PO Box 2345, Beijing 100023, China
www.wjgnet.com
wjg@wjgnet.com

ELSEVIER

World J Gastroenterol 2005;11(41):6407-6408
World Journal of Gastroenterology ISSN 1007-9327

Cycling of antibiotics for the prophylaxis of recurrent spontaneous bacterial peritonitis in a cirrhotic patient

N Assy, S Schlesinger, D Miron, O Hussein

N Assy, S Schlesinger, D Miron, O Hussein, Department of Internal Medicine A, Sieff Government Hospital, Safed, Israel, Technion Institute, Haifa, Israel
Correspondence to: Liver Unit, Sieff Government Hospital, Safed, Israel, Technion Institute, Haifa, Israel. assy.n@ziv.health.gov.il
Received: 2004-11-21 Accepted: 2005-01-01

Assy N, Schlesinger S, Miron D, Hussein O. Cycling of antibiotics for the prophylaxis of recurrent spontaneous bacterial peritonitis in a cirrhotic patient. *World J Gastroenterol* 2005; 11(41): 6407-6408
http://www.wjgnet.com/1007-9327/11/6407.asp

TO THE EDITOR

More than 80% of cirrhotic patients who have been treated successfully for spontaneous bacterial peritonitis (SBP) experience a recurrence[1,2]. Long-term prophylaxis with single daily oral antibiotic has been shown to be cost effective in delaying a recurrence but only for a short time[3]. What has never been tested in this population is the cycling of antibiotics. We report the beneficial use of antibiotic cycling for 36 weeks in a 74-year-old woman with cryptogenic cirrhosis and recurrent SBP.

The patient was admitted because of abdominal pain. Physical examination revealed a malnourished woman with mild jaundice. Blood pressure was 100/60 mmHg, pulse 110 beats /min and temperature 37.4 °C. There was moderate ascites, splenomegaly and multiple signs of chronic liver disease. Plasma levels of urea, creatinine, and electrolytes were within normal limits. Blood platelets were 80 000 per mm³; prothrombin time by international normalized ratio (INR) was1.4; serum albumin, 3.0 g per deciliter; bilirubin, 2.5 mg per deciliter; alanine aminotransferase, 28 U per liter, ascitic protein, 1.0 gr per deciliter and ascitic white blood cells 1500 cell per mm³ with 75% neurophils. Ascitic culture was positive for Escherichia coli bacteria. Blood culture was negative. Abdominal ultrasonography revealed signs of portal hypertension. The patient was on prophylactic therapy with trimethoprim-sulphamethoxazole 160/800 mg daily during the last 3 mo. On admission the patient was treated with intravenous ceftriaxone 1 gr bid for 5 d with good response (ascitic neurophil decreased bellow 200 cell /mm^3). The patient was discharged with a recommendation to be on a prophylactic oral cefuroxime 500 mg qd for 6 wk followed by oral ofloxacin 200 mg qd for 6 wk, followed further by amoxicillin-clavulanic acid 875/125 mg qd for another 6 wk and finally trimethoprim-sulphamethoxazole 160/800 mg for an additional 6 wk (four cycles). The regimen was repeated. Gradually the patient's condition improved, the number of SBP episodes decreased and her ascitic neutrophil count returned to baseline levels (<100 cell/mm^3). Repeated ascitic cultures during follow up of 36 wk was negative for bacteria.

Several strategies have been suggested to prevent or reduce bacterial resistance to antimicrobials, including cycling[4]. This strategy has been studied recently in intensive care units and has resulted in fewer infections and in lower mortality[5]. The basic principle of cycling antibiotics is that a bacterium that becomes resistant (by plasmids, bacteriophages, transposons or integrons) to the first course of treatment would remain susceptible to the second regimen. If it is resistant to the second regimen, the third regimen should cope with the resistance. The selection of antibiotic cycling schedule in this case was arbitrary. Amoxicillin-clavulanic acid eliminates both aerobic and the anaerobic bacteria which could contribute to the development of multi-resistant organism. However, repeated ascites and blood culture were negative for bacteria, so the antibiotic resistance profile and the molecular evidence of bacterial translocation were not performed. Our report suggests the need for a randomized, prospective study of cycling of antibiotic prophylaxis in patients with recurrent SBP. The timing, number and order of cycles directed to prevent selection pressure of bacterial resistance remain to be determined.

REFERENCES

1 **Bleichner G**, Boulanger R, Squara P, Sollet JP, Parent A. Frequency of infections in cirrhotic patients presenting with acute gastrointestinal haemorrhage. *Br J Surg* 1986; **73:** 724-726
2 **Titó L**, Rimola A, Ginès P, Llach J, Arroyo V, Rodés J. Recurrence of spontaneous bacterial peritonitis in cirrhosis: frequency and predictive factors. *Hepatology* 1988; **8:** 27-31
3 **Ginés P**, Rimola A, Planas R, Vargas V, Marco F, Almela M, Forné M, Miranda ML, Llach J, Salmerón JM. Norfloxacin prevents spontaneous bacterial peritonitis recurrence in cirrhosis: results of a double blind, placebo-controlled trial. *Hepatology* 1990; **12: 716-724**
4 **Shlaes DM**, Gerding DN, John JF Jr, Craig WA, Bornstein DL, Duncan RA, Eckman MR, Farrer WE, Greene WH, Lorian

V, Levy S, McGowan JE Jr, Paul SM, Ruskin J, Tenover FC, Watanakunakorn C. Society for Healthcare Epidemiology of America and Infectious Diseases Society of America Joint Committee on the Prevention of Antimicrobial Resistance: guidelines for the prevention of antimicrobial resistance in hospitals. *Infect Control Hosp Epidemiol* 1997; **18: 275-291**

5 **Raymond DP,** Pelletier SJ, Crabtree TD, Gleason TG, Hamm LL, Pruett TL, Sawyer RG. Impact of a rotating empiric antibiotic schedule on infectious mortality in an intensive care unit. *Crit Care Med* 2001; **29: 1101-1108**

Science Editor Li WZ **Language Editor** ELsevier HK

PO Box 2345, Beijing 100023, China
www.wjgnet.com
wjg@wjgnet.com

ELSEVIER

World J Gastroenterol 2005;11(41):6409
World Journal of Gastroenterology ISSN 1007-9327

• *LETTERS TO THE EDITOR* •

Is there an association of microscopic colitis and irritable bowel syndrome-A subgroup analysis of placebo-controlled trials

Ahmed Madisch, Birgit Bethke, Manfred Stolte, Stephan Miehlke

Ahmed Madisch, Stephan Miehlke, Medical Department I, Technical University Hospital Dresden;
Birgit Bethke, Manfred Stolte, Institute for Pathology, Klinikum Bayreuth, Bayreuth, Germany
Correspondence to: Ahmed Madisch, MD, Medical Department I, Technical University Hospital, Fetscherstr. 74, 01307 Dresden, Germany. ahmed.madisch@uniklinikum-dresden.de
Telephone: +49-351-458-4780 Fax: +49-351-458-4394
Received: 2005-06-27 Accepted: 2005-07-14

Key words: Microscopic colitis; Collagenous colitis; Lymphocytic colitis; Irritable bowel syndrome

Madisch A, Bethke B, Stolte M, Miehlke S. Is there an association of microscopic colitis and irritable bowel syndrome-A subgroup analysis of placebo-controlled trials. *World J Gastroenterol* 2005; 11(41): 6409
http://www.wjgnet.com/1007-9327/11/6409.asp

TO THE EDITOR

With great interest we read the recent retrospectice study by Barta *et al* (1) dealing with the clinical presentation of patients with microscopic colitis. They investigated in a cohort of 53 patients with microscopic colitis (46 with collagenous colitis, 7 with lymphocytic colitis) the relationship between microscopic colitis and both constipation and diarrhea. One of their mean finding was that abdominal pain, diarrhea and constipation was a common symptom complex of patients with microscopic colitis, thus the face of microcopic colitis resembles the subgroups of irritable bowel syndrome (IBS).

Irritable bowel syndrome is highly prevalent disorder. Consensus diagnostic criteria (Rome II) based on symptoms have been established to aid the diagnosis of IBS. Microscopic colitis, encompassing collagenous and lymphocytic colitis, is diagnosed by histologic criteria. Since symptoms of microscopic colitis and both diarrhea predominant irritable bowel syndrome or functional diarrhea are similar, a considerable number of patients with micoscopic colitis may be misdiagnosed as IBS or functional diarrhea or a disease overlap could be present in a subgroup of patients.

We would like to confirm the data by Barta *et al*[1] presenting a subgroup analysis of placebo-controlled trials, in which we evaluate the possible symptom overlap between microscopic colitis and IBS. We aimed to assess the proportion of patients with histologically confirmed microscopic colitis who fulfill the Rom-II-criteria for IBS and functional diarrhea[2] .

We selected a large patient cohort with histologically confirmed symptomatic microscopic colitis, who participated in placebo-controlled trials of our group. Baseline gastrointestinal symptoms were assessed by standardized questionnaires and ascertained consistent with Rome-II-criteria (chronic abdominal pain and/or stool abnormalities for at least 12 wk in the preceding 12 mo, no alarm symptoms such as weight loss, no findings in the routine procedures including colonoscopy).

Eighty-two cases of microscopic colitis (74 collagenous, 8 lymphocytic) were included in this analysis. The mean age was 57 years (30-80). Seventy-three % were women. The mean stool frequency per day was 6 (range 3-15). The duration of symptoms prior to histological diagnosis of microscopic colitis ranged between 1 and 156 mo with a mean of 28 mo. Forty-seven patients (57.3%) had concomitant abdominal pain.

Twenty-three patients (28.1%) met the Rome-II-criteria for diarrhea-predominant IBS. Six patients (7.3%) fulfilled the criteria for functional diarrhea. If the criteria for duration of symptoms were excluded from our analysis, the corresponding rates were 65% and 13.4%, respectively These data clearly demonstrate that a considerable group of patients with microscopic colitis have diarrhea-predominant IBS- or functional diarrhea-like symptoms. Thus, patients with microscopic colitis could be misdiagnosed as IBS or functional diarrhea. Additionally, because of the high frequency of IBS, a disease overlap could be present in a subgroup of patients as it was shown between IBS and celiac disease[3]. We conclude that the clinical symptom-based criteria of IBS are not specific enough to rule out the diagnosis of microscopic colitis. Therefore, patients with diarrhea-predominance of IBS-like symptoms should undergo matrix biopsies from the entire colon to investigate for possible microscopic colitis especially biopsies from the right colon are of importance because the left colon sometimes is less involved.

REFERENCES

1 **Barta Z,** Mekkel G, Csípo I, Tóth L, Szakáll S, Szabó GG, Bakó G, Szegedi G, Zeher M. Microscopic colitis: a retrospective study of clinical presentation in 53 patients. *World J Gastroenterol* 2005; **11:** 1351-1355
2 **Thompson WG**, Longstreth GF, Drossman DA, Heaton KW, Irvine EJ, Müller-Lissner SA. Functional bowel disorders and functional abdominal pain. *Gut* 1999; **45** Suppl 2: II43-II47
3 **Wahnschaffe U**, Ullrich R, Riecken EO, Schulzke JD. Celiac disease-like abnormalities in a subgroup of patients with irritable bowel syndrome. *Gastroenterology* 2001; **121**: 1329-1338

Science Editor Guo SY **Language Editor** Elsevier HK

PO Box 2345, Beijing 100023, China
www.wjgnet.com
wjg@wjgnet.com

ELSEVIER

World J Gastroenterol 2005;11(41):6410-6415
World Journal of Gastroenterology ISSN 1007-9327

Distribution of HBV genotypes among HBV carriers in Benin: phylogenetic analysis and virological characteristics of HBV genotype E

Kei Fujiwara, Yasuhito Tanaka, Etsuro Orito, Tomoyoshi Ohno, Takanobu Kato, Kanji Sugihara, Izumi Hasegawa, Mayumi Sakurai, Kiyoaki Ito, Atsushi Ozasa, Yuko Sakamoto, Isao Arita, Ahmed El-Gohary, Agossou Benoit, Sophie I Ogoundele-Akplogan, Namiko Yoshihara, Ryuzo Ueda, Masashi Mizokami

Kei Fujiwara, Etsuro Orito, Tomoyoshi Ohno, Kanji Sugihara, Izumi Hasegawa, Mayumi Sakurai, Kiyoaki Ito, Atsushi Ozasa, Ryuzo Ueda, Department of Internal Medicine and Molecular Science, Nagoya City University Graduate School of Medical Sciences, Nagoya, Japan
Yasuhito Tanaka, Takanobu Kato, Masashi Mizokami, Department of Clinical Molecular Informative Medicine, Nagoya City University Graduate School of Medical Sciences, Nagoya, Japan
Yuko Sakamoto, Namiko Yoshihara, AIDS Research Center, National Institute of Infectious Disease, Tokyo, Japan
Isao Arita, Agency for Cooperation in International Health, Kumamoto, Japan
Ahmed El-Gohary, Clinical Pathology Department, Faculty of Medicine, Suez Canal University, Ismailia, Egypt
Agossou Benoit, Central National Blood Transfusion Center, Cotonou, Benin
Sophie I Ogoundele-Akplogan, Hematology Lab-CNHUC, Cotonou, Benin
Correspondence to: Dr Masashi Mizokami, Department of Clinical Molecular Informative Medicine, Nagoya City University Graduate School of Medical Sciences, 1 Kawasumi, Mizuho, Nagoya 467-8601, Japan. mizokami@med.nagoya-cu.ac.jp
Telephone: +81-52-853-8292 Fax: +81-52-842-0021
Received: 2005-02-15 Accepted: 2005-03-23

Abstract

AIM: To determine the distribution of Hepatitis B virus (HBV) genotypes in Benin, and to clarify the virological characteristics of the dominant genotype.

METHODS: Among 500 blood donors in Benin, 21 HBsAg-positive donors were enrolled in the study. HBV genotypes were determined by enzyme immunoassay and restriction fragment length polymorphism. Complete genome sequences were determined by PCR and direct sequencing.

RESULTS: HBV genotype E (HBV/E) was detected in 20/21 (95.2%), and HBV/A in 1/21 (4.8%). From the age-specific prevalence of HBeAg to anti-HBe seroconversion (SC) in 19 HBV/E subjects, SC was estimated to occur frequently in late teens in HBV/E. The comparison of four complete HBV/E genomes from HBeAg-positive subjects in this study and five HBV/E sequences recruited from the database revealed that HBV/E was distributed throughout West Africa with very low genetic diversity (nucleotide homology 96.7-99.2%). Based on the sequences in the basic core promoter (BCP) to precore region of the nine HBV/E isolates compared to those of the other genotypes, a nucleotide substitution in the BCP, G1757A, was observed in HBV/E.

CONCLUSION: HBV/E is predominant in the Republic of Benin, and SC is estimated to occur in late teens in HBV/E. The specific nucleotide substitution G1757A in BCP, which might influence the virological characteristics, is observed in HBV/E.

Key words: HBV genotype; West Africa; Basic core promoter

Fujiwara K, Tanaka Y, Orito E, Ohno T, Kato T, Sugihara K, Hasegawa I, Sakurai M, Ito K, Ozasa A, Sakamoto Y, Arita I, El-Gohary A, Benoit A, Ogoundele-Akplogan SI, Yoshihara N, Ueda R, Mizokami M. Distribution of HBV genotypes among HBV carriers in Benin: Phylogenetic analysis and virological characteristic of HBV genotype E. *World J Gastroenterol* 2005; 11(41):6410-6415
http://www.wjgnet.com/1007-9327/11/6410.asp

INTRODUCTION

Hepatitis B virus(HBV) is a member of the family *Hepadnaviridae*. This virus is a small DNA virus with a partially double-stranded 3.2-kb genome. HBV has been classified into seven genotypes based on the sequence divergence over the entire genome exceeding 8%[1,2]. The seven genotypes show a distinctive geographical distribution. HBV genotype A (HBV/A) is prevalent in Northwestern Europe, North America, and Africa[3]. HBV/B and HBV/C are characteristics of Asia. HBV/D is predominant in the Mediterranean area, HBV/E in West Africa, and HBV/F in South America.

Recently, virological and clinical differences in genotypes have been reported[4,5]. In addition, subtypes of HBV/B, HBV/Ba, 'a' indicating Asia, and HBV/Bj, 'j' indicating Japan, have been reported[6]. The former has

recombination with HBV/C, but the latter does not, and clinical differences have been shown between them[7]. Furthermore, HBV/A is phylogenetically classified into subtypes, namely HBV/Aa, 'a' indicating Asia/Africa, which is distributed in Asia and Africa, and HBV/Ae, 'e' indicating Europe, which is distributed in Europe[8].

It is now recognized that mutations in basic core promoter (BCP) and precore region regulate hepatitis B e antigen (HBeAg) expression. It was shown in an *in vitro* study that the double mutations in BCP, A1762T and G1764A, downregulate precore mRNA and slightly increase the efficiency of pregenome mRNA and core mRNA[9]. Additionally, the mechanism of HBeAg reduction through subtype-specific nucleotide substitutions just prior to the start of the precore open reading frame (ORF), known as "Kozak sequence" in the African subtype of HBV/A, has been shown in an *in vitro* study[10].

In Africa, the distribution of HBV genotypes is HBV/A in the South, HBV/D in the North, and HBV/E in the West. For HBV/E, only four human HBV/E full genomes have been reported so far, and the virological and clinical characteristics have not yet been sufficiently clarified.

In this study, the distribution of HBV genotypes in the Republic of Benin was investigated for the first time, and the virological and clinical characteristics of the dominant genotype were analyzed.

MATERIALS AND METHODS

Patients

Five hundred blood donors, who visited the National Blood Transfusion Center in the Republic of Benin in 2002, were screened for hepatitis B surface antigen (HBsAg). Twenty-four were positive for HBsAg (4.8%). Sera from 21 donors were available in this study (17 males, 3 females, unknown in 1; mean age, 23.1±6.7 years). All the donors were negative for the antibody to HIV-1 (anti-HIV) and the antibody to human adult leukemia virus 1 (anti-HTLV-1). The antibody to hepatitis C virus (anti-HCV) was positive in one donor. Informed consent was obtained from each patient.

Serological testing

HBsAg, anti-HCV, and anti-HTLV-1 were tested by counting immunoassay (PAMIA, Sysmex, Kobe, Japan). HBeAg and the antibody to HBeAg (anti-HBe) were determined using a commercially available chemiluminescent enzyme immunoassay (EIA, Lumipulse f, Fujirebio Inc., Tokyo, Japan). Aspartate aminotransferase (AST), alanine aminotransferase (ALT), and total bilirubin (T-Bil) were measured in all the samples.

Genotyping

The HBV genotypes were determined in the sera using an EIA with pre-S2 specific mAb[12,13]. When the result of the EIA method was indeterminate, HBV genotypes were detected by restriction fragment length polymorphism, as previously described[14].

PCR amplification and sequencing of HBV

The serum samples were stored at -80 °C until use. Total DNA was extracted from 100 μL of serum using microspin columns (QIAamp Blood kit, Qiagen KK, Tokyo, Japan). Purified DNA was resuspended in 80 μL of distilled water. PCR was carried out by the same protocol as described previously[15]. Nucleotide sequences of the amplified products were determined directly by the dideoxy method, using the ABI Prism BigDye Terminator Cycle Sequencing Ready Reaction kit with a fluorescent 3100 DNA Sequencer (Applied Biosystems, Foster City, CA, USA).

Real-time detection polymerase chain reaction (RTD-PCR)

serum HBV DNA was quantitatively detected by RTD-PCR based on Taqman chemistry as reported previously[16]. Amplification was performed using primers corresponding to conserved sequences of the surface region. A 10-μL aliquot of DNA solution was used for RTD-PCR. A portion of the HBV surface region was amplified using primers: a forward primer HBSF2 (5'-CTTCATCCTGCTGCTATGCCT-3', nucleotide position (nt) 406-426) and a reverse primer HBSR2 (5'-AAAGCCCAGGATGGGAT-3', nt 646-627). A taqman probe was designed as HBSP2 (5'-ATGTTGCCCTTTGTCCTCCTCTAATTCCAG-3', nt 461-488), with an additional G at the 3'-end of HBSP2 in the original method, the detection limit of this system was as low as five DNA copies/assay, and linear standard curve was obtained from 5 to 10^6 DNA copies/assay.

Phylogenetic analysis

Complete sequences of 21 HBV isolates were aligned with the CLUSTAL W software program[17], and the alignment was confirmed by visual inspection. Genetic distances were estimated by the six-parameter method, and phylogenetic trees were constructed by the neighbor-joining method using ODEN program of the National Institutes of Genetics (Mishima, Japan)[18]. To confirm the reliability of the phylogenetic trees, bootstrap resampling tests were performed 1 000 times.

RESULTS

HBV genotypes

Distribution of HBV genotypes among 21 HBV carriers in the Republic of Benin was 20/21 (95.2%) for HBV/E, and 1/21 (4.8%) for HBV/A. HBV/B, C, D, F, and G were not found. HBV/E was the predominant genotype in the Republic of Benin.

Clinical characteristics of asymptomatic HBV carriers in the Republic of Benin

HBeAg was positive for 4/21 (19.0%) subjects, and anti-HBe was positive for 17/21 (81.0%) subjects. The titers of four HBeAg-positive subjects were beyond the upper detection limit. In order to clarify the clinical characteristics of asymptomatic HBV carriers in this country, the clinical and laboratory data between HBeAg-positive patients

Table 1 Comparison of clinical characteristics between HBeAg-positive and anti-HBe-positive subjects

	HBeAg-positive (n = 4)	Anti-HBe-positive (n = 17)	P
Age (yr)	21.25±2.21	23.5±7.42[1]	NS[2]
Sex (M/F)	2/2	1/15[1]	NS[3]
Genotype (A/E)	0/4	1/16	NS[3]
AST (IU/L)	25.8±8.3	18.0±5.4	NS[2]
ALT (IU/L)	11.5±10.3	5.7±1.5	NS[2]
T-Bil (mg/dL)	0.50±0.35	0.57±0.41	NS[2]
HBV DNA (log (copies/mL)	7.76±0.29	<2.6	<0.0005[2]

[1]Sex and age unknown in one subject. [2]P values were calculated by Welch's t-test. [3]P values were calculated by Fisher's exact test. AST, aspartate aminotransferase; ALT, alanine aminotransferase; T-Bil, total bilirubin.

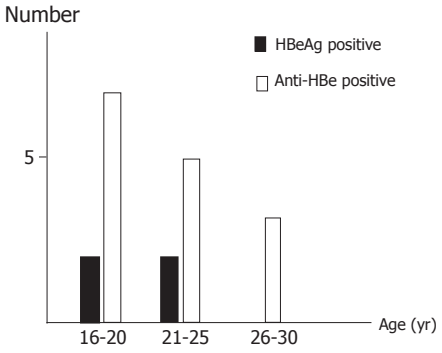

Figure 1 Age-specific prevalence of HBeAg/anti-HBe status in 19 HBV genotype E strains.

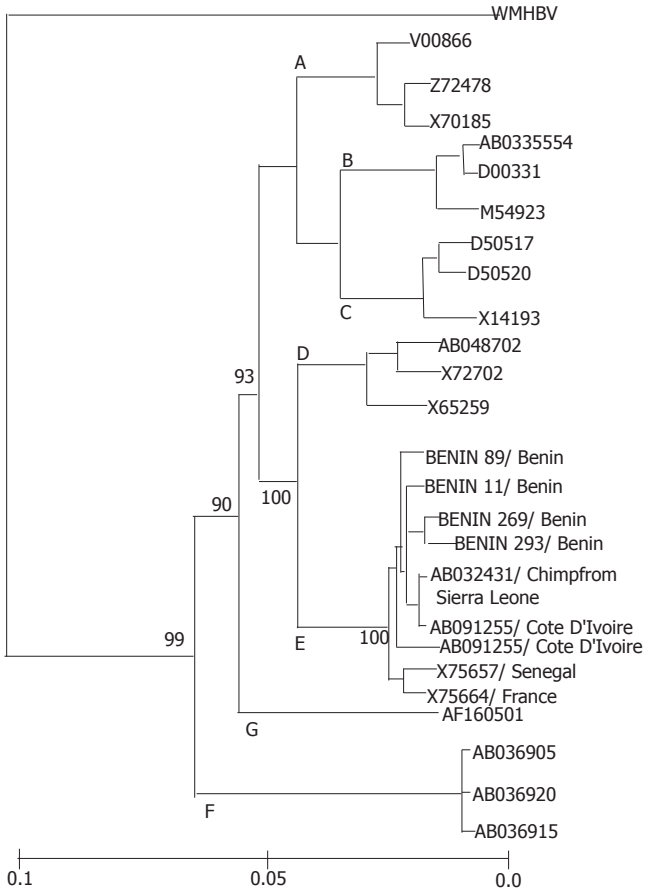

Figure 2 Phylogenetic tree constructed on complete nucleotide sequences of 26 HBV isolates. The nine HBV genotype E isolates were compared along with 16 HBV isolates representative of the other six genotypes **(A–D,** F and **G**), along with woolly monkey hepatitis virus (WMHBV) as an outgroup. The four HBV genotype E isolates determined in this study are indicated in boldface, and the other 22 HBV isolates are specified by accession numbers. The country of origin is indicated after the slash for each HBV isolate of genotype **E.**

and anti-HBe-positive patients were compared (Table 1). The mean age of the HBeAg-positive group was not lower than that of the anti-HBe-positive group. As a matter of course, the difference in the mean HBV DNA titer between the two groups was statistically significant (P<0.0005). HBV DNA titers in anti-HBe-positive subjects were quite low. To examine the correlation between age and HBeAg/anti-HBe status in detail, the age-specific prevalence of the HBeAg/anti-HBe status in 19 HBV/E subjects was analyzed. Seroconversion (SC) during the late teens occurred in 7 of 19 subjects (36.8%, Figure 1). This was the reason why the comparison of age between the two groups was not statistically significant.

Phylogenetic analysis of four strains

HBV full genomes of four HBeAg-positive patients were determined to have a nucleotide length of 3 212 bp. Phylogenetic analysis of the complete genome sequences of these four strains compared to those of 22 HBV strains from the DDBJ/GenBank/EMBL database showed that four strains clustered with five other HBV/E strains (accession numbers: X75657, X75664[2]; and AB032431[19]; AB091255, AB091256[11]) (Figure 2). The nucleotide homology within the HBV/E cluster ranged from 96.7% to 99.2%. In addition, the phylogenetic analysis of four ORFs showed no recombination of HBV/E strains in the Republic of Benin (Figure 3). Genetic diversity among HBV/E strains was very low compared to the other genotypes, excluding HBV/G. The nucleotide sequence data reported in this article will appear in the DDBJ/GenBank/EMBL nucleotide sequence databases with the accession numbers AB201287-90.

Characteristics of nucleotide substitutions in BCP and precore region

In order to find out the HBV/E-specific nucleotide substitution associated with HBe protein production, the BCP to the precore region of nine HBV/E strains and the strains of six genotypes were compared (Figure 4). The representative nucleotide sequences of HBV/A (Aa-Ae), B, C, D, F, and G were determined by aligning five sequences of each genotype, and the consensus nucleotide was deduced, if the identical nucleotide was detected in 60% or more of the sequences. In the BCP, the nucleotide substitution at A1757 was observed in all the strains of HBV/E. This substitution was not found in HBV/A-C, HBV/F, and HBV/G, but was found in more than half of HBV/D[20]. BCP double mutation (T1762/A1764) was not found in the HBV/E strains; however, T1772C substitution was found in all the HBV/E strains as well

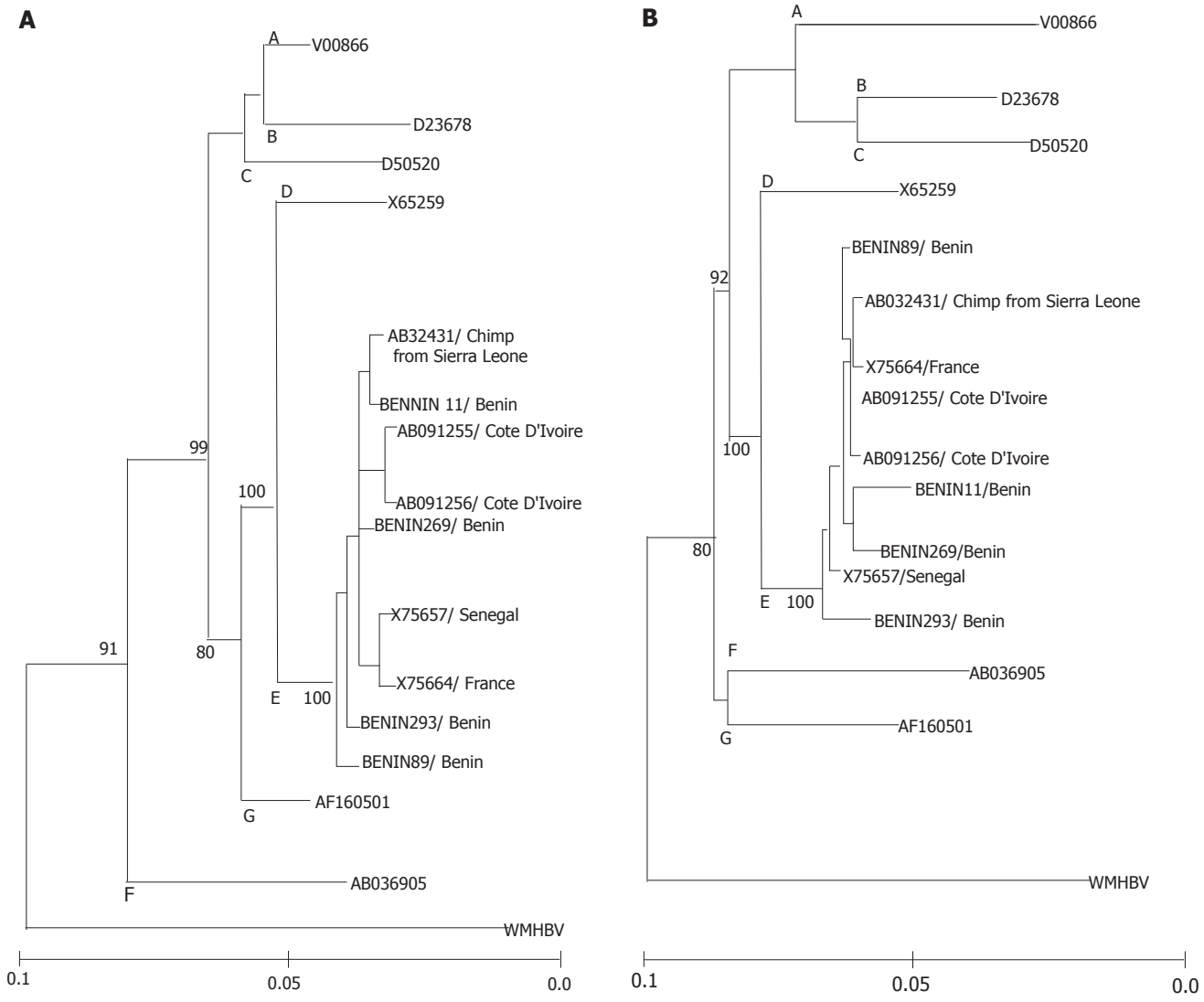

Figure 3 Phylogenetic trees representing the large S gene (**A**), and precore region plus core gene (**B**) along with the strains of the other six genotypes and WMHBV.

as in HBV/B, C and F. Other sequences in the BCP were conserved irrespective of genotypes, except for the above mutations. One HBV/E isolate had T1809 substitution prior to the start of precore ORF, which is recognized as the Kozak sequence frequently found in HBV/Aa. Precore stop mutation (A1896) was not found in the HBV/E.

DISCUSSION

In this study, the distribution of HBV genotypes among blood donors in the Republic of Benin was analyzed for the first time. In Africa, HBV/D is dominant in the Northern region[21], with HBV/A found in South Africa. HBV/E is the major genotype in the Republic of Benin. This agrees with previous reports that HBV/E is prevalent mainly in West Africa[2,11,22]. In addition, the distribution of HBV/E is restricted to West Africa, unlike other genotypes. Though slaves have migrated from West Africa to North America, HBV/E is not found in USA, suggesting that genotype E emerged from the mid to late 19th century[22,23].

East Asia and Sub-Saharan Africa are the two most HBV endemic areas; however, clinical differences have been shown between the two areas. Vertical transmission is the main route in Asia, whereas horizontal transmission is the main route in Africa, and SC occurs much earlier in Africa than in Asia[24,25]. It is important to examine the clinical characteristics of asymptomatic HBV carriers in Benin, which reflect the characteristics of HBV/E, because there are only a few reports concerning the clinical characteristics of HBV/E. As shown in Figure 1, SC is thought to occur at a young age in subjects with HBV/E in Benin. These data might explain one of the reasons why vertical transmission does not occur in West Africa. Recently, the difference in SC between HBV/B and HBV/C in Taiwan was reported[5]. SC occurs a decade earlier in HBV/B patients[26,27] and the mean SC age in HBV/B is approximately 30 years. In comparison with HBV/B, the mean SC age in HBV/E occurs even earlier. These data lead us to speculate that HBV/E has a better prognosis than other genotypes in terms of chronic liver disease.

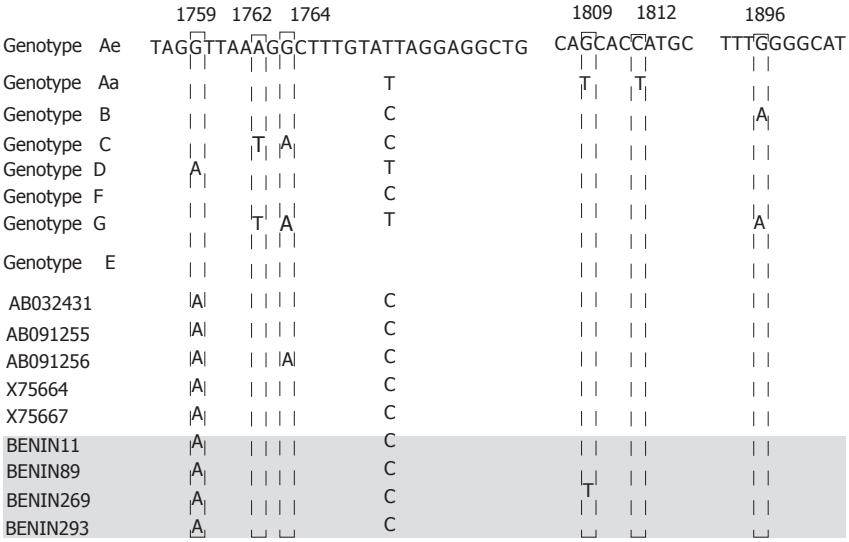

Figure 4 Nucleotide sequences constituting parts of the BCP to the precore of nine HBV genotype E isolates with the consensus sequences of the other six genotypes. The four Benin isolates determined in this study are shaded in gray.

Regarding hepatocellular carcinoma (HCC), a report from Gambia, where HBV/E is the most prevalent, revealed that chronic HBV infection is associated with HCC development at a younger age[28]. Infection with HBV/B is associated with HCC development at a young age in Taiwan[5]. In this sense, HBV/E in West Africa is clinically more similar to HBV/B than HBV/C, and virologically, HBV/E and HBV/B have a high frequency of a precore mutation, G1896A, in common[11,29]. Further information about the clinical characteristics of HBV genotypes might reveal the reason why the age of SC and the age-related HCC incidence differ among genotypes.

So far, only five complete genomes of HBV/E (one from a chimpanzee) have been reported. By adding the four complete genomes reported here, phylogenetic analyses of the full genome and ORFs show much more clearly that HBV/E has a low genetic diversity, as previously reported[11,22,23]. Although subtypes of HBV/B, which have recombination in the BCP to the core region[7] and subtypes of HBV/A[8,30] have been reported, the analysis of nine HBV/E genomes shows neither the possibility of subtypes nor the possibility of recombination.

As mentioned above, HBV/A is divided into two subtypes: HBV/Aa, 'Aa' indicates Asia and Africa, and HBV/Ae, 'Ae' indicates Europe[8,30]. Subtype HBV/Aa has subtype-specific substitutions just before precore start codons, known as the "Kozak sequence". Substitutions reduce the HBeAg expression[10,31]. Hence, genotype- and subtype-specific nucleotide substitutions in the BCP region are crucial, not only in viral replication but also in HBe SC. In this study, we identified the mutation in the BCP, $A^{1757,}$ in HBV/E. Other genotypes have G^{1757} except for HBV/D, in which A^{1757} is observed in about 70%[20]. BCP has been identified as a sequence that regulates both precore and pregenomic messages[32]. The core promoter A1762T and G1764A double mutation is known to downregulate precore mRNA but does not seriously affect pregenome mRNA[33]. The double mutation (1762/1764) occurs over time, as the viral load and HBeAg/anti-HBe status change, and the sequences around the double mutations are conserved irrespective of the genotype so far. However, HBV/E seems to possess 1757A from the early stage of the infection, similar to Kozak sequence substitutions in genotype Aa. Thus, the different functions in relation to nuclear receptor binding between 1757G and 1757A was shown in an *in vitro* study, when the mechanism of suppression of HBV precore RNA transcription by core promoter double mutation was sought. The double mutation in 1762 and 1764 changes the nucleotide sequences of the nuclear-factor binding site of BCP. When the mutation occurs, the nuclear factor known as COUP TF I cannot bind to BCP. Instead, a different nuclear factor, HNF1, binds, and this alters the efficiency of precore and core mRNA transcription. The artificial mutation was created with the intention to create a sequence that neither COUP TF I nor HNF-1 can bind. This mutation is G1757A, and the mutation abolishes both the nuclear factors (COUP TFI and HNF1) binding to BCP in the *in vitro* experiment[34]. This unique mutation and its alteration of nuclear factor binding capacity to the BCP region might influence the clinical characteristics of HBV/E. Further studies, including *in vitro* studies, are expected.

REFERENCES

1 **Okamoto H,** Tsuda F, Sakugawa H, Sastrosoewignjo RI, Imai M, Miyakawa Y, Mayumi M. Typing hepatitis B virus by homology in nucleotide sequence: comparison of surface antigen subtypes. *J Gen Virol* 1988; **69 (**pt 10)**:** 2575-2583

2 **Norder H,** Couroucé AM, Magnius LO. Complete genomes, phylogenetic relatedness, and structural proteins of six strains of the hepatitis B virus, four of which represent two new genotypes. *Virology* 1994; **198:** 489-503

3 **Norder H,** Couroucé AM, Magnius LO. Complete nucleotide sequences of six hepatitis B viral genomes encoding the surface antigen subtypes ayw4, adw4q-, and adrq- and their phylogenetic classification. *Arch Virol Suppl* 1993; **8:** 189-199.

4 **Orito E,** Ichida T, Sakugawa H, Sata M, Horiike N, Hino K,Okita K, Okanoue T, Iino S, Tanaka E, Suzuki K, Watanabe H, Hige S, Mizokami M. Geographic distribution of hepatitis B virus(HBV) genotype in patients with chronic HBV infection in Japan. *Hepatology* 2001; **34:** 590-594

5 **Kao JH,** Chen PJ, Lai MY, Chen DS. Hepatitis B genotypes correlate with clinical outcomes in patients with chronic hepatitis B. *Gastroenterology* 2000; **118:** 554-559

6 **Sugauchi F,** Orito E, Ichida T, Kato H, Sakugawa H, Kakumu S, Ishida T, Chutaputti A, Lai CL, Ueda R, Miyakawa Y, Mizokami M. Hepatitis B virus of genotype B with or without recombination with genotype C over the precore region plus the core gene. *J Virol* 2002; **76:** 5985-5992

7 **Sugauchi F,** Orito E, Ichida T, Kato H, Sakugawa H, Kakumu S, Ishida T, Chutaputti A, Lai CL, Gish RG, Ueda R, Miyakawa Y, Mizokami M. Epidemiologic and virologic characteristics of hepatitis B virus genotype B having the recombination with genotype C. *Gastroenterology* 2003; **124:** 925-932

8 **Sugauchi F,** Kumada H, Acharya SA, Shrestha SM, Gamutan MT, Khan M, Gish RG, Tanaka Y, Kato T, Orito E, Ueda R, Miyakawa Y, Mizokami M. Epidemiological and sequence differences between two subtypes (Ae and Aa) of hepatitis B virus genotype A. *J Gen Virol* 2004; **85:** 811-820.

9 **Buckwold VE**, Xu Z, Chen M, Yen TS, Ou JH. Effects of a naturally occurring mutation in the hepatitis B virus basal core promoter on precore gene expression and viral replication. *J Virol* 1996; **70:** 5845-585

10 **Ahn SH,** Kramvis A, Kawai S, Spangenberg H, Li J, Kimbi G, Kew MC, Wands J, Tong S. Sequence variation upstream of precore translation initiation codon reduces hepatitis B virus e antigen production. *Gastroenterology* 2003; **125:** 1370-1378

11 **Suzuki S,** Sugauchi F, Orito E, Kato H, Usuda S, Siransy L, Arita I, Sakamoto Y, Yoshihara N, El-Gohary A, Ueda R, Mizokami M. Distribution of hepatitis B virus (HBV) genotypes among HBV carriers in the Cote d'Ivoire: complete genome sequence and phylogenetic relatedness of HBV genotype E. *J Med Virol* 2003; **69:** 459-465

12 **Usuda S,** Okamoto H, Iwanari H, Baba K, Tsuda F, Miyakawa Y, Mayumi M. Serological detection of hepatitis B virus genotypes by ELISA with monoclonal antibodies to type-specific epitopes in the preS2-region product. *J Virol Methods* 1999; **80:** 97-112

13 **Usuda S,** Okamoto H, Tanaka T, Kidd-Ljunggren K, Holland PV, Miyakawa Y, Mayumi M. Differentiation of hepatitis B virus genotypes D and E by ELISA using monoclonal antibodies to epitopes on the preS2-region product. *J Virol Methods* 2000; **87:** 81-89

14 **Mizokami M,** Nakano T, Orito E, Tanaka Y, Sakugawa H, Mukaide M, Robertson BH. Hepatitis B virus genotype assignment using restriction fragment length polymorphism patterns. *FEBS Lett* 1999; **450:** 66-71

15 **Sugauchi F,** Mizokami M, Orito E, Ohno T, Kato H, Suzuki S, Kimura Y, Ueda R, Butterworth LA, Cooksley WG. A novel variant genotype C of hepatitis B virus identified in isolates from Australian Aborigines: complete genome sequence and phylogenetic relatedness. *J Gen Virol* 2001; **82:** 883-892

16 **Abe A,** Inoue K, Tanaka T, Kato J, Kajiyama N, Kawaguchi R, Tanaka S, Yoshiba M, Kohara M. Quantitation of hepatitis B virus genomic DNA by real-time detection PCR. *J Clin Microbiol* 1999; **37:** 2899-2903

17 **Thompson JD,** Higgins DG, Gibson TJ. CLUSTAL W: improving the sensitivity of progressive multiple sequence alignment through sequence weighting, position-specific gap penalties and weight matrix choice. *Nucleic Acids Res* 1994; **22:** 4673-4680

18 **Ina Y.** ODEN: a program package for molecular evolutionary analysis and database search of DNA and amino acid sequences. *Comput Appl Biosci* 1994; **10:** 11-12

19 **Takahashi K,** Brotman B, Usuda S, Mishiro S, Prince AM. Full-genome sequence analyses of hepatitis B virus (HBV) strains recovered from chimpanzees infected in the wild: implications for an origin of HBV. *Virology* 2000; **267:** 58-64

20 **Kidd-Ljunggren K,** Oberg M, Kidd AH. Hepatitis B virus X gene 1751 to 1764 mutations: implications for HBeAg status and disease. J Gen Virol 1997; **78** (Pt 6): 1469-78

21 **Saudy N,** Sugauchi F, Tanaka Y, Suzuki S, Aal AA, Zaid MA, Agha S, Mizokami M. Genotypes and phylogenetic characterization of hepatitis B and delta viruses in Egypt. *J Med Virol* 2003; **70:** 529-536

22 **Odemuyiwa SO,** Mulders MN, Oyedele OI, Ola SO, Odaibo GN, Olaleye DO, Muller CP. Phylogenetic analysis of new hepatitis B virus isolates from Nigeria supports endemicity of genotype E in West Africa. *J Med Virol* 2001; **65:** 463-469

23 **Mulders MN,** Venard V, Njayou M, Edorh AP, Bola Oyefolu AO, Kehinde MO, Muyembe Tamfum JJ, Nebie YK, Maiga I, Ammerlaan W, Fack F, Omilabu SA, Le Faou A, Muller CP. Low genetic diversity despite hyperendemicity of hepatitis B virus genotype E throughout West Africa. *J Infect Dis* 2004; **190:** 400-408

24 **Stevens CE,** Beasley RP, Tsui J, Lee WC. Vertical transmission of hepatitis B antigen in Taiwan. *N Engl J Med* 1975; **292:** 771-774

25 **Botha JF,** Ritchie MJ, Dusheiko GM, Mouton HW, Kew MC. Hepatitis B virus carrier state in black children in Ovamboland: role of perinatal and horizontal infection. *Lancet* 1984; **1:** 1210-1212

26 **Chu CJ,** Hussain M, Lok AS. Hepatitis B virus genotype B is associated with earlier HBeAg seroconversion compared with hepatitis B virus genotype C. *Gastroenterology* 2002; **122:** 1756-1762

27 **Kao JH,** Chen PJ, Lai MY, Chen DS. Hepatitis B virus genotypes and spontaneous hepatitis B e antigen seroconversion in Taiwanese hepatitis B carriers. *J Med Virol* 2004; **72:** 363-369.

28 **Kirk GD, Lesi OA,** Mendy M, Akano AO, Sam O, Goedert JJ, Hainaut P, Hall AJ, Whittle H, Montesano R. The Gambia Liver Cancer Study: Infection with hepatitis B and C and the risk of hepatocellular carcinoma in West Africa. *Hepatology* 2004; **39:** 211-219

29 **Orito E,** Mizokami M, Sakugawa H, Michitaka K, Ishikawa K, Ichida T, Okanoue T, Yotsuyanagi H, Iino S. A case-control study for clinical and molecular biological differences between hepatitis B viruses of genotypes B and C. Japan HBV Genotype Research Group. *Hepatology* 2001; **33:** 218-223

30 **Hasegawa I,** Tanaka Y, Kramvis A, Kato T, Sugauchi F, Acharya SK, Orito E, Ueda R, Kew MC, Mizokami M. Novel hepatitis B virus genotype a subtyping assay that distinguishes subtype Aa from Ae and its application in epidemiological studies. *J Virol* 2004; **78:** 7575-7581

31 **Tanaka Y,** Hasegawa I, Kato T, Orito E, Hirashima N, Acharya SK, Gish RG, Kramvis A, Kew MC, Yoshihara N, Shrestha SM, Khan M, Miyakawa Y, Mizokami M. A case-control study for differences among hepatitis B virus infections of genotypes A (subtypes Aa and Ae) and D. *Hepatology* 2004; **40:** 747-755

32 **Yuh CH,** Chang YL, Ting LP. Transcriptional regulation of precore and pregenomic RNAs of hepatitis B virus. *J Virol* 1992; **66:** 4073-4084

33 **Okamoto H,** Tsuda F, Akahane Y, Sugai Y, Yoshiba M, Moriyama K, Tanaka T, Miyakawa Y, Mayumi M. Hepatitis B virus with mutations in the core promoter for an e antigen-negative phenotype in carriers with antibody to e antigen. *J Virol* 1994; **68:** 8102-8110

34 **Li J,** Buckwold VE, Hon MW, Ou JH. Mechanism of suppression of hepatitis B virus precore RNA transcription by a frequent double mutation. *J Virol* 1999; **73:** 1239-1244

Science Editor Wang XL and Guo SY **Language Editor** Elsevier HK

PO Box 2345, Beijing 100023, China
www.wjgnet.com
wjg@wjgnet.com

ELSEVIER

World J Gastroenterol 2005;11(41):6416-6421
World Journal of Gastroenterology ISSN 1007-9327

Integration of hepatitis B virus DNA into chromosomal DNA during acute hepatitis B

Gerald C Kimbi, Anna Kramvis, Michael C Kew

Gerald C Kimbi, Anna Kramvis, Michael C Kew, MRC/University Molecular Hepatology Research Unit, Department of Medicine, University of the Witwatersrand, Parktown 2193, Johannesburg, South Africa
Supported by grants from the Poliomyelitis Research Foundation of South African and the HE Griffin Cancer Trust
Correspondence to: Professor, MC Kew, Department of Medicine, University of the Witwatersrand Medical School, 7 York Road, Parktown 2193, Johannesburg,
South Africa. kewmc@medicine.wits.ac.za
Telephone: +27-11-488-3628 Fax: +27-11-643-4318
Received: 2004-08-26 Accepted: 2004-10-06

Abstract

AIM: To examine the serum from black African patients with acute hepatitis B to ascertain if integrants of viral DNA can be detected in fragments of cellular DNA leaking from damaged hepatocytes into the circulation.

METHODS: DNA was extracted from the sera of five patients with uncomplicated acute hepatitis B and one with fulminant disease. Two subgenomic PCRs designed to amplify the complete genome of HBV were used and the resulting amplicons were cloned and sequenced.

RESULTS: HBV and chromosomal DNA were amplified from the sera of all the patients. In one patient with uncomplicated disease, HBV DNA was integrated into host chromosome 7 q11.23 in the WBSCR1 gene. The viral DNA comprised 200 nucleotides covering the S and X genes in opposite orientation, with a 1 169 nucleotide deletion. The right virus/host junction was situated at nucleotide 1 774 in the cohesive overlap region of the viral genome, at a preferred topoisomerase I cleavage motif. The chromosomal DNA was not rearranged. The patient made a full recovery and seroconverted to anti-HBs- and anti-HBe-positivity. Neither HBV nor chromosomal DNA could be amplified from his serum at that time.

CONCLUSION: Integration of viral DNA into chromosomal DNA may occur rarely during acute hepatitis B and, with clonal propagation of the integrant, might play a role in hepatocarcinogenesis.

Key words: Hepatocellular; Chronic hepatitis B infection; Clonal propagation

Kimbi GC, Kramvis A, Kew MC. Integration of hepatitis B virus DNA into chromosomal DNA during acute hepatitis B. *World J Gastroenterol* 2005; 11(41):6416-6421
http://www.wjgnet.com/1007-9327/11/6416.asp

INTRODUCTION

Hepatitis B Virus (HBV), the prototype member of the family Hepadnaviridae, belongs to the genus Orthohepadnavirus. Compelling evidence supports a causal role for chronic HBV infection in hepatocellular carcinoma (HCC)[1,2]. Less certain is the pathogenesis of HBV-induced HCC. Direct and indirect carcinogenic mechanisms have been implicated, the latter mainly by the frequency with which this tumor co-exists with cirrhosis[3,4]. Evidence for a direct effect is provided by the development of HCC in an otherwise normal liver (in as many as 40% or more of black African patients[5]) and by observations in a variety of animal models. The latter include the development of HCC in the absence of cirrhosis, both in animals that were chronically infected with other members of the family Hepadnaviridae[6-8] and in transgenic mice with HBV DNA incorporated into the germline[9]. Further support comes from the finding of integrated hepadnaviral DNA in cellular DNA in HCCs in animal and human hosts[10-14]. The latter does not, however, prove that insertion of viral DNA is essential for hepatocarcinogenesis. If clonal expansion of integrated HBV DNA proves to be a pivotal step in hepatocarcinogenesis, the timing of integration becomes important. Because HCC typically develops in patients chronically infected with HBV, it has been assumed that DNA insertion occurs at some point during persistent infection. Integration during the short period of viral replication in acute hepatitis B had not been conclusively demonstrated[15-17]. However, in a recent study, integration of HBV DNA was demonstrated in 3 of 19 liver specimens from patients with acute hepatitis B, one of whom had subacute fulminant hepatitis[18]. Moreover, a study in acutely infected ducks showed that insertion of duck HBV (DHBV) DNA into host DNA may occur as early as d 6 after the infection[12]. HCC does not, however, develop in ducks chronically infected with DHBV. The time at which integration occurred was studied in the liver tissue and a similar study could not, for obvious ethical reasons, be performed in human beings with acute hepatitis B.

In a previous study, primers used to amplify the complete genome of HBV were found to amplify

chromosomal DNA also. Taking advantage of this phenomenon and the leakage into the bloodstream of fragments of cellular DNA from damaged hepatocytes during acute liver injury[19,20], we examined the serum of patients with acute hepatitis B for integrated HBV DNA.

MATERIALS AND METHODS

Patients studied

Blood samples were drawn, with informed consent, from six South African blacks suffering from acute hepatitis B during the peak of the disease or shortly thereafter. Permission to undertake this study was given by the Human Ethics Committee of the University of Witwatersrand. In five patients, the illness was uncomplicated, and all recovered completely; the remaining patient had fulminant hepatitis B and died of liver failure. Alanine aminotransferase levels in the early stages of the illness ranged between 799 and 4 747 IU/L. The patients varied in age from 18 to 32 years: 3 were males and 3 females. Serum known to be HBsAg-positive and HBsAg-negative was used as positive- and negative-extraction controls, respectively. The sera were stored at -70 °C until analyzed.

DNA extraction, amplification, cloning, and sequencing

Total DNA was extracted from the sera using the QIAamp DNA Mini Kit (QIAGEN GmbH, Hilden, Germany), according to the manufacturer's instructions. Two subgenomic PCRs designed to amplify the complete genome of HBV were used and the resulting amplicons were cloned and sequenced. A modification of the method of Takahashi K *et al*[21] was used, which involved the amplification of two overlapping fragments of HBV, fragment A (1.35 kb) and fragment B (2.2 kb). However, this amplification designed for amplification of viral DNA also fortuitously, randomly recognized chromosomal DNA, leading to the amplification of genomic DNA in addition to HBV DNA. The sequence of the primers is given in Table 1. The reaction mix for the amplification consisted of 2.25 μL 10× Ex Taq buffer with 20 mmol/L $MgCl_2$ set as subscript, 2 μL 2.5 mmol/L dNTP mix, 1.25 μL each of the appropriate primers (Table 1), 2.5 μL DNA, made up to 22.5 μL with water (SABAX water for injection, Adcock Ingram, Johannesburg, South Africa). The enzyme mix was made up of 1.875 μL water, 0.25 μL 10× Ex Taq and 0.375 μL TaKaRa Ex Taq polymerase [TaKaRa Biotechnology (Dalian) Co., Ltd., Shiga, Japan]. The 22.5μL reaction mix was preheated to 94 °C for 2 min and 2.25 μL TaKaRa Ex Taq enzyme mix was added at the first annealing step. This was followed by 40 cycles of amplification with the cycling profile shown in Table 1. Both HBV-positive and HBV-negative controls were included. The latter consisted of water instead of DNA in the PCR mixture. To avoid cross-contamination and false-positive results, the precautions and procedures suggested by Kwok and Higuchi[22] were strictly adhered to. DNA extraction, PCR amplification, and electrophoresis were performed in physically separated venues.

Amplicons were cloned into a pPCR-ScriptTM Amp SK+ vector (Stratagene, La Jolla, CA, USA) according to the protocol provided by the manufacturer. The positive clones containing either inserts of the correct or shorter size were prepared for direct sequencing using the BigDye Terminator v3.0 Cycle Sequencing Ready Reaction Kit (Applied Biosystems, Foster City, USA) and sequenced on a 377 DNA automated sequencer (Applied Biosystems, Inc.) using primers T3 (5'-AATTAACCCTCACTAAAGG G-3') and T7 (5'-GTAATACGACTCACTATAGGGC-3'). All sequences were analyzed in both forward and reverse directions.

RESULTS

In addition to yielding amplicons of the expected size, i.e., 1.35 kb for fragment A and 2.2 kb for fragment B, the two subgenomic PCRs designed to amplify the complete genome of HBV gave rise to smaller amplicons ranging in size from 100 to 750 bp. These amplicons were successfully cloned into a pPCR-Script^{TM} Amp SK^{+} vector (Figure 1) and a number of clones from each of the six patients were sequenced (Table 2).

The majority of the clones contained HBV DNA only and the detailed analysis of these sequences will be published elsewhere. Fortuitously, the primers designed for the amplification of viral DNA amplified Chromosomal DNA was amplified in 5 patients using primers designed to amplify fragment A (Table 1) and in the remaining patient with primers designed to amplify fragment B. As shown in Table 2, the chromosome number and the lengths

Table 1 Oligonucleotide primers and PCR cycling profiles used in the study

Fragment	Primer	Position[1]	Sequence	Denaturation	Annealing	Extension	Size[2]
A	455(+)	455-474	5'-CAAGGTATGTTGCCCGTTTG-3				1 345
	1 800(–)	1 800-1 773	5'-AGACCAATTTATGCCTACAGCCTCCTA-3'	94 °C 30 s	62 °C 30 s	72 °C 90 s	
B	1 687(+)	1 687-1 708	5'-CGACCGACCTTGAGGCATAC-3'				
	685(-)	704-685	5'-CGAACCACTGAACAAATGGC-3'	94 °C 30 s	63 °C 30 s	72 °C 30 s	2 198

(+) sense (–) anti-sense. [1]Denotes the nucleotide position of HBV adw genome (GenBank accession no. V00866) where the EcoRI cleavage site is position 1[2]. Size of the amplicons in base pairs.

Table 2 Summary of cloning and sequencing results

Patient details			PCR fragment[1]	Number of clones					Chromosome number and length
No.	Sex	Age (yr[2])		Sequenced	With vector DNA	With HBV DNA only	WithHBV/ chromosomal DNA	With chromosomal DNA only	
355	F	18	B	5	1	3	0	1	7 (117 bp)
8225	M	23	A	3	0	2	0	1	1 (278 bp)
			B	4	0	4	0	0	–
28	M	26	A	4	0	2	0	2	4 (512 bp) 16 (140 bp)
			B	4	0	4	0	0	–
4038	F	27	A	6	0	5	0	1	1 (97 bp)
			B	4	0	4	0	0	–
52833	F	32	A	12	2	6	0	4	4 (456 bp) 10 (235 bp) 10 (330 bp) 2 (422 bp)
			B	4	0	4	0	0	–
0962	M	27	A	8	0	4	1	3	1 (300 bp) 14 (410 bp) 17 (410 bp)
			B	5	0	5	0	0	–

[1]Fragment A amplified with primers 455 (+) and 1 800 (–); fragment B amplified with primers 1 687 (+) and 685 (–).[2] yr, years; bp, base pairs; [3]Patient with fulminant hepatitis.

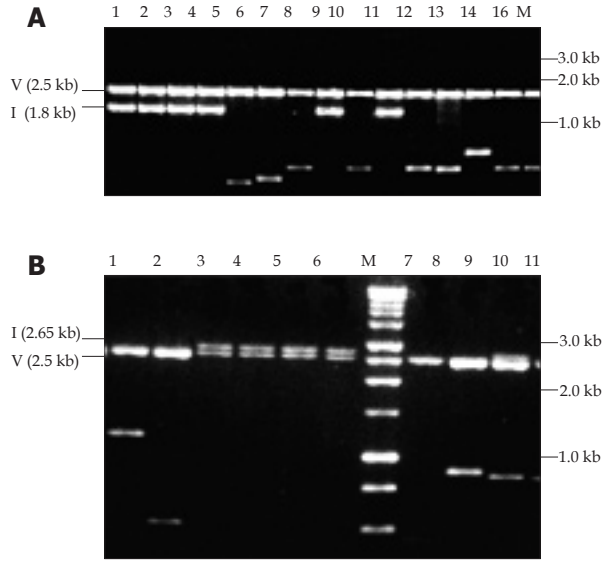

Figure 1 Ethidium bromide stained with 1% agarose gel showing pPCR-Script Amp SK(+) plasmid containing amplicons restricted with PvuII. In panel A, the fragments cloned were amplified with primers 455(+) and 1 800(–). Lanes 1-4, 8, and 10 show the expected size insert of -1.8 kb for fragment A amplicon (1.3 kb) whereas lanes 5-7, 9, and 11-16 show shorter inserts ranging in size 0.6-1.1 kb. In panel B, the fragments cloned were amplified with primers 1 687(+) and 685(–). Lanes 3-6 and 9 show the expected size insert of -2.65 kb for fragment B amplicon (2.2 kb), lane 7 is vector alone and lanes 1, 2, 8-11 show shorter inserts ranging in size 0.5-1.2 kb. M: Promega 1 kb molecular weight marker, V: vector, I: insert of expected size (A and B).

of the fragments varied, although in three cases the fragment amplified corresponded to the sequences from chromosome 1.

In one patient with uncomplicated hepatitis B, HBV DNA was found to be integrated into host chromosome 7q11.23 in the WBSCR1 gene using primers for fragment A. WBSCR1 corresponds to the eukaryotic initiation factor 4H identified in rabbits[23,24] and is within the region encompassing the elastin gene. This region is commonly deleted in patients with Williams–Beuren syndrome, giving rise to loss of heterozygosity[24,25]. The viral DNA comprised 200 nucleotides covering the S and X genes in opposite orientation, with an 1 169 nucleotide deletion (Figure 2). The right virus/host junction was situated at nucleotide 1 774 in the cohesive overlap region of the viral genome, at a preferred topoisomerase I cleavage motif (TAA). The left virus/host junction of the integrant was not identified and, therefore, the length of the integrant could not be determined. Following phylogenetic analysis of the 175 nucleotides of the S region (nucleotides 4-630), the sequence clustered with subgenotype A1 of genotype A, which is the predominant genotype in southern Africa[26-28]. When the 175 nucleotides of the insert covering the S region were translated, starting at nucleotide 3 of the fragment, the amino acid at position 122 was K, which is characteristic of serotype ad. Amino acid 160, which encodes for the w/r determinant, was not included in this fragment and, therefore, we cannot conclusively determine the serotype, although we can probably assume that the determinant is w because the predominant serotype in southern Africa is adw. The nucleotide sequence of the chromosomal DNA (262 bp) was completely conserved and not rearranged. The 3' end was amplified by primer 1 800 (-) (Table 1). A BLAST search[29] revealed that in addition to binding to chromosome 7, the primer 1 800 (–)

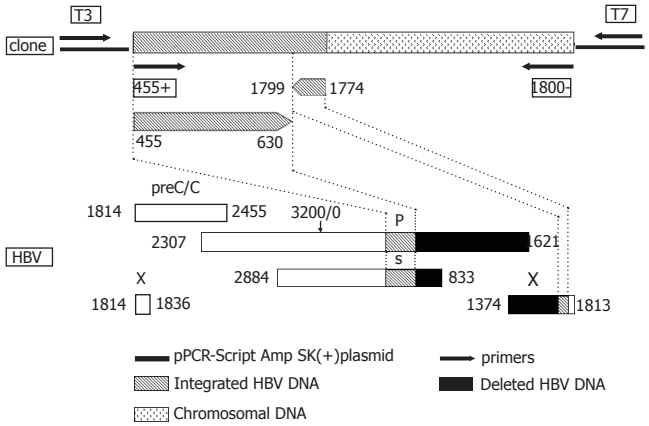

Figure 2 Schematic representation of the HBV DNA integrant amplified from the serum of acute hepatitis patient (#0962) using primers 455 (+) and 1 800 (–) and cloned into pPCR-Script Amp SK (+) plasmid relative to the HBV genome. The lower part of the figure represents the genetic organization of the four open reading frames of HBV, preC/C: precore/core, P: polymerase gene, S: surface gene and X: X gene. Numbering according to nucleotide position of HBV GenBank accession no. V00866 where the EcoRI cleavage site is position 1.

(Table 1) has identical sequences on human chromosomes 2, 3, 12, 13, 20, 22, and Y. The sequence of the integrated HBV DNA and flanking the chromosomal DNA has been deposited in GenBank (accession no. AY223548).

The patient with the integrant was a 27-year-old Xhosa gold-mine laborer, who was previously healthy and presented with the typical clinical features of uncomplicated acute viral hepatitis. When he was first tested, the tests of liver function showed a serum bilirubin concentration of 257 μmol/L (conjugated bilirubin 228 μmol/L), alkaline phosphatase 91 IU/L, γ-glutamyl transferase 94 IU/L, alanine aminotransferase 3 238 IU/L, aspartate aminotransferase 2 781 IU/L, and albumin 4 g/L. HBV surface antigen, e antigen, and IgM core antibody were present in the serum. The patient made an uneventful and complete recovery, with return of biochemical tests to normal and disappearance of surface and e antigens and the appearance of IgG core antibody and antibody to surface and e antigens in his serum. HBV DNA could not be detected in the serum. after he had recovered and cloning and whole genome sequencing were not attempted at that time.

DISCUSSION

Unlike retroviruses, in which insertion of viral DNA into host DNA is integral to the replication cycle, integration does not occur during normal hepadnaviral replication. Integration of hepadnaviral DNA may, however, take place as a result of an illegitimate recombination mechanism mediated by cellular enzymes[12,30]. Clonally propagated integrations have been detected in the majority of HCCs that develop in the presence of chronic hepadnaviral infection[6-10] and have been incriminated in the hepatocarcinogenesis that often complicates persistent infection. HBV DNA insertions are found at random sites in human cellular DNA, although some chromosomes are affected more often than others[31]. In the present study, we detected an integrant in chromosome 7 of an acute hepatitis B patient.

Although we cannot exclude the possibility that the HBV integrant amplified was the result of a PCR artefact, there are a number of observations that argue against this interpretation and support our conviction that this integrant was authentic.

Firstly, the site of integration in chromosome 7q11.23 is within the WBSCR1 gene. This gene corresponds to the eukaryotic initiation factor 4H identified in rabbits[23,24] and the integrant is within the region commonly deleted in patients with Williams-Beuren syndrome, giving rise to loss of heterozygosity[24,25]. Moreover, the WBSCR1 gene contains a high abundance of Alu repeats[24], repetitive elements that have been shown to be the preferred sites for recombination and for HBV DNA insertion[32]. Analogously the sites of integration in the three patients with acute hepatitis B reported by Murakami and coworkers[18] were the intronic sequence of the tumor necrosis factor-induced protein gene and a repetitive sequence in the two patients with a single integrant; and the intronic sequence of a hypothetical protein gene (LOC 169443) and a repetitive sequence in the patient with two integrants.

Secondly, the region of HBV integrated (position 1 774-1 799 from EcoRI site) is a highly preferred site of integration of hepadnaviral DNA, that is, close to the 11-bp direct repeat sequence DR1 (position 1 824-1 834) and within the cohesive overlap region between DR1 and DR2[33].

Thirdly, the one viral DNA/chromosomal DNA junction in the single integrant detected in our patient with acute hepatitis B was located at nucleotide 1 774 of the viral genome, a highly preferred topoisomerase I cleavage motif. Linear hepadnaviral DNA is the primary substrate for integration[12,30], and the circular DNA must first be linearized before integration can take place. Insertion is then accomplished by strand invasion of cellular DNA. Thus, integration of viral DNA into chromosomal DNA requires that the linear DNA be imported into the nucleus of the infected cell[30,34,35]. Wang and Rogler[30] have produced experimental evidence for a key role for the cellular enzyme topoisomerase I in the illegitimate recombination between hepadnaviral and host DNA. A role for this enzyme in illegitimate recombination is supported both by the finding of highly preferred topoisomerase I cleavage motifs in the immediate vicinity of almost all crossover sites in mammalian DNA, and by the observation that integrants in WHV-induced HCC in woodchucks occurred at preferred topoisomerase I cleavage sites[30].Fourthly, the integrated HBV DNA covered the S and X regions, the open reading frames most commonly integrated into chromosomal DNA[36].

Finally, the integrant detected in the serum of our patient with acute hepatitis B conformed in general to the integrants described in HCC developing in the

presence of chronic HBV infection[31]. It contained a long deletion (1 169 nucleotides in length), and the viral DNA between the right end of the deletion and the right virus/chromosome junction was inverted X sequence (Figure 1). One or more deletions or other more complex rearrangements are invariably found in inserted hepadnaviral DNA[10,31], indicating that specific mechanisms for integration of functional viral DNA into chromosomal DNA are not encoded by the virus. Simple microdeletions are most common, probably because the single-stranded ends of viral DNA resulting from topoisomerase I cleavage are sensitive to cellular nucleases. The larger deletions and complex rearrangements of the viral DNA are generally believed to occur after the integration[37], although WHV with extensive rearrangements of DNA has been described in hepatocyte nuclei in woodchucks[38] and there is some evidence in these animals that DNA rearranged in this way may be preferentially integrated[39]. Similarly, Yaginuma *et al*[40] observed features of HBV integration to be common to HCC and patients with chronic active hepatitis and an analogous integrant to the one detected in this study has been described in a 9-year-old child with HCC[41].

Integration of hepadnaviral DNA into host DNA is normally rare, perhaps because recycling of viral DNA into the nucleus is at a low level during productive infection[12]. The frequency of integration of DHBV in experimentally infected ducklings was estimated to be one viral genome per 103-104 cells by 6 d after the infection[12]. It is not known if these recombination events occurred in many cells or if a few cells produced many such events. In keeping with the belief that insertion events are uncommon, we found only a single integrant among many clones in only one of 6 patients with acute hepatitis B. Our finding, and that of others[12,18], of integrated viral DNA in early infection is in accordance with the observation, that importation of linear DNA into the nucleus is necessary for insertion of viral DNA into chromosomal DNA, and that such importation is known to occur in the phase of cccDNA amplification during the initiation of infection[42]. Opportunities for viral integration beyond the early phase of infection would require continued importation of viral DNA into the nucleus, depend on new rounds of infection or loss and replacement of cccDNA by cell turnover[12]. Thus, insertion of linear forms of viral DNA may occur preferentially during early phases of infection or during periods of extensive hepatocyte turnover and/or re-infection, at times when linear viral DNA is imported into the nuclei. Integration may be enhanced during these periods by the availability of DNA ends resulting from DNA replication or damage[43]. Alternatively, interference with the normal replication cycle at some stage in chronic infection may result in the accumulation of linear forms of DNA, and there is some evidence for defective replication of HBV and accumulation of replicative intermediates in patients with HBV-associated HCC[44].

The clinical, biochemical, and serological features of the acute hepatitis B in the patient with the integrant did not differ obviously from those in the other patients with uncomplicated disease. He made a complete clinical and biochemical recovery, and seroconverted to anti-HBs and IgG anti-HBc. At this stage, HBV DNA could no longer be detected in his serum by PCR amplification and further cloning was not attempted. Even if the integrated HBV DNA was still present in hepatocytes, it would not be detected in peripheral blood once healing of hepatocyte cell membranes had taken place. Thus, persistence of the integrated HBV DNA could only have been detected by analysis of liver tissue, and a liver biopsy was not felt to be justified. Although sources other than the liver for the chromosomal DNA amplified in the peripheral blood of the six patients with acute hepatitis B (including the one with fulminant hepatitis) are possible (for example, peripheral blood mononuclear cells), the finding of viral DNA integrated into host DNA in one of the patients favors leakage of chromosomal DNA fragments from damaged hepatocytes during the acute liver injury.

Our finding of an integrant in a patient with acute hepatitis B may have no significance in relation to subsequent HCC development. Clonal expansion of an integrant is required for tumor formation, and the finding of a viral insertion in a tumor may simply reflect the fact that the clonal progenitor of the tumor happened to carry a viral integration[10]. Moreover, integrants may be lost from successive generations of cells[45]. Nevertheless, it is in accordance with the observation made in ducks that hepadnaviral DNA insertion may occur at a very early stage of infection, and raises the possibility that in certain circumstances early integration of HBV DNA might play a role in HBV-induced hepatocarcinogenesis.

ACKNOWLEDGMENTS

The authors are grateful to Dr. Jesse Summers and Dr. Charles Rogler for helpful discussions.

REFERENCES

1 **Kew MC.** Hepatitis B virus in the etiology of hepatocellular carcinoma. In: Tabor E, ed. Viruses and iver cancer. *Amsterdam: Elsevier,* 2002: 17-30
2 **Feitelson MA.** Hepatitis B virus in hepatocarcinogenesis. *J Cell Physiol* 1999; **181:** 188-202
3 **Kew MC,** Popper H. Relationship between hepatocellular carcinoma and cirrhosis. *Semin Liver Dis* 1984; **4:** 136-146
4 **Shikata T.** Primary liver carcinoma and cirrhosis. In: Okuda K PR, ed. Hepatocellular carcinoma. *New York: John Wiley,* 1987: 53-68
5 **Paterson AC,** Kew MC, Herman AA, Becker PJ, Hodkinson J, Isaacson C. Liver morphology in southern African blacks with hepatocellular carcinoma: a study within the urban environment. *Hepatology* 1985; **5:** 72-78
6 **Popper H,** Shih JW, Gerin JL, Wong DC, Hoyer BH, London WT, Sly DL, Purcell RH. Woodchuck hepatitis and hepatocellular carcinoma: correlation of histologic with virologic observations. *Hepatology* 1981; **1:** 91-98
7 **Marion PL,** Knight SS, Salazar FH, Popper H, Robinson WS. Ground squirrel hepatitis virus infection. *Hepatology* 1983; **3:** 519-527
8 **Marion PL,** Knight SS, Ho BK, Guo YY, Robinson WS, Popper H. Liver disease associated with duck hepatitis B virus infection of domestic ducks. *Proc Natl Acad Sci U S A* 1984; **81:** 898-902

9 **Kim CM,** Koike K, Saito I, Miyamura T, Jay G. HBx gene of hepatitis B virus induces liver cancer in transgenic mice. *Nature* 1991;**351:** 317-320

10 **Ogston CW,** Jonak GJ, Rogler CE, Astrin SM, Summers J. Cloning and structural analysis of integrated woodchuck hepatitis virus sequences from hepatocellular carcinomas of woodchucks. *Cell* 1982; **29:** 385-394

11 **Marion PL,** Van Davelaar MJ, Knight SS, Salazar FH, Garcia G, Popper H, Robinson WS. Hepatocellular carcinoma in ground squirrels persistently infected with ground squirrel hepatitis virus. *Proc Natl Acad Sci USA* 1986; **83:** 4543-4546

12 **Yang W,** Summers J. Integration of hepadnavirus DNA in infected liver: evidence for a linear precursor. *J Virol* 1999; **73:** 9710-9717

13 **Bréchot C,** Hadchouel M, Scotto J, Fonck M, Potet F, Vyas GN, Tiollais P. State of hepatitis B virus DNA in hepatocytes of patients with hepatitis B surface antigen-positive and -negative liver diseases. *Proc Natl Acad Sci U S A* 1981; **78:** 3906-3910

14 **Shafritz DA,** Kew MC. Identification of integrated hepatitis B virus DNA sequences in human hepatocellular carcinomas. *Hepatology* 1981; **1:** 1-8

15 **Marconi M,** Scotto J, Laliam M, Hadchouel M, Dazza MC, Larouzé B. A study of liver HBV DNA during follow-up of acute viral hepatitis in children. *J Pediatr Gastroenterol Nutr* 1988; **7:** 507-510

16 **Lugassy C,** Bernuau J, Thiers V, Krosgaard K, Degott C, Wantzin P, Schalm SW, Rueff B, Benhamou JP, Tiollais P. Sequences of hepatitis B virus DNA in the serum and liver of patients with acute benign and fulminant hepatitis. *J Infect Dis* 1987; **155:** 64-71

17 **Yoffe B,** Burns DK, Bhatt HS, Combes B. Extrahepatic hepatitis B virus DNA sequences in patients with acute hepatitis B infection. *Hepatology* 1990; **12:** 187-192

18 **Murakami Y,** Minami M, Daimon Y, Okanoue T. Hepatitis B virus DNA in liver, serum, and peripheral blood mononuclear cells after the clearance of serum hepatitis B virus surface antigen. *J Med Virol* 2004; **72:** 203-214

19 **Tan EM,** Schur PH, Carr RI, Kunkel HG. Deoxybonucleic acid (DNA) and antibodies to DNA in the serum of patients with systemic lupus erythematosus. *J Clin Invest* 1966; **45:** 1732-1740

20 **Jahr S,** Hentze H, Englisch S, Hardt D, Fackelmayer FO, Hesch RD, Knippers R. DNA fragments in the blood plasma of cancer patients:quantitations and evidence for their origin from apoptotic and necrotic cells. *Cancer Res* 2001; **61:** 1659-1665

21 **Takahashi K,** Akahane Y, Hino K, Ohta Y, Mishiro S. Hepatitis B virus genomic sequence in the circulation of hepatocellular carcinoma patients: comparative analysis of 40 full-length isolates. *Arch Virol* 1998; **143:** 2313-2326

22 **Kwok S,** Higuchi R. Avoiding false positives with PCR. *Nature* 1989; **339:** 237-238

23 **Richter-Cook NJ,** Dever TE, Hensold JO, Merrick WC. Purification and characterization of a new eukaryotic protein translation factor. Eukaryotic initiation factor 4H. *J Biol Chem* 1998; **273:** 7579-7587

24 **Martindale DW,** Wilson MD, Wang D, Burke RD, Chen X, Duronio V, Koop BF. Comparative genomic sequence analysis of the Williams syndrome region (LIMK1-RFC2) of human chromosome 7q11.23. *Mamm Genome* 2000; **11:** 890-898

25 **Osborne LR,** Martindale D, Scherer SW, Shi XM, Huizenga J, Heng HH, Costa T, Pober B, Lew L, Brinkman J, Rommens J, Koop B, Tsui LC. Identification of genes from a 500-kb region at 7q11.23 that is commonly deleted in Williams syndrome patients. *Genomics* 1996; **36:** 328-336

26 **Bowyer SM,** van Staden L, Kew MC, Sim JG. A unique segment of the hepatitis B virus group A genotype identified in isolates from South Africa. *J Gen Virol* 1997; **78** (Pt 7)**:** 1719-1729

27 **Kramvis A,** Weitzmann L, Owiredu WK, Kew MC. Analysis of the complete genome of subgroup A' hepatitis B virus isolates from South Africa. *J Gen Virol* 2002; **83:** 835-839

28 **Kimbi GC,** Kramvis A, Kew MC. Distinctive sequence characteristics of subgenotype A1 isolates of hepatitis B virus from South Africa. *J Gen Virol 2004;* **85:** 1211-1220

29 **Altschul SF,** Madden TL, Schäffer AA, Zhang J, Zhang Z, Miller W, Lipman DJ. Gapped BLAST and PSI-BLAST: a new generation of protein database search programs. *Nucleic Acids Res* 1997; **25:** 3389-3402

30 **Wang HP,** Rogler CE. Topoisomerase I-mediated integration of hepadnavirus DNA in vitro. *J Virol* 1991; **65:** 2381-2392

31 **Slagle BL,** Lee TH, Butel JS. Hepatitis B virus and hepatocellular carcinoma. *Prog Med Virol* 1992; **39:**167-203

32 **Shaul Y,** Garcia PD, Schonberg S, Rutter WJ. Integration of hepatitis B virus DNA in chromosome-specific satellite sequences. *J Virol* 1986; **59:** 731-734

33 **Shih C,** Burke K, Chou MJ, Zeldis JB, Yang CS, Lee CS, Isselbacher KJ, Wands JR, Goodman HM. Tight clustering of human hepatitis B virus integration sites in hepatomas near a triple-stranded region. *J Virol* 1987; **61:** 3491-3498

34 **Gong SS,** Jensen AD, Wang H, Rogler CE. Duck hepatitis B virus integrations in LMH chicken hepatoma cells: identification and characterization of new episomally derived integrations. *J Virol* 1995; **69:** 8102-8108

35 **Gong SS,** Jensen AD, Chang CJ, Rogler CE. Double-stranded linear duck hepatitis B virus (DHBV) stably integrates at a higher frequency than wild-type DHBV in LMH chicken hepatoma cells. *J Virol* 1999; **73:** 1492-1502

36 **Unsal H,** Yakicier C, Marçais C, Kew M, Volkmann M, Zentgraf H, Isselbacher KJ, Ozturk M. Genetic heterogeneity of hepatocellular carcinoma. *Proc Natl Acad Sci USA* 1994; **91:** 822-826

37 **Rogler CE,** Summers J. Novel forms of woodchuck hepatitis virus DNA isolated from chronically infected woodchuck liver nuclei. *J Virol* 1982; **44:** 852-863

38 **Rogler CE,** Summers J. Cloning and structural analysis of integrated woodchuck hepatitis virus sequences from a chronically infected liver. *J Virol* 1984; **50:** 832-837

39 **Kew MC,** Miller RH, Chen HS, Tennant BC, Purcell RH. Mutant woodchuck hepatitis virus genomes from virions resemble rearranged hepadnaviral integrants in hepatocellular carcinoma. *Proc Natl Acad Sci U S A* 1993; **90:** 10211-10215

40 **Yaginuma K,** Kobayashi H, Kobayashi M, Morishima T, Matsuyama K, Koike K. Multiple integration site of hepatitis B virus DNA in hepatocellular carcinoma and chronic active hepatitis tissues from children. *J Virol* 1987; **61:** 1808-1813

41 **Tsuei DJ,** Hsu TY, Chen JY, Chang MH, Hsu HC, Yang CS. Analysis of integrated hepatitis B virus DNA and flanking cellular sequences in a childhood hepatocellular carcinoma. *J Med Virol* 1994; **42:** 287-293

42 **Tuttleman JS,** Pourcel C, Summers J. Formation of the pool of covalently closed circular viral DNA in hepadnavirus-infected cells. *Cell* 1986; **47:** 451-460

43 **Petersen J,** Dandri M, Bürkle A, Zhang L, Rogler CE. Increase in the frequency of hepadnavirus DNA integrations by oxidative DNA damage and inhibition of DNA repair. *J Virol* 1997; **71:** 5455-5463

44 **Raimondo G,** Burk RD, Lieberman HM, Muschel J, Hadziyannis SJ, Will H, Kew MC, Dusheiko GM, Shafritz DA. Interrupted replication of hepatitis B virus in liver tissue of HBsAg carriers with hepatocellular carcinoma. *Virology* 1988; **166:** 103-112

45 **Gong SS,** Jensen AD, Rogler CE. Loss and acquisition of duck hepatitis B virus integrations in lineages of LMH-D2 chicken hepatoma cells. *J Virol* 1996; **70:** 2000-2007

Science Editor Wang XL and Li WZ **Language Editor** Elsevier HK

PO Box 2345, Beijing 100023, China
www.wjgnet.com
wjg@wjgnet.com

ELSEVIER

World J Gastroenterol 2005;11(41):6422-6428
World Journal of Gastroenterology ISSN 1007-9327

Changes in lipid metabolism in chronic hepatitis C

Katalin Jármay, Gizella Karácsony, András Nagy, Zsuzsa Schaff

Katalin Jármay, Gizella Karácsony, First Department of Internal Medicine, Albert Szent-Györgyi Medical University, Szeged, Hungary
András Nagy, County Hospital, Department of Cardiology, Kecskemét, Hungary
Zsuzsa Schaff, 2nd Department of Pathology, Semmelweis University, Budapest, Hungary
Supported by the grant from the Hungarian Ministry of Education, No.NKFP-1A/0023/2002 National Research Development Projects and grant from the Hungarian National Scientific Research Fund, No.OTKA T037838
Correspondence to: Dr. Katalin Jármay, First Department of Internal Medicine, Albert Szent-Györgyi Medical University, Szeged, PO Box 469, H-6701, Hungary. jaka@efk.u-szeged.hu
Telephone: +36-62-545-189 Fax: +36-62-545-185
Received: 2004-10-29 Accepted: 2004-11-19

Abstract

AIM: To investigate the relationship between certain biochemical parameters of lipid metabolism in the serum and steatosis in the liver.

METHODS: The grade of steatosis (0-3) and histological activity index (HAI, 0-18) in liver biopsy specimens were correlated with serum alanine aminotransferase (ALT), total cholesterol and triglyceride levels in 142 patients with chronic hepatitis C (CH-C), and 28 patients with non-alcoholic fatty liver disease (NAFLD) without hepatitis C virus (HCV) infection. The serum parameters were further correlated with 1 797 age and sex matched control patients without any liver diseases.

RESULTS: Steatosis was detected in 90 out of 142 specimens (63%) with CH-C. The ALT levels correlated with the grade of steatosis, both in patients with CH-C and NAFLD ($P<0.01$). Inserting the score values of steatosis as part of the HAI, correlation with the ALT level ($P<0.00001$) was found. The triglyceride and cholesterol levels were significantly lower in patients with CH-C (with and without steatosis), compared to the NAFLD group and to the virus-free control groups.

CONCLUSION: Our study confirms the importance of liver steatosis in CH-C which correlates with lower lipid levels in the sera. Inclusion of the score of steatosis into HAI, in case of CH-C might reflect the alterations in the liver tissue more precisely, while correlating with the ALT enzyme elevation.

Key words: Lipid metabolism; Chronic hepatitis C; NAFLD

Jármay K, Karácsony G, Nagy A, Schaff Z. Changes in lipid metabolism in chronic hepatitis C. *World J Gastroenterol* 2005; 11(41):6422-6428
http://www.wjgnet.com/1007-9327/11/6422.asp

INTRODUCTION

Hepatic steatosis is a frequent and characteristic histological finding in patients with chronic hepatitis C (CH-C) in addition to bile duct damage and lymphoid follicles[1-5]. Fat accumulation in hepatocytes has been reported in 30-70% of liver biopsy specimens obtained from patients infected with hepatitis C virus (HCV)[1-4]. Whether steatosis is mainly related to host factors or to the viral cytopathic effect is still uncertain and a matter of dispute[6-15]. The pathogenesis of development of steatosis in CH-C is complex; host factors including alcohol consumption, exposure to other hepatotoxins, obesity, insulin resistance, type 2 diabetes mellitus, hypertriglyceridaemia, hypobetalipoproteinemia have all been identified as determinants[8,12,16-18].

The most important question concerning the clinical significance of steatosis in CH-C is whether lipid accumulation influences the liver disease progression, affects treatment, or is solely an innocent bystander[5,19]. A role of steatosis in the progression of CH-C is suggested by the finding that the severity of fat accumulation correlates with the stage of fibrosis[20,21] and liver cell apoptosis[5]. Treatment with peginterferon or IFNα-2b and ribavirin has been found to reduce steatosis in HCV genotype 3 patients[1]. On the other hand, no significant association between the stage of fibrosis and liver steatosis has been found by others[22]. *In vitro* studies and transgenic mouse model have both shown the HCV core protein to be capable of inducing steatosis by itself[23,24], which suggests a direct effect of specific viral sequences in the pathogenesis of lipid accumulation. An association of nonstructural protein 5A (NS5A) with lipid droplets and apoA1 has also been observed[11].

The aim of the present work was to study the changes in certain parameters of lipid metabolism in patients with CH-C and compare the findings with the accumulation of fat in liver biopsy specimens and with the histology activity index (HAI). For this reason the serum cholesterol and triglyceride levels of CH-C patients were examined. Patients were selected on the basis of the presence or absence of steatosis in their liver biopsy specimens, as well

as the absence of other risk factors for developing steatosis from a broader HCV-positive group referred to our center for treatment of chronic liver diseases. The results were compared to the lipid levels of patients with non-alcoholic fatty liver disease (NAFLD) verified histologically (NAFL, obesity, diabetes mellitus), and with data of a further control group: outpatients from the praxis without clinical and laboratory signs of liver disease, with or without history of alcohol abuse.

MATERIALS AND METHODS

Study population

A total of 142 patients with chronic HCV infection with no history of alcohol consumption were studied before the treatment with antiviral drugs (Table 1). CH-C was diagnosed on the basis of biochemical (serum aminotransferases greater than or equal to 1.5 times the upper normal value for at least 6 mo), serological (positivity for anti-HCV antibody, detection of HCV-RNA in the sera using the Amplicor HCV assay, Roche, Mannheim) and histological findings in liver biopsy specimens. Among the patients, 90 (63%) had micro- or macro-vesicular steatosis in their hepatocytes. This group comprised 46 females (26 patients younger than 44 years, average 38 years; 20 patients older than 45 years, average 52 years) and 44 males (29 patients younger than 44 years, average 38 years; 15 patients older than 45 years, average 51 years). There were 52 CH-C patients without steatosis, and this group comprised 17 females (10 patients younger than 44 years, average: 29 years; 7 patients older than 45 years, average: 53 years) and 45 males (24 patients younger than 44 years, average: 34 years; 11 patients older than 45 years, average: 49 years).

The control group was made up of 28 (16 males and 12 females) patients with NAFLD without HCV infection (Table 1).

A total of 1 797 patients from the outpatient praxis served as another control group which was matched to the CH-C patients with regard to age (Table 1). The 133 patients younger than 44-year-old female patients included 125 non-alcoholic and 8 alcoholic, the 819 patients older than 45-year-old females included 803 non-alcoholic and 16 alcoholic patients. Among the 146 patients younger than 44-year-old males, 60 were non-alcoholic and 86 were alcoholic patients. Out of the 699 patients older than 45-year-old males, 509 were non-alcoholic and 190 were alcoholic patients (Table 1).

Laboratory, virology assessment

Blood samples for the evaluation of alanine aminotransferase (ALT), total cholesterol and triglyceride were obtained after overnight fasting. Routine biochemical tests were carried out using commercially available kits. The HCV-RNA was determined in the sera using an RT-PCR assay (Amplicor, Roche, Mannheim), with a sensitivity of 70 copies/mL.

Histopathological evaluation

Liver biopsy was performed according to the Menghini technique. The biopsy specimens were formalin-fixed and paraffin-embedded, routinely stained with hematoxylin-eosin, picrosirius red, and a Berliner-blue reaction was carried out for the detection of iron. The slides were evaluated by two independent pathologists. A modified Knodell's histological activity index score[25,26] was applied to semiquantitatively score necroinflammatory activity (grade 0-18) and fibrosis (stage 0-4). Steatosis was graded according to the percentage of hepatocytes containing vacuoles in the cytoplasms (macro- or micro-vesicular steatosis). Steatosis was graded as follows, based on the percentage of fat containing hepatocytes[18]: none (0); mild (1: <10% of hepatocytes); moderate (2: 10-30% of hepatocytes); and severe (3: >30% of hepatocytes).

Statistical analysis

One-way analysis of variance was used to differentiate the data among the groups. Pearson's correlation coefficient was applied to measure the degree of association between the variables. $P < 0.05$ values were corrected according to the Bonferroni method. All values were presented as mean ±SD.

RESULTS

Steatosis was detected in 90 out of the 142 specimens (63%) with CH-C. The ALT levels were significantly higher in patients with grade 3 compared to grade 0 steatosis in the CH-C group ($P < 0.01$) (Figure 1). Significant correlation was found between the ALT level and HAI in the CH-C group without steatosis ($r = 0.556$, $P < 0.0002$) (Figure 2A), while this correlation could not be detected in the CH-C with steatosis subgroup (Figure 2B). Inserting the score values of steatosis (0-3) as part of the activity index (HAI)

Table 1 Study population with or without HCV-infection

	Male			Female			Total
	<44 (yr)	>45 (yr)	total	<44 (yr)	>45 (yr)	Total	
HCV-infection:							
With steatosis	29	15	44	26	20	46	90
Without steatosis	24	11	45	10	7	17	52
No HCV-infection							
NAFLD	10	6	16	5	7	12	28
No liver disease:							
Non alcoholic	60	509	569	125	803	928	1 497
Alcoholic	86	190	276	8	16	24	300

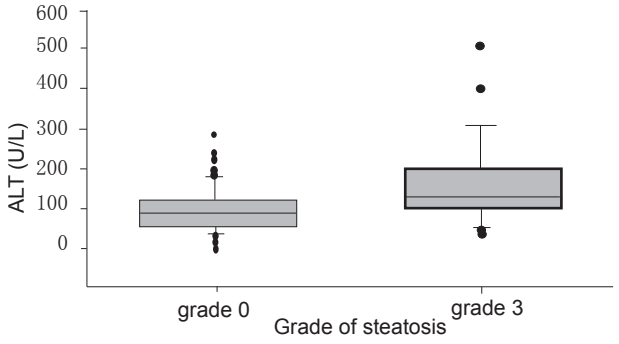

Figure 1 Differences of ALT levels in CH-C patients without steatosis (n = 52, grade 0) and with severe steatosis (n = 28, grade 3) (P < 0.01).

of chronic hepatitis, the correlation between the ALT level and histological scores of inflammatory activity grade was confirmed again in the 142 CH-C patients (r = 0.41, P<0.00001) (Figure 2C). The ALT level also correlated with grade of steatosis in patients without HCV infection (r = 0.533, P<0.005) (Figure 3), similarly to the CH-C patients. Upon comparing the ALT levels in patients with and without steatosis and with steatosis only, the highest ALT level was found in the steatotic CH-C group (Figure 4).

Triglyceride and cholesterol levels of CH-C patients were subgrouped according to age and sex, with and without steatosis. The lipid values of the CH-C groups were compared to the lipid values of the virus-free steatotic patients. The data of these subgroups were further compared based on their average age with the same age and sex group, as well as with the population from the outpatient praxis concerning drinking habits. The lipid levels of CH-C patients with liver steatosis were compared to the levels noted in the drinking outpatients, while these data involving the CH-C patients without liver steatosis were related to the non-drinking outpatients (Figures 5A and B; 6A and B; 7A and B; 8A and B)

The triglyceride levels were low in all the eight separated subgroups with CH-C (with and without steatosis, female, male, young, and elderly patients) (Figures 5A and B; 6A and B). These levels were conspicuously lower compared to the same values of the CH-C virus-free steatotic patients as well as to the drinker or nondrinker population.

Among the same groups, the cholesterol levels showed the same pattern as noted for the triglyceride levels. The only difference was that the young steatotic HCV infected male patients failed to show higher cholesterol levels, as was the case in relation to triglyceride (Figures 7A and B; 8A and B).

DISCUSSION

Liver steatosis is an important hallmark of CH-C[1-4,8,10,13,27-29]. The mechanism of HCV-related steatosis, however, is not exactly clear. Both metabolic[8,16-18,29,30] and viral cytopathic effects[7,10,11,13,24] have been suggested to play a role in the pathogenesis. The HCV viral components, especially the HCV-core protein, have been found in association with steatosis. Lipid droplets on which the core accumulated have been found in HCV-core-transfected cell lines strongly expressing this protein[24]. Hepatic overexpression of the HCV-core protein has been shown to interfere with the hepatic assembly and secretion of triglyceride-rich very low density lipoproteins (VLDL)[31]. Fatty change was detected *in vivo* in core-expressing transgenic mice too[23]. Chimpanzees chronically infected with HCV developed steatosis similarly to human beings[24]. The degree of steatosis in chimpanzees correlated with the amount of viral load and ALT[32].

More recently the NS5A of HCV has been shown in association with lipid droplets and apoA1, suggesting that NS5A may contribute to the pathogenesis of steatosis commonly observed in HCV-infected livers[11]. It has, however, been demonstrated that neither HCV viral load nor HCV genotype is associated with the severity of steatosis in certain studies[29,33].

HCV is a lipid-containing virus which binds to low density lipoprotein, VLDL, IgG and to a minor degree to IgM and high density lipoprotein[34]. This is in correlation with the finding that HCV infection is associated with hypo-β-lipoproteinemia, which occurs in the early stages of HCV infection before the development of cirrhosis[16,35]. The correlation between apo B levels and HCV viral load confirms the interaction between HCV infection and β-lipoprotein metabolism. This suggests that β-lipoproteins competitively inhibit HCV infection, because both HCV and β-lipoprotein use the same LDL receptor[16].

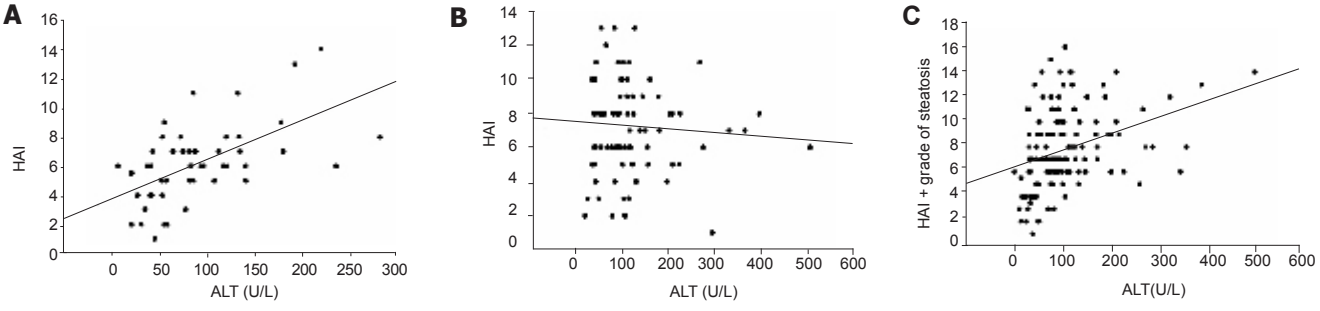

Figure 2 Correlation between ALT levels and HAI/HAI+steatosis in CH-C patients. **A:** without steatosis (n = 52, r = 0.556, P < 0.00002); **B:** with steatosis (n = 90, NS); **C:** in CH-C patients (n = 142, r = 0.41, P < 0.00001).

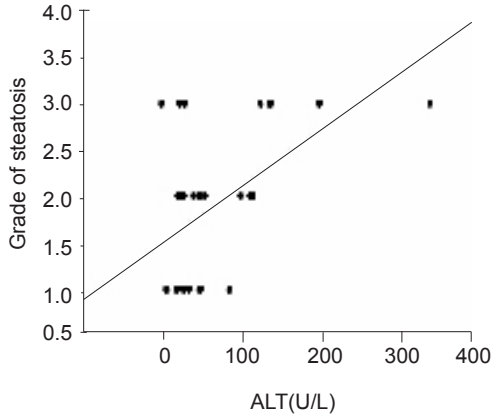

Figure 3 Correlation between ALT levels and grade of steatosis in patients without CH-C (n = 28, r = 0.533, P<0.005).

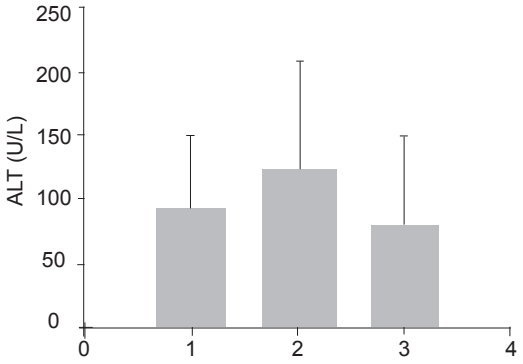

Figure 4 ALT levels in CH-C patients without and with steatosis and in patients with steatosis without CH-C. Bar 1: CH-C patients without steatosis (n = 52). Bar 2: CH-C patients with steatosis (n = 90). Bar 3: Patients with liver steatosis without CH-C (n = 28) Bar 1 P<0.02 *vs* Bar 2. Bar 2 P<0.02 *vs* Bar 3.

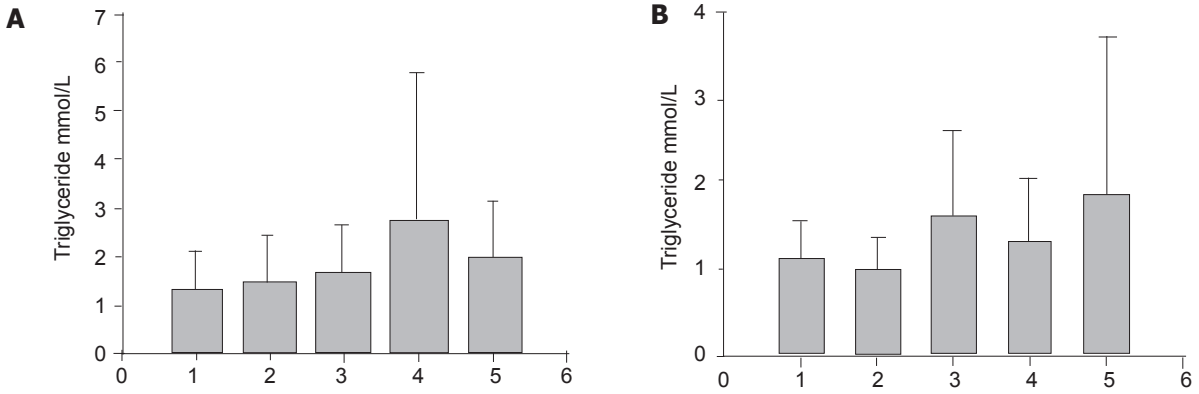

Figure 5 Triglyceride levels in CH-C female patients. **A:** With steatosis compared to outpatients with alcoholic habits;
Bar 1: CH-C young female patients with steatosis (n = 26, average age 38 years); Bar 2: CH-C elderly female patients with steatosis (n = 20, average age 52 years);
Bar 3: Female patients with liver steatosis (n = 12); Bar 4: outpatientswith alcoholic habits (n = 8, age 38 years); Bar 5: outpatients with alcoholic habits (n = 16, age 52 years). Bar 1 Ns *vs* Bar 2. Bar 1 and 2 NS *vs* Bar 3. Bar1 and 2 P<0.004 *vs* Bar 4. **B:** Without steatosis compared to outpatients without alcoholic habits.

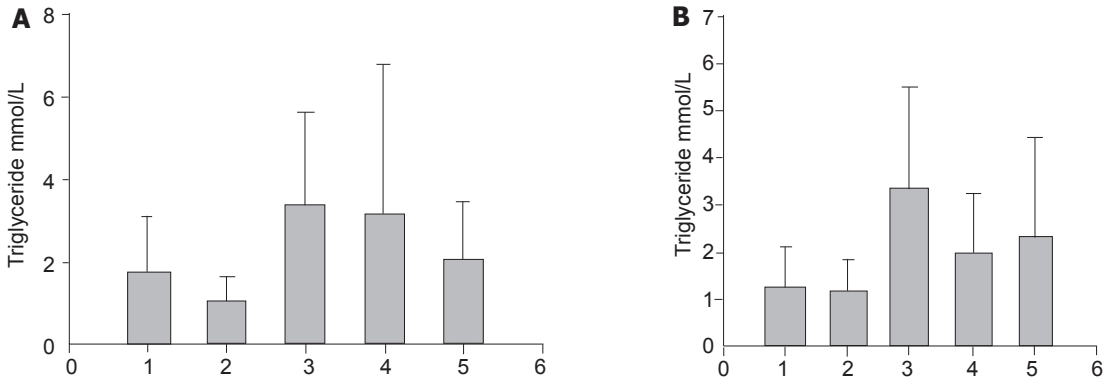

Figure 6 Triglyceride levels in CH-C male patients. **A:** Steatosis compared to outpatients with alcoholic habits; Bar 1: CH-C young male patients with steatosis (n = 29, average age 37 years); Bar 2: CH-C elderly male patients with steatosis (n = 15, average age 52 years); Bar 3: Male patients with liver steatosis (n = 16); Bar 4: Male outpatients with alcoholic habits (n = 86, age 37 years); Bar 5: Male outpatients with alcoholic habits (n = 190, age 52 years). Bar 1 P<0.0001 *vs* Bar 4. Bar 2 P<0.0001 *vs* Bar 4. Bar 4 P<0.0001 *vs* Bar 5. **B:** Without steatosis compared to outpatients without alcoholic habits. Bar 1: CH-C young male patients without steatosis (n = 24, age 37 years); Bar2: CH-C elderly male patients without steatosis (n = 11, average age 49 years); Bar 3: Male patients with liver steatosis (n = 16); Bar 4: Male outpatients without alcoholic habits (n = 60, age 37 years); Bar 5: Male outpatients without alcoholic habits (n = 509, age 49 years). Bar 1 and 2 P<0.0005 *vs* Bar 3. Bar 3 P<0.0005 *vs* Bar 4.

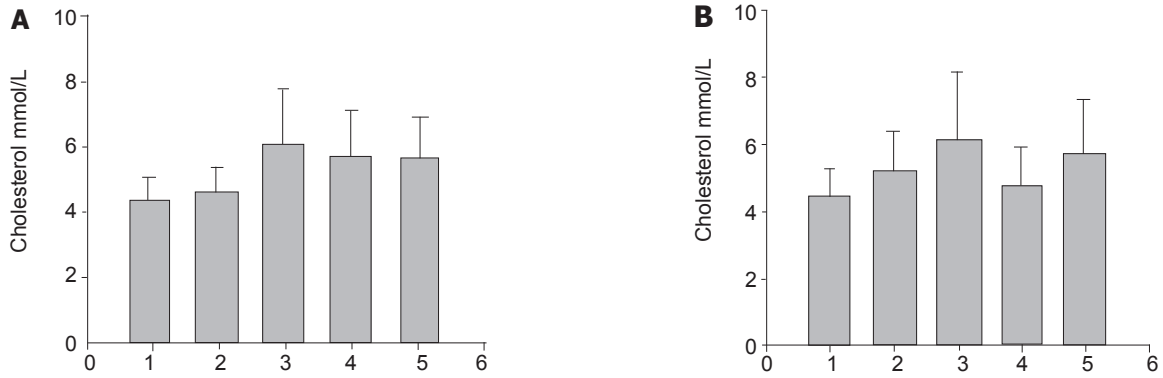

Figure 7 Cholesterol levels in CH-C female patients. **A:** With steatosis compared to outpatients with alcoholic habits; Bar 1: CH-C young female patients with steatosis (*n* = 26, average age 38 years); Bar 2: CH-C elderly female patients with steatosis (*n* = 20,average age 52 years); Bar 3: female patients with liver steatosis (*n* = 12); Bar 4: female outpatients with alcoholic habits (*n* = 8, age 38 years); Bar 5: female outpatients with alcoholic habits (*n* = 16, age 52 years). Bar 1 NS *vs* Bar 2. Bar 1 and 2 *P*<0.0001 *vs* Bar 3. Bar 1 *P*<0.0001 *vs* Bar 4. Bar 1 and 2 *P*<0.0001 *vs* Bar 5. **B:** Without steatosis compared to outpatients without alcoholic habits. Bar 1: CH-C young female patients without steatosis (*n* = 10, average age 29 years); Bar 2: CH-C elderly female patients without steatosis (*n* = 7, average age 53 years); Bar 3: female patients with liver steatosis (*n* = 12); Bar 4: female outpatients without alcoholic habits (*n* = 125, age 29 years); Bar 5: female outpatients without alcoholic habits (*n* = 803, age 53 years). Bar 1 NS *vs* Bar 2. Bar 1 *P* < 0.0001 *vs* Bar 3. Bar 1 *P*<0.0001 *vs* Bar 5. Bar 3 *P* < 0.0001 *vs* Bar 4.

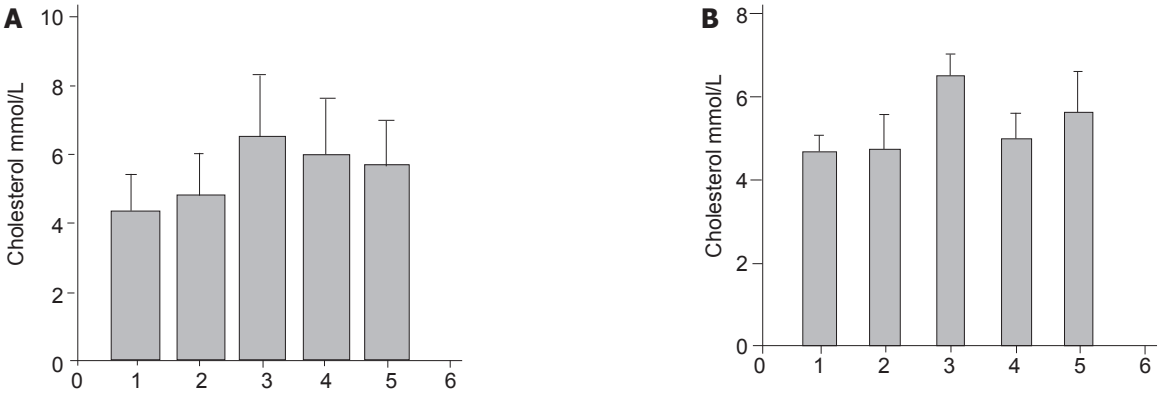

Figure 8 Cholesterol levels in CH-C male patients. **A:** With steatosis compared to outpatients with alcoholic habits; Bar 1: CH-C young male patients with steatosis (*n* = 29, average age 37 years); Bar 2: CH-C elderly male patients with steatosis (*n* = 15, average age 51 years); Bar 3: male patients with liver steatosis (*n* = 16); Bar 4: male outpatients with alcoholic habits (*n* = 86, age 37 years); Bar 5: male outpatients with alcohollic habits (*n* = 190, age 51 years). Bar 1NS *vs* Bar 2. Bar 1 and 2 *P*<0.0001 *vs* Bar 3. Bar 1 and 2 *P*<0.0001 *vs* Bar 4. **B:** Without steatosis compared to outpatients without alcoholic habits. Bar 1: CH-C young male patients without steatosis (*n* = 24, average age 34 years); Bar 2: CH-C elderly male patients without steatosis (*n* = 11, average age 49 years); Bar 3: male patients with liver steatosis (*n* = 16); Bar 4: male outpatients without alcoholic habits (*n* = 60, age 34 years); Bar 5:Male outpatients without alcoholic habits (*n* = 509, age 49 years). Bar1NS *vs* Bar 2. Bar 1 and 2 *P*<0.001 *vs* Bar 3. Bar 1 and 2 *P*<0.001 *vs* Bar 5. Bar 3 P<0.001 *vs* Bar 4.

In certain studies, steatosis was found to accelerate the progression of liver disease and correlate with specific HCV genotype[36]. In our study steatosis was detected in 63% of CH-C patients. The ALT-levels were statistically in correlation with the grade of steatosis. Comparing the HAI and ALT levels, a significant correlation was found in the CH-C cases without steatosis, while no difference was found in the group with steatosis. Inserting the score values of steatosis (0-3) into the score of the grade of necroinflammation, a significant correlation was detected for HAI and ALT levels. This suggests that inclusion of the score of steatosis into the grade, for measuring the necroinflammatory reaction in CH-C, might better reflect the alteration in the liver tissue and correlate with ALT enzyme elevation. Our data strongly suggest the importance of steatosis in the virus related necroinflammatory process. Worsening of steatosis was found as an independent factor in fibrosis progression in CH-C[37].

Regarding the different patient subgroups, the triglyceride levels revealed a marked low degree in the C virus-infected patients in comparison to the levels seen in the non-viral steatotic patients and in the relatively large number of outpatients without clinical signs of liver diseases. This detected phenomenon was observable in relation to the age, sex, and drinking habits of the outpatients of the praxis, too.

The behavior of cholesterol levels was the same as in case of the triglyceride levels, while the young steatotic virus-infected male patients failed to show higher elevated levels.

In conclusion, a recent study has found an association

between liver cell apoptosis and steatosis in CH-C patients, which might contribute to the progression of liver injury and fibrosis in CH-C[5]. Our study confirms the importance of the presence of steatosis, which is associated with higher ALT- and lower lipid levels on the periphery in CH-C patients with steatosis. The peripheral lipid levels, however, do not reflect the severity of steatosis or liver damages. Our study suggests that the grade of steatosis in the liver is a substantial part of the determination of the grade of necroinflammation and should be incorporated into the evaluation of liver biopsy materials in CH-C patients.

REFERENCES

1 **Poynard T,** Ratziu V, McHutchison J, Manns M, Goodman Z, Zeuzem S, Younossi Z, Albrecht J. Effect of treatment with peginterferon or interferon alfa-2b and ribavirin on steatosis in patients infected with hepatitis C. *Hepatology* 2003; **38:** 75-85

2 **Lefkowitch JH,** Schiff ER, Davis GL, Perrillo RP, Lindsay K, Bodenheimer HC Jr, Balart LA, Ortego TJ, Payne J, Dienstag JL, Gibas A, Jakobson IM, Tamburro CH, Carey W, O'Brien C, Sampliner R, Thiel DH, Feit D, Albrecht J, Meschievitz I, Sanghvi B, Vaugham RD. Pathological diagnosis of chronic hepatitis C: A multicenter comparative study with chronic hepatitis B. *Gastroenterol* 1993; **104:** 595-603

3 **Giannini E,** Ceppa P, Botta F, Fasoli A, Romagnoli P, Cresta E, Venturino V, Risso D, Celle G, Testa R. Steatosis and bile duct damage in chronic hepatitis C: distribution and relationships in a group of Northern Italian patients. *Liver* 1999; **19:** 432-437

4 **Scheuer PJ,** Ashrafzadeh P, Sherlock S, Brown D, Dusheiko GM. The pathology of hepatitis C. *Hepatology* 1992; **15:** 567-571

5 **Walsh MJ,** Vanags DM, Clouston AD, Richardson MM, Purdie DM, Jonsson JR, Powell EE. Steatosis and liver cell apoptosis in chronic hepatitis C: Amechanism for increased liver injury. *Hepatology* 2004; **39:** 1230-1238

6 **Fiore G,** Fera G, Napoli N, Vella F, Schiraldi O. Liver steatosis and chronic hepatitis C: a spurious association? *Eur J Gastroenterol Hepatol* 1996; **8:** 125-129

7 **Hui JM,** Kench J, Farrell GC, Lin R, Samarasinghe D, Liddle C, Byth K, George J. Genotype-specific mechanisms for hepatic steatosis in chronic hepatitis C infection. *J Gastroenterol Hepatol* 2002; **17:** 873-881

8 **Sanyal AJ,** Contos MJ, Sterling RK, Luketic VA, Shiffman ML, Stravitz RT, Mills AS. Nonalcoholic fatty liver disease in patients with hepatitis C is associated with features of the metabolic syndrome. *Am J Gastroent* 2003; **98:** 2064-2071

9 **Friedenberg F,** Pungpapong S, Zaeri N, Braitman LE. The impact of diabetes and obesity on liver histology in patients with hepatitis C. *Diabetes Obesity and Metabolism* 2003; **5:** 150-155

10 **Gochee PA,** Jonsson JR, Clouston AD, Pandeya N, Purdie DM, Powell EE. Steatosis in chronic hepatitis C: association with increased messenger RNA expression of collagen I, tumor necrosis factor-alpha and cytochrome P450 2E1. *J Gastroenterol Hepatol* 2003; **18:** 386-392

11 **Shi ST,** Polyak SJ, Tu H, Taylor DR, Gretch DR, Lai MM. Hepatitis C virus NS5A colocalizes with the core protein on lipid droplets and interacts with apolipoproteins. *Virology* 2002; **292:** 198-210

12 **Monto A.** Hepatitis C and steatosis. *Semin Gastrointest Dis* 2002; **13:** 40-46

13 **Kumar D,** Farrell GC, Fung C, George J. Hepatitis C virus genotype 3 is cytopathic to hepatocytes: Reversal of hepatic steatosis after sustained therapeutic response. *Hepatology* 2002; **36:** 1266-1272

14 **Negro,** F. Hepatitis C virus and liver steatosis: Is it the virus? Yes it is, but not always. *Hepatology* 2002; **36:** 1050-1052

15 **Ramalho F.** Hepatitis C virus infection and liver steatosis. *Antiviral Res* 2003; **60:** 125-127

16 **Petit JM,** Bour JB, Galland-Jos C, Minello A, Verges B, Guiguet M, Brun JM, Hillon P. Risk factors for diabetes mellitus and early insulin resistance in chronic hepatitis C. *J Hepatol* 2001; **35:** 279-283

17 **Ratziu V,** Trabut JB, Poynard T. Fat, diabetes, and liver injury in chronic hepatitis C. *Current Gastroenterology Reports* 2004; **6:** 22-29

18 **Serfaty L,** Poujol-Robert A, Carbonell N, Chazouillères O, Poupon RE, Poupon R. Effect of the interaction between steatosis and alcohol intake on liver fibrosis progression in chronic hepatitis C. *Am J Gastroent* 2002; **97:** 1807-1812

19 **Bjoro K,** Bell H, Hellum KB, Skaug K, Raknerud N, Sandvei P, Doskeland B, Maeland A, Lund-Tonnesen S, Myrvang B. Effect of combined interferon-alpha induction therapy and ribavirin on chronic hepatitis C virus infection: a randomized multicentre study. *Scand J Gastroenterol* 2002; **37:** 226-232

20 **Hourigan LF,** Macdonald GA, Purdie D, Whitehall VH, Shorthouse C, Clouston A, Powell EE. Fibrosis in chronic hepatitis C correlates significantly with body mass index and steatosis. *Hepatology* 1999; **29:** 1215-1219

21 **Westin J,** Nordlinder H, Lagging M, Norkrans G, Wejstål R. Steatosis accelerates fibrosis development over time in hepatitis C virus genotype 3 infected patients. *J Hepatol* 2002; **37:** 837-842

22 **Asselah T,** Boyer N, Guimont MC, Cazals-Hatem D, Tubach F, Nahon K, Daïkha H, Vidaud D, Martinot M, Vidaud M, Degott C, Valla D, Marcellin P. Liver fibrosis is not associated with steatosis but with necroinflammation in French patients with chronic hepatitis C. *Gut* 2003; **52:** 1638-1643

23 **Moriya K,** Yotsuyanagi H, Shintani Y, Fujie H, Ishibashi K, Matsuura Y, Miyamura T, Koike K. Hepatitis C virus core protein induces hepatic steatosis in transgenic mice. *J Gen Virol* 1997; **78:** 1527-1531

24 **Barba G,** Harper F, Harada T, Kohara M, Goulinet S, Matsuura Y, Eder G, Schaff Z, Chapman MJ, Miyamura T, Bréchot C. Hepatitis C virus core protein shows a cytoplasmic localization and associates to cellular lipid storage droplets. *Proc Natl Acad Sci USA* 1997; **94:** 1200-1205

25 **Desmet VJ**, Knodell RG**,** Ishak KG, Black WC, Chen TS, Craig R, Kaplowitz N, Kiernan TW, Wollman J. Formulation and application of a numerical scoring system for assessing histological activity in asymptomatic chronic active hepatitis. *Hepatology* 1981; **1:** 431-435

26 **Ishak K,** Baptista A, Bianchi L, Callea F, De Groote J, Gudat F, Denk H, Desmet V, Korb G, MacSween RN. Histological grading and staging of chronic hepatitis. *J Hepatol* 1995; **22:** 696-699

27 **Rubbia-Brandt L,** Quadri R, Abid K, Giostra E, Malé PJ, Mentha G, Spahr L, Zarski JP, Borisch B, Hadengue A, Negro F. Hepatocyte steatosis is a cytopathic effect of hepatitis C virus genotype 3. *J Hepatol* 2000; **33:** 106-115

28 **Rubbia-Brandt L,** Leandro G, Spahr L, Giostra E, Quadri R, Malé PJ, Negro F. Liver steatosis in chronic hepatitis C: a morphological sign suggesting infection with HCV genotype 3. *Histopathology* 2001; **39:** 119-124

29 **Giannini E,** Ceppa P, Botta F, Mastracci L, Romagnoli P, Comino I, Pasini A, Risso D, Lantieri PB, Icardi G, Barreca T, Testa R. Leptin has no role in determining severity of steatosis and fibrosis in patients with chronic hepatitis C. *Am J Gastroenterol* 2000; **95:** 3211-3217

30 **Monto A,** Alonzo J, Watson JJ, Grunfeld C, Wright TL. Steatosis in chronic hepatitis C: Relative contributions of obesity, diabetes mellitus, and alcohol. *Hepatology* 2002; **36:** 729-736

31 **Perlemuter G,** Sabile A, Letteron P, Vona G , Topilco A, Chrétien Y, Koike K, Pessayre D, Chapman J, Barba G, Bréchot C.

Hepatitis C virus core protein inhibits microsomal triglyceride transfer protein activity and very low density lipoprotein secretion: a model of viral-related steatosis. *FASEB J* 2002; **16:** 185-194

32 **Eder G,** Sárosi I, Schaff Zs. Safety testing of blood products in chimpanzees. In: Eder G, Kaiser E, King FA, eds. The role of the chimpanzeein research. Basel: Karger S, 1994: 156-166

33 **Fujie H,** Yotsuyanagi H, Moriya K, Shintani Y, Tsutsumi T, Takayama T, Makuuchi M, Matsuura Y, Miyamura T, Kimura S, Koike K. Steatosis and intrahepatic hepatitis C virus in chronic hepatitis. *J Med Virol* 1999; **59:** 141-145

34 **Thomssen R,** Bonk S, Thiele A. Density heterogeneities of hepatitis C virus in human sera due to the binding of beta-lipoproteins and immunoglobulins. Med Microbiol Immunol 1993; **182:** 329-334

35 **Serfaty L,** Andreani T, Giral P, Carbonell N, Chazouillères O, Poupon R.Hepatitis C virus induced hypobetalipoproteinemia: a possible mechanism for steatosis in chronic hepatitis C. *J Hepatol* 2001; **34:** 428-434

36 **Adinolfi LE,** Gambardella M, Andreana A, Tripodi MF, Utili R, Ruggiero G. Steatosis accelerates the progression of liver damage of chronic hepatitis C patients and correlates with specific HCV genotype and visceral obesity. *Hepatology* 2001; **33:** 1358-1364

37 **Castéra L,** Hézode C, Roudot-Thoraval F, Bastie A, Zafrani ES, Pawlotsky JM, Dhumeaux D. Worsening of steatosis is an independent factor of fibrosis progression in untreated patients with chronic hepatitis C and paired liver biopsies. *Gut* 2003; **52:** 288-292

Science Editor Guo SY **Language Editor** Elsevier HK

PO Box 2345, Beijing 100023, China
www.wjgnet.com
wjg@wjgnet.com

ELSEVIER

world J Gastroenterol 2005;11(41):6429-6432
World Journal of Gastroenterology ISS1007-9327

VP22 fusion protein-based dominant negative mutant can inhibit hepatitis B virus replication

Jun Yi, Wei-Dong Gong, Ling Wang, Rui Ling, Jiang-Hao Chen, Jun Yun

Jun Yi, Ling Wang, Rui Ling, Jiang-Hao Chen, Jun Yun, Department of General Surgery, Xijing Hospital, Fourth Military Medical University, Xi'an 710033, Shaanxi Province, China
Wei-Dong Gong, Oncology Center, Zhujiang Hospital, Southern Medical University, Guangzhou 510282, Guangdong Province, China
Supported by the National Natural Science Foundation of China, No. 30400380
Correspondence to: Wei-Dong Gong, Oncology Center, Zhujiang Hospital, Southern Medical University, Guangzhou 510282, Guangdong Province, China. gongwd70@fmmu.edu.cn.
Telephone: +86-20-83373939
Received: 2004-12-02 Accepted: 2005-02-18

Abstract

AIM: To investigate the inhibitory effect of VP22 fusion protein-based dominant negative (DN) mutant on Hepatitis Bvrus (HBV) replication.

METHODS: Full-length or truncated fragment of VP22 was fused to C terminal of HBV core protein (HBc), and subcloned into pcDNA3.1 (-) vector, yielding eukaryotic expression plasmids of DN mutant. After transfection into HepG2.2.15 cells, the expression of DN mutant was identified by immunofluorescence staining. The inhibitory effect of DN mutant on HBV replication was indexed as the supernatant HBsAg concentration determined by RIA and HBV-DNA content by fluorescent quantification-PCR (FQ-PCR). Meanwhile, metabolism of HepG2.2.15 cells was evaluated by MTT colorimetry.

RESULTS: VP22-based DN mutants and its truncated fragment were expressed in HepG2.2.15 cells, and had no toxic effect on host cells. DN mutants could inhibit HBV replication and the transduction ability of mutant-bearing protein had a stronger inhibitory effect on HBV replication. DN mutants with full length of VP22 had the strongest inhibitory effect on HBV replication, reducing the HBsAg concentration by 81.94%, and the HBV-DNA content by 72.30%. MTT assay suggested that there were no significant differences in cell metabolic activity between the groups.

CONCLUSION: VP22-based DN mutant can inhibit HBV replication effectively.

Key words: Hepatitis B virus; Dominant negative mutant; VP22

Yi J, Gong WD, Wang L, Ling R, Chen JH, Yun J. VP22 fusion protein-based dominant negative mutant can inhibit hepatitis B virus replication. *World J Gastroenterol* 2005; 11(41):6429-6432
http://www.wjgnet.com/1007-9327/11/6429.asp

INTRODUCTION

At present, about 3.5 hundred million people are infected with HBV, and about 1 million people die of Hepatitis Bvrus (HBV) infection or related diseases each year, ranking 9th in disease deaths[1-4]. There are no effective therapies for HBV infection. Although about 40% HBV-infected patients responded to interferon, patients in our country have a poorer response to it. Other antiviral agents, such as nucleoside/nucleotide analogs[5], are quite effective inhibitors of HBV replication[6-9]. However, the rapid development of drug resistance remains a growing concern. Gene therapy provides a novel idea for the treatment of HBV infection, can inhibit replication of HBV at gene level and remove HBV from host cells[10-12]. Expression of dominant negative (DN) mutant in liver cells is one of the most important strategies[13-17].

In 1997, Elliott and O'Hare[18] found that VP22, a structural protein (and its fusion protein) of herpes simplex virus type-1 (HSV-1), can enter into the cells from the medium, and translocate between cells in a contact-independent manner. Here, VP22 was fused to HBV core protein (HBc) and a fusion DN mutant was constructed to enhance the antiviral effect of the DN mutant by utilizing the transduction ability of VP22 protein.

MATERIALS AND METHODS

Materials

Plasmids pVP22/*myc*-His2 and pcDNA3.1(-) were purchased from Invitrogen Co. EBO-HBV, in which 1.3-folds of HBV genome was cloned, and stored in our laboratory. Restriction enzymes and ligations were purchased from TaKaRa Biotech Co., Ltd; mouse anti-HBc or c-myc antibodies were purchased from Santa Cruz Co. FITC-labeled sheep anti-mouse IgG was purchased from BioStar Biotech Co., Ltd. DMEM, fetal bovine serum, and Lipofectamine 2000 were purchased from GIBCO Co. Solid phase radio-immunoassay kit was purchased from Beimian Dongya Biotech Institute, Beijing.

Oligonucleotides and primers

All the oligonucleotides and primers were synthesized

by TaKaRa Biotech Co., Ltd. The underlined sequences indicate restriction enzyme (right) sites, respectively, which were added to the oligonucleotide primers for subsequent cloning of amplified DNA. The capital letters indicate start or stop codon.

HBc1: 5'-gcgcggtaccATGgacatcgaccctt-3' (*Kpn*I)

HBc2: 5'-gcgcctcgagTCAggatccacattgaggttccc-3' (*Xho*I, *Bam*HI)

US: 5'-gcccggatccatgacctctcgctccgtg-3' (*Bam*HI)

UR: 5'-ccccagatctatcgggactcgccatacc-3' (*Bgl*II)

DS: 5'-gccgagatctgacgcggccacggcg-3' (*Bgl*II)

DR: 5'-gggcctcgagTTAcagctaatcctcttctgag-3' (*Xho*I)

c-myc1:5'-gcccggatccgaacaaaaactcatctcagaagaggatctgTAActcgaggggc-3' (*Bam*HI, *Xho*I)

c-myc2:5'-gggcctcgagTTAcagatcctcttctgagatgagtttttgttcggatc
cgccc-3' (*Xho*I, *Bam*HI)

Cell culture

HepG2.2.15 cells integrated with full-length HBV gene[19-21] were cultured in DMEM containing 150 mL/L fetal bovine serum at 37 °C, in 50 mL/L CO_2. G418 was added to screen cells at the final concentration of 100 mg/L. The media were freshened once in every two days and the cells were passaged every six days.

Plasmid constructs

PCR products, amplified from EBO-HBV using HBc1/HBc2 as primers, were cloned into pcDNA3.1(-) after being digested by *Kpn*I/*Xho*I, yielding the vector pHBc (Figure 1).

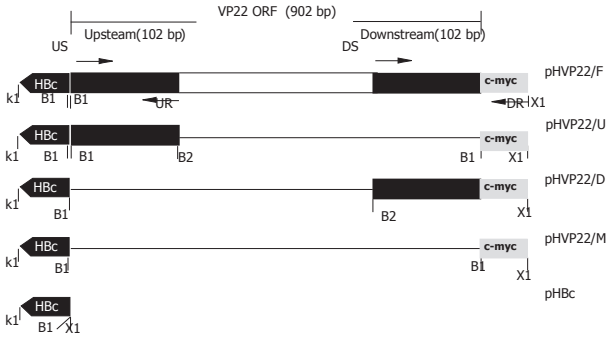

Figure 1 Plasmid constructs used in the experiment. (Dotted lines represent the deleted sequences. The nomenclature of plasmids is listed in the right. The primers, US, UR, DS, and DR, are marked with arrows. Restriction enzymes are expressed in single letters. *K1*, *Kpn*I; *B1*, *Bam*HI; *B2*, *Bgl*II; *X1*, *Xho*I. Downstream sequence of 102 bp is the PTD of VP22).

C-myc1/c-myc2 were dissolved at a concentration of 0.1 g/L and annealed by heating at 100 °C for 5 min, then slowly cooling to room temperature to form double-stranded c-myc digested by *Bam*HI/*Xho*I and cloned into pHBc digested by the same restrictions to produce plasmid pHVP22/M.

The fragment including full-length of VP22 and *c-myc* epitope was amplified from pVP22/*myc*-His2 plasmid (primers US/DR). PCR products were digested by *Bam*HI/*Xho*I and inserted into pHBc to produce pHVP22/F.

The upstream of VP22-coding sequence 102 bp amplified from pVP22/*myc*-His2 (primers US/UR) was digested by *Bam*HI/*Bgl*II and ligated into *Bam*HI site of pHVP22/M restricted with *Bam*HI and dephosphorized. The resulting plasmid bearing directional insertion was called pHVP22/U.

The downstream of VP22-coding sequence 102 bp was amplified from pVP22/*myc*-His2, and PCR products were inserted into pHBc after *Bam*HI/*Xho*I digestion to produce plasmid pHVP22/D.

Transfection

Transfections were performed as described by the provider of Lipofectamine 2000 (Gibco's handbook). Cells (4×10^8 L) were added to a 24-well plate (500 L/well) in which a coverslide was placed in advance. The transfection experiment was divided into seven groups and carried out in triplicate: pHVP22/F, pHVP22/U, pHVP22/D, pHVP22/M, pHBc, pcDNA3.1(-) and MOCK transfection.

Confirmation of transgene expression

After transfection, cells were immediately washed with sterilized PBS (4 °C, pH 8.0), fixed in 20 g/L paraformaldehyde and 1 g/L Triton X-100 diluted in PBS, and put on ice for 30 min. Cells were washed thrice with cold PBS. Non-specific epitopes were blocked with 10 g/L BSA for 10 min at 42 °C. After being washed with cold PBS, cells were incubated with mouse anti-HBc or c-myc mAb (1:500) for 15 min at 42 °C, further incubated with rabbit anti-mouse IgG labeled with FITC (1:1 000). The coverslides were mounted on slides using 50 mL/L glycerol/PBS and observed by fluorescence microscopy.

Antiviral activity

Forty-eight hours after transfection, HBsAg concentration was determined by RIA kit (completed by Nuclear Medicine Department of Xijing Hospital), and HBV-DNA content was quantified by FQ-PCR. The data obtained were analyzed by SPSS software.

MTT assay

The effect of transgene expression on host cells was evaluated by MTT colorimetry.

RESULTS

Plasmid construction

To enhance the antiviral effect of HBc DN mutant, both the full length of VP22 and the truncated version (102 bp upstream or downstream) were fused to C terminals of HBc, respectively (pHVP22/F, pHVP22/U, pHVP22/D), and the effects of anti-HBV replication were detected. All plasmids used here were confirmed by sequencing, which was completed by GeneCore Company (Shanghai, China).

Detection of transgene expression

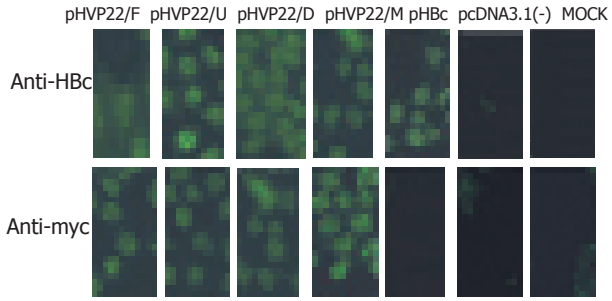

Figure 2 Confirmation of transgene expression in HepG2.2.15 cells.

Table1 MTT results of transfection groups (n=3, mean ±SD)

Group	A_{490}nm	P^1
pHVP22/F	0.425±0.065	>0.05
pHVP22/U	0.465±0.050	>0.05
pHVP22/D	0.410±0.075	>0.05
pHVP22/M	0.438±0.042	>0.05
pHBc	0.413±0.063	>0.05
pcDNA3.1(-)	0.430±0.065	>0.05
MOCK	0.423±0.058	>0.05

[1]*vs* mock.

To identify the expression of transgenes in HepG2.2.15 cells, indirect immunofluorescence was performed using antibody against HBc or c-myc. No fluorescence was found in pcDNA3.1(-) and MOCK transfection, the same results were obtained in pHBc, pcDNA3.1(-) and MOCK transfection. Strong fluorescence was detected in other transfections. The results suggested that transgenes were successfully expressed in HepG2.2.15 cells and recognized by the corresponding antibodies (Figure 2).

Antiviral effect

To investigate the antiviral activity of VP22 fusion DN mutant on HBV replication, the inhibitory effect was determined by HBsAg concentration and HBV-DNA content in the supernatant of HepG2.2.15 cell culture. When compared to MOCK transfection, HBsAg concentrations in pHVP22/F, pHVP22/U, and pHVP22/D transfections decreased by 81.94%, 38.88%, and 63.89%, respectively (Figure 3A, P<0.05), and HBV-DNA content by 72.30%, 29.60%, 46.42%, respectively (Figure 3B, P<0.05), indicating that VP22 fusion DN mutant could inhibit HBV replication effectively. Regardless of taking HBsAg concentration or HBV-DNA content as an index, pHVP22/F, pHVP22/U, and pHVP22/D showed a significant difference between the groups (P<0.05). DN mutant with transduction domains (pHVP22/F and pHVP22/D) had a stronger antiviral activity than that without the domain (pHVP22/U, P<0.05). When compared to DN mutant with full length of VP22 (pHVP22/F), DN mutant with the transduction domain (pHVP22/D) showed a weaker antiviral activity (P<0.05). There was no significant difference between DN mutant based on c-myc epitope (pHVP22/M) and MOCK transfection (P>0.05), suggesting that pHVP22/M could not inhibit HBV replication.

MTT assay

After 48-h incubation, the morphology of cells was observed under inverted microscope and no discernable difference was found between groups. MTT assay showed no significant differences between groups (P>0.05), suggesting that the expression of DN mutants had no effect on the growth of host cells (Table 1).

DISCUSSION

HBV infection is an important health problem worldwide[14], and the investigation about HBV therapy is a long-standing focus. The development of genetic

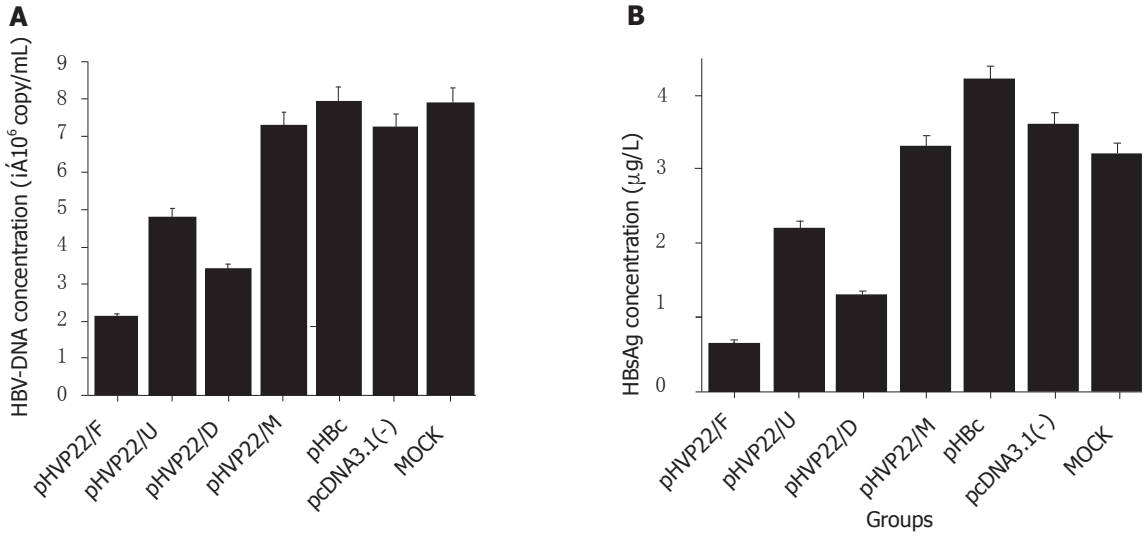

Figure 3 Comparison of HBsAg (**A**) and HBV-DNA (**B**) concentrations between transfection groups.

engineering facilitates the role of gene therapy in anti-HBV therapy[13,14] and DN mutant is one of the important strategies[15-17]. After introduction of mutant gene into the infected cells, the activity of wild-type viral gene is inhibited by the mutant version in a competitive manner, leading to the inhibition of virus replication[22,23]. DN mutant, as a preferential strategy, takes protein as the effector and avoids the problem of HBV mutation, which is one of the obstacles when DNA is used as an effector. But insufficient therapeutic molecules can reach the VP22 protein, bearing protein-transduction ability, to enhance the DN mutant effect and complement the shortage of therapeutic molecules in target cells.

As a structural protein of HSV-1, VP22 (or its fusion protein) has the strong ability to translocate between cells[18]. Proteins fused with the protein transduction domain (PTD), which lies in C terminal of VP22 (34 amino acids), also can translocate into the target cells[24-26]. In this report, HBsAg concentration decreased 63.89% by PTD-HBc fusion based (pHVP22/D) DN mutant, and DN mutant with upstream 34 amino acids of VP22 (pHVP22/U, without PTD) only decreased 38.88%, suggesting that DN mutant with PTD can strongly inhibit the activity of wild-type viral gene than that without PTD, and the transduction domain of VP22 can enhance the antiviral effect of DN mutant. By detecting HBV-DNA concentrations in the supernatant, similar results could be obtained.

DN mutant based on full-length of VP22 (pHVP22/F) decreased HBsAg concentration and HBV-DNA content by 81.94% and 72.30%, respectively (Figures 3A and B), showing a significant difference compared to PTD-based DN mutant (pHVP22/D, $P<0.05$). Due to the different efficiency between the two constructs, the molecular mass of the protein fused to HBc C-terminal is related to the inhibitory effect of DN mutant. The larger the fused molecule, the stronger the antiviral effect of DN mutant. Possible explanations may be related to the stabilization of the larger fusion protein and the steric hindrance is necessary to inhibit proper assembly of the nucleocapsid.

In conclusion, DN mutant-based c-myc epitope (pHVP22/M) cannot inhibit HBV replication. Since c-myc epitope has only 10 amino acids, DN mutant of HBc may mediate antiviral effect through a minimal length of C-terminal. The related experiments are in process.

REFERENCES

1 **Fleming J.** Current treatments for hepatitis. *J Infus Nurs* 2002; **25**: 379-382
2 **elSaadany S**, Tepper M, Mao Y, Semenciw R, Giulivi A. An epidemiologic study of hepatocellular carcinoma in Canada. *Can J Public Health* 2002; **93**: 443-446
3 **Mazumdar TN.** Management of chronic hepatitis B infection: an update. *J Indian Med Assoc* 2001; **99**: 306-308, 310
4 **Ganem D,** Varmus HE. The molecular biology of the hepatitis B viruses. *Annu Rev Biochem* 1987; **56:** 651-693
5 **Tang ZY**. Hepatocellular carcinoma--cause, treatment and metastasis. *World J Gastroenterol* 2001; **7**: 445-454
6 **Wai CT,** Chu CJ, Hussain M, Lok AS. HBV genotype B is associated with better response to interferon therapy in HBeAg(+) chronic hepatitis than genotype C. *Hepatology* 2002; **36**: 1425-1430
7 **Manns MP.** Current state of interferon therapy in the treatment of chronic hepatitis B. *Semin Liver Dis* 2002; **22** Suppl 1: 7-13
8 **Shindo M,** Hamada K, Koya S, Sokawa Y, Okuno T. The clinical significance of core promoter and precore mutations during the natural course and interferon therapy in patients with chronic hepatitis B. *Am J Gastroenterol* 1999; **94**: 2237-2245
9 **Liaw YF.** Therapy of chronic hepatitis B: current challenges and opportunities. *J Viral Hepat* 2002; **9**: 393-399
10 **Wolters LM,** Hansen BE, Niesters HG, de Man RA. Viral dynamics in chronic hepatitis B patients treated with lamivudine, lamivudine-famciclovir or lamivudine-ganciclovir. *Eur J Gastroenterol Hepatol* 2002; **14**: 1007-1011
11 **Santantonio T,** Mazzola M, Iacovazzi T, Miglietta A, Guastadisegni A, Pastore G. Long-term follow-up of patients with anti-HBe/HBV DNA-positive chronic hepatitis B treated for 12 months with lamivudine. *J Hepatol* 2000; **32**: 300-306
12 **Chiou HC,** Lucas MA, Coffin CC, Banaszczyk MG, Ill CR, Lollo CP. Gene therapy strategies for the treatment of chronic viral hepatitis. *Expert Opin Biol Ther* 2001; **1**: 629-639
13 **von Weizsäcker F**, Köck J, Wieland S, Offensperger WB, Blum HE. Dominant negative mutants of the duck hepatitis B virus core protein interfere with RNA pregenome packaging and viral DNA synthesis. *Hepatology* 1999; **30**: 308-315
14 **von Weizsäcker F,** Wieland S, Köck J, Offensperger WB, Offensperger S, Moradpour D, Blum HE. Gene therapy for chronic viral hepatitis: ribozymes, antisense oligonucleotides, and dominant negative mutants. *Hepatology* 1997; **26**: 251-255
15 **Scaglioni P**, Melegari M, Takahashi M, Chowdhury JR, Wands J. Use of dominant negative mutants of the hepadnaviral core protein as antiviral agents. *Hepatology* 1996; **24**: 1010-1017
16 **von Weizsäcker F**, Wieland S, Blum HE. Inhibition of viral replication by genetically engineered mutants of the duck hepatitis B virus core protein. *Hepatology* 1996; **24**: 294-299
17 **Scaglioni PP**, Melegari M, Wands JR. Characterization of hepatitis B virus core mutants that inhibit viral replication. *Virology* 1994; **205**: 112-120
18 **Elliott G,** O'Hare P. Intercellular trafficking and protein delivery by a herpesvirus structural protein. *Cell* 1997; **88**: **223-233**
19 **Sells MA**, Chen ML, Acs G. Production of hepatitis B virus particles in Hep G2 cells transfected with cloned hepatitis B virus DNA. *Proc Natl Acad Sci U S A* 1987; **84**: 1005-1009
20 **Acs G**, Sells MA, Purcell RH, Price P, Engle R, Shapiro M, Popper H. Hepatitis B virus produced by transfected Hep G2 cells causes hepatitis in chimpanzees. *Proc Natl Acad Sci U S A* 1987; **84**: 4641-4644
21 **Sells MA**, Zelent AZ, Shvartsman M, Acs G. Replicative intermediates of hepatitis B virus in HepG2 cells that produce infectious virions. *J Virol* 1988; **62**: 2836-2844
22 Trono D, Feinberg MB, Baltimore D. HIV-1 Gag mutants can dominantly interfere with the replication of the wild-type virus. *Cell* 1989; **59**: 113-120
23 **Malim MH**, Freimuth WW, Liu J, Boyle TJ, Lyerly HK, Cullen BR, Nabel GJ. Stable expression of transdominant Rev protein in human T cells inhibits human immunodeficiency virus replication. *J Exp Med* 1992; **176**: 1197-1201
24 **Elliott G**, O'Hare P. Intercellular trafficking of VP22-GFP fusion proteins. *Gene Ther* 1999; **6**: 149-151
25 **Aints A**, Güven H, Gahrton G, Smith CI, Dilber MS. Mapping of herpes simplex virus-1 VP22 functional domains for inter- and subcellular protein targeting. *Gene Ther* 2001; **8**: 1051-1056
26 **Schwarze SR**, Dowdy SF. *In vivo* protein transduction: intracellular delivery of biologically active proteins, compounds and DNA. *Trends Pharmacol Sci* 2000; **21**: 45-48

Science Editor Guo SY **Language Editor** Elsevier HK

PO Box 2345, Beijing 100023, China
www.wjgnet.com
wjg@wjgnet.com

ELSEVIER

World J Gastroenterol 2005;11(41):6433-6439
World Journal of Gastroenterology ISSN 1007-9327

Hepatitis C virus non-structural 5A protein can enhance full-length core protein-induced nuclear factor-κB activation

Qing-Jiao Liao, Lin-Bai Ye, Khalid Amine Timani, Ying-Long She, Xiao-Jun Yang, Li Ye, Zheng-Hui Wu

Qing-Jiao Liao, Lin-Bai Ye, Khalid Amine Timani, Ying-Long She, Xiao-Jun Yang, Li Ye, Zheng-Hui Wu, State Key Laboratory of Virology, College of Life Sciences, Wuhan University, Wuhan 430072, Hubei Province, China
Supported by the Ph D Program Foundation of Ministry of Education of China, No. 20010486015
Correspondence to: Lin-Bai Ye, Dr., Professor, State Key Laboratory of Virology, College of Life Science, Wuhan University, Wuhan 430072, Hubei Province, China. linbaiye@whu.edu.cn
Telephone: +86-27-68752372 Fax: +86-27-68752372
Received: 2005-03-13 Accepted: 2005-04-30

Abstract

AIM: To study the effects of hepatitis C virus (HCV) core and non-structural 5A (NS5A) proteins on nuclear factor-κB (NF-κB) activity for understanding their biological function on chronic hepatitis caused by HCV infection.

METHODS: Luciferase assay was used to measure the activity of NF-κB in three different cell lines cotransfected with a series of deletion mutants of core protein alone or together with NS5A protein using pNF-κB-Luc as a reporter plasmid. Western blot and indirect immunofluorescence assays were used to confirm the expression of proteins and to detect their subcellular localization, respectively. Furthermore, Western blot was also used to detect the expression levels of NF-κB/p65, NF-κB/p50, and inhibitor κB-a (IκB-a).

RESULTS: The wild-type core protein (C191) and its mutant segments (C173 and C158) could activate NF-κB in Huh7 cells only and activation caused by (C191) could be enhanced by NS5A protein. Moreover, the full-length core protein and its different deletion mutants alone or together with NS5A protein did not enhance the expression level of NF-κB. The NF-κB activity was augmented due to the dissociation of NF-κB-IκB complex and the degradation of IκB-a.

CONCLUSION: NF-κB is the key transcription factor that can activate many genes that are involved in the cellular immune response and inflammation. Coexpression of the full-length core protein along with NS5A can enhance the NF-κB activation, and this activation may play a significant role in chronic liver diseases including hepatocellular carcinoma associated with HCV infection.

Key words: HCV; NS5A; Core protein; NF-κB

Liao QJ, Ye LB, Timani KA, She YL, Yang XJ, Ye L, Wu ZH. Hepatitis C virus non-structural 5A protein can enhance full-length core protein-induced nuclear factor-κB activation. *World J Gastroenterol* 2005; 11(41):6433-6439 http://www.wjgnet.com/1007-9327/11/6433.asp

INTRODUCTION

Hepatitis C virus (HCV) is a major causative agent for acute and chronic hepatitis, which often leads to liver cirrhosis and hepatocellular carcinoma[1,2]. HCV is an enveloped positive-sense RNA virus of the *Flaviviridae* family. The viral genome encodes a single polyprotein precursor of ~3 010 amino acids, which is cleaved by both host and viral proteases to produce three structural proteins at the amino terminus (Core, E1, and E2) and six nonstructural proteins at the carboxyl terminus (NS2, NS3, NS4A, NS4B, non-structural 5A (NS5A), and NS5B)[3-5].

HCV core protein is the viral nucleocapsid protein that binds to and packages the viral RNA genome. Core protein is a multifunctional protein that can interact with many cellular factors such as lymphotoxin-β receptor, tumor necrosis factor receptor (TNFR), heterogeneous nuclear ribonucleoprotein and LZIP[6-10]. Core protein also can modulate the expression of some genes like interleukin-2 (IL-2), p53 and p21[11-14]. NS5A protein is a phosphoprotein that exists in differentially phosphorylated forms of 56 and 58 ku with modifications of serine residues[15]. NS5A protein can directly interact with double-stranded RNA-dependent kinase and inactivate its function, thus modulating the IFN-stimulated antiviral response[16].

Nuclear factor-κB (NF-κB) belongs to a highly conserved Rel-related protein family, which includes RelA (p65), Rel B, c-Rel, NF-κB1 (p105/p50), and NF-κB2 (p100/p52). Of these, the p50/p65 heterodimer, commonly called NF-κB, is the most abundant and ubiquitous. NF-κB is the key transcription factor activating many genes involved in the cellular immune responses and inflammation, such as interferon-β, TNF-α, IL-2, IL-6, and IL-8[17].

Many researchers have reported that HCV core protein can modulate the activity of NF-κB in mammalian cells[18-21]. This phenomenon has also been found in NS5A protein[22-24]. Core protein can interact with NS5A protein both *in vitro* and *in vivo*[25]. However, whether this interaction has effect on NF-κB activation has not yet been determined. In this study, we investigated the effect of core protein and NS5A protein coexpression on NF-κB activity in three different cell lines. Our results showed that NS5A protein could

enhance the effect of full-length core protein on NF-κB activation in Huh7 cell line only. This activation is associated with the degradation of inhibitor κB-α (IκB-α).

MATERIALS AND METHODS

Plasmid construction

The recombinant plasmids with different deletion mutations of HCV core or NS5A genes were constructed by inserting the corresponding DNA fragments into the eukaryotic expression vector pcDNA3 under the immediate early CMV promoter. The DNA fragments were amplified by PCR from pBRTM/HCV1-3011 plasmid (genotype 1a, a generous gift from Dr. Charles M Rice, University of Washington) using primers in Table 1. Primers 1a and 1b were used to generate pcDNA-core (for C191) containing the full-length core protein, 1a and 1c primers were used to generate pcDNA-Δcore519 (for C173) with a deletion of 54 nt at its 3'-end, 1a and 1d primers were used to generate pcDNA-Δcore474 (for C158) with a deletion of 99 nt at its 3'-end, 2a and 1b primers were used to generate pcDNA-Δcore [76-573, for C(26-191)] with a deletion of 75 nt at its 3'-end, 2a and 1d primers were used to generate pcDNA-Δcore [76-474, for C(26-158)] with a 75 and 99 nt deletion at the 5'-end and 3'-end, respectively, 3a and 3b primers were used for pcNS5A with full-length 5A gene. All the constructed plasmids were confirmed by restricted digestion and sequencing.

Table 1 Primers used in this study

Primers	Oligonucleotides
1a	5′-AAG CTT *GAATTC* GCG **ATG** AGC ACG AAT CCT-3′ (*Eco*RI)
1b	5′-GTC GAC *TCTAGA* **CTA** GGC CGA AGC GGG CAC-3′ (*Xba*I)
1c	5′-GTC GAC *TCTAGA* **CTA** AGA GCA ACC AGG AAG-3′ (*Xba*I)
1d	5′-GTC GAC *TCTAGA* **CTA** CAG AAC CCG GAC GCC-3′ (*Xba*I)
2a	5′-AGT ACT *GAATTC* GCG **ATG** GGT GGC GGT CAG-3′ (*Eco*RI)
3a	5′-AGA TCT *AAGCTT* **ATG** GCT TCC GGC TCC TGG-3′ (*Hin*dIII)
3b	5′-TGG TAC *TCTAGA* **TCA** CAT TCA GCA GCA-3′ (*Xba*I)

Italic nucleotides represent the enzymes used for the ligation and the enzymes are also marked in the end of each primer. Bold nucleotides ATG and CTA represent the start and stop codon, respectively.

Cell culture and transfection

Cos-7, HeLa, and Huh7 cell lines were grown in Dulbecco's modified Eagle's medium (Hyclone) with 10% fetal bovine serum (Gibco) at 37 °C in 50 mL/L CO_2. DNA transfection experiment was performed using Lipofectamine™ 2000 (Gibco) according to the manufacturer's instructions.

Luciferase assay

The pNF-κB-Luc (Stratagene) vector containing the *Photinus pyralis* (firefly) luciferase reporter gene driven by a basic promoter element (TATA box) plus five repeats of κB *cis*-enhancer element (TGGGGACTTTCCGC) was used in this experiment. Approximately 5×10^4 cells were seeded into a 24-well tissue culture plate 24 h before transfection. The cells were cotransfected with 0.8 μg plasmids as four kinds of combination: (1) 0.4 μg pNF-κB-Luc and different concentrations (0.1, 0.2, and 0.4 μg) of core mutations or pcNS5A; (2) 0.4 μg pNF-κB-Luc and the same concentration of core mutations (0.2 μg) and pcNS5A (0.2 μg); (3) 0.3 μg pNF-κB-Luc and the same concentration of pcDNA-core (0.2 μg) and different concentrations (0.1, 0.2, and 0.3 μg) of pcNS5A; (4) 0.3 μg pNF-κB-Luc and the same concentration of pcNS5A (0.2 μg) and different concentrations (0.1, 0.2, and 0.3 μg) of pcDNA-core. Cells were cotransfected with pNF-κB-Luc and vector pcDNA3 as a negative control. The total concentration of the transfected plasmids was kept constant with pcDNA3 vector. Cells were harvested at 24 h after transfection and then lysed in the reporter lysis buffer (Promega). The luciferase activity was measured by TD-20/20 luminometer (Turner BioSystems, Sunnyvale, CA, USA), and normalized with respect to the protein concentration of the cell lysates. Each experiment was repeated at least thrice.

Western blot analysis

Twenty-four hours after transfection, the total cell proteins were separated by 15% SDS-polyacrylamide gel electrophoresis (SDS-PAGE) and transferred to a polyvinylidene difluoride membrane. The blots were first blocked with 5% non-fat milk in Tris buffer saline (TBS) containing 1 g/L Tween-20 and then probed with the first antibodies against HCV core protein (ViroStat, Inc., 1851), HCV NS5A protein (a generous gift from Dr. Stephene J Polyak, University of Washington), actin (Santa Cruz Biotechnology, Inc., sc-1616), NF-κB/P65 (Santa Cruz Biotechnology, Inc., sc-800), NF-κB/P50 (Santa Cruz Biotechnology, Inc., sc-114), IκB-α (Santa Cruz Biotechnology, Inc., sc-847) for 1 h at 37 °C After extensive washes, secondary antibodies conjugated with horseradish peroxidase were applied onto the blots for at least 1 h at 37 °C. Blots were washed five times with TBS-1 g/L Tween-20. Reagents for enhanced chemiluminescence were applied to the blots and the light signals were detected by X-ray film.

Indirect immunofluorescence assay

Sterile coverslips were placed in six-well tissue culture plates before the Cos-7 cells were plated on them. Twenty-four hours after transfection, the coverslips were rinsed twice with PBS, and the cells were fixed in methanol-acetone (1:1) at -20 °C for 5 min. After washing thrice with PBS, the fixed cells were covered with anti-core monoclonal or anti-NS5A mAbs for 1 h at 37 °C, and then washed thrice with PBS. Secondary antibodies (FITC-conjugated goat anti-mouse IgG) were then applied on the cells for 1 h at 37 °C in the dark. After washing, the cells were stained with propidium iodide to visualize the nuclear DNA and mounted in antifade mounting medium. The stained cells were visualized under a Leica confocal microscope (TCS NT SN 1500001, Leica Laser Technik, Germany). For the colocalization of full-length core and NS5A proteins, rabbit anti-core polyclonal antibody (produced in our laboratory) and mouse NS5A mAb were used as primary antibodies and TRITC-conjugated goat anti-rabbit IgG and FITC-conjugated goat anti-mouse IgG were used as secondary antibodies, respectively.

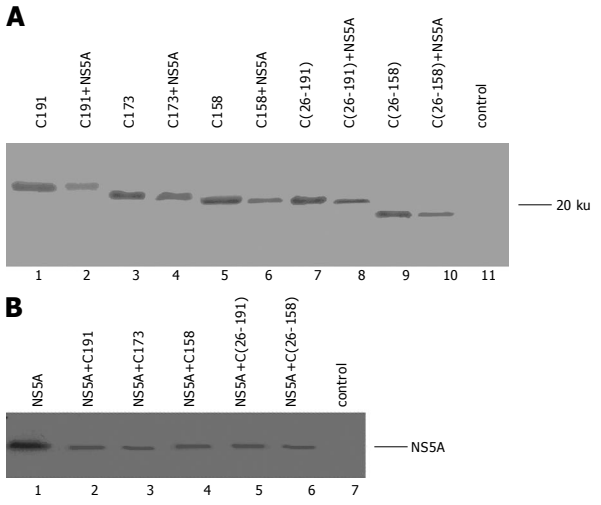

Figure 1 Expression of core mutant fragments **(A)** and NS5A protein **(B)**.

RESULTS

Identification of core mutants and NS5A protein

In this study, four core deletion mutants (C173, C158, C (26-191), C(26-158) were constructed besides the wild-type core protein (C191). C173 is the mature form of core protein with deletion of 18aa at its C-terminus. C158 is a mutant fragment with deletion of the hydrophobic amino acids at its C-terminus. C(26-191) is a mutant fragment without the reported functional domain at its N-terminus. C(26-158) is a mutant fragment without functional and hydrophobic domains at its N- and C-terminus, respectively. The expression of core mutants and NS5A protein in Huh7 was measured by Western blot. As shown in Figure 1A, core mutant fragments were expressed with a correct molecule mass of 21 ku for C191, 19 ku for C173, 18 ku for C158, 18 ku for C(26-191) and 15 ku for C(26-158) in the cells transfected with either core mutation fragments alone (lanes 1, 3, 5, 7, and 9) or together with NS5A protein (lanes 2, 4, 6, 8, and 10). The expression of NS5A protein is shown in Figure 1B. We got the correct band of 56 ku in the cells transfected with NS5A protein alone (lane 1) or together with core mutations (lanes 2-6). This experiment showed that core mutants and NS5A protein were expressed successfully from their respective recombinant plasmids.

HCV core protein activated NF-κB and was enhanced by NS5A protein in Huh7 cells

To study the effect of the coexpression of HCV core and NS5A proteins on NF-κB activity, the expressed plasmids, pcDNA-core, pcDNA-Δcore519, pcDNA-Δcore474, pcDNA-Δcore (75-573), pCDNA-Δcore (75-474), alone or together with pcNS5A were cotransfected with pNF-κB-Luc into three different cell lines Cos-7, HeLa, and Huh7. Luciferase activity was measured 24-h post-transfection. Our results showed a significant change of relative luciferase activity in Huh7 cells (Figure 2A) but not in Cos-7 cells (Figure 2B) or HeLa cells (Figure 2C). In Huh7 cells, the expression of C191 resulted in a significant increase in the NF-κB activity (sevenfold) compared to control cells transfected with vector alone. Expression of C173 and C158 also resulted in an increase in NF-κB activity with about six- and fourfold, respectively, compared to control. Furthermore, the luciferase activity was increased in a dose-dependent manner in core-expressing cells. In contrast, there was no significant change in the relative luciferase activity in the cells transfected with pcDNA-Δcore (75-573) or pcDNA-Δcore (75-474), in which core proteins had 25 amino acids deleted at the N-terminus. This suggested that the N-terminal region (1-25 aa) of core protein is important for its activation on NF-κB, which is consistent with the previous report[20]. The different augmentation of luciferase activity caused by C191, C173, and C158 suggested that

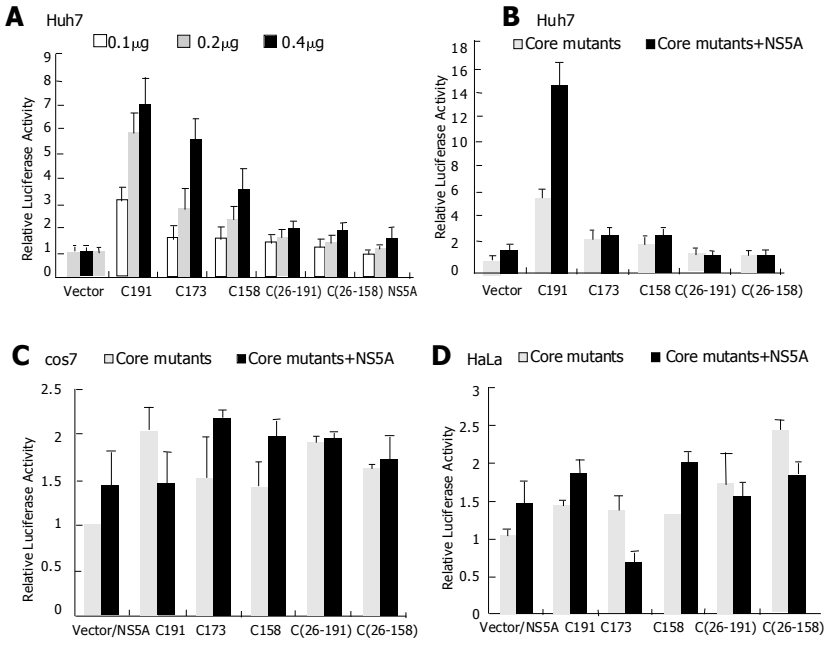

Figure 2 Effect of HCV core and NS5A proteins on NF-κB activity. **A:** NF-κB activation capacity of the core mutant fragments and NS5A protein individually expressing in Huh7 cell line; **B:** NF-κB activation capacity of the core mutants and NS5A protein expressing in Huh7 cells, **C:** Cos-7 cells; **D:** HeLa cells.

the activation of NF-κB by core protein was related to the hydrophobicity of C-terminus of core proteins (C191> C173>C158).

When NS5A protein was expressed alone, it had no effect on NF-κB activation (Figure 2A). But co-expression of C191 and NS5A protein resulted in a significant increase in the luciferase activity with about 15-fold compared to the control and twofold compared to the C191-expressing cells only. However, the relative luciferase activity in the cells co-expressing NS5A protein and other core mutants was not augmented (Figure 2B). These results indicated that NS5A protein could enhance C191-induced NF-κB activation.

NS5A protein enhanced core protein-induced NF-¦ÊB activation in a dose-dependent manner

In order to understand, how NS5A protein affects the NF-κB activation caused by C191 core protein, we designed two kinds of combination between pcNS5A and pcDNA-core expression vectors for luciferase assay. In the first one, 0.2 μg of pcNS5A vector was co-transfected with different concentrations of pcDNA-core (0.1, 0.2, and 0.3 μg), while in the other combination, 0.2 μg of pcDNA-core was co-transfected with different concentrations of pcNS5A (0.1, 0.2, and 0.3 μg). Result is shown in Figure 3. When pcNS5A transfection was certain, more pcDNA-core was transfected, the higher luciferase activity could be detected, while the enhanced increasing of activity in number was almost the same (ninefold) compared to cells expressing C191 alone (Figure 3, right), which meant that the same amount of NS5A protein exerted the same effect on different amounts of C191. When pcDNA-core transfection was certain, more pcNS5A was transfected, higher enhanced increasing of luciferase activity could be detected (Figure 3, left). These results showed that NS5A protein could enhance core protein-induced NF-κB activation in a dose-dependent manner.

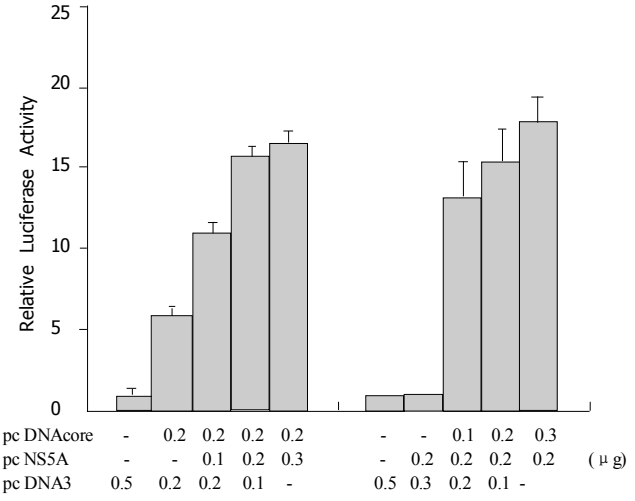

Figure 3 Enhancement of core protein-induced NF-kB activation in a NS5A protein dose-dependent manner.

Activation of NF-κB by core protein and NS5A was associated with IκB−α degradation

We further studied whether NF-κB activation occurred at translational or post-translational levels. To do this, the expression levels of NF-κB/p65, NF-κB/p50, and IκB-α in C191-expressing Huh7 cells either alone or together with NS5A were studied. As shown in Figure 4, at the same concentration of cell lysates as confirmed by actin (Figure 4D), there was no change in the p65 and p50 expression profile (Figures 4A and B). While in case of the IκB-α, the expression level was contrary to the NF-κB activity. In the control, cells transfected with pCDNA3 vector had the highest expression level of IκB-α (Figure 4C, lane 1), while in the cells co-expressing C191 and NS5A with the highest NF-κB activity had the lowest expression of IκB-a (Figure 4C, lane 3). Cells expressing C191 also had a much lower expression of IκB-α (Figure 4C, lane 4), while cells expressing NS5A protein had a much higher expression of IκB-α (Figure 4C, lane 2). It was more likely that when C191 and NS5A protein were co-expressed, they activated IκB kinase (IKK) through some signal pathway, resulted in the phosphorylation and then degradation of IκB, leading to the activation of NF-κB. These results suggested that C191 alone or together with NS5A protein did not enhance the expression of NF-κB. Thus, the NF-κB activity was augmented due to the dissociation of NF-κB¨CIκB complex and IκB degradation.

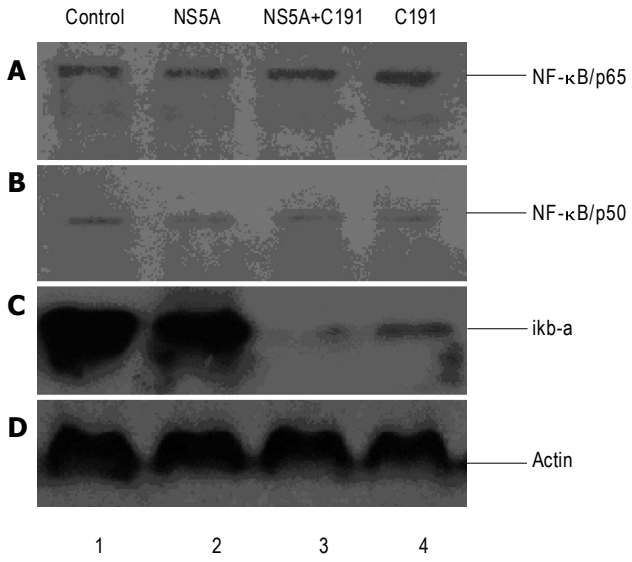

Figure 4 Expression of NF-κB/p65, NF-κB/p50 and IkB-a.

Subcellular localization of C191 and NS5A proteins in Cos-7 cell line

We then analyzed the subcellular localization of C191 and NS5A proteins using indirect immunofluorescence assay in Cos-7 cell line. As shown in Figure 5, C191 was localized predominantly in the cytoplasm (Figures 5A-C). NS5A protein was also localized in the cytoplasm with fluorescence signals surrounded the nuclear membrane (Figures 5D-F). On the other hand, the co-expression of C191 and NS5A proteins did not alter the localization of C191, but redistributed the NS5A protein to the same localization pattern of C191 (Figures 5G-I). All these results are consistent with previous reports[25-27]. Thus, the same

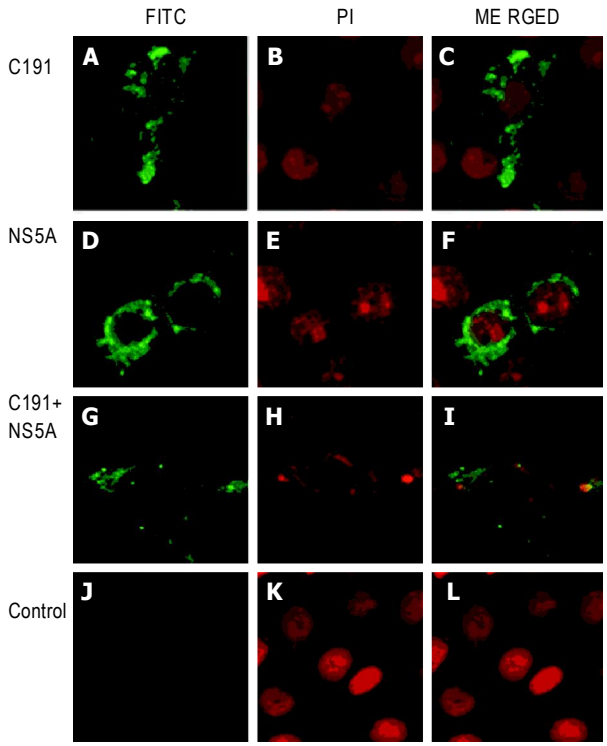

Figure 5 Localization of C191 and NS5A proteins. **A-C:** C191; **D-F**: NS5A protein; **G:** NS5A protein (FITC-labeled); **H:** C191 protein (TRITC-labeled); **I:** merged localization of C191 and NS5A proteins; **J-L:** pcDNA3 vector alone as a negative control.

cytoplasmic localization pattern of C191 and NS5A protein suggested that NF-κB activation caused by co-expression of C191 and NS5A protein was more likely due to a physical interaction between them or the interaction with the same cellular factors.

DISCUSSION

NF-kB is a critical regulator of the immediate early pathogen response, and plays an important role in promoting inflammation and in regulation of cell proliferation and survival[17,28]. NF-κB is highly activated at sites of inflammation in diverse diseases and induces transcription of pro-inflammatory cytokines, chemokines, adhesion molecules, matrix metalloproteinases, cyclooxygenase 2, and inducible nitric oxide synthase[29]. Moreover, NF-κB can also activate the expression of cyclin D1, c-myc, other regulators of the cell cycle and enhance cell survival by switching on genes that inhibit pro-apoptotic signals[30]. Because of the multifunction of NF-κB, many viruses including several human pathogens such as HIV-1, human T-cell leukemia virus, herpes simplex virus, HBV, and Epstein-Barr virus have evolved different strategies to modulate the activity of NF-κB[31-34]. Some of them modulate the NF-κB activity through the binding of the viral particles to their receptor, some of them modulate through viral proteins. The activation of NF-κB may be a strategy of viruses to block apoptosis and prolong survival of the host cells in order to gain time for replication and increase viral progeny production[35].

Since HCV core protein can interact with TNF-α by yeast two-hybrid system[8], NF-κB, the main effective factor in the TNF-α signaling pathway, has become a hot factor in the functional studies of core protein. Core protein can modulate NF-κB at the basal level in many mammalian cell lines, although the modulation is different from HCV genotype and cell lines[19-21].

In this study, we found that core protein could increase the activity of NF-κB only in Huh7 cell line, but not in Cos-7 and HeLa cell lines. This augmentation was in a core protein dose-dependent manner. Core protein can interact with NS5A protein both *in vitro* and *in vivo*[25]. NS5A protein can also modulate the activity of NF-κB[23]. Since this modulation is also different from different cell lines[36], we want to know if this interaction between core and NS5A proteins has certain effect on the regulation of NF-κB. Our results showed that when C191 and NS5A proteins were co-expressed in Huh7 cell line, they activated NF-κB and this activation was in a NS5A protein dose-dependent manner. Moreover, the full-length core protein was required for the interaction between core and NS5A proteins, because no increase in the NF-κB activity was observed in the cells co-expressing any of the core mutant fragments and NS5A protein. Further experiments have confirmed that this activation is associated with the NF-κB-IκB complex dissociation and IκB degradation but not with the change in the expression level of NF-κB.

There are two signaling pathways leading to NF-κB activation. The classical NF-κB pathway, based on IKK-β-dependent IκB degradation, is essential for innate immunity. The alternative NF-κB pathway, based on IKK-α processing of NF-κB2/p100 into NF-κB2/p50, is related to lymphoid organ development and adaptive immunity[29]. The activation of NF-κB caused by co-expression of core and NS5A proteins may occur in the classical NF-κB pathway. Proinflammatory cytokines and pathogen-associated molecular patterns, working through different receptors belonging to the TNFR and Toll-like receptor-IL-1 receptor superfamilies, cause activation of IKK. The activated IKKs, predominantly acting through IKK-β in an IKK-γ-dependent manner, catalyze the phosphorylation of IκBs, polyubiquitination and subsequent degradation by the 26S proteasome[29]. As previously reported, core protein can activate NF-κB through TNF receptor-associated factor 2-IKK-β-dependent pathway[37]. The phosphorylation of I κB-α by IKK-β can be significantly enhanced by HCV core protein expression in a dose-dependent manner. NS5A protein can activate NF-κB by altering intracellular calcium levels and then inducing oxidative stress, through tyrosine phosphorylation of IκB-α at Tyr^{42} and Tyr^{305} residues instead of $Ser^{32,36}$ phosphorylation of IκB-α caused by IKK, thus inducing IκB-α degradation[24]. We found that expression of core protein could activate NF-κB, while this did not happen in case of NS5A protein expression in Huh7 cells. These results of NS5A protein are consistent with one report[38] but inconsistent with other reports[22,24]. This may be due to the different cell lines and/or experimental methods used in their studies. Interestingly, co-expression of C191 and NS5A proteins activated NF-κB significantly.

When NS5A and C191 proteins were co-expressed, this interaction caused the change in the conformation of NS5A protein, which leads to the tyrosine phosphorylation of Iκ B-α, and resulted in core protein-induced NF-κB activation. Further experiments need to be done to elucidate this idea.

HCV causes persistent infection and chronic hepatitis in most infected individuals. Spontaneous recovery following HCV infection is a relatively rare event. The mechanisms responsible for HCV-mediated chronicity and disease progression remain unclear[39]. The activation of NF-κB has been found in both subgenomic replicon and full-length HCV-transfected cells and HCV-infected livers [24,36,39]. This may provide the possible mechanism for HCV pathogenesis.

C191 is produced in the early stage of HCV infection and then cleavaged to its mature form C173 to assist virus assembly[40]. In this study, we found that NS5A protein could enhance C191-induced NF-κB activation but not C173, when NS5A and core proteins were co-expressed in Huh7 cells. Activation of NF-κB always leads to inhibition of apoptosis. In the early stage of HCV infection, NS5A protein functions synergically with C191 on NF-κB activation and this may inhibit apoptosis of host cells; while in late stage of HCV infection, NS5A protein does not function synergically with C173 on NF-κB activation and decreases their ability to inhibit apoptosis of host cells. This may play an important role in the establishment of chronic and persistent liver disease during HCV infection.

ACKNOWLEDGMENTS

The authors thank Dr. Charles M Rice (University of Washington) for providing pBRTM/HCV1-3011 and Dr. Stephene J Polyak (University of Washington) for providing HCV NS5A mAb. The authors thank Jingrong Gao and Changlu Liu for helpful suggestions, and also thank Wei Peng for his technical help in confocal microscopy.

REFERENCES

1 **Farci P,** Choo QL, Kuo G, Weiner AJ, Overby LR, Bradley DW, Houghton M. Isolation of a cDNA clone derived from a blood-borne non-A, non-B viral hepatitis genome. *Science* 1989; **244**: 359-362
2 **Saito I**, Miyamura T, Ohbayashi A, Harada H, Katayama T, Kikuchi S, Watanabe Y, Koi S, Onji M, Ohta Y, Hepatitis C virus infection is associated with the development of hepatocellular carcinoma. *Proc Natl Acad Sci U S A* 1990; **87**: 6547-6549
3 **Hijikata M**, Kato N, Ootsuyama Y, Nakagawa M, Shimotohno K. Gene mapping of the putative structural region of the hepatitis C virus genome by in vitro processing analysis. *Proc Natl Acad Sci U S A* 1991; **88**: 5547-5551
4 **Grakoui A**, Wychowski C, Lin C, Feinstone SM, Rice CM. Expression and identification of hepatitis C virus polyprotein cleavage products. *J Virol* 1993; **67**: 1385-1395
5 **Manabe S**, Fuke I, Tanishita O, Kaji C, Gomi Y, Yoshida S, Mori C, Takamizawa A, Yosida I, Okayama H. Production of nonstructural proteins of hepatitis C virus requires a putative viral protease encoded by NS3. *Virology* 1994; **198**: 636-644
6 **Matsumoto M,** Hsieh TY, Zhu N, VanArsdale T, Hwang SB, Jeng KS, Gorbalenya AE, Lo SY, Ou JH, Ware CF, Lai MM. Hepatitis C virus core protein interacts with the cytoplasmic tail of lymphotoxin-beta receptor. *J Virol* 1997; **71**: 1301-1309
7 **Chen CM,** You LR, Hwang LH, Lee YH. Direct interaction of hepatitis C virus core protein with the cellular lymphotoxin-beta receptor modulates the signal pathway of the lymphotoxin-beta receptor. *J Virol* 1997; **71**: 9417-9426
8 **Zhu N,** Khoshnan A, Schneider R, Matsumoto M, Dennert G, Ware C, Lai MM. Hepatitis C virus core protein binds to the cytoplasmic domain of tumor necrosis factor (TNF) receptor 1 and enhances TNF-induced apoptosis. *J Virol* 1998; **72**: 3691-3697
9 **Hsieh TY,** Matsumoto M, Chou HC, Schneider R, Hwang SB, Lee AS, Lai MM. Hepatitis C virus core protein interacts with heterogeneous nuclear ribonucleoprotein K. *J Biol Chem* 1998; **273**: 17651-17659
10 **Jin DY,** Wang HL, Zhou Y, Chun AC, Kibler KV, Hou YD, Kung H, Jeang KT. Hepatitis C virus core protein-induced loss of LZIP function correlates with cellular transformation. *EMBO J* 2000; **19**: 729-740
11 **Bergqvist A,** Rice CM. Transcriptional activation of the interleukin-2 promoter by hepatitis C virus core protein. *J Virol* 2001; **75**: 772-781
12 **Ray RB,** Steele R, Meyer K, Ray R. Transcriptional repression of p53 promoter by hepatitis C virus core protein. *J Biol Chem* 1997**; 272:** 10983-10986
13 **Jung EY,** Lee MN, Yang HY, Yu D, Jang KL. The repressive activity of hepatitis C virus core protein on the transcription of p21(waf1) is regulated by protein kinase A-mediated phosphorylation. *Virus Res* 2001; **79**: 109-115
14 **Yoshida I,** Oka K, Hidajat R, Nagano-Fujii M, Ishido S, Hotta H. Inhibition of p21/Waf1/Cip1/Sdi1 expression by hepatitis C virus core protein. *Microbiol Immunol* 2001; **45**: 689-697
15 **Hirota M,** Satoh S, Asabe S, Kohara M, Tsukiyama-Kohara K, Kato N, Hijikata M, Shimotohno K. Phosphorylation of nonstructural 5A protein of hepatitis C virus: HCV group-specific hyperphosphorylation. *Virology* 1999; **257**: 130-137
16 **Gale MJ,** Korth MJ, Tang NM, Tan SL, Hopkins DA, Dever TE, Polyak SJ, Gretch DR, Katze MG. Evidence that hepatitis C virus resistance to interferon is mediated through repression of the PKR protein kinase by the nonstructural 5A protein. *Virology* 1997; **230**: 217-227
17 **Li Q,** Verma IM. NF-kappaB regulation in the immune system. *Nat Rev Immunol* 2002; **2**: 725-734
18 **Shrivastava A,** Manna SK, Ray R, Aggarwal BB. Ectopic expression of hepatitis C virus core protein differentially regulates nuclear transcription factors. *J Virol* 1998; **72**: 9722-9728
19 **Marusawa H,** Hijikata M, Chiba T, Shimotohno K. Hepatitis C virus core protein inhibits Fas- and tumor necrosis factor alpha-mediated apoptosis via NF-kappaB activation. *J Virol* 1999; **73**: 4713-4720
20 **Watashi K,** Hijikata M, Marusawa H, Doi T, Shimotohno K. Cytoplasmic localization is important for transcription factor nuclear factor-kappa B activation by hepatitis C virus core protein through its amino terminal region. *Virology* 2001; **286**: 391-402
21 **Ray RB,** Steele R, Basu A, Meyer K, Majumder M, Ghosh AK, Ray R. Distinct functional role of Hepatitis C virus core protein on NF-κappaB regulation is linked to genomic variation. *Virus Res* 2002; **87**: 21-29
22 **Gong G,** Waris G, Tanveer R, Siddiqui A. Human hepatitis C virus NS5A protein alters intracellular calcium levels, induces oxidative stress, and activates STAT-3 and NF-kappa B. *Proc Natl Acad Sci U S A* 2001; **98**: 9599-9604
23 **Park KJ,** Choi SH, Lee SY, Hwang SB, Lai MM. Nonstructural 5A protein of hepatitis C virus modulates tumor necrosis factor alpha-stimulated nuclear factor kappa B activation. *J Biol Chem* 2002; **277**: 13122-13128
24 **Waris G,** Livolsi A, Imbert V, Peyron JF, Siddiqui A. Hepatitis C virus NS5A and subgenomic replicon activate NF-κappaB via tyrosine phosphorylation of IkappaBalpha and its degradation by calpain protease. *J Biol Chem* 2003; **278**: 40778-40787

25 **Goh PY,** Tan YJ, Lim SP, Lim SG, Tan YH, Hong WJ. The hepatitis C virus core protein interacts with NS5A and activates its caspase-mediated proteolytic cleavage. *Virology* 2001; **290**: 224-236
26 **Ide Y,** Zhang L, Chen M, Inchauspe G, Bahl C, Sasaguri Y, Padmanabhan R. Characterization of the nuclear localization signal and subcellular distribution of hepatitis C virus nonstructural protein NS5A. *Gene* 1996; **182**: 203-211
27 **Polyak SJ,** Paschal DM, McArdle S, Gale MJ, Moradpour D, Gretch DR. Characterization of the effects of hepatitis C virus nonstructural 5A protein expression in human cell lines and on interferon-sensitive virus replication. *Hepatology* 1999; **29**: 1262-1271
28 **Karin M,** Cao Y, Greten FR, Li ZW. NF-kappaB in cancer: from innocent bystander to major culprit. *Nat Rev Cancer* 2002; **2**:301-310
29 **Bonizzi G,** Karin M. The two NF-kappaB activation pathways and their role in innate and adaptive immunity. *Trends Immunol* 2004; **25**: 280-288
30 **Karin M,** Lin A. NF-kappaB at the crossroads of life and death. *Nat Immunol* 2002; **3**: 221-227
31 **Bour S,** Perrin C, Akari H, Strebel K. The human immunodeficiency virus type 1 Vpu protein inhibits NF-kappa B activation by interfering with beta TrCP-mediated degradation of Ikappa B. *J Biol Chem* 2001; **276**: 15920-15928
32 **O'Mahony AM**, Montano M, Van Beneden K, Chen LF, Greene WC. Human T-cell lymphotropic virus type 1 tax induction of biologically Active NF-kappaB requires IkappaB kinase-1-mediated phosphorylation of RelA/p65. *J Biol Chem* 2004; **279**:18137-18145
33 **Goodkin ML,** Ting AT, Blaho JA. NF-kappaB is required for apoptosis prevention during herpes simplex virus type 1 infection. *J Virol* 2003; **77**: 7261-7280
34 **Luftig M,** Yasui T, Soni V, Kang MS, Jacobson N, Cahir-McFarland E, Seed B, Kieff E. Epstein-Barr virus latent infection membrane protein 1 TRAF-binding site induces NIK/IKK alpha-dependent noncanonical NF-kappaB activation. *Proc Natl Acad Sci USA* 2004; **101**: 141-146
35 **Santoro MG,** Rossi A, Amici C. NF-kappaB and virus infection: who controls whom. *EMBO J* 2003; **22**: 2552-2560
36 **Soo HM,** Garzino-Demo A, Hong W, Tan YH, Tan YJ, Goh P, Lim SG, Lim SP. Expression of a full-length hepatitis C virus cDNA up-regulates the expression of CC chemokines MCP-1 and RANTES. *Virology* 2002; **303**: 253-77
37 **Chung YM,** Park KJ, Choi SY, Hwang SB, Lee SY. Hepatitis C virus core protein potentiates TNF-alpha-induced NF-kappaB activation through TRAF2-IKK beta-dependent pathway. *Biochem Biophys Res Commun* 2001; **284**: 15-19
38 **Miyasaka Y,** Enomoto N, Kurosaki M, Sakamoto N, Kanazawa N, Kohashi T, Ueda E, Maekawa S, Watanabe H, Izumi N, Sato C, Watanabe M. Hepatitis C virus nonstructural protein 5A inhibits tumor necrosis factor-alpha-mediated apoptosis in Huh7 cells. *J Infect Dis* 2003; **188**: 1537-1544
39 **Tai DI,** Tsai SL, Chen YM, Chuang YL, Peng CY, Sheen IS, Yeh CT, Chang KS, Huang SN, Kuo GC, Liaw YF. Activation of nuclear factor kappaB in hepatitis C virus infection: implications for pathogenesis and hepatocarcinogenesis. *Hepatology* 2000; **31**: 656-664
40 **Yasui K,** Wakita T, Tsukiyama-Kohara K, Funahashi SI, Ichikawa M, Kajita T, Moradpour D, Wands JR, Kohara M. The native form and maturation process of hepatitis C virus core protein. *J Virol* 1998; **72**: 6048-6055

Science Editor Wang XL and Guo SY **Language Editor** ELsevier HK

PO Box 2345, Beijing 100023, China
www.wjgnet.com
wjg@wjgnet.com

ELSEVIER

World J Gastroenterol 2005;11(41):6440-6444
World Journal of Gastroenterology ISSN 1007-9327

Expression and immunoreactivity of HCV/HBV epitopes

Xin-Yu Xiong, Xiao Liu, Yuan-Ding Chen

Xin-Yu Xiong, Xiao Liu, Yuan-Ding Chen, Institute of Medical Biology, Chinese Academy of Medical Sciences and Peking Union Medical College, Kunming 650118, Yunnan Province, China
Supported by the Yunnan Province Natural Science Foundation, No. 2003C0076M
Correspondence to: Professor Yuan-Ding Chen, The key Laboratory, Institute of Medical Biology, Chinese Academy of Medical Sciences and Peking Union Medical College, Kunming 650118, Yunnan Province, China. chenyd@imbcams.com.cn
Telephone: +86-871-8334689 Fax: +86-871-8334483
Received: 2005-03-31 Accepted: 2005-04-30

Abstract

AIM: To develop the epitope-based vaccines to prevent Hepatitis C virus (HCV)/Hepatitis B virus (HBV) infections.

METHODS: The HCV core epitopes C1 STNPKPQRKTKRNTNRRPQD (residuals aa2-21) and C2 VKFPGGGQIVGGVYLLPRR (residuals aa22-40), envelope epitope E GHRMAWDMMMNWSP (residuals aa315-328) and HBsAg epitope S CTTPAQGNSMFPSCCCTKPTDGNC (residuals aa124-147) were displayed in five different sites of the flock house virus capsid protein as a vector, and expressed in *E. coli* cells (pET-3 system). Immunoreactivity of the epitopes with anti-HCV and anti-HBV antibodies in the serum from hepatitis C and hepatitis B patients were determined.

RESULTS: The expressed chimeric protein carrying the HCV epitopes C1, C2, E (two times), L3C1-I2E-L1C2-L2E could react with anti-HCV antibodies. The expressed chimeric protein carrying the HBV epitopes S, I3S could react with anti-HBs antibodies. The expressed chimeric proteins carrying the HCV epitopes C1, C2, E plus HBV epitope S, L3C1-I2E-L1C2-L2E-I3S could react with anti-HCV and anti-HBs antibodies.

CONCLUSION: These epitopes have highly specific and sensitive immunoreaction and are useful in the development of epitope-based vaccines.

Key words: HCV; HBV; Epitope-based vaccine; Recombinant; Immunoreactivity

Xiong XY, Liu X, Chen YD. Expression and immunoreactivity of HCV/HBV epitopes. *World J Gastroenterol* 2005;11(41): 6440-6444

http://www.wjgnet.com/1007-9327/11/6440.asp

INTRODUCTION

hepatitis C virus (HCV) and Hepatitis B virus (HBV) are the causative agents of hepatitis C and B. Exposure to HCV or HBV causes acute hepatitis, leading to chronic hepatitis, liver cirrhosis, hepatocellular carcinoma and even death. The worldwide prevalence is estimated to be around 170 million individuals (3%) infected with HCV and 350 million individuals (7%) infected with HBV[1,2]. HCV and HBV infections are social and economic issues.

HCV is a member of the Flaviviridae family, possessing a linear single-stranded RNA genome of 9.4 kb[3]. The HCV genome contains a single open reading frame (ORF) encoding a polyprotein that is cleaved into the mature viral core, envelope and non-structural proteins[4]. The core protein is the most conserved and contains highly conserved epitopes[5]. The envelope protein E1 is the most variant region and contains the major neutralizing epitopes[6-11]. HBV is a double-stranded circular DNA virus[12]. The surface antigen of HBV (HBsAg), the major antigen protein, consists of large, middle and small proteins encoded by ORF S and preS, and have been successfully used as a hepatitis B vaccine. Since HCV and HBV infections share a similar route, i.e., mainly infected individuals through serum or seral products, it is very important to develop HCV/HBV covalent vaccines to simultaneously protect individuals from HCV and HBV infections.

It has been previously demonstrated that the epitope-presenting system based on the flock house virus (FHV) capsid protein is useful in displaying foreign epitopes[13]. In the present study, epitopes derived from the HCV core, envelope protein and HBsAg were displayed in this system, immunoreactivities were determined, and the possibility to develop epitope-based vaccines was discussed.

MATERIALS AND METHODS

Epitopes and epitope-presenting system

The epitopes studied in this study were derived from the HCV core region residues aa2-21C1 STNPKPQRKTKRNTNRRPQD (C1) and aa22-40, VKFPGGGQIVGGVYLLPRR (C2), the envelope region residues aa315-328, GHRMAWDMMMNWSP (E), and the HBsAg residues aa124-147 CTTPAQGNSMFPSCCCTKPTDGNC (S).

The epitope-presenting system was developed using the

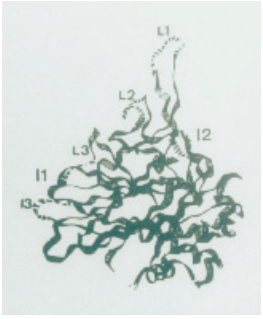

Figure 1 Three-dimensional structure of FHV capsid protein.

FHV capsid protein as a vector (FHV-RNA2 system)[13]. The FHV capsid protein expressed in the recombinant system could self-assemble into virus-like particles (VLPs). Six sites on the vector protein outer surface could be chosen for insertion of foreign epitopes which have little influence on the protein structure (Figure 1). The epitopes were inserted into L3 (C1), I2 (E), L1 (C2), L2 (E) and I3 (S), by means of genetic recombination engineering on plasmid pET-3. Four recombinant plasmids were constructed, pET-Wt carrying the bare vector protein gene, pET-I3S carrying the vector gene and the epitope S, pET-L3C1-I2E-L1C2-L2E carrying the vector gene and the epitopes C1, C2, E, and pET-L3C1-I2E-L1C2-L2E-I3S carrying the vector gene and the epitopes C1, C2, E and S.

Expression of chimeric proteins carrying epitopes

The recombinant plasmids were transformed into *E. coli* BL21(DE3) cells. The chimeric proteins carrying the epitopes were expressed under the control of T7 promotor[14] in TB/ampicillin media at 37 ℃. Cells were harvested by centrifugation at 3 000 r/min for 10 min at 4 ℃ (Beckman rotor type J-20). Cell lysis was accomplished by ultrasonication and centrifuged at 10 000*g* for 30 min. The chimeric proteins in the deposit were dissolved in 8 mol/L urea and analyzed by sodium dodecyl sulfate-polyacrylamide gel electrophoresis (SDS-PAGE). To purify the expressed chimeric proteins, the band containing the chimeric proteins was cut-off from the gel and the proteins were recovered by further electrophoresis procedures. The purified chimeric proteins were stored at -20 ℃ and used as an antigen in ELISA and Western blot tests.

Serum samples

Serum samples used in this study were collected from patients with hepatitis C (anti-HCV positive or HCV-RNA positive) or hepatitis B (anti-HBs positive), from the Kunming Infectious Disease Hospital, Kunming, China.

ELISA

Recombinant chimeric proteins carrying HCV/HBV epitopes purified by PAGE were diluted to 5 mg/L in carbonate/bicarbonate buffer (pH 9.6) and used as coating antigens in ELISA test. One hundred microliters of the protein solution was added to each well of 96-well microtiter plates. The plates were incubated overnight at 4 ℃ and then blocked with 2.5 g/L bovine serum albumin in 10 mmol/L of phosphate-buffered saline containing 0.01% Tween 20 (PBS-T), at 37 ℃ for 1 h and washed five times with (PBS-T). Sera from hepatitis C or B patients were diluted to the ratio 1:10 and 100 μL was added to each well of the blocked plates. The mixture was incubated at 37 ℃ for 1 h. After washing, 100 μL of horseradish peroxidase-conjugated rabbit anti-human immunoglobulin G (Sigma BioSciences, St. Louis, MO, USA) was added to each well, and the plates were incubated for 1 h at 37 ℃. After incubation and washing, ortho-phenylenediamine dihydrochloride (OPD, Sigma BioSciences, St. Louis, MO, USA) was added, and the color was measured at 455 nm with a Titertek plate reader.

When the cut-off value was (SS-NC)/NC ≧ 2, it was defined as positive. In the formula, SS is the OD value of the serum sample, NC is the value of the negative control.

Western blot

In the Western blot test, the expressed chimeric proteins were separated in 10% SDS-PAGE and transferred onto the nitrocellulose membrane. After incubation with the patient's serum (in 1∶400 dilution) and horseradish peroxidase-conjugated rabbit anti-human immunoglobulin G, the immobilized antigens (epitopes) were detected with 3,3-diaminobenzidine tetrahydrochloride (DAB, Sigma BioSciences, St. Louis, MO, USA).

RESULTS

Expression and purification of chimeric proteins

The chimeric proteins Wt, I3S, L3C1-I2E-L1C2-L2E and L3C1-I2E-L1C2-L2E-I3S were expressed in inclusion body form in transformed cells with the corresponding recombinant plasmids pET-Wt, pET-I3S, pET-L3C1-I2E-L1C2-L2E-I3S or pET-L3C1-I2E-L1C2-L2E-I3S, and analyzed by 10% SDS-PAGE (Figure 2). The results showed that the chimeric proteins were highly expressed.

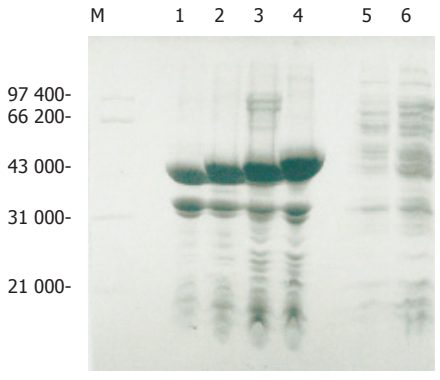

Figure 2 Recombinant proteins expressed in *E. coli* cells. M: protein molecular mass standard; lane 1: recombinant vector protein Wt; lane 2: chimeric protein I3S; lane 3: L3C1-I2E-L1C2-L2E; lane 4: L3C1-I2E-L1C2-L2E-I3S; lane 5: supernatant of BL21 cells transformed by pET-L3C1-I2E-L1C2-L2E; lane 6: non-transformed BL21 cells.

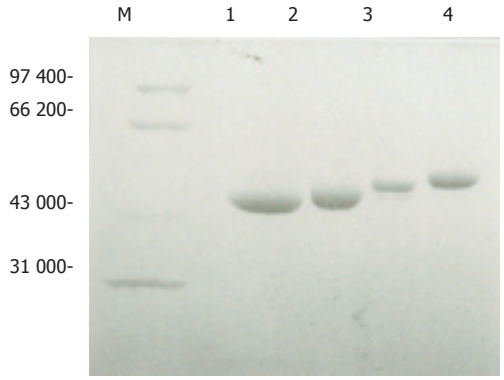

Figure 3 Expression of purified expressed proteins. M: protein molecular mass standard; lane 1: recombinant vector protein Wt; lane 2: chimeric protein I3S; lane 3: L3C1-I2E-L1C2-L2E; lane 4: L3C1-I2E-L1C2-L2E-I3S.

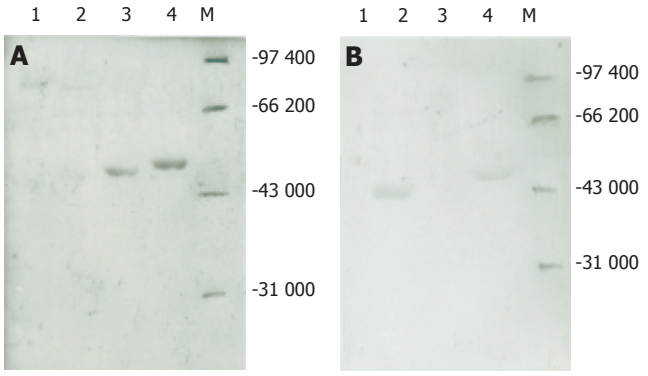

Figure 4 Western blot of expressed proteins using anti-HCV+ **(A)** and anti-HBsAg+ **(B)** sera as detecting antibodies. M: protein molecular mass standard; lane 1: recombinant vector protein W; lane 2: chimeric protein I3S, lane 3: L3C1-I2E-L1C2-L2E; lane 4: L3C1-I2E-L1C2-L2E-I3S.

Table 1 Detection of immunoreaction of expressed proteins as antigen with anti-HCV antibodies in serum from hepatitis C patients by ELISA

Protein	Patients	
	Anti-HCV$^+$/HCV-RNA$^+$ (%)	Anti-HCV$^-$/HCV-RNA$^+$ (%)
Wt	0	0
13S	2/66 (3.1)	1/24 (4.1)
L3C1-12E-L1C2-L2E	63/66 (95.5)	7/24 (29.2)
L3C1-12E-L1C2-L2E-I3S	63/66 (95.5)	9/24 (37.5)

The contents of chimeric proteins were estimated possessing about 35.1% (Wt), 35.5% (I3S), 34.2% (L3C1-I2E-L1C2-L2E), and 39.7% (L3C1-I2E-L1C2-L2E-I3S) of the full cell proteins. After purification, the chimeric proteins possessed about 43.8 kD (Wt), 46.5 kD (I3S), 49.7 kD (L3C1-I2E-L1C2-L2E) and 52.5 kD (L3C1-I2E-L1C2-L2E-I3S) of molecular weight, respectively as expected (Figure 3).

ELISA test

Using purified chimeric proteins as a coating antigen, 66 anti-HCV$^+$/HCV-RNA$^+$ and 24 anti-HCV$^+$/HCV-RNA$^-$ serum samples from hepatitis C patients were determined (Table 1). The results showed that the chimeric proteins carrying HCV epitopes, L3C1-I2E-L1C2-L2E and L3C1-I2E-L1C2-L2E-I3S could react with ant-HCV antibodies with a high specificity and susceptibility. The reactivity rates of chimeric proteins L3C1-I2E-L1C2-L2E and L3C1-I2E-L1C2-L2E-I3S were 95.5% and 95.5% with anti-HCV$^+$/HCV-RNA$^+$ sera, 29.2% and 37.5% with anti-HCV$^+$/HCV-RNA$^-$ sera, respectively. No serum samples reacted with the expressed vector protein Wt. Few serum samples reacted with chimeric protein I3S, implying that the patients were co-infected with HBV

Western blot test

Using sera from patients with hepatitis C (anti-HCV positive by ELISA kit) or B (anti-HBs positive by ELISA kit) as detecting antibody, the chimeric proteins carrying HCV epitopes L3C1-I2E-L1C2-L2E and L3C1-I2E-L1C2-L2E-I3S could be recognized by anti-HCV antibody (Figure 4A), and the chimeric protein carrying HBV epitopes S, I3S and L3C1-I2E-L1C2-L2E-I3S could be recognized by anti-HBV antibody on Western blot (Figure 4B). Ten serum samples from hepatitis C or B patients were detected respectively and the results in each group were similar.

DISCUSSION

Due to the host defense mechanism and virus genome RNA instability, HCV seems to escape immune pressure by mutation and results in high genetic heterogeneity[15,16]. The humoral immune response to neutralizing antibodies appears to be restricted and isolate-specific. HCV isolates obtained can be classified into at least six major clades (clades 1 to 6) and more than 70 subtypes[3]. Development of HCV vaccines is largely hampered for these characteristics of the virus.

Recent studies indicate that when a virus epitope is present in an appropriate vector system, the epitope can be displayed on the exposed surface of the vector protein with high immunogenicity[17]. Sequencing and immunological analysis showed that the residues aa1-40 in HCV core region are the most conserved and the residues aa315-328 in E1 region are highly conserved too[18]. HBsAg is the major antigenic protein of HBV. Mature HBsAg can self-assemble into VLPs and induce effective immune response. The residues aa120-160 of the large protein S exposed on the outer surface of VLPs are defined as a determinant. This determinant induces cross neutralizing antibodies which protect infections against different HBV subtypes[19-21]. Further studies indicate that the "a" determinant is mainly located within a double-looped structure formed by disulfide bridges between cysteines at 124, 137 and at 139-147[22,23]. The epitope S (aa124-147) studied in this report contains the key residues of the "a"

determinant. The epitopes displayed in the FHV-RNA2 system in this study had a high reactivity to specific anti-HCV or anti-HBV antibodies, indicating the importance of these HCV and HBV epitopes.

HCV/HBV epitopes, multiple-presented in a fusion form, cross react with HCV and HBV antibodies[24]. DNA immunization with fusion genes encoding different regions of the HCV E2 fused to the HBsAg gene elicits immune responses to both HCV and HBV. The antibody responses induced by the same epitopes are also demonstrated[25]. These results suggest that these epitopes contribute to the development of epitope-based vaccines.

Since HCV and HBV have a similar infection route with a high co-infection rate, development of HCV/HBV covalent vaccines is of great importance. Previous studies on HIV-1[13], HCV[26] and rotavirus[27-29] single epitopes and the present study demonstrated that the FHV-RNA2 system can be used to study the foreign epitope characteristics and to develop epitope-based vaccines. Since no sustainable cell culture system can be used, whether the antibodies elicited by these epitopes neutralize HCV and HBV infectivity or protect individuals against HCV and HBV infection remains to be studied.

REFERENCES

1 **Koff RS.** Hepatitis vaccines: recent advances. *Int J Parasitol* 2003; **33:** 517-523

2 **El Khouri M,** dos Santos VA. Hepatitis B: epidemiological, immunological, and serological considerations emphasizing mutation. *Rev Hosp Clin Fac Med Sao Paulo* 2004; **59:** 216-224

3 **Robertson B,** Myers G, Howard C, Brettin T, Bukh J, Gaschen B, Gojobori T, Maertens G, Mizokami M, Nainan O, Netesov S, Nishioka K, Shin i T, Simmonds P, Smith D, Stuyver L, Weiner A. Classification, nomenclature, and database development for HCV and related viruses: proposals for standardization. International Committee on Virus Taxonomy. *Arch Virol* 1998; **143:** 2493-2503

4 **Lindenbach BD,** Rice CM. Flaviviridae: the viruses and their replication. In: D. M. Knipe, P. M. Howley, D. E. Griffin, R. A. Lamb, M. A. Martin, B. Roizman, and S. E. Straus (ed.). Fields virology, 4th ed. Philadelphia, Pa. *Lippincott Williams & Wilkins,* 2001; 991-1042

5 **Hadlock KG,** Lanford RE, Perkins S, Rowe J, Yang Q, Levy S, Pileri P, Abrignani S, Foung SK. Human monoclonal antibodies that inhibit binding of hepatitis C virus E2 protein to CD81 and recognize conserved conformational epitopes. *J Virol* 2000; **74:** 10407-10416

6 **Bukh J,** Miller RH, Purcell RH. Genetic heterogeneity of hepatitis C virus: quasispecies and genotypes. *Semin Liver Dis* 1995; **15:** 41-63

7 **Keck ZY,** Op De Beeck A, Hadlock KG, Xia J, Li TK, Dubuisson J, Foung SK. Hepatitis C virus E2 has three immunogenic domains containing conformational epitopes with distinct properties and biological functions. *J Virol* 2004; **78:** 9224-9232

8 **Habersetzer F,** Fournillier A, Dubuisson J, Rosa D, Abrignani S, Wychowski C, Nakano I, Trépo C, Desgranges C, Inchauspé G. Characterization of human monoclonal antibodies specific to the hepatitis C virus glycoprotein E2 with in vitro binding neutralization properties. *Virology* 1998; **249:** 32-41

9 **da Silva Cardoso M,** Siemoneit K, Sturm D, Krone C, Moradpour D, Kubanek B. Isolation and characterization of human monoclonal antibodies against hepatitis C virus envelope glycoproteins. *J Med Virol* 1998; **55:** 28-34

10 **Burioni R,** Plaisant P, Manzin A, Rosa D, Delli Carri V, Bugli F, Solforosi L, Abrignani S, Varaldo PE, Fadda G, Clementi M. Dissection of human humoral immune response against hepatitis C virus E2 glycoprotein by repertoire cloning and generation of recombinant Fab fragments. *Hepatology* 1998; **28:** 810-814

11 **Allander T,** Drakenberg K, Beyene A, Rosa D, Abrignani S, Houghton M, Widell A, Grillner L, Persson MA. Recombinant human monoclonal antibodies against different conformational epitopes of the E2 envelope glycoprotein of hepatitis C virus that inhibit its interaction with CD81. *J Gen Virol* 2000; **81:** 2451-2459

12 **Gust ID,** Burrell CJ, Coulepis AG, Robinson WS, Zuckerman AJ. Taxonomic classification of human hepatitis B virus. *Intervirology* 1986; **25:** 14-29

13 **Tisminetzky SG,** Scodeller EA, Evangelisti P, Chen Y, Schiappacassi M, Porro F, Bizik F, Zacchi T, Lunazzi G, Miertus S. Immunoreactivity of chimeric proteins carrying the HIV-1 epitope IGPGRAF. Correlation between predicted conformation and antigenicity. *FEBS Lett* 1994; **353:** 1-4

14 **Studier FW,** Rosenberg AH, Dunn JJ, Dubendorff JW. Use of T7 RNA polymerase to direct expression of cloned genes. *Methods Enzymol* 1990; **185:** 60-89

15 **Chen YD,** Liu MY, Yu WL, Li JQ, Peng M, Dai Q, Liu X, Zhou ZQ. Hepatitis C virus infections and genotypes in China. *Hepatobiliary Pancreat Dis Int* 2002; **1:** 194-201

16 **Chen YD,** Liu MY, Yu WL, Li JQ, Peng M, Dai Q, Wu J, Liu X, Zhou ZQ. Sequence variability of the 5' UTR in isolates of hepatitis C virus in China. *Hepatobiliary Pancreat Dis Int* 2002; **1:** 541-552

17 **Chen Y,** Dai C. [Current status and strategy of research on epitope-based vaccine] *Zhonghua Yu Fang Yi Xue Za Zhi*. 1999; **33:** 315-316

18 **Bukh J,** Purcell RH, Miller RH. At least 12 genotypes of hepatitis C virus predicted by sequence analysis of the putative E1 gene of isolates collected worldwide. *Proc Natl Acad Sci* U S A 1993; **90:** 8234-8238

19 **Gerin JL,** Alexander H, Shih JW, Purcell RH, Dapolito G, Engle R, Green N, Sutcliffe JG, Shinnick TM, Lerner RA. Chemically synthesized peptides of hepatitis B surface antigen duplicate the d/y specificities and induce subtype-specific antibodies in chimpanzees. *Proc Natl Acad Sci* U S A 1983; **80:** 2365-2369

20 **Moynihan JS,** D'Mello FI, Howard CR. 48-mer synthetic peptide analogue of the hepatitis B virus "a" determinant induces an anti-HBs antibody response after a single injection. *J Med Virol* 2000; **62:** 159-166

21 **Stirk HJ,** Thornton JM, Howard CR. A topological model for hepatitis B surface antigen. *Intervirology* 1992; **33:** 148-158

22 **Berting A,** Hahnen J, Kröger M, Gerlich WH. Computer-aided studies on the spatial structure of the small hepatitis B surface protein. *Intervirology* 1995; **38:** 8-15

23 **Carman WF,** Korula J, Wallace L, MacPhee R, Mimms L, Decker R. Fulminant reactivation of hepatitis B due to envelope protein mutant that escaped detection by monoclonal HBsAg ELISA. *Lancet* 1995; **345:** 1406-1407

24 **Li Q,** Dong C, Wang J, Che Y, Jiang L, Wang J, Sun M, Wang L, Huang J, Ren D. Induction of hepatitis C virus-specific humoral and cellular immune responses in mice and rhesus by artificial multiple epitopes sequence. *Viral Immunol* 2003; **16:** 321-333

25 **Chen YD,** Xiong X, Liu X, Li J, Wen YL, Chen Y, Dai Q, Cao Z, Yu W. Immunoreactivity of HCV/HBV epitopes displayed in an epitope-presenting system. *Mol Immunol* 2006; **43:**436-442 in press

26 **Buratti E,** Di Michele M, Song P, Monti-Bragadin C, Scodeller EA, Baralle FE, Tisminetzky SG. Improved reactivity of hepatitis C virus core protein epitopes in a conformational antigen-presenting system. *Clin Diagn Lab Immunol* 1997; **4:** 117-121

27 **Chen YD,** Liu MY, Zou YJ, Peng M, Dai CB. Induction of neutralizing antibodies by SA11 Vp4-specific epitopes. *Zhongguo Bing du xue* 1997; **12:** 125-131
28 **Chen YD,** Liu MY, Zhao W, Dai CB. Broadly Immunological Reactivities primed by epitopes corresponding to the cleavage region of SA11 Vp4. *Zhongguo Bing du xue* 1998; **13:** 57-63
29 **Liu X,** Li JQ, Xiong XY, Chen YN, Peng M, Dai Q, Wen YL, Chen YD. [Protective efficacy of recombinant rotavirus epitope-based vaccine in mice] *Zhongguo Yixue Kexueyuan Xue bao* 2005; **27:** 216-22

Science Editor Guo SY **Language Editor** Elsevier HK

PO Box 2345, Beijing 100023, China
www.wjgnet.com
wjg@wjgnet.com

ELSEVIER

World J Gastroenterol 2005;11(41):6445-6449
World Journal of Gastroenterology ISSN 1007-9327

• *BASIC RESEARCH* •

Cytochrome P450 2E1 high activity polymorphism in alcohol abuse and end-organ disease

Mark T Cartmell, Hans-Ulrich Schulz, Derek A O'Reilly, Bing-Mei Yang, Volker Kielstein, Simon P Dunlop, Walter Halangk, Andrew G Demaine, Andrew N Kingsnorth

Mark T Cartmell, Derek A O'Reilly, Andrew N Kingsnorth, Department of Surgery, Derriford Hospital, Plymouth, United Kingdom
Simon P Dunlop, Department of Gastroenterology, Derriford Hospital, Plymouth, United Kingdom
Bing-Mei Yang, Andrew G Demaine, Department of Molecular Medicine, Plymouth Postgraduate Medical School, Plymouth, United Kingdom
Hans-Ulrich Schulz, Walter Halangk, Department of Surgery, University of Magdeburg, Magdeburg, Germany
Volker Kielstein, Outpatient Clinic for Addiction Diseases, Magdeburg, Germany
Correspondence to: Mr Mark T Cartmell, c/o Professor Kingsnorth, Derriford Hospital, Plymouth PL6 8DH, United Kingdom. markcartmell@hotmail.com
Telephone : +44-1752-763017 Fax: +44-1752-763007
Received: 2005-03-04 Accepted: 2005-04-02

Abstract

AIM: To investigate a possible role for a recently identified polymorphism in the gene of cytochrome P450 2E1, the presence of which is associated with high activity of the enzyme.

METHODS: Two hundred and thirty-nine alcohol consumers, ICD 10.1/.2 (ALC), and 208 normal controls were studied. PCR amplification of the CYP2E1 gene region was performed to assess polymorphic variation. Fisher's exact test was used to assess the data.

RESULTS: Twelve normal controls (5.8%) possessed the insertion. Five ALC (2.1%) had the insertion; of these 2 of 144 with alcohol induced chronic pancreatitis, none of 28 with alcoholic liver disease and 3 of 67 without end-organ disease had the polymorphism. A significantly Lower frequency of subjects possessed the insertion than normal controls [$P = 0.049$ (genotype analysis $P = 0.03$)]. To further assess, if there was a relationship to alcohol problems *per se* or end-organ disease, we compared patients with alcohol induced end-organ disease *vs* alcoholic controls without end-organ disease *vs* normal controls which again showed a significant difference [$P = 0.045$ (genotype analysis, $P = 0.011$)], further sub-group analysis did not identify which group(s) accounted for these differences.

CONCLUSION: We have shown the frequencies of this high-activity polymorphism in alcohol related patient groups for the first time. The frequency is significantly less in alcoholics than normal controls, as with high activity polymorphisms of alcohol dehydrogenase. The biological significance, and whether the relevance is solely for alcoholism or is there a relationship to end-organ disease, would benefit from the assessment in the populations with a greater frequency of this polymorphism.

Key words: CYP2E1; Alcohol; Chronic pancreatitis; Liver disease; Polymorphism

Cartmell MT, Schulz HU, O'Reilly DA, Yang BM, Kielstein V, Dunlop SP, Halangk W, Demaine AG, Kingsnorth AN. Cytochrome P450 2E1 high activity polymorphism in alcohol abuse and end-organ disease. *World J Gastroenterol* 2005; 11(41):6445-6449
http://www.wjgnet.com/1007-9327/11/6445.asp

INTRODUCTION

Cytochrome P450 2E1 (CYP2E1) is the major component of the microsomal enzyme oxidizing system, which is one of the major pathways of oxidative metabolism of ethanol[1,2] as well as a large number of xenobiotics[3]. CYP2E1 is induced to greater activity by its substrate ethanol, probably *via a* number of mechanisms, including transcriptional, post-transcriptional and post-translational[2,4,5].

CYP2E1 activity is expressed in the liver, at sites of maximal alcohol induced damage[6], and in the pancreas, where it is also induced by chronic alcohol consumption[7,8]. These two are the major sites of damage following chronic consumption of ethanol. In addition, it is found in the brain[9], also a site of ethanol induced damage.

The genetic predisposition to both alcoholism and alcohol induced end-organ damage is an area of debate. Alcohol-induced pancreatitis occurs in approximately 5% of alcoholics[10] while no, or minimal, fibrosis is found in 32% of pancreata of alcoholics[11]. Alcoholic cirrhosis occurs in around 10% and hepatitis in 10-35%[12].

The heterogeneity of the response to alcohol implicates genetic factors. Family and twin studies suggest a genetic component to alcoholism[13,14]. Some evidence suggests that the majority of genetic predisposition to psychosis and liver disease may be accounted for by disposition to alcoholism[14].

Recently, an insertion polymorphism in the promoter

region of the gene coding for the enzyme CYP2E1 has been described; sequencing has shown a 96-bp insertion as a series of eight repeats, as opposed to six in the wild type[15,16]. This corresponds to the restriction fragment length polymorphism, between positions -2270 and -1672. Presence of which is associated with higher CYP2E1 metabolic activity (employing an *in vivo* chlorazoxazone 6-hydroxylation test) in the presence of recently consumed alcohol or obesity[17]. We have therefore analyzed the frequency of this polymorphism in patients with a history of excessive alcohol consumption, with and without end-organ damage, and normal controls.

The 96-bp insertion, previously described, is a 729-bp fragment employing the PCR based analysis of Fritsche *et al*[16]. The wild type allele is 633 bp in length. In addition, a GenBank record also exists for a 48-bp deletion (accession no. J02843), corresponding to 585 bp.

MATERIALS AND METHODS

Subjects

Venous blood samples were drawn from patients giving informed consent and local research ethics committee approval was obtained. We collected samples on 239 Caucasoid subjects (ALC) fulfilling the ICD 10 criteria 10.1 and 10.2, that is harmful use and/or alcohol dependence syndrome. Cut-off for minimal consumption was 80 g alcohol per day (UK patients range 56-400 U/week; median 106 U/week) over a minimum of 2 years (UK range 2-45 years; median 10 years). Age range was 25-73 years, median 47 years. The subjects were sub-divided as follows:

Sixty-seven (36 British and 31 German) subjects without known end-organ disease, AC, collected from clients at alcohol rehabilitation centers.

One hundred and seventy-two with alcohol-related end-organ disease (AEOD). Of which, one hundred and forty-four (39 British and 105 German) patients had alcohol-induced chronic pancreatitis (AICP); all fulfilled the criteria for late- or end-stage AICP, as defined by the Zurich criteria[18]. The twenty-eight patients with alcoholic liver disease (ALD) had biopsy proven cirrhosis or a history, consistent with alcoholic hepatitis, including jaundice associated with excess alcohol consumption without other evident cause.

Two hundred and eight samples of cord blood from Caucasoids with a normal, healthy delivery taken in Derriford Hospital, Plymouth, UK were employed as normal controls.

Laboratory analysis

DNA samples were extracted from peripheral and cord blood samples employing the commercially available Nucleon II DNA extraction kits (Nucleon Biosciences, Lanarkshire, Scotland, UK) or QIAmp DNA Blood Minikits (Qiagen, Hilden, Germany).

DNA amplification was performed for the promoter region of CYP2E1 as previously described[16], employing amplimers 5'-GTG ATG GAA GCC TGA AGA ACA- and 5'-CTT TGG TGG GGT GAG AAC AG-. Reactions were carried out in a volume of 25 μ L employing 100-200 ng of genomic DNA. Following a hot start for 4 min at 94 °C, thirty cycles of: 94 °C (denaturing) for 30 s; 66 °C (annealing) for 2 min and 72 °C (extension) for 2 min were performed. This was followed by 10-min extension at 72 °C.

Products were analyzed on a 1.5% agarose gel stained with 0.01% v/v ethidium bromide, viewed under ultraviolet light and compared to 50 and 100 bp molecular weight ladders (Roche Diagnostics, Lewes, East Sussex, UK).

Statistical analysis

Two-sided Fisher's exact tests were used throughout (SPSS 9.0, SPSS Inc., Chicago, IL, USA). A P value of <0.05 was taken as significant. Where appropriate, multisided contingency tables were employed initially for comparisons, with sub-group analysis only when a statistically significant result was seen in the initial comparison. Individual sub-group analyses for end-organ disease(s) only involved comparison with AC controls. Chi square values, where expected cell numbers are greater than 5, are shown in brackets in tables. A comparison is made for the presence of the insertion polymorphism, which has the functional association[17], and for the genotype of that polymorphism.

RESULTS

Results are displayed in Table 1. of 208 normal controls 12 (5.8%) had the insertion polymorphism, and all were heterozygotes (Figure 1A). In contrast, 5 of 239 ALC subjects (2.1%) had the insertion. In the AICP group two subjects had the insertion and one of these was homozygous for the insertion. In the AC group, three subjects had the insertion. In addition, one AICP and one AC had a band which would correspond to the 48-bp deletion found in GenBank (Figure 1B), as did two normal controls. Results from the British and German groups, all European Caucasoids, were similar: three of the 136 German subjects (2.2%) and 2 of the 103 British (2%) had the insertion; two of the 31 German AC, 1 of the 36 British AC, 1 of the 105 German AICP and 1 of the 39 British AICP.

Comparing ALC to NC for the presence of the insertion polymorphism, showed that it was less abundant in the former than the latter ($P = 0.049$) (Table 2). The same comparison for genotype of the insertion was comparable ($P = 0.030$) (Table 2).

To delineate whether the difference may have been for alcohol problems *per se* or end organ disease we initially employed Fisher's exact test for the presence of the insertion using a three by two contingency table of normal controls, AC and AEOD. This revealed a statistically significant difference ($P = 0.045$), and analysis for insertion genotypes was comparable ($P = 0.011$) (Table 3). Thus, we further analyzed the sub-groups. Comparing AC with NC and comparisons within alcoholic (ALC) subgroups analysis did not reveal any significant differences, as might be expected with such a low frequency in the patient

Table 1 Full genotype data on all subjects

	Normal controls (n = 208)	ALC (n = 239)	Of ALC		Of AEOD	
			AC (n = 67)	AEOD (n = 172)	AICP (n = 144)	ALD (n = 28)
Homozygote wildtype	194	232	63	169	141	28
Heterozygote for insertion	12	4	3	1	1	0
Homozygote for insertion	0	1	0	1	1	0
Heterozygote for deletion	2	2	1	1	1	0

ALC, ICD 10.1/10.2; AC, alcoholic controls; AEOD, alcohol-related end-organ disease; AICP, alcohol induced chronic pancreatitis; ALD, alcoholic liver disease.

Table 2 Normal control and alcoholic figures and comparisons

	Normal controls n = 208 (%)	ALC n = 239 (%)	Fisher's exact test
Presence of insertion polymorphism	12 (5.8)	5 (2.1)	$P = 0.049$ ($\chi^2 = 4.110$, $P = 0.043$)
Genotype for insertion polymorphism			
Heterozygote	12 (5.8)	4 (1.7)	$P = 0.030$
Homozygote	0 (0.0)	1 (0.4)	

ALC, ICD 10.1/10.2.

Table 3 Alcoholic subgroup figures and analyses

	Normal controls n = 208 (%)	Alcoholic controls n = 67 (%)	Alcoholic end organ disease n = 172 (%)	Fisher's exact test
Presence of insertion polymorphism	12 (5.8)	3 (4.5)	2 (1.2)	$P = 0.045$
Genotype for insertion polymorphism				
Heterozygote	12 (5.8)	3 (4.5)	1 (0.6)	$P = 0.011$
Homozygote	0 (0.0)	0 (0.0)	1 (0.6)	

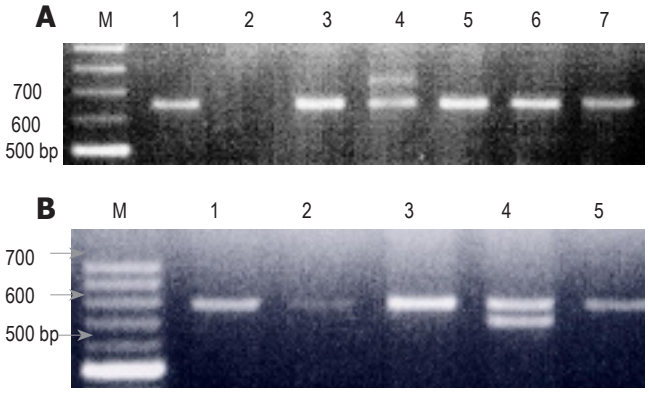

Figure 1 A: Agarose gel showing wild type homozygotes (633 bp, lanes 1, 3, 5–7) and a heterozygote for the insertion polymorphism (729 bp, lane 4). Run alongside a molecular weight marker (M); **B**:Agarose gel showing wild type homozygotes (633 bp, lanes 1–3 and 5) and a heterozygote for the deletion polymorphism (585 bp, lane 4). Run alongside a molecular weight marker (M).

groups. Although genotype analysis for AEOD compared with AC approached significance with $P = 0.068$.

DISCUSSION

Polymorphisms in CYP2E1, other than that studied here, have been looked at in previous studies, though some have used small numbers. Their association with alcoholism has been studied: no association was found for the c1/c2 alleles in most studies[19-23]. A positive association for the D form of the C/D polymorphism was found in Japanese subjects[24]. Although some studies used non-alcoholic controls, in alcohol induced end-organ disease association for these polymorphisms has been found: for ALD and the c2 allele[25-27] and fatty liver and the c2 allele[28]. However, the positive association with end-organ disease has not been found in a number of studies[19,21,29-31] and two studies found an association with the c1 allele[32,33].

The original study describing the polymorphism assessed in this study, showed greater CYP2E1 metabolic activity associated with the 96 bp insertion. In that study chlorazoxazone hydroxylation was higher in the patients with the presence of the polymorphism and who were obese or recent consumers of alcohol[17]; both circumstances when CYP2E1 is induced. The two later descriptions[15,16] delineate the pattern of 8 repeats of 42-60 bp, as opposed to 6 in the wild type. The first sequencing data showed a run of five repeats[34] (accession no. J02843), which had not been seen in the two further studies[15,16], this form would correspond to the smaller band seen in four of our 447 samples (Figure 1B).

Hu *et al*[15] did not find an increased constitutive

expression in luciferase transfection experiments, for the insertion polymorphism, which would agree with McCarver et al[17] findings of increased enzymatic activity only in the induced state (obese subjects and recent alcohol consumers).

To our knowledge, this is the first study to look at this polymorphism in patient groups. In previous studies of healthy groups of American Caucasoids, frequencies of 6.9%[17] and 4.2%[16] are seen. Another previous study found the insertion in only 2.1% of healthy Swedish subjects[15].

At low frequencies these results, on Caucasoid subjects, could all be consistent with the frequencies found in our patient, as well as our control, groups; of 5.8% controls (British), 2.2% German ALC and 2% British ALC. However, in the large numbers in our study our results do indicate a statistically significant difference, which remains when isolating the smaller numbers of only British subjects for insertion genotype between NC and ALC ($P = 0.03$). Population stratification is a confounding factor in all genetic association studies and the possibility of this is recognized, raising the question as to whether our results are biologically as well as statistically significant.

We have shown a significantly lower frequency of this polymorphism, which is associated with increased activity, in the gene coding for the enzyme CYP2E1 when comparing those with alcohol dependence or abuse and normal controls. This could be explained and be analogous to the association found in the functional variations in ADH. It has been shown that high activity forms of ADH (and low activity forms of ALDH) are associated with the protection against alcoholism in a number of studies, as previously reviewed[35]. This is believed to be due to the increased production (or decreased metabolism) of the ethanol metabolite acetaldehyde (and possibly other toxic metabolites), to which associated unpleasant side effects such as flushing are ascribed[35].

Due to the low frequency in our patient populations it was not possible to delineate whether there was only a relationship to alcohol misuse *per se*, or a relationship to end-organ disease. If a lower frequency existed in alcoholics, it could then be expected to be increased in those with end-organ disease compared to alcoholic controls. The sole homozygote was a patient with AICP and genotype analysis of those with end-organ disease *vs* AC approached significance, with $P = 0.068$. However, to infer a finding from such a result would not be justified.

Further analysis in ethnic populations with a frequency of this polymorphism which is sufficiently common to a more likely impact on susceptibility to CYP2E1-related diseases would be useful (e.g. Chinese[15], Taiwanese or African American[16] populations). This would be useful both to confirm or refute the association found here and to delineate any association with end-organ disease, rather than alcoholism *per se*.

In conclusion, the debate regarding a role for CYP2E1 in alcohol misuse and end-organ disease and a genetic component of this is further assessed. We have shown for the first time frequencies of this functional polymorphism in patient groups and there appears to be an association with this high activity polymorphism in the gene coding for cytochrome P450 2E1 and genetic protection against alcohol consumption. However, further studies are required in other populations.

ACKNOWLEDGMENTS

The authors would like to thank David Wright for his statistical input and the staff and clients of Broadreach Drug and Alcohol Treatment Centre, Plymouth.

REFERENCES

1 **Lieber CS**, DeCarli LM. Hepatic microsomal ethanol-oxidizing system. In vitro characteristics and adaptive properties in vivo. *J Biol Chem* 1970; **245: 2**505-2512
2 **Lieber CS**. Cytochrome P-4502E1: its physiological and pathological role. *Physiol Rev* 1997; **77:** 517-544
3 **Parkinson A**. Biotransformation of xenobiotics. In: Klassen CD, Amdur MO, Doull J. eds. Casarett and Doulls' Toxicology: The Basic Science of Poisons. 5th ed. New York: McGraw-Hill, 1996 ; 113-186
4 **Ohnishi K**, Lieber CS. Reconstitution of the microsomal ethanol-oxidizing system. Qualitative and quantitative changes of cytochrome P-450 after chronic ethanol consumption. *J Biol Chem* 1977; **252**: 7124-7131
5 **Takahashi T**, Lasker JM, Rosman AS, Lieber CS. Induction of cytochrome P-4502E1 in the human liver by ethanol is caused by a corresponding increase in encoding messenger RNA. *Hepatology* 1993; **17**: 236-245
6 **Tsutsumi M**, Lasker JM, Shimizu M, Rosman AS, Lieber CS. The intralobular distribution of ethanol-inducible P450IIE1 in rat and human liver. *Hepatology* 1989; **10**: 437-446
7 **Kessova IG**, DeCarli LM, Lieber CS. Inducibility of cytochromes P-4502E1 and P-4501A1 in the rat pancreas. *Alcohol Clin Exp Res* 1998; **22**: 501-504
8 **Norton ID**, Apte MV, Haber PS, McCaughan GW, Pirola RC, Wilson JS. Cytochrome P4502E1 is present in rat pancreas and is induced by chronic ethanol administration. *Gut* 1998; **42**: 426-430
9 **Upadhya SC**, Tirumalai PS, Boyd MR, Mori T, Ravindranath V. Cytochrome P4502E (CYP2E) in brain: constitutive expression, induction by ethanol and localization by fluorescence in situ hybridization. *Arch Biochem Biophys* 2000; **373**: 23-34
10 **Dreiling DA**, Koller M. The natural history of alcoholic pancreatitis: update 1985. *Mt Sinai J Med* 1985; **52:** 340-342
11 **Pitchumoni CS**, Glasser M, Saran RM, Panchacharam P, Thelmo W. Pancreatic fibrosis in chronic alcoholics and nonalcoholics without clinical pancreatitis. *Am J Gastroenterol* 1984; **79**: 382-388
12 **Grant BF**, Dufour MC, Harford TC. Epidemiology of alcoholic liver disease. *Semin Liver Dis* 1988; **8**: 12-25
13 **National Institute of Alcohol Abuse and Alcoholism**. Genetic and psychosocial influences. In: Tenth Special Report to the U. S. Congress on Alcohol and Health. Maryland: NIAAA, 2000; 159-196
14 **Reed T**, Page WF, Viken RJ, Christian JC. Genetic predisposition to organ-specific endpoints of alcoholism. *Alcohol Clin Exp Res* 1996; **20**: 1528-1533
15 **Hu Y**, Hakkola J, Oscarson M, Ingelman-Sundberg M. Structural and functional characterization of the 5'-flanking region of the rat and human cytochrome P450 2E1 genes: identification of a polymorphic repeat in the human gene. *Biochem Biophys Res Commun* 1999; **263**: 286-293
16 **Fritsche E**, Pittman GS, Bell DA. Localization, sequence analysis, and ethnic distribution of a 96-bp insertion in the promoter of the human CYP2E1 gene. *Mutat Res* 2000; **432**: 1-5

17 **McCarver DG**, Byun R, Hines RN, Hichme M, Wegenek W. A genetic polymorphism in the regulatory sequences of human CYP2E1: association with increased chlorzoxazone hydroxylation in the presence of obesity and ethanol intake. *Toxicol Appl Pharmacol* 1998; **152**: 276-281
18 **Ammann RW.** A clinically based classification system for alcoholic chronic pancreatitis: summary of an international workshop on chronic pancreatitis. *Pancreas* 1997; **14:** 215-221
19 **Carr LG**, Hartleroad JY, Liang Y, Mendenhall C, Moritz T, Thomasson H. Polymorphism at the P450IIE1 locus is not associated with alcoholic liver disease in Caucasian men. *Alcohol Clin Exp Res* 1995; **19:** 182-184
20 **Maezawa Y**, Yamauchi M, Toda G, Suzuki H, Sakurai S. Alcohol-metabolizing enzyme polymorphisms and alcoholism in Japan. *Alcohol Clin Exp Res* 1995; **19**: 951-954
21 **Carr LG**, Yi IS, Li TK, Yin SJ. Cytochrome P4502E1 genotypes, alcoholism and alcoholic cirrhosis in Han Chinese and Atayal Natives of Taiwan. *Alcohol Clin Exp Res* 1996; **20**: 43-46
22 **Kee JY**, Kim MO, You IY, Chai JY, Hong ES, An SC, Kim H, Park SM, Youn SJ, Chae HB. [Effects of genetic polymorphisms of ethanol-metabolizing enzymes on alcohol drinking behaviors] *Taehan Kan Hakhoe Chi* 2003; **9:** 89-97
23 **Konishi T**, Luo HR, Calvillo M, Mayo MS, Lin KM, Wan YJ. ADH1B*1, ADH1C*2, DRD2 (-141C Ins), and 5-HTTLPR are associated with alcoholism in Mexican American men living in Los Angeles. *Alcohol Clin Exp Res* 2004; **28:** 1145-1152
24 **Iwahashi K**, Ameno S, Ameno K, Okada N, Kinoshita H, Sakae Y, Nakamura K, Watanabe M, Ijiri I, Harada S. Relationship between alcoholism and CYP2E1 C/D polymorphism. *Neuropsychobiology* 1998; **38**: 218-221
25 **Tsutsumi M**, Takada A, Wang JS. Genetic polymorphisms of cytochrome P4502E1 related to the development of alcoholic liver disease. *Gastroenterology* 1994; **107**: 1430-1435
26 **Tanaka F,** Shiratori Y, Yokosuka O, Imazeki F, Tsukada Y, Omata M. Polymorphism of alcohol-metabolizing genes affects drinking behavior and alcoholic liver disease in Japanese men. *Alcohol Clin Exp Res* 1997; **21:** 596-601
27 **Grove J**, Brown AS, Daly AK, Bassendine MF, James OF, Day CP. The RsaI polymorphism of CYP2E1 and susceptibility to alcoholic liver disease in Caucasians: effect on age of presentation and dependence on alcohol dehydrogenase genotype. *Pharmacogenetics* 1998**; 8**: 335-342
28 **Piao YF**, Li JT, Shi Y. Relationship between genetic polymorphism of cytochrome P450IIE1 and fatty liver. *World J Gastroenterol* 2003; **9**: 2612-2615
29 **Itoga S**, Nomura F, Harada S, Tsutsumi M, Takase S, Nakai T. Mutations in the exons and exon-intron junction regions of human cytochrome P-4502E1 gene and alcoholism. *Alcohol Clin Exp Res* 1999; **23**: 13S-16S
30 **Burim RV**, Canalle R, Martinelli Ade L, Takahashi CS. Polymorphisms in glutathione S-transferases GSTM1, GSTT1 and GSTP1 and cytochromes P450 CYP2E1 and CYP1A1 and susceptibility to cirrhosis or pancreatitis in alcoholics. *Mutagenesis* 2004**; 19:** 291-298
31 **Verlaan M**, Te Morsche RH, Roelofs HM, Laheij RJ, Jansen JB, Peters WH, Drenth JP. Genetic polymorphisms in alcohol-metabolizing enzymes and chronic pancreatitis. *Alcohol Alcohol* 2004; **39:** 20-24
32 **Maezawa Y**, Yamauchi M, Toda G. Association between restriction fragment length polymorphism of the human cytochrome P450IIE1 gene and susceptibility to alcoholic liver cirrhosis. *Am J Gastroenterol* 1994; **89**: 561-565
33 **Kim MS**, Lee DH, Kang HS, Park HS, Jung S, Lee JW, Kwon KS, Kim PS, Kim HG, Shin YW, Kim YS, Baek I, Lee MS. [Genetic polymorphisms of alcohol-metabolizing enzymes and cytokines in patients with alcohol induced pancreatitis and alcoholic liver cirrhosis] *Korean J Gastroenterol* 2004; **43:** 355-363
34 **Umeno M,** McBride OW, Yang CS, Gelboin HV, Gonzalez FJ. Human ethanol-inducible P450IIE1: complete gene sequence, promoter characterization, chromosome mapping, and cDNA-directed expression. *Biochemistry* 1988; **27**: 9006-9013
35 **Bosron WF**, Ehrig T, Li TK. Genetic factors in alcohol metabolism and alcoholism. *Semin Liver Dis* 1993; **13**: 126-135

Science Editor Guo SY **Language Editor** Elsevier HK

PO Box 2345, Beijing 100023, China
www.wjgnet.com
wjg@wjgnet.com

ELSEVIER

World J Gastroenterol 2005;11(41):6450-6458
World Journal of Gastroenterology ISSN 1007-9327

• *BASIC RESEARCH* •

Grapefruit-seed extract attenuates ethanol-and stress-induced gastric lesions *via* activation of prostaglandin, nitric oxide and sensory nerve pathways

Tomasz Brzozowski, Peter C Konturek, Danuta Drozdowicz, Stanislaw J Konturek, Oxana Zayachivska, Robert Pajdo, Slawomir Kwiecien, Wieslaw W Pawlik, Eckhart G Hahn

Tomasz Brzozowski, Danuta Drozdowicz, Stanislaw J Konturek, Robert Pajdo, Slawomir Kwiecien, Wieslaw W Pawlik, Department of Physiology, Jagiellonian University Medical College, Cracow, Poland
Peter C Konturek, Eckhart G Hahn, Department of Medicine I, University of Erlangen-Nuremberg, Erlangen, Germany; Oxana Zayachivska National Medical University, Lviv, Ukraine
Correspondence to: Professor Tomasz Brzozowski, Department of Physiology, Jagiellonian University Medical College, Cracow, Poland. mpbrzozo@cyf-kr.edu.pl
Telephone: +48-12-424-7231 Fax: +48-12-421-1578
Received: 2005-01-06 Accepted: 2005-05-24

Abstract

AIM: Grapefruit-seed extract (GSE) containing flavonoids, possesses antibacterial and antioxidative properties but whether it influences the gastric defense mechanism and gastroprotection against ethanol- and stress-induced gastric lesions remains unknown.

METHODS: We compared the effects of GSE on gastric mucosal lesions induced in rats by topical application of 100% ethanol or 3.5 h of water immersion and restraint stress (WRS) with or without (A) inhibition of cyclooxygenase (COX)-1 activity by indomethacin and rofecoxib, the selective COX-2 inhibitor, (B) suppression of NO-synthase with L-NNA (20 mg/kg ip), and (C) inactivation by capsaicin (125 mg/kg sc) of sensory nerves with or without intragastric (ig) pretreatment with GSE applied 30 min prior to ethanol or WRS. One hour after ethanol and 3.5 h after the end of WRS, the number and area of gastric lesions were measured by planimetry, the gastric blood flow (GBF) was assessed by H_2-gas clearance technique and plasma gastrin levels and the gastric mucosal generation of PGE2, superoxide dismutase (SOD) activity and malonyldialdehyde (MDA) concentration, as an index of lipid peroxidation were determined.

RESULTS: Ethanol and WRS caused gastric lesions accompanied by the significant fall in the GBF and SOD activity and the rise in the mucosal MDA content. Pretreatment with GSE (8-64 mg/kg i g) dose-dependently attenuated gastric lesions induced by 100% ethanol and WRS; the dose reducing these lesions by 50% (ID_{50}) was 25 and 36 mg/kg, respectively, and this protective effect was similar to that obtained with methyl PGE2 analog (5 μg/kg i g). GSE significantly raised the GBF, mucosal generation of PGE_2, SOD activity and plasma gastrin levels while attenuating MDA content. Inhibition of PGE_2 generation with indomethacin or rofecoxib and suppression of NO synthase by L-NNA or capsaicin denervation reversed the GSE-induced protection and the accompanying hyperemia. Co-treatment of exogenous calcitonine gene-related peptide (CGRP) with GSE restored the protection and accompanying hyperemic effects of GSE in rats with capsaicin denervation.

CONCLUSION: GSE exerts a potent gastroprotective activity against ethanol and WRS-induced gastric lesions via an increase in endogenous PG generation, suppression of lipid peroxidation and hyperemia possibly mediated by NO and CGRP released from sensory nerves.

Key words: Grapefriut-seed extract; Gastroprotection; Gastric blood flow; Superoxide dismutase; Prostaglandin; Calcitonine gene-related peptide

Brzozowski T, Konturek PC, Drozdowicz D, Konturek SJ, Zayachivska O, Pajdo R, Kwiecien S, Pawlik WW, Hahn EG. Grapefruit-seed extract attenuates ethanol-and stress-induced gastric lesions via activation of prostaglandin, nitric oxide and sensory nerve pathways . *World J Gastroenterol* 2005; 11(41):6450-6458
http://www.wjgnet.com/1007-9327/11/6450.asp

INTRODUCTION

Grapefruit-seed extract (GSE) containing flavonoids, possesses antibacterial, antiviral and antifungal properties[1-3]. These beneficial actions of GSE have been attributed to the antioxidative activity of grapefruit containing citrous flavonoids such as naringenin[4]. Moreover, grapefruit juice and its major flavonoid exhibited the potent anti-*H pylori* activity *in vitro*[5] and was also recently found to exert the cytoprotection against hepatocyte injury induced by algal toxins[6]. In another study, naringenin showed anti-cancer

activity against human breast cancers[7]. Therapeutic efficacy of citrous fruits such as grapefruits and red grapes has been explained by the content of different classes of polyphenolic flavonoids, that were shown to inhibit platelet aggregation, thus decreasing the risk of coronary thrombosis and myocardial infarction[8]. However, the involvement of grapefruit extracts containing various flavonoids in the mechanism of gastric mucosal defense has been little studied.

Our group demonstrated previously that other flavonoids, namely, meciadanol, a synthetic flavonoid inhibiting histidine decarboxylase (HDC) and decreasing histamine content in the stomach, attenuated gastric mucosal lesions produced by ethanol and aspirin *via* the mechanism unrelated to gastric acid secretion and endogenous prostaglandins (PG)[9]. Furthermore, naringenin, a major citrous flavonoid, was reported to exhibit gastroprotection against the gastric injury induced by absolute ethanol due to the increase in the mucus secretion and that this gastroprotective effect of naringenin and accompanying increase in the mucus secretion, were, in part, attenuated by indomethacin suggesting the involvement of endogenous PG in the mechanism of this flavonoid-induced gastroprotection[10]. It remains unknown, to what extent GSE influences the gastric mucosal injury induced by topical (ethanol) and non-topical ulcerogens (stress) and, if so, what is the mechanism of gastroprotection induced by GSE. Therefore, using animal models of gastric lesions induced by 100% ethanol and water immersion and restraint stress (WRS), we determined the influence of GSE on gastric lesions and the accompanying changes in the gastric blood flow (GBF) in the rat stomach. An attempt was also made to assess the contribution of gastric acid secretion, plasma gastrin levels, PG/cyclooxygenase (COX)-system, nitric oxide (NO) and sensory nerves in the gastroprotective effect of GSE. Finally, we evaluated the effect of pretreatment with GSE on the gene expression and activity of superoxide dismutase (SOD) and lipid peroxidation, as expressed by malonyldialdehyde (MDA) concentration, in rats with or without the pretreatment with GSE.

MATERIALS AND METHODS

Male Wistar rats, weighing 180-220 g and fasted for 24 h before the study were employed in all the studies. This study was approved by the Institutional Animal Care and Use Committee of Jagellonian University School of Medicine in Cracow and run in accordance to the statements of European Union regarding handling of experimental animals.

Gastric secretory studies

The effects of GSE purchased from Herb-Pharma, Welke Dudince, Slovakia on gastric acid secretion were examined in 40 conscious rats equipped about 1 mo earlier with a gastric fistula (GF) as described previously[11]. The animals were fasted overnight but had free access to water 24 h before the experiment and they were placed in individual Bollman type cages to maintain the minimum restraint necessary. The GF was opened; the stomach was rinsed gently with about 5 mL of tap water at 37 ℃. The basal gastric secretion was collected for 60 min and GSE was administered i.g. in gradual doses ranging from 8 to 64mg/kg, each dose being administered on a separate test day. In control tests, vehicle (1 mL of saline, i g) was given in the same volume as in tests with GSE and the collection of gastric juice was continued for the final 120 min. The volume and acid concentration of each collected sample of gastric juice were measured and acid outputs was calculated and expressed in terms of micromoles of acid per 30 min[12].

Induction of ethanol and stress lesions and determination of gastric blood flow (GBF)

Acute gastric lesions were induced by an intragastric (ig) application of 100% ethanol similarly to the method described previously[11,12]. Briefly, 100% ethanol in a volume of 1.5 mL was administered ig to rats by means of a metal orogastric tube. After 60 min, the animals were lightly anesthetized with ether, their abdomen was opened by the midline incision and stomach exposed for the measurement of GBF by means of using the H_2-gas clearance technique as described previously[13]. For this purpose double electrodes of electrolytic regional blood flowmeter (Biotechnical Science, Model RBF-2, Osaka, Japan) were inserted into the gastric mucosa. One of these electrodes was used for the local generation of gaseous H_2 and another for the measurement of tissue H_2. With this method, the H_2 generated locally was carried out by flow of blood, while the polarographic current detector reads out decreasing tissue H_2. The tissue H_2 clearance curve was used to calculate an absolute flow rate (mL/100 g/min) in the oxyntic area as described previously[13]. The measurements were made in three areas of the mucosa and the mean values of the measurements were calculated and expressed as percent changes of those recorded in the vehicle (saline) treated animals. After the GBF measurement, the stomach was removed, rinsed with water and pinned open for macroscopic examination. The area of necrotic lesions in oxyntic mucosa was determined by computerized planimetry (Morphomat, Carl Zeiss, FRG)[12-14] by the person who did not know to which experimental group the animals belonged.

The WRS was induced in the animals that were placed in restraint cages and immersed vertically to the level of the xiphoid process in a water bath of 23 ℃ for 3.5 h[13,14]. After 3.5 h of WRS, the rats were lightly anesthetized with ether, the abdomen was opened and the stomach was exposed. The GBF was measured in the oxyntic gland area of the stomach by means of local H_2-gas clearance method using an electrolytic regional blood flow meter (Biomedical Science, Model RBF-2, Osaka, Japan) as described above. The stomach was removed, opened along the greater curvature and placed flat to count the number of gastric lesions by two investigators, unaware of the treatment given as described in our previous studies[13,14]. The stress lesions were defined as round or linear mucosal defects of at least 0.1 mm in diameter.

Animals with sensory denervation induced by capsaicin

The role of sensory afferent nerves in mechanism of WRS-induced gastric lesions with or without pretreatment with GSE was determined in rats with or without capsaicin induced deactivation of these nerves. For this purpose the animals were pretreated with capsaicin (Sigma Co., St. Louis, MO, USA) injected s.c. for 3 consecutive days at a dose of 25, 50 and 50 mg/kg for about 2 wk, before the experiment[15,16]. All injections of capsaicin were performed under ether anesthesia to counteract the pain reactions and respiratory impairment associated with injection of this agent. To check the effectiveness of the capsaicin denervation, a drop of 0.1 mg/mL solution of capsaicin was instilled into the eye of each rat and the protective counting movements were counted as described previously[16]. Rats with or without capsaicin-denervation received vehicle or GSE (5-80 mg/kg ig) 30 min prior to exposure to 3.5 h of WRS. At the end of WRS, animals were anesthetized and then the GBF and the number of gastric lesions were measured in a similar manner as mentioned above.

Determination of mucosal generation of PGE_2, lipid peroxidation and SOD activity in gastric mucosa exposed to ethanol and WRS with and without GSE

In groups of rats exposed to standard 3.5 h of WRS without or with pretreatment with GSE, the mucosal samples from the gastric mucosa were taken by biopsy (about 200 mg) from oxyntic gland area without mucosal lesions immediately after the animals were killed to determine the mucosal generation of PGE_2 by radioimmunoassay (RIA) as described previously[17]. The capability of the mucosa to generate PGE_2 was expressed in nanograms of wet tissue weight.

Since lipid peroxidation is a well-established mechanism of cellular injury induced by reactive oxygen metabolites, we measured the changes in the MDA as an indicator of this lipid peroxidation in gastric mucosa[18,19] exposed to WRS without and with the treatment with GSE. For the measurement of lipid peroxidation, the tissue was weighed, transferred to the ice-cooled test tube and homogenized in 400 μL of 20 m mol/L Tris buffer pH 7.4 containing 5 mM butylated hydroxytoluene to prevent new lipid peroxidation that can occur during the homogenization. The homogenate was then centrifuged at 4 °C for 10 min and resulted supernatant (200 μL) was stored in -80 °C until an assay of lipid peroxidation. The content of lipid peroxidation was measured at 37 °C by spectrophotometer at a wave length of 586 nm and compared with the absorbance of purified MDA as the standard.

The activity of SOD was measured in the gastric mucosa of rats exposed to WRS with or without pretreatment with GSE using SOD 525 assay kit (OXIS International, Inc., Portland, USA)[19,20]. The gastric tissue was first washed with 0.9% NaCl containing 0.16 mg/mL heparin to remove red blood cells which may interfere with the SOD activity in the gastric specimens. Then the biopsy sample was blotted on the filter paper, weighed and finally homogenized in 400 μL of PBS buffer pH 7.4 using a tissuemizer Ultra Turax (Janke and Kunkel GmbH and Co., Staufen, Germany). The principle of the SOD measurement is based on the SOD-mediated increase in the rate of auto-oxidation of 5, 6, 6a, 11β-tetrahydro-3,9,10-trihydrobenzoflurene in aqueous solution at 37 °C to yield a chromophore with maximum absorbance at 525 nm. Ethanol-chloroform extraction was employed to inactivate Mn-SOD and Fe-SOD and to ensure that the assay is specific for Cu/Zn-SOD.

Determination of SOD transcripts by reverse transcriptase polymerase chain reaction (RT-PCR)

The expression of SOD was determined by RT-PCR in the gastric mucosa of intact rats or following exposure to WRS with or without GSE. Samples of the gastric oxyntic mucosa (about 500 mg) were scraped off on ice using glass slide and then immediately snap frozen in liquid nitrogen, and stored at -80 °C. Total RNA was isolated from the gastric oxyntic mucosa using a rapid guanidinum isothiocyanate/phenol chloroform single step extraction kit from Stratagene (Stratagene GmbH, Heidelberg, Germany)[21,22]. Following precipitation, the RNA was resuspended in RNase-free TE buffer and the concentration was estimated by absorbance at 260 nm wave length. Samples were frozen at -80 °C until analysis.

First strand cDNA was synthesized from total cellular RNA (5 μg) using 200 U Strata Script TM reverse transcriptase (Stratagene GmbH, Heidelberg, Germany) and oligo (dT) primers (Stratagene GmbH, Heidelberg, Germany). After the reverse transcription, the transcriptase activity was destroyed by heating, and the cDNA was stored at -20 °C until PCR.

A 496-bp fragment of SOD was amplified from single-stranded DNA by PCR using two oligonucleotide primers to SOD. The SOD sense primer was 5' CGAGTTATGGCGACGAAG3' and antisense primer was 5'GTCAGCAGTCACATTGCC3'. The primers for SOD and β-actin were synthesized by Biometra (Gottingen, Germany). Concomitantly, amplification of control rat β-actin (Clon Tech, Palo Alto, CA, USA) (764 bp) was performed on the same samples to verify RNA integrity.

DNA amplification was carried out under the following conditions; denaturation at 94 °C for 1 min, annealing at 60 °C for 45 s, and extension at 72 °C for 45 s. The number of amplification cycles was 29 for SOD. Each PCR-product (8 μL) was electrophoresed on 1.5% agarose gel stained with ethidium bromide, and then visualized under UV light. Location of predicted PCR product was confirmed by using a 100-bp ladder (Gibco BRL/Life Technologies, Eggenstein, Germany) as standard marker.

The intensity of bands was quantified in a semi-quantitative manner using densitometry (LKB Ultrascan, Pharmacia, Sweden) as described in detail in our previous studies[22]. Briefly the gel was photographed under UV transillumination. The intensity of PCR products was measured using video image analysis system (Kodak Digital Science). The SOD mRNA signals were standardized against the β-actin mRNA signal for each sample and results were expressed as SOD mRNA/β-actin mRNA ratio.

Statistical analysis

Results are expressed as means±SE. The significance of the difference between means was evaluated using analysis of variance followed by Duncan's test with a level of significance at $P<0.05$.

RESULTS

Effect of GSE on gastric acid secretion and plasma gastrin levels in rats with chronic GF

As shown in Table 1, gastric acid output reached the value of 134±11 μmol/30 min, while fasting plasma gastrin concentration averaged of 53 ± 4 μmol/L in control rats treated with vehicle (saline). GSE applied ig in a dose of 8 mg/kg ig failed to affect significantly the gastric acid output and plasma gastrin levels as compared to those in control animals. GSE applied ig in a dose of 16 mg/kg and higher, produced a significant decrease in the gastric acid output and significantly raised the plasma gastrin levels (Table 1).

Table 1 Effect of vehicle (saline) and GSE applied ig in graded concentrations ranging from 8 up to 64 mg/kg on the gastric acid secretion and plasma gastrin levels. Results are mean±SE from 6 determinations on 6–8 animals

Type of test	Gastric acid output (μmol/30 min)	Plasma gastrin (pmol/L)
Vehicle	134±11	53±4
GSE (mg/kg ig)		
8	131±9	56±6
16	118±9[a]	69±8[a]
32	89±7[a]	75±9[a]
64	64±5[a]	82±10[a]

[a]$P<0.05$ *vs* vehicle.

Effect of GSE on acute gastric lesions induced by ethanol and WRS

Figure 1 shows the effect of topical pretreatment with GSE applied ig in graded concentrations ranging from 8 to 64 mg/kg on the mean area of gastric lesions induced by 100% ethanol and the accompanying changes in the GBF. Ethanol caused typical widespread gastric lesions with an area of 86±5 mm^2 and reduced the GBF by about 38% as compared to that in intact gastric mucosa. Pretreatment with GSE applied in the lowest dose of 8 mg/kg, failed to influence the ethanol lesions but starting from the dose 16 mg/kg up to dose of 64 mg/kg of GSE, a dose-dependent reduction in gastric lesions was observed; the dose that inhibits ethanol damage by 50% (ID_{50}) being 28 mg/kg. This protective effect of GSE applied in graded doses against ethanol damage was accompanied by the significant rise in the GBF. The gastroprotective effect of GSE and accompanying increase in the GBF were similar to those achieved by the pretreatment with methyl analog of PGE_2 applied 30 min before the application of ethanol.

As shown in Figure 2, the pretreatment with GSE applied topically in a doses ranging from 8 to 64 mg/kg caused a significant attenuation of WRS-induced gastric damage; the ID_{50} being 36 mg/kg. The GBF was significantly decreased in rats exposed to 3.5 h of WRS but GSE given 30 min before the exposure of animals to 3.5 h of WRS resulted in a dose-dependent rise in the GBF as compared to that obtained in vehicle-treated animals (Figure 2).

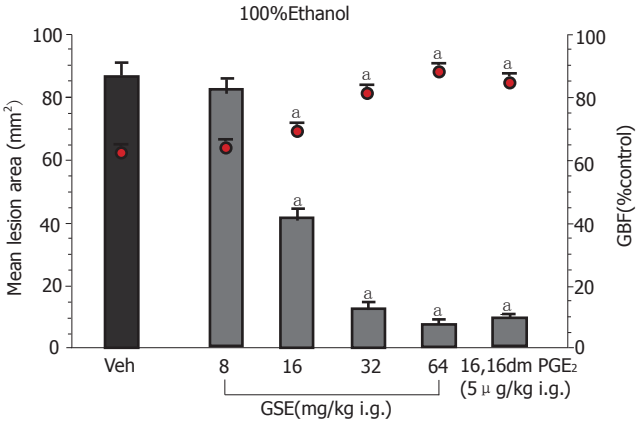

Figure 1 Effect of intragastric (ig) pretreatment with GSE applied in graded doses ranging from 8 mg/kg up to 64 mg/kg or 16,16 dimethyl PGE_2 (5 μg/kg ig) on the mean area of gastric lesions induced by ethanol and accompanying changes in the GBF. Results are mean±SE from 6 to 8 animals per group. [a]$P<0.05$ *vs* vehicle (Veh).

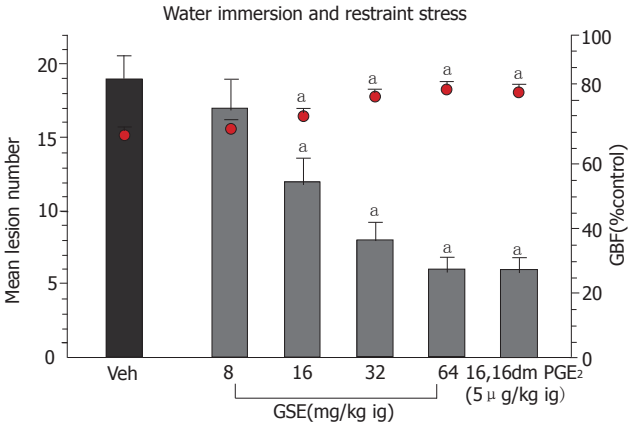

Figure 2 Effect of intragastric (ig) pretreatment with GSE applied in graded doses ranging from 8 mg/kg up to 64 mg/kg or 16,16 dimethyl PGE_2 (5 μg/kg ig) on the mean number of gastric lesions induced by 3.5 h of WRS and accompanying changes in the GBF. Results are mean±SE from 6 to 8 animals per group. [a]$P<0.05$ *vs* vehicle (Veh).

Effect of pretreatment with GSE on the gastric mucosal SOD activity and MDA content in gastric mucosa exposed to ethanol or WRS

Table 2 shows the results of determination of MDA+4HNE as an index of lipid peroxidation in the gastric mucosa or rats exposed to ethanol- or WRS without or with GSE pretreatment. The MDA concentration was significantly increased in vehicle-control gastric mucosa exposed to ethanol or WRS as compared to that in the intact gastric mucosa. Pretreatment with GSE applied ig

in a dose 16 mg/kg or higher, significantly attenuated the MDA concentration in animals exposed to ethanol or WRS (Table 2). The mucosal SOD activity was inhibited in the gastric mucosa of animals exposed to ethanol or WRS as compared to the respective value in intact gastric mucosa (Table 2). In contrast, the pretreatment with GSE applied in i.g. in graded doses ranging from 8 up to 64 mg/kg, which caused a significant attenuation of the damage induced by ethanol or WRS, dose-dependently reversed the deleterious effect of ethanol or WRS on the SOD activity and significantly counteracted the ethanol and WRS-induced rise in the MDA content (Table 2).

Table 2 Effect of vehicle (saline) and GSE applied i.g. in graded concentrations ranging from 8 mg/kg up to 64 mg/kg on the MDA concentration and SOD activity in the gastric mucosa in rats exposed to 100% ethanol or those subjected to 3.5 h of WRS. Results are mean±SE from 6 determinations on 6–8 animals

Type of test	MDA concentration (nmol/g)	SOD activity (unit/g)
Intact	0.5±0.02	733±43
Vehicle+ethanol	14.8±2.3[a]	425±32[a]
Vehicle+WRS	16.8±2.3[a]	425±32[a]
GSE (mg/kg i.g.)+ethanol		
8	13.7±2.3	438±37
16	10.4±2.8[c]	549±38[c]
32	8.3±0.9[c]	675±40[c]
64	6.6±0.7[c]	695±43[c]
GSE (mg/kg i.g.)+WRS		
8	15.7±2.6[c]	438±37[c]
16	13.4±2.3[c]	549±38[c]
32	10.3±1.9[c]	675±40[c]
64	8.6±0.8[c]	695±43[c]

[a]$P<0.05$ *vs* intact, [c]$P<0.05$ *vs* vehicle+ethanol or vehicle+WRS.

Effect of inhibitors of COX and NOS activity on GSE-induced gastroprotection against WRS induced gastric damage and the alterations in GBF

Pretreatment with GSE (32 mg/kg ig) significantly reduced gastric lesions induced by WRS in a manner similar to that presented in Figure 2. The ip administration of indomethacin at a dose of 5 mg/kg which inhibited generation of endogenous PGE_2 by about 85%, aggravated the WRS-induced gastric lesions and significantly decreased GBF as compared to the respective values in animals treated with vehicle. Such pretreatment with indomethacin reversed almost completely the protective effect of GSE against WRS-induced lesions and the accompanying increase in the GBF (Figure 3).

The L-NNA, an inhibitor of NO-synthase by itself failed to affect the area of gastric lesions and the fall in the GBF induced by ethanol or WRS (Table 3, Figure 4). Pretreatment with GSE (32 mg/ kg ig) resulted in a significant reduction of ethanol- or WRS-induced gastric damage and significantly decreased the GBF as compared with the respective values attained in rats without GSE administration. Co-treatment with L-arginine (200 mg/kg ig) but not with D-arginine, added to GSE restored the gastroprotection and the accompanying increase in the GBF induced by this extract in L-NNA treated animals.

Capsaicin-denervation which by themselves aggravated ethanol- and WRS-induced gastric damage significantly attenuated the GSE-induced protection and hyperemia against lesions induced by ethanol or WRS (Table 4, Figure 5). Co-administration of calcitonine gene-related peptide (CGRP) with GSE in rats with capsaicin-denervation restored the protective and hyperemic effects of this extract against ethanol- and WRS-induced gastric lesions.

Table 3 Effect of GSE with or without pretreatment with NG-nitro-L-arginine (L-NNA 20 mg/kg ip) applied with or without the combination with L-arginine (L-Arg, 200 mg/kg ig) or D-arginine (D-Arg, 200 mg/kg ig) on the area of ethanol-induced gastric lesions and accompanying changes in the GBF. Results are mean± SE of 6–8 rats

Type of test	Mean lesion area (mm^2)	GBF (% control)
Without L-NNA		
Vehicle	82±5	63±3
GSE (32 mg/kg i.g.)	8±1.5[a]	81±4[a]
With L-NNA		
Vehicle	88±4	58±3
GSE (32 mg/kg i.g.)	76±3[c]	66±5[c]
L-Arg (200 mg/kg i.g.)		
+GSE (32 mg/kg i.g.)	12±2[e]	79±3[c]
D-Arg (200 mg/kg i.g.)		
+GSE (32 mg/kg i.g.)	72±4	69±3

[a]$P<0.05$ *vs* vehicle, [c]$P<0.05$ *vs* values in respective group without L-NNA, [e]$P<0.05$ *vs* values in respective group with L-NNA but without L-Arg administration.

Gastric mucosal expression of mRNA for SOD in ethanol-treated rats with or without pretreatment with GSE

As shown in Figure 6, mRNA for SOD was detected by RT-PCR as a strong signal in the gastric mucosa of vehicle-control animal not treated with ethanol. In contrast, the signal for the SOD mRNA in the gastric mucosa of ethanol-treated rats was faint. The ratio of SOD mRNA

Table 4 The number of WRS-induced gastric lesions and accompanying changes in the GBF in rats treated with vehicle and GSE (32 mg/kg i.g.) without or with capsaicin denervation. Means ±SE of 6–8 rats

Type of test	Mean lesion number	GBF (% control)
Without capsaicin denervation		
Vehicle	18±3	67±4
GSE (32 mg/kg ig)	8±1.5[a]	78±3[a]
With capsaicin denervation		
Vehicle	28±4[b]	54±3[b]
GSE (32 mg/kg ig)	16±3[b]	64±4[b]
CGRP (10 μg/kg sc)		
+GSE (32 mg/kg ig)	9±1.3[c]	74±3[c]

[a]$P<0.05$ *vs* vehicle, [c]$P<0.05$ *vs* corresponding values obtained in animals without capsaicin denervation, [e]$P<0.05$ *vs* corresponding values obtained in animals with capsaicin denervation without CGRP treatment.

over β-actin mRNA was significantly decreased in ethanol-treated animals as compared to those treated with vehicle only. SOD mRNA was strongly expressed in animals pretreated with various doses of GSE (16-64 mg/kg ig) before the ethanol application. The ratio of mRNA for SOD over the β-actin mRNA was significantly increased in gastric mucosa of rats pretreated with graded doses of GSE as compared to that attained in vehicle-pretreated rats that were given ethanol.

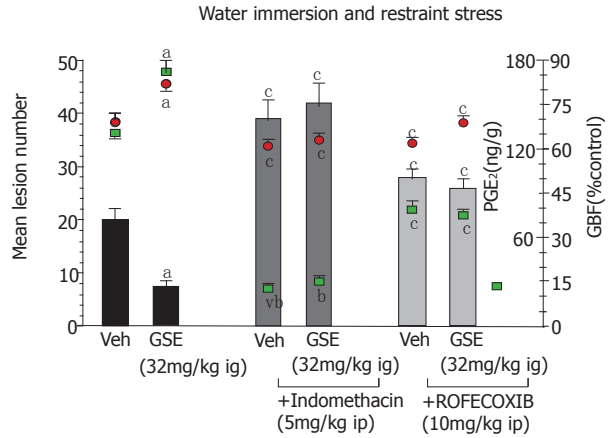

Figure 3 Effect of GSE (32 mg/kg ig) on the mean number of WRS-induced gastric lesions and accompanying alterations in the gastric mucosal PGE2 generation and GBF in rats with or without the pretreatment with indomethacin (5mg/kg ip) or rofecoxib (10 mg/kg ig). Results are mean±SE from 6 to 8 animals per group. $^{a}P<0.05$ *vs* vehicle (Veh), $^{c}P<0.05$ *vs* respective values in animals without indomethacin or rofecoxib pretreatment.

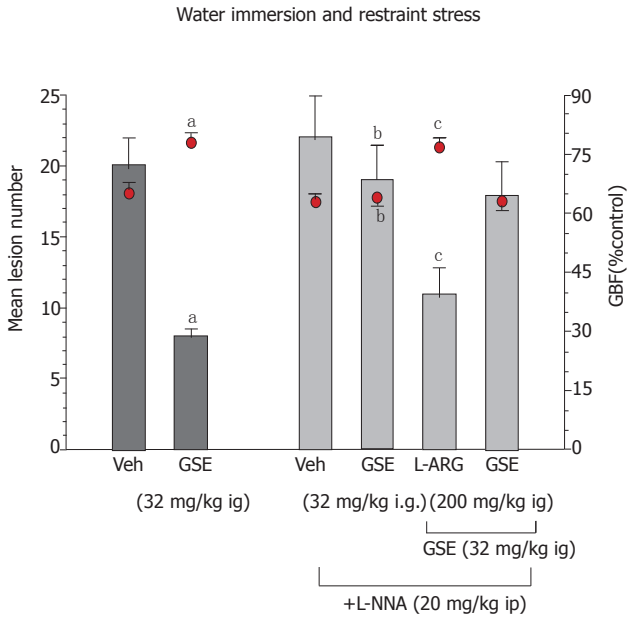

Figure 4 Effect of GSE (32 mg/kg i.g.) on the mean number of WRS-induced gastric lesions and accompanying alterations in the GBF in rats with or without the pretreatment with L-NNA (20 mg/kg i.p.). Results are mean ±SE from 6-8 animals per group. $^{a}P<0.05$ vs vehicle (Veh), $^{b}P<0.01$ *vs* respective values in animals without L-NNA administration, $^{c}P<0.05$ *vs* respective values in animals treated with L-NNA. *vs* vehicle (Veh), $^{b}P<0.01$ *vs* respective values in animals without indomethacin or rofecoxib pretreatment.

DISCUSSION

This study shows that GSE attenuates the lesions in the rat stomach by the intragastric application of noxious agent such as ethanol or those caused by stress and that this protective effect of GSE is accompanied by the increase in the GBF and SOD expression and its activity and reduction of MDA concentration, that is widely considered as an index of lipid peroxidation. The inhibition of acid-dependent lesions caused by WRS can be attributed to the inhibition of acid secretion by this compound as observed in this study using well-conditioned and fully adapted GF rats. This protective and hyperemic activity of GSE against WRS ulcerogenesis was abolished by COX inhibitors such as indomethacin and rofecoxib and significantly reduced by L-NNA. Thus, we conclude that GSE containing citrous flavonoids exerts a potent gastroprotective activity against ethanol- and WRS-induced gastric lesions and this protective effect in the stomach may involve endogenous PG derived from COX-1 and COX-2 activity, suppression of lipid peroxidation and gastric hyperemia mediated by NO and neuropeptides released from afferent sensory nerves.

Previous studies documented that grapefruit seeds are the major depository for limonoids (triterpenoid dilactones chemically related to limonin) of these 77% are neutral while 2% are acidic limonoids[1-3]. Grapefruit contains also many flavonoids that includes glycosides, naringenin, quercetin, kaempferol, hesperetin and apigenin being the most abundant among their aglycones[4]. GSE, containing flavonoids, has been shown to possess antibacterial, antiviral and antifungal properties[2,3]. This beneficial action of GSE was attributed to the antioxidative activity of grapefruit containing citrus flavonoids[4,23], since, for instance, these flavonoids were found to exhibit the potent

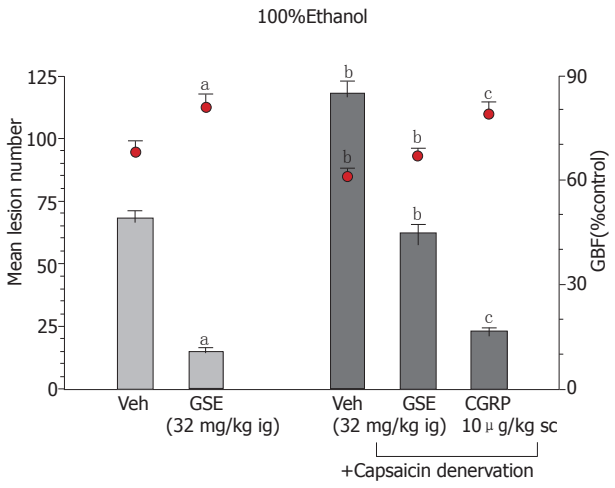

Figure 5 Effect of GSE (32 mg/kg ig) on the mean area of ethanol-induced gastric lesions and accompanying alterations in the GBF in rats with or without capsaicin inactivation of sensory nerves. Results are mean±SE from 6–8 animals per group. $^{a}P<0.05$ *vs* vehicle (Veh), $^{b}P<0.01$ *vs* respective values in animals without capsaicin denervation, $^{c}P<0.05$ *vs* respective values in animals with capsaicin denervation. administration, $^{c}P<0.05$ *vs* respective values in animals treated with L-NNA. *vs* vehicle (Veh), $^{b}P<0.01$ *vs* respective values in animals without indomethacin or rofecoxib pretreatment.

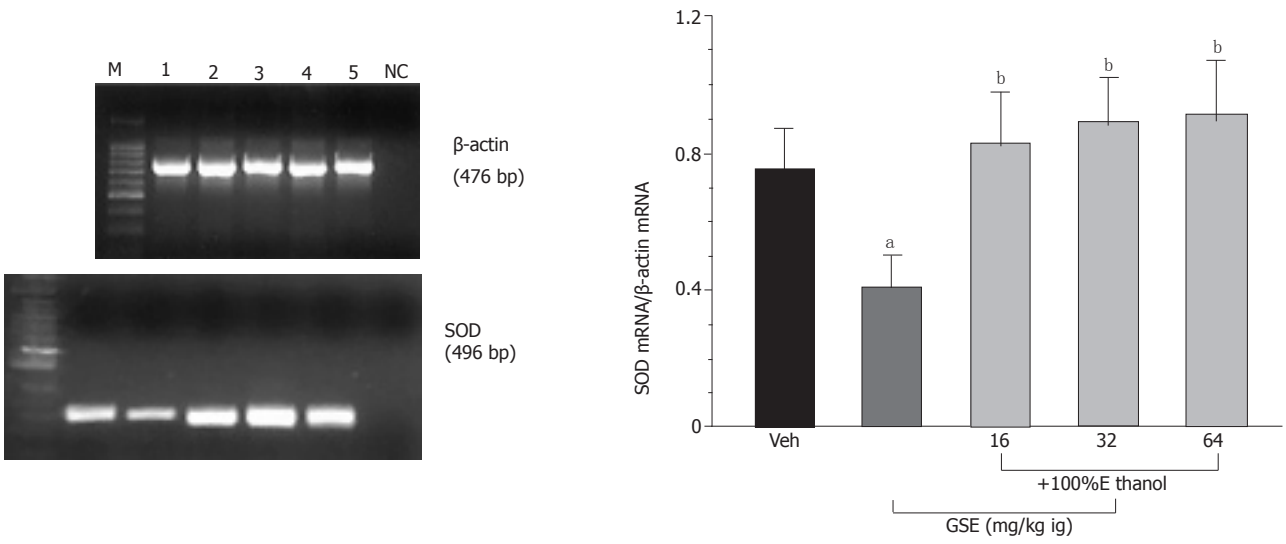

Figure 6 Determination of SOD mRNA (left panel) by RT-PCR and by ratio of SOD mRNA over β -actin (right panel) in the vehicle-control intact gastric mucosa (lane 1) and in those treated with GSE given i.g. in graded doses of 16 mg/kg (lane 2), 32 mg/kg (lane 3) and 64 mg/kg (lane 4) prior to the exposure to ethanol, M-DNA size marker, NC-negative control. Mean±SE of 4–6 rats. $^{a}P<0.05$ *vs* vehicle (Veh), $^{b}P<0.01$ *vs* ethanol alone group. $^{c}P<0.05$ *vs* respective values in animals with capsaicin denervation. administration, $^{c}P<0.05$ *vs* respective values in animals treated with L-NNA. *vs* vehicle (Veh), $^{b}P<0.01$ *vs* respective values in animals without indomethacin or rofecoxib pretreatment.

anti-*H pylori* activity *in vitro*[5,24]. Furthermore, grapefruit containing flavonoids were also recently implicated in cytoprotection against injury induced by algal toxins in isolated hepatocytes[6,25]. Interestingly, GSE in a formulation of Citricidal, was demonstrated to be effective against more than 800 bacterial and vital strains, 100 strains of fungus and a large number of single or multicelled parasites[1]. These antimicrobiological properties against a wide range of Gram-negative and Gram-positive organisms were attributed to the disruption by GSE of the bacterial membrane and the subsequent liberation by this extract of the bacterial cytoplasmic contents within a relatively short time (e.g. 15-20 min). In a similar report, it was reported that GSE-induced antimicrobial action is comparable to that of proven antibacterials[2]. Moreover, naringenin, the bioactive component of GSE, showed anti-cancer activity against human breast cancers[7,26]. The underlying mechanism of the therapeutic efficacy of citrus fruits such as grapefruits and red grapes seems to depend upon the presence of different classes of polyphenolic flavonoids that were shown to inhibit platelet aggregation, thus decreasing the risk of coronary thrombosis and myocardial infarction[27-30].

The involvement of GSE in the mechanism of gastric mucosal defense against the formation of gastric lesions caused by obnoxious substances has been little studied. Herein, we provide evidence that GSE applied topically caused dose-dependent diminution of acute gastric lesions induced by both, 100% ethanol and WRS. Previous studies demonstrated that the damaging action of ethanol and WRS could be attributed to the enhancement in the reactive oxygen substances (ROS) and the ROS-dependent increase in the lipid peroxidation and inhibition of antioxidizing enzyme activity[18,19,21]. We found that GSE dose-dependently attenuated the rise in MDA content in the gastric mucosa injured by ethanol or WRS indicating that this extract can attenuate the process of lipid peroxidation implicated in the pathogenesis of ethanol and WRS-induced gastric damage[18,19]. Moreover, we have demonstrated that ethanol decreased the gene expression and activity of SOD in the gastric mucosa suggesting that the suppression of key mucosal antioxidizing enzyme along with the elevation of lipid peroxidation, play an important role in the pathogenesis of these lesions. This increase in the mucosal lipid peroxidation as well as the fall in SOD expression and its activities were attenuated by GSE, suggesting that the reduction in lipid peroxidation by this seed extract may contribute to the attenuation of the deleterious effect of noxious agents on the gastric mucosa. This is supported by the fact that the GBF was elevated and gastric PGE_2 production were enhanced in animals treated with GSE as compared to those treated with vehicle. Our finding is in accordance with observations that some flavonoids stimulated PGE_2 production by isolated gastric mucosal cells while suppressing gastric acid secretion via direct inhibitory effect on H^+/K^+-ATPase activity[24]. It is not concluded that NO/NOS system is also involved in gastroprotection against ethanol and WRS caused by GSE because both, GSE-induced protection and hyperemia were counteracted by L-NNA, a non-specific inhibitor of NO-synthase and this effect was restored in these animals by the combined treatment with L-arginine and GSE. Thus, our study implies that some natural products of the citrous fruits such as GSE, afford protection against ethanol and stress-induced gastric damage due to

endogenous PG and the preservation of expression and activity of a major antioxidizing enzyme such as SOD.

The mechanism of gastroprotective activity of GSE appears to be dependent on endogenous PG and the functional activity of sensory nerves releasing CGRP. This notion is supported by our findings that indomethacin, a non-selective inhibitor of COX-1 and COX-2 activity or functional ablation of sensory afferent nerves by capsaicin reversed GSE-induced protection and accompanying hyperemia. In addition, co-treatment of exogenous CGRP with GSE, administered to replace the deficit of this peptide in capsaicin-treated animals, restored the protective efficacy of GSE. Interestingly, rofecoxib which is a highly selective COX-2 inhibitor[17], also attenuated the gastroprotective and hyperemic activities of GSE suggesting the involvement of COX-2 derived products in the gastroprotection and increase in the GBF induced by this extract. Further studies assessing the mRNA expression of COX-1 and COX-2 in GSE-treated mucosa should reveal which enzymatic pathway is involved in aforementioned effects of this extract.

This gastroprotective activity of the GSE could be attributed to naringenin, a major GSE flavonoid, because this flavonoid was reported to exhibit gastroprotection against the gastric injury induced by absolute ethanol, predominantly due to the increase in the mucus secretion[10]. It is of interest that this gastroprotective effect of naringenin and accompanying increase in the mucus secretion, were, in part, attenuated by indomethacin, supporting the contribution of endogenous PG to the mechanism of gastroprotection by grapefruit products[10]. As shown in our present study, GSE by itself enhanced the gastric mucosa generation of PGE_2 but our unpublished evidence indicates that this extract can be also effective against aspirin-induced gastric lesions under the conditions, where PG generation is completely suppressed. Therefore, it seems likely, that endogenous PG might not be primary mediators of this protection and other gastroprotective factors such as NO and/or neuropeptides released from sensory afferent nerves could be involved. This was the reason for carrying out the study with L-NNA, a potent NO-synthase inhibitor and with capsaicin, applied in a dose that causes functional ablation of sensory nerves releasing vasoactive neuropeptides such as CGRP. We found that L-NNA and capsaicin denervation inhibited the GSE-induced protection against ethanol- and WRS-induced gastric lesions and accompanying gastric mucosal hyperemia. Our study militates against PG as the primary mediator in the mechanism of GSE-induced gastroprotection and this remains in accordance with our previous report that meciadanol, the synthetic flavonoid inhibiting the activity of HDC, prevented the ethanol- and aspirin-induced injury in rat stomach without altering the mucosal generation of prostacyclin (PGI_2)[9].

Another candidate involved in the GSE-induced protection could be gastrin, which is known to exhibit both, gastroprotective and hyperemic activities[11]. Indeed, we addressed this issue by direct determination of the plasma gastrin levels by specific RIA and we found that gastrin is elevated in GSE-treated animals. This effect could be secondary to the inhibition of gastric acid secretion caused by this compound as demonstrated in our study by the administration of GSE to the chronic, well-adapted rats with chronic GF. Suppression of gastric secretion by GSE might contribute to the protective activity of this extract against WRS, because WRS damage depends upon gastric acidity and becomes exaggerated by acidic conditions in the stomach.

In summary, we have demonstrated in this report that the pretreatment with GSE reduces the ethanol and WRS-induced gastric damage through the preservation of the antioxidizing enzyme (SOD) activity, reduction of free radical-dependent lipid peroxidation, enhancement in the GBF and plasma gastrin levels. Endogenous PG appears to be important mediator of this protection, but other mediators such as NO and neuropeptides released from sensory nerves such as CGRP could be also involved in the gastroprotective and hyperemic activities of this extract. No study, so far has been undertaken to examine the ulcer healing efficacy of GSE, but the fact that this grapefruit seed extract exerts a potent anti-*H pylori* in vitro[30] and profound gastroprotective effects in laboratory animals warrants a further approach for its potential application in healing of chronic ulcerations in human beings.

REFERENCES

1 **Heggers JP,** Cottingham J, Gusman J, Reagor L, McCoy L, Carino E, Cox R, Zhao JG. The effectiveness of processed grapefruit-seed extract as an antibacterial agent: II. Mechanism of action and in vitro toxicity. *J Altern Complement Med* 2002; **8:** 333-340

2 **Reagor L**, Gusman J, McCoy L, Carino E, Heggers JP. The effectiveness of processed grapefruit-seed extract as an antibacterial agent: I. An in vitro agar assay. *J Altern Complement Med* 2002; **8:** 325-332

3 **Proteggente AR**, Pannala AS, Paganga G, Van Buren L, Wagner E, Wiseman S, Van De Put F, Dacombe C, Rice-Evans CA. The antioxidant activity of regularly consumed fruit and vegetables reflects their phenolic and vitamin C composition. *Free Radic Res* 2002; **36**: 217-233

4 **Tirillini B**. Grapefruit: the last decade acquisitions. *Fitoterapia* 2000; **71** Suppl 1: S29-S37

5 **Bae EA**, Han MJ, Kim DH. In vitro anti-Helicobacter pylori activity of some flavonoids and their metabolites. *Planta Med* 1999; **65:** 442-443

6 **Blankson H**, Grotterød EM, Seglen PO. Prevention of toxin-induced cytoskeletal disruption and apoptotic liver cell death by the grapefruit flavonoid, naringin. *Cell Death Differ* 2000; **7:** 739-746

7 **So FV**, Guthrie N, Chambers AF, Moussa M, Carroll KK. Inhibition of human breast cancer cell proliferation and delay of mammary tumorigenesis by flavonoids and citrus juices. *Nutr Cancer* 1996; **26:** 167-181

8 **Keevil JG**, Osman HE, Reed JD, Folts JD. Grape juice, but not orange juice or grapefruit juice, inhibits human platelet aggregation. *J Nutr* 2000; **130**: 53-56

9 **Konturek SJ**, Kitler ME, Brzozowski T, Radecki T. Gastric protection by meciadanol. A new synthetic flavonoid inhibiting histidine decarboxylase. *Dig Dis Sci* 1986; **31**: 847-852

10 10**Motilva V**, Alarcón de la Lastra C, Martín MJ. Ulcer-protecting effects of naringenin on gastric lesions induced by ethanol in rat: role of endogenous prostaglandins. *J Pharm*

Pharmacol 1994; **46:** 91-94

11 **Konturek SJ**, Brzozowski T, Bielanski W, Schally AV. Role of endogenous gastrin in gastroprotection. *Eur J Pharmacol* 1995; **278**: 203-212

12 12 **Brzozowski T**, Konturek SJ, Kwiecień S, Pajdo R, Drozdowicz D, Sliwowski Z, Muramatsu M. SU- 840, a novel synthetic flavonoid derivative of sophoradin, with potent gastroprotective and ulcer healing activity. *J Physiol Pharmacol* 1998; **49**: 83-89

13 **Brzozowski T**, Konturek PC, Sliwowski Z, Drozdowicz D, Hahn EG, Konturek SJ. Importance of nitric oxide and capsaicin-sensitive afferent nerves in healing of stress lesions induced by epidermal growth factor. *J Clin Gastroenterol* 1997; **25** Suppl 1: S28-S38

14 14**Konturek SJ**, Brzozowski T, Konturek PK, Majka J, Dembiński A. Role of salivary glands and epidermal growth factor (EGF) in gastric secretion and mucosal integrity in rats exposed to stress. *Regul Pept* 1991; **32**: 203-215

15 15**Holzer P**, Livingston EH, Saria A, Guth PH. Sensory neurons mediate protective vasodilatation in rat gastric mucosa. *Am J Physiol* 1991; **260:** G363-G370

16 16**Brzozowski T**, Konturek SJ, Sliwowski Z, Pytko-Polończyk J, Szlachcic A, Drozdowicz D. Role of capsaicin-sensitive sensory nerves in gastroprotection against acid-independent and acid-dependent ulcerogens. *Digestion* 1996; **57:** 424-432

17 **Brzozowski T,** Konturek PC, Konturek SJ, Sliwowski Z, Drozdowicz D, Stachura J, Pajdo R, Hahn EG. Role of prostaglandins generated by cyclooxygenase-1 and cyclooxygenase-2 in healing of ischemia-reperfusion-induced gastric lesions. *Eur J Pharmacol* 1999; **385:** 47-61

18 **Kwiecień S,** Brzozowski T, Konturek SJ. Effects of reactive oxygen species action on gastric mucosa in various models of mucosal injury. *J Physiol Pharmacol* 2002; **53:** 39-50

19 **Kwiecień S**, Brzozowski T, Konturek PC, Pawlik MW, Pawlik WW, Kwiecień N, Konturek SJ. The role of reactive oxygen species and capsaicin-sensitive sensory nerves in the pathomechanisms of gastric ulcers induced by stress. *J Physiol Pharmacol* 2003; **54:** 423-437

20 **Kwiecień S,** Brzozowski T, Konturek PC, Pawlik MW, Pawlik WW, Kwiecień N, Konturek SJ. **Gastroprotection by pentoxyfilline** against stress-induced gastric damage. Role of lipid peroxidation, antioxidizing enzymes and proinflammatory cytokines. *J Physiol Pharmacol* 2004; **55:** 337-355

21 **Brzozowski T**, Konturek P, Konturek SJ, Kwiecień S, Sliwowski Z, Pajdo R, Duda A, Ptak A, Hahn EG. Implications of reactive oxygen species and cytokines in gastroprotection against stress-induced gastric damage by nitric oxide releasing aspirin. *Int J Colorectal Dis* 2003; **18:** 320-329

22 **Konturek PC**, Duda A, Brzozowski T, Konturek SJ, Kwiecien S, Drozdowicz D, Pajdo R, Meixner H, Hahn EG. Activation of genes for superoxide dismutase, interleukin-1beta, tumor necrosis factor-alpha, and intercellular adhesion molecule-1 during healing of ischemia-reperfusion-induced gastric injury. *Scand J Gastroenterol* 2000; **35:** 452-463

23 **Lee YS**, Reidenberg MM. **A method for measuring naringenin** in biological fluids and its disposition from grapefruit juice by man. *Pharmacology* 1998; **56**: 314-317

24 **Beil W**, Birkholz C, Sewing KF. Effects of flavonoids on parietal cell acid secretion, gastric mucosal prostaglandin production and Helicobacter pylori growth. *Arzneimittelforschung* 1995; **45:** 697-700

25 **Kanno S,** Shouji A, Asou K, Ishikawa M. Effects of naringin on hydrogen peroxide-induced cytotoxicity and apoptosis in P388 cells. *J Pharmacol Sci* 2003; **92:** 166-170

26 **Guthrie N**, Carroll KK. Inhibition of mammary cancer by citrus flavonoids. *Adv Exp Med Biol* 1998; **439**: 227-236

27 **Nijveldt RJ,** van Nood E, van Hoorn DE, Boelens PG, van Norren K, van Leeuwen PA. Flavonoids: a review of probable mechanisms of action and potential applications. *Am J Clin Nutr* 2001; **74:** 418-425

28 **Folts JD.** Potential health benefits from the flavonoids in grape products on vascular disease. *Adv Exp Med Biol* 2002; **505**: 95-111

29 **Osman HE**, Maalej N, Shanmuganayagam D, Folts JD. Grape juice but not orange or grapefruit juice inhibits platelet activity in dogs and monkeys. *J Nutr* 1998; **128**: 2307-2312

30 **Borrelli F**, Izzo AA. The plant kingdom as a source of anti-ulcer remedies. *Phytother Res* 2000; **14**: 581-591

Science Editor Guo SY **Language Editor** Elsevier HK

PO Box 2345, Beijing 100023, China
www.wjgnet.com
wjg@wjgnet.com

ELSEVIER

World J Gastroenterol 2005;11(41):6459-6465
World Journal of Gastroenterology ISSN 1007-9327

• *BASIC RESEARCH* •

Neutrophil engagement and septic challenge in acute experimental pancreatitis in rats

Stanisław Hać, Marek Dobosz, Jan J Kaczor, Robert Rzepko, Ewa Aleksandrowicz-Wrona, Zdzisław Wajda, Zbigniew Śledziński, Jacek Krajewski

Stanisław Hać, Zbigniew Śledziński, Jacek Krajewski, Department of General Endocrine and Transplant Surgery, Medical University of Gdańsk, Poland
Marek Dobosz, Department of General and Gastroenterological Surgery, St. Vincent a' Paulo Hospital of Gdynia, Poland
Jan J Kaczor, Department of Bioenergetics, J. Śniadecki University School of Physical Education in Gdańsk, Poland
Robert Rzepko, Department of Pathomorphology, Medical University of Gdańsk, Poland
Ewa Aleksandrowicz-Wrona, Department of Clinical Nutrition, Medical University of Gdańsk, Poland
Zdzisław Wajda, II Department of General Gastroenterological and Endocrinological Surgery Medical University of Gdańsk, Poland
Supported by the grant from Medical University of Gdańsk, Poland
Correspondence to: Stanisłasw Hać, MD, PhD, Department of General Endocrine and Transplant Surgery, Medical University of Gdańsk, 7 Dębinki Street, Gdańsk 80-952, Poland. sthac@amg.gda.pl
Telephone: +48-58-3492410 Fax: +48-58-3492410
Received: 2005-03-07 Accepted: 2005-04-04

Abstract

AIM: To investigate the influence of neutrophil adhesion molecule blockade with monoclonal antibody (MoAb CD11b) and *E. coli* lipopolysaccharide (LPS) administration on experimental acute pancreatitis (AP).

METHODS: AP was induced by four ip injections of cerulein (Cn) at 1-h intervals. MoAb CD 11b and LPS were administered at the beginning of the experiment.

RESULTS: The neutrophil count and chemiluminescence were diminished at the beginning of AP. The oxidative stress parameters were found within the pancreatic gland. MoAb CD 11b used for AP resulted in a significant reduction of pancreatic infiltration and pancreatitis oxidative stress parameters. Serum interleukin-6 (IL-6) was not detected in AP animals, whereas high serum IL-6 concentration was noted only in animals receiving LPS.

CONCLUSION: Neutrophils are involved in pancreatic damage in the early stage of AP. Neutrophil infiltration reduction protects the pancreatic gland from destruction during AP. LPS does not change the early course of Cn pancreatitis in rats.

Key words: Acute pancreatitis; Polymorphonuclear cells; Immunomodulation; Septic shock

Hać S, Dobosz M, Kaczor JJ, Rzepko R, Aleksandrowicz-Wrona E, Wajda Z, Śledziński Z, Krajewski J. Neutrophil engagement and septic challenge in acute experimental pancreatitis in rats. *World J Gastroenterol;* 2005;11(41):6459-6465
http://www.wjgnet.com/1007-9327/11/6459.asp

INTRODUCTION

Acute pancreatitis (AP) is an insidious disease. Almost 75% of patients suffer from the mild edematous form of AP. About 25% of patients develop the severe disease with a mortality rate of 30-60%. The reasons of two different courses still remain unclear. One of the discussed reasons of organ dysfunction complicating AP is excessive leukocyte activation. Activation of inflammatory mediators [interleukins, leukotrienes, TNF-α, PAF, and lipopolysaccharide 9LPS)] within the pancreas may result in excessive damage within the pancreas, peripancreatic tissue or even distant organs[1-3]. The suggestion of neutrophil deteriorating role in human AP has largely been suggested. LPS, presented in the Gram-negative bacterial wall, has been studied extensively as an inflammatory stimulating factor contributing to the pathophysiology of conversion from mild to severe form of AP[4-6]. The pathophysiology of inflammatory process in AP leads to the immunomodulation concept. The idea is one of the most promising treatment options in AP nowadays. The early polymorphonuclear (PMN) requirement is well documented in AP.

The aim of this study was to investigate the PMN activation in the early stage of experimental cerulein (Cn) AP and the influence of mAb against adhesion molecule CD 11b on inflammatory response of the disease. Besides, whether LPS aggravated the early experimental AP in rats was also examined. The hypothesis of early aggravation of AP by LPS challenge was investigated.

MATERIALS AND METHODS

The study was performed on male Wistar rats (180-200 g) that were kept on standard rat chow and fasted overnight before the experiment, but with free access to water. AP was induced by four ip injections of Cn at a dose of 15 μg/kg (Sigma Chemical Co., St. Louis, USA) in 1 mL

of saline at 1-h intervals. MoAb CD 11b (POLATOM Świerk, Poland) was given iv once at the beginning of the experiment at a dose of 1 mg/kg. LPS (Sigma Chemical Co., St. Louis, USA) was administered ip at a dose of 10 mg/kg, simultaneously with the first Cn injection. Control animals were injected intravenously with an adequate volume of 0.9% saline solution. Five and nine hours from the beginning of the experiment, rats were anesthetized with sodium pentobarbital (25 mg/kg ip) and thoracolaparotomy was performed. Blood was aspirated into the test tubes on 30 U/mL heparin from left ventricle, the pancreas was excised, and animals were killed by exsanguinations. Pancreas specimen was taken for light microscopy and for determination of malonyldialdehyde (MDA), total sulfhydryl groups (SH) and myeloperoxidase (MPO). The study protocol was approved by The Local Ethic Committee for the Use of Experimental Animals of Medical University (Protocol No. 22/71).

Animals were divided into seven groups: group 1 ($n=14$) control, group 2 ($n=16$) AP, group 3 ($n=11$) AP+MoAb CD 11b, group 4 ($n=11$) AP+LPS, group 5 ($n=8$) AP+MoAb CD 11b+LPS, group 6 ($n=8$) MoAb CD 11b, group 7 ($n=11$) LPS.

Whole blood chemiluminescence (CL) assay

CL assay was performed in 1:200 diluted heparinized whole blood (30 IU/mL) to reduce artefacts. Diluent was prepared with PBS mixed with calcium and magnesium chloride (Biomed, Poland) and glucose (0.1%). Granulocyte CL was started by the phorbol-12-myristate-13-acetate (PMA, ICN Biomedicals Inc., USA). PMA (1 mg) was diluted with 1 mL dimethyl-sulfoxide (DMSO, Sigma) to the final concentration of 1.6×10^{-3} mol/L. PMA solution was diluted with PBS to the final concentration of 1.6×10^{-6} mol/L just before the measurement. Luminol solution was prepared with 1.77 mg dry substance (ICN Biomedicals Inc., USA) combined with 1 mL 0.4% NaOH and filled to 3 mL with PBS to obtain 3×10^{-5} mol/L concentration.

Chemiluminescence measurement

Transparent tubes containing 100 μL heparinized whole blood diluted 1:20 with PBS, 200 μL luminol (3×10^{-5} mol/L), 500 μL PBS and 200 μL PMA (1.6×10^{-5} mol/L) were analyzed in a FB 12 luminometer (Berthold Detection Systems, Germany) at 460-nm light length. The measurement was carried out at 10-s intervals for 20 min. All reagents were kept at 22℃ during the procedure. The CL intensity was calculated in relative light units (RLU) per 2 000 of whole blood PMN cells, per minute (RLU/2 000 PMN ×min).

Serum polymorphonuclear elastase (PMN-E)

The measurement was carried out on the basis of commercial ELISA method (PMN-E, K6840 Immundiagnostic GmbH, Germany). PMN-E serum concentration was expressed as nanogram per milliliter.

Pancreatic myeloperoxidase (MPO)

A part of the pancreatic gland (at least 0.3 g wet mass) was taken during the laparotomy. The tissue was homogenized (Porter-Elvenheim) immediately at 4℃ with PBS (pH 7.4). The volume of PBS was adequate to obtain 5% homogenate solution. Then the sample was centrifuged at 2 400 r/min for 10 min at 4℃. The supernatant was taken for MPO, SH and MDA measurements. Two milliliters of the supernatant was mixed with 0.5 mL of 0.1% phenyl-methyl-sulfo-fluoride (Sigma Chemicals Co.) and 0.5 mL of 0.5% cetrimide (Merck). The mixture was centrifuged again at 2 400 r/min at 4℃. MPO was measured using the ELISA method (Immundiagnostic GmbH, Germany). Pancreatic MPO concentration was expressed as nanogram per one gram of protein.

Sulfhydryl groups (-SH) and malonyldialdehyde (MDA) in pancreatic homogenate

A total of 300 μL of pancreatic homogenate was diluted with sodium phosphate buffer (10 mmol/L) pH 8.0 to obtain 2.5% proteins concentration. Then 300 μL of sodium dodecyl sulfate (10%) was added to the sample to dissolve proteins in order to expose hidden sulfhydryls. Two thousand and four-hundred-microliter PBS was added, mixed and the absorbance was measured at 412 nm (Cecil Super Aquarius CE 9200). Then 300 μL of DTNB was added into the extract or 300 μL of PBS as blank to the reference mixture. Samples were incubated at 37℃ in a water bath for 1 h. The absorbance was measured again. The concentration of SH groups was expressed as nanomole per milliliter.

MDA content was measured by spectrophotometer (LPO-586 Test Kit) assay (OxisResearch, Portland, USA), 600 μL of supernatant was mixed with 1 950 μL of R1 (10.3 nmol/L *N*-methyl-2-phenylindole solved in acetonitrile) and 450 μL 37% HCl. Samples were incubated in a water bath at 45 °C for 1 h, and then centrifuged at 3 500 r/min for 10 min. The absorbance of the supernatant was measured at 586 nm (Cecil Super Aquarius CE 9200).

Plasma α-amylase and lipase activity

The activity of α-amylase was measured using commercial kit RTU 63116 (BioMerieux). Lipase activity was determined using commercial kit Lipase Color 63109 (BioMerieux) in units per liter.

Microscopic findings within the pancreatic gland

Hematoxylin-eosin standard staining was performed. An experienced pathologist performed the light microscopic examination. All samples were estimated with 200× magnification. Edema, vacuolization and necrosis of pancreatic cells were established in modified Spormann scale (0-3 points each parameter). PMN infiltration within the pancreatic parenchyma was calculated as mean number of neutrophils in 10 consecutive microscopic fields by a "blinded" pathologist.

Whole WBC count

Whole WBC and neutrophils were counted in Bürker' s camera following 1∶200 dilution with Türk's solution.

Cells were counted twice by experienced laboratory technician and the mean value was considered as the result.

Interleukin-6 (IL-6) concentration

Serum IL-6 concentration was determined using the commercial ELISA kit Rat-IL-6 (Biosource). The reaction was based on the peroxidation of tetra-methyl-benzydine. The absorbance measurement was made using an automatic reader (Organon Teknika; Reader 200) at 450-nm wave length.

Statistical analysis

Data were expressed as mean±SD. One-way analysis of variance with the *post hoc* analysis was employed to compare the groups. $P<0.05$ was considered statistically significant.

RESULTS

Whole blood chemiluminescence (CL) intensity

CL intensity of peripheral blood neutrophils was significantly lower in Cn AP group after 5 and 9 h of observation than that in control animals. CL was reduced from 1 700 to 1 086 RLU/min ×2 000 PMN in AP group, and from 1 842 to 988 RLU/min ×2 000 PMN after 9 h. MoAb CD 11b given before AP induction did not significantly decrease CL intensity in group 3, but the CL intensity decreased from 1 086 to 1 421 after 5 h and from 988 to 1 408 RLU/2 000 PMN ×min after 9 h of AP induction. No important reduction of CL was observed in AP groups receiving LPS or LPS and MoAb CD 11b. MoAb CD 11b given to healthy animals did not change CL value significantly. LPS given to healthy animals significantly reduced CL from 1 842 to 976 RLU/2 000 PMN ×min after 9 h of experiment (Figure 1).

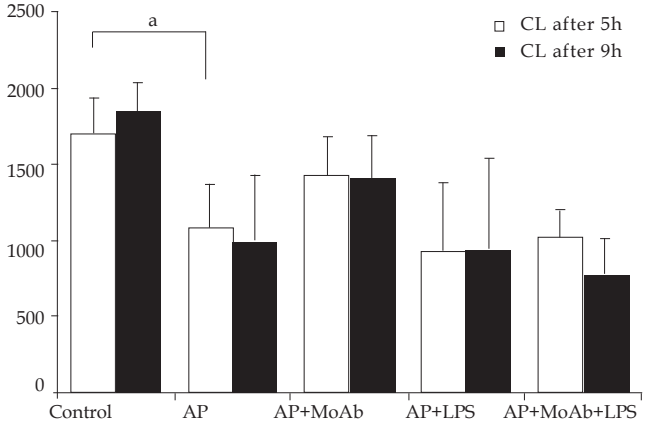

Figure 1 Whole blood CL. [a]$P<0.05$ *vs* control group.

WBC and polymorphonuclear cell (PMN) count

Induction of Cn AP resulted in a significant reduction of peripheral WBC from 5 120 in control group to 2 204 cells/μL in AP group after 5 h of observation. PMN count in peripheral blood reduced from 1 230 to 614 cells/μL during the same period of time. MoAb CD 11b given before AP induction significantly increase WBC/PMN count in peripheral blood (from 2 204/614 to 3 942/2315 after 5 h of observation and from 4 225/1 286 to 4 037/1 120 cells/μL after 9 h of observation). LPS in AP group diminished peripheral WBC count 5 h after AP, while ameliorated their count 9 h after AP induction. LPS given with MoAb CD 11b in AP resulted in a time-dependent decrease of WBC count. MoAb CD 11b given to healthy animals did not change WBC count significantly. LPS given to healthy animals gradually reduced WBC count (Table 1).

Table 1 WBC and PMN cells count (/μL, mean±SD)

Group	WBC after 5 h	WBC after 9 h	PMN after 5 h	PMN after 9 h
	(/μL)	(/μL)	(/μL)	(/μL)
Control	5 120 ±1 220	5 597±1 447	1 230±490	1 434±569
AP	2 204[a]±705[a]	4 225±583	614[a]±229[a]	1 286±598
AP+MoAb	3 942[c]±493[c]	4 037±1 778	2 315[c]±850[c]	1 120±705
AP+LPS	1 678 ±259	6 762[c]±580[c]	1 047±560	5146[c]±1 124[c]
AP+MoAb +LPS	4 087 ±259	5 450±580	1 830±560	3 250±1 124
MoAb	6 587±1 003	3 887±1 612	2 200±502	990±307
LPS	3 771[a]±1 510[a]	4 100±1 824	2 892[a]±1 372[a]	2959[a]±1 553[a]

[a]$P<0.05$ *vs* control group; [c]$P<0.05$ *vs* AP group.

Oxidative stress parameters within pancreatic tissue

Sulfhydryl (-SH) compounds and malonyldialdehyde (MDA) concentration in pancreatic homogenate The concentration of (-SH) groups in pancreatic homogenate reduced from 60.3 nmol/mg protein in control group to 40.2 nmol/mg protein in AP group after 5 h of observation. Depletion of (-SH) compounds accompanied the elevation of MDA concentration in pancreatic homogenate from 0.21 nmol/mg protein in control group to 0.38 nmol/mg protein in AP group in the same period of time. After 9 h of observation concentration of (-SH) groups reduced from 64.7 nmol/mg in control group to 43.5 nmol/mg in AP group. LPS and MoAb CD 11b given together or separately in AP did not change the (-SH) group concentration in both periods of observation in comparison to AP group (group 2). MDA concentration in

Table 2 SH compound and MDA concentration within pancreatic homogenate (nmol/mg protein, mean±SD)

Group	SH after 5 h	SH after 9 h	MDA after 5 h	MDA after 9 h
Control	60.3±7.3	64.7±8.3	0.21±0.02	0.22±0.03
AP	40.2[a]±8.5[a]	43.5[a]±4.3[a]	0.38[a]±0.07[a]	0.39[a]±0.03[a]
AP+MoAb	40.0±6.5	46.7±1.4	0.25[c]±0.06[c]	0.26[c]±0.03[c]
AP+LPS	40.0±6.8	41.1±8.2	0.39±0.07	0.41±0.1
AP+MoAb +LPS	39.0±6.7	40.4±5.0	0.37±0.08	0.35±0.2
MoAb	63.4±8.6	59.4±9.0	0.2±0.03	0.21±0.04
LPS	52.0±9.1	48.6±4.7	0.28±0.04	0.35±0.05

[a]$P<0.05$ *vs* control group; [c]$P<0.05$ vs AP group.

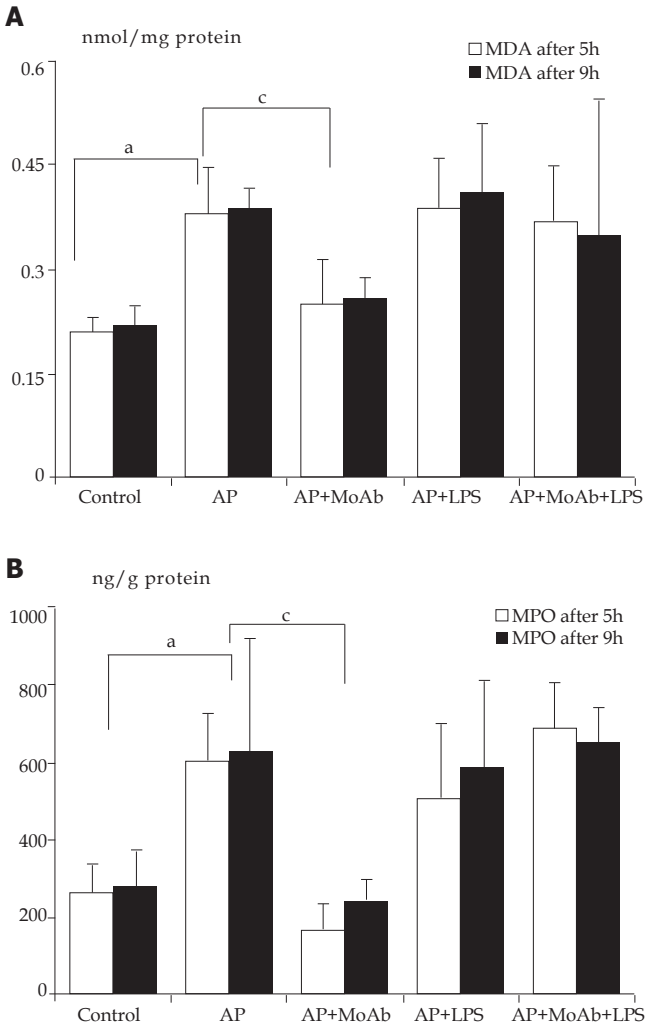

Figure 2 MDA **(A)** and MPO **(B)** level in pancreatic homogenate. [a]*P*<0.05 vs control group; [c]*P*<0.05 *vs* AP group. MDA: malonyldialdehyde; MPO: myeloperoxidase.

AP group treated with MoAb CD 11b reduced significantly from 0.38 to 0.25 after 5 h of observation and from 0.39 to 0.26 nmol/mg protein after 9 h of observation (Figure 2A and Table 2).

Myeloperoxidase (MPO) level in pancreatic homogenate

AP significantly increased pancreatic MPO concentration from 260 in control animals to 602 ng/g protein in AP group after 5 h of observatiozn and from 280 ng/g protein to 626 ng/g protein after 9 h of observation compared to control group. Adhesion molecule blockade with MoAb CD 11b, prior to AP induction, protected the pancreatic gland from MPO elevation after 5 h (from 602 to 168 ng/g protein) and 9 h of observation (626-246 ng/g protein, Figure 2B). LPS or LPS with MoAb CD 11b given to AP groups did not change the course of pancreatic MPO activity (data not shown).

α-Amylase and lipase plasma activity

Cn (15 μg/kg for 4 h) caused transient hyperamylasemia and hyperlipasemia in all AP groups after 5 h of observation (groups 2-5). Animals receiving MoAb CD 11b alone or with LPS in AP (groups 3 and 5) had significantly lower α-amylase and lipase activity after 9 h of experiment compared to other AP groups (groups 2 and 4, Table 3).

Table 3 Plasma α-amylase and lipase activity (U/L, mean±SD)

Group	A-Amylase after 5 h	A-Amylase after 9 h	Lipase after 5 h	Lipase after 9 h
Control	690±120	743±156	6±8	8±9
AP	8 286[a]±143[a]	5 908[a]±640[a]	2 140[a]±1 123[a]	929[a]±252[a]
AP+MoAb	5 119±2 487	2 293[c]±1 739[c]	1 704±731	342[c]±178[c]
AP+LPS	9 310±7 552	4 001±1 638	2 573±2 133	1257±164
AP+MoAb +LPS	12 699[c]±4 978[c]	2 719[c]±634[c]	3 470±1 832	305[c]±65[c]
MoAb	696±151	582±273	21±12	8±4
LPS	584±182	332±93	11±8	8±4

[a]*P*<0.05 *vs* control group; [c]*P*<0.05 *vs* AP group.

Polymorphonuclear elastase (PMN-E) plasma activity

Cn-induced AP caused an elevation of plasma PMN-E in all AP groups (groups 2-5). AP animals receiving MoAb CD 11b alone or with LPS had significantly lower PMN-E activity in both periods compared to other AP groups. LPS given to healthy animals elevated plasma PMN-E in a time-dependent manner (3 ng/mL after 5 h and 8 ng/mL after 9 h of observation, Figure 3).

Interleukin-6 plasma concentration

IL-6 was detectable in high concentration only after 5 h of observation in groups 4, 5, and 7 receiving LPS. AP did not correlate with IL-6 plasma level (Table 4).

Microscopic findings within pancreatic gland

Cn-induced AP caused marked pancreatic interstitial edema and acinar cell vacuolization, neutrophil infiltration and foci of necrosis. mAb given in AP reduced significantly interstitial neutrophil infiltration within the pancreas after 5 h of observation. LPS alone given to healthy animals resulted in a significant acceleration of pancreatic infiltration in comparison to control animals. Lipopolysaccharide given in AP did not result in significant

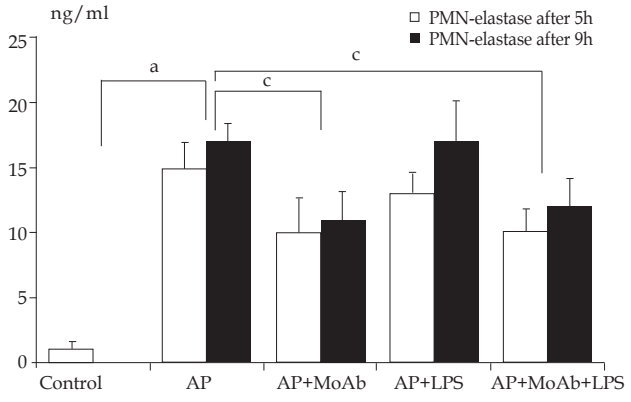

Figure 3 Plasma PMN-E concentration. [a]*P*<0.05 *vs* control group; [c]*P*<0.05 *vs* AP group.

Table 4 Plasma IL-6 concentration (pg/mL, mean ± SD)

Group	IL-6 after 5 h	IL-6 after 9 h
AP	0.6±2.0	0.0±0.0
AP+MoAb	4.7±7.0	0.0±0.0
AP+LPS	982.0[c]±749.0[c]	10.0±20.0
AP+MoAb+LPS	1561.0[c]±493.0[c]	0.0±0.0
Control	0.2±0.3	0.1±0.3
MoAb	0.0±0.0	0.0±0.0
LPS	941.0[a]±756.0[a]	2.0±4.0

[a]*P*<0.05 *vs* control group; [c]*P*<0.05 *vs* AP group.

exacerbation of microscopic findings within the pancreatic gland (Table 5).

DISCUSSION

Cn-induced AP is a widely accepted model of acute edematous pancreatitis in rats. The intraperitoneal route of four doses of Cn (15 μg/kg) at 1-h intervals is as effective as the intravenous route[7-9]. Based on the morphologic criteria of acute edematous pancreatitis including acinar cell vacuolization, interlobar and interstitial edema, leukocyte infiltration and foci of acinar cell necrosis, all animals receiving Cn revealed a remarkable hyperamylasemia and hyperlipasemia at the presented study.

The time of observation was established on the basis of preliminary experiments, maximum effect of Cn and $T_{1/2}$ elimination of MoAb CD11b. The production of highly reactive molecules in PMN, as a result of respiratory burst activation, is an essential step in host defense against micro-organisms. The production of these highly reactive molecules can be measured by CL. CL is the process of light emission derived from the chemical reaction in which excited molecules decay the electronic basic state and emit photons. The CL intensity is directly proportional to cell activation and competence. Measurement of CL is a valuable and simple tool in studying PMN activity[10,11]. CL method is used in experimental and clinical medicine to evaluate the function of different cell types. CL detection is used as a label which allows signal amplification due to the enzyme-catalyzed reaction, thus obtaining a higher sensitivity[11]. The whole blood CL assay requires small blood samples and avoids artefacts due to cell isolation. The disadvantage of whole blood CL measurement is light extinguished by erythrocytes. Thus, highly diluted (final sample dilution 1:200) samples of whole blood are used. The diluted whole blood CL corresponds to individual neutrophil activity, because in this case interaction between cells and plasma is minimal[12].

Neutrophil infiltration is the universal feature of acute and chronic inflammatory process. The adhesion to vessel epithelium is followed by interstitial migration and action in the inflammatory focus[13-15]. This phenomenon is well documented. Neutrophil infiltration is the evidence of cell activation[16-20]. Experimental pancreatitis in the present study resulted in early PMN infiltration within the pancreatic gland. Whole blood white cells and neutrophils, in pancreatitis groups, reduced compared to control animals and also whole blood neutrophil CL reduced in AP groups during the same period of time. The phenomenon of low CL activity in pancreatitis group may be due to the migration of activated cells into interstitial space. After 9 h of experiment, the WBC and PMN count of AP group were similar to control one, because peripheral white cells perhaps were supplemented by immature cells from the bone marrow. However, the CL was still significantly lower, parallel to the results obtained in preliminary investigation[21]. The other possible explanation may be

Table 5 Microscopic findings within the pancreatic gland (mean ± SD)

Houvs	Edema		Vacuolization		Infiltration		Necrosis	
	5	9	5	9	5	9	5	9
Group 1	0.00	0.00	0.00	0.00	1.1	1.21	0.00	0.00
Control	±0.00	±0.00	±0.00	±0.00	±0.9	±1.03	±0.00	±0.00
Group 2	1.91[a]	0.50	2.50[a]	1.00	7.40[a]	14.60[a]	0.17	0.25
AP	±0.90[a]	±0.57	±0.90[a]	±1.41	±5.29[a]	±2.37[a]	±0.38	±0.50
Group 3	2.28	1.50	1.71	1.50	3.87[c]	10.95	0.00	0.00
AP+MoAb CD11b	±0.75	±1.00	±0.4 8	±1.00	±1.69[c]	±0.92	±0.00	±0.00
Group 4	1.28	2.00	1.57	1.25	10.94	17.92	0.14	0.00
AP+LPS	±1.25	±1.15	±1.39	±1.25	±3.02	±5.98	±0.37	±0.00
Group 5	2.50	1.00	2.00	1.00	10.40	15.10	0.00	0.00
AP+MoAbCD11b +LPS	±1.00	±0.00	±1.15	±0.00	±8.30	±6.46	±0.00	±0.00
Group 6	0.25	0.00	0.00	0.00	0.80	0.25	0.00	0.00
Control+MoAb CD11b	±0.50	±0.00	±0.00	±0.00	±1.04	±0.30	±0.00	±0.00
Group 7	0.00	0.00	0.00	0.00	2.45	6.00[a]	0.00	0.00
Control+LPS	±0.00	±0.00	±0.00	±0.00	±2.75	±4.11[a]	±0.00	±0.00

[a]*P*<0.05 *vs* control group; [c]*P*<0.05 *vs* AP group.

the action of plasma anti-inflammatory agents (cytokines: IL-10, IL-11; soluble receptors: IL-1ra, p75 or prostanoids PGE_2 and PGI)[22].

Some data have confirmed that CL intensity is elevated in AP[23,24]. A different methodology of measurement may be the reason. The majority of investigators have analyzed the isolated neutrophils, whereas any isolation technique can change the neutrophil activity status[15,25]. On the other hand, the CL elevation may occur due to infection complicating AP clinical course.

CD11b is a well-known surface adhesion molecule of neutrophils. The use of mAb against CD11b results in competitive binding of specific adhesion molecules. Administration of MoAb CD11b in the present study significantly reduced the neutrophil infiltration within the pancreatic gland in AP animals. The pancreatic MPO tissue level was correlated to pancreatic neutrophil infiltration. Neutrophil depletion may protect pancreas from damage during AP as was observed by several other authors[16-18]. PAF antagonists reduce adhesion molecule expression and may prevent PMN infiltration of the pancreatic gland during AP. Another known pathomechanism of pancreatic damage during AP is oxidative stress. Several other authors documented that free radicals are generated in experimental AP[17-20]. Oxidative stress and lipid peroxidation debris elevated concentration was observed in animals with AP. MoAb CD11b administration during AP in the present study did not change the (-SH) groups concentration within the pancreatic gland, but the significant reduction of pancreatic MDA concentration was observed. The similar result was noticed in preliminary study group[21].

PMNs are the major source of oxygen radicals. Neutrophil NADPH-oxidase activation leads to the production of superoxide radicals during AP. Thus, MoAb 11b protects lipid peroxidation within pancreatic parenchyma in group 3. Our observations suggest that MoAb 11b induces neutrophil depletion in AP[16-20]. Substances which are thought to be effective in AP treatment (i.e., procaine, dextran, NO or heparin) reduce the aggregation of blood cells[14,26-29]. The role of ischemia-reperfusion and xanthine oxidase reaction is also the source of ROS in AP[26,29,30]. The aggregation of neutrophils and platelets may result in vessel obstruction. Kusterer *et al*[14] found that leukocyte adherence can be observed within the first 30 min from AP induction. The early neutrophil requirement determines the early adhesion molecule blockade necessity.

In our investigation, the IL-6 plasma concentration in AP groups was not elevated in both observation periods in comparison to control animals. IL-6 is a marker cytokine in severe human AP. Edematous AP may not demonstrate cytokinemia during the early stage of the disease[31-34]. On the other hand, some data suggest that IL-6 and other pro-inflammatory cytokines are elevated in Cn-induced AP[8,35]. The difference may be related to the different method of measurement. The biological method is not so specific compared to ELISA technique used in the present experiment[34]. On the other hand, IL-6 may be the marker of complications or SIRS but not AP "*per se*". Numerous data have confirmed the early inflammatory process in the pancreatic parenchyma in early AP. Local cytokine concentration is much higher than the peripheral one[33,36]. The liver plays a cardinal role in cytokine clearance in the early stage of the disease. These facts confirm the local characteristic of AP in the edematous form of the disease.

The pathogenesis of AP is the involvement of bacterial LPS. LPS is the universal stimulator of inflammatory process. Digestive tract bacteria are the major source of LPS in AP. Mucosal damage is the reason of LPS detection in early course of AP. The infected pancreatic necrosis foci are responsible for LPS detection in late stage of AP. In the present work, group 7 was the evidence of LPS action on healthy animals. The LPS administered intraperitoneally worked as a systemic inflammatory agent. There was the elevation in peripheral PMN count, pancreatic infiltration and high plasma IL-6 concentration. AP rats receiving LPS (group 4) revealed slight depletion in circulating neutrophils compared to AP group after 5 h of experiment. It could be the consequence of larger neutrophil sequestration. After 9 h of experiment, elevated peripheral blood PMN count was elevated, but the CL intensity was as low as that in AP group. We observed elevation of circulating PMN count in group 4 after 9 h of observation. But CL intensity was not elevated in the same period. The difference in PMN count after 5 and 9 h of experiment might be the result of bone marrow or spleen release. Edematous AP seems to be the local inflammatory process, whereas LPS administration resulted in huge WBC and PMN count elevation after 9 h of observation.

The data confirm the early neutrophil requirement in AP. But surprisingly, the activation of circulating PMN was lower in AP than in control animals. This phenomenon may result from activated cell sequestration within the inflamed pancreatic gland. The adhesion molecule CD11b blockade and neutrophil infiltration reduction can protect the pancreatic parenchyma from damage. The early PMN involvement of PMN makes it difficult to conduct comparable clinical trials. Most AP patients admitted to the hospital have at least few hours of history. The idea of immunomodulation seems to be attractive but needs further investigations.

In conclusion, the circulating neutrophil and activity are reduced in the early period of Cn-induced AP in rats. Adhesion molecule CD11b blockade can prevent pancreatic infiltration and oxidative stress within the pancreatic gland during AP in rats. Lipopolysaccharide septic challenge does not change the early course of Cn-induced AP in rats.

ACKNOWLEDGMENTS

The authors thank Mr. Anselm Berthold from Berthold Detection Systems for professional assistance and help, and Miss Justyna Hirsz for her language assistance.

REFERENCES

1 **Johnson CD**, Kingsnorth AN, Imrie CW, McMahon MJ,

Neoptolemos JP, McKay C, Toh SK, Skaife P, Leeder PC, Wilson P, Larvin M, Curtis LD. Double blind, randomised, placebo controlled study of a platelet activating factor antagonist, lexipafant, in the treatment and prevention of organ failure in predicted severe acute pancreatitis. *Gut* 2001; **48**: 62-69

2 **Kald B**, Kald A, Ihse I, Tagesson C. Release of platelet-activating factor in acute experimental pancreatitis. *Pancreas* 1993; **8**: 440-442

3 **Yamano M,** Umeda M, Miyata K, Yamada T. Protective effects of a PAF receptor antagonist and a neutrophil elastase inhibitor on multiple organ failure induced by cerulein plus lipopolysaccharide in rats. Naunyn Schmiedebergs *Arch Pharmacol* 1998; **358:** 253-263

4 **Soong CV**, Lewis HG, Halliday MI, Rowlands BJ. Intramucosal acidosis and the inflammatory response in acute pancreatitis. *Am J Gastroenterol* 1999; **94**: 2423-2429

5 **Kimura Y,** Hirota M, Okabe A, Inoue K, Kuwata K, Ohmuraya M, Ogawa M. Dynamic aspects of granulocyte activation in rat severe acute pancreatitis. *Pancreas* 2003; **27:** 127-132

6 **Gray KD**, Simovic MO, Chapman WC, Blackwell TS, Christman JW, May AK, Parman KS, Stain SC. Endotoxin potentiates lung injury in cerulein-induced pancreatitis. *Am J Surg* 2003; **186**: 526-530

7 **Frossard JL**, Saluja A, Bhagat L, Lee HS, Bhatia M, Hofbauer B, Steer ML. The role of intercellular adhesion molecule 1 and neutrophils in acute pancreatitis and pancreatitis-associated lung injury. *Gastroenterology* 1999; **116**: 694-701

8 **Norman J**, Franz M, Messina J, Riker A, Fabri PJ, Rosemurgy AS, Gower WR. Interleukin-1 receptor antagonist decreases severity of experimental acute pancreatitis. *Surgery* 1995; **117**: 648-655

9 **Vaccaro MI**, Ropolo A, Grasso D, Calvo EL, Ferreria M, Iovanna JL, Lanosa G. Pancreatic acinar cells submitted to stress activate TNF-alpha gene expression. *Biochem Biophys Res Commun* 2000; **268:** 485-490

10 **Fujisawa M**, Kojima K, Beppu T, Futagawa S, Kuwahara K, Hiramatsu K. Early diagnosis of postoperative infection: assessment of whole blood chemiluminescence. *Surg Today* 2000; **30**: 309-318

11 **Roda A**, Pasini P, Guardigli M, Baraldini M, Musiani M, Mirasoli M. Bio- and chemiluminescence in bioanalysis. *Fresenius J Anal Chem* 2000; **366**: 752-759

12 **Bochev BG**, Magrisso MJ, Bochev PG, Markova VI, Alexandrova ML. Dependence of whole blood luminol chemiluminescence on PMNL and RBC count. *J Biochem Biophys Methods* 1993; **27**: 301-309

13 **Hartwig W,** Jimenez RE, Fernandez-del Castillo C, Kelliher A, Jones R, Warshaw AL. Expression of the adhesion molecules Mac-1 and L-selectin on neutrophils in acute pancreatitis is protease- and complement-dependent. *Ann Surg* 2001; **233:** 371-378

14 **Kusterer K**, Poschmann T, Friedemann A, Enghofer M, Zendler S, Usadel KH. Arterial constriction, ischemia-reperfusion, and leukocyte adherence in acute pancreatitis. *Am J Physiol* 1993; **265**: G165-G171

15 **Larvin M,** Alexander DJ, Switala SF, McMahon MJ. Impaired mononuclear phagocyte function in patients with severe acute pancreatitis: evidence from studies of plasma clearance of trypsin and monocyte phagocytosis. *Dig Dis Sci* 1993; **38:** 18-27

16 **Bhatia M**, Brady M, Shokuhi S, Christmas S, Neoptolemos JP, Slavin J. Inflammatory mediators in acute pancreatitis. *J Pathol* 2000; **190**: 117-125

17 **Dabrowski A,** Chwiećko M. Oxygen radicals mediate depletion of pancreatic sulfhydryl compounds in rats with cerulein-induced acute pancreatitis. *Digestion* 1990; **47:** 15-19

18 **Panés J**, Perry M, Granger DN. Leukocyte-endothelial cell adhesion: avenues for therapeutic intervention. *Br J Pharmacol* 1999; **126**: 537-550

19 **Schulz HU**, Niederau C, Klonowski-Stumpe H, Halangk W, Luthen R, Lippert H. Oxidative stress in acute pancreatitis. *Hepatogastroenterology* 1999; **46**: 2736-2750

20 **Tailor A**, Das AM, Getting SJ, Flower RJ, Perretti M. Subacute treatment of rats with dexamethasone reduces ICAM-1 levels on circulating monocytes. *Biochem Biophys Res Commun* 1997; **231**: 675-678.

21 **Hać S**, Dobosz M, Kaczor J, Rzepko R. Influence of molecule CD 11b blockade on the course of acute ceruleine pancreatitis in rats. *EMP* 2004; **77**: 57-65

22 **McKay C**, Imrie CW, Baxter JN. Mononuclear phagocyte activation and acute pancreatitis. *Scand J Gastroenterol* Suppl 1996; **219**: 32-36

23 **Tsai K**, Wang SS, Chen TS, Kong CW, Chang FY, Lee SD, Lu FJ. Oxidative stress: an important phenomenon with pathogenetic significance in the progression of acute pancreatitis. *Gut* 1998; **42**: 850-855

24 **Widdison AL**, Cunningham S. Immune function early in acute pancreatitis. *Br J Surg* 1996; **83**: 633-636

25 **Pascual C**, Karzai W, Meier-Hellmann A, Bredle DL, Reinhart K. A controlled study of leukocyte activation in septic patients. *Intensive Care Med* 1997; **23**: 743-748

26 **Closa D**, Sabater L, Fernández-Cruz L, Prats N, Gelpí E, Roselló-Catafau J. Activation of alveolar macrophages in lung injury associated with experimental acute pancreatitis is mediated by the liver. *Ann Surg* 1999; **229**: 230-236

27 **Dobosz M**, Hac S, Mionskowska L, Dobrowolski S, Wajda Z. Microcirculatory disturbances of the pancreas in cerulein-induced acute pancreatitis in rats with reference to L-arginine, heparin, and procaine treatment. *Pharmacol Res* 1997; **36**: 123-128

28 **Menger MD**, Bonkhoff H, Vollmar B. Ischemia-reperfusion-induced pancreatic microvascular injury. An intravital fluorescence microscopic study in rats. *Dig Dis Sci* 1996; **41**: 823-830

29 **Sendur R**, Pawlik WW. [Vascular factors in the mechanism of acute pancreatitis] *Przegl Lek* 1996; **53**: 41-45

30 **Dobosz M**, Wajda Z, Hać S, Myśliwska J, Bryl E, Mionskowska L, Roszkiewicz A, Myśliwski A. Nitric oxide, heparin and procaine treatment in experimental ceruleine-induced acute pancreatitis in rats. *Arch Immunol Ther Exp (Warsz)* 1999; **47**: 155-160

31 **Gross V**, Leser HG, Heinisch A, Schölmerich J. Inflammatory mediators and cytokines-new aspects of the pathophysiology and assessment of severity of acute pancreatitis? *Hepatogastroenterology* 1993; **40**: 522-530

32 **Kikuchi Y**, Shimosegawa T, Satoh A, Abe R, Abe T, Koizumi M, Toyota T. The role of nitric oxide in mouse cerulein-induced pancreatitis with and without lipopolysaccharide pretreatment. *Pancreas* 1996; **12**: 68-75

33 **Okabe A**, Hirota M, Nozawa F, Shibata M, Nakano S, Ogawa M. Altered cytokine response in rat acute pancreatitis complicated with endotoxemia. *Pancreas* 2001; **22**: 32-39

34 **Viedma JA**, Pérez-Mateo M, Domínguez JE, Carballo F. Role of interleukin-6 in acute pancreatitis. Comparison with C-reactive protein and phospholipase A. *Gut* 1992; **33**: 1264-1267

35 **de Dios I,** Perez M, de La Mano A, Sevillano S, Orfao A, Ramudo L, Manso MA. Contribution of circulating leukocytes to cytokine production in pancreatic duct obstruction-induced acute pancreatitis in rats. *Cytokine* 2002; **20**: 295-303

36 **Bhatnagar A**, Wig JD, Majumdar S. Expression of activation, adhesion molecules and intracellular cytokines in acute pancreatitis. *Immunol Lett* 2001; **77**: 133-141

Edited by Guo SY **Language Editor** Elsevier HK

PO Box 2345, Beijing 100023, China
www.wjgnet.com
wjg@wjgnet.com

ELSEVIER

World J Gastroenterol 2005;11(41):6466-6471
World Journal of Gastroenterology ISSN 1007-9327

• *BASIC RESEARCH* •

Bile salts inhibit growth and induce apoptosis of culture human normal esophageal mucosal epithelial cells

Ru Zhang, Jun Gong, Hui Wang, Li Wang

Ru Zhang, Jun Gong, Li Wang, the Second Hospital of Xi'an Jiaotong University, Xi'an 710004, Shaanxi Province, China
Hui Wang, Department of Anesthesia, Shaanxi Provincial People's Hospital, Xi'an 710068, Shaanxi Province, China
Supported by the Clinical Key Programs of Ministry of Public Health, China, No. 20012130
Co-first-authors: Ru Zhang and Jun Gong
Co-correspondence: Ru Zhang
Correspondence to: Dr. Jun Gong, Digestive Department of the Second Hospital, Xi'an Jiaotong University, Xi'an 710004, Shaanxi Province, China. zhzhru@sohu.com
Telephone: +86-29-88083495 Fax: +86-29-87678758
Received: 2005-01-07 Accepted: 2005-04-11

Abstract

AIM: To investigate the effect of six bile salts: glycocholate (GC), glycochenodeoxycholate (GCDC), glycodeoxycholate (GDC), taurocholate (TC), taurochenodeoxycholate (TCDC), taurodeoxycholate (TDC), and their mixture on cultured human normal esophageal mucosal epithelial cells.

METHODS: Human normal esophageal mucosal epithelial cells were cultured with serum-free keratinocyte medium. 3-[4,5-Dimethylthiaolyl]-2,5-diphenyl-tetrazolium bromide assay was applied to the detection of cell proliferation. Apoptotic morphology was observed by phase-contrast video microscopy and terminal deoxynucleotidyl transferase-mediated dUTP nick end labeling (TUNEL) assay. Sub-G1 DNA fragmentations and early apoptotic cells were assayed by flow cytometry (FCM) with propidium iodide (PI) staining and annexin V-FITC conjugated with PI staining. Apoptotic DNA ladders on agarose gel electrophoresis were observed.

RESULTS: Except for GC, GCDC, GDC, TC, TCDC, TDC and their mixture could initiate growth inhibition of esophageal mucosal epithelial cells in a dose- and time-dependent manner. TUNEL and FCM assays demonstrated that the bile salts at 500 μmol/L and their mixture at 1 500 μmol/L induced apoptosis except for GC. The percentage of sub-G1 detected by FCM with PI staining was 83.5% in cells treated with 500 μmol/L TC for 2 h, and 19.8%, 20.4%, 25.6%, 13.5%, and 75.8% in cells treated with 500 μmol/L GCDC, TCDC, GDC, TDC, and 1 500 μmol/L mixture for 24 h, respectively, which were higher than that of the control (1.5%). The percentage was 1.4% in cells with 500 μmol/L GC for 24 h. DNA ladders on agarose gel electrophoresis were seen in cells treated with 500 μmol/L TC for 2 h and 1 500 μmol/L mixture for 24 h.

CONCLUSION: All GCDC, GDC, TC, TCDC, TDC and their mixture can inhibit growth and induce apoptosis of cultured human normal esophageal mucosal epithelial cells, but GC is well tolerated by the cells.

Key words: Bile salts; Duodenogastroesophageal reflux; Esophageal mucosal epithelial cells; Apoptosis

Zhang R, Gong J, Wang H, Wang L. Bile salts inhibit growth and induce apoptosis of cultured human normal esophageal mucosal epithelial cells. *World J Gastroenterol* 2005; 11(41): 6466-6471
http://www.wjgnet.com/1007-9327/11/6466.asp

INTRODUCTION

Duodenogastroesophageal reflux (DGER) causes various gastroesophageal reflux diseases (GERD), and is associated with some complications of GERD, such as reflux esophagitis, Barrett's esophagus, and esophageal carcinoma. It is well known that the incidence of adenocarcinoma of the esophagogastric junction has been increasing during the past decade in Western countries[1]. It was also reported that the incidence of GERD is increasing in the developing countries, such as China[2]. The potential contribution of gastroduodenal components to the development of Barrett's esophagus remains unclear. But bile acids, presenting especially frequently in the refluxate of Barrett's esophagus patients, are likely to influence the development and persistence of metaplasia[3–5]. On the other hand, bile salts can enter mucosal cells in their non-ionized lipophilic form, and cause injuries to cell membranes and tight junctions, thus leading to cell necrosis[6]. It has been reported recently that bile acids upregulate the expression of COX-2 in Barrett's esophagus biopsy explant culture systems[7]. Overexpression of COX-2 inhibits apoptosis[8,9]. However, present studies about bile salt-caused cellular injury performed on hepatocytes[10] and colon cancer cell lines[11,12] showed that different bile salts can induce cell apoptosis. Direct oligomerization of the Fas receptor (CD95/Apo-1) has been suggested as the primary causative mechanism of bile salt-mediated hepatocyte apoptosis[13]. Therefore, it is necessary to investigate the injury mechanism of bile salts on human normal esophageal epithelial cells.

There are no studies about bile salt-induced apoptosis in normal human esophageal epithelial cells. In the present study, normal human esophageal epithelial cells were cultured successfully. We characterized the kinetics of different bile salt-inhibited growth and different bile salt-induced apoptosis in cultured normal human esophageal epithelial cells. The specificity of death induction by toxic bile salts was demonstrated.

MATERIALS AND METHODS

Materials

Serum-free keratinocyte medium for culture of human keratinocytes (K-SFM) and dispase were purchased from GIBCO. DMEM was from Hyclone and trypsin was from Sigma, fetal bovine serum (FBS) from Hangzhou Jiangbin Biotechnology Co., Ltd. Glycocholate (GC), glycochenodeoxycholate (GCDC), glycodeoxycholate (GDC), taurocholate (TC), taurochenodeoxycholate (TCDC), and taurodeoxycholate (TDC) were from Sigma. Terminal deoxynucleotidyl transferase-mediated dUTP nick end labeling (TUNEL) kits were purchased from Beijing Zhongshan Golden Bridge Biotechnology Co., Ltd. Annexin V-FITC apoptosis detection kit I was from BD Biosciences.

Cell culture

Human normal esophageal epithelial cells, cultured from normal esophageal epithelium, were obtained from the resected esophagus of a patient suffering from esophageal carcinoma. Tissue for culture was selected just near the edge of the surgical resection specimens and far away from carcinoma lesions. Tissues were confirmed to contain no macroscopic tumor tissue or histologically detectable metaplastic cells or cancer cells[14,15]. Written informed consent was obtained from the patient for surgery and for the usage of his resected samples. Tunica mucosa was separated from the tissues with forceps, and cut into 0.2 cm × 0.5 cm fragments, then the pieces were transferred to a petri dish containing 25 U/mL dispase[16] and incubated for 18-24 h at 4 °C. Epithelial sheets were separated from the full-thickness mucosa with forceps, pooled in PBS containing 0.25% trypsin/0.02% EDTA, and incubated at 37 °C for 15-20 min with gentle pipetting to dissociate aid cells. Trypsin activity was terminated by the addition of DMEM with 10% FBS. The dissociated cells were collected and grown in K-SFM (pH 7.4) in a humidified atmosphere consisting of 50 mL/L CO_2/95% air at 37 °C. K-SFM contained 3 μL epidermal growth factor, and 0.438 g L-glutamine, 0.9 mL bovine pituitary extract per 500 mL, which was based, but modified on the media of esophageal cells[17] and skin keratinocytes[18,19]. The cells were subcultured and those in passages 3-6 were selected to be used in the study. In the following study, different bile salts were added into the K-SFM (pH 7.1-7.3).

Assessment of cell proliferation

3-[4,5-Dimethylthiaolyl]-2,5-diphenyl-tetrazolium bromide (MTT) assay was conducted to determine the cell proliferation. Cells were treated with six bile salts at the concentrations of 500, 250, and 50 μmol/L, and their mixture at the concentrations of 1 500, 1 000, 500, and 250 μmol/L at the ratio 2:2:1:2:2:1.

Cells were seeded on a 96-well plate (4-6×10^4 cells/well). After 24 h of seeding, cells were treated with different bile salts for 3 d and untreated cells served as a control. Prior to the determination, 10 μL of the 2.5 g/L stock solution of MTT was added to each well. After 4 h of incubation, the culture media were discarded followed by addition of 100 mL of DMSO to each well and vibration for 10 min. The absorbance (*A*) was measured at 492 nm with a microplate reader. The percentage of viable cells was calculated as follows: (*A* of experimental group/*A* of control group)×100%.

Flow cytometry by PI staining

Cells from the medium supernatant and adherent cells treated with bile salts were collected and pelleted at 1 200 U/min. The harvested cells were fixed with 1 mL of 75% cold ethanol at -20 °C for a night, and then washed with PBS. Cell pellets were incubated with 10 μg/mL RNAse and stained with 50 μg/mL propidium iodide (PI) for 30 min in the dark. Samples were analyzed using a FACSCalibur flow cytometer (FCM) with an excitation wavelength of 488 nm. The resulting histograms were analyzed by the program CELLQuest. A total of 2104 cells were detected by FCM in each of the samples.

Flow cytometry by annexin V-FITC conjugated with PI staining[20]

Cells from the medium supernatant and adherent cells treated with bile salts were collected and pelleted at 1 200 U/min. Pellets were washed twice with cold PBS and then resuspended in a binding buffer at a concentration of 1×10^6 cells/mL, and two volumes of the 100 μL solution (1×10^5 cells) were transferred to two 5-mL culture tubes. Five microliters of annexin V-FITC and 5 μL of PI were added into each of the 100 μL solution, and the cells were gently vortexed and incubated for 15 min at room temperature in the dark. The samples, to which 400 μL of 1× binding buffer was added, were analyzed by FACSCalibur FCM within 1 h. A total of 2×10^4 cells were detected by FCM in each of the samples.

TUNEL assay

Apoptosis of cells was analyzed using an *in situ* cell apoptosis detection kit based on the TUNEL technique. Cells were grown on chamber glass culture slides and treated with bile salts. To avoid adherence of the apoptotic cells, the slides were coated with poly-lysine. In brief, after the cells were treated with or without bile salts for the indicated time, they were fixed overnight in 100 g/L formaldehyde, then treated with proteinase K and H_2O_2, labeled with dUTP in a humidified box at 37 °C for 1 h. The cells without addition of TdT enzyme were used as a negative control. The positive cells/the total cells were calculated using an

image-analysis system. A mean of 20 adjacent fields, at a magnification of ×400, was analyzed for each section[21].

DNA fragmentation

A total of 10^6-10^7 cells treated with bile salts were collected and low molecular weight DNA was extracted using a cell apoptosis DNA ladder extraction kit (Beijing Dingguo Biotechnology Co., Ltd). Standard loading buffer was added, 20 μL DNA samples was run on an 1% agarose gel containing 0.1% ethidium bromide in TAE buffer (40 mmol/L Tris, 20 mmol/L sodium acetate, and 1 mmol/L EDTA, pH 8.0).

Statistical analysis

All values were expressed as mean±SD. Statistical differences between means were calculated by the Student's *t*-test and the χ^2 test. $P<0.05$ was considered statistically significant.

RESULTS

Human normal esophageal mucosal epithelial cells were cultured with serum-free keratinocyte medium successfully without contamination of fibroblasts, and could be passaged for more than 20 times without senescence. Cells in passages 3-6 were selected for the following research.

Inhibiting growth

The cell viability was determined by MTT assay (Figure 1). Except for GC, the other five bile salts and their mixture inhibited the growth of normal human esophageal mucosal epithelial cells in a dose- and time-dependent manner. The mixture at 1 500 μmol/L had an inhibitory effect of 79% on esophageal mucosal epithelial cells after 24-h treatment. Cell growth was suppressed by 96% after 24-h treatment with TC at 500 μmol/L, higher than that after being treated with other bile salts at the same concentration ($P<0.01$). Cell growth was suppressed by 51%, 58%, 65%, and 24% after 24-h treatment with GCDC, GDC, TCDC, and TDC at 500 μmol/L, respectively.

Apoptosis induced by the mixture of bile salts

The mixture of bile salts induced apoptosis of cultured human normal mucosal epithelial cells. Morphological criteria of cell apoptosis, such as membrane blebbing, cell shrinkage, and nuclear condensation, were assessed 3 h after the addition of the mixture at the concentrations of 1 500 μmol/L by phase-contrast video microscopy (Figure 2A). FCM assays with only PI staining showed that 27.6% and 75.8% of the cells treated with 1 500 μmol/L bile salt mixture for 12 and 24 h, respectively, were in sub-G1, which were higher than that of the control (1.5%, $P<0.01$), and 13.5% of the cells treated with 1 000 μmol/L bile salt mixture for 12 h were in sub-G1 (Figure 2B). Early apoptotic cells, detected by FCM with annexin-V conjugated with PI staining, reached 8.4%, 6 h after being treated with 1 500 μmol/L bile salt mixture, higher than that of the control (2.3%, $P<0.01$, Figure 2C). TUNEL assay also proved that bile salt mixture induced cell apoptosis, because the number of positively stained nuclei was (30±8)% in cells after being treated with 1 500 μmol/L bile salt mixture for 12 h, which was significantly higher than that of the control (3%±2%, $P<0.01$, Figure 2D). DNA laddering, a typical sign of apoptosis, was detectable after being treated with 1 500 μmol/L bile salt mixture for

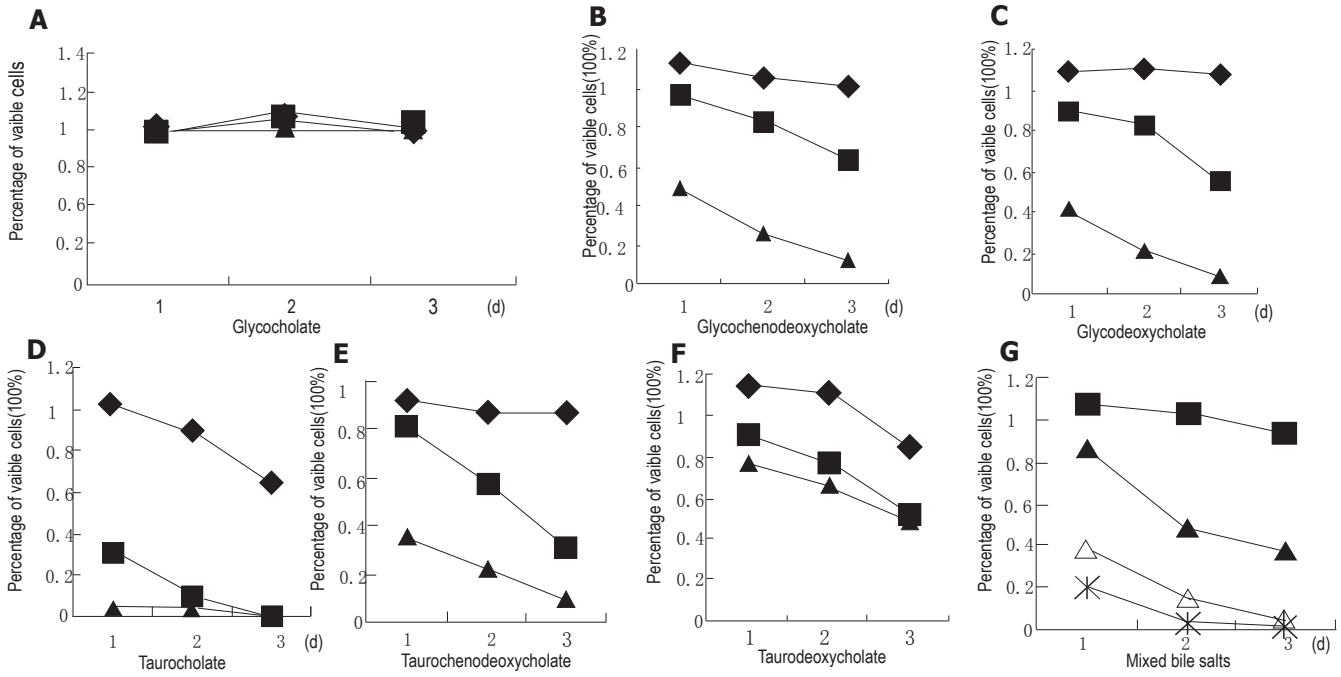

Figure 1 Effect of GC (**A**), GCDC (**B**), GDC (**C**), TC (**D**), TCDC (**E**), TDC (**F**), and mixture (**G**) on the growth of cultured normal human esophageal epithelial cells.◆(at the concentration 50 μmol/L), ■ (250 μmol/L), ▲ (500 μmol/L), △ (1 000 μmol/L), and * (1 500 μmol/L).

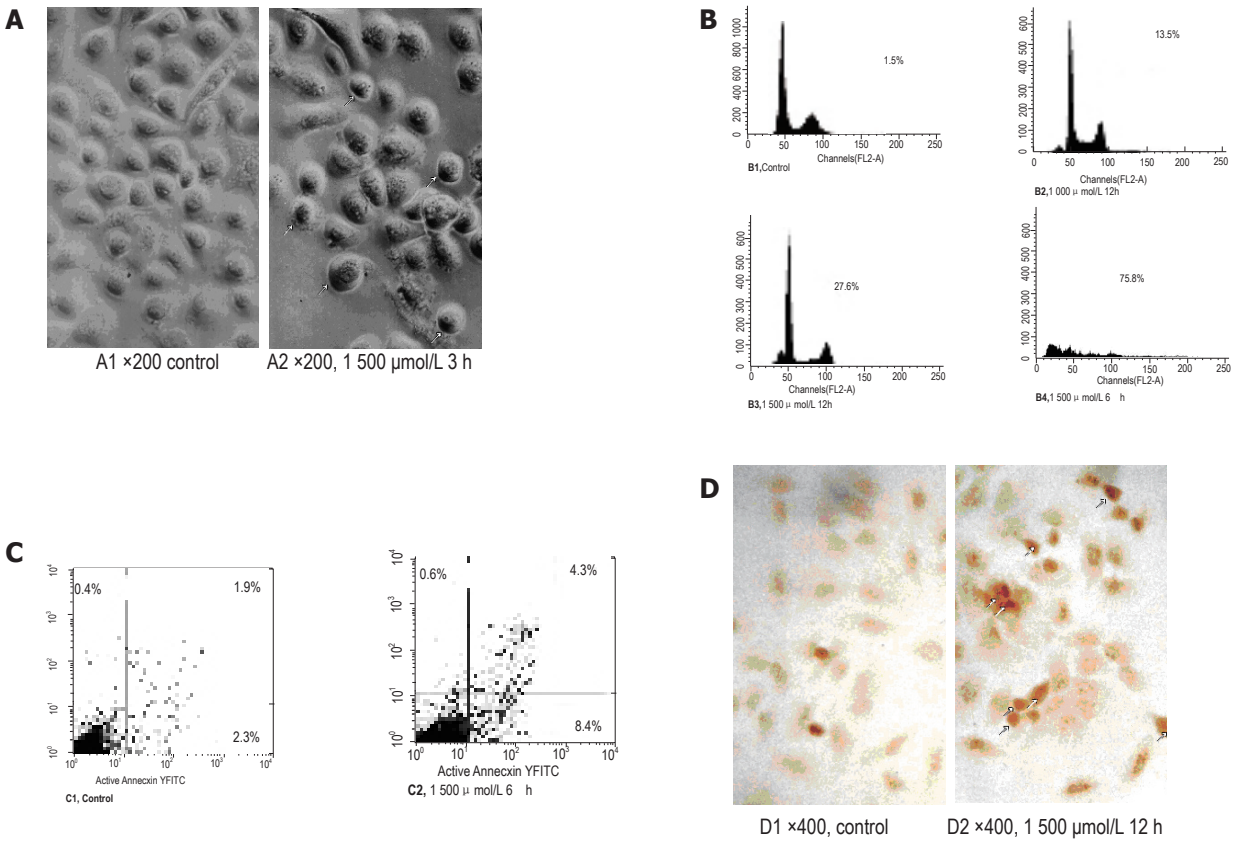

Figure 2 Characterization of bile salt mixture-induced apoptosis of normal esophageal mucosal epithelial cells. **A:** Morphological changes of apoptotic membrane blebbing and cell shrinkage; **B:** apoptotic cells in sub-G1; **C:** early apoptotic cells; **D:** positively stained nuclei.

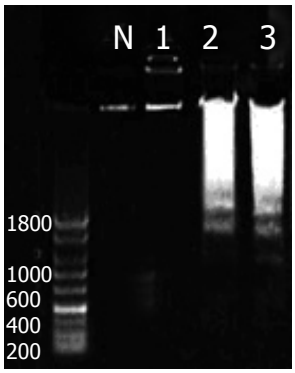

Figure 3 DNA fragments. N: control; lane 1: cells treated with GC; lane 2: cells treated with TC; lane 3: cells treated with mixture.

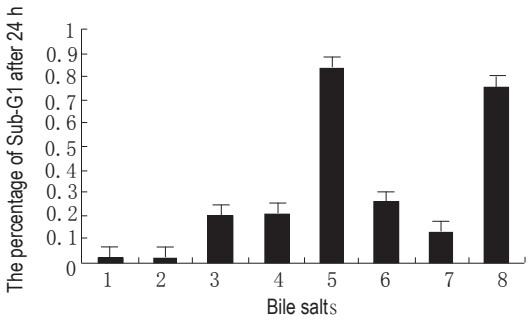

Figure 4 Percentages of apoptotic cells. 1: Control; 2: GC; 3: GCDC; 4: GDC; 5: TC for 2 h; 6: TCDC; 7: TDC; 8: mixture.

24 h (Figure 3).

Effect of GC, GCDC, TCDC, TC, GDC, and TDC

The assays of the six bile salts revealed that the other five bile salts, except for GC, induced apoptosis of esophageal mucosal epithelial cells. The percentages of sub-G1 in cells treated with different bile salts for 24 h are shown in Figure 4. The bile salts induced apoptosis in a time-dependent manner, 83.5% of cells were in sub-G1 treated with 500 μmol/L TC for 2 h, and the percentages were 19.8%, 20.4%, 25.6%, and 13.5% in cells treated with 500 μmol/L GCDC, TCDC, GDC, and TDC for 24 h, respectively. FCM with annexin-V conjugated with PI staining showed that early apoptotic cells reached 24.6% in cells treated with 500 μmol/L TC for 30 min, and 6.8%, 7.6%, 8.3%, and 5.1% in cells treated with 500 μmol/L GCDC, GDC, TCDC, and TDC for 6 h, respectively. They were all higher than that of the control (1.9%, $P<0.05$). The TUNEL assay also revealed that GC did not induce apoptosis, but the other five bile salts did. The positively stained nuclei were (53 ± 8)%, (2 ± 2)%, (20 ± 4)%, (18 ± 3)%, (24 ± 6)%, and (16 ± 3)% in cells treated with 500 μmol/L TC for only 1 h, and 500 μmol/L GC,

GCDC, GDC, TCDC, and TDC for 24 h, respectively. Except for GC, all the others were significantly higher than that of the control (3 ± 2)%, $P < 0.01$). DNA fragments were detected in cells treated with TC at 500 μmol/L for 2 h (Figure 3).

DISCUSSION

The injury mechanism of reflux duodenal components underlying DGER is still controversial. Bile acids and bile salts play a most important role[6]. But the causative mechanism of bile salts has not yet been elucidated in detail.

Bile acids constitute 67% of the normal bile, and are conjugated with glycine or taurine. The normal bile acids consist of 40% cholic acids, 40% chenodeoxycholic acid, and 20% deoxycholic acids, and a minor fraction of lithocholic acid and ursodeoxycholic acid[22]. In the present study, we investigated the effect of GC, GCDC, GDC, TC, TCDC, and TDC in esophageal epithelial cells. In order to speculate the effect of bile in the duodenoesophageal reflux *in vivo*, we also observed the effect of the mixture of these six bile salts. Moreover, the concentrations of bile salts in our study were selected from 25 to 500 μmol/L in the different bile salts and from 50 to 1 500 μmol/L in the mixture. This is because the total bile acid concentration in esophagus of patients suffering from reflux esophagitis is 0.89 mg/mL[23].

MTT assay in this report demonstrated that five bile salts and the mixture, except for GC, could inhibit the growth of cultured human normal esophageal mucosal epithelial cells in a dose- and time-dependent manner. The induced cell death was a major reason for the cell growth inhibition. GCDC, GDC, TC, TCDC, TDC and the mixture caused typical apoptotic alterations including the morphological changes assessed by phase-contrast video microscopy and TUNEL assay, positive cells stained with annexin-V assessed by FCM, apoptotic sub-G1 peak assessed by FCM with PI staining, and DNA fragmentation by agarose gel electrophoresis assay. However, these apoptosis changes were not seen in cells treated with GC.

Differences in the effect of bile salts on cultured normal human esophageal mucosal epithelial cells and hepatocytes and colon cancer cell line death were identified in this study. Studies performed on hepatocytes showed that glycine-conjugated bile acids, such as glycocholic and glycochenodeoxycholic acids, induce hepatocyte apoptosis *in vitro*[24], whereas taurine-conjugated bile acids, such as taurocholic and taurochenodeoxycholic acids, are well tolerated by hepatocytes[25,26]. Cell apoptosis is specifically induced by toxic (hydrophobic) bile salts such as deoxycholate and dihydroxy bile salt, whereas the conjugated bile salt GDC and the trihydroxy bile salt and its conjugate GC do not induce apoptosis of colorectal cancer cell lines[11], which are not in accordance with our results. Conversely, hepatocyte-cytotoxic glycine-conjugated bile acids such as GC, which induce hepatocyte apoptosis *in vitro*[24], do not induce apoptosis in esophageal mucosal epithelial cells. Whereas the hepatocyte-tolerated TC and TCDC[25,26] could induce apoptosis of esophageal mucosal epithelial cells. Our results also showed that TC was the most toxic to esophageal mucosal epithelial cells compared to the other four bile salts. We speculate that the mechanisms of the bile salts-induced apoptosis in human esophageal epithelial cells are different from those in hepatocytes or colorectal cancer cell lines. It was reported that direct oligomerization of the Fas receptor could be suggested as the primary causative mechanism of bile salt-mediated hepatocyte apoptosis[13,27,28]. Some hydrophobic bile acids such as TC could activate PI3K-dependent survival pathways, which prevent their otherwise inherent toxicity in hepatocytes[10,29]. As opposed to hepatocyte death mediated by bile acids, bile salt-induced apoptosis of human colon cancer cell lines involves the mitochondrial transmembrane potential but not the CD95 (Fas/Apo-1) receptor[11,30]. Studies are needed to gain further insight into the effect of bile salts on human esophageal mucosal epithelial cells.

In conclusion, GCDC, GDC, TC, TCDC, and TDC and their mixture inhibit the growth and induce apoptosis of cultured human normal esophageal mucosal epithelial cells in a dose- and time-dependent manner. But GC is not cytotoxic to the esophageal mucosal epithelial cells. Studies are needed to gain further insight into the effect of bile salts on human esophageal mucosal epithelial cells.

ACKNOWLEDGMENTS

We thank Dr. Bingheng Zhang and Dr. Xiaoge Zhao, Central Laboratory for Biomedical Research of Xi'an Jiaotong University Medical School, for their help on the FCM assays.

REFERENCES

1 **Cameron AJ,** Lomboy CT, Pera M, Carpenter HA. Adenocarcinoma of the esophagogastric junction and Barrett's esophagus. *Gastroenterology* 1995; **109:** 1541-1546

2 **Li ZS,** Xu GM, Liu Q. Epidemiology of gastroesophageal reflux disease in Shanghai adults part I: Suggestive symptoms and influencing factors. *Jiefangjun Yixue Zazhi* 1997; **22:** 259-2623

Jankowski JA, Anderson M. Review article: management of oesophageal adenocarcinoma-control of acid, bile and inflammation in intervention strategies for Barrett's oesophagus. *Aliment Pharmacol Ther* 2004; **20** (Suppl 5): 71-80 discussion 95-96

4 **Kondo K,** Kojima H, Akiyama S, Ito K, Takagi H. Pathogenesis of adenocarcinoma induced by gastrojejunostomy in Wistar rats: role of duodenogastric reflux. *Carcinogenesis* 1995; **16:** 1747-1751

5 **Miwa K,** Miyashita T, Hattori T. Reflux of duodenal or gastroduodenal contents induces esophageal carcinoma in rats. *Nippon Rinsho* 2004; **62:** 1433-1438

6 **Stein HJ,** Kauer WK, Feussner H, Siewert JR. Bile acids as components of the duodenogastric refluxate: detection, relationship to bilirubin, mechanism of injury, and clinical relevance. *Hepatogastroenterology* 1999; **46:** 66-73

7 **Shirvani VN,** Ouatu-Lascar R, Kaur BS, Omary MB, Triadafilopoulos G. Cyclooxygenase 2 expression in Barrett's esophagus and adenocarcinoma: Ex vivo induction by bile salts and acid exposure. *Gastroenterology* 2000; **118:** 487-496

8 **Tsujii M,** DuBois RN. Alterations in cellular adhesion and apoptosis in epithelial cells overexpressing prostaglandin endoperoxide synthase 2. *Cell* 1995; **83:** 493-501

9 **Sawaoka H,** Kawano S, Tsuji S, Tsujii M, Gunawan ES, Takei Y, Nagano K, Hori M. Cyclooxygenase-2 inhibitors suppress the growth of gastric cancer xenografts via induction of apoptosis in nude mice. Am J Physiol 1998; **274:** G1061-G1067

10 **Torchia EC,** Stolz A, Agellon LB. Differential modulation of cellular death and survival pathways by conjugated bile acids. *BMC Biochem* 2001; **2**: 11

11 **Schlottman K,** Wachs FP, Krieg RC, Kullmann F, Schölmerich J, Rogler G. Characterization of bile salt-induced apoptosis in colon cancer cell lines. *Cancer Res* 2000; **60:** 4270-4276

12 **Milovic V,** Teller IC, Faust D, Caspary WF, Stein J. Effects of deoxycholate on human colon cancer cells: apoptosis or proliferation. *Eur J Clin Invest* 2002; **32:** 29-34

13 **Sodeman T,** Bronk SF, Roberts PJ, Miyoshi H, Gores GJ. Bile salts mediate hepatocyte apoptosis by increasing cell surface trafficking of Fas. *Am J Physiol Gastrointest Liver Physiol* 2000; **278:** G992-G999

14 **Washington K,** Gottfried MR, Telen MJ. Tissue culture of epithelium derived from Barrett's oesophagus. *Gut* 1994; **35:** 879-883

15 **Kawabe A,** Shimada Y, Soma T, Maeda M, Itami A, Kaganoi J, Kiyono T, Imamura M. Production of prostaglandinE2 via bile acid is enhanced by trypsin and acid in normal human esophageal epithelial cells. *Life Sci* 2004; **75:** 21-34

16 **David AJ,** Paul JB, Darrin DB. Culture of human keratinocytes in defined serum-free mudium. *FOCUS of GIBCO* 1997; **19:** 2-5.

17 **Fitzgerald RC,** Farthing MJ, Triadafilopoulos G. Novel adaptation of brush cytology technique for short-term primary culture of squamous and Barrett's esophageal cells. *Gastrointest Endosc* 2001; **54:** 186-189

18 **Font J,** Braut-Boucher F, Pichon J, Noel-Hudson MS, Muriel MP, Bonnet M, Wepierre J, Aubery M. A new three-dimensional culture of human keratinocytes: optimization of differentiation. *Cell Biol Toxicol* 1994; **10:** 353-359

19 **Harvima IT,** Lappalainen K, Hirvonen MR, Mättö M, Kivinen PK, Hyttinen M, Pelkonen J, Naukkarinen A. Heparin modulates the growth and adherence and augments the growth-inhibitory action of TNF-alpha on cultured human keratinocytes. *J Cell Biochem* 2004; **92:** 372-386

20 **Lecoeur H,** Prévost MC, Gougeon ML. Oncosis is associated with exposure of phosphatidylserine residues on the outside layer of the plasma membrane: a reconsideration of the specificity of the annexin V/propidium iodide assay. *Cytometry* 2001; **44:** 65-72

21 **Coppola D,** Schreiber RH, Mora L, Dalton W, Karl RC. Significance of Fas and retinoblastoma protein expression during the progression of Barrett's metaplasia to adenocarcinoma. *Ann Surg Oncol* 1999; **6:** 298-304

22 **Guoming X,** Meiyun K, Jinyan L. Bile acid reflux related disease. *Shanghai Science and Technology Press* 2002; **9:** 24

23 **Stein HJ,** Feussner H, Kauer W, DeMeester TR, Siewert JR. Alkaline gastroesophageal reflux: assessment by ambulatory esophageal aspiration and pH monitoring. *Am J Surg* 1994; **167:** 163-168

24 **Agellon LB,** Torchia EC. Intracellular transport of bile acids. *Biochim Biophys Acta* 2000; **1486:** 198-209

25 **Torchia EC,** Agellon LB. Bile acid-induced morphological changes in hepatoma cells with elevated sodium-dependent bile acid uptake capacity. *Eur J Cell Biol* 1997; **74:** 190-196

26 **Roberts LR,** Kurosawa H, Bronk SF, Fesmier PJ, Agellon LB, Leung WY, Mao F, Gores GJ. Cathepsin B contributes to bile salt-induced apoptosis of rat hepatocytes. *Gastroenterology* 1997; **113:** 1714-1726

27 **Faubion WA,** Guicciardi ME, Miyoshi H, Bronk SF, Roberts PJ, Svingen PA, Kaufmann SH, Gores GJ. Toxic bile salts induce rodent hepatocyte apoptosis via direct activation of Fas. *J Clin Invest* 1999; **103:** 137-145

28 **Qiao L,** Studer E, Leach K, McKinstry R, Gupta S, Decker R, Kukreja R, Valerie K, Nagarkatti P, El Deiry W, Molkentin J, Schmidt-Ullrich R, Fisher PB, Grant S, Hylemon PB, Dent P. Deoxycholic acid (DCA) causes ligand-independent activation of epidermal growth factor receptor (EGFR) and FAS receptor in primary hepatocytes: inhibition of EGFR/mitogen-activated protein kinase-signaling module enhances DCA-induced apoptosis. *Mol Biol Cell* 2001; **12:** 2629-2645

29 **Rust C**, Karnitz LM, Paya CV, Moscat J, Simari RD, Gores GJ. The bile acid taurochenodeoxycholate activates a phosphatidylinositol 3-kinase-dependent survival signaling cascade. *J Biol Chem* 2000; **275:** 20210-20216

30 **Wachs FP,** Krieg RC, Rodrigues CM, Messmann H, Kullmann F, Knüchel-Clarke R, Schölmerich J, Rogler G, Schlottmann K. Bile salt-induced apoptosis in human colon cancer cell lines involves the mitochondrial transmembrane potential but not the CD95 (Fas/Apo-1) receptor. *Int J Colorectal Dis* 2005; **20:** 103-113

Science Editor Wang XL **Language Editor** Elsevier HK

PO Box 2345, Beijing 100023, China
www.wjgnet.com
wjg@wjgnet.com

ELSEVIER

World J Gastroenterol 2005;11(41):6472-6476
World Journal of Gastroenterology ISSN 1007-9327

• *BASIC RESEARCH* •

Effect of acupuncture at different meridian acupoints on changes of related factors for rabbit gastric mucosal injury

Jie Yan, Ren-Da Yang, Jun-Feng He, Shou-Xiang Yi, Xiao-Rong Chang, Ya-Ping Lin

Jie Yan, Ren-Da Yang, Jun-Feng He, Shou-Xiang Yi, Xiao-Rong Chang, Ya-Ping Lin, Department of Acupuncture and Moxibustion, Hunan College of Traditional Chinese Medicine, Changsha 410007, Hunan Province, China
Supported by the National Natural Science Foundation of China, NO. 90209023
Correspondence to: Professor Jie Yan, Department of Acupuncture and Moxibustion, Hunan College of Traditional Chinese Medicine, Changsha 410007, Hunan Province, China. yj5381159@yahoo.com.cn
Telephone: +86-731-5381159 Fax: +86-731-5381159
Received: 2005-03-01 Accepted: 2005-04-02

Abstract

AIM: To explore the regularity of multi-meridians controlling a same viscus (MMCSV).

METHODS: The rabbit gastric ulcer model was established by ethanol intragastric instillation. Fifty-six rabbits were randomly divided into normal group, model group (MG), model plus acupuncture at Foot Yangming Meridian group (YMG), model plus acupuncture at Foot Taiyin Meridian group (TYG), model plus acupuncture at Foot Shaoyang Meridian group (SYG), model plus acupuncture at Foot Jueyin Meridian group (JYG), model plus acupuncture at Foot Taiyang Meridian group (TYMG), with eight rabbits in each group. Gastric mucosal nitric oxide (NO) and nitric oxide synthase (NOS) were assayed by the nitric acid reductase method, and prostaglandin E2 (PGE2) and epidermal growth factor (EGF) were measured by radioimmunoassay. The comprehensive effects were analyzed by weighing method.

RESULTS: Compared to MG, SYG, JYG and TYMG, the rabbits gastric mucosal injury index (GMII) reduced very significantly in YMG ($P<0.01$). Compared to MG, the GMII also reduced significantly in TYG ($P<0.05$). NO, NOS, PGE2 and EGF increased very significantly in YMG ($P<0.01$). The EGF in YMG also increased significantly than that in TYG compared to those in MG, SYG, JYG and TYMG ($P<0.05$). The PGE2 and EGF also increased very significantly in TYG than those in MG, JYG and TYMG ($P<0.01$). While compared to SYG, the NOS increased significantly in TYG ($P<0.05$). NOS was the highest in YMG ($P<0.01$), and was higher in TYG than in MG ($P<0.01$).

CONCLUSION: MMCSV is common. The Foot Yangming Meridian is most closely related to the stomach, followed by Foot Taiyin Meridian, Foot Shaoyang Meridian and Foot Jueyin Meridian. Foot Taiyang Meridian has no correlation with the stomach.

Key words: Relationship between Meridian and Viscus; Gastric mucosal injury/acupuncture effects; MMCSV

Yan J, Yang RD, He JF, Yi SX, Chang XR, Lin YP. Effect of acupuncture at different meridian acupoints on changes of related factors for rabbit gastric mucosal injury. *World J Gastroenterol* 2005;11(41):6472-6476
http://www.wjgnet.com/1007-9327/11/6472.asp

INTRODUCTION

According to the meridian theory, the meridians in the body connections are sealed. Qi and blood flow recurrently, the meridians connect with each other directly or indirectly. Therefore, it is the underlying theory of multi-meridians controlling a same viscus (MMCSV)[1]. Previous studies are focused on one meridian controlling one viscus[2-4], while MMCSV is seldom referred to. In general, NO, NOS, PGE2 and EGF are regarded as protective factors involved in repairing gastric mucosal injury. Based on our previous research on MMCSV[5,6], in this study, we focused on the Foot Yangming Meridian (FYM) controlling the stomach. The Foot Shaoyang Meridian (FSY), Foot Jueyin Meridian (FJY), Foot Taiyin Meridian (FTY), as well as Foot Taiyang Meridian (FTYM) were selected to explore the regularity of MMCSV and meridian speciality for the Stomach.

MATERIALS AND METHODS

Animals

Fifty-six New Zealand 3-4 mo old pure rabbits, weighing 1.5-2.5 kg, were supplied by the Experimental Animal Center of Hunan College of Traditional Chinese Medicine (Permission number: 20030316).

Animal model and groups

The rabbit gastric ulcer model was established by ethanol intragastric instillation[7]. Fifty-six rabbits were divided into normal group (NG), model group (MG), model plus acupuncture at Foot Yangming Meridian group (YMG), model plus acupuncture at Foot Taiyin Meridian group (TYG), model plus acupuncture at Foot Shaoyang Meridian group (SYG), model plus acupuncture at Foot

Jueyin Meridian group (JYG), and model plus acupuncture at Foot Taiyang Meridian group (TYMG), with eight rabbits in each group. All the animals were fasted for 48 h before ulcer model-making. Rabbits in NG were given normal saline by intragastric instillation (2.35 mL/kg). Rabbits in other groups were given ethanol intragastrically (2.35 mL/kg). Twenty-four hours later, all animals were allowed free access to normal food. Except for rabbits in NG and MG groups, the animals received acupuncture therapy.

Acupuncture method

Acupoints were selected based on the (Modern Acupuncturolgy)[8] and anthropomorphic method[6] as well as on our previous research results[5,6]. In the FYM, Neiting (ST 44), Jiexi (ST 41), Zusanli (ST36), Liangqiu (ST 34), Tianshu (ST 25) and Liangmen (ST 21) were selected for gastric ulcer therapy. The other acupoints of different meridians were almost in the same horizontal level to the FYM. In the FSY, Jiaxi (GB 43), Qiuxu (GB 40), Yanglingquan (GB 34), Xiyangguan (GB 33), Daimai (GB 26) and Jingmen (GB 25) were selected. In the FJY, the selected acupoints were Xingjian (LR 2), Zhongfeng (LR 4), Xiguan (LR 7), Yinbao (LR 9), Zhangmen (LR 13) and Qimen (LR 14). In the FTY, Dadu (SP 2), Shangqiu (SP 5), Yinlingquan (SP 9), Xuehai (SP 10), Dahen (SP 15) and Fu'ai (SP 16) were selected. In the FTYM, Tonggu (BL 66), Shenmai (BL 62), Chengjin (BL 56), Fuxi (BL 38), Beixiadian and Beishangdian were selected.

Consecutive acupoint-stimulation in one meridian was applied by Xuanshou Meridian Dredging Apparatus (China Peace Economy Technology Consultation Company)[6]. Parameters for manipulation were as follows: single way running, six steps, at 0.5 s intervals; double direction narrow impulse and consecutive wave, 50 Hz, 0.5 ms wave width. The apparatus output was connected to the needle (diameter 0.25 mm, length 25 mm) which was inserted into the acupoints. Just mimicking human's obeying meridian to propaganda sense, the excited order was from low leg to trunk, and the output strength was controlled within 2-3 intensity. Acupuncture stimulation was manipulated once a day, for seven days, 30 s each time. All the selected acupoints were in the left lateral body throughout the experiment.

Determination of gastric mucosal injury index (GMII)

After seven days, the animals were killed with their stomachs removed and opened along the greater curvature. The content in the stomach was washed with running water, mucus attached to gastric mucosa was removed by the brusher. Then the mucosa was extended in a flat plate. GMII was calculated by the Guth method[9] with a general magnifier.

Determination of NO, NOS, PGE2 and EGF in gastric mucosa

NO and NOS kit were supplied by Nanjing Jincheng Bioengineering Institute. EGF radioimmunoassay kit was provided by Beijing Huaying Radioimmunoassay Institute. [3H]PGE2 radioimmunoassay kit was obtained from Beijing Furui Bioengineer Co. Gastric mucosal NO and NOS were assayed by the nitric acid reductase method, and PGE2 and EGF were measured by radioimmunoassay. All assays were carried out according to the manufacturer's instructions.

Statistical analysis

All the results were expressed as mean±SD. Comparison between groups was made using one-way analysis of variance (ANOVA). Differences were considered statistically significant, if the *P* value was less than 0.05. Software SPSS 10.0 was used in all statistical tests.

RESULTS

Gastric mucosal injury condition and index (Table1)

There were some dots and strips of injury under the magnifier. The highest GMII was observed in MG and the lowest GMII in NG. There was a very significant difference between them ($P<0.01$), demonstrating that the ulcer model was successful. Compared to MG, GMII in YMG and TYG reduced significantly ($P<0.05$ or $P<0.01$), and the GMII in YMG was better than that in TYG. While the GMII in SYG, JYG and TYMG had no significant difference compared to that in MG ($P>0.05$). The GMII in YMG had a significant difference compared to that in SYG, JYG and TYMG ($P<0.01$). The GMII in TYG also had a significant difference compared to that in TYGM ($P<0.05$).

Table 1 Gastric mucosal injury index comparison (mean±SD)

Groups	*n*	GMII
NG	8	8.50±2.98[b]
MG	8	24.88±6.29[df]
YMG	8	10.88±3.23[b]
SYG	8	19.38±3.66[d]
JYG	8	20.38±4.03[d]
TYG	8	14.62±3.20[a]
TYMG	8	24.13±1.64[dc]

[a]$P<0.05$, [b]$P<0.01$ *vs* MG; [d]$P<0.01$ *vs* YMG; [c]$P<0.05$, [f]$P<0.01$ *vs* TYG.

NO and NOS changes in gastric mucosa (Table 2)

Gastric mucosal NO and NOS in NG were both higher than those in MG ($P<0.01$). The highest NO content was found in YMG, than TYG, JYG and TYMG, while the lowest NO content was observed in SYG. The NO was higher in YMG than in MG, SYG, JYG and TYMG, and there was a very significant difference between YMG and MG, SYG, JYG, TYMG, respectively ($P<0.01$). However, no significant difference was found between YMG and TYG ($P>0.05$). The highest NOS content was observed in YMG, the lowest NOS content was found in TYMG. The NOS was higher in YMG and TYG than in

Table 2 NO and NOS changes in gastric mucosa (mean ± SD)

Groups	*n*	NO (μ mot/gprot)	NOS (u/mgprot)
NG	8	1.48±0.54[b]	2081.4±482.6[b]
MG	8	0.45±0.20[d]	762.1±156.3[d,f]
YMG	8	1.38±0.27[b]	1931.5±612.6[b]
SYG	8	0.45±0.19[d]	1327.0±319.4[bdc]
JYG	8	0.76±0.25[d]	987.2±365.1[d,f]
TYG	8	1.25±0.68	1728.2±213.2[b]
TYMG	8	0.57±0.24[d]	750.9±254.3[d,f]

[a]*P* <0.05, [b]*P* <0.01 *vs* MG; [d]*P* <0.01 *vs* YMG; [c]*P* <0.05, [f]*P* <0.01 *vs* TYG.

MG, SYG, JYG and TYMG (*P*<0.05 or <0.01). The NOS was also higher in SYG than in MG, and there was a very significant difference between them (*P*<0.01).

PGE2 and EGF changes in gastric mucosa (Table 3)

Gastric mucosal PGE2 and EGF were both higher in NG than in MG (*P*<0.01). The PGE2 was higher in YMG and TYG than that in NG and other acupuncture therapy groups (*P*<0.01). The highest EGF was found in YMG, compared to MG and other acupuncture therapy groups, and there were very significant differences between YMG and other groups respectively (*P*<0.01), demonstrating that acupuncture can raise gastric mucosal PGE2 and EGF content in YMG, while acupuncture could only raise gastric mucosal PGE2 content in TYG ulcer rabbits.

Table 3 PGE2 and EGF changes in gastric mucosa (mean±SD, ng/L)

Groups	*n*	PGE2	EGF
NG	8	2 624.8±336.2[b]	91.3±14.9[b]
MG	8	1 629.2±406.7[d,f]	73.6±14.8[d]
YMG	8	2 708.8±526.2[b]	92.2±6.7[b]
SYG	8	1 763.8±371.5[d,f]	74.9±9.0[d]
JYG	8	1 663.4±258.0[d,f]	72.7±12.4[d]
TYG	8	2 383.6±547.5[b]	68.5±14.1[d]
TYMG	8	1 748.6±594.9[d,f]	65.4±12.8[d]

[b]*P* <0.01 *vs* MG; [d]*P* <0.01 *vs* YMG; [f]*P* <0.01 *vs* TYG.

Summarization of effects of acupuncture at different meridian acupoints (Table 4)

To compare the protective effects of acupuncture at different meridian acupoints on the gastric mucosal injury, we ranked the intensity of effects. From the summarization in Table 4, we could see the comprehensive protection of acupuncture therapy against gastric mucosal injury of experimental rabbits was the best in YMG, followed by TYG, JYG or SYG, and TYMG.

Comprehensive protective effects of acupuncture at different meridian acupoints in gastric mucosa (Table 5)

In order to compare the comprehensive effects of acupuncture at different meridian acupoints on gastric mucosa, weight method was used to analyze the differences.

According to the importance of gastric mucosal protective factors including NO, NOS, PGE2 and EGF, the whole weight was set at 10, NO at 2.5, NOS at 1.25, EGF at 3.75 and PGE2 at 2.5. The comprehensive effect value (CEV) was made in the following process: NO, NOS, EGF and PGE2 content were multiplied with their own weight respectively, then added. ANOVA was used to compare the difference in the acupuncture therapy groups. The highest CEV was found in YMG followed by TYG, SYG, JYG, TYMG, and MG. The statistics showed that there was a very significant difference in CEV between YMG and other groups (*P*<0.01). In addition, CEV was also higher in TYG than in SYG, JYG, TYMG, and MG, respectively (*P*< 0.01).

Table 4 Summarization of effects on items after acupuncture therapy

Items	Order sequence				
	1	2	3	4	5
GMII	YMG	TYG	SYG	JYG	TYMG
NO	YMG	TYG	JYG	TYMG	SYG
NOS	YMG	TYG	SYG	JYG	TYMG
EGF	YMG	SYG	JYG	TYG	TYMG
PGE2	YMG	TYG	SYG	TYMG	JYG

Order sequence refers to the effect intensity from strong to weak.

Table 5 Comprehensive protective effects of different meridian acupuncture on gastric mucosa (mean±SD)

Groups	*n*	WEV
NG	8	9 542.1±851.4[b]
MG	8	5 298.5±963.8[d,f]
YMG	8	9 653.5±1 064.7[b]
SYG	8	6 344.6±1 013.8[d,f],
JYG	8	5 660.7±919.4[d,f]
TYG	8	8 391.1±1 466.1[b,d]
TYMG	8	5 550.4±1 501.4[d,f]

[b]*P* <0.01 *vs* MG; [d]*P* <0.01 *vs* YMG; [f]*P* <0.01 *vs* TYG.

DISCUSSION

Excessive ethanol ingestion can result in gastritis characterized by mucosal edema, subepithelial hemorrhages, cellular exfoliation and inflammatory cell infiltration[6]. Ethanol intragastric instillation breaks the gastric mucosal barrier and increases histamine release and pepsinogen output, thus leading to the damage in the gastric mucosa at least in part via hyperosmolarity[7]. In the present study, after ethanol intragastric instillation, the highest GMII was found in MG, demonstrating that the model of gastric mucosal injury is reliable. It is known that neuronal modulating processes such as release of vasoactive mediators are crucial for the gastric mucosa to resist the continual onslaught of aggressive agents[8,9]. Endothelial cells also release a highly labile humoral vasodilator

substance, now known as NO that mediates the vascular relaxation induced by vagal stimulation[10]. NO could protect the gastric mucosa by increasing gastric mucosal blood flow[11,12], suggesting that gastroprotection can be induced by low level of central vagal stimulation and the consequent release of NO, and that NO plays a role also in ulcer healing by stimulating the formation of growth factors, such as epithelial proliferation and angiogenesis[13]. NOS is a limited enzyme for NO synthesis. Studies have shown that chronic nitric oxide synthase inhibitor L-NAME enhances ulcerogenesis by decreasing mucosal resistance due to reduced mucosal blood perfusion[14–16]. When the specific iNOS inhibitor L-N6-(1-iminoethyl) lysine (L-NIL) is given intravenously to rats, the blood flow increase in response to luminal acid is attenuated[17]. Therefore, NOS is important for maintaining mucosal resistance through increasing the gastric mucosal blood flow. PGE2 is also involved in protecting gastric mucosa. PGE2 inhibits ethanol-induced apoptosis and increases cell viability in a dose-dependent manner in primary cultures of guinea pig gastric mucosal cells. PGE2 also inhibits hydrogen peroxide-induced apoptosis[18]. EGF is also a key to the protection against mucosal injury. Since acute gastric lesions are induced by cold-restraint stress, the ulcer score is significantly reduced after intraperitoneal and intragastric administration of EGF solution[19]. When EGF is added to primary monolayer cultures of guinea pig gastric mucous cells, the cytoprotection induced by EGF can be demonstrated. Mucin biosynthesis and PGE2 release are both significantly increased by EGF[20]. EGF promotes gastric mucosal restitution by activating Na^+/H^+ exchange of epithelial cells[21]. In the present study, the comprehensive effects of different meridian acupuncture on gastric mucosal protective factors including NO, NOS, PGE2 and EGF, the relationship between meridian and viscus were revealed.

MMCSV is common in the theory of meridian and viscus correlation, manifested in two aspects. On the one hand, multiple meridians have different connections with the same viscus, and the function of meridians is complex. For example, there are five meridians connecting the stomach, namely Hand Taiyin Meridian (HTY), FTY, FJY, Hand Taiyang Meridian (HTY), FYM. On the other hand, stimulating different meridian acupoints could regulate the same viscus physical function, which is the underlying theory for treating diseases. For example, moxibustion at Neiguan (PC 6) of Hand Jueyin Meridian, Yangfu (GB 38) of FSY, as well as Shangqiu (SP 5) of FTY, can be selected for stomachache therapy.

Though MMCSV is common, the meridians do have some speciality. It could be explained by the following two reasons. One is that since different meridian acupoints have a relative speciality, and meridian is composed of acupoints, it is no doubt that the meridian has some speciality. In addition, the meridian and viscus match theory also can explain the meridian's speciality. Since FYM is the responsible meridian to stomach, acupuncture at FYM could regulate the stomach physical function and improve pathological conditions. According to viscus-viscus match theory, the stomach is matched with the spleen; since the FTY is responsible for the spleen, acupuncture at FTY also has good effects on the stomach function regulation. Gallbladder's bile secretion from gallbladder could help the stomach to digest, while the secretion depends on the liver dredging function. Since the FSY is responsible for gallbladder, and FJY for the liver, acupuncture at FSY and FJY also has some effects on the stomach function regulation. In the present study, FYM had the best effect on stomach function regulation, followed by FTY, FSY and FJY, while the FTYM had no effect.

MMCSV is the unification for universality and speciality of meridian and viscus theory. In the present study, the protective effects of acupuncture at different meridian acupoints on gastric mucosa were various. For example, except for acupuncture at FTY, GMII decreased in all acupuncture therapy groups, while acupuncture at FYM, FTY and FSY, increased the NOS, suggesting that MMCSV is common. Acupuncture at FYM achieved the best intensity and width of protective effects on gastric mucosa. FJY had almost no effects on NO, NOS, PGE2, and EGF. FTYM has no significant effects on NO, NOS, PGE2, and EGF.

In summary, the FYM is most closely related to the stomach, followed by FTY, FSY, FJY, while FTYM has no correlation with the stomach.

REFERENCES

1 **Bing Z.** Zhenjiu De Kexue Jichu. 1th edition. Qingdao: Qingdao Press, 1998:323
2 **Sun DY,** Huan YX, Gao W, Chu ZH, Wang QL. Mechanism of electroacupuncture of Zusanli in protecting gastric mucosa of dogs. *Guangzhou Zhongyiydao Daxue Xuebao* 2002; **19**: 192-194
3 **Sun DY,** Huan YX, Gao W, Chu ZH, Wang QL. Effects of electroacupuncture on plasma and gastric mucosal levels of ET in dogs. *Zhenci Yanjiu* 2002; **27**: 197-200
4 **Yan J,** Li JS, Chang XR, Yi SX, Lin YP. Effect of electroacupuncture at acupoints of the Foot-Yangming meridian on gastric motion function in normal rabbits. *Chinese J Cur Tra West Med* 2003; **1:** 193-194
5 **Zhang H,** Yi SX, Yan J,Chang XR, Liu YQ, Lin YP,Deng YJ. A comparative study on the effect of electroacupuncture to the points of three yang meridians of foot on brain-gut peptide of rabbits. *Zhongguo Linchuang Kangfu* 2004; **8:** 2290-2291
6 **Yi SX,** Lin YP, Yan J, Chang XR, Yang Y. Effect of electro-acupuncture on gastric motility, substance P (SP) and motilin (MTL) in rats. *Shijie Huaren Xiaohua Zazhi* 2001; **9:** 284-287
7 **Miao M.** Shiyan Dongwu He Dongwu Shiyan Jishu. Beijing: Zhongguo Zhongyiyao Chubanshe, 1997: 219
8 **Lin WZ,** Wang P. Modern Acupuncturolgy. 1th edition. Beijing: *Shanghai Kexue Jishu Chubanse* 1999: 278-281
9 **Guth PH,** Aures D, Paulsen G. Topical aspirin plus HCl gastric lesions in the rat. Cytoprotective effect of prostaglandin, cimetidine, and probanthine. *Gastroenterology* 1979; **76:** 88-93
10 **Ko JK,** Cho CH, Lam SK. Adaptive cytoprotection through modulation of nitric oxide in ethanol-evoked gastritis. *World J Gastroenterol* 2004; **10:** 2503-2508
11 **Puurunen J,** Huttunen P, Hirvonen J. Is ethanol-induced damage of the gastric mucosa a hyperosmotic effect? Comparative studies on the effects of ethanol, some other hyperosmotic solutions and acetylsalicylic acid on rat gastric mucosa. *Acta Pharmacol Toxicol (Copenh)* 1980; **47:** 321-327
12 **Yonei Y,** Holzer P, Guth PH. Laparotomy-induced gastric

protection against ethanol injury is mediated by capsaicin-sensitive sensory neurons. *Gastroenterology* 1990; **99:** 3-9
13 **Whittle BJ,** Lopez-Belmonte J, Moncada S. Regulation of gastric mucosal integrity by endogenous nitric oxide: interactions with prostanoids and sensory neuropeptides in the rat. *Br J Pharmacol* 1990; **99:** 607-611
14 **Palmer RM,** Ferrige AG, Moncada S. Nitric oxide release accounts for the biological activity of endothelium-derived relaxing factor. *Nature* 1987; **327:** 524-526
15 **Holzer P.** Neural emergency system in the stomach. *Gastroenterology* 1998; **114**: 823-839
16 **Wallace JL,** Miller MJ. Nitric oxide in mucosal defense: a little goes a long way. *Gastroenterology* 2000; **119:** 512-520
17 **Gyires K.** Gastric mucosal protection: from prostaglandins to gene-therapy.*Curr Med Chem* 2005; **12:** 203-215
18 **Qiu BS,** Pfeiffer CJ, Cho CH. Effects of chronic nitric oxide synthase inhibition in cold-restraint and ethanol-induced gastric mucosal damage in rats. *Digestion* 1996; **57:** 60-66
19 **Kim H,** Hwan Kim K. Role of nitric oxide and mucus in ischemia/reperfusion-induced gastric mucosal injury in rats. *Pharmacology* 2001; **62:** 200-207
20 **Lippe IT,** Holzer P. Participation of endothelium-derived nitric oxide but not prostacyclin in the gastric mucosal hyperaemia due to acid back-diffusion. *Br J Pharmacol* 1992; **105:** 708-714
21 **Phillipson M,** Henriksnäs J, Holstad M, Sandler S, Holm L. Inducible nitric oxide synthase is involved in acid-induced gastric hyperemia in rats and mice. *Am J Physiol Gastrointest Liver Physiol* 2003; **285:** G154-G162

Science Editor Wang XL and Guo SY **Language Editor** ELsevier HK

PO Box 2345, Beijing 100023, China
www.wjgnet.com
wjg@wjgnet.com

ELSEVIER

World J Gastroenterol 2005;11(41):6477-6482
World Journal of Gastroenterology ISSN 1007-9327

• *BASIC RESEARCH* •

Acid fibroblast growth factor reduces rat intestinal mucosal damage caused by ischemia-reperfusion insult

Wei Chen, Xiao-Bing Fu, Shi-Li Ge, Tong-Zhu Sun, Wen-Juan Li, Zhi-Yong Sheng

Wei Chen, Xiao-Bing Fu, Tong-Zhu Sun, Wen-Juan Li, Zhi-Yong Sheng, Wound Healing and Cell Biology Laboratory, Burns Institute, 304th Clinical Department, General Hospital of PLA, Beijing 100037, China
Shi-Li Ge, Institute of Radiation Medicine, Academy of Military Medicine Sciences, Beijing 100850, China
Supported by the National Natural Science Foundation of China, No. 30400172 and 30230370 and "973" programm NO.2005CB52203
Correspondence to: Professor Xiao-Bing Fu, Wound Healing and Cell Biology Laboratory, Burns Institute, 304th Clinical Department, General Hospital of PLA, 51 Fu Cheng Road, Beijing 100037, China. fuxb@cgw.net.cn
Telephone: +86-10-66867396 Fax: +86-10-88416390
Received: 2004-12-28 Accepted: 2005-03-24

Abstract

AIM: To detect the effects of acid fibroblast growth factor (aFGF) on apoptosis and proliferation of intestinal epithelial cells in differentiation or proliferation status to explore the protective mechanisms of aFGF.

METHODS: Wistar rats were randomly divided into sham-operated control group (C, $n = 6$), intestinal ischemia group (I, $n = 6$), aFGF treatment group (A, $n = 48$) and intestinal ischemia-reperfusion group (R, $n = 48$). Apoptosis of intestinal mucosal cells was determined with terminal deoxynucleotidyl transferase-mediated dUTP-biotin nick-end labeling (TUNEL) technique. Proliferating cell nuclear antigen (PCNA) protein expression and distribution were detected with immunohistochemical method. Plasma levels of D-lactate were determined with modified Brandts method.

RESULTS: In A group, administration of exogenous aFGF could improve intestinal histological structure and decrease plasma D-lactate levels at 2-12 h after the reperfusion compared with R group. The apoptotic rates and PCNA protein expressions were not increased until 2 h after reperfusion and were maximal at 12 h. After reperfusion for 2-12 h, the apoptotic rates were gradually augmented along the length of jejunal crypt-villus units. Administration of aFGF could significantly reduce the apoptotic response at 2-12 h after reperfusion ($P<0.05$). Apoptosis rates in villus and crypt epithelial cells in A group at 12 h after reperfusion were (62.5±5.5)% and (73.2±18.6)% of those in R group, respectively. Treatment of aFGF could apparently induce protein expression of PCNA in intestinal mucosal cells of A group compared with R group during 2-12 h after reperfusion ($P<0.05$). There were approximately 1.3- and 1.5-times increments of PCNA expression levels in villus and crypt cells in A group at 12 h after reperfusion compared with R group, respectively.

CONCLUSION: Intestinal I/R insult could lead to histological structure change and apoptotic rate increment. The protective effects of aFGF against ischemia/reperfusion in rat intestinal mucosa might be partially due to its ability to inhibit ischemia/reperfusion-induced apoptosis and to promote cell proliferation of crypt cells and villus epithelial cells.

Key words: Acid fibroblast growth; Ischemia; Reperfusion; Intestine; Crypt; Villus

Chen W, Fu XB, Ge SL, Sun TZ, Li WJ, Sheng ZY. Acid fibroblast growth factor reduces rat intestinal mucosal damage caused by ischemia-reperfusion insult. *World J Gastroenterol* 2005; 11(41): 6477-6482
http://www.wjgnet.com/1007-9327/11/6477.asp

INTRODUCTION

An ischemic insult decreases oxygen and nutrient delivery and causes post mitotic cell lineages in the brain, myocardium, muscle and adrenal cortex to undergo apoptosis. Paradoxically, the introduction of oxygen during reperfusion of ischemic tissues exacerbates the damage of these tissues[1-5]. These tissues do not allow evaluation of the effects of proliferative status or state of differentiation on the apoptotic response to this inductive stimulus. The intestinal epithelium provides an excellent system for such an analysis. Renewal of intestinal epithelium takes place continuously in anatomically distinct crypt-villus units. Proliferation is restricted to mucosal invaginations known as crypts. All epithelial cells in each crypt are derived from an uncertain number of multipotent stem cells located at or near the base of the crypt[6-8]. These crypt stem cells divided to produce daughter stem cells as well as more rapidly replicating transit cells, which in turn undergo 4-6 rapid cell divisions in the proliferative zone located in the lower half of each crypt[9,10]. The small intestine is highly sensitive to ischemia-reperfusion (I/R). It has been demonstrated that occlusion of the superior mesenteric artery (SMA) followed by reperfusion can cause apoptosis in the intestinal epithelium[11].

Acid fibroblast growth factor (aFGF) is a mitogen *in vitro* for most of the ectodermal- and mesodermal-derived cell lines. In addition, this factor shows a wide range of endocrine-like activities[12,13]. As a multiple function growth factor, aFGF is involved in embryo development and tissue repair[14-16]. However, the protective mechanisms of aFGF on intestinal I/R injury remain unknown. Given the anatomically well-defined stratification of proliferation and differentiation programs along its crypt-villus axis, the self-renewing intestinal epithelium provides an opportunity to consider, whether aFGF protects intestinal mucosa from I/R injury through inducing proliferation of cells located in crypt or inhibiting apoptosis of epithelial cells distributed in villus or adopting both these two procedures.

In the present article, we have clarified the mechanism of aFGF protection following I/R injury in the small intestinal mucosa of rats by evaluating changes in apoptosis of epithelial cells along gut crypt-villus axis. We evaluated the expression of proliferating cell nuclear antigen (PCNA). The expressive level of this protein is frequently used to evaluate the regenerative ability of epithelial tissue[17]. We also estimated the integrity of small intestinal mucosa by measuring the levels of plasma D-lactate. This study will lead to a better understanding of the repair mechanisms of small intestinal mucosa induced by aFGF treatment after I/R injury.

MATERIALS AND METHODS

Animal model and experimental design

Healthy male Wistar rats weighing 220 ± 20 g (Animal Centre, Academy of Military Medical Science, Beijing) were used in this study. Animals were housed in wire-bottomed cages placed in a room illuminated from 08:00 am to 08:00 pm (12:12 h light-dark cycle) and maintained at 21±1 °C. Rats were allowed to access water and chow *ad libitum*. The animals were anesthetized by using 3% sodium pentobarbital (40 mg/kg), and a laparotomy was performed. The SMA was identified and freed by blunt dissection. A micro-bulldog clamp was placed at the root of SMA to cause complete cessation of blood flow for 45 min, and thereafter the clamp was loosened to form reperfusion injury. The animals were randomly divided into sham-operated control group (C, $n = 6$), intestinal ischemia group (I, $n = 6$), aFGF treatment group (A) and intestinal ischemia-reperfusion group (R). According to the different periods after reperfusion, groups R and A were further divided into 0.25, 0.5, 1, 2, 6, 12, 24 and 48 h subgroups, respectively ($n = 6$, each subgroup). In group I, the animals were killed after 45 min of SMA occlusion, while in groups R and A, the rats sustained 45 min of SMA occlusion and were treated with 0.15 mL normal saline and 0.15 mL saline plus 20 μg/kg aFGF (R&D Systems, Inc.) injected from tail vein, respectively, then sustained 0.25, 0.5, 1, 2, 6, 12, 24 and 48 h of reperfusion, respectively. In C group, SMA was separated, but without occlusion, and the samples were taken after exposure of SMA for 45 min. In groups R and A, rats were killed at different time points after reperfusion. Blood samples and intestinal tissue biopsies were taken. Blood samples were centrifuged and serum was frozen to measure plasma levels of D-lactate. Tissue biopsies were fixed with 10% neutral buffered formalin for detection of intestinal epithelial apoptosis, and protein expression of PCNA.

In situ detection of cell death

The apoptotic cells in intestinal tissues were detected with the terminal deoxynucleotidyl transferase (TdT)-mediated dUTP-biotin nick-end labeling (TUNEL) method. Specimens were dewaxed and immersed in phosphate-buffered saline containing 0.3% hydrogen peroxide for 10 min at room temperature and then incubated with 20 μg/mL proteinase K for 15 min. Seventy-five microliters of the equilibration buffer was applied directly onto the specimens for 10 min at room temperature, followed by 55 μL of TdT enzyme and incubation, which were then incubated at 37 ℃ for 1 h. The reaction was terminated by transferring the slides to prewarmed stop/wash buffer for 30 min at 37 ℃. The specimens were covered with a few drops of rabbit serum and incubated for 20 min at room temperature and then covered with 55 μL of anti-digoxigenin peroxidase and incubated for 30 min at room temperature. Specimens were then soaked in Tris buffer containing 0.02% diaminobenzidine and 0.02% hydrogen peroxide for 1 min to achieve color development. Finally, the specimens were counterstained by immersion in hematoxylin. The cells with clear nuclear labeling were defined as TUNEL-positive cells. The results of positive cells and their distribution were observed under 400 times microscope. Sixty intestinal villi and crypts per time point were required for counting, and then the apoptotic ratios were calculated and analyzed, respectively.

Immunohistochemistry

Immunostaining for PCNA was performed in paraffin sections with a high-temperature antigen-unmasking method in citrate buffer and ABC peroxidase, using monoclonal mouse antibody (Zymed Corp., ZM-0213) against antigen (1 ∶ 100 in PBS). Tissues were fixed overnight in 4% paraformaldehyde, dehydrated, and embedded in paraffin. Sections of 5 μm thickness were deparaffinized and rehydrated using graded alcohol concentrations. Antigen retrieval was performed by incubation in 100 mmol/L sodium citrate, pH 6.0, at 90 ℃ for 20 min. Then, sections were blocked with 5% normal swine serum in PBS for 30 min at 25 ℃, followed by incubation with primary antibodies at a concentration of 5 μg/mL overnight at 4 ℃. Control slides were incubated with PBS without primary antibodies. Tissues sections were then incubated for 60 min with biotinylated secondary antibody. After washing in PBS, the sections were exposed to acidin-biotin complex for 60 min. The sections were reacted with 0.05% (wt/vol) DAB in 50mol/L Tris-HCl (pH 7.4) with 0.1% (vol/vol) hydrogen peroxide for 5 min and counterstained with hematoxylin. The results of positive staining cells and their distribution were observed under 400 times microscope. Sixty intestinal villi and crypts per time point were required for counting,

and then the ratio of positive cells were calculated and analyzed, respectively.

Measurement of plasma D-lactate

The levels of plasma D-lactate were measured with modified Brandts method[18,19]. Briefly, heparinized blood was centrifuged at 3 200 r/min for 10 min and 2 mL of the plasma was deproteinized with 0.2 mL perchloric acid (1/10 vol), mixed and kept in an ice bath for 10 min. The denatured protein solution was centrifuged at 3 200 r/min for 10 min and the supernatant was removed. To 1.4 mL of supernatant, 0.12 mL KON was added and they were mixed for 20 s. Precipitant $KCLO_4$ was removed by centrifugation at 3 200 r/min for 10 min. The supernatant and neutralized-protein-free plasma were used to measure the absorbency at 304 nm. Plasma D-lactate concentrations were expressed as μg/mL.

Statistical analysis

All values were expressed as mean±SD. Differences in mean values were compared using SPSS 11.0 by one-way ANOVA and Student-Newman-Keul (SNK) test. $P<0.05$ as considered as statistically significant.

RESULTS

Change of cellular apoptotic rates

After the SMA was clamped near its origin from the aorta, the damage to the small intestine in the 45-min ischemia group was small. At 2 h after reperfusion, the partial loss of the mucosa could be observed. During 6-12 h after reperfusion, the damage of intestinal epithelial cells, hemorrhage and necrosis could be found, the crypt-villus structure was seriously spoiled. In the period of 24-48 h after reperfusion, the mucosal integrity was partially restored. The protective function of aFGF on intestinal mucosa was the most effective during 2-12 h after reperfusion. The structures of crypt and villus were both guarded, with less damage of the intestinal mucosa (Figure 1). Apoptosis was measured and quantified by TUNEL assay in serial sections prepared from the middle quarter of the small intestine (jejunum). The time animals were killed after a 45 min SMA occlusion followed by reperfusion was varied to further define the apoptotic response. Statistically significant increases in TUNEL-positive cells were not detectable until 2 h after reperfusion and were maximal at 12 h. The augmentation of the cellular apoptotic rates was evident along the length of jejunal crypt-villus units after reperfusion for 2-12 h; i.e., the average increase was 2.3 times for villi [84.0±6.2 (12 h after reperfusion) *vs* 37.3±6.6 (C group $P<0.05$)] and 1.9 times for crypts [28.2±3.9 (12 h after reperfusion) *vs* 14.4±3.8 (C group $P<0.05$; Table 1)]. Highest levels of apoptosis were noted in the upper quarter of the villus. In no matter villus and crypt, the apoptotic rates were restored to the levels of C group after reperfusion for 24 and 48 h. Administration of aFGF could significantly reduce the apoptotic response observed 2-12 h after reperfusion ($P<0.05$). Apoptosis rates in villus and crypt epithelial cells of A group at 12 h after reperfusion were (62.5±5.5)% and (73.2±18.6)% of those in their littermates of R group, respectively (Table 1, Figure 2).

Table 1 Effect of aFGF on the apoptotic rates in intestinal villi and crypts after ischemia-reperfusion insult ($n=6$, mean±SD, %)

Groups	Villus		Crypt	
	R group	A group	R group	A group
C group	37.3±8.6	37.3±8.6	14.4±3.8	14.4±3.8
I group	40.0±6.9	40.0±6.9	13.7±4.1	13.7±4.1
0.25 h after reperfusion	45.3±5.7	35.2±6.7[c]	15.0±3.2	11.8±2.6
0.5 h after reperfusion	46.3±8.3	37.8±7.4	16.2±4.7	13.0±3.5
1 h after reperfusion	49.5±5.3	45.3±7.4	19.3±5.6	16.2±3.3
2 h after reperfusion	70.2±6.5[a]	50.5±5.3[ac]	23.5±6.2[a]	17.8±4.1[c]
6 h after reperfusion	76.8±4.7[a]	49.2±5.0[a,c]	27.2±4.8[a]	19.3±5.0[a,c]
12 h after reperfusion	84.0±6.2[a]	52.5±4.6[a,c]	28.0±3.9[a]	20.5±5.2[a,c]
24 h after reperfusion	41.8±5.4	35.2±5.2	14.2±4.3	9.3±3.6
48 h after reperfusion	33.7±4.8	34.3±6.2	13.3±2.9	11.0±4.3

[a]$P<0.05$ *vs* C group; [c]$P<0.05$ *vs* R group at matched time points.

Expression characteristics of PCNA protein

Quantitative immunohistochemical results for PCNA protein were evaluated in Table 2 and Figure 3. PCNA was weakly expressed in the sham-operated intestinal tissues and ischemic tissues, with positive particles mostly

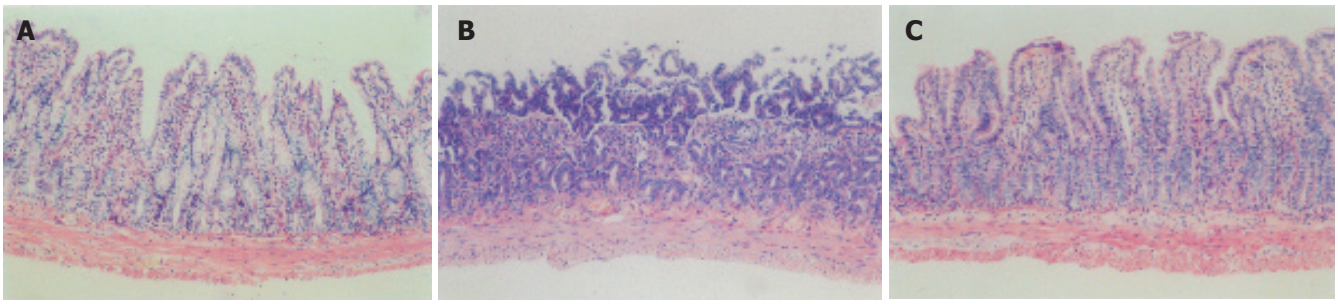

Figure 1 The histological structure of intestine in sham-operated control group **(A)**, 6 h after ischemia-reperfusion in R group **(B)** and 6 h after ischemia-reperfusion in A group **(C)** (100×). Anatomic structures of villi and crypts of intestine in control group were intact. In R group, at 6 h after reperfusion, the crypt-villus structure was seriously spoiled, accompanied by inflammatory cells infiltrating into the intestinal wall. In A group, the structures of crypt and villi were both protected, with less damage of the intestinal mucosa.

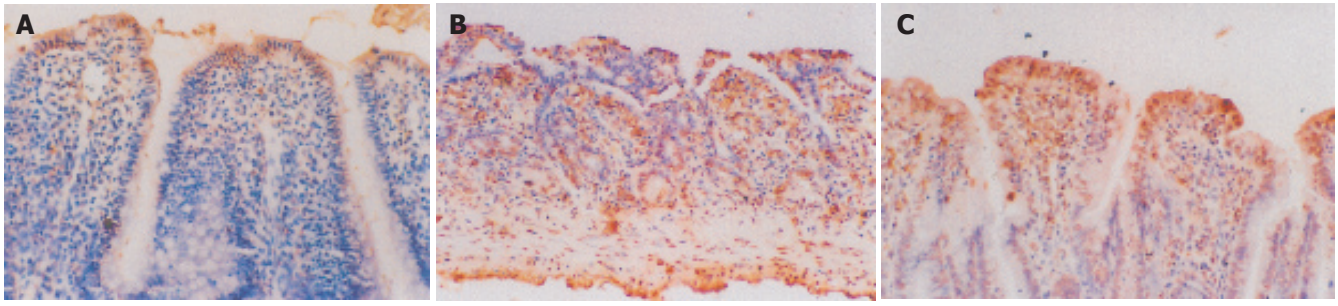

Figure 2 The cellular apoptotic rates in sham-operated control group **(A)**, 6 h after ischemia-reperfusion in R group **(B)** and 6 h after ischemia-reperfusion in A group **(C)** (200×). Cellular apoptotic rates were less in sham-operated control group and were significantly increased in villi and crypts at 6 h after reperfusion. The augmentation of the cellular apoptotic rates was evident along the length of jejunal crypt-villus units. The cellular apoptotic rates both decreased remarkably at 6 h after reperfusion in villi and crypts of A group *vs* those of R group.

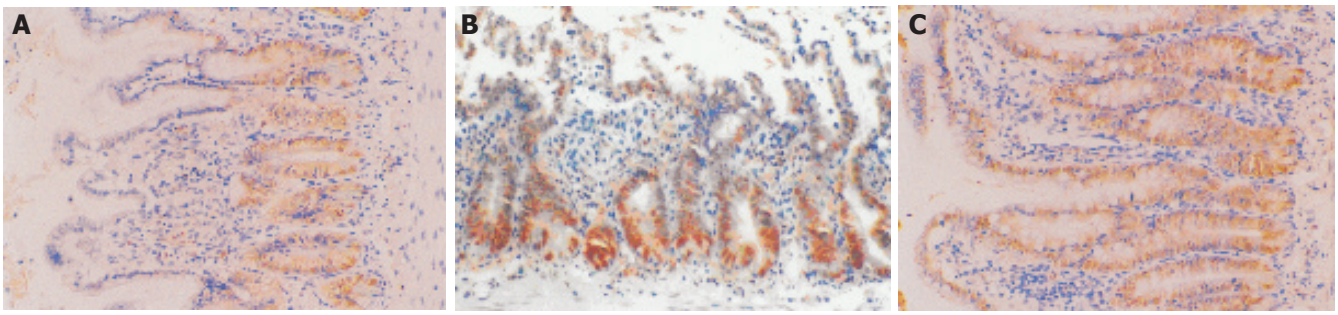

Figure 3 The expression of PCNA protein in sham-operated control group **(A)**, 6 h after ischemia-reperfusion in R group **(B)** and 6 h after ischemia-reperfusion in A group **(C)** (200×). PCNA was weakly expressed in sham-operated control group, with positive particles mostly distributing in the nuclei of the lower third of crypt cells. Protein contents of PCNA were significantly increased in villi and crypts at 6 h after reperfusion compared with control group. The contents of PCNA increased remarkably in villi and crypts at 6 h after reperfusion in A group *vs* R group.

Table 2 Effect of aFGF on protein expression of PCNA in intestinal villi and crypts after ischemia-reperfusion (n=6, mean±SD, %)

Groups	Villus		Crypt	
	R group	A group	R group	A group
C group	8.5±5.0	8.5±5.0	31.5±5.2	31.5±5.2
I group	8.8±5.3	8.8±5.3	33.3±4.1	33.3±4.1
0.25 h after reperfusion	10.5±5.1	10.7±4.9	39.7±5.4	36.0±5.6
0.5 h after reperfusion	11.5±3.8	14.7±4.3	41.0±4.7[a]	43.8±5.2[a]
1 h after reperfusion	12.3±6.2	11.3±5.4	44.3±4.6[a]	51.5±6.0[a]
2 h after reperfusion	16.7±4.5[a]	23.3±5.1[ac]	48.2±5.3[a]	67.8±5.3[ac]
6 h after reperfusion	18.2±3.5[a]	25.0±6.4[ac]	47.3±5.5[a]	76.0±3.8[ac]
12 h after reperfusion	19.0±5.4[a]	25.3±4.5[ac]	52.1±5.1[a]	79.8±5.2[ac]
24 h after reperfusion	8.7±4.7	11.2±2.3	43.7±5.4	44.8±6.2
48 h after reperfusion	6.7±2.9	9.2±4.0	38.5±6.1	42.7±4.9

[a]P<0.05 *vs* C group; [c]P<0.05 *vs* R group at matched time points.

distributing in the nuclei of the lower third of crypt cells. However, the positive cellular rate elevated with the increment of duration after reperfusion injury. In the period after reperfusion, marked PCNA immunoreactivities were observed in the nuclei of crypt and villus cell. At 12 h after reperfusion, the positive cellular rates were maximal, the average increase was 2.2 times for villi [19.0±5.4 *vs* 8.5±5.0 (P<0.05)] and 1.7 times for crypts [52.1±5.1 *vs* 31.5±5.2 (P<0.05; Table 2)]. The positive cellular rates of PCNA were restored to the levels of sham-operated tissues at 24 and 48 h after reperfusion. During 2-12 h after reperfusion, treatment of aFGF could apparently induce protein expression of PCNA in intestinal mucosal epithelial cells from villi and crypts in comparison with R group at different matched times (P<0.05) (Table 2). There are approximately 1.3- and 1.5-time increments of PCNA expressive levels in both villus and crypts in rats of A group after reperfusion for 12 h compared with their littermates of R group, respectively. After reperfusion for 24 and 48 h, the positive signals of this protein had no substantial change in A group in comparison with R group (P>0.05).

The changes of plasma levels of D-lactate

As shown in Table 3, 45 min of ischemia followed by reperfusion in intestinal mucosa could result in plasma D-lactate level elevation. Plasma D-lactate level was significantly elevated from 30 min after reperfusion in R group, and reach its peak at 12 h, which was 1.5-folds of that in sham-operated group ((0.299±0.025) μg/mL *vs* (0.201±0.008) μg/mL, P<0.05), and then returned to the level of sham-operated group (P>0.05). Administration of aFGF produced decreases in the plasmas D-lactate level compared with R group during 0.25-12 h after reperfusion, except for 1 h after reperfusion, leading to statistically significant reduction of D-lactate contents (P<0.05). No significant decreases were observed at 24 and 48 h after reperfusion in A group compared with R group

Table 3 Effect of aFGF on plasma D-lactate levels after intestinal ischemia-reperfusion (n=6, mean±SD, μg/mL)

Groups	R group	A group
C group	0.201±0.008	0.201±0.008
I group	0.212±0.011	0.212±0.011
0.25 h after reperfusion	0.247±0.011	0.225±0.016[c]
0.5 h after reperfusion	0.281±0.036[a]	0.222±0.020[c]
1 h after reperfusion	0.285±0.068[a]	0.233±0.022
2 h after reperfusion	0.283±0.031[a]	0.232±0.018[ac]
6 h after reperfusion	0.293±0.033[a]	0.252±0.014[ac]
12 h after reperfusion	0.299±0.025[a]	0.250±0.018[ac]
24 h after reperfusion	0.228±0.012	0.223±0.015
48 h after reperfusion	0.231±0.004	0.224±0.009

[a]P<0.05 *vs* C group; [c]P<0.05 *vs* R group at matched time points.

(P>0.05, Table 3).

DISCUSSION

The major clinical disorders involving gastrointestinal circulation are hemorrhage and ischemia. It is well recognized that the small intestine is very sensitive to the deleterious effects of I/R and it has been clearly demonstrated that I/R causes mucosal injury within the small intestine. Several recent studies have proposed that ischemia-reperfusion can induce an apoptotic response in the adult rat intestinal epithelium, although they did not quantitate this response along the crypt-villus axis[11,20]. In the current study, we found that I/R, following occlusion of the SMA, led to statistically significant increment of apoptosis in undifferentiated epithelial cells located in the proliferative compartment of the adult rat's small intestine, as well as in differentiated epithelial cells distributed in the villus at 2-12 h after reperfusion. The most apoptotic rates in the upper portion of the villus are the region, which is farthest from submucosal vessels that supply blood to the mesenchymal core of the villus. The asymmetric distribution of apoptosis may reflect the fact that hypoxia and deficient nutrient generated by SMA occlusion are greater in epithelial cells located in the upper villus compared with crypts. However, it is also possible that the signaling pathways that mediate the induction differ qualitatively or quantitatively between undifferentiated proliferating cells in the crypt and postmitotic differentiated cells in the upper villus. The actual mechanism needs to be deeply explored. Our studies displayed that administration of exogenous aFGF produced an approximately 1.5-fold reduction in the number of TUNEL positive cells that appear following transient SMA occlusion in proliferating undifferentiated crypt epithelial lineage as well as their postmitotic differentiated villus descendants. These results are compatible with the notion that exogenous aFGF might protect from intestinal injury caused by I/R insult through an identical mechanism in villus and crypt epithelial cells.

D(-)-lactate is the stereoisomer of mammalian L(+)-lactate. Mammalian tissue cannot produce D(-)-lactate and can only slowly metabolize it. It is a strict product of bacterial fermentation. Since intestinal I/R injury can cause mucosal injury and subsequent bacterial proliferation, D(-)-lactate releasing from the gut into the host blood circulation, the change of plasma D(-)-lactate level was used as a predictor of intestinal I/R injury[21,22]. In the present study, it was shown that plasma D(-)-lactate levels began to increase in rat's intestinal villus subjected to 45 min of ischemia followed by 30 min of reperfusion, maximal at 12 h after reperfusion. In the aFGF treated group, it was significantly decreased during 2-12 h after reperfusion compared with normal saline treated group, which was corroborated with the data obtained by the TUNEL method, indicating that aFGF exerts a positive protective effect on the mucosal barrier and decreases the intestinal permeability.

Our study also found that apoptosis occurred at 2 h post-reperfusion fδllowed by a return to baseline values by 24 h suggestsing that I/R induction of intestinal apoptosis and mucosal recovery were rapid processes. The reason for this interesting kinetics of induction of mucosal cell death and restoration was unclear. PCNA is a significant cell-cycle regulated nuclear protein for DNA-polymerase. PCNA-labeled nuclei identify cells in the late G1 and early S phases of the cell cycle, as well as cells undergoing DNA repair[23,24]. Our current study demonstrated that the expressing levels of PCNA at 2-12 h after reperfusion were significantly higher than the levels of C control in both crypt and villus epithelial cells. These findings indicated that the repair process of small intestinal mucosa was initiated by I/R and cellular regeneration continued for 12 h following reperfusion. At the same time, the PCNA protein was mainly located in the nuclei of proliferative cells in crypts. Administration of exogenous aFGF could induce protein expression of PCNA in mucosal cells, especially in crypt epithelial cells. At 2-12 h after reperfusion, PCNA was strongly expressed both in undifferentiated crypt epithelial cells as well as differentiated villus cells in comparison with normal saline treated group. These results suggest that aFGF treatment could inhibit cellular apoptosis of mucosal cells and induced cell proliferation, especially cells in crypt, to accelerate regeneration and repair of small intestinal mucosa after ischemia-reperfusion insult. Ischemia of the adult human small intestine could result in high mortality[25]. Because administration of exogenous aFGF can ameliorate the reperfusion injury that accompanies intestinal transplantation or the epithelial wound brought about by sepsis, interventions that elevate aFGF levels or enhance its activity may be useful for reducing the damage produced by ischemia-reperfusion insult.

In conclusion, the present study provided the primary evidence that the protective effects of aFGF against ischemia/reperfusion in rat's intestinal villus might be partially due to its abilities to inhibit ischemia/reperfusion-induced apoptosis and to promote crypt and villus epithelial cell proliferation. The precise mechanism for the attenuation of intestinal ischemia/reperfusion injury and acceleration of mucosal regeneration afforded by aFGF

requires further investigation.

REFERENCES

1 **Chang TH,** Liu XY, Zhang XH, Wang HL. Effects of dl-praeruptorin A on interleukin-6 level and Fas, bax, bcl-2 protein expression in ischemia-reperfusion myocardium. *Acta Pharmacol Sin* 2002; **23:** 769-774

2 **Zhou H,** Ma Y, Zhou Y, Liu Z, Wang K, Chen G. Effects of magnesium sulfate on neuron apoptosis and expression of caspase-3, bax and bcl-2 after cerebral ischemia-reperfusion injury. *Chin Med J (Engl)* 2003; **116:** 1532-1534

3 **Wang Y,** Hayashi T, Chang CF, Chiang YH, Tao LI, Su TP, Borlongan C, Lin SZ. Methamphetamine potentiates ischemia/reperfusion insults after transient middle cerebral artery ligation. *Stroke 2001;* **32:** 775-782

4 **Hatoko M,** Tanaka A, Kuwahara M, Yurugi S, Iioka H, Niitsuma K. Difference of molecular response to ischemia-reperfusion of rat skeletal muscle as a function of ischemic time: study of the expression of p53, p21(WAF-1), Bax protein, and apoptosis. *Ann Plast Surg 2002;* **48:** 68-74

5 **Baskin DS,** Ngo H, Didenko VV. Thimerosal induces DNA breaks, caspase-3 activation, membrane damage, and cell death in cultured human neurons and fibroblasts. *Toxicol Sci* 2003; **74:** 361-368

6 **Loeffler M,** Bratke T, Paulus U, Li YQ, Potten CS. Clonality and life cycles of intestinal crypts explained by a state dependent stochastic model of epithelial stem cell organization. *J Theor Biol* 1997; **186:** 41-54

7 **Fu XB,** Xing F, Yang YH, Sun TZ, Guo BC. Activation of phosphorylating-p38 mitogen-activated protein kinase and its relationship with localization of intestinal stem cells in rats after ischemia-reperfusion injury. *World J Gastroenterol* 2003, **9:** 2036-2039

8 **Fu XB,** Yang YH, Sun TZ, Chen W, Li JY, Sheng ZY. Rapid mitogen-activated protein kinase by basic fibroblast growth factor in rat intestine after ischemia/reperfusion injury. *World J Gastroenterol* 2003; **9:** 1312-1317

9 **Potten CS,** Booth C, Pritchard DM. The intestinal epithelial stem cell: the mucosal governor. *Int J Exp Pathol* 1997; **78:** 219-243

10 **Wang ZH,** Chang XT, Fu XB, Sun TZ, Yang YH, Chen W, Zhao ZL. Expression of protooncogene c-jun, p38 and proliferating cell nuclear antigen in intestinal epithelial cells in rats different development stages. *Chin Crit Care Med* 2003; **15:** 77-80

11 **Noda T, I**wakiri R, Fujimoto K, Matsuo S, Aw TY. Programmed cell death induced by ischemia-reperfusion in rat intestinal mucosa. *Am J Physiol* 1998; **274:** G270-G276

12 **Cuevas P,** Carceller F, Martinez-Coso V, Asin-Cardiel E, Giménez-Gallego G. Fibroblast growth factor cardioprotection against ischemia-reperfusion injury may involve K+ ATP channels. *Eur J Med Res* 2000; **5:** 145-149

13 **Cuevas P,** Carceller F, Martinez-Coso V, Cuevas B, Fernandez-Ayerdi A, Reimers D, Asin-Cardiel E, Gimenez-Gallego G. Cardioprotection from ischemia by fibroblast growth factor: role of inducible nitric oxide synthase. *Eur J Med Res* 1999; *4:* 517-524

14 **Chen W, F**u XB, Zhou G, Jiang D, Sun T, Sheng ZY. Gene expression of fibroblast growth factors and their receptors in proliferative and mature hypertrophic scars. *Chin J Exp Surg* 2004; **21:** 1111-1113

15 **Weng LX,** Fu XB, Li XX, Sun TZ, Zheng SY, Chen W. [Effects of acidi fibroblast growth factor on hepatic and renal functions after intestinal ischemia/reperfusion injury] *Zhongguo Wei Zhong Bing Ji Jiu Yi Xue* 2004; **16:** 19-21

16 **Fu X,** Cuevas P, Gimenez-Gallego G, Sheng Z, Tian H. Acidic fibroblast growth factor reduces rat skeletal muscle damage caused by ischemia and reperfusion. *Chin Med J* 1995; **108:** 209-214

17 **Itoh H,** Yagi M, Hasebe K, Fushida S, Tani T, Hashimoto T, Shimizu K, Miwa K. Regeneration of small intestinal mucosa after acute ischemia-reperfusion injury. *Dig Dis Sci* 2002; **47:** 2704-2710

18 **Li JY,** Sun D, Lu Y, Jin H, Jiang XG, Hu S, Sheng ZY. [Change in intestinal function in sepsis in rat] *Zhongguo Weizhongbingji jiu Yixue* 2004; **16:** 352-354

19 **Li JY,** Sun D, Lu Y, Jin H, Hu S, Sheng ZY, Effect of intestinal ischemia-reperfusion on gut barrier, absorption, penetration and transmission. *Shijie Huaren Xiaohua Zazhi* 2004; **12:** 464-466

20 **Fu X,** Sheng Z, Wang Y, Ye Y, Xu M, Sun T, Zhou B. Basic fibroblast growth factor reduces the gut and liver morphologic and functional injuries after ischemia and reperfusion. *J Trauma* 1997; **42:** 1080-1085

21 **Murray MJ,** Barbose JJ, Cobb CF. Serum D (-)-lactate levels as a predictor of acute intestinal ischemia in a rat model. *J Surg Res* 1993; **54:** 507-509

22 **Murray MJ,** Gonze MD, Nowak LR, Cobb CF. Serum D (-)-lactate levels as an aid to diagnosing acute intestinal ischemia. *Am J Surg* 1994; **167:** 575-578

23 **Itoh H,** Yagi M, Fushida S, Tani T, Hashimoto T, Shimizu K, Miwa K. Activation of immediate early gene, c-fos, and c-jun in the rat small intestine after ischemia/reperfusion. *Transplantation* 2000; **69:** 598-604

24 **Chen W,** Fu XB, Sun TZ, Zhao Z, Yang Y, Sheng ZY. Characteristics of proliferating cell nuclear antigen and P53 expression in fetal and postnatal skins and their biological significance. *Chin Criti Care Med* 2002; **14:** 654-657.

25 **Chen W,** Fu XB, Ge SL, Sun TZ, Zhao JY, Du YR, Sheng ZY. Effects of extrogenous aFGF on bax and bcl-2 expression in intestine cells after ischemia/reperfusion. *Shijie Huaren Xiaohua Zazhi* 2004; **12:** 2599-2604.

Science Edited Wang XL and Guo SY **Language Editor** ELsevier HK

PO Box 2345, Beijing 100023, China
www.wjgnet.com
wjg@wjgnet.com

ELSEVIER

World J Gastroenterol 2005;11(41):6483-6488
World Journal of Gastroenterology ISSN 1007-9327

• *BASIC RESEARCH* •

Pathological mechanisms of alcohol-induced hepatic portal hypertension in early stage fibrosis rat model

Jian Li, Jian-Zhao Niu, Ji-Feng Wang, Yu Li, Xiao-Hua Tao

Jian Li, Jian-Zhao Niu, Ji-Feng Wang, Yu Li, Xiao-Hua Tao, Cell Biochemistry Laboratory, Basic Medicine College, Beijing University of Traditional Chinese Medicine, Beijing 100029, China
Supported by National Natural Science Foundation of China, No. 30130220 and Program for Changjiang Scholars and Innovative Research Team in University (2004)
Correspondence to: Jian-Zhao Niu, Basic Medicine College, Beijing University of Traditional Chinese Medicine, Beijing 100029, China. niujjzz@263.net
Telephone: +86-10-64287538 Fax: +86-10-64286716
Received: 2005-05-09 Accepted: 2005-06-24

Abstract

AIM: To study the role of hepatic sinusoidal capillarization and perisinusoidal fibrosis in rats with alcohol-induced portal hypertension and to discuss the pathological mechanisms of alcohol-induced hepatic portal hypertension.

METHODS: Fifty SD rats were divided into control group (n=20) and model group (n=30). Alcoholic liver fibrosis rat model was induced by intragastric infusion of a mixture containing alcohol, corn oil and pyrazole (1 000:250:3). Fifteen rats in each group were killed at wk 16. The diameter and pressure of portal vein were measured. Plasma hyaluronic acid (HA), type IV collagen (CoIV) and laminin (LN) were determined by radioimmunoassay. Liver tissue was fixed in formalin (10%) and 6-μm thick sections were routinely stained with Mallory and Sirius Red. Liver tissue was treated with rabbit polyclonal antibody against LN and ColIV. Hepatic non-parenchymal cells were isolated, total protein was extracted and separated by SDS-PAGE. MMP-2 and TIMP-1 protein expression was estimated by Western blotting.

RESULTS: The diameter (2.207 ± 0.096 *vs* 1.528 ± 0.054 mm, P<0.01) and pressure (11.014±0.395 *vs* 8.533±0.274 mmHg, P<0.01) of portal vein were significantly higher in model group than those in the control group. Plasma HA (129.97±16.10 *vs* 73.09±2.38 ng/mL, P<0.01), ColIV (210.49±4.36 *vs* 89.65±4.42 ng/mL, P<0.01) and LN (105.00±7.29 *vs* 55.70±4.32 ng/mL, P<0.01) were upregulated in model group. Abundant collagen deposited around the central vein of lobules, hepatic sinusoids and hepatocytes in model group. ColI and ColIII increased remarkably and perisinusoids were almost surrounded by ColIII. Immunohistochemical staining showed that ColIV protein level (0.130±0.007 *vs* 0.032±0.004, P<0.01) and LN protein level (0.152±0.005 *vs* 0.029±0.005, P<0.01) were up-regulated remarkably in model group. MMP-2 protein expression (2.306±1.089 *vs* 0.612±0.081, P<0.01) and TIMP-1 protein expression (3.015±1.364 *vs* 0.446±0.009, P<0.01) in freshly isolated hepatic non-parenchymal cells were up-regulated in model group and TIMP-1 protein expression was evidently higher than MMP-2 protein expression (2.669±0.170 *vs* 1.695±0.008, P<0.05).

CONCLUSION: Hepatic sinusoidal capillarization and peri-sinusoidal fibrosis are responsible for alcohol-induced portal hypertension in rats.

Key words: Alcoholic liver fibrosis; Portal hypertension; Hepatic sinusoidal capillarization; Perisinusoidal fibrosis

Li J, Niu JZ, Wang JF, Li Y, Tao XH. Pathological mechanisms of alcohol-induced hepatic portal hypertension in early stage fibrosis rat model. *World J Gastroenterol* 2005; 11(41):6483-6488
http://www.wjgnet.com/1007-9327/11/6483.asp

INTRODUCTION

In China, the number of patients with alcoholic liver fibrosis is increasing. It has been reported that about 20% of people with 10-20 years of alcohol drinking might develop alcoholic liver fibrosis[1]. Portal hypertension is a major complication of liver fibrosis and cirrhosis, which can lead to variceal bleeding, fluid retention and reduced renal blood flow, *etc.* being a major cause of death in patients with liver fibrosis. The pathological mechanisms of portal hypertension remain unclear. Recently, it has been found that pathological changes of hepatic microvasculature play a major role in the formation of portal hypertension[2]. Wang *et al*[3]. pointed out that alcohol might cause microvasculature obstruction and capillarization of hepatic sinusoids. Capillarization of the sinusoids is an early event in liver fibrogenesis, which is gradually formed by deposition of type IV collagen and LN in the perisinusoidal space and finally forms a complete and thick basement membrane[4]. When liver fibrosis occurs, it affects normal material exchange between blood and hepatocytes while the blood flow

resistance and portal hypertension ensue. Studies on the relation between alcoholic liver injury and portal hypertension are rarely available and the pathological mechanisms are still controversial. One of the popular hypotheses is that hepatic non-parenchymal cells might synthesize basement membrane proteins and take part in the formation of extra-cellular matrix (ECM)[5].

In order to understand the pathological mechanisms of alcohol-induced portal hypertension, we explored the possible changing rule by which ECM of perisinusoid basement membrane (types I, III and IV collagen and LN) abides. Moreover, the synthesis of MMP-2 and TIMP-1 protein in freshly isolated hepatic non-parenchymal cells and their correlation with portal hypertension were also investigated. Hopefully, this may provide new insights for the prevention of alcoholic liver fibrosis.

MATERIALS AND METHODS

Materials

Male SD rats weighing 160±10 g, were purchased from Vital River Experimental Animal Company (eligible certificate number: SCXK2002-2003). Pyrazole was purchased from Aldrich Chemical Company. Alcohol was purchased from Beijing Red Star Alcohol Ltd (concentration: 52%). Conventional corn oil was from the supermarket. Rabbit immunoglobulins directed against mouse ColIV, LN, MMP-2, and TIMP-1 were from Santa Cruz (USA). Secondary antibody (PV-6001) and DAB kit were purchased from Beijing Zhongshan Company. Unless specifically indicated, all other reagents were purchased from Beijing Chemical Agent Company.

Modeling alcoholic liver fibrosis

Fifty rats were divided into control group (n = 20) and model group (n = 30). Alcoholic liver fibrosis model was induced by intra-gastric infusion of a mixture containing alcohol, corn oil and pyrazole (1 000:250:3) as previously described[6,7]. The control rats received intra-gastric infusion of saline solution and had normal diet. Fifteen animals in each group were killed at wk 16.

Measurement of portal vein diameter and pressure

Rats were anesthetized with sodium pentobarbital (40 mg/kg, ip) and the abdomen was opened to expose the portal vein. Portal vein diameter and pressure were measured. The numerical value was recorded as previously described[8].

Radioimmunoassay of HA, ColIV and LN

Blood samples were obtained by abdominal aortic artery puncture for radioimmunoassay of HA, ColIV and LN using a standardized and optimized commercial radioimmunoassay kit.

Liver tissue collagen staining

Liver tissue was fixed in buffered formalin (10%) and embedded in paraffin. Sections (6-μm thick) were routinely stained with Mallory and Sirius Red, then observed under ordinary optical and polarization microscope.

Liver tissue immunohistochemical staining

Liver tissue sections were treated with 1% hydrogen peroxide, 0.1% proteinase K and 1% Triton X-100. The sections were reacted with 1:150 diluted rabbit polyclonal antibody against LN and ColIV overnight at 4 °C, then with PV-6001 kits for 2 h at room temperature (SP method).

Isolation of hepatic nonparenchymal cells

Hepatic non-parenchymal cells were isolated from male SD rats with proteinase E and collagenase digestion as described previously[9]. Following perfusion, hepatocytes were removed by low-speed centrifugation. Hepatic non-parenchymal cells were separated by density centrifugation in a Nycodenz (33%) gradient. Hepatic sinusoidal cells, Kupffer cells and hepatic stellate cells were harvested.

Western blotting

Hepatic non-parenchymal cells were treated with RIPA (50 mmol/L TrisHCl, 150mmol/L NaCl, 0.025% NaN_3, 0.1% SDS, 100 μg/mL PMSF, 1 mmol/L NaF, 1% NP-40, 2 mmol/L Na_3VO_4, 50mmol/L Hepes, 1% Triton X-100) to extract total protein. Total protein was detected with the BCA protein assay method. Total protein(12μg) was loaded into each lane. Cell extracts were separated by SDS-PAGE using a 12% gel and transferred onto a PVDF membrane. The membranes were blocked for 1 h at room temperature in 10 g/L BSA and incubated overnight at 4°C with surviving antibody(MMP-2 and TIMP-1), then with sheep anti-rabbit second antibody conjugated to horseradish peroxidase for 2 h. Finally the membranes were developed with DAB and incubated until color developed sufficiently. An equal amount of proteins was loaded onto the stocking gel, β-actin expression was simultaneously estimated in each sample as the internal marker by Western blotting using anti-actin monoclonal antibody.

Image analysis of immunohistochemical staining and Western blot results

Immunohistochemical staining results were analyzed by "5-point sampling" method using the Motic patho-image analysis system on 7 sections for each group. Under the same magnification (10×20), we collected 35 samples from each group, then measured the average facio-density (average facio-density = whole area of positive reaction grains/whole area of visual field). Western blotting results were analyzed by the Motic gel analysis system. We compared the gray scale value of target protein and internal marker to gain the relative optical density value.

Statistical analysis

SPSS version 10.0 was used. Data were analyzed using test and one-way ANOVA. All values were expressed as mean±SE. $P<0.05$ or <0.01 was considered statistically significant.

RESULTS

Changes of portal vein diameter and pressure

All data of portal vein diameter and pressure were collected and analyzed by a computer. The results are shown in Table 1. Portal vein diameter and pressure were significantly higher in model group than in control group ($^bP<0.01$)

Table 1 Comparison of portal vein diameter and pressure in control and model groups (mean±SE)

Group	*n*	Portal vein diameter (mm)	Portal vein pressure (mmHg)
Control	10	1.528 ± 0.054	8.533 ± 0.274 [b]
Model	10	2.207 ± 0.096	11.014 ± 0.395[b]

[b]*P*<0.01 *vs* control.

Plasma HA, ColIV and LN assay

Plasma HA, ColIV and LN levels were detectable by radioimmunoassay. The levels of plasma HA (129.97±16.10 *vs* 73.09±2.38 ng/mL), ColIV(210.49±4.36 *vs* 89.65±4.42 ng/mL) and LN(105.00 ±7.29 *vs* 55.70±4.32 ng/mL) were all up-regulated in model group compared to control group(*P*<0.01, Figure 1).

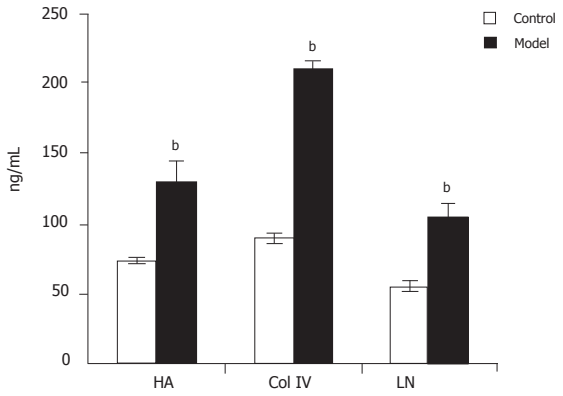

Figure1 Levels of plasma HA, ColIV and LN in model and control groups [b]*P*<0.01 *vs* control.

Results of Mallory and Sirius Red staining

More collagen was stained with Mallory in model group than in control group. Optical microscopy showed that there was only a little collagen around the central vein of lobules in control rats (Figure 2A). On the contrary, abundant collagen deposited around the central vein of lobules, hepatic sinusoids and hepatocytes in model group, which interweaved to form a net-shape pattern and connected with each other (Figure 2B). Polarization microscopy showed that ColIV was red or yellow while ColIV was green, suggesting that there was a small quantity of ColIV around the central vein of lobules in control rats (Figure 2C). But in model rats, ColIV and ColIV increased remarkably and perisinusoids were almost surrounded by increased ColIV (Figure 2D).

Immunohistochemical staining

The immune reaction for ColIV in normal liver was detected only at the level of portal tract and around the major central vein of lobules (Figure 2E). In alcoholic liver fibrosis tissue, positive ColIV was detected at the level of portal tract and in the central vein of lobules or in the Disse space between the sinusoid cells and hepatocytes (Figure 2F). Image analysis showed that the average facio-density of positive granules in ColIV of alcoholic liver fibrosis tissue was upregulated remarkably compared to the normal liver tissue (0.130±0.007 *vs* 0.032±0.004, *P*<0.01, Figure 3).

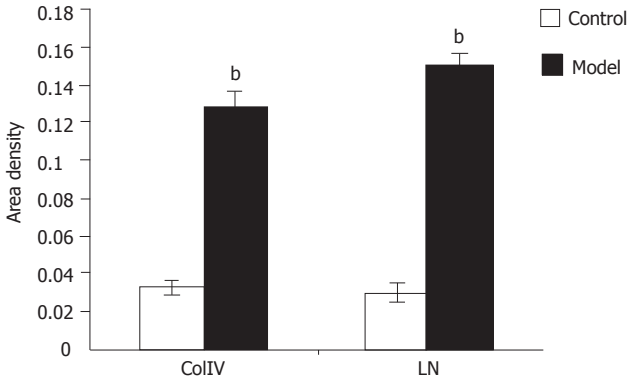

Figure 3 Density of ColIV and LN in positive granule area [b]*P*<0.01 *vs* control in model and co.

In normal liver tissue, a few LN positive cells were detected (Figure 2G). However, the LN positivity increased significantly in alcoholic liver fibrosis tissue. The LN positive granules deposited not only in the cytoplasm but also in the perisinusoidal area (Figure 2H). Image analysis showed that the average facio-density of positive granules in LN was upregulated remarkably compared to the normal liver tissue (0.1518±0.0058 *vs* 0.0299±0.0058, *P*<0.01, Figure 3).

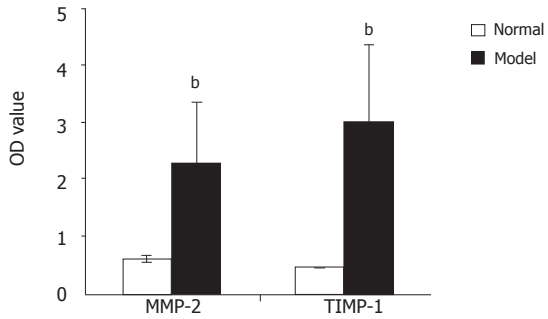

Figure 4 Comparison of MMP-2 and TIMP-1 protein expression in hepatic non-parenchymal cells between model and control groups[b]*P*<0.01, model group *vs* control group; [c]*P*<0.05, TIMP-1 *vs* MMP-2.

Western blotting analysis

Western blotting analysis showed that MMP-2 and

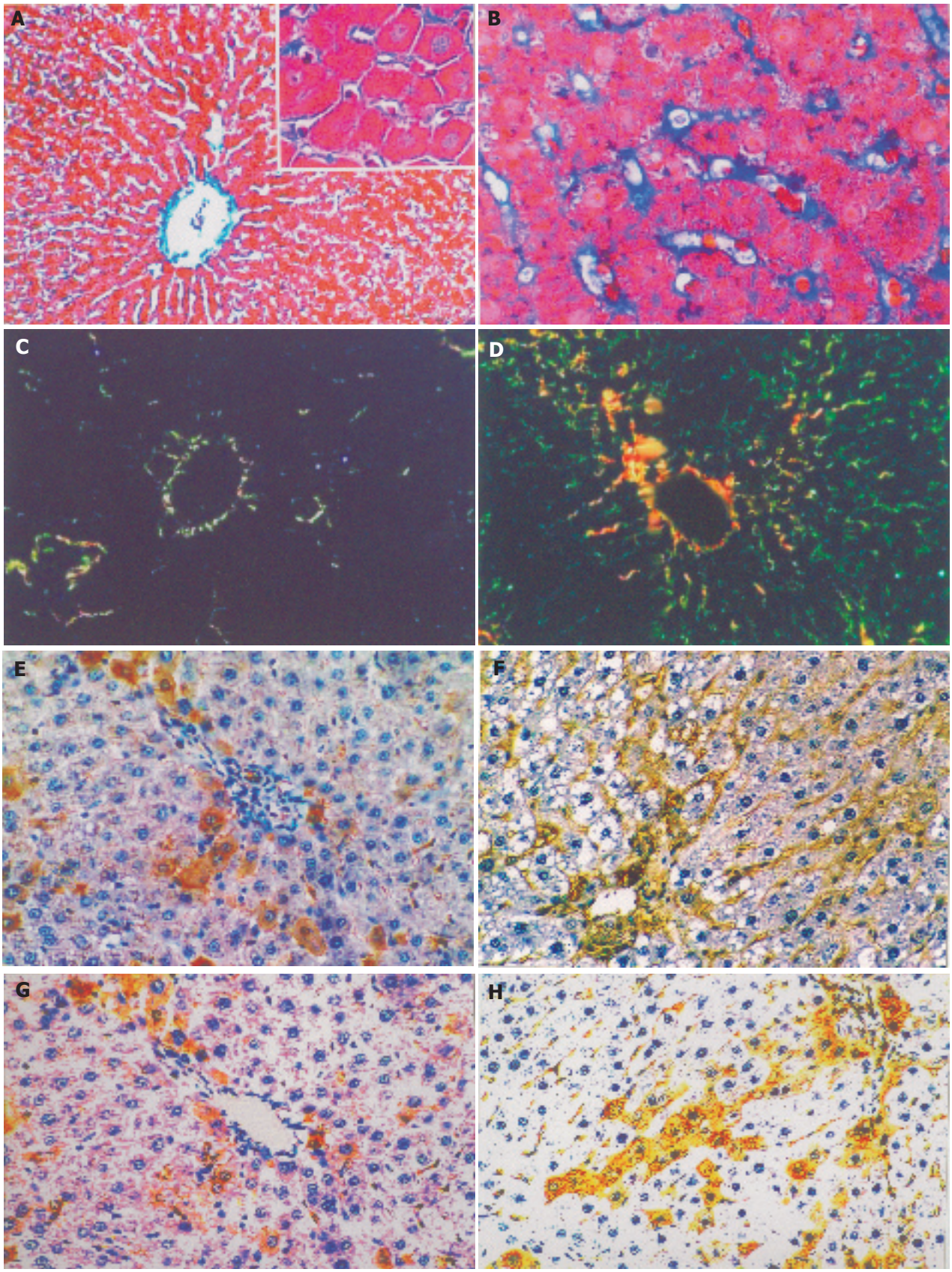

Figure 2 Mallory, Sirius Red and immunohistochemical staining of liver tissue. **A:** Mallory staining of normal rat liver tissue, ×200 **B:** Mallory staining of rat alcoholic fibrosis liver tissue, ×400 **C:** Sirius Red staining of normal rat liver tissue and polarization microscopy, ×200 **D:** Sirius Red staining of rat alcoholic fibrosis liver tissue and polarization microscopy, ×200 **E:** Immunohistochemical staining of the first antibody of ColIV of normal rat liver tissue, ×200 **F:** Immunohistochemical staining of the first antibody of ColIV rat alcoholic liver fibrosis tissue, ×200 **G:** Immunohistochemistry staining of the first antibody of LN in normal rat liver tissue, ×200 **H:** Immunohistochemical staining of the first antibody of LN in rat alcoholic liver fibrosis tissue, ×200.

TIMP-1 proteins were significantly up-regulated in rat fibrosis liver tissue compared to control group (2.306±1.089 *vs* 0.612±0.081 and 3.015±1.364 *vs* 0.446±0.009, $P<0.01$). Image analysis of rat fibrosis liver tissue showed that protein expression was higher in TIMP-1 than in MMP-2 (2.669±0.170 *vs* 1.695±0.008, $P<0.05$, Figure 4).

DISCUSSION

In this study, portal vein pressure increased significantly in the early stage of alcoholic liver fibrosis. ColI, ColIII, ColIV and LN levels were increased in the ECM of basement membrane. Furthermore, TIMP-1 protein level was increased in hepatic non-parenchymal cells isolated from alcoholic liver fibrotic tissue, suggesting that the major pathological changes are capillarization of hepatic sinusoids and perisinusoidal fibrosis in early stage of alcoholic liver fibrosis.

Some studies demonstrated that kupffer cells, hepatic stellate cells (HSC) and sinusoidal endothelial cells (SEC) play a key role in the synthesis or decomposition of extra cellular matrix (ECM)[10,11]. Others believe that the levels of serum hyaluronate are strongly related to SEC injury and hepatic microcirculation disorders[12]. Serum hyaluronate is a better index of morphological and functional changes in SECs. Our results showed that the level of rat serum hyaluronate increased remarkably in the early stage of alcoholic liver fibrosis, indicating that SECs are severely injured. When SECs get injured, a large number of inflammatory leucocytes move to the injured sinusoids and trigger the self-recovery process. Therefore, the ECM of basement membrane increases and enwraps the injured sinusoids in order to defend against inflammatory leucocytes. After repeated injury, over-recovery emerges and the ECM of basement membrane including type I, III, IV collagen and LN is over-deposited in perisinusoid[13,14]. Deposition of type I, III, IV collagen and LN reduces hepatic sinusoidal penetration and causes sinusoidal capillarization[15].

Hepatic sinusoids are special capillaries that are limited by fenestrated endothelial cells without a genuine basement membrane and surrounded by perisinusoidal cells storing vitamin A and Kupffer cells as well as pit cells, resident macrophages and large granular lymphocytes[16]. Hepatic sinusoidal capillarization includes a series of pathological changes, in which SECs lose fenestrae, basement membrane develops and sinusoidal outlets collapse[17]. All these pathological changes disable the normal sinusoid intrinsic functions[18]. Capillarization of the sinusoid may cause a disturbance in the exchange of many bioactive substances between the sinusoidal blood and hepatocytes across the Disse space, contributing to the pathogenesis of alcoholic liver fibrosis. On the other hand, with the occurrence of sinusoidal capillarization, the sinusoidal space is significantly narrowed and the sinusoidal endothelial fenestrations are decreased in size and number or disappear in the end. All these pathological changes increase resistance of the hepatic vascular bed and pressure of hepatic portal vein.

Additionally, the breakdown of ECM is essential for tissue remodeling. The matrix metalloproteinases (MMPs), also called matrixins, are thought to play a central role in these processes[19]. The activities of MMPs are precisely controlled during the activation from their precursors and inhibited by tissue inhibitors of metalloproteinases (TIMPs)[20]. MMP-2 is secreted from Kupffer cells and HSCs as they become activated. Also, the activation of MMP-2 is in turn inhibited by TIMP-1. Generally, TIMP-1 and MMP-2 affect biological functions by non-covalent bond [20]. At the early stage of alcoholic liver fibrosis, with the activation of Kupffer cells and HSCs, the level of MMP-2 expression increases. MMP-2 can decompose type I, III, IV collagen and assist Kupffer cells, HSCs and SECs to activate and transfer. Emmanouil *et al*[21]. showed that increased MMP-2 could decompose the basal membrane of neighboring SECs. The signal of injured SECs triggers the mechanisms of TIMP synthesis to balance the levels of MMPs. However, while repeated injury occurs, the synthesis of ECM becomes stronger than decomposition[22,23]. We examined the expression of MMP-2 and TIMP-1 protein in freshly isolated hepatic non-parenchymal cells of normal and fibrotic rats by Western blotting. The results showed that the levels of MMP-2 and TIMP-1 protein expression were upregulated in the early stage of alcoholic liver fibrosis, the level of TIMP-1 was significantly higher than that of MMP-2, suggesting that the synthesis of basal membrane collagen is stronger than decomposition and more and more ECMs of the basement membrane are synthesized due to the inhibition deposit around SECs and hepatocytes of MMPS[24]. This in turn induces perisinusoidal fibrosis and causes aggravating portal hypertension[25,26]. The therapy of alcohol-induced liver disease varies according to the severity of histological liver damage and clinically overt portal hypertension and hepatic dysfunction[27,28]. Only a few studies have been conducted on alcohol-induced portal hypertension in the past decades[29,30]. Our experimental results showed that hepatic portal hypertension occurred earlier than alcohol-induced cirrhosis, suggesting that hepatic portal hypertension plays a potential role in cirrhosis.

In conclusion, hepatic sinusoidal capillarization and perisinusoidal fibrosis are the vital causes for alcohol-induced portal hypertension in rats. A thorough evaluation of hepatic microcirculation and anti-capillarization may provide the basis for new therapeutic avenues.

REFERENCES

1 **Lu XL,** Luo JY, Tao M, Gen Y, Zhao P, Zhao HL, Zhang XD, Dong N. Risk factors for alcoholic liver disease in China. *World J Gastroenterol* 2004; **10:** 2423-2426
2 **Wang Xb,** Liu P, Tang ZP, Lu X, Liu CH, Hu YY, Xu LM, Gu H-T, Liu CH. Study on the mechanisms of development of hepatic sinusoidal capillarization. *Zhonghua Xiaohua Zazhi* 2004; **24:** 289-292
3 **Wang BY,** Fu BY, Zhang J, Ju XH, Cao YX. The influence of alcohol on the liver sinusoids endothelial cell fenestrae of rats *Zhonghua Gan Zang Bing Za Zhi* 2004; **12:** 479-481
4 **Xu GF,** Wang XY, Ge GL, Li PT, Jia X, Tian DL, Jiang LD,

Yang JX. Dynamic changes of capillarization and peri-sinusoid fibrosis in alcoholic liver diseases. *World J Gastroenterol* 2004; **10:** 238-243

5 **Neubauer K,** Kruger M, Quondamatteo F, Knittel T, Saile B, Ramadori G. Transforming growth factor-beta1 stimulates the synthesis of basement membrane proteins laminin, collagen type IV and entactin in rat liver sinusoidal endothelial cells. *J Hepatol* 1999; **31:** 692-702

6 **Lin H,** Lu M, Zhang YX, Wang BY, Fu BY. Induction of a rat model of alcoholic liver diseases. *Shijie Huaren Xiaohua Zazhi* 2001; **9:** 24-28

7 **Ding X,** Meng YC, Ben CE, Tian DL. Induction of alcoholic liver fibrosis animal model. *Zhongguo Zhongyi Jichu Yixue Zazhi* 1999; **5:** 47-48

8 **Scorticati C,** Prestifilippo JP, Eizayaga FX, Castro JL, Romay S, Fernández MA, Lemberg A, Perazzo JC. Hyperammonemia, brain edema and blood-brain barrier alterations in prehepatic portal hypertensive rats and paracetamol intoxication. *World J Gastroenterol* 2004; **10:** 1321-1324

9 **Zhang X,** Yu WP, Gao L, Wei KB, Ju JL, Xu JZ. Effects of lipopolysaccharides stimulated Kupffer cells on activation of rat hepatic stellate cells. *World J Gastroenterol* 2004; **10:** 610-613

10 **Zimmermann A,** Zhao D, Reichen J. Myofibroblasts in the cirrhotic rat liver reflect hepatic remodeling and correlate with fibrosis and sinusoidal capillarization. *J Hepatol* 1999; **30:** 646-652

11 **Kimura H,** Mochida S, Inao M, Matsui A, Fujiwara K. Angiopoietin/tie receptors system may play a role during reconstruction and capillarization of the hepatic sinusoids after partial hepatectomy and liver necrosis in rats. *Hepatol Res* 2004; **29:** 51-59

12 **Hao JH,** Shi J, Ren WH, Han GQ, Zhang JR, Wang WZ, Wang SY, Wang YH. The relationship between serum hyaluronate level and hepatic microcirculation status. *Linchuang Ganbing Zazhi* 2002; **18:** 35-37

13 **Xu GF,** Tian DL. Progressive of hepatic sinusoidal capillarization. *Zhongguo Zhongxiyi Jiehe Zazhi* 2002; **10:** 314-316

14 **Jia YT,** Zeng MD. Progressive on hepatic sinusoidal capillarization. Guowai Yixue: Xiaohuadao Jibing 2000; 20: 86-90

15 **Reichen J.** The role of the sinusoidal endothelium in liver function. *News Physiol Sci* 1999; **14:** 117-121

16 **Paolo Onori,** Sergio Morini, Antonio Franchitto, Robert Sferra, Domenico Alvaro, Eugenio Gaudio. Hepatic microvascular features in experimental cirrhosis: a structural and morphometrical study in CCl4-treated rats. *J Hepatol* 2000; **33:** 555-563

17 **Xiao W,** Wang Y, Liu X. The coordinated expression of laminin and its integrin receptor in hepatic sinusoidal capillarization. *Zhonghua Neike Zazhi* 2001; **40:** 618-620

18 **Nakashima O,** Kurogi M, Yamaguchi R, Miyaaki H, Fujimoto M, Yano H, Kumabe T, Hayabuchi N, Hisatomi J, Sata M, Kojiro M. Unique hypervascular nodules in alcoholic liver cirrhosis: identical to focal nodular hyperplasia-like nodules? *J Hepatol* 2004; **41:** 992-998

19 **Arthur MJ.** Fibrogenesis II. Metalloproteinases and their inhibitors in liver fibrosis. *Am J Physiol Gastrointest Liver Physiol* 2000; **279:** G245-G249

20 **Nagase H,** Woessner JF. Matrix metalloproteinases. *J Biol Chem* 1999; **274:** 21491-21494

21 **Karagiannis ED,** Popel AS. A theoretical model of type I collagen proteolysis by matrix metalloproteinase 2 and membrane type 1 MMP in the presence of tissue inhibitor of metalloproteinase 2. *J Biol Chem* 2004; **279:** 39105-39114

22 **Vaillant B,** Chiaramonte MG, Cheever AW, Soloway PD, Wynn TA. Regulation of hepatic fibrosis and extracellular matrix genes by the th response: new insight into the role of tissue inhibitors of matrix metalloproteinases. *J Immunol* 2001; **167:** 7017-7026

23 **Murphy FR,** Issa R, Zhou X, Ratnarajah S, Nagase H, Arthur MJ, Benyon C, Iredale JP. Inhibition of apoptosis of activated hepatic stellate cells by tissue inhibitor of metalloproteinase-1 is mediated via effects on matrix metalloproteinase inhibition: implications for reversibility of liver fibrosis. *J Biol Chem* 2002; **277:** 11069-11076

24 **Li J,** Niu JZ, Zeng Y, Yang MJ, Tao XH, Wang JF. Effects of FFBJRGP on collagen deposition in hepatic Disse space in alcohol induced liver fibrosis in rat. *Jiefangjun Yixue Zazhi* 2004; **29:** 567-570

25 **Lu X,** Liu P, Xu GF, Liu CH, Li FH, Liu C. The role of hepatic sinusoid capillarization during the formation of portal hypertension in fibrotic rats induced by dimethylnitrosamine *Zhonghua Gan Zang Bing Za Zhi* 2003; **11:** 595-598

26 **Zhang RP,** Zhang WH, Xue DB, Wei YW. Morphology of portal hypertension at the early stage of liver damage induced by CCl4: an experimental study with dogs *Zhonghua Yi Xue Za Zhi* 2004; **84:** 1118-1121

27 **Xu B,** Broome U, Uzunel M, Nava S, Ge X, Kumagai-Braesch M, Hultenby K, Christensson B, Ericzon BG, Holgersson J, Sumitran-Holgersson S. Capillarization of hepatic sinusoid by liver endothelial cell-reactive autoantibodies in patients with cirrhosis and chronic hepatitis. *Am J Pathol* 2003; **163:** 1275-1289

28 **Patch D,** Armonis A, Sabin C, Christopoulou K, Greenslade L, McCormick A, Dick R, Burroughs AK. Single portal pressure measurement predicts survival in cirrhotic patients with recent bleeding. *Gut* 1999; **44:** 264-269

29 **Mookerjee RP,** Sen S, Davies NA, Hodges SJ, Williams R, Jalan R. Tumor necrosis factorα is an important mediator of portal and systemic haemodynamic derangements in alcoholic hepatitis. *Gut* 2003; **52:** 1182-1187

30 **Diehl AM.** Liver disease in alcohol abusers: clinical perspective. *Alcohol* 2002; **27:** 7-11

Science Editor Wang XL and Guo SY **Language Editor** Elsevier HK

PO Box 2345, Beijing 100023, China
www.wjgnet.com
wjg@wjgnet.com

ELSEVIER

World J Gastroenterol 2005;11(41):6489-6494
World Journal of Gastroenterology ISSN 1007-9327

• *BASIC RESEARCH* •

Effects of angiotensin II receptor antagonist, Losartan on the apoptosis, proliferation and migration of the human pancreatic stellate cells

Wen-Bin Liu, Xing-Peng Wang, Kai Wu, Ru-Ling Zhang

Wen-Bin Liu, Xing-Peng Wang, Kai Wu, Ru-Ling Zhang, Shanghai No. 1 People's Hospital, Shanghai Jiaotong University, Shanghai 200080, China
Supported by Shanghai Sanitary Bureau Foundation, No. 40306
Correspondence to: Xing-Peng Wang, Shanghai No. 1 People's Hospital, Shanghai Jiaotong University, Shanghai 200080, China. wangxp1965@yahoo.com.cn
Telephone: +86-21-63240090-4706 Fax: +86-21-63240825
Received: 2004-12-30 Accepted: 2005-02-18

Abstract

AIM: To investigate the effects of AT_1 (Type 1 angiotensin II receptor) antagonist (Losartan) on the apoptosis, proliferation and migration of the human pancreatic stellate cells (hPSCs).

METHODS: hPSCs were isolated from pancreatic sample of patients with pancreatic carcinoma using radioimmunoassay (RIA) technique to detect the concentration of AngII in culture media and cell homogenate. Immunocytochemistry (ICC) and *in situ* hybridization (ISH) methods were utilized to test AT_1 expression in hPSCs. Effects of Losartan on hPSCs proliferation, apoptosis and migration were investigated using BrdU incorporation, TUNEL, flow cytometry (FCM), and phase-contrast microscope separately when cells treated with Losartan. Immunofluorescence and Western blot were applied to quantify the expression of type I collagen in hPSCs.

RESULTS: There exists AT_1 expression in hPSCs, while no AngII was detected in culture media and cell homogenate. Losartan induces cell apoptosis in a dose- and time-dependent manner (apparently at 10^{-5} mol/L), no pro-proliferative effect was observed in the same condition. Corresponding dosage of Losartan can also alleviate the motion capability and type I collagen content of hPSCs compared with AngII treatment and non-treatment control groups.

CONCLUSION: These findings suggest that paracrine not autocrine functions of AngII may have effects on hPSCs, which was mediated by AT_1 expressed on cells, while Losartan may exert anti-fibrotic effects by inhibiting hPSCs motion and partly by inducing apoptosis.

Key words: Pancreatic stellate cell; Angiotensin II receptor; Antagonist; Losartan

Liu WB, Wang XP, Wu K, Zhang RL. Effects of angiotensin II receptor antagonist, Losartan on the apoptosis, proliferation and migration of the human pancreatic stellate cells. *World J Gastroenterol* 2005; 11(41):6489-6494
http://www.wjgnet.com/1007-9327/11/6489.asp

INTRODUCTION

Fibrosis is a dynamic process in which both altered matrix degradation and abnormal extracellular matrix (ECM) protein synthesis play key roles[1,2]. Chronic pancreatitis is accompanied by progressive fibrosis that is characterized by the loss of functional tissue and its replacement by ECM, while the molecular mechanisms of pancreatic fibrogenesis remain to be elucidated.

In 1998, star-shaped cells in the pancreas, namely PSCs, were identified and characterized[3,4]. These cells like their counterparts, hepatic stellate cells (HSCs) and pancreatic stellate cells (PSCs) are responsible for the development of pancreatic fibrosis. Meanwhile, many of the morphological and metabolic changes associated with the activation of PSCs in animal models of fibrosis also occur when these cells are grown in culture on plastics. Therefore, a culture of primary PSCs on plastics has been accepted as a model that mimics the *in vivo* process of PSC activation following pancreatic injury[5].

Numerous studies have emphasized the important role of the local Renin-angiotensin system (RAS) in the fibrogenesis that occurs in the setting of chronic kidney or cardiac diseases and the antifibrogenic effect of therapies with AT_1 blockers or angiotensin-converting enzyme (ACE) inhibitors in this condition. Recent study has shown that AngII may induce apoptosis in some type of cells triggered by the interaction with AT_1[6]. Also, AngII can promote cell migration even though the mechanism is still unclear. A local RAS has been described in the pancreas[7-9]. Though apoptosis, migration and proliferation of human pancreatic stellate cells (hPSCs) might affect the pancreatic fibrotic process, it has reason to hypothesize that AngII and AT_1 may participate in this process by different mechanisms.

The present study attempts to investigate the effects of Losartan, an antagonist of AT_1 on hPSCs, providing laboratory data for interfering pancreatic fibrosis.

MATERIALS AND METHODS

Cell isolation and culture

hPSCs were isolated from pancreatic sample of patients

with pancreatic carcinoma (kindly gifted by Prof. Bachem MG)[4], culturing in a 95% air and 50 mL/L CO_2 incubator at 37 ℃ with DMEM containing 10% FCS supplemented with 100 U/mL penicillin,100 μg/mL streptomycin and 2 mmol/L L-glutamine.

AngII level in culture media and cell homogenate

Cell homogenate and culture media were taken and kept at -30 ℃ for assays. The levels of AngII were determined by radioimmunoassay (RIA) method following the company directions (Northern Biot Co, China).

ICC Staining of AT_1

For analysis of AT_1 expression, cells were fixed with acetone for 5 min, exposed to a rabbit anti-human AT_1 antibody (4 ℃ overnight, 1∶200 in PBS, Boster, Wuhan, China), washing and incubating with an anti-rabbit secondary antibody (37 ℃, 2 h, 1∶200 in PBS, Dako, USA) and with the substrate solution (DAB in H_2O_2 in Tris buffer pH 7.4) for 15 min after repeating the above-mentioned steps. Pictures were visualized and taken with microscope (Olympus, Japan) and camera (Japan). For control staining, PBS was used instead of the primary antibody.

ISH for AT_1

In situ hybridization (ISH) kit (Boster, Wuhan, China) was used to detect AT_1 expression in hPSCs, Briefly, slides were incubated with the probe and a biotinylated secondary antibody subsequently. The bound antibody was visualized with an indirect biotin streptavidin system coupled to alkaline phosphatase and were detected by the DAB reagent. Human heart tissue was used as a positive control and the sense probes (included in kit) were used as a negative control.

Apoptosis evaluation of hPSCs

Immunocytochemistry (ICC) detection of apoptotic cells was carried out with the use of TUNEL, in which residues of digoxigenin-labeled dUTP are catalytically incorporated into the DNA by terminal deoxynucleotidyl transferase II. After treatment with Losartan (Merck & Co, New Jersey, USA) in different concentrations (10^{-9}, 10^{-7}, 10^{-5} and 10^{-3} mol/L), the slides were fixed and washed thrice in 0.01 mol/L PBS, the following procedures were performed according to the manufacturer's guidance (Boster, Wuhan, China). The positive particles of DAB staining were viewed with a microscope (Olympus Japan). The number of apoptotic cells was counted and expressed as a percentage of total hPSCs population. Next, after a certain concentration of Losartan treatment, harvested cells were washed twice with PBS (0.01 mmol/L, pH 7.4), and the cells were resuspended in bind buffer to a final concentration of 1×10^6 cells/mL. Annexin-V FITC/PI solution (Roche, Germany) was added, which can stain the damaged DNA in apoptotic cells, and then the cells were kept in a dark place at room temperature for 15 min. Quantitative analysis for apoptosis was performed with regular flow cytometry (FCM)[10].

Cell proliferation assessment

The effect of Losartan on hPSCs proliferation was determined by BrdU incorporation and cell counting. After being cultured for 3 d on glass slides, hPSCs were incubated with Losartan (a series of final concentrations 10^{-9}, 10^{-8}, 10^{-7} mol/L) for 48 h. Each concentration included six wells, cells being cultured for 48 h firstly, and then supplemented with BrdU (Boster, Wuhan, China) at 1×10^{-5} mmol/L. After 24 h, slides were stained according to the protocol. Positive signals were visualized by DAB reagent plus substrate intensifier. Five random areas of the slides were chosen for counting stained and unstained hPSCs nuclei [positive cells/(negative+positive cells)×100].

Migration study

Cell migration was assessed by an *in vitro* wound-healing assay. For the wound-healing assay, hPSCs were cultured until confluence on 35 mm-diameter culture dishes. Cells were serum-starved for 24 h, and a 2-mm wide linear wound was cleared. Cells were then incubated with AngII (10^{-8}mol/L, Sigma, USA), AngII (10^{-8} mol/L) plus Losartan (10^{-7} mol/L) for 24 h[11]. Cells migrating into the wound were detected using a phase-contrast microscope.

Western blotting

Western blotting was performed under standard conditions. Briefly, hPSCs (1×10^6) were cultured in 60 mm culture dishes, and were stimulated with AngII (10^{-7} mol/L) and AngII plus Losartan (10^{-6} mol/L) separately for 24 h, 4 mL of the cell media as precipitated with 0.76 g of sodium sulfite at 4 ℃ for 4 h and then centrifuged at 12 000 *g* for 30 min. Pellets were resuspended in buffer (containing 50 mmoL Tris-Cl, 50 mmol DTT, 2% SDS, 0.1% bromophenol blue, 10% glycerol), protein concentrations were determined by BCA protein assay (Pierce, IL). Protein samples were heated for 5 min at 100 ℃ and were subjected to electrophoresis on a 8% acrylamide gel, and transferred to PVDF membrane (Schleicher&Schuell, Germany). The membrane was blocked in 50 mL/L non-fat dried milk in TBS buffer for 2 h at 20 ℃, then membrane was incubated overnight at 4 ℃ with rabbit anti-human collagen type I antibody (diluted 1∶200 in TBS buffer; Boster, Wuhan China) and for 60 min with corresponding horseradish-conjugated secondary antibodies (Santa Cruz, USA) at room temperature. Membrane was washed thrice in Tris-buffered saline containing 1% Tween-20 for 10 min after each of the steps. The protein bands were visualized with ECL chemiluminescence system.

Immunofluorescent staining for collagen type I

hPSCs grew in chamber slides fixed with 2% paraformaldehyde, permeabilized by 0.1% Triton X-100. For non-specific binding site blocking, 1∶50 normal goat serum was applied for 10 min, and then incubated with primary antibody for type collagen I (Boster, Wuhan, China) at 4 ℃ overnight, biotinylated secondary antibody and streptavidin-conjugated FITC (Southern Biotechnology Association, Birmingham, USA) were used to intensify the images. Images were taken by fluorescent microscope (Olympus, Japan).

Statistical analysis

Data values we expressed as mean±SD, these experiments were performed in triplicate for each of the six samples.

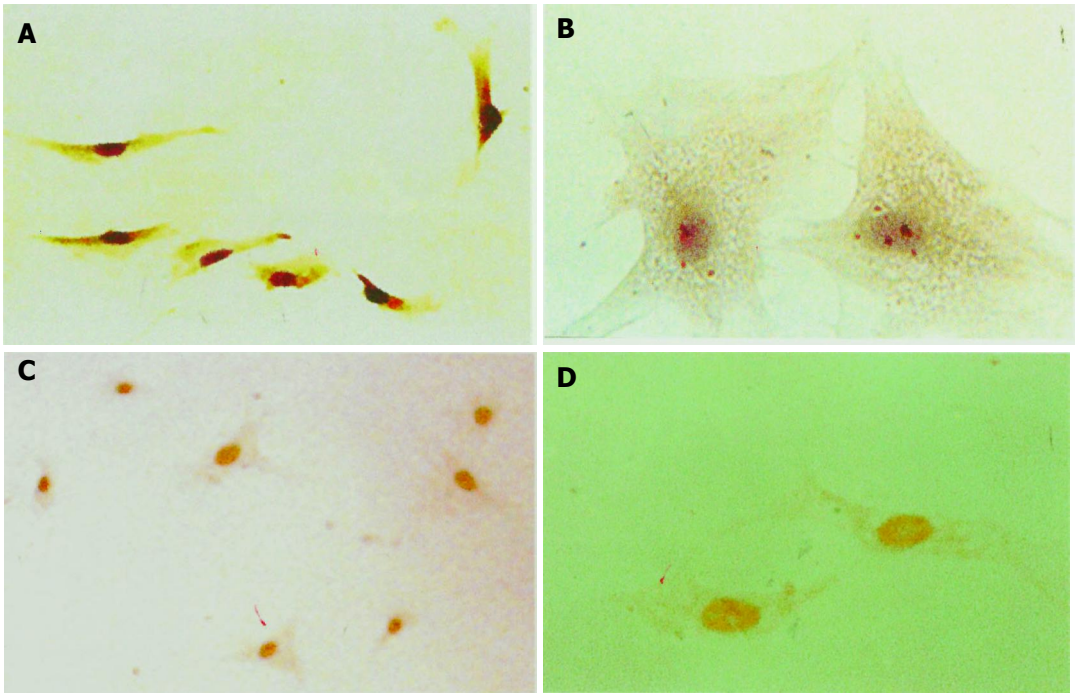

Figure 1 Immunocytochemistry and ISH detection of AT_1 in hPSCs at protein and mRNA levels. Immunostaining positive particles were located in plasm, **A** (magnification ×100); **B** (magnification ×400). ISH positive signals were located in nuclei **C** (magnification ×100); **D** (magnification ×400).

Statistical analysis was performed with a two-tailed Student's *t* test, and $P<0.05$ was considered statistically significant.

RESULTS

AT_1 expression and AngII concentration in hPSCs

hPSCs were cultured for 14 d (activated PSCs), immunostaining revealed that positive signals for AT_1 were located in cell plasm as shown (in Figures 1A and B). ISH assay shows positive nuclei in hPSCs at mRNA level, and representative examples of ISH staining are shown (in Figures 1C and D). AngII was not detected in the culture media or cell homogenate by RIA.

Effects of Losartan on hPSCs

TUNEL staining results suggest a marked increase in apoptotic cell death in Losartan treatment groups in a dosage-dependent manner compared to PBS treatment group (Figure 2).

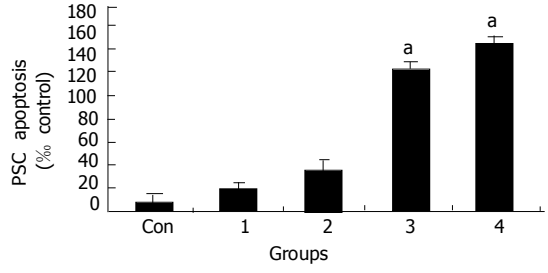

Figure 2 Dose-dependent induction of apoptosis by Losartan at different concentrations. (Con, 1 = 10^{-9}, 2 = 10^{-7}, 3 = 10^{-5}, 4 = 10^{-3} mol/L; $^aP < 0.05$ *vs* different from all groups).

The percentage of apoptotic cell induced by Losartan (Figure 3) was achieved using FCM (EpicsXL Coulter, USA). In the two-dimensional histogram the horizontal axis shows Annexin-V binding and the vertical axis shows PI uptake. The percentage of cells are indicated in the apoptotic quadrant (bottom right). Apoptosis began 24 h after certain dosage of Losartan (10^{-5} mol/L) treatment, and the percentage of apoptotic hPSCs rose from 3.7% (24 h) to 13.1% (72 h) during treatment.

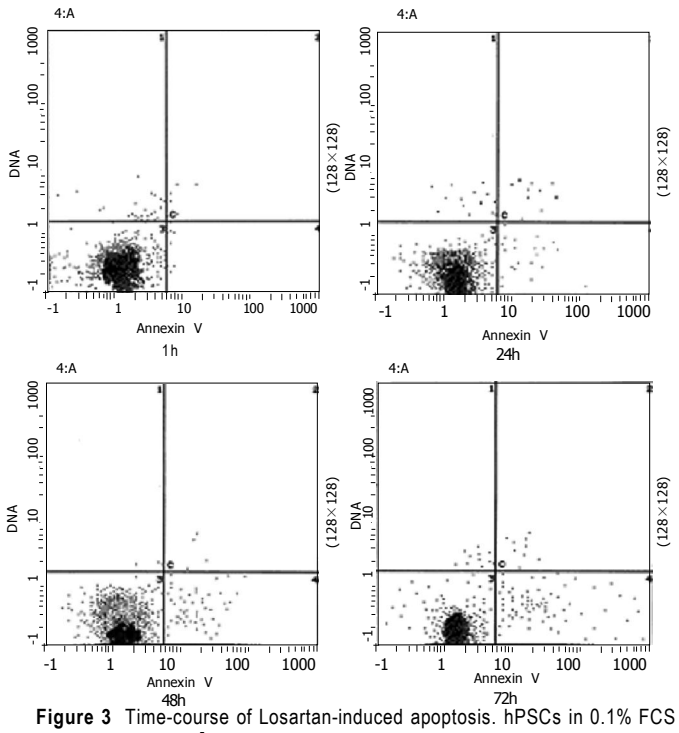

Figure 3 Time-course of Losartan-induced apoptosis. hPSCs in 0.1% FCS were exposed to 10^{-5} mol/L Losartan, and was assessd at 24, 48,72 h. Results indicate that Losartan induces apoptosis in a time-dependent manner.

The BrdU labeling index in control cells was 3.5±0.8%. Treatment with Losartan did not increase the labeling indices (4.7±1.1%, 3.6±0.7%, 4.3±0.5%, Figure 4).

Migration of hPSCs was assessed with an *in vitro* wound-healing assay. AngII (10^{-8} mol/L) and 10% FCS induced migration of hPSCs into the wound. This effect might be inhibited by Losartan (10^{-7} mol/L)[10], as demonstrated by the assay. Images are representative of this experiment (Figure 5).

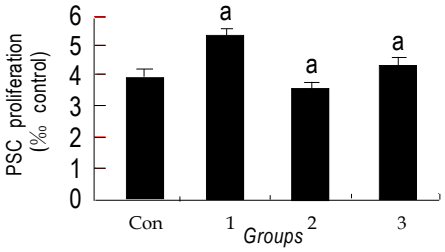

Figure 4 Effects of Losartan on hPSCs proliferation assessed with BrdU incorporation. Losartan itself did not affect cell proliferation compared to control group. (^aP>0.05 different from all the groups).

Western blotting and immunofluorescence assay for collagen type I

The collagen type I level was substantially down-regulated after 10^{-6} mol/L Losartan treatment in hPSCs. In contrast, levels of collagen were higher in control groups, and the same results were shown by immunofluorescence assay (Figure 6).

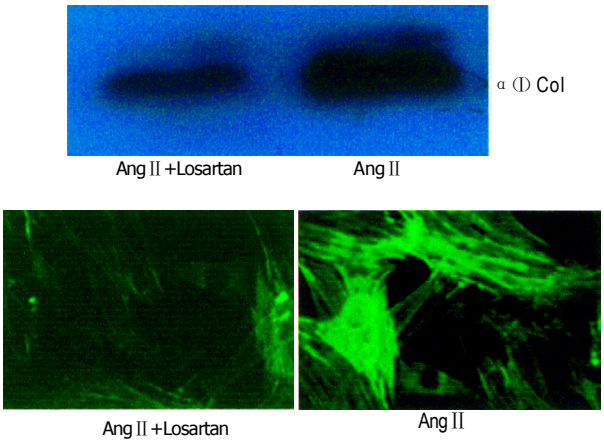

Figure 6 Losartan down-regulated collagen I protein expression by western blot and immunofluoresence. hPSCs were incubated with 10^{-6} mol/L Losartan. Samples were exposed to certain concentration of Losartan+AngII and AngII for 24 h.

DISCUSSION

Chronic pancreatitis is an irreversible progressive disease characterized by the destruction of acinar and ductule cells. Increased accumulation of ECM is a histologic characteristic of chronic pancreatitis that results in pancreatic fibrosis[12,13].

The molecular mechanisms resulting in the fibrosis in pancreas remain unknown. PSCs may participate in matrix remodeling through the regulation of ECM production and matrix degradation. Like his counterpart HSCs, it is now

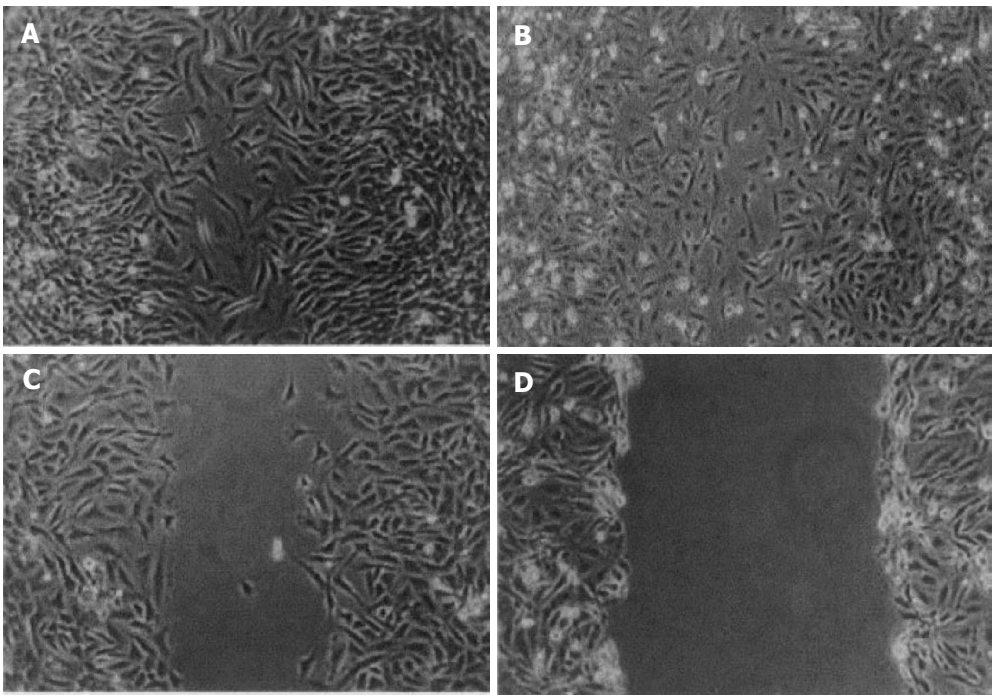

Figure 5 AngII accelerates *in vitro* wound healing confluent, culture-activated PSCs were serum deprived for 48 h. A wound was produced in the monolayer with a pipette tip, and the cells were exposed to (**A**) AngII (10^{-8} mol/L), (**B**) 10% fetal bovine serum, (**C**) AngII + Losartan, (**D**) serum-free medium along 24 h later, the cells were photographed.

generally accepted that PSCs are major ECM producing cells in the pancreas[14,15]. On activation by different stimuli, such as growth factor, cytokines, ethanol, oxidative stress, PSCs produce a large amount of ECM proteins. Increasing synthesis of ECM results from the number of PSCs, determined by the balance of cell proliferation and apoptosis, or cells migrating from non-injured areas to injured areas. Apoptosis, proliferation and migration of PSCs must play a crucial role in pancreatic fibrotic process.

Recent evidence indicates that AngII plays a role in liver fibrogenesis[16]. The AngII is locally expressed in injured livers, and AngII inhibition attenuates experimental liver fibrosis[17]. AngII is able to induce contraction and proliferation of HSCs[18], and also increase the expression of collagen I in lung fibroblasts[19]. Recently, it was shown that ACE inhibitor suppressed progression of hepatic fibrosis in rats[18]. In addition, AngII and AT_1 interaction results in hepatic fibrosis, which could be suppressed by AT_1 antagonist *in vivo* and *in vitro*[16]. Since the pathophysiologic process of pancreatic fibrosis is similar to hepatic fibrosis, and the hPSCs are a counterpart of HSCs, we hypothesize that AngII participates in pancreatic fibrogenesis, though the mechanisms underlying the fibrogenic action of AngII in the pancreas merit further investigation. We speculated that AngII and AT_1 also play an important role in the fibrogenesis of pancreas, so the expression of AT_1 in PSCs was assessed in our study.

It is reported that increased AngII may affect activation and proliferation of PSCs[20]. Therefore, we propose a link between AngII and PSCs during pancreatic fibrosis. While the effects of AngII on cells are mediated by interaction with its receptor (mainly AT_1), we here present evidence that hPSCs express AT_1 at protein and mRNA level, this finding suggests that AngII could exert biological actions in these cells. Moreover we found that no AngII was detected by RIA either in culture media or in hPSCs homogenate, indicating that it is paracrine but not autocrine function of AngII interacting with AT_1 in hPSCs, which plays a role in pancreatic fibrosis. In injured areas of pancreas, the level of AngII alleviate apparently. We observed that AngII derived from exogenous pathway could promote hPSCs migration, which is an important way for increasing hPSCs number in these areas, and this process can be blocked with certain concentration of Losartan. We know that AngII may modulate the re-organization of actin and vinculin through Paxillin and other downstream molecules such as small Rho family members after combining to a certain membrane receptor, leading to cell polarity and migration[21,22]. hPSCs migrating from uninjured areas accumulate in the injured area, and participate in ECM secretion and fibrotic formation[23,24]. The inhibitory effect of Losartan might be attributed to AngII receptor intervention. However, the precise modulating mechanisms still need to be elucidated.

It is well accepted that AngII can induce apoptosis through AT_1 in some cell types, and this apoptotic process could be alleviated with Losartan[25]. AT_1 and AT_2 are two subtypes receptor of AngII. The AT_1 regulates vasoconstriction and sodium and water re-absorption, as well as promote cell growth, proliferation, and collagen matrix deposition. The AT_2 appears to counterbalance the AT_1 by increasing the production of bradykinin, nitric oxide, and cyclic guanosine monophosphate-mediating vasodilation and by promoting cell differentiation, anti-proliferation, and apoptosis. It is meaningful that our results suggest that Losartan itself can induce hPSCs apoptosis in a dose- and time-dependent manner clarified by TUNEL and FCM assays, while there are no marked effects on hPSCs proliferation. We made a serial concentration of Losartan firstly in order to ascertain the adaptable pro-apoptotic dosage, and found that 10^{-5} mol/L had significant pro-apoptotic effect. Also we chose 0.1% FCS in time-course apoptotic test in order to decrease the serum's effect on anti-apoptosis. Based on this result, we used 10^{-6} mol/L in pro-proliferation study in order to avoid pro-apoptotic effect. Apoptosis is a physiological mechanism of deleting cells that regulates cell mass and architecture in many tissues. Inducing PSCs apoptosis or inhibiting PSCs proliferation are always hope-giving methods for complete treatment of pancreatic fibrosis. The regulatory mechanisms and signaling pathways in this process are poorly defined. However, how can we explain this paradox? Actually, AngII is also a potent anti-apoptotic factor, capable of reversing the effects of NO as well as the response to serum withdrawal-induced apoptosis was noted at concentrations as low as 10 nmol/L[26]. The observation that AngII inhibits cGMP analog-induced apoptosis suggests that the survival signal is downstream from the activation of cGMP protein kinase[26]. Given the pleiotropic effects of AngII on a variety of second messenger systems, such as calcium, protein kinase C, mitogen-activated protein kinase, and other tyrosine kinases, there are many potential mechanisms by which AngII may stimulate a cell survival signal[27,28]. It has been reported that AngII inhibits apoptosis mainly via the stimulation of the AT_1[26]. Other anti-apoptotic mechanism might be associated with down-regulation of iNOS expression and requires an intact phosphatidylinositol 3-kinase-Akt survival signal pathway[29]. Whether the interaction between Losartan and AT_1 could activate downstream molecular signals inducing apoptosis is worthy of further investigation. Losartan treatment also lowers the content of collagen I in culture media and hPSCs compared to control group determined by Western blot and immunofluorescence. This contention coincides with other reports that the specific blockade of AT_1 causes a reduction in collagen I.

It is demonstrated that PSCs possessing AT_1, have a possible impact on the pathogenesis of acute and chronic pancreatitis. In the injured pancreas, AngII production by the local RAS may contribute to an impaired microcirculation, resulting in increased intrapancreatic vascular resistance, reduced pancreatic juice efflux, and fibrotic reorganization[30]. Kuno *et al*.[12] recently demonstrated in an *in vivo* model of chronic pancreatitis that inhibition of the ACE attenuates pancreatic inflammation and fibrosis, further corroborating the view that AngII and AT_1 may play an important role in pancreatic pathophysiology. Taken together, our data provide evidence to support that Losartan has direct anti-migration, antifibrotic and pro-apoptotic effects on hPSCs *in vitro*, these processes might be mediated in part, by interaction with AT_1. These findings have important implications for

understanding the role of AT_1 and its antagonist in pancreatic fibrosis. If this is confirmed, the inhibition of AT_1 by Losartan could represent a novel approach to inhibit fibrogenesis in patients with chronic pancreatic disease.

REFERENCES

1 **Valderrama R,** Navarro S, Lopez JM, Caballeria J, Gimenez A, Pares A, Adrian MJ, Fernandez-Cruz L, Teres J. Synthesis and degradation of collagen in pancreatic fibrogenesis. *Pancreas* 1999; **18**: 34-38

2 **Wang XP,** Zhang R, Wu K, Wu L, Dong Y. Angiotensin II mediates acinar cell apoptosis during the development of rat pancreatic fibrosis by AT_1R. *Pancreas* 2004; **29**: 264-270

3 **Masamune A,** Satoh M, Kikuta K, Suzuki N, Shimosegawa T. Establishment and characterization of a rat pancreatic stellate cell line by spontaneous immortalization. *World J Gastroenterol* 2003; **9**: 2751-2758

4 **Bachem MG,** Schneider E, Gross H, Weidenbach H, Schmid RM, Menke A, Siech M, Beger H, Grunert A, Adler G. Identification, culture, and characterization of pancreatic stellate cells in rats and humans. *Gastroenterology* 1998; **115**: 421-432

5 **Ohnishi N,** Miyata T, Ohnishi H, Yasuda H, Tamada K, Ueda N, Mashima H, Sugano K. Activin A is an autocrine activator of rat pancreatic stellate cells: potential therapeutic role of follistatin for pancreatic fibrosis. *Gut* 2003; **52**: 1487-1493

6 **Kajstura J,** Cigola E, Malhotra A, Li P, Cheng W, Meggs LG, Anversa P. Angiotensin II induces apoptosis of adult ventricular myocytes *in vitro*. *J Mol Cell Cardiol* 1997; **29**: 859-870

7 **Chan WP,** Fung ML, Nobiling R, Leung PS. Activation of local renin-angiotensin system by chronic hypoxia in rat pancreas. *Mol Cell Endocrinol* 2000; **160**: 107-114

8 **Regoli M,** Bendayan M, Fonzi L, Sernia C, Bertelli E. Angiotensinogen localization and secretion in the rat pancreas. *J Endocrinol* 2003; **179**: 81-89

9 **Ohta T,** Amaya K, Yi S, Kitagawa H, Kayahara M, Ninomiya I, Fushida S, Fujimura T, Nishimura G, Shimizu K, Miwa K. Angiotensin converting enzyme-independent, local angiotensin II-generation in human pancreatic ductal cancer tissues. *Int J Oncol* 2003; **23**: 593-598

10 **Vermes I,** Haanen C, Steffens-Nakken H, Reutelingsperger C. A novel assay for apoptosis. Flow cytometric detection of phosphatidylserine expression on early apoptotic cells using fluorescein labelled Annexin V. *J Immunol Methods* 1995 ; **184**: 39-51

11 **Bataller R,** Schwabe RF, Choi YH, Yang L, Paik YH, Lindquist J, Qian T, Schoonhoven R, Hagedorn CH, Lemasters JJ, Brenner DA. NADPH oxidase signal transduces angiotensin II in hepatic stellate cells and is critical in hepatic fibrosis. *J Clin Invest* 2003; **112**: 1383-1394

12 **Kuno A,** Yamada T, Masuda K, Ogawa K, Sogawa M, Nakamura S, Nakazawa T, Ohara H, Nomura T, Joh T, Shirai T, Itoh M. Angiotensin-converting enzyme inhibitor attenuates pancreatic inflammation and fibrosis in male Wistar Bonn/Kobori rats. *Gastroenterology* 2003; **124**: 1010-1019

13 **Tsang SW,** Cheng CH, Leung PS. The role of the pancreatic renin-angiotensin system in acinar digestive enzyme secretion and in acute pancreatitis. *Regul Pept* 2004; **119**: 213-219

14 **Haber PS,** Keogh GW, Apte MV, Moran CS, Stewart NL, Crawford DH, Pirola RC, McCaughan GW, Ramm GA, Wilson JS. Activation of pancreatic stellate cells in human and experimental pancreatic fibrosis. *Am J Pathol* 1999; **155**: 1087-1095

15 **Lam KY,** Leung PS. Regulation and expression of a renin-angiotensin system in human pancreas and pancreatic endocrine tumours. *Eur J Endocrinol* 2002; **146**: 567-572

16 **Yoshiji H,** Kuriyama S, Yoshii J, Ikenaka Y, Noguchi R, Nakatani T, Tsujinoue H, Fukui H.Angiotensin-II type 1 receptor interaction is a major regulator for liver fibrosis development in rats. *Hepatology* 2001; **34**: 745-750

17 **Jonsson JR,** Clouston AD, Ando Y, Kelemen LI, Horn MJ, Adamson MD, Purdie DM, Powell EE. Angiotensin-converting enzyme inhibition attenuates the progression of rat hepatic fibrosis.*Gastroenterology* 2001; **121**: 148-155

18 **Bataller R,** Gines P, Nicolas JM, Gorbig MN, Garcia-Ramallo E, Gasull X, Bosch J, Arroyo V, Rodes J. Angiotensin II induces contraction and proliferation of human hepatic stellate cells. *Gastroenterology* 2000; **118**: 1149-1156

19 **Marshall RP,** McAnulty RJ, Laurent GJ. Angiotensin II is mitogenic for human lung fibroblasts via activation of the type 1 receptor. *Am J Respir Crit Care Med* 2000; **161**: 1999-2004

20 **Nagashio Y,** Asaumi H, Watanabe S, Nomiyama Y, Taguchi M, Tashiro M, Sugaya T, Otsuki M. Angiotensin II type 1 receptor interaction is an important regulator for the development of pancreatic fibrosis in mice. *Am J Physiol Gastrointest Liver Physiol* 2004; **287**: G170-G177

21 **Ishida T,** Ishida M, Suero J, Takahashi M, Berk BC. Agonist-stimulated cytoskeletal reorganization and signal transduction at focal adhesions in vascular smooth muscle cells require c-Src. *J Clin Invest* 1999; **103**: 789-797

22 **Amaya K,** Ohta T, Kitagawa H, Kayahara M, Takamura H, Fujimura T, Nishimura G, Shimizu K, Miwa K. Angiotensin II activates MAP kinase and NF-kappaB through angiotensin II type I receptor in human pancreatic cancer cells. *Int J Oncol* 2004; **25**: 849-856

23 **Klonowski-Stumpe H,** Reinehr R, Fischer R, Warskulat U, Luthen R, Haussinger D. Production and effects of endothelin-1 in rat pancreatic stellate cells. *Pancreas* 2003; **27**: 67-74

24 **Phillips PA,** Wu MJ, Kumar RK, Doherty E, McCarroll JA, Park S, Pirola RC, Wilson JS, Apte MV. Cell migration: a novel aspect of pancreatic stellate cell biology. *Gut* 2003; **52**: 677-682

25 **Gonzalez A,** Lopez B, Ravassa S, Querejeta R, Larman M, Diez J, Fortuno MA. Stimulation of cardiac apoptosis in essential hypertension: potential role of angiotensin II. *Hypertension* 2002; **39**: 75-80

26 **Pollman MJ,** Yamada T, Horiuchi M, Gibbons GH. Vasoactive substances regulate vascular smooth muscle cell apoptosis. Countervailing influences of nitric oxide and angiotensin II. *Circ Res* 1996; **79**: 748-756

27 **Griendling KK,** Alexander RW. The angiotensin (AT1) receptor. *Semin Nephrol* 1993; **13**: 558-566

28 **Ip SP,** Tsang SW, Wong TP, Che CT, Leung PS. Saralasin, a nonspecific angiotensin II receptor antagonist, attenuates oxidative stress and tissue injury in cerulein-induced acute pancreatitis. *Pancreas* 2003; **26**: 224-229

29 **Tian B,** Liu J, Bitterman P, Bache RJ. Angiotensin II modulates nitric oxide-induced cardiac fibroblast apoptosis by activation of AKT/PKB. *Am J Physiol Heart Circ Physiol* 2003; **285**: H1105-H1112

30 **Reinehr R,** Zoller S, Klonowski-Stumpe H, Kordes C, Haussinger D. Effects of angiotensin II on rat pancreatic stellate cells. *Pancreas* 2004; **28**: 129-137

Science Editor Guo SY **Language Editor** Elsevier HK

PO Box 2345, Beijing 100023, China
www.wjgnet.com
wjg@wjgnet.com

ELSEVIER

World J Gastroenterol 2005;11(41):6495-6502
World Journal of Gastroenterology ISSN 1007-9327

• *BASIC RESEARCH* •

Differential effects of glutamate receptor antagonists on dorsal horn neurons responding to colorectal distension in a neonatal colon irritation rat model

Chun Lin, Elie D Al-Chaer

Chun Lin, Elie D Al-Chaer, Laboratory of Elie D Al-Chaer (ACELAB), Center for Pain Research (CPR), University of Texas Medical Branch, Galveston, TX 77555-0632, United States
Chun Lin, Center for Neubiological Research, Department of Physiology and Pathophysiology, Fujian Medical University, Fuzhou 350004, Fujian Province, China
Supported by NIH grant 40434
Correspondence to: Elie D Al-Chaer, MS, Ph D, JD, Associate Professor of Pediatrics, Neurobiology and Developmental Sciences, College of Medicine, University of Arkansas for Medical Sciences, 4301 West Markham, Slot 842, Little Rock, AR 72205-842, United States. ealchaer@uams.edu
Telephone: +1-501- 526-7828 Fax: +1-501- 526-7862
Received: 2005-05-10 Accepted: 2005-06-18

Abstract

AIM: To investigate and compare the effects of spinal D-(-)-2-amino-7-phosphonoheptanoic acid (AP-7) and 6-cyano-7-nitroquinoxaline-2,3-dione disodium (CNQX), two glutamate receptor antagonists, on the responses of dorsal horn neurons to colorectal distension (CRD) in adult rats exposed to neonatal colon irritation (CI).

METHODS: Hypersensitive SD rats were generated by CI during postnatal days 8, 10 and 12. Experiments on adult rats were performed using extracellular single-unit recording. The effects of spinal application of AP-7 (0.001, 0.01, 0.1, 1 mmoL) were tested on the CRD-evoked neuronal responses in 16 controls and 17 CI rats. The effects of CNQX (0.2, 2, 5, 10 μmoL) were also tested on the CRD-evoked responses of 17 controls and 18 CI neurons.

RESULTS: (1) The average responses of lumbosacral neurons to all intensities of CRD in CI rats were significantly higher than those in control rats; (2) In control rats, AP-7（0.01 mmoL）had no significant effect on the neuronal response to all intensities of CRD (20, 40, 60, 80 mmHg); while AP-7 (0.1 mmoL) inhibited the neuronal response to 80-mmHg CRD. By contrast, in CI rats, AP-7 (0.01-1 mmoL) attenuated the CRD-evoked neuronal responses to all distention pressures in a dose-dependent manner; (3) In control rats, CNQX (2 μmoL) had no significantly effect on the neuronal response to all intensities of CRD; however, CNQX (5 μmoL) significantly attenuated the responses to CRD in the 40-80 mmHg range. By contrast, CNQX (2-10 μmoL) significantly decreased the neuronal responses in CI rats to non-noxious and noxious CRD in a dose-dependent manner.

CONCLUSION: Our results suggest that spinal *N*-methyl-D-aspartate (NMDA) and non-NMDA receptors may contribute to the processing of central sensitivity in a neonatal CI rat model, but they may play different roles in it.

Key words: Chronic visceral hypersensitivity; Dorsal horn neurons; Irritable bowel syndrome; NMDA receptors; Non-NMDA receptors

Lin C, Al-Chaer ED. Differential effects of glutamate receptor antagonists on dorsal horn neurons responding to colorectal distension in a neonatal colon irritation rat model. *World J Gastroenterol* 2005; 11(41): 6495-6502
http://www.wjgnet.com/1007-9327/11/6495.asp

INTRODUCTION

Chronic pain is frequently associated with increased neuronal excitability in the spinal cord, a phenomenon often referred to as central sensitization. Central sensitization can be induced by a number of sensitizing stimuli, including repeated mechanical stimulation and peripheral tissue injury, triggering burst of activities in nociceptors that alter the strength of synaptic connections between the nociceptors and the neurons of the spinal cord. In functional pain disorders, the peripheral stimulus is mostly lacking, and the prevalent hypothesis is that hypersensitivity is caused by functional changes (plasticity) in the nervous system, including central sensitization[1]. A key step in the development of central sensitization is activation and modulation of the *N*-methyl-D-aspartate (NMDA) receptor in those dorsal horn neurons of the spinal cord that receive primary afferent input[2,3]. NMDA receptors have a voltage-dependent magnesium ion (Mg^{2+}) channel block at resting membrane potential[4] and, therefore, do not seem to contribute to transient pain transmission[5-7]. Transient pain transmission occurs through the release of glutamate from the nociceptor afferent neurons acting via the AMPA/kainate receptors at the dorsal horn, which do not have a Mg^{2+} block, resulting

in membrane depolarization. However, stimulation of nociceptive afferents following injury/inflammation causes an increased and sustained release of glutamate from the central terminals of nociceptor afferents in the dorsal horn; this results in depolarization beyond a critical threshold, with the removal of the Mg^{2+} block, activation of NMDA receptors and a consequent amplification of pain[8,9]. This phenomenon of NMDA receptor-mediated central sensitization is a well-established mechanism in both animal and human models of somatic pain hypersensitivity and is attenuated by NMDA receptor antagonists[10,11].

Persistent or inflammatory visceral stimuli also produce central sensitization via NMDA receptors. Spinal administration of NMDA aggravates behavioral and neural responses to both noxious and innocuous intensities of CRD; these responses can be blocked by NMDA receptor antagonists[12,13]. Visceral hyperalgesia produced by colonic inflammation is mediated by NMDA and non-NMDA spinal receptors[14,15]. However, to our knowledge, little is known about the role of NMDA or non-NMDA glutamate receptors in the central sensitization of chronic visceral pain.

Previous work done by our group has shown that colon irritation (CI) in neonates can engender chronic visceral hypersensitivity in adult rats with associated peripheral and central neuronal sensitization in the absence of identifiable peripheral pathology[1,16]. The present study investigated and compared the effects of spinal D-(-)-2-amino-7-phosphonoheptanoic acid (AP-7, TOCRIS), an NMDA receptor antagonist, and 6-cyano-7-nitroquinoxaline-2, 3-dione disodium (CNQX, TOCRIS), a non-NMDA receptor antagonist, on the responses of dorsal horn neurons responding to colorectal distension (CRD) in rats with neonatal CI and in controls. Part of these data have been reported in abstract[17].

MATERIALS AND METHODS

Experiments were performed on 68 adult male Sprague-Dawley rats (weight, 250-350 g) obtained as pre-weanling neonates (younger than 5 d) from Harlan Sprague-Dawley (Indianapolis, IN). Thirty five rats received colon irritation (CI) as neonates and 33 rats served as controls (see below). Rats were housed in plastic cages containing corn chip bedding (Sani-Chips; PJ Murphy Forest Products, Montville, NJ) and maintained on a 12:12 h light-dark cycle (lights on at 7 am). The irritation procedures and the experimental testing were conducted during the light component of the cycle. The neonates were housed 10 per cage with 1 mo until they were 28-d-old. The adult females were accessed to food and water *ad libitum*. After separation, the male young rats were housed 4 per cage with access to food and water *ad libitum*. The rats were observed daily, and their weights were measured at least once a week. Adequate measures were taken to minimize pain and discomfort. All studies were performed in accordance with the proposal of the Committee for Research and Ethical Issues of the International Association for the Study of Pain[18] and were approved by the Institutional Animal Care and Use Committee at the University of Texas Medical Branch in accordance with the guidelines provided by the USA National Institute of Health Guide for the Care and Use of Laboratory Animals (NIH Publications No. 80-23) revised in 1996.

Neonatal colon irritation

Neonatal colon irritation (CI) was applied using colorectal distension (CRD) during postnatal development. The CRD procedure was modified from a previous report by Al-Chaer *et al*[1]. Briefly, the rats (8-d-old) were divided into two groups for the purposes of two different treatments: Group 1 (CI rats) received CRD once on postnatal (PN) days 8, 10, and 12. The distention was applied using an angioplasty balloon (Advanced Polymers Inc., length: 20.0 mm; diameter: 3 mm), inserted rectally into the descending colon in awake neonates. The balloon was distended with 0.3 mL of water, exerting a pressure of 60 mmHg (as measured with a sphygmomanometer) for 1 min and then deflated and withdrawn. Group 2 (which served as controls) was handled in a way similar to group 1 except that no colonic insertion was made. Rats in this group were separated from the dams, gently held and touched on the perianal area on a schedule similar to that described for group 1. Above experiments were done by the same investigator. No treatment, procedures or further interventions were done by the investigator until the testing date.

Electrophysiological preparations

Animal preparation and surgical procedures Experiments were carried out on anesthetized and paralyzed adult rats (> 2 mo). Anesthesia for adult rats in both groups was induced by 5% halothane. The depth of anesthesia during surgery was maintained by ~2.5 % halothane, which was adjusted by monitoring withdrawal responses to pinch. During electrophysiological recording, anesthesia was maintained by ~1.0 % halothane. Once a stable level of anesthesia was reached, the rats were paralyzed with pancuronium bromide (0.3 mg/kg iv) and artificially ventilated. The adequacy of the depth of anesthesia during recordings was monitored by frequent examination of the pupillary reflexes and assessing stability of the level of end-tidal CO_2, which was kept between 3.5% and 4.5% by adjusting the respiratory parameters. Body temperature was monitored and maintained at 37 °C by a servo-controlled heating blanket. The L_6-S_1 segments of the spinal cord were exposed by laminectomy. The rat was placed in a head holder and suspended with thoracic vertebral and ishial clamps. The dura matter was carefully removed and the spinal cord was bathed in artificial cerebral spinal fluid (ACSF)[19].

Colon stimulation Colon stimulation in adult rats consisted of graded colorectal distension (CRD) produced by inflating a balloon inside the descending colon and rectum. The balloon was 4 cm in length and made of the

finger of a latex glove. It was attached to polyethylene tubing and inserted through the anus into the rectum and descending colon. The open end of the balloon was secured to the tubing with thread and wrapped with tape (1 cm wide). The balloon was inserted so that the thread was approximately 1 cm proximal to the anal sphincter, and was held in place by taping the tubing to the tail. The tubing was attached via a T-connector to a sphygmomanometer pump and a pressure gauge. Prior to use, the balloon was inflated and left overnight so that the latex stretched and the balloon became compliant. CRD was produced by rapidly inflating the balloon to the desired pressure (20, 40, 60 or 80 mmHg) for a duration of 10 s. Stimuli applied in an ascending graded manner (spaced by 4 min). To decrease the "human factor" bias to the minimum possible, the same stimulation paradigm was used in every rat. Colon stimulation was applied accurately according to the pressure gauge without observation of the oscilloscope or computerized record so that the experimenter was unaware of the response magnitude.

Electrophysiological recording Tungsten microelectrodes (2-6 MΩ Micro Probe Inc.) were used for extracellular single-unit recording in the L_6-S_2 spinal segments, 0-1.5 mm lateral to midline, 0.2-1.1 mm from the spinal cord dorsum. The search stimulus consisted of brushing the ipsilateral perianal/scrotal area with a small paint brush[20] and CRD (60 mmHg)[21]. When a neuron responsive to the cutaneous stimuli was identified, the colon was distended for several seconds to test whether the neuron was responsive to CRD. The electrophysiological recordings were conducted by an investigator blinded to the type of rats. Action potentials were fed into a window discriminator and monitored continuously by analog delay and displayed on a storage oscilloscope after initial amplification through a low-noise AC differential amplifier (DAM 80i). The output of the amplifier and window discriminator were fed into a data collection system (CED 1401 +) and Spike2 for Windows software (Cambridge Electronic design, UK) to compile rate histograms or wavemark files. Single units were differentiated on- and off-line. Only cells that had an excitatory response to CRD were chosen for the study. Care was taken to insure that noise was not captured by the window discriminator.

Experimental protocols

Each CRD-responsive neuron was tested with the same method (20, 40, 60, and 80 mmHg) before drug administration to establish a baseline response of the neuron. Drugs were dissolved in ACSF and 20 μL was applied spinally to the surface of the spinal cord[19]. The effects of spinal application of AP-7 (0.001, 0.01, 0.1, 1 mmoL) were tested on the CRD-evoked responses of 16 controls and 17 CI neurons. The effects of spinally administered CNQX (0.2, 2, 5, 10 μmoL) were tested on the CRD-evoked responses of 17 controls and 18 CI neurons. The drug was removed by tissue wick prior to application of the next dose. Only one neuron was studied in each animal. The reported doses were the applied dose, not a cumulative dose. A drug effect was described as a change by more than 20% in the response to CRD after the drug was applied, compared to baseline response recorded before drug application. Responses of LS neurons to CRD were recorded 15 min after each drug administration.

The responses to CRD were recorded and calculated as the difference between the rate of firing during the stimulus application and that during the baseline recording. The responses of CI rats were compared to those of controls for statistical significance. Drug effect was tested by recording responses of neurons to CRD before and after the drug application in controls and CI rats. For control purposes, the spinal cord was bathed in ACSF before the drug application. The effects of drugs on the baseline and the responses to CRD were analyzed within each group and were compared between the controls and CI groups for any statistical significance. At the end of the experiments, the rats were euthanized with an overdose of halothane.

Statistical analysis

The spontaneous activity of a neuron was measured for 20 s before CRD, and the response of a neuron to CRD was determined as the average increase in discharge during distention above the average spontaneous activity. The responses recorded in CI rats were compared to those recorded in control rats for statistical significance. Unless otherwise indicated, data were expressed as mean ± SE. The CRD data was analyzed using repeated measures analysis of variance (RM ANOVA). A model with the repeated factors of intensity, group, and the (intensity x group) interaction was used to examine significant intensity effects, group effects and (intensity x group) interactions. Significant group and interaction effects meant that responses in the corresponding groups increased in a significantly different manner (*i.e.,* responses of CI group were significantly different from responses of control group). For non-parametric data, the Mann Whitney rank sum test was used. $P<0.05$ was considered statistically significant in all cases.

RESULTS

Responses to CRD

The neuronal responses to CRD recorded in the controls or CI rats were stimulus-locked. In both controls and CI rats, responses of lumbosacral (LS) neurons to CRD were graded with stimulus intensity. A model with the repeated factors of intensity, group, and the (intensity x group) interaction showed that there was a significant intensity effect ($P<0.05$), group effect ($P<0.05$) and (intensity x group) interaction ($P<0.05$). The interpretation of these results is that there was a significant increase in the magnitude of neuronal responses with increasing levels of CRD in both groups (Figure 1). Also, the average responses of LS neurons to all intensities of CRD in CI rats were significantly higher than those in control rats (Figure 1).

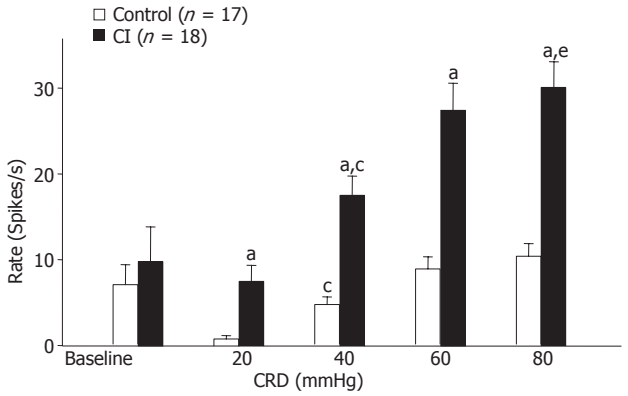

Figure 1 Average responses of LS neurons to CRD (20, 40, 60, 80 mmHg). Bar graph summarizes the average background activity (baseline; control, n = 17; CI, n = 18) and the responses of LS neurons to all intensities of CRD in control and CI rats. The responses to CRD are reported as the mean increase in firing rate above baseline. Responses recorded in CI rats were significantly higher than those recorded in control rats. [a]P<0.05 *vs* the values of normal rats with the same intensity; [c]P<0.05 *vs* 20 mmHg CRD in each group; [e]P<0.05 *vs* 40mmHg CRD in CI rats.

Effect of spinal AP-7 on LS neuronal response to CRD

Percentage of LS neurons inhibited by spinal AP-7 Generally, the effect of AP-7 occurred during 5-30 min after the drug administration.

In control rats, 4 of the 16 neurons (25%) were inhibited by AP-7 (0.001 mmoL); these responded to all graded CRD. Eight of the 16 neurons (50%) responded to CRD (20-60 mmHg); these were inhibited by AP-7 (1 mmoL). Thirteen of the 16 neurons (81.2%) that responded to CRD (80 mmHg) were inhibited by AP-7 (1 mmoL). The effect of AP-7 appeared to be incremental with dose and stimulus intensity with maximum effect seen on the response to 80 mmHg CRD in control rats (Table 1).

In CI rats, 6 of the 15 neurons (40%) that responded to all intensities of CRD were inhibited by AP-7 (0.001 mmoL). All nine neurons (100%) that responded to all intensities of CRD were inhibited by AP-7 (1 mmoL) (Table 1).

The effect of AP-7 on neuronal response to all intensities of CRD was more pronounced in CI rats compared to control rats. AP-7 dose-dependently attenuated the CRD-evoked responses at all distention pressures in all nine (100%) CI neurons.

Effect of spinal AP-7 on the average responses of LS neurons to CRD No significant changes were seen in the responses of 11 control neurons to intensities of CRD following spinal administration of AP-7 (0.01 mmoL) (Figure 2A). On the other hand, AP-7 (0.1 mmoL) significantly attenuated the average response to high intensity of CRD (80 mmHg) (n = 12) and AP-7 (1 mmoL) significantly attenuated the average responses to CRD (40-80 mmHg) in controls (n = 16) (Figure 3A).

AP-7 (0.01 mmoL) significantly attenuated the average responses to intensities of CRD in CI rats in a dose-dependant manner (Figures 2B and 3B).

Table 1 Percentage attenuation of responses to graded CRD of LS neurons by AP-7 in control and CI rats

Dose	20 (%)	40 (%)	60 (%)	80 (mmHg%)
Controls				
0.001 mmoL	25 (4/16)	25 (4/16)	25 (4/16)	25 (4/16)
0.01 mmoL	36.3 (4/11)	36.3 (4/11)	36.3 (4/11)	45.4 (5/11)
0.1 mmoL	41.6 (5/12)	50 (6/12)	58.3 (7/12)	75 (9/12)
1 mmoL	50 (8/16)	50 (8/16)	50 (8/16)	81.2 (13/16)
CI rats				
0.001 mmoL	40 (6/15)	40 (6/15)	40(6/15)	40 (6/15)
0.01 mmoL	60 (6/10)	60 (6/10)	60 (6/10)	60 (6/10)
0.1 mmoL	81.8 (9/11)	81.8 (9/11)	81.8 (9/11)	81.8 (9/11)
1 mmoL	100 (9/9)	100 (9/9)	100 (9/9)	100 (9/9)

Denominators in parentheses indicate the total number of LS neurons treated with AP-7 and numerators indicate the number of neurons affected by AP-7 at the same dose level in control and CI rats. A drug effect is described as a change by more than 20% in the response to CRD after the drug was applied, compared to baseline response recorded before the use of drug.

Table 2 Percentage attenuation of responses to graded CRD of LS neurons by CNQX in control and CI rats

Dose	20 (%)	40 (%)	60 (%)	80 (mmHg%)
Controls				
0.2 μmoL	23.5 (4/17)	23.5 (4/17)	23.5 (4/17)	23.5 (4/17)
2 μmoL	44.4 (4/9)	44.4 (4/9)	44.4 (4/9)	44.4 (4/9)
5 μmoL	50 (4/8)	62.5 (5/8)	62.5 (5/8)	62.5 (5/8)
10 μmoL	71.4 (5/7)	75 (6/8)	75 (6/8)	75 (6/8)
CI rats				
0.2 μmoL	45.4 (5/11)	45.4(5/11)	45.4 (5/11)	45.4 (5/11)
2 μmoL	77.8 (7/9)	77.8 (7/9)	77.8 (7/9)	77.8 (7/9)
5 μmoL	83.3 (5/6)	83.3 (5/6)	83.3 (5/6)	83.3 (5/6)
10 μmoL	100 (8/8)	100 (8/8)	100 (8/8)	100 (8/8)

Denominators in parentheses indicate the total number of LS neurons treated with CNQX and numerators indicate the number of neurons affected by CNQX at the same dose level in control and CI rats. The effect of CNQX on neuronal response to all intensities of CRD was more pronounced in CI rats than that in control rats. CNQX dose-dependently attenuated the CRD-evoked responses at all distention pressures in all 8 (100%) CI neurons.

Effect of spinal CNQX on LS neuronal response to CRD (20-80 mmHg)

Percentage of LS neurons inhibited by CNQX In general, the effect of CNQX occurred during about 10 min after the drug administration.

In control rats, spinal CNQX (0.2 μmoL) inhibited the responses of 4 of the 17 neurons (23.5%) that responded to intensities of CRD. At a higher dose, CNQX (10 μmoL) inhibited the responses of 6 of 8 neurons (75%) that responded to CRD (40-80 mmHg), (Table 2).

In CI rats, spinal CNQX (0.2 μmoL) inhibited the responses of 5 of the 11 neurons (45.4%) that responded to intensities of CRD. At a higher dose, CNQX (10 μmoL) inhibited the responses of all 8 neurons (100%) that responded to intensities of CRD (Table2). Thus, CNQX dose-dependently attenuated the CRD-evoked responses at all distention pressures in CI neurons. The effect of CNQX on neuronal response to all intensities of CRD was more pronounced in the CI rats compared to the control rats.

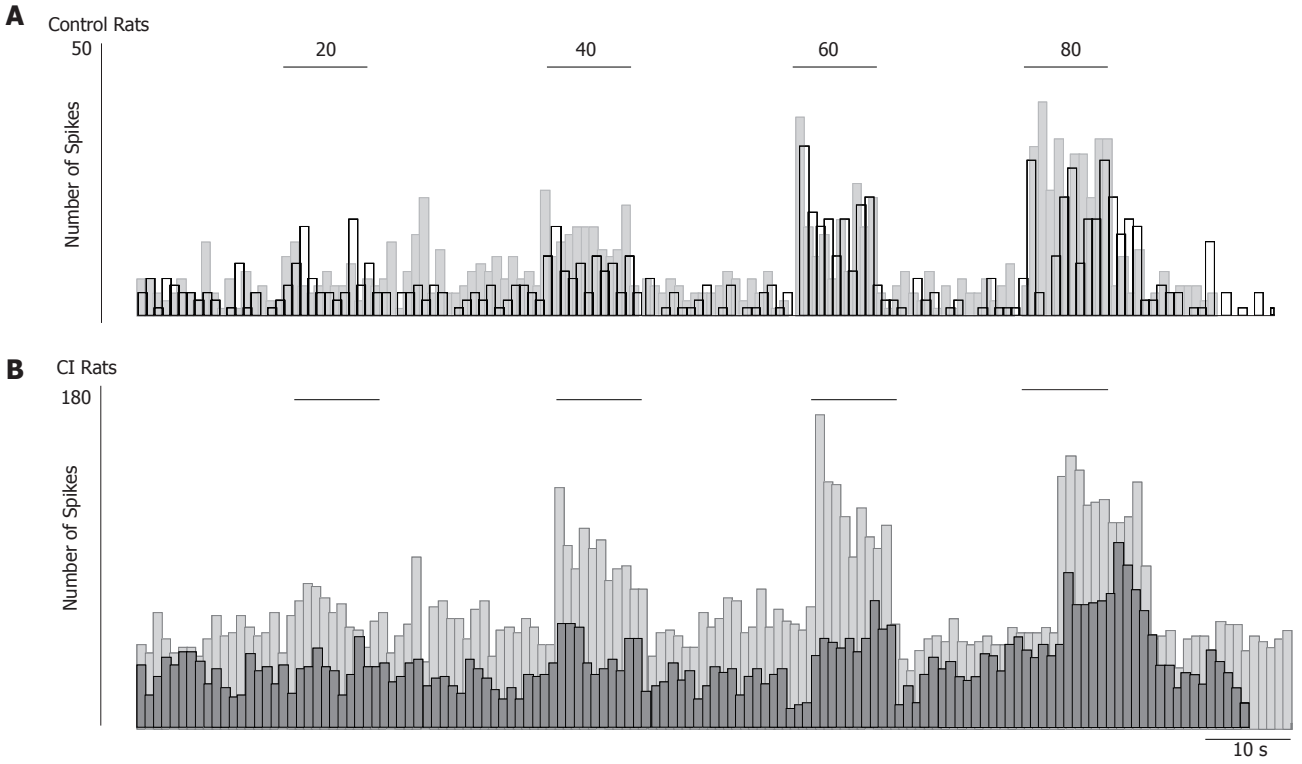

Figure 2 Effect of AP7 (0.01 mmoL) on dorsal horn neuronal responses to CRD in control or CI rats. Rate histograms illustrate the responses of a dorsal horn neuron isolated from a control rat (**A**) and of another neuron isolated from a CI rat (**B**) before (grey) and after (black) spinal administration of AP-7 (0.01 mmoL). Horizontal bars indicate the timing and duration (10 s) of CRD (20- 80 mmHg).

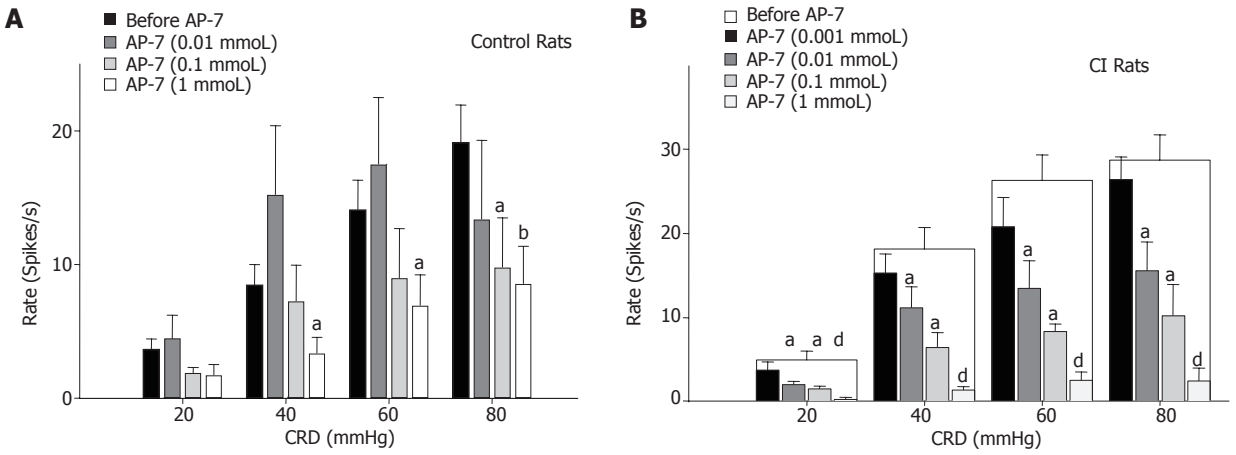

Figure 3 Effect of spinal AP7 on average responses of LS neurons to CRD. Bar graphs illustrate the responses of LS neurons to CRD (20-80 mmHg) recorded in control rats (A; left panel) or CI rats (B; right panel) before and after spinal administration of AP7. **A:** AP-7 (0.1 mmoL) significantly attenuated the average response to high intensity CRD (80 mmHg) and AP-7 (1 mmoL) significantly attenuated the responses to CRD (40-80 mmHg) in controls; **B:** AP-7 (0.01 mmoL) significantly attenuated the average responses to graded CRD in CI rats in a dose-dependant manner. [a]*P*<0.05, [b]*P*<0.01, [d]*P*<0.001 *vs* before AP-7 application at that distention pressure in each group.

Effect of spinal CNQX on the average responses of LS neurons to CRD CNQX (2 μmoL) had no significant effect on the responses of 9 control neurons to all intensities of CRD (Figure 4A). However, CNQX (5 μmoL) significantly attenuated the responses to CRD in the 40-80 mmHg range and CNQX (10 μmoL) significantly attenuated the response to all intensities of CRD in control rats (n = 8) (Figure 5A).

By contrast, CNQX (2 μmoL) significantly attenuated the average response of 9 CI neurons to all intensities of CRD (Figure 4B). In general CNQX (2-10 μmoL) decreased the neuronal responses in CI rats to non-noxious and noxious CRD in a dose-dependant manner (Figure 5B).

DISCUSSION

Injury and pain in neonates can have severe developmental

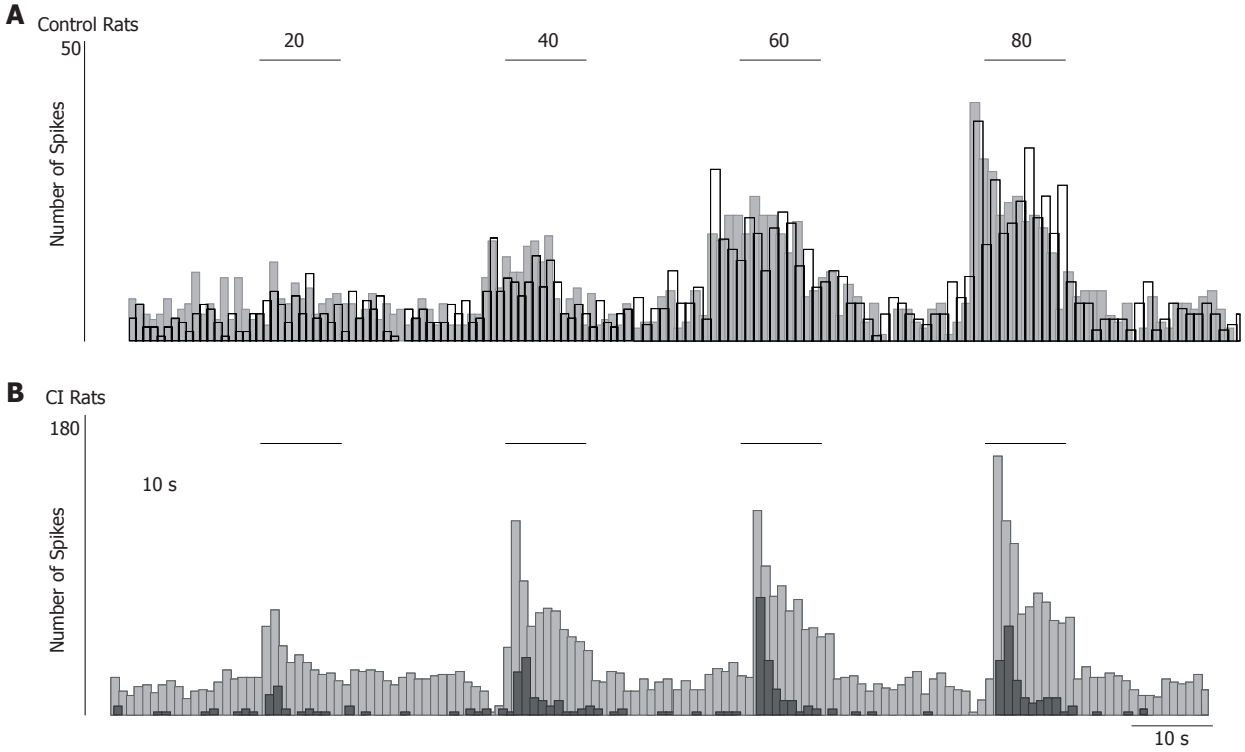

Figure 4 Effect of CNQX (2 μmoL) on dorsal horn neuronal responses to CRD in control or CI rats. Rate histograms illustrate the responses of a dorsal horn neuron isolated from a control rat (**A**) and of another neuron isolated from a CI rat (**B**) before (grey) and after (black) spinal administration of CNQX (2 μmoL).

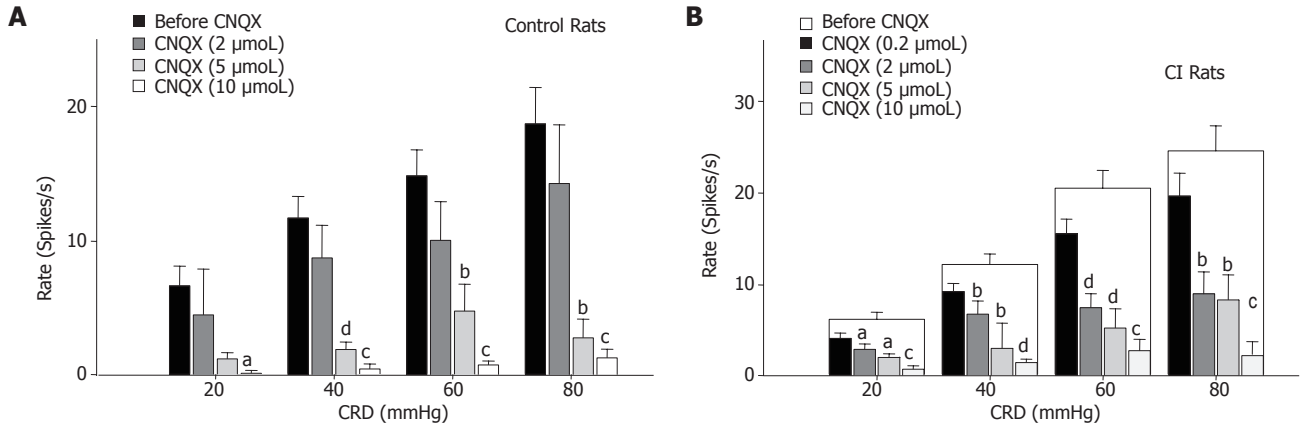

Figure 5 Effect of spinal CNQX on average responses of LS neurons to CRD. Bar graphs illustrate the responses of LS neurons to graded CRD (20-80 mmHg) recorded in control rats (A; left panel) or CI rats (B; right panel) before and after spinal administration of CNQX. **A:** In control rats, CNQX (5 μmoL) significantly attenuated the responses to CRD in the 40-80 mmHg range and CNQX (10 μmoL) significantly attenuated the response to all intensities of CRD; **B:** In CI rats, CNQX (2-10 μmoL) significantly decreased the response to all intensities of CRD in a dose-dependent manner. [a]*P*<0.05, [b]*P*<0.01, [d]*P*<0.001 *vs* before CNQX application at that distention pressure in each group; [c]*P* <0.05 *vs* 2 μmoL CNQX.

repercussions that may often alter the physiological and functional profile of the adult. In previous studies, our group has shown that colon pain in neonatal rats can cause long-term visceral hypersensitivity associated with central neuronal and peripheral sensitization, despite the lack of inflammation signs in the colon[1,16]. This chronic colorectal hyperalgesia can be blocked by a peripheral NMDA receptor antagonist (AP7)[22]. In this study, we showed that spinal application of AP-7 or CNQX attenuated the neuronal response to graded CRD in both control and CI rats with a more pronounced effect in CI rats. Thus, both spinal NMDA and non-NMDA receptors contribute to the central sensitization seen in adult rats with chronic visceral hypersensitivity.

Neonatal injury and central sensitization

Significant development of nociceptive neural circuits occurs during early postnatal life[9]. Painful or stressful stimuli, which are normally absent or limited during this critical developmental period, represent a unique sensory

experience that may result in permanent alterations in the afferent pathways of the newborn organism[23-28]. In human neonates, sensitization can be produced by repeated mechanical stimulation or heel lances and as a consequence of circumcision or surgery[29,30]. The neonatal nervous system appears particularly vulnerable and susceptible to plastic changes.

Our group has previously shown that neonatal colon pain or inflammation in rats can have a devastating effect on the physiology and function of the adult. Colon hypersensitivity, characterized by allodynia and hyperalgesia, could be observed two months after the initial injury despite the lack of an obvious pathology in the colon tissue. This hypersensitivity was shown to be associated with central neural and peripheral sensitization characterized by increased neuronal responses to CRD and a reduction in the thresholds of visceral nociceptors[1,16]. This was consistent with the work of others who have demonstrated the presence of central plastic changes in both somatic and visceral nociceptive systems[31-33], and also consistent with our earlier work on central processing of visceral nociception[34-36].

Generally, pelvic visceral input converges onto spinal neurons in the lumbosacral (LS) segments[37, 38] and hypogastric input onto thoracolumbar (TL) segments of the spinal cord. Many experiments have demonstrated that nociceptive afferent discharges in visceral afferents evoke profound central changes[31,32,39].

NMDA receptors and CRD

In somatic tissue, NMDA receptors contribute to the generation of central sensitization following tissue injury and inflammation[2,3]. Transient distension of the ureter evokes a pressor response that is inhibited by NMDA receptor antagonists[40]. Rice and McMahon[41] investigated the role of spinal NMDA receptors in central sensitization in an animal model of persistent visceral pain[12]. Likewise, NMDA receptor antagonists attenuated primary afferent[22,42] and spinal neuron responses to acute noxious and innocuous colorectal stimuli[13,43,44]. Our results indicated that, in control animals (without colon hypersensitivity), the lower doses of AP-7 had no effect on the neuronal response to noxious and innocuous CRD; while the higher dose of AP-7 lowered the neuronal response to noxious CRD. However, in chronic colon hypersensitivity rats in the absence of inflammation, lower doses of AP-7 significantly decreased the response to graded CRD as compared to the controls. These data support the proposition that spinal NMDA receptors contribute to chronic visceral hypersensitivity.

Non-NMDA receptors and CRD

Intrathecal administration of non-NMDA receptor antagonist, DNQX, was reported to attenuate enhanced reflex responses to mechanical stimulation of an inflamed colon, but was ineffective in non-inflamed rats[14]. On the other hand, systemically-administered DNQX attenuated spinal dorsal horn neuronal responses to noxious CRD in normal rats[45]. Our experiments showed that the response to noxious and innocuous CRD was dose-dependently attenuated by CNQX in 75% (6/8) and 71.4% (5/7) control neurons. But, the effect of CNQX on neuronal response to all intensities of CRD was more pronounced in CI rats than that in control rats. These results further support a role for spinal non-NMDA receptors in visceral sensory processing[19,35,46] .

In summary, a possible shift in the role of spinal NMDA and non-NMDA receptors residual to the neonatal injury may underlie the differential effects of AP-7 and CNQX between rats with neonatal CI and controls. These results further support the assertion that both spinal NMDA and non-NMDA receptors contribute to the central sensitization seen in adult rats with chronic visceral hypersensitivity and the conjecture that IBS pain may be associated with NMDA and non-NMDA receptors.

ACKNOWLEDGMENTS

The authors thank Ms. Kirsten Garner for administrative assistance with the manuscript and publication fee supported by FJGXY grant 04009.

REFERENCES

1 **Al-Chaer ED**, Kawasaki M, Pasricha PJ. A new model of chronic visceral hypersensitivity in adult rats induced by colon irritation during postnatal development. *Gastroenterology* 2000; **119:** 1276-1285
2 **Haley JE**, Sullivan AF, Dickenson AH. Evidence for spinal N-methyl-D-aspartate receptor involvement in prolonged chemical nociception in the rat. *Brain Res* 1990; **518:** 218-226
3 **Woolf CJ,** Thompson SW. The induction and maintenance of central sensitization is dependent on N-methyl-D-aspartic acid receptor activation; implications for the treatment of post-injury pain hypersensitivity states. *Pain* 1991; **44**: 293-299
4 **Mayer ML,** Westbrook GL, Guthrie PB. Voltage-dependent block by Mg2+ of NMDA responses in spinal cord neurons. *Nature* 1984; **309:** 261-263
5 **Dickenson AH,** Sullivan AF. Evidence for a role of the NMDA receptor in the frequency dependent potentiation of deep rat dorsal horn nociceptive neurones following C fibre stimulation. *Neuropharmacology* 1987; **26**: 1235-1238
6 **Dickenson AH.** A cure for wind up: NMDA receptor antagonists as potential analgesics. *Trends Pharmacol Sci* 1990; **11:** 307-309
7 **Dubner R,** Ruda MA. Activity-dependent neuronal plasticity following tissue injury and inflammation. *Trends Neurosci* 1992; **15**: 96-103
8 **Woolf CJ**, Costigan M. Transcriptional and posttranslational plasticity and the generation of inflammatory pain. *Proc Natl Acad Sci U S A* 1999; **96:** 7723-7730
9 **Woolf CJ,** Salter MW. Neuronal plasticity: increasing the gain in pain. *Science* 2000; **288**: 1765-1769
10 **Graven-Nielsen T**, Aspegren Kendall S, Henriksson KG, Bengtsson M, Sörensen J, Johnson A, Gerdle B, Arendt-Nielsen L. Ketamine reduces muscle pain, temporal summation and referred pain in fibromyalgia patients. *Pain* 2000; **85:** 483-491
11 **Park KM**, Max MB, Robinovitz E, Gracely RH, Bennett GJ. Effects of intravenous ketamine, alfentanil, or placebo on pain, pinprick hyperalgesia, and allodynia produced by intradermal capsaicin in human subjects. *Pain* 1995; **63:** 163-172
12 **Kolhekar R**, Gebhart GF.Modulation of spinal visceral nociceptive transmission by NMDA receptor activation in the rat. *J Neurophysiol* 1996; **75**: 2344-2353
13 **Zhai QZ**, Traub RJ. The NMDA receptor antagonist MK-801

attenuates c-Fos expression in the lumbosacral spinal cord following repetitive noxious and non-noxious colorectal distention. *Pain* 1999; **83**: 321-329

14 **Coutinho SV**, Meller ST, Gebhart GF. Intracolonic zymosan produces visceral hyperalgesia in the rat that is mediated by spinal NMDA and non-NMDA receptors. *Brain Res* 1996; **736:** 7-15

15 **Silva E**, Cleland CL, Gebhart GF. Contributions of glutamate receptors to the maintenance of mustard oil-induced hyperalgesia in spinalized rats. *Exp Brain Res* 1997; **117:** 379-388

16 **Lin C**, Al-Chaer ED. Long-term sensitization of primary afferents in adult rats exposed to neonatal colon pain. *Brain Res* 2003; **971:** 73-82

17 **Lin C**, Al-Chaer ED. Differential effects of glutamate receptor antagonists on dorsal horn neurons responding to colorectal distension in a neonatal colon irritation rat model. *World J Gastroenterol* 2005;**11**:6495-6502

18 **Zimmermann M**. Ethical guidelines for investigations of experimental pain in conscious animals. Pain 1983; 16: 109-110

19 Ji Y, Traub RJ. Differential effects of spinal CNQX on two populations of dorsal horn neurons responding to colorectal distension in the rat. *Pain* 2002; **99:** 217-222

20 **Takahashi Y,** Nakajima Y, Sakamoto T. Dermatome mapping in the rat hindlimb by electrical stimulation of the spinal nerves. *Neurosci Lett* 1994; **168**: 85-88

21 **Ness TJ,** Gebhart GF. Colorectal distension as a noxious visceral stimulus: physiologic and pharmacologic characterization of pseudaffective reflexes in the rat. *Brain Res* 1988; **450:** 153-169

22 **Lin C,** Al-Chaer ED. Primary afferent sensitization in an animal model of chronic visceral pain. *The Journal of Pain* 2002; **3:** 27, #706. American Pain Society, 2002

23 **Anand KJ,** Coskun V, Thrivikraman KV, Nemeroff CB, Plotsky PM. Long-term behavioral effects of repetitive pain in neonatal rat pups. *Physiol Behav* 1999; **66:** 627-637

24 **Anand KJ**, Scalzo FM. Can adverse neonatal experiences alter brain development and subsequent behavior? *Biol Neonate* 2000; **77:** 69-82

25 **Coutinho SV**, Plotsky PM, Sablad M, Miller JC, Zhou H, Bayati AI, McRoberts JA, Mayer EA. Neonatal maternal separation alters stress-induced responses to viscerosomatic nociceptive stimuli in rat. *Am J Physiol Gastrointest Liver Physiol* 2002 ; **282**: G307-G316

26 **Fitzgerald M**, Beggs S. The neurobiology of pain: developmental aspects, *Neuroscientist* 2001; **7:** 246-257

27 **Lidow MS**, Song ZM, Ren K. Long-term effects of short-lasting early local inflammatory insult. *Neuroreport* 2001; 12: 399-403

28 Ruda MA, Ling QD, Hohmann AG, Peng YB, Tachibana T. Altered nociceptive neuronal circuits after neonatal peripheral inflammation. *Science* 2000; **289:** 628-631

29 **Taddio A**, Katz J, Ilersich AL, Koren G. Effect of neonatal circumcision on pain response during subsequent routine vaccination. *Lancet* 1997; **349:** 599-603

30 **Taddio A**, Shah V, Gilbert-MacLeod C, Katz J. Conditioning and hyperalgesia in newborns exposed to repeated heel lances. *JAMA* 2002; **288:** 857-861

31 **Pozo MA**, Cervero F. Neurons in the rat spinal trigeminal complex driven by corneal nociceptors: receptive-field properties and effects of noxious stimulation of the cornea. *J Neurophysiol* 1993; **70**: 2370-2378

32 **Traub RJ**. The spinal contribution of substance P to the generation and maintenance of inflammatory hyperalgesia in the rat. Pain 1996; 67: 151-161 33 Woolf CJ. Evidence for a central component of post-injury pain hypersensitivity. *Nature* 1983; **306**: 686-688

33 **Woolf CJ**. Evidence for a central component of post-injury pain hypersensitivity. *Nature* 1983;**306**:686-688

34 **Al-Chaer ED**, Feng Y, Willis WD. Comparative study of viscerosomatic input onto postsynaptic dorsal column and spinothalamic tract neurons in the primate. *J Neurophysiol* 1999; **82:** 1876-1882

35 **Al-Chaer ED**, Lawand NB, Westlund KN, Willis WD. Pelvic visceral input into the nucleus gracilis is largely mediated by the postsynaptic dorsal column pathway. *J Neurophysiol* 1996; **76:** 2675-2690

36 **Al-Chaer ED**, Westlund KN, Willis WD. Sensitization of postsynaptic dorsal column neuronal responses by colon inflammation. *Neuroreport* 1997; **8**: 3267-3273

37 **Honda CN**. Visceral and somatic afferent convergence onto neurons near the central canal in the sacral spinal cord of the cat. *J Neurophysiol* 1985; **53**: 1059-1078

38 **Ness TJ**, Gebhart GF. Characterization of neuronal responses to noxious visceral and somatic stimuli in the medial lumbosacral spinal cord of the rat. *J Neurophysiol* 1987; **57:** 1867-1892

39 **Cervero F,** Laird JM, Pozo MA. Selective changes of receptive field properties of spinal nociceptive neurones induced by noxious visceral stimulation in the cat. *Pain* 1992; **51:** 335-342

40 **Olivar T**, Laird JM. Differential effects of N-methyl-D-aspartate receptor blockade on nociceptive somatic and visceral reflexes. *Pain* 1999; **79:** 67-73

41 **Rice AS,** McMahon SB. Pre-emptive intrathecal administration of an NMDA receptor antagonist (AP-5) prevents hyper-reflexia in a model of persistent visceral pain. *Pain* 1994; **57**: 335-340

42 **McRoberts JA**, Coutinho SV, Marvizón JC, Grady EF, Tognetto M, Sengupta JN, Ennes HS, Chaban VV, Amadesi S, Creminon C, Lanthorn T, Geppetti P, Bunnett NW, Mayer EA. Role of peripheral N-methyl-D-aspartate (NMDA) receptors in visceral nociception in rats. *Gastroenterology* 2001; **120:** 1737-1748

43 **Ji Y**, Traub RJ. Spinal NMDA receptors contribute to neuronal processing of acute noxious and nonnoxious colorectal stimulation in the rat. *J Neurophysiol* 2001; **86**: 1783-1791

44 **Traub RJ**, Zhai Q, Ji Y, Kovalenko M. NMDA receptor antagonists attenuate noxious and nonnoxious colorectal distention-induced Fos expression in the spinal cord and the visceromotor reflex. *Neuroscience* 2002; **113:** 205-211

45 **Kozlowski CM**, Bountra C, Grundy D. The effect of fentanyl, DNQX and MK-801 on dorsal horn neurones responsive to colorectal distension in the anaesthetized rat. *Neurogastroenterol Motil* 2000; **12:** 239-247

46 **Song XJ,** Zhao ZQ. Involvement of NMDA and non-NMDA receptors in transmission of spinal visceral nociception in cat. *Zhonggua Yi Xue Za Zhi* 1999; **79**: 308-312

Science Editor Guo SY **Language Editor** Elsevier HK

PO Box 2345, Beijing 100023, China
www.wjgnet.com
wjg@wjgnet.com

World J Gastroenterol 2005;11(41):6503-6507
World Journal of Gastroenterology ISSN 1007-9327

• *CLINICAL RESEARCH* •

Narrow portion of the terminal choledochus is a cause of upstream biliary dilatation in patients with anomalous union of the pancreatic and biliary ducts

Tatsuya Nomura, Yoshio Shirai, Toshifumi Wakai, Naoyuki Yokoyama, Jun Sakata, Katsuyoshi Hatakeyama

Tatsuya Nomura, Yoshio Shirai, Toshifumi Wakai, Naoyuki Yokoyama, Jun Sakata, Katsuyoshi Hatakeyama, Division of Digestive and General Surgery, Niigata University Graduate School of Medical and Dental Sciences, 1 Asahimachi-dori, Niigata, 951-8510, Japan
Correspondence to: Dr. Yoshio Shirai, Division of Digestive and General Surgery, Niigata University Graduate School of Medical and Dental Sciences, 1 Asahimachi-dori, Niigata, 951-8510, Japan. shiray@med.niigata-u.ac.jp
Telephone: +81-25-227-2228 Fax: +81-25-227-0779
Received: 2005-04-13 Accepted: 2005-04-30

Abstract

AIM: To clarify the pathogenesis of biliary dilatation associated with anomalous union of the pancreatic and biliary ducts (AUPBD).

METHODS: Direct cholangiopancreatograms of 350 adult patients with or with suspicion of hepatobiliary or pancreatic disorders were reviewed. AUPBD was diagnosed cholangiopancreatographically, when the pancreaticobiliary ductal union was located above the narrow distal segment of the bile duct, which represents the action of the sphincter of Oddi. The narrow portion of the terminal choledochus was defined as symmetrical stricture of the common bile duct just above the pancreaticobiliary ductal union.

RESULTS: AUPBD was found in 36 patients. Among cholangiopancreatographic features, the narrow portion of the terminal choledochus was the most pathognomonic for AUPBD (accuracy, 98%); it was present in 29 (81%) patients with AUPBD, but was not found in any patients without AUPBD. Among patients with AUPBD, biliary dilatation (>10 mm) was more frequent in those with the narrow portion of the terminal choledochus (23/29) than in those without (2/7; P = 0.018) AUPBD. Among the patients with both AUPBD and the narrow portion of the terminal choledochus, there was a strong negative correlation between the minimum diameter of the narrow portion and the maximum diameter of the choledochus (r = -0.78, P<0.001), suggesting that the degree of biliary narrowing at the narrow portion correlates with that of upstream biliary dilatation.

CONCLUSION: The narrow portion of the terminal choledochus, a pathognomonic radiologic feature of AUPBD, may be a cause of biliary dilatation in patients with AUPBD.

Key words: Anomalous; Biliary dilatation; Congenital biliary dilatation; Congenital choledochal cyst; Terminal choledochus; Cholangiopancreatography

Nomura T, Shirai Y, Wakai T, Yokoyama N, Sakata J, Hatakeyama K. Narrow portion of the terminal choledochus is a cause of upstream biliary dilatation in patients with anomalous union of the pancreatic and biliary ducts. *World J Gastroenterol* 2005; 11(41):6503-6507
http://www.wjgnet.com/1007-9327/11/6503.asp

INTRODUCTION

Anomalous union of the pancreatic and biliary ducts (AUPBD) is an uncommon congenital condition, which predisposes to various pancreaticobiliary disorders including congenital choledochal cyst[1-5], biliary cancer[6-8], and pancreatitis[9-12], and is more commonly seen in Asian than in Western countries[13]. This anomaly is defined as the pancreaticobiliary ductal union located above the action of the sphincter of Oddi as first described by Babbitt[1]. Although direct cholang-iopancreatography is the most reliable means of detecting this anomaly[14-16], the pathognomonic cholangiopancreatographic features of AUPBD have not been fully delineated.

AUPBD is frequently accompanied by biliary dilatation[1-5], but some patients with AUPBD show no biliary dilatation[8,17]. The causal relationship between AUPBD and biliary dilatation associated with this anomaly has not been fully established.

The aims of this study were to elucidate the cholang-iopancreatographic features specific to AUPBD and to clarify the pathogenesis of biliary dilatation associated with AUPBD, by analyzing direct cholangiopancreatograms of 350 Japanese adult patients with or without AUPBD.

MATERIALS AND METHODS

Patients

From January 1988 to July 1999, 535 consecutive adult patients with or with suspicion of hepatobiliary or pancreatic disorders underwent direct cholangiopancrea-

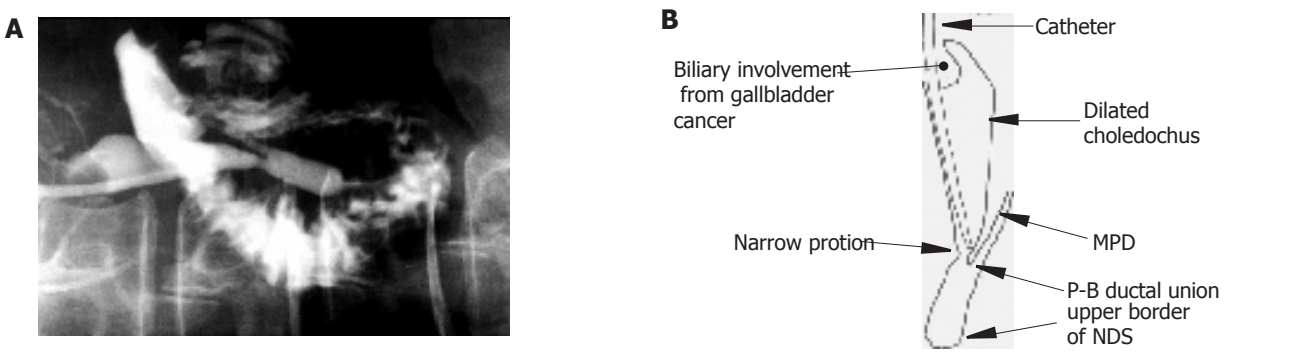

Figure 1 Endoscopic retrograde cholangiopancreatogram in a 55-year-old woman with gallbladder cancer associated with AUPBD and cylindrical biliary dilatation (**A**). Diagram of the cholangiopancreatogram (**B**). The minimum diameter of the narrow portion of the terminal choledochus is 4 mm, and the maximum diameter of the upstream choledochus is 15 mm. AUPBD: anomalous union of the pancreatic and biliary ducts; NDS: narrow distal segment; P-B ductal union: pancreaticobiliary ductal union; narrow portion: narrow portion of the terminal choledochus; MPD: main pancreatic duct.

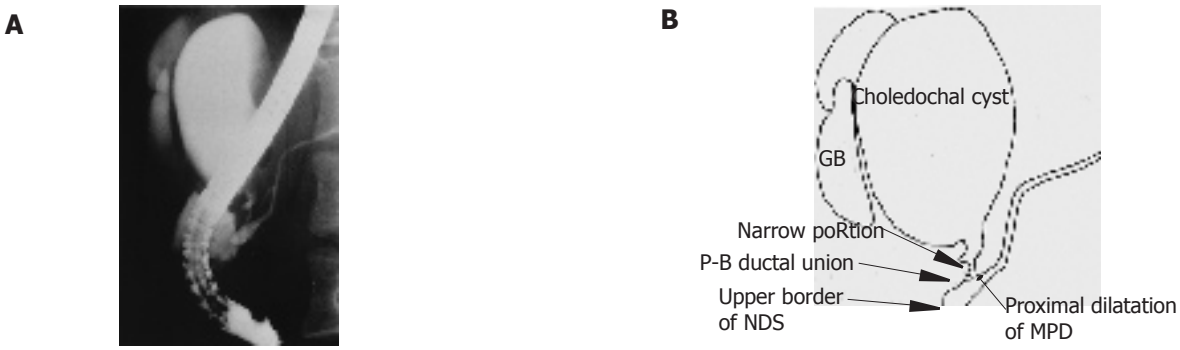

Figure 2 Endoscopic retrograde cholangiopancreatogram in a 21-year-old woman with AUPBD and cystic biliary dilatation (**A**). Diagram of the cholangiopancreatogram (**B**). The minimum diameter of the narrow portion of the terminal choledochus is 1.5 mm, and the maximum diameter of the upstream choledochus is 57 mm. Proximal dilatation of the MPD is also seen. AUPBD: anomalous union of the pancreatic and biliary ducts; NDS: narrow distal segment; P-B ductal union: pancreaticobiliary ductal union; narrow portion: narrow portion of the terminal choledochus; GB: gallbladder; MPD: main pancreatic duct.

tography before surgical intervention in our hospital. All were Japanese. Direct cholangiopancreatography included endoscopic retrograde cholangiopancreatography (ERCP) and percutaneous transhepatic cholangiography (PTC). One hundred and seventy-six patients were excluded due to biliary involvement from pancreaticobiliary malignancies which precluded opacification of the pancreaticobiliary ductal union, lack of opacification of one or both ducts, or failure to localize the pancreaticobiliary ductal union despite opacification of both ductal systems. Nine patients in whom the common bile and main pancreatic ducts entered separately into the duodenum were also excluded. The remaining 350 patients, in whom ERCP ($n = 324$) or PTC ($n = 26$) opacified the pancreaticobiliary ductal union, formed the basis of this retrospective study, including 174 women and 176 men with ages ranging from 18 to 86 years (median, 61 years). They included 118 patients with biliary malignancy, 118 with gallstone disease, 27 with liver tumor, 17 with pancreatic cancer, 16 with congenital choledochal cyst, 11 with chronic pancreatitis, and 43 with miscellaneous disorders.

Cholangiopancreatographic diagnosis of AUPBD

Although the criteria for AUPBD have not been standardized, the essential feature of this condition is the pancreaticobiliary ductal union located above the action of the sphincter of Oddi as first described by Babbitt[1]. Thus, in this study, AUPBD was diagnosed cholangiopancreatographically when the pancreaticobiliary ductal union was located above the narrow distal segment (NDS), which represents the functional region of the sphincter of Oddi (Figures 1 and 2)[8,16,17].

Terminology of cholangiopancreatographic features

Direct cholangiopancreatograms were reviewed in each of our patients to elucidate the presence or absence of the following major radiologic features: narrow portion of the terminal choledochus, biliary dilatation, and proximal dilatation of the main pancreatic duct.

The narrow portion of the terminal choledochus was defined as symmetrical stricture of the common bile duct just above the pancreaticobiliary ductal union and is a synonym for "stenosis of the distal choledochus"[3], "narrow segment distal to the common bile duct"[18], "narrow segment of the terminal bile duct"[19], "narrow portion of the choledochus"[20], "narrow segment of the common bile duct distal to choledochal cyst"[21], and "narrowed duct segment distal to the biliary cyst"[22]. The narrow portion of the terminal choledochus was always located just below choledochal cysts, when cysts were

Table 1 Diagnostic accuracy of cholangiopancreatographic features for the detection of AUPBD

Cholangiopancreatographic feature	Sensitivity(%)	Specificity(%)	Positive predictive value (%)	Negative predictive value (%)	Accuracy(%)
Narrow portion of the terminal choledochus (n = 29)	81	100	100	98	98
Biliary dilatation (>10 mm) (n = 25)	69	68	20	95	68
Proximal dilatation of the main pancreatic duct (>5 mm) (n = 7)	19	100	100	91	92

AUPBD: anomalous union of the pancreatic and biliary ducts.

present. The minimum diameter of the narrow portion of the terminal choledochus (if any) and the maximum diameter of the upstream choledochus were measured on cholangiopancreatograms in each patient (Figures 1 and 2).

Biliary dilatation was defined as a diameter exceeding 10 mm[17]. Biliary dilatation was classified as cystic, fusiform, or cylindrical based on its contours on cholangiopancreatogram[23].

Proximal dilatation of the main pancreatic duct was defined as the proximal portion of the main pancreatic duct with a diameter exceeding 5 mm[24,25].

Kune first demonstrated that the NDS of the bile duct as visualized on cholagiopancreatography represents the functional region of the sphincter of Oddi[26-28]. The NDS was defined as the region lying between the upper border of the "notch" of the bile duct, sudden narrowing of the choledochal lumen just above the ampulla of Vater[29], and the orifice of the ampulla of Vater (Figures 1 and 2).

Statistical analysis

Statistics were calculated with the SPSS 9.0 J software package for Windows (SPSS Japan Inc., Tokyo, Japan). Fisher's exact test and the Spearman's rank correlation were used for data analysis. P values of <0.05 were accepted as statistically significant.

RESULTS

AUPBD was diagnosed in 36 patients (10%) on direct cholangiopancreatograms, including 27 women and 9 men. They had concomitant pancreaticobiliary disorders, including congenital choledochal cyst (n = 16), gallbladder cancer (n = 13), benign gallbladder polyps (n = 3), chronic pancreatitis (n = 2), carcinoma of the common bile duct (n = 1), and adenomyomatosis of the gallbladder (n = 1).

Cholangiopancreatographic features specific to AUPBD

The accuracy of cholangiopancreatographic features for the detection of AUPBD is summarized in Table 1. The narrow portion of the terminal choledochus was present in 29 (81%) patients with AUPBD, but was not found in any patients without AUPBD.

Relationship between the narrow portion of the terminal choledochus and upstream biliary dilatation

In 36 patients with AUPBD, biliary dilatation was more frequent in patients with the narrow portion of the terminal choledochus (23/29, 79%) than in those without (2/7, 28%; P = 0.018) AUPBD. Thus, the presence of the narrow portion of the terminal choledochus was associated with upstream biliary dilatation.

Among the 29 patients with both AUPBD and the narrow portion of the terminal choledochus, there was a strong negative correlation between the minimum diameter of the narrow portion of the terminal choledochus and the maximum diameter of the upstream choledochus (r = -0.78, P < 0.001) (Figure 3). Thus, the degree of biliary narrowing at the narrow portion of the terminal choledochus correlated with that of upstream biliary dilatation.

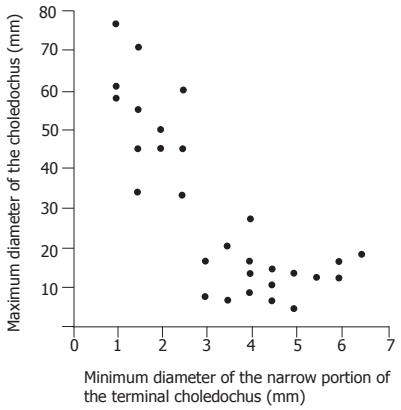

Figure 3 There was a strong negative correlation between the minimum diameter of the narrow portion of the terminal choledochus and the maximum diameter of the upstream choledochus (r = -0.78, P < 0.001).

Also, among the 29 patients with both AUPBD and the narrow portion of the terminal choledochus, a strong positive correlation was noted between patient's age and the minimum diameter of the narrow portion of the terminal

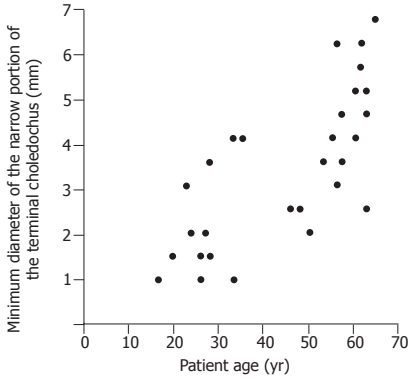

Figure 4 Patient's age was strongly correlated with the minimum diameter of the narrow portion of the terminal choledochus (r = 0.78, P<0.001).

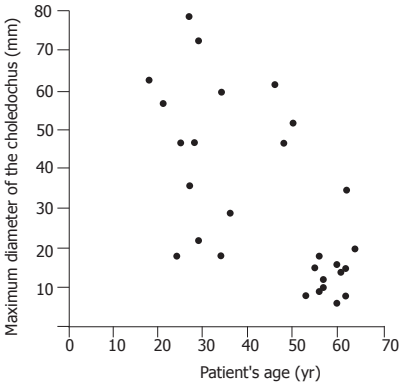

Figure 5 Patient's age was negatively correlated with the maximum diameter of the choledochus (r = –0.53, P = 0.001).

choledochus (r = 0.78, P < 0.001) (Figure 4), whereas there was a negative correlation between patient's age and the maximum diameter of the choledochus(r = -0.53, P = 0.001) (Figure 5). Thus, younger the patient, the more marked were the biliary narrowing at the narrow portion of the terminal choledochus and upstream biliary dilatation.

DISCUSSION

The narrow portion of the terminal choledochus is a characteristic feature of congenital biliary dilatation[18-22]. The current study demonstrated that it is also a pathognomonic feature of AUPBD. AUPBD is often associated with congenital biliary dilatation[2-5]. Thus, we hypothesized that the narrow portion of the terminal choledochus contributes to the development of upstream biliary dilatation frequently seen in AUPBD patients.

Previous studies from Japan reported a prevalence of AUPBD on ERCP ranging from 1.5% to 3.2%[6,10,30]. The extremely high prevalence of AUPBD in our series (10%) may be explained by the fact that our hospital is a tertiary referral center and that only surgical patients were included in this study.

While pancreaticobiliary ductal union located above the sphincteric action[16,17,31], long common channel[10,30], and concomitant cystic biliary dilatation[2-5] have been advocated as characteristic radiologic findings, the diagnostic significance of the narrow portion of the terminal choledochus has not been emphasized. The current study revealed that the narrow portion is present in most adult patients with AUPBD and is a pathognomonic radiologic feature of AUPBD. The narrow portion of the terminal choledochus is an important finding when diagnosing AUPBD by direct cholangiopancreatography.

Previous studies suggested that the narrow portion of the terminal choledochus may lead to the development of congenital biliary dilatation in pediatric patients[18,32,33]. Ito *et al*[18] reported that the length rather than the width of the narrow portion of the terminal choledochus is positively correlated with the degree of upstream choledochal dilatation in children with congenital biliary dilatation. Experimental studies revealed that bile duct obstruction causes cystic biliary dilatation in young animals, while it leads to cylindrical, not cystic, biliary dilatation in adult animals[32,34,35], suggesting that increased intraluminal pressure leads to cystic dilatation of the bile duct, only if the ductal wall is immature. This may explain the fact that cystic biliary dilatation is more common in pediatric patients[6,36] and that the degree of biliary dilatation was more marked in younger patients in our series. The current study is the first demonstration that biliary narrowing at the narrow portion correlates with upstream biliary dilatation even in adult patients with AUPBD. In summary, increased intraluminal pressure due to the narrow portion of the terminal choledochus may cause upstream biliary dilatation in both pediatric and adult patients with AUPBD, although the form of upstream biliary dilatation appears to differ between pediatric and adult patients.

Another possible cause of biliary dilatation in patients with AUPBD is the reflux of pancreatic juice into the bile duct. It has been reported that the refluxed pancreatic juice into the bile duct may lead to increased intraluminal pressure and dilatation of the bile duct[1,37,38]. However, the strong negative correlation between the minimum diameter of the narrow portion of the terminal choledochus and the maximum diameter of the upstream choledochus in the current study suggests that increased intraluminal pressure due to biliary narrowing, rather than refluxed pancreatic juice, may cause upstream biliary dilatation in patients with AUPBD.

Kusunoki *et al*[20,39] reported the presence of "oligoganglio-nosis" in the choledochal wall just below the cystic dilatation in patients with congenital choledochal cyst, suggesting that autonomic dysfunction at the "oligoganglionic" segment of the bile duct may play a role in the development of upstream biliary dilatation. This "oligoganglionic" segment appears to correspond to the narrow portion of the terminal choledochus, as defined in the current study, and may functionally obstruct biliary passage through the segment. It is unknown, however, whether the "oligoganglionosis" was present in our patients because histologic specimens of the narrow portion of the terminal choledochus were not available in any of our patients.

The limitations of the current study include the fact that it was retrospective, and that 176 patients were excluded due to inadequate opacification of the pancreaticobiliary ductal system. However, we feel that these limitations did not significantly influence the outcome of the study because the correlations between variables were too marked to have resulted from chance. The current results are the clearest demonstration to date of the causal relationship between the narrow portion of the terminal choledochus and upstream biliary dilatation in patients with AUPBD.

In conclusion, the narrow portion of the terminal choledochus is a pathognomonic radiologic feature of AUPBD and may be a cause of biliary dilatation in patients with AUPBD.

REFERENCES

1 **Babbitt DP.** Congenital choledochal cysts: new etiological concept based on anomalous relationships of the common bile duct and pancreatic bulb. *Ann Radiol* 1969; **12:** 231-240
2 **Kimura K,** Ohto M, Ono T, Tsuchiya Y, Saisho H, Kawamura K, Yogi Y, Karasawa E, Okuda K. Congenital cystic dilatation of the common bile duct: relationship to anomalous pancreaticobiliary ductal union. *Am J Roentgenol* 1977; **128:** 571-577
3 **Todani T,** Watanabe Y, Fujii T, Uemura S. Anomalous arrangement of the pancreatobiliary ductal system in patients with a choledochal cyst. *Am J Surg* 1984; **147:** 672-676
4 **Okada A,** Nakamura T, Higaki J, Okumura K, Kamata S, Oguchi Y. Congenital dilatation of the bile duct in 100 instances and its relationship with anomalous junction. *Surg Gynecol Obstet* 1990; **171:** 291-298
5 **Lipsett PA,** Pitt HA, Colombani PM, Boitnott JK, Cameron JL. Choledochal cyst disease. A changing pattern of presentation. *Ann Surg* 1994; **220:** 644-652
6 **Kimura K,** Ohto M, Saisho H, Unozawa T, Tsuchiya Y, Morita M, Ebara M, Matsutani S, Okuda K. Association of gallbladder carcinoma and anomalous pancreaticobiliary ductal union. *Gastroenterology* 1985; **89:** 1258-1265
7 **Misra SP,** Gulati P, Thorat VK, Vij JC, Anand BS. Pancreaticobiliary ductal union in biliary diseases. An endoscopic retrograde cholangiopancreatographic study. *Gastroenterology* 1989; **96:** 907-912
8 **Sandoh N,** Shirai Y, Hatakeyama K. Incidence of anomalous union of the pancreaticobiliary ductal system in biliary cancer. *Hepatogastroenterology* 1997; **44:** 1580-1583
9 **Misra SP,** Dwivedi M. Pancreaticobiliary ductal union. *Gut* 1990; **31:** 1141-1149
10 **Sugiyama M,** Atomi Y, Kuroda A. Pancreatic disorders associated with anomalous pancreaticobiliary junction. *Surgery* 1999; **126:** 492-497
11 **Guelrud M,** Morera C, Rodriguez M, Prados JG, Jaén D. Normal and anomalous pancreaticobiliary union in children and adolescents. *Gastrointest Endosc* 1999; **50:** 189-193
12 **Guelrud M,** Morera C, Rodriguez M, Jaen D, Pierre R. Sphincter of Oddi dysfunction in children with recurrent pancreatitis and anomalous pancreaticobiliary union: an etiologic concept. *Gastrointest Endosc* 1999; **50:** 194-199
13 **Sautereau D,** Sava P, Dupuy JF, Cessot F, Cubertafond P, Claude R, Pillegand B. Cancer des voies biliaires extra-hépatiques et anomalie de la jonction bilio-pancréatique. *Gastroenterol Clin Biol* 1989; **13:** 298-301
14 **Yamao K,** Mizutani S, Nakazawa S, Inui K, Kanemaki N, Miyoshi H, Segawa K, Zenda H, Kato T. Prospective study of the detection of anomalous connections of pancreatobiliary ducts during routine medical examinations. *Hepatogastroenterology* 1996; **43:** 1238-1245
15 **Matos C,** Nicaise N, Deviére J, Cassart M, Metens T, Struyven J, Cremer M. Choledochal cysts: comparison of findings at MR cholangiopancreatography and endoscopic retrograde cholangiopancreatography in eight patients. *Radiology* 1998; **209:** 443-448
16 **Nomura T,** Shirai Y, Sandoh N, Nagakura S, Hatakeyama K. Cholangiographic criteria for anomalous union of the pancreatic and biliary ducts. *Gastrointest Endosc* 2002; **55:** 204-208
17 **Mori K,** Nagakawa T, Ohta T, Nakano T, Kayahara M, Kanno M, Ueno K, Izumi R, Miyazaki I. Association between gallbladder cancer and anomalous union of the pancreaticobiliary ductal system. *Hepatogastroenterology* 1993; **40:** 56-60
18 **Ito T,** Ando H, Nagaya M, Sugito T. Congenital dilatation of the common bile duct in children.-- The etiologic significance of the narrow segment distal to the dilated common bile duct. *Z Kinderchir* 1984; **39:** 40-45
19 **Matsumoto Y,** Uchida K, Nakase A, Honjo I. Clinicopathologic classification of congenital cystic dilatation of the common bile duct. *Am J Surg* 1977; **134:** 569-574
20 **Kusunoki M,** Saitoh N, Yamamura T, Fujita S, Takahashi T, Utsunomiya J. Choledochal cysts. Oligoganglionosis in the narrow portion of the choledochus. *Arch Surg* 1988; **123:** 984-986
21 **Suda K,** Matsumoto Y, Miyano T. Narrow duct segment distal to choledochal cyst. *Am J Gastroenterol* 1991; **86:** 1259-1263
22 **Matsumoto Y,** Fujii H, Itakura J, Mogaki MA, Matsuda M, Morozumi A, Fujino M, Suda K. Pancreaticobiliary maljunction: etiologic concepts on radiologic aspects. *Gastrointest Endosc* 2001; **53:** 614-619
23 **Todani T,** Watanabe Y, Narusue M, Tabuchi K, Okajima K. Congenital bile duct cysts. Classification, operative procedures, and review of thirty-seven cases including cancer arising from choledochal cyst. *Am J Surg* 1977; **134:** 263-269
24 **Rattner DW,** Schapiro RH, Warshaw AL. Abnormalities of the pancreatic and biliary ducts in adult patients with choledochal cysts. *Arch Surg* 1983; **118:** 1068-1073
25 **Wiedmeyer DA,** Stewart ET, Dodds WJ, Geenen JE, Vennes JA, Taylor AJ. Choledochal cyst : findings on cholangiopancreatography with emphasis on ectasia of the common channel. *Am J Roentgenol* 1989; **153:** 969-972
26 **Kune GA.** Surgical anatomy of common bile duct. *Arch Surg* 1964; **89:** 995-1004
27 **Kune GA.** The influence of structure and function in the surgery of the biliary tract. *Ann R Coll Surg Engl* 1970; **47:** 78-91
28 **Kune GA,** Sali A. The practice of biliary surgery. 2nd ed. Oxford: *Blackwell Sci Pub* 1980: 1-31
29 **Hand BH.** An anatomical study of the choledochoduodenal area. *Br J Surg* 1963; **50:** 486-494
30 **Kato O,** Hattori K, Suzuki T, Tachino F, Yuasa T. Clinical significance of anomalous pancreaticobiliary union. *Gastrointest Endosc* 1983; **29:** 94-98
31 **Nagata E,** Sakai K, Kinoshita H, Kobayashi Y. The relation between carcinoma of the gallbladder and an anomalous connection between the choledochus and the pancreatic duct. *Ann Surg* 1985; **202:** 182-190
32 **Miyano T,** Suruga K, Suda K. Abnormal choledocho-pancreatico ductal junction related to the etiology of infantile obstructive jaundice diseases. *J Pediatr Surg* 1979; **14:** 16-26
33 **Shimotake T,** Iwai N, Yanagihara J, Inoue K, Fushiki S. Innervation patterns in congenital biliary dilatation. *Eur J Pediatr Surg* 1995; **5:** 265-270
34 **Kato T,** Asakura Y, Kasai M. An attempt to produce choledochal cyst in puppies. *J Pediatr Surg* 1974; **9:** 509-513
35 **Spitz L.** Experimental production of cystic dilatation of the common bile duct in neonatal lambs. *J Pediatr Surg* 1977; **12:** 39-42
36 **Chaudhary A,** Dhar P, Sachdev A, Kumar N, Vij JC, Sarin SK, Broor SL, Sharma SS. Choledochal cysts - differences in children and adults. *Br J Surg* 1996; **83:** 186-188
37 **Ohkawa H,** Sawaguchi S, Yamazaki Y, Ishikawa A, Kikuchi M. Experimental analysis of the ill effect of anomalous pancreaticobiliary ductal union. *J Pediatr Surg* 1982; **17:** 7-13
38 **Oguchi Y,** Okada A, Nakamura T, Okumura K, Miyata M, Nakao K, Kawashima Y. Histopathologic studies of congenital dilatation of the bile duct as related to an anomalous junction of the pancreaticobiliary ductal system: clinical and experimental studies. *Surgery* 1988; **103:** 168-173
39 **Kusunoki M,** Yamamura T, Takahashi T, Kantoh M, Ishikawa Y, Utsunomiya J. Choledochal cyst. Its possible autonomic involvement in the bile duct. *Arch Surg* 1987; **122:** 997-1000

Science Editor Ma JY and Guo SY **Language Editor** Elsevier HK

PO Box 2345, Beijing 100023, China
www.wjgnet.com
wjg@wjgnet.com

ELSEVIER

World J Gastroenterol 2005;11(41):6508-6511
World Journal of Gastroenterology ISSN 1007-9327

• *RAPID COMMUNICATION* •

Prevalence of gallstone disease in first-degree relatives of patients with cholelithiasis

Adolfo Francesco Attili, Adriano De Santis, Fabia Attili, Enrico Roda, Davide Festi, Nicola Carulli

Adolfo Francesco Attili, Adriano De Santis, Fabia Attili, GI Unit, Department of Clinical Medicine, University of Roma "La Sapienza", Italy
Enrico Roda, Davide Festi, Department of Internal Medicine, University of Bologna, Italy
Nicola Carulli, Department of Internal Medicine, University of Modena, Italy
Supported by the SANOFI-Synthelabo SpA
Correspondence to: Adolfo Francesco Attili, GI Unit, Department of Clinical Medicine, Policlinico Umberto I, Rome 00185 , Italy. adolfo.attili@uniroma1.it
Telephone: +39-6-491671
Received: 2004-11-23 Accepted: 2004-12-20

Abstract

AIM: To evaluate the influence of familiality on the prevalence of gallstone disease (GD) in Italy.

METHODS: Families of 79 subjects with gallstones (cases) and of 79 subjects without gallstones (controls) were investigated for the presence of gallstones by ultrasonography. Index cases and index controls were matched for age, sex, and operative unit. Sixty-three and sixty-two husbands and wives of index cases and index controls, respectively, were also studied.

RESULTS: Overall,the prevalence of GD was significantly higher (χ^2=14.52, P<0.001) in the 202 first-degree relatives of subjects with gallstones than that in the 201 first-degree relatives of subjects without gallstones (28.6% *vs* 12.4%, relative risk (RR) 1.80, 95% confidence interval (CI) 1.29-2.63). In particular, prevalence of GD was significantly higher in mothers, fathers, and sisters of index cases than that in the respective family members of index controls. The highest RR was observed in mothers (RR=2.35, 95%CI 1.38-4.3). Prevalence of GD was not obviously different in brothers and also in husbands and wives of index cases and index controls. Family members of index cases did not differ from family members of control cases with respect to the most important risk factors for gallstones (age, diabetes, BMI, and number of pregnancies) with an exception of a higher prevalence of diabetes in fathers of index controls than in fathers of index cases.

CONCLUSION: This study confirms that familiality plays a very important role in the pathogenesis of gallstones.

Key words: Gallstones; Familiality

Attili AF, De Santis A, Attili F, Roda E, Festi D, Carulli N. Prevalence of gallstone disease in first-degree relatives of patients with cholelithiasis. *World J Gastroenterol* 2005;11(41): 6508-6511
http://www.wjgnet.com/1007-9327/11/6508.asp

INTRODUCTION

Gallstone disease (GD) is very common among the Western civilized countries. Nonetheless the literature concerning family inheritance is scarce, although consistent. Körner[1] collected 74 family pedigrees of probands with gallbladder disease and showed that gallstones were five times more common in families of affected individuals than in families of his control group. Van der Linden and Lindelöf[2] investigated the presence of gallstones in wives and husbands of subjects with gallstones and also in siblings of the same sex of the wife or husband, demonstrating the data of a clear 2:1 ratio in favor of familial occurrence. Because familial occurrence does not necessarily reflect genetic factors, Van der Linden and Westlin[3] studied the occurrence of GD in spouses who had lived together continuously and presumably shared the same environment, especially diet, during adult life. They found that women married to subjects with gallstones do not suffer more often from the disease than do other women.

The importance of familiality has been well identified also in epidemiological studies. Jorgensen[4] in Denmark demonstrated a relative risk (RR) of 2:1 in first degree relatives of gallstone patients. The Sirmione study[5] found a RR of 3.3:1 in sons of subjects with gallstones with respect to sons of subjects without gallstones. Similarly, in Israel[6] and in India[7] too, an elevated prevalence of gallstones has been demonstrated in family members of subjects with gallstones with respect to family members of subjects without gallstones. The MICOL study[8] demonstrated that subjects with a family history of GD are at an increased risk for the presence of gallstones in their gallbladder. To our knowledge, a formal family study for gallstones is lacking in Italy. We, therefore, aimed to evaluate the influence of familiality on the prevalence of GD in Italy.

MATERIALS AND METHODS

This study was performed in 16 operative units (5 in the north, 5 in the center and 6 in the south of Italy). Each operative unit was equipped with an ultrasonographic apparatus of similar characteristics (i.e., equipped with a 3.5-MHz linear transducer) and was instructed to follow an identical protocol (all the subjects were examined in the supine and left decubitus position).

Seventy-nine families of cases and 79 families of controls were enrolled in the study. All subjects with gallstones consecutively observed by the medical staff of the operative units were included as cases (case subjects), if at least one parent and a sibling were living and gave their consent to participate in the study. For each case subject, a control subject matching the sex and age (±3 years) was selected among those who attended the outpatient echographic services of the single operative unit and did not show any presence of gallstones or were previously submitted to cholecystectomy. Cases and controls were matched not only for age and sex, but they did not differ also for the other most important risk factors for gallstones: BMI, number of pregnancies (for females) and prevalence of diabetes (Table 1). Families without a matching family within the same operative unit were excluded from the calculations.

Table 1 Levels of the most important risk factors for gallstones in cases with or without gallstones

	Cases $n=79$	Controls $n=79$	*P*
Male/female (*n*)	30/49	30/49	NS
Age (yr); mean (CI)	48.6 (45.8–51.4)	48.5 (45.7–51.4)	NS
BMI; mean (CI)	25.5 (24,9–26.4)	25.7 (24.7–26.7)	NS
Number of pregnancies (females); mean (CI)	1.71 (1.29–2.13)	1.47 (1.04–1.89)	NS

All the available first degree relatives of cases were invited to participate in the study. Husbands and spouses were also studied, when available. Participations among living first degree relatives of cases and controls were 82% and 80%, respectively; among living spouses and husbands of cases and controls were 88% and 89%, respectively. A precoded questionnaire regarding personal, physiological and pathological history, dietary habits and number of pregnancies (females) was administered by a member of the medical staff to all the family members. Each family subject was also submitted to anthropometric measurements (weight and height) and ultrasonographic examination of the biliary tract. BMI was calculated by dividing the weight (kg) by the square of height (m).

Subjects were considered as having GD, if they showed presence of gallstones in their gallbladder or had already been submitted to cholecystectomy.

Statistical analysis

All statistical analyses were carried out with the NCSS statistical software program, 329 North 1000 East Kaysville, UT 84037, USA. The Student's *t*-test and the χ^2 test were used when appropriate. A *P* value less than 0.05 was considered statistically significant. We computed Mantel-Haenszel estimates of RR with 95% confidence intervals (CI).

RESULTS

Overall, prevalence of GD was significantly higher (χ^2=14.52, *P*<0.001) in the 202 first-degree relatives of subjects with gallstones than that in the 201 first-degree relatives of subjects without gallstones (28.6% *vs* 12.4%, RR 1.80, 95%CI 1.29-2.63)(Table 1).

In particular, 13 of the 31 (41.9%) fathers of the index cases and 6 of the 34 fathers of the index controls had GD. The difference was significant according the χ^2 test although the lower limit of the 95%CI of the RR was below 1 (Table 2). Fathers of cases and controls did not differ for age and BMI, but fathers of controls had a significantly higher prevalence of diabetes (Table 2).

Prevalence of GD was significantly higher among the 51 mothers of index cases as compared to the 51 mothers of index controls (56.9% *vs* 21.6%, RR 2.35 95%CI 1.38-4.3, Table 2). Mothers of cases did not differ from mothers of controls as far as the most important risk factors for gallstones were concerned, i.e. age, BMI, prevalence of diabetes, and number of pregnancies.

Brothers of cases and brothers of controls (Table 3) showed similar prevalences of GD and similar levels of risk factors for gallstones, i.e. age, BMI, and prevalence of diabetes. Among the sisters, prevalence of GD

Table 2 Prevalence of GD and levels of the most important risk factors for gallstones in fathers and mothers of subjects with or without gallstones

	Fathers of		Mothers of	
	Cases $n=31$	Controls $n=34$	Cases $n=51$	Controls $n=51$
Age (yr); mean (CI)	70.0 (66.7-73.4)	70.9 (67.6-74.2)	72.4 (69.2-75.5)	71.8 (71.8-74.8)
BMI; mean (CI)	25.7 (24.4-27.0)	27.5 (26.3-28.6)	26.3 (25.1-27.6)	26.3 (25.4-27.3)
Diabetes (%)	3.4[a]	20.6	20.0	21.2
Number. of pregnancies; mean (CI)	-	-	2.9 (2.4-3.4)	2.9 (2.5-3.4)
GD (%)	41.9[c]	17.6	56.9[b]	21.6

[a]*P*<0.05 *vs* controls (χ^2=4.15); [c]*P*<0.05 *vs* controls (χ^2=4.66; RR=1.75 (0.98-2.6 95% CI); [b]*P*<0.001 *vs* controls (χ^2=13.32; RR=2.35 (1.38-4.3 95% CI).

Table 3 Prevalence of GD and levels of the most important risk factors for gallstones in brothers and sisters of subjects with or without gallstones

	Brothers of		Sisters of	
	Cases $n=50$	Controls $n=47$	Cases $n=39$	Controls $n=44$
Age (yr); mean (CI)	48.5 (45.4-51.6)	44.9 (41.4-48.3)	43.9 (39.0-48.8)	48.9 (44.9-52.8)
BMI ; mean (CI)	25.6 (24.6-26.5)	25.5 (24.4-26.6)	24.8 (23.4-26.1)	25.8 (24.5-27.1)
Diabetes (%)	5.9	0	2.7	11.4
No. of pregnancies; mean (CI)	-	-	1.3 (0.9-1.7)	1.5 (1.0-1.9)
GD (%)	10.0	8.5	25.6[a]	9.1

[a]$P<0.05$ *vs* controls ($\chi^2=4.04$; RR = 2.03 [0.94-6.22 95%CI])

was significantly higher among the sisters of index cases as compared to the sisters of controls (25.6% *vs* 9.1%; $\chi^2=4.04$, $P<0.05$), but the lower limit of the RR confidence interval was below 1 [RR = 2.03 (0.94-6.22 95%CI)]. The sisters of cases and sisters of controls did not differ in age, BMI, prevalence of diabetes, and number of pregnancies.

None of the sons of the cases and controls had GD.

No significant difference was observed in prevalence of GD among husbands and spouses of the index cases and controls (Table 4). Husbands and wives of index cases or controls also did not differ for the most important risk factors for gallstones (Table 4).

Table 4 Prevalence of GD and levels of the most important risk factors for gallstones in husbands and wives of subjects with or without gallstones

	Husbands and wives of		*P*
	Cases $n=63$	Controls $n=62$	
Males/females	40/23	39/23	NS
Age (yr); mean (CI)	50.2 (48.8-51.4)	50.6 (48.9-51.7)	NS
BMI ; mean (CI)	25.9 (24.9-26.6)	26.0 (24.9-27.0)	NS
No. of pregnancies (female); mean (CI)	1.5 (1.0-2.2)	1.6 (0.8-2.1)	NS
Diabetes (%)	4.8	3.2	NS
GD (%)	9.5	11.2	NS

DISCUSSION

This study confirms that genetic factors play a very important role in the pathogenesis of GD. Overall, the prevalence of GD was significantly higher in the first-degree relatives of subjects with gallstones than in those of subjects without gallstones. The highest relative risks were found in female family members (mothers and sisters). This finding might be explained by the fact that GD is inherited as a sex-linked dominant trait. One might argue that an increased familial prevalence of gallstones might not necessarily involve a genetic defect, but rather reflects a common environmental risk factor. However, our results regarding the prevalence of GD in husbands and wives of index cases and index controls were in agreement with previous data by Van Der Linden and Westlin[3] and Leoci *et al*[9]. On the other hand, family members of index cases and control cases had similar levels of the most important risk factors for GD. These results support the hypothesis that the differences in GD prevalences were due to genetic rather than to environmental factors.

The results of our study further confirmed that a positive family history of GD might be included among the variables that can be used in order to select populations with a higher prevalence of gallstones than that predicted simply on the basis of age and sex. Using a similar approach[10], we were able to demonstrate that selection of subjects with multiple factors associated with gallstones increases the a priori probability of gallstone diagnosis by a factor 2 in females and 3 in males.

Some studies have identified genes (Lith1 on Chr 2, Lith 2 on Chr 19, Lith 3 on Chr 17) that are resporsible for increased gallstone formation in mice[11-18]. Although there is no evidence yet, that any of the Lith genes in the mouse is important in human gallstone susceptibility, some are likely to be and an era of "pre-gallstone disease" identification and possibly prevention seems open.

ACKNOWLEDGMENTS

Participating Operative Units are as follows: (1). Correggio (Reggio Emilia) - Ospedale Civile, Marchi M; (2). Parma -Ospedale Civile, Colla G; (3). Faenza (Ravenna)-Ospedale degli Infermi, Stefanini G; (4). Abano Terme (Padova)-Presidio Ospedaliero USSL 16, Parisi G; (5). Genova, Cattedra di Gastroenterologia, Celle G; (6). Castel Fiorentino (Firenze)-Ospedale Civile. Tafi A; (7). Livorno-Ospedale Civile, Vivaldi I; (8). Pisa-Ospedale Cisanello, Bresci G; (9). Roma - Campus Biomedico, Cicala M; (10). Roma-Policlinico Umberto I, De Santis A; (11). Enna-Ospedale Umberto I, Trimarchi M; (12). Lecce-Ospedale Civile Delle Fonti Di Scorano, Paiano A; (13). Foggia-Ospedali Riuniti Di Foggia, Vinelli F; (14). Salerno -Ospedale Civile S Leonardo, Romano M; (15). Mercato S Severino (Salerno)-Ospedale Civile, Maurano A; (16). Reggio Calabria-Ospedale Morelli, Polimeni N.

REFERENCES

1 **Körner G.** Über die familiare harfung den gallenblasenkrankh eitern. *Z Mensch Vererb Konstitutionsl* 1937; **20:** 526-582

2 **Van der Linden W,** Lindelöf G. The familial occurrence of

gallstone disease. *Acta Genet Stat Med.* 1965; **15 :** 159-164
3 **Van der Linden W,** Westlin N. The familial occurrence of gallstone disease II. Occurrence in husbands and wives. ***Acta Genet Stat Med*** 1966; **16:** 377-382
4 **Jørgensen T.** Gallstones in a Danish population: familial occurrence and social factors. *J Biosoc Sci* 1988; **20:** 111-120
5 **Barbara L,** Sama C, Morselli Labate AM, Taroni F, Rusticali AG, Festi D, Sapio C, Roda E, Banterle C, Puci A. A population study on the prevalence of gallstone disease: the Sirmione Study. *Hepatology* 1987; **7:** 913-917
6 **Gilat T,** Feldman C, Halpern Z, Dan M, Bar Meir S. An increased familial frequency of gallstones. *Gastroenterology* 1983; **84:** 242-246
7 **Sarin SK,** Negi VS, Dewan R, Sasan S, Saraya A. High familial prevalence of gallstones in the first-degree relatives of gallstone patients. *Hepatology* 1995; **22:** 138-141
8 **Attili AF,** Capocaccia R, Carulli N, Festi D, Roda E, Barbara L, Capocaccia L, Menotti A, Okolicsanyi L, Ricci G, Lalloni L, Mariotti S, Sama C, Scafato E. Factors associated with gallstone disease in the MICOL experience. Multicenter Italian Study on Epidemiology of Cholelithiasis. *Hepatology* 1997; **26:** 809-818
9 **Leoci C,** Chiloiro M, Guerra V, Misciagna G. [Genetic epidemiology of cholelithiasis. A case-control study of a population] *Minerva Gastroenterol Dietol* 1991; **37:** 35-39
10 **Attili AF,** Pazzi P, Galeazzi R. Prevalence of previously undiagnosed gallstones in a population with multiple risk factors. *Dig Dis Sci* 1995; **40:** 1770-1774
11 **Khanuja B,** Cheah YC, Hunt M, Nishina PM, Wang DQ, Chen HW, Billheimer JT, Carey MC, Paigen B. Lith1, a major gene affecting cholesterol gallstone formation among inbred strains of mice. *Proc Natl Acad Sci United States* 1995; **92:** 7729-7733
12 **Lammert F,** Wang DQ, Wittenburg H, Bouchard G, Hillebrandt S, Taenzler B, Carey MC, Paigen B. Lith genes control mucin accumulation, cholesterol crystallization, and gallstone formation in A/J and AKR/J inbred mice. *Hepatology* 2002; **36:** 1145-1154
13 **Wittenburg H,** Lammert F, Wang DQ, Churchill GA, Li R, Bouchard G, Carey MC, Paigen B. Interacting QTLs for cholesterol gallstones and gallbladder mucin in AKR and SWR strains of mice. *Physiol Genomics* 2002; **8:** 67-77
14 **van Erpecum KJ,** Wang DQ, Lammert F, Paigen B, Groen AK, Carey MC. Phenotypic characterization of Lith genes that determine susceptibility to cholesterol cholelithiasis in inbred mice: soluble pronucleating proteins in gallbladder and hepatic biles. *J Hepatol* 2001; **35:** 444-451
15 **Paigen B,** Schork NJ, Svenson KL, Cheah YC, Mu JL, Lammert F, Wang DQ, Bouchard G, Carey MC. Quantitative trait loci mapping for cholesterol gallstones in AKR/J and C57L/J strains of mice. *Physiol Genomics* 2000; **4:** 59-65
16 **Lammert F,** Wang DQ, Paigen B, Carey MC. Phenotypic characterization of Lith genes that determine susceptibility to cholesterol cholelithiasis in inbred mice: integrated activities of hepatic lipid regulatory enzymes. *J Lipid Res* 1999; **40:** 2080-2090
17 **Wang DQ,** Lammert F, Paigen B, Carey MC. Phenotypic characterization of lith genes that determine susceptibility to cholesterol cholelithiasis in inbred mice. Pathophysiology Of biliary lipid secretion. *J Lipid Res* 1999; **40:** 2066-2079
18 **Wang DQ,** Paigen B, Carey MC. Phenotypic characterization of Lith genes that determine susceptibility to cholesterol cholelithiasis in inbred mice: physical-chemistry of gallbladder bile. *J Lipid Res* 1997; **38:** 1395-1411

Sciencel Editor Kumar M and Guo SY **Language Editor** ELsevier HK

PO Box 2345, Beijing 100023, China
www.wjgnet.com
wjg@wjgnet.com

ELSEVIER

World J Gastroenterol 2005;11(41):6512-6517
World Journal of Gastroenterology ISSN 1007-9327

• *RAPID COMMUNICATION* •

Genistein inhibits invasive potential of human hepatocellular carcinoma by altering cell cycle, apoptosis, and angiogenesis

Yan Gu, Chen-Fang Zhu, Hitoshi Iwamoto, Ji-Sheng Chen

Yan Gu, Chen-Fang Zhu, Department of General Surgery, The Ninth People's Hospital, Shanghai Second Medical University, Shanghai 200011, China
Hitoshi Iwamoto, Fifth Department of Surgery, Tokyo Medical University, Tokyo 193-8639, Japan
Ji-Sheng Chen, Department of Hepatobiliary Surgery, Sun Yat-Sen Memorial Hospital, Sun Yat-Sen University, Guangzhou 510120, China
Supported by the Basic Research Key Project of the Science Foundation of Shanghai Municipal Commission of Science and Technology, No. 02JC14001
Correspondence to: Yan Gu, Division of Liver and Pancreas Transplantation, The Dumont-UCLA Transplant Center, Los Angeles, CA 90095, United Stutes. yguchina@ucla.edu
Telephone: +1-323-397-8941
Received: 2005-03-18 Accepted: 2005-04-11

Abstract

AIM: To study the *in vitro* and *in vivo* inhibitory effects of genistein on invasive potential of Bel 7402 hepatocellular carcinoma (HCC) cells and to explore the underlying mechanism.

METHODS: Bel 7402 HCC cells were exposed to genistein. The invasive activity of tumor cells was assayed in transwell cell culture chamber. $p125^{FAK}$ expression and cell cycle were evaluated by a functional assay. Cell apoptosis analysis was performed with TUNEL method. In addition, bilateral subrenal capsule xenograft transplantation of HCC was performed in 10 nude mice. Genistein was injected and the invasion of HCC into the renal parenchyma was observed. Microvessels with immunohistochemical staining were detected.

RESULTS: Genistein significantly inhibited the growth of Bel 7402 cells, the inhibitory rate of tumor cells was 26–42%. The invasive potential of Bel 7402 cells *in vitro* was significantly inhibited, the inhibitory rate was 11–28%. Genistein caused G2/M cell cycle arrest, S phase decreased significantly. The occurrence of apoptosis in genistein group increased significantly. The expression of $p125^{FAK}$ in 5 μg/mL genistein group (15.26±0.16%) and 10 μg/mL genistein group (12.89±0.36%) was significantly lower than that in the control group (19.75±1.12%, $P<0.05$). Tumor growth in genistein-treated nude mice was significantly retarded in comparison to control mice, the inhibitory rate of tumor growth was about 20%. Genistein also significantly inhibited the invasion of Bel 7402 cells into the renal parenchyma of nude mice with xenograft transplant. The positive unit value of microvessels in genistein-treated group (10.422 ± 0.807) was significantly lower than that in control group (22.330 ± 5.696, $P < 0.01$).

CONCLUSION: Genistein can effectively inhibit the invasive potential of Bel 7402 HCC cells by altering cell cycle, apoptosis and angiogenesis, inhibition of focal adhesion kinase may play a significant role in this process.

Key words: Genistein; Human hepatocellular carcinoma; Invasion; Cell cycle; Apoptosis; Angiogenesis

Gu Y, Zhu CF, Iwamoto H, Chen JS. Genistein inhibits invasive potential of human hepatocellular carcinoma by altering cell cycle, apoptosis, and angiogenesis. *World J Gastroenterol* 2005; 11(41): 6512-6517
http://www.wjgnet.com/1007-9327/11/6512.asp

INTRODUCTION

Genistein (5,7,4'-trihydroxyisoflavone), an isoflavinoid in soy beans, has been identified as a potential cause for the low incidence of certain types of tumor such as breast cancer, gastric cancer, colon cancer, prostate cancer, *etc.*[1-4]. As a natural tyrosine kinase inhibitor[5-7], genistein can suppress the formation and development of these tumors[8-11]. However, only limited data are available to demonstrate the effects of genistein on human HCC. The purpose of this study was to investigate the invasive potential and apoptotic effects of genistein *in vitro* and *in vivo* on HCC cells and to gain insights regarding the underlying mechanism mediating the effects of genistein.

MATERIALS AND METHODS

Cell culture and genistein

The human HCC cell line, Bel 7402, was obtained from Cancer Institute of Sun Yat-Sen University in Guangzhou. The cells were maintained in RPMI 1640 medium supplemented with 10% fetal bovine serum (FBS), penicillin (100 U/mL), and streptomycin (100 μg/mL) and cultured at 37 °C in a humidified atmosphere containing 50 mL/L CO_2 in air. Genistein purchased from Sigma

Chemical Co. was suspended in dimethylsulfoxide (DMSO) for the experiments.

In vitro assays of Bel 7402 cell growth and viability

The cells were seeded at the density of 1×10^4 cells with 1mL of medium/well onto 24 plates and incubated with or without genistein for 6 d. On the indicated day thereafter, cells were trypsinized and the number of cells was scored. An equivalent volume of DMSO was added to control cultures.

Cell viability was assayed using methyl thiazol tetrazolium (MTT) method. A 96-well plate was incubated with exponentially growing cells at the density of 1×10^4/well, following incubation of Bel 7402 cells with or without genistein in different columns of 96-well microtiter plates on d 1, 3, 5, and 7, MTT was added to each well and incubated at 37 °C for further 4 h before 595 nm absorbance (A_{595nm}) was detected. Each assay was performed in quadruplicate.

Inhibitory rate of tumor cell growth = (average $A_{595\ nm}$ value of control group-average $A_{595\ nm}$ value of genistein group)/average $A_{595\ nm}$ value of control group[12].

In vitro assays of Bel 7402 cell adhesion and invasion

Ninety-six-well microtiter plates were precoated with 20 mg/L fibronectin and incubated at 4 °C overnight. Wells were blocked with 2% BSA for 45 min at 37 °C. The cells were cultured in 2% serum-containing medium for 24 h, harvested at about 70% confluency, resuspended in serum-free RPMI 1640 medium supplemented with 0.1% BSA and distributed to wells (8×10^4/well). The cells were incubated at 37 °C in a 50 mL/L CO_2 atmosphere for 20, 40, 60, and 90 min with or without genistein. The wells were washed thrice with PBS to remove unattached cells, then the attached cells were incubated with MTT and the absorbance was measured at 595 nm. Each assay was performed in triplicate.

Adhesion rate = average $A_{595\ nm}$ value of genistein group/average $A_{595\ nm}$ value of control group×100%.

Inhibitory rate of adhesion = (average $A_{595\ nm}$ value of control group-average A595 nm value of genistein group)/average A595 nm value of control group×100%.

The invasive activity of Bel 7402 cells was assayed in transwell cell chambers (Corning Inc., USA), according to the method reported by Kido *et al*[13]. The basement membrane Matrigel was obtained from the Department of Cell Biology, Peking University Health Science Center. Polyvinylpyrrolidone-free polycarbonate filters with an 8.0-μm pore size were precoated with 5 μg of fibronectin in a volume of 50 μL on the lower surface. The Matrigel was diluted to 100 μg/mL with cold PBS and applied to the upper surface of the filters (5 μg/filter), and dried overnight under a hood at room temperature. The coated filters were washed extensively in PBS, and then dried immediately before use. Log-phase cell cultures of Bel 7402 cells were harvested and washed thrice with serum-free RPMI 1640, and resuspended to a final concentration of 2×10^6/mL in RPMI 1640 with 0.1% BSA. Cell suspensions (100 μL) with or without genistein were added to the upper compartment and incubated for 10-20 h at 37°C in a 50 mL/L CO_2 atmosphere. The filters were fixed with methanol and stained with Giemsa. The cells on the upper surface of the filters were removed by wiping with cotton swabs. The cells invading the lower surface of the filter through Matrigel and filter were manually counted under a microscope at a magnification of ×400, and each assay was performed in triplicate.

Invasion rate = average cell numbers invading the lower surface of the filter in genistein group/average cell numbers invading the lower surface of the filter in control group×100%.

Inhibitory rate of invasion=(average cell numbers invading the lower surface of the filter in control group-average cell numbers invading the lower surface of the filter in genistein group)/average cell numbers invading the lower surface of the filter in control group×100%.

Cell cycle analysis

Bel 7402 cells were seeded at the density of 5×10^5/well in six-dishes. After 24 h, the cells were treated with or without genistein for 72 h and harvested by trypsinization. The cells were then centrifuged at 300 r/min for 10 min, washed in PBS, and resuspended in cold 70% ethanol. The cells were then subjected to flow cytometric analysis on a FACScan cytofluorimeter (Becton Dickinson) after propidium iodide labeling.

Detection of focal adhesion kinase expression by flow cytometry assay

On d 3 of cell culture, control and genistein-treated Bel 7402 cells were centrifuged at 300 r/min for 10 min, washed and fixed in 1 mL 70% ethanol at 4 °C, treated with 0.1% Triton X-100 and 1% FBS, and anti-focal adhesion kinase (FAK C-20 sc-558, Santa Cruz Biotechnology, Inc., USA) and IgG1 (1 ∶ 100) were added. Cells were then treated with RNAse (1 mg/mL, Sigma, USA) and propidium iodide (10 μg/mL) for 30 min at room temperature. FAK expression was measured using a FACScan cytofluorimeter (Becton Dickinson).

Terminal deoxynucleotidyl transferase-mediated dUTP nick end-labeling (TUNEL) assay

Control cells and genistein-treated cells were harvested at 72 h by trypsinization and collected by centrifugation. Cells were washed twice in PBS-0.1% bovine serum albumin and prepared for TUNEL assay. Cells were fixed for 30 min in 4% paraformaldehyde, washed twice in PBS, and then permeabilized in 0.1% Triton-X 100 and 0.1% sodium citrate. Cells were labeled with terminal deoxynucleotidyl transferase for 60 min at 37 °C in a dark humidified incubator. The samples were washed twice, resuspended in 500 μL of PBS, and then analyzed on a FACScan cytofluorimeter (Becton Dickinson).

In vivo experiments

Six-week-old male BALB/C nu/nu mice were obtained from the Medical Laboratory Animal Center, Sun Yat-Sen University, China. They were kept under sterile conditions

in autoclaved cages with filter bonnets in laminar flow units and fed with sterilized MF pellets and distilled water. The mice were maintained in accordance with institutional accredited guidelines.

Bel 7402 cells were grown to 80-90% of confluence and detached with 0.25% trypsin. The cells were washed twice, counted, and resuspended in PBS at 1×10^7/mL (viability over 95%). Cells (0.3 mL) were injected into the male nude mice. Each animal received two injections, one on each side of the neck. Animals were killed 3 wk after tumor inoculation, when the largest tumors reached about 10 mm in diameter. Surgical excision of primary tumor was carried out, and tumor tissues were cut into 1-mm^3 pieces for bilateral subrenal capsule xenograft transplantation in next 10 nude mice anesthetized with chloral hydrate. The xenograft volume was assessed and calculated by the formula: length×width×depth×0.5236.

Mice bearing subrenal capsule xenograft transplant were randomly selected for the treatment with genistein ($n = 5$) and those without genistein treatment served as control ($n = 5$). Genistein (50 mg/kg) was administered ip daily to each mouse in genistein group for 15 d, while control animals were given the same vehicle. The animals were killed by cervical dislocation 16 d after transplantation of the tissues. Autopsies were performed and the kidney was excised, fixed, and embedded in paraffin, and examined histologically. The inhibitory rate of transplant growth was calculated by comparing the changes in xenograft transplant volume[15,16]. The criteria for invasive capacity of tumor cells in subrenal capsule xenograft transplant were as previously described[14,16,17].

Immunohistochemical determination of angiogenesis

After deparaffinization, dehydration, and washing, sections from xenograft transplant were incubated with trypsin at 37 °C for 30 min, quenched with 0.3% H_2O_2-methanol for 30 min, and blocked with 10% normal goat serum in a buffer containing 100 mL of PBS, 1.0 g of BSA, and 0.1 mL of Tween-20. The sections were treated with a rabbit polyclonal antibody against human factor VIII-related antigen at a 1∶100 dilution with the PBS-BSA-Tween-20 buffer, followed by a biotinylated universal antibody at a 1∶100 dilution. The sections were then treated with avidin-biotin complex followed by 3,3-diaminobenzidine as a substrate for staining. Positive unit (PU) of the microvessels with staining was tested and calculated according to the method described by Shen[17].

Statistical analysis

The statistical significance of difference between the groups was determined by applying the one-way ANOVA and χ^2 using the Stata 6.0 program.

RESULTS

In vitro effects of genistein on Bel 7402 cell growth

Genistein significantly inhibited Bel 7402 cell growth over the 7 d of experiment. The inhibitory rate of tumor cell growth in 5 and 10 μg/mL genistein groups was 26.71%±10.2% and 42.64±16.1%, respectively. The inhibitory rate of tumor cell growth in 10 μg/mL genistein group was significantly higher than that in 5 μg/mL genistein group ($P<0.01$). The dose-dependent effects of genistein on Bel 7402 cell growth are presented in Figure 1.

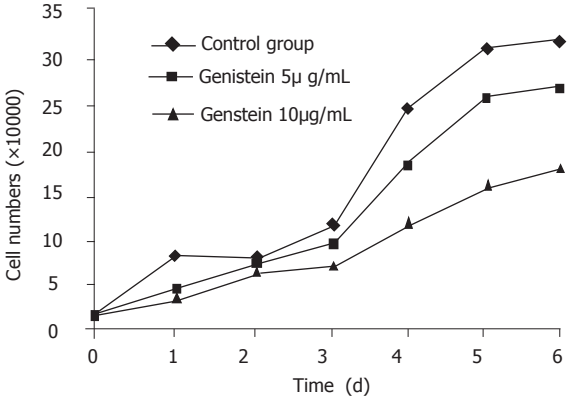

Figure 1 Effects of genistein on Bel 7402 cell proliferation *In vitro* effects of genistein on adhesion and invasion of Bel 7402 cells.

The adhesion rate of Bel 7402 cells for 20, 40, 60, and 90 min was 30.61%, 56.48%, 61.89% and 81.55% in 5 μg/mL genistein group, and 17.78%, 15.82%, 42.98% and 64.48% in 10 μg/mL genistein group. The inhibitory rate of Bel 7402 cells for 20, 40, 60, and 90 min was 69.39%, 43.52%, 38.11%, and 18.45% in 5 μg/mL genistein group, and 82.22%, 84.18%, 57.02%, and 35.52% in 10 μg/mL genistein group. Our results showed that genistein could inhibit tumor cell adhesion to fibronectin-coated substrates in a concentration-dependent fashion, and more potent inhibitory effect of genistein on adhesion occurred within 40 min.

We also investigated the capability of metastatic tumor cells through reconstituted basement membrane Matrigel. The cells invading the lower surface of the filter through Matrigel in control group, 5 μg/mL genistein group, and 10 μg/mL genistein group were 243.7±12.6/filed, 216.7±21.3/filed, and 174.5±9.6/filed, respectively. The invasion rate in 5 and 10 μg/mL genistein group was 88% and 71%, respectively, the inhibitory rate of invasion was 11% and 28%, respectively. Our results showed that genistein could inhibit the in vitro invasion of Bel 7402 cells, the inhibitory effect on invasion of Bel 7402 cells in 10 μg/mL genistein group was more significant than that in 5 μg/mL genistein group ($P<0.05$).

In vitro effects of genistein on cell cycle progression

Bel 7402 cells treated with genistein in the G0/G1 and G2/M phases increased significantly than cells in control group, the increase of cells in G0/G1 and G2/M phases was more remarkable in 10 μg/mL genistein group than in 5 μg/mL genistein group ($P<0.05$). S fractions decreased significantly in cells treated with genistein ($P<0.05$). Percentage of apoptotic cells in genistein-treated

group increased significantly compared to that in control group (P<0.05). The results of cell cycle analysis by flow cytometry in Bel 7402 cells are presented in Table 1.

Table 1 Effects of genistein on cell cycle progression in Bel 7402 cell line (mean±SD)

Treatment	Cell cycle phase			Apoptosis (%)
	G0/G1 (%)	G2/M (%)	S (%)	
Control	64.58±8.46	0.78±0.02	34.64±1.36	0.47±0.01
Genistein 5 μg/mL	71.74±4.46	2.75±0.03[b]	25.50±2.28[b]	1.02±0.06[a]
Genistein 10 μg/mL	75.27±6.12[ac]	6.37±0.08[d]	18.36±1.53[b]	2.12±0.12[b]

[a]P<0.05 *vs* control; [b]P<0.01 *vs* control; [c]P<0.05 *vs* 5 μg/mL genistein; [d]P<0.01 *vs* control and 5 μg/mL genistein.

Effects of genistein on induction of apoptosis of Bel 7402 cells

TUNEL assay in our studies showed that the percentage of cells undergoing apoptosis was significantly higher in 10 μg/mL genistein group (1.05±0.09%) and 5 μg/mL genistein group (0.80±0.12%) than in control group (0.43±0.08%, P<0.01 and P<0.05, respectively) being consistent with genistein's ability to induce apoptosis observed in cell cycle analysis.

Evaluation of expression of p125^{FAK} protein

We investigated whether genistein could modulate protein expression of the signal transduction molecule-p125FAK. After 72-h treatment with genistein, p125FAK expression in 10 μg/mL genistein group (12.89±0.36)% was significantly lower than that in control group (19.75%±1.12%, P<0.05). p125FAK expression in 5 μg/mL genistein group (15.26±0.16)% also decreased, but there was no statistically significant difference between 5 μg/mL genistein group and control group (P>0.05).

Effects of genistein on growth of subrenal capsule xenograft transplant

The anti-tumor activity of genistein was evaluated in nude mice bearing subrenal capsule xenograft transplant. Treatment with genistein inhibited the local tumor growth significantly compared to the control group. At the end of the treatment (15 d post implantation), the increase of tumor volume in genistein group (63.32±8.96 mm^3) was significantly less than that in control group (79.25±6.85 mm^3, P<0.05). Tumors in mice treated with genistein reduced in volume by 20% compared to the control group.

Effects of genistein on in vivo tumor invasion

The criteria for invasive capacity of tumor cells in subrenal capsule xenograft transplant were as previously described[17]. The 0-IV invasion rank to renal parenchyma was recorded[14,16]. In the control group, invasion rank 0 was observed in 1 of 10 mice (1/10), invasion rank I in 8 of 10 mice (8/10), and invasion rank II in 1 of 10 mice (1/10). In genistein-treated group, invasion rank 0 was observed in 8/10, rank I in 2/10 and rank II in 0/10 mice. No rank III or rank IV invasion was observed in both groups. Our results showed that treatment with genistein could significantly inhibit the invasion of Bel 7402 cells to the renal parenchyma (P<0.05). Hematoxylin-eosin stained specimens are shown in Figure 2.

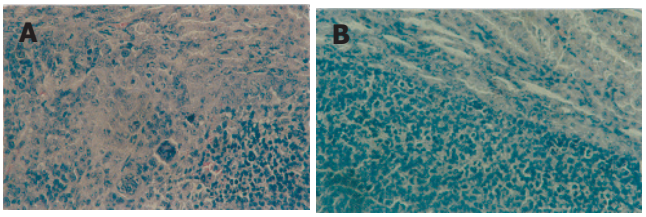

Figure 2 Tumor invasion of renal parenchyma in control (**A**) and genistein-treated nude mice (**B**). HE, magnification ×200.

Effects of genistein on tumor angiogenesis

In untreated tumor tissues, tumor cells were arranged in large nests with plenty of blood sinusoids. Whereas, in genistein-treated tumor tissue, tumor cells were characterized by small cancerous nests with scanty blood vessels. PU value of microvessels in the subrenal capsule xenograft transplant, as a marker of tumor angiogenesis, significantly decreased in genistein group (10.422±0.807) compared to that in control group (22.330±5.696, P<0.01). Immunohistochemical staining for the determination of angiogenesis in subrenal capsule xenograft transplant of the nude mice is shown in Figure 3.

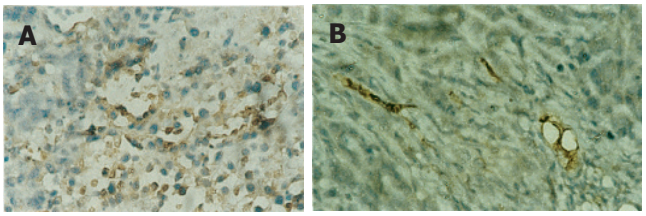

Figure 3 Tumor tissue with plenty of blood vessels (**A**) and scanty blood vessels (**B**) in control and genistein-treated nude mice. HE, magnification ×200.

DISCUSSION

Invasion and metastasis are the most devastating aspects of cancer. Advances in surgical techniques and adjuvant therapies have been proved to be useful in the treatment of primary tumors[18]. However, invasion and metastasis remain a major cause of poor prognosis and death in cancer patients. Reports from epidemiological and experimental studies indicate that genistein plays an important role in the prevention and inhibition of tumors such as breast cancer, prostate cancer, colon cancer, leukemia, melanoma, *etc*.[19]. However, there are still a few reports of studies on the correlation between genistein and the invasion and metastasis of human HCC. Our data provide evidence that genistein can also inhibit HCC cell proliferation and invasion.

In this report, we haveshould for the first time that genistein could significantly inhibit the growth and

viability of Bel 7402 cells. The inhibitory rate of tumor cell growth was about 26%-42%. We also found that genistein induced cell cycle arrest in the G0/G1 and G2/M phases. These findings are in agreement with other reports[19-24]. Although the exact mechanisms of genistein await further elucidation, induction of apoptosis may be partly responsible[25-27]. In our studies with TUNEL assay, the percentage of Bel 7402 cells undergoing apoptosis was significantly higher in genistein group than in control group, which is consistent with those found in other studies[28,29].

The adhesion and invasiveness of tumor cells represent some important properties necessary for the formation of metastases. We investigated the effect of genistein on the adhesive properties of Bel 7402 cells, and found that genistein could inhibit tumor cell adhesion to fibronectin-coated substrates, the most potent inhibitory effect of genistein on adhesion occurred within 40 min, demonstrating that reduction in cell adhesion after the treatment with genistein may account for the ability of Bel 7402 cells to transgress normal tissue boundaries and disperse to the adjacent sites. The invasion assay both *in vitro* and *in vivo* was further performed in our experiments. Bel 7402 cells invading the lower surface of the filter through Matrigel was significantly inhibited in genistein-treated groups compared to control group. Our experiments with the subrenal capsule xenograft transplant of nude mice showed that the treatment with genistein could significantly inhibit the invasion of Bel 7402 cells to the renal parenchyma, which was correlated with the biological behavior *in vitro*.

Inhibition of angiogenesis was observed in our studies. Angiogenesis is virtually absent in the healthy adult organism and is restricted to a few conditions including wound healing, placenta, endometrium, etc., representing the ordered and self-limited processes[30,31]. In certain pathological conditions, angiogenesis is dramatically enhanced and is no longer self-limited[30]. The most important manifestation of pathological angiogenesis is induced by solid tumors[32]. In our immunohistochemical studies, tumor cells were characterized by small cancerous nests with scanty blood vessels in genistein-treated mice. The PU value of microvessels was significantly decreased in genistein group compared to the control group. As angiogenesis is an important step in the invasion and metastasis process of tumors[33,34], the changes in angiogenesis caused by genistein may play a crucial role in inhibition of the invasiveness of Bel 7402 cells.

FAK is a cytoplasmic tyrosine kinase that plays an important role in integrin-mediated signal transduction pathways closely related to cell adhesion, motility, and growth[35-39]. Upregulation of FAK expression is associated with oncogenesis[40-43] and decrease in FAK is associated with the loss of ability to attach, decreased migration and induction of apoptosis[44-48]. We have reported that FAK is overexpressed in HCC, the expression of FAK in invasive or metastatic HCC is significantly higher than that in non-invasive or non-metastatic HCC[16]. Therefore, FAK seems to be an important pharmacologic target site[49]. In the present study, a significant downregulation of p125FAK after genistein treatment was observed, suggesting that genistein may serve as a potential important anticancer agent for HCC progression by blocking the FAK signaling process, which play a crucial role in angiogenesis and apoptosis.

In summary, our results provide the preliminary evidence that genistein is an effective chemopreventive agent for HCC. Further in-depth studies coupled with clinical trials are needed to establish the scientific basis for the use of genistein in the prevention and treatment of HCC.

REFERENCES

1 **Park OJ,** Surh YJ. Chemopreventive potential of epigallocatechin gallate and genistein: evidence from epidemiological and laboratory studies. *Toxicol Lett* 2004; **150:** 43-56

2 **Magee PJ,** Rowland IR. Phyto-oestrogens, their mechanism of action: current evidence for a role in breast and prostate cancer. *Br J Nutr* 2004; **91:** 513-531

3 **Sarkar FH,** Li Y. Soy isoflavones and cancer prevention. *Cancer Invest* 2003; **21:** 744-757

4 **Sarkar FH,** Li Y. Mechanisms of cancer chemoprevention by soy isoflavone genistein. *Cancer Metastasis Rev* 2002; **21:** 265-280

5 **Adlercreutz CH,** Goldin BR, Gorbach SL, Höckerstedt KA, Watanabe S, Hämäläinen EK, Markkanen MH, Mäkelä TH, Wähälä KT, Adlercreutz T. Soybean phytoestrogen intake and cancer risk. *J Nutr* 1995: s757-s770

6 **Spinozzi F,** Pagliacci MC, Migliorati G, Moraca R, Grignani F, Riccardi C, Nicoletti I. The natural tyrosine kinase inhibitor genistein produces cell cycle arrest and apoptosis in Jurkat T-leukemia cells. *Leukemia Res* 1994; **18:** 431-439

7 **Liu XJ,** Yang L, Mao YQ, Wang Q, Huang MH, Wang YP, Wu HB. Effects of the tyrosine protein kinase inhibitor genistein on the proliferation, activation of cultured rat hepatic stellate cells. *World J Gastroenterol* 2002; **8:** 739-745

8 **Burke TR,** Yao ZJ, Liu DG, Voigt J, Gao Y. Phosphoryltyrosyl mimetics in the design of peptide-based signal transduction inhibitors. *Biopolymers* 2001; **60:** 32-44

9 **Suthar AC,** Banavalikar MM, Biyani MK. Pharmacological activities of Genistein, an isoflavone from soy. *Indian J Exp Biol* 2001; **39:** 511-519

10 **Dixon RA,** Ferreira D. Genistein. *Phytochemistry* 2002; **60:** 205-211

11 **Schweigerer L,** Christeleit K, Fleischmann G, Adlercreutz H, Wähälä K, Hase T, Schwab M, Ludwig R, Fotsis T. Identification in human urine of a natural growth inhibitor for cells derived from solid paediatric tumours. *Eur J Clin Invest* 1992; **22:** 260-264

12 **Gu Y,** Chen JS, Zhou XD. Inhibitory effects of antisense focal adhesion kinase oligodeoxynucleotides on the invasion of Bel 7402 hepatocellular carcinoma cells. *Zhonghua Ganzangbin Zazhi* 2003, **10:** 612-615

13 **Kido A,** Krueger S, Haeckel C, Roessner A. Inhibitory effect of antisense aminopeptidase N (APN/CD13) cDNA transfection on the invasive potential of osteosarcoma cells. *Clin Exp Metastasis* 2003; **20:** 585-592

14 **Wang JJ,** Gao Y, XU Q. Progress of mechanism, diagnosis and treatment of tumor metastasis. 1st. Shanghai: *Second Military Medical Press* , 2002: 217

15 **Gu Y,** Hao QJ, Chen JS, Zhou XD,Gao JS. Effects of antisense FAK ODN transfection on xenograft hepatocellular carcinoma in nude mice. *Zhonghua Shiyan Waike Zazhi* 2003; **20:** 616-618

16 **Gu Y,** Chen JS, Zhou XD,Gao JS. Overexpression of focal

adhesion kinase (FAK) and its relationship with the invasion and metastasis of human hepatocellular carcinoma. *Zhonghua Shiyan Waike Zazhi* 2003; **20:** 4-5
17 **Shen H.** Study on the quantitative method of immuneohistochemistry (III). *Zhongguo Zuzhi Huaxue Yu Xibao Huaxue Zazhi* 1995; **4:** 89-92
18 **Entschladen F,** Drell TL, Lang K, Joseph J, Zaenker KS. Tumour-cell migration, invasion, and metastasis: navigation by neurotransmitters. *Lancet Oncol* 2004; **5:** 254-258
19 **Powis G,** Hill SR, Frew TJ, Sherrill KW. Inhibitors of phospholipid intracellular signaling as antiproliferative agents. *Med Res Rev* 1995; **15:** 121-138
20 **Toi M,** Mukaida H, Wada T, Hirabayashi N, Toge T, Hori T, Umezawa K. Antineoplastic effect of erbstatin on human mammary and esophageal tumors in athymic nude mice. *Eur J Cancer* 1990; **26:** 722-724
21 **Constantinou A,** Kiguchi K, Huberman E. Induction of differentiation and DNA strand breakage in human HL-60 and K-562 leukemia cells by genistein. *Cancer Res* 1990; **50:** 2618-2624
22 **Yamashita Y,** Kawada S, Nakano H. Induction of mammalian topoisomerase II dependent DNA cleavage by nonintercalative flavonoids, genistein and orobol. *Biochem Pharmacol* 1990; **39:** 737-744
23 **Alhasan SA,** Pietrasczkiwicz H, Alonso MD, Ensley J, Sarkar FH. Genistein-induced cell cycle arrest and apoptosis in a head and neck squamous cell carcinoma cell line. *Nutr Cancer* 1999; **34:** 12-19
24 **Li Y,** Upadhyay S, Bhuiyan M, Sarkar FH. Induction of apoptosis in breast cancer cells MDA-MB-231 by genistein. *Oncogene* 1999; **18:** 3166-3172
25 **Yanagihara K,** Ito A, Toge T, Numoto M. Antiproliferative effects of isoflavones on human cancer cell lines established from the gastrointestinal tract. *Cancer Res* 1993; **53:** 5815-5821
26 **Pagliacci MC,** Smacchia M, Migliorati G, Grignani F, Riccardi C, Nicoletti I. Growth-inhibitory effects of the natural phyto-oestrogen genistein in MCF-7 human breast cancer cells. *Eur J Cancer* 1994; **30:** 1675-1682
27 **Yousefi S,** Blaser K, Simon HU. Activation of signaling pathways and prevention of apoptosis by cytokines in eosinophils. *Int Arch Allergy Immunol* 1997; **112:** 9-12
28 **Matsukawa Y,** Marui N, Sakai T, Satomi Y, Yoshida M, Matsumoto K, Nishino H, Aoike A. Genistein arrests cell cycle progression at G2-M. *Cancer Res* 1993; **53:** 1328-1331
29 **Kyle E,** Neckers L, Takimoto C, Curt G, Bergan R. Genistein induced apoptosis of prostate cancer cells is preceded by a specific decrease in focal adhesion kinase activity. *Mol Pharmacol* 1997; **51:** 193-200
30 **Denekamp J.** Vascular attack as a therapeutic strategy for cancer. *Cancer Metastasis Rev* 1990; **9:** 267-282
31 **Kreuter M,** Bielenberg D, Hida Y, Hida K, Klagsbrun M. Role of neuropilins and semaphorins in angiogenesis and cancer. *Ann Hematol* 2002; **81** Suppl 2**:** S74
32 **Folkman J.** Tumor angiogenesis. *Adv Cancer Res* 1985; **43:** 175-203
33 **Fotsis T,** Pepper MS, Aktas E, Breit S, Rasku S, Adlercreutz H, Wahala K, Montesano R, Schweigerer L. Flavonoids, dietary-derived inhibitors of cell proliferation and in vitro angiogenesis. *Cancer Res* 1997; **57:** 2916-2921
34 **Fotsis T,** Pepper M, Adlercreutz H, Hase T, Montesano R, Schweigerer L. Genistein, a dietary-ingested isoflavonoid, inhibits cell proliferation and in vitro angiogenesis. *J Nutr* 1995; **125:** 790S-797S
35 **Hynes RO.** Integrins: versatility, modulation, and signaling in cell adhesion. *Cell* 1992; **69:** 11-25
36 **Weimar IS,** de Jong D, Muller EJ, Nakamura T, van Gorp JM, de Gast GC, Gerritsen WR. Hepatocyte growth factor/scatter factor promotes adhesion of lymphoma cells to extracellular matrix molecules via alpha 4 beta 1 and alpha 5 beta 1 integrins. *Blood* 1997; **89:** 990-1000
37 **Hedin U,** Thyberg J, Roy J, Dumitrescu A, Tran PK. Role of tyrosine kinases in extracellular matrix-mediated modulation of arterial smooth muscle cell phenotype. *Arterioscler Thromb Vasc Biol* 1997; **17:** 1977-1984
38 **Schlaepfer DD,** Hauck CR, Sieg DJ. Signaling through focal adhesion kinase. *Prog Biophys Mol Biol* 1999; **71:** 435-478
39 **Schaller MD,** Borgman CA, Cobb BS, Vines RR, Reynolds AB, Parsons JT. pp125FAK a structurally distinctive protein-tyrosine kinase associated with focal adhesions. *Proc Natl Acad Sci* U S A 1992; **89:** 5192-5196
40 **Hill TD,** Dean NM, Mordan LJ, Lau AF, Kanemitsu MY, Boynton AL. PDGF-induced activation of phospholipase C is not required for induction of DNA synthesis. *Science* 1990; **248:** 1660-1663
41 **Hollenberg MD.** Tyrosine kinase-mediated signal transduction pathways and the actions of polypeptide growth factors and G-protein-coupled agonists in smooth muscle. *Mol Cell Biochem* 1995; **149-150:** 77-85
42 **Bergan R,** Kyle E, Nguyen P, Trepel J, Ingui C, Neckers L. Genistein-stimulated adherence of focal adhesion kinase to beta-1-integrin. *Clin Exp Metastasis* 1996; **14:** 389-398
43 **Agochiya M,** Brunton VG, Owens DW, Parkinson EK, Paraskeva C, Keith WN, Frame MC. Increased dosage and amplification of the focal adhesion kinase gene in human cancer cells. *Oncogene* 1999; **18:** 5646-5653
44 **Fotsis T,** Pepper M, Adlercreutz H, Fleischmann G, Hase T, Montesano R, Schweigerer L. Genistein, a dietary derived inhibitor of in vitro angiogenesis. *Proc Natl Acad Sci* USA 1993; **90:** 2690-2694
45 **Ogawara H,** Akiyama T, Watanabe S, Ito N, Kobori M, Seoda Y. Inhibition of tyrosine protein kinase activity by synthetic isoflavones and flavones. *J Antibiot (Tokyo)* 1989; **42:** 340-343
46 **Xu LH,** Owens LV, Sturge GC, Yang X, Liu ET, Craven RJ, Cance WG.. Attenuation of the expression of the focal adhesion kinase induces apoptosis in tumor cells. *Cell Growth Differ* 1996; **7:** 413-418
47 **Hunter T.** The proteins of oncogenes. *Sci Am* 1984; **251:** 70-79
48 **Peterson G.** Evaluation of the biochemical targets of genistein in tumor cells. *J Nutr* 1995; **125:** 784S-789S
49 **Perandones CE**, Illera VA, Peckham D, Stunz LL, Ashman RF. Regulation of apoptosis in vitro in mature murine spleen T cells. *J Immunol* 1993; **151:** 3521-3529

Science Editor Wang XL and Guo SY **Language Editor** Elsevier

PO Box 2345, Beijing 100023, China
www.wjgnet.com
wjg@wjgnet.com

ELSEVIER

World J Gastroenterol 2005;11(41):6518-6520
World Journal of Gastroenterology ISSN 1007-9327

• *RAPID COMMUNICATION* •

Effects of *Helicobacter pylori* eradication on atrophic gastritis and intestinal metaplasia: A 3-year follow-up study

Bin Lu, Ming-Tao Chen, Yi-Hong Fan, Yan Liu, Li-Na Meng

Bin Lu, Ming-Tao Chen, Yi-Hong Fan, Yan Liu, Li-Na Meng, Department of Gastroenterology, Affiliated Hospital of Zhejiang Traditional Chinese Medicine College, Hangzhou 310006, Zhejiang Province, China
Supported by the Scientific Research Fund of the Health Bureau of Zhejiang Province, No. 2001QN012
Correspondence to: Dr. Bin Lu, Department of Gastroenterology, Affiliated Hospital of Zhejiang Traditional Chinese Medicine College, Hangzhou 310006, Zhejiang Province China. lvbin@medmail.com.cn
Telephone: +86-571-87032028 Fax: +86-571-87077785
Received: 2004-12-28 Accepted: 2005-03-24

Abstract

AIM: To investigate the effect of *H pylori* eradication on atrophic gastritis and intestinal metaplasia (IM).

METHODS: Two hundred and fifty-nine patients with atrophic gastritis in the antrum were included in the study, 154 patients were selected for *H pylori* eradication therapy and the remaining 105 patients served as untreated group. Gastroscopy and biopsies were performed both at the beginning and at the end of a 3-year follow-up study. Gastritis was graded according to the updated Sydney system.

RESULTS: One hundred and seventy-nine patients completed the follow-up, 92 of them received *H pylori* eradication therapy and the remaining 87 *H pylori*-infected patients were in the untreated group. Chronic gastritis, active gastritis and the grade of atrophy significantly decreased in *H pylori* eradication group ($P<0.01$). However, the grade of IM increased in *H pylori* -infected group ($P<0.05$).

CONCLUSION: *H pylori* eradication may improve gastric mucosal inflammation, atrophy and prevent the progression of IM.

Key words: *H pylori*; Atrophic gastritis; Intestinal metaplasia

Lu B, Chen MT, Fan YH, Liu Y, Meng LN. Effects of *H pylori* eradication on atrophic gastritis and intestinal metaplasia: A 3-year follow-up study. *World J Gastroenterol* 2005; 11(41): 6518-6520
http://www.wjgnet.com/1007-9327/11/6518.asp

INTRODUCTION

H pylori-infected gastric mucosa evolves through stages of chronic gastritis, glandular atrophy (GA) and intestinal metaplasia (IM) which is a main cause of intestinal type of gastric adenocarcinoma. *H pylori* infection induces gastric epicyte apoptosis. The index of apoptosis and proliferation decrease after *H pylori* eradication[1,2]. *H pylori* eradication can prevent gastric cancer. Whether the precancerous lesions are reversed or terminated after *H pylori* eradication is crucial to evaluate this therapy for a preventive purpose. To investigate the histological changes in the gastric mucosa, we followed up chronic atrophic gastritis patients who received *H pylori* eradication therapy for 3 years.

MATERIALS AND METHODS

A total of 259 *H pylori*-infected patients, who were diagnosed as having antral atrophic gastritis (without organic gastropathy, e.g., ulcer, tumor, etc.) by gastroscopy and biopsy in our hospital during 1997 to 1999, were followed up in our study; 154 of them received *H pylori* eradication therapy and the remaining 105 did not receive *H pylori* eradication therapy. Patients who failed to respond to *H pylori* eradication therapy and had uncertain *H pylori* infection were excluded. Patients who did not return for re-evaluation or became *H pylori* negative without receiving *H pylori* eradication therapy were also excluded. A total of 179 patients including 82 men and 97 women aged 30-74 years (92 in the *H pylori* eradicated group and 87 in the control group) completed the 3-year follow-up study.

All the subjects underwent gastroscopy when they entered the study and fulfilled the 3-year follow-up; some patients underwent gastroscopy every year. During gastroscopy, 3 antral biopsy specimens (from the greater and lesser curvatures 2-3 cm from the pylorus) were taken. One antral biopsy specimen was submitted to rapid urease test (RUT) and the other two were cut into sections for histological examination.

The patients were confirmed to have *H pylori* infection only when both RUT and histological stain (modified Giemsa stain) produced positive results. Otherwise they were considered as non-*H pylori*-infected healthy volunteers. Uncertain cases that were positive in one test and negative in the other test should be excluded. After they were treated for more than 4 wk, *H pylori* status was determined by ^{14}C-urea breath test.

Biopsy specimens were stained with H&E. A single pathologist, who was unaware of the conditions of the patients and assigned treatment of biopsies, performed

the histological assessment. The gastritis was graded using the visual analog scales of the updated Sydney system[3] as none (0), mild (1), moderate (2), or marked (3). Histological grading of the same subject before and 3 years after the therapy was compared and classified as improvement, no improvement, or exacerbation.

To eradicate *H pylori* infection, the patients received omeprazole (20 mg) or lansoprazole (30 mg), clarithromycin (500 mg), amoxicillin (1 g) or furazolidone (0.1 g), twice daily for 1 wk. During the whole follow-up period, two group patients received expectant treatment.

Statistical analysis

The results of histology score were expressed as mean. The differences between the two groups before treatment with respect to histological grades were calculated using Mann-Whitney *U* test. Changes in histological grading in *H pylori* eradication and control groups before and 3 years after the treatment were compared by Stuart-Maxwell test. Differences in the proportions of histological grading with improvement, no improvement and exacerbation between two groups were made using the χ^2 test. $P<0.05$ was considered statistically significant (two-sided).

RESULTS

The *H pylori* eradicated group and control group were comparable in age and sex ratio ($P>0.05$). At entry into the study, the percentage of mild and moderate GA was 75% in *H pylori*-eradiated group and 25% in control group. The percentage of mild, moderate and marked GA was 77%, 21.8% and 1.2%, respectively. IM was 51% in *H pylori*-eradicated group and 58.6% in control group.

Active (AI) and chronic inflammation (CI) were found in both groups. Overall, the pretreatment histological scores were comparable in two treatment groups (Table 1).

Histological scores in paired samples before and after 3-year treatment in two groups are shown in Table 2.

After cure of infection, scoring of CI, AI and GA decreased significantly ($P<0.01$) and that of IM increased slightly with no significant difference ($P>0.05$). In control group, scoring of IM increased significantly ($P<0.05$), but that of other pathologic changes had no statistical significance ($P>0.05$).

The histological changes in paired samples before and after 3-year treatment in *H pylori*-eradicated group and control group are shown in Figure 1. CI and AI were improved by 38.04% and 63.04% in *H pylori*-eradicated group, but only by 17.24% and 21.84% in the control group ($P<0.01$). The GA was improved by 28.26% in the treatment group and 14.94% in the control group. GA was exacerbated by 4.35% in treatment group and 4.6% in control group ($P>0.05$). IM was improved by 23.91% and exacerbated by 31.52% in *H pylori*-eradicated group, and by 20.69% and 33.33% in the control group ($P>0.05$).

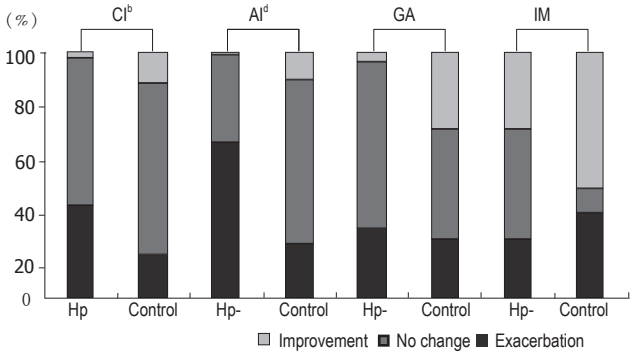

Figure 1 Percentage changes in gastric histology 3 years after treatment in *H pylori*-eradicated group and control group. [b]$P<0.01$, [d]$P<0.001$ *vs* baseline. CI: chronic inflammation; AI: active inflammation; GA: glandular atrophy; IM: intestinal metaplasia; *Hp-*: *H pylori*-eradicated group; Control: the control group.

DISCUSSION

H pylori is one of the causative factors for gastric cancer. Its eradication may play an important role in the prevention of gastric cancer. GA and IM are pre-cancerous lesions, but data on the effects of anti-*H pylori* therapy on GA and IM are conflicting. Vander Hulst *et al*[4] reported that the severity of GA and IM does not change after treatment. Forbes *et al*[5]showed that no changes in GA and IM are to be found after *H pylori* eradication treatment.

Sung *et al*[6] showed that IM in the gastric antrum is slightly improved in *H pylori*-eradicated patients and GA in the corpus is significantly improved in *H pylori*- infected patients. Ohkusa *et al*[7]demonstrated that 89% of GA and 61% of IM are improved. Ito *et al*[8] have reported a marked decrease in the average grade of IM and GA after treatment. Correa *et al*[9]reported the proportions of GA and IM are increased significantly in *H pylori*-eradicated

Table 1 Histological scores at entry of study in *H pylori*-eradicated group and control group (mean±SD)

	H pylori-eradicated group ($n=92$)	Control group ($n=87$)
Chronic inflammation	1.95±0.40	1.97±0.32
Active inflammation	1.84±0.41	1.90±0.40
Glandular atrophy	1.25±0.44	1.24±0.46
Intestinal metaplasia	0.64±0.76	0.63±0.57

Table 2 Histological scores at baseline and 3 yr after treatment (mean±SD)

	H pylori-eradicated group ($n=92$)		Control group ($n=87$)	
	Baseline	3-yr	Baseline	3-yr
Chronic inflammation	1.95±0.40	1.56±0.53[b]	1.97±0.32	1.91±0.47
Active inflammation	1.84±0.41	0.39±0.19[d]	1.90±0.40	1.78±0.44
Glandular atrophy	1.25±0.44	0.97±0.83[b]	1.24±0.46	1.19±0.82
Intestinal metaplasia	0.64±0.76	0.73±0.77	0.63±0.57	0.83±0.87[a]

[a]$P<0.05$, [b]$P<0.01$, [d]$P<0.001$ *vs* baseline

patients. Ruiz *et al*[10] showed that GA in the antrum improves significantly after *H pylori* eradication, but no significant change is observed by standard visual scoring method.

In our study, after a 3-year follow-up the scoring of GA decreased significantly in *H pylori*-eradicated group, while no significant change was found in control group ($P<0.01$). The proportion of change in GA was higher in *H pylori*-eradicated group than in control group (28.26% *vs* 14.94%), but it was not statistically significant ($P>0.05$). Though the GA grade in our study was mild and moderate, the results showed that eradication of *H pylori* was beneficial to some patients with GA in the antrum. Compared with GA, IM had no significant change after *H pylori* eradication. But the scoring of IM in the control group demonstrated that eradication of *H pylori* could prevent the further development of IM.

The reasons for these discrepancies may be due to the difference in sample size, follow-up time, histological standard, quantity and location of biopsy specimens and other gastric diseases. But the normal subjects or atrophic gastritis patients may cause deviation in statistics leading to different conclusions. Therefore, patients with different lesions (e.g., GA and IM) should be observed at different grades and at different times to demonstrate the possibility of reversal.

Whether GA and IM could be reversed is controversial, since bile reflux and other bacterial infections can also cause GA and IM. Moreover, age and dietary structure influence gastric mucosa lesions. Therefore, eradication of *H pylori* cannot cure all GA and IM.

Kokkola *et al*[11] reported that inflammation, GA and IM decrease significantly in patients with severe atrophic gastritis, including that GA and IM can be reversed by *H pylori* eradication. Dixon[12] considered that it is impossible to reverse GA and IM by *H pylori* eradication.

Our follow-up study demonstrated that gastritis activity and CI severity decreased significantly in *H pylori*-eradicated group but not in control group, suggesting that *H pylori* eradication can effectively treat gastritis. If we eradicate *H pylori* at the stage of gastric mucosa inflammation, the lesions can be reserved and will not develop into GA and IM. Therefore, in order to prevent gastric carcinoma, eradication of *H pylori* infection will be more beneficial, if the therapy is given at the early stage of lesions, i.e. before the formation of pre-cancerous lesions.

REFERENCES

1 **Lu B**, Wang HP, Xiang BK, Meng LN , Zhu LX. The effect of Helicobacter pylori infection on gastric epithelial cell apoptosis and oncogen expression. *Zhonghua Neike Zazhi* 2000; **39:** 255-258

2 **Liu WZ**, Zheng X, Dong QJ, Shi Y,Xiao SD. Effect of Helicobacter pylori infection on gastric epithelial proliferation in progression from normal mucosa to gastriccarcinoma. *World J Gastroenterol* 1998;**4**:246-248

3 **Dixon MF,** Genta RM, Yardley JH, Correa P. Classification and grading of gastritis. The updated Sydney System. International Workshop on the Histopathology of Gastritis, Houston 1994. *Am J Surg Pathol* 1996; **20:** 1161-1181

4 **van der Hulst RW,** van der Ende A, Dekker FW, Ten Kate FJ, Weel JF, Keller JJ, Kruizinga SP, Dankert J, Tytgat GN. Effect of Helicobacter pylori eradication on gastritis in relation to cagA: a prospective 1-year follow-up study. *Gastroenterology* 1997; **113:** 25-30

5 **Forbes GM,** Warren JR, Glaser ME, Cullen DJ, Marshall BJ, Collins BJ. Long-term follow-up of gastric histology after Helicobacter pylori eradication. *J Gastroenterol Hepatol* 1996; **11:** 670-673

6 **Sung JJ**, Lin SR, Ching JY, Zhou LY, To KF, Wang RT, Leung WK, Ng EK, Lau JY, Lee YT, Yeung CK, Chao W, Chung SC. Atrophy and intestinal metaplasia one year after cure of *H pylori* infection: a prospective, randomized study. *Gastroenterology* 2000; **119**: 7-14

7 **Ohkusa T**, Fujiki K, Takashimizu I, Kumagai J, Tanizawa T, Eishi Y, Yokoyama T, Watanabe M. Improvements in atrophy gastritis and intestinal metaplasia in patients in whom helicobacter pylori was eradicated. *Ann Intern Med* 2001; **134**; 380-386.

8 **Ito M**, Haruma K, Kamada T, Mihara M, Kim S, Kitadai Y, Sumii M, Tanaka S, Yoshihara M, Chayama K. Helicobacter pylori eradication therapy improves atrophic gastritis and intestinal metaplasia: a 5-year prospective study of patients with atrophic gastritis. *Aliment Pharmacol Ther* 2002; **16**: 1449-1456

9 **Correa P,** Fontham ET, Bravo JC, Bravo LE, Ruiz B, Zarama G, Realpe JL, Malcom GT, Li D, Johnson WD, Mera R. Chemoprevention of gastric dysplasia: randomized trial of antioxidant supplements and anti-helicobacter pylori therapy. *J Natl Cancer Inst* 2000; **92:** 1881-1888

10 **Ruiz B,** Garay J, Correa P, Fontham ET, Bravo JC, Bravo LE, Realpe JL, Mera R. Morphometric evaluation of gastric antral atrophy: improvement after cure of Helicobacter pylori infection. *Am J Gastroenterol* 2001; **96:** 3281-3287

11 **Kokkola A**, Sipponen P, Rautelin H, Härkönen M, Kosunen TU, Haapiainen R, Puolakkainen P. The effect of Helicobacter pylori eradication on the natural course of atrophic gastritis with dysplasia. *Aliment Pharmacol Ther* 2002; **16:** 515-520

12 **Dixon MF**. Prospects for intervention in gastric carcinogenesis: reversibility of gastric atrophy and intestinal metaplasia. *Gut*

Science Editor Wang XL **Language Editor** Elsevier HK

PO Box 2345, Beijing 100023, China
www.wjgnet.com
wjg@wjgnet.com

ELSEVIER

World J Gastroenterol 2005;11(41):6521-6524
World Journal of Gastroenterology ISSN 1007-9327

• *RAPID COMMUNICATION* •

Significance and relationship between infiltrating inflammatory cell and tumor angiogenesis in hepatocellular carcinoma tissues

Shao-Hua Peng, Hong Deng, Jian-Feng Yang, Ping-Ping Xie, Cheng Li, Hao Li, De-Yun Feng

Shao-Hua Peng, Hong Deng, Jian-Feng Yang, Ping-Ping Xie, Cheng Li, Hao Li, Department of Pathology, Medical College, Hunan Normal University, Changsha 410006, Hunan Province, China
De-Yun Feng, Department of Pathology, Xiangya School of Medicine, Central South University, Changsha 410078, Hunan Province, China
Supported by the Hunan Provincial Natural Science Foundation of China, No. 03-JJY5031
Co-first authors: Shao-Hua Peng and Hong Deng
Co-correspondent: De-Yun Feng
Correspondence to: Shao-Hua Peng, Department of Pathology, Medical College, Hunan Normal University, Changsha 410006, Hunan Province, China. pengshaohua2004@sina.com
Telephone: +86-731-8630309
Received: 2004-09-13 Accepted: 2004-12-26

Abstract

AIM: To investigate the relationship between infiltrating inflammatory cell and tumor angiogenesis in hepatocellular carcinoma (HCC) tissues and their clinicopathological features.

METHODS: The paraffin-embedded specimens from 70 cases with HCC were stained using EliVision immunohistochemistry with mAbs against CD68, tryptase, and CD34. The counts of tumor-associated macrophage (TAM), mast cell (MC) and tumor microvessel (MV) were performed in the tissue sections.

RESULTS: The mean counts of TAM, MC, and MV in HCC tissues were significantly higher than those in pericarcinomatous liver tissues (TAM: 69.31 ± 11.58 *vs* 40.23 ± 10.36; MC: 16.74 ± 5.67 *vs* 7.59 ± 4.18; MV: 70.11 ± 12.45 *vs* 38.52 ± 11.16, $P<0.01$). The MV count in the patients with metastasis was markedly higher than that with non-metastasis ($P<0.01$). In addition, the MC count in the patients with poorly differentiated HCC was obviously higher than that with well differentiated HCC ($P<0.01$). The correlation analysis showed that the TAM count was significantly correlated with the count of MV ($r=0.712$, $P<0.01$), and the MC count was obviously correlated with the MV count ($r=0.336$, $P<0.05$).

CONCLUSION: TAM and MC might be closely related to the enhancement of tumor angiogenesis. The MV count might be associated with tumor invasion and metastasis. Moreover, the MC count might be associated with tumor differentiation and prognosis of HCC.

Key words: Hepatocellular carcinoma; Mast cell; Microvessel; Macrophage

Peng SH, Deng H, Yang JF, Xie PP, Li C, Li H, Feng DY. Significance and relationship between infiltrating inflammatory cell and tumor angiogenesis in hepatocellular carcinoma tissues. *World J Gastroenterol* 2005; 11(41):6521-6524
http://www.wjgnet.com/1007-9327/11/6521.asp

INTRODUCTION

Tumor angiogenesis is one of the fundamental requirements for tumor growth and proliferation, and the regulatory mechanisms of tumor angiogenesis are very complicated. The tumor neovascularization and its controlling factors have become investigative hot points in current tumor studies[1-5]. Tumor infiltrating inflammatory cells in the microenvironment plays very important functions in tumor angiogenesis[6-8]. Hepatocellular carcinoma (HCC) is a kind of a familiar malignant tumor in our country, though the treatment of HCC has obtained the substantial advance, the total treatment results are still unsatisfactory[9-12]. Until recently, there is some lack of knowledge in literature regarding the relationship among the count of tumor-associated macrophage (TAM), mast cell (MC), and microvessel (MV)_ in HCC tissues and their relation to the clinicopathological characteristics of HCC. In this study, we applied immunohistochemical method to detect the count of TAM, MC, and MV in HCC, and to investigate their relation to the clinicopathological characteristics of HCC, so that we could understand the regulating function of microenvironment in tumor angiogenesis. We believed that this study would offer some new clues for tumor angiogenesis research and biological therapeutic approach, such as suppressing tumor angiogenesis.

MATERIALS AND METHODS

Materials

Fresh surgical specimens were obtained from 70 HCC

patients (all specimens contained pericarcinomatous liver tissues) who had undergone partial hepatectomy during the period from January 1996 to February 2003 in Xiangya Hospital. All specimens were fixed in 40 g/L formaldehyde, embedded in paraffin, sliced into consecutive sections, and pathologically diagnosed explicitly. Of 70 HCC patients, 53 were males and 17 were females with average age of 53.4 years (range, 27-68 years). The size of tumors was less than 5 cm in 25 cases, 5.1-10 cm in 29 cases and larger than 10 cm in 16 cases. Among all cases, 19 cases contained several tumor tubercles in liver tissues. None of the patients received any preoperative treatment, such as radiotherapy and chemotherapy. The HCC tissues were graded according to the Edmondson standard. Of them, 11 cases had grade I, 31 cases grade II, 23 cases grade III, and 5 cases grade IV tumors. All the pericarcinomatous liver tissues had liver fibrosis with cirrhosis of different degrees and 22 pericarcinomatous liver tissues had dysplasia. The antibodies against CD68, trypsin of MC and CD34, and "two step" EliVisions reagent box were all obtained from Maixin Biochemical Development Company of Fuzhou.

Immunohistochemical staining

Briefly, after the sections were deparaffinized, the endogenous peroxidase was blocked by incubation with 30mL/L hydrogen peroxide for 30 min, followed by carrying out the two-step method of immunohistochemistry according to the manufacturer's instructions. The sections were incubated with the primary antibodies at room temperature overnight. For negative control, the primary antibodies were replaced with PBS.

Brown-yellow staining was observed in the cytoplasm of TAM, whereas brown-yellow grains were observed both in the cytoplasm and nucleus of MC. According to the count method of Molin *et al*[13], we chose five random microscopic fields in each section under high power, counting the number of TAM and MC in each visual field, respectively. In addition, in the same visual field, we counted the number of MC that had the phenomenon of taking-off grains. MV and its endothelial cells showed brown-yellow staining. Similarly, according to the count method of Weidner *et al*[14], we chose five random microscopic fields in each section under high power, counting the number of MV in each visual field.

Statistical analysis

The data were analyzed using *t* test and relativity analyses in the statistical computer software SPSS10.0. A *P* value less than 0.05 was considered statistically significant.

RESULTS

Expressional characteristics of CD68, MC, CD34

The cytoplasm of CD68-positive cells was stained with brown-yellow color. We could observe in all the sections, that most of the CD68-positive cells had the characteristic of microphage in appearance and the TAM was primarily distributed in the perimeter of tumor cells. Moreover, brown-yellow grains were observed in the cytoplasm and nucleus of MC. In the relatively normal areas, MC was circular or oval with complete cell membrane, clear outline, abnormally dyed grains in cytoplasm and some of the MCs appearing to have the phenomenon of taking-off grains. But in the HCC tissue and its adjacent areas, the number of MC was obviously increased, the physical volume enlarged with a different appearance, and the majority of MC appeared to have the phenomenon of taking-off grains. The CD34 staining was located in the cytoplasm of vascular endothelial cells. We could observe a single endothelial cell or a cluster of cells in some areas containing partly irregular tube cavity and irregular MV distribution, which could mostly be seen in the perimeter areas of the tumor.

Counts of TAM, MC, and MV

The counts of TAM, MC, and MV were all obviously higher in HCC tissues compared with the pericarcinomatous liver tissues ($P<0.01$, Table 1).

Table 1 Counts of TAM, MC, and MV in HCC tissues and pericarcinomatous liver tissues (mean±SD)

	TAM	MC	MV
HCC tissues	69.31± 11.58	16.74±5.67	70.11±12.45
Pericarcinomatous liver tissues	40.23±10.36[b]	7.59±4.18[b]	38.52±11.16[b]

[b]$P<0.01$ *vs* HCC tissues

Relationship between the counts of TAM, MC, and MV and the clinicopathological characteristics of HCC

The counts of TAM, MC, and MV were significantly higher in metastatic HCC than that in non-metastatic HCC, and the count of MC in low grade HCC tissues was markedly higher compared to high grade HCC tissues ($P<0.05$). In addition, we also discovered that MC having the phenomenon of taking-off grains was more and more

Table 2 Relationship of the counts of TAM, MC, and MV with the clinicopathological characteristics of HCC (mean±SD)

Pathologic characteristics	*n*	TAM	MC	MV
Stage of HCC				
I	11	68.86±10.23	13.68±5.21	65.86±12.05
II	31	68.95±9.82	17.03±6.11	67.84±11.54
III	23	70.11±13.16	19.95±4.29[a]	72.11±10.84
IV	5	69.84±12.57	23.56±3.86[a]	68.70±9.53
Tumor size				
≤5 cm	25	69.32±10.17	16.57±5.56	66.56±11.84
5.1–10 cm	29	71.35±9.54	16.98±4.81	65.84±10.53
>10 cm	16	70.83±12.11	17.02±6.12	73.13±11.30
Metastasis				
Yes	29	68.36±12.17	16.99±6.49	73.49±12.32[c]
No	41	69.14±11.69	16.76±6.88	64.39±13.17

[a]$P<0.05$ *vs* stage I; [c]$P<0.05$ *vs* non-transferred.

familiar in low grade HCC tissues. However, no obvious relationship was found between the counts of TAM, MC, and MV and the clinicopathological characteristics of HCC (Table 2).

Relationship of the counts of TAM and MC with the count of MV in HCC tissues

Using the relativity analyses of the counts of TAM and MC with the count of MV in HCC tissues, we found that the TAM count and MV count in HCC tissues had a close and positive relationship of high degree ($r=0.712$, $P<0.01$), and the MC count and MV count in HCC tissues had a close and positive relationship ($r=0.336$, $P<0.05$).

DISCUSSION

Tumor growth and proliferation are highly dependent on tumor neovascularization. Tumor angiogenesis is mediated by tumor-secreted angiogenic factors that interact with their surface receptors expressed on endothelial cells[15-19]. In fact, the mechanisms of regulation of tumor angiogenesis have become one of the investigative hot points in current tumor studies[1-5]. Our study showed that the MV count was significantly higher in HCC tissues as compared with the pericarcinomatous liver tissues, and also higher in the metastatic HCC compared with the metastatic HCC, suggesting that tumor angiogenesis has a crucial role in the development and metastasis of HCC.

Tumor angiogenesis is a complicated process, including many regulating factors[20-24]. The angiogenic response in the microvasculature is associated with the changes in cellular adhesive interactions between adjacent endothelial cells, pericytes and surrounding extracellular matrix. In addition, the infiltrating inflammatory cells in tumor are closely related with tumor angiogenesis. The infiltrating inflammatory cells in tumor, such as neutrophil, microphage, lymphocyte, eosinophil, MC, *etc*., can produce various cell factors and enzymes which participate in the growth and spread of tumor. Microphage is a main composition of the infiltrating inflammatory cells in the tumor and usually belongs to TAM in tumor tissues[23-28]. On one hand, it can produce several growth-stimulating and repressing factors, and albumen hydrolyze enzymes, such as fibroblast growth factor, vascular endothelial growth factor, etc. and thereby plays an important role in chain responding of tumor angiogenesis. On the other hand, tumor cells also can produce various chemoattractant factors, such as monocyte chemoattractant proteins, macrophage colony-stimulating factor etc, which have an important effect on the activation and migration of macrophage. These TAMs, being closely related to microvessel density, also have something to do with tumor angiogenesis, metastasis, and prognosis. In this study, we found that the count of TAM was obviously higher in HCC tissues as compared with the pericarcinomatous liver tissues, suggesting that TAM plays an important role in the development of HCC. In addition, the TAM count and the MV count in HCC tissues had a close and positive relationship, which suggested that TAM might promote tumor angiogenesis.

Several studies have shown that MCs in the local milieu may have something to do with the growth, invasion, metastasis, and neovascularization of malignant tumor[29-30]. Our results showed that the MC count was obviously higher in HCC tissues as compared with the pericarcinomatous liver tissues, suggesting an important role of MC in the development of HCC. We also found that the MC count in the lower grade HCC tissues was higher than that in the higher grade HCC, which suggested that the high MC count might be related to the low grade and poor prognosis of HCC. In addition, we observed that MC showing the phenomenon of taking-off grains was more and more familiar in low grade HCC tissues; however, its concrete relationship still needs further research. The counts of MC and MV in HCC tissues had a close and positive relationship, which revealed that MC might promote HCC angiogenesis.

REFERENCES

1 **Saaristo A,** Karpanen T, Alitalo K. Mechanisms of angiogenesis and their use in the inhibition of tumor growth and metastasis. *Oncogene* 2000; **19:** 6122-6129
2 **Lutsenko SV,** Kiselev SM, Severin SE. Molecular mechanisms of tumor angiogenesis. *Biochemistry(Mosc)* 2003; **68:** 286-300
3 **Boudreau N,** Myers C. Breast cancer-induced angiogenesis: multiple mechanisms and the role of the microenvironment. Breast *Cancer Res* 2003; **5:** 140-146
4 **Rofstad EK,** Halsør EF. Vascular endothelial growth factor, interleukin 8, platelet-derived endothelial cell growth factor, and basic fibroblast growth factor promote angiogenesis and metastasis in human melanoma xenografts. *Cancer Res* 2000; **60:** 4932-4938
5 **Zheng S,** Han MY, Xiao ZX, Peng JP, Dong Q. Clinical significance of vascular endothelial growth factor expression and neovascularization in colorectal carcinoma. *World J Gastroenterol* 2003; **9:** 1227-1230
6 **Kataki A,** Scheid P, Piet M, Marie B, Martinet N, Martinet Y, Vignaud JM. Tumor infiltrating lymphocytes and macrophages have a potential dual role in lung cancer by supporting both host-defense and tumor progression. *J Lab Clin Med* 2002; **140:** 320-328
7 **Yu JL,** Rak JW. Host microenvironment in breast cancer development: inflammatory and immune cells in tumour angiogenesis and arteriogenesis. Breast *Cancer Res* 2003; **5:** 83-88
8 **Elpek GO,** Gelen T, Aksoy NH, Erdoğan A, Dertsiz L, Demircan A, Keleş N. The prognostic relevance of angiogenesis and mast cells in squamous cell carcinoma of the oesophagus.*J Clin Pathol* 2001; **54:** 940-944
9 **Lu SY,** Sui YF, Li ZS, Ye J, Dong HL, Qu P, Zhang XM, Wang WY, Li YS. Superantigen-SEA gene modified tumor vaccine for hepatocellular carcinoma: an in vitro study. *World J Gastroenterol* 2004; **10:** 53-57
10 **Harris AL,** Reusch P, Barleon B, Hang C, Dobbs N, Marme D. Soluble Tie2 and Flt1 extracellular domains in serum of patients with renal cancer and response to antiangiogenic therapy. *Clin Cancer Res* 2001; **7:** 1992-1997
11 **Zhao WH,** Ma ZM, Zhou XR, Feng YZ, Fang BS. Prediction of recurrence and prognosis in patients with hepatocellular carcinoma after resection by use of CLIP score. *World J Gastroenterol* 2002; **8:** 237-242
12 **Qin LX,** Tang ZY. The prognostic molecular markers in hepatocellular carcinoma. *World J Gastroenterol* 2002; **8:** 385-392
13 **Molin D,** Edström A, Glimelius I, Glimelius B, Nilsson G,

Sundström C, Enblad G. Mast cell infiltration correlates with poor prognosis in Hodgkin's lymphoma. *Br J Haematol* 2002; **119:** 122-124

14 **Weidner N,** Carroll PR, Flax J, Blumenfeld W, Folkman J. Tumor angiogenesis correlates with metastasis in invasive prostate carcinoma. *Am J Pathol* 1993; **143:** 401-409

15 **Strohmeyer D,** Rössing C, Bauerfeind A, Kaufmann O, Schlechte H, Bartsch G, Loening S. Vascular endothelial growth factor and its correlation with angiogenesis and p53 expression in prostate cancer. *Prostate* 2000; **45:** 216-224

16 **Guang-Wu H,** Sunagawa M, Jie-En L, Shimada S, Gang Z, Tokeshi Y, Kosugi T. The relationship between microvessel density, the expression of vascular endothelial growth factor (VEGF), and the extension of nasopharyngeal carcinoma. *Laryngoscope* 2000; **110:** 2066-2069

17 **Fidler IJ.** Angiogenesis and cancer metastasis. *Cancer* J 2000; **6 Suppl 2:** S134-S141

18 **Streit M,** Detmar M. Angiogenesis, lymphangiogenesis, and melanoma metastasis. *Oncogene* 2003; **22:** 3172-3179

19 **Yamaguchi R,** Yano H, Nakashima Y, Ogasawara S, Higaki K, Akiba J, Hicklin DJ, Kojiro M. Expression and localization of vascular endothelial growth factor receptors in human hepatocellular carcinoma and non-HCC tissues. *Oncol Rep* 2000; **7:** 725-729

20 **Etoh T,** Inoue H, Tanaka S, Barnard GF, Kitano S, Mori M. Angiopoietin-2 is related to tumor angiogenesis in gastric carcinoma: possible in vivo regulation via induction of proteases. *Cancer Res* 2001; **61:** 2145-2153

21 **Yudoh K,** Kanamori M, Ohmori K, Yasuda T, Aoki M, Kimura T. Concentration of vascular endothelial growth factor in the tumour tissue as a prognostic factor of soft tissue sarcomas.*Br J Cancer* 2001; **84:** 1610-1615

22 **Mitsuhashi N,**Shimizu H, Ohtsuka M, Wakabayashi Y, Ito H, Kimura F, Yoshidome H, Kato A, Nukui Y, Miyazaki M. Angiopoietins and Tie-2 expression in angiogenesis and proliferation of human hepatocellular carcinoma. *Hepatology* 2003; **37:** 1105-1113

23 **Feoktistov I,** Ryzhov S, Goldstein AE, Biaggioni I. Mast cell mediated stimulation of angiogenesis: cooperative interaction between A2B and A3 adenosine receptors. *Circ Res* 2003; **92:** 485-492

24 **Aoki M,** Pawankar R, Niimi Y, Kawana S. Mast cells in basal cell carcinoma express VEGF, IL-8 and RANTES. *Int Arch Allergy Immunol* 2003; **130:** 216-223

25 **Torisu H,** Ono M, Kiryu H, Furue M, Ohmoto Y, Nakayama J, Nishioka Y, Sone S, Kuwano M. Macrophage infiltration correlates with tumor stage and angiogenesis in human malignant melanoma: possible involvement of TNFalpha and IL-1alpha. *Int J Cancer* 2000; **85:** 182-188

26 **Ishigami S,** Natsugoe S, Tokuda K, Nakajo A, Okumura H, Matsumoto M, Miyazono F, Hokita S, Aikou T. Tumor-associated macrophage (TAM) infiltration in gastric cancer. *Anticancer Res* 2003; **23:** 4079-4083

27 **Li C,** Shintani S, Terakado N, Nakashiro K, Hamakawa H. Infiltration of tumor-associated macrophages in human oral squamous cell carcinoma. *Oncol Rep* 2002; **9:** 1219-1223

28 **Ono M,** Torisu H, Fukushi J, Nishie A, Kuwano M. Biological implications of macrophage infiltration in human tumor angiogenesis. *Cancer Chemother Pharmacol* 1999; **43:** S69-71

29 **Hiromatsu Y,** Toda S. Mast cells and angiogenesis. *Microsc Res Tech* 2003; **60:** 64-69

30 **Ribatti D,** Ennas MG, Vacca A, Ferreli F, Nico B, Orru S, Sirigu P. Tumor vascularity and tryptase-positive mast cells correlate with a poor prognosis in melanoma. *Eur J Clin Invest* 2003; **33:** 420-425

Science Editor Guo SY **Language Editor** Elsevier HK

PO Box 2345, Beijing 100023, China
www.wjgnet.com
wjg@wjgnet.com

ELSEVIER

World J Gastroenterol 2005;11(41):6525-6529
World Journal of Gastroenterology ISSN 1007-9327

• *RAPID COMMUNICATION* •

Clinical characteristics and distribution of hepatitis B virus genotypes in Guangxi Zhuang population

Zhong-Min Huang, Qi-Wen Huang, Ya-Qin Qin, Chun-He Huang, Hou-Ji Qin, Yiao-Nan Zhou, Xiang Xu, Chun-Lei Lu

Zhong-Min Huang, Qi-Wen Huang, Ya-Qin Qin, Chun-He Huang, Hou-Ji Qin, Yiao-Nan Zhou, Xiang Xu, Chun-Lei Lu, Department of Infectious Diseases, The Affiliated Hospital of Youjiang Medical College for Minority Nationalities, Baise 533000, Guangxi Zhuang Autonomous Region, China
Supported by the Natural Science Foundation of Guangxi Zhuang Autonomous Region, No. 49 (2002), Key Program of Youjiang Medical College for Minority Nationalities, No. (2004) 86
Co-Correspondence: Ya-Qin Qin and Zhang-Min Huang
Correspondence to: Dr. Ya-Qin Qin Department of Infectious Diseases, The Affiliated Hospital of Youjiang Medical College for Minority Nationalities, Baise 533000, Guangxi Zhuang Autonomous Region,
China. zhongminhuang@msn.com
Telephone: +86-776-2836942 Fax: +86-776-2825603
Received: 2004-09-23 Accepted: 2004-11-04

Abstract

AIM: To investigate the distribution of HBV genotypes and their YMDD mutations in Guangxi Zhuang population, China, and to study the relationship between HBV genotypes and clinical types of HB, ALT, HBV DNA, HBe system as well as the curative effect of Lamivudine (LAM) on hepatitis B.

METHODS: A total of 156 cases were randomly chosen as study subjects from 317 patients with chronic hepatitis B (CHB). HBV genotypes were determined by PCR-microcosmic nucleic acid cross-ELISA. YMDD mutations were detected by microcosmic nucleic acid cross-nucleic acid quantitative determination. HBV DNA was detected by fluorescence ratio PCR analysis. LAM was given to 81 cases and its curative effect was observed by measuring ALT, HBV DNA load, HBeAg, and HBeAg/HBeAb conversion rate.

RESULTS: HBV genotypes B, C, D, and non-classified genotypes were found in Guangxi Zhuang population. accounting for 25.6%, 47.4%, 58.3%, and 16.0%, respectively. Seventy-four cases were CD-, CB-, BD-mixed genotypes (47.7%). Forty-six (29.5%) cases had YMDD mutations. Genotype B was mostly found in mild and moderate CHB patients. Genotypes C, D and mixed genotype mostly occurred in severe CHB cases. Genotypes D and CD HBV-infected patients had higher ALT and HBV DNA than patients with other types of HBV infection. There was no significant difference among the genotypes in YMDD mutations, clinical types, ALT and HBV DNA level. Non-classified types geno had a significantly lower positive rate of HBeAg than other genotypes (χ^2=12.841, P<0.05). There was no significant difference in ALT recovery rate, HBV DNA load, HBeAg, and HBeAg/HBeAb conversion rate, 48 wk after LAM treatment between groups of genotypes D, CD, and non-classified type.

CONCLUSION: Genotypes B, C, and D, non-classified and mixed genotype of HBV are identified in the Guangxi Zhuang population. Variations in genotypes are associated with clinical severity and serum ALT levels, but not with YMDD mutation or HBV DNA load. Therapeutic effects of LAM on clinical parameters are not influenced by differences in genotypes. Further studies are needed to gain an in-depth understanding of the relationship between HBV genotypes and serum HBeAb and HBeAg.

Key words: Hepatitis B virus; Chronic hepatitis; Genotype; YMDD mutation; Lamivudine; Zhuang nationality

Huang ZM, Huang QW, Qin YQ, Huang CH, Qin HJ, Zhou YN, Xu X, Lu CL. Clinical characteristics and distribution of hepatitis B virus genotypes in Guangxi Zhuang population. *World J Gastroenterol* 2005; 11(41):6525-6529
http://www.wjgnet.com/1007-9327/11/6525.asp

INTRODUCTION

Guangxi Zhuang Autonomous Region is an endemic area of HBV infection. To examine the distribution of HBV genotypes and their associations with clinical characteristics of hepatitis B (HB) in Zhuang population, a total of 156 cases selected randomly from chronic hepatitis B (CHB) 317 patients without any previous antiviral treatment were studied, and some cases were given Lamivudine (LAM) treatment. The results reported are as follows.

MATERIALS AND METHODS

General data of patients

A total of 156 patients, 89 males and 67 females, aged 15-70 years, were selected randomly from CHB 317 patients from out-patient and in-patient departments of our hospital during January 2001 to June 2003. These patients received no previous LAM treatment or any antiviral treatment within a year. Their serum HBsAg, HBeAg or HBcAb and HBV DNA were positive. Those

infected with HCV, HDV, and HIV were excluded. All cases fulfilled the diagnostic criteria modified at the Tenth Viral Hepatitis Conference of Chinese Medical Association[1].

Detection of HBV genotypes

HBV DNA genotypes were detected by PCR-microcosmic nucleic acid cross-ELISA. One hundred microliters of serum samples was mixed with a reaction solution in a 0.5 mL centrifuge tube, heated to 100 °C for 15 min, and centrifuged at 12 000 *g* for 5 min. Twelve-microliter supernatant from the previous step was centrifuged at 10 000 *g* for 10 s before being placed in a PCR reactor, pre-denatured at 94 °C for 2 min, amplified for 35 cycles (at 94 °C for 50 s, at 53 °C for 50 s, and at 72 °C for 65 s), followed by extension at 72 °C for min and a final extension at 98 °C for 10 min. The samples were chilled immediately in an ice-bath for 10 min. Package was pinked at the microcosmic openings at 37 °C for 14 min in $NaHCO_3$ solution (pH 9.6). Nonspecific conjugate at the microcosmic openings was sealed by seal reagent. Ninety microliters of (three drops) hybridization liquid, 20 μL denatured output, 23 μL each nucleic pink (one kind was added to one opening) were added to different reaction openings, mixed up lightly and put into 50 °C water bath for 60 min, and poured completely. Then, 200 μL (eight drops) lotion was added at 37 °C for 3-5 min, poured completely and baptized once again. One hundred microliters of enzyme-antibody liquid (two drops) was added and kept at 37 °C for 30 min, poured and dried by water absorber, 200 μL (eight drops) lotion was added and kept at room temperature for 3-5 min, baptized twice, then color reagents A and B (one drop) were added, respectively, kept at room temperature in the dark for 10 min. Then, 2 mol/L H_2SO_4 solution (one drop) was added and the photoabsorption degree value (A) was detected at 450 nm. HBV DNA was considered positive, if P/N≥2.1 and negative if P/N<2.1. Positive result in hybridization indicated the virus gene

Detection of YMDD mutation

Reagent kits were provided by Biomedicine Diagnosis and Research Center of Basic Medicine Department of the First Military Medical University. YMDD mutations were detected by PCR. Twenty-five specimens were tested in Biomedicine Diagnosis and Research Center of Basic Medicine Department of the First Military Medical University, and the other 131 specimens were tested according to the manual of the kits and results were evaluated by experts at the Central Laboratory of our hospital.

Quantitative determination of HBV DNA

FX990 micro-fluorometer and HBV-PCR fluoroscopy reagent kits (detection limit is 103 copies/mL) were used to detect HBV DNA according to the instructions of the kits and results were evaluated by experienced experts.

Detection of HBVM

HBVM was detected by ELISA. Reagent kits were provided by Zhongshan Bioengineering Co., Ltd, Guangdong, China. The function of the liver was examined by the method of Laishi, and the normal level of ALT was lower than 40 U/L

Treatment

According to the common clinical practice[2], LAM (10 mg/d.p.o.) was given to 30 patients with single genotypes B, C, or D, and 35 patients with mixed genotypes CD, CB, or DB, and 16 non-classified types. HBV DNA and ALT were high, and HBeAg was positive in all cases selected. Twenty-eight cases had YMDD mutation. Liver function, HBVM and HBV DNA load were detected every 4 wk, for 48 wk.

Statistical analysis

The incidence rate of YMDD mutations, the rate of various clinical types of HB, the abnormal rate of ALT, the high loading rate of HBV DNA, and the positive rate of HBeAg in different genotypes of HBV were compared before and after LAM treatment by χ^2 using SAS statistical software. $P<0.05$ was considered statistically significant.

RESULTS

HBV genotypes in 156 CHB patients

Genotypes in 156 selected cases included B, C, D, mixed, and non-classified types. Genotypes A, E, and F were tested but not discovered. Genotype D accounted for 58.3% (91/156), type C 47.4% (74/156), type B 25.6% (40/156), and non-classified type 16.0% (25/156), mixed types (CD, CB, and BD) 47.4% (74/156). Single genotypes (B, C, or D) accounted for 36.5% (57/156, Table 1)

Table 1 Distribution of HBV genotypes in 156 cases

Patterns of genotype	A	B	C	D	E	F	CD	CB	BD	Non-A–F
n	–	9	15	33	–	–	43	16	15	25
Incidence rate (%)	–	5.8	9.6	21.2	–	–	27.6	10.3	9.6	16.0

Relationship between different HBV genotypes and YMDD mutations, clinical types of CHB, ALT, and HBV DNA, and HBe system

Natural YMDD mutations occurred in 46 cases (29.5%). Genotype B had no YMDD mutation. Genotypes had a different incidence rate of YMDD mutations, but there was no significant difference among them. Genotype B was seen mostly in mild and moderate CHB patients, while genotypes C, D and mixed types of CD, BD occurred mostly in severe CHB patients. The abnormal rate of ALT and the high loading rate of HBV DNA in genotypes D, and CD were higher than those in other genotypes, but there was no significant difference. The positive rate of HBeAg in non-classified genotype was low, and there was a significant difference between non-classified and other genotypes ($\chi^2 = 12.841$, $P<0.05$, Table 2).

Table 2 Relationship between different HBV genotypes and YMDD mutations, clinical types of CHB, ALT, and HBV DNA level, HBe system

Genotypes	*n*	Rate of YMDD mutation (%)	Clinical type of CHB		Clinical test		
			Mild and moderate CHB (%)	SevereCHB (%)	Abnormal rate of ALT (%)	HBV DNA >105 copies/mL (%)	HBeAg(+)/HBeAb(–)
B	9	–	8 (88.9)	1 (11.1)	3 (33.3)	4 (44.4)	7/2
C	15	6 (40.0)	4 (26.7)	11 (73.3)	8 (53.3)	9 (60.0)	10/5
D	33	7 (21.2)	14 (42.4)	19 (57.6)	23 (69.7)	22 (66.7)	23/10
CD	43	15 (34.9)	19 (44.2)	24 (55.8)	32 (74.4)	30 (69.8)	28/15
CB	16	6 (37.5)	9 (56.3)	7 (43.7)	9 (56.3)	10 (62.5)	12/4
BD	15	4 (26.7)	7 (46.7)	8 (53.3)	8 (53.3)	9 (60.0)	9/6
Non-A–F	25	8 (32.0)	15 (60.0)	10 (40.0)	12 (48.0)	10 (40.0)	8/17
χ^2		2.788	11.272		9.858	7.448	12.841
P		>0.05	>0.05		>0.05	>0.05	<0.05

Table 3 Curative effect after 48 weeks of LAM treatment

Group	*n*	Recovery rate of ALT (%)	HBV DNA level <103 copies/mL (%)	HBeAg negative conversion rate (%)	HBeAg/HBeAb conversion rate (%)
Single genotypes	30	23 (76.7)	24 (80.0)	16 (53.3)	11 (36.7)
Mixed genotypes	35	28 (80.0)	29 (82.9)	18 (51.4)	12 (34.3)
Non-classified genotypes	16	13 (81.3)	14 (87.5)	10 (62.5)	6 (37.5)
χ^2		0.168	0.411	0.561	0.065
P		>0.05	>0.05	>0.05	>0.05

Observation of curative effects of LAM

ALT and HBV DNA level in all genotypes decreased in different degrees, 4 wk after LAM treatment. There was no significant difference in ALT recovery rate, HBV DNA level, HBeAg, and HBeAg/HBeAb conversion rate 48 weeks after treatment between the groups (Table 3). Twenty-eight cases showed natural mutations of single mixed and non-classified genotypes. After 48 weeks, HBV DNA level decreased in 22 cases to a level <103 copies/mL and ALT became normal. Rebound of HBV DNA level and base line of ALT were not found. HBeAg became negative in 15 cases and 10 cases had HBeAg/HBeAb conversion 48 weeks after the treatment.

DISCUSSION

Research data indicate that HBV can be divided into eight genotypes[3], ranging from A to H. Genotype A is frequently found in northwest Europe and Africa. Genotypes B and C are common in Asia, while genotype D is prevalent in the Mediterranean and Near East. Genotype E is restricted to Sub-Saharan Africa, and F is localized in American aboriginal population. Genotype G has been found in France and USA, and genotypes A –H[4] have been found in patients with HBV infection in San Francisco. The distribution of HBV genotypes is related to immigration[5–7] and race background of the carriers. In China, genotypes B and C are predominant, while genotypes A and D are rare. But type D has a high percentage in minority nationalities. In our study, HBV genotypes were determined in 156 Zhuang CHB patients by PCR-microcosmic nucleic acid cross-ELISA. Genotypes B–D and non-classified type were identified. HBV genotype D was mostly found (58.3%), followed by genotypes C (47.4%), and B (25.6%). Non-classified type (16.0%) was significantly higher than that reported in Taiwan[8]. The distribution of genotypes B and C is consistent with most reports[9–11] in China. Type D is the predominant genotype in Zhuang population, which is different from other reports[11]. It may be related to the geographical and ethnic characteristics of Zhuang population. There was a high rate (47.4%) of mixed

genotypes. The mixed infection occurred between genotypes B and C or B and D, but mostly between genotypes D and C, which is also different from other reports[9] in China. The reasons may be as follows: (1) super infection and mixed infection, patients are easily treated, (2) gene mutation, detection methods, recombination of different genotypes[12]. Our study did not rule out the possibility of recombination of different genotypes. Further studies are needed to explore whether it is related to the special genobackground of Zhuang population or random mechanism.

YMDD motif, located in the C-domain of the catalytic site of the polymerase gene, is also the binding site of the antiviral drug LAM. Long-term treatment with LAM induces mutation of the YMDD motif; however, it was reported recently that YMDD mutations are occurring naturally[13-16]. Original research considered that the natural occurrence of YMDD mutant strains is associated with a great amount of HBV existing in patients[13]. Further research revealed that YMDD mutations occur spontaneously as they gain fitness without any particular cause[17]. The detection rate (29.5%) of mutant strains in our study is in accordance with that reported by Zhang *et al*[15]. showing that wild YMDD mutant strains exist in HBV DNA. There were differences of incidence rate of HBV YMDD wild mutant strains in HBV genotypes D, C, non-classified, and mixed genotypes of CD, BC, and CB. Although no significant difference was found among these genotypes, we cannot exclude the relation between YMDD mutations and HBV genotypes because of the limited samples in our study.

The virus gene controls antigen expression, leading to different genotypes and disease spectrum after infection. However, the conclusions are controversial. It was reported that genotype A is related to chronic active hepatitis, genotype D is related to acute self-limited hepatitis[18], and HBV-D is related to chronic symptomatic carriers[19]. All chronic HBV infections found in Jeju Island are genotype C[20]. But most scholars[21–23] found that genotype C is related to severe hepatitis or the aggravation of illness. Yuen *et al*[24] reported that genotype B has a higher mortality than genotype C because of decompensation of liver function. Our study showed that genotype A was not found in 156 CHB patients, while genotype D was predominant. This may be associated with uneven distribution of genotypes and simple clinical type, or the ethnic background. Genotype B was mainly found in chronic mild and moderate HBV patients, while genotypes C and D were mainly in chronic severe HBV patients. They seemed to increase with the progression of the illness. But there was no statistical significance. Studies on whether mixed genotype infection can worsen liver diseases are available[25–27], but the conclusion is controversial. In our study, mixed genotype CD and BD infections were mainly found in patients with chronic severe HBV infection, indicating that mixed genotype infection can lead to liver disease.

More attention has been paid to the relationship between HBV genotype and HBe, ALT, and HBV DNA. In our study, genotypes of CD and D had higher levels of ALT and HBV DNA than other genotypes, indicating that different genotypes are related with the level of ALT and HBV DNA. Compared to HBeAg-positive rate, there was a significant difference between non-classified and other genotypes ($P<0.05$), indicating that HBV genotype is related with HBe. Further studies are needed.

LAM is one of the first-line medicines for CHB patients[28,29]. Whether the effect of LAM treatment is influenced by HBV genotype is a topic of the researchers. Some studies showed that the effect of LAM treatment is not influenced by HBV genotype[30–32]. In our study, the effect of LAM treatment was not influenced by HBV genotype, suggesting that determination of HBV genotype cannot predict antiviral effect before LAM treatment[30]. Among the 28 cases with YMDD mutations, after 48 weeks of LAM treatment, HBV DNA levels in 22 cases decreased to below 103 copies/mL, and ALT became normal, and HBeAg became negative in 15 cases and 10 cases had HBeAg/HBeAb conversion, showing that LAM has a short-term effect in patients with YMDD wild mutation. This may be associated with the fact that wild viral strains are in the dominant side, while YMDD mutational strains are in the weak side and have a lower duplication activity and weaker pathogenicity.

In short, there are some unique characteristics in the distribution of HBV genotypes of Guangxi Zhuang population. This may be related to the geographic location and ethnics. HBV genotypes are not correlated with YMDD mutation, ALT, and HBV DNA level. The effect of LAM is not influenced by these factors. Further studies are needed to examine the relationship between the characteristics of HBV genotype, the mutation of pre-C-zone and different genotypes, as well as the conversion and prognosis of the disease.

REFERENCES

1 **Hepatology branch-conference of infectious diseases,** parasitic diseases association of Chinese medical association. Schemes of prevention and cure for viral hepatitis. *Zhonghua Ganzangbing Zazhi* 2000; **8:** 324-329

2 **Lamivudine Clinical Practice Group.** Lamivudine treatment consensus from relative experts in 2003. *Zhonghua Ganzangbing Zazhi* 2003; **11:** 497-499

3 **Miyakawa Y,** Mizokami M. Classifying hepatitis B virus genotypes. *Intervirology* 2003; **46:** 329-338

4 **Kato H,** Gish RG, Bzowej N, Newsom M, Sugauchi F, Tanaka Y, Kato T, Orito E, Usuda S, Ueda R, Miyakawa Y, Mizokami M. Eight genotypes (A-H) of hepatitis B virus infecting patients from San Francisco and their demographic, clinical, and virological characteristics. *J Med Virol* 2004; **73:** 516-521

5 **Yuen MF,** Sablon E, Tanaka Y, Kato T, Mizokami M, Doutreloigne J, Yuan HJ, Wong DK, Sum SM, Lai CL. Epidemiological study of hepatitis B virus genotypes, core promoter and precore mutations of chronic hepatitis B infection in Hong Kong. *J Hepatol* 2004; **41:** 119-125

6 **Sallam TA,** William Tong CY. African links and hepatitis B virus genotypes in the Republic of Yemen. *J Med Virol* 2004; **73:** 23-28

7 **Chu CJ,** Keeffe EB, Han SH, Perrillo RP, Min AD, Soldevila-Pico C, Carey W, Brown RS, Luketic VA, Terrault N, Lok AS. Hepatitis B virus genotypes in the United States: results of a

nationwide study. *Gastroenterology* 2003; **125:** 444-451
8 **Lee CM**, Chen CH, Lu SN, Tung HD, Chou WJ, Wang JH, Chen TM, Hung CH, Huang CC, Chen WJ. Prevalence and clinical implications of hepatitis B virus genotypes in southern Taiwan. *Scand J Gastroenterol* 2003; **38:** 95-101
9 **Zhu B,** Luo K, Hu Z. Establishment of a method for classification of HBV genome and it's application *Zhonghua Shi Yan He Lin Chuang Bing Du Xue Za Zhi* 1999; **13:** 309-313
10 **Xia G,** Nainan OV, Jia Z. Characterization and distribution of hepatitis B virus genotypes and subtypes in 4 provinces of China *Zhonghua Liu Xing Bing Xue Za Zhi* 2001; **22:** 348-351
11 **Ge XM,** Li DY, Fang ZL, Huang GY, Jiang SQ, Pan HD, Du Y, Wang CY, Ding X, Masashi M. Distribution of hepatitis B virus genotypes and its clinical significance in Guangxi *Zhonghua Shi Yan He Lin Chuang Bing Du Xue Za Zhi* 2003; **17:** 174-179
12 **Sugauchi F,** Mizokami M, Orito E, Ohno T, Kato H, Suzuki S, Kimura Y, Ueda R, Butterworth LA, Cooksley WG. A novel variant genotype C of hepatitis B virus identified in isolates from Australian Aborigines: complete genome sequence and phylogenetic relatedness. *J Gen Virol* 2001; **82:** 883-892
13 **Kobayashi S,** Ide T, Sata M. Detection of YMDD motif mutations in some lamivudine-untreated asymptomatic hepatitis B virus carriers. *J Hepatol* 2001; **34:** 584-586
14 **Yan MH,** Zhang C, Ling Q, Zhou RF. Detection of YMDD motif mutations in lamivudine-untreated patients with chronic hepatitis B *Zhonghua Gan Zang Bing Za Zhi* 2003; **11:** 430-431
15 **Zhang XH,** Zhang YX, Sun LR, Wen Q, Zhou LQ, Fan GX, Zhang X, Yang DG. Study of gene chips in the detection of YMDD mutations in the region of HBV polymeras *Zhonghua Yi Xue Za Zhi* 2003; **83:** 459-462
16 **Matsuda M,** Suzuki F, Suzuki Y, Tsubota A, Akuta N, Hosaka T, Someya T, Kobayashi M, Saitoh S, Arase Y, Satoh J, Takagi K, Kobayashi M, Ikeda K, Kumada H. Low rate of YMDD motif mutations in polymerase gene of hepatitis B virus in chronically infected patients not treated with lamivudine. *J Gastroenterol* 2004; **39:** 34-40
17 **Kobayashi S.** Clinical characteristics of asymptomatic hepatitis B virus carriers with YMDD mutant not treated with lamivudine. *Kurume Med J* 2003; **50:** 87-90
18 **Mayerat C,** Mantegani A, Frei PC. Does hepatitis B virus (HBV) genotype influence the clinical outcome of HBV infection? *J Viral Hepat* 1999; **6:** 299-304
19 **Duong TN,** Horiike N, Michitaka K, Yan C, Mizokami M, Tanaka Y, Jyoko K, Yamamoto K, Miyaoka H, Yamashita Y, Ohno N, Onji M. Comparison of genotypes C and D of the hepatitis B virus in Japan: a clinical and molecular biological study. *J Med Virol* 2004; **72:** 551-557
20 **Kim BJ,** Song BC. Distribution of hepatitis B virus genotypes according to the clinical outcomes in patients with chronic hepatitis B virus infection in Jeju island. *Korean J Gastroenterol* 2003; **42:** 496-501
21 **Wang Y,** Zhou G, Li X, Zhou Z, Zhou S, Ruan L, Chen M, Deng W. Genotyping of hepatitis B virus and clinical investigation *Zhonghua Shi Yan He Lin Chuang Bing Du Xue Za Zhi* 2002; **16:** 367-369
22 **Ding X,** Mizokami M, Yao G, Xu B, Orito E, Ueda R, Nakanishi M. Hepatitis B virus genotype distribution among chronic hepatitis B virus carriers in Shanghai, China. *Intervirology* 2001; **44:** 43-47
23 **Kao JH,** Chen PJ, Lai MY, Chen DS. Hepatitis B genotypes correlate with clinical outcomes in patients with chronic hepatitis B. *Gastroenterology* 2000; **118:** 554-559
24 **Yuen MF,** Sablon E, Wong DK, Yuan HJ, Wong BC, Chan AO, Lai CL. Role of hepatitis B virus genotypes in chronic hepatitis B exacerbation. *Clin Infect Dis* 2003; **37:** 593-597
25 **Kato H,** Orito E, Gish RG, Bzowej N, Newsom M, Sugauchi F, Suzuki S, Ueda R, Miyakawa Y, Mizokami M.Hepatitis B e antigen in sera from individuals infected with hepatitis B virus of genotype G. *Hepatology* 2002; **35:** 922-929
26 **Kao JH,** Chen PJ, Lai MY, Chen DS.Clinical and virological aspects of blood donors infected with hepatitis B virus genotypes B and C. *J Clin Microbiol* 2002; **40:** 22-25
27 **Kao JH,** Chen PJ, Lai MY, Chen DS. Acute exacerbations of chronic hepatitis B are rarely associated with superinfection of hepatitis B virus. *Hepatology* 2001; **34:** 817-823
28 **Pramoolsinsup C.** Management of viral hepatitis B. *J Gastroenterol Hepatol* 2002; **17** Suppl**:** S125-S145
29 **Alberti A,** Brunetto MR, Colombo M, Craxì A. Recent progress and new trends in the treatment of hepatitis B. *J Med Virol* 2002; **67:** 458-462
30 **Yuen MF,** Wong DK, Sablon E, Yuan HJ, Sum SM, Hui CK, Chan AO, Wang BC, Lai CL. Hepatitis B virus genotypes B and C do not affect the antiviral response to lamivudine. *Antivir Ther* 2003; **8:** 531-534
31 **Yuen MF,** Tanaka Y, Lai CL. Hepatitis B genotypes in chronic hepatitis B and lamivudine therapy. *Intervirology* 2003; **46:** 373-376
32 **Akuta N,** Suzuki F, Kobayashi M, Tsubota A, Suzuki Y, Hosaka T, Someya T, Kobayashi M, Saitoh S, Arase Y, Ikeda K, Kumada H.The influence of hepatitis B virus genotype on the development of lamivudine resistance during long-term treatment. *J Hepatol* 2003; **38:** 315-321

Science Editor Wang XL and Zhu LH **Language Editor** Elsevier HK

PO Box 2345, Beijing 100023, China
www.wjgnet.com
wjg@wjgnet.com

ELSEVIER

World J Gastroenterol 2005;11(41):6530-6534
World Journal of Gastroenterology ISSN 1007-9327

• *RAPID COMMUNICATION* •

Correlation between CK18 gene and gastric carcinoma micrometastasis

Wei Xu, Ming-Wei Zhang, Jing Huang, Xin Wang, Shu-Fen Xu, Yan Li, Shu-Jie Wang

Wei Xu, Jing Huang, Xin Wang, Shu-Fen Xu, Yan Li, Shu-Jie Wang, Department of Laboratory, The First Hospital of Jilin University, Changchun 130021, Jilin Province, China
Ming-Wei Zhang, Department of General Surgery, The Second Hospital of Jilin University, Changchun 130041, Jilin Province, China
Supported by the Natural Science Foundation of Jilin Province, No. 20010594
Correspondence to: Wei Xu, Department of Laboratory, The First Hospital of Jilin University, Changchun 130021, Jilin Province, China. xuwei0210@sina.com
Telephone: +86-431-5612622 Fax: +86-431-5612622
Received: 2005-03-18 Accepted: 2005-04-30

Abstract

AIM: To explore the biological behavior of gastric carcinoma micrometastasis (MM) with a marker of cytokeratin 18 (CK18) and to evaluate the clinical stage of gastric carcinoma and its prognosis.

METHODS: Reverse transcription-polymerase chain reaction (RT-PCR) was used to examine the expression of CK18 mRNA in 298 lymph nodes from 35 patients with gastric carcinoma and 20 lymph nodes from 10 patients with chronic peptic ulcer and gastric perforation diagnosed by pathological examination and surgery. CK18 mRNA expression of peripheral blood from 54 patients with gastric carcinoma and 10 healthy people were also examined.

RESULTS: Expression of CK18 mRNA was not found in 10 patients with benign pathological changes. CK18 mRNA expression in gastric carcinoma tissues was strongly positive. In gastric carcinoma patients, pathological examination revealed that 99 of 298 (33.2%) lymph nodes were positive, while RT-PCR showed that 133 of 298 (44.6%) lymph nodes had expression of CK18 mRNA. The difference was significant ($P < 0.05$). Among the 199 negative lymph nodes identified by pathological examinations, 34 (17.1%) displayed positive expression of CK18 mRNA by RT-PCR. The positive expression of CK18 mRNA was associated with lymph node micrometastasis (LMM) of gastric carcinoma. CK18 mRNA was negatively expressed in all 10 healthy cases and positively expressed in 38.9% of 54 blood specimens from gastric carcinoma patients. The positive rate was not correlated with tumor invasion of gastric carcinoma, but was significantly associated with TNM stage, lymph node metastasis ($P = 0.0290$, $P < 0.05$) and tumor differentiation ($P = 0.2956$, $P<0.05$).

CONCLUSION: RT-PCR with CK18 mRNA as a molecular marker is highly sensitive and specific in detecting LMM of gastric carcinoma. It can benefit the diagnosis of MM and guide studies on biological behavior, clinical phase, and therapy as well as relapse monitoring.

Key words: Gastric carcinoma; CK18; RT-PCR; Biological behavior

Xu W, Zhang MW, Huang J, Wang X, Xu SF, Li Y, Wang SJ. Correlation between CK18 gene and gastric carcinoma micrometastasis. *World J Gastroenterol* 2005;11(41):6530-6534
http://www.wjgnet.com/1007-9327/11/6530.asp

INTRODUCTION

Gastric carcinoma ranks second in alimentary canal diseases and third in all tumors in China. Metastasis and relapse are two major reasons for the death of patients. The two important metastatic pathways of gastric carcinoma are lymph nodes and peripheral blood, which are important factors for the prognosis of patients after curative surgery. This study used reverse transcription-polymerase chain reaction (RT-PCR) to detect the expression of cytokeratin 18 (ck18) mRNA and to explore its correlation with gastric carcinoma micrometastasis (MM).

MATERIALS AND METHODS

Patients and tissue samples

Enrolled in this study were 54 patients (24 females, 30 males) undergone curative gastrectomy for gastric carcinoma at the First and Second Hospitals of Jilin University between October 2001 and August 2002. The patients' age ranged from 34 to 74 years (mean age of 51.2 years). Control group I included 10 patients with peptic ulcer, control group II consisted of 10 healthy people.

A total of 298 lymph nodes were obtained from 54 patients with gastric carcinoma. Lymph nodes were divided into two parts: one for pathological examination and the other stored at -80 °C for use.

Five milliliters of peripheral blood was collected from 54 patients with gastric carcinoma. Blood specimens were anti-coagulated with heparin. Peripheral blood

mononuclear cells (PBMC) were separated from the whole blood by Ficoll-Hypaque density-gradient centrifugation and stored at -70 °C for use. Five milliliters of peripheral blood was collected from negative controls.

Preparation of RNA samples and RT-PCR

RNA was isolated from PBMC and lymph nodes with TRIzol reagent. Lymph nodes were collected from normal controls and gastric carcinoma patients in 1 mL of TRIzol reagent per 100 mg of tissue using power homogenizer. RNA pellet was dried and RNA dissolved in RNase-free water was stored at -70 °C for use. RNA was used as a template for amplification. Oligonucleotides as specific primers and probes for CK18 were synthesized by a company (Biotechnology, Dalian, China). As a PCR control reaction, β-actin was also detected in each run. The sequences of primers are as follows: CK18: 5' -PCR primer AAGAAAACCCGAAGAGG, 3'-PCR primer CTGACTCAAGGTGCAGC; β-actin: 5'-PCR primer GTGGGGCGCCCCAGGCACCA, 3'-PCR primer CTTCCTTAATGTCACGCACGATTTC. The expected sizes of PCR products were 402 bp for CK18 and 540 bp for β-actin. Complementary (c) DNA was synthesized using Rous-associated virus reverse transcriptase (TAKARA Biomedicals).

PCR was performed following the procedure: briefly 130 ng of RNA was used for RT-PCR. For cDNA synthesis, 130 ng in 4 μL of sample RNA solution and 2 μL of oligo dT were heated at 70 °C for 5 min and cooled rapidly. After adding 1 μL of a ribonuclease inhibitor (Takara, Dalian, China), 4 μL of 2.5 mmol/L dNTP (dATP, dCTP, dGTP, dTTP, Takara, Dalian, China) and 4 μL of Rous-associated virus reverse transcriptase (Takara, Dalian, China), 10 μL of 5×PCR buffer, 25 μL of DEPC-water, the mixture was incubated at 65 °C for 60 min, and then at 95 °C for 5 min. The PCR mixture contained 25 μL of cDNA , 7.5 μL of 10×PCR buffer, 6μL of 25 mmol/L $MgCl_2$,8 μL of 2.5 mmol/L dNTP, 50 μL of DEPC-water , 2 μL of 5'- and 3'-PCR primer , 0.5 μL of μ-actin and 1.0 μL of thermostable Taq polymerase (Takara, Dalian, China). The amplification was done with a DNA thermal cycler (Geneam PCR System 2400). After denaturation at 94 °C for 4 min, the amplification was conducted for 35 cycles at 94 °C for 45 s, at 55 °C for 45 s, and at 72 °C for 60 s. This was followed by a final extension for 1 min at 72 °C. Ten microliter aliquots of the product was analyzed by electrophoresis on a 2% agarose gel and visualized by UV fluorescence after being stained with ethidium bromide.

Standard of result assessment

The expected sizes of PCR products were 402 bp for CK18 and 540 bp for β-actin. CK18 mRNA expression of two DNA bands in the corresponding location was positive. CK18 mRNA expression of one 540 bp band was negative (Figure 1).

Statistical analysis

Data were analyzed by χ^2 test using Instat software. $P<0.05$ was considered statistically significant.

Classification standard for lymph node metastasis

According to the 1997 International Union Contrele Cancer (UICC)/American Joint Committee on Cancer (AJCC) pN classification, PN0: without lymph node metastasis, PN1: 1-6 lymph node metastases, PN2: 7-15 lymph node metastases, PN3: >15 lymph node metastases.

RESULTS

Expressions of CK18 mRNA in lymph nodes and peripheral blood are shown in Figure 1.

Lymph node MM, correlation between CK18 mRNA expression in lymph nodes, peripheral blood and tissue differentiation, tumor stage and invasion are summarized in Tables 1-3.

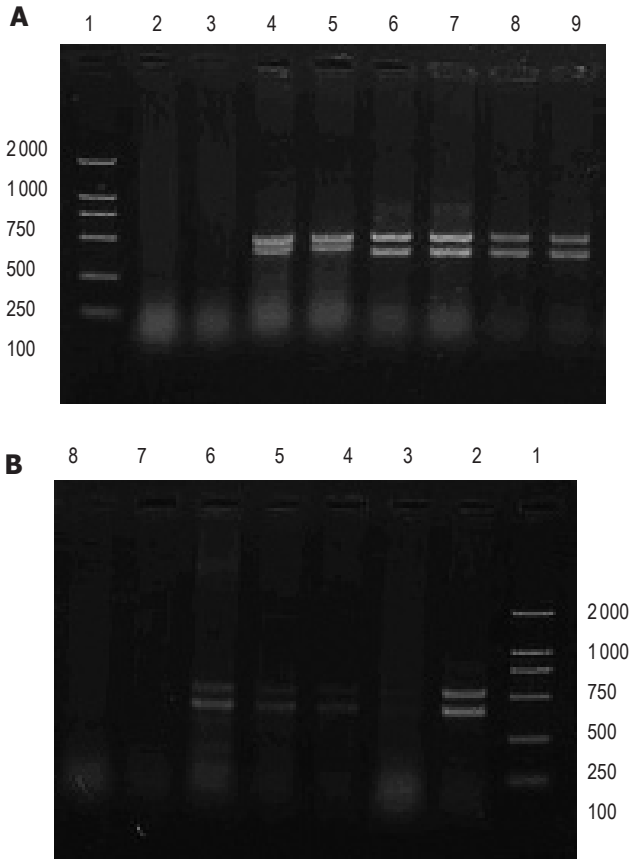

Figure 1 Expression of CK18 mRNA gene in lymph nodes **(A)** and peripheral blood **(B)**. Lane 1: 2-kb DNA ladder marker; lane 2: positive gastric carcinoma tissue; lanes 3-6: positive peripheral blood specimens; lanes 7 and 8: negative lymph nodes.

Table 1 Lymph node MM

Pathological diagnosis of lymph nodes (carcinoma cells)	RT-PCR(CK18 mRNA)		Sum
	Positive	Negative	
Positive	99	0	99
Negative	34	165	199
Sum	133	165	298

Table 2 Correlation between expression of CK18 mRNA in lymph nodes, peripheral blood and TNM stage

Pathologic	Lymph nodes				Peripheral blood			
parameters	*n*	+	–	*P*	*n*	+	–	*P*
Tissue				>0.05				<0.05
differentiation	15	4	11		29	7	22	
Well-moderate	20	10	10		25	14	11	
Poor				<0.05				>0.05
Tumor invasion	11	1	10		23	6	17	
Muscularis	24	13	11		31	15	16	
Serosa				<0.05				<0.05
Lymph node	14	2	12		20	3	17	
metastasis	21	12	9		34	18	16	
Yes				>0.05				<0.05
No	15	4	11		21	4	17	
TNM stage	20	11	9		33	17	16	
I+II								
III+IV								

+: positive cases; –: negative cases.

Table 3 Correlation between expression of CK18 mRNA in lymph nodes, tissue differentiation and tumor invasion

Pathologic parameters	CK18 mRNA expression of lymph nodes			*P*
	n	Positive	Negative	
Tissue differentiation				>0.05
Well-moderate	31	11	20	
Poor	267	122	145	
Tumor invasion				<0.05
Muscularis (T_1+T_2)	62	12	50	
Serosa (T_3+T_4)	236	121	115	

DISCUSSION

Micrometastasis

MM spreads from primary tumor to distant secondary tumors in lymph system, blood circulation, bone marrow, liver, kidney, lung, and other organs during the development of malignant neoplasm in non-hematopoietic system. It often has no clinical symptoms[1,2]. Gastric carcinoma is one of the most common malignant neoplasms in China. Many patients showing lymph node metastasis of gastric carcinoma experience relapse and eventually die after curative surgery. Even those with no metastasis of gastric carcinoma ultimately die in the relapse of metastasis. The essential reason is MM, that cannot be detected. MM has become the focus in recent studies on malignant neoplasm. The growth and metastasis of gastric carcinoma are a complicated process with a variety of gene mutations. Although most carcinoma cells entering into circulation are destroyed through mechanisms such as immunization, the residual carcinoma cells can disseminate through a number of mechanisms, such as changes of cell modulation, excretion of protease, growth of blood vessels, and increase of cell dynamics[3]. MM of malignant tumor is controlled by the positive and negative functions of a number of genes at molecule level. Successful clones of "correlating genes of tumor metastasis" and "restraining genes of tumor metastasis" are related with tumor metastasis. Genes at molecule level such as c-met, ras, myc and HER-2/neu, and restraining genes of tumor metastasis such as nm23, p53 and CD44 are related to tumor metastasis[4]. Loss, mutation and abnormal expression of the genes are correlated with invasive metastasis of tumor. Lymph node MM is the main pathway of gastric carcinoma MM. Lymph node MM has been considered as cancer metastasis that cannot be detected by traditional pathological methods[4]. MM foci of lymph node could be easily ignored or missed. Amplifying tumor- or tissue-specific mRNA by RT-PCR can detect tumor cells from 106 to 107 normal cells, and further detect the MM foci of lymph nodes. Patients with MM identified by RT-PCR are often in the developing stage of the disease, and symptoms are likely to turn out to be negative after the therapy. Therefore, lymph node metastasis is not only a prognosis indicator but also an indicator for assessing the effectiveness of therapy and monitoring early relapse[5]. Lymph node metastasis was not only an index of dys-outcome, but also has curative effect and monitoring earlier period relapse[3]. The hematogenous dissemination is another pathway of gastric carcinoma MM. Although the presence of carcinoma cells in blood does not necessarily lead to metastasis, entry of carcinoma cells into blood is the first step for the occurrence of tumor transfer in remote areas. Tumor cells shedding from pro-foci in perioperative or postoperative periods have spread to blood, lymph nodes, marrow or other organs even before pro-foci formation. However, it is difficult to detect metastasis in patients without clinical symptoms by traditional methods such as imaging and clinical pathology. Therefore, many researchers are dedicated in searching sensitive and specific methods to detect MM.

CK18 as a marker for micrometastasis

Cytokeratins (CKs) constitute the cytoskeleton of intermediate filament type in most epithelial cells. They consist of at least 20 members, designated as CK1–CK20 according to their molecular weights and isoelectric points[6,7]. Each type of epithelial cells has a rather stable CK composition, termed as CK pattern, which has been used in the identification of different epithelial tissues and their neoplasms[7]. CKs are expressed in the epithelial tissues, but not in the intermediate filament tissues (blood vessel, nerve, lymph tissues). They are continuously expressed in epithelial cells during malignant transformation and tumor formation, but not in normal lymph nodes, which provides the basis for applying CKs in diagnosing gastric carcinoma MM[8]. Molecular markers of malignant tumor MM from epithelial tissues have been explored recently[9–11]. For example, Liu *et al*[9] from abroad used CK20 mRNA as a marker to examine large intestine carcinoma with RT-PCR. With CK19 mRNA as a marker Ueda *et al*[10] examined lung carcinoma with RT-

PCR. Noguchi *et al*[11] examined CK19 mRNA in lymph nodes from 10 cases of gastric carcinoma with RT-PCR. Domestic researchers have detected lymph node MM of gastric carcinoma by targeting CK19, CK20 with RT-PCR technique[12,13]. Lymph node MM of gastric carcinoma by choosing CK7, CK8 with immunofluorescence stain and immunocyte chemical technique[1]. Different from other CKs, CK18 has a stricter specific distribution in epithelial cells and a specific expression in cells from glandular epithelium[14]. Therefore, if CK18 mRNA is expressed in lymph nodes from gastric carcinoma patients, it indicates the existence of tumor metastasis in lymph nodes; If CK18 mRNA is expressed in peripheral blood from gastric carcinoma patients, it indicates the possibility that metastasis has been transferred to other distant organs.

Correlation between gastric carcinoma micrometastasis and CK18 expression

RT-PCR was used in this study to detect CK18 mRNA. Results from analyzing 298 lymph nodes of gastric carcinoma and 20 lymph nodes from control group I indicate that: (1) In contrast to the findings of negative expression in all the benign pathological changes of lymph nodes, CK18 mRNA showed positive expression in gastric carcinoma tissues, indicating that RT-PCR technique has a high specificity for detecting CK18 mRNA. Expression of CK18 mRNA was detected in lymph nodes from patients with gastric carcinoma, indicating that the cancer is transferred. CK18 mRNA was positively expressed in 34 of 199 lymph nodes (17.1%), showing that RT-PCR has a high sensitivity for detecting lymph node metastasis of gastric carcinoma. As lymph node metastasis of gastric carcinoma directly affects the prognosis of gastric carcinoma patients, lymph nodes around gastric carcinoma tissues should be removed. According to UICC/AJCC new classification of lymph node metastasis of gastric carcinoma in 1997[15], 199 lymph nodes with PN0 from 35 patients with gastric carcinoma demonstrated by pathological examination in postoperative, contained 17.1% lymph node micrometastases by RT-PCR that should be classified into PN1. The main risk factors for lymph node metastasis include the size of primitive tumor, the degree of differentiation and depth of invasion[16]. Fukagawa *et al*[17] have found that metastasis occurs more often from tumescent growth tumors than from invasive growth tumors. The current study has revealed that lymph node MM is highly correlated with the depth of invasion (T)[18]. It was reported that patients (PT3N0) without lymph node metastasis detected by routine pathological examination have lymph node metastasis (PT3N1) detected by RT-PCR[19]. Suggesting that MM examination should be conducted for PN0 to improve the accuracy of clinical stage of gastric carcinoma, MM in peripheral blood does not necessarily develop clinical symptoms, but it correlates with biological behavior of gastric carcinoma. Zhang *et al*[20] demonstrated that CK20 mRNA is a marker of gastric carcinoma MM. Chausovsky *et al*[21] used CK20 mRNA as a target gene to examine MM of gastric carcinoma in peripheral blood from 116 patients with malignant neoplasm, and found that CK20 mRNA is a target gene for MM of epithelial tumor. Majima *et al*[22] took CK19 and CK20 mRNA as target genes to examine MM in peripheral blood from 52 patients with gastric carcinoma and found that CK19 mRNA is better than CK20 mRNA as a marker. The current study detected the expression of CK18 mRNA in peripheral blood from 54 patients with gastric carcinoma and found that the positive expression was 38.9% (21/54) compared to control group II, suggesting that patients with gastric carcinoma develop MM in peripheral blood. Suppressed by the organic defense mechanism, carcinoma cells in peripheral blood are in dormant status after they disseminate into the organs. However, carcinoma cells can grow and reproduce again due to multiple factors such as aggravation of the disease which eventually lead to clinical metastasis and relapse, thus influencing prognosis. Therefore, examination of MM in peripheral blood among patients with gastric carcinoma is recommended. It helps to determine relevant assistant therapy and to evaluate prognosis.

In conclusion, RT-PCR has a high specificity and sensitivity in detecting CK18 mRNA in gastric carcinoma patients and can be used to evaluate metastasis of gastric carcinoma at the molecule level.

REFERENCES

1 **Chen XM,** Chen GY, Zhang X. The cytological examination of cancer cells in peripheral blood of patients with gastric cancer. *Zhonghua Xiaohua Zazhi* 2002; **22:** 481-484

2 **Zheng JJ,** Hu P, F JX. Clinical significance and detection of micrometastasis with gastric carcinoma. *Fubu Waike* 2002; **15:** 63

3 **Liu Y.** The evaluation of PCR in diagnosis of genes with gastric carcinoma. *Xibei Minzu Zazhi* 2002; **23:** 50-51

4 **Weng DS,**Ding YQ. Studying progression of gene controlling of tumor metastasis. *Yixue Zongshu* 2003; **9:** 131-133

5 **Xiao WD,** Peng CH, Wang ML, Zhou YQ, Cheng H, Zhu PQ. Detecting micrometastasis of pathology negative lymph nodes with gastric carcinoma by RT-PCR. *Zhongguo Puwai Jichu yu Linchuang Zazhi* 2003; **10:** 487-488

6 **Gong YL,** Zhou QH. Study progression of moleculor diagnosis of lung carcinoma micrometastasis. *Zhongguo Feiai Zazhi* 2002; **3:** 75

7 **Moll R,** Löwe A, Laufer J, Franke WW. Cytokeratin 20 in human carcinomas. A new histodiagnostic marker detected by monoclonal antibodies. *Am J Pathol* 1992; **140:** 427-447

8 **Yang XW,** Liu HW. Studying progression of lymph nodes with gastric carcinoma.*Yixue Zongshu*,2001; **7:** 645

9 **Lowe A,** Laufer J, Franke WW. Cytokeratin 20 in human carcinomas. A new histodiagnostic marker detected by monoclonal antibodies. *Chin Med J* 2002, **115:** 529-531

10 **Ueda Y,** Fujita J, Bandoh S, Hojo S, Yamaji Y, Ohtsuki Y, Dobashi N, Takahara J. Expression of cytokeratin 19 mRNA in human lung cancer cell lines. *Int J Cancer* 1999, **81:** 939-943

11 **Noguchi S,**Hiratsuka M, Furukawa H, Aihara T, Kasugai T, Tamura S, Imaoka S, Koyama H, Iwanaga T. Detection of gastric cancer micrometastases in lymph nodes by amplification of keratin 19 mRNA with reverse transcriptase-polymerase chain reaction. *Jpn J Cancer Res* 1996; **87:** 650-654

12 **Dong Q,** Zhang YCh, Hong HQ,J BC, Xu J,Qian HQ. Detecting lymph nodes micrometastasis with gastric carcinoma by reverse transcriptase-polymerase chain reaction. *Zhonghua Waike Zazhi* 2000, **38:** 621

13 **Lu J,** Wu YG, Mu QL,Wu TH. Studying of micrometastasis of peripheral blood preoperative and postoperative with gastric carcinoma. *Shandong Yiyao* 2002; **42:** 1-3
14 **Chen YD,** Liu FK, Qi XP,Li JT. The studing of bone marrow micrometastasis and proliferation in gastric carcinoma. *Yixue Yanjiusheng Bao* 2001; **14:** 297-298
15 **Roder JD,** Böttcher K**,** Busch R, Wittekind C, Hermanek P, Siewert JR. Classification of regional lymph node metastasis from gastric carcinoma. German Gastric Cancer Study Group. *Cancer* 1998; **82:** 621-631
16 **Maehara Y,**Orita H,Okuyama T,Moriguchi S,Tsujitani S, Korenaga D,Sugimachi K.Predictors of lymph node metastasis in early gastric cancer. *Br J Surg* 1992; **79:** 245-247
17 **Fukagawa T,** Sasako M, Mann GB, Sano T, Katai H, Maruyama K, Nakanishi Y, Shimoda T. Immunohistochemically detected micrometastases of the lymph nodes in patients with gastric carcinoma. *Cancer* 2001; **92:** 753-760
18 **Ishida K,**Katsuyama T,Sugiyama A,Kawasaki S. Immunohistochemical evaluation of lymph node micrometastases from gastric carcinomas. *Cancer* 1997; **79:** 1069-1076.
19 **Matsumoto M.**Detecting lymph nodes and lymph location drawing with PN0 gastric carcinoma by reverse transcriptase-polymerase chain reaction(British). *Guowai Yixue Waikexue Fence* 2003; **1:** 62-63
20 **Zhang XW,** Fan P, Yang HY, Yang L, Chen GY. Significance of detecting disseminated tumor cells in peripheral blood of gastric and colorectal cancer patients. *Zhonghua Zhongliu Zazhi* 2003; **25:** 66-68
21 **Chausovsky G,** Luchansky M, Figer A, Shapira J, Gottfried M, Novis B, Bogelman G, Zemer R, Zimlichman S, Klein A. Expression of cytokeratin 20 in the blood of patients with disseminated carcinoma of the pancreas, colon, stomach, and lung. *Cancer* 1999; **86:** 2398-2405
22 **Majima T,** Ichikura T, Takayama E, Chochi K, Mochizuki H. Detecting circulating cancer cells using reverse transcriptase-polymerase chain reaction for cytokeratin mRNA in peripheral blood from patients with gastric cancer. *Jpn J Clin Oncol* 2000; **30:** 499-503

Science Editor Wang XL and Guo SY **Language Editor** ELsevier HK

PO Box 2345, Beijing 100023, China
www.wjgnet.com
wjg@wjgnet.com

ELSEVIER

World J Gastroenterol 2005;11(41):6535-6537
World Journal of Gastroenterology ISSN 1007-9327

• *RAPID COMMUNICATION* •

Quantitative evaluation of diffusion-weighted magnetic resonance imaging of focal hepatic lesions

Xi-Jie Sun, Xian-Yue Quan, Fan-Heng Huang, Yi-Kai Xu

Xi-Jie Sun, Xian-Yue Quan, Fan-Heng Huang, Imaging Center, Affiliated Zhujiang Hospital of Southern Medical University, Guangzhou 510282, Guangdong Province, China
Yi-Kai Xu, Imaging Center, Affiliated Nanfang Hospital of Southern Medical University, Guangzhou 510515, Guangdong Province, China
Supported by the Natural Science Foundation of Guangdong Province, China, No. 32830 and 101595
Correspondence to: Dr. Xian-Yue Quan, Imaging Center, Affiliated Zhujiang Hospital of Southern Medical University, Guangzhou 510282, Guangdong Province, China. qxy1318@sina.com
Telephone: +86-20-61643460 Fax: +86-20-61643460
Received: 2005-01-12 Accepted: 2005-01-26

Abstract

AIM: To explore the quantitative analysis of diffusion-weighted magnetic resonance imaging (DWMRI) in differential diagnosis of focal hepatic lesions.

METHODS: DWMRI was performed in 149 hepatic lesions, including hepatocellular carcinoma (34 cases), hepatic metastases (37 cases), cavernous hemangioma (42 cases), hepatic cyst (36 cases). Apparent diffusion coefficient (ADC) values were evaluated using four different *b* values in different sequences. The ratio of ADC values of lesion/liver in hepatocellular carcinoma and hepatic metastases was also calculated.

RESULTS: The mean ADC values of hepatic lesions were as follows: hepatocellular carcinoma $(0.95 \pm 0.11) \times 10^{-3}$ mm^2/s, hepatic metastasis $(1.13 \pm 0.21) \times 10^{-3}$ mm^2/s, cavernous hemangioma $(1.86 \pm 0.36) \times 10^{-3}$ mm^2/s, hepatic cyst $(3.14 \pm 0.31) \times 10^{-3}$ mm^2/s. The ratio of ADC values in lesion/liver in hepatocellular carcinoma was 0.91 ± 0.11, being significantly different from that in hepatic metastasis (1.21 ± 0.18, $P < 0.05$).

CONCLUSION: ADC values and quantitative analysis of focal hepatic lesions are of significant values in differential diagnosis of focal hepatic lesions.

Key words: Diffusion-weighed magnetic resonance imaging; Hepatic lesion; Quantitative analysis

Sun XJ, Quan XY, Huang FH, Xu YK. Quantitative evaluation of diffusion-weighted magnetic resonance imaging of focal hepatic lesions. *World J Gastroenterol* 2005; 11(41): 6535-6537
http://www.wjgnet.com/1007-9327/11/6535.asp

INTRODUCTION

Diffusion-weighted magnetic resonance imaging (DWMRI) is a new technique of magnetic resonance imaging (MRI) at the level of molecular movements and can reflect the functions and structures of the body without trauma. It has been used to diagnose diseases in the central nervous system[1-3]. Radiologists have paid more attention to its values in differential diagnosis of focal hepatic lesions[4-6]. This study was to evaluate the value of DWMRI in differential diagnosis of focal hepatic lesions by quantifying apparent diffusion coefficient (ADC) values.

MATERIALS AND METHODS

In this study, DWMRI was performed in 149 patients with focal hepatic lesions (31 women and 109 men, aged 24-89 years, mean 52.37 years), including 34 hepatocellular carcinomas, 37 hepatic metastases, 42 cavernous hemangiomas, 36 hepatic cysts. The diameter of the above lesions was 1.1-20.5, 0.8-25.8, 0.9-8.6, and 0.8-2.7 cm, respectively.

The criteria for selecting the patients were as follows: (1) The diagnosis of all cases of hepatocellular carcinoma was confirmed by α-fetal protein, clinical data, ultrasound, CT or/and MR imaging, and pathology. (2) All cases of hepatic metastasis of primary malignant tumors were surgically confirmed. (3) The diagnosis of all the cases of cavernous hemangioma and hepatic cyst was confirmed by clinical data, ultrasound, CT or/and MR imaging, and follow-up observation.

DWMRI was performed by 1.5 T MR scanner with a body coil (Signa, Horizon LX, GE, USA). All data were measured in control console. All lesions were scanned with spin-echo (SE) T1WI and fast SE T2WI in the axial plane. The imaging parameters of DWMRI with SE-echo planar imaging (EPI) sequence were set as follows: repetition time ms/echo time ms: 10 000/90; matrix: 128×128; field of view: 36 cm×36 cm; section thickness: 8 mm; gap: 2 mm; slice number: 10-15; one signal. Four different *b* values (b=0 mm^2/s, 100, 500, 1 000 mm^2/s) and three directions were used, total acquisition time was 40 s.

The standards of measurement of signal intensities in hepatic lesions on DWMRI were as follows: the largest diameter of lesions was measured, three regions of interest in each lesion were marked off and measured, the regions of blood vessels and artifacts were rejected, the edges of parenchyma in the lesion were measured, when apparent necrosis was present, and regions of interest should involve parenchyma and the diameter of it should be longer than 1 cm, the same area of the section should be chosen for the measurement of different sequences, the signal intensity of each ROI was measured thrice and a mean value of SI was acquired for ADC calculation.

ADC values were evaluated with the following formula: $ADC=(\ln[S_l+S_h])/(b_h-b_l)$, where ln is the natural logarithm, S_l and S_h are the signal intensities of low b value and high b value, respectively.

All data were expressed as mean±SD. Statistical analysis was performed by t-test using SPSS software 10.0. $P<0.05$ was considered statistically significant.

RESULTS

In this study, 149 focal hepatic lesions were detected by DWMRI, the DWMRI sensitivity was 100%. We used four different b values ($b=0$, 100, 500, and 1 000 mm^2/s). The higher the b values on the DWMRI ($b=1\ 000$ mm^2/s). The lower the b values on DWMRI ($b=100$ mm^2/s), the higher the ADC values. Thus, we measured the highest b value ($b=1\ 000$ mm^2/s) on DWMRI. Table 1 shows the ADC values in focal hepatic lesions.

Table 1 ADC values in focal hepatic lesions (×10^{-3} mm^2/s)

Hepatic lesion	$b=100$	$b=500$	$b=1\ 000$
Hepatocellular carcinoma	0.56-1.33	0.60-1.31	0.57-1.23
Hepatic metastases	0.75-1.62	0.71-1.59	0.72-1.35
Cavernous hemangioma	1.26-2.54	1.32-2.36	1.37-2.21
Hepatic cyst	2.70-3.85	2.73-3.71	2.78-3.51

The ADC values in hepatic cyst were significantly higher than those in hepatic hemangioma, metastasis, and hepatocellular carcinoma, respectively; the t-test value was 2.329-3.237 ($P<0.01$). There was a significant difference in ADC values of hepatic hemangioma, hepatic metastasis, and hepatocellular carcinoma, respectively, with the t-test value being 1.139-3.467 ($P<0.05$). No significant difference was demonstrated between hepatic metastasis and hepatocellular carcinoma with the t-test value being 1.432 (Table 2).

Table 2 ADC value in focal hepatic lesions ($b=1\ 000$ mm^2/s, mean±SD)

Hepatic lesion	ADC value (×10-3 mm^2/s)
Hepatocellular carcinoma	0.95±0.11
Hepatic metastases	1.13±0.21
Cavernous hemangioma	1.86±0.36
Hepatic cyst	3.14±0.31

The ratio of ADC values of lesion/liver between hepatocellular carcinoma and hepatic metastasis was significantly different with the t-test value being 2.328 (Table 3).

Table 3 Ratio of ADC values of lesion/liver between hepatocellular carcinoma and hepatic metastasis (mean±SD)

Hepatic lesion	Coverage	Ratio of ADC values of lesion/liver
Hepatocellular carcinoma	0.73-1.05	0.91±0.11
Hepatic metastases	1.07-1.43	1.21±0.18

DISCUSSION

Diffusion is known as the Brownian motion caused by thermal movement of molecules, and is arbitrary and irregular. The effect of molecular diffusion movement is weak, but it can result in MR signal missing converge, the attenuation degree lies on MR gradient intensity and amplitude of molecular movement[7,8]. DWMRI is an imaging method to observe microcosmic molecular movement using macroscopical flowing phase displacement theory. Body diffusion coefficient is affected by microcirculation factors[9], such as humoral flowing, cellular osmosis and temperature, perfusion of capillary vessels, glutinous degree and proportion of intra- and extra-cellular water, direction of cellular membrane transition. It is also affected simultaneously by macro factors and circadian function, such as breath, pulsate, and peristalsis. In fact, apparent diffusion coefficient (ADC) regularly replaces the diffusion coefficient, and is always greater than the latter[10,11].

In theory, ADC value can be obtained by one pulsate sequence using two different b values. In experimental researches and clinical applications, ADC values are constantly related to the kinds and quantities of b value in sequences and perfusion of tissue[12-14]. The bigger the b value, the more accurately the ADC value. We measured the four different b values in different sequences (b=0, 100, 500, and 1 000 mm^2/s), and found that ADC values had higher stabilization with higher b values. The technique of EPI, which has a more rapid imaging speed and higher section efficiency, could complete signal collection of single images in several milliseconds and freeze-up artifact of physiological functions. Therefore, it is the commonly used diffusion imaging sequence[15-17]. We adopted images of 1 000 mm^2/s as a reference to give enough attention to attenuation degrees of four different lesions.

Animal experiments and clinical researches indicate that ADC value depends on imaging materials and molecular spatial distribution[18,19]. Cavernous hemangioma and hepatic cyst are mainly composed of liquid component, which has more movement freedom in the two lesions; ADC values are greater than those in hepatic parenchymatous mass. Cavernous hemangioma often presents fiber septation, scar, and hemorrhage, and the blood glutinous degree is higher than that of hydatid fluid in hepatic cyst. This is why the ADC value in hepatic cyst is lower than that in cavernous hemangioma[20-22]. Thus,

entity mass, cavernous hemangioma and hepatic cyst have significantly different ADC values. These findings are consistent with the results in our study.

Our results indicate that the different ADC values in DWMRI could differentiate hepatic cyst and cavernous hemangioma from other hepatic entity masses[23]. We also analyzed the ratio of ADC values of the lesion/liver. Statistical analysis demonstrated that ADC ratio was different between hepatocellular carcinoma and hepatic metastasis.

We believe that the ratio of ADC value of lesion/liver could differentiate hepatocellular carcinoma from hepatic metastasis, and provide some information for the diagnosis of focal hepatic lesions that are less than 3 cm in diameter. This theory is based on the situation in our country that hepatocellular carcinoma generally results from cirrhosis, but hepatic metastasis is not the case[24-26]. Although the ADC values in hepatic metastasis foci are slightly greater than those in hepatocellular carcinoma foci, the ADC values in liver parenchyma with hepatic metastasis are lower than those in hepatocellular carcinoma. Patients with hepatic metastasis have a higher ratio of ADC values of lesion/liver than those with hepatocellular carcinoma.

In conclusion, DWMRI is a new functional MRI technique, and is of great value in the differential diagnosis of focal hepatic lesions.

REFERENCES

1 **F**urukawa M, Terae S, Chu BC, Kaneko K, Kamada H, Miyasaka K. MRI in seven cases of tacrolimus (FK-506) encephalopathy: utility of FLAIR and diffusion-weighted imaging. Neuroradiology 2001; 43: 615-621

2 Berman JI, Berger MS, Mukherjee P, Henry RG.. Diffusion-tensor imaging-guided tracking of fibers of the pyramidal tract combined with intraoperative cortical stimulation mapping in patients with gliomas. J Neurosurg 2004; 101: 66-72

3 Takeuchi M, Harada M, Hisaoka S, Nishitani H, Mori K, Sakama M. Magnetic resonance imaging and proton MR spectroscopy of the brain in a patient with carbohydrate-deficient glycoprotein syndrome type I. J Magn Reson Imaging 2003; 17: 722-725

4 Boulanger Y, Amara M, Lepanto L, Beaudoin G, Nguyen BN, Allaire G, Poliquin M, Nicolet V. Diffusion-weighted MR imaging of the liver of hepatitis C patients. NMR Biomed 2003 ; 16: 132-136

5 Bianco F, Fattapposta F, Locuratolo N, Pierallini A, Rossi M, Ruberto F, Bozzao L. Reversible diffusion MRI abnormalities and transient mutism after liver transplantation. Neurology 2004; 62: 981-983

6 Geschwind JF, Artemov D, Abraham S, Omdal D, Huncharek MS, McGee C, Arepally A, Lambert D, Venbrux AC, Lund GB. Chemoembolization of liver tumor in a rabbit model: assessment of tumor cell death with diffusion-weighted MR imaging and histologic analysis. J Vasc Interv Radiol 2000; 11: 1245-1255

7 Flemming K, Ulmer S, Duisberg B, Hahn A, Jansen O. MR spectroscopic findings in a case of Alpers-Huttenlocher syndrome. AJNR Am J Neuroradiol 2002; 23: 1421-1423

8 McCabe K, Tyler K, Tanabe J. Diffusion-weighted MRI abnormalities as a clue to the diagnosis of herpes simplex encephalitis. Neurology 2003; 61: 1015-1016

9 Au WL, Lim TC, Seow DC, Koh PL, Loh NK, Lim MS, Tan IK, Yee WC. Serial diffusion-weighted magnetic resonance imaging in adult-onset citrullinaemia. J Neurol Science 2003; 209: 101-104

10 Inoha S, Inamura T, Nakamizo A, Ikezaki K, Amano T, Fukui M. Magnetic resonance imaging in cases with encephalopathy secondary to immunosuppressive agents. J Clin Neurosci 2002; 9: 305-307

11 Cheryauka AB, Lee JN, Samsonov AA, Defrise M, Gullberg GT. MRI diffusion tensor reconstruction with PROPELLER data acquisition. Magn Reson Imaging 2004; 22: 139-148

12 Hori M, Ichikawa T, Sou H, Tsukamoto T, Kitamura T, Okubo T, Araki T, Amemiya Y, Okamoto E, Obara M. [Improving diffusion-weighted imaging of liver with SENSE technique: a preliminary study] Nippon Igaku Hoshasen Gakkai Zasshi 2003; 63: 177-179

13 Eastwood JD, Vollmer RT, Provenzale JM. Diffusion-weighted imaging in a patient with vertebral and epidural abscesses. AJNR Am J Neuroradiol 2002; 23: 496-498

14 Byun WM, Shin SO, Chang Y, Lee SJ, Finsterbusch J, Frahm J. Diffusion-weighted MR imaging of metastatic disease of the spine: assessment of response to therapy. AJNR Am J Neuroradiol 2002 :23: 906-912

15 Chow LC, Bammer R, Moseley ME, Sommer FG. Single breath-hold diffusion-weighted imaging of the abdomen. J Magn Reson Imaging 2003 ; 18: 377-382

16 Ulmer S, Flemming K, Hahn A, Stephani U, Jansen O. Detection of acute cytotoxic changes in progressive neuronal degeneration of childhood with liver disease (Alpers-Huttenlocher syndrome) using diffusion-weighted MRI and MR spectroscopy. J Comput Assist Tomogr 2002 ; 26: 641-646

17 Blomqvist L. Preoperative staging of colorectal cancer-computed tomography and magnetic resonance imaging. Scand J Surg 2003; 92: 35-43

18 Colagrande S, Politi LS, Messerini L, Mascalchi M, Villari N. Solitary necrotic nodule of the liver: imaging and correlation with pathologic features. Abdom Imaging 2003; 28: 41-44

19 Kamel IR, Bluemke DA, Ramsey D, Abusedera M, Torbenson M, Eng J, Szarf G, Geschwind JF. Role of diffusion-weighted imaging in estimating tumor necrosis after chemoembolization of hepatocellular carcinoma. AJR Am J Roentgenol 2003 ;181: 708-710

20 Lodi R, Tonon C, Stracciari A, Weiger M, Camaggi V, Iotti S, Donati G, Guarino M, Bolondi L, Barbiroli B. Diffusion MRI shows increased water apparent diffusion coefficient in the brains of cirrhotics. Neurology 2004; 62: 762-766

21 Chan JH, Tsui EY, Luk SH, Fung AS, Yuen MK, Szeto ML, Cheung YK, Wong KP. Diffusion-weighted MR imaging of the liver: distinguishing hepatic abscess from cystic or necrotic tumor. Abdom Imaging 2001; 26: 161-165

22 Aubé C, Racineux PX, Lebigot J, Oberti F, Croquet V, Argaud C, Calès P, Caron C. [Diagnosis and quantification of hepatic fibrosis with diffusion weighted MR imaging: preliminary results] J Radiology 2004 ; 85: 301-306

23 Moteki T, Horikoshi H, Oya N, Aoki J, Endo K. Evaluation of hepatic lesions and hepatic parenchyma using diffusion-weighted reordered turboFLASH magnetic resonance images. J Magn Reson Imaging 2002; 15: 564-572

24 Glass NL, Lee L. Isolation of Neurospora crassa A mating type mutants by repeat induced point (RIP) mutation. Genetics 1992; 132: 125-33

25 Sun XJ, Quan XY, Liang W, Wen ZB, Zeng S, Huang FH, Tang M. [Quantitative study of diffusion weighted imaging on magnetic resonance imaging in focal hepatic lesions less than 3 cm] Zhonghua Zhong liu za zhi 2004; 26:165-167

26 Mürtz P, Flacke S, Träber F, van den Brink JS, Gieseke J, Schild HH. Abdomen: diffusion-weighted MR imaging with pulse-triggered single-shot sequences. Radiology 2002; 224: 258-264

Science Editor Kumar M and Guo SY **Language Editor** Elsevier HK

PO Box 2345, Beijing 100023, China
www.wjgnet.com
wjg@wjgnet.com

ELSEVIER

World J Gastroenterol 2005;11(41):6538-6542
World Journal of Gastroenterology ISSN 1007-9327

• *RAPID COMMUNICATION* •

Dual effects of 8-Br-cAMP on differentiation and apoptosis of human esophageal cancer cell line Eca-109

Hong-Mei Wang, Nai-Gang Zheng, Jing-Lan Wu, Cui-Cui Gong, Yi-Ling Wang

Hong-Mei Wang, Department of Laboratory Medicine, First Affiliated Hospital of Zhengzhou University, Zhengzhou 450052, Henan Province, China
Nai-Gang Zheng, Jing-Lan Wu, Yi-Ling Wang, Molecular Cell Biology Research Center, Zhengzhou University, Zhengzhou 450052, Henan Province, China
Cui-Cui Gong, Laboratory Medicine Center, PLA No. 153 Hospital, Zhengzhou 450042, Henan Province, China
Supported by the Research Science Foundation of Henan Province, No. 2000180007
Correspondence to: Dr. Jing-Lan Wu, Molecular Cell Biology Research Center, Zhengzhou University, Zhengzhou 450052, Henan Province, China. jlwu@zzu.edu.cn
Telephone: +86-371-66117733
Received: 2004-09-18 Accepted: 2004-12-26

Abstract

AIM: To investigate the effects of 8-Br-cAMP on differentiation and apoptosis of human esophageal cancer cell line Eca-109, and the related gene expression.

METHODS: The cultured Eca-109 cells were divided into four groups: E1 group (co-cultured with 8-Br-cAMP for 24 h); E2 group (co-cultured with 8-Br-cAMP for 48 h); C1 group (treated without 8-Br-cAMP for 24 h); and C2 group (treated without 8-Br-cAMP for 48 h). The same concentration of cell suspension of each group was dropped separately onto the slides and nitrocellulose membranes (NCM). The biotin-labeled cDNA probes for c-myc, wild-type (wt) p53, bcl-2 and iNOS were prepared for *in situ* hybridization. The expressions of epidermal growth factor receptor (EGFR), p38 kinase, FAS, FasL and caspase-3 were detected using immunocytochemistry, and the NOS activity and the ratio of differentiated cells/proliferating cells were examined by cytochemistry. Immunocytochemistry, cytochemistry, and *in situ* hybridization were separately carried out on both slides and NCM specimens for each group. In addition, TUNEL was used to detect the cell apoptosis rate in each group.

RESULTS: The apoptotic rate of E2 group was significantly higher compared to E1 group, while there was no difference in the ratio of differentiated cells/proliferating cells between E1 and E2 groups. The signals of wt p53 and iNOS were markedly stronger, while the signals of c-myc and EGFR were obviously weaker in E1 group than those in C1 group ($P<0.05$). Moreover, the signals of wt p53, iNOS, p38 kinase, caspase-3 and NOS activity were significantly stronger, whereas, the signals of bcl-2, c-myc and Fas/FasL were markedly weaker in E2 group than those in C2 group ($P<0.05$).

CONCLUSION: The differentiation and apoptosis of human esophageal cancer cell Eca-109 can be induced after 24- and 48-h treatment with 8-Br-cAMP, respectively. Upregulation of wt p53, iNOS and downregulation of c-myc may be associated with differentiation and apoptosis of Eca-109 cells. Furthermore, upregulation of FasL, p38 kinase and caspase-3 as well as downregulation of bcl-2, and Fas may be involved in the apoptosis of Eca-109 cells.

Key words: Differentiation; Apoptosis; Gene expression; 8-Br-cAMP; Eca-109 cell line

Wang HM, Zheng NG, Wu JL, Gong CC, Wang YL. Dual effects of 8-Br-cAMP on differentiation and apoptosis of human esophageal cancer cell line Eca-109. *World J Gastroenterol* 2005;11(41): 6538-6542
http://www.wjgnet.com/1007-9327/11/6538.asp

INTRODUCTION

There are two isoforms of cAMP receptor proteins, type I (PKAI) and type II (PKAII). PKAI can stimulate cell growth, while PKAII can inhibit it. Cho-Chung[1] have reported that the nontoxic 8-Br-cAMP is one of the site-selective cAMP analogs to combine with the PKAII attractively and 8-Br-cAMP could induce cancer cell differentiation via regulatory balance of the intracellular signal transducers of cAMP. It was reported that cAMP analogs or upregulation of cAMP/PKA pathway could suppress tumor malignancy through growth inhibition and differentiation induction[2,3]. In our previous studies, we found that 8-Br-cAMP could inhibit growth-related gene expressions in Eca-109 cells mainly through regulation of c-myc, epidermal growth factor receptor (EGFR), c-fos and wild-type (wt) p53 expressions; and facilitate retinoblastoma Rb44 cell differentiation mainly through iNOS gene expression[4,5]. Some studies demonstrated that the acid-denatured and methyl green-pyronin stain could be used for the identification of differentiated non-proliferating cells[6-8]. It is known that the oncogene/proto-oncogene, EGFR and c-myc can enforce cell proliferation, while the anti-oncogene, wt p53, can inhibit it; iNOS,

p38 kinase, Fas/FasL and caspase-3 are mainly associated with apoptosis, while bcl-2 is of anti-apoptotic; besides, different expression levels of the same gene may result in different effects. In this study, we aimed to investigate the effects of 8-Br-cAMP on differentiation and apoptosis of human Eca-109 cells, and to examine the alteration of related gene expressions by using *in situ* hybridization, immunocytochemistry and cytochemistry.

MATERIALS AND METHODS

Cell culture

The human esophageal cancer cell line Eca-109 was cultured in DMEM (Gibco BRL, USA) supplemented with 100 mL/L fetal bovine serum. The Eca-109 cells were cultured with 2×10^{-5} mol/L of 8-Bromo-cAMP (Sigma, USA) for 24 h as the experimental 1 (E1) group and for 48 h as the experimental 2 (E2) group. The Eca-109 cells were cultured with the same medium without any drug for 24 h as the control 1 (C1) group and for 48 h as the control 2 (C2) group.

Preparation of specimen

The cultured cell suspension (1×10^6 cells) of each group was dropped onto the pretreated slides and then the slides were dried, followed by fixation with 20-40 g/L paraformaldehyde and stored at -20 °C.

Furthermore, the cultured cell suspension (1×10^6 cells) of each group was dropped onto the nitrocellulose membrane (NCM, Protran™, USA) pretreated with 20 × SSC for dot blot hybridization or with RNase-free water for immunodot blotting, and then NCM specimens were dried and stored at -20 °C.

Labeling and sensitivity detection of cDNA probes

The denatured cDNAs of wt p53, c-myc, bcl-2, and iNOS were labeled with biotin-11-dUTP (Sigma, USA) by random primer system (Promega, USA), and the sensitivity of each probe was detected using DNA dot blotting.

In situ hybridization

After being pretreated with 5 mg/mL final concentration of proteinase K (Promega, USA) for 10 min, post-fixation with paraformaldehyde and pre-hybridization without the cDNA probes for 3 h, the slide specimens of each group were hybridized with each kind of cDNA probes in final concentration of 0.5 μg/mL at 42 °C overnight. Then the slides were stringently washed four times with 0.1× SSC at 42 °C for 15 min. The streptavidin-alkaline phosphatase (dilution 1:1 000, Promega, USA) was added onto the slides after blocking with 10 g/L acetylated BSA. The nitroblue tetrazolium and 5-bromo 4-chloro 3-indole phosphate (NBT-BCIP, Promega, USA) were used as the substrate to develop the signals in bluish-violet color. For detection of intact cell using dot blot hybridization, the NCM specimens were first rinsed rapidly with chloroform, followed by treating at 80 °C under vacuum for 2 h and subsequently treated basically as aforementioned procedures for the slides.

Immunocytochemistry

The slide specimens of respective groups were treated with 3 g/L Triton X-100/PBS for 10 min, 30 mL/L H_2O_2 5 min, 0.01 mol/L citrate buffer (pH 6.0) at 95 °C for 10 min, washed with 1× PBS after each step. The slides were treated with 100 mL/L normal goat serum for 20 min, followed by incubation with the primary mAbs against EGFR (Sigma, USA) for E1 and C1 groups, and against p38 kinase and caspase-3 (Invitrogen, USA) for E2 and C2 groups at a dilution of 1:100 at 4 °C overnight. The HRP-labeled or alkaline phosphatase-labeled goat anti-mouse serum was added onto the slides for 1 h as the secondary antibody. The slides were thoroughly washed with PBS after treatment with respective antibodies. The DAB/H_2O_2 was used as the substrate to develop the positive signals in brownish color, while NBT/BCIP was used as the substrate to develop bluish-violet color. The specific primary antibodies were replaced by PBS for the negative controls. For detection of immunodot blotting, the NCM specimens were treated using the above procedures except for substitution of 0.5 g/L Tween 20 in TBS (Tris-Cl buffer saline) for PBS.

Cytochemistry

The slides of each group were incubated with phosphate buffer (PB) containing 1.0 mg/mL reduced form of NAD 1 (co-enzyme 1) and 0.5 mg/mL NBT at 37 °C for 1.5 h. The negative control was performed simultaneously except for the addition of PB alone.

Ratio of differentiated cells/proliferating cells

The slides of each group were re-fixed with ice-cold Carnoy' s fixative for 15 min, followed by digestion of intra-nuclear DNA with 1 mol/L HCL in 800 mL/L ethanol for 5 min. The slides were stained with 5 g/L methyl green and pyronin GS (BDH, UK) in an acetate buffer (pH 4.8) for 5-7 min, subsequently washed with D.H_2O and acetone.

Detection of apoptosis rate by TUNEL

The slides of each group were treated with 50 mg/mL levamizol in ethanol for 15 min, followed by digestion with proteinase K and post-fixation with paraformaldehyde. Then the slides were incubated with 1 mg/mL terminal deoxyribonucleotidyl transferase (TdT, Promega, USA), biotin-11-UTP (Sigma, USA) and dNTP in TdT buffer at 4 °C overnight. The following procedures were performed similarly as those for *in situ* hybridization. The negative control was carried out at the same time except for incubation with TdT buffer alone in the total incubation substrate.

Statistical analysis

Each kind of dot blotting was repeated six times. The dot blotting in violet color was scanned at 560 nm by thin-layer chromatography scanner (Shimada, Japan), and that in brownish color was scanned at 420 nm. The signal intensity in slide specimens was calculated as

total integration value in more than 100 cells under oil-microscope. The data were analyzed with SSPS 10. A *P* value less than 0.05 was considered statistically significant.

RESULTS

The sensitivity of each kind of biotin-labeled cDNA probe, including wt p53, c-myc, bcl-2, and iNOS, could approach to 1.0 ng/L as detected by DNA dot blotting. The apoptotic signals in violet color were localized in the nuclei mostly translocated towards cell periphery. The cell apoptosis rate and the ratio of differentiated cells (D)/proliferating cells (P) in each group are shown in Table 1 and Figures 1 A-D.

Table 1 Apoptosis rate and ratio of differentiated cells (D)/proliferating cells (P) in each group

	E1 group	C1 group	E2 group	C2 group
Apoptosis rate	16%[a]	3.0%	54%[c]	4.0%
Ratio of D/P	1.7 (63/37)[e]	0.2 (17/83)	2.3 (70/30)[g]	0.16 (14/86)

Apoptosis rate: [a]$P<0.05$ *vs* C1 and E2 groups; [c]$P<0.05$ *vs* C2 group. Ratio of D/P:[e]$P<0.05$ *vs* C1, [g]$P<0.05$ *vs* C2.

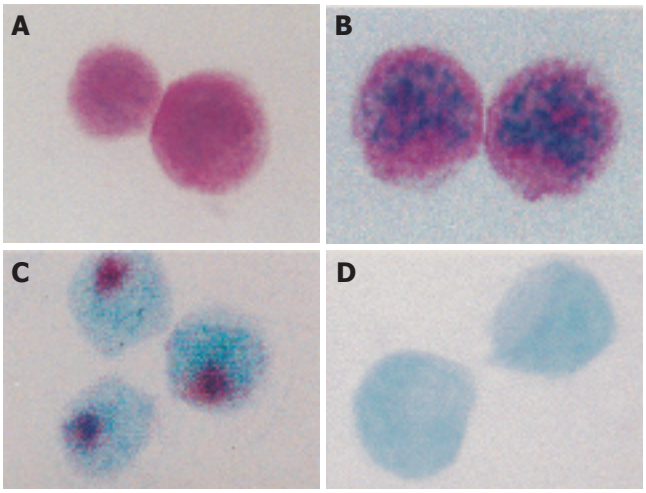

Figure 1 A :HCl denaturation and methyl green-pyronin staining of differentiated Eca-109 cells (×1 000); **B:** HCl denaturation and methyl green-pyronin staining of proliferating Eca-109 cells (×1 000); **C:** TUNEL assay showing apoptotic Eca-109 cells (×1 000); **D:**TUNEL assay showing non-apoptotic Eca-109 cells (×1 000).

The results showed that there was a significant difference in apoptosis whereas no significant difference in differentiation between E1 and E2 groups.The signals of both *in situ* hybridization (gene transcription of c-myc, wt p53 and iNOS) and EGFR-immunoreactivity (IR) were all localized in the cytoplasm. The hybridization signals appeared as violet color granules; the signal intensity of wt p53 and iNOS in E1 group was markedly higher than that in the C1 group, whereas that of c-myc and EGFR in E1 group was significantly lower than that in the C1 group. The scanning values on NCM specimens for each kind of signals are shown in Table 2.

Table 2 Comparison of signal scanning values on NCM between E1 group and C1 group (mean±SD)

Groups	c-myc mRNA	Wt p53 mRNA	iNOS mRNA	EGFR-IR
E1 group	3.38±0.99	2.74±0.83	4.52±0.74	2.37±1.05
C1 group	5.18±1.39	0.38±0.27	2.63±0.13	4.38±0.48

$P<0.05$, E1 *vs* C1 for each signal.

The hybridization signals in violet-colored granules of c-myc, wt p53 and iNOS were localized in the cytoplasm, while that of Fas-IR and FasL-IR were located surrounding the cytomembrane. The signal intensity of bcl-2, c-myc gene expression and Fas/FasL-IR was obviously decreased in E2 group as compared to C2 group, while that of wt p53 and iNOS was markedly increased in E2 group as compared to C2 group. The scanning values of each signal on NCM specimens are shown in Table 3.

Table 3 Comparison of signal scanning values on NCM between E2 group and C2 group (mean±SD)

Groups	bcl-2	c-myc	iNOS	Wt p53	Fas/FasL-I
	mRNA	mRNA	mRNA	mRNA	R
E2 group	1.36±0.54	1.72±0.76	5.47±0.35	4.76±1.28	2.69±0.73
C2 group	3.49±1.53	5.22±1.44	2.65±1.22	0.42±0.28	4.17±0.92

$P<0.05$, E2 *vs* C2 for each signal.

The brownish-colored granules of caspase-3 IR were scattered in the cytoplasm, the signal intensity of E2 group was obviously higher than that of C2 group. In C2 group, the p38-IR staining appeared as yellow-brownish colored granules in the cytoplasm, while in E2 group, the p38-IR staining with stronger intensity was mostly located in the nuclei (the activated p38 kinase translocated from cytoplasm into nuclei). The violet-colored NOS activity located in the cytoplasm was markedly increased in E2 group as compared to C2 group (Table 4).

Table 4 Comparison of total integration of signal intensities for p38-IR, caspase-3-IR and NOS activity between E2 and C2 groups

Group	p38-IR	Caspase-3 IR	NOS activity
E2 group	184	348	302
C2 group	122	207	138

$P<0.05$, E2 *vs* C2 for each signal.

DISCUSSION

It is well known that DNA can be stained by methyl green, and RNA by pyronin in cytochemistry. Sen *et al*[8] demonstrated that the proliferating cells were differentially stained by methyl green in bluish-

green color and the differentiated cells were stained mainly by pyronin in red color, since the nuclear DNA of proliferating cells was less sensitive to hydrolysis with hydrochloric acid as compared to the differentiated cells. In this study, the ratio of differentiated cells/proliferating cells had no significant difference between E1 and E2 groups, the effect of cell differentiation or proliferation inhibition could be demonstrated earlier in E1 group induced with 8-Br-cAMP for 24 h. However, there was a significant difference in the apoptosis rate between E1 and E2 groups.

It was reported that the activation of EGFR, c-myc oncogene, and inactivation of wt p53 tumor suppressor gene could be detected in the development of squamous cell carcinoma of the esophagus[9]. The wt p53 encoded by wt p53 tumor suppressor gene antagonized cell cycle progression to inhibit cell growth with contrary effect to EGFR and c-myc through $p21^{waf1}$, which was elucidated in our previous study[4]. It is known that the EGF receptor in the esophageal cancer, homologous to v-erbB, is a truncated form of EGFR with deletion of extra-cellular ligand domain, and a persistent tyrosine kinase activity displayed to stimulate the cancer cell growth independent of EGF ligand. The c-myc proto-oncogene encodes transcriptional regulator; upregulation of myc enforces cell growth; while abrupt downregulation of myc or withdrawal of any growth cytokine from environmental factors may have an association with cell differentiation and apoptosis[10]. In this experiment, downregulation of myc may be associated with decreased expression of EGFR. The precise mechanism of myc-induced pathways to contribute to apoptotic response is still largely unsolved[11].

It was found that multifunctional gene p53 could be involved in cell differentiation and apoptosis in malignant tumors[12]. Schwartz *et al*[13] reported that the osteoblasts in an osteosarcoma cell line could be induced by p53 to produce osteocalcin product. Tsumamoto *et al*[14] indicated that NO could induce cell differentiation in the rat retinal ganglion cells. Our previous study showed that NO and NOS could induce the retinoblastoma HXO-Rb44 cells towards differentiation with enhanced enolase expression[5]. The wt p53 could be upregulated by NO[15]; and apoptosis of human carcinoma cells could be induced by inducible NOS expression[16,17]. The exogenous wt p53 at higher level could inhibit proliferation of K562 cells and induce apoptosis; but could induce the cell differentiation at lower p53 level[18]. Similarly, the NO, product of NOS, in a small amount could involve cell protection, while a great amount of NO could cause cytotoxicity or apoptosis[19]. Interestingly, in this study, we observed that downregulation of EGFR and c-myc and upregulation of wt p53 and iNOS in E1 group (after treatment with 8-Br-cAMP for 24 h) might be associated with differentiation; and further downregulation of c-myc and upregulation of wt p53 and iNOS in E2 group (after treatment with 8-Br-cAMP for 48 h) might be associated with apoptosis in Eca-109 cells.

Our previous study demonstrated that the decreased ratio of bcl-2/bax expression was associated with inhibition of cell apoptosis. The downregulation of anti-apoptotic bcl-2 could cause the cells sensitive to apoptosis, and p53 could inhibit the bcl-2 expression and promote expression of pro-apoptotic Fas; besides, bcl-2 could participate in NO-mediated and p53-mediated apoptosis[14]. The Fas has been shown as a target gene for transcription and activation by p53[20]. The combination of Fas with FasL could participate in apoptosis of tumors, such as ovarian cancer, etc.[21]. In this experiment, the decreased Fas/FasL ratio implicated that the decreased Fas with increased FasL might be induced by 8-Br-cAMP after 48 h of treatment.

Among the mitogen-activated protein kinase (MAPK) family, the p38-MAPK has been reported to be involved in apoptosis, while ERK-1 oppositely stimulated cell growth; and the p53 could be activated by p38 through N-terminal serine in p53 phosphorylated by p38-MAPK[22]. Kim *et al*[23] indicated that NO-induced p38 kinase activity was an induction signal for apoptosis of chondrocytes in association of p53 accumulation, caspase-3 activation and differentiation status. The caspase-3 is a downstream effector member in the caspase family, playing a role in the final common pathway of apoptosis. It was reported that Fas could induce apoptosis through caspase effector pathway directly, not necessary to be gene-mediated[24]. Our results suggested that 8-Br-cAMP-induced Eca-109 cell apoptosis might mainly be mediated through downregulation of bcl-2 by wt p53 and upregulation of wt p53 by p38 kinase; or wt p53-mediated Fas/NO effector pathway may finally come to the common pathway of activated caspase-3. Hence, upregulation of wt p53 may play an important role, synergistically in combination with regulation of related gene expressions to form a regulatory network involved in Eca-109 cell differentiation and apoptosis. Understanding of the regulatory network may contribute to providing novel strategy and bright insight for cancer therapy.

REFERENCES

1 **Cho-Chung YS**. Role of cyclic AMP receptor proteins in growth, differentiation, and suppression of malignancy: new approaches to therapy. *Cancer Res* 1990; **50:** 7093-7100

2 **Carlson CC,** Burnham LL, Shanks RA, Dransfield DT. 8-Cl-adenosine induces differentiation in LS174T cells. *Dig Dis Sci* 2001; **46**: 757-764

3 **Chen TC,** Hinton DR, Zidovetzki R, Hofman FM. Up-regulation of the cAMP/PKA pathway inhibits proliferation, induces differentiation, and leads to apoptosis in malignant gliomas. *Lab Invest* 1998; **78**: 165-174

4 **Chen KS,** Zheng NG, Wu JL, Ding Y, Wang YL. Effects of 8-Br-cAMP on growth related gene expressions in human esophageal cancer Eca-109 cells. *Acta Anatomica Sinica* 1999; **30**: 227-229

5 **Deng X**, Wu J, Guo X, Han X, Ding X. Effect of 8-bromo-cyclic AMP on neuron specific enolase, heat shock protein, nitric oxide, nitric oxide synthase and nitric oxide synthase mRNA in human retinoblastoma HXO-Rb44 cells and cell differentiation. *Chin Med J* (Engl) 2000; **113:** 198-200

6 **Iseki S**, Mori T. Methyl green-pyronin stain distinguishes proliferating from differentiated nonproliferating cell nuclei

after acid denaturation of DNA. *J Histochem Cytochem* 1986; **34**: 683-687
7 **Chen KS**, Zhang LQ,**Wang HM, Wang YL, Wu JL. Effects of** 8-Br-cAMP on human esophageal cancer Eca-109 cell growth and differentiation, *J Henan Med Univ* 1998; **33**: 99-101
8 **Sen JY,** Huang QY, Gao HY, Liu YL, Cheng CF. Modification and application of methyl green-pyronin stain after acid denaturation of DNA. *Progress Anat Sci* 1999; **5:** 272-273
9 **Mandard AM,** Hainaut P, Hollstein M. Genetic steps in the development of squamous cell carcinoma of the esophagus. *Mutat Res* 2000; **462:** 335-342
10 **Mata-Greenwood E**, Cuendet M, Sher D, Gustin D, Stock W, Pezzuto JM. Brusatol-mediated induction of leukemic cell differentiation and G(1) arrest is associated with down-regulation of c-myc. *Leukemia* 2002; **16:** 2275-2284
11 **Nilsson JA**, Cleveland JL. Myc pathways provoking cell suicide and cancer. *Oncogene* 2003; **22**: 9007-9021
12 **Mezencev R**, Kohút A. [Apoptosis, tumor phenotype and pathogenesis of malignant tumors] *Cesk Fysiol* 2004; **53:** 48-65
13 **Schwartz KA,** Lanciloti NJ, Moore MK, Campione AL, Chandar N. p53 transactivity during in vitro osteoblast differentiation in a rat osteosarcoma cell line. *Mol Carcinog* 1999; **25**: 132-138
14 **Tsumamoto Y,** Yamashita K, Takumida M, Okada K, Mukai S, Shinya M, Yamashita H, Mishima HK. In situ localization of nitric oxide synthase and direct evidence of NO production in rat retinal ganglion cells. *Brain Res* 2002; **933**: 118-129
15 **Kitamura Y,** Kamoshima W, Shimohama S, Nomura Y, Taniguchi T. Nitric oxide donor-induced p53-sensitive cell death is enhanced by Bcl-2 reduction in human neuroblastoma cells. *Neurochem Int* 1998; **32**: 93-102
16 **Hajri A**, Metzger E, Vallat F, Coffy S, Flatter E, Evrard S, Marescaux J, Aprahamian M. Role of nitric oxide in pancreatic tumour growth: in vivo and in vitro studies. *Br J Cancer* 1998; **78**: 841-849
17 **Li L**, Heldin NE, Grawé J, Ulmsten U, Fu X. Induction of apoptosis or necrosis in human endometrial carcinoma cells by 2-methoxyestradiol. *Anticancer Res* 2004; **24:** 3983-3990
18 **Liang M**, Chen YZ, Wu Y, Yang XW, Lu LH. [Effects of Exogenous Wild-Type p53 Gene on K562 Cells] *Zhongguo Shi Yan Xue Ye Xue Za Zhi* 2001; **9:** 119-123
19 **Alexander B.** The role of nitric oxide in hepatic metabolism. *Nutrition* 1998; **14**: 376-390
20 **Kannan K**, Amariglio N, Rechavi G, Givol D. Profile of gene expression regulated by induced p53: connection to the TGF-beta family. *FEBS Lett* 2000; **470:** 77-82
21 **Ghahremani M**, Foghi A, Dorrington JH. Activation of Fas ligand/receptor system kills ovarian cancer cell lines by an apoptotic mechanism. G*ynecol Oncol* 1998; **70**: 275-281
22 **Sanchez-Prieto R**, Rojas JM, Taya Y, Gutkind JS. A role for the p38 mitogen-acitvated protein kinase pathway in the transcriptional activation of p53 on genotoxic stress by chemotherapeutic agents. *Cancer Res* 2000; **60:** 2464-2472
23 **Kim SJ**, Ju JW, Oh CD, Yoon YM, Song WK, Kim JH, Yoo YJ, Bang OS, Kang SS, Chun JS. ERK-1/2 and p38 kinase oppositely regulate nitric oxide-induced apoptosis of chondrocytes in association with p53, caspase-3, and differentiation status. *J Biol Chem* 2002; **277**: 1332-1339
24 **Fridman JS,** Lowe SW. Control of apoptosis by p53. *Oncogene* 2003; **22**: 9030-9040

Science Editor Kumar M , Li WZ and Guo SY **Language Editor** Elsevier HK

PO Box 2345, Beijing 100023, China
www.wjgnet.com
wjg@wjgnet.com

ELSEVIER

World J Gastroenterol 2005;11(41):6543-6548
World Journal of Gastroenterology ISSN 1007-9327

• *RAPID COMMUNICATION* •

Discovery and analysis of pancreatic adenocarcinoma genes using cDNA microarrays

Gang Jin, Xian-Gui Hu, Kang Ying, Yan Tang, Rui Liu, Yi-Jie Zhang, Zai-Ping Jing, Yi Xie, Yu-Min Mao

Gang Jin, Xian-Gui Hu, Yan Tang, Rui Liu, Yi-Jie Zhang, Zai-Ping Jing, Department of General Surgery, Changhai Hospital, Second Military Medical University, Shanghai 200433, China
Kang Ying, Yi Xie, Yu-Min Mao, State Key Laboratory of Genetic Engineering, Institute of Genetics, School of Life Science, Fudan University, Shanghai 200433, China
Supported by the National Natural Science Foundation of China, No. 30000160
Correspondence to: Jin Gang, Department of General Surgery, Changhai Hospital, Second Military Medical University, Shanghai 200433, China. jingang@sh163.net
Telephone: +86-21-25070566 Fax: +86-21-65492727
Received: 2004-12-07 Accepted: 2005-01-05

Abstract

AIM: To study the pathogenetic processes and the role of gene expression by microarray analyses in expediting our understanding of the molecular pathophysiology of pancreatic adenocarcinoma, and to identify the novel cancer-associated genes.

METHODS: Nine histologically defined pancreatic head adenocarcinoma specimens associated with clinical data were studied. Total RNA and mRNA were isolated and labeled by reverse transcription reaction with Cy5 and Cy3 for cDNA probe. The cDNA microarrays that represent a set of 4 096 human genes were hybridized with labeled cDNA probe and screened for molecular profiling analyses.

RESULTS: Using this methodology, 184 genes were screened out for differences in gene expression level after nine couples of hybridizations. Of the 184 genes, 87 were upregulated and 97 downregulated, including 11 novel human genes. In pancreatic adenocarcinoma tissue, several invasion and metastasis related genes showed their high expression levels, suggesting that poor prognosis of pancreatic adenocarcinoma might have a solid molecular biological basis.

CONCLUSION: The application of cDNA microarray technique for analysis of gene expression patterns is a powerful strategy to identify novel cancer-associated genes, and to rapidly explore their role in clinical pancreatic adenocarcinoma. Microarray profiles provide us new insights into the carcinogenesis and invasive process of pancreatic adenocarcinoma. Our results suggest that a highly organized and structured process of tumor invasion exists in the pancreas.

Key words: Pancreatic adenocarcinoma; cDNA microarrays; Cancer-associated genes

Jin G, Hu XG, Ying K, Tang Y, Liu R, Zhang YJ, Jing ZP, Xie Y, Mao YM. Discovery and analysis of pancreatic adenocarcinoma genes using cDNA microarrays. *World J Gastroenterol* 2005;11(41): 6543-6548
http://www.wignet.com/1007-9327/11/6543.asp

INTRODUCTION

Pancreatic carcinoma is the 12th most common cause of cancer death in China, which is one of the most aggressive form of human tumors and is virtually incurable. Its incidence and mortality rates are almost identical, even after receiving surgical resection and adjuvant chemo-radiotherapy, the overall 5-year survival rate is only 4.1%[1]. The etiology of pancreatic carcinoma is still unknown. There is clearly a need for novel and more effective diagnostic and therapeutic methods.

Oncogenesis and development of neoplasm is a complex multiphase process, which involves overexpression of oncogenes or inactivation of tumor suppressor genes, mutation or depletion of normal genes, pleiotropic effects and immunologic function. The genes are involved in vital processes of life, such as gene expression accommodation, immunology or cell differentiation, which are arranged in some gene clusters, in which all the members are being controlled in unity[2]. In the process of oncogenesis, there may exist some different clusters of tumor-related genes. Hence, it is important to find such unique gene clusters involved in carcinogenesis, invasion and metastasis processing.

Current focus of molecular profiling is the large-scale analysis of gene expression using new DNA array technology[3]. This powerful technology is being used to study many biological processes. The experimental or clinical goals range from insights to pathogenesis, cancer diagnosis and prediction of clinical outcome for identification of therapeutic targets. In this way, DNA array analysis is providing the first glimpse of a substantial improvement in our understanding of cancer biology and diagnosis. Identifying and sequencing a set of full-length cDNAs that represent all human genes would help in both gene discovery and functional analysis. It offers a

great opportunity to study the pathogenetic processes and molecular pathophysiology of pancreatic carcinoma.

In this study, we analyzed nine pancreatic adenocarcinomas using the cDNA microarray containing 4 096 human genes with the aim of understanding expression patterns and searching for carcinogenesis-related gene clusters and novel useful markers for the malignant potential of pancreatic carcinoma at the molecular level.

MATERIALS AND METHODS

Patients and tissue specimens

We analyzed samples of pancreatic head adenocarcinoma from nine patients (five males, four females, 51-71 years) who underwent pancreaticoduodenectomy at Changhai Hospital, Shanghai, China, between November 1999 and May 2000. All samples were collected with informed consent and Ethics Committee approval. Samples were grossly dissected and snap-frozen in liquid nitrogen within 10 min of removal and stored at -80 °C. Initial diagnosis of each sample from the frozen section was later confirmed by detailed analysis of paraffin-embedded sections. Following the fourth Japanese edition of the Classification of Pancreatic Carcinoma (Japan Pancreas Society, 1993), the nine tumors were staged, including two stage I, two stage II, four stage III and one stage IVa. We isolated and purified total RNA from pooled, noncancerous, male adult human pancreas tissues and used as a reference "normal" sample for each microarray experiment.

RNA isolation

Tumor and normal tissue samples were ground into a fine powder in a 10-cm ceramic mortar (RNase-free) and total RNA was extracted according to the original single-step extraction procedure with slight modifications. Ground tissue was homogenized in Solution D containing 1% ß-mercaptoethanol. After centrifugation, the supernatant was extracted twice with an equal volume of phenol: chloroform (1:1) and once with an equal volume of acidic phenol:chloroform (5:1), discarding the organic phase each time. The aqueous phase was then precipitated by an equal volume of isopropylalcohol at 4 °C, centrifuged to pellet the RNA and dissolved in deionized (Milli-Q) H_2O. mRNA was purified using an Oligotex-dT mRNA Midi Kit (Qiagen, Inc., Carlsbad, CA, USA), following the manufacturer's instructions. The RNA concentration was measured by using spectrophotometry, and its integrity was assessed by electrophoresis on formaldehyde-agarosegel.

Microarrays

The construction of the microarrays was carried out following Stanford University's method[4]. The microarrays consist of 4 096 sequences, including full-length and partial complementary DNAs (cDNAs) representing novel, known and control genes provided by United Gene Holdings, Ltd. The known genes were selected from NCBI UniGene set and cloned into a plasmid vector. The novel genes were obtained through systematic full-length cloning efforts carried out at United Gene Holding, Ltd. The control spots of non-human origin in 4 096 chip included the rice U2 RNA gene (8 spots), hepatitis C virus (HCV) coat protein gene (8 spots), and spotting solution alone without DNA (32 spots). The cDNA inserts were amplified by PCR using universal primers and then purified. All PCR products were examined by electrophoresis on an agarose gel to ensure the quality and identity of amplified clones as expected. Then the amplified PCR products were dissolved in a buffer containing 3× SSC solution. The solutions with amplified PCR products were spotted onto silylated slides (CEL Associates, Houston, TX, USA) using a Cartesian PixSys 7 500 motion control robot (Cartesian Technologies, Irvine, CA, USA) fitted with ChipMaker Micro-Spotting Technology (TeleChem International, Sunnyvale, CA, USA). Glass slides with spotted cDNA were then hydrated for 2 h in 70% humidity, dried for 0.5 h at room temperature, and UV cross-linked at a dose of 65 mJ/cm. They were further treated with 2 g/L sodium dodecyl sulfate (SDS) for 10 min, distilled H_2O for 10 min, and 2 g/L sodium borohydride ($NaBH_4$) for 10 min at room temperature. The slides were dried again and made ready for use.

Probe preparation and hybridization

The fluorescent cDNA probes were prepared through reverse transcription of the isolated mRNAs and then purified. The RNA samples from healthy individuals were labeled with Cy3-dUTP and those from cancerous patients with Cy5-dUTP. The two color probes were then mixed, precipitated with ethanol and dissolved in 20 μL of hybridization solution. Microarrays were pre-hybridized with hybridization solution containing 0.5 mg/mL denatured salmon sperm DNA at 42 °C for 6 h. Fluorescent probe mixtures were denatured at 95 °C for 5 min, and the denatured probe mixtures were applied onto the pre-hybridized chip under a cover glass. Chips were hybridized at 42 °C for 15-17 h. The hybridized chips were then washed at 60 °C for 10 min each in solutions of 2× SSC and 2 g/L SDS, 0.1× SSC and 2 g/L SDS, and 0.1× SSC, and then dried at room temperature.

Data analysis

The chips were scanned with a ScanArray 3000 (GSI Lumonics, Billerica, MA, USA) at two wavelengths to detect emission from both Cy3 and Cy5. The acquired images were analyzed using ImaGene 3.0 software (BioDiscovery, Inc., Los Angeles, CA, USA). The intensities of each spot at the two wavelengths represent the quantity of Cy3-dUTP and Cy5-dUTP, respectively, hybridized to each spot. Ratios of Cy3-Cy5 were computed for each location on each microarray. Overall intensities were normalized with a correction coefficient obtained using the ratios of 40 housekeeping genes (available at http://www.biodoor.com/).

We used the threshold value to define significant relative expression changes, which set at 2.0 for overexpression and at 0.50 for underexpression on the

basis of both the experimental variability in our data and the manufacturer's established performance criteria. Data filtering with this algorithm identified the genes overexpressed at least by twofold and underexpressed at least by 50% across, more than 66.7% (6/9) of all specimens. To minimize artifacts arising from low expression values, only the genes with raw intensity values for both Cy3 and Cy5 of >600 counts were chosen for differential analysis.

RESULTS

Sensitivity and reproducibility of the microarray system

The purity and concentration of isolated RNA were analyzed first by using UV spectrophotometer at absorbance wavelengths of 260 and 280 nm (A_{260} and A_{280}). The average A_{260}/A_{280} ratio was higher than 1.9. Furthermore, the integrity of the RNA sample was verified by electrophoresis on 10 g/L agarose gel stained with ethidium bromide. The quality of the RNA was assessed by the visualization of the 28S and 18S ribosomal RNA bands. The bands were distinct and sharp, without being diffused and smeared. The results indicated that mRNA preparation expressed continuous polyadenylated transcripts between 0.9 and 4.0 kb in length.

In order to access the "noise" in the differential expression assay, we employed self-comparison experiments. A sample of mRNA from a single fetal liver tissue was divided into two equal aliquots and labeled with Cy3-dUTP and Cy5-dUTP, respectively. The labeled samples were then mixed together and hybridized to the microarray. The results revealed that approximately 1% of the 4 096 cDNA clones showed more than 2.0-fold difference in signal intensity between the two channels. Furthermore, this "noise" in the data was shown upon analysis to occur at random array positions in each microarray experiment. Figure 1 shows the scatter plots of the within-slide normalization experiment. The Cy3/Cy5 log ratios from the different print tip groups were centered around zero, indicating that the types of systematic errors were minimized. The spots in the experiments showed a highly concordant distribution pattern. Besides, hybridization experiments with probes prepared from human mRNA produced little or no signal at the positions of the negative controls (data not shown).

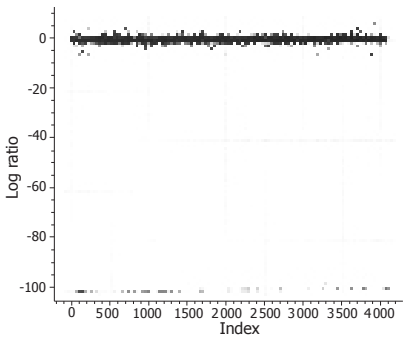

Figure 1 Scatter plots of average ratio/spot label distribution.

Gene expression analysis in patients with pancreatic adenocarcinoma

The hybridizations for each individual were repeated twice. Of all the 4 096 human genes analyzed through microarray experiments, a total of 184 genes (4.5%) revealed differential expression in more than 60.66% (6/9) of the pancreatic adenocarcinoma specimens using a fold ratio of >2 as criteria for cut-off. Of 184 genes, the expression of 87 genes (47.3%) was markedly increased in pancreatic adenocarcinoma tissues as compared with the normal pancreas tissues (Figure 1). In addition, the expression of 97 genes (52.7%) was significantly decreased in pancreatic adenocarcinoma tissues as compared with normal pancreatic tissues (Figure 2). The 184 genes corresponded to 173 genes represented in the GenBank and 11 novel sequences which have not been found in the GenBank. Scatter plots with cancerous tissues showed a wide distribution pattern (Figure 2), suggesting that genes are expressed differentially in cancer cells when compared with the normal cells. Scatter plot of the values of Cy3 and Cy5 fluorescent signals also revealed a pattern of tight distribution and clustered in an almost 45° diagonal line as expected.

In the 11 novel genes screened by our microarray experiments, an overexpressed clone in pancreatic adenocarcinomas was identified. The average Cy5/Cy3 ratio of the clone is 4.92. As we have reported recently[5], this clone is the full-length cDNA of the human gene S100P (GenBank accession number AF539739). The sequence is of 1 297 bp and encodes a protein identical to previously characterized human S100P, but it is much longer than the previously reported 439 bp. The cDNA is near full-length as confirmed by Northern blot analysis. We examined its distribution in tissues by using Northern blot and RT-PCR analysis, and found that it was abundantly expressed in many tissues including placenta, unlike the expression pattern of other S100 family genes.

DISCUSSION

DNA microarray technology has offered us a new insight into the secrets of life by monitoring the activities and

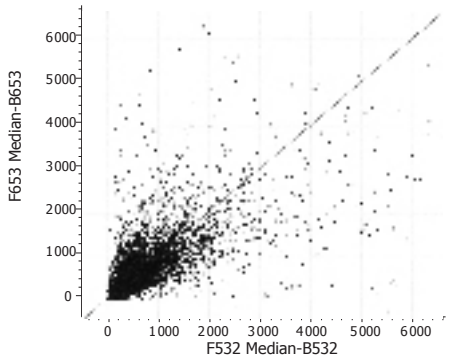

Figure 2 Microarray scatter plot for pancreatic adenocarcinoma mRNA labeled with Cy5 and normal pancreas mRNA labeled with Cy3. The "sameness line" drawn at a 45° angle denotes a 1:1 ratio of signal intensity between the Cy3 dye (*Y* axis) and the Cy5 dye (*X* axis) at each position on the array.

profiles of thousands clones simultaneously. The gene expression profiles can led us to mapping a cross-section of genetic activities and biological entity[6].

In this experiment, the genes identified as differentially expressed in microarrays revealed a wealth of information that pancreatic adenocarcinomas are complex tumors, as evidenced by the wide range of investigations[7-9]. However, these findings not only provide novel insight into the biology of pancreatic carcinoma, but also serve to identify numerous new targets for development into serologic markers or therapeutic target. The differentially expressed genes in pancreatic adenocarcinomas included oncogenes and tumor suppression genes, cell-cycle-related genes, signal transduction factors, extracellular matrix and skeleton related genes, transcription factors, DNA damage and repair related genes and apoptosis-related genes (Tables1 and 2).

The screened genes with good concordance in these pancreatic adenocarcinoma patients may have the potential to become candidates for tumor markers and the molecular target for gene therapy, whereas genes that show concordance in a patient subset may reflect different disease stages or physiological and genetic differences between the patients.

Griffin *et al*[10] reported that more than 70% of pancreatic adenocarcinomas possessed consistent chromosome abnormalities. The most frequent whole chromosomal gains were chromosomes 20 and 7, and

Table 1 Representative list of highly expressed genes in pancreatic carcinoma

Categories	Accessions	Descriptions	Symbols	Gene map locus	Average ratios
Oncogenes	AF183421	RAB22b, RAS oncogene family	Rab22b	18p11.3	3.530
Cell cycle	NM_001175	Rho GDP dissociation inhibitor	Rho GDI	12p12.3	4.504
	NM_001788	Cell division cycle 10	CDC10	7p14.3-14.1	3.219
	NM_001798	Cyclin-dependent kinase 2	CDK2	12q13	2.853
	NM_002592	Proliferating cell nuclear antigen	PCNA	20pter-p12	3.388
Signal transduction	NM_002835	Protein tyrosine phosphatase, non-receptor type 12	PTPN12	7q11.23	4.236
	NM_007039	Protein tyrosine phosphatase, non-receptor type 21	PTPN21	14q31.3	2.65
	NM_004721	Mitogen-activated protein kinase kinase kinase 13	MAPK13	3q25-29	2.361
	NM_000876	Insulin-like growth factor 2 receptor	IGF2R	6q26	2.192
	NM_000700	Annexin I	ANXA1	9q12-21.2	4.092
Extracellular matrix	NM_002345	Lumican	LUM	12q21.3-22	9.892
	NM_000089	α 2 type I collagen	COL1A2	7q22.1	11.638
	NM_000090	α 1 type III collagen	COL3A1	2q31	18.165
	M26576	α 1 type IV collagen preproprotein	COL4A1	13q34	4.171
	NM_000393	α 2 type V collagen preproprotein	COL5A2	2q14-32	3.677
	NM_001920	Decorin	DCN	12q13.2	3.633
	NM_000582	Secreted phosphoprotein 1	SPP1	4q21-25	5.033
	NM_004385	Chondroitin sulfate proteoglycan 2	CSPG2	5q14.3	6.073
	NM_003380	Vimentin	VIM	10p13	2.543
	NM_033138	Caldesmon 1	CALD1	7q33	5.097
	NM_002026	Fibronectin 1	FN1	q34	18.298
	NM_003254	Tissue inhibitor of metalloproteinase1	TIMP1	Xp11.3-p11.23	13.791
Cytoskeleton and	NM_001613	α 2 actin	ACTa2	10q23.3	2.79
motility	NM_006009	Tubulin, α 3	TUBA3	12q12-14.3	2.647
	NM_005717	Actin related protein complex subunit 5	TPM1	15q22.1	2.113
Cell surface antigen	NM_002659	Plasminogen activator, urokinase receptor	UPAR	19q13	6.073
	NM_001769	CD9 antigen	CD9	12p13	2.614
Enzymes	NM_000396	Cathepsin K preproprotein	CTSK	1q21	2.809
	NM_002654	Pyruvate kinase, muscle	PKM2	15q22	3.186
Cytokines	NM_005534	Interferon γ receptor 2	IFNGR2	21q22.11	2.492
	NM_003641	Interferon-induced transmembrane protein 1	IFITM1	11	3.187
	NM_006435	Interferon-induced transmembrane protein 2	IFITM2	11p15.5	4.149
Transcription factor	NM_007315	Signal transducer and activator of transcription 1	STAT1	2q32.2-32.3	2.945
	BC007874	Fructose bisphosphatase 3	FBP3	9q34.2	2.35
	NM_001530	Hypoxia-inducible factor 1, α	HIF1α	14q21-24	2.796
	NM_006940	SRY-box 5 isoform A	SOX5	12p12.1	2.671
	AF332192	Regulatory factor X, 4	RFX4	12q	2.094

Table 2 Representative list of downregulated genes in pancreatic carcinoma

Categories	Accessions	Descriptions	Symbols	Gene map locus	Average ratios
DNA injury and repair	NM_006763	BTG family, member 2	BTG2	1q32	0.141
	NM_014877	Helicase with zinc finger domain	HELZ	17q24.2	0.337
	NM_014140	SWI/SNF-related matrix-associated actin regulator of chromatin a like 1	SMARCAL1	2q34-36	0.397
Tumor suppressor	NM_000551	Von Hippel–Lindau syndrome gene	VHL	3p25	0.4
Apoptosis	NM_001229	Caspase 9 isoform α preproprotein	CASP9	1p36.3-36.1	0.29
	NM_022173	TIA1 protein isoform 1	TIA1	2p13	0.413
Cell-cycle dependent	NM_002923	Regulator of G-protein signaling 2	RGS2	1q31	0.186
	NM_005381	Nucleolin	NCL	2q12	0.411
	NM_006341	MAD2 homolog 2	MAD2L2	1p36	0.348
Adhesive molecule	NM_001078	Vascular cell adhesion molecule 1	VCAM	1p32-31	0.363
	NM_000216	Kallmann syndrome 1 protein	KAL	Xp22.32	0.444
	NM_005655	TGFB inducible early growth response	TIEG	8q22.2	0.431
Ribosomal protein	BC001365	Ribosomal protein L4	RPL4	15q22	0.399
	NM_005617	Ribosomal protein S14	RPS14	5q31-33	0.319
	NM_000969	Ribosomal protein L5	RPL5	1p21.3	0.375
	NM_033301	Ribosomal protein L8	RPL8	8q24.3	0.398
	NM_002950	Ribophorin I	RPN1	3q21.3-25.2	0.314
Guanine nucleotide exchange factor	NM_001268	RCC1-like G exchanging factor	CHC1L	13q14.3	0.363
	NM_001960	Eukaryotic translation elongation factor 1- δ	EEF1D	19p13.13	0.242
	NM_001959	Eukaryotic translation elongation factor 1- β 2	EEF1B2	2q33-34	0.305
Transcription factor	NM_014390	EBNA-2 co-activator (100 ku)	p100	7q31.3	0.322
	NM_005080	X-box binding protein 1	XBP-1	22q12.1	0.325
	NM_001880	Activating transcription factor 2	ATF2	2q32	0.314
	NM_012082	Transcription factor GATA4	FOG2	8q23	0.348
Signal transduction	NM_004301	BRG1-associated factorBAF53a		3q27.1	0.25
	NM_004236	Thyroid receptor interacting protein 15	SGN2	15q21.2	0.377
	NM_002825	Pleiotrophin	PTN	7q33-34	0.355
	NM_002928	Regulator of G-protein signaling 16	RGS16	1q25-31	0.422
	NM_005645	TBP-associated factor 13	TAF2K	1p13.1	0.462
	NM_000596	Insulin-like growth factor binding protein 1	IGFBP1	7p13-12	0.365
	NM_002514	IGFBP9	IGFBP9	8q24.1	0.376
Enzymes	NM_001979	Epoxide hydrolase 2	EPHX2	8p21-12	0.315
	NM_001482	Glycine amidinotransferase	GATM	15q15.3	0.179
	NM_000170	Glycine dehydrogenase	GLDC	9p22	0.428
	NM_000382	Aldehyde dehydrogenase 3 family, member A2	ALDH3A2	17p11.2	0.393
	NM_005600	Nitrilase 1	NIT1	1q21-22	0.358
	NM_004990	Methionine-tRNA synthetase	MARS	12q13.2	0.438
	NM_001064	Transketolase	TKT	3p14.3	0.317
	NM_000221	Ketohexokinase	KHK	2p23.3-2	0.309

the chromosomal losses were much more frequent in chromosomes 18, 13, 12, 17, and 6. Structural abnormalities were frequently involved in chromosomes 1p, 6q, 7q, 17p, 1q, 3p, 11p, and 19q. From our microarrays, we found that the overexpressed genes in pancreatic adenocarcinomas are mainly located in chromosomes 1, 2q, 7q, 9q, 12, 14q, 15q, and 21q, and the downexpressed genes are mainly located in chromosomes 1, 2, 3, 7q, 8q, 15q, 17, 19, and 22q, which are similar to the previous reports. This phenomenon suggests the existence of acquired genomic alterations in pancreatic carcinomas.

Among the genes overexpressed in pancreatic adenocarcinomas, RAB22B and Rho GDP dissociation inhibitor (Rho GDI) are the members of Ras superfamily, whose Cy3/Cy3 ratios are 3.53 and 4.504, respectively. As it is well known that many pancreatic carcinoma cells show "addiction" to K-ras mutation, while normal cells appear resistant to suppression of K-ras-mediated signaling by antisense K-ras RNA expression adenoviral vector[11]. So, overexpressed RAB22B may be the result of K-ras mutation in pancreatic adenocarcinoma. The Rho family proteins were found to reorganize cytoskeletons and regulate the cell migration via the activation of effector proteins. GTP-bound Rho is an active form, whereas the GDP-bound form is inactive. Rho GDI can block the conversion between the GTP- and GDP-bound forms. Expression of Rho family molecules has recently been reported in breast, lung, pancreas and colon carcinomas, and testicular germ cell tumors[12]. Moreover, three guanine nucleotide exchange factors (RCC1-like G

exchanging factor, eukaryotic translation elongation factor 1-δ, eukaryotic translation elongation factor 1-β2) were downexpressed in our microarrays, which implied that GDP-bound forms might be related to tumorigenesis of pancreatic adenocarcinoma. Furthermore, VHL gene, which has been confirmed as a tumor suppressor gene[13], was also downexpressed in pancreatic adenocarcinoma.

The result showed that pancreatic carcinoma cells are much more active than normal cells in many steps of multiple pathways of signal transduction. The stable state of normal somatic cells depends on the dynamic equilibrium of apoptosis and proliferation. Apoptosis-related genes were downexpressed in cancer. These findings revealed that the phenotypical similarities among different cancers are also reflected at the molecular level.

Gene expression profiling of pancreatic carcinoma has also provided new insights into the process of tumor invasion. In pancreatic carcinoma tissue, many invasion and metastasis related genes, such as ECM and cell skeleton related genes (type I collagen, type III collagen, type IV collagen, decorin, secreted phosphoprotein 1, vimentin, tissue inhibitor of matrix metalloproteinase 1, fibronectin 1,α2-actin, tubulin, tropomyosin 1, *etc.*), showed high expression level, reflecting the cellular components of the host stromal response seen in the presence of infiltrating carcinoma. Moreover, the urokinase-type plasminogen activator receptor (uPAR) was found highly expressed in pancreatic adenocarcinomas, which is a key molecule in the regulation of cell-surface plasminogen activation and, as such, plays an important role in many normal as well as pathologic processes[14]. Memarzadeh *et al*[15] concluded that uPAR is a useful prognostic marker for biologically aggressive forms of endometrial cancer. These phenomena suggest that poor prognosis of pancreatic carcinoma may have a solid molecular biological basis, and also indicate that a highly organized and structured process of tumor invasion exists in the pancreas.

The downregulated genes in the patients with pancreatic adenocarcinoma are also divided into distinct functional categories. Reduced expression was observed in genes encoding products that function in the apoptosis, immune system, cell regulation, DNA injury and repair processing and GTP/GDP signaling, which were in agreement with the previous reports[16,17].

In conclusion, the application of cDNA microarray technique for analysis of gene expression patterns is a powerful strategy to identify novel cancer-associated genes, and can rapidly explore their role in clinical pancreatic adenocarcinomas. Microarray profiles provide us new insights into the carcinogenesis and invasive process in pancreatic adenocarcinoma. Our results suggest that a highly organized and structured process of tumor invasion exists in the pancreas.

REFERENCES

1 **Yeo CJ,** Cameron JL, Sohn TA, Lillemoe KD, Pitt HA, Talamini MA, Hruban RH, Ord SE, Sauter PK, Coleman J, Zahurak ML, Grochow LB, Abrams RA. Six hundred fifty consecutive pancr eaticoduodenectomies in the 1990s: pathology, complications, and outcomes. *Ann Surg* 1997; **226:** 248-57; discussion 257-260

2 **Holland EC.** Regulation of translation and cancer. *Cell Cycle* 2004; **3**: 452-455

3 **Wulfkuhle J**, Espina V, Liotta L, Petricoin E. Genomic and proteomic technologies for individualisation and improvement of cancer treatment. *Eur J Cancer* 2004; **40**: 2623-2632

4 **Shalon D**, Smith SJ, Brown PO. A DNA microarray system for analyzing complex DNA samples using two-color fluorescent probe hybridization. *Genome Res* 1996; **6**: 639-645

5 **Jin G**, Wang S, Hu X, Jing Z, Chen J, Ying K, Xie Y, Mao Y. Characterization of the tissue-specific expression of the s100P gene which encodes an EF-hand Ca2+-binding protein. *Mol Biol Rep* 2003; **30**: 243-248

6 **van de Vijver** MJ, He YD, van't Veer LJ, Dai H, Hart AA, Voskuil DW, Schreiber GJ, Peterse JL, Roberts C, Marton MJ, Parrish M, Atsma D, Witteveen A, Glas A, Delahaye L, van der Velde T, Bartelink H, Rodenhuis S, Rutgers ET, Friend SH, Bernards R. A gene-expression signature as a predictor of survival in breast cancer. *N Engl J Med* 2002; **347**: 1999-2009

7 **Missiaglia E**, Blaveri E, Terris B, Wang YH, Costello E, Neoptolemos JP, Crnogorac-Jurcevic T, Lemoine NR. Analysis of gene expression in cancer cell lines identifies candidate markers for pancreatic tumorigenesis and metastasis. *Int J Cancer* 2004; **112**: 100-112

8 **Ryu B**, Jones J, Blades NJ, Parmigiani G, Hollingsworth MA, Hruban RH, Kern SE. Relationships and differentially expressed genes among pancreatic cancers examined by large-scale serial analysis of gene expression. *Cancer Res* 2002; **62**: 819-826

9 **Tarbé N**, Lösch S, Burtscher H, Jarsch M, Weidle UH. Identification of rat pancreatic carcinoma genes associated with lymphogenous metastasis. *Anticancer Res* 2002; **22**: 2015-2027

10 **Griffin CA**, Hruban RH, Morsberger LA, Ellingham T, Long PP, Jaffee EM, Hauda KM, Bohlander SK, Yeo CJ. Consistent chromosome abnormalities in adenocarcinoma of the pancreas. *Cancer Res* 1995; **55**: 2394-2399

11 **Yoshida T**, Ohnami S, Aoki K. Development of gene therapy to target pancreatic cancer. *Cancer Sci* 2004; **95**: 283-289

12 **Aznar S**, Fernández-Valerón P, Espina C, Lacal JC. Rho GTPases: potential candidates for anticancer therapy. *Cancer Lett* 2004; **206**: 181-191

13 **Maynard MA**, Ohh M. Von Hippel-Lindau tumor suppressor protein and hypoxia-inducible factor in kidney cancer. *Am J Nephrol* 2004; **24**: 1-13

14 **Choong PF,** Nadesapillai AP. Urokinase plasminogen activator system: a multifunctional role in tumor progression and metastasis. *Clin Orthop Relat Res* 2003; : S46-S58

15 **Memarzadeh S**, Kozak KR, Chang L, Natarajan S, Shintaku P, Reddy ST, Farias-Eisner R. Urokinase plasminogen activator receptor: Prognostic biomarker for endometrial cancer. *Proc Natl Acad Sci USA* 2002; **99:** 10647-10652

16 **Grützmann R**, Foerder M, Alldinger I, Staub E, Brümmendorf T, Röpcke S, Li X, Kristiansen G, Jesenofsky R, Sipos B, Löhr M, Lüttges J, Ockert D, Klöppel G, Saeger HD, Pilarsky C. Gene expression profiles of microdissected pancreatic ductal adenocarcinoma. *Virchows Arch* 2003; **443**: 508-517

17 **Logsdon CD**, Simeone DM, Binkley C, Arumugam T, Greenson JK, Giordano TJ, Misek DE, Kuick R, Hanash S. Molecular profiling of pancreatic adenocarcinoma and chronic pancreatitis identifies multiple genes differentially regulated in pancreatic cancer. *Cancer Res* 2003; **63**: 2649-2657

Science Editor Kumar M, Li WZ and Guo SY **Language Editor** Elsevier HK

PO Box 2345, Beijing 100023, China
www.wjgnet.com
wjg@wjgnet.com

ELSEVIER

World J Gastroenterol 2005;11(41):6549-6553
World Journal of Gastroenterology ISSN 1007-9327

• *RAPID COMMUNICATION* •

No relationship between IL-1B gene polymorphism and gastric acid secretion in younger healthy volunteers

Sheng Hu, Qi-Bing Song, Ping-Fang Yao, Qing-Long Hu, Ping-Jin Hu, Zhi-Rong Zeng, Rui-Ping Pang

Sheng Hu, Qi-Bing Song, Ping-Fang Yao, Qing-Long Hu, Zhi-Rong Zeng, Rui-Ping Pang, Institute of Cancer, the Cancer Hospital of Hubei Province, Wuhan 430079, Hubei Province, China
Qing-Long Hu, Department of Pathology, Creighton University Medical Center, 30th Street, Omaha NE 68131, United States
Ping-Jin Hu, Zhi-Rong Zeng, Rui-Ping Pang, Department of Gastroenterology, the First Affiliated Hospital of Sun Yat-Sen University of Medical Science, Guangzhou 510080, Guangdong Province, China
Correspondence to: Hu Sheng, Institute of Cancer, the Cancer Hospital of Hubei Province, Wuhan 430079, Hubei Province, China. ehusmn@yahoo.com.cn
Telephone: +86-27-87670057
Received: 2005-01-12 Accepted: 2005-04-18

Abstract

AIM: To investigate the influence of IL-1B-511 gene polymorphism on IL-1B mRNA expression and gastric acid output in individual with or without *Helicobacter pylori (H pylori)* infection.

METHODS: IL-1B mRNA expression and gastric acid secretion in 117 health volunteers were assayed using semi-quantitative RT-PCR and gastric juice assay, respectively. Pepsinogen (PG) I and II of 255 subjects (including 117 health volunteers) were also examined.

RESULTS: T/T genotype individuals with *H pylori* infection had a more decreased PG I/II ratio. In gastric antrum mucosa, the individuals with *H pylori* infection had higher IL-1B expression than those without *H pylori* infection, but there was no obvious difference among each genotype. In gastric corpus, the individuals with *H pylori* infection had a significantly higher IL-1B expression than those without *H pylori* infection. IL-1B-511T/T genotype was markedly higher as compared with the other two genotypes. Both maximal acid output and basic acid output were similar among each genotype in IL-1B-511 gene locus, regardless of *H pylori* infection.

CONCLUSION: IL-1B-511 T allele does not decrease gastric acid output, although it has a stimulated influence on IL-1B expression. Consequently, the pathway, through which IL-1B plays a central role in gastric cancer development, might not depend on low acid, but on the other regulation mechanisms.

Key words: IL-1; Polymorphism; Stomach neoplasm; Gastric acid; *Helicobacter pylori* (*H pylori*)

Hu S, Song QB, Yao PF, Hu QL, Hu PJ, Zeng ZR, Pang RP. No relationship between IL-1B gene polymorphism and gastric acid secretion in younger healthy volunteers. *World J Gastroenterol* 2005; 11(41):6549-6553
http://www.wjgnet.com/1007-9327/11/6549.asp

INTRODUCTION

Gastric cancer development is a multifactor and multi-step process. Clinical and epidemiological studies have suggested that environmental effects and dietary habits, such as smoking, alcohol consumption, low intake of fruits or vegetables and *Helicobacter pylori (H pylori)* infection, were the primary causes for the occurrence of carcinogenesis[1,2]. Furthermore, decades of researches have built up a variety of evidence that genetic risk factors also play an important role in cancer development[3]. Recently, through a case-control study, El-Omar *et al*[4] discovered that there was a strong relationship between IL-1 gene polymorphism and gastric cancer in the Polish population. The association between IL-1B-511 T allele and gastric carcinoma or atrophic gastritis was discovered by Machado *et al*[5] and Furuta *et al*[6] respectively. The results of several studies are in agreement with ours on Chinese population[7].

The epidemiological studies mentioned above were based on a hypothesis that IL-1B-511 and -31 gene polymorphisms contributed to stomach cancer development through T allele upregulating IL-1B mRNA expression, and then inhibiting directly gastric acid secretion. Low gastric acid was reported as a risk factor for cancer, because it resulted in a change of the colonized place of *H pylori* from gastric antrum to the corpus[8,9]; unfortunately, corpus-predominant gastritis with bacterial overgrowth was at increased risk of atrophic gastritis (with several biomarkers, such as pepsinogen (PG)I, II or I/II ratio)[6,10] and even gastric cancer. Both increased intragastric pH value and *H pylori* infection could significantly enhance N-nitroso compounds concentration, which is a putative promoter of carcinogenesis and tumor progression[11]. Svendsen *et al*[12] discovered 5 gastric cancer patients among 114 patients with low gastric acid secretion in a long-term follow-up (mean 8.4 years) study. However, this model was only supported by animal studies[4,13]. It is unknown now whether IL-1B gene polymorphism increased IL-1β protein level and resulted in human hypochlorhydria and atrophic gastritis *in vivo*. In the present study, we investigated the effects of IL-1B-511 genetic polymorphism on IL-1β mRNA expression and gastric acid secretion in the gastric mucosa of human beings with or without *H pylori* infection.

MATERIALS AND METHODS

Subjects

A total of 255 students (121 females and 132 males) from the Sun Yat-Sen University of Medical Sciences were enrolled in this study (Table 1). All subjects belonged to the ethnic group of Han and their age ranged from 19 to 24 years (mean 21.4±1.5 years). None of them had the histories of systemic lupus erythematosis, diabetes mellitus, rheumatoid arthritis, and inflammatory bowel disease. None of the subjects had received treatment for *H pylori* infection. Subjects with a family history of gastric cancer were also excluded.

Table 1 Relationship between IL-1B-511 genotypes and *H pylori* status

Loci	Genotype	*H pylori*+ (*n*=96)	*H pylori*– (*n*=159)	Total (*n*=255)
IL-1B-511	C/C	34	63	97
	C/T	46	75	121
	T/T	16	21[1]	37 (14.1%)
IL-1B-31	C/C	72	120	192
	C/T	22	37	59
	T/T	2	2[2]	4 (1.6%)

[1]*H pylori*+ *vs H pylori*–: x^2=0.6; [2]*H pylori*+ *vs H pylori*–: x^2=0.3

After genotyping of IL-1B gene and test of *H pylori* antibody IgG, 117 subjects were randomly selected for the second step study on IL-1B-511 locus, but IL-1B-31 T/T genotype frequency is too low to be researched (Tables 1 and 2). Three biopsy specimens were collected from the antrum (two specimens for RNA extraction and another one for urease test) and two biopsy specimens from corpus for RNA extraction. In each genotypical group, no statistical difference in *H pylori* prevalence, sex, and age was observed (Table 2).

Table 2 Common characteristics of 117 subjects (*n*, mean±SD)

	IL-1B-511 genotype (*n* =117)		
	T/T (*n* =37)	C/T (*n* =40)	C/C (*n* =40)
H pylori+	14	15	18[1]
Sex (F/M)	16/21	18/22	19/21[2]
Age (yr)	21.9±1.5	22.1±1.6	22.3±1.6[3]

[1]x^2=0.6; [2]x^2=0.1, [3]F=1.4

Examination of pepsinogen I and II

Using ELISA assay, PG I and II of 255 subjects were examined. Blood samples were obtained after 10-h fasting, and then coagulated at room temperature for 30 min to extract serum. Finally, the ELISA assay was performed according to the manufacturer's instructions (Orion Diagnostica Company). All analysis was done in duplicate and with an internal standard. The mean absorbance (A_{450}) of each specimen was tested at 450 nm.

DNA extraction

DNA was isolated from peripheral blood using the NaI method[14]. Briefly, heparinized whole blood (100 mL) was added to twofold volume of 6 mol/L NaI and fourfold volume of chloroform:isoamyl alcohol (24:1) and centrifuged at 5 000 r/min for 5 min. The aqueous layer was removed and isopropanol was added to the pellet to deposit DNA (centrifugation at 5 000 r/min for 5 min). Extracted DNA was rinsed 2-3 times with 700 mL/L alcohol and resuspended in 40 μL TE buffer (pH 8.0).

Genotyping of IL-1B-511 and -31 loci polymorphism

Polymorphism of IL-1B-511 and -31 that encodes IL-1B was genotyped by polymerase chain reaction-restriction fragment length polymorphism (PCR-RFLP)

A fragment containing the AvaI polymorphic site at position -511 of the IL-1B gene was amplified using PCR. The oligonucleotides, 5'-GCCTGAACCCTGCATACCGT-3' and 5'-GCCAATAGCCCTCCCTTCT-3', flanking this region were used as primers. AluI polymorphic site at position -31 was amplified using primers: 5'-AGAAGCTTCCACCAATACTC-3' and 5'-ACCACCTAGTTGTAAGGAAG-3'. PCR was carried out as described previously by Zeng *et al*[7] PCR fragments were separated by electrophoresis on 30 g/L agarose with ethidium bromide staining. The C allele was designated, if two bands of 92 and 63 bp were obtained, and T allele was designated, if a single band of the undigested 155 bp was obtained. The genotype was designated as follows: C/C, 2 bands of 92 and 63 bp; C/T, 3 bands of 155, 92, and 63 bp; T/T, a single band of 155 bp.

Detection of IL-1B mRNA expression

The biopsy specimens (5-10 mg) were mixed with 1 000 μL TRIzol (Invitrogen) and then homogenized for RNA extraction. RNA was resuspended in 40 μL TE buffer (RNase-free).

RNA solution (5 μL) was diluted 10-fold and $A_{260}/_{280}$ ratio was examined. The total RNA was calculated as follows: $RNA_{total}=A_{260}\times40\times N$.

IL-1B amplification was performed using the primers: IL-1B primers, P1 5'-gatgaagtgctccttccaggac-'3, P2 5'-tggagcaacaagtggtgttctcca-'3 (480 bp); and GAPDH primers, P1 5'-cacagtccatgccatcactg-'3, P2 5'-tactccttggaggccatgtg-'3 (480 bp).

RT-PCR amplification was performed in a volume of 50 μL containing 2× AccessQuick™ Master mixture (Promega Company). The final PCR aliquot (10 μL) was analyzed by electrophoresis on 30 g/L agarose with ethidium bromide staining.

Measurement of gastric acid secretion

Gastric acid secretion was detected in 117 subjects following pentagastrin injection. For this, all subjects received no medication (e.g. antiacid, etc.) for 24 h and no food for 12 h before the test. On the morning of the test, a tube was passed into the stomach through the nose. The tube was securely fastened and subjects were made to lie

on their left-side. The gastric juices were then collected by applying continuous suction (at 30-50 mmHg below atmospheric pressure) to the tube.

Statistical analyses

Hardy–Weinberg equilibrium at individual loci was assessed using χ^2 test in the statistics program SPSS (version 12.0, Chicago, IL, USA). Comparison of genotype frequencies between cases and controls was assessed by χ^2 test. ANOVA or *t*-test was used for analysis of means. All *P* values were two-sided and considered statistically significant at $P<0.05$.

RESULTS

Analysis of pepsinogen I and I/II ratio in different IL1-1B-511 genotypes

In *H pylori*-positive cases, T/T genotype individuals had markedly decreased PGI/II ratio as compared with the other genotypes ($F = 3.7$, $P = 0.03$). On the contrary, no significant difference in PGI/II ratio was observed among the genotypical groups without *H pylori* infection. PGI level was similar in the three genotypes of infected subjects or non-infected subjects, although PGI level was lower in *H pylori*-positive subjects than that in negative subjects (Table 3).

Table 3 PG I and I/II ratio in different genotypes with or without *Helicobacter pylori* (*H pylori)* infection (mean±SD)

		IL-1B-511 genotype		
		C/C (*n* = 97)	C/T (*n* = 121)	T/T (*n* = 37)
H pylori+	PGI	38.5 ± 6.7	40.3 ± 7.2	38.0 ± 6.7
(*n*=96)	PGI/II	4.9 ± 0.4	5.0 ± 0.4	4.7 ± 0.31
H pylori–	PGI	23.6 ± 4.3	24.0 ± 5.0	23.5 ± 3.5
(*n*=159)	PGI/II	5.0 ± 0.3	4.9 ± 0.3	4.9 ± 0.4

$F = 3.7$, $P = 0.03$ ($P_{T/TvsC/T} = 0.008$, $P_{T/TvsC/C} = 0.04$).

Relationship between IL-1B-511 gene polymorphism and IL-1B mRNA expression

In *H pylori*-negative individuals, the levels of IL-1B mRNA expression were markedly decreased in the gastric antrum, and similar among each genotype. However, in *H pylori*-positive subjects, IL-1β mRNA expression was significantly increased, but there was no difference among C/C, C/T, or T/T genotype (Figures 1 and 2)

Furthermore, in the individuals without *H pylori*-infected corpus, no significant difference was detected in the expression of IL-1β mRNA among the genotype in IL-1B-511 single nucleotide polymorphism. In *H pylori* infection corpus, however, the level of IL-1β mRNA was higher. Individuals with T/T genotype had remarkably increased IL-1B mRNA than those with C/C or C/T genotype. No difference in IL-1B mRNA levels was observed between C/C and C/T genotypes. Meantime, we discovered a carrier of both IL-1B-511 T/T and –31 T/T genotypes, which had the highest IL-1B gene expression among all the subjects (Figures 1 and 2).

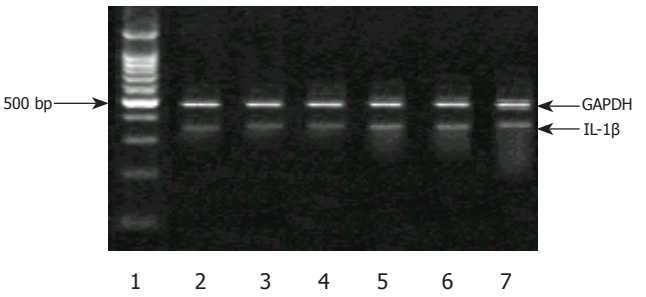

Figure 1 Expression of IL-1βmRNA in antrum Lane 1: a standard DNA ladder, lane 2: C/C genotype without *H pylori* infection, lane 3: C/T genotype without *H pylori* infection, lane 4: T/T genotype without *H pylori* infection, lane 5: C/C genotype with *H pylori* infection, lane 6: C/T genotype with *H pylori* infection, lane 7: T/T genotype with *H pylori* infection.

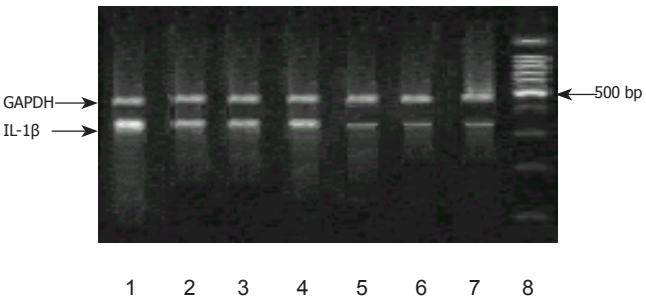

Figure 2 Expression of IL-1βmRNA in corpus. Lane 8: a standard DNA ladder, lane 7: C/C genotype without *H pylori* infection, lane 6: C/T genotype without *H pylori* infection, lane 5: T/T genotype without *H pylori* infection, lane 4: C/C genotype with *H pylori* infection, lane 3: C/T genotype with *H pylori* infection, lane 2: T/T genotype with *H pylori* infection, lane 1: T/T genotype of -511 and -31 with *H pylori* infection.

IL-1B-511 genotype and gastric fluid analysis

In basic condition (basic acid output), gastric acid secretion was similar between *H pylori*-negative and -positive subjects (5.1±1.0 *vs* 5.2±1.1 mmol/h, $t = 0.48$), and also among three different genotypes (six groups comparison, $F = 0.2$, Figure 3). After a pentagastrin stimulation, there was no significant difference for maximal acid output between *H pylori*-negative and -positive subjects (18.3±2.3 *vs* 18.4±2.0 mmol/h, $t = 0.1$), and among three different genotypes (six groups comparison, $F = 0.7$, Figure 4).

pH values of basic gastric juice and stimulated gastric fluid were 4.8±1.1 and 1.4±0.4, respectively. There was a slight increased pH value in *H pylori* infection subjects. Nevertheless, the individuals with T/T genotype did not show a much weaker ability to secrete hydrogen ion (Figure 5, $F = 0.13$ and 0.35).

DISCUSSION

Several studies revealed that hypochlorhydria induced

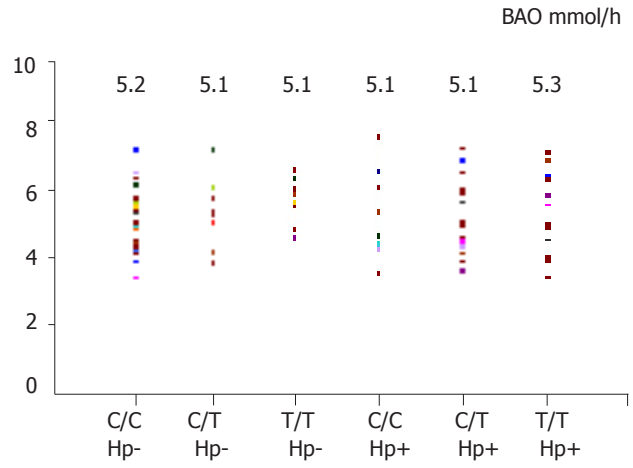

Figure 3 BAO in different genotype or *H pylori* status

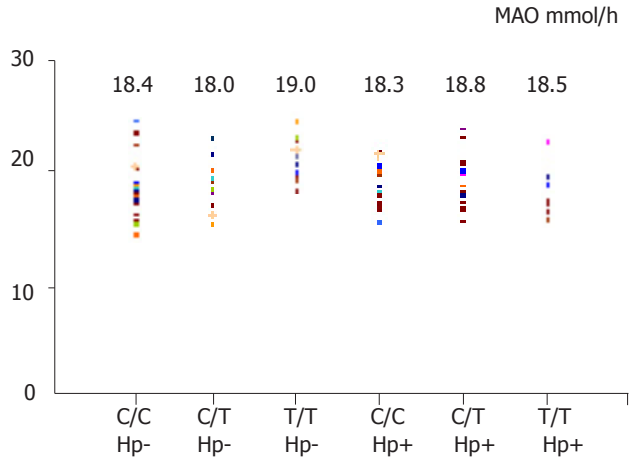

Figure 4 MAO in different genotypes or *H pylori* status

by overexpression of IL-1B was regarded as a bridge to link IL-1 gene polymorphism to gastric cancer[4–7]. The ability of mucosa to secrete gastric acid has been considered as a critical factor to decide clinical outcomes and bacterial description of *H pylori* infection[14,15]. *H pylori* implanted predominantly in the antrum mucosa, a

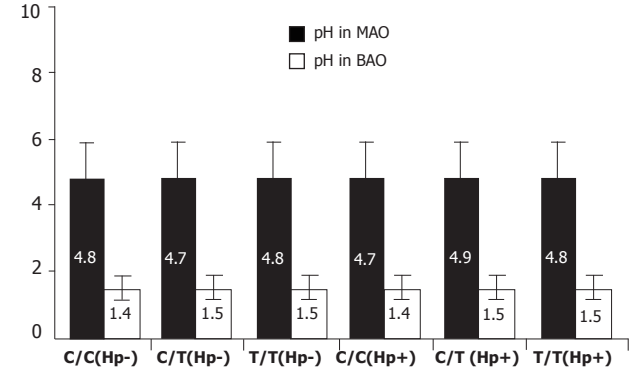

Figure 5 pH value of BAO and MAO in different genotypes or *H pylori* status.

place with a higher pH value, contrarily increased acid environment of corpus mucosa that resulted from a large number of B lymphocytes provides a habitat for *H pylori* to grow. However, for some special individuals with genetic hypochlorhydria, *H pylori* has a chance to migrate from antrum to the corpus. As a result, a large ulcer area resulted in a decreased acid level, which accumulates gastric atrophy or stomach carcinoma development[9]. Schepp *et al*[16] reported that rat parietal cells express IL-1 receptors mediating inhibition of H+ production. The antisecretory effect of IL-1B may contribute to hypoacidity secondary to acute *H pylori* infection or during chronic colonization by *H pylori* preferring the fundic mucosa. Another study reported that the efficacy of IL-1B to inhibit parietal cell H+ production was 100-fold and 6 000-fold higher as compared to proton pump inhibitors and H2 antagonists, respectively[17]. Recently, it has been identified that IL-1B exerts a potent function of gastric acid secretion through the other molecules and protein kinase pathway[18,19].

Until recently, however, no research has provided unambiguous and direct proofs suggesting that lower acid output resulted from higher IL-1B level in the human body except from a rodent model.

In this study, we discovered that T/T genotype individuals infected with *H pylori* had a more decreased PGI/II ratio as compared with the other genotypes, which is partly consistent with the results reported by Furuta *et al*[6] suggesting that IL-1B-511 gene polymorphism might be a risk factor for gastric carcinoma. IL-1B mRNA expression in subjects without *H pylori* infection was not remarkable, and was similar in each genotype, showing that there might be a very low level of IL-1B mRNA expression in normal mucosa. In contrast, the results are more complex in *H pylori*-positive individuals. There was a remarkable upregulation in the antrum, but no relationship with genotype was observed. In the corpus mucosa, however, the level of IL-1B mRNA was markedly higher than that in the antrum mucosa. Furthermore, IL-1B-511 T/T genotype individual had a mild increased IL-1B mRNA level as compared with C/T and C/C genotype. So, these results indicated that this mutation of IL-1B-511 C→T might upregulate IL-1B mRNA expression in corpus but not in the antrum, as these results are consistent to the results reported by Hwang *et al*[20]

The association of IL-1B-31 locus and IL-1B expression is not investigated because genetically mutated subject is too small (about 1%) to be collected. Fortunately, we found one female subject with *H pylori* positive and IL-1B-511 T/T and -31 T/T genotypes simultaneously had a markedly increased IL-1B mRNA level in corpus but not in the antrum. These results suggested a cooperative effect between –511 and –31 locus in IL-1B mRNA expression. These findings are also in agreement with the previous results reported by El-Omar *et al*[4] and Hwang *et al*[20]

We discovered that in basic or pentagastrin stimulation condition, gastric acid secretion was similar between *H pylori*-negative and -positive subjects. Acid secretion function did not show a marked heterogeneity among

three different genotypes of IL-1B-511. This data denoted that higher IL-1B level does not make a strong impact on gastric acid output. So, previous hypothesis that *H pylori* infection leads to IL-1B mRNA overexpression in IL-1B-511 T/T genotype, thereby directly inhibits gastric acid secretion is impossible, at least *in vivo*, in low gastric cancer prevalence region.

Hence, we inferred that the other pathways (such as chronic inflammatory process[21]), but not low acid secretion regulated by IL-1B (a pre-inflammatory factor), lead to mucosal atrophy. Our results, also taking into consideration the reports of several studies, suggested that IL-1B gene polymorphism was a susceptibility factor to gastric carcinoma in population-based studies. Furthermore, Lundell *et al*[21,22] have reported that acid-suppressive therapy maintained for 3 years facilitates neither the development of gastric glandular atrophy of the corpus mucosa nor the occurrence of intestinal metaplasia in *H pylori*-infected GERD patients. Fox *et al*[23] argued that coca leaf chewers (added with slaked lime or ash) did not have a higher prevalence of *H pylori* infection, or a higher rate of progression to gastric atrophy. So, we propose a new hypothesis that IL-1B gene polymorphism acts as a gastric cancer risk factor via upregulating IL-1B expression but downregulating acid secretion.

The individuals included in our study had a strong physiological captivity of acid output in the gastric mucosa as their age ranged from 19 to 24 years. This might be the reason that acid secretion levels were not seen significantly different between upregulated IL-1B mRNA and unchanged IL-1B mRNA groups. But using younger population in the present study is not unreasonable. As we know *H pylori* infection and genetic background play crucial roles in carcinogenesis beginning from early age. Further studies, however, should focus on larger age-range subjects or on other races to identify our results.

REFERENCES

1 **Stadtländer CT,** Waterbor JW. Molecular epidemiology, pathogenesis and prevention of gastric cancer. *Carcinogenesis* 1999; **20:** 2195-2208

2 **Hohenberger P,** Gretschel S. Gastric cancer. *Lancet* 2003; **362:** 305-315

3 **Rhyu MG.** Genetic events underlying morphological complexity of gastric carcinoma. *J Korean Med Sci* 1998; **13:** 339-349

4 **El-Omar EM,** Carrington M, Chow WH, McColl KE, Bream JH, Young HA, Herrera J, Lissowska J, Yuan CC, Rothman N, Lanyon G, Martin M, Fraumeni JF, Rabkin CS. Interleukin-1 polymorphisms associated with increased risk of gastric cancer. *Nature* 2000; **404:** 398-402

5 **Machado JC,** Pharoah P, Sousa S, Carvalho R, Oliveira C, Figueiredo C, Amorim A, Seruca R, Caldas C, Carneiro F, Sobrinho-Simões M. Interleukin 1B and interleukin 1RN polymorphisms are associated with increased risk of gastric carcinoma. *Gastroenterology* 2001; **121:** 823-829

6 **Furuta T,** El-Omar EM, Xiao F, Shirai N, Takashima M, Sugimura H. Interleukin 1beta polymorphisms increase risk of hypochlorhydria and atrophic gastritis and reduce risk of duodenal ulcer recurrence in Japan. *Gastroenterology* 2002; **123:** 92-105

7 **Zeng ZR,** Hu PJ, Hu S, Pang RP, Chen MH, Ng M, Sung JJ. Association of interleukin 1B gene polymorphism and gastric cancers in high and low prevalence regions in China. *Gut* 2003; **52:** 1684-1689

8 **El-Omar EM,** Oien K, El-Nujumi A, Gillen D, Wirz A, Dahill S, Williams C, Ardill JE, McColl KE. Helicobacter pylori infection and chronic gastric acid hyposecretion. *Gastroenterology* 1997; **113:** 15-24

9 **Xu GP,** Reed PI. N-nitroso compounds in fresh gastric juice and their relation to intragastric pH and nitrite employing an improved analytical method. *Carcinogenesis* 1993;**14:** 2547-2551

10 **Broutet N,** Plebani M, Sakarovitch C, Sipponen P, Mégraud F. Pepsinogen A, pepsinogen C, and gastrin as markers of atrophic chronic gastritis in European dyspeptics. *Br J Cancer* 2003; **88:** 1239-1247

11 **Stockbruegger RW.** Bacterial overgrowth as a consequence of reduced gastric acidity. *Scand J Gastroenterol* Suppl 1985; **111:** 7-16

12 **Svendsen JH,** Dahl C, Svendsen LB, Christiansen PM. Gastric cancer risk in achlorhydric patients. A long-term follow-up study. *Scand J Gastroenterol* 1986; **21:** 16-20

13 **Beales IL,** Calam J. Inhibition of carbachol stimulated acid secretion by interleukin 1beta in rabbit parietal cells requires protein kinase C. *Gut* 2001; **48:** 782-789

14 **Loparev VN,** Cartas MA, Monken CE, Velpandi A, Srinivasan A. An efficient and simple method of DNA extraction from whole blood and cell lines to identify infectious agents. *J Virol Methods* 1991; **34:** 105-112

15 **McColl KE,** el-Omar E, Gillen D. Helicobacter pylori gastritis and gastric physiology. *Gastroenterol Clin North Am* 2000; **29:** 687-703, viii

16 **Schepp W,** Dehne K, Herrmuth H, Pfeffer K, Prinz C. Identification and functional importance of IL-1 receptors on rat parietal cells. *Am J Physiol* 1998; **275:** G1094-G1105

17 **Wolfe MM,** Nompleggi DJ. Cytokine inhibition of gastric acid secretion-a little goes a long way. *Gastroenterology* 1992; **102:** 2177-2178

18 **Mahr S,** Neumayer N, Gerhard M, Classen M, Prinz C. IL-1beta-induced apoptosis in rat gastric enterochromaffin-like cells is mediated by iNOS, NF-kappaB, and Bax protein. *Gastroenterology* 2000; **118:** 515-524

19 **Beales IL,** Calam J. Interleukin 1 beta and tumour necrosis factor alpha inhibit acid secretion in cultured rabbit parietal cells by multiple pathways. *Gut* 1998; **42:** 227-234

20 **Hwang IR,** Kodama T, Kikuchi S, Sakai K, Peterson LE, Graham DY, Yamaoka Y. Effect of interleukin 1 polymorphisms on gastric mucosal interleukin 1beta production in Helicobacter pylori infection. *Gastroenterology* 2002;**123:** 1793-1803

21 **Lundell L,** Miettinen P, Myrvold HE, Pedersen SA, Thor K, Andersson A, Hattlebakk J, Havu N, Janatuinen E, Levander K, Liedman B, Nyström P. Lack of effect of acid suppression therapy on gastric atrophy. Nordic Gerd Study Group. *Gastroenterology* 1999;**117:** 319-326

22 **Coussens LM,** Werb Z. Inflammation and cancer. *Nature* 2002; **420:** 860-867

23 **Fox JG,** Wang TC. Reply to "The 'African enigma' - another explanation". *Nat Med* 2000; **6:** 1297-1298

Science Editor Kumar M and Guo SY **Language Editor** Elsevier HK

PO Box 2345, Beijing 100023, China
www.wjgnet.com
wjg@wjgnet.com

ELSEVIER

World J Gastroenterol 2005;11(41):6554-6556
World Journal of Gastroenterology ISSN 1007-9327

•*CASE REPORT*•

Peroral cholangioscopy for non-invasive papillary cholangiocarcinoma with extensive superficial ductal spread

Toshifumi Wakai, Yoshio Shirai, Katsuyoshi Hatakeyama

Toshifumi Wakai, Yoshio Shirai, Katsuyoshi Hatakeyama, Division of Digestive and General Surgery, Niigata University Graduate School of Medical and Dental Sciences, Niigata, Japan
Correspondence to: Yoshio Shirai, MD, PhD, Division of Digestive and General Surgery, Niigata University Graduate School of Medical and Dental Sciences, 1-757 Asahimachi-dori, Niigata, Niigata 951-8510, Japan. shiray@med.niigata-u.ac.jp
Telephone: +81-25-227-2228 Fax: +81-25-227-0779
Received: 2005-01-06 Accepted: 2005-01-26

Abstract

Papillary carcinoma arising from the extrahepatic bile duct often shows superficial ductal spread. We report herein the case of a patient with extensive superficial spread of non-invasive papillary cholangiocarcinoma, which was depicted with peroral cholangioscopy. A 65-year-old woman presented with the sudden-onset of severe epigastric pain. Ultrasonography revealed acute acalculous cholecystitis. Endoscopic retrograde cholangiography found small protruding lesions around the confluence of the cystic duct, suggestive of a cholangiocarcinoma. As the contour of the middle and upper bile ducts it was slightly irregular on the cholangiogram, the presence of superficial ductal spread was suspected. Peroral cholangioscopy revealed small papillary lesions around the confluence of the cystic duct and fine granular mucosal lesions in the middle and upper bile ducts and the right hepatic duct, suggesting a superficially spreading tumor. A right hepatectomy with bile duct resection was performed and no residual tumor was found. Histological examination revealed a non-invasive papillary carcinoma arising from the cystic duct with extensive superficial spread. Our experience of this case and a review of the literature suggest that a fine granular or fine papillary appearance of the ductal mucosae on cholangioscopy indicates superficial spread of papillary cholangiocarcinoma, for which peroral cholangioscopy is an efficient diagnostic option.

Key words: Cholangiocarcinoma; Bile duct neoplasms; Peroral cholangioscopy; Papillary carcinoma; Superficial ductal spread; Surgery

Wakai T, Shirai Y, Hatakeyama K. Peroral cholangioscopy for non-invasive papillary cholangiocarcinoma with extensive superficial ductal spread. *World J Gastroenterol* 2005; 11(41): 6554-6556
http://www.wjgnet.com/1007-9327/11/6554.asp

INTRODUCTION

Papillary carcinoma arising from the extrahepatic bile duct often shows superficial ductal spread[1]. Peroral cholangioscopy, introduced in the 1970s by Rosch *et al*[2] and Nakajima *et al*[3], provides direct visualization of the biliary ducts. We report herein the case of a patient with extensive superficial ductal spread of non-invasive papillary cholangiocarcinoma, which was depicted with peroral cholangioscopy.

CASE REPORT

A 65-year-old woman presented with the sudden-onset of severe epigastric pain. No jaundice was observed on physical examination, and the serum total bilirubin level was 0.6 mg/dL (reference range: 0.3-0.9 mg/dL). The serum levels of carcinoembryonic antigen and carbohydrate antigen 19-9 were 0.7 ng/mL (reference range: 0-6 ng/mL) and 6 U/mL (reference range: 0-37 U/mL), respectively.

Ultrasonography revealed acute acalculous cholecystitis, for which percutaneous cholecystostomy was performed. Endoscopic retrograde cholangiography found small protruding lesions around the confluence of the cystic duct, suggestive of a cholangiocarcinoma (Figure 1). Smear cytology of the ductal bile aspirated during endoscopic retrograde cholangiography revealed that exfoliated cells were categorized into Papanicolaou class II. As the contour of the middle and upper bile ducts was slightly irregular on the cholangiogram, the presence of superficial ductal spread was suspected. In order to confirm this, peroral cholangioscopy using a fiberoptic endoscope (CHF-B20QY, Olympus, Tokyo, Japan) was performed, and both small papillary lesions around the confluence of the cystic duct (Figure 2) and fine granular mucosal lesions, brownish in color, in the middle and upper bile ducts were revealed, suggesting a superficially spreading tumor. Such mucosal lesions were also seen in the right hepatic duct (Figure 3).

After laparotomy, a bile duct resection with regional lymphadenectomy was performed. As the resection margin at the right hepatic duct was positive for *in situ* carcinoma on frozen-section examination, a right hepatectomy was additionally performed and no residual tumor was found. Histological examination of the resected specimen revealed a non-invasive papillary carcinoma arising from the cystic duct, with superficial spread extending up to the right anterior sectoral duct (pathologic T1N0M0, Stage IA, according to the tumor-node-metastasis staging system[4]).

Fine granular mucosal lesions on peroral cholangioscopy (Figure 3) corresponded to papillary *in situ* carcinoma histologically, whereas the flat mucosae between the fine granular mucosal lesions, which appeared normal on cholangioscopy (Figure 3), corresponded to non-papillary *in situ* carcinoma. The patient remains healthy, with no evidence of recurrence 7 years after the resection.

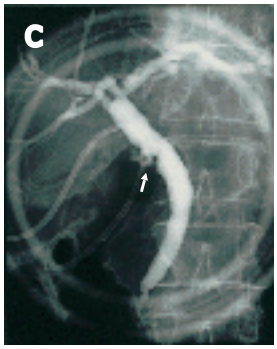

Figure 1 Endoscopic retrograde cholangiography. The cystic duct is poorly opacified with small protruding lesions around the confluence of the cystic duct (arrow). An 8-Fr pig-tail catheter **(C)** is inserted into the gallbladder.

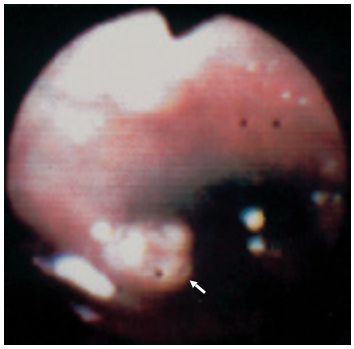

Figure 2 Peroral cholangioscopy shows a small papillary lesion (arrow) around the confluence of the cystic duct.

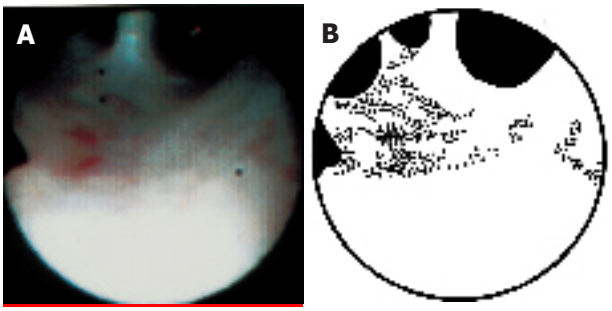

Figure 3 Peroral cholangioscopy of the interior of the right hepatic duct. **A:** Fine granular mucosal lesions, brownish in color, are scattered, suggesting the presence of papillary *in situ* carcinoma. The flat mucosae between the fine granular lesions, which appear normal on cholangioscopy, corresponded to non-papillary *in situ* carcinoma histologically. The lower part of this figure is fogged owing to halation. **B:** Schematic representation. The dotted areas indicate the fine granular lesions.

DISCUSSION

Nimura and Kamiya[5,6] demonstrated, by means of percutaneous transhepatic cholangioscopy, that a fine granular or fine papillary appearance of the ductal mucosae indicates superficial spread of cholangiocarcinoma. In the current case, the fine granular mucosal appearance on cholangioscopy corresponded to papillary *in situ* carcinoma histologically. It is very likely that a fine granular or fine papillary mucosal appearance on cholangioscopy is pathognomonic of superficial ductal spread of papillary cholangiocarcinoma.

The ductal resection margin status is an established prognostic factor in patients with extrahepatic cholangiocarcinoma[7,8]. Although intraductal ultrasonography is helpful in discerning T category of biliary malignancies[9], the extent of the superficial spread of cholangiocarcinoma is difficult to determine preoperatively on imaging studies[5,10,11]. In the current case, although peroral cholangioscopy detected papillary *in situ* carcinoma in the form of fine granular lesions, it did not detect the non-papillary *in situ* carcinoma between the lesions, suggesting that cholangioscopy is incapable of detecting flat ductal spread of *in situ* carcinoma. Intraoperative frozen-section examination is indispensable in assessing the ductal resection margin status.

In conclusion, a fine granular or fine papillary appearance of the ductal mucosae on cholangioscopy suggests superficial spread of papillary cholangiocarcinoma, for which peroral cholangioscopy is an efficient diagnostic option, unless the superficial lesions are flat.

REFERENCES

1 **Sakamoto E,** Nimura Y, Hayakawa N, Kamiya J, Kondo S, Nagino M, Kanai M, Miyachi M, Uesaka K. The pattern of infiltration at the proximal border of hilar bile duct carcinoma: a histologic analysis of 62 resected cases. *Ann Surg* 1998; **227**: 405-411
2 **Rosch W,** Koch H, Demling L. Peroral cholangioscopy. *Endoscopy* 1976; **8**: 172-175
3 **Nakajima M,** Akasaka Y, Fukumoto K, Mitsuyoshi Y, Kawai K. Peroral cholangiopancreatosocopy (PCPS) under duodenoscopic guidance. *Am J Gastroenterol* 1976; **66**: 241-247
4 **Greene FL,** Page DL, Fleming ID, Fritz AG, Balch CM, Haller DG, Morrow M. *American Joint Committee on Cancer Staging Manual* (6th edition). New York: Springer-Verlag, 2002: 131-138
5 **Nimura Y.** Staging of biliary carcinoma: cholangiography and cholangioscopy. *Endoscopy* 1993; **25**: 76-80
6 **Nimura Y,** Kamiya J. Cholangioscopy. *Endoscopy* 1996; **28**: 138-146
7 **Wakai T,** Shirai Y, Moroda T, Yokoyama N, Hatakeyama K. Impact of ductal resection margin status on long-term survival in patients undergoing resection for extrahepatic cholangiocarcinoma. *Cancer* 2005; **103**: 1210-1216
8 **Burke EC,** Jarnagin WR, Hochwald SN, Pisters PW, Fong Y, Blumgart LH. Hilar Cholangiocarcinoma: patterns of spread, the importance of hepatic resection for curative operation, and a presurgical clinical staging system. *Ann Surg* 1998; **228**: 385-394
9 **Menzel J,** Poremba C, Dietl KH, Domschke W. Preoperative diagnosis of bile duct strictures--comparison of intraductal

ultrasonography with conventional endosonography. *Scand J Gastroenterol* 2000; **35**: 77-82

10 **Barish MA,** Yucel EK, Ferrucci JT. Magnetic resonance cholangiopancreatography. *N Engl J Med* 1999; **341**: 258-264

11 **Tamada K,** Ido K, Ueno N, Kimura K, Ichiyama M, Tomiyama T. Preoperative staging of extrahepatic bile duct cancer with intraductal ultrasonography. *Am J Gastroenterol* 1995; **90**: 239-246

Science Editor Wang XL and Guo SY **Language Editor** Elsevier HK

PO Box 2345, Beijing 100023, China
www.wjgnet.com
wjg@wjgnet.com

ELSEVIER

World J Gastroenterol 2005;11(41):6557-6559
World Journal of Gastroenterology ISSN 1007-9327

• *CASE REPORT* •

Left paraduodenal hernia presenting as recurrent small bowel obstruction

Yu-Min Huang, Andy Shau-Bin Chou, Yung-Kang Wu, Chao-Chuan Wu, Ming-Che Lee, Haw-Tzong Chen, Yao-Jen Chang

Yu-Min Huang, Yung-Kang Wu, Chao-Chuan Wu, Ming-Che Lee, Haw-Tzong Chen, Yao-Jen Chang, Department of Surgery, Buddhist Tzu Chi General Hospital, Hualien, Taiwan, China
Andy Shau-Bin Chou, Department of Radiology, Buddhist Tzu Chi General Hospital, Hualien, Taiwan, China
Correspondence to: Dr. Yao-Jen Chang, Department of Surgery, Buddhist Tzu-Chi General Hospital, No. 707, Sec. 3, Chung Yang Road, Hualien City, Hualien County 970, Taiwan, China. y.m.huang@yahoo.com.tw
Telephone: +886-3-8561825-2229 Fax: +886-3-8577161
Received: 2005-04-07 Accepted: 2005-04-30

Abstract

Internal herniation of the small bowel is a relatively rare cause of intestinal obstruction. Left paraduodenal hernia resulting from abnormal rotation of the midgut during embryonic development is the most common form of congenital internal hernia. We report our experience in the diagnosis and management of a young male with left paraduodenal hernia presenting as recurrent intestinal obstruction. Correct preoperative diagnosis of left paraduodenal hernia had been difficult due to non-specific clinical presentations, but the advent of modern imaging technology makes early and correct diagnosis possible. Due to the risk of obstruction and strangulation, surgical treatment is indicated; however, timely intervention increases the likelihood of a favorable outcome.

Key words: Internal hernia; Paraduodenal hernia; Small bowel obstruction

Huang YM, Chou ASB, Wu YK, Wu CC, Lee MC, Chen HT, Chang YJ. Left paraduodenal hernia presenting as recurrent small bowel obstruction. *World J Gastroenterol* 2005; 11(41): 6557-6559
http://www.wjgnet.com/1007-9327/11/6557.asp

INTRODUCTION

congenital internal hernias, paraduodenal hernias are the most common and account for 25%-53% of all cases[2]. Paraduodenal hernias result from abnormal rotation of the midgut during embryonic development and can be divided into two subtypes, left and right paraduodenal hernias, according to their distinct pathogenesis and the resultant anatomical derangement. Correct preoperative diagnosis of paraduodenal hernia was once difficult, because of its non-specific presentations; however, with the advent of modern imaging technology, more information can be gained regarding the anatomical characteristics of the underlying lesion and allow for better treatment planning. We present our experience in the diagnosis and management of a patient with left paraduodenal hernia presenting as recurrent intestinal obstruction, as well as a brief review of the literature.

CASE REPORT

The patient was a slim 24-year-old male who visited our emergency room because of intermittent epigastric abdominal pain associated with bilious vomitus during the previous few hours. He had no history of previous abdominal surgery, but had a similar episode with pain and vomiting about 6 mo before. He had lost about 10 kg during that period. Physical examination revealed a non-tender, mildly distended abdomen with hyperactive bowel sounds. The only remarkable finding on plain abdominal film was loops of a dilated small bowel. Initial abdominal computed tomography (CT) revealed a mass lesion of soft tissue density located between the stomach, the pancreas, and the transverse colon (Figure 1A). For better elucidation

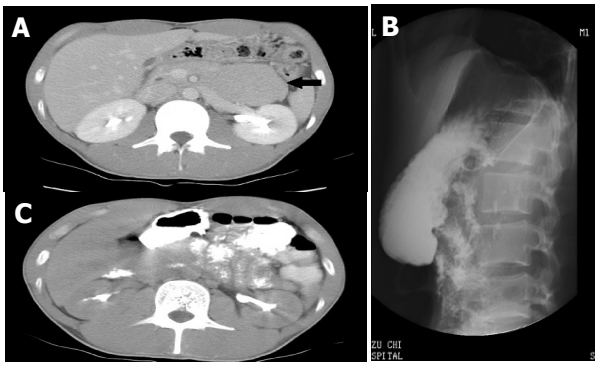

Figure 1 A: Computed tomography (CT) showing a soft tissue mass between the stomach, the pancreas, and the transverse colon (arrow); **B:** Upper gastrointestinal series showing a cluster of jejunum interposing between the stomach and the spine; **C:** The mass proved to be a cluster of intestinal loop after ingestion of contrast medium.

of the character of the mass lesion, we performed an upper gastrointestinal series with small intestinal follow-through, which revealed loops of jejunum clumping over the left upper quadrant of the abdomen (Figure 1B). The mass lesion proved to be a cluster of jejunum on follow-up CT (Figure 1C). The patient underwent surgery with a tentative diagnosis of left paraduodenal hernia with small bowel obstruction. Exploratory laparoscopy and laparotomy revealed that the jejunum did not emerge from the usual position at the base of transverse mesocolon; instead, only loops of the small bowel were visualized behind a thin layer of peritoneum (Figure 2A). Further exploration revealed that the jejunum exited from an aperture of about 15 cm caudal to the usual location of Treitz's ligament. The initial 10 cm of intraperitoneal jejunum ran parallel and was adherent to both the inferior mesenteric artery (IMA) and the inferior mesenteric vein (IMV), which constitute the anterior rim of the orifice (Figure 2B). A 25 cm long segment of jejunum had herniated through the orifice into the space behind the descending mesocolon. We manually reduced the herniated bowel loops after opening the anterior wall of the hernial sac by dividing the adhesion between the jejunum and the IMV. We then closed the orifice of the hernial sac around the jejunum with interrupted 3-0 silk sutures (Figure 2C). The patient tolerated the procedure well and recovery was uneventful postoperatively. Follow-up upper gastrointestinal series revealed the smooth passage of contrast medium without evidence of abnormal aggregation of the small bowel.

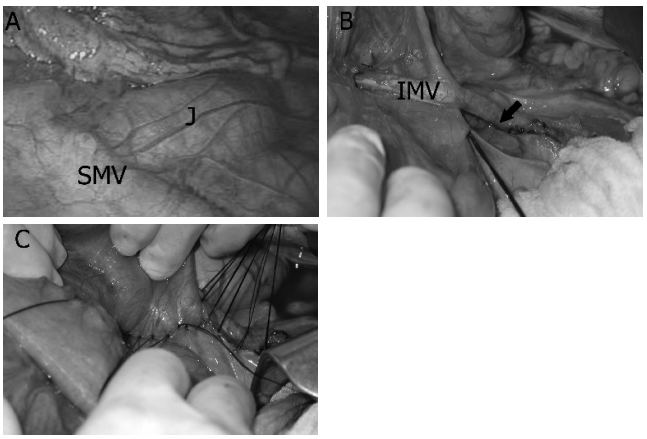

Figure 2 **A:** Loops of small bowel behind the mesocolon. Treitz's ligament was not seen. SMV: superior mesenteric vein, J: jejunum; **B:** the orifice through which the small bowel herniated (arrow). IMV: inferior mesenteric vein; **C:** completion of the repair.

DISCUSSION

Left paraduodenal hernia is about three times more frequent than its right counterpart, and is reported to occur three times more often in men[3]. As mentioned previously, left paraduodenal hernia usually results from abnormal rotation of the midgut. In the 5th wk of embryonic development, the rapidly elongating midgut herniates into the umbilical cord. Later, the herniated midgut undergoes a counter clockwise rotation of 90° around the superior mesenteric artery (SMA), leaving the prearterial limb on the left side. The herniated intestinal loop, first the prearterial then the postarterial limb, returns to the abdominal cavity by the 10th week. During this process, the intestinal loop undergoes another 180° countercloc kwise rotation. In the end, the prearterial limb lies left to the SMA and the postarterial limb lies superior and right to the SMA[4]. Under normal circumstances, fusion of the mesocolon with the peritoneum of the body wall follows this process. Failure of the fusion to take place in time leaves a potential space (the fossa of Landzert) behind the mesocolon. A leftparaduodenal hernia results from invagination of the small intestine into this unsupported area through an opening bound anteriorly by the IMV and is established as the descending colon that seeks its normal attachment[2].

Although the left paraduodenal hernia is congenital, most patients are recognized between the 4th and 6th decades of life, and the mean age at the time of diagnosis is 38.5 years[3]. The most common presentations are those associated with small bowel obstruction and are nonspecific[5], ranging in severity from recurrent vague abdominal pain, nausea, and vomiting in partial, reversible obstruction to acute abdomen in cases of incarceration and strangulation.

Physical examination is usually unrevealing except for such nonspecific findings as abdominal tenderness, distension, and the occasional presence of a mass. Correct preoperative diagnosis has been difficult in the past, due to these ambiguous presentations; therefore, it is mandatory to maintain a high index of suspicion in patients with pertinent unexplained complaints. Under emergent settings, diagnosis is only possible at the time of surgery. In the absence of an abdominal emergency, however, a variety of diagnostic tools is available to help establish the correct diagnosis before surgery. Because of the ambiguous clinical presentation of this disease, a CT scan may be the initial tool of investigation. A characteristic finding is a cluster of small bowel loops between the stomach and pancreas[6,7]. In case that the trapped loops are collapsed and oral contrast is not used, the hernia contents may be mistaken for a soft tissue mass. A high index of suspicion is again required to avoid inadvertent invasive diagnostic procedures such as CT-guided biopsy, which may be disastrous under such circumstances. An upper gastrointestinal series with small bowel follow-through demonstrates contrast-filled loops of small bowel clustering over the left upper aspect of the abdomen, as is seen in our patient. Abdominal ultrasonography might also aid in the diagnosis of paraduodenal hernia. Suggestive findings include a cluster of bowel loops or a well-defined mass. Peristalsis of the bowel loops can be appreciated and made more obvious with the ingestion of water[8].

In earlier reports, the diagnosis and treatment of left paraduodenal hernia tended to be delayed and the result of treatment seemed to be less satisfactory[5]. With the diagnostic tools available today, correct diagnoses are

possible even in the absence of acute symptoms, and treatment can commence promptly. Once diagnosed, left paraduodenal hernia should be surgically repaired because 50% of them cause intestinal obstruction[5,9]. The procedure consists of a manual reduction of the hernia contents followed by repair of the defect. If the herniated intestine is difficult to reduce because of its bulky size or adhesions within the sac, an incision can be made in the avascular portion of the hernial sac to the right of the inferior mesenteric vessels to enlarge the opening[2]. During this procedure, it is important to consider the relationship of the inferior mesenteric vessels to the sac opening and to take care to avoid injury to these structures. Although Bartlett indicated that these vessels can be divided without compromising blood supply to the colon[1], they should be preserved whenever possible. Intestinal resection is necessary in cases of strangulation and gangrene. In addition to the conventional "open" approach, successful laparoscopic repair of left paraduodenal hernia has been reported by Uematsu *et al*[10].

In conclusion, although relatively uncommon, left paraduodenal hernia should be included in the differential diagnosis of small bowel obstruction in patients who are relatively young, who have repetitive attacks, and who lack any history of previous abdominal surgery. The combination of a high index of suspicion, familiarity with this disease entity, and modern imaging technology make preoperative diagnosis easier today. Timely surgical intervention effectively relieves the patient's complaints and prevents further complications.

REFERENCES

1 **Bartlett MK,** Wang C, Williams WH. The surgical management of paraduodenal hernia. *Ann Surg* 1968; **168:** 249-254

2 **Brigham RA,** Fallon WF, Saunders JR, Harmon JW, d'Avis JC. Paraduodenal hernia: diagnosis and surgical management. *Surgery* 1984; **96:** 498-502

3 **Khan MA,** Lo AY, Vande Maele DM. Paraduodenal hernia. *Am Surg* 1998; **64:** 1218-1222

4 **Berardi RS.** Paraduodenal hernias. *Surg Gynecol Obstet* 1981; **152:** 99-110

5 **Newsom BD,** Kukora JS. Congenital and acquired internal hernias: unusual causes of small bowel obstruction. *Am J Surg* 1986; **152:** 279-285

6 **Olazabal A,** Guasch I, Casas D. Case report: CT diagnosis of nonobstructive left paraduodenal hernia. *Clin Radiol* 1992; **46:** 288-289

7 **Warshauer DM,** Mauro MA. CT diagnosis of paraduodenal hernia. *Gastrointest Radiol* 1992; **17:** 13-15

8 **Wachsberg RH,** Helinek TG, Merton DA. Internal abdominal hernia: diagnosis with ultrasonography. *Can Assoc Radiol J* 1994; **45:** 223-224

9 **Isabel L,** Birrell S, Patkin M. Paraduodenal hernia. *Aust N Z J Surg* 1995; **65:** 64-66

10 **Uematsu T,** Kitamura H, Iwase M, Yamashita K, Ogura H, Nakamuka T, Oguri H. Laparoscopic repair of a paraduodenal hernia. *Surg Endosc* 1998; **12:** 50-52

Science Editor Guo SY **Language Editor** Elsevier HK

PO Box 2345, Beijing 100023, China
www.wjgnet.com
wjg@wjgnet.com

ELSEVIER

World J Gastroenterol 2005;11(41):6560-6562
World Journal of Gastroenterology ISSN 1007-9327

• *CASE REPORT* •

Splenic angiosarcoma metastasis to small bowel presented with gastrointestinal bleeding

Jun-Te Hsu, Chin-Yew Lin, Ting-Jun Wu, Han-Ming Chen, Tsann-Long Hwang, Yi-Yin Jan

Jun-Te Hsu, Ting-Jun Wu, Han-Ming Chen, Tsann-Long Hwang, Yi-Yin Jan, Department of General Surgery, Chang Gung Memorial Hospital, Taoyuan, Taiwan, China
Chin-Yew Lin, Department of Pathology, Chang Gung Memorial Hospital, Keelung, Taiwan, China
Correspondence to: Dr. Han-Ming Chen, Department of General Surgery, Chang Gung Memorial Hospital, 5, Fushing Street, Kweishan Shiang, Taoyuan 333, Taiwan
China. ming1838@yahoo.com
Telephone: +886-3-3281200-3219 Fax: +886-3-3285818
Received: 2005-04-25 Accepted: 2005-05-12

Abstract

Primary splenic angiosarcoma is a very rare, aggressive neoplasm with a high metastatic rate and dismal prognosis. This neoplasm usually presents with abdominal pain, splenomegaly, anemia, and thrombocytopenia. Splenic angiosarcoma with bleeding gastrointestinal metastases is extremely rare. The literature contains only two case reports. This study reported a 44-year-old male patient with splenic angiosarcoma with sustained repeated gastrointestinal bleeding due to small bowel metastases. Salvage surgery was performed by splenectomy and resection of the metastatic small bowel tumors. The post-operative course was uneventful; the patient survived with the disease and had no GI bleeding, 7 mo after surgery.

Key words: Gastrointestinal bleeding; Metastasis; Small bowel; Splenectomy; Splenic angiosarcoma

Hsu JT, Lin CY, Wu TJ, Chen HM, Hwang TL, Jan YY. Splenic angiosarcoma metastasis to small bowel presented with gastrointestinal bleeding. *World J Gastroenterol* 2005;11(41): 6560-6562
http://www.wjgnet.com/1007-9327/11/6560.asp

INTRODUCTION

Primary splenic angiosarcoma is a very rare neoplasm with a high metastatic rate and dismal prognosis. Langhans[1] first identified this disease in 1879. Presentations of splenic angiosarcoma are extremely variable and frequently cause diagnostic difficulties. The disease usually manifests with abdominal mass, abdominal pain, splenomegaly, and anemia. Distant metastases can occur in the liver, lung, lymph node, and bone, and soft tissue[2]. To our knowledge, splenic angiosarcoma with bleeding gastrointestinal (GI) metastases is extremely rare. The literature contains only two case reports[3,4]. The present case is the first report of splenic angiosarcoma metastasis to the small bowel. This work describes the experience of the authors in the management of the splenic angiosarcoma with bleeding GI metastases.

CASE REPORT

A 44-year-old male patient was admitted to Chang Gung Memorial Hospital on July 1, 2004, complaining of severe lower back pain and progressively weakness in his bilateral lower legs for 1 mo. Subconjunctiva hemorrhage and gingival bleedings were noted during initial examination mild pale conjunctiva, hepatomegaly, and splenomegaly. The hematogram measured hemoglobin at 108 g/L and platelet at 137 000/cm^3. Prothrombin and activated partial thromboplastin times were normal. Magnetic resonance imaging of the spine identified abnormal enhancement at multiple bodies in the thoracic, lumbar, and sacral spines, which were assumed to be metastatic lesions. Unfortunately, the patient developed hematochezia 9 d after admission. Persistent passage of tarry stools resulted in severe anemia (the lowest hemoglobin level was 43 g/L) and an episode of syncope. The patient received transfusions of packed RBC to a total of 12 U, before surgery. Both endoscopy and colonscopy failed to detect the site of bleeding. Abdominal computed tomography showed a diffusely heterogeneous density infiltrating the whole spleen (Figure 1) and did not detect any GI tumors. The scan of Tc-99m RBC revealed evidence of active bleeding in the left mid-abdominal region. The patient then underwent an exploratory laparotomy on July 17, 2004. During surgery, the spleen was enlarged with multiple dark-red nodules on its surface (Figure 2). Intra-operative endoscopy failed to identify any site of bleeding. The serosa of the small intestine was intact and multiple small hemorrhagic patches (number >5) were observed at the jejunum and ileum (Figure 3). Splenectomy and resection of the small intestine containing hemorrhagic patches were then performed.

Macroscopically, the surgical specimen of the spleen measured 14 cm×10 cm×9 cm with a weight of 400 g, and the splenic parenchyma was diffusely scattered with multiple, irregular sized and dark-red color nodules. Mucosal tumors (size <1 cm) were identified at the resected small intestine. Microscopically, the spleen revealed neoplastic sinusoidal endothelial cells with

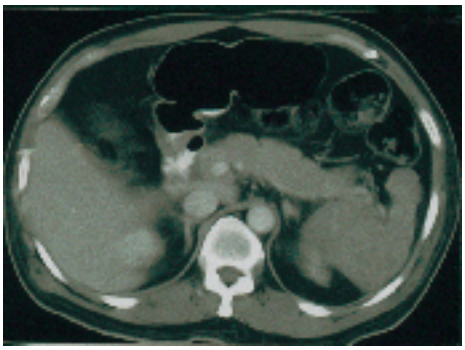

Figure 1 Abdominal computed tomography identifies an enlarged spleen with a heterogeneous density involving the whole spleen.

Figure 3 Multiple small hemorrhagic patches are identified at the jejunum and ileum.

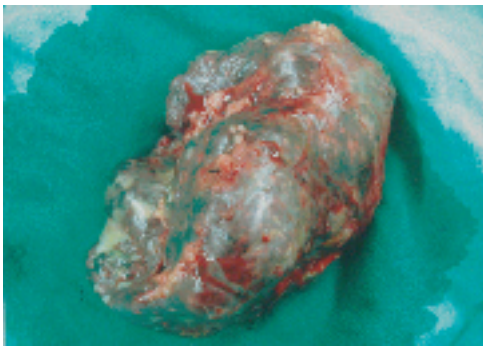

Figure 2 The splenic parenchyma is diffusely scattered with multiple, irregular sized and dark-red nodules.

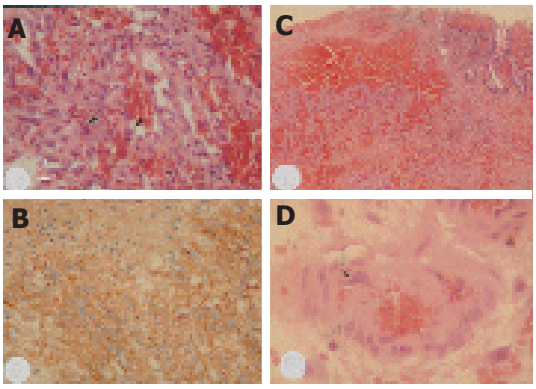

Figure 4A Photomicrography of the spleen reveals neoplastic sinusoidal endothelial cells with marked cytological atypia (arrowhead) lining the congested sinusoid spaces (hematoxylin and eosin staining, 200×); **B:** immunohistochemical staining of the neoplastic cells is positive for factor XIII associated antigen (immunostain, 200×); **C:** histological examination of the specimen of small intestine shows metastatic neoplastic cells primarily distributed within the submucosal layer and focally extending to the mucosal layer (hematoxylin and eosin staining, 100 ×); **D:** photomicrography of the intestinal vessel reveals presence of individual neoplastic cells (arrowhead) within the vascular lumen (hematoxylin and eosin staining, 400×).

marked cytological atypia lining the congested sinusoid spaces (Figure 4A). The tumor cells were immunoreactive to factor XIII associated antigen (polyclonal, 1:500, Calbiochem Novabiochem, CA, USA, Figure 4B). The neoplastic cells of the small intestine only involved the mucosal and submucosal layers (Figure 4C); the muscular layer and serosa were intact and free of malignancy. They formed anastomosing network of sinusoids lined by pleomorphic endothelial cells, similar to those seen in the spleen. In addition, individual tumor cells were identified within the small vessels (Figure 4D). The diagnosis of primary splenic angiosarcoma with metastases of bones and small intestine was confirmed.

The patient had an uneventful post-operative course. He received external beam radiation therapy for his bone pain postoperatively. He did not experience GI bleeding again and survived with the disease 7 mo after surgery.

DISCUSSION

PATIENTS WITH splenic angiosarcoma may occur at any age[2,5–7]. The mean age of the reported patients was 50-60 years[2,5,6]. The pathogenesis of splenic angiosarcoma remains unknown. Reported causes are exposed to ionizing radiation[8] or chemotherapy for lymphoma[9]. However, some authors believed that splenic angiosarcoma develops from a previously existing benign counterparts of the splenic tumors such as hemangioma or hemangioendothelioma[7,8]. In this case, no such risk factors were noted.

Splenomegaly with left-side upper abdominal pain occurs in over 70% of patients with splenic angiosarcoma[2,5]. Anemia and thrombocytopenia are the frequent findings of hematogram and are reported in more than 70% of cases[5,6]. Spontaneous splenic rupture presenting with acute abdominal pain has been reported in 13%-32% of patients[2,5,10]. Other systemic symptoms such as body weight loss, gum bleeding, fatigue, weakness, fever, chest pain, and GI bleeding have also been observed[2,5].

Metastases of the splenic angiosarcoma are frequent, occurring in 69–100% of cases[2,5]. The most common metastasis sites are the liver, lung, lymph node, bone, bone marrow, and soft tissue. To the best of our knowledge, the present patient is the first case report of splenic angiosarcoma metastasis to the small bowel.

Table 1 Primary splenic angiosarcoma with bleeding gastrointestinal metastases

Author/yr	Age/sex	Site of GI metastasis	Treatment	Status and time of follow-up
Chung[3] 1999	54/M	ND	Splenectomy	DOD, 10 mo
Jimenez-Heffernan[4] 1999	71/F	Colon (splenic flexure)	Splenectomy, left hemicolectomy, radiation	DOD, 9 mo
Hsu, present	45/M	Small bowel	Splenectomy, resection of small bowel metastases, radiation	AWD, 7 mo

AWD; alive with disease; DOD, dead of disease; GI, gastrointestinal; mo, months; ND, not described.

Malignancies of the small bowel can be either primary or metastatic. Primary small bowel malignant tumors are rare with the incidence of about 1 per 100000 and a prevalence of 0.6%[11]. Secondary neoplastic involvement of the small bowel is more frequent than primary small bowel neoplasm by hematogenous spread, direct invasion or intraperitoneal seeding[12]. Metastatic malignant tumors from the colon, ovary, uterus, and stomach generally invade the small bowel via direct invasion or intraperitoneal spread. The breast cancer, lung cancer, and melanoma usually metastasize to the small bowel hematogenously. Based on the operative and histopathologic findings, this case is the first report of small bowel metastases from the splenic angiosarcoma via hematogenous route.

The prognosis for splenic angiosarcoma is typically very dismal with a 6-mo survival for only 20% of cases[2,4]. Notably, survival of pediatric patients was reported as extremely poor ranging from less than 1 mo to 2 years[13]. However, Falk *et al*[5] had reported that two adults survived at the last follow-up, 1 with disease at 8 years and the other disease-free at 10 years. Survival is favorable for early diagnosis with splenectomy before rupture[4,10]. Montemayor and Caggiano[14] also found that patients with splenic angiosarcoma had longer survival, if splenectomy was performed prior to rupture compared to after rupture (14.4 *vs* 4.4 mo).

Table 1 shows only three cases including this case that have experienced GI bleeding due to GI metastasis from the splenic angiosarcoma (Table 1). In patients with either primary or metastatic GI angiosarcoma, repeated GI bleeding and the need for blood transfusion made them hospitalization-dependent and debilitated. These patients frequently die of uncontrolled GI bleeding[15]. The survival of these patients in Allison's study ranges from 1 wk to 3 years after resection of the foci[15]. No consensus yet exists regarding the need to treat patients with disseminated metastases aggressively. Nevertheless, salvage surgery (resection of small bowel metastases) combined with splenectomy to control bleeding and confirm diagnosis was justified in the present case. The patient survived with the disease, 7 mo after surgery without evidence of GI bleeding.

In conclusion, splenic angiosarcoma with bleeding GI metastases is extremely rare. This case is the first report of metastatic small bowel malignancy from the splenic angiosarcoma. Salvage surgery to control bleeding due to the GI metastases is justified in this case.

REFERENCES

1 **Langhans T**. Pulsating cavernous neoplasm of the spleen with metastatic nodules to the liver. *Vichows Arch Pathol Anat* 1879; **75:** 273-291

2 **Neuhauser TS,** Derringer GA, Thompson LD, Fanburg-Smith JC, Miettinen M, Saaristo A, Abbondanzo SL. Splenic angiosarcoma: a clinicopathologic and immunophenotypic study of 28 cases. *Mod Pathol* 2000; **13**: 978-987

3 **Chung YF**, Busmanis I, Hong GS, Soo KC. Splenic angiosarcoma--an unusual cause of bleeding gastrointestinal tract. *Singapore Med J* 1999; **40:** 106-108

4 **Jimenez-Heffernan JA,** Hardisson D, Prieto-Nieto MI, Burgos E. Ruptured primary splenic angiosarcoma into the colon. Presentation as anal bleeding. *Acta Gastroenterol Belg* 1999; **62:** 248-251

5 **Falk S,** Krishnan J, Meis JM. Primary angiosarcoma of the spleen. A clinicopathologic study of 40 cases. *Am J Surg Pathol* 1993; **17:** 959-970

6 **Chen KT,** Bolles JC, Gilbert EF. Angiosarcoma of the spleen: a report of two cases and review of the literature. *Arch Pathol Lab Med* 1979; **103:** 122-124

7 **Alt B,** Hafez GR, Trigg M, Shahidi NT, Gilbert EF. Angiosarcoma of the liver and spleen in an infant. *Pediatr Pathol* 1985; **4:** 331-339

8 **Sordillo EM,** Sordillo PP, Hajdu SI. Primary hemangiosarcoma of the spleen: report of four cases. *Med Pediatr Oncol* 1981; **9:** 319-324

9 **Zwi LJ,** Evans DJ, Wechsler AL, Catovsky D. Splenic angiosarcoma following chemotherapy for follicular lymphoma. *Hum Pathol* 1986; **17:** 528-530

10 **Autry JR,** Weitzner S. Hemangiosarcoma of spleen with spontaneous rupture. *Cancer* 1975; **35:** 534-539

11 **Attanoos R**, Williams GT. Epithelial and neuroendocrine tumors of the duodenum. *Semin Diagn Pathol* 1991; **8:** 149-162

12 **Gill SS**, Heuman DM, Mihas AA. Small intestinal neoplasms. *J Clin Gastroenterol* 2001; **33:** 267-282

13 **Kren L,** Kaur P, Goncharuk VN, Dolezel Z, Krenova Z. Primary angiosarcoma of the spleen in a child. *Med Pediatr Oncol* 2003; **40:** 411-412

14 **Montemayor P,** Caggiano V. Primary hemangiosarcoma of the spleen associated with leukocytosis and abnormal spleen scan. *Int Surg* 1980; **65:** 369-373

15 **Allison KH,** Yoder BJ, Bronner MP, Goldblum JR, Rubin BP. Angiosarcoma involving the gastrointestinal tract: a series of primary and metastatic cases. *Am J Surg Pathol* 2004; **28**: 298-307

Science Editor Guo SY **Language Editor** Elsevier HK

PO Box 2345, Beijing 100023, China
www.wjgnet.com
wjg@wjgnet.com

ELSEVIER

World J Gastroenterol 2005;11(41):6563-6565
World Journal of Gastroenterology ISSN 1007-9327

• *CASE REPORT* •

Esophageal rupture due to Sengstaken-Blakemore tube misplacement

Chee-Fah Chong

Chee-Fah Chong, Emergency Department, Shin-Kong Wu Ho-Su Memorial Hospital, Taipei, Taiwan, China
Correspondence to: Dr Chee-Fah Chong, School of Medicine, Fu Jen Catholic University, No. 510 Chung-Cheng Road, Hsin-Chuang Hsih, Taipei Hsien, Taipei 24205, Taiwan, China. m002202@ms.skh.org.tw
Telephone: +886-2-29053490 Fax: +886-2-29052096
Received: 2005-04-21 Accepted: 2005-05-24

Abstract

The author presents three cases of esophageal rupture during the treatment of massive esophageal variceal bleeding with Sengstaken-Blakemore (SB) tube. In each case, simple auscultation was used to guide SB tube insertion, with chest radiograph obtained only after complete inflation of the gastric balloon. Two patients died of hemorrhagic shock and one died of mediastinitis. The author suggests that confirmation of SB tube placement by auscultation alone may not be adequate. Routine chest radiographs should be obtained before and after full inflation of the gastric balloon to confirm tube position and to detect tube dislocation.

Key words: Chest radiograph; Esophageal rupture; Sengstaken-Blakemore tube

Chong CF. Esophageal rupture due to Sengstaken-Blakemore tube misplacement. *World J Gastroenterol* 2005; 11(41): 6563-6565
http://www.wjgnet.com/1007-9327/11/6563.asp

INTRODUCTION

Esophageal rupture is a well-known but rarely reported fatal complication of the management of bleeding esophageal varices with the Sengstaken-Blakemore (SB) tube[1]. Described below are three cases of fatal esophageal rupture with striking radiographs showing the gastric balloon of the SB tube inflated in the thoracic cavity. A routine pre-inflation chest radiograph should have prevented esophageal perforation due to malposition of the SB tube in these cases.

CASE REPORTS

Case 1

A 38-year-old man was admitted with massive hematemesis. On physical examination, his blood pressure, pulse rate, respiratory rate, and temperature were 86/50 mmHg, 126 bpm, 24/min, and 37.3 °C, respectively. Pale conjunctivae, icteric sclera, splenomegaly, and spider angiomata were also observed. Resuscitation was started with normal saline, packed red cells and platelet concentrates. When stabilized, an emergency esophago-gastroduodenoscopy was performed, which revealed active bleeding from ruptured esophageal varices.

Despite aggressive therapies with fluids, blood components and full-dose terlipressin, the patient deteriorated into coma due to hemorrhagic shock. He was moved to the intensive care unit (ICU) for insertion of an SB tube. Endotracheal intubation was accomplished to secure airway before the procedure. A chest radiograph taken soon after tracheal intubation and inflation of the gastric balloon to 300 mL showed a radiolucent area behind the heart (Figure 1). The gastric balloon was immediately deflated and the SB tube removed (2 h after insertion). A repeated chest radiograph revealed massive left hemothorax. As the patient was deemed unfit for surgery, he was treated conservatively. The patient died when a further episode of massive hematemesis developed 44 h after admission.

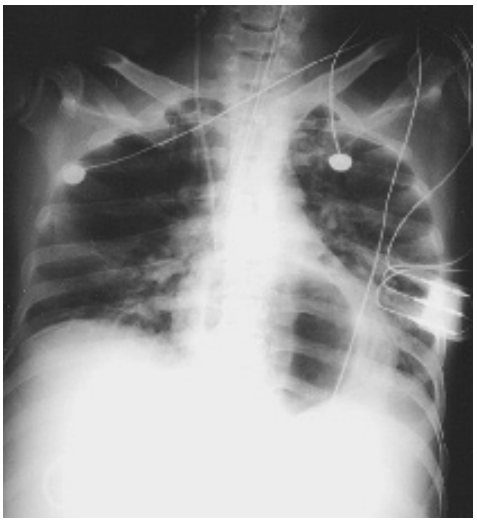

Figure 1 Chest radiographs indicating gastric balloon of SB tube, behind the heart shadow.

Case 2

A 49-year-old man was admitted to the ICU due to uncontrolled hematemesis from ruptured esophageal varices and hepatic encephalopathy. Physical examination showed that he was in deep coma (Glasgow coma scale of E2M1V1) and severe hypotension (BP 60/40 mmHg). Rapid endotracheal intubation followed by insertion of an SB tube was performed without difficulties. However, a chest radiograph ordered to check tube positions demonstrated a radiolucent circle (the gastric balloon) within the left hemithorax (Figure 2). The patient died of shock-related multiple organ failure on the third day of admission.

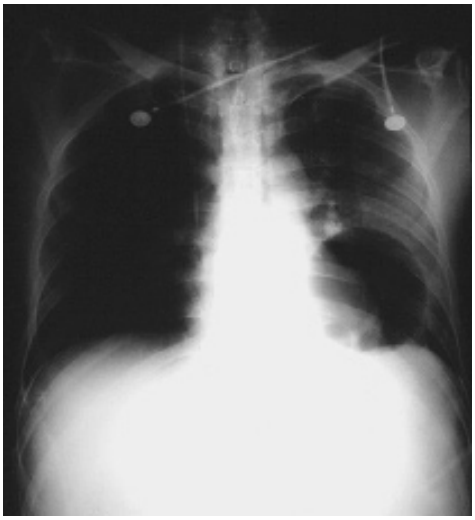

Figure 2 Chest radiographs indicating gastric balloon of SB tube, within the left lower hemithorax.

Case 3

A 43-year-old male alcoholic was treated in the ICU for convulsions due to decompensated hepatic cirrhosis with grade IV encephalopathy. He was tracheally intubated with a Glasgow coma scale of E2M2VT. His vital signs were within the normal limits. However, he suffered a massive hematemesis on the third day of admission, which was the result of ruptured esophageal varices. An SB tube was inserted and a chest radiograph later showed a radiolucent area within the lower mediastinum (Figure 3). The patient developed fever, leukocytosis and shock in the following days and a chest computer tomography (CT) revealed findings compatible with mediastinitis. He died of sepsis 12 d after the admission.

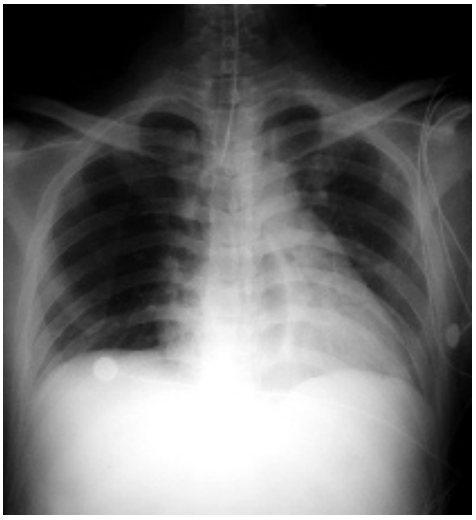

Figure 3 Chest radiographs indicating gastric balloon of SB tube, in the lower mediastinum.

DISCUSSION

The management of acute bleeding episodes from ruptured esophageal varices consists of volume replacement, pharmacological, mechanical (balloon tamponade), and surgical modes of arresting hemorrhage. While balloon tamponade using SB tube is effective in achieving initial hemostasis, it has a significant complication rate. The most common complications of esophageal balloon therapy for varices include aspiration, esophageal perforation, and pressure necrosis of the mucosa[2]. The exact incidence of complications is difficult to determine, as it varies with the skill and experience of the surgical team, the duration of treatment, and the status of the patient. Aspiration of secretions is the most common complication of balloon tamponade, occurring in approximately 10%-20% of cases[3].

As described in past literature, cases with esophageal perforation can occur as a result of difficult SB tube insertion[4], retching and vomiting[5], and repeated endoscopic sclerotherapy[6]. In each of our cases, the SB tube was inserted without documented difficulties. Intragastric position was confirmed with auscultation. A radiographic localization of the SB tube before full inflation of the gastric balloon was ignored. The diagnosis of esophageal perforation in each case was confirmed by a follow-up chest radiograph taken after full inflation of the gastric balloon. Though uncommon, esophageal rupture due to SB tube misplacement carries a high incidence of mortality from hemothorax or septic mediastinitis, as demonstrated in our patients.

In conclusion, following insertion of the SB tube, confirmation of tube placement by auscultation alone may not be adequate. Routine chest radiographs should be obtained before and after full inflation of the gastric balloon to confirm correct tube position and to detect tube dislocation as soon as possible.

REFERENCES

1 **McGrath RB.** Inadvertent gastric balloon inflation within the chest in the management of esophageal varices. *Crit Care Med* 1986; **14:** 580-582

2 **Vlavianos P,** Gimson AE, Westaby D, Williams R. Balloon tamponade in variceal bleeding: use and misuse. *BMJ* 1989; **298:** 1158

3 **Avgerinos A,** Armonis A. Balloon tamponade technique and

efficacy in variceal haemorrhage. *Scand J Gastroenterol Suppl* 1994; **207:** 11-16
4 **Hamm DD,** Papp JP. Rupture of esophagus during use of Sengstaken-Blakemore tube. *Postgrad Med* 1974; **56:** 199-200
5 **Zeid SS,** Young Pc, Reeves Jt. Rupture of the esophagus after introduction of the Sengstaken-Blakemore tube. *Gastroenterology* 1959; **36:** 128-131
6 **Crerar-Gilbert A.** Oesophageal rupture in the course of conservative treatment of bleeding oesophageal varices. *J Accid Emerg Med* 1996; **13:** 225-227

Science Editor Guo SY **Language Editor** Elsevier HK

PO Box 2345, Beijing 100023, China
www.wjgnet.com
wjg@wjgnet.com

ELSEVIER

World J Gastroenterol 2005;11(42):6571-6576
World Journal of Gastroenterology ISSN 1007-9327

• *REVIEW* •

Immunological treatment of liver tumors

Maurizio Chiriva-Internati, Fabio Grizzi, Cynthia A Jumper, Everardo Cobos, Paul L Hermonat, Eldo E Frezza

Maurizio Chiriva-Internati, Department of Microbiology and Immunology, Texas Tech University Health Sciences Center and Southwest Cancer Treatment and Research Center, Lubbock, TX 79430, United States
Fabio Grizzi, Scientific Direction, Istituto Clinico Humanitas, 20089 Rozzano, and Foundation "M. Rodriguez" – Institute for Quantitative Measures in Medicine, 20100 Milan, Italy
Cynthia A Jumper, Department of Internal Medicine, Texas Tech University Health Sciences Center and Southwest Cancer Treatment and Research Center, Lubbock, TX 79430, United States
Everardo Cobos, Department of Internal Medicine, Texas Tech University Health Sciences Center and Southwest Cancer Treatment and Research Center, Lubbock, TX 79430, United States
Paul L Hermonat, Department of Internal Medicine, University of Arkansas for Medical Sciences, Little Rock, Arkansas 72205, United States
Eldo E Frezza, Department of Surgery, Texas Tech University Health Sciences Center and Southwest Cancer Treatment and Research Center, Lubbock, TX 79430, United States
Correspondence to: Maurizio Chiriva-Internati, PhD, Department of Microbiology and Immunology, Texas Tech University Health Sciences Center, Room 5B191, Lubbock, TX 79430-6591, United States. maurizio.chirivainternati@ttushc.edu
Telephone: +1-806-743-4057 Fax: +1-806-743-2334
Received: 2005-01-22 Accepted: 2005-02-18

Abstract

Although multiple options for the treatment of liver tumors have often been described in the past, including liver resection, radiofrequency ablation with or without hepatic pump insertion, laparoscopic liver resection and the use of chemotherapy, the potential of immunotherapy and gene manipulation is still largely unexplored. Immunological therapy by gene manipulation is based on the interaction between virus-based gene delivery systems and dendritic cells. Using viruses as vectors, it is possible to transduce dendritic cells with genes encoding tumor-associated antigens, thus inducing strong humoral and cellular immunity against the antigens themselves. Both chemotherapy and radiation therapy have the disadvantage of destroying healthy cells, thus causing severe side-effects. We need more precisely targeted therapies capable of killing cancer cells while sparing healthy cells. Our goal is to establish a new treatment for solid liver tumors based on the concept of cytoreduction, and propose an innovative algorithm.

Key words: Liver; Tumors; Surgery; Dendritic cell; Cytoreduction; Immunotherapy; Gene manipulation

Chiriva-Internati M, Grizzi F, Jumper CA, Cobos E, Hermonat PL, Frezza EE. Immunological treatment of liver tumors. *World J Gastroenterol* 2005; 11(42): 6571-6576
http://www.wjgnet.com/1007-9327/11/6571.asp

HEPATIC TUMORS

Although relatively uncommon in Western countries, hepatocellular carcinoma (HCC) is probably the most common solid cancer in the world, with an estimated incidence of at least one million new patients per year[1,2]. The optimal treatment for HCC is surgical excision with a curative intent, but only 5-15% of newly diagnosed patients undergo potentially curative resection[3]. Patients with disease confined to the liver may not be candidates for resection because of multifocal disease, or an inadequate hepatic functional reserve capacity related to co-existent cirrhosis may contraindicate resection. As there are few other curative treatment options for patients with unresectable liver disease, HCC is one of the most lethal human malignancies, with a mortality rate of 94%[4].

The liver is second only to lymph nodes as a site of metastases from other solid cancers[5], and may be the only site of metastatic disease particularly in patients with colorectal adenocarcinoma[6]. However, fewer than 10-15% of patients with liver metastases are candidates for resection for the same reasons as those regarding HCC. The majority of patients with primary or metastatic hepatic malignancies who are not candidates for complete surgical resection therefore require novel treatment modalities to control and potentially cure their disease[2,7].

Cirrhosis may be another variable that places such patients at the highest risk[2]. Patients in class C of the Child-Pugh Classification (Table 1) have the highest mortality and morbidity rate following all treatments, particularly surgical procedures[8,9], and so most centers have shifted away from open liver surgery and are attempting other approaches. The treatment of hepatic tumors in cirrhotic and non-cirrhotic patients is a major decision-making issue for oncologists and surgeons, and the high mortality rate of open liver surgery in cirrhotic patients has spurred physicians to seek new modalities[10].

We here outline the immunological and genetic techniques available for the treatment of liver tumors, and propose a new immunologico-clinical algorithm using immunological therapy to debulk the mass, kill micrometastases, and allow a lower dose of chemotherapy to achieve better cytoreduction.

Table 1 Child-Pugh classification

	A	B	C
Ascites	None	Controlled	Uncontrolled
Bilirubin (mmol/L)	<2.0	2.0-2.5	>3.0
Encephalopathy	None	Minimal	Advanced
PT (s prolonged)	<4.0	4.0-6.0	>6.0
INR	<2.0	2.0-3.0	>3
Albumin (g/L)	>3.5	3.0-3.5	<3.0

WHAT IS THE ROLE OF SURGERY?

Open surgery

Complete surgical resection of primary or secondary liver tumors is the gold standard of surgical therapy[2,8,9], but it has fallen out of favor because of complications related to bleeding and liver failure. Furthermore, the time of the associated hospitalization is not cost-effective in the context of the new health plan insurance capitation systems.

Underlying anatomical and physiological limitations may exclude the use of complete surgical resection but, when complete or partial resection is plausible, the approach of choice is either the traditional open technique (wedge resection, segmentectomy or major lobectomy) or the laparoscopic technique. Laparoscopic liver surgery has become feasible with the improvement in laparoscopic techniques and the development of new and dedicated technologies[9]. There are benefits common to all endoscopic procedures, and the choice of the approach to hepatic resection is usually made by both the surgeon and the patient.

Laparoscopic surgery

The laparoscopic method is useful in oncological therapy, as it allows abdominal exploration and the visualization of the tumor itself. Specimen collection is another key benefit, and can range from a lymph node biopsy in the peritoneum or retro-peritoneum, to scraping the peritoneum in the abdominal wall. Laparoscopy allows direct visualization of the organs and biopsy. The liver is a large organ, and can therefore be visualized quite well, particularly the anterior section, although it is laparoscopically more difficult to visualize the posterior section of the retroperitoneal area of the right lobe. Anatomically, the left side of the liver is not hard to mobilize by dissecting the left triangular ligament and flipping the left side of the liver over the midline, but it is more complicated to achieve the same result on the right side where segments VI and VII (the lateral segments) and segment VIII are harder to visualize posteriorly, and so intraoperative ultrasound has been introduced to improve the visualization of tumors in these segments[9].

Radiofrequency ablation

This is a thermal technique designed to cause localized tumor destruction by heating the tumoral tissue to temperatures of more than 50 °C. The methodology has been previously described by our group[8,11], and has been found to be safe and effective in the treatment of single tumors of <5 cm with curative intent, or the cytoreduction of multiple or larger tumors.

Percutaneous ethanol injection (PEI)

This is usually performed under transabdominal ultrasonographic guidance, and consists of intra-tumorally injecting 5-10 mL of ethanol twice a week. Patient compliance has been a problem because of the number of injections required and the associated pain. As PEI requires multiple treatment sessions and is associated with a high local recurrence rate, it should only be considered in the case of tumors with a diameter of less than 1.5 cm.

Cryosurgery

This has been used to treat patients with unresectable primary and metastatic liver tumors for the last 20 years. Most of the scientific data concerning local tumor recurrences and complications after cryosurgery comes from patients treated for colorectal cancer liver metastases[8].

CLINICAL ALGORITHM FOR SOLID LIVER TUMORS

The pros and cons of liver surgery and the new clinical algorithm used for the treatment of liver tumors will be briefly discussed[8], considering only the patients with Child –Pugh class A or B cirrhosis, because those with advanced liver cirrhosis (Child–Pugh class C) would probably receive no survival benefit and would be at a disproportionately increased risk of interventional therapy. The patients in the two groups will belong to one of the following four categories: (1) Those with stage I, primary liver tumors will be evaluated for liver resection or radiofrequency ablation (RFA); (2) Those with stage II and III primary liver tumors will undergo complete resection, if anatomically possible, or partial resection with RFA, or RFA alone; the patients with vascular invasion will also receive a hepatic arterial pump (HAP); (3) The patients with stage IV primary liver tumors or liver metastases of other than colorectal origin (endocrine, breast) will only be treated with RFA and a HAP; (4) The patients with colorectal metastases will undergo complete resection if possible, or partial resection with RFA, or RFA alone, and all will receive a HAP.

After a median follow-up of 20 mo in patients with unresectable liver disease, the addition of adjuvant HAP therapy to cryoreduction decreased all recurrences from 77% to 49% and decreased liver recurrences from 67% to 38%. This, and other multi-approaches (RFA and HAP therapy) to the treatment of partially resectable or unresectable liver disease, is promising and deserves further investigation.

IMMUNOTHERAPY AND NEOPLASTIC LIVER DISEASE

Most cancer patients are currently treated with some combination of surgery, radiation therapy and

chemotherapy, but both chemo- and radiation-therapy have the disadvantage of destroying healthy cells and this causes severe side effects. The possibility of destroying more cancer cells by increasing the chemotherapeutic dose or radiation exposure is limited by the non-specific organ toxicity of these therapies and the relatively old age of most patients. We therefore need more precisely targeted therapies capable of killing cancer cells while sparing healthy cells.

One possible answer is immunological therapy, which is not only more specific and less toxic, but may also induce memory responses that could yield long-term tumor immunosurveillance and reduce the incidence of relapses, thus increasing long-term disease-free survival. Immunological therapy may be adoptive[10,12] in which case the patients' white blood cells are coupled with a naturally producing growth factor to enhance their cancer fighting capacity, or passive[13], with immunity being acquired as a result of the transfer of antibodies from a healthy donor. However, the possibility of successfully implementing these therapies rests on the existence of tumor-specific antigens, and suitable antigens have been hard to come by because of the complex process required to validate them[14–18].

Immunotherapy refers to any approach aimed at mobilizing or manipulating a patient's immune system to treat or cure disease[19], and immunological therapy by means of gene manipulation is based on the interaction between virus-based gene delivery systems and dendritic cells (DCs). Using viruses as vectors, it is possible to transduce DCs with genes encoding tumor-associated antigens (TAA), thus inducing a robust immune response[20,21].

A number of studies have established the role played by DCs in the immune system, and provided a rationale for using them as natural adjuvants for cancer immunotherapy[20-22]. Previous studies have concentrated on identifying the proliferating progenitors of DCs within the small CD34+ sub-fraction of cells in human blood[23]. These cells can be stimulated by cytokines (particularly by GM-CSF and TNF-alpha) to differentiate into DCs *in vitro* over a period of 1 wk[24]. It has also been more recently found that the combination of GM-CSF and IL-4 facilitates the generation of significantly larger numbers of DCs from monocytes/macrophages, which have equal or greater stimulatory activity in mixed lymphocyte reactions, and a greater capacity to present soluble protein antigens than CD34+ cell-derived DCs[23,24].

Gene manipulation

Gene manipulation transmits new genes/DNA into target cells infected with the viral vector, and has been most widely used to treat genetic diseases. The vector unloads its genetic material containing the therapeutic human gene into the target cell, which is finally restored to its normal state as a result of the generation of a functional protein encoded by the therapeutic gene[24,25]. The technique can be used in cancer to activate self and non-self antigens and enhance T cell responses. Some of the different types of viruses used as gene therapy vectors are listed in Table 2.

There are also various non-viral options for gene delivery. The simplest method is to introduce therapeutic DNA directly into target cells, but its application is limited by the fact that it can only be used with certain tissues and requires large amounts of DNA. Another non-viral approach involves creating a liposome (an artificial lipid sphere with an aqueous core), which is capable of shuttling the therapeutic DNA through the target cell's membrane, and a further delivery system is based on electroporation[25-28].

Problems in applying gene therapy

Whenever a foreign body (antigen, bacteria, *etc.*) enters the human tissue, the immune system is prompted to attack the invader, and so there is a risk of stimulating an immune response and reducing the effectiveness of gene manipulation. Furthermore, the immune system's enhanced response to previously encountered invaders makes it difficult for gene therapy to be repeated.

Viruses are the carriers of choice in most gene therapy studies, but they can give rise to a number of potential problems relating to toxicity, immune and inflammatory responses, gene control, and targeting. The main concern is that, once inside the patients, the viral vector may somehow recover its ability to cause disease, which is why we decided to use virus vectors with little or no replicative capacity, such as adeno-associated viruses (AAV)[29-31].

Viral delivery of antigen genes into dendritic cells

There are various ways of inserting antigen genes and proteins into DCs via protein pulses or viral vector loading[27-32]. Recombinant retroviruses, adenoviruses, and poxviruses can all efficiently transduce DCs[29-31],

Table 2 Commonest viruses used as gene therapy vectors

Retroviruses	Adenoviruses	Adeno-associated virus (AAV)	Herpes virus
8kb, RNA enveloped	35 kb, DNA, non-enveloped	5 kb, single stranded DNA, non-enveloped	61 kb, double-stranded DNA
Activate proto-oncogene by insertional mutagenesis	Episomal, transient	Stable integration, high infectivity	Infect mainly neurons
Cause lymphoma	Highly immunogenic, causing inflammation and anaphylactic shock	Non-pathogenic; requires helper viruses such as Adenoviruses for replication and packaging in mammalian cells.	Cause cold sores or blisters in the genital areas
Inactivation of transgene *in vivo*	One case of death	Long-term expression *in vivo*	Cutaneous skin lesions

but they all have well-known and serious disadvantages. Retroviruses can integrate chromosomally, but any residual contaminating wild-type virus can lead to significant disease and malignancy in the host. Furthermore, as they can also integrate gonadally and alter the germ line, their use may be restricted by the FDA[30,31].

Adenoviruses carry many genes in addition to the transgene, and the viral particle contains several proteins; the delivered antigen gene would therefore be only one of the many genes/proteins and epitopes to which a CTL response would be generated.

Unlike these viruses, AAVs are non-pathogenic, and various studies have shown that they are effective gene delivery vectors for both immortalized tissue culture cells and primary hematopoietic cells[33-36]. The helper-dependent parvovirus AAV can latently infect cells via stable chromosomal integration. Early studies demonstrated that 15-30% of immortalized cells could be latently infected with wild-type AAV, and the AAV genome was chromosomally integrated[21]. After the mapping of AAV genes and their functions[32-34], recombinant AAV virus vectors proved to have a similar capacity in immortalized tissue culture cells[33,34], and the recombinant AAV transduction of primary hematopoietic stem cells was achieved in 1988[35].

We have demonstrated that AAVs can be highly efficiently (>90%) used to transduce antigen genes into primary human monocytes (Mo) and Mo-derived DCs[36,37]. Unlike cells transduced using adenoviruses, retroviruses and other pathogenic viruses, AAV-transduced cells are not usually significant targets of the host immune system[37]. The use of the rAAV-based DC loading of human papillomavirus type 16, E6, and E7 antigen genes leads to robust and rapid antigen-specific, MHC class I-restricted CTL responses with one stimulation (one DC addition) and a 7-10 d co-incubation period[37,38]. Our data therefore strongly suggest that AAVs may be effective vectors for manipulating DCs[20,36,39].

DISCUSSION

Experimental algorithm for solid liver tumors

The key to the new evolution toward immunotherapy is to set up an algorithm for patients who will not respond to surgery. As shown in Figure 1, the liver tumor of selected patients is staged and the patients are directed to follow the clinical[8] or immunological algorithm. The experimental option is designed by taking specimens, with the tumor being preferably harvested laparoscopically or by means of the open technique. The next step is to insert modified antigens with carriers into the neoplastic cells. At this point, the choice is whether to inject them with DCs after leukopheresis, or by means of a virus (AAV). Both injections can be performed laparoscopically, thus allowing minimally invasive surgery, the introduction of the antigen inside the area of the tumor, and the initiation of a cell-mediated reaction designed to ensure immunological cytoreduction or debulking. An ultrasound-guided needle is placed into the abdomen, and a biopsy of the tumor can be taken.

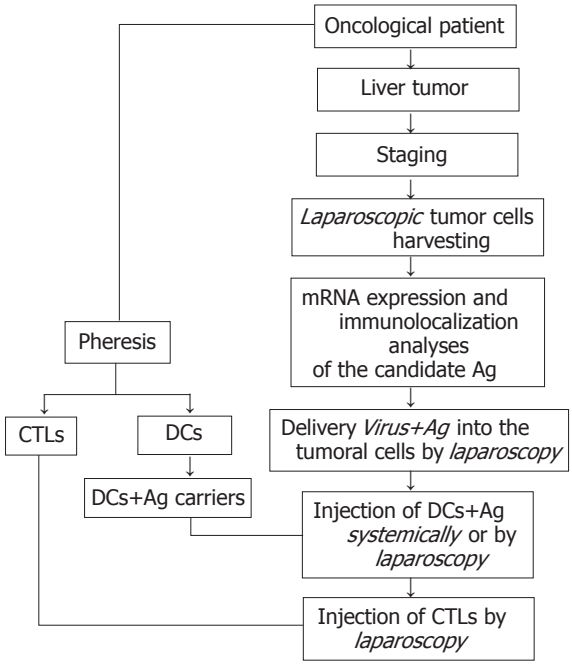

Figure 1 Relationships between laparoscopic surgery and immunotherapy for treatment of primary and secondary liver tumors. CTLs: cytotoxic T lymphocytes; DCs: dendritic cells; Ag: antigen.

As laparoscopy is a widely used surgical technique, most surgeons can easily adopt the procedure of injecting antigens, CTLs and DCs directly into the primary or secondary tumor in order to increase tumor immunogenicity and kill the remaining tumor cells by means of a local injection of CTLs and DCs for better cytoreduction. A port should be placed inside the internal jugular or subclavian artery in order to allow the retrieval of blood for leukopheresis; this port can be accessed quite easily using an external needle.

Improving cytoreduction: our new approach

The most widely used treatment is tumor resection, and so the main role of surgeons and oncologists is to decrease tumor bulk or mass in order to improve survival or allow the possibility of chemotherapy. Some liver tumors are so large that they are either inoperable or require such extensive surgery as to increase the incidence of death, but the introduction of cryoablation, alcohol injection, and radiofrequency ablation means that surgeons can reduce the amount of tumor in the liver, thus allowing chemotherapy to work on fewer tumor cells. The theory is that shrinking the tumor should lead to better chemotherapeutic results. Chemotherapy usually not only kills the tumoral cells remaining after radiofrequency, but also eliminates the satellite cells present in the liver or liver vessels together with good and normally replicating cells. We strongly believe that immunological therapy could become the new standard treatment for liver tumors. It not only debulks the tumor mass while destroying the tumor by means of a cell-mediated response, but its cell-

specific nature should enable it to kill satellite lesions and micro-metastases more efficiently (thus leading to better cytoreduction) without killing normal cells, and allow the use of low-dose chemotherapy to avoid or reduce undesirable side effects. Furthermore, the possible activation of memory responses could lead to much-needed long-term tumor immunosurveillance, which should reduce the incidence of relapses.

CONCLUSIONS

Evidence of practical immunotherapy treatment

Our initial clinical results suggest that there is an urgent need to explore further therapeutic options for liver tumors. This study introduces several innovations and a methodology that will help establish critical clinical assays for assessing immune responses targeting liver tissue, and verify the relationship between host response and liver tumor regression/progression.

Relevance to liver cancer research

We believe that immunological therapy can improve our overall understanding of how the host immune system interacts with primary and secondary liver cancer tissue, and will further elucidate useful methods for assessing this potential interaction.

Relevance to tumor immunology/immunotherapy

The importance of breaking host tolerance in order to achieve a tissue-specific mediated response and facilitate a favorable response to antitumor immunotherapy has recently been stressed in the literature[40]. For this reason, we believe that the use of a mini-invasive surgical approach, the immunotherapy and a clinical treatment will have a significant impact on liver tumors.

Costs and applications

Immunological therapy seems a very promising treatment for liver tumors. However, its specificity and cost makes it indicated for patients with tumors that cannot be resected by any of the different ablation methods, and small tumors in cirrhotic patients who are unsuitable candidates for standard surgery.

Improved cytoreduction

We believe that immunological therapy could become a new standard treatment of liver tumor for mainly three reasons: (1) it can debulk the tumor mass, while destroying the tumor by means of a cellular response; (2) it should be able to control the satellite lesions and micro-metastases more efficiently because of its more cell-specific nature, thus improving cytoreduction, avoiding the killing of normal cells, and reducing the use of chemotherapy and therefore its side effects; and (3) the possible activation of memory responses could lead to much-needed long-term tumor immunosurveillance, and thus reduce the incidence of relapses.

REFERENCES

1 **Di Bisceglie AM,** Rustgi VK, Hoofnagle JH, Dusheiko GM, Lotze MT. NIH conference. Hepatocellular carcinoma. *Ann Intern Med* 1988; **108:** 390-401
2 **Carr BI.** Hepatocellular carcinoma: current management and future trends. *Gastroenterology* 2004; **127:** S218-S224
3 **Tsuzuki T,** Sugioka A, Ueda M, Iida S, Kanai T, Yoshii H, Nakayasu K. Hepatic resection for hepatocellular carcinoma. *Surgery* 1990; **107:** 511-520
4 **Di Bisceglie AM.** Hepatocellular carcinoma: molecular biology of its growth and relationship to hepatitis B virus infection. *Med Clin North Am* 1989; **73:** 985-997
5 **Liu LX,** Zhang WH, Jiang HC. Current treatment for liver metastases from colorectal cancer. *World J Gastroenterol* 2003; **9:** 193-200
6 **Arya SC,** Ashraf SJ, Parande CM, Tobeiqi MS, Ageel AR. Hepatitis B and delta markers in primary hepatocellular carcinoma patients in the Gizan area of Saudi Arabia. *APMIS* Suppl 1988; **3:** 30-34
7 **Curley SA,** Izzo F, Delrio P, Ellis LM, Granchi J, Vallone P, Fiore F, Pignata S, Daniele B, Cremona F. Radiofrequency ablation of unresectable primary and metastatic hepatic malignancies: results in 123 patients. *Ann Surg* 1999; **230:** 1-8
8 **Frezza EE.** Therapeutic management algorithm in cirrhotic and noncirrhotic patients in primary or secondary liver masses. *Dig Dis Sci* 2004; **49:** 876-871
9 **Frezza EE.** Extensive liver resection: can it be applicable to laparoscopic surgery? *J Laparoendosc Adv Surg Tech A* 2001; **11:** 141-145
10 **Sun HC,** Tang ZY. Preventive treatments for recurrence after curative resection of hepatocellular carcinoma--a literature review of randomized control trials. *World J Gastroenterol* 2003; **9:** 635-640
11 **Frezza EE.** Laparoscopic radiofrequency ablation of solitary hepatic gastrinoma metastases. *Dig Dis Sci* 2004; **49:** 224-227
12 **Butterfield LH.** Immunotherapeutic strategies for hepatocellular carcinoma. *Gastroenterology* 2004; **127:** S232-S241
13 **Haigwood NL,** Montefiori DC, Sutton WF, McClure J, Watson AJ, Voss G, Hirsch VM, Richardson BA, Letvin NL, Hu SL, Johnson PR. Passive immunotherapy in simian immunodeficiency virus-infected macaques accelerates the development of neutralizing antibodies. *J Virol* 2004; **78:** 5983-5995
14 **Zhao L,** Mou DC, Leng XS, Peng JR, Wang WX, Huang L, Li S, Zhu JY. Expression of cancer-testis antigens in hepatocellular carcinoma. *World J Gastroenterol* 2004; **10:** 2034-2038
15 **Chiriva-Internati M,** Wang Z, Salati E, Bumm K, Barlogie B, Lim SH. Sperm protein 17 (Sp17) is a suitable target for immunotherapy of multiple myeloma. *Blood* 2002; **100:** 961-965
16 **Chiriva-Internati M,** Wang Z, Salati E, Timmins P, Lim SH. Tumor vaccine for ovarian carcinoma targeting sperm protein. *Cancer* 2002; **94:** 2447-2453
17 **Kast WM,** Levitsky H, Marincola FM. Synopsis of the 6th Walker's Cay Colloquium on Cancer Vaccines and Immunotherapy. *J Transl Med* 2004; **2:** 20
18 **Chiriva-Internati M,** Grizzi F, Bright RK, Martin Kast W. Cancer immunotherapy: avoiding the road to perdition. *J Transl Med* 2004; **2:** 26
19 **Steinman RM,** Mellman I. Immunotherapy: bewitched, bothered, and bewildered no more. *Science* 2004; **305:** 197-200
20 **Chiriva-Internati M,** Liu Y, Salati E, Zhou W, Wang Z, Grizzi F, Roman JJ, Lim SH, Hermonat PL. Efficient generation of cytotoxic T lymphocytes against cervical cancer cells by adeno-associated virus/human papillomavirus type 16 E7 antigen gene transduction into dendritic cells. *Eur J Immunol* 2002; **32:** 30-38
21 **Fisher-Adams G,** Wong KK Jr, Podsakoff G, Forman SJ, Chatterjee S. Integration of adeno-associated virus vectors in CD34+ human hematopoietic progenitor cells after

transduction. *Blood* 1996; **88:** 492-504
22 **Steinman RM.** The dendritic cell system and its role in immunogenicity. *Annu Rev Immunol* 1991; **9:** 271-296
23 **Romani N,** Gruner S, Brang D, Kampgen E, Lenz A, Trockenbacher B, Konwalinka G, Fritsch PO, Steinman RM, Schuler G. Proliferating dendritic cell progenitors in human blood. *J Exp Med* 1994; **180:** 83-93
24 **Sallusto F,** Lanzavecchia A. Efficient presentation of soluble antigen by cultured human dendritic cells is maintained by granulocyte/macrophage colony-stimulating factor plus interleukin 4 and downregulated by tumor necrosis factor alpha. *J Exp Med* 1994; **17:** 1109-1118
25 **Arthur JF,** Butterfield LH, Roth MD, Bui LA, Kiertscher SM, Lau R, Dubinett S, Glaspy J, McBride WH, Economou JS. A comparison of gene transfer methods in human dendritic cells. *Cancer Gene Ther* 1997; **4:** 17-25
26 **Meyer zum Buschenfelde C,** Nicklisch N, Rose-John S, Peschel C, Bernhard H. Generation of tumor-reactive CTL against the tumor-associated antigen HER2 using retrovirally transduced dendritic cells derived from CD34+ hemopoietic progenitor cells. *J Immunol* 2000; **165:** 4133-4140
27 **Szabolcs P,** Gallardo HF, Ciocon DH, Sadelain M, Young JW. Retrovirally transduced human dendritic cells express a normal phenotype and potent T-cell stimulatory capacity. *Blood* 1997; **90:** 2160-2167
28 **Yoshida J,** Mizuno M. Clinical gene therapy for brain tumors. Liposomal delivery of anticancer molecule to glioma. *J Neurooncol* 2003; **65:** 261-267
29 **Grimm D,** Kay MA. From virus evolution to vector revolution: use of naturally occurring serotypes of adeno-associated virus (AAV) as novel vectors for human gene therapy. *Curr Gene Ther* 2003; **3:** 281-304
30 **Ponnazhagan S.** Parvovirus vectors for cancer gene therapy. *Expert Opin Biol Ther* 2004; **4:** 53-64
31 **Shih A,** Coutavas EE, Rush MG. Evolutionary implications of primate endogenous retroviruses. Virology 1991; **182:** 495-502
32 **Daly TM.** Overview of adeno-associated viral vectors. *Methods Mol Biol* 2004; **246:** 157-165
33 **Hermonat PL,** Labow MA, Wright R, Berns KI, Muzyczka N. Genetics of adeno-associated virus: isolation and preliminary characterization of adeno-associated virus type 2 mutants. *J Virol* 1984; **51:** 329-339
34 **Tratschin JD,** Miller IL, Carter BJ. Genetic analysis of adeno-associated virus: properties of deletion mutants constructed in vitro and evidence for an adeno-associated virus replication function. *J Virol* 1984; **51:** 611-619
35 **LaFace D,** Hermonat P, Wakeland E, Peck A. Gene transfer into hematopoietic progenitor cells mediated by an adeno-associated virus vector. *Virology* 1988; **162:** 483-486
36 **Chiriva-Internati M,** Liu Y, Weidanz JA, Grizzi F, You H, Zhou W, Bumm K, Barlogie B, Mehta JL, Hermonat PL. Testing recombinant adeno-associated virus-gene loading of dendritic cells for generating potent cytotoxic T lymphocytes against a prototype self-antigen, multiple myeloma HM1.24. *Blood* 2003; **102:** 3100-3107
37 **Liu Y,** Santin AD, Mane M, Chiriva-Internati M, Parham GP, Ravaggi A, Hermonat PL. Transduction and utility of the granulocyte-macrophage colony-stimulating factor gene into monocytes and dendritic cells by adeno-associated virus. *J Interferon Cytokine Res* 2000; **20:** 21-30
38 **Tillman BW,** Hayes TL, DeGruijl TD, Douglas JT, Curiel DT. Adenoviral vectors targeted to CD40 enhance the efficacy of dendritic cell-based vaccination against human papillomavirus 16-induced tumor cells in a murine model. *Cancer Res* 2000; **60:** 5456-5463
39 **Liu Y,** Chiriva-Internati M, You C, Luo R, You H, Prasad CK, Grizzi F, Cobos E, Klimberg VS, Kay H, Mehta JL, Hermonat PL. Use and specificity of breast cancer antigen/milk protein BA46 for generating anti-self-cytotoxic T lymphocytes by recombinant adeno-associated virus-based gene loading of dendritic cells. *Cancer Gene Ther* 2005; **12:** 304-312
40 **Crittenden MR,** Thanarajasingam U, Vile RG, Gough MJ. Intratumoral immunotherapy: using the tumour against itself. *Immunology* 2005; **114:** 11-22

Science Editor Guo SY **Language Editor** Elsevier HK

PO Box 2345, Beijing 100023, China
www.wjgnet.com
wjg@wjgnet.com

ELSEVIER

World J Gastroenterol 2005;11(42):6577-6581
World Journal of Gastroenterology ISSN 1007-9327

• *REVIEW* •

Management of functional dyspepsia: Unsolved problems and new perspectives

Ahmed Madisch, Stephan Miehlke, Joachim Labenz

Ahmed Madisch, Stephan Miehlke, Medical Department I, Technical University Hospital Dresden, Germany
Joachim Labenz, Medical Department, Ev. Jung-Stilling-Hospital, Academic Teaching Hospital of the University of Bonn, Siegen, Germany
Correspondence to: Ahmed Madisch, MD, Medical Department I, Technical University Hospital, Fetscherstrasse 74, D-01307 Dresden, Germany. ahmed.madisch@uniklinikum-dresden.de
Telephone: +49-351-4584780 Fax: +49-351-4584394
Received: 2004-11-12 Accepted: 2005-02-18

Key words: Dyspepsia; Functional dyspepsia; Definition; Diagnosis; Management; Drug efficacy; Clinical trials; Outcome measurements; Herbal drugs

Madisch A, Miehlke S, Labenz J. Management of functional dyspepsia: Unsolved problems and new perspectives. *World J Gastroenterol* 2005; 11(42): 6577-6581
http://www.wjgnet.com/1007-9327/11/6577.asp

Abstract

The common characteristic criteria of all functional gastrointestinal (GI) disorders are the persistence and recurrence of variable gastrointestinal symptoms that cannot be explained by any structural or biochemical abnormalities. Functional dyspepsia (FD) represents one of the important GI disorders in Western countries because of its remarkably high prevalence in general population and its impact on quality of life. Due to its dependence on both subjective determinants and diverse country-specific circumstances, the definition and management strategies of FD are still variably stated. Clinical trials with several drug classes (e.g., proton pump inhibitors, H2-blockers, prokinetic drugs) have been performed frequently without validated disease-specific test instruments for the outcome measurements. Therefore, the interpretation of such trials remains difficult and controversial with respect to comparability and evaluation of drug efficacy, and definite conclusions can be drawn neither for diagnostic management nor for efficacious drug therapy so far. In view of these unsolved problems, guidelines both on the clinical management of FD and on the performance of clinical trials are needed. In recent years, increasing research work has been done in this area. Clinical trials conducted in adequately diagnosed patients that provided validated outcome measurements may result in better insights leading to more effective treatment strategies. Encouraging perspectives have been recently performed by methodologically well-designed treatment studies with herbal drug preparations. Herbal drugs, given their proven efficacy in clinical trials, offer a safe therapeutic alternative in the treatment of FD which is often favored by both patients and physicians. A fixed combination of peppermint oil and caraway oil in patients suffering from FD could be proven effective by well-designed clinical trials.

INTRODUCTION

Symptoms of upper gastrointestinal distress are of world-wide interest and very common in the general population. In developing countries the important form of dyspepsia is organic dyspepsia, whereas the problem of functional dyspepsia (FD) seems to be mainly confined to industrialized Western countries though convincing data for underdeveloped countries are still lacking[1]. It is estimated that the annual prevalence of recurrent upper abdominal discomfort in the United States and other Western countries is approximately 25%, about 2% to 5% of all primary care consultations are related to dyspeptic symptoms[2]. For many patients the symptoms are of short duration or mild severity[3] and are therefore self-manageable. Less than half of these patients consult their general practitioner[2]. Moreover, patients with upper gastrointestinal problems frequently suffer from recurrent affections. However, several long-term studies showed that high percentages of patients with dyspeptic symptoms at entry report similar symptoms of dyspepsia after some years[3,4]. Repetitive diagnostic measures and medical treatments with low success rates lead to high costs and frustrating results. Thus, FD represents not only a clinical challenge but also a major socio-economical problem. In recent years, a lot of efforts have been made by national and international consensus meetings to work out precise definitions as well as adequate management strategies for dyspepsia. Still unsolved problems and new perspectives for both research work and disease management in clinical practice are summarized and discussed in more detail in this review.

Definition of functional dyspepsia

Several definitions of dyspepsia have been proposed in the past decades[5] demonstrating the difficulties in categorizing

dyspepsia as a clearly pathologically defined entity based on the variability of symptoms. According to the proposition of an international committee meeting in Rome in 1991, the term "dyspepsia" refers to pain or discomfort centered in the upper abdomen[6] while discomfort refers to a subjective negative (or aversive) feeling that is distinct from pain. Discomfort may include several specific bothersome but non-painful symptoms, such as early satiety, fullness, bloating and nausea (the so-called Rome criteria). In Rome I and more recent Rome II reports[1,7-9], the symptoms of heartburn, acid regurgitation, and belching are excluded from the definition of dyspepsia because they are more likely related to gastroesophageal reflux disease (GERD) and aerophagia[1,9]. It is important to distinguish subjects with uninvestigated dyspepsia from patients with dyspepsia after adequate diagnostic procedure. Patients who have neither definite structural or biochemical explanation for their symptoms are considered to have FD. Thus, FD is defined as a persistent or recurrent dyspepsia for at least 12 wk in the preceding 12 mo if there is no evidence for organic disease (including upper endoscopy) that could cause the symptoms. The Rome II definitions of FD also exclude patients who report a relief of symptoms by defecation or symptoms associated with the onset of a change in stool frequency or stool form[9]. In the latter case, irritable bowel syndrome (IBS) is the diagnosis by definition. Coexistence of FD and IBS can be considered if there is pain or discomfort in the upper abdomen that is unrelated to bowel pattern and if there is other pain or discomfort that is related to bowel pattern[7].

Management of dyspepsia

Due to geographical, cultural, educational, social, and psychological aspects, universally applicable guidelines on diagnostic and therapeutical measures are difficult to implement[1,10]. Management strategies should be individualized and developed for each major community taking into account the prevalence of risk factors for gut diseases such as prevalence of *H pylori* infection, use of non-steroidal anti-inflammatory drugs, dietary habits, tobacco smoking and alcohol consumption[1,10]. Beyond these patient-related factors, the available financial and technical resources in each particular country may dictate the individual steps in the management of dyspepsia[1].

Nevertheless, useful recommendations regarding the management of dyspepsia are concluded in a recent systematic review of the literature[11]. To date, five management strategies can be offered to the physicians treating dyspeptic patients: (1) wait and see-strategy without diagnostic and therapeutic interventions; (2) empiric medical therapy with any subsequent investigation reserved for treatment failures; (3) immediate diagnostic evaluation in all cases; (4) testing for *H pylori* infection and reserving endoscopy for *H pylori*-positive cases to look for organic diseases (test-and-scope strategy); and (5) testing for *H pylori* infection by serology or urea breath test and treating all positive cases with *H pylori* eradication therapy (test-and-treat strategy).

For adult patients in Western countries with new onset of dyspepsia, endoscopy is the gold standard approach providing a firm diagnosis and facilitating decisions on treating or excluding organic diseases. In elderly patients or in those with alarm symptoms such as weight loss, immediate endoscopy is strongly advised. In respect of cost-effectiveness, a repeated endoscopy in those with an initially negative result should be avoided. An alternative management strategy in young dyspeptic patients under 45 years is non-invasive testing for *H pylori* infection and antibacterial treatment of positive cases[10-12]. Because of many substantial disadvantages such as antibiotic resistance, overtreatment, or undertreatment, there is ongoing discussion about the benefit of this strategy.

Management of functional dyspepsia

Patients with FD typically present an array of painful and non-painful symptoms demonstrating the multifactorial nature of this syndrome[13,14]. In order to identify pathophysiological abnormalities with subsequent targeted treatment and to promote more homogeneity, patients can be subdivided into ulcer-like, dysmotility-like and unspecified dyspepsia subgroups based on the concept of a cluster of symptoms[13,15]. Several studies have shown that this arbitrary classification seems to be unsustainable because of the considerable overlap of the subgroups, the lack of stability over time, and the inconsistent responses to therapy[13,16]. Currently, the existence of subgroups among dyspeptic patients is neither endorsed nor categorically disproved[7,8,13].

Another approach to a subdivision of patients with FD is the sus pected association with *H pylori* infection. Between 30% and 60% of patients suffering from FD have *H pylori*-induced gastritis. However, *H pylori* infection is also common in the asymptomatic background population[17,18]. Even most recent trials with prolonged follow-up, analyzing the association between *H pylori* status and specific symptom profiles in FD have produced inconsistent and conflicting results. To date, there is no convincing evidence for the relief of specific dyspeptic symptoms after an eradication therapy[5,13,19,20]. Thus, a benefit of anti- *H pylori* therapy in FD is not established [5,11,19].

Drug therapy for functional dyspepsia

The wide range of therapies reflects the uncertainty about the pathogenesis and the lack of satisfactory treatment. The pathophysiology of FD remains inadequately understood, even though various mechanisms may play a role in the development of symptoms. As yet, there is no cure for this disorder and available treatments are aimed at the relief of symptoms. Even though the efficacy of some currently established treatments (e.g., antisecretory agents or prokinetics) has been proven in placebo-controlled trials, these treatments yield sufficient relief of symptoms only in a proportion of patients[5].

In ulcer-like (pain predominating) functional dyspepsia, H_2-receptor antagonists have produced inconsistent response rates[21]. Patients with dysmotility-like symptoms

(upper abdominal discomfort predominating) may benefit from prokinetic drug treatment[22-24]. Proton pump inhibitors appear to be efficacious especially in patients with ulcer-like pain and accompanying reflux symptoms. The majority of controlled clinical trials have shown only minor advantages of these drugs compared to placebo[25,26].

Thus, efforts should be made to identify and develop new effective treatments. Various herbal medications are used in many countries for the treatment of patients with FD. While some clinicians believe that clinical experience appears to support the use of these remedies, randomized controlled studies supporting the efficacy of these treatments have been lacking in the past decades. Recently, several well-designed placebo-controlled clinical trials have provided evidence for the efficacy of herbal preparations used in the treatment of dyspepsia[27]. Particularly, patients with dysmotility-like dyspeptic symptoms, such as postprandial sensations of fullness, premature feelings of repleteness, non-acid eructation, or epigastric pain, experience a notable amelioration of their complaints[28,29].

Problems with evaluating drug efficacy in functional dyspepsia

Clinical trials in functional GI disorders remain a challenge due to a variable placebo response ranging 20-60%[30], marked spontaneous fluctuations of symptoms and a lack of widely accepted primary response variables. In addition, patients recruited at tertiary referral centers may represent a highly selected population that is less likely to respond to therapy[31]. It is likely that patients with FD present to general practitioners when their symptoms are worse. Therefore, spontaneous improvement may partially explain at least part of the placebo response[18].

Beside these well-known problems, the differences in the design of clinical drug trials in FD call for caution when interpreting their results. A systematic analysis of more than fifty eligible published placebo-controlled clinical trials testing prokinetics[32-35], cytoprotectives[36,37] or anti-ulcer agents[38-40] and other drugs[36,37] used in the treatment of functional dyspepsia revealed that single substantial items for the consistency of clinical studies such as inclusion and exclusion criteria for trial design and outcome measures are common but differ quite definitively in specific determinations[41]. Particularly, it is of importance how investigators deal with symptomatic GERD and other organic diseases. In 50% of the analyzed studies other upper GI disorders such as esophagitis and duodenal or gastric ulcer were not excluded; only 27% of the trials exclude or account for patients with overt irritable bowel syndrome as an overlapping functional disorder. The study design varies from parallel group, cross-over to multiple cross-over design[41]. The majority of analyzed trials fail to fulfill the indispensable requirement for efficacy evaluation and comparability of drug classes, i.e. use of clearly defined patient groups according to the consensual definition of FD and the use of validated outcome measures regarding described symptoms, their severity, and quality of life yielded with validated categorical and visual analog scales (VAS). Thus, the authors concluded that convincing conclusions for efficacious drug therapy in the treatment of FD cannot be drawn.

Promising outcome measures for clinical trials

Although some research work has been done to develop validated outcome measures of symptoms[42] which can be used in FD, no generally accepted scales are available. Categorical scales (often referred to as Likert Scales) and VAS (horizontal line, usually 10 cm with endpoints on which the patient must place a mark) have been extensively applied[29,39,43-45] and qualified as most eligible measurement scales by their reproducibility and ability to detect changes in a wide variety of clinical trials of different diseases. The usefulness of a reasonable combination of a categorical scale and a VAS is demonstrated by the dyspeptic discomfort score (DDS) which records the existence, frequency and severity of the symptoms of functional dyspepsia[28,29]. Integrating the dyspeptic, intestinal and extraintestinal autonomic discomforts assessed by means of numerical scales, the DDS seems to consider the entire complexity of this syndrome. Nevertheless, the DDS has not been validated yet.

A noteworthy measurement instrument to be mentioned is the clinical global impression (CGI) scale consisting of three items, namely severity of illness, global improvement and efficacy index. The first and second items are rated on a point scale while the third is a rating of the interaction of therapeutic effectiveness and adverse reactions. Originally conceived for schizophrenic studies, the CGI scale facilitates prognosis, survey and assessment of drug efficacy during the treatment period[28,29,44].

During the last years, attention has been drawn to the fact that in diseases without obvious biological or clinical markers such as functional dyspepsia, the use of quality of life instruments and psychometric documentation as an outcome measure can reflect treatment efficacy evaluated by its impact on symptoms as well as on patient well-being and functioning[41,46]. The underlying philosophy is that quality of life is affected by the severity of disease-specific symptoms. Hence, the reciprocal conclusion can be drawn by any change of symptom severity. Recently, validation data of the new disease-specific Nepean dyspepsia index (NDI)[46,47] and the quality of life in reflux and dyspepsia patient (QOLRAD) questionnaire[48] measuring frequency, intensity, and bothersomeness of upper gastrointestinal symptoms have been presented. The remarkable feature of the NDI is the consideration not only of a subject's ability to perform or engage in an aspect of life but also the enjoyment of that aspect of life. In a systematic review of full-length publications during 1980-2002 reporting studies in patients with FD and measuring health-related quality of life, none of the studies used dyspepsia-specific health-related quality of life instruments[49]. However, recently a first methodologically well-designed clinical study proving efficacy of the study drug by use of the NDI was reported by Holtmann and colleagues[50], which demonstrates a

statistically significant and clinically relevant superiority of a fixed combination of peppermint oil and caraway oil (PCC) in comparison to placebo. The reported outcome confirms the results formerly obtained with this herbal preparation in placebo-controlled clinical trials[28,44] and in a double-blind equivalence study with the prokinetic drug cisapride[29], measured by VAS, CGI and the DDS.

Recommendations for future trials

In view of the mentioned weaknesses in present trials, the most essential recommendations are summarized as follows.

According to the consensus for a diagnosis of FD, a minimum set of diagnostic measures including upper endoscopy, an abdominal ultrasound and basic laboratory is obligatory[6]. At the time of enrolment for a treatment study, eligible patients must have persistent symptoms that are of a sufficient degree to seek medical attention. Any definite structural abnormalities of the upper GI tract, explaining the symptoms, e.g., peptic ulcer confirmed by endoscopic evidence and biochemical agents such as daily use of NSAID or high dose aspirin must be excluded. To avoid an overlap with gastroesophageal reflux disease, patients in whom heartburn or acid regurgitation are the predominant symptoms or patients suffering from irritable bowel syndrome and other known organic diseases that might explain the dyspepsia symptoms must not be enrolled.

Despite some well recognized problems such as the occurrence of period-by-treatment interactions of cross-over trials resulting in ambiguous interpretation of data, the randomized, double-blind, placebo-controlled parallel group design is strongly advocated as the trial design of choice.

It is not to deny that even among physicians there is great variation in the definitions of common dyspeptic symptoms. In addition, terminology and possibly also the sensations experienced vary between cultures and countries. Therefore, it is advisable that clinical investigators use definitions of symptoms suggested by the Rome Working Party report and accommodated to common parlance in the respective study population.

As validated outcome measures like the NDI and the QOLRAD questionnaire are now available, their use is strongly recommended regarding described symptoms, their severity, and aspects of quality of life. In order to support the results obtained with these validated disease specific questionnaires, categorical scales, VAS and the CGI could be used as secondary outcome measures. Promising outcome measures such as DDS, should be validated soon in order to broaden the range of appropriate devices for evaluating drug efficacy in functional dyspepsia.

Further research using well-validated outcome instruments for measurement of individual symptoms as well as their severity and their impact on quality of life may perhaps result in a valid symptom-related categorization of functional dyspepsia that may be used to improve treatment strategies.

Causally determined by the aforementioned unsolved problems concerning the definition and management of FD as well as the listed weaknesses in trial methodology of present treatment studies, convincing conclusions for efficacious drug therapy cannot be drawn yet. However, it is very likely that effective drug therapies are av-ailable. Further research on well-validated measurement instruments for outcome data permitting comparability of drug classes may perhaps result in better insights with respect to effective treatment strategies. Quite recently, new perspectives have been arising from presented efficacy of a fixed peppermint oil/caraway oil preparation in a methodologically adequate clinical trial.

ACKNOWLEDGMENT

This paper is dedicated to Professor Jürgen Hotz, a friend, colleague, and academic teacher, who passed away in 2002.

REFERENCES

1 **Malfertheiner P.** Current concepts in dyspepsia: a world perspective. *Eur J Gastroenterol Hepatol* 1999; **11** Suppl 1: S25-S29
2 **Knill-Jones RP.** Geographical differences in the prevalence of dyspepsia. *Scand J Gastroenterol* Suppl 1991; **182:** 17-24
3 **Johannessen T,** Petersen H, Kristensen P, Kleveland PM, Dybdahl J, Sandvik AK, Brenna E, Waldum H. The intensity and variability of symptoms in dyspepsia. *Scand J Prim Health Care* 1993; **11:** 50-55
4 **Jones R,** Lydeard S. Dyspepsia in the community: a follow-up study. *Br J Clin Pract* 1992; **46:** 95-97
5 **Talley NJ.** Helicobacter pylori and dyspepsia. *Yale J Biol Med* 1999; **72:** 145-151
6 **Talley NJ,** Stanghellini V, Heading RC, Koch KL, Malagelada JR, Tytgat GN. Functional gastroduodenal disorders. *Gut* 1999; **45** Suppl 2: II37-II42
7 **Talley NJ,** Stanghellini V, Heading RC, Koch KL, Malagelada JR, Tytgat GN. Functional gastroduodenal disorders. *Gut* 1999; **45** Suppl 2: II37-II42
8 **Thompson WG,** Longstreth GF, Drossman DA, Heaton KW, Irvine EJ, Muller-Lissner SA. Functional bowel disorders and functional abdominal pain. *Gut* 1999; **45** Suppl 2: II43-II47
9 **Spiller R.** Rome II: the functional gastrointestinal disorders. Diagnosis, pathophysiology and treatment: a multinational consensus. *Gut* 2000; **46:** 741B
10 **Mullins PD,** Colin-Jones DG. Guidelines for the management of dyspepsia. *Eur J Gastroenterol Hepatol* 1999; **11:** 215-217
11 **Talley NJ,** Silverstein MD, Agreus L, Nyren O, Sonnenberg A, Holtmann G. AGA technical review: evaluation of dyspepsia. American Gastroenterological Association. *Gastroenterology* 1998; **114:** 582-595
12 **Moayyedi P,** Zilles A, Clough M, Hemingbrough E, Chalmers DM, Axon AT. The effectiveness of screening and treating Helicobacter pylori in the management of dyspepsia. *Eur J Gastroenterol Hepatol* 1999; **11:** 1245-1250
13 **Holtmann G,** Stanghellini V, Talley NJ. Nomenclature of dyspepsia, dyspepsia subgroups and functional dyspepsia: clarifying the concepts. *Baillieres Clin Gastroenterol* 1998; **12:** 417-433
14 **Mansi C,** Mela GS, Pasini D, Grosso M, Corti L, Moretti M, Celle G. Patterns of dyspepsia in patients with no clinical evidence of organic diseases. *Dig Dis Sci* 1990; **35:** 1452-1458
15 **Gotthard R,** Bodemar G, Brodin U, Jonsson KA. Treatment with cimetidine, antacid, or placebo in patients with dyspepsia of unknown origin. *Scand J Gastroenterol* 1988; **23:** 7-18
16 **Talley NJ,** Weaver AL, Tesmer DL, Zinsmeister AR. Lack of

discriminant value of dyspepsia subgroups in patients referred for upper endoscopy. *Gastroenterology* 1993; **105:** 1378-1386
17 **Verdu EF,** Armstrong D, Idstrom JP, Labenz J, Stolte M, Borsch G, Blum AL. Intragastric pH during treatment with omeprazole: role of Helicobacter pylori and H pylori-associated gastritis. *Scand J Gastroenterol* 1996; **31:** 1151-1156
18 **Talley NJ,** Hunt RH. What role does Helicobacter pylori play in nonulcer dyspepsia? Arguments for and against H. pylori being associated with dyspeptic symptoms. *Gastroenterology* 1997; **113**: S67-S77
19 **Talley NJ.** A critique of therapeutic trials in Helicobacter pylori-positive functional dyspepsia. *Gastroenterology* 1994; **106:** 1174-1183
20 **El-Omar EM,** Oien K, El-Nujumi A, Gillen D, Wirz A, Dahill S, Williams C, Ardill JE, McColl KE. Helicobacter pylori infection and chronic gastric acid hyposecretion. *Gastroenterology* 1997; **113:** 15-24
21. **Farup PG,** Wetterhus S, Osnes M, Ulshagen K. Ranitidine effectively relieves symptoms in a subset of patients with functional dyspepsia. *Scand J Gastroenterol* 1997; **32:** 755-759
22 **Holtmann G,** Gschossmann J, Karaus M, Fischer T, Becker B, Mayr P, Gerken G. Randomised double-blind comparison of simethicone with cisapride in functional dyspepsia. *Aliment Pharmacol Ther* 1999; **13:** 1459-1465
23 **Halter F,** Staub P, Hammer B, Guyot J, Miazza BM. Study with two prokinetics in functional dyspepsia and GORD: domperidone vs. cisapride. *J Physiol Pharmacol* 1997; **48:** 185-192
24 **Carvalhinhos A,** Fidalgo P, Freire A, Matos L. Cisapride compared with ranitidine in the treatment of functional dyspepsia. *Eur J Gastroenterol Hepatol* 1995; **7:** 411-417
25 **Hansen JM,** Bytzer P, Schaffalitzky de Muckadell OB. Placebo-controlled trial of cisapride and nizatidine in unselected patients with functional dyspepsia. *Am J Gastroenterol* 1998; **93:** 368-374
26 **Talley NJ,** Meineche-Schmidt V, Pare P, Duckworth M, Raisanen P, Pap A, Kordecki H, Schmid V. Efficacy of omeprazole in functional dyspepsia: double-blind, randomized, placebo-controlled trials (the Bond and Opera studies). *Aliment Pharmacol Ther* 1998; **12:** 1055-1065
27 **Pu RT,** Osmani SA. Mitotic destruction of the cell cycle regulated NIMA protein kinase of Aspergillus nidulans is required for mitotic exit. *EMBO J* 1995; **14:** 995-1003
28 **May B,** Kohler S, Schneider B. Efficacy and tolerability of a fixed combination of peppermint oil and caraway oil in patients suffering from functional dyspepsia. *Aliment Pharmacol Ther* 2000; **14:** 1671-1677
29 **Madisch A,** Heydenreich CJ, Wieland V, Hufnagel R, Hotz J. Treatment of functional dyspepsia with a fixed peppermint oil and caraway oil combination preparation as compared to cisapride. A multicenter, reference-controlled double-blind equivalence study. *Arzneimittelforschung* 1999; **49:** 925-932
30 **Talley NJ,** Phillips SF. Non-ulcer dyspepsia: potential causes and pathophysiology. *Ann Intern Med* 1988; **108:** 865-879
31 **Veldhuyzen van Zanten SJ,** Talley NJ, Bytzer P, Klein KB, Whorwell PJ, Zinsmeister AR. Design of treatment trials for functional gastrointestinal disorders. *Gut* 1999; **45** Suppl 2: II69-II77
32 **Hausken T,** Berstad A. Wide gastric antrum in patients with non-ulcer dyspepsia. Effect of cisapride. *Scand J Gastroenterol* 1992; **27:** 427-432
33 **Hausken T,** Berstad A. Cisapride treatment of patients with non-ulcer dyspepsia and erosive prepyloric changes. A double-blind, placebo-controlled trial. *Scand J Gastroenterol* 1992; **27:** 213-217
34 **Sarin SK,** Sharma P, Chawla YK, Gopinath P, Nundy S. Clinical trial on the effect of domperidone on non-ulcer dyspepsia. *Indian J Med Res* 1986; **83:** 623-628
35 **De Loore I,** Van Ravensteyn H, Ameryckx L. Domperidone drops in the symptomatic treatment of chronic paediatric vomiting and regurgitation. A comparison with metoclopramide. *Postgrad Med J* 1979; **55** Suppl 1: 40-2
36 **Hausken T,** Stene-Larsen G, Lange O, Aronsen O, Nerdrum T, Hegbom F, Schulz T, Berstad A. Misoprostol treatment exacerbates abdominal discomfort in patients with non-ulcer dyspepsia and erosive prepyloric changes. A double-blind, placebo-controlled, multicentre study. *Scand J Gastroenterol* 1990; **25:** 1028-1033
37 **Skoubo-Kristensen E,** Funch-Jensen P, Kruse A, Hanberg-Sorensen F, Amdrup E. Controlled clinical trial with sucralfate in the treatment of macroscopic gastritis. *Scand J Gastroenterol* 1989; **24:** 716-720
38 **Johannessen T,** Kristensen P, Petersen H, Fosstvedt D, Loge I, Kleveland PM, Dybdahl J. The symptomatic effect of 1-day treatment periods with cimetidine in dyspepsia. Combined results from randomized, controlled, single-subject trials. *Scand J Gastroenterol* 1991; **26:** 974-980
39 **Farup PG,** Larsen S, Ulshagen K, Osnes M. Ranitidine for non-ulcer dyspepsia. A clinical study of the symptomatic effect of ranitidine and a classification and characterization of the responders to treatment. *Scand J Gastroenterol* 1991; **26:** 1209-1216
40 **Smith PM,** Troughton AH, Gleeson F, Walters J, McCarthy CF. Pirenzepine in non-ulcer dyspepsia: a double-blind multicentre trial. *J Int Med Res* 1990; **18:** 16-20
41 **Veldhuyzen van Zanten SJ,** Cleary C, Talley NJ, Peterson TC, Nyren O, Bradley LA, Verlinden M, Tytgat GN. Drug treatment of functional dyspepsia: a systematic analysis of trial methodology with recommendations for design of future trials. *Am J Gastroenterol* 1996; **91:** 660-673
42 **Leidy NK,** Farup C, Rentz AM, Ganoczy D, Koch KL. Patient-based assessment in dyspepsia: development and validation of Dyspepsia Symptom Severity Index (DSSI). *Dig Dis Sci* 2000; **45:** 1172-1179
43 **Madisch A,** Melderis H, Mayr G, Sassin I, Hotz J. A plant extract and its modified preparation in functional dyspepsia. Results of a double-blind placebo controlled comparative study. *Z Gastroenterol* 2001; **39:** 511-517
44 **May B,** Kuntz HD, Kieser M, Kohler S. Efficacy of a fixed peppermint oil/caraway oil combination in non-ulcer dyspepsia. *Arzneimittelforschung* 1996; **46:** 1149-1153
45 **Corazza GR,** Biagi F, Albano O, Porro GB, Cheli R, Mazzacca G, Miglio F, Naccarato R, Quaglino D, Surrenti C, Verme G, Gasbarrini G. Levosulpiride in functional dyspepsia: a multicentric, double-blind, controlled trial. *Ital J Gastroenterol* 1996; **28:** 317-323
46 **Talley NJ,** Haque M, Wyeth JW, Stace NH, Tytgat GN, Stanghellini V, Holtmann G, Verlinden M, Jones M. Development of a new dyspepsia impact scale: the Nepean Dyspepsia Index. *Aliment Pharmacol Ther* 1999; **13:** 225-235
47 **Talley NJ,** Verlinden M, Jones M. Validity of a new quality of life scale for functional dyspepsia: a United States multicenter trial of the Nepean Dyspepsia Index. *Am J Gastroenterol* 1999; **94:** 2390-2397
48 **Wiklund IK,** Junghard O, Grace E, Talley NJ, Kamm M, Veldhuyzen van Zanten S, Pare P, Chiba N, Leddin DS, Bigard MA, Colin R, Schoenfeld P. Quality of Life in Reflux and Dyspepsia patients. Psychometric documentation of a new disease-specific questionnaire (QOLRAD). *Eur J Surg Suppl* 1998; **583:** 41-49
49 **El-Serag HB,** Talley NJ. Health-related quality of life in functional dyspepsia. *Aliment Pharmacol Ther* 2003; **18:** 387-393
50 **Holtmann G,** Haag S, Adam B, Funk P, Wieland V, Heydenreich CJ. Effects of a fixed combination of peppermint oil and caraway oil on symptoms and quality of life in patients suffering from functional dyspepsia. *Phytomedicine* 2003; **10** Suppl 4: 56-57

Science Editor Wang XL and Guo SY **Language Editor** Elsevier HK

PO Box 2345, Beijing 100023, China
www.wjgnet.com
wjg@wjgnet.com

ELSEVIER

World J Gastroenterol 2005;11(42):6582-6586
World Journal of Gastroenterology ISSN 1007-9327

Adenovirus expressing p27^{kip1} suppresses growth of established esophageal carcinoma xenografts

Wei-Guo Zhang, Qing-Ming Wu, Jie-Ping Yu, Qiang Tong, Guo-Jian Xie, Xiao-Hu Wang, Sheng-Bao Li

Wei-Guo Zhang, Qing-Ming Wu, Qiang Tong, Guo-Jian Xie, Xiao-Hu Wang, Sheng-Bao Li, Digestive Department, Taihe Hospital, Yunyang Medical College, Shiyan 442000, Hubei Province, China
Jie-Ping Yu, Digestive Department, Renmin Hospital of Wuhan University, Wuhan 430060, Hubei Province, China
Correspondence to: Dr. Qing-Ming Wu, Digestive Department, Taihe Hospital, Yunyang Medical College, 29 Renmin Nanlu, Shiyan 442000, Hubei Province, China. zwg789@sina.com
Telephone: +86-719-8801431
Received: 2004-05-27 Accepted: 2004-06-12

Abstract

AIM: To investigate the growth suppression of adenovirus expressing p27^{kip1} on established esophageal tumors in nude mice.

METHODS: Esophageal carcinoma xenografts in nude mice were established by tumor tissue mass transplantation. The successfully constructed recombinant adenoviral vectors carrying p27^{kip1} gene (Ad-p27^{kip1}) were directly injected into the esophageal tumors in nude mice. Compared to control group, the growth curve of tumor was drawn and the growth inhibition rate of tumor was calculated. The histology of tumors was examined by hematoxylin and eosin (H&E) staining. The expression of p27^{kip1} and survivin was detected in tumors by immunohistochemical technique.

RESULTS: The growth of tumors in gene therapy group with Ad-p27^{kip1} was obviously suppressed compared to control group (0.42±0.08 g *vs* 1.17±0.30 g, t=6.39, P<0.01), the inhibition rate of tumor growth reached 64.1%. Pathological detection showed that the tumors in nude mice were poorly differentiated esophageal squamous carcinoma. In addition, the expression of p27^{kip1} was increased, while the expression of survivin was decreased in tumors after being transfected with Ad-p27^{kip1}.

CONCLUSION: p27^{kip1} gene therapy mediated by adenovirus vector has a significant inhibitory effect on esophageal carcinoma *in vivo*. Up-regulated p27^{kip1} expression and down-regulated survivin expression may be its important mechanisms.

Key words: p27^{kip1} gene; Esophageal carcinoma; Xenograft; Nude mice; Survivin gene

Zhang WG, Wu QM, Yu JP, Tong Q, Xie GJ, Wang XH, Li SB. Adenovirus expressing p27^{kip1} suppresses growth of established esophageal carcinoma xenografts. *World J Gastroenterol* 2005; 11(42): 6582-6586
http://www.wjgnet.com/1007-9327/11/6582.asp

INTRODUCTION

p27^{kip1} is an anti-oncogene with the function of negative regulation of cell cycle[1], and is also involved in the inhibitory reaction of cytokines, induction of cell differentiation and apoptosis, increase of cell adherence and regulation of resistance to drugs for noumenal tumors[2-6]. Our earlier investigation indicates that p27^{kip1} gene transfer mediated by adenovirus can obviously inhibit the growth of esophageal carcinoma cells[7]. Whether this gene therapy has the same effectiveness *in vivo* is worth further investigation. In this study, we explored the growth suppression of adenovirus expressing p27^{kip1} on established esophageal tumor in nude mice in order to find a new strategy for esophageal carcinoma therapy.

MATERIALS AND METHODS

Materials

The esophageal carcinoma cell strain EC109 and 4-week-old nude mice (Balb/C) of both sexes bred under specific pathogen-free conditions were purchased from Cancer Institute, Chinese Academy of Medical Sciences. pCMV5p27^{kip1} was presented by Dr. Gang Wang, Urinary Surgery Research Institute of the First Hospital of Beijing Medical University. pAACCMVpLpA and pJM17 were presented by academician Zu-Ze Wu, No. 2 Research Institute of Academy of Military Medical Sciences. DH$_{5a}$ was presented by Dr. Xu Peng, Heart Disease Department of the First Hospital of Beijing Medical University. Recombinant adenovirus was constructed by Molecular Biology Laboratory of Taihe Hospital. p27^{kip1}cDNA and adenovirus PCR primer were designed and synthesized by Saibaisheng Biological Company (Beijing, China). RPMI 1640 medium was purchased from Gibco BRL (NY, USA). Polyclonal goat antibody of survivin was purchased from Santa Cruz Biotechnology (CA, USA). Monoclonal mouse antibody of p27^{kip1}, ultra sensitive S-P kit, and 3,3-diaminobenzidine (DAB) kit were purchased from Fuzhou Maixin Biotechnology Co. Ltd (Fuzhou, China).

Construction of recombinant adenovirus Ad-p27^{kip1}

The process was the same as described in our previous work[7].

Cell culture

Human esophageal carcinoma cell strain EC109 was maintained in RPMI 1640 medium supplemented with 100 mL/L fetal calf serum (FCS), 100 kU/L penicillin, 100 mg/L streptomycin, 2 mmol/L L-glutamine, and 50 mL/L CO_2 in a humidified incubator at 37 ℃. The medium was changed every 2-3 d.

Establishment of esophageal carcinoma xenografts

EC109 cells growing exponentially were selected. The final concentration was adjusted to 10^7 cells/mL. Nude mice (Balb/C) of 4 wk old received injections into the dorsal midline in a 100 mL volume to establish tumors. The transplanted tumors were reproduced among the animals continually when the original grafts were growing well. Then esophageal carcinoma xenografts were established by transplanting the tumor tissue mass into the subcutaneous tissue of 36 nude mice. They were ready for use when the tumor diameter reached about 0.7 cm.

Therapeutic effect of intratumoral injection of Ad-p27^{kip1} into established tumors

The animals were randomized into three groups, and each group had seven mice with comparable tumor size within and among the groups. Intratumoral injection of Ad-p27^{kip1}, Ad-LacZ (1.0×10^{10} pfu) or PBS was made every other day for totally four times. The growth curve of tumor was drawn and the growth inhibitory rate of tumor was calculated after the animals were killed at wk 4. Tumor sizes were calculated by the formula: tumor volume = 1/2 ×length×width^2. The growth inhibitory rate of tumor was calculated by the formula: inhibitory rate = (tumor mass of control group–tumor mass of experimental group)/ tumor mass of control group.

Histology

The tumor tissues were fixed in 10% neutral formalin and embedded in paraffin. Sections of 5 μm thickness were used for morphological and immunohistochemical examinations. Paraffin sections were stained with hematoxylin and eosin (H&E) to demonstrate esophageal carcinoma tissue components.

Expression of p27^{kip1}

The paraffin sections were washed with phosphate-buffered saline (PBS, pH 7.4) and incubated in 3% hydrogen peroxide for 10 min to block endogenous peroxidase. After being heated for 10 min in 0.01 mol/L citrate buffer (pH 6.0) using a microwave oven, the sections were incubated with normal animal serum for 10 min and then with monoclonal mouse antibody of p27^{kip1} overnight at 4 ℃. Biotinylated antimouse immunoglobulin and streptavidin conjugated to horseradish peroxidase were subsequently applied. Finally, DAB was used for color development, and hematoxylin was used for counterstaining. As a negative control, the sections were processed in the absence of primary antibody. A scoring method was used to quantitate the p27^{kip1} expression in samples examined. A mean percentage of positive tumor cells was determined in at least five areas at 400-fold magnification. Samples with scores less than 50% were defined as low expression, otherwise as high expression[8]. These scorings were performed in a blinded fashion.

Expression of survivin

The sections carrying survivin protein were stained according to SP immunohistochemical staining method as aforementioned. The primary antibody was polyclonal goat antibody of survivin (dilution 1:200). The mean percentage of positive cells for the expression of survivin was determined in at least five areas at 400-fold magnification, and the samples with less than 10% positively stained cells were defined as negative. Samples with 10-29% positively stained cells were defined as +, 30-59% as ++, and 60% or more than 60% as +++[9].

Statistical analysis

The data were expressed as mean±SD. The difference between each group was analyzed by *t*-test. $P<0.05$ was considered statistically significant.

RESULTS

Growth suppression of established esophageal carcinoma xenografts by intratumoral injection of Ad-p27^{kip1}

Intratumoral injection of Ad-p27^{kip1} into established tumors induced partial growth suppression. The growth of tumors in gene therapy group with p27^{kip1} was obviously suppressed, being significantly different from that in control group and Ad-LacZ group ($P<0.01$). The growth inhibitory rate (IR) of tumor reached 64.1% (Figures 1 and 2, Table 1).

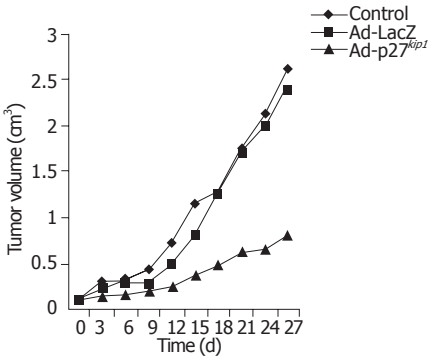

Figure 1 The growth curves of tumor.

Histological evaluation

The result of hematoxylin and eosin staining showed poorly differentiated esophageal squamous carcinoma (Figure 3).

Table 1 Tumor mass of three groups treated with Ad-p27^{kip1}, Ad-LacZ (1.0×10^{10} pfu) or PBS at wk 4

Groups (%)	Tumor mass (g)								IR
	1	2	3	4	5	6	7	mean±SD	
Control	1.02	0.93	1.31	1.47	0.86	1.63	0.95	1.17±0.30	
Ad-LacZ	0.72	1.36	1.12	0.87	0.92	1.23	0.85	1.00±0.23	
Ad-p27^{kip1}	0.32	0.46	0.35	0.43	0.57	0.38	0.40	0.42±0.08^{b}	64.1

$t = 6.39$, $^{b}P<0.01$ *vs* control group. IR: inhibition rate.

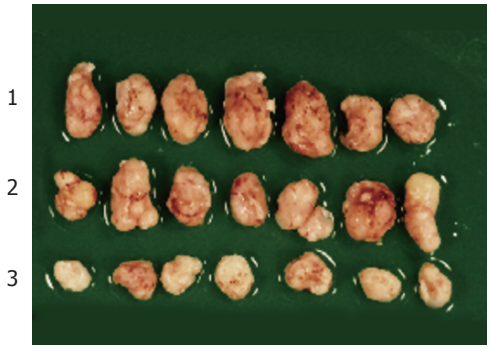

Figure 2 Growth suppression of Ad-p27^{kip1} on established esophageal carcinoma xenografts. 1: control group; 2: Ad-LacZ group; 3: Ad-p27^{kip1} group.

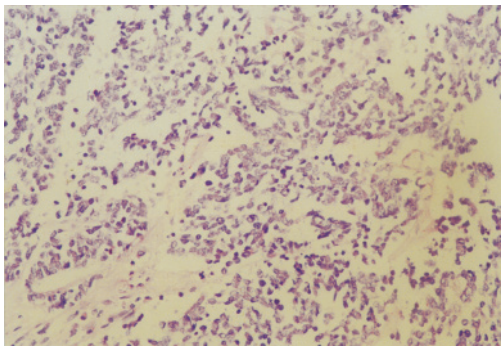

Figure 3 Hematoxylin and eosin (H&E) staining of established esophageal carcinoma xenografts (×200).

Expression of p27^{kip1}

Immunohistochemical staining showed that the expression of p27^{kip1} was increased in established esophageal carcinoma xenografts after being transfected with Ad-p27^{kip1} (Figure 4).

Expression of survivin

Survivin was prominently found in control group by immunohistochemistry and decreased in established esophageal carcinoma xenografts after being transfected with Ad-p27^{kip1} (Figure 5).

DISCUSSION

p27^{kip1} has been mapped to the short arm of chromosome 12 at the 12p12-12p13.1 boundary containing two introns and two exons[10]. Mutations of gene p27^{kip1} occur rarely in human tumors and the decrease in p27^{kip1} expression in tumor tissues is due to post-transcriptional degradation[11]. p27^{kip1} protein belongs to the family of proteins called cyclin-dependent kinase inhibitors (CDKIs). These proteins play an important role as negative regulators of cell cycle-dependent kinases during the progression of cell cycle. p27^{kip1} regulates the progression from G_1 into S phase by binding to and inhibiting the cyclin E/Cdk2 complex, which is required for entry into the S phase. It also interacts with various other cyclin complexes and is therefore designated as a universal CDKI[12-16]. p27^{kip1} expression decreases in esophageal cancer and may correlate with the histologic differentiation. Reduction of p27^{kip1} is considered to be an independent prognostic indicator of esophageal cancer[17-20].

In this study, we found that the growth of established esophageal carcinoma xenografts was obviously depressed and the inhibitory rate reached 64.1% after transfection with Ad-p27^{kip1}. The result of immunohistochemical staining demonstrated that Ad-p27^{kip1} could efficiently express p27^{kip1} in esophageal carcinoma. Ad-p27^{kip1} constructed in the present study is a kind of replication defective adenoviral vector, which has only one opportunity for infection in target cells without any dup-lication ability to fulfill the functions of adenoviral carrier, thus avoiding damage of adenovirus itself to target cells and reaching gene conversion.

We also observed that the expression of survivin was decreased in tumors of nude mice, indicating that p27^{kip1} might downregulate survivin expression. Survivin is a newly identified gene in inhibitors of apoptosis protein (IAP) family and is characterized by a unique structure with a single baculovirus IAP repeat and no zinc-binding domain known as Ring finger[21-23]. Survivin is an oncogene, which has been implicated in inhibition of apoptosis and control of mitotic progression. It is not usually detectable in normal adult tissues, but is prominently expressed in almost all common human cancers and most transformed cell lines. It is a short-lived protein degraded by ubiquitin proteasome pathway and interferes with the activation of caspases, called "cell death executioners"[24-28]. Disruption of survivin-microtubule interactions results in loss of survivin's anti-apoptosis function and increase of caspase-3 activity, a mechanism involved in cell death during mitosis. Survivin functions as a dimer and is regulated in a cell-cycle-dependent manner, peaking at G_2/M, nearly not detectable at G_1, and is associated with the mitotic spindle, centromeres, and the midbody in dividing cells[29-31]. p27^{kip1}, a down-regulating survivin may be associated with G1 blocking of p27^{kip1}, which has been identified in our previous studies[7].

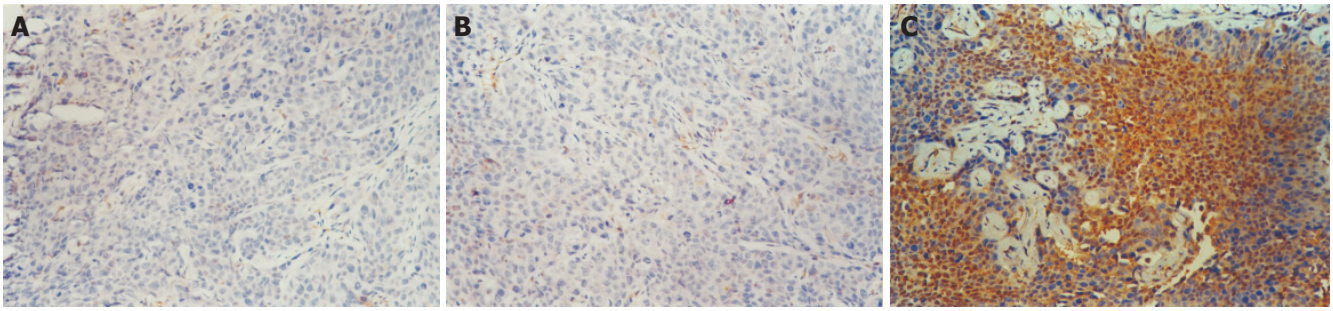

Figure 4 Result of immunohistochemical staining of tumors in nude mice. **A:** control group. p27^{kip1} protein located in cytoplasm of a few cells showing low expression; **B:** Ad-LacZ group. The result showed low expression also; **C:** Ad-p27^{kip1} group. p27^{kip1} protein located in cytoplasm and nucleus showing high expression (×200).

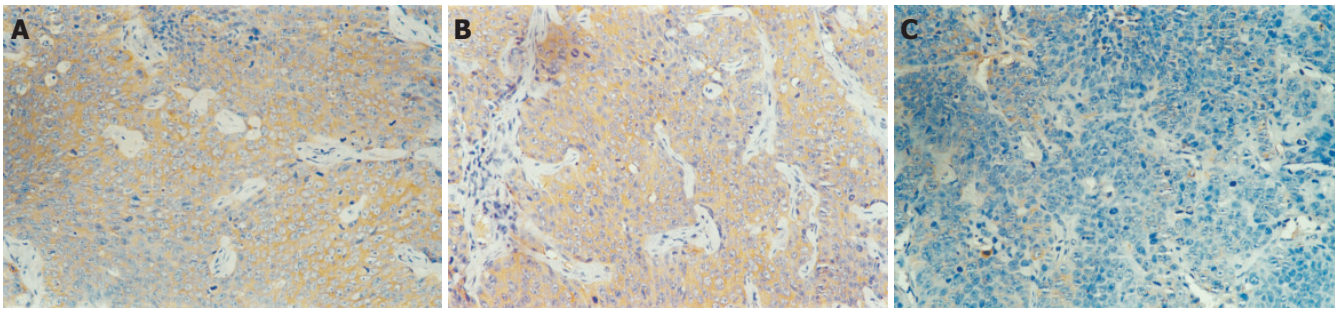

Figure 5 Result of immunohistochemical staining of tumors in nude mice. **A:** control group. Survivin protein located in cytoplasm showing high expression; **B:** Ad-LacZ group. The result showed high expression also; **C:** Ad-p27^{kip1} group. Survivin protein located in cytoplasm of a few cells showing low expression (×200).

In conclusion, p27^{kip1} gene therapy mediated by adenovirus vector has significant inhibitory effect on esophageal carcinoma *in vivo*. Upregulated p27^{kip1} expression and downregulated survivin expression may be its important mechanisms.

REFERENCES

1 **Polyak K,** Kato JY, Solomon MJ, Sherr CJ, Massague J, Roberts JM, Koff A. p27*Kip1*, a cyclin-CDK inhibitor, links transforming growth factor-beta and contact inhibition to cell cycle arrest. *Genes Dev* 1994; **8:** 9-22

2 **Zhang WG,** Wu QM, Tong Q, Yu JP, Wang XH, Xie GJ. The effect of p27*kip1* mediated by adenovirus on the cell cycle and DNA synthesis in gastric cancer cells. *Weichang Bingxue* 2003; **8:** 210-214

3 **Kiyokawa H,** Kineman RD, Manova-Todorova KO, Soares VC, Hoffman ES, Ono M, Khanam D, Hayday AC, Frohman LA, Koff A. Enhanced growth of mice lacking the cyclin-dependent kinase inhibitor function of p27(*Kip1*). *Cell* 1996; **85:** 721-732

4 **Eguchi H,** Carpentier S, Kim SS, Moss SF. P27*kip1* regulates the apoptotic response of gastric epithelial cells to Helicobacter pylori. *Gut* 2004; **53:** 797-804

5 **Ghanem MA,** Van der Kwast TH, Sudaryo MK, Mathoera RB, van den Heuvel MM, Al-Doray AA, Nijman RM, van Steenbrugge GJ. MIB-1 (KI-67) proliferation index and cyclin-dependent kinase inhibitor p27(*Kip1*) protein expression in nephroblastoma. *Clin Cancer Res* 2004; **10:** 591-597

6 **Center DM,** Cruikshank WW, Zhang Y. Nuclear pro-IL-16 regulation of T cell proliferation: p27(*KIP1*)-dependent G0/G1 arrest mediated by inhibition of Skp2 transcription. *J Immunol* 2004; **172:** 1654-1660

7 **Zhang WG,** Wu QM, Tong Q, Yu JP, Wang XH, Xie GJ, Wang WM. Effect of p27*kip1* gene transfere mediated by adenovirus on cell cycle of esophageal carcinoma cells. *Zhongguo Yishi Zazhi* 2004; **6:** 456-458

8 **Singh SP,** Lipman J, Goldman H, Ellis FH Jr, Aizenman L, Cangi MG, Signoretti S, Chiaur DS, Pagano M, Loda M. Loss or altered subcellular localization of p27 in Barrett's associated adenocarcinoma. *Cancer Res* 1998; **58:** 1730-1735

9 **Zhang WG,** Wu QM, Wang XH, Xie GJ, Yu JP. Relationship between expression of Survivin gene and biological character in esophageal carcinoma. *Zhongguo Yishi Zazhi* 2003; **5:** 1378-1380

10 **Ponce-Castaneda MV,** Lee MH, Latres E, Polyak K, Lacombe L, Montgomery K, Mathew S, Krauter K, Sheinfeld J, Massague J. p27*Kip1*: chromosomal mapping to 12p12-12p13.1 and absence of mutations in human tumors. *Cancer Res* 1995; **55:** 1211-1214

11 **Shin JY,** Kim HS, Lee KS, Kim J, Park JB, Won MH, Chae SW, Choi YH, Choi KC, Park YE, Lee JY. Mutation and expression of the p27*KIP1* and p57*KIP2* genes in human gastric cancer. *Exp Mol Med* 2000; **32:** 79-83

12 **Dimberg A,** Bahram F, Karlberg I, Larsson LG, Nilsson K, Oberg F. Retinoic acid-induced cell cycle arrest of human myeloid cell lines is associated with sequential down-regulation of c-Myc and cyclin E and posttranscriptional up-regulation of p27(*Kip1*). *Blood* 2002; **99:** 2199-2206

13 **Lim MS,** Adamson A, Lin Z, Perez-Ordonez B, Jordan RC, Tripp S, Perkins SL, Elenitoba-Johnson KS. Expression of Skp2, a p27(*Kip1*) ubiquitin ligase, in malignant lymphoma: correlation with p27(*Kip1*) and proliferation index. *Blood* 2002; **100:** 2950-2956

14 **Taguchi T,** Kato Y, Baba Y, Nishimura G, Tanigaki Y, Horiuchi C, Mochimatsu I, Tsukuda M. Protein levels of p21, p27, cyclin E and Bax predict sensitivity to cisplatin and paclitaxel in head and neck squamous cell carcinomas. *Oncol Rep* 2004; **11:** 421-426

15 **Leung-Pineda V,** Pan Y, Chen H, Kilberg MS. Induction of

p21 and p27 expression by amino acid deprivation of HepG2 human hepatoma cells involves mRNA stabilization. *Biochem J* 2004; **379:** 79-88

16 **Sekimoto T,** Fukumoto M, Yoneda Y. 14-3-3 suppresses the nuclear localization of threonine 157-phosphorylated p27(*Kip1*). *EMBO J* 2004; **23:** 1934-1942

17 **Yasunaga M,** Tabira Y, Nakano K, Iida S, Ichimaru N, Nagamoto N, Sakaguchi T. Accelerated growth signals and low tumor-infiltrating lymphocyte levels predict poor outcome in T4 esophageal squamous cell carcinoma. *Ann Thorac Surg* 2000; **70:** 1634-1640

18 **Shamma A,** Doki Y, Tsujinaka T, Shiozaki H, Inoue M, Yano M, Kawanishi K, Monden M. Loss of p27(*KIP1*) expression predicts poor prognosis in patients with esophageal squamous cell carcinoma. *Oncology* 2000; **58:** 152-158

19 **Shibata H,** Matsubara O, Wakiyama H, Tanaka S. The role of cyclin-dependent kinase inhibitor p27 in squamous cell carcinoma of the esophagus. *Pathol Res Pract* 2001; **197:** 157-164

20 **Taniere P,** Martel-Planche G, Saurin JC, Lombard-Bohas C, Berger F, Scoazec JY, Hainaut P. TP53 mutations, amplification of P63 and expression of cell cycle proteins in squamous cell carcinoma of the oesophagus from a low incidence area in Western Europe. *Br J Cancer* 2001; **85:** 721-726

21 **Ambrosini G,** Adida C, Altieri DC. A novel anti-apoptosis gene, survivin, expressed in cancer and lymphoma. *Nat Med* 1997; **3:** 917-921

22 **Verdecia MA,** Huang H, Dutil E, Kaiser DA, Hunter T, Noel JP. Structure of the human anti-apoptotic protein survivin reveals a dimeric arrangement. *Nat Struct Biol* 2000; **7:** 602-608

23 **Muchmore SW,** Chen J, Jakob C, Zakula D, Matayoshi ED, Wu W, Zhang H, Li F, Ng SC, Altieri DC. Crystal structure and mutagenic analysis of the inhibitor-of-apoptosis protein survivin. *Mol Cell* 2000; **6:** 173-182

24 **Shariat SF,** Lotan Y, Saboorian H, Khoddami SM, Roehrborn CG, Slawin KM, Ashfaq R. Survivin expression is associated with features of biologically aggressive prostate carcinoma. *Cancer* 2004; **100:** 751-757

25 **Pennati M,** Binda M, Colella G, Zoppe' M, Folini M, Vignati S, Valentini A, Citti L, De Cesare M, Pratesi G, Giacca M, Daidone MG, Zaffaroni N. Ribozyme-mediated inhibition of survivin expression increases spontaneous and drug-induced apoptosis and decreases the tumorigenic potential of human prostate cancer cells. *Oncogene* 2004; **23:** 386-394

26 **Lo Muzio L,** Pannone G, Staibano S, Mignogna MD, Rubini C, Mariggio MA, Procaccini M, Ferrari F, De Rosa G, Altieri DC. Survivin expression in oral squamous cell carcinoma. *Br J Cancer* 2003; **89:** 2244-2248

27 **Altieri DC.** Survivin, versatile modulation of cell division and apoptosis in cancer. *Oncogene* 2003; **22:** 8581-8589

28 **Carter BZ,** Kornblau SM, Tsao T, Wang RY, Schober WD, Milella M, Sung HG, Reed JC, Andreeff M. Caspase-independent cell death in AML: caspase inhibition in vitro with pan-caspase inhibitors or in vivo by XIAP or Survivin does not affect cell survival or prognosis. *Blood* 2003; **102:** 4179-4186

29 **Li F,** Ambrosini G, Chu EY, Plescia J, Tognin S, Marchisio PC, Altieri DC. Control of apoptosis and mitotic spindle checkpoint by survivin. *Nature* 1998; **396:** 580-584

30 **Fukuda S,** Pelus LM. Regulation of the inhibitor-of-apoptosis family member survivin in normal cord blood and bone marrow CD34(+) cells by hematopoietic growth factors: implication of survivin expression in normal hematopoiesis. *Blood* 2001; **98:** 2091-2100

31 **Song Z,** Liu S, He H, Hoti N, Wang Y, Feng S, Wu M. A single amino acid change (Asp 53 --> Ala53) converts Survivin from anti-apoptotic to pro-apoptotic. *Mol Biol Cell* 2004; **15:** 1287-1296

Science Editor Wang XL and Zhu LH **Language Editor** Elsevier HK

PO Box 2345, Beijing 100023, China
www.wjgnet.com
wjg@wjgnet.com

ELSEVIER

World J Gastroenterol 2005;11(42):6587-6592
World Journal of Gastroenterology ISSN 1007-9327

Clinical significance of CT-defined minimal ascites in patients with gastric cancer

Dong Kyung Chang, Ji Won Kim, Byung Kwan Kim, Kook Lae Lee, Chi Sung Song, Joon Koo Han, In Sung Song

Dong Kyung Chang, Ji Won Kim, Byung Kwan Kim, Kook Lae Lee, Chi Sung Song, In Sung Song, Department of Internal Medicine, Seoul National University, College of Medicine, Seoul National University Hospital, and Seoul Municipal Boramae Hospital, Seoul, Korea
Joon Koo Han, Department of Radiology, Seoul National University, College of Medicine, Seoul National University Hospital, and Seoul Municipal Boramae Hospital, Seoul, Korea
Correspondence to: Ji Won Kim, MD, Department of Internal Medicine, Seoul Municipal Boramae Hospital, 395, Shindaebang 2-Dong, Dongjak-Gu, Seoul, Korea. giwkim@hanmail.net
Telephone: +82-2-840-2414 Fax:+82-2-831-0714
Received: 2005-03-17 Accepted: 2005-05-12

Abstract

AIM: To study the clinical significance of minimal ascites, which was only defined by the CT and whose nature was not determined preoperatively, in the relationship with the peritoneal carcinomatosis.

METHODS: The medical records and the dynamic CT films of 118 patients with gastric cancer were reviewed. Factors associated with peritoneal carcinomatosis were analyzed in 40 patients who had CT-defined ascites of which the nature was surgically confirmed.

RESULTS: Only 12.5-25% of the CT-defined minimal ascites, whose volume was estimated to be less than 50 mL, were associated with peritoneal carcinomatosis. When the estimated CT-defined ascitic volume was 50 mL or more, peritoneal carcinomatosis was identified in 75–100%. When CT-defined lymph node enlargements were not found beyond the regional gastric area, perigastric invasions were not suspected, and the size of tumor was less than 3 cm, peritoneal carcinomatosis seemed significantly less accompanied at the univariate analysis. However, except for the minimal volume of CT-defined ascites in comparison with the mild or more, other factors were not confirmed multivariately.

CONCLUSION: In the patients with gastric cancer, CT-defined minimal ascites alone is rarely associated with peritoneal carcinomatosis, if it does not accompany other signs suggestive of malignant seeding. Therefore, consideration of active curative resection should not be hesitated, if CT-defined minimal ascites is the only delusive sign.

Key words: Ascites; Peritoneal carcinomatosis; Gastric cancer

Chang DK, Kim JW, Kim BK, Lee KL, Song CS, Han JK, Song IS. Clinical significance of CT-defined minimal ascites in patients with gastric cancer. *World J Gastroenterol* 2005; 11(42): 6587-6592
http://www.wjgnet.com/1007-9327/11/6587.asp

INTRODUCTION

Gastric cancer, quite uncommon in the developed countries, is still the second leading cause of cancer death in the world[1]. Surgical resection is the only effective therapy to secure curability of this fatal disease. Therefore, overestimation of the stage to render surgery being given up is critically hazardous, as it could deprive a patient of a chance for cure.

The two most frequent conditions in which gastric cancer is regarded incurable are when distant metastasis and malignant peritoneal seeding are demonstrated[2]. Dynamic CT is an excellent modality in clinical staging for gastric cancer and reliably detects metastasis to distant organs such as liver or lung[3,4]. However, the accuracy of dynamic CT in assessing malignant peritoneal involvement is somewhat questionable[4]. The presence of ascites, intestinal wall thickening, contrast-enhanced density in peritoneal adipose tissues, or implanted peritoneal, mesenteric or omental nodules are commonly stated CT findings suggestive of peritoneal carcinomatosis[5,6]. Among these, ascites is assumed to be the most frequently occurring clue for malignant seeding[5].

The nature of ascites is easily disclosed by aspiration cytology as long as the quantity of intra-abdominal fluid enables paracentesis[7,8]. Even small amount of ascites could be recovered for analysis by ultrasonography-guided needle aspiration[9,10]. However, dynamic CT has now become extremely sensitive and may occasionally detect subtle and equivocal amount of ascites in the pelvis, too little for preoperative aspiration-based examination. Without a cytological study or other strong evidences of peritoneal carcinomatosis, the significance of CT-defined minimal ascites might be ambiguous.

In clinical practice, some degree of hesitation is unavoidable in proceeding to surgery, when peritoneal seeding is equivocally suspected. The aim of this study is to make obvious whether the minimal ascites, which was

only defined by CT and whose nature was not practically feasible to characterize preoperatively, is related to genuine peritoneal carcinomatosis. We intend to draw a reasonable perception about 'minimal' ascites in view of clinical significance.

MATERIALS AND METHODS

Patients

Between January 2002 and December 2002, 118 consecutive patients were diagnosed for gastric cancer based on the histological examination of a gastroscopic biopsy and were also examined by dynamic CT at Boramae hospital. Their medical records and CT films were retrospectively reviewed. Out of these, 11 patients did not complete all necessary diagnostic and therapeutic procedures and were excluded from the study. One patient with massive ascites caused by decompensated hepatic cirrhosis was also excluded. Finally, a total of 106 patients remained for an initial analysis (BRM02) for overall frequency of ascites, peritoneal carcinomatosis, and distant metastasis.

The nature of ascites was often unexplored in the patients with metastatic diseases, because curative surgery was not indicated for them and thus characterization of ascites was practically unnecessary. Therefore, when analyzing the clinical implications of CT-defined ascites, we excluded 17 metastatic cases. In the remaining 89 cases (BRM02-NoMeta), the relationships between CT-defined ascites, surgery- or aspiration-recovered ascites, and peritoneal carcinomatosis were analyzed.

Thereafter, we tried to find factors predicting the absence of peritoneal carcinomatosis in the patients with CT-defined ascites, whose nature could not be evaluated preoperatively. To obtain sufficient number of cases for statistical analysis, we extended the study subjects to the cases of Boramae Hospital and of Seoul National University Hospital during the periods between March 1998 and December 2002. We reviewed 2 365 CT reports of the cases who had undergone open abdominal surgery, so whose ascitic natures were confirmed. In this screening step based on the reports, we collected 40 operated cases in which the patients had CT-defined ascites of undetermined nature at preoperative phase and had no definite evidence of distant metastasis or apparent peritoneal seeding (BRM-SNU group). Their medical records and CT films were reviewed in detail.

Radiologic analysis

Dynamic CT studies were performed with Somatom plus-4 scanner (Siemens Medical System, Erlangen, Germany). The abdomen and pelvis were scanned with helical technique and the image was reconstructed at 1-cm-thick sections. Patients were asked not to drink or eat anything for 8 h before CT examination. A total of 500-1 000 mL of tap water was given by mouth, immediately before scanning. A total of 80-120 mL of iopromide contrast medium (Ultravist370®, Schering, Berlin, Germany) was administrated by Mark V dedicated CT injector (Medrad, Pittsburgh, PA, USA) at a flow rate of 3 mL/s, through 18-gauge angiographic catheter placed in the antecubital vein.

Ascites was defined at CT images by at least two experienced radiologists, when the reasonably low radiologic density of 10 or less Hounsfield number was found within the pelvic cavity outside intra-abdominal or pelvic organs. Volume of ascites was estimated by the ruler grids applied on CT images. For example, the area of ascites was measured about 3.5 cm^2 in Figure 1A and 16 cm^2 in Figure 1B and these respectively corresponded with the estimated volumes of 3.5 mL (3.5 $cm^2 \times 1$ cm) and 16 mL (16 $cm^2 \times 1$ cm), because the interval between the serial images obtained in the study was 1 cm. When fluid densities were detected in more than one image, the volumes at each image were added up.

'Minimal' ascites was defined, when the volume of ascites was estimated to be less than 50 mL, and ascites of 50-300 mL was defined as 'mild'. Because we focused on the small amount of ascites which could not be easily evaluated by conventional measures at the preoperative stage, definition about moderate to severe ascites was not considered.

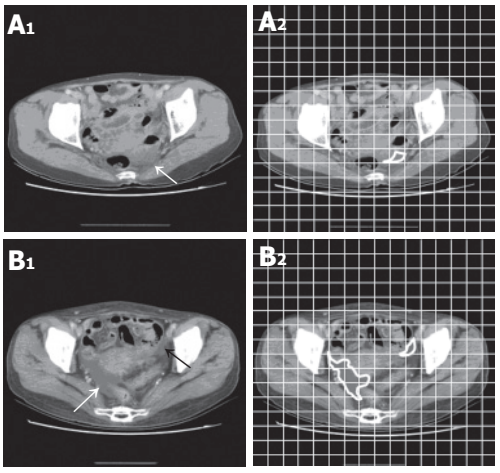

Figure 1 To estimate the volume of ascites by applying grids. Arrows indicate ascitic density (**A1-2**-**B1-2**).

Obliteration of a fat plane between the stomach and adjacent organs or apparent infiltration shown in the CT images was regarded as tumor invasion. Lymph nodes were considered significantly enlarged, when the long diameter was more than 1 cm. The lymph nodes were classified as 'regional' when they were located along the lesser or the greater curvatures of stomach, or at the left gastric, common hepatic, celiac, or splenic arteries. Other intra-abdominal nodes beyond these regions, such as the hepatoduodenal, retropancreatic, mesenteric, or para-aortic area, were defined as distant lymph nodes.

Statistical analysis

Data were analyzed by SPSS (11.5th version) software. Chi-square test was used for categorical data analysis, and the

univariate analysis and the multivariate logistic regression modeling were employed for assessing the predictive factors for the absence of peritoneal carcinomatosis in patients with CT-defined ascites.

RESULTS

Overall proportion of CT-defined ascites, peritoneal carcinomatosis and distant metastasis in the patients with gastric cancer (BRM02 group)

One hundred and six patients committed to the initial analysis consisted of 70 men and 36 women with a mean age of 63.3 years. The stage of gastric cancer at diagnosis was stage I, 23.6%; stage II, 7.5%; stage III, 34.0%; and stage IV, 34.9%. Patients with early gastric cancers were 27.4%.

Of the BRM02 patients, 22 (20.7%) had ascites defined by CT images. Based on the estimated volume of ascites, 12 patients belonged to the category of minimal ascites and 10 patients had mild or more ascites (11.3% and 9.4% of all patients, respectively).

Twenty patients out of the 106 BRM02 group (18.9%) were found to have peritoneal carcinomatosis that was confirmed by preoperative aspiration cytology or laparotomy no matter, whether they had CT-defined ascites or not. Seventeen patients (16%) had metastatic diseases to distant organs. Among these, four patients (3.8%) were confirmed to have both distant metastasis and malignant peritoneal seeding (Table 1).

Clinical realities of CT-defined ascites in the metastasis-free patients (BRM02-NoMeta)

Out of the remaining 89 patients (BRM02-NoMeta) after excluding those with metastatic diseases, 8 had minimal ascites, and 7 had mild ascites. There were no patients having ascites greater than mild category in the metastasis-free group. The nature of ascites was explored by surgery, in all 8 cases with minimal ascites, and in 5 out of 7 cases with mild ascites. The remaining two patients' ascites were proven malignant by aspiration cytology, and surgery was not performed.

Ascites defined by CT images were not always identified as peritoneal fluid on surgery. As for the CT-defined minimal ascites, ascitic fluid was recovered at the surgical field in only one (12.5%) of the cases. However, as CT-estimated ascitic volume was higher, surgical correlation improved. In the cases of 'mild' ascites which had more volume than 'minimal', the concordance rate between CT-defined ascites and surgery- or aspiration-recovered ascites was as high as 85.7% (6 out of 7). On the other hand, 5 (6.8%) out of 74 patients who had no CT-identified ascites preoperatively demonstrated ascites at the time of surgery (Table 2A).

The relationship between CT-defined ascites and peritoneal carcinomatosis was analyzed (Table 2B). Among the patients who did not show ascites at the CT images, seven (9.5%) had peritoneal carcinomatosis on surgery. Seven out of sixteen (43.8%) patients with peritoneal carcinomatosis did not demonstrate radiological signs of ascites at the preoperative CT. In the patients with CT-defined 'minimal' ascites, only 25% were concluded by surgery to have peritoneal carcinomatosis. This was contrast to the cases with CT-defined 'mild' ascites, in which all of the CT-defined ascites turned out to have occurred in the association with peritoneal carcinomatosis.

The presence of surgery- or aspiration-recovered ascites was not always accompanied with malignant peritoneal seeding, too. Four out of twelve patients (33.3%) with surgically or cytologically recovered ascites did not accompany peritoneal carcinomatosis, and 8% of ascites-free patients were actually positive for malignant peritoneal seeding (Table 2C).

Factors favoring absence of peritoneal carcinomatosis

Table 1 Proportion of peritoneal carcinomatosis, distant metastasis, and CT-defined ascites in the patients with gastric cancer that completed diagnostic work-up including dynamic CT in January 2002–December 2002 at Boramae Hospital (BRM02)

	Peritoneal carcinomatosis			
Distant metastasis	Negative	Positive	Unknown	Total
Negative	73 (67/6/0)[1]	11 (6/2/3)	0	84 (73/8/3)
Positive	5 (4/1/0)	4 (1/0/3)	8 (5/3/0)	17 (10/4/3)
Unknown	0	5 (1/0/4)	0	5 (1/0/4)
Total	78 (71/7/0)	20 (8/2/10)	8 (5/3/0)	106 (84/12/10)

[1]CT-defined ascites (none/minimal/more than minimal).

Table 2 Clinical realities of CT-defined, preoperatively malignancy-undetermined ascites in the metastasis-free patients (BRM02-NoMeta)[1]

a

	Surgery- or aspiration-recovered ascites			
CT-defined ascites	Negative (%)	Positive (%)	Unknown (%)	Total (%)
No	68 (91.9)	5 (6.8)	1 (1.4)	74 (100)
Minimal	7 (87.5)	1 (12.5)	0 (0.0)	8 (100)
Mild	0 (0.0)	6 (85.7)	1 (14.3)	7 (100)
Total	75	12	2	89

b

	Peritoneal carcinomatosis		
CT-defined ascites	Negative (%)	Positive (%)	Total (%)
No	67 (90.5)	7 (9.5)	74 (100)
Minimal	6 (75.0)	2 (25.0)	8 (100)
Mild	0 (0.0)	7 (100)	7 (100)
Total	73	16	89

c

	Peritoneal carcinomatosis		
Surgery- or aspiration-Recovered ascites	Negative (%)	Positive (%)	Total (%)
Negative	69 (92.0)	6 (8.0)	75 (100)
Positive	4 (33.3)	8 (66.7)	12 (100)
Unknown	0 (0.0)	21 (100)	2 (100)
Total	73	16	89

[1]Presence of ascites was not examined because operation was immediately ceased following observation of malignant omental cakes.

in the patients with CT-defined ascites which was not yet determined whether malignant or not.

We tried to search factors favoring absence of peritoneal carcinomatosis in the gastric cancer patients with CT-defined ascites in the larger number of cases. The sex and age distributions in these 40 patients (BRM-SNU) were not statistically different from those of the initial 106 gastric cancer patients (BRM02).

Majority of CT-defined ascites, of which the nature could not be preoperatively characterized, had volumes of less than 10 mL with a left-skewed pattern (Skewness = 2.768, Figure 2). The range of volume was 1-300 mL; the mean was 34.8 mL and the median was 9.9 mL. Thirty-two cases were categorized as 'minimal' ascites and the rest eight were 'mild' ascites. Age and sex were not related to the volume of CT-defined ascites (data not shown), but the stage of cancer seemed lower in the patients with minimal ascites than those with mild ascites (Table 3).

The CT-defined 'minimal' ascites were associated with peritoneal carcinomatosis in only 12.5% and demonstrated surgically recovered ascites in only 9.4% (Table 4). These data confirmatively reproduced the results obtained from the fewer cases in BRM02 (Table 2). Contrary to the CT-defined 'minimal' ascites, the CT-defined 'mild' ascites were accompanied with peritoneal carcinomatosis in as high as 75%, and were proved to have genuine fluid collection in 62.5%.

In addition to the ascitic volume, several other factors suggestive of negative peritoneal carcinomatosis were tested by the univariate analysis in the patients with CT-defined minimal or mild ascites (Table 5). When enlargement of peritoneal lymph nodes were absent or confined to the regional perigastric area at the CT images, the negative predictive value for peritoneal carcinomatosis was 88.9%. Free of CT-defined perigastric invasion also negatively predicted peritoneal carcinomatosis in 90.9%. None of the patients with tumors with less than 3 cm were accompanied with malignant peritoneal seeding. However, except for the CT-defined 'minimal' ascites in comparison with the more abundant ascites, none of the above factors obtained statistical significance by multivariate analysis as an independent predictor for absence of malignant seeding.

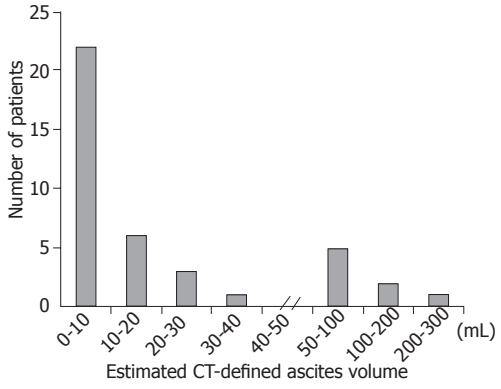

Figure 2 Frequency of patients based on the estimated CT-defined ascites volume.

Table 3 Proportion of the minimal or mild CT-defined ascites at each UICC stage of gastric cancer

Stage	Minimal ascites (%)	Mild ascites (%)
1	9 (28.1)	0 (0)
2	4 (12.5)	1 (12.5)
3	5 (15.6)	1 (12.5)
4	14 (43.8)	6 (75.0)
Total	32 (100)	8 (100)

DISCUSSION

CT has been established as the most popular staging modality in gastric cancer although conventional or endoscopic ultrasonography, or laparoscopy can also be used[3,4,10-14]. The role of CT in detecting distant metastasis has been particularly well recognized; overall sensitivity for assessing liver metastasis reached about 62-89%[4,13,14].

However, CT is less reliable in identifying ascites or peritoneal carcinomatosis; the sensitivity was merely

Table 4 Peritoneal carcinomatosis and surgically recovered ascites in the patients with minimal or mild CT-defined ascites

CT-defined ascites	Peritoneal carcinomatosis		Significance	Predictive value
	Negative	Positive		
Minimal	28 (27/1)[1]	4 (2/2)		NPV: 87.5%[2]
Mild	2 (1/1)	6 (2/4)	$P<0.01$	

[1]Surgically recovered ascites (negative/positive). [2]NPV: negative predictive value of CT-defined 'minimal' ascites for peritoneal carcinomatosis, in comparison with CT-defined 'mild' ascites.

Table 5 Peritoneal carcinomatosis in the patients with CT-defined, yet preoperatively malignancy-undetermined ascites. Univariate analysis

	Peritoneal carcinomatosis		Significance	Predictive value
	Negative	Positive		
CT-defined enlarged lymph node (L/N)				
None or Regional L/N	24	3		NPV: 88.9%[1]
Distant L/N	6	7	$P<0.01$	
CT-defined perigastric invasion				
Negative	20	2		NPV: 90.9%
Positive	10	8	$P<0.05$	
Tumor size defined by endoscopy or UGIS				
<3 cm	10	0		NPV: 100%
3-10 cm	16	6		
>10 cm	4	4	$P<0.05$	
EGC *vs* AGC[2]				
EGC	7	0		NPV: 100%
AGC	23	10	NS	

[1]NPV: negative predictive value for peritoneal carcinomatosis. [2]EGC: early gastric cancer; AGC: advanced gastric cancer.

36-46.7% for ascites and was 13-30% for malignant peritoneal seeding[4,12,14,15]. While the full blown peritoneal carcinomatosis demonstrating all the relevant radiologic features is diagnosed unambiguously, early and tiny malignant implantation cannot be easily decided. Although ascites has been regarded an important sign suggesting peritoneal carcinomatosis[5], the meaning of ascites may become ambiguous, as the dynamic CT detects subtle amounts of peritoneal fluid collection with increased sensitivity.

Then, what is the clinical significance of minimal ascites found in the CT image? Our data showed that minimal amounts of suspicious ascites defined by the dynamic CT were associated by peritoneal carcinomatosis in only 12.5-25%. This data may suggest that the patients need not hesitate to go through surgery, if the CT-defined minimal ascites is the only delusive clue for peritoneal seeding.

In the past, these amounts of minimal ascites might have never been detected by the CT and, therefore, might have never become a clinical issue. It may be argued whether the CT-defined minimal ascites is true or false-positive. However, this kind of question seems clinically out of point. Confirmation of real ascites may hardly be possible. Even surgery cannot be a gold standard in judging the presence of ascites because some blood or irrigated saline might be inevitably mixed with minimal, if any, ascites during surgery. Moreover, peritoneal cavity physiologically contains small amount of serous fluid which has been produced by permeable mesothelium[16], although this disperses diffusely in the peritoneal cavity and is not usually detected by the CT. It remains uncertain, if our CT-defined 'minimal' ascites is exaggerated physiologic fluid, or pathologic ascites.

On the other hand, high index of suspicion may have rendered observers to detect phantom radiologic ascites in the cancer patients. However, an article by Chen *et al*. also reported that small amounts of ascites were detected at the perigastric area in 39% of patients with gastric cancers by endoscopic ultrasonography and they were not significantly correlated with macroscopic peritoneal carcinomatosis[17]. Revealing the mechanism in the development of minimal ascites may be beyond the scope of this study.

No matter whether CT-defined minimal ascites is true or false, the apparent existence of minimal ascites reasonably defined by the dynamic CT may confuse a physician in determining the patient's operability. This may be particularly critical in the patients with marginally poor condition. It is possible that, for example, elderly patients may give up radical surgery, when they are imprudently suggested the worse prognosis, because of the suspicious ascites. Adoption of laparoscopic staging in patients with CT-defined minimal ascites is another issue. Although laparoscopic examination may reveal the nature of minimal ascites more clearly[12], this procedure is not always routinely available at every hospital. In the most common practice setting, a physician cannot help but judge the operability according to the CT finding and other clinical manifestations.

If CT-defined minimal ascites has just low probability of peritoneal carcinomatosis, what additional factors could enhance the possibility of free peritoneum? Of course, it should be explored first whether peritoneal nodules, fat strands, pleated soft tissue, thickening of omental, mesentery and/or bowel wall, or other radiologic clues for malignant seeding were accompanied with or not. As our data suggested, when CT-defined lymph node enlargements were not found beyond the regional gastric area, CT-defined perigastric invasions were not detected, and the size of tumor was less than 3 cm, the probability of true peritoneal carcinomatosis may be very low, at least based on the univariate analysis.

In conclusion, majority of malignancy-undetermined CT-defined minimal ascites that was estimated to be less than 50 mL at the preoperative phase are not significantly related to the peritoneal carcinomatosis. Therefore, if the peritoneal carcinomatosis was not definitely established, passive therapeutic strategy should not be applied to those patients simply because ascites is suspected. Definite meaning of CT-defined minimal ascites may need to be reinterpreted by the final effect on survival after long-term follow-up, and this study is under way.

ACKNOWLEDGMENTS

We thank Dr. Yaron Niv for helpful discussion and critical reading of the manuscript; and Dr. Ajay Goel for editing the manuscript.

REFERENCES

1 **Plummer M,** Franceschi S, Munoz N. Epidemiology of gastric cancer. *IARC Sci Publ* 2004; **157:** 311-326
2 **Adachi Y,** Kitano S, Sugimachi K. Surgery for gastric cancer: 10-year experience worldwide. *Gastric Cancer* 2001; **4:** 166-174
3 **Paramo JC,** Gomez G. Dynamic CT in the preoperative evaluation of patients with gastric cancer: correlation with surgical findings and pathology. *Ann Surg Oncol* 1999; **6:** 379-384
4 **D'Elia F,** Zingarelli A, Palli D, Grani M. Hydro-dynamic CT preoperative staging of gastric cancer: correlation with pathological findings. A prospective study of 107 cases. *Eur Radiol* 2000; **10:** 1877-1885
5 **Yoshikawa T,** Kanari M, Tsuburaya A, Kobayahi O, Sairenji M, Motohashi H. Clinical and diagnostic significance of abdominal CT for peritoneal metastases in patients with primary gastric cancer. *Gan To Kagaku Ryoho* 2002; **29:** 1925-1928
6 **Villanueva A,** Perez C, Sabate JM, Llauger J, Gimenez A, Sanchis E, Garcia T, Moreno A. Peritoneal carcinomatosis. Review of CT findings in 107 cases. *Rev Esp Enferm Dig* 1995; **87:** 707-714
7 **Nakajima T,** Harashima S, Hirata M, Kajitani T. Prognostic and therapeutic values of peritoneal cytology in gastric cancer. *Acta Cytol* 1978; **22:** 225-229
8 **Kodera Y,** Nakanishi H, Yamamura Y, Shimizu Y, Torii A, Hirai T, Yasui K, Morimoto T, Kato T, Kito T, Tatematsu M.. Prognostic value and clinical implication of disseminated cancer cells in the peritoneal cavity detected by reverse transcriptase-polymerase chain reaction and cytology. *Int. J. Cancer* 1998: **79:** 429-433
9 **Doust BD.** The use of ultrasound in the diagnosis of gastroenterological disease. *Gastroenterology* 1976; **70:** 602-610

10 **Habermann CR,** Weiss F, Riecken R, Honarpisheh H, ohnacker S, Staedtler C, Dieckmann C, Schoder V, Adam G. Preoperative staging of gastric adenocarcinoma: comparison of helical CT and endoscopic US. *Radiology* 2004; **230:** 465-471

11 **Lavonius MI,** Gullichsen R, Salo S, Sonninen P, Ovaska J. Staging of gastric cancer: a study with spiral computed tomography, ultrasonography, laparoscopy, and laparoscopic ultrasonography. *Surg Laparosc Endosc Percutan Tech* 2002; **12:** 77-81

12 **Stell DA,** Carter CR, Stewart I, Anderson JR. Prospective comparison of laparoscopy, ultrasonography and computed tomography in the staging of gastric cancer. *Br J Surg* 1996; **83:** 1260-1262

13 **Adachi Y,** Sakino I, Matsumata T, Iso Y, Yoh R, Kitano S, Okudaira Y. Preoperative assessment of advanced gastric carcinoma using computed tomography. *Am J Gastroenterol* 1997; **92:** 872-875

14 **Kayaalp C,** Arda K, Orug T, Ozcay N. Value of computed tomography in addition to ultrasound for preoperative staging of gastric cancer. *Eur J Surg Oncol* 2002; **28:** 540-543.

15 **Nozoe T,** Matsumata T, Sugimachi K. Usefulness of preoperative transvaginal ultrasonography for women with advanced gastric carcinoma. *Am J Gastroenterol* 1999; **94:** 2509-2512

16 **Nance FC.** Diseases of the peritoneum, retroperitoneum, mesentery, and omentum. In: Haubrich WS, Schaffner F, Berk JE, eds. Bockus Gastroenterology. 5th ed. Philadelphia: W.B. Saunders, 1995: 3061-3096

17 **Chen CH,** Yang CC, Yeh YH. Preoperative staging of gastric cancer by endoscopic ultrasound: the prognostic usefulness of ascites detected by endoscopic ultrasound. *J Clin Gastroenterol* 2002; **35:** 321-327

Science Editor Pravda J and Guo SY **Language Editor** Elsevier HK

PO Box 2345, Beijing 100023, China
www.wjgnet.com
wjg@wjgnet.com

ELSEVIER

World J Gastroenterol 2005;11(42):6593-6600
World Journal of Gastroenterology ISSN 1007-9327

• *GASTRIC CANCER* •

Polymorphisms of DNA repair genes *XRCC1* and *XRCC3*, interaction with environmental exposure and risk of chronic gastritis and gastric cancer

Márcia Cristina Duarte, Jucimara Colombo, Andrea Regina Baptista Rossit, Alaor Caetano, Aldenis Albaneze Borim, Durval Wornrath, Ana Elizabete Silva

Márcia Cristina Duarte, Jucimara Colombo, Ana Elizabete Silva, UNESP - São Paulo State University, Department of Biology, Campus São José do Rio Preto, SP, Brazil
Andrea Regina Baptista Rossit, FAMERP- São José do Rio Preto School of Medicine, Microorganism Investigation Center, São José do Rio Preto, SP, Brazil
Alaor Caetano, Aldenis Albaneze Borim, FAMERP- São José do Rio Preto School of Medicine, Hospital de Base, São José do Rio Preto, SP, Brazil
Durval Wornrath, Pio XII Foundation, Barretos, SP, Brazil
Supported by Brazilian Agency CAPES
Correspondence to: Ana Elizabete Silva, Departamento de Biologia, UNESP, Rua Cristóvão Colombo, 2265, Jardim Nazareth, CEP: 15054-000, São José do Rio Preto, SP, Brazil. anabete@ibilce.unesp.br
Telephone: +55-17-32212384 Fax: +55-17-32212390
Received: 2005-02-24 Accepted: 2005-04-09

Abstract

AIM: To evaluate the association between polymorphisms *XRCC1* Arg194Trp and Arg399Gln and *XRCC3* Thr241Met and the risk for chronic gastritis and gastric cancer, in a Southeastern Brazilian population.

METHODS: Genotyping by PCR-RFLP was carried out on 202 patients with chronic gastritis (CG) and 160 patients with gastric cancer (GC), matched to 202 (C1) and 150 (C2) controls, respectively.

RESULTS: No differences were observed among the studied groups with regard to the genotype distribution of *XRCC1* codons 194 and 399 and of *XRCC3* codon 241. However, the combined analyses of the three variant alleles (194Trp, 399Gln and 241Met) showed an increased risk for chronic gastritis when compared to the GC group. Moreover, an interaction between the polymorphic alleles and demographic and environmental factors was observed in the CG and GC groups. *XRCC1* 194Trp was associated with smoking in the CG group, while the variant alleles *XRCC1* 399Gln and *XRCC3* 241Met were related with gender, smoking, drinking and *H pylori* infection in the CG and GC groups.

CONCLUSION: Our results showed no evidence of a rela-tionship between the polymorphisms *XRCC1* Arg194Trp and Arg399Gln and *XRCC3* Thr241Met and the risk of chronic gastritis and gastric cancer in the Brazilian population, but the combined effect of these variants may interact to increase the risk for chronic gastritis, considered a premalignant lesion. Our data also indicate a gene-environment interaction in the susceptibility to chronic gastritis and gastric cancer.

Key words: Gastric cancer; Gastritis; *XRCC1*; *XRCC3*; Polymorphism; Environmental exposure

Duarte MC, Colombo J, Rossit ARB, Caetano A, Borim AA, Wornrath D, Silva AE. Polymorphisms of DNA repair genes *XRCC1* and *XRCC3*, interaction with environmental exposure and risk of chronic gastritis and gastric cancer. *World J Gastroenterol* 2005; 11(42): 6593-6600
http://www.wjgnet.com/1007-9327/11/6593.asp

INTRODUCTION

DNA repair pathways are responsible for maintaining the integrity of the genome in face of environmental insults and general DNA replication errors, playing a role in protecting it against mutations that lead to cancer[1]. So, polymorphisms of DNA repair enzymes, which may alter the function or efficiency of the DNA repair, may contribute to an increased risk of environmental carcinogenesis[2]. These low-penetrance susceptibility genes have common variants and interact with environmental factors, contributing as a major factor to the populational incidence of cancer[3]. Several polymorphisms in genes that participate in different DNA repair pathways, such as *XPD*, *XPF*, *ERCC1*, *XRCC1*, *XRCC3*[4], *hOGG1*[5], *XPA*, *XPB*[6] and *XPC*[7], have been identified and related to cancer susceptibility.

The *XRCC1* gene is responsible for a scaffolding protein that directly associates with other proteins such as DNA polymerase β, PARP (ADP-ribose polymerase) and DNA ligase III in a complex, to facilitate the processes of base excision repair (BER) or single-strand break repair[8]. The BER pathway repairs DNA damage caused by a variety of endogenous and exogenous factors, including oxidation, alkylating agents and ionizing radiation[1,9]. The *XRCC1* protein can bind directly to both gapped and nicked DNA, as well as to gapped DNA associated with DNA

polymerase β, suggesting that this protein might be independently involved in DNA damage recognition[10]. Two polymorphisms, more often found in *XRCC1'* conserved sites, lead to a C→T substitution at codon 194 in exon 6 and to a G→A substitution at codon 399 in exon 10 of the gene, leading to the amino acid alterations arginine (Arg) to tryptophan (Trp) and arginine (Arg) to glutamine (Gln), respectively. These changes in conserved protein sites may alter the BER capacity, increasing the chances of DNA damage[4].

The Arg399Gln variant is more frequent and has been associated mainly with head and neck[11], colorectal[12], gastric[13], esophageal[14,15], breast[16] and lung[17,18] cancers. The Arg194Trp polymorphism has been related to colorectal[12], gastric[13], head and neck[19] and skin[20] cancers.

Protein *XRCC3* functions in the DNA double-strand break (DSB) and cross-link repair[21] and interacts and stabilizes Rad51[22], one of the key components of the homologous repair (HR) pathway. The HR pathway uses a second intact copy of a homologous chromosome as a template to copy the information lost at the DSB site, resulting in a high-fidelity process and preventing chromosomal aberrations[9]. The main polymorphism in this gene involves the change of threonine (Thr) to methionine (Met) at codon 241 in exon 7[4]. Little is known about the functional consequences of this variation, although some studies observed a positive relation between the Thr241Met polymorphism and an increased risk for skin[23], bladder[24], breast[25] and lung[26] cancers.

So far, the investigations about interactions between *XRCC1* and *XRCC3* polymorphisms and environmental carcinogenesis have produced scarce and conflicting results[27,28,29,30], showing the functional complexity of these variants, that can include their interaction with environmental factors, thus modulating the susceptibility to cancer. Regarding gastric cancer, only a few studies were conducted to investigate its association with *XRCC1* and *XRCC3* variants[13, 27,29,31].

In Brazil, gastric cancer is still one of the most frequent types of cancer. The estimate for 2005 points to the fourth place in incidence and mortality, with about 23 000 new cases and 12 000 deaths[32]. However, multiple factors are thought to play a role in gastric carcinogenesis, including diet[33], lifestyle[34], pathological changes in the stomach such as chronic gastritis[35], and genetic alterations[36,37], besides the infection by *Helicobacter pylori*, the first bacterium to be termed as a definitive cause of cancer[38].

Thus, we conducted a study to evaluate the association between the polymorphisms *XRCC1* Arg194Trp and Arg399Gln and *XRCC3* Thr241Met and the risk of chronic gastritis and gastric cancer in a Brazilian population, as well as the interaction between these polymorphisms and environmental factors involved in gastric carcinogenesis.

MATERIALS AND METHODS

Subjects

This was a case-control study on chronic gastritis and gastric cancer. The case groups comprised 202 patients with a histopathologically confirmed diagnosis of chronic gastritis (100 men and 102 women), with a mean age of 52 years (range 19-86 years), and 160 patients with a histopathologically confirmed diagnosis of gastric adenocarcinoma (118 men and 42 women), with a mean age of 61 years (range 28-93 years). All subjects were recruited from the Hospital de Base in São José do Rio Preto, SP, and from the Pio XII Foundation in Barretos, SP, Brazil. Gastric adenocarcinomas were classified as diffuse or intestinal types, according to the classification proposed by Lauren[39], and the chronic gastritis cases according to the Sidney System[40]. *H pylori* infection was histologically established by the Giemsa staining technique. Two cancer-free control groups with no previous history of gastric disease were matched to the case groups with respect to age, gender and ethnicity. The control group for chronic gastritis (C1) was composed of 202 healthy individuals (100 men and 102 women) with a mean age of 51 years (range 20-85 years), and the control group for gastric cancer (C2) consisted of 150 healthy volunteers (108 men and 42 women) with a mean age of 59 years (range 22-93 years). Epidemiological data on the study population were collected using a standard interviewer-administered questionnaire, with questions about current and past occupation, smoking habits, alcohol intake and family history of cancer. This work was approved by the National Research Ethics Committee and written informed consent was obtained from all individuals.

DNA extraction and genotype analyses

About 5 mL of whole blood were collected from all study participants in sterile EDTA-coated vacutainers. The samples were assigned a unique identifier code. DNA was extracted according to Abdel-Rahman *et al.*[41] and stored at -20 ºC until used for genotyping.

Genotypic analyses of the *XRCC1* gene were carried out by multiplex PCR-RFLP, using primers for codons 399 (F 5' -TTGTGCTTTCTCTGTGTCCA-3' and R 5'-TCCTCCAGCC TTTTCTGATA-3') and 194 (F 5'-GCCCCGTCCCAGGTA-3' and R 5'-AGCCCCAAGACCCTTTCACT-3'), which generate a fragment of 615 and 491 bp, respectively, as previously described[12] with modifications. Briefly, PCR was performed in 25 μL reaction buffer containing 12.5 pmol each primer, 0.2 mmol/L of dNTPs, 3 mmol/L of $MgCl_2$, about 100 ng DNA and 1 U of Taq DNA polymerase. The PCR products were digested overnight with 10 U of *Msp*I at 37 ºC. The wild-type Arg allele for codon 194 is identified by the presence of a 293 bp band, and the mutant Trp allele by the presence of a 313 bp band (indicative of the absence of the *Msp*I cutting site). For codon 399, the presence of two bands of 375 and 240 bp, respectively, identifies the wild-type Arg allele, while the uncut 615 bp band identifies the mutant Gln allele (indicative of the absence of the *Msp*I cutting site). A 178 bp band, resulting from an additional invariant *Msp*I cutting site in the 491 bp amplified fragment, is always present and serves as an internal control for complete enzyme digestion.

Polymorphism of the *XRCC3* gene was deter-

mined by PCR-RFLP, using codon 241 primers (F- 5' GCCTGGTGGTCATCGACTC 3' e R- 5' ACAGGGCTCTGGAAGGCACT GCTCAGCTCACGCACC 3'), as previously described by David-Beabes *et al.*[42]. The 25 µL PCR mixture contained about 100 ng of DNA, 12.5 pmol of each primer, 0.2 mmol/L of dNTPs, 2 mmol/L of $MgCl_2$ and 1 U of Taq DNA polymerase. The 552 bp amplified product was digested overnight with 5 U of *Nla*III at 37 ºC. The wild-type allele Thr was identified by the presence of two 239 and 313 bp bands, while the mutant allele Met was represented by 105, 208, and 239 bp bands.

Statistical analysis

Chi-square or Fisher's exact tests were utilized to compare the groups with regard to genotype frequencies and putative risk factors such as age, gender, ethnicity, smoking, drinking, *H pylori* infection and histological type of adenocarcinoma. To investigate the gene-environment interactions, the odds ratios (OR) and their 95% confidence intervals (95% CI) were calculated, according to a combination of the *XRCC1* and *XRCC3* polymorphisms with putative risk factors. The statistical analyses were performed using Statidisk and GraphPad InStat computer software programs. A probability level (*P*) of less than 0.05 was used as criterion of significance.

RESULTS

Cases and controls did not show any statistically significant difference with regard to age, gender and ethnicity, indicating a well-matched study population. Gastric cancer (GC) patients were more likely to be cigarette smokers or alcohol drinkers than chronic gastritis (CG) patients and controls (C2), and this difference was statistically significant ($P<0.05$), the same occurring with CG patients when compared to controls (C1).

The *XRCC1* and *XRCC3* genotypes and the allele frequency distributions among cases and controls are presented in Table 1. The allele frequencies of polymorphisms 194Trp, 399Gln and 241Met were similar in cases and controls, not showing any statistically significant

Table 1 *XRCC1* and *XRCC3* allele frequencies in patients with chronic gastritis (CG) and gastric cancer (GC) and in the respective control groups C1 and C2

	Genotypes	CG (*n* = 202) *n* (%)	C1 (*n* = 202) *n* (%)	*P*	GC (*n* = 160) *n* (%)	C2 (*n* = 150) *n* (%)	*P*
XRCC1	Arg/Arg	176 (87.1)	183 (90.6)		140 (87.5)	130 (86.7)	
Codon 194	Arg/Trp	24 (11.9)	19 (9.4)		20 (12.5)	19 (12.7)	
	Trp/Trp	2 (1.0)	0 (0.0)		0 (0.0)	1 (0.6)	
	Arg/Trp+Trp/Trp	26 (12.9)	19 (9.4)	0.2683	20 (12.5)	20 (13.3)	0.8269
	Allele frequency	0.07	0.05		0.06	0.07	
XRCC1	Arg/Arg	98 (48.5)	95 (47)		73 (45.6)	70 (46.7)	
Codon 399	Arg/Gln	91 (45.0)	82 (40.6)		67 (41.9)	57 (38.0)	
	Gln/Gln	13 (6.5)	25 (12.4)	0.7651	20 (12.5)	23 (15.3)	0.5035
	Arg/Gln+Gln/Gln	104 (51.5)	107 (53.0)		87 (54.4)	80 (53.3)	
	Allele frequency	0.29	0.33		0.33	0.34	
XRCC3	Thr/Thr	92 (45.5)	84 (41.6)		84 (52.5)	67 (44.7)	
Codon 241	Thr/Met	81 (40.1)	89 (44.1)		53 (33.1)	60 (40.0)	
	Met/Met	29 (14.4)	29 (14.3)	0.4221	23 (14.4)	23 (15.3)	0.1679
	Thr/Met+Met/Met	110 (54.5)	118 (58.4)		76 (47.5)	83 (55.3)	
	Allele frequency	0.34	0.36		0.31	0.35	

Table 2 Association between *XRCC1* and *XRCC3* genotype profiles and risk for chronic gastritis (CG) and gastric cancer (GC)

XRCC1		*XRCC3*										Groups			
Codon 194	Codon 399	Codon 241	CG	GC	OR (95%CI)	*P*	CG	C1	OR (95%CI)	*P*	GC	C2	OR (95%CI)	*P*
All wide-type genotypes														
Arg	Arg	Thr	33	32	1.0 (reference)		33	34	1.0 (reference)		32	23	1.0 (reference)	
One variant polymorphism														
Trp	Arg	Thr	5	8	0.6 (0.17-2.04)	0.5469	5	6	1.2 (0.32-4.16)	1.0000	8	6	1.1 (0.32-3.44)	1.0000
Arg	Gln	Thr	51	38	1.4 (0.68-2.50)	0.5124	51	42	0.8 (0.42-1.51)	0.5234	38	34	1.2 (0.61-2.56)	0.5918
Arg	Arg	Met	50	27	2.0 (0.91-3.57)	0.1237	50	49	1.0 (0.51-1.75)	1.0000	27	34	2,0 (0.83-3.70)	0.1426
Two variant polymorphisms														
Trp	Gln	Thr	3	5	0.6 (0.13-2.63)	0.7106	3	2	0.6 (0.1-4.16)	1.0000	5	4	1.1 (0.16-4.54)	1.0000
Arg	Gln	Met	43	43	1.0 (0.50-1.85)	1.0000	43	58	1.4 (0.69-2.43)	0.4309	43	39	1.2 (0.63-2.50)	0.5389
Trp	Arg	Met	10	6	1.6 (0.52-5.00)	0.5771	10	6	0.6 (0.19-1.78)	0.4106	6	7	1.6 (0.48-5.55)	0.5999
Three variant polymorphisms														
Trp	Gln	Met	8	1	8.3 (0.91-100)	0.0372	8	5	0.6 (0.17-2.04)	0.5400	1	3	5.0 (0.40-50.0)	0.3113

differences ($P>0.05$). However, a combined analysis of the *XRCC1* Arg194Trp and Arg399Gln polymorphisms and the *XRCC3* Thr241Met polymorphism (Table 2), and the assessment of the inter- and intra-gene interactions of these three polymorphisms revealed a statistically significant ($P = 0.0372$) association when the three variant alleles interacted in the chronic gastritis group, as compared to the gastric cancer group. Other combinations did not show any significant difference. The banding patterns of *XRCC1* Arg194Trp and Arg399Gln and of *XRCC3* Thr241Met are represented in Figure 1.

Table 3 shows the associations of the different genotypes with the variables gender, smoking, drinking and *H pylori* infection, among the groups. For this analysis, we combined the heterozygous and mutant homozygous genotypes. Allele 194Trp was associated with smoking, with an increased OR for chronic gastritis (4.16, 95%CI = 1.16-16.66), when we compared the CG and C1 groups. The comparison between the CG and GC groups revealed that in men who were smokers and drinkers there was an association with increased OR's for gastric cancer in the individuals with the alleles *XRCC1* 399Gln (3.03,

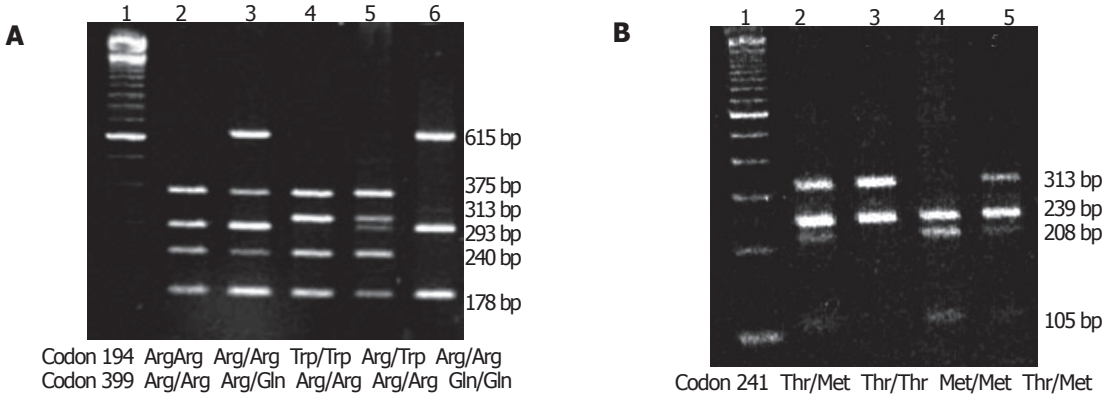

Figure 1 PCR-RFLP of XRCC1 and XRCC3 genes. **A:** *XRCC1* gene. Lane 1: molecular weight marker. Lane 2: wild-type homozygous codons 194 and 399. Lane 3: wild-type homozygous codon 194 and heterozygous codon 399. Lane 4: mutant homozygous codon 194 and wild-type homozygous codon 399. Lane 5: heterozygous codon 194 and wild type-homozygous codon 399. Lane 6: wild-type homozygous codon 194 and mutant homozygous codon 399; **B:** *XRCC3* gene. Lane 1: molecular weight marker. Lanes 2 and 5: heterozygous codon 241. Lane 3: wild-type homozygous codon 241. Lane 4: mutant homozygous codon 241.

Table 3 Association of heterozygous and mutant homozygous to the polymorphisms of codons 194 and 399 of the *XRCC1* gene and to the codon 241 of the *XRCC3* gene with demographic and environmental risk factors in chronic gastritis (CG) and gastric cancer (GC) patients and the respective control groups C1 and C2

	Groups	Variable							
		Gender		Smoke		Drink		*H pylori* infection	
		Male	Female	No	Yes	No	Yes	Positive	Negative
		n (%)	*n* (%)	*n* (%)	*n* (%)	*n* (%)	*n* (%)	*n* (%)	*n* (%)
XRCC1	CG	11 (42.3)	15 (57.7)	9 (34.6)	17 (65.4)	20 (77)	6 (23)		
Arg194Trp									
+	C1	10 (52.6)	9 (47.4)	13 (68.4)	6 (31.6)	17 (89.5)	2 (10.5)		
Trp194Trp		$P = 0.4929$		$P = 0.0250$		$P = 0.4355$			
XRCC1	CG	55 (53)	49 (47)	48 (46.2)	56 (53.8)	71 (68.3)	33 (31.7)	45 (53.6)	39 (46.4)
Arg399Gln	GC	67 (77)	20 (23)	24 (27.6)	63 (72.4)	35 (40.2)	52 (59.8)	9 (23.7)	29 (76.3)
+		$P = 0.0005$		$P = 0.0084$		$P = 0.0001$		$P = 0.0021$	
Gln399Gln	CG	55 (52.9)	49 (47.1)	48 (46.2)	56 (53.8)	71 (68.3)	33 (31.7)		
	C1	52 (48.5)	55 (51.4)	68 (63.6)	39 (36.4)	91 (85)	16 (15)		
		$P = 0.5335$		$P = 0.0111$		$P = 0.0039$			
	GC	67 (77)	20 (23)	24 (27.6)	63 (72.4)	35 (40.2)	52 (59.8)		
	C2	56 (70)	24 (30)	46 (57.5)	34 (42.5)	63 (78.8)	17 (21.2)		
		$P = 0.3042$		$P = 0.0001$		$P = 0.0000$			
XRCC3	CG	57 (51.8)	53 (48.2)	46 (41.8)	64 (58.2)	77 (70)	33 (30)	44 (52.4)	40 (47.6)
Thr241Met	GC	59 (77.6)	17 (22.4)	21 (27.6)	55 (72.4)	36 (47.4)	40 (52.6)	10 (28.6)	25 (71.4)
+		$P = 0.0004$		$P = 0.0494$		$P = 0.0019$		$P = 0.0175$	
Met241Met	CG	57 (51.8)	53 (48.2)	46 (41.8)	64 (58.2)	77 (47.4)	33 (52.6)		
	C1	59 (50)	59 (50)	75 (63.6)	43 (36.4)	98 (79.6)	20 (20.4)		
		$P = 0.7838$		$P = 0.0010$		$P = 0.0110$			
	GC	59 (77.6)	17 (22.4)	21 (27.6)	55 (72.4)	36 (47.4)	40 (52.6)		
	C2	59 (71.1)	24 (28.9)	42 (50.6)	41 (49.4)	66 (79.6)	17 (20.5)		
		$P = 0.3458$		$P = 0.0031$		$P = 0.0000$			

95%CI = 1.58-5.55; 2.27, 95%CI = 1.22-4.16 and 3.22, 95%CI = 1.75-5.88, respectively) and *XRCC3* 241Met (3.22, 95%CI = 1.66-6.25; 1.88, 95%CI = 1.01-3.57 and 2.63, 95%CI = 1.41-4.76, respectively). Comparing the CG and GC groups further, we found increased OR' s for gastric cancer in the association between *H pylori*-negative subjects and the alleles *XRCC1* 399Gln (0.26, 95%CI = 0.11-0.63) and *XRCC3* 241Met (0.36, 95%CI = 0.15-0.85). An association between smoking and drinking and the polymorphisms 399Gln (2.04, 95%CI = 1.17-3.57 and 2.63, 95%CI = 1.35-5.26, respectively) and 241Met (2.44, 95%CI = 1.42-4.16 and 2.13, 95%CI = 1.10-4.00, respectively) was observed when we compared the CG and C1 groups, with increased OR' s for chronic gastritis. Likewise, when we compared GC and C2, we observed an association between smoking and drinking, with an increased OR for stomach cancer, and alleles 399Gln (3.57, 95%CI = 1.85-6.66 and 5.55, 95%CI = 2.77-10.99) and 241Met (2.70, 95%CI = 1.38-5.26 and 4.34, 95%CI = 2.17-9.09). The other evaluated parameters as age and ethnicity, presented no association with the studied polymorphisms.

DISCUSSION

There is increasing evidence that genetic variation leads to different DNA repair capacities in the human population. So, common polymorphisms can play a role in the individual genetic susceptibility to cancer[43]. Very few studies have investigated the role of polymorphisms of the DNA repair genes *XRCC1* and *XRCC3* in the risk of gastric cancer, and, to our knowledge, so far no study examined both gene polymorphisms in this type of cancer and in chronic gastritis. We conducted the first case-control study to investigate the relationship between the polymorphisms *XRCC1* Arg194Trp and Arg399Gln and *XRCC3* Thr241Met and the risk of chronic gastritis and gastric cancer, in a Southeastern Brazilian population.

Our data showed no association between the *XRCC1* and *XRCC3* polymorphisms and an increased risk for chronic gastritis and gastric cancer. To date, there are three published reports on investigations of the association between *XRCC1* polymorphisms and gastric cancer risk[13,27,31], and only one that examined the influence of an *XRCC3* polymorphism[29], with conflicting results. While Shen *et al.*[13] found the wild-genotype Arg194Arg and the mutant-genotype Arg399Gln in the *XRCC1* gene to be associated with an increased risk of gastric cardia cancer, Ratnasinghe *et al.*[27] observed a significant reduction in the risk of this type of cancer, both in Chinese populations. Similarly, Lee *et al.*[31] did not find any association with the risk of gastric cancer in a Korean population, but suggested that the 194Trp allele might be a protective allele with regard to gastric antral cancer. The only study that investigated the role of the *XRCC3* polymorphism in gastric cancer in a Chinese population found no evidence of an association between this polymorphism and an increased risk of gastric cancer[29].

The differences observed in these reports may be due to the different types of gastric cancer studied (cardia and antrum), which may have a distinct pathogenesis and ethnical differences[31]. In the Brazilian population, most gastric cancers are located in the antral region, as in the Korean population, and are commonly associated with H. pylori infection. We also found that in the gastric cancer group the variant allele frequency of 194Trp was lower (0.06) and those of 399Gln and 241Met were higher (0.33 and 0.31, respectively) than those reported in Asian popula tions[13,27,29,31].

These differences can yet be due to the presence of variants of the common susceptibility polymorphisms, not just a single one, but DNA repair genes or activation and detoxification genes may jointly contribute to the susceptibility of gastric and other cancers. Thus, it is important to include more gene polymorphisms for the same or other DNA repair pathways to verify the gene-gene interactions, as well as the gene-environment interactions that may be important in the etiology of the disease.

When we assessed the association of *XRCC1* Arg194trp and Arg399Gln and *XRCC3* Thr241Met with the risk of chronic gastritis and gastric cancer, we found an increased risk for chronic gastritis when all three variant alleles were present at the same time, supporting the hypothesis of an additive effect of these three polymorphisms. There are no studies on chronic gastritis regarding its association with DNA repair gene polymorphisms, as there are for several metabolizing genes, such as *GSTM1*, *GSTT1* and *CYP2E1*, in Brazilian[44] and Chinese[45] populations. Chronic gastritis, a frequent inflammation of the stomach[46], is considered a premalignant lesion[47]. Gastritis may start after an *H pylori* infection and progress over time from an initially superficial form to more severe forms, including severe atrophic gastritis with intestinal metaplasia[48]. About 10% of patients with gastric atrophy develop gastric cancer within a time period of 15 years[46]. Therefore, a reduced DNA repair capacity due to variant alleles may allow mutations to accumulate in the DNA of the epithelial cells of the stomach, resulting from the inflammatory process caused by *H pylori* or from environmental factors such as dietary habits and lifestyle, increasing the risk of gastric cancer.

Gastric cancer has a complex etiology in which genetic and environmental factors play an important role. In this study, we observed a statistically significant association between variant alleles and demographic and environmental factors such as gender, smoking, drinking and *H pylori* infection.

It is known that *H pylori* infection has a very important role in the development of chronic gastritis and in its development into gastric cancer[48]. Various mechanisms were proposed for *H pylori*-associated carcinogenesis, such as the formation of DNA adducts, the generation of free radicals, and a dysregulation of the gastric epithelial cell cycle[49,50]. So, these factors, associated with a decreased DNA repair capacity, may increase the risk for gastric cancer. Differently from these findings, we found a high frequency of variants 399Gln and 241Met

in *H pylori*-negative gastric cancer patients, as compared to chronic gastritis patients. However, these data must have been influenced by the great number of *H pylori*-negative individuals, as compared to the H. pylori-positive individuals found in the gastric cancer group, probably due to an underestimate of the histological diagnosis in these patients.

In smokers, the presence of *XRCC1* 194Trp was more frequent in chronic gastritis cases, while polymorphisms *XRCC1* 399Gln and *XRCC3* 241Met were more frequent in both the chronic gastritis and the gastric cancer groups, compared with healthy controls. Whether the mechanisms of tobacco carcinogens act in human gastric cancer is currently uncertain. The main carcinogens contained in tobacco smoke include polyaromatic hydrocarbons (PAH), *N*-nitrosamines and aromatic amines. Cigarette smoking increases the number of single-strand breaks and DNA adducts, which, if left unrepaired, can lead to gene mutation[51]. These DNA damages can be repaired by BER, in which the *XRCC1* protein has an important role. Functional studies of *XRCC1* variants observed a significantly elevated level of sister chromatid exchange (SCE) in peripheral blood lymphocytes after *in vitro* exposure to the tobacco-specific NNK in carriers of the 399Gln allele, but the same was not observed for the 194Trp polymorphism[52]. Duell *et al*.[53] reported higher frequencies of SCE for current smokers with the 399Gln polymorphism than for smokers with the Arg/Arg genotype.

Protein *XRCC3* participates in the DSB repair by the homologous repair pathway and the 241Met variant may lead to biological implications for the enzyme's function and/or the interaction with other proteins involved in DNA damage repair. Matullo *et al*.[54] associated the 241Met polymorphism with ^{32}P-DNA adduct levels, indicating a possible role of the *XRCC3* gene in the repair of bulky DNA adducts. Thus, variations in DNA repair capacity caused by polymorphisms of DNA repair genes may modulate the genotoxic effect of tobacco smoking.

Excessive alcohol consumption can also lead to DNA damage through the production of free radical intermediates, such as reactive oxygen species, which are produced during the ethanol metabolism[55]. The frequency of DNA single-strand breaks also increases with chronic exposure to alcohol[56]. We observed an association with alcohol consumption in the patients with chronic gastritis and gastric cancer, and found an increased risk for these diseases when polymorphisms *XRCC1* 399Gln and *XRCC3* 241Met were present.

In conclusion, in the Brazilian population studied, we did not find evidence of a relationship between the polymorphisms *XRCC1* Arg194Trp and Arg399Gln and *XRCC3* Thr241Met and the development of chronic gastritis and gastric cancer. However, intra- and inter-gene interactions may contribute to the development of chronic gastritis, a precursor lesion of stomach cancer. We also verified a gene-environment interaction between the *XRCC1* and *XRCC3* polymorphisms, mainly with the habits of smoking and drinking, in the chronic gastritis and gastric cancer patients. Our study is an important addition to the small number of previously published reports on DNA repair gene variants in gastric cancer and shows the need for further studies in different populations, to elucidate the role of these polymorphisms in carcinogenesis.

ACKNOWLEDGMENTS

We thank Prof. Dr. Antonio José Manzato for assistance with the statistical analysis.

REFERENCES

1 **Lindahl T.** Suppression of spontaneous mutagenesis in human cells by DNA base excision-repair. *Mutat Res* 2000; **462**: 129-135
2 **Mohrenweiser HW,** Jones IM. Variation in DNA repair is a factor in cancer susceptibility: a paradigm for the promises and perils of individual and population risk estimation? *Mutat Res* 1998; **400**: 15-24
3 **Shields PG,** Harris CC. Cancer risk and low-penetrance susceptibility genes in gene-environment interactions. *J Clin Oncol* 2000; **18**: 2309-2315
4 **Shen MR,** Jones IM, Mohrenweiser H. Nonconservative amino acid substitution variants exist at polymorphic frequency in DNA repair genes in healthy humans. *Cancer Res* 1998; **58**: 604-608
5 **Ishida T,** Takashima R, Fukayama M, Hamada C, Hippo Y, Fujii T, Moriyama S, Matsuba C, Nakahori Y, Morita H, Yazaki Y, Kodama T, Nishimura S, Aburatani H. New DNA polymorphisms of human MMH/OGG1 gene: prevalence of one polymorphism among lung-adenocarcinoma patients in Japanese. *Int J Cancer* 1999; **80**: 18-21
6 **Butkiewicz D,** Rusin M, Harris CC, Chorazy M. Identification of four single nucleotide polymorphisms in DNA repair genes: XPA and XPB (ERCC3) in Polish population. *Hum Mutat* 2000; **15**: 577-578
7 **Chavanne F,** Broughton BC, Pietra D, Nardo T, Browitt A, Lehmann AR, Stefanini M. Mutations in the XPC gene in families with xeroderma pigmentosum and consequences at the cell, protein, and transcript levels. *Cancer Res* 2000; **60**: 1974-1982
8 **Caldecott KW,** Aoufouchi S, Johnson P, Shall S. XRCC1 polypeptide interacts with DNA polymerase beta and possibly poly (ADP-ribose) polymerase, and DNA ligase III is a novel molecular 'nick-sensor' in vitro. *Nucleic Acids Res* 1996; **24**: 4387-4394
9 **Christmann M,** Tomicic MT, Roos WP, Kaina B. Mechanisms of human DNA repair: an update. *Toxicology* 2003; **193**: 3-34
10 **Marintchev A,** Mullen MA, Maciejewski MW, Pan B, Gryk MR, Mullen GP. Solution structure of the single-strand break repair protein XRCC1 N-terminal domain. *Nat Struct Biol* 1999; **6**: 884-893
11 **Sturgis EM,** Castillo EJ, Li L, Zheng R, Eicher SA, Clayman GL, Strom SS, Spitz MR, Wei Q. Polymorphisms of DNA repair gene XRCC1 in squamous cell carcinoma of the head and neck. *Carcinogenesis* 1999; **20**: 2125-2129
12 **Abdel-Rahman SZ,** Soliman AS, Bondy ML, Omar S, El-Badawy SA, Khaled HM, Seifeldin IA, Levin B. Inheritance of the 194Trp and the 399Gln variant alleles of the DNA repair gene XRCC1 are associated with increased risk of early-onset colorectal carcinoma in Egypt. *Cancer Lett* 2000; **159**: 79-86
13 **Shen H,** Xu Y, Qian Y, Yu R, Qin Y, Zhou L, Wang X, Spitz MR, Wei Q. Polymorphisms of the DNA repair gene XRCC1 and risk of gastric cancer in a Chinese population. *Int J Cancer* 2000; **88**: 601-606
14 **Lee JM,** Lee YC, Yang SY, Yang PW, Luh SP, Lee CJ, Chen CJ, Wu MT. Genetic polymorphisms of XRCC1 and risk of the

esophageal cancer. *Int J Cancer* 2001; **95**: 240-246
15 **Yu HP,** Zhang XY, Wang XL, Shi LY, Li YY, Li F, Su YH, Wang YJ, Lu B, Sun X, Lu WH, Xu SQ. DNA repair gene XRCC1 polymorphisms, smoking, and esophageal cancer risk. *Cancer Detect Prev* 2004; **28**: 194-199
16 **Duell EJ,** Millikan RC, Pittman GS, Winkel S, Lunn RM, Tse CK, Eaton A, Mohrenweiser HW, Newman B, Bell DA. Polymorphisms in the DNA repair gene XRCC1 and breast cancer. *Cancer Epidemiol Biomarkers Prev* 2001; **10**: 217-222
17 **Divine KK,** Gilliland FD, Crowell RE, Stidley CA, Bocklage TJ, Cook DL, Belinsky SA. The XRCC1 399 glutamine allele is a risk factor for adenocarcinoma of the lung. *Mutat Res* 2001; **461**: 273-278
18 **Zhou W,** Liu G, Miller DP, Thurston SW, Xu LL, Wain JC, Lynch TJ, Su L, Christiani DC. Polymorphisms in the DNA repair genes XRCC1 and ERCC2, smoking, and lung cancer risk. *Cancer Epidemiol Biomarkers Prev* 2003; **12**: 359-365
19 **Olshan AF**, Watson MA, Weissler MC, Bell DA. XRCC1 polymorphisms and head and neck cancer. *Cancer Lett* 2002; **178**: 181-186
20 **Han** J, Hankinson SE, Colditz GA, Hunter DJ. Genetic variation in XRCC1, sun exposure, and risk of skin cancer. *Br J Cancer* 2004; **91**: 1604-1609
21 **Thompson LH,** Schild D. Recombinational DNA repair and human disease. *Mutat Res* 2002; **509**: 49-78
22 **Schild D,** Lio YC, Collins DW, Tsomondo T, Chen DJ. Evidence for simultaneous protein interactions between human Rad51 paralogs. *J Biol Chem* 2000; **275:** 16443-16449
23 **Winsey SL,** Haldar NA, Marsh HP, Bunce M, Marshall SE, Harris AL, Wojnarowska F, Welsh KI. A variant within the DNA repair gene XRCC3 is associated with the development of melanoma skin cancer. *Cancer Res* 2000; **60**: 5612-5616
24 **Matullo G,** Guarrera S, Carturan S, Peluso M, Malaveille C, Davico L, Piazza A, Vineis P. DNA repair gene polymorphisms, bulky DNA adducts in white blood cells and bladder cancer in a case-control study. *Int J Cancer* 2001; **92**: 562-567
25 **Smith TR,** Miller MS, Lohman K, Lange EM, Case LD, Mohrenweiser HW, Hu JJ. Polymorphisms of XRCC1 and XRCC3 genes and susceptibility to breast cancer. *Cancer Lett* 2003; **190**: 183-190
26 **Jacobsen NR,** Raaschou-Nielsen O, Nexo B, Wallin H, Overvad K, Tjonneland A, Vogel U. XRCC3 polymorphisms and risk of lung cancer. *Cancer Lett* 2004; **213**: 67-72
27 **Ratnasinghe LD,** Abnet C, Qiao YL, Modali R, Stolzenberg-Solomon R, Dong ZW, Dawsey SM, Mark SD, Taylor PR. Polymorphisms of XRCC1 and risk of esophageal and gastric cardia cancer. *Cancer Lett* 2004; **216**: 157-64
28 **Duan Z,** Shen H, Lee JE, Gershenwald JE, Ross MI, Mansfield PF, Duvic M, Strom SS, Spitz MR, Wei Q. DNA repair gene XRCC3 241Met variant is not associated with risk of cutaneous malignant melanoma. *Cancer Epidemiol Biomarkers Prev* 2002; **11**: 1142-1143
29 **Shen H,** Wang X, Hu Z, Zhang Z, Xu Y, Hu X, Guo J, Wei Q. Polymorphisms of DNA repair gene XRCC3 Thr241Met and risk of gastric cancer in a Chinese population. *Cancer Lett* 2004; **206**: 51-58
30 **Sanyal S,** Festa F, Sakano S, Zhang Z, Steineck G, Norming U, Wijkstrom H, Larsson P, Kumar R, Hemminki K. Polymorphisms in DNA repair and metabolic genes in bladder cancer. *Carcinogenesis* 2004; **25**: 729-734
31 **Lee SG,** Kim B, Choi J, Kim C, Lee I, Song K. Genetic polymorphisms of XRCC1 and risk of gastric cancer. *Cancer Lett* 2002; **187**: 53-60
32 **INCA** – Instituto Nacional do Câncer, Ministério da Saúde. Estimativa 2005 – Estimativas de incidência por câncer no Brasil, 2004. Disponível em http://www.inca.org.br.
33 **Kobayashi M,** Tsubono Y, Sasazuki S, Sasaki S, Tsugane S. Vegetables, fruit and risk of gastric cancer in Japan: a 10-year follow-up of the JPHC Study Cohort I. *Int J Cancer* 2002; **102**: 39-44
34 **Sasazuki S,** Sasaki S, Tsugane S. Cigarette smoking, alcohol consumption and subsequent gastric cancer risk by subsite and histologic type. *Int J Cancer* 2002; **101**: 560-566
35 **Correa P.** Human gastric carcinogenesis: a multistep and multifactorial process--First American Cancer Society Award Lecture on Cancer Epidemiology and Prevention. *Cancer Res* 1992; **52**: 6735-6740
36 **Chen X,** Leung SY, Yuen ST, Chu KM, Ji J, Li R, Chan AS, Law S, Troyanskaya OG, Wong J, So S, Botstein D, Brown PO. Variation in gene expression patterns in human gastric cancers. *Mol Biol Cell* 2003; **14**: 3208-3215
37 **Tahara E.** Genetic pathways of two types of gastric cancer. *IARC Sci Publ* 2004; **157**: 327-349
38 **IARC**–Working Group on the Evaluation of Carcinogenic Risks to Humans. Lyon, 7-14 June 1994. Schistosomes, liver flukes and Helicobacter pylori. *IARC Monogr Eval Carcinog Risks Hum* 1994; **61:** 1-241
39 **Lauren P.** The two histological main types of gastric carcinoma: diffuse and so-called intestinal-type carcinoma. an attempt at a histo-clinical classification. *Acta Pathol Microbiol Scand* 1965; **64:** 31-49
40 **Price AB.** The Sydney System: histological division. *J Gastroenterol Hepatol* 1991; **6**: 209-222
41 **Abdel-Rahman SZ,** Nouraldeen AM, Ahmed AE. Molecular interaction of [2,3-14C] acrylonitrile with DNA in gastric tissue of rat. *J Biochem Toxicol* 1994; **9**: 191-198
42 **David-Beabes GL,** Lunn RM, London SJ. No association between the XPD (Lys751G1n) polymorphism or the XRCC3 (Thr241Met) polymorphism and lung cancer risk. *Cancer Epidemiol Biomarkers Prev* 2001; **10**: 911-912
43 **Hu JJ,** Mohrenweiser HW, Bell DA, Leadon SA, Miller MS. Symposium overview: genetic polymorphisms in DNA repair and cancer risk. *Toxicol Appl Pharmacol* 2002; **185**: 64-73
44 **Colombo J,** Rossit AR, Caetano A, Borim AA, Wornrath DR, Silva AE. GSTT1, GSTM1 and CYP2E1 genetic polymorphisms in gastric cancer and chronic gastritis in a Brazilian population. *World J Gastroenterol* 2004; **10**: 1240-1245
45 **Setiawan VW,** Zhang ZF, Yu GP, Li YL, Lu ML, Tsai CJ, Cordova D, Wang MR, Guo CH, Yu SZ, Kurtz RC. GSTT1 and GSTM1 null genotypes and the risk of gastric cancer: a case-control study in a Chinese population. *Cancer Epidemiol Biomarkers Prev* 2000; **9**: 73-80
46 **Cheli R,** Giacosa A. Chronic atrophic gastritis and gastric mucosal atrophy--one and the same. *Gastrointest Endosc* 1983; **29**: 23-25
47 **Genta RM.** Review article: Gastric atrophy and atrophic gastritis--nebulous concepts in search of a definition. *Aliment Pharmacol Ther* 1998; **12** Suppl 1: 17-23
48 **Correa P.** Helicobacter pylori and gastric carcinogenesis. *Am J Surg Pathol* 1995; **19** Suppl 1: S37-S43
49 **Moss SF.** The carcinogenic effect of H. pylori on the gastric epithelial cell. *J Physiol Pharmacol* 1999; **50**: 847-856
50 **Zhang ZW,** Patchett SE, Farthing MJ. Role of Helicobacter pylori and p53 in regulation of gastric epithelial cell cycle phase progression. *Dig Dis Sci* 2002; **47**: 987-995
51 **Newcomb PA,** Carbone PP. The health consequences of smoking. Cancer. *Med Clin North Am* 1992; **76**: 305-331
52 **Abdel-Rahman SZ,** El-Zein RA. The 399Gln polymorphism in the DNA repair gene XRCC1 modulates the genotoxic response induced in human lymphocytes by the tobacco-specific nitrosamine NNK. *Cancer Lett* 2000; **159**: 63-71
53 **Duell EJ,** Wiencke JK, Cheng TJ, Varkonyi A, Zuo ZF, Ashok TD, Mark EJ, Wain JC, Christiani DC, Kelsey KT. Polymorphisms in the DNA repair genes XRCC1 and ERCC2 and biomarkers of DNA damage in human blood mononuclear cells. *Carcinogenesis* 2000; **21**: 965-971
54 **Matullo G,** Palli D, Peluso M, Guarrera S, Carturan S, Celentano E, Krogh V, Munnia A, Tumino R, Polidoro S, Piazza A, Vineis P. XRCC1, XRCC3, XPD gene polymorphisms, smoking and (32)P-DNA adducts in a sample of healthy subjects. *Carcinogenesis* 2001; **22**: 1437-1445
55 **Brooks PJ.** DNA damage, DNA repair, and alcohol toxicity - a review. *Alcohol Clin Exp Res* 1997; **21**: 1073-1082

56 **Daiker DH,** Shipp BK, Schoenfeld HA, Klimpel GR, Witz G, Moslen MT, Ward JB Jr. Effect of CYP2E1 induction by ethanol on the immunotoxicity and genotoxicity of extended low-level benzene exposure. *J Toxicol Environ Health A* 2000; **59**: 181-196

Science Editor Guo SY **Language Editor** Elsevier HK

PO Box 2345, Beijing 100023, China
www.wjgnet.com
wjg@wjgnet.com

ELSEVIER

World J Gastroenterol 2005;11(42):6601-6606
World Journal of Gastroenterology ISSN 1007-9327

Expression and significance of CD44s, CD44v6, and nm23 mRNA in human cancer

Yong-Jun Liu, Pei-Song Yan, Jun Li, Jing-Fen Jia

Yong-Jun Liu, College of Environmental and Municipal Engineering, Xi'an University of Architecture and Technology, Xi'an 710055, Shaanxi Province, China
Pei-Song Yan, Department of Pathology, Xijing Hospital, Fourth Military Medical University, Xi'an 710033, Shaanxi Province, China
Yong-Jun Liu, Jun Li, Center of Basic Research, Shaan'xi Chaoying Biomedicine R&D Limited Company, Xi'an 710061, Shaanxi Province, China
Jing-Fen Jia, College of Life Science, North-west University, Xi' an 710069, Shaanxi Province, China
Supported by the National Key Development Programs of West China during the 10th Five-Year Plan Period, No. 2001BA901A44
Correspondence to: Dr. Yong-Jun Liu, College of Environmental and Municipal Engineering, Xi'an University of Architecture and Technology, 13 Yanta Road, Xi'an 710055, Shaanxi Province, China. liuyj6984@hotmail.com
Telephone: +86-29-85530179 Fax: +86-29-82202541
Received: 2005-01-31 Accepted: 2005-04-30

Abstract

AIM: To investigate the relationship between the expression levels of nm23 mRNA, CD44s, and CD44v6, and oncogenesis, development and metastasis of human gastric adenocarcinoma, colorectal adenocarcinoma, intraductal carcinoma of breast, and lung cancer.

METHODS: Using tissue microarray by immu-histochemical (IHC) staining and *in situ* hybri-dization (ISH), we examined the expression levels of nm23 mRNA, CD44s, and CD44v6 in 62 specimens of human gastric adenocarcinoma and 62 specimens of colorectal adenocarcinoma; the expression of CD44s and CD44v6 in 120 specimens of intraductal carcinoma of breast and 20 specimens of normal breast tissue; the expression of nm23 mRNA in 72 specimens of human lung cancer and 23 specimens of normal tissue adjacent to cancer.

RESULTS: The expression of nm23 mRNA in the tissues of gastric and colorectal adenocarcinoma was not significantly different from that in the normal tissues adjacent to cancer ($P>0.05$), and was not associated with the invasion of tumor and the pathology grade of adenocarcinoma ($P>0.05$). However, the expression of nm23 mRNA was correlated negatively to the lymph node metastasis of gastric and colorectal adenocarcinoma ($r = -0.49$, $P<0.01$; $r = -4.93$, $P<0.01$). The expression of CD44s in the tissues of gastric and colorectal adenocarcinoma was significantly different from that in the normal tissues adjacent to cancer ($P<0.05$; $P<0.01$). CD44v6 was expressed in the tissues of gastric and colorectal adenocarcinoma only, the expression of CD44v6 was significantly associated with the lymph node metastasis, invasion and pathological grade of the tumor ($r = 0.47$, $P<0.01$; $r = 5.04$, $P<0.01$). CD44s and CD44v6 were expressed in intraductal carcinoma of breast, the expression of CD44s and CD44v6 was significantly associated with lymph node metastases and invasion ($P<0.01$). However, neither of them was expressed in the normal breast tissue. In addition, the expression of CD44v6 was closely related to the degree of cell differentiation of intraductal carcinoma of breast ($\chi^2 = 5.68$, $P<0.05$). The expressional level of nm23 mRNA was closely related to the degree of cell differentiation ($P<0.05$) and lymph node metastasis ($P<0.01$), but the expression of nm23 gene was not related to sex, age, and type of histological classification ($P>0.05$).

CONCLUSION: Patients with overexpression of CD44s and CD44v6 and low expression of nm23 mRNA have a higher lymph node metastatic rate and invasion. In addition, overexpression of CD44v6 is closely related to the degree of cell differentiation. Detection of the three genes is able to provide a reliable index to evaluate the invasion and metastasis of tumor cells.

Key words: Tissue microarray; Nm23 mRNA; CD44s; CD44v6; Gastric adenocarcinoma; Colorectal adeno-carcinoma; Intraductal carcinoma of breast; Lung cancer

Liu YJ, Yan PS, Li J, Jia JF. Expression and significance of CD44s, CD44v6, and nm23 mRNA in human cancer. *World J Gastroenterol* 2005; 11(42): 6601-6606
http://www.wjgnet.com/1007-9327/11/6601.asp

INTRODUCTION

Tissue microarray (TMA) technology is a new method used to analyze hundreds of tumor samples on a single slide, allowing high resolution analysis of genes and proteins on a large cohort. TMA is ideally suitable for genomics-based diagnosis and drug target locating. Oncogenesis, development and metastasis of tumor are triggered by many genes and factors. In recent years, research on the molecular mechanism of oncogenesis and metastasis and the diagnosis of the correlated mark of tumor are

important objects in clinical research in oncology. CD44 is one of the transmembrane proteins on the surface of cells. Its distribution is very extensive and can be detected in lymphocytes and fibroblasts[1]. The expression of CD44v, which is related to the progression, metastasis and prognosis of tumor, has been detected in lung cancer, carcinoma of colon, esophageal cancer, carcinoma of breast, carcinoma of urinary bladder, liver cancer, cervix cancer, carcinoma of kidney and reticulosarcoma[2-5]. Nm23 was first found by Steeg in 1988. Lower expression of nm23 is related to the metastasis of tumors, such as carcinoma of breast, lung cancer, gastric carcinoma, malignant melanoma, and ovary cancer, and has been regarded as the gene of transfer inhibition. In order to investigate the relationship between the expression level of nm23 mRNA, CD44s and CD44v6 and the oncogenesis, pathological grade, invasion, and metastasis of tumor, we detected the expression of nm23 mRNA, CD44s, and CD44v6 in tissues of human gastric adenocarcinoma, colorectal adenocarcinoma, intraductal carcinoma of breast and lung cancer, and also in tissues adjacent to cancer using tissue microarray by immunohistochemical (IHC) staining and *in situ* hybridization (ISH).

MATERIALS AND METHODS

Tissue specimens

The following tissue specimens were enrolled in this study: 40 specimens of colorectal adenocarcinoma (including 16 specimens of moderately differentiated colorectal adenocarcinoma, 24 poorly differentiated adenocarcinoma, 14 lymph node metastatic carcinoma, and 17 invasive carcinoma) and 22 specimens of normal colorectal tissue, 40 specimens of gastric adenocarcinoma (including 20 specimens of moderately differentiated gastric adenocarcinoma, 20 poorly differentiated adenocarcinoma, 15 lymph node metastatic carcinoma, and 23 invasive carcinoma) and 22 specimens of normal gastric tissue, 120 specimens of intraductal carcinoma of breast (including 86 specimens of moderately differentiated intraductal carcinoma, 34 poorly differentiated intraductal carcinoma, 30 lymph node metastatic carcinoma and 58 invasive carcinoma) and 20 specimens of normal breast tissue, 72 specimens of lung cancer (including 13 specimens of moderately differentiated carcinoma, 19 poorly differentiated carcinoma, 24 lymph node metastatic carcinoma) and 23 specimens of normal lung tissue. All patients underwent surgery at Xijing Hospital of the Fourth Military University, China in 2003. The resected specimens were fixed in 10% formaldehyde.

Reagents

CD44s and CD44v6 monoclonal antibodies were obtained from MBI. SABC kit was bought from Sina-America Biotechnology Company. nm23 oligonucleotide probe and CSA test kit were purchased from Boshide Biotechnology Company. Biotin labeled anti-digitoxin (DIG) antibody was obtained from Sigma.

Tissue microarray

Samples were fixed in buffered formaldehyde and subsequently paraffin-embedded. Histological sections (5 μm) were prepared from the specimens, and then diagnosed and labeled by the pathologist. Tissue microarray was performed on the instrument of microarray from Beecher, USA. A hole (diameter 0.5 mm) was made on the recipient block (blank paraffin block), then the tissue core was taken on the supply block (labeled tissue block) and put in the hole. The former procedure was repeated and tissue microarray was completed. Histological sections (3-5 μm) were prepared with the instrument of Leica, Germany, and then rediagnosed by the pathologist.

Immunohistochemical analysis

The sections for tissue microarray were dewaxed in water by normal technique, and then the antigen was restored in high pressure (at 121 °C for 10 min). Immunohistochemistry was performed with the SABC kit. The primary antibodies were CD44s and CD44v6 monoclonal antibodies. Staining was performed following the instructions of SABC kit.

Detection of nm23 mRNA expression by in situ hybridization

All reagents and containers were treated by diethylprocarbonate (DEPC). In brief, the sections for tissue microarray were dewaxed in water by normal technique, immersed into 3% H_2O_2 at room temperature for 10 min, and then washed twice with distilled water. Twenty microgram per milliliter of freshly diluted protease K was added and digested for 20 min at 37 °C to expose mRNA nucleic acid segments. Twenty milliliter of glycerine (20%) was added to the dry bottom of the test kits to keep humidity, 20 μL of the pre-hybridization solution was added to each section and kept at 37 °C for 4 h. Then the supernumerary liquid was absorbed without washing, hybridization solution was added as mentioned above. The sections were then covered with protective membrane and put in homeothermia at 40 °C overnight. After the coverglass was removed, the sections were washed twice at 37 °C in 2×SSC for 5 min, once in 0.5×SSC for 15 min, once in 0.2×SSC for 15 min, and kept in 3% BSA at 37 °C for 30 min and in seal solution at 37 °C for 30 min. After being washed with 0.5 mol/L PBS, the biotin labeled anti-digitoxin antibody was added for 60 min at 37 °C, followed by biotin-peroxidase for 20 min at 37 °C and then washed with PBS. Color was showed by DAB. Finally, the sections were restained, dehydrated, pellucidated, and sealed. Negative controls were designed.

Assessment of immunohistochemical staining and in situ hybridization

Specimens were considered positive when >50% of the tissue components were immunohistochemically stained brown-yellow in appropriate cellular compartment. Specimens were considered positive for ISH when >50% of the tissue components were stained blue in appropriate cellular compartment.

Statistical analysis

Statistical analysis was performed with χ^2 test. $P<0.05$ was considered statistically significant.

RESULTS

Relationship between expression of CD44s, CD44v6, nm23 mRNA, and clinical pathology of human colorectal adenocarcinoma

The expression of CD44s in tissues of colorectal adenocarcinoma and normal colorectal mucosa was 42.0% (17/40) and 13.6% (3/22), respectively (Figures 1A and B), and there was a significant difference between them ($\chi^2 = 5.18$, $P<0.05$). In addition, there was a statistical significance between colorectal adenocarcinoma of with and without invasion ($\chi^2 = 10.52$, $P<0.01$), as well as with and without lymph node metastasis ($\chi^2 = 12.48$, $P<0.01$). However, there was no statistical significance between moderately and poorly differentiated colorectal adenocarcinoma ($P>0.05$), indicating that the expression of CD44s was related to the oncogenesis and development of colorectal adenocarcinoma. The expression of CD44v6 in tissues of colorectal adenocarcinoma and normal colorectal mucosa was 55.8% (22/40) and 0% (0/22), respectively (Figure 1C). There was a statistical significance between moderately and poorly differentiated colorectal adenocarcinoma ($P<0.05$) with and without invasion ($P<0.05$), as well as with and without lymph node metastasis ($\chi^2 = 9.22$, $P<0.01$). The results showed that the expression of CD44v6 was related not only to the invasion of colorectal carcinoma, but also to the metastasis. The expression of nm23 mRNA in tissues of colorectal adenocarcinoma and normal colorectal mucosa was 45.0% (18/40) and 40.9% (9/22), respectively (Figure 1D), and there was no statistically significant difference ($P>0.05$). However, the expression of nm23 mRNA in gastric adenocarcinoma with/without lymph node metastasis was 28.5% (4/14) and 53.8% (14/26), respectively. The difference was statistically significant ($\chi^2 = 8.47$, $P<0.05$). In addition, the expression of CD44v6 in colorectal adenocarcinoma was related to the invasion ($P<0.05$), but not to the pathological grade ($P>0.05$, Table 1).

Relationship between expression of CD44s, CD44v6, and nm23 mRNA in human colorectal adenocarcinoma

Expression of CD44s and CD44v6 was associated with invasion and lymph node metastasis of colorectal adenocarcinoma ($r = 0.47$, $P<0.05$). However, expression of nm23 mRNA was not associated with invasion and lymph node metastasis of colorectal adenocarcinoma ($r = -0.49$, $P<0.05$), suggesting that CD44s, CD44v6 and nm23 mRNA could regulate invasion and lymph node metastasis of colorectal adenocarcinoma. In addition, the expression level of nm23 mRNA, CD44s and CD44v6 was not associated with the age and sex of patients ($P>0.05$, Table 1).

Relationship between expression of CD44s, CD44v6, nm23 mRNA, and clinical pathology of human gastric adenocarcinoma

The expression of CD44s in tissues of gastric adenocarcinoma and normal gastric mucosa was 48% (19/40) and 13.6% (3/22), respectively (Figures 2A and B), and there was a significant difference between them ($\chi^2 = 10.29$, $P<0.01$). However, the expression of CD44s was not significantly associated with lymph node metastasis. There was no statistical significance between moderately and poorly differentiated gastric

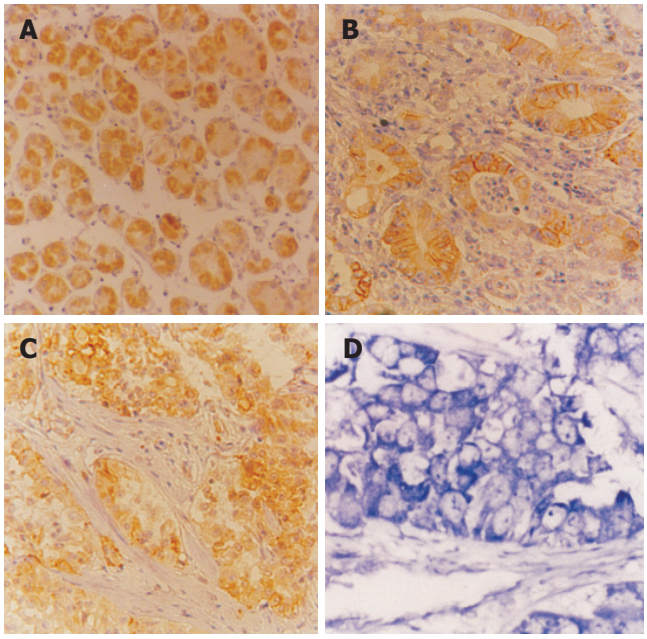

Figure 1 Expression of CD44s in human normal colorectal and adenocarcinoma tissue (**A**, **B**) and expression of CD44v6 (**C**) and nm23 mRNA (**D**) in human colorectal adenocarcinoma.

Table 1 Relationship between expression of CD44s, CD44v6, nm23 mRNA and pathologic feature of human colorectal adenocarcinoma

Pathologic feature	*n*	CD44s Positive (%)	CD44s *P*	CD44v6 Positive (%)	CD44v6 *P*	nm23 mRNA Positive (%)	nm23 mRNA *P*
Grade			>0.05		<0.05[a]		>0.05
II	16	7(43.7)		11(68.7)		8(50.0)	
I	24	10(41.6)		11(45.8)		10(41.6)	
Invasion			<0.01[b]		<0.01[b]		<0.05[c]
+	17	11(64.7)		12(70.5)		5(29.4)	
–	23	6(26)		10(43.4)		13(56.5)	
Metastasis			<0.0[d]		<0.05[e]		<0.05[e]
+	14	9(64.2)		10(71.4)		4(28.5)	
–	26	8(30.7)		12(46.1)		4(53.8)	
Age/yr			>0.05		>0.05		>0.05
>60	19	8(42.1)		10(52.6)		8(42.1)	
<60	21	9(42.8)		12(57.1)		10(47.6)	
Sex			>0.05		>0.05		>0.05
M	26	10(38.4)		14(53.8)		12(46.1)	
F	14	7(50)		8(57.1)		6(42.8)	
Normal	22	4(18.1)		0(0)		9(40.9)	

[a]$P<0.05$ *vs* poorly differentiated colorectal adenocarcinoma; [c]$P<0.05$, [b]$P<0.01$ *vs* without invasion; [e]$P<0.05$, [d]$P<0.01$ *vs* without metastasis.

adenocarcinoma with/without invasion (P>0.05). The expression of CD44v6 in tissues of gastric adenocarcinoma and normal gastric mucosa was 63.3% (25/40) and 0% (0/22), respectively (Figure 2C). There was a statistical significance between moderately and poorly differentiated gastric adenocarcinoma (χ^2 = 9.19, P<0.01) with and without invasion (χ^2 = 22.22, P<0.01), as well as with and without lymph node metastasis (χ^2 = 10.36, P<0.01). The expression of nm23 mRNA in tissues of gastric adenocarcinoma and normal gastric mucosa was 47% (19/40) and 43% (9/22), respectively (Figure 2D) and there was no statistically significant difference between them (P>0.05). However, the expression of nm23 mRNA in gastric adenocarcinoma with/without lymph node metastasis was 26.7% (4/15) and 60% (15/25) respectively, the difference was significant (χ^2 = 18.47, P<0.01, Table 2).

Relationship between expression of CD44v6 and nm23mRNA in human gastric adenocarcinoma

The expression of CD44v6 was associated with lymph node metastasis of gastric adenocarcinoma (r = 5.04). However, the expression of nm23 mRNA was not associated with lymph node metastasis of gastric adenocarcinoma (r = -4.93, Table 2).

Relationship between the expression of CD44s, CD44v6, and clinical pathology of human intraductal carcinoma of breast

The expression of CD44s and CD44v6 in tissues of intraductal carcinoma of breast was 45.8% (55/120) and 53.3% (64/120), respectively (Figures 3A and B), but neither of them was expressed in normal breast tissue. The expression of CD44s and CD44v6 in intraductal breast carcinoma with and without invasion had a significant statistical difference (χ^2 = 9.52, P<0.01; χ^2 = 22.89, P<0.001), as well as with and without lymph node metastasis (χ^2 = 9.41, P<0.01; χ^2 = 8.75, P<0.01). Furthermore, the expression of CD44s was not significantly associated with moderately and poorly differentiated intraductal breast carcinoma (P>0.05). However, the expression of CD44v6 was not only related to invasion and lymph node metastasis of intraductal breast carcinoma, but also related to its pathological grade (χ^2 = 5.68, P<0.05, Table 3).

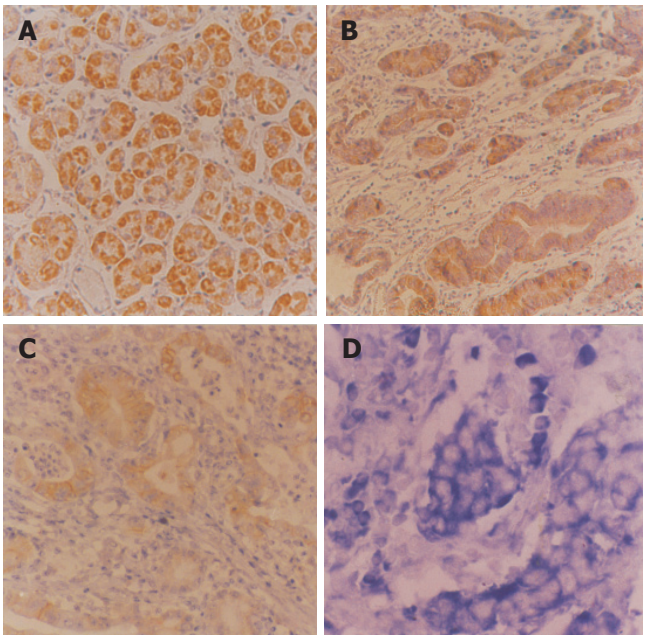

Figure 2 Expression of CD44s in human normal gastric tissue (**A, B**) and expression CD44v6 (**C**) and nm23 mRNA (**D**) in human gastric adenocarcinoma

Relationship between expression of nm23 mRNA and clinical pathology of human lung cancer

The expression of nm23 mRNA in tissues of lung cancer and normal lung tissues was 55.2% (40/72) and 82.6% (19/23), respectively (Figure 4), and there was a significant difference between them (χ^2 = 5.42, P<0.05). The expression of nm23 mRNA in tissues of lung cancer with and without lymph node metastasis was 25.0% (6/24) and 70.8% (34/48), respectively and there was a significant difference between them (χ^2 = 13.61, P<0.001), as well as between moderately and poorly differentiated lung cancer (χ^2 = 9.61, P<0.01), indicating that the expression of nm23 mRNA was associated with the oncogenesis, lymph node metastasis and pathological grade of lung cancer. In addition, the expression of nm23 mRNA in lung cancer was not associated with the age and sex of patients and the pathologic feature of lung cancer (P>0.05, Table 4).

DISCUSSION

CD44s, a hyaluronic acid receptor, is important in regulating invasion and metastasis of tumor[3-7]. Previous studies demonstrated that the expression of CD44s is an important biological marker for predicting metastatic potential. Invasion and metastasis of tumor are a very complicated process, which is regulated by many correlated genes. CD44v6 may take part in the invasion and meta-

Table 2 Relationship between expression of CD44s, CD44v6, nm23 mRNA, and pathologic feature of human gastric adenocarcinoma

Pathologic feature	n	CD44s			CD44v6			nm23 mRNA		
		Positive	%	P	Positive	%	P	Positive	%	P
Grade				>0.05			[b]<0.01			>0.05
II	20	8	40.0		10	50.0		9	45.0	
III	20	10	50.0		15	75.0		10	50.0	
Invasion				>0.05			[d]<0.01			>0.05
+	23	11	47.8		18	78.2		11	47.8	
-	17	7	41.1		7	41.0		8	47.1	
Metastasis				>0.05			[f]<0.01			[f]<0.01
+	15	6	40.0		12	80.0		4	26.7	
-	25	12	48.0		13	52.0		15	60.0	
Age/year				>0.05			>0.05			>0.05
>60	21	10	47.2		13	61.9		9	42.9	
<60	19	8	42.1		12	63.1		10	52.6	
Normal	22	3	13.6		0	0		9	43.0	

[b]P <0.01 *vs* well-differentiated gastric adenocarcinoma; [d]P <0.01 *vs* without invasion; [f]P <0.01 *vs* without metastasis.

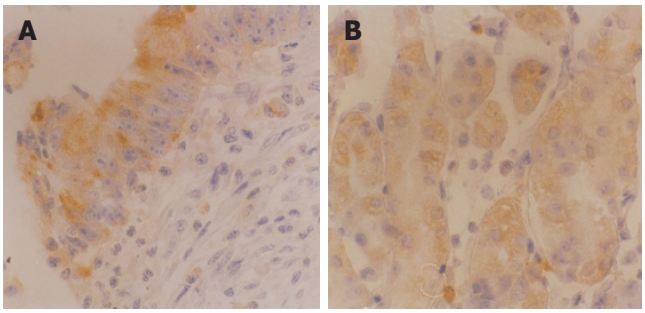

Figure 3 Expression of CD44s (**A**) and CD44v6 (**B**) in human intraductal breast carcinoma.

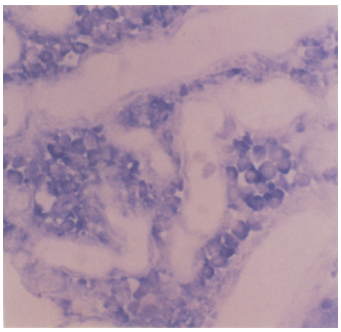

Figure 4 Expression of nm23 mRNA in human lung cancer.

Table 3 Relationship between the expression of CD44s and CD44v6 and pathologic feature of human intraductal breast carcinoma

Pathologic features	*n*	CD44s			CD44v6		
		Positive	%	*P*	Positive	%	*P*
Grade				>0.05			<0.05[a]
II	86	38	44.2		40	46.5	
III	34	17	50		24	70.1	
Invasion				<0.01[b]			<0.01[b]
+	58	35	60.3		44	75.9	
−	62	20	32.3		20	32.3	
Metastasis				<0.01[d]			<0.01[d]
+	30	21	70		23	76.7	
−	90	34	37.8		41	45.6	
Age(yr)				>0.05			>0.05
>50	66	31	47.1		34	51.5	
<50	54	24	44.4		30	55.6	
Normal	20	0	0		0	0	

[a]*P*<0.05 *vs* well-differentiated intraductal breast carcinoma; [b]*P*<0.01 *vs* without invasion; [d]*P*<0.01 *vs* without metastasis.

Table 4 Relationship between expression of nm23 mRNA and pathologic feature of lung cancer

Pathologic feature	*n*	nm23 mRNA		
		Positive	%	*P*
Grade				<0.01[b]
I	19	3	15.8	
II	13	7	53.8	
III	20	17	85	
Metastasis				<0.01[d]
+	24	6	25	
−	48	34	70.8	
Sex				>0.05
M	51	28	54.9	
F	21	12	57.1	
Age(yr)				>0.05
>55	42	22	52.3	
<55	30	18	60	
Normal	23	19	82.6	

[b]*P*<0.01 *vs* moderately and well-differentiated lung cancer; [d]*P*<0.01 *vs* without metastasis.

stasis of tumor, but it is not the necessary factor for tumor invasion and metastasis. When CD44v6 produces a marked effect, it must be restricted by many factors in vivo. It has been proved that CD44v6 is correlated to tumor invasion and metastasis in experiments of cultured cells and animals. But consistent view has not been reached so far with respect to the relationship between expression of CD44v6 and human tumor invasion and metastasis.

It was reported that CD44v mRNA is expressed in human colorectal carcinoma as detected by RT-PCR[8-10]. Zalewski *et al*.[11] reported that the expression of CD44 is associated with the size of tumor, age, and sex of patients. In our current study, CD44 and CD44v6 were expressed in colorectal carcinoma and normal colorectal tissues respectively, indicating that the expression of CD44 and CD44v6 is associated with the invasion and metastasis of colorectal carcinoma, but not associated with the age and sex of colorectal carcinoma patients. In addition, the expression of CD44v6 was related to the pathological grade of tumor. Other studies reported that the expression of CD44 is not associated with the clinical pathological feature of colorectal carcinoma[12,13]. Whether the expression level of CD44 can be seen as a marker of tumor histopathology requires further research.

Using reverse transcription polymerase chain reaction followed by Southern blotting, Yamamichi *et al*.[14] examined the expression of the standard and variant forms (v6 and v9) of CD44 mRNA in 73 cases of gastric cancer, and found that the expression status of the standard form of CD44 mRNA is correlated with peritoneal dissemination only, and that of CD44v9 mRNA does not significantly correlate with any clinicopathologic factor. Li *et al*.[15] reported that 74% gastric cancers and 80% invasive carcinomas are positive for CD44v6, implying that CD44v6 is also a useful marker of tumor invasion and metastasis. In the present study, the expression of CD44v6 was significantly correlated with tumor differentiation, lymph node metastasis and invasion of tumor. The expression of CD44s and CD44v6 in gastric cancer was much higher than that in normal stomach and was associated with genesis, metastasis and clinically aggressive behavior of gastric adenocarcinoma.

The aberrant activation of two or more genes plays a different role during different stages of genesis, progression and metastasis of malignant tumor. These genes synergically facilitate carcinoma change. Our studies showed that the expression of nm23 mRNA in colorectal adenocarcinoma was negatively correlated with that of

CD44 and CD44v6, which was closely associated with the invasion and metastasis of colorectal adenocarcinoma. These results indicate that nm23 and CD44v6 synergically play positive and negative roles during lymph node metastasis of colorectal, and gastric adenocarcinoma. Further studies are needed to investigate the relationship between nm23 and CD44v6, which is important for tumor metastasis.

Mammary cancer is one of the most common malignant tumors. Although 50% of mammary cancers are surgically curable, 50% patients have metastasis within 5 years after surgery. Kaufmann *et al*.[16] reported that the positive expression rate of CD44v6 is 80% in primary tumor and 100% in focal tumor, but no expression is found in normal mammary tissue. The patients with positive expression of CD44v6 have a poor prognosis. There are still many correlative reports[17–20]. Our results showed that the expression of CD44s and CD44v6 in intraductal carcinoma was related with tumor invasion and metastasis, but not with the age and sex of patients.

Since the gene of nm23 was found, lower expression of nm23 has been found to be associated with high metastatic potential and poor prognosis of human mammary cancer, gastric cancer, lung cancer, melanoma, and ovary cancer. Nm23H1 is more important than nm23H2. Gazzeri *et al*.[21] reported that the expression of nm23H1 is not associated with clinicopathological features of adenocarcinoma, while it is associated with the development of squamous carcinoma. Lai *et al*.[22] reported that the expression of nm23H1 is positively correlated with tumor metastasis and prognosis. The lower the nm23H1 expression is, the poorer the prognosis is. Our studies showed that the expression of nm23 mRNA was correlated with lymph node metastasis (r = -4.93). The expression of nm23 mRNA was gradually reduced in normal lung tissue adjacent to cancer. In conclusion, nm23H1 may take part in the regulation of metastasis as a prohibitive gene, and may become a valuable target in the evaluation of tumor development and prognosis.

REFERENCES

1 **Gu H,** Ni C, Zhan R. The expression of CD15 mRNA CD44v6 mRNA and nm23H1 mRNA in breast cancer and their clinical significance. *Zhonghua Yixue Zazhi* 2000; **80:** 854-857

2 **Wang FL,** Wei LX. Expression of CD44 variant exon 6 in lung cancers. *Zhongguo Yixue Kexueyuan Xuebao* 2001; **23:** 401-402

3 **Yan RL,** Qian XH, Xin XY, Jin M, Hui HX, Wang DT, Wang J. Experimental study of anti-VEGF hairpin ribozyme gene inhibiting expression of VEGF and proliferation of ovarian cancer cells. *Ai Zheng* 2002; **21:** 39-44

4 **Ylagan LR,** Scholes J, Demopoulos R. Cd44: a marker of squamous differentiation in adenosquamous neoplasms. *Arch Pathol Lab Med* 2000; **124:** 212-215

5 **Shimabukuro K,** Toyama-Sorimachi N, Ozaki Y, Goi T, Furukawa K, Miyasaka M, Aso T. The expression patterns of standard and variant CD44 molecules in normal uterine cervix and cervical cancer. *Gynecol Oncol* 1997; **64:** 26-34

6 **Frank S,** Rihs HP, Stocker W, Muller J, Dumont B, Baur X, Schackert HK, Schackert G. Combined detection of CD44 isoforms by exon-specific RT-PCR and immunohistochemistry in primary human brain tumors and brain metastases. *Biochem Biophys Res Commun* 1996; **222:** 794-801

7 **Montgomery E,** Abraham SC, Fisher C, Deasel MR, Amr SS, Sheikh SS, House M, Lilliemoe K, Choti M, Brock M, Ephron DT, Zahuruk M, Chadburn A. CD44 loss in gastric stromal tumors as a prognostic marker. *Am J Surg Pathol* 2004; **28:** 168-177

8 **Kuniyasu H,** Oue N, Tsutsumi M, Tahara E, Yasui W. Heparan sulfate enhances invasion by human colon carcinoma cell lines through expression of CD44 variant exon 3. *Clin Cancer Res* 2001; **7:** 4067-4072

9 **Yamada Y,** Itano N, Narimatsu H, Kudo T, Hirohashi S, Ochiai A, Tohnai I, Ueda M, Kimata K. CD44 variant exon 6 expressions in colon cancer assessed by quantitative analysis using real time reverse transcriptase-polymerase chain reaction. *Oncol Rep* 2003; **10:** 1919-1924

10 **Masaki T,** Goto A, Sugiyama M, Matsuoka H, Abe N, Sakamoto A, Atomi Y. Possible contribution of CD44 variant 6 and nuclear beta-catenin expression to the formation of budding tumor cells in patients with T1 colorectal carcinoma. *Cancer* 2001; **92:** 2539-2546

11 **Zalewski B,** Famulski W, Sulkowska M, Sobaniec-Lotowska M, Piotrowski Z, Kisielewski W, Sulkowski S. CD44 expression in colorectal cancer. An immunohistochemical study including correlation with cathepsin D immunoreactivity and some tumour clinicopathological features. *Folia Histochem Cytobio*l 2001; **39** Suppl 2: 152-153

12 **Sokmen S,** Lebe B, Sarioglu S, Fuzun M, Terzi C, Kupelioglu A, Ellidokuz H. Prognostic value of CD44 expression in colorectal carcinomas. *Anticancer Res* 2001; **21:** 4121-4126

13 **Ishida T.** Immunohistochemical expression of the CD44 variant 6 in colorectal adenocarcinoma. *Surg Today* 2000; **30:** 28-32

14 **Yamamichi K,** Uehara Y, Kitamura N, Nakane Y, Hioki K. Increased expression of CD44v6 mRNA significantly correlates with distant metastasis and poor prognosis in gastric cancer. *Int J Cancer* 1998; **79:** 256-262

15 **Li H,** Li J, Guo L. Characteristics of expression of CD44v and receptor for HA-mediated motility (RHAMM) in multi-step gastrocarcinogenesis. *Zhonghua Zhongliu Zazhi* 1999; **21:** 329-331

16 **Kaufmann M,** Heider KH, Sinn HP, von Minckwitz G, Ponta H, Herrlich P. CD44 variant exon epitopes in primary breast cancer and length of survival. *Lancet* 1995; **345:** 615-619

17 **Kopp R,** Classen S, Wolf H, Gholam P, Possinger K, Wilmanns W. Predictive relevance of soluble CD44v6 serum levels for the responsiveness to second line hormone- or chemotherapy in patients with metastatic breast cancer. *Anticancer Res* 2001; **21:** 2995-3000

18 **Saddik M,** Lai R. CD44s as a surrogate marker for distinguishing intraductal papilloma from papillary carcinoma of the breast. *J Clin Pathol* 1999; **52:** 862-864

19 **Sanchez Lockhart M,** Hajos SE, Basilio FM, Mongini C, Alvarez E. Splice variant expression of CD44 in patients with breast and ovarian cancer. *Oncol Rep* 2001; **8:** 145-151

20 **Berner HS,** Nesland JM. Expression of CD44 isoforms in infiltrating lobular carcinoma of the breast. *Breast Cancer Res Treat* 2001; **65:** 23-29

21 **Gazzeri S,** Brambilla E, Negoescu A, Thoraval D, Veron M, Moro D, Brambilla C.Overexpression of nucleoside diphosphate/kinase A/nm23-H1 protein in human lung tumors:association with tumor progression in squamous carcinoma. *Lab Invest* 1996; **74:** 158-167

22 **Lai WW,** Wu MH, Yan JJ, Chen FF. Immunohistochemical analysis of nm23-H1 in stage I non-small cell lung cancer: a useful marker in prediction of metastases. *Ann Thorac Surg* 1996; **62:** 1500-1504

Science Editor Wang XL and Guo SY **Language Editor** Elsevier HK

PO Box 2345, Beijing 100023, China
www.wjgnet.com
wjg@wjgnet.com

ELSEVIER

World J Gastroenterol 2005;11(42):6607-6612
World Journal of Gastroenterology ISSN 1007-9327

Assessment of KL-6 as a tumor marker in patients with hepatocellular carcinoma

Amal Gad, Eiji Tanaka, Akihiro Matsumoto, Moushira Abd-el Wahab, Abd el-Hamid Serwah, Fawzy Attia, Khalil Ali, Howayda Hassouba, Abd el-Raoof el-Deeb, Tetsuya Ichijyo, Takeji Umemura, Hidetomo Muto, Kaname Yoshizawa, Kendo Kiyosawa

Amal Gad, Eiji Tanaka, Akihiro Matsumoto, Moushira Abd-el Wahab, Tetsuya Ichijyo, Takeji Umemura, Hidetomo Muto, Kaname Yoshizawa, Kendo Kiyosawa, Second Department of Internal Medicine, Shinshu University School of Medicine, Matsumoto, Japan
Amal Gad, Abd el-Hamid Serwah, Fawzy Attia, Khalil Ali, Howayda Hassouba, Abd el-Raoof el-Deeb, Suez Canal University School of Medicine, Ismailia, Egypt
Kendo Kiyosawa, Shinshu University Graduate School of Medicine, Institutes of Organ Transplants, Reconstructive Medicine and Tissue Engineering, Matsumoto, Japan
Supported by the Takeda Foundation, Osaka, Japan
Correspondence to: Eiji Tanaka, MD, Second Department of Internal Medicine, Shinshu University School of Medicine, 3-1-1 Asahi, Matsumoto 390-8621,
Japan. etanaka@hsp.md.shinshu-u.ac.jp
Telephone: +81-263-37-2634 Fax: +81-263-32-9412
Received: 2005-03-13 Accepted: 2005-04-30

Abstract

AIM: To investigate the clinical significance of KL-6 as a tumor marker of HCC in two different ethnic groups with chronic liver disease consecutively encountered at outpatient clinics.

METHODS: Serum KL-6 was measured by the sandwich enzyme immunoassay method using the KL-6 antibody (Ab) as both the capture and tracer Ab according to the manufacturer's instructions (Eisai, Tokyo, Japan). Assessment of alpha fetoprotein (AFP) and protein induced vitamin K deficiency or absence (PIVKA-II) was performed in both groups using commercially available kits.

RESULTS: A significantly higher mean serum KL-6 (556±467 U/L) was found in HCC in comparison with non-HCC groups either with (391±176 U/L; P<0.001) or without (361±161 U/L; P<0.001) liver cirrhosis (LC). Serum KL-6 level did not correlate with either AFP or PIVKA-II serU/Levels. Using receiver operating curve analysis for KL-6 as a predictor for HCC showed that the area under the curve was 0.574 (95%CI = 0.50-0.64) and the KL-6 level that gave the best sensitivity (61%) was found to be 334 U/L but according to the manufacturer's instructions; a cut-off point of 500 U/L was used that showed the highest specificity (80%) in comparison with AFP and PIVKA-II (78% *vs* 72% respectively). Combining the values of the three markers improved specificity of AFP for HCC diagnosis from 78% for AFP alone; 93% for AFP plus PIVKA-II to 99% for both plus KL-6 value (P<0.001). Mean serum alkaline phosphatase level was significantly higher in KL-6 positive (564±475) in comparison with KL-6 negative (505±469) HCC patients (P = 0.021), but such a difference was not found among non-HCC corresponding groups.

CONCLUSION: KL-6 is suggested as a tumor for HCC. Its positivity may reflect HCC-associated cholestasis and/or local tumor invasion.

Key words: Tumor markers; Liver disease; Hepatocellular carcinoma

Gad A, Tanaka E, Matsumoto A, Wahab MA, Serwah AeH, Attia F, Ali K, Hassouba H, el-Deeb AeR, Ichijyo T, Umemura T, Muto H, Yoshizawa K, Kiyosawa K. Assessment of KL-6 as a tumor marker in patients with hepatocellular carcinoma. *World J Gastroenterol* 2005; 11(42): 6607-6612
http://www.wjgnet.com/1007-9327/11/6607.asp

INTRODUCTION

Hepatocellular carcinoma (HCC) is the 4th most common cancer worldwide, and it is a well-known complication of chronic hepatitis[1,2]. Asymptomatic patients diagnosed as HCC through screening programs are more likely to be candidates for curative treatment and have improved short- and medium-term survival[3,4]. Although serum alpha-fetoprotein (AFP) had been shown to be associated with HCC since 1963[5], unfortunately it is also elevated in a wide variety of non-hepatic malignancies[6,7] and benign hepatic conditions[8,9]. Moreover, it is uncertain whether serum AFP is a useful marker for HCV-related HCC in some ethnic groups e.g., North American patients of African origin[10]. Thus, searching another tumor marker, that together with AFP could improve the diagnostic utility of the later, seemed to be justified. KL-6 was originally found using a murine monoclonal antibody that recognized an undefined sialylated carbohydrate chain on a mucin-like glycoprotein[11] which was also defined as MUC1[12]. The cell membrane MUC1 was found to regulate cell adhesion properties[13]. KL-6 has been first shown to be

Table 1 Background data of the study groups

	Egyptian			Japanese		
	HCC (+)	HCC (-)	*P*	HCC (+)	HCC (-)	*P*
	n = 65	*n* = 106		*n* = 45	*n* = 128	
Mean age (SD, yr)	57±11[b]	47±9	<0.001	66±10[b]	63±10	NS
Age <50 yr	16 (25)[d]	65 (61)	<0.001	3 (7)[d]	17 (13)	NS
Male	50 (77)	82 (77)	NS	38 (84)	87 (68)	0.024
Liver disease						
Viral	61 (94)	96 (91)		44 (98)	107 (84)	
HCV-related	59 (91)	92 (87)	NS	36 (80)	81 (63)	0.031
HBV-related	2 (3)[1]	4 (4)	NS	8 (18)[1]	28 (22)	NS
Non-viral	4 (6)	10 (9)	NS	1 (2)	20 (16)	0.010
Cirrhosis	46 (71)	45 (42)	<0.001	40 (89)	40 (31)	<0.001
Child's C	25 (38)[f]	17 (16)	0.001	4 (9)[f]	1 (1)	0.017
Mean±(SD)						
ALT (IU/L)	73±95	66±45	0.08	55±35	50±39	NS
Serum Albumin (g/L)	3.0±0.7	3.0±0.5	NS	3.6 ±0.5	4.2±0.4	<0.001
Platelet count×1 000/mL^3	186±107[h]	89±53	0.001	130±51[h]	170±71	<0.001
AFP >10 ng/mL (+)	64 (99)	28 (26)	<0.001	30 (67)	23 (18)	<0.001
PIVIKA>40 mAU/L (+)	51 (79)	38 (36)	<0.001	16 (36)	27 (21)	0.047

[b]P<0.001, [d]P<0.001, [f]P<0.001, [h]P<0.001 *vs* Japannese, [1]P = 0.001.

elevated in patients with interstitial pneumonia[14]. It was also reported to have a high positive rate in different non-hepatic malignancies and its expression was also correlated with metastatic potential of the primary tumor in some of them[15-17]. It has also been studied as a fibrosis marker in patients with HCV-related chronic liver disease[18] and was found to correlate with the degree of irregular regeneration of hepatocytes[19]. A recent study addressed its clinical significance as a tumor marker in HCV-related HCC[20]. However, all these studies investigated KL-6 in HCV-related disease only so that its actual significance as a marker for screening HCC in patients with different chronic liver disease is not yet fully understood. In this study, we aimed to investigate KL-6 as a tumor marker in consecutive patients with chronic liver disease seen at outpatient settings in two different ethnic groups of possible different risk factors for HCC, so that we could get a wider spectrum of disease in order to assess KL-6 validity for HCC screening.

MATERIALS AND METHODS

Study population

We conducted a cross-sectional study between October 2001 and November 2002. Data were gathered from two Affiliations; Shinshu University (Japan) and Suez Canal University (Egypt) Hospitals. A total of 334 consecutive patients with chronic liver disease seen at outpatient liver clinics in the two settings (who met our inclusion/exclusion criteria) were included; of them: 110 patients were diagnosed as HCC with a mean age of 61±11 years and M:F (4:1). Sixty-five were Egyptians and 45 Japanese with viral-related liver disease accounting for 94% and 98% of them respectively. Non-HCC patients were 234 with a mean age of 56±13 years; M:F (7/3). One hundred and six were Egyptians and 128 Japanese with viral-related liver disease accounting for 91% and 84% of them respectively (Table 1).

Chronic liver disease and cirrhosis were identified and diagnosed according to liver biopsy findings, clinical and/or radiological evidence of portal hypertension. HCC was excluded by imaging studies (abdominal ultrasound (US), computed tomography (CT), magnetic resonance imaging (MRI) and/or hepatic angiography), one of which must have been performed at least 6 months following the measurement of AFP.

HCC was diagnosed when meeting our inclusion criteria of positive cytology and/or histology or by the presence of characteristic hepatic masses on liver CT, MRI and/or hepatic angiography (i.e., enlarging tumors and/or tumors with typical arterial vascularization).

We excluded patients with alcoholic and schistosomal liver diseases from our study populations. We had also excluded patients known from their medical history to have interstitial lung fibrosis or any other lung disease from our study population.

Tumor markers measurement

Serum KL-6 was measured by the sandwich enzyme immunoassay method using the KL-6 antibody (Ab) as both the capture and tracer Ab (14) according to the manufacturer's instructions (Eisai, Tokyo, Japan). KL-6 cut-off point was set at 500 U/L for this study. Assessment of alpha fetoprotein (AFP) and protein-induced vitamin K deficiency or absence (PIVKA-II) was performed using commercially available kits. Cut-off points were set at 10 ng/mL for AFP and 40 mAU/L for PIVKA-II.

Statistical analysis

Univariate statistical analysis was performed using Student's *t*-test for quantitative and χ^2 test with Yates' correction for qualitative data. Fisher's exact test was used

for comparison of small numbers; statistical significant level was set at $P<0.05$. Statistical analysis was performed using a computer software (SPSS, version 6.0).

RESULTS

Population background

A difference in mean age, prevalence of advanced Child class and HBV infection was observed between Egyptian and Japanese patients with HCC (Table 1). However, no difference in tumor characteristics was found between the two studied populations (Table 2).

KL-6 and other tumor markers in HCC

A significantly higher mean serum KL-6 (556±467) was found in HCC in comparison with non-HCC groups of patients with (391±176; $P<0.001$) and without (361±161; $P<0.001$) liver cirrhosis (LC). Serum KL-6 level did not correlate with either AFP (Figure 1) or PIVKA-II (Figure 1) serU/Levels. Using receiver operation characteristic (ROC) curve, the KL-6 level that gave the best sensitivity (61%) was found to be 334 U/L with a specificity of 50%, while PIVKA-II and AFP showed a sensitivity/specificity of (60/72)% and (80/78)% respectively. However, according to the manufacturer's instructions; a cut-off point of 500 U/L was used in this study that showed the highest specificity (80%) for KL-6 in comparison with the other two markers. Combining the values of KL-6; AFP and PIVKA-II resulted in improvement in the specificity of AFP for HCC diagnosis from 78% for AFP alone; 93% for AFP plus PIVKA-II to 99% for both plus KL-6 ($P<0.001$) (Table 3).

Table 2 Comparison of background tumor characteristics between Egyptian and Japanese HCC patients

Tumor characteristic	Egyptian (n = 65)	Japanese (n = 45)	P
Tumor multiplicity			
Solitary	25 (38)	22 (49)	>0.2
Multiple	40 (62)	23 (51)	0.06
Tumor size			
<3 cm	32 (49)	20 (44)	>0.2
3:< 5cm	15 (23)	14 (31)	>0.2
⩾5 cm	18 (28)	11 (25)	0.13
Metastases	01 (2)	>0.2	
Tumor grade[1]			
Well differentiated	5 (16)	2 (8)	>0.2
Poorly differentiated	5 (16)	4 (16)	>0.2

[1]Tumor grade is analyzed in 32 of the Egyptian and 22 of the Japanese groups who passed HCC resection operation during the study period.

Factors associated with positive KL-6 in the study population

Univariate analysis (Table 4) of possible factors that could be associated with elevated serum KL-6 in our study group showed that elevated AFP ($P<0.001$), Child's class C ($P = 0.002$), Egyptian race ($P = 0.003$) and HCC ($P = 0.008$) were significantly associated with positive serum KL-6. Also mean serum alkaline phosphatase level was significantly higher in KL-6 positive (564±475) in comparison with KL-6 negative (505±469) HCC patients ($P = 0.021$), but such a difference was not found among non-HCC corresponding group (Table 5). Mean serum bilirubin was found to be higher in KL-6 positive subgroups in both HCC and non-HCC ($P = 0.077$, 0.023) respectively, while mean serum albumin was significantly lower in both groups ($P = 0.029$, 0.041), respectively (Table 5).

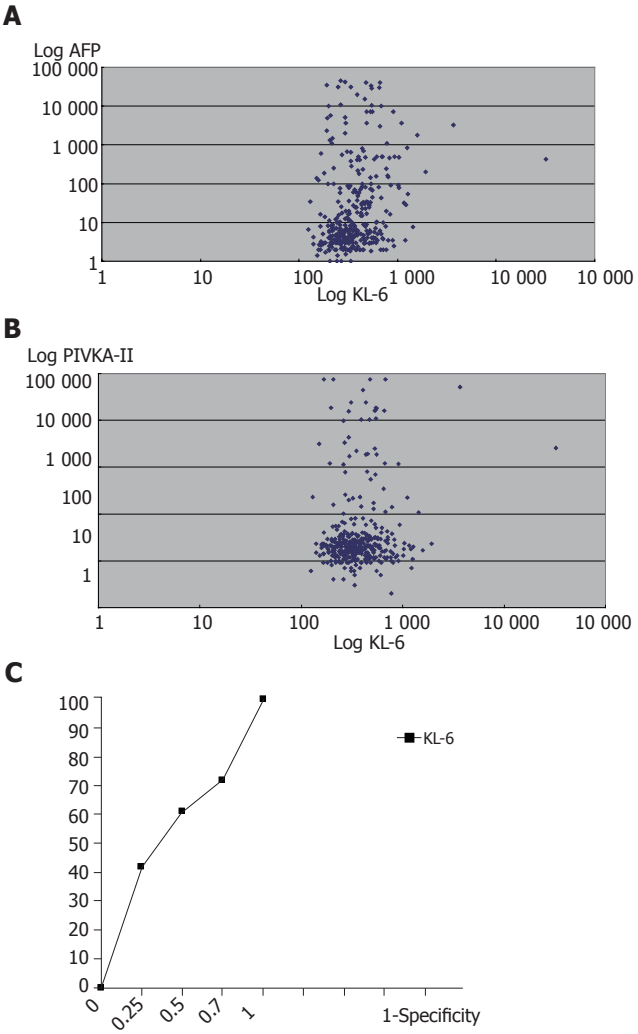

Figure 1 A: Correlation between KL-6 U/L and AFP ng/ml serU/Levels in the study population. $C = 0.04$, $P>0.1$. The Log values of both markers are shown; **B:** Correlation between KL-6 U/L and PIVKA-II mAU/L serU/Levels in the study population. $C = 0.03$, $P>0.5$. The Log values of both markers are shown; **C:** Receiver operating characteristic curves for KL-6 as predictors of HCC. The area under the ROC was found to be 0.574 (95%CI = 0.50–0.64). The best KL-6 sensitivity was obtained at a cut-off point = 334 U/L.

KL-6 in Egyptian vs Japanese

Mean KL-6 was significantly higher in Egyptians (576±522) in comparison with Japanese (510±300) HCC

Table 3 Comparison of the result of different tumor markers between HCC and non-HCC group

Tumor marker (cut-off point)	Sensitivity %	Specificity %
AFP (10 ng/mL)	86	78
PIVKA-II (35 mAU/L)	61	72
KL-6 (500 U/L)	34	80
AFP+PIVKA-II	86[1]	93
AFP+KL-6	87[2]	94
AFP+PIVKA-II+KL-6	87	99

[1]All PIVKA-II (+) HCC patients are AFP (+). [2]One KL-6 (+) HCC patient is AFP (–).

Table 4 Factors associated with KL-6 positivity in the study population

Factors	Total	KL-6 (+)	KL-6 (–)
Age (yr)			
>=50	244	60 (24)	184 (75)
<50	100	24(24)	76 (76)
P	NS		
Sex			
Male	257	61 (24)	196 (76)
Female	87	23 (26)	64 (73)
P	NS		
Ethnicity			
Egyptian	171	53 (31)	118 (69)
Japanese	173	31 (18)	142 (82)
P	0.003		
Underlying liver disease			
HCV-related	267	71 (27)	196 (73)
HBV-related	42	5 (12)	37 (88)
Non-viral	35	8 (23)	27 (77)
P	NS		
Cirrhosis			
(+)	169	46 (27)	123 (73)
(–)	175	38 (22)	137 (78)
P	NS		
Child's class			
C	47	20 (43)	27 (57)
A&B	297	64 (21)	233 (78)
P	0.002		
HCC:			
(+)	110	37 (34)	73 (66)
(–)	234	47 (20)	187 (80)
P	0.008		
AFP			
(+)	145	49 (34)	96 (66)
(–)	199	35 (17)	164 (82)
P	<0.001		

patients ($P = 0.041$) (Table 6). Although a significant difference in mean KL-6 level between HCC and non-HCC was observed in both Egyptian and Japanese patients with chronic liver disease ($P<0.001$ respectively), the difference was not statistically significant among Japanese patients with HCV-related disease (Table 6). No difference in mean KL-6 level was found between cirrhotic and non-cirrhotic in either HCC or non-HCC patients.

KL-6 and tumor characteristics

In the HCC groups of both Egyptian and Japanese patients; KL-6 showed no significant association with tumor site, echogenicity or multiplicity. However, a significantly lower mean KL-6 (Table 7) was noticed in larger size tumors of >5 cm (371±168 U/L) in comparison with tumors of less than or equal to 5 cm (537±323) ($P<0.05$ in the Japanese group).

DISCUSSION

KL-6 was studied as a tumor marker in different malignancies like breast, lung and pancreatic cancer and it was reported to be elevated in up to 50% of these malignancies[14]. Two previous studies by Moriyama *et al*.[19, 20] addressed KL-6 as a tumor marker for HCC in patients with HCV-related chronic liver disease, and his results showed that the estimated cumulative incidence of HCC development in HCV-related chronic liver disease patients was significantly greater in patients with positive KL-6[19] and suggested KL-6 to be used as a serological marker for HCC development in HCV-positive patients[20]. In our study, we included consecutive patients with chronic liver disease seen at outpatient settings in two different ethnic groups of possible different risk factors for HCC[22, 23] in order to have a wider spectrum of disease to judge KL-6 validity as a diagnostic test for HCC; however, one limitation was that most of the encountered patients in the two settings were actually with HCV-related disease with low proportion of HBV and non-viral-related disease. Our results showed a significantly higher mean KL-6 in HCC compared with non-HCC; either with or without LC; in addition no difference in mean KL-6 was found among HCC patients with and without LC; such findings together point to KL-6 association with HCC independent on the presence or absence of LC. A significantly higher mean KL-6 level was found in HBV-related in comparison with HCV-related HCC in both Egyptian and Japanese populations; a finding that deserves future study on a larger population of HBV-related disease. Our results also showed a significantly higher mean KL-6 level in HCC patients of Egyptian compared with Japanese race. The finding of a difference in the clinical background between both in terms of lower mean age and lower prevalence of HBV-related HCC could reflect a difference in the risk factors for HCC in both groups. Also, a higher prevalence of advanced Child class in the HCC Egyptian patients was observed that could stand behind the finding of higher mean KL-6 level in this group compared to their corresponding Japanese group. Although we excluded patients with overt schistosomal from this study, still some Egyptian patients had a past history of schistosomiasis with US evidence of hepatic periportal fibrosis (denoting a background of schistosomal liver disease) that could also explain the finding of higher mean KL-6 level in Egyptian HCC patients, if we consider the possibility that KL-6 could be a fibrosis marker too[21]. This topic is highly suggested for future study.

Table 5 Comparison of the clinical profile of KL-6 positive and negative patients with and without HCC

	HCC (+)			HCC (–)		
	KL-6 (+)	KL-6 (–)	*P*	KL-6 (+)	KL-6 (–)	*P*
	n = 37	*n* = 73		*n* = 47	*n* = 187	
Mean age (yr)[1]	59±12	62±10	NS	57±12	56±13	NS
Cirrhosis	39 (81)	55 (76)	NS	16 (34)	65 (35)	NS
Child's C	13 (35)	15 (21)	NS	7 (15)	11 (6)	0.045
Mean ALT	74±101	62±61	NS	59±33	57±45	NS
Serum						
Albumin (g/L)[1]	2.9±0.7	3.3±0.7	0.029	3.5±0.9	3.8±0.8	0.041
Bilirubin (mmol/L)[1]	2.7±2.8	2.5±3.0	0.077	2.4±2.9	1.4±1.9	0.023
ALP (IU/L)[1]	564±475	505±469	0.021	316±139	299±152	NS
AFP (+)	36 (97)	58 (80)	0.013	13 (28)	37 (20)	NS
PIVIKA (+)	23 (62)	44 (60)	NS	14 (30)	50 (27)	NS

[1]Data is shown as mean±SD. Other data is shown as *n* (%).

Table 6 Comparison of mean serum KL-6 level among different study sub-groups

	Egyptian			Japanese		
	HCC (+)	HCC (-)	*P*	HCC (+)	HCC (-)	*P*
Chronic liver disease[1]:	576 (522)	398 (185)	0.001	510 (300)	350 (147)	<0.001
HCV-related	558 (524)	400 (172)	0.008	356 (290)	382 (209)	>0.2
HBV-related	778 (663)	246 (72)	>0.2	877 (292)	340 (163)	<0.001
Non-viral	729 (538)	446 (309)	>0.2	262[2] ()	357 (160)	–
Cirrhotics	599 (586)	406 (159)	0.035	510 (350)	374 (196)	0.035
Non-cirrhotics	518 (325)	398 (185)	0.045	225 (73)	349 (222)	<0.001

[1]The KL-6 values are shown as mean (SD) U/L. [2]Only one patient's data.

Table 7 Difference in mean KL-6 level according to HCC size

	Egyptian	*P*[1] value	Japanese	*P* value
	(*n* = 65)		(*n* = 45)	
Tumor size				
<3 cm	485±227		618±361	
3:<5 cm	643±685	>0.1	456±285	0.17
⩾5 cm	581±420	>0.1	371±168	0.04

[1]*P* value is shown for the difference group (<3 cm) and the other two groups.

We used a cut-off point of 500 U/L for KL-6 positivity in this study; however, applying the ROC analysis showed that a cut-off point of 334 U/L would give the best sensitivity in our study population of 60% compared with only 32% for a cut-off (500 U/L); however, the best specificity was obtained using the later. Moriyama *et al*. used a cut-off point of 300 U/L in his analysis of KL-6 in HCV-related disease[19,20]. KL-6 serU/Level did not correlate with either serum AFP or PIVKA-II levels, which points to its behavior independently from either of them and this may justify its clinical significance as an independent tumor marker for HCC diagnosis when considered with both AFP and PIVKA-II. Our results also supported this finding as AFP specificity for HCC diagnosis improved from 78% for AFP alone and 93% of both AFP and PIVKA-II to 99% when combined with KL-6. Univariate analysis showed that low serum albumin, hyperbilirubinemia and elevated ALP were significantly associated with positive KL-6 in HCC patients, while KL-6 showed no association with LC in turn, and this denotes a possible association between positive KL-6 and deterioration of hepatic condition in HCC patients independent from their cirrhotic status; a finding that might point to KL-6 as a predictor of tumor aggression and/or local or systemic metastasizing potential. A follow-up study is needed to confirm its exact role in this regard.

ACKNOWLEDGMENTS

We would like to thank Takeda Foundation, Osaka, Japan for their financial support. We also thank Dr. Alla Sad, Dr. Essam Abd Alla, Dr. Khaled Gad for their help with various laboratory techniques.

REFERENCES

1 **Sherman M.** Hepatocellular carcinoma: epidemiology, risk factors, and screening. *Semin Liver Dis* 2005; **25:** 143-154
2 **Szilagyi A,** Alpert L. Clinical and histopathological variation in hepatocellular carcinoma. *Am J Gastroenterol* 1995; **90:** 15-23
3 **Yuen MF,** Cheng CC, Lauder IJ, Lam SK, Ooi CG, Lai CL. Early detection of hepatocellular carcinoma increases the chance of treatment: Hong Kong experience. *Hepatology* 2000; **31:** 330-335
4 **Wong LL,** Limm WM, Severino R, Wong LM. Improved survival with screening for hepatocellular carcinoma. *Liver Transpl* 2000; **6:** 320-325
5 **Johnson PJ.** The role of serum alpha-fetoprotein estimation in the diagnosis and management of hepatocellular carcinoma.

Clin Liver Dis 2001; **5:** 145-159

6 **Iwai M,** Kashiwadani M, Takino T, Ibata Y. Demonstration by light and ultrastructural immunoperoxidase study of alpha-fetoprotein-positive non-hepatoma cells and hepatoma cells during 3'-methyl-4-dimethylaminoazobenzene hepatocarcinogenesis. *Virchows Arch B Cell Pathol Incl Mol Pathol* 1988; **55:** 117-123

7 **McIntire KR,** Waldmann TA, Moertel CG, Go VL, Serum alpha-fetoprotein in patients with neoplasms of the gastrointestinal tract. *Cancer Res* 1975; **35:** 991-996

8 **Gallo V,** Cerutti E, Riberi A, Re M, Petrino R, Pecchio F. Alpha-fetoprotein and tissue polypeptide antigen in non neoplastic hepatic disorders. *J Nucl Med Allied Sci* 1989; **33:** 89-93

9 **Alpert E,** Feller ER. Alpha-fetoprotein (AFP) in benign liver disease. Evidence that normal liver regeneration does not induce AFP synthesis. *Gastroenterology* 1978; **74:** 856-858

10 **Nguyen MH,** Garcia RT, Simpson PW, Wright TL, Keeffe EB. Racial differences in effectiveness of alpha-fetoprotein for diagnosis of hepatocellular carcinoma in hepatitis C virus cirrhosis. *Hepatology* 2002; **36:** 410-417

11 **Kohno N,** Kyoizumi S, Awaya Y, Fukuhara H, Yamakido M, Akiyama M. New serum indicator of interstitial pneumonitis activity. Sialylated carbohydrate antigen KL-6. *Chest* 1989; **96:** 68-73

12 **Stahel RA,** Gilks WR, Lehmann HP, Schenker T. Third International Workshop on Lung Tumor and Differentiation Antigens: overview of the results of the central data analysis. *Int J Cancer Suppl* 1994; **8:** 6-26

13 **Wesseling J,** van der Valk SW, Vos HL, Sonnenberg A, Hilkens J. Episialin (MUC1) overexpression inhibits integrin-mediated cell adhesion to extracellular matrix components. *J Cell Biol* 1995; **129:** 255-265

14 **Kohno N.** Serum marker KL-6/MUC1 for the diagnosis and management of interstitial pneumonitis. *J Med Invest* 1999; **46:** 151-158

15 **Sagara M,** Yonezawa S, Nagata K, Tezuka Y, Natsugoe S, Xing PX, McKenzie IF, Aikou T, Sato E. Expression of mucin 1 (MUC1) in esophageal squamous-cell carcinoma: its relationship with prognosis. *Int J Cancer* 1999; **84:** 251-257

16 **Utsunomiya T,** Yonezawa S, Sakamoto H, Kitamura H, Hokita S, Aiko T, Tanaka S, Irimura T, Kim YS, Sato E. Expression of MUC1 and MUC2 mucins in gastric carcinomas: its relationship with the prognosis of the patients. *Clin Cancer Res* 1998; **4:** 2605-2614

17 **Tanimoto T,** Tanaka S, Haruma K, Yoshihara M, Sumii K, Kajiyama G, Shimamoto F, Kohno N. MUC1 expression in intramucosal colorectal neoplasms. Possible involvement in histogenesis and progression. *Oncology* 1999; **56:** 223-231

18 **Suzuki K,** Takada H, Oka S, Kanouzawa S, Iimuro M, Kitazumi Y, Arima T, Ohyama R, Kuwayama H. Clinical significance of KL-6, a marker of interstitial pneumonia, in cases of HCV-associated chronic liver disease. *Intern Med* 2003; **42:** 650-654

19 **Moriyama M,** Matsumura H, Mikuni M, Arkawa Y, Ohshiro S, Aoki H, Yamagami H, Kaneko M, Shioda A, Saito H, Tanaka N, Arakawa Y. The clinical significance of serum KL-6 levels in patients with type C liver diseases. *Hepatol Res* 2003; **25:** 385-395

20 **Moriyama M,** Matsumura H, Watanabe A, Nakamura H, Arakawa Y, Oshiro S, Aoki H, Shimizu T, Yamagami H, Kaneko M, Shioda A, Tanaka N, Arakawa Y. Detection of serum and intrahepatic KL-6 in anti-HCV positive patients with hepatocellular carcinoma. *Hepatol Res* 2004; **30:** 24-33

21 **Hirasawa Y,** Kohno N, Yokoyama A, Inoue Y, Abe M, Hiwada K. KL-6, a human MUC1 mucin, is chemotactic for human fibroblasts. *Am J Respir Cell Mol Biol* 1997; **17:** 501-507

22 **Hassan MM,** Zaghloul AS, El-Serag HB, Soliman O, Patt YZ, Chappell CL, Beasley RP, Hwang LY. The role of hepatitis C in hepatocellular carcinoma: a case control study among Egyptian patients. *J Clin Gastroenterol* 2001; **33:** 123-126

23 **Tanaka K,** Sakai H, Hashizume M, Hirohata T. A long-term follow-up study on risk factors for hepatocellular carcinoma among Japanese patients with liver cirrhosis. *Jpn J Cancer Res* 1998; **89:** 1241-1250

Science Editor Guo SY **Language Editor** Elsevier HK

PO Box 2345, Beijing 100023, China
www.wjgnet.com
wjg@wjgnet.com

ELSEVIER

World J Gastroenterol 2005;11(42):6613-6619
World Journal of Gastroenterology ISSN 1007-9327

Modulation of gene expression in MHCC97 cells by interferon alpha

Wei-Zhong Wu, Hui-Chuan Sun, Lu Wang, Jie Chen, Kang-Da Liu, Zhao-You Tang

Wei-Zhong Wu, Hui-Chuan Sun, Lu Wang, Jie Chen, Kang-Da Liu, Zhao-You Tang, Liver Cancer Institute and Zhongshan Hospital, Fudan University, 136 Yi Xue Yuan Road, Shanghai 200032, China
Supported by the Key Projects for the Clinical Medicine from the Ministry of Public Health of China (2002–2005)
Correspondence to: Zhao-You Tang, Liver Cancer Institute and Zhongshan Hospital, Fudan University, 136 Yi Xue Yuan Road, Shanghai 200032, China. zytang@srcap.stc.sh.cn
Telephone: +86-21-6403-7181 Fax: +86-21-6403-7181
Received: 2005-03-17 Accepted: 2005-04-30

Abstract

AIM: To elucidate the molecular mechanisms of the inhibitory effects of IFN-α on tumor growth and metastasis in MHCC97 xenografts.

METHODS: Three thousand international units per milliliter of IFN-α-treated and -untreated MHCC97 cells were enrolled for gene expression analysis using cDNA microarray. The mRNA levels of several differentially expressed genes in cDNA microarray were further identified by Northern blot and RT-PCR.

RESULTS: A total of 190 differentially expressed genes including 151 IFN-α-repressed and 39 -stimulated genes or expressed sequence tags from 8 464 known human genes were found to be regulated by IFN-α in MHCC97. With a few exceptions, mRNA levels of the selected genes in RT-PCR and Northern blot were in good agreement with those in cDNA microarray.

CONCLUSION: IFN-α might exert its complicated anti-tumor effects on MHCC97 xenografts by regulating the expression of functional genes involved in cell metabolism, proliferation, morphogenesis, angiogenesis, and signaling.

Key words: Interferon α; cDNA microarray; Gene expression profile; HCC

Wu WZ, Sun HC, Wang L, Chen J, Liu KD, Tang ZY. Modulation of gene expression in MHCC97 cells by interferon alpha. *World J Gastroenterol* 2005; 11(42): 6613-6619
http://www.wjgnet.com/1007-9327/11/6613.asp

INTRODUCTION

Human hepatocellular carcinoma (HCC) is one of the most prevalent malignancies in China. Patients with HCC often die of tumor metastasis and recurrence even after curative resection. Recently, a metastatic human HCC model in nude mice (LCI-D20) and a series of HCC cell lines (MHCC97, MHCC97-H, MHCC97-L) with different metastatic potentials derived from LCI-D20 have been established in our institute[1,2]. Using this model, IFN-α significantly inhibits tumor growth and metastasis of MHCC97 xenografts has been found[3-5]. However, the underlying molecular mechanisms are still unclear.

IFN-α is a multifunctional cytokine capable of interfering with viral infection, inhibiting cell proliferation, regulating cell differentiation, as well as modulating immune response[6-9]. It is well known that these pleiotropic effects of IFN-α are mediated primarily through the transcriptional regulation of many different functional genes. Thanks to the rapid progress in human genetic projects; many functional human genes and expressed sequence tags (ESTs) are identified and released, which make us possible to use cDNA microarray to survey IFN-α-modulated genes in MHCC97 cells. In this study, we identified 190 differentially expressed genes from 8 464 known human genes, which might mediate various biological functions of IFN-α. These data provide us useful clues for further studying the anti-tumor mechanisms of IFN-α and finding the IFN-α mimics for HCC therapy.

MATERIALS AND METHODS

Cell culture

MHCC97, a metastatic HCC cell line derived from LCI-D20 xenografts, was cultured in high glucose Dulbecco's modified Eagle's medium (Gibco-BRL, NY, USA) supplemented with 10% fetal calf serum (Hyclone, UT, USA), 100 U/mL penicillin and 100 μg/mL streptomycin in 20-cm^2 tissue culture flasks. Cells were grown at 37 °C in a humidified atmosphere of 50 mL/L CO_2 and passaged every 3 d.

cDNA microarray analysis

A total of 8 464 cDNAs of known human genes (United Gene Holding, Ltd, Shanghai) were amplified by polymerase chain reaction (PCR) using universal primers and spotted onto silylated slides (CEL Associates,

Houston, TX, USA) using a Cartesian PixSys 7500 motion control robot (Cartesian Tech, Irvine, CA, USA) fitted with ChipMaker micro-spotting technology (TeleChem, Sunnyvale, CA, USA). After being hydrated, dried, cross linked and washed, the microarray was ready for use. Total RNA was isolated from IFN-α-treated and untreated (3 000 IU/mL, 16 h) cells using TRIzol (Gibco-BRL). cDNA probes were prepared by reverse transcription and purified according to the methods described by Schena *et al*.[10]. Then equal amount of cDNA from IFN-α-untreated and treated MHCC97 cells was labeled with Cy3-dUTP and Cy5-dUTP, respectively. The mixed Cy3/Cy5 probes were purified and dissolved in 20 μL of hybridization solution (0.75 mol/L NaCl, 0.075 mol/L sodium citrate, 0.4% SDS, 50% formamide, 0.1% Ficoll, 0.1% polyvinylpyrrolidone and 0.1% BSA). Microarrays were pre-hybridized with 0.5 mg/mL salmon sperm DNA at 42 °C for 6 h. After being extensively washed, the denatured (95 °C, 5 min) fluorescent-labeled probe mixture was applied onto the pre-hybridized chips and further hybridized at 42 °C for 15-17 h under a cover glass. Subsequently, chips were sequentially washed for 10 min at 60 °C with 2×SSC+0.2% SDS, 0.1×SSC+0.2% SDS and 0.1×SSC solutions and dried at room temperature (1× SSC: 150 mmol/L NaCl, 15 mmol/L sodium citrate). Both Cy3 and Cy5 fluorescent signals of hybridized chips were scanned by ScanArray 4000 (GSI Lumonics, MA, USA) and analyzed using Genepix Pro 3.0 software (BioDiscovery Inc., CA, USA). To minimize artifacts arising from low expression, only genes whose Cy3 and Cy5 fluorescent intensities were both over 200 counts, or genes whose Cy3 or Cy5 fluorescent intensity was over 800 were selected for calculating the normalization cofactor (ln(Cy5/Cy3)). Genes were identified as differentially expressed, if the ratio of Cy5/(Cy3×normalization cofactor) (Cy5/Cy3*) was more than 2 or less than 0.5.

Reverse transcription and polymerase chain reaction

MHCC97 cells (106) cultured in 20-cm^2 flasks were treated with 3 000 IU/mL IFN-α (Roche, Shanghai) for 0 or 16 h, and total RNA was extracted (RNeasy Mini Kit, QIAGEN Inc., CA, USA). One microgram RNA was used to set-up reverse transcription reactions (Gibco-BRL, NY, USA). Nine differentially expressed genes identified by cDNA microarray were selected for analysis by semi-quantitative PCR. Appropriate primers were designed using Primer3 software (http://www-genome.wi.mit.edu). γ-Actin was used as an internal standard. PCR reaction conditions and primer sequences are summarized in Table 1.

Northern blot analysis

Total RNA of 3 000 IU/mL IFN-α-treated or untreated MHCC97 cells was isolated as described above. Thirty microgram was separated by 1% agarose formaldehyde gel electrophoresis and transferred to a nylon membrane (Millipore, MA, USA) in 10×SSC by capillary blotting. The membrane was hybridized with the appropriate cDNA probe prepared from the human library of cDNA clones (Biostar Genechip Inc., Shanghai) and labeled with [α-^{32}P]dCTP (Yahui Biomedical, Beijing) using random primer (Ambion Inc., Austin, TX, USA).

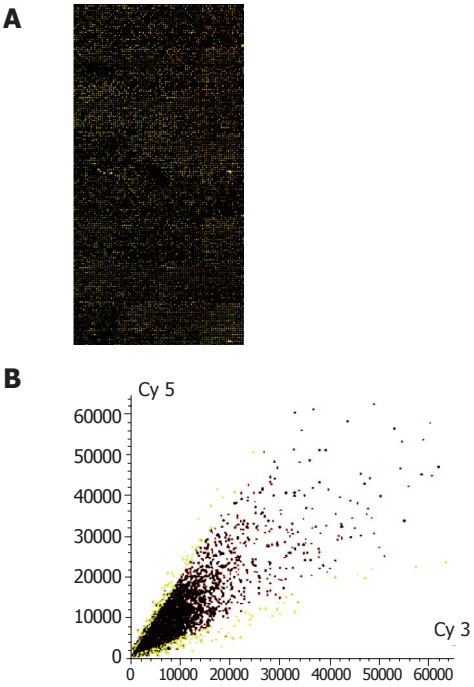

Figure 1 Representative hybrid result (**A**) and scatter plots (**B**) of cDNA microarray analysis in IFN-α treated MHCC97.

RESULTS

Gene expression profile identified by cDNA microarray

It is well known that the gene expression pattern of cells often varies with time and differentiation status and that cells derived from different individuals often have different genetic expression profiles. As a result, it is often difficult to extract useful information on the possible causes of phenotypic differences by comparing the genetic expression profiles of different cell lines. To minimize such complicated factors, we compared the gene expression profiles in 3 000 IU/mL IFN-α-treated and untreated (0 IU/mL) MHCC97 cells in two independent cDNA microarray analyses. We reasoned that such an internally consistent comparison might provide useful information on explaining the anti-tumor molecular mechanism of IFN-α in MHCC97 xenografts.

In 8 464 tested genes and ESTs, 190 genes were identified to be modulated by 3 000 IU/mL IFN-α treatment in MHCC97 cells. Among them the ex-pression of 151 genes was downregulated by IFN-α and the expression of 39 genes was upregulated by IFN-α. All differentially expressed genes are listed in Table 2 and the gene expression profiles obtained by cDNA microarray analysis are shown in Figure 1.

Nine differentially expressed genes evaluated by RT-PCR and Northern blot

To validate the results of cDNA microarray, we selected

Table 1 Primer sequence and condition for PCR analysis of selected genes

Category	Gene	Sense and antisense primers	Annealing (°C)	Cycles	Size (bp)
Cytoskeletal gene	Neutral calponin	5′-TGGCACCAGCTAGAAAACCT-3′; 5′-CAGGGACATGGAGGAGTTGT-3′	56	26	498
Proliferative gene	hMCM2	5′-ACCGAGACAATGACCTACGG-3′; 5′-CTAGCTGTCTGCCCCTTGTC-3′	56	30	382
Angiogenic gene	VEGF165 receptor	5′-GAAGCACCGAGAGAACAAGG-3; 5′-CACCTGTGAGCTGGAAGTCA-3′	56	30	359
IFN-α-induced genes	9-27	5′-TTGGTCCCTGGCTAATTCAC-3′; 5′-ATGAGGATGCCCAGAATCAG-3′	53	35	491
	ISG-56 ku	5′-AAAAGCCCACATTTGAGGTG-3′; 5′-GGCTGATATCTGGGTGCCTA-3′	54	30	451
MAPK pathway-related genes	ERK activator kinase (MEK2)	5′-CGAAAGGATCTCAGAGCTGG-3′; 5′-GTGCTTCTCTCGGAGGTACG-3′	56	26	349
	G3BP2	5′-GCAGAACCTGTTTCTCTGCC-3′; 5′-CACCACCACCTCTGGTTTCT-3′	56	30	475
	CHED	5′-TCCTTGGCGAACTCTTCACT-3′; 5′-TGCCATAAAGGGAGATCTGG-3′	56	30	336
cAMP/PI3 pathway-related gene	Adenylyl cyclase	5′-CCAGGAGCCTGAAGAATGAG-3′; 5′-GGCTTCTGAGCTCCAATCAC-3′	53	35	439
Housekeeping gene	γ-Actin	5′-ATGGAAGAAGAAATCGCCGC-3′; 5′-ACACGCAGCTCGTTGTAGAA-3′	55	25	287

nine genes whose expressions were clearly altered by IFN-α and evaluated their expressions by PCR and Northern blot. We enrolled IFN-α-regulated genes and found that the results were consistent with the previous reports[11,12].

For PCR analysis, we synthesized primers as indicated in Table 1 and performed semi-quantitative RT-PCR as outlined under "Materials and methods" after treatment of MHCC97 cells with 3 000 IU/mL IFN-α for 0 or 16 h. The transcription patterns of the same genes were also analyzed by Northern blot. Among the nine selected genes, seven downregulated genes were proved by cDNA microarray, six by RT-PCR and five by Northern blot analysis. Two stimulated genes, ISG-56 ku and 9-27 were proved by cDNA microarray, RT-PCR and Northern blot analysis. ERK activator kinase (MEK2), one repressed gene in cDNA microarray, was not changed in RT-PCR or Northern blot analysis. Thus, with a few exceptions, the results of RT-PCR and Northern blot were in good agreement with those of cDNA microarray analysis (Figure 2).

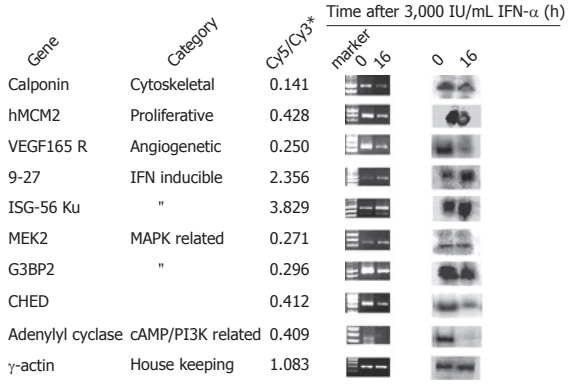

Figure 2 Confirmation of gene expression profiles in cDNA microarray analysis with RT-PCR and Northern blot.

DISCUSSION

cDNA microarray is a useful technique for rapid screening of gene expressions in cells, although the results need to be further confirmed by other molecular methods. Using this method, we found 211 hybrid dots, whose Cy5/Cy3* ratio was either more than 2 or less than 0.5 in IFN-α-treated MHCC97. Blasting the cDNA sequences in public database showed that these dots represented 190 different human genes or ESTs due to the redundant hybrids. Based on the results of RT-PCR and Northern blot, we believe that our cDNA microarray data are reliable. These differentially expressed genes might mediate the multiple biological functions of IFN-α directly or indirectly in MHCC97. We have artificially categorized these genes into nine functional clusters (Table 2).

IFN-α might interfere with cellular metabolisms by downregulating metabolic gene expression. In detail, IFN-α can inhibit glycolysis, glycogen degradation, gluconeogenesis as well as creatine or glucose transportation by repressing the expressions of liver-type phosphofructokinase (hPFKL), M2-type pyruvate kinase, brain glycogen phosphorylase, 2-oxoglutarate dehydrogenase, glucose transporter glycoprotein (SGLT) and cytosolic thyroid hormone-binding protein[13]. IFN-α can also inhibit lipolysis by reducing the expression of delta7-sterol reductase and pristanoyl-CoA oxidase, two key enzymes in lipid metabolism[14,15]. In addition, IFN-α reduces purine and pyridine biosynthesis by repressing the expression of GARs-AIRs-GART and serine hydroxymethyltransferase 2 (SHMT2). All these indicate that IFN-α-treated MHCC97 can result in lower ATP production and DNA synthesis, and slow down cell proliferation.

Many proliferation-, apoptosis- and cell cycle-regulating genes are modulated by IFN-α in MHCC97.

Table 2 Gene expression profile of MHCC97 cells induced by IFN-α

Category	GenBank ID	Gene description	Cy5/Cy3* (average)
2.1 Metabolism related genes	HUMCRTR	Creatine transporter	0.251
	HSGAGMR	GARs-AIRs-GART	0.289
	HUM2OGDH	2-Oxoglutarate dehydrogenase	0.298
	AF034544	Delta7-sterol reductase	0.318
	HUMTK	Thymidine kinase	0.333
	HSU12778	Acyl-CoA dehydrogenase	0.341
	HUMTHBP	Thyroid hormone-binding protein(p55)	0.349
	AF067127	7-Dehydrocholesterol reductase (DHCR)	0.356
	HSPRCOX	Pristanoyl-CoA oxidase	0.364
	AF035429	Cytochrome oxidase subunit 1	0.372
	AF070544	Glucose transporter glycoprotein (SGLT)	0.379
	HSPFKLA	Liver-type1-phosphofructokianse (PFKL)	0.392
	HUMSHMT	Serine hydroxymethyltransferase 2 (SHMT2)	0.407
	HUMMGPHB	Brain glycogen phosphorylase	0.413
	HUMTCBA	Cytosolic thyroid hormone-binding protein (p58)	0.415
	D88152	Acetyl-coenzyme A transporter	0.451
	HUMPKM2L	M2-type pyruvate kinase	0.456
	HSLDHBR	Lactate dehydrogenase B	2.156
	AF108211	Inorganic pyrophosphatase	2.25
	HSCOXVII	Cytochrome C oxidase VII	2.279
	HUMCYCPSK	Cytochrome C (HS7)	2.574
	HUMDBI	Diazepam binding inhibitor	2.628
2.2 Proliferation, apoptosis and damaged DNA repairing related genes	HSATPBR	Na/K ATPase beta subunit	0.208
	HUMP53T	Mutant p53 protein	0.233
	HSMITG	Mitochondrial DNA	0.309
	HSNUMAMR	Nuclear mitotic apparatus protein	0.325
	HSDNALIG3	DNA ligase III	0.34
	G28520	STS HSGC-31478 (homolog to Rad23a)	0.341
	AF096870	Estrogen-responsive B box protein	0.352
	AF001609	EXT like protein 3	0.367
	AF015283	Selenoprotein W	0.369
	AF011905	Putative checkpoint control protein hRad1	0.398
	HUMHMAM2	Minichromosome maintenance 2	0.408
	HUMRNAPII	RNA polymerase II 23 ku subunit	0.408
	AF007790	Inversely correlated with estrogen receptor Expression (ICERE-1)	0.413
	HSU78310	Pescadillo	0.43
	AF004162	Nickel-specific induction protein (Cap43)	0.434
	HSU3298	UV-damaged DNA binding factor	0.437
	HUMP1CDC47	P1cdc47	0.442
	HSU72649	B cell translocation gene 2	0.444
	AF031523	bcl-xL/bcl-2 associated death promoter (BAD)	0.481
	AF132973	CGI-39 (homolog to GRIM-19)	2.079
2.3 Morphogenesis, adhesion, and cytoskeleton remodeling related genes	D38735	Neutral calponin	0.141
	AF006082	Actin-related protein Arp2	0.197
	U01244	Fibulin 1D	0.212
	AF070593	Beta tublin	0.236
	HSU35622	EWS-E1A-F chimeric protein	0.255
	AF049259	Keratin 13	0.335
	HSPRO4HY	Prolyl 4-hydoxylase beta	0.337
	HUMCN4GEL	Collagenase type IV	0.36
	AF005654	Actin-binding double zinc-finger protein	0.378
	HSTEST	Testican	0.379
	HUMEPSURAN	Surface antigen	0.389
	AF004841	CAM-related/down-regulated by oncogenes	0.398
	HUMGLBA	Co-beta-glucosidase	0.402
	HUMCA1XIA	Alpha-1 type XI collagen	0.423
	HUMMCPGV	Macrophage capping protein	0.461
	HUMNID	Nidogen	0.497
	HSTUMP	Translationally controlled tumor protein	2.022
2.4 Signal transmitting related genes	HUMEPHT2R	Protein tyrosine kinase (NET PTK)	0.248
	HUMMEK2NF	ERK activator kinase (MEK2)	0.271
	HUMBADPTA	Beta-adaptin	0.273
	HUMP2A	Alpha-PR65	0.282
	HUMHRGAA	rab GDI alpha	0.285
	AF053535	ras-GAP/RNA binding protein G3BP2	0.296
	HSRING3GE	RING 3	0.316
	HSU45973	Pt Ins (4,5) P(2) 5-phosphatase	0.324
	HSU07139	Voltage-gated calcium channel beta	0.329
	HUMFTPB	Farnesyl-protein transferase beta	0.345
	HSU33053	Lipid-activated protein kinase (PRK1)	0.352
	HUMHK1A	Calcium-ATPase (HK1)	0.386
	HSU66406	EPH-related PTK receptor ligand LERK-8	0.386
	HSPP15	Placental protein 15	0.387
	HSADCYCL	Adenylyl cyclase	0.409
	HUMCHED	cdc2-related protein kinase (CHED)	0.412
	AF093265	Homer 3	0.415
	HSU40282	Integrin-linked kinase	0.416
	HUMGKAS	Stimulatory G protein	0.416
	HSU43939	Nuclear transport factor 2	0.429
	HUMCAK	Tyrosine protein kinase (CAK)	0.439
	HUMGNOS48	Endothelial nitric oxide synthase	0.443
	HUMCDPKIV	Calmodulin-dependent protein kinase IV	0.449
	HSPKX1MR	Protein kinase, PKX1	0.469
	D83760	Mother against dpp (Mad) related protein	0.472
	HUMEGFGRBA	EGF receptor binding protein GRB2	0.481
	HSU51004	Protein kinase C inhibitor (PKCI-1)	2.223
2.5 Tumor angiogenesis related genes	HUMRNAMBPE	Golli-mbp	0.236
	AF016050	VEGF 165 receptor/ neuropilin	0.25
	AF001307	Aryl hydrocarbon receptor nuclear translocator	0.27
	HSU64791	Golgi membrane sialoglycoprotein MG 160	0.355
	HUMPTPRZ	Protein tyrosine phosphatase Zeta-polypeptide	0.363
	HSU28811	Cysteine-rich FGFR (CFR1)	0.414
	HSU20758	Osteopontin	2.193

	HUMTR107	DNA-binding protein, TAXREB107	2.24
	HUMNEPPON	Nephropontin	2.413
2.6 Transcriptional activity related genes	S66431	Retinoblastoma binding protein 2	0.182
	HUMANT61K	Medium antigen-associated 61 ku protein	0.183
	HSU58197	Interleukin enhancer binging factor 2	0.226
	HSUBP	Upstream binding factor	0.266
	4758315	ets-related molecule, ETV5	0.267
	AF099013	Glucocorticoid modulatory element binding protein 1	0.309
	HSU72621	Lost on transformation 1(LOT1)	0.313
	HUMFOS	Oncogene protein, c-fos	0.361
	AB019524	Nuclear receptor co-repressor	0.369
	HS14AGGRE	Conserved gene telomeric to alpha globin cluster	0.398
	HSU74667	tat interactive protein (tip60)	0.404
	AF114816	KRAB-zinc finger protein SZF1-1	0.406
	HSU80456	Drosophila single-minded, SIM2	0.409
	AF117756	TRAP 150	0.41
	HSU15306	Cysteine rich DNA binding protein NFX1	0.417
	S57153	Retinoblastoma binding protein 1	0.469
	HUM56KDAPR	IEF SSP 9502	2.183
	HUMTR107	DNA binding protein. TAXREB 107	2.24
	HUMMSS1	Mammalian suppressor of sgv 1, MSS 1	2.313
2.7 mRNA and protein processing, secretory, proteolysis related genes	HSU39412	Alpha SNAP	0.141
	HSU47927	Isopeptidase T (ISOT)	0.229
	HSU72355	hsp27 ERE-TATA bind protein, HET	0.231
	AF077039	TIM17 homolog	0.238
	HUMHRH1	RNA helicase, HRH1	0.251
	AF206402	U5 SnRNP 100 ku protein	0.255
	D85429	Heat shock protein 40	0.344
	HSU85946	hSec 10p	0.378
	HSY10806	Arginine methyltransferase	0.412
	AB002135	Glycophosphatidylinositol anchor attachment 1	0.428
	AB007510	PRP8 protein	0.436
	HSU24105	Coatomer protein (COPA)	0.455
	HSCANPX	Calpain-like protease (CANPX)	0.456
	HSRBPRL7A	Ribosomal protein L7	2.067
	D89678	A+U-rich element RNA-binding protein	2.069
	HSU14966	Ribosomal protein L5	2.113
	HSRPL31	Ribosomal protein L31	2.142
	HUMPSC9	Proteasome subunit HC9	2.179
	HSU26312	Heterochromatin protein HP1 HS-gamma	2.182
	HUMRPS7A	Ribosomal protein S7	2.289
	AF106622	TIM17a	2.312
	HSUCEH3	Ubiquitin-conjugated enzyme UbCH2	2.323
	HUMRPS7A	Ribosomal protein S7	2.289
	AF106622	TIM17a	2.312
	HSUCEH3	Ubiquitin-conjugated enzyme UbCH2	2.323
	HUMRPS25	Ribosomal protein S25	2.326
	HUMRPSA3A	Ribosomal protein S3a	2.328
	HSRNASMG	Sm protein G	2.334
	HUMRPS18	Ribosomal protein S18	2.341
	HUMRP4SX	Ribosomal protein S4 isoform	2.346
	HUMPSC3	Proteasome subunit HC3	2.368
	HUMTCP20	Chaperonin protein, TCP20	2.572
	4504522	Chaperonin protein, hsp10	2.686
2.8 Tumor antigen processing, anti-viral infection related genes	HUMSAPC1	Cerebroside sulfate activator protein	0.211
	AF077011	Interleukin 16	0.23
	AF057307	Prosaposin	0.26
	HUMSIATA	Sialyltransferase	0.26
	AF055008	Epithelin 1 and 2	0.363
	HSU58766	FX protein	0.393
	HUMOSF1	OSF1	0.407
	HSU46194	RAGE 4	0.43
	HSU18121	136 ku double-stranded RNA binding protein	0.469
	AF021315	Reverse transcriptase	0.483
	S74095	Preproenkephalin A	2.115
	HUM927A	Interferon inducible protein 9-27	2.356
	HSIFI56R	Interferon inducible protein 56 ku	3.829
	HUMHCAMAP1	Interferon inducible protein 44 ku	4.03
2.9 Genes with unknown biological functions	D50928	KIAA0138	0.23
	AF132942	CGI08	0.269
	AB020677	KIAA0870	0.271
	AB011110	KIAA0538	0.277
	AB028956	KIAA1033	0.28
	HSU10362	GB36b glycoprotein	0.335
	4579277	A homolog of proteasome regulatory S2	0.352
	AB002356	KIAA0358	0.371
	4505130	A homolog of MCM3	0.371
	AB029020	KIAA1097	0.381
	HS130N43		0.383
	HSU66406	Eplg8	0.386
	HSNIPSNA1	NIPSNAP1 protein	0.391
	AB002378	KIAA0380	0.405
	HSU90907	Regulatory subunit of P55 PIK	0.407
	AB208959	KIAA1036	0.414
	AB020658	KIAA0851	0.416
	AF035282		0.416
	AF000136		0.419
	HUMORFFA	KIAA0120	0.424
	D13699	KIAA0019	0.43
	HUMORFB1	KIAA0123	0.432
	AF151830	CGI72	0.436
	AB007900	KIAA0440	0.437
	AB014595	KIAA0695	0.439
	HSM800064		0.439
	HUMORFA04	KIAA0115	0.457
	HSU79287		0.462
	AF007149		0.473
	AF007135		2.147
	AF151875	CGI117	2.184
	AF151857	CGI99	2.326
	HUMRSC508	KIAA0020	2.45

Downregulating the expression of mutant p53, mitochondrial DNA, nuclear mitotic apparatus protein (NuMA), and RNA polymerase II 23 ku subunit (polR2) might cause cell cycle arrest[16,17]. Downregulating the expression of DNA ligase III, hRad1, minichromosome maintenance 2 (hMCM2) as well as UV-damaged DNA binding factor might hinder damaged DNA repairing[18,19]. Stimulating retinoid-IFN-induced mortality 19 (GRIM-19) expression might promote IFN-α-induced apoptosis[20].

Several genes functionally related to cell morphogenesis,

adhesion, and cytoskeleton remodeling are also modulated by IFN-α in MHCC97. For example, decreasing the expression of calponin, actin-related protein 2 (Arp2), fibulin 1D, beta-tublin and epidermal surface antigen (ESA), *etc.*, might damage mitotic spindle formation and might interfere with actin-based cell motility, migration, adhesion and morphogenesis[21-24]. Reducing the expression of prolyl 4-hydroxylase beta, a key enzyme in collagen biosynthesis and type IV collagenase, a tumor-derived extracellular matrix metalloproteases might block tumor invasion and metastasis. Although most genes in this category were first identified as IFN-α regulating genes, their roles in mediating IFN-α functions need to be further studied.

In this study, we found that many genes functionally related to signal transmitting were affected by IFN-α in MHCC97. By repressing the expressions of discoidin domain receptor, integrin-linked kinase, EPH-related tyrosine kinase (EPT2) and MEK2, *etc.*, IFN-α might block cellular signaling initiated by tyrosine-kinase receptors[25,26]. By modulating the expressions of Rab GDI, Ras-related GTP-binding proteins and farnesyl-protein transferase and nuclear transport factor (NTF2) and G3BP2, a Ras-GAP/RNA binding protein, IFN-α might interfere with GTP/GDP exchange and nuclear import, thus influencing the recycles and activities of ras and its homologs[27-29]. By attenuating the expressions of adenylyl cyclase (AC) and phosphatidylinositol 4,5-bisphosphate 5-phosphatase (PtdIns (4,5)P(2)5- phospharase), a catalyzer of phosphatidylinositol 4,5-bisphosphate and PRK1, IFN-α might decrease inositol polyphosphate levels in cytosol and might inhibit the serine/threonine-kinase activities through cAMP/ PI3P signal pathway[30,31]. All these changes might exert inhibitory effects of IFN-α on MAPK and PI3K signaling. In addition, other signaling pathways such as Ca(2+), NO and TGFβ/hMAD-dependent signaling pathways are suppressed by IFN-α as well[32,33]. Plausibly Jak/STATs pathway, the most important IFN-α signaling pathway, is confirmed not to be regulated in IFN-α-treated MHCC97. The deficient expression of p48 (ISGF3γ) in this cell line may be the possible mechanism for the non-response of IFN-α priming via Jak/STATs pathway (data not shown).

In this study, we found that many angiogenic-related genes were regulated by IFN-α. By attenuating the expressions of Golli-MBP[34], VEGF 165 receptor and aryl hydrocarbon receptor nuclear translocator (ARNT)[35] as well as Golgi membrane sialoglycoprotein MG 160, a bFGF binding protein and cysteine-rich FGF receptor (CFR-1)[36], IFN-α may destroy the balance between pro- and anti-angiogenic factors and exert its inhibitory effects on tumor angiogenesis.

It is well known that cells usually respond to various stimuli by rapidly shifting the functions of transcriptional factors. Using this strategy, IFN-α might impose its anti-proliferative functions and hormone response by fluctuating the expression of several transcriptional factors or their cofactors such as retinoblastoma binding protein2 (RBP2), interleukin enhancer binding factor 2, lost on transformation 1 (LOT1) and KRAB-zinc finger protein (SZF1)[37-40].

In addition, IFN-α might hinder with mRNA/rRNA spicing and maturation by downregulating RNA helicase (HRH1), U5 snRNP[41] and affect protein transportation, secretion and proteolysis by downregulating alpha SNAP, GPAA1, hSec10p, hsp40 and isopeptidase T, a putative molecular in ubiquitin–proteasome pathway[42-44]. Meanwhile IFN-α might evoke anti-viral or tumor immune response by upregulating 9-27, 56 ku protein and p44 expressions.

Except for functionally definite genes, many ESTs with unknown functions were identified as IFN-α-regulated genes in our study (Table 2). In conclusion, cDNA microarray is a useful, rapid method for screening transcriptome of cells and potentially paves a way for elucidating IFN-α effects on tumor growth and metastasis.

ACKNOWLEDGMENT

We thank Shanghai Biostar Genechip Inc. for cDNA microarray service.

REFERENCES

1 **Sun FX,** Tang ZY, Liu KD, Ye SL, Xue Q, Gao DM, Ma ZC. Establishment of a metastatic model of human hepatocellular carcinoma in nude mice via orthotopic implantation of histologically intact tissue. *Int J Cancer* 1996; **66:** 239-243

2 **Tian J,** Tang ZY, Ye SL, Liu YK, Lin ZY, Chen J, Xue Q. New human hepatocellular carcinoma (HCC) cell line with highly metastatic potential (MHCC97) and its expressions of the factors associated with metastasis. *Br J Cancer* 1999; **81:** 814-821

3 **Wang L,** Tang ZY, Qin LX, Wu XF, Sun HC, Xue Q, Ye SL. High-dose and long-term therapy with interferon-alfa inhibits tumor growth and recurrence in nude mice bearing human hepatocellular carcinoma xenografts with high metastatic potential. *Hepatology* 2000; **32:** 43-48

4 **Wu WZ,** Sun HC, Gao YQ, Li Y, Wang L, Zhou K, Liu KD, Iliakis G, Tang ZY. Reduction in p48-ISGFgamma levels confers resistance to interferon-alpha2a in MHCC97 cells. *Oncology* 2004; **67:** 428-440

5 **Wu WZ,** Sun HC, Shen YF, Chen J, Wang L, Tang ZY, Iliakis G, Liu KD. Interferon alpha 2a downregulates VEGF expression through PI3 kinase and MAP kinase signaling pathways. *J Cancer Res Clin Oncol* 2005; **131:** 169-178

6 **Tough DF,** Borrow P, Sprent J. Induction of bystander T cell proliferation by viruses and type I interferon in vivo. *Science* 1996; **272:** 1947-1950

7 **Albini A,** Marchisone C, Del Grosso F, Benelli R, Masiello L, Tacchetti C, Bono M, Ferrantini M, Rozera C, Truini M, Belardelli F, Santi L, Noonan DM. Inhibition of angiogenesis and vascular tumor growth by interferon-producing cells: A gene therapy approach. *Am J Pathol* 2000; **156:** 1381-1393

8 **Slaton JW,** Perrotte P, Inoue K, Dinney CPN, Fidler IJ. Interferon- α -mediated down-regulation of angiogenesis-related genes and therapy of bladder cancer are dependent on optimization of biological dose and schedule. *Clin Cancer Res* 1999; **5:** 2726-2734

9 **Hong YK,** Chung DS, Joe YA, Yang YJ, Kim KM, Park YS, Yung WK, Kang JK. Efficient inhibition of in vivo human malignant glioma growth and angiogenesis by interferon-beta treatment at early stage of tumor development. *Clin Cancer Res* 2000; **6:** 3354-3360

10 **Schena M,** Shalon D, Davis RW, Brown PO. Quantitative monitoring of gene expression patterns with a complementary DNA microarray. *Science* 1995; **270:** 467-470

11 **Elco CP,** Guenther JM, Williams BR, Sen GC. Analysis of

genes induced by Sendai virus infection of mutant cell lines reveals essential roles of interferon regulatory factor 3, NF-kappaB, and interferon but not toll-like receptor 3. *J Virol* 2005; **79:** 3920-3929

12 **Martensen PM,** Justesen J. Small ISGs coming forward. *J Interferon Cytokine Res* 2004; **24:** 1-19

13 **Ishikawa N,** Oguri T, Isobe T, Fujitaka K, Kohno N. SGLT gene expression in primary lung cancers and their metastatic lesions. *Jpn J Cancer Res* 2001; **92:** 874-879

14 **Witsch-Baumgartner M,** Loffler J, Utermann G. Mutations in the human DHCR7 gene. *Hum Mutat* 2001; **17:** 172-182

15 **Jia Y,** Qi C, Zhang Z, Hashimoto T, Rao MS, Huyghe S, Suzuki Y, Van Veldhoven PP, Baes M, Reddy JK. Overexpression of peroxisome proliferator-activated receptor-alpha (PPARalpha)-regulated genes in liver in the absence of peroxisome proliferation in mice deficient in both L- and D-forms of enoyl-CoA hydratase/dehydrogenase enzymes of peroxisomal beta-oxidation system. *J Biol Chem* 2003; **278:** 47232-47239

16 **Wang J,** Silva JP, Gustafsson CM, Rustin P, Larsson NG. Increased in vivo apoptosis in cells lacking mitochondrial DNA gene expression. *Proc Natl Acad Sci U S A* 2001; **98:** 4038-4043

17 **Taimen P,** Viljamaa M, Kallajoki M. Preferential expression of NuMA in the nuclei of proliferating cells. *Exp Cell Res* 2000; **256:** 140-149

18 **Maiorano D,** Lemaitre JM, Mechali M. Stepwise regulated chromatin assembly of MCM2-7 proteins. *J Biol Chem* 2000; **275:** 8426-8431

19 **Brand M,** Moggs JG, Oulad-Abdelghani M, Lejeune F, Dilworth FJ, Stevenin J, Almouzni G, Tora L. UV-damaged DNA-binding protein in the TFTC complex links DNA damage recognition to nucleosome acetylation. *EMBO J* 2001; **20:** 3187-3196

20 **Chidambaram NV,** Angell JE, Ling W, Hofmann ER, Kalvakolanu DV. Chromosomal localization of human GRIM-19, a novel IFN-beta and retinoic acid-activated regulator of cell death. *J Interferon Cytokine Res* 2000; **20:** 661-665

21 **Curtis M,** Nikolopoulos SN, Turner CE. Actopaxin is phosphorylated during mitosis and is a substrate for cyclin B1/cdc2 kinase. *Biochem J* 2002; **363:** 233-242

22 **Kovacs EM,** Goodwin M, Ali RG, Paterson AD, Yap AS. Cadherin-directed actin assembly: E-cadherin physically associates with the Arp2/3 complex to direct actin assembly in nascent adhesive contacts. *Curr Biol* 2002; **12:** 379-382

23 **Roof DJ,** Hayes A, Adamian M, Chishti AH, Li T. Molecular characterization of abLIM, a novel actin-binding and double zinc finger protein. *J Cell Biol* 1997; **138:** 575-588

24 **Bickel PE,** Scherer PE, Schnitzer JE, Oh P, Lisanti MP, Lodish HF. Flotillin and epidermal surface antigen define a new family of caveolae-associated integral membrane proteins. *J Biol Chem* 1997; **272:** 13793-13802

25 **Hannigan GE,** Leung-Hagesteijn C, Fitz-Gibbon L, Coppolino MG, Radeva G, Filmus J, Bell JC, Dedhar S. Regulation of cell adhesion and anchorage-dependent growth by a new beta 1-integrin-linked protein kinase. *Nature* 1996; **379:** 91-96

26 **Tang XX,** Biegel JA, Nycum LM, Yoshioka A, Brodeur GM, Pleasure DE, Ikegaki N. cDNA cloning, molecular characterization, and chromosomal localization of NET(EPHT2), a human EPH-related receptor protein-tyrosine kinase gene preferentially expressed in brain. *Genomics* 1995; **29:** 426-437

27 **Ishizaki H,** Miyoshi J, Kamiya H, Togawa A, Tanaka M, Sasaki T, Endo K, Mizoguchi A, Ozawa S, Takai Y. Role of rab GDP dissociation inhibitor alpha in regulating plasticity of hippocampal neurotransmission. *Proc Natl Acad Sci USA* 2000; **97:** 11587-11592

28 **Prigent M,** Barlat I, Langen H, Dargemont C. IkappaBalpha and IkappaBalpha /NF-kappa B complexes are retained in the cytoplasm through interaction with a novel partner, RasGAP SH3-binding protein 2. *J Biol Chem* 2000; **275:** 36441-36449

29 **Brassard DL,** English JM, Malkowski M, Kirschmeier P, Nagabhushan TL, Bishop WR. Inhibitors of farnesyl protein transferase and MEK1,2 induce apoptosis in fibroblasts transformed with farnesylated but not geranylgeranylated H-Ras. *Exp Cell Res* 2002; **273:** 138-146

30 **Tu JC,** Xiao B, Yuan JP, Lanahan AA, Leoffert K, Li M, Linden DJ, Worley PF. Homer binds a novel proline-rich motif and links group 1 metabotropic glutamate receptors with IP3 receptors. *Neuron* 1998; **21:** 717-726

31 **Di Pasquale G,** Stacey SN. Adeno-associated virus Rep78 protein interacts with protein kinase A and its homolog PRKX and inhibits CREB-dependent transcriptional activation. *J Virol* 1998; **72:** 7916-7925

32 **Tamura N,** Tai Y, Sugimoto K, Kobayashi R, Konishi R, Nishioka M, Masaki T, Nagahata S, Tokuda M. Enhanced expression and activation of Ca(2+)/calmodulin-dependent protein kinase IV in hepatocellular carcinoma. *Cancer* 2000; **89:** 1910-1916

33 **Mostert V,** Dreher I, Kohrle J, Wolff S, Abel J. Modulation of selenoprotein P expression by TGF-beta(1) is mediated by Smad proteins. *Biofactors* 2001; **14:** 135-142

34 **Baron P,** Constantin G, Meda L, Scarpini E, Scarlato G, Trinchieri G, Monastra G, Rossi F, Cassatella MA. Cultured human monocytes release proinflammatory cytokines in response to myelin basic protein. *Neurosci Lett* 1998; **252:** 151-154

35 **Onita T,** Ji PG, Xuan JW, Sakai H, Kanetake H, Maxwell PH, Fong GH, Gabril MY, Moussa M, Chin JL. Hypoxia-induced, perinecrotic expression of endothelial Per-ARNT-Sim domain protein-1/hypoxia-inducible factor-2alpha correlates with tumor progression, vascularization, and focal macrophage infiltration in bladder cancer. *Clin Cancer Res* 2002; **8:** 471-480

36 **Shen B,** Arese M, Gualandris A, Rifkin DB. Intracellular association of FGF-2 with the ribosomal protein L6/TAXREB107. *Biochem Biophys Res Commun* 1998; **252:** 524-528

37 **Lopez-Fernandez LA,** Parraga M, del Mazo J. Ilf2 is regulated during meiosis and associated to transcriptionally active chromatin. *Mech Dev* 2002; **111:** 153-157

38 **Cao X,** Sudhof TC. A transcriptionally [correction of transcriptively] active complex of APP with Fe65 and histone acetyltransferase Tip60. *Science* 2001; **293:** 115-120

39 **Peng H,** Begg GE, Harper SL, Friedman JR, Speicher DW, Rauscher FJ 3rd. Biochemical analysis of the Kruppel-associated box (KRAB) transcriptional repression domain. *J Biol Chem* 2000; **275:** 18000-18010

40 **Woods SL,** Whitelaw ML. Differential activities of murine single minded 1 (SIM1) and SIM2 on a hypoxic response element. Cross-talk between basic helix-loop-helix/per-Arnt-Sim homology transcription factors. *J Biol Chem* 2002; **277:** 10236-10243

41 **Teigelkamp S,** Mundt C, Achsel T, Will CL, Luhrmann R. The human U5 snRNP-specific 100-kD protein is an RS domain-containing, putative RNA helicase with significant homology to the yeast splicing factor Prp28p. *RNA* 1997; **3:** 1313-1326

42 **Moro F,** Sirrenberg C, Schneider HC, Neupert W, Brunner M. The TIM17.23 preprotein translocase of mitochondria: composition and function in protein transport into the matrix. *EMBO J* 1999; **18:** 3667-3675

43 **Hiroi Y,** Chen R, Sawa H, Hosoda T, Kudoh S, Kobayashi Y, Aburatani H, Nagashima K, Nagai R, Yazaki Y, Medof ME, Komuro I. Cloning of murine glycosyl phosphatidylinositol anchor attachment protein, GPAA1. *Am J Physiol Cell Physiol* 2000; **279:** C205-C212

44 **Hernandez MP,** Chadli A, Toft DO. HSP40 binding is the first step in the HSP90 chaperoning pathway for the progesterone receptor. *J Biol Chem* 2002; **277:** 11873-11881

Science Editor Wang XL and Guo SY **Language Editor** Elsevier HK

PO Box 2345, Beijing 100023, China
www.wjgnet.com
wjg@wjgnet.com

ELSEVIER

World J Gastroenterol 2005;11(42):6620-6623
World Journal of Gastroenterology ISSN 1007-9327

Detection of germline mutations of *hMLH1* and *hMSH2* based on cDNA sequencing in China

Chao-Fu Wang, Xiao-Yan Zhou, Tai-Ming Zhang, Meng-Hong Sun, Da-Ren Shi

Chao-Fu Wang, Xiao-Yan Zhou, Tai-Ming Zhang, Meng-Hong Sun, Da-Ren Shi, Laboratory of Molecular Pathology, Cancer Hospital of Fudan University; Department of Oncology, Shanghai Medical College of Fudan University, Shanghai 200032, China
Supported by the Key Programs of Shanghai Medical Subjects, No. 05 III 004
Correspondence to: Dr. Xiao-Yan Zhou, Laboratory of Molecular Pathology, Cancer Hospital of Fudan University, 270 Dongan Road, Shanghai 20032, China. xyzhou100@yahoo.com
Telephone: +86-21-64175590-3646
Received: 2005-03-18 Accepted: 2005-04-18

Abstract

AIM: To detect the germline mutations of *hMLH1* and *hMSH2* based on mRNA sequencing to identify hereditary non-polyposis colorectal cancer (HNPCC) families.

METHODS: Total RNA was extracted from peripheral blood of 14 members from 12 different families fulfilling Amsterdam criteria II. mRNA of *hMLH1* and *hMSH2* was reversed with special primers and heat-resistant reverse transcriptase. cDNA was amplified with expand long template PCR and cDNA sequencing analysis was followed.

RESULT: Seven germline mutations were found in 6 families (6/12, 50%), in 4 *hMLH1* and 3 *hMSH2* mutations (4/12, 33.3%); (3/12, 25%). The mutation types involved 4 missense, 1 silent and 1 frame shift mutations as well as 1 mutation in the non-coding area. Four out of the seven mutations have not been reported previously. The 4 *hMLH1* mutations were distributed in exons 8, 12, 16, and 19. The 3 *hMSH2* mutations were distributed in exons 1 and 2. Six out of the 7 mutations were pathological, which were distributed in 5 HNPCC families.

CONCLUSION: Germline mutations of *hMLH1* and *hMSH2* can be found based on cDNA sequencing so as to identify HNPCC family, which is highly sensitive and has the advantages of cost and time saving.

Key words: *hMLH1*; *hMSH2*; Colorectal cancer; Hereditary non-polyposis; Reverse transcription; Germline mutation

Wang CF, Zhou XY, Zhang TM, Sun MH, Shi DR. Detection of germline mutations of *hMLH1* and *hMSH2* based on cDNA sequencing in China. *World J Gastroenterol* 2005; 11(42): 6620-6623

http://www.wjgnet.com/1007-9327/11/6620.asp

INTRODUCTION

hMLH1 and *hMSH2* are the two most important genes for HNPCC, which is the most common hereditary colon syndrome accounting for 10% of all colorectal cancers. It is autosomally dominant with a penetrance rate of 80-90%. HNPCC occurrence is closely associated with deficiency or loss of function of mismatch repair (MMR) genes. Affected individuals have an approximately 70% lifetime risk of colon cancer with a mean onset age of 44 years and an approximately 40% lifetime risk of endometrial cancer in females. At least 5 MMR genes, *hMLH1, hMSH2, hMSH6, hPMS1,* and *hPMS2*, have been implicated in HNPCC[1,2]. Information of genetic linkage analysis shows that germline mutations of *hMLH1* and *hMSH2* account for nearly 90% of all germline mutations found in HNPCC[3]. Germline mutations in MMR genes predispose to colorectal and other HNPCC associated epithelial cancers. Identification of MMR gene germline mutations has direct clinical implications in counseling and management of HNPCC.

Methods such as microsatellite instability (MSI), immunohistochemistry (IHC)[4-6], and sequencing of genes are employed to screen HNPCC. The most specific method is to detect the germline mutations of MMR. Its cost and sensitivity limitations can be overcome at least in part by RNA-based analysis[7]. It is the first time in China that we identified HNPCC families by detecting germline mutations of *hMLH1* and *hMSH2* genes based on cDNA sequencing with special primers and heat-resistant reverse transcriptase.

MATERIALS AND METHODS

Subjects

Fourteen anticipants from 12 unrelated families fulfilling Amsterdam criteria II for HNPCC were studied. Personal and family cancer history was obtained from the patients and their relatives. Pathological diagnosis and death were confirmed by review of medical records, pathological reports or death certificates.

Samples

Three microliters of peripheral blood was taken from each participant. Total RNA was extracted using TRIzol (Sigma Company) according to the manufacturer's instructions.

RT-PCR

cDNA was synthesized with transcriptor reverse transcriptase (Roche Diagnostics) using 0.5 μg of total RNA and specific primers complementary to the 3' end of *hMLH1* (2484-TATGTTAAGACACATCTATTTATTTA-2459) and to the 3' end of *hMSH2* (3145-CCACCAAACTACA TGATTTTATTTATAAAATTC-3114). RT was performed at 60 °C for 60 min.

cDNA of *hMLH1* and *hMSH2* was amplified in two overlapping fragments using primers (Table 1) to generate products of ~2 000 bp. PCR was performed using expand long template PCR (Roche Diagnostics) at 94 °C for 5 min; then 10 cycles at 94 °C for 30 s, at 59 °C for 30 s, at 68 °C for 3 min; 32 cycles at 94 °C for 30 s, at 57 °C for 30 s, at 68 °C for 3 min with a final elongation at 68 °C for 7 min.

PCR products were size fractionated by agarose gel electrophoresis and analyzed by ethidium bromide staining.

Sequencing

Purified PCR fragments were sequenced directly using a DNA sequencing kit according to Applied Biosystems from USA with BigDye Terminators on an ABI3700 automated DNA sequencer.

cDNA of *hMLH1* (2 484 bp) was sequenced in six overlapping fragments and cDNA of *hMSH2* (3 145 bp) was sequenced in eight overlapping fragments using primers (Table 2).

Table 1 Sequence and localization of primers used for amplification of cDNA of *hMLH1* and *hMSH2*

Sense	Antisense
hMLH1-1F(1-18)	*hMLH1*-5R(2198-2175)
CTTGGCTCTTCTGGCGCC	GAGCGCAAGGCTTTATAGACAATG
hMLH1-4F(1333-1353)	*hMLH1*-6R(2484-2459)
GCTGAAGTGGCTGCCAAAAAT	TATGTTAAGACACATCTATTTATTTA
hMSH2-1F(1-21)	*hMSH2*-7R(2753-2732)
GGCGGGAAACAGCTTAGTGGG	GGGCATTTGTTTCACCTTGGAC
hMSH2-6F(1898-1920)	*hMSH2*-8R(3145-3114)
CGTGTCAAATGGAGCACCTGTTC	CCACAAACTACATGATTTTATTTATAAAATTC

RESULTS

The sizes of amplified *hMLH1* and *hMSH2* segments were respected (Figure 1). Seven germline mutations were found in 6 out of 12 families, 4 *hMLH1* and 3 *hMSH2* mutations (4/12, 33.3%); (3/12, 25%). The mutation types involved 4 missense, 1 silent and 1 frame shift mutations as well as 1 mutation in non-coding area, including *hMLH1* mutation in family H2 at 649 codon 217 exon 8: CGC→TGC; *hMLH1* mutation in family H31 at 1742 codon 581 exon 16: CCG→CTG; *hMLH1* missense mutation in family H114 at 1151 codon 384 exon 12: GTT→GAT; family H111 *hMLH1* non-coding area at 2438 exon 19: A→C; family H11 *hMSH2* at 14 codon 5: CCG→CAG; family H38 hMSH2 mutations at 295 and 296 codon 99 exon 2: 295: A→C, 296:del.G (Table 3, Figure 2).

DISCUSSION

Colorectal cancer (CRC) is one of the most common malignant tumors and its incidence is increasing gradually. According to the different molecular mechanism, CRC is divided into sporadic and genetic types. The latter type HNPCC is characterized by its early onset[8-10], location in the proximal colon and an increased risk of neoplasms in extracolonic organs including endometrium, stomach, urothelium, small intestine, ovary and multiple

Table 2 *hMLH1* and *hMSH2* primers used for sequencing of cDNA

Sense		Antisense	
hMLH1-1F	CCTGGCTCTTCTGGCGCC	*hMLH1*-1R	CTTTTCTCCTCGTGGCTATGTTGT
hMLH1-2F	ATGTGCTGGCAATCAAGGGA	*hMLH1*-2R	GGTGCACATTAACATCCACATTCT
hMLH1-3F	CCAAAAACACACACCCATTCCT	*hMLH1*-3R	CCTTTGTTGTATCCCCCTCCA
hMLH1-4F	GCTGAAGTGGCTGCCAAAAAT	*hMLH1*-4R	CATCTTCCTCTGTCCAGCCACTC
hMLH1-5F	TTGCCATGCTTGCCTTAGATAGTC	*hMLH1*-5R	GAGCGCAAGGCTTTATAGACAATG
hMLH1-6F	GCTCCATTCCAAACTCCT	*hMLH1*-6R	TATGTTAAGACACATCTATTTATTTA
hMSH2-1F	GGCGGGAAACAGCTTAGTGGG	*hMSH2*-1R	CTCTGGCCATCAACTGCGGAC
hMSH2-2F	GGCTTCTCCTGGCAATCTCTCTCA	*hMSH2*-2R	CTTGATTACCGCAGACAGTGATGAAAC
hMSH2-3F	GCAAAAAGGGAGAGCAGATGAATAGTG	*hMSH2*-3R	GGCAAGTCGGTTAAGATCTGGGAAT
hMSH2-4F	AGATGCAGAATTGAGGCAGACTTTACA	*hMSH2*-4R	GGACTTTTTCTTCCTTACAGGTTACACG
hMSH2-5F	CAGAGATCTTGGCTTGGACCCT	*hMSH2*-5R	TTCAACACAAGCATGCCTGGAT
hMSH2-6F	CGTGTCAAATGGAGCACCTGTTC	*hMSH2*-6R	GATTGGCCAAGGCAGTAAGTTCAT
hMSH2-7F	AATCATAGATGAATTGGGAAGAGGAACT	*hMSH2*-7R	GGGCATTTGTTTCACCTTGGAC
hMSH2-8F	CTATCTGGAAAGAGAGCAAGGTGAA	*hMSH2*-8R	CCACAAACTACATGATTTTATTTATAAAATTC

Table 3 *hMLH1* and *hMSH2* mutations detected by cDNA sequencing

Families	Genes	Exon	Codons affected	DNA change	Amino acid change	Mutation types
H31	*hMLH1*	16	581	T>C, at 1742	Pro→Leu	Missense
H111	*hMLH1*	19	Non-coding area	A>T, at 2438		
H114	*hMLH1*	12	384	T→A, at 1151	Val→Asp	Missense
H2	*hMLH1*	8	217	T->C, at 649	Arg→Cyc	Missense
H11	*hMLH1*	1	5	A>C, at 14	Pro→His	Missense
H38	*hMLH1*	2	99	A>C, at 295	Arg→Arg	Silent
H38	*hMLH1*	2	99	Del G, at 296	Frame shift	Frame shift

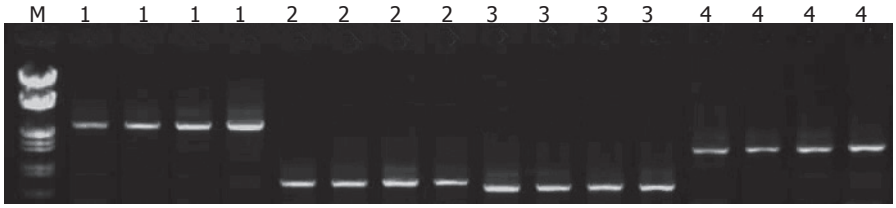

Figure 1 Amplified segments of *hMLH1* and *hMSH2*. "M" is mark. Lanes 1-4 sizes of segments.

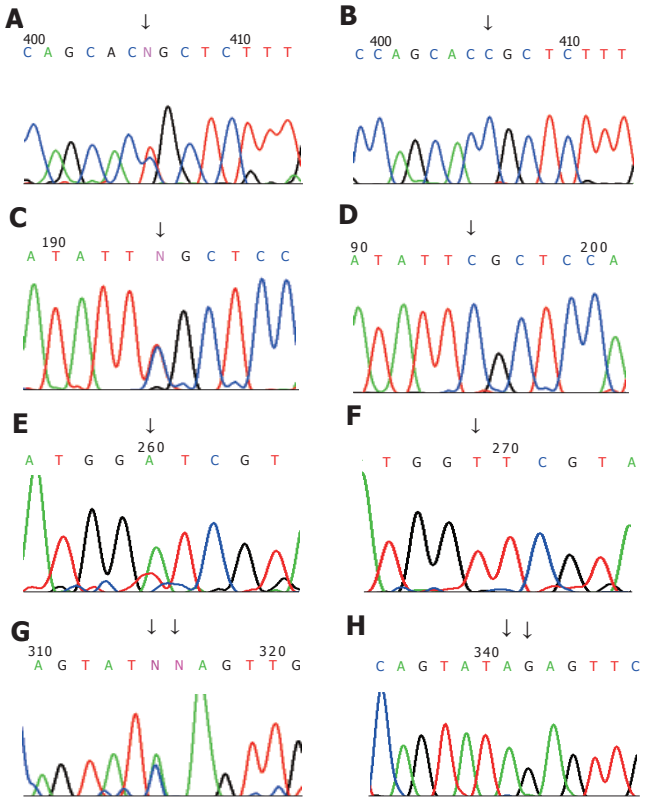

Figure 2 *hMLH1* and *hMSH2* mutations (**A, C, E, G**) and wild-type sequence (**B, D, F, H**) in families H31, H2, H114, and H38 at different codons. Arrows indicate the corresponding sites of mutation.

metachronous CRCs[9,11-14]. Its prognosis is better than sporadic type of CRC[15]. HNPCC is closely associated with the deficiency or loss of MMR gene function. Identification of MMR gene germline mutations has direct clinical implications in counseling and management of HNPCC.

Methods are available for the identification of HNPCC. The most specific method is to detect the germline mutations of MMR genes. Up to now, the germline mutations are mainly detected by genomic DNA-based sequencing (gDNA). A lot of information shows that the germline mutations of MMR genes associated with HNPCC are mainly localized in exons[3,5,7,13]. The gDNA-based sequencing is invariably affected by introns. cDNA-based sequencing of MMR genes has been reported recently. The new technique utilizes specific primers and heat-resistant reverse trancriptase to specifically synthesize cDNA of MMR genes, then full-length cDNA is amplified in two over fragments using specific primers followed by sequencing analysis of cDNA. The technique can successfully avoid the influence of introns. Additionally, it is well known that RNA is easily decayed. If RNA samples are stored too long, reverse transcription with random primers and common reverse transcription enzyme often fails, while the new technique employs specific primers and heat-resistant reverse trancriptase, the limitations can be overcome at least in part, thus improving the specificity and efficiency. Anna *et al*.[7] compared the two techniques and found that cDNA-based sequencing not only has the advantage of specificity and efficiency, but also a lower cost, being 2.5-3 times less expensive than gDNA-based sequencing. We used 35 pair primers to amplify the two genes in the past, and only 4 pair primers were used in the present study, the procedure is greatly simplified.

We detected 7 germline mutations in 14 anticipants with HNPCC from 12 different families employing the new technique. The 3 mutations, at sites 1151, 14, and 217 in *hMLH1* reported, the first two have been verified to be pathological. Moreover, the mutation at 1151 in *hMLH1* has been found only in Japan and Korea, which is likely to be a hot mutation site in East Asia. The mutation at site 217 in *hMLH1* occurs at a less conserved region is in 80 healthy Japanese. Whether it is pathological or not needs further study. None of the 4 unreported mutations belongs to polymorphism[17]. The 6 pathological mutations (2 reported, 4 unreported) were distributed in 5 HNPCC families in our study.

Of course, all mutations cannot be detected by the improved technique. For example, mutations in the promoter and 3'-untranslated regions of *hMLH1* and *hMSH2* cannot be detected. Sequencing of individual exons of gDNA also has such limitations.

Up to now, there is no optimal method to screen HNPCC patients or their families. The new technique can be utilized to screen HNPCC patients and their families, which may achieve a better result.

REFERENCES

1 **Huang D,** Chen C, Sun W, Strom CM, Bender RA. High-throughput gene sequencing assay development for hereditary nonpolyposis colon cancer. *Clin Colorectal Cancer* 2004; **4:** 275-279

2 **Wijnen J,** de Leeuw W, Vasen H, van der Klift H, Moller P, Stormorken A, Meijers-Heijboer H, Lindhout D, Menko F, Vossen S, Moslein G, Tops C, Brocker-Vriends A, Wu Y, Hofstra R, Sijmons R, Cornelisse C, Morreau H, Fodde R. Familial endometrial cancer in female carriers of MSH6

germline mutations. *Nat Genet* 1999; **23:** 142-144
3 **Peltomaki P,** Vasen H. Mutations associated with HNPCC predisposition -- Update of ICG-HNPCC/INSiGHT mutation database. *Dis Markers* 2004; **20:** 269-276
4 **Shin KH,** Shin JH, Kim JH, Park JG. Mutational analysis of promoters of mismatch repair genes hMSH2 and hMLH1 in hereditary nonpolyposis colorectal cancer and early onset colorectal cancer patients: identification of three novel germline mutations in promoter of the hMSH2 gene. *Cancer Res* 2002; **62:** 38-42
5 **Peltomaki P,** Gao X, Mecklin JP. Genotype and phenotype in hereditary nonpolyposis colon cancer: a study of families with different vs. shared predisposing mutations. *Fam Cancer* 2001; **1:** 9-15
6 **Wahlberg SS,** Schmeits J, Thomas G, Loda M, Garber J, Syngal S, Kolodner RD, Fox E. Evaluation of microsatellite instability and immunohistochemistry for the prediction of germ-line MSH2 and MLH1 mutations in hereditary nonpolyposis colon cancer families. *Cancer Res* 2002; **62:** 3485-3492
7 **Jakubowska A,** Gorski B, Kurzawski G, Debniak T, Hadaczek P, Cybulski C, Kladny J, Oszurek O, Scott RJ, Lubinski J. Optimization of experimental conditions for RNA-Based sequencing of MLH1 and MSH2 Genes. *Hum Mutat* 2001; **17:** 52-60
8 **Anwar S,** Hall C, White J, Deakin M, Farrell W, Elder JB. Hereditary non-polyposis colorectal cancer: an updated review. *Eur J Surg Oncol* 2000; **26:** 635-645
9 **Jass JR.** HNPCC and sporadic MSI-H colorectal cancer: a review of the morphological similarities and differences. *Fam Cancer* 2004; **3:** 93-100
10 **Aarnio M,** Sankila R, Pukkala E, Salovaara R, Aaltonen LA, de la Chapelle A, Peltomaki P, Mecklin JP, Jarvinen HJ. Cancer risk in mutation carriers of DNA-mismatch-repair genes. *Int J Cancer* 1999; **81:** 214-218
11 **Lucci-Cordisco E,** Zito I, Gensini F, Genuardi M. Hereditary nonpolyposis colorectal cancer and related conditions. *Am J Med Genet A* 2003; **122:** 325-334
12 **Park YJ,** Shin KH, Park JG. Risk of gastric cancer in hereditary nonpolyposis colorectal cancer in Korea. *Clin Cancer Res* 2000; **6:** 2994-2998
13 **Ericson K,** Halvarsson B, Nagel J, Rambech E, Planck M, Piotrowska Z, Olsson H, Nilbert M. Defective mismatch-repair in patients with multiple primary tumours including colorectal cancer. *Eur J Cancer* 2003; **39:** 240-248
14 **Lynch HT,** de la Chapelle A. Genetic susceptibility to non-polyposis colorectal cancer. *J Med Genet* 1999; **36:** 801-818
15 **Watson P,** Lin KM, Rodriguez-Bigas MA, Smyrk T, Lemon S, Shashidharan M, Franklin B, Karr B, Thorson A, Lynch HT. Colorectal carcinoma survival among hereditary nonpolyposis colorectal carcinoma family members. *Cancer* 1998; **83:** 259-266
16 **Wang Y,** Friedl W, Lamberti C, Nothen MM, Kruse R, Propping P. A novel missense mutation in the DNA mismatch repair gene hMLH1 present among East Asians but not among Europeans. *Hum Hered* 1998; **48:** 87-91
17 **Peltomaki P,** Vasen HF. Mutations predisposing to hereditary nonpolyposis colorectal cancer: database and results of a collaborative study. The International Collaborative Group on Hereditary Nonpolyposis Colorectal Cancer. *Gastroenterology* 1997; **113:** 1146-1158

Science Editor Wang XL and Guo SY **Language Editor** Elsevier HK

PO Box 2345, Beijing 100023, China
www.wjgnet.com
wjg@wjgnet.com

ELSEVIER

World J Gastroenterol 2005;11(42):6624-6630
World Journal of Gastroenterology ISSN 1007-9327

Cytokine profile in Egyptian hepatitis C virus genotype-4 in relation to liver disease progression

Abdel-Rahman N Zekri, Mohammed S El-Din Ashour, Ahmed Hassan, Hanaa M Alam El-Din, Amal MR El-Shehaby, Maha A Abu-Shady

Abdel-Rahman N Zekri, Hanaa M Alam El-Din, Virology and Immunology Unit, Cancer Biology Department, National Cancer Institute, Cairo University, Egypt
Mohammed S El-Din Ashour, Maha A Abu-Shady, Microbiology Department, Faculty of Pharmacy, Azhar University, Egypt
Ahmed Hassan, Microbiology and Immunology Department, Sohag Faculty of Medicine, South Valley University, Egypt
Amal MR El-Shehaby, Biochemistry Department, El-Kaser El-Aini School of Medicine, Cairo University, Egypt
Supported by the USA project BIO-8-002-009 and by the Grant office of National Cancer Institute, Cairo University
Correspondence to: Abdel-Rahman N Zekri, MSc, PhD, Virology and Immunology Unit, Cancer Biology Department, National Cancer Institute, Fom El-Khalig, Cairo 11796, Egypt. ncizakri@starnet.com.eg
Telephone: +20-10-1413-521 Fax: +20-2-3644-720
Received: 2004-05-25 Accepted: 2004-07-19

Abstract

AIM: To observe the imbalance between T helper cell Th1 and Th2 cytokines in several chronic hepatitis disease at different stages of disease progression.

METHODS: We measured the cytokine levels of Th1 (IL-2 and IL-2R), Th2 (IL-10) and the pro-inflammatory cytokines (IL-6 and IL-6R and TNF and TNF-RI and II) by the ELISA technique in the sera of 33 hepatocellular carcinoma (HCC) patients and 20 chronic liver disease (CLD) patients. In addition, 20 asymptomatic hepatitis C virus carriers and 20 healthy subjects negative for hepatitis C virus(HCV) markers served as controls.

RESULTS: Anti-HCV antibodies were found to be positive in 94% of HCC cases and 75% of CLD cases. On the other hand, HCV viremia was detected using RT-PCR in 67% of HCC cases and 65% of CLD cases. HBsAg was positive in 9% of HCC cases and 30% of CLD cases. Also bilharzial-Ab was positive in 55% of HCC cases, 65% of CLD cases and in 70% of asymptomatic carriers (ASC). HCC patients had significantly higher values of IL-2R, TNF-RII (P<0.001), and TNF-RI (P>0.05), but lower TNFα (P<0.001) and IL-6 (P = 0.032) in comparison to ASC. But, in comparison to non-cancer controls, HCC patients had higher values of IL-2R, IL-6R, TNF-RI and TNF-RII, but lower TNF-α (P<0.001). CLD patients had higher IL-2R, TNF-RI, and TNF-RII (P<0.001) than ASC. But, in comparison to non-cancer controls, CLD patients had higher values of IL-2R, TNF-RI and TNF-RII, but lower TNF-α (P<0.001). IL-10 was higher (though not significantly) in HCC and CLD patients than in symptomatic carriers and non-cancer controls.

CONCLUSION: Liver disease progression from CLD to HCC due to HCV genotype-4 infection is associated with an imbalance between Th1 and Th2 cytokines. IL-2R, TNF-RI, and TNF-RII could be used as potential markers.

Key words: Cytokine; HCV; Genotype-4; Liver disease

Zekri ARN, Ashour MSE, Hassan A, Alam El-Din MA, El-Shehaby AMR, Abu-Shady MA. Cytokine profile in Egyptian HCV genotype-4 in relation to liver disease progression. *World J Gastroenterol* 2005; 11(42): 6624-6630
http://www.wjgnet.com/1007-9327/11/6624.asp

INTRODUCTION

Hepatitis C virus(HCV) is a common cause of hepatocellular injury that is associated with complex and vigorous immunologic mechanisms. Both humoral and cell-mediated immune responses participate in the host defense against HCV infection, but it is increasingly recognized that cellmediated response to the cytokine system plays a role in the im-munopathogenesis of chronic hepatitis C[1].

Cytokines constitute a complex network of molecules involved in the regulation of the inflammatory response and the homeostasis of organ functions. Moreover, cytokines coordinate physiologic and pathologic processes going on in the liver, such as liver growth and regeneration, inflammatory processes including viral liver disease, liver fibrosis and cirrhosis. Liver growth and regeneration are regulated by several cytokines. The cell-mediated immune response plays a central role in hepatocellular necrosis and in the immunopathogenic mechanisms involved in viral clearance and persistence in liver disease of viral etiology[2].

T lymphocytes and immunoregulatory cytokines are of critical importance in the host defense against HCV infection. T-helper type 1 (Th1) cytokines (interleukin-2 [IL-2], interferon-γ [IFN-γ]) are required for host anti-viral responses, while T-helper type 2 (Th2) cytokines (IL-4, IL-10) can inhibit the development of these effectors[3]. It has been demonstrated that pro-inflammatory IL-6 is able

to influence hepatocarcinoma progression in patients with liver cancer[4]. Tumor necrosis factor (TNF) plays a role in the pathogenesis of chronic hepatitis C[5]. Also, chronic HCV infection is associated with an increase in the levels of soluble TNF receptors I and II[6].

Screening high-risk populations with ultrasonography and serum αFP levels produces diagnosis of only 40-60% of patients with hepatocellular carcinoma (HCC) at a stage where the tumor can be resected or treated with curative intent[7].

In this study, we aimed to characterize serum cytokine levels of IL-2 and its receptor (IL-2R), IL-6 and its receptor (IL-6R), IL-10, TNF-α and its soluble receptors (TNF-RI and TNF-RII) by enzyme immunosorbent assay in HCC patients, chronic liver disease (CLD) patients, and HCV asymptomatic carriers (ASC), to figure out the possible imbalance between Th1 and Th2-like cytokines and their possible relation to hepatocarcinogenesis, as well as to evaluate the clinical significance of these cytokines in different stages of HCV infection, and their possible use as markers of disease progression, since there are no reliable markers for disease progression from CLD to HCC.

PATIENTS AND METHODS

Patients and controls

This study was conducted on 33 histologically proven HCC and 20 CLD patients (i.e., chronic active hepatitis with or without cirrhosis). All patients were presented before treatment to the specialized liver clinic of the National Cancer Institute (NCI), Cairo University, between April 2000 and June 2001. The study also included 40 control subjects: 20 asymptomatic carriers of HCV infection (ASC) as positive controls (positive for both HCV-AB and HCV RT-PCR), and 20 subjects without infection with HCV (NC) as negative controls (negative for HCV by both anti-HCV-Ab and HCV RT-PCR). The criteria for inclusion in the study groups were as follows: (a) ASC group: persistently normal alanine aminotransferase (ALT) values for 6 mo and no detectable liver changes by sonography except for a bright fatty liver, which is common in the Egyptian population. (b) CLD group: (1) persistent increase of the ALT values more than three times the normal value for atleast 6 mo; (2) exclusion of other causes of CLD such as alcoholism or hepatotoxic drugs; (3) histopathological examination of core needle biopsies. Accordingly, patients were classified into 8 mild, 7 moderate, and 5 severe cases of CLD. (c) HCC group: HCC neoplastic cells were identified histopathologically in H&E-stained sections of a core needle biopsy. Cases were classified into G1 (8 cases), G2 (22 cases) and G3 (3 cases). A detailed history and physical examination of the patients were carried out with special emphasis on history of bilharzias, prior parenteral therapy, infective hepatitis and jaundice or other signs of liver cell failure. Complete clinical examination, which includes the manifestations of hepatitis and liver cell failure such as jaundice, hepatomegaly, tenderness in the right hypochondrium, ascites, spleenomegaly, lower limb edema as well as abdominal ultrasonography was also done side by side with routine laboratory investigations including complete blood picture, liver and kidney function tests.

ELISA and HA assays

Sera collected from 5 mL of coagulated blood was aliquoted and stored at -80 ℃ until use. All the sera of patients and controls were tested for HCV antibody and HBsAg by the third-generation ELISA using kits from Innogenetics (Belgium) and the Equipar (Saronno, Italy). They were also tested for antibodies of Schistosomal infestation by quantitative indirect hemagglutination kits from Fumouze Laboratories (Paris, France). All tests were done according to the manufacturer's instructions.

RT-PCR of HCV

Nucleic acid extraction was done by QIAGEN viral RNA Mini-extraction kit (QIAGEN) using 140 μL of patient serum according to the manufacturer's procedure.

RT and PCR were done as previously described by Zekri *et al.*[8]. After completion of the amplification reaction, 10 μL of each PCR reaction product was analyzed by electrophoresis through an agarose 1.2% gel stained by ethidium bromide in Tris-acetate-EDTA buffer (pH 8.0) and DNA was transferred from the gel onto a nitrocellulose filter with alkaline buffer (4 N NaOH). The transferred DNA was cross-linked by incubation for 2-3 h at 80 ℃ and the blot was then hybridized with an internal probe[8].

HCV genotyping

The line immuno-probe assay was used to determine the HCV genotype as described previously[9] using INNO-LiPA II and III provided by Innogenetics (Belgium).

ELISA for cytokine assay

The following cytokines were assayed for all study groups using quantitative ELISA plate method: IL-2 (Quantikine, R&D Systems, Inc., Minneapolis, USA), soluble IL-2 receptor (sIL-2R) (Diaclone Research, France), IL-10 (Quantikine R&D Systems, Inc., Minneapolis, USA), IL-6 (Accucyte, Cytimmune Sciences Inc., MD, USA), soluble IL-6 receptor (sIL-6R) (Diaclone Research, France), tumor necrosis factor alpha (TNF-α) (Accucyte, Cytimmune Sciences Inc., MD, USA), as well as their soluble receptors (sTNF-RI, sTNF-RII; Immunotech, France). We considered the cut-off values for the studied cytokines as mean+2SD of the negative controls.

Histological studies of liver

Liver core needle biopsies (atleast 10 mm long) from CAH and HCC patients who participated in the study were examined by two independent pathologists. Biopsy specimens were assessed for fibrosis (score 0-4) and activity (score 0-18) according to the scoring system of

Knodell. Chronic hepatitis C was defined as mild, if the total score was 6, moderate, if the score was between 6 and 9, and severe, if the score was 9.

Statistical analysis

SPSS package (version 10) was used. Mean and standard deviation were estimates of quantitative data. Non-parametric *t* test (Mann-Whitney test) or non-parametric ANOVA (Kruskal-Wallis test) was used to compare means of more than two independent groups. Fisher's exact and chi-square tests were used to validate the hypothesis of proportional independency. Correlation analysis was used to detect the association between quantitative data.

RESULTS

The clinical characteristics of the studied groups are shown in Table 1. HCC patients had significantly higher cirrhosis, irregular surface of liver, jaundice, serum AST and HCV-Ab positivity than in CLD cases (0.05, 0.007, 0.002, 0.006, and 0.05 respectively) and only HCC patients had significantly lower HBsAg than CLD patients. All the studied cases showed HCV genotype-4 by INNO-LiPA.

No significant difference was found in the history of bilharziasis, prior to the parenteral anti-bilharzial therapy, smoking, diabetes and hypertension in relation to the presence of HCV-Ab was found in HCC and CLD patients. HCV viremia by RT-PCR was positive in 22 of 31 (71%) HCV-Ab positive HCC cases, and in 11 of 15 (73%) HCV-Ab positive CLD cases.

Scatter diagram representing the values of IL-2, IL-2R, IL-6, IL-6R, IL-10, TNF-α and their soluble receptors TNF-RI and TNF-RII in HCC, CLD cases, ASC and normal controls around the cut-off value are shown in Figures 1A-G.

Concentrations of IL-2R, IL-6R and IL-10 were higher in HCC patients than in other groups (16.7±5.4 ng/mL, 56.5±17.97 ng/mL, 9±26.07 pg/mL respectively). On the other hand, the mean concentrations of TNF-RI and TNF-RII were higher (1.87±1.5 and 9.160±0.4 ng/mL) in CLD patients than in other groups. Schistosomal-Ab and TNF-α were higher (1205±120 and 811±5.8 ng/mL) in asymptomatic HCV carriers than in other groups. IL-6R was significantly higher in HCC, CLD and ASC than NC group and there is a consistent increase in the IL-10 level with the disease progression from NC to HCC (Table 2).

In HCC group, positive HCV-RT-PCR cases had higher values of IL-2R, IL-6, IL-10 and TNF-RII (P = 0.689, P = 0.925, P = 0.636 and P = 0.05 respectively) than non-viremic cases, whereas positive HCV-RT-PCR in CLD cases had higher values of IL-6R, IL-10 and TNF-α (P = 0.28, P = 0.08 and P = 0.966) (results not shown).

No significant difference was noticed in any of the clinical characteristics of the patients with cytokine values above the cut-off, when compared to those below the cut-off in both HCC and CLD patients (results not shown). Scatter diagram representing the values of IL-1, IL-2R, IL-6, IL-6R, IL-10, TNF-RI and TNF-RII in HCC, CLD cases, ASC and non-cancer controls (NC) around the cut-off value are shown in Figures 1A-G. Mean serum cytokine levels in the different study groups are shown in Table 2. Regarding IL-2, no difference in its level was observed among the four groups. However, HCC patients had significantly higher values of IL-2R, TNFRII (P<0.001), and TNF RI (P>0.05), but lower TNF-α (P<0.001) and IL-6 (P = 0.032) in comparison to ASC.

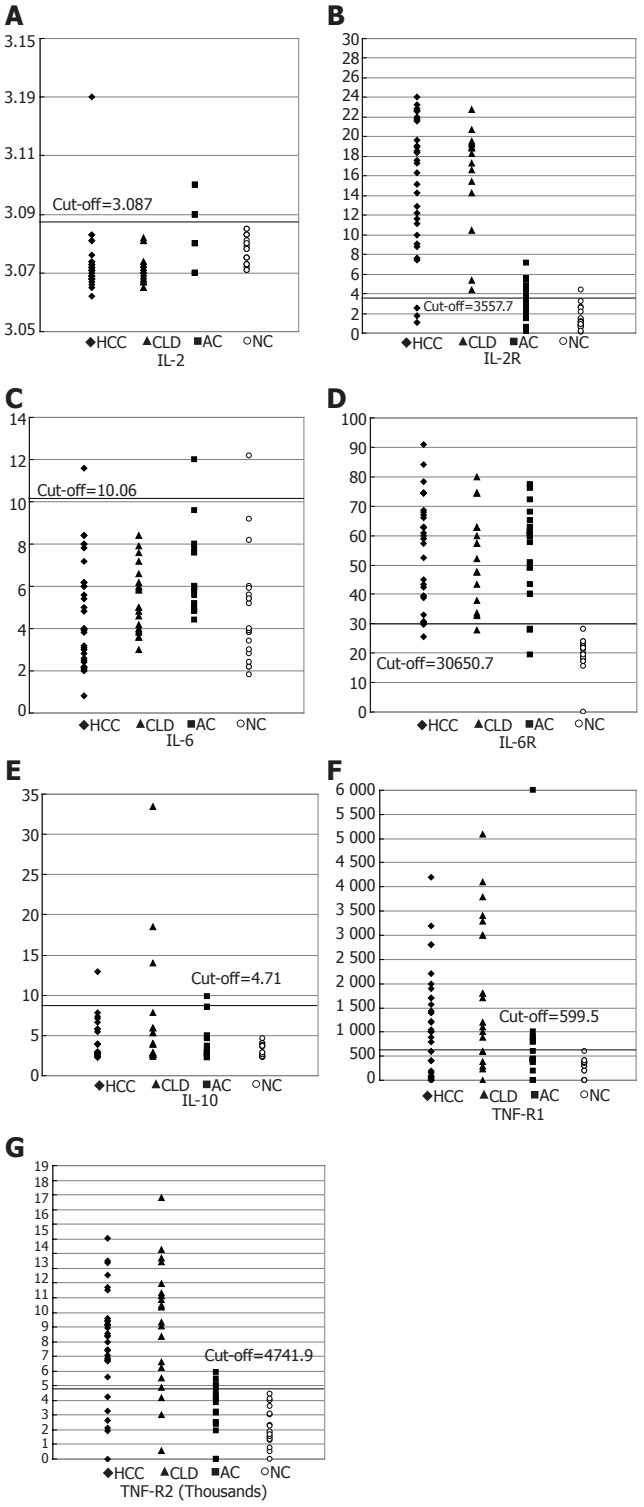

Figure 1 Scatter diagram represents the distribution value of (**A**) IL-2, (**B**) IL-2R (**C**) IL-6, (**D**) IL-6R, (**E**) IL-10, (**F**) TNF-R1, (**G**) TNF-R2 in HCC, CLD, ASC and normal controls around the cut-off value.

Table 1 Clinical features of study groups

Variables	HCC (n = 33)	CLD (n = 20)	ASC (n = 20)	NC (n = 20)	P
Age (mean±SD)	55.3±10.1	63.3±8.3	34±7.7	31.7±11.8	
Gender (M/F)	27/6	14/6	14/6	12/8	
Liver state:					
Cirrhosis	30 (91%)	14 (70%)	0	0	0.05
Irregular surface	30 (91%)	12 (60%)	0	0	0.007
Ascites	13 (39.4%)	11 (55%)	0	0	0.27
Jaundice	27 (81.8%)	8 (40%)	0	0	0.002
LL edema1	19 (57.6%)	11 (55%)	0	0	0.85
Megaly	33 (100%)	19 (95%)	0	0	0.38
Spleenomegaly	19 (57.6%)	13 (65%)	0	0	0.59
Schistosomal-Ab	18 (54.5%)	13 (65%)	14 (70%)	1 (5%)	0.45
HCV-Ab	31 (93.9%)	15 (75%)	20 (100%)	1 (5%)	0.05
HBsAg	3 (9%)	6 (30%)	4 (20%)	0	0.05
HCV-RNA	22 (66.7%)	14 (70%)	20 (100%)	0	0.8
Liver function tests					
ALT (mean±SD)	67.2±43.3	48±33.1	27.2±(7.0)	25.3±(4.2)	0.06
AST (mean±SD)	126.4±57.4	83.6±54.1	26.1±(5.0)	19.1±(5.0)	0.006
Alk ph (mean±SD)	260.4±193.4	221±126.7	70±26.1	65±24.2	0.414
Bil (mean±SD)	2.28±2.1	2.02±1.9	1.0±0.2	0.9±0.1	0.34

[1]LL edema: lower limb edema. P<0.05 difference is statistically significant.

Table 2 Serum levels of cytokines in the study groups (mean±SD)

Cytokine	HCC (n = 33)	CLD(n = 20)	ASC(n = 20)	NC(n = 20)	P
IL-2	3.07±0.01	3.07±0.005	3.07±0.009	3.08±0.004	>0.05
Cut-off=3.087 pg/mL					
Number of positive cases	1 (3%)	0	6 (30%)	0	
IL-2R	16.67±5.44	16.28±5.28	3.42±1.85	1.39±1.09	<0.001
Cut-off=3.5 ng/mL					
Number of positive cases	30 (91%)	16 (80%)	9 (45%)	1 (5%)	
IL-6	4.71±2.49	5.2±1.68	6.4±1.9	4.82±2.62	0.032
Cut-off=10.06 ng/mL					
Number of positive cases	1 (3%)	0	1 (5%)	1 (5%)	
IL-6R	56.48±17.97	54.47±16.72	54.13±16.35	19.62±5.52	<0.001
Cut-off=30.65 ng/mL					
Number of positive cases	29 (88%)	19 (95%)	17 (85%)	0	
IL-10	9±26.07	6.59±7.57	3.96±2.24	3.13±0.79	>0.05
Cut-off=4.71 pg/mL					
Number of positive cases	9 (31%)	8 (40%)	3 (15%)	0	
TNF-α	4.77±3.2	5.53±1.9	811±5.8	58±196	<0.001
Cut-off=17.2 ng/mL					
Number of positive cases	0	0	20 (100%)	1 (5%)	
TNF-α RI	1.27±0.98	1.87±1.50	0.56±0.23	0.29±0.16	<0.001
Cut-off=0.599 ng/mL					
Number of positive cases	24 (72%)	16 (80%)	7 (35%)	1 (5%)	
TNF-α RII	7.89±3.57	9.16±4.26	3.42±1.72	2.17±1.29	<0.001
Cut-off=4.74 ng/mL					
Number of positive cases	25 (81%)	17 (85%)	4 (20%)	0	

[1]Cut-off=mean±2 SD of non-cancer controls. P<0.05 difference is statistically significant.

But, in comparison to non-cancer controls, HCC patients had higher values of IL-2R, IL-6R, TNF-RI and TNF-RII, but less TNF-α (P<0.001). CLD patients had higher IL-2R, TNF-RI and TNF-RII (P<0.001) than in ASC. But, in comparison to non-cancer controls, CLD patients had higher IL-2R, TNF-RI and TNF-RII, but lower TNF-α (P<0.001). IL-10 was higher (though not significantly) in HCC and CLD patients than in symptomatic carriers and non-cancer controls. No significant difference was noticed in any of the clinical characteristics of patients with cytokines values above the cut-off, when compared with those below the cut-off in both HCC and CLD patients.

The most sensitive cytokines as markers for disease progression in HCV-infected patients were IL-2R (91% of HCC and 80% of CLD patients had values above the cut-off), IL-6R (88%, 95%, and 85% of HCC, CLD and ASC respectively, had values above the cut-off) and also TNF-RII (81% of HCC and 85% of CLD cases had values above the cut-off).

DISCUSSION

It has been reported that hepatotropic viruses HBV, HDV, HCV are associated with HCC, and more than 80% of HCCs that occur worldwide are thought to be associated with chronic viral hepatitis[10]. In our series, the prevalence of anti-HCV antibodies by the third-generation ELISA was 93.9% in HCC patients. HCV-AB

was positive in 86.5% of 37 HCC patients in our previous study[11]. However, this ratio is higher than those reported by other researchers[12,13]. The present study showed that the prevalence of anti-HCV antibodies was 75% in CLD patients, which is also higher than those reported by other researchers[14,15].

The HCV viremia in our HCV-serpositive HCC cases was also higher than those reported by other researchers[11,16,17]. This discrepancy might be explained by the fluctuations of the amount of the viruses in the serum[18]; or the discrepancy of RT-PCR methods used by the different series[8].

In our study, HBsAg was found in 9% of HCC cases, which is similar to that in our previous studies[11,12]. HBsAg was found in 30% of our CLD cases, which is higher than that reported by Angelico *et al*.[14]. In the present study, history of bilharziasis and prior anti-bilharzial parenteral therapy was found in 51.6% and 41.9% of HCC patients and in 73.3% and 60% of CLD patients respectively, indicating that history of parenteral anti-schistosomal therapy is a major risk factor for transmitting HCV infection.

Anti-bilharzial antibodies were found in 55% of HCC patients in our study, which is higher than that reported in our previous studies[11]. This high incidence could be attributed to the fact that most of our HCC patients (66.7%) came from rural areas. Rural populations in both Egypt and other African areas have a higher incidence of viral hepatitis. In the rural areas, many individuals may become infected due to tattooing[19].

A characteristic feature of HCV infection is a high frequency of persistence and progression to CLD. Persistent infection upsets the balance between immunostimulatory and inhibitory cytokines, which can prolong inflammation and lead to necrosis, fibrosis, and CLD[1]. Elevated concentrations of cytokines also represent a characteristic feature of CLD, regardless of underlying etiology, which may represent a consequence of liver dysfunction instead of inflammatory disorder[20].

Missale *et al*.[2] and Cacciarelli *et al*.[3] found that serum IL-2 is significantly elevated in HCV chronically HCV-infected patients. However, Simsek and Kadayifci[21] found that serum IL-2 has no significant change in the same group of patients. In contrast, our study showed no significant change in the levels of IL-2 among the different groups. The high level of sIL-2R might explain the apparently normal level of IL-2 in our patients as low IL-2 level could therefore be due to soluble receptor binding to IL-2. This theory is also supported by Sismek and Kadayifci[21]. On the other hand, Izzo *et al*.[22] found that serum levels of sIL-2R correlate with the histological severity of liver damage in patients with chronic HCV infection and may be used as a marker in patients at high risk of getting HCC and the highest levels of soluble IL-2R occur in patients with HCC[23]. We could not, however, correlate serum levels of sIL-2R with the different clinical and biochemical findings in HCC in this study.

Thus, sIL-2R may play a role in the pathogenesis of chronic active hepatitis and HCC, and could be considered as a good marker for disease progress in chronic HCV-infected patients. IL-2R was above normal in 91% of HCC and in 80% of CLD cases in our study.

Interleukin-6, a multifunctional cytokine produced by a variety of cells, plays a central role in regulating the immune system, hematopoiesis, and acute phase reaction. It interacts with a receptor complex consisting of a specific ligand-binding protein (IL-6R, gp80) and a signal transduction protein (gp130)[24,25]. Serum IL-6 levels are higher in patients with chronic HCV infection in comparison to healthy adults[26,27]. In contrast, our results showed that IL-6 was slightly higher only in asymptomatic HCV carriers than in non-cancer controls, but apparently normal in both HCC and CLD patients, which is in accordance with that reported by Tovey *et al*.[28]. Altered IL-6 gene expression is a characteristic feature of advanced stage of severe liver disease. McGuinness *et al*.[29] also found that IL-6 mRNA is down-regulated in chronic HCV-infected patients.

On the other hand, Steffen *et al*.[30] revealed that IL-6 is inversely correlated with sIL-6R, as IL-6 may play a role in the decrease of sIL-6R either by the direct inhibitory effect on the expression of the IL-6R gene or by the formation of IL-6R/sIL-6R complexes followed by their internalization in target cells. This might partially explain the apparently normal levels of IL-6 in our HCC and CLD patients by the increase in their sIL-6R levels.

The pro-inflammatory cytokine tumor necrosis factor-α plays an important role in the pathophysiology of liver disease. Specific antagonists of this cytokine have been found in recent years. TNF soluble receptors p55 and p57 derived from the cell surface are naturally occurring substances that inhibit the biological effects of tumor necrosis factor.

The striking elevation of pro-inflammatory cytokine TNF-α in asymptomatic HCV carriers may reflect both insufficiency of HCV elimination and a failure to control the cytokine cascade. Our result is opposite to those reported by Goyal A[20] and Toyoda *et al*.[31]. This could be attributed also to the difference in the epitopes of the ELISA system used by the different groups or to the difference in genotypes. All our cases showed HCV genotype-4.

The promoter in the IL-6 gene has been shown to contain regulatory regions to which DNA-binding proteins can bind. These DNA-binding proteins, induced by IL-1 and TNF-α, stimulate transcription of the IL-6 gene. Thus, as IL-1 and TNF-α levels increase, production of IL-6 also increases[32]. Our result is in accordance with the above findings, and the decrease in TNF-α is associated with a decrease in IL-6 in HCC and CLD cases.

In our study, HCC cases had significantly higher values of TNF-RII and TNF-RII ($P<0.001$) than ASC and NC subjects. Thus, the rise in concentrations of TNF receptors I and II in our patients suggests that HCV-related liver disease involves immunological mechanisms including activation of the TNF system and may reflect the degree of inflammation and development of HCC. These results are in accordance with other studies[33,34].

Tai *et al*.[5] also showed that sTNF-RI levels correlate with liver inflammation in all patients, whereas this correlation cannot be found with sTNF-RII, IL-2, IL-10 and TNF-α.

Accordingly, we can use TNF-RII as a marker in HCV-infected cases at high risk of getting CLD and HCC.

Delpuech *et al*. [35] showed that even if the infection of H9 T cell line with HCV does not result in any viral progeny, HCV induces the activation of IL-10 secretion, which supports the role of IL-10 in HCV pathogenesis. Cacciarelli *et al*.[3] and Kakumu *et al*.[33] found that serum IL-10 levels are significantly higher in all CLD groups than in controls, indicating that IL-10 reflects the degree of inflammation in the liver and may be related to the development of HCC. In our series, IL-10 levels were increased (though not significantly) in HCC, CLD in comparison to non-cancer controls. The positive HCV-viremic CLD cases also had higher values of IL-10 ($P = 0.08$) than non-viremic cases. In addition to the production at the site of inflammatory changes with activated infiltrating mononuclear cells in the liver, the high serum IL-10 levels in patients with HCC presumably also result from the secretion of IL-10 by tumor cells. Its secretion by human hepatocellular tumors has been observed previously[36]. Thus, a high IL-10 level is suggested to contribute to a relative state of immuno-suppression, and in patients with HCC, may help the tumor cells escape host immune surveillance and potentiate tumor cells to metastasize[37].

It has been postulated that an imbalance between Th1 and Th2 cytokine production is implicated in disease progression or inability to clear infections. It was reported that HCV-infected patients who develop chronicity have a predominant Th2 response, but a weak Th1 response, suggesting that this immune response imbalance can result from HCV interaction with dendritic cell functions[38]. These results agree with ours and support the notion that Th-lymphocyte polarization may play an important pathophysiologic role in influencing the outcome of HCV infection. All these immunological findings are mostly due to HCV infection rather than schistosomal infection, because patients with no schistosomal antibody had the same elevation of the same cytokines, late Schistosoma mansoni cases showed a suppressed cell-mediated immunity and a significant depletion of T-helper/inducer subset[39].

In conclusion, the most sensitive cytokines as markers for disease progression in HCV-infected patients are IL-2R, IL-6R and TNF-RII. Accordingly, we may use serum IL-2R, IL-6R, TNF-RII as markers in HCV-infected cases at high risk of getting CLD and HCC. Thus, disease progression due to HCV infection is associated with decrease of circulating Th1 cytokines (IL-2) and increase of Th2 cytokine (IL-10). Persistent infection upsets the balance between immunostimulatory and inhibitory cytokines, which can prolong inflammation and lead to necrosis, fibrosis, and CLD.

REFERENCES

1 **Jacobson Brown PM,** Neuman MG. Immunopathogenesis of hepatitis C viral infection: Th1/Th2 responses and the role of cytokines. *Clin Biochem* 2001; **34:** 167-171

2 **Missale G,** Ferrari C, Fiaccadori F. Cytokine mediators in acute inflammation and chronic course of viral hepatitis. *Ann Ital Med Int* 1995; **10:** 14-18

3 **Cacciarelli TV,** Martinez OM, Gish RG, Villanueva JC, Krams SM. Immunoregulatory cytokines in chronic hepatitis C virus infection: pre- and posttreatment with interferon alfa. *Hepatology* 1996; **24:** 6-9

4 **Malaguarnera M,** Trovato BA, Laurino A, Di Fazio I, Romeo MA, Motta M. Interleukin-6 in hepatitis C cirrhosis. *Med* 1996; **38:** 207-210

5 **Tai DI,** Tsai SL, Chen TC, Lo SK, Chang YH, Liaw YF. Modulation of tumor necrosis factor receptors 1 and 2 in chronic hepatitis B and C: the differences and implications in pathogenesis. *J Biomed Sci* 2001; **8:** 321-327

6 **Realdon S,** Pontisso P, Adami F, Trentin L, Noventa F, Ferrari A, Migliorato I, Gatta A, Alberti A. High levels of soluble tumor necrosis factor superfamily receptors in patients with hepatitis C virus infection and lymphoproliferative disorders. *J Hepatol* 2001; **34:** 723-729

7 **Curely SA,** Levin B, Rish TA. Liver and Bile ducts. In: Clinical oncology. Abdeloff, MD, Armitage, JO, Lichter, AS and Niederhuber, J E (eds.), Churchill livingstone, USA, 1995; 1305-1372

8 **Zekri AR,** Bahnassy AA, Ramadan AS, El-Bassuoni M, Badran A, Madwar MA. Hepatitis C virus genotyping versus serotyping in Egyptian patients. *Infection* 2001; **29:** 24-26

9 **Zekri AR,** Bahnassy AA, Shaarawy SM, Mansour OA, Maduar MA, Khaled HM, El-Ahmadi O. Hepatitis C virus genotyping in relation to neu-oncoprotein overexpression and the development of hepatocellular carcinoma. *J Med Microbiol* 2000; **49:** 89-95

10 **Brooks GF,** Butel JS, Morse SA. Hepatitis viruses. In: Medical microbiology. Brooks, GF, Butel, JS, and Morse, S A (eds.). Twenty-second edition, Lange medical books. McGraw-Hill, USA 2001

11 **Zekri AR,** Sedkey L, el-Din HM, Abdel-Aziz AO, Viazov S. The pattern of transmission transfusion virus infection in Egyptian patients. *Int J Infect Dis* 2002; **18:** 107-110

12 **Hassan MM,** Zaghloul AS, El-Serag HB, Soliman O, Patt YZ, Chappell CL, Beasley RP, Hwang LY. The role of hepatitis C in hepatocellular carcinoma: a case control study among Egyptian patients. *J Clin Gastroenterol* 2001; **33:** 123-126

13 **Waked IA,** Saleh SM, Moustafa MS, Raouf AA, Thomas DL, Strickland GT. High prevalence of hepatitis C in Egyptian patients with chronic liver disease. *Gut* 1995; **37:** 105-107

14 **Angelico M,** Renganathan E, Gandin C, Fathy M, Profili MC, Refai W, De Santis A, Nagi A, Amin G, Capocaccia L, Callea F, Rapicetta M, Badr G, Rocchi G. Chronic liver disease in the Alexandria governorate, Egypt: contribution of schistosomiasis and hepatitis virus infections. *J Hepatol* 1997; **26:** 236-243

15 **El-Medany OM,** El-Din Abdel Wahab KS, Abu Shady EA, Gad El-Hak N. Chronic liver disease and hepatitis C virus in Egyptian patients. *Hepatogastroenterology* 1999; **46:** 1895-1903

16 **Mabrouk GM.** Prevalence of hepatitis C infection and schistosomiasis in Egyptian patients with hepatocellular carcinoma. *Dis Markers* 1997; **13:** 177-182

17 **Yates SC,** Hafez M, Beld M, Lukashov VV, Hassan Z, Carboni G, Khaled H, McMorrow M, Attia M, Goudsmit J. Hepatocellular carcinoma in Egyptians with and without a history of hepatitis B virus infection: association with hepatitis C virus (HCV) infection but not with (HCV) RNA level. *Am J Trop Med Hyg* 1999; **60:** 714-720

18 **Brechot C.** Polymerase chain reaction for the diagnosis of hepatitis B and C viral hepatitis. *J Hepatol* 1993; **17** Suppl 3:

S35-S41
19 **Attia MA.** Prevalence of hepatitis B and C in Egypt and Africa. In: "Therapies for viral hepatitis". Schinazi R F , Sommadossi J P and Thomas H C (eds.), International Medical Press. London, UK, 1998: 15-24
20 **Goyal A,** Kazim SN, Sakhuja P, Malhotra V, Arora N, Sarin SK. Association of TNF-beta polymorphism with disease severity among patients infected with hepatitis C virus. *J Med Virol* 2004; **72:** 60-65
21 **Simsek H,** Kadayifci A. Serum interleukin 2 and soluble interleukin 2 receptor in chronic active hepatitis C: effect of interferon therapy. *J Int Med Res* 1996; **24:** 239-245
22 **Izzo F,** Curley S, Maio P, Leonardi E, Imparato L, Giglio S, Cremona F, Castello G. Correlation of soluble interleukin-2 receptor levels with severity of chronic hepatitis C virus liver injury and development of hepatocellular cancer. *Surgery* 1996; **120:** 100-105
23 **Izzo F,** Cremona F, Delrio P, Leonardi E, Castello G, Pignata S, Daniele B, Curley SA. Soluble interleukin-2 receptor levels in hepatocellular cancer: a more sensitive marker than alfa fetoprotein. *Ann Surg Oncol* 1999; **6:** 178-185
24 **Blum AM,** Metwali A, Elliott D, Li J, Sandor M, Weinstock JV. IL-6 deficient mice form granulomas in murine schistosomiasis that exhibit an altered B cell response. *Cell Immunol* 1998; **188:** 64-72
25 **Giannitrapani L,** Cervello M, Soresi M, Notarbartolo M, La Rosa M, Virruso L, D'Alessandro N, Montalto G. Circulating IL-6 and sIL-6R in patients with hepatocellular carcinoma. *Ann N Y Acad Sci* 2002; **963:** 46-52
26 **Malaguarnera M,** Di Fazio I, Romeo MA, Restuccia S, Laurino A, Trovato BA. Elevation of interleukin 6 levels in patients with chronic hepatitis due to hepatitis C virus. *J Gastroenterol* 1997; **32:** 211-215
27 **Oyanagi Y,** Takahashi T, Matsui S, Takahashi S, Boku S, Takahashi K, Furukawa K, Arai F, Asakura H. Enhanced expression of interleukin-6 in chronic hepatitis C. *Liver* 1999; **19:** 464-472
28 **Tovey MG,** Gugenheim J, Guymarho J, Blanchard B, Vanden Broecke C, Gresser I, Bismuth H, Reynes M. Genes for interleukin-1, interleukin-6, and tumor necrosis factor are expressed at markedly reduced levels in the livers of patients with severe liver disease. *Autoimmunity* 1991; **10:** 297-310
29 **McGuinness PH,** Painter D, Davies S, McCaughan GW. Increases in intrahepatic CD68 positive cells MAC387 positive cells, and proinflammatory cytokines (particularly interleukin 18) in chronic hepatitis C infection. *Gut* 2000; **46:** 260-269
30 **Steffen M,** Pichlmeier U, Zander A. Inverse correlation of interleukin-6 with soluble interleukin-6 receptor after transplantation of bone marrow or peripheral blood stem cells. *Bone Marrow Transplant* 1997; **20:** 715-720
31 **Toyoda M,** Kakizaki S, Horiguchi N, Sato K, Takayama H, Takagi H, Nagamine T, Mori M. Role of serum soluble Fas/soluble Fas ligand and TNF-alpha on response to interferon-alpha therapy in chronic hepatitis C. *Liver* 2000; **20:** 305-311
32 **Akira S,** Taga T, Kishimoto T. Interleukin-6 in biology and medicine. *Adv Immunol* 1993; **54:** 1-78
33 **Kakumu S,** Okumura A, Ishikawa T, Yano M, Enomoto A, Nishimura H, Yoshioka K, Yoshika Y. Serum levels of IL-10, IL-15 and soluble tumour necrosis factor-alpha (TNF-alpha) receptors in type C chronic liver disease. *Clin Exp Immunol* 1997; **109:** 458-463
34 **Zylberberg H,** Rimaniol AC, Pol S, Masson A, De Groote D, Berthelot P, Bach JF, Brechot C, Zavala F. Soluble tumor necrosis factor receptors in chronic hepatitis C: a correlation with histological fibrosis and activity. *J Hepatol* 1999; **30:** 185-191
35 **Delpuech O,** Buffello-Le Guillou DB, Rubinstein E, Feray C, Petit MA. The hepatitis C virus (HCV) induces a long-term increase in interleukin-10 production by human CD4+ T cells (H9). *Eur Cytokines Netw* 2001; **12:** 69-77
36 **Matsuguchi I,** Okamura S, Kawasaki C, Niho Y. Production of interleukin 6 from human liver cell lines: production of interleukin 6 is not concurrent with the production of alpha-fetoprotein. *Cancer Res* 1990; **50:** 7457-7459
37 **Chau GY,** Wu CW, Lui WY, Chang TJ, Kao HL, Wu LH, King KL, Loong CC, Hsia CY, Chi CW. Serum interleukin-10 but not interleukin-6 is related to clinical outcome in patients with resectable hepatocellular carcinoma. *Ann Surg* 2000; **231:** 552-558
38 **Stoll-Keller F,** Schvoerer E, Thumann C, Navas MC, Aubertin AM. Immunomodulating effect of HCV during the development of chronic hepatitis C: toward new therapeutic approaches. *Bull Acad Natl Med* 2003; **187:** 1147-1160 discussion 1160-1
39 **Elrefaei M,** El-Sheikh N, Kamal K, Cao H. HCV-specific CD27- CD28- memory T cells are depleted in hepatitis C virus and Schistosoma mansoni co-infection. *Immunology* 2003; **110:** 513-518

Science Editor Wang XL and Ma JY **Language Editor** Elsevier HK

PO Box 2345, Beijing 100023, China
www.wjgnet.com
wjg@wjgnet.com

ELSEVIER

World J Gastroenterol 2005;11(42):6631-6637
World Journal of Gastroenterology ISSN 1007-9327

Toll-like receptor 4 plays an anti-HBV role in a murine model of acute hepatitis B virus expression

Wen-Wei Chang, Ih-Jen Su, Ming-Derg Lai, Wen-Tsan Chang, Wenya Huang, Huan-Yao Lei

Wen-Wei Chang, Institute of Basic Medical Science, National Cheng Kung University Medicine College, Tainan, Taiwan, China
Ih-Jen Su, Division of Clinical Research, National Health Research Institute, Tainan, Taiwan, China
Ming-Derg Lai, Wen-Tsan Chang, Department of Biochemistry, National Cheng Kung University Medicine College, Tainan, Taiwan, China
Wenya Huang, Department of Medical Laboratory Science and Biotechnology, National Cheng Kung University Medicine College, Tainan, Taiwan, China
Huan-Yao Lei, Department of Microbiology and Immunology, National Cheng Kung University Medicine College, Tainan, Taiwan, China
Supported by grant form National Science Council of Taiwan, No. NSC 93-2320-B006-026
Correspondence to: Dr. Huan-Yao Lei, Department of Microbiology and Immunology, College of Medicine, National Cheng Kung University, Tainan, Taiwan, China. hylei@mail.ncku.edu.tw
Telephone: +886-6-2353535 Ext. 5643 Fax: +886-6-2097825
Received: 2005-04-29 Accepted: 2005-06-18

Abstract

AIM: Toll-like receptor 4 (TLR4) has been shown to be important for bacterial infection, especially to lipopolysaccharide signaling. Its possible role in HBV infection is studied in the present study.

MATERIALS AND METHODS: pHBV3.6 plasmid, containing full-length HBV genome was used in the murine model of acute HBV expression by hydrodynamics *in vivo* transfection. TLR4 normal or mutant mouse strain was compared to investigate the possible role of TLR4 in acute HBV expression.

RESULTS: After pHBV3.6 injection, the infiltrating leukocytes expressed TLR4 were observed nearby the HBsAg-expressing hepatocytes. The HBV antigenemia as well as the replication and transcription were higher in TLR4-mutant C3H/HeJ mice than in normal C3H/HeN mice. The HBV-specific immune responses were impaired in the liver or spleen of the C3H/HeJ mice. Their inducible nitric oxide synthase (iNOS) expression on the hepatic infiltrating cells was also impaired. When adoptively transferring splenocytes from C3H/HeN mice to C3H/HeJ mice, the HBV replication was inhibited to the level as that of C3H/HeN.

CONCLUSION: These results suggest that TLR4 plays an anti-HBV role *in vivo* through the induction of iNOS expression and HBV-specific immune responses after HBV expression.

Key words: TLR4; Rodent; HBV; iNOS; Liver

Chang WW, Su IJ, Lai MD, Chang WT, Huang W, Lei HY. Toll-like receptor 4 plays an anti-HBV role in a murine model of acute hepatitis B virus expression. *World J Gastroenterol* 2005; 11(42): 6631-6637
http://www.wjgnet.com/1007-9327/11/6631.asp

INTRODUCTION

Hepatitis B virus (HBV) is an enveloped, double-strand DNA virus, and its replication is through an RNA intermediate that requires reverse transcriptase activity[1]. HBV infection in human beings can cause chronic hepatitis and is associated with liver cirrhosis and hepatocellular carcinoma[2,3]. One-third of the global population has been infected with HBV and about 350 million people are chronic carriers of HBV[4]. HBV is non-cytopathic to hepatocytes and the hepatitis it causes is thought to be mediated by immune mechanism. However, the innate immune response to HBV infection is not fully understood.

Toll receptors are type I membrane proteins that was first identified in Drosophila and play a key role in antifungal immunity of Drosophila[5]. The mammalian homologs of Drosophila Toll protein are called Toll-like receptors (TLRs), and there are 10 human (TLR1 to TLR10) and murine TLRs (TLR 1 to TLR9 and TLR11)[5,6]. TLRs play a key role in host defense against microbial infection by regulating both innate and acquired immunity[7,8]. For example, TLR4 is the receptor of Gram-negative bacterial lipopolysaccharide (LPS). After binding, the MyD88, interleukin-1 receptor-associated kinase, and tumor necrosis factor receptor associated factor 6 are activated, and then through MAP kinases and NF-κB transcription factors[6,9] to turn on the genes expression, which were involved in the inflammatory responses[10]. TLR4 also plays a role in viral infections. Respiratory syncytial virus (RSV) persists longer in the lung of TLR4-deficient mice than normal mice, and RSV fusion protein can activate the human monocytes through TLR4[11].

Hydrodynamics-based *in vivo* transfection has been

recently described. With this procedure, naked DNA can be introduced and expressed significantly in liver[12,13]. This property allows investigators to develop hepatitis virus infection model in mouse[14]. Recently, a murine acute HBV expression model was generated by hydrodynamics-based injection of plasmid containing full-length HBV genome by our group[15] or others[16]. After hydrodynamic injection of pHBV3.6, including full-length HBV genome, the HBV transcript and replicative intermediate were induced in the liver whereas the HBV-antigens, HBV-DNA, and HBV-specific antibody were detected in the sera[15].

We are interested in the role of TLR4 during HBV infection. Using the murine model of acute HBV expression in this study, we reported that HBV expression-induced TLR4 expression has anti-HBV activity by upregulating the iNOS expression and HBV-specific immune response to help clearing the virus.

MATERIALS AND METHODS

Mice

Breeder mice of C3H/HeN and C3H/HeJ strain were purchased from The Jackson Laboratory (Bar Harbor, ME, USA) or Charles River Japan, Inc. (Atsugi, Japan). They were fed standard laboratory chow and water *ad libitum* in the animal facility. The animals were raised and cared for according to the guidelines set up by the National Science Council of the Republic of China. Eight- to twelve-week-old male mice were used in all experiments.

Plasmids

pHBV3.6 containing all HBV open-reading frames was provided by Dr LP Ting (Department of Microbiology and Immunology, National Yang-Ming University), p(3A)SAg that encodes HBsAg was provided by Dr CC Lu (Department of Pathology, National Cheng Kung University) and pHBV^PSX that encodes HBcAg was provided by Dr SJ Lo (Department of Microbiology and Immunology, National Yang-Ming University). pEGFP-N1 was obtained from Clontech (Palo Alto, CA, USA). All plasmids were prepared with Hi-speed Plasmid Midi Kit (Qiagen, Hilden, Germany).

Cells and transfection

The C3H/He bladder cancer cell line, MBT-2, was kindly provided by Dr MD Lai (Department of Biochemistry, National Cheng Kung University). Cells were maintained in Dulbecco's modified Eagle medium (Gibco BRL, Grand Island, NY, USA) and 10% fetal bovine serum (HyClone, Logan, UT, USA) at 37 ℃ under 50 mL/L CO_2. The cells were plated at a density of 3×10^5 cells/well in six well-culture plate. One day later, cells were transfected with 1 μg of p(3A)SAg and pHBV^PSX using Lipofectamine 2000 (Invitrogen, Carlsbad, CA, USA) according to the manufacturer's protocol. The medium was replaced with a fresh medium 8 h after transfection, and cells were used for T cell stimulation at 36 h after transfection.

Hydrodynamics-based in vivo transfection

Ten micrograms of plasmid, dissolved in Ringer's solution (NaCl 0.154 mol/L, KCl 5.63 mmol/L, $CaCl_2$ 2.25 mmol/L), were injected in the mouse tail vein, within 5 to 7 s, at a 12% of mouse bodyweight (around 3.0 mL) following the hydrodynamics-based transfection protocol described previously[15].

Immunohistochemical analysis of HBsAg, TLR4, and iNOS expression

Mouse liver tissues were embedded in OCT compound (Miles Inc., Elkhart, IN, USA) and frozen in liquid nitrogen. Four micrometer cryosections were made using cryostats (Leica CM 1800, Nussloch, Germany). For TLR4 and HBsAg double staining, sections were fixed by 3.7% formaldehyde/PBS and then firstly stained with sheep-anti-HBsAg antibody (Serotec, Oxford, UK) and FITC-conjugated donkey-anti-sheep antibody (Jackson Laboratories, West Grove, PA, USA). After washing with PBS, the sections were further stained with rat-anti-mouse TLR4 antibody (Santa Cruz Biotechnology, Inc., Santa Cruz, CA, USA) and Rhodamine-conjugated donkey-anti-rat antibody (Jackson Laboratories, West Grove, PA, USA). The nucleuses were stained by Hoecsht 33258. For HBsAg and iNOS staining, the sections were fixed by cold acetone and endogenous peroxidase was inhibited by 3% H_2O_2/PBS. HBsAg and iNOS were detected with sheep polyclonal anti-HBs (Serotec, Oxford, UK) and rabbit polyclonal anti-iNOS antibodies (Chemicon, Temecula, CA, USA), respectively. Secondary antibody used was either biotinylated anti-sheep or anti-rabbit, and then incubated with avidin-peroxidase complex (Vector Laboratories, Burlingame, CA, USA). Peroxidase stain of red color was developed by aminoethyl carbazole substrate (Zymed Laboratories, San Francisco, CA, USA) and counterstained with Mayer's hematoxylin (Merck, Darmstadt, Germany).

Northern and Southern blot hybridization of HBV transcription and replication

Total RNA was purified from mouse liver by TRI Reagent (Molecular Research Center, Inc, Cincinnati, OH, USA). The cytoplasmic DNA of mouse liver was purified as described previously by Guidotti *et al*.[17]. Thirty micrograms of total RNA or cytoplasmic DNA isolated from 30 mg of liver tissue were run on agarose gel electrophoresis, transferred to a nylon membrane and hybridized with biotin labeled HBV specific DNA probe, which was prepared by PCR amplication with the primers as: HBV1806: 5'-CCGGAAAGCTTGAGCT CTTCAAAAAGTATGGTGCTGG-3' ; HBV1821: 5' -CCGGAAAGCTTCTTTTTCACCTCTGCCTAATCA-3', at 45 ℃ overnight. To verify the transfection efficiency, we injected pEGFP-N1 with pHBV3.6 simultaneously and detected by a specific biotin labeled DNA probe. The hybridized bands were detected by Detector AP Chemiluminescent Blotting Kit (KPL, Inc., Gaithersburg, MD, USA) and visualized by X-ray films.

HBV DNA detection in mouse sera

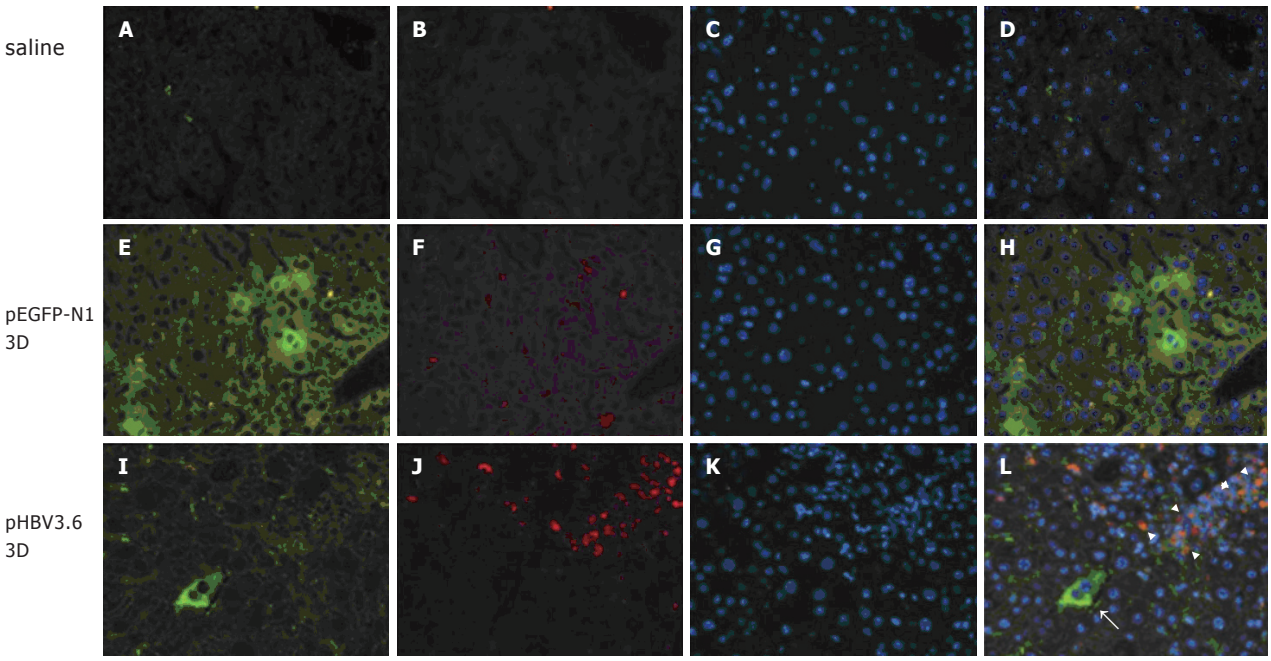

Figure 1 TLR4 expression in the liver of C3H/HeN mice after hydro-dynamic injection of pHBV3.6. Groups of four C3H/HeN mice were injected intravenously with 10 μg of plasmid by hydrodynamics-based transfection. The liver tissues were collected at day 3 post injection and 4-μm cryosections were made, stained with anti-HBsAg-FITC and anti-TLR4-PE antibody. The green represents EGFP-positive (**E**) or HBsAg-positive cells (**I**) and the red represents TLR4-positive cells (**B, F, J**). The blue represents counter staining by Hoechst 33258 dye (**C, G, K**). **A-D:** naïve; **E-H:** pEGFP-N1; **I–L:** pHBV3.6. The arrows indicate the HBsAg positive hepatocytes and the arrowheads indicate the TLR4 positive immune cells (original magnification ×200)

Two hundred microliters of mouse serum was treated with 20 U DNase I for at least 12 h to remove retaining plasmid. After DNase I treatment, the serum DNA was purified by Viral DNA/RNA Isolation Kit (Maxim Biotech, INC., San Francisco, CA, USA). Five microliters of isolated DNA solution was used to detect the HBV DNA by PCR analysis. The preS2 region of surface antigen gene was amplified and visualized on an agarose gel as described previously[18].

Detection of HBsAg and HBeAg in mouse sera

The level of HBsAg and HBeAg were determined using enzyme-linked immunosorbent assay (ELISA) kits (General Biological Corp., Taiwan, ROC) following the manufacturer's protocol.

ELISA for detecting cytokines

The intrahepatic lymphocytes (IHLs) were isolated as described previously[15] with further removing the adhering cells. The IHLs or splenocytes were co-cultured with mitomycin C-treated (100 μg/mL at 37 ℃ for 90 min) MBT-2[19] or p(3A)SAg and pHBV^PSX transfected, MBT-2 (MBT-2-SC) at a ratio of 10:1 for 48 h The co-cultured supernatants were harvested and assayed by sandwich ELISA for mouse IFN-γ, TNF-α or IL-12 (R&D Systems, Minneapolis, MN, USA).

RESULTS

Infiltrating cells in the liver expressed TLR4 after transfection of HBV gene

To investigate the association of TLR4 and HBV expression, the plasmid pHBV3.6, containing the full-length HBV genome was administrated to C3H/HeN mice by hydrodynamics *in vivo* transfection. As shown in Figure 1, the TLR4 expression could be detected on infiltrating leukocytes at day 3 post-injection (Figures 1I-L). But it was not detected in the liver of naïve C3H/HeN mice (Figures 1A-D) or pEGFP-N1 injected mice (Figures 1E-H). These results indicate that TLR4 expressed on leukocytes might involve the acute HBV expression.

HBV antigenemia and replication was higher in C3H/HeJ than in C3H/HeN

In C3H/HeJ mice, a missense mutation in the cytoplasmic domain of TLR4 impaired its ability to respond to lipopolysaccharide (LPS)[20]. To further investigate the role of TLR4 in HBV expression, we compared the response in C3H/HeN (TLR4 normal) and C3H/HeJ (TLR4 mutation) after the pHBV3.6 *in vivo* transfection. As shown in Figure 2, the serum HBsAg (Figure 2A) or HBeAg (Figure 2B) level was higher in C3H/HeJ than in C3H/HeN mice. By Northern and Southern blot analyses, the specific HBV transcripts or HBV replication fragments were also higher in the liver of C3H/HeJ than C3H/HeN mice under similar transfection efficiency that was verified by co-injection of pEGFP-N1 (Figure 2C). Using viral DNA isolation and PCR analysis, the serum HBV-DNA showed higher level in C3H/HeJ than in C3H/HeN mice (Figure 2D). These results suggest that TLR4 is involved

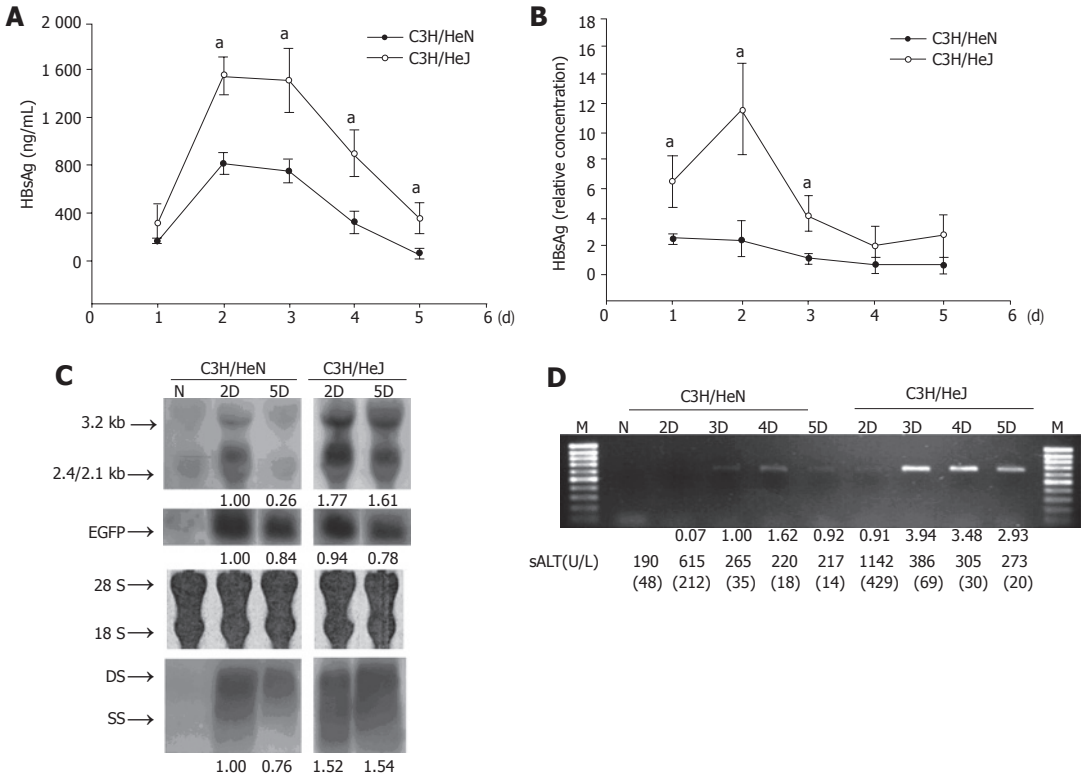

Figure 2 HBV antigenemia and replication in TLR4-mutant C3H/HeJ mice or normal C3H/HeN mice. Groups of four C3H/HeN or C3H/HeJ mice were injected intravenously with 10 μg of pHBV3.6 and 10 μg of pEGFP-N1 that was used as control of transfection efficiency by hydrodynamics-based transfection. The HBsAg (**A**) or HBeAg (**B**) in the serum was detected by ELISA kits as described in Materials and methods. [a]*P*<0.05. (**C**) The total RNA or cytoplasmic DNA was purified from liver and hybridized with HBV specific probes to analyze the HBV transcription or replication. The number below each land of Northern or Southern blot was represented as the relative fold of expression comparing to d2 result of C3H/HeN mice. N, naïve C3H/HeN. (**D**) The serum DNA was purified after treatment with 20 U DNase I and the HBV-DNA was detected by PCR method. The number below each land was represented as the relative fold of expression comparing to d3 result of C3H/HeN mice. M, 100-bp DNA ladder; N, naïve C3H/HeN. The sALT level was represented as mean (SD).

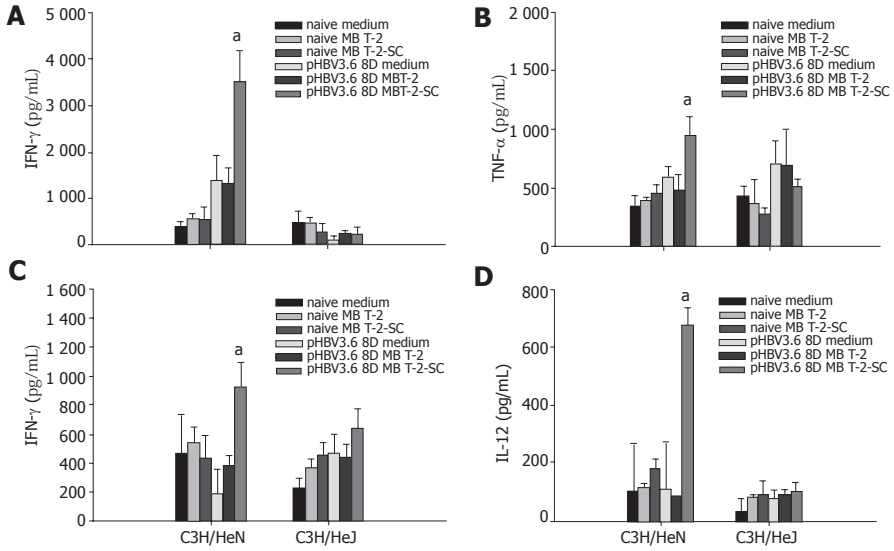

Figure 3 HBV-specific immune responses in the liver or spleen of C3H/HeN or C3H/HeJ mice after hydrodynamic-injection of pHBV3.6. Groups of four C3H/HeN or C3H/HeJ mice were injected intravenously with 10 μg of pHBV3.6 by hydrodynamics-based transfection. The intrahepatic lymphocytes (**A** and **B**) or splenocytes (**C** and **D**) were isolated at d 8 post injection. After being co-cultured with HBsAg and HBcAg expressing syngenic MBT-2 cells (MBT-2-SC) for 48 h, the IFN-γ (**A** and **C**), TNF-α (**B**) or IL-12 (**D**) in the culture supernatant was analyzed by ELISA method. [a]*P*<0.05 *vs* naïve MBT-2-SC group.

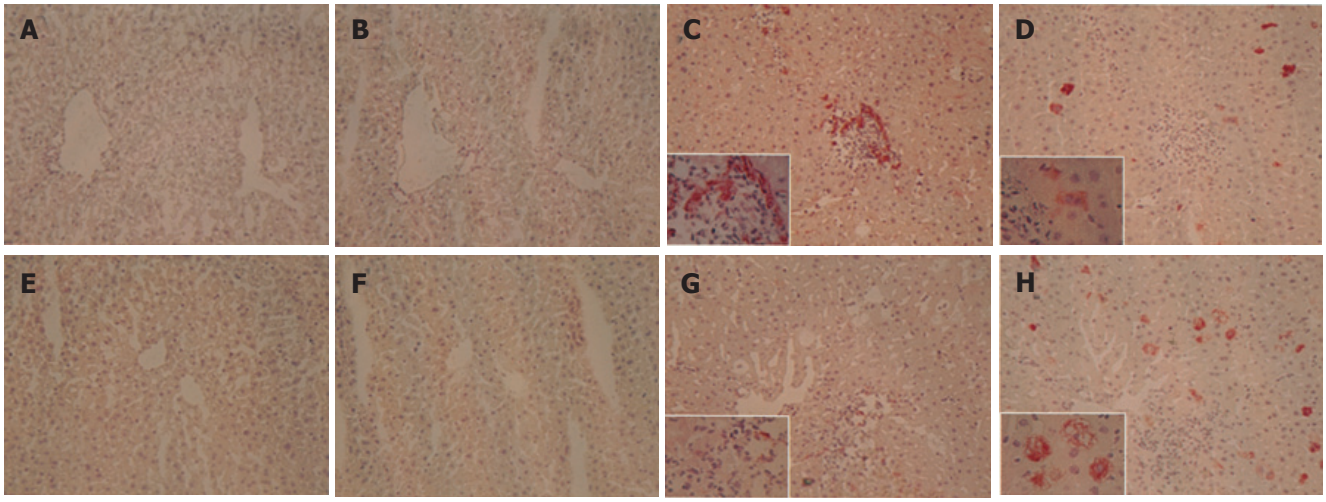

Figure 4 iNOS expression in the liver of C3H/HeN or C3H/HeJ mice after hydrodynamic-injection of pHBV3.6. Groups of four C3H/HeN (**C, D**) or C3H/HeJ (**G, H**) mice were injected intravenously with 10 μg of pHBV3.6 by hydrodynamics-based transfection. Serial sections of frozen liver tissue were made and stained with anti-HBs antibody (**B, D, F, H**) or anti-iNOS antibody (**A, C, E, G**). Red color was developed and indicated the positive staining. The insets in (**C**), (**D**), (**G**), and (**H**) represent twofold magnification of positive staining. **A, B, E, F,** saline injected control mice; **C, D, G, H,** day 2 post injection (original magnification ×200).

in host responses to HBV replication and a mutation in C3H/HeJ impaired its ability to clear the HBV virus.

HBV-specific immune responses were defective in TLR4 mutant C3H/HeJ mice after hydrodynamic injection of pHBV3.6

To investigate the effect of TLR4 on immune responses to HBV, intrahepatic lymphocytes (IHLs) or splenocytes from pHBV3.6-injected C3H/HeN or C3H/HeJ mice were isolated and stimulated with HBsAg- and HBcAg-expressing syngenic MBT-2 cells. The IFN-γ and TNF-α production of IHLs from C3H/HeN mice was significantly increased at 48 h after HBsAg and HBcAg stimulation. But this was not observed in IHLs from C3H/HeJ mice (Figures 3A and B). The IFN-γ and IL-12 production of splenocytes of C3H/HeN mice was also significantly increased in C3H/HeN mice, but not in C3H/HeJ mice (Figures 3C and D). These data suggest that TLR4 mutation in C3H/HeJ affects the HBV specific immune responses (IFN-γ and TNF-α production in liver or IFN-γ and IL-12 production in spleen).

Induction of iNOS was also defective in TLR4 mutant C3H/HeJ mice after hydrodynamic injection of pHBV3.6

It was reported that the activation of TLR4 signaling can induce the iNOS expression[21], and we also reported that iNOS plays an anti-HBV role in acute HBV expression[15]. Therefore, the iNOS expressed was compared in wild type and TLR4 mutant mice after pHBV3.6 transfection. The HBsAg-expressing hepatocytes were equivalent among C3H/HeN and C3H/HeJ mice after pHBV3.6 injection, indicating the transfection efficiency was similar in both strains of mice. But iNOS stainings were detected on the infiltrating leukocytes nearby the HBsAg-expressing hepatocytes in the liver of pHBV3.6-injected C3H/HeN (Figures 4C and D) whereas the expression of iNOS on infiltrating leukocytes was impaired in the liver of C3H/HeJ mice (Figures 4G and H). These data suggested that the mutation of TLR4 influences the induction of iNOS expression during acute HBV expression and may further affect the clearance of HBV.

HBV replication was reduced in C3H/HeJ mice after adoptive transfer of splenocytes from C3H/HeN mice

To further confirm, if TLR4-expressing immune cells provide the protection role to HBV expression, the splenocytes from C3H/HeN mice were injected into C3H/HeJ mice intravenously at the day before pHBV3.6 injection. The HBsAg antigenemia was higher in C3H/HeJ than in C3H/HeN mice, but the adoptive transfer of C3H/HeN splenocytes into the C3H/HeJ mice reduced the serum HBsAg to the level similar to that in C3H/HeN mice (Figure 5A). The HBV transcription or replication in liver (Figure 5B) or HBV-DNA in sera (Figure 5C) was also reduced as well under similar transfection efficiency as verified by co-injection of pEGFP-N1. But when adoptive transfer of splenocytes from C3H/HeJ mice to C3H/HeN mice was carried out, there was no effect to HBsAg in sera (Figure 5A), HBV replication in liver (Figure 5B), or HBV-DNA in sera (Figure 5C). These results indicate that the TLR4 enhances the immune functions to help clear the HBV replication.

DISCUSSION

In this study, we investigated the role of TLR4 in a murine acute HBV expression model. The HBV antigenemia, serum HBV-DNA, as well as HBV transcription and replication in liver were higher in TLR4 mutant C3H/HeJ than TLR4 normal C3H/HeN. This is probably caused by the impaired induction of iNOS and HBV specific immune response because of TLR4 mutation in C3H/

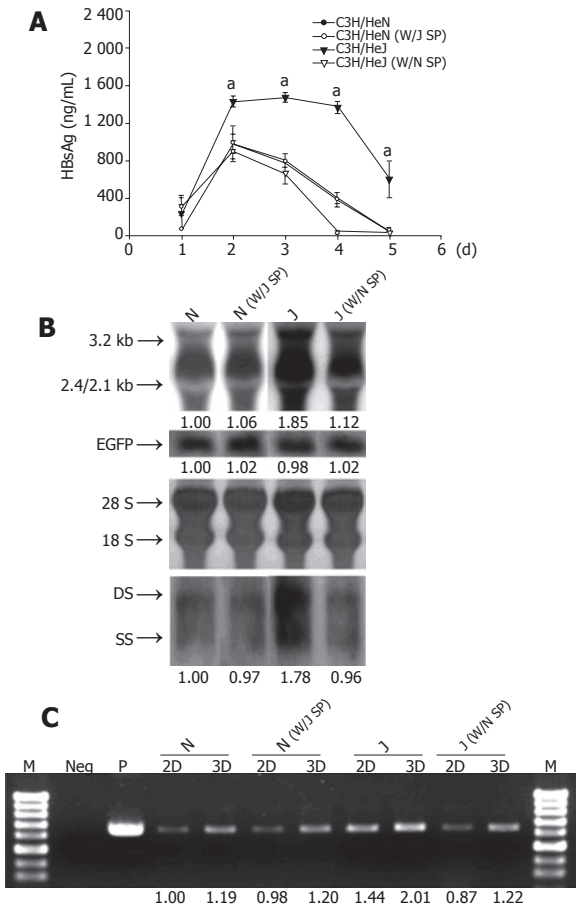

Figure 5 HBV replication was reduced in C3H/HeJ mice after adoptive transfer of splenocytes from C3H/HeN mice. 5×10^6 splenocytes from C3H/HeN or C3H/HeJ mice were injected into C3H/HeJ or C3H/HeN mice intravenously at the day before pHBV3.6 injection, respectively. (**A**) The HBsAg in sera was detected as indicated day by ELISA. $^aP<0.05$. (**B**) The total RNA or cytoplasmic DNA of liver was isolated at day 3 and was further analyzed for HBV transcription or replication by Northern or Southern blot. The transfection efficiency was verified by co-injection of pEGFP-N1 and EGFP RNA confirmation. The number below each land of Northern or Southern blot was represented as the relative fold of expression comparing to C3H/HeN mice. N, C3H/HeN; J, C3H/HeJ; SP, splenocytes. (**C**) The HBV-DNA in sera was isolated as on the indicated day and detected by PCR method. The number below each land was represented as the relative fold of expression comparing to day 2 result of C3H/HeN mice. M, 100-bp DNA ladder; Neg, no template control; P, pHBV3.6 5 ng; N, C3H/HeN; J, C3H/HeJ; SP, splenocytes.

HeJ mice, and suggests that TLR4 plays an antiviral role in HBV replication. Recently, Isogawa *et al*. reported that TLR signaling which includes TLR4 could inhibit HBV replication in transgenic mice model and the mechanism might be through the induction of type I interferon[22]. Our finding of iNOS and HBV specific immune response has increased further understanding on anti-HBV response in addition to the induction of type I interferon.

The TLRs are pattern-recognition receptors that have an important role in mammalian immunity[7,8]. At least 10 TLRs are expressed on a variety of cell types including immune cells, endothelial cells[23], cardiac myocytes[24], and intestinal epithelial cells[25]. Most TLR ligands are conserved pathogen-associated molecular patterns of microbes and the TLR signals serve as a sensor to the presence of infection[13]. TLR4 is the first identified mammalian TLR that expresses predominantly on macrophages and dendritic cells (DCs)[5]. A point mutation ($His^{712}\rightarrow Pro^{712}$) in the Toll/interleukine-1 receptor domain of TLR4 gene causes the C3H/HeJ mice to become defective after LPS challenge[20,26]. TLR4 has been shown to initiate a response to the fusion protein of RSV[11]. Prolonged RSV infection was found in TLR4-deficient mice because of the impaired recruitment of natural killer cells and $CD14^+$ cells in the lung tissue as well as the impaired IL-12 production[27]. Two vaccinia virus ORFs, A46R, and A52R, have been shown to share amino acid sequence similarity to TIR domain, and these two proteins can partially or potentially inhibit the IL-1 and TLR4 mediated NF- κ B activation[28]. These reports indicate that TLR4 also has anti-virus activity in addition to its anti-bacterial function.

In our study, the IHLs nearby the HBsAg-positive hepatocytes (which represented HBV-replicating hepatocytes) expressed TLR4 post pHBV3.6 hydrodynamic transfection (Figure 1). The HBV replication was higher in TLR4 mutant C3H/HeJ than C3H/HeN mice (Figure 2). This is probably caused by the impaired specific anti-HBV immunity in liver or spleen (Figure 3). When adoptively transferring splenocytes from TLR4 normal C3H/HeN mice to TLR4 mutant C3H/HeJ mice, the anti-HBV responses could be upregulated (Figure 5). These results indicate that anti-HBV specific immune responses may be initiated by TLR4 activation. Activation of DCs by LPS through TLR4 has been found to induce IL-12 production and elicit the Th1 responses against intracellular pathogens[29]. In our study, the IL-12 production in splenocytes after HBsAg or HBcAg stimulation (Figure 3D) and IFN-γ production in IHLs (Figure 3A) was also impaired in the C3H/HeJ mice. These results correlated with the impaired function of TLR4 in the C3H/HeJ mice.

TLR4 can signal to induce iNOS expression. After TLR4 agonist stimulation, iNOS gene could be induced through MyD88-dependent (NF-κB) or -independent (IFN-β and STAT-1) pathway in murine macrophage cell line[21]. We have also reported the role of iNOS in anti-HBV response[15]. The iNOS induction in the infiltrating immune cells was impaired in C3H/HeJ mice (Figure 4). Therefore, the iNOS may also involve in the TLR4-mediated anti-HBV responses. In conclusion, the present study reports that TLR4 plays an anti-HBV role in acute HBV expression through induction of iNOS expression and specific anti-HBV immune responses.

ACKNOWLEDGMENT

We thank M. Theron for editorial assistance.

REFERENCES

1 **Nassal M,** Schaller H. Hepatitis B virus replication. *Trends Microbiol* 1993; **1:** 221-228
2 **Arbuthnot P,** Kew M. Hepatitis B virus and hepatocellular carcinoma. *Int J Exp Pathol* 2001; 2:77-100
3 **Feltelson MA.** Hepatitis B virus in hepatocarcinogenesis. *J Cell Physiol* 1999; **181:** 188-202
4 **Lee WM.** Hepatitis B virus infection. *N Engl J Med* 1997; **337:**

1733-1745
5 **Lien E,** Ingalls RR. Toll-like receptors. *Crit Care Med* 2002; **30:** S1-S11
6 **Zhang D,** Zhang G, Hayden MS, Greenblatt MB, Bussey C, Flavell RA, Ghosh S. A toll-like receptor that prevents infection by uropathogenic bacteria. *Science* 2004; **303:** 1522-1526
7 **Akira S,** Takeda K, Kaisho T. Toll-like receptors: critical proteins linking innate and acquired immunity. *Nat Immunol* 2001; **2:** 675-680
8 **Aderem A,** Ulevitch RJ. Toll-like receptors in the induction of the innate immune response. *Nature* 2000; **406:** 782-787
9 **Barton GM,** Medzhitov R. Toll-like receptor signaling pathways. *Science* 2003; **300:** 1524-1525
10 **Ghosh S,** May MJ, Kopp EB. NF-kappa B and Rel proteins: evolutionarily conserved mediators of immune responses. *Annu Rev Immunol* 1998; **16:** 225-260
11 **Kurt-Jones EA,** Popova L, Kwinn L, Haynes LM, Jones LP, Tripp RA, Walsh EE, Freeman MW, Golenbock DT, Anderson LJ, Finberg RW. Pattern recognition receptors TLR4 and CD14 mediate response to respiratory syncytial virus. *Nat Immunol* 2000; **1:** 398-401
12 **Liu F,** Song YK, Liu D. Hydrodynamics-based transfection in animals by systemic administration of plasmid DNA. *Gene Ther* 1999; **6:** 1258-1266
13 **Zhang G,** Budker V, Wolff JA. High levels of foreign gene expression in hepatocytes after tail vein injections of naked plasmid DNA. *Hum Gene Ther* 1999; **10:** 1735-1737
14 **Chang J,** Sigal LJ, Lerro A, Taylor J. Replication of the human hepatitis delta virus genome Is initiated in mouse hepatocytes following intravenous injection of naked DNA or RNA sequences. *J Virol* 2001; **75:** 3469-3473
15 **Chang WW,** Su IJ, Lai MD, Chang WT, Huang W, Lei HY. The role of inducible nitric oxide synthase in a murine acute hepatitis B virus (HBV) infection model induced by hydrodynamics-based in vivo transfection of HBV-DNA. *J Hepatol* **39:** 834-842
16 **Yang PL,** Althage A, Chung J, Chisari FV. Hydrodynamic injection of viral DNA: A mouse model of acute hepatitis B virus infection. *Proc Natl Acad Sci USA* 2002; **99:** 13825-13830
17 **Guidotti LG,** Matzke B, Schaller H, Chisari FV. High level hepatitis B virus replication in transgenic mice. *J Virol* 1995; **69:** 6158-6169
18 **Fan YF,** Lu CC, Chen WC, Yao WJ, Wang HC, Chang TT, Lei HY, Shiau AL, Su IJ. Prevalence and significance of hepatitis B virus (HBV) pre-S mutants in serum and liver at different replicative stages of chronic HBV infection. *Hepatology* 2001; **33:** 277-286
19 **Eto M,** Harada M, Tamada K, Tokuda N, Koikawa Y, Nakamura M, Nomoto K, Naito S. Antitumor activity of interleukin-12 against murine bladder cancer. *J Urol* 2000; **163:** 1549-1552
20 **Poltorak A,** He X, Smirnova I, Liu MY, Van Huffel C, Du X, Birdwell D, Alejos E, Silva M, Galanos C, Freudenberg M, Ricciardi-Castagnoli P, Layton B, Beutler B. Defective LPS signaling in C3H/HeJ and C57BL/10ScCr mice: mutations in Tlr4 gene. *Science* 1998; **282:** 2085-2088
21 **Schilling D,** Thomas K, Nixdorff K, Vogel SN, Fenton MJ. Toll-like receptor 4 and Toll-IL-1 receptor domain-containing adapter protein (TIRAP)/myeloid differentiation protein 88 adapter-like (Mal) contribute to maximal IL-6 expression in macrophages. *J Immunol* 2002; **169:** 5874-5880
22 **Isogawa M,** Robek MD, Furuichi Y, Chisari FV. Toll-like receptor signaling inhibits hepatitis B virus replication in vivo. *J Virol* 2005; **79:** 7269-72
23 **Faure E,** Thomas L, Xu H, Medvedev A, Equils O, Arditi M. Bacterial lipopolysaccharide and IFN-gamma induce Toll-like receptor 2 and Toll-like receptor 4 expression in human endothelial cells: role of NF-kappa B activation. *J Immunol* 2001; **166:** 2018-2024
24 **Frantz S,** Kelly RA, Bourcier T. Role of TLR-2 in the activation of nuclear factor kappaB by oxidative stress in cardiac myocytes. *J Biol Chem* 2001; **276:** 5197-5203
25 **Cario E,** Rosenberg IM, Brandwein SL, Beck PL, Reinecker HC, Podolsky DK. Lipopolysaccharide activates distinct signaling pathways in intestinal epithelial cell lines expressing Toll-like receptors. *J Immunol* 2000; **164:** 966-972
26 **Hoshino K,** Takeuchi O, Kawai T, Sanjo H, Ogawa T, Takeda Y, Takeda K, *et al*. Toll-like receptor 4 (TLR4)-deficient mice are hyporesponsive to lipopolysaccharide: evidence for TLR4 as the Lps gene product. *J Immunol* 1999; **162:** 3749-3752
27 **Haynes LM,** Moore DD, Kurt-Jones EA, Finberg RW, Anderson LJ, Tripp RA. Involvement of toll-like receptor 4 in innate immunity to respiratory syncytial virus. *J Virol* 2001; **75:** 10730-10737
28 **Bowie A,** Kiss-Toth E, Symons JA, Smith GL, Dower SK, O'Neill LA. A46R and A52R from vaccinia virus are antagonists of host IL-1 and toll-like receptor signaling. *Proc Natl Acad Sci U S A* 2000; **97:** 10162-10167
29 **Agrawal S,** Agrawal A, Doughty B, Gerwitz A, Blenis J, Van Dyke T, Pulendran B. Different Toll-like receptor agonists instruct dendritic cells to induce distinct Th responses via differential modulation of extracellular signal-regulated kinase-mitogen-activated protein kinase and c-Fos. *J Immunol* 2003; **171:** 4984-4989

Science Editor Guo SY **Language Editor** Elsevier HK

PO Box 2345, Beijing 100023, China
www.wjgnet.com
wjg@wjgnet.com

ELSEVIER

World J Gastroenterol 2005;11(42):6638-6643
World Journal of Gastroenterology ISSN 1007-9327

He Jie Tang in the treatment of chronic hepatitis B patients

Ze-Xiong Chen, Shi-Jun Zhang, Shao-Xian Lao, Hong-Tao Hu, Cui-Yi Zhang, Shi-He Guan, Yan-Li Gu

Ze-Xiong Chen, Shi-Jun Zhang, Hong-Tao Hu, Cui-Yi Zhang, Department of Traditional Chinese Medicine, First Affiliated Hospital, Sun Yat-Sen University, Guangzhou 510080, Guangdong Province, China
Shao-Xian Lao, Institute of Digestive Diseases, Traditional Chinese Medicine University of Guangzhou, Guangzhou 510405, Guangdong Province, China
Shi-He Guan, Institute of virus, University of Essen, Hufelandstrasse 55, 45122 Essen, Germany
Yan-Li Gu, Department of General Surgery, University of Essen, Hufelandstrasse 55, 45122 Essen, Germany
Supported by the Administrative Bureau of TCM and Chinese Drugs of Guangdong Province, No. 98374 and No. 100108
Co-first-authors: Ze-Xiong Chen and Shi-Jun Zhang
Co-correspondence: Ze-Xiong Chen
Correspondence to: Dr. Shi-Jun Zhang, Department of Traditional Chinese Medicine, First Affiliated Hospital, Sun Yat-Sen University, Guangzhou 510080, Guangdong Province, China. zhsjun1967@hotmail.com
Telephone: +86-20-87334505 Fax: +86-20-87334505
Received: 2005-01-25 Accepted: 2005-04-11

Abstract

AIM: To explore the effect of He Jie Tang (decoction for medication) on serum levels of T lymphocyte subsets, NK cell activity and cytokines in chronic hepatitis B patients.

METHODS: Eighty-five patients with chronic hepatitis B were divided randomly into two groups. Fifty patients in group I were treated with He Jie Tang (HJT) and 35 patients in group II were treated with combined medication. The levels of T-lymphocyte subsets (CD_3^+, CD_4^+, CD_8^+), NK cell activity, cytokines (TNF-α, IL-8, sIL-2R) were observed before and after the treatment. Another 20 normal persons served as group 3.

RESULTS: The level of CD_4^+ cells and NK cell activity were lower, whereas the level of CD_8^+ cells in patients was higher than that in normal persons (t = 2.685, 3.172, and 2.754 respectively; P<0.01). The levels of TNF-α, IL-8, and sIL-2R in chronic hepatitis B patients were higher than those in normal persons (t = 3.526, 3.170, and 2.876 respectively; P<0.01). After 6 months of treatment, ALT, AST, and TB levels in the two groups were obviously decreased (t = 3.421, 3.106, and 2.857 respectively; P<0.01). The level of CD_4^+ cells and NK cell activity were increased whereas the level of CD_8^+ cells decreased (t = 2.179, 2.423, and 2.677 respectively; P<0.05) in group I. The levels of TNF-α, IL-8, and sIL-2R in group I were decreased significantly after the treatment (t = 2.611, 2.275, and 2.480 respectively; P<0.05) but had no significant difference in group II after the treatment (t = 1.906, 1.833, and 2.029 respectively; P>0.05). The total effective rate had no significant difference between the two groups (χ^2 = 2.882, P>0.05) but the markedly effective rate was significantly different between the two groups (χ^2 = 5.340, P<0.05).

CONCLUSION: HJT is effective in treating chronic hepatitis B. HJT seems to exert its effect by improving the cellular immune function and decreasing inflammatory cytokines in chronic hepatitis B patients. The function of HJT in protecting liver function in the process of eliminating virus needs to be further studied.

Key words: He Jie Tang; Lymphocyte subsets; NK cell; Cytokines; Chronic hepatitis B

Chen ZX, Zhang SJ, Lao SX, Hu HT, Zhang CY, Guan SH, Gu YL. He Jie Tang in the treatment of chronic hepatitis B patients. *World J Gastroenterol* 2005; 11(42): 6638-6643
http://www.wjgnet.com/1007-9327/11/6638.asp

INTRODUCTION

Chronic hepatitis B virus (HBV) infection is a serious clinical problem worldwide and may lead to end-stage liver disease, cirrhosis, and hepatocellular carcinoma (HCC), *etc.*[1-3]. The pathogenesis of hepatitis B is very complex and has not been clarified. Generally, HBV itself does not directly damages hepatocytes, but results in dysfunction of cell-mediated immunity[3-5]. Peripheral blood mononuclear cells (PBMCs), which are aggregated immunologically competent cells, such as T lymphocytes, natural, and lymphokine-activated killer cells, likely play an important role in anti-HBV infection.

Some agents such as interferon (INF) and lamivudine have been proved to be effective for chronic hepatitis B, but their efficacy is limited to a small percentage of highly selected patients[6-13]. The management of chronic hepatitis B remains a clinical challenge.

Traditional Chinese medicine (TCM) has a long history in treating hepatitis, and has been proven to have good curative effects and fewer side effects in treating acute and chronic liver diseases. HJT is a recipe for chronic hepatitis B, which can improve liver function and immunity of chronic hepatitis B patients as the seroconversion rate of HBeAg[14]. In order to analyze the immunoregulatory mechanisms of HJT, we treated chronic hepatitis B patients with HJT from June 1999 to March 2003 and

observed the clinical effect of HJT on T lymphocyte subset level, NK cell activity as well as TNF-α, IL-8, and sIL-2R level.

MATERIALS AND METHODS

Patients

A total of 85 patients with chronic hepatitis B were enrolled in this study and randomly divided into two groups. There were 27 males and 23 females aged 18-60 years (mean 36.9±9.5 years) in group I. There were 19 males and 16 females aged 18-60 years (mean 38.5±9.1 years) in group II. The difference in clinical data between the two groups was insignificant. Twenty age-matched healthy donors from the Blood Center of our hospital were assigned as group III. This prospective study was approved by the local ethics committee and written consent was obtained from the participants.

Diagnostic criteria

Patients with a history of hepatitis B or HBsAg carriers for at least 6 mo, who still had symptoms and signs of hepatitis as well as abnormal liver function and positive HBsAg, HBeAg and HBV-DNA, were diagnosed as chronic hepatitis B in the present study.

Criteria for enrollment

Patients, aged 18-60 years with their serum alanine aminotransferase (ALT) level being 80-240 μ/L and who had positive serum HBeAg and HBV-DNA, were enrolled. The diagnosis of hepatitis B was made in accordance with the standards for chronic viral hepatitis issued in the Fifth National Conference on Infectious Diseases and Parasitosis (Beijing, China, 1995).

Criteria for exclusion

Patients aged over 60 years or less than 18 years, patients in pregnancy or in breast feeding period; patients who had hepatitis C or other hepatic viral infection, autoimmune hepatitis and drug-induced hepatitis or alcoholic hepatitis; patients with severe complications of the cardiovascular, renal or hematopoietic system and patients with mental diseases, were excluded.

Group I was treated with HJT that consisted of 10 g Radix Bupleuri, 12 g Radix Scutellariae, 9 g Rhizoma Pinelliae, 30 g Radix Codonopsis Pilosulae, 6 g Radix Glycyrrhizae Praeparata, 9 g Fructus Ziziphi Jujubae, 30 g Rhizoma Polygoni Cuspidati, 8 g Radix Morindae Officinalis, 30 g Herba Hedyotis Diffusae. One dose was taken per day for 6 mo. Group II was treated with oxymatrine (200 mg, t.i.d.), compound vitamin B (2 tablets, t.i.d.), vitamin C (100 mg, t.i.d.), vitamin E (50 mg, t.i.d.), and ester capsule (2 tablets, t.i.d.) for 6 mo.

Patients who had normal serum ALT and sero-conversion of HBeAg and HBV DNA (quantitative PCR) after treatment were defined as responders while those with negative results as non-responders.

Recording and observation of symptoms and signs

The symptoms and signs of patients were recorded in detail using the "Clinical Observation Table" once a month before and during the treatment.

Etiological markers of hepatitis B

HBV-M and anti-HAV, anti-HCV, anti-HDV, and anti-EBV marks were detected by enzyme-linked immunosorbent assay (ELISA). HBV-DNA was detected by quantitative polymerized chain reaction (PCR).

Liver function

The patients had liver function examination every month during the treatment, including contents of serum proteins, total bilirubin (TB) and activities of ALT and AST (aspartate aminotransferase).

T-lymphocyte subsets and NK cell activity

T-lymphocyte subsets were detected by the single clone antibody APAAP method, NK cell activity was assayed by MTT colorimetry.

Detection of cytokines

The levels of TNF-α, sIL-2R, and IL-8 were detected by double antibody sandwich ELISA.

Statistical analysis

All statistical analyses were performed by χ^2 test and Wilcoxon rank sum test using SPSS software. $P<0.05$ was considered statistically significant.

RESULTS

Standard for efficacy evaluation

The clinical efficacy of treatment was evaluated according to the following standards. Markedly effective: chief symptoms including right upper abdomen pain, poor appetite, and abdominal distention disappeared; HBeAg and HBV-DNA turned negative; serum levels of ALT, AST, and TBIL restored to normal. Effective: chief symptoms were alleviated or improved; the level of HBV-DNA decreased; HBeAg did not turn negative; serum levels of ALT, AST, and TBIL decreased by >50% of the original levels. Ineffective: the chief symptoms or the serum levels of ALT, AST, and TBIL or HBeAg and HBV-DNA did not show any improvement.

Clinical efficacy of treatment

In group I, treatment was markedly effective in 7 cases, effective in 41 and ineffective in 2, the total effective rate being 96.0%. In group II, treatment was markedly effective in 0 cases, effective in 30, and ineffective in 5, the total effective rate being 85.7%. The difference in total effective rate was insignificant between the two groups ($P>0.05$) and the markedly effective rate was significantly different between the two groups ($P<0.05$).

Levels of ALT, AST, TB, and HBV-DNA before and after the treatment

After 6 mo of treatment, the levels of ALT, AST, and TB in two groups were obviously decreased ($P<0.01$). HBV-DNA level in group I was obviously decreased ($P<0.05$). HBV-DNA and HBeAg turned negative in seven patients and HBeAg turned negative in two patients but HBV-DNA did not turn negative. HBeAg turned negative in two patients of group II but HBV-DNA did not turn negative (Table 1).

T lymphocyte subsets before and after the treatment

The level of CD_4^+ cells was lower whereas the level of CD_8^+ cells (groups I and II) was higher in patients than in normal persons (group III) ($P<0.01$). There was no significant difference between the levels of CD_3^+ cells in patients and normal persons ($P>0.05$). After 6 mo of treatment, the level of CD_4^+ cells increased, whereas the level of CD_8^+ cells decreased ($P<0.05$) in group I. However, the levels of CD_4^+ and CD_8^+ cells had no significant difference in group II ($P>0.05$, Table 2).

Serum levels of TNF-α, sIL-2R, and IL-8 as well as NK activity before and after the treatment

The NK cell activity was lower whereas the levels of TNF-α, sIL-2R, and IL-8 was higher in patients (groups I and II) than in normal persons (group III) ($P<0.01$). After 6 mo of treatment, NK cell activity was significantly increased, whereas the levels of TNF-α, sIL-2R, and IL-8 decreased ($P<0.05$) in group I. However, there was no significant difference in group II ($P>0.05$, Table 3).

T lymphocyte subsets and NK activity of responders and non-responders of group I before and after the treatment

The levels of CD_3^+, CD_4^+, and CD_8^+ cells and NK cell activity in the two groups had no significant difference before treatment ($P>0.05$). After 6 mo of treatment, the level of CD_4^+ cells and NK cell activity increased, whereas the level of CD_8^+ cells decreased in responders ($P<0.05$). NK cell activity and the level of CD_4^+ and CD_8^+ cells in the non-responders had no significant difference after treatment ($P>0.05$, Table 4).

DISCUSSION

Though the pathogenesis of chronic hepatitis B remains unclear, a great many studies have shown that chronic hepatitis B patients are usually accompanied with disorder of immune function and hepatocyte damage is mainly caused by immunological injury[15–19]. Alterations of T

Table 1 Levels of ALT, AST, TB, and HBV-DNA before and after the treatment (mean±SD)

		n	ALT (U/L)	AST (U/L)	TB (μmol/L)	HBV-DNA (copy/mL)
Group III		20	21.52±8.90	15.56±7.65	11.75±5.71	<1 000
Group I	Pre-T	50	232.52±12.25	139.65±9.62	43.35±5.86	$(1.62\pm0.81)\times10^{8.31}$
	Post-T	50	33.26±9.35[b]	35.18±8.26[b]	19.95±5.12[b]	$(9.25\pm1.90)\times10^{5.02a}$
Group II	Pre-T	35	225.70±11.61	135.45±9.21	41.45±5.85	$(1.47\pm0.65)\times10^{8.22}$
	Post-T	35	30.86±8.95[b]	65.68±8.82[b]	29.55±546[b]	$(8.26\pm2.20)\times10^{7.62}$

Pre-T: before treatment; Post-T: after treatment; [a]$P<0.05$ *vs* before treatment in the same group; [b]$P<0.01$ *vs* before treatment in the same group.

Table 2 T lymphocyte subsets before and after the treatment (mean±SD)

		n	CD_3(%)	CD_4(%)	CD_8(%)	CD_4/CD_8
Group III		20	68.10±9.25	39.27±8.70	30.96±6.82	1.70±0.72
Group I	Pre-T	50	65.55±8.22	35.06±5.38[b]	34.80±4.36[b]	1.10±0.35[b]
	Post-T	50	67.35±8.85	37.60±8.52[a]	31.95±5.61[a]	1.31±0.42[a]
Group II	Pre-T	35	65.86±9.21	35.15±6.01[b]	35.10±6.56[b]	1.07±0.46[b]
	Post-T	35	66.71±9.56	35.92±8.55	34.66±6.25	1.12±0.36

Pre-T: before treatment; Post-T: after treatment; [b]$P<0.01$ *vs* group III ; [a]$P<0.05$ *vs* before treatment in the same group.

Table 3 Serum levels of TNF-α, sIL-2R, and IL-8 as well as NK activity before and after the treatment (mean±SD)

		n	TNF-a (mg/L)	sIL-2R (kU/L)	IL-8 (μg/L)	NK (%)
Group III		20	0.58±0.23	310.0±30.7	0.72±0.2	59.65±7.5
Group I	Pre-T	50	18.8±8.9[b]	390.9±12.0[b]	2.42±0.8[b]	43.12±6.5[b]
	Post-T	50	10.5±6.8[a]	310.22±8.9[a]	1.12±0.5[a]	52.90±7.0[a]
Group II	Pre-T	35	19.0±7.2[b]	395.7±16.5[b]	2.45±0.8[b]	43.02±6.8[b]
	Post-T	35	15.62±7.9	355.6±9.5	1.80±0.7	46.54±6.9

αPre-T: before treatment; Post-T: after treatment; [a]$P<0.05$ *vs* before treatment in the same group; [b]$P<0.01$ *vs* group III.

Table 4 T lymphocyte subsets in responders and non-responders of group I before and after the treatment (mean±SD)

		n	CD_3 (%)	CD_4 (%)	CD_8 (%)	NK (%)
Responders	Pre-T	7	66.02±8.86	35.10±4.76[b]	34.92±4.36[b]	43.52±7.1[b]
	Post-T	7	67.80±9.11	38.85±8.85[a]	30.15±5.82[a]	55.60±8.2[a]
Non-responders	Pre-T	43	65.50±9.08	34.92±6.30[b]	34.77±6.56[b]	42.93±6.7[b]
	Post-T	43	66.09±9.35	35.99±8.70	34.25±5.52	45.60±6.5
Group III		20	68.10±9.25	39.27±8.70	30.96±6.82	59.65±7.5

[a]$P<0.05$ *vs* before treatment in the same group; [b]$P<0.01$ *vs* group III.

lymphocyte subsets and NK cells are important reasons for the disorder of immune function due to HBV infection, TNF-α, IL-8, and sIL-2R are important cytokines associated with liver damage. Therefore, the importance of T lymphocytes and NK cells as well as cytokines in the occurrence of chronic HBV infection has received more and more attention.

CD_3^+, CD_4^+, and CD_8^+ cells are major function subgroups of T cells. An antiviral cellular immune response of CD_4^+ and CD_8^+ is the important mechanism of hepatocyte injury induced by HBV, the specific response of CD_4^+ and CD_8^+ to the virus antigen is closely related with the elimination of the virus[6,20,21]. NK cells play a critical role in host innate defense against viruses and are partly responsible for liver injury in the process of erasing viruses[22-28]. Recent studies found that NK cells are potent activators of dendritic cells (DCs), which have an impact on the magnitude and direction of DC activation of T cells under the conditions of chronic viral infection, activated NK cells can release cytokines and prevent virus from reproducing[23,29]. Therefore, T-lymphocyte subsets and NK activity can be considered as an appropriate response of immune system to inhibit viral replication and HBV eradication. In the present study, we discovered that in the outbreak period of chronic hepatitis B, NK activity and level of CD_4^+ cells were lower, whereas the level of CD_8^+ cells was higher in patients than in normal persons, suggesting that disorders of cellular immune function and pathologic damages occur in chronic hepatitis B patients.

The serum NK activity and CD_4^+ cell level in non-responders were lower than those in normal persons, whereas the level of CD_8^+ cells in non-responders was higher than that of normal persons. After treatment, the NK activity and CD_4^+ cell level were increased in seven patients with the conversion of HBV-DNA and HBeAg and the liver function resumed to normal. The results suggest that T-lymphocyte subsets and NK activity are depressed rather than activated in viral hepatitis B, but levels of T lymphocyte subsets and NK activity are closely related with different courses of hepatitis B. At the same time, levels of T lymphocyte subsets and NK activity in some patients were still low in palliative period, indicating that the chance of recrudescence might increase. T lymphocyte subsets and NK cells play a critical role in response to HBV infection and their level and mutual relation can be used to identify the cellular immune level in patients with chronic hepatitis B[11,38].

TNF-α plays an indispensable role in liver injury mediated by specific immune response to HBV infection[30]. Pretreatment with anti-TNF-α mAb in animal model strongly blocks Th1 cell-induced hepatocyte necrosis and apoptosis[32]. However, it was reported that TNF-α exerts its antiviral effects without destruction of hepatocytes[33]. IL-8 is a chemotactic factor of neutrophils and T cells and plays a role in hepatic injury in patients with chronic viral hepatitis. Remarkable increase of IL-8 leads to accumulation of cytotoxic T lymphocytes, which get direct and immediate access to the target hepatocytes and the resident intrahepatic macrophages, subsequently causing the damage of hepatocytes[34-36]. Release of sIL-2R from activated T lymphocytes may occur as a result of proteolysis of mIL-2R or as a result of alternative mRNA process. High level of sIL-2R in chronic HBV infection appears directly related to the activity of liver diseases; therefore, serum sIL-2R levels can be used to indicate the degree of liver damage in patients with chronic HBV infection[31,37,38].

In the present study, we discovered that in the outbreak period of chronic hepatitis B, the levels of IL-8, TNF-α, and sIL-2R were higher in patients than in normal persons during and after HJT treatment, significantly increased suggesting that cytokines and immunocytes may play a role in the pathogenesis of chronic hepatitis B.

HJT is a recipe for treating hepatitis in which cold and warm drugs are used to eliminate evils and restore healthy energy. Former research indicates that HJT can protect the liver from injury[20,21]. We discovered that HJT could improve liver function and NK activity, regulate T cellular immune function in chronic hepatitis B patients. The results suggest that HJT exerts its effect by improving the cellular immune function and decreasing inflammatory cytokines in chronic hepatitis B patients.

REFERENCES

1 **Kagawa T**, Watanabe N, Kanouda H, Takayama I, Shiba T, Kanai T, Kawazoe K, Takashimizu S, Kumaki N, Shimamura K, Matsuzaki S, Mine T. Fatal liver failure due to reactivation of lamivudine-resistant HBV mutant. *World J Gastroenterol* 2004; **10**: 1686-1687

2 **Ohata K**, Hamasaki K, Toriyama K, Ishikawa H, Nakao K, Eguchi K. High viral load is a risk factor for hepatocellular carcinoma in patients with chronic hepatitis B virus infection. *J Gastroenterol Hepatol* 2004; **19**: 670-675

3 **Ikeda K,** Kobayashi M, Saitoh S, Someya T, Hosaka T, Akuta N, Suzuki Y, Suzuki F, Tsubota A, Arase Y, Kumada H. Significance of hepatitis B virus DNA clearance and early prediction of hepatocellular carcinogenesis in patients with cirrhosis undergoing interferon therapy: long-term follow up of a pilot study. *J Gastroenterol Hepatol* 2005; **20**: 95-102

4 **Ikeda K**, Arase Y, Kobayashi M, Someya T, Saitoh S, Suzuki Y, Suzuki F, Tsubota A, Akuta N, Kumada H. Consistently low hepatitis B virus DNA saves patients from hepatocellular carcinogenesis in HBV-related cirrhosis. A nested case-control study using 96 untreated patients. *Intervirology* 2003; **46**: 96-104

5 **Torre F**, Cramp M, Owsianka A, Dornan E, Marsden H, Carman W, Williams R, Naoumov NV. Direct evidence that naturally occurring mutations within hepatitis B core epitope alter CD4+ T-cell reactivity. *J Med Virol* 2004; **72**: 370-376

6 **Mutimer D.** Hepatitis B virus antiviral drug resistance: from the laboratory to the patient. *Antivir Ther* 1998; **3**: 243-246

7 **Jang MK**, Chung YH, Choi MH, Kim JA, Ryu SH, Shin JW, Kim IS, Park NH, Lee HC, Lee YS, Suh DJ. Combination of alpha-interferon with lamivudine reduces viral breakthrough during long-term therapy. *J Gastroenterol Hepatol* 2004; **19**: 1363-1368

8 **Jang MK,** Chung YH, Choi MH, Kim JA, Ryu SH, Shin JW, Kim IS, Park NH, Lee HC, Lee YS, Suh DJ. Combination of alpha-interferon with lamivudine reduces viral breakthrough during long-term therapy. *J Gastroenterol Hepatol* 2004; **19:** 1363-1368

9 **Mutimer D**. Hepatitis B virus infection: resistance to antiviral agents. *J Clin Virol* 2001; **21**: 239-242

10 **Leung N.** Treatment of chronic hepatitis B: case selection and duration of therapy. *J Gastroenterol Hepatol* 2002; **17**: 409-414

11 **Fischer KP,** Gutfreund KS, Tyrrell DL. Lamivudine resistance in hepatitis B: mechanisms and clinical implications. *Drug Resist Updat* 2001; **4**: 118-128

12 **Fung SK**, Lok AS. Treatment of chronic hepatitis B: who to treat, what to use, and for how long? *Clin Gastroenterol Hepatol* 2004; **2**: 839-848

13 **Schiefke I**, Klecker C, Maier M, Oesen U, Etzrodt G, Tannapfel A, Liebert UG, Berr F. Sequential combination therapy of HBe antigen-negative/virus-DNA-positive chronic hepatitis B with famciclovir or lamivudine and interferon-alpha-2a. *Liver Int* 2004; **24**: 98-104

14 **Zhang SJ,** Chen ZX, Huang BJ. Effect of hejie decoction on T-cell receptor V beta 7 gene expression in patients of chronic hepatitis B. *Zhongguo Zhongxi Yijiehe Zazhi* 2002; **22**: 499-501

15 **Mancini-Bourgine M,** Fontaine H, Scott-Algara D, Pol S, Brechot C, Michel ML. Induction or expansion of T-cell responses by a hepatitis B DNA vaccine administered to chronic HBV carriers. *Hepatology* 2004; **40**: 874-882

16 **Shimada N,** Yamamoto K, Kuroda MJ, Terada R, Hakoda T, Shimomura H, Hata H, Nakayama E, Shiratori Y. HBcAg-specific CD8 T cells play an important role in virus suppression, and acute flare-up is associated with the expansion of activated memory T cells. *J Clin Immunol* 2003; **23**: 223-232

17 **Hasebe A**, Akbar SM, Furukawa S, Horiike N, Onji M. Impaired functional capacities of liver dendritic cells from murine hepatitis B virus (HBV) carriers: relevance to low HBV-specific immune responses. *Clin Exp Immunol* 2005; **139**: 35-42

18 **Kondo Y,** Kobayashi K, Asabe S, Shiina M, Niitsuma H, Ueno Y, Kobayashi T, Shimosegawa T. Vigorous response of cytotoxic T lymphocytes associated with systemic activation of CD8 T lymphocytes in fulminant hepatitis B. *Liver Int* 2004; **24**: 561-567

19 **Lee CK,** Suh JH, Cho YS, Han KH, Chung JB, Chon CY, Moon YM. Direct analysis of HBV-specific CD8+ lymphocyte by tetrameric HLA-A2/core 18-27 complex in chronic Hepatitis B. *Taehan Kan Hakhoe Chi* 2002; **8**: 139-148

20 **Xuan SY**, Sun Y, Zhang J. The influence to the function of cellular immunity after being infected by HBV in the PBMC in chronic hepatitis B. *Zhonghua Liuxing Bingxue Zazhi* 1997; **18**: 80-82

21 **Ahn DS,** Jang HC, Ahn JK, Yim CY, Kim DG. Impaired interleukin-2 receptor expression on lymphocytes from patients with chronic active hepatitis type B. *Korean J Intern Med* 1989; **4**: 34-40

22 **Dong Z,** Wei H, Sun R, Hu Z, Gao B, Tian Z. Involvement of natural killer cells in PolyI: C-induced liver injury. *J Hepatol* 2004; **41**: 966-973

23 **Jinushi M**, Takehara T, Tatsumi T, Kanto T, Miyagi T, Suzuki T, Kanazawa Y, Hiramatsu N, Hayashi N. Negative regulation of NK cell activities by inhibitory receptor CD94/NKG2A leads to altered NK cell-induced modulation of dendritic cell functions in chronic hepatitis C virus infection. *J Immunol* 2004; **173**: 6072-6081

24 **Sun R**, Gao B. Negative regulation of liver regeneration by innate immunity (natural killer cells/interferon-gamma). *Gastroenterology* 2004; **127**: 1525-1539

25 **Kakimi K**, Guidotti LG, Koezuka Y, Chisari FV. Natural killer T cell activation inhibits hepatitis B virus replication in vivo. *J Exp Med* 2000; **192**: 921-930

26 **Echevarria S**, Casafont F, Miera M, Lozano JL, de la Cruz F, San Miguel G, Pons Romero F. Interleukin-2 and natural killer activity in acute type B hepatitis. *Hepatogastroenterology* 1991; **38**: 307-310

27 **Chemello L**, Mondelli M, Bortolotti F, Schiavon E, Pontisso P, Alberti A, Rondanelli EG, Realdi G. Natural killer activity in patients with acute viral hepatitis. *Clin Exp Immunol* 1986; **64**: 59-64

28 **Lehoux M**, Jacques A, Lusignan S, Lamontagne L. Murine viral hepatitis involves NK cell depletion associated with virus-induced apoptosis. *Clin Exp Immunol* 2004; **137**: 41-51

29 **Li Y**, Zhang T, Ho C, Orange JS, Douglas SD, Ho WZ. Natural killer cells inhibit hepatitis C virus expression. *J Leukoc Biol* 2004; **76**: 1171-1179

30 **Bozkaya H,** Bozdayi M, Turkyilmaz R, Sarioglu M, Cetinkaya H, Cinar K, Kose K, Yurdaydin C, Uzunalimoglu O. Circulating IL-2, IL-10 and TNF-alpha in chronic hepatitis B: their relations to HBeAg status and the activity of liver disease. *Hepatogastroenterology* 2000; **47**: 1675-1679

31 **Monsalve-De Castillo F**, Romero TA, Estevez J, Costa LL, Atencio R, Porto L, Callejas D. Concentrations of cytokines, soluble interleukin-2 receptor, and soluble CD30 in sera of patients with hepatitis B virus infection during acute and convalescent phases. *Clin Diagn Lab Immunol* 2002; **9**: 1372-1375

32 **Tanaka Y**, Takahashi A, Watanabe K, Takayama K, Yahata T, Habu S, Nishimura T. A pivotal role of IL-12 in Th1-dependent mouse liver injury. *Int Immunol* 1996; **8**: 569-576

33 **Guidotti LG,** Chisari FV. Noncytolytic control of viral infections by the innate and adaptive immune response. *Annu Rev Immunol* 2001; **19**: 65-91

34 **Mahe Y**, Mukaida N, Kuno K, Akiyama M, Ikeda N, Matsushima K, Murakami S. Hepatitis B virus X protein transactivates human interleukin-8 gene through acting on nuclear factor kB and CCAAT/enhancer-binding protein-like cis-elements. *J Biol Chem* 1991; **266**: 13759-13763

35 **Masumoto T**, Ohkubo K, Yamamoto K, Ninomiya T, Abe M, Akbar SM, Michitaka K, Horiike N, Onji M. Serum IL-8 levels and localization of IL-8 in liver from patients with chronic viral hepatitis. *Hepatogastroenterology* 1998; **45**: 1630-1634

36 **Nobili V**, Marcellini M, Giovannelli L, Girolami E, Muratori F, Giannone G, Devito R, De Benedetti F. Association of serum interleukin-8 levels with the degree of fibrosis in infants with chronic liver disease. *J Pediatr Gastroenterol Nutr* 2004; **39**: 540-544

37 **Sawayama Y**, Hayashi J, Kawakami Y, Furusyo N, Ariyama I, Kishihara Y, Ueno K, Kashiwagi S. Serum soluble interleukin-2 receptor levels before and during interferon treatment in

patients with chronic hepatitis B virus infection. *Dig Dis Sci* 1999; **44**: 163-169
38 **Xuan SY**, Sun Y, Zhang J. The influence to the function of cellular immunity after being infected by HBV in the PBMC in chronic hepatitis B. *Zhonghua Liuxing Bingxue Zazhi* 1997; **18**: 80-82

Science Editor Wang XL and Guo SY **Language Editor** Elsevier HK

PO Box 2345, Beijing 100023, China
www.wjgnet.com
wjg@wjgnet.com

ELSEVIER

World J Gastroenterol 2005;11(42):6644-6649
World Journal of Gastroenterology ISSN 1007-9327

• *BRIEF REPORTS* •

Herpes simplex virus type 1 in peptic ulcer disease: An inverse association with *Helicobacter pylori*

Klisthenis Tsamakidis, Efstathia Panotopoulou, Dimitrios Dimitroulopoulos, Dimitrios Xinopoulos, Maria Christodoulou, Alexandra Papadokostopoulou, Ioannis Karagiannis, Elias Kouroumalis, Emmanuel Paraskevas

Klisthenis Tsamakidis, Dimitrios Dimitroulopoulos, Dimitrios Xinopoulos, Alexandra Papadokostopoulou, Ioannis Karagiannis, Emmanuel Paraskevas, Department of Gastroenterology, "Agios Savvas" Anticancer Hospital, Athens, Greece
Efstathia Panotopoulou, Maria Christodoulou, Papanicolaou Research Center of Oncology and Experiment Surgery, Athens, Greece
Elias Kouroumalis, Department of Gastroenterology, University Hospital, Heraklion, Crete, Greece
Correspondence to: Dr D Dimitroulopoulos, Department of Gastroenterology, "Agios Savvas" Hospital, Parnasou 35, GR-152 34 Athens, Greece. dimdim@otenet.gr
Telephone: +30-210-6892460 Fax: +30-210-6420146
Received: 2005-04-14 Accepted: 2005-05-12

Abstract

AIM: To assess the frequency of herpes simplex virus type I in upper gastrointestinal tract ulcers and normal mucosa with the modern and better assays and also with a larger number of well characterized patients and controls and its relationship to *Helicobacter pylori*(H *pylori)*.

METHODS: Biopsy specimens from 90 patients (34 with gastric ulcer of the prepyloric area and 56 with duodenal ulcer) were evaluated. Biopsies from 50 patients with endoscopically healthy mucosa were considered as the control group. The method used to identify herpes simplex virus-1 (HSV-1) was polymerase chain reaction. *H pylori* was detected by the CLO-test and by histological method.

RESULTS: Herpes simplex virus-1 was detected in 28 of 90 patients with peptic ulcer (31%) [11 of 34 patients with gastric ulcer (32.4%) and 17 of 56 with duodenal ulcer (30.4%)] exclusively close to the ulcerous lesion. All control group samples were negative for HSV-1. The likelihood of *H pylori* negativity among peptic ulcer patients was significantly higher in HSV-1 positive cases than in HSV-1 negative cases (P = 0.009). Gastric ulcer patients with HSV-1 positivity were strongly associated with an increased possibility of *Helicobacter pylori* negativity compared to duodenal ulcer patients (P = 0.010).

CONCLUSION: HSV-1 is frequent in upper gastrointestinal tract ulcers but not in normal gastric and duodenal mucosa. There is an inverse association between HSV-1 and *H pylori* infection.

Key words: HSV-1; Herpes simplex virus type 1; Peptic ulcer; Duodenal ulcer; Gastric ulcer; PCR; Polymerase chain reaction; *H pylori*; Non-steroidal anti-inflammatory drugs

Tsamakidis K, Panotopoulou E, Dimitroulopoulos D, Xinopoulos D, Christodoulou M, Papadokostopoulou A, Karagiannis I, Kouroumalis E, Paraskevas E. Herpes simplex virus type 1 in peptic ulcer disease: An inverse association with *H pylori*. *World J Gastroenterol* 2005; 11(42): 6644-6649
http://www.wjgnet.com/1007-9327/11/6644.asp

INTRODUCTION

During the last two decades, a significant progress has been made in the role of *Helicobacter pylori*(*H pylori*) in the pathogenesis of peptic ulcers, while the invention of new powerful antisecretory drugs has changed dramatically the treatment of the disease. However, the exact etiopathogenesis of peptic ulcer disease is still under investigation.

The significant role of gastric acidity and inflammation of mucosa due to *H pylori* cannot be disputed, but a multifactorial etiology for peptic ulcer disease seems to be emerging[1-3].

The idea of a possible correlation between HSV-1 and peptic ulcers has appeared almost 40 years before[4,5], due to many common characteristics observed in the clinical picture and the natural history of both diseases[4-7].

A possible involvement of HSV-1 in peptic ulcer disease was reported from several investigators, but a firm conclusion has not yet been reached. The vast majority of these studies are based on the detection of antibodies against the virus in the serum and the duodenal juice of patients with peptic ulcer[8-12], a finding also common in the apparent healthy population. There are only two studies that report the presence of HSV-1 in tissue samples obtained from gastric and duodenal ulcers, using polymerase chain reaction (PCR) methods, but the number of the examined populations is small[13,14]. On the other hand, in the studies reported above, a possible correlation between HSV-1 and *H pylori* has been investigated in the

pathogenesis of peptic ulcer disease.

DNA of HSV-1 has been detected also in human vagal[15] and celiac ganglia[16], which provide the nerve network to gastric tissue. Theoretically, since vagotomy is used to treat peptic ulcer disease, the same treatment may interrupt the migration of activated HSV-1 from ganglia to gastric mucosa, thus preventing the recurrence of ulcer.

The purpose of this study was to investigate the possible relationship between HSV-1 and peptic ulcer and whether viral infection of ulcer patients is related to the presence of *H pylori* infection.

MATERIALS AND METHODS

Patients and biopsies

All patients who underwent esophagogastroduodenoscopy at our institution from September 1999 to September 2002 were recruited. The first group included 56 patients (31 men and 25 women) with active duodenal ulcer (average 53.5±15 years, range from 19 to 83 years). The second group included 34 patients (22 men and 12 women) with active ulcer of the prepyloric area of the stomach (mean of 61.5±16.2 years, range from 22 to 89 years) and the third group that formed the control group, consisted of 50 patients (28 men and 22 women) with no evidence of pathologic findings (mean of 54.8±16.7 years, range from 21 to 86 years).

Tissue samples were taken from all 90 patients with peptic ulcer for the detection of HSV-1 in duplicate, from the following areas: the base and the rim of the ulcer; the adjacent area of the ulcer at a distance of 3 cm (minimal and maximal distance from the crater 3 and 5 cm respectively). For this reason, in the duodenal ulcer group a second duodenal biopsy was obtained; an endoscopically normal area of the stomach (the corpus in gastric ulcer cases and the antrum in duodenal ulcer cases).

Two samples were also taken from endoscopically healthy areas of the antrum and corpus of the stomach in all 50 controls.

Two samples from the antrum and two from the corpus of the stomach were taken for the detection of *H pylori* using the rapid urease test (CLO-test) and routine histology.

Finally, specimens from the gastric ulcers were examined histopathologically to exclude malignancy.

Risk factors probably involved in the pathogenesis of peptic ulcer, such as non-steroidal anti-inflammatory drugs (NSAIDs), smoking, alcohol, history of herpes labialis, family history of peptic ulcer, and ulcer site, were recorded and analyzed.

DNA extraction

Genomic DNA was extracted using the QIAamp DNA mini kit, following the protocol supplied for purification from fresh tissues. DNA was finally dissolved in 50–100 μL of TE buffer depending on the size of DNA pellets and stored at -20 °C until amplification.

Primer design

For the nested PCR assay, oligonucleotides deduced from the published sequence of the RL2 gene-coding region from HSV-1 were used[17]. For the control DNA assay, oligonucleotides for b-actin gene were used. The primer sequences and characteristics are shown in Table 1.

Table 1 Characteristics and nucleotide base sequences of primers used for nested PCR and control assays

Gene target	GenBank accession number	Product size (bp)	Sequences[1]	T_m (°C)
HSV-1: RL2	X14112	450	Outer sense agcagcgactctgaggcggagaccg	69.1
			Outer antisense tgcgggtctgggggtcgttcacga	71.4
		110	Inner sense cccggcagttgcgggggcgc	73.4
			Inner antisense aaggtgtcgcagcggcaggtg	60.8
b-actin		200	Forward gtgatctccttctgcatcc	53.2
			Reverse ctcttccagccttccttc	52.7

T_m, melting temperature. [1]Sequences shown are in the 5′ to 3′ direction.

Nested PCR amplification and detection assay of HSV-1

B-actin PCR generating a 200-bp product was performed to determine the DNA integrity of the samples. For the quality control PCR assay, the following program was used 1 cycle at 94 °C for 2 min; 35 cycles at 94 °C for 30 s, at 58 °C for 30 s, at 72 °C for 30 s; and a final cycle at 72 °C for 7 min.

PCR detection of HSV-1 was carried out in a 50 μL reaction mixture containing 25 μL of Taq PCR master mix solution (Qiagen), 13 μL of double-distilled DNase-free water, 1 μmol/L concentration of each primer and 10 μL of the extracted sample. PCR was performed on a PE 9 600 thermocycler (Perkin-Elmer Cetus, Branchburd, NJ, USA). The cycling conditions were at 94 °C for 1 min, 5 cycles at 94 °C for 5 s and at 72 °C for 4 min; 5 cycles at 94 °C for 5 s and at 70 °C for 4 min; 30 cycles at 94 °C for 5 s and at 68 °C for 4 min. After the final cycle, tubes were incubated for an additional 10 min at 72 °C. Nested PCR amplification was done with a 0.5 μL aliquot from the first run, 25 μL of Taq PCR master mix solution, 18 μL of double-distilled DNase-free water and 1 μmol/L concentration of each inner primer under the following cycling conditions: at 94 °C for 2 min; 35 cycles at 90 °C for 30 s, at 68 °C for 30 s, at 72 °C for 30 s and a final extension at

72 °C for 10 min. Each amplification run contained one negative and one positive control. The negative control consisted of blank reagent and water. For the positive control, HSV-1 genomic DNA provided by Sigma was used. Consistent PCR analyses were repeated twice or more.

The PCR products were analyzed by 2% agarose gel electrophoresis in 0.5×Tris–borate EDTA buffer along with ethidium bromide. A molecular weight marker (Φ× 174/Hae III, Sigma) was also run simultaneously to identify the molecular size of the PCR products. The DNA bands were visualized by UV transillumination and analyzed using a gel-documentation system. None of the PU and the control samples were negative in the b-actin test ultimately leaving 90 PU and 50 controls that were subjected to HSV-1 PCR analysis.

Helicobacter pylori testing

For the detection of *H pylori*, a CLO-test was used with high sensitivity and specificity (Kimberly-Clark CLO test, Ballard Medical products, Draper, UT 84020, USA)[18,19].

An experienced pathologist also assessed the histological sections with Giemsa stain[20].

Statistical analysis

All associations between parameters of interest were examined either by Fisher's exact test or Pearson's *chi square* test with continuity correction.

Multivariate analysis was performed using the stepwise logistic regression model to assess the contribution of the common risk factors to peptic ulcer development and *H pylori* detection.

$P<0.05$ was considered statistically significant.

RESULTS

Polymerase chain reaction

The genome of HSV-1 was present in 28 of the 90 patients with peptic ulcer (31.1%), contrary to the control group in which no positive detections were found (0%, $P<0.0005$, Figures 1-3). There was an equal prevalence in the two subgroups of patients, 17 of 56 patients with duodenal ulcer (30.4%) and 11 of 34 with gastric ulcer (32.4%) were tested positive ($P = 0.843$). In all HSV-1 positive cases, the viral genome was detected from the tissue samples obtained from the crater of the ulcer as from the samples obtained from the rim, while all samples from adjacent and distant areas were negative.

CLO test

All the *H pylori* positive subjects by CLO test from both groups were also positive for the bacteria with histology.

The incidence of *H pylori* was significantly higher in peptic ulcer patients (76/90, 84.4%) than in controls (30/50, 60%) ($P = 0.002$). A statistically significant difference was also found between patients with duodenal ulcer and those with gastric ulcer ($P = 0.036$). Negative *H pylori* was more frequently observed in patients with gastric ulcer (26.5%) than in patients with duodenal ulcer (8.9%, Table 2).

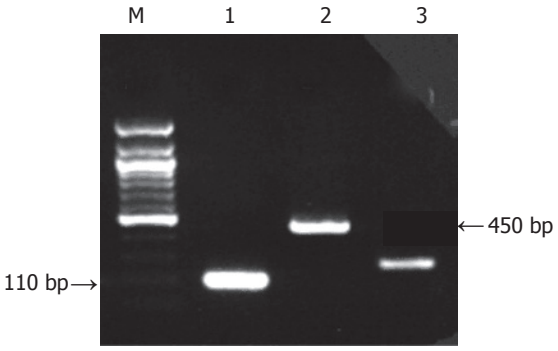

Figure 1 Nested PCR with HSV-1 outer and inner primers (450- and 110-bp amplicons: arrows) on 2% agarose gel, by ethidium bromide staining. Lane M: DNA molecular weight marker Φ×174/*Hae* III, lane 1: HSV-1 positive control (second run of nested PCR), lane 2: HSV-1 positive control (first run of nested PCR), lane 3: b-actin quality control PCR peptic ulcer sample.

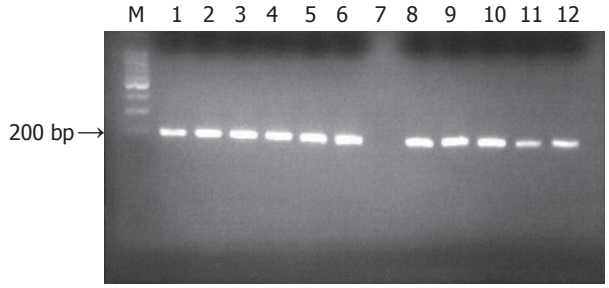

Figure 2 PCR quality assay control. Lane M: DNA molecular weight marker Φ ×174/Hae III, lanes 1-6: positive b-actin peptic ulcer samples; lane 7: negative control (without template); lanes 8-12: positive b-actin peptic ulcer samples.

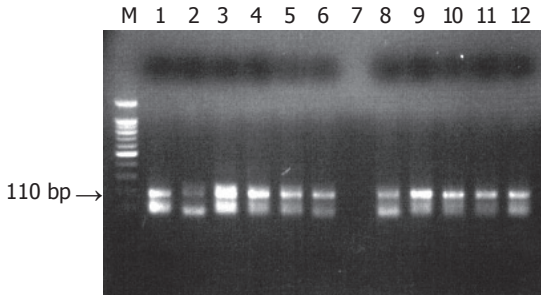

Figure 3 Nested PCR amplification of HSV-1 in samples of patients with peptic ulcer. Lane M: DNA molecular weight marker Φ×174/Hae III, lane 1: HSV-1 positive control (HSV-1 genomic DNA by Sigma), lanes 2-6: positive samples from patients with peptic ulcer, lane 7: negative control (without template), lanes 8-11: positive samples from patients with peptic ulcer, lane 12: HSV-1 positive control.

PCR and CLO test were significantly associated with respect to *H pylori* detection in all 90 peptic ulcer patients. Negative *H pylori* was more frequently detected in positive PCR samples (32.1%) than in negative PCR samples (8.1%) ($P = 0.009$) (Table 2). In the group of duodenal ulcer patients, *H pylori* negativity was more frequently observed in positive PCR samples (11.8%), than in negative PCR samples (7.7%). However, this difference was not

Table 2 Association between *H pylori* and HSV-1 in patients with peptic ulcer

	H pylori (+), %	*H pylori* (–)	*P*	Odds ratio (95%CI)
Peptic ulcer	76/90 (84.4)	14/90		
Controls	30/50 (60)	20/50	0.002	3.7 (1.6–8.1)
Gastric ulcer	25/34 (73.5)	9/34		
Duodenal ulcer	51/56 (91.1)	5/56	0.036	3.67 (1.1–12.11)
HSV-1 (+)	19/28 (67.9)	9/28		
HSV-1 (–)	57/62 (91.9)	5/62	0.009	5.4 (1.61–18.11)
HSV-1 (+)/GU	4/11 (36.4)	7/11		
HSV-1 (–)/ GU	21/23 (91.3)	2/23	0.002	18.37 (2.75–122.94)
HSV-1 (+)/ Duodenal ulcer	15/17 (88.2)	2/17		
HSV-1(–)/ Duodenal ulcer	36/39 (92.3)	3/39	0.634	-

HSV-1 (+)/gastric ulcer, patients with gastric ulcer positive for HSV-1; HSV-1 (–)/gastric ulcer, patients with gastric ulcer negative for HSV-1; HSV-1 (+)/duodenal ulcer, patients with duodenal ulcer positive for HSV-1; HSV-1 (–)/duodenal ulcer, patients with duodenal ulcer negative for HSV-1; CI, confidence interval.

Table 3 Association between *H pylori* and HSV-1 in relation with the site of peptic ulcer

	H pylori (+), %	*H pylori* (-)	*P*-value	Odds ratio (95% CI)
HSV-1(+)/ gastric ulcer	4/11 (36.4)	5/11	0.010	13.13 (1.92–89.5)
HSV-1(–)/ duodenal ulcer	15/17 (88.2)	2/17		

HSV-1 (+), patients positive for HSV-1; CI, confidence interval.

statistically significant ($P = 0.634$) (Table 2) whereas it was statistically significant in the subgroup of gastric ulcer patients ($P = 0.002$). In the gastric ulcer subgroup, *H pylori,* negative cases were observed in 63.6% of positive PCR samples and in 8.7% of negative PCR samples (Table 2). Finally, the likelihood of negative *H pylori* in HSV-1 positive samples in the group of gastric ulcer patients was significantly higher than that in the group of duodenal ulcer patients ($P = 0.010$) (Table 3).

Statistical analysis of other parameters

We also studied some of the common risk factors for the development of peptic ulcer disease. No statistically significant difference was found between patients and controls regarding family history of upper gastrointestinal ulcer, history of *Herpes labialis*, alcohol consumption, and use of NSAIDs (Table 4).

As expected, tobacco smoking was the only statistically significant risk factor for the development of peptic ulcers between patients and control population ($P = 0.019$). Smokers were associated with a 2.57-fold increase risk of peptic ulcer development.

The performed multivariate analysis also confirmed that *H pylori* and tobacco smoking (OR: 3.320 and 2.619 respectively) were more likely to induce peptic ulcer (Table 5).

Table 4 Risk factors and peptic ulcer disease

	Peptic ulcer patients (%)	Controls (%)	Odds ratio	*P*
History of *H labialis*				
Yes	24/90 (26.7)	9/50 (18.0)	-	0.302
No	66/90 (73.3)	41/50 (82.0)		
Alcohol consumption				
Yes	32/90 (35.6)	14/50 (28.0)	-	0.469
No	58/90 (64.4)	36/50 (72.0)		
NSAID use				
Yes	23/90 (25.6)	8/50 (16.0)	-	0.275
No	67/90 (74.4)	42/50 (84.0)		
Smoking				
Yes	45/90 (50.0)	14/50 (28.0)	2–57	0.019
No	45/90 (50.0)	36/50 (72.0)		
Family history of peptic ulcer				
Yes	30/90 (33.3)	9/50 (18.0)	2.3	0.076
No	60/90 (66.7)	41/50 (82.0)		

Table 5 Contribution of other risk factors to peptic ulcer development

	B	S.E	df	Sig.	Odds ratio	95%CI for Odds ratio
Smoking	0.963	0.394	1	0.015	2.619	1.209–5.673
H pylori infection	1.2	0.473	1	0.011	3.32	1.313–8.389
Age	0.011	0.014	1	0.432		
Sex	0.144	0.442	1	0.745		
History of *H labialis*	0.721	0.484	1	0.137		
Alcohol	0.021	0.492	1	0.966		
NSAID use	0.286	0.494	1	0.562		
Family history	0.44	0.48	1	0.359		
Constant	–0.741	0.393	1	0.06		

CI, confidence interval.

DISCUSSION

Despite the progress during the last 20 years in the understanding of the pathogenesis of peptic ulcer disease, it is clear that gastroduodenal ulcer is the result of a multifactorial process.

H pylori infection and NSAIDs have been recognized as the two most important causes of peptic ulcer disease. The proportion of peptic ulcers not associated with *H pylori* infection or the use of NSAIDs is increasing. Yet several studies have shown that 4.1-44% of peptic ulcers are not related to either of the two factors[21-25].

The possible involvement of HSV-1 in the process is a field of interest for several investigators, but a firm conclusion has not been reached. The presence of viral DNA in tissue samples obtained from the ulcer site is 9.5-18%[13,14]. The possible explanation for this finding is that the HSV-1 expression is prompted either by the ulcer injury or by immune cells[14,16] or HSV-1 itself might cause the ulcerative lesion by directly infecting the mucosal cells[13] or finally that HSV-1 expression is induced by the ulcer treatment[26-28].

In the present study, in a substantially larger number of patients than in the studies reported above (90 *vs* 22 and 21 respectively), the positivity for HSV-1 DNA was expressed using PCR in a greater percentage of samples (31% *vs* 9.5% and 18% respectively).

It should be noted that viral DNA was detected only in the tissue samples obtained from the base and the rim of the lesions, whereas all the other examined samples obtained from the adjacent ulcer areas and endoscopically healthy mucosa from the patients and the control group were negative for the viral genome.

This finding can be explained as follows. The HSV-1 may have initially entered the vagus ganglia through the oral pharynx or other peripheral connecting sites. Upon activation, the virus would travel down the vagal nerve to the potential site of peptic ulcer lesion. HSV-1 itself might cause ulcerative lesion in selected cases of a subset of peptic ulcer diseases by directly infecting the mucosal cells in the stomach and duodenum following virus release from neuroendocrine cells or vagal nerve terminals or both. Alternatively, peptic ulcer might activate latent HSV-1 in vagal ganglia, making replication of HSV-1, a contributing but not an initiating factor of ulcer[13].

The detection percentage of positive HSV-1 was similar between the group of patients with gastric and the group of patients with duodenal ulcer (32.4% and 30.4% respectively), in contrast to previous studies, where the viral DNA is demonstrated only in tissue samples from gastric ulcers[13,14]. The exact cellular localization of HSV-1 DNA could not be identified.

On the other hand, investigating a possible association between *H pylori* and HSV-1 in pathogenesis of a subset of gastroduodenal ulcers, our data suggest that the PCR HSV-1 positivity is associated with a 5.4-fold increase in negative *H pylori* detection. Moreover, the patients with ulcer lesions infected with HSV-1 presented a similar prevalence of *H pylori* infection as the control group, which was significantly lower than that in the HSV-1 negative ulcer cases ($P = 0.09$). This finding requires further investigation.

Possible interpretations for the increased HSV-1 DNA positive detection rate in *H pylori* negative ulcers include the following. *H pylori* negativity is influenced by the viral expression, HSV-1 negativity influences *H pylori* infection and the virus independently causes some gastroduodenal ulcers.

According to our results, in the subgroup of patients with duodenal ulcers, the risk of *H pylori* infection was independent from HSV-1 DNA expression ($P = 0.634$). On the other hand, in the subgroup of patients with gastric ulcer disease, the possibility of *H pylori* negativity was 18.5-fold higher ($P = 0.002$). These data are in accordance with those reported by Lohr *et al*.[13].

Additionally, according to our results, there was not any correlation between peptic ulcer disease and age, sex, ulcer site, family history of gastroduodenal ulcers, history of *H. labialis*, alcohol consumption and NSAIDs use. On the contrary, statistically significant difference ($P = 0.019$) was observed between patients with peptic ulcers and controls, as far as smoking was concerned.

Our results indicate an involvement of HSV-1 in the pathogenesis of peptic ulcer disease. Although an opportunistic infection with the virus in the ulcer site cannot be excluded, the inverse relationship between HSV-1 detection and *H pylori* infection indicates a possible implication of this virus in the formation of the ulcer crater, at least in a subgroup of patients. Furthermore, experimental data support this[13,15,16,30,31]. The exact localization of the virus in ulcer tissue cells should be precisely determined in order to clarify whether the lesion is caused by HSV-1 or the virus opportunistically is established, especially in immunocompromised patients[32].

REFERENCES

1 **Wirth HP.** Gastroduodenal ulcer disease: update on pathogenesis. *Schweiz Rundsch Med Prax* 1995; **84:** 570-580
2 **Brooks MJ,** Maxson CJ, Rubin W. The infectious etiology of peptic ulcer disease. Diagnosis and implications for therapy. *Prim Care* 1996; **23:** 443-454
3 **Peura DA.** Ulcerogenesis: integrating the roles of *Helicobacter pylori* and acid secretion in duodenal ulcer. *Am J Gastroenterol* 1997; **92:** 8S-13S; discussion 13S-16S
4 **Knyvett AF.** Herpes simplex in peptic ulceration? *Lancet (Letter)* 1967; ii: 1040.
5 **Neumann HH.** Herpes simplex in peptic ulceration? *Lancet (Letter)* 1967; ii: 779.
6 **Editorial.** Viruses and duodenal ulcer. *Lancet* 1981; **1;** 705-706
7 **Bader C,** Crumpacker CS, Schnipper LE, Ransil B, Clark JE, Arndt K, Freedberg IM. The natural history of recurrent facial-oral infection with herpes simplex virus. *J Infect Dis* 1978; **138:** 897-905
8 **Rand KH,** Jacobson DG, Cottrell CR, Koch KL, Guild RT, McGuigan JE. Antibodies to herpes simplex type 1 in patients with active duodenal ulcer. *Arch Intern Med* 1983; **143:** 1917-1920
9 **Kottaridis SD,** Mihas TA, Goula I, Mihas AA. Herpes viruses and duodenal ulcer disease. *J Med Virol* 1989; **29:** 224-226
10 **Archimandritis A,** Markoulatos P, Tjivras M, Alexiou A, Kordossi A, Kordossis T, Fertakis A. Herpes simplex virus types 1 and 2 and cytomegalovirus in peptic ulcer disease and non-ulcer dyspepsia. *Hepatogastroenterology* 1992; **39:** 540-541
11 **Rune SJ,** Vestergaard BF. IgA antibodies to herpes simplex virus type 1 in duodenal juice and saliva from patients with peptic ulcer and non-ulcer controls. *Scand J Gastroenterol* 1984; **19:** 81-84
12 **Hari VR,** Ananthakrishnan N, Kate V, Badrinath S. Can duodenal ulcer perforation be linked to herpes simplex virus infection? *Indian J Gastroenterol* 2004; **23:** 5-7
13 **Lohr JM,** Nelson JA, Oldstone MB. Is herpes simplex virus associated with peptic ulcer disease? *J Virol* 1990; **64:** 2168-2174
14 **Kemker BP Jr,** Docherty JJ, De Lucia A, Ruf W, Lewis RD. Herpes simplex virus: a possible etiologic agent in some gastroduodenal ulcer disease. *Am Surg* 1992; **58:** 775-778
15 **Warren KG,** Brown SM, Wroblewska Z, Gilden D, Koprowski H, Subak-Sharpe J. Isolation of latent herpes simplex virus from the superior cervical and vagus ganglions of human beings. *N Engl J Med* 1978; **298:** 1068-1069
16 **Rand KH,** Berns KI, Rayfield MA. Recovery of herpes simplex type 1 from the celiac ganglion after renal transplantation. *South Med J* 1984; **77:** 403-404
17 **McGeoch DJ,** Dalrymple MA, Dolan A, McNab D, Perry LJ, Taylor P, Challberg MD. Structures of herpes simplex virus type 1 genes required for replication of virus DNA. *J Virol* 1988; **62:** 444-453

18 **Marshall BJ,** Warren JR, Francis GJ, Langton SR, Goodwin CS, Blincow ED. Rapid urease test in the management of Campylobacter pyloridis-associated gastritis. *Am J Gastroenterol* 1987; **82:** 200-210

19 **Thillainayagam AV,** Arvind AS, Cook RS, Harrison IG, Tabaqchali S, Farthing MJ. Diagnostic efficiency of an ultrarapid endoscopy room test for Helicobacter pylori. *Gut* 1991; **32:** 467-469

20 **Stevens A.** Micro-organisms. In: Bancroft J, Stevens A, eds. Theory and Practice of Histological Techniques, 3rd ed. Edinburg-London: Churchill Livingston, 1990: 289-308.

21 **Kurata JH,** Nogawa AN. Meta-analysis of risk factors for peptic ulcer. Nonsteroidal antiinflammatory drugs, Helicobacter pylori, and smoking. *J Clin Gastroenterol* 1997; **24:** 2-17

22 **Sprung DJ,** Apter MN. What is the role of *Helicobacter pylori* in peptic ulcer and gastric cancer outside the big cities? *J Clin Gastroenterol* 1998; **26:** 60-63

23 **Ciociola AA,** McSorley DJ, Turner K, Sykes D, Palmer JB. *Helicobacter pylori* infection rates in duodenal ulcer patients in the United States may be lower than previously estimated. *Am J Gastroenterol* 1999; **94:** 1834-1840

24 **Chan HL,** Wu JC, Chan FK, Choi CL, Ching JY, Lee YT, Leung WK, Lau JY, Chung SC, Sung JJ. Is non-*Helicobacter pylori*, non-NSAID peptic ulcer a common cause of upper GI bleeding? A prospective study of 977 patients. *Gastrointest Endosc* 2001; **53:** 438-442

25 **Xia HH,** Wong BC, Wong KW, Wong SY, Wong WM, Lai KC, Hu WH, Chan CK, Lam SK. Clinical and endoscopic characteristics of non-*Helicobacter pylori*, non-NSAID duodenal ulcers: a long-term prospective study. *Aliment Pharmacol Ther* 2001; **15:** 1875-1882

26 **Dargan DJ,** Subak-Sharpe JH. The effect of triterpenoid compounds on uninfected and herpes simplex virus infected cells in culture. I. Effect on cell growth, virus particles and virus replication. *J Gen Virol* 1985; **66** (Pt 8): 1771-1784

27 **Poswillo DE,** Roberts GJ. Topical carbenoxolone for orofacial herpes simplex infections. *Lancet* 1981; **2:** 143-144

28 **Van der Spuy S,** Levy DW, Levin W. Cimetidine in the treatment of herpesvirus infections. *S Afr Med J* 1980; **58:** 112-116

29 **Wiley CA,** Schrier RD, Denaro FJ, Nelson JA, Lampert PW, Oldstone MB. Localization of cytomegalovirus proteins and genome during fulminant central nervous system infection in an AIDS patient. *J Neuropathol Exp Neurol* 1986; **45:** 127-139

30 **Alexiu O,** David S, Cajal N, Gruia M, Gologan R, Nicolescu P. Gastroduodenal ulcer obtained by experimental herpes virus inoculation. *Virologie* 1976; **27:** 61-62

31 **Gesser RM,** Valyi-Nagy T, Fraser NW, Altschuler SM. Oral inoculation of SCID mice with an attenuated herpes simplex virus-1 strain causes persistent enteric nervous system infection and gastric ulcers without direct mucosal infection. *Lab Invest* 1995; **73:** 880-889

32 **Howiler W,** Goldberg HI. Gastroesophageal involvement in herpes simplex. *Gastroenterology* 1976; **70:** 775-778

Science Editor Wang XL and Guo SY **Language Editor** Elsevier HK

PO Box 2345, Beijing 100023, China
www.wjgnet.com
wjg@wjgnet.com

ELSEVIER

World J Gastroenterol 2005;11(42):6650-6655
World Journal of Gastroenterology ISSN 1007-9327

• *BRIEF REPORTS* •

Endoscopic mucosal resection for high-grade dysplasia and intramucosal carcinoma in Barrett's esophagus: An Italian experience

Massimo Conio, Alessandro Repici, Renzo Cestari, Sabrina Blanchi, Gabriella Lapertosa, Guido Missale, Domenico Della Casa, Vincenzo Villanacci, Pier Gigi Calandri, Rosangela Filiberti

Massimo Conio, Department of Gastroenterology, Sanremo, Italy
Alessandro Repici, Department of Gastroenterology, Molinette Hospital, Torino, Italy
Renzo Cestari, Guido Missale, Domenico Della Casa, Department of Surgical-Surgery Endoscopy, Spedali Civili, University of Brescia, Italy
Sabrina Blanchi, Department of Internal Medicine, University of Genova, Italy
Gabriella Lapertosa, Division of Pathology, University of Genova, Italy
Vincenzo Villanacci, 2nd Department of Pathology, Spedali Civili, University of Brescia, Italy
Pier Gigi Calandri, Anesthesia and Resuscitation Unit, National Institute for Cancer Research, Genova, Italy
Rosangela Filiberti, Epidemiology and Biostatistics, National Institute for Cancer Research, Genova, Italy
Correspondence to: Massimo Conio, MD, Department of Gastroenterology, Sanremo Hospital, 18038 Sanremo (IM), Italy. mxconio@tin.it
Telephone: +39-0184-536873 Fax: +39-0184-536873
Received: 2004-12-11 Accepted: 2005-02-18

Abstract

AIM: To evaluate endoscopic mucosal resection (EMR) in patients with high-grade dysplasia (HGD) and/or intramucosal cancer (IMC) in Barrett's esophagus (BE).

METHODS: Between June 2000 and December 2003, 39 consecutive patients with HGD (35) and/or IMC (4) underwent EMR. BE >30 mm was present in 27 patients. In three patients with short segment BE (25.0%), HGD was detected in a normal appearing BE. Lesions had a mean diameter of 14.8±10.3 mm. Mucosal resection was carried out using the cap method.

RESULTS: The average size of resections was 19.7±9.4×14.6±8.2 mm. Histopathologic assessment post-resection revealed 5 low-grade dysplasia (LGD) (12.8%), 27 HGD (69.2%), 2 IMC (5.1%), and 5 SMC (-12.8%). EMR changed the pre-treatment diagnosis in 10 patients (25.6%). Three patients with SMC underwent surgery. Histology of the surgical specimen revealed 1 T0N0 and 2 T1N0 lesions. The remaining two patients were cancer free at 32.5 and 45.6 mo, respectively. A metachronous lesion was detected after 25 mo in one patient with HGD. Intra-procedural bleeding, controlled at endoscopy, occurred in four patients (10.3%). After a median follow-up of 34.9 mo, all patients remained in remission.

CONCLUSION: In the medium term, EMR is effective and safe to treat HGD and/or IMC within BE and is a valuable staging method. It could become an alternative to surgery.

Key words: Endoscopic mucosal resection; Barrett's esophagus; High-grade dysplasia; Intramucosal cancer

Conio M, Repici A, Cestari R, Blanchi S, Lapertosa G, Missale G, Della Casa D, Villanacci V, Calandri PG, Filiberti R. Endoscopic mucosal resection for high-grade dysplasia and intramucosal carcinoma in Barrett's esophagus: An Italian experience. *World J Gastroenterol* 2005; 11(42): 6650-6655
http://www.wjgnet.com/1007-9327/11/6650.asp

INTRODUCTION

The incidence of adenocarcinoma (AC) of the esophagus has increased in the last three decades in the Western world[1-3]. Most esophageal adenocarcinomas arise in a precursor lesion, Barrett's esophagus (BE). The esophageal cancer risk in BE patients is about 1 cancer per 200 patient-years, or 0.5% per year[4,5]. The prognosis is poor for the typical patient who presents with invasive cancer, with a 5-year survival rate of under 10%[6].

Dysplasia arising in BE is a marker of progression toward invasive cancer. High-grade dysplasia (HGD) is an uncommon but a serious problem. In 16-60% of patients found to have HGD, invasive cancer was diagnosed in the next 5-7 years[6,7], although spontaneous regression of HGD can also occur[8]. Following surgical esophagectomy for HGD, 10-50% of cases had previously undetected foci of invasive cancer found in the resected specimen[9,10].

When HGD is detected, the three options that are available are: endoscopic surveillance, esophagectomy, and endotherapy.

Surveillance in patients with HGD is controversial. The uncertainty of natural history of HGD and its slow progression rate, could justify a contemplative attitude. Schnell *et al.* evaluated the long-term outcome of 75 patients with HGD who were enrolled in an endoscopic

surveillance program. After a mean follow-up of 7 years, AC occurred in 12 (16%) patients[7].

Esophagectomy has been the standard treatment of HGD and early cancer in BE. However esophagectomy is associated with surgical morbidity of 20-50% and mortality of about 3%, even at high-volume centers. In patients older than 70 years, mortality was 11%[11,12]. A less invasive treatment would be desirable. A newer alternative to esophagectomy is endoscopic mucosal resection (EMR). Improved diagnosis of early malignancy in BE, including endoscopic ultrasound (EUS), may change the therapeutic approach. The superficial lesions of HGD and intramucosal cancer (IMC), with minimal risk of lymph node metastasis, can be removed by EMR. This procedure allows adequate histologic assessment and definitive treatment.

The use of EMR to treat HGD and IMC in BE is increasing, but the number of published series remains less. Our aim was to evaluate EMR in the treatment of HGD and IMC in Barrett's patients in terms of complications and recurrence rate.

PATIENTS AND METHODS

Patients

Between June 2000 and December 2003, 39 consecutive patients (mean age 62.8±11.4 years) with histologically confirmed HGD (35) or IMC (4) in BE underwent EMR in three Departments of Gastroenterology acting as regional referral centers. All patients were previously identified by endoscopic examination performed in our centers or referred from other hospitals. In this case, the original histologic slides were re-evaluated by two expert pathologists (G.L., V.V.) on BE before EMR.

This study was approved by our institutional review board. All patients gave written informed consent to endoscopic therapy. Patients were evaluated and treated using the same protocol by one of the authors representing each of the three institutions.

At endoscopy, superficial lesions were defined using the following classification: slightly elevated (0-IIa), flat (0-IIb), and slightly depressed (0-IIc)[13]. Endoscopy was performed with standard diagnostic videoendoscopes (GIF-Q145, Olympus Optical Co. Ltd., Tokyo, Japan). Patients with ulcerated lesions seen on endoscopy were excluded.

Before EMR, EUS with mechanical rotating transducer, using the water-filling method (GF-UMQ130, 7.5-20 MHz, Olympus Optical Co. Ltd.), was routinely performed to assess lesion depth and mediastinal lymph node status. All patients had a CT scan of the thorax. Only lesions confined to the mucosal layer with no apparent lymph node metastases were considered for EMR.

Deep sedation with propofol was used. EMR was performed using a plastic cap (MH-594, Olympus Optical Co. Ltd, Tokyo, Japan) preloaded on the tip of a standard diagnostic forward-viewing endoscope. The cap had an outer diameter of 13 mm and a length of 15 mm. Inside the distal end of the cap was a gutter, which positions the opened polypectomy snare. A 2-mm segment of the gutter was removed with a scalpel before placement on the endoscope tip. This modification was then aligned with the operative channel to avoid interference by the injection needle or other devices (hemoclips, biopsy forceps). Submucosal injection of epinephrine solution (1:60.000-1:100.000) to create a fluid cushion was performed using variceal injection needles (VIN-23, Wilson Cook Medical Inc; Variject Contrast Injection Needle, Boston Scientific) in all patients. Injected volume ranged between 8 and 30 mL, depending on the lesion diameter. Methylene blue was added to the solution for visual enhancement of the fluid cushion in contrast to the lesion. The cap was next applied against the lesion, which was aspirated into it. A monofilament polypectomy snare (SD-221U-25, Olympus Optical Co. Ltd, Tokyo, Japan) was then firmly secured around the tissue and resection was performed. Resection was performed by endocut mode only, using the ERBE-ICC 200 cautery device (ERBE Elektromedizin GmbH, Tubingen, Germany). The output setting predefined by the manufacturer was adopted: cut 120 W, coagulation 60 W. To minimize interobserver variability among the three endoscopists performing EMR, the diameter of the lesion and the resected areas were estimated by placing an open polypectomy snare around the lesion. In patients with lesions ⩽12 mm wide "en-bloc" resection was performed. For larger lesions, piecemeal resection was completed by applying the cap close to the previously resected area. Specimens were aspirated into the cap and all materials were retrieved for histopathologic assessment. To complete EMR, multiple withdrawals and re-intubations were needed. No overtube was used.

Intra-procedural bleeding (during the EMR) was controlled by epinephrine-saline injections (1:10.000) and, when required, by placing hemoclips (HX-600-090L; rotatable clip fixing device HX-6UR-1, Olympus Optical Co., Ltd).

All patients were hospitalized for 48 h. They were kept fasting for 24 h, then a soft diet was advised for the next two weeks. After EMR, an intravenous PPI (omeprazole, 40 mg/d) was administered for 24 h, followed by a maintenance oral dose of 40 mg/d.

Surveillance

Following EMR, patients were contacted by phone weekly in the first fifteen days, then monthly, to monitor for symptoms such as dysphagia. Endoscopy was repeated at 3, 6, and 12 mo and then yearly, with multiple biopsies from the EMR site, and four-quadrant biopsies from the residual BE.

Complete remission was defined, when well demarcated areas of squamous re-epithelialization without mucosal irregularities, were observed. A lesion was considered metachronous, when diagnosed more than 12 mo from the EMR, irrespective of its location.

Histology

Following the WHO guidelines, we defined HGD by cytologic and architectural changes confined to the

mucosa. IMC was defined by cytologic and architectural changes confined to the lamina propria. Invasive cancers were considered to be those infiltrating the submucosa (SMC)[14,15].

Statistical analysis

Statistical data were expressed as mean±SD. The Kruskal-Wallis test was used to compare histologic severity with lesion size. A P value of 0.05 or less was considered statistically significant.

RESULTS

EMR was performed in 39 patients, 34 males and 5 females. Their mean age was 62.8±11.4 years. Thirty-six patients had type 0-IIa mucosal abnormalities and three had HGD detected by random biopsies in a normal appearing BE.

Mean Barrett's length was 4.3±2.5 cm. Long segment BE (LSBE, ⩾3 cm) was present in 27 patients. The three patients with non-visible lesions had short segment BE (SSBE). These patients underwent EMR with the aim of completely removing the metaplastic epithelium.

Lesions had a mean diameter of 14.8±10.3 mm. Histologic severity did not correlate with lesion size. The average size of reconstructed resected specimens was 19.7±9.4×14.6±8.2 mm. In all patients the EMR was completed in one session. "En-bloc" resection was performed in 19 cases with lesions of ⩽12 mm. The size of the first resected specimen by EMR-C method ranged between 8 and 12 mm.

Following EMR, the pre-treatment histology was re-classified in 10/39 patients (25.6%). Among the 35 initially diagnosed as HGD, five were found to have only LGD, but three had SMC. Of the four patients initially diagnosed as IMC, two were re-classified as SMC. EUS did not help to identify submucosal infiltration.

Table 1 shows the characteristics of patients and lesions according to the histology found in the EMR resection specimens.

Table 1 Characteristics of patients and lesions according to histology of mucosa resected at EMR (mean±SD)

	LGD	HGD	IMC	SMC (no surgery)
Age (yr)	60.6±8.8	61.76±11.8	56±4.2	73.6±8.3
BE length (cm)	6.6±4.1	3.6±1.8	3.7±1.8	5.8±3.1
Size of lesion (mm)	22.5±8.7	13±10.2	16±5.7	17.6±11.9
Metachronous lesion (%)				
No	5 (100)	24 (88.9)	2 (100)	2 (100)
Yes	-	1 (3.7)	-	-
No follow-up endoscopy (%)	-	2 (7.4)	-	-
Total	5	27	2	2

LGD: low-grade dysplasia; HGD: high-grade dysplasia; IMC: intramucosal cancer; SMC: submucosal cancer; BE: Barrett's esophagus.

Cancers

The five patients with SMC had a mean age of 73.6± 8.3 years. The mean BE length was 5.8±3.1 cm, and lesion size ranged from 5 to 30 mm. The lesions were type IIa (superficial elevated). Histologic assessment detected tiny areas of low-grade differentiation, and in two of them, lymphatic permeation. Three (7.7% of all patients) underwent esophagectomy and the histopathologic assessment showed one T0N0 and two T1N0. The remaining two patients were considered unfit for surgery due to advanced age (81 and 84 years) and/or comorbidities (cardiovascular disease). They were included in the surveillance program.

Complications

Intra-procedural bleeding occurred in four patients (10.3%), and was controlled with epinephrine injections in two, and with epinephrine plus clipping in the other two. Delayed bleeding was not seen. No patient needed blood transfusion. No perforations occurred. Retrosternal pain was present in one patient. An esophageal stenosis developed 8 mo later in a patient with LSBE (7 cm). He had a 30 mm HGD lesion and the diameter of the EMR area was 40 mm. He was successfully treated by a single bougienage.

Surveillance

Follow-up endoscopy was performed in 32 of the 34 patients without invasive cancer (94.1%), two patients declining repeat examination. The follow-up ranged from 16.3 to 72.1 mo (median 34.9 mo). In one patient (3.1%), with an original lesion of 20 mm (HGD), a metachronous lesion was detected after 25 mo. It was easily removed by EMR, and the histology showed HGD. One of the two patients with SMC, who did not undergo surgery died of cardiovascular disease 45.6 mo later, and the other was alive and cancer free at a 32.5 mo surveillance.

EUS was repeated at 3 and 6 mo after EMR. CT of the thorax and upper abdomen were also performed after 6 mo, and then after 1 year to evaluate the lymph node status and the presence of metastases. Figures 1A and 1B show endoscopic appearance of a SSBE with HGD before and three months after EMR.

DISCUSSION

The use of EMR for EC in the digestive tract was described by Inoue *et al*.[16]. We employed EMR to remove 39 focal esophageal HGD and IMC lesions of 3-30 mm size in BE, with few complications. Most lesions were flat mucosal abnormalities. Systematic biopsies were taken from the remainder of the BE to exclude non-visible multifocal lesions.

The data reported in the present study represent the first experience of EMR in BE, in Italy. Three major referral centers joined in the effort of evaluating the clinical outcome of EMR. In a period of three years a relatively small number of patients has been included in our study, especially when compared with the series

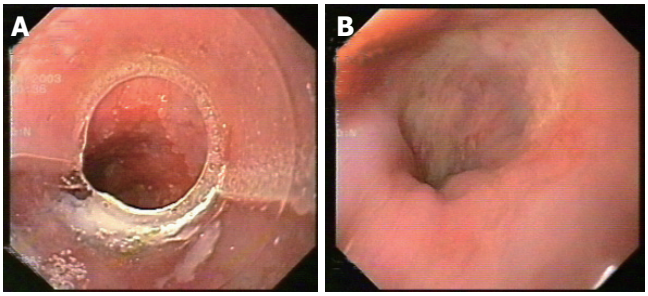

Figure 1 Endoscopic appearance of SSBE with HGD before (**A**) and 3 mo after EMR (**B**).

reported by German authors[17]. This difference is attributable to the still limited number of patients with early neoplastic lesions in BE, detected in endoscopic centers. Furthermore, as surgery is still the gold standard treatment for HGD and IM, the majority of these patients is referred for esophagectomy.

EMR could become a management option for HGD, and also for IMC, where the risk of lymph node involvement is from 0% to 4%[18,19]. Unfortunately, in cases with SMC, the incidence of regional lymph-node metastasis is 15-50%[20-22]. Current data support surgical resection in the setting of submucosal infiltration by AC, unless comorbidity or advanced patient age precluded it.

Table 2 displays data from selected studies on EMR in BE since 2000. Most published studies report EMR of endoscopically visible areas of HGD. Some of these studies differ in methodology and it is difficult to compare them. However, our results are in accordance with the data reported by other authors. EMR provides greater diagnostic precision than endoscopic biopsy, despite endoscopy with biopsies and standard EUS before EMR in all patients. In five of 39 cases, undetected SMC was found on histological examination of the resected specimen. Reclassification of the histology after EMR occurred in 26% of our patients. Other authors have reported reclassification in 0% to 75% of cases after EMR (Table 2). Causes may include biopsy sampling error and observer interpretation variability.

Bleeding is the most frequent adverse event with EMR, reported in a median 10% of patients. Intra-procedural bleeding also occurred in 10% of our patients and was managed endoscopically without transfusion. Esophageal stenosis is a late complication of EMR, reported in 0-30% of cases (Table 3). In our study, one patient (2.5%) developed stenosis. Larger EMR resections may increase the risk; in a study of 137 patients, stenosis was seen only when EMR involved more than two-thirds of the esophageal circumference[23]. However, in one report of circumferential EMR, only two of 12 patients developed stenosis[24]. The perforation risk is generally less than 1%. No perforations occurred in our series. Overall, complications seem fewer for EMR than for surgical resection. In one study, complications occurred in 48% of esophagectomies *vs* 16% for EMR combined with photodynamic therapy (PDT)[25].

A recent controlled study of 100 mucosectomies compared the cap method and a ligation method for suction EMR. The diameter of the removed specimen, the diameter of the resected area, and the complication rate showed no significant differences between the two groups, and no severe complications occurred[26].

There is limited information on the long-term effectiveness of EMR. May *et al.* followed 70 patients with HGD or early AC for a mean of 34 mo after EMR. Ten percent had minor complications. During follow-up, 21/70 patients were found to have locally recurrent or metachronous disease, treated endoscopically with success in all but one case. The only death from Barrett's AC was in a patient who had surgery for SMC[17]. In our series, follow-up for a median 35 mo was available in 94.1% of patients. One of the 39 patients (2.6%) had a metachronous lesion after 25 mo, successfully treated with another EMR. According to other authors, malignant transformation of HGD is about 34% in 6-54 mo[27], corresponding to our follow-up period. In this time range we did not find invasive AC. In our two patients with SMC who did not undergo surgery, no histologic evidence of disease was detected.

Table 2 Selected studies on EMR in Barrett's esophagus

Author	Number of patiens	Size of lesions cm (mean)	Technique	Histology pre-EMR	Histology post-EMR	Change in diagnosis (%)	Complications	Follow-up months (mean)	Recurrence
Seewald *et al*. 2003 Germany[24]	12	Median 5	EUS Snare	5 HGD/ IMC (visible) 7 IMC (non-visible)	2 BE 1 LGD 5 HGD AC 4	75%	Bl: 33% Stricture:17%	Median: 9	0
Ahmad *et al*. 2002 USA[33]	19/101	0.5-3	EUS EMR-C Snare injection	AC 6 HGD 6 NOS 7	AC 8 HGD 4 LGD 1 Benign 6	58%	Bl: 11%	>=24	0
May *et al*. 2002 Germany[17]	80	Nos	EUS EMR±PDT	HGD 7 EC 73	AC: 11/80	Nos	Bl: 6% Stricture: 4%	34	24/78

Table 3 Selected studies on EMR in Barrett's esophagus

Author	Number of pts	Size of lesions cm (mean)	Technique	Histology pre-EMR	Histology post-EMR	Change in diagnosis (%)	Complications	Follow-up Months (mean)	Recurrence
Buttar *et al*. 2001 USA[34]	17	8	EUS VLD-PDT Injection	IMC: 7 AC: 10	IMC: 7 AC: 10	47%	Bl: 6% Stricture: 30%	13	HGD (1)[1] AC (1)
Nijhawan *et al*. 2000 USA[35]	25	7	EUS Lift-and-cut VLD Injection	2 BE 8 LGD 5 HGD 9 AC 1 other	2 BE 3 LGD 5 HGD 13 AC 2 other	48%	0	14.6	0
Ell *et al*. 2000 Germany[36]	35	0.9	EUS EMR± injection	HGD: 3 EC: 32	HGD: 3 EC: 32	0	Bl: 20%	12	11%

Pts: patients; EMR: endoscopic mucosal resection; EUS: endoscopic ultrasonography; HGD: high-grade dysplasia; IMC: intramucosal carcinoma; BE: Barrett's esophagus; LGD: low-grade dysplasia; AC: invasive adenocarcinoma; Bl: bleeding; EMR-C: EMR with cap; PDT: photodynamic therapy; Nos: not otherwise specified; VLD: variceal ligator device; EC: early cancer; [1]persistence of HGD.

We used EMR to remove focal lesions, but did not attempt to resect long circumferential segments of Barrett mucosa. This might seem a logical extension of the use of EMR. Removing both focal lesions and also the remainder of the BE might give greater assurance that no neoplasia or columnar mucosa remained than with PDT or thermal methods, as well as providing complete histological assessment of the mucosa. Potential risks and technical difficulties have so far limited the use of circumferential EMR, but this has now been tried. Experimentally, we assessed the feasibility of 3 cm circumferential EMR in a porcine model using EMRC. One out of four pigs developed a severe stenosis[28]. This work was advanced by Rajan *et al*. who performed more extensive EMR without complications[29]. In the clinical setting, Satodate *et al*. resected an entire 5 cm circumferential BE, together with 2 cm of gastric mucosa. The patient had early multifocal AC, with one small area of submucosal invasion. EMR was performed using the cap method in a single session, 30 separate pieces of the mucosa being removed. Following dilatations for esophageal stenosis, at 10 mo he was asymptomatic and endoscopy showed no stenosis, no recurrent cancer, and no remaining BE[30]. Seewald *et al*. performed circumferential EMR in 12 patients with HGD and IMC. Seven had no visible lesions. A monofilament polypectomy snare without a cap was used. In each case, the entire BE (median length 5 cm) was completely removed in 1-5 sessions, with a median number of 5 snare resections per endoscopic session. Four patients had minor bleeding, and two required esophageal dilations[24].

Recent advances in techniques as chromoendoscopy with methylene-blue and high-magnification endoscopy may help in identifying non-visible dysplastic lesions and in recognizing their width in Barrett's esophagus. Chromoendoscopy with methylene-blue may be useful to detect dysplastic mucosal areas. In fact, about 90% of these areas are unstained[31]. High-magnification endoscopy allows the identification of specific pit-patterns of the esophageal epithelium. Dysplasia seems to distort this pattern[32]. In our three patients with non-visible lesion in SSBE, we did not use these techniques because we performed EMR with the aim to completely remove the metaplastic epithelium.

Our study confirms that EMR is a feasible, low risk procedure to treat focal HGD and IMC within BE. Given encouraging short and medium-term results, endoscopic therapy is more often being considered as primary treatment[17]. However, controlled studies comparing EMR and esophagectomy are not available. Further experience is needed to determine the place of total removal of Barrett' s mucosa by a more extensive EMR.

REFERENCES

1 **Blot WJ**, Devesa SS, Kneller RW, Fraumeni JF Jr. Rising incidence of adenocarcinoma of the esophagus and gastric cardia. *JAMA* 1991; **265**: 1287-1289

2 **Bollschweiler E**, Wolfgarten E, Gutschow C, Holscher AH. Demographic variations in the rising incidence of esophageal adenocarcinoma in white males. *Cancer* 2001; **92**: 549-555

3 **Conio M**, Lapertosa G, Blanchi S, Filiberti R. Barrett's esophagus: an update. *Crit Rev Oncol Hematol* 2003; **46**: 187-206

4 **Conio M**, Blanchi S, Lapertosa G, Ferraris R, Sablich R, Marchi S, D'Onofrio V, Lacchin T, Iaquinto G, Missale G, Ravelli P, Cestari R, Benedetti G, Macri G, Fiocca R, Munizzi F, Filiberti R. Long-term endoscopic surveillance of patients with Barrett' s esophagus. Incidence of dysplasia and adenocarcinoma: a prospective study. *Am J Gastroenterol* 2003; **98**: 1931-1939

5 **Shaheen NJ**, Crosby MA, Bozymski EM, Sandler RS. Is there publication bias in the reporting of cancer risk in Barrett's esophagus? *Gastroenterology* 2000; **119**: 333-338

6 **Reid BJ**, Levine DS, Longton G, Blount PL, Rabinovitch PS. Predictors of progression to cancer in Barrett's esophagus: baseline histology and flow cytometry identify low- and high-risk patient subsets. *Am J Gastroenterol* 2000; **95:** 1669-1676

7 **Schnell TG**, Sontag SJ, Chejfec G, Aranha G, Metz A, O' Connell S, Seidel UJ, Sonnenberg A. Long-term nonsurgical management of Barrett's esophagus with high-grade dysplasia. *Gastroenterology* 2001; **120**: 1607-1619

8 **Weston AP**, Sharma P, Topalovski M, Richards R, Cherian R, Dixon A. Long-term follow-up of Barrett's high-grade dysplasia. *Am J Gastroenterol* 2000; **95**: 1888-1893

9 **Cameron AJ**, Carpenter HA. Barrett's esophagus, high-grade dysplasia and early adenocarcinoma: a pathologic study. *Am J Gastroenterol* 1997; **92**: 586-591

10 **Korst RJ**, Altorki NK. High-grade dysplasia: surveillance, mucosal ablation, or resection? *World J Surg* 2003; **27**: 1030-1034

11 **Collard JM.** High-grade dysplasia in Barrett's esophagus. The case for esophagectomy. *Chest Surg Clin N Am* 2002; **12:** 77-92

12 **McCulloch P,** Ward J, Tekkis PP. Mortality and morbidity in gastro-oesophageal cancer surgery: initial results of ASCOT multicentre prospective cohort study. *BMJ* 2003; **327:** 1192-1197

13 **Schlemper RJ**, Hirata I, Dixon MF. The macroscopic classification of early neoplasia of the digestive tract. *Endoscopy* 2002; **34**: 163-168

14 **Jass JR**, Sobin LH, Watanabe H. The World Health Organization's histologic classification of gastrointestinal tumors. A commentary on the second edition. *Cancer* 1990; **66**: 2162-2167

15 **Schlemper RJ**, Riddell RH, Kato Y, Borchard F, Cooper HS, Dawsey SM, Dixon MF, Fenoglio-Preiser CM, Flejou JF, Geboes K, Hattori T, Hirota T, Itabashi M, Iwafuchi M, Iwashita A, Kim YI, Kirchner T, Klimpfinger M, Koike M, Lauwers GY, Lewin KJ, Oberhuber G, Offner F, Price AB, Rubio CA, Shimizu M, Shimoda T, Sipponen P, Solcia E, Stolte M, Watanabe H, Yamabe H. The Vienna classification of gastrointestinal epithelial neoplasia. *Gut* 2000; **47**: 251-255

16 **Inoue H**, Takeshita K, Hori H, Muraoka Y, Yoneshima H, Endo M. Endoscopic mucosal resection with a cap-fitted panendoscope for esophagus, stomach, and colon mucosal lesions. *Gastrointest Endosc* 1993; **39**: 58-62

17 **May A**, Gossner L, Pech O, Fritz A, Gunter E, Mayer G, Muller H, Seitz G, Vieth M, Stolte M, Ell C. Local endoscopic therapy for intraepithelial high-grade neoplasia and early adenocarcinoma in Barrett's oesophagus: acute-phase and intermediate results of a new treatment approach. *Eur J Gastroenterol Hepatol* 2002; **14**: 1085-1091

18 **Baba H**, Maehara Y, Okuyama T, Orita H, Anai H, Akazawa K, Sugimachi K. Lymph node metastasis and macroscopic features in early gastric cancer. *Hepatogastroenterology* 1994; **41**: 380-383

19 **Nigro JJ,** Hagen JA, DeMeester TR, DeMeester SR, Theisen J, Peters JH, Kiyabu M. Occult esophageal adenocarcinoma: extent of disease and implications for effective therapy. *Ann Surg* 1999; **230:** 433-8; discussion 438-40

20 **Stein HJ**, Feith M, Mueller J, Werner M, Siewert JR. Limited resection for early adenocarcinoma in Barrett's esophagus. *Ann Surg* 2000; **232**: 733-742

21 **Holscher AH**, Bollschweiler E, Schneider PM, Siewert JR. Early adenocarcinoma in Barrett's oesophagus. *Br J Surg* 1997; **84**: 1470-1473

22 **Nigro JJ**, Hagen JA, DeMeester TR, DeMeester SR, Peters JH, Oberg S, Theisen J, Kiyabu M, Crookes PF, Bremner CG. Prevalence and location of nodal metastases in distal esophageal adenocarcinoma confined to the wall: implications for therapy. *J Thorac Cardiovasc Surg* 1999; **117**: 16-23; discussion 23-25

23 **Katada C**, Muto M, Manabe T, Boku N, Ohtsu A, Yoshida S. Esophageal stenosis after endoscopic mucosal resection of superficial esophageal lesions. *Gastrointest Endosc* 2003; **57**: 165-169

24 **Seewald S,** Akaraviputh T, Seitz U, Brand B, Groth S, Mendoza G, He X, Thonke F, Stolte M, Schroeder S, Soehendra N. Circumferential EMR and complete removal of Barrett' s epithelium: a new approach to management of Barrett's esophagus containing high-grade intraepithelial neoplasia and intramucosal carcinoma. *Gastrointest Endosc* 2003; **57**: 854-859

25 **Pacifico RJ**, Wang KK, Wongkeesong LM, Buttar NS, Lutzke LS. Combined endoscopic mucosal resection and photodynamic therapy versus esophagectomy for management of early adenocarcinoma in Barrett's esophagus. *Clin Gastroenterol Hepatol* 2003; **1**: 252-257

26 **May A**, Gossner L, Behrens A, Kohnen R, Vieth M, Stolte M, Ell C. A prospective randomized trial of two different endoscopic resection techniques for early stage cancer of the esophagus. *Gastrointest Endosc* 2003; **58**: 167-175

27 **Sampliner RE**. Practice guidelines on the diagnosis, surveillance, and therapy of Barrett's esophagus. The Practice Parameters Committee of the American College of Gastroenterology. *Am J Gastroenterol* 1998; **93**: 1028-1032

28 **Conio M**, Sorbi D, Batts KP, Gostout CJ. Endoscopic circumferential esophageal mucosectomy in a porcine model: an assessment of technical feasibility, safety and outcome. *Endoscopy* 2001; **33**: 791-794

29 **Rajan E**, Gostout CJ. Widespread endoscopic mucosal resection. *Gastrointest Endosc Clin N Am* 2001; **11:** 489-497

30 **Satodate H,** Inoue H, Yoshida T, Usui S, Iwashita M, Fukami N, Shiokawa A, Kudo SE. Circumferential EMR of carcinoma arising in Barrett's esophagus: case report. *Gastrointest Endosc* 2003; **58:** 288-292

31 **Canto MI**, Setrakian S, Willis JE, Chak A, Petras RE, Sivak MV. Methylene blue staining of dysplastic and nondysplastic Barrett's esophagus: an in vivo and ex vivo study. *Endoscopy* 2001; **33:** 391-400

32 **Sharma P**, Weston AP, Topalovski M, Cherian R, Bhattacharyya A, Sampliner RE. Magnification chromoendoscopy for the detection of intestinal metaplasia and dysplasia in Barrett's oesophagus. *Gut* 2003; **52**: 24-27

33 **Ahmad NA**, Kochman ML, Long WB, Furth EE, Ginsberg GG. Efficacy, safety, and clinical outcomes of endoscopic mucosal resection: a study of 101 cases. *Gastrointest Endosc* 2002; **55**: 390-396

34 **Buttar NS**, Wang KK, Lutzke LS, Krishnadath KK, Anderson MA. Combined endoscopic mucosal resection and photodynamic therapy for esophageal neoplasia within Barrett's esophagus. *Gastrointest Endosc* 2001; **54**: 682-688

35 **Nijhawan PK**, Wang KK. Endoscopic mucosal resection for lesions with endoscopic features suggestive of malignancy and high-grade dysplasia within Barrett's esophagus. *Gastrointest Endosc* 2000; **52**: 328-332

36 **Ell C**, May A, Gossner L, Pech O, Gunter E, Mayer G, Henrich R, Vieth M, Muller H, Seitz G, Stolte M. Endoscopic mucosal resection of early cancer and high-grade dysplasia in Barrett's esophagus. *Gastroenterology* 2000; **118**: 670-677

Science Editor Wang XL and Guo SY **Language Editor** Elsevier HK

PO Box 2345, Beijing 100023, China
www.wjgnet.com
wjg@wjgnet.com

ELSEVIER

World J Gastroenterol 2005;11(42):6656-6661
World Journal of Gastroenterology ISSN 1007-9327

• *BRIEF REPORTS* •

Effect of cytokine gene polymorphism on histological activity index, viral load and response to treatment in patients with chronic hepatitis C genotype 3

Zaigham Abbas, Tariq Moatter, Akber Hussainy, Wasim Jafri

Zaigham Abbas, Wasim Jafri, Department of Medicine, The Aga Khan University Hospital, Karachi, Pakistan
Tariq Moatter, Akber Hussainy, Department of Pathology, The Aga Khan University Hospital, Karachi, Pakistan
Correspondence to: Dr. Zaigham Abbas, Consultant Gastroenterologist, The Aga Khan University Hospital, Stadium Road, Karachi, Pakistan. zaigham@akunet.org
Telephone: +92-21-4930051 Fax: +92-21-4934294
Received: 2005-02-07 Accepted: 2005-04-09

Abstract

AIM: To investigate the association between cytokine gene polymorphism and disease status in chronic hepatitis C genotype 3 by liver biopsy, ALT, HCV RNA levels and response to treatment.

METHODS: Patients with chronic hepatitis C genotype 3 were analyzed for single nucleotide polymorphisms of interleukin (IL)-10, IL-1 beta, interferon-gamma (IFN-γ), tumor necrosis factor-alpha (TNF-α) and transforming growth factor-beta (TGF-β) by polymerase chain reaction using sequence-specific oligonucleotide primers. Liver biopsies were assessed by modified histological activity index (HAI) scoring system using a scale of 0–18 for grading the necro-inflammatory activity and 0–6 for staging the fibrosis. HCV RNA levels were determined by bDNA assay. The patients were treated with interferon alpha and ribavirin for 6 mo. Sustained virological response was assessed 6 mo after the completion of the treatment.

RESULTS: Out of the 40 patients analyzed, 26 were males. Mean age was 40.5±12.5 years (range 18–65 years). The frequencies of different dimorphic polymorphisms based on single nucleotide substitution were as follows: IL-10-1082 G/A 85%, A/A 12.5%, G/G 2.5%; IL-10-819 A/C 87.5%, C/C 10%, A/A 2.5%; IL-10-592 C/A 72.5%, C/C 27.5%; IL-1 C 90%, U 10%; IFN-874 T/A 50%, T/T 27.5%, A/A 22.5%; TNF-308 A/G 95%, G/G 5%; TGF-10 T/C 52.5%, C/C 35%, T/T 12.5%. The mean grades of necro-inflammatory activity of different genotypes of IL-10 at promoter site -1082 were A/A = 3.6, A/G = 5.0, and G/G = 10.0 and the difference was significant (P = 0.029). The difference in the stage of disease at a scale of 0–6 was A/A 0.8, A/G 2.3, and G/G 4.0 (P = 0.079). The difference in the HAI seemed to be related to the presence of allele -1082G. For IL-10 -819 genotypes, mean scores of fibrosis were A/A = 6.0, A/C = 2.2, and C/C = 1.0 (P = 0.020) though the inflammatory activity was not much different. No significant differences in HAI were noted among polymorphisms of other cytokines. Moreover, ALT and HCV RNA levels were not significantly different among different cytokine polymorphisms. There was a significant correlation of HAI and HCV RNA levels with the duration of disease. TGFβ -10 genotype CC patients had a better end of treatment response than those with other genotypes (P = 0.020). Sustained virological response to the treatment was not influenced by the cytokine polymorphism. No effect of other factors like viral load, degree of fibrosis, gender, steatosis, was observed on sustained virological response in this population infected with genotype 3.

CONCLUSION: There is no significant correlation between cytokine polymorphisms and HAI except for the polymorphisms of anti-inflammatory cytokine IL-10, which may influence hepatic inflammatory activity and fibrosis in patients with chronic hepatitis C genotype 3. Sustained virological response in this genotype does not seem to be influenced by cytokine gene polymorphisms.

Key words: Interleukin; Interferon gamma; Tumor necrosis factor alpha; Transforming growth factor; Cytokines; Gene polymorphism; Hepatitis C; Alanine aminotransferase; Liver biopsy

Abbas Z, Moatter T, Hussainy A, Jafri W. Effect of cytokine gene polymorphism on histological activity index, viral load and response to treatment in patients with chronic hepatitis C genotype 3. *World J Gastroenterol* 2005; 11(42): 6656-6661
http://www.wjgnet.com/1007-9327/11/6656.asp

INTRODUCTION

HCV infection is a leading cause of chronic liver disease worldwide. The infection leads to viral persistence and chronic disease in a very high proportion of cases. Pathogenesis of liver injury is not fully understood. There is a complex relationship between HCV and its host. Liver lesions could be the result of immune

responses or cytopathic action of the virus. Cytotoxic T cells and cytokines produced by both CD4+ (T helper) and cytotoxic T cells may be responsible for much of the damage that occurs in the livers of infected patients[1].

Two distinct patterns of cytokine production may occur[2]. Type 1 responses are characterized by production of interleukin-2 (IL-2), tumor necrosis factor-alpha (TNF-α) and interferon-gamma (IFN-γ), which are prime and maintain antigen-specific cellular immunity[3,4] and are important in defense against viruses. Type 2 responses are characterized by IL-4, IL-5, and IL-10, which promote humoral immune responses. An imbalance in helper T-cell type 1 (Th1) and type 2 (Th2) cytokines is suggested to play an important role in the pathogenesis of chronic hepatitis C. The progressive liver injury seen in chronic HCV infection is associated with the upregulation of intrahepatic Th1-like cytokines. Intrahepatic IFN-γ and IL-2 mRNA expression is upregulated in chronic hepatitis C, while the expression of IL-10, a Th2-like cytokine, is downregulated[5] .

Intrahepatic CD4+ T cells play a pathogenetic role in the hepatic injury of HCV infection[6]. Vigorous HCV-specific CD4+ Th1 response, particularly against the nonstructural proteins of the virus, may be associated with viral clearance and protection from disease progression[7]. Patients without viremia after HCV infection frequently have strong Th lymphocyte responses of the Th1 type to multiple HCV antigens many years after the onset of infection, whereas antibody responses are less marked. These results suggest that control of HCV replication may depend on effective Th lymphocyte activation[8,9]. There is also an enhanced Th2 response during chronic HCV infection, which may partly be responsible for the persistence of HCV infection.

In addition to the altered intrahepatic cytokine expression, there might be a significant correlation between circulating cytokines and degree of inflammation in the liver. One study has shown such a correlation between baseline TNF levels and histologic grading score of hepatitis[10]. The maximal capacity of cytokine production varies between individuals and may correlate with polymorphism in cytokine gene promoters. The objectives of our study were to analyze the role of allelic or genotype variations of IL-10, IL-1 beta, IFN-γ, TNF-α and TGF-β and its association with hepatocellular injury as suggested by liver biopsy and ALT and treatment outcome. We selected genotype 3 for this study which is the main genotype in our country.

MATERIALS AND METHODS

Out of the 40 patients analyzed, 26 were males. Mean age was 40.5±12.5 years (range 18-65 years). The participants did not receive interferon therapy and had neither co-infection with human immunodeficiency virus and hepatitis B virus nor other associated forms of chronic liver disease.

Quantitative serum HCV RNA was determined by bDNA assay (Bayer, USA) according to the manufacturer's instructions. The minimum quantification limit of the assay was 3 000 HCV RNA copies/mL serum. HCV genotyping was performed using PCR and reverse hybridization assay (Innogenetics, Belgium). All patients included in this study were of HCV genotype 3. For cytokine gene polymorphism, DNA was extracted by proteinase K digestion from peripheral mononuclear cells, followed by phenol chloroform extraction and ethanol precipitation. After amplification polymorphisms in IL-10 (592, 819, 1082), IL-1β (-511), IFNγ (874), TNFα (308) and TGF (codon25) were examined as described previously[11-13]. The number in parenthesis indicates the location of the polymorphism on the DNA sequence. Briefly, single nucleotide polymorphisms (SNPs) were determined using sequence specific oligonucleotide primers. Each PCR reaction consisted of 1× PCR buffer, 0.2 mmol dNTPs. Concentration of $MgCl_2$ varied with the type of SNP examined, 50 ng of each polymorphism specific primer, 1 U of *Taq* polymerase in a final volume of 10 μL. To monitor PCR inhibition, growth hormone gene was simultaneously amplified as an internal control. Thermal cycling was performed in a Perkin-Elmer 9700 thermal cycler. Following PCR amplification, amplicons were stained with ethidium bromide and visualized on a UV transilluminator. The size of product generated in each PCR assay was ascertained and scored as positive/negative for the presence/absence of a particular polymorphism. The PCR product obtained with IL-1β-511 specific primers was digested with the restriction enzyme *Ava*II. The digested product was then visualized for the presence of restriction fragments.

Liver biopsy specimens were analyzed by a single pathologist, who was unaware of the patient's identity, treatment regimen, response, or timing of the biopsy relative to the treatment. Liver biopsies were assessed by modified histological activity index (HAI) scoring system[14] using a scale of 0-18 for grading and 0-6 for staging. Degree of steatosis was scored at a scale of 0-3. Presence or absence of lymph follicles was also documented.

Duration of disease was determined by calculating time interval from the exposure to a possible risk factor. Patients were treated with standard doses of interferon alpha (3 mega units subcutaneous, thrice a week) and ribavirin (800-1 200 mg/d) for 6 mo and followed up for another 6 mo. HCV RNA was repeated 6 mo after the treatment to document sustained response.

Statistical analysis

Statistical analysis was performed by two-tailed tests. *P* values were calculated by one-way analysis of variance (ANOVA), Pearson's χ^2 and Spearman's rho correlation tests. $P<0.05$ was considered statistically significant.

RESULTS

The frequencies of different dimorphic polymorphisms based on single nucleotide substitution were as follows:

IL10-1082 G/A 85%, A/A 12.5%, G/G 2.5%; IL10-819 A/C 87.5%, C/C 10%, A/A 2.5%; IL10-592 C/A 72.5%, C/C 27.5%; IL-1 C 90%, U 10%; IFN-874 T/A 50%, T/T 27.5%, A/A 22.5%; TNF-308 A/G 95%, G/G 5%; TGF-10 T/C 52.5%, C/C 35%, T/T 12.5%. The mean grades of necro-inflammatory activity at a scale of 0-18 for different genotypes of IL10 at promoter site -1082 were A/A = 3.6, A/G = 5.0, and G/G = 10.0 and the difference was significant (P = 0.029). The difference in the stage of disease at a scale of 0-6 was A/A 0.8, A/G 2.3, and G/G 4.0 (P = 0.079). This difference in the HAI seemed to be related to the presence of allele -1082G. For IL 10 -819 genotypes the mean scores of fibrosis were A/A = 6.0, A/C = 2.2, and C/C = 1.0 (P = 0.020) though the inflammatory activity was not much different.

No significant differences in the degree of necro-inflammatory activity and fibrosis were noted among the polymorphisms of other cytokines (Table 1). Moreover, ALT and HCV RNA levels were not significantly different among different cytokine polymorphisms. There was a significant correlation of duration of disease with grade and stage of disease and HCV RNA levels (P = 0.017, 0.018, and 0.015 respectively with Spearman's rho test).

Out of the 40 patients, 34 remained under the follow-up. These patients completed the 6-mo treatment with interferon and ribavirin. HCV RNA was repeated 6 mo after the treatment to document the sustained response and the effect of cytokine gene polymorphism. TGFβ -10 genotype CC patients had a better end of treatment response than those with other genotypes (P = 0.020), though there was no difference in the sustained virological response. No effect of other factors like viral load, degree of fibrosis, gender, steatosis, was observed on the sustained virological response in this population infected with genotype 3.

DISCUSSION

Approximately 80-90% of patients acutely infected with hepatitis C virus develop persistent infection, about one-half of them have elevated transaminases indicative of ongoing liver inflammation[15]. In the context of an inflammatory response against the virus, variable cytokine response of the host may be responsible for the variable liver damage. Moreover, the cause of viral persistence during HCV infection may be the development of a weak antiviral immune response to the viral antigens, with corresponding inability to eradicate infected cells or insensitivity of the virus to such cytokines or insufficient production of cytokines[16]. Thus, the continuing inflammation results in liver damage in the absence of complete virologic recovery[17].

Studies have shown that active liver injury in chronic hepatitis C patients is associated with increased circulating Th1 cytokine IL-2 but not with Th2 cytokine IL-10[18]. It has also been shown by some workers that serum alanine transaminase and the hepatic fibrosis levels are related directly to the frequencies of peripheral memory effector CD8(+) T cells producing IFN-γ (Tc1), but inversely to the frequencies of those producing both IL-4 and IL-10 (Tc2)[19]. Moreover, most liver-infiltrating T cells in chronic hepatitis C are type 1 cells. Studies to date in liver tissue showed that intrahepatic mRNA for type 1-like cytokines, such as IL-1β, IL-2, IL-6, IL-8, TNF-α, and IFN-γ were upregulated in chronic HCV infection[20]. The level of expression of type 1 cytokines, such as IL-2 and IFN-γ, is correlated with the degree of histologic injury as well as the likelihood of non-responsiveness to IFN-α therapy[21]. The presence of an ongoing cellular immune response probably also contributes to the process of hepatic fibrosis. Kupffer cells can be activated by the production of cytokines such as TNF-α, which in turn produce TGF-β[22].

Serum levels of different cytokines may not give the true picture of what is going on in the liver. For example, the mean IL2Rs and IFN serum levels are much higher in patients with anti-HCV than in the control group,

Table 1 Statistical significance of effects of cytokine gene polymorphisms on different parameters

Cytokine gene polymorphism	ALT (upper limit normal)	HCV RNA level	Grade of inflammation (0-18)	Stage of fibrosis (0-6)	Steatosis (0-3)	Lymph follicles	End of treatment response	Sustained response
IL 10 -1082 (GA, AA, GG)	0.636	0.241	0.029	0.079	0.267	0.848	0.078	0.331
IL 10 -819 (AC, CC, AA)	0.794	0.781	0.412	0.020	0.57	0.295	0.063	0.331
IL 10 -592 (CA, CC)	0.582	0.198	0.243	0.281	0.551	0.626	0.416	0.283
IFNγ -874 (AA, TT, TA)	0.389	0.848	0.919	0.921	0.955	0.382	0.21	0.933
TNFα -308 (AG, GG)	0.952	0.436	0.777	0.307	0.32	0.85	0.674	0.451
TGFβ -10 (CC, TC, TT)	0.734	0.72	0.386	0.959	0.232	0.643	0.026	0.206
IL 1 (C/U)	0.144	0.591	0.964	0.826	0.326	0.836	1.00	1.00

P values were calculated by ANOVA and Pearson' s χ^2 test. Statistically significant values. IL: interleukin; IFNγ: interferon gamma; TNFα: tumor necrosis factor alpha; TGFβ: transforming growth factor beta.

whereas the mean IL4 and IL6 levels are lower in patients infected with HCV[23]. Another study shows the higher levels of serum IL-1β, IL-4 and IL-6 (0.221, 0.104 and 1.393 pg/mL) in all HCV patients than in healthy adults (0.188, 0.025 and 0.600 pg/mL)[24].

Sustained response to interferon and ribavirin, defined as undetectable HCV RNA at 6 mo after discontinuation of therapy, is achievable in 30-60% of treated patients[25,26]. Predictors of response include viral factors such as viral genotypes, viral load and early disappearance of HCV RNA after initiation of therapy, while the host factors include gender, age and degree of fibrosis[25-27]. In recent years, increasing attention has been drawn to the role of host variation in cytokine levels in inflammatory and immune responses. Polymorphisms in genes encoding immunoregulatory proteins, proinflammatory cytokines, and fibrogenic factors may affect the production of these factors and influence disease progression in patients with chronic liver disease due to alcohol, primary biliary cirrhosis, or hepatitis C[28].

There might be an association of cytokine gene polymorphism and susceptibility to hepatitis C infection. Hohler *et al*.[29] have reported such an association with the polymorphism at the TNFα promoter. The TNF promoter variants TNF2 (-238A) and TNF3 (-308A) confer a 3.2-fold and 5.1-fold risk of cirrhosis respectively (P = 0.03 for both). Reciprocal effects have been observed with several TNF alleles and haplotypes defined by the -238 G/A and -308 G/A dimorphic sequences, thus polymorphisms in the TNF alpha promoter appear to be associated with the variability in the histological severity of chronic hepatitis C infection[30]. In our study done on hepatitis C genotype 3 patients, no such effect of TNFα -308 variability was observed.

Interleukin (IL)-10 is a cytokine that downregulates the proinflammatory response and has a modulatory effect on hepatic fibrogenesis and is a potent anti-inflammatory Th2 cytokine that downregulates the expression of major histocompatibility complex (MHC) class I and class II molecules, as well as the production of Th1 cytokines[31-36]. IL-10 levels differ widely between individuals, possibly because of polymorphisms in the promoter region of the IL-10 gene[37,38]. Specifically, three SNPs in the promoter (at positions -1082, -819, and -592 relative to the transcription start site) form three SNP combinations (ATA, ACC, GCC), which are associated with differential IL-10 expression[38-40]. It is reasonable to assume that hepatitis C patients who produce high levels of IL-10 have less hepatocellular injury and less ability to control infection and patients with low secretion of IL-10 have a better ability to eliminate the hepatitis infection. Perhaps low IL-10 production can skew the immune system into the Th1 type of response, facilitating the clearance of viral load. -1082A allele is associated with reduced IL-10 production *in vitro*[39]. In our study, individuals who were homozygous for IL-10 AA at position -1082 had a lower HAI.

It has been shown that hepatitis C patients, genotyped as high IL-10 producers, have a poor response to IFN-α therapy[40]. Such polymorphisms may also predict the sustained viral response to antiviral therapy[41]. These patients may benefit from additional treatment strategies designed to enhance T-helper type 1 (Th1) response. In one study, the interleukin-10 -1082 G/G genotype was identified more frequently in patients than in controls (P = 0.048). The patients exhibiting transforming growth factor-beta 1+29 (codon 10) C/C genotype variables were less likely to respond to treatment than patients with the T/T or T/C genotypes[42]. Liver transplant recipients, who are genotyped as having a low production profile of IL-10, are more prone to rejection and less likely to have hepatitis C recurrence[43]. The IL-1beta-31 genotype T/T or the IL-1beta-511/-31 haplotype C/T is associated with the presence of HCC in Japanese patients with chronic HCV infection[44].

However, not all the studies favor such effect of polymorphisms. Three members of the interleukin-1 gene family (IL-1A, IL-1B and IL-1RN), three polymorphic sites in the interleukin-10 gene promoter (-1082, -819, -592) and two in the TNF-α promoter (-308, -238) were studied in two independent DNA banks, each with appropriate controls. Standard PCR-based genotyping techniques were used. No significant difference in the distribution of any of the polymorphisms has been found in either study set[45].

We, in this study, determined SNP at position -1082, -819 and -592 in case of IL-10, -874 for IFN-γ, -308 for TNF-α, -10 for TGF-β and IL-1 C/ U and analyzed the frequency of their distribution and correlation with the ALT and HCV RNA levels, HAI and response to treatment. In our series, we selected genotype 3 patients because this is the main genotype in our region and not enough data are available on the influence of host cytokine gene polymorphisms of this viral genotype. Another reason of selecting a single genotype was to make the group uniform as different genotypes have different response rates to antiviral therapy and influence of cytokines may also be different. We could not find any significant difference in the cytokine genotype profile while analyzing different variables except for some influence of polymorphisms of IL-10 on liver histology. These polymorphisms did not modulate the response to interferon plus ribavirin therapy. This may be due to the small sample size or the fact that viral genotype 3 is easy to treat genotype in any case.

REFERENCES

1 **Pawlotsky JM.** Hepatitis C virus infection: virus/host interactions. *J Viral Hepat* 1998; **5** Suppl 1: 3-8
2 **Mosmann TR,** Sad S. The expanding universe of T-cell subsets: Th1, Th2 and more. *Immunol Today* 1996; **17**: 138-146
3 **Biron CA.** Cytokines in the generation of immune responses to, and resolution of virus infection. *Curr Opin Immunol* 1994; **6**: 530-538
4 **Tough DF,** Borrow P, Sprent J. Induction of bystander T cell proliferation by viruses and type I interferon in vivo. *Science* 1996; **272**: 1947-1950
5 **Napoli J,** Bishop GA, McGuinness PH, Painter DM, McCaughan GW. Progressive liver injury in chronic hepatitis

C infection correlates with increased intrahepatic expression of Th1-associated cytokines. *Hepatology* 1996; **24**: 759-765

6 **Sobue S,** Nomura T, Ishikawa T, Ito S, Saso K, Ohara H, Joh T, Itoh M, Kakumu S. Th1/Th2 cytokine profiles and their relationship to clinical features in patients with chronic hepatitis C virus infection. *J Gastroenterol* 2001; **36**: 544-551

7 **Rosen HR,** Miner C, Sasaki AW, Lewinsohn DM, Conrad AJ, Bakke A, Bouwer HG, Hinrichs DJ. Frequencies of HCV-specific effector CD4+ T cells by flow cytometry: correlation with clinical disease stages. *Hepatology* 2002; **35**: 190-198

8 **Cramp ME,** Carucci P, Rossol S, Chokshi S, Maertens G, Williams R, Naoumov NV. Hepatitis C virus (HCV) specific immune responses in anti-HCV positive patients without hepatitis C viraemia. *Gut* 1999; **44**: 424-429

9 **Chang KM,** Thimme R, Melpolder JJ, Oldach D, Pemberton J, Moorhead-Loudis J, McHutchison JG, Alter HJ, Chisari FV. Differential CD4(+) and CD8(+) T-cell responsiveness in hepatitis C virus infection. *Hepatology* 2001; **33**: 267-276

10 **Fabris C,** Soardo G, Falleti E, Toniutto P, Vitulli D, Federico E, Del Forno M, Mattiuzzo M, Gonano F, Pirisi M. Relationship among hepatic inflammatory changes, circulating levels of cytokines, and response to IFN-alpha in chronic hepatitis C. *J Interferon Cytokine Res* 1998; **18**: 705-709

11 **Kato S,** Onda M, Yamada S, Matsuda N, Tokunaga A, Matsukura N. Association of the interleukin-1 beta genetic polymorphism and gastric cancer risk in Japanese. *J Gastroenterol* 2001; **36**: 696-699

12 **di Giovine FS,** Takhsh E, Blakemore AI, Duff GW. Single base polymorphism at -511 in the human interleukin-1 beta gene (IL1 beta). *Hum Mol Genet* 1992; **1**: 450

13 **Perrey C,** Turner SJ, Pravica V, Howell WM, Hutchinson IV. ARMS-PCR methodologies to determine IL-10, TNF-alpha, TNF-beta and TGF-beta 1 gene polymorphisms. *Transpl Immunol* 1999; 7: 127-128

14 **Ishak K,** Baptista A, Bianchi L, Callea F, De Groote J, Gudat F, Denk H, Desmet V, Korb G, MacSween RN. Histological grading and staging of chronic hepatitis. *J Hepatol* 1995; **22**: 696-699

15 **Alter MJ,** Mast EE, Moyer LA, Margolis HS. Hepatitis C. *Infect Dis Clin North Am* 1998; **12**: 13-26

16 **Cerny A,** Chisari FV. Pathogenesis of chronic hepatitis C: immunological features of hepatic injury and viral persistence. *Hepatology* 1999; **30**: 595-601

17 **Koziel MJ.** The role of immune responses in the pathogenesis of hepatitis C virus infection. *J Viral Hepat* 1997; **4** Suppl 2: 31-41

18 **Bozkaya H,** Bozdayi AM, Aslan N, Turkay C, Sarioglu M, Cetinkaya H, Akdogan M, Cinar K, Erden E, Kose K, Senturk H, Akkiz H, Karayalcin S, Yurdaydin C, Uzunalimoglu O. Circulating IL-2 and IL-10 in chronic active hepatitis C with respect to the response to IFN treatment. *Infection* 2000; **28**: 309-313

19 **Prezzi C,** Casciaro MA, Francavilla V, Schiaffella E, Finocchi L, Chircu LV, Bruno G, Sette A, Abrignani S, Barnaba V. Virus-specific CD8(+) T cells with type 1 or type 2 cytokine profile are related to different disease activity in chronic hepatitis C virus infection. *Eur J Immunol* 2001; **31**: 894-906

20 **Llorent L,** Richaud-Patin Y, Alcocer-Castillejos N, Ruiz-Soto R, Mercado MA, Orozco H, Gamboa-Dominguez A, Alcocer-Varela J. Cytokine gene expression in cirrhotic and non-cirrhotic human liver. *J Hepatol* 1996; **24**: 555-563

21 **Fukuda R,** Ishimura N, Ishihara S, Chowdhury A, Morlyama N, Nogami C, Miyake T, Niigaki M, Tokuda A, Satoh S, Sakai S, Akagi S, Watanabe M, Fukumoto S. Intrahepatic expression of pro-inflammatory cytokine mRNAs and interferon efficacy in chronic hepatitis C. *Liver* 1996; **16**: 390-399

22 **Roulot D,** Durand H, Coste T, Rautureau J, Strosberg AD, Benarous R, Marullo S. Quantitative analysis of transforming growth factor beta 1 messenger RNA in the liver of patients with chronic hepatitis C: absence of correlation between high levels and severity of disease. *Hepatology* 1995; **21**: 298-304

23 **Cribier B,** Schmitt C, Rey D, Lang JM, Kirn A, Stoll-Keller F. Production of cytokines in patients infected by hepatitis C virus. *J Med Virol* 1998; **55**: 89-91

24 **Lapinski TW.** The levels of IL-1beta, IL-4 and IL-6 in the serum and the liver tissue of chronic HCV-infected patients. *Arch Immunol Ther Exp (Warsz)* 2001; **49**: 311-316

25 **Poynard T,** Marcellin P, Lee SS, Niederau C, Minuk GS, Ideo G, Bain V, Heathcote J, Zeuzem S, Trepo C, Albrecht J. Randomised trial of interferon alpha2b plus ribavirin for weeks or for 24 weeks versus interferon alpha2b plus placebo for 48 weeks for treatment of chronic infection with hepatitis C virus. *International Hepatitis Interventional Therapy Group (IHIT) Lancet* 1998; **352**: 1426-1432

26 **McHutchison JG,** Gordon SC, Schiff ER, Shiffman ML, Lee WM, Rustgi VK, Goodman ZD, Ling MH, Cort S, Albrecht JK. Interferon alfa-2b alone or in combination with ribavirin as initial treatment for chronic hepatitis C. Hepatitis Interventional Therapy Group. *N Engl J Med* 1998; **339**: 1485-1492

27 **Brouwer JT,** Hansen BE, Niesters HG, Schalm SW. Early prediction of response in interferon monotherapy and in interferon-ribavirin combination therapy for chronic hepatitis C: HCV RNA at 4 wk versus ALT. *J Hepatol* 1999; **30**: 192-198

28 **Bataller R,** North KE, Brenner DA. Genetic polymorphisms and the progression of liver fibrosis: a critical appraisal. *Hepatology* 2003; **37**: 493-503

29 **Hohler T,** Kruger A, Gerken G, Schneider PM, Meyer zum Buschenfelde KH, Rittner C. Tumor necrosis factor alpha promoter polymorphism at position -238 is associated with chronic active hepatitis C infection. *J Med Virol* 1998; **54**: 173-177

30 **Yee LJ,** Tang J, Herrera J, Kaslow RA, van Leeuwen DJ. Tumor necrosis factor gene polymorphisms in patients with cirrhosis from chronic hepatitis C virus infection. *Genes Immun* 2000; **1**: 386-390

31 **Fiorentino DF,** Zlotnik A, Vieira P, Mosmann TR, Howard M, Moore KW, O'Garra A. IL-10 acts on the antigen-presenting cell to inhibit cytokine production by Th1 cells. *J Immunol* 1991; **146**: 3444-3451

32 **Yue FY,** Dummer R, Geertsen R, Hofbauer G, Laine E, Manolio S, Burg G. Interleukin-10 is a growth factor for human melanoma cells and down-regulates HLA class-I, HLA class-II and ICAM-1 molecules. *Int J Cancer* 1997; **71**: 630-637

33 **Tsuruma T,** Yagihashi A, Torigoe T, Sato N, Kikuchi K, Watanabe N, Hirata K. Interleukin-10 reduces natural killer sensitivity and downregulates MHC class I expression on H-ras-transformed cells. *Cell Immunol* 1998; **184**: 121-128

34 **Zeller JC,** Panoskaltsis-Mortari A, Murphy WJ, Ruscetti FW, Narula S, Roncarolo MG, Blazar BR. Induction of CD4+ T cell alloantigen-specific hyporesponsiveness by IL-10 and TGF-beta. *J Immunol* 1999; **163**: 3684-3691

35 **de Waal Malefyt R,** Haanen J, Spits H, Roncarolo MG, te Velde A, Figdor C, Johnson K, Kastelein R, Yssel H, de Vries JE. Interleukin 10 (IL-10) and viral IL-10 strongly reduce antigen-specific human T cell proliferation by diminishing the antigen-presenting capacity of monocytes via downregulation of class II major histocompatibility complex expression. *J Exp Med* 1991; **174**: 915-924

36 **de Waal Malefyt R,** Abrams J, Bennett B, Figdor CG, de Vries JE. Interleukin 10(IL-10) inhibits cytokine synthesis by human monocytes: an autoregulatory role of IL-10 produced by monocytes. *J Exp Med* 1991; **174**: 1209-1220

37 **Eskdale J,** Gallagher G, Verweij CL, Keijsers V, Westendorp RG, Huizinga TW. Interleukin 10 secretion in relation to human IL-10 locus haplotypes. *Proc Natl Acad Sci USA* 1998; **95**: 9465-9470

38 **Eskdale J,** Keijsers V, Huizinga T, Gallagher G. Microsatellite alleles and single nucleotide polymorphisms (SNP) combine to form four major haplotype families at the human interleukin-10 (IL-10) locus. *Genes Immun* 1999; **1**: 151-155

39 **Turner DM,** Williams DM, Sankaran D, Lazarus M, Sinnott

PJ, Hutchinson IV. An investigation of polymorphism in the interleukin-10 gene promoter. *Eur J Immunogenet* 1997; **24**: 1-8

40 **Edwards-Smith CJ,** Jonsson JR, Purdie DM, Bansal A, Shorthouse C, Powell EE. Interleukin-10 promoter polymorphism predicts initial response of chronic hepatitis C to interferon alfa. *Hepatology* 1999; **30**: 526-530

41 **Yee LJ,** Tang J, Gibson AW, Kimberly R, Van Leeuwen DJ, Kaslow RA. Interleukin 10 polymorphisms as predictors of sustained response in antiviral therapy for chronic hepatitis C infection. *Hepatology* 2001; **33**: 708-712

42 **Vidigal PG,** Germer JJ, Zein NN. Polymorphisms in the interleukin-10, tumor necrosis factor-alpha, and transforming growth factor-beta1 genes in chronic hepatitis C patients treated with interferon and ribavirin. *J Hepatol* 2002; **36**: 271-277

43 **Tambur AR,** Ortegel JW, Ben-Ari Z, Shabtai E, Klein T, Michowiz R, Tur-Kaspa R, Mor E. Role of cytokine gene polymorphism in hepatitis C recurrence and allograft rejection among liver transplant recipients. *Transplantation* 2001; **71**: 1475-1480

44 **Wang Y,** Kato N, Hoshida Y, Yoshida H, Taniguchi H, Goto T, Moriyama M, Otsuka M, Shiina S, Shiratori Y, Ito Y, Omata M. Interleukin-1beta gene polymorphisms associated with hepatocellular carcinoma in hepatitis C virus infection. *Hepatology* 2003; **37**: 65-71

45 **Constantini PK,** Wawrzynowicz-Syczewska M, Clare M, Boron-Kaczmarska A, McFarlane IG, Cramp ME, Donaldson PT. Interleukin-1, interleukin-10 and tumour necrosis factor-alpha gene polymorphisms in hepatitis C virus infection: an investigation of the relationships with spontaneous viral clearance and response to alpha-interferon therapy. *Liver* 2002; **22**: 404-412

Science Editor Wang XL and Guo SY **Language Editor** Elsevier HK

PO Box 2345, Beijing 100023, China
www.wjgnet.com
wjg@wjgnet.com

ELSEVIER

World J Gastroenterol 2005;11(42):6662-6666
World Journal of Gastroenterology ISSN 1007-9327

• *BRIEF REPORTS* •

Gastroprotective activity of *Nigella sativa* L oil and its constituent, thymoquinone against acute alcohol-induced gastric mucosal injury in rats

Mehmet Kanter, Halit Demir, Cengiz Karakaya, Hanefi Ozbek

Mehmet Kanter, Department of Histology and Embryology, Faculty of Medicine, Trakya University, Edirne, Turkey
Halit Demir, Department of Chemistry, Faculty of Art and Science, Yuzuncu Yil University, Van, Turkey
Cengiz Karakaya, Department of Biochemistry, Faculty of Medicine, , Yuzuncu Yil University, Van, Turkey
Hanefi Ozbek, Department of Pharmacology, Faculty of Medicine, Yuzuncu Yil University, Van, Turkey
Correspondes to: Dr. Mehmet Kanter, Department of Histology and Embryology, Faculty of Medicine, Trakya University, Edirne, Turkey. mehmetkanter65@hotmail.com
Telephone: +902842357641 Fax: +902842352730
Received: 2004-07-23 Accepted: 2004-05-17

Abstract

AIM: To evaluate the role of reactive oxygen species in the pathogenesis of acute ethanol-induced gastric mucosal lesions and the effect of *Nigella sativa* L oil (NS) and its constituent thymoquinone (TQ) in an experimental model.

METHODS: Male Wistar albino rats were assigned into 4 groups. Control group was given physiologic saline orally (10 mL/kg body weight) as the vehicle (gavage); ethanol group was administrated 1 mL (per rat) absolute alcohol by gavage; the third and fourth groups were given NS (10 mL/kg body weight) and TQ (10 mg/kg body weight p.o) respectively 1 h prior to alcohol intake. One hour after ethanol administration, stomach tissues were excised for macroscopic examination and biochemical analysis.

RESULTS: NS and TQ could protect gastric mucosa against the injurious effect of absolute alcohol and promote ulcer healing as evidenced from the ulcer index (UI) values. NS prevented alcohol-induced increase in thiobarbituric acid-reactive substances (TBARS), an index of lipid peroxidation. NS also increased gastric glutathione content (GSH), enzymatic activities of gastric superoxide dismutase (SOD) and glutathione-S-transferase (GST). Likewise, TQ protected against the ulcerating effect of alcohol and mitigated most of the biochemical adverse effects induced by alcohol in gastric mucosa, but to a lesser extent than NS. Neither NS nor TQ affected catalase activity in gastric tissue.

CONCLUSION: Both NS and TQ, particularly NS can partly protect gastric mucosa from acute alcohol-induced mucosal injury, and these gastroprotective effects might be induced, at least partly by their radical scavenging activity.

Key words: *Nigella sativa*; Thymoquinone; Ulcer; Antioxidant; Rat

Kanter M, Demir H, Karakaya C, Ozbek H. Gastroprotective activity of Nigella sativa L oil and its constituent, thymoquinone against acute alcohol-induced gastric mucosal injury in rats. *World J Gastroenterol* 2005; 11(42); 6662-6666
http://www.wjgnet.com/1007-9327/11/6662.asp

INTRODUCTION

Intragastric application of absolute ethanol has long been used as a reproducible method to induce gastric lesions in experimental animals[1]. Gastric lesion is accompanied with the formation of free radicals (FRs) and reactive oxygen species (ROS)[2-4]. These radicals in particular seem to play an important role in ulcerative and erosive lesions of the gastrointestinal tract[5], as they attack and damage many biological molecules. Therefore, treatment with antioxidants and FR scavengers can decrease ethanol-induced gastric mucosal damage[6,7].

The black seed, *Nigella sativa* L (NS), a member of the family of ranunculaceae, contains more than 30% of fixed oil and 0.4-0.45 % wt/wt of volatile oil. The volatile oil contains 18.4-24% thymoquinone (TQ) and 46% many monoterpenes such as *p*-cymene and α-piene[8]. Recently, clinical and animal studies have shown that extract of the black seeds have many therapeutic effects such as immunomodilative[9], antibacterial[10], hypotensive[11], hepatoprotective[12] and antidiabetic effects[13]. Ohkawa *et al*.[14] also reported that NS oil and its derivative TQ inhibit eicosanoid generation in leukocytes and membrane lipid peroxidation. However, the gastroprotective effect of this plant and its major constituent against ethanol-induced gastric mucosal injury remains unclear.

In the present investigation, we studied the influence of NS on gastric mucosal lesions and the redox state induced by ethanol and to compare its actions with those of its constituent TQ.

MATERIALS AND METHODS

Plant materials and extraction procedure

The NS seeds were purchased from a local herb store, Van, Turkey. Voucher specimens were kept at the Department of Biochemistry, Yuzuncuyil University, Van, Turkey, for the future reference. The seeds of NS were powdered in a mixer, placed in a distillation flask and the volatile oil with 0.2% yield was collected by steam distillation. TQ 2-isopropyl-5-methyl-1,4-benzoquinone, was purchased from Sigma (St. Louis, MO, USA).

Treatment of rats

Forty male Wistar albino rats, weighing 200-250 g (aged 4 mo), were supplied by The Center of Medical Investigations of Yuzuncu Yil University. The animals were fed with a standard rat chaw (Murat Food Factory, Ankara, Turkey) and allowed to drink water *ad libitum*, but they were deprived of food 12 h before the experiment. The animals were housed in a single temperature controlled (20-25 °C) cage in dark/light cycle. All procedures were performed in sterilized conditions. All animals received human care according to the criteria outlined in the "Guide for the Care and Use of Laboratory Animals" prepared by the National Academy of Sciences and published by the National Institutes of Health.

Rats were assigned into 4 groups (each containing 10 animals). Control group was given physiologic saline orally (10 mL/kg body weight) as the vehicle (gavage), ethanol group was administrated 1 mL (per rat) absolute alcohol by gavage. The third and fourth groups were given NS (10 mL/kg body weight) and TQ (10 mg /kg body weight p.o) respectively 1 h prior to alcohol intake. One hour after ethanol administration, the animals were euthanized by cervical dislocation. The stomach was excised, cut along the greater curvature, and gently rinsed in tap water. The stomach was stretched on a piece of cork with mucosal surface up, and then examined in a standard position for macroscopic examination. Scoring of ulcer was performed with the help of magnifying glass. Lesion size (mm) was determined by measuring each lesion and its greatest diameter was recorded in the case of petechial lesions. Four such lesions were considered to be the equivalent of an 1 mm ulcer. The sum of the total severity scores in each group of rats divided by the number of animals, was expressed as the mean ulcer index (UI).

Biochemical analysis

Stomachs were cut into small pieces and homogenized in 0.15 mol/L ice-cold KCl using Heidolf Diax 900, type 595 (Germany) to give 20% homogenates. The homogenates were then made into aliquots and used for the assessment of antioxidant parameters.

MDA levels were determined as previously described[15]. Less than 0.2 mL of 10% (w/v) tissue homogenate, 0.2 mL of 8.1% sodium dodecyl sulfate (SDS), 1.5 mL of 20% acetic acid solution adjusted to pH 3.5 with NaOH, and 1.5 mL of 0.8% aqueous solution thiobarbituric acid (TBA) were added into the sample. The mixture was made up to 4.0 mL with distilled water, and heated at 95 ^{0}C for 60 min. After cooling, 1.0 mL of distilled water and 5.0 mL of the mixture of *n*-buthanol and pyridine (15:1, v/v) were added and shaken vigorously. After centrifugation at 4 000 r/min for 10 min, the organic layer was taken and its absorbance at 532 nm was measured. Total TBA-reactive materials were expressed as MDA, using a molar extinction coefficient for MDA of 1.56×10^5 cm/mol/L. MDA level was expressed as nmol/g.

Reduced glutathione (GSH) was determined according to the method described by Sun[16]. The GSH concentration (μmol/g) was computed from a standard curve constructed using different concentrations of standard GSH.

Stomach homogenate (20%) was centrifuged at 10 000 *g* for 10 min for 30 min at 4 ^{0}C (Beckman XL-70, USA). Following centrifugation, the supernatant (cytosolic fraction) was carefully removed from the pellet and used directly for assay of the enzymatic activities of SOD, GST and CAT.

SOD activity was detected according to Sun and Habig[17]. One SOD unit was defined as the enzyme amount causing 50% inhibition in the $NBTH_2$ reduction rate. SOD activity was also expressed as U/mg protein of stomach tissue sediment.

Gastric GST activity was determined according to the method of Clairborne *et al*.[18]. In brief, the GST activity toward 1-chloro-2,4-dinitrobenzene in the presence of glutathione as a co-substrate was measured specrophotometrically at 25 °C. The enzyme activity was determined by monitoring the changes in the absorbance at 340 nm for 4 min at 1-min intervals. The enzymatic activity was expressed as nmol min/g tissue.

CAT activity was determined according to the method of Lowry[19]. In short, the supernatant (50 μL) was added to a quartz cuvette containing 2.95 mL of 19 mmol/L H_2O_2 solution prepared in potassium phosphate buffer (0.1mol/L, pH 7.4). The change in absorbance was monitored at 240 nm over a 5-min period using a spectrophotometer (Shimadzu UV-1201, Japan). Commercially available CAT was used as the standard. CAT activity was expressed as U/g tissue.

The amount of protein was determined by the Lowry method[20].

Statistical analysis

The data were expressed as mean±SD and analyzed by repeated measures of variance (ANOVA). Tukey test was used to test for differences among means for which ANOVA indicated a significant ($P<0.05$) F ratio.

RESULTS

Oral administration of absolute ethanol produced multiple mucosal lesions in the rat stomach. Pretreatment with NS and TQ inhibited the ethanol-induced gastric mucosal injury in rats. Pretreatment with single oral dose of NS significantly reduced the ulcer index compared to alcohol

($P<0.01$). TQ also significantly inhibited ethanol-induced gastric lesions ($P<0.05$). Ulcer index (UI) is shown in Figure 1.

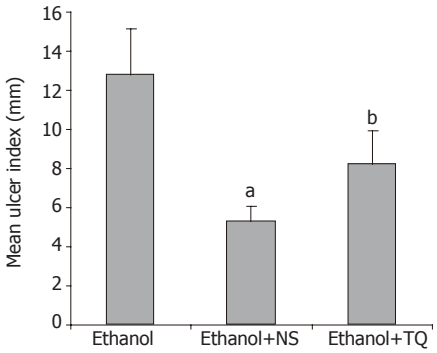

Figure 1 Mean UI in ethanol, ethanol + NS and ethanol + TQ treated rats. $^{b}P<0.01$, $^{a}P<0.05$ *vs* ethanol group

Administration of ethanol increased the MDA level in rat gastric tissue. In contrast, pretreatment with NS significantly decreased the MDA levels as compared to ethanol. TQ also significantly decreased the gastric MDA content, but to a lesser extent than NS. GSH activity decreased in the gastric tissue after ethanol administration, but pretreatment with NS or TQ increased the GSH activity gastric tissue compared to ethanol (Table 1). Prior administration of NS to rats markedly increased the gastric activity of SOD. Likewise, TQ increased the enzymatic activity of SOD compared to alcohol (Table 1). Pretreatment with either NS or TQ increased the enzyme activity of gastric GST. Neither NS nor TQ had any effect on the CAT activity of gastric mucosa (Table 1).

DISCUSSION

ROS are continuously produced during normal physiologic events, and removed by antioxidant defence mechanisim[21]. In pathological conditions, ROS are over produced and result in lipid peroxidation and oxidative damage. The imbalance between ROS and antioxidant defence mechanisms leads to oxidative modification in the cellular membrane or intracellular molecules[22]. Recent studies showed that ROS are one of the important factors in the pathogenesis of ethanol-induced mucosal damage[7,23,24]. Some ROS scavengers or inhibitors such as melatonin have protective effects on indomethacin- or ethanol-induced acute gastric injury in rats[25,26]. The cytoprotective role of antioxidants in the prevention and healing of gastric lesions has been widely investigated in a number of studies[24,27].

In the present study, administration of absolute alcohol by gastric gavage induced marked damage to the gastric mucosa that was obvious by macroscopic examination. The lesions were elongated hemorrhage and confined to the glandular portion with the highest subjective ulcer-scoring rate.

It was reported that alcohol causes severe oxidative stress in gastric tissue manifested as stimulated lipid peroxidation by increasing MDA content and decreasing of gastric GSH content[3,24,27].

The gastric activities of SOD and GST notably decreased following alcohol intake. The CAT activity, however, was unchanged. These results are in line with previous reports that demonstrated marked alterations in the enzymatic antioxidants following acute administration of alcohol to rats[3,28]. Depletion of non-protein sulfhydryl concentrations[1], modulation of nitric oxide sytem[29], reduction of mucosal blood flow[30], and autonomic nervous system regulation[31], are involved in the development of gastric lesions. One of the major mechanisms underlying the induction of gastric erosions by absolute alcohol is the oxidative damage with its dual events of lipid peroxidation and oxygen reactive species generation. Actually, oxygen-derived radicals have been implicated in the pathogenesis of gastric tissue damage and ulcerogenesis[6,32,33].

Pretreatment with a single oral dose of NS could partly reduce the ulcer index and promote healing of gastric lesions induced by acute intake of alcohol in rats. NS significantly decreased the gastric MDA content while it increased the gastric level of GSH compared to alcohol. The gastric activities of both SOD and GST were markedly elevated following administration of NS, whereas the CAT activity was not altered. Likewise, prior administration of TQ to animals could protect gastric mucosa and ameliorate most of the biochemical adverse effects induced by alcohol application, but to a lesser extent than NS.

These findings are in good agreement with a recent study by El-Denshary *et al.*[34]. The anti-ulcerogenic effects of NS can be attributed to the improvement of

Table 1 Effects of alcohol intake alone and following administration of either NS or TQ on the contents of MDA and GSH and activities of SOD, GSH and CAT in rat gastric tissue (means ± SD)

Parameters	Control	Ethanol	Eth + NS	Eth + TQ
MDA (nmol/g proteine)	136.33 ± 11.42	329.43 ± 19.80[a]	112 ± 17.16[c]	201.15 ± 29.11[c]
GSH (μmol/g proteine)	0.84 ± 0.04	0.44 ± 0.03[a]	0.54 ± 0.05[c]	0.42 ± 0.02
SOD (U/g proteine)	47.39 ± 5.74	17.75 ± 3.02[a]	56.88 ± 4.09[c]	51.08 ± 3.17[c]
GST (nmol/min/g proteine)	4.39 ± 0.29	1.81 ± 0.32[a]	4.02 ± 0.31[c]	4.07 ± 0.28[c]
CAT (U/g proteine)	56.45 ± 3.30	59.5 ± 7.99	55.63 ± 6.52	54.18 ± 10.19

$^{a}P<0.05$ *vs* control group. $^{c}P<0.05$ *vs* alcohol group.

the antioxidant status of animals due to an increase in mucin content of the gastric mucosa[34], or the presence of FR scavenging substances such as TQ[35]. It was also reported that NS given to sensitized quinea pigs, inhibits FR generation, and increases serum levels of SOD and glutathione[14]. NS could protect the gastric mucosa by increasing the bioavailability of arachidonic acid, resulting in biosynthesis of the cytoprotective prostaglandins in the stomach[36]. NS has also been reported to produce a marked inhibition on the release of leukotrienes, which cause mucosal tissue injury and hypoxemia[37]. Therefore, it may alter the delicate balance between prostaglandins and leukotrienes in the gastric mucosa favoring cytoprotection. TQ is the main active component of NS, and is able to inhibit lipid peroxidation[14]. Moreover, its ability to preserve the cell membrane integrity can be proven by the restoration.

In conclusion, pretreatment with NS and TQ, particularly NS can partly protect the gastric mucosa against the injurious effects of absolute ethanol and promote ulcer healing. NS or TQ can also mitigate most of the biochemical adverse effects induced by alcohol instillation in gastric tissue. Further studies are required to clarify the anti- ulcer and antioxidant action of NS or TQ.

REFERENCES

1 **Szabo S,** Trier JS, Frankel PW. Sulfhydryl compounds may mediate gastric cytoprotection. *Science* 1981; **214:** 200-202
2 **Cho CH,** Pfeiffer CJ, Misra HP. Ulcerogenic mechanism of ethanol and the action of sulphanilyl fluoride on the rat stomach *in-vivo*. *J Pharm Pharmacol* 1991; **43:** 495-498
3 **Lutnicki K,** Wrobel J, Ledwozyw A, Trebas-Pietras E. The effect of calcium ions on the intensity of peroxidation processes and the severity of ethanol-induced injury to the rat's gastric mucosa. *Arch Vet Pol* 1992; **32:** 125-132
4 **Bast A,** Haenen GR, Doelman CJ. Oxidants and antioxidants: state of the art. *Am J Med* 1991; **91:** 2S-13S
5 **Hirokawa M,** Miura S, Yoshida H, Kurose I, Shigematsu T, Hokari R, Higuchi H, Watanabe N, Yokoyama Y, Kimura H, Kato S, Ishii H. Oxidative stress and mitochondrial damage precedes gastric mucosal cell death induced by ethanol administration. *Alcohol Clin Exp Res* 1998; **22:** 111S-114S
6 **La Casa C,** Villegas I, Alarcon de la Lastra C, Motilva V, Martin Calero MJ. Evidence for protective and antioxidant properties of rutin, a natural flavone, against ethanol induced gastric lesions. *J Ethnopharmocal* 2000; **71:** 45-53
7 **el Tahir KE,** Ashour MM, al-Harbi MM. The respiratory effects of the volatile oil of the black seed (Nigella sativa) in guinea-pigs: elucidation of the mechanism(s) of action. *Gen Pharmacol* 1993; **24:** 1115-1122
8 **El-Kadi A,** Kandil O. The black seed (Nigella sativa) and immunity: its effect on human T cell subset. *Fed Proc* 1987; **46:** 1222
9 **Hanafy MS,** Hatem ME. Studies on the antimicrobial activity of Nigella sativa seed (black cumin). *J Ethnopharmacol* 1991; **34:** 275-278
10 **Zaoui A,** Cherrah Y, Lacaille-Dubois MA, Settaf A, Amarouch H, Hassar M. Diuretic and hypotensive effects of Nigella sativa in the spontaneously hypertensive rat. *Therapie* 2000; **55:** 379-382
11 **Turkdogan MK,** Agaoglu Z, Yener Z, Sekeroglu R, Akkan HA, Avci ME. The role of antioxidant vitamins (C and E), selenium and Nigella sativa in the prevention of liver fibrosis and cirrhosis in rabbits: new hopes. *Dtsch Tierarztl Wochenschr* 2001; **108:** 71-73
12 **Kanter M,** Meral I, Yener Z, Ozbek H, Demir H. Partial regeneration/proliferation of the beta-cells in the islets of Langerhans by Nigella sativa L. in streptozotocin-induced diabetic rats. *Tohoku J Exp Med* 2003; **201:** 213-219
13 **Houghton PJ,** Zarka R, de las Heras B, Hoult JR. Fixed oil of Nigella sativa and derived thymoquinone inhibit eicosanoid generation in leukocytes and membrane lipid peroxidation. *Planta Med* 1995; **61:** 33-36
14 **Ohkawa H,** Ohishi N, Yagi K. Reaction of linoleic acid hydroperoxide with thiobarbituric acid. *J Lipid Res* 1978; **19:** 1053-1057
15 **Ellman GL.** Tissue sulfhydryl groups. *Arch Biochem Biophys* 1959; **82:** 214-226
16 **Sun Y,** Oberley LW, Li Y. A simple method for clinical assay of superoxide dismutase. *Clin Chem* 1988; **34:** 497-500
17 **Habig WH,** Pabst MJ, Jakoby WB. Glutathione S-transferases. The first enzymatic step in mercapturic acid formation. *J Biol Chem* 1974; **249:** 7130-7139
18 **Clairborne A.** Catalase activity. In: Greenwald RA, editor. Handbook of Methods for Oxygen Radical Research. *Boca Raton*, FL 1985; 383-384
19 **Lowry OH,** Rosebrough NJ, Farr AL, Randall RJ. Protein measurement with the Folin phenol reagent. *J Biol Chem* 1951; **193:** 265-275
20 **Halliwell B,** Gutteridge JM, Cross CE. Free radicals, antioxidants, and human disease: where are we now? *J Lab Clin Med* 1992; **119:** 598-620
21 **El-Habit OH,** Saada HN, Azab KS, Abdel-Rahman M, El-Malah DF. The modifying effect of beta-carotene on gamma radiation-induced elevation of oxidative reactions and genotoxicity in male rats. *Mutat Res* 2000; **466:** 179-186
22 **Tuncel N,** Erkasap N, Sahinturk V, Ak DD, Tuncel M. The protective effect of vasoactive intestinal peptide (VIP) on stress-induced gastric ulceration in rats. *Ann N Y Acad Sci* 1998; **865:** 309-322
23 **Suzuki Y,** Ishihara M, Segami T, Ito M. Anti-ulcer effects of antioxidants, quercetin, alpha-tocopherol, nifedipine and tetracycline in rats. *Jpn J Pharmacol* 1998; **78:** 435-441
24 **Brzozowski T,** Konturek PC, Konturek SJ, Pajdo R, Bielanski W, Brzozowska I, Stachura J, Hahn EG. The role of melatonin and L-tryptophan in prevention of acute gastric lesions induced by stress, ethanol, ischemia, and aspirin. *J Pineal Res* 1997; **23:** 79-89
25 **Alarcon de la Lastra C,** Motilva V, Martin MJ, Nieto A, Barranco MD, Cabeza J, Herrerias JM. Protective effect of melatonin on indomethacin-induced gastric injury in rats. *J Pineal Res* 1999; **26:** 101-107
26 **Bilici D,** Suleyman H, Banoglu ZN, Kiziltunc A, Avci B, Ciftcioglu A, Bilici S. Melatonin prevents ethanol-induced gastric mucosal damage possibly due to its antioxidant effect. *Dig Dis Sci* 2002; **47:** 856-861
27 **El-Missiry MA,** El-Sayed IH, Othman AI. Protection by metal complexes with SOD-mimetic activity against oxidative gastric injury induced by indomethacin and ethanol in rats. *Ann Clin Biochem* 2001; **38:** 694-700
28 **Kato S,** Kitamura M, Korolkiewicz RP, Takeuchi K. Role of nitric oxide in regulation of gastric acid secretion in rats: effects of NO donors and NO synthase inhibitor. *Br J Pharmacol* 1998; **123:** 839-846
29 **Holzer P,** Livingston EH, Saria A, Guth PH. Sensory neurons mediate protective vasodilatation in rat gastric mucosa. *Am J Physiol* 1981; **260:** 363-370
30 **Ko JK,** Cho CH, Ogle CW. The vagus nerve and its non-cholinergic mechanism in the modulation of ethanol-induced gastric mucosal damage in rats. *J Pharm Pharmacol* 1994; **46:** 29-33
31 **Cho CH,** Pfeiffer CJ, Misra HP. Ethanol and the antioxidant defense in the gastrointestinal tract. *Acta Physiol Hung* 1992; **80:** 99-105
32 **Ligumsky M,** Sestieri M, Okon E, Ginsburg I. Antioxidants

inhibit ethanol-induced gastric injury in the rat. Role of manganese, glycine, and carotene. *Scand J Gastroenterol* 1995; **30:** 854-860

33 **El-Dakhakhny M,** Barakat M, El-Halim MA, Aly SM. Effects of Nigella sativa oil on gastric secretion and ethanol induced ulcer in rats. *J Ethnopharmacol* 2000; **72:** 299-304

34 **Saleh S,** El-Denshary EMS, Mahran LG, Salah N. Anti-inflammatory and antioxidant effect of *Nigella sativa* oil in sensitized animals. The 25th International Conference on Science and Technology, New Delhi 2000

35 **Campbell WB,** Halushka PV. Lipid-derived autacoids. Eicosanoids and platelet-activating factors. In: Hardman JG, Limbird LE, Molinoff PB, Ruddon RW, Gilman AG. Goodman and Gilman's. The Pharmacol Basis of Therapeutics, McGraw-Hill, New York 1996; 601-616

36 **Tsuji S,** Kawano S, Sato N, Kamada T. Mucosal blood flow stasis and hypoxemia as the pathogenesis of acute gastric mucosal injury: role of endogenous leukotrienes and prostaglandins. *J Clin Gastroenterol* 1990; **12** Suppl 1: S85-S91

37 **Mansour MA.** Protective effects of thymoquinone and desferrioxamine against hepatotoxicity of carbon tetrachloride in mice. *Life Sci* 2000; **66:** 2583-2591

Science Editor Wang XL and Guo SY **Language Editor** Elsevier HK

PO Box 2345, Beijing 100023, China
www.wjgnet.com
wjg@wjgnet.com

ELSEVIER

World J Gastroenterol 2005;11(42):6667-6670
World Journal of Gastroenterology ISSN 1007-9327

• *BRIEF REPORTS* •

Giardiasis in patients with dyspeptic symptoms

Javed Yakoob, Wasim Jafri, Shahab Abid, Nadim Jafri, Saeed Hamid, Hasnain Ali Shah, Lubna Rizvi, Muhammad Islam, Hizbullah Shaikh

Javed Yakoob, Wasim Jafri, Shahab Abid, Nadim Jafri, Saeed Hamid, Hasnain Ali Shah, Lubna Rizvi, Muhammad Islam, Section of Gastroenterology, Department of Medicine, Aga Khan University Hospital, Karachi 74800, Sindh, Pakistan
Hizbullah Shaikh, Department of Pathology, Aga Khan University Hospital, Karachi 74800, Sindh, Pakistan
Co-first author: Wasim Jafri
Co-correspondence: Wasim Jafri
Correspondence to: Dr. Javed Yakoob, MBBS, PhD, Section of Gastroenterology, Department of Medicine, Aga Khan University Hospital, Stadium Road, Karachi 74800, Pakistan. yakoobjaved@hotmail.com
Telephone: +92-21-48594661 Fax: +92-21-4934294
Received: 2005-03-10 Accepted: 2005-04-09

Abstract

AIM: To investigate the prevalence of giardiasis in patients with dyspeptic symptoms.

METHODS: Clinical records of consecutive patients who attended Gastroenterology Department at Aga Khan University Hospital from January 2000 to June 2003 and had esophagogastroduodenoscopy (EGD) with duodenal biopsies and international classification of diseases 9th revision with clinical modifications (ICD-9-CM) coded with giardiasis were studied.

RESULTS: Two hundred and twenty patients fulfilled the above criteria. There were 44% (96/220) patients who were giardiasis positive, 72% (69/96) of them were males and 28% (27/96) of them were females. There were 65% (81/124) males and 35% (43/124) females who were giardiasis negative. The mean age of patients with giardiasis was 28±17 years, while that of giardiasis negative patients was 40±18 years (P<0.001). In patients with giardiasis, abdominal pain was present in 71% (68/96) of patients (P = 0.02) and diarrhea in 29% (28/96) (P = 0.005); duodenitis in 25% (24/96) on EGD (P = 0.006) and in 68% (65/96) on histopathology (P = 0.002).

CONCLUSION: Giardiasis occurs significantly in young people with abdominal pain, while endoscopic duodenitis is seen in only 25% of giardiasis positive cases, which supports routine duodenal biopsy.

Key words: Abdominal pain; Giardiasis; Stool examination; EGD; Duodenal biopsy

Yakoob J, Jafri W, Abid S, Jafri N, Hamid S, Shah HA, Rizvi L, Islam M, Shaikh H. Giardiasis in patients with dyspeptic symptoms. *World J Gastroenterol* 2005; 11(42): 6667-6670
http://www.wjgnet.com/1007-9327/11/6667.asp

INTRODUCTION

Giardia lamblia is the most common protozoan isolated from the gastrointestinal tract[1]. Worldwide incidence is believed to range from 20% to 60%[2]. The incidence rate is 2-7% in industrialized nations[3]. Patients with giardiasis typically present with diarrhea, vague abdominal discomfort, nausea and distention together with mild weight loss and lassitude. The absence of these symptoms may result in a low clinical index of suspicion for the diagnosis. Giardiasis is diagnosed by signs and symptoms, as well as the presence of giardia cysts and trophozoites in the stool. Stool examination can be unreliable, as organisms may be excreted at irregular intervals which can produce a false negative test result[4]. There is no gold standard for the diagnosis of giardiasis. The initial method of diagnosis is by demonstration of the trophozoite or cysts of *G lamblia* in the stool by microscopy or stool antigen detection by ELISA. Other methods of diagnosis include examination of duodenal contents by aspiration or biopsy with endoscopy. A definitive diagnosis may require repeated stool examinations, fecal immunoassays, or even sampling of the upper intestinal contents. Two stool examinations can detect 80-90% of infections, while three samples detect >90%[5]. About 20% of infestations are symptomatic, and do not continue for more than 3 mo along with the passage of cysts[2]. Difficulties are often encountered in finding the underlying cause of recurrent abdominal pain. Giardiasis is considered as an infrequent cause of dyspepsia[6], but this might not be true in a third world country. Prevalence of giardiasis is the highest in areas of poor sanitation and drinking water treatment. It is transmitted by eating and drinking contaminated food and water or fecal-oral contact. In immunocompetent patient, small bowel biopsy may show normal histology or villous architecture, but increased intraepithelial lymphocytes and plasma cells in the lamina propria or villous atrophy and inflammatory cells[7]. Giardia trophozoites can be found on the surface or penetrating the epithelium down to the lamina propria[7]. The aim of this study was to investigate the prevalence of giardiasis in patients with dyspeptic symptoms.

MATERIALS AND METHODS

Patients

We carried out a retrospective analysis of medical records of all the patients who attended endoscopy unit of gastrointestinal section at the Aga Khan University Hospital from January 2000 to June 2003 consecutively for dyspeptic symptoms. They had an esophagogastrodu odenoscopy (EGD) with duodenal biopsies after routine examination including stool examination. The giardiasis negative group consisted of the patients who had a stool examination and an EGD with duodenal biopsy and were not diagnosed as giardiasis. The giardiasis positive group consisted of the patients who had positive EGD with duodenal biopsy and stool examination for giardia cysts or trophozoites. Clinical symptoms at the time of presentation, diagnosis, drug treatment dosage and duration, past history of giardiasis, neutrophil and lymphocyte counts from complete blood picture, random blood glucose and stool examination were noted. Patients with diagnosis of celiac disease were excluded from the analysis.

Stool examination

Stool parasitological analysis of samples collected from spontaneous bowel movement was performed. Samples were collected in a sterile container and transported soon after to the laboratory for examination. Microscopically each stool specimen was examined in a fresh normal saline smear and Lugol's iodine preparation.

Esophagogastroduodenoscopy

All endoscopic examinations were performed by staff-members of our hospital's gastroenterology section, using an Olympus video scope GIF xQ 140. Duodenitis was diagnosed when scattered. Reddened raised non-eroded mucosal patches were endoscopically identified in the duodenal bulb and descending duodenum.

Histopathology

Hematoxylin and eosin (HE) staining of duodenal biopsy was used for pathological confirmation of giardia trophozoites. Most organisms were tangentially cut and many were seen as small sickle-shaped objects near the epithelial surface.

Statistical analysis

The SPSS (Release 11.5.0, standard version, copyright © SPSS; 1989-02) was used for data analysis. Descriptive analysis was done for demographic and clinical features. Results were presented as mean±SD for continuous variables, and number (percentage) for categorical variables. Univariate analysis was performed by using the independent sample *t*-test for continuous variables and Pearson's chi-square test for categorical variables to assess the demographic and clinical parameters associated with giardiasis. Odds ratio (OR) estimates with their 95% confidence interval (CIs) and *P* values were calculated (Table 1). $P \leqslant 0.05$ was considered statistically significant. All *P* values were two sided.

RESULTS

Patients

Two hundred and twenty patients fulfilled the criteria. There were 44% (96/220) patients who were giardiasis positive and 56% (124/220) were giardiasis negative. In patients with giardiasis, 72% (69/96) were males and 28% (27/96) were females. The mean age of patients with giardiasis was 28±17 years, while that of patients without giardiasis was 40±18 years ($P<0.001$). Abdominal pain was present in 71% (68/96) patients with giardiasis and in 56% (69/124) patients without giardiasis ($P = 0.02$), diarrhea was present in 29% (28/96) patients with giardiasis and in 14% (17/124) patients without giardiasis ($P = 0.005$, Table 1).

Table 1 Clinical details of patients with and without endoscopic giardiasis

Variables	Giardiasis positive (n = 96) (%)	Giardiasis negative (n = 124) (%)	*P*	OR (95%CI)
Age groups (yr)				
<22	34 (35)	21 (17)		1
22–31	29 (30)	27 (22)		0.7 (0.3–1.5)
32–48	20 (21)	35 (28)		0.4 (0.2–0.9)
>48	13 (14)	41 (33)	<0.001	0.2 (0.1–0.5)
Gender				
Female	27 (28)	43 (35)		
Male	69 (72)	81 (65)	0.301	1.4 (0.8–2.4)
Abdominal pain	68 (71)	69 (56)	0.021	1.9 (1.1–3.4)
Diarrhea	28 (29)	17 (14)	0.005	2.6 (1.3–5.1)
Weight loss	9 (9.4)	6 (5)	0.186	2.0 (0.7–5.9)
Endo-duodenitis	24 (25)	53 (43)	0.007	0.4 (0.2–0.8)
Histological duodenitis	65 (68)	58 (46)	0.002	2.5 (1.4–4.4)
Lamina propria inflammation	73 (76)	53 (42)	<0.001	4.4 (2.4–8.1)
Villus shortening	5 (5)	–	–	–

Results are presented as number (percentage), Odds ratio (95%CI).

Stool examination

Stool examination was carried out in 88.5% (85/96) cases, 6% (5/85) were positive for giardia cysts and trophozoites.

Endoscopy

On EGD, antral gastritis was present in 46% (44/96) patients with giardiasis and in 75% (93/124) patients without giardiasis ($P<0.001$); duodenitis was present in 25% (24/96) patients with giardiasis and in 50% (53/124) patients without giardiasis ($P = 0.006$); duodenal ulcer was present in 4% (4/96) patients with giardiasis and in 72% (89/124) patients without giardiasis ($P<0.001$, Table 1).

Histopathology

On histopathology of gastric antral biopsy, *H. pylori* was seen in 42% (40/96) patients with giardiasis and in 54% (67/124) patients without giardiasis ($P = 0.06$); antral gastritis was found in 53% (51/96) patients with giardiasis and in 81% (100/124) patients without giardiasis ($P<0.001$). Duodenitis was seen in 68% (65/96) patients with giardiasis and in 46% (58/124) patients without giardiasis ($P = 0.002$); villus shortening was seen in 5% (5/96) patients with giardiasis and absent in patients giardiasis negative; lamina propria inflammatory infiltration with increased intraepithelial lymphocytes and plasma cells was seen in 76% (73/96) patients with giardiasis and in 42% (53/124) patients without giardiasis ($P<0.001$, Table 1).

DISCUSSION

It is sometimes difficult to establish the diagnosis of giardiasis. Tests for parasitic antigen in stool are at least as sensitive and specific as good microscopic examination and are easier to perform. All these methods occasionally yield false-negative results.

The implications of this study are that no symptom complex is associated with the giardiasis. Giardiasis may present with abdominal pain alone and it should be considered even in the absence of diarrhea. Abdominal pain is the most common presentation and diagnosis, and investigations carried out are more often for gastritis or peptic ulcer disease with or without *H pylori* infection. Abdominal pain has also been previously found to be significantly associated with the presence of giardiasis[8]. In our study, the incidence of giardiasis was higher in males, which is in agreement with the other studies[9-11]. However, the mean age of our patients was lower and might be attributed to more frequent exposure to this water borne infection because of social activities that involve frequent restaurants beside others. Diarrhea was seen in only 29% of cases. *G lamblia* infestation or other infectious causes were not considered because of the absence of diarrhea in most of these cases and hence a single stool examination was carried out. It is generally held that giardiasis may present with atypical gastrointestinal symptoms but this would be expected in combination with diarrhea[12]. The sensitivity for examination of a single random stool specimen is only 30-50%[13-14]. Hence this might explain the 6% low yield of stool examination in the cases for giardia cysts and trophozoites. Microscopic examination of a single stool sample cannot exclude *G lamblia* infection; therefore, at least three stool specimens should be examined before other diagnostic procedures. As only saline or Lugol's iodine examination of fecal smear was employed, it may have been insufficient in the absence of numerous parasites[14]. Other useful methods such as zinc sulfate floatation, a concentration technique for cysts, were also not employed in our study.

Duodenal ulcer is not a feature of giardiasis, while duodenitis was seen in 25% on endoscopy and in 68% on histology ($P = 0.002$). EGD with duodenal biopsy helps ruling out peptic ulcer as the only cause of symptoms. Giardiasis was associated with the normal endoscopic findings in the duodenum in 75% cases (Table 1). Hence duodenal biopsy should be considered with EGD in patients with abdominal pain as antral biopsy alone may prove inadequate for determining the cause of abdominal pain in a developing country. This is in agreement with the opinion held by some investigators that routine duodenal biopsies should be done in patients undergoing upper intestinal endoscopy[15,16]. In this study, most of our cases on EGD showed normal duodenal mucosa but duodenal biopsy with H&E staining demonstrated *G lamblia* trophozoites (Table 1). Although special stains such as Giemsa or phosphotungstic acid hematoxylin can occasionally be helpful, routine hematoxylin and eosin staining is almost always satisfactory[17].

The data suggesting the role of giardiasis in dyspeptic patients are in contradiction to a previous prospective study[17]. Carr *et al*.[18] carried out a study in an area which is not endemic for Giardia, and demonstrated Giardia in 15.5% of patients presenting with dyspepsia and its prevalence is similar with or without obvious lesions at endoscopy. In their study, only 52% patients presented with abdominal pain, and patients with vomiting and diarrhea as presentation had a significantly increased prevalence of Giardia. However, our data originates from a developing country located in an area endemic for the acquisition of Giardia. In our study, patients more commonly presented with abdominal pain than diarrhea (Table 1). The discrepancy describing a lower frequency of endoscopic duodenitis and higher frequency of histologic duodenitis in infected patients than in non-infected group might be due to a higher prevalence of *H pylori* infection in the latter. However, this was a retrospective observational study with its selection bias and limitations in diagnostic methods. Serial stool examinations were not carried in all patients.

The presentation of giardiasis varies and for diagnosis it requires a high degree of suspicion in the appropriate clinical setting. Examination of duodenal biopsy from patients presenting with abdominal pain should be considered so as to prevent missing diagnosis of giardiasis. Giardiasis is diagnosed more often on EGD with duodenal biopsy rather than on stool examination. As cyst excretion is variable and may be undetectable at times, repeated

examination of properly preserved stool samples and biopsy of the small intestine may be required to detect the parasites. A prospective study is under way to confirm the results of this study.

REFERENCES

1 **Eckmann L,** Gillin FD. Microbes and microbial toxins: paradigms for microbial-mucosal interactions I. Pathophysiological aspects of enteric infections with the lumen-dwelling protozoan pathogen Giardia lamblia. *Am J Physiol Gastrointest Liver Physiol* 2001; **280:** G1-G6

2 **Tripathi DM,** Gupta N, Lakshmi V, Saxena KC, Agrawal AK. Antigiardial and immunostimulatory effect of Piper longum on giardiasis due to Giardia lamblia. *Phytother Res* 1999; **13:** 561-565

3 **Upcroft P**, Upcroft JA. Drug targets and mechanisms of resistance in the anaerobic protozoa. *Clin Microbiol Rev* 2001; **14:** 150-164

4 **Beers MH**, Berkow R. The Merk Manual. NJ: Whitehouse Station. Merck Research Laboratories; 1999: 1257-1258.

5 **Gardner TB**, Hill DR. Treatment of giardiasis. *Clin Microbiol Rev* 2001; **14:** 114-128

6 **Heikkinen M**, Pikkarainen P, Takala J, Rasanen H, Julkunen R. Etiology of dyspepsia: four hundred unselected consecutive patients in general practice. *Scand J Gastroenterol* 1995; **30:** 519-523

7 **Ferguson A**, Gillon J, Munro G. Pathology and pathogenesis of the intestinal mucosal damage in giardiasis. In: Meyer EA, ed. *Giardiasis*. New York: Elsevier Publishing Co, 1990: 55-173.

8 **Minvielle MC**, Pezzani BC, Cordoba MA, De Luca MM, Apezteguia MC, Basualdo JA. Epidemiological survey of Giardia spp. and Blastocystis hominis in an Argentinian rural community. *Korean J Parasitol* 2004; **42:** 121-127

9 **Zafar MN**, Baqai R, Lodi TZ, Ahmad S, Ahmed W, Qureshi H**,** Zuberi SJ, Jamal Q, Alam SM**.** Giardia lamblia in patients undergoing upper G.I. endoscopy. *J Pak Med Assoc* 1991; **41:** 74-75

10 **Abbas Z**, Qureshi AA, Sheikh H, Jafri SM, Khan AH. Peculiar histopathological features of giardiasis in distal duodenal biopsies. *J Pak Med Assoc* 1994; **44:** 206-209

11 **Shenoy S**, Urs S, Prabhu G, Mathew B, Antony G, Bharati B. Giardiasis in the adult population of Dakshina Kannada district of south India. *Trop Doct* 1998; **28:** 40-42

12 **Kori M**, Gladish V, Ziv-Sokolovskaya N, Huszar M, Beer-Gabel M, Reifen R. The significance of routine duodenal biopsies in pediatric patients undergoing upper intestinal endoscopy. *J Clin Gastroenterol* 2003; **37:** 39-41

13 **Farrar WE**. Giardiasis. In: Farrar WE, Wood MJ, eds. Atlas of Gastrointestinal and Hepatobiliary infections. London: Gower Medical Publishing, 1992: 62-65.

14 **Smith HV**. Intestinal protozoa. In: Gillespie SH, Hawkey PM, eds. Medical parasitology: a practical approach. Oxford: Oxford University Press, 1995: 79-118.

15 **Hopper AD**, Cross SS, McAlindon ME, Sanders DS. Symptomatic giardiasis without diarrhea: further evidence to support the routine duodenal biopsy? *Gastrointest Endosc* 2003; **58:** 120-122

16 **Hanson KL**, Cartwright CP. Use of an enzyme immunoassay does not eliminate the need to analyze multiple stool specimens for sensitive detection of *Giardia lamblia*. *J Clin Microbiol* 2001; **39:** 474-477

17 **Yardley JH**. Pathology of chronic gastritis and duodenitis. In: Goldman H, Appelman HD, Kaufman N, eds. Gastrointestinal Pathology. Washington DC: Williams and Wilkins, 1995: 69-143

18 **Carr MF Jr,** Ma J, Green PHR. *Giardia lamblia* in patients undergoing endoscopy: lack of evidence for a role in nonulcer dyspepsia. *Gastroenterology* 1988; **95:** 972-974

Science Editor Wang XL and Guo SY **Language Editor** Elsevier HK

PO Box 2345, Beijing 100023, China
www.wjgnet.com
wjg@wjgnet.com

ELSEVIER

World J Gastroenterol 2005;11(42):6671-6675
World Journal of Gastroenterology ISSN 1007-9327

• *BRIEF REPORTS* •

Plasma carnitine ester profile in adult celiac disease patients maintained on long-term gluten free diet

Judit Bene, Katalin Komlósi, Beáta Gasztonyi, Márk Juhász, Zsolt Tulassay, Béla Melegh

Judit Bene, Katalin Komlósi, Béla Melegh, Department of Medical Genetics and Child Development, School of Medicine, University of Pécs, Hungary
Judit Bene, MTA PTE Clinical Genetics Research Group of Hungarian Academy of Sciences at the University of Pécs, Hungary
Beáta Gasztonyi, 1st Department of Medicine, School of Medicine, University of Pécs, Hungary
Márk Juhász, Zsolt Tulassay, 2nd Department of Medicine, Semmelweis University, Budapest, Hungary
Supported by the grant of Hungarian Science Foundation OTKA T 35026, T 49589 and by the grant of Ministry of Health ETT 325/2003
Correspondence to: Dr. Béla Melegh, Professor of Medical Genetics and Pediatrics, Department of Medical Genetics and Child Development, University of Pécs, H-7624 Pécs, Szigeti 12., Hungary. bela.melegh@aok.pte.hu
Telephone: +36-72-536-427 Fax: +36-72-536-427
Received: 2005-01-12 Accepted: 2005-04-30

Abstract

AIM: To determine the fasting plasma carnitine ester in patients with celiac disease.

METHODS: We determined the fasting plasma carnitine ester profile using ESI triple quadrupol mass spectrometry in 33 adult patients with biopsy-confirmed maturity onset celiac disease maintained on long term gluten free diet.

RESULTS: The level of free carnitine did not differ as the celiac disease patients were compared with the healthy controls, whereas the acetylcarnitine level was markedly reduced (4.703 ± 0.205 *vs* 10.227 ± 0.368 nmol/mL, $P<0.01$). The level of propionylcarnitine was 61.5%, butyrylcarnitine 56.9%, hexanoylcarnitine 75%, octanoylcarnitine 71.1%, octenoylcarnitine 52.1%, decanoylcarnitine 73.1%, cecenoylcarnitine 58.3%, lauroylcarnitine 61.5%, miristoylcarnitine 66.7%, miristoleylcarnitine 62.5% and oleylcarnitine 81.1% in the celiac disease patients compared to the control values, respectively ($P<0.01$).

CONCLUSION: The marked decrease of circulating acetylcarnitine with 50-80 % decrease of 11 other carnitine esters shows that the carnitine ester metabolism can be influenced even in clinically asymptomatic and well being adult celiac disease patients, and gluten withdrawal alone does not necessarily normalize all elements of the disturbed carnitine homeostasis.

Key words: Plasma carnitine ester profile; Celiac disease

Bene J, Komlósi K, Gasztonyi B, Juhász M, Tulassay Zs, Melegh B. Plasma carnitine ester profile in adult celiac disease patients maintained on long-term gluten free diet. *World J Gastroenterol* 2005; 11(42): 6671-6675
http://www.wjgnet.com/1007-9327/11/6671.asp

INTRODUCTION

The adult celiac disease (CD) is a complex autoimmune type of gastrointestinal disorder which can be induced by gluten as a nutritional etiological factor in genetically susceptible persons[1,2]. Metabolism of lipids and lipoproteins is disturbed in the disease[3-7]. The therapy includes withdrawal of the alimentary gluten, introduction of the diet usually results in dramatic clinical improvement and normalization of numerous metabolic deteriorations[1-3]. However, in the case of certain nutriments the diet alone is not enough and supplementation is also necessary.

The primary biochemical function of carnitine is related to its ester-forming capability[8]. In addition to its involvement in ß-oxidation of the long-chain fatty acids, it can form ester with several medium- and short-chain endogenous or exogenous fatty acids[8,9]. In mammals, the body stores of carnitine have exogenous and endogenous origin[10,11]. Several lines of evidence suggest that in human carnitine should be considered as a vitamin-like compound, since the majority of the body stores are of exogenous origin[10,12,13]. The sites of absorption are located in the small intestine[14,15]. These considerations prompted us to obtain information on plasma carnitine esters in patients with CD using tandem mass spectrometry profiling.

MATERIALS AND METHODS

Patients

We examined 33 patients with classic form of celiac disease (9 males, 24 females, mean age: 32.2 ± 2.5 years) and 35 carefully selected clinically healthy age, sex, weight and height matched control subjects (22 males, 13 females, mean age: 31.0 ± 1.9 years; Table 1).

The diagnostic criteria of established CD in our patients included: verification of the specific histological features in small intestinal biopsy specimens, according to

Table 1 Selected clinical and laboratory parameters of patients with celiac disease and control subjects (means ± SE)

	Celiac disease patients $n = 33$		Controls $n = 35$
Females/males	24/9		13 / 22
	at diagnosis	*in current study*	
Age (yrs)	27.4 ± 3.0	32.2 ± 2.5	31.0 ± 1.9
Iron (μmol/L)	13.0 ± 1.5[a]	17.6±1.3[c]	23.1 ± 2.1
Hb (g/dL)	12.6 ± 0.4[a]	13.9±0.3[c]	15.8 ± 0.5
MCV (fL)	85.5 ± 1.7[a]	88.4±1.0[c]	94.3 ± 2.7
RDW (%)	15.7 ± 0.6	14.4±0.4	13.9 ± 0.5
BMI (kg/m^2)	20.0 ± 0.7[a]	22.8±0.6	23.1 ± 1.1

[a]$P < 0.05$ *vs* same group and controls at the time of the study. [c]$P < 0.05$ *vs* controls

the modified Marsh classification[16], positive serological results (antiendomysial antibody and tissue transglutaminase), unequivocally favorable clinical response to the administration of gluten free diet. Patients with any of the rare manifestations of the disease were excluded. All the CD patients were at least 17 years old upon diagnosis, and adhered to gluten free diet for at least one year. All patients received long-term oral iron replacement therapy. Exclusion criteria in both groups were as follows: secondary causes of intestinal atrophy, systemic diseases, any malformations, endocrine disorders, consumption of any drugs, evidence of intestinal bacterial infection, history or evidence for any inherited metabolic disease including those with impairment of glucose and lipid metabolism, smoking, hepatic or renal disease, and pregnancy.

The clinical and laboratory data from the time of diagnosis were from the records of the patients, while the actual results of the current study were from measurements performed from sample aliquots of a blood collection done after an overnight fast precisely between 8:00 and 8:30 AM, both in the celiac disease patients and in the healthy control subjects. This strict postailmental time scheduling was introduced to prevent the diet or fasting time induced dynamic changes of carnitine esters in the circulation[17].

Informed consent was obtained from each participant of the study and the study design was approved by the departmental ethics committee.

Methods

Plasma calcium, iron and albumin levels were determined by routine methods. The blood pictures, including hemoglobin (Hb), mean corpuscular volume (MCV), red blood cell distribution width (RDW) were measured by automated analysis (SYSMEX XE 2100, Japan). The body mass index (BMI) was calculated as body weight/height^2 (in kilograms/m^2).

Acylcarnitines were analyzed as butyl esters using a Micromass Quattro Ultima ESI triple-quadrupole mass spectrometer, combined with a Waters 2795 HPLC system for sample introduction. The procedure was a modified method described previously by Vreken *et al*.[18]. Essentially, 10 μL plasma was first spotted and dried onto a filter paper, then the plasma dot was excised and the excised piece was placed into an Eppendorf tube. Then 200 μL of methanolic stock solution of internal deuterated standards (containing 0.76 μmol/L [^{2}H$_3$]-free carnitine, 0.04 μmol/L [^{2}H$_3$]-propionylcarnitine, 0.04 μmol/L [^{2}H$_3$]-octanoylcarnitine and 0.08 μmol/L [^{2}H$_3$]-palmitoylcarnitine) was added. After 20 min of agitation the supernatant was dried under nitrogen at 40 °C. Derivatization was carried out at 65 °C for 15 min with an addition of 100 μL 3mol/L butanolic HCl. The resulting mixtures were dried again under nitrogen at 40 °C and redissolved in 100 μL mobile phase (acetonitrile:water 80:20). With the help of the autosampler 10 μL of sample aliquots was injected into the mass spectrometer. During the ESI-MS/MS analysis free carnitine and acylcarnitines were measured by positive precursor ion scan of m/z 85, with a scan range of m/z: 200-550. The applied capillary voltage, cone voltage and collision energy were 2.52 kV, 55 V and 26 eV, respectively. The flow rate was 100 μL/min and the total analysis time was 4 min per sample. For each sample the measurements were performed in triplicates beginning with the injection step and the means of the three determinations were used for further calculations.

For statistics Student's t test for unpaired samples was used. The values were expressed as means ± SE, in three decimals for the carnitine esters with respect to the low levels of the long-chain carnitine esters.

RESULTS

Major clinical and laboratory parameters, including those regarded generally as activity markers of CD[19-23] are shown in Table 1. The levels of plasma iron and Hb, and the value of MCV and BMI determined at the time of diagnosis were significantly lower in patients with CD as compared either to the values of the CD patients in the present study, or to the control subjects. In the current study all the previous parameters increased compared with the initial values, but decreased for the plasma iron, Hb and MCV (Table 1).

The plasma circulating carnitine ester profiles are shown in Table 2. The plasma level of free carnitine did not differ between CD patients and controls. By contrast, a marked decrease was found in the acetylcarnitine level in CD patients, which corresponded to 46% of the control value. A significant decrease was also found in the levels of propionyl- (61.5%), butyryl- (56.9%), hexanoyl- (75%), octanoyl- (71.1%), octenoyl- (52.1%), decanoyl- (73.1%) cecenoyl- (58.3%), lauroyl- (61.5%), miristoyl- (66.7%), miristoleyl- (62.5%) and oleylcarnitine (81.1%) in the CD patients as compared with the controls (the rates of decrease are expressed throughout as percent in parentheses taking the controls as 100%).

As a result of the decrease of individual carnitine esters, the plasma level of total esters was lower in CD patients than in controls (6.087 ± 0.571 *vs* 12.166 ± 0.978, $P<0.001$). The ratio of acetylcarnitine/total carnitine esters was 0.773 in the patients and was 0.841 in the controls.

DISCUSSION

We found a marked decrease in acetylcarnitine concentration and a significant decrease in the level of 11 further carnitine esters in plasma of CD patients on long-term gluten free diet. The pattern of the carnitine ester profile found in our patients differs from that found during fasting[17] and differs from the features seen in any of the known metabolic diseases[18,24,25]. The changes observed in the present study could be the result of impaired carnitine homeostasis, consequence of influenced metabolism of the acyl groups derived mainly from the fatty acid metabolism, and combination of thereof.

Damage of the intestinal mucosa can play a central role in the events leading to the changes observed in the current work. Majority of the carnitine reserves are derived from alimentary sources[26,27], the site of the absorption is located in the small intestines[14,15]. The epithelial cells are actively involved in the carnitine- and carnitine ester: contain different carnitine acyltransferases[8] such as the OCTN2 carnitine transporter[28] and the first three enzymes of the mammalian carnitine biosynthesis[29]: trimethyllysine hydroxylase, EC 1.14.11.8; hydroxytrimethyllysine aldolase, EC 4.1.2.'X'; and trimethylaminobutyraldehyde dehydrogenase, EC 1.2.1.47. On the other hand, the mucosa in the small intestine participates in the absorption of triglycerides and plays a complex role in the metabolism of lipoproteins, including chylomicrons, very-low-density lipoproteins, high-density lipoproteins and various apolipoproteins[30-34]. The mucosal damage in CD is classically known to cause fat malabsorption[1,2]. Untreated patients with the classic form of celiac disease may be malnourished and have impaired dietary substrate utilization, including impairment of the metabolism of fats and lipoproteins. It should be noted, that the long-term gluten free diet leads to improvement of several parameters of lipid metabolism[3]. However, the recovery is not necessarily complete for a number of metabolites of lipid metabolism[35,36].

Paradoxically, though the knowledge is growing on the circulating carnitine ester profile features in various disease conditions, very little is known about its normal regulation. Carnitine releases into the circulation by the liver primarily as acetylcarnitine[37] and the actual ester pattern is a result of the uptake/release action of the peripheral tissues. In the present study mainly the short-chain and medium chain carnitine esters were affected. Except for the propionylcarnitine, which can be also derived from the catabolism of amino acids methionine, valine and isoleucine, these acyl groups are mainly degradation products of the longer chain fatty acid oxidation[17], altered profile of the esters found in our asymptomatic patients likely reflects the still affected fatty acid metabolism.

Lipid and lipoprotein metabolism has been extensively investigated in CD, but carnitine homeostasis has hardly been studied. In 1994, Lerner *et al*.[38] investigated the carnitine concentrations in sera of pediatric CD subjects, and found that the total serum carnitine concentration is decreased in patients with active disease as compared with

Table 2 Plasma carnitine ester profiles in celiac disease patients and controls (mean±SE, μmol/L)

	Patients $n = 33$	Controls $n = 35$
Free carnitine (C0)	27.191 ± 1.194	30.029 ± 1.902
Short-chain acylcarnitines		
Acetylcarnitine (C2)	4.703 ± 0.205[b]	10.227 ± 0.368
Propionylcarnitine (C3)	0.247 ± 0.014[b]	0.400 ± 0.021
Butyrylcarnitine (C4)	0.152 ± 0.011[b]	0.267 ± 0.013
Isovalerylcarnitine (C5)	0.111 ± 0.010	0.138 ± 0.010
Tiglylcarnitine (C5:1)	0.034 ± 0.002	0.033 ± 0.003
Medium-chain acylcarnitines		
Hexanoylcarnitine (C6)	0.060 ± 0.004[b]	0.080 ± 0.006
Octanoylcarnitine (C8)	0.086 ± 0.006[b]	0.121 ± 0.009
Octenoylcarnitine (C8:1)	0.037 ± 0.003[b]	0.071 ± 0.008
Decanoylcarnitine (C10)	0.103 ± 0.008[b]	0.141 ± 0.009
Cecenoylcarnitine (C10:1)	0.063 ± 0.005[b]	0.108 ± 0.010
Lauroylcarnitine (C12)	0.032 ± 0.002[b]	0.052 ± 0.004
Long-chain acylcarnitines		
Myristoylcarnitine (C14)	0.016 ± 0.001[b]	0.024 ± 0.001
Myristoleylcarnitine (C14:1)	0.025 ± 0.002[b]	0.040 ± 0.004
Palmitoylcarnitine (C16)	0.097 ± 0.006	0.113 ± 0.006
Palmitoleylcarnitine (C16:1)	0.037 ± 0.003	0.032 ± 0.002
Stearoylcarnitine (C18)	0.076 ± 0.004	0.080 ± 0.004
Oleylcarnitine (C18:1)	0.137 ± 0.007[b]	0.169 ± 0.008
Hydroxymyristoylcarnitine (C14OH)	0.007 ± 0.001	0.005 ± 0.001
Hydroxypalmitoylcarnitine (C16OH)	0.022 ± 0.001	0.023 ± 0.002
Hydroxypalmitoleylcarnitine (C16:1OH)	0.026 ± 0.002	0.029 ± 0.002
Hydroxyoleylcarnitine (C18:1OH)	0.016 ± 0.002	0.013 ± 0.002

[b]$P < 0.01$ *vs* controls

normal subjects, while it was unchanged in CD patients with gluten withdrawal - associated non-active disease[38]. The decrease of carnitine reserves in active disease is likely secondary to the mucosal injury associated damage of the absorption. Albeit similar study on adult subjects is not presented in the literature, after this single pediatric paper the possible development of carnitine deficiency in untreated CD has become widely accepted[39].

In our patients the decrease of total carnitine esters could also reflect shortening of the reserves. It is known that even in patients strictly adhering to a gluten free diet the recovering mucosa can exhibit functional limitations. Therefore, carnitine absorption can be influenced on the one side. On the other side, the mucosa also participates in the trimethyllysine-butyrobetaine conversion, since the first three enzymes of the carnitine biosynthesis are expressed in it[29]. Residual damage can influence this procedure. In addition, trymethyllysine hydroxylase requires Fe^{2+} ion as cofactor[11]. Our patients had improvement after iron replacement therapy, but their plasma iron, Hb and MCV remained decreased. This phenomenon is common in the disease[22]. The decreased tissue iron reserves can also theoretically act on the enzyme activity.

In the recent years there has been increasing recognition that besides the classical major presentations of CD with a malabsorption syndrome and a flat jejunal mucosa, a broad spectrum of metabolic alterations can associate primarily or secondarily with the disease[40,41]. Some of them can be theoretically an early hallmark and predisposing factor for a clinical symptom manifested at a later stage of CD. Inhibition of oxidative metabolism of fatty acids, leading to myopathy with hypotonia and hyporeflexia, hypoglycemia, cardiomyopathy, encephalopathy and disturbed liver function, which are also among the rare extraintestinal manifestation of CD, may be results of carnitine insufficiency[42]. Whether supplementation of carnitine has rationale in the treatment of the disease similar to other metabolic nutriments used routinely in clinical practice[43] remains to be elucidated.

ACKNOWLEDGMENTS

The authors are grateful to Tamás Zágoni, Miklós Tóth and Ilona Szántó for their help in the management of the study.

REFERENCES

1 **Green PH**, Jabri B. Coeliac disease. *Lancet* 2003; **362**: 383-391
2 **Shamir R**. Advances in celiac disease. *Gastroenterol Clin North Am* 2003; **32**: 931-947
3 **Capristo E**, Addolorato G, Mingrone G, De Gaetano A, Greco AV, Tataranni PA, Gasbarrini G. Changes in body composition, substrate oxidation, and resting metabolic rate in adult celiac disease patients after a 1-y gluten-free diet treatment. *Am J Clin Nutr* 2000; **72**: 76-81
4 **Capristo E**, Addolorato G, Mingrone G, Scarfone A, Greco AV, Gasbarrini G. Low-serum high-density lipoprotein-cholesterol concentration as a sign of celiac disease. *Am J Gastroenterol* 2000; **95**: 3331-3332
5 **Vuoristo M**, Kesaniemi YA, Gylling H, Miettinen TA. Metabolism of cholesterol and apolipoprotein B in celiac disease. *Metabolism* 1993; **42**: 1386-1391
6 **Ciampolini M**, Bini S. Serum lipids in celiac children. *J Pediatr Gastroenterol Nutr* 1991; **12**: 459-460
7 **Rosenthal E**, Hoffman R, Aviram M, Benderly A, Erde P, Brook JG. Serum lipoprotein profile in children with celiac disease. *J Pediatr Gastroenterol Nutr* 1990; **11**: 58-62
8 **Bieber LL**. Carnitine. *Annu Rev Biochem* 1988; **57**: 261-283
9 **Melegh B**, Kerner J, Bieber LL. Pivampicillin-promoted excretion of pivaloylcarnitine in humans. *Biochem Pharmacol* 1987; **36**: 3405-3409
10 **Kerner J**, Hoppel C. Genetic disorders of carnitine metabolism and their nutritional management. *Annu Rev Nutr* 1998; **18**: 179-206
11 **Vaz FM**, Wanders RJ. Carnitine biosynthesis in mammals. *Biochem J* 2002; **361**: 417-429
12 **Melegh B**, Hermann R, Bock I. Generation of hydroxytrimethyllysine from trimethyllysine limits the carnitine biosynthesis in premature infants. *Acta Paediatr* 1996; **85**: 345-350
13 **Vaz FM**, Melegh B, Bene J, Cuebas D, Gage DA, Bootsma A, Vreken P, van Gennip AH, Bieber LL, Wanders RJ. Analysis of carnitine biosynthesis metabolites in urine by HPLC-electrospray tandem mass spectrometry. *Clin Chem* 2002; **48**: 826-834
14 **Hamilton JW**, Li BU, Shug AL, Olsen WA. Carnitine transport in human intestinal biopsy specimens. Demonstration of an active transport system. *Gastroenterology* 1986; **91**: 10-16
15 **McCloud E**, Ma TY, Grant KE, Mathis RK, Said HM. Uptake of L-carnitine by a human intestinal epithelial cell line, Caco-2. *Gastroenterology* 1996; **111**: 1534-1540
16 **Oberhuber G**, Granditsch G, Vogelsang H. The histopathology of coeliac disease: time for a standardized report scheme for pathologists. *Eur J Gastroenterol Hepatol* 1999; **11**: 1185-1194
17 **Costa CC**, de Almeida IT, Jakobs C, Poll-The BT, Duran M. Dynamic changes of plasma acylcarnitine levels induced by fasting and sunflower oil challenge test in children. *Pediatr Res* 1999; **46**: 440-444
18 **Vreken P**, van Lint AE, Bootsma AH, Overmars H, Wanders RJ, van Gennip AH. Quantitative plasma acylcarnitine analysis using electrospray tandem mass spectrometry for the diagnosis of organic acidaemias and fatty acid oxidation defects. *J Inherit Metab Dis* 1999; **22**: 302-306
19 **Stahlberg MR**, Savilahti E, Siimes MA. Iron deficiency in coeliac disease is mild and it is detected and corrected by gluten-free diet. *Acta Paediatr Scand* 1991; **80**: 190-193
20 **Sategna Guidetti C**, Scaglione N, Martini S. Red cell distribution width as a marker of coeliac disease: a prospective study. *Eur J Gastroenterol Hepatol* 2002; **14**: 177-181
21 **Dickey W**, Bodkin S. Prospective study of body mass index in patients with coeliac disease. *BMJ* 1998; **317**: 1290
22 **Mody RJ**, Brown PI, Wechsler DS. Refractory iron deficiency anemia as the primary clinical manifestation of celiac disease. *J Pediatr Hematol Oncol* 2003; **25**: 169-172
23 **Hjelt K**, Krasilnikoff PA. The impact of gluten on haematological status, dietary intakes of haemopoietic nutrients and vitamin B12 and folic acid absorption in children with coeliac disease. *Acta Paediatr Scand* 1990; **79**: 911-919
24 **Chace DH**, Kalas TA, Naylor EW. Use of tandem mass spectrometry for multianalyte screening of dried blood specimens from newborns. *Clin Chem* 2003; **49**: 1797-1817
25 **Schulze A**, Lindner M, Kohlmuller D, Olgemoller K, Mayatepek E, Hoffmann GF. Expanded newborn screening for inborn errors of metabolism by electrospray ionization-tandem mass spectrometry: results, outcome, and implications. *Pediatrics* 2003; **111**: 1399-1406
26 **Li B**, Lloyd ML, Gudjonsson H, Shug AL, Olsen WA. The effect of enteral carnitine administration in humans. *Am J Clin Nutr* 1992; **55**: 838-845
27 **Baker H**, Frank O, DeAngelis B, Baker ER. Absorption and excretion of L-carnitine during single or multiple dosings in

humans. *Int J Vitam Nutr Res* 1993; **63**: 22-26
28 **Tamai I**, Ohashi R, Nezu J, Yabuuchi H, Oku A, Shimane M, Sai Y, Tsuji A. Molecular and functional identification of sodium ion-dependent, high affinity human carnitine transporter OCTN2. *J Biol Chem* 1998; **273**: 20378-20382
29 **Zaspel BJ**, Sheridan KJ, Henderson LM. Transport and metabolism of carnitine precursors in various organs of the rat. *Biochim Biophys Acta* 1980; **631**: 192-202
30 **Green PH**, Glickman RM. Intestinal lipoprotein metabolism. *J Lipid Res* 1981; **22**: 1153-1173
31 **Field FJ**, Mathur SN. Intestinal lipoprotein synthesis and secretion. *Prog Lipid Res* 1995; **34**: 185-198
32 **Cartwright IJ**, Higgins JA. Molecular and intracellular events in the assembly and secretion of chylomicrons by enterocytes. *Biochem Soc Trans* 1998; **26**: 211-216
33 **Raybould HE**. Nutrient tasting and signaling mechanisms in the gut. I. Sensing of lipid by the intestinal mucosa. *Am J Physiol* 1999; **277**: G751-G755
34 **Tso P**, Nauli A, Lo CM. Enterocyte fatty acid uptake and intestinal fatty acid-binding protein. *Biochem Soc Trans* 2004; **32**: 75-78
35 **Mediene S**, Hakem S, Bard JM, Medjaoui I, Benhamamouch S, Lebel P, Fruchart JC, Clavey V. Serum lipoprotein profile in Algerian patients with celiac disease. *Clin Chim Acta* 1995; **235**: 189-196
36 **Pillan MN**, Spandrio S, Sleiman I, Meini A, Scalvini T, Balestrieri GP. Effects of a gluten-free diet on serum lipids and lipoprotein (a) levels in a group of patients with celiac disease. *J Pediatr Gastroenterol Nutr* 1994; **18**: 183-185
37 **Sandor A**, Kispal G, Melegh B, Alkonyi I. Ester composition of carnitine in the perfusate of liver and in the plasma of donor rats. *Eur J Biochem* 1987; **170**: 443-445
38 **Lerner A**, Gruener N, Iancu TC. Serum carnitine concentrations in coeliac disease. *Gut* 1993; **34**: 933-935
39 **Fitzgerald JF**, Troncone R, Roggero P, Pozzi E, Garavaglia B, Parini R, Carissimi E, Santus F, Piemontese P, Cataliotti E, Mosca F, Carnelli V. Clinical quiz. Secondary carnitine deficiency due to celiac disease. *J Pediatr Gastroenterol Nutr* 2003; 36: **636**, 646
40 **Hardoff D**, Sharf B, Berger A. Myopathy as a presentation of coeliac disease. *Dev Med Child Neurol* 1980; **22**: 781-783
41 **Rossi T**. Celiac disease. *Adolesc Med Clin* 2004; **15**: 91-103
42 **Hoppel C**. The role of carnitine in normal and altered fatty acid metabolism. *Am J Kidney Dis* 2003; **41**: S4-12
43 **Abdulkarim AS**, Murray JA. Review article: The diagnosis of coeliac disease. *Aliment Pharmacol Ther* 2003; **17**: 987-995

Science Editor Wang XL and Guo SY **Language Editor** Elsevier HK

PO Box 2345, Beijing 100023, China
www.wjgnet.com
wjg@wjgnet.com

ELSEVIER

World J Gastroenterol 2005;11(42):6676-6680
World Journal of Gastroenterology ISSN 1007-9327

• *BRIEF REPORTS* •

Investigation of fundo-antral reflex in human beings

Satish SC Rao, Anjana Kumar, Brent Harris, Bruce Brown, Konrad S Schulze

Satish SC Rao, Anjana Kumar, Brent Harris, Bruce Brown, Konrad S Schulze, Department of Internal Medicine, University of Iowa Carver College of Medicine, Iowa City, Iowa, United States
Supported in part by an American College of Gastroenterology Clinical Research Grant, RR00059 and by General Clinical Research Centers Program, R01DK57100-03, National Institutes of Health
Correspondence to: Satish SC Rao, MD, PhD, FRCP, Department of Internal Medicine, University of Iowa Hospitals and Clinics, 200 Hawkins Drive, 4612 JCP, Iowa City 52242, Iowa, United States. satish-rao@uiowa.edu
Telephone: +1-319-353-6602 Fax: +1-319-353-6399
Received: 2005-03-12 Accepted: 2005-04-09

Abstract

AIM: To examine the sensory and motor response(s) of the stomach following fundic distention and to assess whether cholinergic mechanisms influence these responses.

METHODS: Fundic tone, gastric sensory responses and antral motility were evaluated in eight healthy volunteers after a probe with two sensors was placed in the antrum and a highly compliant balloon in the fundus. Isobaric balloon distentions were performed with a barostat. Study was repeated in six volunteers after intravenous atropine was given.

RESULTS: Fundic distention induced large amplitude antral contractions in all subjects. The area under the curve was higher ($P<0.05$) during fundic distention. First sensation was reported at 12±4 mmHg, moderate sensation at 18±4 mmHg and discomfort at 21±4 mmHg. Discomfort was associated with a decrease in antral motility. After atropine was given, the area under the curve of pressure waves and fundic tone decreased ($P<0.05$). Sensory thresholds were not affected.

CONCLUSIONS: Fundic balloon distention induces an antral motor response, the fundo-antral reflex, which in part may be mediated by cholinergic mechanisms.

Key words: Gastric motility; Reflex; Fundo-antral reflex; Sensation

Rao S SC, Kumar A, Harris B, Brown B, Schulze KS. Investigation of fundo-antral reflex in human beings. *World J Gastroenterol* 2005; 11(42): 6676-6680

http://www.wjgnet.com/1007-9327/11/.asp

INTRODUCTION

The stomach performs several important functions. It subserves the function of accommodation and thereby acts as a storage organ. It also functions as a grinder that triturates food into smaller particles and as a pump that transports chyme into the small bowel in a controlled fashion[1]. These functions depend on a complex mix of neurohumoral mechanisms, visceral sensation, intrinsic reflexes, intragastric transport, nutrient composition, particulate size, and the coordinated motor activity of the gastroduodenal unit[2,3].

In ferrets, distension of the corpus produces phasic activity in the antrum, a response termed as excitatory corporo-antral reflex. This is probably mediated by cholinergic mechanisms and intramural gastric pathways[4,5]. Intramural excitatory and inhibitory reflexes have also been demonstrated in isolated gastric preparations[6–9]. Recent studies have suggested that balloon distention of the stomach may increase phasic activity in the antrum and duodenum[10,11]. Whether this phasic activity represents an intrinsic gastro-gastric reflex has not been well characterized.

Furthermore, previous studies have assessed some of the individual components of gastric function[12,13]; whereas an integrated assessment of the biomechanical and sensory properties of the stomach has been scarcely performed. Also, there is very little information regarding the integrated role of the stomach as a sensory, motor and reflex organ. Our hypothesis is that fundic balloon distention may induce reflex antral pressure activity and this response may be mediated by cholinergic mechanisms.

Our objectives were to examine the antral motor responses during step-wise balloon distentions of the fundus, to simultaneously assess the sensory and tone responses of the stomach and to examine if the sensory and motor effects were mediated by cholinergic mechanisms.

METHODS

Study population

Eight healthy volunteers (m/f = 4/4) were recruited for this study. Their mean age was 32±4.95 years. None of them had a history of gastrointestinal or systemic ailments and none was using any medications. All had a normal physical examination. All participants gave written

informed consent and the study protocol was approved by the Human Investigation Review Board of the University of Iowa College of Medicine.

Manometry and barostat assembly

A double lumen plastic-probe (6 mm in diameter) containing a 10 cm long, highly-compliant balloon was used (MUI Scientific; Toronto, ON, Canada). The capacity of the balloon was 600 mL. The balloon was connected to a barostat (GMB Distender II; G&J Electronics Inc., Toronto, Canada). The probe had two perfusion side holes, 5 and 8 cm from the distal end of the balloon. These holes were perfused with gas-free distilled water at a rate of 0.2 mL/min (15 psi) using a low-compliance pneumohydraulic perfusion system (Arndorfer Medical Specialties, Inc., Milwaukee, WI, USA) that connected to transducers (Medex Inc.; MX860-G8618, Hilliard, OH, USA). Intraluminal pressures were relayed to an analog data recorder/amplifier (Medtronics Polygraph, Medtronics Functional Diagnostics; MN, USA) and displayed on a computer monitor using a software program (Polygram for Windows; Synectics Medical AB). The balloon volume and pressure data from the barostat were fed to the polygraph via an interface (Golden Gate; G&J Electronics Inc.).

Thus, the computer display consisted of the intragastric balloon volume, intra-balloon pressure as well as the intraluminal pressure changes in the antrum. The manometric data and the ultrasound images were simultaneously fed into a digital splitter (American Dynamics Ao1479, Orangeburg, NY, USA).

The ultrasonographic image of the cross-sectional diameter of the gastric antrum allowed visualization of antral contractions and assurance that the probe was properly positioned (Acuson 128XP with a 3 mHz sector transducer). The digital splitter synchronized the two images and displayed these images on a monitor screen (VM-17; Javelin, Los Angeles, CA, USA) such that one half of the screen showed the combined manometry and barostat recording and the other half displayed the ultrasound image. These images were recorded on a VHS tape for future analysis.

Study protocol

After an overnight fast, the oropharynx was sprayed with a local anesthetic, pontocaine (Abbott Laboratories, North Chicago, IL, USA). Then the probe with the balloon was placed through the mouth into the stomach. The volunteers were asked to sit in a semi-recumbent position, such that the head end was elevated by 45°. The balloon was distended with 250 mL of air and the probe was slowly retracted until a "tug" was felt signaling that the proximal end of the balloon was located in the fundus. Subsequently, ultrasound images were obtained to check the probe location. The location of pressure sensors in the antrum was also confirmed by the occurrence of typical antral motor pattern consisting of 3-cycle/min activity. The balloon was deflated and the probe was anchored to the cheek with a tape.

After a rest period of 15 min, the balloon was distended by 1 mmHg increments to assess the minimum distending pressure, a pressure at which diaphragmatic oscillations are clearly visible[14]. The intraoperating pressure (IOP) was set at a value of 2 mmHg above the minimum distending pressure using previous criteria[9-11]. Subsequently, a baseline recording of intragastric tone was performed for a period of 20 min. Then isobaric balloon distentions were performed at 3 mmHg increments. Each distention was maintained for 8 min followed by a rest period of 8 min. Thirty seconds after each distention, the subject was asked to rate their sensation on a scale of 0-6 as published previously[14], 0 = no sensation, 1 = vague perception of mild sensation, 2 = definite perception of mild sensation, 3 = vague perception of moderate sensation, 4 = definite perception of moderate sensation, 5 = discomfort, and 6 = pain. If the subject reported discomfort at two incremental distentions or pain at any one distention, the balloon distentions were discontinued. Abdominal ultrasonography was performed intermittently to visualize the antral configuration and morphology. Blood pressure and heart rate were monitored throughout the study.

We administered intravenously 0.6 mg of atropine sulfate in six volunteers (4 m/2 f) after a rest period of 60 min. Five minutes after administration of atropine, the balloon distentions were repeated as described above. Ultrasound images were obtained once again to confirm the location of antral sensors.

Manometric responses

Manometric recordings from the two antral pressure sensors were analyzed visually and manually with the assistance of Polygram for Windows software (Synectics Medical AB). Pressure waves that were $\geqslant$8 mmHg and $\geqslant$3 s in duration were included in the analysis. Artifacts were identified and excluded. There was good quality pressure activity at both channels in approximately 50% of the recordings and therefore an average of the pressure activity at the two antral channels was used. In the rest of the recordings, the pressure activity was more prominent in one of the antral channels and this channel was used for data analysis. The maximum amplitude, duration and area under the curve of each wave were calculated. We also measured the time interval between balloon distention and the onset of the first antral pressure wave as well as the total number of propagating pressure waves in the antrum during each inflation and deflation periods. Propagating waves were defined as pressure waves, which migrated across the antral leads within 6 s of each other and were categorized as either antegrade or retrograde depending on which of the two leads they first appeared in. A similar analysis of the antral pressure waves was performed after atropine injection.

Barostat responses

Gastric tone was assessed by measuring the area under the curve of the gastric volume during isobaric balloon

distentions as previously described[15-17]. The tone changes during and after distention were compared. Likewise, the tone changes obtained during the baseline study were compared with those after atropine injection.

Visceral sensory responses

During intragastric balloon distention, the minimum distending pressure that induced the first perception (a sensation of fullness and discomfort) were calculated. Likewise the sensory responses obtained after administration of atropine were compared to those obtained during the baseline study.

Statistical analysis

The data were presented as mean±SE. The number of pressure waves in the antrum during and after each balloon distention as well as before and after atropine injection was compared using Student's *t*-test. The thresholds for sensory perception and the gastric tone changes before and after atropine injection were compared using ANOVA.

RESULTS

Effects of fundic distention on antral pressure activity

Fundic balloon distention induced antral pressure waves, typically with an amplitude of ⩾50 mmHg (Figure 1). Occasionally, the distention-induced pressure activity persisted for several seconds even after the balloon was deflated, but in most instances the pressure activity ceased after deflation. Incremental balloon distention was associated with a steady increase in antral motility of up to 15 mmHg, but thereafter and particularly at 18 mmHg pressure there was a decrease in antral motility (Figure 2). Interestingly, during successive deflation periods, there was a trend towards progressive decrease in the area under the curve of pressure waves possibly reflecting a recovery of muscle tone.

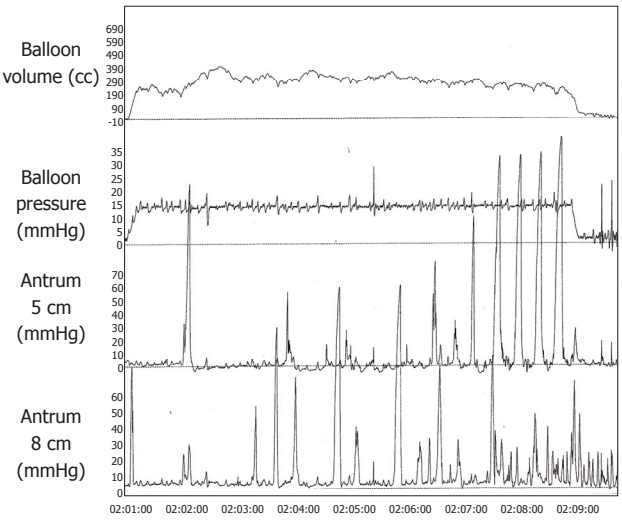

Figure 1 Typical example of the fundo-antral reflex. Channel 1: the fundic balloon volume; channel 2: the balloon pressure; channels 3 and 4: the pressure changes in the antrum.

The mean amplitude of antral pressure waves was also higher ($P<0.05$) during balloon distention than during balloon deflation. For example at balloon distending pressures of 6, 12, and 15 mmHg, the amplitudes were (inflation *vs* deflation) 60(11) *vs* 42(9), 70(14) *vs* 33(7), and 65(11) *vs* 23(7) mmHg respectively. The area under the curve (AUC) of the pressure waves was also significantly higher ($P<0.05$) during balloon distention (Figure 2A).

Visceral sensory responses

The subjects reported a first sensation at distending pressures ranging from 6 to 15 mmHg, a definite perception between 6 and 18 mmHg, a vague perception of moderate sensation between 11 and 21 mmHg, a definite sensation of moderate fullness between 12 and 24 mmHg and definite discomfort between 15 and 28 mmHg (Figure 2B).

Effects of atropine on gastric motor and sensory function

Visceral sensory responses The thresholds for first perception, fullness, and discomfort tended to be lower after administration of atropine but the difference was not significant (Figure 2C).

Antral pressure activity The area under the curve of pressure waves was significantly lower ($P<0.05$) after administration of atropine, particularly at balloon pressures of 6, 9, and 15 mmHg, but not at higher distending pressures (Figure 2D).

Fundic tone responses After administration of atropine, there was a significant increase ($P<0.05$) in balloon volume (Figure 2E) for the same corresponding level of intra balloon pressure, suggesting a decrease in fundic tone.

Cardiovascular responses The mean heart rate/min increased significantly ($P<0.05$) after administration of atropine during most of the distention except at 18 mmHg. There was no significant change in blood pressure.

DISCUSSION

We found that graded balloon distentions of the fundus induced antral pressure waves starting at thresholds that were not perceived by our healthy volunteers. This response was seen in all of our subjects. The area under the curve of pressure waves was significantly higher during the balloon inflation period than during the baseline period or the deflation period. Typically, the waves were ⩾50 mmHg in amplitude. Ultrasound images confirmed that these pressure events were often lumen-occluding contractions. The contractions began within a few seconds after balloon distention. These features suggest the existence of an excitatory gastro-gastric reflex in human beings, wherein distention of the fundus induces antral contractions. In a previous uncontrolled pilot study, we showed that fundic balloon distention may induce antral and duodenal phasic activity[10]. However, in the previous study, gastric visceral sensation or tone was not assessed and likewise the possible role of cholinergic mechanism(s) was not explored.

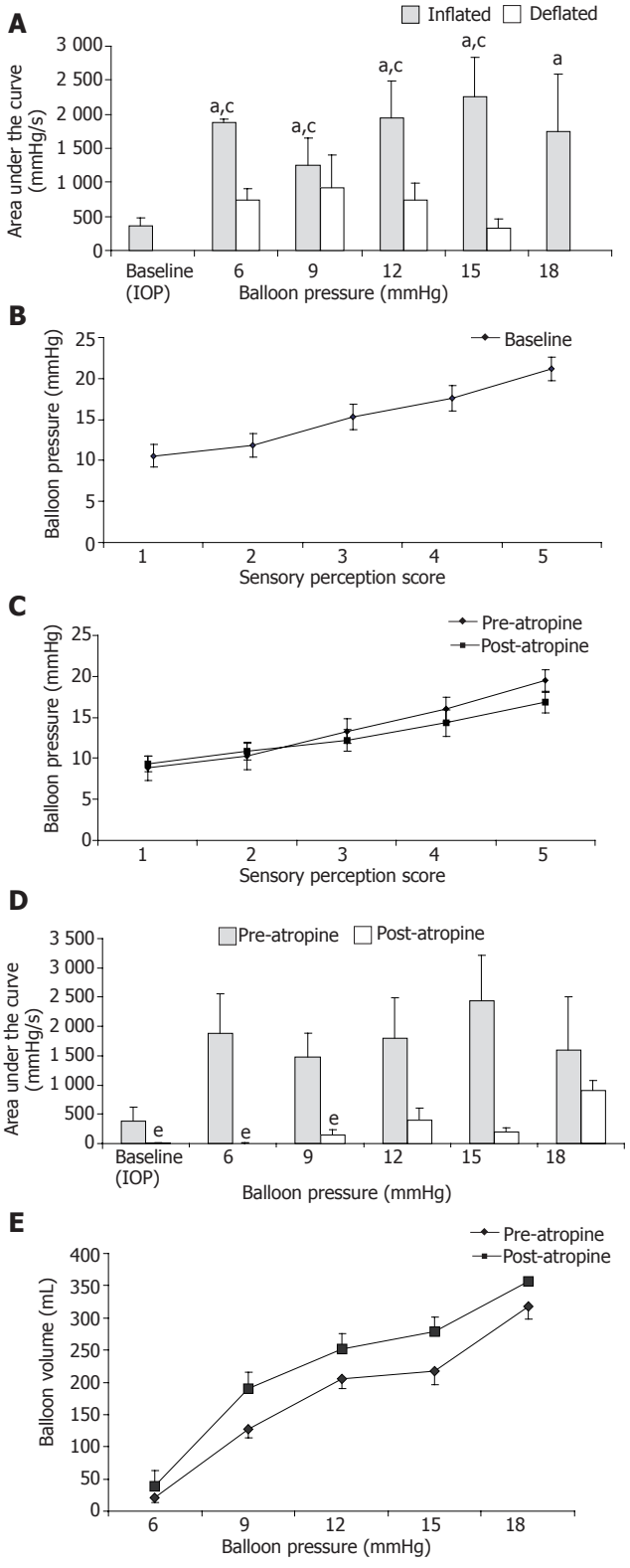

Figure 2 [a]*P*<0.05 inflation *vs* deflation. [c]*P*<0.05 baseline *vs* balloon inflation, [e]*P*<0.05 pre- *vs post*-atropine (**A-E**).

One of the limitations of our study is that we recorded motility from only two antral pressure sensors and it is possible that some of the antral activities may have been missed. However, the number of distention-induced contractions and the area under the curve of pressure waves gradually increased to a distending pressure of 15 mmHg, but thereafter their incidence declined, suggesting that there appears to be some correlation of antral motor responses with the visceral sensory responses. All of our subjects tolerated balloon distentions up to a pressure of 15 mmHg above IOP. Beyond this level of distention, some subjects reported discomfort or pain which was associated with a decrease in pressure activity. Thus, it appears that fundic distention at either subthreshold levels of perception or at thresholds that produce first sensation or fullness may induce reflex antral contractions, whereas higher distending pressures that induce discomfort or pain may cause an attenuation of this response.

After administration of atropine, there was a significant increase in heart rate and decrease in the resting gastric tone. Furthermore, the antral motor activity was also significantly attenuated, particularly at lower levels of balloon distention. At higher distending pressures ($\geqslant$12 mm Hg), some antral pressure activities were seen, though its incidence was lower than those observed before administration of atropine, suggesting that there is an adequate anti-cholinergic response and that the fundo-antral reflex may be partially mediated by cholinergic mechanisms[15]. However, we used a single dose of atropine and it is possible that over time there may have been a loss of anti-cholinergic effect. Also, there was no placebo arm, which is a limitation of this study. Nonetheless, these features suggest that either neuronal or drug-induced inhibition of cholinergic neurotransmission may partly affect gastric motor function. The sensory thresholds were either unchanged or somewhat decreased after administration of atropine, suggesting that gastric sensory responses may not be affected by cholinergic mechanisms, though the study was underpowered to assess this more completely.

Our study showed the possible existence of an intrinsic gastro-gastric reflex that can be induced by fundic distention. This response is different from the fundic relaxation that can be induced by antral distention[7,8] and appears to be partially mediated by cholinergic mechanisms and may in part be related to gastric sensation. Furthermore, unlike the Starling's Law which states that distention of an intestinal segment is associated with proximal contraction and distal relaxation, our result shows that in the human stomach, distention of the fundus is not necessarily associated with antral relaxation. Whether this response plays a role in the trituration of food or in the transport of gastric contents remains to be examined. Also, whether an attenuated or absent fundo-antral reflex plays a role in the pathogenesis of diabetic gastroparesis or functional dyspepsia remains to be explored.

REFERENCES

1 **Rao SSC**, Schulze-Delrieu K. The stomach, pylorus and duodenum. 2nd ed. London: Churchill Livingstone, 1993. 373-392
2 **Quigley EM**. Gastric and small intestinal motility in health and disease. *Gastroenterol Clin North Am* 1996; **25:** 113-145
3 **Malagelada JR**, Azpiroz F. Determinants of gastric emptying

and transit in the small intestine. Bethesda (Maryland): American Physiological Society, 1989: 909-937
4 **Andrews PL**, Grundy D, Scratcherd T. Reflex excitation of antral motility induced by gastric distension in the ferret. *J Physiol* 1980; **298:** 79-84
5 **Grundy D**, Hutson D, Scratcherd T. A permissive role for the vagus nerves in the genesis of antro-antral reflexes in the anaesthetized ferret. *J Physiol* 1986; **381:** 377-384
6 **Hennig GW**, Brookes SJ, Costa M. Excitatory and inhibitory motor reflexes in the isolated guinea-pig stomach. *J Physiol* 1997; **501:** 197-212
7 **Stadaas J**, Aune S, Haffner JF. Effects of proximal gastric vagotomy on intragastric pressure and adaptation in pigs. *Scand J Gastroenterol* 1974; **9;** 479-485
8 **Haffner JF**, Stadaas J. Pressure responses to cholinergic and adrenergic agents in the fundus, corpus, and antrum of isolated rabbit stomachs. *Acta Chir Scand* 1972; **138:** 713-719
9 **Leclere PG**, Lefebvre RA. Investigation of the interaction between cholinergic and nitrergic neurotransmission in the pig gastric fundus. *Br J Pharmacol* 1998; **125:** 1779-1787
10 **Rao SS**, Vemuri S, Harris B, Schulze K. Fundic balloon distension stimulates antral and duodenal motility in man. *Dig Dis Sci* 2002; **47:** 1015-1019
11 **Piessevaux H**, Tack J, Geubel A, Janssens J. Influence of fundic distension on fasting antro-duodenal manometric patterns in man. *Gastroenterology* 1998; **114:** G3374
12 **Tack J**, Piessevaux H, Coulie B, Caenepeel P, Janssens J. Role of impaired gastric accommodation to a meal in functional dyspepsia. *Gastroenterology* 1998; **115:** 1346-1352
13 **Camilleri M**, Malagelada JR. Abnormal intestinal motility in diabetics with the gastroparesis syndrome. *Eur J Clin Invest* 1984; **14:** 420-427
14 **Azpiroz F**, Malagelada JR. Perception and reflex relaxation of the stomach in response to gut distention. *Gastroenterology* 1990; **98:** 1193-1198
15 **Azpiroz F**, Malagelada JR. Gastric tone measured by an electronic barostat in health and postsurgical gastroparesis. *Gastroenterology* 1987; **92:** 934-943
16 **Sarnelli G**, Vos R, Cuomo R, Janssens J, Tack J. Reproducibility of gastric barostat studies in healthy controls and in dyspeptic patients. *Am J Gastroenterol* 2001; **96:** 1047-1053
17 **Lidums I**, Hebbard GS, Holloway RH. Effect of atropine on proximal gastric motor and sensory function in normal subjects. *Gut* 2000; **47:** 30-36

Science Editor Wang XL and Guo SY **Language Editor** Elsevier HK

PO Box 2345, Beijing 100023, China
www.wjgnet.com
wjg@wjgnet.com

ELSEVIER

World J Gastroenterol 2005;11(42):6681-6683
World Journal of Gastroenterology ISSN 1007-9327

• *BRIEF REPORTS* •

Validation of four *Helicobacter pylori* rapid blood tests in a multi-ethnic Asian population

Lee-Guan Lim, Khay-Guan Yeoh, Bow Ho, Seng-Gee Lim

Lee-Guan Lim, Khay-Guan Yeoh, Seng-Gee Lim, Department of Gastroenterology and Hepatology, National University Hospital, 5 Lower Kent Ridge Road, Singapore 119074, Republic of Singapore
Bow Ho, Department of Microbiology, National University of Singapore, Lower Kent Ridge Road, Singapore 119260, Republic of Singapore
Correspondence to: Associate Professor Khay-Guan Yeoh, Department of Gastroenterology and Hepatology, National University Hospital, 5 Lower Kent Ridge Road, Singapore 119074, Republic of Singapore. mdcykg@nus.edu.sg
Telephone: +65-67724353 Fax: +65-67794112
Received: 2005-01-19 Accepted: 2005-04-26

Abstract

AIM: To validate the accuracy of four rapid blood tests in the diagnosis of *Helicobacter pylori*.

METHODS: Consecutive dyspeptic patients scheduled for endoscopy at the National University Hospital, Singapore, were interviewed and had blood drawn for serology. The first 109 patients were tested with BM-test (BM), Pyloriset Screen (PS) and QuickVue (QV), and the next 99 subjects were tested with PS and Unigold (UG). Endoscopies were performed blinded to rapid blood test results and biopsies were taken for culture and rapid urease test. Urea breath tests were performed after endoscopies. The rapid blood test results were compared with four reference tests (rapid urease test, culture, serology, and breath test).

RESULTS: The study population composed of 208 patients (mean age 43.1 years; range 18-73 years; 119 males; 174 Chinese). The number of evaluable patients for BM, QV, UG and PS were 102, 102, 95, and 197, respectively. The sensitivity and specificity, respectively were: PS 80.2%, 95.8%; UG 55.9%, 100%; QV 43.3%, 100%; BM 67.2%, 97.1%.

CONCLUSION: The rapid blood test kits showed high specificity and positive predictive value (97-100%), while sensitivity and negative predictive value ranged widely (43%-80% and 47%-73%, respectively). Among test kits, PS showed the best sensitivity (80%), best negative predictive value (73%) and best negative likelihood ratio (0.207). PS had a specificity of 96%, positive predictive value of 97% and positive likelihood ratio of 19.1.

Key words: *Helicobacter pylori*; Rapid blood test

Lim LG, Yeoh KG, Ho B, Lim SG. Validation of four *Helicobacter pylori* rapid blood tests in a multi-ethnic Asian population. *World J Gastroenterol* 2005; 11(42): 6681-6683
http://www.wjgnet.com/1007-9327/11/6681.asp

INTRODUCTION

There are a variety of methods available for the detection of *Helicobacter pylori (H pylori)*, but many of these are invasive (such as biopsies for rapid urease test, culture, histology, and polymerase chain reaction) or require laboratories (such as urea breath test and serology). Recently, *H pylori* rapid test kits have become available. Rapid blood tests detect *H pylori* antibodies in whole or capillary blood, are easy to use, and yield results in a few minutes, making it a convenient point-of-care test for screening *H pylori*.

The 1997 Asia Pacific Consensus Conference on the management of *H pylori* infection[1] recommended that any blood test must be locally validated, with two or more alternative means of testing, before its widespread application.

Rapid blood test kits have not been widely validated in the Asian populations[2-5]. Local validation is important because the performance characteristics of blood test kits and population prevalence of *H pylori* vary in different populations. In Asian countries, the prevalence of *H pylori* infection is generally higher than in the developed Western nations (such as the United Kingdom, Australia, and France)[6]. In addition, the test performance of rapid blood kits may vary because local *H pylori* strains may be different[7,8].

Our prospective study aimed to validate four rapid blood test kits in the diagnosis of *H pylori* infection in a multi-ethnic Asian population. Amongst the Asian studies till date[2-5], none was conducted in a multi-ethnic population, and all were tested with less than four rapid blood test kits.

MATERIALS AND METHODS

Consecutive patients who were referred from general practice or outpatient clinics and scheduled for endoscopy for initial evaluation of dyspepsia at the National University Hospital, Singapore, were included for the

study. Exclusion criteria included patients with known peptic ulcer or gastric cancer, subjects with prior *H pylori* treatment, and those who had taken antibiotics, bismuth or proton pump inhibitors in the previous one month.

At entry, patients were interviewed using a standard questionnaire. Ten cubic centimeter of blood was drawn from each patient for serology. Each of the first 109 patients were tested with BM-test (BM, Boehringer Mannheim, East Essex, UK), QuickVue (QV, Quidel, CA, USA) and Pyloriset Screen (PS, Orion Diagnostica, Espoo, Finland). The kit with the best sensitivity was retained for continued testing in the next 99 patients together with an additional kit, Unigold (UG, Trinity Biotech, NY, USA). Endoscopy was then performed in the routine fashion by experienced endoscopists blinded to earlier results and three antral biopsy specimens were taken from each patient. Two biopsy specimens were sent for culture and one specimen was sent for the rapid urease test.

A ^{13}C urea breath test was performed directly after endoscopy. The technician doing the urea breath test was blinded to the results of the endoscopy. The results from the rapid blood test, rapid urease test, serology, culture, urea breath test and endoscopy were recorded on a standard data form.

The results of the rapid blood tests were compared with four reference tests: serology using HEL-p Test kit (AMRAD Operations Pty. Ltd, Australia), which had been validated locally[9], culture, rapid urease test, and urea breath test. *H pylori* infection was diagnosed, if any two reference tests were positive. If all the four reference tests were negative, it was assumed that infection was absent. Patients with a single positive test out of the four reference tests were classified as having indeterminate results.

Sample size was estimated based on reference tables[10]. Based on sensitivity of 80% and specificity of 90%, absolute precision of 0.10 and confidence interval of 95%, we needed a minimum of 62 *H pylori*-positive and 35 *H pylori*-negative patients.

The study was approved by the Research and Ethics Committee, National University Hospital, Singapore.

RESULTS

The characteristics of recruited patients are described in Table 1. One hundred and nine patients were tested with BM, QV, and PS (102 evaluable, 7 indeterminate results), and the next 99 subjects with PS and UG (95 evaluable, 4 indeterminate results).

Table 2 shows the sensitivity, specificity, predictive values and likelihood ratios of the respective rapid blood tests for *H pylori*. The rapid blood kits tested all showed specificities above 95% and very good positive predictive values exceeding 97%. There was a wide range in sensitivity between 43% and 80%, negative predictive value ranged from 48% to 73%, and negative likelihood ratios ranged from 0.207 to 0.567. PS had the best sensitivity of 80%, the best negative predictive value of 73%, and the best negative likelihood ratio of 0.207. PS had a high specificity of 96%, a good positive predictive value of 97.1% and a high positive likelihood ratio of 19.1.

Table 1 Characteristics of recruited patients

Kits used	PS, QV, BM	PS, UG	All
Number	109	99	208
Male:female	56:53	63:36	119:89
C:I:M:O[1]	91:12:4:2	83:7:6:3	174:19:10:5
Mean age (range)	44.7 (18–73)	41.3 (20–68)	43.1 (18–73)
H pylori positive	67	59	126
H pylori negative	35	36	71
Indeterminate results	7	4	11

[1]C = Chinese; I = Indian; M = Malay; O = Others.

Table 2 Sensitivity, specificity, predictive values, and likelihood ratios of rapid blood test for *H pylori* infection

Performance characteristics	BM	QV	UG	PS
Sensitivity (%)	67.2	43.3	55.9	80.2
Specificity (%)	97.1	99	99	95.8
Positive predictive value (%)	97.8	98	99	97.1
Negative predictive value (%)	60.7	47.9	58.1	73.1
Positive likelihood ratio	23.2	31.2	41.3	19.1
Negative likelihood ratio	0.338	0.567	0.441	0.207

DISCUSSION

Among the kits tested in our study, PS showed the best sensitivity (84%). Our study showed a wide range in the performance characteristics of the rapid tests. This may be attributable to the antigens used[11] or test kit designs.

The same rapid blood test kit might vary in performance between different populations. For example, QV's sensitivity for *H pylori* was 43.3% in our Singapore population, compared with 81% in Europe[12] and 82% in America[13]. These factors make it important that kits are locally tested and validated before use. A meta-analysis had shown that rapid tests are less accurate than reference tests, with sensitivity and specificity averaging 80-85% and 75-80%, respectively[14].

We conducted this study in an institution. For better evaluation of the potential of rapid blood test as a screening method in primary care, local studies conducted in general practice would be needed. Talley *et al.* reported that when used in general practice in Australia, rapid blood test had a sensitivity of 60% and specificity of 90%[15] Data on the performance characteristics of *H pylori* rapid blood test kits in general practice in the Asian population is lacking.

The Maastricht 2-2000 Consensus report[16] recommended a 'test and treat' approach in the primary care for *H pylori* infection. However, there is a strong association between *H pylori* infection and gastric cancer, especially in the Asian population, which has a high incidence of gastric cancer. Therefore, the use of 'test and treat' approach in Asians remains controversial and awaits further study. PS had a good sensitivity and specificity for the detection of *H pylori* infection, with the positive likelihood ratio of above 10, providing convincing diagnostic evidence, and negative likelihood ratio of 0.2, giving a strong diagnostic evidence. PS might therefore be potentially useful for 'test

and referral' strategy in general practice. Our study, which validated the point-of-care rapid blood test kits in a multi-ethnic Asian population, is an important step for future studies in this area.

In conclusion, there was a wide range in the performance characteristics of rapid blood test, making it important for the kits to be tested and validated locally before being used. Of the rapid blood kits tested, the best sensitivity for *H pylori* detection was 80% (PS). The validation of rapid blood test kits in the local population facilitates future studies on the 'test and treat' or 'test and referral' approach in the Asian population.

ACKNOWLEDGMENTS

We would like to thank Mrs Lim Thiew Peng who performed the *H pylori* serology and our research nurse Ms Lai Shuet Ting, for their kind assistance.

REFERENCES

1 **Lam SK**, Talley NJ. Report of the 1997 Asia Pacific Consensus Conference on the management of *Helicobacter pylori* infection. *J Gastroenterol Hepatol* 1998; **13:** 1-12

2 **Leung WK**, Chan FK, Falk MS, Suen R, Sung JJ. Comparison of two rapid whole-blood tests for *Helicobacter pylori* infection in Chinese patients. *J Clin Microbiol* 1998; **36:** 3441-3442

3 **Wong BC**, Wong W, Tang VS, Lai K, Yuen S, Hu WH, Chan C, Lau GK, Lai C, Lam S. An evaluation of whole blood testing for *Helicobacter pylori* infection in the Chinese population. *Aliment Pharmacol Ther* 2000; **14:** 331-335

4 **Chen TS**, Chang FY, Lee SD. No difference of accuracy between capillary and venous blood in rapid whole blood test for dia-gnosis of *Helicobacter pylori* infection. *Dig Dis Sci* 2002; **47:** 2519-2522

5 **Wong WM**, Lam SK, Xia HH, Tang VS, Lai KC, Hu WH, Chan CK, Cheung KL, Wong BC. Accuracy of a new near patient test for the diagnosis of *Helicobacter pylori* infection in Chinese. J *Gastroenterol Hepatol 2002*; **17:** 1272-1277

6 **Graham DY**. *Helicobacter pylori:* its epidemiology and its role in duodenal ulcer disease. *J Gastroenterol Hepatol* 1991; **6:** 105-113

7 **Hua J**, Ng HC, Yeoh KG, Ho KY, Ho B. Characterization of clinical isolates of *Helicobacter pylori* in Singapore. *Microbios* 1998; **94:** 71-81

8 **Hook-Nikanne J**, Perez-Perez GI, Blaser MJ. Antigenic characterization of Helicobacter pylori strains from different parts of the world. *Clin Diagn Lab Immunol* 1997; **4:** 592-597

9 **Kang JY**, Yeoh KG, Ho KY, Guan R, Lim TP, Quak SH, Wee A, Teo D, Ong YW. Racial differences in *Helicobacter pylori* seroprevalence in Singapore: correlation with differences in peptic ulcer frequency. *J Gastroenterol Hepatol* 1997; **12:** 655-659

10 **Browner WS**, Black D, Newman TB, Hulley SB. Estimating sample size and power. In: Hulley SB, Cummings SR, editors. Designing clinical research: an epidemiological approach. 1st ed. Williams and Wilkins, 1988: 139-150

11 **Feldman RA**, Evans SJ. Accuracy of diagnostic methods used for epidemiological studies of *Helicobacter pylori*. *Aliment Pharmacol Ther* 1995; **9** Suppl 2: 21-31

12 **Hawthorne AB**, Morgan S, Westmoreland D, Stenson R, Thomas GA, Newcombe RG. A comparison of two rapid whole blood tests and laboratory serology, in the diagnosis of *Helicobacter pylori* infection. *Eur J Gastroenterol Hepatol* 1999; **11:** 863-865

13 **Chey WD**, Murthy U, Shaw S, Zawadski A, Montague J, Linscheer W, Laine L. A comparison of three fingerprick, whole blood antibody tests for *Helicobacter pylori* infection: A United States, multicenter trial. *Am J Gastroenterol* 1999; **94:** 1512-1516

14 **Glupczynski Y**. Microbiological and serological diagnostic tests for Helicobacter pylori: an overview. *Br Med Bull* 1998; **54:** 175-186

15 **Talley NJ**, Lambert JR, Howell S, Xia HH, Lin SK, Agreus L. An evaluation of whole blood testing for *Helicobacter pylori* in general practice. *Aliment Pharmacol Ther* 1998; **12:** 641-645

16 **Malfertheiner P**, Megraud F, O'Morain C, Hungin AP, Jones R, Axon A, Graham DY, Tytgat G. Current concepts in the management of Helicobacter pylori infection--the Maastricht 2-2000 Consensus Report. *Aliment Pharmacol Ther* 2002; **16:** 167-180

Science Editor Guo SY **Language Editor** Elsevier HK

PO Box 2345, Beijing 100023, China
www.wjgnet.com
wjg@wjgnet.com

ELSEVIER

World J Gastroenterol 2005;11(42):6684-6688
World Journal of Gastroenterology ISSN 1007-9327

• *BRIEF REPORTS* •

Hepatoprotective effects of *Nigella sativa* L and *Urtica dioica* L on lipid peroxidation, antioxidant enzyme systems and liver enzymes in carbon tetrachloride-treated rats

Mehmet Kanter, Omer Coskun, Mustafa Budancamanak

Mehmet Kanter, Omer Coskun, Department of Histology and Embryology, Faculty of Medicine, Trakya University, Edirne, Turkey
Mustafa Budancamanak, Department of Rheumatology, Faculty of Medicine, Yuzuncu Yil University, Van, Turkey
Correspondes to: Dr. Mehmet Kanter, Department of Histology and Embryology, Faculty of Medicine, Trakya University, Edirne, Turkey. mehmetkanter65@hotmail.com
Telephone: +90-284-2357641 Fax: +90-284-2352730
Received: 2004-07-23 Accepted: 2004-09-27

Abstract

AIM: To investigate the effects of *Nigella sativa* L (NS) and *Urtica dioica* L (UD) on lipid peroxidation, antioxidant enzyme systems and liver enzymes in CCl_4-treated rats.

METHODS: Fifty-six healthy male Wistar albino rats were used in this study. The rats were randomly allotted into one of the four experimental groups: A (CCl_4-only treated), B (CCl_4+UD treated), C (CCl_4+NS treated) and D (CCl_4+UD+NS treated), each containing 14 animals. All groups received CCl_4 (0.8 mL/kg of body weight, sc, twice a week for 60 d). In addition, B, C and D groups also received daily i.p. injections of 0.2 mL/kg NS or/and 2 mL/kg UD oils for 60 d. Group A, on the other hand, received only 2 mL/kg normal saline solution for 60 d. Blood samples for the biochemical analysis were taken by cardiac puncture from randomly chosen-seven rats in each treatment group at beginning and on the 60th d of the experiment.

RESULTS: The CCl_4 treatment for 60 d increased the lipid peroxidation and liver enzymes, and also decreased the antioxidant enzyme levels. NS or UD treatment (alone or combination) for 60 d decreased the elevated lipid peroxidation and liver enzyme levels and also increased the reduced antioxidant enzyme levels. The weight of rats decreased in group A, and increased in groups B, C and D.

CONCLUSION: NS and UD decrease the lipid peroxidation and liver enzymes, and increase the antioxidant defense system activity in the CCl_4-treated rats.

Key words: CCl_4; Nigella sativa L.; Urtica dioica L.; Lipid peroxidation; Antioxidant enzymes; Rat

Kanter M, Coskun O, Budancamanak M. Hepatoprotective effects of *Nigella sativa* L and *Urtica dioica* L on lipid peroxidation, antioxidant enzyme systems and liver enzymes in carbon tetrachloride-treated rats. *World J Gastroenterol* 2005; 11(42): 6684-6688
http://www.wjgnet.com/1007-9327/11/6684.asp

INTRODUCTION

Carbon tetrachloride (CCl_4) is one of the oldest and most widely used toxins for experimental induction of liver fibrosis in laboratory animals[1]. This model has been used in various studies on examined the deposition of extracellular matrix in the fibrotic and cirrhotic liver[2,3].

CCl_4 is a selective hepatotoxic chemical agent. CCl_4-induced reactive free radicals initiate cell damage through two different mechanisms of covalent binding to the membrane proteins and cause lipid peroxidation. A number of investigators have utilized this chemical to produce liver cirrhosis in experimental animals[4]. Production of reactive oxygen species and lipid peroxidation induced by iron overload[5], cholestatic injury[6] and intoxication by ethanol[7] and CCl_4[4] is associated with liver fibrosis and cirrhosis. These effects are partially prevented by antioxidant compounds including α-tocopherol[4,8], silymarin[9] and salvianolic acid[10].

The seed of *Nigella sativa* L (NS), an annual *Ranunculaceae* herbaceous plant, has been used traditionally for centuries in the Middle East, Northern Africa, Far East and Asia for the treatment of asthma. NS contains more than 30 of a fixed oil and 0.40-0.45 w/w of a volatile oil. The volatile oil has been shown to contain 18.4-24% thymoquinone and 46% many monoterpenes such as p-cymene, and α-pinene[11]. Recently conducted clinical and experimental researches have shown many therapeutic effects of NS extracts such as immunomodulator[12], anti-inflammatory[13] and anti-tumour agents[14].

Urtica dioica L (UD) is a plant belonging to the plant family *Urticaceae*. Its seeds are widely used in folk medicine in many parts of Turkey, especially in the therapy of advanced cancer patients. Polar extract of the UD contains lignans (+)-neoolivil, (-)-secoisolariciresinol, dehydrodiconiferyl alcohol, isolariciresinol, pinoresinol, and 3,4-divanillyltetrahydrofuran, and has antiinflammatory

effects[15] and stimulates the proliferation of human lymphocytes[16].

The present study aimed to investigate the preventive effects of NS and UD on lipid peroxidation, antioxidant enzyme systems and some liver enzymes in CCl_4-treated rats.

MATERIALS AND METHODS

Plant materials and extraction procedure

The NS and UD seeds were purchased from a local herb store, Zonguldak, Turkey. Voucher specimens were kept at the Department of Biochemistry, Zonguldak Karaelmas University, Zonguldak, Turkey for the future reference. The seeds of NS were powdered in a mixer, placed in a distillation flask and the volatile oil with 0.2 % yield was collected by a steam distillation. The fixed oil of UD was extracted with the help of a rotary evaporator using diethyl ether as solvent.

Treatment of rats

Fifty-six male Wistar albino rats, weighing 150-200 g, averaging 16 wk old, were used in this study. The rats were randomly allotted into one of the four experimental groups: A (CCl_4-only treated), B (CCl_4+UD treated), C (CCl_4+NS treated) and D (CCl_4+UD+NS treated), each containing 14 animals. All groups received CCl_4 (Merck; 153.82 g/moL, 1.59 kg, Germany, 0.8 mL/kg of body weight, sc, twice a week for 60 d). In addition, B, C and D groups also received the daily ip injection of 0.2 mL/kg NS or/and 2 mL/kg UD oils for 60 d. Group A, on the other hand, received only 2 mL/kg normal saline solution for 60 d. The animals were housed in macrolon cages under standard laboratory conditions (light period 7.00 a.m. to 7.00 p.m., 21±1 °C, rat chow and tap water freely available). All animals received human care according to the criteria outlined in the "Guide for the Care and Use of Laboratory Animals" prepared by the National Academy of Sciences and published by the National Institutes of Health. The experiment lasted for 60 d.

Biochemical analysis

Blood samples for the biochemical analysis were taken from each treatment group at beginning and on the 60th d of the experiment. Rats from which blood samples were taken were excluded from the experiment to eliminate the haemorrhage- and stress-induced complications. At the end of the experiment, rats in all groups were starved overnight, and sacrificed under chloralhydrate (6 mL of 7% chloralhydrate/kg, Sigma, St. Louis, MO, USA) anaesthesia. Blood samples were collected by cardiac puncture using heparinised syringes. Leukocytes and plasma components were seperated by centrifugation of the blood. Erythrocytes were washed three times with 0.9% NaCl solution and packed, and then stored at -70 °C until study.

Blood MDA (mmol/L) was determined by the double heating method of Draper and Hadley[17]. The principle of the method is spectrophotometric measurement of the colour produced during the reaction to thiobarbituric acid (TBA) with MDA. For this purpose, 2.5 mL of 100 g/L trichloroacetic acid solution was added to 0.5 mL erythrocytes in each centrifuge tube and placed in a boiling water bath for 15 min. After cooled in tap water, the mixture was centrifuged at 1 000 r/min for 10 min, and 2 mL of the supernatant was added to 1 mL of 6.7 g/L TBA solution in a test tube and placed in a boiling water bath for 15 min. The solution was then cooled in tap water and its absorbance was measured using a Shimadzu UV-1601 (Japan) spectrophotometer at 532 nm. The concentration of MDA was calculated by the absorbance coefficient of MDA-TBA complex 1.56×10^5 /cm, and expressed in μmol/g Hb erythrocytes and μmol/g tissue protein.

Blood GSH concentration was measured by the method described by Beutler *et al.*[18]. Briefly, 200 μL of whole blood was added to 1.8 mL of distilled water. Three ml of the precipitating solution was mixed with the hemolysate. The mixture was allowed to stand for approximately 5 min and then filtered. Two milliliters of filtrate were taken and added into another tube, and then, 8 mL of the phosphate solution and 1 mL of the DTNB [5,5'dithiobis-(2-nitrobenzoic acid)] were added. A blank was prepared with 8 mL of the phosphate solution, 2 mL of the diluted precipitating solution (three parts to two parts of the distilled water), and 1 mL of the DTNB reagent. A standard solution of glutathione was prepared (40 mg/100 mL). The optical density was measured at 412 nm with a spectrophotometer.

Serum ceruloplasmin *p*-phenylenediamine (PPD) oxidase activity was measured according to Sunderman and Nomoto[19]. At pH 5.4, ceruloplasmin catalyze the oxidation of PPD to yield a colored product. The rate of formation of the colored oxidation product was proportional to the concentration of serum ceruloplasmin if a correction was made for nonenzymatic oxidation of PPD.

Vitamin E was analyzed colorimetrically with 2,4,6-tripridyl-s-triazin and $FeCl_3$ after the extraction with absolute ethanol and xylene[20]. Serum vitamin C level was determined after derivatisation with 2,4-dinitrophenylhydrazine[21]. The levels of β-carotene at 425 nm and retinol at 325 nm were detected after the reaction of serum : ethanol : hexane at the ratio of 1 : 1 : 3 respectively[22].

Alanine aminotransferase (ALT), aspartate aminotransferase (AST) and alkaline phosphatase (ALP) levels were determined by an autoanalyzer (Roche-Hittachi, Japan) using commercial kits (Roche, Basel, Switzerland).

Statistical analysis

The data were expressed as mean±SD and analysed by repeated measures of variance. Tukey test was used to test for differences among means when ANOVA indicated a significant ($P\leqslant0.05$) F ratio.

Table 1 Blood MDA level (nmol/mL erythrocytes) in CCl_4+NaCl-treated (A), CCl_4+UD treated (B), CCl_4+NS treated (C) and CCl_4+UD+NS treated (D) rats (mean±SD)

Groups(d)	A	B	C	D
0	1.23±0.09	1.18±0.14	1.21±0.12	1.25±0.03
60	2.81±0.05	1.35±0.07	1.41±0.09	1.28±0.12

Table 2 Serum antioxidant levels (mg/dL) in CCl_4+NaCl-treated(A), CCl_4+UD treated (B), CCl_4+NS treated (C) and CCl_4+UD+NS treated (D) rats (mean±SD)

Groups(d)	A	B	C	D
GSH				
0	50.76±0.72	47.14±1.02	47.72±1.25	49.36±0.93
60	40.21±2.38	55.44±3.32	50.63±3.41	61.12±8.26
Ceruloplasmin				
0	18.72±0.82	18.47±0.89	17.36±1.13	19.23±0.59
60	12.92±0.49	29.33±0.64	25.90±1.61	30.22±1.23
Vitamin E				
0	0.20±0.12	0.19±0.01	0.18±0.01	0.20±0.13
60	0.11±0.02	0.34±0.03	0.24±0.02	0.45±0.01
Vitamin C				
0	0.53±0.01	0.51±0.01	0.52±0.01	0.54±0.01
60	0.40±0.01	0.61±0.02	0.54±0.02	0.89±0.01
Beta-karoten				
0	26.49±0.85	25.28±0.44	26.41±0.37	25.15±0.83
60	19.28±1.23	25.21±1.55	26.73±1.53	25.25±1.27
Retinol				
0	50.33±0.87	52.72±0.66	51.22±0.39	52.64±0.55
60	44.98±1.18	56.19±0.37	53.52±0.63	61.69±1.69

Table 3 Serum liver enzyme levels (U/L) in CCl4+NaCl-treated (A), CCl4+UD treated (B), CCl4+NS treated (C) and CCl4+UD+NS treated (D) rats (mean±SD)

Groups(d)	A	B	C	D
ALP				
0	957±23.62	961±16.64	987±13.64	1028±36.51
60	1354±32.58	692±24.21	637.82±31.21	772.57±91.45
ALT				
0	89.3±4.86	78.21±17.35	80.14±20.12	83.17±11.21
60	2762±42.45	553±60.29	425±42.24	253±39.27
AST				
0	143.29±6.43	141.28±16.26	143.50±7.85	144.27±20.44
60	2342.25±34.06	554.23±14.83	1031.44±92.68	672.17±58.42

Table 4 Weights (g) of rats in CCl_4+NaCl-treated (A), CCl_4+UD treated (B), CCl_4+NS treated (C) and CCl_4+UD+NS treated (D) rats (mean±SD)

Groups(d)	A	B	C	D
0	189±6.21	181.43±12.21	187.21±4.33	189.63±3.21
60	171.73±3.90	204.02±12.09	214.76±12.72	217.50±11.52

RESULTS

The levels of blood MDA, antioxidants of all groups and the levels of serum liver enzymes are shown in Table 1-3, respectively. The CCl_4 treatment for 60 d significantly ($P<0.05$) increased the MDA and liver enzymes, and also decreased ($P<0.05$) the antioxidant levels. NS or UD treatment (alone or in combination) for 60 d significantly ($P<0.05$) decreased the elevated MDA and liver enzyme levels and also increased ($P<0.05$) the reduced antioxidant levels. The weight of rats decreased ($P<0.05$) in group A, and increased ($P<0.05$) in groups B, C, and D (Table 4).

DISCUSSION

Treatment of animals with CCl_4 is known to cause severe hepatic injury[23]. In our study, we showed that repeated CCl_4 treatment for 60 d increased the lipid peroxidation and liver enzymes, and also decreased the antioxidant enzyme levels. It has been suggested that the lipid peroxidation may be a link between tissue injury and liver fibrosis by modulating collagen gene expression[24]. It was reported that CCl_4 is suitable to induce lipid peroxidation in experimental animals within a few minutes after administration and its long-term use results in liver fibrosis and cirrhosis by lipid peroxidation pathway[25]. It is generally thought that CCl_4 toxicity is due to reactive free radical (CCl_3.), which is generated by its reductive metabolism by hepatic cytochrome P450. The reactive intermediate is believed to cause lipid peroxidation and breakdown of cellular membranes[26].

Recent experimental studies have investigated the role of antioxidative vitamins, minerals, drugs and plant-derived compounds in the prevention and therapy of liver fibrosis. Parola *et al*.[4] showed that an increased liver content of vitamin E leads to a significant degree of protection against carbon tetrachloride-induced chronic liver damage and cirrhosis in rats. Ianas *et al*.[27] have described the all-round beneficial action of a selenium preparation upon the organism in rats exposed to CCl_4 as well as a strong antioxidative effect, confirming the essential role of selenium in maintaining cellular integrity.

Several plant derived compounds such as colchicine (Colchicum dispert), silymarin (Slybum marianum), polyenylphosphatidyl choline (soy bean), ellagic acid (cruciferous vegetables), Gingko biloba composita and recently Sho-saiko-to (extract of seven herbs in Chinese folk medicine) have been proposed as antioxidants and antifibrotics in the treatment of chronic liver disease[28-30]. The antioxidative and hepatoprotective effects of chitosan against CCl_4-induced liver toxicity in rats have been under investigation by measuring thiobarbituric acid reactive substances (TBARS) and antioxidant enzyme activities[31]. The antioxidant systems such as antioxidant vitamins (A, C, and E), superoxide dismutase (SOD), catalase, glutathione (GSH), ceruloplasmin and glutathione peroxidase (GSH-Px) protect the cells against lipid peroxidation, which is the base of many pathologic processes [32,33].

In our study, we found that NS or UD treatment (alone or combination) for 60 d decreased the elevated MDA and liver enzyme levels and also increased the reduced antioxidant enzyme levels in CCl_4-treated rats. Previously performed clinical and experimental investigations have shown that NS has a protective effect against oxidative damage in isolated rat hepatocytes[34]. It was found that the fixed oil of NS has both antioxidant and anti-eicosanoid effects greater than thymoquinone which is its active

constituent[13]. Furthermore, NS has antioxidant activity by suppressing the chemiluminescence in phagocytes[35].

Recently, Turkdogan *et al.*[36] observed that NS has a significant hepatoprotective effect in CCl_4-administrated rabbits, ans that hepatocellular degenerative and necrotic changes are slight without advanced fibrosis and cirrhotic process in NS-treated group. However, Turkdogan *et al.*[37] found that NS can prevent liver fibrosis and cirrhosis, suggesting that NS protects liver against fibrosis possibly through immunomodulator and antioxidant activities.

There are no comprehensive studies on the therapeutic effects of UD. Only one study reported that UD extract can inhibit *in vitro* prostate cancer cell proliferation[38]. It has been suggested that the extract of UD is effective in inducing glutathione S-transferase, SOD and catalase activity in the forestomach and SOD and CAT activity in the lung at both dose levels[39]. However, Turkdogan *et al.*[36] showed that NS and UD can significantly prevent CCl_4-induced hepatotoxicity in rats. Our biochemical results demonstrated that NS and UD treatment prevented CCl_4-induced hepatotoxicity in rats by decreasing the lipid peroxidation and increasing the antioxidant defense system activity. However, Kanter *et al.*[40] also showed the NS and UD increase the antioxidant defense system activity in experimentally CCl_4-treated rats.

In conclusion, NS and UD decrease lipid peroxidation and liver enzymes, and increase antioxidant defense system activity in the CCl_4-treated rats. They also prevent weight lose induced by the CCl_4 treatment. Further studies are required to evaluate the possible hepatoprotective effect of NS and UD which are traditionally used as a medicine for many complaints including liver diseases.

REFERENCES

1 **Tsukamoto H,** Matsuoka M, French SW. Experimental models of hepatic fibrosis: a review. *Seminar in Liver Disease* 1990; **10:** 56-65

2 **Hernandez-Munoz R,** Diaz-Munoz M, Chagoya de Sanchez V. Possible role of cell redox state on collagen metabolism in carbon tetrachloride-induced cirrhosis as evidenced by adenosine administration to rats. *Biochim Biophys Acta* 1994; **1200:** 93-99

3 **Muriel P.** Nitric oxide protection of rat liver from lipid peroxidation, collagen accumulation, and liver damage induced by carbon tetrachloride. *Biochemical Pharmacology* 1998; **56:** 773-779

4 **Parola M,** Leonarduzzi G, Biasi F, Albano E, Biocca ME, Poli G, Dianzani MU. Vitamin E dietary supplementation protects against carbon tetrachloride-induced chronic liver damage and cirrhosis. *Hepatology* 1992; **16:** 1014-1021

5 **Bacon BR,** Britton RS. The pathology of hepatic iron overload: a free radical-mediated process? *Hepatology* 1990; **11:** 127-137

6 **Parola M,** Leonarduzzi G, Robino G, Albano E, Poli G, Dianzani MU. On the role of lipid peroxidation in the pathogenesis of liver damage induced by long-standing cholestasis. *Free Radic Biol Med* 1996; **20:** 351-359

7 **Kamimura S,** Gaal K, Britton RS, Bacon BR, Triadafilopoulos G, Tsukamoto H. Increased 4-hydroxynonenal levels in experimental alcoholic liver disease: association of lipid peroxidation with liver fibrogenesis. *Hepatology* 1992; **16:** 448-453

8 **Halim AB,** El-Ahmady O, Hassab-Allah S, Abdel-Galil F, Hafez Y, Darwish A. Biochemical effect of antioxidants on lipids and liver function in experimentally-induced liver damage. *Ann Clin Biochem* 1997; **34** (Pt 6): 656-663

9 **Mourelle M,** Muriel P, Favari L, Franco T. Prevention of CCl_4-induced liver cirrhosis by silymarin. *Fundam Clin Pharmacol* 1989; **3:** 183-191

10 **Hu YY,** Liu P, Liu C, Xu LM, Liu CH, Zhu DY, Huang MF. Actions of salvianolic acid A on CCl_4-poisoned liver injury and fibrosis in rats. *Zhongguo Yaoli Xuebao* 1997; **18:** 478-480

11 **El Tahir KE,** Ashour MM, al-Harbi MM. The respiratory effects of the volatile oil of the black seed (Nigella sativa) in guinea-pigs: elucidation of the mechanism(s) of action. *Gen Pharmacol* 1993; **24:** 1115-1122

12 **El-Kadi A,** Kandil O. The black seed (Nigella sativa) and immunity: its effect on human T cell subset. *Fed Proc* 1987; **46:** 1222

13 **Houghton PJ,** Zarka R, de las Heras B, Hoult JR. Fixed oil of Nigella sativa and derived thymoquinone inhibit eicosanoid generation in leukocytes and membrane lipid peroxidation. *Planta Med* 1995; **61:** 33-36

14 **El Daly ES.** Protective effect of cysteine and vitamin E, Crocus sativus and Nigella sativa extracts on cisplatin-induced toxicity in rats. *J Pharm Belg* 1998; **53:** 87-93; discussion 93-5

15 **Riehemann K,** Behnke B, Schulze-Osthoff K. Plant extracts from stinging nettle (Urtica dioica), an antirheumatic remedy, inhibit the proinflammatory transcription factor NF-kappaB. *FEBS Lett* 1999; **442:** 89-94

16 **Wagner H,** Willer F, Kreher B. Biologically active compounds from the aqueous extract of Urtica dioica. *Planta Med* 1989; **55:** 452-454

17 **Draper HH,** Hadley M. Malondialdehyde determination as index of lipid peroxidation. *Methods Enzymol* 1990; **186:** 421-431

18 **Buetler E,** Dubon O, Kelly BM. Improved metod fot the determination of blood glutathione. *J Lab Clin Med* 1963; **61:** 882-888

19 **Sunderman FW Jr,** Nomoto S. Measurement of human serum ceruloplasmin by its p-phenylenediamine oxidase activity. *Clin Chem* 1970; **16:** 903-910

20 **Martinek RG.** Method for the determination of vjitamin E (total tocopherols) in serum. *Clin Chem* 1964; **10:** 1078-1086

21 **Omaye ST,** Turnbull JD, Sauberlich HE.Selected methods for the determination of ascorbic acid in animal cells, tissues, and fluids. *Methods Enzymol* 1979; **62:** 3-11

22 **Suzuki J,** Katoh N. A simple and cheap methods for measuring serum vitamin A in cattle using only a spectrophotometer. *Nippon Juigaku Zasshi* 1990; **52:** 1281-1283

23 **Terblanche J,** Hickman R. Animal models of fulminant hepatic failure. *Dig Dis Sci* 1991; **36:** 770-774

24 **Parola M,** Pinzani M, Casini A, Albano E, Poli G, Gentilini A, Gentilini P, Dianzani MU. Stimulation of lipid peroxidation or 4-hydroxynonenal treatment increases procollagen alpha 1 (I) gene expression in human liver fat-storing cells. *Biochem Biophys Res Commun* 1993; **194:** 1044-1050

25 **Sherlock S.** [Drugs and the liver] *G Clin Med* 1970; **51:** 753-759

26 **De Groot H,** Sies H. Cytochrome P-450, reductive metabolism, and cell injury. *Drug Metab Rev* 1989; **20:** 275-284

27 **Ianas O,** Olinescu R, Badescu I, Simionescu L, Popovici D. The influence of "selenium organicum" upon the hepatic function of carbon tetrachloride poisoned rats. *Rom J Intern Med* 1995; **33:** 113-120

28 **Seitz HK,** Pöschl G. Antioxidant drugs and colchicine in the treatment of alcoholic liver disease. In: Arroyo, V., Bosch, J., Rodes, J., eds. Treatments in Hepatology. First ed. *Barcelone Masson* 1995; 271-276

29 **Schuppan D,** Hahn EG. Clinical studies with silymarin: fibrosis progression is the end point. *Hepatology* 2001; **33:** 483-484

30 **Shimizu I.** Sho-saiko-to: Japanese herbal medicine for protection against hepatic fibrosis and carcinoma. *J Gastroenterol Hepatol* 2000; **15** Suppl: D84-90

31 **Jeon TI,** Hwang SG, Park NG, Jung YR, Shin SI, Choi SD,

Park DK. Antioxidative effect of chitosan on chronic carbon tetrachloride induced hepatic injury in rats. *Toxicology* 2003; **187:** 67-73

32 **Williams RJ.** Zinc: what is its role in biology? *Endeavour* 1984; **8:** 65-70

33 **Bray TM,** Bettger WJ. The physiological role of zinc as an antioxidant. *Free Radic Biol Med* 1990; **8:** 281-291

34 **Daba MH,** Abdel-Rahman MS. Hepatoprotective activity of thymoquinone in isolated rat hepatocytes. *Toxicol Lett* 1998; **95:** 23-29

35 **Haq A,** Abdullatif M, Lobo PI, Khabar KS, Sheth KV, al-Sedairy ST. Nigella sativa: effect on human lymphocytes and polymorphonuclear leukocyte phagocytic activity. *Immunopharmacology* 1995; **30:** 147-155

36 **Turkdogan MK,** Ozbek H, Yener Z, Tuncer I, Uygan I, Ceylan E. The role of Urtica dioica and Nigella sativa in the prevention of carbon tetrachloride-induced hepatotoxicity in rats. *Phytother Res* 2003; **17:** 942-946

37 **Turkdogan MK,** Agaoglu Z, Yener Z, Sekeroglu R, Akkan HA, Avci ME. The role of antioxidant vitamins (C and E), selenium and Nigella sativa in the prevention of liver fibrosis and cirrhosis in rabbits: new hopes. *Dtsch Tierarztl Wochenschr* 2001; **108:** 71-73

38 **Konrad L,** Muller HH, Lenz C, Laubinger H, Aumuller G, Lichius JJ. Antiproliferative effect on human prostate cancer cells by a stinging nettle root (Urtica dioica) extract. *Planta Med* 2000; **66:** 44-47

39 **Ozen T,** Korkmaz H. Modulatory effect of Urtica dioica L. (Urticaceae) leaf extract on biotransformation enzyme systems, antioxidant enzymes, lactate dehydrogenase and lipid peroxidation in mice. *Phytomedicine* 2003; **10:** 405-415

40 **Kanter M,** Meral I, Dede S, Gunduz H, Cemek M, Ozbek H, Uygan I. Effects of Nigella sativa L. and Urtica dioica L. on lipid peroxidation, antioxidant enzyme systems and some liver enzymes in CCl4-treated rats. *J Vet Med A Physiol Pathol Clin Med* 2003; **50:** 264-268

Science Editor Wang XL and Guo SY **Language Editor** Elsevier HK

PO Box 2345, Beijing 100023, China
www.wjgnet.com
wjg@wjgnet.com

ELSEVIER

World J Gastroenterol 2005;11(42):6689-6693
World Journal of Gastroenterology ISSN 1007-9327

• *BRIEF REPORTS* •

Preoperative sorting of circulating T lymphocytes in patients with esophageal squamous cell carcinoma: Its prognostic significance

Tadahiro Nozoe, Yoshihiko Maehara, Keizo Sugimachi

Tadahiro Nozoe, Department of Surgery, Fukuoka Higashi Medical Center, Koga, Japan
Yoshihiko Maehara, Department of Surgery and Science, Graduate School of Medical Sciences, Kyushu University, Fukuoka, Japan
Keizo Sugimachi, Kyushu Central Hospital
Correspondence to: Tadahiro Nozoe, Department of Surgery, Fukuoka Higashi Medical Center, 1-1-1, Chidori, Koga 811-3195, Japan. ntvb@med.uoeh-u.ac.jp
Fax: +81-92-943-8775
Received: 2004-04-07 Accepted: 2005-02-15

Abstract

AIM: To elucidate the immunologic parameters for the outcome of patients with malignant tumors, especially esophageal squamous cell carcinoma (ESCC) associated with high malignant potential.

METHODS: Clinicopathologic features were compared between patients with lower and higher CD4 and CD8 values as well as CD4/CD8 ratio in peripheral blood.

RESULTS: The survival rate of patients with higher CD4 value was significantly better than that in patients with lower CD4 value (P = 0.039). The survival rate of patients with higher CD8 value was significantly worse than that of patients with lower CD8 value (P = 0.026). Similarly, the survival rate of patients with higher CD4/CD8 ratio was significantly better than that of patients with lower CD4/CD8 ratio (P = 0.042). Additionally, multivariate analysis demonstrated that lower CD8 and lower CD4/CD8 ratio were factors independently associated with worse prognosis of patients.

CONCLUSION: All the immunologic parameters can predict the outcome of patients with ESCC.

Key words: Lymphocyte sub-population; Esophagus; Squamous cell carcinoma; Prognostic indicator

Nozoe T, Maehara Y, Sugimachi K. Preoperative sorting of circulating T lymphocytes in patients with esophageal squamous cell carcinoma: Its prognostic significance. *World J Gastroenterol* 2005; 11(42): 6689-6693
http://www.wjgnet.com/1007-9327/11/6689.asp

INTRODUCTION

Impaired immunity is well known to be correlated with the tumorigenesis and/or progressive behavior of human tumors[1-3]. Therefore, it is important to assess the immunologic dynamics of patients with malignant tumors, especially esophageal carcinoma.

We have reported the significance of preoperative assessment of such immunological parameters as serum C-reactive protein concentration[4], prognostic nutritional index[5], and phytohemagglutinin (PHA) response test[6] as a prognostic indicator in esophageal carcinoma.

CD8+, cytotoxic T lymphocytes, plays an immunologic role as the specific tumor terminator and CD4+, helper T lymphocyte, serves the function of controlling CD8+ T-cell-dependent tumor termination[7]. However, only a few investigations are available on the clinicopathologic significance of these lymphocytes in controlling esophageal carcinoma[8-10].

It was reported that lower CD4/CD8 ratio in peripheral blood can be used as an indicator for worse prognosis of patients with esophageal carcinoma[11]. In the current study, we investigated the clinical significance of the serum values of CD4 and CD8, and the CD4/CD8 ratio in patients with esophageal squamous cell carcinoma (ESCC).

MATERIALS AND METHODS

One hundred and thirty-four patients (118 men and 16 women) with ESCC, who underwent esophageal resection and reconstruction of the digestive tract in our institute between 1990 and 1997, were enrolled in this study. The patients had a median age of 62 years (range, 41-82 years).

Follow-up was continued until their death. The interval of follow-up ranged from 29 d to 8 years and 9 mo averaged 2 years and 11 mo. Serum values of lymphocyte sub-populations, CD4 and CD8, were measured as previously described[11].

Pathological features were presented according to the guidelines for clinical and pathologic studies on carcinoma of the esophagus established by the Japanese Society for Esophageal Diseases[12], and clinical stages were determined by the TNM classification of malignant tumors approved by the International Union Against Cancer[13]. Clinicopathologic features were compared between patients with lower and higher values of CD4 and

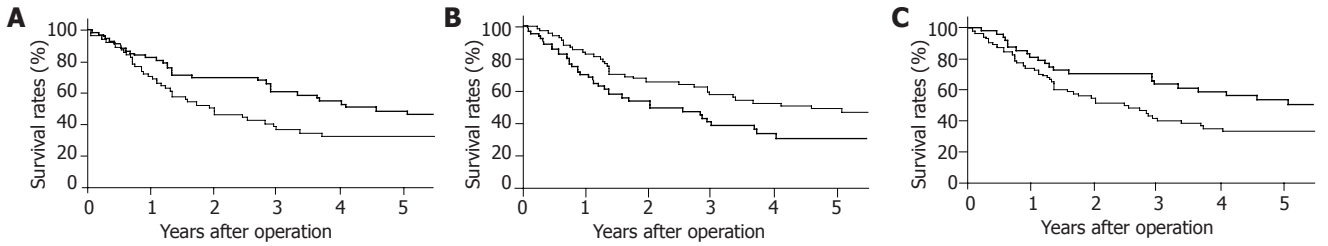

Figure 1 **A:** Survival rate in group H-CD4 (thick line) and group L-CD4 (thin line, *P*=0.039); **B:** Survival rate in group H-CD8 (thick line) and group L-CD8 (thin line, *P*=0.026); **C:** Survival rate in group H-CD4/8 (thick line) and group L-CD4/8 (thin line, *P*=0.042).

Table 1 Relationship between serum CD4 value and clinicopathological features (mean±SD), *n* (%)

Variables	Group H-CD4 (*n* = 68)	Group L-CD4 (*n* = 66)	*P*
Gender			
Male	57 (83.8)	61 (92.4)	0.205
Female	11 (16.2)	5 (7.6)	
Age	60.9±8.8	64.1+9.6	0.046
Location of tumor			
Upper	12 (17.6)	11 (16.7)	0.845
Middle	38 (55.9)	40 (60.6)	
Lower	18 (26.5)	15 (22.7)	
Degree of differentiation			
Well	4 (5.9)	6 (9.1)	0.620
Moderately	57 (83.8)	51 (77.3)	
Poorly	7 (10.3)	9 (13.6)	
Tumor size (cm)	5.3+2.7	5.4+2.5	0.970
Depth of tumor			
Tis	2 (2.9)	2 (3.0)	0.051
T1a	6 (8.8)	5 (7.6)	
T1b	15 (22.1)	9 (13.6)	
T2	14 (20.6)	9 (13.6)	
T3	15 (22.1)	33 (50.0)	
T4	16 (23.5)	8 (12.2)	
Lymph nodes metastasis			
Positive	24 (35.3)	31 (53.0)	0.231
Negative	44 (64.7)	35 (47.0)	
Lymphatic invasion			
Positive	12 (17.6)	18 (27.3)	0.259
Negative	56 (82.4)	48 (72.7)	
Venous invasion			
Positive	5 (7.4)	11 (16.7)	0.163
Negative	63 (92.6)	55 (83.3)	
TNM stage			
0	2 (2.9)	2 (3.0)	0.749
I	17 (25.0)	11 (16.7)	
IIA	16 (23.5)	18 (27.3)	
IIB	10 (14.7)	8 (12.2)	
III	23 (33.8)	27 (40.8)	
Curability			
Curative resection	52 (76.5)	56 (84.8)	0.314
Non curative resection	16 (23.5)	10 (15.2)	

Well = well differentiated squamous cell carcinoma; Moderately = moderately differentiated squamous cell carcinoma; Poorly = poorly differentiated squamous cell carcinoma.

CD8 as well as CD4/CD8 ratio.

Chi-square test and Student's *t* test were used to compare the clinicopathologic data. The cumulative survival rates were calculated by the Kaplan-Meier method and the survival curves were tested by the Mantel-Cox method. $P<0.05$ was considered statistically significant.

RESULTS

Among the clinicopathologic factors, the mean age of patients with higher CD4 value (group H-CD4) was significantly lower than that of patients with lower CD4 value (group L-CD4, $P = 0.046$). However, no significant difference was observed in other factors including tumor-related factors (Table 1). The 1-, 3-, and 5-year survival rates were 82.2%, 60.4% and 48.4%, respectively, in group H-CD4 and 70.8%, 36.9% and 32.7%, respectively, in group L-CD4 ($P = 0.039$, Figure 1A).

No significant difference was found in the clinicopathologic factors between patients with higher (group H-CD8) and lower CD8 value (group L-CD8, Table 2). The 1-, 3-, and 5-year survival rates were 69.7%, 38.5% and 30.0%, respectively, in group H-CD8 and 82.7%, 57.7%, and 49.0%, respectively, in group L-CD8 ($P = 0.026$, Figure 1B).

Significant difference between patients with higher (group H-CD4/8) and lower CD4/CD8 ratio (group L-CD4/8) was observed only in gender proportion ($P = 0.036$, Table 3). The 1-, 3-, and 5-year survival rates were 80.9%, 62.9%, and 52.9%, respectively, in group H-CD4/8 and 74.0%, 40.3% and 33.0%, respectively, in group L-CD4/8 ($P = 0.042$, Figure 1C).

Multivariate analysis demonstrated that lower CD8 (95%CI, 2.07, 1.26–3.38; $P = 0.004$) and lower CD4/CD8 ratio (95%CI, 1.73, 1.02-2.93; $P = 0.043$) were factors independently associated with worse prognosis of patients.

DISCUSSION

With the development of monoclonal antibodies in detecting lymphocytes subpopulation[14], lymphocyte subtypes in peripheral blood were examined to investigate their functions in immune-surveillance. Among the subpopulations of lymphocytes, investigations of cancer immunology have been focused on CD8, suppressor/

Table 2 Relationship between serum CD8 value and clinico-pathological features (mean±SD), *n* (%)

Variables	Group H-CD8 (*n* = 64)	Group L-CD8 (*n* = 70)	*P*
Gender			
Male	58 (90.6)	60 (85.7)	0.543
Female	6 (9.4)	10 (14.3)	
Age	63.4+9.6	61.6+9.1	0.265
Location of tumor			
Upper	9 (14.1)	14 (20.0)	0.635
Middle	38 (59.4)	40 (57.1)	
Lower	17 (26.5)	16 (22.9)	
Degree of differentiation			
Well	4 (6.3)	6 (8.6)	0.810
Moderately	53 (82.8)	55 (78.6)	
Poorly	7 (10.9)	9 (12.8)	
Tumor size (cm)	5.4+2.4	5.3+2.8	0.930
Depth of tumor			
Tis	2 (3.1)	2 (2.8)	0.899
T1a	4 (6.3)	7 (10.0)	
T1b	11 (17.2)	13 (18.6)	
T2	10 (15.6)	13 (18.6)	
T3	26 (40.6)	22 (31.4)	
T4	11 (17.2)	13 (18.6)	
Lymph nodes metastasis			
Positive	29 (45.3)	26 (37.1)	0.382
Negative	35 (54.7)	44 (62.9)	
Lymphatic invasion			
Positive	11 (17.2)	19 (27.1)	0.241
Negative	53 (82.8)	51 (72.9)	
Venous invasion			
Positive	9 (14.1)	7 (10.0)	0.647
Negative	55 (85.9)	63 (90.0)	
TNM stage			
0	2 (3.1)	2 (2.8)	0.858
I	12 (18.8)	16 (22.9)	
IIA	15 (23.4)	19 (27.1)	
IIB	8 (12.5)	10 (14.3)	
III	27 (42.2)	23 (32.9)	
Curability			
Curative resection	51 (79.7)	57 (81.4)	0.830
Non curative resection	13 (20.3)	13 (18.6)	

Well = well differentiated squamous cell carcinoma; Moderately = moderately differentiated squamous cell carcinoma; Poorly = poorly differentiated squamous cell carcinoma.

Table 3 Relationship between serum CD4/CD8 ratio and clinico-pathological features (mean±SD), *n* (%)

Variables	Group H-CD4/8 (*n* = 48)	Group L-CD4/8 (*n* = 86)	*P*
Gender			
Male	38 (79.2)	80 (93.0)	0.036
Female	10 (20.8)	6 (7.0)	
Age	61.4+8.9	63.0+9.6	0.322
Location of tumor			
Upper	10 (20.8)	13 (15.1)	0.675
Middle	26 (54.2)	52 (60.5)	
Lower	12 (25.0)	21 (24.4)	
Degree of differentiation			
Well	5 (10.4)	5 (5.8)	0.459
Moderately	36 (75.0)	72 (83.7)	
Poorly	7 (14.6)	9 (10.5)	
Tumor size (cm)	4.9+2.5	5.6+2.7	0.125
Depth of tumor			
Tis	2 (4.2)	2 (2.3)	0.213
T1a	4 (8.3)	7 (8.1)	
T1b	11 (22.9)	13 (15.1)	
T2	8 (16.7)	15 (17.5)	
T3	11 (22.9)	37 (43.0)	
T4	12 (25.0)	12 (14.0)	
Lymph nodes metastasis			
Positive	16 (33.3)	39 (34.9)	0.241
Negative	32 (66.7)	47 (65.1)	
Lymphatic invasion			
Positive	12 (25.0)	18 (20.9)	0.745
Negative	36 (75.0)	68 (79.1)	
Venous invasion			
Positive	5 (10.4)	11 (12.8)	0.647
Negative	43 (89.6)	75 (87.2)	
TNM stage			
0	2 (4.2)	2 (2.3)	0.858
I	13 (27.1)	15 (17.5)	
IIA	11 (22.9)	23 (26.7)	
IIB	6 (12.5)	12 (14.0)	
III	16 (33.3)	34 (39.5)	
Curability			
Curative resection	36 (75.0)	72 (83.7)	0.830
Non curative resection	12 (25.0)	14 (16.3)	

Well = well differentiated squamous cell carcinoma; Moderately = moderately differentiated squamous cell carcinoma; Poorly = poorly differentiated squamous cell carcinoma.

cytotoxic T lymphocyte responses. Attention has also been paid to CD4, helper/inducer T lymphocytes, as a critical component of the anti-tumor immune response[15].

Tumor-specific immune response depends on the function of activated CD4 cells[16], and therefore the deficiency in the function of activated CD4 cells might be directly correlated with the immune-deficiency of the host. CD4 helper/inducer T lymphocytes produce lymphokines, thus promoting the cytotoxic activity of CD8 T lymphocytes[17,18]. Therefore, activation of both CD4 and CD8 can exert a synergistic immune response to the termination of tumor cells.

Though some investigations have demonstrated an immunologic anti-tumor effect of CD4 and CD8[8], the clinical significance of CD4/CD8 ratio in tumor infiltrating lymphocytes and/or in peripheral blood as an indicator of progressive gastrointestinal tumor and/or worse prognosis of patients has been occasionally reported[19-21]. Diederichsen *et al.*[19] reported that low CD4/CD8 ratio in tumor infiltrating lymphocytes is an independent prognostic indicator in patients with colorectal carcinoma. Decrease of the CD4/CD8 ratio is correlated with progressive behavior of the tumor indicated by such tumor-related factors as stage of the tumor, tumor invasion, lymph node metastasis, and size of the tumor in gastric cancer[20]. Moreover, severe pre-

operative cellular immune-suppression, where CD4/CD8 ratio was less than 1.0, is a predictive parameter for mortality in patients with gastric cancer[21].

CD8 expression in TIL in tumor tissue can serve the function of suppressing the proliferation of ESCC[9], and similarly CD8 infiltration into the tumor is an independent prognostic indicator for ESCC[10]. Recently, increase of the number of CD4 and CD8 T lymphocytes in tumor nests and stroma has been found to be an independent indicator of favorable prognosis of patients with ESCC[8].

These results suggest that CD8 T-lymphocyte infiltration, as have been investigated in some other tumors[22,23], plays a pivotal role in immune-potential against ESCCs.

However, it was reported that the prognosis of patients with lung carcinoma associated with more CD8 expressing T cells within cancer nests is significantly worse than that of patients with tumors of fewer CD8 expressing T cells[24]. High percentage of activated CD8-positive cells in postoperative peripheral blood is an indicator of worse prognosis for renal cell carcinoma[25].

The different methods used to evaluate the value or expression of CD8, histological type of the tumor, or balance between immunologic dynamics of the tumor and the host might explain this possible discrepancy in the significance of CD8 T lymphocytes in anti-tumor immune.

In the current study, the decreased CD4/CD8 ratio as well as the increased CD8 and the decreased CD4 in peripheral blood could predict the worse prognosis in patients with ESCCs. Preoperative coexistence of impaired immunity could influence the postoperative complications[5]. The incidence of postoperative complications is an independent indicator of worse prognosis in patients with esophageal carcinoma[26]. Therefore, preoperative impaired immunity seems not to be negligible as the cause of death, other than esophageal carcinoma.

Assessment of preoperative immunity in patients seems to be of great importance in predicting the subsequent outcome of patients with ESCCs.

REFERENCES

1 **Neuner A,** Schindel M, Wildenberg U, Muley T, Lahm H, Fischer JR. Prognostic significance of cytokine modulation in non-small cell lung cancer. *Int J Cancer* 2002; **101:** 287-292

2 **Takagi K,** Yamamori H, Morishima Y, Toyoda Y, Nakajima N, Tashiro T. Preoperative immunosuppression: its relationship with high morbidity and mortality in patients receiving thoracic esophagectomy. *Nutrition* 2001; **17:** 13-17

3 **Eilber FR,** Morton DL. Impaired immunologic reactivity and recurrence following cancer surgery. *Cancer* 1970; **25:** 362-367

4 **Nozoe T,** Saeki H, Sugimachi K. Significance of preoperative elevation of serum C-reactive protein as an indicator of prognosis in esophageal carcinoma. *Am J Surg* 2001; **182:** 197-201

5 **Nozoe T,** Kimura Y, Ishida M, Saeki H, Korenaga D, Sugimachi K. Correlation of pre-operative nutritional condition with post-operative complications in surgical treatment for oesophageal carcinoma. *Eur J Surg Oncol* 2002; **28:** 396-400

6 **Nozoe T,** Korenaga D, Ohga T, Futatsugi M, Maehara Y. Suppression of phytohemagglutinin response to lymphocytes is an independent prognosticator in patients with squamous cell carcinoma of the esophagus. *Ann Thorac Surg* 2003; **76:** 260-265

7 **Shiku H.** Importance of CD4+ helper T-cells in antitumor immunity. *Int J Hematol* 2003; **77:** 435-438

8 **Cho Y,** Miyamoto M, Kato K, Fukunaga A, Shichinohe T, Kawarada Y, Hida Y, Oshikiri T, Kurokawa T, Suzuoki M, Nakakubo Y, Hiraoka K, Murakami S, Shinohara T, Itoh T, Okushiba S, Kondo S, Katoh H. CD4+ and CD8+ T cells cooperate to improve prognosis of patients with esophageal squamous cell carcinoma. *Cancer Res* 2003; **63:** 1555-1559

9 **Takeno S,** Noguchi T, Kikuchi R, Wada S, Sato T, Uchida Y. Immunohistochemical study of leukocyte infiltration and expression of hsp70 in esophageal squamous cell carcinoma. *Oncol Rep* 2001; **8:** 585-590

10 **Schumacher K,** Haensch W, Roefzaad C, Schlag PM. Prognostic significance of activated CD8(+) T cell infiltrations within esophageal carcinomas. *Cancer Res* 2001; **61:** 3932-3936

11 **Tsutsui S,** Sonoda K, Sumiyoshi K, Kitamura K, Toh Y, Kitamura M, Kuwano H, Sugimachi K, Okamura S. Prognostic significance of immunological parameters in patients with esophageal cancer. *Hepatogastroenterology* 1996; **43:** 501-509

12 Japanese Society for Esophageal Diseases. Guide lines for the clinical and pathological studies on carcinoma of the esophagus, 9th ed. Tokyo: Kanehara Company, 1999

13 **LH Sobin,** Wittekind C, editors. International Union Against Cancer. TNM classification of malignant tumours, 5th ed. New York: Wiley-Liss, 1997: p 54-58

14 **Reinherz EL,** Kung PC, Goldstein G, Schlossman SF. Separation of functional subsets of human T cells by a monoclonal antibody. *Proc Natl Acad Sci USA* 1979; **76:** 4061-4065

15 **Pardoll DM,** Topalian SL. The role of CD4+ T cell responses in antitumor immunity. *Curr Opin Immunol* 1998; **10:** 588-594

16 **Chen L,** Linsley PS, Hellstrom KE. Costimulation of T cells for tumor immunity. *Immunol Today* 1993; **14:** 483-486

17 **Toes RE,** Ossendorp F, Offringa R, Melief CJ. CD4 T cells and their role in antitumor immune responses. *J Exp Med* 1999; **189:** 753-756

18 **Qin Z,** Richter G, Schuler T, Ibe S, Cao X, Blankenstein T. B cells inhibit induction of T cell-dependent tumor immunity. *Nat Med* 1998; **4:** 627-630

19 **Diederichsen AC,** Hjelmborg JB, Christensen PB, Zeuthen J, Fenger C. Prognostic value of the CD4+/CD8+ ratio of tumour infiltrating lymphocytes in colorectal cancer and HLA-DR expression on tumour cells. *Cancer Immunol Immunother* 2003; **52:** 423-428

20 **Lee WJ,** Chang KJ, Lee CS, Chen KM. Selective depression of T-lymphocyte subsets in gastric cancer patients: an implication of immunotherapy. *J Surg Oncol* 1994; **55:** 165-169

21 **Rey-Ferro M,** Castano R, Orozco O, Serna A, Moreno A. Nutritional and immunologic evaluation of patients with gastric cancer before and after surgery. *Nutrition* 1997; **13:** 878-881

22 **Oshikiri T,** Miyamoto M, Shichinohe T, Suzuoki M, Hiraoka K, Nakakubo Y, Shinohara T, Itoh T, Kondo S, Katoh H. Prognostic value of intratumoral CD8+ T lymphocyte in extrahepatic bile duct carcinoma as essential immune response. *J Surg Oncol* 2003; **84:** 224-228

23 **Naito Y,** Saito K, Shiiba K, Ohuchi A, Saigenji K, Nagura H, Ohtani H. CD8+ T cells infiltrated within cancer cell nests as a prognostic factor in human colorectal cancer. *Cancer Res* 1998; **58:** 3491-3494

24 **Wakabayashi O,** Yamazaki K, Oizumi S, Hommura F, Kinoshita I, Ogura S, Dosaka-Akita H, Nishimura M. CD4(+) T cells in cancer stroma, not CD8(+) T cells in cancer cell nests, are associated with favorable prognosis in human non-small cell lung cancers. *Cancer Sci* 2003; **94:** 1003-1009

25 **Arima K,** Nakagawa M, Yanagawa M, Sugimura Y, Tochigi

H, Kawamura J. Prognostic factors of peripheral blood lymphocyte subsets in patients with renal cell carcinoma. *Urol Int* 1996; **57:** 5-10

26 **Nozoe T,** Miyazaki M, Saeki H, Ohga T, Sugimachi K. Significance of allogenic blood transfusion on decreased survival in patients with esophageal carcinoma. *Cancer* 2001; **92:** 1913-1918

Science Editor Wang XL and Guo SY **Language Editor** Elsevier HK

PO Box 2345, Beijing 100023, China
www.wjgnet.com
wjg@wjgnet.com

ELSEVIER

World J Gastroenterol 2005;11(42):6694-6700
World Journal of Gastroenterology ISSN 1007-9327

• *BRIEF REPORTS* •

DNA end binding activity and Ku70/80 heterodimer expression in human colorectal tumor

Paola Mazzarelli, Paola Parrella, Davide Seripa, Emanuela Signori, Giuseppe Perrone, Carla Rabitti, Domenico Borzomati, Armando Gabbrielli, Maria Giovanna Matera, Carolina Gravina, Marco Caricato, Maria Luana Poeta, Monica Rinaldi, Sergio Valeri, Roberto Coppola, Vito Michele Fazio

Paola Mazzarelli, Emanuela Signori, Maria Luana Poeta, Vito Michele Fazio, Laboratory of Molecular Medicine and Biotechnology, Interdisciplinary Center for Biomedical Research, Università Campus Bio-Medico, Rome 00155, Italy
Paola Parrella, Davide Seripa, Maria Giovanna Matera, Carolina Gravina, Vito Michele Fazio, Laboratory of Gene Therapy and Oncology, IRCCS "Casa Sollievo della Sofferenza" Hospital, San Giovanni Rotondo (FG) 71013, Italy
Giuseppe Perrone, Carla Rabitti, Service of Histopathology, Università Campus Bio-Medico, Rome 00155, Italy
Domenico Borzomati, Marco Caricato, Sergio Valeri, Roberto Coppola, Department of General Surgery, Università Campus Bio-Medico, Rome 00155, Italy
Armando Gabbrielli, Department of Digestive Disease, Università Campus Bio-Medico, Rome 00155, Italy
Emanuela Signori, Monica Rinaldi, Vito Michele Fazio, CNR Gene-Medicine Division, Section of Molecular Medicine, Institute of Neurobiology and Molecular Medicine, Rome 00133, Italy
Supported by Italian Ministero della Salute, IRCCS, RC0302TG13, and by Ministero dell'Istruzione, Università e Ricerca scientifica e tecnologica (MIUR), COFIN2002, to the Università Campus Bio-Medico
Correspondence to: Professor Vito Michele Fazio, Laboratory of Molecular Medicine and Biotechnology, Università Campus Bio-Medico, Via Longoni, 83, Rome 00155, Italy. fazio@unicampus.it
Telephone: +39-06-22541780 Fax: +39-06-22541780
Received: 2005-02-01 Accepted: 2005-04-26

Abstract

AIM: To determine the DNA binding activity and protein levels of the Ku70/80 heterodimer, the functional mediator of the NHEJ activity, in human colorectal carcinogenesis.

METHODS: The Ku70/80 DNA-binding activity was determined by electrophoretic mobility shift assays in 20 colon adenoma and 15 colorectal cancer samples as well as matched normal colonic tissues. Nuclear and cytoplasmic protein expression was determined by immunohistochemistry and Western blot analysis.

RESULTS: A statistically significant difference was found in both adenomas and carcinomas as compared to matched normal colonic mucosa (P<0.00). However, changes in binding activity were not homogenous with approximately 50% of the tumors showing a clear increase in the binding activity, 30% displaying a modest increase and 15% showing a decrease of the activity. Tumors, with increased DNA-binding activity, also showed a statistically significant increase in Ku70 and Ku86 nuclear expression, as determined by Western blot and immunohistochemical analyses (P<0.001). Cytoplasmic protein expression was found in pathological samples, but not in normal tissues either from tumor patients or from healthy subjects.

CONCLUSION: Overall, our DNA-binding activity and protein level are consistent with a substantial activation of the NHEJ pathway in colorectal tumors. Since the NHEJ is an error prone mechanism, its abnormal activation can result in chromosomal instability and ultimately lead to tumorigenesis.

Key words: Colorectal cancer; Colon adenoma; DNA-dependent protein kinase; Ku70/80 heterodimer; Mismatch repair; Non-homologous end joining; Double strand break repair; Chromosomal instability

Mazzarelli P, Parrella P, Seripa D, Signori E, Perrone G, Rabitti C, Borzomati D, Gabbrielli A, Matera MG, Gravina C, Caricato M, Poeta ML, Rinaldi M, Valeri S, Coppola R, Fazio VM. DNA end binding activity and Ku70/80 heterodimer expression in human colorectal tumor. *World J Gastroenterol* 2005; 11(42): 6694-6700
http://www.wjgnet.com/1007-9327/11/6694.asp

INTRODUCTION

Colorectal cancer is a significant cause of morbidity and mortality in Western populations[1]. This cancer progresses through a series of defined histopathological stages, going from a small benign tumor (adenomatous polyps) to a malignant cancer (carcinoma)[2]. During tumor progression, a stepwise accumulation of genetic changes is observed, leading to inactivation of tumor suppressor genes (e.g. APC, p53) and activation of oncogenes (e.g. K-ras, β-catenin)[2]. The number of genomic alterations in cancer appears to exceed the level possibly due to the accumulation of mutations in cells with normal mutation rates. A number of intricate networks have evolved in eukaryotic cells to respond to exogenous and endogenous genotoxic stimuli[3]. Genes involved in these pathways play

a crucial role in maintaining DNA integrity and a defect in these processes may result in hypersensitivity to DNA damaging agents and genomic instability[4]. Two main forms of genetic instability are associated with tumors. One arises from the inactivation of DNA mismatch repair (MMR) genes[5], leading to instability at the nucleotide sequence level (microsatellite instability, MSI). The other results from a disruption of the pathways intending to protect the cells from chromosomal breakage (double-strand breaks, DSBs), which leads to gross chromosomal rearrangements (chromosomal instability, CIN)[6]. Of the many types of DNA damage, DSBs are the most dangerous, because of the intrinsic difficulty of their repair as compared to other types of DNA damage[6]. In physiological conditions, DNA-DSBs are generated by homologous recombination (HR) during meiosis and occur in other events, such as V(D)J recombination and immunoglobulin class switch[6]. In addition, DSBs can result from both exogenous agents such as ionizing radiation or chemotherapeutic agents and endogenously generated reactive oxygen species[6]. Erroneous rejoining of the broken DNA-DSBs may cause loss or amplification of chromosomal material and even translocations, ultimately leading to tumorigenesis[4].

There are two distinct and complementary mechanisms for DNA-DSB repair: the NHEJ and the HR[4]. Recently, a caretaker role in preventing carcinogenesis has been proposed for the NHEJ pathway[7-9]. At present, five proteins involved in the NHEJ pathway have been identified; namely, the ligase IV and its associated protein XRCC1, and the three components of the DNA-dependent protein kinase (DNA-PK) complex, Ku70, Ku86, and the catalytic subunit PKcs[10]. Mutational analysis has shown that activation of the DNA-PK well correlates with Ku protein heterodimerization and DNA-end binding[11]. Once anchored to the DNA, the Ku70/80 heterodimer translocates along the molecule and facilitates recruitment of the catalytic subunit to the site of the break, to form an activated DNA-PK complex[11]. Numerous studies have investigated the role of MMR pathway in colorectal carcinogenesis, but little is known about the involvement of the DSB repair pathway in the adenoma/carcinoma sequence[11-13]. In the attempt to better understand this role, we analyzed the DNA-binding activity of the Ku70/80 heterodimer and the protein expression of the two Ku subunits in colon adenomas, colorectal cancers and matched normal tissues. Ku70/80 DNA binding activity was increased in approximately 50% of adenoma and carcinoma samples, as compared to matched normal tissues. In tumors with increased DNA-binding activity, Ku70 and Ku86 protein expression correlated with the heterodimer binding activity.

MATERIALS AND METHODS

Patients characteristics and tissue samples

Twenty patients with colon adenoma and 15 patients with colorectal carcinoma were recruited in the study. The patients underwent endoscopic polypectomy or surgical resection between 1999 and 2002, at the Departments of Gastroenterology and General Surgery, Campus Bio-Medico University of Rome, Italy. None of the patients were affected by familial polyposis or HNPCC. Subjects included 20 males (57%) and 15 females (43%), with a mean age of 69.5±12 years (range 35-82 years). None had pre-operative chemotherapy or irradiation. All the patients gave informed consent for the study. Thirty-one lesions (89% including adenomas and carcinomas) were located in the colon and 4 (11%) in the rectum. Adenomas were classified according to the National Polyp Study Cohort and WHO recommendations on the basis of size and grade of dysplasia[14,15]. Clinical staging of colorectal cancer was assessed according to the Dukes' classification[13].

Preparation of cell and nuclear extracts

Following surgical resection, tissue samples were immediately frozen at -80 °C. For each case, before protein extraction, one 3-μm hematoxylin-eosin stained slide was analyzed to ensure that tumor samples contained at least 70% cancer cells. Protein extraction was performed as previously described[16-18]. Briefly, frozen samples were mechanically fractionated to obtain a cellular suspension. Nuclear and cytoplasmic fractions were separated by centrifugation at 10 000 *g* and stored at -80 °C.

Protein content in nuclear and cytoplasmic extracts was determined in triplicate by Bradford assay (Bio-Rad Protein Assay, Bio-Rad Laboratories, Munchen).

Gel-shift assay

Electrophoretic mobility shift assay (EMSA) was performed as described previously[18,19]. Briefly, DNA binding reactions contained 50 000 cpm of the labeled probe, nuclear (2 μg) or cytoplasmic (5 μg) extracts with closed circular plasmid DNA pUC-19 (1 μg) as the unspecific competitor. For each sample, three single shift assays were performed. As controls, 33 normal human tissues from patients without colon tumor were analyzed (mammary gland $n = 8$, bladder mucosa $n = 8$, and skin $n = 17$).

To normalize all the samples, electrophoretic mobility shift assays were performed by incubating the nuclear extracts (3 μg) with 50 000 cpm/sample of ^{32}P-end labeled Sp-1 oligonucleotide (Promega Corporation, Madison, WI, USA) in a binding buffer, with 1 μg of poly (dI-dC) as the unspecific competitor. The correction factor (CF) was calculated as follows: *SP1 binding activity in the sample/mean SP1 binding activity*. Data were normalized using the following formula: *Mean Ku70/80 binding activity/CF*[20].

For gel supershift experiments, goat polyclonal anti-Ku70 and anti-Ku86 antibodies (M-19, M-20: Santa Cruz Biotechnologies Inc., CA, USA) were incubated with protein extracts for 30 min at room temperature, before the other components were added to the binding reaction. Complexes were separated on 6% non-denaturing polyacrylamide gels and exposed to X-ray films (Amersham-Pharmacia Biotech, England HP7 9NA).

The optical densities (OD) were obtained by scanning densitometry using colon carcinoma cell line CaCo-2 (ATCC) as internal control (OD = 10.7±6.4).

Supershift control experiments confirmed the specificity of the results in each gelshift assay experiment.

Immunohistochemistry

Paraffin sections from matched normal colonic mucosa were available for all the colon cancer cases entered in the study, whereas paraffin embedded blocks from matched normal tissues were available only for 10 adenomas. Paraffin sections from five subjects who showed normal colonic mucosa at colonoscopy were also analyzed. Consecutive two micron sections were immunostained for Ku70 and Ku86 following the streptavidin-biotin method, as described previously[20] . In brief, sections were deparaffinized, rehydrated in decreasing alcohol and microwave treated. Endogenous peroxidase activity was quenched by treatment with 0.03% hydrogen peroxide in absolute methanol for 30 min at room temperature. The primary antibodies were goat polyclonal anti-Ku70 and anti-Ku86 antibodies specifically validated for immunohistochemical analysis of paraffin embedded tissues (M-19, M-20: Santa Cruz Biotechnology Inc., CA, USA), in a 1:200 dilution. Biotinylated swine antigoat/mouse/rabbit IgG (Dako A/S, Denmark) was used as secondary antibody. After washing, sections were treated with streptavidin-peroxidase reagent (Dakopatts A\S, Denmark), incubated with diaminobenzidine (DAB) and counterstained with hematoxylin. Slides were examined under a two-head microscope by two pathologists, unaware of the clinical data and molecular results. No discrepant results were identified. Results of the nuclear immunostaining were expressed as percentage of positively stained cells. For cytoplasmic staining the microscopic analysis was not able to discriminate one cell from another. Thus the immunoreactivity was classified into four staining levels (SL): 0 SL (no staining); 1 SL (1-33% of positively stained area); 2 SL (33-66% of the area), and 3 SL (66-99% of the area)[21].

Western blotting

Protein extracts (10 μg) were separated in 10% SDS-PAGE, transferred to a PVDF membrane (Hybond-P, Amersham-Pharmacia Biotech, UK HP7 9NA) using an electroblotting apparatus, and incubated for 1 h at room temperature in 1% BSA, 1% skim milk (Difco Lab., Detroit, MI, USA), and 0.5% Tween 20 (USB, Cleveland, OH, USA). Membranes were stained with Ponceau S dye, to check for equal loading and homogeneous transfer. Immunodetection experiments were performed as described previously[17]. Filters were reprobed with anti β-actin (Sigma-Aldrich, St. Louis, MO 63103, USA) mouse IgG_1 monoclonal antibody, to normalize the nuclear protein levels. Filters were washed and developed using an enhanced chemiluminescence system (ECL, Amersham-Pharmacia Biotech, UK HP7 9NA). The optical densities (OD) were obtained by scanning densitometric analysis of the bands normalized for the β-actin levels, as reference protein.

Statistical analysis

All values provided in the text and figures are means of three independent experiments±standard deviations (SD). Variation rates (VR) were defined by the following formula: [(*pathological sample value–normal sample value)/pathological sample value*]×100. Mean values were compared using the one- or two-tailed Student's *t*-test, for independent samples. $P<0.05$ was considered statistically significant.

RESULTS

Nuclear and cytoplasmic Ku70/80 DNA-binding activity

EMSA were performed on nuclear extracts of colon tissues, to compare the DNA binding activity of the Ku70/80 heterodimer in adenoma and carcinoma samples as well as matched normal colonic mucosa samples (Figure 1A). We found that adenoma and carcinoma samples had an overall increase in DNA binding activity as compared to matched normal samples ($P<0.01$, Table 1). However, these variations were not homogeneous among the tumors that were tested. Since the overall increase in binding activity compared to normal was approximately 50% (Table 1), we set this value as the cut-off for better classifying our pathological samples. Of the 20 adenomas, 11 (55%) showed an increase in DNA binding activity higher than 50% ($P = 0.000$) (Figure 1A, Group I), 6 (30%) displayed an increase in DNA binding activity lower than 50% (P = NS) (Figure 2A, Group II), and 3 (15%) showed reduced levels of activity ($P = 0.04$) (Figure 2A, Group III). Of the 15 carcinomas, 7 (47%) displayed an increase in DNA binding activity higher than 50% (Figure 2B, Group I), 6 (40%) showed an increase in DNA binding activity lower than 50% ($P<0.02$) (Figure 2B, Group II), and 2 (13%) showed reduced levels of activity (P = ND) (Figure 2B, Group III).

No significant differences were found when the Ku70/80 DNA-binding activity was compared in adenoma and carcinoma samples (Table 1). We also determined, if functional Ku70/80 heterodimer was present in cytoplasmic protein extracts. Cytoplasmic Ku70/80 DNA binding activity was only found in three colorectal cancers, whereas adenomas did not show cytoplasmic activity (Figure 1B). No statistically significant correlation was found when results of nuclear and cytoplasmic Ku70/80 DNA-binding activity were compared with clinical parameters.

Table 1 Statistical summary of Ku70/80 DNA binding activity and Ku70 protein expression in pathological samples and matched normal tissues (mean±SD)

Colon	Ku70/80 DNA binding activity			Ku70 protein expression		
Tissue	Normal	Tumor	*P*	Normal	Tumor	*P*
Adenomas	2.66±2.32	5.01±3.15	<0.01	0.88±0.59	1.28±0.45	<0.01
Carcinomas	2.99±2.84	5.35±2.75	<0.001	1.09±0.80	1.77±0.83	<0.01

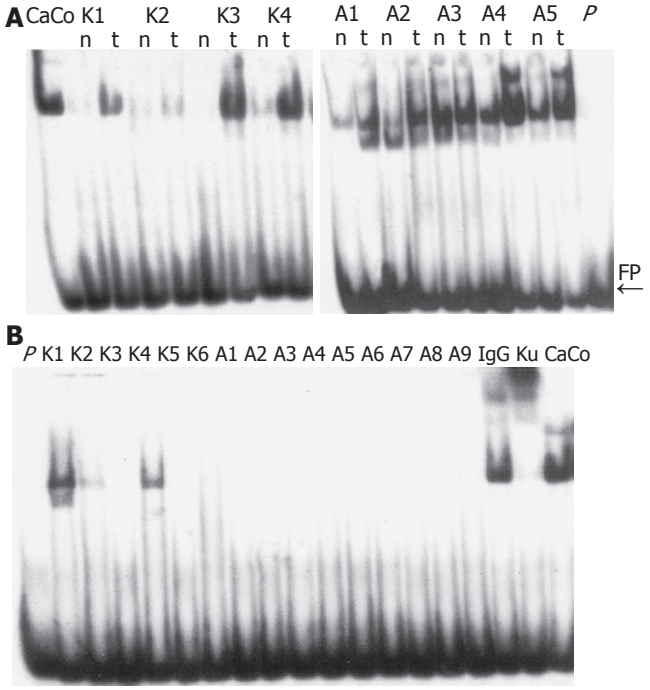

Figure 1 Representative gel shift experiments on nuclear (**A**) and cytoplasmic (**B**) extracts from human colon tissues. Panel A: Normal (n) and pathologic (t) nuclear extracts, obtained from four colorectal cancer (K1-K4) and five adenoma (A1-A5) patients, were analyzed by EMSA as described in "Materials and methods". The positions of Ku band-shifts and of the free probe (FP) are indicated. The binding activity in nuclear extracts from the CaCo-2 cell line (CaCo) has been used as a standard in order to compare the activity in the different gels. Lane P: free probe without protein extract. Panel B: EMSA was performed on pathologic cytoplasmic extracts from colorectal cancer (K1-K6) and adenoma (A1-A9) patients. Lane P: free probe without protein extract.

Ku70 and Ku86 expression in nuclear and cytoplasmic protein extracts

In adenomas and carcinomas with increased DNA-binding activity, the Ku70 nuclear levels were markedly increased as compared to matched normal samples ($P<0.000$) (Figures 3A and B, Group I), whereas protein level changes were not statistically significant in tumors with minimal increases or reduced binding activity (Figures 3A and B, Groups II and III). Representative results are shown in Figure 4.

In all the samples, Ku86 protein levels were always lower than Ku70 and in most cases it was undetectable (data not shown). Analysis of cytoplasmic protein extracts showed barely detectable Ku70 protein in normal colon tissues and a significant increase in pathologic samples with increased DNA binding activity (0.22±0.3 OD and 0.80±0.2 OD, respectively, $P = 0.001$) (data not shown). Ku86 protein subunit was undetectable by Western blot analysis on cytoplasmic extracts.

Ku70 and Ku86 immunohistochemical analysis

A significant increase in the percentage of stained nuclei was found for Ku70 and Ku86 subunits in all adenoma and carcinoma samples, as compared to matched normal tissues ($P<0.000$) but no statistically significant differences were found between adenoma and carcinoma samples (Table 3). In all cases, Ku subunits were not detected in the cytoplasm of normal colonic mucosa ($n = 25$) from patients or healthy donors ($n = 5$) (SL 0). For Ku70, a low level (SL 1) of cytoplasmic staining was detected in 11 of the 20 adenomas (55%), and in 3 of the 15 carcinomas

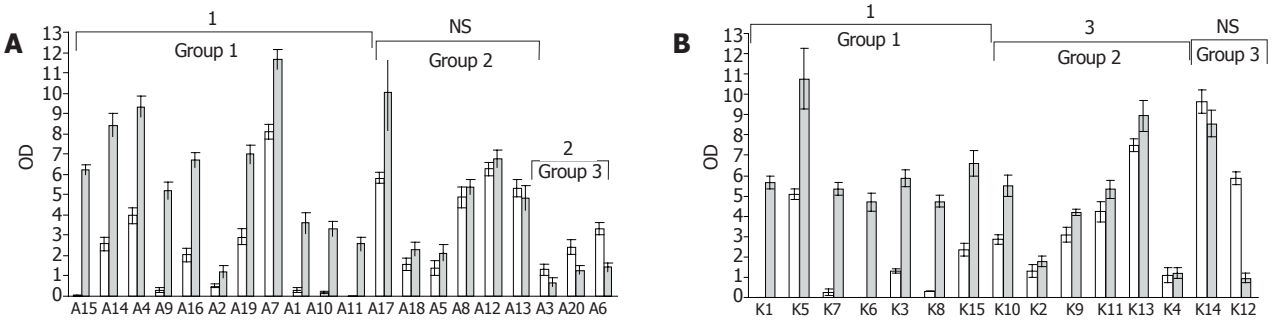

Figure 2 Changes in Ku70/Ku80 heterodimer DNA binding activity in adenoma (**A**) and carcinoma (**B**) compared to matched normal colonic mucosa. □ Normal; ▨ Tumor; vertical bars indicate standard deviation from the mean of three independent experiments. Adenomas (**A**) and carcinomas (**B**) samples characterize by: Group 1 more than 50% increase in DNA binding activity; Group 2 modest increase in binding activity; Group 3 reduced binding activity, $^1P<0.000$ *vs* group 1; $^2P<0.04$ *vs* group 3; $^3P<0.02$ *vs* group 2.

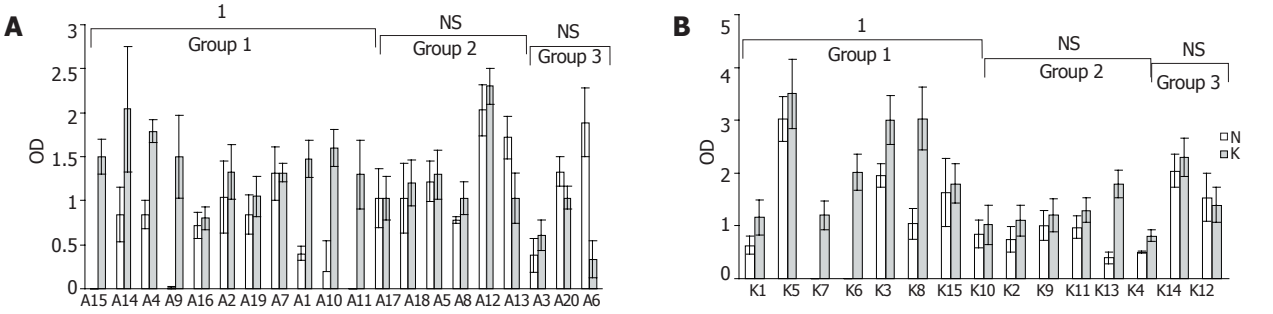

Figure 3 Changes in Ku70 protein levels determined by Western blot analysis in adenoma (**A**) and carcinoma (**B**) compared to matched normal colonic mucosa. □ Normal; ▨ Tumor; vertical bars indicate standard deviation from the mean of three independent experiments. Adenomas (**A**) and carcinomas (**B**) are grouped according to the criteria described in Figure 2, $^1P<0.000$ *vs* group 1.

(20%, $P = 0.089$). For Ku86, 17 of the 20 adenomas (85%) showed medium levels of cytoplasmic staining (SL 2-3), and 5 of the 15 carcinomas (34%) displayed cytoplasmic staining with SL 1-2 ($P = 0.004$). Ku86 cytoplasmic staining showed a typical granular pattern, probably due to the presence of protein subunit in cytoplasmic vesicles (Figure 5).

DISCUSSION

The NHEJ pathway plays a pivotal role in the repair of DSBs. Several studies on cell lines and knock-out mice suggest that a non-functional NHEJ can induce an increased level of genomic instability and lead to cancer progression[22-24]. In a previous study, we found a downregulation of the Ku70/80 DNA binding activity in advanced breast and bladder human cancers, as compared to non-invasive or low stage tumors[17]. This observation was also confirmed in a patient affected by sporadic multiple basal cell carcinoma, where we demonstrated a differential modulation of the NHEJ pathway in non-aggressive and aggressive tumors, showing that the first is an upregulation system, and the latter a strong downregulation system[20].

In the present study, we investigated the involvement of the ku70/80 heterodimer during progression from adenoma to carcinoma. Our results indicated that the NHEJ pathway was activated in approximately half of the cases, with no differences in binding activity between adenomas and carcinomas. In these tumors, the increase in DNA binding activity correlated with protein levels of the Ku subunits as determined by Western blot and immunohistochemical analysis. Moreover the cytoplasmic accumulation of the Ku70 and Ku86 protein subunits only in neoplastic tissues is also indicative of an upregulation of the NHEJ system. The NHEJ pathway repairs DSBs by modifying the two DNA broken ends prior to rejoining, and few nucleotides at each end of the DNA break are lost during this process[23]. Thus, the repair through the NHEJ can potentially lead to chromosomal alterations. Rothkamm *et al*.[25] found that after X-ray exposure, NHEJ-proficient cells form misrejoinings and multiple DSBs more frequently than NHEJ deficient cells. Also, myeloid leukemia cells characterized by gross chromosomal abnormalities show a higher end-joining efficiency but a lower DSB repair fidelity, as compared to lymphocytes from healthy donors[24]. Thus, the upregulation of the NHEJ system in adenoma and colon carcinoma may be

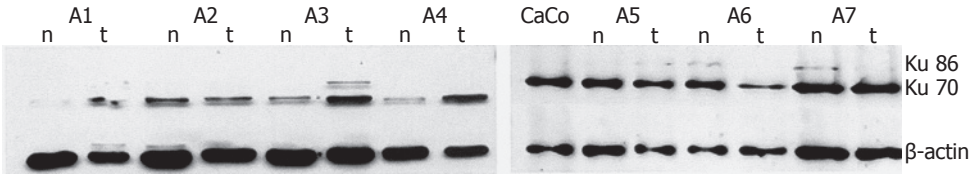

Figure 4 Representative immunoblot experiments on nuclear extracts from adenoma cases p70 and p86 protein expression was evaluated by Western blot, on normal (n) and pathologic (t) nuclear extracts from adenoma patients (A1-A7). The p86 protein was slightly detectable on this and on the other filters analyzed. CaCo-2 cell line nuclear extracts (CaCo) were used as internal standard. Filters were reprobed with anti-β-actin monoclonal antibody to normalize the protein levels.

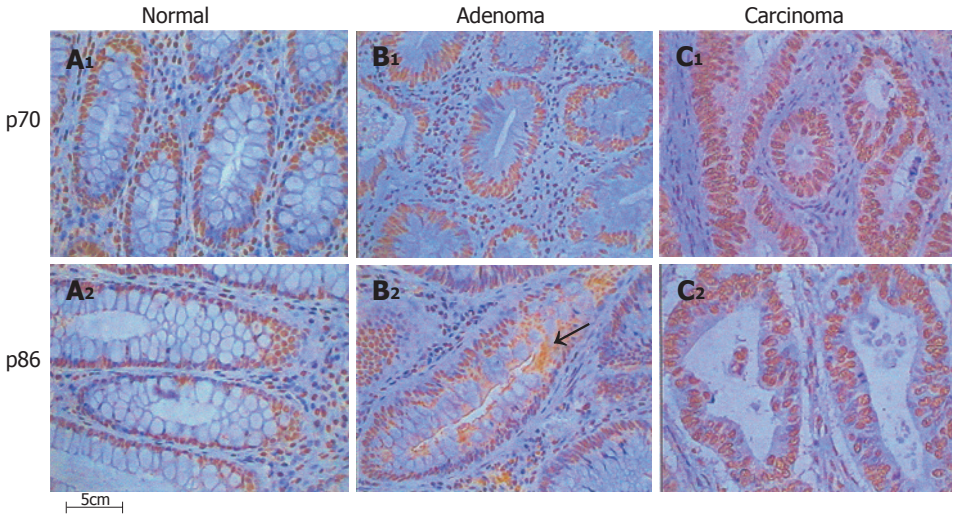

Figure 5 Expression of DNA-PK protein subunits in human colon tissues. Tissue sections were stained by immunohistochemistry for Ku70 and Ku86 proteins, as described in "Materials and methods". The increase of positively stained cells is evident in the nuclei of adenoma and carcinoma sections, respect to the normal controls. Ku70 nuclear expression is uniform and displays a higher intensity of staining as compared with p86, as described in the text. No cytoplasmic expression is evident in the normal mucosa sections for any of the protein subunits, whereas it is clearly visible in the pathologic tissues. Ku86 was expressed in the cytoplasm following a speckled pattern of staining, as evident on the adenoma section (arrow). Original magnification ×400. **A**$_{1\text{-}2}$: Normal; **B**$_{1\text{-}2}$: Adenoma; **C**$_{1\text{-}2}$: Carcinoma.

Table 2 Ku70 and Ku86 nuclear immunostaining in adenomas and matched normal tissues

Adenomas	Ku70		Ku86	
	Normal	Tumor	Normal	Tumor
A1	61	93	40	81
A2	65	81	33	70
A3	60	83	31	63
A4	61	82	35	71
A5	65	79	32	75
A6	58	68	39	62
A7	64	74	26	62
A16	51	75	25	71
A17	79	92	24	63
A19	61	87	29	62
Carcinomas				
K1	66	95	27	78
K2	48	76	37	62
K3	66	84	26	71
K4	47	86	40	86
K5	72	85	34	70
K6	76	86	26	61
K7	72	88	28	76
K8	51	92	17	79
K9	62	96	44	65
K10	65	90	51	71
K11	56	94	51	66
K12	52	82	34	73
K13	65	85	25	66
K14	52	92	18	64
K15	65	73	28	65

responsible for an increase in genomic rearrangements and chromosomal defects, contributing to tumor progression.

Although increase in DNA binding activity was the more frequent abnormality detected in our series of adenomas and carcinomas, we also identified a subset of colon neoplasia (approximately 15%) that showed reduced levels of DNA binding activity. Rigas *et al*.[26] have previously analyzed protein expression of the DNA-PK subunits in adenomas and colorectal cancers by IHC assay. By using a score that correlates the intensity of staining to the percentage of stained cells, a decrease in protein expression levels is demonstrated for all DNA-PK subunits in adenoma and carcinoma samples, as compared to normal tissues[26]. In our study the reduction in DNA binding activity did not correlate completely with Ku subunit protein levels. While three of the adenomas and one of the cancers showed a decrease of Ku70 expression by Western blot analysis, the remaining adenoma and carcinoma samples displayed an increase in protein expression. IHC data also showed an increase in the percentage of nuclear stained cells in the tumor as compared to the normal colonic mucosa. We can speculate that in this subset of tumors the NHEJ proteins are expressed and localized in the nuclei, but they are not functional, due to post-translational regulation mechanisms or mutations in one or more components of the NHEJ pathway.

Overall, our results indicate that the NHEJ pathway

Table 3 Statistical summary of Ku70 and Ku86 nuclear immunostaining in pathological samples and matched normal tissues (mean±SD)

Colon tissue	Ku70			Ku86		
	Normal	Tumor	*P*	Normal	Tumor	*P*
Adenomas	63.39±7.72	80.22±7.52	0.000	30.48±5.43	67.57±7.64	0.000
Carcinomas	61.42±9.66	87.34±6.97	0.000	32.86±11.29	70.36±7.55	0.000
Healthy	74.20±6.38	-	-	32.00±5.10	-	-

is activated in colon adenoma and carcinoma, with only a subset of tumors showing decreased binding activity. These results however do not exclude an involvement of the NHEJ pathway in colon carcinogenesis, rather suggest the presence of colon cancer subsets that may differ in their biological behavior. Since Ku70 and Ku80 protein levels are correlated to tumor radiosensitivity and response to chemotherapy in human colorectal cancer and experimental models[27–30], the clarification of the mechanisms involved in DNA repair may ultimately lead to an improved management of colorectal cancer patients.

ACKNOWLEDGMENT

The authors thank Miss Simona Virga for skilful help with artwork and manuscript preparation.

REFERENCES

1 **DeVita VT Jr**, Hellmann S, Rosemberg SA, eds. Cancer. Principles and Practice of Oncology. Philadelphia, New York: Lippincott-Raven, 1997: 1144-97.
2 **Fearon ER**, Vogelstein B. A genetic model for colorectal tumorigenesis. *Cell* 1990; **61**: 759-767
3 **Rouse J,** Jackson SP. Interfaces between the detection, signaling, and repair of DNA damage. *Science* 2002; **297**: 547-551
4 **Khanna KK,** Jackson SP. DNA double-strand breaks: signaling, repair and the cancer connection. *Nat Genet* 2001; **27**: 247-254
5 **Loeb LA.** A mutator phenotype in cancer. *Cancer Res* 2001; **61**: 3230-3239
6 **van Gent DC,** Hoeijmakers JH, Kanaar R. Chromosomal stability and the DNA double-stranded break connection. *Nat Rev Genet* 2001; **2**: 196-206
7 **Difilippantonio MJ**, Zhu J, Chen HT, Meffre E, Nussenzweig MC, Max EE, Ried T, Nussenzweig A. DNA repair protein Ku80 suppresses chromosomal aberrations and malignant transformation. *Nature* 2000; **404**: 510-514
8 **Ferguson DO**, Sekiguchi JM, Chang S, Frank KM, Gao Y, DePinho RA, Alt FW. The nonhomologous end-joining pathway of DNA repair is required for genomic stability and the suppression of translocations. *Proc Natl Acad Sci USA* 2000; **97**: 6630-6633
9 **Gao Y**, Ferguson DO, Xie W, Manis JP, Sekiguchi J, Frank KM, Chaudhuri J, Horner J, DePinho RA, Alt FW. Interplay of p53 and DNA-repair protein XRCC4 in tumorigenesis, genomic stability and development. *Nature* 2000; **404**: 897-900
10 **Jackson SP**. Sensing and repairing DNA double-strand breaks. *Carcinogenesis* 2002; **23**: 687-696
11 **Wang J**, Dong X, Reeves WH. A model for Ku heterodimer assembly and interaction with DNA. Implications for the function of Ku antigen. *J Biol Chem* 1998; **273**: 31068-31074
12 **Jin S,** Weaver DT. Double-strand break repair by Ku70 requires heterodimerization with Ku80 and DNA binding

functions. *EMBO J* 1997; **16**: 6874-6885
13 **Li GC**, He F, Shao X, Urano M, Shen L, Kim D, Borrelli M, Leibel SA, Gutin PH, Ling CC. Adenovirus-mediated heat-activated antisense Ku70 expression radiosensitizes tumor cells in vitro and in vivo. *Cancer Res* 2003; **63**: 3268-3274
14 **O'Brien MJ**, Winawer SJ, Zauber AG, Gottlieb LS, Sternberg SS, Diaz B, Dickersin GR, Ewing S, Geller S, Kasimian D. The National Polyp Study. Patient and polyp characteristics associated with high-grade dysplasia in colorectal adenomas. *Gastroenterology* 1990; **98**: 371-379
15 **Jass JR** and Sobin LH. Histological typing of intestinal tumours: World Health Organization. 1989. Springer, Berlin.
16 **Dignam JD**, Lebovitz RM, Roeder RG. Accurate transcription initiation by RNA polymerase II in a soluble extract from isolated mammalian nuclei. *Nucleic Acids Res* 1983; **1**: 1475-1489
17 **Pucci S**, Mazzarelli P, Rabitti C, Giai M, Gallucci M, Flammia G, Alcini A, Altomare V, Fazio VM. Tumor specific modulation of KU70/80 DNA binding activity in breast and bladder human tumor biopsies. *Oncogene* 2001; **20**: 739-747
18 **Lahiri DK**, Ge Y. Electrophoretic mobility shift assay for the detection of specific DNA-protein complex in nuclear extracts from the cultured cells and frozen autopsy human brain tissue. *Brain Res Brain Res Protoc* 2000; **5**: 257-265
19 **Frasca D**, Barattini P, Goso C, Pucci S, Rizzo G, Bartoloni C, Costanzo M, Errani A, Guidi L, Antico L, Tricerri A, Doria G. Cell proliferation and ku protein expression in ageing humans. *Mech Ageing Dev* 1998; **100**: 197-208
20 **Mazzarelli P**, Rabitti C, Parrella P, Seripa D, Persichetti P, Marangi GF, Perrone G, Poeta ML, Delfino M, Fazio VM. Differential modulation of Ku70/80 DNA-binding activity in a patient with multiple basal cell carcinomas. *J Invest Dermatol* 2003; **121**: 628-633
21 **Kumagai I**, Masuda T, Sato S, Ishikawa K. Immunoreactivity to monoclonal antibody, Hep Par 1, in human hepatocellular carcinomas according to histopathological grade and histological pattern. *Hepatol Res* 2001; **20**: 312-319
22 **Lanuszewska J**, Widlak P. The truncation of Ku86 in human lymphocytes. *Cancer Lett* 2004; **205:** 197-205
23 **Lieber MR**, Ma Y, Pannicke U, Schwarz K. Mechanism and regulation of human non-homologous DNA end-joining. *Nat Rev Mol Cell Biol* 2003; **4**: 712-720
24 **Choi EK**, Lee YH, Choi YS, Kwon HM, Choi MS, Ro JY, Park SK, Yu E. Heterogeneous expression of Ku70 in human tissues is associated with morphological and functional alterations of the nucleus. *J Pathol* 2002; **198**: 121-130
25 **Rothkamm K,** Lobrich M. Evidence for a lack of DNA double-strand break repair in human cells exposed to very low x-ray doses. *Proc Natl Acad Sci U S A* 2003; **100**: 5057-5062
26 **Rigas B,** Borgo S, Elhosseiny A, Balatsos V, Manika Z, Shinya H, Kurihara N, Go M, Lipkin M. Decreased expression of DNA-dependent protein kinase, a DNA repair protein, during human colon carcinogenesis. *Cancer Res* 2001; **61**: 8381-8384
27 **Komuro Y**, Watanabe T, Hosoi Y, Matsumoto Y, Nakagawa K, Tsuno N, Kazama S, Kitayama J, Suzuki N, Nagawa H. The expression pattern of Ku correlates with tumor radiosensitivity and disease free survival in patients with rectal carcinoma. *Cancer* 2002; **95**: 1199-1205
28 **Komuro Y**, Watanabe T, Hosoi Y, Matsumoto Y, Nakagawa K, Saito S, Ishihara S, Kazama S, Tsuno N, Kitayama J, Suzuki N, Tsurita G, Muto T, Nagawa H. Prediction of tumor radiosensitivity in rectal carcinoma based on p53 and Ku70 expression. *J Exp Clin Cancer Res* 2003; **22**: 223-228
29 **Achanta G**, Pelicano H, Feng L, Plunkett W, Huang P. Interaction of p53 and DNA-PK in response to nucleoside analogues: potential role as a sensor complex for DNA damage. *Cancer Res* 2001; **61**: 8723-8729
30 **Muller C**, Christodoulopoulos G, Salles B, Panasci L. DNA-Dependent protein kinase activity correlates with clinical and in vitro sensitivity of chronic lymphocytic leukemia lymphocytes to nitrogen mustards. *Blood* 1998; **92**: 2213-2219

Science Editor Wang XL and Guo SY **Language Editor** Elsevier HK

PO Box 2345, Beijing 100023, China
www.wjgnet.com
wjg@wjgnet.com

ELSEVIER

World J Gastroenterol 2005;11(42):6701-6706
World Journal of Gastroenterology ISSN 1007-9327

• *BRIEF REPORTS* •

Correlation and prognostic significance of beta-galactoside alpha-2,6-sialyltransferase and serum monosialylated alpha-fetoprotein in hepatocellular carcinoma

Terence CW Poon, Clarissa HS Chiu, Paul BS Lai, Tony SK Mok, Benny Zee, Anthony TC Chan, Joseph JY Sung, Philip J Johnson

Terence CW Poon, Joseph JY Sung, Department of Medicine and Therapeutics, Sir YK Pao Cancer Centre, the Chinese University of Hong Kong, Prince of Wales Hospital, NT, Hong Kong, China
Clarissa HS Chiu, Tony SK Mok, Benny Zee, Anthony TC Chan, Department of Clinical Oncology, Sir YK Pao Cancer Centre, the Chinese University of Hong Kong, Prince of Wales Hospital, NT, Hong Kong, China
Paul BS Lai, Department of Surgery, Sir YK Pao Cancer Centre, the Chinese University of Hong Kong, Prince of Wales Hospital, NT, Hong Kong, China
Philip J Johnson, Cancer Research UK Institute for Cancer Studies, University of Birmingham, Vincent Drive, Edgbaston, Birmingham B15 2TT, United Kingdom
Supported by Central Allocation Grant CUHK 2/02C from the University Grants Committee of Hong Kong, and the Direct Grant for Research (2040750) from the Chinese University of Hong Kong
Co-first authors: Terence CW Poon and Clarissa HS Chiu
Correspondence to: Terence CW Poon, PhD, Assistant Professor, Department of Medicine and Therapeutics, the Chinese University of Hong Kong, Prince of Wales Hospital, Shatin, Hong Kong, China. tcwpoon@cuhk.edu.hk
Telephone: +852-2632-1205 Fax: +852-2648-8842
Received: 2005-02-26 Accepted: 2005-06-02

Abstract

AIM: To investigate the correlation between tissue ST6Gal I and serum msAFP in HCC patients, and to investigate their prognostic significance.

METHODS: Preoperative sera, paired tumorous and non-tumorous tissues were collected from 19 consecutive patients who had undergone surgical resection of HCC. ST6Gal I activities in the tissues were measured by an *in vitro* microsomal enzyme activity assay. The percentages of tumor-specific msAFP in the sera were also estimated by an isoelectric focusing-immunoblotting assay.

RESULTS: The tumor ST6Gal I activity was negatively correlated with serum msAFP percentage (r = -0.53, P = 0.019). Both decreased tumor ST6Gal I activity and increased serum msAFP percentage were associated with poor tumor cell differentiation. Univariate analyses showed that both decreased tumor ST6Gal I activity (P = 0.028), increased serum msAFP percentage (P = 0.034) and poor tumor cell differentiation (P = 0.031) were associated with shorter overall survival. Multivariate analysis using the Cox regression model showed that the preoperative serum msAFP percentage (P = 0.022) and tumor cell differentiation status (P = 0.048) were independent prognostic indicators for patient overall survival.

CONCLUSION: Our results indicate that the presence of msAFP in blood circulation is associated with a decreased activity of ST6Gal I activity in HCC. Both tissue ST6Gal I and serum msAFP are potential prognostic markers for patients with operable HCC.

Key words: Alpha-fetoprotein; Beta-galactoside alpha-2,6-sialyltransferase; Hepatocellular carcinoma; Patient survival; Cell differentiation

Poon T CW, Chiu C HS, Lai P BS, Mok T SK, Zee B, Chan A TC, Sung J JY, Johnson P J. Correlation and prognostic significance of beta-galactoside alpha-2,6-sialyltransferase and serum monosialylated alpha-fetoprotein in hepatocellular carcinoma. *World J Gastroenterol* 2005; 11(42): 6701-6706
http://www.wjgnet.com/1007-9327/11/6701.asp

INTRODUCTION

Beta-galactoside alpha-2,6-sialyltransferase (ST6Gal I) is the key enzyme for the production of alpha-2,6-linked sialoglycoconjugates. Both ST6Gal I and alpha-2,6-linked sialoglycoconjugates have been suggested to play important roles in oncogenic transformation and metastasis[1-3]. Upregulated expression of ST6Gal I has been shown in colorectal cancer[4,5], breast cancer[6], cervical cancer[7], and choriocarcinoma[8]. However, elevated alpha-2,6 sialylation inhibited formation of glioma *in vivo*[9]. Expression of ST6Gal I may have different effects in different cancer types.

Serum alpha-fetoprotein (AFP) is a conventional marker for the diagnosis of hepatocellular carcinoma. Eighty to ninety percent of patients with HCC will have levels above the reference range[10-12]. A serum concentration >500 μg/L, in an area with high incidence of HCC,

and in the appropriate clinical setting, is usually considered diagnostic of HCC. However, modestly raised levels of AFP (10-500 μg/L) are also common in non-malignant chronic liver disease, so that the specificity of the AFP test for HCC tends to be low[10,13-15]. Recent studies have shown that monosialylated AFP (msAFP), which is a hyposialylated isoform of alpha-fetoprotein (AFP), is specific to hepatocellular carcinoma (HCC)[16,17]. msAFP can be identified, measured quantitatively by isoelectrofocusing electrophoresis approach or by glycosylation immunosorbent assay[18]. msAFP percentage (msAFP%) relative to total AFP can be used as a serum marker to differentiate HCC patients with non-diagnostic total AFP from patients with chronic liver diseases[18].

Sialylation of AFP is mediated by cellular ST6Gal I. We hypothesize that downregulation of ST6Gal I plays an important role in the HCC pathogenesis, and causes the presence of msAFP in blood circulation of HCC patients. In the present study, we examined the enzyme activity and mRNA expression of ST6Gal I in the paired tumorous and non-tumorous tissues from patients with HCC. The correlation among ST6Gal I activity, serum msAFP percentage and their clinical implications were investigated.

MATERIALS AND METHODS

Clinical materials

Between December 1999 and January 2001, 19 consecutive patients who had undergone surgical resection of HCC, which contained viable tumor cells as shown by histological examination, and with serum AFP levels higher than 20 ng/mL were recruited into this study. Informed consent was obtained for using the resected tissues and sera for research studies. The patients were followed up for 2 years or until death. Preoperative sera, paired tumorous and non-tumorous tissues were collected. Sera were stored at -20 °C until further analysis. The tissues were cut into small pieces, snap frozen with liquid nitrogen, and stored at -70 °C. The AFP levels in the serum samples were quantified with a commercial sandwich-type ELISA (DAKO, Glostrup, Denmark). This study was approved by the Joint CUHK-NTEC Clinical Research Ethics Committee.

Preparation of tissue microsomal fraction

The tissues were homogenized on ice in 1 mL of sodium phosphate buffer (PBS, 10 mmol/L $NaPO_4$, 150 mmol/L NaCl, pH 7.4), containing 0.8 mmol/L protease inhibitor (Pefabloc® SC PLUS, Boehringer Mannheim, Roche Diagnostics, Germany), with a Polytron-Aggregate (Kinetica, Switzerland) using a 11-mm cutting probe at a speed setting of 5 for 15 s. After centrifugation at 4 °C for 10 min at 1 000 r/min, the supernatant fraction was saved and centrifuged again at 13 000 *g* for 30 min at 4 °C. The microsomal pellet obtained after centrifugation was then resuspended in Tris-HCl buffer (15 mmol/L Tris-HCl, pH 6.0) and stored at -70 °C until analyzed. The protein content was measured by the Bradford Coomassie Dye-Binding Protein Assay.

ST6Gal I activity assay

The assay was similar to the method described by Pousset *et al*. and Halliday *et al*. It was based on the specific binding property of *Sambucus nigra agglutinin* (SNA, Calibiochem, San Diego, USA) that preferentially binds sialic acid residues attached to terminal Galβ1, 4GlcNAc units on *N*-glycan in alpha-2,6, but not 2,3 or 2,8 linkage[19,20].

Briefly, the microsomal preparation was used as a source of alpha-2,6-sialyltransferase, and the *N*-glycan on asialofetuin (ASF) (Sigma, St. Louis, USA) was used as a sialic acid acceptor. The ST6Gal I activity assay was carried out in a mixture containing 10 μg of tissue microsome preparation, 125 μg ASF, 125 μmol/L CMP-sialic acid and 0.25 μCi CMP-[^{3}H]-sialic acid in reaction buffer (0.1% BSA, 0.1% Triton X-100, 45 mmol/L NaCl, 15 mmol/L Tris-HCl, pH 6.0) with a final volume of 20 μL. The mixture was added to 30 μL of SNA-sepharose (1 mg SNA covalently linked to 0.3 g of CNBr activated Sepharose 4B gel), mixed, and incubated at 37 °C overnight. After washing the gels four times with washing buffer (PBS containing 0.5% Tween 20), the molecules bound to the SNA-Sepharose were released by vortexing the gel in 300 μL of 1 mol/L H_2SO_4 for 30 s. Two hundred and eighty-five microliters of the supernatant was transferred to a vial, and 5 mL scintillant solution was added. The amount of radiolabeled ASF was then measured with a liquid scintillation counter. Commercial rat ST6Gal I (Sigma) was used as the calibration standard. One unit of the commercial rat ST6Gal I is defined as the amount that will transfer 1.0 μmol of sialic acid from CMP-sialic acid to asialomucin per minute at pH 6.5.

Semi-quantitation of ST6Gal I mRNA by RT-PCR-ELISA

Ten to thirty milligrams of frozen tumorous or non-tumorous liver tissue was disrupted and homogenized using a mortar and pestle (Kontes, Vineland, NJ, USA). Total RNA was extracted from the tissue sample using the RNeasy Mini Kit (Qiagen, GmbH, Germany), and reverse transcribed into cDNA by using a 1st strand cDNA Synthesis Kit (AMV, Roche Diagnostic, Boehringer Mannheim, Germany) with the oligo-$p(dT)_{15}$ primer provided. The cDNA was then used as the template for PCR amplification with primers specific to ST6Gal I (forward: 5'-CCTGAACAATTCCAGCCT GCTCCTTT-3' and reverse: 5'-GACGATGTTTCCA ATCCCCTGTACCA-3') or β-actin gene (forward, 5' -CTTCTACAATGAGCTGCGT-3' and reverse: 5'-TCAT GAGGTAGTCAGTCAG-3'). In the PCR for ST6Gal I, the cDNA, diluted in Tris–EDTA buffer (10 mmol/L Tris-HCl, 1 mmol/L EDTA, pH 8.0), was mixed with 1×PCR buffer, 2 mmol/L DIG-labeled dNTP, 2.5 mmol/L $MgCl_2$, 1 μmol/L of each primer, 0.83 U *Taq* DNA polymerase, 0.022 μmol/L TaqStart Antibody, 0.8 U uracil glycosylase in a final volume of 20 μL. The mixture was incubated at room temperature for 10 min. Then an initial denaturation step of 2 min at 94 °C was done, followed by repeating

cycles of 1 min at 94 °C, 1 min at 63 °C for primer annealing, and 1 min at 72 °C for extension. A final extension run of 7 min at 72 °C was performed to ensure complete elongation of all amplicons. In the PCR for β-actin gene, 3.5 mmol/L of $MgCl_2$ was used instead of 2.5 mmol/L, and the primer annealing temperature in each PCR cycle was 60 °C instead of 63 °C. In the initial attempts, 40 cycles of PCR were performed. The specificity of the PCR amplication was checked by agarose gel electrophoresis to see if the sizes of the amplicons were the same as the expected values, 421 bp for ST6Gal I cDNA and 305 bp for β-actin gene. A commercially available cDNA preparation of human normal liver tissues, pooled from two male/female Caucasians, was used as positive control (Clontech Laboratories, Inc., CA, USA).

For the semi-quantitative assay, 25 cycles of PCR were performed in the presence of DIG-labeled dNTP. The concentrations of the DIG-labeled amplicons were measured with the PCR ELISA (DIG-detection) kit (Roche Diagnostics), according to the manufacturer's instruction. Briefly, the DIG-labeled amplicons were first denatured, and hybridized with 7.5 pmol biotinylated DNA probe specific for the ST6Gal I (biotin-5'-TGCATTGGGC ACAATTGTAA-3') or β-actin gene (biotin-5'-GTCCAGA CGCAGGATGGCAT-3'). The DNA-probe hybrids were then captured onto an avidin-coated microplate. After washing, the amount of the DNA-probe hybrids bound to the microplate was determined by incubating with anti-DIG-HRP conjugate at 37 °C for 30 min, followed by adding the BM Blue peroxidase substrate (Roche Diagnostics). One hundred microliters of 1 mol/L H_2SO_4 was added to stop the colorimetric reaction. The optical density of the wells was determined at 450 nm with a reference wavelength of 690 nm. The ST6Gal I/β-actin mRNA ratios were calculated as the mRNA values of the tissue ST6Gal I.

Semi-quantitation of msAFP percentage by IEF-immunoblotting assay

The semi-quantitative analysis of msAFP was performed as previously reported by us[18]. AFP isoforms in the serum samples were separated by IEF on a polyacrylamide gel, which were pre-swollen with a solution containing 5 mol/L urea and 1:16 Pharmalyte 4.5-5.4 (Amersham Pharmacia Biotech, Uppsala, Sweden) in double distilled water. One microliter of pre-diluted serum samples or standard containing 5 or 10 ng/mL AFP. The total AFP was applied to the anode side of the gel after prefocusing (2 000 V, 2.0 mA, 3.5 W, 10 °C, 75 V.h). The sample was applied for 15 V.h (200 V, 2.0 mA, 3.5 W, 10 °C). The final isoelectric separation step was done for 450 V.h (2 000 V, 5.0 mA, 3.5 W, 10 °C). The focused proteins were transferred to nitrocellulose membrane, and then incubated with polyclonal rabbit anti-human AFP (DAKO), followed by horseradish peroxidase conjugated polyclonal swine anti-rabbit immunoglobulin (DAKO). After washing, the enhanced chemiluminescence detection system (ECL, Amersham Pharmacia Biotech) was used to visualize the AFP protein bands. The image of each band was scanned with a densitometer (GS-700, Bio-Rad, CA, USA), and the intensity of each band was expressed as a percentage of the total intensity of all AFP bands.

Statistical analysis

The Wilcoxon signed rank test was used to compare the differences between the paired tumor and non-tumor groups. The Mann–Whitney rank sum test and Fisher's exact test were used to compare the differences between other study groups. Correlations between the study parameters were analyzed by the Spearman's rank order correlation test. The log-rank test and Cox proportional hazards model were applied for survival analyses.

RESULTS

Two HCC subgroups with increased and decreased tumor ST6Gal I activities

The clinical features of the 19 patients with primary HCC are summarized in Table 1. The tumor ST6Gal I activity was compared to that of the paired non-tumorous tissue. Seven HCC patients fell into a group with decreased ST6Gal I activity in the tumorous tissue, whereas 12 HCC patients fell into a group with increased ST6Gal I activity in the tumorous tissue (Table 2). The tumor ST6Gal I activities in the decreased group were significantly lower than the values in the increased group ($P = 0.005$).

Absence of correlation between ST6Gal I activity and mRNA level in HCC

The specificity of the RT-PCR reaction was checked by subjecting the RT-PCR product to agarose gel electrophoresis. In all cases including the positive control (normal human liver cDNA), the RT-PCR product appeared as a single DNA band with the expected size of 421 bp for ST6Gal I, or 305 bp for β-actin. The electrophoresis results indicated that the RT-PCR amplifications were specific. Our data also confirmed that ST6Gal I gene was expressed in all the HCC tissues and the non-tumorous liver tissues (Figure 1). Two cases were omitted for the RT-PCR ELISA to measure ST6Gal I mRNA level owing to insufficient tissue materials. The measured ST6Gal I mRNA level of individual tissues was normalized by expressing the data as a ratio of β-actin mRNA level. In the non-tumorous tissues, the ST6Gal I mRNA level positively correlated with the ST6Gal I activity ($r = 0.49$, $P = 0.039$). In the tumorous tissues, no significant correlation was found between the enzyme activity ($r = -0.093$, $P = 0.72$).

Correlation between tumor ST6Gal I enzyme activity and serum msAFP

The percentages of tumor-specific msAFP (relative to total intensity of AFP isoforms) in the preoperative sera of the HCC patients were estimated, and the results of the patient groups with increased and decreased tumor ST6Gal I enzyme activity are shown in Table 2. Comparison of the

Table 1 Clinical features of the studied subjects with operable HCC

Case	Sex	Age	HBs Ag positivity	Cirrhosis	Tumor stage		Tumor size	Tumor differentiation	Encapsulation	Capsule invasion	Vascular invasion	Preoperative serum AFP (ng/mL)
					ALTSG	AJCC	(cm)					
1	F	51	Yes	Yes	T2	T2	2.4	Moderate	Yes	Yes	No	20
2	M	75	Yes	Yes	T2	T2	3.4	Moderate	Yes	Yes	No	25
3	M	52	Yes	No	T3	T2	10	Moderate	Yes	No	No	64
4	M	44	Yes	Yes	T3	T3	4	Well	Yes	Yes	Yes	69
5	M	44	No	Yes	T2	T2	2.6	Poor	Yes	Yes	No	73
6	M	53	Yes	Yes	T3	T2	8.3	Poor	Uncertain	Uncertain	No	100
7	M	65	No	Yes	T2	T2	4.4	Moderate	Yes	No	No	150
8	F	41	Yes	Yes	T3	T2	7	Well	Yes	Yes	No	151
9	M	57	No	Yes	T3	T2	6	Poor	Yes	Yes	Yes	152
10	M	46	Yes	Yes	T1	T1	1.2	Moderate	Yes	Yes	No	365
11	M	60	Yes	Yes	T2	T2	2.2	Poor	Yes	Yes	No	618
12	M	67	Yes	Yes	T2	T2	2.5	Moderate	Yes	Yes	No	1 057
13	M	48	Yes	No	T2	T2	4	Moderate	Yes	No	No	1 427
14	M	43	Yes	No	T2	T2	2.5	Moderate	Yes	Yes	No	1 500
15	F	31	Yes	Yes	T2	T2	2	Moderate	Yes	No	No	2 726
16	M	40	Yes	No	T2	T2	1.6	Moderate	No	No	No	3 338
17	M	35	Yes	No	T3	T2	8	Poor	Yes	No	No	5 505
18	M	42	Yes	Yes	T2	T2	3.4	Poor	Yes	Yes	No	12 185
19	M	72	Yes	No	T3	T3	6.5	Poor	Yes	Yes	No	42 837

Table 2 The average values of relative ST6Gal I activity, the relative ST6Gal I mRNA level, serum msAFP percentage in the patients with decreased (group 1) and increased (group 2) tumor ST6Gal I activity compared to that of non-tumorous tissue

	Group 1: decreased ST6Gal (n = 7)	Group 2: increased ST6Gal (n = 12)	P[1]
Tumor ST6Gal I activity (mU/mg of protein)	0.57 (0.47, 0.37-0.59)	1.76 (1.21, 0.94-1.93)	0.005
Relative tumor ST6Gal I activity (against non-tumor ST6Gal I activity)	0.46 (0.42, 0.25-0.71)[2]	2.04 (1.51, 1.35-1.88)	<0.001
Tumor ST6Gal I mRNA level[3]	1.78 (0.64, 0.24-1.7)	1.51 (1.08, 0.68-2.6)	N.S[4]
Serum AFP level (ng/mL)	7687 (680, 246-145045)	739 (161, 72-1 197)	N.S.
Serum msAFP percentage (%)	35 (41, 23-45)	18 (13, 11-17)	0.031

[1]Mann–Whitney test; [2]mean (median, 25th-75th percentile); [3]group 1: n = 6, group 2: n = 11; [4]N.S., not significant.

two groups shows that the percentage of msAFP in the patient group with decreased tumor enzyme activity was significantly higher than those in the group with increased activity (P = 0.031), whereas the serum total AFP levels were not significantly different. Furthermore, the msAFP percentage was negatively correlated with the relative tumor ST6Gal I enzyme activity (r = -0.53, P = 0.019).

Associations with poorly differentiated HCC

The relationships between ST6Gal I activity, msAFP percentage and various patient clinical parameters, including HBV status, tumor stage (ALTSG and AJCC), tumor size, differentiation status, vascular invasion, encapsulation, capsule invasion, metastasis and recurrent, were investigated. More cases with poorly differentiated tumor were found in the patient groups with decreased enzyme activity (P = 0.045, Figure 2). Similar to tumor ST6Gal I activity, but in an opposite manner, more cases with poorly differentiated tumor were found in the patient group with higher (>20%) msAFP percentage (P = 0.045, Figure 2).

Associations with poor overall survival

During the 2 years follow-up period, 8 out of the 19 patients died. The absolute/relative tumor ST6Gal I activity, serum msAFP percentage, serum AFP level and various patient clinical parameters were subjected to survival analyses. In univariate analyses using the Cox regression model, the preoperative serum msAFP percentage (P = 0.034), the relative tumor ST6Gal I activity (P = 0.028) and the tumor differentiation status (P = 0.031) were shown to be predictors for patient overall survival. The log-rank test results showed that the patient group with decreased tumor ST6Gal I activity had an overall survival (P = 0.0099, Figure 3A) shorter than the group with increased activity. When the cases were divided into two groups based on the preoperative serum msAFP percentage at a cut-off value of 20%, the log-rank test results showed that higher preoperative serum msAFP percentage was associated with poorer patient overall survival (P = 0.0031, Figure 3B). The log-rank test results also showed that patients with poorly differentiated tumor had poorer overall survival (P = 0.0063). In a multivariate analysis using the Cox regression model, among all the

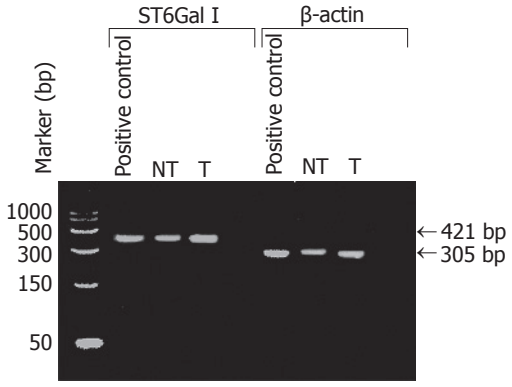

Figure 1 Electrophoresis of RT-PCR products amplified from the total RNA preparations of the tumor (T) and non-tumor liver (NT) tissues from HCC patients. For both tumor and non-tumor total RNA preparations, the RT-PCR products corresponding to ST6Gal I and β-Actin DNA showing the expected sizes (421 bp and 305 bp respectively) were obtained. Commercially available human normal liver cDNA was used as the positive control. Similar DIG-labeled RT-PCR products with the same sizes were obtained when DIG-dNTPs were used.

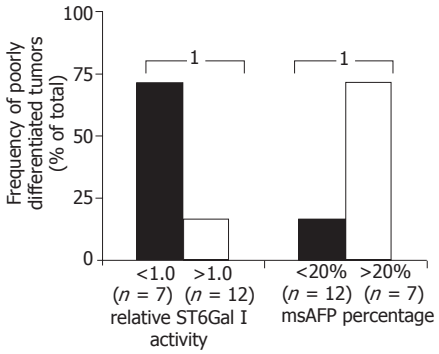

Figure 2 The frequency of poorly differentiated tumors among the 19 HCC patients with different relative tumor ST6Gal I activity or with different preoperative serum msAFP percentage. Differences between the study groups were tested by Fisher's exact test. $^1P = 0.045$.

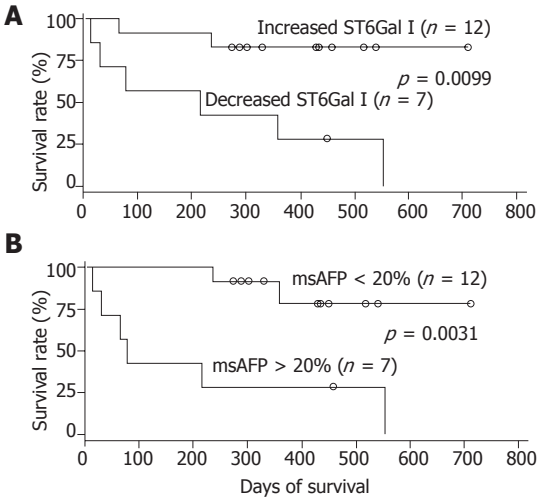

Figure 3 Survival curves of 19 patients with operable hepatocellular carcinoma after surgical resection according to relative tumor ST6Gal I activity (**A**) and preoperative serum msAFP percentage (**B**). Censored cases (○).

clinical features, only the preoperative serum msAFP percentage ($P = 0.022$) and tumor cell differentiation status ($P = 0.048$) were found to be independent prognostic indicators for patient overall survival.

DISCUSSION

Both ST6Gal I and alpha-2,6-linked sialoglycoconjugates play important roles in oncogenic transformation and metastasis in various cancers[21]. However, information about the influence of ST6Gal I in human HCC tissue has been very limited. The results of the present study were consistent to the findings reported by Cao *et al*. and Dall' Olio *et al*.[22,23]. Dalli'Olio *et al*. observed that both ST6Gal I activity can undergo up- or down-regulation in different HCC patients. The present study confirmed Dalli'Olio *et al*.'s observation. Compared to non-tumorous tissue, the HCC patients could be divided into two groups with increased and decreased ST6Gal I activity in the tumorous tissue. By immunohistochemical staining, Cao *et al*. showed that expression levels of ST6Gal were decreased in poorly differentiated HCC. This is also consistent to our observation that poorly differentiated HCCs had lower ST6Gal I activities.

The present study provided additional information about ST6Gal I in HCC. We showed that changes of ST6Gal I activity in HCC positively correlated with the presence of msAFP in blood circulation. As sialylation of AFP is mediated by ST6Gal I, probably the presence of hyposialyled AFP variants in blood circulation is caused by decreased ST6Gal I activity. Furthermore, our data suggests that tissue ST6Gal I and serum msAFP are potential prognostic markers for patients with operable HCC.

In the non-tumorous tissues, ST6Gal I mRNA level positively correlated with ST6Gal I activity. This result is consistent to the observation of Svensson *et al*. when studying normal liver[24]. This result therefore could be served as a positive control to confirm the validity of our measurements of tissue ST6Gal I activity and mRNA level. No significant correlation was found in the tumorous tissues. This suggests that ST6Gal I activity in HCC is regulated at post-transcriptional level.

The present study and the studies from Cao *et al*. and Dall'Olio *et al*. strongly indicate that the functional roles of ST6Gal I in HCC are different from those in colorectal cancer and in breast cancer. An *in vitro* antisense DNA experiment has shown that upregulation of ST6Gal I plays an important role in the invasive potential of human colon carcinoma HT29 cells[3]. Furthermore, high expression levels of ST6Gal I have been correlated with poor survival in colorectal cancer patients[25]. In breast cancers, high ST6Gal I expression was associated with histoprognostic grade III, and negatively correlated to progesterone receptor expression[26]. However, no ST6Gal I expression was found in malignant gliomas or in medulloblastomas[26]. It is worth noting that elevated alpha-2,6 sialylation

inhibited formation of glioma *in vivo*[9]. All these findings indicate that expression of ST6Gal may have different effects in different cancer types.

In conclusion, HCC can be divided into two subtypes, one with decreased tumor ST6Gal I activity and one with increased tumor ST6Gal I activity. The ST6Gal I activity in HCC is not regulated at the transcription level. Downregulation of tumor ST6Gal I activity and an increase in msAFP percentage in preoperative serum are associated with poorly differentiated tumors and poor patient survival. Both ST6Gal I and msAFP percentage are potential prognostic markers for HCC. The presence of msAFP in the blood circulation probably reflects the downregulation of ST6Gal I activity in the HCC tissue.

REFERENCES

1 **Collard JG,** Schijven JF, Bikker A, La Riviere G, Bolscher JG, Roos E. Cell surface sialic acid and the invasive and metastatic potential of T-cell hybridomas. *Cancer Res* 1986; **46:** 3521-3527

2 **Le Marer N,** Laudet V, Svensson EC, Cazlaris H, Van Hille B, Lagrou C, Stehelin D, Montreuil J, Verbert A, Delannoy P. The c-Ha-ras oncogene induces increased expression of beta-galactoside alpha-2, 6-sialyltransferase in rat fibroblast (FR3T3) cells. *Glycobiology* 1992; **2:** 49-56

3 **Zhu Y**, Srivatana U, Ullah A, Gagneja H, Berenson CS, Lance P. Suppression of a sialyltransferase by antisense DNA reduces invasiveness of human colon cancer cells in vitro. *Biochim Biophys Acta* 2001; **1536**: 148-160

4 **Dall'Olio F,** Malagolini N, Serafini-Cessi F. Enhanced CMP-NeuAc:Gal beta 1,4GlcNAc-R alpha 2,6 sialyltransferase activity of human colon cancer xenografts in athymic nude mice and of xenograft-derived cell lines. *Int J Cancer* 1992; **50**: 325-330

5 **Bresalier RS**, Ho SB, Schoeppner HL, Kim YS, Sleisenger MH, Brodt P, Byrd JV. Enhanced sialylation of mucin-associated carbohydrate structures in human colon cancer metastasis. *Gastroenterology* 1996; **110**: 1354-1367

6 **Recchi MA**, Hebbar M, Hornez L, Harduin-Lepers A, Peyrat JP, Delannoy P. Multiplex reverse transcription polymerase chain reaction assessment of sialyltransferase expression in human breast cancer. *Cancer Res* 1998; **58**: 4066-4070

7 **Wang PH**, Li YF, Juang CM, Lee YR, Chao HT, Tsai YC, Yuan CC. Altered mRNA expression of sialyltransferase in squamous cell carcinomas of the cervix. *Gynecol Oncol* 2001; **83**: 121-127

8 **Fukushima K**, Hara-Kuge S, Seko A, Ikehara Y, Yamashita K. Elevation of alpha2-->6 sialyltransferase and alpha1-->2 fucosyltransferase activities in human choriocarcinoma. *Cancer Res* 1998; **58**: 4301-4306

9 **Yamamoto H**, Oviedo A, Sweeley C, Saito T, Moskal JR. Alpha2,6-sialylation of cell-surface N-glycans inhibits glioma formation in vivo. *Cancer Res* 2001; **61**: 6822-6829

10 **Johnson PJ**, Portmann B, Williams R. Alpha-fetoprotein concentrations measured by radioimmunoassay in diagnosing and excluding hepatocellular carcinoma. *Br Med J* 1978; **2**: 661-663

11 **Sheu JC**, Sung JL, Chen DS, Yang PM, Lai MY, Lee CS, Hsu HC, Chuang CN, Yang PC, Wang TH. Growth rate of asymptomatic hepatocellular carcinoma and its clinical implications. *Gastroenterology* 1985; **89**: 259-266

12 **Nomura F**, Ohnishi K, Tanabe Y. Clinical features and prognosis of hepatocellular carcinoma with reference to serum alpha-fetoprotein levels. Analysis of 606 patients. *Cancer* 1989; **64**: 1700-1707

13 **Lok AS**, Lai CL. alpha-Fetoprotein monitoring in Chinese patients with chronic hepatitis B virus infection: role in the early detection of hepatocellular carcinoma. *Hepatology* 1989; **9**: 110-115

14 **Okuda K**. Early recognition of hepatocellular carcinoma. *Hepatology* 1986; **6**: 729-738

15 **Trevisani F**, D'Intino PE, Morselli-Labate AM, Mazzella G, Accogli E, Caraceni P, Domenicali M, De Notariis S, Roda E, Bernardi M. Serum alpha-fetoprotein for diagnosis of hepatocellular carcinoma in patients with chronic liver disease: influence of HBsAg and anti-HCV status. *J Hepatol* 2001; **34**: 570-575

16 **Johnson PJ**, Poon TCW, Hjelm NM, Ho CS, Ho SK, Welby C, Stevenson D, Patel T, Parekh R, Townsend RR**.** Glycan composition of serum alpha-fetoprotein in patients with hepatocellular carcinoma and non-seminomatous germ cell tumour. *Br J Cancer* 1999; **81**: 1188-1195

17 **Johnson PJ**, Poon TC, Hjelm NM, Ho CS, Blake C, Ho SK. Structures of disease-specific serum alpha-fetoprotein isoforms. *Br J Cancer* 2000; **83**: 1330-1337

18 **Poon TC**, Mok TS, Chan AT, Chan CM, Leong V, Tsui SH, Leung TW, Wong HT, Ho SK, Johnson PJ. Quantification and utility of monosialylated alpha-fetoprotein in the diagnosis of hepatocellular carcinoma with nondiagnostic serum total alpha-fetoprotein. *Clin Chem* 2002; **48**: 1021-1027

19 **Pousset D**, Piller V, Bureaud N, Monsigny M, Piller F. Increased alpha2,6 sialylation of N-glycans in a transgenic mouse model of hepatocellular carcinoma. *Cancer Res* 1997; **57**: 4249-4256

20 **Halliday JA**, Franks AH, Ramsdale TE, Martin R, Palant E. A rapid, semi-automated method for detection of Galbeta1-4GlcNAc alpha2,6-sialyltransferase (EC 2.4.99.1) activity using the lectin Sambucus nigra agglutinin. *Glycobiology* 2001; **11**: 557-564

21 **Dall'Olio F,** Chiricolo M. Sialyltransferases in cancer. *Glycoconj J* 2001; **18**: 841-850

22 **Cao Y**, Merling A, Crocker PR, Keller R, Schwartz-Albiez R. Differential expression of beta-galactoside alpha2,6 sialyltransferase and sialoglycans in normal and cirrhotic liver and hepatocellular carcinoma. *Lab Invest* 2002; **82**: 1515-1524

23 **Dall'Olio F,** Chiricolo M, D'Errico A, Gruppioni E, Altimari A, Fiorentino M, Grigioni WF. Expression of beta-galactoside alpha2,6 sialyltransferase and of alpha2,6-sialylated glyco-conjugates in normal human liver, hepatocarcinoma, and cirrhosis. *Glycobiology* 2004; **14**: 39-49

24 **Svensson EC**, Conley PB, Paulson JC. Regulated expression of alpha 2,6-sialyltransferase by the liver-enriched transcription factors HNF-1, DBP, and LAP. *J Biol Chem* 1992; **267**: 3466-3472

25 **Lise M**, Belluco C, Perera SP, Patel R, Thomas P, Ganguly A. Clinical correlations of alpha2,6-sialyltransferase expression in colorectal cancer patients. *Hybridoma* 2000; **19**: 281-286

26 **Kaneko Y**, Yamamoto H, Kersey DS, Colley KJ, Leestma JE, Moskal JR. The expression of Gal beta 1,4GlcNAc alpha 2,6 sialyltransferase and alpha 2,6-linked sialoglycoconjugates in human brain tumors. *Acta Neuropathol (Berl)* 1996; **91**: 284-292

Science Editor Guo SY **Language Editor** Elsevier HK

PO Box 2345, Beijing 100023, China
www.wjgnet.com
wjg@wjgnet.com

ELSEVIER

World J Gastroenterol 2005;11(42):6707-6712
World Journal of Gastroenterology ISSN 1007-9327

• *BRIEF REPORTS* •

Cysteamine increases expression and activity of H^+-K^+-ATPase of gastric mucosal cells in weaning piglets

Zhi-Min Shi, Gai-Mei Du, Xi-Hui Wei, Lei Zhang, Jie Chen, Ru-Qian Zhao

Zhi-Min Shi, Gai-Mei Du, Xi-Hui Wei, Lei Zhang, Jie Chen, Ru-Qian Zhao, Key Laboratory of Animal Physiology and Biochemistry, Ministry of Agriculture, Nanjing Agricultural University, Nanjing 210095, Jiangsu Province, China
Supported by the National Natural Science Foundation of China, No. 30270975 and National Basic Research Program of China, No. 2004CB117505
Correspondence to: Professor Ru-Qian Zhao, Key Laboratory of Animal Physiology and Biochemistry, Nanjing Agricultural University, Nanjing 210095, Jiangsu Province, China. yzwj@public1.ptt.js.cn
Telephone: +86-25-84395047 Fax: +86-25-84398669
Received: 2005-01-24 Accepted: 2005-04-30

Abstract

AIM: To determine the *in vivo* and *in vivo* effects of cysteamine (CS) on expression and activity of H^+-K^+-ATPase of gastric mucosal cells in weaning piglets.

METHODS: Eighteen litters of newborn Xinhuai piglets were employed in the *in vivo* experiment and allocated to control and treatment groups. From 12 d of age (D12), piglets in control group were fed basal diet, while the treatment group received basal diet supplemented with 120 mg/kg CS. Piglets were weaned on D35 in both groups. Six piglets from each group (n = 6) were slaughtered on D28 (one week before weaning), D35 (weaning), D36.5, D38, D42, and D45 (36 h, 72 h, one week and 10 d after weaning), respectively. Semi-quantitative RT-PCR was performed to determine the levels of H^+-K^+-ATPase mRNA in gastric mucosa. H^+-K^+-ATPase activity in gastric mucosa homogenate was also determined. Gastric mucosal epithelial cells from piglets through primary cultures were used to further elucidate the effect of CS on expression and activity of H^+-K^+-ATPase *in vivo*. Cells were treated for 20 h with 0.001, 0.01, and 0.1 mg/mL of CS (n = 4), respectively. The mRNA expression of H^+-K^+-ATPase and somatostatin (SS) as well as the H^+-K^+-ATPase activity were determined.

RESULTS: *in vivo*, both mRNA expression and activity of H^+-K^+-ATPase in gastric mucosa of control group exhibited a trend to increase from D28 to D45, reaching a peak on D45, but did not show significant age differences. Furthermore, neither the mRNA expression nor the activity of H^+-K^+-ATPase was affected significantly by weaning. CS increased the mRNA expression of H^+-K^+-ATPase by 73%, 53%, 30% and 39% on D28 (P = 0.014), D35 (P = 0.017), D42 (P = 0.013) and D45 (P = 0.046), respectively. In accordance with the mRNA expression, H^+-K^+-ATPase activities were significantly higher in treatment group than in control group on D35 (P = 0.043) and D45 (P = 0.040). *In vivo*, CS exhibited a dose-dependent effect on mRNA expression and activity of H^+-K^+-ATPase. Both H^+-K^+-ATPase mRNA expression and activity in gastric mucosal epithelial cells were significantly elevated after 20 h of exposure to the moderate (H^+-K^+-ATPase expression: P=0.03; H^+-K^+-ATPase activity: P = 0.014) and high concentrations (H^+-K^+-ATPase expression: P=0.017; H^+-K^+-ATPase activity: P = 0.022) of CS. Significant increases in SS mRNA expression were observed to accompany the elevation of H^+-K^+-ATPase expression and activity induced by the moderate (P = 0.024) and high concentrations (P = 0.022) of CS. Low concentration of CS exerted no effects either on expression and activity of H^+-K^+-ATPase or on SS mRNA expression in cultured gastric mucosal epithelial cells.

CONCLUSION: No significant changes are observed in mRNA expression and activity of H^+-K^+-ATPase in gastric mucosa of piglets around weaning from D28 to D45. CS increases expression and activity of gastric H^+-K^+-ATPase *in vivo* and *in vivo*. SS is involved in mediating the effect of CS on gastric H^+-K^+-ATPase expression and activity in weaning piglets.

Key words: Cysteamine; Weaning piglets; H^+-K^+-ATPase; Gastric mucosal cells; Somatostatin

Shi ZM, Du GM, Wei XH, Zhang L, Chen J, Zhao RQ. Cysteamine increases expression and activity of H^+-K^+-ATPase of gastric mucosal cells in weaning piglets. *World J Gastroenterol* 2005; 11(42): 6707-6712
http://www.wjgnet.com/1007-9327/11/6707.asp

INTRODUCTION

The proton pump, H^+-K^+-ATPase consisting of α- and β-subunits, is the molecular base of gastric acid production and the final common pathway mediating secretion of hydrochloric acid by gastric parietal cells. The enzyme, which is typically located in the parietal cells, mediates the electroneutral exchange of intracellular H^+ and extracellular K^+ to achieve acid secretion when parietal cells are under the stimulation of secretagogues[1]. In H^+-K^+-ATPase α-

or β-subunit deficiency mice, achlorhydria and destruction of parietal cells have been observed[2,3]. The capability of gastric acid secretion is dependent on the gastric H^+-K^+-ATPase activity[4]. Therefore, H^+-K^+-ATPase activity can serve as an accurate indicator for evaluating the ability of gastric acid secretion from parietal cells.

Gastric acid secretion is regulated by stimulatory factors such as gastrin, histamine and acetylcholine, as well as inhibitory factors including somatostatin (SS). SS is a typical brain-gut-peptide releasing from D cells in the mucous membrane of stomach. Numerous publications reported that SS inhibits gastric acid secretion directly or indirectly by inhibiting the stimulatory effects of gastrin and histamine[5,6]. We found in our previous study that gastric expression of SS mRNA is upregulated in weaning piglets[7], and that gastric acid secretion is low in piglets[8]. Therefore, it is presumed that the increased inhibitory tone of SS is responsible for retarded gastric function development and insufficient gastric acid secretion which contribute, atleast partly, to diarrhea, poor growth and even death in newborn and early-weaning piglets.

Cysteamine (CS), which is able to deplete tissue SS, induces a profound loss of biological and immunological activities of SS both *in vivo* and *in vitro*[9,10]. CS is known to increase gastric acid secretion in rats, and is often used to produce the clinical model of gastric ulcer[11-13]. CS is approved to use as a feed additive in animal production to promote growth rate and improve feed efficiency[14]. However, CS application in pig production is mostly restricted to growing and fattening stages[15]. Up to now, the possible effect of CS on gastric acid secretion in weaning piglets remains unknown. Therefore, the present study was designed to examine the effect of CS on gastric acid secretion both *in vivo* and *in vitro*, the mRNA expression and activity of H^+-K^+-ATPase in gastric mucosa tissue and cultured mucosal epithelial cells were determined as response criteria. In addition, the change of SS mRNA expression in mucosal epithelial cells responding to CS exposure was also measured for elucidating the possible mechanisms underlying the CS action.

MATERIALS AND METHODS

Animals and sampling

Eighteen litters of newborn piglets from the 2nd or 3rd farrowing Xinhuai sows were employed in the *in vivo* experiment and allocated to control and treatment groups. From 12 d of age (D12), piglets in control group were fed basal diet, while the treatment group received basal diet supplemented with 120 mg/kg CS. The diet was formulated according to the requirement of piglets and provided *ad libitum*. Piglets were weaned on D35 in both groups. Six piglets from each group were slaughtered on D28 (one week before weaning), D35 (weaning), D36.5, D38, D42 and D45 (36 h, 72 h, one week and 10 d after weaning), respectively. Samples of the gastric fundic mucosa were frozen in liquid nitrogen immediately and then stored at -70 ºC until RNA extraction.

For *in vitro* experiment, four piglets at the age of D28 were killed to collect gastric mucosa for primary cell culture. DMEM (high glucose) and HEPES were products of Gibco, Hyclone, respectively. Trypsin was bought from Sigma and fetal bovine serum was purchased from Hangzhou Sijiqing Company, China.

Cells were dispersed from freshly obtained gastric mucosa of piglets as described previously[16], with minor modifications. Briefly, the gastric mucosa was washed in D-Hank's solution containing 400 U/mL penicillin, 400 μg/mL streptomycin and dipped in D-Hank's solution for 30 min. Then the tissues were dispersed by trypsin (0.15 mg/mL) at 37 °C for 1 h, filtrated and centrifuged (1 000 r/min, 5 min). Viability of the cells exceeded 95% as judged by trypan blue exclusion. Then cells at the density of 1×10^6/mL were cultured (37 °C, 50 mL/L CO_2) in a six-well plate containing DMEM (high glucose) with 10% fetal bovine serum, 15 mmol/L HEPES buffer, and 100 U/mL penicillin, 100 μg/mL streptomycin. After 24 h, the culture medium was refreshed by a new medium containing 0, 0.001, 0.01 and 0.1 mg/mL CS, respectively. The cells were continuously cultured for 20 h, and then collected for RNA extraction and H^+-K^+-ATPase activity determination.

The experiments were undertaken following the guidelines of the regional Animal Ethics Committee.

RNA extraction and analysis

Total RNA was extracted from the tissue samples with the single-step method of RNA extraction by acid guanidinium thiocyanate-phenol-chloroform[17]. Total RNA concentration was then quantified by measuring the absorbance at 260 nm in a photometer (Eppendorf Biophotometer). Ratios of absorption (260/280 nm) of all preparations were between 1.8 and 2.0. Aliquots of RNA samples were subjected to electrophoresis through a 1.4% agarose-formaldehyde gel to verify their integrity.

Two micrograms of total RNA was reverse transcribed by incubation at 42 °C for 1 h in a 25 μL mixture consisting of 10 U avian myeloblastosis virus reverse transcriptase, 10 U RNase inhibitor, 12 μmol/L random primers, 50 mmol/L Tris-HCl (pH 8.3), 10 mmol/L $MgCl_2$, 50 mmol/L KCl, 10 mmol/L DDT, 0.5 mmol/L spermidine and 0.8 mmol/L each dNTP. The reaction was terminated by heating at 95 °C for 5 min and quickly cooling on ice.

The primers for H^+-K^+-ATPase were designed according to the cDNA sequence published on GenBank (M22724): 5'-gagaaccaccacctacaag-3' as sense primer, and 5'-caacagcgaactccaag-3' as anti-sense primer, the predicted PCR product being 362 bp in size. The SS primers were designed according to the coding region of porcine SS genomic DNA sequence (GenBank, U36385): sense, 5'-agctgctgtctgaacccaac-3' and anti-sense, 5'-gaaattcttgcagccagctt-3', the expected PCR product being 161 bp in size. The PCR primers were designed using Primer Premier 5.0 and synthesized by Haojia Biotech. Ltd, China. The Quantum RNA 18S Internal Standards

kit (catalogue no. 1716, Ambion Inc., Austin, TX, USA), containing primers and competitors, was used to normalize variations in pipetting and amplification.

Different controls were set to monitor the possible contaminations of genomic DNA and environment DNA both at the stage of RT and RCR. The pooled samples made by mixing equal quantity of total RNA from all samples were used for optimizing the PCR condition and normalizing the intra-assay variations. PCR conditions were established as follows: for H^+-K^+-ATPase, the total volume of reaction was 25 μL, including 0.5 U Taq DNA polymerase (Promega, Shanghai), 5 mmol/L Tris-HCl (pH 9.0), 10 mmol/L NaCl, 0.1 mmol/L DDT, 0.01 mmol/L EDTA, 5% (w/v) glycerol, 0.1% (w/v) Triton X-100, 0.2 mmol/L each dNTP, 1.5 mmol/L $MgCl_2$, 0.7 μmol/L specific primers, 1.0–2.6 μL 18S rRNA. The program is set as: denaturation at 94 °C for 5 min, 20 cycles (for *in vivo* samples), 24 cycles (for *in vitro* samples) at 94 °C for 30 s, at 52 °C for 30 s, at 72 °C for 60 s, and a final extension at 72 °C for 8 min; for SS, the reaction mix contained 0.5 U Taq DNA polymerase, 5 mmol/L Tris-HCl (pH 9.0), 10 mmol/L NaCl, 0.1 mmol/L DDT, 0.01 mmol/L EDTA, 5% (w/v) glycerol, 0.1% (w/v) Triton X-100, 0.2 mmol/L each dNTP, 1.5 mmol/L $MgCl_2$, 1.6 μmol/L specific primers, 1.0-2.6 μL 18S rRNA. The program is set as: denaturation at 94 °C for 5 min, 26 cycles at 94 °C for 30 s, at 54 °C for 30 s, at 72 °C for 30 s, and a final extension at 72 °C for 8 min. All samples were included in the same run of PCR on GeneAmp PCR system 9600 (Perkin Elmer, USA) and repeated atleast thrice.

Twenty microliters of PCR products was analyzed by 2% agarose gel electrophoresis. The gels were stained with ethidium bromide and photographed with a digital camera. The net intensities of individual bands were measured using Kodak Digital Science 1D software (Eastman Kodak Company, Rochester, NY, USA). The ratio of band density for target genes to that for 18S rRNA was used to represent the abundance of H^+-K^+-ATPase and SS mRNA expression.

H^+-K^+-ATPase activity assay

H^+-K^+-ATPase activity was measured according to the method described by Hervatin *et al*.[18]. H^+-K^+-ATPase activity was evaluated as the amount of inorganic phosphate released from ATP by the method of Sanui[19]. The reaction was initiated at 37 °C by addition of 2 mmol/L ATP-Mg^{2+} salt as substrate and proceeded in a total volume of 1.0 mL containing 60 mmol/L Tris-1,4-piperzine-bis (ethanesulfonic acid) (pH 7.4), 0.1 mmol/L ouabain, 90 mmol/L sucrose, 100 μL sample and either 15 mmol/L KCl or 30 mmol/L sucrose. It was terminated after 10 min by addition of 1.5 mL of ice-cold 14% trichloroacetic acid. Ouabain was included to avoid Na^+-K^+-ATPase activity. The ATPase activity measured without K^+ was taken as the basal Mg^{2+}-ATPase activity. The difference between the activities measured with and without K^+ was defined as H^+-K^+-ATPase activity. Bradford[20] assay was employed to determine the tissue protein content and the activity of H^+-K^+-ATPase was expressed as the amount of inorganic phosphate released per milligram of protein per hour (μmol Pi/mg prot/h).

Statistical analysis

All data were expressed as mean±SE. The data were analyzed by *t*-test for independent samples or ANOVA with Statistical Packages for the Social Sciences (2000). $P<0.05$ was considered statistically significant.

RESULTS

Expression and activity of H^+-K^+-ATPase in vivo

H^+-K^+-ATPase mRNA expression and H^+-K^+-ATPase activity in control group exhibited a trend to increase from D28 to D45, reaching a peak on D45, but did not show significant age differences (Figure 1). Furthermore, neither the mRNA expression nor the activity of H^+-K^+-ATPase was affected significantly by weaning.

Effects of CS on expression and activity of H^+-K^+-ATPase in vivo

As shown in Figure 1, CS increased the level of H^+-K^+-

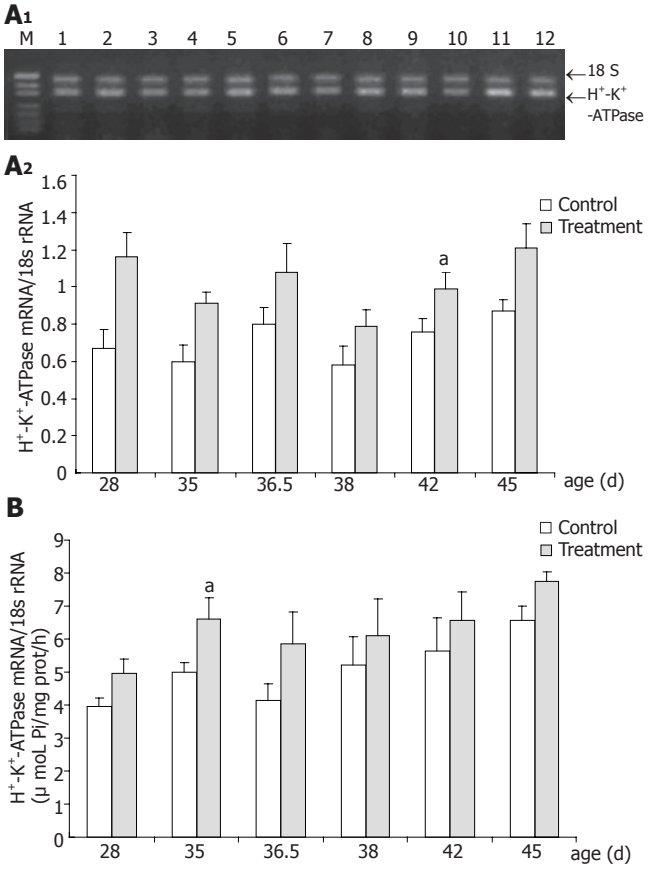

Figure 1 Expression (**A**1-2) and activity (**B**) of H+-K+-ATPase in vivo. Lane M: PUC19 marker; lanes 1-6: piglets at 28, 35, 36.5, 38, 42, 45 d of age in control group, respectively; lanes 7-12: piglets at 28, 35, 36.5, 38, 42, 45 d of age in treatment, respectively. Bars without a common superscript representing significant differences between age groups (small letters a and b for control group and capital letters A and B for treatment group); $^aP<0.05$ indicating differences between control and treatment groups at the same age.

ATPase mRNA expression and the differences were significant on D28 (P = 0.014), D35 (P = 0.017), D42 (P = 0.013) and D45 (P = 0.046), respectively. Relative abundances of H^+-K^+-ATPase mRNA expression were significantly increased by 73%, 53%, 30%, and 39% in treatment group compared with control at the same age. CS supplementation increased markedly H^+-K^+-ATPase activity by 32.3% on D35 (P = 0.043) and 18.3% on D45 (P = 0.040), respectively, compared with that of the control counterparts.

Effects of CS on expression and activity of H^+-K^+-ATPase in vitro

As shown in Figure 2, low concentration of CS exhibited no effects on both mRNA expression and activity of H^+-K^+-ATPase, while moderate and high concentrations of CS markedly increased H^+-K^+-ATPase mRNA expression by 61% (P = 0.03) and 65% (P = 0.014), and H^+-K^+-ATPase activity by 48% (P = 0.017) and 50% (P = 0.022), respectively.

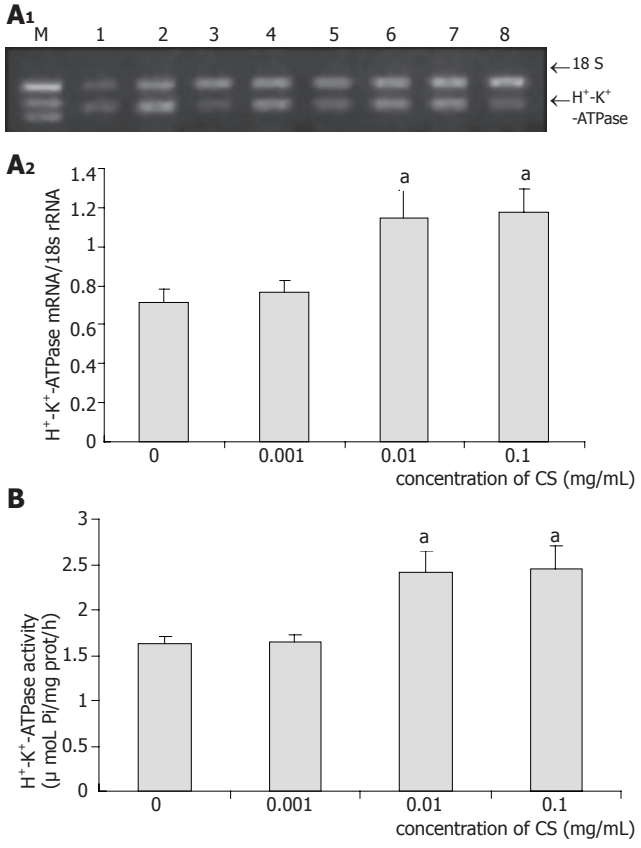

Figure 2 Effect of CS on expression (**A**$_{1\text{-}2}$) and activity (**B**) of H+-K+-ATPase in vitro. Lane M: PUC19 marker, lanes 1-2: control; lanes 3-4: low concentration group; lanes 5-6: moderate concentration group; lanes 7-8: high concentration group. [a]P<0.05 *vs* 0 mg/mL of CS.

Effects of CS on SS mRNA expression in vitro

Low concentration of CS had no influence on SS mRNA expression, whereas SS mRNA expression was markedly increased by 56% (P = 0.024) in moderate concentrations of CS and 64% (P = 0.022) in high concentrations of CS (Figure 3).

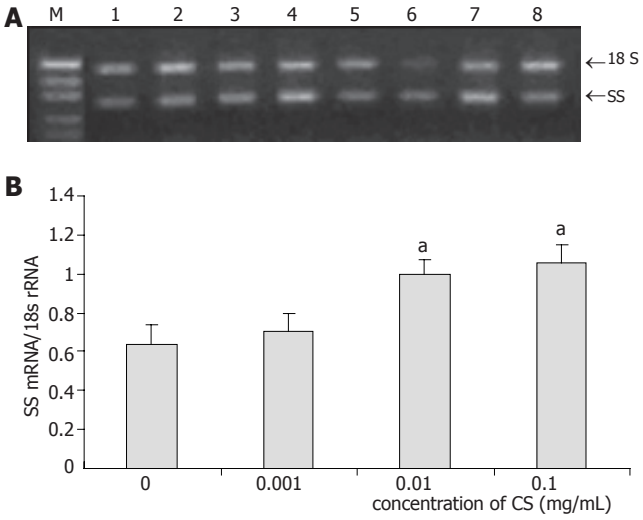

Figure 3 Effect of CS on SS mRNA expression *in vitro*. Lane M: PUC19 marker, lanes 1 and 2: control; lanes 3 and 4: low concentration group; lanes 5 and 6: moderate concentration group; lanes 7 and 8: high concentration group (**A**,**B**). [a]P<0.05 *vs* 0 mg/mL of CS.

DISCUSSION

The developmental pattern of H^+-K^+-ATPase was found to be in agreement with that of gastric acid secretion capacity, both at the level of mRNA expression and enzyme activity. Yang *et al*.[21] reported that H^+-K^+-ATPase mRNA expression and activity in fundic gland keep increasing with age from gestational day 19.5 to week 18 of postnatal age in rats. The developmental pattern of human gastric H^+-K^+-ATPase from week 25 of gestation by Western blot analysis agrees with that of gastric pH recorded in preterm infants[22]. Furthermore, the H^+-K^+-ATPase mRNA content in rat fundus increases with age from one week to six weeks of age and the change parallels the developmental change of acid secretion capacity[23]. However, the developmental pattern of H^+-K^+-ATPase expression and activity in pigs has not been reported. In contrary to the reported data, the present study failed to show significant developmental change in both the expression and the activity of H^+-K^+-ATPase in piglets around weaning throughout the period of observation. It seems that the developmental pattern of H^+-K^+-ATPase is species-specific. In addition, it is documented that gastrin is involved in the regulation of H^+-K^+-ATPase expression. In ovine fetus, developmental pattern of gastrin mRNA agrees with that of H^+-K^+-ATPase expression[24]. Gastrin can stimulate H^+-K^+-ATPase expression[25] and improve its activity by increasing the intracellular Ca^{2+} concentration to initiate the phosphorization of H^+-K^+-ATPase in parietal cells[26]. In accordance with our findings, gastrin contents in gastric tissues are stable from 4 to 6 wk of age in piglets[27].

Since the period of observation was limited to less than 3 wk from D28 to D45 in the present study, the possibility that H^+-K^+-ATPase expression and activity subjected to change during growth in a longer term cannot be excluded.

Until now no report is available describing the effect of weaning stress on expression and activity of H^+-K^+-ATPase. Our results indicated that weaning stress exhibited no effect on expression and activity of H^+-K^+-ATPase, which might be attributed to the relatively mature age of weaning on D35. This explanation is supported by the study of Efird *et al*.[28], who found that gastric acid secretion of piglets weaned after 35 d of age is not easily affected by weaning.

Our earlier publication reported that the inhibition of gastric acid secretion agrees with the upregulation of gastric SS expression in pre-weaning piglets[7]. Read *et al*.[24] reported that the developmental pattern of gastric SS mRNA is on the contrary to the patterns of gastrin mRNA and H^+-K^+-ATPase mRNA in ovine. *In vitro* studies have provided further evidence that endogenous SS plays a role as a strong inhibitory factor in gastric acid secretion, since SS antiserum significantly increases gastric acid release from perfused stomach of sheep[29].

CS possesses the ability to deplete tissue SS. Szabo and Reichlin[9] found that, in rats, CS administration brings about a prompt depletion of radioimmunoassayable SS in plasma, stomach, duodenum, pancreas, and hypothalamus. Some researches showed that gastrin plays a significant role in CS-induced hypersecretion of gastric acid. Intravenous infusion of CS in the perfused rat stomach results in a significant increase in acid secretion, which is accompanied with a marked increase in plasma gastrin concentration. The injection of anti-gastrin rabbit serum completely blocks CS-induced acid increase, and infusion of a gastrin receptor antagonist also suppresses CS-induced increase in acid secretion[13]. Van de Brug *et al*.[12] also found that intravenous bolus administration of CS induces increase in serum gastrin concentration and gastric acid outputs. However, there is no report concerning the effect of CS on expression and activity of H^+-K^+-ATPase. In the present study, we found that CS significantly increased both the expression and activity of H^+-K^+-ATPase *in vivo*. To further affirm the effect of CS on H^+-K^+-ATPase, we added CS to the culture medium of gastric mucosal epithelial cells *in vitro*. The results indicated that moderate and high concentrations of CS increased significantly both the expression and activity of H^+-K^+-ATPase, accompanied with a marked increase in the expression of SS. The upregulation of SS mRNA expression might be the consequence of SS depletion. The signal of SS depletion feeds back to the cells to boost SS synthesis in order to maintain homeostasis. Kanayama and Liddle[30] also found that the content of SS mRNA in duodenum is reduced after SS perfusion in rats. However, this upregulation might be temporal, since SS mRNA in stomach and brain significantly increases, then reduces after perfusion of CS in rats[31]. These authors presumed that SS mRNA upregulation results from SS depletion, and the subsequent SS mRNA downregulation is caused by direct effect of CS on SS expression.

In conclusion, the present experiments provide evidence that the mRNA expression and activity of H^+-K^+-ATPase in gastric mucosa remain relatively constant in piglets around weaning from D28 to D45. CS increases gastric expression and activity of H^+-K^+-ATPase both *in vivo* and *in vitro*. In addition, SS is involved in mediating the effect of CS on gastric H^+-K^+-ATPase expression and activity in weaning piglets, although the complex effect of CS on SS mRNA expression awaits further investigation.

REFERENCES

1 **Yao X,** Forte JG. Cell biology of acid secretion by the parietal cell. *Annu Rev Physiol* 2003; **65:** 103-131
2 **Spicer Z,** Miller ML, Andringa A, Riddle TM, Duffy JJ, Doetschman T, Shull GE. Stomachs of mice lacking the gastric H,K-ATPase alpha -subunit have achlorhydria, abnormal parietal cells, and ciliated metaplasia. *J Biol Chem* 2000; **275:** 21555-21565
3 **Scarff KL,** Judd LM, Toh BH, Gleeson PA, Van Driel IR. Gastric H(+),K(+)-adenosine triphosphatase beta subunit is required for normal function, development, and membrane structure of mouse parietal cells. *Gastroenterology* 1999; **117:** 605-618
4 **Wallmark B,** Larsson H, Humble L. The relationship between gastric acid secretion and gastric H+,K+-ATPase activity. *J Biol Chem* 1985; **260:** 13681-13684
5 **Park J,** Chiba T, Yamada T. Mechanisms for direct inhibition of canine gastric parietal cells by somatostatin. *J Biol Chem* 1987; **262:** 14190-14196
6 **Zaki M,** Harrington L, McCuen R, Coy DH, Arimura A, Schubert ML. Somatostatin receptor subtype 2 mediates inhibition of gastrin and histamine secretion from human, dog, and rat antrum. *Gastroenterology* 1996; **111:** 919-924
7 **Xia D,** Zhao RQ, Wei XH, Xu QF, Chen J. Developmental patterns of GHr and SS mRNA expression in porcine gastric tissue. *World J Gastroenterol* 2003; **9:** 1058-1062
8 **Xu RJ,** Cranwell PD. Development of gastric acid secretion in pigs from birth to thirty six days of age: the response to pentagastrin. *J Dev Physiol* 1990; **13:** 315-326
9 **Szabo S,** Reichlin S. Somatostatin in rat tissues is depleted by cysteamine administration. *Endocrinology* 1981; **109:** 2255-2257
10 **Widmann R,** Sperk G. Cysteamine-induced decrease of somatostatin in rat brain synaptosomes in vitro. *Endocrinology* 1987; **121:** 1383-1389
11 **Drago F,** Montoneri C. Influence of growth hormone on cysteamine-induced gastro-duodenal lesions in rats: the involvement of somatostatin. *Life Sci* 1997; **61:** 21-28
12 **van de Brug FJ,** Jansen JB, Kuijpers IJ, Lamers CB. Contribution of gastrin to cysteamine-induced gastric acid secretion in rats. *Life Sci* 1993; **52:** 1861-1867
13 **Shiratori K,** Shimizu K, Ikeda M, Watanabe S, Hayashi N. Evidence for a significant role of gastrin in cysteamine-induced hypersecretion of gastric acid. *J Clin Gastroenterol* 1997; **25** Suppl 1: S84-S88
14 **Wang C.** Researches and applications of somatostatin and cysteamine. *Shouyao Yu Siliao Tianjiaji* 2003; **8:** 20-23
15 **CHEN AG,** WU LY, HONG QH. Effects of cysteamine on carcass characteristics of growing finishing pigs and approach to the mechanism. *Zhongguo Xumu Zhazhi* 2004; **40:** 11-13
16 **Terano A,** Ivey KJ, Stachura J, Sekhon S, Hosojima H, McKenzie WN Jr, Krause WJ, Wyche J H. Cell culture of rat gastric fundic mucosa. *Gastroenterology* 1982; **83:** 1280-1291
17 **Chomczynski P,** Sacchi N. Single-step method of RNA isolation by acid guanidinium thiocyanate-phenol-chloroform extraction. *Anal Biochem* 1987; **162:** 156-159
18 **Hervatin F,** Moreau E, Ducroc R, Garzon B, Avril P, Millet P,

Geloso JP. Ontogeny of rat gastric H^+-K^+-ATPase activity. *Am J Physiol* 1987; **252:** G28-G32

19 **Sanui H.** Measurement of inorganic orthophosphate in biological materials: extraction properties of butyl acetate. *Anal Biochem* 1974; **60:** 489-504

20 **Bradford MM.** A rapid and sensitive method for the quantitation of microgram quantities of protein utilizing the principle of protein-dye binding. *Anal Biochem* 1976; **72:** 248-254

21 **Yang DH,** Tsuyama S, Murata F. The expression of gastric H+-K+-ATPase mRNA and protein in developing rat fundic gland. *Histochem J* 2001; **33:** 159-166

22 **Grahnquist L,** Ruuska T, Finkel Y. Early development of human gastric H,K-adenosine triphosphatase. *J Pediatr Gastroenterol Nutr* 2000; **30:** 533-537

23 **Marino LR,** Muglia BH, Yamada T. H(+)-K(+)-ATPase and carbonic anhydrase II gene expression in the developing rat fundus. *Am J Physiol* 1990; **259:** G108-G115

24 **Read MA,** Chick P, Hardy KJ, Shulkes A. Ontogeny of gastrin, somatostatin, and the H+/K(+)-ATPase in the ovine fetus. *Endocrinology* 1992; **130:** 1688-1697

25 **Campbell VW,** Yamada T. Acid secretagogue-induced stimulation of gastric parietal cell gene expression. *J Biol Chem* 1989; **264:** 11381-11386

26 **Geibel J,** Abraham R, Modlin I, Sachs G. Gastrin-stimulated changes in Ca2+ concentration in parietal cells depends on adenosine 3',5'-cyclic monophosphate levels. *Gastroenterology* 1995; **109:** 1060-1067

27 **Xu RJ,** Cranwell PD. Gastrin in fetal and neonatal pigs. *Comp Biochem Physiol B* 1991; **98:** 615-621

28 **Efird RC,** Armstrong WD, Herman DL. The development of digestive capacity in young pigs: effects of age and weaning system. *J Anim Sci* 1982; **55:** 1380-1387

29 **Westbrook SL,** McDowell GH, Hardy KJ, Shulkes A. Active immunization against somatostatin alters regulation of gastrin in response to gastric acid secretagogues. *Am J Physiol* 1998; **274:** G751-G756

30 **Kanayama S,** Liddle RA. Somatostatin regulates duodenal cholecystokinin and somatostatin messenger RNA. *Am J Physiol* 1990; **258:** G358-G364

31 **Papachristou DN,** Liu JL, Patel YC. Cysteamine-induced reduction in tissue somatostatin immunoreactivity is associated with alterations in somatostatin mRNA. *Regul Pept* 1994; **49:** 237-247

Science Editor Wang XL and Guo SY **Language Editor** Elsevier HK

PO Box 2345, Beijing 100023, China
www.wjgnet.com
wjg@wjgnet.com

ELSEVIER

World J Gastroenterol 2005;11(42):6713-6715
World Journal of Gastroenterology ISSN 1007-9327

• *BRIEF REPORTS* •

Hepatitis E virus chimeric DNA vaccine elicits immunologic response in mice

Yan Hong, Bing Ruan, Lian-Hua Yang, Yong Chen, Luo Jing, Yi-Ting Wang, Hua-Jun Hu

Yan Hong, Lian-Hua Yang, Yong Chen, Luo Jing, Yi-Ting Wang, Hua-Jun Hu, Institute of Bioengineering, Zhejiang Academy of Medical Sciences, Hangzhou 310013, Zhejiang Province, China
Bing Ruan, Zhejiang University Medical School, Hangzhou 310003, Zhejiang Province, China
Supported by the Grants from the Natural Science Foundation of Zhejiang Province, No. RC01054, Science and Technology Department of Zhejiang Province, No. F11023 and Key Project of Health Bureau of Zhejiang Province
Correspondence to: Dr. Yong Chen, Institute of Bioengineering, Zhejiang Academy of Medical Sciences, Hangzhou 310013, Zhejiang Province, China. cmlong93@yahoo.com.cn
Telephone: +86-0571-88862228 Fax: +86-0571-88075447
Received: 2005-03-12 Accepted: 2005-04-11

Abstract

AIM: To construct the plasmid pcHEV23 containing fragments of HEV ORF2 and ORF3 chimeric gene and to assess its ability to elicit specific immunologic response in mice.

METHODS: The gene encoding the structural protein of HEV ORF2 fragment and full-length ORF3 was amplified by PCR. The PCR products were cloned into an eucaryotic expression plasmid pcDNA3. The resulting plasmid pcHEV23 was used as a DNA vaccine to inoculate BALB/c mice intramuscularly thrice at a dose of 100 or 200 μg. Mice injected with empty pcDNA3 DNA or saline served as control and then specific immune responses in the mice were detected.

RESULTS: After 2-3 times of inoculation, all mice injected with pcHEV23 had anti-HEV IgG seroconversion and specific T lymphocyte proliferation. The lymphocyte stimulation index in the group immunized with pcHEV23 (3.1±0.49) was higher than that in the control group (0.787±0.12, $P<0.01$). None in the control group had a detectable level of anti-HEV IgG.

CONCLUSION: DNA vaccine containing HEV ORF2 and ORF3 chimeric gene can successfully induce specific humoral and cellular immune response in mice.

Hong Y, Ruan B, Yang LH, Chen Y, Jing L, Wang YT, Hu HJ. Hepatitis E virus chimeric DNA vaccine elicits immunologic response in mice. *World J Gastroenterol* 2005; 11(42): 6713-6715

http://www.wjgnet.com/1007-9327/11/6713.asp

INTRODUCTION

Hepatitis E virus (HEV) is an unclassified, non-enveloped RNA virus, a causative agent of acute hepatitis E transmitted principally via the fecal-oral route. The virus can cause large water-borne epidemics of the disease and sporadic cases as well. Hepatitis E occurs predominantly in developing countries usually affecting young adults with a fatality rate of 15-20% in pregnant women[1]. However, no effective treatment is currently available for hepatitis E and there are no commercial vaccines for hepatitis E in the world. Although at least four major genotypes of HEV have been identified, only one serotype of HEV is recognized. DNA vaccine can synthesize viral proteins within the host cells and induce humoral and cellular immune responses[2,3]. In this study, we constructed eucaryotic expression plasmid containing HEV ORF2 fragment and full-length ORF3 (DNA vaccine) chimeric gene and inoculated it to BALB/c mice to detect the specific humoral and cellular immune responses in mice.

MATERIALS AND METHODS

Construction of plasmid

All PCR primers were designed according to the nucleotide sequence of a Chinese HEV isolate (DDBJ accession number D11092)[4]. HEV mRNA was extracted from the feces of a patient with hepatitis E in Hangzhou, Zhejiang Province. The HEV ORF2 fragment and full-length ORF3 chimeric gene were amplified by RT-PCR. The PCR product was inserted into an eucaryotic expression plasmid pcDNA3 to form a recombinant plasmid pcHEV23 (DNA vaccine) (Figure 1).

DNA inoculation protocol

Thirty-two female BALB/c mice (18-20 g) provided by Zhejiang Experimental Animal Center were used for immunization and divided into four groups: Group 1 was injected with 100 μL saline solution as control. Group 2 was injected with 100 μg/100 μL vector pcDNA3 as control. Group 3 was injected with 100 μg/100 μL pcHEV23 plasmid. Group 4 was injected with 200 μg/100 μL pcHEV23 plasmid. Three weeks after the first injection, mice were bled and then boosted by same method. After another 3 wk, mice were boosted again for the second time (Table 1).

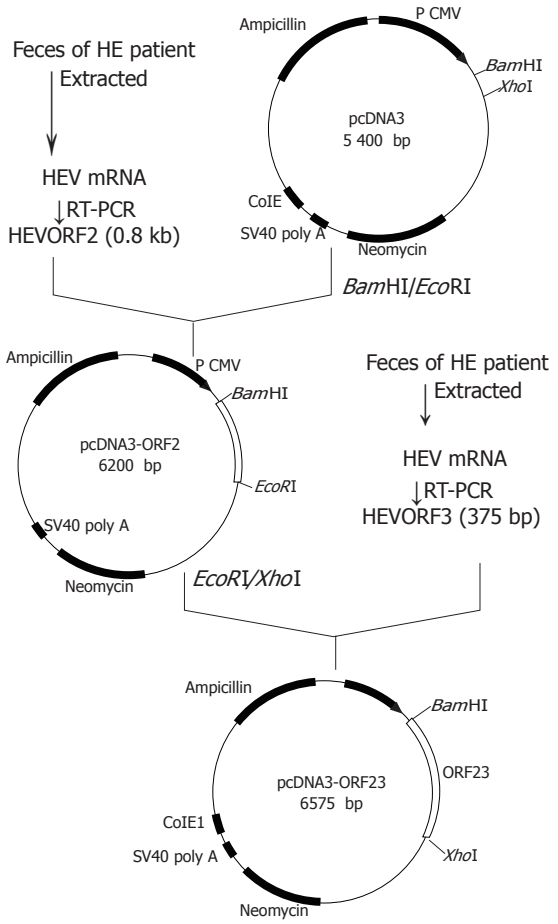

Figure 1 Construction of pcHEV23 plasmid (pcDNA3-ORF23).

Table 1 Protocol of DNA injection

Group	Mice (*n*)	Immunogen	Time of injection (wk)		
1	8	Saline	0	3	6
2	8	pcDNA3(100 μg/100 μL)	0	3	6
3	8	pcHEV23(100 μg/100 μL)	0	3	6
4	8	pcHEV23(200 μg/100 μL)	0	3	6

Serological test

Two weeks after the first three injections, blood samples were collected. All serum specimens were tested for anti-HEV IgG by EIA. In brief, microwell plates (Nunc, Roskilde, Denmark) were coated overnight at 4 °C with purified HEV ORF23 proteins (expressed *in E coli*) at 1 μg/mL in carbonate–bicarbonate buffer (pH 9.6). The wells were washed thrice with 0.05% Tween 20 in PBS (PBS-T) and then blocked with 2% BSA in PBS-T at 37 °C for 1 h. Following three washes with PBS-T, serum samples diluted in 2% BSA were added to the plates and incubated at 37 °C for 1 h. Following five washes, HRP-conjugated anti-human IgG (Sigma) diluted 2 000-fold in PBS-T was added to detect the bound antibodies. Following incubation at 37 °C for 1 h, the plates were washed as above and the substrate tetramethylbenzidine solution (Sigma) was added to the wells. After incubation at room temperature for 15 min, color development was stopped by adding 2 mol/L H_2SO_4. Optical density (OD) at 450 nm was determined with an ELISA reader. The cut-off values were set for each test as 2.1 times the mean value of negative control samples.

Table 2 Anti-HEV IgG titers after the third injection (mean±SD)

Group	1	2	3	4
Mean±SD	0.116±0.009[b]	0.210±0.028[b]	0.353±0.085[b]	0.336±0.066[b]

[b]$P<0.01$ *vs* control.

Table 3 Result of assay of T-cell proliferation (mean±SD)

Group	1	2	3	4
	0.787±0.12[b]	1.54±0.25[b]	3.1±0.49[b]	2.85±0.59[b]

[b]$P<0.01$ *vs* control.

T-lymphocyte proliferation

All the animals were killed 14 d after the last injection to analyze cellular immune responses. Single cell suspension of splenocytes was prepared for each individual animal. Splenocytes were immediately cultured in the presence of HEV ORF23 (20 μg/mL, expressed in *E coli*). Sixty-eighth day after culture, MTT was then added to the cells to measure antigen-specific proliferation. Lymphocyte stimulation index (SI) was measured according to formula: SI = A_{570} (antigen stimulation)/A_{570} (control).

RESULTS

Construction of pcHEV23 plasmid

The sequencing data indicated that the pcHEV23 construct (Figure 1) contained the correct orientation of the HEV ORF2 and ORF3 fragments (sequencing data not shown).

Analysis of anti-HEV response in pcHEV23-inoculated mice

None of the mice had seroconversion after the initial injection of pcHEV23. Following the third dose of pcHEV23, anti-HEV IgG titers in groups 3 and 4 was higher than those in groups 1 and 2 ($P<0.01$, Table 2).

T-lymphocyte proliferation assay

The lymphocyte SI in the group immunized with pcHEV23 was higher than that in saline group and pcDNA3 in control DNA group ($P<0.01$). Results are shown in Table 3.

DISCUSSION

DNA vaccines represent a new and potentially powerful approach for the development of subunit vaccines. DNA vaccines induce a broad range of immune responses due to efficient priming of T lymphocytes[5]. This novel approach to vaccination is attractive as it offers several

desirable features. First, DNA is not infectious and does not replicate and encodes only the protein or proteins of interest. Second, DNA is stable and can be made inexpensively in large quantities at a high level of purity. Third, plasmid DNA does not contain any heterologous protein components compared to a recombinant virus vaccine. Fourth, DNA vaccine can induce both cell-mediated and humoral immunity. Finally, antigen expression persists after DNA vaccination, promoting the induction of long-lived memory immune cells[6]. DNA immunization can be defined as a physical delivery of nucleic acids *in vivo* to express antigenic proteins and elicit specific immune responses. Direct naked DNA inoculation obviates the requirement of purified antigens. Pathogenic antigens synthesized inside the inoculated host cells can be processed in a natural form to develop classes I and II-regulated immune responses, mimicking the aspects of live attenuated virus.

Epitope mapping demonstrates that there are at least 7 immunodominant epitopes in HEV ORF2 region and four epitopes in HEV ORF3 region[7,8]. In this study, the full length of HEV ORF3 cDNA and partial HEV ORF2 cDNA were combined and used as an antigen-coding sequence for construction of HEV DNA vaccine.

In conclusion, direct injection of pcHEV23 is able to induce specific anti-HEV IgG and T-lymphocyte proliferation. HEV DNA vaccine constructed by us can successfully induce both humoral and cellular immune responses and appears to be a viable alternative to the recombinant protein subunit vaccine candidate.

REFERENCES

1 **Wang L**, Zhuang H. Hepatitis E: an overview and recent advances in vaccine research. *World J Gastroenterol* 2004; **10:** 2157-2162
2 **Tang DC**, DeVit M, Johnston SA. Genetic immunization is a simple method for eliciting an immune response. *Nature* 1992; **356**: 152-154
3 **Wolff JA**, Malone RW, Williams P, Chong W, Acsadi G, Jani A, Felgner PL. Direct gene transfer into mouse muscle in vivo. *Science* 1990; **247**: 1465-1468
4 **Bi SL**, Purdy MA, McCaustland KA, Margolis HS, Bradley DW. The sequence of hepatitis E virus isolated directly from a single source during an outbreak in China. *Virus Res* 1993; **28**: 233-247
5 **Sarzotti M,** Dean TA, Remington MP, Ly CD, Furth PA, Robbins DS. Induction of cytotoxic T cell responses in newborn mice by DNA immunization. *Vaccine* 1997; **15**: 795-797
6 **Pardoll DM**, Beckerleg AM. Exposing the immunology of naked DNA vaccines. *Immunity* 1995; **3**: 165-169
7 **Khudyakov YE**, Khudyakova NS, Fields HA, Jue D, Starling C, Favorov MO, Krawczynski K, Polish L, Mast E, Margolis H. Epitope mapping in proteins of hepatitis E virus. *Virology* 1993; **194**: 89-96
8 **Khudyakov YuE,** Favorov MO, Jue DL, Hine TK, Fields HA. Immunodominant antigenic regions in a structural protein of the hepatitis E virus. *Virology* 1994; **198**: 390-393

Science Editor Wang XL and Guo SY **Language Editor** Elsevier HK

PO Box 2345, Beijing 100023, China
www.wjgnet.com
wjg@wjgnet.com

ELSEVIER

World J Gastroenterol 2005;11(42):6716-6721
World Journal of Gastroenterology ISSN 1007-9327

• *BRIEF REPORTS* •

Relation of overexpression of S phase kinase-associated protein 2 with reduced expression of p27 and PTEN in human gastric carcinoma

Xiu-Mei Ma, Ying Liu, Jian-Wen Guo, Jiang-Hui Liu, Lian-Fu Zuo

Xiu-Mei Ma, Ying Liu, Jian-Wen Guo, Jiang-Hui Liu, Lian-Fu Zuo. The Fourth Affiliated Hospital of Hebei Medical University, Shijiazhuang 050011, Hebei Province, China
Correspondence to: Lian-Fu Zuo, Hebei Provincial Tumor Institute, the Fourth Affiliated Hospital of Hebei Medical University, Shijiazhuang 050011, Hebei Province, China. maxiumei0471@yahoo.com.cn
Telephone: +86-0311-86033941-337
Received: 2005-01-24 Accepted: 2005-05-25

Abstract

AIM: To investigate the significance of S phase kinase-associated protein 2 (Skp2) expression in human gastric carcinoma and the relation between expressions of Skp2, p27 and PTEN.

METHODS: Immunohistochemical analysis was performed on 138 gastric carcinoma specimens, their paired adjacent mucosa specimens, 102 paired lymphatic metastatic carcinoma tissue specimens, 30 dysplasia specimens, 30 intestinal metaplasia specimens, 10 chronic superficial gastritis specimens and 5 normal gastric mucosa specimens for Skp2 expression and on 138 gastric carcinoma specimens for p27 and PTEN expression.

RESULTS: Skp2 labeling frequency was significantly higher in intestinal metaplasia (12.68±0.86) and adjacent mucosa (19.32±1.22) than in normal gastric mucosa (0.53±0.13) and chronic superficial gastritis (0.47±0.19) (P = 0.000); in dysplasia (16.74±0.82) than in intestinal metaplasia (P = 0.000); in gastric primary carcinoma (31.34±2.17) than in dysplasia and adjacent mucosa (P = 0.000); in metastasis gastric carcinoma in lymph nodes (39.76±2.00) than in primary gastric carcinoma (P = 0.037), respectively. Skp2 labeling frequency was positively associated with differentiation degree (*rho* = 0.315, P = 0.000), vessel invasion (*rho* = 0.303, P = 0.000) and lymph node metastasis (*rho* = 0.254, P = 0.000) of gastric cancer. Expression of Skp2 was negatively associated with p27 (*rho* = -0.451, P = 0.000) and PTEN (*rho* = -0.480, P = 0.000) expression in gastric carcinoma. p27 expression was positively associated with PTEN expression in gastric carcinoma (*rho* = 0.642, P = 0.000).

CONCLUSION: Skp2 overexpression may be involved in carcinogenesis and progression of human gastric carcinoma *in vivo*, possibly via p27 proteolysis. PTEN may regulate the expression of p27 by negatively regulating Skp2 expression.

Key words: Gastric carcinoma; Skp2; p27; PTEN

Ma XM, Liu Y, Guo JW, Liu JH, Zuo LF. Relation of overexpression of S phase kinase-associated protein 2 with reduced expression of p27 and PTEN in human gastric carcinoma. *World J Gastroenterol* 2005; 11(42): 6716-6721
http://www.wjgnet.com/1007-9327/11/6716.asp

INTRODUCTION

Dysregulation of the cell cycle is required for the formation of most malignant tumors. Progression of the cell cycle is controlled by interactions between cell cycle control proteins (cyclins) and their catalytically active cyclin-dependent kinase (CDKs). The activity of each cyclin-CDK complex is in turn regulated by several different mechanisms; the most important being negative regulation by CDK inhibitors[1]. p27 is an inhibitor of cyclinE-CDK2 and cyclinA-CDK2, which drive cells from G_1 to S phase of the cell division cycle[2,3]. Loss of p27 function therefore accelerates cell cycle progression and predisposes cells to malignant transformation, as is well illustrated by the observation of increased tumor incidence in hemizygous and homozygous p27-deleted mutant mice after carcinogen exposure[4,5]. Many clinical studies also indicate that low levels of p27 are associated with high aggressiveness and poor prognosis in a large variety of malignant tumors[2,3], including breast carcinoma[6,7], colorectal carcinoma[8], lung cancer[9], prostate cancer[10] and gastric carcinoma[11].

The amount of p27 is mainly regulated by post-translational ubiquitin-proteasome-mediated proteolysis[12]. Cell cycle-dependent degradation of p27 is dependent on phosphorylation at Thr^{187} in late G_1 phase by CDK2 under positive regulation by cyclinE. Thr^{187} phosphorylation is a necessary prerequisite for the sequential addition of ubiquitin molecules by an ubiquitin ligase complex, SCF^{skp2} composed of Skp1, Cull, Rbx1 and the F-box protein Skp2[3]. Polyubiquitination of p27 then targets p27 for degradation in proteasome, thus removing the p27 cell

cycle "brake" and allowing cells to transition from G_1 to S phase[13].

Some investigations have shown that Skp2 is a specific substrate-recognition subunit of SCF^{skp2}, expression of Skp2 is required for the ubiquitination and subsequent degradation of p27 *in vitro*[20-22], and Skp2 knock-out cells show high levels of p27[16]. The level of p27 has also been reported to be inversely related to that of Skp2 in lymphoma[24], oral squamous cell carcinoma[18,19] and colorectal carcinoma[20].

Recently, Mamillapalli *et al*.[21] reported that PTEN, a tumor suppressor, regulates the ubiquitin-dependent degradation of p27 through SCF^{Skp2}. Yang *et al*.[22] suggested that induction of Skp2 may be causally linked with decreased levels of p27 in prostate cancer and implicate PTEN in the regulation of Skp2 expression *in vivo*.

Recent studies have shown that Skp2 has oncogenic potential in breast epithelial cells and is overexpressed in a subset of breast carcinomas (ER- and Her-2 negative)[23] and Skp2 can mediate transformation and is upregulated during oral epithelial carcinogenesis[18]. Recently, a line of evidence also indicates a possible relationship between Skp2 expression and the malignancy of tumors. Skp2 expression has been shown to be greatly increased in malignantly transformed cell lines including oral squamous cell carcinoma[18] and correlates directly with the grade of malignancy of lymphoma[17] and oral squamous cell carcinoma[18]. Kudo *et al*.[19] reported that high Skp2 expression is also correlated with poor prognosis in oral squamous cell carcinoma. Thus, Skp2 may have a great significance in human carcinogenesis. However, few studies are available regarding the significance of Skp2 expression in human gastric carcinomas *in vivo* and there are no studies regarding the relationship between Skp2, p27 and PTEN expression. We therefore investigated the significance of Skp2 expression in human gastric carcinomas and the relationship between Skp2, p27 and PTEN expression *in vivo*.

MATERIALS AND METHODS

Patients and gastric specimens

One hundred and thirty-eight surgically resected gastric carcinoma specimens, paired adjacent mucosa specimens and paired 102 lymphatic gastric carcinoma tissue specimens metastatically selected from the Fourth Affiliated Hospital of Hebei Medical University were used in this study. All gastric carcinoma patients underwent total or subtotal gastrectomy and no patient received any treatment for cancer before surgery. All regional lymph nodes were removed. The patients comprised 111 males and 27 females with a mean age of 58.5 years and a median age of 60 years (from 36 to 78 years). After surgery, gastric specimens were fixed in 40 g/L neutral-buffered formaldehyde and embedded in paraffin. Additionally, 75 biopsy cases (5 cases of normal gastric mucosa, 10 cases of chronic superficial gastritis, 30 cases of intestinal metaplasia and 30 cases of dysplasia) were included in this study as well. To avoid evaluator variability, all pathological diagnoses were done by two pathologists. Clinical stage was done according to the International Union Contrele Cancer criteria published in 1997.

Immunohistochemistry

A standard Non-Biotin HRP two-step immunohistochemical method (Zymed) was used. Four-micrometer-thick sections were deparaffinized and rehydrated. Endogenous peroxidase in sections was inactivated in 30 mL/L hydrogen peroxide (H_2O_2) in ethanol for 15 min at room temperature. The sections were washed thrice for 5 min with 0.01 mol/L phosphate-buffered saline (PBS) and then heated in a citrate buffer (0.01 mol/L, pH 6.4) for PTEN and p27 or in a EDTA buffer (1 mmol/L, pH 8.0) for Skp2 in an 800-W microwave oven for 12 min for antigen retrieval. The sections were incubated with mouse monoclonal antibody to Skp2 (1:50 dilution, Zymed), p27 (1:50 dilution, Santa Cruz) and PTEN (1:50 dilution, Zymed) overnight at 4 °C, washed thrice for 5 min with 0.01 mol/L PBS 3 and then incubated with common IgG (Fab fraction)-HRP complex for 30 min at room temperature. Immunoreactive products were visualized using 3,3'-diaminobenzidine/H_2O_2, and finally the sections were counterstained with hematoxylin. Some sections were incubated with PBS instead of primary antibody as negative control to verify the specificity of the immunoreactions. Vascular endothelial cells showed strong PTEN expression with a nuclear predominance and served as an internal positive control for PTEN in this study. The positive breast adenocarcinoma served as a positive control for Skp2 and p27.

Immunohistochemical quantitation

Immunostaining of nuclear Skp2, p27 and PTEN in each specimen was evaluated microscopically and recorded as the percentage of Skp2, p27, and PTEN-positive cells (labeling frequency), after at least 1 000 nuclei at the lesion site were calculated in at least five high-power fields (×400). All specimens were evaluated without any knowledge of the patients' clinical information.

Statistical analysis

The differences in Skp2 labeling frequencies among specimens of normal gastric mucosa, chronic superficial gastritis, intestinal metaplasia, dysplasia, gastric adenocarcinoma, adjacent mucosa and lymphatic metastatic gastric carcinoma were compared by Mann-Whitney *U* test. The relation between Skp2 expression and the clinical and pathological variables was evaluated using the Spearman correlation coefficient. The Spearman's correlation coefficient testing was also used to determine the relation between Skp2, PTEN and p27 as well as between PTEN and p27. $P<0.05$ was considered statistically significant. All analyses were performed using SPSS 11.0 statistical software.

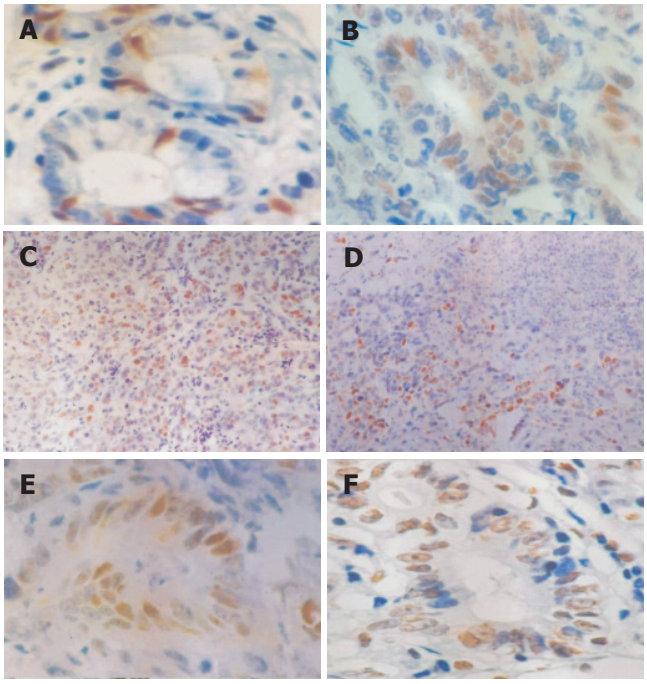

Figure 1 Skp2, p27 and PTEN expression in different gastric tissues (DAB and hematoxylin stain). **A:** Positive Skp2 in nuclei of intestinal metaplasia and dysplasia cells (original magnification ×400); **B:** Positive Skp2 in nuclei of well-differentiated gastric carcinoma cells (original magnification ×400); **C:** Positive Skp2 in nuclei of poorly differentiated gastric carcinoma cells (original magnification ×100); **D:** Positive Skp2 in lymphatic metastatic gastric carcinoma cells (original magnification ×100); **E:** Positive p27 in nuclei of well-differentiated gastric carcinoma cells (original magnification ×400); **F:** Positive PTEN in nuclei of well-differentiated gastric carcinoma cells (original magnification ×400).

RESULTS

Expression of Skp2 in human gastric specimen

The Skp2 immunoreactivity was predominantly localized in the nuclei of gastric cells (Figure 1). In 5% of the cancer specimens examined, a weak or moderate cytoplasmic immunoreactivity could be seen in addition to the predominant nuclear reactivity in cancer cells. Skp2 labeling frequency in normal gastric mucosa, intestinal metaplasia, dysplasia, primary gastric carcinoma and lymphatic metastatic gastric carcinoma was significantly higher than in normal gastric mucosa and chronic superficial gastritis ($P = 0.000$); it was in dysplasia than in intestinal metaplasia ($P = 0.000$); in primary gastric carcinoma than in dysplasia ($P = 0.000$); in lymphatic metastatic gastric carcinoma than in primary gastric carcinoma ($P = 0.037$, Table 1).

Relation between Skp2 labeling frequency and clinicopathological features in gastric carcinoma

Relation between Skp2 labeling frequency and clinicopathological variables including age, gender, histological differentiation, depth of invasion, vessel invasion, lymphatic metastasis, distant metastasis as well as clinical stage is summarized in Table 2. Skp2 labeling frequency was negatively associated with age, gender, depth of invasion, distant metastasis as well as clinical stage. A significant correlation was found between the

Table 1 Skp2 protein expression in human gastric tissues

Tissue	Specimens (*n*)	Skp2 labeling frequency(%) Median	Mean±SE
Normal gastric mucosa	5	0.00	0.47±0.19
Chronic superficial gastritis	10	0.00	0.53±0.13
Intestinal metaplasia	30	12.00	12.68±0.86
Dysplasia	30	19.00	16.74±0.82
Primary gastric carcinoma	138	29.00	31.34±2.17
Adjacent mucosa	138	16.00[6]	19.32±1.22
Metastasis tumor tissue in lymph node	102	39.50[7]	39.76±2.00

[1,2,3,4]Frequency was significantly higher than in normal gastric tissue and chronic superficial gastritis ($P = 0.000$,all the same; Mann-Whitney U test). [2]Frequency was significantly higher than in intestinal metaplasia ($P = 0.000$; Mann-Whitney U test). [3]Frequency was significantly higher than in intestinal metaplasia and dysplasia, ($P = 0.000$,all the same; Mann-Whitney U test). [5]Frequency was Significantly higher than in primary tumors (P = 0.037; Mann-Whitney U test).

Table 2 Skp2 protein expression in 138 human gastric cancers

Clinicopathological feature	Specimens (*n*)	Skp2 labeling frequency (%) Mean±SE	rho	*P*
Patients	138	36.32±1.22		
Age (yr)	138	58.50	0.190	0.833
<60	66	34.25±3.58		
⩾60	72	34.41±2.63		
Gender			0.119	0.179
Females	27	24.96±5.21		
Males	111	32.90±2.37		
Differentiation grade			0.315	0.000
Well/Moderate	63	22.41±2.59		
Poor	75	38.85±3.10		
Depth of invasion			0.001	0.986
Serosal	24	25.84±2.45		
Outside soft tissue	114	29.25±4.87		
Vessel invasion			0.303	0.000
Absent	120	27.89±2.11		
Present	18	54.39±6.84		
Lymph node metastasis			0.254	0.000
Absent	36	27.94±3.38		
Present	102	37.14±2.69		
Distant metastasis			0.091	0.307
Absent	26	22.77±6.92		
Present	12	31.79±2.38		
Clinical stage			0.069	0.440
0	0			
Ia	0			
Ib	3	22.78±6.92		
II	36	29.81±3.14		
IIIa	12	44.67±6.78		
IIIb	66	34.50±3.55		
IV	9	53.00±0.57		

[1,2,3]Skp2 labeling frequency was positively correlated with differentiated degree (rho = 0.315, $P = 0.000$), vessel invasion (rho = 0.303, $P = 0.000$), and lymph node metastasis (rho = 0.254, $P = 0.000$) in gastric carcinoma, respectively. [4]Because clinical staging could not be performed due to the lack of accurate records about lymph node in operation, data of 12 cases were cancelled in statistical analysis.

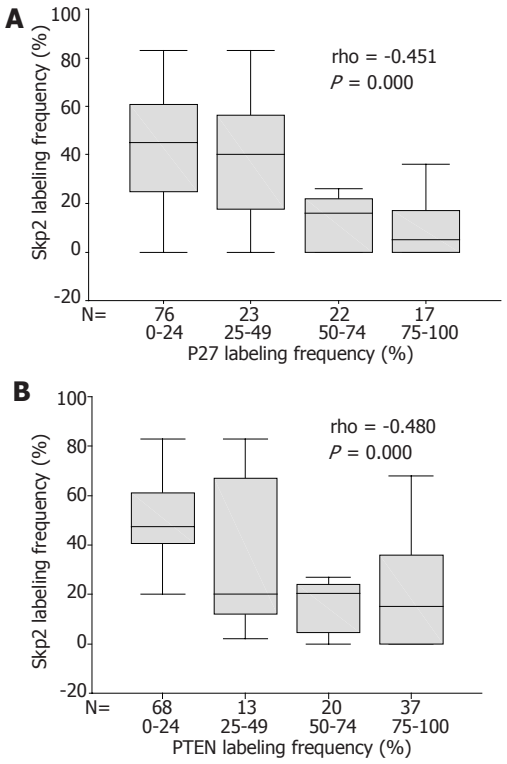

Figure 2 Correlation of Skp2 with p27 (**A**) and PTEN (**B**) protein levels. Each box and the associated bars represent the values of middle 50% and the range of the data respectively. The dark line within a box denotes the median.

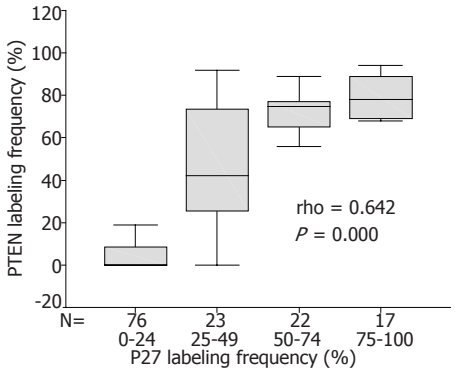

Figure 3 Correlation of p27 and PTEN expression in human gastric carcinoma. Each box and the associated bars represent the values of middle 50% and the range of the data respectively. The dark line within a box denotes the median.

Skp2 labeling frequency and differentiation degree (*rho* = 0.315, *P* = 0.000), vessel invasion (*rho* = 0.303, *P* = 0.000) and lymphatic metastasis (*rho* = 0.254, *P* = 0.000). Poorly differentiated gastric carcinoma, gastric carcinoma with vessel invasion and gastric carcinoma with lymphatic metastasis tended to have a higher Skp2 labeling frequency.

Relation between Skp2, p27 and PTEN expression in gastric carcinoma

Given the biochemical link between Skp2 and p27, we asked whether there was a correlation between Skp2 and p27 levels in gastric carcinoma using the same set of gastric carcinoma specimens used for the Skp2 analysis. A statistically significant inverse relation between p27 and Skp2 labeling frequency was evident (*rho* = -0.451, *P* = 0.000; Figure 2A). *In vitro* study linking loss of PTEN with increased Skp2 levels led us[29] to also compare the expression of PTEN and Skp2 using the same set of gastric carcinoma specimens. Interestingly, we found that increased Skp2 expression was significantly correlated with loss and decrease of PTEN expression in gastric carcinoma (*rho* = -0.480, *P* = 0.000; Figure 2B). Additionally, a positive relation between p27 and PTEN expression was observed in gastric carcinoma (*rho* = 0.642, *P* = 0.000; Figure 3).

DISCUSSION

Protein degradation by the ubiquitin–proteasome pathway plays a fundamental role in the regulation of eukaryotic cell cycle. Proteolysis of G_1 regulatory proteins is mediated by SCF ubiquitin ligase complex (SCF^{Skps}) composed of four major subunits, Skp1, Cul1, Rbx1/Roc1 and one of the F-box proteins (Fbps)[24]. There are 11 Fbps in budding yeast, 22 in Drosophila[25] and 38 in human beings[26,27]. Skp2 is a Fbp first identified together with Skp1 as an interactor of the cyclinA-Cdk2 complex which drives cells from G_1 to S phase, hence it is named as S phase kinase-associated protein 2 (Skp2)[24].

In this study, we found that Skp2 immunoreactivity was rare in normal gastric mucosa and chronic superficial gastritis, but Skp2 labeling frequency was significantly increased during the course of intestinal metaplasia, dysplasia and primary gastric carcinoma. From pathological point of view, development of gastric adenocarcinoma involves progression through a well-defined series of histological steps initiated by the change of normal mucosa to chronic superficial gastritis, followed by the appearance of atrophic gastritis and intestinal metaplasia, then dysplasia and finally adenocarcinoma[28]. These results suggest that Skp2 may have oncogenic potential in gastric carcinoma and is involved in gastric carcinogenesis. It may become a new biomarker in gastric carcinogenesis. Additionally, we found that Skp2 labeling frequency in adjacent mucosa of gastric carcinoma was significantly higher than that in normal gastric mucosa, suggesting that some adjacent mucosae of gastric carcinoma have normal histological structure, but the expression of some proteins is changed.

In this study, we found that Skp2 labeling frequency was positively correlated with differentiation degree, lymphatic metastasis and vessel invasion of gastric carcinoma. Poorly differentiated gastric carcinoma and gastric carcinoma with lymphatic metastasis and vessel invasion tended to have a higher Skp2 labeling frequency. Skp2 labeling frequency was higher in lymphatic metastatic gastric carcinoma than in primary gastric carcinoma. The overexpression of Skp2 could modulate the malignant phenotype of gastric carcinoma cells, suggesting that overexpression of Skp2 may be associated with metastasis

potential of gastric carcinoma cells. Further studies need to be done to clarify their mechanism.

In the present study, we also found that Skp2 expression was inversely correlated with the expression of p27, which is consistent with the results reported in other studies[18,19,21]. These results suggest that Skp2 overexpression is associated with p27 protein degradation in cancer tissue, which may be a reason why Skp2 overexpression is involved in carcinogenesis and progression of cancer. Furthermore, Skp2 expression was also inversely correlated with PTEN expression and p27 expression was positively related with PTEN expression in gastric carcinoma. PTEN tumor suppressor acts as a phosphatase of phosphatidylinositol-3,4,5-trisphosphate (PIP3) and negatively controls the G_1/S cell cycle transition and regulates the levels of p27[29]. Mamillapalli *et al*.[21] showed that PTEN deficiency in mouse embryonic stem cells decreases p27 level while increases Skp2 level. Conversely, in human glioblastoma cells, ectopic PTEN expression leads to p27 accumulation accompanied with a reduction of Skp2 and ectopic expression of Skp2 alone is sufficient to reverse PTEN-induced p27 accumulation, restore the kinase activity of cyclin E/CDK2 and partially overcome the PTEN-induced G_1 cell cycle arrest. Recombinant SCF^{Skp2} complex or Skp2 protein alone can rescue the defect in p27 ubiquitination in extracts from cells treated with a PI 3-kinase inhibitor. Yang *et al*.[30] showed that loss of expression or reduced expression of PTEN protein contributes to carcinogenesis and progression of gastric carcinoma. Myung *et al*.[31] reported that reduced expression of cyclin-dependent kinase inhibitor p27 is associated with advanced stage and invasiveness of gastric carcinoma. Additionally, Yang *et al*.[22] also found that elevated Skp2 protein expression in human prostate cancer is associated with loss of p27 and PTEN expression. Thus, all these findings suggest that PTEN functions as a negative regulator of the Skp2 pathway that is normally used to control S-phase entry through the regulation of p27 in gastric carcinoma and the effects of Skp2, p27 and PTEN together play an important role in carcinogenesis and progression of gastric carcinoma. These results also suggest that Skp2 functions as a critical component in the PTEN/PI3-kinase pathway for the regulation of p27.

In conclusion, alterations in the levels of proteins controlled by the ubiquitin–proteasome pathway during transformation are likely to be common. Further studies that define how such posttranscriptional control pathways are altered during transformation may provide additional biomarkers or facilitate the identification of novel therapeutic targets. The finding that Skp2 is induced in a number of different cancers suggests that drugs directed at this molecule may provide a more selective target for therapeutic development.

REFERENCES

1 **Sherr CJ.** Cancer cell cycles. *Science* 1996; **274**: 1672-1677
2 **Philipp-Staheli J,** Payne SR, Kemp CJ. p27(Kip1): regulation and function of a haploinsufficient tumor suppressor and its misregulation in cancer. *Exp Cell Res* 2001; **264**: 148-168
3 **Slingerland J,** Pagano M. Regulation of the cdk inhibitor p27 and its deregulation in cancer. *J Cell Physiol* 2000; **183**: 10-17
4 **Fero ML**, Randel E, Gurley KE, Roberts JM, Kemp CJ. The murine gene p27Kip1 is haplo-insufficient for tumour suppression. *Nature* 1998; **396**: 177-180
5 **Nakayama K,** Ishida N, Shirane M, Inomata A, Inoue T, Shishido N, Hori I, Loh DY, Nakayama K. Mice lacking p27(Kip1) display increased body size, multiple organ hyperplasia, retinal dysplasia, and pituitary tumors. *Cell* 1996; **85**: 707-720
6 **Tan P,** Cady B, Wanner M, Worland P, Cukor B, Magi-Galluzzi C, Lavin P, Draetta G, Pagano M, Loda M. The cell cycle inhibitor p27 is an independent prognostic marker in small (T1a,b) invasive breast carcinomas. *Cancer Res* 1997; **57**: 1259-1263
7 **Catzavelos C**, Bhattacharya N, Ung YC, Wilson JA, Roncari L, Sandhu C, Shaw P, Yeger H, Morava-Protzner I, Kapusta L, Franssen E, Pritchard KI, Slingerland JM. Decreased levels of the cell-cycle inhibitor p27Kip1 protein: prognostic implications in primary breast cancer. *Nat Med* 1997; **3**: 227-230
8 **Loda M,** Cukor B, Tam SW, Lavin P, Fiorentino M, Draetta GF, Jessup JM, Pagano M. Increased proteasome-dependent degradation of the cyclin-dependent kinase inhibitor p27 in aggressive colorectal carcinomas. *Nat Med* 1997; **3**: 231-234
9 **Esposito V,** Baldi A, De Luca A, Groger AM, Loda M, Giordano GG, Caputi M, Baldi F, Pagano M, Giordano A. Prognostic role of the cyclin-dependent kinase inhibitor p27 in non-small cell lung cancer. *Cancer Res* 1997; **57**: 3381-3385
10 **Tsihlias J,** Kapusta LR, DeBoer G, Morava-Protzner I, Zbieranowski I, Bhattacharya N, Catzavelos GC, Klotz LH, Slingerland JM. Loss of cyclin-dependent kinase inhibitor p27Kip1 is a novel prognostic factor in localized human prostate adenocarcinoma. *Cancer Res* 1998; **58:** 542-548
11 **Ohtani M,** Isozaki H, Fujii K, Nomura E, Niki M, Mabuchi H, Nishiguchi K, Toyoda M, Ishibashi T, Tanigawa N. Impact of the expression of cyclin-dependent kinase inhibitor p27Kip1 and apoptosis in tumor cells on the overall survival of patients with non-early stage gastric carcinoma. *Cancer* 1999; **85**: 1711-1718
12 **Pagano M,** Tam SW, Theodoras AM, Beer-Romero P, Del Sal G, Chau V, Yew PR, Draetta GF, Rolfe M. Role of the ubiquitin-proteasome pathway in regulating abundance of the cyclin-dependent kinase inhibitor p27. *Science* 1995; **269:** 682-685
13 **Eguchi H,** Herschenhous N, Kuzushita N, Moss SF. Helicobacter pylori increases proteasome-mediated degradation of p27(kip1) in gastric epithelial cells. *Cancer Res* 2003; **63**: 4739-4746
14 **Carrano AC,** Eytan E, Hershko A, Pagano M. SKP2 is required for ubiquitin-mediated degradation of the CDK inhibitor p27. *Nat Cell Biol* 1999; **1**: 193-199
15 **Tsvetkov LM,** Yeh KH, Lee SJ, Sun H, Zhang H. p27(Kip1) ubiquitination and degradation is regulated by the SCF(Skp2) complex through phosphorylated Thr187 in p27. *Curr Biol* 1999; **9**: 661-664
16 **Nakayama K**, Nagahama H, Minamishima YA, Matsumoto M, Nakamichi I, Kitagawa K, Shirane M, Tsunematsu R, Tsukiyama T, Ishida N, Kitagawa M, Nakayama K, Hatakeyama S. Targeted disruption of Skp2 results in accumulation of cyclin E and p27(Kip1), polyploidy and centrosome overduplication. *EMBO J* 2000; **19**: 2069-2081
17 **Latres E**, Chiarle R, Schulman BA, Pavletich NP, Pellicer A, Inghirami G, Pagano M. Role of the F-box protein Skp2 in lymphomagenesis. *Proc Natl Acad Sci USA* 2001; **98**: 2515-2520
18 **Gstaiger M,** Jordan R, Lim M, Catzavelos C, Mestan J, Slingerland J, Krek W. Skp2 is oncogenic and overexpressed in human cancers. *Proc Natl Acad Sci USA* 2001; **98**: 5043-5048
19 **Kudo Y,** Kitajima S, Sato S, Miyauchi M, Ogawa I, Takata T. High expression of S-phase kinase-interacting protein 2, human F-box protein, correlates with poor prognosis in oral squamous cell carcinomas. *Cancer Res* 2001; **61**: 7044-7047

20 **Hershko D,** Bornstein G, Ben-Izhak O, Carrano A, Pagano M, Krausz MM, Hershko A. Inverse relation between levels of p27(Kip1) and of its ubiquitin ligase subunit Skp2 in colorectal carcinomas. *Cancer* 2001; **91**: 1745-1751

21 **Mamillapalli R,** Gavrilova N, Mihaylova VT, Tsvetkov LM, Wu H, Zhang H, Sun H. PTEN regulates the ubiquitin-dependent degradation of the CDK inhibitor p27(KIP1) through the ubiquitin E3 ligase SCF(SKP2). *Curr Biol* 2001; **11**: 263-267

22 **Yang G,** Ayala G, De Marzo A, Tian W, Frolov A, Wheeler TM, Thompson TC, Harper JW. Elevated Skp2 protein expression in human prostate cancer: association with loss of the cyclin-dependent kinase inhibitor p27 and PTEN and with reduced recurrence-free survival. *Clin Cancer Res* 2002; **8:** 3419-3426

23 **Signoretti S**, Di Marcotullio L, Richardson A, Ramaswamy S, Isaac B, Rue M, Monti F, Loda M, Pagano M. Oncogenic role of the ubiquitin ligase subunit Skp2 in human breast cancer. *J Clin Invest* 2002; **110**: 633-641

24 **Carrano AC,** Pagano M. Role of the F-box protein Skp2 in adhesion-dependent cell cycle progression. *J Cell Biol* 2001; **153**: 1381-1390

25 **Rubin GM**, Yandell MD, Wortman JR, Gabor Miklos GL, Nelson CR, Hariharan IK, Fortini ME, Li PW, Apweiler R, Fleischmann W, Cherry JM, Henikoff S, Skupski MP, Misra S, Ashburner M, Birney E, Boguski MS, Brody T, Brokstein P, Celniker SE, Chervitz SA, Coates D, Cravchik A, Gabrielian A, Galle RF, Gelbart WM, George RA, Goldstein LS, Gong F, Guan P, Harris NL, Hay BA, Hoskins RA, Li J, Li Z, Hynes RO, Jones SJ, Kuehl PM, Lemaitre B, Littleton JT, Morrison DK, Mungall C, O'Farrell PH, Pickeral OK, Shue C, Vosshall LB, Zhang J, Zhao Q, Zheng XH, Lewis S. Comparative genomics of the eukaryotes. *Science* 2000; **287**: 2204-2215

26 **Cenciarelli C,** Chiaur DS, Guardavaccaro D, Parks W, Vidal M, Pagano M. Identification of a family of human F-box proteins. *Curr Biol* 1999; **9**: 1177-1179

27 **Winston JT,** Koepp DM, Zhu C, Elledge SJ, Harper JW. A family of mammalian F-box proteins. *Curr Biol* 1999; **9**: 1180-1182

28 **Konturek PC,** Kania J, Konturek JW, Nikiforuk A, Konturek SJ, Hahn EG. H.pylori infection, atrophic gastritis, cytokines, gastrin, COX-2, PPAR gamma and impaired apoptosis in gastric carcinogenesis. *Med Sci Monit* 2003; **9**: SR53-SR66

29 **Gottschalk AR,** Basila D, Wong M, Dean NM, Brandts CH, Stokoe D, Haas-Kogan DA. p27Kip1 is required for PTEN-induced G1 growth arrest. *Cancer Res* 2001; **61**: 2105-2111

30 **Yang L**, Kuang LG, Zheng HC, Li JY, Wu DY, Zhang SM, Xin Y. PTEN encoding product: a marker for tumorigenesis and progression of gastric carcinoma. *World J Gastroenterol* 2003; **9**: 35-39

31 **Myung N,** Kim MR, Chung IP, Kim H, Jang JJ. Loss of p16 and p27 is associated with progression of human gastric cancer. *Cancer Lett* 2000; **153:** 129-136

Science Editor Wang XL and Guo SY **Language Editor** Elsevier HK

PO Box 2345, Beijing 100023, China
www.wjgnet.com
wjg@wjgnet.com

ELSEVIER

World J Gastroenterol 2005;11(42):6722-6724
World Journal of Gastroenterology ISSN 1007-9327

• *CASE REPORT* •

Regression of hepatocellular carcinoma during vitamin K administration

Kazuhiro Nouso, Shuji Uematsu, Kunihiro Shiraga, Ryoichi Okamoto, Ryo Harada, Shoko Takayama, Wakako Kawai, Shigeru Kimura, Toru Ueki, Nobuaki Okano, Masahiro Nakagawa, Motowo Mizuno, Yasuyuki Araki, Yasushi Shiratori

Kazuhiro Nouso, Shuji Uematsu, Kunihiro Shiraga, Ryoichi Okamoto, Ryo Harada, Shoko Takayama, Wakako Kawai, Shigeru Kimura, Toru Ueki, Nobuaki Okano, Masahiro Nakagawa, Motowo Mizuno, Yasuyuki Araki, Department of Internal Medicine, Hiroshima City Hospital, Hiroshima 730-8518, Japan

Yasushi Shiratori, Department of Medicine and Medical Science, Okayama University Graduate School of Medicine and Dentistry, Okayama 700-8558, Japan

Correspondence to: Kazuhiro Nouso, MD, PhD, Department of Internal Medicine, Hiroshima City Hospital, 7-33 Motomachi, Naka-ku, Hiroshima-city, Hiroshima 730-8518, Japan. nouso@cc.okayama-u.ac.jp

Telephone: +81-82-221-2291 Fax: +81-82-223-1447
Received: 2005-01-24 Accepted: 2005-02-18

Abstract

An 85-year-old man with HCV infection and diabetes mellitus was diagnosed as having hepatocellular carcinoma (HCC, 13 cm in diameter) based on high serum alpha-fetoprotein (AFP), AFP-L3, and des-γ-carboxy prothrombin levels as well as typical enhancement pattern on contrast-enhanced CT. The patient did not receive any interventional treatments because of advanced age and the advanced stage of HCC. He chose to take vitamin K, which was reported to suppress the growth of HCC *in vitro*. Three months after starting vitamin K, all three tumor markers were normalized and HCC was markedly regressed, showing no enhancement in the early arterial phase on CT. Here we present the report describing the regression of HCC during the administration of vitamin K.

Key words: Hepatocellular carcinoma; Vitamin K; Regression

Nouso K, Uematsu S, Shiraga K, Okamoto R, Harada R, Takayama S, Kawai W, Kimura S, Ueki T, Okano N, Nakagawa M, Mizuno M, Araki Y, Shiratori Y. Regression of hepatocellular carcinoma during vitamin K administration. *World J Gastroenterol* 2005; 11(42): 6722-6724
http://www.wjgnet.com/1007-9327/11/6722.asp

INTRODUCTION

Hepatocellular carcinoma (HCC) is one of the most common cancers worldwide[1]. HCC is developed mainly in patients with chronic hepatitis C or B virus infections and the screening of this high risk group makes it possible to detect HCC at the early stage. However, many patients are still diagnosed at the advanced stage and the prognosis is poor. Transcatheter chemoembolization or chemotherapies are performed in cases of advance HCC[1-3]. These treatments are sometimes very effective, but are harmful to the background liver and accelerate the progression of pre-existing chronic liver injury. Therefore, these therapies cannot be performed in patients with severe liver cirrhosis. In addition, severe side effects often impair the quality of life. Thus, the development of new low-invasive therapies is needed.

Vitamin K is a factor in blood coagulation and is used for the treatment of osteoporosis[4]. Vitamin K is also known to inhibit the growth of cancer cell lines, but its clinical usefulness in the treatment of human cancer remains controversial[5-7]. In this report, we present a case of advanced HCC in which marked regression during the administration of vitamin K has been documented.

CASE REPORT

In July 2003, an 85-year-old man with liver cirrhosis due to HCV and diabetes mellitus was admitted to our hospital because of giant liver tumors. The patient had no history of alcohol drinking or blood transfusion. He did not smoke and was not taking any medicine, but was under intermediate-acting insulin (12 U/d) injection. He had undergone surgery for prostate hypertrophy 3 years before the present admission. Routine laboratory studies showed Hb 13.8 g/L, platelet count 101 000/mm^3, albumin 3.2 g/L, total bilirubin 0.6 mg/dL, aspartate aminotransferase and alanine aminotransferase 232 U/L and 102 U/L respectively, γ-glutamyl transpeptidase 93 IU/L, fasting blood glucose 126 mg/dL, HbA1c 11.1%. Serum alpha-fetoprotein (AFP), lentil lectin-A-reactive AFP (AFP-L3), and des-γ-carboxy prothrombin (DCP) were 1 212 ng/mL, 76.9%, and 51 300 mAU/mL, respectively. The patient was positive for HCV antibody and hepatitis B virus core antigen but negative for hepatitis B virus surface antibody. There were no esophageal or gastric varices observed during gastro-intestinal endoscopy. Although the patient did not complain of abdominal pain, gastric ulcer was detected by endoscopy and administration of the proton pump inhibitor was started.

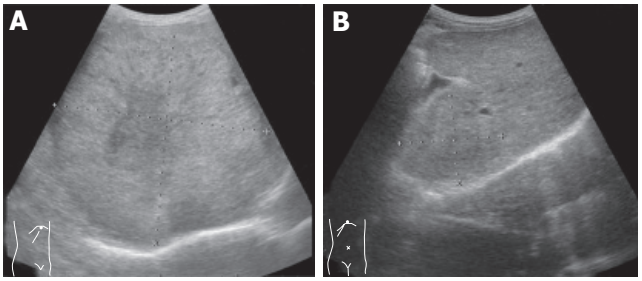

Figure 1 Giant tumor with central hypoechoic area dominated the right lobe of the liver (**A**) and remarkable regression of tumor with obscure margin after administration of vitamin K (**B**).

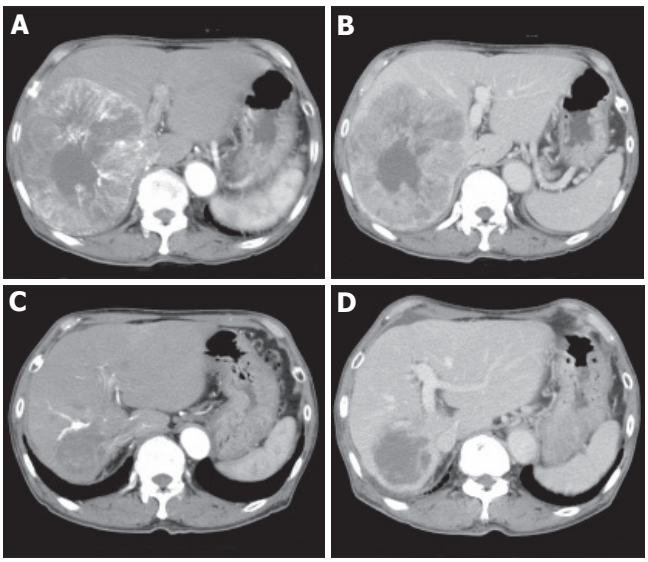

Figure 2 Enhancement of peripheral portion of tumor during early arterial phase (**A**) and hypoattenuation during portal phase (**B**) as well as remarkable tumor regression and no enhancement during early arterial phase (**C**) and portal phase (**D**) 5 mo after administration of vitamin K.

Abdominal ultrasonography (US) demonstrated that a large hyperechoic mass (13 cm in diameter) with central hypoechoic area dominated the right lobe of the liver (Figure 1A). At least four nodules about 2 cm in diameter surrounded the main nodule and another nodule (5 cm in diameter) existed at segment 4. Portal vein (PV) in the right lobe was replaced by tumor except for the PV in segments 5 and 8 in which faint blood flow was observed. Right hepatic vein was replaced and the middle hepatic vein was stretched by the tumor. Enhancement during the early arterial phase and defect during portal phase were observed by contrast enhanced-computed tomography (CE-CT, Figures 2A and B). Based on typical imaging features and elevated HCC tumor markers, the liver tumors were diagnosed as HCC. There was no distant metastasis observed by chest X-ray or abdominal CT.

Because of the patient's advanced age and advanced stage of HCC, the patient declined interventional therapies or angiography. Thereafter, we prescribed oral vitamin K_2 (45 mg daily), which was reported to inhibit cancer growth

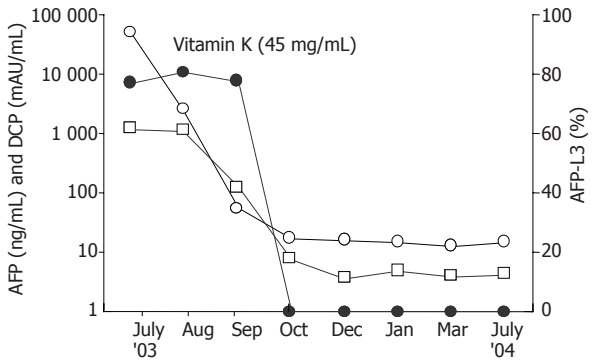

Figure 3 Clinical course of the patient.

in vitro[4,5]. The recommended dose for osteoporosis therapy was used. Informed consent for the administration of vitamin K was obtained from the patient and his family. Soon after the administration of vitamin K, AFP as well as DCP decreased and finally normalized in the 3rd month. AFP-L3 also decreased to below the detectable level from 76.9% to 0% (Figure 3). CE-CT, 5 months after starting vitamin K, demonstrated that the tumor sizes were remarkably decreased and the diameter of the main tumor was 5.5 cm (Figures 2C and D). Enhancement during the early arterial phase had disappeared in all nodules. US demonstrated that the tumor regressed and the margin of the tumor became obscure (Figure 1B). Twenty-two months have passed and there are no signs of recurrence observed to date. All three tumor markers have remained within the normal limits.

DISCUSSION

Vitamin K is known to inhibit the growth of many cancer cell lines including HCC[5–7]. The mechanisms of the anticancer action of vitamin K are not precisely understood, but several candidates including the induction of apoptosis, differentiation, and cell cycle inhibition have been proposed[4]. Recent research has demonstrated that the anticancer action of vitamin K may occur at the level of tyrosine kinases and phosphatase, modulating various transcription factors. In addition to the *in vitro* analysis, there are several case reports that described the usefulness of vitamin K for the treatment of human cancers including myelodysplastic syndrome (MDS)[6,7]. In a clinical trial of vitamin K for MDS and post-MDS acute myeloid leukemia, hematological improvement is reported in four of nine patients[8]. Recently, Koike *et al.* demonstrated that the development of PV tumor thrombus is inhibited and patient's survival is improved in patients with HCC following administration of vitamin K (unpublished data). These reports suggest that vitamin K is an anticancer agent for HCC.

Spontaneous regression of cancer is rare and estimated to occur once in 60 000-100 000 patients with cancer[9]. At least 27 cases of spontaneous regression of HCC have been reported[10-14]. There were no apparent clinical

characteristics discriminating the patient with spontaneous regression of HCC from others and various causes of regression have been documented (e.g. lack of blood supply due to arterial infarction or rapid growth of HCC, withdrawal from steroids, abstinence of alcohol consumption, administration of herbal medicines, and immunological activation due to high fever or sepsis)[10,15]. Hepatic angiography was performed in some cases and blood shortage due to the intimal damage induced by micro catheters could also be the cause of regression. In this report, the speed of tumor growth was uncertain because the patient was not followed up before admission. Other than that, he did not have any of the background factors reported previously. Therefore, possible reasons for regression are limited in this case; spontaneous regression due to blood shortage induced by rapid tumor growth or regression due to vitamin K administration, which was reported to inhibit tumor growth.

Although we could not conclude that administration of vitamin K was the cause of the regression in this case, this is a case report documenting regression of HCC during the administration of vitamin K. Further prospective study is needed to confirm the efficacy of vitamin K for the treatment of HCC.

REFERENCES

1 **Llovet JM**, Burroughs A, Bruix J. Hepatocellular carcinoma. *Lancet* 2003; **362**: 1907-1917
2 **Leung TW**, Johnson PJ. Systemic therapy for hepatocellular carcinoma. *Semin Oncol* 2001; **28**: 514-520
3 **Anthony PP**. Hepatocellular carcinoma: an overview. *Histopathology* 2001; **39**: 109-118
4 **Lamson DW**, Plaza SM. The anticancer effects of vitamin K. *Altern Med Rev* 2003; **8**: 303-318
5 **Wang Z**, Wang M, Finn F, Carr BI. The growth inhibitory effects of vitamins K and their actions on gene expression. *Hepatology* 1995; **22**: 876-882
6 **Yaguchi M**, Miyazawa K, Otawa M, Katagiri T, Nishimaki J, Uchida Y, Iwase O, Gotoh A. Kawanishi Y, Toyama K. Vitamin K2 selectively induces apoptosis of blastic cells in myelodysplastic syndrome: flow cytometric detection of apoptotic cells using APO2.7 monoclonal antibody. *Leukemia* 1998; **12**: 1392-1397
7 **Nishimaki J**, Miyazawa K, Yaguchi M, Katagiri T, Kawanishi Y, Toyama K, Ohyashiki K, Hashimoto S, Nakaya K, Takiguchi T. Vitamin K2 induces apoptosis of a novel cell line established from a patient with myelodysplastic syndrome in blastic transformation. *Leukemia* 1999; **13**: 1399-1405
8 **Miyazawa K**, Nishimaki J, Ohyashiki K, Enomoto S, Kuriya S, Fukuda R, Hotta T, Teramura M, Mizoguchi H, Uchiyama T. Omine M. Vitamin K2 therapy for myelodysplastic syndromes (MDS) and post-MDS acute myeloid leukemia: information through a questionnaire survey of multi-center pilot studies in Japan. *Leukemia* 2000; **14**: 1156-1157
9 **WH C**. Efforts to explain spontaneous regression of cancer. *J Surg Oncol* 1981; **17**: 201-209
10 **Lin TJ**, Liao LY, Lin CL, Shih LS, Chang TA, Tu HY, Chen RC, Wang CS. Spontaneous regression of hepatocellular carcinoma: a case report and literature review. *Hepatogastroenterology* 2004; **51**: 579-582
11 **Iiai T**, Sato Y, Nabatame N, Yamamoto S, Makino S, Hatakeyama K. Spontaneous complete regression of hepatocellular carcinoma with portal vein tumor thrombus. *Hepatogastroenterology* 2003; **50**: 1628-1630
12 **Morimoto Y**, Tanaka Y, Itoh T, Yamamoto S, Mizuno H, Fushimi H. Spontaneous necrosis of hepatocellular carcinoma: a case report. *Dig Surg* 2002; **19**: 413-418
13 **Abiru S**, Kato Y, Hamasaki K, Nakao K, Nakata K, Eguchi K. Spontaneous regression of hepatocellular carcinoma associated with elevated levels of interleukin 18. *Am J Gastroenterol* 2002; **97**: 774-775
14 **Ikeda M**, Okada S, Ueno H, Okusaka T, Kuriyama H. Spontaneous regression of hepatocellular carcinoma with multiple lung metastases: a case report. *Jpn J Clin Oncol* 2001; **31**: 454-458
15 **Takeda Y**, Togashi H, Shinzawa H, Miyano S, Ishii R, Karasawa T, Saito T, Saito K, Haga H, Matsuo T, Aoki M, Mitsuhashi H, Watanabe H, Takahashi T. Spontaneous regression of hepatocellular carcinoma and review of literature. *J Gastroenterol Hepatol* 2000; **15**: 1079-1086

Science Editor Wang XL and Guo SY **Language Editor** Elsevier HK

PO Box 2345, Beijing 100023, China
www.wjgnet.com
wjg@wjgnet.com

ELSEVIER

World J Gastroenterol 2005;11(42):6725-6727
World Journal of Gastroenterology ISSN 1007-9327

• *CASE REPORT* •

Unicentric Castleman's disease of the pancreas with massive central calcification

Oliver Goetze, Matthias Banasch, Klaus Junker, Wolfgang E. Schmidt, Christian Szymanski

Oliver Goetze, Matthias Banasch, Wolfgang E. Schmidt, Christian Szymanski, Department of Medicine, St. Josef-Hospital, Ruhr-University Bochum, Germany
Klaus Junker, Institute of Pathology, Bergmannsheil University Hospital, Ruhr-University, Bochum, Germany
Correspondence to: Oliver Goetze, MD, Department of Medicine, St. Josef-Hospital, Ruhr-University, Bochum, Germany Gudrunstr, 5644791 Bochum, Germany. oliver.goetze@rub.de
Telephone: +49-234-509-1 Fax: +49-234-509-2309
Received: 2005-01-29 Accepted: 2005-04-18

Abstract

Unicentric Castleman's disease of the pancreas is extremely rare, with only six cases described in the worldwide literature. An asymptomatic case of unicentric, hyaline, vascular-type Castleman's disease (UCD) localized to the tail of the pancreas with central calcification imitating a primary neoplasm of the pancreas is presented. This is the first description of endosonographic and endoscopic retrograde pancreatographic findings of pancreatic UCD. Additionally, computed tomography, histological and serologic findings are reported.

Key words: Unicentric Castleman's disease; Calcification; Pancreas; Endoscopic ultrasound

Goetze O, Banasch M, Junker K, Schmidt WE, Szymanski C. Unicentric Castleman's disease of the pancreas with massive central calcification. *World J Gastroenterol* 2005; 11(42): 6725-6727
http://www.wjgnet.com/1007-9327/11/6725.asp

INTRODUCTION

Unicentric Castleman's disease (UCD), also called giant lymph node hyperplasia, follicular lymphoreticuloma or angiofollicular mediastinal lymph node hyperplasia, is a rare lymphoproliferative disorder of unknown aetiology. UCD was first described and defined by Benjamin Castleman in 1956 in tumors of the thymus with asymptomatic mediastinal lymph node hyperplasia, which could be separated histologically from thymomas and other neoplastic lymph node disorders[1]. Flendrig and Schillings distinguished two basic pathologic types and one mixed variant[2], while Keller *et al.* designated hyaline-vascular, plasma cell, and hyaline-vascular plasma cell type[3]. UCD typically presents as indolent benign disease in young adults with a median age of approximately 35 years and is equally distributed between males and females[2,3]. A subset of patients with plasma cell variant may have systemic symptoms. UCD in the abdomen and pelvis has been only described in the radiology literature as a focal enhancing mass of varying locations, including the retroperitoneum, mesentery, and hepatic porta[4].

CASE REPORT

A 53-year-old man was well until one week before admission with renal colic with an onset of pain strongest at the right paravertebral region and radiating in the right iliac crest. Excretion urography performed in another hospital showed a slight pyelectasis of the right kidney and a left renal duplication with ureter bifidus, while, incidentally, abdominal ultrasound showed a calcified mass (3.4 cm × 3.4 cm) in the left hilar region of the kidney. Then the patient was subsequently referred to our tertiary care centre for further evaluation and treatment .

On physical examination the patient was afebrile and appeared well. The pulse was 80 bpm and the blood pressure 130/70 mm Hg. No lymphadenopathy was found. A non-tender liver edge descended 2 to 3 cm below the right costal margin; the spleen was not felt. Peripheral blood counts, liver function tests, cancer antigen (CA 19-9), carcinoembryonic antigen (CEA) and β-2 microglobulin were within normal levels. Immunologic tests for hepatitis A, B, C were negative. An ELISA for human immunodeficiency virus antibodies was negative. A postoperative ELISA (assay against viral latency-associated nuclear antigen) and a polymerase-chain-reaction test for herpes simplex virus 8 was negative and the serum interleukin 6 level was normal.

The patient had undergone a thorough systematic investigation, which included abdominal ultrasonography, computed tomography (CT), endoscopic ultrasound with fine-needle aspiration and endoscopic retrograde pancreatography (ERP). A spiral abdominal CT examination showed a well-circumscribed (5.5 cm × 4.5 cm × 4.5 cm) hypervascularized mass of soft tissue density with focal calcification in the tail of the pancreas without evidence of invasion of surrounding structures or vessels (Figure 1A). A thoracic and neck CT was normal. Endoscopic ultrasound revealed a solid, well defined, slightly heterogeneous, hypoechogenic soft-tissue mass with central calcification. Local lymph nodes were not enlarged (Figure 1B). The cytological evaluation of

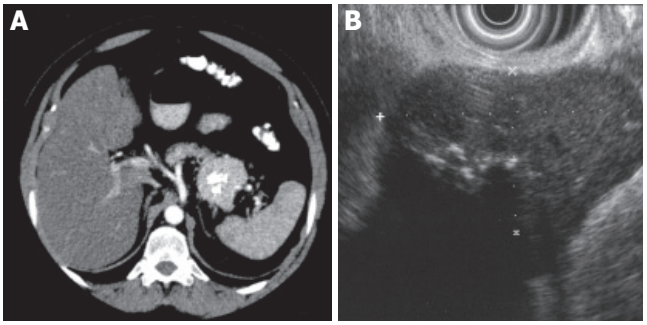

Figure 1 A: Enhanced CT shows a well-circumscribed hypervascular mass of soft tissue density with focal calcification in the tail of pancreas; **B:** 7.5 MHz endosonography shows a well-circumscribed hypoechogenic mass (2.8 x 4.9 cm) with focal hyperechogenicity and without signs of infiltration.

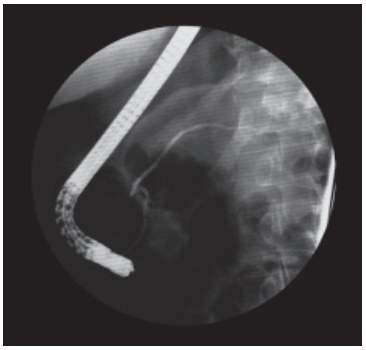

Figure 2 Endoscopic retrograde pancreatography (ERP) shows no malignant stricture of the pancreatic duct and a slight parenchymography in the tail of the pancreas.

endosonography controlled fine-needle aspiration biopsy disclosed lymphatic tissue with focal sclerosis. In ERP (Figure 2) a malignant stricture of the pancreatic duct could be ruled out and a slight parenchymography in the tail of the pancreas with circular calcification of the tumor projecting around the pancreatic duct was shown. Postoperative microscopical examination of a specimen of bone marrow obtained by needle aspiration biopsy disclosed only slight hypercellularity.

Then the patient subsequently underwent left hemipancreatectomy with splenectomy. The specimen of hemipancreatectomy had a spheroidal tumor mass measuring up to 4.6 cm, which was demarcated by a fibrous pseudocapsule (partially with tumor infiltration) from normal tumor-free pancreas tail tissue (12 cm × 7 cm × 4 cm, 367 g). Remarkably, there was a central calcification 3.2 cm in diameter (Figures 1A and 3B). Microscopic examination of the mass revealed germinal centres *with hyalinized venules* originating from a hypervascular mantle zone surrounded by small lymphocytes in a concentric onionskin pattern with focal hyaline deposits, which is characteristic for hyaline-vascular type of Castleman's disease (Figures 3A and 3B). The interfollicular stroma showed few plasma cells expressing light chains and IgM. The patient's

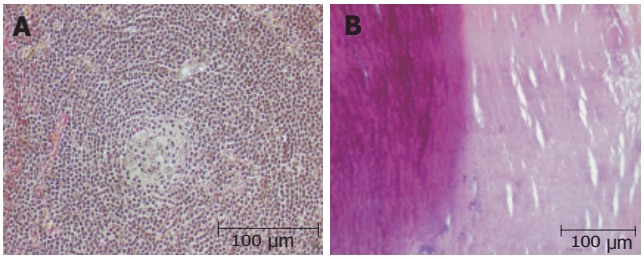

Figure 3 A: Germinal centers with hyalinized venules originating from a hypervascular mantle zone surrounded by small lymphocytes in a concentric onionskin pattern (hematoxylin and eosin); **B:** Areas of heterotopic calcification of the central part of the tumor (left panel) and hyaline deposits (right panel) (hematoxylin and eosin).

postoperative course was without complications and no recurrence has occurred after a two year follow up period in our patient.

DISCUSSION

Unicentric Castleman's disease commonly occurs in the mediastinum (over 50 %), but has also been identified in multiple anatomic locations, including the neck, the pelvis and the axilla[5]. So far, UCD in the abdomen and pelvis has been described in the radiology literature as a focal enhancing mass of varying location, whereas UCD in the pancreas constitutes an extremely rare entity, which can imitate a tumor originating from pancreatic tissue[4]. Prior to this report, endoscopic retrograde cholangiopancreatography and endoscopic ultrasound findings of pancreatic Castleman's are not available. The patient had no systemic symptoms, the pancreatic mass was well defined and hypoechogenic on endoscopic ultrasonography and showed no contact between the main pancreatic duct with circular calcification projecting around the pancreatic tail at ERP. On abdominal CT homogeneous enhancement with central pattern of calcification was found, as described in the literature[4,6,7]. Hence, possible differential diagnoses of this indeterminate tumor of the pancreatic tail containing central calcifications were acinar cell carcinoma, solid and papillary epithelial neoplasm, solid cystic tumor, serous cystadenoma or cystic teratomas of the pancreas, which are all known as well defined tumors with calcification patterns[8,9]. Castleman's disease in the abdomen and pelvis displays a variety of calcification patterns, including punctuate, coarse, peripheral, and "arborizing". In a recently published retrospective review of 16 cases of abdominal and pelvic manifestations, 31% showed calcification, one with an arborizing pattern and the remaining lesions with punctuate calcification[4]. Calcification with a diameter of 3.2 cm in a case of monocentric or multicentric disease has as yet not been observed.

Patients with the hyaline-vascular subtype are usually clinical asymptomatic, as was our patient. Only 3% of the patients present with systemic complaints[3] and less

than 10% (usually patients with plasma cell variant) have disease associated syndromes like myasthenia gravis, erythema nodosum, Horton's arteritis or Moschcowitz' s disease[5,10-13]. In contrast, the multicentric type of Castleman disease (MCD) is accompanied by a general lymphadenopathy, systemic symptoms, laboratory abnormalities, organomegaly and progressive clinical course with potential for malignancy and was not recognized until 1978[14]. Understanding of MCD has greatly expanded since the identification of its association with HIV and HHV-8 infection[15-17]. However, the sources of the immune activation in the unicentric form and the HHV-8 and HIV negative multicentric form are still unidentified. In retrospective studies, complete surgical resection for patients with unicentric hyaline vascular Castleman's disease has been associated with the best chance of cure [18].

REFERENCES

1 **Castleman B,** Iverson L, Menendez VP. Localized mediastinal lymphnode hyperplasia resembling thymoma. *Cancer* 1956; **9:** 822-830

2 **Flendrig JA.** Benign giant lymphoma: clinicopathologic correlation study. In: Clark RL, Cumle RW, eds. The year book of cancer. Chicago: Year Book Medical Publishers, 1970: 296-299

3 **Keller AR,** Hochholzer L, Castleman B. Hyaline-vascular and plasma-cell types of giant lymph node hyperplasia of the mediastinum and other locations. *Cancer* 1972; **29:** 670-683

4 **Meador TL,** McLarney JK. CT features of Castleman disease of the abdomen and pelvis. *AJR Am J Roentgenol* 2000; **175:** 115-118

5 **Frizzera G.** Castleman's disease and related disorders. *Semin Diagn Pathol* 1988; **5:** 346-364

6 **Lepke RA,** Pagani JJ. Pancreatic Castleman disease simulating pancreatic carcinoma on computed tomography. *J Comput Assist Tomogr* 1982; **6:** 1193-1195

7 **Rahmouni A,** Golli M, Mathieu D, Anglade MC, Charlotte F, Vasile N. Castleman disease mimicking liver tumor: CT and MR features. *J Comput Assist Tomogr* 1992; **16:** 699-703

8 **Nakamura S,** Okayama Y, Imai H, Aoki S, Kobayashi S, Hattori T, Shiraki S, Goto K, Sano H, Ohara H, Nomura T, Joh T, Yoshifumi Y, Itoh M. A solid cystic tumor of the pancreas with ossification and possible malignancy, coexisting nonfusion of the pancreatic ducts. *J Clin Gastroenterol* 2001; **33:** 333-336

9 **Chiou YY,** Chiang JH, Hwang JI, Yen CH, Tsay SH, Chang CY. Acinar cell carcinoma of the pancreas: clinical and computed tomography manifestations. *J Comput Assist Tomogr* 2004; **28:** 180-186

10 **Hartmeier SH,** Steurer J, Christen R, Fehr J, Schleiffenbaum B. Castleman's disease--a rare cause of a febrile state with lymphadenopathy. *Dtsch Med Wochenschr* 1997; **122:** 1141-1146

11 **Herrada J,** Cabanillas F, Rice L, Manning J, Pugh W. The clinical behavior of localized and multicentric Castleman disease. *Ann Intern Med* 1998; **128:** 657-662

12 **Hineman VL,** Phyliky RL, Banks PM. Angiofollicular lymph node hyperplasia and peripheral neuropathy: association with monoclonal gammopathy. *Mayo Clin Proc* 1982; **57:** 379-382

13 **Massey GV,** Kornstein MJ, Wahl D, Huang XL, McCrady CW, Carchman RA. Angiofollicular lymph node hyperplasia (Castleman's disease) in an adolescent female. Clinical and immunologic findings. *Cancer* 1991; **68:** 1365-1372

14 **Gaba AR, Stein RS,** Sweet DL, Variakojis D. Multicentric giant lymph node hyperplasia. *Am J Clin Pathol* 1978; **69:** 86-90

15 **Soulier J,** Grollet L, Oksenhendler E, Cacoub P, Cazals-Hatem D, Babinet P, d'Agay MF, Clauvel JP, Raphael M, Degos L. Kaposi's sarcoma-associated herpesvirus-like DNA sequences in multicentric Castleman's disease. *Blood* 1995; **86:** 1276-1280

16 **Dupin N,** Gorin I, Deleuze J, Agut H, Huraux JM, Escande JP. Herpes-like DNA sequences, AIDS-related tumors, and Castleman's disease. *N Engl J Med* 1995; **333:** 798-799 author reply 798-799

17 **Yamasaki S,** Iino T, Nakamura M, Henzan H, Ohshima K, Kikuchi M, Otsuka T, Harada M. Detection of human herpesvirus-8 in peripheral blood mononuclear cells from adult Japanese patients with multicentric Castleman's disease. *Br J Haematol* 2003; **120:** 471-477

18 **Bowne WB**, Lewis JJ, Filippa DA, Niesvizky R, Brooks AD, Burt ME, Brennan MF. The management of unicentric and multicentric Castleman's disease: a report of 16 cases and a review of the literature. *Cancer* 1999; **85:** 706-717

Science Editor Guo SY **Language Editor** Elsevier HK

PO Box 2345, Beijing 100023, China
www.wjgnet.com
wjg@wjgnet.com

ELSEVIER

World J Gastroenterol 2005;11(42):6728-6729
World Journal of Gastroenterology ISSN 1007-9327

• *CASE REPORTS* •

Bile peritonitis due to intra-hepatic bile duct rupture

R Lochan, BV Joypaul

R Lochan, BV Joypaul, Department of Surgery, South Tyneside District General Hospital, South Shields, NE34 0PL United Kingdom
Correspondence to: R Lochan, Research Fellow, HPB Unit, Department of Surgery (level 4 Secretaries Office), Freeman Hospital, Newcastle upon Tyne NE7 7DN, United Kingdom. rajiv.lochan@nuth.northy.nhs.uk
Telephone: +44-191-2448427 Fax: +44-191-2231483
Received: 2004-08-13 Accepted: 2004-12-14

Abstract

Generalized biliary peritonitis is a serious intra-abdominal emergency. Most of them occur due to duodenal ulcer perforation and rapidly evolve into bacterial peritonitis due to contamination by gut organisms and food. In this situation, recognition of the pathology and its treatment is straightforward and is usually associated with a good outcome. There are a few unusual causes of biliary peritonitis, of which rupture of the biliary tree is one. We describe a rare case of biliary peritonitis due to rupture of an intra-hepatic biliary radical. Unusual causes of peritonitis do interrupt our daily routine emergency surgical experience. Rapid recognition of the presence of peritonitis, adequate resuscitation, recognition of operative findings, establishment of biliary anatomy, and performance of a meticulous surgical procedure resulted in a good outcome.

Key words: Biliary peritonitis; Intra-hepatic biliary radicle; Rupture

Lochan R, Joypaul BV. Bile peritonitis due to intra-hepatic bile duct rupture. *World J Gastroenterol* 2005; 11(42): 6728-6729
http://www.wjgnet.com/1007-9327/11/6728.asp

INTRODUCTION

Rupture of an intra-hepatic biliary duct leading to biliary peritonitis is a rare occurrence, with only few cases reported in the literature[1-4]. This case report reinforces the necessity of complete and meticulous operative assessment of the biliary system in every case of bile peritonitis.

CASE REPORT

A 78-year-old male with severe spondyloarthropathy presented with a 12-h history of upper abdominal pain, nausea and vomiting. He was shocked (BP 80/40, pulse 120/min) and clinical examination revealed guarding, tenderness with rebound in the upper abdomen and absence of bowel sounds. A diagnosis of peritonitis was made and he was appropriately resuscitated. He responded well to the treatment and became hemodynamically stable. His hematological blood profile as well as his urea and electrolytes were unremarkable. He had conjugated hyperbilirubinemia with raised alkaline phosphatase and alanine transaminase. Plain radiology (erect CXR and abdominal films) did not demonstrate any pneumoperitoneum.

When the patient was optimized, he underwent surgery. At laparotomy, there was no evidence of gastrointestinal perforation; however, free intra-peritoneal bile was found. The extra hepatic biliary system was grossly dilated due to obvious obstruction at the distal common bile duct by an impacted calculus. The gall bladder contained calculi and was thick walled. There was a perforated superficial biliary radicle in the left lobe of the liver, which was the source of the free bile in the peritoneal cavity.

A cholecystectomy was performed and the CBD was explored. The calculus in the distal CBD needed to be extracted through a trans-duodenal sphincterotomy. Post exploratory choledochoscopy and on-table cholangiography confirmed clearance of the bile ducts. The common bile duct was drained with a T-tube and at the end of the operation the ruptured biliary radicle stopped leaking bile. It was however reinforced with two interrupted 3/0 prolene sutures. The right sub-hepatic space was drained and the abdomen was closed as per standard.

The patient was transferred to the high dependency unit for immediate care. He made a slow, but steady post-operative recovery. T-tube cholangiogram performed on day 14 (post-op) confirmed free passage of contrast into the duodenum and absence of residual CBD stones; thus allowing its removal. The patient was discharged 34 days following surgery and he is still healthy with normal liver function tests when last reviewed 2 years following surgery.

DISCUSSION

Peritonitis requiring surgical intervention is caused by perforated peptic ulcer in about 40% cases (duodenum: gastric: 3:1), appendicitis in 20%, gangrene of the small bowel or gall bladder in 15%, post-operative complications in 10% and miscellaneous causes in 15% cases[5]. Most commonly, peritonitis in the clinical setting is due to microorganisms, though the initial insult is usually chemical as in peptic ulcer perforation where bile, pancreatic

enzymes, blood, etc., gain access into the peritoneal cavity.

The peritoneum can be contaminated with bile through a number of routes. The commonest is post-cholecystectomy. This is usually due to the division of small bile channels between the gall bladder and liver, imperfect clipping of the cystic duct, residual CBD stones causing raised intrabiliary pressure and inadvertent division of an accessory hepatic duct. The latter is potentially serious usually requiring biliary reconstruction. Other causes include post liver transplant biliary peritonitis, spontaneous hepatic rupture in pregnancy and trauma to the extra-hepatic biliary system such as that following minimal access renal surgery[6].

Perforation of the biliary tract secondary to rupture of the gall bladder (empyema/gangrene) is well documented. However, spontaneous rupture of the CBD is exceedingly rare and here the etiologies are increased intra-ductal pressure, calculus erosion and necrosis of the duct wall secondary to thrombosis[7]. Spontaneous perforation of extra hepatic ducts is also a very rare cause of jaundice in infancy[8]. The commonest site is the confluence of the cystic and common hepatic ducts[9]. Biliary peritonitis secondary to intra-hepatic duct rupture is rarely reported in the literature; the causes are calculus disease of the biliary ducts (as in this case), stenosis of the papilla and Caroli's disease[10].

The clinical picture associated with biliary peritonitis varies and the correct pre-operative diagnosis is difficult. This combined with the associated comorbidity of the patient population (mainly elderly) significantly contributes to a mortality rate of 30–50%[11]. Though the initial insult by bile is chemical, secondary bacterial infection is the usual sequelae. Furthermore, it has been clearly shown that, in the presence of bacteria, bile further impairs local host defense mechanism through its detergent lytic effects[12]. Paralytic ileus is also a frequent complication. Laboratory findings are usually non-contributory but biliary peritonitis should always be suspected in any patient with unexplained abdominal symptoms.

The aim of treatment is to prevent sepsis in the abdominal cavity and thus prompt recognition of the condition and control of source of the contamination with appropriate drainage/reconstruction of the biliary system is of paramount importance. The type of surgery is dependent upon the general condition of the patient as well as on biliary anatomy. Regardless, biliary peritonitis requires some form of drainage, either externally via the percutaneous route or internally via the endoscopic/open surgery route. In our patient, the intra-hepatic duct rupture was presumably due to a very high pressure in the biliary system secondary to calculus obstruction in the distal common bile duct. Transduodenal sphincterotomy and extraction of the impacted calculus along with 'T' tube drainage resulted in an uneventful resolution. Prompt recognition of this condition before biliary/systemic sepsis supervened played a major role in the positive outcome for this patient. In conclusion, prompt laparotomy in a well-resuscitated patient and an adequately tailored operation depending on the operative findings are the mainstay to avoid local and systemic sepsis and long-term morbidity in these cases of peritonitis.

REFERENCES

1 **Somorjai B**, Orosz E, Horvath T, Krasznay P. Non-traumatic intrahepatic bile-duct perforation in an adult. *Orvasi Hetilap* 1994; **135:** 361-363

2 **Raza H,** Hussain AM. Biliary peritonitis, due to rupture of intrahepatic duct. *Post graduate Medical Journal* 1991; **67:** 490

3 **Nobusawa S,** Adachi T, Miyazaki A, Nakajima A, Takeno Y, Ogawa S, Sakamoto A. A case report of biliary peritonitis--spontaneous perforation of an intrahepatic duct. *Am J Gastroenterol* 1986; **81:** 568-571

4 **Veselov VS**, Sukharev VF. Spontaneous rupture of the intrahepatic bile ducts as a cause of biliary peritonitis. *Vestn Khir Im I I Grek* 1983; **131:** 60-62

5 **Crawford E**, Ellis H. Generalised peritonitis--the changing spectrum. A report of 100 consecutive cases. *Br J Clin Pract* 1985; 39: 177-8, 184

6 **Kontothanassis D**, Bissas A. Biliary peritonitis complicating percutaneous nephrostomy. *Int Urol Nephrol* 1997; **29:** 529-531

7 **Kerstein MD**, McSwain NE. Spontaneous rupture of the common bile duct. *Am J Gastroenterol* 1985; **80:** 469-471

8 **Chardot C**, Iskandarani F, De Dreuzy O, Duquesne B, Pariente D, Bernard O, Gauthier F, Valayer J. Spontaneous perforation of the biliary tract in infancy: a series of 11 cases. *Eur J Pediatr Surg* 1996; **6:** 341-346

9 **Lilly JR**, Weintraub WH, Altman RP. Spontaneous perforation of the extrahepatic bile ducts and bile peritonitis in infancy. *Surgery* 1974; **75:** 664-673

10 **Chalasani N**, Nguyen CC, Gitlin N. Spontaneous rupture of a bile duct and its endoscopic management in a patient with Caroli's syndrome. *Am J Gastroenterol* 1997; **92:** 1062-1063

11 **Borghese M**, Caramanico L, Anelli L, De Cesare A, Farrocco G, Spallone G. Etiopathogenetic and physiopathological considerations on biliary peritonitis. *Minerva Med* 1986; **77:** 735-738

12 **Andersson R**, Tranberg KG, Bengmark S. Roles of bile and bacteria in biliary peritonitis. *Br J Surg* 1990; **77:** 36-39

Science Editor Wang XL and Guo SY **Language Editor** Elsevier HK

ELSEVIER

World Journal of Gastroenterology®

Supported by NSFC 2005-2006

Volume 11 Number 43
November 21, 2005

National Journal Award 2005

Contents

World Journal of Gastroenterology®
Volume 11 **Number** 43 **November 21**, 2005

Contents

World Journal of Gastroenterology®
Volume 11 **Number** 43 **November 21**, 2005

Contents

Editorial Coordinator for this issue: Anitha Kumaran

World Journal of Gastroenterology (*World J Gastroenterol , WJG*), a leading international journal in gastroenterology and hepatology, has an established reputation for publishing first class research on esophageal cancer, gastric cancer, liver cancer, viral hepatitis, colorectal cancer, and *Helicobacter pylori* infection, providing a forum for both clinicians and scientists, and has been indexed and abstracted in Index Medicus, MEDLINE, PubMed, Chemical Abstracts, EMBASE, Abstracts Journals, Nature Clinical Practice Gastroenterology and Hepatology, CAB Abstracts and Global Health. *WJG* is a weekly journal published jointly by The *WJG* Press and Elsevier Inc. The publication date is on 7th, 14th, 21st, and 28th every month. The *WJG* is supported by The National Natural Science Foundation of China, No. 30224801 and No.30424812, which was founded with a name of *China National Journal of New Gastroenterology* on October 1,1995, and renamed as *WJG* on January 25, 1998.

PUBLISHED JOINTLY BY
The WJG Press and Elsevier Inc.

PRINTING GROUP
Printed in Beijing on acid-free paper by Beijing Kexin Printing House

 Print ISSN 1007-9327 CN 14-1219/R.

EDITORIAL OFFICE
Editor: *World Journal of Gastroenterology*,
The WJG Press, Apartment 1066 Yishou Garden, 58 North Langxinzhuang Road, PO Box 2345, Beijing 100023, China
Telephone: +86-(0)10-85381901-1023
Fax: +86-10-85381893
E-mail: wjg@wjgnet.com
http://www.wjgnet.com

Public Relationship Manager
Shi-Yu Guo
The WJG Press, Apartment 1066 Yishou Garden, 58 North Langxinzhuang Road, PO Box 2345, Beijing 100023, China
Telephone: +86-(0)10-85381901-1023
Fax: +86-10-8538 1893
E-mail: s.y.guo@wjgnet.com
http://www.wjgnet.com

SUBSCRIPTION INFORMATION
Foreign
Elsevier (Singapore) Pte Ltd, 3 Killiney Road
#08-01, Winsland House I, Singapore 239519
Telephone: +65-6349 0200
Fax: +65-6733 1817
E-mail: r.garcia@elsevier.com
http://asia.elsevierhealth.com
Institutional Rates Print-2005 rates: USD1 500.00
Personal Rates Print-2005 rates: USD700.00

Domestic
Local Post Offices Code No. BM 82-261

Author Reprints
The WJG Press, Apartment 1066 Yishou Garden, 58 North Langxinzhuang Road, PO Box 2345, Beijing 100023, China
Telephone: +86-(0)10-85381901-1023
Fax: +86-10-85381893
E-mail: wjg@wjgnet.com
http://www.wjgnet.com

ADVERTISING
Rosalia Da Carcia
Elsevier Science
Journals Marketing & Society Relations Health Science Asia
3 Killiney Road #08-01, Winsland House 1
Singapore 239519
Telephone: +65-6349 0200
Fax +65- 6733 1817
E-mail: r.garcia@elsevier.com
http://asia.elsevierhealth.com

INSTRUCTIONS TO AUTHORS
Full instructions are available online at http://www.wjgnet.com/wjg/help/instructions.jsp If you do not have web access please contact the editorial office.

PO Box 2345, Beijing 100023, China
www.wjgnet.com
wjg@wjgnet.com

ELSEVIER

World J Gastroenterol 2005;11(43):6735-6739
World Journal of Gastroenterology ISSN 1007-9327

• *REVIEW* •

Enzyme inhibition assay for pyruvate dehydrogenase complex: Clinical utility for the diagnosis of primary biliary cirrhosis

Katsuhisa Omagari , Hiroaki Hazama, Shigeru Kohno

Katsuhisa Omagari , Hiroaki Hazama, Shigeru Kohno, Second Department of Internal Medicine, Nagasaki University School of Medicine, 1-7-1 Sakamoto, Nagasaki 852-8501, Japan
Correspondence to: Katsuhisa Omagari, MD, Second Department of Internal Medicine, Nagasaki University School of Medicine, 1-7-1 Sakamoto, Nagasaki 852-8501, Japan. omagari@net.nagasaki-u.ac.jp
Telephone: +81-95-849-7281 Fax: +81-95-849-7285
Received: 2005-04-25 Accepted: 2005-06-02

Abstract
Primary biliary cirrhosis (PBC) is usually diagnosed by the presence of characteristic histopathological features of the liver and/or antimitochondrial antibodies (AMA) in the serum traditionally detected by immunofluorescence. Recently, new and more accurate serological assays for the detection of AMA, such as enzyme-linked immunosorbent assay (ELISA), immunoblotting, and enzyme inhibition assay, have been developed. Of these, the enzyme inhibition assay for the detection of anti-pyruvate dehydrogenase complex (PDC) antibodies offers certain advantages such as objectivity, rapidity, simplicity, and low cost. Since this assay has almost 100% specificity, it may have particular applicability in screening the at-risk segment of the population in developing countries. Moreover, this assay could be also used for monitoring the disease course in PBC. Almost all sera of PBC-suspected patients can be confirmed for PBC or non-PBC by the combination results of immunoblotting and enzyme inhibition assay without histopathological examination. For the development of a "complete" or "gold standard" diagnostic assay for PBC, similar assays of the enzyme inhibition for anti-2-oxoglutarate dehydrogenase complex (OGDC) and anti-branched chain oxo-acid dehydrogenase complex (BCOADC) antibodies will be needed in future.

Key words: Primary biliary cirrhosis; Enzyme inhibition assay; Antimitochondrial antibody; 2-oxo-acid dehydrogenase complex

Omagari K, Hazama H, Kohno S. Enzyme inhibition assay for pyruvate dehydrogenase complex: Clinical utility for the diagnosis of primary biliary cirrhosis. *World J Gastroenterol* 2005; 11(43): 6735-6739
http://www.wjgnet.com/1007-9327/11/6735.asp

INTRODUCTION
Primary biliary cirrhosis (PBC) is a chronic autoimmune cholestatic liver disease characterized by the destruction of small and medium-sized bile ducts and the presence of antimitochondrial antibodies (AMA) in the serum traditionally detected by immunofluorescence[1,2]. The "gold standard" procedure for the diagnosis of PBC is histopathological examination of liver tissue. However, the characteristic histopathological changes of PBC are not always evident in biopsy specimens. Therefore, serological examination such as AMA is useful for the diagnosis of PBC because this is non-invasive and therefore can be repeated throughout the course of the disease. The major mitochondrial autoantigens recognized in the sera of PBC patients are members of 2-oxo-acid dehydrogenase complex (2-OADC) family, including E2 subunit of pyruvate dehydrogenase complex (PDC-E2), E2 subunit of branched chain oxo-acid dehydrogenase complex (BCOADC-E2), and E2 subunit of 2-oxoglutarate dehydrogenase complex (OGDC-E2)[1,3]. Unfortunately, however, there is so far no "gold standard" assay (i.e., with 100% sensitivity and 100% specificity) for the detection of AMA in PBC.

PBC is present among various ethnic and racial populations, but its incidence and prevalence varies quite widely, from the highest among Northern European populations to vanishingly low in certain parts of Asia[3]. This difference may be due, at least in part, to the diagnostic awareness of physicians for asymptomatic cases. Therefore, reliable and easy-to-use tool for screening PBC in general population is needed.

Serological assays for the detection of AMA
AMA is one of the most diagnostically useful of all autoimmune markers, since both the sensitivity and specificity for the diagnosis of PBC are acceptably high[1]. Indirect immunofluorescence assay using either Hep-2 cells or mouse kidney/stomach sections as the substrate and enzyme-linked immunosorbent assay (ELISA) using semipurified PDC as the antigen source are now widely used in clinical laboratories. Traditional indirect immunofluorescence assay has high sensitivity, and can detect reactivity to all 2-OADC enzymes. However, this assay is non-automated and labor-intensive, and the "readout" is subjective. The reactivity of serum with mitochondrial antigens other than PBC specific 2-OADC enzymes and nonspecific staining or high background could influence its specificity and sensitivity[3]. The

sensitivity, specificity, positive predictive value, negative predictive value, and accuracy determined in our previous study were 89%, 99%, 98%, 94%, and 95%, respectively[4].

Recently, new and more accurate serological assays for the detection of anti-2-OADC, such as ELISA, immunoblotting, and enzyme inhibition assay, has been developed. ELISA can detect more precisely the reactivity to a single 2-OADC enzyme in each run, and is non-subjective readout. Recently, more sensitive ELISAs using PDC-E2, BCOADC-E2 and OGDC-E2 as coating antigens have been developed[5-8]. In ELISA using commercially available MESACUP-2 Test Mitochondria M2 kit (Medical & Biological Laboratories Co., Nagoya, Japan), the sensitivity, specificity, positive predictive value, negative predictive value, and accuracy are 90%, 98%, 95%, 96%, and 94%, respectively[9]. Immunoblotting has been reported to have almost 100% sensitivity, and can detect individual reactivity to 2-OADC enzymes[10,11]. In our immunoblotting assay condition, the sensitivity, specificity, positive predictive value, negative predictive value, and accuracy were 99%, 86%, 89%, 99%, and 93%, respectively[11]. However, this assay is labor intensive, and can only be performed in specialized laboratories. Moreover, its specificity has not been well established[12]. The enzyme inhibition assay, which measures the capacity of PBC sera to inhibit the catalytic activity of PDC, is non-subjective compared to immunofluorescence, is more rapid and technically simpler than immunoblotting and ELISA. This assay has almost 100% specificity[6,13-16], but the sensitivity has been reported to be around 80%[6,15,16]. This lower sensitivity can be explained by the fact that this assay does not detect the inhibitory activity of sera to 2-OADC enzymes other than PDC, such as BCOADC or OGDC.

Enzyme inhibition assay

A striking property of AMA in PBC sera is their capacity to rapidly inactivate the catalytic function of 2-OADC *in vitro*[17]. Enzyme inhibition assay has been utilized to demonstrate a population of autoantibodies in PBC sera that inhibit enzyme function, and a miniaturized semiautomated enzyme inhibition assay was developed for the detection of anti-PDC antibodies in PBC in 1991[18] (Figure 1). Several subsequent studies have assessed its objectivity, rapidity, simplicity, and costeffectiveness, by comparing these parameters to other assays such as immunofluorescence, ELISA, and immunoblotting[13,15]. Immunoblotting might be the most expensive, and enzyme inhibition assay might have most cost-effectiveness in many countries. Recently, an automated enzyme inhibition assay kit, TRACE enzymatic mitochondrial Antibody (M2) assay (EMA) kit (Thermo Trace, Victoria, australia), became available commercially. In principle, the "Substrate reagent" (250 μL) containing sodium pyruvate, magnesium acetate, cocarboxylase, coenzyme A, and nicotinamide adenine dinucleotide (NAD), is placed in flat-bottomed microtiter wells. Thereafter, 4 μL of undiluted test serum is added to each well and incubated for 1 min at 37 °C before adding 50 μL of the "Enzyme reagent" containing

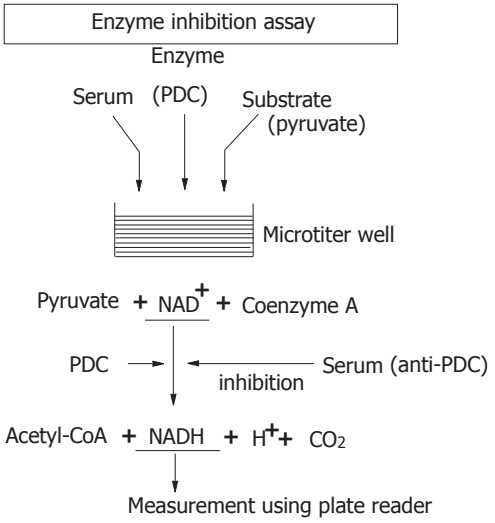

Figure 1 Principle of enzyme inhibition assay.

pyruvate dehydrogenase and dithiothreitol. After 30 s of lag time, the rate of reaction is monitored by measuring the rate of increase in absorbance at 340 nm in a microplate reader. The reaction rate (RR) is calculated using the absorbance values at 0 and 2 min based on the following formula: (final absorbance - initial absorbance)/time. The units of activity (%) are derived from the formula: (test RR/standard RR) x 100. The standard RR is derived from the "Calibrator" wells that contain anti-PDC antibody-free serum (100% activity). The unit of PDC activity of less than 70% is considered as anti-PDC positive with sensitivity and specificity of 82% and 100%, respectively, based on the information provided by the manufacturer[16] (Figure 2). By using this kit, Schmit *et al.*[14] tested the enzyme inhibition assay for 23 sera from patients with AMA-positive PBC and 92 sera from non-PBC including healthy controls, and compared the results to those of immunofluorescence and in-house ELISA. They reported that the sensitivity and specificity of EMA were quite sufficient compared to other assays. Our previous

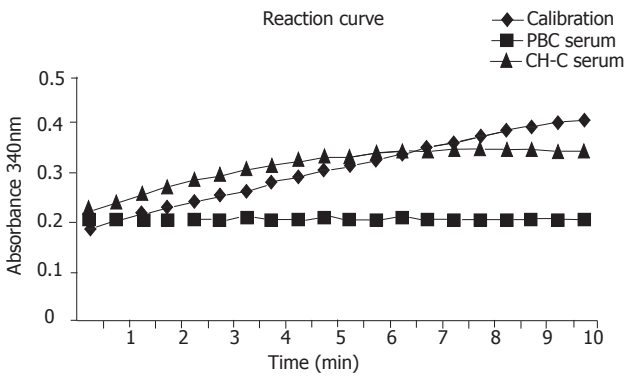

Figure 2 Representative reaction curve of automated enzyme inhibition assay using TRACE enzymatic mitochondrial antibody (M2) assay (EMA) kit. PBC; primary biliary cirrhosis, CH-C; chronic hepatitis C.

Table 1 Detection of enzymatic inhibitory antibody to PDC by enzyme inhibition assay in non-PBC s

First author	Year	Case studied	Antigen source	Serum amount (μL)	Serum dilution	Positivity rate (%)[1]
Teoh	1991	Normal subject, AIH, ALD, RA, SLE	Commercial PDC	100[2]	1:500	0 / 62 (<1.7)
Teoh	1994	Healthy subject, immunopathic diseases	Commercial PDC	100[2]	1:500	0 / 42 (<2.4)
Omagari	1996	Adult blood donors, healthy women	Commercial PDC	2	Undiluted	0 / 186 (<0.6)
Schmit	1999	Healthy controls, viral hepatitis, AIH	TRACE EMA kit	4	Undiluted	0 / 92 (<1.1)
Jois	2000	Normal subject, AIC, AIH, ALD, RA, SLE, etc.	Commercial PDC	2	Undilute	4 / 1055 (0.4)
Hazama	2000	Healthy subject, ALD, viral hepatitis, fatty liver	TRACE EMA kit	4	Undiluted	0 / 50 (<2.0)
Jensen	2000	AIH, abnormal LFT patients, Normal blood donors, etc.	TRACE EMA kit	4	Undiluted	0 / 250 (<0.4)
Masuda	2002	Healthy subject, ALD, viral hepatitis, fatty liver, etc.	TRACE EMA kit	4	Undiluted	0 / 130 (<0.8)
Hazama	2002	Healthy subject, ALD, viral hepatitis, fatty liver, etc.	TRACE EMA kit	4	Undiluted	0 / 97 (<1.1)

[1]When the numerator is zero, the percentage is calculated as a nominal value of <1.
[2]100 μL of doubling dilutions of serum from 1:500 in phosphate-buffered saline solution. PDC, pyruvate dehydrogenase complex; PBC, primary biliary cirrhosis; AIH, autoimmune hepatitis; ALD, alcoholic liver disease; RA, rheumatoid arthritis; SLE, systemic lupus erythematosus; EMA kit,Enzymatic mitochondrial Antibody (M2) Assay kit; AIC, autoimmune cholangitis; LFT; liver function tests.

study of EMA indicated sensitivity, specificity, positive predictive value, negative predictive value, and accuracy of 72%, 100%, 100%, 87%, and 90%, respectively. We also concluded that EMA is useful for the diagnosis of AMA-positive PBC and could be used to monitor the disease course of PBC, particularly due to the small amount of serum requested, objective read-out, and rapid turnaround time[16,19]. Jensen *et al.*[6] also reported that the sensitivity and specificity of EMA were 83% and 100%, respectively, and the EMA compared favorably against commercial ELISA methods.

Clinical utility of enzyme inhibition assay in PBC

Enzyme inhibition assay including commercially available EMA kit has the advantages of few procedural steps, small amount of test serum requested (only 4 μL of undiluted test serum), rapid turnaround time (approximately 6 min for 10 serum samples), and non-subjective readout[14,19]. Moreover, this assay has almost 100% specificity (Table 1). This means that if the serum is positive for enzymatic inhibitory antibody to PDC by enzyme inhibition assay, the diagnosis of PBC is almost confirmed. The result from our laboratory is in line with this finding because none of 245 non-PBC sera was positive for enzymatic inhibitory antibody to PDC by enzyme inhibition assay, whereas 96 (76%) of 127 PBC sera were positive (detailed data are not shown). Therefore, enzyme inhibition assay may have particular applicability in screening the at-risk segment of the population, middle-aged to elderly females[15]. This assay is also applicable in developing countries due to its objectivity, rapidity, simplicity, and low cost. However, this assay may not be suitable for screening in a particular country or area such as Japan. This assay has relatively low sensitivity compared with that of immunofluorescence and immunoblotting due to the lower frequency of autoantibodies to PDC-E2 among the Japanese compared with Caucasian patients with PBC, and a correspondingly higher frequency of antibodies to E2 subunits of the other 2-OADC enzymes[20].

This assay could also be used for monitoring the disease course in PBC. In our previous study, we determined the serial changes in enzymatic inhibitory antibody to PDC by enzyme inhibition assay using EMA kit in Japanese patients with PBC[19]. The units of PDC activity by EMA correlated significantly and inversely with AMA titers by immunofluorescence, and serum reactivity to PDC-E2 by immunoblotting, respectively. Indeed, in three patients who showed a decrease in AMA titers by immunofluorescence, AMA titers correlated more with EMA results than immunoblotting. Moreover, in a patient with fluctuating AMA titers by immunofluorescence, the units of PDC activity by EMA paralleled AMA titers[19] (Figure 3). These data suggested that PBC disease course might influence the EMA results.

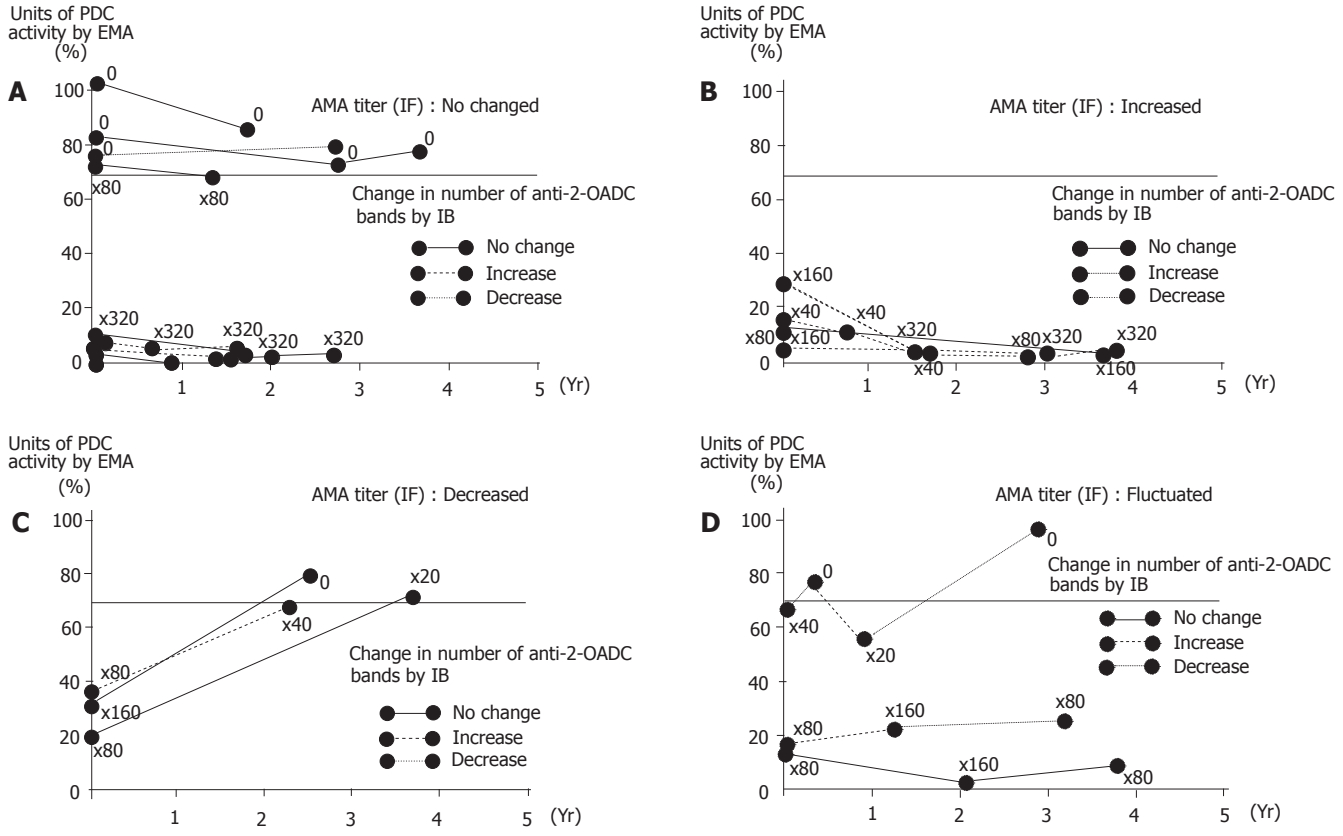

Figure 3 The units of pyruvate dehydrogenase complex (PDC) activity by enzymatic mitochondrial antibody (M2) assay (EMA) did not significantly vary in all the 9 patients in whom the titer of antimitochondrial antibodies (AMA) by immunofluorescence (IF) did not change during the course of follow-up. However, the number of anti-2-oxo-acid dehydrogenase complex (anti-2-OADC) bands by immunoblotting (IB) changed in 4 of these patients (2 increased and 2 decreased) (**A**). The units of PDC activity by EMA decreased in all 4 patients whose AMA titers by IF had increased, but the number of anti-2-OADC bands by IB did not change in 1 patient (**B**). The units of PDC activity by EMA increased in all 3 patients in whom AMA titers by IF had decreased, but the number of anti-2-OADC bands by IB in these patients did not decrease (**C**). Of the 3 patients in whom AMA titers by IF showed some fluctuation, one showed fluctuation in the units of PDC activity by EMA and two showed fluctuation in the number of anti-2-OADC bands by IB (**D**).

Table 2 Interpretation of detection of anti-2-OADC by immunoblotting and enzyme inhibition assay

Immunoblotting (IgG/IgM/IgA)	Enzyme inhibition assay	Interpretation	Estimated percentage (%)
Positive	Positive	PBC	72 - 83
Positive	Negative	Non-anti-PDC positive PBC	10 - 25
		Immunoblotting false positive?	10 - 15
Negative	Positive	Enzyme inhibition assay false positive?	Very rare
Negative	Negative	Non-PBC	Very rare

These data are based on our results that the sensitivity of immunoblotting for PBC is almost 100%, and the specificity of enzyme inhibition assay for PBC is nearly 100%, i.e., when the result by immunoblotting is negative, the serum is not from PBC, and when the result of enzyme inhibition assay is positive, the serum should be from the patient with PBC. 2-OADC, 2-oxo-acid dehydrogenase complex; PBC, primary biliary cirrhosis; PDC, pyruvate dehydrogenase complex.

Interpretation of detection of anti-2-OADC by immunoblotting and enzyme inhibition assay in PBC

Clinically, the serological diagnosis of PBC is in most instances based on the detection of AMA by indirect immunofluorescence and/or ELISA. As mentioned above, however, these two assays are not yet the "gold standard" (i.e., with 100% sensitivity and 100% specificity) for the detection of AMA in PBC, although both the sensitivity and specificity of these two assays are acceptably high. Based on the fact that immunoblotting has almost 100% sensitivity, and enzyme inhibition assay has almost 100% specificity, interpretation of anti-2-OADC results by combination of these two assays in PBC sera can be established. For example, since the negative predictive value of immunoblotting is 99%, a negative result by immunoblotting means that the serum is not from a patient with PBC. Since a positive predictive value of enzyme inhibition assay is 100%, a positive result by enzyme inhibition assay means that the serum should be from a patient with PBC. When the serum sample is positive for anti-2-OADC by immunoblotting but negative for anti-PDC by enzyme inhibition assay, it can be from non-anti-PDC positive PBC or the result of immunoblotting may be false positive. Conversely, when the serum is negative for anti-2-OADC by immunoblotting but positive for anti-PDC by enzyme inhibition assay, the result of enzyme inhibition assay may be false positive (Table 2). Thus, almost all sera from PBC-suspected patients can be confirmed for PBC or non-PBC by the combination results of immunoblotting and enzyme

inhibition assay without histopathological examination. For the development of a "complete" or "gold standard" (100% sensitivity and 100% specificity) diagnostic assay for PBC, similar assays of the enzyme inhibition for anti-OGDC and anti-BCOADC antibodies (or one-step assay for anti-PDC, OGDC, and BCOADC antibodies) will be needed in the future.

Conclusions

For the diagnosis of PBC, enzyme inhibition assay may have particular applicability in screening the at-risk segment of the population since this assay has almost 100% specificity. This assay is also applicable in developing countries due to its objectivity, rapidity, simplicity, and low cost.

REFERENCES

1 **Kaplan MM**. Primary biliary cirrhosis. *N Engl J Med* 1996; **335**: 1570-1580

2 **Talwalkar JA**, Lindor KD. Primary biliary cirrhosis. *Lancet* 2003; **362**: 53-61

3 **Gershwin ME**, Mackay I, Coppel R, Nakanuma Y. Clinical, immunologic and molecular features of primary biliary cirrhosis. *Semin Clin Immunol* 1994; **7**: 5-16

4 **Kadokawa Y**, Omagari K, Ohba K, Masuda J, Hazama H,Kinoshita H, Ohnita K, Mizuta Y, Tanioka H, Imanishi T, Kohno S. Does the diagnosis of primary biliary cirrhosis or autoimmune cholangitis depend on the "phase" of the disease? *Liver Int* 2005: **25**: 317-324

5 **Moteki S**, Leung PSC, Coppel RL, Dickson ER, Kaplan MM, MunozS, Gershwin ME. Use of a designer triple expression hybrid clone for three different lipoyl domains for the detection of antimitochondrial autoantibodies. *Hepatology* 1996; **24**: 97-103

6 **Jensen WA**, Jois JA, Murphy P, De Giorgio J, Brown B, Rowley MJ, Mackay IR. Automated enzymatic mitochondrial antibody assay for the diagnosis of primary biliary cirrhosis. *Clin Chem Lab Med* 2000; **38**: 753-758

7 **Miyakawa H**, Tanaka A, Kikuchi K, Matsushita M, Kitazawa E, Kawaguchi N, Fujikawa H, Gershwin ME. Detection of antimitochondrial autoantibodies in immunofluorescent AMA-negative patients with primary biliary cirrhosis using recombinant autoantigens. *Hepatology* 2001; **34**: 243-248

8 **Kadokawa Y**, Omagari K, Hazama H, Ohba K, Masuda J, Kinoshita H, Hayashida K, Isomoto H, Mizuta Y, Murase K, Murata I, Kohno S. Evaluation of newly developed ELISA using "MESACUP-2 Test Mitochondrial M2" kit for the diagnosis of primary biliary cirrhosis. *Clin Biochem* 2003; **36**: 203-210

9 **Takemura M**, Ohya K, Kojima K. Fundamental evaluation of "MESACUP-2 Test Mitochondrial M2". *Jpn J Med Pharm Sci* 2001; **46**: 809-816 (in Japanese)

10 **Kitami N**, Komada T, Ishii H, Shimizu H, Adachi H, Yamaguchi Y, Kitamura T, Oide H, Miyazaki A, Ishikawa M, Endo K, Watanabe S, Yokoi Y, Sato N. Immunological study of anti-M2 in antimitochondrial antibody-negative primary biliary cirrhosis. *Intern Med* 1995; **34**: 496-501

11 **Kinoshita H**, Omagari K, Matsuo I, Yamaguchi K, Ikuno N, Kohno S. Frequency of IgG, IgM, and IgA class autoantibodies against 2-oxo-acid dehydrogenase complex in 102 Japanese patients with primary biliary cirrhosis. *Hepatol Res* 1999; **15**: 163-171

12 **Masuda J**, Omagari K, Miyakawa H, Hazama H, Ohba K, Kinoshita H, Matsuo I, Isomoto H, Murata I, Kohno S. Clinical significance of positive immunoblotting but negative immunofluorescence for antimitochondrial antibodies in patients with liver diseases other than primary biliary cirrhosis. *Autoimmunity* 2002; **35**: 135-141

13 **Teoh K-L**, Rowley MJ, Zafirakis H, Dickson ER, Wiesner RH, Gershwin ME, Mackay IR. Enzyme inhibitory autoantibodies to pyruvate dehydrogenase complex in primary biliary cirrhosis: Applications of a semiautomated assay. *Hepatology* 1994; **20**: 1220-1224

14 **Schmit P**, Gilson G, Humbel RL. Evaluation of an automated enzyme inhibition assay for the detection of anti-mitochondrial M2 autoantibodies. *Clin Chem* 1999; **45**: 2287-2289

15 **Jois J**, Omagari K, Rowley MJ, Anderson J, Mackay IR. Enzyme inhibitory antibody to pyruvate dehydrogenase: diagnostic utility in primary biliary cirrhosis. *Ann Clin Biochem* 2000; **37**: 67-73

16 **Hazama H**, Omagari K, Masuda J, Ohba K, Kinoshita H, Matsuo I, Isomoto H, Mizuta Y, Murase K, Murata I, Kohno S. Automated enzymatic mitochondrial antibody assay for the diagnosis of primary biliary cirrhosis: applications of a routine diagnostic tool for the detection of antimitochondrial antibodies. *J Gastroenterol Hepatol* 2002; **17**: 316-323

17 **Bassendine MF**, Jones DEJ. Antimitochondrial and other autoantibodies in primary biliary cirrhosis. In: Krawitt EL, Wiesner RH, Nishioka M. Autoimmune Liver Diseases. *Amsterdam: Elsevier Science BV*, 1998; 287-304

18 **Teoh K-L**, Rowley MJ, Mackay IR. An automated microassay for enzyme inhibitory effects of M2 antibodies in primary biliary cirrhosis. *Liver* 1991; **11**: 287-291

19 **Hazama H**, Omagari K, Masuda J, Kinoshita H, Ohba K, Sakimura K, Matsuo I, Isomoto H, Murase K, Murata I, Kohno S. Serial changes in enzyme inhibitory antibody to pyruvate dehydrogenase complex during the course of primary biliary cirrhosis. *J Clin Lab Anal*. 2000; **14**: 208-213

20 **Omagari K**, Rowley MJ, Jois JA, Feeney SJ, Komatsu K, Maeda T, Onishi S, Yamazaki K, Suzuki K, Galperin C, Mackay IR. Immunoreactivity of antimitochondrial autoantibodies in patients with primary biliary cirrhosis. *J Gastroenterol* 1996; **31**: 61-68

Science Editor Guo SY **Language Editor** Elsevier HK

PO Box 2345, Beijing 100023, China
www.wjgnet.com
wjg@wjgnet.com

ELSEVIER

World J Gastroenterol 2005;11(43):6740-6744
World Journal of Gastroenterology ISSN 1007-9327

• *REVIEW*•

Loss of heterozygosity analyzed by single nucleotide polymorphism array in cancer

Hai-Tao Zheng, Zhi-Hai Peng, Sheng Li, Lin He

Hai-Tao Zheng, Zhi-Hai Peng, Department of General Surgery, Shanghai First People's Hospital, Shanghai Jiaotong University, Shanghai 200080, China
Sheng Li, Lin He, Shanghai Institutes for Nutrition Science, Chinese Academy of Sciences, Shanghai 200031, China
Supported by the National Natural Science Foundation of China, No. 30080016 and 30470977
Correspondence to: Zhi-Hai Peng, MD, Professor, Department of General Surgery, Shanghai First People's Hospital, Shanghai Jiaotong University, Shanghai 200080, China. pengpzh@hotmail.com
Telephone: +86-21-63240090-4312 Fax: +86-21-63240090
Received: 2005-01-31 Accepted: 2005-02-03

Abstract
Neoplastic progression is generally characterized by the accumulation of multiple genetic alterations including loss of tumor suppression gene function. Loss of heterozygosity (LOH) has been used to identify genomic regions that harbor tumor suppressor genes and to characterize different tumor types, pathological stages and progression. LOH pattern has been detected by allelotyping using restriction fragment length polymorphism, and later by simple sequence length polymorphisms (SSLPs or microsatellite) for 10 years. This paper reviews the detection of LOH by recently developed single nucleotide polymorphism (SNP) arrays (all analyzed by Affymetrix array); furthermore, its advantage and disadvantage were analyzed in several kinds of cancer.

Key words: Loss of heterozygosity; Single nucleotide polymorphism; Array; Cancer

Zheng HT, Peng ZH, Li S, He L. Loss of heterozygosity analyzed by single nucleotide polymorphism array in cancer. *World J Gastroenterol* 2005; 11(43): 6740-6744
http://www.wjgnet.com/1007-9327/11/6740.asp

INTRODUCTION
Cancer arises from the accumulation of inherited polymorphism (i.e. SNPs) and mutation and/or sporadic somatic polymorphism (i.e. non-germline polymorphism) in cell cycle, DNA repair, and growth signaling genes[1]. Neoplastic progression is generally characterized by the accumulation of multiple somatic-cell genetic alterations as the tumor progresses to advanced stages[2-6]. The classic mechanism of tumor suppressor gene inactivation is described by the two-hit mode in which one allele is mutated (or promoter hypermethylation or a small intragenic deletion) and the other allele is lost through a number of possible mechanisms, resulting in the loss of heterozygosity (LOH) at multiple loci[7-11]. Loss of heterozygosity is the most common molecular genetic alteration observed in human cancers. In the model of colorectal tumorigenesis, mutational inactivation of tumor suppressor genes predominates[12].

Loss of heterozygosity and studying methods
LOH is caused by a variety of genetic mechanisms, including physical deletion of chromosome nondisjunction, mitotic nondisjunction followed by republication of the remaining chromosomes, mitotic recombination, and gene conversion. The mechanisms of LOH are remarkably chromosome-specific. Some chromosomes display complete loss. However, more than half of the losses are associated with the loss of only a part of the chromosome rather than the whole chromosome[13]. LOH is also a common form of allelic imbalance and the detection of LOH has been used to identify genomic regions that harbor tumor suppressor genes and to characterize different tumor types, pathological stages, and progression[14,15].

In addition to the inherited and sporadic polymorphisms, many tumors exhibit aneuploidy and chromosomal instability in which the diploid structure of the genome is corrupted. A modest increase in copy number (such as trisomy for a region) would not give rise to allelic imbalance in the SNP assay. Allelic imbalance in the SNP assay should thus usually indicate true LOH, except in the case of extreme amplification[16].

Global patterns of LOH can be analyzed through allelotyping of tumors with polymorphic genetic markers from each chromosomal arm[17]. Most investigations have concentrated on defining the minimal regions of loss of specific chromosomes in various cancers in an effort to identify the putative tumor suppressor genes targeted by the losses. Two allele RFLPs and Southern analysis give way to simple sequence length polymorphisms such as PCR-based microsatellite, and both have been proved to be reliable genetic markers for studying LOH[18]. RFLP markers have low heterozygosity rates and are available in small number, gel-based microsatellite assay is difficult to automate and not readily scalable[19]. Microsatellite markers are reliable genetic markers for studying LOH, but only

a modest number of SSLPs are used in LOH studies because the genotyping procedure is rather tedious and difficult to automate and are not readily scalable.

As a result, most genome-wide scans for LOH have been conducted at low resolution with a relatively small number of polymorphic markers. Previous allelotyping analysis of cancer by many groups was restricted to particular chromosomal regions or arms, or else used a relatively low density of markers. For example, an average of 120 microsatellites has been used to determine the allelotype of multiple different human neoplasms in a series of studies since 1995, and the highest density microsatellite allelotype is ~280 polymorphic markers before the year 2000[20-24].

We conducted a genome-wide LOH study of 83 tumor samples obtained from Chinese patients in sporadic colorectal cancer. We employed 400 fluorescence-labeled microsatellite marker primers to amplify the corresponding loci of genomic DNA and then electrophoresed the polymerase chain reaction products and analyzed the fluorescent signals. The LOH frequencies were high (>35%) but not associated with the tumor stage and progression in 20 loci. Loss of other loci, including two narrow regions on chromosome 2, was related to the tumor stage[25,26]. In some loci, we performed detailed deletion mapping to narrow the loss region.

SNPs are the most common form of sequence variation in human genome, occurring approximately in every 1 200 bp[27]. SNPs may occur at more than 2 million sites in the genome, thus making it possible to place SNPs at high density along the genome[28].

High-throughput polymorphism detection technologies hold great promise for the characterization of complex diseases including cancer. High-density mapping of genetic losses reveals potential tumor suppressor loci and might be useful in the clinical classification of individual tumors. SNP array has been introduced recently for genome-wide screening of chromosome imbalance.

Higher density SNP array can be used effectively to detect small regions of chromosomal changes and provide more information regarding the boundaries of loss regions. In addition, more markers increase confidence in a detected event. If multiple adjacent SNPs show a consistent change, the confidence in the call is much higher than when it is based on a single SNP[15].

HuSNP chip (the first generation of SNP chip), an array of oligonucleotide probes for 1494 SNP loci, is distributed in all human chromosomes with an average of 2.57 cm between each SNP markers. A recent study using microarray has demonstrated a 97% accuracy on 65% of the SNPs surveyed[29]. The Affymetrix 10K SNP array (the second generation) contains 11 560 SNP alleles with high frequency of heterozygosity (average 36% based on Affymetrix in-house data). The Affymetrix 100K SNP array, a new SNP array platform, provides a high accuracy (99.5%), a reproducibility (91.1%) and a high call (heterozygous or homozygous) rate (95%)[30]. The average accuracy is calculated as 81% at 95% significance with a median inter-SNP distance of 105 kb in osteosarcoma using 10K array[30].

The HuSNP chip call rate does not differ between normal and tumor samples[16]. The genotyping accuracy of the chip calls is estimated at 95.4% on the basis of validation of random SNPs in normal and tumor samples by gel-based length multiplex single-base extension (LM-SBE)[16].

Tumor sample purity mixing experiment

LOH involves complete loss of one of the two alleles at a locus, but normal cell contamination can confound the distinction between true LOH and other mechanisms of allelic imbalance[31]. However, studies using flow-cytometrically purified samples have shown that complete LOH can be detected in tissue samples[32,33].

Tumor sample purity mixing experiment showed that samples with 90% tumor purity give essentially identical results than those with 100% tumor purity, when the purity decreases to 80%; it results in an increase in "uncertain" calls and a few false positive "retention". Accuracy decreases steeply when the purity is 70% or lower, because the lost allele contains 15% or more of contaminated samples. Although tumor purity is dependent on tumor type, a purity of 80% can often be achieved using gross dissection or microdissection[16,34]. With the SNP arrays, Mei *et al*.[15] found that chromosomal changes are detectable in heterogeneous samples with a background of up to 50% normal DNA.

The DNA fragment that occurs with formalin fixation does not seem to affect HuSNP array analysis result[35]. However, it is believed that formalin reduces the size of PCR segments that may be amplified from a sample[36]. There is significant agreement between the LOH result obtained from formalin-fixed paraffin embedded prostate tumor sections and those for freshly cultured cancer cells[34].

SNP array principle and methods

DNA sample is subjected to 24 multiplex PCR reactions, the resulting products are pooled, hybridized to the SNP array, stained with streptavidin-phycoerythrin, and assayed by fluorescence detection.

Briefly, the detector for each SNP locus contains four rows of 25-mer oligonucleotides, two of which contain oligonucleotides that perfectly match either SNP allele A or SNP allele B, whereas the other two contain single-base mismatches at various positions. The allelotype at a locus is determined by fluorescence intensity ratios in an automated fashion. Affymetrix HuSNP mapping system is used to determine tumor and normal allelotypes.

A general scanner scans chips and genotyped "call" is made from the collected hybridization signals using Affymetrix HuSNP 3.1 software. Tumor and normal samples are allelotyped on separate chips. For each patient's tumor, each SNP locus is scored as LOH, retention of heterozygosity, uninformative, or uncertain by comparing the genotype calls for tumor and normal (autologous) pairs. The possible SNP calls made by Affymetrix genotyping software are A, B, AB, AB_A (i.e,

AB or A), AB_B (i.e, AB or B), and "no call". "no call", AB_A, AB_B calls are considered to be noninformative[15].

Both amplified and unamplified DNA give similar results in terms of SNP call and LOH[30]. LOH can be established or inferred from 10K SNP array data using only amplified tumor DNA with the Affymetrix Genechip chromosome copy number tool.

SNP array application in LOH detection

Using SNP detection array, Wang *et al*.[37] found that breast cancer is highly heterogeneous, with the proportion of LOH ranging widely from 0.3% to >60% of heterozygous markers.

The call rate is 74.9-83.2% over all samples, yielding 1 120–1 205 SNPs scored per sample using HuSNP array[8,14,34,37,38]. The median of heterozygous loci is 341-349 with an average coverage of one SNP per 7.9-8.7cm[14,37]. Using 10K SNP array, the call rate is 91.1% over all samples[39]. In lung and breast cancer, the average call rate does not vary significantly between the lymphoblastoid and tumor cell lines[8,37].

LOH result comparison between SNP array and microsatellite

Very few reports have presented allelotyping data on multiple sites in the same tumor using two different methods, LOH between SNP array and microsatellite is concordant in the majority of analyzed kinds of cancer samples[16,34,37]. Most affected LOH regions are consistent with those in previous LOH studies, lending validity to both the method and results[34].

The range of consistency between two methods in different loci varies from 50% to 100% in bladder cancer[14]. Moreover, when the two methods are compared by chromosome arms, the concordance is very robust[14]. In osteosarcoma assay, 14 of 18 microsatellite markers have associated SNPs with LOH[30].

By comparing the microsatellite results in selected areas of several chromosomes with SNP array-based detection of allelic imbalance, in 69 sites, 60 microsatellite markers correlate, but nine microsatellite markers do not correlate with adjacent HuSNP markers[35].

Janne *et al*.[8] found that neither HuSNP nor SSLP is perfect. Using two methods together, the combined informative rate is 84%, and both methods provide calls for loci that were not informative by the other methods. However, a combined analysis is unlikely to be practical for future studies.

The comparison shows that, given a sufficient number of polymorphic markers, the SNP array can be used to screen both small and large chromosomal losses. But neither technique is currently infallible in identifying LOH[14].

LOH conflict between SNP array and microsatellite

Lindblad-Toh *et al*.[16] examined a number of instances of apparent conflict between SSLPs and SNP-based analysis by repeating the analysis and found that discordance is slightly more often due to the errors in SSLP rather than in SNP genotyping. SNP genotyping thus appears to be at least as accurate as the SSLP approach.

SNPs associated with the remaining four microsatellite markers do not show any LOH[30]. Allelic imbalance has been detected in microsatellite analysis but not detected by the SNP, which is probably caused by a no-signal genotype call either in the tumor or in normal DNA or in both. This problem can be solved by increasing the number of SNPs for the specific loci and by developing a more sensitive method for the generation of calls[14].

Possible reason of discrepancy

Because of the lower average heterozygosity rate of SNPs (0.33) compared to microsatellite, approximately a threefold SNPs is required for an equivalent resolution.

It is difficult to determine whether the apparent discordance is due to the technical limitation or if the microsatellite markers recognize a smaller region with a different allelic loss pattern compared to the adjacent regions scored by SNP[35].

The possible reasons are as follows: limitation of mapping data; differences in resolution, amplification efficiency, and differential sensitivity between microsatellite and SNP, technical limitations such as a genotype call by the Affymetrix softwares, the presence of bad SNPs in the array[14,30].

Cancer classification by LOH pattern using SNP array

Finding unique LOH pattern by SNP array in different groups of breast cancer, in part defined by expression signature, adds confidence to newer schemes of molecular classification. Furthermore, exclusive association between biological subclasses and restricted LOH event provide rationale to search for targeted genes[37]. Janne *et al*.[8] demonstrate that clustering of LOH data can distinguish SCLC from NSCLC with reasonable accuracy.

Advantage of SNP array

SNP array assay is accurate, automatic, and readily adaptable to the clinical setting and high-density mapping. Analysis of genetic alterations with HuSNP assay saves considerable time over microsatellite analysis. The assay involves multiplex amplification and other methods that can be completed in one day. The SNP array method is also a molecular technique that allows the detection of chromosomal imbalance in tumor DNA. A minimal quantity (120-135 ng) of sample DNA is needed for each SNP assay. The amplification step makes it possible to use only a small amount of genomic DNA, which is often essential when working with limited clinical materials[14,15].

The 10K array also provides calls (either LOH or retention) for 71.7% and 22.3% of the loci identified as non-informative by HuSNP and SSLP, respectively. The proximal and distal ends of the deletion are clearly identified and single LOH events identified using SSLP fall within these regions. The mapping 10K array can identify more than twice the number of LOH regions compared to SSLP or HuSNP. The minimum, mean, and median sizes of these regions are substantially smaller by the mapping 10K array than by the other two methods. The maximum

size of the LOH regions is similar by the three methods[8]. Disadvantage of SNP array is.

SNP array is difficult to distinguish all polymorphisms and to detect low level polymorphism and requires PCR amplification.

The average proportion of LOH informative markers out of callable markers is 31–33%, which is a considerably lower heterozygosity rate than that of SSLPs (typically 70%), but can readily increase to about 50% by selecting SNP with higher heterozygosity[14,16].

High false positive rate (11-21%) and false negative rates (19.9%) have been observed with this technology, limiting its utility in both SNP and tumor analysis[30,41].

Array-based methods of SNP detection may have a certain degree of inaccuracy ("noise"), and moreover, the precise genomic mapping of each SNP is still not completely stable. Thus, "true" regions of LOH can be interrupted by apparently false positively "retained" SNP alleles. Conversely, true regions of retention of heterozygosity may be interrupted by false LOH calls[42].

In summary, with the increasing number of SNPs available and technical progression[43], it is possible to probe the entire genome, and specific regions at much higher resolution. SNP array hybridization is an accurate and efficient method for evaluating genome-wide tumor LOH at present.

REFERENCES

1 **Kirk BW**, Feinsod M, Favis R, Kliman RM, Barany F. Single nucleotide polymorphism seeking long term association with complex disease. *Nucleic Acids Res* 2002; **30:** 3295-3311
2 **Fults D**, Pedone CA, Thomas GA, White R. Allelotype of human malignant astrocytoma. *Cancer Res* 1990; **50:** 5784-5789
3 **Sato T**, Tanigami A, Yamakawa K, Akiyama F, Kasumi F, Sakamoto G, Nakamura Y. Allelotype of breast cancer: cumulative allele losses promote tumor progression in primary breast cancer. *Cancer Res* 1990; **50:** 7184-7189
4 **Tsuchiya E**, Nakamura Y, Weng SY, Nakagawa K, Tsuchiya S, Sugano H, Kitagawa T. Allelotype of non-small cell lung carcinoma--comparison between loss of heterozygosity in squamous cell carcinoma and adenocarcinoma. *Cancer Res* 1992; **52:** 2478-2481
5 **Yamaguchi T**, Toguchida J, Yamamuro T, Kotoura Y, Takada N, Kawaguchi N, Kaneko Y, Nakamura Y, Sasaki MS, Ishizaki K. Allelotype analysis in osteosarcomas: frequent allele loss on 3q, 13q, 17p, and 18q. *Cancer Res* 1992; **52:** 2419-2423
6 **Thrash-Bingham CA**, Greenberg RE, Howard S, Bruzel A, Bremer M, Goll A, Salazar H, Freed JJ, Tartof KD. Comprehensive allelotyping of human renal cell carcinomas using microsatellite DNA probes. *Proc Natl Acad Sci U S A* 1995; **92:** 2854-2858
7 **Knudson AG Jr**, Nakahara memorial lecture. Hereditary cancer, oncogenes, and anti-oncogenes. *Princess Takamatsu Symp* 1989; **20:** 15-29
8 **Janne PA**, Li C, Zhao X, Girard L, Chen TH, Minna J, Christiani DC, Johnson BE, Meyerson M. High-resolution single-nucleotide polymorphism array and clustering analysis of loss of heterozygosity in human lung cancer cell lines. *Oncogene* 2004; **23:** 2716-2726
9 **Knudson AG Jr**, Mutation and cancer: statistical study of retinoblastoma. *Proc Natl Acad Sci U S A* 1971; **68:** 820-823
10 **Hansen MF**, Cavenee WK. Genetics of cancer predisposition. *Cancer Res* 1987; **47:** 5518-5527
11 Brown MA, Tumor suppressor genes and human cancer. *Adv Genet* 1997; **36:** 45-135
12 **Fearon ER**, Vogelstein B. A genetic model for colorectal tumorigenesis. *Cell* 1990; **61:** 759-767
13 **Thiagalingam S**, Laken S, Willson JK, Markowitz SD, Kinzler KW, Vogelstein B, Lengauer C. Mechanisms underlying losses of heterozygosity in human colorectal cancers. *Proc Natl Acad Sci U S A* 2001; **98:** 2698-2702
14 **Hoque MO**, Lee CC, Cairns P, Schoenberg M, Sidransky D. Genome-wide genetic characterization of bladder cancer: a comparison of high-density single-nucleotide polymorphism arrays and PCR-based microsatellite analysis. *Cancer Res* 2003; **63:** 2216-2222
15 **Mei R**, Galipeau PC, Prass C, Berno A, Ghandour G, Patil N, Wolff RK, Chee MS, Reid BJ, Lockhart DJ. Genome-wide detection of allelic imbalance using human SNPs and high-density DNA arrays. *Genome Res* 2000; **10:** 1126-1137
16 **Lindblad-Toh K**, Tanenbaum DM, Daly MJ, Winchester E, Lui WO, Villapakkam A, Stanton SE, Larsson C, Hudson TJ, Johnson BE, Lander ES, Meyerson M. Loss-of-heterozygosity analysis of small-cell lung carcinomas using single-nucleotide polymorphism arrays. *Nat Biotechnol* 2000; **18:** 1001-1005
17 **Vogelstein B**, Fearon ER, Kern SE, Hamilton SR, Preisinger AC, Nakamura Y, White R. Allelotype of colorectal carcinomas. *Science* 1989; **244:** 207-211
18 **Weissenbach J**, Gyapay G, Dib C, Vignal A, Morissette J, Millasseau P, Vaysseix G, Lathrop M. A second-generation linkage map of the human genome. *Nature* 1992; **359:** 794-801
19 **Gruis NA**, Abeln EC, Bardoel AF, Devilee P, Frants RR, Cornelisse CJ. PCR-based microsatellite polymorphisms in the detection of loss of heterozygosity in fresh and archival tumour tissue. *Br J Cancer* 1993; **68:** 308-313
20 **Hatta Y**, Yamada Y, Tomonaga M, Said JW, Miyosi I, Koeffler HP. Allelotype analysis of adult T-cell leukemia. *Blood* 1998; **92:** 2113-2117
21 **Piao Z**, Park C, Park JH, Kim H. Allelotype analysis of hepatocellular carcinoma. *Int J Cancer* 1998; **75:** 29-33
22 **Shih YC**, Kerr J, Hurst TG, Khoo SK, Ward BG, Chenevix-Trench G. No evidence for microsatellite instability from allelotype analysis of benign and low malignant potential ovarian neoplasms. *Gynecol Oncol* 1998; ***69:*** 210-213
23 **Mao X**, Barfoot R, Hamoudi RA, Easton DF, Flanagan AM, Stratton MR. Allelotype of uterine leiomyomas. *Cancer Genet Cytogenet* 1999; **114:** 89-95
24 **Yustein AS**, Harper JC, Petroni GR, Cummings OW, Moskaluk CA, Powell SM. Allelotype of gastric adenocarcinoma. *Cancer Res* 1999; **59:** 1437-1441
25 **Peng Z**, Zhang F, Zhou C, Ling Y, Bai S, Liu W, Qiu G, He L, Wang L, Wei D, Lin E, Xie K. Genome-wide search for loss of heterozygosity in Chinese patients with sporadic colorectal cancer. *Int J Gastrointest Cancer* 2003; **34:** 39-48
26 **Peng Z**, Zhou C, Zhang F, Ling Y, Tang H, Bai S, Liu W, Qiu G, He L. Loss of heterozygosity of chromosome 20 in sporadic colorectal cancer. *Chin Med J (Engl)* 2002; **115:** 1529-1532
27 **Sachidanandam R**, Weissman D, Schmidt SC, Kakol JM, Stein LD, Marth G, Sherry S, Mullikin JC, Mortimore BJ, Willey DL, Hunt SE, Cole CG, Coggill PC, Rice CM, Ning Z, Rogers J, Bentley DR, Kwok PY, Mardis ER, Yeh RT, Schultz B, Cook L, Davenport R, Dante M, Fulton L, Hillier L, Waterston RH, McPherson JD, Gilman B, Schaffner S, Van Etten WJ, Reich D, Higgins J, Daly MJ, Blumenstiel B, Baldwin J, Stange-Thomann N, Zody MC, Linton L, Lander ES, Altshuler D. A map of human genome sequence variation containing 1.42 million single nucleotide polymorphisms. *Nature* 2001; **409:** 928-933
28 **Marth G**, Yeh R, Minton M, Donaldson R, Li Q, Duan S, Davenport R, Miller RD, Kwok PY. Single-nucleotide polymorphisms in the public domain: how useful are they? *Nat Genet* 2001; **27:** 371-372
29 **Patil N**, Berno AJ, Hinds DA, Barrett WA, Doshi JM, Hacker CR, Kautzer CR, Lee DH, Marjoribanks C, McDonough DP, Nguyen BT, Norris MC, Sheehan JB, Shen N, Stern D, Stokowski RP, Thomas DJ, Trulson MO, Vyas KR, Frazer

KA, Fodor SP, Cox DR. Blocks of limited haplotype diversity revealed by high-resolution scanning of human chromosome 21. *Science* 2001; **294:** 1719-1723

30 **Wong KK**, Tsang YT, Shen J, Cheng RS, Chang YM, Man TK, Lau CC. Allelic imbalance analysis by high-density single-nucleotide polymorphic allele (SNP) array with whole genome amplified DNA. *Nucleic Acids Res* 2004; **32:** e69

31 **Hahn SA**, Seymour AB, Hoque AT, Schutte M, da Costa LT, Redston MS, Caldas C, Weinstein CL, Fischer A, Yeo CJ. Allelotype of pancreatic adenocarcinoma using xenograft enrichment. *Cancer Res* 1995; **55:** 4670-4675

32 **Barrett MT**, Galipeau PC, Sanchez CA, Emond MJ, Reid BJ. Determination of the frequency of loss of heterozygosity in esophageal adenocarcinoma by cell sorting, whole genome amplification and microsatellite polymorphisms. *Oncogene* 1996; **12:** 1873-1878

33 **Paulson TG**, Galipeau PC, Reid BJ. Loss of heterozygosity analysis using whole genome amplification, cell sorting, and fluorescence-based PCR. *Genome Res* 1999; **9:** 482-491

34 **Dumur CI**, Dechsukhum C, Ware JL, Cofield SS, Best AM, Wilkinson DS, Garrett CT, Ferreira-Gonzalez A. Genome-wide detection of LOH in prostate cancer using human SNP microarray technology. *Genomics* 2003; **81:** 260-269

35 **Zhao X**, Li C, Paez JG, Chin K, Janne PA, Chen TH, Girard L, Minna J, Christiani D, Leo C, Gray JW, Sellers WR, Meyerson M. An integrated view of copy number and allelic alterations in the cancer genome using single nucleotide polymorphism arrays. *Cancer Res* 2004; **64:** 3060-3071

36 **Greer CE**, Lund JK, Manos MM. PCR amplification from paraffin-embedded tissues: recommendations on fixatives for long-term storage and prospective studies. *PCR Methods Appl* 1991; **1:** 46-50

37 **Wang ZC**, Lin M, Wei LJ, Li C, Miron A, Lodeiro G, Harris L, Ramaswamy S, Tanenbaum DM, Meyerson M, Iglehart JD, Richardson A. Loss of heterozygosity and its correlation with expression profiles in subclasses of invasive breast cancers. *Cancer Res* 2004; **64:** 64-71

38 **Lieberfarb ME**, Lin M, Lechpammer M, Li C, Tanenbaum DM, Febbo PG, Wright RL, Shim J, Kantoff PW, Loda M, Meyerson M, Sellers WR. Genome-wide loss of heterozygosity analysis from laser capture microdissected prostate cancer using single nucleotide polymorphic allele (SNP) arrays and a novel bioinformatics platform dChipSNP. *Cancer Res* 2003; **63:** 4781-4785

39 **Zhou X**, Mok SC, Chen Z, Li Y, Wong DT. Concurrent analysis of loss of heterozygosity (LOH) and copy number abnormality (CNA) for oral premalignancy progression using the Affymetrix 10K SNP mapping array. *Hum Genet* 2004; **115:** 327-330

40 **Primdahl H**, Wikman FP, von der Maase H, Zhou XG, Wolf H, Orntoft TF. Allelic imbalances in human bladder cancer: genome-wide detection with high-density single-nucleotide polymorphism arrays. *J Natl Cancer Inst* 2002; **94:** 216-223

41 **Halushka MK**, Fan JB, Bentley K, Hsie L, Shen N, Weder A, Cooper R, Lipshutz R, Chakravarti A. Patterns of single-nucleotide polymorphisms in candidate genes for blood-pressure homeostasis. *Nat Genet* 1999; **22:** 239-247

42 **Lieberfarb ME**, Lin M, Lechpammer M, Li C, Tanenbaum DM, Febbo PG, Wright RL, Shim J, Kantoff PW, Loda M, Meyerson M, Sellers WR. Genome-wide loss of heterozygosity analysis from laser capture microdissected prostate cancer using single nucleotide polymorphic allele (SNP) arrays and a novel bioinformatics platform dChipSNP. *Cancer Res* 2003; **63:** 4781-4785

43 **Lin M**, Wei LJ, Sellers WR, Lieberfarb M, Wong WH, Li C. dChipSNP: significance curve and clustering of SNP-array-based loss-of-heterozygosity data. *Bioinformatics* 2004; **20:** 1233-1240

Science Editor Wang XL and Guo SY **Language Editor** Elsevier HK

PO Box 2345, Beijing 100023, China
www.wjgnet.com
wjg@wjgnet.com

ELSEVIER

World J Gastroenterol 2005;11(43):6745-6750
World Journal of Gastroenterology ISSN 1007-9327

Soluble adhesion molecules ICAM-1, VCAM-1, P-selectin in children with *Helicobacter pylori* infection

Elzbieta Maciorkowska, Maciej Kaczmarski, Anatol Panasiuk, Katarzyna Kondej-Muszynska, Andrzej Kemonai

Elzbieta Maciorkowska, Department of Pediatric Nursing, Medical University of Bialystok, Poland
Katarzyna Kondej-Muszynska, Maciej Kaczmarski, 3rd Department of Children's Diseases, Medical University of Bialystok, Poland
Anatol Panasiuk, Department of Infectious Diseases, Medical University of Bialystok, Poland
Andrzej Kemona, Department of Pathomorphology, Medical University of Bialystok, Poland
Correspondence to: Elzbieta Maciorkowska, MD, Department of Pediatric Nursing, Medical University of Bialystok, Waszyngtona Str., 15, 15-274 Bialystok, Poland. emaciorkowska@o2.pl
Telephone: +48-85-7-450-565 Fax: +48-85-7-450-568
Received: 2005-03-01 Accepted: 2005-04-30

Abstract

AIM: To assess the sICAM-1, sVCAM-1, and sP-selectin levels in children with *Helicobacter pylori* (*H pylori*) infection and to evaluate their significance for the morphological changes found in gastric mucosa.

METHODS: The study included 106 children: 59 children (55.7%) with chronic gastritis and positive IgG against *H pylori*, 29 children (27.3%) after previous *H pylori* infection without the bacterium colonization but with positive IgG against *H pylori*, and 18 children (17%) with functional disorders of the gastrointestinal system but with normal IgG against *H pylori*. Endoscopic and histopathological evaluation of gastric mucosa was performed based on the Sydney System classification. The evaluation of sP-selectin, sICAM-1, sVCAM-1 levels in the sera of children was carried out using ELISA test.

RESULTS: The assessment of gastritis activity degrees indicated statistically significant values in the antrum and corpus ($P<0.001$) of children examined. Serum sVCAM-1 levels were higher in group with gastritis due to *H pylori* infection than in group without infection and differed statistically ($P<0.05$). Serum sVCAM-1 levels proved to be the highest among other adhesive molecules in infected children and decreased after eradication of *H pylori*. Serum sICAM-1 levels were similar in all examined groups. Serum sP-selectin levels were similar in children with and without *H pylori* infection.

CONCLUSION: Assessment of adhesive molecules (sP-selectin, sICAM-1, sVCAM-1) in the sera of children with active *H pylori* infection can show the participation of sVCAM-1 in the pathogenesis of gastric mucosal inflammation. sP-selectin and sICAM-1 concentrations in the sera of children with *H pylori* infection after eradication cannot reveal any significant differences as compared to healthy children.

Key words: sVCAM-1; sICAM-1; sP-selectin; *Helicobacter pylori*

Maciorkowska E, Kaczmarski M, Panasiuk A, Kondej-Muszynska K, Kemona A. Soluble adhesion molecules ICAM-1, VCAM-1, P-selectin in children with *Helicobacter pylori* infection. *World J Gastroenterol* 2005; 11(43): 6745-6750
http://www.wjgnet.com/1007-9327/11/6745.asp

INTRODUCTION

In the course of *Helicobacter pylori* (*H pylori*) infection, a selective recruitment of neutrophils, monocytes, macrophages, mast cells, T and B lymphocytes takes place[1]. Additionally, infiltrating cells synthesize and release mediating cells, which influence the recruitment and activation of further inflammatory cells and increase the triggering activity of cytokines and chemokines. For example, neutrophils are the source of IL-1, IL-8, TNF-α[2], and macrophages – MIP-1α[1]. Adhesion molecules (selectins, their ligands, integrins, immunoglobulin-like molecules) take part in a selective recruitment of leukocytes[3–8]. Selectins are transmembrane molecules with numerous extracellular domains, containing lectin domain at the N-end – hence their name, L selectin (CD62L) – leukocyte, E selectin (CD62E) – endothelial cell, P-selectin (CD62P) – platelet. Saccharic residues combined with sialic acid [blood group antigen Lewis X (CD15) and its isoforms] expressing numerous leukocytes are ligands for L, E, and P selectins.

Glycosaminoglycans, such as heparin sulfate and carbohydrate residues on platelets and neutrophils, are ligands for L- and P-selectin[9,10]. A soluble form of P-selectin binds to the same ligand on granulocytes as its membrane form. It does not inhibit intergrins of granulocytes but supports agonists stimulating polymorphonuclear leukocytes, their function of secretion, PAF synthesis and LTB4 synthesis, and secretion. Thus, a soluble form does not differ in its activity from a membrane form. Its high serum levels (1-20 μg/mL) are significantly higher in the inflammatory process than in a healthy condition (36-250 ng/mL)[11].

Soluble forms of ICAM-1 (sICAM) were described

in 1991 and are derived basically from mononuclear cells. Epithelial cells are unlikely to be their source[12]. They can be found in the serum, in molecular forms: 240 ku, 430 ku, and mainly 500 ku[13]. A functionally soluble ICAM-1 form can be regulated by cytokines and is able to bind to LFA-1 ligand. Thus, sICAM may compete with leukocytic ligands for binding and decrease leukocyte adhesion to endothelial cells and may even promote their de-adhesion. sICAM-1 may be regarded as a marker of inflammation, because its levels increase significantly in the serum in the course of inflammation, at tissue damage or during the activity of proteolytic enzymes[14]. In healthy individuals, ICAM-1 occurs in small amounts on surfaces of many cells, like leukocytes, endothelial vascular cells, fibroblasts, epithelial cells whereas in the course of inflammation correlates with chronic inflammatory phase as well as the occurrence of ulceration in the course of *H pylori* infection. ICAM-1 is considered to be a marker of chronic immunological stimulation and thus it is potentially responsible for chronic course of a disease. A vascular adhesion molecule (VCAM-1) requires about 8-96 h to be activated and expressed on cells *in vitro*. Its expression is enhanced especially by TNF-α, IL- 4, and IL-13[13]. Since VLA-4 is its ligand, it binds only to mononuclear leukocytes (lymphocytes and monocytes). Normal gastric mucosa is free of leukocytes. Abundant infiltrations of poly- and mono-nuclear cells and lymphatic follicles can be found in the course of *H pylori* infection.

The aim of the study was to evaluate the levels of adhesion molecules sICAM-1, sVCAM-1 and sP-selectin in the sera of children with *H pylori* infection and to determine their significance for morphological changes in gastric mucosa.

MATERIALS AND METHODS

Patients

The study included 106 patients, who were divided into three groups with regard to the presence and course of *H pylori* infection. Group I : 59 children (55.7%) with chronic gastritis in the course of *H pylori* infection with a positive titer of IgG antibodies against *H pylori*, including 29 girls (49.2%) and 30 boys (50.8%). The children's age ranged from 2 to 19 years, the mean age was 12.2±4.6 years.

Group II : 29 children (27.3%) after previous *H pylori* infection, without the bacterium colonization of the gastric mucosa but with a positive titer of IgG antibodies against *H pylori*, including 14 girls (14%) and 15 boys (51.7%). The children's age ranged from 3 to 19 years and the mean age was 11.0±4.1 years.

Group III : 18 children (17 %) with functional disorders of the gastrointestinal tract, without *H pylori* infection but with normal IgG level against *H pylori*, 12 girls (66.7%) and 6 boys (33.3%). The children's age ranged from 5 to 17 years, and the mean age was 10.7±3.6 years (Table 1).

Ethical approval for the research was obtained from local Ethics Committee in Medical University.

Table 1 Age of examined children (yr)

Groups	*n* (g/b)[1]	Min. value	Max. value	Mean arithmetic	Median	SD	Lower quartile	Upper quartile
Group I	46 (30/29)	2.0	19.0	12.2	13.0	4.6	9	16
Group II	17 (14/15)	3.0	19.0	11.0	11.0	4.2	8	14
Group III	18 (12/6)	5.0	17.0	10.7	10.0	3.6	8	13

[1]g/b – girls/boys.

Methods

Endoscopic examination of the upper gastrointestinal tract with gastric mucosa samples (corpus and antrum) was performed in 88 children with positive IgG against *H pylori* and 18 children with negative IgG against *H pylori*. Endoscopic and histopathological evaluation was performed based on the Sydney System[16]. Chronic stomachache indicated the need for endoscopy. The assessment of sP-selectin (sP-selectin, Bender MedSystems, Austria), sICAM-1 (sICAM, Bender MedSystem) and sVCAM-1 (sVCAM, Bender MedSystems) levels in the serum samples was performed using ELISA method. The materials for the examination and assessment of individual parameters were prepared according to the manufacturer's instructions. The results were read in a spectrophotometer at 450 nm wavelength. The minimum detection threshold in the method used equaled 1.3 ng/mL for sP-selectin, 0.5 ng/mL for sICAM-1, and 0.9 ng/mL for sVCAM-1.

Statistical analysis

The results of laboratory analysis were processed using appropriate calculating techniques and statistical tests. Descriptive statistics with central deviation measure including arithmetic mean (χ), median and mode, and measure of dispersion including standard deviation (SD), variations and values of the upper and lower quartiles were given to each variable (feature) measured and group of patients. The distribution of empirical data matching the normal distribution was checked using χ^2 test and the Kolmogorow–Smirnow test. The results enabled to determine the direction of further statistical analysis and to use parametric tests or their non-parametric equivalents in statistical analysis. Since in most cases, formal normality tests proved that variations differed significantly from assumed theoretical distribution, the Mann–Whitney *U* test was used to examine the significance of difference in the feature intensity between the groups examined. $P<0.05$ was considered statistically significant. Receiver operating characteristic (ROC) curves were applied to the estimation of the usability of individual diagnostic parameters.

RESULTS

While evaluating the activity of antrum gastritis in groups, we showed the largest changes in children with *H pylori* infection (group I). The severe degree activity was found in 69.5% of this group and the moderate degree activity in 30.5% of the infected children. In children with previous infection and after bacteria eradication (group II), no severe or moderate degree activity was found, whereas mild degree activity was revealed only in 20.7% of this group (Figure 1A).

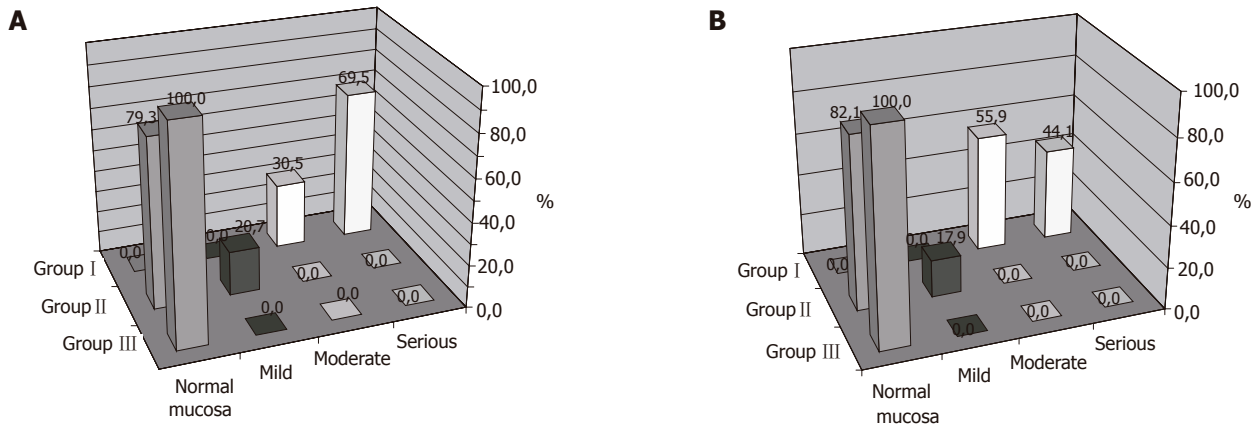

Figure 1 Gastritis activity in antrum (**A**) and corpus (**B**) of examined children (according to the Sydney System).

The analysis of antral gastritis activity by χ^2 test proved a statistical significance (P<0.001) in examined groups. While the corpus mucosa in children with *H pylori* infection (group I) was assessed, the moderate degree activity was found in 55.9% of children and the severe degree activity was revealed in 44.1% of children. In children after *H pylori* eradication (group II), the mild degree activity was established only in 17.9%. No severe or moderate degree activity was reported (Figure 1B). The histopathological evaluation of the corpus gastritis differed statistically significant in particular groups (P<0.001).

sP-selectin levels equaled 339.2±122.9 ng/mL in the sera of children with *H pylori* infection (group I). The similar levels of sP-selectin were observed in children after *H pylori* eradication (group II) and in controls. Therefore, no statistically significant differences were found between the groups examined (Table 2). Based on the results of ROC analysis of sP-selectin levels in serum, the usefulness of this parameter was not confirmed (AUC = 0.62±0.08). The highest accuracy was obtained when the level of 1 288.2 ng/mL was taken as the criterion of sP-selectin concentration. The sensitivity was 87.2% and the specificity was 52.9% for this value (Figure 2A).

Soluble ICAM level was 482.3±143.2 ng/mL in children with *H pylori* infection (group I). Similar sICAM-1 levels were observed in children after *H pylori* eradication (group II) and in controls. No statistically significant differences of sICAM levels were proved between/among the groups (Table 3). A linear correlation was proved between the age of children with *H pylori* infection (group I) and sICAM levels. A negative value of a slope of a line (b = –9.43±3.98) (according to the Sydney System) indicates that sICAM levels decreased in the serum as the age increased. The value of the line equaled 597.18±51.91 ng/mL. This correlation was statistically significant (P<0.05) (Figure 3A).

Soluble VCAM-1 levels in the sera of children with *H pylori* infection equaled 1 032.7±267.5 ng/mL. A statistically significant difference was proved between the levels of group I and group II (P<0.05) (Table 4). In children with *H pylori* infection, a statistically significant dependence (P<0.001) was revealed between the age of children examined and sVCAM-1 levels in their sera. This dependence can be described by a general formula: y =

Table 2 Serum sP-selectin levels in serum of examined children (ng/mL), Mann–Whitney *U* test

Groups	*n*	Min. value	Max. value	Mean arithmetic	Median	Mode	SD	Lower quartile	Upper quartile
Group I	46	158	612	339.2	312.0	343	122.9	248	380
Group II	17	127	624	389.1	375.2	–	151.5	283	509
Group III	3	215	330	283.7	306.0	–	60.7	261	318

Table 3 Serum sICAM-1 levels in examined children (ng/mL), Mann–Whitney *U* test

Groups	*n*	Min. value	Max. value	Mean arithmetic	Median	Mode	SD	Lower quartile	Upper quartile
Group I	55	232	887	482.3	478.0	514	143.2	399	548
Group II	23	176	930	490.5	487.7	–	164.7	412	580
Group III	5	304	705	475.3	446.0	–	168.1	394	527

Table 4 Serum sVCAM-1 levels in examined children (ng/mL), Mann–Whitney *U* test

Groups	*n*	Min. value	Max.value	Mean arithmetic	Median	Mode	SD	Lower quartile	Upper quartile
Group I	47	612	1 921	1 032.7	1 018.0	819	267.5	819.0	1 183.0
Group II	23	176	930	490.5	487.7	–	164.7	412.0	580.0
Group III	5	367	523	422.1	400.2	–	59.7	398.3	421.2

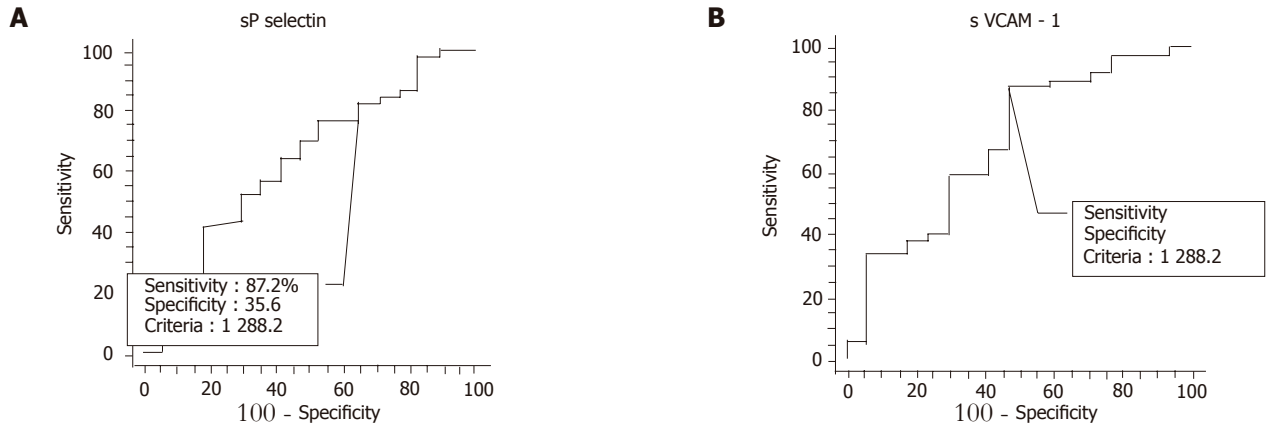

Figure 2 ROC curve for serum sP-selectin (**A**) and sVCAM-1 (**B**) levels.

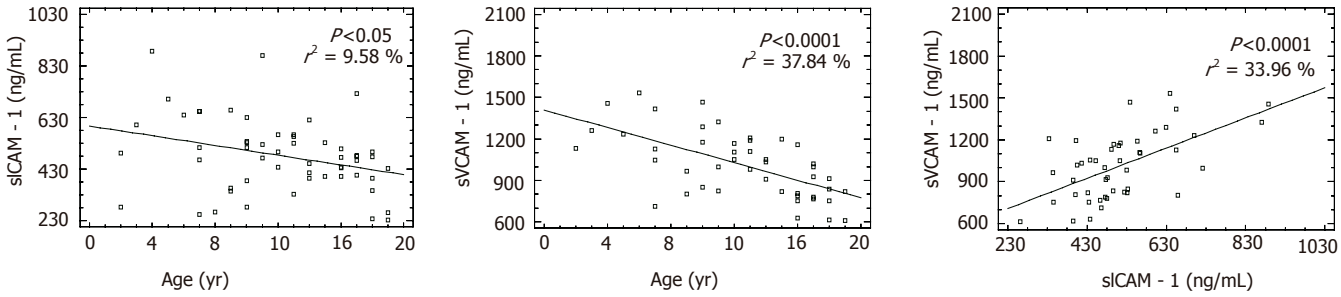

Figure 3 Correlation between age and sICAM-1 (**A**) between age and sVCAM-1 (**B**), and between sICAM-1 and sVCAM-1 (**C**) levels in serum of children with *H pylori* infection (group I).

$a+b\times x$. A negative value of a slope of a line ($b = -31.67\pm -5.18$) means that the value of sVCAM-1 levels decreased as the age of children increased (Figure 3B). Based on the results of ROC analysis of sVCAM levels in the serum, the usefulness of this parameter in *H pylori* infection and eradication was not confirmed (AUC = 0.69±0.08). In case of sVCAM-1 levels, the highest accuracy of diagnosis was obtained at the criterion of 1 288.2 ng/mL. The sensitivity was 87.2% and the specificity was 52.9% (Figure 2B).

In children with *H pylori* infection, a linear dependence ($y = a+b+x$) was proved between sICAM-1 and sVCAM-1 levels in the serum. A positive value of a slope of a line
(b = 1.08±0.23) indicates that sICAM-1 levels increased simultaneously with sVCAM-1 levels (Figure 3C).

DISCUSSION

The evaluation of soluble adhesion molecule levels in serum can confirm their presence and assess their levels quickly and therefore may be of better use in the diagnosis of *H pylori* infection or eradication than time-consuming immunohistochemical methods.

The levels of sVCAM-1 were higher in the sera of patients with gastritis of *H pylori* etiology than in patients without infection and differed significantly ($P<0.05$). The levels of sICAM in the sera were similar in all groups examined. The levels of sP-selectin were similar in the groups with or without *H pylori* infection but were twice as high as in controls. Similar results were presented in studies evaluating ICAM-1, VCAM-1 molecules on the surface of gastric epithelium[17-19].

Later studies in patients with chronic gastritis in the course of *H pylori* infection have proved that the predominant increase in ICAM-1 expression on vascular epithelial cells and inflammatory cells (lymphocytes, granulocytes) in lamina propria is connected with a massive inflammatory infiltrate and the expression of HLA-DR, LFA-1, and Mac-1 on cells presenting antigen[7,20]. No ICAM-1 expression was found on endothelial lymphocytes and epithelial cells. Similar to our study, no correlation with the degree of gastritis was proved. A decrease in the level of adhesion molecules examined was observed after effective eradication of *H pylori*.

Hatz *et al*.[21] have proved that ICAM-1 expression increases on endothelial cells. Moreover, they observed an increase in VCAM - expression in lymphatic follicles, though they neither found an increase in P-selectin expression nor any E-selectin expression. According to the authors, constant P-selectin levels (no increase) may be due to a quick metabolism of this molecule (*in vitro* it is decomposed after a few minutes after its exposition on epithelial cells) and undetectable changes of its levels in immunohistopathological examination. As stated by Hatz *et al*.[21], the increased levels of proinflammatory

cytokines such as IL-1b and TNF-α and the increased quantity of $CD4^+$ and CD45RO lymphocytes in lamina propria might contribute to the upregulated expression of ICAM-1 and VCAM-1. However, studies examining ICAM-1, VLA-4, and CD44 expressions on the surface of mononuclear cells in the serum have proved their increased quantity together with the expression of the molecules mentioned above in patients with *H pylori* infection but without ulceration and in healthy people[3,5]. Polymorphonuclear cells react similarly. The enhanced adhesion of these cells to the epithelial cells of the human navel vein exposed to *H pylori* antigens has been shown in laboratory tests evaluating ICAM-1, VCAM-1, E-selectin expression on neutrophils[6].

Innocenti *et al*.[4] found that not all *H pylori* strains are able to activate epithelial cells of gastric mucosa to the expression of adhesion molecules (ICAM-1, VCAM-1, E-selectin) and chemokines for neutrophils. But the authors failed to prove whether combination of bacterial antigens (CagPaI, Lewis, BabA, VacA) could influence *H pylori* capability of activating epithelial cells. According to these authors, bacterial proteins not described so far take part in the activation of epithelial cells.

While the interdependence was evaluated between adhesion molecules, a strong correlation was found between the serum levels of sICAM and sVCAM-1 ($P<0.001$) in children with *H pylori* infection, indicating that the increase in sICAM-1 levels is accompanied with the increase in sVCAM-1 levels. Such a correlation may point to the simultaneous and proportional contribution of both adhesion molecules in inflammation.

In our study, while the correlation of sICAM-1 and sVCAM-1 levels with the age of children examined in groups I and II was evaluated, the highest levels were found in the youngest children, whereas they decreased gradually as the age of patients increased. The correlation was statistically significant in both groups (I and II) for sICAM ($P<0.05$), whereas for sVCAM in group I ($P<0.0001$) and in group II ($P<0.05$). The variability of sICAM-1 and sVCAM levels in serum regarding the age may suggest a greater maturity of children's immunological system and its reaction to bacterial antigens.

The results of our study and other studies indicate that adhesion molecules play an important role in immuno-inflammatory response in patients with gastritis due to *H pylori* infection. The levels of adhesion molecules increase in inflammatory process. In our study, such a correlation was proved for sP-selectin.

The quantity of adhesion molecules in inflammatory infiltrating cells or the increased levels of their soluble forms in the serum correlate with the intensity of inflammatory process.

REFERENCES

1 **Kusugami K**, Ando T, Imada A, Ina K, Ohsuga M, Shimizu T, Sakai T, Konagaya T, Kaneko H. Mucosal macrophage inflammatory protein-1alpha activity in Helicobacter pylori infection. *J Gastroenterol Hepatol* 1999; **14:** 20-26

2 **Kim JS**, Jung HC, Kim JM, Song IS, Kim CY. Interleukin-8 expression by human neutrophils activated by Helicobacter pylori soluble proteins. *Scand J Gastroenterol* 1998; **33:** 1249-1255

3 **Ohara T**, Arakawa T, Higuchi K, Kaneda K. Overexpression of co-stimulatory molecules in peripheral mononuclear cells of Helicobacter pylori-positive peptic ulcer patients: possible difference in host responsiveness compared with non-ulcer patients. *Eur J Gastroenterol Hepatol* 2001; **13:** 11-18

4 **Innocenti M**, Thoreson AC, Ferrero RL, Stromberg E, Bolin I, Eriksson L, Svennerholm AM, Quiding-Jarbrink M. Helicobacter pylori-induced activation of human endothelial cells. *Infect Immun* 2002; **70:** 4581-4590

5 **Fan XG**, Fan XJ, Xia HX, Keeling PW, Kelleher D. Up-regulation of CD44 and ICAM-1 expression on gastric epithelial cells by H. pylori. *APMIS* 1995; **103:** 744-748

6 **Byrne MF**, Corcoran PA, Atherton JC, Sheehan KM, Murray FE, Fitzgerald DJ, Murphy JF. Stimulation of adhesion molecule expression by Helicobacter pylori and increased neutrophil adhesion to human umbilical vein endothelial cells. *FEBS Lett* 2002; **532:** 411-414

7 **Dobretsov GE**, Kharitonenkov IG, Mishiev VE, Vladimirov IuA. [Relation between fluorescence and circular dichroism of the complex of the fluorescence probe 4-dimethylaminochalcone with serum albumin] *Biofizika* 1975; **20:** 215-221

8 **Hatz RA**, Rieder G, Stolte M, Bayerdorffer E, Meimarakis G, Schildberg FW, Enders G. Pattern of adhesion molecule expression on vascular endothelium in Helicobacter pylori-associated antral gastritis. *Gastroenterology* 1997; **112:** 1908-1919

9 **Mayadas TN**, Johnson RC, Rayburn H, Hynes RO, Wagner DD. Leukocyte rolling and extravasation are severely compromised in P selectin-deficient mice. *Cell* 1993; **74:** 541-554

10 **Moore KL**, Structure and function of P-selectin glycoprotein ligand-1. *Leuk Lymphoma* 1998; **29:** 1-15

11 **Lorant DE**, Topham MK, Whatley RE, McEver RP, McIntyre TM, Prescott SM, Zimmerman GA. Inflammatory roles of P-selectin. *J Clin Invest* 1993; **92:** 559-570

12 **Marlin SD**, Springer TA. Purified intercellular adhesion molecule-1 (ICAM-1) is a ligand for lymphocyte function-associated antigen 1 (LFA-1). *Cell* 1987; **51:** 813-819

13 **Seth R**, Raymond FD, Makgoba MW. Circulating ICAM-1 isoforms: diagnostic prospects for inflammatory and immune disorders. *Lancet* 1991; **338:** 83-84

14 **Rothlein R**, Mainolfi EA, Czajkowski M, Marlin SD. A form of circulating ICAM-1 in human serum. *J Immunol* 1991; **147:** 3788-3793

15 **Kotowicz K**, Dixon GL, Klein NJ, Peters MJ, Callard RE. Biological function of CD40 on human endothelial cells: costimulation with CD40 ligand and interleukin-4 selectively induces expression of vascular cell adhesion molecule-1 and P-selectin resulting in preferential adhesion of lymphocytes. *Immunology* 2000; **100:** 441-448

16 **Dixon MF**, Genta RM, Yardley JH, Correa P. Classification and grading of gastritis. The updated Sydney System. International Workshop on the Histopathology of Gastritis, Houston 1994. *Am J Surg Pathol* 1996; **20:** 1161-1181

17 **Enders G**, Brooks W, von Jan N, Lehn N, Bayerdorffer E, Hatz R. Expression of adhesion molecules on human granulocytes after stimulation with Helicobacter pylori membrane proteins: comparison with membrane proteins from other bacteria. *Infect Immun* 1995; **63:** 2473-2477

18 **Scheynius A**, Engstrand L. Gastric epithelial cells in Helicobacter pylori-associated gastritis express HLA-DR but not ICAM-1. *Scand J Immunol* 1991; **33:** 237-241

19 **Fan X**, Long A, Fan X, Keeling PW, Kelleher D. Adhesion molecule expression on gastric intra-epithelial lymphocytes of patients with Helicobacter pylori infection. *Eur J Gastroenterol Hepatol* 1995; **7:** 541-546

20 **Archimandritis A**, Sougioultzis S, Foukas PG, Tzivras M, Davaris P, Moutsopoulos HM. Expression of HLA-DR, costimulatory molecules B7-1, B7-2, intercellular adhesion molecule-1 (ICAM-1) and Fas ligand (FasL) on gastric

epithelial cells in Helicobacter pylori gastritis; influence of H. pylori eradication. *Clin Exp Immunol* 2000; **119:** 464-471
21 **Hatz RA**, Meimarakis G, Bayerdorffer E, Stolte M, Kirchner T, Enders G. Characterization of lymphocytic infiltrates in Helicobacter pylori-associated gastritis. *Scand J Gastroenterol* 1996; **31:** 222-228

Science Editor Wang XL and Guo SY **Language Editor** Elsevier HK

PO Box 2345, Beijing 100023, China
www.wjgnet.com
wjg@wjgnet.com

ELSEVIER

World J Gastroenterol 2005;11(43):6751-6756
World Journal of Gastroenterology ISSN 1007-9327

Concentrations of gastric mucosal cytokines in children with food allergy and *Helicobacter pylori* infection

Elżbieta Maciorkowska, Anatol Panasiuk, Maciej Kaczmarski

Elżbieta Maciorkowska, Department of Pediatric Nursing, Medical University of Bialystok, Poland
Anatol Panasiuk, Department of Infectious Diseases, Medical University of Bialystok, Poland
Maciej Kaczmarski, 3rd Department of Children's Diseases, Medical University of Bialystok, Poland
Correspondence to: Elżbieta Maciorkowska, MD, Department of Pediatric Nursing, Medical University of Bialystok, Waszyngtona Str. 15, 15-274 Bialystok, Poland. emaciorkowska@o2.pl
Telephone: +48-85-7450565 Fax: +48-85-7450568
Received: 2005-03-2 Accepted: 2005-04-09

Abstract

AIM: To measure the concentrations of chosen cytokines in the antrum mucosa depending on the kind of harmful pathogenic factors and to compare the concentrations with the values of controls without allergy and coexisting *Helicobacter pylori* (*H pylori*) infection.

METHODS: The patients (97 children) were divided into three groups according to the data obtained from the case history, to the main cause of the disease and to the dominant clinical symptoms. Group I: children with food allergy (Fa); group II: children infected with *H pylori*; group III (control group): children with functional disorders of the alimentary tract (without Fa and Hp infection). *H pylori* infection was determined by the presence of anti-Hp antibodies in serum (ELISA method) and urease test performed during endoscopic examination. Cytokine concentration in homogenates of gastric mucosa was detected by ELISA method.

RESULTS: The IL-2 concentration in gastric mucosa bioptates was the highest in children with Hp infection (116.5±179.5 pg/mg of the protein) and Fa and Hp infection (98.1±101.0 pg/mg), while decreased in children with Fa (44.8±50.3 pg/mg) and controls (45.7±23.5 pg/mg). The lowest mean concentration of IFN-γ was observed in children with Hp infection (18.9±16.4 pg/mg), with Fa and Hp infection (25.5±27.7 pg/mg), with Fa (40.6±39.7 pg/mg) and controls (49.9±33.4 pg/mg). The highest IL-4 concentrations were observed in children with Hp infection (35.3±52.8 pg/mg) and in children with Fa and Hp infection (37.2±51.7 pg/mg), while lower IL-4 concentration (23.6±35.8 pg/mg) was found in children with Fa compared to the controls (22.7±13.8 pg/mg). The analysis of IL-4 concentrations in children with Hp infection regarding the intensity of gastritis showed the highest value (62.2±61.2 pg/mg) in mild and moderate gastritis. The concentrations of IL-5 in the gastric mucosa of children with or without Fa did not differ significantly and were comparable to the control group. The highest mean IL-8 value was observed in Hp-infected children with or without Fa. The highest concentration of mucosal IL-10 was detected in children with Hp infection (79.3±41.2 pg/mg) and decreased in children with Fa and Hp infection (50.1±18.8 pg/mg) and in children with Fa (39.9±35.5 pg/mg). The intensity and activity of the inflammation did not affect IL-10 concentrations in the gastric mucosa. In children with Hp infection, TNF-α concentration was the highest (45.9±49.3 pg/mg) and in children with Fa and Hp infection was low (45.3±32.6 pg/mg), whereas decreased in children with Fa (21.7±34.2 pg/mg) and in controls (31.6±14.5 pg/mg).

CONCLUSION: The morphological changes of the gastric mucosa in children with Hp infection are comparable to those in children with Fa and coexisting Hp infection. Cytokine concentration in children with Fa and Hp infection is significantly different in IFN-γ, IL-2, IL-8, and TNF-α.

Key words: Mucosal cytokines; Food allergy; *Helicobacter pylori* dehydrogenase complex

Maciorkowska E, Panasiuk A, Kaczmarski M. Concentrations of gastric mucosal cytokines in children with food allergy and *Helicobacter pylori* infection. *World J Gastroenterol* 2005; 11(43): 6751-6756
http://www.wjgnet.com/1007-9327/11/6751.asp

INTRODUCTION

Many medical research centers dealing with food allergy (Fa) have assessed the morphological changes of gastric mucosa in children with hypersensitivity. Endoscopic evaluation of the alimentary tract and allergical and immunological examinations of food hypersensitivity are valuable diagnostic examination and pathogenetic inquiry element[1,2]. Numerous mast cells releasing histamine and triptase as well as the phenomenon of the selective accumulation of eosinophils and neutrophils have been observed in various parts of the alimentary tract of patients sensitive to food[3-6]. Erosive gastritis and ulceration may occur periodically in the gastric and/or

duodenal mucosa, whereas chronic intestinal disorders are usually recurrent with stomachache or diarrhea with abundant mucus and sometimes bloody secretion.

Besides allergy, *Helicobacter pylori* (*H pylori)* infection is another factor triggering inflammatory changes in the gastric and duodenal mucosa of children. Czinn *et al*.[7] are the first to show the connection of inflammatory changes of the gastric pylorus mucosa with Hp in children. The presence of Hp in the stomach leads to diminishment of the mucous protective layer due to the inhibition of mucus production caused by epithelial cells. The bacteria settle in the stomach, locating in and under the layer of epithelial cells, around intercellular epithelial connections and on the surface by producing special adherence structures, the so-called "bridge attachment". The number of bacteria is the main factor conditioning the epithelial damage degree[8-10]. Inflammatory changes in the gastric mucosa dependent on Hp may persist for several years giving neutrophilic infiltrations in the acute phase and lymphoplasmatic, macrophagic, and eosinophilic infiltrations in the chronic phase of the inflammation. The size of leukocytic infiltration correlates with the degree of colonization and mucosal damage. A small amount of B lymphocytes can be observed in an inflammatory infiltrate. The inflammatory process is developed due to a smaller number of CD8+ lymphocytes when compared to helping lymphocytes CD4+[11-13].

Abnormal IgE production in response to allergens is a characteristic feature of atopy. IL-4, IL-13 and IFN-γ are the most important cytokines regulating IgE production. IL-4 and IL-13 are responsible for the change of immunoglobulins produced by B lymphocytes from IgG and IgM towards IgE and IgG4[14-16]. IFN-γ reacts adversely and inhibits IL-4 effect on B lymphocytes, which secretes specific anti-antigen antibodies. Other cytokines, IL-2, IL-5, and IL-6 have an adjunctive activity to IL-4. They increase IgE production induced by IL-4, whereas IL-12 blocks IgE production induced by IL-4[17-19].

In case of infectious factors or toxins, the first contact cells are the cells of the monocyte/macrophage system. After activation, the cells produce and secrete proinflammatory cytokines, namely IL-1, IL-6, and TNF-α. Biologically, the cell activity occurs through endocrine paths and concerns remote organs, i.e. the liver (acute phase protein production), hypothalamus (pyrogenic effect) and adrenal glands (inflammatory process eradication)[20]. In Hp infection, cytokines also play an important role in the pathogenesis of gastritis. Hp infection is connected with the upregulated production of mucosal inflammatory cytokines: TNF-α, IL-1β, IL-2, IL-6, IL-7, and IL-8[10,21–24].

The purpose of the present study was to assess the concentrations of chosen cytokines in the gastric mucosa of children with Fa and Hp infection and to compare the concentrations obtained by the group of children without Fa and coexisting Hp infection.

MATERIALS AND METHODS

Examinations were conducted in 97 patients with dyspeptic symptoms, including recurrent or chronic stomachache, disorexia, recurrent diarrhea, nausea, vomiting, and loss of body weight. The symptoms were indications for gastroscopy. The patients were divided into three groups according to the cause and clinical symptoms observed.

Group I consisted of 48 children (49.5%) with Fa including 22 girls (45.8%) and 26 boys (54.2%) aged 4.6-18.4 years (mean 10.6±3.6 years). The case history, clinical complaints and the results of the upper alimentary tract endoscopic and histopathological examinations were the qualifying criteria for the further morphologic and biochemical analysis of the patients. The children with Fa were chosen on the basis of the clinical picture, positive immunological and allergical examinations, and inflammatory changes of gastric mucosa after Hp and giardiasis exclusion.

Group II comprised 34 children (35%) with Hp infection including 17 girls (50%) and 17 boys (50%). Fa and simultaneous Hp infection (Fa+Hp) were revealed in 16 (47%) children aged 3.3-16.2 years (mean 11.0±3.8 years). The rest of the 18 patients (52.9%) suffered from Hp infection without Fa. The age of the patients ranged from 5.0 to 18 years (mean 12.8±4.1 years). Children with Fa or without Fa and Hp infection were chosen on the basis of the same criteria as in group I and the positive results urease test (CLO-test) performed during endoscopy. The presence of Hp in the gastric antrum and corpus mucosa specimens was confirmed by hematoxylin and eosin staining (H+E) and the Giemsa method. Moreover, anti-Hp antibodies were determined by ELISA method (RecomWell Helicobacter IgG, Mikrogen, Germany). The amount of the bacteria as well as gastric antrum and corpus inflammatory activities were the decisive factors defining the severity of infection[24].

Group III included 15 children (9 girls -60%, 6 boys-40%) aged 4.9-14.9 years (mean 10.1±3.2 years) with functional disorders of the alimentary tract. The patients did not complain of allergy and showed no Fa symptoms. Hp infection was also excluded and endoscopy was carried out due to clinical symptoms mentioned above. The group constituted the control group (C). During gastroscopy, three specimens were collected from the prepyloric part of the stomach. Biopsies were weighed on an analytical scale immediately after the collection and then put in 1 mL of phosphatic buffer (molality 0.05 and pH 7.4) and placed in a thermos with ice.

Biopsies were homogenized using a tissue homogenizer. The protein was determined by Lowry method (mg/100 mL). Homogenates were divided into portions of 200 mL each, then frozen and stored at -20 °C for further examinations. Determination was conducted separately for each homogenate sample after gradual warming up to the room temperature. The concentrations of tumor necrosis factor (TNF-α), IL-2, IL-4, IL-5, IL-8, IL-10, and INF-γ in homogenates of the gastric mucosa were determined by ELISA method using ENDOGEN standard kits (Cambridge, USA) according to the manufacturer's instructions. Absorbance reading was performed spectrophotometrically with the wavelength

recommended by the manufacturer. The concentrations of cytokines examined (in pg/mL) were calculated on the basis of the standard curve. The results were expressed in milligram of protein in homogenate of the tissue examined.

Statistical analysis

Statistical analysis included the arithmetic mean±SD, the minimum result (min), and the maximum result (max). The levels of parameters examined were compared using Student's *t*-test for independent or paired trials. The differences were significant at $P<0.05$. The interdependence between measurable features was evaluated with Pearson's linear correlation coefficient, of which significance was assessed using Student's *t*-test for each correlation. The interdependence between non-measurable features evaluated using an independence test χ^2 or Fisher's exact test is presented in the correlation tables.

RESULTS

The histopathological evaluation of the gastric mucosa in patients could distinguish the following categories of changes: normal mucous membrane, mucosa at the borderline of the norm (a slightly decreased number of mononuclear cells in superficial layers of the mucous membrane) and chronic inflammation. In children with Fa, normal gastric mucosa was observed in 43.7%, mucosa at the edge of the norm in 35.4% and chronic inflammation in 20.8% of children. In children with Fa and Hp infection and in those without Fa, morphological changes of the antrum mucosa resembled chronic inflammation in 100%. According to the Sydney System, three stages of gastritis could be distinguished: mild, moderate, and severe. The severe stage of antrum mucosal inflammation was observed in 55% of children with Hp infection and in 31.2% of children with Fa and Hp infection (Table 1). Moderate antrum gastritis concerned children with Fa and Hp infection (50%) and children with Hp infection (44.4%). Mild gastritis was revealed in 18.7% (group I) of children with Fa and in 18.7% of children with Fa coexisting Hp infection. Morphometric analysis regarding the severity of inflammation showed statistically significant pathological changes in the antrum ($P<0.001$). The evaluation of antral gastritis activity according to the Sydney System also presented a statistical significance ($P<0.001$). Severe antral gastritis was observed in 72.2% of children with Hp infection and in 68.7% of children with Fa and Hp infection (Table 2). The moderate activity was found in children with Fa and Hp infection (31.2%), in children with Hp infection (27.7%) and in children with Fa (6.2%). Group I showed the moderate activity in 6.2% of children. Histopathological examinations of the corpus mucosa were evaluated in the same way, i.e. in three categories of changes: normal mucosa, mucosa at the edge of the norm,and chronic inflammation.

Group I showed chronic corpus gastritis in 16.6% of children, whereas the second category of changes was observed in 37.7% and normal mucosa was reported in 45.8% of children in this group. Chronic corpus gastritis was diagnosed in 100% of children with Hp infection. In children with Fa and Hp infection, 93.7% of children had chronic inflammation and 6.2% had mucosa at the edge of the norm. Severe corpus gastritis was observed in 12.5% of children with Fa and Hp infection and in 5.5% of children without Fa but with Hp infection (Table 1). The moderate corpus gastritis occurred in 50% of children with Hp infection and in 50% of those with Fa and coexisting Hp infection. Only 2% of children with Fa had moderate corpus gastritis. Mild gastritis was observed in children with Hp infection (44.4%) and in 31.2% of children with Fa and Hp infection. Severe activity of the corpus mucosa was found in 38% of children infected with Hp and in 37.5% of allergic children infected with Hp. The moderate activity was observed in 61.1% of children with Hp infection, 56.2% of allergic children with Hp infection and 6.2% of children with Fa.

Gastric mucosal biopsies showed the highest IL-2 concentration in children infected with Hp (116.5±179.5 pg/mg of the protein) and slightly lower level in allergic children with Hp infection (98.1±101.0 pg/mg). The levels were statistically significantly different from those in the control group ($P<0.01$). The lowest IL-2 concentration was observed in children with Fa (44.8±50.3 pg/mg), which was comparable to that in the controls (45.7±23.5 pg/mg;

Table 1 Severity of corpus and antrum mucosa gastritis in children examined according to Sydney System[25] *n* (%)

Stage of corpus mucosa gastritis				
Group	*n*	Mild	Moderate	Severe
Fa	48	6 (12.5)	1 (2)	0 (0)
Hp	18	8 (44.4)	9 (50)	1 (5.5)
Fa+Hp	16	5 (31.2)	8 (50)	2 (12.5)
C	15	0 (0)	0 (0)	0 (0)
Stage of antrum mucosa gastritis				
Fa	48	9 (18.7)	1 (2)	0 (0)
Hp	18	1 (5.5)	8 (44.4)	9 (55)
Fa+Hp	16	3 (18.7)	8 (50)	5 (31.2)
C	15	0 (0)	0 (0)	0 (0)

Fa, food allergy; Hp, *H pylori*; C, control group.

Table 2 Activation of corpus and antrum mucosa gastritis in children examined according to Sydney System[25] *n* (%)

		Activity of corpus gastritis			
Group examined	*n*	Mild	Moderate	Severe	Lack
Fa	48	4 (8.3)	3 (6.2)	0 (0)	41 (85.4)
Hp	18	0 (0)	11 (61.1)	7 (38.8)	0 (0)
Fa+Hp	16	0 (0)	9 (56.2)	6 (37.5)	1 (6.2)
C	15	0 (0)	0 (0)	0 (0)	15 (100)
Activity of antrum gastritis					
Fa	48	7 (14.5)	3 (6.2)	0 (0)	38 (79.1)
Hp	18	0 (0)	5 (27.7)	13 (72.2)	0 (0)
Fa+Hp	16	0 (0)	5 (31.2)	11 (68.7)	0 (0)
C	15	0 (0)	0 (0)	0 (0)	15 (100)

Fa, food allergy; Hp, *H pylori*, C, control group.

Table 3 Cytokine concentration in gastric mucosa of children examined, according to Sydney System[25] (pg/mg)

Group	IL-2	IL-4	IL-5	IL-8	IL-10	IFN-γ	TNF-α
Fa	44.8	23.6	35.5	59.9	39.9	40.6	21.7
Hp	116.5[b]	35.3	34.1	88.0[b]	79.3[b]	18.9[b]	45.9[b]
Fa+Hp	98.1[d,f]	37.2	29.9	101.2[d]	50.1	25.5[f]	45.3[d,f]
C	45.7[h]	22.7	30.8	93.8[f]	40.4[h]	49.9[h]	31.6[j]

[b]P<0.01 *vs* Fa and Hp, [d]P<0.01 *vs* Fa and Fa+Hp, [f]P<0.01 *vs* Fa and C, [h]P<0.01 *vs* Hp and C, [j]P<0.01 *vs* Fa+Hp and C.

Table 3). The highest IL-2 concentration in the gastric mucosa with regard to the intensity of inflammation (mild+moderate) was observed in the antrum of children with Hp (184.4±227.8 pg/mg) and the allergic process with coexisting Hp infection (125.4±109.4 pg/mg). The highest IL-2 concentration in relation to gastric mucosa inflammation activity was found in children with severe Hp infection (187.6±232.6 pg/mg), being statistically significant when compared to the control group (P<0.01; Tables 4 and 5). IFN-γ concentrations in the gastric mucosa ranged from undetermined levels to 188.2 pg/mg of the protein. The lowest mean concentration of IFN-γ was observed in children infected with Hp (18.9±16.4 pg/mg of the protein) and differed significantly when compared to the controls (P<0.01). In allergic children with Hp infection, the mean concentration of IFN-γ in the gastric mucosa was slightly higher (25.5±27.7 pg/mg, P<0.01; Table 3).

The mean concentration of IFN-γ was 40.6±39.7 pg/mg of the protein in children with Fa and was close to that in the controls (49.9 ±33.4 pg/mg). In Hp infected children with mild and moderate gastric mucosal inflammation, IFN-γ concentration was the lowest (13.1±16.5 pg/mg), being significantly different from that in the controls (P<0.01; Tables 4 and 5).

The values of IL-4 ranged from undetectable to 208.4 pg/mg in biopsies of the gastric mucosa. The highest IL-4 concentration was observed in Hp infected children. IL-4 concentration was 37.2±51.7 pg/mg in allergic and Hp infected children and 35.3±52.8 pg/mg in those without Fa.

The mean concentration of IL-4 was 23.6±35.8 pg/mg in children with Fa, being comparable with the control group (22.7±13.8 pg/mg). The highest IL-4 concentration in children with Hp infection regarding the intensity of gastritis was 62.2±61.2 pg/mg in mild and moderate gastritis (P<0.01).

The IL-5 concentration ranged from 6.7 to 250.9 pg/mg in the biopsies and was 35.5±50.9 pg/mg in allergic children, being not significantly different from that in the controls. The mean concentration of IL-5 in the gastric mucosa of children with or without Fa did not differ significantly and was comparable to that in the control group.

IL-8 concentration ranged from 10.5 to 618.8 pg/mg in

Table 4 Concentrations of cytokines in gastric mucosa of children examined depending on inflammation stage according to Sydney System[25]

Cytokines (pg/mg of the protein)	Fa		Hp				Fa+Hp			
	Antrum	Corpus	Antrum		Corpus		Antrum		Corpus	
	Mild+moderate	Mild+moderate	Mild+moderate	Severe	Mild	Moderate+severe	Mild+moderate	Severe	Mild	Moderate+severe
IL-2	17.7	17.9	184.4[b]	38.8	77.7	150.4[b]	125.4[b]	38.3	106.7 [b]	98.6
IFN-γ	54.9	46.6	13.1[b]	24.1	17.8[b]	19.7[b]	21.9	34.3	23.1	27.1
IL-4	15.4	6.7[b]	62.2[b]	3.9[a]	37.6	32.7	44.3	1.7	32.1	46.4
IL-5	24.5	25.5	–	–	–	–	29.7	–	–	33.0
IL-8	37.5	37.5	101.2	72.9	93.6	83.1	98.0	108.2	71.1	118.3
IL-10	30.4	24.4	–	–	–	–	44.6	–	–	58.9
TNF-α	20.6	4.8	65.2	24.1	48.7	43.3	54.8[b]	24.3	49.0	44.8

[b]P<0.01, cytokine concentrations statistically significantly different from controls. Fa, food allergy; Hp, *H pylori*; C, control group.

Table 5 Cytokine concentrations in gastric mucosa of children examined depending on the inflammation activity according to Sydney System[25]

Cytokines (pg/mg protein)	Fa		Hp				Fa+Hp			
	Antrum	Corpus	Antrum		Corpus		Antrum		Corpus	
	Mild+moderate	Mild+moderate	Mild+moderate	Severe	Mild+moderate	Severe	Mild+moderate	Severe	Mild	Moderate+severe
IL-2	17.7	17.9	204.3[b]	72.5	69.0	187.6[b]	70.1	110.9	119.3	74.3
IFN-γ	54.9	46.6	20.4	18.4	21.8[b]	14.6[b]	25.6	25.4	22.4	33.4
IL-4	15.4	6.7[b]	81.1[b]	6.7[b]	30.0	47.8	52.0	29.8	39.9	39.9
IL-5	24.5	25.0	–	–	–	–	–	–	–	–
IL-8	37.5	37.5	83.5	90.2	86.9	89.6	69.8	115.5	83.2	131.6
IL-10	30.4	24.0	–	–	–	–	–	–	–	–
TNF-α	20.6	4.8	76.0	33.3	37.4	57.9	24.6	54.6	60.4	24.9

[b]P<0.01 *vs* cytokine concentrations statistically significantly different from controls. Fa, food allergy; Hp, *H pylori*; C, control group.

gastric mucosal biopsies before the treatment. The highest mean IL-8 value was observed in Hp infected children (with or without Fa). The mean IL-8 concentration was 101.2 ±68.3 pg/mg in allergic children with Hp infection. This value was statistically significant ($P<0.005$) in comparison to that in allergic children. In children with Hp infection, the mean gastric mucosa IL-8 concentration was 88.0± 40.4 pg/mg, being statistically significant ($P<0.005$) in comparison to that in children with Fa. The evaluation of mucosa IL-8 concentration with regard to the intensity and activity of inflammatory process in the gastric mucosa did not show any statistically significant dependence (Tables 4 and 5).

In gastric mucosal biopsies, IL-10 concentration ranged from undetectable to 141.8 pg/mg. The highest mean concentration of mucosa IL-10 was detected in children with Hp infection (79.3±41.2 pg/mg) and in allergic children with Hp infection (50.1±18.8 pg/mg).

The mean IL-10 concentration was 39.9±35.5 pg/mg in children with Fa, being statistically significantly different from that in children with Hp infection ($P<0.01$, Table 3). The intensity and activity of inflammation did not affect IL-10 concentration in the gastric mucosa (Tables 4 and 5).

TNF-α concentration ranged from undetectable to 208.4 pg/mg in gastric mucosal biopsies. The mean TNF-α concentration was the highest in children with Hp infection and 45.9±49.3 pg/mg, in children without Fa compared to that in the controls ($P<0.06$). Infection revealed the mean TNF-α concentration of 45.3±32.6 pg/mg in allergic children with coexisting Hp infection, being statistically different from controls ($P<0.01$). The mean TNF-α concentration was 21.7±34.2 pg/mg in allergic children and showed statistically significant difference ($P<0.003$) in comparison to children with Hp infection or with Fa and coexisting Hp infection ($P<0.004$). The analysis of TNF-α concentration in the gastric mucosa with regard to the intensity and activity of the inflammation showed no statistically significant differences.

DISCUSSION

Our study proved that the pathogenic factors like harmful food could induce certain morphological changes of the gastric mucosa. They are smaller with regard to the percentage and "depth" than in the combined activity of allergy and Hp. It seems essential to check the intensity of the changes and their dynamics by assessing their characteristics and size as well as local properties of cytokines produced. The concentration of chosen cytokines in the antrum mucosa in children with Fa was comparable to that in the controls. However, IL-4 concentration was statistically significantly different from the control group. IL-4 is secreted by antigen- or mitogen-inactivated lymphocytes Th2 and by mast cells in the gastric mucosa infiltrates in children with Fa.

Another frequent etiological factor, Hp infection leading to gastritis, was observed besides the allergic one affecting the gastric mucosa. Histopathological changes induced by the activity of this factor were far greater than those observed in children with Fa.

It should be assumed that the intensified local production of many inflammatory cytokines, including IL-2, takes place in Hp infection where gastric mucosa is infiltrated by such cells as neutrophils, lymphocytes, monocytes/macrophages and cytoplasmic cells. The IL-2 concentration was the highest in the gastric mucosa of children with Hp infection (116.5 pg/mg) and slightly lower in children with Fa and Hp infection (98.1 pg/mg). The values were statistically significant when compared to the control group.

IL-8 is another cytokine, whose chemotactic properties are directed selectively towards neutrophils. The activity of IL-8 on neutrophils is triggered by binding to a specific receptor, which can be found on the surface of the cells (5 ku)[10,25-27]. A population of children with Fa and coexisting Hp infection was included additionally in our study. The mean concentration of IL-8 in the gastric mucosa of children with Hp infection was 88.0 pg/mg, being statistically significantly different ($P<0.01$) in comparison to 59.9 pg/mg in allergic children. The mean IL-8 concentration was even higher (101.2 pg/mg) in allergic children with Hp infection.

Another cytokine with a wide range of biological actions is IL-4 secreted by antigen-inactivated Th lymphocytes (Th2) and mast cells[28-31]. We evaluated IL-4 concentration in particular groups of children and found IL-4 levels were increased in allergic patients, though the values were not statistically different from those in the controls.

TNF-α is one of the most potent cytokines activating numerous functions of neutrophils. It stimulates directly oxygenic metabolite release by neutrophils and the effectiveness of this phenomenon depends on the doses used[32-34]. Isolauri *et al*.[35] and Majamaa *et al*.[36] showed that TNF-α is elevated in feces of allergic children, which is thought to be a delayed reaction type to food challenge. Children with immediate reaction have a significant increase in α1-antitripsin and eosinophil cationic protein (ECP) in their feces as compared to patients who do not respond to food challenge.

The relatively low TNF-α concentration in the antrum mucosa (21.7 pg/mg) of allergic children may be due to the fact that a marked percentage of the patients revealed IgE-dependent mediators engaged in allergic reactions. TNF-α assessed in biopsies of the alimentary tract mucosa or excrements feces seems to be a good factor for active immunological reactions to food allergens ingested by children who react to food without IgE participation. Isolauri *et al*.[35] showed that TNF-α can be equally used as a factor of pathogenic process activation and food hypersensitivity as cationic protein (ECP) and α1-antitripsin in case of patients whose cytokines secreted by T lymphocytes are responsible for clinical symptoms.

In conclusion, the pathogenic process is individually different with regard to morphological examinations and proinflammatory and proallergic cytokine production. Concentrations of IFN-γ, IL-2, IL-8, and TNF-α in the gastric mucosa of children with Fa and those with Hp infection (without Fa) are different.

REFERENCES

1 **Burks AW**, Sampson HA. Diagnostic approaches to the patient with suspected food allergies. *J Pediatr* 1992; **121:** S 64-S 71
2 **Hourihane JO**. Prevalence and severity of food allergy--need for control. *Allergy* 1998; **53**: (suppl. 46): 84-88
3 **Leal-Berumen I**, Conlon P, Marshall JS. IL-6 production by rat peritoneal mast cells is not necessarily preceded by histamine release and can be induced by bacterial lipopolysaccharide. *J Immunol* 1994; **152:** 5468-5476
4 **Schwartz LB**. Tryptase, a mediator of human mast cells. *J Allergy Clin Immunol* 1990; **86:** 594-598
5 **Tharp MD**, Thirlby R, Sullivan TJ. Gastrin induces histamine release from human cutaneous mast cells. *J Allergy Clin Immunol* 1984; **74:** 159-165
6 **Katz AJ**, Goldman H, Grand RJ. Gastric mucosal biopsy in eosinophilic (allergic) gastroenteritis. *Gastroenterology* 1977; **73:** 705-709
7 **Czinn SJ**, Dahms BB, Jacobs GH, Kaplan B, Rothstein FC. Campylobacter-like organisms in association with symptomatic gastritis in children. *J Pediatr* 1986; **109:** 80-83
8 **Chan WY**, Hui PK, Leung KM, Thomas TM. Modes of Helicobacter colonization and gastric epithelial damage. *Histopathology* 1992; **21:** 521-528
9 **Crabtree JE**. Immune and inflammatory responses to Helicobacter pylori infection. *Scand J Gastroenterol Suppl* 1996; **215:** 3-10
10. **Crabtree JE**, Peichl P, Wyatt JI, Stachl U, Lindley IJ. Gastric interleukin-8 and IgA IL-8 autoantibodies in Helicobacter pylori infection. *Scand J Immunol* 1993; **37:** 65-70
11 **Atherton JC**, Peek RM Jr, Tham KT, Cover TL, Blaser MJ. Clinical and pathological importance of heterogeneity in vacA, the vacuolating cytotoxin gene of Helicobacter pylori. *Gastroenterology* 1997; **112:** 92-99
12 **Harris PR**, Mobley HL, Perez-Perez GI, Blaser MJ, Smith PD. Helicobacter pylori urease is a potent stimulus of mononuclear phagocyte activation and inflammatory cytokine production. *Gastroenterology* 1996; **111:** 419-425
13 **Mai UE**, Perez-Perez GI, Allen JB, Wahl SM, Blaser MJ, Smith PD. Surface proteins from Helicobacter pylori exhibit chemotactic activity for human leukocytes and are present in gastric mucosa. *J Exp Med* 1992; **175:** 517-525
14 **Andre F**, Pene J, Andre C. Interleukin-4 and interferon-gamma production by peripheral blood mononuclear cells from food-allergic patients. *Allergy* 1996; **51:** 350-355
15 **Kiniwa M**, Gately M, Gubler U, Chizzonite R, Fargeas C, Delespesse G. Recombinant interleukin - 12 suppresses the synthesis of immunoglobulin E by interleukin-4 stimulated human lymphocytes. *J Clin Invest* 1992; **90:** 262-266
16 **Zurawski G**, de Vries JE. Interleukin 13, an interleukin 4-like cytokine that acts on monocytes and B cells, but not on T cells. *Immunol Today* 1994; **15:** 19-26
17 **Chandra RK**, Kumari S. Nutrition and immunity: an overview. *J Nutr* 1994; **124:** 1433-1435
18 **Pene J**, Rousset F, Briere F, Chretien I, Wideman J, Bonnefoy JY, De Vries JE. Interleukin 5 enhances interleukin 4-induced IgE production by normal human B cells. The role of soluble CD23 antigen. *Eur J Immunol* 1988; **18:** 929-935
19 **Schroeder JT**, MacGlashan DW Jr. New concepts: the basophil. *J Allergy Clin Immunol* 1997; **99:** 429-433
20 **Baggiolini M**, Dahinden CA. CC chemokines in allergic inflammation. *Immunol Today* 1994; **15:** 127-133
21 **Yamaoka Y**, Kita M, Kodama T, Sawai N, Kashima K, Imanishi J. Expression of cytokine mRNA in gastric mucosa with Helicobacter pylori infection. *Scand J Gastroenterol* 1995; **30:** 511-519
22 **Yamaoka Y**, Kita M, Kodama T, Sawai N, Kashima K, Imanishi J. Expression of cytokine mRNA in gastric mucosa with Hp infection. *Scand J Gastroenterol* 1995; **30:** 1153-1159
23 **Ishihara S**, Fukuda R, Fukumoto S. Cytokine gene expression in the gastric mucosa: its role in chronic gastritis. *J Gastroenterol* 1996; **31:** 485-490
24 **Dixon MF**, Genta RM, Yardley JH, Correa P. Classification and grading of gastritis. The updated Sydney System. International Workshop on the Histopathology of Gastritis, Houston 1994. *Am J Surg Pathol* 1996; **20:** 1161-1181
25 **Abreu-Martin MT**, Vidrich A, Lynch DH, Targan SR. Divergent induction of apoptosis and IL-8 secretion in HT-29 cells in response to TNF-alpha and ligation of Fas antigen. *J Immunol* 1995; **155:** 4147-4154
26 ***Nishi Y***, Isomoto H, Uotani S, Wen CY, Shikuwa S, Ohnita K, Mizuta Y, Kawaguchi A, Inoue K, Kohno S. Enhanced production of leptin in gastric fundic mucosa with Helicobacter pylori infection. *World J Gastroenterol* 2005; **11:** 695-699
27 **Wang KX**, Chen L. Helicobacter pylori L-form and patients with chronic gastritis. *World J Gastroenterol* 2004; **10:** 1306-1309
28 **Chen CC**, Manning AM. TGF-beta 1, IL-10 and IL-4 differentially modulate the cytokine-induced expression of IL-6 and IL-8 in human endothelial cells. *Cytokine* 1996; **8:** 58-65
29 **Huang H**, Hu-Li J, Chen H, Ben-Sasson SZ, Paul WE. IL-4 and IL-13 production in differentiated T helper type 2 cells is not IL-4 dependent. *J Immunol* 1997; **159:** 3731-3738
30 **Joyce DA**, Steer JH. IL-4, IL-10 and IFN-gamma have distinct, but interacting, effects on differentiation-induced changes in TNF-alpha and TNF receptor release by cultured human monocytes. *Cytokine* 1996; **8:** 49-57
31 **Ji SL**, Cui HF, Shi F, Chi YQ, Cao JC, Geng MY, Guan HS. Inhibitory effect of heparin-derived oligosaccharides on secretion of interleukin-4 and interleukin-5 from human peripheral blood T lymphocytes. *World J Gastroenterol* 2004; **10:** 3490-3494
32 **Gordon JR**, Galli SJ. Mast cells as a source of both preformed and immunologically inducible TNF-alpha/cachectin. *Nature* 1990; **346:** 274-276
33 **Hernandez-Pando R**, Rook GA. The role of TNF-alpha in T-cell-mediated inflammation depends on the Th1/Th2 cytokine balance. *Immunology* 1994; **82:** 591-595
34 **Marie C**, Pitton C, Fitting C, Cavaillon JM. IL-10 and IL-4 synergize with TNF-alpha to induce IL-1ra production by human neutrophils. *Cytokine* 1996; **8:** 147-151
35 **Isolauri E**, Suomalainen H, Kaila M, Jalonen T, Soppi E, Virtanen E, Arvilommi H. Local immune response in patients with cow milk allergy: follow-up of patients retaining allergy or becoming tolerant. *J Pediatr* 1992; **120:** 9-15
36 **Majamaa H**, Miettinen A, Laine S, Isolauri E. Intestinal inflammation in children with atopic eczema: faecal eosinophil cationic protein and tumour necrosis factor-alpha as non-invasive indicators of food allergy. *Clin Exp Allergy* 1996; **26:** 181-187

Science Editor Wang XL and Guo SY **Language Editor** Elsevier HK

PO Box 2345, Beijing 100023, China
www.wjgnet.com
wjg@wjgnet.com

ELSEVIER

World J Gastroenterol 2005;11(43):6757-6764
World Journal of Gastroenterology ISSN 1007-9327

• *BASIC RESEARCH* •

Effect of bombesin and neurotensin on gut barrier function in partially hepatectomized rats

Stelios F Assimakopoulos, Ilias H Alexandris, Chrisoula D Scopa, Panagiotis G Mylonas, Konstantinos C Thomopoulos, Christos D Georgiou, Vassiliki N Nikolopoulou, Constantine E Vagianos

Stelios F Assimakopoulos, Department of Internal Medicine, School of Medicine, University of Patras, Patras, Greece
Ilias H Alexandris, Constantine E Vagianos, Department of Surgery, School of Medicine, University of Patras, Patras, Greece
Chrisoula D Scopa, Department of Pathology, School of Medicine, University of Patras, Patras, Greece
Panagiotis G Mylonas, Department of Internal Medicine, Division of Endocrinology, School of Medicine, University of Patras, Patras, Greece
Konstantinos C Thomopoulos, Vassiliki N Nikolopoulou, Department of Internal Medicine, Division of Gastroenterology, School of Medicine, University of Patras, Patras, Greece
Christos D Georgiou, Department of Biology, Division of Genetics, Cell and Developmental Biology, University of Patras, Patras, Greece
Correspondence to: Constantine E Vagianos, MD, Associate Professor, Department of Surgery, University of Patras, Medical School, Rion University Hospital, 26500 Patras, Greece. vagian@otenet.gr
Telephone: +30-2610-999 779 Fax: +30-2610-993 984
Received: 2005-03-28 Accepted: 2005-04-26

Abstract

AIM: To investigate the effect of regulatory peptides bombesin (BBS) and neurotensin (NT) on intestinal barrier function in partially hepatectomized rats.

METHODS: Ninety male Wistar rats were randomly divided into five groups: I (*n* = 10): controls, II (*n* = 20): sham operated, III (*n* = 20): partial hepatectomy 70% (PHx), IV (*n* = 20): PHx+BBS (30 μg/kg/d), V (*n* = 20): PHx+NT (300 μg/kg/d). Groups IV and V were treated for 8 days before PHx and 48 h post surgery. At the end of the experiment, on day 10, intestinal barrier function was assessed by measuring endotoxin concentrations in portal and aortic blood. Tissue sections of the terminal ileum were examined histologically and villus density, mucosal thickness, mitotic activity and apoptosis in crypts were assessed. In addition, ileal mucosa was analyzed for DNA and protein content and microbiological analysis was performed in cecal contents. To estimate intestinal oxidative stress, lipid peroxidation was determined on tissue homogenates from terminal ileum.

RESULTS: BBS or NT administration significantly reduced portal and systemic endotoxemia observed 48 h after partial hepatectomy. In hepatectomized rats (group III), a trend towards induction of mucosal atrophy was observed, demonstrated by the reduction of villus density, mucosal thickness, protein content and significant reduction of DNA, while these alterations were reversed by regulatory peptides administration. This trophic effect of BBS and NT was accompanied by induction of mitoses above control levels and a significant reduction of apoptosis in intestinal crypts. Intestinal lipid peroxidation was found significantly lower in PHx group and regulatory peptides exerted an antioxidant action, further decreasing this parameter of oxidative stress. The bacterial population of *E. coli* and aerobic Gram (+) cocci was increased in cecal content of hepatectomized rats, while this parameter was not affected by the administration of BBS or NT.

CONCLUSION: Gut regulatory peptides BBS and NT improve intestinal barrier function and reduce endotoxemia in experimental partial hepatectomy. This effect is, at least in part, mediated by their trophic, antiapoptotic, mitogenic, and antioxidant effect on the intestinal epithelium. This observation might be of potential value in patients undergoing liver resection.

Key words: Hepatectomy; Rats; Bombesin; Neurotensin; Intestinal barrier; Apoptosis; Oxidative stress

Assimakopoulos SF, Alexandris IH, Scopa CD, Mylonas PG, Thomopoulos KC, Georgiou CD, Nikolopoulou VN, Vagianos CE. Effect of bombesin and neurotensin on gut barrier function in partially hepatectomized rats. *World J Gastroenterol* 2005; 11(43): 6757-6764
http://www.wjgnet.com/1007-9327/11/6757.asp

INTRODUCTION

Despite current advances in the safety of hepatic resection and perioperative care, which have led to a significant reduction of perioperative mortality, septic events remain still an important problem complicating the outcome of hepatectomized patients[1]. It has been previously shown that enteric bacteria and endotoxins passing through the intestinal barrier to extraintestinal sites and the systemic circulation result in intra-abdominal abscess formation, pulmonary infections, sepsis and multiple organ dysfunction in patients and rats after liver resection[1,2]. A

compromised gut barrier function promotes the escape of enteric bacteria and endotoxins into portal circulation, while the reduction of the functional reticuloendothelial volume after hepatectomies permits their systemic spread[3].

Bombesin (BBS), a tetradecapeptide originally isolated from the skin of the European frog *Bombina bombina* is analogous to gastrin-releasing peptide found in mammalians[4]. BBS stimulates the release of various gut hormones and peptides e.g, gastrin, cholecystokinine, insulin, glucagons, somatostatin, motilin, pancreatic polypeptide, neurotensin and exerts a trophic effect on intestinal and gastric mucosa and pancreas, while it stimulates intestinal motility[5,6]. It has been previously shown that BBS improves intestinal integrity in experimental models of gut barrier dysfunction, such as after elemental diets, methotrexate administration, chemically induced colitis and burns[5,7-9].

Neurotensin (NT), a tridecapeptide originally isolated from the bovine hypothalamus, is additionally found in the gut mucosal endocrine cells (N cells), especially in the ileum[10]. NT stimulates pancreaticobiliary secretions, intestinal blood flow and colonic motility, while it inhibits small intestinal and gastric motility. It is a potent trophic agent for small and large intestine, gastric mucosa and pancreas[11-14]. NT has been shown to prevent intestinal atrophy induced by feeding rats an elemental diet, restores mucosal ulceration after radiation therapy and enhances intestinal regeneration after small bowel resection[7,15,16].

We have recently shown that BBS and NT improve intestinal barrier function in experimental obstructive jaundice by exerting mitogenic, antiapoptotic, and antioxidant effects on the intestinal epithelium[17]. The present study was undertaken to investigate the effect of exogenous administration of BBS and NT on gut barrier function after partial hepatectomy in rats.

MATERIALS AND METHODS

Animals

Ninety male albino Wistar rats, weighing 250-320 g, were used. They were housed in stainless-steel cages, three rats per cage, under controlled temperature (23 °C) and humidity conditions, with 12-h dark/light cycles, and maintained on standard laboratory diet with tap water *ad libitum* throughout the experiment, except for an overnight fast before surgery.

The experiments were carried out according to the guidelines set forth by the Ethics Committee of Patras University Hospital, Patras, Greece.

Experimental design

Animals were divided randomly into five groups: Group I (n = 10): non-operated controls, group II (n = 20): sham operated, group III (n = 20): partial hepatectomy (70%), group IV (n = 20): partial hepatectomy and BBS administration, group V (n = 20): partial hepatectomy and NT administration.

Starting on d 0, the animals of groups IV and V were treated daily with BBS (10 μg/kg, subcutaneously, thrice a day) and NT (300 μg/kg, intraperitoneally, once a day), respectively, while the animals of groups I, II, and III were divided to receive daily either three subcutaneous or one intraperitoneal injection of 0.5 mL normal saline. Previous pilot studies showed that the way of saline administration does not affect the results. On the 8th day, animals from groups III, IV, and V underwent laparotomy and partial hepatectomy (almost 70%) as described by Higgins and Andersson[18], while animals in group II underwent laparotomy and mobilization of the liver. The abdominal incision was closed in two layers with chromic 4-0 cat gut and 4-0 silk. All surgical procedures were performed under strict sterile conditions, using light ether anesthesia. Administration of BBS, NT, and normal saline was continued for 48 h after surgery. On the 10th d, all animals were operated (group I) or reoperated (groups II, III, IV, and V), again under strict sterile conditions. Samples were obtained according to the experimental protocol, after which the rats were killed by exsanguination.

Peptides preparation

A stock solution of BBS (Sigma Chemical Co, St. Louis, MO, USA) was prepared by first dissolving the amount of peptide needed for the study in 1 mL sterile water containing 0.1% (w/v) bovine serum albumin and then diluted with normal saline containing 1% (w/v) bovine serum albumin, so that the amount of BBS needed for each injection to be contained in a volume of 0.1 mL. This solution was divided into equal aliquots of 0.1 mL that were stored in plastic tubes at -20 °C. At the time of administration, in order to prolong absorption, each aliquot was mixed with 0.4 mL of a solution of 8% (w/v) hydrolyzed gelatin (Sigma Chemical Co, St. Louis, MO, USA). A final volume of 0.5 mL, containing 10 μg BBS/kg body weight, was injected subcutaneously thrice daily.

A stock solution of NT (Sigma Chemical Co, St. Louis, MO, USA) was prepared by first dissolving the amount of peptide needed for the study in 1 mL sterile water containing 0.1% (w/v) bovine serum albumin and then diluted with normal saline containing 0.1% (w/v) bovine serum albumin, so that the dose of NT needed for each injection to be contained in a volume of 0.1 mL. This solution was divided into equal aliquots of 0.1 mL that were stored in glass vials at -20 °C. At the time of administration, each aliquot was further diluted with 0.4 mL sterile saline to a final volume of 0.5 mL and was given intraperitoneally as a bolus injection containing 300 μg NT/kg body weight.

Endotoxin measurements

For the determination of endotoxin concentrations, a laparotomy was performed in all groups, the portal vein and the abdominal aorta were punctured and samples of 1 and 2 mL of blood were obtained, respectively. Endotoxin concentration was determined by the quantitative chromogenic Limulus amebocyte lysate test according to the manufacturer's instructions (QCL-1 000, BioWhittaker, Walkersville, USA) and expressed in EU/mL.

Measurements of mucosal DNA and protein

DNA and protein content in the terminal ileal mucosa were determined in all animals. A 1-cm long sample of the terminal ileum was excised, opened by longitudinal incision and washed with cold normal saline. Using a clean glass slide the mucosa was removed and homogenized in 1 mL NaOH 1 N, by means of a polytron homogenizer. The protein was measured according to Lowry's method[19] using a commercial kit (Sigma Diagnostics, Deisenhofen, Germany) and the DNA was determined according to a modified Barton technique[20].

Histological evaluation

For histological examination, tissue samples from the terminal ileum were obtained from all animals. The ileal samples were fixed in 10% neutral buffered formalin, embedded in paraffin, sectioned at 4 μm and stained with hematoxylin and eosin. In each ileal specimen, several histologic features were evaluated and recorded. These features included architectural distortion, villous blunting, surface and crypt epithelial injury, presence and cell type of inflammation of the lamina propria, surface and cryptal intraepithelial infiltration, lamina propria fibrosis and granulation tissue formation. Ileal mucosal morphometric characteristics were studied by measurements of villus density, defined as the number of villi per centimeter (V/cm), and villus height (Vh) in micrometers (μm). Villus height was measured with a micrometer eyepiece affixed to a Reichert–Jung light microscope and at least 20 well-preserved villi were estimated in each sample. In addition, the number of mitoses and apoptotic bodies per crypt were also counted. Apoptotic bodies of the cryptal epithelium were identified and tallied using a morphometric analysis, which has been described in detail elsewhere[21]. Apoptotic bodies were defined as rounded vacuoles with fragments of karyorrhectic nuclear debris and were differentiated from small isolated fragments of nuclear chromatin and intraepithelial neutrophils. Apoptotic bodies and mitoses were counted in all architecturally successive crypts included in the specimen, regardless of crypt orientation, and their total number was divided by the number of the crypts. The number of apoptotic bodies per crypt is referred to as the apoptotic body count (ABC).

Cecal bacterial population

Collection of cecal contents for microbiological analysis, was performed by the following technique: the ascending colon was ligated below the hepatic flexure, and a 21-gauge needle mounted on a 5 mL syringe was introduced into the cecum through the ileocecal valve, after puncturing the terminal ileum. Two milliliters of sterile saline was infused in the cecum, after which the needle was withdrawn and the terminal ileum was ligated. The cecal content was manually mollified for 2 min and after a good mixture was achieved, 1 mL of colonic content was removed; serial tenfold dilutions were performed and 0.001 mL of each sample was inoculated into 5% blood and McConkey's agar plates for recovery of aerobic bacteria and Gram-negative/nonspore-forming agar plates for anaerobes. After 24 and 48 h of incubation at 37 °C, for aerobic and anaerobic cultures respectively, colonies were identified and counted. Quantitative culture results were expressed as the number of colony-forming units (CFU) per milliliter or per gram of the cecal samples, calculated from the dilutions of colonic content. *E coli* was identified by Gram stain and a standard biochemical identification system (API-20E, Biomérieux, Marcy-l'Etoile, France, according to the analytical profile index).

Intestinal lipid peroxidation

A 1-cm long tissue sample of the terminal ileum of each animal was excised, washed in 9 g/L of NaCl and was homogenized in a porcelain mortar in liquid nitrogen. Intestinal homogenates were processed for the determination of lipid peroxidation, according to a modified [2-thiobarbituric acid (TBA)]-based method, as reported previously[22]. Lipid peroxidation was expressed in pmoles malondialdehyde (MDA)/mg total protein.

Statistical analysis

The results are expressed as mean (SD). Comparisons among multiple groups were performed using the one-way ANOVA, followed by Bonferroni's *post hoc* test, when variances across groups were equal or by Dunnett's T3 *post hoc* test, when variances were not equal. Variance equality was tested by Levene statistical analysis. Differences were considered significant, when $P<0.05$.

RESULTS

Portal and aortic endotoxin concentrations

Hepatectomized animals (group III) presented significantly elevated endotoxin concentrations in portal and aortic blood compared with groups I and II ($P<0.001$, respectively). Treatment with BBS or NT led to significantly lower endotoxin values both in portal vein ($P<0.001$ *vs* group III, respectively) and aorta ($P<0.001$ and $P<0.01$ *vs* group III, respectively) (Figure 1).

Mucosal DNA and protein

DNA content of the intestinal mucosa was significantly decreased in partially hepatectomized rats as compared to controls ($P<0.01$) and increased in BBS and NT treated rats ($P<0.05$ and $P<0.01$ *vs* group III, respectively)

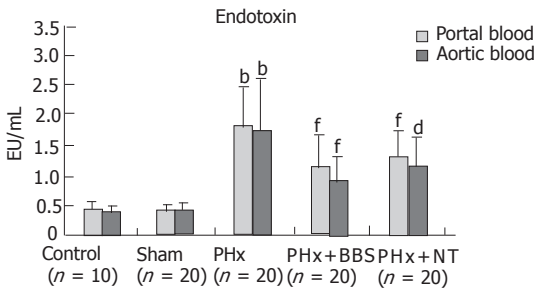

Figure 1 Portal and aortic endotoxin concentrations. Values are mean±SD. [b]$P<0.001$ *vs* sham, [d]$P<0.01$ and [f]$P<0.001$ *vs* PHx. PHx, partial hepatectomy; BBS, bombesin; NT, neurotensin.

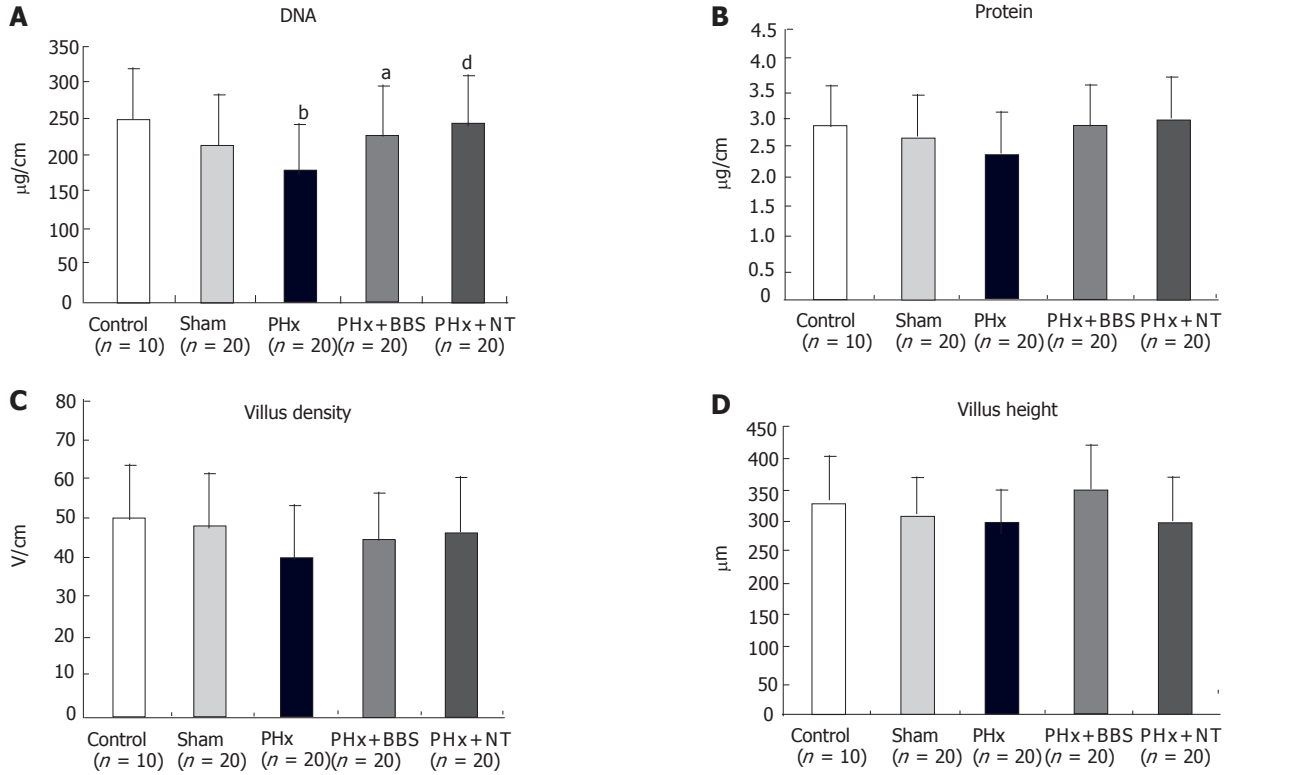

Figure 2 Indices of ileal mucosa trophic state. Values are mean±SD. [b]*P*<0.01 *vs* control, [a]*P*<0.05 and [d]*P*<0.01 *vs* PHx. PHx, partial hepatectomy; BBS, bombesin; NT, neurotensin(**A-D**).

(Figure 2A). Protein content was also decreased in hepatectomized rats and increased to normal levels after peptides administration, but these differences did not reach statistical significant levels (Figure 2B).

Intestinal morphology

Overall, the ileal architecture remained intact and epithelial continuity was retained, in all specimens studied. The ileal biopsies from group III demonstrated a reduction in the number of villi per centimeter (Figure 2C) and in villus height (Figure 2D), which were increased towards control values in rats treated with BBS or NT; however, the differences among groups were not significant. Intestinal crypt mitotic activity was reduced in hepatectomized rats, though not to significant levels, and increased above normal levels after BBS or NT administration (Figure 3A). Crypt epithelial apoptosis was present in all intestinal samples evaluated. The ABC in ileal specimens from control group was significantly lower compared with group III ($P<0.001$) (Figure 3B). After BBS or NT administration the ABC was significantly reduced ($P<0.05$ and $P<0.01$, compared to PHx, respectively).

Cecal bacterial population

Table 1 provides the quantitative culture results of the cecal contents for aerobic and anaerobic bacteria. In partially hepatectomized rats (group III) there was a significant increase in Gram (+) cocci and *E coli* cecal count as compared with group I ($P<0.05$, respectively). Neurotensin presented a trend towards reduction of aerobic and anaerobic bacterial populations, which reached significant levels for Gram (+) anaerobic bacteria ($P<0.001$ *vs* group III).

Table 1 Bacterial cecal population (CFU×10^5/mL)

Groups	*n*	Aerobic bacteria		Anaerobic bacteria	
		Gram (+) cocci	*E coli*	Gram (+)	Gram (–)
Control	10	6.70 (1.62)	1.04 (0.88)	9 (2.74)	4.64 (1.99)
Sham	20	9.45 (4.92)	1.60 (2.07)	13.34 (5.62)	6.5 (4.35)
PHx	20	11.09 (5.71)[a]	6.43 (6.38)[a]	13.17 (3.88)	5.48 (4.57)
PHx+BBS	20	11.70 (6.41)	6.31 (6.20)	10 (4.29)	4.45 (2.86)
PHx+NT	20	6.76 (4.31)	2.77 (3.92)	6.76 (5.64)[b]	3.08 (4.48)

Data expressed as mean (SD). [a]*P*<0.05 *vs* control, [b]*P*<0.001 *vs* PHx. PHx, partial hepatectomy; BBS, bombesin; NT, neurotensin.

Intestinal lipid peroxidation

Liver resection resulted in decreased intestinal lipid peroxidation ($P<0.001$ *vs* group II), while administration of BBS or NT led to further significant decrease of this index of oxidative stress ($P<0.01$ and $P<0.001$ *vs* group III, respectively, Figure 4).

DISCUSSION

An intact intestinal barrier function effectively separates potentially harmful intraluminal elements such as bacteria and endotoxins from extraintestinal tissues and the systemic circulation. Major liver resection has been shown to compromise the anatomic and functional integrity of the gut barrier resulting in the translocation of indigenous bacteria and endotoxins to remote organs and

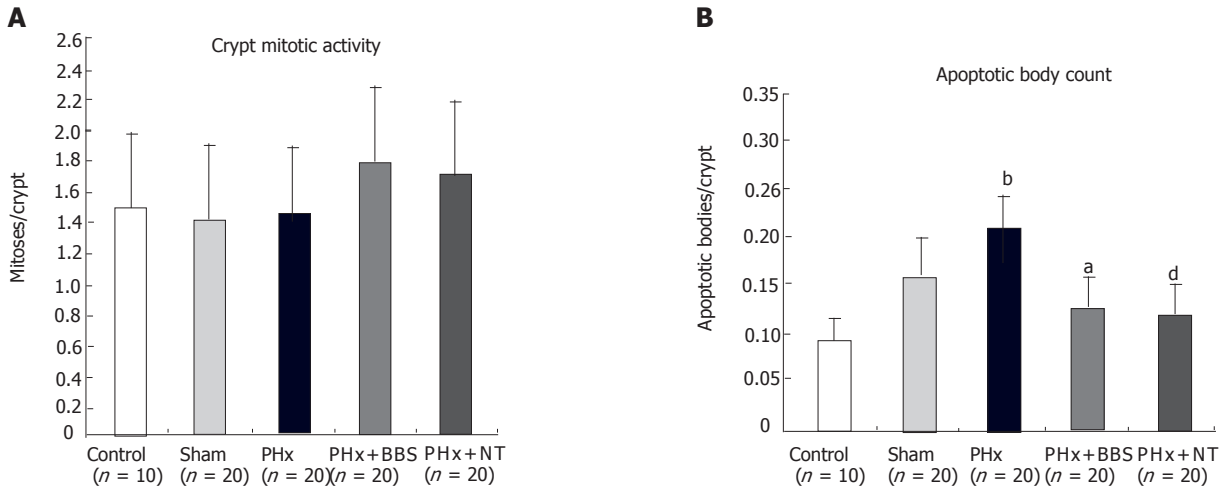

Figure 3 Crypt epithelial cell proliferation and apoptosis. Values are mean±SD. $^{b}P<0.001$ *vs* control, $^{a}P<0.05$ and $^{d}P<0.01$ *vs* PHx. PHx, partial hepatectomy; BBS, bombesin; NT, neurotensin(**A**, **B**).

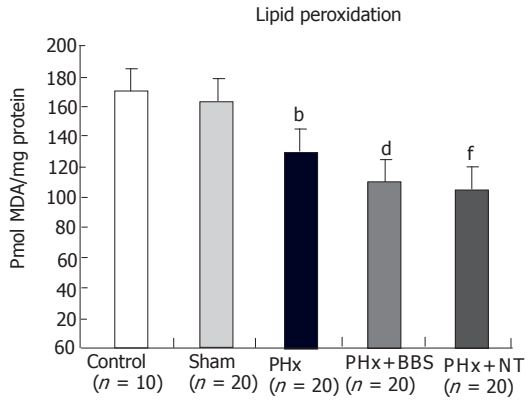

Figure 4 Lipid peroxidation in the intestine. Values are mean±SD. $^{b}P<0.001$ *vs* sham, $^{d}P<0.01$ and $^{f}P<0.001$ *vs* PHx. PHx, partial hepatectomy; BBS, bombesin; NT, neurotensin.

tissues[3,23]. Systemic endotoxemia plays a pivotal role in the development of septic complications and dysfunction of remote organs after liver resections through activation of a systemic inflammatory response, which is associated with structural and functional deleterious effects on vital organs[24]. Failure of the gut barrier leads to bacterial and endotoxin translocation and the pathogenesis of the so-called "gut-derived sepsis"[25]. However, the mechanisms implicated in intestinal barrier failure after liver resection have not been fully elucidated.

Physical injury to the intestinal mucosa is one of the mechanisms postulated to promote bacterial translocation. In our study, the ileal architecture remained intact and epithelial continuity was retained in hepatectomized rats. Previous experimental studies have shown that 70% hepatectomy induces trophic changes on the distal ileum after 30 d, causing atrophy of the ileum wall and a drop in villus thickness[26]. The present study shows that 48 h after partial liver resection there is a trend for decreased villous density and mucosal thickness that does not reach statistical significant levels. Diminished bile production and secretion to the duodenum, after partial hepatectomy, deprives partly the gut from its trophic action thus promoting mucosal atrophy. On the other hand, the plethora of enterotrophic growth factors and cytokines that are elaborated after liver resection exert the opposite effect[27]. The combinatory action of these factors seems to produce a balanced adaptive intestinal response, 48 h after partial hepatectomy.

The balance between cell proliferation and death in intestinal crypts is crucial for epithelial homeostasis because the total of epithelial cells lining villi originate from stem cells located in the proliferation zone of the crypt. Apoptosis was the only histologic parameter that altered significantly in the present study. Definite evidence of apoptosis is seen in the crypt, where apoptotic cells are seen once in every 5^{th}-10^{th} crypt section[28]. Occasional apoptotic bodies found in the rapidly proliferating epithelial cells of the normal gastrointestinal mucosa, help to maintain a steady-state in cellular populations[29]. Control animals presented this basal level of apoptotic activity known as spontaneous apoptosis, which serves to remove either occasionally overproduced stem cells or stem cells with minor DNA damage caused by external factors. Two-thirds hepatectomy resulted in a significant increase of apoptosis in the crypt, which may explain the trend for induction of mucosal atrophy without alterations in the mitotic activity of the intestinal epithelium. In addition, increase of the apoptotic process in the intestinal epithelium may partly contribute to the decrease of mucosal DNA content. Apoptotic cells have a lower DNA content than the G0/G1 value and this hypo-diploid DNA is a hallmark to show apoptosis[30].

Apoptosis is a morphologically distinct, gene-directed, form of cell death that contributes to both physiological and pathological processes[31]. Although in gastrointestinal epithelium it has been associated with several conditions[17,21,32], the biological significance of intestinal apoptosis after liver resection is not clear till

date. The responsible mechanism could reflect primary immunologic events following hepatectomy (apoptosis has been shown to be induced by a variety of triggers, including proinflammatory cytokines such as TNF, IL-1, and IL-6, or by cytotoxic T lymphocytes that act through either granzyme B or Fas receptor pathways) or a direct action of bacterial toxins[31,33,34].

Another factor associated with bacterial translocation is intestinal flora disturbances. In our study hepatectomized rats presented a significant increase of cecal aerobic bacteria [*E coli* and Gram (+) cocci]. Diminished bile production and disturbances of interdigestive motility may have led to bacterial overgrowth. Bile salts have a constraining role on the indigenous microflora, while secretory *IgA* contained in bile modulates the local immunological milieu[35]. In addition, delayed intestinal transit time in experimental liver resection seem to be implicated in intestinal bacterial overgrowth and increased bacterial translocation[36]. A correlation between cecal overgrowth of a specific organism and bacterial translocation of the same organism is well documented[37]. Overgrowth of *E coli* detected in our study and diminished biliary *IgA* may lead to increased attachment of this bacterial strain to the intestinal mucosa, predisposing to bacterial translocation and previous studies have shown that *E coli* is usually cultured from the mesenteric lymph nodes of hepatectomized rats[2].

Another parameter we have addressed in our study is intestinal oxidative stress estimated by quantification of lipid peroxidation, which is a common indicator of oxidative stress. Our data show that 48 h after partial hepatectomy decreased levels of lipid peroxidation were measured in the intestine. This may be attributed to liver regeneration and release of several growth factors and hormones that may influence intestinal oxidative stress[27]. In addition, previous studies demonstrate evidence for activation of the intestinal cytosolic antioxidant enzyme glutathione *S*-transferase after hepatectomy[38]. Another explanation might be that the removal of a large portion of the liver could result in a decrease of oxidants originating from the liver, therefore lowering lipid peroxidation. The liver and gut are considered as an anatomic and functional unit with inseparable and interdependent functions and from this point of view liver regeneration under low oxidative stress[39] may be associated with similar oxidant alterations in the intestine. A question that rose is if low oxidative stress is compatible with increased apoptosis. Whether a cell will enter or not the apoptotic process is determined by a variety of stimuli and intrinsic pathways and it seems that apoptosis of enterocytes after partial hepatectomy is not mediated by oxidative stress.

The present study has further investigated the role of gut regulatory peptides BBS and NT on gut barrier function in experimental partial hepatectomy. To the best of our knowledge, our results demonstrate for the first time that administration of BBS or NT improves gut barrier function after partial hepatectomy, leading to significantly lower portal and aortic endotoxin concentrations. Treatment with these factors reversed the decrease of intestinal morphometric characteristics and preserved mucosal DNA and protein content to control levels. Although these alterations were statistically significant only for DNA, they show a trend for induction of a trophic effect on the intestinal mucosa. This effect was accompanied by the increase of cell proliferation beyond control levels and inhibition of programmed cell death in intestinal crypts. The mitogenic effect of BBS and NT may be a direct receptor-mediated effect, since intestinal epithelial cells express receptors for both peptides[40-42] and it is known that BBS and NT are potent cellular growth factors whose binding to their receptors activates a mitogenic signal to the nucleus[43]. An indirect mechanism may be related to a further reduction of intestinal lipid peroxidation since oxidative state is involved in the modulation of cell proliferation and death[44]. The antiapoptotic effect of BBS and NT may be mediated by the reduction of endotoxemia and amelioration of the subsequent systemic inflammatory response, characterized by the release of numerous cytokines and proinflammatory mediators, such as tumor necrosis factor-alpha, which may activate the apoptotic process. Another explanation of their antiapoptotic action may be provided through induction of vasodilation[45,46], which improves intestinal microcirculation thus preventing enterocytes hypoxia, energy depletion and activation of apoptotic pathways.

Apart from their antiapoptotic action on the intestinal epithelium, BBS and NT exerted an antioxidant effect as well, further decreasing intestinal lipid peroxidation. The compromise of the intestinal barrier function, after partial hepatectomy, shows that intestinal compensatory response, which may be partly expressed by low oxidative stress, is relatively insufficient to overwhelm the noxious effect of hepatectomy on the intestinal epithelium. From this point of view, the additional decrease of intestinal oxidative stress achieved by peptides treatment may contribute to the enhancement of intestinal barrier. The results of this study are consistent with our previous work demonstrating the antioxidant effect of BBS and NT on the intestinal epithelium of bile duct ligated rats[17]. Possible explanations of their antioxidant action is the reduction of systemic endotoxemia, which is associated with generation of oxygen free radicals via a xanthine oxidase depended pathway, improvement of oxygen supply to enterocytes through vasodilation, or receptor-mediated activation of intracellular antioxidant pathways. It has been shown that binding of regulatory peptides to their specific G-protein coupled receptors is followed by a pivotal activation of protein kinase C[43]. Increased cellular PKC activity promotes the mitochondrial translocation and organization in a catalytically active form of a representative isoform of glutathione *S*-transferases, which are an important antioxidant enzyme system[47].

In conclusion, the present study shows that the gut regulatory peptides BBS and NT improve the intestinal barrier function and reduce endotoxemia, in experimental partial hepatectomy. This effect is, at least in part, mediated by their antiapoptotic, mitogenic and antioxidant effect on the intestinal epithelium. Although laboratory results

should not be easily extrapolated to the clinical situation, we feel that BBS and NT merit consideration, as potential therapeutic agents, for the improvement of gut barrier function in cases of liver resection.

ACKNOWLEDGMENT

The authors wish to express their thanks to Dr I Spiliopoulou, Department of Microbiology of Patras University Medical School, for her excellent work in microbiological analyses.

REFERENCES

1 **Jarnagin WR**, Gonen M, Fong Y, DeMatteo RP, Ben-Porat L, Little S, Corvera C, Weber S, Blumgart LH. Improvement in perioperative outcome after hepatic resection: analysis of 1,803 consecutive cases over the past decade. *Ann Surg* 2002; **236:** 397-406; discussion 406-407
2 **Wang X**, Andersson R, Soltesz V, Bengmark S. Bacterial translocation after major hepatectomy in patients and rats. *Arch Surg* 1992; **127:** 1101-1106
3 **Wang XD**, Parsson H, Andersson R, Soltesz V, Johansson K, Bengmark S. Bacterial translocation, intestinal ultrastructure and cell membrane permeability early after major liver resection in the rat. *Br J Surg* 1994; **81:** 579-584
4 **Anastasi A**, Erspamer V, Bucci M. Isolation and structure of bombesin and alytesin, 2 analogous active peptides from the skin of the European amphibians Bombina and Alytes. *Experientia* 1971; **27:** 166-167
5 **Chu KU**, Evers BM, Ishizuka J, Townsend CM Jr, Thompson JC. Role of bombesin on gut mucosal growth. *Ann Surg* 1995; **222:** 94-100
6 **Chu KU**, Higashide S, Evers BM, Ishizuka J, Townsend CM, Jr., Thompson JC. Bombesin stimulates mucosal growth in jejunal and ileal Thiry-Vella fistulas. *Ann Surg* 1995; **221:** 602-609; discussion 609-611
7 **Evers BM**, Izukura M, Townsend CM, Jr., Uchida T, Thompson JC. Differential effects of gut hormones on pancreatic and intestinal growth during administration of an elemental diet. *Ann Surg* 1990; **211:** 630-636; discussion 636-638
8 **Gulluoglu BM**, Kurtel H, Gulluoglu MG, Aktan AO, Yegen BC, Dizdaroglu F, Yalin R, Yegen BC. Bombesin ameliorates colonic damage in experimental colitis. *Dig Dis Sci* 1999; **44:** 1531-1538
9 **Alican I**, Unluer EE, Yegen C, Yegen BC. Bombesin improves burn-induced intestinal injury in the rat. *Peptides* 2000; **21:** 1265-1269
10 **Polak JM**, Sullivan SN, Bloom SR, Buchan AM, Facer P, Brown MR, Pearse AG. Specific localisation of neurotensin to the N cell in human intestine by radioimmunoassay and immunocytochemistry. *Nature* 1977; **270:** 183-184
11 **Chung DH**, Evers BM, Shimoda I, Townsend CM Jr, Rajaraman S, Thompson JC. Effect of neurotensin on gut mucosal growth in rats with jejunal and ileal Thiry-Vella fistulas. *Gastroenterology* 1992; **103:** 1254-1259
12 **Wood JG**, Hoang HD, Bussjaeger LJ, Solomon TE. Neurotensin stimulates growth of small intestine in rats. *Am J Physiol* 1988; **255:** G813-G817
13 **Evers BM**, Izukura M, Chung DH, Parekh D, Yoshinaga K, Greeley GH Jr, Uchida T, Townsend CM Jr, Thompson JC. Neurotensin stimulates growth of colonic mucosa in young and aged rats. *Gastroenterology* 1992; **103:** 86-91
14 **Feurle GE**, Muller B, Rix E. Neurotensin induces hyperplasia of the pancreas and growth of the gastric antrum in rats. *Gut* 1987; **28 Suppl:** 19-23
15 **Vagianos C**, Karatzas T, Scopa CD, Panagopoulos C, Tsoni I, Spiliopoulou I, Kalfarentzos F. Neurotensin reduces microbial translocation and improves intestinal mucosa integrity after abdominal radiation. *Eur Surg Res* 1992; **24:** 77-83
16 **Olsen PS**, Pedersen JH, Poulsen SS, Yamashita Y, Kirkegaard P. Neurotensin-like immunoreactivity after intestinal resection in the rat. *Gut* 1987; **28:** 1107-1111
17 **Assimakopoulos SF**, Scopa CD, Zervoudakis G, Mylonas PG, Georgiou C, Nikolopoulou V, Vagianos CE. Bombesin and neurotensin reduce endotoxemia, intestinal oxidative stress, and apoptosis in experimental obstructive jaundice. *Ann Surg* 2005; **241:** 159-167
18 **Higgins G**, Andersson RM. Experimental pathology of the liver. I. Restoration of the liver of the white rat following partial surgical removal. *Arch Pathol* 1931; **12:** 186-202
19 **LOWRY OH**, ROSEBROUGH NJ, FARR AL, RANDALL RJ. Protein measurement with the Folin phenol reagent. *J Biol Chem* 1951; **193:** 265-275
20 **Giles K**, Myers M. Improved diphenylamine method for estimation of DNA. *Nature* 1965; **206:** 93-95
21 **Lee RG**, Nakamura K, Tsamandas AC, Abu-Elmagd K, Furukawa H, Hutson WR, Reyes J, Tabasco-Minguillan JS, Todo S, Demetris AJ. Pathology of human intestinal transplantation. *Gastroenterology* 1996; **110:** 1820-1834
22 **Georgiou CD**, Zervoudakis G, Tairis N, Kornaros M. beta-Carotene production and its role in sclerotial differentiation of Sclerotium rolfsii. *Fungal Genet Biol* 2001; **34:** 11-20
23 **Kakkos SK**, Kirkilesis J, Scopa CD, Arvaniti A, Alexandrides T, Vagianos CE. Nonabsorbable antibiotics reduce bacterial and endotoxin translocation in hepatectomised rats. *HPB Surg* 1997; **10:** 283-289; discussion 289-291
24 **Boermeester MA**, Houdijk AP, Meyer S, Cuesta MA, Appelmelk BJ, Wesdorp RI, Hack CE, Van Leeuwen PA. Liver failure induces a systemic inflammatory response. Prevention by recombinant N-terminal bactericidal/permeability-increasing protein. *Am J Pathol* 1995; **147:** 1428-1440
25 **Deitch EA**. The role of intestinal barrier failure and bacterial translocation in the development of systemic infection and multiple organ failure. *Arch Surg* 1990; **125:** 403-404
26 **Rodriguez Sanz MB**, Alarcon Garcia J, del Riego Tomas FJ, Vaquero Puerta C. Effects of partial hepatectomy on the distal ileum in rats. *Rev Esp Enferm Dig* 2004; **96:** 185-190
27 **Michalopoulos GK**, DeFrances MC. Liver regeneration. *Science* 1997; **276:** 60-66
28 **Pritchard DM**, Watson AJ. Apoptosis and gastrointestinal pharmacology. *Pharmacol Ther* 1996; **72:** 149-169
29 **Lee FD**. Importance of apoptosis in the histopathology of drug related lesions in the large intestine. *J Clin Pathol* 1993; **46:** 118-122
30 **Suen YK**, Fung KP, Choy YM, Lee CY, Chan CW, Kong SK. Concanavalin A induced apoptosis in murine macrophage PU5-1.8 cells through clustering of mitochondria and release of cytochrome c. *Apoptosis* 2000; **5:** 369-377
31 **Cummings MC**, Winterford CM, Walker NI. Apoptosis. *Am J Surg Pathol* 1997; **21:** 88-101
32 **Potten CS**, Merritt A, Hickman J, Hall P, Faranda A. Characterization of radiation-induced apoptosis in the small intestine and its biological implications. *Int J Radiat Biol* 1994; **65:** 71-78
33 **Bemelmans MH**, Gouma DJ, Greve JW, Buurman WA. Cytokines tumor necrosis factor and interleukin-6 in experimental biliary obstruction in mice. *Hepatology* 1992; **15:** 1132-1136
34 **Thompson CB**, Apoptosis in the pathogenesis and treatment of disease. *Science* 1995; **267:** 1456-1462
35 **Deitch EA**, Sittig K, Li M, Berg R, Specian RD. Obstructive jaundice promotes bacterial translocation from the gut. *Am J Surg* 1990; **159:** 79-84
36 **Wang XD**, Soltesz V, Andersson R. Cisapride prevents enteric bacterial overgrowth and translocation by improvement of intestinal motility in rats with acute liver failure. *Eur Surg Res* 1996; **28:** 402-412
37 **Guarner C**, Runyon BA, Young S, Heck M, Sheikh MY. Intestinal bacterial overgrowth and bacterial translocation in cirrhotic rats with ascites. *J Hepatol* 1997; **26:** 1372-1378
38 **Carnovale CE**, Monti JA, Favre C, Scapini C, Carrillo MC. Is

intestinal cytosolic glutathione S-transferase an alternative detoxification pathway in two-thirds hepatectomized rats? *Life Sci* 1995; **57:** 903-910

39 **Alexandris IH**, Assimakopoulos SF, Vagianos CE, Patsoukis N, Georgiou C, Nikolopoulou V, Scopa CD. Oxidative state in intestine and liver after partial hepatectomy in rats. Effect of bombesin and neurotensin. *Clin Biochem* 2004; **37:** 350-356

40 **Chang EB**, Brown DR, Wang NS, Field M. Secretagogue-induced changes in membrane calcium permeability in chicken and chinchilla ileal mucosa. Selective inhibition by loperamide. *J Clin Invest* 1986; **78:** 281-287

41 **Seybold VS**, Treder BG, Aanonsen LM, Parsons A, Brown DR. Neurotensin binding sites in porcine jejunum: biochemical characterization and intramural localization. *Synapse* 1990; **6:** 81-90

42 **Seybold VS**, Parsons AM, Aanonsen LM, Brown DR. Characterization and autoradiographic localization of gastrin releasing peptide receptors in the porcine gut. *Peptides* 1990; **11:** 779-787

43 **Rozengurt E**, Signal transduction pathways in the mitogenic response to G protein-coupled neuropeptide receptor agonists. *J Cell Physiol* 1998; **177:** 507-517

44 **Schafer FQ**, Buettner GR. Redox environment of the cell as viewed through the redox state of the glutathione disulfide/glutathione couple. *Free Radic Biol Med* 2001; **30:** 1191-1212

45 **Heuser M**, Pfaar O, Gralla O, Grone HJ, Nustede R, Post S. Impact of gastrin-releasing peptide on intestinal microcirculation after ischemia-reperfusion in rats. *Digestion* 2000; **61:** 172-180

46 **Harper SL**, Barrowman JA, Kvietys PR, Granger DN. Effect of neurotensin on intestinal capillary permeability and blood flow. *Am J Physiol* 1984; **247:** G161-G166

47 **Robin MA**, Prabu SK, Raza H, Anandatheerthavarada HK, Avadhani NG. Phosphorylation enhances mitochondrial targeting of GSTA4-4 through increased affinity for binding to cytoplasmic Hsp70. *J Biol Chem* 2003; **278:** 18960-18970

Science Editor Guo SY **Language Editor** Elsevier HK

PO Box 2345, Beijing 100023, China
www.wjgnet.com
wjg@wjgnet.com

ELSEVIER

World J Gastroenterol 2005;11(43):6765-6769
World Journal of Gastroenterology ISSN 1007-9327

• *BASIC RESEARCH* •

Expression of Ki-67, p53, and K-*ras* in chronic pancreatitis and pancreatic ductal adenocarcinoma

Seok Jeong, Don Haeng Lee, Jung Il Lee, Jin-Woo Lee, Kye Sook Kwon, Pum-Soo Kim, Hyung Gil Kim, Yong Woon Shin, Young Soo Kim, Young Bae Kim

Seok Jeong, Don Haeng Lee, Jung Il Lee, Jin-Woo Lee, Kye Sook Kwon, Pum-Soo Kim, Hyung Gil Kim, Yong Woon Shin, Young Soo Kim, Division of Gastroenterology, Department of Internal Medicine, Inha University College of Medicine, Incheon, Korea
Young Bae Kim, Department of Pathology, Ajou University College of Medicine, Suwon, Korea
Supported by the Inha University Research Grant 2005
Correspondence to: Professor Don Haeng Lee, Division of Gastroenterology, Department of Internal Medicine, Inha University Hospital, 7-206, 3-Ga, Sinheung-Dong, Jung-Gu, Incheon 400-711, South Korea. ldh@inha.ac.kr
Telephone: +82-32-8902548 Fax: +82-32-8902549
Received: 2005-03-18 Accepted: 2005-05-24

Abstract

AIM: To examine surgical specimens of pancreas with either chronic pancreatitis or pancreatic cancer in order to study whether ductal hyperplasia and dysplasia in pancreas represent precursor lesions for pancreatic cancer.

METHODS: We examined expression of Ki-67, CEA, p53, and K-*ras*, in the surgical specimens of pancreas with adenocarcinomas (n = 11) and chronic pancreatitis (n = 12). Cellular proliferation was assessed by Ki-67 proliferation index using the proliferation marker Ki-67. In specimens with pancreas cancer, we divided pancreas epithelium into normal (n = 7), ductal hyperplasia (n = 3), dysplasia (n = 4), and cancerous lesion (n = 11) after hematoxylin and eosin staining, Ki-67, and CEA immunohistochemical staining. In cases with chronic pancreatitis, the specimen was pathologically examined as in cases with pancreas cancer, and they were also determined as normal (n = 10), ductal hyperplasia (n = 4), or dysplasia (n = 5). p53 and K-*ras* expression were also studied by immunohistochemical staining.

RESULTS: In pancreatic cancer, the Ki-67 index was 3.73±3.58 in normal site, 6.62±4.39 in ductal hyperplasia, 13.47±4.02 in dysplasia and 37.03±10.05 in cancer tissue, respectively. Overall, p53 was positive in normal ducts, ductal hyperplasia, dysplasia, and carcinoma cells in 0 of 14 (0%), 0 of 7 (0%), 7 of 9 (78%), and 10 of 11 (91%), respectively, and K-*ras* was positive in 0 of 8 (0%), 1 of 3 (33%), 4 of 6 (67%), 4 of 5 (80%), respectively.

CONCLUSION: Our results favorably support the hypothesis that ductal hyperplasia and dysplasia of the pancreas might be precursor lesions for pancreas cancer. Further evaluation of oncogenes by the molecular study is needed.

Key words: Ki-67; p53; K-*ras*; Chronic pancreatitis; Pancreatic ductal adenocarcinoma

Jeong S, Lee DH, Lee JI, Lee JW, Kwon KS, Kim PS,Kim HG, Shin YW, Kim YS, Kim YB. Expression of Ki-67, p53, and K-*ras* in chronic pancreatitis and pancreatic ductal adenocarcinoma *World J Gastroenterol;* 2005; 11(43): 6765-6769
http://www.wjgnet.com/1007-9327/11/6765.asp

INTRODUCTION

The pancreatic cancer has the poorest prognosis among various cancers with a 5-year survival rate of 3%, making it the fourth most common cause of cancer-related mortality rate[1-3]. Although the surgical resection offers the only chance for cure, only 10-30% of patients have resectable tumor[4]. Since early diagnosis followed by complete resection is the only way to the complete recovery, understanding the pathogenesis of pancreatic cancer seems to be of great value.

The ductal hyperplasia of pancreas is defined by abnormally increased number of epithelial cells of pancreatic duct. It may be detected in both normal and chronically inflamed pancreatic tissues, and its incidence is generally increased with age[5]. However, the patients with chronic pancreatitis and ductal hyperplasia have been reported to be associated with the development of pancreas cancer[5-8]. In addition, there has been an investigation suggesting three times higher incidence of papillary hyperplasia of pancreatic duct epithelium in patients with pancreatic cancer compared with the control group[6]. There is also a report that 41% of patients with pancreatic cancer showed hyperplasia of pancreatic duct epithelium when 9% of the control group have that pathological finding[7].

In an effort to search for the pathogenesis of pancreatic cancer, mutations of K-*ras*, p53, and overexpression of HER-2/neu were found in human pancreatic ductal adenocarcinoma[9].

Currently, the hypothesis of multistep carcinogenesis

that states cumulative genetic mutations in the normal pancreas might have progressed into pancreatic cancer is mostly accepted. However, detailed explanation for each step of carcinogenesis needs further investigation. In the current study, we performed histological examination of pancreas and detected normal epithelium and that with ductal hyperplasia, dysplasia, or cancerous lesions. Then we immunohistochemically determined the expression of Ki-67, K-*ras*, and p53 to identify if ductal hyperplasia and dysplasia of pancreas might be precancerous lesion.

MATERIALS AND METHODS

Subjects

The study was performed in 11 patients with pancreatic ductal adenocarcinoma and 12 patients with chronic pancreatitis, the total 23 patients went through surgical pancreatic resection at Inha University Hospital. The mean age of patients was 67 years (range 40-74 years) for pancreatic cancer and 61 years (range 37-67 years) for chronic pancreatitis. Male to female ratio was 6:5 for pancreatic cancer and 10:2 for chronic pancreatitis.

Histologic classification

The degree of pancreatic ductal lesion was classified morphologically according to Cubilla and Fitzgerald[6], and the pancreatic carcinoma according to Kloppel[10]. Most pancreatic duct epitheliums are composed of cuboidal and low columnar cells, their cytoplasm filled with mucous components. They are surrounded by loose fibrous connective tissue. Hyperplasia of pancreatic duct epithelium is divided into either flat or papillary type. However, recent studies show that there is no difference in genetic mutations between these two forms of hyperplasia[9]. Therefore, we considered these two different forms of hyperplasia in the same tissue in this study. Dysplasia was classified according to flattening, papillary hyperplasia of ductal epithelium, increased nucleus/cytoplasm ratio as the epithelium changes into atypical form, loss of nuclear polarity, morphologic form, and aggregation. A little evidence of cellular division was also considered as dysplasia. The degree of hyperplasia was evaluated objectively by counting the numbers of hyperplasia using the method of Ki-67 (Immunotec, France) immunohistochemical staining. To see whether dysplasia develops or not, we performed CEA immunohistochemical staining in the area of hyperplasia stained with Ki-67 using double staining method and classified them into different categories, so that we can minimize the errors arising from differential classification of pancreatic tissue.

Immunohistochemical staining

After 10% of surgically resected pancreatic tissue was fixed in neutral formalin, paraffin-embedded tissue was sliced to the thickness of 4 μm continuously. One slice was stained with hematoxylin-eosin (H&E), and the others were stuck to the slide with poly-L-lysine for immunohistochemical staining. After all the slices went through autoclave (120 °C, 15 lb) for 15 min to expose the antigens fixed by formalin, we treated with H_2O_2 for 30 min to eliminate intrinsic peroxidase. For immunohistochemical staining, CEA monoclonal antibody (Ab) (DAKO, Carpenteria, CA, USA) and Ki-67 monoclonal Ab (Immunotech, Marseille, Cedex, France) were diluted to 1:150 and 1:100, respectively, then incubated at room temperature for 3 h. Labeled streptavidin biotin kit (LSAB kit, DAKO) and 3',3-diaminobenzidine (DAB) were used for staining. Also p53 monoclonal Ab (Novocastra, Newcastle, UK) was diluted to 1:150 and incubated at 4 °C for one day. Then alkaline phosphatase, anti-alkaline phosphatase kit (APAAP kit, DAKO) was used for staining and fast red (DAKO) for expression. For K-*ras* staining, $p21^{ras}$ monoclonal Ab (Oncogene Research Products, Calbiochem, Germany) was diluted to 1:50. The serially sliced tissues were examined morphologically at the same area using H&E staining for histologic diagnosis, and then were compared with the results of immunohistochemical staining in response to CEA, p53, K-*ras*, and Ki-67. The following Ki-67 proliferation index was expressed as the percent of Ki-67-positive cells of 1 000 pancreatic duct epithelial cells. The double staining was performed using Ki-67 and CEA monoclonal Ab to ascertain the presence of dysplasia. Dysplasia was classified using CEA+p53 and CEA+Ki-67 staining.

RESULTS

Histology

Hematoxylin and eosin staining Normal pancreatic duct epithelium is composed of mainly cuboidal and low columnar cells and surrounded by fibrous connective tissues (Figure 1A). We detected basally located nuclei, aggregation and intraductal papillary proliferation of pancreatic duct epithelial cells in ductal hyperplasia (Figure 1C). Dysplasia of the pancreatic duct showed an

Table 1 Summary of immunohistochemical staining in each group of patients

	Case of study *n* (%)	Ki-67 index	*p*53 *n* (%)	K-*ras* *n* (%)
Overall				
Normal	17/23 (74)	2.35±2.79	0/14 (0)	0/8 (0)
Hyperplasia	7/16 (44)	9.07±5.39	0/7 (0)	1/3 (33)
Dysplasia	9/16 (56)	10.79±5.51	7/9 (78)	4/6 (67)
Carcinoma	11/23 (48)	37.03±10.05	10/11 (91)	4/5 (80)
Pancreatic cancer				
Normal	7/11 (64)	3.73±3.58	0/6 (0)	0/5 (0)
Hyperplasia	3/7 (43)	6.62±4.39	0/3 (0)	1/3 (33)
Dysplasia	4/7 (57)	13.47±4.02	4/4 (100)	2/3 (67)
Carcinoma	11/11 (100)	37.03±10.05	10/11 (91)	4/5 (80)
Chronic pancreatitis				
Normal	10/13 (77)	2.35±2.79	0/8 (0)	0/3 (0)
Hyperplasia[1]	4/9 (44)	7.66±5.58	0/4 (0)	
Dysplasia	5/9 (56)	8.64±5.51	3/5 (60)	2/3 (67)

[1]Fails to stain.

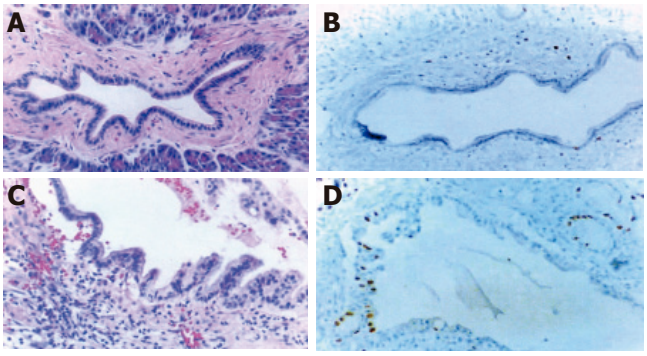

Figure 1 H&E and immunohistochemical staining of normal pancreatic and ductal hyperplasia tissues. **A:** Normal interlobular duct surrounded by fibrous tissue is illustrated. Small cuboidal cells with basally located nuclei having intact nuclear polarity are seen in the inset. H&E stain, ×100; **B:** Ki-67 monoclonal Ab does not show reaction to almost epithelial cells. DAB and hematoxylin counter stain, ×100; **C:** Pancreatic duct hyperplasia with uniformly large columnar epithelial cells, which are more than twice as long as cytoplasm of normal cells and have mucinous metaplasia of the cytoplasm. The nuclei are small and basally located without atypia. H&E stain, ×100; **D:** Ki-67 monoclonal Ab shows a few proliferating nuclei of hyperplastic ductal epithelium. DAB and hematoxylin counter stain, ×100.

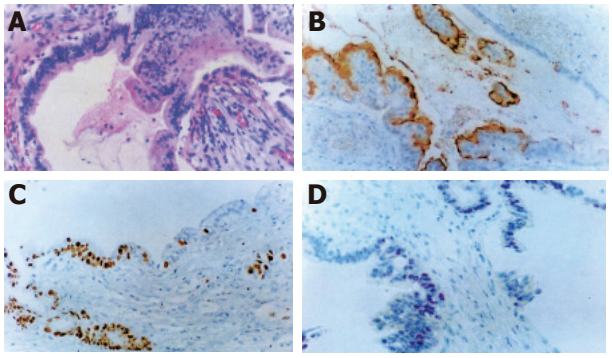

Figure 2 H&E and immunohistochemical staining of dysplastic tissues of the pancreatic duct. **A:** The nuclear enlargement, increased nuclear-to-cytoplasmic ratio, loss of nuclear polarity, pleomorphism, and nuclear overcrowding are seen. Several mitotic figures including atypical form are present. H&E stain, ×100; **B:** CEA monoclonal antibody shows positive reaction in the cytoplasmic membranes of dysplastic cells. DAB and hematoxylin counter stain, ×100; **C:** Ki-67 monoclonal antibody shows focally increased proliferating nuclei of dysplastic cells. DAB and hematoxylin counter stain, ×100; **D:** p53 monoclonal antibody shows focally positive reaction in the nuclei of dysplastic cells. AEC and hematoxylin counter stain, × 100.

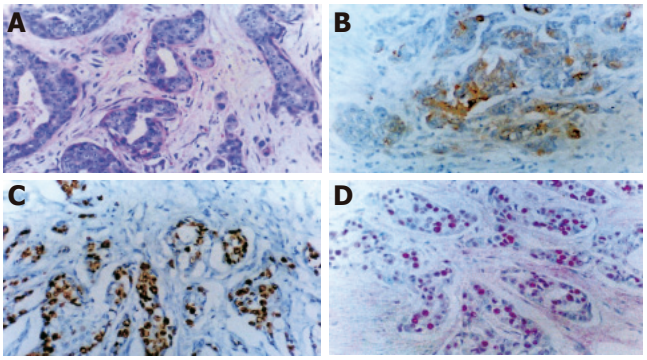

Figure 3 H&E and immunohistochemical staining of pancreatic cancer. **A**: Moderate to poorly differentiated pancreatic adenocarcinoma with desmoplastic background. H&E stain, ×200; **B**: Immunohistochemical staining using CEA monoclonal antibody shows positive reaction in the cytoplasms of tumor cells. DAB and hematoxylin counter stain, ×200; **C**: Ki-67 monoclonal antibody shows significantly increased proliferation of nuclei of tumor cells. DAB and hematoxylin counter stain, ×200; **D**: Intense nuclear immunohistochemical staining of p53 in an invasive pancreatic adenocarcinoma. AEC and hematoxylin counter stain, ×200.

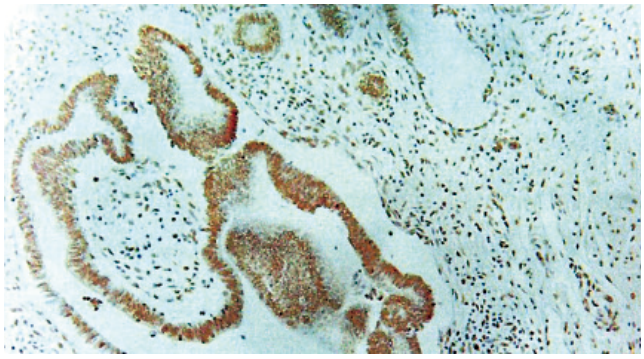

Figure 4 Cytoplasmic staining with K-*ras* is illustrated in both ductal hyperplasia and adjacent invasive adenocarcinoma. K-*ras* immunohistochemical stain, ×200.

increased nuclear to cytoplasm ratio and loss of nuclear polarity (Figure 2A). The tissue of pancreatic duct showed numerous cell divisions, an increased nuclear-to-cytoplasm ratio, and loss of cellular polarity (Figure 3A).

Immunohistochemical staining Normal pancreatic duct showed negative reaction to Ki-67, CEA, p53, K-*ras* staining (Figure 1B), whereas in hyperplasia, the nuclei were stained by Ki-67 (Figure 1D), cellular membrane by CEA and cytoplasm by K-*ras*, respectively. In dysplasia, the nuclei were stained by Ki-67, p53, and cell membrane by CEA respectively (Figures 2B-D). Focal, weak positive reaction to CEA was also detected in the cytoplasm. In pancreatic cancer, the nuclei were stained by Ki-67 and p53, whereas both cell membrane and cytoplasm showed strong positive reaction to CEA (Figures 3B-D). K-*ras* showed negative reaction to K-*ras* (Table 1, Figure 4).

Ki-67 proliferation index

Pancreatic cancer tissue Ki-67 proliferation index of pancreatic cancer tissue based on the histologic classification was 3.73±3.58, 6.62±4.39, 13.47±4.02, and 37.03±10.05 in normal, ductal hyperplasia, dysplasia, and cancer site respectively.

Chronic pancreatitis tissue Ki-67 proliferation index based on the histologic classification in chronic pancreatitis tissue was 2.35±2.79, 7.66±5.78, and 8.64±5.51 in normal, ductal hyperplasia, and dysplasia, respectively.

Results based on random histologic classification Ki-67 proliferation index based on random histologic classification was 2.35±2.79, 9.07±5.39, 10.79±5.51, and 37.03±10.05 in normal, hyperplasia, dysplasia, and cancer area, respectively.

Expression of p53 protein

In all 11 pancreatic cancer tissues, the expression of p53 protein was observed in all dysplasia (4/4), but not in all normal sites. The expression of p53 protein was also observed in 91% of cancer area that involved lesions.

In 12 samples of all chronic pancreatitis tissues, the expression of p53 protein was negative in both normal and hyperplasia sites, whereas positive in 60% of dysplasia site. Overall, the expression of p53 protein was negative in all normal sites and pancreatic epithelial hyperplasia, whereas positive in 78% of dysplasia and 91% of cancer sites.

Expression of K-ras protein

The positive reaction to K-*ras* protein seen in cytoplasm was observed in 33% of hyperplasia sites and 67% of dysplasia sites, but not in normal tissue in the pancreatic cancer patients. The positive staining to K-*ras* was in 80% of cancer tissue. The character and intensity in staining was not proportional to the differentiation of cancer. In chronic pancreatitis, K-*ras* was expressed in 67% of dysplasia, but not in normal sites. Overall, K-*ras* was expressed in 33% of pancreatic duct hyperplasia, 67% of dysplasia and 80% of cancerous sites, but no expression of K-*ras* could be detected in any normal sites.

DISCUSSION

It is generally accepted that three to seven accumulated mutations might be required for a normal cell to transform into a neoplastic cell[11]. A famous example of multistep development of malignancy has been reported in colorectal carcinoma[12], and similar multiple mutational steps seem to be associated in the development of pancreatic cancer[13]. Chronic pancreatitis is accepted as a precancerous lesion of pancreatic cancer, although a detailed mechanism regarding this is yet to be delineated. Several possible mechanisms have been proposed. There has been a study suggesting that ductal hyperplasia might play an important role[6,8]. Unfortunately, this hypothesis is hard to be tested since ductal hyperplasia could not be objectively determined on general means of pathological examination. Moreover, morphologically and functionally different kinds of pancreatic tissue tend to be mixed together which makes statistical analysis difficult. All these problems are partly due to the ambiguous pathologic terms and definitions; for example, the pancreatic duct hyperplasia, dysplasia, atypical ductal hyperplasia, intraductal tumor, carcinoma *in situ*, adenomatous hyperplasia, and atypical adenomatous hyperplasia[7,14].

In the present study, we only used the term, hyperplasia and dysplasia, since there are similar lesions, morphologically and cytologically, in other parts of the gastrointestinal tract. In order to objectively determine pancreatic duct hyperplasia, we used Ki-67 proliferation index. In evaluation of atypical hyperplasia, we used CEA immunohistochemical study.

The p53 gene is a tumor suppressor gene that involves regulation of the cell cycle and its mutation is most common in human cancers[15]. Mutated p53 in tumor cell accumulates nuclear p53 proteins and this overexpression is used as a marker for immunohistochemical staining[15,18]. It is reported that mutation of p53 has been reported to be detected in at least 50-70% of pancreatic adenocarcinoma[15-17]. In this study, p53 overexpression was most frequently shown in the cancerous lesion, rarely in the dysplastic cells and not at all in hyperplastic and normal cells. Therefore, it seems that the overexpression of p53 is implied to be the last phenomenon in the tumorigenesis. The fact that overexpression of p53 is shown more frequently in cancer tissues, regardless of the cell differentiation, suggests that it would be a useful marker in detecting activated dysplasia from well-differentiated cancer.

$P21^{K\text{-}ras}$ protein, synthesized by K-*ras* gene, accumulates in the cytoplasm[12], and found to be strongly stained in cytoplasm of most of the cancer cells[19]. The pancreas cancer originated from the exocrine gland showed 75-95% incidence of K-*ras* activation[20-24]. High incidence of K-*ras* mutation in pancreatic cancer implicates that this mutation might be a basic step of carcinogenesis. However, the earliest pancreatic lesion in which K-*ras* mutation can be found is not clearly known. As for the reports on the detection of K-*ras* mutation in the hyperplastic pancreatic duct of chronic pancreatitis patients, there have been some discrepancies. The current study immunohistochemically examined oncogene protein expressions in various pancreatic lesions. Although the presence of mutated gene needs to be confirmed at the molecular level, we found the possible continuity between pancreas diseases through protein expressions of oncogene. K-*ras* was strongly and frequently expressed in dysplastic and cancerous tissues compared with that of hyperplastic tissue. These results indicate that the overexpression of K-*ras* is associated with the pancreatic duct dysplasia in the carcinogenesis. Results in chronic pancreatitis were also similar to pancreatic cancer, suggesting that ductal dysplasia may be the precancerous lesion.

In our study, we found the possibility of the existence of stepwise mutation in the progression of advanced cancer from normal pancreatic cell. First, in the pancreatic cancer tissues, we found tissues presumed to be precancerous lesion, histologically different from normal epithelial cells. Second, this premalignant lesion was found more frequently in the tissues of pancreatic cancer compared with that of other disease states. Third, in the dysplastic and cancer tissues, the excessive expression of oncogene product was shown more frequently than in normal tissues. Fourth, K-*ras* protein overexpression developed in earlier stage of carcinogenesis, while the overexpression of p53 protein mostly occurred in advanced steps such as dysplasia or cancer. Finally, in chronic pancreatitis, some hyperplastic and dysplastic tissues showed the overexpression of oncogenic proteins similar to pancreatic cancer, although at low percentage. Therefore, chronic pancreatitis patients with protein overexpression of oncogene would have higher risk of cancer. Consequently, these results suggest that there is a correlation between the protein overexpression by genetic alteration and histological changes. Although we investigated mutation of only two important genes using low-sensitive immunohistochemical staining method, we believe that this study would be useful in the future

researches on the pathogenesis of pancreatic cancer.

REFERENCES

1 **Warshaw AL,** Fernandez-del Castillo C. Pancreatic carcinoma. *N Engl J Med* 1992; **326**: 455-465
2 **Boyle P,** Hsieh CC, Maisonneuve P, La Vecchia C, Macfarlane GJ, Walker AM, Trichopoulos D. Epidemiology of pancreas cancer (1988). *Int J Pancreatol* 1989; **5**: 327-346
3 **Wingo PA,** Tong T, Bolden S. Cancer statistics, 1995. *CA Cancer J Clin* 1995; **45:** 8-30
4 **Crist DW,** Cameron JL. The current status of the Whipple operation for periampullary carcinoma. *Adv Surg* 1992; **25**: 21-49
5 **Lowenfels AB,** Maisonneuve P, Cavallini G, Ammann RW, Lankisch PG, Andersen JR, Dimagno EP, Andren-Sandberg A, Domellof L. Pancreatitis and the risk of pancreatic cancer. International Pancreatitis Study Group. *N Engl J Med* 1993; **328**: 1433-1437
6 **Cubilla AL,** Fitzgerald PJ. Morphological lesions associated with human primary invasive nonendocrine pancreas cancer. *Cancer Res* 1976; **36**: 2690-2698
7 **Kozuka S,** Sassa R, Taki T, Masamoto K, Nagasawa S, Saga S, Hasegawa K, Takeuchi M. Relation of pancreatic duct hyperplasia to carcinoma. *Cancer* 1979; 43: 1418-1428
8 **SOMMERS SC,** MURPHY SA, WARREN S. Pancreatic duct hyperplasia and cancer. *Gastroenterology* 1954; **27:** 629-640
9 **Apple SK,** Hecht JR, Lewin DN, Jahromi SA, Grody WW, Nieberg RK. Immunohistochemical evaluation of K-*ras*, p53, and HER-2/neu expression in hyperplastic, dysplastic, and carcinomatous lesions of the pancreas: evidence for multistep carcinogenesis. *Hum Pathol* 1999; **30**: 123-129
10 **Kloppel G.** Pancreatic Pathology. Edinburg, Scotland: *Churchill Livingstone,* 1984: 79-113
11 **Fearon ER,** Vogelstein B. A genetic model for colorectal tumorigenesis. *Cell* 1990; **61**: 759-767
12 **Vogelstein B,** Fearon ER, Hamilton SR, Kern SE, Preisinger AC, Leppert M, Nakamura Y, White R, Smits AM, Bos JL. Genetic alterations during colorectal-tumor development. *N Engl J Med* 1988; **319**: 525-532
13 **Chen J,** Baithun SI, Ramsay MA. Histogenesis of pancreatic carcinomas: a study based on 248 cases. *J Pathol* 1985; **146**: 65-76
14 **Kloppel G.** The pancreas: biology, pathobiology, and disease. 2nd ed. New York: *Raven Press,* 1993: 871-898
15 **Greenblatt MS,** Bennett WP, Hollstein M, Harris CC. Mutations in the p53 tumor suppressor gene: clues to cancer etiology and molecular pathogenesis. *Cancer Res* 1994; **54**: 4855-4878
16 **DiGiuseppe JA,** Hruban RH, Goodman SN, Polak M, van den Berg FM, Allison DC, Cameron JL, Offerhaus GJ. Overexpression of p53 protein in adenocarcinoma of the pancreas. *Am J Clin Pathol* 1994; **101**: 684-688
17 **Pellegata NS,** Sessa F, Renault B, Bonato M, Leone BE, Solcia E, Ranzani GN. K-*ras* and p53 gene mutations in pancreatic cancer: ductal and nonductal tumors progress through different genetic lesions. *Cancer Res* 1994; **54**: 1556-1560
18 **Yokoyama M,** Yamanaka Y, Friess H, Buchler M, Korc M. p53 expression in human pancreatic cancer correlates with enhanced biological aggressiveness. *Anticancer Res* 1994; **14**: 2477-2483
19 **Sakorafas GH,** Lazaris A, Tsiotou AG, Koullias G, Glinatsis MT, Golematis BC. Oncogenes in cancer of the pancreas. *Eur J Surg Oncol* 1995; **21**: 251-253
20 **Berrozpe G,** Schaeffer J, Peinado MA, Real FX, Perucho M. Comparative analysis of mutations in the p53 and K-*ras* genes in pancreatic cancer. *Int J Cancer* 1994; **58**: 185-191
21 **Almoguera C,** Shibata D, Forrester K, Martin J, Arnheim N, Perucho M. Most human carcinomas of the exocrine pancreas contain mutant c-K-*ras* genes. *Cell* 1988; **53**: 549-554
22 **Motojima K,** Tsunoda T, Kanematsu T, Nagata Y, Urano T, Shiku H. Distinguishing pancreatic carcinoma from other periampullary carcinomas by analysis of mutations in the Kirsten-*ras* oncogene. *Ann Surg* 1991; **214**: 657-662
23 **Motojima K,** Urano T, Nagata Y, Shiku H, Tsurifune T, Kanematsu T. Detection of point mutations in the Kirsten-*ras* oncogene provides evidence for the multicentricity of pancreatic carcinoma. *Ann Surg* 1993; **217**: 138-143
24 **Tabata T,** Fujimori T, Maeda S, Yamamoto M, Saitoh Y. The role of *Ras* mutation in pancreatic cancer, precancerous lesions, and chronic pancreatitis. *Int J Pancreatol* 1993; **14**: 237-244

Sciencel Editor Wang XL and Guo SY **Language Editor** Elsevier HK

PO Box 2345, Beijing 100023, China
www.wjgnet.com
wjg@wjgnet.com

ELSEVIER

World J Gastroenterol 2005;11(43):6770-6774
World Journal of Gastroenterology ISSN 1007-9327

• *BASIC RESEARCH* •

Effect of IL-4 on altered expression of complement activation regulators in rat pancreatic cells during severe acute pancreatitis

Cheng Zhang, Chun-Lin Ge, Ren-Xuan Guo, San-Guang He

Cheng Zhang, Chun-Lin Ge, Ren-Xuan Guo, San-Guang He, Department of General Surgery, No. 1 Hospital of China Medical University, Shenyang 110001, Liaoning Province, China
Supported by the Research Program of Science and Technology Technology Commission Foundation of Liaoning Province, No. 2001225001-17
Correspondence to: Dr. Cheng Zhang, Department of General Surgery, 201 Hospital of Chinese PLA, Liaoyang 111000, Liaoning Province, China. zc1971@hotmail.com
Telephone: +86-419-2314433
Received: 2005-02-02 Accepted: 2005-04-11

Abstract

AIM: To investigate the effect of IL-4 on the altered expression of complement activation regulators in pancreas and pancreatic necrosis during experimental severe acute pancreatitis (SAP).

METHODS: SAP model of rats was established by retrograde injection of 5% sodium taurocholate (1 mL/kg) into the pancreatic duct. We immunohistochemically assayed the expression of three complement activation regulators: decay accelerating factor (DAF; CD55), 20 ku homologous restriction factor (HRF20; CD59) and membrane cofactor protein (MCP; CD46), in the pancreatic acinar cells of rats at 0, 3, 6, 12, and 24 h after the induction of SAP model. Meanwhile the levels of amylase and lipase were determined, and morphological examination was performed. Then, 61 rats were randomly divided into three groups. Group A (n = 21) received no treatment after the SAP model was established; group B (n = 20) was given IL-4 (8 μg/animal) intraperitoneally 0.5 h before the SAP model was established; group C (n = 20) was given IL-4 (8 μg/animal) intraperitoneally 0.5 h after the SAP model was established. Plasma amylase and lipase, extent of pancreatic necrosis and expression of complement activation regulators were investigated 6 h after the induction of SAP model.

RESULTS: Three complement activation regulators were all expressed in pancreatic acinar cells. MCP was not found on the basolateral surface as reported. Contrary to the gradually increasing plasma level of amylase and lipase, expression of complement activation regulators decreased after SAP model was set up. At the same time, the severity of pancreatic necrosis was enhanced. A strong negative correlation was found between the expression of MCP, DAF, CD59 in pancreatic acinar cells and the severity of pancreatic necrosis (r = –0.748, –0.827, –0.723; P<0.01). In the second series of experiments, no matter when the treatment of IL-4 was given (before or after the induction of SAP model), the serum level of amylase or lipase was decreased and the extent of pancreatic necrosis was ameliorated significantly. Compared to SAP control group, the expression of DAF and CD59 in pancreas was reinforced when IL-4 was given before the induction of SAP model (P<0.01, P<0.05), but the expression of MCP was not influenced (P>0.05). The expression of DAF was enhanced, when IL-4 was given after the induction of SAP model (P<0.05), but the expression of CD59 and MCP did not change (P>0.05).

CONCLUSION: Complement activation regulators may participate in the pathogenesis of pancreatic inflammation. Downregulation of complement activation regulators expression may be one of the causes of pancreatic necrosis. IL-4 treatment may control SAP aggravation by enhancing expression of DAF and CD59 in pancreas and decreasing pancreatic necrosis. Moreover, DAF and CD59 may play an important role in the regulation of complement activation regulators during SAP.

Key words: Severe acute pancreatitis; Complement activation regulators; Interleukin-4

Zhang C, Ge CL, Guo RX, He SG. Effect of IL-4 on altered expression of complement activation regulators in rat pancreatic cells during severe acute pancreatitis. *World J Gastroenterol* 2005; 11(43): 6770-6774
http://www.wjgnet.com/1007-9327/11/6770.asp

INTRODUCTION

During activation of complement, fragments of complement proteins may be deposited on non-target cells[1], thereby causing tissue injury. In order to prevent this, several proteins on cell membranes inhibit the activation of the complement cascade[2]. These proteins include decay accelerating factor (DAF; CD55) which inhibits the formation of C3 and C5 convertases and promotes their catabolism[3,4], 20 ku homologous restriction factor (HRF20; CD59) which inhibits the formation

of terminal complement complexes by preventing the polymerization of C9 on C5b-8[5,6], and membrane cofactor protein (MCP; CD46) which functions as a cofactor in the factor I-mediated inactivation of C3b and C4b[7]. These proteins, which are widely distributed in normal tissues[8-10], are thought to protect host tissues from autologous complement-mediated damage.

Expression of these three proteins has been described in the gastrointestinal tract of human beings[11-14]. In normal colonic and gastric mucosa, DAF and CD59 have been found only on the apical surface of epithelial cells, whereas MCP is localized on the basolateral surface of these cells[11,13-15]. In patients with ulcerative colitis (UC) and chronic gastritis, the expression of DAF in colonic and gastric epithelial cells was markedly enhanced and was proportional to the severity of mucosal inflammation[14,15]. Expression of these complement activation regulators has not been assayed in more severe types of inflammation. Being one of the main causes of pancreatic necrosis, activation of complement in the process of SAP has been proved by other authors[16,17]. We therefore examined the distribution of DAF, CD59, and MCP in pancreatic acinar cells and the relationship between the expression of these proteins and the severity of pancreatic necrosis during SAP. In addition, we investigated the therapeutic effects of IL-4 on the expression of complement activation regulators and pancreatic necrosis in order to clarify the role of IL-4 and three membrane inhibitors of complement during SAP.

MATERIALS AND METHODS

Animals and model of severe acute pancreatitis

Male Wistar rats (250-300 g) were used in this study. Animals were allowed to have free access to water before the experiment. Anesthesia was induced with an intraperitoneal injection of 6% sodium pentobarbital (Northeast Drug Manufactory, China) (0.1 mL/100 g body weight). After midline laparotomy and transduodenal cannulation of the pancreatic duct, the hepatic duct was closed by a small bulldog clamp, and then 5% sodium taurocholate (Sigma, USA) in saline was infused at a rate of 0.1 mL/min. Control animals received an infusion of 0.9% saline solution.

Experimental design

In the first series of experiments, animals were killed at 3, 6, 12, and 24 h after the induction of pancreatitis (n = 10 per group). Pancreatic tissues were removed and processed as indicated below.

In the second series of experiments, to test the effect of IL-4 on complement activation regulators, 61 rats were randomly divided into three groups. Group A (n = 21) received no treatment after the SAP model was established, group B (n = 20) was given IL-4 (Peprotech, UK) (8 μg/animal)[18-20] intraperitoneally 0.5 h before the SAP model was established, group C (n = 20) was given IL-4 (8 μg/animal) intraperitoneally 0.5 h after the SAP model was established. Animals were killed at 6 h after the induction of pancreatitis model.

Pancreatic tissue was immediately frozen in liquid N_2 and embedded in OCT embedding medium. All blood samples were centrifuged at 3 000 r/min for 5 min. Supernatant was stored at -70 ℃.

The serum levels of amylase and lipase were determined by a colorimetric kinetic method and nephelometry method respectively.

Tissue immunohistochemistry staining

Cryostat sections were serially cut at 6 μm, and fixed in acetone for 10 min. After being washed with phosphate-buffered saline (PBS), the sections were treated with 30 mL/L H_2O_2 for 15 min at room temperature to inactivate endogenous peroxidase, and then with a 1:10 dilution of non-immune goat serum for 20 min to block non-specific immunoglobulin binding sites. After the excess serum was blotted, the sections were incubated with each of the primary antibodies (dilution 1:150 in PBS) [MCP (sc-7056), DAF (sc-9156), CD59 (sc-9157), Santa Cruz, USA] for 2 h at room temperature, control sections were incubated with PBS. Unbound antibody was washed from the tissue thrice in PBS for 5 min, incubated with the secondary biotin-labeled goat anti-mouse IgG antibody for 20 min, and then washed thrice for 5 min with PBS. Subsequently, the sections were incubated with peroxidase-labeled streptavidin-biotin for 20 min (ABC kit; Boster, Wuhan, China). After being washed with PBS for four times, the sections were stained with 0.02% (w/v) 3,3'-diaminobenzidine tetrahydrochloride (Boster, Wuhan, China). The sections were counterstained with hematoxylin, washed with PBS, dehydrated in graded concentrations of ethanol, and mounted.

Vascular endothelial cells were used as a positive control for DAF, MCP, and CD59. Expression of complement activation regulators in pancreatic acinar cells was scored on a scale of (-) to (+3)[15], where (-) denotes faint or no staining; (1+) specific staining in 10-50% of cells; (2+) specific staining of 50-90% of the cells; (3+) specific staining of 90-100% of cells.

Evaluation of pancreatitis severity

The extent of pancreatic acinar cell necrosis was quantitated morphometrically by an observer who was not aware of the sample identity, as described by Kusske *et al.* [21]. For these studies, cryostat sections were stained with hematoxylin and eosin. Ten randomly chosen microscopic fields (×200) were examined for each tissue sample, and the extent of acinar cell injury/necrosis was expressed as a percentage of total acinar tissue.

Statistical analysis

Data were presented as mean±SE. Differences between groups were compared using analysis of variance followed by Student's t-test. Correlation between the expression of complement activation regulators and pancreatic necrosis was analyzed using Spearman's rank correlation test. Correlation between IL-4 intervention and the expression of complement membrane inhibitors was analyzed using

Table 1 Serum amylase and lipase activities (u/L) and histological scores of pancreatic necrosis in the first series of experiment (mean±SE)

	Control group	Pancreatitis group			
		3 h	6 h	12 h	24 h
Serum amylase	1360±259	4715±1 120[b]	7527±1 595[b]	13321±3 848[b]	13686±4 175[b]
Serum lipase	2.52±0.35	11.09±2.93[b]	31.17±5.66[b]	40.39±9.04[b]	38.06±9.67[b]
Scores of pancreatic necrosis	0.00±0.00	0.30±0.48[b]	1.40±0.70[b]	2.70±0.48[b]	2.80±0.79[b]

[b]P<0.01 *vs* control.

Table 3 Serum amylase and lipase activities (u/L) and histological scores of pancreatic necrosis in the second series of experiment (mean±SE)

Group	n	Serum amylase	Serum lipase	Scores of pancreatic necrosis
A	21	7 393±1 433	32.15±5.42	1.52±0.75
B	20	4 482±1 224[a]	11.75±4.42[a]	0.45±0.69[a]
C	20	5 947±1 503[a]	22.28±7.10[a]	0.95±0.76[a]

[a]P<0.05 *vs* group A.

the χ^2-test. P<0.05 was considered statistically significant.

RESULTS

Serum levels of amylase and lipase

Tables 1 and 3 summarize the changes of serum amylase and lipase activities in experiments 1 and 2.

Evaluation of morphology

In the first series of experiments, the morphological changes varied with the time elapsed after sodium taurocholate injection. By gross examination, the ductal tree became hemorrhagic immediately after injection, and the whole pancreas became edematous and brownish red in color within the next 5-10 min. As time elapsed, edema, hemorrhages, acinar cell necrosis (Table 1), amount of ascitic fluid and inflammatory cell infiltration aggravated gradually. At 24 h, the color of pancreas was pale and slightly yellowish. Many animals had marked distension of the stomach.

In the second series of experiments, pancreatic necrosis was significantly reduced, when IL-4 was administered either prophylactically or therapeutically (P<0.01), (Table 3).

Expression of complement activation regulators

At the microscopic level, we observed the expression of DAF, CD59, and MCP on the luminal surface of pancreatic acinar cells. We did not find positive staining of MCP on the basolateral surface of pancreatic acinar cells, though staining for MCP was positive on the basolateral surface of gastric and colonic epithelial cells[14,15]. Although DAF, CD59, and MCP were well recognized as membrane binding proteins, immunostaining of these proteins was also detected in the cytoplasm[15]. No staining was observed when samples were treated with control PBS. Expression of complement activation regulators decreased gradually after SAP model was set up. We also examined the relationship between the expression of three complement inhibitors and the pancreatic necrosis. We found a strong negative correlation between the expression of MCP, DAF, and CD59 in pancreatic acinar cells and the severity of pancreatic necrosis (r = -0.748, -0.827, and -0.723; P<0.01), (Table 2). In the second series of experiments, compared to SAP control group, the expression of DAF and CD59 in pancreas was reinforced when IL-4 was given before the induction of SAP model (P<0.01, P<0.05), but the expression of MCP was not influenced (P>0.05). The expression of DAF was enhanced when IL-4 was given after the induction of SAP model (P<0.05), but the expression of CD59 and MCP did not change (P>0.05) (Table 4).

Table 2 Correlation between expression of DAF, CD59, MCP, and pancreatic necrosis

		Histological scores of pancreatic necrosis				
		0	1	2	3	4
MCP	–	1	5	6	12	2
	+	8	3	3	0	0
	++	6	2	0	0	0
	+++	2	0	0	0	0
DAF	–	0	6	7	12	2
	+	6	4	2	0	0
	++	10	0	0	0	0
	+++	1	0	0	0	0
CD59	–	2	6	6	12	2
	+	5	3	3	0	0
	++	7	1	0	0	0
	+++	3	0	0	0	0

Table 4 Effects of IL-4 on expression of MCP, DAF, and CD59 in pancreas during SAP

Group	n	Expression intensity of DAF			Expression intensity of CD59			Expression intensity of MCP		
		–	+	++	–	+	++	–	+	++
A	21	12	7	2	12	6	3	11	6	4
B	20	2	7	11[b]	3	7	10[a]	5	8	7[c]
C	20	4	8	8[a]	9	6	5[c]	7	7	6[c]

[a]P<0.05, [b]P<0.01, [c]P>0.05 *vs* group A.

DISCUSSION

Severe acute pancreatitis is a common acute abdominal disorder. Since angiorrhexis and hemorrhage in pancreas are frequent during severe acute pancreatitis, and the complement system is activated by trypsin[16,17], it is possible that inflammation may result in constant exposure of pancreatic acinar cells to activated complement

fragments in the blood. Then, severe pancreatic necrosis is inevitable. Being the membrane inhibitors, complement activation regulators in the acinar cells may be important for local defense system during SAP. We investigated the role of RCA in the process of SAP and then attempted to attenuate inflammatory reaction by regulating the expression of complement activation regulators.

It has been reported that expression of DAF on gastric epithelial cells and colonic epithelial cells is strongly enhanced during gastritis and ulcerative colitis, and a strong positive correlation between DAF expression and degree of inflammation (extent of inflammatory cell infiltration) has been found[14,15]. At the same time, other researches revealed that expression of MCP and CD59 in alveolar epithelial cells is conspicuously enhanced during acute lung injury, but is greatly decreased during acute respiratory distress syndrome[22]. These results suggest that complement activation regulators play a different role in these inflammatory diseases.

We utilized immunohistochemical methods to assay the expression of DAF, CD59, and MCP in normal and pathological pancreatic specimens. We found that MCP, DAF, and CD59, which are glycosyl phosphatidylinositol (GPI) anchored membrane proteins, were present on the apical side of pancreatic acinar cells[23], whereas MCP, a transmembrane protein, was not distributed in these cells as in epithelial cells of the colonic and gastric mucosa[14,15]. While complement activation regulators were slightly or moderately expressed in the acinar cells of normal pancreatic tissue, their expression in pancreatic acinar cells decreased gradually after the model of SAP was induced. These phenomena are similar to those in ARDS[22]. Although there are differences in the inflammatory process between pancreatic and pulmonary epithelial cells, the lower expression of complement activation regulators detected in the inflammatory cells suggests that complement activation regulators play an important role in the regulation of complement activation in epithelia during severe inflammation. In this study, a strong negative correlation was observed between the expression of complement activation regulators and inflammation (pancreatic necrosis). It is not clear, which of MCP, DAF, and CD59 is the most important factor in the regulation of complement activation during SAP. Although the precise mechanism by which the repression of complement activation regulators is regulated remains to be elucidated, it is clear that these proteins are important in the regulation of the inflammatory process of the pancreas.

In general, the expression of membrane inhibitors of complement is mediated by various cytokines[24-27]. Being an anti-inflammatory mediator, IL-4 has been proven to enhance the expression of DAF in small intestine epithelial cells and vascular endothelial cells *in vitro*[24-28]. We applied IL-4 to rats with severe acute pancreatitis to testify its therapeutic effects on the expression of complement activation regulators and pancreatic necrosis *in vivo*. We found that the expression of DAF and CD59 was upregulated when IL-4 was administered prophylactically (given before the model was established), but the expression of MCP did not change significantly. When IL-4 was administered therapeutically (given after the model was established), only DAF was upregulated. Compared to control group, the serum amylase and lipase activities and the extent of pancreatic necrosis were significantly reduced when IL-4 was administered either prophylactically or therapeutically. These findings suggest that activation of complement during severe acute pancreatitis may be mediated primarily by DAF and CD59, and IL-4 treatment may be a valuable strategy for severe acute pancreatitis. Considering the therapeutic value of IL-4, some other biological activities of IL-4 should be mentioned. It has been reported that IL-4 displays its anti-inflammatory feature by inhibiting the activation and accumulation of macrophages[29], preventing the production of TNF-α and IL-1β[30], upregulating the expression of IL-1 receptor antagonist[31], stimulating 15-lipoxidase activity of macrophages[32]. These functions are important to control systemic inflammation reaction that is common during SAP.

In conclusion, complement activation regulators may play an important role in the regulation of complement activation, and downregulation of complement activation regulators may be one of the causes of pancreatic necrosis. IL-4 treatment provides a new therapeutic strategy for controlling systemic inflammatory reaction during severe acute pancreatitis.

ACKNOWLEDGMENT

The authors thank Professor San-Guang He for helpful advice and discussions.

REFERENCES

1 **Davitz MA.** Decay-accelerating factor (DAF): a review of its function and structure. *Acta Med Scand Suppl* 1987; **715:** 111-121
2 **Kinoshita T**. Biology of complement: the overture. *Immunol Today* 1991; **12:** 291-295.
3 **Nicholson-Weller A,** Burge J, Fearon DT, Weller PF, Austen KF. Isolation of a human erythrocyte membrane glycoprotein with decay-accelerating activity for C3 convertases of the complement system. *J Immunol* 1982; **129:** 184-189
4 **Fujita T, Inoue T,** Ogawa K, Iida K, Tamura N. The mechanism of action of decay-accelerating factor (DAF). DAF inhibits the assembly of C3 convertases by dissociating C2a and Bb. *J Exp Med* 1987; **166:** 1221-1228
5 **Okada N,** Harada R, Fujita T, Okada H. A novel membrane glycoprotein capable of inhibiting membrane attack by homologous complement. *Int Immunol* 1989; **1:** 205-208
6 **Rollins SA, Sims PJ**. The complement-inhibitory activity of CD59 resides in its capacity to block incorporation of C9 into membrane C5b-9. *J Immunol* 1990; **144:** 3478-3483.
7 **Seya T**, Turner JR, Atkinson JP. Purification and characterization of a membrane protein (gp45-70) that is a cofactor for cleavage of C3b and C4b. *J Exp Med* 1986; **163:** 837-855.
8 **Nose M,** Katoh M, Okada N, Kyogoku M, Okada H. Tissue distribution of HRF20, a novel factor preventing the membrane attack of homologous complement, and its predominant expression on endothelial cells in vivo. *Immunology* 1990; **70:** 145-149
9 **McNearney T,** Ballard L, Seya T, Atkinson JP. Membrane

cofactor protein of complement is present on human fibroblast, epithelial, and endothelial cells. *J Clin Invest* 1989; **84:** 538-545

10 **Medof ME,** Walter EI, Rutgers JL, Knowles DM, Nussenzweig V. Identification of the complement decay-accelerating factor (DAF) on epithelium and glandular cells and in body fluids. *J Exp Med* 1987; **165:** 848-864

11 **Koretz K,** Bruderlein S, Henne C, Moller P. **Decay-accelerating** factor (DAF, CD55) in normal colorectal mucosa, adenomas and carcinomas. *Br J Cancer* 1992; **66:** 810-814

12 **Koretz K,** Bruderlein S, Henne C, Moller P. **Expression of** CD59, a complement regulator protein and a second ligand of the CD2 molecule, and CD46 in normal and neoplastic colorectal epithelium. *Br J Cancer* 1993; **68:** 926-931.

13 **Inoue H,** Mizuno M, Uesu T, Ueki T, Tsuji T. Distribution of complement regulatory proteins, decay-accelerating factor, CD59/homologous restriction factor 20 and membrane cofactor protein in human colorectal adenoma and cancer. *Acta Med Okayama* 1994; **48:** 271-777

14 **Uesu T,** Mizuno M, Inoue H, Tomoda J, Tsuji T. Enhanced expression of decay accelerating factor and CD59/homologous restriction factor 20 on the colonic epithelium of ulcerative colitis. *Lab Invest* 1995; **72:** 587-591

15 **Sasaki M,** Joh T, Tada T, Okada N, Yokoyama Y, Itoh M. Altered expression of membrane inhibitors of complement in human gastric epithelium during Helicobacter-associated gastritis. *Histopathology* 1998; **33:** 554-560

16 **Roxvall L,** Bengtson A, Sennerby L, Heideman M. Activation of the complement cascade by trypsin. *Biol Chem Hoppe Seyler* 1991; **372:** 273-278

17 **Bhatia M,** Saluja AK, Singh VP, Frossard JL, Lee HS, Bhagat L, Gerard C, Steer ML. Complement factor C5a exerts an anti-inflammatory effect in acute pancreatitis and associated lung injury. *Am J Physiol Gastrointest Liver Physiol* 2001; **280:** G974-978

18 **Tam FW,** Smith J, Karkar AM, Pusey CD, Rees AJ. Interleukin-4 ameliorates experimental glomerulonephritis and up-regulates glomerular gene expression of IL-1 decoy receptor. *Kidney Int* 1997; **52:** 1224-31

19 **He XY,** Chen J, Verma N, Plain K, Tran G, Hall BM. Treatment with interleukin-4 prolongs allogeneic neonatal heart graft survival by inducing T helper 2 responses. *Transplantation* 1998; **65:** 1145-1152

20 **Erwig LP,** Stewart K, Rees AJ. Macrophages from inflamed but not normal glomeruli are unresponsive to anti-inflammatory cytokines. *Am J Pathol* 2000; **156:** 295-301

21 **Kusske AM,** Rongione AJ, Ashley SW, McFadden DW, Reber HA. Interleukin-10 prevents death in lethal necrotizing pancreatitis in mice. *Surgery* 1996; **120:** 284-289

22 **Yang Kang,** LIU Wei-Yong. **CD59 and CD46 expression in** lungs of cats with traumatic ALI or ARDS. *Disi Junyi Daxue Xuebao* 2000; **21**: 624-626.

23 **Johnstone RW**, Loveland BE, McKenzie IF. Identification and quantification of complement regulator CD46 on normal human tissues. *Immunology* 1993; **79**: 341-347

24 **Moutabarrik A,** Nakanishi I, Namiki M, Hara T, Matsumoto M, Ishibashi M, Okuyama A, Zaid D, Seya T. Cytokine-mediated regulation of the surface expression of complement regulatory proteins, CD46(MCP), CD55(DAF), and CD59 on human vascular endothelial cells. *Lymphokine Cytokine Res* 1993; **12:** 167-172

25 **Mason JC,** Lidington EA, Yarwood H, Lublin DM, Haskard DO. Induction of endothelial cell decay-accelerating factor by vascular endothelial growth factor: a mechanism for cytoprotection against complement-mediated injury during inflammatory angiogenesis. *Arthritis Rheum* 2001; **44:** 138-150

26 **Spiller OB,** Criado-Garcia O, Rodriguez De Cordoba S, Morgan BP. Cytokine-mediated up-regulation of CD55 and CD59 protects human hepatoma cells from complement attack. *Clin Exp Immunol* 2000; **121:** 234-241

27 **Bjorge L**, Jensen TS, Matre R. Characterisation of the complement-regulatory proteins decay-accelerating factor (DAF, CD55) and membrane cofactor protein (MCP, CD46) on a human colonic adenocarcinoma cell line. *Cancer Immunol Immunother* 1996; **42:** 185-192.

28 **Andoh A,** Fujiyama Y, Sumiyoshi K, Sakumoto H, Bamba T. Interleukin 4 acts as an inducer of decay-accelerating factor gene expression in human intestinal epithelial cells. *Gastroenterology* 1996; **111:** 911-918

29 **Cook HT,** Singh SJ, Wembridge DE, Smith J, Tam FW, Pusey CD. Interleukin-4 ameliorates crescentic glomerulonephritis in Wistar Kyoto rats. *Kidney Int* 1999; **55:** 1319-1326

30 **Hart PH**, Vitti GF, Burgess DR, Whitty GA, Piccoli DS, Hamilton JA. Potential antiinflammatory effects of interleukin 4: suppression of human monocyte tumor necrosis factor alpha, interleukin 1, and prostaglandin E_2. *Proc Natl Acad Sci U S A* 1989; **86**: 3803-3807

31 **Vannier E**, Miller LC, Dinarello CA. Coordinated antiinflammatory effects of interleukin 4: interleukin 4 suppresses interleukin 1 production but up-regulates gene expression and synthesis of interleukin 1 receptor antagonist. *Proc Natl Acad Sci U S A* 1992; **89**: 4076-4080

32 **Katoh T,** Lakkis FG, Makita N, Badr KF. Co-regulated expression of glomerular 12/15-lipoxygenase and interleukin-4 mRNAs in rat nephrotoxic nephritis. *Kidney Int* 1994; **46**: 341-349

Sciencel Editor Wang XL and Guo SY **Language Editor** Elsevier HK

PO Box 2345, Beijing 100023, China
www.wjgnet.com
wjg@wjgnet.com

ELSEVIER

World J Gastroenterol 2005;11(43):6775-6779
World Journal of Gastroenterology ISSN 1007-9327

• *BASIC RESEARCH* •

Effects of nuclear factor-kappaB on rat hepatocyte regeneration and apoptosis after 70% portal branch ligation

Wen-Jun Yang, Qi-Yu Zhang, Zheng-Ping Yu, Qi-Tong Song, Hua-Ping Liang, Xiang Xu, Guan-Bao Zhu, Fei-Zhao Jiang, Hong-Qi Shi

Wen-Jun Yang, Qi-Yu Zhang, Zheng-Ping Yu, Qi-Tong Song, Guan-Bao Zhu, Fei-Zhao Jiang, Hong-Qi Shi, Department of General Surgery, the First Affiliated Hospital, Wenzhou Medical College, Zhejiang Province, China
Hua-Ping Liang, Xiang Xu, Research Institute of Surgery, 3rd Military Medical University, Chongqing, China
Correspondence to: Dr Wen-Jun Yang, Department of General Surgery, the First Affiliated Hospital, Wenzhou Medical College, Wenzhou 325000, Zhejiang Province, China. yangwenjun165@sohu.com
Telephone: +86-577-88069208
Received: 2005-03-18 Accepted: 2005-04-30

Key words: Portal branch ligation; Nuclear factor-kappaB; Regeneration; Apoptosis

Yang WJ, Zhang QY, Yu ZP, Song QT, Liang HP, Xu X, Zhu GB, Jiang FZ, Shi HQ. Effects of nuclear factor-kappaB on rat hepatocyte regeneration and apoptosis after 70% portal branch ligation. *World J Gastroenterol* 2005; 11(43): 6775-6779
http://www.wjgnet.com/1007-9327/11/6775.asp

Abstract

AIM: To detect the DNA binding activity of nuclear factor-kappaB (NF-κB) in rat hepatocyte and to investigate the effects of NF-κB on rat hepatocyte regeneration and apoptosis after 70% portal branch ligation.

METHODS: Sixty Wistar rats were randomly divided into control group and portal branch ligation group. The animals were killed 12 h, 1, 2, 3, 7, and 14 d after surgery to determine the contents of plasma ALT. Hepatocytes were isolated and nuclear protein was extracted. DNA binding activity of NF-κB was measured by EMSA. Hepatocyte regeneration and apoptosis were observed under microscope by TUNEL staining. The ultrastructural changes of liver were observed under electron microscope.

RESULTS: Seventy percent portal branch ligation produced atrophy of the ligated lobes and the perfused lobes underwent compensatory regeneration, the total liver weight and plasma ALT levels were maintained at the level of sham-operated animals throughout the experiment. After 2 d of portal branch ligation, DNA binding activity of NF-κB in hepatocyte increased and reached its peak, the number of apoptotic hepatocyte in the ligated lobes and the number of mitotic hepatocyte in the perfused lobes also reached their peak. Typical apoptotic changes and evident fibrotic changes in the ligated lobes were observed under electron microscope.

CONCLUSION: After 70% portal branch ligation, DNA binding activity of NF-κB in hepatocyte is significantly increased and NF-κB plays an important role in hepatocyte regeneration and apoptosis.

INTRODUCTION

Portal branch ligation (PBL) or embolization is widely used in the treatment of liver carcinoma, especially in the treatment of patients who have already missed the surgical opportunity[1-3]. PBL or embolization could produce atrophy of the ligated lobes and the perfused lobes undergo compensatory regeneration, while the liver structure and function maintained normal. But the mechanism is still unclear.

It is demonstrated that nuclear factor-kappaB (NF-κB) plays an important role in cell regeneration and apoptosis after partial hepatectomy[4-6]. To study its effects on hepatocyte regeneration and apoptosis, we observed the changes of DNA binding activity of NF-κB in rat liver and its relations to hepatocyte regeneration and apoptosis after 70% PBL.

MATERIALS AND METHODS

Animals

Sixty Wistar rats, weighing 200-240 g, were obtained from the Animal Center of the Third Military University and used in all experiments. All animals were kept in a temperature- and humidity-controlled environment in a 12-h light/dark cycle and allowed free access to water and standard food-pellet diet.

Surgical procedure and experimental design

All surgical procedures were carried out under sodium pentobarbital (40 mg/kg intraperitoneally) anesthesia at room air between 9:00 and 12:00 a.m. with a clean but not sterile technique. The 70% PBL model used was based on the Bilodeau method[7]. In 70% PBL, a median laparotomy was performed, and the branch of the portal vein feeding the anterior and lateral lobes was carefully dissected under

an operating microscope and completely ligated with a 7-0 suture. Care was taken not to injure the hepatic artery and the bile duct and to avoid hemorrhage. In sham-operated rats, a laparotomy followed by dissection of the relevant ligaments without ligature was performed. The animals had free access to water and food after surgery. The animals were killed 12 h, 1, 2, 3, 7, and 14 d after surgery.

Electrophoretic mobility shift assay

Nuclear extracts were prepared separately from the anterior (ligated) and posterior (nonligated) lobes as previously described[8]. Protein concentration was determined using the Bradford method. Double-stranded NF-κB consensus oligonucleotides (5'-AGT TGA GGG GAC TTT CCC AGG C-3', 3'-TCA ACT CCC CTG AAA GGG TCC G-5', Promega Co., USA) were end-labeled[5] with [γ-^{32}P] ATP (Beijing Yahui Biomed Inc., Beijing, China) using T4 polynucleotide kinase (Promega Co.). After the probe was purified, 5 μg of nuclear proteins was preincubated for 10 min at room temperature with 2 μg poly (dI-dC) (Sigma Co., USA) in the binding buffer. Double-stranded oligonucleotides were ^{32}P end-labeled with [γ-^{32}P] ATP and added to the extracts. The mixture was further incubated for 30 min at room temperature and then electrophoresed (200 V, 2 h) on a 5% polyacrylamide gel in a 0.5× TBE buffer. Then the gel was subjected to gamma autoradiography at -70 ℃ for 12 h, and analyzed with gel imaging system (Biorad Co., USA).

Liver morphologic structure

The rat liver color and quality were observed. Both ligated and nonligated lobes were weighed separately for measurement of their absolute and relative weights (the ratio of liver weight/body weight), and their percent in the whole liver was calculated.

Serum ALT level

Serum ALT level was measured with the biochemical multi-analyzer in Biochemistry Department of our hospital.

Histological studies and mitotic activity

Liver sections were derived from formaldehyde-fixed tissues embedded in paraffin and stained with hematoxylin –phloxin–saffron. Mitotic activity in stained sections was determined. Mitotic hepatocytes were sought in 100 consecutive high-power fields (×400), and mitotic index was expressed as per 1 000 hepatic nuclei. Prophases before dissolution of nuclear membrane and late telophases were excluded.

In situ determination of hepatocyte apoptosis (TUNEL stain)

Tissue sections of rat liver were dewaxed in toluene and alcohol. After rehydration with phosphate-buffered saline, they were incubated with proteinase K (25 μg/mL) for 15 min at room temperature and then with terminal deoxyribonucleotidyl transferase (1 U/mL) and digoxigenin-tagged dUTP (10 μmol/L) at 37 ℃ for 1 h in 0.2 mol/L sodium cacodylate, 30 mmol/L Tris (pH 7.2), 1 mmol/L $CoCl_2$, and 0.25 mg/mL bovine serum albumin. The sections were exposed to anti-digoxigenin antibodies labeled with alkaline phosphatase for 30 min at room temperature in 50 mmol/L Tris (pH 7.4) and 150 mmol/L NaCl. The binding of the antibody was revealed with 4-nitroblue tetrazolium chloride and 5-bromo-4-chloro-3-indolyl-phosphate reagents. Slides were counterstained with 1% eosin.

Ultrastructural study

The rat liver was cut into sections as large as 1 mm× 1 mm×1 mm, which were embedded in Epon618 resin and stained with uranyl acetate and lead citrate. H-2000 transmission electron microscope was used to study the ultrastructure.

Statistical analysis

Results were expressed as mean±SD. The statistical difference between the groups was tested using the one-way analysis of variance (ANOVA). $P<0.05$ was considered statistically significant.

RESULTS

Activation of NF-κB in hepatocyte after 70% PBL

After 12 h of 70% PBL, DNA binding activity of NF-κB both in ligated and nonligated lobes increased and reached its peak on d 2, and returned to normal on d 7. The changes of DNA binding activity of NF-κB in the ligated lobes were more obvious than those in the perfused lobes. No NF-κB binding was observed in nuclear extracts from control animals (Figure 1).

Changes in liver morphologic structure

The liver lobes deprived of portal flow were darkened, rapid and progressive atrophy occurred, with their proportion being reduced gradually in the whole liver. At the same time, the nonligated lobes were progressively enlarged, the total liver weight was maintained at the level of sham-PBL controls at each time interval (Figure 2A).

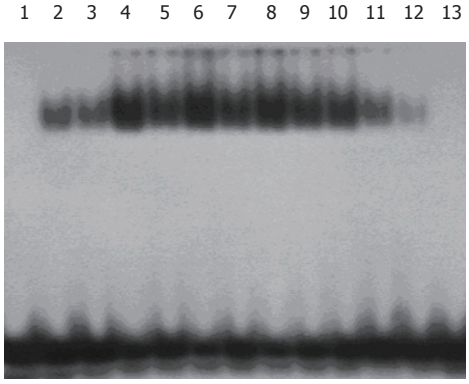

Figure 1 Changes of NF-κB binding activity in rat liver at different time points after 70% PBL by EMSA. Lane 1: control group; lanes 2, 4, 6, 8, 10, 12: 0.5, 1, 2, 3, 7, 14 d ligated liver lobes in PBL group; lanes 3, 5, 7, 9, 11, 13: 0.5, 1, 2, 3, 7, 14 d nonligated liver lobes in PBL group.

Changes in serum ALT level

There were no changes of serum ALT level in control group. After 70% PBL, the serum ALT level only increased slightly 1 d after surgery and then returned to normal (Table 1).

Table 1 Changes of serum ALT level after 70% PBL (U/L) (mean ± SD)

Group	0.5 d	1 d	2 d	3 d	7 d	14 d
Control	55.6±8.9	43.7±10.4	38.5±7.8	40.1±9.4	36.4±11.3	42.0±13.7
PBL	59.7±17.3	67.9±15.7[a]	44.6±9.8	42.6±7.8	38.9±12.1	41.3±7.9

[a]$P<0.05$ *vs* control group.

Histological studies and mitotic activity quantification

No apparent changes were found at light microscopic examination in the control liver. One day after 70% PBL, mild necrosis was found in the ligated lobes, mainly around the central vein. The cytoplasm was homogenous, and the nuclear pyknosis inside the necrosis and neutrophils was seen in some lesions. After 3 d, the necrosis was partly resorbed, and many monocytes were seen inside them. The lobules were small, with portal areas lying near each other. One to two weeks after ligation, the necrosis was completely disappeared, and the lobules became small. Fibrosis appeared around larger portal and hepatic veins, and bile ducts were collapsed with low epithelium.

Remarkable hepatocyte regeneration was observed in the nonligated lobes 12 h after 70% PBL and reached its peak 2 d later, and was still high after 7 d. The liver structure was almost normal (Figure 2B).

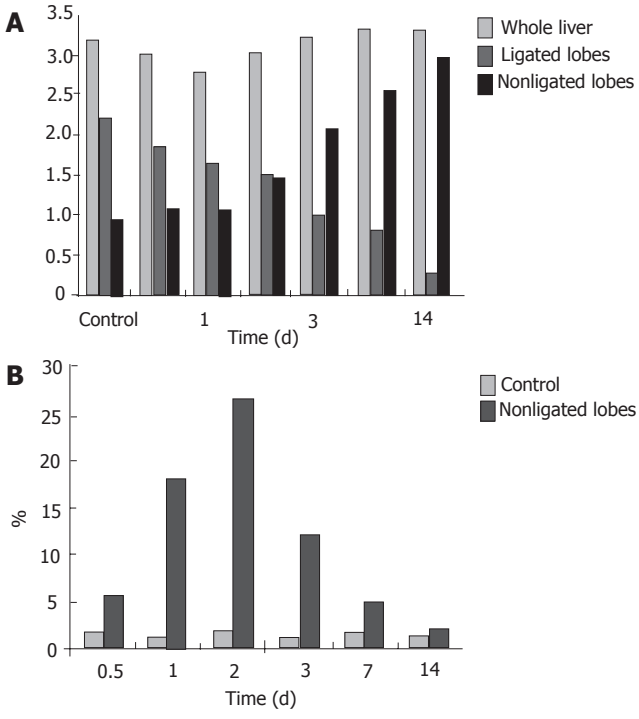

Figure 2 Changes in weight of rat liver (**A**), Changes of mitogenetic index of rat hepatocyte (**B**) after 70% PBL.

Hepatocyte apoptosis assay

There were only few apoptotic hepatocytes in the liver of control animals and in the nonligated lobes after 70% PBL. Many apoptotic hepatocytes were found in the ligated lobes 1 d after 70% portal branch ligation, and reached its peak 2 d later. These cells were mainly present around the central veins with necrosis (Figures 3A-E).

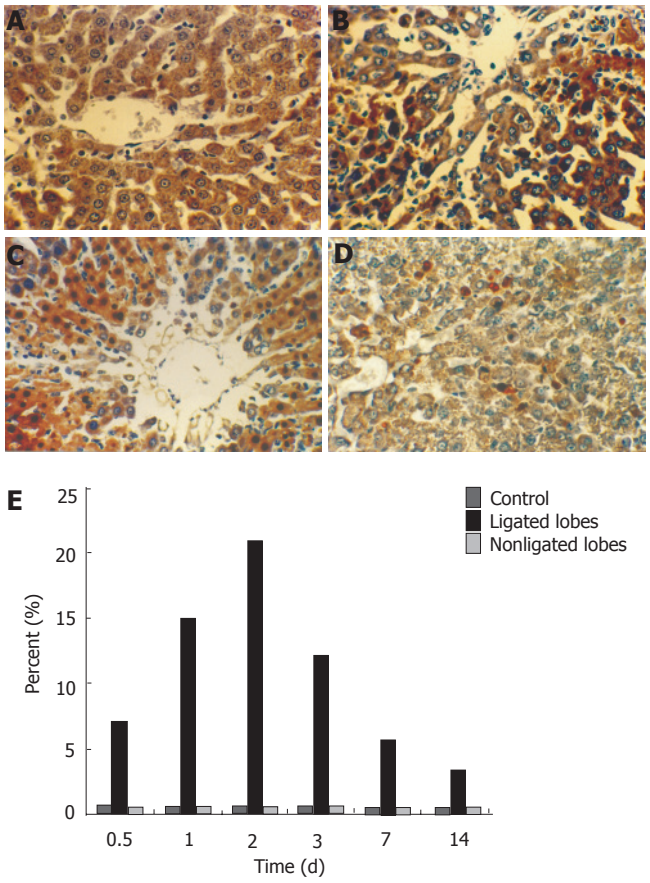

Figure 3 Apoptotic hepatocytes in control group (**A**), in rat ligated liver lobes 1 d (**B**), 2 d (**C**), 7 d (**D**), and hepatocyte apoptotic index (**E**) after 70% PBL.

Ultrastructural changes

The liver ultrastructure was normal in control animals and was almost normal in the ligated lobes early after 70% PBL, and only wild necrosis was found in some local areas. One day after 70% PBL, many apoptotic hepatocytes were found in the ligated lobes. Histological evidence for apoptosis included disappearance of the nuclear membrane, condensation, and margin of karyoplasms or chromatin, pieces of nuclei. There were no morphological changes in the mitochondriae and other intracellular structures (Figure 4). A number of apoptotic hepatocytes reached its peak 2 d later. Collagen was deposited in the Disse space and hepatic sinus became narrow 7 d after 70% PBL. Evident fibrotic changes were found in the ligated lobes 14 d after 70% PBL. A lot of collagens were deposited in the Disse space and portal areas, between hepatocytes and in hepatocytes.

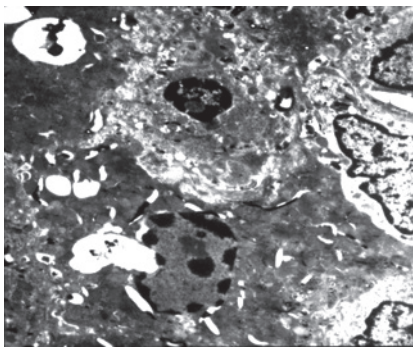

Figure 4 Ultrastructure of rat ligated liver lobes 2 d after 70% PBL (EM ×6 000)

DISCUSSION

PBL or embolization is widely used in the treatment of liver carcinoma, especially in the treatment of patients who have missed the opportunity of surgery[1-3]. It was verified in our experiment that PBL could produce atrophy of the ligated lobes, whereas the perfused lobes underwent compensatory regeneration, the liver structure and function maintained normal. Therefore, it is safe and practicable to ligate 70% portal vein branch in normal rat liver.

The 70% PBL could produce atrophy of the ligated lobes through hepatocyte apoptosis; whereas the perfused lobes undergo compensatory regeneration through hepatocyte mitosis. The total liver weight and function maintained normal. The mechanism of rat liver is still unclear. We observed the changes of DNA binding activity of NF-κB in liver through EMSA. After 70% PBL, DNA binding activity of NF-κB significantly increased both in ligated lobes and nonligated lobes, which was positively correlated with hepatocyte regeneration and apoptosis. Therefore, we could conclude that NF-κB plays an important role in hepatocyte regeneration and apoptosis after 70% PBL.

NF-κB, as a universal nuclear transcriptional factor, plays an important role in the regulation of genes relative to cell regeneration and apoptosis[9,10]. In most cells, NF-κB heterodimers are present in the cytoplasm forming an active complex by interacting with the IκB family of proteins. In response to a variety of activators, IκB-α, the prototypic member of this family of inhibitors, is phosphorylated at series 32 and 36, rendering the factor susceptible to proteolysis via the ubiquitin–proteasome pathway. This event unmasks a nuclear localization sequence of the transactivating heterodimers, allowing NF-κB translocation to nuclei. Therefore, the complex binds to κB consensus motifs in DNA, upregulating the transcription of many genes[11-14].

NF-κB plays an important role on hepatocyte regeneration in nonligated lobes by inhibiting hepatocyte apoptosis and accelerating hepatocyte regeneration. NF-κB can inhibit hepatocyte apoptosis by regulating relative cytokine transcription and expression[15-17], inducing antiapoptotic genes in Bcl-2 family[18], regulating the expression of TRAF and IAP at transcription and translation level and inhibiting the activation of caspase-8, a key enzyme in cell apoptosis[19-21], activating the apoptotic inhibitors[22,23]. NF-κB, which takes part in hepatocyte regeneration, may be mediated by regulating the transcription and expression of relative genes. NF-κB can activate the transcription and expression of TNF-α, increased TNF-α can stimulate secretion of IL-6, which can activate STAT3 through combining with IL-6R on the surface of hepatocyte, and accelerate hepatocyte regeneration[24-27].

We observed that the changes of DNA binding activity of NF-κB in the ligated lobes were more obvious than those in the perfused lobes. One reason is that compensatory response to the excessive hepatocyte apoptosis could maintain the relative weight and function of the liver. The other reason is that NF-κB plays an important role in accelerating hepatocyte apoptosis. Kuhnel *et al*.[28] reported that NF-κB mediates hepatocyte apoptosis through transcriptional activation of Fas (CD95) in adenoviral hepatitis. Recently the induction of NF-κB through the double-stranded RNA-dependent protein kinase has been suggested as a principal mechanism of virus-mediated apoptotic cell death[29].

In conclusion, NF-κB plays a completely different role in the ligated lobes and nonligated lobes through different stimulating factors and different signal transduction pathways. This may have important significance in maintaining liver structure and function after 70% PBL.

REFERENCES

1 **Tanaka H**, Hirohashi K, Kubo S, Shuto T, Higaki I, Kinoshita H. Preoperative portal vein embolization improves prognosis after right hepatectomy for hepatocellular carcinoma in patients with impaired hepatic function. *Br J Surg* 2000; **87:** 879-882

2 **Hatsuno T**, Kaneko T, Inoue S, Sugimoto H, Takeda S, Nakao A. Changes in hepatic lobe volume in hepatocellular carcinoma after transcatheter arterial and percutaneous transhepatic portal embolization. *Hepatogastroenterology* 2004; **51:** 1820-1824

3 **Kokudo N**, Makuuchi M. Current role of portal vein embolization/hepatic artery chemoembolization. *Surg Clin North Am* 2004; **84:** 643-657

4 **Riggins RB**, Zwart A, Nehra R, Clarke R. The nuclear factor kappa B inhibitor parthenolide restores ICI 182,780 (Faslodex; fulvestrant)-induced apoptosis in antiestrogen-resistant breast cancer cells. *Mol Cancer Ther* 2005; **4:** 33-41

5 **Singh RP**, Mallikarjuna GU, Sharma G, Dhanalakshmi S, Tyagi AK, Chan DC, Agarwal C, Agarwal R. Oral silibinin inhibits lung tumor growth in athymic nude mice and forms a novel chemocombination with doxorubicin targeting nuclear factor kappaB-mediated inducible chemoresistance. *Clin Cancer Res* 2004; **10:** 8641-8647

6 **Djavaheri-Mergny M**, Javelaud D, Wietzerbin J, Besancon F. NF-kappaB activation prevents apoptotic oxidative stress via an increase of both thioredoxin and MnSOD levels in TNFalpha-treated Ewing sarcoma cells. *FEBS Lett* 2004; **578:** 111-115

7 **Bilodeau M**, Aubry MC, Houle R, Burnes PN, Ethier C. Evaluation of hepatocyte injury following partial ligation of the left portal vein. *J Hepatol* 1999; **30:** 29-37

8 **Kawamura I**, Morishita R, Tsujimoto S, Manda T, Tomoi M, Tomita N, Goto T, Ogihara T, Kaneda Y. Intravenous injection of oligodeoxynucleotides to the NF-kappaB binding site inhibits hepatic metastasis of M5076 reticulosarcoma in mice. *Gene Ther* 2001; **8:** 905-912

9 **Tang JB**, Xu Y, Wang XT. Tendon healing in vitro: activation

of NIK, IKKalpha, IKKbeta, and NF- kappaB genes in signal pathway and proliferation of tenocytes. *Plast Reconstr Surg* 2004; 113: 1703-1711

10 **Sanchez A**, Factor VM, Schroeder IS, Nagy P, Thorgeirsson SS. Activation of NF-kappaB and STAT3 in rat oval cells during 2-acetylaminofluorene/partial hepatectomy-induced liver regeneration. *Hepatology* 2004; **39:** 376-385

11 **Buss H**, Dorrie A, Schmitz ML, Frank R, Livingstone M, Resch K, Kracht M. Phosphorylation of serine 468 by GSK-3beta negatively regulates basal p65 NF-kappaB activity. *J Biol Chem* 2004; **279:** 49571-39574

12 **Natarajan R**, Fisher BJ, Jones DG, Fowler AA 3rd. Atypical mechanism of NF-kappaB activation during reoxygenation stress in microvascular endothelium: a role for tyrosine kinases. *Free Radic Biol Med* 2002; **33:** 962

13 **Li Q**, Verma IM. NF-kappaB regulation in the immune system. *Nat Rev Immunol* 2002; **2:** 725-734

14 **Schooley K**, Zhu P, Dower SK, Qwarnstrom EE. Regulation of nuclear translocation of nuclear factor-kappaB relA: evidence for complex dynamics at the single-cell level. *Biochem J* 2003; **369:** 331-339

15 **Zong WX**, Edelstein LC, Chen C, Bash J, Gelinas C. The prosurvival Bcl-2 homolog Bfl-1/A1 is a direct transcriptional target of NF-kappaB that blocks TNFalpha-induced apoptosis. *Genes Dev* 1999; **13:** 382-387

16 **Shah RD**, Gonzales F, Golez E, Augustin D, Caudillo S, Abbott A, Morello J, McDonough PM, Paolini PJ, Shubeita HE. The antidiabetic agent rosiglitazone upregulates SERCA2 and enhances TNF-alpha- and LPS-induced NF-kappaB-dependent transcription and TNF-alpha-induced IL-6 secretion in ventricular myocytes. *Cell Physiol Biochem* 2005; **15:** 41-50

17 **Takada I**, Suzawa M, Kato S. Nuclear receptors as targets for drug development: crosstalk between peroxisome proliferator-activated receptor gamma and cytokines in bone marrow-derived mesenchymal stem cells. *J Pharmacol Sci* 2005; **97:** 184-189

18 **Wang CY**, Guttridge DC, Mayo MW, Baldwin AS Jr. NF-kappaB induces expression of the Bcl-2 homologue A1/Bfl-1 to preferentially suppress chemotherapy-induced apoptosis. *Mol Cell Biol* 1999; **19:** 5923-5929

19 **Wang CY**, Mayo MW, Korneluk RG, Goeddel DV, Baldwin AS Jr. NF-kappaB antiapoptosis: induction of TRAF1 and TRAF2 and c-IAP1 and c-IAP2 to suppress caspase-8 activation. *Science* 1998; **281:** 1680-1683

20 **Kreuz S**, Siegmund D, Rumpf JJ, Samel D, Leverkus M, Janssen O, Hacker G, Dittrich-Breiholz O, Kracht M, Scheurich P, Wajant H. NFkappaB activation by Fas is mediated through FADD, caspase-8, and RIP and is inhibited by FLIP. *J Cell Biol* 2004; **166:** 369-380

21 **Rathore N**, Matta H, Chaudhary PM. An evolutionary conserved pathway of nuclear factor-kappaB activation involving caspase-mediated cleavage and N-end rule pathway-mediated degradation of IkappaBalpha. *J Biol Chem* 2004; **279:** 39358-39365

22 **Wu MX**, Ao Z, Prasad KV, Wu R, Schlossman SF. IEX-1L, an apoptosis inhibitor involved in NF-kappaB-mediated cell survival. *Science* 1998; **281:** 998-1001

23 **Islam S**, Hassan F, Mu MM, Ito H, Koide N, Mori I, Yoshida T, Yokochi T. Piceatannol prevents lipopolysaccharide (LPS)-induced nitric oxide (NO) production and nuclear factor (NF)-kappaB activation by inhibiting IkappaB kinase (IKK). *Microbiol Immunol* 2004; **48:** 729-736

24 **Cressman DE**, Greenbaum LE, DeAngelis RA, Ciliberto G, Furth EE, Poli V, Taub R. Liver failure and defective hepatocyte regeneration in interleukin-6-deficient mice. *Science* 1996; **274:** 1379-1383

25 **Legendre F**, Dudhia J, Pujol JP, Bogdanowicz P. JAK/STAT but not ERK1/ERK2 pathway mediates interleukin (IL)-6/soluble IL-6R down-regulation of Type II collagen, aggrecan core, and link protein transcription in articular chondrocytes. Association with a down-regulation of SOX9 expression. *J Biol Chem* 2003; **278:** 2903-2912

26 **Waris G**, Huh KW, Siddiqui A. Mitochondrially associated hepatitis B virus X protein constitutively activates transcription factors STAT-3 and NF-kappa B via oxidative stress. *Mol Cell Biol* 2001; **21:** 7721-7730

27 **Chaisson ML**, Brooling JT, Ladiges W, Tsai S, Fausto N. Hepatocyte-specific inhibition of NF-kappaB leads to apoptosis after TNF treatment, but not after partial hepatectomy. *J Clin Invest* 2002; **110:** 193-202

28 **Kuhnel F**, Zender L, Paul Y, Tietze MK, Trautwein C, Manns M, Kubicka S. NFkappaB mediates apoptosis through transcriptional activation of Fas (CD95) in adenoviral hepatitis. *J Biol Chem* 2000; **275:** 6421-6427

29 **Gil J**, Alcami J, Esteban M. Induction of apoptosis by double-stranded-RNA-dependent protein kinase (PKR) involves the alpha subunit of eukaryotic translation initiation factor 2 and NF-kappaB. *Mol Cell Biol* 1999; **19:** 4653-4663

Science Editor Wang XL and Guo SY **Language Editor** Elsevier HK

PO Box 2345, Beijing 100023, China
www.wjgnet.com
wjg@wjgnet.com

ELSEVIER

World J Gastroenterol 2005;11(43):6780-6786
World Journal of Gastroenterology ISSN 1007-9327

• *BASIC RESEARCH* •

Effects of different ingredients of zedoary on gene expression of HSC-T6 cells

Yuan Jiang, Ze-Song Li, Fu-Sheng Jiang, Xin Deng, Cong-Shun Yao, Guang Nie

Yuan Jiang, Shenzhen Shajing People's Hospital, Shenzhen 518104, Guangdong Province, China
Ze-Song Li, Shenzhen Yishengtang Biology Enterprise Company, Shenzhen 518126, Guangdong Province, China
Fu-Sheng Jiang, Xin Deng, Guang Nie, Shenzhen Donghu Hospital, Shenzhen 518020, Guangdong Province, China
Cong-Shun Yao, Teaching pharmacology and Research Section of Shenyang Pharmaceutial University, Shenyang 110000, Liaoning Province, China
Supported by Guandong Traditional Chinese Medicine Bureau No.102135 and Shenzhen Technology Bureau No.200204187,
Co-first-author: Yuan Jiang
Co-Correspondent: Yuan Jiang
Correspondence to: Professor Guang Nie, Shenzhen Donghu Hospital, Shenzhen 518020, Guangdong Province, China. fqng1008@163.com
Telephone: +86-755-25634729 Fax: +86-755-27205055
Received: 2004-12-25 Accepted: 2005-02-18

Abstract

AIM: To investigate the effects of four different ingredients of zedoary (Curcuma aromatica oil, Curcumol, β-elemence, and Curcumin) on the gene expressions of hepatic stellate cells (HSCs), and to explore the molecular mechanism of zedoary against hepatic fibrosis at gene network level.

METHODS: We detected the mRNA sequences of 50 liver fibrosis-related genes in GenBank and designed oligonucleotide probes. We synthesized oligonucleotides with PE8909 DNA synthesizing instrument, and carried out oligonucleotide microarray with OGR-04 dropping instrument and aldehyded glass chip. Cultured HSC-T6 cells were treated with different concentrations of Colchicine, Curcuma aromatica oil, Curcumol, β-elemence, and Curcumin. According to the experiment of cell toxicity, we took the appropriate concentrations of medicines that resulted in over 50% of cell survival as experiment concentrations. We collected the cells at 1, 6, 12, and 24 h, and extracted total RNA with TRIzol reagent, then labeled cDNAs with Cy3-dUTP and Cy5-dUTP. These labeled cDNAs were hybridized to an oligonucleotide microarray which was washed several times and scanned by scanner GenePix 4000B. Different gene expressions of HSC-T6 cells were analyzed by ImaGene 4.2 software.

RESULTS: After HSC-T6 cells were cultured in a medium containing 6.25 μg/mL Colchicine for 12 h, expression of TIMP-1 decreased 2.2-folds. After HSC-T6 cells were cultured in a medium containing 78.125 μg/mL of Curcuma aromatica oil for 24 h, the expression of TIMP-2 and IL-6 decreased 2.3- and 2.2-folds, respectively. Moreover, after HSC-T6 cells were cultured in a medium containing 1.5625 μg/mL of Curcumol for 12 h, the expression of TGFβ1 and P450a decreased 2.3- and 2.1-folds, respectively.

CONCLUSION: Our results may show the possible molecular mechanism of Curcuma aromatica oil and Curcumol against hepatic fibrosis.

Key words: DNA microarray; Curcuma aromatica oil; Curcumol; Hepatic stellate cells; Hepatic fibrosis

Jiang Y, Li ZS, Jiang FS, Deng X, Yao CS, Nie G. Effects of different ingredients of zedoary on gene expression of HSC-T6 cells. *World J Gastroenterol* 2005; 11(43): 6780-6786
http://www.wjgnet.com/1007-9327/11/6780.asp

INTRODUCTION

In the past 10 years or more, great progress has been made in treating liver fibrosis with Chinese herbal medicines such as compound 861[1] and Fuzheng Huayu Decoction[2] and Tidu Hugan Decoction[3] as well as single herbal medicines as red sage root, zedoary, Chinese caterpillar fungus, hanfangchin A, extracts from peach seeds. Although many medicines can be used to treat liver fibrosis, effective medicines are still hard to find. Herbal medicines have the characteristics of multiple targets and poly-functioning routes, but genes in the organisms alone form a strict and complicated network. Therefore, study of herbal medicines should focus on the molecular mechanism at the level of genetic network based on the integral bio-system. Genetic chip technology is characterized by high communication, low consumption and miniaturization, thus providing a technological platform to study the mechanism of herbal medicines against liver fibrosis[4].

We found that zedoary could inhibit the proliferation of hepatic stellate cells (HSCs). Curcumin can be used to treat inflammation and tumors and Curcuma aromatica oil functions as an anti-inflammation, anti-virus, anti-tumor and anti-thrombus agent. Now more than 20 chemical ingredients such as Curcumol, Epicurzerenone, β-elemence, Camphene, Isoborneol, Borneol, Cineole, and 4-methyl-pyrazine have been identified from Curcuma

aromatica oil. It was reported that Curcumol and Elemence can function as anti-tumor and virus agents[5, 6]. Xi *et al*.[7] found that zedoary could protect hepatic cells against necrosis and degeneration as well as proliferation of fibrous tissues.

To study the molecular mechanism of zedoary against liver fibrosis, we used the genetic expression spectrum chips to represent 50 genes related to liver fibrosis and substituted HSC-T6 for original HSCs, and investigated the effects of four different ingredients of zedoary (Curcuma aromatica oil, Curcumol, β- elemence, Curcumin) on the gene expression of activated HSCs.

MATERIALS AND METHODS

Materials

Colchicine was purchased from American ALEXIS Co, Elemence injection and Curcumin were obtained from Jingang Pharmaceutic Corporation Ltd, Dalian, China. Curcumol and Curcuma aromatica oil were from Pharmaceutical University, Shenyang, China. HSC-T6 was provided by the Insititute of Hepatology, Shanghai University of Traditional Chinese Medicine and pharmacology. AXSys Probe Punctum-controlling software was purchased from Cartesian Technologies Co., and ImaGene 4.2 figure-analyzing softwares was from American Biodiscovery Co.

Preparatin of gene probes

Design of oligonucleotide probe Oligonucleotide probes were designed by the design software of oligonucleotide probe . The coding region near the 3 end was selected for BLAST analysis. One or two probes related to liver fibrosis whose homology was less than 70% were used as spare probes.

Synthesis of oligonucleotide Oligonucleotides were synthesized by the chemical method of standard subphosphorus imide using PE8909 DNA synthesizer. *N*-MMTr-6- ammonia-2-cyanogen-*N* and *N*-diisopropyl-subimide ammonia were modified by 5- or 3-amino-group. Dense ammonia was deprotected at 55 ℃ and incised for 15 h, and purified by ordinary portland cement column.

Preparation of probes In brief, 0.5 μg/μL oligonucleotide probe was resolved into 3×SSC solution, glass chip was aldehyded and stayed overnight, processed with 2 g/L SDS de-ion water for 10 min, and then dried for later use.

Preparation of medical culture medium Colchicine was dissolved in double-vaporing water to get the original solution (3.2 mg/mL). Curcumin was mixed with 950 mL/L alcohol to get the original solution (320 mg/L). Curcumol was mixed with 950 mL/L alcohol plus Tween-80 to get the original solution (3.2 mg/mL). Curcuma aromatica oil was mixed with Tween-80 (ratio, 1:10) plus 950 mL/L alcohol to get the original solution (2.5 mg/mL). Elemence injection (5 mg/mL) was used. All the medicines were filtrated through 0.45 micropores and stored at 4 ℃.

Culture of HSC-T6 cells

The ampoule was taken out of the liquid nitrogen jar (wearing protective glasses and gloves) and put into a porcelain enamel vessel containing 36-37 ℃ water with shaking. The pocket was cut and the ampoule was taken out, sterilized with 700 mL/L alcohol. The cell suspension was aspirated and put into centrifuge tube, then 10 mL culture medium was added, centrifuged for 5 min at 500-1 000 r/min and rinsed . The culture medium was changed on the next day.

Test of cytotoxicity (MTT assay[8])

The 96-well plates were incubated at 37 °C until HSC-T6 cells were grown in a single layer. The culture medium was incubated for 48 h, and then 5 mg/mL MTT was added and incubated for 48 h. The A value of the solution was tested in enzymatic marking instrument (wave length on the light-filtrating slice is 492 nm). According to the experiment of cell toxicity, we took the appropriate concentrations of medicines that resulted in over 50% of cell survival. The formula of cell survival rate: cell survival rate (%) = (medicine group/control group)×100%.

Incubation of HSC-T6 cells with medicines at different times

HSC-T6 cells were incubated with different concentrations of Colchicine, Curcuma aromatica oil, Curcumol, β-elemence, and Curcumin, followed by collecting them at 1, 6, 12, and 24 h, respectively.

Extraction and evaluation of cellular tRNA

Extraction of cellular tRNA HSC-T6 cells were washed softly with germ-free PBS. One-milliliter of TRIzol reagent was used to blow the cells and to make them dissolve completely. Then 0.2 mL of methylene trichloride was added, followed by centrifugation at 12 000 *g* for 15 min at 4 ℃. The supernatant was aspirated with 200 μL tip (dealt with DEPC) and moved to another EP tube. Then 0.5 mL of isopropylalcohol was added and put aside for 15 min, and centrifuged at 12 000 *g* for 10 min at 4 ℃. The RNA was washed with 750 mL/L alcohol (dealt with DEPC), and then 1 mL of 750 mL/L alcohol (dealt with DEPC) was added, centrifuged at 7 500 r/min for 5 min at 4 ℃, and stored at -20 ℃.

Evaluation of purity DEPC water was added to 2 μL of RNA to make a total volume of 100 μL. Ultraviolet spectrophotometer was used to measure the value of A_{260} and A_{280} as well as A_{260}/A_{280}. The formula of concentration of RNA: RNA (μg/μL) = A_{260}×40× dilution multiple/1 000.

Evaluation of integrity Five-microliter of RNA samples were put into 10 mL/L formaldehyde degeneration sepharose for cataphoresis, followed by painting with EB and examination under ultraviolet light.

Reverse transcription system and the labeling and purification of cDNA

Reverse transcription system and conditions Ten-microliter of TRNA (10 μg/μL), 0.3 μL of positive control, 4.0 μL of oligo (dT)16 (0.5 μg/μL) and 0.5 μL of

Table 1 Genetic probe matrix related to liver fibrosis

Genetic probe matrix											
TIMP1	TIMP1	TIMP2	TIMP2	TIMP3	TIMP3	MMP2	MMP2	MMP8	MMP8	TGFβ1	TGFβ1
PDGFA	PDGFA	PDGFC	PDGFC	MMP3	MMP3	IL-6	IL-6	IL-10	IL-10	IL-1	IL-1
HGF2	HGF2	HGF1	HGF1	VEGFA	VEGFA	VEGFB	VEGFB	VEGFC	VEGFC	VEGFD	VEGFD
IGF2	IGF2	IGF1	IGF1	TGFβR Ⅰ	TGFβR Ⅰ	TGFβR Ⅱ	TGFβR Ⅱ	PDGFRα	PDGFRα	PDGFRβ	PDGFRβ
N	N	P	P	N	N	P	P	N	N	P	P
C-myc	C-myc	P-450d	P-450d	P-450a	P-450a	P-450e	P-450e	P450-4A3	P450-4A	P-450-LA	P-450-LA
TNFα	TNFα	TNFR1	TNFR1	CJUNB	CJUNB	CJUND	CJUND	ETRA	ETRA	ET-1	ET-1
CYP2D4	CYP2D4	CYP1B1	CYP1B1	ESTSUL	ESTSUL	FGF1	FGF1	STAA	STAA	FGF2	FGF2
ICAM-1	ICAM-1	PAFR	PAFR	VCAM-1	VCAM-1	MIP-2	MIP-2	MCP-1	MCP-1	PAF	PAF
β-actin	β-actin	GAPDH	GAPDH								

RNase inhibitor (40 U/μL) were mixed together, incubated for 10 min and then put into ice bath. Then 5.0 μL of 5× first chain buffer, 2.0 μL of DTT (0.1 mol/L), 1.0 μL of Cy3-dUTP or Cy5-dUTP (1 mmol/L), 0.5 μL of dTTP (10 mmol/L, and 0.1 μL of each dATP, dCTP and dGTP (100 mmol/L) were mixed together and incubated for 2 min at 42 ℃. Then 1.0 μL of SuperScript II RNase H-transcriptase (10 U/μL) was added and incubated for 2 h. Then 1.0 μL of RNaseH was added and incubated for 0.5 h at 30 ℃, followed by inactivation of anti-transcriptase at 70 ℃ for 15 min. Then 5.0 μL of NaOH (1 mol/L) was added and incubated at 65 ℃ for 1 h, followed by addition of 5.0 μL of 1 mol/L HCl (pH 6.8) and 6.0 μL of 5 mol/L NaCl. The sediment was stayed overnight at –20 ℃, centrifuged at 12 000 *g* for 10 min at 4 ℃. The supernatant was abandoned, the sedimentation was washed once with 750 mL/L alcohol and then dried, followed by resolving in 2 μL of aseptic water and stored at -20 ℃.

Evaluation of cDNA One-microliter of the above product of reverse transcription was put into 10 mL/L formaldehyde degeneration sepharose for cataphoresis, and then the quality of probes was evaluated.

Hybridization and wash

Two microliters of probes labeled by fluorescence were diluted to 8 μL for hybridization, and the hybridization liquor was moved onto the cover glass chip with the density of 2 μL/cm^2. The solution was put onto the carry sheet glass chip equally by the capillarity between cover glass chip and carry sheet glass chip. Then the glass chips were put into a hybridization box and 5 μL of 3× SSC was added to keep the humidity. The probe washing temperatures varied according to the different probes, usually under room temperature. The order of washing liquor was lotion A–C.

Analysis of data from fluorescence

After hybridization, the genetic chips were scanned by Scanner Genepix 4 000B, ImaGene4.2 was used to analyze the ratio of Cy3, Cy5 and the intensity of two kinds of fluorescence signals.Housekeeping gene and positive control were taken to balance the data of fluorescence of Cy3 and Cy5. Ratio of Cy3, Cy5>2 or <0.5 was used to evaluate the differences of genetic expression.

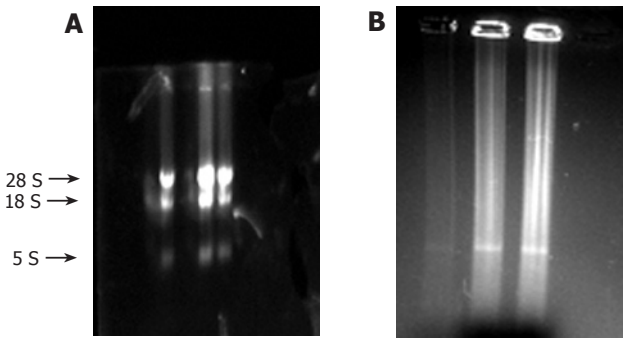

Figure 1 Influence of ingredients of zedoary on genetic expression of HSCs. **A:** tRNA formaldehyde degeneration; **B:** products of reverse transcription.

RESULTS

Effects of different medicines on the growth of HSCs

After treatment of HSC-T6 cells with different concentrations of Colchicine, Curcuma aromatica oil, Curcumol, β-elemence, and Curcumin for 48 h, along with deduction of the concentrations, the survival ratio of HSC-T6 increased.

Influence of four different ingredients of zedoary on the genetic expression of HSCs

RNA was put on 10 mL/L formaldehyde agarose gels for cataphoresis, and the results were recorded with gel photography. Three strips (28S, 18S, and 5S) can be seen in Figure 1A. After the analysis by software, the ratio of 28S and 18S was found to be between 1.5 and 2.0, showing that the RNA was integral and without degradation. Using ultraviolet spectrophotometer, the value of A_{260}/A_{280} was found to be between 1.7 and 2.0, showing that the RNA was pure and without protein pollution or phenol.

In addition, most of the cDNAs were observed between 0.5 and 2 kb (Figure 1B). Distribution of probes is shown in Table 1.

Hybridization

In the hybridization scanning figures of probes (Figures 2A, 3A, and 4A), the green spots represent the locations of downregulated genetic expression. ImaGene 4.2 software was used to analyze the intensity and ratio of Cy3 and Cy5. After correction of housekeeping gene and positive

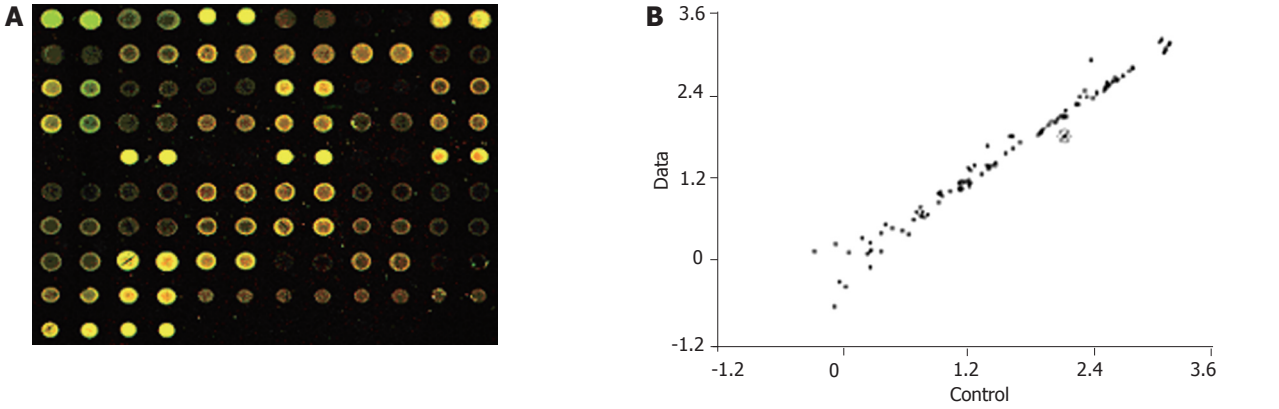

Figure 2 Effects of 6.25 μg/mL Colchicines on genetic expression of HSC-T6 cells after 12 h. **A:** Scanning diagram; **B:** scattering diagram.

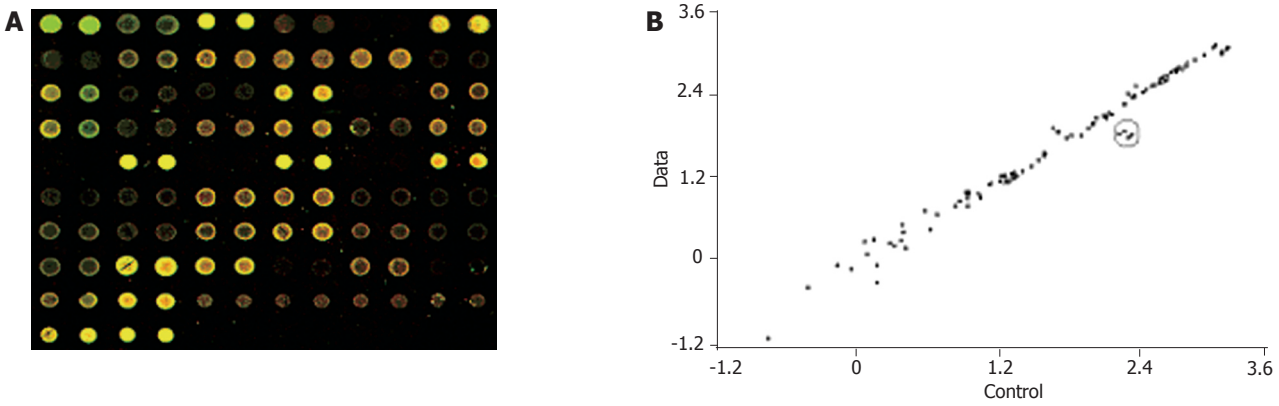

Figure 3 Effects of 78.125 μg/mL Curcuma aromatica oil on genetic expression of HSC-T6 cells after 24 h. **A:** Scanning diagram; **B:** scattering diagram.

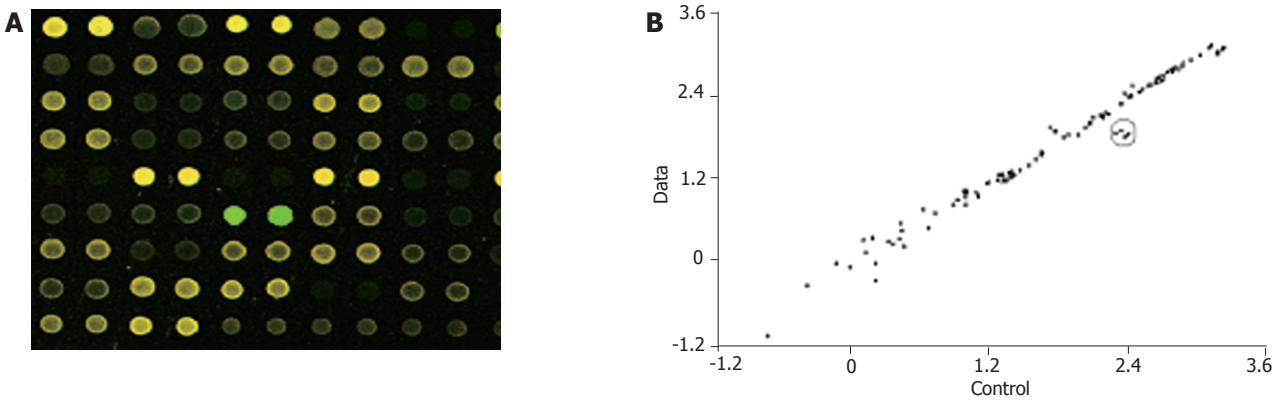

Figure 4 Effects of 1.5625 μg/mL Curcumol on genetic expression of HSC-T6 cells after12 h. **A:** Scanning diagram; **B:** scattering diagram.

control, the two conditions were taken to evaluate the difference of genetic expression as follows: (1) the ratio of Cy3 and Cy5 >2 or <0.5; and (2) one of Cy3 and Cy5 >1 000. In the scattering diagram (Figures 2B, 3B, and 4B), the spots on the opposite angles show that the intensity of two groups (treatment group and control group) was the same. The farther they depart from the opposite angles, the bigger the difference of genetic expression would be. The different effects of medicines on genetic expression are shown in Tables 2-4. After culture of HSC-T6 cells in a medium containing 6.25 μg/mL of Colchicine for 12 h, the expression of TIMP-1 decreased 2.2-folds, which was in agreement with a previous report[9], suggesting that the genetic probe testing system in the experiment was dependable. Furthermore, Figures 3 and 4 stand for the scattering diagram and the scattering diagram of Curcuma aromatica oil group and Curcumol group, respectively, and the data of analysis are shown in Tables 3 and 4.

Table 2 Genetic expression difference of HSC-T6 cells treated with Colchicines (6.25μg/mL) for 12 h

Gene	GenBank	Ratio
TIMP-1	U06179	2.20

Table 3 Genetic expression difference of HSC-T6 cells treated with Curcuma aromatica oil (78.125 μg/mL) for 24 h

Gene	GenBank	Ratio
TIMP-2	NM-021989	2.30
IL-6	M26744	2.20

Table 4 Gene expression difference of HSC-T6 cells treated with Curcumol (1.5625 μg/mL) for12 h

Gene	GenBank	Ratio
TGFβ1	NM-021578	2.30
P-450a	J02669	2.10

These results showed that after HSC-T6 cells were cultured in a medium containing 6.25 μg/mL Colchicine for 12 h, the expression of TIMP-1 decreased 2.2-folds. The expression of TIMP-2 and IL-6 decreased 2.3- and 2.2-folds, respectively, after HSC-T6 cells were cultured in a medium containing 78.125 μg/mL of Curcuma aromatica oil for 24 h. Moreover, the expression of TGFβ1 and p450a decreased 2.3- and 2.1-folds, respectively, after HSC-T6 cells were cultured in a medium containing 1.5625 μg/mL Curcumol for 12 h. Other concentrations of neither Curcuma aromatica oil nor Curcumol could bring forth gene expression differences, nor did β-elemence and Curcumin.

DISCUSSION

Genetic chip technology is characterized by high communication, low consumption and miniaturization[10-13], providing a technological platform to study the mechanism of herbal medicines against liver fibrosis. Genetic expression spectrum chips can be categorized into two kinds, namely cDNA chips and oligonucleotide chips, the probe of the former is cDNA, the probe of the latter is fragment of oligonucleotide. To study medicines with genetic expression spectrum chips can help us acknowledge the target genes of herbal medicines, western medicine and some foods with medical functions. It is also an effective way to study the toxicity of medicines, and the mechanism of causing deformity and genetic mutation of medicines.

According to the key role of HSCs in hepatic fibrosis, 50 genes related to liver fibrosis are chosen. They can be categorized into five groups as follows: (1) expressing cytokines and receptors of cytokines, such as transforming growth factor β1 (TGF β1), platelet-derived growth factor A (PDGFA), platelet-derived growth factor C (PDGFC), interleukin-1, interleukin-6, interleukin-10, hepatocyte growth factor 1 (HGF1), hepatocyte growth factor 2 (HGF2), vascular endothelial growth factor A (VEGFA), vascular endothelial growth factor B (VEGFB), vascular endothelial growth factor C (VEGFC), vascular endothelial growth factor D (VEGFD), fibroblast growth factor 1 (FGF1), fibroblast growth factor 2 (FGF2), platelet-activating factor (PAF), tumor necrosis factor α (TNFα), insulin-like growth factor 1 (IGF1), insulin-like growth factor 2 (IGF2), endothelin 1 (ET-1), intercellular adhesion molecule 1 (ICAM-1), vascular cell adhesion molecule 1 (VCAM-1), murine macrophage inflammatory protein 2 (MIP-2), monocyte chemotactic protein 1 (MCP-1), transforming growth factor β receptor I (TGFβRI), transforming growth factor β receptor II (TGFβRII), platelet-derived growth factor receptor α (PDGFRα), platelet-derived growth factor receptor β (PDGFRβ), tumor necrosis factor α receptor 1 (TNFαR1), platelet-activating factor receptor (PAFR), and endothelin receptor A (ETRA). TGFβ1 is the strongest factor which promotes the synthesis of extracellular matrix (ECM). PDGF can accelerate the proliferation of HSCs; (2) expressing MMPs (matrix metalloproteinases) and TIMPs (tissue inhibitor of metalloproteinases), such as MMP2, MMP3, MMP8, TIMP-1, TIMP-2, and TIMP-3, which take part in the degradation of ECM; (3) gene expression related to the preliminary activation of HSCs, such as c-myc, Ets-1, STAT1, c-jun B, c-jun D; (4) involving in gene expression related to the biological oxidation[14], such as cytochrome P450d, cytochrome P450a, cytochrome P450e, cytochrome P450-LA, and cytochrome P450 (4A3), CYP1B1, CYP2D4; and (5) house keeping gene, such as β-actin and GAPDH.

How to choose the genes related to liver fibrosis is the key of the design of oligonucleotide probes. The mRNA sequences which contain 40 amino acids are selected and then oligonucleotide probes are designed using the design software of oligonucleotide probe. By and large, the length of oligonucleotide probe is 15-80 nt, the content of GC is 45-55%. Probes of the coding region approaching end 3 are chosen for BLAST analysis. One to two probes whose homology of sequences was less than 70% are chosen as gene distinctive oligonucleotide probes.

Because some sequences of mRNA related to collagen I, III, IV are so short, the probes designed through software are easy to cause cross reactions which may result in false positive results, and such genes, therefore, cannot be chosen. However, the aforementioned 50 genes, in general, can represent approximately the changes which take place in the process of preliminary and persistent activation of HSCs in liver fibrosis.

HSC-T6 cells are SV40 transfected HSCs of Sprague-Dawley rats. The cells can be steadily cultured and their phenotype is activated HSCs which can express high-level collagen I and TIMP-1 mRNA, etc. In our study, HSC-T6 was substituted for the original HSC. Yin *et al.*[15,16] took HSC-T6 as model cells to investigate the influence of compound 861 on the gene expression of MMP-3 and TIMP-1 and they found that 0.25, 0.5, and 1.0 mg/mL of compound 861 could increase the expression of MMP3 and inhibit the expression of TIMP1.

TIMPs can prevent MMPs from degrading ECM[17-21]. Using genetic chip technology, we found that after HSC-T6 cells were cultured in a medium containing 6.25 μg/mL

Colchicine for 12 h, the expression of TIMP-1 decreased 2.2-folds. Expression of TIMP-2 decreased 2.3-folds after HSC-T6 cells were cultured in a medium containing 78.125 μg/mL Curcuma aromatica oil for 24 h. These results showed that Curcuma aromatica oil, like Colchicines, can also inhibit the expression of TIMPs and reduce the inhibition of MMPs which, in turn, help MMPs to degrade ECM. This may be one of the mechanisms for zedoary against liver fibrosis.

IL-6 is also called hepatic cell stimulating factor which can directly stimulate hepatic cells proliferation, induce the expression of IL-6 receptors in liver, and stimulate fibroblastic cells to synthesize collagens[22–26]. In our study, 78.125 μg/mL Curcuma aromatica oil could decrease the expressions of IL-6, TIMP1 and other genes related to hepatic fibrosis, thereby enhancing MMPs to degrade ECM. It might be another mechanism of zedoary against hepatic fibrosis.

TGFβ1 plays an important role in hepatic fibrosis which can activate HSCs and, as a transcription factor of collagen, accelerate its expression[27]. In our study, the expression of TGFβ1 decreased 2.3-folds after culture of HSC-T6 cells in a medium containing 1.5625 μg/L Curcumol for 12 h, suggesting that Curcumol can inhibit the synthesis of ECM through the inhibition of TGFβ1 which might be an another important mechanism of zedoary against hepatic fibrosis.

Cytochrome P450 (or Cyt P450) involves in the synthesis of steroid hormone, bile acid and bile pigments as well as the process of the bio-transformation of medicine and poison[14]. Yang *et al*.[28] have shown that lipid peroxidation takes part in the activation of HSCs. Svegliati Baroni *et al*.[29] have indicated that HCM/Fe might induce a significant increase in collagen type I accumulation in HSC culture media, and HSCs proliferation may be associated with changes in the Na^+/H^+ exchanger activity. Nieto *et al*.[30] transfected CYP2E1 to HSC-T6 cells, and found that there was an increase in the level of reactive oxygen species and type I collagen mRNA. It has been reported that when HSCs were cultured with HepG2 cells which overexpress CYP2E1 together, the level of collagen markedly increased, suggesting that the solved oxidants can activate HSCs[31]. In our study, we found that after culture of HSC-T6 cells in a medium containing 1.5625 μg/mL Curcumol for 12 h, the expression of P450a decreased 2.1-folds, suggesting that the metabolism of Curcumol in HSC-T6 cells might bring forth oxidation-conjugation reaction through the P450 enzyme system, induce a decline of oxidative stress and lipid peroxidation, and thus inhibit the activation of HSCs. This may be one of the mechanisms of zedoary against hepatic fibrosis.

In conclusion, two different ingredients of zedoary (Curcuma aromatica oil, Curcumol), when treated with HSC-T6 cells for 24 and 12 h, can decrease the expression of TIMP-2, IL-6, TGFβ1 and P450a by different degrees, indicating the molecular mechanisms of zedoary against hepatic fibrosis at gene network level. But the changes of genes and the expression of proteins might not be the same events. Along with the development of protein histology, further research needs to testify the proteins related to liver fibrosis, for example, to examine the content of type I collagen using ELISA or investigate the influence of Curcuma aromatica oil and Curcumol on protein expression of HSC-T6 cells by protein chip technology.

REFERENCES

1 **Wang L**, Wang J, Wang BE, Xiao PG, Qiao YJ, Tan XH. Effects of herbal compound 861 on human hepatic stellate cell proliferation and activation. *World J Gastroenterol* 2004; **10**: 2831-2835

2 **Liu C**, Wang X, Liu P. Serapharmacological effect of fuzheng huayu 319 Decoction on expression of type I collagen and transforming growth factor beta 1 in hepatic stellate cells. *Zhongguo Zhongxiyi Jiehe Zazhi* 1999; **19**: 412-414

3 **Zhu QJ**, Nie G, Li HW, Xiao L, Hu CQ, Yang L, Ming AP, Wang BX.Inhibitory effect of Tidu Hugan Decoction on experimental hepatic fibrosis in ducks. *Zhongxiyi Jiehe Ganbing Zazhi* 1998; **8**: 84-87

4 **Abelson PH**. *A third technological revolution.Science* 1998; **279**: 2019

5 **Wang Y**, Wang MZ. Reseach of commonly used Chinese traditional medicine: Curcuma categories. *Zhongguo Yaoxue Zazhi* 2001; **36**: 80

6 **Li GD**, Xiu F, Shen AJ. Reseach of Curcuma aramatica oil. *Zhongguo Yaoxue Zazhi* 2002; **37**: 806-809

7 **Xi ZT**, Shan CM, Jiang XL, Luan XY, Li KK.Experimental study of Sparganium stoloniferum and zedoary on immunological hepatic fibrosis in rats. *Zhongguo Zhongyao Zazhi* 2002; **27**: 929-932

8 **Bian XY**, Yin XN.The method and application of MTT assay. *Gouwai Yixue Linchuang Shengwu Huaxue Yu Jianyanxue Fence* 1998; **19**: 83-85

9 **Yang CQ**, Hu GL, Zhou WH.Effect of Colchicine on Matrix metalloproteinase-1 and tissue inhibitor of metalloproteinase-1 expression in rat liver fibrosis. *Zhonghua Chuanran Bing Zazhi* 2000; **18**: 176-179

10 **Schena M**, Heller RA, Theriault TP, Konrad K, Lachenmeier E, Davis RW. Microarrays: biotechnology's discovery platform for functional genomics. *Trends Biotechnol* 1998; **16**: 301-306

11 **Persidis A**. Biochips. *Nature Biotechol* 1998; **16**: 981-983

12 **Schena M**, Shalon D, Heller R, Chai A, Brown PO, Davis RW.Parallel human genome analysis: microarray-based expression monitoring of 1000 genes. *Proc Natl Acad Sci USA* 1996; **93**: 10614-10619

13 **Debouck C**, Goodfellow PN.DNA microarrays in drug discovery and development. *Nat Genet* 1999; **21** (suppl): 48-50

14 **Zhou AR**. Biochemistry. Fifth edition. *Beijing: Renming Weisheng Chuban She* 2001: 160

15 **Yin CH**, Ma H, Wang AM, Ma XM, Jia JD, Wang BE.Effect of compound 861 on tissue inhibitor of metalloprotenase 1 gene expression of HSC-T6 cells . *Zhonghua Ganzang Bing Zazhi* 2002; **10**: 197-199

16 **Yin C**, Ma H, Wang A, Ma X, Jia J, Wang B.Effect of compound 861 on stromelysin gene expression of HSC-T6 cells. *Linchuang Gandanbing Zazhi* 2002; **18**: 168-170

17 **Iredale JP**.Tissue inhibitors of metalloproteinases in liver fibrosis. *Int J Biochem Cell Biol* 1997; **29**: 43-54

18 **McCrudden R**, Iredale JP. Liver fibrosis, the hepatic stellate cell and tissue inhibitors of metalloproteinases. *Histol Histopathol* 2000; **15**: 1159-1168

19 **Murawaki Y**, Ikuta Y, Koda M, Okamoto K, Mimura K. The pro MMP-2 activation rate in patients with chronic viral liver disease. *Clin Chim Acta* 2002; **324**: 99-103

20 **Nie QH**, Zhou YX, Xie YM, Chen YQ.The localization and

expression of TIMP-2 in experi mental hepatic fibrosis in rats. *Jiefangjun Yixue Zazhi* 2002; **27**: 208-209
21 **Luo XD**, Nie QH.The value of tissue inhibitors of metalloproteinases in the study of hepatic fibrosis. *Ganzang* 2003; **8**: 40-42
22 **Li D**, Zhang LJ, Chen ZX, Huang YH, Wang XZ. Effects of TNFα, IL-6 and IL-10 on the development of experimental rat liver fibrosis. *Shijie Huaren Xiaohua Zazhi* 2001; **9**: 1242-1245
23 **Llorent L**, Richaud-Patin Y, Alcocer-Castillejos N, Ruiz-Soto R, Mercado MA, Orozco H, Gamboa-Dominguez A, Alcocer-Varela J. Cytokine gene expression in cirrhotic and non-cirrhotic human liver. *J Hepatol* 1996; **24**: 555-563
24 **Liu HL**, Li XH, Wang DY, Yang SP. Matrix metalloproteinase-2 and tissue inhibitor of metalloproteinase-1 expression in fibrotic rat liver. *World J Gastroenterol* 2000; **6**: 881-884
25 **Ramadori G**, Christ B. Cytokines and the hepatic acute-phase response. *Semi Liver Dis* 1999; **19**: 141-155
26 **Moshage H**. Cytokines and the hepatic acute phase response. *J Pathol* 1997; **181**: 257-266
27 **Wang LS**, Chen YW, Li DG. Activation of TGF-β1 and liver fibrosis. *Gouwai Yixue Xiaohua Xitong Fence* 2003; **23**: 222-225
28 **Yang WF**, Chen HC, Jiang YP.Factors in hepatic stellate cells activation. *Zhonghua Ganzang Bing Zazhi* 2004; **12**: 121-123
29 **Svegliati Baroni G**, D'Ambrosio L, Ferretti G, Casini A, Di Sario A, Salzano R, Ridolfi F, Saccomanno S, Jezequel AM, Benedetti A. Fibrogenic effect of oxidative stress on rat hepatic stellate cells. *Hepatology* 1998; **27**: 720-726
30 **Nieto N**, Friedman SL, Greenwel P, Cederbaum AI. CYP2E1-mediated oxidative stress induces collagen type I expression in rat hepatic stellate cells. *Hepatology* 1999; **30**: 987-996
31 **Mari M**, Cederbaum Al. Induction of catalase, alpha, and microsomal glutathione S-transferase in CYP2E1 overexpressing HepG2 cells and protection against short-term oxidative stress. *Hepatology* 2001; **33**: 652-661

Science Editor Kumar M, Wang XL and Guo SY **Language Editor** Elsevier HK

PO Box 2345, Beijing 100023, China
www.wjgnet.com
wjg@wjgnet.com

ELSEVIER

World J Gastroenterol 2005;11(43):6787-6791
World Journal of Gastroenterology ISSN 1007-9327

• *CLINICAL RESEARCH* •

Changes of duplex parameters and splenic size in liver transplant recipients during a long period of observation

Bita Boozari, Michael Gebel, Mathias J Bahr, Michael P Manns, Christian P Strassburg, Joerg S Bleck, J Klempnauer, Bjoern Nashan

Bita Boozari, Michael Gebel, Mathias J Bahr, Michael P Manns, Christian P Strassburg, Joerg S Bleck, Department of Gastroenterology, Hepatology and Endocrinology, Medical School of Hannover, Carl-Neuberg-Str. 1, 30625 Hannover, Germany
J Klempnauer, Department of Visceral and Transplant Surgery, Medical School of Hannover, Carl-Neuberg-Str. 1, 30625 Hannover, Germany
Bjoern Nashan, Department of Transplant Surgery, Dalhousie University, QEII HSC, VG Site 6S-202, 1278 Tower Road, Halifax, Nova Scotia B3H 2Y9, Canada
Correspondence to: Dr Med. B Boozari, Department of Gastroenterology, Hepatology and Endocrinology, Medical School of Hannover, Carl-Neuberg-Str. 1, 30625 Hannover, Germany. bita.boozari@t-online.de
Telephone: +49-511-532-9203 Fax: +49-511-532-9405
Received: 2004-11-28 Accepted: 2005-01-26

Abstract

AIM: To assess the changes of portal and arterial velocities, resistance index, spleen and liver size during a long observation period (13.7 years) after orthotopic liver transplantation (OLT).

METHODS: Two hundred and sixty patients were recruited retrospectively for this study and divided into groups with defined time intervals after OLT. The cross-sectional changes of portal and arterial velocities, resistance index, spleen and liver size between the defined time intervals were studied. The complications detected by ultrasound were compared to gold standard methods.

RESULTS: The mean values for liver size were all within the normal range. The splenic size decreased between the time intervals 100 and 1 000 d after OLT (*t*; $P<0.01$). While portal and arterial flow velocities decreased up to 5.5 years (*t*; portal velocity $P<0.01$, maximal systolic velocity $P = 0.05$, maximal end diastolic velocity $P<0.01$), RI increased during this interval (*t*: $P<0.01$). Higher RI values were found in older patients ($r = 0.24$, $P<0.001$).

CONCLUSION: The arterial and portal velocities show adaptation processes continuing over the course of many years after OLT and are reported for the first time. The vascular complications detected by ultrasound occur mostly up to 100 d after OLT.

Key words: Ultrasound; Color Doppler; Liver transplantation; Monitoring

Boozari B, Gebel M, Bahr MJ, Manns MP, Strassburg CP, Bleck JS, Klempnauer J, Nashan B. Changes of duplex parameters and splenic size in liver transplant recipients during a long period of observation. *World J Gastroenterol* 2005; 11 (43): 6787-6791
http://www.wjgnet.com/1007-9327/11/6787.asp

INTRODUCTION

Since the 1980s, OLT has become a standard therapy for patients with end-stage liver disease[1] and till date, the outcome of this therapy depends on the early diagnosis and appropriate treatment of complications[2]. Vascular complications are a frequent cause of early graft failure[3]. Graft damage can be either directly caused by hypoxemia or indirectly by biliary ischemia during graft handling which equally leads to chronic biliary damage[4,5]. Time-dependent changes of splanchnic hemodynamics in liver graft recipients have been reported[6]. Based on these data, it is likely that an understanding and interpretation of splanchnic hemodynamics may lead to the prevention and diagnosis of vascular complications[6].

Apart from physical examination and biochemical work-up, routine and diagnostic imaging procedures are recommended to detect post-OLT vascular complications[7-9]. B-mode and especially color Doppler sonography have played a central role in the monitoring of post-transplantation patients. The use of ultrasound allows for the early diagnosis of hepatic arterial as well as biliary complications[3,9,10] and contributes to a better understanding of splanchnic hemodynamic changes[6].

Long-term follow-up studies of splanchnic hemodynamic changes after OLT are time consuming and therefore not applicable. The aim of this study was to assess the post-transplantation changes of duplex parameter as well as liver and splenic size in liver graft recipients for a long period of observation. This study was performed retrospectively as a cross-sectional analysis in a large cohort of OLT patients. The secondary objective of this study was to assess the post-transplantation complications detected by ultrasound during this observation time.

MATERIALS AND METHODS

All the liver graft recipients received routine ultrasound

examinations in our sonography department. For this study, we chose a sample of all OLT patients (with or without clinical problems) who received ultrasound examinations between February 2000 and December 2001. Five hundred and eighteen ultrasound examinations on 282 patients were performed during this period. Patients who received at least one ultrasound examination after liver transplantation were included in this study. In the case of multiple ultrasound examinations, one examination was chosen randomly in order to prevent dependencies, due to multiple measurements of a single case. Patients who had acute cardiac or renal failure were excluded (n = 2). Two hundred and sixty consecutive patients were included, and their clinical characteristics are shown in Tables 1 and 2.

All patients were examined with high-end ultrasound equipment Power Vision 8000 (Toshiba, Japan) and Elegra Sonoline Advanced (Siemens, Germany) using convex arrays 3.5C40H (Siemens, Germany) and C 3-6 MHz (Toshiba, Japan) as well as sector array 3-6 MHz (Toshiba, Japan). The patients were examined by two gastroenterologists with more than 20 years of experience in the field of ultrasound.

Systematic B-mode examination of all abdominal organs including the retroperitoneum was performed following the recommendations of the German Association of Ultrasound in Medicine (DEGUM). Liver size was measured by the diameter of the right lobe in the mid clavicular line (MCL). The spleen length was measured from upper to lower pole in an oblique intercostal array position. The normal liver size was defined as 13±0.5 cm[11]. The normal spleen size was defined as 11±0.5 cm[11]. In addition, the portal vein and the bile duct anastomosis were examined in the proximal and distal portion.

The maximum velocity of the portal vein [(P)V_{max}], the maximum systolic velocity [(A)V_{max}], the maximum end diastolic velocity [(A)V_{min}] and the resistance index of the hepatic artery (RI) were measured before and after the anastomosis in each case after an overnight fasting. Settings such as gain, filter, and pulse-repetition frequencies were adjusted as needed for optimal signal detection to prevent artifacts. Segmental arterial stenosis was considered to be present when circumscript aliasing was visualized by color Doppler sonography using the maximal pulse repetition frequency (PRF) as well as the presence of a V_{max} exceeding 170 cm/s. Alternatively, in case of the absence of a segmental stenosis, the detection of a tardus-parvus duplex spectrum with a cut off RI below 0.5 in addition to a V_{max}>170 cm/s was required for the definition of a stenosis. Stenosis of the portal vein required a two-fold increase of flow velocity in the stenosis. Dilated intrahepatic and extrahepatic bile ducts were defined as exceeding 3 and 10 mm in diameter (DEGUM guidelines), respectively.

The complications detected by ultrasound were confirmed by following the gold standard methods. In all patients with suspected stenosis or thrombosis of the hepatic artery by ultrasound examination, a CT-angiography was performed to confirm the diagnosis. Most of the biliary complications such as bile duct dilatation, thickening, stricture, and calculi in the bile duct system were confirmed by endoscopic retrograde cholangiopancreatic ography (ERCP) in patients with chocholedochostomy[12] and by percutaneous transhepatic cholangiography (PTC) in patients with status after hepaticojejunostomy. The occurrence of intrahepatic abscesses was confirmed by biopsy. Liver biopsies after OLT were available from 94 patients (n = 45 acute rejections, n = 2 chronic rejections, n = 2 ischemia, n = 21 viral re-infection, n = 21 fibrosis, n = 7 cirrhosis, n = 33 cholangitis).

Statistical evaluation was performed using the SPSS 11.5 software package for Windows™. Mean values and standard errors of the means (mean±SE) as well as frequencies were calculated. Correlations were done using Spearman's (S) rank correlation coefficient. We also analyzed the changes of the velocity values as well as organ sizes in the course of time. Due to different time points of ultrasound examinations after OLT, we divided the patients in groups with defined time intervals after OLT. The time points were days 100 (1), 1 000 (2), 2 000 (3), 3 000 (4), 4 000 (5) and 5 000 (6) after OLT. The number of patients at the defined time intervals was as follows: n = 20 (1), n = 120 (2), n = 81 (3), n = 48 (4), n = 25 (5), n = 11 (6). At these time points, the data of patients before the defined

Table 1 Clinical characteristics of the patients included in this study

Parameter	Value
Gender (M/F)	165/95
Age (yr)	49.8±0.8
Age (yr)	18.5–74.5
Mean time after OLT (d)	1 523.3±97.6
Mean US evaluation time after OLT (d)	2–8 912
Full size OLT (n)	244
Split liver OLT (n)	16

Table 2 Etiologies of liver diseases leading to OLT

Etiology	Cases (n)
Chronic hepatitis B	37
Primary sclerosing cholangitis	36
Chronic hepatitis C	33
Chronic hepatitis and hepatocellular carcinoma	24
Primary biliary cirrhosis	18
Cryptogenic liver disease	18
Cystic liver degeneration	12
Autoimmune hepatitis	12
Budd-Chiari syndrome	12
Alcoholic cirrhosis	10
Primary hepatocellular carcinoma	8
Wilson's disease	8
Others[1]	32

[1]Includes: Oxalosis n = 1 (0.4%), acute hepatitis A, n = 1 (0.4%), CMV infection, n = 1 (0.4%), veno occlusive disease, n = 1 (0.4%), Halothane induced hepatic failure, n = 1 (0.4%), cystic fibrosis, n = 1 (0.4%), tyrosinemia, n = 1 (0.4%), amyloidosis, n = 2 (0.8%), hemochromatosis, n = 2 (0.8%), toxic liver failure, n = 2 (0.8%), secondary sclerosing cholangitis, n = 3 (1.2%), alpha 1 antitrypsin deficiency, n = 3 (1.2%), Caroli's syndrome, n = 3 (1.2%), adenomatosis of the liver, n = 3 (1.2%), carcinoid disease, n = 3 (1.2%), biliary atresia, n = 4 (1.5%).

time point (days after transplantation) were compared with the data of patients after this time point. Mean values of the parameters were calculated and compared for significance using the *t*-test. Therefore, our data reflected only the changes of the studied parameters at these time points. The changes of the parameters in the group of patients before the defined time points were graphically demonstrated. The graphs were assembled using the Prism 3.0 software package.

Correlations as well as the mean values were calculated with and without extremes. The extremes were defined as stenosis or thrombosis of the portal vein and/or the hepatic artery ($n = 8$).

RESULTS

Frequencies of ultrasound-detected B-mode findings/ complications after OLT

Vascular complications over a 13.7-year observation period were detected in one case (0.4%) of thrombosis and five cases (1.9%) of stenosis of the hepatic artery and in seven cases (2.7%) of stenosis of the portal vein by ultrasound (Table 3). All cases were confirmed by CT angiography.

In a 13.7-year observation period by ultrasound examination, 58 (22.3%) patients showed biliary complications, of them 33 (56.9%) had either ERCP or PTC. In 29 patients (87.9%), ultrasound diagnosis was confirmed either by ERCP or PTC. Nine patients (3.5%) had extrahepatic dilatation and 37 cases (14.2%) had intrahepatic dilatation of the bile ducts. One patient (0.4%) had calculi, 14 (5.4%) patients had sludge in the intra- and extra-hepatic bile ducts. Eighteen patients (6.9%) showed a thickening of intra- and extra-hepatic bile duct walls, two cases (0.8%) had intrahepatic abscesses, one patient (0.4%) had stricture of the main hepatic bile duct, 114 patients (43.8%) had splenomegaly after OLT, and 14 patients (5.4%) had detectable ascites (Table 3).

Changes in organ size after liver transplantation

The mean liver size after OLT was 12.2±0.2 cm in MCL. The mean splenic size after liver transplantation was 12.9 ±0.2 cm (Table 4). Women had a smaller spleen than men (12.2±0.3 cm *vs* 13.4±0.2 cm, *t*; $P<0.01$).

Table 3 Ultrasound findings and complications in liver graft recipients

US findings	US frequency in this study (%)	Reported frequency (%)
Thrombosis of the hepatic artery	0.4	12 [21]
Stenosis of the hepatic artery	1.9	3–5 [8]
Stenosis of the portal vein	2.7	1–6.2 [3,17]
Biliary complications generally	22.3	18 [22]
Bile duct dilatations	17.7	7.3–48.8 [20]
Thickening of bile ducts	6.9	
Abscess	0.8	
Calculi of biliary system	6.2	36.6 [20]
Bile duct stricture	0.4	5–14 [21]
Ascites	5.4	
Splenomegaly	43.8	

US, ultrasound.

Table 4 Ultrasound data (mean±SE)

Parameter	Value	Unit
(P) V_{max}	30.0±1.5	cm/s
(A) V_{max}	67.1±4.2	cm/s
(A) V_{min}	20.4±1.6	cm/s
RI	0.69±0.01	
Spleen size	12.9±0.2	cm
Liver size in MCL	12.2±0.2	cm

The changes of mean values for liver and splenic size 100, 1 000, 2 000, 3 000, 4 000, and 5 000 d after OLT were calculated. The mean values for liver size after OLT were all within the normal range and did not change significantly between the studied time intervals. In contrast, the splenic size decreased between the intervals 100 and 1 000 d after OLT. After this interval, the splenic size increased. Consequently, the spleens in the patients more than 1 000 d after OLT were significantly larger than those in the patients less than 1 000 d after OLT (13.6±0.3 cm *vs* 12.2±0.3 cm, *t*; $P<0.01$). The mean splenic size remained higher than the normal range throughout the observed time in this study.

Dynamics of color Doppler parameters in patients after liver transplantation

The mean value of color Doppler data for all patients is shown in Table 4. There was an inverse correlation between (P) V_{max} and time after OLT ($r = -0.41$, $P<0.001$). After exclusion of patients with stenosis and thrombosis of the arterial and portal vein anastomosis in order to eliminate the velocity extremes, the correlation coefficients still remained high ($r = 0.38$, $P<0.001$). There was also an inverse correlation between (A) V_{max} and (A) V_{min} of the hepatic artery and time after OLT [for (A) V_{max} $r = 0.21$, $P<0.01$ and for (A) V_{min} $r = 0.23$, $P<0.01$]. After exclusion of extremes, the correlation persisted [for (A) V_{max} $r = 0.21$, $P<0.01$ and for (A) V_{min} $r = 0.22$, $P<0.01$]. We could not observe a correlation between RI and time after OLT, but we confirmed a significant correlation between RI and age of the patients ($r = 0.24$, $P<0.001$).

The changes of mean values of all color Doppler parameters were calculated 100, 1 000, 2 000, 3 000, 4 000, and 5 000 d post OLT after exclusion of extremes. (P) V_{max} decreased between the time points 100 and 3 000 d after OLT. It was stabilized at a level of 23 cm/s between the time points 3 000 and 4 000 d after OLT and dropped again from day 4 000 (Figure 1A). (A) V_{max} decreased from 100 up to 4 000 d after OLT (Figure 1B). (A) V_{min} decreased from 2 000 d after OLT (Figure 1B). RI increased between 100 and 2 000 d after OLT. From this time point on, we observed a decrease of RI which was stabilized at a level of 0.70 from time point 4 000 d after OLT to the end of the observation time (Figure 1A).

DISCUSSION

All vascular complications detected by duplex measurements in this study occurred within the first 100 d after

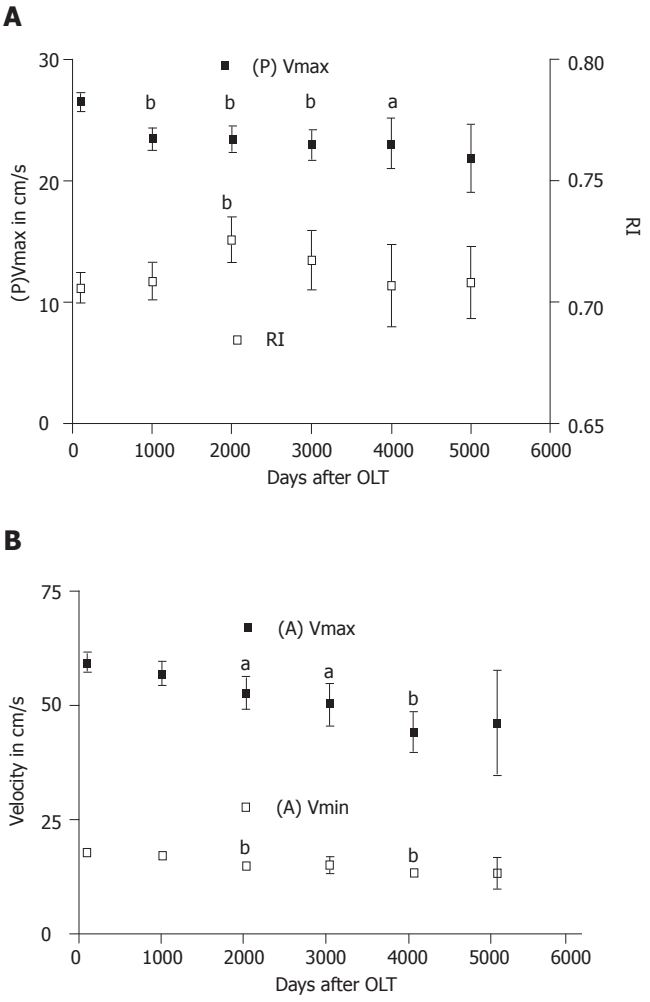

Figure 1 Changes in portal flow velocity and resistance index **(A)** and arterial velocities (A)V_{max} and (A)V_{min} after OLT **(B)** during the course of time after liver transplantation in 260 patients. ($^{a}P<0.05$; $^{b}P<0.01$ *vs* others).

Table 5 Reasons of vascular complications after liver transplantation

Arterial system	
Reperfusion damage	(n = 2)
Thrombosis of the celiac trunk	(n = 1)
Thrombosis of the hepatic artery[1]	(n = 1)
Dissection of the common hepatic artery	(n = 1)
Unknown	(n = 1)
Portal system	
Over average length of the portal anastomosis	(n = 3)
Intraoperative thrombectomy[2]	(n = 2)
Intraoperative thrombectomy of malign thrombus[3]	(n = 1)
Leakage of the biliary anastomosis and consequently	(n = 1)
Systemic infection leading to portal thrombosis	

[1]The patient suffered from fulminant acute hepatitis A with thrombosis of the arterial and portal vascular system at the time of OLT. [2]The patients had Budd-Chiari syndrome as an underlying liver disease. [3]In this particular case, infiltration of a tumor thrombus in the portal venous trunk was observed which led to portal vein stenosis after OLT.

liver transplantation (Table 5). Due to this information as well as the fact that complications such as rejection appear mostly during the early phase after OLT, drastic long-term hemodynamic changes in these patients are not expected. All vascular complications were initially diagnosed by ultrasound examination. Interestingly, a satisfactory blood flow was observed intraoperatively, but these patients developed stenosis after OLT. Routine and protocol ultrasound examinations during this interval are therefore recommended[13,14]. The flow characteristics of patients early after OLT have been reported in prospective studies[6,15]. We therefore focused our study on the long-term changes of these parameters.

The long-term hemodynamic changes in these patients seem to be influenced by factors in the graft itself or alteration of the vascular track. The prospective study of Bolognesi *et al.*[6] is the largest follow-up study investigating the hemodynamic changes in patients after OLT. Compared to this study, our study showed a more heterogeneous spectrum of the underlying liver diseases. Our findings showed that the mean liver size remained within the normal range, independent of the complications, even many years after OLT. Based on the results of liver biopsies after OLT, at least 20% of the patients included in this study had parenchymal changes such as cirrhosis or fibrosis which consequently leads to a smaller liver size. Interestingly, the mean values of liver size still remained stable in the course of studied time points. The mean splenic size was smaller than that of previously reported[6] which may be explained by the heterogeneity of liver diseases with a considerable amount of transplantations without portal hypertension.

Depending on the evaluation time after OLT, an initial increase in portal blood flow in patients with cirrhosis has been reported, which was normalized within 2 years[6]. We observed a decrease of portal blood flow from 100 d to 8.2 years after OLT. This stable decrease may also be influenced by the low prevalence of portal stenosis and thrombosis in our patients. We also detected a decrease of arterial velocities over a long period of time after OLT. This could be caused by the normalization of hyperdynamic circulatory syndromes of patients with cirrhosis at the time of OLT. While the role of arterial RI in patients after kidney transplantation has been extensively studied, the RI changes in liver graft recipients are still unclear. It was reported that a high arterial RI after kidney transplantation is associated with poor subsequent allograft performance and death[16]. In liver graft recipients, an early increase in hepatic arterial resistance has been reported[6,17], which is related to older donor age and prolonged period of ischemia. Higher RI values were found in older patients in our study. RI increase is also attributed to the elevation of portal blood flow early after OLT[6]. In our study, RI did not correlate with portal flow.

Our data have confirmed the reported rate of ultrasound detected complications in patients after liver transplantation. However, the sensitivity of ultrasound for detection of biliary complications is better than that of previously reported[12]. Arterial thrombosis after transplantation has an estimated incidence of 12%[8]. In our patients, thrombosis of the hepatic artery was detected by ultrasound in 0.4% of cases. Since the majority of arterial thromboses occur during the early post-transplantation

period[3] and most of our examinations were performed 100 or more days after OLT, the low prevalence of arterial thrombosis in this study may be related to the time point of investigation. The detection rate of hepatic artery stenosis as well as portal vein thrombosis in our study was comparable to the reported incidence[8,18,7]. The detection rate of biliary tract complications in this study (22.3%) is higher than the reported incidence approaching 18%[19]. Regarding the cases, which were confirmed by ERCP or PTC in our study, ultrasound has a sensitivity of 88%[12].

This study provides an insight into time point of vascular complications as well as hemodynamic and parenchymal adaptive processes present in liver graft recipients. The cross sectional characteristic of our study did not allow a continuous assessment of hemodynamic changes in the course of time, but it enables the analysis of a very long observation period. These data can serve as an orientation for the examining physicians to have a better understanding and interpretation of duplex changes in these patients.

REFERENCES

1 **Nashan B**, Luck R, Becker T, Grannas G, Strassburg C, Schneider A, Melter M, Strassburg A, Klempnauer J. **Expansion** of the donor pool in liver transplantation: the Hannover experience 1996-2002. *Clin Transpl* 2002**; : 221-228**

2 **Brems JJ**, Hiatt JR, Colonna JO 2nd, el-Khoury G, Quinones WJ, Ramming KP, Ziomek S, Busuttil RW. **Variables** influencing the outcome following orthotopic liver transplantation. *Arch Surg* 1987; **122**: 1109-1111

3 **De Gaetano AM**, Cotroneo AR, Maresca G, Di Stasi C, Evangelisti R, Gui B, Agnes S. **Color Doppler sonography in the** diagnosis and monitoring of arterial complications after liver transplantation. *J Clin Ultrasound* 2000; **28:** 373-380

4 **Langnas AN**, Marujo W, Stratta RJ, Wood RP, Shaw BW Jr. Vascular complications after orthotopic liver transplantation. *Am J Surg* 1991**; 161:** 76-82; discussion 82-83

5 **Greif F**, Bronsther OL, Van Thiel DH, Casavilla A, Iwatsuki S, Tzakis A, Todo S, Fung JJ, Starzl TE. **The incidence, timing,** and management of biliary tract complications after orthotopic liver transplantation. *Ann Surg* 1994**; 219:** 40-**45**

6 **Bolognesi M**, Sacerdoti D, Bombonato G, Merkel C, Sartori G, Merenda R, Nava V, Angeli P, Feltracco P, Gatta A.**Change in** portal flow after liver transplantation: effect on hepatic arterial resistance indices and role of spleen size. *Hepatology* 2002; **35**: 601-608

7 **Kok T**, Boeve WJ, Prins TR, Baarslag HJ, Woesthuis M, Slooff MJ, Haagsma EB, Bijleveld CM, van der Jagt EJ. **Arteriography** and portal venography on routine follow-up after orthotopic liver transplantation. *Invest Radiol* 2000; **35:** 653-660

8 **Pinna AD**, Smith CV, Furukawa H, Starzl TE, Fung JJ. **Urgent** revascularization of liver allografts after early hepatic artery thrombosis. *Transplantation* 1996; **62:** 1584-1587

9 **Dalgic A**, Dalgic B, Demirogullari B, Ozbay F, Latifoglu O, Ersoy E, Mahli A, Ilgit E, Ozdemir H, Arac M, Akyol G, Tatlicioglu E.**Clinical approach to graft hepatic artery thrombosis** following living related liver transplantation. *Pediatr Transplant* 2003; **7:** 149-152

10 **Shaw AS**, Ryan SM, Beese RC, Sidhu PS. **Ultrasound of non-**vascular complications in the post liver transplant patient. *Clin Radiol* 2003**; 58:** 672-**680**

11 **Schmidt G**. Ultraschall Kursbuch. 4 ed. Stuttgart: Thieme Verlag, 2003

12 **Hussaini SH**, Sheridan MB, Davies M. **The predictive value** of transabdominal ultrasonography in the diagnosis of biliary tract complications after orthotopic liver transplantation. *Gut* 1999; **45:** 900-903

13 **Heffron TG**, Emond JC, Whitington PF, Thistlethwaite JR Jr, Stevens L, Piper J, Whitington S, Broelsch CE.**Biliary** complications in pediatric liver transplantation. A comparison of reduced-size and whole grafts. *Transplantation* 1992; **53:** 391-395

14 **Nishida S**, Kato T, Levi D, Naveen M, Thierry B, Vianna R, Selvaggi G, Buitorago E, Al-Niami A, Nakamura N, Vaidya A, Nery J, Tzakis A. **Effect of protocol Doppler ultrasonography** and urgent revascularization on early hepatic artery thrombosis after pediatric liver transplantation. *Arch Surg* 2002 137; **11**: 1279-**1283**

15 **Piscaglia F**, Zironi G, Gaiani S, Mazziotti A, Cavallari A, Gramantieri L, Valgimigli M, Bolondi L.**Systemic and splanchnic** hemodynamic changes after liver transplantation for cirrhosis: a long-term prospective study. *Hepatology* 1999; **30;** 58-64

16 **Radermacher J**, Mengel M, Ellis S, Stuht S, Hiss M, Schwarz A, Eisenberger U, Burg M, Luft FC, Gwinner W, Haller H. **The** renal arterial resistance index and renal allograft survival. *N Engl J Med* 2003; **349**: 115-124

17 **Garcia-Criado A**, Gilabert R, Salmeron JM, Nicolau C, Vilana R, Bianchi L, Bunesch L, Garcia-Valdecasas JC, Rimola A, Bru C.**Significance of and contributing factors for a high** resistive index on Doppler sonography of the hepatic artery immediately after surgery: prognostic implications for liver transplant recipients. *AJR Am J Roentgenol* 2003; **181**: 831-838

18 **Molmenti EP**, Levy MF, Molmenti H, Casey D, Fasola CG, Hamilton WM, Jung G, Marubashi S, Gogel BM, Goldstein RM, Gonwa TA, Klintmalm GB.**Correlation between** intraoperative blood flows and hepatic artery strictures in liver transplantation. *Liver Transpl* 2002; **8**: 160-163

19 **Gomez R**, Moreno E, Castellon C, Gonzalez-Pinto I, Loinaz C, Garcia I.**Choledochocholedochostomy conversion to** hepaticojejunostomy due to biliary obstruction in liver transplantation. *World J Surg* 2001**; 25**: 1308-**1312**

20 **Huang DZ**, Le GR, Zhang QP, Li KY, Ye QF, Zhu W, Chen YC.**The value of color Doppler ultrasonography in monitoring** normal orthotopic liver transplantation and postoperative complications. *Hepatobiliary Pancreat Dis Int* 2003; **2**: 54-58

21 **Sanchez-Urdazpal L**, Gores GJ, Ward EM, Maus TP, Wahlstrom HE, Moore SB, Wiesner RH, Krom RA.Ischemic-type biliary complications after orthotopic liver transplantation. *Hepatology* 1992; **16**: 49-53

22 **Busuttil RW**, Goldstein LI, Danovitch GM, Ament ME, Memsic LD. **Liver transplantation today.** *Ann Intern Med* 1986; **104**: 377-389

23 **Wolfsen HC**, Porayko MK, Hughes RH, Gostout CJ, Krom RA, Wiesner RH. **Role of endoscopic retrograde cholangiop-**ancreatography after orthotopic liver transplantation. *Am J Gastroenterol* 1992; **87:** 955-960

Science Editor Wang XL and Guo SY **Language Editor** Elsevier HK

PO Box 2345, Beijing 100023, China
www.wjgnet.com
wjg@wjgnet.com

ELSEVIER

World J Gastroenterol 2005;11(43):6792-6799
World Journal of Gastroenterology ISSN 1007-9327

• *CLINICAL RESEARCH* •

Improvement of regional cerebral blood flow after oral intake of branched-chain amino acids in patients with cirrhosis

Mika Yamamoto, Motoh Iwasa, Kaname Matsumura, Yuri Nakagawa, Naoki Fujita, Yoshinao Kobayashi, Masahiko Kaito, Kan Takeda, Yukihiko Adachi

Mika Yamamoto, Motoh Iwasa, Naoki Fujita, Yoshinao Kobayashi, Masahiko Kaito, Yukihiko Adachi, Department of Internal Medicine, Division of Gastroenterology and Hepatology, Mie University School of Medicine, Tsu, Japan
Kaname Matsumura, Yuri Nakagawa, Kan Takeda, Department of Radiology, Mie University School of Medicine, Tsu, Japan
Correspondence to: Motoh Iwasa, MD, Department of Internal Medicine, Division of Gastroenterology and Hepatology, Mie University School of Medicine, Edobashi 2-174, Tsu, Mie 514-8507, Japan. motoh@clin.medic.mie-u.ac.jp
Fax: +81-59-231-5223
Received: 2005-02-17 Accepted: 2005-06-02

Key words: Liver cirrhosis; Cerebral blood flow; Branched-chain amino acids

Yamamoto M, Iwasa M, Matsumura K, Nakagawa Y, Fujita N, Kobayashi Y, Kaito M, Takeda K, Adachi Y. Improvement of regional cerebral blood flow after oral intake of branched-chain amino acids in patients with cirrhosis. *World J Gastroenterol* 2005; 11(43): 6792-6799
http://www.wjgnet.com/1007-9327/11/6792.asp

Abstract

AIM: To evaluate the effect of oral intake of branched-chain amino acids (BCAA) on brain perfusion in patients with liver cirrhosis.

METHODS: Single photon emission computed tomography scans were performed in 43 patients with cirrhosis and in 15 age-matched healthy subjects. Twenty-nine out of forty-three patients were randomly treated with either BCAA granules or placebo, and single photon emission computed tomography was performed before and after the treatment. We measured the regional cerebral blood flow values using a three-dimensional stereotaxic region of interest template.

RESULTS: Cirrhotic patients had regions of significant hypoperfusion in the bilateral central (right $P = 0.039$, $P<0.05$; left $P = 0.006$ $P<0.01$), parietal (right $P = 0.018$, $P<0.05$; left $P = 0.009$, $P<0.01$), angular (right $P = 0.039$, $P<0.05$; left $P = 0.008$, $P<0.01$), and left pericallosal segments ($P = 0.038$ P<0.05) as compared with healthy subjects. A significant increase in cerebral perfusion was observed 70 min after the oral intake of BCAA in the angular (right $P = 0.012$, $P<0.05$; left $P = 0.049$, $P<0.05$), temporal (right $P = 0.012$, $P<0.05$; left $P=0.038$, $P<0.05$), pericallosal segments (right $P = 0.025$, $P<0.05$; left $P = 0.049$, $P<0.05$) and left precentral ($P = 0.044$, $P<0.05$), parietal ($P = 0.040$, $P<0.05$) and thalamus ($P = 0.033$, $P<0.05$). No significant change in perfusion was observed in the placebo group.

CONCLUSION: Administration of BCAA rapidly improves cerebral perfusion.

INTRODUCTION

Beneficial effects of branched-chain amino acids (BCAA) supplementation on hepatic encephalopathy (HE) have been previously reported[1-3]. Recently, Marchestini *et al.* carried out a large multicenter, randomized controlled trial with BCAA-enriched dietary supplements in comparison with lactoalbumin or maltodextrin dietary supplementation[4]. The results of this study showed reduced hospital admission rate in patients treated with BCAA compared with the control group[4]. Thus, BCAA therapy may be effective for the treatment of HE, which is a common cause of hospital admission.

Some cirrhotic patients with apparently normal mental status may have abnormalities in cognitive function when they are examined with sensitive and quantitative neuropsychological tests[5,6]. This group of patients is considered to have minimal HE[7]. This HE-associated cognitive impairment may be sometimes associated with a poor quality of life[8-10] and thus early diagnosis and treatment of this condition is important[8]. It has been reported that therapy with lactulose improves neuropsychological functions[11]. However, there are no data on whether BCAA supplementation ameliorates cerebral disturbance in cirrhotic patients.

Single photon emission computed tomography (SPECT) and positron emission tomography studies can demonstrate alterations in regional cerebral blood flow (CBF) and cerebral glucose metabolism in cirrhotic patients[12-19]. We previously reported that administration of solutions enriched with BCAA improves cerebral perfusion in patients with cirrhosis[20]. However, the BCAA-rich solutions used in this previous study in cirrhotic patients contained L-arginine, which is a precursor of nitric oxide, a potent vasodilator[21]. The dose of L-arginine used in previous study might have increased blood flow in the brain[21].

The main aim of the present study was to confirm regional differences in CBF in patients with liver cirrhosis and to evaluate whether alterations in CBF is reversed by the oral administration of BCAA. In this study, we used granules containing only BCAA and a three-dimensional stereotaxic region of interest template (SRT) for objective estimation of anatomically standardized CBF SPECT images[22,23].

MATERIALS AND METHODS

Subjects

Forty-three Japanese patients with liver cirrhosis (30 men and 13 women, mean age 63±8 years) were enrolled in this study. The diagnosis of cirrhosis was based on the results of liver function tests, ultrasonography, computed tomography imaging, laparoscopy and liver biopsy. The cause of liver cirrhosis was viral infection in the majority of patients (n = 37). No patient with alcoholic liver disease was included in the study. In six patients, the cause of liver cirrhosis was unclear. None of the patients had overt HE (grade I or more) at the time of the examination, and none of them exhibited neuropsychiatric signs or symptoms on standard bedside clinical assessment. Patients with focal brain lesions, severe brain atrophy, abnormalities on computed tomography or magnetic resonance images, or neurological or psychiatric disorders were excluded from the study. None of the patients were receiving psychoactive drugs. Twenty-nine out of forty-three patients were randomized into two groups: one group received BCAA granules orally (16 patients) and another group received placebo (13 patients). We have previously reported that the ratio of serum BCAA to tyrosine increases nearly twofold, 1 h after the administration of oral BCAA and that it decreases to basal values after 10 h[24]. The clinical and biochemical characteristics of the patients are summarized in Table 1.

Control SPECT images were obtained from 15 subjects (11 men and 4 women; mean age, 62±9 years) referred to our neurology department for minor subjective symptoms. These subjects were free of liver disease, neurological disorder or dementia and had normal brain magnetic resonance images. The control subjects were not taking any medication.

Informed consent was obtained from all subjects, and the study was performed in accordance with the Helsinki Declaration. The Ethics Committee of Mie University School of Medicine approved the protocol of this study.

Table 1 Patients' clinical characteristics

Age (yr)	63 ± 8	(48 - 74)
Sex ratio, M/F	30/13	
Etiology of cirrhosis, HBV/HCV/unknown	5/32/6	
Previous history of overt hepatic encephalopathy,		
None/Chronic	39/4	
Child-Pugh score	8.0 ± 2.2	(5 -13)
Laboratory examinations		
Platelet (10^4 μL)	7.5 ± 5.1	(8 - 31.4)
Albumin (g/dL)	2.9 ± 0.5	(1.9 - 3.9)
Total bilirubin (mg/dL)	2.0 ± 2.3	(0.5 - 13.8)
Cholinesterase (ΔpH)	0.36 ± 0.19	(0.11 - 0.97)
Plasma ammonia (μmol/L)	38 ± 23	(4 - 104)
Prothrombin time (%)	69.1 ± 12.8	(31.3 - 93.5)
BCAA to tyrosine ratio	3.3 ± 1.3	(1.32 - 6.95)
Neuropsychological test		
Trail making test (s)	54 ± 26	(28 - 160)
Digit symbol test (gross point)	35 ± 10	(12 - 54)

BCAA, branched-chain amino acids.

Scan acquisition and image processing

Each subject received 278 MBq of technetium-99 m L,L-ethyl cysteinate dimer (ECD) by intravenous injection in the morning after an overnight fast. Ten minutes after the injection of ECD, brain SPECT images were acquired using a three-head gammacamera system (GCA-9300A/DI, Toshiba, Tokyo, Japan) equipped with low-energy, high-resolution fanbeam collimators. The projection data were obtained using a matrix size of 128×128. SPECT images were reconstructed by filtered back-projection using a ramp filter follower by postprocessing with a Butterworth filter. Attenuation correction was performed using Chang's method[25]. The triple-energy window technique was employed for scatter correction. After baseline SPECT, the patients were orally treated with BCAA granules (8 g BCAA, 8 g protein, 32 kcal, Ajinomoto, Tokyo, Japan: L-isoleucine 1 904 mg, L-leucine 3 808 mg, L-valine 2 288 mg), or placebo (cornstarch, 8 g protein, 32 kcal). After 60 min, 278 MBq of ECD was intravenously administered, and 10 min later a second SPECT acquisition was performed. The methods are briefly summarized in Figure 1.

Image analysis

The spatial normalization was performed using linear and non-linear transformation and SPECT template in the statistical parametric mapping (SPM) 99 (Wellcome Department of Cognitive Neurology, London, UK)

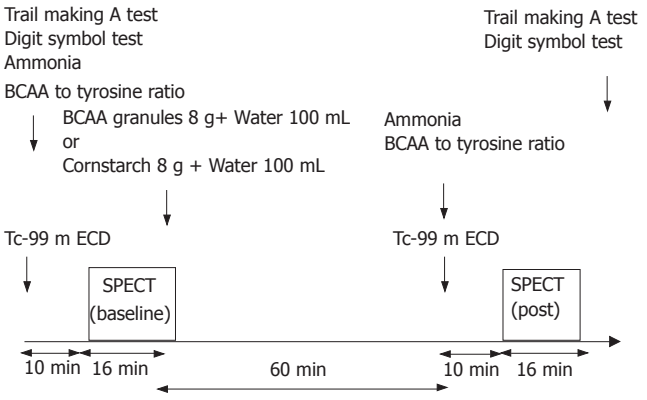

Figure 1 Study protocol. Baseline SPECT imaging was taken 10 min after the injection of 278 MBq ECD. After baseline SPECT, BCAA granules or placebo were orally administered. Sixty minutes later, another 278 MBq of technetium-99 m ECD was intravenously administered and a second SPECT acquisition was performed 10 min after the injection of ECD. Laboratory and neuropsychological tests were taken before and after the administration of BCAA or placebo. SPECT, single photon emission computed tomography; ECD, ethyl cysteinate dimer; BCAA, branched-chain amino acid

program. Smoothing was performed using 12 mm full width at half maximum Gaussian filter in SPM99. To obtain post-BCAA counts, baseline mean SPECT counts were subtracted from the second SPECT counts, multiplied by a correction factor, which is the coefficient of the decay of technetium-99 m between the baseline and post-treatment measurement. In each hemisphere, we estimated the regional CBF values of 270 constant regions of interest (ROI, three-dimensional SRT) grouped into 12 segments as follows: callosomarginal, 48 ROI; precentral, 45 ROI; central, 28 ROI; parietal, 14 ROI; angular, 8 ROI; temporal, 27 ROI; posterior cerebral, 33 ROI; pericallosal, 16 ROI; lenticular nucleus, 12 ROI; thalamus, 11 ROI; hippocampus, 17 ROI; and cerebellum, 11 ROI; and the segmental CBF was calculated as the area-weighed mean value for each of the 12 segments based on the regional CBF of each ROI[22,23].

Semiquantitative analysis was performed to obtain region-to-reference ratios for each segmental CBF value. The CBF value in cerebellum was selected as the reference region, because cerebellar abnormalities were not detected in SPECT images, computed tomography or magnetic resonance images.

Neuropsychological tests and laboratory examinations

The trail making A test (number connection test) and digit symbol test (revised Wechsler adult intelligence scale) were performed as neuropsychological tests. Laboratory examinations included plasma ammonia and BCAA to tyrosine ratio. These data were taken before and after the administration of BCAA or placebo (Figure 1).

Statistical analysis

Results were expressed as the mean±SD of the mean and range. The Mann–Whitney *U* test was used to evaluate the statistical difference in clinical or laboratory variables between BCAA and placebo groups and in CBF between patients and healthy subjects. The analysis of variance with Bonferroni's correction for multiple comparisons in the three groups was analyzed. The Wilcoxon was used to compare pre-, post-BCAA or -placebo values in the same group of patients. A $P<0.05$ was considered as statistical significance.

RESULTS

Baseline study

Cirrhotic patients ($n = 43$) had regions of significant hypoperfusion in the bilateral central (right, $P<0.05$; left, $P<0.01$), parietal (both, $P<0.05$), angular (right, $P<0.05$; left, $P<0.01$), and left pericallosal segments ($P<0.05$) as compared with healthy subjects ($n = 15$, Figure 2).

The influence of the clinical profile on regional CBF was also evaluated. There were no significant differences in cerebral perfusion between the mild (Child–Pugh A, $n = 13$), moderate/severe (Child–Pugh B+C, $n = 30$) liver dysfunction groups and healthy subjects (data not shown). In cirrhotic patients with hyperammonemia (i.e., more than 50 μm/L, $n = 15$), SRT showed regions of significant hypoperfusion in the right parietal ($P<0.05$) and left callosomarginal ($P<0.05$), central ($P<0.01$), angular ($P<0.01$) and pericallosal segments ($P<0.01$) as compared to healthy subjects (Figure 3A, right hemisphere is not shown). Likewise, in cirrhotic patients with severe decrease of serum BCAA to tyrosine ratio (i.e., <3, $n = 19$), SRT showed regions of significant hypoperfusion in the angular (right, $P<0.05$; left, $P<0.01$) and right parietal ($P<0.05$) and left callosomarginal ($P<0.01$), central ($P<001$) and pericallosal segments ($P<0.01$) as compared to healthy subjects (Figure 3B, right hemisphere is not shown).

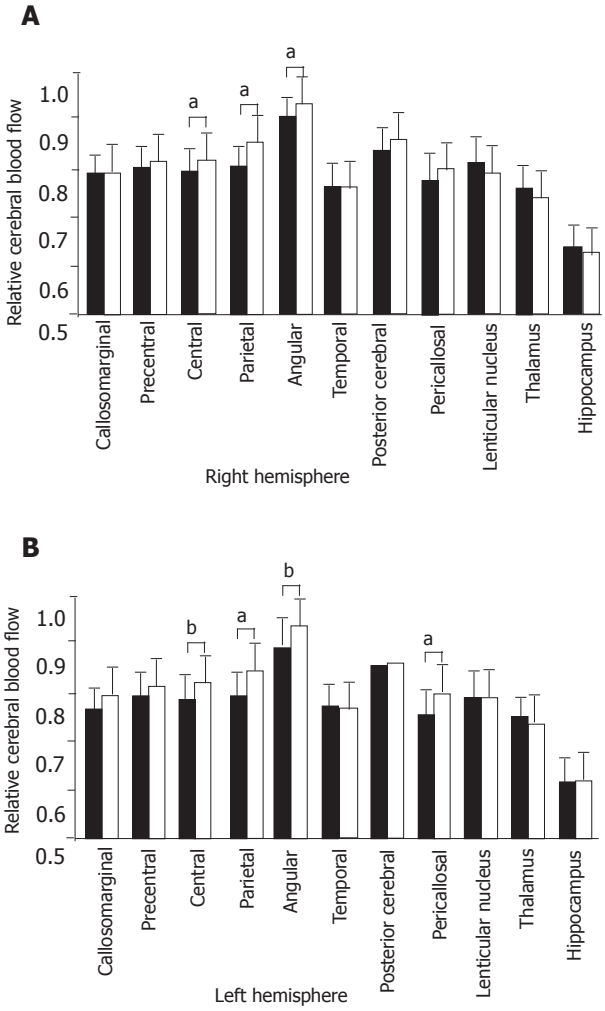

Figure 2 Relative CBF of different brain regions. Comparison of patients with liver cirrhosis (closed bars) and healthy subjects (open bars). Data were expressed as the mean±SD. [a]$P<0.05$, [b]$P<0.01$, [d]$P<0.001$. CBF, cerebral blood flow.

Abnormalities in neuropsychological tests [values more than two SD from the mean values for the age-matched healthy subjects at our hospital (i.e., more than 50 s on the trail making A test and less than 30 points on digit symbol test)] were considered to be indicative of minimal HE. Among cirrhotic patients, 10 showed abnormalities in both neurological tests and thus they were considered to have minimal HE. In patients with abnormalities in neurological tests ($n = 10$), SRT showed significant hypoperfusion in the left parietal ($P<0.01$), pericallosal ($P<0.01$), lenticular nucleus ($P<0.01$) and hippocampus ($P<0.05$) regions as compared to patients with grade-0 HE ($n = 14$, Figure 3C,

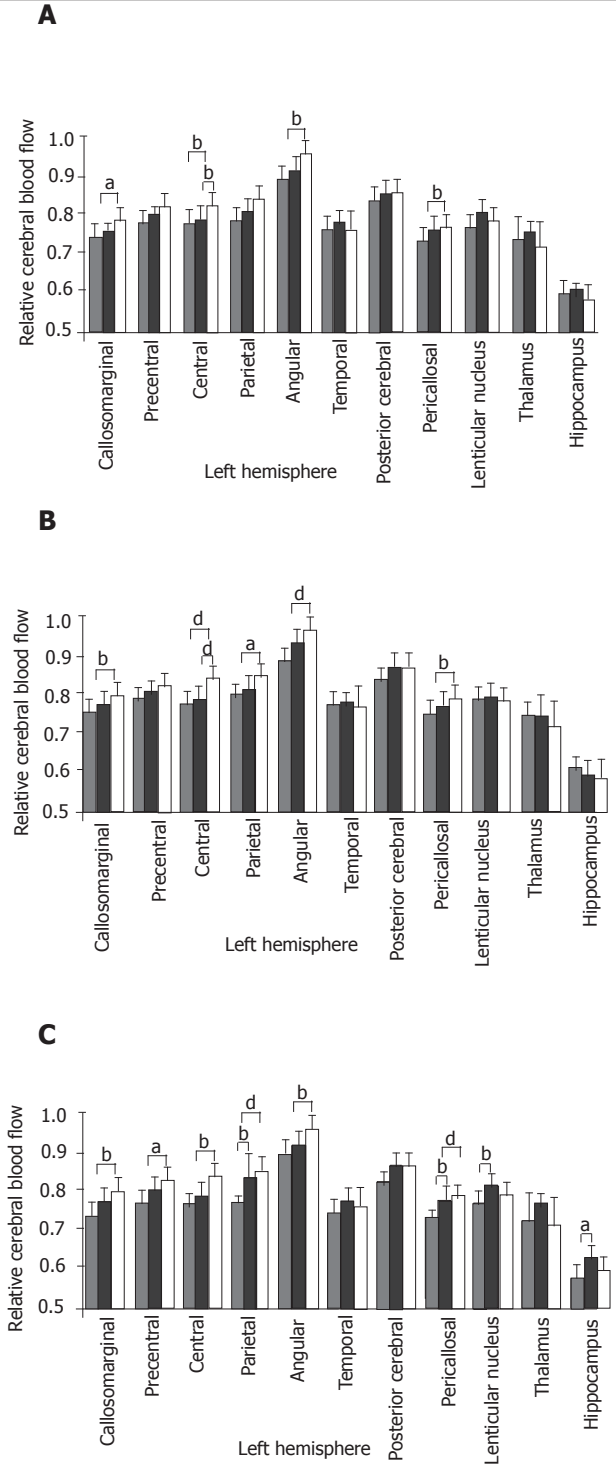

Figure 3 Relative CBF of different brain regions. **A:** Comparison of cirrhotic patients with hyperammonemia (gray bars), normal ammonemia (dashed bars) and healthy subjects (open bars); **B:** Comparison of cirrhotic patients with severe decrease in the levels of serum BCAA to tyrosine ratio (gray bars), with mild decrease in serum BCAA to tyrosine ratio (dashed bars) and healthy subjects (open bars); **C:** Comparison of patients with minimal encephalopathy (gray bars), with grade-0 encephalopathy (dashed bars) and healthy subjects (open bars).

right hemisphere is not shown).

Effect of BCAA

At entry, there was no difference in clinical or laboratory variables between BCAA (n = 16) and placebo (n = 13) groups (Table 2). A significant increase in cerebral perfusion was observed 70 min after oral intake of BCAA in the angular (both regions, P<0.05, Figure 4C), temporal (both regions, P<0.05, Figure 4D), pericallosal segments (both regions, P<0.05, Figure 4E) and left precentral (P<0.05, Figure 4A), parietal (P<0.05, Figure 4B) and thalamus (P<0.05, Figure 4F). In addition, after the administration of oral BCAA, the values of relative CBF improved in almost all segments, reaching values observed in healthy subjects. There were no significant differences in cerebral perfusion between cirrhotic patients after oral intake of BCAA and healthy subjects. No significant change in relative CBF values was observed in the placebo group (Figure 5). In the BCAA group, the serum BCAA to tyrosine ratio increased fourfold, 86 min after the administration of oral BCAA (P<0.01). No significant change in plasma ammonia levels or in neuropsychological tests was observed in BCAA and placebo groups (Table 3).

DISCUSSION

Functional imaging techniques such as CBF SPECT and positron emission tomography can demonstrate abnormalities in patients with cirrhosis[12-19]. In the present study, cirrhotic patients had regions of significant hypoperfusion in central, parietal, angular and pericallosal segments as compared to healthy subjects. These areas included parts of the frontal and parietal associated areas of the cortex and cingulum. Impaired flow and oxygen metabolism in the frontal, parietal and cingulate cortices in cirrhotic patients have also been reported[12-14,16-18]. Cognitive impairment, especially defect in attention is an important feature of HE[26,27]. The anterior cingulate gyri may provide an important connection between widely divergent aspects of attention and visual location[28]. The internal organization of the anterior cingulate gyri shows alternating bands of cells with close connections to the dorsolateral frontal cortex and the posterior parietal lobe[29]. The results of studies using N-13 ammonia positron emission tomography of cerebral ammonia metabolism in patients with cirrhosis and minimal encephalopathy coincide well with these regional differences[30]. This regional hypoperfusion may be the pathophysiological basis for the minimal cerebral dysfunction that is often detected by neuropsychological tests in patients with cirrhosis.

We found no significant relationship between cerebral perfusion and severity of liver disease, as assessed by the Child–Pugh scores. This observation may be due to the fact that non-hepatic factors, such as neurotoxins produced in the gut or toxic agents that cross the blood-brain barrier such as ammonia, contribute to impairment of cerebral function. Although no single metabolic derangement can account for the occurrence of HE, the plasma level of ammonia is believed to be an important causative factor of HE. Lockwood *et al*. reported regional metabolic abnormalities in cirrhotic patients with hyperammonemia[16]. They also reported increased permeability of the blood-brain barrier to ammonia and suggested that ammonia might be responsible for cerebral dysfunction in HE[31]. In

Table 2 Clinical characteristics of BCAA and placebo groups

	BCAA group		Placebo group	
Age (yr)	64 ± 9	(50 - 72)	65 ± 8	(51 - 74)
Sex ratio, M/F	10/6		9/4	
Etiology of cirrhosis, HBV/HCV/unknown	1/11/4		0/12/1	
Previous history of overt hepatic encephalopathy, None/Chronic	14/2		12/1	
Child-Pugh score	8.1 ± 2.5	(5 - 13)	7.8 ± 2	(5 - 11)
Laboratory examinations				
Platelet (10^4 μL)	8.3 ± 6.8	(3.4 - 31.4)	7.6 ± 3.1	(2.8 – 12.3)
Albumin (g/dL)	2.8 ± 0.5	(2.1 - 3.9)	2.9 ± 0.4	(2.4 - 3.9)
Total bilirubin (mg/dL)	2.2 ± 3.2	(0.8 - 13.8)	1.9 ± 1.8	(0.5 – 6.9)
Cholinesterase (ΔpH)	0.32 ± 0.16	(0.12 - 0.64)	0.38 ± 0.12	(0.17 - 0.55)
Plasma ammonia (μmol/L)	35 ± 20	(9 - 79)	34 ± 18	(7 - 74)
Prothrombin time (%)	68.9 ± 14.4	(31.3 - 93.5)	71.1 ± 13.4	(51.8 – 89.2)
BCAA to tyrosine ratio	3.7 ± 1.2	(2.3 - 7)	3 ± 1.3	(1.3 – 5.6)
Neuropsychological test				
Trail making test (s)	49 ± 16	(34 - 77)	50 ± 16	(25 - 72)
Digit symbol test (gross point)	38 ± 10	(21 - 53)	37 ± 15	(19 - 63)

BCAA, branched-chain amino acids.

Table 3 Changes in laboratory and neuropsychological tests after BCAA and placebo administration

	BCAA group				Placebo group			
	Before		After		Before		After	
Laboratory variables								
Plasma ammonia (μM/L)	35 ± 20	(9 - 79)	31 ± 14	(8 - 54)	36 ± 20	(7 - 74)	37 ± 14	(17 - 58)
BCAA to tyrosine ratio	3.7 ± 1.2	(2.3 - 7)	16.7 ± 3.4[b]	(13.1 - 24.6)	3 ± 1.3	(1.3 - 5.6)	3.1 ± 1.3	(1.6 - 5.7)
Neuropsychological test								
Trail making test (s)	49 ± 16	(34 - 77)	47 ± 13	(30 - 72)	50 ± 16	(25 - 72)	51 ± 15	(29 - 75)
Digit symbol test (goss point)	38 ± 10	(21 - 53)	45 ± 14	(21 - 71)	37 ± 15	(19 - 63)	40 ± 14	(23 - 61)

[b]$P < 0.01$ BCAA, branched-chain amino acids

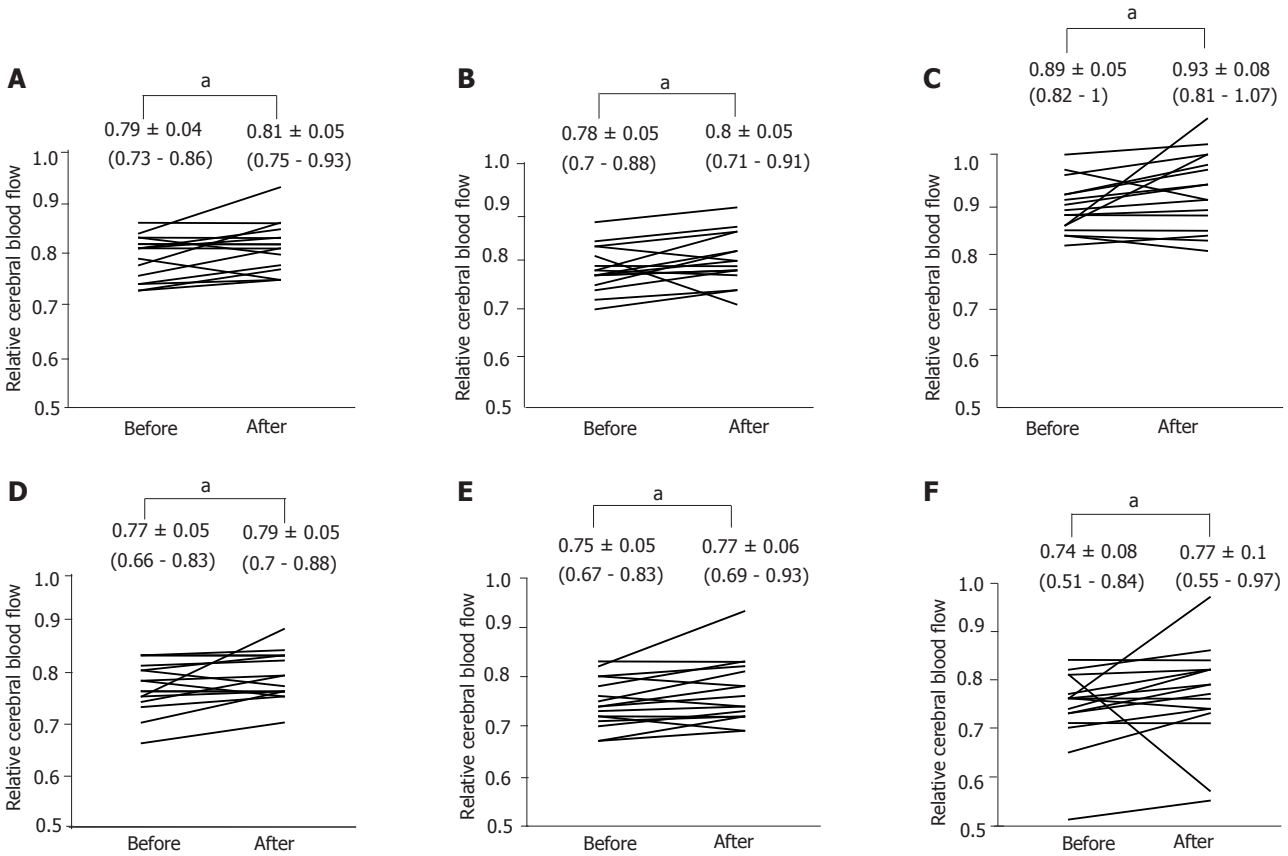

Figure 4 Changes in relative CBF of different brain regions. CBF was compared before and after BCAA. **A:** Left precentral; **B:** left parietal; **C:** left angular; **D:** left temporal; **E:** left pericallosal; **F:** left thalamus. Data were expressed as the mean±SD and range. [a]$P<0.05$V *vs* CBF, cerebral blood flow; BCAA, branched-chain amino acid.

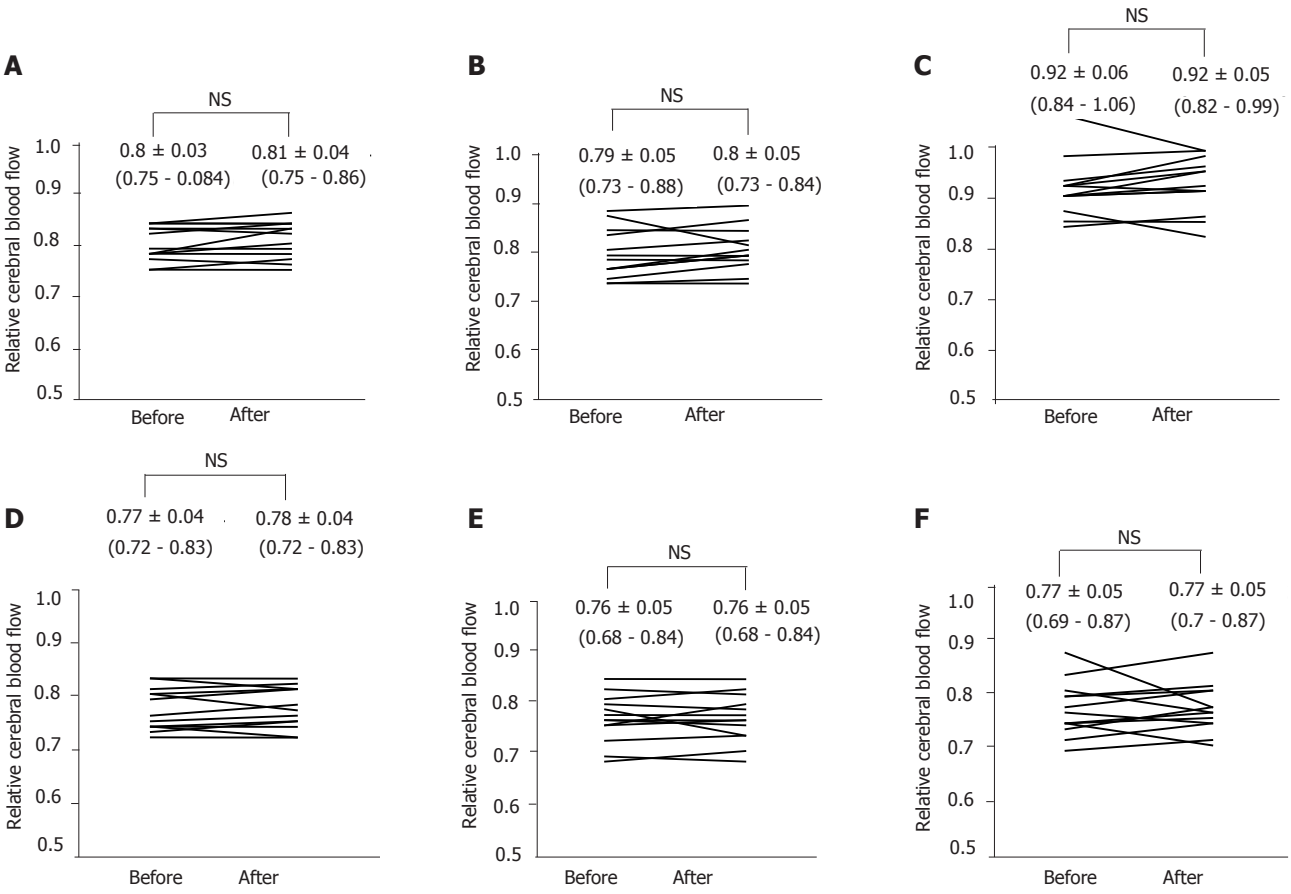

Figure 5 Changes in relative CBF of different brain regions. CBF was compared before and after placebo. **A:** Left precentral; **B:** left parietal; **C:** left angular; **D:** left temporal; **E:** left pericallosal; **F:** left thalamus. Data were expressed as the mean±SD and range. CBF, cerebral blood flow.

our patients with hyperammonemia, SRT analysis showed several segments, including the cingulum, with significant decreased perfusion as compared to healthy subjects. This finding supports the hypothesis of Lockwood *et al*. In addition, SPECT with SRT analysis showed a significant reduction in relative CBF values in cirrhotic patients with minimal HE as compared to patients with grade-0 HE and normal subjects. This result is also consistent with the observation of Lockwood *et al*.[18]. Moreover, we found that the relative CBF values are significantly correlated with the baseline venous BCAA to tyrosine ratio. Relationship between CBF values and the serum BCAA to tyrosine ratio has not been previously assessed.

There are several studies in which stereotaxic ROI analysis was used[32,33], but in all of them the ROI values were transformed to fit the subjects' individual anatomical arrangements. Inter-individual anatomical variations may exist giving non-consistent relationship between ROI location and anatomy. In the present study, we used a fully automated regional CBF quantification software, SRT. This incorporates an anatomical standardization engine transplant into SPM99 and ROI for quantification on the Montreal Neurological Institute space of the magnetic resonance image anatomically standardized by SPM99. We believe that our results are valid due to the accuracy of the SRT analysis.

We took the cerebellum as reference for the semiquantitative analysis, because brain segments of cirrhotic patients exhibit variable perfusion values whose distribution may affect the validity of the uptake ratios. We previously reported that there is no alteration in cerebellar perfusion in cirrhotic patients as analyzed by SPM with ECD SPECT[13]. In addition, the absence of symptoms and the normal appearance of cerebellar perfusion in our patients led us to consider the cerebellum as the best reference to evaluate regional CBF. However, cerebellar hypermetabolism has been observed in cirrhotic patients with cerebellar degeneration[30], and thus it may be difficult to deal with methodological limitations in such region-to-cerebellar ratios as it was in this study. To evaluate the effect of BCAA, repeated SPECT studies are necessary. In the pre/post studies, the assumption is that the original distribution pattern is still the same during the second SPECT image. Moretti *et al*. reported that during the 50-120 min postinjection period, the regional structures are washing out at the same rate[3]; however, there might be differences between cirrhotic and normal brain. This may be a potential pitfall in split-dose and sequential SPECT method with ECD.

The mechanism by which BCAA granules rapidly improve relative CBF in cirrhotic patients without overt HE is unknown. The rationale for BCAA therapy is based

on the results of studies showing that the use of solutions rich in BCAA reversed the abnormal blood levels of amino acids and led to mental recovery from acute HE in patients with cirrhosis[35,36]. Mental recovery is observed immediately after the treatment with BCAA solution. One of the proposed mechanisms of HE is the interference of cerebral metabolism by ammonia, including depletion of operational rates of tricarboxylic acid cycle by removing α-ketoglutarate for ammonia detoxification[37]. Decreased brain levels of glutamate have been reported in various models of HE. Glutamate is an integral component of malate-aspartate shuttle. It is therefore possible that reduced glutamate levels contribute to impaired cerebral energy metabolism in HE[38]. BCAA is known to cross rapidly the blood-brain barrier and to serve as an energy source in the brain[39,40]. It has been previously shown in animal models of chronic HE that decreased brain BCAA concentrations is normalized and that acceleration of ammonia metabolism occurs by stimulated glutamine synthesis, after intravenous infusion of BCAA[41]. Thus, it is possible that administration of BCAA blocks the vicious cycle of cerebral energy metabolism in HE by providing the amino group for glutamate synthesis from a-ketoglutarate in astrocytes.

In the present study, we found that cirrhotic patients increased thalamic perfusion after the administration of oral BCAA. According to current knowledge, information coming from the cortex passes through the striatopallidal system to the thalamus and then returns to the cortex. Alterations of neurotransmission within the pallidum and thalamus therefore may lead to impairment of cortical function, as in HE[42]. Catafau *et al.* reported that thalamic CBF increases in proportion to neuropsychological deficits as a compensatory effect[12]. Supplementation with BCAA may be effective in the treatment of cirrhotic patients for improving thalamic CBF.

A number of studies have reported association between minimal HE and impairment of quality of life[5,6,8-10]. It has also been suggested that the ability to drive a car is impaired in patients with cirrhosis and minimal HE[43]. Therefore, it is important to initiate therapy to improve neuropsychological function. Protein restriction may not be beneficial for long-term therapy in patients with protein malnutrition. Oral BCAA supplementation may be one of the candidates for the initial treatment of minimal HE. In the present study, there was no significant change in the results of neuropsychological test after the administration of BCAA. Additional study is necessary to clarify the time course of regional CBF changes after oral administration of BCAA. Neuropsychological performance and cerebral perfusion after long-term oral administration of BCAA also needs further evaluation.

In conclusion, this study shows that patients with cirrhosis and no neurologic symptoms have widespread reduction in relative CBF and that this is restored after oral intake of BCAA. These findings suggest that oral supplementation with BCAA may be a therapeutic adjunct of conventional therapy for the treatment of cirrhotic patients for its beneficial action on regional CBF.

ACKNOWLEDGMENTS

The authors thank Tokio Kitano, Masakazu Gotoh, and Katsunori Iijima for their technical assistance in the nuclear medicine studies and data analysis.

REFERENCES

1 **Plauth M**, Egberts EH, Hamster W, Torok M, Muller PH, Brand O, Furst P, Dolle W. Long-term treatment of latent portosystemic encephalopathy with branched-chain amino acids. A double-blind placebo-controlled crossover study. *J Hepatol* 1993; **17:** 308-314

2 **Marchesini G**, Dioguardi FS, Bianchi GP, Zoli M, Bellati G,Roffi L, Martines D, Abbiati R. Long-term oral branched-chain amino acid treatment in chronic hepatic encephalopathy. A randomized double-blind casein-controlled trial. The Italian Multicenter Study Group. *J Hepatol*; **11**: 92-101

3 **Egberts EH**, Schomerus H, Hamster W, Jurgens P. Branched chain amino acids in the treatment of latent portosystemic encephalopathy. A double-blind placebo-controlled crossover study. *Gastroenterology* 1985; **88:** 887-895

4 **Marchesini G**, Bianchi G, Merli M, Amodio P, Panella C, Loguercio C, Rossi Fanelli F, Abbiati R. Nutritional supplementation with branched-chain amino acids in advanced cirrhosis: a double-blind, randomized trial. *Gastroenterology* 2003; **124:** 1792-1801

5 **Li YY**, Nie YQ, Sha WH, Zeng Z, Yang FY, Ping L, Jia L. Prevalence of subclinical hepatic encephalopathy in cirrhotic patients in China. *World J Gastroenterol* 2004; **10:** 2397-2401

6 **vom Dahl S**, Kircheis G, Haussinger D. Hepatic encephalopathy as a complication of liver disease. *World J Gastroenterol* 2001; **7:** 152-156

7 **Ferenci P**, Lockwood A, Mullen K, Tarter R, Weissenborn K, Blei AT. Hepatic encephalopathy--definition, nomenclature, diagnosis, and quantification: final report of the working party at the 11th World Congresses of Gastroenterology, Vienna, 1998. *Hepatology* 2002; **35:** 716-721

8 **Gu S**, Li L, Li Z, He D. Analysis on clinical features of hepatic encephalopathy of 108 cases. *World J Gastroenterol* 1998; **4:** tk 101abstract

9 **Groeneweg M**, Quero JC, De Bruijn I, Hartmann IJ, Essink-bot ML, Hop WC, Schalm SW. Subclinical hepatic encephalopathy impairs daily functioning. *Hepatology* 1998; **28:** 45-49

10 **Marchesini G**, Bianchi G, Amodio P, Salerno F, Merli M, Panella C, Loguercio C, Apolone G, Niero M, Abbiati R. Factors associated with poor health-related quality of life of patients with cirrhosis. *Gastroenterology* 2001; **120:** 170-178

11 **Horsmans Y**, Solbreux PM, Daenens C, Desager JP, Geubel AP. Lactulose improves psychometric testing in cirrhotic patients with subclinical encephalopathy. *Aliment Pharmacol Ther* 1997; **11:** 165-170

12 **Catafau AM**, Kulisevsky J, Berna L, Pujol J, Martin JC, Otermin P, Balanzo J, Carrio I. Relationship between cerebral perfusion in frontal-limbic-basal ganglia circuits and neuropsychologic impairment in patients with subclinical hepatic encephalopathy. *J Nucl Med* 2000; **41:** 405-410

13 **Nakagawa Y**, Matsumura K, Iwasa M, Kaito M, Adachi Y, Takeda K. Single photon emission computed tomography and statistical parametric mapping analysis in cirrhotic patients with and without minimal hepatic encephalopathy. *Ann Nucl Med* 2004; **18:** 123-129

14 **O'Carroll RE**, Hayes PC, Ebmeier KP, Dougall N, Murray C, Best JJ, Bouchier IA, Goodwin GM. Regional cerebral blood flow and cognitive function in patients with chronic liver disease. *Lancet* 1991; **337**: 1250-1253

15 **Iwasa M**, Matsumura K, Kaito M, Ikoma J, Kobayashi Y, Nakagawa N, Watanabe S, Takeda K, Adachi Y. Decrease of regional cerebral blood flow in liver cirrhosis. *Eur J Gastroenterol Hepatol* 2000; **12:** 1001-1006

16 **Lockwood AH**, Murphy BW, Donnelly KZ, Mahl TC, Perini S.

Positron-emission tomographic localization of abnormalities of brain metabolism in patients with minimal hepatic encephalopathy. *Hepatology* 1993; **18:** 1061-1068
17 **Trzepacz PT**, Tarter RE, Shah A, Tringali R, Faett DG, Van Thiel DH. SPECT scan and cognitive findings in subclinical hepatic encephalopathy. *J Neuropsychiatry Clin Neurosci* 1994; **6:** 170-175
18 **Lockwood AH**, Weissenborn K, Bokemeyer M, Tietge U, Burchert W. Correlations between cerebral glucose metabolism and neuropsychological test performance in nonalcoholic cirrhotics. *Metab Brain Dis* 2002; **17:** 29-40
19 **Dam M**, Burra P, Tedeschi U, Cagnin A, Chierichetti F, Ermani M, Ferlin G, Naccarato R, Pizzolato G. Regional cerebral blood flow changes in patients with cirrhosis assessed with 99mTc-HM-PAO single-photon emission computed tomography: effect of liver transplantation. *J Hepatol* 1998; **29:** 78-84
20 **Iwasa M**, Matsumura K, Watanabe Y, Yamamoto M, Kaito M, Ikoma J, Gabazza EC, Takeda K, Adachi Y. Improvement of regional cerebral blood flow after treatment with branched-chain amino acid solutions in patients with cirrhosis. *Eur J Gastroenterol Hepatol* 2003; **15:** 733-737
21 **Reutens DC**, McHugh MD, Toussaint PJ, Evans AC, Gjedde A, Meyer E, Stewart DJ. L-arginine infusion increases basal but not activated cerebral blood flow in humans. *J Cereb Blood Flow Metab* 1997; **17:** 309-315
22 **Takeuchi R**, Matsuda H, Yoshioka K, Yonekura Y. Cerebral blood flow SPET in transient global amnesia with automated ROI analysis by 3DSRT. *Eur J Nucl Med Mol Imaging* 2004; **31:** 578-589
23 **Takeuchi R**, Yonekura Y, Matsuda H, Konishi J. Usefulness of a three-dimensional stereotaxic ROI template on anatomically standardised 99mTc-ECD SPET. *Eur J Nucl Med Mol Imaging* 2002; **29:** 331-341
24 **Kawamura-Yasui N**, Kaito M, Nakagawa N, Fujita N, Ikoma J, Gabazza EC, Watanabe S, Adachi Y. Evaluating response to nutritional therapy using the branched-chain amino acid/tyrosine ratio in patients with chronic liver disease. *J Clin Lab Anal* 1999; **13:** 31-34
25 **Chang LT**. A method for attenuation correction in radionuclide computed tomography. *IEEE Trans Nucl Sci Soc* 1979; **25:** 638-643
26 **Gilberstadt SJ**, Gilberstadt H, Zieve L, Buegel B, Collier RO Jr, McClain CJ. Psychomotor performance defects in cirrhotic patients without overt encephalopathy. *Arch Intern Med* 1980; **140:** 519-521
27 **Tarter RE**, Hegedus AM, Van Thiel DH, Schade RR, Gavaler JS, Starzl TE. Nonalcoholic cirrhosis associated with neuropsychological dysfunction in the absence of overt evidence of hepatic encephalopathy. *Gastroenterology* 1984; **86:** 1421-1427
28 **Posner MI**. Attention in cognitive neuroscience: An overview. The cognitive neurosciences. Gazzangia MS. Cambridge Massachusetts; MIT Press, 1995: 615-624
29 **Goldman-Rakic PS**. Topography of cognition: parallel distributed networks in primate association cortex. *Annu Rev Neurosci* 1988; **11:** 137-156
30 **Ahl B**, Weissenborn K, van den Hoff J, Fischer-Wasels D, Kostler H, Hecker H, Burchert W. Regional differences in cerebral blood flow and cerebral ammonia metabolism in patients with cirrhosis. *Hepatology* 2004; **40:** 73-79
31 **Lockwood AH**, Yap EW, Wong WH. Cerebral ammonia metabolism in patients with severe liver disease and minimal hepatic encephalopathy. *J Cereb Blood Flow Metab* 1991; **11:** 337-341
32 **Hooper HR**, McEwan AJ, Lentle BC, Kotchon TL, Hooper PM. Interactive three-dimensional region of interest analysis of HMPAO SPECT brain studies. *J Nucl Med* 1990; **31:** 2046-2051
33 **San Pedro EC**, Deutsch G, Liu HG, Mountz JM. Frontotemporal decreases in rCBF correlate with degree of dysnomia in primary progressive aphasia. *J Nucl Med* 2000; **41:** 228-233
34 **Moretti JL**, Tamgac F, Weinmann P, Caillat-Vigneron N, Belin CA, Cesaro P, Holman BL, Defer G. Early and delayed brain SPECT with technetium-99m-ECD and iodine-123-IMP in subacute strokes. *J Nucl Med* 1994; **35:** 1444-1449
35 **Naylor CD**, O'Rourke K, Detsky AS, Baker JP. Parenteral nutrition with branched-chain amino acids in hepatic encephalopathy. A meta-analysis. *Gastroenterology* 1989; **97:** 1033-1042
36 **Rossi Fanelli F**, Cangiano C, Capocaccia L, Cascino A, Ceci F, Muscaritoli M, Giunchi G. Use of branched chain amino acids for treating hepatic encephalopathy: clinical experiences. *Gut* 1986; **27 Suppl 1:** 111-115
37 **Bessman SP**, Paul N. The Krebs's cycle depletion theory of hepatic coma. Urea Cycle, New York, Wiley; 1976: 83-89.
38 **Hindfelt B**, Plum F, Duffy TE. Effect of acute ammonia intoxication on cerebral metabolism in rats with portacaval shunts. *J Clin Invest* 1977; **59:** 386-396
39 **Chaplin ER**, Goldberg AL, Diamond I. Leucine oxidation in brain slices and nerve endings. J Neurochem 1976; 26: 710-717
40 Oldendorf WH. Brain uptake of radiolabeled amino acids, amines, and hexoses after arterial injection. *Am J Physiol* 1971; **221:** 1629-1639
41 ***Fraser CL***, Arieff AI. Hepatic encephalopathy. *N Engl J Med* 1985; **313:** 865-873
42 **Weissenborn K**, Kolbe H. The basal ganglia and portal-systemic encephalopathy. *Metab Brain Dis* 1998; **13:** 261-272
43 **Wein C**, Koch H, Popp B, Oehler G, Schauder P. Minimal hepatic encephalopathy impairs fitness to drive. *Hepatology* 2004; **39:** 739-745

Science Editor Guo SY **Language Editor** Elsevier HK

PO Box 2345, Beijing 100023, China
www.wjgnet.com
wjg@wjgnet.com

ELSEVIER

World J Gastroenterol 2005;11(43):6800-6806
World Journal of Gastroenterology ISSN 1007-9327

• *CLINICAL RESEARCH* •

Pregnancy is not a risk factor for gallstone disease: Results of a randomly selected population sample

Thomas Walcher, Mark Martin Haenle, Martina Kron, Birgit Hay, Richard Andrew Mason, Alexa Friederike Alice von Schmiesing, Armin Imhof, Wolfgang Koenig, Peter Kern, Bernhard Otto Boehm, Wolfgang Kratzer

Thomas Walcher, Mark Martin Haenle, Richard Andrew Mason, Alexa Friederike Alice von Schmiesing, Bernhard Otto Boehm, Wolfgang Kratzer, Department of Internal Medicine I, University Hospital Ulm, Ulm, Germany
Martina Kron, Birgit Hay, Department of Biometry and Medical Documentation, University of Ulm, Ulm, Germany
Armin Imhof, Wolfgang Koenig, Department of Internal Medicine II, University Hospital Ulm, Ulm, Germany
Peter Kern, Department of Internal Medicine III, Section of Infectious Diseases and Clinical Immunology, University Hospital Ulm, Ulm, Germany
Co-first-authors: Thomas Walcher and Mark Martin Haenle
Correspondence to: W. Kratzer, PD Dr Med., University Hospital Ulm, Department of Internal Medicine I, Robert-Koch-Str. 8, D-89081 Ulm,
Germany. wolfgang.kratzer@medizin.uni-ulm.de.
Telephone: +49-731-50024536 Fax: +49-731-50024867
Received: 2005-04-11 Accepted: 2005-05-24

Abstract

AIM: To investigate the prevalence, risk factors, and selection of the study population for cholecystolithiasis in an urban population in Germany, in relation to our own findings and to the results in the international literature.

METHODS: A total of 2 147 persons (1 111 females, age 42.8 ± 12.7 years; 1 036 males, age 42.3 ± 13.1 years) participating in an investigation on the prevalence of *Echinococcus multilocularis* were studied for risk factors and prevalence of gallbladder stone disease. Risk factors were assessed by means of a standardized interview and calculation of body mass index (BMI). A diagnostic ultrasound examination of the gallbladder was performed. Data were analyzed by multiple logistic regression, using the SAS statistical software package.

RESULTS: Gallbladder stones were detected in 171 study participants (8.0%, *n* = 2 147). Risk factors for the development of gallbladder stone disease included age, sex, BMI, and positive family history. In a separate analysis of female study participants, pregnancy (yes/no) and number of pregnancies did not exert any influence.

CONCLUSION: Findings of the present study confirm that age, female sex, BMI, and positive family history are risk factors for the development of gallbladder stone disease. Pregnancy and the number of pregnancies, however, could not be shown to be risk factors. There seem to be no differences in the respective prevalence for gallbladder stone disease in urban and rural populations.

Key words: Cholecystolithiasis; Pregnancy; Risk factors; Selection bias; Ultrasonography

Walcher T, Haenle MM, Kron M, Hay B, Mason RA, von Schmiesing AFA, Imhof A, Koenig W, Kern P, Boehm BO, Kratzer W. Pregnancy is not a risk factor for gallstone disease: Results of a randomly selected population sample. *World J Gastroenterol* 2005; 11(43): 6800-6806
http://www.wjgnet.com/1007-9327/11/6800.asp

INTRODUCTION

Disorders of the gallbladder are a major cause of morbidity and a leading indication for hospital admissions in the United States[1-4] and in Europe[5,6]. In these developed nations, the economic impact of gallstone disease is high[1-5]. In the United States, more than 500 000 cholecystectomies are performed annually and direct costs for the diagnosis and treatment of gallbladder stones are estimated at 5 billion US Dollar per year[7,8]. For the treatment of gallstone disease in Germany, 200 inpatient hospital days per 10 000 health insured persons accumulate every year[9]. This creates costs of more than ½ billion[10]. Gallstone disease is not only an unsolved problem in Western industrialized nations but also in African nations[11,12] as well as in Asian countries like China, India, Bangladesh, and Japan[13-17]. Cholelithiasis is one of the commonest surgical diseases in China and accounted for 11.5% of overall hospitalized patients during the period from 1985 to 1995[18].

The most important risk factors for the development of gallstone disease currently being discussed in the literature include age[19-23], female gender[14,20-22,24], obesity[6,25-28] and heredity[19,20,29-31]. Other factors like pregnancy or number of pregnancies are still discussed are contradictory[12,21,32-34].

To our knowledge, there are no publications that assess the influence of the selection of study population on gallstone disease prevalence.

The present prospective ultrasound-based survey investigates the prevalence and risk factors for cholecystolithiasis in an urban population and also addresses the effect of selection of study population on the different risk factors.

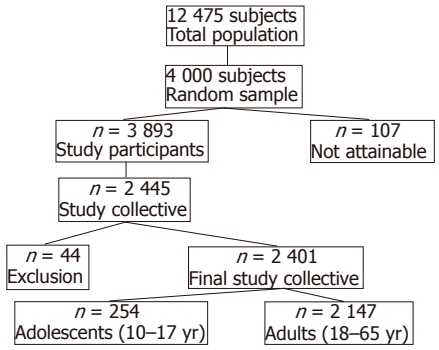

Figure 1 Study collective and participation.

METHODS

Study collective and participation

A random sample of 4 000 subjects was selected from the population of a city in southwestern Germany (total population: 12 475) for participation in a seroprevalence study for *Echinococcus multilocularis*. Of the 4 000 randomly selected and invited subjects, 107 could not be included in the final evaluation due to factors such as non-response to repeated invitations or incompetent legal status (n = 39), or moved away with no forwarding address (n = 68), resulting in a total random sample size of 3 893 subjects. Out of this pool, a total of 2 445 persons actually participated in the study (response rate: 62.8%). The following inclusion and exclusion criteria determined the composition of the collective studied for gallbladder stone disease (Figure 1):

Only persons in the age of 10-65 years were included into the study. Written consent for the examination and collection of personal health information was required.

Failure to visualize and assess the gallbladder or poor or restricted examination conditions lead to the exclusion from the study collective (n = 26 subjects). Significant contraction of the gallbladder following an inadequate fasting period (when no clinical signs of cholecystitis were identified) (n = 9 subjects), a history of cholecystectomy for gallbladder polyps or cholecystectomy of unknown reason (n = 4 subjects) or subject's refusal to undergo examination (n = 1 subject) also constituted exclusion criteria. Missing or invalid data acquisition (n = 4 subjects). Patients with prior cholecystectomy for gallbladder stones were added in the calculations of the gallbladder stone prevalence.

The total collective of subjects undergoing ultrasound examination of the gallbladder was 2 401 persons. In order to enhance comparability with published studies, we explicitly examined adult subjects aged 18-65 years. This non-selected adult collective consisted of 2 147 subjects (1 036 males, 48.3%; 1 111 females, 51.7%).

Subjects' informed written consent was obtained for examination and collection of personal health information. The study met the international agreements of the Helsinki Declaration from 1996 and was approved by the research Ethics Committee of the Baden-Württemberg General Medical Council (Landesärztekammer Baden-Württemberg).

Questionnaire and physical examination

Under the guidance of a trained interviewer, each subject completed a comprehensive questionnaire covering the following parameters: Demographic information (age, sex, nationality, marital status, education, occupation), recreational activities (sports, exercise), medical history (gallbladder stones, gastrointestinal, hepatic, cardiovascular, respiratory, endocrine, renal, rheumatic, or malignant diseases), dietary behavior (meal patterns including intake of certain foods; fluid intake including alcohol, use of tobacco products), family history (gall bladder stone disease, diabetes mellitus, overweight, history of cancer) and medication history.

Based on the recommendations of the WHO[35] for anthropometric measurements, patients then underwent determination of body height and weight and waist and hip circumference. BMI was calculated according to the common formula[35].

Ultrasound examination

Study participants were asked to present for the examination following a 4-h fasting period. All subjects underwent ultrasound examination of the upper abdomen under standard conditions to assure exact evaluation of the gallbladder. In order to enhance visualization of the gallbladder, subjects were asked to raise their right arm over their head, which increases both the intercostal spaces and the distance between the lower margin of the rib cage and the iliac crest. Examination was performed upon deep inspiration and with outward pressure on the abdominal wall.

The gallbladder was examined in three planes (longitudinal, cross-sectional and diagonal), providing the examiner with a three-dimensional impression of the organ. In cases in which cholecystolithiasis was present, the mobility of the stone(s) was assessed. Subjects, in whom differentiation between mobile stones and wall-adhering polyps was difficult, were examined again in standing position in order to reliably distinguish between stone and polyps on the basis of their mobility. The thickness of the gallbladder wall was measured and, in subjects with gallbladder stones, the number, size, and localization of stones before mobilization were determined. Ultrasound examinations were performed by a group of six examiners trained in gallbladder sonography. These examiners worked under supervision of an experienced specialist (>4 000 examinations per year), who also reviewed all questionable findings. Examinations were performed using four identical, state-of-the-art HDI-5000 ultrasound scanners (Advanced Technology Laboratories Ultrasound, Philips Medical Systems, Bothell, WA, USA).

Criteria for the diagnosis of gallstones were as follows: one or more hyperechoic structure(s) in the gallbladder with dorsal shadow; one or more hyperechoic structure(s) in the gallbladder without dorsal shadow but which by means of examination in multiple planes and/or attempt at mobilization can be certainly distinguished from a gallbladder septum, Heister's valve or a gallbladder polyp; a strongly hyperechoic structure with dorsal shadow in

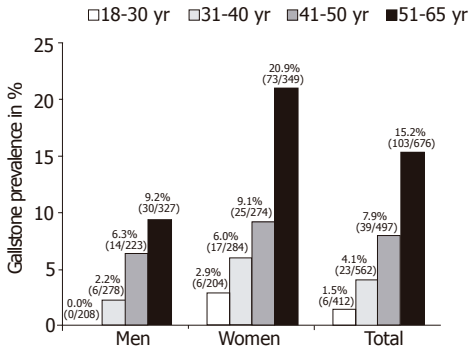

Figure 2 Distribution of gallbladder stone prevalence in relation to sex and age.

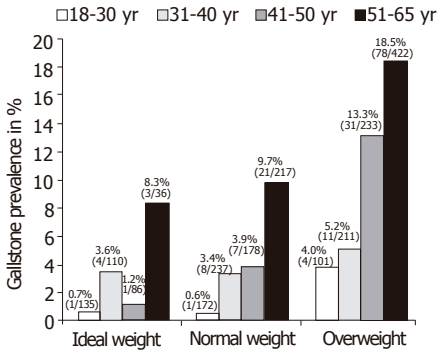

Figure 3 Prevalence of gallbladder stones in relation to BMI and age.

the anatomic location of gallbladder, with no or only slight visualization of residual gallbladder lumen; failure to delineate the gallbladder lumen in patients who have undergone prior cholecystectomy and who demonstrate corresponding surgical incisions in the right upper abdominal quadrant; presence of a significant amount of gallbladder sludge filling at least one-quarter of the gall bladder lumen with corresponding dorsal shadow.

Subjects, who because of recent food intake or other reasons, such as overlying intestinal gas, presented unfavorable examination conditions, were excluded from the study.

Statistical analysis

Multiple logistic regression[36] was performed to assess the impact of the known risk factors age, sex, BMI, and positive family history on the development of gallbladder stones. Two further multiple logistic regression models were fitted for female study participants in order to assess the impact of pregnancy and number of pregnancy, whereby in both models odds ratios were adjusted for the known risk factors like age, BMI, and positive family history for gallbladder stones. Odds ratios with 95% confidence interval and corresponding *P*-value are given. Statistical analyses were performed using the SAS statistical software package (version 8.02).

RESULTS

Prevalence in relation to age and sex

Gallbladder stones were detected at upper abdominal ultrasound examination in 87 of 2 147 subjects examined (4.1%), while gallbladder sludge was identified in two subjects (0.1%). A further 84 subjects (3.9%) had undergone prior cholecystectomy for the treatment of gallbladder stone disease. Thus, 171 subjects satisfied the inclusion criteria for cholecystolithiasis, representing an overall prevalence of cholecystolithiasis of 8.0% in the study population.

Among females, the proportion of subjects with current or prior gallbladder stone disease stood at 10.9% (121 of 1 111 subjects), while 4.8% of males (50 of 1 036 subjects) fulfilled the criteria for the diagnosis of cholecystolithiasis. The prevalence of gallbladder stone disease was higher for females than for males in all age classes. The highest prevalence was found in the group of females aged 51-65 years (20.9%; 73 of 349 subjects; Figure 2). Overall, the prevalence of gallbladder stones (defined as current and past cholecystolithiasis) increases with advancing age from 1.5% among subjects aged 18-30 years to 15.2% in the 51-65 years age group.

Prevalence in relation to BMI

BMI was calculated in 99.6% of study participants (n = 2 138). Mean BMI for the subcollective of subjects without gallbladder stone disease was 25.8±4.9 kg/m^2 (median 25.1 kg/m^2; range: 14.1-52.6 kg/m^2). Corresponding value for subjects with current or prior cholecystolithiasis was 29.2±5.9 kg/m^2 (median 28.7 kg/m^2; range: 17.6-51.5 kg/m^2). For description, BMI results were assigned to one of three classes defined according to the recommendations of the World Health Organization (WHO; Figure 3).

Class I, defined as at or below a subject's respective ideal weight (BMI <21 kg/m^2 in females and <22 kg/m^2 in males), included 367 subjects (17.2%). Class II (BMI 21-25 kg/m^2 in females and 22-26 kg/m^2 in males) included 804 subjects (37.6%), while 967 subjects (45.2%) met the criteria for Class III (BMI >25 kg/m^2 in females and BMI >26 kg/m^2 in males), and thus were considered as overweight. Only 9 subjects (2.5%) in BMI Class I exhibited evidence of gallbladder stone disease compared to 37 subjects (4.6%) in Class II and 124 subjects (12.8%) in Class III (Figure 3).

Prevalence in relation to positive family history of gallbladder stones

Of 2 147 subjects, 105 (4.9%) were unable to provide information on their biological parents; thus, evaluation of the influence of hereditary predisposition was limited to a subcollective of 2 042 subjects. Gallbladder stones were diagnosed more frequently in subjects with a positive family history of cholecystolithiasis. In subjects with a positive family history involving one biological parent, the prevalence of gallbladder stones stood at 12.6% (51 of 405 subjects) and at 14.3% (3 of 21 subjects) in subjects, both of whose biological parents suffered from gallbladder stone disease. In the remaining 1 616 subjects with negative family history of gallbladder stone disease, prevalence of cholecystolithiasis stood at only 6.3% (n = 102).

Table 1 Classical risk factors of cholecystolithiasis in multiple logistic regression

Classical risk factors	Odds ratio (OR)	95%CI	*P*
Age (per yr)	1.06	1.05–1.08	<0.001
Female sex	2.78	1.91–4.07	<0.001
BMI (per kg/m^2)	1.12	1.08–1.15	<0.001
Positive family history	1.89	1.30–2.75	<0.001

Table 2 History of pregnancy and the number of prior pregnancies in the multiple logistic regression model (only females)

Factor tested	Odds ratio (OR)	95%CI	*P*
Age (per yr)	1.06	1.04–1.08	<0.001
BMI (per kg/m^2)	1.11	1.07–1.15	<0.001
Positive family history	1.99	1.28–3.07	0.002
Positive history of pregnancy	0.76	0.44–1.31	0.321

Prevalence in relation to pregnancy

All female study subjects were questioned about their pregnancy status. Fifteen women declined to provide information on prior pregnancy. Of the remaining 1 096 subjects included in this analysis, 26.3% (n = 288) reported never having been pregnant. The group of women with positive history of pregnancy (n = 808, 73.7%) was broken down into the group with one to two pregnancies (560 women, 51.1%) and those with three or more pregnancies (248 women, 22.6%). Gallbladder stones were detected in 22 of 288 nulliparae (7.6%). In the group of 560 women with one or two pregnancies, 55 subjects (9.8%) were positive for past or present cholecystolithiasis, compared to 43 subjects (17.3%) in the group of patients with three or more pregnancies.

Multiple logistic regression analysis

Multiple logistic regression showed a strong association of the factor "age" with the development of gallbladder stones (OR 1.11 per year of age; 95%CI: 1.05-1.08; P<0.001; Table 1). The comparison of females to males yielded an odds ratio of 2.78 (95%CI: 1.91-4.07; P<0.001; Table 1). Body mass index (BMI in kg/m^2) also was an important risk factor (OR 1.12 per-unit; 95%CI: 1.08-1.15; P<0.001; Table 1). Compared to study subjects without known gallbladder stone disease in the biological parents, persons with a positive parental history of cholecystolithiasis showed an odds ratio of 1.89 (95%CI: 1.30-2.75; P<0.001; Table 1).

In separate logistic regression models for females including the risk factors age, BMI, and family history, neither pregnancy nor number of pregnancies showed an association with the development of gallbladder stone disease. The first model revealed an OR of 0.76 for pregnancy yes *vs* no (95%CI: 0.44-1.31; P = 0.321; Table 2) and the second model an OR of 0.65 for one or two pregnancies *vs* no pregnancy and an OR of 1.04 for three or more pregnancies *vs* no pregnancy (95%CI: 0.37-1.15 and 0.56-1.94; P = 0.104; Table 3).

Table 3 Number of pregnancies in the multiple logistic regression model (only females)

Factor tested	Odds ratio (OR)	95%CI	*P*
Age (per yr)	1.06	1.04–1.08	<0.001
BMI (per kg/m^2)	1.11	1.07–1.15	<0.001
Positive family history	2.09	1.34–3.25	<0.001
Number of pregnancies			0.104
One or two *vs* none	0.65	0.37–1.15	
Three or more *vs* none	1.04	0.56–1.94	

DISCUSSION

The present ultrasound-based epidemiological survey is, to our knowledge, the first study conducted in a collective drawn from an urban population in Germany. The prevalence of gallbladder stone disease in our unselected collective stands at 8.0%. Our findings are comparable, on one hand, with those documented in a rural population and in a collective of blood donors in Germany[19,20], and, on the other, with the prevalence figures reported from Italian, British, and Danish studies[21,27,33,37], but our results are not comparable with the low prevalences from Eastern countries such as China, India, Japan, Taiwan, and Thailand[14,16,17,23,38] (Figure 4).

The prevalence of gallbladder stone disease (predominantly cholesterol gallstones) reported from a majority of European and American studies shows a clear female dominance. In Asian countries with a higher prevalence of pigment gallstones, the female dominance is less distinct[6,23,38]. In the present study, female sex was also found to be a clear risk factor (OR = 2.78; 95%CI: 1.91-4.07; P<0.001) and the ratio of males with gallbladder stone disease to females stood at 1 to 2.3. Due to the great importance of the risk factors, age and especially female sex, the selection modalities of study collectives gain paramount importance[6,37]. Comparing gallbladder stone prevalence in women in relation to the method of selecting the study population, the highest prevalence is observed in studies conducted as a cross sectional sample of the total population[20–22] or large random samples[14,24] (Table 4). Most large European studies were conducted either as random samples[24,39,40] or as surveys of entire factories or governmental departments[32,41] (Table 4).

Our findings from Leutkirch (total prevalence 8.0%) are comparable to those reported for populations in Römerstein (7.8%) and blood donors in Ulm (6.0%) as well as to Italian studies conducted in Sirmione (6.9%) and Chianciano (5.9%), all of which were conducted as cross-sectional sample of the total population[19–22] (Figure 4).

The prevalence of gallbladder stones in our study collective is lower in younger persons than in those belonging to older age groups. Similar trends toward higher gallbladder stone prevalence in older persons have been described in nearly all sonographic studies[6,19,20,23,25], as well as in autopsy studies[37] and in studies based on clinical symptoms[42] (Figure 4).

Using multiple regression analysis under consideration

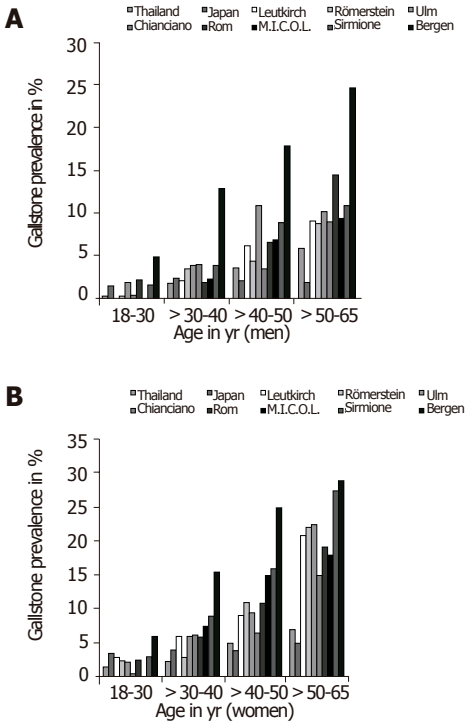

Figure 4 Age adjusted gallbladder stone prevalence in males and females in comparable large studies. **A:** in men; **B:** in women.

of the known risk factors age, sex, and family history, we found an association with study participants' current BMI (OR 1.12/unit; 95%CI: 1.08-1.15; $P<0.0001$). As in most other European studies, our findings showed an increased prevalence of gallbladder stone disease in overweight subjects[6,25–28]. The prevalence of gallbladder stones in subjects with a positive family history in the biological parents (12.7%) is more than twice as high as that in subjects with negative family history (6.3%). Our findings point to a strong effect for genetic factors in the pathogenesis of cholecystolithiasis (OR = 1.89; 95%CI: 1.30-2.75; $P<0.001$), although the mechanism of inheritance is not known. A familial accumulation of cholecystolithiasis cases has been observed in other sonographic screening studies in first-degree relatives of persons suffering from gallbladder stones[6,29-31,39].

The multiple logistic regression model failed to show an increased prevalence of gallbladder stones for female subjects with prior pregnancy (prevalence 12.1% *vs* 7.6%). One reason might be the much lower average age of the nulliparae (33.6±13.7 years) compared to women who had borne children (46.0±10.7 years), suggesting that the higher prevalence may actually be an age-related phenomenon. This effect is also apparent in the increased prevalence of gallbladder stones in women with three or more pregnancies (average age 48.9±9.7 years) compared with women who had been pregnant only one or two times (average age 44.7±10.9 years). The analysis of pregnancy as a risk factor for cholecystolithiasis has lead to different results in the literature[12,21,32–34] which range from no effect to a prevalence that is reduced by a factor of 40 in comparison of nulliparae to women who have been pregnant[15,43] (Table 5). The old clinical experience of an increased prevalence of gallbladder stones in women who have borne children could not be substantiated by the findings of the present study.

Table 4 Relative risk for gall bladder stones in relation to selection of study population

Place/region	Population selection	*n*	Sex distribution male:female
Chiayi[23]	Random sample	923	1:1.0
Rome[32]	Factory	2 325	1:1.1
Bergen[40]	Random sample	1 371	1:1.1
Ulm[19]	Blood donors	1 116	1:1.1
Copenhagen[44]	Random sample	4 807	1:1.4
Chiang Mai[38]	Random sample	6 146	1:1.5
Schwedt[41]	Factory	1 616	1:1.6
Okinawa[17]	Inhabitants of an island	2 584	1:1.7
Jiaotong[14]	Random sample	15 856	1:2.0
M.I.C.O.L[24]	Random sample	29 739	1:2.0
Römerstein[20]	Total survey	2 498	1:2.1
Sirmione[21]	Total survey	1 911	1:2.2
Cianciano[22]	Total survey	1 804	1:2.3
Leutkirch	Random sample	2 401	1:2.3

In conclusion, the classical risk factors age, female sex, body mass index (BMI), and positive family history have been confirmed by the findings of the present study. The female-specific factors of prior pregnancy and number of prior pregnancies, however, could not be shown to exert measurable influence on the prevalence of gallbladder stones. The selection of study populations affects study results i.e. the strength of the effect of female sex on the development of gallbladder stones. There does not appear to be a difference between the prevalence of gallbladder stones in urban and rural populations.

ACKNOWLEDGMENTS

The study was initiated by the Government of the state of Baden-Württemberg, Germany. Financial support was granted via the work of the Baden-Württemberg state health office, District Government Stuttgart, Germany as well as the regional health office from Ravensburg, Germany. Further support was granted by the administration of the city of Leutkirch, Germany. Vials for blood samples and part of the laboratory testing were supplied by Sarstedt AG & Co., Nürnbrecht, Germany. BOB is supported by the German Research Council (GRK 1041). The authors wish to express their gratitude to Mr. Walter Feucht of the ULDO Backwaren Company, Neu-Ulm, Germany for his generous support of this study. Without his participation, the rapid evaluation and prompt analysis of the data would not have been possible. The following members of the EMIL-Study-Group contributed to the accomplishment of this study: Adler G, Armsen A, Banzhaf H-M, Bauerdick M, Bertling U, Boehm BO, Brandner BO, Brockmann SO, Deckert M, Dingler C, Eggink S, Fuchs M, Gaus W, Goussis H, Gruenert A, Haenle MM, Hampl W, Haug C, Hay B, Huetter M-L, Imhof A, Kern P, Kimmig P, Kirch A, Klass D, Koenig

Table 5 Review of published studies addressing the effect of the factor "pregnancy" on the prevalence of gallbladder stones

Factor by which the prevalence of gallstone disease in women with prior pregnancy is increased	1.0–1.5 times	1.6–2.5 times	2.6–10 times	11 – 50 times
Studies showing a quantitative relation between cholecystolithiasis and pregnancy	1966 Framingham[42] 1988 Sirmione[21] 1985 San Antonio[45] 1985 Maastricht[46]	1982 Oxford[47] 1982 Kopenhagen[44]	1979 Stockholm[48] 1982 Rom[32] 1986 Schwedt[41] 1986 Chianciano[22] 1991 Santiago[49]	1988 Srinagar[15]
Studies not showing a quantitative relation between cholecystolithiasis and pregnancy	1956 Birmingham[50] 1970 Pima reservation[51] 1980 Boston[52] 1982 Oberpfuss[53] 1983 Oxford[54] 1984 Adelaide[55] 1989 Soweto[12] 1990 Dublin[43] 1995 Ulm[19] 1996 Römerstein[20] 2002 Leutkirch			

W, Kratzer W, Kron M, Manfras B, Meitinger K, Mertens T, Oehme R, Pfaff G, Piechotowski I, Reuter S, Romig T, von Schmiesing AFA, Steinbach G, Tourbier M, Voegtle A, Walcher T, Wolff S.

REFERENCES

1 National Institutes of Health Consensus Development Conference Statement on Gallstones and Laparoscopic Cholecystectomy. *Am J Surg* 1993; 165: 390-398
2 **Russo MW,** Wei JT, Thiny MT, Gangarosa LM, Brown A, Ringel Y, Shaheen NJ, Sandler RS. Digestive and liver diseases statistics, 2004. *Gastroenterology* 2004; **126**: 1448-1453
3 **Diehl AK.** Epidemiology and natural history of gallstone disease. *Gastroenterol Clin North Am* 1991; **20**: 1-19
4 **Sandler RS,** Everhart JE, Donowitz M, Adams E, Cronin K, Goodman C, Gemmen E, Shah S, Avdic A, Rubin R. The burden of selected digestive diseases in the United States. *Gastroenterology* 2002; **122**: 1500-1511
5 **Kang JY,** Ellis C, Majeed A, Hoare J, Tinto A, Williamson RC, Tibbs CJ, Maxwell JD. Gallstones--an increasing problem: a study of hospital admissions in England between 1989/1990 and 1999/2000. *Aliment Pharmacol Ther* 2003; **17:** 561-569
6 **Kratzer W,** Mason RA, Kachele V. Prevalence of gallstones in sonographic surveys worldwide. *J Clin Ultrasound* 1999; **27**: 1-7
7 **Everhart JE**. US government printing office. *US government printing* 1994; 647-649
8 National Center for Health Statistics. National Hospital Discharge Survey. Advance Data from Vital and Health Statistics No 329, Hyatsville, MD 2002
9 Bundesministerium für Gesundheit. Morbidität - Krankenhausfälle und Arbeitsunfähigkeit. In: Der Bundesminister für Gesundheit, editor. Daten des Gesundheitswesens. Baden-Baden: Nomos, 1993: 34-43
10 Bundesministerium für Gesundheit. Gallensteine (ICD 574). In: Der Bundesminister für Gesundheit, editor. Ernährungsabhängige Krankheiten und ihre Kosten. Baden-Baden: Nomos, 1993: 187-193
11 **Safer L,** Bdioui F, Braham A, Ben Salem K, Soltani MS, Bchir A, Saffar H. [Epidemiology of cholelithiasis in central Tunisia. Prevalence and associated factors in a nonselected population] *Gastroenterol Clin Biol* 2000; **24:** 883-887
12 **Walker AR,** Segal I, Posner R, Shein H, Tsotetsi NG, Walker AJ. Prevalence of gallstones in elderly black women in Soweto, Johannesburg, as assessed by ultrasound. *Am J Gastroenterol* 1989; **84**: 1383-1385
13 **Shi JS,** Ma JY, Zhu LH, Pan BR, Wang ZR and Ma LS. Studies on gallstone in China. *World J Gastroenterol* 2001; **7**: 593-596
14 **Zhao Y,** Zhang R, Hu Y, Li R, Liang L, Gang Y. An epidemiological survey of gallstones with gray-scale ultrasound *Huaxi Yike Daxue Xuebao* 1990; **21:** 217-220
15 **Khuroo MS,** Mahajan R, Zargar SA, Javid G, Sapru S. Prevalence of biliary tract disease in India: a sonographic study in adult population in Kashmir. *Gut* 1989; **30:** 201-205
16 **Dhar SC,** Ansari S, Saha M, Ahmad MM, Rahman MT, Hasan M, Khan AK. Gallstone disease in a rural Bangladeshi community. *Indian J Gastroenterol* 2001; **20:** 223-6
17 **Nomura H,** Kashiwagi S, Hayashi J, Kajiyama W, Ikematsu H, Noguchi A, Tani S, Goto M. Prevalence of gallstone disease in a general population of Okinawa, *Japan. Am J Epidemiol* 1988; **128:** 598-605
18 **Zhu X,** Zhang S, Huang Z. [The trend of the gallstone disease in China over the past decade] *Zhonghua Waike Zazhi* 1995; **33:** 652-658
19 **Kratzer W,** Kachele V, Mason RA, Hill V, Hay B, Haug C, Adler G, Beckh K. Gallstone prevalence in Germany: the Ulm Gallbladder Stone Study. *Dig Dis Sci* 1998; **43**: 1285-1291
20 **Kratzer W,** Kron M, Hay B, Pfeiffer MM, Kachele V. Prevalence of cholecystolithiasis in South Germany--an ultrasound study of 2,498 persons of a rural population. *Z Gastroenterol* 1999; **37**: 1157-1162
21 **Barbara L,** Sama C, Morselli Labate AM, Taroni F, Rusticali AG, Festi D, Sapio C, Roda E, Banterle C, Puci A. A population study on the prevalence of gallstone disease: the Sirmione Study. *Hepatology* 1987; **7:** 913-917
22 **Loria P,** Dilengite MA, Bozzoli M, Carubbi F, Messora R, Sassatelli R et al. Prevalence rates of gallstone disease in Italy. The Chianciano population study. *Eur J Epidemiol* 1994; **10**: 143-150
23 **Lu SN,** Chang WY, Wang LY, Hsieh MY, Chuang WL, Chen SC, Su WP, Tai TY, Wu MM, Chen CJ. Risk factors for gallstones among Chinese in Taiwan. A community sonographic survey. *J Clin Gastroenterol* 1990; **12:** 542-526
24 **Attili AF,** Carulli N, Roda E, Barbara B, Capocaccia L, Menotti A, Okoliksanyi L, Ricci G, Capocaccia R, Festi D. Epidemiology of gallstone disease in Italy: prevalence data of the Multicenter Italian Study on Cholelithiasis (M.I.COL.) *Am J Epidemiol* 1995; **141:** 158-165
25 **Mendez-Sanchez N,** Chavez-Tapia NC, Motola-Kuba D, Sanchez-Lara K, Ponciano-Rodriguez G, Baptista H, Ramos MH, Uribe M. Metabolic syndrome as a risk factor for gallstone disease. *World J Gastroenterol* 2005; **11:** 1653-7
26 **Kono S,** Shinchi K, Todoroki I, Honjo S, Sakurai Y, Wakabayashi K, Imanishi K, Nishikawa H, Ogawa S, Katsurada M. Gallstone disease among Japanese men in relation to obesity,

glucose intolerance, exercise, alcohol use, and smoking. *Scand J Gastroenterol* 1995; **30**: 372-376
27 **Heaton KW,** Braddon FE, Mountford RA, Hughes AO, Emmett PM. Symptomatic and silent gall stones in the community. *Gut* 1991; **32**: 316-320
28 **Kodama H,** Kono S, Todoroki I, Honjo S, Sakurai Y, Wakabayashi K, Nishiwaki M, Hamada H, Nishikawa H, Koga H, Ogawa S, Nakagawa K. Gallstone disease risk in relation to body mass index and waist-to-hip ratio in Japanese men. *Int J Obes Relat Metab Disord* 1999; **23**: 211-216
29 **Barbara L,** Festi D, Morselli AM, Labate, Roda E, Rusticali AG et al. The sirmione study: familial frequency of gallstone disease. *Hepatology* 1984; **4**:1086
30 **Nurnberg D,** Berndt H, Pannwitz H. [Familial incidence of gallstones]. *Dtsch Med Wochenschr* 1989; **114**: 1059-1063
31 **Sarin SK,** Negi VS, Dewan R, Sasan S, Saraya A. High familial prevalence of gallstones in the first-degree relatives of gallstone patients. *Hepatology* 1995; **22**: 138-141
32 Prevalence of gallstone disease in an Italian adult female population. Rome Group for the Epidemiology and Prevention of Cholelithiasis (GREPCO). *Am J Epidemiol* 1984; **119**: 796-805
33 **Jorgensen T.** Gall stones in a Danish population: fertility period, pregnancies, and exogenous female sex hormones. *Gut* 1988; **29**: 433-439
34 **Hossain GA,** Islam SM, Mahmood S, Chakrabarty RK, Akhter N. Gall stone in pregnancy. *Mymensingh Med J* 2003; **12**: 112-116
35 WHO Expert Committee on Physical Status: the Use and Interpretation of Anthropometry: report of a WHO expert committee (WHO technical report series). *Genf: World Health Organization* 1995; 427-437
36 **Hosmer DWJr**, Lemeshow S. Applied logistic regression. *New York: Wiley*; 1989
37 **Brett M,** Barker DJ. The world distribution of gallstones. *Int J Epidemiol* 1976; **5**: 335-341
38 **Prathnadi P,** Miki M, Suprasert S. Incidence of cholelithiasis in the northern part of Thailand. J Med Assoc Thai 1992; 75: 462-470
39 **Jorgensen T.** Gallstones in a Danish population: familial occurrence and social factors. *J Biosoc Sci* 1988; **20**: 111-120
40 **Glambek I,** Kvaale G, Arnesjo B, Soreide O. Prevalence of gallstones in a Norwegian population. *Scand J Gastroenterol* 1987; **22**: 1089-1094
41 **Berndt H,** Nurnberg D, Pannwitz H. [Prevalence of cholelithiasis. Results of an epidemiologic study using sonography in East Germany] *Z Gastroenterol* 1989; **27**: 662-666
42 **Friedman GD,** Kannel WB, Dawber TR. The epidemiology of gallbladder disease: observations in the Framingham Study. *J Chronic Dis* 1966; **19**: 273-292
43 **Basso L,** McCollum PT, Darling MR, Tocchi A, Tanner WA. A study of cholelithiasis during pregnancy and its relationship with age, parity, menarche, breast-feeding, dysmenorrhea, oral contraception and a maternal history of cholelithiasis. *Surg Gynecol Obstet* 1992; **175**: 41-46
44 **Jorgensen T.** Prevalence of gallstones in a Danish population. *Am J Epidemiol* 1987; **126**: 912-921
45 **Diehl AK,** Rosenthal M, Hazuda HP, Comeaux PJ, Stern MP. Socioeconomic status and the prevalence of clinical gallbladder disease. *J Chronic Dis* 1985; **38**:1019-1026
46 **Thijs C,** Knipschild P, Leffers P. Pregnancy and gallstone disease: an empiric demonstration of the importance of specification of risk periods. *Am J Epidemiol* 1991; **134**: 186-195
47 **Layde PM,** Vessey MP, Yeates D. Risk factors for gall-bladder disease: a cohort study of young women attending family planning clinics. *J Epidemiol Community Health* 1982; **36**: 274-278
48 **Ahlberg J,** Angelin B, Einarsson K, Hellstrom K, Leijd B. Prevalence of gallbladder disease in hyperlipoproteinemia. *Dig Dis Sci* 1979; **24**: 459-464
49 **Valdivieso V,** Covarrubias C, Siegel F, Cruz F. Pregnancy and cholelithiasis: pathogenesis and natural course of gallstones diagnosed in early puerperium. *Hepatology* 1993; **17**: 1-4
50 **Horn G.** Observations on the aetiology of cholelithiasis. *Br Med J* 1956; **12**: 732-737
51 **Sampliner RE,** Bennett PH, Comess LJ, Rose FA, Burch TA. Gallbladder disease in pima indians. Demonstration of high prevalence and early onset by cholecystography. *N Engl J Med* 1970; **283**: 1358-1364
52 **Maclure KM,** Hayes KC, Colditz GA, Stampfer MJ, Speizer FE, Willett WC. Weight, diet, and the risk of symptomatic gallstones in middle-aged women. *N Engl J Med* 1989; **321**: 563-569
53 **Rhomberg HP,** Judmair G, Lochs A. How common are gallstones? *Br Med J (Clin Res Ed)* 1984; **289**: 1002
54 **Pixley F,** Wilson D, McPherson K, Mann J. Effect of vegetarianism on development of gall stones in women. *Br Med J (Clin Res Ed)* 1985; **291**: 11-12
55 **Scragg RK,** McMichael AJ, Seamark RF. Oral contraceptives, pregnancy, and endogenous oestrogen in gall stone disease--a case-control study. *Br Med J (Clin Res Ed)* 1984; **288**: 1795-1799

Science Editor Guo SY **Language Editor** Elsevier HK

PO Box 2345, Beijing 100023, China
www.wjgnet.com
wjg@wjgnet.com

ELSEVIER

World J Gastroenterol 2005;11(43):6807-6814
World Journal of Gastroenterology ISSN 1007-9327

• *CLINICAL RESEARCH* •

Characteristics of patients with columnar-lined Barrett's esophagus and risk factors for progression to esophageal adenocarcinoma

Kamal E Bani-Hani, Bayan K Bani-Hani, Iain G Martin

Kamal E Bani-Hani, Bayan K Bani-Hani, Department of Surgery, Faculty of Medicine, Jordan University of Science and Technology, Irbid, Jordan
Iain G Martin, Academic Surgical Unit and Center for Digestive Diseases, The General Infirmary, Leeds LS1 3EX, United Kindom
Correspondence to: Kamal E Bani-Hani, Professor of Surgery, Department of Surgery, Faculty of Medicine, Jordan University of Science and Technology, Irbid 22110, PO Box 3030, Jordan. banihani@yahoo.com
Telephone: +962-2-7060200 Fax: +962-2-7095010
Received: 2005-03-26 Accepted: 2005-04-30

Abstract

AIM: To determine the risk factors for the development of esophageal adenocarcinoma in these patients with columnar-lined esophagus (CLE).

METHODS: Data collected retrospectively on 597 consecutive patients diagnosed at endoscopy and histology to have CLE at Leeds General Infirmary between 1984 and 1995 were analyzed. Factors evaluated included age, sex, length of columnar segment, smoking, and drinking habits, history of non-steroidal ingestion, presence of endoscopic esophagitis, ulceration or benign strictures and presence of *Helicobacter pylori* in esophageal biopsies. Univariate and multivariate analyses were performed to identify risk factors for the development of adenocarcinoma.

RESULTS: Forty-four patients presented or developed esophageal adenocarcinoma during follow-up. Independent risk factors for the development of adenocarcinoma in patients with CLE were males (OR 5.12, 95%CI 2.04–12.84, $P = 0.0005$), and benign esophageal stricture (OR 4.37, 95%CI 2.02–9.45, $P = 0.0002$). Male subjects and patients who developed benign esophageal stricture constituted 86% ($n = 38$) of all patients who presented or developed esophageal adenocarcinoma. The presence of esophagitis was associated with a significant reduction in the development of esophageal carcinoma (OR 0.28, 95%CI 0.13–0.57, $P = 0.0006$). No other clinical characteristics differentiate between the non-malignant and malignant group.

CONCLUSION: In patients with CLE, endoscopic surveillance for the early detection of adenocarcinoma may be restricted to male subjects, as well as patients who develop benign esophageal strictures.

Key words: Barrett's esophagus; Adenocarcinoma; Risk factors; Esophageal adenocarcinoma; Esophageal stricture

Bani-Hani KE, Bani-Hani BK, Martin IG. Characteristics of patients with columnar-lined Barrett's esophagus and risk factors for progression to esophageal adenocarcinoma. *World J Gastroenterol* 2005; 11(43): 6807-6814
http://www.wjgnet.com/1007-9327/11/6807.asp

INTRODUCTION

Columnar-lined (Barrett's) esophagus (CLE) is defined as the replacement of the normal squamous lining of the lower esophagus by a unique metaplastic columnar epithelium usually as a consequence of chronic gastro-esophageal reflux (GER). The prevalence of CLE has been estimated to occur in 1 in 400 of the general population[1], and in 10–16% of patients with reflux esophagitis[2,3]. Cameron *et al.* suggested that there are 20 times as many cases of CLE in the general population as are clinically diagnosed[4].

Patients with CLE are at increased risk of esophageal adenocarcinoma[5]. The incidence of the latter varies between one in 46 to one in 441 patient-years follow-up[6,7] with an annual incidence of 1%, and is increasing more rapidly than any other type of malignancy[8,9]. Endoscopic surveillance programs are therefore instituted. Nonetheless, the increased cost and workload associated with the surveillance adds to the pressures on available resources. The identification of risk factors for the development of adenocarcinoma in these patients may allow for the selection of patients for intense endoscopic surveillance and a more efficient utilization of health care services and resources.

The current paper examines our experience with 597 consecutive patients diagnosed to have CLE for over a 11-year period. Our aim was to determine clinical factors, which could identify a subgroup of patients who are at a higher risk for the development of adenocarcinoma and who therefore would benefit most from being in a surveillance program. Examining the characteristics of

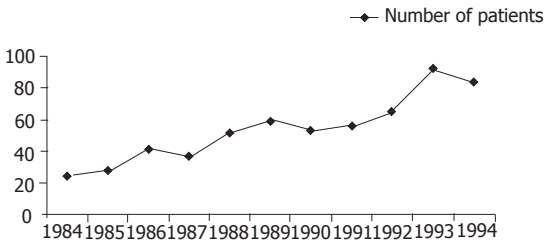

Figure 1 Number of patients diagnosed with columnar-lined esophagus during the study period.

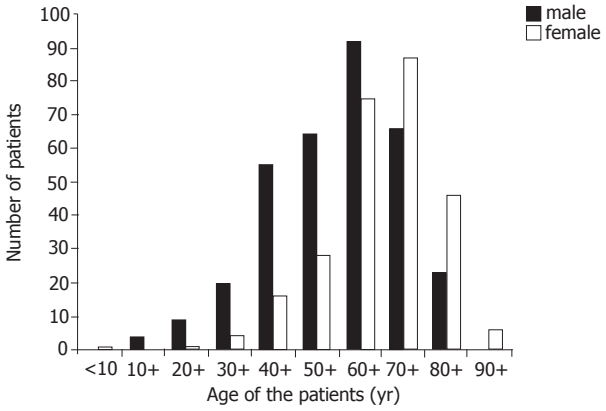

Figure 2 Age of patients at the time of diagnosis of columnar-lined esophagus.

patients with CLE and comparing them between the non-malignant group and both the prevalence and incident cases of adenocarcinoma might serve this purpose.

PATIENTS AND METHODS

Between January 1984 and December 1995, 626 consecutive patients were diagnosed at endoscopy and histology to have a CLE under the care of the Center for Digestive Diseases at the General Infirmary at Leeds. Patients were identified from a computer registry at the Institute of Pathology and their records were retrospectively reviewed. Data, including patient demographic characteristics, endoscopic findings, and histology reports were entered into a computer database.

Columnar-lined esophagus was defined as the presence of columnar-lined epithelium at least 3 cm above the endoscopically determined gastro-esophageal junction or the presence of specialized columnar epithelium (SCE) anywhere in the esophagus. Twenty-nine patients were excluded from this study; 17 patients did not fulfill the definition criteria mentioned above and the medical records of 12 patients could not be located.

Factors that may be associated with increased risk of development of adenocarcinoma were examined. These included age, sex, smoking, regular alcohol use, the ingestion of non-steroidal anti-inflammatory drugs (NSAIDs), length of columnar segment, the presence of hiatul hernia, esophagitis, benign esophageal stricture or ulcers at endoscopy, and the presence of SCE or *H pylori* in esophageal biopsies. Mean follow-up was 43 (range 1-155 mo) mo. Data related to the size of hiatul hernia and body mass index of the patients were incomplete and excluded from analysis. Data related to the result of the surveillance program for these patients were published elsewhere[6].

Patients were defined as smokers if they regularly smoked more than 10 cigarettes per day for at least one year at any time before the diagnosis of CLE. Patients were defined as regular alcohol users if they have a history of drinking 10 units of alcohol or more weekly for at least one year at any time before the diagnosis of CLE. Patients who have a history of regular ingestion of NSAIDs for at least 6 mo at any time before the diagnosis of CLE were regarded as NSAIDs users. *H pylori* colonization was determined upon the basis of hematoxylin and eosin and the use of a modified Giemsa stain of esophageal and gastric biopsy specimens.

All cases with malignant stricture were not regarded as cases of benign esophageal stricture and were not considered for the analysis. Only cases where the stricture was away from the cancer and histologically not involved with cancer were regarded as benign esophageal ulcer.

Statistical analysis

Univariate analysis was performed utilizing the χ^2 test and the Mann–Whitney *U* test as appropriate. Statistical significance was accepted at a $P<0.05$. Stepwise logistic regression analysis was used to identify independent risk factors. Statistical analyses were performed using SPSS for Windows version 10.

RESULTS

Five hundred and ninety-seven patients with histologically confirmed diagnosis of CLE were seen at our institute from 31st January 1984 to 31st January 1995. The number of new patients diagnosed each year during the study period showed an increasing trend (Figure 1). There were 333 (56%) males and 264 (44%) females. The mean age for the total group was 63.4 years (SD 14.86; range 2-94 years). Seventy-three percent of the male patients (244/333) had their diagnosis below the age of 70, while 81% (214/264) of female patients were diagnosed when they were above 60 years of age (Figure 2).

Of the 597 patients included in the analysis, 31 (5.2%) presented or developed adenocarcinoma within 6 mo of initial diagnosis of CLE and 13 (2.2%) developed adenocarcinoma after a mean follow-up of 55 mo (range 8-155 mo). Patients were divided into two groups: Non-malignant group: 553 patients had no esophageal adenocarcinoma either at initial presentation or during follow-up. There were 299 (54%) males and 254 (46%) females. Malignant group: 44 patients presented (31 patients) or developed (13 patients) esophageal adenocarcinoma. There were 34 (77%) males and 10 (23%) females.

Table 1 summarizes the details of patients and the results of the univariate analysis of the risk factors studied. Table 2 summarizes the results of multivariable analysis.

Table 1 Univariate analysis of potential risk factors for the development of esophageal adenocarcinoma in patients with columnar-lined esophagus

	Non-malignant group (n = 553)	Malignant group (n = 44)	P
Age			
<60 (yr: *n,* %)	189 (34.2)	13 (29.5)	0.532
>60 (yr: *n,* %)	364 (65.8)	31 (70.5)	
Sex: male (%)	299 (54.1)	34 (77.3)	0.003
Smoking+: *n* (%)	161 (45.2)	21 (51.2)	0.466
Regular alcohol use±: *n* (%)	52 (15.2)	8 (20)	0.430
NSAIDs: *n* (%)	304 (55)	25 (56.8)	0.813
Specialized epithelium: *n* (%)	467 (84.4)	42 (95.5)	0.047
Length of CLE Median (cm)	5	6	0.001
Hiatul hernia: *n* (%)	314 (56.8)	22 (50)	0.383
Esophagitis: *n* (%)	330 (59.7)	13 (29.5)	<0.0001
Esophageal ulcer	117 (21.2)	11 (25)	0.550
Esophageal stricture	77 (13.9)	16 (36.4)	<0.0001
Hp in esophageal biopsy	42 (7.6)	2 (4.5)	0.456

CLE – columnar-lined esophagus; NSAIDs – non-steroidal anti-inflammatory drugs; Hp – *Helicobacter pylori*. +Information regarding smoking was available in only 356 patients of the non-malignant group and 41 patients of the malignant group; ‡information regarding alcohol consumption was available in only 342 patients of the non-malignant group and 40 patients of the malignant group.

Table 2 Risk factors associated with the development of adenocarcinoma in patients with CLE; results of multivariable regression analysis

Risk factors	Odds ratio	95%CI for Odds ratio	P
Age ≥60 yr	1.65	0.75–3.64	0.216
Male sex	5.12	2.04–12.84	0.0005
Regular alcohol use	1.15	0.46–2.90	0.760
NSAIDs	1.41	0.68–2.93	0.352
Esophagitis	0.28	0.13–0.57	0.0006
Esophageal stricture	4.37	2.02–9.45	0.0002

CLE – columnar lined esophagus; NSAIDs – non-steroidal anti-inflammatory drugs

Significant independent risk factors for the development of esophageal adenocarcinoma in patients with CLE were male sex, and benign esophageal stricture. Male subjects and patients who developed benign esophageal stricture constituted 86% (n = 38) of all patients who presented or developed esophageal adenocarcinoma. Among the 24 patients who presented with esophageal adenocarcinoma, 9 patients had histologically proven benign peptic stricture above and away from the cancer and the strictures were located at the junction of the columnar mucosa with the squamous epithelium. Among the seven patients who developed esophageal adenocarcinoma within 6 mo after the diagnosis of CLE, four of them had histologically proven benign peptic stricture at the time of diagnosis of CLE. Among the 13 patients who developed esophageal adenocarcinoma after a mean follow-up of 55 (range 8-155 mo) mo, three patients had histologically proven benign peptic stricture at the time of diagnosis of CLE, and these three patients developed adenocarcinoma 17, 24, and 35 mo after the diagnosis of CLE, respectively.

The presence of esophagitis was associated with a significant reduction in the development of esophageal carcinoma. Although univariate analysis identified the length of columnar-lined esophageal segment and the presence of SCE on endoscopic biopsies as significant variables (P = 0.001, P = 0.047 respectively), these did not reach significance on multivariable analysis. Age >60 years, smoking, alcohol consumption, the presence of hiatul hernia or esophageal ulcer, and the presence of *H pylori* in the esophageal biopsies were insignificant risk factors for malignant progression.

Symptoms as a risk factor

For the purpose of comparison between the two groups, the main principal symptom for each patient was considered at the time of diagnosis, although many patients had more than one symptom. In the non-malignant group, the main symptoms at presentation were as follows: In 259 patients (46.8%), the main symptoms were those of GER (heartburn, regurgitation) or dyspepsia. Anemia or gastro-intestinal bleeding was the main symptom in 137 patients (24.8%). Dysphagia was the main symptom in 111 patients (20%) and chest pain was the main symptom in 26 patients (4.7%). Weight loss was the main symptom in only 20 patients (3.6%). Ninety-four patients (17%) in the non-malignant group had no esophageal symptoms at the time of diagnosis and CLE was diagnosed when endoscopy was performed to investigate iron deficiency anemia. In the malignant group, the main symptom was dysphagia in 21 patients (47.7%). Anemia or gastrointestinal bleeding was the main symptom in nine patients (20.5%). GER symptoms were the main symptoms in 10 patients (22.7%). Weight loss was the main symptom in four patients (9%). Dysphagia rather than reflux symptom was the main complaint of the patients in the malignant group at the time of diagnosis. This was mainly due to dysphagia being prominent in the prevalent adenocarcinoma cases (61%; 19/31) as would be expected; in contrast among the 13 patients who developed adenocarcinoma during follow-up, dysphagia was the main symptom in only two patients (15%; 2/13).

Length of the columnar segment

The length of the columnar segments for all patients is shown in Figure 3. Twenty-three patients had short segment (<3 cm) of SCE; none of this group were adenocarcinoma patients. The mean length of the columnar segment in the non-malignant group was 5.8 cm; range 2-20 cm and for the malignant group was 7.2 cm; range 3-15 cm. There was no correlation between the extent of the columnar segment and the presence or absence of symptoms of GER.

Esophageal and gastric H pylori

Forty-four patients only (7.4%) had *H pylori* detected in their esophageal biopsies. Only 234 patients of this series had gastric biopsies in addition to their esophageal specimens. Among this subgroup who had biopsy demonstrated CLE and from whom concomitant gastric biopsies were taken, 77 patients (32.9%) had *H pylori* in

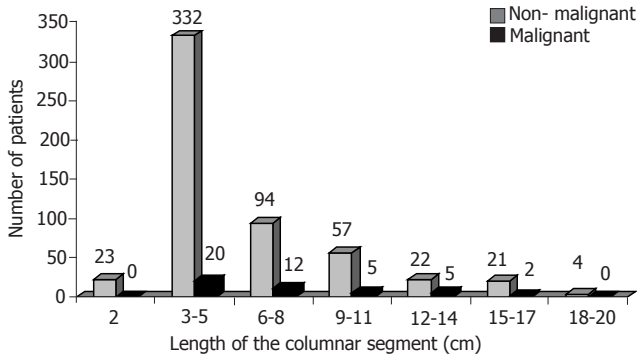

Figure 3 Length of the columnar segments in all patients.

their gastric biopsies, 20 of them had *H pylori* in both the esophageal and gastric specimens. The finding of *H pylori* in CLE biopsies was not associated with increase in the prevalence of esophagitis (52% *vs* 58%), esophageal strictures (11% *vs* 16%), esophageal ulcers (23% *vs* 21%) or esophageal adenocarcinoma (4.5% *vs* 7.6%).

DISCUSSION

The present series confirms the findings of other studies[10,11] that the prevalence of CLE increases with age and reaches a peak in late middle age. Eighty-two percent of our patients (487/597) were diagnosed when they were over 50 years of age. The high prevalence of CLE occurs mainly in later middle age and the elderly as shown by our population with a mean age of 59 in males and 68 in females, although it can be seen in younger patients also. However, only 2.5% of patients (15/597) were under 30 years of age at the time of diagnosis. One patient had a diagnosis of CLE below the age of 10 and this was a 3-year old girl who presented with repeated vomiting. Endoscopic and histological examination confirmed the diagnosis of CLE and anti-reflux surgery was performed on this patient at the age of four. This case could be explained on the basis of the few cases of congenital Barrett's esophagus reported previously[12].

Although there were slightly more males than females in the whole of our series (56% *vs* 44%), we have found that below the age of 60, there is a clear male predominance of 3:1. In contradiction to other published data, which showed either a male predominance[13] or an equal sex distribution[10,14], we observed a female predominance of 1.5:1 in patients above the age of 70.

A large proportion of patients with CLE in the general population will remain undiagnosed unless complications or carcinoma develop. CLE itself causes no symptoms[15] whereas the main symptoms, which bring patients to medical attention, are related to the reflux symptoms or complications of CLE such as ulceration, stricture, bleeding or adenocarcinoma. There is no correlation between severity of symptoms and histological findings, as about 17% of our patients with CLE had no esophageal symptoms. It is clear therefore that the selection of patients for a surveillance program cannot be based on symptomatology. This conclusion was also made in earlier patient series[10,16,17].

Our study confirms that patients with CLE have an increased incidence of esophageal adenocarcinoma. There were 7 patients who developed adenocarcinoma within 6 mo of initial diagnosis, before their first annual review endoscopy. This is likely to reflect the presence of undetected malignancy at the time of initial endoscopy. This probably represents a sampling error in the biopsies taken and therefore these seven patients were included in the prevalence rather than the incidence data[6].

This study identified male sex, and benign esophageal stricture to be independent risk factors (at least four-fold increased risk) for the development of esophageal adenocarcinoma in patients with CLE. Male patients with benign esophageal stricture constituted 86% of all patients who developed esophageal malignancy. The risk of malignancy was not related to the age of the patients, smoking, presence of SCE, length of columnar-lined segment, or the presence of esophageal ulceration or hiatul hernia on endoscopy or *H pylori* in esophageal or gastric biopsies. Previous reports identified white ethnicity[18], older age[19], male sex[13,14,20], SCE[21,22], long columnar segment[10,19,23-28], large hiatal hernia size[26,27], esophageal ulcer or stricture[10,29-31], severe acid reflux[26,32], obesity[33,34] and smoking and alcohol[20,35] to be associated with the progression from columnar epithelium to adenocarcinoma. However, some of these reports were based on observations or univariate analyses, and did not control for other variables as in the current study.

There was no significant association between age >60 years and the risk of malignant progression. Most patients are diagnosed with CLE in their sixth or seventh decade of life. Patients with Barrett's are often reported to be of the same age as those who develop cancer[26]. On the other hand, other studies have reported that the risk of esophageal adenocarcinoma increases with age. Gopal *et al.* reported that the risk of dysplasia increased by 3.3% per year of age[19]. A potential problem is that the mean age of patients with dysplasia is quite high, increasing the expected operative mortality and tending to preclude operative intervention. Clearly, surveillance should be offered only for those patients in whom esophagectomy is considered as a therapeutic option, if early carcinoma is detected. On the other hand, with the availability of ablation therapy, one can argue that even patients who are not fit for esophagectomy will benefit from the treatment of their high-grade dysplasia or early adenocarcinoma using photoablation irrespective of their age.

The increased susceptibility of male subjects with CLE to the development of esophageal malignancy has been reported previously[20,36,37]. In these series, men constituted 67–100% of all patients who developed esophageal adenocarcinoma (77% in this report). Our finding that benign stricture formation, which complicated 16% of all patients with CLE, was a risk factor for malignant transformation that supports previous reports[10,30,31,38,39]. Careful endoscopic surveillance of patients with benign

esophageal strictures is therefore required, despite the fact that malignant progression occurred in only one in eight patients.

We found no evidence to support the suggestion that a longer CLE segment is associated with a greater risk of carcinoma. Although the length of columnar segment was significantly greater in patients who developed esophageal adenocarcinoma compared with those who did not, this was not an independent risk factor for malignant transformation. This finding is in concordance with that of Robertson *et al*. who showed that the progression of the metaplastic epithelium up the esophagus, which occurred in 20% of their patients, was not associated with an increased risk of malignancy, as out of the 11 patients who had progression up to 6 cm, only 1 developed carcinoma[16]. Additionally, the marked association between adenocarcinoma of the gastroesophageal junction and 'short-segment' Barrett's mucosa[21,22,25,40] underscores the importance of the 'short-segment', and calls for follow-up program similar to that of longer segments of CLE. Rudolph *et al*. reported that segment length was not related to cancer risk in the full cohort of patients with CLE, and when patients with high-grade dysplasia at baseline were excluded; however, a non-significant trend was observed; a 5 cm difference in segment length was associated with a 1.7-fold increase in cancer risk. These authors concluded that the risk for esophageal adenocarcinoma in patients with short-segment Barrett esophagus was not substantially lower than that in patients with longer segments. They suggested that until more data are available, the frequency of endoscopic surveillance should be selected without regard to segment length[28].

There are some indications that the risk of cancer is proportionate to the anatomic extent of CLE[19,26,27]. A few studies have shown that the risk of adenocarcinoma increases with the length of the columnar segment and they suggested considering patients with CLE of more than 8 or 10 cm in length for surveillance. For example, Iftikhar *et al*.[24] reported that among 102 patients with CLE, 12 were found to have dysplasia; all of them had a columnar segment of 8 cm or more at the time of diagnosis and no patient with a columnar segment of less than 8 cm was found to have dysplasia or adenocarcinoma. In two retrospective studies conducted by Harle *et al*.[41] and Rosenberg *et al*.[42], 94% and 88% of patients with adenocarcinoma had long segments (>10 cm) of columnar epithelium. Both series suggested that an extended length of Barrett's esophagus is associated with a higher risk of malignant progression. Schnell *et al*.[23] reported a series of 238 patients with CLE. Adenocarcinoma was found in 7% of the 129 patients with segments less than 2 cm in length, in 12% of 50 patients with 3-5 cm segments, in 31% of 45 patients with 6-10 cm Barrett's segments and in 43% of the 14 patients who had segments of more than 10 cm in length. They concluded that there is a strong association between the length of CLE and risk of adenocarcinoma. Gopal *et al*. reported that the risk of dysplasia increased by 14%/cm of increased length[19], and similarly Avidan *et al*. reported that each 1-cm elongation of Barrett's mucosa carried with it a 17% increase in the risk of developing high-grade dysplasia or carcinoma[26]. On the other hand, other studies have suggested that shorter lengths of CLE may have been obscured by the tumor and therefore missed at resection. For example, Hamilton *et al*.[40] found that 64% of the resected specimens of adenocarcinoma of the esophagus and GEJ were associated with Barrett' s esophagus although the Barrett's mucosa was identified by endoscopic biopsies in only 38% of cases. When adenocarcinoma develops in a short segment of specialized epithelium, the tumor may destroy the area of specialized epithelium leaving no trace of such epithelium. Schnell *et al*.[21] did indeed report four patients with adenocarcinoma in short segment of specialized epithelium. Cameron *et al*.[22] reported that SCE was found in 9 of 9 (100%) cases of esophageal adenocarcinomas and in 10 of 24 (42%) of cases of junctional adenocarcinomas. SCE was found in 8 of 12 (67%) of junctional adenocarcinoma of 6 cm or less in length but in only 2 of 12 (17%) of larger tumors. Again they concluded that junctional adenocarcinomas are associated with both short and long segments of Barrett' s esophagus and larger tumors probably overgrow and conceal the underlying SCE from which they arise. In 38% of the patients who developed cancer, the metaplastic segment was less than 3 cm[43] Schnell *et al*.[21] emphasizes that patients with short segments should be considered at risk and should be followed in the same way as their counterparts with longer segments of CLE. The above studies clearly demonstrate that carcinoma can develop in short as well as long segment of CLE. It is now established that short segment CLE does carry a risk of malignant progression, *albeit* currently this is difficult to quantify[44].

Specialized epithelium is the most common and distinctive type of columnar epithelium found in CLE. Although dysplasia and carcinoma develop mainly in the presence of SCE, we cannot regard this type of epithelium as the sole indication for surveillance because histology has shown that it is present in most patients with CLE. Indeed nowadays its presence is rather a criterion to establish the diagnosis of CLE. There are, however, a few cases of adenocarcinoma, which can develop in columnar epithelium of other histological types (junctional or fundic type).

The reported data concerning the influence of alcohol consumption on the malignant progression of CLE is controversial. Most published reports including the current study suggest that alcohol ingestion has no or only little effect[26]. The reported decline in the incidence of oral cavity and pharynx cancers, which are traditionally, related to alcohol consumption contrasts with the increase in the incidence of esophageal adenocarcinoma[45]. Gammon *et al*. reported a decrease in the risk associated with wine drinking and no increase in the risk by the use of other alcoholic beverages[46]. Similarly, Garridou *et al*. reported that wine might have a protective effect[47]. On the other hand, other investigators have reported an increased risk of esophageal adenocarcinoma with high alcohol intake[20,35,48-50]. Zhang *et al*. reported a statistically not significant twofold increase in the risk of esophageal

adenocarcinoma in those who consume alcohol when compared with nondrinkers[48]. Kabat *et al*. reported that only hard liquor intake was associated with esophageal adenocarcinoma in males, and only daily beer intake was associated with adenocarcinoma in females[49]. Barrett's esophagus was reported to occur more frequently among subjects who consume large amounts of alcohol and alcohol consumption was also a risk factor for an increased length of Barrett's mucosa[51,52]. There is a well-known association between alcohol intake and risk of upper digestive tract cancers from epidemiological studies[53]. One possible mechanism is that this increased risk is due to a direct exposure of the esophageal mucosa to high alcohol concentrations but systemic effects could also be important.

There were no differences between smokers and non-smokers with regard to the length of the columnar segment and the presence or absence of Barrett's complications such as ulcer, stricture or adenocarcinoma. Several reports[26,54,55], as well as the current one, did not support the suggested increased risk of malignant transformation with smoking. Cooper and Barbezat[54] reported a series of 52 patients with CLE and 25 of them were smokers or ex-smokers. They also found no difference in the clinical characteristics between the smokers and non-smokers. Other investigators have shown a higher proportion of smokers in patients with CLE[56] and some suggested that the malignant progression of Barrett's metaplasia was higher in patients who smoked[20,35,50]. On the other hand, Levi *et al*.[55] evaluated the relationship between tobacco, alcohol and the risk of esophageal adenocarcinoma in CLE in an endoscopy-clinic-based case-control study of 30 cases of adenocarcinoma and 140 controls with non-malignant CLE. Among the cases, 18 (60%) were non-smokers and 14 (47%) non-drinkers, the corresponding proportions in the controls being 52% and 44%. Thus, there was no apparent relation between tobacco, alcohol and the risk of esophageal adenocarcinoma. They suggested that the findings of their study, although based on a limited number of cases, indicate that alcohol and tobacco are unlikely to play a major role in the etiology of adenocarcinoma in CLE. Overall, alcohol and tobacco may be risk factors for esophageal adenocarcinoma, but are not as important as they are in the etiology of esophageal squamous cell carcinoma[57].

Esophagitis and hiatal hernia were more common in the non-malignant group than the malignant group. But these differences have no clinical value, as it will not differentiate between the two groups. The apparent protective effect of esophagitis against malignant progression reflects the natural history of the disease. Esophagitis precedes the replacement of squamous with columnar epithelium, which in turn may become progressively dysplastic with final transformation into adenocarcinoma[12,58,59]. Additionally, columnar epithelium, unlike squamous, is less sensitive to injury secondary to GER and thus more resistant to inflammation[60].

There was an association between the prevalence of esophagitis and esophageal ulcerations with the history of NSAIDs ingestion within the non-cancer patients; however, there was no significant difference between the non-malignant group and malignant group regarding the prevalence of NSAIDs ingestion. It is likely that NSAIDs are prescribed or self-prescribed for esophagitis. Fifty-five percent of patients in the non-malignant group were taking these drugs at the time of diagnosis and 62% of them were found to have esophagitis or esophageal ulcerations. Cooper and Barbezat[54] reported similar findings and suggested that patients with CLE should avoid taking NSAIDs. However, NSAIDs are now proposed in intervention trials for patients with CLE. Increased expression of the cyclooxygenase 2 enzyme is proposed to be central to the development of esophageal cancer. Since this enzyme is inhibited by NSAIDs, these drugs hold promise as cancer chemopreventive agents in Barrett's esophagus patients[61]. Several preventive strategies against esophageal adenocarcinoma are under investigation using NSAIDs[62].

We found that esophageal ulcerations were present in 25% of patients in the carcinoma group (11/44) and in 21% of the patients who had no carcinoma (117/553); a difference that was not statistically significant. No case of esophageal perforation due to these ulcers was found in our series. These findings disagree with previous series, which suggested that the risk of developing carcinoma is increased in the presence of esophageal ulcers[10,29–31].

In concordance with previous work suggesting that stricture formation in CLE is a risk factor of malignant progression[10,30,31,39], we observed that esophageal strictures were present in 36% of patients in the carcinoma group (16/44) and in only 14% of the patients without carcinoma (77/553); a difference that was statistically significant. Theoretically it is possible that some of the strictures of the patients who presented or developed adenocarcinoma within 6 mo of CLE diagnoses could be malignant strictures (missed cancers) which were not detected histologically due to sampling error.

We found that *H pylori* colonization of the esophagus was not a risk factor for malignant progression. Our data indicate that *H pylori* can colonize the CLE, but its prevalence rate in the esophageal biopsies of these patients or in the subgroups that had complications or carcinoma is low and it is unlikely that *H pylori* has a significant role in the pathogenesis of CLE or its complications. Similar conclusion was reported before[63,64]. The prevalence rate of *H pylori* in the gastric biopsies of the same patients is similar or less than that in the normal population. Weston *et al*.[65] found that Barrett's high-grade dysplasia and adenocarcinoma were significantly more prevalent in patients who are not infected with *H pylori*. They suggested that *H pylori* appear to have a protective effect against the development of Barrett's adenocarcinoma.

While the role of endoscopic surveillance in low-risk patients with CLE is controversial, efficient and effective screening would target high-risk patients. This study suggests that such programs may be largely directed to male subjects and those who develop benign esophageal strictures. We have previously shown that

immunohistochemical detection of cyclin D1 in esophageal biopsies of patients with CLE is a sensitive tool for identifying subgroup of patients who may be at a higher risk[66]. But given that multiple genetic alterations, which are implicated in the natural history of esophageal adenocarcinoma, a combination of clinical risk factors and carefully validated biomarkers including cyclin D1, might improve still further the predictive value of the molecular approach[66,67].

In conclusion, we have found that 44 patients presented or developed esophageal adenocarcinoma of which 34 (77%) were males. Independent risk factors for progression from columnar metaplasia to esophageal adenocarcinoma were male sex, and the development of benign esophageal stricture. No other clinical characteristics differentiate between the non-malignant and malignant group. Most esophageal adenocarcinoma occurs in men with specialized epithelium. This subgroup may constitute a clinically recognized group at a high risk of cancer and particularly suitable for endoscopic surveillance. In patients with CLE, endoscopic surveillance for the early detection of adenocarcinoma may be restricted to male subjects, as well as patients who develop benign esophageal strictures. A large proportion of patients with CLE have no esophageal symptoms making recruitment into endoscopic surveillance programs problematic.

REFERENCES

1 **Stein HJ,** Siewert JR. Barrett's esophagus: pathogenesis, epidemiology, functional abnormalities, malignant degeneration, and surgical management. *Dysphagia* 1993; **8:** 276-288

2 **Naef AP,** Savary M, Ozzello L. Columnar-lined lower esophagus: an acquired lesion with malignant predisposition. Report on 140 cases of Barrett's esophagus with 12 adenocarcinomas. *J Thorac Cardiovasc Surg* 1975; **70:** 826-835

3 **Bartlesman JF,** Hameeteman W, Tytgat GN. Barrett's oesophagus. *Eur J Cancer Prev* 1992; **1:** 323-325

4 **Cameron AJ,** Zinsmeister AR, Ballard DJ, Carney JA. Prevalence of columnar-lined (Barrett's) esophagus. Comparison of population-based clinical and autopsy findings. *Gastroenterology* 1990; **99:** 918-922

5 **Spechler SJ**. Endoscopic surveillance for patients with Barrett' s esophagus: Does the cancer risk justify the practice? *Ann Intern Med* 1987; **106:** 902-904

6 **Bani-Hani K,** Sue-Ling H, Johnston D, Axon AT, Martin IG. Barrett's oesophagus: results from a 13-year surveillance programme. *Eur J Gastroenterol Hepatol* 2000; **12:** 649-654

7 **Cameron AJ**, Ott BJ, Payne WS. The incidence of adenocarcinoma in columnar-lined (Barrett's) esophagus. *N Engl J Med* 1985; **313:** 857-859

8 **Spechler SJ.** The frequency of cancer in patients with Barrett's esophagus. *Acta Endoscopica* 1992; **22:** 541-4

9 **Blot WJ**, Devesa SS, Kneller RW, Fraumeni JF Jr. Rising incidence of adenocarcinoma of the esophagus and gastric cardia. *JAMA* 1991; **265:** 1287-1289

10 **Macdonald CE,** Wicks AC, Playford RJ. Ten years' experience of screening patients with Barrett's oesophagus in a university teaching hospital. *Gut* 1997; **41:** 303-307

11 **Cameron AJ**, Lomboy CT. Barrett's esophagus: age, prevalence, and extent of columnar epithelium. *Gastroenterology* 1992; **103:** 1241-1245

12 **Borrie J**, Goldwater L. Columnar cell-lined esophagus: assessment of etiology and treatment. A 22 year experience. *J Thorac Cardiovasc Surg* 1976; **71:** 825-834

13 **Wright TA**, Gray MR, Morris AI, Gilmore IT, Ellis A, Smart HL, Myskow M, Nash J, Donnelly RJ, Kingsnorth AN. Cost effectiveness of detecting Barrett's cancer. *Gut* 1996; **39:** 574-579

14 **Menke-Pluymers MB,** Hop WC, Dees J, van Blankenstein M, Tilanus HW. Risk factors for the development of an adenocarcinoma in columnar-lined (Barrett) esophagus. The Rotterdam Esophageal Tumor Study Group. *Cancer* 1993; **72:**1155-1158

15 **Sjogren RW Jr**, Johnson LF. Barrett's esophagus: a review. *Am J Med* 1983; **74:** 313-321

16 **Robertson CS**, Mayberry JF, Nicholson DA, James PD, Atkinson M. Value of endoscopic surveillance in the detection of neoplastic change in Barrett's oesophagus. *Br J Surg* 1988; **75:** 760-763

17 **Achkar E**, Carey W. The cost of surveillance for adenocarcinoma complicating Barrett's esophagus. *Am J Gastroenterol* 1988; **83:** 291-294

18 **Rogers EL**, Goldkind SF, Iseri OA, Bustin M, Goldkind L, Hamilton SR, Smith RL. Adenocarcinoma of the lower esophagus. A disease primarily of white men with Barrett's esophagus. *J Clin Gastroenterol* 1986; **8:** 613-618

19 **Gopal DV**, Lieberman DA, Magaret N, Fennerty MB, Sampliner RE, Garewal HS, Falk GW, Faigel DO. Risk factors for dysplasia in patients with Barrett's esophagus (BE): results from a multicenter consortium. *Dig Dis Sci* 2003; *48:* 1537-1541

20 **Skinner DB,** Walther BC, Riddell RH, Schmidt H, Iascone C, DeMeester TR. Barrett's esophagus. Comparison of benign and malignant cases. *Ann Surg* 1983; **198:** 554-566

21 **Schnell TG,** Sontag SJ, Chejfec G. Adenocarcinomas arising in tongues or short segments of Barrett's esophagus. *Dig Dis Sci* 1992; **37:** 137-143

22 **Cameron AJ,** Lomboy CT, Pera M, Carpenter HA. Adenocarcinoma of the esophagogastric junction and Barrett's esophagus. *Gastroenterology* 1995; **109:** 1541-1546

23 **Schnell T**, Sontag S, Chejfec G, Miller T, Kurucar C, O' Connell S, Brand L. Does length (L) of Barrett's esophagus (BE) correlate with age, cigarette or alcohol consumption or risk of adenocarcinoma (adCa) (abstract)? *Gastroenterology* 1990; **98:** A120.

24 **Iftikhar SY,** James PD, Steele RJ, Hardcastle JD, Atkinson M. Length of Barrett's oesophagus: an important factor in the development of dysplasia and adenocarcinoma. *Gut* 1992; **33:** 1155-1158

25 **Clark GW,** Smyrk TC, Burdiles P, Hoeft SF, Peters JH, Kiyabu M, Hinder RA, Bremner CG, DeMeester TR. Is Barrett's metaplasia the source of adenocarcinomas of the cardia? *Arch Surg* 1994; **129:** 609-614

26 **Avidan B**, Sonnenberg A, Schnell TG, Chejfec G, Metz A, Sontag SJ. Hiatal hernia size, Barrett's length, and severity of acid reflux are all risk factors for esophageal adenocarcinoma. *Am J Gastroenterol* 2002; **97:** 1930-1936

27 **Weston AP**, Badr AS, Hassanein RS. Prospective multivariate analysis of clinical, endoscopic, and histological factors predictive of the development of Barrett's multifocal high-grade dysplasia or adenocarcinoma. *Am J Gastroenterol* 1999; **94:** 3413-3419

28 **Rudolph RE**, Vaughan TL, Storer BE, Haggitt RC, Rabinovitch PS, Levine DS, Reid BJ. Effect of segment length on risk for neoplastic progression in patients with Barrett esophagus. *Ann Intern Med* 2000; **132:** 612-620

29 **Van der Veen AH**, Dees J, Blankensteijn JD, Van Blankenstein M. Adenocarcinoma in Barrett's oesophagus: an overrated risk. *Gut* 1989; 30: 14-18

30 **Moghissi K,** Sharpe DA, Pender D. Adenocarcinoma and Barrett's oesophagus. A clinico-pathological study. *Eur J Cardiothorac Surg* 1993; **7:** 126-131

31 **Lerut T,** Coosemans W, Van Raemdonck D, Dillemans B, De Leyn P, Marnette JM, Geboes K. Surgical treatment of Barrett's carcinoma. Correlations between morphologic findings and prognosis. *J Thorac Cardiovasc Surg* 1994; **107:** 1059-65;

discussion 1065-1066
32 **Lagergren J**, Bergstrom R, Lindgren A, Nyren O. Symptomatic gastroesophageal reflux as a risk factor for esophageal adenocarcinoma. *N Engl J Med* 1999; **340:** 825-831
33 **Brown LM,** Swanson CA, Gridley G, Swanson GM, Schoenberg JB, Greenberg RS, Silverman DT, Pottern LM, Hayes RB, Schwartz AG. Adenocarcinoma of the esophagus: role of obesity and diet. *J Natl Cancer Inst* 1995; **87:** 104-109
34 **Lagergren J**, Bergstrom R, Nyren O. Association between body mass and adenocarcinoma of the esophagus and gastric cardia. *Ann Intern Med* 1999; 130: 883-890
35 **Gray MR,** Donnelly RJ, Kingsnorth AN. The role of smoking and alcohol in metaplasia and cancer risk in Barrett's columnar lined oesophagus. *Gut* 1993; **34:** 727-731
36 **Allison PR,** Johnstone AS. The oesophagus lined with gastric mucous membrane. *Thorax* 1953; **8:** 87-101
37 **Haggitt RC**, Tryzelaar J, Ellis FH, Colcher H. Adenocarcinoma complicating columnar epithelium-lined (Barrett's) esophagus. *Am J Clin Pathol* 1978; 70: 1-5
38 **Chow WH,** Finkle WD, McLaughlin JK, Frankl H, Ziel HK, Fraumeni JF Jr. The relation of gastroesophageal reflux disease and its treatment to adenocarcinomas of the esophagus and gastric cardia. *JAMA* 1995; **274:** 474-477
39 **van der Burgh A,** Dees J, Hop WC, van Blankenstein M. Oesophageal cancer is an uncommon cause of death in patients with Barrett's oesophagus. *Gut* 1996; **39:** 5-8
40 **Hamilton SR,** Smith RR, Cameron JL. Prevalence and characteristics of Barrett's esophagus in patients with adenocarcinoma of the esophagus or esophagogastric junction. *Hum Pathol* 1988; **19:** 942-948
41 **Harle IA**, Finley RJ, Belsheim M, Bondy DC, Booth M, Lloyd D, McDonald JW, Sullivan S, Valberg LS, Watson WC, *et al*. Management of adenocarcinoma in a columnar-lined esophagus. *Ann Thorac Surg* 1985; **40:** 330-336
42 **Rosenberg JC**, Budev H, Edwards RC, Singal S, Steiger Z, Sundareson AS. Analysis of adenocarcinoma in Barrett' s esophagus utilizing a staging system. *Cancer* 1985; **55:** 1353-1360
43 **Levine DS**, Haggitt RC, Blount PL, Rabinovitch PS, Rusch VW, Reid BJ. An endoscopic biopsy protocol can differentiate high-grade dysplasia from early adenocarcinoma in Barrett's esophagus. *Gastroenterology* 1993; **105:** 40-50
44 **Sharma P**. Short segment Barrett esophagus and specialized columnar mucosa at the gastroesophageal junction. *Mayo Clin Proc* 2001; **76:** 331-334
45 **Reynolds JC**, Rahimi P, Hirschl D. Barrett's esophagus: clinical characteristics. *Gastroenterol Clin North Am* 2002; **31:** 441-460
46 **Gammon MD**, Schoenberg JB, Ahsan H, Risch HA, Vaughan TL, Chow WH, Rotterdam H, West AB, Dubrow R, Stanford JL, Mayne ST, Farrow DC, Niwa S, Blot WJ, Fraumeni JF Jr. Tobacco, alcohol, and socioeconomic status and adenocarcinomas of the esophagus and gastric cardia. *J Natl Cancer Inst* 1997; **89:** 1277-1284
47 **Garidou A**, Tzonou A, Lipworth L, Signorello LB, Kalapothaki V, Trichopoulos D. Life-style factors and medical conditions in relation to esophageal cancer by histologic type in a low-risk population. *Int J Cancer* 1996; **68:** 295-299
48 **Zhang ZF**, Kurtz RC, Sun M, Karpeh M Jr, Yu GP, Gargon N, Fein JS, Georgopoulos SK, Harlap S. Adenocarcinomas of the esophagus and gastric cardia: medical conditions, tobacco, alcohol, and socioeconomic factors. *Cancer Epidemiol Biomarkers Prev* 1996; **5:** 761-768
49 **Kabat GC**, Ng SK, Wynder EL. Tobacco, alcohol intake, and diet in relation to adenocarcinoma of the esophagus and gastric cardia. *Cancer Causes Control* 1993; **4:** 123-132
50 **Spechler SJ,** Robbins AH, Rubins HB, Vincent ME, Heeren T, Doos WG, Colton T, Schimmel EM. Adenocarcinoma and Barrett's esophagus. An overrated risk? *Gastroenterology* 1984; **87:** 927-933
51 **Avidan B**, Sonnenberg A, Schnell TG, Sontag SJ. Hiatal hernia and acid reflux frequency predict presence and length of Barrett's esophagus. *Dig Dis Sci* 2002; **47:** 256-264
52 **Conio M,** Filiberti R, Blanchi S, Ferraris R, Marchi S, Ravelli P, Lapertosa G, Iaquinto G, Sablich R, Gusmaroli R, Aste H, Giacosa A. Risk factors for Barrett's esophagus: a case-control study. *Int J Cancer* 2002; **97:** 225-229
53 **Gronbaek M**, Becker U, Johansen D, Tonnesen H, Jensen G, Sorensen TI. Population based cohort study of the association between alcohol intake and cancer of the upper digestive tract. *BMJ* 1998; **317:** 844-847
54 **Cooper BT,** Barbezat GO. Barrett's oesophagus: a clinical study of 52 patients. *Q J Med* 1987; **62:** 97-108
55 **Levi F**, Ollyo JB, La Vecchia C, Boyle P, Monnier P, Savary M. The consumption of tobacco, alcohol and the risk of adenocarcinoma in Barrett's oesophagus. *Int J Cancer* 1990; **45:** 852-854
56 **Herlihy KJ**, Orlando RC, Bryson JC, Bozymski EM, Carney CN, Powell DW. Barrett's esophagus: clinical, endoscopic, histologic, manometric, and electrical potential difference characteristics. *Gastroenterology* 1984; **86:** 436-443
57 **Day NE**, Munoz N. Esophagus. In: Schottenfeld D, Fraumeni JF Jr, eds. Cancer epidemiology and prevention Philadelphia: WB Saunders Co, 1982: 596-623
58 **Goldman MC,** Beckman RC. Barrett syndrome. Case report with discussion about concepts of pathogenesis. *Gastroenterology* 1960; **39:** 104-110
59 **Halvorsen JF**, Semb BK. The "Barrett syndrome" (the columnar-lined lower oesophagus): an acquired condition secondary to reflux oesophagitis. A case report with discussion of pathogenesis. *Acta Chir Scand* 1975; **141:** 683-687
60 **Jankowski J**. Gene expression in Barrett's mucosa: acute and chronic adaptive responses in the oesophagus. *Gut* 1993; **34:** 1649-1650
61 **Morgan G**, Vainio H. Barrett's oesophagus, oesophageal cancer and colon cancer: an explanation of the association and cancer chemopreventive potential of non-steroidal anti-inflammatory drugs. *Eur J Cancer Prev* 1998; 7: 195-199
62 **Heath EI,** Limburg PJ, Hawk ET, Forastiere AA. Adenocarcinoma of the esophagus: risk factors and prevention. *Oncology (Williston Park)* 2000; **14:** 507-14; discussion 518-520, 522-523
63 **Paull G**, Yardley JH. Gastric and esophageal Campylobacter pylori in patients with Barrett's esophagus. *Gastroenterology* 1988; **95:** 216-218
64 **Talley NJ**, Cameron AJ, Shorter RG, Zinsmeister AR, Phillips SF. Campylobacter pylori and Barrett's esophagus. *Mayo Clin Proc* 1988; **63:** 1176-1180
65 **Weston AP**, Badr AS, Topalovski M, Cherian R, Dixon A, Hassanein RS. Prospective evaluation of the prevalence of gastric Helicobacter pylori infection in patients with GERD, Barrett's esophagus, Barrett's dysplasia, and Barrett's adenocarcinoma. *Am J Gastroenterol* 2000; **95:** 387-394
66 **Bani-Hani K**, Martin IG, Hardie LJ, Mapstone N, Briggs JA, Forman D, Wild CP. Prospective study of cyclin D1 overexpression in Barrett's esophagus: association with increased risk of adenocarcinoma. *J Natl Cancer Inst* 2000; **92:** 1316-1321
67 **Wild CP,** Forman D. Surveillance for Barrett's oesophagus. It is too early to dismiss surveillance programmes. *BMJ* 2001; **322:** 1125; author reply 1126

Science Editor Guo SY **Language Editor** Elsevier HK

PO Box 2345, Beijing 100023, China
www.wjgnet.com
wjg@wjgnet.com

ELSEVIER

World J Gastroenterol 2005;11(43):6815-6822
World Journal of Gastroenterology ISSN 1007-9327

•*CLINICAL RESEARCH*•

Association between cag-pathogenicity island in *Helicobacter pylori* isolates from peptic ulcer, gastric carcinoma, and non-ulcer dyspepsia subjects with histological changes

Mahaboob Ali, Aleem A Khan, Santosh K Tiwari, Niyaz Ahmed, L Venkateswar Rao, CM Habibullah

Mahaboob Ali, Aleem A Khan, Santosh K Tiwari, CM Habibullah, Center for Liver Research and Diagnostics, Deccan College of Medical Sciences, Kanchanbagh, Hyderabad 500 058, Andhra Pradesh, India
Niyaz Ahmed, Pathogen Evolution Group, Centre for DNA Fingerprinting and Diagnostics, Nacharam Main Road, Hyderabad 500 076, Andhra Pradesh, India
Mahaboob Ali, L Venkateswar Rao, Department of Microbiology, Osmania University, Hyderabad 500 007, Andhra Pradesh, India
Supported by the Department of Biotechnology, Government of India , NO. BT/PR2473/Med/13/106/2001
Co-correspondence: Mahaboob Ali
Correspondence to: Professor L Venkateswar Rao, Head of the Department, Department of Microbiology, Osmania University, Hyderabad 500 007, Andhra Pradesh, India. vrlinga@yahoo.com
Telephone: +91-40-27090661 Fax: +91-40-27090661
Received: 2005-03-24 Accepted: 2005-04-30

Abstract

AIM: To investigate the presence of the *cag*-pathogenicity island and the associated histological damage caused by strains with complete *cag*-PAI and with partial deletions in correlation to the disease status.

METHODS: We analyzed the complete *cag*-PAI of 174 representative *Helicobacter pylori* (*H pylori*) clinical isolates obtained from patients with duodenal ulcer, gastric ulcer, gastric cancer, and non-ulcer dyspepsia using eight different oligonucleotide primers viz *cag*A1, *cag*A2, *cag*AP1, *cag*AP2, *cag*E, *cag*T, LEC-1, LEC-2 spanning five different loci of the whole *cag*-PAI by polymerase chain reaction (PCR).

RESULTS: The complete screening of the genes comprising the *cag*-PAI showed that larger proportions of subjects with gastric ulcer (97.8%) inhabited strains with complete *cag*-PAI, followed by gastric cancer (85.7%), non-ulcer dyspepsia (7.1%), and duodenal ulcer (6.9%), significant differences were found in the percentage distribution of the genes in all the clinical groups studied. It was found that strains with complete *cag*-PAI were able to cause severe histological damage than with the partially deleted ones.

CONCLUSION: The *cag*-PAI is a strong virulent marker in the disease pathogenesis as it is shown that a large number of those infected with strain with complete *cag*-PAI had one or the other of the irreversible gastric pathologies and interestingly 18.5% of them developed gastric carcinoma. The presence of an intact *cag*-PAI correlates with the development of more severe pathology, and such strains were found more frequently in patients with severe gastroduodenal disease. Partial deletions of the *cag*-PAI appear to be sufficient to render the organism less pathogenic.

Key words: *Helicobacter pylori*; *cag*-pathogenicity island; Genetic diversity; Gastro-duodenal diseases

Ali M, Khan AA, Tiwari SK, Ahmed N, Rao LV, Habibullah C. Association between *cag*-pathogenicity island in *Helicobacter pylori* isolates from peptic ulcer, gastric carcinoma, and non-ulcer dyspepsia subjects with histological changes. *World J Gastroenterol* 2005; 11(43): 6815-6822
http://www.wjgnet.com/1007-9327/11/6815.asp

INTRODUCTION

Gastric cancer is the second most deadly malignant neoplasia worldwide. According to the presently available statistics, approximately 74% of those diagnosed succumb to this disease every year[1]; this is because of poor prognosis as it is often made when the disease has assaulted the muscularis propria. Evidences show that the pathogenesis of gastric cancer is a multistep process[2,3]. This 'cascade' is believed to be triggered by *Helicobacter pylori* (*H pylori*) infection, a Gram negative pathogen. Chronic infection with this gastric pathogen is known to be the major factor driving the precancerous process via mechanisms including direct transformation of cells, induction of immunosuppression with consequently reduced cancer immunosurveillance, or by causing chronic inflammation[4,5]. In 1994, the International Agency for Research on Cancer (IARC) declared *H pylori* a Class 1 (definite) carcinogen based on the epidemiological and interventional studies in human beings[6] and convinced that this bacterial infection indeed plays a key role in the initiation of the neoplastic process in the stomach.

Although many attempts in the past have been made to understand and associate the causal link between *H pylori* infection and the sequelae that leads to gastric carcinoma[7,8], there are conflicting data in the literature due

to differences in the study population and designs[9,10].

In the past few years, many *H pylori* virulence factors have been described that contribute to the survival of this pathogen in an extremely hostile acidic milieu of the stomach and its colonization in that organ[11,12]. Other putative virulence determinants such as vacuolating cytotoxin gene A (vacA), cytotoxin associated gene pathogenicity island (*cag*-PAI) and induced by contact with epithelium gene A (iceA) are not present in all *H pylori* strains or are known to exhibit different allelic variations[13]. The cytotoxin-associated gene island also referred to as the *cag*-PAI is an approximately 40-kb cluster of genes and is the most studied marker of the *H pylori*. In many studies[20,22,24], this large fragment has been a criterion of typing *H pylori* into pathogenic and non-pathogenic strains (Type I and Type II). Studies emphasizing on the functional importance of this island have reported that strains possessing *cag*-PAI induce more notable phenotypic changes *in vivo*, such as higher levels of IL-8 production than *cag*-PAI negative ones[30]. Recent studies made from within our institute[14,15] and other parts of the world[16,17] have mainly focused on the presence of this large fragment and its association with the disease status. Therefore, in a continuing attempt to further establish a strong epidemiologic relation between the *cag*-PAI and the disease conditions with reference to the histopathologic changes lead to the inception of the present study. As it is reported[18] that the presence of *cag* island and the consequent *cag* instability may produce differences in the pathogenicity and host adaptability within a bacterial strain, detailed analyses of the genes of the *cag* island in human beings isolates with reference to histologic damage and disease outcome would be essential. Therefore, compelled by these observations, the present study was designed to identify the distribution of different genes of the *cag*-PAI in clinical *H pylori* isolates by assessing the presence of representative genes located in different segments of the *cag*-island and its correlation with the histologic changes and disease status.

MATERIALS AND METHODS

Patients and sampling

The study population consisted of 174 patients (100 males and 74 females) with a mean age of 48.4 years (range 21-73 years). The patients were classified at the time of endoscopy into those suffering from active ulcers disease [duodenal ulcers (n = 58), gastric ulcers (n = 46), gastric carcinoma (n = 14)] and those with no evidence of mucosal ulcer and gastritis, but suffering from mild or severe dyspeptic symptoms, i.e. non-ulcer dyspepsia (n = 56). None of the patients included in the study had received NSAIDs or antibiotics within the previous 2 mo. Informed consents were taken from the patients who underwent upper gastrointestinal endoscopy at the department of gastroenterology, Deccan College of Medical Sciences, Hyderabad.

Four gastric biopsies were collected: one in urea solution for the rapid urease test (RUT), one in supplemented broth for isolating culture, one in phosphate-buffered saline (PBS) for testing by PCR assay, and one in 10% buffered formalin for histological examination by modified Giemsa stain for the presence of *H pylori*.

H pylori strains

A total of 174 clinical *H pylori* strains were screened for the presence of *cag*-PAI genes. These strains were recovered from individual subjects undergoing upper gastrointestinal endoscopy presenting with various symptoms. This included 43 live strains and 131 genomic DNA isolated from the gastric biopsy.

Extraction of genomic DNA

H pylori culture and DNA extraction from the culture and biopsy was carried out as described elsewhere[19].

PCR analysis of the *cag*-PAI genes

The genes of the *cag*-PAI were PCR amplified under the conditions described by Ikenoue *et al*.[20]. One microliter of the extracted genomic DNA was used in a 20 μL reaction volume containing 1´ PCR buffer, 1 U Taq DNA polymerase, 1.5 mmol/L $Mg2^{+}$, 200 μmol/L each dNTP and 10 pmol/L of each primer.

The cycling parameters were optimized and are as follows: Initial denaturation at 95 °C for 5 min, followed by 40 cycles each of denaturation at 94 °C for 30 s, annealing at 52 °C for 30 s and extension at 72 °C for 1.5 min and finally after the last cycle, extension was continued for another 7 min.

Eight sets of oligonucleotide primers spanning the 40 kb *cag*-PAI were used in the study. Appropriate positive and negative controls were included in each set to avoid misinterpretation of results. The details of the primers used with their product sizes are enlisted in Table 1. Amplicons were separated by electrophoresis on 2% agarose gel and stained by ethidium bromide.

Histopathological analysis

The biopsy specimen collected from the gastric antrum was used for histopathologic examination to grade

Table 1 List of primers

Target gene	Primer	Sequence (5'- 3')	Product size (bp)
	CagA-F1	AACAGGACAAGTAGCTAGCC	
CagA1	CagA-R1	TATTAATGCGTGTGTGGCTG	701
	CagA-F2	GATAACAGGCAAGCTTTTGA	
CagA2	CagA-R2	CTGCAAAAGATTGTTTGGCAGA	349
	CagAP-F1	GTGGGTAAAAATGTGAATCG	
CagAP1	CagA-R1	TATTAATGCGTGTGTGGCTG	730
	CagAP-F2	CTACTTGTCCCAACCATTTT	
CagAP2	CagA-R2	CTGCAAAAGATTGTTTGGCAGA	1 181
	CagE-F1	GCGATTGTTATTGTGCTTGTAG	
CagE	CagE-R1	GAAGTGGTTAAAAAATCAATGCCCC	329
	CagT-F1	CCATGTTTATACGCCTGTGT	
CagT	CagT-R1	CATCACCACACCCTTTTGAT	301
	LEC-F1	ACATTTTGGCTAAATAAACGCTG	
LEC-1	LEC-R1	TCTCCATGTTGCCATTATGCT	384
	LEC-F2	ATAGCGTTTTGTGCATAGAA	
LEC-2	LEC-R2	ATCTTTAGTCTCTTTAGCTT	877

the severity of disease after they were embedded in paraffin and stained with hematoxylin and eosin. A single experienced pathologist (ZA), who was blinded to the patient's history and molecular data of the isolate, evaluated all histological data. The grade of gastritis was determined on the basis of the updated Sydney system[21].

Statistical analysis

The data were analyzed by means of χ^2 test and the Mann –Whitney *U* test.

RESULTS

In a total of 174 isolates screened, only 65 (37.4%) was found to carry the complete *cag*-PAI, while 109 (62.6%) carried the *cag*-PAI with partial deletions. No isolate was found with completely deleted *cag*-PAI (Table 2).

With reference to the clinical status, we found majority of the duodenal ulcer (DU) isolates and non-ulcer dyspepsia (NUD) isolates to possess partially deleted *cag*-PAI, while on the contrary we found ~97.8% of the gastric ulcer (GU) isolates and 85.7% of the gastric carcinoma (GC) isolates possessed the intact *cag*-PAI. The details of the results obtained are given in Table 2 and Figure 1. Statistically these differences were highly significant.

Table 2 Relationship between the presence of cag-PAI and the clinical status

Clinical status (*n*)	Intact PAI (%)	*cag*-PAI type Partially deleted PAI (%)	Completely deleted PAI (%)
DU (58)	4 (6.9)	54 (93.1)	0
GU (46)	45 (97.8)	1 (2.2)	0
NUD (56)	4 (7.1)	52 (92.9)	0
GC (14)	12 (85.7)	2 (14.3)	0
Total (174)	65 (37.4)	109 (62.6)	0

χ^2=130.71 .

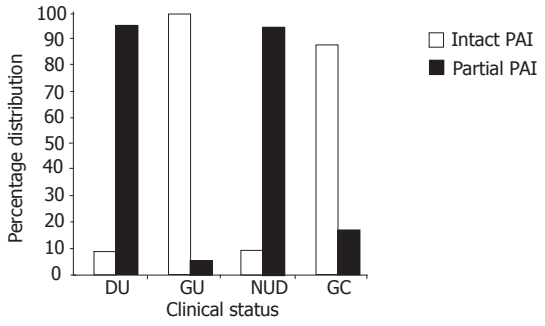

Figure 1 Distribution of *cag*-PAI in dyspeptic subjects.

When checked for the presence of each locus, we could find that the total *cag*A gene (i.e. with promoters) to be present in 69 (39.7%) of all the isolates screened, 4 (2.3%) isolates had total deletion of the gene and 101 (58%) were carrying partial deletions. Of the 69-*cag*A positive isolates, prevalence of *cag*A gene was predominant among gastric ulcer (GU) and gastric carcinoma (GC) strains (Table 3 and Figure 2) simultaneously *cag*A gene with partial deletions were more prevalent among *H pylori* isolated from duodenal ulcer (DU) and non-ulcer dyspepsia (NUD) subjects.

Table 3 *cag*A status of *H pylori* isolates

Clinical status (*n*)	*cagA* +ve (%)	Partial *cagA* +ve (%)	*cagA* –ve (%)
DU (58)	8 (13.8)	46 (79.3)	4 (6.9)
GU (46)	45 (97.8)	1 (2.2)	0
NUD (56)	4 (7.1)	52 (92.9)	0
GC (14)	12 (85.7)	2 (14.3)	0
Total (174)	69 (39.7)	101 (58)	4 (2.3)

DU *vs* GU, DU *vs* GC, GU *vs* NUD and NUD *vs* GC combinations are highly significant at 0.1% level. DU *vs* NUD and GU *vs* GC combinations are not significant at 0.1% level.

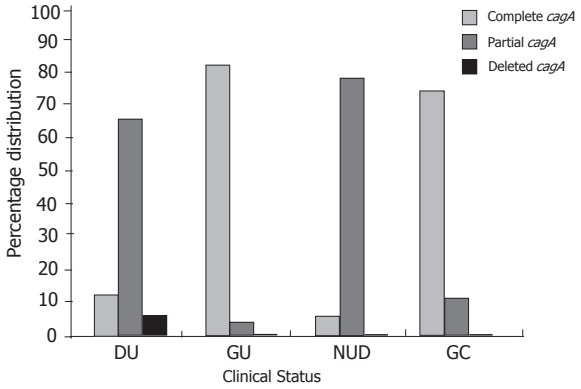

Figure 2 Distribution of *cag*A in clinical isolates.

Observing the prevalence patterns of *cag*A deletion mutant strains, we further analyzed the predominance of deletions in the promoter and body part of the *cag*A gene. The body part of *cag*A gene (i.e. A1+A2) was present in a maximum number of isolates i.e. 134 (77%), among which a considerable number of isolates lacked the promoter region (i.e. AP1+AP2) (Table 4).

Screening of the *cag*II region of the *cag*-PAI revealed *cag*E, *cag*T, LEC-1, and LEC-2 to be present in 143 (82.1%), 145 (87.3%), 142 (81.6%) and 111 (63.7%) of the total isolates, respectively. The distribution of these genes with reference to disease status is illustrated in detail in Table 5 and Figure 3. We found the difference between DU and GU, GU and NUD, GC and NUD to be highly significant statistically.

In the present study, histopathological examination of antral biopsies from a total of 174 subjects was carried out

Table 4 Distribution of *cag*A gene and *cag*A promoter in *H pylori* isolates

Clinical status (*n*)	A1+A2 (%)	AP1+AP2 (%)
DU (58)	43 (74.1)	8 (13.8)
GU (46)	45 (97.8)	46 (100)
NUD (56)	32 (57.1)	6 (10.7)
GC (14)	14 (100)	12 (85.7)
Total (174)	134 (77)	72 (41.4)

Table 5 Distribution of *cag*E, T, LEC1, and LEC2 in *H pylori* isolates

Clinical status (*n*)	*cag*E (%)	*cag*T (%)	LEC1 (%)	LEC2 (%)
DU (58)	47 (81)	56 (96.5)	44 (75.8)	33 (56.8)
GU (46)	46 (100)	46 (100)	46 (100)	46 (100)
NUD (56)	36 (64.2)	36 (64.2)	38 (67.8)	18 (32.1)
GC (14)	14 (100)	14 (100)	14 (100)	14 (100)
Total (174)	143 (82.1)	152 (87.3)	142 (81.6)	111 (63.7)

For *cag*E, GU *vs* NUD is highly significant at 0.1% level ($P<0.001$), DU *vs* GU, NUD *vs* GC combinations are significant at 1% level ($P<0.01$), DU *vs* NUD combination is significant at 5% level ($P<0.05$) and DU *vs* GC . For *cag*T, DU *vs* NUD, GU *vs* NUD combinations are highly significant at 0.1% level ($P<0.001$), NUD *vs* GC combination is significant at 1% level ($P<0.01$) and DU *vs* GU, DU *vs* GC, GU *vs* GC are not significant at 1% level. For LEC1, DU *vs* GU, GU *vs* NUD combinations are highly significant at 0.1% level ($P<0.001$), NUD *vs* GC is significant at 1% level ($P<0.01$), DU *vs* GC is significant at 5% level ($P<0.05$). For LEC2, DU *vs* GU, GU *vs* NUD, NUD *vs* GC combinations are highly significant at 0.1% level ($P<0.001$), DU *vs* NUD, DU *vs* GC combinations are significant at 1% level ($P<0.01$) and GU *vs* GC is not significant at 1% level.

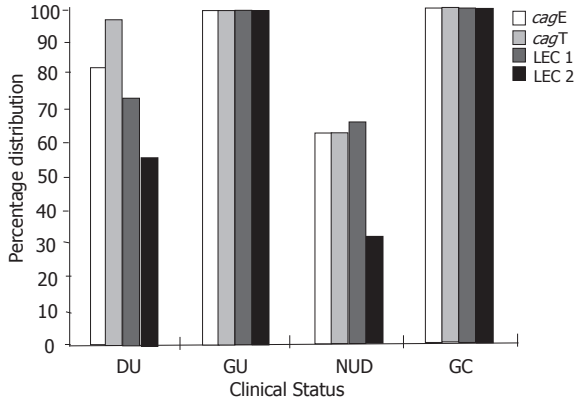

Figure 3 Distribution of *cag*E, T, LEC1, LEC2

to check the grade of gastritis and the differences between the pathologies of intact *cag*-PAI and partial *cag*-PAI infection. Of the 174 subjects included for the study, we screened 160 subjects as 14 of them had endoscopically proven gastric carcinoma and hence histopathology confirmed features of carcinoma. Out of the 160 subjects screened, all showed chronic gastritis and on further screening for any other advanced type of gastritis, we found 112 (70%) of the total 160 to possess topographic chronic superficial gastritis, 20 (12.5%) showed atrophic changes, whereas 18 (11.25%) and 10 (6.25%) of the subjects showed IM and dysplasia respectively (Table 6). When each of these histological lesions were scored individually in relation to their respective clinical status, we found that among the 58 duodenal ulcer cases, 52 (89.7%) showed chronic superficial gastritis, 2 (3.4%) showed atrophy and 4 (6.9%) showed intestinal metaplasia while none of the subjects had dysplasia (Table 6).

In the gastric ulcer category, we found that 9 (19.6%) showed chronic superficial gastritis, 13 (28.3%) showed atrophy, 14 (30.4%) showed intestinal metaplasia and 10 (21.7%) showed dysplasia. For atrophy, metaplasia and dysplasia, the difference between GU and DU was statistically highly significant ($P<0.001$, Table 6).

In the NUD category, we found that 51 (91.1%) showed chronic superficial gastritis and 5 (8.9%) showed atrophic gastritis while none had intestinal metaplasia and dysplasia. For metaplasia and dysplasia, the difference between GU and NUD, was statistically highly significant ($P<0.001$, Table 6).

Table 6 Frequency of atrophy, metaplasia, and dysplasia in chronic gastritis subjects

Clinical status (*n*)	Acute gastritis (%)	Chronic gastritis			
		Superficial gastritis	Gastritis with atrophy (%)	Gastritis with metaplasia (%)	Gastritis with dysplasia (%)
DU (58)	0	52 (89.7)	2 (3.4)	4 (6.9)	0
GU (46)	0	9 (19.6)	13 (28.3)	14 (30.4)	10 (21.7)
NUD (56)	0	51 (91.1)	5 (8.9)	0	0
Total (160)	0	112 (70)	20 (12.5)	18 (11.25)	10 (6.25)

For atrophy, DU *vs* GU combination is highly significant at 0.1% level ($P<0.001$), GU *vs* NUD is significant at 1% level ($P<0.01$) and DU *vs* NUD combination is not significant at 1% level. For metaplasia, DU *vs* GU, GU *vs* NUD combinations are highly significant at 0.1% level ($P<0.001$) and DU *vs* NUD combination is significant at 5% level ($P<0.05$). For dysplasia, DU *vs* GU, GU *vs* NUD combinations are highly significant at 0.1% level ($P<0.001$) and DU *vs* NUD combination is not significant at any level.

When we analyzed the histological status, with reference to the strain infecting with either intact PAI or partially deleted ones, we found a significant difference among them. As evidenced from Table 7, we found that, of the 65 subjects infected with intact PAI, 8 (12.3%) showed chronic superficial gastritis, 17 (26.1%) showed atrophic changes, 18 (27.7%) showed intestinal metaplasia (all of them were Type III), 10 (15.4%) showed high grade dysplastic changes and 12 (18.5%) showed intestinal type gastric carcinoma. On the contrary, when we checked those subjects, who inhabited partially deleted strains, we found 104 (95.4%) to possess chronic superficial gastritis, 3 (2.8%) showed atrophy while 2 (1.8%) showed gastric carcinoma and these differences were statistically very significant ($P<0.001$, Table 7).

When a correlation between the histological status of the subjects infected with either intact *cag*-PAI or partially deleted strains isolated from subjects with varied disease status was made, we found that among 58 DU subjects, 4 had intact *cag*-PAI and all of them were Type III intestinal metaplasia, among the remaining 54, which had partial deletions in the *cag*-PAI, 52 (96.3%) showed chronic superficial gastritis and 2 (3.7%) showed atrophic changes. Among the GU subjects, of the 46 infected, 45 were known to possess the *cag*-PAI and 8 (17.8%) of them showed chronic superficial gastritis, 13 (28.9%) showed atrophic gastritis, 14 (31.1%) showed Type III intestinal metaplasia and 10 (22.2%) showed high grade dysplastic changes (Table 8). Among the 56 NUD subjects, 4 with intact *cag*-PAI showed atrophic changes and of the rest with partial deletions 51 (98.1%) showed chronic superficial gastritis and 1 (1.9%) showed atrophic gastritis (Table 8) while among the 14 isolated from

Table 7 Histological status of subjects with intact *cag*-PAI (*n* = 65) and partial *cag*-PAI (*n* = 109)

Cag-type	Chronic gastritis							Gastric carcinoma	
(*n*)	Superficial gastritis	Gastritis with atrophy	Gastritis with metaplasia (%)			Gastritis with dysplasia(%)		Intestinal (%)	Diffuse (%)
	(%)	(%)	Ty-1	Ty-2	Ty-3	Low grade	High grade		
Intact (65)	8 (12.3)	17 (26.1)[b]	0	0	18 (27.7)	0	10 (15.4)	12[b] (18.5)	0
Partial (109)	104 (95.4)	3 (2.8)	0	0	0	0	0	2 (1.8)	0

[b]*P*<0. 001 *vs* others.

Table 8 Correlation of the histological status of the subjects with intact and partially deleted *cag*-PAI from varied disease status

Clinical status	Chronic gastritis								Gastric carcinoma	
(*n*)	cag status	Superficial gastritis	Gastritis with atrophy (%)	Gastritis with metaplasia (%)			Gastritis with dysplasia (%)		Intestinal (%)	Diffuse (%)
	(*n*)	(%)		Ty-1	Ty-2	Ty-3	Low grade	High grade		
DU (58)	Intact (4)	0	0	0	0	4 (100)	0	0	0	0
	Partial (54)	52 (96.3)	2 (3.7)	0	0	0	0	0	0	0
GU (46)	Intact (45)	8(17.8)[a]	13 (28.9)	0	0	14 (31.1)	0	10 (22.2)	0	0
	Partial (1)	1 (100)	0	0	0	0	0	0	0	0
NUD (56)	Intact (4)	0	4(100)[a]	0	0	0	0	0	0	0
	Partial (52)	51 (98.1)	1 (1.9)	0	0	0	0	0	0	0
GC (14)	Intact (12)	0	0	0	0	0	0	0	12 (100)[b]	0
	Partial (2)	0	0	0	0	0	0	0	2 (100)	0

[a]*P* <0.05, [b]*P* <0.001 *vs* others.

gastric carcinoma 12 had intact *cag*-PAI while the other 2 partial deletions and when scored for the type of gastric carcinoma all of them showed intestinal type of carcinoma (Table 8).

DISCUSSION

The *cag*-PAI is an approximately 40-kb cluster of genes in *H pylori* chromosome, and a quite conservative entity. Censini *et al*.[22] in 1996 first identified strains with partially deleted *cag*-PAIs. The molecular mechanism of these genetic rearrangements was explained by incorporation of an insertion element, IS605, in *cag*-PAI. Recently, the composition of the *cag*-PAI in clinical *H pylori* isolates has been studied in different populations by various methods, including PCR, dot blotting and long distance PCR[20,23,24].

In the present study, we used simple PCR for structural screening of *cag*-PAI in clinical isolates of *H pylori*. Out of the 174 clinical isolates, we found only 37.4% were carrying the complete *cag*-PAI (Table 2), whereas Mukhopadhyay *et al*.[25] reported more than 96% in Calcutta strains of peptic ulcer and non-ulcer dyspepsia. In our study, 97.8% of gastric ulcer and 85.7% (Table 2 and Figure 1) of the gastric carcinoma strains were carrying complete PAI, which are considered to be severe forms of the gastro-duodenal diseases. Even though duodenal ulcer is also considered to be a severe form of the gastro-duodenal disease, the proportion of DU strains that carried was just 6.9%. Jenks *et al*.[23] reported that the presence of certain genes (*cag*A, *cag*E, *cag*M, T, ORF 6, 10, 13) in the *cag*-PAI is highly associated with duodenal ulcers. We too found a similar type of observation, but not for all the seven genes which they selected. We observed the same kind of correlation with only two genes i.e. *cag*E and *cag*T, where DU cases carried *cag*E with 81% and *cag*T with 96.5% (Table 5 and Figure 3). Whereas NUD isolates were carrying the genes with an average of 65% (Table 5 and Figure 3). Further, Day *et al*.[26] revealed that isolates containing *cag*E were associated with duodenal ulceration.

Among non-ulcer dyspepsia strains, we found 7.1% to carry the complete *cag*-PAI, which is statistically almost equal to DU percentage, and a report from Sweden[27] showed 58% of *cag*-PAI positivity in NUD isolates. In the same report, the authors showed that 5% of isolates from severe pathology i.e. gastric carcinoma and duodenal ulcer, and 15% of the isolates from NUD lacking the *cag*-PAI. Not only the data from other continents, but from the same Indian sub-continent showed total deletions from ulcer group and non-ulcer group[25], whereas we could not come across a single isolate with entirely deleted *cag*-PAI from any of the disease condition indicating strain diversity. This kind of diversity, i.e. absence of completely deleted PAIs and presence of just 6.9% complete *cag*-PAIs in duodenal ulcer cases, might be particularly true for the south Indian of Telugu linguistic group who are mainly Dravidian and married consanguineously for millennia[28]. Their genetic separation from other Indian communities during much of the human history has already been reported[29].

Strains with intermediate genotypes, lacking parts of the *cag*-PAI, were found in 62.6% (Table 2) and more frequently found in patients with non-ulcer dyspepsia and duodenal ulcer (Figure 1). A probable mechanism for the establishment of these internal deletions within the *cag*-PAI would be that the short repeated sequences found by Nilsson *et al*.[27] may serve as homologies enabling slipped strand mispairing and consequently excision of the enclosed DNA fragment especially in DU and NUD subjects. Moreover, in our observation, the partially deleted *cag*-PAI represented a genotype more common than a complete *cag*-PAI and no strain was found with completely

deleted *cag*-PAI.

Conventionally *cag*A was used and is still used as a marker for the presence of an intact *cag*-PAI and for virulence. Recently, Backert *et al*.[30] showed a good correlation of *cag*A with the presence of *cag*-PAI. In this study, we found that 39.7% of the strains carried the complete *cag*A gene (Table 3) and the presence of *cag*A gene did not correlate with the genetic presence of complete *cag*-PAI. Further, for - 4 kb *cag*A gene, we used four sets of primers i.e. two primers for body of the gene and two primers for promoter, designed from various locations of the body region and promoter, whereas other studies taken up earlier had used a single set of primer for complete *cag*-PAI. This might be the reason for the correlation, which they obtained. The typical observation was when 77% of the isolates were carrying the body region (A1+A2) only 41.4% of them carried promoter region (Table 4), which means that in our isolates even though the strains carried the *cag*A gene, most of them lacked the promoter of the gene, without which *cag*A is not functional. Further, four isolates i.e. 2.3% completely lacked the *cag*A gene and all the four isolates belonged to duodenal ulcer cases.

Among many virulence markers present in the *H pylori* genome, *cag*-PAI is the major virulence factor and is associated with severe gastroduodenal pathology[31,32] that includes both duodenal and gastric ulcers along with carcinomas. Some studies have identified a correlation between an intact *cag*-PAI and development of disease[20,23,24,27], as we are trying to show with this present study in Indian scenario, whereas others could not find such a relationship[33,34].

"Infection with *H pylori* always causes chronic active gastritis"[35]. This phrase has become true in our observation. As it is observed in Table 6, there are no acute gastritis subjects. Moreover, the subjects infected with *cag*-PAI positive strains were found to show severe forms of histopathological changes, like atrophic gastritis, intestinal metaplasia, and neoplasia. This might be the reason for IARC-WHO to designate *H pylori* a class I (definite) carcinogen[6].

Out of the 174 isolates, 65 (37.4%) had complete *cag*-PAI and 109 (62.6%) had partial deletions in the *cag*-PAI (Table 2). As evident from Table 7, it can be observed that subjects infected with *H pylori* strains with intact *cag*-PAI had many remarkable histopathological changes, when compared to those who had partially deleted *cag*-PAI. It is quite clear from the statistics ($P<0.001$) that among 65 *H pylori* strains with intact *cag*-PAI, 18.5% subjects had advanced cancerous lesions, while only 1.8% of the 109 subjects, who harbored *H pylori* with partial *cag*-PAI had advanced to carcinoma thus allowing us to delineate that persons with intact *cag*-PAI are 10-fold more prone to develop carcinoma in comparison to the partially deleted *cag*-PAI strains.

Parallelly, a small group of population, i.e. 12.3% with intact *cag*-PAI, were shown to have only chronic superficial gastritis, but according to Ohkuma *et al*.[36] *H pylori* positive cases with chronic gastritis have increased risk of atrophy and intestinal metaplasia. On the other hand, partial *cag*-PAI subjects were also shown to have chronic gastritis (Table 6), but the percentage of disease progression was very high among *cag*-PAI positive subjects (Table 7) than those with partially deleted ones. Moreover, Type-3 metaplasia and high-grade dysplasia were seen only in *cag*-PAI positive subjects, where Type-3 metaplasia is closely linked to carcinoma[37] and dysplasia is nothing but a non-invasive type of neoplasia[38]. The results of this study are in contrast to those obtained by Keates *et al*.[39] who determined that gene products of the *cag* pathogenicity island are required for maximal activation of mitogen-activated protein kinases (MAPK) in gastric epithelial cells, which regulate cell proliferation, differentiation, inflammatory responses, stress, and programmed death, leading to induce gastroduodenal inflammation, ulceration and neoplasia. Further, Naumann *et al*.[40] stated that the integrity of whole *cag*-PAI is also a pre-requisite for efficient activation of early transcription factor AP-1, which is known for its immuno-stimulatory function.

In relation with disease status, among DU, GU, and NUD, gastric ulcers are considered to be more prone to the gastric carcinoma[41]. The observations of this study are in correlation to that obtained by Hansson *et al*.[41]. When we compare GU subjects with DU and NUD, the percentage of predisposing factors was much more among GU subjects. Recently, Wanatabe *et al*.[42] proved this in animal models. In their study at 26 wk, Mongolian gerbils developed chronic gastritis, ulceration and metaplasia. At 62 wk, 31% of them developed adenocarcinoma. Interestingly the inoculum used for the infection was obtained from a patient with gastric ulcer. Moreover, there have been reports that gastric cancer mortality rates bear an inverse relationship to duodenal ulcer disease rates[43], suggesting that they are directly relating with gastric ulcer in ulcer groups.

Further, in partial *cag*-PAI subjects, 2.8% showed atrophy, 1.8% showed carcinoma (Table 7) suggesting the role of other virulence genes and risk factors. Parallelly high incidence rate of gastric carcinoma among the gastric ulcer cases might be true, but it should not be assigned to a single determinant such as *cag*-PAI, but it is a result of many factors such as host genetic factors, environment, low socio-economic status, irregular dietary habits in addition to *H. pylori* with complete *cag*-PAI[44].

Hence, we can suggest that the *cag*-PAI is a strong virulent marker in the disease pathogenesis because more than 85% of the *cag*-PAI positive subjects were shown to have one or the other of the irreversible gastric pathologies and interestingly 18.5% of them developed gastric carcinoma and GU is the major risk/predisposing factor for the gastric carcinoma. Moreover, duodenal ulcer is not at all a risk factor for severe gastric pathologies and it is not a severe kind of disease, like gastric ulcer in our population.

REFERENCES

1 **Leung WK**, Lin SR, Ching JY, To KF, Ng EK, Chan FK, Lau

JY, Sung JJ. Factors predicting progression of gastric intestinal metaplasia: results of a randomised trial on Helicobacter pylori eradication. *Gut* 2004; **53:** 1244-1249

2 **Correa P**. Human gastric carcinogenesis: a multistep and multifactorial process--First American Cancer Society Award Lecture on Cancer Epidemiology and Prevention. *Cancer Res* 1992; **52:** 6735-6740

3 **Kuipers EJ**, Uyterlinde AM, Pena AS, Roosendaal R, Pals G, Nelis GF, Festen HP, Meuwissen SG. Long-term sequelae of Helicobacter pylori gastritis. *Lancet* 1995; **345:** 1525-1528

4 **Correa P**. Is gastric cancer preventable? *Gut* 2004; **53:** 1217-1219

5 **Shimoyama T**, Fukuda S, Liu Q, Nakaji S, Fukuda Y, Sugawara K. Helicobacter pylori water soluble surface proteins prime human neutrophils for enhanced production of reactive oxygen species and stimulate chemokine production. *J Clin Pathol* 2003; **56:** 348-351

6 International Agency for Research on Cancer. IARC monographs on the evaluation of carcinogenic risks to humans, vol. **61:** Schistosomes, liver flukes and *Helicobacter pylori*. Lyons, France: IARC, 1994

7 **Wong BCY**, Ching CK, Lam SK. Helicobacter pylori and gastric cancer. *Hong Kong Med J* 1999; **5 :** 175-179

8 **Blaser MJ**. Linking Helicobacter pylori to gastric cancer. *Nat Med* 2000; **6:** 376-377

9 ***Uemura N***, Mukai T, Okamoto S, Yamaguchi S, Mashiba H, Taniyama K, Sasaki N, Haruma K, Sumii K, Kajiyama G. Effect of Helicobacter pylori eradication on subsequent development of cancer after endoscopic resection of early gastric cancer. *Cancer Epidemiol Biomarkers Prev* 1997; **6:** 639-642

10 **Sung JJY**, Lin S-R, Ching JYL, Zhou L–Y, To KF, Wang R–T, Leung WK, NG EKW, Lau JYW, Lee YT, Yeung CK, Chao W, Chung SCS. Atrophy and intestinal metaplasia one year after cure of *H pylori* infection: a prospective, randomized study. *Gastroenterology* 2000; **119:** 7-14

11 **Koehler CI**, Mues MB, Dienes HP, Kriegsmann J, Schirmacher P, Odenthal M. Helicobacter pylori genotyping in gastric adenocarcinoma and MALT lymphoma by multiplex PCR analyses of paraffin wax embedded tissues. *Mol Pathol* 2003; **56:** 36-42

12 **Suerbaum S**, Michetti P. Helicobacter pylori infection. *N Engl J Med* 2002; ***347:*** 1175-1185

13 **Covacci A**, Telford JL, Del Giudice G, Parsonnet J, Rappuoli R. Helicobacter pylori virulence and genetic geography. *Science* 1999; **284:** 1328-1333

14 **Tiwari SK**, Khan AA, Ahmed KS, Ali M, Ahmed I, Habeeb A, Kauser F, Hussain MA, Ahmed N and Habibullah CM. PCR based analysis of Helicobacter pylori isolated from saliva: An approach for rapid molecular genotyping in correlation with disease status. *J Gastroenterol Hepatol* (In press).

15 **Kauser F**, Khan AA, Hussain MA, Carroll IM, Ahmad N, Tiwari S, Shouche Y, Das B, Alam M, Ali SM, Habibullah CM, Sierra R, Megraud F, Sechi LA, Ahmed N. The cag pathogenicity island of Helicobacter pylori is disrupted in the majority of patient isolates from different human populations. *J Clin Microbiol* 2004; **42:** 5302-5308

16 **Covacci A**, Falkow S, Berg DE, Rappuoli R. Did the inheritance of a pathogenicity island modify the virulence of Helicobacter pylori? *Trends Microbiol* 1997; **5:** 205-208

17 **Occhialini A**, Marais A, Urdaci M, Sierra R, Munoz N, Covacci A, Megraud F. Composition and gene expression of the cag pathogenicity island in Helicobacter pylori strains isolated from gastric carcinoma and gastritis patients in Costa Rica. *Infect Immun* 2001; **69:** 1902-1908

18 **Tomasini ML**, Zanussi S, Sozzi M, Tedeschi R, Basaglia G, De Paoli P. Heterogeneity of cag genotypes in Helicobacter pylori isolates from human biopsy specimens. *J Clin Microbiol* 2003; **41:** 976-890

19 **Li C**, Musich PR, Ha T, Ferguson DA Jr, Patel NR, Chi DS, Thomas E. High prevalence of Helicobacter pylori in saliva demonstrated by a novel PCR assay. *J Clin Pathol* 1995; **48:** 662-666

20 **Ikenoue T**, Maeda S, Ogura K, Akanuma M, Mitsuno Y, Imai Y, Yoshida H, Shiratori Y, Omata M. Determination of Helicobacter pylori virulence by simple gene analysis of the cag pathogenicity island. *Clin Diagn Lab Immunol* 2001; **8:** 181-186

21 **Dixon MF**, Genta RM, Yardley JH, Correa P. Classification and grading of gastritis. The updated Sydney System. International Workshop on the Histopathology of Gastritis, Houston 1994. *Am J Surg Pathol* 1996; **20:** 1161-1181

22 **Censini S**, Lange C, Xiang Z, Crabtree JE, Ghiara P, Borodovsky M, Rappuoli R, Covacci A. cag, a pathogenicity island of Helicobacter pylori, encodes type I-specific and diseaseassociated virulence factors. *Proc Natl Acad Sci USA* 1996; **93:** 14648-14653

23 **Jenks PJ**, Megraud F, Labigne A. Clinical outcome after infection with Helicobacter pylori does not appear to be reliably predicted by the presence of any of the genes of the cag pathogenicity island. *Gut* 1998; **43:** 752-758

24 **Maeda S**, Yoshida H, Ikenoue T, Ogura K, Kanai F, Kato N, Shiratori Y, Omata M. Structure of cag pathogenicity island in Japanese Helicobacter pylori isolates. *Gut* 1999; **44:** 336-341

25 **Mukhopadhyay AK**, Kersulyte D, Jeong JY, Datta S, Ito Y, Chowdhury A, Chowdhury S, Santra A, Bhattacharya SK, Azuma T, Nair GB, Berg DE. Distinctiveness of genotypes of Helicobacter pylori in Calcutta, India. *J Bacteriol* 2000; **182:** 3219-3227

26 **Day AS**, Jones NL, Lynett JT, Jennings HA, Fallone CA, Beech R, Sherman PM. cagE is a virulence factor associated with Helicobacter pylori-induced duodenal ulceration in children. *J Infect Dis* 2000; **181:** 1370-1375

27 **Nilsson C**, Sillen A, Eriksson L, Strand ML, Enroth H, Normark S, Falk P, Engstrand L. Correlation between cag pathogenicity island composition and Helicobacter pylori-associated gastroduodenal disease. *Infect Immun* 2003; **71:** 6573-581

28 **Ahmed N**, Khan AA, Alvi A, Tiwari S, Jyothirmayee CS, Kauser F, Ali M, Habibullah CM. Genomic analysis of Helicobacter pylori from Andhra Pradesh, South India: molecular evidence for three major genetic clusters. *Current Sci* 2003; **85 :** 1579-1586

29 **Bamshad M**, Fraley AE, Crawford MH, Cann RL, Busi BR, Naidu JM, Jorde LB. mtDNA variation in caste populations of Andhra Pradesh, India. *Hum Biol* 1996; **68:** 1-28

30 **Backert S**, Schwarz T, Miehlke S, Kirsch C, Sommer C, Kwok T, Gerhard M, Goebel UB, Lehn N, Koenig W, Meyer TF. Functional analysis of the cag pathogenicity island in Helicobacter pylori isolates from patients with gastritis, peptic ulcer, and gastric cancer. *Infect Immun* 2004; **72:** 1043-56

31 **Crabtree JE**, Kersulyte D, Li SD, Lindley IJ, Berg DE. Modulation of Helicobacter pylori induced IL-8 synthesis in gastric epithelia cells mediated by cag-PAI encoded VirD4 homologoue. *J Clin Pathol* 1999; **52:** 653-657

32 **Guillemin K**, Salama NR, Tompkins LS, Falkow S. Cag pathogenicity island-specific responses of gastric epithelial cells to Helicobacter pylori infection. *Proc Natl Acad Sci USA* 2002; **99:** 15136-15141

33 **Audibert C**, Burucoa C, Janvier B, Fauchere JL. implication of the structure of the Helicobacter pylori cag pathogenicity island in induction of interleukin-8 secretion. *Infect Immun* 2001; **69:** 1625-1629

34 **Peters TM**, Owen RJ, Slater E, Varea R, Teare EL, Saverymuttu S. Genetic diversity in the Helicobacter pylori cag pathogenicity island and effect on expression of anti-CagA serum antibody in UK patients with dyspepsia. *J Clin Pathol* 2001; **54:** 219-223

35 **Meining A**, Riedl B, Stolte M. Features of gastritis predisposing to gastric adenoma and early gastric cancer. *J Clin Pathol* 2002; **55:** 770-773

36 **Ohkuma K**, Okada M, Murayama H, Seo M, Maeda K, Kanda M, Okabe N. Association of Helicobacter pylori infection with atrophic gastritis and intestinal metaplasia. *J Gastroenterol*

Hepatol 2000; ***15:*** 1105-1112

37 **Rokkas T**, Filipe MI, Sladen GE. Detection of an increased incidence of early gastric cancer in patients with intestinal metaplasia type III who are closely followed up. *Gut* 1991; **32:** 1110-1113

38 **Rugge M**, Correa P, Dixon MF, Hattori T, Leandro G, Lewin K, Riddell RH, Sipponen P, Watanabe H. Gastric dysplasia: the Padova international classification. *Am J Surg Pathol* 2000; **24:** 167-176

39 **Keates S**, Keates AC, Warny M, Peek RM Jr, Murray PG, Kelly CP. Differential activation of mitogen-activated protein kinases in AGS gastric epithelial cells by cag+ and cag- Helicobacter pylori. *J Immunol* 1999; **163:** 5552-559

40 **Naumann M**, Wessler S, Bartsch C, Wieland B, Covacci A, Haas R, Meyer TF. Activation of activator protein 1 and stress response kinases in epithelial cells colonized by Helicobacter pylori encoding the cag pathogenicity island. *J Biol Chem* 1999; **274:** 31655-662

41 **Hansson LE**, Nyren O, Hsing AW, Bergstrom R, Josefsson S, Chow WH, Fraumeni JF Jr, Adami HO. The risk of stomach cancer in patients with gastric or duodenal ulcer disease. *N Engl J Med* 1996; **335:** 242–249

42 **Wanatabe T**, Tada M, Hirofumi N, Sasaki S, Nakao M. Helicobacter pylori infection induces gastric cancer in Mongolian gerbils. *Gastroenterology* 1998; **115:** 642-648

43 **Suerbaum S**, Michetti P. Helicobacter pylori infection. *N Engl J Med* 2002; ***347:*** 1175-1186

44 **Sipponen P**, Hyvarinen H, Seppala K, Blaser MJ. Review article: Pathogenesis of the transformation from gastritis to malignancy. *Aliment Pharmacol* Ther 1998; **12 Suppl 1:** 61-71

Science Editor Pravda J and Guo SY **Language Editor** Elsevier HK

PO Box 2345, Beijing 100023, China
www.wjgnet.com
wjg@wjgnet.com

ELSEVIER

World J Gastroenterol 2005;11(43):6823-6827
World Journal of Gastroenterology ISSN 1007-9327

• *CLINICAL RESEARCH* •

Single daily amikacin versus cefotaxime in the short-course treatment of spontaneous bacterial peritonitis in cirrhotics

Tai-An Chen, Gin-Ho Lo, Kwok-Hung Lai, Whey-Jen Lin

Tai-An Chen, Gin-Ho Lo, Kwok-Hung Lai, Whey-Jen Lin, Division of Gastroenterology, Department of Internal Medicine, Kaohsiung Veterans General Hospital, Taiwan, China
Correspondence to: Dr. Gin-Ho Lo, Division of Gastroenterology, Kaohsiung Veterans General Hospital, 386 Ta-Chung 1st Road, Kaohsiung 813, Taiwan, China. ghlo@isca.vghks.gov.tw
Telephone: +886-7-3468078 Fax: +886-7-3468237
Received: 2005-01-18 Accepted: 2005-07-01

Abstract

AIM: To compare the efficacy and safety of single daily amikacin *vs*. cefotaxime in the 5-d treatment of spontaneous bacterial peritonitis (SBP).

METHODS: Thirty-seven cirrhotic patients with SBP, 19 in group A and 18 in group B, were studied. Group A received 1 g of cefotaxime every 6 h, and group B received 500 mg of amikacin qd. Both antibiotics were administered up to 5 d and the responses were compared.

RESULTS: Infection was cured in 15 of 19 patients (78.9%) treated with cefotaxime and in 11 of 18 (61.1%) treated with amikacin. Four patients of the Cefotaxime group (21.1%) and five patients of the Amikacin group (27.8%) died. Two in each group (10.5% *vs* 11.1%) had renal impairment during study period. One in each group (5.3% *vs* 5.6%) may be considered to suffer from nephrotoxicity due to increased urinary β_2-microglobulin concentration.

CONCLUSION: In this study, single daily doses of amikacin in the treatment of SBP in cirrhotics were not associated with an increased incidence of renal impairment or nephrotoxicity. However, a 5-d regimen of amikacin is less effective than a 5-d regimen of cefotaxime in the SBP treatment.

Key words: Spontaneous bacterial peritonitis; Amikacin; Cefotaxime

Chen TA, Lo GH, Lai KH, Lin WJ. Single daily amikacin versus cefotaxime in the short-course treatment of spontaneous bacterial peritonitis in cirrhotics. *World J Gastroenterol* 2005; 11(43): 6823-6827
http://www.wjgnet.com/1007-9327/11/6823.asp

INTRODUCTION

Some studies have suggested that liver disease is a risk factor for aminoglycoside-induced nephrotoxicity[1-4]. However, aminoglycosides are still frequently used to treat sepsis in patients with liver disease[5]. In recent studies[6-8], single daily parenteral aminoglycoside administrations have shown some benefits as compared with multiple daily doses. These benefits include reduced toxicity, possible enhanced efficacy, greater convenience, and reduced costs. However, results of single daily aminoglycoside treatments of bacterial infections in cirrhotics have not been evaluated.

Spontaneous bacterial peritonitis (SBP) is a common complication of cirrhotic ascites. In a recent study, 5-d cefotaxime treatment of SBP was as efficacious as a 10-d course[9].

Because of these reasons, we have designed this prospective randomized study to compare the efficacy and nephrotoxicity of single daily amikacin dosage versus that of cefotaxime in the 5-d treatment of SBP in cirrhotics.

MATERIALS AND METHODS

Materials

Between July 2000 and June 2002, patients admitted to the Kaohsiung Veterans General Hospital who fulfilled all of the following criteria were enrolled into this study: (1) had liver cirrhosis; (2) had an ascitic fluid absolute neutrophil count > 500 cells/mm^3 with SBP as the only suspected cause. Patients were excluded from the study for any of the following reasons: (1) had a history of allergy to penicillins, cephalosporins, or aminoglycoside; (2) considered to be a terminal or critical case with life expectancy of less than one month; (3) had secondary peritonitis or tumor rupture; (4) had a serum creatinine level >2 mg/dL; (5) had an antibiotic treatment during previous 2 wk.

Methods

Patients were randomly allocated into two different therapeutic groups. Group A received 1 g of cefotaxime every 6 h. Group B received 500 mg of amikacin qd or 8 mg/kg of body weight qd if patient's body weight was less than 60 kg. The subsequent dosages of amikacin were adjusted according to renal function so that the trough level of plasma amikacin remained ≤30 μg/mL Both antibiotics were administered by intravenous infusion for 30 min. The antibiotics were not changed in any case during the first 72 h unless a nonsusceptible organism was isolated in the initial cultures. Antibiotics

were administered up to 5 d to patients who responded to the treatment. For patients who did not respond to the treatment after 5 d, antibiotic treatment was changed according to antibiotic susceptibility tests when a resistant organism was isolated, or empirically when the causative bacteria was not cultured.

Blood, urine, and ascites samples were obtained for culture, routine cell counts, and chemistry screening before initiation of antibiotic treatment. Other body fluids were cultured when indicated.

Abdominal paracentesis was repeated every 72 h until the culture became sterile and the ascitic fluid neutrophil count decreased to <250 cells/mm^3. Clinical signs and symptoms of infection, e.g., fever, chills, abdominal pain, abdominal tenderness, ileus, and mental status change, were recorded daily. Patients infected by organisms resistant to cefotaxime or amikacin were treated with appropriate alternative antibiotics according to the culture result and susceptibility tests. Two days after completion of antibiotic therapy, abdominal paracentesis was performed for culture test and cell count. Blood culture was repeated if bacteremia had been documented previously. If signs or symptoms of infection developed after discontinuation of the antibiotic, paracentesis for cell count and culture of blood were also repeated.

Infection was considered cured when all clinical and laboratory signs of infection disappeared during therapeutic period and cultures performed 2 d after antibiotic withdrawal were negative. Antibiotic treatment was considered a failure when the symptoms and signs of infection did not improve, or worsened, or when a nonsusceptible bacteria was isolated in the initial cultures. Patients discharged alive were followed closely throughout their illness for 4 wk after completion of treatment. Recurrence within 4 wk after discontinuation of therapy was defined as recurrent SBP or bacteremia. Relapse within 4 wk after discontinuation of therapy was defined as recurrent infection of ascitic fluid or blood with the same organism (identical species) that caused the initial infection. Reinfection within 4 wk after discontinuation of therapy was defined as recurrent bacteremia or recurrence of SBP with an organism different from the original pathogen. Superinfection was defined as development of SBP or bacteremia caused by a different pathogenic bacterium from the original organism during therapy. Infection-related mortality was defined as death caused by bacterial infection of ascitic fluid or blood, with clinical or bacteriologic evidence of uncontrolled infection. Hospitalization mortality was defined as death due to any cause during the hospitalization. In evaluating antibiotic efficacy, patients who died within the first 3 d after inclusion in the study were not considered.

Serum and urine creatinine levels were measured before treatment, every 2 d during treatment, and 24 h after completion of therapy. The 24-h urine was collected every 2 d for assessment of the creatinine clearance.

For patients who were treated with amikacin, blood and ascites samples for the determination of the trough and peak levels of amikacin were obtained 30 min before and one hour after administration of the drugs for every alternate day during treatment. The samples were stored at - 30 ^{o}C until assay. The amikacin levels were measured by radioimmunoassay.

According to previous investigations[4], urinary β_2-microglobulin is a useful test to discriminate antibiotic-induced nephrotoxicity from functional renal failure (or hepatorenal syndrome) in cirrhotic patients. Therefore, in the current study, the urinary concentration of β_2-microglobulin was measured in all patients studied before therapy, 3 d after initiation of treatment, and 2 d after antibiotic withdrawal. Fresh urine samples were collected and stored at pH 6 to 7 (with the addition of 1 N sodium hydroxide) and at - 30 ^{o}C until assayed. The analysis was performed using a commercial radioimmunoassay. Results of β_2-microglobulin were not available during the study.

In this study, renal impairment was defined as a rise in serum creatinine of 0.5 mg/dL or a ≥50% fall in creatinine clearance during the period. In the absence of other possible causes of renal tubular damage, renal impairment was considered to be secondary to nephrotoxicity if urinary β_2-microglobulin concentration increased from normal values (before treatment) to more than 2 000 mg/L (during treatment). Otherwise, renal impairment was considered functional. Patient who died within the first 3 d after inclusion in the study were not considered in evaluating the incidence of nephrotoxicity.

The *t*-test with Yates' correction, χ^2 with Fisher's exact test, or the nonparametric Mann-Whitney *U* test were used for statistical analysis. Data are presented as mean±SD. In each instance a two-tailed test was used. A *P* value of < 0.05 was considered significant.

RESULTS

A total of fifty- seven patients met inclusion criteria. Twelve patients were excluded because of either critical case with shock on presentation (4), prior treatment with antibiotics (2), initial serum creatinine concentration > 2 mg/dL (4), evidence of secondary peritonitis (1), or tumor rupture (1). Forty-five patients were eligible for the study and were randomized. Twenty-two patients were randomized to cefotaxime treatment and twenty-three patients to amikacin treatment. Two patients in amikacin group were later disqualified, because secondary peritonitis and tuberculous peritonitis were diagnosed after evaluation. Three patients in each group were not considered in the analysis of the result, because they died or fled against medical advice within 48 h after entry into the study. The remaining 37 patients, 19 in cefotaxime group and 18 in amikacin group, were the subjects of this analysis.

There was no significant difference between patients of the two groups (Table 1), in relation to sex, age, etiology of cirrhosis, severity of cirrhosis as expressed by Child-Pugh score, and renal function before treatment (expressed by serum creatinine level). In each group only one patient was Child-Pugh class B. The others were class C. Only 22 patients (59.5%) had normal serum creatinine level

Table 1 Comparison of clinical and laboratory characteristics of the patients

Characteristics	Treatment regimen		
	Cefotaxime	Amikacin	*P*
Number of patients	19	18	
Male/female	17/2	11/7	NS
Age(yr)[1]	54 ± 17	58 ± 11	NS
Etiologies of cirrhosis (%)[2]			NS
Alcoholism	3 (16)	2 (11)	
Chronic hepatitis B	14 (74)	11 (61)	
Chronic hepatitis C	1 (5)	4 (22)	
Child-Pugh score[1]	11.4 ± 1.2	11.1 ± 1.1	NS
Serum creatinine(mg/dL)[1]	1.5 ± 0.5	1.4 ± 0.4	NS

[1]Data are presented as mean ± SD. [2]Data are presented as number and percentage of total. NS: not significant

(<1.5 mg/dL) before treatment.

Nine (24%) of the 37 patients grew a pathogen from their ascitic fluid, and 8 (21.6%) were bacteremic. The ascites and blood isolates were similar between the two groups (Table 2). Two pathogens in the blood (group B *Streptococcus* and *Vibrio amalonaticus*) were resistant to cefotaxime and amikacin. Although the clinical signs of infection disappeared during therapeutic period with cefotaxime, crystal penicillin and tetracycline were given according to the susceptibility tests since the sixth day. The other isolates were sensitive to cefotaxime and amikacin.

Table 2 Flora of ascites and blood

	Treatment regimen		
	Cefotaxime (%)	Amikacin (%)	*P*
Ascites			
Escherichia coli	4 (21)	3 (17)	NS
Klebsiella pneumoniae	0	1 (6)	NS
Citrobacter diversus	0	1 (6)	NS
Blood			
Escherichia coli	2 (11)	1 (6)	NS
Klebsiella pneumoniae	1 (5)	2 (11)	NS
Streptococcus group B	1 (5)	0	NS
Vibrio amalonaticus	1 (5)	0	NS

Data are presented as number and percentage of total. NS: not significant.

The clinical response to treatment and survival were similar between the groups (Table 3). Infection was cured in 15 of 19 patients (78.9%) treated with cefotaxime and in 11 of 18 (61.1%) treated with amikacin. However, there was no statistic significance between these two groups. Three patients in cefotaxime group had recurrent infection within 4 wk after completion of treatment. One was considered relapse due to recurrent bacteremia with the same organism that caused the initial bacteremia. The other two also suffered from bacteremia, but the previous infection episode was not bacteremic. Recurrent SBP concurrent with new episodes of bacteremia rather than relapse were considered in these two patients. Among the 8 bacteremic patients in the initial treatment, 2 in the cefotaxime group had resistant isolates. Although they became well during the initial therapeutic period and cured without recurrence within 4 wk after changing antibiotics, treatment failure was still considered according to the study's design. The other 6 bacteremic patients were bacteriologically cured by repeated culture after 5-d of antibiotic treatment. Only one patient (16.6%) in the cefotaxime group had relapse 10 d after completion of treatment.

Table 3 Results of treatment

	Treatment regimen		
	Cefotaxime (%)	Amikacin (%)	*P*
Number of patients	19	18	
Cure[2]	15 (78.9)	11 (61.1)	NS
Normalized PMN count[2]	18 (94.7)	15 (83.3)	NS
Serum creatinine(mg/dL)[1]	1.3 ± 0.8	1.5 ± 1.1	NS
Afebril in 72 h[2]	18 (94.7)	15 (83.3)	NS
Pain-free in 72 h[2]	19 (100)	17 (94.4)	NS
Recurrence[2]	3(15.8)	0	NS
Superinfection[2]	0	0	NS
Infection-related mortality[2]	0	3 (16.7)	0.105
Hospitalization mortality[2]	4 (21.1)	5 (27.8)	NS
Days of hospitalization[1]	12 ± 8	13 ± 9	NS

[1]Data are presented as mean ± SD. [2]Data are presented as number and percentage of total. NS: not significant

There was no significant difference between these two groups in the mortality rate. During the whole hospitalization period, 4 patients of the cefotaxime group (21.1%) and 5 patients of the amikacin group (27.8%) died. Although for most patients the cause of death was multifactorial, in three cases of the amikacin group infection was considered to be the main cause of death due to no other major event or infection identified.

There was no significant difference in the incidence of renal impairment or nephrotoxicity between patients treated with cefotaxime or amikacin (Table 4). Two in each group (10.5% *vs* 11.1%) had renal impairment during study period. The urinary β_2-microglobulin concentration increased in both groups during treatment and decreased after antibiotics withdrawal. One in each group (5.3% *vs* 5.6%) may be considered nephrotoxicity due to increased urinary β_2-microglobulin concentration from normal values (before treatment) to more than 2 000 mg/L (during treatment). The patient who developed nephrotoxicity in the amikacin group died on the 6th d of the study period.

Table 4 Evaluation of nephrotoxicity

	Treatment regimen		
	Cefotaxime(%)	Amikacin(%)	*P*
Number of patients	19	18	
Renal impairment (%)[2]	2 (10.5)	2 (11.1)	NS
Urinary β^2-microglobulin (mg/L)			
Before treatment[1]	402 ± 80	1220 ± 392	NS
3 d after initiation[1]	779 ± 2465	612 ± 814	NS
2 d after withdrawal[1]	126 ± 119	173 ± 44	NS
increase > 2 000 mg/L (%)[2]	1 (5.3)	1 (5.6)	NS

[1]Data are presented as mean ± SD. [2]Data are presented as number and percentage of total. NS: not significant.

The mortality was considered infection-related. The patient in the cefotaxime group died on the 5th d due to hepatic and renal failure even though the infection appeared under controlled.

Wide range of peak and trough levels of amikacin in patients treated with amikacin was noted in this study (Table 5).

Table 5 Amikacin concentration (mean ± SD)

Blood peak level (μg/mL)	19.6 – 127.3 (40 ± 32)
Blood trough level (μg/mL)	1.3 – 73.7 (12 ± 22)
Ascites peak level (μg/mL)	4.3 – 80.1 (20 ± 25)
Ascites trough level(μg/mL)	1.2 – 78.9 (15 ± 26)

DISCUSSION

The aminoglycosides are potent antibiotics, with peak concentration-dependent bactericidal activity against Gram-negative pathogens and staphylococci. They display trough concentration-dependent nephrotoxicity and ototoxicity. Aminoglycosides exhibit enduring antibacterial activity (especially against Gram-negative bacilli) many hours after tissue concentrations become negligible. Appreciation of this postantibiotic effect leads to replacement of conventional multiple daily doses by large single daily doses. The latter regimens confer at least equivalent efficacy and less risk of nephrotoxicity[7]. Among the aminoglycosides available in our hospital, we used amikacin in this study, because it is the least susceptible to degradation by bacterial enzymes and causes less nephrotoxicity than gentamicin and tobramycin[7]. Because some studies have suggested that liver disease is a risk factor for nephrotoxicity in patients treated with aminoglycoside[1-4], we used only about half of the recommended single daily dosage of amikacin (15 mg/kg q24 h in usual study[7]) in this study.

The optimal duration of antibiotic treatment for SBP had been investigated recently. Ten to fourteen days intravenous therapy had been recommended[10-12]. However, it had been argued that, because SBP had a low bacterial load (often only 1 organism/mm^3 of ascitic fluid), a shorter duration of treatment might suffice. A recent randomized controlled study comparing 5 d *vs* 10 d treatment with cefotaxime found no difference in efficacy and mortality rate [9].

In this study the cure rate was higher in the group of patients treated with cefotaxime (78.9%) than in the group of patients treated with amikacin (61.1%), although there was no significant difference. Larger sample sizes in further studies may confirm this finding. The cure rate for SBP in patients treated with cefotaxime in this study is similar to the previous studies. In Runyon's study[9], the cure rate for SBP treated by 5-d cefotaxime is 93.1%. On the other hand, the cure rate in patients treated with amikacin in this study is also similar to the previous studies that treated cirrhotic patients with severe infection using aminoglycosides combining with other antibiotics. In Felisart's study which compared cefotaxime *vs.* ampicillin-tobramycin in cirrhotics with severe infections (most were peritonitis), the cure rates were 85% and 56% respectively[13]. The response rate in the McCormick's study which used netilmicin plus mezlocillin in the empirical therapy of presumed sepsis in cirrhotic patients was 56%[5]. Single daily dosage of aminoglycoside in the treatment of infections in cirrhotic patients seemed as effective as combining with other antibiotics in traditional dosages but less effective than cefotaxime.

It is well known that in traditional dosages, the serum, the tissue and the body fluid levels of aminoglycosides are unpredictable, varying from one patient to another[14, 15]. We conducted this study by using a single daily dose of aminoglycoside for easy monitoring of the drug level. Just like previous reports, our study also showed that there were wide ranges of drug levels in blood and ascites between the patients regardless of whether their renal function were normal or not. Some levels might not achieve the bactericidal levels. For example, the MIC of amikacin for *E coli* was 2 mg/mL in this study. Only 13 of the 18 patients (72%) had 4-fold or higher for their peak level of ascites. On the other hand, it is well established that cefotaxime has a wide range between therapeutic and toxic dosages. Also, the ascitic fluid concentration of cefotaxime is several-fold higher than the MIC of most susceptible organisms at any time throughout the treatment[16]. This may explain the difference of efficacy of treatment between cefotaxime and amikacin.

The incidence of nephrotoxicity in this present study was 5.6% in patients treated with amikacin. This was similar with the Felisart's study in patients treated with ampicillin-tobramycin (7%)[13], but almost six times lower than the Cabrera's study in patients treated with cephalothin-gentamicin or cephalothin-tobramycin (32%)[4]. Previous investigations have suggested that combined therapy, i.e. cephalothin, might enhance the nephrotoxicity of aminoglycosides[17, 18]. Although some study suggested that the risk for aminoglycoside nephrotoxicity was 5 times higher in a patient with liver disease than without[2], we found that a single daily dosage of amikacin did not cause marked nephrotoxicity in cirrhotic patient in this study. The incidence was between 3% and 11% in patients treated with aminoglycosides, similar with previous reports[19, 20].

In this study, eight patients (22%) had positive blood culture concurrent with SBP. Two of them were resistant isolates to cefotaxime and had other antibiotic treatment. Six patients were all bacteriologic cured after 5-d of treatment. This was confirmed by negative culture result repeated after treatment. However, one of the six patients (17%) who was treated with cefotaxime had bacteremic relapse 10 d after completion of treatment. In Runyon's study, 9 bacteremic patients treated with 5-d cefotaxime were documented to become sterile during the first 72 h of therapy. No relapse was mentioned. 9 Because bacteremia in cirrhosis is a severe prognostic sign, it has been considered common practice to treat it for 10 to 14 d[21]. Do patients with SBP in addition to bacteremia require longer treatments than patients without bacteremia? Is a

5-d course adequate for treating bacteremia in cirrhotic patients? These issues remain to be clarified.

In spite of the lower antibiotic efficacy of amikacin, the hospitalization mortality rate resulting from this antibiotic regimen was similar to that observed in patients treated with cefotaxime. This may be explained by the fact that both groups of cirrhotics had a similar degree of liver failure. Most mortalities were related to infective complications in patients treated with amikacin and to noninfective complications in patients treated with cefotaxime.

In summary, we found that single daily doses of amikacin in the treatment of SBP in cirrhotics were not associated with an increased incidence of renal impairment or nephrotoxicity. However, the efficacy of a 5-d regimen of amikacin is less than a 5-d regiimen of cefotaxime in SBP treatment.

REFERENCES

1 **Garcia-Tsao G**. Current management of the complications of cirrhosis and portal hypertension: variceal hemorrhage, ascites, and spontaneous bacterial peritonitis. *Gastroenterology* 2001; **120:** 726-748

2 **Mowat C**, Stanley AJ. Review article: spontaneous bacterial peritonitis--diagnosis, treatment and prevention. *Aliment Pharmacol Ther* 2001; **15:** 1851-1859

3 **Follo A**, Llovet JM, Navasa M, Planas R, Forns X, Francitorra A, Rimola A, Gassull MA, Arroyo V, Rodes J. Renal impairment after spontaneous bacterial peritonitis in cirrhosis: incidence, clinical course, predictive factors and prognosis. *Hepatology* 1994; **20:** 1495-1501

4 **Cabrera J**, Arroyo V, Ballesta AM, Rimola A, Gual J, Elena M, Rodes J. Aminoglycoside nephrotoxicity in cirrhosis. Value of urinary beta 2-microglobulin to discriminate functional renal failure from acute tubular damage. *Gastroenterology* 1982; **82:** 97-105

5 **McCormick PA**, Greenslade L, Kibbler CC, Chin JK, Burroughs AK, McIntyre N. A prospective randomized trial of ceftazidime versus netilmicin plus mezlocillin in the empirical therapy of presumed sepsis in cirrhotic patients. *Hepatology* 1997; **25:** 833-836

6 **Prins JM**, Buller HR, Kuijper EJ, Tange RA, Speelman P. Once versus thrice daily gentamicin in patients with serious infections. *Lancet* 1993; **341:** 335-339

7 **Kumana CR**, Yuen KY. Parenteral aminoglycoside therapy. Selection, administration and monitoring. *Drugs* 1994; **47:** 902-913

8 **Mauracher EH**, Lau WY, Kartowisastro H, Ong KH, Genato VX, Limson B, Yusi GM, Liu CY, Suwangool P. Comparison of once-daily and thrice-daily netilmicin regimens in serious systemic infections: a multicenter study in six Asian countries. *Clin Ther* 1989; **11:** 604-613

9 **Runyon BA**, McHutchison JG, Antillon MR, Akriviadis EA, Montano AA. Short-course versus long-course antibiotic treatment of spontaneous bacterial peritonitis. A randomized controlled study of 100 patients. *Gastroenterology* 1991; **100:** 1737-1742

10 **Holland DJ**, Sorrell TC. Antimicrobial therapy and prevention of spontaneous bacterial peritonitis. *J Gastroenterol Hepatol* 1993; **8:** 370-374

11 **Bhuva M**, Ganger D, Jensen D. Spontaneous bacterial peritonitis: an update on evaluation, management, and prevention. *Am J Med* 1994; **97:** 169-175

12 **Garcia-Tsao G**. Spontaneous bacterial peritonitis. *Gastroenterol Clin North Am* 1992; **21:** 257-275

13 **Felisart J**, Rimola A, Arroyo V, Perez-Ayuso RM, Quintero E, Gines P, Rodes J. Cefotaxime is more effective than is ampicillin-tobramycin in cirrhotics with severe infections. *Hepatology* 1985; **5:** 457-462

14 **Kaye D**, Levison ME, Labovitz ED. The unpredictability of serum concentrations of gentamicin: pharmacokinetics of gentamicin in patients with normal and abnormal renal function. *J Infect Dis* 1974; **130:** 150-154

15 **Moore RD**, Lietman PS, Smith CR. Clinical response to aminoglycoside therapy: importance of the ratio of peak concentration to minimal inhibitory concentration. *J Infect Dis* 1987; **155:** 93-99

16 **Moreau L**, Durand H, Biclet P. Cefotaxime concentrations in ascites. J Antimicrob Chemother 1980; **6 Suppl A:** 121-122

17 Wade JC, Schimpff SC, Wiernik PH. Antibiotic combination-associated nephrotoxicity in granulocytopenic patients with cancer. *Arch Intern Med* 1981; **141:** 1789-1793

18 **Wade JC**, Smith CR, Petty BG, Lipsky JJ, Conrad G, Ellner J, Lietman PS. Cephalothin plus an aminoglycoside is more nephrotoxic than methicillin plus an aminoglycoside. *Lancet* 1978; **2:** 604-606

19 **Appel GB**, Neu HC. The nephrotoxicity of antimicrobial agents (second of three parts). *N Engl J Med* 1977; **296:** 722-728

20 **Kahlmeter G**, Dahlager JI. Aminoglycoside toxicity - a review of clinical studies published between 1975 and 1982. *J Antimicrob Chemother* 1984; **13 Suppl A:** suppl A 9-22

21 **Graudal N**, Hubeck B, Bonde J, Thomsen AC. The prognostic significance of bacteremia in hepatic cirrhosis. *Liver* 1987; **7:** 138-141

Science Editor Guo SY **Language Editor** Elsevier HK

PO Box 2345, Beijing 100023, China
www.wjgnet.com
wjg@wjgnet.com

ELSEVIER

World J Gastroenterol 2005;11(43):6828-6832
World Journal of Gastroenterology ISSN 1007-9327

• *RAPID COMMUNICATION* •

Scattered and rapid intrahepatic recurrences after radio frequency ablation for hepatocellular carcinoma

Kazuhiro Kotoh, Munechika Enjoji, Eiichirou Arimura, Shusuke Morizono, Motoyuki Kohjima, Hironori Sakai, Makoto Nakamuta

Kazuhiro Kotoh, Munechika Enjoji, Shusuke Morizono, Motoyuki Kohjima, Makoto Nakamuta, Department of Medicine and Bioregulatory Science, Graduate School of Medical Sciences, Kyushu University, Fukuoka, Japan
Eiichirou Arimura, Hironori Sakai, Department of Gastroenterology, National Hospital Organization Kyushu Medical Center, Fukuoka, Japan
Correspondence to: Munechika Enjoji, MD, PhD, Department of Medicine and Bioregulatory Science, Graduate School of Medical Sciences, Kyushu University, 3-1-1 Maidashi, Higashi-ku, Fukuoka 812-8582,
Japan. enjoji@intmed3.med.kyushu-u.ac.jp
Telephone: +81-92-642-5282 Fax: +81-92-642-5287
Received: 2005-04-11 Accepted: 2005-06-09

Abstract

AIM: To evaluate a series of patients with hepatocellular carcinoma (HCC) treated with several different protocols and devices.

METHODS: We treated 138 patients [chronic hepatitis/liver cirrhosis (Child–Pugh A/B/C), 3/135 (107/25/3)] with two different devices and protocols: cool-tip needle [initial ablation at 60 W (standard method) (n = 37) or at 40 W (modified method) (n = 28)] or; ablation with a LeVeen needle using a standard single-step, full expansion (single-step) method (n = 39) or a multi-step, incremental expansion (multi-step) method.

RESULTS: Eleven patients experienced rapid and scattered recurrences 1 to 7 mo after the ablation. Nine patients were treated by the cool-tip original protocol (60 W) (9/37 = 24%) and the other two by the LeVeen single-step method (2/39 = 5%). The location of the recurrence was surrounding and limited to the site of ablation segment in three cases, and spread over one lobule or both lobules in the other eight cases. There was no recurrence in the patients treated with the modified cool-tip modified method (40 W) or the LeVeen multi-step method.

CONCLUSION: There is a risk of rapid and scattered recurrence after RFA, especially when the standard cool-tip procedure is used. Because such recurrence would worsen the prognosis, we recommend that modified protocols for the cool-tip and LeVeen needle methods should be used in clinical practice.

Key words: Radio frequency ablation; Hepatocellular carcinoma; Cool-tip needle; LeVeen needle; Recurrence

Kotoh K, Enjoji M, Arimura E, Morizono S, Kohjima M, Sakai H, Nakamuta M. Scattered and rapid intrahepatic recurrences after radio frequency ablation for hepatocellular carcinoma. *World J Gastroenterol* 2005; 11(43): 6828-6832
http://www.wjgnet.com/1007-9327/11/6828.asp

INTRODUCTION

Image-guided radio frequency ablation (RFA) is an emerging technique for the treatment of hepatocellular carcinoma (HCC)[1-5], as well as for metastatic liver tumors[6]. The procedure has been adopted worldwide as a safe and effective method, and is replacing percutaneous ethanol injection therapy (PEIT) as the treatment of choice. Livraghi *et al*.[7] and Lencioni *et al*.[8] have compared RFA and PEIT for the treatment of small-sized HCC. Although both studies concluded that RFA resulted in a higher rate of complete necrosis, Livraghi *et al*.[7] also indicated that the complication rate was higher with RFA than with PEIT.

A number of reports have described complications associated with RFA[9-14]. The major complications reported were peritoneal bleeding, hepatic abscess, hemothorax, perforation of the gastrointestinal wall, and rapid hepatic decompensation. These complications occurred during or just after RFA, however, and delayed complications have been reported much less frequently. Takada *et al*.[15] described two cases in which rapid and aggressive recurrence accompanied by portal thrombus occurred 4 to 6 mo after RFA. Nicoli *et al*.[16] described a peculiar form of recurrence after RFA for HCC that was characterized by numerous and equally-sized recurrence nodules and which occurred after only one month post-treatment. More recently, Ruzzenente *et al*.[17] also described a series of patients with rapidly spreading recurrence after RFA.

In the past several years, we have observed cases similar to those presented by Nicoli *et al*.[16]. We have previously reported a significant increase in pressure in the ablated area during RFA[18], and concluded that scattered recurrence is attributable to an explosion caused by excessive increases in intra-tumor pressure. In our experience, intra-operative complications are easily avoidable by confirming the safety of a puncture route

before the treatment, whereas a rapid recurrence after RFA is a serious clinical problem that can influence the prognosis of patients.

In this report, we have evaluated a series of HCC cases treated by RFA with different devices and protocols, and have analyzed cases with rapid and scattered recurrence after RFA.

PATIENTS AND METHODS

RFA

Between April 2000 and December 2004, 138 patients with HCC were treated with the RFA procedure in Kyushu University Hospital or National Hospital Organization Kyushu Medical Center. Characteristics of the candidates are shown in Table 1. They consisted of 79 males and 59 females, aged 40 to 83 years with a mean of 68.2 years. All of them had chronic liver damage; 121 patients were hepatitis C virus (HCV) positive and 17 were hepatitis B virus (HBV) positive. Among them, 135 patients were diagnosed with liver cirrhosis by liver biopsy, clinical laboratory data, ultrasonography and/or computed tomography. According to the hepatic functional reserve evaluation for the cirrhotic patients just before RFA, 107, 25, and 3 were classified as Child–Pugh's class A, B, and C, respectively. The diagnosis of HCC was confirmed by aspiration tumor biopsy for all patients prior to treatment.

RFA was performed with either a LeVeen™ multipolar array needle in combination with an RF 2000 generator™ (Radio Therapeutics Corporation, Mountain View, CA, USA) or a Cool-tip™ RF System (3.0 cm exposure length) (Radionics, Burlington, MA, USA). One of the two devices was selected randomly for RFA. All procedures were performed by hepatologists who had at least 10 years of experience performing image-guided *in situ* tumor ablation therapy. The original standard protocol was used for cool-tip needle RFA until December 2002, and the modified protocol was used thereafter. For LeVeen needle RFA, the original standard protocol was used until April 2002, and the modified method was used thereafter. The details of each protocol are described below.

Original procedure with cool-tip needle: Cool-tip electrode with 3 cm of exposed tip was used to deliver RF (radio frequency) energy to the tumors. RF energy was delivered as described previously[19]. In short, after needle puncture of the tumor, generator output was increased to 100–120 W and maintained at this level until the end of the procedure. If an increase in impedance equal to or greater than 10 Ω above baseline was observed, the current was reduced, until stable impedance was observed and then increased again.

Modified procedure with cool-tip needle: The needle used was the same type as was used for the original procedure. The method differed from the original procedure in that the ablation was started at a low voltage of 40 W, and the electric power was increased by 10 W every minute. The maximum of electric power was 120 W, and the RF energy delivery was continued, until the impedance increased beyond the limit of the generator.

Original procedure with LeVeen needle: The electrode used for this procedure was a 3 or 3.5 cm LeVeen needle depending on the tumor size. Before delivery of RF power, the tumor was punctured with a needle and the ten tines were then fully expanded. The ablation was started at 40 W (3-cm needle) or 50 W (3.5-cm needle) RF power and was further increased by 10 W/min up to 75 W (3-cm needle) or 90 W (3.5-cm needle). If the impedance had not increased after 10 min, the RF power was again increased by 10 W increments. The procedure was terminated when a marked increase in impedance ("roll off") occurred.

Modified procedure with LeVeen needle: The needle used was the same type as was used for the original procedure. In the modified version, the tines of the electrode were expanded step by step in 10 steps, and at every step, the length of tine expansion was one-tenth of the full expansion length. Ablation at each step was continued, until the impedance increased to "roll off". Furthermore, at the first step, the ablation was started at a low voltage of 30 W. If it took more than 30 s for "roll off" at a step, the power was increased by 10 W before starting the next step. The maximum electric power for this protocol was 75 W (3-cm needle) or 90 W (3.5-cm needle), which was maintained until the final step.

After RFA treatment, all of the patients were followed up every one or two months with US or CT. When recurrence was detected by imaging examination, additional treatment was instituted with RFA, PEIT, transarterial chemoembolization (TACE) or a combination of these therapies. The prognosis was based on the data obtained up to December 2004.

Statistical analysis

Baseline characteristics of the patients prior to RFA treatment are shown as mean±SD and statistical comparisons were performed using χ^2 test for categorical data and non-paired *t*-test for numerical data.

Table 1 Characteristics of the patients

	Scattered recurrence (–)	Scattered recurrence (+)	Total
n	127	11	138
Age	67.5±8.6	69.2±8.1	67.6±8.5
Sex (male/female)	71/56	8/3	79/59
Virus (HBV/HCV)	14/113	3/8	17/121
Tumor size (mm)	24.3±13.7	20.1±5.7	24.0±13.5
Albumin (g/dL)	3.65±0.38	3.52±0.57	3.64±0.39
Bilirubin (mg/dL)	0.86±0.51	1.02±0.44	0.87±0.50
ALT (U/L)	48.4±28.3	56.0±17.8	49.0±28.5
Platelet (x10^4/mL)	10.9±5.5	9.0±3.6	10.7±5.5
Child–Pugh (CH[1]/A/B/C)[a]	3/102/20/2	0/5/5/1	3/107/25/3
Device and Protocol[b]			
Original cool-tip	28	9	37
Modified cool-tip	28	0	28
Single-step LeVeen	37	2	39
Multi-step LeVeen	34	0	34
Prognosis (alive/death)[b]	87/40	3/8	90/48
Observation period (mo)	27.1±11.0	24.0±11.5	26.9±11.1

[a]$P<0.05$, [b]$P<0.01$ between the patients with and without scattered recurrences (χ^2 test). [1]CH: chronic hepatitis.

Table 2 Details of the patients with scattered recurrence

n	Sex	Age	Background	Liver function (Child-Pugh)	Location/ Size (mm)	Device	Protocol	Form of recurrence	Interval between RFA and recurrence (mo)	Prognosis after RFA (mo)
1	F	75	LC (HCV)	C	S8/15	LeVeen	Original	Bilobular	3	Death (15)
2	M	61	LC (HBV)	A	S7/20	Cool-tip	Original	Bilobular	3	Alive (42)
3	F	79	LC (HCV)	B	S2/25	Cool-tip	Original	Bilobular	2	Death (36)
4	M	63	LC (HBV)	A	S4/15	Cool-tip	Original	Surrounding	7	Death (24)
5	M	69	LC (HCV)	B	S7/26	Cool-tip	Original	Bilobular	4	Death (27)
6	M	73	LC (HCV)	B	S5/13	Cool-tip	Original	Bilobular	5	Death (20)
7	M	74	LC (HCV)	A	S4/18	Cool-tip	Original	Bilobular	4	Death (7)
8	M	70	LC (HCV)	A	S8/30	Cool-tip	Original	Surrounding	5	Alive (36)
9	M	70	LC (HCV)	B	S8/25	Cool-tip	Original	Bilobular	6	Death (16)
10	M	51	LC (HBV)	B	S6/20	LeVeen	Original	Surrounding	2	Death (10)
11	F	76	LC (HCV)	A	S3/14	Cool-tip	Original	Lobular	7	Alive (31)

RESULTS

Eleven patients suffered from rapid and scattered intrahepatic recurrences, which occurred between one month and seven months after ablation. These 11 cases consisted of eight males and three females, ranging in age from 51 to 79 years. The ablated tumors were located variably in either lobe of the liver. Among the baseline characteristics of patients prior to RFA treatment, the cirrhosis stage was significantly more advanced in patients without scattered recurrences (Table 1). Of the patients with scattered recurrences, nine were treated with the cool-tip device according to the original protocol and the other two with the LeVeen needle and original full-expansion method (Tables 1 and 2). After switching from the original to the modified protocols, no scattered recurrences were observed.

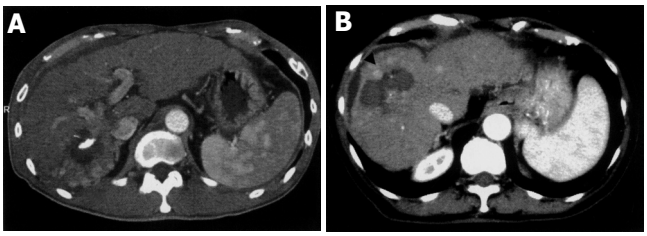

Figure 1 CT images of scattered recurrences after RFA. **A:** Recurrences around the ablated tumor after RFA (case 10 in Table 2); **B:** Multiple recurrences scattered over the whole liver after RFA (case 6 in Table 2). The white arrows indicate the ablated area without enhancement by contrast medium, and the black arrowheads indicate scattered recurrence with enhancement.

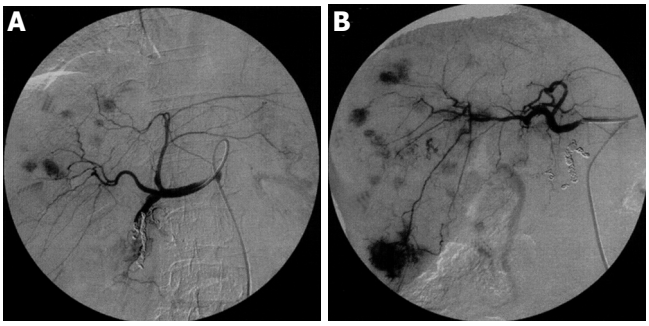

Figure 2 Angiographic images of scattered recurrences after RFA, which were treated by TACE in most of the cases. **A:** Multiple recurrences were located surrounding the ablated tumor (case 8 in Table 2). **B:** Multiple recurrences were scattered in the whole liver (case 9 in Table 2). In both patterns, recurrent tumors were almost equal in size.

Scattered recurrent tumors occurred in two different patterns. One pattern consisted of scattered tumors that were located in a single lobe (three patients). This pattern is shown in Figures 1A (CT) and 2A (angiography), appearing as multiple tumors around the ablated tumor that were localized in the segment. The other pattern consisted of tumors spread over a single lobule in the several segments (one patient) or both lobules (Figures 1B and 2B) (seven patients). Regardless of the scattering pattern, the tumors were roughly equal in diameter. When recurrences were found, neither tumor thrombus nor extrahepatic metastasis was observed by CT or US imaging.

Follow-up of patients to December 2004 showed that the prognosis was significantly worse for patients with scattered recurrences. Among the 127 patients without scattered recurrences, 40 patients died within the observation period; 8 due to liver failure caused by progression of liver cirrhosis, 2 from variceal rupture, and the remainder due to the progression of HCC. In contrast, 8 of 11 patients with scattered recurrences died and all had advanced HCC.

DISCUSSION

There are several common characteristics among the cases described in this study. First, recurrence occurred rapidly following RFA. Most of these cases were detected within 6 mo. Second, multiple recurrent tumors were almost equal in diameter. Finally, the recurrent tumors were either scattered around the ablated tumor or all over the lobe(s), and the location had no relation to the puncture route used for RFA.

Nicoli *et al.*[16] recently reported a similar form of recurrence that is, rapid and numerous bilobular recurrent tumors, and proposed that this type of recurrence would result from new communication formed between two vascular regions (arterial and venous-portal) as a result of RFA needle puncture. It was also suggested that the new communication facilitated the migration of tumor cells

from a high pressure arterial regions to a low pressure portal liver regions. However, we disagree with this speculation because the tumor treated with RFA in that study was only 3.5 cm in diameter, and the feeding artery would not likely have sufficient pressure to spread the malignant cells throughout the lobes. Ruzzenente *et al*.[17] also identified a series of patients with similar recurrences and suggested that increased intra-tumor pressure might be the cause.

In recent *in vitro* and *in vivo* experiments, we demonstrated that the pressure in an ablated area can increase drastically during RFA[18]. We assumed that the peculiar scattered recurrence was caused by an explosion due to increased intra-tumor pressure. The explosion could strew the malignant cells, as a large cluster, which would enable the metastatic tumors to grow in a short time.

A substantial increase in pressure would be necessary for the tumor to explode during RFA, and in rider for this to occur either of the two different conditions would be necessary; namely a fibrotic capsule around the tumor, or parenchymal fibrosis surrounding the tumor accompanied by cirrhosis. Without these conditions, the pressure produced by ablation would easily escape through the microvasculature or sinusoids adjacent to the ablated tumor. In our study, all of the patients with scattered recurrences also had liver cirrhosis, and the rate of advanced-stage cirrhosis was higher in patients with recurrence. This suggests that accumulated collagens in the liver of patients with cirrhosis could form a wall that traps in pressure.

Once a scattered recurrence occurs, focal treatment such as ablation therapy can no longer be used, and the only remaining treatment options are TACE or systemic chemotherapy. The incidence of recurrent tumors is also associated with a poor prognosis. We found that within the observation period, the mortality rate of patients with scattered recurrences was higher than that of patients without scattered recurrences.

In order to avoid scattered recurrences, we believe that modified protocols for RFA should be used. After changing to the modified protocols, we found no cases of scattered recurrence associated with either the cool-tip or LeVeen needle procedures. Another way to avoid scattered recurrence is to use alternative procedures to RFA such as ablation by PEIT, which is performed with a thinner needle than that used for RFA and has a lower risk of complications[7,8,20]. There are no reports that we are aware of to indicate that PEIT can cause scattered recurrences. PEIT is generally considered to be inferior to RFA for the following two reasons. First, in contrast with RFA, PEIT requires multiple sessions. Second, local recurrence following PEIT may be more likely when the surgeon is inexperienced, while a highly-skilled surgeon can achieve complete tumor necrosis.

We conclude that critical complications of rapid and scattered recurrences after RFA can be avoided by the use of modified protocols. If the need arises, it is also necessary to select PEIT, not to cling to use RFA procedure. In some cases, PEIT should be considered as a suitable alternative to RFA.

REFERENCES

1 **Giorgio A**, Francica G, Tarantino L, de Stefano G. Radio-frequency ablation of hepatocellular carcinoma lesions. *Radiology* 2001; **218:** 918-919

2 **Gazelle GS**, Goldberg SN, Solbiati L, Livraghi T. Tumor ablation with radio-frequency energy. *Radiology* 2000; **217:** 633-646

3 **Denys AL**, De Baere T, Mahe C, Sabourin JC, Sa Cunha A, Germain S, Roche A. Radio-frequency tissue ablation of the liver: effects of vascular occlusion on lesion diameter and biliary and portal damages in a pig model. *Eur Radiol* 2001; **11:** 2102-2108

4 **Maluf D**, Fisher RA, Maroney T, Cotterell A, Fulcher A, Tisnado J, Contos M, Luketic V, Stravitz R, Shiffman M, Sterling R, Posner M. Non-resective ablation and liver transplantation in patients with cirrhosis and hepatocellular carcinoma (HCC): safety and efficacy. *Am J Transplant* 2003; **3:** 312-317

5 **Livraghi T**. Treatment of hepatocellular carcinoma by interventional methods. *Eur Radiol* 2001; **11:** 2207-2219

6 **Solbiati L**, Livraghi T, Goldberg SN, Ierace T, Meloni F, Dellanoce M, Cova L, Halpern EF, Gazelle GS. Percutaneous radio-frequency ablation of hepatic metastases from colorectal cancer: long-term results in 117 patients. *Radiology* 2001; **221:** 159-166

7 **Livraghi T**, Goldberg SN, Lazzaroni S, Meloni F, Solbiati L, Gazelle GS. Small hepatocellular carcinoma: treatment with radio-frequency ablation versus ethanol injection. *Radiology* 1999; **210:** 655-661

8 **Lencioni RA**, Allgaier HP, Cioni D, Olschewski M, Deibert P, Crocetti L, Frings H, Laubenberger J, Zuber I, Blum HE, Bartolozzi C. Small hepatocellular carcinoma in cirrhosis: randomized comparison of radio-frequency thermal ablation versus percutaneous ethanol injection. *Radiology* 2003; **228:** 235-240

9 **Francica G**, Marone G, Solbiati L, D'Angelo V, Siani A. Hemobilia, intrahepatic hematoma and acute thrombosis with cavernomatous transformation of the portal vein after percutaneous thermoablation of a liver metastasis. *Eur Radiol* 2000; **10:** 926-929

10 **Choi H**, Loyer EM, DuBrow RA, Kaur H, David CL, Huang S, Curley S, Charnsangavej C. Radio-frequency ablation of liver tumors: assessment of therapeutic response and complications. *Radiographics* 2001; **21 Spec No:** S41-S54

11 **Dromain C**, de Baere T, Elias D, Kuoch V, Ducreux M, Boige V, Petrow P, Roche A, Sigal R. Hepatic tumors treated with percutaneous radio-frequency ablation: CT and MR imaging follow-up. *Radiology* 2002; **223:** 255-262

12 **Livraghi T**, Solbiati L, Meloni MF, Gazelle GS, Halpern EF, Goldberg SN. Treatment of focal liver tumors with percutaneous radio-frequency ablation: complications encountered in a multicenter study. *Radiology* 2003; **226:** 441-451

13 **Tamai F**, Furuse J, Maru Y, Yoshino M. Intrahepatic pseudoaneurysm: a complication following radio-frequency ablation therapy for hepatocellular carcinoma. *Eur J Radiol* 2002; **44:** 40-43

14 **Koda M**, Maeda Y, Matsunaga Y, Mimura K, Murawaki Y, Horie Y. Hepatocellular carcinoma with sarcomatous change arising after radiofrequency ablation for well-differentiated hepatocellular carcinoma. *Hepatol Res* 2003; **27:** 163-167

15 **Takada Y**, Kurata M, Ohkohchi N. Rapid and aggressive recurrence accompanied by portal tumor thrombus after radiofrequency ablation for hepatocellular carcinoma. *Int J Clin Oncol* 2003; **8:** 332-335

16 **Nicoli N**, Casaril A, Hilal MA, Mangiante G, Marchiori L, Ciola M, Invernizzi L, Campagnaro T, Mansueto G. A case of rapid intrahepatic dissemination of hepatocellular carcinoma after radiofrequency thermal ablation. *Am J Surg* 2004; **188:** 165-167

17 **Ruzzenente A**, Manzoni GD, Molfetta M, Pachera S, Genco B, Donataccio M, Guglielmi A. Rapid progression of hepatocellular carcinoma after Radiofrequency Ablation. *World J Gastroenterol* 2004; **10:** 1137-1140

18 **Kotoh K**, Nakamuta M, Morizono S, Kohjima M, Arimura E, Fukushima M, Enjoji M, Sakai H, Nawata H. A multi-step, incremental expansion method for radio frequency ablation: optimization of the procedure to prevent increases in intra-tumor pressure and to reduce the ablation time. *Liver Int*, in press

19 **Poon RT**, Ng KK, Lam CM, Ai V, Yuen J, Fan ST. Radiofrequency ablation for subcapsular hepatocellular carcinoma. *Ann Surg Oncol* 2004; **11:** 281-289

20 **Caturelli E**. Percutaneous ablative therapies for small hepatocellular carcinoma: radio-frequency or percutaneous ethanol injection? *Radiology* 2000; **216:** 304-306

Science Editor Guo SY **Language Editor** Elsevier HK

PO Box 2345, Beijing 100023, China
www.wjgnet.com
wjg@wjgnet.com

ELSEVIER

World J Gastroenterol 2005;11(43):6833-6838
World Journal of Gastroenterology ISSN 1007-9327

• *RAPID COMMUNICATION* •

Effect of pegylated interferon alpha 2b plus ribavirin treatment on plasma transforming growth factor-β1, metalloproteinase-1, and tissue metalloproteinase inhibitor-1 in patients with chronic hepatitis C

Robert Flisiak, Jerzy Jaroszewicz, Tadeusz W Łapiński, Iwona Flisiak, Danuta Prokopowiczi

Robert Flisiak, Jerzy Jaroszewicz, Tadeusz W Łapiński, Danuta Prokopowicz, Department of Infectious Diseases, Medical University of Bialystok, Poland
Iwona Flisiak, Department of Dermatology and Venereology, Medical University of Bialystok, Poland
Correspondence to: Professor Robert Flisiak, Department of Infectious Diseases, Medical University of Bialystok, 15-540 Bialystok, Zurawia str., 14, Poland. flisiakr@priv.onet.pl
Telephone: +4885-7409481 Fax: +4885-7434613
Received: 2005-04-07 Accepted: 2005-05-12

Abstract

AIM: To evaluate the effect of antiviral treatment on plasma levels of transforming growth factor-β1 (TGF-β1), metalloproteinase 1 (MMP-1), and tissue inhibitor of metalloproteinase-1 (TIMP-1) in patients with chronic hepatitis C.

METHODS: TGF-β1, MMP-1, and TIMP-1 plasma concentrations were measured by an enzyme immunoassay in 28 patients, during 48 wk of treatment with pegylated interferon-alpha 2b (PEG-IFN-α2b) plus ribavirin (RBV) and after 24 wk of follow-up. Patients were divided into two groups: responders (R) and non-responders (NR) related to achieved sustained virologic response. Normal values were evaluated in plasma samples of 13 healthy volunteers.

RESULTS: Baseline plasma concentrations of TGF-β1 and TIMP-1 (30.9±3.7 and 1 506±61 ng/mL respectively) measured in all subjects significantly exceeded the normal values (TGF-β1: 18.3±1.6 ng/mL and TIMP-1: 1 102±67 ng/mL). In contrast, pretreatment MMP-1 mean level (6.5±0.9 ng/mL) was significantly lower than normal values (11.9±0.9 ng/mL). Response to the treatment was observed in 12 patients (43%). TGF-β1 mean concentration measured during the treatment phase decreased to the control level in both groups. However at wk 72, values of NR patients increased and became significantly higher than in R group. TIMP-1 concentrations in R group decreased during the treatment to the level similar to normal. In NR group, TIMP-1 remained significantly elevated during treatment and follow-up phase and significant difference between both groups was demonstrated at wk 48 and 72. MMP-1 levels were significantly decreased in both groups at baseline. Treatment caused rise of its concentration only in the R group, whereas values in NR group remained on the level similar to baseline. Statistically significant difference between groups was noted at wk 48 and 72.

CONCLUSION: These findings support the usefulness of TGF-β1, TIMP-1, and MMP-1 in the management of chronic hepatitis C. Elevated TIMP-1 and low MMP-1 plasma concentrations during antiviral therapy may indicate medication failure.

Key words: HCV; Hepatitis; Liver; Interferons; Fibrosis

Flisiak R, Jaroszewicz J, Lapinski TW, Flisiak I, Prokopowicz D. Effect of pegylated interferon alpha 2b plus ribavirin treatment on plasma transforming growth factor-β1, metalloproteinase-1, and tissue metalloproteinase inhibitor-1 in patients with chronic hepatitis C. *World J Gastroenterol* 2005; 11(43): 6833-6838
http://www.wjgnet.com/1007-9327/11/6833.asp

INTRODUCTION

Transforming growth factor-β1 (TGF-β1) is considered as a pivotal inducer of liver fibrosis acting through activation of hepatic stellate cells (HSCs) and their transformation to myofibroblasts, which are the main source of extracellular matrix (ECM) proteins[1,2]. Moreover, TGF-β1 stimulates the production of tissue inhibitor of TIMP-1 that inhibits MMP activity. This effect is responsible for the inhibition of ECM protein breakdown and its accumulation[3]. TGF-β1 inhibits DNA synthesis serving as a terminator of regenerative cell proliferation and induces apoptosis of hepatocytes[4]. Additionally, TGF-β1 may inhibit stellate cell apoptosis and promote their survival, at least in part as a result of anti-apoptotic effect of TIMP-1[5,6]. On the other hand, TGF-β1 exerts regulatory, mostly immunosuppressive effects on the immune system and as demonstrated recently can also suppress hepatitis C virus (HCV) replication[7,8]. Since HCV infection is related to an immune response, cell proliferation and fibrosis as well as modulation of TGF-β1 can affect the course of chronic hepatitis C. As demonstrated recently, HCV core and

nonstructural proteins regulate biological functions in HSC and increase the secretion of TGF-β1 and the expression of ECM proteins in both HSCs and parenchymal hepatic cells[9,10]. The possible role of TGF-β1, TIMP-1, and MMP-1 as predictive biomarkers of chronic hepatitis activity and progression is supported by recent clinical studies[11-19]. These studies demonstrated association with hepatic function impairment or fibrosis, and only few evaluated possible effects of antiviral treatment on growth factors, but they did not include possible metalloproteinase involvement[20,21].

We undertook this study to evaluate the effect of pegylated interferon-α2b plus ribavirin (PEG-IFN-α2b/RBV) treatment on plasma TGF-β1, TIMP-1, and MMP-1 levels in patients with chronic hepatitis C.

MATERIALS AND METHODS

Patients

Ethical approval for the study was obtained from the Bioethical Committee of the Medical University of Bialystok. Informed consent was obtained from 28 patients (8 females and 20 males, mean age 49±12 years) with chronic hepatitis C, who were included into the protocol of PEG-IFN-α2b (Pegintron™, Schering-Plough) and RBV (Rebetol™, Schering-Plough) treatment. All patients had proven chronic hepatitis C through the presence of anti-HCV antibodies with elevated ALT activities demonstrated at least twice during a 6-mo observation period. Additionally, the disease activity was confirmed by the presence of viral replication and liver biopsy (Hepafix System, Braun, Melsungen, Germany). Patients with HBV infection and a history of alcohol abuse or psychiatric disorders were excluded from the study. Patients received combination therapy with weekly doses of 100 μg PEG-IFN-α2b administered subcutaneously and RBV administered orally at daily doses of 1 000 or 1 200 mg/d based on body weight <75 or ≥75 kg, respectively. The total duration of treatment was 48 wk. Liver biopsy was performed before and after antiviral therapy. Patients were divided into two groups related to sustained virologic response (SVR), defined as undetectable HCV RNA, 24 wk after the end of therapy. Patients who achieved SVR were included into the responder group (R) and those without SVR into non-responder group (NR). Paraffin-embedded biopsy specimens were stained and evaluated using the scoring system according to Scheuer[22]. TGF-β1, TIMP-1, and MMP-1 plasma concentrations were measured at baseline, 24 and 48 wk after treatment and additionally 24 wk after the termination of the treatment (wk 72). Serum liver function tests and scored histological changes were investigated for the possible correlation with TGF-β1, TIMP-1, and MMP-1. Normal values of TGF-β1, TIMP-1, and MMP-1 were collected from 13 healthy volunteers (5 females and 7 males , mean age: 48± 6 years).

Methods

Venous blood for plasma TGF-β1, TIMP-1, and MMP-1 was collected on ice using tubes with EDTA. Samples for TGF-β1 were immediately activated with acetic acid and urea and assayed with ELISA using recombinant human TGF-β soluble receptor Type II (TbR-II) as a solid phase precoated onto a microplate (Quantikine®, R&D Systems Inc., Minneapolis, USA) as described previously[23]. TIMP-1 and MMP-1 were assayed by the two-site ELISA sandwich technique (Amersham Pharmacia Biotech, Little Chalfont, Buckinghamshire, UK) using specific antibodies as a solid phase. MMP-1 assay recognized total human MMP-1, namely free and complexed with TIMP-1. TIMP-1 assay recognized total human TIMP-1, including free and complexed with any of the metalloproteinases bound to the solid phase. TIMP-1 or MMP-1 bound to the solid phase was detected by peroxidase-labeled antibodies. There was no cross-reactivity between TIMP-1 and MMP-1 in these assays. Alanine and aspartate aminotransferase (ALT and AST) activity and bilirubin concentration were measured in serum using a Cobas Mira instrument (Roche).

Statistical analysis

Values were expressed as mean±SE. The significance of the difference was calculated by two-tailed Student's *t* test. For correlation analysis, the Pearson's product moment correlation was performed. $P<0.05$ was considered statistically significant.

RESULTS

Plasma concentrations of TGF-β1 and TIMP-1 measured before PEG-IFN-α2b/RBV treatment (mean: 30.9±3.7 and 1 506±61 ng/mL respectively) significantly exceeded the normal values (18.3±1.6 and 1 102±67 ng/mL respectively). Treatment resulted in a significant decrease of TGF-β1 by wk 24, and its further decline at the end of the treatment as well as 24 wk after its completion to the level similar to normal (Table 1). TIMP-1 plasma mean concentration also decreased, but did not differ significantly from baseline. Moreover, it remained on the level significantly exceeding controls during treatment and follow-up period (Table 1). Mean MMP-1 baseline level (6.5±0.9 ng/mL) was significantly lower than normal (11.9±0.9 ng/mL) but increased during the treatment. After treatment, its level still remained lower than normal but the difference was not significant (Table 1). There was a significant positive correlation between TIMP-1 and aminotransferases as well as between TGF-β1 and AST at baseline (Table 2). A significant correlation was also demonstrated between baseline TGF-β1 or TIMP-1 concentrations and scored fibrosis in pre-treatment liver biopsy specimens (Table 3). No association was

Table 1 Plasma concentrations of TGF-β1, TIMP-1, and MMP-1 during treatment (mean±SE)

	Controls	Weeks after starting treatment			
		0	24	48	72
TGF-β1 (ng/mL)	18.3±1.6	30.9±3.7[a]	21.2±2.8[c]	17.9±2.0[c]	21.0±2.5[c]
TIMP-1 (ng/mL)	1 102±67	1 506±61[a]	1 372±70[a]	1 389±51[a]	1410±66[a]
MMP-1 (ng/mL)	11.9±0.9	6.5±0.9[a]	7.2±1.5[a]	7.5±2.6	8.0±1.6

[a]$P<0.05$ *vs* normal, [c]$P<0.05$ *vs* baseline.

Table 2 Correlation expressed by r-value between biochemical indices of liver injury and TGF-β1, TIMP-1, or MMP-1 in chronic hepatitis C patients before treatment

	Bilirubin	ALT	AST
TGF-β1 (ng/mL)	0.240	0.163	0.388[a]
TIMP-1 (ng/mL)	0.023	0.393[a]	0.370[a]
MMP-1 (ng/mL)	–0.192	–0.130	–0.299

[a]$P<0.05$ biochemical indices *vs* TGF-β1, TIMP-1, and MMP-1.

Table 3 Correlation expressed by r-value between scored histological picture and TGF-β1, TIMP-1, or MMP-1 in chronic hepatitis C patients before treatmen

	Inflammation		Fibrosis
	Portal	Lobular	
TGF-β1 (ng/mL)	0.088	–0.132	0.495[a]
TIMP-1 (ng/mL)	0.091	0.326	0.404[a]
MMP-1 (ng/mL)	0.229	0.360	–0.018

[a]$P<0.05$ histological score *vs* TGF-β1, TIMP-1, and MMP-1

demonstrated between MMP-1 and biochemical or histological signs of liver injury (Tables 2 and 3).

SVR was observed in 12 among 28 patients (43%). Evaluation of baseline liver function tests showed no statistically significant differences between R and NR groups (Table 4). Treatment did not affect bilirubin levels in both groups. Responders demonstrated a significant decrease of ALT and AST activities during the treatment and follow-up. Decline of aminotransferases activity in NR group was only temporal and rose to values significantly higher than in R group after discontinuation of the treatment (Table 4). As demonstrated in Figure 1, scored values of histologic changes were similar before the treatment. There were no significant differences between biopsies preformed before and after the treatment in NR group. In contrast, responders demonstrated improvement after the treatment; however, statistically significant difference between score values at wk 0 and 48 was noted only in respect to portal inflammation.

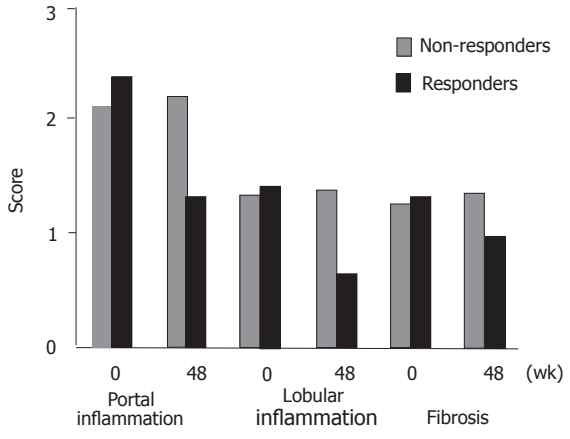

Figure 1 Mean score values of histologic changes in liver biopsy specimens before (wk 0) and after (wk 48) treatment. Statistically significant difference is indicated with arrows.

Table 4 Values of biochemical indices of liver injury during treatment (0, 24, and 48 wk) and 24 wk after its completion (wk 72) in both groups

		Weeks after the beginning of treatment			
		0	24	48	72
Bilirubin	Non-responders	1±0.1	1±0.1	0.7±0.1	0.9±0.1
(mg%)	Responders	1.1±0.1	1.1±0.1	0.9±0.1	1.0±0.1
ALT(U/L)	Non-responders	101±15	40±6[c]	55±20	98±18[a]
	Responders	96±13	35±9[c]	24±5[c]	22±2[c]
AST(U/L)	Non-responders	58±8	30±4[c]	34±6[a,c]	64±10[a]
	Responders	48±6	26±3[c]	20±1[c]	19±2[c]

[a]$P<0.05$ responders *vs* non-responders, [c]$P<0.05$ *vs* baseline.

There were no statistically significant differences in TGF-β1, TIMP-1, and MMP-1 concentrations between R and NR groups at the baseline and 24 wk after the treatment. As demonstrated in Figure 2A, TGF-β1 mean concentration decreased to the control level during treatment in both groups. However, 24 wk after the treatment (wk 72), values in NR patients increased (23.2± 2.3 ng/mL) and became significantly higher than those in R group (18.6±3.7 ng/mL). As shown in Figure 2B, mean concentration of TIMP-1 decreased during the treatment only in R group and there were no statistically significant differences in comparison with controls at wk 24, 48, and 72. In contrast, TIMP-1 concentration in NR group remained significantly elevated (above 1 500 ng/mL) during treatment and follow-up (Figure 2B). Significant difference between both groups was demonstrated at wk 48 and 72. As shown in Figure 2C, MMP-1 levels were significantly decreased in both groups at baseline. Treatment caused rise of its concentration only in the R group, whereas the values in NR group remained on the level similar to baseline. Statistically significant difference between groups was noted at wk 48 and 72 (Figure 2C).

DISCUSSION

The effect of TGF-β1 on liver fibrosis is at least in part related to stimulation of TIMP-1 that affects MMP activity and is responsible for inhibition of ECM protein breakdown[3]. The pivotal role of TGF-β1 in fibrogenesis is initially proved in transgenic mice with overexpression of TGF-β1, causing increase of its plasma levels up to 700 ng/mL and a marked upregulation of TIMP-1 gene expression[24-26]. Recent studies demonstrated that HCV proteins can stimulate secretion of TGF-β1 and production of ECM proteins by HSCs[9,10]. On the other hand, Murata *et al*.[8] showed that TGF-β suppresses viral HCV-RNA replication and can affect the mechanism of liver disease caused by HCV. Chronic liver injury leading to fibrosis displays diminished ECM degradation mainly through TIMP induction following MMP inhibition[3]. As demonstrated recently, TIMP-1 recombinant plasmid has inhibitory effects on the production of types I and III collagens secreted by activated rHSCs *in vitro*[27].

The most important factor affecting TGF-β1 measurement in human beings is from platelets which are an important source of this cytokine[28]. The Quantikine ELISA System is recommended because

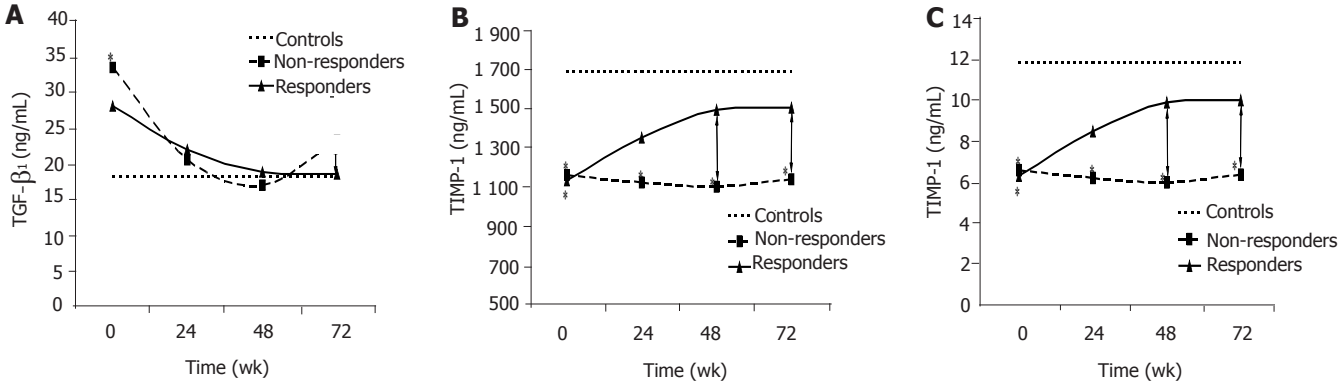

Figure 2 Mean TGF-β1 (**A**), TIMP-1 (**B**), and MMP-1 (**C**) plasma concentrations before and during IFN-α plus RBV therapy as well as 24 wk after its completion (wk 72) in respect to the treatment efficacy. Statistical significance in comparison to normal values is indicated with asterisks and between groups with arrows.

of quick and simple activation with acid and urea that disrupt the majority of TGF-β1 complexes. Mean plasma concentration of TGF-β1 measured in our healthy controls with this method is consistent with the range from more than 20 studies reviewed by Grainger *et al*.[28].

According to our previous research, TGF-β1 and TIMP-1 correlate with the degree of liver insufficiency, hepatocyte injury and degree of fibrosis in human beings with liver cirrhosis and chronic viral hepatitis[12,23,29]. Association between TGF-β1 mRNA in liver specimens and fibrogenic activity in chronic hepatitis is demonstrated for the first time by Castilla *et al*.[30]. Ten years after the association between circulating or tissue TGF-β and liver fibrosis in HCV infection has been confirmed by Kanzler *et al*.[13]. As demonstrated by Yoo *et al*.[31] and Lee *et al*.[32], HBV antigens also stimulate TGF-β1 synthesis. According to Neuman *et al*.[20,33], serum TNF-α reflects the progression of inflammation, whereas TGF-β reflects the degree of fibrosis in HCV patients. A similar relationship has been demonstrated with respect to primary biliary cirrhosis and alcoholic liver disease[34]. Our previous study showed that a positive predictive value of TGF-β1 plasma levels exceeding the upper normal range reaches 96% for liver cirrhosis[23]. According to Boeker *et al*.[11] measurement of plasma TIMP-1 detects cirrhosis with 100% sensitivity but a lower specificity. Lichtinghagen *et al*.[14] demonstrated that MMP-1 mRNA expression increases steadily with fibrosis progression during the course of chronic hepatitis C. Walsh *et al*.[17] who studied liver histology in patients with chronic hepatitis C have underlined the high sensitivity of TIMP-1 and TIMP-2 in detecting advanced liver disease. According to Nie *et al*.[35], there is a significant correlation between circulating and liver levels of TIMP-1 in cirrhotics, indicating that its measurement in plasma may be useful in fibrosis management. These observations indicate the usefulness of both TGF-β1 and TIMP-1 as possible early non-invasive biomarkers for liver fibrosis.

In this study, we confirmed the association between the degree of hepatocyte injury or liver fibrosis and plasma TGF-β1 or TIMP-1 levels in patients with chronic hepatitis C. As the levels of TGF-β1 showed a similar behavior in both groups during therapy, it is unclear whether its decrease is a direct effect of medication on the expression or an effect caused by HCV inhibition. However, measurement carried out 24 wk after treatment demonstrated an association with treatment efficiency. Similar effects on plasma TGF-β1 have been observed by Castilla *et al*.[30] and Neuman *et al*.[20] and in our previous study of chronic hepatitis B[29]. TIMP-1 and MMP-1 concentrations demonstrated significant differences between groups at the end of the treatment and after 24 wk of follow-up. Since plasma TIMP-1 and MMP-1 remained on the baseline level in non-responder group only, lack of their normalization should be considered as a possible indicator of ineffective antiviral therapy. Results of the present study are in accordance with our previous findings, demonstrating the strong association between TGF-β1 or TIMP-1 plasma levels and scored hepatic fibrosis evaluated in biopsy specimens of patients with chronic hepatitis B and C[12]. Since the findings of increased TGF-β1 and TIMP-1 are accompanied with an elevation in plasma carboxyterminal cross-linked telopeptide of type 1 procollagen (ICTP), indicating type I collagen degradation, collagenolytic mechanisms precede TGF-β1/TIMP-1 dependent stimulation of liver fibrosis[12]. Low MMP-1 plasma levels before the treatment in the present study are consistent with this observation as well as in accordance with Murawaki *et al*.[15] who demonstrated a decrease in MMP-1 concentration during histological progression of chronic hepatitis. Moreover, significantly decreased baseline plasma MMP-1 followed by an increase during treatment supports the role of TGF-β1/TIMP-1 dependent mechanism of liver fibrosis in patients with active chronic hepatitis C. Similar effects on MMP-1 and TIMP-1 in patients with chronic hepatitis C have been observed by Ninomiya *et al*.[16] who showed improvement of liver histology after treatment with IFN-α alone. Downregulation of the mechanism causing an increase of MMP-1 activity should be considered as the probable reason for this effect. As we demonstrated recently, treatment of chronic hepatitis B with lamivudine affects TGF-β1, TIMP-1, and MMP-1 plasma levels in a similar way and this mechanism should be recognized as an effect of response to the antiviral treatment,

irrespective of the etiology[29].

Results of this study support the role of TIMP-1 and MMP-1 balance in the TGF-β1 dependent mechanism of liver fibrosis related to HCV infection. Association between hepatic injury and antiviral treatment efficacy suggests their possible usefulness in chronic hepatitis C management. Elevated TIMP-1 and low MMP-1 plasma concentrations during antiviral therapy may indicate medication failure.

REFERENCES

1 **Knittel T**, Janneck T, Muller L, Fellmer P, Ramadori G. Transforming growth factor beta 1-regulated gene expression of Ito cells. *Hepatology* 1996; **24:** 352-360
2 **Williams EJ**, Gaca MD, Brigstock DR, Arthur MJ, Benyon RC. Increased expression of connective tissue growth factor in fibrotic human liver and in activated hepatic stellate cells. *J Hepatol* 2000; **32:** 754-761
3 **Knittel T**, Mehde M, Kobold D, Saile B, Dinter C, Ramadori G. Expression patterns of matrix metalloproteinases and their inhibitors in parenchymal and non-parenchymal cells of rat liver: regulation by TNF-alpha and TGF-beta1. *J Hepatol* 1999; **30:** 48-60
4 **Fausto N**, Liver regeneration. *J Hepatol* 2000; **32:** 19-31
5 **Saile B**, Matthes N, Knittel T, Ramadori G. Transforming growth factor beta and tumor necrosis factor alpha inhibit both apoptosis and proliferation of activated rat hepatic stellate cells. *Hepatology* 1999; **30:** 196-202
6 **Murphy FR**, Issa R, Zhou X, Ratnarajah S, Nagase H, Arthur MJ, Benyon C, Iredale JP. Inhibition of apoptosis of activated hepatic stellate cells by tissue inhibitor of metalloproteinase-1 is mediated via effects on matrix metalloproteinase inhibition: implications for reversibility of liver fibrosis. **J Biol Chem** 2002; **277:** 11069-11076
7 **Prud'homme GJ**, Piccirillo CA. The inhibitory effects of transforming growth factor-beta-1 (TGF-beta1) in autoimmune diseases. *J Autoimmun* 2000; **14:** 23-42
8 **Murata T**, Ohshima T, Yamaji M, Hosaka M, Miyanari Y, Hijikata M, Shimotohno K. Suppression of hepatitis C virus replicon by TGF-beta. *Virology* 2005; ***331:*** 407-417
9 **Bataller R**, Paik YH, Lindquist JN, Lemasters JJ, Brenner DA. Hepatitis C virus core and nonstructural proteins induce fibrogenic effects in hepatic stellate cells. *Gastroenterology* 2004; **126:** 529-540
10 **Taniguchi H**, Kato N, Otsuka M, Goto T, Yoshida H, Shiratori Y, Omata M. Hepatitis C virus core protein upregulates transforming growth factor-beta 1 transcription. *J Med Virol* 2004; **72:** 52-59
11 **Boeker KH**, Haberkorn CI, Michels D, Flemming P, Manns MP, Lichtinghagen R. Diagnostic potential of circulating TIMP-1 and MMP-2 as markers of liver fibrosis in patients with chronic hepatitis C. *Clin Chim Acta* 2002; **316:** 71-81
12 **Flisiak R**, Maxwell P, Prokopowicz D, Timms PM, Panasiuk A. Plasma tissue inhibitor of metalloproteinases-1 and transforming growth factor beta 1--possible non-invasive biomarkers of hepatic fibrosis in patients with chronic B and C hepatitis. *Hepatogastroenterology* 2002; **49:** 1369-1372
13 **Kanzler S**, Baumann M, Schirmacher P, Dries V, Bayer E, Gerken G, Dienes HP, Lohse AW. Prediction of progressive liver fibrosis in hepatitis C infection by serum and tissue levels of transforming growth factor-beta. *J Viral Hepat* 2001; **8:** 430-437
14 **Lichtinghagen R**, Bahr MJ, Wehmeier M, Michels D, Haberkorn CI, Arndt B, Flemming P, Manns MP, Boeker KH. Expression and coordinated regulation of matrix metalloproteinases in chronic hepatitis C and hepatitis C virus-induced liver cirrhosis. *Clin Sci* 2003; **105:** 373-382
15 **Murawaki Y**, Ikuta Y, Idobe Y, Kawasaki H. Serum matrix metalloproteinase-1 in patients with chronic viral hepatitis. *J Gastroenterol Hepatol* 1999; **14:** 138-145
16 **Ninomiya T**, Yoon S, Nagano H, Kumon Y, Seo Y, Kasuga M, Yano Y, Nakaji M, Hayashi Y. Significance of serum matrix metalloproteinases and their inhibitors on the antifibrogenetic effect of interferon-alfa in chronic hepatitis C patients. *Intervirology* 2001; **44:** 227-231
17 **Walsh KM**, Timms P, Campbell S, MacSween RN, Morris AJ. Plasma levels of matrix metalloproteinase-2 (MMP-2) and tissue inhibitors of metalloproteinases -1 and -2 (TIMP-1 and TIMP-2) as noninvasive markers of liver disease in chronic hepatitis C: comparison using ROC analysis. *Dig Dis Sci* 1999; **44:** 624-630
18 **Patel K**, Gordon SC, Jacobson I, Hezode C, Oh E, Smith KM, Pawlotsky JM, McHutchison JG. Evaluation of a panel of non-invasive serum markers to differentiate mild from moderate-to-advanced liver fibrosis in chronic hepatitis C patients. *J Hepatol* 2004; **41:** 935-942
19 **Leroy V**, Monier F, Bottari S, Trocme C, Sturm N, Hilleret MN, Morel F, Zarski JP. Circulating matrix metalloproteinases 1, 2, 9 and their inhibitors TIMP-1 and TIMP-2 as serum markers of liver fibrosis in patients with chronic hepatitis C: comparison with PIIINP and hyaluronic acid. *Am J Gastroenterol* 2004; **99:** 271-279
20 **Neuman MG**, Benhamou JP, Bourliere M, Ibrahim A, Malkiewicz I, Asselah T, Martinot-Peignoux M, Shear NH, Katz GG, Akremi R, Benali S, Boyer N, Lecomte L, Le Breton V, Le Guludec G, Marcellin P. Serum tumour necrosis factor-alpha and transforming growth factor-beta levels in chronic hepatitis C patients are immunomodulated by therapy. *Cytokine* 2002; **17:** 108-117
21 **Anatol P**, Robert F, Danuta P. Effect of interferon alpha2b plus ribavirin treatment on selected growth factors in respect to inflammation and fibrosis in chronic hepatitis C. *World J Gastroenterol* 2005; **11:** 1854-1858
22 **Scheuer PJ**. Classification of chronic viral hepatitis: a need for reassessment. *J Hepatol* 1991; **13:** 372-374
23 **Flisiak R**, Pytel-Krolczuk B, Prokopowicz D. Circulating transforming growth factor beta(1) as an indicator of hepatic function impairment in liver cirrhosis. *Cytokine* 2000; **12:** 677-681
24 **Kanzler S**, Lohse AW, Keil A, Henninger J, Dienes HP, Schirmacher P, Rose-John S, zum Buschenfelde KH, Blessing M. TGF-beta1 in liver fibrosis: an inducible transgenic mouse model to study liver fibrogenesis. *Am J Physiol* 1999; **276:** G1059-G1068
25 **Sanderson N**, Factor V, Nagy P, Kopp J, Kondaiah P, Wakefield L, Roberts AB, Sporn MB, Thorgeirsson SS. Hepatic expression of mature transforming growth factor beta 1 in transgenic mice results in multiple tissue lesions. *Proc Natl Acad Sci USA* 1995; **92:** 2572-2576
26 **Clouthier DE**, Comerford SA, Hammer RE. Hepatic fibrosis, glomerulosclerosis, and a lipodystrophy-like syndrome in PEPCK-TGF-beta1 transgenic mice. *J Clin Invest* 1997; **100:** 2697-2713
27 **Liu WB**, Yang CQ, Jiang W, Wang YQ, Guo JS, He BM, Wang JY. Inhibition on the production of collagen type I, III of activated hepatic stellate cells by antisense TIMP-1 recombinant plasmid. *World J Gastroenterol* 2003; **9:** 316-319
28 **Grainger DJ**, Mosedale DE, Metcalfe JC. TGF-beta in blood: a complex problem. *Cytokine Growth Factor Rev* 2000; **11:** 133-145
29 **Flisiak R**, Al-Kadasi H, Jaroszewicz J, Prokopowicz D, Flisiak I. Effect of lamivudine treatment on plasma levels of transforming growth factor beta1, tissue inhibitor of metalloproteinases-1 and metalloproteinase-1 in patients with chronic hepatitis B. *World J Gastroenterol* 2004; **10:** 2661-2665
30 **Castilla A**, Prieto J, Fausto N. Transforming growth factors beta 1 and alpha in chronic liver disease. Effects of interferon alfa therapy. *N Engl J Med* 1991; **324:** 933-940
31 **Yoo YD**, Ueda H, Park K, Flanders KC, Lee YI, Jay G, Kim SJ. Regulation of transforming growth factor-beta 1 expression

by the hepatitis B virus (HBV) X transactivator. Role in HBV pathogenesis. *J Clin Invest* 1996; **97:** 388-395

32 **Lee DK**, Park SH, Yi Y, Choi SG, Lee C, Parks WT, Cho H, de Caestecker MP, Shaul Y, Roberts AB, Kim SJ. The hepatitis B virus encoded oncoprotein pX amplifies TGF-beta family signaling through direct interaction with Smad4: potential mechanism of hepatitis B virus-induced liver fibrosis. *Genes Dev* 2001; **15:** 455-466

33 **Neuman MG**, Benhamou JP, Malkiewicz IM, Ibrahim A, Valla DC, Martinot-Peignoux M, Asselah T, Bourliere M, Katz GG, Shear NH, Marcellin P. Kinetics of serum cytokines reflect changes in the severity of chronic hepatitis C presenting minimal fibrosis. *J Viral Hepat* 2002; **9:** 134-140

34 **Neuman M**, Angulo P, Malkiewicz I, Jorgensen R, Shear N, Dickson ER, Haber J, Katz G, Lindor K. Tumor necrosis factor-alpha and transforming growth factor-beta reflect severity of liver damage in primary biliary cirrhosis. *J Gastroenterol Hepatol* 2002; **17:** 196-202

35 **Nie QH**, Cheng YQ, Xie YM, Zhou YX, Bai XG, Cao YZ. Methodologic research on TIMP-1, TIMP-2 detection as a new diagnostic index for hepatic fibrosis and its significance. *World J Gastroenterol* 2002; **8:** 282-287

Science Editor Wang XL and Guo SY **Language Editor** Elsevier HK

PO Box 2345, Beijing 100023, China
www.wjgnet.com
wjg@wjgnet.com

ELSEVIER

World J Gastroenterol 2005;11(43):6839-6842
World Journal of Gastroenterology ISSN 1007-9327

• *RAPID COMMUNICATION* •

Prevalence and risk factors of stress-induced gastrointestinal bleeding in critically ill children

Chookhuan Nithiwathanapong, Sanit Reungrongrat, Nuthapong Ukarapol

Chookhuan Nithiwathanapong, Sanit Reungrongrat, Nuthapong Ukarapol, Department of Pediatrics, Faculty of Medicine, Chiang Mai University, Chiang Mai 50200, Thailand
Correspondence to: Nuthapong Ukarapol, MD, Division of Pediatric Gastroenterology/Hepatology, Department of Pediatrics, Chiang Mai University, Chiang Mai 50200, Thailand. nukarapo@chiangmai.ac.th
Telephone: +66-53-945412 Fax: +66-53-946461
Received: 2005-03-31 Accepted: 2005-05-04

Abstract

AIM: To assess the frequency and the risk factors of stress-induced gastrointestinal (GI) bleeding in children admitted to a pediatric intensive care unit (PICU).

METHODS: The medical records of children aged between 1 month and 15 years admitted to the PICU between January 2002 and December 2002 were reviewed. Demographic data, indications for PICU admission, principle diagnosis, and basic laboratory investigations were recorded. Previously described factors for stress ulcer bleeding (mechanical ventilation, sepsis, acute respiratory distress syndrome, renal insufficiency, coagulopathy, thrombocytopenia, and intracranial pathology) were used as independent variables in a multivariate analysis.

RESULTS: One hundred and seventy of two hundred and five medical records were eligible for review. The most common indication for PICU admission was respiratory failure (48.8%). Twenty-five children received stress ulcer bleeding prophylaxis with ranitidine. The incidence of stress ulcer bleeding was 43.5%, in which 5.3% were clinically significant bleeding. Only mechanical ventilation and thrombocytopenia were significantly associated with stress ulcer bleeding using the univariate analysis. The odds ratio and 95% confidence intervals were 5.13 (1.86-14.12) and 2.26 (1.07-4.74), respectively. However, the logistic regression analysis showed that mechanical ventilation was the only significant risk factor with the odds ratio of 14.1.

CONCLUSION: The incidence of gastrointestinal bleeding was high in critically ill children. Mechanical ventilation was an important risk factor for gastrointestinal bleeding.

Key words: Gastrointestinal; Hemorrhage; Stress; Risk factor; Child

Nithiwathanapong C, Reungrongrat S, Ukarapol N. Prevalence and risk factors of stress-induced gastrointestinal bleeding in critically ill children. *World J Gastroenterol* 2005;11(43):6839-6842
http://www.wjgnet.com/1007-9327/11/6839.asp

INTRODUCTION

Stress ulcer bleeding is one of the common complications in critically ill patients admitted to the intensive care unit. Its incidence in adults ranges from 0.17% to 14%, depending on the diagnostic criteria, patient selection, and methods of investigation[1-4]. There have been a few reports of this condition in pediatric populations with the incidence varying from 10% in a pediatric intensive care unit to 53% in a neonatal intensive care unit[5,6]. This study was designed to assess the frequency and the risk factors of stress-induced upper gastrointestinal bleeding in critically ill children admitted to a pediatric intensive care unit.

MATERIALS AND METHODS

Patients

All medical records of children younger than 15 years admitted to the PICU between January 2002 and December 2002 at Chiang Mai University Hospital were retrospectively reviewed. Our hospital is a tertiary care center with a facility of six-bed PICU, taking care of approximately 83% of medical and 17% of surgical pediatric patients. The general indications for admission included respiratory/cardiovascular failure, shock, coma, post-operative care, and patients requiring intensive monitoring. The patients with duration of admission in PICU shorter than 48 h, positive previous history of GI bleeding, recent GI tract surgery, brain death, and epistaxis/oropharyngeal bleeding were excluded. Demographic data, indications for PICU admission, and principle diagnosis as well as basic laboratory investigations including hemoglobin level, platelet count, coagulation studies, blood urea nitrogen (BUN), creatinine (Cr), and liver function tests were recorded. Upper GI bleeding during PICU admission was categorized as overt and clinically significant bleeding. Overt GI bleeding (OB) was diagnosed, if there was evidence of hematemesis, coffee ground gastric content, or melena;

whereas clinically significant bleeding (CSB) was defined as overt GI bleeding associated with major changes in vital signs, namely a decrease in blood pressure greater than 20 mmHg, an increase in heart rate of >20 beats above the baseline value, and a decrease in hemoglobin level of more than 2 g/dL. Based on previous studies in adults, potential risk factors were used. These were the use of mechanical ventilation, sepsis, acute respiratory distress syndrome (ARDS), renal insufficiency, coagulopathy, thrombocytopenia, and intracranial pathology. The diagnostic criteria for these conditions were: sepsis-at least two of the following, body temperature >38 °C or <36 ° C, heart rate >160/min (infant) or >150/min (child) or >90/min (adolescent), WBC >15 000 or <4000/mm^3, and band form >10% or there was a positive blood culture; ARDS - positive alveolar infiltration in both lungs on chest X-ray and PaO_2/FiO_2 <200 without evidence of left-sided heart failure; *renal insufficiency* - Cr >2 mg/dL, or requiring dialysis; *coagulopathy* - prothrombin time (PT) >3s and partial thromboplastin time (PTT) >10 s above the control value; *thrombocytopenia* -'platelet count<100 000/mm^3; *intracranial pathology* - abnormal imaging study, meningitis, or encephalitis. This study protocol was approved by the Research Ethic Committee of Chiang Mai University.

Statistical analysis

All data were assessed by SPSS program. Cross-tabulations were analyzed using the χ^2 test, presented as the odds ratio and 95% confidence interval, in which a $P<0.05$ was considered statistically significant. Multivariate analysis of various independent variables was performed using logistic regression modeling.

RESULTS

Over the 12-month period, 205 of 258 medical records were available for review (53 records were missing). Thirty-five cases were excluded for the following reasons: duration of admission shorter than 48 h (n = 28), incomplete medical records (n = 3), epistaxis (n = 2), brain death (n = 1), and recent gastrointestinal surgery (n = 1). Therefore, a total of 170 charts were eligibly reviewed. There were 89 males (52.4%) with an average age of 3.8 years. The total duration of admission was 7.2 d (2-35 d). The most common indication for PICU admission was respiratory failure (48.8%). The demographic data of children with and without bleeding are shown in Table 1. Twenty-five children received stress ulcer bleeding prophylaxis, in which ranitidine was used in 22 cases with a dosage of 3 mg/kg/d; whereas the other three patients received antacids. In the subgroup of children who received stress ulcer prophylaxis, 14 cases developed upper GI hemorrhage (3 CSB and 11 OB); whereas stress ulcer bleeding occurred in 60 of 145 cases who did not receive the prophylactic treatment (6 CSB and 54 OB). GI bleeding complicated 43.5% of cases admitted to the PICU and 5.3% had clinically significant bleeding. Twenty-two percent of patients with CSB were diagnosed as dengue hemorrhagic fever, compared to none in the patients without bleeding.

Table 1 Demographic data of children with and without stress-induced GI bleeding

Characteristic	Bleeding (n = 74)	No bleeding (n = 96)	P
Age (yr)[1]	3.82 (0.44)	3.84 (0.40)	0.977
Sex, male	41	48	0.484
Duration of admission (d)[1]	8.23 (0.78)	6.41 (0.58)	0.062
Underlying diseases			
Respiratory system	8	15	0.445
Cardiovascular system	9	18	
Neurological system	19	25	
Hemato/oncologic system	11	11	
Infections/HIV	14	9	
Gastrointestinal system	5	6	
Others	8	12	

[1]Presented as mean±SE.

Among the independent variables, only mechanical ventilation and thrombocytopenia were significantly associated with stress ulcer bleeding using the univariate analysis. The odds ratio and 95%CI were 5.13 (1.86-14.12) and 2.26 (1.07-4.74), respectively (Table 2). Using multivariate analysis, only mechanical ventilation was found to be significantly associated with the development of gastrointestinal bleeding in critically ill patients ($P<0.05$). In our study, stress ulcer prophylaxis did not reduce the risk of bleeding. The overall mortality rate was 18.8%. Gastrointestinal bleeding and transfusion requirements were associated with high mortality ($P<0.05$).

DISCUSSION

Stress-induced gastrointestinal lesions, including gastritis, erosions, gastric, and duodenal ulcers, can result in significant upper gastrointestinal hemorrhage, increased morbidity and mortality[2]. The prevalence varies between studies[1-6]. In our series, 5% of the cases developed clinically significant bleeding which is considerably higher than that in previous studies performed in pediatric population[5,7]. This might result from a relatively high prevalence of hemorrhagic fever which commonly causes thrombocytopenia and subsequent gastrointestinal bleeding in our region. As noted in our report, 22% of the cases with CSB were diagnosed as dengue hemorrhagic fever. Additionally, we did not routinely use stress ulcer prophylaxis in all patients, and patients with ranitidine prophylaxis did not receive the recommended dose of 6 mg/kg/d[8]. This may explain the poor beneficial prophylactic effect noted in our study. Apart from clinically significant bleeding, we also found a high prevalence of overt upper gastrointestinal bleeding (38.2%), which is comparable to the retrospective report section from Kuusela *et al.* in neonates[6]. However, this figure could be exceptionally high due to a possibility of inclusion of traumatic nasogastric tube injuries which are very difficult to be documented in such a retrospective design and we did not routinely perform endoscopy in all children to delineate the cause of upper GI bleeding during the study period. Although we believe that the prevalence

Table 2 Risk factors for stress-induced GI bleeding in children (*n* = 170)

Risk factors		*n*	Gastrointestinal bleeding (%)	Odds ratio (95%CI) simple regression	Odds ratio (95%CI) multiple regression
Mechanical ventilation	Yes	139	49.6	5.126 (1.861–14.118)	14.096 (2.205–90.112)
	No	31	16.1	*P* = 0.001	*P* = 0.005
Thrombocytopenia	Yes	37	59.4	2.256 (1.073–4.745)	3.462 (0.843–14.216)
	No	132	39.4	*P* = 0.030	*P* = 0.085
Renal insufficiency	Yes	9	77.8	4.858 (0.978–24.124)	2.763 (0.326–23.426)
	No	160	43.1	*P* = 0.035	*P* = 0.351
Prolonged PT	Yes	34	64.7	2.292 (0.946–5.551)	1.222 (0.289–5.161)
	No	32	44.4	*P* = 0.064	*P* = 0.785
Prolonged PTT	Yes	37	62.2	2.071 (0.876–4.899)	1.198 (2.640–5.446)
	No	52	44.2	*P* = 0.095	*P* = 0.815
ARDS	Yes	96	46.9	2.050 (0.912–4.610)	0.772 (0.171–3.487)
	No	54	38.5	*P* = 0.080	*P* = 0.737
Sepsis	Yes	69	49.3	1.481 (0.799–2.748)	1.234 (0.325–4.691)
	No	101	39.6	*P* = 0.212	*P* = 0.757
Intracranial pathology	Yes	32	46.8	1.181 (0.546–2.556)	1.192 (0.283–5.010)
	No	138	42.8	*P* = 0.672	*P* = 0.811

reported in this study might be over-estimated, it discerns a significant magnitude of the problem that requires careful medical attention. Similar to previous studies in adults and children, the mechanical ventilation was found to be the most significant risk factor for stress-induced gastrointestinal bleeding in our study[1,2,5,6]. Although coagulopathy is also noted as a significant independent risk factor in some studies[1,2,5,7], this was not observed in our series using multivariate analysis. A further prospective study with a larger sample size is needed.

Imbalance between protective and destructive factors has been postulated as a basic pathophysiology of GI bleeding. Increased acid production and decreased gastric blood flow, secondary to hypotension and metabolic acidosis, are composed of major physiologic responses leading to mucosal injuries. Hemorrhagic gastritis affects mainly the gastric body as it is the most vulnerable area for ischemic injury[4]. As a result, prophylactic strategies with H_2RA and cytoprotective agents have been widely prescribed to the critically ill patients admitted to the intensive care unit. Lacroix *et al.*[9] have reported a significant increase in the gastric pH following cimetidine prophylaxis stress ulcer bleeding in children, but no prophylactic benefit was demonstrated in their study. Kuusela *et al.*[10] showed that short-term prophylactic ranitidine treatment could prevent gastric mucosal lesions in newborn infants under stress. Cook *et al.*[11] performed a meta-analysis and showed that H_2RA significantly reduces clinically important bleeding over sucralfate and antacids. However, overgrowth of Gram-negative bacteria following the increase of gastric pH by antisecretory agents can be associated with ventilator-associated pneumonia (VAP)[12,13]. Lopriore *et al.*[14] reported that 8.4% of mechanically ventilated children develop VAP. Among these, more children prophylactically treated with ranitidine tend to be associated with VAP than those in the control group (11.1% *vs* 6.2%), despite no statistical significance. The use of sucralfate, since its introduction, seems logically useful in preventing this complication. Unfortunately, this hypothesis was not supported by the large meta-analysis study[11].

Ben-Menachem *et al.*[15] did a cost-effective analysis on stress ulcer prophylaxis and suggested that the cost of prophylaxis is substantial and may be prohibitive in ICU patients at low risk of developing stress-related hemorrhage. Therefore, several authors have recently suggested that such prophylaxis should be selective and may be indicated only for patients at high risk, particularly in those with mechanical ventilation and coagulopathy[2,7]. However, the cost estimation in PICU on this issue has not been well studied.

In conclusion, the incidence of gastrointestinal bleeding is high in critically ill children. Mechanical ventilation is a significant risk factor for gastrointestinal bleeding.

REFERENCES

1 **Schuster DP**, Rowley H, Feinstein S, McGue MK, Zuckerman GR. Prospective evaluation of the risk of upper gastrointestinal bleeding after admission to a medical intensive care unit. *Am J Med* 1984; **76**: 623-630

2 **Cook DJ,** Fuller HD, Guyatt GH, Marshall JC, Leasa D, Hall R, Winton TL, Rutledge F, Todd TJ, Roy P. Risk factors for gastrointestinal bleeding in critically ill patients. Canadian Critical Care Trials Group. *N Engl J Med* 1994; **330:** 377-381

3 **Pimentel M**, Roberts DE, Bernstein CN, Hoppensack M, Duerksen DR. **Clinically significant gastrointestinal bleeding in** critically ill patients in an era of prophylaxis. *Am J Gastroenterol* 2000; **95**: 2801-2806

4 **Fusamoto H**, Hagiwara H, Meren H, Kasahara A, Hayashi N, Kawano S, SugimotoT, Kamada T. A clinical study of acute gastrointestinal hemorrhage associated with various shock states. *Am J Gastroenterol* 1991; **86**: 429-433

5 **Chaibou M**, Tucci M, Dugas MA, Farrell CA, Proulx F, Lacroix J. Clinically significant upper gastrointestinal bleeding

acquired in a pediatric intensive care unit: a prospective study. *Pediatrics* 1998; **102**: 933-938

6 **Kuusela AL**, Maki M, Ruuska T, Laippala P. Stress-induced gastric findings in critically ill newborn infants: frequency and risk factors. *Intensive Care Med* 2000; **26**: 1501-1506

7 **Lacroix J**, Nadeau D, Laberge S, Gauthier M, Lapierre G, Farrell CA. Frequency of upper gastrointestinal bleeding in a pediatric intensive care unit. *Crit Care Med* 1992; **20**: 35-42

8 **Harrison AM**, Lugo RA, Vernon DD. Gastric pH control in critically ill children receiving intravenous ranitidine. *Crit Care Med* 1998; **26**: 1433-1436

9 **Lacroix J**, Infante-Rivard C, Gauthier M, Rousseau E, van Doesburg N. Upper gastrointestinal tract bleeding acquired in a pediatric intensive care unit: prophylaxis trial with cimetidine. *J Pediatr* 1986; **108**: 1015-1018

10 **Kuusela AL**, Ruuska T, Karikoski R, Laippala P, Ikonen RS, Janas M, Maki M. A randomized, controlled study of prophylactic ranitidine in preventing stress-induced gastric mucosal lesions in neonatal intensive care unit patients. *Crit Care Med* 1997; **25**: 346-351

11 **Cook DJ**, Reeve BK, Guyatt GH, Heyland DK, Griffith LE, Buckingham L, Tryba M. Stress ulcer prophylaxis in critically ill patients: Resolving discordant meta-analyses. *JAMA* 1996; **275**: 308-314

12 **Tryba M**. Risk of acute stress bleeding and nosocomial pneumonia in ventilated intensive care unit patients: sucralfate versus antacids. *Am J Med* 1987; **83** :117-124

13 **Prod'hom G**, Leuenberger P, Koerfer J, Blum A, Chiolero R, Schaller MD, Perret C, Spinnler O, Blondel J, Siegrist H, Saghafi L, Blanc D, Francioli P. Nosocomial pneumonia in mechanically ventilated patients receiving antacid, ranitidine, or sucralfate as prophylaxis for stress ulcer. A randomized controlled trial. Ann Intern Med 1994; **120:** 653-662

14 **Lopriore E**, Markhorst DG, Gemke RJ. Ventilator-associated pneumonia and upper airway colonisation with Gram negative bacilli: the role of stress ulcer prophylaxis in children. *Intensive Care Med* 2002; **28**: 763-767

15 **Ben-Menachem T**, McCarthy BD, Fogel R, Schiffman RM, Patel RV, Zarowitz BJ, Nerenz DR, Bresalier RS. Prophylaxis for stress-related gastrointestinal hemorrhage: a cost effectiveness analysis. *Crit Care Med* 1996; **24**: 338-345

Sciencel Editor Wang XL and Guo SY **Language Editor** Elsevier HK

PO Box 2345, Beijing 100023, China
www.wjgnet.com
wjg@wjgnet.com

ELSEVIER

World J Gastroenterol 2005;11(43):6843-6847
World Journal of Gastroenterology ISSN 1007-9327

• *RAPID COMMUNICATION* •

Favorable response to subcutaneous administration of infliximab in rats with experimental colitis

John K Triantafillidis, Apostolos E Papalois, Aikaterini Parasi, Emmanuel Anagnostakis, Stavros Burnazos, Aristofanis Gikas, Emmanuel G Merikas, Emmanuel Douzinas, Maria Karagianni, Helen Sotiriou

John K Triantafillidis, Emmanuel Anagnostakis, Aristofanis Gikas, Emmanuel G Merikas, Department of Gastroenterology, "Saint Panteleimon" General State Hospital, Nicea, Greece
Apostolos E Papalois, Stavros Burnazos, Emmanuel Douzinas, Experimental Research Unit, ELPEN Company, Athens, Greece
John K. Triantafillidis, Apostolos E. Papalois, Aristofanis Gikas, Research Group of the Hellenic Society of Gastrointestinal Oncology, Greece
Aikaterini Parasi, Maria Karagianni, Helen Sotiriou, Department of Pathology, "Saint Panteleimon" General State Hospital, Nicea, Greece
Correspondence to: John K Triantafillidis MD, 8, Kerasountos Street, 12461, Haidari, Athens, Greece. jkt@panafonet.gr
Telephone: +210-5819481 Fax: +210-5810790
Received: 2005-03-23 Accepted: 2005-04-30

Abstract

AIM: To investigate the influence of infliximab (Remicade) on experimental colitis produced by 2,4,6,trinitrobenzene sulfonic acid (TNBS) in rats.

METHODS: Thirty-six Wistar rats were allocated into four groups (three groups of six animals each and a fourth of 12 animals). Six more healthy animals served as normal controls (Group 5). Group 1: colitis was induced by intracolonic installation of 25 mg of TNBS dissolved in 0.25 mL of 50% ethanol and infliximab was subcutaneously administered at a dose of 5 mg/kg BW; Group 2: colitis was induced and infliximab was subcutaneously administered at a dose of 10 mg/kg BW; Group 3: colitis was induced and infliximab was subcutaneously administered at a dose of 15 mg/kg BW; Group 4: colitis was induced without treatment with infliximab. Infliximab was administered on d 2–6. On the 7th d, all animals were killed. The colon was fixed in 10% buffered formalin and examined by light microscopy for the presence and activity of colitis and the extent of tissue damage. Tumor necrosis factor-alpha (TNF-α) and malondialdehyde (MDA) were also measured.

RESULTS: Significant differences concerning the presence of reparable lesions and the extent of bowel mucosa without active inflammation in all groups of animals treated with infliximab compared with controls were found. Significant reduction of the tissue levels of TNF-α in all groups of treated animals as compared with the untreated ones was found (0.47±0.44, 1.09±0.86, 0.43±0.31 *vs* 18.73±10.53 respectively). Significant reduction in the tissue levels of MDA was noticed in group 1 as compared to group 4, as well as between groups 2 and 4.

CONCLUSION: Subcutaneous administration of infliximab reduces the inflammatory activity as well as tissue TNF-α and MDA levels in chemical colitis in rats. Infliximab at a dose of 5 mg/kg BW achieves better histological results and produces higher reduction of the levels of TNF-α than at a dose of 10 mg/kg BW. Infliximab at a dose of 5 mg/kg BW produces higher reduction of tissue MDA levels than at a dose of 15 mg/kg BW.

Key words: Experimental colitis; Infliximab; Inflammatory bowel disease; Tumor necrosis factor-alpha; Malondialdehyde; Ulcerative colitis

Triantafillidis JK, Papalois AE, Parasi A, Anagnostakis E, Burnazos S, Gikas A, Merikas EG, Douzinas E, Karagianni M, Sotiriou H. Favorable response to subcutaneous administration of infliximab in rats with experimental colitis. *World J Gastroenterol* 2005; 11(43):6843-6847
http://www.wjgnet.com/1007-9327/11/6843.asp

INTRODUCTION

Ulcerative colitis is a chronic relapsing inflammatory condition involving the large bowel of unknown etiology. Clinical manifestations are considered to be the result of an imbalance between proinflammatory and inflammatory cytokines, resulting in inflammation and clinical symptoms. Activated T-lymphocytes release cytokines, thereby recruiting a large number of inflammatory cells in the mucosa. Activation of these cells causes further production of cytokines, cell recruitment and inflammation. In addition to cytokines, leukotrienes, thromboxane, and reactive oxygen species are released from activated mucosal cells[1]. This uncontrolled immune system activation results in the sustained overproduction of reactive metabolites of oxygen and nitrogen[2]. It has been suggested that self-sustaining cycles of oxidant formation may amplify flare-ups of inflammation and mucosal injury in ulcerative colitis[3]. Treatment of ulcerative colitis includes a wide range of anti-inflammatory and immunosuppressant drugs

with satisfactory results.

TNF-α is a pleiotropic cytokine with important proinflammatory and immunomodulatory properties. This cytokine plays a significant role in a number of inflammatory disorders including inflammatory bowel disease[4]. It has been shown that administration of the chimeric anti-TNF-α antibody in patients with active Crohn's disease results in a dramatic improvement of many clinical and laboratory parameters[5,6]. One of the most striking findings of the initially performed clinical trials is the observation that infliximab administered at a dose of 5 mg/kg BW results in better patients' improvement than at the dose of 10 or 15 mg/kg BW. Infliximab has also been administered in severe ulcerative colitis patients with promising results[7-9], though the clinical benefit is not prominent in patients refractory to previous administration of steroids[10,11]. Experimental evidence suggests that TNF-α may also play a role in the pathogenesis of experimental colitis[12].

The aim of this study was to investigate the influence of infliximab on experimental colitis in rats, produced by TNBS and to estimate its influence on the oxidative stress accompanying this model of colitis.

METHODS

The experimental procedures described below were approved by the Animal Care Committee according to the European Union Act and Greek Law 160, A-64, May, 1991.

General preparation

Adult male Wistar rats weighing 200-240 g were allowed to adapt to our laboratory conditions 1 wk prior to the experiment. They were housed individually in cages at a constant temperature (22 °C) and in a 12-h d/night cycle with free access to food and water. A total number of 36 rats were used. They were randomly allocated into five groups. *Group 1*: experimental colitis was induced and infliximab was subcutaneously administered at a dose of 5 mg/kg BW ("Infliximab 5"); *Group 2*: experimental colitis was induced and infliximab was subcutaneously administered at a dose of 10 mg/kg BW ("Infliximab 10"); *Group 3*: experimental colitis was induced and infliximab was subcutaneously administered at a dose of 15 mg/kg BW ("Infliximab 15"); *Group 4*: experimental colitis was induced without treatment with infliximab (12 animals) ("Untreated"). Six more healthy animals served as controls (Group 5). On the 7th d, all animals were killed and the colon was removed. The same part of rat's colon was used for histology as well as for MDA and TNF-α estimation.

Induction of experimental colitis

Distal colitis was induced by intracolonic installation of 25 mg of TNBS dissolved in 0.25 mL of 50% ethanol. The solution was injected into the colon 8 cm proximal to the anus with a PE-50 cannula. In order to ensure that TNBS-ethanol solution was not immediately expelled by the rat, the cannula was left in place for 15 s prior to its removal.

Drug administration

Infliximab was administered subcutaneously only in groups 1, 2, and 3 on d 2-6 at the doses of 5, 10 and 15 mg/kg BW, respectively. The subcutaneous administration has not previously been tried in both men and animals. We chose to administer the drug for five consecutive d and not to follow the usual scheme of administration of infliximab in patients with Crohn's disease because we were unable to predict the exact serum levels of the drug following the subcutaneous administration. A second reason was the fact that in this model of experimental colitis, the recommended time to kill the animals was 7 d. Following two or more weeks, the macro- and microscopic lesions were usually not detectable in the survived animals. Healthy control animals were given a subcutaneous dose of normal saline from d 2 to 6.

Histology

Specimens were fixed in 10% buffered formalin and embedded in paraffin blocks (3-4 blocks for each case). Then hematoxylin-eosin stained sections were blindly examined by two pathologists. In each case, the extent of lesions (expressed as a percentage of tissue damage of the whole bowel length) was estimated. The histological lesions such as active ulcers and erosions and reparable lesions (newly re-epithelized lesions or granulation tissue beneath cylindrical epithelium) were estimated. The extent of mucosa without signs of active inflammation was also estimated as previously described[13-16].

Tissue malondialdehyde (MDA) estimation

The MDA measurement was based on the reaction of a chromogenic reagent, *N*-methyl-2-phenylindole (MPI), with MDA at 45°C. One molecule of MDA reacted with two molecules of MPI to yield a stable chromophore with maximum absorbance at 586 nm. The reagents used included Reagent MPI, 10.3 mmol/L *N*-methyl-2-phenylindole in acetonitrile, MDA standard, 10 mmol/L 1,1,3,3-tetramethoxypropane in 20 mmol/L Tris-HCl, 500 mmol/L butylated-hydroxytoluene, in acetonitrile, 20 mmol/L Tris buffer pH 7.4, 0.9% NaCl, 37% (12 mol/L) HCl, methanol, HPLC grade, acetonitrile and HPLC grade. Before the procedure, three volumes of the MPI reagent were diluted with one volume of 100% methanol. Tissue samples were rinsed with ice-cold isotonic saline before homogenization which was carried-out using Tris buffer 20 mmol/L pH 7.4 and an ULTRA-TURRAX (IKA-Labortecnik) blender. One milliliter buffer was used for 0.1 g of tissue. Ten milliliters of 500 mmol/L BHT was added to 1 mL of tissue homogenate to prevent sample oxidation. The homogenate was centrifuged at 3 000 r/min at 4 °C for 10 min. Then 0.2 mL of sample (plasma or supernatant of tissue homogenate) and 0.65 mL of diluted MPI reagent were added to a polypropylene microcentrifuge tube. The mixture was vortexed and then 0.15 mL of 12 mol/L HCl was added. Tubes were incubated at 45 °C for 60 min and centrifuged at 6 000 r/min.

Table 1 Comparison of histological lesions in treated and untreated groups of animals (mean±SD)

Group	Active ulcers and erosions	*P* value	Reparative lesions	*P* value
1 (Infliximab 5, *n* = 6)	0.07±0.12	0.30	0.38±0.12	0.0001
2 (Infliximab 10, *n* = 6)	3.77±5.07	0.42	0.80±0.14	0.0001
3 (Infliximab 15, *n* = 6)	25.02±38.90	1.00	1.00±0.47	0.0001
4 (Untreated, *n* = 12)	25.00±38.91		15.00±5.48	

Table 2 Percentage of bowel area without active inflammation in treated and untreated groups of animals (mean±SD)

Group	Percentage of mucosa without active inflammation	*P* value
1 (Infliximab 5)	99.55±0.19	0.049
2 (Infliximab 10)	95.43±5.15	0.088
3 (Infliximab 15)	73.98±39.29	0.705
4 (Untreated)	60.00±37.18	

Table 3 Tissue TNF-α levels in treated and untreated groups of animals (mean±SD)

Group	Tissue TNF-α (pg/mL)	*P* value
1 (Infliximab 5)	0.47±0.44	<0.0001
2 (Infliximab 10)	1.09±0.86	<0.0001
3 (Infliximab 15)	0.43±0.31	<0.0001
4 (Untreated)	18.73±10.53	
5 (Healthy animals)	0.00+/–0.0	

Table 4 Mean value of tissue malondialdehyde in treated and untreated groups of animals (mean±SD)

Group	Serum malondialdehyde (μmol/l)	*P* value
1 (Infliximab 5)	1.85±0.20	0.017
2 (Infliximab 10)	1.84±0.37	0.011
3 (Infliximab 15)	2.29±0.56	0.272
4 (Untreated)	2.73±0.46	
5 (Healthy animals)	1.11+/–0.19	

for 15 min. Then 0.8 mL of the supernatant was measured at 586 nm. MDA standards for the standard curve were made by dilutions of the stock 10 mm TMOP solution. The final concentrations were 2.08, 4.16, 8.33, 12.5 and 16.66 μmol/L and the assay procedure was followed as for the samples. The absorbance was 0.059, 0.124, 0.264, 0.4, and 0.545 respectively.

Tissue TNF-α estimation

TNF-α was determined after tissue homogenization by ELISA. In order to avoid errors in the interpretation of results, a specific rat antibody was used (antirat, DIACLONE Research) instead of human antibody against TNF-α.

Statistical analysis

Data were presented as mean±SD. Statistical comparisons between groups were made by one-way ANOVA followed by Dunnett's (two-sided) test. A difference between treated (1-3 groups) and untreated (group 4) animals was considered statistically significant at the level of $P<0.05$. Computations were done using the statistical package SPSS (version 11.0).

RESULTS

Histology

Table 1 shows the percentage of bowel area with the presence of active ulcers and erosions and reparative lesions observed in the treated and untreated groups of animals. Significant differences concerning the presence of reparable lesions between all groups of animals treated with infliximab compared to the untreated ones were found. Though differences were obvious between groups 1 and 2, they did not reach statistical significance (Table 1).

Table 2 shows the extent of mucosa without active inflammation in all groups of animals expressed as a percentage (mean value). Significant differences between the three groups of treated animals compared to the untreated ones were observed.

TNF-α tissue levels (pg/mL) (mean value)

The levels of tissue TNF-α in all groups are shown in Table 3. A significant reduction of the tissue levels of TNF-α was found in all groups of treated animals compared to the untreated ones.

Tissue malondialdehyde levels (μM)

The levels of tissue MDA in the treated and untreated animals are shown in Table 4. A significant reduction was noticed in group 1 compared to group 4, as well as between groups 2 and 4. No significant differences between groups 3 and 4 were noticed.

DISCUSSION

The findings of this experimental study in rats suggested that subcutaneous administration of infliximab was biologically effective; infliximab at doses of 5, 10, and 15 mg/kg BW could reduce the histological changes as observed in this particular experimental model; infliximab could significantly reduce tissue levels of TNF-α and MDA; suggesting that this molecule has probably antioxidant properties though the latter could be the consequence of its anti-inflammatory action.

In more details, subcutaneous administration of infliximab resulted in a significant amelioration of inflammatory histological lesions, a finding which was more prominent in the group of animals receiving 5 mg/kg per d. Administration of the drug resulted in a statistically significantly smaller area of large bowel with reparable lesions compared to the untreated group of animals, although the percentage of bowel area with active ulcers and erosions did not differ significantly between treated and untreated animals. It was also shown that the percentage of bowel area with normal mucosa was

significantly larger only in the group treated with 5 mg/kg BW of infliximab as compared to untreated animals. The percentage of bowel area with normal mucosa did not differ significantly between groups receiving 10 and 15 mg/kg BW and the untreated group of animals. Wooddruff *et al*.[17] also showed that a single IV dose of infliximab before the induction of experimental colitis results in a significant reduction of the severity of the lesions.

In our study, all doses of infliximab significantly reduced the tissue levels of TNF-α, suggesting that TNF-α plays a significant pathogenetic role in this model of colitis as well. The IV dose of 5 mg/kg BW is the currently recommended one for the treatment of patients with active Crohn's disease. The beneficial effect of infliximab observed in this experimental model is in accordance with clinical observations showing beneficial clinical effects on some patients with severe ulcerative colitis[7-9]. TNF-α is a 17-ku proinflammatory cytokine produced by monocytes, macrophages, and T cells. The biological actions of this cytokine include induction of acute-phase response, cachexia, and potentially lethal shock[18]. Furthermore, TNF-α stimulates secretion of IL-1 and IL-6, expression of adhesive molecules and fibroblast proliferation. Release of TNF-α is mediated by a specific metalloproteinase (TNF-α convertase). After secretion, TNF-α binds as a soluble ligand to two cell-bound transmembrane TNF receptors, namely TNFR1 and TNFR2[19]. Chronic inflammation in Crohn's disease can be attributed mainly to the production of proinflammatory cytokines, especially TNF-α. This cytokine is considerably increased in the histologically normal as well as inflamed large bowel mucosa of patients with Crohn's disease. It has been described that thalidomide, a drug with well-known anti-TNF-α action, significantly reduces colonic inflammation induced by iodoacetamide, probably via the inhibition of TNF-α[20]. This experiment is another paradigm of amelioration of colitis by a drug with inhibitory influence of TNF-α.

An important finding of this study is the increased tissue levels of tissue MDA in the untreated rats and the reduced tissue levels of MDA in the groups treated with 5 and 10 mg/kg BW. However, the animals treated with 15 mg/kg BW did not show any statistically significant difference from the untreated ones. There is no obvious explanation for that, though it seems that the reduction of MDA levels could not be a phenomenon related to quantity of the reactive elements. We must emphasize that the results of the 5 and 10 mg/kg BW administration of infliximab on MDA levels were quite similar with the results concerning the corresponding histological lesions. We suppose that the reduction in lipid peroxidation and cellular damage originating from oxidative stress following the administration of infliximab is an important factor contributing to amelioration of experimental colitis. A growing number of data suggests that in experimentally-induced colitis, the colon may be subjected to considerable oxidative stress[21]. Oxidative stress leads to the extension and propagation of crypt abscesses either through direct membrane disruption by lipid peroxidation or through generation of secondary toxic oxidants such as chloramines. Subsequently, chemotactic products of lipid peroxidation provide positive feedback to accelerate the inflammatory/oxidative process[22]. Colonic mucosa may be overwhelmed during active inflammation resulting in intestinal inflammation due to the inability of the mucosa to ameliorate the generating stress because of the small amount of antioxidant enzymes contained in it. It could be possible that colonic injury and dysfunction observed in inflammatory bowel disease are due to the elaboration of these reactive species. Infliximab may have antioxidant properties as well, as it can be suggested by the significant reduction of MDA levels observed in all treated groups of animals though this could simply be the consequence of its anti-inflammatory action.

Another point of interest of this study is the fact that subcutaneous administration of the drug resulted in the reduction of inflammation and tissue damage. The recommended route of administration of infliximab is the IV route. The beneficial effect observed in this model suggests that the other routes of administration of the drug could be effective in human beings as well.

In conclusion, the results of the present study suggest that subcutaneous administration of infliximab reduces the inflammatory activity, as well as tissue TNF-α and MDA levels in chemical colitis in rats. Moreover, infliximab at a dose of 5 mg/kg BW achieves better histological results and produces higher reduction of the levels of TNF-α than at a dose 10 mg/kg BW. Finally, infliximab at a dose of 5 mg/kg BW produces higher reduction of tissue MDA levels than at a dose of 15 mg/kg BW. The administration of infliximab in rats with chemical colitis supports the clinical observations that the dose of 5mg/kg BW produces better results than the dose of 10 or 15 mg/kg BW. The possible antioxidant properties of infliximab must be further investigated both from clinical and experimental points of view.

REFERENCES

1 **Nassif A,** Longo WE, Mazuski JE, Vernava AM, Kaminski DL. **Role of cytokines and platelet-activating factor in** inflammatory bowel disease. Implications for therapy. *Dis Colon Rectum* 1996; **39**: 217-223

2 **Pavlick KP,** Laroux FS, Fuseler J, Wolf RE, Gray L, Hoffman J, Grisham MB. Role of reactive metabolites of oxygen and nitrogen in inflammatory bowel disease. *Free Radic Biol Med* 2002; **33**: 311-322

3 **Kruidenier L,** Verspaget HW. Review article: oxidative stress as a pathogenic factor in inflammatory bowel disease: radicals or ridiculous? *Aliment Pharmacol Ther* 2002; **16**: 1997-2015

4 **Holtmann MH,** Schuchmann M, Zeller G, Galle PR, Neurath MF. **The emerging distinct role of TNF-receptor 2 (p80)** signaling in chronic inflammatory disorders. *Arch Immunol Ther Exp (Warsz)*. 2002; **50**: 279-288

5 **Targan SR,** Hanauer SB, van Deventer SJ, Mayer L, Present DH, Braakman T, DeWoody KL, Schaible TF, Rutgeerts PJ. A short-term study of chimeric monoclonal antibody cA2 to tumor necrosis factor alpha for Crohn's disease. Crohn's Disease cA2 Study Group. *N Engl J Med* 1997; **337**: 1029-1035

6 **Rutgeerts P,** D'Haens G, Targan S, Vasiliauskas E, Hanauer

SB, Present DH, Mayer L, Van Hogezand RA, Braakman T, DeWoody KL, Schaible TF, Van Deventer SJ. Efficacy and safety of retreatment with anti-tumor necrosis factor antibody (infliximab) to maintain remission in Crohn's disease. *Gastroenterology* 1999; **117**: 761-769

7 **Chey WY**. Infliximab for patients with refractory ulcerative colitis. *Inflamm Bowel Dis* 2001; **7** Suppl 1:S30-S33

8 **Kohn A**, Prantera C, Pera A, Cosintino R, Sostegni R, Daperno M. Anti-tumor necrosis factor alpha (infliximab) in the treatment of severe ulcerative colitis: result of an open study on 13 patients. *Dig Liver Dis* 2002; **34:** 626-630

9 **Actis GC,** Bruno M, Pinna-Pintor M, Rossini FP, Rizzetto M. Infliximab for treatment of steroid-refractory ulcerative colitis. *Dig Liver Dis* 2002; **34:** 631-634

10 **Su C,** Salzberg BA, Lewis JD, Deren JJ, Kornbluth A, Katzka DA, Stein RB, Adler DR, Lichtenstein GR. Efficacy of anti-tumor necrosis factor therapy in patients with ulcerative colitis. *Am J Gastroenterol* 2002; **97**: 2577-2584

11 **Probert CS,** Hearing SD, Schreiber S, Kuhbacher T, Ghosh S, Arnott ID, Forbes A. Infliximab in moderately severe glucocorticoid resistant ulcerative colitis: a randomised controlled trial. *Gut* 2003; **52**: 998-1002

12 **Andreadou I,** Papalois A, Triantafillidis JK, Demonakou M, Govosdis V, Vidali M, Anagnostakis E, Kourounakis PN. Beneficial effect of a novel non-steroidal anti-inflammatory agent with basic character and antioxidant properties on experimental colitis in rats. *Eur J Pharmacol* 2002; **441**: 209-214

13 **Jenkins D,** Balsitis M, Gallivan S, Dixon MF, Gilmour HM, Shepherd NA, Theodossi A, Williams GT. Guidelines for the initial biopsy diagnosis of suspected chronic idiopathic inflammatory bowel disease. The British Society of Gastroenterology Initiative. *J Clin Pathol* 1997; **50:** 93-105

14 **Robinson JW**, Mirkovitch V, Winistorfer B, Saegesser F. Response of the intestinal mucosa to ischaemia. *Gut* 1981; **22**: 512-527

15 **Burns BJ,** Brandt LJ. Intestinal ischemia. *Gastroenterol Clin North Am* 2003; **32:** 1127-1143

16 **Geboes K,** Riddell R, Ost A, Jensfelt B, Persson T, Lofberg R. A reproducible grading scale for histological assessment of inflammation in ulcerative colitis. *Gut* 2000; **47**: 404-409

17 **Wooddruff TM,** Arumugam TV, Shiels IA, Reid RC, Fairlie DP, Taylor SM. A potent human C5a receptor antagonist protects aginst disease pathology in a rat model of inflammatory bowel disease. *J Immunol* 2003; **171**: 5514-5520

18 **Hehlgans T,** Pfeffer K. The intriguing biology of the tumour necrosis factor/tumour necrosis factor receptor superfamily: players, rules and the games. *Immunology* 2005; **115**: 1-20

19 **Mizoguchi E**, Mizoguchi A, Takedatsu H, Cario E, de Jong YP, Ooi CJ, Xavier RJ, Terhorst C, Podolsky DK, Bhan AK. Role of tumor necrosis factor receptor 2 (TNFR2) in colonic epithelial hyperplasia and chronic intestinal inflammation in mice. *Gastroenterology* 2002; **122**: 134-144

20 **Kenet G,** Wardi J, Avni Y, Aeed H, Shirin H, Zaidel L, Hershkoviz R, Bruck R. Amelioration of experimental colitis by thalidomide. *Isr Med Assoc J* 2001; **3**: 644-648.

21 **Thiele GM,** Worrall S, Tuma DJ, Klassen LW, Wyatt TA, Nagata N. The chemistry and biological effects of malondialdehyde-acetaldehyde adducts. Alcohol Clin Exp Res 2001; **25**: 218S-224S.

22 **Yamada T,** Grisham MB. Role of neutrophil-derived oxidants in the pathogenesis of intestinal inflammation. *Klin Wochenschr* 1991; **69**: 988-994.

Sciencel Editor Wang XL and Guo SY **Language Editor** Elsevier HK

PO Box 2345, Beijing 100023, China
www.wjgnet.com
wjg@wjgnet.com

ELSEVIER

World J Gastroenterol 2005;11(43):6848-6852
World Journal of Gastroenterology ISSN 1007-9327

• RAPID COMMUNICATION •

Relative predictive factors for hepatocellular carcinoma after HBeAg seroconversion in HBV infection

Kazumoto Murata, Kazushi Sugimoto, Katsuya Shiraki, Takeshi Nakano

Kazumoto Murata, Kazushi Sugimoto, Katsuya Shiraki, Takeshi Nakano, the First Department of Internal Medicine, Mie University School of Medicine, 2-174 Edobashi Tsu Mie 514-8507, Japan
Correspondence to: Kazumoto Murata, MD, PhD, the First Department of Internal Medicine, Mie University School of Medicine, 2-174 Edobashi Tsu Mie 514-8507, Japan. atarum@clin.medic.mie-u.ac.jp
Telephone: +81-59-231-5015 Fax: +81-59-231-5201
Received: 2005-01-20 Accepted: 2005-04-09

Abstract

AIM: To determine the predictive factors for hepatocellular carcinoma (HCC) development in patients after spontaneous or therapeutic HBeAg seroconversion.

METHODS: In 48 patients who seroconverted to anti-HBe positive during follow-up, the background factors for HCC development were analyzed.

RESULTS: HCC was developed in six patients during follow-up (average follow-up after HBeAg seroconversion: 10.9±5.4 years). The incidence of HCC evaluated by Kaplan–Meier analysis was significantly higher in patients with abnormal aspartate aminotransferase (AST> 40 IU/L) level, lower platelet counts (PLT<10×10^4/μL), lower albumin level (Alb<30 g/L), positive HBV-DNA or older age at seroconversion (>40 years). However, lower platelet count was the only predictive factor for HCC development shown by multivariate proportional-hazard analysis.

CONCLUSION: Active hepatitis or advanced hepatitis at HBeAg seroconversion or progressive hepatitis even after HBeAg seroconversion would be the risk factors for HCC development. These predictive factors should be taken into account in determining the frequency of biochemical study or imaging studies for HCC surveillance.

Key words: HBeAg seroconversion; Hepatocellular carcinoma; Predictive factors

Murata K, Sugimoto K, Shiraki K, Nakano T. Relative predictive factors for hepatocellular carcinoma after HBeAg seroconversion in HBV infection. *World J Gastroenterol* 2005; 11(43): 6848-6852
http://www.wjgnet.com/1007-9327/11/6848.asp

INTRODUCTION

Hepatitis B virus

Hepatitis B virus (HBV) in Japan, where genotype C is dominant, is generally infected during delivery or early childhood with immature immune systems, and those children become HBV carriers before HBV vaccine was introduced. In adolescents, hepatitis e antigen (HBeAg) seroconversion to its antibody (anti-HBe) often occurs after multiple exacerbations, which coincide with subsidence of hepatic inflammatory activities[1,2]. The failure of seroconversion usually results in chronic progressive liver diseases and hepatocellular carcinoma (HCC). The calculated annual incidence of acute exacerbation was two times higher in patients with positive HBeAg or HBV-DNA than those without these markers[3]. The patients who have recurrent episodes of acute exacerbations with bridging hepatic necrosis are more likely to develop cirrhosis[4]. These observations suggest that HBeAg seroconversion to anti-HBe confers favorable long-term outcomes. On the other hand, most HCC occurred in HBeAg-negative patients with undetectable HBV-DNA[5,6], suggesting that all HBV patients should be carefully followed-up for HCC even after HBeAg seroconversion. However, there seems to be some predictive factors for HCC in our clinical experiences. Previous reports demonstrated the natural history of anti-HBe positive patients. However, they included patients with spontaneous reactivation, which may be the major cause of progressive hepatic damage[7,8]. To our knowledge, there are no reports about incidences of HCC that selected only patients who seroconverted to anti-HBe during follow-up. Therefore, we focused on anti-HBe-positive patients without any reactivation of HBeAg and tried to determine the risk factors for HCC development to select high risk group for HCC.

MATERIALS AND METHODS

Three hundred and thirty-one HBsAg-positive patients were followed-up in our hospital between 1990 and 2004. Inclusion criteria in this study were: (1) follow-up until death or October 2004; (2) sufficient data to evaluate; and (3) careful follow-up for HCC with evaluation of both tumor markers (alpha-fetoprotein or des-gamma-carboxyprothrombin) and image studies (USG or CT) every 3-6 mo. HBeAg serocoversion was determined if anti-HBe completely became positive and HBeAg was never recovered retrospectively. We excluded the cases that showed fluctuation of HBeAg or anti-HBe levels.

None of the patients had any other viral infections, such as hepatitis C virus (HCV) or human immunodeficiency virus (HIV). Patients were followed-up by biochemical studies and image studies for at least 3-6 mo intervals. The biochemical tests were measured using routine automated techniques. HBsAg, HBeAg, and anti-HBe were assayed using commercial enzyme immunoassay kits (Abbott Japan, Tokyo). HBV-DNA was determined by a transcription-mediated amplification (TMA) method. The detection sensitivity of this assay is 3.7 LGE/mL. All HCC were initially found by USG or CT and confirmed by CT during abdominal angiography.

Statistical analysis

Fisher's exact test or the χ^2 test was used to compare patients' backgrounds. Kaplan–Meier analysis and log-rank test were performed to test a cumulative incidence of HCC in each group. Multivariate proportional-hazards survival analysis was used to determine the important risk factors for HCC. $P<0.05$ was considered statistically significant.

RESULTS

One hundred and thirty-four out of the 331 HBV patients were enrolled in this study. Forty six patients (M:F = 34:12) were HBeAg-positive and 88 (M:F = 64:24) patients were anti-HBe-positive. There were no patients who had positive tests for both HBeAg and anti-HBe. Regarding the patients' backgrounds, age, sex, platelet counts, albumin level and AST level were similar in both HBeAg-positive and anti-HBe-positive patients. However, ALT level was significantly higher in HBeAg-positive patients as compared with anti-HBe-positive patients (P = 0.001, Table 1). HCC developed in 15 HBeAg-positive patients and in 11 anti-HBe-positive patients during follow-up. The average age for the appearance of HCC was similar in both groups (55±8 years in HBeAg-positive and 53±12 years in anti-HBe-positive patients). The cumulative incidence of HCC was significantly higher in HBeAg-positive patients than in anti-HBe-positive patients as previously reported (P = 0.016, Figure 1). However, the incidence of HCC was found to be increased with age even in patients with anti-HBe, especially in those who were over 70 years. Out of 88 patients with anti-HBe, the time of HBeAg seroconversion was observed in 48 patients. Other 40 patients already showed anti-HBe positive when the patients first presented. The current study focused on these 48 patients. The average age of 48 patients was 50

Table 1 Patients' characteristics

Feature	HBeAg	Anti-HBe	*P*
n	46	88	NS
Age	53±12	54±14	NS
Male sex	34 (74%)	64 (73%)	NS
Platelet ($\times10^4/\mu L$)	14.3±6.6	18.7±6.4	NS
Alb (g/dL)	4.0±0.5	4.1±0.5	*NS*
AST (IU/L)	56±33	41±36	NS
ALT (IU/L)	62±57	36±27	0.001

NS: not significant.

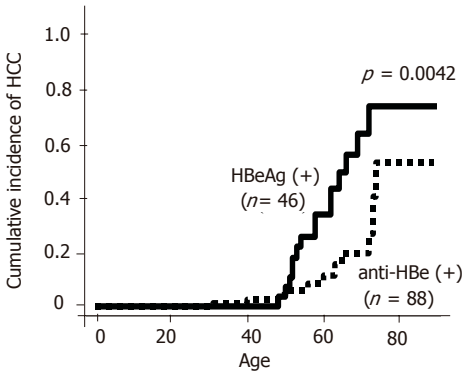

Figure 1 Cumulative incidence of HCC in patients with HBeAg or anti-HBe (Kaplan –Meier analysis and log-rank test). The incidence of HCC in both groups was increasing after the age of 50. The incidence of HCC was significantly higher in the patients with HBeAg positive (solid line) than those with anti-HBe positive (dot line) (P=0.0042).

±14 years (M:F = 34:14). The average age at HBeAg seroconversion was 40±12 years (range, 16-67 years). HBeAg seroconversion occurred spontaneously in 75% (36/48), by IFN in 18.8% (9/48) and by propagermanium in 6.2% (3/48) cases. HBV-DNA was detectable by TMA methods in 27.1% (13/48) patients. The average follow-up periods after HBeAg seroconversion were 10.9±5.4 years (range, 1-25 years). Six patients developed HCC during follow-up. All six patients were male and the average age of HCC development was 57±13 years (14.0±5.1 years after HBeAg seroconversion). The incidence of HCC evaluated by Kaplan–Meier analysis was significantly higher in patients with abnormal AST (>40 IU/L) level (P = 0.007, Figure 2A), suggesting that active hepatitis even after seroconversion may be one of the risk factors for HCC. However, there were no differences in ALT levels (Figure 2B). Low platelet count ($<10\times10^4/\mu L$) ($P<0.0001$) or low albumin level (Alb<30 g/L) (P = 0.009) was another risk factor for HCC, suggesting that HCC may develop in patients with advanced liver diseases at HBeAg seroconversion or with progressive liver diseases even after seroconversion (Figures 2C and D). Positive HBV-DNA (P = 0.014) increased the incidence of HCC as well (Figure 2E). The incidence of HCC tended to be non-significantly higher in the patients with HBeAg seroconversion by therapy as compared with the spontaneous seroconversion (Figure 3A). The cumulative incidence of HCC was significantly higher in the patients with HBeAg seroconversion after 40 years of age (Figure 3B). Multivariate proportional-hazards analysis demonstrated that low platelet counts ($<10\times10^4/\mu L$) was the only predictive factor for HCC (P = 0.032, hazard ratio = 21.6), whereas serum albumin and AST levels and HBV-DNA positivity could not be determined as predictive factors for HCC (Table 2). Furthermore, the incidence of HCC was not observed in the patients with both normal platelet counts ($>10\times10^4/\mu L$) and normal AST level (<40 IU/L) during follow-up in our study. In contrast, the incidence of HCC was annually increasing after HBeAg seroconversion in patients with either lower platelet counts ($<10\times10^4/\mu L$) or abnormal AST level (>40 IU/L) (Figure 4).

DISCUSSION

The present study demonstrated that low platelet counts ($<10\times10^4/\mu L$), low albumin level (<30 g/L), abnormal AST level (>40 IU/L), older age at HBeAg seroconversion (>40 years) and positive HBV-DNA were the predictive factors for HCC after HBeAg seroconversion. Multivariate proportional-hazard analysis demonstrated that platelet count was the only significant risk factor. These observations suggested that active hepatitis or progression of liver disease even after HBeAg seroconversion or advanced hepatitis at HBeAg seroconversion would be the predictive factors for HCC. In other words, patients without any of these factors after HBeAg seroconversion would be at low risk for HCC development.

In patients with chronic hepatitis C virus (HCV) infection, we should focus on patients with advanced

Table 2 Predictve Features of HCC

Variable	Hazard ratio	95%CI	*P*
Platelet counts ($<10^5$ *vs* $\geq10^5$/mL)	21.6	1.3 – 354.8	0.032
Alb (< 3.0 *vs* ≥ 3.0 g/dL)	0.4	0.1 – 3.4	0.376
AST (> 40 *vs* ≤ 40 IU/L)	3.6	0.2 – 51.3	0.351
HBV-DNA (+ *vs* -)	0.1	0.1 – 10.4	0.912

Multivariate proportional-hazards analysis.

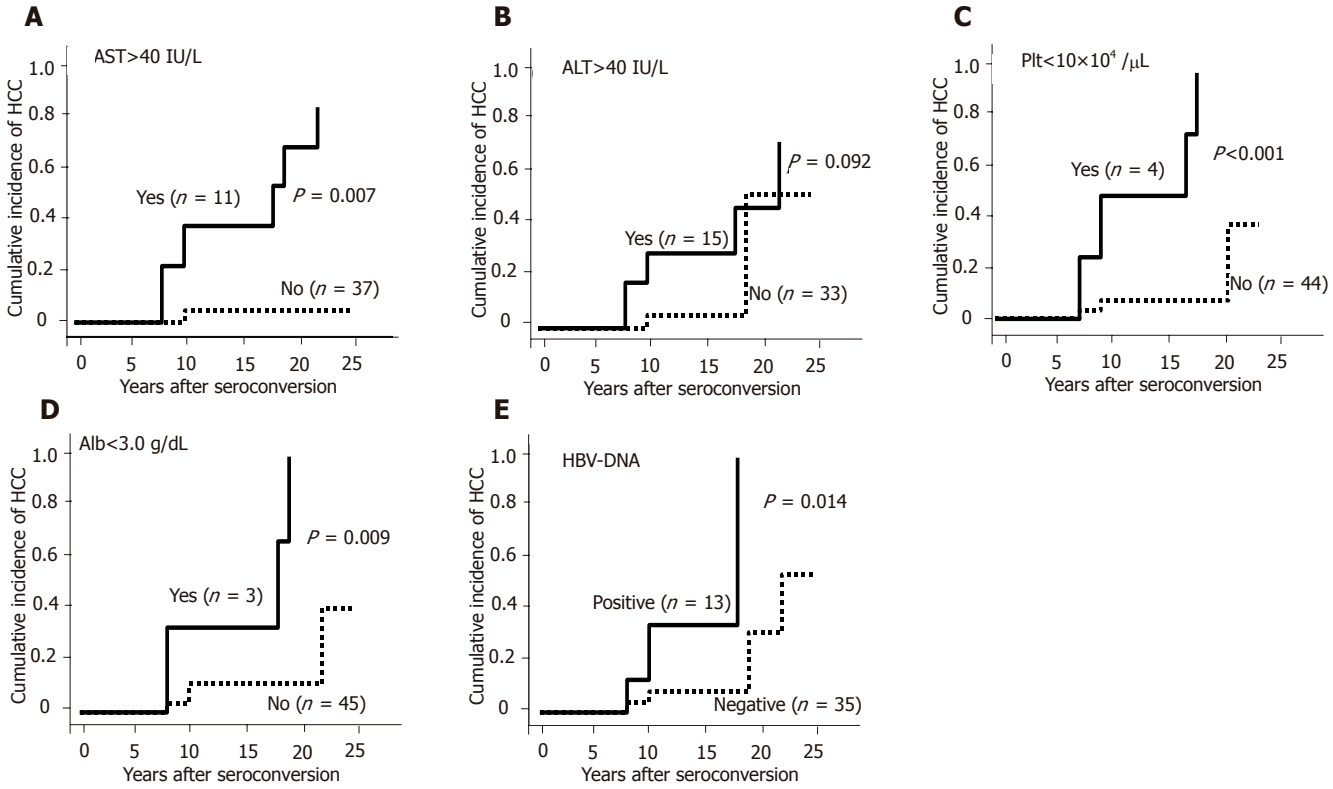

Figure 2 Cumulative incidence of HCC in patients with different parameters (Kaplan–Meier analysis and log-rank test). **A:** AST level (>40 or ≤40 IU/L); **B:** ALT level (>40 or ≤40 IU/L); **C:** platelet counts ($<10\times10^4$ or $\geq10\times10^4/\mu L$): **D:** albumin level (<30 or ≥30 g/L); **E:** HBV-DNA (positive or negative).

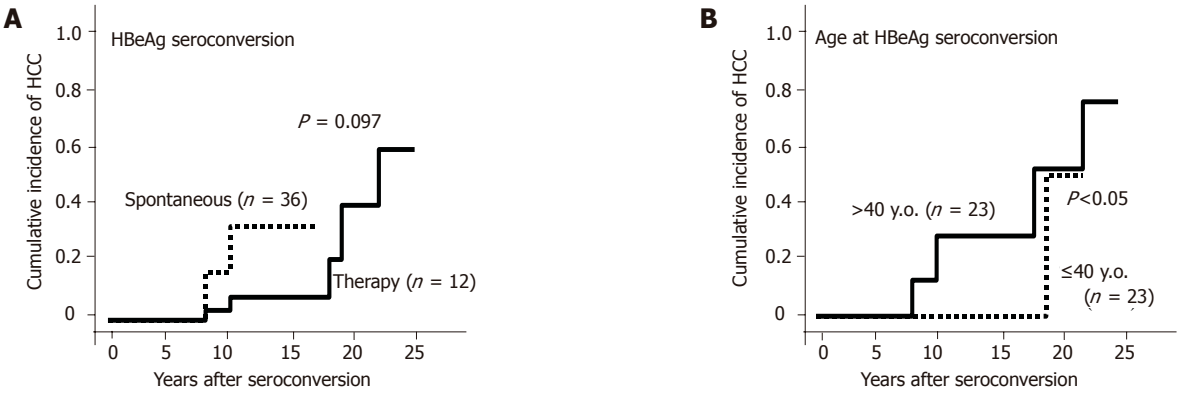

Figure 3 Cumulative incidence of HCC in patients after seroconversion (Kaplan–Meier analysis and log-rank test). **A:** Spontaneous or post-therapeutic seroconversion; **B:** age at seroconversion (>40 or ≤40 years).

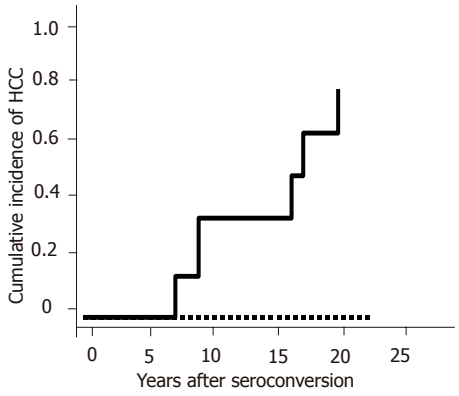

Figure 4 Cumulative incidence of HCC in patients with or without risk factors (Kaplan–Meier analysis and log-rank test). Solid line: either platelet counts<10×10^4/μL or AST>40 IU/L; dot line: both platelet counts≥10×10^4/μL, and AST<40 IU/L.

chronic hepatitis or cirrhosis as high risk group for HCC development and follow-up with tight observation for biochemical studies, tumor markers and image studies since HCC is usually accompanied with the progression of liver diseases. In patients with chronic HBV infection, however, HCC sometimes develops not only in liver cirrhosis, but even in mild hepatitis[9,10]. So, it is more difficult to select high risk patients for HCC in chronic HBV infection than that in HCV infection. Of course, positive HBeAg or reactivation after HBeAg seroconversion with active hepatitis is one of the risk factors for cirrhosis[7,8], HCC[3,11] or survival[12]. However, the cumulative incidence of HCC in our study was high even in anti-HBe-positive patients, especially in older patients (Figure 1). Therefore, we conducted this study to determine the predictive factors for HCC in patients with anti-HBe.

We found that the cumulative incidence of HCC was significantly higher in patients with abnormal AST (Figure 2A), suggesting that active hepatitis even after HBeAg seroconversion was one of the risk factors. This result was consistent with previous reports that progression to cirrhosis or HCC occurred in patients with HBeAg negative hepatitis without reversion to HBeAg[11,13]. Furthermore, the incidence of HCC was significantly reduced in HBeAg-negative chronic hepatitis or cirrhotic patients who maintained virological response by lamivudine[14] or interferon (IFN)[15,16]. These previous reports support our observation that therapy for transaminase control may reduce the risk of HCC development in our patients with abnormal AST level. On the other hand, the cumulative incidence of HCC was not statistically different in ALT levels. We, therefore, hypothesized that ALT elevation might be observed in patients with fatty liver as well as necroinflammatory liver disease.

Other risk factors for HCC development in anti-HBe-positive patients were lower platelet counts and low albumin level. Interestingly, multivariate proportional-hazards analysis showed that low platelet counts (<10×10^4/μL) was the only risk factor for HCC development, suggesting that HCC may develop in patients with progressive liver disease even after HBeAg seroconversion or advanced liver diseases before HBeAg seroconversion. Since multiple exacerbations usually occurred before HBeAg seroconversion, necroinflammation occurs more frequently in patients with delayed HBeAg seroconversion, which results in progression to liver cirrhosis or HCC[13]. Our results show that the cumulative incidence of HCC was significantly higher in patients with delayed HBeAg seroconversion (older than 40 years) are consistent with the previous reports. Furthermore, the cumulative incidence of HCC in our study was annually increasing in the patients with either low platelet counts (<10×10^4/μL) or abnormal AST (>40 IU/L) after HBeAg seroconversion, whereas no HCC was observed in patients with both normal platelet counts (≥10×10^4/μL) and normal AST (<40 IU/L) during follow-up (median follow-up period: 11±5 years).

In this study, we observed a relatively higher incidence of HCC in patients with anti-HBe as compared with the previous reports. This might be because our study was not a prospective study and we might have lost the patients with relative low risk of active hepatitis or fibrosis during follow-up. It is possible that there might be a bias, in which the patients with relative high risk (high AST or ALT) were accumulated in our study. Prospective and large-scale studies need to determine the predictive factors for HCC in patients with anti-HBe.

In conclusion, in anti-HBe-positive patients, lower platelet counts, lower albumin, abnormal AST and positive HBV-DNA are the predictive factors for HCC. In other words, anti-HBe-positive patients without any of these factors are at low risk for HCC. In the follow-up of anti-HBe-positive patients, those predictive factors, especially platelet counts, should be taken into account for determining the frequency of biochemical study or imaging studies. Moreover, to reduce the risk for HCC development, we should induce HBeAg seroconversion before progression to advanced liver diseases and control AST level within the normal range using lamivudine or IFN. These results may be supported by our clinical experiences. However, to our knowledge, there are no reports to clarify the high risk group in anti-HBe positive patients with known time of HBeAg seroconversion.

REFERENCES

1 **Hoofnagle JH**, Dusheiko GM, Seeff LB, Jones EA, Waggoner JG, Bales ZB. Seroconversion from hepatitis B e antigen to antibody in chronic type B hepatitis. *Ann Intern Med* 1981; **94:** 744-748
2 **Realdi G**, Alberri M, Rugge M, Borrolotti F, Rigoli AM, Tremolada F, Ruol A. Seroconversion from hepatitis B e antigen to anti-HBe in chronic hepatitis B virus infection. *Gastroenterology* 1980; **79:** 195-199
3 **Liaw YF**, Lin DY, Chen TJ, Chu CM. Natural course after the development of cirrhosis in patients with chronic type B hepatitis: a prospective study. *Liver* 1989; **9:** 235-241
4 **Chu CM**, Natural history of chronic hepatitis B virus infection in adults emphasis on the occurrence of cirrhosis and hepatocellular carcinoma. *J Gastroenterol Hepatol* 2000; **15:** E25-30

5 **Lok AS**, Prevention of hepatitis B virus-related hepatocellular carcinoma. *Gastroenterology* 2004; **127:** S303-S309
6 **Yuen MF**, Lai CL. Natural history of chronic hepatitis B virus infection. *J Gastroenterol Hepatol* 2000; **15:** E20-24
7 **Fattovich G**, Brollo L, Alberti A, Realdi G, Pontisso P, Giustina G, Ruol A. Spontaneous reactivation of hepatitis B virus infection in patients with chronic type B hepatitis. *Liver* 1990; **10:** 141-146
8 **Takano S**, Yokosuka O, Imazeki F, Tagawa M, Omata M. Incidence of hepatocellular carcinoma in chronic hepatitis B and C: a prospective study of 251 patients. *Hepatology* 1995; **21:** 230-235
9 **Di Bisceglie AM**, Rustgi VK, Hoofnagle JH, Dusheiko GM, Lotze MT. NIH conference. Hepatocellular carcinoma. *Ann Intern Med* 1988; **108:** 390-401
10 **Takano S**, Yokosuka O, Imazeki F, Tagawa M, Omata M. Incidence of hepatocellular carcinoma in chronic hepatitis B and C: a prospective study of 251 patients. *Hepatology* 1995; **21:** 650-655
11 **Hsu YS**, Chien RN, Yeh CT, Sheen IS, Chiou HY, Chu CM, Liaw YF. Long-term outcome after spontaneous HBeAg seroconversion in patients with chronic hepatitis B. *Hepatology* 2002; **35:** 1522-1527
12 **Niederau C**, Heintges T, Lange S, Goldmann G, Niederau CM, Mohr L, Haussinger D. Long-term follow-up of HBeAg-positive patients treated with interferon alfa for chronic hepatitis B. *N Eng J Med* 1996; **334:** 1422-1427
13 **Chu CM**, Hung SJ, Lin J, Tai DI, Liaw YF. Natural history of hepatitis B e antigen to antibody seroconversion in patients with normal serum aminotransferase levels. *Am J Med* 2004; **116:** 829-834
14 **Marco VD**, Marzano A, Lampertico P, Andreone P, Santantonio T, Almasio PL, Rizzetto M, Craxi A for the Italian Association for the Study of the Liver (AISF) Lamivudine Study Group. Clinical outcome of HBeAg-negative chronic hepatitis B in relation to virological response to lamivudine. *Hepatology* 2004; **40:** 883-891
15 **Marco VD**, Iacono OL, Camma C, Vaccaro A, Giunta M, Martorana G, Fuschi P, Almasio PL, Craxi A. The long-term course of chronic hepatitis B. *Hepatology* 1999; **30:** 257-264
16 **Paratheodoridis GV**, Manesis E, Hadziyannis SJ. The long-term outcome of interferon-a treated and untreated patients with HBeAg-negative chronic hepatitis B. *J Hepatol* 2001; **34:** 306-313

Science Editor Kumar M and Guo SY **Language Editor** Elsevier HK

PO Box 2345, Beijing 100023, China
www.wjgnet.com
wjg@wjgnet.com

ELSEVIER

World J Gastroenterol 2005;11(43):6853-6857
World Journal of Gastroenterology ISSN 1007-9327

• RAPID COMMUNICATION •

Evaluation of liver tissue by polymerase chain reaction for hepatitis B virus in patients with negative viremia

Fouad Thakeb, Magdy El-Serafy, Soheir Zakaria, Bahaa Monir, Sahar Lashin, Raghda Marzaban, Mostafa El-Awady

Fouad Thakeb, Magdy El-Serafy, Soheir Zakaria, Tropical Medicine Department, Cairo University, Egypt
Bahaa Monir, Sahar Lashin, Raghda Marzaban, Pathology Department, Cairo University, Egypt
Mostafa El-Awady, Department of Biomedical Technology, National Research Center, Cairo, Egypt
Correspondence to: Dr Mostafa K El-Awady, Department of Biomedical Technology, National Research Center, Tahrir Street, Dokki, Cairo, Egypt. mkawady@yahoo.com
Telephone: +20123132640
Received: 2005-02-04 Accepted: 2005-04-01

Abstract

AIM: To assess the clinical significance of Hepatitis B virus (HBV) DNA localization in the liver tissue of patients with positive HBsAg and negative viremia.

METHODS: HBV virological parameters of 33 HBsAg positive chronic hepatitis patients, including seromarkers and HBV DNA amplification in both sera and liver biopsies, were evaluated.

RESULTS: Ten patients had negative viremia and positive HBV DNA in their liver biopsies. Most of them had HBeAg-negative/HBeAb-positive chronic hepatitis. Their liver biochemical and histopathological profiles were different from the viremic patients. Their disease pattern was designated as "hepatitis B *in situ*".

CONCLUSION: Hepatitis B *in situ* is a consequential entity which can be missed in clinical practice. It is a new clinical pattern of chronic HBV infection that considers HBV in liver biopsy and adds a new indication for antiviral therapy.

Key words: Hepatitis B *in situ*; Antiviral therapy; HBV DNA; Chronic hepatitis

Thakeb F, El-Serafy M, Zakaria S, Monir B, Lashin S, Marzaban R, El-Awady M. Evaluation of liver tissue by polymerase chain reaction for hepatitis B virus in patients with negative viremia. *World J Gastroenterol* 2005; 11(43): 6853-6857
http://www.wjgnet.com/1007-9327/11/6853.asp

INTRODUCTION

Hepatitis B virus is a virus that infects 350 million people worldwide with a clinical spectrum of acute hepatitis, the healthy carrier state, cirrhosis, and hepatocellular carcinoma. The outcome of infection is the result of complicated viral-host interactions. As in other infections with non-cytopathic viruses, the immune response is thought to play a crucial role in disease pathogenesis. However, there are increasing evidences that varieties of viral mechanisms, some depending on the function of virally encoded proteins, have a profound impact on the infected hepatocytes, the liver microenvironment and host antiviral responses[1].

Occult HBV infection is characterized by undetectable HBsAg. Serum HBV DNA level is usually less than 10^4 copies/mL in these patients. Diagnosis requires a sensitive HBV-DNA assay[2]. To our knowledge, no data are available about the amount of HBV genomes in the liver of patients with chronic HBV infection. However, it has been reported that cases with suppressed HBV activity, despite the very low level of viremia, maintain a relatively high amount of intrahepatic viral genomes. This virus reservoir is likely involved in HBV reactivation, which is usually observed after stopping lamivudine treatment[3].

The detection of HBV genomes in nested PCR-based assays appears to be the most reliable methods for monitoring infection and assessing response to antiviral treatment[4]. The majority of patients with HBsAg in serum have HBV DNA present in serum as well. Some patients have HBsAg but no HBV DNA in serum. These are chronic carriers with normal transaminases[5]. On the other hand, HBV DNA can be detected in serum and liver by PCR in patients who have lost their HBsAg. In addition, hepatic HBV DNA can be detected in cirrhotic liver in the absence of serum HBV DNA[5,6]. HBV DNA can be treated as a sign of HBV activity[7], without ignoring the facts that HBV DNA levels fluctuate in patients with chronic HBV infection and that the correlation between serum HBV DNA levels and histologic activity is poor[8].

In this study, we evaluated the clinical significance of the localization of HBV in liver tissue of chronic HBV patients with negative viremia and elevated ALT.

PATIENTS AND METHODS

This prospective study included chronic liver disease patients who attended the out-patient clinic of the

Endemic Medicine Department, Cairo University during the period between September 2002 and July 2003. All patients with data suggestive of liver affection were evaluated, and those with positive HBsAg and elevated ALT were selected as the candidates for this study.

Exclusion criteria were HCV infection, advanced liver disease, alcohol consumption, autoimmune hepatitis, drug-induced hepatitis, hepatic schistosomiasis, evidence of acute hepatitis in the last 6 mo, presence of HDVAb, hepatocellular carcinoma, and advanced co-morbid conditions such as cardiac or renal disease.

Selected patients were subjected to clinical evaluation and laboratory investigations including viral serologic tests using enzyme immunoassay technique applying the Abbott System®. These assays included the detection of HBsAg, HBsAb, HBcAb (total), HBeAg, HBeAb, and HCVAb (total) by 3rd generation ELISA assay (Sorin®, Italy). Abdominal ultrasonography and liver biopsy were performed. The modified HAI score was used to stage and grade liver disease[9]. For the detection of hepatic total HBV DNA (integration plus CCC form), part of the liver sample was incubated at 56 °C for 3 h with 270 μL of phosphate buffer saline containing 160 μg of proteinase K (Promega, Madison, WI, USA) and 30 μL of 10 buffer. Serum HBV DNA was extracted by incubation at 56 °C for 3 h with 270 μL of serum plus 30 μL of 10×buffer containing 160 μg proteinase K. DNA extraction was purified by phenol: chloroform (300 μL, 1:1 V/V) extraction, ethanol/0.2 mol/L sodium acetate precipitation. Qualitative PCR testing for HBV in serum and liver tissue was carried out using nested PCR technique[10]. Total genomic DNA was extracted from serum or liver tissue using phenol/chloroform extraction after proteinase K digestion. Purified DNA (1–2 μg) was utilized as a template in the polymerase chain reaction using two rounds of amplification with nested primers as follows:
Outer primers: B1 5' AAGGTCTTACATAAGAGGAC 3' (nt 1 644–1 663), B2 5' CTAACATTGAGATTCCCGAG ATTGAGA 3' (nt 2 458–2 432);
Inner primers: B3 5' GGCTGTAGGCATAAATTGGTC-TG 3' (nt 1 781–1 803), B4 5' TTGCCTGAGTGCAGTA-TGGT 3' (nt 2 075–2 056).

The PCR reactions were performed in 50 μL reaction volume containing 10 μmol/L dNTPs, 50 pmol from each primer, and 2 U of Taq. The amplification protocol for the two nested rounds consisted of 35 cycles, each cycle contained a denaturation at 94 °C for 30 s, annealing at 52 °C for 1 min, and extension at 72 °C for 2 min, followed by a single cycle with final extension at 72 °C for 7 min. Positive samples infected with HBV DNA produced a amplified product of 295 bp in length.

Statistical analysis

Patients' data were tabulated, and then processed using the software SPSS for Windows 9 version 10.0®. Quantitative variables were expressed as mean±SD and compared using Student's *t* test. Qualitative variables were compared using Fisher's exact test. A $P<0.05$ was considered statistically significant.

RESULTS

Out of the 670 patients with chronic liver disease, 44 were seropositive for HBsAg. Eleven of the forty-four HBsAg seropositive patients were excluded because of normal liver enzymes. The study was then conducted on the remaining 33 patients (26 males and 7 females; mean age 32.8±12.0 years, range 18–60 years). Fifteen patients were originally from urban areas and 18 from rural areas (10 from Nile Delta, and 8 from Upper Egypt).

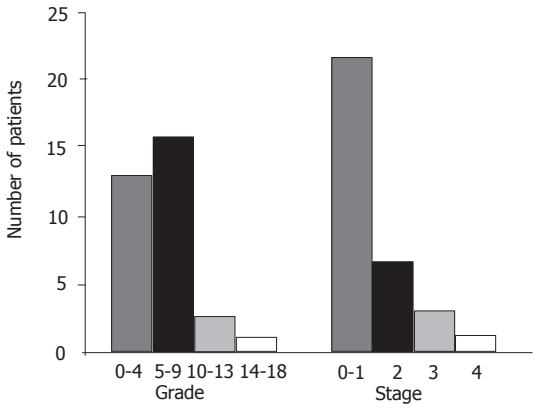

Figure 1 Histopathological grading and staging

According to the modified HAI grading and staging, histopathological findings are shown in Figure 1. Ground glass pattern of the hepatocytes was detected in 21 patients, steatosis was found in 14 patients, while cholestasis was detected in two cases.

HBV markers were spread into Poynard's table of classification of HBV infected patients[10]. Seventeen patients were fit with the "chronic carrier, pre-core mutant type", and six with the "chronic carrier, wild type" definitions. Ten patients remained uncategorized, showing a unique pattern (Table 1).

These 10 patients (group 1) were compared to the remaining 23 chronic hepatitis B patients (group 2) as shown in Tables 2 and 3. No statistically significant differences were observed regarding the liver biochemical or histological parameters. In this study, we found five possible permutations of the HBV seromarkers, which were grouped according to the HBV DNA results (Table 4). Among the HBcAb-negative patients, three patients were also negative for HBeAg and HBeAb. HBV DNA was detectable in

Table 1 Characteristics of patients uncategorized in Poynard (2000) classification

	HBsAg	HBsAb	HBeAg	HBeAb	HBcAb *IgG*	HBcAb *IgM*	DNA serum	DNA liver	Symptom	ALT	HAI/fibrosis	No. of patients
Uncategorized	+	+/–	–/+	+/–	+	–	–	+	+/–	+	+	10

Table 2 Hepatic biochemical tests in group I *vs* group II patients

	Group I (n = 10)	Group II (n = 23)	P values
Serum bilirubin (mg/dL)	1.36±1.31	1.44±2.1	0.9
AST (IU/L)	63.9±24.1	82.0±51.3	0.3
ALT (IU/L)	62.6±27.4		0.2
Serum albumin (g/dL)	3.9±0.50	4.0±0.57	0.4
INR	1.25±0.22	1.23±0.14	0.7

Table 3 Hepatic histopathologic parameters in group I *vs* group II patients

		Group I (n = 10)	Group II (n = 23)	P values
Grading	0–9	8	20	0.4
	10–18	2	3	
Staging	0–2	9	19	0.9
	3–6	1	4	

Table 4 HBV seromarker pattern according to HBV DNA testing

Marker pattern	n	HBV DNA status			
		+ve serum +ve liver	–ve serum –ve liver	+ve serum –ve liver	–ve serum +ve liver
cAb+eAg–eAb+	18	7	1	3	7
cAb+eAg+eAb–	7	5	–	1	1
cAb–eAg–/+eAb–/+	5	2	2	1	–
cAb+eAg–eAb–	2	1	–	–	1
cAb+eAg+eAb+	1	–	–	–	1
Total	33	15	3	5	10

cAb: hepatitis B core antibody; eAg: hepatitis B envelope (e) antigen; eAb: hepatitis B antibody against envelope (e) antigen.

six patients with positive HBsAb (four with detectable viral DNA in both serum and liver tissue, while two with detectable viral DNA only in liver tissue). Although four of the HBeAg-negative cases had higher HAI score (10–18) compared to none of the HBeAg-positive chronic hepatitis cases, the two groups showed no significant difference in either biochemical or histological parameters.

DISCUSSION

HBV infection varies widely from high (>8%, e.g., Africa, Asia, and the Western Pacific) to intermediate (2–7%, e.g., Southern and Eastern Europe) to low (<2%, e.g., Western Europe, North America, and Australia) prevalence areas. Egypt lies in the intermediate prevalence region[10]. HBV DNA is a good marker of the level of viremia and can be correlated with serum transaminase levels. The majority of patients with HBsAg in serum have HBV DNA. However, some patients are positive for HBV DNA in serum even in the absence of HBsAg, while some others have HBsAg but not HBV DNA in serum[5]. The presence of HBV genome is associated with ongoing necroinflammation[8]. In the presence of HBeAg, the diagnosis of replicating chronic HBV can be made whatever the viral load is. In contrast, the interpretation of HBV DNA quantification is difficult in HBeAg-negative/HBeAb-positive patients (pre-core mutant HBV) who generally have lower replication levels than HBeAg-positive patients. Active HBV replication is associated with a significant risk of progression to chronic hepatitis B complications[11]. The presence of HBV DNA is the single most important indication to start antiviral therapy[12]. This work aimed at evaluating the clinical significance of localizing HBV DNA in the liver in case of negative viremia. Patients with HBsAg and elevated ALT were selected among patients who presented at the outpatient clinic of the Tropical Medicine Department, suffering from a variety of chronic liver diseases.

Of 670 patients, the prevalence of HBsAg-positive patients among those with chronic liver disease was 6.6% (44/670). This figure represented both the carriage rate and the infection rate among chronic liver disease patients, whatever the causes were. The prevalence of HBV chronic hepatitis among chronic liver disease patients was 4.9% (33/670). The prevalences of HBV infection in Egypt have been found to be variable among different studies, ranging from 3.2% to 21%[13–19], depending on the number of patients. The higher figures studied the prevalence among cirrhotic patients, the lowest figures were found among school children in certain villages. Thirty-three patients eligible for the present study were considered to have chronic hepatitis B. NASH was not totally excluded. Fourteen liver biopsies showed prominent steatosis. The prevalence of steatosis in Egypt is expected to be quite high. It is known that 35% of the Egyptians are considered obese[20]. Moreover, high comorbid factors are recorded among Egyptians, such as diabetes, pollution, etc. It is worth mentioning that none of our 33 patients had a BMI >29 kg/m^2, and we had two diabetic patients.

In this study, the histopathological results showed that most of our patients had relatively mild disease, with an HAI score between 0 and 9, and a fibrosis score between 0 and 2. Conversely, the HBsAb-positive patients had a higher HAI score as compared with the HBsAb-negative patients. This might be explained by a stronger reaction to HBV infection in the former subgroup. The co-existence of both HBsAg and HBsAb has been previously described, and it is thought that HBsAb in such a situation is unable to neutralize the virus[21]. It has also been postulated that infection with multiple types of HBV is another explanation for this finding[22]. Most of our patients (78.8%) were HBeAg-negative chronic hepatitis B. It is known that the core promoter mutants are predominant in Egypt[23]. Compared to the HBeAg-negative chronic hepatitis B, the HBeAg-positive patients had a milder disease histopathologically, which was in agreement with previous reports[23–25]. We observed that the detection of HBV viremia was more in HBeAg-positive patients, which is expected, because of the formerly documented strong correlation between HBV DNA and HBeAg[26]. Characteristically, five patients (15.2%) were negative for both HBeAg and HBeAb, and five patients were negative for HBcAb. Three patients were negative for all seromarkers except HBsAg. These unusual patterns of serological profile can be explained either by mutations or viral DNA integration. Absence of cytotoxic T-lymphocyte (CTL) recognition of epitopes in HBeAg, HBsAg, and other viral proteins contributes to viral persistence. Failure of antigen presentation to CD4 helper T cells, failure of CD4

proliferating responses, immune modulation by secreted proteins, viral mutation, and integration of viral DNA into the cellular genome are all mechanisms involved in viral persistence[27]. Three patients had undetectable HBV DNA in either serum or liver tissue. This might be explained by an enhanced immunological response to HBV DNA, and extraordinarily low viral DNA copy number[28], or by the integration phenomenon affecting the primer orientation used in PCR technique[29]. Another explanation stands on HBV infection being a dynamic process, so that some of these patients might have been in the immune clearance phase[23]. Five patients had negative HBV DNA in the liver tissue, but positive in serum. This can be explained by the liver being a vast size organ, and hence, substantial viremia can result even if each cell produces only a few numbers of virions per day. This hypothesis has been proposed by Branch *et al*.[31] on HCV infection. In our opinion, it can also be applied on HBV infection if the viral genome is present in a very low level to be detected by biopsy. Ten patients (30.3%) did not fulfill any of the clinical criteria identified in literature. They could not classically fit in the Poynard's 2002 classification. They had one common serological profile, which is, detection of HBV DNA in the liver tissues but not in the sera (negative viremia). The disease burden as evidenced by hepatic biochemical profile and the spectrum of HAI and fibrosis was not different in this group of patients from those with the classic chronic HBV infection. This group has been named in this study as "hepatitis B *in situ*". Seven out of the eighteen patients, showing a classic unequivocal pattern of HBeAg-negative chronic hepatitis, had hepatitis B *in situ*. This implies that the reliance on mere testing of serum HBV DNA would have missed viral replication in such condition. On the other hand, HBeAg-positive hepatitis showed viremia in most cases.

In conclusion, a significant number of patients with chronic hepatitis B fail to show viremia, yet HBV DNA can be detected in their liver tissues. Hepatitis B *in situ* is a term used to describe the detection of total HBV DNA (Integrated plus CCC form) in liver tissue of patients with positive HBsAg and negative viremia. It is particularly frequent in the HBeAg-negative variety of chronic hepatitis B. The bearing of "hepatitis B *in situ*" on the liver is no less than the viremic form; serious sequelae are thus liable to take place. The recognition of this form of the disease may have its impact on the choice of therapy, since such patients should not be denied the chance to receive antiviral treatment.

REFERENCES

1 **Rapicetta M**, Ferrari C, Levrero M. Viral determinants and host immune responses in the pathogenesis of HBV infection. *J Med Virol* 2002; **67:** 454-457

2 **Fong TL**, Di Bisceglie AM, Gerber MA, Waggoner JG, Hoofnagle JH. Persistence of hepatitis B virus DNA in the liver after loss of HBsAg in chronic hepatitis B. *Hepatology* 1993; **18:** 1313-1318

3 **Cacciola I**, Pollicino T, Squadrito G, Cerenzia G, Villari D, de Franchis R, Santantonio T, Brancatelli S, Colucci G, Raimondo G. Quantification of intrahepatic hepatitis B virus (HBV) DNA in patients with chronic HBV infection. *Hepatology* 2000; **31:** 507-512

4 **Pawlotsky JM**, Bastie A, Hezode C, Lonjon I, Darthuy F, Remire J, Dhumeaux D. Routine detection and quantification of hepatitis B virus DNA in clinical laboratories: performance of three commercial assays. *J Virol Methods* 2000; **85:** 11-21

5 **Kaneko S**, Miller RH, Di Bisceglie AM, Feinstone SM, Hoofnagle JH, Purcell RH. Detection of hepatitis B virus DNA in serum by polymerase chain reaction. Application for clinical diagnosis. *Gastroenterology* 1990; **99:** 799-804

6 **Lee CZ**, Huang GT, Yang PM, Sheu JC, Lai MY, Chen DS. Correlation of HBV DNA levels in serum and liver of chronic hepatitis B patients with cirrhosis. *Liver* 2002; **22:** 130-135

7 **Meng Q**, Wong C, Rangachari A, Tamatsukuri S, Sasaki M, Fiss E, Cheng L, Ramankutty T, Clarke D, Yawata H, Sakakura Y, Hirose T, Impraim C. Automated multiplex assay system for simultaneous detection of hepatitis B virus DNA, hepatitis C virus RNA, and human immunodeficiency virus type 1 RNA. *J Clin Microbiol* 2001; **39:** 2937-2945

8 **Chu CJ**, Lok AS. Clinical utility in quantifying serum HBV DNA levels using PCR assays. *J Hepatol* 2002; **36:** 549-551

9 **Ishak K**, Baptista A, Bianchi L, Callea F, De Groote J, Gudat F, Denk H, Desmet V, Korb G, MacSween RN. Histological grading and staging of chronic hepatitis. *J Hepatol* 1995; **22:** 696-699

10 **De Castro L**, Niel C, Gomes SA. Low frequency of mutations in the core promoter and precore regions of hepatitis B virus in anti-HBe positive Brazilian carriers. *BMC Microbiol* 2001; **1:** 10

11 **Poynard T**. Hepatitis B. In Hepatitis B and C: management and treatment. 1st ed. Mobipocket ebooks. 2002: 63 http://www.ebookmall.com/ebook/88983-ebook.htm

12 **Pawlotsky JM**. Molecular diagnosis of viral hepatitis. *Gastroenterology* 2002; **122:** 1554-1568

13 **Tsai NC**. Practical management of chronic hepatitis B infection. *Semin Liver Dis* 2004; **24 Suppl 1:** 71-76

14 **Sherif MM**, Abou-Aita BA, Abou-Elew MH, el-Kafrawi AO. Hepatitis B virus infection in upper and lower Egypt. *J Med Virol* 1985; **15:** 129-135

15 **Kamel MA**, Miller FD, el Masry AG, Zakaria S, Khattab M, Essmat G, Ghaffar YA. The epidemiology of Schistosoma mansoni, hepatitis B and hepatitis C infection in Egypt. *Ann Trop Med Parasitol* 1994; **88:** 501-509

16 **Attia MA**. Prevalence of hepatitis B and C in Egypt and Africa. *Antivir Ther* 1998; **3:** 1-9

17 **Andre F**. Hepatitis B epidemiology in Asia, the Middle East and Africa. *Vaccine* 2000; **18 Suppl 1:** S20-S22

18 **Angelico M**, Renganathan E, Gandin C, Fathy M, Profili MC, Refai W, De Santis A, Nagi A, Amin G, Capocaccia L, Callea F, Rapicetta M, Badr G, Rocchi G. Chronic liver disease in the Alexandria governorate, Egypt: contribution of schistosomiasis and hepatitis virus infections. *J Hepatol* 1997; **26:** 236-243

19 **Zaki A**, Bassili A, Amin G, Aref T, Kandil M, Abou Basha LM. Morbidity of schistosomiasis mansoni in rural Alexandria, Egypt. *J Egypt Soc Parasitol* 2003; **33:** 695-710

20 **Reda AA**, Arafa MA, Youssry AA, Wandan EH, Ab de Ati M, Daebees H. Epidemiologic evaluation of the immunity against hepatitis B in Alexandria, Egypt. *Eur J Epidemiol* 2003; **18:** 1007-1011

21 http://www.tribuneindia.com/2000/20000917/world.htm#6

22 **Park LC**, Maruyama T, Kamiya N, Goto M, Kuma H, Hamasaki N. Mutation detection in the drug-resistant hepatitis B virus polymerase gene using nanostructured reverse micelles. *Anal Sci* 2004; **20:** 1609-1611

23 **Saudy N**, Sugauchi F, Tanaka Y, Suzuki S, Aal AA, Zaid MA, Agha S, Mizokami M. Genotypes and phylogenetic characterization of hepatitis B and delta viruses in Egypt. *J Med Virol* 2003; **70:** 529-536

24 **Fattovich G**. Natural history and prognosis of hepatitis B. *Semin Liver Dis* 2003; **23:** 47-58

25 **Hadziyannis SJ**, Vassilopoulos D. Hepatitis B e antigen-negative chronic hepatitis B. *Hepatology* 2001; **34:** 617-624
26 **Yalcin K**, Degertekin H, Yildiz F, Celik Y. Markers of disease activity in chronic hepatitis B virus infection. *Clin Invest Med* 2003; **26:** 27-34
27 **Zhang L**, Zhu J, Ma Y, Zhang H. Nucleic acid quantifying assay of hepatitis B virus. *Zhonghua Ganzangbing Zazhi* 2002; **10:** 49-51
28 **Carman WF**, Thomas HC, Zuckermann AJ. Molecular variants of hepatitis B. In: viral hepatitis. Zuckermann A, Thomas HC, eds. 2nd ed. *Churchill Livingstone*. 1998; **Section III:** 141-172
29 **Kuhns M**, McNamara A, Mason A, Campbell C, Perrillo R. Serum and liver hepatitis B virus DNA in chronic hepatitis B after sustained loss of surface antigen. *Gastroenterology* 1992; **103:** 1649-1656
30 **Balderas-Renteria I**, Munoz-Espinosa LE, Dector-Carrillo MA, Martinez-Martinez FJ, Barrera-Saldana HA. Detection of hepatitis B virus in seropositive and seronegative patients with chronic liver disease using DNA amplification by PCR. *Arch Med Res 2002*; **33:** 566-571
31 **Branch AD**, Seeff LB. Afterword: HCV in the decades ahead. *Semin Liver Dis* 2000; **20:** 233-237

Science Editor Kumar M and Guo SY **Language Editor** Elsevier HK

PO Box 2345, Beijing 100023, China
www.wjgnet.com
wjg@wjgnet.com

ELSEVIER

World J Gastroenterol 2005;11(43):6858-6862
World Journal of Gastroenterology ISSN 1007-9327

• *RAPID COMMUNICATION* •

Effect of transjugular intrahepatic portosystemic shunt on pulmonary gas exchange in patients with portal hypertension and hepatopulmonary syndrome

Graciela Martínez-Pallí, Britt B Drake, Joan-Carles García-Pagán, Joan-Albert Barberà, Miguel R Arguedas, Robert Rodriguez-Roisin, Jaume Bosch, Michael B Fallon

Graciela Martínez-Pallí, Servei d'Anestesiologia i Reanimació. Hospital Clínic, Institut d'Investigacions Biomèdiques August Pi i Sunyer (IDIBAPS), Universitat de Barcelona, Barcelona, Spain
Britt B Drake, Miguel R Arguedas, Michael B Fallon, University of Alabama at Birmingham Liver Center, 290 MCLM, 1918 University Blvd., Birmingham, AL 35294-0005, United States
Joan-Carles García-Pagán, Jaume Bosch, Hepatic Hemodynamic Laboratory, Liver Unit, Institut de Malalties Digestives, Hospital Clínic, IDIBAPS, Universitat de Barcelona, Barcelona, Spain
Robert Rodriguez-Roisin, Joan-Albert Barberà, Servei de Pneumologia i Al·lèrgia Respiratòria, Institut Clinic de Pneumologia I Cirurgia Toràcica , Hospital Clínic, IDIBAPS, Universitat de Barcelona, Barcelona, Spain
Supported by FIS 02/0692 and 02/0739 from the Fondo de Investigaciones Sanitarias, SGR 2001 SGR00286 from the Generalitat de Catalunya (DURSI), and CO 3/02 and CO 3/11 from the Instituto de Salud Carlos III
Correspondence to: Joan-Carles García-Pagán, Hepatic Hemodynamic Laboratory, Hospital Clínic, Villarroel 170, 08036 Barcelona, Spain. jcgarcia@clinic.ub.es
Telephone: +34-93-2275400 -2824 Fax: +34-93-4515272
Received: 2005-02-04 Accepted: 2005-05-12

Abstract

AIM: To assess the impact of transjugular intrahepatic portosystemic shunt (TIPS) on pulmonary gas exchange and to evaluate the use of TIPS for the treatment of hepatopulmonary syndrome (HPS).

METHODS: Seven patients, three of them with advanced HPS, in whom detailed pulmonary function tests were performed before and after TIPS placement at the University of Alabama Hospital and at the Hospital Clinic, Barcelona, were considered.

RESULTS: TIPS patency was confirmed by hemodynamic evaluation. No changes in arterial blood gases were observed in the overall subset of patients. Transient arterial oxygenation improvement was observed in only one HPS patient, early after TIPS, but this was not sustained 4 mo later.

CONCLUSION: TIPS neither improved nor worsened pulmonary gas exchange in patients with portal hypertension. This data does not support the use of TIPS as a specific treatment for HPS. However, it does reinforce the view that TIPS can be safely performed for the treatment of other complications of portal hypertension in patients with HPS.

Key words: Portal hypertension; Transjugular intrahepatic portosystemic shunt; Pulmonary gas exchange; Hepatopulmonary syndrome

Martínez-Pallí G, Drake BB, García-Pagán JC, Barberà JA, Arguedas MR, Rodriguez-Roisin R, Bosch J, Fallon MB. Effect of transjugular intrahepatic portosystemic shunt on pulmonary gas exchange in patients with portal hypertension and hepatopulmonary syndrome. *World J Gastroenterol* 2005; 11(43): 6858-6862
http://www.wjgnet.com/1007-9327/11/6858.asp

INTRODUCTION

Transjugular intrahepatic portosystemic shunt (TIPS) has been used increasingly in patients with cirrhosis complicated by bleeding varices and refractory ascites[1]. Recently, TIPS has also been proposed as a potential treatment for pulmonary vasodilatation associated with cirrhosis, the so-called hepatopulmonary syndrome (HPS)[2-7]. However, both hemodynamic and metabolic effects of TIPS have been widely studied, little data exists on the effects of TIPS on pulmonary gas exchange in patients with portal hypertension.

HPS occurs when intrapulmonary vasodilatation causes abnormal pulmonary gas exchange in the setting of liver disease[8]. The abnormalities in pulmonary gas exchange result from microvascular dilatation and involve varying degrees of ventilation-perfusion imbalance, oxygen diffusion limitation (diffusion-perfusion defect), and increased intrapulmonary shunting[9]. Although the natural history of HPS is poorly understood, pulmonary gas exchange abnormalities are generally progressive, even in the setting of clinically stable hepatic dysfunction[10]. Currently, liver transplantation is the only therapeutic approach that can resolve HPS. However, perioperative mortality remains high (16-38% within 1 year) and appears to be greatest in those with more advanced HPS[11,12].

HPS has been described most commonly in patients

with cirrhosis of the liver, although it has also been reported in patients with severe acute hepatitis and in non-cirrhotic portal hypertension[13-15]. These findings suggest that portal hypertension plays an important role in the development of intrapulmonary vasodilatation and in the occurrence of HPS. TIPS, by correcting portal hypertension[1], could improve HPS. Indeed, TIPS may be an attractive alternative therapeutic option in selected patients with advanced HPS who are not transplant candidates or in whom liver function is well preserved, particularly if HPS is of sufficient severity to increase transplant mortality or if the waiting time for transplantation is expected to be prolonged. However, the small number of case reports published to date have had variable clinical features and results, and the majority TIPS placement was performed for an acute indication other than HPS[2–7]. Therefore, it is difficult to determine if TIPS specifically improves HPS. In addition, TIPS is known to further exacerbate the hyperdynamic circulation present in patients with cirrhosis and portal hypertension, a fact that might trigger or increase pulmonary vasodilatation and adversely effect pulmonary gas exchange[16-19].

Accordingly, in the present study, we aimed to assess the impact of TIPS on pulmonary gas exchange in patients with portal hypertension and to evaluate the use of TIPS for the treatment of HPS.

MATERIALS AND METHODS

Patients submitted to TIPS treatment at the University of Alabama Hospital and at the Hospital Clínic, Barcelona, were reviewed and the characteristics of patients in whom pulmonary function was evaluated in a period of less than 6 mo before TIPS placement and no more than 1 year after, were included. In three of these patients, TIPS was placed specifically for the treatment of HPS. The diagnosis of HPS was made on the basis of established criteria: the presence of an increase of alveolar-arterial oxygen difference ($AaPO_2$ >15 mmHg); with or without hypoxemia; and evidence of pulmonary vascular dilatation by means of contrast-enhanced echocardiography and/or nuclear isotope lung perfusion scanning, in the context of liver disease[8-10]. The presence of mild intrinsic cardiopulmonary disease was not considered as an exclusion criterion for the diagnosis of HPS[20,21].

Before TIPS placement, all patients underwent measurements of forced spirometry, plethysmography, and single-breath carbon monoxide diffusing capacity (DL_{CO}) after correcting appropriately for hemoglobin concentration. Arterial blood gases were collected while breathing room air in the upright position. The $AaPO_2$ was calculated according to the alveolar gas standard equation using 0.8 as the standard respiratory exchange ratio. Arterial blood gases were repeated after a 20-min period of 100% oxygen breathing in an upright position in patients with HPS.

The TIPS procedure was similar in both institutions and has been previously described[1]. After TIPS, patients underwent close follow-up with US-Doppler and hemodynamic evaluation of TIPS patency. Clinical and biochemical evolution, pulmonary gas exchange analysis, and systemic and pulmonary hemodynamics after TIPS placement were recorded for at least 1 mo following TIPS.

RESULTS

Pulmonary gas exchange was assessed before and after TIPS placement in seven patients. Three patients had HPS and the specific indication for TIPS in each of these patients was treatment of HPS. The remaining four patients had no HPS, but one of them had mild hypoxemia due to a moderate obstructive ventilatory pattern, and the indication for TIPS in these patients was variceal bleeding in three and refractory ascites in one. Demographic and clinical data are summarized in Table 1. TIPS substantially reduced the portal pressure gradient (PPG) (from 15±2 to 5±2 mmHg). In each case, the PPG immediately after TIPS was below 12 mmHg. In addition, during follow-up, TIPS patency, defined as a PPG <12 mmHg, was confirmed by hemodynamic evaluation. The clinical course of pulmonary function in patients without HPS was stable during all the study period. Pulmonary function tests and gas exchange data before and at least 3 mo after TIPS placement in patients with normal gas exchange prior to placement are shown in Table 2. As shown, TIPS neither influenced arterial blood gases nor pulmonary function tests in these patients.

Individual data of patients with HPS are shown in Table 3. All patients had advanced HPS as evidenced by PaO_2<60 mmHg with low $PaCO_2$ values; only Patient #2 responded favorably to 100% oxygen administration. Patients #1 and #2 had a mild restrictive ventilatory pattern possibly related to a coexistent diffuse interstitial

Table 1 Demographic and clinical characteristics (mean±SD, *n*)

	HPS (*n* = 3)	Non-HPS (*n* = 4)
Sex (M/F)	2/1	4/–
Age (yr)	50±22	48±10
Smoking (*n*)	1	4
Current	-	2
Past	1	2
Etiology of chronic liver disease (*n*)		
Hepatitis C	1	1
Alcohol abuse	1	3
Idiopathic portal hypertension	1	
Child–Pugh score A/B/C (*n*)	1/2/–	1/2/1
Presence of esophageal varices	3	4
Gastrointestinal bleeding	2	3
Ascites	1	1
Hepatic encephalopathy	–	–
Cutaneous spider nevi	3	3
Concomitant respiratory symptoms		
Digital clubbing	3	–
Dyspnea	3	1
Cyanosis	3	–
Indication of TIPS		
Variceal bleeding	–	3
Refractory ascites	–	1
Hepatopulmonary syndrome	3	–

TIPS: transjugular intrahepatic portosystemic shunt ; Query: please check the change made.

lung disease (Patient #1) and unilateral pleural fibrosis (Patient #2), respectively. Pulmonary angiography excluded the presence of arterio-venous communications. Ventilation-perfusion (V_A/Q) studies in these two patients, using the multiple inert gas elimination technique[22], was consistent with HPS, showing increased intrapulmonary shunt (43% and 11% of cardiac output) with a mild to moderate degree of V_A/Q mismatch, characterized by areas with low V_A/Q units (6.4% and 0.1% of cardiac output). All three patients exhibited a very severely reduced diffusing capacity (<25% predicted). Transient improvement in arterial oxygenation was observed in only one patient early after TIPS placement (Patient #1) but this was not maintained 4 mo later despite TIPS patency. In the other two patients, no improvement in gas exchange was observed early after TIPS and progressive deterioration in arterial oxygen saturation was evident at 4 mo in Patient #2 and at 4 wk in Patient #3 after TIPS. Patient #1 was excluded for liver transplantation because of the potential coexistence of diffuse interstitial pulmonary disease and severe hypoxemia with a poor response to 100% oxygen breathing. He died of progressive deterioration of pulmonary, hepatic, and renal function. Patient #2 was transplanted, 8 mo after TIPS placement. At the time of liver transplantation, he had persistent severe oxygenation abnormalities. Ten months after orthotopic liver transplant (OLT), pulmonary gas exchange was markedly improved with normal arterial oxygenation and contrast-enhanced echocardiography confirmed resolution of intrapulmonary vasodilatation. Patient #3 was excluded for liver transplantation due to severe hypoxemia. Subsequently, she developed progressive hypoxemia 4 wk after TIPS and died of multisystem organ failure one week later.

Table 2 Pulmonary gas exchange before and after TIPS placement in patients without HPS (mean±SD)

	Pre-TIPS	Post-TIPS
PaO_2 (mmHg)	95±16	95±27
$PaCO_2$ (mmHg)	29±6	31±7
$AaPO_2$ (mmHg)	18±12	18±20
FEV1 (% pred)	72±9	74±5
FVC (% pred)	76±6	80±2
FEV1/FVC	75±10	76±8
DLCO (mL/(min×mmHg))	22±4	20±5
DLCO (% pred)	67±13	63±9

PaO_2: partial pressure of arterial oxygen; $PaCO_2$: partial pressure of arterial carbon dioxide; $AaPO_2$: alveolar to arterial oxygen partial pressure gradient; FEV1: forced expiratory volume at 1 s; FVC: forced vital capacity; FEV1/FVC: ratio of forced expiratory volume at 1 s to forced vital capacity; DL_{CO}: single-breath carbon monoxide diffusing capacity.

DISCUSSION

Portal hypertension is characteristically associated with a hyperkinetic circulation reflected by an increased cardiac output and splanchnic and peripheral vasodilatation[23]. A number of mechanisms contribute to these hemodynamic changes including increased bioavailability of vasodilators, such as nitric oxide[23]. HPS is most commonly observed in the setting of portal hypertension and likely appears to result from a disequilibrium between vasodilator and vasoconstrictor factors in the pulmonary microcirculation. Increased production of nitric oxide has also been proposed as one major determinant of pulmonary vascular dilatation in human HPS[24]. However, whether the same mechanisms that drive the splanchnic and peripheral vasodilatation are operative in the pulmonary microvasculature in HPS is still unknown.

Since HPS is associated with the presence of portal hypertension, portal pressure reduction through TIPS placement may be a useful therapeutic alternative. Till date, six case reports have evaluated the effects of TIPS on gas exchange in HPS[2–7]. Surprisingly, five demonstrated some

Table 3 Pulmonary gas exchange and hemodynamics before and after TIPS placement in patients with HPS

	Pre-TIPS			Post-TIPS <1 mo			Post-TIPS >4 mo		
Patients	# 1	# 2	# 3	# 1	# 2	# 3	# 1	# 2	# 3
FEV1 (% pred)	69	77	100						
FVC (% pred)	66	77	113						
FEV1/FVC	77	80	82						
TLC (% pred)	68	70	83						
DLCO (% pred)	21.3	24	8						
PaO_2 (mmHg)	32	59	28	58	61	31	33	34	–
$PaCO_2$ (mmHg)	27	28	35	31	27	38	26	34	–
$AaPO_2$ (mmHg)	88	54	78	53	69	71	87	73	–
PaO_2 100% O_2 breathing (mmHg)	64	606	86	–	–	–	–	–	–
PAP (mmHg)	14.5	9	18	–	8	22	20	8	–
PVR (dyn.s/cm5)	49	31	111	–	21	82	38	18	–
SVR (dyn.s/cm5)	773	415	1 174	–	400	922	549	560	–
QT (L/min)	9.0	10.4	6.47	–	11.2	7.8	10.5	11.3	–
PP (mmHg)	22	16	19	14	11	22	18.5	11	–
IVCP (mmHg)	5	4	3	7	2.5	19	8	2.5	–
PPG (mmHg)	17	12	16	7	8.5	3	10.5	8.5	–

FEV_1: forced expiratory volume at 1 s; FVC: forced vital capacity; TLC: total lung capacity; DL_{CO}: single-breath carbon monoxide diffusing capacity; PaO_2: partial pressure of arterial oxygen; $PaCO_2$: partial pressure of arterial carbon dioxide; $AaPO_2$: alveolar to arterial oxygen partial pressure gradient; PAP: mean pulmonary artery pressure; PVR: pulmonary vascular resistance; SVR: systemic vascular resistance; Q_T: cardiac output; PP: portal pressure; IVCP: inferior vena cava pressure; PPG: portocaval pressure gradient.

degree of improvement in oxygenation. However, short-term (<1 mo) duration of follow-up in two patients[2,3] and the presence of coexistent hepatic hydrothorax in the third one[4] limit the evaluation of the utility of TIPS for hypoxemia in these cases. In two other reports[5,6], with a longer follow-up (>7 mo), arterial desaturation improved after TIPS and in one of these, a 11 year-old female with biliary atresia, gas exchange improvement was associated with a remarkable reduction in intrapulmonary shunt[6]. In the sixth report[7], TIPS failed to improve arterial hypoxemia in one patient. Altogether these reports suggest that portal pressure reduction *per se* does not consistently improve pulmonary gas exchange in HPS.

Portal pressure reduction after TIPS is also associated with an exacerbation of the hyperdynamic circulatory state, an effect that persists for at least 3 mo following TIPS placement[16-19]. During this time, pulmonary vascular resistance may also decline[17,18,25]. The mechanisms by which TIPS accentuate the hyperdynamic circulation are not well understood but may involve porto-systemic shunting of vasoactive substances through the TIPS which alter NO production[17,26-28]. The net result could enhance pulmonary vasodilation, thereby resulting in the development and/or worsening of HPS. In two of our patients with HPS who underwent TIPS, we confirmed obviously decreased systemic and pulmonary vascular resistance early after placement. Despite these hemodynamic changes, arterial oxygenation did not significantly deteriorate. In addition, in our four other patients without HPS who underwent successful TIPS, no changes in gas exchange were shown following TIPS placement. These findings complement and extend the findings of prior reports and support that the exacerbation of the hyperdynamic state following TIPS placement is not associated with arterial oxygenation worsening.

The portal pressure gradient (PPG) was reduced below 10 mmHg in each of our patients who underwent TIPS for HPS. Despite this, none of them had a sustained improvement in arterial blood gases. One patient did have a transient improvement in arterial oxygenation early after TIPS placement. Conceivably, one explanation for this improvement could be improved ventilation-perfusion matching induced by a rise in cardiac output resulting in increased blood flow, selective redistribution to the upper lobes of the lung, where vasodilatation is typically less severe in HPS. A similar mechanism may have been operative in the study by Selim *et al.*[4] where oxygenation improved after TIPS in association with a rise in cardiac output despite significant persistent intrapulmonary shunting. Alternatively, the increased cardiac output may improve PaO_2 through increased mixed venous PO_2, other things being equal. Our study and patients were different from prior case reports in that our group represented patients who specifically underwent TIPS for HPS. In four of the six prior reports, another acute indication for TIPS was present, including variceal bleeding and hepatic hydrothorax. The presence and resolution of other major complications of portal hypertension could have influenced favorably arterial blood gases in these cases. In addition, our patients had more severe gas exchange abnormalities than those in prior studies and it is unknown whether or not the severity of pulmonary vasodilatation may modulate the response to TIPS. Finally, our findings are clearly different from the report by Paramesh *et al.*[7], where TIPS placement resulted in a sustained and dramatic improvement in both pulmonary vasodilatation and arterial oxygenation. However, this case involved a child with biliary atresia and whether pathophysiologic mechanisms and responses to portal decompression in this setting are applicable to adults with other causes of liver disease is unknown[7].

In summary, our findings suggest that treatment with TIPS in patients with portal hypertension has no deleterious effects on pulmonary gas exchange, despite coexisting exacerbation of the hyperdynamic circulatory state. However, portal decompression with TIPS as a specific therapy for HPS is ineffective. This data supports the use of TIPS in patients with HPS for the treatment of other accepted indications for TIPS, but not as a specific therapy to improve arterial oxygenation defects in HPS.

REFERENCES

1 **Casado M**, Bosch J, Garcia-Pagan JC, Bru C, Banares R, Bandi JC, Escorsell A, Rodriguez-Laiz JM, Gilabert R, Feu F, Schorlemer C, Echenagusia A, Rodes J. Clinical events after transjugular intrahepatic portosystemic shunt: correlation with hemodynamic findings. *Gastroenterology* 1998; **114**: 1296-1303

2 **Riegler JL**, Lang KA, Johnson SP, Westerman JH. Transjugular intrahepatic portosystemic shunt improves oxygenation in hepatopulmonary syndrome. *Gastroenterology* 1995; **109**: 978-983

3 **Lasch HM**, Fried MW, Zacks SL, Odell P, Johnson MW, Gerber DA, Sandhu FS, Fair JH, Shrestha R. Use of transjugular intrahepatic portosystemic shunt as a bridge to liver transplantation in a patient with severe hepatopulmonary syndrome. *Liver Transpl* 2001; **7**: 147-149

4 **Selim KM**, Akriviadis EA, Zuckerman E, Chen D, Reynolds TB. Transjugular intrahepatic portosystemic shunt: a successful treatment for hepatopulmonary syndrome. *Am J Gastroenterol* 1998; **93**: 455-458

5 **Allgaier HP**, Haag K, Ochs A, Hausentein KH, Jeserich M, Krause T, Heilmann C, Gerok W, Rossle M. Hepato-pulmonary syndrome: succesful treatment by transjugular intrahepatic portosystemic shunt (TIPS) (letter). *J Hepatoly* 1995; **23**: 102-105

6 **Corley DA**, Scharschmidt B, Bass N, Somberg K, Gold W. Lack of efficacy of TIPS for hepatopulmonary syndrome *Gastroenterology* 1997; **113**: 728-730

7 **Paramesh AS**, Husain SZ, Shneider B, Guller J, Tokat I, Gondolesi GE, Moyer S, Emre S. Improvement of hepatopulmonary syndrome after transjugular portosystemic shunting : case report and review of literature. *Pediatric transplant* 2003;**7**: 157-162

8 **Rodriguez-Roisin R**, Krowka MJ, Herve P, Fallon MB. Pulmonary-Hepatic vascular Disorders (PHD). *Eur Respir J* 2004; **24**: 861-880

9 **Fallon MB**, Abrams GA. Pulmonary dysfunction in chronic liver disease. *Hepatology* 2000; **32**: 859-865

10 **Martínez GP**, Barbera JA, Visa J, Rimola A, Pare JC, Roca J, Navasa M, Rodes J, Rodriguez-Roisin R. Hepatopulmonary syndrome in candidates for liver transplantation. *J Hepatol* 2001; **34**: 651-657

11 **Arguedas MR**, Abrams GA, Krowka MJ, Fallon MB. Prospective evaluation of outcomes and predictors of mortality

in patients with hepatopulmonary syndrome undergoing liver transplantation. *Hepatology* 2003; **37**: 192-197

12 **Krowka MJ**, Porayko MK, Plevak DJ, Pappas C, Steers JL, Krom RAF, Wiesner RH. Hepatopulmonary syndrome with progressive hypoxemia as an indication for liver transplantation: case reports and literature review. *Mayo Clin Proc* 1997; **72**: 44-53

13 **Babbs C**, Warners TW, Haboubi NY. Non cirrhotic portal hypertension with hypoxemia. *Gut* 1988; **29**:129-131.

14 **De BK**, Sen S, Biswas PK, Mandal SK, Das D, Das U, Guru S, Bandyopadhyay K. Occurrence of hepatopulmonary syndrome in Budd-Chiari syndrome and the role of venous decompression. *Gastroenterology* 2002; **122**: 897-903

15 **Abrams GA**, Fallon MB. The hepatopulmonary syndrome. *Clin Liver Dis* 1997; **1**: 185-200

16 **Azoulay D**, Castaing D, Dennison A, Martino W, Eyraud D, Bismuth H. Transjugular intrahepatic portosystemic shunt worsens the hyperdynamic circulatory state of the cirrhotic patient: preliminary report of a prospective study. *Hepatology* 1994; **19**: 129-132

17 **Rodriguez-Laiz JM**, Banares R, Echenagusia A, Casado M, Camunez F, Perez-Roldan F, de Diego A, Cos E, Clemente G. Effects of transjugular intrahepatic portasystemic shunt (TIPS) on splanchnic and systemic hemodynamics, and hepatic function in patients with portal hypertension. Preliminary results. *Dig Dis Sci* 1995; **40**: 2121-2127

18 **Van Der Linden P**, Le Moine O, Ghysels M, Ortinez M, Deviere J. Pulmonary hypertension after transjugular intrahepatic portosystemic shunt: effects on right ventricular function. *Hepatology* 1996; **23**: 982-987

19 **Francois E**, Garcia-Pagan JC, Bru C, Feu F, Gilabert R, Escorsell A, Bosch J, Rodes J. Effects of percutaneous intrahepatic portosystemic shunt on splanchnic and systemic hemodynamics in patients with portal hypertension. *Gastroenterol Hepatol* 1997; **20**: 11-14

20 **Martinez-Pallí G**, Barbera JA, Navasa M, Roca J, Visa J, Rodriguez-Roisin R. Hepatopulmonary syndrome associated with cardiorespiratory disease. *J Hepatol* 1999; **30**: 882-889

21 **Krowka MJ**. Caveats concerning hepatopulmonary syndrome. *J Hepatol* 2001; **34**: 756-758

22 **Roca J**, Wagner PD. Contribution of multiple inert gas elimination technique to pulmonary medicine. 1. Principles and information content of the multiple inert gas elimination technique. *Thorax* 1994; **49**: 815-824

23 **Bosch J**, García-Pagán JC. Complications of cirrhosis. I. Portal hypertension. *J Hepatol* 2000; **32S**: 141-156

24 **Cremona G**, Higenbottam TW, Mayoral V, Alexander G, Demoncheaux E, Borland C, Roe P, Jones GJ. Elevated exhaled nitric oxide in patients with hepatopulmonary syndrome. *Eur Respir J* 1995; **8**: 1883-1885

25 **Lotterer E**, Wengert A, Fleig WE. Transjugular intrahepatic portosystemic shunt: short term and lshort-term effects on hepatic and systemic hemodynamics in patients with cirrhosis. *Hepatology* 1999; **29**: 632-639

26 **Bernadich C**, Bandi JC, Melin P, Bosch J. Effects of F-180, a new selective vasoconstrictor peptide, compared with terlipressin and vasopressin on systemic and splanchnic hemodynamics in a rat model of portal hypertension. *Hepatology* 1997; **26**: 262-267

27 **Jalan R**, Damink SO, Deutz N, Redhead D, Lee A. Increased cerebral and peripheral vasodilation, and whole body nitric oxide (NO) production after insertion of a transjugular intrahepatic portosystemic stent-shunt (TIPSS) in patient with cirrhosis. *J Hepatol* 2002; **36**: A178:55

28 Colombato LA, Spahr L, Martinet JP, Dufresne MP, Lafortune M, Fenyves D, Pomier-Layrargues G. Haemodynamic adaptation two months after transjugular intrahepatic portosystemic shunt (TIPS) in cirrhotic patients. *Gut* 1996; **39**: 600-604

Science Editor Kumar M and Guo SY **Language Editor** Elsevier HK

PO Box 2345, Beijing 100023, China
www.wjgnet.com
wjg@wjgnet.com

ELSEVIER

World J Gastroenterol 2005;11(43):6863-6866
World Journal of Gastroenterology ISSN 1007-9327

• *RAPID COMMUNICATION* •

Incidence and localization of lymphoid follicles in early colorectal neoplasms

Kuang-I Fu, Yasushi Sano, Shigeharu Kato, Takahiro Fujii, Ikuro Koba, Takayuki Yoshino, Atsushi Ochiai, Shigeaki Yoshida, Takahiro Fujimori

Kuang-I Fu, Yasushi Sano, Shigeharu Kato, Takahiro Fujii, Ikuro Koba, Takayuki Yoshino, Shigeaki Yoshida, Division of Gastrointestinal Oncology and Digestive Endoscopy, National Cancer Center Hospital East, Kashiwa, Chiba 277-8577, Japan
Atsushi Ochiai, Division of Pathology, National Cancer Center Research Institute East, Kashiwa, Japan
Kuang-I Fu, Takahiro Fujimori, Department of Surgical and Molecular Pathology, Dokkyo University School of Medicine, 880 Kitakobaysashi, Mibu, Shimotuga, Tochigi 321-0293, Japan
Correspondence to: Kuang-I Fu, MD, Department of Surgical and Molecular Pathology, Dokkyo University School of Medicine, 880 Kitakobayashi, Mibu, Shimotuga, Tochigi, 321-0193, Japan. fukuangi@hotmail.com
Telephone: +81-282-86-1111 Fax: +81-282-86-5678
Received: 2004-02-21 Accepted: 2005-04-02

Abstract

AIM: To investigate the incidence and localizations of lymphoid follicles (LFs) in early colorectal neoplasms in human beings.

METHODS: From July 1992 to September 1999, a total of 1 324 early colorectal neoplasms were removed endoscopically or surgically at our hospital; 1 031 (77.9%) were available for analysis in this study. Localization of LFs was defined histologically: as submucosal LFs, if located under the muscularis mucosa; and as intramucosal LFs, if located across or over the muscularis mucosa.

RESULTS: Histologically, the materials included 903 intramucosal neoplasms and 128 submucosal cancers. Overall incidence of LFs was 27.2% (280/1 031). The incidence of LFs was significantly higher in females (33.6% *vs* 24.9%, $P = 0.0064$), the right-sided colon (32.2% *vs* 25.6%, $P = 0.0403$) and in flat or depressed type lesions (34.6% *vs* 25.2%, $P<0.0001$) as compared to males, left-sided colon and protruding type lesions, respectively. The incidences of intramucosal neoplasms and submucosal cancers were 24.3% and 43.8%, respectively ($P<0.0001$). Localizations of LFs (intramucosal LF/submucosal LF) in depressed, flat, and protruding types were 1/24, 14/36, and 131/74, respectively.

CONCLUSION: The incidence of LFs in early human colorectal neoplasms significantly differs by gender, location, macroscopic type, and histology. Moreover, localization significantly differs by macroscopic type.

Key words: Lymphoid follicle; Early colorectal neoplasm; Carcinogenesis

Fu KI, Sano Y, Kato S, Fujii T, Koba I, Yoshino T, Ochiai A, Yoshida S, Fujimori T. Incidence and localization of lymphoid follicles in early colorectal neoplasms. *World J Gastroenterol* 2005; 11(43): 6863-6866
http://www.wjgnet.com/1007-9327/11/6863.asp

INTRODUCTION

Several reports have investigated the association between lymphoid aggregates and colonic tumors in rodents[1-4]. The results indicate that colonic crypts overlying lymphoid follicles (LFs) show a significantly higher proliferative activity. These results also showed that the risk of carcinoma increased in the colonic mucosa on LFs compared to mucosa without LFs. Consequently, it was considered that factors from LFs promote carcinogenesis in the epithelium in rodents. Rubio *et al*.[5] also investigated the incidence of LFs in early stage adenomas and adenocarcinomas in Swedish and Japanese patients, showing that 38% of 174 consecutive non-polypoid adenomas and flat incipient adenocarcinomas had subjacent LFs. Moreover, they observed a higher incidence of LFs in non-polypoid neoplasms as compared to polypoid neoplasms in rats[6].

Recently, advances in endoscopic techniques and equipment have enabled much smaller flat and depressed colorectal neoplasms to be detected[7-11]. We have also microscopically encountered LFs and found that their incidence and localization tended to be different according to their macroscopic features in early colorectal neoplasms. In this study, we, therefore, aimed to investigate the incidence and localization of LFs revealed in early human colorectal neoplasms.

MATERIALS AND METHODS

Subjects

From July 1992 to September 1999, a total of 1 324 early colorectal neoplasms, including adenoma with high-grade

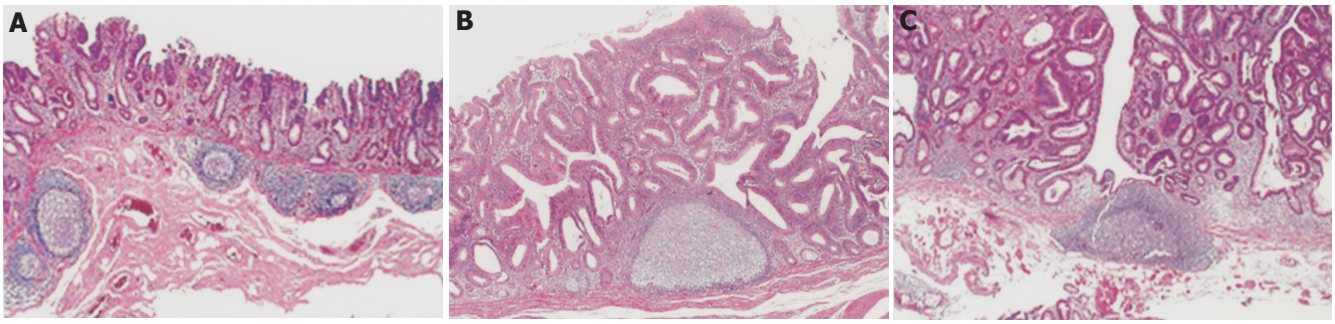

Figure 1 Localizations of LFs in early colorectal neoplasms. **A:** Submucosal LF in intramucosal carcinoma; **B:** intramucosal LFs in adenoma with moderate atypia; **C**: intermucosal LFs in adenoma with moderate atypia.

atypia, intramucosal cancer and submucosal invasive cancer, were removed endoscopically or surgically in our hospital. Of the 1 324 lesions, 293 (22.1%) were excluded from this study because the histology had been damaged by endoscopic procedures and they were judged inappropriate for analysis. The lesions of patients with familial polyposis, hereditary non-polyposis colorectal cancer, and inflammatory bowel disease were also excluded.

Location

The locations of the lesions were categorized into two groups at the splenic flexure: right-sided colon (including the cecum, ascending colon, and transverse colon); and left-sided colon (including descending colon, sigmoid colon, and rectum).

Macroscopic type

Macroscopically, colorectal lesions were classified into three groups according to the criteria of the Japanese Research Society for Cancer of the Colon and Rectum (JRSCCR): depressed (D) type; flat (F) type; and protruding (P) type.

Evaluation

Histological examinations of the available lesions were performed with hematoxylin-and-eosin (HE) staining. The pathological definitions of the lesions were as established by the JRSCCR. We defined a lymphoglandular complex with an enlarged germinal center as a LF. The localizations of LFs were classified into two groups: LFs located beyond the muscularis mucosa were defined as "submucosal LFs" (Figure 1A); and LFs located across or above the muscularis mucosa were defined as "intramucosal LFs" (Figures 1B and C). The presence and localization of LFs were investigated histologically.

Statistical analysis

Using χ^2 test and Fisher's exact probability test, we compared the clinicopathological characteristics and the incidence and localization of LFs in early human colorectal neoplasms. Correlations between lesion size and the presence or absence of LFs in each macroscopic type were evaluated by using Spearman's rank correlation. A value of $P<0.05$ was considered statistically significant.

RESULTS

The details of the clinicopathological characteristics of the subjects are shown in Table 1. A total of 1 031 lesions, including 903 intramucosal neoplasms and 128 submucosal cancers, were investigated histologically. Endoscopically, 60 were depressed type, 157 flat type, and 814 protruding type.

Incidence of LFs

LFs were present in 280 of the 1 031 lesions, an overall incidence of 27.2%. The incidence of LFs was significantly higher in females (89/265, 33.6%) compared to males (191/766, 24.9%) ($P = 0.0064$). The incidence of LFs was markedly higher in the right-sided colon (32.2%, 79/166) than in the left-sided colon (25.6%, 201/786, $P = 0.0403$). In addition, the incidence of LFs in submucosal cancers (43.8%, 56/128) was significantly higher than in intramucosal neoplasms (24.3%, 224/903, $P<0.0001$). The incidences of LFs in submucosal cancers with or without lymph node metastasis were 8.9% (5/56) and 8.3% (6/72), respectively, showing no significant correlation between the presence of LFs and lymph node metastasis in submucosal cancers. LFs were present in 41.7% (25/60) of D type, 31.8% (50/157) of F type, and 25.2% (205/814) of P type lesions. The incidence of LFs in F and D type (34.6%, 75/217) was significantly higher than in P type (25.2%, 205/814) ($P<0.0001$, Table 1).

Localization of LFs

Of the 280 lesions with LFs, 146 were classified as intramucosal and 134 as submucosal. In addition, the localizations of LFs (intramucosal/submucosal) were also different according to macroscopic types: 1/24 in D, 14/36 in F, and 131/74 in P types (Table 2). The D and F type lesions harboring LFs also showed a significantly higher incidence of submucosal LFs as compared to the P type lesions ($P<0.0001$).

Correlation between the presence of LFs and tumor size

The mean tumor sizes of the early colorectal neoplasms with or without LFs in each macroscopic type were 12.3±6.3 and 8.0±5.7 mm in D type, 14.8±10.6 and 8.6±5.1 mm in F type, and 17.9±12.0 and 12.8±8.3 mm in P type, respectively,

Table 1 Correlations between clinicopathological characteristics and the presence or absence of lymphoid follicles

		LF[1] present (%)	LF absent (%)	*P*
Total cases	1 031	280 (27.2)	51 (72.8)	
Gender				
Male	766	191 (24.9)	575 (75.1)	
Female	265	89 (33.6)	176 (66.4)	0.0064
Location				
Right - sided colon	245	79 (32.2)	166 (67.8)	
Left - sided colon	786	201 (25.6)	585 (74.4)	0.0403
Size (mean)(mm)				
Depressed + Flat	10.3 ± 3.4	13.9 ± 6.3	8.5 ± 5.3	
Protruding	14.1 ± 9.6	17.9 ± 12.0	12.8 ± 8.3	0.0095
Macroscopic type				
Depressed + Flat	217	75 (34.6)	142 (65.4)	
Protruding	814	205 (25.2)	609 (74.8)	0.0133
Histology				
Intramucosal neoplasias	903	224 (24.8)	679 (75.2)	
Submucosal cancer	128	56 (43.8)	72 (56.2)	<0.0001

[1]Lymphoid follicle.

Table 2 Localizations of the lymphoid follicles in each macroscopic types

	Intramucosal LF[1] (%)	Submucosal LF (%)	Total
Depressed	1 (4)	24 (96)	25
Flat	14 (28)	36 (72)	50
Protruding	131 (64)	74 (36)	205

[1]Lymphoid follicle

which showed that the mean tumor size in each macroscopic type with LFs was obviously larger compared to the macroscopic type without LFs ($P<0.0001$), and the mean tumor sizes of D and F types with LFs were markedly smaller than that of P type ($P = 0.0095$).

DISCUSSION

We believe that this study is the first report to describe the incidence and localization of LFs subjacent to early colorectal neoplasms in human beings. Rubio *et al*.[5,6] concluded that there appeared to be a genuine association between LFs and non-polypoid adenomas, not only in rodents but also in human beings; however, they did not mention depressed type lesions. Recently, with advances in endoscopic instruments and techniques, concerns have arisen about depressed and flat type early colorectal neoplasms that have increasingly been found worldwide[7-11]. To clarify the characteristics of these depressed and flat type lesions, we investigated the incidence of LFs not only of protruding, but also of depressed and flat type lesions.

Our present results showed that the incidence of LFs differed according to the macroscopic features of early colorectal neoplasms, being especially high in depressed type lesions (41.7%). We also observed that the localizations of LFs seen in early colorectal neoplasms were different according to macroscopic type: 96% (24/25) of depressed and 72% (36/50) of flat lesions-associated LFs were located under the muscularis mucosa (submucosal LF), while 36% (74/205) of protruding lesions harboring LFs were located over or across the muscularis mucosa (intramucosal LF). To the best of our knowledge, no other reports on the localization of LFs in early colorectal neoplasms have been published as yet.

Depressed lesions are known to demonstrate invasive tendencies despite their smaller size[7-9]. Furthermore, flat lesions are reported to be 10 times more likely to contain high-grade dysplasia than protruding ones[12]. In this study, the depressed or flat lesions were found to have a significantly higher incidence of LFs and submucosal LFs compared to the protruding lesions. Based on reports of the aggressive growth patterns of depressed and flat lesions, we speculate that the differences in incidence and location of LFs between flat or depressed and protruding lesions might reflect the host physical defense against neoplasms in human beings; that the submucosal LFs might prevent depressed or flat lesions from downward growth; and that LFs might act against the upward growth of protruding lesions. However, the results from experimental colon cancer studies indicated that aggregates of LFs might promote the development of adenocarcinomas[1-4]. On the other hand, studies in experimental animals have also shown that the intestinal lymphoid system plays an important role in the immunologic defense mechanisms; that is, antigenic stimuli result in germinal center formation, subsequently antibody production, and finally enlargement of the follicles[13]. *In vivo*, the presence of tumor-infiltrating lymphocytes is associated with improved prognosis in colorectal cancers, as does the presence of high level DNA microsatellite instability[14-15]. Carcinomas with lymphoid stroma in various organs are also reported to be associated with better prognosis[16]. Thus, these results suggest LFs in early colorectal neoplasms play an important role in defense rather than promotion.

In our study, the incidence of LFs was markedly higher in submucosal invasive cancers than in intramucosal lesions, and it was also more frequently observed in depressed or flat lesions and in larger sizes of each macroscopic type. We observed significant correlations

among the incidence of LFs and the invasive tendencies and size of early colorectal lesions. Mortality rates for colorectal cancer in Japan tend to be lower in females than males. Our results also showed a significant higher incidence of LFs in females compared to males (33.6% *vs* 24.9%). Taking these results together, we suggest that LFs in early colorectal neoplasms are signs of a possible early physical defense event against neoplastic cells.

Submucosal cancers are reported to show lymph node metastasis in 3.6–16.2%[17-20]. However, in this study, we could not find a significant difference between the presence of LFs and lymph node metastasis in submucosal cancers. This might be due to the small numbers of submucosal cancers (8.6%, 11/128) harboring lymph node metastasis. Another explanation is that LFs may have defense only against the process of tumor invasion but not that of metastasis.

In conclusion, significant differences exist in the incidence and localization of LFs in early colorectal neoplasms in human beings. We suggest that LFs in early colorectal neoplasms might be considered as a sign of the host physical defense against neoplastic cells. Further studies, including experimental and clinical analyses, will be necessary to confirm this phenomenon.

REFERENCES

1 **Nauss KM**, Locniskar M, Pavlina T, Newberne PM. Morphology and distribution of 1,2-dimethylhydrazine dihydrochloride-induced colon tumors and their relationship to gut-associated lymphoid tissue in the rat. *J Natl Cancer Inst* 1984; **73**: 915-924

2 **Hardman WE**, Cameron IL. Colonoic crypts located over lymphoid nodules of 1,2-dimethylhydrazine-treated rats are hyperplastic and at high risk of forming adenocarcinoma. *Carcinogenesis* 1994; **15**: 2353-2361

3 **Ward JM**. Morphogenesis of chemically induced neoplasms of the colon and small intestine in rats. *Lab Invest* 1974; **30**: 505-513

4 **Martin MS**, Hammann A, Matin F. Gut-associated lymphoid tissue and 1,2-dimethylhydrazine intestinal tumors in the rat: a histological immunoenzymatic study. *Int J Cancer* 1986; **38**: 75-80

5 **Rubio CA**, Kumagai J, Kanamori T, Nakamura K. Apoptosis in flat neoplasias of the colorectal mucosa. *In Vivo* 1995; **9:** 173-176

6 **Rubio CA**, Shetye J, Jaramillo E. Non-polypoid adenomas of the colon are associated with subjacent lymphoid nodules. An experimental study in rats. *Scand J Gastroenterol* 1999; **34**: 504-508

7 **Kudo S**, Tamura S, Hirota S, Sano Y, Yamano H, Serizawa M, Fukuoka T, Mitsuoka H, Nakajima T, Kusaka H. The problem of de novo colorectal carcinoma. *Eur J Cancer* 1995; **31A:** 1118-1120

8 **Kudo S**, Tamura S, Nakajima T, Hirota S, Asano M, Ito O, Kusaka H. Depressed type of colorectal cancer. *Endoscopy* 1995; **27**: 54-57

9 **Fujii T**, Rembacken BJ, Dixon MF, Yoshida S, Axon AT. Flat adenomas in the United Kingdom: are treatable cancers being missed? *Endoscopy* 1998; **30**: 437-443

10 **Hart AR**, Kudo S, Mackay EH, Mayberry JF, Atkin WS. Flat adenomas exist in asymptomatic people: important implications for colorectal cancer screening programmes. *Gut* 1998; **43:** 229-231

11 **Rembacken BJ**, Fujii T, Cairns A, Dixon MF, Yoshida S, Chalmers DM, Axon AT. Flat and depressed colonic neoplasms: a prospective study of 1000 colonoscopies in the UK. *Lancet* 2000; **355:** 1211-1214

12 **Wolber RA**, Owen DA. Flat adenoma of the colon. *Hum Pathol* 1991; **34**: 981-986

13 **O'Leary AD**, Sweeney EC. Lymphoglandular complexes of the colon: structure and distribution. *Histopathology* 1986; **10:** 267-283

14 **Ropponen KM**, Eskelinen MJ, Lipponen PK, Alhava E, Kosma VM. Prognostic value of tumour-infiltrating lymphocytes (TILs) in colorectal cancer. *J Pathol* 1997; **182:** 318-324

15 **Michael-Robinson JM**, Biemer-Huttman A-E, Purdie DM, Walsh MD, Simms LA, Biden KG, Young JP, Leggett BA, Jass JR, Radford-Smith GL. Tumor infiltrating lymphocytes and apoptosis are independent features in colorectal cancer stratified according to microsatellite instability status. *Gut* 2001; **48:** 360-366

16 **Minamoto T**, Mai M, Watanabe K, Ooi A, Kitamura T, Takahashi Y, Ueda H, Ogino T, Nakanishi I. Medullary carcinoma with lymphocytic infiltration of the stomach – Clinicopathologic study of 27 cases and immunohistochemical analysis of the subpopulations of infiltrating lymphocytes in the tumor. *Cancer* 1990; **66:** 945-952

17 **Kyzer S**, Begin LR, Gordon PH, Mitmaker B. The care of patients with colorectal polyps that contain invasive adenocarcinoma. Endoscopic polypectomy or colectomy? *Cancer* 1992; **70:** 2044-2050

18 **Minamoto T**, Mai M, Ogino T, Sawaguchi K, Ohta T, Fujimoto T, Takahashi Y. Early invasive colorectal carcinomas metastatic to the lymph node with attention to their nonpolypoid development. *Am J Gastroenterol* 1993; **88**: 1035-1039

19 **Tanaka S**, Yokota T, Saito D, Okamoto S, Oguro Y, Yoshida S. Clinicopathologic features of early rectal carcinoma and indications for endoscopic treatment. *Dis Colon Rectum* 1995; **38**: 959-963

20 **Tanaka S**, Haruma K, Teixeira CR, Tatsuta S, Ohtsu N, Hiraga Y, Yoshihara M, Sumii K, Kajiyama G, Shimamoto F. Endoscopic treatment of submucosal invasive colorectal carcinoma with special reference to risk factors for lymph node metastasis. *J Gastroenterol* 1995; **30:** 710-717

Science Editor Kumar K and Guo SY **Language Editor** Elsevier HK

PO Box 2345, Beijing 100023, China
www.wjgnet.com
wjg@wjgnet.com

ELSEVIER

World J Gastroenterol 2005;11(43):6867-6870
World Journal of Gastroenterology ISSN 1007-9327

• RAPID COMMUNICATION •

MSX2 overexpression inhibits gemcitabine-induced caspase-3 activity in pancreatic cancer cells

Shin Hamada, Kennichi Satoh, Kenji Kimura, Atsushi Kanno, Atsushi Masamune, Tooru Shimosegawa

Shin Hamada, Kennichi Satoh, Kenji Kimura, Atsushi Kanno, Atsushi Masamune, Tooru Shimosegawa, Division of Gastroenterology, Tohoku University Graduate School of Medicine, 1-1, Seiryo-machi, Aobaku, Sendai city, Miyagi 980-8574, Japan
Supported by the grant-in-aid from the Ministry of Education, Science, Sports and Culture in Japan, No. 14370172 and 15590615
Correspondence to: Kennichi Satoh, Division of Gastroenterology, Tohoku University Graduate School of Medicine, 1-1, Seiryo-machi, Aobaku, Sendai city, Miyagi 980-8574, Japan. ksatoh@mail.tains.tohoku.ac.jp
Telephone: +81-22-717-7171 Fax: +81-22-717-7177
Received: 2005-04-11 Accepted: 2005 -04-30

Abstract

AIM: To evaluate the effect of MSX2 on gemcitabine-induced caspase-3 activation in pancreatic cancer cell line Panc-1.

METHODS: Using V5-tagged MSX2 expression vector, stable transfectant of MSX2 was generated from Panc-1 cells (Px14 cells). Cell viability under gemcitabine administration was determined by MTT assay relative to control cell line (empty-vector transfected Panc-1 cells; P-3EV cells). Hoechst staining was used for the detection of apoptotic cell. Activation of caspase-3 was assessed using Western blotting analysis and direct measurement of caspase-3 specific activities.

RESULTS: MSX2 overexpression in Panc-1 cells resulted in decreased gemcitabine-induced caspase-3 activation and increased cell viability under gemcitabine treatment in Px14 cells.

CONCLUSION: MSX2 exerts repressive effects on gemcitabine-induced apoptotic pathway. This novel apoptosis-regulating function of MSX2 may provide a new therapeutic target for pancreatic cancer.

Key words: MSX2; Caspase-3; Gemcitabine

Hamada S, Satoh K, Kimura K, Kanno A, Masamune A, Shimosegawa T. MSX2 overexpression inhibits gemcitabine-induced caspase-3 activity in pancreatic cancer cells. *World J Gastroenterol* 2005; 11(43): 6867-6870
http://www.wjgnet.com/1007-9327/11/6867.asp

INTRODUCTION

Pancreatic cancer is known as a cancer with poor prognosis. Surgical resection of pancreatic cancer is available only in 15-20% of all patients[1], while medical approaches, such as chemotherapy or radiation, have no cure. The resistance of pancreatic cancer to chemotherapeutic agents is one of the serious problems in clinical situation. Gemcitabine (2',2'-difluoro-2'-deoxycytidine) is a widely used chemotherapeutic agent for unresectable pancreatic cancer treatment, and its administration triggers apoptosis in pancreatic cancer cell line[2]. On the other hand, previous report showed that acquired gemcitabine resistance was accompanied by altered expression of apoptosis regulatory genes[3]. The mechanisms how cancer cells evade apoptotic signals are beginning to come to light, but its upstream regulators are not fully understood as yet.

We have previously demonstrated that overexpression of homeobox gene MSX2 accelerated proliferation of pancreatic cancer cell lines, combined with epithelial-mesenchymal transition (EMT)-like phenotypic changes *in vitro* (Satoh *et al*., submitted). In addition, forced expression of MSX2 increased anchorage-independent growth of pancreatic cancer cells, indicating enhanced aggressive biological behavior. Recent studies have demonstrated that MSX2 is a downstream target of the Wnt signaling pathway in several cancer cell lines[4,5]. The upregulation of Wnt signaling is reported in various cancer cell lines, and its target genes are closely related to cancer cell growth and survival[6–9]. At this point of view, we hypothesized that MSX2 might affect apoptotic signaling pathway, which leads to the chemoresistance of pancreatic cancer cells.

In this study, we generated MSX2-overexpressing pancreatic cancer cell line Px14, and this cell line revealed resistance to the gemcitabine treatment. When cells were treated with gemcitabine, the caspase-3 activation was significantly upregulated in empty vector-transfected control cells, but not in Px14 cells compared to basal control cells. Taken together, MSX2 might act as a negative regulator of apoptosis in this cell line. This new upstream regulator of apoptotic signaling pathway may provide a novel therapeutic target of chemotherapy-resistant pancreatic cancer.

MATERIALS AND METHODS

Cell line and cell culture

Panc-1, a human pancreatic cancer cell line, was maintained in Dulbecco's modified Eagle's medium (DMEM)

supplemented with 100 mL/L fetal bovine serum (FBS), and incubated at 37 °C in a humidified atmosphere containing 50 mL/L CO_2 in air.

Chemical substances

Gemcitabine (Gemzar; Eli Lilly Co., Indianapolis, IN, USA) was dissolved in phosphate buffered saline (PBS) at various concentrations of 0.1, 1, 10, 100 μg/mL and 1 mg/mL as stock solutions. In cell culture, vehicle and these stock solutions were used in 1:100 dilutions.

Plasmids, gene transduction and expression

Expression vector, pcDNA3.1-MSX2V5, was generated as described previously (Satoh *et al*. submitted). Panc-1 cells were plated in six-well plates and cultured until reaching a subconfluent state. Cells were transfected with 1 μg of pcDNA3.1-V5His (empty vector) or pcDNA3.1-MSX2V5 using FuGENE6 transfection reagent (Roche Diagnostics, Basel, Switzerland) in normal growth medium. Three days later, cells were plated on 10-cm dishes and cultured until reaching a confluent state. After G418 selection, clones were subjected to Western blot analysis with a specific anti-V5 antibody (Invitrogen, Carlsbad, CA, USA).

Cell proliferation and cell viability assays

For cell proliferation assay, 6 000 cells were seeded per well in triplicate in 96-well plates in normal growth media. After 24-h (d1) and 72-h (d3) incubation, cell proliferation assay was performed using cell proliferation ELISA, BrdU (5-bromo-2-deoxyuridine) kit (Roche Diagnostics) according to the manufacturer's instructions. Cell proliferation ratio at d3 was normalized by that of d1. For cell viability assay, 10 000 cells were seeded per well in triplicate in 96-well plates in normal growth media. After 24-h incubation, cells were incubated with gemcitabine at various concentrations. After 48-h incubation, cell viability was measured by using 3-(4,5-dimethylthiazol-2-yl)-2,5-diphenyltetrazolium bromide (MTT) assay. Cells were treated with MTT solution at a concentration of 0.5 mg/mL for 2 h, and then solubilized in dimethylsulfoxide (DMSO). Color reaction was measured by a spectrometer at a wavelength of 570 nm. Each experiment was repeated at least twice.

Detection of apoptotic cells

Apoptosis was determined by staining with Hoechst. Cells were plated at 1×10^4 on culture slide (Becton Dickinson, Franklin Lakes, NJ, USA) and allowed to adhere to the slide overnight. Gemcitabine (1 μg/mL) was added and incubated for an additional 24 h. The cells were fixed with 40 g/L paraformaldehyde for 20 min, followed by Hoechst 33342 (Calbiochem-Novabiochem, La Jolla, CA, USA) staining in these cells for 30 min. Then the cells were analyzed under a fluorescence microscope (Leica, Cambridge, UK). Between the incubations, the specimens were washed thrice with PBS. Chromatin condensation, nuclear shrinkage, and nucleosomal fragmentation were considered to be morphological markers of apoptosis.

Measurement of caspase-3 activities

APOCYTO Caspase-3 Colorimetric Assay Kit (MBL, Nagoya, Japan) was used for the detection of caspase-3 activity following the manufacturer's protocol. The subconfluent state cells in 10-cm dishes were harvested after 24-h incubation with gemcitabine (1 μg/mL), and subjected to caspase-3 activity detection.

Western blotting analysis

Cells were lysed by the addition of lysis buffer containing 150 mmol/L NaCl, 50 mmol/L Tris–HCl, 10 mL/L Nonidet P40 and 5 g/L sodium deoxycholate. Cell lysates were cleared by centrifugation at 16 000 *g* at 4 °C for 15 min. Cleared lysates were boiled for 5 min at 100 °C after the addition of 5× sample loading buffer containing 1 mol/L Tris–HCl (pH 6.8), sodium dodecyl sulfate, glycerol, and bromophenol blue. Samples were electrophoresed at 200 V on 125 g/L polyacrylamide gels and transferred to nitrocellulose membranes (Bio-Rad, Hercules, CA, USA), blocked with 50 g/L nonfat dry milk, and then incubated with primary antibodies, such as anti-caspase-3 antibody (BD610322), anti-v5 antibody (R960-25, Invitrogen) and anti-α-tubulin antibody (sc-8035, Santa Cruz Biotechnology, Santa Cruz, CA, USA). Horseradish peroxidase-conjugated anti-mouse antibody (NA931, Amersham, Buckinghamshire, UK) was used as secondary antibody. Reactive bands were detected using ECL™ Western Blotting Detection Reagents (Amersham).

Statistical analysis

The unpaired *t*-test and one-way ANOVA were used for statistical comparison. Calculations were made with the help of Microsoft Excel computer software (Microsoft, Redmond, WA, USA). $P<0.05$ was considered statistically significant.

RESULTS

Forced MSX2 expression in human pancreatic cancer cell line Panc-1

To evaluate whether MSX2 expression correlates with gemcitabine resistance in pancreatic cancer cells, we generated MSX2 stable transfectant cell line. As described previously (Hamada *et al*., submitted), V5-tagged MSX2 expression vector was transfected in Panc-1 cells. MSX2-expressing clone (Px14) was selected and subjected to further analysis (Figure 1A). Panc-1 cells transfected with empty vector were maintained with the culture media containing G418, and used as control cell line (P-3EV). BrdU incorporation assay showed no significant difference in cell growth between two cell lines, but there was a tendency of slightly increased proliferation ratio in Px14 cells ($P = 0.074$, Figure 1B) relative to control cells (P-3EV cells), which was compatible to our previous report (Satoh *et al*., submitted).

Decrease of gemcitabine sensitivity in Panc-1 cells by MSX2 overexpression

Gemcitabine administration at a concentration of 10 μg/mL

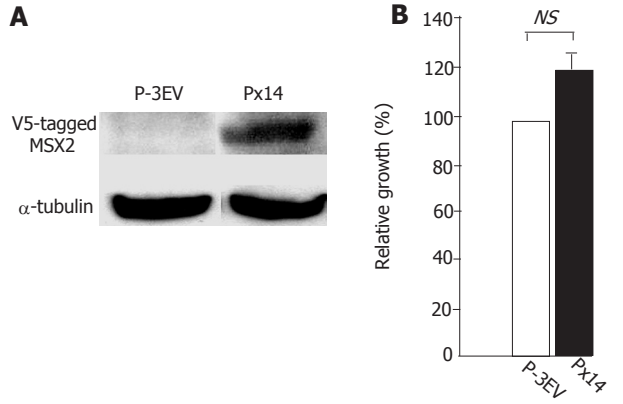

Figure 1 A: Western blotting analysis of V5-tagged MSX2 expression in Px14 cells; **B:** detection of cell proliferation of P-3EV and Px14 by BrdU incorporation assay. No significant difference was observed in these two cell lines, but slight increase of proliferation ratio was observed in Px14 cells (unpaired *t*-test, $n = 3$).

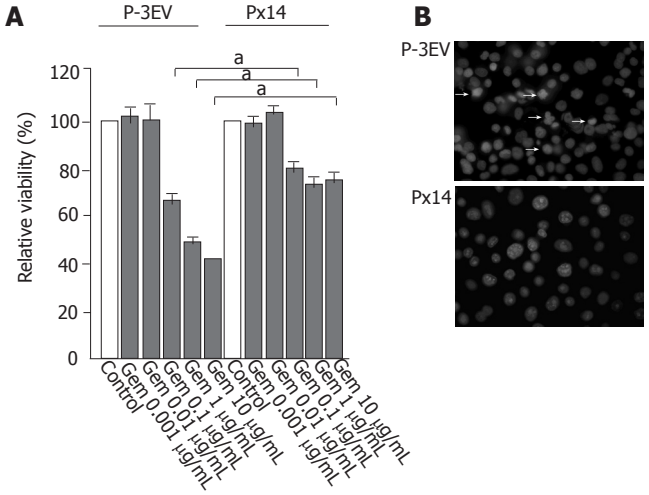

Figure 2 A: Cell viability of P-3EV and Px14 cell lines after 24 h of gemcitabine treatment at various concentrations. Gemcitabine reduced cell viability in a dose-dependent manner. At a concentration of 0.1 μg/mL or above, Px14 cells exhibited higher viability relative to P-3EV cells (one-way ANOVA, $n = 3$, $^aP<0.05$ *vs* others); **B:** Hoechst staining of P-3EV and Px14 cell lines. After 24 h of gemcitabine treatment at a concentration of 1 μg/mL, apoptotic changes (nuclear chromatin condensation and nuclear fragmentation) were obviously observed in P-3EV cells (arrow), but not in Px14 cells.

for 48 h decreased the viability of P-3EV cells by 60%, whereas that of Px14 cells only by 30% (Figure 2A). Px14 cells also depicted gemcitabine resistance at concentrations of 1 and 0.1 μg/mL (Figure 2A). Since Px14 cells were thought to be resistant to gemcitabine cytotoxicity, we analyzed gemcitabine-induced morphological alteration in P-3EV cells and Px14 cells. Gemcitabine-treated P-3EV cells at a concentration of 1 μg/mL for 24 h showed obvious apoptotic characteristics such as nuclear fragmentation and chromatin condensation, while these morphological changes were unremarkable in Px14 cells (Figure 2B).

Gemcitabine-induced caspase-3 activation in P-3EV cells and Px14 cells

Gemcitabine treatment led P-3EV cells to apoptotic state,

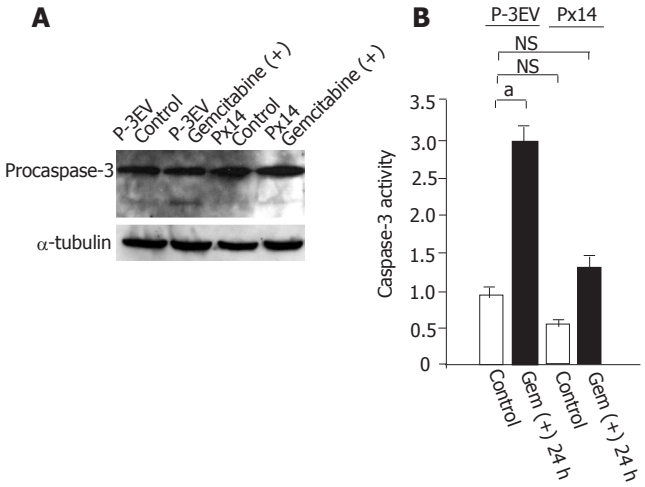

Figure 3 A: Western blotting analysis for caspase-3 activation. Cells were harvested 24 h after gemcitabine (1 g/mL) or vehicle administration. In P-3EV cells, active caspase-3 (cleaved form) was detected after gemcitabine treatment (arrow), whereas in Px14 cells, cleaved form of caspase-3 was undetectable with or without gemcitabine; **B:** direct caspase-3 activity measurements by APOCYTO Caspase-3 Colorimetric Assay Kit. Gemcitabine (1 μg/mL) treatment significantly enhanced caspase-3 specific activity in P-3EV cells, but not in Px14 cells. No significant differences in caspase-3 activities were detected between vehicle-treated P-3EV cells and Px14 cells, even after gemcitabine treatment (one-way ANOVA, $n = 3$, $^aP<0.05$ *vs* others).

thus we examined caspase-3 activation in P-3EV and Px14 cells. Gemcitabine administration at a concentration of 1 μg/mL clearly induced active (cleaved) form of caspase-3 in P-3EV cells, but not in Px14 cells (Figure 3A). Caspase-3 activation is a critical event in apoptosis induction; therefore, we hypothesized that gemcitabine resistance in Px14 cells might be due to suppressed caspase-3 activity. To evaluate this hypothesis, we conducted direct measurements of caspase-3 activities in P-3EV cells and Px14 cells, with or without gemcitabine treatment. The basal activities of caspase-3 in these cells were not significantly different (Figure 3B). However, gemcitabine treatment at a concentration of 1 μg/mL significantly increased caspase-3 activity in P-3EV cells but not in Px14 cells as compared with its basal activity in control cells.

DISCUSSION

Even in pancreatic cancer cells, apoptotic signal does exist, but the signal is considered to be overwhelmed by inhibitor of apoptosis[10]. In our experiment, gemcitabine treatment induced apoptotic changes in P-3EV cells, whereas this effect was attenuated by MSX2 overexpression. Studies have shown that the ability of evasion from apoptosis is one of the critical steps for tumor progression. For example, interference of X-linked inhibitor of apoptosis (XIAP) expression in MDA-MB-231 mammary cancer cell line increases sensitivity to several chemotherapeutic agents[11]. The expression level of survivin in pancreatic cancer tissue is significantly associated with the reduction of the apoptotic index of tumor cells[12] and is also reported to be correlated with the prognosis of patients[13],

indicating that anti-apoptotic effectors directly affect clinical outcomes.

MSX2 overexpression enhanced cell proliferation in pancreatic cancer cell line BxPC-3 (Satoh K *et al.*, submitted), and tended to stimulate the Panc-1 cell growth in the current study, indicating that MSX2 enhances the proliferation effect rather than the pro-apoptotic effect in pancreatic cancer cells. Association of MSX2 with cell proliferation has also been shown in facial mesenchyme[14] and in skeletogenic mesenchyme[15], suggesting that the downstream targets of this homeobox gene may include regulators of cell proliferation. In addition, MSX2 itself and/or BMP-induced MSX2 has shown to lead the pancreatic cancer cells to epithelial-mesenchymal transition (EMT) state (Satoh *et al.*, Hamada *et al.*, submitted), indicating the enhancement of malignant phenotype of pancreatic cancer cells by MSX2. In this study, we clearly demonstrated that forced expression of MSX2 in pancreatic cancer cells produced the resistance to gemcitabine-induced apoptosis via the suppression of caspase-3 activity, which is an additional new aspect of MSX2 to accelerate the pancreatic cancer cell malignancy. Although further detailed investigations would be required to clarify how MSX2 inhibits caspase-3 activation in pancreatic cancer cells, the involvement of this gene in the development of gemcitabine resistance provides us some clues for further understanding of the cancerous cell nature and a novel therapeutic target.

REFERENCES

1 **Li D,** Xie K, Wolff R, Abbruzzese JL. Pancreatic cancer. *Lancet* 2004; **363:** 1049-1057

2 **Chandler NM**, Canete JJ, Callery MP. Caspase-3 drives apoptosis in pancreatic cancer cells after treatment with gemcitabine. *J Gastrointest Surg* 2004; **8:** 1072-1078

3 **Schniewind B**, Christgen M, Kurdow R, Haye S, Kremer B, Kalthoff H, Ungefroren H. Resistance of pancreatic cancer to gemcitabine treatment is dependent on mitochondria-mediated apoptosis. *Int J Cancer* 2004; **109:** 182-188

4 **Hussein SM**, Duff EK, Sirard C. Smad4 and beta-catenin co-activators functionally interact with lymphoid-enhancing factor to regulate graded expression of Msx2. *J Biol Chem* 2003; **278:** 48805-48814

5 **Schwartz DR**, Wu R, Kardia SL, Levin AM, Huang CC, Shedden KA, Kuick R, Misek DE, Hanash SM, Taylor JM, Reed H, Hendrix N, Zhai Y, Fearon ER, Cho KR. Novel candidate targets of beta-catenin/T-cell factor signaling identified by gene expression profiling of ovarian endometrioid adenocarcinomas. *Cancer Res* 2003; **63:** 2913-2922

6 **Tetsu O**, McCormick F. Beta-catenin regulates expression of cyclin D1 in colon carcinoma cells. *Nature* 1999; **398:** 422-426

7 **Shtutman M**, Zhurinsky J, Simcha I, Albanese C, D'Amico M, Pestell R, Ben-Ze'ev A. The cyclin D1 gene is a target of the beta-catenin/LEF-1 pathway. *Proc Natl Acad Sci USA* 1999; **96:** 5522-5527

8 **He TC**, Sparks AB, Rago C, Hermeking H, Zawel L, da Costa LT, Morin PJ, Vogelstein B, Kinzler KW. Identification of c-MYC as a target of the APC pathway. *Science* 1998; **281:** 1509-1512

9 **Zhang T**, Otevrel T, Gao Z, Gao Z, Ehrlich SM, Fields JZ, Boman BM. Evidence that APC regulates survivin expression: a possible mechanism contributing to the stem cell origin of colon cancer. *Cancer Res* 2001; **61:** 8664-8667

10 **Yang L**, Cao Z, Yan H, Wood WC. Coexistence of high levels of apoptotic signaling and inhibitor of apoptosis proteins in human tumor cells: implication for cancer specific therapy. *Cancer Res* 2003; **63:** 6815-6824

11 **McManus DC**, Lefebvre CA, Cherton-Horvat G, St-Jean M, Kandimalla ER, Agrawal S, Morris SJ, Durkin JP, Lacasse EC. Loss of XIAP protein expression by RNAi and antisense approaches sensitizes cancer cells to functionally diverse chemotherapeutics. *Oncogene* 2004; **23:** 8105-8117

12 **Satoh K**, Kaneko, K, Hirota, M, Masamune, A, Satoh, A, and Shimosegawa, T. Expression of survivin is correlated with cancer cell apoptosis and is involved in the development of human pancreatic duct cell tumors. *Cancer* 2001; **92:** 271-278

13 **Kami K**, Doi R, Koizumi M, Toyoda E, Mori T, Ito D, Fujimoto K, Wada M, Miyatake S, Imamura M. Survivin expression is a prognostic marker in pancreatic cancer patients. *Surgery* 2004; **136**: 443-448

14 **Ashique AM**, Fu K, Richman JM. Endogenous bone morphogenetic proteins regulate outgrowth and epithelial survival during avian lip fusion. *Development* 2002; **129**: 4647-4660

15 **Ishii M**, Merrill AE, Chan YS, Gitelman I, Rice DP, Sucov HM, Maxson RE Jr. Msx2 and Twist cooperatively control the development of the neural crest-derived skeletogenic mesenchyme of the murine skull vault. *Development* 2003; **130**: 6131-6142

Science Editor Kumar M and Guo SY **Language Editor** Elsevier HK

PO Box 2345, Beijing 100023, China
www.wjgnet.com
wjg@wjgnet.com

ELSEVIER

World J Gastroenterol 2005;11(43):6871-6874
World Journal of Gastroenterology ISSN 1007-9327

• *RAPID COMMUNICATION* •

Association of *Helicobacter pylori Ig*A antibodies with the risk of peptic ulcer disease and gastric cancer

Timo U Kosunen, Kari Seppälä, Seppo Sarna, Arpo Aromaa, Paul Knekt, Jarmo Virtamo, Anniina Salomaa-Räsänen, Hilpi Rautelin

Timo U Kosunen, Anniina Salomaa-Räsänen, Department of Bacteriology and Immunology, Haartman Institute, University of Helsinki, FIN-00014 Helsinki, Finland
Kari Seppälä, Gastroenterological Research Unit, Department of Medicine, University of Helsinki, FIN-00029 Helsinki, Finland
Seppo Sarna, Department of Public Health, University of Helsinki, FIN-00014 Helsinki, Finland
Arpo Aromaa, Paul Knekt, Jarmo Virtamo, National Public Health Institute, FIN-00300 Helsinki, Finland
Hilpi Rautelin, Department of Bacteriology and Immunology, Haartman Institute, University of Helsinki, FIN-00014 Helsinki, Finland, and HUSLAB, Helsinki University Central Hospital Laboratory, FIN-00029 Helsinki, Finland
Supported by the University of Helsinki, the Helsinki University Central Hospital and the Finnish Cancer Organisations, Helsinki, Finland
Correspondence to: Dr.Timo U Kosunen, Department of Bacteriology and Immunology, University of Helsinki, PO Box 21, FIN-00014 Helsinki, Finland. timo.kosunen@helsinki.fi
Telephone: +358-9-19126298 Fax: +358-9-19126382
Received: 2005-04-21 Accepted: 2005-05-12

Abstract

AIM: To compare the prevalence of *Helicobacter pylori (H pylori) Ig*G and *Ig*A antibodies between adult subjects, with defined gastric diseases, nondefined gastric disorders and those representing the population.

METHODS: Data on *H pylori Ig*G and *Ig*A antibodies, determined by enzyme immunoassay, were analyzed in 3 252 subjects with DGD including 482 patients with gastric ulcer, 882 patients with duodenal ulcer, 1 525 patients with chronic gastritis only and 363 subjects with subsequent gastric cancer, 19 145 patients with NoDg and 4 854 POPUL subjects. The age-adjusted prevalences were calculated for 1- and 20-year age cohorts.

RESULTS: The prevalences of *Ig*G antibodies were equally high (89-96%) in all 20-year age cohorts of the DGD groups, whereas the prevalences of *Ig*G antibodies were lower and increased by age in the POPUL and NoDg groups. The prevalences of *Ig*A antibodies were also higher in the DGD groups; among them CA (84-89%) and GU groups (78-91%) showed significantly higher prevalences than DU (68-77%) and CG patients (59-74%) (OR 2.49, 95%CI 1.86-3.34 between the GU and DU groups). In the CA, GU, and DU groups, the *Ig*A prevalences showed only minor variation according to age, while they increased by age in the CG, POPUL, and NoDg groups ($P \leqslant 0.0001$). The *Ig*A response, but not the *Ig*G response, was associated with an increased risk of CA (OR 2.41, 95%CI 1.79-3.53) and GU (OR 2.57, 95%CI 1.95-3.39) in comparison with CG patients.

CONCLUSION: An *Ig*A antibody response during *H pylori* infection is significantly more common in CA and GU patients as compared with CG patients.

Key words: *Helicobacter pylori*; *Ig*A antibodies; Gastric cancer; Gastric ulcer; Duodenal ulcer; Chronic gastritis

Kosunen TU, Seppälä K, Sarna S, Aromaa A, Knekt P, Virtamo J, Salomaa-Räsänen A, Rautelin H. Association of *Helicobacter pylori Ig*A antibodies with the risk of peptic ulcer disease and gastric cancer. *World J Gastroenterol* 2005; 11(43): 6871-6874
http://www.wjgnet.com/1007-9327/11/6871.asp

INTRODUCTION

Helicobacter pylori (*H pylori*), the causative agent of chronic gastritis[1], is also the most important risk factor for peptic ulcer disease[25] and distal gastric cancer[4,5]. The presence of *H pylori* antibodies signify this chronic infection and their prevalence increases with age in all populations, mainly due to the birth of cohort phenomenon[6,7]. The optimal serological tests for *Ig*G antibodies to *H pylori* show a sensitivity and a specificity of over 95%[8-10]. Antibodies of the *Ig*A class are usually detected in combination with elevated *Ig*G antibodies in approximately two-thirds of infected subjects[8,11,12]. They are diagnostically useful in the 2-7% of *H pylori* patients who do not have elevated *Ig*G levels[7,8,12-15]. *Ig*A antibodies have been shown to be a sensitive indicator of an increased risk for gastric cancer[14]. In this context, it may be important that subjects with CagA antibodies have more often *H pylori* antibodies of the *Ig*A class as compared with those who are CagA antibody-negative[15], since CagA-positive infections have been associated with an increased risk of both peptic ulcer disease and gastric cancer[16,17].

In the present study, we analyzed the prevalences of *H pylori* antibodies determined in our laboratory from 1986 to 2000 in clinical samples taken from patients with endoscopically verified or undefined gastric disorders and

in samples collected from the Finnish population.

MATERIALS AND METHODS

Study subjects

Serum samples for this study were obtained from 1986 to 2000 from the following patient groups: 3 252 patients with defined gastric diseases (DGD), including 482 patients with an endoscopically confirmed gastric ulcer (GU) (mean age 60.79 years, SD±12.59 years), 882 patients with an endoscopically confirmed duodenal ulcer (DU) (mean age 53.80 years, SD±13.64 years), 1 525 patients with a histologically verified chronic gastritis (CG) (mean age 50.58 years, SD±15.95 years) and 363 subjects with subsequent gastric cancer (CA) (mean age at the time of the serum sampling 57.23 years, SD±10.91 years). Sera from GU, DU, and CG patients were collected on the day of the endoscopy, those from CA patients between 2 wk to 24 years before the diagnosis of cancer was made (reported in part earlier[5,14]). In the GU, DU, and CG groups, patients who had prior successful eradication therapy were excluded from the study. In addition, serum samples were obtained from 4 854 subjects participating in a population study in Vammala, Finland (POPUL) (mean age 41.73 years, SD±20.60 years), reported in part earlier[7] and from 19 145 patients whose sera were sent by general practitioners, Municipal Health Centers or Hospitals to our diagnostic laboratory for *H pylori* antibody tests without any information on possible gastric disorders (NoDg) (mean age 51.47 years, SD±16.97 years).

Ethics

The study was approved by the Ethics Committee for Epidemiology and Public Health of the Helsinki and Uusimaa Hospital district.

Laboratory assessment

H pylori *Ig*G and *Ig*A antibody titers were determined by in-house enzyme immunoassays[8,10].The antigen used was an acid glycine extract from *H pylori* strain NCTC 11637. During the study period, the sensitivity and specificity of the *Ig*G test were 95-99% and 93-97%, respectively, and those of the *Ig*A test were 64-67% and 92-98%, respectively, as determined in patients in whom the presence of *H pylori* infection had been verified by culture and histology of gastric biopsies[8,10].

Statistical analysis

The trend in changes in the prevalences of *Ig*G and *Ig*A antibodies by age was studied using the linear trend test. The comparisons of prevalences of *Ig*A and *Ig*G antibodies between the groups were analyzed using the logistic regression model adjusting for age based on 1-year age cohorts. For an overview, the prevalences were determined for 20-year age-adjusted cohorts (15-34, 35-54, 55-74, and 75-94 years), each including at least 50 subjects. The association of *Ig*A and *Ig*G responses with the risk of serious complications (CA, GU, and DU) was analyzed using a logistic regression model by comparing the number of subjects in each antibody response and complication category to that in CG patients, who are regarded to present the basic disease caused by *H pylori*. Statistical analyses were carried out using the SPSS 12.0 software package (SPSS Inc., Chicago, IL, USA). $P<0.05$ was considered statistically significant.

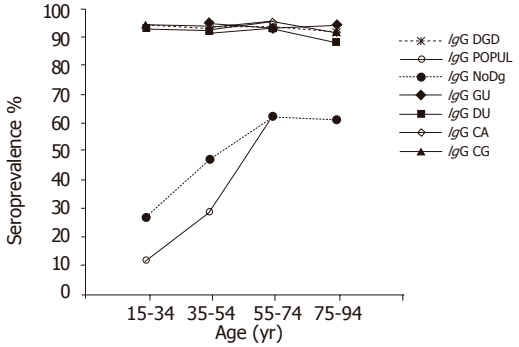

Figure 1 Prevalence of *H pylori* *Ig*G antibodies by 20-year age cohorts in the Finnish population and patients with different gastric disorders. (Only cohorts including at least 50 subjects are shown).

RESULT

Of the 27 251 subjects, 13 939 (51.2%) were positive for *H pylori* antibodies. Of the antibody-positive subjects, 61.8% were positive for both *Ig*G and *Ig*A antibodies, 34.9% for *Ig*G antibodies only and 3.3% for *Ig*A antibodies only.

IgG antibody prevalences

Among the subjects in the DGD groups, 88.6-95.7% had *H pylori* antibodies of the *Ig*G class in all 20-year age cohorts (Figure 1). In contrast, among the subjects representing the POPUL and NoDg groups, significantly lower seroprevalences were observed (OR 19.73, 95%CI 16.15-24.10 and OR 14.11, 95%CI 12.28-16.21, respectively) (Figure 1). Furthermore, the prevalence was seen to increase by age from 12% in the youngest cohort to 63% in the 55-74-year-old cohort in the POPUL group ($P<0.0001$; trend test), and from 27% to 62%, respectively, in the NoDg patients ($P<0.0001$; trend test). The prevalence of *Ig*G antibodies was significantly higher in the NoDg patients than in the POPUL group (OR 2.18, 95%CI 2.00-2.36) (Figure 1).

Within the DGD group, the prevalences did not differ between the GU, DU, CG, and CA groups, nor did they show any significant variation by age (trend test).

IgA antibody prevalences

The prevalence of *Ig*A antibodies group in all age cohorts was significantly higher in the DGD group than in the POPUL (OR 9.61; 95%CI 8.20-11.26) and NoDg groups (OR 5.00; 95%CI 4.59-5.44) (Figure 2). Within the DGD group, the highest prevalences were found in the GU and CA groups in all 20-year cohorts (77.7-90.7% and 84.3-88.6%, respectively) (Figure 2) without a significant difference between these two groups (OR 1.09, 95%CI

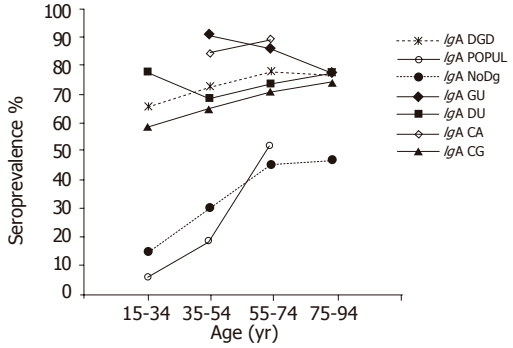

Figure 2 Prevalence of *H pylori IgA* antibodies by 20-year age cohorts in the Finnish population and patients with different gastric disorders. (Only cohorts including at least 50 subjects are shown.)

0.75-1.58). Although the GU patients showed a small decrease of *Ig*A-positive subjects by increasing age ($P = 0.016$; trend test), the prevalence was markedly higher than in DU (68.4-77.4%, OR 2.49; 95%CI 1.86-3.34) and CG patients (58.7-74.2%, OR 2.57, 95%CI 1.95-3.39). In the DU patients, the *Ig*A prevalence showed no significant trend by age (trend test), whereas a significantly increased trend by age was found in CG patients ($P = 0.0001$; trend test); the overall prevalences did not differ significantly between these two groups (OR 1.13; 95%CI 0.95-1.35) (Figure 2, Table 1).

In the subjects representing the POPUL and NoDg groups, the prevalence of *Ig*A antibodies increased by age from the lowest rates (6.5% and 15.1%, respectively) to significantly higher rates in the 55-74-year-old cohorts (52.1% and 45.6%, respectively; $P<0.0001$; trend test) (Figure 2). The overall prevalence of *Ig*A antibodies was higher in the NoDg patients than that in the POPUL group (OR 1.93, 95%CI 1.73-2.10).

Association of IgG and IgA responses with the risk of CA, GU, and DU in comparison with CG

*Ig*A response was more common in CA and GU groups as compared with CG patients (OR 2.41, 95%CI 1.79-3.53 and OR 2.57, 95%CI 1.95-3.39, respectively); however, this difference was not significant in DU patients (Table 1). The number of *Ig*G responders in CA and GU groups did not differ significantly as compared with the CG patients (Table 1), whereas it was even slightly lower in DU patients as compared with the CG patients (OR 0.72, 95%CI 0.55-0.99).

DISCUSSION

In the present study, we analyzed, according to age cohorts, a large body of serological data collected during a 15-year period. DGD subjects with gastric disorders known to be associated with *H pylori* infection showed a high and rather a constant prevalence of *H pylori Ig*G antibodies in all the 20-year age cohorts. Based on the prevalence of *Ig*A antibodies, the DGD group could be divided into two categories: in GU-CA-category, the age-adjusted *Ig*A prevalences ranged from 78% to 91%; whereas in DU-CG-category, the age-adjusted *Ig*A prevalences remained significantly lower. With the exception of CG patients, the *Ig*A antibody rates also remained rather constant throughout the age range. In contrast, the infected subjects in the POPUL and NoDg groups showed significantly lower *Ig*G and *Ig*A rates than those in the DGD group and that increased significantly by age. The CG patients formed a special intermediate group with overall *Ig*G and *Ig*A antibody prevalences at the same level as those of the DU patients, but with a significantly increasing trend by age in the prevalence of *Ig*A antibodies.

Table 1 Association of *H pylori Ig*A and *Ig*G antibodies with the risk of CA, GU or DU in comparison to CG

Subjects	*Ig*A		*Ig*G	
with	OR	95%CI	OR	95%CI
CG	1		1	
CA	2.41	1.79–3.53	1.28	0.81–2.02
GU	2.57	1.95–3.39	0.69	0.46–1.03
DU	1.13	0.95–1.35	0.72	0.55–0.99

The importance of the *Ig*A response increases when considered in connection with our earlier findings showing the association of *H pylori* antibodies of the *Ig*A class with a CagA-positive infection[15], as well as with other reports showing an increased risk of peptic ulcer disease and gastric cancer in CagA-positive infection[16,17]. The present results imply that an *Ig*A response during *H pylori* infection might be regarded as an indicator of an increased risk not only for gastric cancer[14] but also for gastric ulcer disease. In these comparisons, that we carried out using the data from patients with chronic gastritis as baseline values, we found that the higher *Ig*A response rate seen in DU patients did not reach significance.

By using the data obtained in prospective gastric cancer studies, we wanted to avoid the bias caused by severe atrophic gastritis, regarded as a precancerous process[18]. Severe atrophic gastritis may progress to a disease stage when *Helicobacters* first gradually decrease in number, then disappear and finally also *Helicobacter* antibodies, the longest lasting indicators of the infection, fall to a normal level[19]. In particular, in elderly subjects with non-cardia cancer, there may be several individuals who at the time of diagnosis may have lost all direct indicators of their burnt out *Helicobacter* infection.

Our large materials and the high sensitivity and specificity of our antibody tests also gave an opportunity to compare the prevalence of *H pylori* antibodies between the POPUL and NoDg groups. It is tempting to speculate that the higher *H pylori* prevalence in the two youngest cohorts (by 15% and 18% units in antibodies of *Ig*G class in the order of increasing age) in NoDg patients would preferentially reflect the strength of gastric symptoms driving patients to clinical consultations.

In conclusion, irrespective of age, practically all DGD subjects have *H pylori Ig*G antibody. The prevalence of *Ig*A antibodies highest in CA and GU patients, second highest in DU and CG patients, and lowest in the NoDg patients and POPUL subjects. An *Ig*A response is associated with serious sequelae of *H pylori* infection.

REFERENCES

1 **Marshall BJ**, Armstrong JA, McGechie DB, Glancy RJ. Attempt to fulfil Koch's postulates for pyloric *Campylobacter*. *Med J Aust* 1985; **142**: 436-439
2 **Rauws EA,** Tytgat GN. Cure of duodenal ulcer associated with eradication of *Helicobacter pylori*. *Lancet* 1990; **335**: 1233-1235
3 **Marshall BJ.** *Helicobacter pylori*. *Am J Gastroenterol* 1994; **89**: S116-128
4 Infection with *Helicobacter pylori*. *IARC Monogr Eval Carcinog Risks Hum* 1994; **61**: 177-240
5 Helicobacter and Cancer Collaborative Group. Gastric cancer and Helicobacter pylori: a combined analysis of 12 case control studies nested within prospective cohorts. *Gut* 2001; **49**: 347-353
6 **Talley NJ,** Noack KB. The woldwide prevalence of *Helicobacter pylori*: Asymptomatic infection and clical states associated with infection in adults. In: Goodwin CS, Worsley BW, eds. *Helicobacter pylori: Biology and clinical practice*. Boca Raton, Florida: CRC Press Inc. 1993; 63-83
7 **Kosunen TU,** Aromaa A, Knekt P, Salomaa A, Rautelin H, Lohi P, Heinonen OP. Helicobacter antibodies in 1973 and 1994 in the adult population of Vammala, Finland. *Epidemiol Infect* 1997; **119**: 29-34
8 **Kosunen, TU**, Seppälä K, Sarna S, Sipponen P. Diagnostic value of decreasing IgG, IgA, and IgM antibody titres after eradication of *Helicobacter pylori*. *Lancet* 1992; **339**: 893-895
9 **Feldman RA,** Deeks JJ, Evans SJ. Multi-laboratory comparison of eight commercially available *Helicobacter pylori* serology kits. *Helicobacter pylori* Serology Study Group. *Eur J Clin Microbiol Infect Dis* 1995; **14**: 428-433
10 **Oksanen A,** Veijola L, Sipponen P, Schauman KO, Rautelin H. Evaluation of Pyloriset Screen, a rapid whole-blood diagnostic test for *Helicobacter pylori* infection. *J Clin Microbiol* 1998; **36**: 955-957
11 **Kosunen TU,** Höök J, Rautelin HI, Myllylä G. Age-dependent increase of *Campylobacter pylori* antibodies in blood donors. *Scand J Gastroenterol* 1989; **24**: 110-114
12 **Andersen LP,** Rosenstock SJ, Bonnevie O, Jorgensen T. Seroprevalence of immunoglobulin G, M, and A antibodies to *Helicobacter pylori* in an unselected Danish population. *Am J Epidemiol* 1996; **143**: 1157-1164
13 **Jaskowski TD**, Martins TB, Hill HR, Litwin CM. Immunoglobulin A antibodies to *Helicobacter pylori*. *J Clin Microbiol* 1997; **35**: 2999-3000
14 **Aromaa A,** Kosunen TU, Knekt P, Maatela J, Teppo L, Heinonen OP, Harkonen M, Hakama MK. Circulating anti-Helicobacter pylori immunoglobulin A antibodies and low serum pepsinogen I level are associated with increased risk of gastric cancer. *Am J Epidemiol* 1996; **144**: 142-149
15 **Rautelin HI,** Oksanen AM, Karttunen RA, Seppala KM, Virtamo JR, Aromaa AJ, Kosunen TU. Association of CagA-positive infection with Helicobacter pylori antibodies of IgA class. *Ann Med* 2000; **32**: 652-656
16 **Cover TL,** Glupczynski Y, Lage AP, Burette A, Tummuru MK, Perez-Perez GI, Blaser MJ. Serologic detection of infection with cagA$^+$ *Helicobacter pylori* strains. *J Clin Microbiol* 1995; **33**: 1496-1500
17 **Parsonnet J,** Friedman GD, Orentreich N, Vogelman H. Risk for gastric cancer in people with CagA positive or CagA negative *Helicobacter pylori* infection. *Gut* 1997; **40**: 297-301
18 **Correa P,** Haenszel W, Cuello C, Zavala D, Fontham E, Zarama G, Tannenbaum S, Collazos T, Ruiz B. Gastric precancerous process in a high risk population: cohort follow-up. *Cancer Research* 1990; **50**: 4737-4740
19 **Kokkola A,** Kosunen TU, Puolakkainen P, Sipponen P, Harkonen M, Laxen F, Virtamo J, Haapiainen R, Rautelin H. Spontaneous disappearance of Helicobacter pylori antibodies in patients with advanced atrophic corpus gastritis. *APMIS* 2003; **111**: 619-624

Science Editor Kumar M and Guo SY **Language Editor** Elsevier HK

PO Box 2345, Beijing 100023, China
www.wjgnet.com
wjg@wjgnet.com

ELSEVIER

World J Gastroenterol 2005;11(43):6875-6879
World Journal of Gastroenterology ISSN 1007-9327

• *RAPID COMMUNICATION* •

Polymorphisms in sulfotransferase 1A1 and glutathione *S*-transferase P1 genes in relation to colorectal cancer risk and patients' survival

Xiao-Feng Sun, Ahmad Ahmadi, Gunnar Arbman, Åsa Wallin, Daniel Asklid, Hong Zhang

Xiao-Feng Sun, Åsa Wallin, Department of Oncology, Institute of Biomedicine and Surgery, University of Linköping, Linköping, Sweden
Ahmad Ahmadi, Daniel Asklid, Hong Zhang, Department of Cell Biology, Institute of Biomedicine and Surgery, University of Linköping, Linköping, Sweden
Gunnar Arbman, Department of Surgery, Vrinnevi Hospital, Norrköping, Sweden
Supported by grants from the Swedish Cancer Foundation and the Health Research Council in the South-East of Sweden
Correspondence to: Xiao-Feng Sun, Professor, MD, PhD, Department of Oncology, Institute of Biomedicine and Surgery, University of Linköping, S-581 85 Linköping, Sweden. xiasu@ibk.liu.se
Telephone: +46-13-222066 Fax: +46-13-222846
Received: 2005-03-09 Accepted: 2005-04-02

Abstract

AIM: To examine whether polymorphisms in SULT1A1 and GSTP1 genes contribute to colorectal cancer development and whether they are associated with clinicopathological variables are not well identified.

METHODS: We examined the genotypes of 125 colorectal cancer patients and 666 healthy controls in a Swedish population by using PCR-restriction fragment length polymorphism (RFLP).

RESULTS: SULT1A1 *2/*2 genotype (OR = 2.49, 95%CI = 1.48-4.19, P = 0.0002) and *2 allele (OR = 1.56, 95%CI = 1.16-2.10, P = 0.002) had an effect on colorectal cancer susceptibility, while GSTP1 genotype was without effect. However, GSTP1 G-type predicted a worse prognosis in the patients independently of gender, age, Dukes' stage, growth pattern, and differentiation (P = 0.03).

CONCLUSION: Polymorphism in SULT1A1 may predispose to colorectal cancer and GSTP1 may be a biological indicator of prognosis in the patients.

Key words: GSTP1; SULT1A1; Survival; Colorectal cancer; PCR-RFLP

Sun XF, Ahmadi A, Arbman G, Wallin Å, Asklid D, Zhang H. Polymorphisms in sulfotransferase 1A1 and glutathione *S*-transferase P1 genes in relation to colorectal cancer risk and patients' survival. *World J Gastroenterol* 2005; 11(43): 6875-6879
http://www.wjgnet.com/1007-9327/11/6875.asp

INTRODUCTION

Sulfotransferase 1A1 (SULT1A1), a major sulfotransferase enzyme in human beings, is an important component in the detoxification pathway of numerous xenobiotics. The enzyme also plays an important role in the metabolism and bioactivation of many dietary and environmental mutagens, including heterocyclic amines implicated in carcinogenesis of colorectal and other cancers[1]. *SULT1A1* is polymorphic with the most common variant allele, *SULT1A1**2, where a G→A change occurs at nucleotide 638, resulting in an arg213→his213 change. This allele codes for an allozyme with low enzyme activity and stability compared to the *SULT1A1**1 variant. Therefore, *SULT1A1* genotype may influence susceptibility to mutagens following exposure to heterocyclic amines and other environmental toxins[1]. However, regarding the results of the *SULT1A1* polymorphism in relation to colorectal cancer risk was inconsistent[2-4].

Glutathione *S*-transferase P1 (GSTP1) plays a central role in the inactivation of toxic and carcinogenenic electrophiles[5]. The A to G polymorphism at nucleotide 313 in the *GSTP1* gene results in an isoleucine to valine change at residue 105, which reduces the catalytic activity of the enzyme. The polymorphism of lower activity allele of *GSTP1* was related to several types of cancers including bladder, testicular, and lung cancer, but not to colorectal cancer[5-10].

There was no study on the polymorphisms of *SULT1A1* and *GSTP1* in patients with colorectal cancer in comparison with healthy controls in Sweden; we, therefore, investigated the polymorphisms in this population in order to clarify whether the polymorphisms were related to colorectal cancer risk, and further to analyze whether the polymorphisms had any clinicopathological significance. We analyzed genomic DNA of normal colorectal mucosa from 125 colorectal cancer patients and of blood samples from 666 healthy controls by using PCR-restriction-fragment length polymorphism (RFLP).

MATERIALS AND METHODS

Materials

Normal colorectal mucosal samples and colorectal cancer tissue were obtained from 125 patients with primary colorectal adenocarcinomas diagnosed at the Department of Pathology, Vrinnevi Hospital, Norrköping, Sweden, during the period between 1990 and 2001. All patients were Caucasians. Patients' gender, age, tumor site, Dukes' stage and the grade of differentiation were obtained from their surgical and pathological records and reviewed by two authors. Normal colorectal mucosa was taken from the distant resection margin and the corresponding tumor tissue from the colorectal cancer. The patients with colon cancers in Dukes' stage C/advanced tumor received chemotherapy (the influence on survival was less than 20%), and some patients with rectal cancers received adjuvant preoperative radiotherapy (the treatment has a marginal influence on survival). The patients were followed up until the end of October 2003, and 32 deaths due to the cancer had been registered.

Control population comprised 666 individuals from the same residential area as the patients. The individuals had neither gastrointestinal diseases nor history of tumors. DNA samples were extracted from the peripheral leukocytes.

Methods

DNA extraction Genomic DNA was isolated from frozen normal colorectal mucosa and tumor from colorectal cancer patients by a modified proteinase K digestion and phenol/chloroform extraction technique. In brief, the tissue (about 200 mg) was cut into small pieces and dissolved in a cell lysis buffer (40 μL of 20% SDS, 40 μL of 10 mg/mL proteinase K, 400 μL TEN buffer, 0.1 mol/L NaCl, 10 mmol/L Tris-HCl, 1 mmol/L EDTA, pH 8.4). Samples were kept in a shaking water bath at 55 °C overnight. The digestive step was repeated by the addition of half of the volume of the cell lysis solution (above), until the sample solution turned completely clear. DNA was extracted with phenol, phenol/chloroform and chloroform, precipitated with ice-cold ethanol, washed with 70% ethanol, and redissolved in double distilled water. The amount of purified DNA was measured by a DU 640 spectrophotometer (Beckman, Fullerton, USA), and the DNA concentration was calculated. Genomic DNA from the controls was extracted from peripheral leukocytes by means of the Wizard Genome Purification Kit (Promega Inc., Madison, USA) according to the manufacturer's instructions.

PCR-RFLP Two sets of primers were used respectively for determining the polymorphisms of the *SULT1A1* (A1VIIF: GTT GGC TCT GCA GGG TCT CTA GGA GAG and 1A1VIIR: CCC AAA CCC CCG TAC TGG CCA GCA CCC) and *GSTP1* (P105F: ACC CCA GGG CTC TAT GGG AA and P105R: TGA GGG CAC AAG AAG CCC CT). PCR reactions were performed in a total volume 20-80 μL of a solution containing PCR buffer (2 mmol/L $MgCl_2$, 50 mmol/L KCl, 10 mmol/L Tris-HCl, pH 8.4, 1.2 μL DMSO (only for SULT1A1)), 0.2 mmol/L each of dATP, dCTP, dGTP, and dTTP (Pharmacia Biotech, Uppsala, Sweden) and 0.4-1.0 U of Taq DNA polymerase (Sigma Chemical, St. Louis, USA). The reaction started with 94 °C for 3 min, followed by 35-39 cycles consisting of denaturation (at 94 °C for 0.5-3 min), annealing (SULT1A1: at 63 °C for 1 min and GSTP1: 55 °C for 0.5 min), and extension (at 70-72 °C for 0.5-5 min). PCR products were checked by electrophoresis on a 1.5-2% agarose gel (Invitrogen Life Technologies, Groningen, The Netherlands) with 0.2 μg/mL ethidium bromide. A negative control (PCR without template) was included in each set of PCR reactions. All PCR reactions were repeated at least three times for confirmation and to ensure reproducibility.

Hae II (New England BioLabs) was applied to identify *SULT1A1* genotypes[11] and Alw26I (New England Biolabs, Hertfordshire, UK) for *GSTP1* genotypes[8]. The PCR products were digested with the restriction enzymes and separated in a 3.5% agarose gel or in a 4% of 3:1 NuSieve GTG agarose (BioWhittaker Molecular Applications, Rockland, ME, USA)/agarose, stained with ethidium bromide to visualize the bands.

Genotyping and grouping Genotyping and grouping of genotypes in the present study were based on their effect on carcinogenic metabolism and commonly used classifications in previous other studies. For *SULT1A1,* three genotypes of *1/*1, *1/*2, and *2/*2 were classified[2,11-13]. To analyze the relationship of *SULT1A1* genotype with clinicopathological factors, we combined *SULT1A1**1/* with *1/*2 as one group *vs* *SULT1A1**2/*2 group. The polymorphisms of *GSTP1* were confirmed to be A/A, A/G, and G/G. *GSTP1* A type was referred to A/A, and G type was referred to both A/G and G/G[6,14,15].

Statistical analysis

The χ^2 method was used to test the frequencies of genotypes/allele in colorectal cancer patients with the control population and various clinicopathological variables. McNemar's method was used for testing the differences of the genotype/allele frequency in normal colorectal mucosa and tumor tissue. The odds ratio (OR), an estimate of the relative risk, with 95% confidence intervals (CI) was computed to assess the relationship of the genotypes/allele to the risk of colorectal cancer. Cox's Proportional Hazard Model was used to test the relationship between the polymorphisms and the survival of patients. Survival curves were computed according to the Kaplan-Meier method. All *P* values cited were two-sided and *P* values <0.05 were judged as statistically significant.

RESULTS

We examined the polymorphisms of *SULT1A1* in 109 colorectal cancer patients and 666 healthy individuals. As shown in Table 1, the frequencies of *SULT1A1* *2/*2

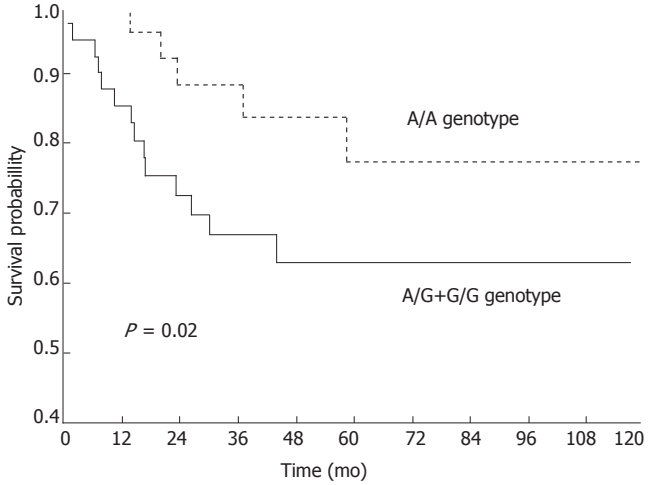

Figure 1 Colorectal cancer patients with G-type genotype (A/G+G/G) of the *GSTP1* gene had a worse prognosis than those with A/A genotype (A/A) ($P = 0.02$).

Table 1 Polymorphisms of SULT1A1 and GSTP1 in colorectal cancer patients and healthy controls

Gene	Patients (%)	Controls (%)	Odds ratio (95%CI)	*P*
SULT1A1				
*1/*1	43 (39)	266 (40)	1.0	
*1/*2	27 (25)	303 (45)	0.55 (0.32–0.94)	
*2/*2	39 (36)	97 (15)	2.49 (1.48–4.19)	0.0002[1]
Allele *1	113 (52)	835 (63)	1.0	
Allele *2	105 (48)	497 (37)	1.56 (1.16–2.10)	0.002
GSTP1				
A/A	59 (47)	127 (50)	1.0	
A/G	51 (41)	101 (40)	1.09 (0.67–1.76)	
G/G	15 (12)	27 (10)	1.20 (0.56–2.55)	0.63[2]
A allele	169 (68)	355 (70)	1.0	
G allele	81(32)	155 (30)	1.10 (0.78–1.54)	0.57

[1]SULT1A1: *2/*2 *vs* *1/*1+*1/*2, [2]GSTP1: G type (G/G+A/G) *vs* A type (A/A).

genotype (36% *vs* 15%, OR = 2.49, 95%CI = 1.48-4.19, $P = 0.0002$) and *2 allele (48% *vs* 37%, OR = 1.56, 95% CI = 1.16-2.10, $P = 0.002$) in the patients were significantly higher than in the controls. The *SULT1A1*2/*2* was still related to the risk for developing colorectal cancer when we did age-matched analyses of case-control, age ≤70 ($P = 0.04$), ≤80 ($P<0.0001$) and >70 years ($P<0.0001$). The status did not change when the tests were performed in different tumor sites (proximal or distal) in comparison with the control group ($P>0.05$).

The genotypes and allele frequency of the *GSTP1* gene were determined in 125 patients and 255 healthy controls. *GSTP1* G type was referred to both A/G and G/G. As shown in Table 1, there was no significant difference between the patients and controls based on G type (53% *vs* 50%, OR = 0.90, 95%CI = 0.57-1.41, $P = 0.63$) or allele frequency (32% *vs* 30%, OR = 1.10, 95%CI = 0.78-1.54, $P = 0.57$), neither in the subgroups of the age and tumor location ($P>0.05$).

The patients with *GSTP1* G-type genotype had a worse prognosis than those with *GSTP1* A (A/A) type genotype ($P = 0.02$, Figure 1). Even in multivariate analysis, the genotype was still related to survival, independent of gender, age, tumor location, Dukes' stage, growth pattern, and differentiation ($P = 0.03$, Table 2). Besides, there was no relationship of genotype/allele frequency with any of the clinicopathological variables studied in the patients ($P>0.05$).

Table 2 Multivariate analysis of GSTP1, gender, age, site, Dukes' stage, growth pattern, and histological type in relation to survival in colorectal cancer

Variable	Number	Cancer death Rate ratio	95%CI	*P*
GSTP1 genotype				
A/A	14	1.0	–	0.03
A/G+G/G	26	5.3	1.26–19.53	
Gender				0.09
Male	25	1.0	–	
Female	15	0.2	0.05–1.18	
Age				0.37
≤70	15	1.0	–	
>70	25	1.9	0.51–7.94	
Tumor location				1.00
Colon	21	1.0	–	
Rectum	19	1.0	0.26–3.98	
Dukes' stage				1.16
A+B	19	1.0	–	
C+D	21	2.7	0.69–10.72	
Growth pattern				0.08
Expansive	24	1.0	–	
Infiltration	16	4.1	0.85–19.45	
Histological type				0.02
Non-mucinous	27	1.0	–	
Mucinous	13	7.1	1.39–32.07	

In order to check whether there was a difference between normal colorectal mucosa and tumor regarding the two polymorphisms, we isolated DNA from the tumors in the same patients and analyzed the genotype/allele frequencies of *SULT1A1* and *GSTP1* polymorphisms by using the same protocol. Neither genotype nor allele frequency of the polymorphisms in the tumors differed from that of the polymorphisms determined in normal mucosal samples ($P>0.05$).

DISCUSSION

In the present study, we demonstrated that the patients with colorectal cancer, comparing with the controls, had significantly higher frequencies of *SULT1A1*2/*2* genotype (36% *vs* 15%) and *2 allele (48% *vs* 37%), indicating that *SULT1A1*2/*2* allele was related to colorectal cancer risk. Our results supported previous findings in colorectal, esophagus, breast and lung cancer studies, where *SULT1A1* *2/*2 genotype was associated with an increased risk for the tumor development[2,16-18]. It has been observed that a G to A transition at nucleotide 638 in *SULT1A1* gene causes an Arg213 to His substitution associated with a low SULT activity. Thus, these results suggest that low activity of SULT1A1*2 allozyme lacks a protection against dietary and/or environmental chemicals involved in the carcinogenesis of colorectal cancer.

It has been demonstrated that individuals with *GSTP1* G/G alleles had a lower catalytic activity compared with individuals with *GSTP1* A/A. An intermediate activity was reported for heterozygotes[19,20]. In the present study, the frequencies of genotype and allele in the control (50% for A/A, 40% for A/G, 10% for G/G, and 70% for A allele) and in the patients (47%, 41%, 12%, and 68%, respectively) were similar to the frequencies raised by other studies in Caucasian controls (40-52%, 39-48%, 7-11%, and 67%, respectively) and colorectal cancer patients (37-49%, 42-55%, 8-12%, and 70%, respectively)[7,8,10,14,21]. We failed to find any evidence supporting an association between the allelic variants of *GSTP1* and susceptibility to colorectal cancer or certain clinicopathological factors including gender, age, tumor location, Dukes' stage and differentiation, which is supportive to previous findings[6,7,9,21].

Interestingly, we found that patients with *GSTP1* G-type had a worse prognosis than the patients with *GSTP1* A-type, even after adjustment for gender, age, tumor location, Dukes' stage, and differentiation. A study in breast cancer found that a significantly higher proportion of breast cancer patients with a *GSTP1* G-type had more frequency of p53 mutations and loss of heterozygosity at the TPp53 gene locus, compared with *GSTP1* A-genotype[22]. It has been widely accepted that altered p53 predicts a poor prognosis in breast cancer patients, although there is not a direct evidence of *GSTP1* in relation to survival in their study. It seems that *GSTP1*, through the A→G polymorphism, may reduce its effect on the inactivation of toxic and carcinogenic electrophiles[5]. In contrast, Stoehlmacher *et al*.[21] demonstrated that the *GSTP1* A→G polymorphism was associated in a dose-dependent fashion with increased survival of patients with advanced colorectal cancers receiving 5-FU/oxaliplatin chemotherapy. They suggest that the effect of certain chemotherapeutic drugs might be altered when enzymes that could enhance the elimination of these drugs show a reduced activity. The opposite results related to survival in colorectal cancer patients may be due to different characteristics of patients included in the two studies. We included all Dukes' stages with a proper stratification (A = 12, B = 46, C = 34, and D = 17); among them, the cases with colon cancers in Dukes' stage C or advanced tumors received chemotherapy, and some patients with rectal cancer received adjuvant preoperative radiotherapy. All patients in their study had a metastasis and received 5-FU/oxaliplatin combination chemotherapy. Furthermore, we had a longer follow-up period than theirs (median month: 33 *vs* 10.9). Comparing with their data, we have more Caucasians (100% *vs* 72%) and older patients (median: 73 *vs* 60 years).

In conclusion, our results suggest that *SULT1A1* may predispose to colorectal cancer, and *GSTP1* may be used as a prognostic factor to predict the patients' survival.

ACKNOWLEDGMENT

The authors are grateful to Dr. Kornelia Polyak (Department of Medical Oncology, Dana-Farber Cancer Institute, Harvard Medical School, Boston, MA, USA) for valuable discussions and the linguistic revision.

REFERENCES

1 **Glatt H**. Sulfotransferases in the bioactivation of xenobiotics. *Chem Biol Interact* 2000; **129:** 141-170
2 Rommelspacher H. Unravelling genetic modifiers of anxiety and depressiveness in psychiatric disorders. Pharmacogenetics 2001; **11:** 679-685
3 **Wong CF**, Liyou N, Leggett B, Young J, Johnson A, McManus ME. Association of the SULT1A1 R213H polymorphism with colorectal cancer. *Clin Exp Pharmacol Physiol* 2002; **29:** 754-758
4 **Nowell S**, Coles B, Sinha R, . MacLeod S, Luke Ratnasinghe D, Stotts C, Kadlubar FF, Ambrosone CB, Lang NP. Analysis of total meat intake and exposure to individual heterocyclic amines in a case-control study of colorectal cancer: contribution of metabolic variation to risk. *Mutat Res* 2002; **506-503:** 175-185
5 **Hengstler JG**, Arand M, Herrero ME, Oesch,F. Polymorphisms of N-acetyltransferases, glutathione S-transferases, microsomal epoxide hydrolase and sulfotransferases: influence on cancer susceptibility. Recent Results Cancer Res 1998; **154:** 47-85
6 **Katoh T,** Kaneko S, Takasawa S, Nagata N, Inatomi H, Ikemura K, Itoh H, Matsumoto T, Kawamoto T, Bell DA. Human glutathione S-transferase P1 polymorphism and susceptibility to smoking related epithelial cancer; oral, lung, gastric, colorectal and urothelial cancer. Pharmacogenetics 1999; **9:** 165-169
7 **Loktionov A**, Watson MA, Gunter M, Stebbings WS, Speakman CT, Bingham SA. Glutathione-S-transferase gene polymorphisms in colorectal cancer patients: interaction between GSTM1 and GSTM3 allele variants as a risk-modulating factor. *Carcinogenesis* 2001; **22:** 1053-1060
8 **Harries LW**, Stubbins MJ, Forman D, Howard GC, Wolf CR. Identification of genetic polymorphisms at the glutathione S-transferase Pi locus and association with susceptibility to bladder, testicular and prostate cancer. *Carcinogenesis* 1997; **18:** 641-644
9 **Harris MJ**, Coggan M, Langton L, Wilson SR, Board PG. Polymorphism of the Pi class glutathione S-transferase in normal populations and cancer patients. *Pharmacogenetics* 1998; **8:** 27-31
10 **Welfare M**, Monesola Adeokun A, Bassendine MF, Daly AK. Polymorphisms in GSTP1, GSTM1, and GSTT1 and susceptibility to colorectal cancer. *Cancer Epidemiol Biomarkers Prev* 1999; **8:** 289-292
11 **Coughtrie MW**, Gilissen RA, Shek B, Strange RC, Fryer AA, Jones PW, Bamber DE. Phenol sulphotransferase SULT1A1 polymorphism: molecular diagnosis and allele frequencies in Caucasian and African populations. *Biochem J* 1999; **337**(pt 1)**:** 45-49
12 **Seth P**, Lunetta KL, Bell DW, Gray H, Nasser SM, Rhei E, Kaelin CM, Iglehart DJ, Marks JR, Garber JE, Haber DA, Polyak K. Phenol sulfotransferases: hormonal regulation, polymorphism, and age of onset of breast cancer. *Cancer Res* 2000; **60:** 6859-6863
13 **Stone J,** Wade JA, Cauch-Dudek K, Ng C, Lindor KD, Heathcote EJ. Human leukocyte antigen Class II associations in serum antimitochondrial antibodies (AMA)-positive and AMA-negative primary biliary cirrhosis. J Hepatol **2002; 35:** 137-142
14 **Ryberg D**, Skaug V, Hewer A, Phillips DH, Harries LW, Wolf CR, Ogreid D, Ulvik A, Vu P, Haugen A. Genotypes of glutathione transferase M1 and P1 and their significance for lung DNA adduct levels and cancer risk. *Carcinogenesis* 1997; **18:** 1285-1289
15 **Yoshioka M**, Katoh T, Nakano M, Takasawa S, Nagata N, Itoh H. Glutathione S-transferase (GST) M1, T1, P1, N-acetyltransferase (NAT) 1 and 2 genetic polymorphisms and

susceptibility to colorectal cancer. *J UOFH* 1999; **21:** 133-147
16 **Wu MT**, Wang YT, Ho CK, Wu DC, Lee YC, Hsu HK, Kao EL, Lee JM. SULT1A1 polymorphism and esophageal cancer in males. *Int J Cancer* 2003; **103:** 101-104
17 **Han DF**, Zhou X, Hu MB, Wang CH, Xie W, Tan XD, Zheng F, Liu F. Sulfotransferase 1A1 (SULT1A1) polymorphism and breast cancer risk in Chinese women. *Toxicol Lett* 2004; **150:** 167-177
18 **Liang G,** Miao X, Zhou Y, Tan W, Lin D. A functional polymorphism in the SULT1A1 gene (G638A) is associated with risk of lung cancer in relation to tobacco smoking. *Carcinogenesis* 2004; **25**: 773-778
19 **Watson MA**, Stewart RK, Smith GB, Massey TE, Bell DA. Human glutathione S-transferase P1 polymorphisms: relationship to lung tissue enzyme activity and population frequency distribution. *Carcinogenesis* 1998; **19:** 275-280
20 **Srivastava SK**, Singhal SS, Hu X, Awasthi YC, Zimniak P, Singh SV. Differential catalytic efficiency of allelic variants of human glutathione S-transferase Pi in catalyzing the glutathione conjugation of thiotepa. *Arch Biochem Biophys* 1999; **366:** 89-94
21 **Stoehlmacher J**, Park DJ, Zhang W, Groshen S, Tsao-Wei DD, Yu MC, Lenz HJ. Association between glutathione S-transferase P1, T1, and M1 genetic polymorphism and survival of patients with metastatic colorectal cancer. *J Natl Cancer Inst* 2002; **94:** 936-942
22 **Nedelcheva Kristensen V**, Andersen TI, Erikstein B, Geitvik G, Skovlund E, Nesland JM, Borresen-Dale AL. Single tube multiplex polymerase chain reaction genotype analysis of GSTM1, GSTT1 and GSTP1: relation of genotypes to TP53 tumor status and clinicopathological variables in breast cancer patients. *Pharmacogenetics* 1998; **8:** 441-447

Sciencel Editor Wang XL and Guo SY **Language Editor** Elsevier HK

PO Box 2345, Beijing 100023, China
www.wjgnet.com
wjg@wjgnet.com

ELSEVIER

World J Gastroenterol 2005;11(43):6880-6883
World Journal of Gastroenterology ISSN 1007-9327

• *RAPID COMMUNICATION* •

Immunoproteomics of membrane proteins of *Shigella flexneri* 2a 2457T

Tian-Yi Ying, Jun-Jun Wang, Heng-Liang Wang, Er-Ling Feng, Kai-Hua Wei, Liu-Yu Huang, Pei-Tang Huang, Cui-Fen Huang

Tian-Yi Ying, Jun-Jun Wang, Heng-Liang Wang, Er-Ling Feng, Kai-Hua Wei, Liu-Yu Huang, Pei-Tang Huang, Cui-Fen Huang, Beijing Institute of Biotechnology, State Key Lab of Pathogen and Biosecurity, Beijing 100071, China
Tian-Yi Ying, Beijing Institute of Pharmaceutical Chemistry, Beijing 102205, China
Supported by the Capital "248" Key Innovation Project, No. H010210360119, State Basic Research Development Program of China No. 973 Program, G1999054103 and 2005CB22904 and National Natural Science Foundation of China No. 30470101
Correspondence to: Dr Heng-Liang Wang, Institute of Biotechnology, State Key Lab of Pathogen and Biosecurity, 20 Dongdajie Street, Fengtai District, Beijing 100071, China. wanghl@nic.bmi.ac.cn
Telephone: +86-10-66948836
Received: 2005-04-12 Accepted: 2005-04-30

Abstract

AIM: To screen the immunogenic membrane proteins of *Shigella flexneri* 2a 2457T.

METHODS: The routine two-dimensional polyacrylamide gel electrophoresis (2-DE) and Western blotting were combined to screen immunogenic proteins of *S. flexneri* 2a 2457T. Serum was gained from rabbits immunized with the same bacteria. Immunogenic spots were cut out from the polyacrylamide gel and digested by trypsin in-gel. Matrix-assisted laser desorption/ionization time of flight-mass spectrometry (MALDI-TOF-MS) was performed to determine the molecular weight of peptides. Electrospray ionization (ESI-MS/MS) was performed to determine the sequences of the interesting peptides.

RESULTS: A total of 20 spots were successfully identified from Coomassie brilliant blue stained gels representing 13 protein entries, 5 known antigens and 8 novel antigens. A hypothetical protein (YaeT) was detected, which might be a candidate target of vaccine.

CONCLUSION: Membrane proteins of *S. flexneri* 2a 2457T were successfully observed by 2-DE. Several known and novel antigens were identified by mass spectrum.

Key words: *Shigella flexneri* 2a 2457T; Immunoproteomics; Membrane proteins

Ying TY, Wang JJ, Wang HL, Feng EL, Wei KH, Huang LY, Huang PT, Huang CF. Immunoproteomics of membrane proteins of *Shigella flexneri* 2a 2457T. *World J Gastroenterol* 2005; 11(43): 6880-6883
http://www.wjgnet.com/1007-9327/11/6880.asp

INTRODUCTION

The genus *Shigella* spp. is a group of Gram-negative enteric bacilli which cause bacillary dysentery in human beings, accounting for 20% of the 4.6 million diarrhea-associated deaths among children[1]. Though the LPS can induce a good immune response in human beings, the role of proteins (especially the membrane proteins) in conferring immunity to shigellosis is at best speculative. Considering outer membrane proteins of *Shigella* spp. function as a dynamic interface between the cell and its surroundings, it is possible to develop new antigens from them. Due to the methodology limitations of protein separation and identification, it is difficult to identify the immunogenic proteins in bands on 1-D gel. With the improvement of 2-DE in recent years much valuable information is available and immunoproteomics has been built around 2-DE and routine immunologic technologies.

S. flexneri 2a is the dominant serotype causing shigellosis in China. Our laboratory has finished a two-dimensional electrophoresis reference map and a proteomic database of *S. flexneri* 2a 2457T[2], but only a few of membrane proteins can be identified in that database. In order to develop new protective antigens against *S. flexneri* and to understand their immune mechanism, we applied immunoproteomic technologies in screening new antigens of *S. flexneri* 2a 2457T.

MATERIALS AND METHODS

Bacterial strains and growth conditions

S. flexneri 2a 2457T was aerobically cultured in LB overnight at 37 °C. Overnight cultures were diluted 1:100 and shaken at 250 r/min. Growth was stopped at the early stationary phase at an A_{600} of 3.3.

Membrane protein preparation

Cells were harvested and centrifuged for 15 min at 2 000 r/min (Sigma 3K12, No. 12150; St. Louis, MO, USA) at 4 °C. The pellet was washed thrice for 10 min at 2 000 r/min with low-

salt washing buffer (3 mmol/L KCl, 1.5 mmol/L KH_2PO_4, 68 mmol/L NaCl, 9 mmol/L NaH_2PO_4)[3]. Proteins were extracted using the ReadyPrep™ protein extraction kit (Membrane I) (BioRad, USA). Integral membrane proteins were separated from hydrophilic proteins using the nonionic detergent Triton X-114.

Two-dimensional electrophoresis

Eighteen-centimeter immobilized pH gradient (IPG) strips (pH ranges, 4-7) (Amersham Pharmacia Biotech, Sweden) were used. Isoelectric focusing (IEF) was conducted for 60 000 Vh (IPGphor, Amersham Pharmacia Biotech). Vertical slab SDS-PAGE (12.5%) was run at 30 mA/gel for the second dimension. Gels were stained with Colloidal Coomassie Blue[4]. Image analysis was performed with Image-Master 2D Elite Version 3.1.

Preparation of antisera against 2457T

S. flexneri 2a 2457T was aerobically cultured in LB overnight at 37 °C. Rabbits were immunized six times with culture solution intravenously at intervals of 5 d. The doses were (5, 7.5, 10, 15, 20, 20)×10^8 CFU, respectively. Eight days after the last immunization, blood was collected from the tested animals and the sera were separated. Antibody titers 1:5 120 was measured by microaggalutination test and ELISA.

Immunoblot assay

After two-dimensional electrophoresis, the gels were electroblotted onto Hybond™ECL™ nitrocellulose membrane (Amersham Pharmacia Biotech) using a semi-dry transfer unit (Hoefer™ TE 77, Amersham Pharmacia Biotech, Sweden). Before immunodetection, the membranes were stained for 10 min with 5 g/L Ponceau S in 10 mL/L acetic acid and the positions of some selected spots were marked by clean needles. Western blotting was performed as previously described[5]. Then antigen-antibody complexes were detected with peroxidase-labeled goat anti-rabbit IgGs and substrate.

In-gel protein digestion and MALDI-TOF-MS protein identification

In-gel protein digestion was performed as previously described[6]. All MALDI-MS measurements were performed on a Bruker Reflex. III MALDI-TOF-MS (Bruker Daltonik, Bremen, Germany) operating in reflectron mode.

Nanospray ESI-MS/MS

The peptide solution after in-gel protein digestion was desalted with ZipTip C18™ pipette tips (Millipore, Bedford, MA, USA). Electrospray ionization (ESI-MS/MS) was carried out with a hybrid quadrupole orthogonal acceleration tandem mass spectrometer (Q-TOF2) (Micromass, Manchester, UK)[2].

Peptide mass fingerprinting

Peptide mass fingerprinting searches were performed using the program Mascot developed by Matrix Science Ltd (http://www.matrixscience.com). For protein identification, peptide mass searches against the database of 2457T by Mascot licensed in-house and the searches against the NCBInr database with free access on the internet were done. A peptide mass accuracy of 0.3 Da was defined.

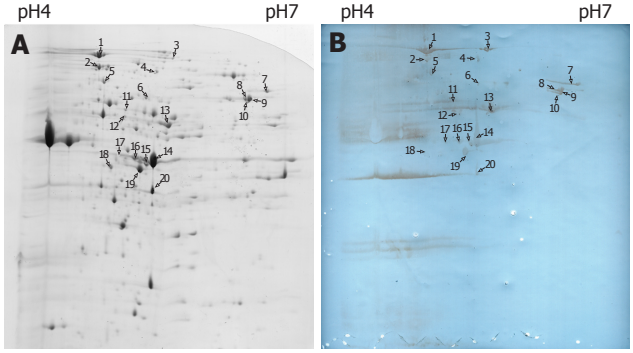

Figure 1 A: Two-dimensional electrophoresis profile of *S. flexneri* 2a 2457T membrane proteins, stained with Colloidal Coomassie Blue; **B:** Western blot of membrane proteins of *S. flexneri* 2a 2457T. Gel equal to Figure 1A was electroblotted onto nitrocellulose membrane using a semi-dry transfer unit.

RESULTS

The sample was prepared on the basis of the separation of membrane proteins by temperature-dependent phase partitioning using Triton X-114 detergent. Proteins anchored to the membrane or containing one or two transmembrane domains were efficiently partitioned to the detergent-rich phase. In order to solubilize the protein thoroughly, thiourea was used. In pH 4-7 gradient 2-DE map, 148 spots were cut and 111 spots were successfully identified by MALDI-TOF-MS presenting 82 protein entries. Twenty-five proteins were not observed/identified in our previous work[2]. The majority of these 25 proteins (data not shown) were hydrophobic and associated with the membrane. The relative abundance of membrane-associated proteins identified in this study was higher than that in our previous study[2].

On the basis of the established immunoproteomic map of soluble proteins of *S. flexneri* 2a 2457T (unpublished), we described a group of spots in a 2-DE map of immunogenic proteins from hydrophobic proteins in this study. Five hundred micrograms of protein sample was used to perform the 2-DE. One of the parallel gels was electroblotted onto nitrocellulose membrane and the other was stained with Coomassie brilliant blue G-250. We successfully identified 20 immunoreactive spots from Coomassie brilliant blue stained gels using sera from immunized rabbits, which represented 13 protein entries, 5 known antigens and 8 novel antigens. The 20 spots were marked on the 2-D gel and corresponding blotting membrane (Figure 1). Table 1 lists all the identified proteins. ESI-MS/MS was used to confirm the protein marked as spot 1. Figure 2 shows the result of ESI-MS/MS identification.

Table 1 List of immunoreactive proteins of membrane proteins

Spot ID	Gene symbol	Protein common name	NCBI GI identifier	Cellular role
1	YaeT	Hypothetical protein	gi|30061734	Cell envelope
2	DnaK	Chaperone Hsp70; autoregulated heat shock protein	gi|30061584	Protein fate
3	ClpB	Heat shock protein	gi|30063993	Protein fate
4/14/16/17/ 20	OmpA	Outer membrane protein 3a (II*; G; d)	gi|30062494	Cell envelope
5	MopA	GroEL, chaperone Hsp60, peptide-dependent ATPase, heat shock protein	gi|30065518	Protein fate
6	Pgm	Phosphoglucomutase	gi|30062137	Energy metabolism
7	OppA	Periplasmic oligopeptide binding protein	gi|30062764	Protein fate
8/9	AtpA	Membrane-bound ATP synthase, F1 sector, alpha-subunit	gi|30064961	Energy metabolism
10	LpdA	Lipoamide dehydrogenase (NADH)	gi|30061682	Energy metabolism
11	Gnd	Gluconate-6-phosphate dehydrogenase	gi|30063478	Energy metabolism
12/13/18	TufB	Protein chain elongation factor EF-Tu	gi|30064737	Protein synthesis
15	Tsf	Protein chain elongation factor EF-Ts	gi|30061727	Protein synthesis
19	MglB	Galactose-binding transport protein; receptor for galactose taxis	gi|30063593	Transport and binding proteins

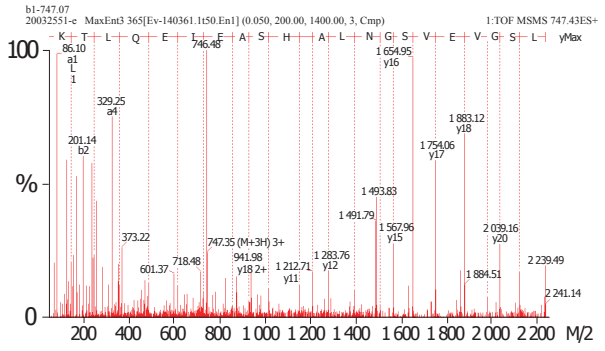

Figure 2 Mass spectra showing the determination of a partial peptide sequence of the *hypothetical* protein (spot 1).

DISCUSSION

Known antigens

Our results are in accordance with other studies[7-11].The outer membrane protein 3a (II*; G; d) is a precursor of OmpA, a major and highly conserved outer membrane protein of Gram-negative bacteria. Due to its high copies per cell[12], multiple charged isoforms[13] and its strong immunogenecity, identification of OmpA was performed several times during the immunoproteomics analysis. All these proteins were observed in our other works (unpublished).

Novel antigens

Besides the above confirmatory findings, the study detected several new immunoreactive proteins (AtpA, OppA, MglB, LpdA, ClpB, Gnd, Pgm, YaeT). AtpA, LpdA, Gnd, and Pgm are components of the energy metabolism system. ATP synthesis/hydrolysis occurs in the ATP synthase F1 sector which lies at the surface of cytoplasmic membrane. LpdA codes for an outer membrane lipoamide dehydrogenase that is highly immunogenic. It is an *in vivo*-induced antigen in *Mycobacterium tuberculosis*[14]. Since LpdA is a functional subunit of both pyruvate dehydrogenase (aceEF) and alpha-ketoglutarate dehydrogenase (sucAB), a lpdA mutant of *H. influenzae* can be significantly attenuated[15]. Gnd is an important component of pentose phosphate pathway. Phosphoglucomutase (pgm) is associated with virulence of *Brucella abortus* because the deltapgm strain is unable to assemble the O side chain in the complete LPS. Vaccination with the deltapgm strain induces effective protection[16]. The periplasmic oligopeptide binding protein OppA is part of the oligopeptide transport system. In addition to the function mentioned above, it also plays a role in mediating the adhesion or interactions of bacteria to different substrates, tissues or environments[17-19]. OppA and periplasmic galactose-binding protein MglB also display some chaperone-like functions, suggesting that they are probably involved in protein folding and protection against stress in periplasm[20]. ClpB is also a heat shock protein. The proteins described above have not been reported as antigens and may serve as candidate markers for bacterial infection though they are unlikely to be protective.

A hypothetical protein (YaeT) detected is of high homology to Oma90 of *S. flexneri* M90T (serotype 5)[21]. We also detected this protein in another study (unpublished), which is verified by ESI-MS/MS. Since it has an enhanced expression in a murine model and exhibits strong homology to genes encoding *Haemophilus influenzae* D15 and *Pasteurella multocida* Oma87, its role in Shigella infection and immunoreaction is worthy to be clarified.

REFERENCES

1 **Ahmed F,** Ansaruzzaman M, Haque E, Rao MR, Clemens JD. Epidemiology of postshigellosis persistent diarrhea in young children. *Pediatr Infect Dis J* 2001; **20:** 525-530
2 **Liao X,** Ying T, Wang H, Wang J, Shi Z, Feng E, Wei K, Wang Y, Zhang X, Huang L, Su G, Huang P. A two-dimensional proteome map of Shigella flexneri. *Electrophoresis* 2003; **24:** 2864-2882
3 **Humphery-Smith I,** Guyonnet F, Chastel C. Polypeptide cartography of Spiroplasma taiwanense. *Electrophoresis* 1994; **15:** 1212-1217
4 **Cordwell SJ.** Acquisition and archiving of information for bacterial proteomics: from sample preparation to database. *Methods Enzymol* 2002; B 207-227
5 **Wu M,** Stockley PG, Martin WJ 2nd. An improved western blotting technique effectively reduces background. *Electrophoresis* 2002; **23:** 2373-2376
6 **Liao X,** Ying TY, Wang HL, Wang J, Wei KH, Huang LY, Huang PT. A modified method of in-gel digestion of Coomassie brilliant blue-stained 2-D gels. *Shengwu Jishu Tongxun* 2003; **14:** 509-511

7 **Sanchez-Campillo M,** Bini L, Comanducci M, Raggiaschi R, Marzocchi B, Pallini V, Ratti G. Identification of immunoreactive proteins of Chlamydia trachomatis by Western blot analysis of a two-dimensional electrophoresis map with patient sera. *Electrophoresis* 1999; **20:** 2269-2279

8 **Bini L,** Sanchez-Campillo M, Santucci A, Magi B, Marzocchi B, Comanducci M, Christiansen G, Birkelund S, Cevenini R, Vretou E, Ratti G, Pallini V. Mapping of Chlamydia trachomatis proteins by immobiline-polyacrylamide two-dimensional electrophoresis: spot identification by N-terminal sequencing and immunoblotting. *Electrophoresis* 1996; **17:** 185-190

9 **Pardo M,** Ward M, Pitarch A, Sanchez M, Nombela C, Blackstock W, Gil C. Cross-species identification of novel Candida albicans immunogenic proteins by combination of two-dimensional polyacrylamide gel electrophoresis and mass spectrometry. *Electrophoresis* 2000; **21:** 2651-2659

10 **McAtee CP,** Lim MY, Fung K, Velligan M, Fry K, Chow T, Berg DE. Identification of potential diagnostic and vaccine candidates of Helicobacter pylori by two-dimensional gel electrophoresis, sequence analysis, and serum profiling. *Clin Diagn Lab Immunol* 1998; **5:** 537-542

11 **Haas G,** Karaali G, Ebermayer K, Metzger WG, Lamer S, Zimny-Arndt U, Diescher S, Goebel UB, Vogt K, Roznowski AB, Wiedenmann BJ, Meyer TF, Aebischer T, Jungblut PR. Immunoproteomics of Helicobacter pylori infection and relation to gastric disease. *Proteomics* 2002; **2:** 313-324

12 **Nikaido H.** Outer membrane. In: Neidhardt FC. Escherichia coli and Salmonella: Cellular and molecular biology. Washington DC: *ASM Press*, 1996: 29-47

13 **Molloy MP,** Herbert BR, Slade MB, Rabilloud T, Nouwens AS, Williams KL, Gooley AA. Proteomic analysis of the Escherichia coli outer membrane. *Eur J Biochem* 2000; **267:** 2871-2881

14 **Deb DK,** Dahiya P, Srivastava KK, Srivastava R, Srivastava BS. Selective identification of new therapeutic targets of Mycobacterium tuberculosis by IVIAT approach. *Tuberculosis* 2002; **82:** 175-182

15 **Herbert M,** Kraiss A, Hilpert AK, Schlor S, Reidl J. Aerobic growth deficient Haemophilus influenzae mutants are non-virulent: implications on metabolism. *Int J Med Microbiol* 2003; **293:** 145-152

16 **Ugalde JE,** Comerci DJ, Leguizamon MS, Ugalde RA. Evaluation of Brucella abortus phosphoglucomutase (pgm) mutant as a new live rough-phenotype vaccine. *Infect Immun* 2003; **71:** 6264-6269

17 **Sutcliffe IC,** Russell RR. Lipoproteins of gram-positive bacteria. *J Bacteriol* 1995; **177:** 1123-1128

18 **Higgins CF,** Hardie MM. Periplasmic protein associated with the oligopeptide permeases of Salmonella typhimurium and Escherichia coli. *J Bacteriol* 1983; **155:** 1434–1438

19 **Fenno JC,** Tamura M, Hannam PM, Wong GW, Chan RA, McBride BC. Identification of a Treponema denticola OppA homologue that binds host proteins present in the subgingival environment. *Infect Immun* 2000; **68:** 1884-1892

20 **Richarme G,** Caldas TD. Chaperone properties of the bacterial periplasmic substrate-binding proteins. *J Biol Chem* 1997; **272:** 15607-15612

21 **Robb CW,** Orihuela CJ, Ekkelenkamp MB, Niesel DW. Identification and characterization of an in vivo regulated D15/Oma87 homologue in Shigella flexneri using differential display polymerase chain reaction. *Gene* 2001; **262:** 169-177

Science Editor Wang XL and Guo SY **Language Editor** Elsevier HK

PO Box 2345, Beijing 100023, China
www.wjgnet.com
wjg@wjgnet.com

ELSEVIER

World J Gastroenterol 2005;11(43):6884-6887
World Journal of Gastroenterology ISSN 1007-9327

• *CASE REPORT* •

Non-parasitic splenic cysts: A report of three cases

A Macheras, EP Misiakos, T Liakakos, D Mpistarakis, C Fotiadis, G Karatzas

A Macheras, EP Misiakos, T Liakakos, D Mpistarakis, C Fotiadis, G Karatzas, 3rd Department of Surgery, University of Athens, School of Medicine, Attikon University Hospital, Haidari, Athens, Greece
Correspondence to: Evangelos P Misiakos, MD, Lecturer in Surgery, University of Athens, School of Medicine, 19 Giavasi Street, Agia Paraskevi, Athens 15341,
Greece. misiakos@med.uoa.gr
Telephone: +11-30210-5326419 Fax: +11-30210-5326420
Received: 2005-03-12 Accepted: 2005-04-02

Abstract

Primary splenic cyst is a relatively rare disease, and the majority of cases are classified as epithelial cysts. Three cases with nonparasitic splenic cysts are presented: two epithelial and one pseudocyst. All cases had an atypical symptomatology, consisted mainly of fullness in the left upper abdomen and a palpable mass. Preoperative diagnosis was established with ultrasonography and computerized tomography. Two cases with large cysts located in the splenic hilum were treated with open complete splenectomy. The most recent case, a pseudocyst, was managed laparoscopically with partial cystectomy. All cases did not have any problems or recurrence during follow-up. Laparoscopic partial cystectomy is an acceptable procedure for the treatment of splenic cysts, because it cures the disease preserving the splenic tissue. Complete splenectomy is reserved for cases in which cyst excision cannot be done otherwise.

Key words: Spleen; Epithelial cyst; Surgery; Laparoscopy

Macheras A, Misiakos EP, Liakakos T, Mpistarakis D, Fotiadis C, Karatzas G. Non-parasitic splenic cysts: A report of three cases. *World J Gastroenterol* 2005; 11(43): 6884-6887
http://www.wjgnet.com/1007-9327/11/6884.asp

INTRODUCTION

Splenic cysts are unusual in everyday surgical practice. They can be parasitic (hydatid), caused by the parasite *Echinococcus granulosus*, or nonparasitic[1,2]. Non-parasitic cysts are classified as primary (true, epithelial), lined by an epithelial cover (epidermoid, dermoid, and mesothelial) or endothelial cover (hemangioma, lymphangioma), and secondary (pseudocysts, non-epithelial), which are usually of post-traumatic origin[3,4].

Primary splenic cysts comprise 30-40% of the total and are encountered more commonly in children and young adults[5,6]. Most of the cysts are asymptomatic, and they are incidental findings during abdominal ultrasonography. The number of diagnosed splenic cysts seems to rise because of the increased use of abdominal imaging techniques[7].

Laparotomy with splenectomy has been the method of choice for the treatment of primary splenic cysts[5,8]. Today, performance of more conservative surgical procedures has been advised, especially in children and young adults, in order to avoid overwhelming postsplenectomy infection[4,8]. Herein, we present three cases with non-parasitic splenic cysts, their diagnostic evaluation and surgical management.

CASE REPORTS

Case 1

A 15-year-old girl was admitted to our Department with a chief complaint of abdominal fullness. An elastic, hard mass of approximately 15 cm in diameter was palpable in the left upper abdomen. A chest X-ray showed a mild elevation of the left hemidiaphragm. Ultrasonography of the upper abdomen showed a giant cystic lesion with irregular echoic patterns. Computerized tomography confirmed the splenic localization of the cyst and demonstrated almost total displacement of the remaining splenic parenchyma.

At laparotomy, a huge splenic cyst of approximately 15 cm of maximal diameter was revealed, located in the middle of the splenic parenchyma, displacing it towards the splenic poles. First, reduction of the cyst with intraoperative drainage of 1 000 mL of serous fluid was done. However, due to the cyst location, preservation of the spleen was considered impossible, and complete splenectomy followed. The aspirated cystic fluid showed no evidence of malignancy. Histology report revealed that the cyst wall consisted of dense fibrous tissue, covered by stratified squamous or cuboid epithelium. Thus, the diagnosis of a primary epidermoid splenic cyst was established. The postoperative clinical course of the patient was satisfactory and was discharged on postoperative d 7. She received a pneumococcal vaccine and chemoprophylaxis with oral penicillin at a dose of 1 500 000 IU twice daily, for a period of 6 months. Today, the patient is in excellent condition, 8 years after surgery.

Case 2

A 27-year-old woman presented with mild dyspeptic symptoms, an atypical pain and a sensation of fullness in the epigastrium. Past medical history was negative,

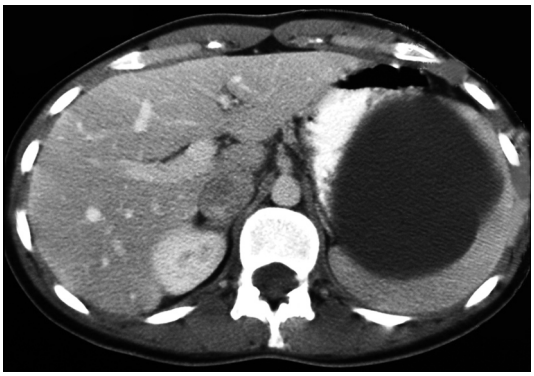

Figure 1 Plain abdominal CT scan showing the splenic localization of a large cyst displacing the remaining splenic parenchyma, the so-called "beak-sign".

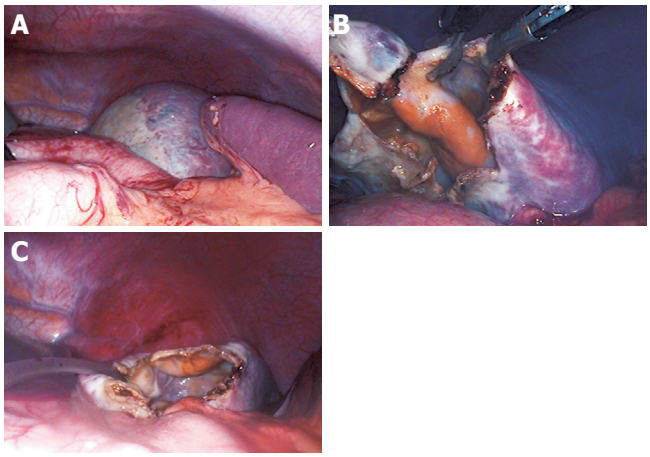

Figure 2 Laparoscopic view of the cyst. Most parts of the cyst are covered with a thin layer of splenic tissue; only a small portion in the upper pole of the spleen displays a "white roof" **(A)**. The cyst was punctured and evacuated and a 3 cm× 3 cm portion of the cyst was excised using the monopolar scissor **(B)**. A drainage tube was inserted in the remaining cavity **(C)**.

and physical examination revealed a 6-7 cm palpable mass in the left upper quadrant of her abdomen. All laboratory tests were normal, and serological tests gave no evidence of parasitic infection with *Echinococcus granulosus*. Plain abdominal films of the abdomen were negative. Ultrasound and computerized tomography of the abdomen showed a solitary cystic mass in the splenic hilum with a maximum diameter of 8 cm, displacing the splenic parenchyma (Figure 1). Endoscopic examination of the upper gastrointestinal tract did not reveal any significant findings.

The diagnosis of a splenic cyst was confirmed and the patient was subjected to exploratory laparotomy. On exploration, there was a medium-sized splenic cyst located in the hilum, which made splenectomy inevitable. Postoperative recovery was uneventful. Histological examination of the specimen showed a normal splenic parenchyma and an epidermoid splenic cyst with a fibrous wall lined by epithelial cells. The patient had no problems after surgery and she received pneumococcal vaccine and oral penicillin for 6 months. Today she is in good clinical condition, 4 years postoperatively.

Case 3

A 24-year-old female presented with an asymptomatic lump in the left hypochondriac region, since 2 years. The patient did not have any specific symptoms except for a mild abdominal discomfort and a sensation of fullness in her left upper abdomen. She had a negative medical history. On physical examination, a cystic mass was palpable under the left costal margin, which was moving according to the respiratory movements. The routine hematological and biochemical tests were normal. Casoni's skin test and complement fixation test for hydatid disease were negative. A clinical diagnosis of cystic splenomegaly was made and the patient was subjected to radiological investigations. Ultrasonography of the upper abdomen revealed a single unilocular spherical cystic lesion in the anterior surface of the spleen. Computerized tomography confirmed the ultrasound findings of a subcapsular cystic lesion with an almost 10 cm of maximal diameter within the spleen with attenuation value near that of water with a non-calcified wall.

With a preoperative diagnosis of a splenic cyst, the patient was subjected to laparoscopy. Before starting with the procedure, a thorough video-guided inspection of the peritoneal cavity was performed. After focusing on the left upper quadrant, the greater omentum was pulled down, and the cyst was clearly visible in the upper pole of the spleen (Figure 2A). The cyst roof was punctured and about 700 mL of yellowish (serous) fluid was aspirated and sent for culture and cytological examination. A 3 cm ×3 cm portion of the collapsed cyst wall was then excised with monopolar scissors, paying attention to remove the cyst wall segment free of splenic parenchyma (Figure 2B). Thus, there was minimal blood loss and unroofing of the cyst wall was accomplished. The specimen was extracted through a 10-mm port and sent for histological examination. The tip of an elastic drainage tube was left inside the remaining cavity (Figure 2C). The postoperative course was uneventful. The patient resumed oral diet on the first postoperative day, and was discharged on the second postoperative day after the drain was removed.

Bacteriological cultures of the fluid were negative. Cytological examination of the fluid showed a few lymphocytes and histiocytes. Histological examination of the cyst wall revealed the presence of dense cytopenic connective tissue without any epithelial lining, and confirmed the diagnosis of a splenic pseudocyst. The patient is in good clinical condition, one year after surgery, and on follow-up tomographic scan had no evidence of recurrence.

DISCUSSION

Benign true non-parasitic splenic cysts cannot be clinically distinguished from other types of splenic cysts. They have an inner lining of epithelial cells and are usually of congenital etiology[3,6]. Pseudocysts have an inner lining of connective tissue and are usually secondary to blunt trauma or hemorrhage in the splenic parenchyma, but

they may also be of infectious and degenerative origin[9,10]. Both types of splenic cysts do not produce any specific symptoms, until they reach a significant size. Large cysts may cause atypical pain and heaviness in the left hypochondriac region, due to distension of the capsule or space-occupying mechanisms within the abdominal cavity, or they may present as a palpable mass[3,5,9]. Indeed, in our patients, symptomatology was atypical with a sensation of fullness and a palpable mass in the left upper abdominal quadrant, as well as mild dyspeptic symptoms. Symptoms secondary to pressure on surrounding organs, such as nausea, vomiting, flatulence, and diarrhea may gradually appear. Also, pressure in the cardiorespiratory system may cause pleuritic pain or dyspnea, and irritation of the left diaphragm may cause persistent cough[10]. Occasionally splenic cysts may present with complications, such as infection, rupture and hemorrhage[9,11].

When a lump is detected in the left upper quadrant of the abdomen, it is necessary to exclude any disease associated with splenomegaly, mononucleosis, fever of unknown origin, hemolytic anemia, chronic leukemias, collagen vascular disease, and liver diseases[12]. Serological studies are useful in excluding most of the above-mentioned diagnosis. In our cases hematological, biochemical, and serological investigations were negative. Angiography is useful in differentiating a splenic cyst, which is usually avascular, from solid malignant tumors (lymphoma, sarcoma), which usually have neoplastic vasculature in a disorganized pattern[10,13]. Ultrasonography is able to see that the cysts are either anechoic or hypoechoic and they have a smooth thin wall[14], whereas solid tumors are either isoechoic or hypoechoic. In addition, computerized tomography and magnetic resonance imaging may give most of the necessary information, regarding the morphology of the cyst, the composition of the cystic fluid, the location in the spleen, the position of the cyst and its relationship with the surrounding tissues[5,7,10]. Calcifications of both the primary and secondary cysts are frequently found, which are useful in diagnosing cysts from other causes of splenomegaly[5]. In our cases, ultrasonography and computerized tomography had preoperatively set the diagnosis of solitary unilocular noncalcified splenic cysts.

Due to the increased risk of complications in splenic cysts with a diameter larger than 4-5 cm should be managed surgically[9,11,15], because conservative options, such as percutaneous aspiration or sclerosis, do not result in long-term control[5,8,16]. There are different types of surgical treatment according to the patient's age and the size, location and nature of the cyst. The classical approach to splenic cysts has been open complete splenectomy[5,8,17]. However, there was a trend towards more conservative surgery after the 1970s, because of the appearance of overwhelming life-threatening septicemia, especially in children who underwent splenectomy[5,10,18]. Indeed, the spleen plays an important role in hematopoiesis, immune function, and protection against infections and malignancies[5,19]. Today the optimal treatment options are partial splenectomy, total cystectomy, marsupialization, or cyst decapsulation (unroofing), accessed either by open laparotomy or laparoscopy[5,11,19,20,21].

Partial splenectomy preserves more than 25% of splenic parenchyma, which is the minimal splenic tissue to preserve immunologic protection without increasing the risk of recurrence[5,20]. Partial splenectomy can be performed safely with the laparoscopic approach[4,11,20,21]. This procedure is recommended, if the cyst is located in the poles of the spleen, or if the cyst cavity is deep, due to the higher risk of recurrence[5,8]. Incision of the splenic capsule and hemostasis is performed with the ultrasonic or the monopolar scissors[5,11]. A more conservative option could be a partial cystectomy (unroofing) of the cyst. However, it has yet to be determined how much of the cyst wall should be resected, and whether unroofing should be partial or radical. It is supported that as much of the cyst wall as possible should be resected to prevent reclosure of the cyst[11,15].

Marsupialization of the cyst is another conservative option recommended for superficial splenic cysts, and can be performed safely with the laparoscopic method. This approach reduces the duration of the operation and carries no risk of recurrence[5,8]. In general, the laparoscopic management of splenic cysts offers the benefits of minimally invasive surgery: minimal postoperative pain, faster recovery, shorter hospital stay, and reduced morbidity and recovery[21].

However, any type of conservative procedure is difficult to perform, if the cyst is very large, is located in the splenic hilum, or is covered completely by the splenic parenchyma (intrasplenic cyst), or if there are multiple cysts (polycystic cases): in these cases, a complete splenectomy should be performed either using the open or the laparoscopic appro ach[1,21,22,23].

In all our cases, the cysts were of significant size and had produced clinical manifestations. Therefore, surgical treatment was absolutely indicated. Our first and second cases have been treated earlier, when laparoscopic splenectomy was not performed routinely in our center. In both the cases, we had to treat large cysts located in the splenic hilum, whereas the splenic parenchyma consisted of a rim of tissue pushed to the periphery. Therefore, both indications were met, location and dimension, and a successful open complete splenectomy was accomplished. In both cases the cysts were proved to be true epithelial cysts.

In the third case, there was a large subcapsular cyst located in the lower pole of the spleen, and thus a laparoscopic cystectomy looked as a feasible option. A partial cystectomy was done using the monopolar scissors followed by placement of a drainage tube in the remaining cavity. In this case, histology revealed a cyst without an epithelial lining (pseudocyst), and thus recurrence is not expectable[15,24]. Since there was no history of trauma, this cyst was probably of degenerative origin. We conclude that laparoscopic partial cystectomy is considered as an adequate procedure in cysts devoid of epithelial lining[24], as was our third case. No neoplastic growth has been found in any of our cases.

In conclusion, splenic cysts larger than 5 cm or symptomatic ones should be treated surgically, trying to preserve as much of splenic parenchyma as possible. If the cyst is very large and almost completely covered by splenic parenchyma, or if it is located in the splenic hilum, complete splenectomy is recommended, because of the risk of intractable bleeding from the spleen. Partial cystectomy (unroofing) could be an acceptable procedure in the majority of other cases. The laparoscopic approach seems to be a safe procedure, having all the benefits of minimally invasive surgery.

REFERENCES

1 **Avital S**, Kashtan H. A large epithelial splenic cyst. *N Engl J Med* 2003; **349**: 2173-2174
2 **Safioleas M**, Misiakos E, Manti C. Surgical treatment for splenic hydatidosis. *World J Surg* 1997; **21**: 374-378 discussion
3 **Reddi VR**, Reddy MK, Srinivas B, Sekhar CC, Ramesh O. Mesothelial splenic cyst-a case report. *Ann Acad Med Singapore* 1998; **27**: 880-882
4 **Heidenreich A**, Canero A, di Pasquo A. Laparoscopic approach for treatment of a primary splenic cyst. *Surg Laparosc Endosc* 1996; **6**: 243-246
5 **Hansen MB**, Moller AC. Splenic cysts. *Surg Laparosc Endosc percutan Tech* 2004; **14**: 316-322
6 **Ough YD**, Nash HR, Wood DA. Mesothelial cysts of the spleen with squamous metaplasia. *Am J Clin Pathol* 1981; **76**: 666-669
7 **Robertson F**, Leander P, Ekberg O. Radiology of the spleen. *Eur Radiol* 2001; **11**: 80-95
8 **Smith ST**, Scott DJ, Burdick JS, Rege RV, Jones DB. Laparoscopic marsupialization and hemisplenectomy for splenic cysts. *J Laparoendosc Adv Surg Tech A* 2001; **11**: 243-249
9 **Trompetas V**, Panagopoulos E, Priovolou-Papaevangelou M, Ramantanis G. Giant benign true cyst of the spleen with high serum level of CA 19-9. *Eur J Gastroenterol Hepatol* 2002; **14**: 85-88
10 **Labruzzo C**, Haritopoulos KN, EL Tayar AR, Hakim NS. Posttraumatic cyst of the spleen: a case report and review of the literature. *Int Surg* 2002; **87**: 152-156
11 **Till H,** Schaarschmidt K. Partial laparoscopic decapsulation of congenital splenic cysts. *Surg Endosc* 2004; **18;** 626-628
12 **Knudson P,** Coon W, Schnitzer B, Liepman M. Splenomegaly without an apparent cause. Surg Gynecol Obstetr 1982; **155:** 705-708
13 **Nakashima A,** Nakashima K, Seto H, Kamei T, Kakishita M, Kitagawa M. Primary splenic lymphoma presenting as a large cyst. *Radiat Med* 1994; **12:** 42-45
14 **Siniluoto TM,** Paivansalo MJ, Lahde ST, Alavaikko MJ, Lohela PK, Typpo AB, Suramo IJ. Nonparasitic splenic cysts. Ultrasonographic features and follow-up. *Acta Radiol* 1994; **35:** 447-451
15 **Morgenstern L.** Nonparasitic splenic cysts: pathogenesis, classification and treatment. *J Am Coll Surg* 2002; **194:** 306-314
16 **Cowles RA,** Yahanda AM. Epidermoid cyst of the spleen. *Am J Surg* 2000; **180:** 227
17 **Desai MB,** Kamdar MS, Bapat R, Modhe JM, Medhekar ST, Kokal KC, Abraham P. Splenic cysts: (report of 2 cases and review of the literature). *J Postgrad Med* 1981; **27:** 251-252
18 **Grinblat J,** Gilboa Y. Overwhelming pneumococcal sepsis 25 years after splenectomy. *Am J Med Sci* 1975; **270:** 523-524
19 **Sakamoto Y**, Yunotani S, Edakuni G, Mori M, Iyama A, Miyazaki K. Laparoscopic splenectomy for a giant splenic epidermoid cyst: report of a case. *Surg Today* 1999; **29:** 1268-1272
20 **Touloukian RJ**, Maharaj A, Ghoussoub R, Reyes M. Partial decapsulation of splenic epithelial cysts: studies on etiology and outcome. *J Pediatr Surg* 1997; **32**: 272-274
21 **Tagaya N,** Oda N, Furihata M, Nemoto T, Suzuki N, Kubota K. Experience with laparoscopic management of solitary symptomatic splenic cysts. *Surg Laparosc Endosc* Percutan Tech 2002; **12:** 279-282
22 **Birmole BJ**, Kulkarni BK, Vaidya MM, Borwankar SS. Splenic cyst. *J Postgrad Med* 1993; **39**: 40-41
23 **Yagi S,** Isaji S, Iida T, Mizuno S, Tabata M, Yamagiwa K, Yokoi H, Imai H, Uemoto S. Laparoscopic splenectomy for a huge splenic cyst without preoperative drainage: report of a case. *Surg Laparosc Endosc Percutan Tech* **2003; 13:** 397-400
24 **Losanoff JE,** Richman BW, Jones JW. Laparoscopic management of splenic cysts. *Surg Laparosc Endosc Percutan Tech* 2003; **13:** 63-**64; author reply 64**

Science Editor Guo SY **Language Editor** Elsevier HK

PO Box 2345, Beijing 100023, China
www.wjgnet.com
wjg@wjgnet.com

ELSEVIER

World J Gastroenterol 2005;11(43):6888-6890
World Journal of Gastroenterology ISSN 1007-9327

• *CASE REPORT* •

Secondary pouchitis in a post-operative patient with ulcerative colitis, successfully treated by salvage surgery

Yuji Toiyama, Toshimitsu Araki, Shigeyuki Yoshiyama, Chikao Miki, Masato Kusunoki

Yuji Toiyama, Toshimitsu Araki, Shigeyuki Yoshiyama, Chikao Miki, Masato Kusunoki, The Second Department of Surgery, Mie University School of Medicine, 2-174 Edobashi, Tsu, Mie 514-8507, Japan
Correspondence to: Dr Masato Kusunoki, The Second Department of Surgery, Mie University School of Medicine, 2-174 Edobashi, Tsu, Mie 514-8507,
Japan. kusunoki@clin.medic.mie-u.ac.jp
Telephone: +81-59-2315294 Fax: +81-59-2326968
Received: 2005-03-22 Accepted: 2005-04-26

Abstract

We report a case of secondary pouchitis, defined as a mucosal inflammatory lesion in the ileal reservoir provoked by pouch-related complication following total colectomy and pouch anal anastomosis, which was successfully treated by salvage surgery. A 20-year-old woman with ulcerative colitis developed acute severe bloody diarrhea following proctocolectomy, ileal pouch-anal anastomosis and diverting ileostomy. She was diagnosed as having a secondary pouchitis mainly caused by a peripouch abscess and partly concerned with the abnormal pouch formation. The remnant rectum and ileal pouch were excised and ileal pouch-anal anastomosis and diverting ileostomy were constructed. The postoperative course was uneventful with no sign of pouchitis. Salvage surgery may be indicated to treat secondary pouchitis when caused by surgery-related complications.

Key words: Ulcerative colitis; Ileal pouch-anal anastomosis; Secondary pouchitis; Salvage operation

Toiyama Y, Araki T, Yoshiyama S, Miki C, Kusunoki M. Secondary pouchitis in a post-operative patient with ulcerative colitis, successfully treated by salvage surgery. *World J Gastroenterol* 2005; 11(43): 6888-6890
http://www.wjgnet.com/1007-9327/11/6888.asp

INTRODUCTION

Restorative proctocolectomy with ileal pouch-anal anastomosis (IPAA) is the current treatment of surgical choice for ulcerative colitis and for selected familial adenomatous polyposis[1,2]. One of the main long-term complications after IPAA is inflammation of the pouch (pouchitis). Symptomatic inflammation of the ileal pouch develops in 7-40% of patients who undergo IPAA[3-6]. The etiology of pouchitis is probably a multifactorial event involving genetic, immune, microbial, and toxic mediators, but is poorly understood. Heusten first identified "secondary pouchitis" caused by surgical complication specific to the ileal reservoir and pouch anal anastomosis[7]. Most cases of pouchitis are primary with an acute course and show a good response to medical therapy, but patients with secondary pouchitis underlying surgical complications need surgical management because medical treatment alone is ineffective. In this report, we described a case of secondary pouchitis due to a peripouch abscess, blind loop formation, which had no response to medical treatment, and so we selected a surgical procedure suitable to the disease state.

CASE REPORT

This case was about a 20-year-old woman who had been diagnosed as having an ulcerative colitis when she was 12 years old. She had been controlled in remission with medical therapy (prednisone and 5-aminosalicylic acid), but on July 2001, she relapsed to severe colitis and was admitted in another hospital. She was treated there with intravenous fluids, broad spectrum parenteral antibiotics, systemic steroids (prednisone 60 mg/d), and granulocytapheresis (GCAP). Despite this conservative therapy, her condition deteriorated and she had underwent laparoscopic total colectomy, ileal pouch-anal anastomosis and diverting ileostomy.

About 3 mo after the primary operation, she had episodes 10 times a day of continuous severe bloody diarrhea. Colonoscopy showed inflammatory mucosa spontaneously bleeding from the anal verge to the ileal J pouch; and was diagnosed as severe pouchitis. She received metronidazole in the form of enemas, but did not respond.

On admission to our hospital, she was not pale, afebrile with a pulse rate of 90 beats/min, and had an anal bloody mucus discharge of 5-10 times per day. Laboratory studies showed that all parameters were almost normal. Culture analysis of the bloody mucus discharge showed multiplication of streptococcus agalactiae and Gram-negative rods. Pouchoscopy showed easy bleeding, inflammatory mucosa with ulcer formation, apical bride formation in the ileal J pouch and edematous colonic mucosa with inflammation from the anal verge to the anastomosis (Figure 1). A pouchogram showed an about

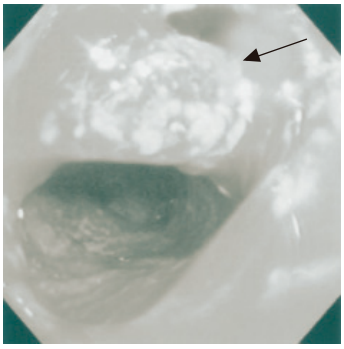

Figure 1 Pouchoscopy shows inflamed hemorrhagic mucosa. An apical bridge is seen (arrow head).

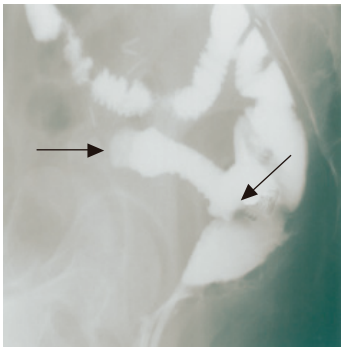

Figure 2 Pouchography shows a blind loop 10 cm in length (arrow head) and apical bridge formation (arrow).

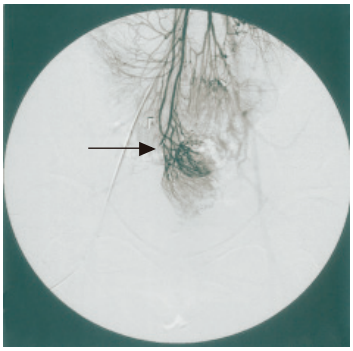

Figure 3 Superior mesenteric arteriography shows a marginal disconnection of the arcade (superior mesenteric artery–ileocolic artery) (arrow).

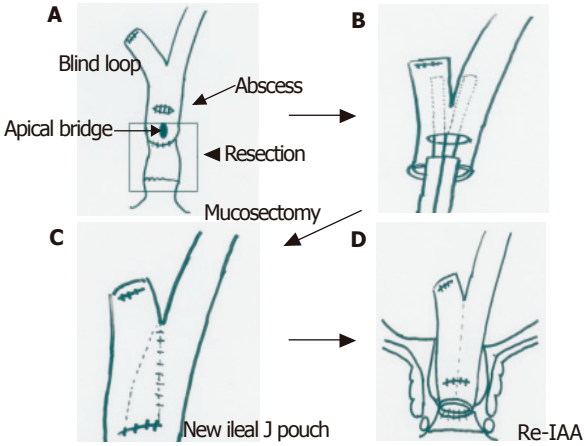

Figure 4 A: Mucosectomy and ileal pouch excision; **B:** side to side anastomosis of blind loop by linear stapler; **C:** reconstruction of a new ileal pouch; **D:** re-ileal pouch anal anastomosis.

10-cm blind loop formation of the ileal J pouch and apical bridge formation (Figure 2). Since we assumed that the operative procedures had not causally affected the outcomes, conservative therapy using metronidasole enemas, steroid enemas, and leukocytapheresis was undertaken for 1 mo.

However, no improvement of clinical symptoms or endoscopic findings was obtained. We attempted to re-evaluate using more extensive examinations. Abdominal CT showed that bilateral ovarian cysts but no remarkable intrapelvic abscess was recognized. Superior mesenteric arterial angiography showed that the ileal J pouch was supplied from the superior mesenteric artery (SMA) and the ileocolic artery (ICA), but that the arcades of these arteries were divided (Figure 3). These findings suggested that the pathogenesis of the disease was secondary pouchitis, due to abnormal formation of the ileal J pouch constructed apical bridge and blind loop or/and ischemic change of the pouch.

On 27 February 2002, she underwent laparotomy. At laparotomy, adhesion in the intra-abdominal space was recognized, but no ascites was seen. From the dentate line, rectal mucosectomy and ileal J pouch excision was performed at first. A peripouch abscess was recognized on the posterior wall of the pouch, and was tightly adhesive to the sacrum. Pouch mucosa on the site of the abscess had erosion and was partly deficient. We diagnosed secondary pouchitis due to a late peripouch abscess. We undertook abscess drainage, excision of the remnant rectum and ileal J pouch including the apical bridge. Side to side anastomosis of the blind loop was performed using a linear stapler into the site of the wall deficiency. After re-ileoanal anastomosis was performed, a covering ileostomy was constructed (Figures 4A-D).

There was a sustained clinical improvement in the patient after this re-operation without any complications. She was discharged on March 25, 2002. Three months later, ileostomy closure was performed. She remains well, with no sign of pouchitis, and has complete continence with bowel movements, 5 times per day.

DISCUSSION

Pouchitis is a term coined by Kock[8] that described the reservoir ileitis that developed in a number of patients with ulcerative colitis who underwent continent ileostomy operations. In 1980, proctocolectomy with ileal reservoir and anal anastomosis was described by Parks[9] and this operation, when performed for ulcerative colitis,

also produced pouchitis in a number of patients. The causes of the pouchitis have been poorly understood. Possible causes advanced include fecal stases resulting in bacterial overgrowth and infection[10], ischemia[11], oxygen free radical injury[12] and deprivation of short chain fatty acids[13].

Data on incidence and prevalence of pouchitis in the literature shows great disparities[14,15]. One reason for this disparity is related to the varying durations and modes of follow-up, the lack of a commonly accepted definition of pouchitis, and the lack of valid scoring for estimating the severity of inflammation[16-20]. Another reason is that pouchitis caused by surgical complication is not widely recognized. Heuschen[7] coined the term "secondary pouchitis" caused by surgical complication specific to the ileal reservoir and pouch-anal anastomosis. These surgical complications can cause clinical symptoms, such as an elevated frequency of defecation, hematochesia, fever, and malaise, which are very similar to those of idiopathic pouchitis. Nonspecific medical treatment of these symptoms as with primary pouchitis appears to be totally inadequate.

In our case, the patient had inflammatory changes in ileal J pouch mucosa with a defunctioned pouch. Pouch formation was abnormal with an apical pouch bridge[21] and an about 10-cm blind loop of the ileal pouch. Furthermore, medical treatment such as with metronidazole, topical steroids in the form of enemas, and GCAP were not effective. SMA angiography could suspect ischemic changes of the pouch mucosa because of the dividing of the arcades of SMA and ICA. However, a resected specimen (remnant rectum and ileal pouch) near the abscess formation showed extensive erosion and diffuse thickening. So we diagnosed that this secondary pouchitis was mainly caused by a peripouch abscess and was partly concerned with the abnormal pouch formation.

Moreover, crucial elements in our salvaged surgery were the initial resection of the peripouch abscess and the damaged portion of the pouch, and then the reconstruction of the pouch and re-IAA; thus improving hopes of curability.

In conclusion, salvage surgery might be indicated as a first choice treatment for secondary pouchitis caused by surgery-related complications. A surgical procedure suitable for the state of the disease should be selected after instituting a comprehensive series of examinations[22].

REFERENCES

1 **Williams NS.** Restorative proctocolectomy is the first choice elective surgical treatment for ulcerative colitis. *Br J Surg* 1989; **76**: 1109-1110

2 **Ambroze WL** Jr, Dozois RR, Pemberton JH, Beart RW Jr, Ilstrup DM. Familial adenomatous polyposis: results following ileal pouch-anal anastomosis and ileorectostomy. *Dis Colon Rectum* 1992; **35**: 12-15

3 **Nicholls RJ,** Belliveau P, Neill M, Wilks M, Tabaqchali S. Restorative proctocolectomy with ileal reservoir: a pathophysiological assessment. *Gut* 1981; **22**: 462-468

4 **Keighley MR.** Review article: the management of pouchitis. *Aliment Pharmacol Ther* 1996; **10**: 449-457

5 **Zuccaro G Jr**, Fazio VW, Church JM, Lavery IC, Ruderman WB, Farmer RG. Pouch ileitis. *Dig Dis Sci* 1989; **34**: 1505-1510

6 **Tytgat GN**, van Deventer SJ. Pouchitis. *Int J Colorectal Dis* 1988; **3**: 226-228

7 **Heuschen UA**, Autschbach F, Allemeyer EH, Zollinger AM, Heuschen G, Uehlein T, Herfarth C, Stern J. Long-term follow-up after ileoanal pouch procedure: algorithm for diagnosis, classification, and management of pouchitis. *Dis Colon Rectum* 2001;**44**:487-499

8 **Kock NG**, Darle N, Hulten L, Kewenter J, Myrvold H, Philipson B. ileostomy. *Curr Probl Surg* 1977; **14**: 1-52

9 **Parks AG**, Nicholls RJ, Belliveau P. Proctocolectomy with ileal reservoir and anal anastomosis. *Br J Surg* 1980; **67**: 553-558

10 **Fonkalsrud EW**, Phillips JD. Reconstruction of malfunctioning ileoanal pouch procedures as an alternative to permanent ileostomy. *Am J Surg* 1990; **227**: 245-251

11 **Chaussade S**, Denizot Y, Valleur P, Nicoli J, Raibaud P, Guerre J, Hautefeuille P, Couturier D, Benveniste J. Presence of PAF-acether in stool of patients with pouch ileoanal anastomosis and pouchitis. *Gastroenterology* 1991; **100**: 1509-1514

12 **Levin KE**, Pemberton JH, Phillips SF, Zinsmeister AR, Pezim ME. Role of oxygen free radicals in the etiology of pouchitis. *Dis Colon Rectum* 1992; **35**: 452-456

13 **Clausen MR**, Tvede M, Mortensen PB. Short-chain fatty acids in pouch contents from patients with and without pouchitis after ileal pouch-anal anastomosis. *Gastroenterology* 1992; **103**: 1144-1153

14 **Sandborn WJ.** Pouchitis following ileal pouch-anal anastomosis: definition, pathogenesis, and treatment. *Gastroenterology* 1994; **107**: 1856-1860

15 **Kuhbacher T**, Schreiber S, Runkel N. Pouchitis: pathophysiology and treatment. *Int J Colorectal Dis* 1998; **13**: 196-207

16 **Rauh SM**, Schoetz DJ Jr, Roberts PL, Murray JJ, Coller JA, Veidenheimer MC. Pouchitis--is it a wastebasket diagnosis? *Dis Colon Rectum* 1991; **34**: 685-689

17 **Dozois RR**, Kelly KA, Welling DR, Gordon H, Beart RW Jr, Wolff BG, Pemberton JH, Ilstrup DM. Ileal pouch-anal anastomosis: comparison of results in familial adenomatous polyposis and chronic ulcerative colitis. *Ann Surg* 1989; **210:** 268-71; discussion 272-273

18 **Luukkonen P**, Jarvinen H, Tanskanen M, Kahri A. Pouchitis--recurrence of the inflammatory bowel disease? *Gut* 1994; **35**: 243-246

19 **Keranen U**, Luukkonen P, Jarvinen H. Functional results after restorative proctocolectomy complicated by pouchitis. *Dis Colon Rectum* 1997; **40**: 764-769

20 **Svaninger G**, Nordgren S, Oresland T, Hulten L. Incidence and characteristics of pouchitis in the Kock continent ileostomy and the pelvic pouch. *Scand J Gastroenterol* 1993; **28**: 695-700

21 **Sakanoue Y**, Shoji Y, Kusunoki M, Utsunomiya J. Transanal division of an apical pouch bridge after restorative proctocolectomy with a J shaped reservoir. *Br J Surg* 1993; **80**: 248

22 **Thoeni RF**, Fell SC, Engelstad B, Schrock TB. Ileoanal pouches: comparison of CT, scintigraphy, and contrast enemas for diagnosing postsurgical complications. *Am J Roentgenol* 1990; **154**: 73-78

Science Editor Pravda J and Guo SY **Language Editor** Elsevier HK

PO Box 2345, Beijing 100023, China
www.wjgnet.com
wjg@wjgnet.com

ELSEVIER

World J Gastroenterol 2005;11(43):6891-6893
World Journal of Gastroenterology ISSN 1007-9327

• *CASE REPORT* •

Crohn's disease and recurrent appendicitis: A case report

Ron Shaoul, Yosi Rimar, Aurora Toubi, Jorge Mogilner, Reuven Polak, Michael Jaffe

Ron Shaoul, Yosi Rimar, Jorge Mogilner, Reuven Polak, Michael Jaffe, Department of Pediatrics, Bnai Zion Medical Center, Faculty of Medicine, Technion – Israel Institute of Technology, Haifa, Israel
Aurora Toubi, Department of Radiology, Bnai Zion Medical Center, Faculty of Medicine, Technion – Israel Institute of Technology, Haifa, Israel
Jorge Mogilner, Department of Pediatric Surgery, Bnai Zion Medical Center, Faculty of Medicine, Technion – Israel Institute of Technology, Haifa, Israel
Correspondence to: Ron Shaoul, MD, Head, Pediatric Day Care Unit, Department of Pediatrics, Bnai Zion Medical Center, 47 Golomb St. POB 4940, Haifa 31048, Israel. shaoul_r@012.net.il
Telephone: +972-4-8359662 Fax: +972-4-8371393
Received: 2005-04-10 Accepted: 2005-04-26

Abstract

The clinical diagnosis of classic Crohn's disease (CD) of the small bowel is based on a typical history, tender right lower quadrant fullness or mass, and characteristic radiographic findings of the terminal ileum. Appendicitis may as well present with chronic or recurrent symptoms and this presentation may be confused with CD. We herein describe the case of a young teenage girl with a presumptive diagnosis of CD, who was ultimately diagnosed as having chronic nongranulomatous appendicitis. The literature on the subject is reviewed.

Key words: Chronic appendicitis; Crohn's disease; Diagnosis; Terminal ileitis; Adolescent

Shaoul R, Rimar Y, Toubi A, Mogilner J, Polak R, Jaffe M. Crohn's disease and recurrent appendicitis: A case report. *World J Gastroenterol* 2005; 11(43): 6891-6893
http://www.wjgnet.com/1007-9327/11/6891.asp

INTRODUCTION

Crohn's disease (CD) is a chronic transmural inflammation, which may involve any part of the alimentary tract from mouth to the anus. CD typically affects the ileum, colon, or perianal region[1]. The clinical diagnosis of classic CD of the small bowel is based on a typical history, tender right lower quadrant fullness or mass, characteristic radiographic findings of the terminal ileum and endoscopic findings. Although granulomas are regarded as the characteristic feature of CD, their absence does not rule out the diagnosis[1]. Only half of the documented cases of CD reveal epithelioid granulomas in surgical specimens[1]. CD can involve the appendix by extension from the terminal ileum or the cecum and present as an acute or subacute appendicitis. About 25% of patients with ileal CD and 50% of those with colonic Crohn's disease have appendiceal involvement[2]. A clinical picture similar to acute appendicitis is not an uncommon presentation of Crohn's disease.

Among the inflammatory diseases of the right lower quadrant that may mimic CD, acute appendicitis is the most common and potentially the most dangerous one. The principal distinguishing features of acute appendicitis are its onset without any pre-existing history of chronic bowel symptoms and the change in the location of pain and tenderness from epigastrium to the right lower quadrant (RLQ)[1]. Appendicitis, however, may present with chronic or recurrent symptoms and this presentation may be confused with CD. Although an entity of recurrent attacks of RLQ pain, apparently self-limiting, is not infrequently encountered, the entity of chronic or recurrent appendicitis is controversial[3-7]. Nevertheless, it is probably an authentic clinical and pathologic entity[3-15]. Intermittent bouts of obstruction of the appendiceal lumen with spontaneous remission may be the cause[4]. True chronic inflammation of the appendix is difficult to define as a pathologic entity, although occasionally granulation tissue and fibrosis associated with acute and chronic inflammation of the appendix are demonstrated, suggesting an organizing acute appendicitis[16]. In the pediatric population, children with cystic fibrosis can develop chronic appendicitis due to mucous engorgement of the lumen. The occurrence of chronic appendicitis in otherwise healthy children is nevertheless debatable[6].

Herein, we have described the case of a young teenage girl with a presumptive diagnosis of CD, who was ultimately diagnosed as having chronic non-granulomatous appendicitis. The literature on the subject has been reviewed.

CASE REPORT

A 17-year-old girl presented to our pediatric emergency room because of persistent RLQ abdominal pain. She had been previously healthy. Three weeks prior to admission, she was admitted to another hospital for severe RLQ pain. A computerized tomography (CT) scan of the abdomen with barium contrast showed a bowel conglomerate in the cecal area and a stricture of the distal ileum. A presumptive diagnosis of CD was made and the patient was discharged

Table 1 Laboratory values

	1st admission	2nd admission	3rd admission	4th admission	Normal values
HB	12	12.4	13.2	13.8	11.5–16.5 g/dL
WBC	8.0	17.7	5.7	9.1	4.0–11.0×109/L
PLT	322	197	371	309	150–400×109/L
ESR	NA	20	53	6	0–20 mm/h
CRP	2.4	27	0	0.28	0–1 mg/L
ALB	3.7	3.6	4.4	4.8	3.2–5 g/dL
AST	27	15	65	17	10–40 U/L
ALT	18	46	61	15	10–40 U/L
GGT	10	16	105	47	7–33 U/L

HB: hemoglobin; WBC: white blood cells; PLT: platelets; ESR: erythrocyte sedimentation rate; CRP: C reactive protein; ALB: albumin; AST: aspartate aminotransferase; ALT: alanine aminotransferase; GGT: gamma-glutamyl transpeptidase.

Figure 1 Upper gastrointestinal and barium follow-through study showing a stricture of an ileal loop without involvement of the terminal ileum (arrow).

Figure 2 Abdominal CT with contrast media showing a bowel conglomerate in the cecal area and a stricture of the distal ileum (arrow).

on 5-ASA, antibiotics and steroids. Colonoscopy, performed a week later, showed no gross pathology and the treatment was discontinued. Biopsy samples from the colon and terminal ileum were normal.

She was admitted to our Pediatric Department because of the continuation of RLQ abdominal pain, recurrent non-bilious vomiting and a 6-kg weight loss over 2 wk.

Physical examination revealed a well-looking young girl with 45 kg body weight and 167 cm height. Diffuse tenderness of the abdomen and right flank was noted. Rectal examination revealed no masses, normal stools and no localized tenderness.

Laboratory results are shown in Table 1 (1st admission). Abdominal ultrasound (US) was normal; a gynecological US showed a left ovarian cyst and a tubular structure in the RLQ. An upper gastrointestinal and barium follow-through study showed a stricture of an ileal loop without involvement of the terminal ileum. This finding was considered to be compatible with CD (Figure 1). Gastroscopy showed gastritis with hemorrhagic areas in the body and antrum. A quick urease test for *H pylori* was negative. Biopsies from the antral mucosa showed remodeling of the foveolar layer, regeneration, atypia, and mild chronic inflammation. Biopsies from the small bowel, gastric corpus and esophagus were normal.

Despite the absence of characteristic histological findings of CD, the clinical presentation and the radiological findings were thought to be compatible with CD and therefore oral steroids and omeprazole were prescribed with resolution of symptoms.

Four weeks later, she was readmitted because of a 24-h history of abdominal pain mainly over the RLQ, fever of 39 °C and non-bilious vomiting.

Physical examination revealed a sick-looking girl having 37.8 °C temperature, 47.5 kg body weight and severe diffuse tenderness over the right lower abdomen. Laboratory results are shown in Table 1 (2nd admission). Abdominal X-ray was normal. Abdominal US showed a thickened bowel loop located over the RLQ. A repeat CT of the abdomen with contrast media showed a bowel conglomerate in the cecal area and a stricture of the distal ileum similar to the findings previously demonstrated. No signs of appendicitis or periappendicular abscess were noted (Figure 2). After 5 d of intravenous treatment with steroids, ciprofloxacin, and metronidazole, the patient's symptoms and clinical signs improved and she was discharged on oral steroids and azathioprine.

For the following 2 mo, the patient was asymptomatic. She was gradually weaned from steroids and maintained on azathioprine. She was then readmitted because of abdominal pain and non-bilious vomiting for 10 d. She had no fever or diarrhea, her appetite was poor and had a 1 kg weight loss. Her physical examination revealed severe diffuse tenderness over the right abdomen. Laboratory results are shown in Table 1 (3rd admission). Budesonide was started and the azathioprine dose was decreased due to abnormal liver enzymes. She was discharged after a clinical improvement but readmitted a week later due to vomiting and epigastric and RLQ pain for 4 d. Laboratory results are shown in Table 1 (4th admission). Gastroscopy showed a mild inflammation with normal antral and duodenal biopsies. A diagnostic laparoscopy showed a phlegmonous appendicitis and an appendectomy was performed. No other abnormality was noted and the ileum appeared to be normal. Histological examination of the appendix and terminal ileum showed periappendicular inflammation and normal small bowel. No granulomata were found. A diagnosis of chronic appendicitis mimicking CD was made. Follow-up of 4 years showed a healthy asymptomatic girl.

DISCUSSION

Controversy and skepticism surround the diagnoses of chronic and recurrent appendicitis[3-6]. Nevertheless, a sufficient histological and radiological evidence to support that this entity exists[3-16].

Chronic appendicitis is defined as lower abdominal pain lasting for 3 wk with radiological and pathological findings of appendicitis. Recurrent appendicitis is defined as recurring episodes of right lower abdominal pain with radiological or pathological finding of appendicitis[17].

Five to ten percent of patients suffering from acute appendicitis describe prior episodes of RLQ pain resolving spontaneously. USG studies have demonstrated a spontaneous resolution of acute appendicitis, in as many as 1 in 13 patients suffering from symptoms of acute appendicitis. The recurrence rate, however, was 38%, mostly in the year following the initial episode[9]. The CT diagnosis of acute appendicitis includes distended or thickened appendix with or without appendicolith, greater than approximately 5-7 mm in size. The wall of the inflamed appendix is circumferentially thickened and may appear as a "halo" or "target." CT findings of periappendiceal inflammation would also support the diagnosis of appendicitis[4,18]. Moreover, CT findings of appendices in patients suffering from prolonged (more than 3 wk) abdominal pain as well as recurring episodes of abdominal pain are identical to those of patients suffering from acute appendicitis[17]. None of these findings were present in the CT done in our patient. It is important to mention that advances in CT with high-resolution techniques have yielded a sensitivity as high as 100% and specificity as high as 98% for the diagnosis of acute appendicitis[18]. The yield of CT in the diagnosis of CD is not good.

Mattei *et al*.[14] reviewed a series of seven patients matching the criteria of chronic or recurrent appendicitis and concluded that recurrent and chronic appendicitis should be considered in the differential diagnosis of recurrent or non-resolving lower abdominal pain. Barber *et al*.[3], in their retrospective study encompassing 1 084 patients who had inflamed appendices removed, found that 6.5% of them had attended the emergency ward prior to their operation for symptoms compatible with recurrent appendicitis. Our patient had clinical and radiological findings compatible with Crohn's ileitis, without evidence of acute or chronic appendicitis on US and CT. It has been suggested that these modalities can aid diagnosis in questionable situations[1]. Although there was no histopathological evidence of CD at biopsy, the clinical manifestations, the radiological findings and the response to treatment supported the diagnosis.

Consideration was also given to the diagnosis of isolated CD of the appendice, an uncommon chronic appendicitis with histological findings (granulomas) resembling a CD[2]. This rare presentation of CD is confined to the appendice and progression to systemic disease is rarely noted. The reluctance to intervene surgically in a patient with a suspected CD is another barrier to diagnosis.

Considering the data presented, chronic or recurrent appendicitis seemed to be the probable diagnosis. It must be considered in every case of unexplained long-standing or recurrent abdominal pain over RLQ. The great improvements in laparoscopic techniques should be valuable in those cases where endoscopical, histological and radiological findings do not provide a definitive answer.

REFERENCES

1 **Kornbluth A**, Sachar DB, Salomon P. Crohn's disease. In: Feldman M, Scharschmidt BF, Sleisenger MH, Klein S, editors. Sleisenger & Fordtran's Gastrointestinal and Liver Disease. 6th ed. W. B. Saunders Company, 1998: 1708-1734

2 Case records of the Massachusetts General Hospital. Weekly clinicopathological exercises. Case 10-1996. A 36-year-old man with right-lower-quadrant pain of two years' duration. *N Engl J Med* 1996; **334:** 849-854

3 **Barber MD**, McLaren J, Rainey JB. Recurrent appendicitis. *Br J Surg* 1997; **84**: 110-112

4 **Lally KP**, Cox CS, Andrassy RJ. Appendicitis. In: Townsend CM, Beauchamp RD, Evers BM, Mattox KL, editors. Sabiston Textbook of Surgery. 16th ed. W. B. Saunders Company, 2001: 918-926

5 **Leardi S**, Delmonaco S, Ventura T, **Chiominto A, De Rubeis G,** Simi M. Recurrent abdominal pain and "chronic appendicitis". *Minerva Chir* 2000; **55**: 39-44

6 **Schrock TR**. Appendicitis. In: Feldman M, Scharschmidt BF, Sleisenger MH, Klein S, editors. Sleisenger & Fordtran' s Gastrointestinal and Liver Disease. 6th ed. W. B. Saunders Company, 1998: 1778-1787

7 **Seidman JD,** Andersen DK, Ulrich S, Hoy GR, Chun B. Recurrent abdominal pain due to chronic appendiceal disease. *South Med J* 1991; **84:** 913-916

8 **Babb RR,** Trollope ML. Recurrent appendicitis. Uncommon, but it does occur. *Postgrad Med* 1999; **106:** 135-138

9 **Cobben LP**, de Van Otterloo AM, Puylaert JB. Spontaneously resolving appendicitis: frequency and natural history in 60 patients. *Radiology* 2000; **215**: 349-352

10 **Crabbe MM,** Norwood SH, Robertson HD, Silva JS. Recurrent and chronic appendicitis. *Surg Gynecol Obstet* 1986; **163:** 11-13

11 **Falk S**, Schutze U, Guth H, Stutte HJ. Chronic recurrent appendicitis. A clinicopathologic study of 47 cases. *Eur J Pediatr Surg* 1991; **1**: 277-281

12 **Fayez JA**, Toy NJ, Flanagan TM. The appendix as the cause of chronic lower abdominal pain. *Am J Obstet Gynecol* 1995; **172**: 122-123

13 **Graham D**. Chronic appendicitis: it does exist. *Tenn Med* 2001; **94**: 23-24

14 **Mattei P**, Sola JE, Yeo CJ. Chronic and recurrent appendicitis are uncommon entities often misdiagnosed. *J Am Coll Surg* 1994; **178**: 385-389

15 **Van Winter JT**, Wilkinson JM, Goerss MW, Davis PM. Chronic appendicitis: does it exist? *J Fam Pract* 1998; **46**: 507-509

16 **Crawford JM**. The Gastrointestinal tract. In: Cotran RS, Kumar V, Collins T, editors. Robbins Pathologic Basis of Disease. 6th ed. W.B. Saunders Company, 1999: 775-844

17 **Rao PM**, Rhea JT, Novelline RA, McCabe CJ. The computed tomography appearance of recurrent and chronic appendicitis. *Am J Emerg Med* 1998; **16**: 26-33

18 **Pena BM**, Taylor GA, Fishman SJ, Mandl KD. Costs and effectiveness of ultrasonography and limited computed tomography for diagnosing appendicitis in children. *Pediatrics* 2000; **106**: 672-676

Science Editor Kumar M and Guo SY **Language Editor** Elsevier HK

PO Box 2345, Beijing 100023, China
www.wjgnet.com
wjg@wjgnet.com

ELSEVIER

World J Gastroenterol 2005;11(43):6894
World Journal of Gastroenterology ISSN 1007-9327

Acknowledgments to Reviewers of World Journal of *Gastroenterology*

Many reviewers have contributed their expertise and time to the peer review, a critical process to ensure the quality of *World Journal of Gastroenterology*. The editors and authors of the articles submitted to the journal are grateful to the following reviewers for evaluating the articles (including those were published and those were rejected in this issue) during the last editing period of time.

Chi-Hin Cho, Chair and Professor
Departmentof Pharmacology, The University of Hong Kong, 21 Sassoon Road, Hong Kong, China

Vincent Coghlan, Professor
Neurological Sciences Institute, 505 NW 185th Avenue, Beaverton, Oregon 97006, United States

Da-Jun Deng, Professor
Department of Cancer Etiology, Peking University School of Oncology, 1 Da-Hong-Luo-Chang Street, Western District, Beijing 100034, China

Erpecum Karel van Erpecum, Dr
Department of Gastroenterology and Hepatology, University Hospital Utrecht, PO Box 855003508 GA, Utrecht, The Netherlands

Sheung-Tat Fan, Professor
Department of Surgery and Center for the Study of Liver Disease, The University of Hong Kong, Queen Mary Hospital, 102 Pokfulam Road, Hong Kong, China

Robert John Lovat Fraser, Associate Professor
Investigations and Procedures Unit, Repatriation General Hospital, Daw Park, Australia

Takahiro Fujimori, MD, PhD, Professor
Department of Surgical and Molecular Pathology, Dokkyo Univesity School of Medicine, 880 Kitakobayashi, Mibu, Shimotsuga, Tochigi 321-0293, Japan

Subrata Ghosh, Professor
Department of Gastroenterology, Imperial College London, Hammersmith Hospital, 9 Lady Aylesford Avenue, Stanmore, Middlesex, London HA7 4FG, United Kingdom

Axel M Gressner, Professor
Institut für Klinische Chemie und Pathobiochemie sowie Klinisch-Chemisches Zentrallaboratorium, Universitätsklinikum Aachen, Pauwelsstr. 30, Aachen 52074, Germany

De-Wu Han, Professor
Institute of Hepatology, Shanxi Medical University, 86 Xinjian South Road, Taiyuan 030001, China

Naohiko Harada, PhD
Department of Gastroenterology, Fukuoka Higashi Medical Center, Chidori 1-1-1, Koga, Fukuoka 811-3195, Japan

Yik-Hong Ho, Professor
Department of Surgery, School of Medicine, James Cook University, Townsville 4811, Australia

Hiromi Ishibashi, Professor
Director General, Clinical Research Center, National Hospital Organization Nagasaki Medical Center, Professor, Department of Hepatology, Nagasaki University Graduate School of Biomedical Sciences, Kubara 2-1001-1 Kubara Omura, Nagasaki 856-8562, Japan

Hiroaki Itoh, MD
First Department of Internal Medicine, Akita University Scool of Medicine,1-1-1,Hondou, Akita City 010-8543, Japan

Dusan M Jovanovic, Professor
Institute of Oncology, Institutski Put 4, Sremska Kamenica 21204, Yugoslavia

Elias A Kouroumalis, Professor
Department of Gastroenterology, University of Crete, Medical School, Department of Gastroenterology, University Hospital, PO Box 1352, Heraklion, Crete 71110, Greece

Zahariy Krastev, Professor
Department of Gastroneterology, Universiti Hospital "St. Ivan Rilski",#15, blvd "Acad. Ivan Geshov", Sofia 1431, Bulgaria

Joachim Labenz, Associate Professor
Jung-Stilling Hospital, Wichernstr. 40, Siegen 57074, Germany

Edward V Loftus, Jr, Associate Professor
Division of Gastroenterology and Hepatology, Mayo Clinic College of Medicine, 200 First Street, SW, Rochester, MN 55905, United States

Reza Malekzadeh, Professor
Director , Digestive Disease Research Center, Tehran University of Medical Sciences, Shariati Hospital, Kargar Shomali Avenue, 19119 Tehran, Iran

Sasa Markovic, Professor
Head, Department of Gastroenterology, Univercity Clinical Center Ljubljana, 2 Japljeva 1525 Ljubljana, Slovenia

James Neuberger, Professor
Liver Unit, Queen Elizabeth Hospital, Birmingham B15 2TH, United Kingdom

Masayuki Ohta, MD
Department of Surgery I, Oita University Faculty of Medicine, 1-1 Idaigaoka, Hasama-machi, Oita 879-5593, Japan

Ulrich KS Peitz, MD
Department of Gastroenterology Hepatology and Infectious Disease, Otto-von-Guericke University Magdeburg, Leipziger Str. 44, D 39120 Magdeburg, Germany

Jesus Prieto, Professor
Clinica Universitaria, University of Navarra, Avda, Pio XII, 36, Pamplona 31080, Spain

Bashkim Resuli, MD
Department of Internal Medicine and University Service of Gastrohepatology, University Hospital Center " Mother Theresa", Medical Faculty of Tirana, Tirana, Albania

Jose Sahel, Professor
Hepato-gastroenterology, Hospital sainti Marevenite, I270 Boolevard AE Sainti Margrenise, Marseille 13009, France

Simon D Taylor-Robinson, MD
Department of Medicine A, Imperial College London, Hammersmith Hospital, Du Cane Road, London W12 0HS, United Kingdom

Harry HX Xia, MD
Department of Medicine, The University of Hong Kong, Pokfulam Road, Hong Kong, China

Jian-Zhong Zhang, Professor
Department of Pathology and Laboratory Medicine, Beijing 306 Hospital, 9 North Anxiang Road, PO Box 9720, Beijing 100101, China

PO Box 2345, Beijing 100023, China
www.wjgnet.com
wjg@wjgnet.com

ELSEVIER

World J Gastroenterol 2005;11(43):6895
World Journal of Gastroenterology ISSN 1007-9327

Meetings

MAJOR MEETINGS COMING UP

American College of Gastroenterology Annual Scientific Meeting
October 28 -November 2, 2005
annualmeeting@acg.gi.org
www.acg.gi.org

EVENTS AND MEETINGS IN THE UPCOMING 6 MONTHS

ISGCON2005
November 11-15, 2005
isgcon2005@yahoo.co.in
isgcon2005.com

II Latvian Gastroenterology Congress
November 29, 2005
gec@stradini.lv
www.gastroenterologs.lv

70th ACG Annual Scientific Meeting and Postgraduate Course
October 28-November 2, 2005

Advanced Capsule Endoscopy Users Course
November 18-19, 2005
www.asge.org/education

2005 CCFA National Research and Clinical Conference - 4th Annual Advances in the Inflammatory Bowel Diseases
December 1-3, 2005
c.chase@imedex.com
www.imedex.com/calendars/therapeutic.htm

EVENTS AND MEETINGS IN 2005

XIII Argentine Hepatology Congress
XIII Congreso Argentino de HepatologÃa
June 10-13, 2005
mci@mcimeetings.com
www.hepatologia.org

9th Annual Coolum Update in Gastroenterology & Hepatology
June 11-13, 2005
info@e-Kiddna.com.au

Canadian Digestive Disease Week Conference
February 26-March 6, 2005
www.cag-acg.org

2005 World Congress of Gastroenterology
September 12-14, 2005
wcog2005@congrex.nl

International Colorectal Disease Symposium 2005
February 3-5, 2005
info@icds-hk.org

15th World Congress of the International Association of Surgeons and Gastroenterologists
September 7-10, 2005
iasg2005@guarant.cz
www.iasg2005.cz

7th International Workshop on Therapeutic Endoscopy
September 10-12, 2005
alfa@alfamedical.com
www.alfamedical.com

EASL 2005 the 40th annual meeting
April 13-17, 2005
www.easl.ch/easl2005/

ISGCON2005
November 11-15, 2005
isgcon2005@yahoo.co.in
isgcon2005.com

Pediatric Gastroenterology, Hepatology and Nutrition
March 13, 2005

II Latvian Gastroenterology Congress
November 29, 2005
gec@stradini.lv
www.gastroenterologs.lv

21st annual international congress of Pakistan society of Gastroenterology & GI Endoscopy
March 25-27, 2005
psgc05@hotmail.com
www.psgc2005.com

8th Congress of the Asian Society of HepatoBiliary Pancreatic Surgery
February 10-13, 2005

1º Workshop de Gastrenterologia para Clínica Geral
April 29, 2005
luis.m.lopes@sapo.pt

APDW 2005 - Asia Pacific Digestive Week 2005
September 25-28, 2005
asiapdw@kornet.net
www.apdw2005.org

World Congress on Gastrointestinal Cancer
June 15-18, 2005
meetings@imedex.com

British Society of Gastroenterology Conference
March 14-17, 2005
www.bsg.org.uk

Training Director's Workshop:Developing and Teaching Principles in the New Era of GI Training
February 4-6, 2005
www.asge.org/education

The Pharmacological, Surgical and Endoscopic Management of GERD
April 8-9, 2005
www.asge.org/education

Digestive Disease Week
DDW 106th Annual Meeting
May 15-18, 2005
ddwadmin@gastr.org
www.ddw.org

ASGE Advanced Endscopy Skills Hands-on Sessions
May 15, 2005
www.asge.org/education

ASGE GERD Hands-on Session
May 17, 2005
www.asge.org/education

Annual Postgraduate Course
May 18-19, 2005
www.asge.org/education

Advanced Capsule Endoscopy Users Course
June 4-5, 2005
www.asge.org/education

Advanced Capsule Endoscopy Users Course
August 12-13, 2005
www.asge.org/education

GI Practice Management Symposium: Solutions for a Successful Practice
August 18, 2005
www.asge.org/education

70th ACG Annual Scientific Meeting and Postgraduate Course
October 28-November 2, 2005

Advanced Capsule Endoscopy Users Course
November 18-19, 2005
www.asge.org/education

2005 CCFA National Research and Clinical Conference - 4th Annual Advances in the Inflammatory Bowel Diseases
December 1-3, 2005
c.chase@imedex.com
www.imedex.com/calendars/therapeutic.htm

EVENTS AND MEETINGS IN 2006

10th World Congress of the International Society for Diseases of the Esophagus
February 22-25, 2006
isde@sapmea.asn.au
www.isde.net

Easl 2006 - The 41st Annual Meeting
April 26-30, 2006

Canadian Digestive Disease Week Conference
March 4-12, 2006
www.cag-acg.org

XXX pan-american congress of digestive diseases
XXX congreso panamericano de anfermedades digestivas
November 25-December 1, 2006
amg@gastro.org.mx
www.gastro.org.mx

World Congress on Gastrointestinal Cancer
June 14-17, 2006
c.chase@imedex.com

7th World Congress of the International Hepato-Pancreato-Biliary Association
September 3-7, 2006
convention@edinburgh.org
www.edinburgh.org/conference

Annual Postgraduate Course
May 25-26, 2006
www.asge.org/education

71st ACG Annual Scientific Meeting and Postgraduate Course
October 20-25, 2006

PO Box 2345, Beijing 100023, China
www.wjgnet.com
wjg@wjgnet.com

ELSEVIER

World J Gastroenterol 2005;11(43):6896-6897
World Journal of Gastroenterology ISSN 1007-9327

Instructions to authors

GENERAL INFORMATION

World Journal of Gastroenterology (*WJG,* ISSN 1007-9327 CN 14-1219/R) is a weekly journal of more than 48 000 circulation, published on the 7th, 14th, 21st and 28th of every month.

Original Research, Clinical Trials, Reviews, Comments, and Case Reports in esophageal cancer, gastric cancer, colon cancer, liver cancer, viral liver diseases, *etc*., from all over the world are welcome on the condition that they have not been published previously and have not been submitted simultaneously elsewhere.

Published jointly by
The WJG Press and Elsevier Inc.

SUBMISSION OF MANUSCRIPTS

Manuscripts should be typed double-spaced on A4 (297×210 mm) white paper with outer margins of 2.5 cm. Number all pages consecutively, and start each of the following sections on a new page: Title Page , Abstract, Introduction, Materials and Methods, Results, Discussion, Acknowledgements, References, Tables, Figures and Figure Legends. Neither the Editors nor the Publisher is responsible for the opinions expressed by contributors. Manuscripts formally accepted for publication become the permanent property of The WJG Press and Elsevier Inc., and may not be reproduced by any means, in whole or in part without the written permission of both the Authors and the Publisher. We reserve the right to put onto our website and copy-edit accepted manuscripts. Authors should also follow the guidelines for the care and use of laboratory animals of their institution or national animal welfare committee.

Authors should retain one copy of the text, tables, photographs and illustrations, as rejected manuscripts will not be returned to the author(s) and the editors will not be responsible for the loss or damage to photographs and illustrations.

Online submission
Online submission is strongly advised. Manuscripts should be submitted through the Online Submission System at: http://www.wjgnet.com/index.jsp. Authors are highly recommended to consult the ONLINE INSTRUCTIONS TO AUTHORS (http://www.wjgnet.com/wjg/help/instructions.jsp) before attempting to submit online. Authors encountering problems with the Online Submission System may send an email describing the problem to wjg@wjgnet.com for assistance. If you submit manuscript online, do not make a postal contribution. A repeated online submission for the same manuscript is strictly prohibited.

Postal submission
Send 3 duplicate hard copies of the full-text manuscript typed double-spaced on A4(297×210 mm) white paper together with any original photographs or illustrations and a 3.5 inch computer diskette or CD-ROM containing an electronic copy of the manuscript including all the figures, graphs and tables in native Microsoft Word format or *.rtf format to:

World Journal of Gastroenterology
Apartment 1066 Yishou Garden,
58 North Langxinzhuang Road,
PO Box 2345, Beijing 100023, China
E-mail: wjg@wjgnet.com
http: //www.wjgnet.com

MANUSCRIPT PREPARATION

All contributions should be written in English. All articles must be submitted using a word-processing software. All submissions must be typed in 1.5 line spacing and in word size 12 with ample margins. The letter font is Tahoma. For authors originating from China, one copy of the Chinese translation of the manuscript is also required (excluding references). Style should conform to our house format. Required information for each of the manuscript sections is as follows:

Title page
Full manuscript title, running title, all author(s) name(s), affiliations, institution(s) and/or department(s) where the work was accomplished, disclosure of any financial support for the research, and the name, full address, telephone and fax numbers and email address of the corresponding author should be involved. Titles should be concise and informative (removing all unnecessary words), emphasize what is NEW, and avoid abbreviations. A short running title of less than 40 letters should be provided. List the author(s)' name(s) as follows: initials and/or first name, middle name or initial(s) and full family name.

Abstract
An informative, structured abstract of no more than 250 words should accompany each manuscript. Abstracts for original contributions should be structured into the following sections: AIM: Only the purpose should be included. METHODS: The materials, techniques, instruments and equipments, and the experimental procedures should be included. RESULTS: The observatory and experimental results, including data, effects, outcome, *etc*. should be included. Authors should present *P* value where necessary, and the significant data should accompany. CONCLUSION: Accurate view and the value of the results should be included.

The format of structured abstracts is at: http://www.wjgnet.com/wjg/help/11.doc

Key words
Please list 3-10 key words that could reflect content of the study.

Text
For most article types, the main text should be structured into the following sections: INTRODUCTION, MATERIALS AND METHODS, RESULTS and DISCUSSION, and should include appropriate Figures and Tables. Data should be presented in the body text or Figures and Tables, not both.

Illustrations
Figures should be numbered as 1, 2, 3 and so on, and mentioned clearly in the main text. Provide a brief title for each figure on a separate page. No detailed legend should be involved under the figures. This part should add into the text where the figures are applicable. Digital images: black and white photographs should be scanned and saved in TIFF format at a resolution of 300 dpi; color images should be saved as CMYK (print files) and not RGB (screen-viewing files). Place each photograph in a separate file. Print images: supply images of size no smaller than 126× 76 mm printed on smooth surface paper; label the image by writing the Figure number and orientation using an arrow. Photomicrographs: indicate the original magnification and stain in the legend. Digital Drawings: supply files in EPS if created by Freehand and Illustrator, or TIFF from Photoshop. EPS files must be accompanied by a version in native file format for editing purposes. Scans of existing line drawings should be scanned at a resolution of 1200 dpi and as close as possible to the size at which they will appear when printed, not smaller. Please use uniform legends for the same subjects. For example: Figure 1 Pathological changes of atrophic gastritis after treatment. A: ...; B: ...;C: ...; D: ...; E: ...; F: ...; G: ...

Tables
Three-line tables should be numbered as 1, 2, 3 and so on, and mentioned clearly in the main text. Provide a brief title for each table. No detailed legend should be involved under the tables. This part should add into the text where the tables are applicable. The information should complement but not duplicate that contained in the text. Use one horizontal line under the title, a second under the column heads, and a third below the Table, above any footnotes. Vertical and italic lines should be omitted.

Notes in tables and illustrations
Data which is not statistically significant should not be noted. $^{a}P<0.05$, $^{b}P<0.01$ ($P>0.05$ should not be noted). If there are other series of *P* values, $^{c}P<0.05$ and $^{d}P<0.01$ are used; Third series of *P* values can be expressed as $^{e}P<0.05$ and $^{f}P<0.01$. Other notes in tables or under illustrations should be expressed as ^{1}F, ^{2}F, ^{3}F; or some other symbols with a superscript (Arabic

numerals) in the upper left corner. In a multi-curve illustration, each curve should be labeled with ●, ○, ■, □, ▲, △, *etc*. in a certain sequence.

Acknowledgments

Brief acknowledgments of persons who have made genuine contributions to the manuscripts and who endorse the data and conclusions are included. Authors are responsible for obtaining written permission to use any copyrighted text and/or illustrations.

References

Cited references should mainly be drawn from journals covered in the Science Citation Index (http://www.isinet.com) and/or Index Medicus (http://www.ncbi.nlm.nih.gov/PubMed) databases. Mention all references in the text, tables and figure legends, and set off by consecutive, superscripted Arabic numerals. References should be numbered consecutively in the order in which they appear in the text. Abbreviate journal title names according to the Index Medicus style (http://www.ncbi.nlm.nih.gov/entrez/query.fcgi?db=journals). Unpublished observations and personal communications are not listed as references. The style and punctuation of the references conform to ISO standard and the Vancouver style (5th edition); see examples below. Reference lists not conforming to this style could lead to delayed or even rejected publication status. Examples:

Standard jounal article (list all authors and include the PubMed ID [PMID] where applicable)

1 **Das KM,** Farag SA. Current medical therapy of inflammatory bowel disease. *World J Gastroenterol* 2000; 6: 483-489 [PMID: 11819634]

2 **Pan BR**, Hodgson HJF, Kalsi J. Hyperglobulinemia in chronic liver disease: Relationships between *in vitro* immunoglobulin synthesis, short lived suppressor cell activity and serum immunoglobulin levels. *Clin Exp Immunol* 1984; 55: 546-551 [PMID: 6231144]

3 **Lin GZ,** Wang XZ, Wang P, Lin J, Yang FD. Immunologic effect of Jianpi Yishen decoction in treatment of Pixu-diarrhoea. *Shijie Huaren Xiaohua Zazhi* 1999; 7: 285-287 [CMFAID:1082371101835979]

Books and other monographs (list all authors)

4 **Sherlock S,** Dooley J. Diseases of the liver and billiary system. 9th ed. Oxford: Blackwell Sci Pub, 1993: 258-296

Chapter in a book (list all authors)

5 **Lam SK.** Academic investigator's perspectives of medical treatment for peptic ulcer. In: Swabb EA, Azabo S. Ulcer disease: investigation and basis for therapy. New York: Marcel Dekker, 1991: 431-450

Electronic journal (list all authors)

6 **Morse SS.** Factors in the emergence of infectious diseases. Emerg Infect Dis serial online, 1995-01-03, cited 1996-06-05; 1(1):24 screens. Available from: URL: http//www.cdc.gov/ncidod/EID/eid.htm

PMID requirement

From the full reference list, please submit a separate list of those references embodied in PubMed, keeping the same order as in the full reference list, with the following information only: (1) abbreviated journal name and citation (e.g. *World J Gastroenterol* 2003;9(11):2400-2403; (2) article title (e.g. Epidemiology of gastroenterologic cancer in Henan Province, China; (3) full author list (e.g. Lu JB, Sun XB, Dai DX, Zhu SK, Chang QL, Liu SZ, Duan WJ; (4) PMID (e.g. 14606064). Provide the full abstracts of these references, as quoted from PubMed on a 3.5 inch disk or CD-ROM in Microsoft Word format and send by post to The *WJG* Press. For those references taken from journals not indexed by *Index Medicus*, a printed copy of the first page of the full reference should be submitted. Attach these references to the end of the manuscript in their order of appearance in the text.

Inappropriate references

Authors should always cite references that are relevant to their article, and avoid any inappropriate references. Inappropriate references include those that are linked with a hyphen and the difference between the two numbers at two sides of the hyphen is more than 5. For example, [1-6], [2-14] and [1, 3, 4-10, 22] are all considered as inappropriate references. Authors should not cite their own unrelated published articles.

Statistical data

Present as mean±SD and mean±SE.

Statistical expression

Express *t* test as *t*(in italics), *F* test as *F*(in italics), chi square test as χ^2(in Greek), related coefficient as *r*(in italics), degree of freedom as γ (in Greek), sample number as *n*(in italics), and probability as *P*(in italics).

Units

Use SI units. For example: body mass, m(B) = 78 kg; blood pressure, p(B)=16.2/12.3 kPa; incubation time, t(incubation)=96 h, blood glucose concentration, c(glucose) 6.4±2.1 mmol/L; blood CEA mass concentration, p(CEA) = 8.6 24.5 μg/L; CO_2 volume fraction, 50 mL/L CO_2 not 5% CO_2; likewise for 40 g/L formaldehyde, not 10% formalin; and mass fraction, 8 ng/g, *etc*. Arabic numerals such as 23,243,641 should be read 23 243 641.

The format about how to accurately write common units and quantum is at: http://www.wjgnet.com/wjg/help/15.doc

Abbreviations

Standard abbreviations should be defined in the abstract and on first mention in the text. In general, terms should not be abbreviated unless they are used repeatedly and the abbreviation is helpful to the reader. Permissible abbreviations are listed in Units, Symbols and Abbreviations: A Guide for Biological and Medical Editors and Authors (Ed. Baron DN, 1988) published by The Royal Society of Medicine, London. Certain commonly used abbreviations, such as DNA, RNA, HIV, LD50, PCR, HBV, ECG, WBC, RBC, CT, ESR, CSF, IgG, ELISA, PBS, ATP, EDTA, mAb, can be used directly without further mention.

Italicization

Quantities: *t* time or temperature, *c* concentration, *A* area, *l* length, *m* mass, *V* volume.

Genotypes: *gyr*A, *arg* 1, *c myc*, *c fos*, *etc*.

Restriction enzymes: *Eco*RI, *Hin*dI, *Bam*HI, *Kbo* I, *Kpn* I, *etc*.

Biology: *Helicobacter pylori, H pylori, E coli, etc*.

SUBMISSION OF THE REVISED MANUSCRIPTS AFTER ACCEPTED

Please revise your article according to the revision policies of *WJG*. The revised version including manuscript and high-resolution image figures (if any) should be copied on a floppy or compact disk. Author should send the revised manuscript, along with printed high-resolution color or black and white photos, copyright transfer letter, the final check list for authors, and responses to reviewers by a courier (such as EMS) (submission of revised manuscript by e-mail or on the WJG Editorial Office Online System is NOT available at present).

Language evaluation

The language of a manuscript will be graded before sending for revision. (1) Grade A: priority publishing; (2) Grade B: minor language polishing; (3) Grade C: a great deal of language polishing; (4) Grade D: rejected. The revised articles should be in grade B or grade A.

Copyright assignment form

It is the policy of WJG to acquire copyright in all contributions. Papers accepted for publication become the copyright of WJG and authors will be asked to sign a transfer of copyright form. All authors must read and agree to the conditions outlined in the Copyright Assignment Form (which can be downloaded from http://www.wjgnet.com/wjg/help/9.doc).

Final check list for authors

The format is at: http://www.wjgnet.com/wjg/help/13.doc

Responses to reviewers

Please revise your article according to the comments/suggestions of reviewers. The format for responses to the reviewers' comments is at: http://www.wjgnet.com/wjg/help/10.doc

Proof of financial support

For paper supported by a foundation, authors should provide a copy of the document and serial number of the foundation.

Publication fee

Authors of accepted articles must pay publication fee.

PO Box 2345, Beijing 100023, China
www.wjgnet.com
wjg@wjgnet.com

ELSEVIER

World J Gastroenterol 2005;11(43):6898
World Journal of Gastroenterology ISSN 1007-9327

World Journal of Gastroenterology standard of quantities and units

Number	Nonstandard	Standard	Notice
1	4 days	4 d	In figures, tables and numerical narration
2	4 days	four days	In text narration
3	day	d	After Arabic numerals
4	Four d	Four days	At the beginning of a sentence
5	2 hours	2 h	After Arabic numerals
6	2 hs	2 h	After Arabic numerals
7	hr, hrs,	h	After Arabic numerals
8	10 seconds	10 s	After Arabic numerals
9	10 year	10 years	In text narration
10	Ten yr	Ten years	At the beginning of a sentence
11	0,1,2 years	0,1,2 yr	In figures and tables
12	0,1,2 year	0,1,2 yr	In figures and tables
13	4 weeks	4 wk	
14	Four wk	Four weeks	At the beginning of a sentence
15	2 months	2 mo	In figures and tables
16	Two mo	Two months	At the beginning of a sentence
17	10 minutes	10 min	
18	Ten min	Ten minutes	At the beginning of a sentence
19	50% (*V/V*)	500 mL/L	
20	50% (m/*V*)	500 g/L	
21	1 M	1 mol/L	
22	10 μM	10 μmol/L	
23	1N HCl	1 mol/L HCl	
24	1N H_2SO_4	0.5 mol/L H_2SO_4	
25	4rd edition	4^{th} edition	
26	15 year experience	15- year experience	
27	18.5 kDa	18.5 ku,18 500u or M_r18 500	
28	25 $g.kg^{-1}/d^{-1}$	25 g/(kg·d) or 25 g/kg per day	
29	6900	6 900	
30	1000 rpm	1 000 r/min	
31	sec	s	After Arabic numerals
32	1 pg $\cdot L^{-1}$	1 pg/L	
33	10 kilograms	10 kg	
34	13 000 rpm	13 000 *g*	High speed; *g* should be in italic and suitable conversion.
35	1000 *g*	1 000 r/min	Low speed. *g* cannot be used.
36	Gene bank	GenBank	International classified genetic materials collection bank
37	Ten L	Ten liters	At the beginning of a sentence
38	Ten mL	Ten milliliters	At the beginning of a sentence
39	umol	μmol	
40	30 sec	30 s	
41	1 g/dl	10 g/L	10-fold conversion
42	OD_{260}	A_{260}	"OD" has been abandoned.
43	One g/L	One microgram per liter	At the beginning of a sentence
44	*A*260 nm	A_{260} nm	*A* should be in italic.
	$^bP<0.05$	$^aP<0.05$	In Table, no note is needed if there is no significance in statistics: $^aP<0.05$, $^bP<0.01$ (no note if $P>0.05$). If there is a second set of *P* value in the same table, $^cP<0.05$ and $^dP<0.01$ are used for a third set: $^eP<0.05$, $^fP<0.01$.
45	**F*=9.87, $^§F$=25.9, $^{\#}F$=67.4	^1F=9.87,^2F=25.9, ^3F=67.4	Notices in or under a table
46	KM	km	kilometer
47	CM	cm	centimeter
48	MM	mm	millimeter
49	Kg, KG	kg	kilogram
50	Gm, gr	g	gram
51	nt	N	newton
52	l	L	liter
53	db	dB	decibel
54	rpm	r/min	rotation per minute
55	bq	Bq	becquerel, a unit symbol
56	amp	A	ampere
57	coul	C	coulomb
58	HZ	Hz	
59	w	W	watt
60	KPa	kPa	kilo-pascal
61	p	Pa	pascal
62	ev	EV	volt (electronic unit)
63	Jonle	J	joule
64	J/mmol	kJ/mol	kilojoule per mole
65	10×10×10cm^3	10 cm×10 cm×10 cm	
66	N·km	KN·m	moment
67	$\bar{x}\pm s$	mean±SD	In figures, tables or text narration
68	– Mean±SEM	mean±SE	In figures, tables or text narration
69	*im*	im	intramuscular injection
70	*iv*	iv	intravenous injection
71	Wang et al	Wang *et al.*	
72	EcoRI	*Eco*RI	*Eco* in italic and RI in positive. Restriction endonuclease has its prescript form of writing.
73	Ecoli	*E.coli*	Bacteria and other biologic terms have their specific expression.
74	Hp	*H pylori*	
75	Iga	*Iga*	writing form of genes
76	*igA*	IgA	writing form of proteins
77	-70 kDa	~70 ku	

PO Box 2345, Beijing 100023, China
www.wjgnet.com
wjg@wjgnet.com

ELSEVIER

World J Gastroenterol 2005;11(44):6899-6904
World Journal of Gastroenterology ISSN 1007-9327

Clinicopathological study of cardiac tamponade due to pericardial metastasis originating from gastric cancer

Michiya Kobayashi, Takehiro Okabayashi, Ken Okamoto, Tsutomu Namikawa, Keijiro Araki

Michiya Kobayashi, Takehiro Okabayashi, Ken Okamoto, Tsutomu Namikawa, Keijiro Araki, Department of Tumor Surgery, Kochi Medical School, Nankoku 783-8505, Japan
Supported by KOBAYASHI MAGOBE Memorial Medical Foundation
Correspondence to: Michiya Kobayashi, MD, PhD, Department of Tumor Surgery, Kochi Medical School, Oko-cho, Nankoku, Kochi 783-8505, Japan. kobayasm@kochi-ms.ac.jp
Telephone: +81-888-80-2370 Fax: +81-888-80-2371
Received: 2005-05-02 Accepted: 2005-07-19

Key words: Gastric cancer; Pericarditis carcinomatosa; Cardiac tamponade; Chemotherapy

Kobayashi M, Okabayashi T, Okamoto K, Namikawa T, Araki K. Clinicopathological study of cardiac tamponade due to pericardial metastasis originating from gastric cancer. *World J Gastroenterol* 2005; 11(44): 6899-6904
http://www.wjgnet.com/1007-9327/11/6899.asp

Abstract

AIM: To review the cases reported in the literature, examined their clinicopathological features, and evaluated the efficacy of different therapeutic modalities for this rare condition.

METHODS: A search of the MEDLINE database revealed 16 cases of pericarditis carcinomatosa (PC) originating from GC reported in the literature between 1982 and 2005. Additional detailed data were obtained from the authors of these studies for subsequent clinicopathological investigation. We have also described about a case study from our own clinic.

RESULTS: The mean age of cases with pericarditis carcinomatosa originating from GC was 54 years. Females were diagnosed at a younger age (46.3 years) compared to males (58 years). The mean survival period after diagnosis was 4.5 mo. No statistical differences in the length of survival time were found between different therapeutic modalities, such as drainage, and local and/or systemic chemotherapy after drainage. However, three cases who underwent systemic chemotherapy survived for more than 10 mo. Cases that developed metachronous cardiac tamponade for more than 2 years after the diagnosis of GC generally survived for a longer period of time, although this was not statistically significant. Multivariate analysis revealed that low levels of carcinoembryonic antigen (CEA), and CEA and/or cancer antigen 19-9 (CA 19-9) were associated with longer survival.

CONCLUSION: Cases with low levels of CEA, and CEA and/or CA 19-9 should undergo systemic chemotherapy with or without local chemotherapy after drainage.

INTRODUCTION

Malignant pericardial effusion typically develops slowly and can spontaneously regress or remain stable. Some cases, however, may progress to cardiac tamponade[1]. Pericardial effusion can be caused by common primary malignancies that metastasize to the pericardium, such as lung cancer, lymphoma, breast cancer, and leukemia[2-4]. Cardiac tamponade due to pericarditis carcinomatosa (PC) originating from a primary gastric cancer (GC) is a rare condition. It is usually detected during the terminal stages of GC; however, it is also detected during cardiac emergencies. There are several reports of cardiac tamponade due to GC; however, most of them are only case reports. Due to the limited number of cases seen in a single institute, we performed a clinicopathological study of the cases of PC originating from GC reported in the literature, including a case from our hospital, and investigated the best therapeutic modality for this rare condition.

MATERIALS AND METHODS

A search of the MEDLINE database revealed 16 cases of PC originating from GC reported in the literature and meeting proceedings between 1982 and 2005 (Table 1)[5-15]. Cases in which PC was synchronous with GC and its recurrence were included. In addition, we asked the authors of these studies to review the available medical records to obtain more information about the cases.

A 36-year-old female patient, diagnosed with Kruckenberg's tumor, who consulted our clinic for further examination, was included in this case study. Endoscopic examination revealed GC of the antrum. The patient underwent distal gastrectomy with lymph node dissection. Histological examination showed that signet-ring cell carcinoma was mostly confined within the mucosal layer and had slightly invaded the muscular layer. Histology also showed lymph node metastases in a wide area with

Table 1 Reported cases of cardiac tamponade due to pericarditis carcinomatosa from gastric cancer.

Case	Author	Year	Sex	Age	Hist[1]	T	ly	v	n	Time interval[2]	Symptom	AST	ALT	ALP	LDH	CEA	CA19-9	Treatment[3]	Survival[4]
1	Ohtomo	1982	F	33	ud	2	3	NA	NA	0	Cough	31	26	297	365	NA	NA	D	5.0
2	Koide	1984	M	67	NA	NA	NA	NA	NA	NA	NA	NA	NA	NA	NA	NA	NA	D	2.0
3		1984	F	65	NA	NA	NA	NA	NA	NA	NA	NA	NA	NA	NA	NA	NA	D	5.0
4	Usami	1989	F	44	NA	NA	NA	NA	NA	NA	NA	NA	NA	NA	NA	NA	NA	L	1.3
5	Moriyama	1995	M	64	por	>2	NA	NA	>1	2.5 mo	Chest pain	38	11	4.2KA	832	240.1	26.7	S + L	1.5
6	Orihata	1996	M	51	sig	2	0	0	0	27.5 mo	Dyspnea	417	283	281	921	2.3	1 100	L	3.0
7	Sakusabe	1998	M	42	por	2	2	0	0	77 mo	Hypotension	25	35	142	154	0.6	2.7	L	3.5
8	Unno	1998	F	48	sig	NA	NA	NA	NA	7 mo	Dyspnea	51	56	503	235	0.7	47	L	1.5
9	Sakai	1999	M	45	sig	1	3	NA	3	0	Dyspnea	14	18	299	211	1.7	8.6	D	2.5
10	Kobayashi	2000	M	44	sig	1	2	1	2	19 mo	Dyspnea	22	94	456	216	2.5	56	S + L	5.0
11	Hiramatsu	2002	M	51	por	2	2	1	2	26 mo	Fatigue	1 224	1 087	NA	NA	3.0	27.9	S	10.0
12	Saitoh	2003	M	68	tub1	1	2	0	2	4 mo	Hypotension	NA	NA	NA	NA	12.5	238	S	2.5
13		2003	M	69	sig	2	3	3	2	50 mo	Cough	44	58	307	377	3.6	15.5	S + L	14.0
14	Sakusabe	2005	M	69	tub1	2	1	2	0	13 mo	Dyspnea	NOR	NOR	NOR	NOR	5.7		S	2.5
15	Suto	2003	F	52	sig	2	3	2	1	26 mo	Dyspnea	N	N	N	N	N	178.4	D	4.0
16		2003	M	68	tub2	3	3	2	3	32 mo	Dyspnea	N	N	N	N	41.6	894.1	D	1.0
17	Author		F	36	sig	2	2	1	2	27.5 mo	Vomit	95	152	312	272	0.76	9.78	S + L	13.0

NA: data not available, NOR: within normal range

[1]Hist: Histology, ud: undifferentiated carcinoma, por: poorly differentiated adenocarcinoma, sig: signet-ring cell carcinoma, tub1: well differentiated tubular adenocarcinoma, tub2: moderately differentiated tubular adenocarcinoma

[2]Time interval: time interval from the diagnosis of gastric cancer to the onset of cardiac tamponade

[3]D: drainage only, L: local chemotherapy, S: systemic chemotherapy

[4]Survival: survival after onset of cardiac tamponade (months)

Cases 11, 13 and 14 were cited from meeting proceedings.

massive permeation into the lymphatic vessels. The patient underwent postoperative chemotherapy of sequential methotrexate plus 5-fluorouracil. Twenty-seven and a half months after the operation, she developed nausea and laboratory data showed elevated levels of aspartate aminotransferase (95 IU/L), alanine aminotransferase (152 IU/L) and alkaline phosphatase (312 IU/L). An abdominal CT scan revealed massive pericardial effusion and left pleural effusion. The patient underwent pericardiocentesis and left pleural centesis. Cytological examination of the fluid revealed signet-cell carcinoma. After drainage, 10 mg of cisplatin was infused into the pericardial space. The pericardial effusion subsequently disappeared. She underwent injection chemotherapy into the pleural space (135 mg cisplatin) and systemic chemotherapy (cisplatin and sequential methotrexate plus 5-fluorouracil) until the pericardial effusion reappeared 9.5 mo later. Pericardiocentesis was performed again and 150 mg cisplatin was infused into the pericardial space. She also underwent systemic chemotherapy, however, died 13 months after the onset of PC.

Survival curves were generated using the Kaplan-Meier method and compared using the log-rank test. Multivariate Cox regression analysis was used to identify factors independently associated with mortality. For multivariate analysis, all factors were dichotomized: gender (male, female), time interval between diagnosis of gastric cancer and diagnosis of cardiac tamponade (<24 mo including synchronous cases, >24 mo), carcinoembryonic antigen (CEA) levels (<5.0, >5.0 ng/mL), cancer antigen 19-9 (CA 19-9, <40 U/mL, >40 U/mL), and systemic chemotherapy (done, not done). Using the Pearson's χ^2 test, differences in proportions were evaluated. $P<0.05$ was considered statistically significant.

RESULTS

The clinicopathological features of cardiac tamponade due to PC originating from GC are presented in Table 2. More than half of the patients were males, an occurrence similar to that generally seen in GC. The mean age of the 17 cases was 54 years (range, 33-69 years). Females diagnosed with cardiac tamponade tended to be younger (mean, 46.3 years; range, 33-65 years) as compared with the males (mean, 58 years; range, 42-69 years). Of the 17 cases, 14 died within 6 mo of diagnosis. Figure 1 shows the Kaplan-Meier survival curve for all the 17 cases. The mean survival after the diagnosis of PC was 4.5 mo (range: 1.0-14.0 mo). Histological data was obtained for 12 of the cases. Of these, 11 were of the less differentiated type. Eleven of the twelve cases also showed lymphatic permeation, and nine showed lymph node metastasis.

The different treatments used after the diagnosis of cardiac tamponade and the survival of the corresponding cases are shown in Table 3. Six cases underwent pericardiocentesis only, and the mean survival after the diagnosis of cardiac tamponade was 3.3 mo. Eleven cases underwent local infusion chemotherapy targeting the pericardial space and/or systemic chemotherapy following pericardiocentesis. The mean survival periods of the cases treated with local chemotherapy, systemic chemotherapy, and combined local and systemic chemotherapy were

Table 2 Clinicopathological analysis of cardiac tamponade due to PC from GC

Male:female	11:6
Mean age (yr; *n* = 17)	54.0 (range: 33-6)
Male	58.0 (range: 42-69)
Female	46.3 (range: 33-65)
Histological types (*n* = 14)	
sig	7
por	3
ud	1
tub	3
T (*n* = 13)	
1	3
2	9
3	1
ly (*n* = 12)	
0	1
1	1
2	5
3	5
v (*n* = 10)	
0	3
1	3
2	3
3	1
n (*n* = 12)	
0	3
1	2
2	5
3	2

The histological types, "T", "ly", "v", and "n", are defined in the General Rules for the Gastric Cancer Study by Japanese Research Society for Gastric Cancer[26]. sig: signet-ring cell carcinoma; por: poorly differentiated carcinoma; ud: undifferentiated carcinoma; and tub: tubular adenocarcinoma.

For T which represents depth of cancer invasion, 1: mucosal and submucosal layer; 2: proper muscular and subserosal layer; 3: expose to serosal layer; and 4: invasion to the adjacent organ.

For ly and v which represent lymphatic permeation and venous permeation, respectively, 0: none; 1: slight; 2: moderate; and 3: massive.

Table 3 Treatment and corresponding mean survival time after the diagnosis of cardiac tamponade

Modalities	*n*	Mean survival (mo)
Drainage only	6	3.3
Drainage+chemotherapy		
Local only	4	2.3
Systemic+local	4	8.4
Systemic only	3	5.0

Local: local infusion chemotherapy into pericardial space.

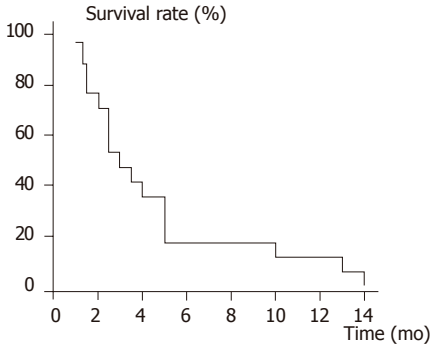

Figure 1 Kaplan-Meier survival curve of all cases (*n* = 17).

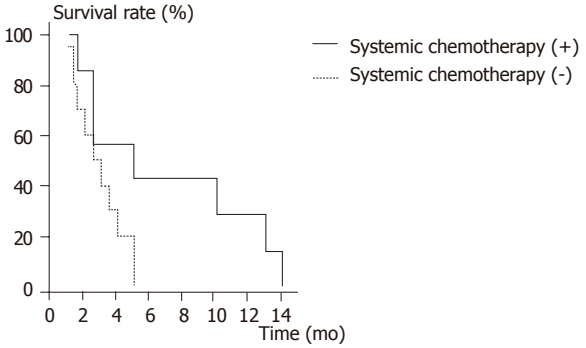

Figure 2 Kaplan-Meier survival curve according to administration of systemic chemotherapy. The cases treated with systemic chemotherapy were more likely to survive longer (*P* = 0.0579) than those who were not treated with systemic chemotherapy.

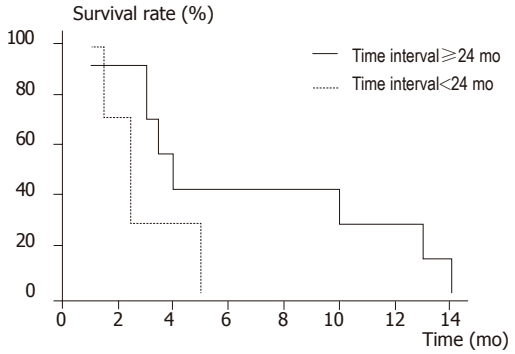

Figure 3 Kaplan-Meier survival curve according to time period between the diagnosis of gastric cancer and diagnosis of cardiac tamponade. The cases in whom cardiac tamponades were diagnosed for more than 24 mo after the diagnosis with gastric cancer were more likely to survive longer than those in whom cardiac tamponade was diagnosed for less than 24 mo after the initial diagnosis of gastric cancer. However, there was no statistical difference between the two groups (*P* = 0.1130).

2.3, 5.0, and 8.4 mo, respectively. All the three cases who had survived for more than 10 mo underwent systemic chemotherapy (two cases: local and systemic; one case: systemic only).

Statistical analyses of the prognostic factors are presented in Table 4. Cases treated with systemic chemotherapy tended to survive longer (6.9 mo) than those who were not treated with systemic chemotherapy (*P* = 0.0579; Figure 2). The mean survival period of the cases that developed cardiac tamponade within 2 years after the diagnosis of primary GC, including one synchronous case, was 2.9 mo. This was shorter than the cases in which the onset of cardiac tamponade occurred 2 years after the diagnosis of GC (6.9 mo). However, there were no statistical differences between the two groups (*P* = 0.1130; Figure 3). The mean

Table 4 Clinical characteristics of cardiac tamponade due to pericarditis carcinomatosa from GC

Characteristics	*n*	Survival rate (%) 1 mo	5 mo	10 mo	Median survival in months (range)	*P* values
Overall	17	94.2	17.7	11.8	4.5 (1.0-14.0)	
Gender						
Male	11	90.9	18.2	9.1	4.3 (1.0-14.0)	
Female	6	-	16.7	-	5.0 (1.3-13.0)	0.7614
Time interval						
<24 mo	7	-	0.0	0.0	2.9 (1.5-5.0)	
>24 mo	7	85.7	-	28.5	6.9 (1.0-14.0)	0.1130
CEA (ng/mL)						
<5	9	-	-	22.2	6.3 (1.5-14.0)	
>5	4	75.0	0.0	0.0	1.9 (1.0-2.5)	0.0071
CA 19-9 (U/mL)						
<40	6	-	33.3	16.7	7.4 (1.5-14.0)	
>40	6	-	0.0	0.0	2.8 (1.0-5.0)	0.1074
CEA and/or CA 19-9						
Normal	5	-	0.0	0.0	8.6 (2.5-14.0)	
High	8	87.5	0.0	0.0	2.6 (1.0-5.0)	0.0244
Systemic chemotherapy						
Done	7	-	42.9	28.6	6.9 (1.5-14.0)	
Not done	7	90.0	0.0	0.0	2.8 (1.0-5.0)	0.0579

Table 5 Relative risk of death as analyzed by Cox proportional Hazards model

Variables	*B* value	Relative risk (95%CI)	*P* values
CEA			
<5.0 ng/mL			
>5.0 ng/mL	1.9	6.7 (1.2–36.6)	0.029
CEA and/or CA-19-9			
<5.0 ng/mL, <40 U/mL			
>5.0 ng/mL, >40 U/mL	1.6	4.9 (1.0-23.7)	0.049

95%CI: confidence interval.

survival periods of cases with high levels (>5.0 ng/mL) and normal levels (<5.0 ng/mL) of CEA were 6.3 and 1.9 months, respectively (P = 0.0071; Figure 4). The mean survival periods of cases with high levels (>40 U/mL) and normal levels (<40 U/mL) of CA 19-9 were 2.8 and 7.4 months, respectively (P = 0.1074). The cases in which either CEA and/or CA 19-9 were elevated at the time of cardiac tamponade had shorter survival periods (2.6 mo) as compared with the cases without CEA and/or CA 19-9 elevation (8.6 mo) (P = 0.0244). Multivariate analysis also revealed that high levels of CEA and CEA and/or CA 19-9 were associated with poor survival (P = 0.029 and 0.049, respectively; Table 5).

DISCUSSION

Secondary tumors of the heart and/or pericardium are rarely diagnosed in clinical practice. However, it is not uncommon to find these during autopsy cases. Secondary cardiac metastases most frequently arise from primary lung tumors. Primary GC rarely metastasize to the heart, with 4.3-7.7%[16-19] reported from autopsy investigations.

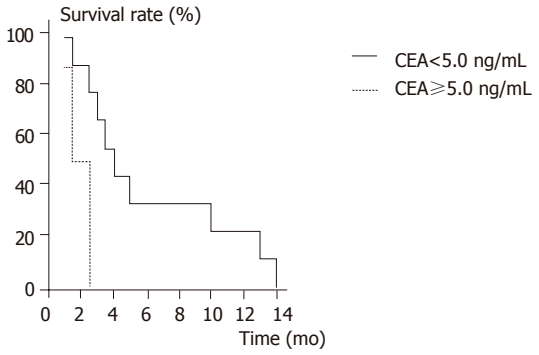

Figure 4 Kaplan-Meier survival curve according to CEA levels. The cases with normal CEA levels had a longer survival period as compared to those with high CEA levels (P = 0.0071).

We investigated 17 reported cases of cardiac tamponade due to PC originating from GC, and observed several characteristics specific to this condition. The mean age of the patients was 54 years, which was slightly younger than the average age reported for GC. Females tended to be diagnosed at a younger age than males. Histopathological results of 11 out of the 12 cases showed less differentiated tumors with massive lymphatic involvement. Raven[20] and Hanfling[21] reported that the hematogenous route was the most common metastatic pathway to the heart, while Warren and Gates[22] and Kline[23] believed that the cardiac lymphatic system was the major metastatic pathway to the heart. The fact that almost all cases showed massive lymphatic permeation suggested that the mechanism of pericardial metastasis might be through the lymphatic system.

There is no defined therapy for pericardial metastasis. Most reports describing therapeutic modalities for cardiac tamponade due to malignant pericarditis were based on cases in which lung cancer was the primary tumor. Drainage of the malignant effusion either by percutaneous pericardiocentesis or by pericardiectomy should be performed if this condition is diagnosed. The prognosis of cardiac tamponade caused by malignant pericarditis is grave and survival is limited. Fraser *et al*.[24] reported the prognosis of 21 cases and more than half of the 21 cases originated from lung cancer. Seven patients treated with pericardiocentesis and provided with supportive care had a median survival time of 3 wk. Eight patients treated with pericardiocentesis and either radiotherapy and/or intrapericardial or systemic chemotherapy had a median survival period of 3.5 mo. Six patients treated with pericardiocentesis and pericardiectomy with or without radio- or chemotherapy had a median survival period of 6 mo. Moreover, Appelqvist *et al*.[1] reported the prognosis of three cases of pericardiectomy. Among them, two cases had primary lung cancer, while the primary tumor was of unknown origin in the third case. The case who did not undergo treatment only survived for 5 wk, the case treated with radiotherapy survived for 7 wk, and the case treated with systemic chemotherapy survived for 9 mo[1].

To our knowledge, there are no reports investigating the different therapeutic modalities available for the treatment of cardiac tamponade originating from GC. Our review of the literature showed that the therapeutic modalities in 6 cases were only the drainage of malignant effusion, while the 10 cases underwent chemotherapy after the drainage. In addition, the chemotherapy treatment varied in the cases with the routes of administration of anti-cancer agents (e.g., intrapericardial infusion and/or systemic administration), the type of anti-cancer agents, and the dose of anti-cancer agents. More than half of the cases treated with local chemotherapy received various doses of cisplatin. We found that there were no complications caused by local chemotherapy in our review of the literature, and cisplatin was the most frequently used agent for local chemotherapy. The agents used for local chemotherapy should be less irritable to the heart. As the number of cases was limited, we were unable to determine which treatment was the most effective for this condition. However, we did find that cases treated with systemic chemotherapy tended to survive longer than those who were not ($P = 0.0579$).

The period of time from the diagnosis of gastric cancer to the onset of cardiac tamponade may influence prognosis. When the time period was less than 2 years, the survival was 2.9 mo, and if the time period was over 2 years, the survival increased to 6.9 mo. The cases with high levels of either of the tumor markers CEA or CA 19-9 had a shorter survival period than those with low levels of either of these markers.

Honda *et al*.[25] reported a case of cardiac tamponade originating from lung cancer, in which the malignant cardiac effusion was controlled by weekly paclitaxel therapy. Sakusabe *et al*.[15] also reported that weekly administration of paclitaxel was effective for the control of malignant pericardial effusion originating from GC. There are many reports demonstrating that malignant ascites arising from GC can be controlled by paclitaxel in patients diagnosed with peritonitis carcinomatosa of GC. We confirmed that the level of paclitaxel in malignant ascites remained effective until 72 h after systemic administration (submitted for publication). Paclitaxel may, therefore, be a promising agent for systemic chemotherapy, and should be considered for the treatment of malignant pericardial effusion.

In summary, we were unable to reveal which therapy was the best for extending the life expectancy in cases of PC originating from GC. However, the cases with systemic chemotherapy survived for a longer period of time compared to the cases treated with drainage only or with local chemotherapy. The cases that developed cardiac tamponade due to PC arising from GC more than 2 years after the diagnosis, and the cases in which the levels of CEA and CA 19-9 were not elevated may have a possibility of surviving for a longer period of time. Such cases should undergo chemotherapy following emergency pericardiocentesis. While a specific chemotherapeutic strategy has not yet been developed for these cases, the use of paclitaxel for systemic, and cisplatin for local chemotherapy may be promising for the treatment of cardiac tamponade caused by PC arising from GC.

REFERENCES

1 **Appelqvist P,** Maamies T, Gröhn P. Emergency pericardiotomy as primary diagnostic and therapeutic procedure in malignant pericardial tamponade: report of three cases and review of the literature. *J Surg Oncol* 1982; **21:** 18-22

2 **Thurber DL,** Edwards JE, Achor RW. Secondary malignant tumors of the pericardium. *Circulation* 1962; **26:** 228-241

3 **Kusnoor VS,** D'Souza RS, Bhandarkar SD, Golwalla AF. Malignant pericardial effusion. Report of 2 cases. *J Assoc Physicians India* 1973; **21:** 101-104

4 **Theologides A.** Neoplastic cardiac tamponade. *Semin Oncol* 1978; **5:** 181-192

5 **Ohtomo T,** Sakanaka M, Urano S, Shimizu I, Kitamura H, Kunishige H, Andachi H. Superficial spreading carcinoma of the stomach presenting as neoplastic cardiac tamponade: report of a case with autopsy findings. *Matsushita Med J* 1982; **20:** 28-35

6 **Koide S,** Kawada S, Inoue H, Ogawa J, Fukuda T, Inamura S. Shohtsu A, Hoshiai M. Cardiac tamponade - especially with subxiphoid pericardial window. *Heart* 1984; **16:** 504-511

7 **Usami I,** Kato M, Hayashi Y, Kuroki H, Hanaki H, Furutani M, Yamada Y, Takeuchi T. Local treatment of cancerous pericarditis by cisplatin. *Jpn J Lung Cancer* 1989; **29:** 127-131

8 **Moriyama A,** Murata I, Kuroda T, Yoshikawa I, Tabaru A, Ogami Y, Otsuki M. Pericardiac metastasis from advanced gastric cancer. *J Gastroenterol* 1995; **30:** 512-516

9 **Orihata M,** Hata M, Hase Y, Nakagawa H, Kidokoro T, Yamanaka O, Sagawa F. A case of cardiac tamponade induced by cardiac metastasis of a gastric cancer two years after a surgical treatment. *J Jpn Surg Assoc* 1996; **57:** 862-866

10 **Unno J,** Yasunami T, Ishiko T, Koizumi M, Ichikawa K, Arai S, Okuyama H, Hayashida N, Kouda S, Tadokoro M. A case study of gastric carcinoma presenting as carcinomatous pericarditis and meningeal carcinomatosis. *Gan no Rinsho* 1998; **44:** 1555-1559

11 **Sakusabe M,** Yoshioka H, Niwa M. A case of cardiac tamponade secondary to gastric cancer after curative gastrectomy. *J Jpn Surg Assoc* 1998; **59:** 2578-2581

12 **Sakai Y,** Minouchi K, Ohta H, Annen Y, Sugimoto T. Cardiac tamponade originating from primary gastric signet ring cell carcinoma. *J Gastroenterol* 1999; **34:** 250-252

13 **Hiramatsu K,** Matsuura Y, Kono H, Kitagawa Y, Yamanaka H. A recurrent case of gastric cancer presented with carcinomatous pericarditis. *J Jpn Surg Assoc* 2002; **63:** 333-336

14 **Suto K,** Ichikawa W, Tsuji Y, Arai E, Shimizu M, Hirayama R. Two cases of pericardial metastasis from gastric cancer with cardiac tamponade. *J Jpn Surg Assoc* 2003; **64:** 2414-2417

15 **Sakusabe M,** Ouchi S, Seki H, Kumagai Y, Kamata S, Kotanagi H. A case of effective weekly paclitaxel administration for gastric cancer recurrence with carcinomatous pericarditis. *Gan To Kagaku Ryoho* 2005; **32:** 77-79

16 **Tabata Y,** Nakato H, Nakamura Z, Sasaki A, Shoji K, Yokoyama H, Tanji Y, Saito K, Uehara H. Metastatic cancer to the heart: a clinicopathological analysis of 64 autopsy cases. *Respir Circ* 1983; **31:** 569-573

17 **Klatt EC,** Heitz DR. Cardiac metastases. *Cancer* 1990; **65:** 1456-1459

18 **Nakayama R,** Yoneyama T, Takatani O, Kimura K. A study of metastatic tumors to the heart, pericardium and great vessels. I. Incidences of metastases to the heart, pericardium and great vessels. *Jpn Heart J* 1966; **7:** 227-234

19 **Mukai K,** Shinkai T, Tominaga K, Shimosato Y. The incidence of secondary tumors of the heart and pericardium: a 10-year study. *Jpn J Clin Oncol* 1988; **18:** 195-201

20 **Raven RW.** Secondary malignant disease of the heart. *Br J*

Cancer 1948; **2:** 1-7
21 **Hanfling SM.** Metastatic cancer to the heart. Review of the literature and report of 127 cases. *Circulation* 1960; **22:** 474-483
22 **Warren S,** Gates O. Lung Cancer and Metastasis. *Arch Pathol* 1964; **78:** 467-473
23 **Kline IK.** Cardiac lymphatic involvement by metastatic tumor. *Cancer* 1972; **29:** 799-808
24 **Fraser RS,** Viloria JB, Wang NS. Cardiac tamponade as a presentation of extracardiac malignancy. *Cancer* 1980; **45:** 1697-1704
25 **Honda K,** Oura S, Hirai I, Yoshimasu T, Kokawa Y, Sasaki R, Okamura Y. Successful management of malignant pericardial effusion with weekly paclitaxel therapy in a lung adenocarcinoma patient. *Gan To Kagaku Ryoho* 2003; **30:** 1317-20
26 **Japanese Gastric Cancer Association.** Japanese classification of gastric carcinoma -2nd English edition-. *Gastric Cancer* 1998; **1:** 10-24

Science Editor Kumar M and Guo SY **Language Editor** Elsevier HK

PO Box 2345, Beijing 100023, China
www.wjgnet.com
wjg@wjgnet.com

ELSEVIER

World J Gastroenterol 2005;11(44):6905-6909
World Journal of Gastroenterology ISSN 1007-9327

Significance of a novel sucrose permeability test using serum in the diagnosis of early gastric cancer

Tadayuki Shishido, Taketo Yamaguchi, Takeo Odaka, Masanori Seimiya, Hiromitsu Saisho, Fumio Nomura

Tadayuki Shishido, Taketo Yam aguchi, Takeo Odaka, Hiromitsu Saisho, Department of Medicine and Clinical Oncology, Graduate School of Medicine, Chiba University, 1-8-1 Inohana, Chuo-ku, Chiba-city, Chiba 260-8677, Japan
Masanori Seimiya, Fumio Nomura, Department of Molecular Diagnosis, Graduate School of Medicine, Chiba University, 1-8-1 Inohana, Chuo-ku, Chiba-city, Chiba 260-8677, Japan
Correspondence to: Taketo Yamaguchi, Department of Medicine and Clinical Oncology, Graduate School of Medicine, Chiba University, 1-8-1 Inohana, Chuo-ku, Chiba-city, Chiba 260-8677, Japan. yamaguch-cib@umin.ac.jp
Telephone: +43-226-2083 Fax: +43-226-2088
Received: 2005-04-25 Accepted: 2005-05-24

Abstract

AIM: To investigate the usefulness of sucrose permeability test using serum in the diagnosis of gastric diseases, with special reference to early gastric cancer (EGC).

METHODS: A total of 63 subjects, including 11 patients with gastric ulcer, 20 patients with gastric cancer (13, early; 7, advanced) and 32 healthy controls, were studied. Blood and urine samples were collected repeatedly for 5 h before and after the sucrose loading. Sucrose levels were measured by a newly developed enzymatic method.

RESULTS: Serum sucrose levels started to increase 15 min after loading, and peaked at 60 min in the gastric disease groups. The levels for gastric ulcer, EGC and advanced gastric cancer (AGC) at 60 min were significantly higher than that in the healthy controls (26.9±2.4, 34.4±5.0, and 71.8±15.6 *vs* 7.9±0.7 mol/L, respectively, $P<0.01$). The cut-off level set at 15.4 mol/L (60 min) offered the best distinction between EGC patients and healthy controls; and the sensitivity and specificity were 92.3% and 93.8%, respectively, while those of the urine method were 76.9% and 93.8%, respectively.

CONCLUSIONS: The gastric permeability test using serum is reliable for the detection of EGC, and this test can provide results much earlier than the conventional urine method. This test may offer a useful alternative to more invasive tests for EGC.

Key words: Sucrose test; Gastric permeability; Early gastric cancer; Advanced gastric cancer; Gastric ulcer

Shishido T, Yamaguchi T, Odaka T, Seimiya M, Saisho H, Nomura F. Significance of a novel sucrose permeability test using serum in the diagnosis of early gastric cancer. *World J Gastroenterol* 2005; 11(44): 6905-6909
http://www.wjgnet.com/1007-9327/11/6905.asp

INTRODUCTION

In 1993, Meddings *et al.*[1], proposed the sucrose permeability test as a new non-invasive test for evaluating gastroduodenal injury. This test is based on the principle that sucrose does not permeate the healthy gastric mucosa and is rapidly dissolved in the small intestine, whereas it permeates and is absorbed through sites of injury in the stomach, enters the bloodstream and is excreted into the urine. It is reported that this test is useful for diagnosing gastric ulcer or gastroduodenal injury caused by NSAIDs or steroids[2-6]. Furthermore, it has been demonstrated that sucrose permeability is elevated by infection with *H pylori* or celiac disease, reflecting mucosal injury associated with inflammatory cell infiltration; thus, the usefulness of this test in evaluating gastroduodenal injury has been established[4,7,8].

However, the conventional method is not practical for outpatients or for health screenings because urine must be collected for 5 h or longer after the sucrose loading. If the sucrose test could be done in a shorter period of time, its clinical usefulness would increase.

We recently developed a novel enzymatic assay that is sensitive enough to determine serum levels of sucrose accurately[9]. The changes of serum sucrose levels after ingestion in patients with gastric diseases, as in healthy subjects, are unknown. Therefore, the first aim of this study was to investigate the changes of serum sucrose levels in healthy subjects, patients with gastric ulcer and gastric cancer. The second aim was to identify the most suitable time to collect serum samples for the detection of gastric disease.

There are reports that gastric mucosal permeability is elevated in patients with advanced gastric cancer (AGC), but none regarding those with early gastric cancer (EGC). The third aim of this study was to evaluate the diagnostic value of the sucrose test using serum in patients with EGC.

MATERIALS AND METHODS

Patients

The subjects studied included: (1) 32 healthy volunteers (HV: 15 men and 17 women; mean age 51.0 years, range 35-65 years) without symptoms or a history of gastrointestinal disease, who had not been prescribed any medicine that might have affected the gastrointestinal system; and (2) a gastric disease patient group composed of 31 patients, including 11 with gastric ulcers (GU: 5 men and 6 women; mean age 55.5 years, range 24-80 years; mean long diameter 1.4 cm, range 0.8-2.0 cm), 13 with EGC (11 men and 2 women; mean age 73.5 years, range 61-87 years; depth of invasion Tis in 11, T1 in 2; mean long diameter 1.55 cm, range 0.8-3.5 cm), and 7 with AGC (3 men and 4 women; mean age 65.0 years, range 48-75 years; depth of invasion T2 in 3, T3 in 2, and unknown in 2; mean long diameter 7.7 cm, range 4.3 cm-whole stomach). The depth of invasion of the gastric cancer was judged by pathological exploration of the resected mucosal specimens and the surgical specimens (Table 1).

Table 1 Clinical data of subjects studied

	HV (n = 32)	GU (n = 11)	EGC (n = 13)	AGC (n = 7)
Age (yr)	51 (35-65)	55.5 (24-80)	73.5 (61-87)	65 (48-75)
Gender (M:F)	17:15	5: 6	11: 2	3: 4
Size (cm)	-	1.4 (0.8-2.0)	1.55 (0.8-3.5)	7.7 (4.3-whole stomach)
Invasive Depth	-	-	Tis:T1=11:2	T2:T3:unknown = 3:2:2

HV: healthy volunteers, GU: Gastric ulcers, EGC: early gastric cancers, AGC: advanced gastric cancers.
Tis = mucosa, T1 = submucosa, T2 = proper muscle and subserosa, T3 = serosa.

The gastric mucosa was resected in patients with EGC, when considered, on the basis of endoscopic diagnosis including endoscopic ultrasonography, to be an intramucosal lesion. In two cases of EGC that were judged to have invaded as far as the deep submucosa, and in five cases of AGC, surgery was performed, while the remaining two cases were treated non-surgically. Two cases in which the depth of invasion could not be determined histopathologically were diagnosed endoscopically as AGC. Patients with diabetes mellitus or reduced renal function were excluded.

Informed consent was obtained from every subject. This study was performed with the approval of the Ethical Committee of Chiba University School of Medicine, Japan.

Gastric permeability

After an overnight fast, patients and HV were given a solution composed of 100 g sucrose and 450 mL water for 15 min. Blood samples were collected before and at 15, 30, 45, 60, 75, 90, 120, 180, 240, and 300 min after the sucrose loading. The blood samples were immediately centrifuged and the sera were obtained. Simultaneously, urine was collected for over a period of 5 h after the sucrose loading and the amount of sucrose excreted during the 5-h period was obtained from the volume of urine and the concentration of sucrose. Sera and urine were stored at -20 °C until the assay.

Assay

Sucrose was phosphorylated by the action of sucrose phosphorylase. The subsequent reaction in the presence of phosphoglucomutase and glucose-1, 6-diphosphate formed glucose-6-phosphate. Finally, the sucrose of the monad formed the dyad thio-NADPH. The reaction was monitored by changes in absorbance at 405 nm. The details of the assay procedures are published elsewhere[9].

Statistical analysis

Data were expressed as mean±SE. Using ANOVA, the serum sucrose concentration before and after the administration of sucrose in each group was compared. Serum sucrose concentrations at each sampling time within each group and comparison by the urine collection method within each group were compared using Tukey's method. Comparison of diagnostic ability based on areas under the receiver operator characteristics (ROC) curve at each sampling point was carried out using Hanley's method[10]. Cut-off points based on the ROC curve at each time point were set to obtain sensitivity, specificity, and accuracy. The surface area of GC was calculated using the formula (1/4×π×long diameter×short diameter) on the assumption that the tumor was elliptical. The relationship between the surface area of EGC and the serum sucrose level was determined. A two-sided P value <0.05 was considered statistically significant.

RESULTS

Baseline serum sucrose concentrations were 2.4±0.4, 2.9±0.8, 1.4±0.7, and 1.6±1.4 μmol/L for the HV, GU, EGC and AGC, respectively, which showed no significant intergroup differences. The peak serum sucrose level for the HV was 8.5±0.8 μmol/L at 120 min after the sucrose loading. Serum sucrose levels for the GU, EGC and AGC, which increased 15 min after the sucrose loading (P<0.01), peaked between 45 and 120 min, and then gradually decreased (Figure 1). Serum sucrose levels for GU, EGC and AGC showed a significant difference from the HV (P<0.01) between 60 and 240 min. Between 15 and 300 min, serum sucrose levels for AGC showed a significant difference from those for EGC or GU (P<0.01). However, there was no significant difference between the serum sucrose levels for EGC and GU at any time point from 15 to 300 min.

The amounts of sucrose excreted into the urine in HV, GU, EGC and AGC were 50.5±4.4, 172.9±19.1, 165.1±27.2, and 464.5±78.9 mg, respectively, showing significantly higher values in GU, EGC and AGC as compared to the HV. In addition, the amount of sucrose excreted into the urine in AGC showed a significantly higher value than that

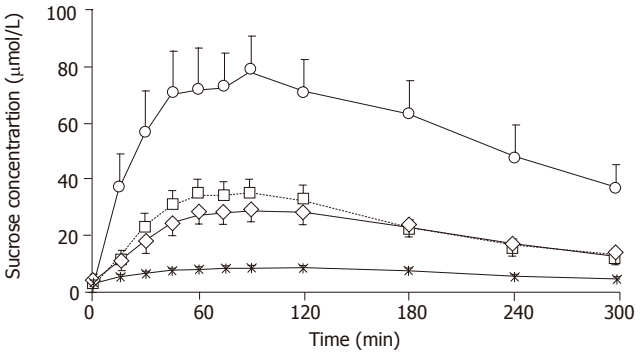

Figure1 Changes in serum sucrose level in HV, GU, EGC, and AGC groups (mean ±SE). The serum sucrose level in EGC group (□) showed a significant difference between 30 and 300 min after the sucrose loading as compared to the HV group (⁎) between 30 and 240 min (P<0.01) and 30 and 300 min (P<0.05). The serum sucrose level of AGC (○) patients showed a significant difference from HV (⁎) between 15 and 300 min after sucrose loading, GU (◇) and EGC (□) (P<0.01). GU patients (◇) showed a significant difference from the HV group ( ) between 45 and 240 min after sucrose loading (45 min, P<0.05; from 60 to 240 min, P<0.01). However, there was no significant difference in serum sucrose level in HV group from 15 to 300 min after loading as compared with either EGC (◇) or GU (□) group.

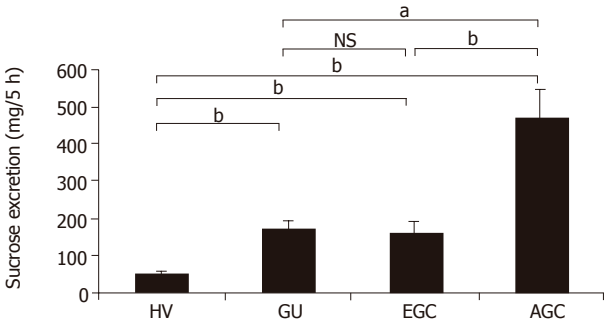

Figure 2 Amounts of sucrose excreted into urine in HV, GU, EGC and AGC groups (mean±SE). Even in the urine collection method, the amount of sucrose excreted in GU, EGC and AGC groups showed a significant difference (^bP<0.01) as compared with the HV group, and AGC group showed a significant difference (^bP<0.01) from both GU and EGC groups. However, no significant difference was seen in either EGC; NS: no significant difference.

in GU or EGC (Figure 2).

The diagnostic value of the sucrose test in gastric disease (GU, EGC and AGC) in relation to HV was compared between the serum method and the urine collection method using ROC curves (Figure 3). The areas under the curve (AUC) in the serum method at 15 and 60 min, and in the urine collection method were 0.876 (95%CI 0.783-0.968), 0.992 (95%CI 0.978-1.006), and 0.980

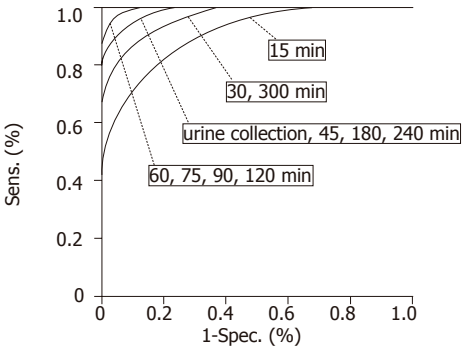

	AUC	SE	95% CI	
			Lower limit	Upper limit
Urine (5 h)	0.98	0.014	0.953	1.006
0 min	0.366	0.072	0.226	0.506
15 min	0.876	0.047	0.783	0.968
30 min	0.951	0.024	0.904	0.998
45 min	0.979	0.014	0.952	1.005
60 min	0.992	0.007	0.978	1.006
75 min	0.994	0.006	0.983	1.005
90 min	0.993	0.006	0.981	1.006
120 min	0.989	0.01	0.97	1.008
180 min	0.971	0.017	0.937	1.005
240 min	0.973	0.016	0.941	1.004
300 min	0.959	0.022	0.917	1.002

Figure 3 Receiver operator characteristics (ROC) curve and AUC of ROC curve. Comparison of the ROC curve of the sucrose test and AUC at each time point. There was no significant difference between the urine collection method and the serum method from 30 to 300 min. AUC: Area under the ROC curve; SE: standard error; CI: confidence interval.

(95%CI 0.953-1.006), respectively (Figure 3). Comparison of the AUC between the urine collection method and the serum method at every time point showed no significant difference. The diagnostic values of the urine collection method and the serum method were comparable from 30 min onward at each sampling time.

Cut-off points for the detection of gastric disease at each sampling time in the serum method were obtained from the ROC curves, and the diagnostic value of this method was also obtained. Similarly, cut-off points and diagnostic values were obtained by the urine collection method (Table 2). The cut-off points for the detection of gastric disease by the serum method over 60 min was 15.4 μmol/L and that of the urine collection method was 95 mg. Serum sucrose levels of the four studied groups at 60 min are shown in Table 3.

The sensitivity, specificity, and overall accuracy of the urine collection method for detecting gastric disease were 90.3%, 93.8%, and 92.1%, respectively, while those

Table 2 Cut-off points and diagnostic values of sucrose test at each time point for detection of gastric disease (gastric ulcer and gastric cancer)

Time (min)	Urine	15	30	45	60	75	90	120	180	240	300
Cut-off points[1]	95	7.4	10.2	11.8	15.2	16.8	16	14	11	8.2	6.5
Sensitivity (%)	90.3	80.6	83.9	93.5	96.8	96.8	96.8	96.8	93.5	93.5	90.3
Specificity (%)	93.8	87.5	93.8	90.6	93.8	96.9	93.8	93.8	90.6	90.6	90.6
Accuracy (%)	92.1	84.1	88.9	92.1	95.2	96.8	95.2	95.2	92.1	92.1	90.5

[1] Cut-off points: Urine as mg/5 h, Serum as μmol/L

Table 3 Sucrose concentrations at 60 min of the 4 groups

	HV	GU	EGC	AGC
Mean (μmol/L)	7.6	26.9	34.4	71.8
SE (μmol/L)	0.7	2.4	5.0	15.6

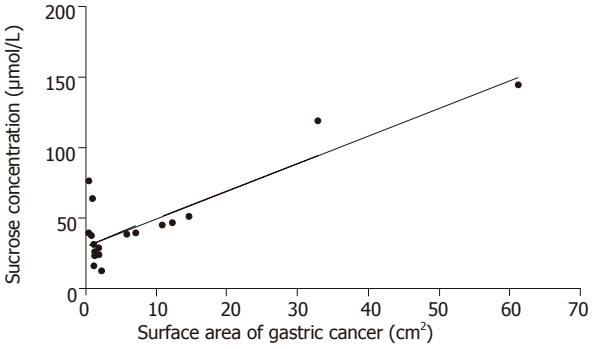

Figure 4 Relationship between serum sucrose level at 60 min and surface area of gastric cancer. The serum sucrose level at 60 min was closely correlated with the surface area of the gastric cancer (r = 0.83, P<0.01).

for the serum method (over 60 min) were 96.8%, 93.8%, and 95.2% (Table 4), indicating that the serum method was superior to the urine collection method, but not so significantly.

Sensitivity in detecting GU and AGC was 100% by using both the methods. Sensitivity in detecting EGC was 76.9% by the urine collection method, but 92.3% by the serum method (60 min), which was relatively high, but again without a significant difference.

There was a significant correlation between the surface area of GC and the serum sucrose level (60 min) (r = 0.83) (Figure 4).

DISCUSSION

The sucrose permeability test is a valuable noninvasive test for detecting gastroduodenal injury[1-8,11-13]. The conventional method involves measuring the amount of sucrose excreted into the urine for over a period of as long as 5 h following the administration of sucrose. If this test could be done more quickly, its clinical usefulness would increase greatly.

Vinet *et al*.[14] reported that the serum concentrations of sucrose after sucrose loading in volunteers whose stomachs had been injured by NSAIDs or alcohol clearly increased, and that this occurred only after 15-45 min. We considered that it might be useful in clinical practice to measure the sucrose concentration in the serum instead of the urine. However, the pattern of the changes of serum sucrose levels after sucrose ingestion either in healthy subjects or in patients with gastric diseases was unknown. Moreover, the appropriate time point for collecting serum samples was not known, nor was the usefulness of serum testing for detecting gastric diseases. We conducted this fundamental study for these reasons.

We took advantage of a novel enzymatic method that we had recently developed for measuring serum sucrose levels. Previously, the concentration of sucrose in biological fluids was measured by high-performance liquid chromatography (HPLC) with an electrochemical technique for detection[1-7,11], or by an enzymatic assay[8,14,15] in which invertase hydrolyzes sucrose to fructose and glucose, and then the glucose is measured using a hexokinase procedure with reduced nicotinamide adenine dinucleotide phosphate formation. But the invertase method is not applicable to serum samples because of interference by the glucose in the samples. The HPLC method is accurate and widely used, but is labor-intensive, costly, and time-consuming.

We collected blood specimens at 11 different sampling times from 63 individuals and examined the changes in serum sucrose and the time point appropriate for the detection of mucosal injury. There was no significant difference in diagnostic value between the urine collection method and the serum method at any determined time point between 30 and 300 min. Thus, it may be possible to detect a gastroduodenal injury using serum at any determined point between 30 and 300 min after sucrose loading. In particular, because the accuracy at 60, 75, 90, and 120 min was greater than 95%, which was higher than that for the urine collection method, it should be satisfactory to carry out sampling for the serum method only at 60 min in order to obtain more reliable results more quickly. On the basis of these results, we were able to shorten the sucrose test, and to increase its diagnostic accuracy.

All cases of GU were detected when the serum method was carried out for 60 min. Although GU is a benign disease, medical treatment is essential, and GU must be distinguished from cancer. In this respect, the high detection rate of GU by the serum method will not reduce the significance of this test for the screening of gastric cancer.

The average age of patients with GC in this study was higher than those of HV and GU patients, but there was no significant age-related difference in the sucrose level within each group (data not shown), because the inter-group age differences had little effect on the outcome.

Table 4 Sensitivity of sucrose permeability test for each gastric disease

Time (min)	Urine	15	30	45	60	75	90	120	180	240	300
Cut-off points[1]	95	7.4	10.2	11.8	15.2	16.8	16	14	11	8.2	6.5
GU	100	72.7	81.8	100	100	100	100	100	100	100	90.9
EGC	84.6	76.9	76.9	84.6	92.3	92.3	92.3	92.3	92.3	84.6	84.6
AGC	100	100	100	100	100	100	100	100	100	100	100

[1]Cut-off points: Urine, as mg/5 h; serum, as μmol/L

We observed a significant relationship between the surface area of the gastric cancer and sucrose permeability even in cases without ulcer formation. This observation is exceedingly interesting and indicates some process of active absorption of sucrose through unhealthy gastric mucosa. This finding should be tested *in vitro*.

Using the conventional urine collection test for sucrose permeability, Kawabata *et al*.[11] reported an abnormally high sucrose permeability in 11 of 12 patients with advanced gastric cancer, which was significantly higher than that of a healthy control group. However, the diagnostic significance of this test for patients with early gastric cancer has not been elucidated. The results of our study clearly demonstrated that the sucrose test can detect not only AGC but also EGC.

When early gastric cancers are limited to the mucosal layer, they are frequently subjected to endoscopic submucosal dissection (ESD), and can be treated without conventional surgery[16,17]. In this study, 10 of the 11 patients who underwent ESD showed positive results with the sucrose test.

Gastric cancer is the second largest cause of cancer death throughout the world[18]. Contrast-enhanced upper gastrointestinal radiography has been widely used as the screening test for gastric cancer in Japan, but its diagnostic value regarding EGC is considered to be low[19]. The serum pepsinogen method is a new screening test for gastric cancer, but it was reported that the test failed to detect a considerable proportion of patients with advanced gastric cancer[19,20]. In this study, our results clearly demonstrated that the sucrose test on the serum had a higher sensitivity rate for EGC than any other non-invasive test reportedly used for screening purposes. Furthermore, the diagnostic sensitivity of the test for AGC was 100%.

In conclusion, the sucrose test conducted on the serum is a very promising screening test for gastric cancer. Since the serum method can be performed much more easily with an automatic analyzer, it can be used for mass screening of a large number of samples. Confirmatory large-scale prospective studies comparing this method with other methods used in mass screenings are still needed before definite recommendations can be made regarding the significance of the test in screening for gastric cancer, especially EGC.

ACKNOWLEDGMENTS

We thank Shino-Test Corporation for the supply of enzymatic assay reagents.

REFERENCES

1 **Meddings JB,** Sutherland LR, Byles NI, Wallace JL. Sucrose: a novel permeability marker for gastroduodenal disease. *Gastroenterology* 1993; **104:** 1619-1926
2 **Sutherland LR,** Verhoef M, Wallace JL, Van Rosendaal G, Crutcher R, Meddings JB. A simple, non-invasive marker of gastric damage: sucrose permeability. *Lancet* 1994; **343:** 998-1000
3 **Meddings JB,** Kirk D, Olson ME. Noninvasive detection of nonsteroidal anti-inflammatory drug-induced gastropathy in dogs. *Am J Vet Res* 1995; **56:** 977-981
4 **Rabassa AA,** Goodgame R, Sutton FM, Ou CN, Rognerud C, Graham DY. Effects of aspirin and Helicobacter pylori on the gastroduodenal mucosal permeability to sucrose. *Gut* 1996; **39:** 159-163
5 **Smecuol E,** Bai JC, Sugai E, Vazquez H, Niveloni S, Pedreira S, Maurino E, Meddings J. Acute gastrointestinal permeability responses to different non-steroidal anti-inflammatory drugs. *Gut* 2001; **49:** 650-655
6 **Kiziltas S,** Imeryuz N, Gurcan T, Siva A, Saip S, Dumankar A, Kalayci C, Ulusoy NB. Corticosteroid therapy augments gastroduodenal permeability to sucrose. *Am J Gastroenterol* 1998; **93:** 2420-2425
7 **Goodgame RW,** Malaty HM, el-Zimaity HM, Graham DY. Decrease in gastric permeability to sucrose following cure of Helicobacter pylori infection. *Helicobacter* 1997; **2:** 44-47
8 **Vogelsang H,** Oberhuber G, Wyatt J. Lymphocytic gastritis and gastric permeability in patients with celiac disease. *Gastroenterology* 1996; **111:** 73-77
9 **Seimiya M,** Osawa S, Hisae N, Shishido T, Yamaguchi T, Nomura F. A sensitive enzymatic assay for the determination of sucrose in serum and urine. *Clin Chim Acta* 2004; **343:** 195-199
10 **Hanley JA,** McNeil BJ. The meaning and use of the area under a receiver operating characteristic (ROC) curve. *Radiology* 1982; **143:** 29-36
11 **Kawabata H,** Meddings JB, Uchida Y, Matsuda K, Sasahara K, Nishioka M. Sucrose permeability as a means of detecting diseases of the upper digestive tract. *J Gastroenterol Hepatol* 1998; **13:** 1002-1006
12 **Fukuda Y,** Bamba H, Okui M, Tamura K, Tanida N, Satomi M, Shimoyama T, Nishigami T. Helicobacter pylori infection increases mucosal permeability of the stomach and intestine. *Digestion* 2001; 63 (*Suppl*) **1:** 93-96
13 **Gotteland M,** Cruchet S, Verbeke S. Effect of Lactobacillus ingestion on the gastrointestinal mucosal barrier alterations induced by indometacin in humans. *Aliment Pharmacol Ther* 2001; **15:** 11-17
14 **Vinet B,** Panzini B, Boucher M, Massicotte J. Automated enzymatic assay for the determination of sucrose in serum and urine and its use as a marker of gastric damage. *Clin Chem* 1998; **44:** 2369-2371
15 **Birnberg PR,** Brenner ML. A one-step enzymatic assay for sucrose with sucrose phosphorylase. *Anal Biochem* 1984; **142:** 556-561
16 **Noda M,** Kodama T, Atsumi M, Nakajima M, Sawai N, Kashima K, Pignatelli M. Possibilities and limitations of endoscopic resection for early gastric cancer. *Endoscopy* 1997; **29:** 361-365
17 **Ono H,** Kondo H, Gotoda T, Shirao K, Yamaguchi H, Saito D, Hosokawa K, Shimoda T, Yoshida S. Endoscopic mucosal resection for treatment of early gastric cancer. *Gut* 2001; **48:** 225-229
18 **Hohenberger P,** Gretschel S. Gastric cancer. *Lancet* 2003; **362:** 305-315
19 **Miki K,** Morita M, Sasajima M, Hoshina R, Kanda E, Urita Y. Usefulness of gastric cancer screening using the serum pepsinogen test method. *Am J Gastroenterol* 2003; **98:** 735-739
20 **Kitahara F,** Kobayashi K, Sato T, Kojima Y, Araki T, Fujino MA. Accuracy of screening for gastric cancer using serum pepsinogen concentrations. *Gut* 1999; **44:** 693-697

Science Editor Kumar M and Guo SY **Language Editor** Elsevier HK

PO Box 2345, Beijing 100023, China
www.wjgnet.com
wjg@wjgnet.com

ELSEVIER

World J Gastroenterol 2005;11(44):6910-6919
World Journal of Gastroenterology ISSN 1007-9327

Bifunctional chimeric SuperCD suicide gene -YCD: YUPRT fusion is highly effective in a rat hepatoma model

Florian Graepler, Marie-Luise Lemken, Wolfgang A Wybranietz, Ulrike Schmidt, Irina Smirnow, Christine D Groß, Martin Spiegel, Andrea Schenk, Hansjörg Graf, Ulrike A Lauer, Reinhard Vonthein, Michael Gregor, Sorin Armeanu, Michael Bitzer, Ulrich M. Lauer

Florian Graepler, Marie-Luise Lemken, Wolfgang A. Wybranietz, Ulrike Schmidt, Irina Smirnow, Christine D. Groß, Martin Spiegel, Andrea Schenk, Michael Gregor, Sorin Armeanu, Michael Bitzer, Ulrich M. Lauer, Department of Internal Medicine I, University Clinic Tübingen, Tübingen D-72076, Germany
Hansjörg Graf, Ulrike A. Lauer, Section of Experimental Radiology, University Clinic Tübingen, Tübingen D-72076, Germany
Reinhard Vonthein, Department of Medical Biometry, University Clinic Tübingen, Tübingen D-72076, Germany
Supported by grants from German Research Foundation (LA649-20-2), Federal Ministry of Education, Science, Research and Technology (Fö. 01KS9602, Fö. 01KV9532), Interdisciplinary Clinical Research Center (IZKF) Tübingen, and the fortüne-program of the Medical Faculty of Eberhard-Karls-University Tübingen (F.1281127). W.A.W. supported by a scholarship from Pinguin Foundation (Henkel KGaA)
Correspondence to: Dr Florian Graepler, Department of Internal Medicine I, Medical University Clinic Tübingen, Otfried-Müller-Str. 10, Tübingen D-72076,
Germany. florian.graepler@uni-tuebingen.de
Telephone: +49-7071-2980651 Fax: +49-7071-294630
Received: 2005-04-26 Accepted: 2005-05-24

Abstract

AIM: To investigate the effects of catalytically superior gene-directed enzyme prodrug therapy systems on a rat hepatoma model.

METHODS: To increase hepatoma cell chemosensitivity for the prodrug 5-fluorocytosine (5-FC), we generated a chimeric bifunctional SuperCD suicide gene, a fusion of the yeast cytosine deaminase (YCD) and the yeast uracil phosphoribosyltransferase (YUPRT) gene.

RESULTS: *In vitro* stably transduced Morris rat hepatoma cells (MH) expressing the bifunctional SuperCD suicide gene (MH SuperCD) showed a clearly marked enhancement in cell killing when incubated with 5-FC as compared with MH cells stably expressing YCD solely (MH YCD) or the cytosine deaminase gene of bacterial origin (MH BCD), respectively. *In vivo*, MH SuperCD tumors implanted both subcutaneously as well as orthotopically into the livers of syngeneic ACI rats demonstrated significant tumor regressions ($P<0.01$) under both high dose as well as low dose systemic 5-FC application, whereas MH tumors without transgene expression (MH naïve) showed rapid progression. For the first time, an order of *in vivo* suicide gene effectiveness (SuperCD>> YCD>>BCD>>>negative control) was defined as a result of a direct *in vivo* comparison of all three suicide genes.

CONCLUSION: Bifunctional SuperCD suicide gene expression is highly effective in a rat hepatoma model, thereby significantly improving both the therapeutic index and the efficacy of hepatocellular carcinoma killing by fluorocytosine.

Key words: YCD/YUPRT fusion; Cytosine deaminase; GDEPT; Suicide gene therapy; Hepatoma therapy

Graepler F, Lemken ML, Wybranietz WA, Schmidt U, Smirnow I, Groß CD, Spiegel M, Schenk A, Graf H, Lauer UA, Vonthein R, Gregor M, Armeanu S, Bitzer M, Lauer UM. Bifunctional chimeric SuperCD suicide gene -YCD: YUPRT fusion is highly effective in a rat hepatoma model. *World J Gastroenterol* 2005; 11(44): 6910-6919
http://www.wjgnet.com/1007-9327/11/6910.asp

INTRODUCTION

Suicide gene therapy involves the transfer of genes into tumor cells to render them specifically sensitive to prodrugs that are relatively nontoxic to normal tissues. Cytosine deaminase (CD) enzyme is found in many bacteria, yeast and fungi, where it deaminates cytosine to uracil[1]. It also deaminates the relatively nontoxic prodrug 5-fluorocytosine (5-FC) to the highly toxic chemotherapeutic compound 5-fluorouracil (5-FU), used in the treatment of malignant tumors (Figure 1A)[2]. Transduction of the CD gene into tumor cells combined with systemic administration of 5-FC has been shown to have anticancer effects in various animal models[3-7]. Due to their inherent bystander effect, toxic 5-FU metabolites (Figure 1A) also reach non-transduced neighboring cells[8-10]. In contrast to the herpes simplex virus type 1 thymidine kinase/ganciclovir system, this bystander effect does not depend on gap junctional intercellular communication channels[11].

In this work, we focused on the optimization of the CD suicide gene system for hepatoma treatment. We

compared both *in vitro* and *in vivo* therapeutic efficiency of stable expression of: (1) a new bifunctional chimeric SuperCD suicide gene, composed of the yeast cytosine deaminase (YCD) suicide gene directly fused to a 5'-terminally deleted yeast uracil phosphoribosyltransferase (YUPRT) gene[12]; (2) YCD suicide gene; and (3) bacterial cytosine deaminase (BCD) suicide gene in the MH 3924A animal model[13].

MATERIALS AND METHODS

Retroviral vector construction

Genomic DNA of *Saccharomyces cerevisiae*, strain KFY159 (kindly provided by K.-U. Fröhlich, Physiologisch-Chemisches Institut, Eberhard-Karls-University, Tübingen, Germany), was employed to amplify YCD and YUPRT using polymerase chain reaction technique. YCD (*S. cerevisiae* gene FCY-1) was amplified with primers: 5'-G GGGTACCGCCACCATGGTGACAGGGGGAAT GGCAAG-3' (primer #1) and 5'-GGGCGGCCGCCT CACTCACCAATATCTTCAAA CCAATC-3' (primer #2). Alternatively, primer #3 (5'-GGGAATTCTCACC AATATCTTCAAACCAATC-3') was used as a reverse primer in combination with primer #1 to amplify the yeast FCY-1 gene. The latter YCD fragment was subsequently joined to a PCR product amplifying the yeast FUR-1 gene (YUPRT). While omitting the N-terminal domain, the remaining domains of the YUPRT open reading frame, enzymatically sufficient for efficiently transferring the phosphoribosyl residue to the deaminated 5-FC[14], were amplified with primers: 5'-CCGAATTCGGAACCATTTA AGAACGTC-3' (primer #4) and 5'-CCGCGGCCGCCTT AAACACAGTAGTATCTGTCACC-3' (primer #5). Both PCR fragments were purified for subsequent ligation as recently described elsewhere[15]. Subsequently, both YCD and YUPRT PCR amplification products were combined in a three-fragment ligation procedure employing a pUC-based cloning vehicle as a backbone. This intermediate construct was used to remove the *Eco*RI site between the YCD and YUPRT sequences and at the same time to generate the bifunctional SuperCD suicide fusion gene employing a site-directed mutagenesis using the Promega QuikChange method (Promega, Mannheim, Germany). With sense and anti-sense mutagenesis primers (sense sequence: 5'-ATGGTTTCCGAAGCCTCACCAATAT CT-3'), the two enzymatic moieties were joined in-frame, resulting in an Ala residue linking the two yeast ORFs (now with the YUPRT gene starting at the natural S38 codon). Subsequently, the following retroviral constructs were generated (Figure 1B): (1) pLXSN-BCD contains the *E. coli* cytosine deaminase (BCD) suicide gene under the control of the retroviral 5´LTR in basic retroviral vector pLXSN[16] (kindly provided by R.M. Blaese, NIH, Bethesda, MD, USA; originally denominated as pCD2)[17]; (2) pLXSN-YCD harboring the YCD suicide gene was generated by the insertion of the YCD PCR amplification product into basic vector pLXSN-GreeN (derivative of vector pLXSN, in which we exchanged the neo^r gene by a bifunctional EGFP/neo^r fusion gene); (3) pLXSN-SuperCD harboring the bifunctional SuperCD suicide fusion gene was generated by insertion of the YCD/YUPRT in-frame fusion fragment into basic vector pLXSN-GreeN.

Cell culture

Morris hepatoma (MH 3924A) cells were purchased from the German Cancer Research Center (DKFZ) Tumor Collection, Heidelberg, Germany, and maintained in DMEM supplemented with 50 mL/L fetal calf serum (FCS) in a humidified incubator containing 50 mL/L CO_2 at 37 °C.

Generation of stable BCD, YCD and SuperCD expressing Morris hepatoma 3924A cell lines

For the generation of suicide gene transducing retroviral particles, 5×10^5 PE501 ecotropic packaging cells were seeded on 60-mm diameter petri dishes. After 24 h, using lipofectAMINE reagent (Invitrogen), cells were transiently transfected with 3 μg of each retroviral vector DNA. Forty-eight hours later, the supernatant was employed for transduction of 3×10^5 naïve MH cells. Following G418 selection (600 μg/mL), resistant clones were analyzed for EGFP marker gene expression by fluorescence microscopy, followed by functional characterization of suicide gene expression in the sulforhodamin B (SRB) cytotoxicity assay. Cell clones exhibiting the highest cytotoxic effect were selected and named as MH BCD, MH YCD, and MH SuperCD.

Western blot analysis

Cells were lysed in SDS sample buffer and proteins were separated on 100 g/L SDS-PAGE and transferred to PVDF membranes[18]. Polyclonal rabbit antiserum directed against YCD (a generous gift from Transgene SA, Strasbourg, France), a polyclonal rabbit anti-BCD antibody (a generous gift from C. Richards, Glaxo-Wellcome, RTP, NC, USA)[19] and goat anti-rabbit IgG-horseradish peroxidase conjugates (BioRad, München, Germany) were used. Detection of reactive bands was facilitated using horseradish peroxidase-linked secondary conjugate and ECL detection reagents (Amersham Pharmacia, Freiburg, Germany).

SRB cytotoxicity assay

MH (naïve) as well as MH BCD, MH YCD, MH SuperCD cells were seeded in 24-well plates (1×10^4 cells/well). The next day 5-FC containing medium was added (a generous gift from Roche, Basel, Switzerland) and the cells were incubated for 4 d in order to allow untreated cells to reach confluence. Growth inhibition was evaluated by the SRB cytotoxicity assay[20] using a microtiter plate reader (Dynatech MR7000, Denkendorf, Germany) at 550 nm.

In vivo experiments

All animal experiments were performed in concordance with the laws of the German Government concerning the conduction of animal experimentation. Surgical and imaging procedures were performed under intraperitoneally applied anesthesia with ketamine hydrochloride (Ketanest,

Parke-Davis, Berlin, Germany; 100 mg/kg body weight) and xylazine hydrochloride (Rompun, Bayer, Leverkusen, Germany; 10 mg/kg body weight).

The subcutaneous MH naïve and MH SuperCD tumors were established by injecting 1×10^7 cells (in 70 μL PBS) at the dorsum of 6-wk-old male syngeneic ACI rats (Harlan Winkelmann, Borchen, Germany). Eleven days later the rats were randomized into two groups (3 rats/group), and were treated twice daily with ip injections of 5-FC (283 mg/kg body weight) or saline (0.9% NaCl) for 7 d. Tumor sizes were measured with calipers. Tumor volumes were calculated in cubic centimeter using the formula recommended by Carlsson *et al*.[21]: tumor volume (mm^3)=largest diameter (mm)×[smallest diameter (mm)]^2/2.

In order to monitor 5-FC serum levels by HPLC quantification, blood was taken via tail vein puncture on d 5 of the 5-FC application period. On d 8 of the treatment period, the animals were killed, and tumors were explanted and measured for tumor weight and volume. Tumor samples were analyzed for (1) the presence of SuperCD DNA and (2) the endurance of the SuperCD suicide gene functional activity. For PCR analysis, tumor sample DNA was extracted using DNeasy Tissue Kit (Qiagen, Hilden, Germany). MH SuperCD DNA was amplified using primers 5'-CGACCCCGCCTCGATCCTCC-3' (primer #6) and 5'-CTGCTGGGGAGCCTGGGGAC-3' (primer #7). PCR products were separated by electrophoresis on a 10 g/L agarose gel. For the functional testing of continuous suicide gene presence following the *in vivo* growth period of MH SuperCD tumors, tumor tissues were minced, placed into six-well plates and cultivated in DMEM medium containing 50 mL/L FCS, supplemented with 1% penicillin-streptomycin. Three days later, stably transduced MH SuperCD cells were selected by continuous addition of G418 (600 μg/mL). Two weeks later, the cells were analyzed for functional SuperCD gene activity employing the SRB cytotoxicity assay.

Orthotopic tumor implantation within the liver was performed as described elsewhere[13]. Twenty-one days later, tumor sizes were measured by magnetic resonance imaging (MRI). Subsequently, the rats were randomized into two groups (six rats/group) and were treated twice daily with ip injections of 5-FC (283 mg/kg body weight) or saline. On d 31, tumor sizes were again measured by MRI. Animals were killed, livers explanted and analyzed macroscopically for the presence of tumor tissue.

MRI measurements

Monitoring of tumor growth was performed by sequential MRI studies, using a 1.5 Tesla MR tomograph (VISION, Siemens, Erlangen, Germany). A turbospinecho sequence was applied to acquire T2 weighed images using the following parameters: 3.5 s repetition time, 96 ms echo time, field of view of 200 mm×100 mm. Fifteen slices with an in-plane resolution of 0.75 mm×0.75 mm, a slice thickness of 2 mm and a gap of 0.3 mm between the slices were acquired with six signal averages. Maximum areas of the tumors were determined by the identification of the tumor slice exhibiting largest diameters (main diameter *a* and minor diameter *b*), followed by the calculation of the respective area ($a/2\times b/2\times\pi$).

Statisticial analysis

Viability was explained by cell line, 5-FU concentration, and their interaction in analyses of variance. Square roots of counts were used as Box-Cox analyses and normal quantile-plots of residuals suggested so. Means and 95% confidence intervals were transformed back and divided by the fitted value of MH naïve cells. The *in vivo* experiment with four cell lines was analyzed by the analysis of covariance of logarithms of tumor sizes (considered censored at 30 mm² when below) with variable time factors, cell line and individual and different slopes for the cell lines. The hypotheses were: all four mean growth rates are equal, and mean growth rates of YCD and SuperCD cells are equal. As intra-individual comparison of cell lines was possible, all six possible combinations were implanted as in a balanced incomplete block plan. Sample size was planned to guarantee multiple power of more than 0.8 at effect size 30% and coefficient of variation 30%, while the multiple significance level was 0.05.

RESULTS

Through its toxic metabolites, 5-FU kills cells by binding to the thymidylate synthase, thereby causing a blockade of DNA synthesis as well as by directly interfering with the cellular RNA metabolism (Figure 1A). Because 5-FU is able to diffuse passively through cell membranes, it not only affects transduced cells, but also neighboring cells (so-called bystander cells). However, the conversion of 5-FU to 5-FUMP constitutes a rate-limiting step at least in some tumor cells[22]. In the context of suicide gene transfer, it is hypothesized that an additional encoding of the UPRT gene not only enhances tumor cell sensitivity to 5-FU, but also augments the sensitivity of tumor cells to 5-FC, when such cells are enabled to simultaneously express a CD gene (Figure 1A). Since also low tumor transduction efficiencies are recognized as a major limitation in liver tumor suicide gene therapy[23,24], 5-FC/CD/UPRT-based suicide gene systems could not only help to improve the effectiveness of 5-FC toxification, but also enhance the effectiveness of bystander killing, thereby helping to compensate for currently still low efficiencies of direct liver tumor suicide gene transfer. In this work, we therefore investigated whether hepatoma cell chemosensitivity for 5-FC could be enhanced by simultaneously addressing the two major steps of 5-FC metabolism. For this purpose, we first generated a so-called SuperCD fusion gene which combines the (1) enzymatic function of yeast CD (YCD) with (2) YUPRT-mediated phosphorylation of 5-FU to 5-FUMP (Figures 1A and B).

Construction of SuperCD/YCD/BCD suicide gene expressing retroviral vectors, and analysis of stably transduced Morris rat hepatoma cells

We employed genomic DNA of *S. cerevisiae* to amplify both yeast CD as well as yeast UPRT genes by PCR[22].

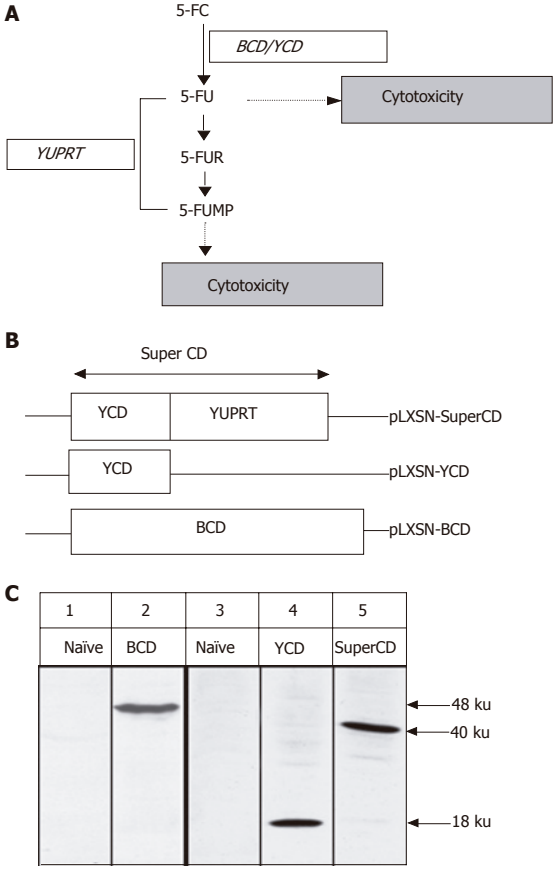

Figure 1 Mode of action of SuperCD (YCD::YUPRT) fusion. Panel **A**: Schematic representation of biological pathways resulting in cytotoxicity following cytosine deaminase/uracil phosphoribosyltransferase (UPRT)-mediated toxification of the prodrug 5-FC. 5-FC: 5-fluorocytosine; 5-FU: 5-fluorouracil; 5-FUR: 5-fluorouridine; 5-FUMP: 5-fluorouridine 5'-monophosphate; CD: cytosine deaminase; YUPRT: yeast uracil phosphoribosyltransferase. Panel **B**: Schematic representation of retroviral vectors used, in which suicide gene expression was placed under the retroviral 5' LTR. Panel **C**: Western blot detection of suicide gene expression in retrovirally generated stable SuperCD/YCD/BCD-expressing Morris hepatoma (MH) cell lines employing polyclonal rabbit antisera directed against BCD (lanes 1 and 2) and YCD (for detection of both SuperCD and YCD; lanes 3-5). Lane 1: MH naïve cells (negative control); lane 2: MH BCD cells, exhibiting a 48-ku band specific for BCD; lane 3: MH naïve cells (negative control); lane 4: MH YCD cells, exhibiting a 18-ku band specific for YCD; lane 5: MH SuperCD cells, exhibiting a 40-ku band specific for the YCD::YUPRT fusion, i.e. SuperCD. Numbers on the right hand side indicate the sizes of the expected proteins.

Subsequently, both genes were linked in-frame using a site-directed mutagenesis scheme, resulting in generation of a bifunctional suicide fusion gene which was named as SuperCD. Next, the SuperCD DNA sequence was inserted into basic retroviral vector pLXSN[16], resulting in generation of pLXSN-SuperCD (Figure 1B, upper construct), in which transgene expression is driven by the retroviral 5´LTR. For comparison of cytotoxic effectiveness, we likewise generated retroviral vectors pLXSN-YCD (Figure 1B, middle construct; solely encoding the YCD cDNA) and pLXSN-BCD (Figure 1B, lower construct; solely encoding the BCD cDNA)[25]. Employing all three constructs, PE501 ecotropic packaging cells were transiently transfected. Subsequently, respective

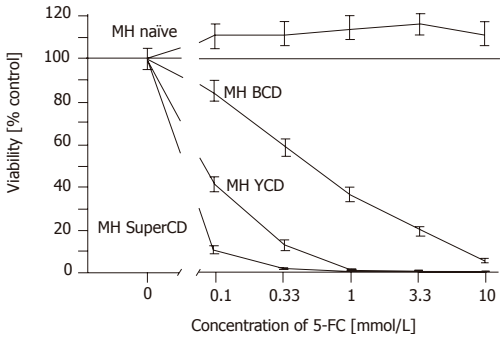

Figure 2 SRB cytotoxicity assay with stable BCD, YCD, SuperCD expressing Morris hepatoma (MH) cell lines generated by retroviral transduction. Untransduced MH3924A cells (MH naïve) and stably transduced Morris hepatoma cell lines (MH BCD, MH YCD, MH SuperCD) were seeded on 24-well plates. After 4 d of 5-FC treatment, the growth inhibition was determined by SRB staining and measured at 550 nm. All values were referred to that of the untransduced control cells without the addition of 5-FC and are given as percentage of surviving cells (control: 100%). All experiments were carried out at least in quadruplicate. Viability values plotted represent fitted medians and 95%CI.

supernatants containing recombinant retroviruses were used for transduction of MH 3924A cells. G418 selection gave rise to neo^r resistant clones (MH SuperCD, MH YCD, and MH BCD), which stably expressed suicide genes SuperCD, YCD, or BCD at comparable levels as detected by Western blotting (Figure 1C). Next, a SRB cytotoxicity assay was performed to compare the suicidal efficiencies of the different transgenes in the context of stable cell lines. As shown in Figure 2, a clear order of efficacy of the different suicide transgenes was found: in the SuperCD expressing cell line (MH SuperCD) even at a 5-FC concentration as low as 0.1 mmol/L, a very low cell survival of only 8% was observed. In contrast, sole expression of YCD (MH YCD) was much less efficient, resulting in a nearly 5-fold higher cell survival (38% at 0.1 mmol/L 5-FC). Finally, sole expression of BCD had only a minor cytotoxic effect (>80% cell survival at 0.1 mmol/L 5-FC). Thereby, convincing *in vitro* evidence was provided that the YUPRT component implemented within the SuperCD fusion gene is highly functional in the context of hepatoma cells. This corresponds to observations made by others with cell lines derived from non-liver tumor tissues (e.g. human colon cancer cells, human pancreas tumor cells, human breast cancer cells, human glioblastoma cells)[22,26]. The efficacy of much lower 5-FC doses has to be regarded as an important finding when transferring the 5-FC/SuperCD system to the preclinical/clinical situation: in the mammalian organism, 5-FC is also metabolized by the bacteria of the gut flora. An increased intestinal production of 5-FU can lead to dramatic unwanted side effects which are feared greatly in the context of 5-FU chemotherapeutic regimes[27].

Subcutaneously implanted MH SuperCD tumors demonstrate a complete tumor regression under systemic 5-FC application

A first *in vivo* testing of the SuperCD-enhanced suicide

gene effect was performed in six animals who received two sc tumor cell injections each: (1) MH SuperCD cells into the right dorsum; and (2) as a control in the same animals MH naïve cells into the left dorsum. On d 11, when tumors had reached a measurable size, rats were randomized into two groups and treated for one week with twice daily ip injections of 5-FC or saline (control group). 5-FC serum levels of treated animals as determined by HPLC ranged from 1 to 2.6 μg/mL, whereas control animals receiving saline displayed background levels only (data not shown). During the treatment period, tumor volume increased constantly in the saline-treated negative control group, irrespectively of the tumor type implanted. In contrast, in all the three 5-FC treated animals, the MH SuperCD tumors disappeared completely, whereas the MH naïve tumors grown on the opposite dorsum further increased in volume until d 18, when the animals were killed (Table1). At post mortem examination of 5-FC-treated animals, no residual tumor tissue was found on the right dorsum in which the MH SuperCD tumors originally had grown, whereas large MH SuperCD tumors, weighing between 1.8 and 2.7 g, were found in the saline-treated animals. As expected, all animals displayed large MH naïve tumors on the opposite site, independent of 5-FC or saline treatment.

Molecular and functional analysis of subcutaneously grown control tumors explanted on d 18

In vivo selective pressure for transgene-negative tumor cells and silencing of transgenes by methylation events are well-known phenomena[28]. We, therefore, extracted DNA from subcutaneously grown xenograft tumors for PCR analysis. In all three SuperCD tumor samples obtained from saline-treated animals, a 1 143-bp SuperCD-specific PCR amplification product was detected (Figure 3A, lanes #1-#3). Thus, *in vivo* passage of SuperCD-expressing tumor cells does not cause a relevant selective pressure against the presence of the SuperCD transgene. From the same subcutaneously grown tumors explanted at d 18, we further performed a functional analysis on recultured tumor cells (saline-treated MH SuperCD/MH naïve tumors) by applying the SRB cytotoxicity assay (Figure 3B). A 4-d treatment with 5-FC had no toxic effect on *in vivo* passaged MH naïve cells (control). However, all three MH SuperCD cell cultures (#1-#3) obtained after *in vivo* passage demonstrated a profound 5-FC-induced cytotoxic effect (Figure 3B, lower curves). The cytotoxic effect following *in vivo* passage was found to be comparable with MH tumor cells that had not undergone an *in vivo* passage (compared with Figure 2). These results demonstrated that, irrespective of an 18-d *in vivo* passage, MH SuperCD tumor cells continuously exerted a strong suicide gene effect at low 5-FC prodrug levels, which is of importance for further preclinical and clinical suicide gene therapy approaches.

Orthotopically implanted MH SuperCD tumors demonstrate a profound tumor regression under systemic 5-FC application

Based on the overwhelming efficacy of 5-FC treatment

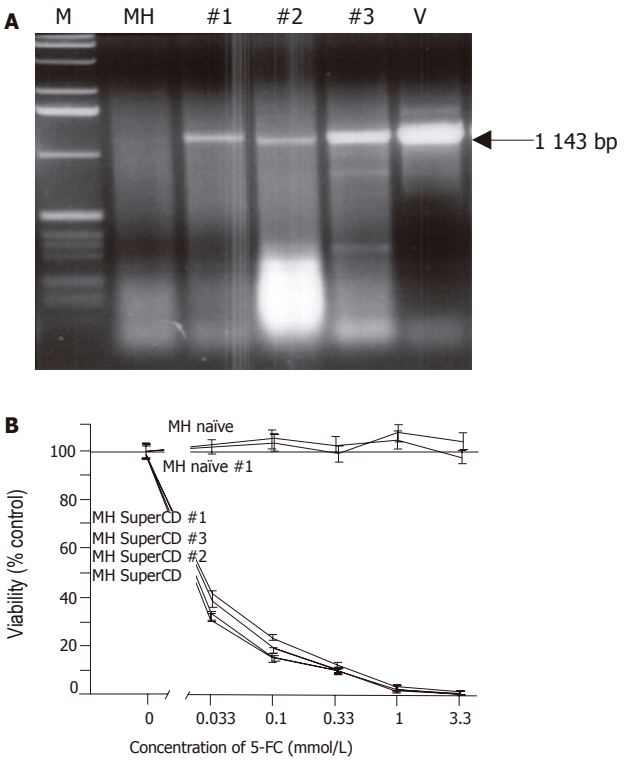

Figure 3 Molecular and functional analysis of subcutaneously grown control tumors explanted on d 18 (saline-treated MH SuperCD/MH naïve tumors).
A: Agarose gel electrophoresis of SuperCD DNA-specific PCR products. Lane M: marker DNA ladder; lane MH: MH parental cell line (no transgene; negative control; PCR performed with 1 μg of DNA); lanes 1-3: PCR amplifications performed on MH SuperCD tumor tissues of animals 1, 2, 3 (PCR performed with 1–3 μg of DNA); lane V: vector control lane (PCR performed with 1 pg of pLXSN-SuperCD). Arrow: indicates 1 143-bp SuperCD-specific amplification product. **B:** SRB cytotoxicity assay with recultured tumor cells explanted after 18 d of subcutaneous growth. As in Figure 2, cytotoxicity was measured after 5-FC treatment for 4 d *in vitro*. MH naïve: negative control with MH parental cell line (no transgene; no animal passage); MH naïve, #1: MH naïve tumor explanted from a saline-treated animal (control); MH SuperCD, cell line: MH SuperCD parental cell line (control; no animal passage); MH SuperCD 1, 2, 3, tumor passage: MH SuperCD tumors explanted from saline-treated animals 1, 2, 3. All values were referred to that of the untransduced control cells and are given as percentage of surviving cells (control: 100%). All experiments were carried out in quadruplicate. Viability values plotted represent fitted medians and 95%CI.

observed in subcutaneously grown MH SuperCD tumors, we next treated orthotopic liver tumors in the same rat hepatoma model in a larger number of animals, thereby investigating the statistical relevance of SuperCD suicide protein expression. As caliper measurement of small intrahepatic tumors is impossible, this study was based on non-invasive MRI imaging. Twenty-one days after the implantation of solitary MH SuperCD tumors into the livers of recipient animals, a first MRI was performed. Maximum tumor areas were analyzed. Rats with tumor areas ranging from 20 to 156 mm^2 (representative day 21 MRI images shown in Figures 4B and C, respectively, column 1 "untreated") were then randomized into two groups with six rats in each, and treated twice daily with ip injections of 5-FC or saline for 10 d.

MRI-based measurement of tumor sizes at the end of

Table 1 Effect of 5-FC treatment on subcutaneous MH tumor growth

		Suicide gene	
		None (control)	SuperCD
Treatment	5-FC	1.4 g	n.d.
		3.2 g	n.d.
		1.8 g	n.d.
	Saline (control)	2.5 g	1.8 g
		2.9 g	1.9 g
		3.7 g	2.7 g

Six animals received two sc tumor cell injections (1×10^7 cells in 70 μL PBS/animal). On d 11, tumor-bearing rats were randomized into two groups and treatment started with twice daily ip injections of 5-FC (283 mg/kg body weight) or saline (control). At the end of 5-FC treatment (d 18), animals were killed, tumors were harvested and weighed. Complete regression of tumors was observed only in the 5-FC-treated SuperCD tumors (n.d.: no detectable tumors).

the treatment (d 31) revealed a persistent orthotopic tumor growth for saline-treated control animals (Figure 4A, solid lines). In contrast, all six animals treated systemically for 10 d with 5-FC exhibited a clear decline of tumor sizes, either complete regressions or dramatic reductions (Figure 4A, broken lines). Ranking area differences revealed a significant difference between the untreated and the treated groups (*U*-test, $P = 0.0051$). Thus, bifunctional SuperCD suicide gene expression was found to be highly effective against a rat hepatoma model under both subcutaneous and orthotopic implantation conditions.

Low dose 5-FC application found to be sufficient to achieve complete tumor regressions of orthotopically implanted MH SuperCD cells

Anticipating an enhanced SuperCD suicide gene effect, we already had started to administer twice daily with 5-FC dosage of 283 mg/kg body weight, which is only half of the dosage of about 500 mg/kg body weight used by others[6,29-33]. Since this prodrug dosing regimen was found to be highly efficient for the eradication of both subcutaneous (Table 1) and orthotopic (Figure 4) MH SuperCD hepatomas, we aimed next at further decreasing the 5-FC dose by reducing the application frequency. Thereby, side effects due to 5-FU metabolites resulting from unwanted routes of "collateral" gut toxification could be even further reduced.

We tested this hypothesis on three animals with small MH SuperCD liver tumors (#7, #8, #9) having received saline only as control animals during the first treatment period. The other animals had to be euthanized due to their tumor burden. In these animals, low dose treatment was started on d 31 with only twice weekly ip injections of 5-FC (283 mg/kg body weight) for 28 d. When MRI was again performed at d 59, all MH SuperCD tumors had completely disappeared (Figure 5, right column). In none of these three animals, any solid tumor tissue was found at autopsy. Instead, only small yellowish fatty "scars" were visible. Thereby, bifunctional SuperCD suicide gene expression was found to be highly effective in a rat hepatoma model under both subcutaneous and orthotopic growth conditions, even when a strongly reduced 5-FC dosing regime was applied.

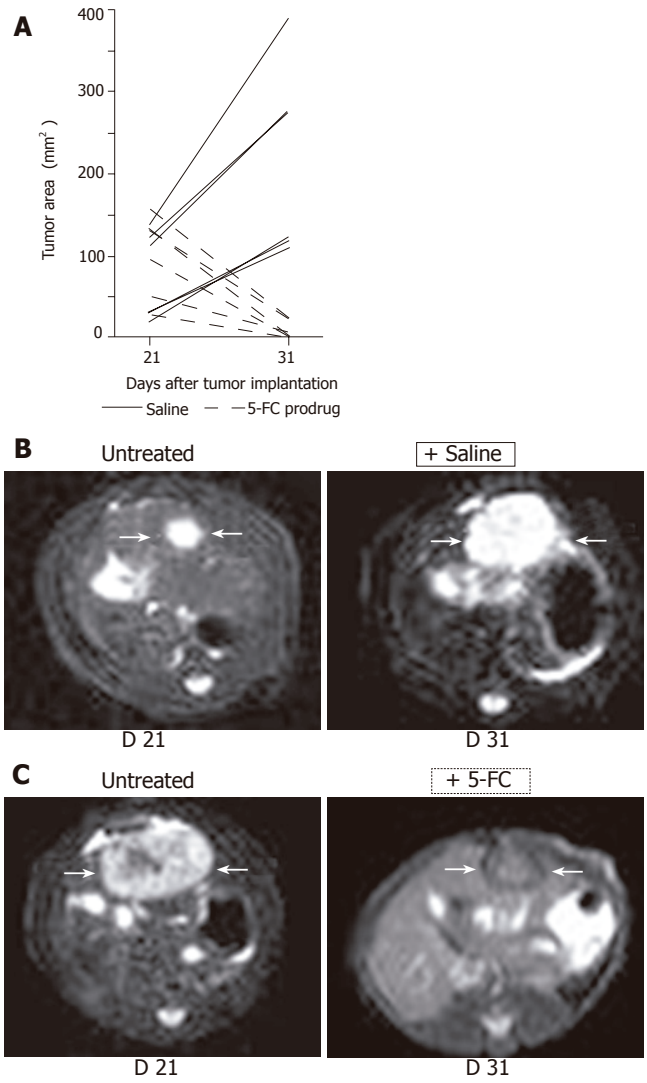

Figure 4 Non-invasive MRI detection of tumor growth of orthotopically implanted MH SuperCD hepatomas (saline *vs* 5-FC prodrug treatment). Animals with MRI detectable liver tumors in T2 weighed images were randomized into two groups (6 rats/group) and treated twice daily with ip injections of saline or 5-FC (283 mg/kg body weight) over a 10-d period. Panel A: Maximum tumor areas (mm^2) at d 21 and d 31; solid lines: tumor growth of control animals (saline-treated); broken lines: tumor regression of serum animals (5-FC-treated). Panel B: Representative MRI tumor images of the saline-treated control animal exhibiting the smallest tumor area at d 21 (left); and a dramatic tumor growth was observed at d 31 (right). Panel C: Representative MRI tumor images of the serum animal (treated with 5-FC) exhibiting the largest tumor area at d 21 (left); and a dramatic tumor regression was measured at d 31 (right).

Determination of in vivo suicide gene effectiveness by direct in vivo comparison of suicide genes SuperCD vs YCD vs BCD

Until now, no study encompassing a direct *in vivo* comparison of different suicide genes (SuperCD *vs* YCD *vs* BCD) has been performed. Therefore, 1×10^7 cells of the four cell-lines (1) MH naïve (negative control), (2) MH BCD, (3) MH YCD, and (iv) MH SuperCD were injected subcutaneously into ACI rats. In this course, each animal

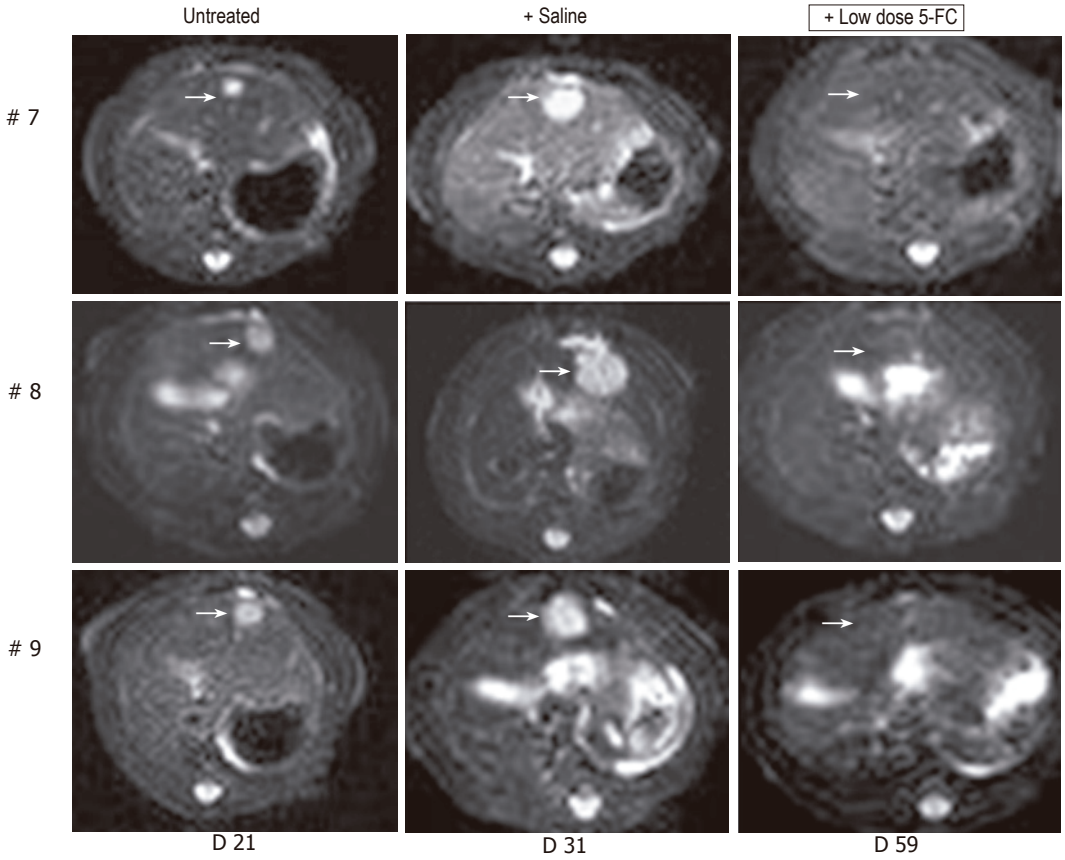

Figure 5 MRI detection of tumor growth of orthotopically implanted MH SuperCD hepatomas treated under a low-dose 5-FC regimen. Animals #7, #8, #9 (column 1: tumor size at d 21), which first had been treated with saline only for over a 7-d period and thereafter, uniformly exhibiting a substantial tumor growth (column 2: tumor size at d 31), were then treated by a low-dose 5-FC regimen [twice weekly ip injections of 5-FC (283 mg/kg body weight)] over a 28-d period until d 59. Analysis of subsequent MRI sections did not reveal any MH SuperCD tumors (column 3, d 59: +low dose 5-FC); T2 weighed images are depicted; arrows in column 3 point out to places of former tumor localizations before the onset of 5-FC treatment.

received two injections with two different cell-lines, one inoculated at the left dorsum, and the other one at the right dorsum. Based on a balanced incomplete block plan, the six possible pairs of cell lines were implanted into six groups, each comprising eight animals. Tumor volumes were determined by caliper measurement. At d 15 after hepatoma cell inoculation, prodrug therapy with twice weekly ip injections of 283 mg 5-FC/kg body weight (low dose regime) was started. Interestingly, 8 out of 18 MH SuperCD tumors on d 28 and 11 out of 18 MH SuperCD-tumors on d 31 had shrunken to an immeasurable size (Figure 6A, right panel). A subsequent analysis of covariance of log tumor volumes revealed a significant reduction in median tumor volumes under our low dose 5-FC application scheme only for the MH SuperCD tumors. The reduction in median tumor volume was almost complete (95%CI for the reduction between d 14 and 31 from 98.7% to 99.6%) (Figure 6B). The maximum likelihood ratio χ^2 test of the global hypothesis was significant $\chi^2 = 264$; 3 df; $P = 6\times10^{-57}$). Thus, for the first time *in vivo* evidence was provided demonstrating that the SuperCD *in vivo* suicide gene effect might be superior to the one of YCD ($P < 10^{-10}$), which itself was superior to BCD (Figures 6A and B).

DISCUSSION

Although the study described here demonstrated that the expression of YCD and YUPRT as a fusion protein with 5-FC administration exerted a striking antitumor effect on solid tumors like hepatomas, further improvements are needed for clinical applications. Current limitations of *in vivo* liver tumor transduction efficiencies could be further compensated with the help of intercellular cargo proteins (e.g. VP22, our own work[18,34], and Refs. [35,36]). At the moment, we are evaluating the properties of VP22-SuperCD/SuperCD-VP22 fusion proteins to further potentiate suicide gene therapy efficiencies in our rat hepatoma model, thereby improving the intratumoral distribution of enzymatically enhanced suicide genes. Other promising approaches rely on the employment of strong hepatoma-specific promoters which are suitable to achieve high levels of hepatoma-specific SuperCD expression *in vivo* (e.g. the cell growth-related midkine promoter)[37]. Most importantly, gene transfer systems have to be identified, which are suitable to provide a significant increase of the accessibility of liver tumor cells to systemically applied gene transfer vectors. In a recent study, herpes thymidine kinase suicide gene transducing liposomes, based on the hemagglutinating

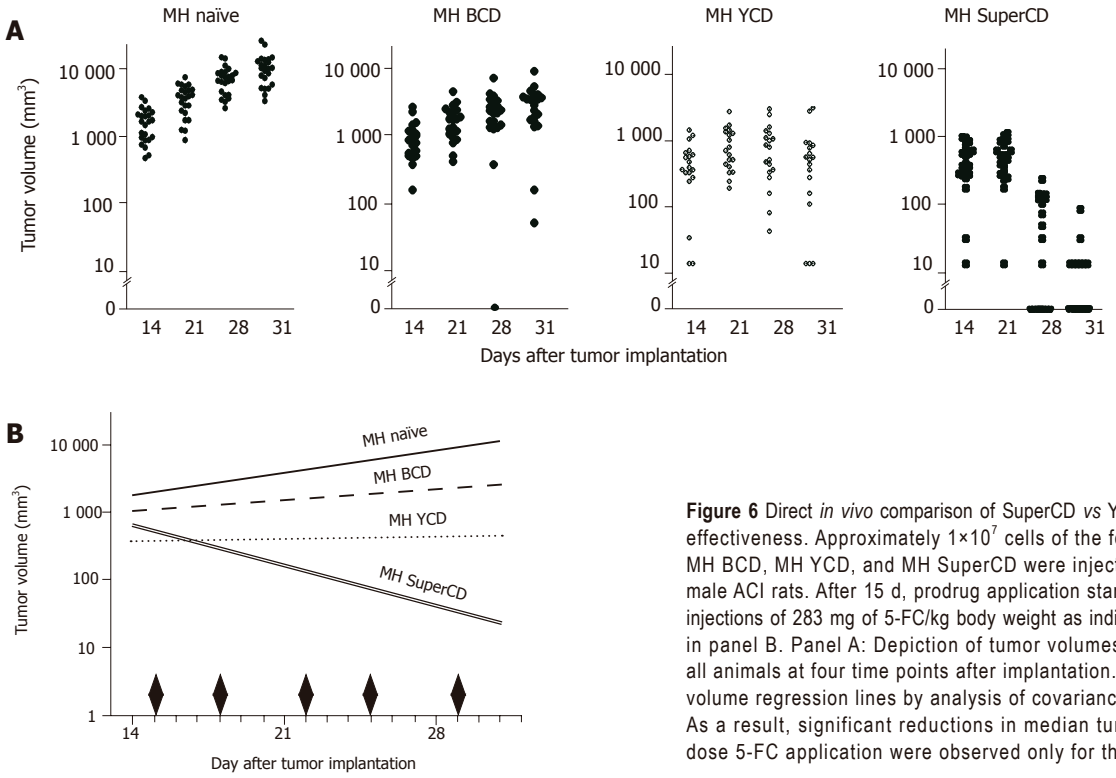

Figure 6 Direct *in vivo* comparison of SuperCD *vs* YCD *vs* BCD suicide gene effectiveness. Approximately 1×10^7 cells of the four cell-lines MH naïve, MH BCD, MH YCD, and MH SuperCD were injected subcutaneously into male ACI rats. After 15 d, prodrug application started with twice weekly ip injections of 283 mg of 5-FC/kg body weight as indicated by black diamonds in panel B. Panel A: Depiction of tumor volumes of all four cell lines in all animals at four time points after implantation. Panel B: Median tumor volume regression lines by analysis of covariance of log tumor volumes. As a result, significant reductions in median tumor volumes under low dose 5-FC application were observed only for the MH SuperCD tumors.

virus of Japan, were injected directly into the portal vein of severe combined immunodeficiency mice, and reported to be as an efficient tool for the transduction of multilocalized HUH7 human hepatocellular carcinomas in this animal model[38]. Thus, transduction properties of hemagglutinating virus of Japan (also defined as Sendai virus) seem to favor transduction of liver tumors. Concluding from this, also recombinant Sendai virus vectors[39,40] encoding optimized suicide genes might be suitable to overcome the liver tumor transduction barrier[41,42]. HIV-derived lentiviral vectors have also been successfully used for suicide gene therapy in hepatocellular carcinoma[43]. In addition, newly developed replication-competent vectors/oncolytic vectors[42,44-47] could be used to cope with the liver tumor transduction barrier.

Concerning our current knowledge on severe gene therapeutic side effects employing state-of-the-art retroviral[48], adenoviral[49], or adeno-associated virus vectors[50], a reduction of vector dosages might become possible with the SuperCD suicide gene. This would constitute an important additional safety factor for further clinical gene therapy applications. Subsequent *in vivo* studies will compare application of the therapeutic SuperCD suicide gene by virtue of direct (injection), systemic (iv) or regional (ia) gene transfer and treatment with 5-FC.

In summary, a combination of synergistic strategies as described above may allow a further enhancement of the suicide gene effect in the near future. Thus, further refinements may help to make suicide gene therapy a feasible treatment modality for solid malignant tumors in human beings.

REFERENCES

1 **Danielsen S,** Kilstrup M, Barilla K, Jochimsen B, Neuhard J. Characterization of the Escherichia coli codBA operon encoding cytosine permease and cytosine deaminase. *Mol Microbiol* 1992; **6:** 1335-1344
2 **Austin EA,** Huber BE. A first step in the development of gene therapy for colorectal carcinoma: cloning, sequencing, and expression of Escherichia coli cytosine deaminase. *Mol Pharmacol* 1993; **43:** 380-387
3 **Kanai F,** Lan KH, Shiratori Y, Tanaka T, Ohashi M, Okudaira T, Yoshida Y, Wakimoto H, Hamada H, Nakabayashi H, Tamaoki T, Omata M. *In vivo* gene therapy for alpha-fetoprotein-producing hepatocellular carcinoma by adenovirus-mediated transfer of cytosine deaminase gene. *Cancer Res* 1997; **57:** 461-465
4 **Ohwada A,** Hirschowitz EA, Crystal RG. Regional delivery of an adenovirus vector containing the Escherichia coli cytosine deaminase gene to provide local activation of 5-fluorocytosine to suppress the growth of colon carcinoma metastatic to liver. *Hum Gene Ther* 1996; **7:** 1567-1576
5 **Richards CA,** Austin EA, Huber BE. Transcriptional regulatory sequences of carcinoembryonic antigen: identification and use with cytosine deaminase for tumor-specific gene therapy. *Hum Gene Ther* 1995; **6:** 881-893
6 **Adachi Y,** Tamiya T, Ichikawa T, Terada K, Ono Y, Matsumoto K, Furuta T, Hamada H, Ohmoto T. Experimental gene therapy for brain tumors using adenovirus-mediated transfer of cytosine deaminase gene and uracil phosphoribosyltransfer ase gene with 5-fluorocytosine. *Hum Gene Ther* 2000; **11:** 77-89
7 **Miller CR,** Williams CR, Buchsbaum DJ, Gillespie GY. Intratumoral 5-fluorouracil produced by cytosine deaminase/5-fluorocytosine gene therapy is effective for experimental human glioblastomas. *Cancer Res* 2002; **62:** 773-780
8 **Uckert W,** Kammertons T, Haack K, Qin Z, Gebert J, Schendel DJ, Blankenstein T. Double suicide gene (cytosine deaminase and herpes simplex virus thymidine kinase) but not single

gene transfer allows reliable elimination of tumor cells *in vivo*. *Hum Gene Ther* 1998; **9:** 855-865

9 **Hirschowitz EA,** Ohwada A, Pascal WR, Russi TJ, Crystal RG. *In vivo* adenovirus-mediated gene transfer of the Escherichia coli cytosine deaminase gene to human colon carcinoma-derived tumors induces chemosensitivity to 5-fluorocytosine. *Hum Gene Ther* 1995; **6:** 1055-1063

10 **Huber BE,** Austin EA, Richards CA, Davis ST, Good SS. Metabolism of 5-fluorocytosine to 5-fluorouracil in human colorectal tumor cells transduced with the cytosine deaminase gene: significant antitumor effects when only a small percentage of tumor cells express cytosine deaminase. *Proc Natl Acad Sci USA* 1994; **91:** 8302-8306

11 **Trinh QT,** Austin EA, Murray DM, Knick VC, Huber BE. Enzyme/prodrug gene therapy: comparison of cytosine deaminase/5-fluorocytosine versus thymidine kinase/ganciclovir enzyme/prodrug systems in a human colorectal carcinoma cell line. *Cancer Res* 1995; **55:** 4808-4812

12 **Tiraby M,** Cazaux C, Baron M, Drocourt D, Reynes JP, Tiraby G. Concomitant expression of E. coli cytosine deaminase and uracil phosphoribosyltransferase improves the cytotoxicity of 5-fluorocytosine. *FEMS Microbiol Lett* 1998; **167:** 41-49

13 **Trubenbach J,** Graepler F, Pereira PL, Ruck P, Lauer U, Gregor M, Claussen CD, Huppert PE. Growth characteristics and imaging properties of the morris hepatoma 3924A in ACI rats: a suitable model for transarterial chemoembolization. *Cardiovasc Intervent Radiol* 2000; **23:** 211-217

14 **Kern L,** de Montigny J, Jund R, Lacroute F. The FUR1 gene of Saccharomyces cerevisiae: cloning, structure and expression of wild-type and mutant alleles. *Gene* 1990; **88:** 149-157

15 **Wybranietz WA,** Lauer U. Distinct combination of purification methods dramatically improves cohesive-end subcloning of PCR products. *Biotechniques* 1998; **24:** 578-580

16 **Miller AD,** Rosman GJ. Improved retroviral vectors for gene transfer and expression. *Biotechniques* 1989; **7:** 980-982, 984-986, 989-990

17 **Mullen CA,** Kilstrup M, Blaese RM. Transfer of the bacterial gene for cytosine deaminase to mammalian cells confers lethal sensitivity to 5-fluorocytosine: a negative selection system. *Proc Natl Acad Sci USA* 1992; **89:** 33-37

18 **Wybranietz WA,** Prinz F, Spiegel M, Schenk A, Bitzer M, Gregor M, Lauer UM. Quantification of VP22-GFP spread by direct fluorescence in 15 commonly used cell lines. *J Gene Med* 1999; **1:** 265-274

19 **Rogulski KR,** Kim JH, Kim SH, Freytag SO. Glioma cells transduced with an Escherichia coli CD/HSV-1 TK fusion gene exhibit enhanced metabolic suicide and radiosensitivity. *Hum Gene Ther* 1997; **8:** 73-85

20 **Skehan P,** Storeng R, Scudiero D, Monks A, McMahon J, Vistica D, Warren JT, Bokesch H, Kenney S, Boyd MR. New colorimetric cytotoxicity assay for anticancer-drug screening. *J Natl Cancer Inst* 1990; **82:** 1107-1112

21 **Carlsson G,** Gullberg B, Hafstrom L. Estimation of liver tumor volume using different formulas - an experimental study in rats. *J Cancer Res Clin Oncol* 1983; **105:** 20-23

22 **Erbs P,** Regulier E, Kintz J, Leroy P, Poitevin Y, Exinger F, Jund R, Mehtali M. *In vivo* cancer gene therapy by adenovirus-mediated transfer of a bifunctional yeast cytosine deaminase/uracil phosphoribosyltransferase fusion gene. *Cancer Res* 2000; **60:** 3813-3822

23 **Maron DJ,** Tada H, Moscioni AD, Tazelaar J, Fraker DL, Wilson JM, Spitz FR. Intra-arterial delivery of a recombinant adenovirus does not increase gene transfer to tumor cells in a rat model of metastatic colorectal carcinoma. *Mol Ther* 2001; 4: 29-35

24 **Yoon SK,** Armentano D, Wands JR, Mohr L. Adenovirus-mediated gene transfer to orthotopic hepatocellular carcinomas in athymic nude mice. *Cancer Gene Ther* 2001; **8:** 573-579

25 **Mullen CA,** Kilstrup M, Blaese RM. Transfer of the bacterial gene for cytosine deaminase to mammalian cells confers lethal sensitivity to 5-fluorocytosine: a negative selection system. *Proc Natl Acad Sci United States* 1992; **89:** 33-37

26 **Kievit E,** Nyati MK, Ng E, Stegman LD, Parsels J, Ross BD, Rehemtulla A, Lawrence TS. Yeast cytosine deaminase improves radiosensitization and bystander effect by 5-fluorocytosine of human colorectal cancer xenografts. *Cancer Res* 2000; **60:** 6649-6655

27 **Diasio RB,** Lakings DE, Bennett JE. Evidence for conversion of 5-fluorocytosine to 5-fluorouracil in humans: possible factor in 5-fluorocytosine clinical toxicity. *Antimicrob Agents Chemother* 1978; **14:** 903-908

28 **Roncarolo MG,** Levings MK, Mangia P, Bordignon C, Marktel S, Bonini C, Traversar C. Characterization and modulation of the undesirable T cell-mediated responses to transgenes. *Mol Ther* 2002: S399

29 **Kanyama H,** Tomita N, Yamano T, Aihara T, Miyoshi Y, Ohue M, Sekimoto M, Sakita I, Tamaki Y, Kaneda Y, Senter PD, Monden M. Usefulness of repeated direct intratumoral gene transfer using hemagglutinating virus of Japan-liposome method for cytosine deaminase suicide gene therapy. *Cancer Res* 2001; **61:** 14-18

30 **Kievit E,** Bershad E, Ng E, Sethna P, Dev I, Lawrence TS, Rehemtulla A. Superiority of yeast over bacterial cytosine deaminase for enzyme/prodrug gene therapy in colon cancer xenografts. *Cancer Res* 1999; **59:** 1417-1421

31 **Chung-Faye GA,** Chen MJ, Green NK, Burton A, Anderson D, Mautner V, Searle PF, Kerr DJ. *In vivo* gene therapy for colon cancer using adenovirus-mediated, transfer of the fusion gene cytosine deaminase and uracil phosphoribosyltransferase. *Gene Ther* 2001; **8:** 1547-1554

32 **Hamstra DA,** Rice DJ, Fahmy S, Ross BD, Rehemtulla A. Enzyme/prodrug therapy for head and neck cancer using a catalytically superior cytosine deaminase. *Hum Gene Ther* 1999; **10:** 1993-2003

33 **Block A,** Freund CT, Chen SH, Nguyen KP, Finegold M, Windler E, Woo SL. Gene therapy of metastatic colon carcinoma: regression of multiple hepatic metastases by adenoviral expression of bacterial cytosine deaminase. *Cancer Gene Ther* 2000; **7:** 438-445

34 **Wybranietz WA,** Gross CD, Phelan A, O'Hare P, Spiegel M, Graepler F, Bitzer M, Stahler P, Gregor M, Lauer UM. Enhanced suicide gene effect by adenoviral transduction of a VP22-cytosine deaminase (CD) fusion gene. *Gene Ther* 2001; **8:** 1654-1664

35 **Liu CS,** Kong B, Xia HH, Ellem KA, Wei MQ. VP22 enhanced intercellular trafficking of HSV thymidine kinase reduced the level of ganciclovir needed to cause suicide cell death. *J Gene Med* 2001; **3:** 145-152

36 **Ford KG,** Souberbielle BE, Darling D, Farzaneh F. Protein transduction: an alternative to genetic intervention? *Gene Ther* 2001; **8:** 1-4

37 **Tomizawa M,** Yu L, Wada A, Tamaoki T, Kadomatsu K, Muramatsu T, Matsubara S, Watanabe K, Ebara M, Saisho H, Sakiyama S, Tagawa M. A promoter region of the midkine gene that is frequently expressed in human hepatocellular carcinoma can activate a suicide gene as effectively as the alpha-fetoprotein promoter. *Br J Cancer* 2003; **89:** 1086-1090

38 **Hirano T,** Kaneko S, Kaneda Y, Saito I, Tamaoki T, Furuyama J, Tamaoki T, Kobayashi K, Ueki T, Fujimoto J. HVJ-liposome-mediated transfection of HSVtk gene driven by AFP promoter inhibits hepatic tumor growth of hepatocellular carcinoma in SCID mice. *Gene Ther* 2001; **8:** 80-83

39 **Yonemitsu Y,** Kitson C, Ferrari S, Farley R, Griesenbach U, Judd D, Steel R, Scheid P, Zhu J, Jeffery PK, Kato A, Hasan MK, Nagai Y, Masaki I, Fukumura M, Hasegawa M, Geddes DM, Alton EW. Efficient gene transfer to airway epithelium using recombinant Sendai virus. *Nat Biotechnol* 2000; **18:** 970-973

40 **Sedlmeier R,** Neubert WJ. The replicative complex of

paramyxoviruses: structure and function. *Adv Virus Res* 1998; **50:** 101-139

41 **Bilbao R,** Bustos M, Alzuguren P, Pajares MJ, Drozdzik M, Qian C, Prieto J. A blood-tumor barrier limits gene transfer to experimental liver cancer: the effect of vasoactive compounds. *Gene Ther* 2000; **7:** 1824-1832

42 **Shayakhmetov DM,** Li ZY, Ni S, Lieber A. Targeting of adenovirus vectors to tumor cells does not enable efficient transduction of breast cancer metastases. *Cancer Res* 2002; **62:** 1063-1068

43 **Gerolami R,** Uch R, Faivre J, Garcia S, Hardwigsen J, Cardoso J, Mathieu S, Bagnis C, Brechot C, Mannoni P. Herpes simplex virus thymidine kinase-mediated suicide gene therapy for hepatocellular carcinoma using HIV-1-derived lentiviral vectors. *J Hepatol* 2004; ***40:*** 291-297

44 **Ohashi M,** Kanai F, Tateishi K, Taniguchi H, Marignani PA, Yoshida Y, Shiratori Y, Hamada H, Omata M. Target gene therapy for alpha-fetoprotein-producing hepatocellular carcinoma by E1B55k-attenuated adenovirus. *Biochem Biophys Res Commun* 2001; **282:** 529-535

45 **Rogulski KR,** Wing MS, Paielli DL, Gilbert JD, Kim JH, Freytag SO. Double suicide gene therapy augments the antitumor activity of a replication-competent lytic adenovirus through enhanced cytotoxicity and radiosensitization. *Hum Gene Ther* 2000; **11:** 67-76

46 **Bitzer M,** Lauer UM. [Oncolytic viruses for genetic therapy of gastrointestinal tumors] *Z Gastroenterol* 2003; **41:** 667-674

47 **Kirn D,** Martuza RL, Zwiebel J. Replication-selective virotherapy for cancer: Biological principles, risk management and future directions. *Nat Med* 2001; **7:** 781-787

48 **Hacein-Bey-Abina S,** Le Deist F, Carlier F, Bouneaud C, Hue C, De Villartay JP, Thrasher AJ, Wulffraat N, Sorensen R, Dupuis-Girod S, Fischer A, Davies EG, Kuis W, Leiva L, Cavazzana-Calvo M. Sustained correction of X-linked severe combined immunodeficiency by ex vivo gene therapy. *N Engl J Med* 2002; **346:** 1185-1193

49 **Somia N,** Verma IM. Gene therapy: trials and tribulations. *Nat Rev Genet* 2000; **1:** 91-99

50 **Arruda VR,** Fields PA, Milner R, Wainwright L, De Miguel MP, Donovan PJ, Herzog RW, Nichols TC, Biegel JA, Razavi M, Dake M, Huff D, Flake AW, Couto L, Kay MA, High KA. Lack of germline transmission of vector sequences following systemic administration of recombinant AAV-2 vector in males. *Mol Ther* 2001; **4:** 586-592

Science Editor Kumar M and Guo SY **Language Editor** Elsevier HK

PO Box 2345, Beijing 100023, China
www.wjgnet.com
wjg@wjgnet.com

ELSEVIER

World J Gastroenterol 2005;11(44):6920-6925
World Journal of Gastroenterology ISSN 1007-9327

Role of blood AFP mRNA and tumor grade in the preoperative prognostic evaluation of patients with hepatocellular carcinoma

Umberto Cillo, Alessandro Vitale, Filippo Navaglia, Daniela Basso, Umberto Montin, Marco Bassanello, Francesco D'Amico, Francesco Antonio Ciarleglio, Alberto Brolese, Giacomo Zanus, Vito De Pascale, Mario Plebani, Davide Francesco D'Amico

Umberto Cillo, Alessandro Vitale, Umberto Montin, Marco Bassanello, Francesco D'Amico, Francesco Antonio Ciarleglio, Alberto Brolese, Giacomo Zanus, Davide Francesco D'Amico, Clinica Chirurgica I, Dipartimento di Scienze Chirurgiche e Gastroenterologiche, Università degli Studi di Padova, Italy
Filippo Navaglia, Daniela Basso, Mario Plebani, Dipartimento di Medicina di Laboratorio, Università degli Studi di Padova, Italy
Vito De Pascale, Dipartimento Assistenziale di Chirurgia Generale ed Emergenze Chirurgiche, II Università degli Studi di Napoli, Italy
Correspondence to: Alessandro Vitale, MD, Clinica Chirurgica I - Dipartimento di Scienze Chirurgiche e Gastroenterologiche - Università degli Studi di Padova - Via Giustiniani 2, Policlinico III piano, 35128 Padova, Italy. alessandro.vitale@unipd.it
Telephone: +39-49-8212210 Fax: +39-49-656145
Received: 2005-02-17 Accepted: 2005-04-26

Abstract

AIM: To explore the potential prognostic role of preoperative tumor grade and blood AFP mRNA in a cohort of patients with hepatocellular carcinoma (HCC) eligible for radical therapies according to a well-defined treatment algorithm not including nodule size and number as absolute selection criteria.

METHODS: Fifty patients with a diagnosis of HCC were prospectively enrolled in the study. Inclusion criteria were: (1) histological assessment of tumor grade by means of percutaneous biopsies; (2) determination of AFP mRNA status in the blood; (3) patient's eligibility for radical therapies.

RESULTS: At preoperative evaluation, 54% of the study group had a well-differentiated HCC, 42% had AFP mRNA in the blood, 40% had a tumor larger than 5 cm and 56% had more than one nodule. Surgery (resection or liver transplantation) was performed in 29 patients, while 21 had percutaneous ablation procedures. After a median follow-up of 28 mo, 12-, 24-, and 36-mo survival rates were 78%, 58%, and 51%, respectively. Surgical therapy, performance status and three tumor-related variables (AFP mRNA, HCC grade and gross vascular invasion) resulted as significant survival predictors at univariate analysis. Nodule size and number did not perform as significant prognosticators. Multivariate study selected only surgical therapy and a biologically early HCC profile (AFP mRNA negative and well-differentiated tumor without gross vascular invasion) as independent survival variables.

CONCLUSION: The preoperative determination of tumor grade and blood AFP mRNA status may potentially refine the prognostic evaluation of HCC patients and improve the selection process for radical therapies.

Key words: Hepatocellular carcinoma; Prognosis; Treatment policy; Biomarker; Tumor biology

Cillo U, Vitale A, Navaglia F, Basso D, Montin U, Bassanello M, D'Amico F, Ciarleglio FA, Brolese A, Zanus G, De Pascale V, Plebani M, D'Amico DF. Role of blood AFP mRNA and tumor grade in the preoperative prognostic evaluation of patients with hepatocellular carcinoma. *World J Gastroenterol* 2005; 11(44): 6920-6925
http://www.wjgnet.com/1007-9327/11/6920.asp

INTRODUCTION

Liver transplantation (LT), hepatic resection and percutaneous treatments[1-3] are commonly considered as potential radical therapies for patients with hepatocellular carcinoma (HCC). Macroscopic tumor characteristics detected by imaging studies (nodule size and number) undoubtedly identify a subgroup of HCC patients at an early stage of hepatic disease (single nodule <5 cm, <3 nodules, and <3 cm) able to achieve long-term survival figures when radically treated[4,5]. Large pathologic retrospective studies[6-9], however, have shown that these macro-morphological features are indirect markers of specific tumor histological characteristics such as grade of differentiation and microscopic vascular invasion which have therefore the potential to refine the HCC prognostic assessment[10-12]. On the other hand, many molecular biological factors have been studied and related to the HCC biological aggressiveness[13]. However, preoperatively detectable biomarkers (histological and/or hematic) have not yet been introduced in the

routine HCC prognostic evaluation. In our experience, the preoperative determination of the HCC grade by means of percutaneous biopsy performed as a valid tool in the selection of unresectable HCC patients for transplantation[14]. Moreover, we retrospectively showed that some patients with morphologically advanced but well-differentiated HCC may benefit of potentially radical therapies[15]. Among the proposed HCC molecular markers, alpha-fetoprotein messenger RNA (AFP mRNA), detected in the blood by reverse-transcription polymerase chain reaction (RT-PCR), has been the most diffusely studied in last years[16-19]. Our preliminary experience with this marker showed its significance and promising correlation with HCC invasiveness parameters[16]. However, the prognostic utility of AFP mRNA when detected before the treatment remains controversial[20-22]. In this prospective study, a group of HCC patients were selected for radical therapies according to a precise treatment schedule. In addition to conventional HCC parameters, their preoperative study also included the determination of tumor grade and AFP mRNA status in the blood. The enrolled patients were prospectively followed in order to identify the main preoperative predictors of survival.

MATERIALS AND METHODS

Patient enrolment

Between April 2001 and October 2002, 50 patients with a diagnosis of HCC were prospectively enrolled in the study. Patients were eligible for inclusion if they met the following criteria: (1) HCC diagnosis histologically confirmed by the examination of liver specimens obtained by percutaneous biopsies. Pathological grading was contextually assessed in all the patients according to Edmonson's classification; (2) patient's informed consent to provide blood samples for AFP mRNA determination; (3) patient's eligibility for radical therapies according to a published schedule[14,23].

Hepatic resection was considered for HCC patients with preserved liver function (Child-Pugh A-B) and a technically resectable liver tumor without extra hepatic metastasis. If resection was not feasible, patients were considered for LT. The following exclusion criteria for LT were established as previously reported[14]: general contraindications to transplant (age, severe extrahepatic diseases, recent malignancies, and compliance), extra hepatic spread or gross vascular invasion (preoperatively evident or suspected), poorly-differentiated HCC (G3) at pre-OLT percutaneous biopsy. Size and number of nodules were not considered as absolute selection criteria. Patients not fulfilling the criteria for any surgical procedure were assessed for other loco-regional treatments such as percutaneous radiofrequency (RF) or ethanol injection (PEI), and transarterial chemoembolization (TACE).

After discharge, the patients were followed up regularly according to the main treatment received. To detect tumor recurrence after surgery, patients received clinical and laboratory assessment every month, and US and CT every 3rd and 6th mo, respectively. When HCC recurrence was noted, patients were further treated with the most appropriate procedure according to our treatment schedule. After PEI, RF or TACE, dynamic CT examinations were performed to determine therapy efficacy and, when residual staining was noted, these procedures were repeated and the outcome was examined. None of the enrolled patients were lost during follow-up or died within 30 d after first observation or treatment. Therefore, all the 50 patients initially entering the study were available for the survival analysis.

Detection of AFP mRNA in nucleated cells

The AFP mRNA status in the blood was determined in each enrolled patient within 3 mo from treatment application. In brief, total RNA was extracted from 7 mL of peripheral blood and converted to complementary DNA. A nested polymerase chain reaction (PCR) protocol was performed as previously reported[16]. Positive results were evidenced as a 282-bp band in agarose gel stained with ethidium-bromide. As a positive control, cDNA obtained from human hepatocyte was used in each run. Negative controls for each step were also always included.

Statistical analysis

All variables were described by statistical characteristics: categorical data were described by frequency and percentage, whereas continuous data by median (range). Comparison between groups was done by using the χ^2 test or the Fisher's exact test for qualitative variables and the logistic regression for quantitative variables. Follow-up length and survival are expressed as median (range). Recruitment of follow-up data was closed on December 31, 2004. Twenty-four preoperative variables were assessed in the univariate survival analysis: age, sex, performance status, presence of cirrhosis, etiology of cirrhosis, clinical evidence of portal hypertension (presence of esophageal varices, splenomegaly with a platelet count <100 000/mm^3, or ascites), Child-Pugh's classification[24], bilirubin, albumin, prothrombin activity, alkaline phosphatase, gamma-glutamyl transpeptidase, creatinin, aspartate, and alanine aminotransferase, AFP, AFP mRNA blood-status, tumor morphology at preoperative imaging study (TNM, bilobarity, number and size of nodules, gross vascular invasion), differentiation degree at preoperative liver biopsy, and type of treatment. For continuous variables, the cut-off level was their median value. Univariate survival analysis was performed including each variable in a Cox regression model and calculating its related likelihood-ratio of χ^2 and *P* value. Survival curves were calculated using the Kaplan-Meier method and compared by means of the log-rank test. All variables significantly influencing survival in the univariate analysis were analyzed together in a Cox's proportional hazard regression model (multivariate analysis) with the aim of studying the independent contribution of each variable in explaining survivorship. The results of the Cox regression were expressed using both the risk ratios with its related confidence interval and the likelihood ratio of χ^2 with its related *P* value. Analyses were performed using the SAS Institute statistical package

(JMP). Differences were considered significant at $P<0.05$.

RESULTS

The main characteristics of the study group are shown in Table 1. At presentation, only 20% of patients had a compromised general condition due to cancer-related symptoms (PST ⩾1), 63% had a Child B-C cirrhosis and 62% had a clinically relevant portal hypertension. As for tumor characteristics, 52% of patients had a T3-T4 HCC; the tumor was larger than 5 cm in 20 patients (40%), while 28 (56%) had more than one nodule; macroscopic vascular invasion was detected in 12 patients (24%) and 27 patients (54%) had a well-differentiated HCC. AFP mRNA was found in the blood of 21 HCC patients (42%). As previously reported[16], the presence of AFP mRNA in blood was significantly related to cholestatic indices, gross vascular invasion, nodule size, and G2-G3 tumors (Table 1). Surgery was performed in 29 patients (58%), including 22 liver resections and 7 OLT, while 21 patients (42%) had percutaneous ablation procedures eventually associated with TACE.

Survival analysis

As at December 31st 2004, the median follow-up for the whole HCC group (50 patients) was 28 months (range 1-45 mo). Overall mortality was 48% (24 cases) and 12-, 24-, and 36-mo survival rates were 78%, 58%, and 51%, respectively (Figure 1A). Five out of the twenty-four variables had predictive prognostic value for survival in the univariate analysis (Table 1): PST, AFP mRNA, gross vascular invasion, histological grade, and surgical therapy.

A first multivariate study including these five variables selected only surgical treatment as independent survival predictor (Table 2, Figure 1B). Taking into account the strict correlation between AFP mRNA, vascular invasion and HCC grade in the study group[16], in a further analysis we combined these three tumor-related variables in a single parameter defined early HCC (AFP mRNA negative and well-differentiated tumor without gross vascular invasion). This second multivariate study selected tumor early biological status as the most important prognostic factor (Table 2 and Figure 1C).

DISCUSSION

Prognostic prediction and therapeutic decision for HCC patients are currently based in most centers on macroscopic tumor characteristics detected by imaging studies (nodule size and number). In the last decade, an empirical rule

Table 1 Preoperative characteristics of the 50 enrolled HCC patients and univariate survival analysis

Variables	Study group (50 patients)	Likelihood-ratio χ^2 (*P* value)
Median age (yr)	62 (22-88)	2.23 (NS)
Sex (M/F)	41/9	1.35 (NS)
Performance status (PST) ⩾1	10	4.06 (.0438)
Cirrhosis	43	1.12 (NS)
Etiology: HCV/HBV/alcohol/other	29/6/5/10	
viral	35	1.7 (NS)
Portal hypertension	31	0.17 (NS)
Child-Pugh score (A/B/C)	16/24/3	2.31 (NS)
Analytical data		
Bilirubin (μmol/L)	20 (7-233)	0.02 (NS)
Serum albumin (g/L)	35 (21-46)	0.49 (NS)
Prothrombin activity (%)	77 (39-109)	0.02 (NS)
[1]Alkaline phosphatase (U/L)	113 (42-395)	1.33 (NS)
[1]GGT (U/L)	64 (21-864)	3.25 (NS)
Creatinin (μmol/L)	83 (63-166)	1.47 (NS)
AST (U/L)	95 (20-492)	0.48 (NS)
ALT (U/L)	78 (12-469)	0.19 (NS)
Median AFP level (ng/L)	17 (4-1 400)	0.69 (NS)
Positive AFP mRNA	21	5.96 (0.0146)
TNM T3/T4	26	2.8 (NS)
Bilobar	7	2.38 (NS)
Number of nodules (1/2 or 3/>3)	22/23/5	
Multinodular	28	0.99 (NS)
[1]Median nodule size (cm)	4 (1-18)	2.76 (NS)
Nodule >5 cm	20	1.62 (NS)
[1]Gross vascular invasion	12	4.42 (0.0354)
[1,2]Histological grade (I/II/III)	27/16/7	
II-III	23	4.10 (0.0490)
Type of treatment		
Resection/LT/loco-regional therapies	22/7/21	
Surgery	29	16.40 (0.0001)

HCV: hepatitis C virus; HBV: hepatitis B virus; AFP: alpha-fetoprotein; TNM: tumor node metastasis classification; LT: liver transplantation.
[1]Variables significantly related to the presence of AFP mRNA in blood. [2]I: well; II: moderately; and III: poorly differentiated HCC.

Table 2 Multivariate survival analysis in the 50 enrolled HCC patients. Only variables significantly influencing survival at univariate analysis were introduced in the Cox proportional hazard model

Variables	RR (95%CI)	Likelihood-ratio χ^2	*P*
Assessing single variables			
Surgery	2.72 (1.59-5.03)	14.07	0.0002
AFP mRNA	2.00 (0.90-4.82)	2.83	NS
Moderately or poorly differentiated grade	1.20 (0.55-2.41)	0.23	NS
Gross vascular invasion	0.86 (0.48-1.59)	0.24	NS
Performance status >1	1.21(0.64-2.46)	0.31	NS
Combining tumor related variables			
Surgery	5.84 (2.23-17.32)	13.23	0.0003
[1]Early HCC	5.84 (2.23-17.32)	13.60	0.0002
Performance status >1	1.18 (0.41-3.09)	0.11	NS

RR: risk ratio; CI: confidence interval.

[1]AFP mRNA negative and well-differentiated HCC without gross vascular invasion.

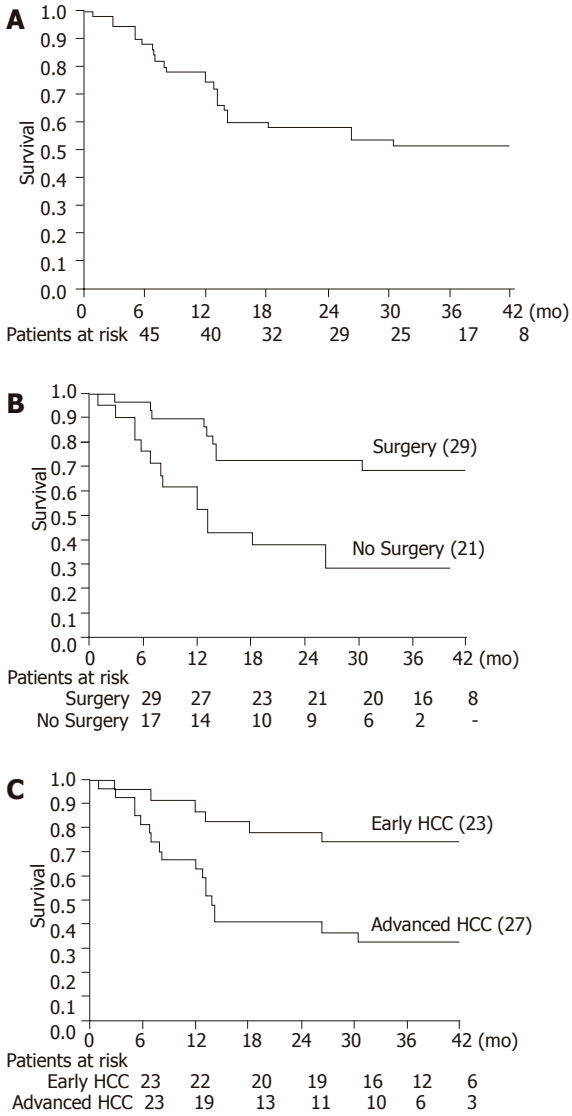

Figure 1 Subject **A:** Overall probability of survival of the 50 enrolled HCC patients; **B:** Overall probability of survival of the 50 enrolled HCC patients, dividing them in the two main treatment groups (surgery *vs* no surgery). Log rank test = 0.0015; **C:** Overall probability of survival of the 50 enrolled HCC patients, dividing them according to tumor biological status (early *vs* advanced HCC). Log rank test = 0.0042. Early HCC = AFP mRNA negative and well-differentiated HCC without gross vascular invasion.

of single nodule smaller than 5 cm in diameter and of multiple nodules (2 or 3) smaller than 3 cm has been used to define early HCC, reflecting the excellent outcomes achieved after LT[25,26]. Although the use of these strict selection criteria for the treatment has undoubtedly improved survival rates of a subgroup of HCC patients in the previous years[4,5], such a diffuse therapeutic policy has dramatically reduced the use of potentially radical therapies for those HCC patients not meeting the same criteria. In virtue of such a tight selection philosophy, on one hand it has obtained an important reallocation of resources but on the other it has faced the concrete risk that a considerable proportion of HCC patients have been unfairly excluded from radical treatment[6-8]. In this context, the identification of new reliable prognostic factors may play a crucial role in improving the treatment criteria process of HCC patients[27].

This study was designed to identify prospectively the main preoperative HCC predictors of survival with particular reference to the prognostic utility of preoperative AFP mRNA and tumor grade. In order to avoid the bias associated to predefined selection criteria, less restrictive enrollment criteria for radical treatment in terms of both tumor status and liver function were deliberately used. If on one hand such a selection policy may account for the relatively unsatisfactory outcome of the 50 enrolled patients (Figure 1A), on the other it allowed us to develop an effective analysis of predictive factors for survival. Moreover, in spite of the relatively low number of enrolled patients, our study has the advantage of a monocentric, prospective analysis in which a well-defined treatment algorithm was used[14,23].

According to other studies[28,29], tumor biological parameters appeared as the most relevant prognostic factors selecting those patients achieving the best survival outcome when radically treated (Tables 1 and 2). In the present study, macro-morphological parameters failed in defining early HCC, since they showed a marginal impact on survival in our group of patients (Table 1). On the contrary, other tumor characteristics such as AFP mRNA in the blood, histological grade and vascular involvement served as more adequate markers of HCC biological

aggressiveness.

In this context, the independent prognostic power of surgical treatment (Table 2 and Figure 1B) may not be misinterpreted as a therapeutic disadvantage in using other loco-regional options. It is not the aim of the present study, in fact, to make a comparison between treatment options since such an analysis may be correctly performed only in the experimental setting of a randomized clinical trial.

This study, in fact, showed that some HCC biological features such as grading, AFP mRNA status in the blood and gross vascular invasion influence patient prognosis independently from the type of adopted therapy (Table 2). A prognostic stratification of the study group in two main tumor stages according to significantly predictive variables was obtained (Figure 1C). A favorable biological picture of HCC (AFP mRNA negative, well-differentiated and without gross vascular invasion) appeared hierarchically as the most relevant factor in determining patient prognosis. Conversely, liver function parameters, such as Child-Pugh classification, bilirubin and portal pressure, did not reach a significant impact on survival in our small study group suggesting a secondary prognostic role when compared to tumor features. In this view, our study does not claim to provide a new definition of early HCC but it wants to simply and strongly underline the urgent need to readdress the focus of the HCC patients selection process for radical treatment more on tumor biological aggressiveness rather than on size and number of tumor nodules.

Concerning the single HCC parameters selected from survival analysis, tumor grade is a well recognized prognostic factor for HCC patients as showed by many large retrospective pathological analyses[1,6,11]. There are, however, no studies evaluating the prognostic role of preoperative determined HCC grading in a prospective setting.

Previous experiences exploring the prognostic role of preoperative AFP mRNA showed controversial results[30-32]. It is likely that this biologic HCC parameter alone does not reach an adequate prognostic power in highly selected populations undergoing radical therapies. In this view, the present study suggests that in the context of a larger population basis, AFP mRNA may be probably useful in identifying morphologically advanced HCC suitable for radical therapies. The introduction of appropriate molecular methods to quantify AFP mRNA in the blood in perspective will further improve the prognostic power of this promising biomarker.

In conclusion, this study showed that the preoperative determination of tumor grade and blood AFP mRNA may potentially refine the prognostic evaluation of HCC patients. On a purely preliminary basis, these two parameters may probably help the treatment decision process for that group of HCC patients suitable for radical therapies consequently improving the currently used restrictive selection criteria.

REFERENCES

1 **Jonas S,** Bechstein WO, Steinmuller T, Herrmann M, Radke C, Berg T, Settmacher U, Neuhaus P. Vascular invasion and histopathologic grading determine outcome after liver transplantation for hepatocellular carcinoma in cirrhosis. *Hepatology* 2001; **33:** 1080-1086

2 **Ikeda K,** Saitoh S, Tsubota A, Arase Y, Chayama K, Kumada H, Watanabe G, Tsurumaru M. Risk factors for tumor recurrence and prognosis after curative resection of hepatocellular carcinoma. *Cancer* 1993; **71:** 19-25

3 **Koda M,** Murawaki Y, Mitsuda A, Ohyama K, Horie Y, Suou T, Kawasaki H, Ikawa S. Predictive factors for intrahepatic recurrence after percutaneous ethanol injection therapy for small hepatocellular carcinoma. *Cancer* 2000; **88:** 529-537

4 **Bruix J,** Llovet JM. Prognostic prediction and treatment strategy in hepatocellular carcinoma. *Hepatology* 2002; **35:** 519-524

5 **Befeler AS,** Di Bisceglie AM. Hepatocellular carcinoma: diagnosis and treatment. *Gastroenterology* 2002; **122:** 1609-1619

6 **Klintmalm GB.** Liver transplantation for hepatocellular carcinoma: a registry report of the impact of tumor characteristics on outcome. *Ann Surg* 1998; **228:** 479-490

7 **Poon RT,** Fan ST, Ng IO, Wong J. Prognosis after hepatic resection for stage IVA hepatocellular carcinoma: a need for reclassification. *Ann Surg* 2003; **237:** 376-383

8 **Regimbeau JM,** Farges O, Shen BY, Sauvanet A, Belghiti J. Is surgery for large hepatocellular carcinoma justified? *J Hepatol* 1999; **31:** 1062-1068

9 **Vauthey JN,** Lauwers GY, Esnaola NF, Do KA, Belghiti J, Mirza N, Curley SA, Ellis LM, Regimbeau JM, Rashid A, Cleary KR, Nagorney DM. Simplified staging for hepatocellular carcinoma. *J Clin Oncol* 2002; **20:** 1527-1536

10 **Ercolani G,** Grazi GL, Ravaioli M, Del Gaudio M, Gardini A, Cescon M, Varotti G, Cetta F, Cavallari A. Liver resection for hepatocellular carcinoma on cirrhosis: univariate and multivariate analysis of risk factors for intrahepatic recurrence. *Ann Surg* 2003; **237:** 536-543

11 **Esnaola NF,** Lauwers GY, Mirza NQ, Nagorney DM, Doherty D, Ikai I, Yamaoka Y, Regimbeau JM, Belghiti J, Curley SA, Ellis LM, Vauthey JN. Predictors of microvascular invasion in patients with hepatocellular carcinoma who are candidates for orthotopic liver transplantation. *J Gastrointest Surg* 2002; **6:** 224-232; discussion 232

12 **Yao FY,** Ferrell L, Bass NM, Watson JJ, Bacchetti P, Venook A, Ascher NL, Roberts JP. Liver transplantation for hepatocellular carcinoma: expansion of the tumor size limits does not adversely impact survival. *Hepatology* 2001; **33:** 1394-1403

13 **Qin LX,** Tang ZY. The prognostic molecular markers in hepatocellular carcinoma. *World J Gastroenterol* 2002; **8:** 385-392

14 **Cillo U,** Vitale A, Bassanello M, Boccagni P, Brolese A, Zanus G, Burra P, Fagiuoli S, Farinati F, Rugge M, D'Amico DF. Liver transplantation for the treatment of moderately or well-differentiated hepatocellular carcinoma. *Ann Surg* 2004; **239:** 150-159

15 **Bassanello M,** Cillo U, Vitale A, Lumachi F, Ciarleglio FA, Boccagni P, Brolese A, Zanus G, D'Amico F, Senzolo M, D'Amico DF. Multimodal approach and its impact on survival for patients with hepatocellular carcinoma. *Anticancer Res* 2003; **23:** 4047-4053

16 **Cillo U,** Navaglia F, Vitale A, Molari A, Basso D, Bassanello M, Brolese A, Zanus G, Montin U, D'Amico F, Ciarleglio FA, Carraro A, Bridda A, Burra P, Carraro P, Plebani M, D'Amico DF. Clinical significance of alpha-fetoprotein mRNA in blood of patients with hepatocellular carcinoma. *Clin Chim Acta* 2004; **347:** 129-138

17 **Matsumura M,** Niwa Y, Kato N, Komatsu Y, Shiina S, Kawabe T, Kawase T, Toyoshima H, Ihori M, Shiratori Y. Detection of alpha-fetoprotein mRNA, an indicator of hematogenous spreading hepatocellular carcinoma, in the circulation: a possible predictor of metastatic hepatocellular carcinoma. *Hepatology* 1994; **20:** 1418-1425

18 **Funaki NO,** Tanaka J, Seto SI, Kasamatsu T, Kaido T,

Imamura M. Hematogenous spreading of hepatocellular carcinoma cells: possible participation in recurrence in the liver. *Hepatology* 1997; **25:** 564-568

19 **Louha M,** Poussin K, Ganne N, Zylberberg H, Nalpas B, Nicolet J, Capron F, Soubrane O, Vons C, Pol S, Beaugrand M, Berthelot P, Franco D, Trinchet JC, Brechot C, Paterlini P. Spontaneous and iatrogenic spreading of liver-derived cells into peripheral blood of patients with primary liver cancer. *Hepatology* 1997; **26:** 998-1005

20 **Matsumura M,** Shiratori Y, Niwa Y, Tanaka T, Ogura K, Okudaira T, Imamura M, Okano K, Shiina S, Omata M. Presence of alpha-fetoprotein mRNA in blood correlates with outcome in patients with hepatocellular carcinoma. *J Hepatol* 1999; **31:** 332-339

21 **Minata M,** Nishida N, Komeda T, Azechi H, Katsuma H, Nishimura T, Kuno M, Ito T, Yamamoto Y, Ikai I, Yamaoka Y, Fukuda Y, Nakao K. Postoperative detection of alpha-fetoprotein mRNA in blood as a predictor for metastatic recurrence of hepatocellular carcinoma. *J Gastroenterol Hepatol* 2001; **16:** 445-451

22 **Ijichi M,** Takayama T, Matsumura M, Shiratori Y, Omata M, Makuuchi M. alpha-Fetoprotein mRNA in the circulation as a predictor of postsurgical recurrence of hepatocellular carcinoma: a prospective study. *Hepatology* 2002; **35:** 853-860

23 **Cillo U,** Bassanello M, Vitale A, Grigoletto FA, Burra P, Fagiuoli S, D'Amico F, Ciarleglio FA, Boccagni P, Brolese A, Zanus G, D'Amico DF. The critical issue of hepatocellular carcinoma prognostic classification: which is the best tool available? *J Hepatol* 2004; **40:** 124-131

24 **Pugh RN,** Murray-Lyon IM, Dawson JL, Pietroni MC, Williams R. Transection of the oesophagus for bleeding oesophageal varices. *Br J Surg* 1973; **60:** 646-649

25 **Bismuth H,** Chiche L, Adam R, Castaing D, Diamond T, Dennison A. Liver resection versus transplantation for hepatocellular carcinoma in cirrhotic patients. *Ann Surg* 1993; **218:** 145-151

26 **Mazzaferro V,** Regalia E, Doci R, Andreola S, Pulvirenti A, Bozzetti F, Montalto F, Ammatuna M, Morabito A, Gennari L. Liver transplantation for the treatment of small hepatocellular carcinomas in patients with cirrhosis. *N Engl J Med* 1996; **334:** 693-699

27 **Cillo U,** Vitale A, Bassanello M, Grigoletto F, Burra P, D' Amico DF. The two faces of HCC prognostic evaluation: 'observational' or 'pragmatic' approach? *J Hepatol* 2004; **40:** 1042-1043

28 **Llovet JM,** Bru C, Bruix J. Prognosis of hepatocellular carcinoma: the BCLC staging classification. *Semin Liver Dis* 1999; **19:** 329-338

29 **Bruix J,** Sherman M, Llovet JM, Beaugrand M, Lencioni R, Burroughs AK, Christensen E, Pagliaro L, Colombo M, Rodes J. Clinical management of hepatocellular carcinoma. Conclusions of the Barcelona-2000 EASL conference. European Association for the Study of the Liver. *J Hepatol* 2001; **35:** 421-430

30 **Lemoine A,** Le Bricon T, Salvucci M, Azoulay D, Pham P, Raccuia J, Bismuth H, Debuire B. Prospective evaluation of circulating hepatocytes by alpha-fetoprotein mRNA in humans during liver surgery. *Ann Surg* 1997; **226:** 43-50

31 **Witzigmann H,** Geissler F, Benedix F, Thiery J, Uhlmann D, Tannapfel A, Wittekind C, Hauss J. Prospective evaluation of circulating hepatocytes by alpha-fetoprotein messenger RNA in patients with hepatocellular carcinoma. *Surgery* 2002; **131:** 34-43

32 **Sheen IS,** Jeng KS, Shih SC, Wang PC, Chang WH, Wang HY, Shyung LR, Lin SC, Kao CR, Tsai YC, Wu TY. Does surgical resection of hepatocellular carcinoma accelerate cancer dissemination? *World J Gastroenterol* 2004; **10:** 31-36

Science Editor Guo SY **Language Editor** Elsevier HK

PO Box 2345, Beijing 100023, China
www.wjgnet.com
wjg@wjgnet.com

ELSEVIER

World J Gastroenterol 2005;11(44):6926-6931
World Journal of Gastroenterology ISSN 1007-9327

Etiology and functional status of liver cirrhosis by ^{31}P MR spectroscopy

Monika Dezortova, Pavel Taimr, Antonin Skoch, Julius Spicak, Milan Hajek

Monika Dezortova, Antonin Skoch, Milan Hajek: MR Unit, Department of Diagnostic and Interventional Radiology; Institute for Clinical and Experimental Medicine, Prague, Czech Republic
Pavel Taimr, Julius Spicak: Department of Hepatogastroenterology; Institute for Clinical and Experimental Medicine, Prague, Czech Republic
Supported by grant from Ministry of Health IGA 7853-3, and MZO 00023001, Czech Republic
Correspondence to: Monika Dezortova, PhD, MR-Unit, ZRIR, IKEM, Videnska 1958/9, 140 21 Prague 4,
Czech Republic. mode@medicon.cz
Telephone: +420-241717729 Fax: +420-241717729
Received: 2005-03-03 Accepted: 2005-04-08

Abstract

AIM: To assess the functional status and etiology of liver cirrhosis by quantitative ^{31}P magnetic resonance spectroscopy (MRS).

METHODS: A total of 80 patients with liver cirrhosis of different etiology and functional status described by Child-Pugh score were examined and compared to 11 healthy volunteers. MR examination was performed on a 1.5 T imager using a ^{1}H/^{31}P surface coil by the 2D chemical shift imaging technique. Absolute concentrations of phosphomonoesters (PME), phosphodiesters (PDE), inorganic phosphate (Pi) and adenosine triphosphate (ATP) were measured.

RESULTS: MRS changes reflected the degree of liver dysfunction in all the patients as well as in individual etiological groups. The most important change was a decrease of PDE. It was possible to distinguish alcoholic, viral and cholestatic etiologies based on MR spectra. Alcoholic and viral etiology differed in PDE (alcoholic, viral, controls: 6.5±2.3, 6.5±3.1, 10.8±2.7 mmol/L, P<0.001) and ATP (alcoholic, viral, controls: 2.9±0.8, 2.8 ±0.9, 3.7±1.0 mmol/L, P<0.01) from the control group. Unlike viral etiology, patients with alcoholic etiology also differed in Pi (alcoholic, controls: 1.2±0.4, 1.6±0.6 mmol/L, P<0.05) from controls. No significant changes were found in patients with cholestatic disease and controls; nevertheless, this group differed from both alcoholic and viral groups (cholestatic, alcoholic, viral: 9.4 ±2.7, 6.5±2.3, 6.5±3.1 mmol/L, P<0.005) in PDE.

CONCLUSION: ^{31}P MRS can significantly help in non-invasive separation of different etiological groups leading to liver cirrhosis. In addition, MRS changes reflect functional liver injury.

Key words: Liver cirrhosis; ^{31}P MR spectroscopy; Absolute concentration; Child-Pugh score; Etiology

Dezortova M, Taimr P, Skoch A, Spicak J, Hajek M. Etiology and functional status of liver cirrhosis by ^{31}P MR spectroscopy. *World J Gastroenterol* 2005; 11(44): 6926-6931
http://www.wjgnet.com/1007-9327/11/6926.asp

INTRODUCTION

Cirrhosis is the final stage of various liver diseases. Regardless of etiology (i.e., viral, alcoholic, autoimmune, metabolic and others), the liver injury leads to the excessive accumulation of extracellular matrix and to nodular regeneration of parenchyma. Information about the etiology and degree of liver derangement is indispensable and usually needs to be verified by means of liver biopsy. This procedure is invasive, uncomfortable for the patient and sometimes not without serious complications. Therefore, efforts have been made to non-invasively obtain information concerning liver injury.

Additional important information is the degree of functional limitation of the liver. In clinical settings, this is usually described by a Child-Pugh score (CPS), which is calculated from clinical and laboratory tests[1-3]. As clinicians need to determine the specific etiological diagnosis of liver cirrhosis, all possible additional information is valuable in clinical practice to find an appropriate treatment[4]. Imaging examinations, which are capable of improving the diagnostic process, are very helpful.

One of the promising techniques is the application of magnetic resonance (MR) spectroscopy[5]. Phosphorus (^{31}P) MR spectroscopy has been used to study liver metabolism *in vivo* for several years[6-9]. It enables the observation of energy metabolism and intracellular compartmentation through the signals of phosphomonoesters (PME), phosphodiesters (PDE), inorganic phosphate (Pi) and nucleotide triphosphates, mainly adenosine triphosphate (ATP). The PME and PDE signals are multicomponent with phosphorylcholine and phosphorylethanolamine which are the main contributors to PME as well as

glycerophosphorylcholine and glycerophosphorylethanola mine which are the main contributors to PDE [10]. The final typical signal of ^{31}P MR spectra *in vivo* is phosphocreatine (PCr). Although it is a dominant signal in muscles, it is not readily observable in spectra of the liver because of its low contribution to hepatic metabolic processes. Its presence indicates some contribution of signals from abdominal wall muscle as a partial volume effect.

In this study we investigated whether quantitative ^{31}P MR spectroscopy can distinguish different etiologies of liver cirrhosis and assess the functional severity of liver injury. The main goal of the study was to describe the relationship between the concentration of phosphorylated metabolites in the liver and the different etiological groups of liver cirrhosis.

METHODS

Subjects

A group of 80 patients (49.7 ± 11.5 years) with confirmed liver cirrhosis of different etiology (alcoholic cirrhosis in 33 cases, viral hepatitis in 22 cases (B virus in three cases, C virus in 17 cases, combined B+C in two cases), cholestatic liver disease in 16 cases (primary biliary cirrhosis in six cases, one case of secondary biliary cirrhosis, primary sclerosing cholangitis in eight cases and one case of biliary atresia), and other etiologies in nine cases (one Budd-Chiari, two congenital fibrosis, two autoimmune, and four cryptogenic cases) were examined. The last nine patients were excluded from etiological evaluations because of their etiological diversity and small number. Patients with combined etiologies (especially viral and alcoholic) were strictly excluded from the study as well as another 19 patients with insufficient resolution or low signal to noise ratio due to technical problems. Results were compared to those of a group of 11 healthy volunteers (40.5 ± 10.9 years). Liver biopsy was performed in all cirrhotic patients except for those whose clinical, laboratory, endoscopic and imaging studies (abdominal ultrasound and CT) were typical and without any doubt for severe liver cirrhosis. Etiological diagnosis was made using standard diagnostic rules. All alcoholic patients admitted had a previous regular drinking of alcohol more than 80 g/d, patients with viral hepatitis B and C were confirmed by specific antibodies and/or PCR DNA/RNA positivity. Patients with primary biliary cirrhosis were AMA positive, patients with primary sclerosing cholangitis had typical cholangiography, all cholestatic patients were confirmed by liver biopsy. Similarly strict criteria were used for other etiologies. All patients were originally examined for the liver transplantation program and six-month alcohol abstinence in alcoholic patients was proved by independent observers, i.e. family members, primary care physicians and psychiatrists trained in substance abuse treatment. All subjects, including the healthy volunteers, abstained from alcohol during 48 h before MR examination and underwent standard clinical biochemical testing just before the MR examination which was performed in early morning after an overnight fast (at least 8 h of fasting). A Child-Pugh score [1-3] was obtained in all patients (mean CPS = 9.3) and patients were distributed into groups A, B, and/or C for statistical evaluation. MELD score was not used because of its main application in donor allocations. The subjects were fully informed and signed the protocol of the examination in accordance with rules approved by the ethical committee, which conform to the ethical guidelines of the 1975 Declaration of Helsinki.

MR examination

MR examination was performed on a Siemens Vision (Erlangen, Germany) whole-body MR imager operating at 1.5 Tesla equipped with a commercial dual ^{1}H/^{31}P surface coil. The subjects were examined in a prone position with the liver centered on the surface coil. Neither ECG nor breathing monitoring due to this position was found to be necessary. No tremor because of encephalopathy which might also influence the quality of MR examination was observed. Basic MR images in all orientations were obtained for the localization of voxels (Figure 1). ^{31}P MR spectra were measured using a standard two-dimensional chemical shift imaging (CSI) technique[5] in the transversal plane with the following parameters: TR = 323 ms, TE = 2.3 ms, matrix 16 × 16, field of view (FOV) = 480 mm, flip angle = 90º, slice thickness = 4 cm, voxel volumes were 3 cm × 3 cm × 4 cm, 12 acquisitions, acquisition time = 16 min.

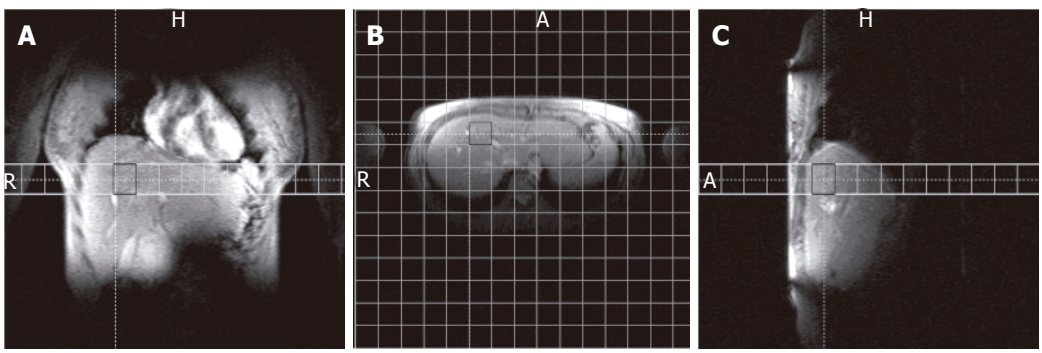

Figure 1 MR images of a healthy volunteer in all orientations with selected matrix for spectroscopic measurement and indicated volume of interest for spectra evaluation.

Spectra evaluation

Approximately 12 voxels (in the normal size of the liver) were selected from a whole CSI matrix (256 voxels). The most appropriate voxel for the quantitative evaluation[11] had to fulfill two conditions: (1) no visible PCr signal characterizing the presence of abdominal muscles; (2) no visible large intrahepatic blood vessels (portal vein truncus and its left and right lobar branches, inferior vena cava and large branches of hepatic veins). Such voxel was chosen using a standard postprocessing method (the movement of the whole CSI matrix) and considered as volume of interest (VOI) for quantitative evaluation. However, the contribution of small hepatic veins to measured signal intensities could not be excluded.

Spectra were evaluated using standard Siemens Numaris software (Gauss apodization with halfwidth = 30 ms, manual phase and spline baseline correction, Fourier transformation and curve fitting with the assumption of Gaussian line shapes). We used Pi chemical shift = 5 ppm as a standard frequency for the assignment of observed signals. Signal intensities of PME, Pi, PDE and β ATP (αATP and γATP signals were not used for the evaluation because of overlap with signals of other compounds) were used for the measurement of absolute molar concentrations. The methodology of the absolute quantification using the CSI sequence was published previously[11,12]. The signal intensity ratios were not used because of the signal intensity dependence on the distance of the VOI from the center of the surface coil.

Statistical analysis

The comparison of several neighboring voxels from different places in the liver was performed and a VOI of 36 mL was found to be large enough to disregard structural heterogeneities. All data represented three independent evaluations and were expressed as mean ± SD unless otherwise indicated.

Statistical analysis was performed using paired *t* tests and the technique of "contrast analysis" in the ANOVA module of STATISTICA 6[13] for multiple comparisons. Pattern recognition analysis of data was performed by principal component analysis (PCA) using the Multivariate Explanatory Techniques module of the STATISTICA software and by linear and nonlinear discriminant analyses (LDA and NDA, respectively)[14] using MaZda B11[15].

A Levene's test of homogeneity of variances in groups confirmed that there was no effect at $P<0.05$. This means data had the same variance and could be compared by standard t test. The null hypothesis H_0 (group means are not different from the control group) was rejected if $P<0.05$ (5 % error level).

RESULTS

Figure 2 shows typical examples of phosphorus spectra from healthy and cirrhotic liver tissue. The altered hepatic phosphorus metabolism in cirrhosis could be described by calculated molar concentrations of selected compounds in the liver tissue. The spectroscopic data of patients and controls together with Child-Pugh score are summarized in Table 1. Compared to controls, molar concentrations of PDE and ATP were significantly lower in all patients with liver cirrhosis. We divided patients into three groups according to CPS, independent of etiology. In this case, no significant differences were found between controls and patients with mild cirrhosis status (CPS-A) whereas groups CPS-B and CPS-C showed statistical differences to the control group in PDE ($P<0.001$) and ATP ($P<0.02$). If groups of patients were compared to each other, differences in patients within the CPS-A grouping increased for PDE as CPS worsened, no statistical differences were found in ATP. The relationship between calculated molar concentrations and the known etiology of liver cirrhosis is summarized in Table 2.

Spectroscopic data (PME, Pi, PDE and ATP concentrations) were also evaluated by various pattern recognition methods. We found similar levels of misclassification of subjects by using PCA, LDA and NDA procedures[15]. For demonstration and graphical output we used PCA plots from STATISTICA software[13], LDA and NDA results were not shown. To distinguish the different etiology and functional status of the liver cirrhosis from the controls, we highlighted individual subgroups of patients in PCA plots. If individual etiological groups were projected together with a control group, trends demonstrating the functional status of the liver were highlighted, i.e. the distance from the control area directly depended on CPS. The alcoholic group differed from

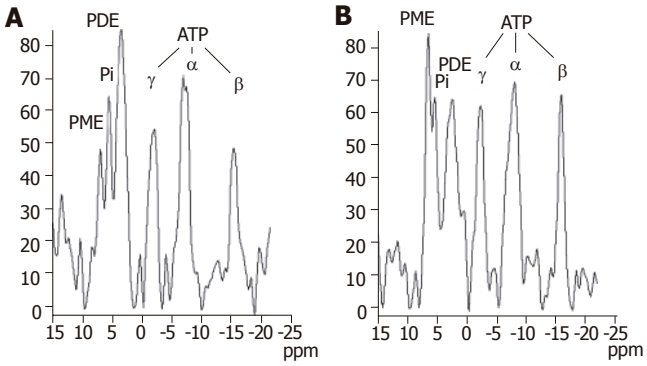

Figure 2 ^{31}P MR spectra of the liver in a healthy volunteer (**A**) and in a patient with liver cirrhosis (**B**). PME - phosphomonoesters; Pi - inorganic phosphate; PDE - phosphodiesters; γATP, αATP, βATP - γ, α and β phosphates of adenosine triphosphate.

Table 1 Concentrations of ^{31}P visible metabolites (mmol/L) in the liver according to the degree of liver injury

	n	PME	Pi	PDE	ATP
Controls	11	3.09±1.45	1.63±0.55	10.83±2.68	3.72±0.99
All patients	80	3.53±1.45	1.33±0.61	7.16±2.88[d]	2.95±0.84[b]
CPS-A	18	3.64±1.68	1.37±0.56	9.16±2.32	3.24±0.85
CPS-B	25	3.60±1.31	1.31±0.57	7.31±2.62[d]	2.93±0.78[a]
CPS-C	37	3.44±1.46	1.33±0.66	6.07±2.80[d,f]	2.83±0.87[b]

[a]$P<0.05$, [b]$P<0.01$, [d]$P<0.001$ *vs* the control group; [f]$P<0.01$ *vs* the CPS-A group.

Table 2 Concentrations (mmol/L) of ^{31}P visible metabolites in the liver according to different etiologies and CPS

	n	PME	Pi	PDE	ATP	CPS	*n*	PME	Pi	PDE	ATP
Controls	11	3.09±1.45	1.63±0.55	10.83±2.68	3.72±0.99	-	-	-	-	-	-
Alcohol	33	3.48±1.53	1.19±0.39[a,c]	6.52±2.29[d,f]	2.86±0.80b	A	5	3.87±2.05	1.17±0.32	8.35±1.26	3.43±0.53
						B	6	3.50±1.32	1.17±0.35	6.22±2.01[c]	2.92±0.55
						C	22	3.38±1.51	1.21±0.43a	6.18±2.40[c]	2.71±0.87[b]
Viral	22	3.64±1.55	1.57±0.77[c]	6.47±3.13[d,f]	2.84±0.92b	A	7	3.47±1.92	1.54±0.69	8.95±2.37	3.27±1.20
						B	8	3.99±1.51	1.51±0.63	6.23±2.72[c]	2.59±0.74[b]
						C	7	3.40±1.41	1.66±1.04	4.26±2.66c	2.69±0.74[a]
[1]Cholestatic	16	3.59±1.31	1.43±0.63	9.36±2.70	3.27±0.90	A	2	-	-	-	-
						B	10	3.44±1.26	1.26±0.66	8.94±2.34	3.24±0.89
						C	4	-	-	-	-

[a]P<0.05, [b]P<0.01, [d]P<0.001 *vs* the control group; [c]P<0.05 between alcohol and viral etiological groups; [f]P<0.001 *vs* the cholestatic group.
[1]The cholestatic group was not divided into subgroups reflecting CPS because of the insufficient number in groups CPS-A and CPS-C.

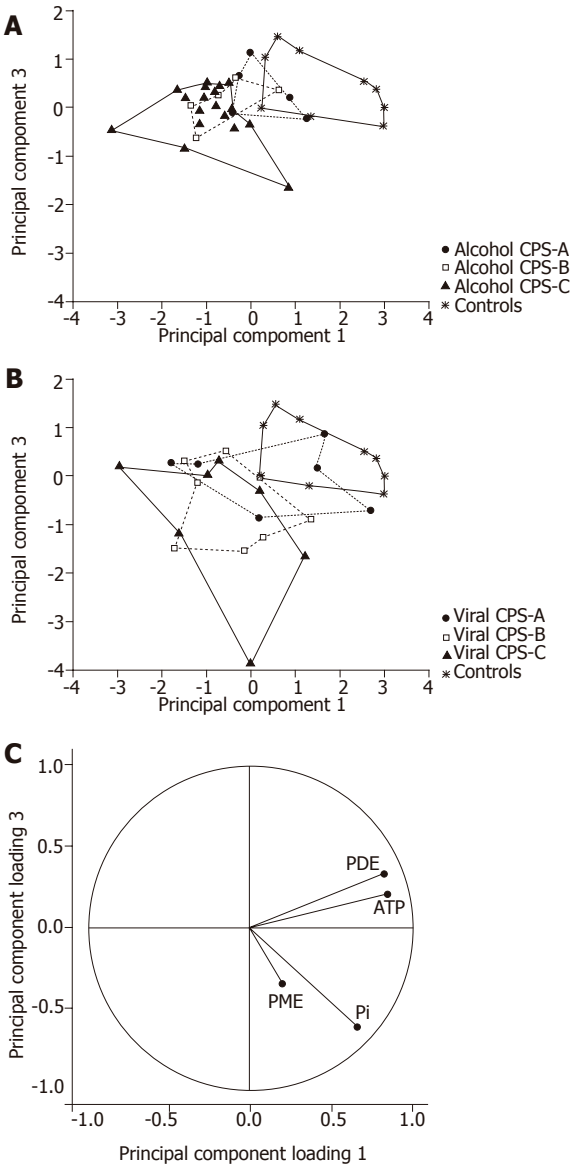

Figure 3 Results of principal component analysis (CPS). Individual positions of spectra displayed on the PCA scatterplots. Principal components are standardized (centered and scaled to unit variance). Principal component 1 explains 47 % of total variance, principal component explains 3 16% of total variance. (**A**) Patients with only alcoholic etiology and controls; (**B**) patients with only viral etiology and controls. Child-Pugh score subgroups (**A, B,** and **C**) and controls are bounded. (**C**) Projection of the principal component loadings on the planes 1 and 3.

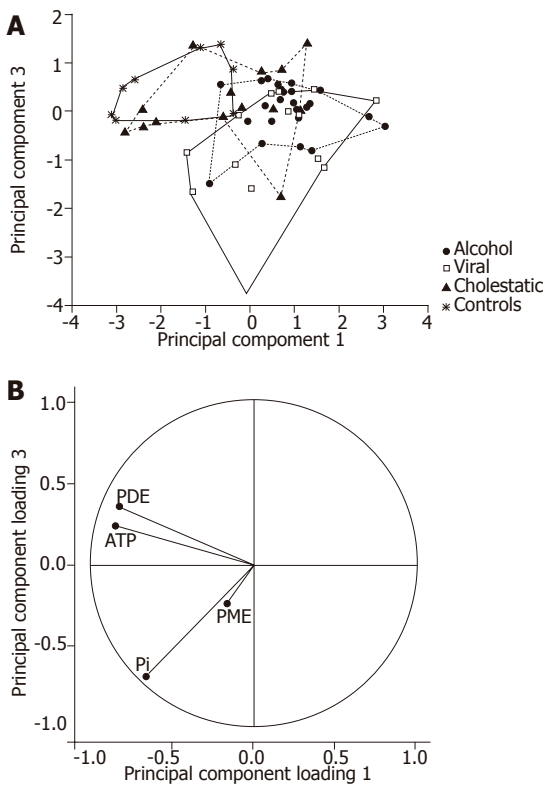

Figure 4 Results of principal component analysis (etiology). (**A**) Individual positions of spectra of patients with CPS-B and C together with a control group are displayed on the PCA plot. Etiological groups (alcoholic, viral and cholestatic) and controls are bounded. Principal component 1 explains 46 % of total variance, principal component 3 explains 17% of total variance; (**B**) Projection of the principal component loadings on the planes 1 and 3.

controls in the CPS-C area, whereas the viral group differed in the CPS-B area (Figure 3). Because of the insufficient number of cholestatic patients in the CPS-A and CPS-C groups, that plot was not presented.

As data from the CPS-A groups overlapped with controls, we used patients with CPS-B or CPS-C liver status for another statistical analysis (Figure 4). In this case, principal component analysis confirmed clear separation of viral patients from controls. Partial overlap was seen between alcoholic patients and controls. Finally, the group

of cholestatic patients overlapped all groups.

By comparing differences in ^{31}P MR spectra of patients to controls we could distinguish alcoholic, viral and cholestatic etiologies of liver cirrhosis. Patients with alcoholic and viral etiology differed in PDE and ATP from the control group. Unlike viral etiology, patients with alcoholic etiology also differed from the control group in Pi (P<0.05). No significant changes were found in patients with cholestatic disease and the control group; however, this group differed from both alcoholic and viral groups in PDE.

DISCUSSION

Diagnosis of liver cirrhosis is mainly based on invasive methods such as liver biopsy, laparoscopy, various radiological examinations and other clinical tests. The functional severity of liver cirrhosis is usually described by CPS which is partially based on subjective parameters. Thus, this description is not fully sufficient and can impair accuracy. On the other hand, signals from ^{31}P MR spectroscopy reflect intracellular and membrane metabolism *in vivo* non-invasively and they are objective parameters[6,7,8,10].

From our data above, we are able to conclude: (1) three basic etiologies can be distinguished by using correlation with metabolite concentrations; (2) there exists a correlation between the Child-Pugh score and the concentration of PDE and ATP, which is also observable in single etiologies.

The majority of published ^{31}P MR spectroscopic studies have dealt with quantification of relative signal intensities characterized by ratios such as PCr/Pi, Pi/ATP etc. Unlike previous studies, where only relative signal ratios were used, we measured absolute concentration of the metabolites[11]. Absolute quantification of metabolites in mmol/L is not often used because of technical problems[12,16]. However, we believe that only relative quantification using signal intensity ratios cannot fully describe metabolic changes and absolute quantification should be taken into account even if a number of correction factors must be calculated. For example, if two or more compounds increase or decrease together, only the absolute quantification of independent metabolites accurately describes the event as signal ratios may remain unchanged.

PCA analysis of PME, Pi, PDE and ATP concentrations showed different localization of the etiological groups and trends in accordance with the CPS (Figures 3 and 4). Projection of the variables confirmed the similarities of ATP and PDE spectroscopic parameters. The best separation was obtained in the projection on the principal component-planes 1 and 3 despite losing some information available in the projections 1 and 2. The principal component 2 correlated specifically with PME. Nevertheless, in our study PME had high variation so that we did not use the projection on the component-plane 1 and 2.

Standard statistic tests confirmed the trends observable in PCA graphs. Data show a mean decrease of about 23% in ATP in patients with alcohol etiology versus the control group. A similar decrease of ATP concentration was also observed in the group of patients with viral etiology. In both groups we found that the decrease strongly depend on the CPS. Nevertheless, the higher difference was foud between CPS group A and CPS groups B and C. A very small difference was observed between CPS groups B and C which could be explained by the overall severity of hepatocyte dysfunction. Contrary to the alcoholic and viral groups, no statistically significant changes were found in ATP concentration in the cholestatic group.

Our findings in the group of alcoholic patients correspond to the results of animal studies. A number of reports show decreased levels of ATP in the liver of animals chronically fed ethanol. ATP levels could be measured using the intragastric feeding model[17,18]. In rats feeding a high-fat, low protein diet plus alcohol (similar to the diet of malnourished human alcoholics) levels of ATP decreased and remained constant at 35 % lower than levels of ATP in control animals. Hypoxia resulted in a decrease in hepatic levels of ATP in both ethanol-fed and control rats, but the magnitude of the decrease was significantly greater in the ethanol-fed group. Levels of adenosine monophosphate (AMP) and adenosine diphosphate (ADP) were not changed.

The most important change was a decreased concentration of PDE which is considered to be an indicator of membrane phospholipids and catabolic processes. The rate of PDE change was different in various etiologies. When etiological groups were compared to the control group regardless of CPS status (Table 2), mean PDE values were found to be about 60% in alcoholic and viral patients (P<0.001 to controls, and P<0.005 compared to the cholestatic group) and about 86% in the cholestatic group (without statistical significance). Moreover, in CPS-C groups, PDE concentration decreased to 39% of the control value in viral patients (58% in CPS-B) whereas in alcoholic patients PDE did not further decrease (57% of control PDE value in CPS-B and CPS-C). The fact that the changes are already significant in milder stages of cirrhosis (CPS-B) can improve the diagnostic effectiveness of this method. Unlike a previous study[9], our results were more pronounced in more severely affected patients.

We also studied PME concentration, which mainly represents intermediates on the phospholipid biosynthesis pathway. Although some other studies describe an increased PME signal[7,9,19-21], our data only show a statistically non-significant trend.

The last measured concentration - inorganic phosphate Pi - has been found to change only in alcoholic patients (P<0.05). Thus, inorganic phosphate concentration could be used to separate patients with alcoholic and viral etiology.

Observed signals in ^{31}P MR spectra describe many metabolites in intra and extracellular liver tissue. It is known that many types of cells (hepatocytes, cholangiocytes, vascular wall cells, hepatic stellate cells macrophages and others) contribute to liver metabolism depending on their status. Changes in extracellular matrix also influence the concentration of energetic metabolites. Although ^{31}P MR signals from the liver represent whole parenchymal tissue, the results of our study have confirmed previous

findings that metabolic changes in energetic phospholipid metabolism are observable by ^{31}P MRS in patients with decompensated cirrhosis in contrast to patients with compensated cirrhosis. In addition, different concentrations of metabolites in various etiologies indicate different damages of liver parenchyma.

In conclusion, according to differences in ^{31}P MR spectra of patients and controls, we can differentiate various etiologies of liver cirrhosis, i.e. alcoholic, viral and cholestatic. Patients with alcoholic etiology differed in all selected metabolites except for PME from the control group. Patients with viral etiology differed from controls only in PDE and ATP, and no significant changes were found in patients with cholestatic disease. We suppose that this reflects different pathophysiological mechanisms of various liver diseases.

The importance of a larger, multicentric study to delineate ranges, borders and significant parameters for different cirrhotic groups (etiological and/or functional) in the nearest future is advisable. That will be the only way to assess the clinical relevance and usefulness of ^{31}P MRS in liver cirrhosis. The application of this noninvasive method in liver patients will increase. The ultimate goal is the use of ^{31}P MRS as a standard tool in the armamentarium of clinical hepatologists.

ACKNOWLEDGMENTS

The authors thank Dr Karoly Heberger, Chemical Research Center, Hungarian Academy of Sciences, for the helpful discussion of the results.

REFERENCES

1 **Child CG,** Turcotte JG. Surgery and portal hypertension. In child CG. The liver and portal hypertension. 1st ed. Philadelphia. WB Saunders Co. 1968: 50-72
2 **Pugh RN,** Murray-Lyon IM, Dawson JL, Pietroni MC, Williams R. Transection of the oesophagus for bleeding oesophageal varices. *Br J Surg* 1973; **60:** 646-649
3 **Christensen E,** Schlichting P, Fauerholdt L, Gluud C, Andersen PK, Juhl E, Poulsen H, Tygstrup N. Prognostic value of Child-Turcotte criteria in medically treated cirrhosis. *Hepatology* 1984; **4:** 430-435
4 **Montgomery Bissel D,** Maher JJ. Hepatic fibrosis and cirrhosis. In: Zakim D, Boyer TD. Hepatology, a textbook of liver disease. 4th ed. Philadelphia: Saunders, 2002: 395-416
5 **de Graff RA.** In vivo NMR Spectroscopy: Principles and Techniques. 1st ed. Chichester: John Wiley & Sons, 1998
6 **Meyerhoff DJ,** Boska MD, Thomas AM, Weiner MW. Alcoholic liver disease: quantitative image-guided P-31 MR spectroscopy. *Radiology* 1989; **173:** 393-400
7 **Munakata T,** Griffiths RD, Martin PA, Jenkins SA, Shields R, Edwards RH. An in vivo 31P MRS study of patients with liver cirrhosis: progress towards a non-invasive assessment of disease severity. *NMR Biomed* 1993; **6:** 168-172
8 **Angus PW,** Dixon RM, Rajagopalan B, Ryley NG, Simpson KJ, Peters TJ, Jewell DP, Radda GK. A study of patients with alcoholic liver disease by 31P nuclear magnetic resonance spectroscopy. *Clin Sci (Lond)* 1990; **78:** 33-38
9 **Menon DK,** Sargentoni J, Taylor-Robinson SD, Bell JD, Cox IJ, Bryant DJ, Coutts GA, Rolles K, Burroughs AK, Morgan MY. Effect of functional grade and etiology on in vivo hepatic phosphorus-31 magnetic resonance spectroscopy in cirrhosis: biochemical basis of spectral appearances. *Hepatology* 1995; **21:** 417-427
10 **Taylor-Robinson SD,** Sargentoni J, Bell JD, Saeed N, Changani KK, Davidson BR, Rolles K, Burroughs AK, Hodgson HJ, Foster CS, Cox IJ. In vivo and in vitro he patic 31P magnetic resonance spectroscopy and electron microscopy of the cirrhotic liver. *Liver* 1997; **17:** 198-209
11 **Tosner Z,** Dezortova M, Tintera J, Hajek M. Application of two-dimensional CSI for absolute quantification of phosphorus metabolites in the human liver. *MAGMA* 2001; **13:** 40-46
12 **Murphy-Boesch J,** Jiang H, Stoyanova R, Brown TR. Quantification of phosphorus metabolites from chemical shift imaging spectra with corrections for point spread effects and B1 inhomogeneity. *Magn Reson Med* 1998; **39:** 429-438
13 http://www.statsoft.com/textbook/stathome.html
14 **Meloun M,** Militky J. Statisticka analyza experimentalnich dat. (Cz) (Statistical analysis of experimental data.) 1st ed. Academia, 2004
15 http://www.eletel.P.lodz.pl/cost/cost_project.html
16 **Sijens PE,** Dagnelie PC, Halfwerk S, van Dijk P, Wicklow K, Oudkerk M. Understanding the discrepancies between 31P MR spectroscopy assessed liver metabolite concentrations from different institutions. *Magn Reson Imaging* 1998; **16:** 205-211
17 **Miyamoto K,** French SW. Hepatic adenine nucleotide metabolism measured in vivo in rats fed ethanol and a high fat-low protein diet. *Hepatology* 1988; **8:** 53-60
18 **Corbin IR,** Buist R, Peeling J, Zhang M, Uhanova J, Minuk GY. Hepatic 31P MRS in rat models of chronic liver disease: assessing the extent and progression of disease. *Gut* 2003; **52:** 1046-1053
19 **Jalan R,** Taylor-Robinson SD, Hodgson HJ. In vivo hepatic magnetic resonance spectroscopy: clinical or research tool? *J Hepatol* 1996; **25:** 414-424
20 **Kiyono K,** Shibata A, Sone S, Watanabe T, Oguchi M, Shikama N, Ichijo T, Kiyosawa K, Sodeyama T. Relationship of 31P MR spectroscopy to the histopathological grading of chronic hepatitis and response to therapy. *Acta Radiol* 1998; **39:** 309-314
21 **Lim AK,** Patel N, Hamilton G, Hajnal JV, Goldin RD, Taylor-Robinson SD. The relationship of in vivo 31P MR spectroscopy to histology in chronic hepatitis C. *Hepatology* 2003; **37:** 788-794

Science Editor Wang XL and Guo SY **Language Editor** Elsevier HK

PO Box 2345, Beijing 100023, China
www.wjgnet.com
wjg@wjgnet.com

ELSEVIER

World J Gastroenterol 2005;11(44):6932-6935
World Journal of Gastroenterology ISSN 1007-9327

• *COLORECTAL CANCER* •

Three-dimensional computed tomography in laparoscopic surgery for colorectal carcinoma

Hiroshi Ohtani, Kohei Ohta, Yuichi Arimoto, Eui-Chul Kim, Hiroko Oba, Kenji Adachi, Shoichi Terakawa, Mitsuo Tsubakimoto

Hiroshi Ohtani, Kohei Ohta, Yuichi Arimoto, Eui-Chul Kim, Department of Surgery, Osaka City Sumiyoshi Hospital, 1-2-16 Higashikagaya, Suminoe-ku, Osaka 559-0012, Japan
Hiroko Oba, Kenji Adachi, Department of Gastroenterology, Osaka City Sumiyoshi Hospital, 1-2-16 Higashikagaya, Suminoe-ku, Osaka 559-0012, Japan
Shoichi Terakawa, Mitsuo Tsubakimoto, Department of Radiology, Osaka City Sumiyoshi Hospital, 1-2-16 Higashikagaya, Suminoe-ku, Osaka 559-0012, Japan
Co-first-author: Hiroshi Ohtani
Co-correspondence: Hiroshi Ohtani
Correspondence to: Dr Hiroshi Ohtani, Department of Surgery, Osaka City Sumiyoshi Hospital, 1-2-16 Higashikagaya, Suminoe-ku, Osaka 559-0012, Japan. m5051923@msic.med.osaka-cu.ac.jp
Telephone: +81-6-6681-1000 Fax: +81-6-6686-1547
Received: 2005-04-24 Accepted: 2005-05-24

Abstract

AIM: To evaluate the usefulness of three-dimensional computed tomography (3DCT) in laparoscopic surgery for colorectal carcinoma.

METHODS: Seventy-two patients with colorectal cancer who underwent curative operation at our hospital were enrolled in this study. They were classified into two groups by operative procedures. Sixteen patients underwent laparoscopic surgery, laparoscopic group (LG), while 56 patients underwent conventional open surgery, open group (OG). At our institution, contrast-enhanced CT is routinely performed as part of intra-abdominal screening and the 3D images of the major regional vessels are described. We have previously described about the preoperative visualization of the inferior mesenteric artery (IMA) by 3DCT. This time we newly acquired 3D images of the superior mesenteric artery (SMA)/superior mesenteric vein (SMV), ileocecal artery (ICA), middle colic artery (MCA), and inferior mesenteric vein (IMV). We have compared our two study groups with regard to five items, including clinical anastomotic leakage. We have discussed here the role of 3DCT in laparoscopic surgery for colorectal carcinoma.

RESULTS: The mean length of the incision in LG was 4.625±0.89 cm, which was significantly shorter than that in OG (P<0.001). The association between ICA and SMV and SMA was described in the right-sided colectomy. The preoperative imaging of IMA and IMV was created in the rectosigmoidectomy. There was no significant difference in anastomotic leakage between the two groups, but no patients in LG experienced anastomotic leakage.

CONCLUSION: Most of the patients are satisfied with the shorter incisional length following laparoscopic surgery. Preoperative visualization of the major regional vessels may be helpful for the secure treatment of the anastomosis in laparoscopic surgery for colorectal carcinoma.

Key words: Three-dimensional computed tomography; Laparoscopic colorectal surgery; Colorectal cancer

Ohtani H, Ohta K, Arimoto Y, Kim EC, Oba H, Adachi K, Terakawa S, Tsubakimoto M. Three-dimensional computed tomography in laparoscopic surgery for colorectal carcinoma. *World J Gastroenterol* 2005; 11 (44): 6932-6935
http://www.wjgnet.com/1007-9327/11/6932.asp

INTRODUCTION

Laparoscopic colectomy has been generally accepted, and the instruments and techniques have been developed considerably. The advantages of laparoscopic approaches include shorter hospital stay, quicker return of gastrointestinal function, less pain, fewer wound complications, and quicker recovery[1-6]. However, laparoscopic colorectal surgery for malignancies requires the use of advanced surgical techniques that entail a long learning curve[7,8]. In right-sided colon cancer, the regional anatomy is relatively complicated[9]. In the lymph node dissection around the surgical trunk, it is important to recognize two patterns in the relationship between the ileocecal artery (ICA) and the superior mesenteric vein (SMV). One pattern is that the ICA is in front of SMV (Type A), and the other is that ICA is in back of SMV (Type B)[10]. A previous study have described about the risk of more anastomotic leakage in the converted laparoscopic colorectal surgery compared to the conventional open surgery[11]. In laparoscopic colorectal surgery, understanding of the anatomical orientation, including the regional vessels, is important. We have previously reported that preoperative visualization of the inferior mesenteric artery (IMA) by three-dimensional computed tomography (3DCT) is useful in colorectal surgery[12]. In this study, we have described about the three-dimensional (3D) images of the other major visceral vessels, such as the superior mesenteric artery (SMA), SMV, ICA, middle colic artery (MCA), and inferior mesenteric vein (IMV). Here, we have

evaluated the efficacy of 3DCT in performing laparoscopic colorectal surgery for carcinoma.

MATERIALS AND METHODS

Patients

Between April 2002 and March 2005, 72 patients with colorectal cancer underwent curative surgery at our hospital. Operative procedures were laparoscopic colorectal surgery [laparoscopic group (LG); 16 patients: 5 men and 11 women] and open colorectal surgery [open group (OG); 56 patients: 32 men and 14 women]. The mean age was 66.6±7.4 years (range, 52-83 years) in LG and 68.2±11.3 years (range, 36-91 years) in OG. The following data were examined and compared between LG and OG: (1) patient's age and gender; (2) Duke's staging; (3) presence of the postoperative ileus; (4) length of incision for exteriorization and resection of the specimen; (5) wound infection; and (6) clinical anastomotic leakage.

Methods

Contrast-enhanced CT is routinely performed to screen for intra-abdominal malignancies before the surgery at our hospital. Dual-phase helical CT was performed with a high-speed scanner [multi-detector CT (MDCT); Aquilion M8, Toshiba Medical Systems Co., Ltd, Tokyo, Japan] on the patients. During each phase, scanning was performed in a single breath-hold. Dual-phase helical CT data were then transferred to a Zio M900 workstation (Ziosoft, Inc., Morgan Hill, CA, USA), and 3DCT images of the major visceral vessels, such as SMA, SMV, ICA, IMA, and IMV, were reconstructed. The detailed imaging techniques have been described in the previous literatures[12,13]. In right-sided colectomy, the association between ICA and SMV, the variation of the right colic artery (RCA) and the image of the middle colic artery were confirmed by 3DCT before the surgery. In the resectioning of advanced sigmoid colon and rectal cancer, we routinely dissect the lymph nodes around the root of IMA while preserving the left colic artery (LCA), because resection of the root of IMA occasionally causes ischemia of the oral side of the sigmoid colon, sometimes leading to anastomotic leakage[12].

Statistical analysis

Data were expressed as the mean±SD. Statistical analysis was performed using Mann-Whitney *U* test, χ^2 and Student's *t*-test. *P* values of less than 0.05 were considered statistically significant.

RESULTS

There was no significant difference in age, gender, Duke's staging, presence of the postoperative ileus or wound infection between the LG and the OG (Tables 1 and 2). The mean length of incision in the LG (4.625± 0.885 cm) was significantly shorter, than that in OG (15.91 ±2.51 cm, $P<0.001$). Three patients in OG experienced anastomotic leakage, while no patients in LG experienced it. However, there was no statistically significant difference in anastomotic leakage between these two groups. Two of the three patients undergoing anastomotic leakage in OG suffered from advanced rectal cancer. The root of IMA was resected because of the wide-ranging lymph node metastasis. In one of the two patients, lymph node metastasis spread around the marginal vessels of the sigmoid colon.

Table 1 Characteristics of patients in the two groups

	LG (*n* = 16)	OG (*n* = 56)	*P*
Age (yr)	66.6±7.4 (52–83)	68.2±11.3 (36–91)	NS
Male/female	5/11	32/14	NS
Duke's staging			NS
A	7	12	
B	6	24	
C	3	20	

NS: not statistically significant

Table 2 Complications of surgery

	LG (*n* = 16)	OG (*n* = 56)	*P*
Postoperative ileus	0	5	NS
Wound infection	2	13	NS
Anastomotic leakage	0	3	NS

Preoperative visualization of the ICA in front of the SMV (Type A) and that in back of the SMV (Type B) is shown in Figures 1A and 2A, respectively. The variation of the RCA and MCA was evaluated. Intraoperative findings of the association between ICA and SMV are shown in Figures 1B, 2B and C. Figure 3 shows the MCA diverging at a more peripheral portion of SMA than usual. The image of IMA and LCA to be preserved can be seen (Figure 4A). The intraoperative findings are shown in Figure 4B. Preoperative visualization of the essential vessels was described in all the patients undergoing contrast-enhanced CT.

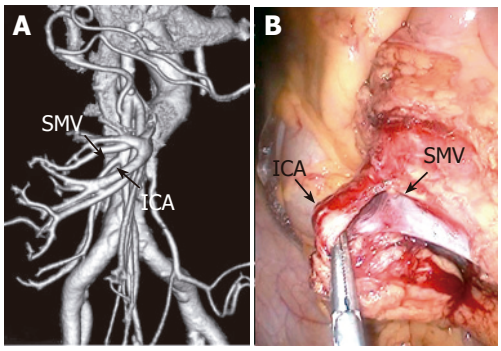

Figure 1 ICA situated in front of SMV at 3DCT (**A**) and at intraoperative findings (**B**).

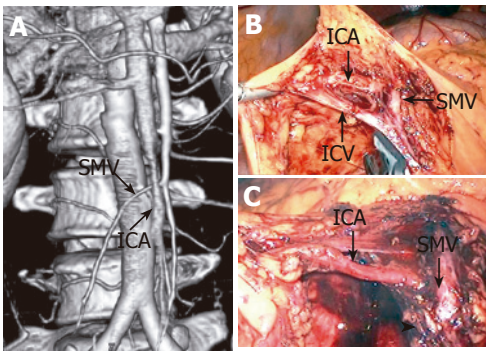

Figure 2 ICA situated in back of SMV at 3DCT (**A**) and at intraoperative findings (**B**); **C**: ICA existed after the ileocecal vein (ICV) had been resected. The arrow head shows the cut end of the ICV.

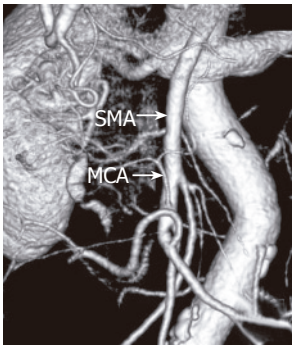

Figure 3 Preoperative visualization of the SMA showing the MCA to branch at a more peripheral portion of the SMA than usual.

DISCUSSION

Laparoscopic approaches have been widely applied, but laparoscopic colorectal surgery for carcinoma is not yet a proven operation[1]. There exists some controversies about the safety of the operation[14,15], the oncological results[16,17] and the long-term survival rate[18]. Recently, a number of studies have shown a favorable outcome of laparoscopic surgery for colon cancer[19-23]. There appears to be no significant differences in perioperative complications between laparoscopic and open colorectal surgery[24]. In our study, we acquired the same results in the presence of postoperative ileus and wound infection. The mean length of the wound used for the extraction of specimens in LG was significantly shorter than that in OG. Most of the patients in LG were satisfied with the shortness of the incisional length during the perioperative period and the subtlety of the incisional scar during the follow-up period, as they had said[25]. In addition, laparoscopic surgery has been found to be associated with significantly decreased intraoperative blood loss and postoperative complications[19,26]. The anastomotic leak rate reported in a larger series of laparoscopic anterior resection was considerably less than 10%, which was comparable to that of conventional open anterior resection[18,27]. To date, the laparoscopic approach for colorectal surgery is not associated with a higher risk of anastomotic leaks[28].

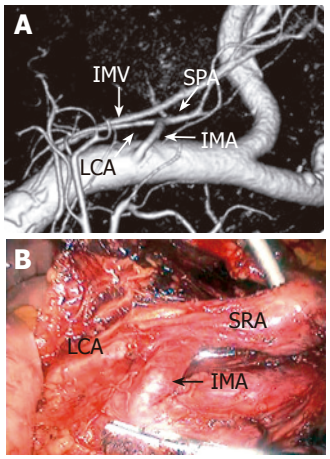

Figure 4 Three-dimensional images of the IMA, the IMV, the LCA and the superior rectal artery (SRA) were obtained (**A**) and were helpful in resecting the SRA (**B**).

In a previous report, four instances (25%) of clinical anastomotic leakage occurred in patients in whom the laparoscopic dissection had been difficult[11]. For the prevention of leakage, it is essential that there is a good supply to the colorectal anastomosis site[29]. Therefore, we preserve the LCA when dissecting lymph nodes around the root of IMA. Understanding the vascular anatomy of the regional vessels is important[12]. Preoperative visualization of SMA/SMV, ICA, MCA or IMA/IMV is crucial when performing a right-sided colectomy or a rectosigmoidectomy. Recently, a new generation of MDCT has been used in clinical practice[30]. At our hospital, MDCT has been performed not only to examine intra-abdominal malignancies, but also to provide preoperative visualization of the regional vessels. At our institution, no patients in LG had experienced anastomotic leakage, while three patients in OG experienced so. Ischemia of the oral side colon may have caused anastomotic leakage. There was no significant difference in anastomotic leakage between LG and OG, suggesting that preoperative visualization in laparoscopic surgery may be helpful in the prevention of anastomotic leakage. MDCT scanning is performed in a single breath-hold during each phase. In the past, there was a significant delay before roentgen engineers could show us the 3D images of the regional vessels, but now they are able to provide 3D images promptly after CT scanning. Having 3D images of SMA/SMV, ICA, MCA, and IMA/IMV lead to a more secure treatment of the regional vessels in laparoscopic surgery for carcinoma.

In conclusion, we suggest that preoperative visualization of the major regional vessels may have advantages in laparoscopic surgery for colorectal carcinoma.

REFERENCES

1 **Kieran JA,** Curet MJ. Laparoscopic colon resection for colon cancer. *J Surg Res* 2004; **117:** 79-91
2 **Franklin ME Jr,** Rosenthal D, Abrego-Medina D, Dorman JP, Glass JL, Norem R, Diaz A. Prospective comparison of

open vs. laparoscopic colon surgery for carcinoma. Five-year results. *Dis Colon Rectum* 1996; **39:** S35-46
3 **Hoffman GC,** Baker JW, Doxey JB, Hubbard GW, Ruffin WK, Wishner JA. Minimally invasive surgery for colorectal cancer. Initial follow-up. *Ann Surg* 1996; **223:** 790-798
4 **Milsom JW,** Bohm B, Hammerhofer KA, Fazio V, Steiger E, Elson P. A prospective, randomized trial comparing laparoscopic versus conventional techniques in colorectal cancer surgery: a preliminary report. *J Am Coll Surg* 1998; **187:** 46-55
5 **Stocchi L,** Nelson H. Laparoscopic colectomy for colon cancer: trial update. *J Surg Oncol* 1998; **68:** 255-267
6 **Falk PM,** Beart RW Jr, Wexner SD, Thorson AG, Jagelman DG, Lavery IC, Johansen OB, Fitzgibbons RJ Jr. Laparoscopic colectomy: a critical appraisal. *Dis Colon Rectum* 1993; **36:** 28-34
7 **Bennett CL,** Stryker SJ, Ferreira MR, Adams J, Beart RW Jr. The learning curve for laparoscopic colorectal surgery. Preliminary results from a prospective analysis of 1194 laparoscopic-assisted colectomies. *Arch Surg* 1997; **132:** 41-45
8 **Agachan F,** Joo JS, Sher M, Weiss EG, Nogueras JJ, Wexner SD. Laparoscopic colorectal surgery. Do we get faster? *Surg Endosc* 1997; **11:** 331-335
9 **Zheng MH,** Feng B, Lu AG, Li JW, Wang ML, Mao ZH, Hu YY, Dong F, Hu WG, Li DH, Zang L, Peng YF, Yu BM. Laparoscopic versus open right hemicolectomy with curative intent for colon carcinoma. *World J Gastroenterol* 2005; **11:** 323-326
10 **Okuda J,** Tanigawa N. [Laparoscopic surgery for rectal and sigmoid colon cancer] *Nippon Rinsho* 2003; 61**:** 391-395
11 **Slim K,** Pezet D, Riff Y, Clark E, Chipponi J. High morbidity rate after converted laparoscopic colorectal surgery. *Br J Surg* 1995; **82:** 1406-1408
12 **Ohtani H,** Kawajiri H, Arimoto Y, Ohno K, Fujimoto Y, Oba H, Adachi K, Hirano M, Terakawa S, Tsubakimoto M. Efficacy of multislice computed tomography for gastroenteric and hepatic surgeries. *World J Gastroenterol* 2005; **11:** 1532-1534
13 **Kim T,** Murakami T, Hori M, Takamura M, Takahashi S, Okada A, Kawata S, Cruz M, Federle MP, Nakamura H. Small hypervascular hepatocellular carcinoma revealed by double arterial phase CT performed with single breath-hold scanning and automatic bolus tracking. *AJR Am J Roentgenol* 2002; **178:** 899-904
14 **Larach SW,** Patankar SK, Ferrara A, Williamson PR, Perozo SE, Lord AS. Complications of laparoscopic colorectal surgery. Analysis and comparison of early vs. latter experience. *Dis Colon Rectum* 1997; **40:** 592-596
15 **Degiuli M,** Mineccia M, Bertone A, Arrigoni A, Pennazio M, Spandre M, Cavallero M, Calvo F. Outcome of laparoscopic colorectal resection. *Surg Endosc* 2004; **18:** 427-432
16 **Yamamoto S,** Watanabe M, Hasegawa H, Kitajima M. Oncologic outcome of laparoscopic versus open surgery for advanced colorectal cancer. *Hepatogastroenterology* 2001; **48:** 1248-1251
17 **Braga M,** Vignali A, Zuliani W, Radaelli G, Gianotti L, Toussoun G, Carlo V. Training period in laparoscopic colorectal surgery. *Surg Endosc* 2002; **16:** 31-35
18 **Scheidbach H,** Schneider C, Huegel O, Barlehner E, Konradt K, Wittekind C, Kockerling F. Laparoscopic sigmoid resection for cancer: curative resection and preliminary medium-term results. *Dis Colon Rectum* 2002; **45:** 1641-1647
19 **Hasegawa H,** Kabeshima Y, Watanabe M, Yamamoto S, Kitajima M. Randomized controlled trial of laparoscopic versus open colectomy for advanced colorectal cancer. *Surg Endosc* 2003; **17:** 636-640
20 **Leung KL,** Kwok SP, Lam SC, Lee JF, Yiu RY, Ng SS, Lai PB, Lau WY. Laparoscopic resection of rectosigmoid carcinoma: prospective randomised trial. *Lancet* 2004; **363:** 1187-1192
21 **Braga M,** Vignali A, Gianotti L, Zuliani W, Radaelli G, Gruarin P, Dellabona P, Di Carlo V. Laparoscopic versus open colorectal surgery: a randomized trial on short-term outcome. *Ann Surg* 2002; **236:** 759-767
22 **Stage JG,** Schulze S, Moller P, Overgaard H, Andersen M, Rebsdorf-Pedersen VB, Nielsen HJ. Prospective randomized study of laparoscopic versus open colonic resection for adenocarcinoma. *Br J Surg* 1997; **84:** 391-396
23 Clinical Outcomes of Surgical Therapy Study Group.A comparison of laparoscopically assisted and open colectomy for colon cancer. *N Engl J Med* 2004; **350:** 2050-2059
24 **Tomita H,** Marcello PW, Milsom JW. Laparoscopic surgery of the colon and rectum. *World J Surg* 1999; **23:** 397-405
25 **Adachi Y,** Sato K, Kakisako K, Inomata M, Shiraishi N, Kitano S. Quality of life after laparoscopic or open colonic resection for cancer. *Hepatogastroenterology* 2003; **50:** 1348-1351
26 **Lacy AM,** Garcia-Valdecasas JC, Delgado S, Castells A, Taura P, Pique JM, Visa J. Laparoscopy-assisted colectomy versus open colectomy for treatment of non-metastatic colon cancer: a randomised trial. *Lancet* 2002; **359:** 2224-2229
27 **Pera M,** Delgado S, Garcia-Valdecasas JC, Pera M, Castells A, Pique JM, Bombuy E, Lacy AM. The management of leaking rectal anastomoses by minimally invasive techniques. S*urg Endosc* 2002; **16:** 603-606
28 **Kockerling F,** Rose J, Schneider C, Scheidbach H, Scheuerlein H, Reymond MA, Reck T, Konradt J, Bruch HP, Zornig C, Barlehner E, Kuthe A, Szinicz G, Richter HA, Hohenberger W. Laparoscopic colorectal anastomosis: risk of postoperative leakage. Results of a multicenter study. Laparoscopic Colorectal Surgery Study Group (LCSSG). *Surg Endosc* 1999; **13:** 639-644
29 **Wu WX,** Sun YM, Hua YB, Shen LZ. Laparoscopic versus conventional open resection of rectal carcinoma: A clinical comparative study. *World J Gastroenterol* 2004; **10:** 1167-1170
30 **Zheng XH,** Guan YS, Zhou XP, Huang J, Sun L, Li X, Liu Y. Detection of hypervascular hepatocellular carcinoma: Comparison of multi-detector CT with digital subtraction angiography and Lipiodol CT. *World J Gastroenterol* 2005; **11:** 200-203

Science Editor Kumar M and Guo SY **Language Editor** Elsevier HK

PO Box 2345, Beijing 100023, China
www.wjgnet.com
wjg@wjgnet.com

ELSEVIER

World J Gastroenterol 2005;11(44):6936-6940
World Journal of Gastroenterology ISSN 1007-9327

Fibrinogen-like protein 2 fibroleukin expression and its correlation with disease progression in murine hepatitis virus type 3-induced fulminant hepatitis and in patients with severe viral hepatitis B

Chuan-Long Zhu, Wei-Ming Yan, Fan Zhu, Yong-Fen Zhu, Dong Xi, De-Ying Tian, Gary Levy, Xiao-Ping Luo, Qin Ning

Chuan-Long Zhu, Wei-Ming Yan, Fan Zhu, Yong-Fen Zhu, Dong Xi, De-Ying Tian, Xiao-Ping Luo, Qin Ning, Tongji Hospital of Tongji Medical College, Huazhong University of Science and Technology, Wuhan 430030, Hubei Province, China
Gary Levy, Toronto General Hospital of University of Toronto, Toronto M5G 2N2, Canada
Supported by the National Natural Science Foundation of China for Distinguished Young Scholars, No. 30225040 for Dr Ning Q, No. 30123019 for Dr Luo XP
Co-first-authors: Chuan-Long Zhu and Wei-Ming Yan
Correspondence to: Dr Qin Ning, Laboratory of Infectious Immunology and Department of Infectious Disease, Tongji Hospital, 1095 Jie Fang Avenue, Wuhan 430030, Hubei Province, China. qning@tjh.tjmu.edu.cn
Telephone: +86-27-83662391 Fax: +86-10-85381893
Received: 2005-04-28 Accepted: 2005-05-25

Abstract

AIM: To evaluate the expression of fibrinogen-like protein 2 (fgl2) and its correlation with disease progression in both mice and patients with severe viral hepatitis.

METHODS: Balb/cJ or A/J mice were infected intraperitoneally (ip) with 100 PFU of murine hepatitis virus type 3 (MHV-3), liver and serum were harvested at 24, 48, and 72 h post infection for further use. Liver tissues were obtained from 23 patients with severe acute chronic (AOC) hepatitis B and 13 patients with mild chronic hepatitis B. Fourteen patients with mild chronic hepatitis B with cirrhosis and 4 liver donors served as normal controls. In addition, peripheral blood mononuclear cells (PBMC) were isolated from 30 patients (unpaired) with severe AOC hepatitis B and 10 healthy volunteers as controls. Procoagulant activity representing functional prothrombinase activity in PBMC and white blood cells was also assayed. A polyclonal antibody against fgl2 was used to detect the expression of both mouse and human fgl2 protein in liver samples as well as in PBMC by immunohistochemistry staining in a separate set of studies. Alanine aminotransferase (ALT) and total bilirubin (TBil) in serum were measured to assess the severity of liver injury.

RESULTS: Histological changes were found in liver sections 12-24 h post MHV-3 infection in Balb/cJ mice. In association with changes in liver histology, marked elevations in serum ALT and TBil were observed. Mouse fgl2 (mfgl2) protein was detected in the endothelium of intrahepatic veins and hepatic sinusoids within the liver 24 h after MHV-3 infection. Liver tissues from the patients with severe AOC hepatitis B had classical pathological features of acute necroinflammation. Human fgl2 (hfgl2) was detected in 21 of 23 patients (91.30%) with severe AOC hepatitis B, while only 1 of 13 patients (7.69%) with mild chronic hepatitis B and cirrhosis had hfgl2 mRNA or protein expression. Twenty-eight of thirty patients (93.33%) with severe AOC hepatitis B and 1 of 10 with mild chronic hepatitis B had detectable hfgl2 expression in PBMC. No hfgl2 expression was found either in the liver tissue or in the PBMC from normal donors. There was a positive correlation between hfgl2 expression and the severity of the liver disease as indicated by the levels of TBil. PCA significantly increased in PBMC in patients with severe AOC hepatitis B.

CONCLUSION: The molecular and cellular results reported here in both mice and patients with severe viral hepatitis suggest that virus-induced hfgl2 prothrombinase/fibroleukin expression and the coagulation activity associated with the encoded fgl2 protein play a pivotal role in initiating severe hepatitis. The measurement of hfgl2/fibroleukin expression in PBMC may serve as a useful marker to monitor the severity of AOC hepatitis B and a target for therapeutic intervention.

Key words: Viral hepatitis; Fgl2; Murine hepatitis virus; Gene expression

Zhu CL, Yan WM, Zhu F, Zhu YF, Xi D, Tian DY, Levy G, Luo XP, Ning Q. Fibrinogen-like protein 2 fibroleukin expression and its correlation with disease progression in murine hepatitis virus type 3-induced fulminant hepatitis and in patients with severe viral hepatitis B. *World J Gastroenterol* 2005; 11(44): 6936-6940
http://www.wjgnet.com/1007-9327/11/6936.asp

INTRODUCTION

Viral hepatitis remains a major public health problem and the most common type of liver disease worldwide[1,2]. There are an increasing number of patients with chronic hepatitis B who develop acute hepatitis on chronic condition (AOC) and die of acute hepatic failure both as a result of our lack of understanding of the pathogenesis of the disease and lack of effective treatment[3]. The hallmark of AOC is the extreme rapidity of the necro-microinflammatory process resulting in widespread or total hepatocellular necrosis in weeks or even in days[3]. Our previous studies have shown that macrophage activation and expression of fgl2, encoding a serine protease capable of directly cleaving prothrombin to thrombin, result in widespread fibrin deposition within the liver and hepatocyte necrosis[3-6]. The present study was designed to assess the expression of fgl2 and its correlation with disease progression in both mice and patients with severe viral hepatitis.

MATERIALS AND METHODS

Virus

MHV-3 was purchased from the American Type Culture Collection (ATCC), plaque was purified on monolayers of DBT cells and grown to a titer of 1×10^6 PFU/mL in 17 CL cells. Viral titers were determined on monolayers of L2 cells by a standard plaque assay as described elsewhere[5].

Animals

Female Balb/cJ mice, 8-10 wk of age and weighing 20-22 g, were purchased from Hubei Provincial Institute of Science and Technology. Female A/J mice, 8-10 wk of age and weighing 20-22 g, were purchased from Jackson Laboratory (Bar Harbor, ME, USA).

Main reagents

The affinity-purified polyclonal antibody to both murine and human fgl2 prothrombinases was produced by 21 repeated injections into rabbits with a 14-amino-acid hydrophilic peptide (CKLQADDHRDPGGN) from exon 1 of the fgl2 prothrombinase coupled to keyhole limpet hemocyanin. Rabbit brain thromboplastin was purchased from Sigma Chemical Company (St. Louis, MO, USA).

Murine hepatitis model

All animal experiments were carried out according to the guidelines of the Chinese Council on Animal Care and approved by the Tongji Hospital of Tongji Medical College Committees on Animal Experimentation. The research protocol was reviewed and approved by the Hospital Institutional Review Board of Tongji Hospital, Huazhong University of Science and Technology, Wuhan, China. All mice were housed in the animal facility in Tongji Hospital. Mice received 100 PFU of MHV-3 by intraperitoneal injection. The liver and serum were collected from both Balb/cJ and A/J mice 0, 24, 48, and 72 h after intraperitoneal injection of MHV-3.

Patients

Biochemical, histological, and clinical features were used to define patients with severe AOC hepatitis B or mild chronic viral hepatitis B and compensated cirrhosis. The patients with chronic viral hepatitis B were evaluated on the basis of a thorough history and physical examination with special emphasis on risk factors for co-infection (with hepatitis C, D, or HIV), alcohol use, family history of viral hepatitis B and liver cancer. Liver tissues were obtained by biopsies from patients in 1995-2001, including 23 severe AOC hepatitis B patients (20 males and 3 females, 36.0±7.8 years on average with a mortality of 82% ALT 586.0±570.2 IU/L, TBil 452.9±227.2 μmol/L, and PT 35±10 s), 13 mild chronic hepatitis B patients (11 males and 2 females, 43.8±5.6 years on average, ALT 300.5±325.2 IU/L, TBil 78.3±175.4 μmol/L, and PT 12±1 s), 14 compensated cirrhosis hepatitis B patients (all males, 45.0±8.6 years on average, ALT 265.3±215.8 IU/L and TBil 46.6±27.6 μmol/L, PT 14±2 s). All mild chronic hepatitis B and compensated cirrhotic hepatitis B patients recovered from the disease. There were no significant differences in HBV DNA levels among different groups of patients. Liver biopsies were performed within 30 min after the patients died of acute hepatic failure. Liver samples were also obtained from four liver donors as normal controls. PBMCs were freshly isolated from 30 patients (all males, 37.7±9.1 years on average) with severe AOC hepatitis B, elevated ALT (108.9±75.2 IU/L) and TBil (389.3±116.9 μmol/L), elevated PT (40±31 s). Ten mild chronic hepatitis B patients (8 males and 2 females, 34.0±10.5 years on average) had normal ALT and TBil. The isolated PBMCs were smeared on slides and kept at -80 ℃ for further study. Liver tissue histological sections were stained with hemotoxylin and eosin.

Immunohistochemical staining

Immunohistochemical staining was performed with a rabbit polyclonal antibody against the fgl2 prothrombinase as described previously[3,6].

Procoagulant activity (PCA)

PBMC and white blood cells (WBC) were evaluated for functional PCA in a one-stage clotting assay. Freshly isolated PBMC and WBC were washed twice with PBS (pH 7.0) and resuspended at a concentration of 10^6/mL. Samples were assayed for the ability to shorten the spontaneous clotting time of normal citrated human platelet-poor plasma. Milliunits of PCA were assigned by reference to a standard curve generated with serial log dilutions of a standard rabbit brain thromboplastin as described previously[2].

Statistical analysis

Quantitative data were expressed as mean±SD. Statistical analysis was carried out by one-way analysis of variance. $P<0.05$ was considered statistically significant.

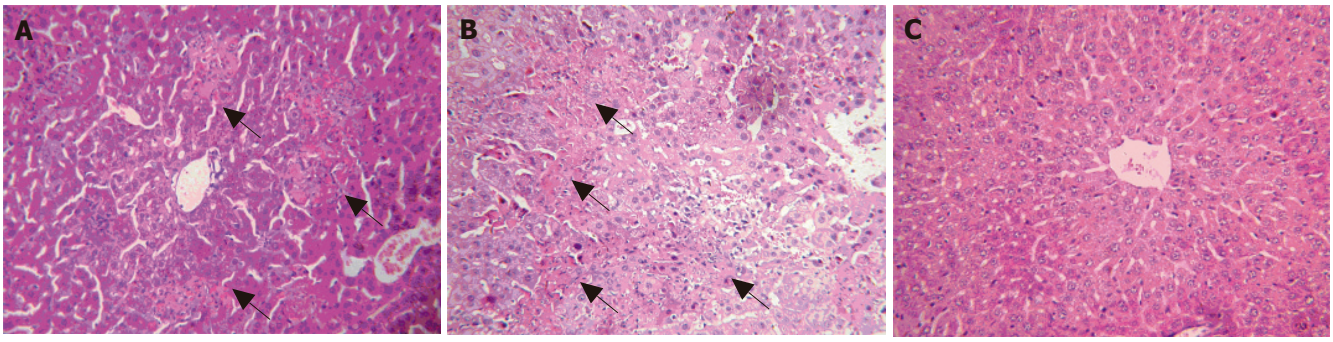

Figure 1 HE staining of liver tissue 48 h (**A**) and 72 h (**B**) after MHV-3 infection in Balb/cJ mice and 72 h (**C**) after MHV-3 infection in A/J mice. Arrows represent areas of hepatocyte necrosis.

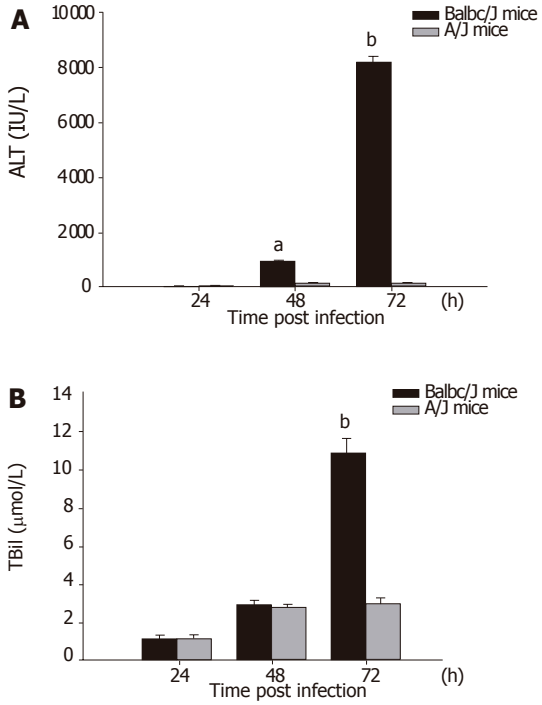

Figure 2 Serum ALT (**A**) and TBil (**B**) levels in MHV-3 infected Balb/cJ and A/J mice. $^{b}P<0.01$ *vs* A/J mice group.

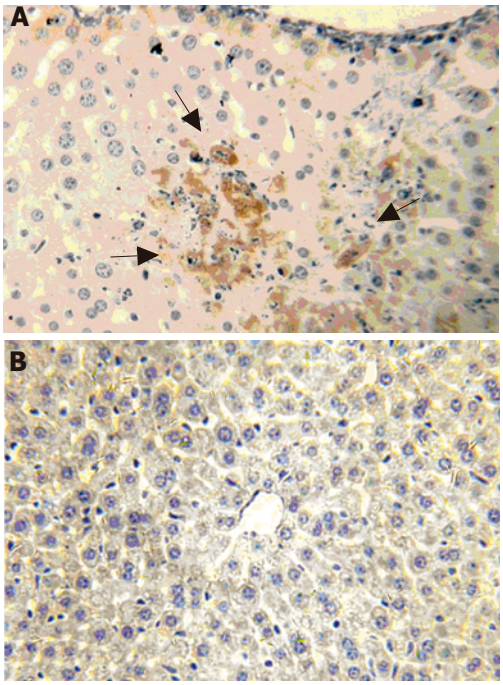

Figure 3 Mfgl2 expression in liver 24 h after MHV-3 infection Balb/cJ (**A**) and A/J (**B**) mice by immunohistochemical staining. Arrows represent mfgl2 positive cells.

RESULTS

Peritoneal administration of MHV-3-induced fulminant viral hepatitis in Balb/cJ mice

Small and discrete foci of necrosis with sparse polymorphonuclear leukocyte infiltrates were seen 12-24 h after MHV-3 infection. After 48 h, the area of these lesions enlarged and became confluent necroses (Figures 1A and 1B). There was no evidence of necrosis in the livers of MHV-3 infected A/J mice (Figure 1C). In Balb/cJ mice, serum ALT and TBil levels increased after 16-24 h, peaked at 72 h and remained elevated thereafter, while there were no significant ALT and TBil changes in MHV-3-infected A/J mice (Figures 2A and 2B).

Elevated expression of mfgl2 prothrombinase in MHV-3-infected Balb/cJ mice

mfgl2 prothrombinase expression increased in MHV-3-infected Balb/cJ mice starting from 12 to 24 h (Figure 3A) and was sustained until the animals died days after infection (data not shown). There was no evidence of mfgl2 staining in normal Balb/cJ mice (data not shown) or MHV-3-infected A/J mice (Figure 3B).

Increased hfgl2 prothrombinase and PCA in patients with severe AOC hepatitis B

Hfgl2 was detected in 21 of 23 patients (91.30%) with severe AOC hepatitis B (Figure 4A), while only 1 of 13 patients (7.69%) with mild chronic hepatitis B and cirrhosis (no evidence of active disease) had hfgl2 mRNA or protein expression. Twenty-eight of thirty patients with severe AOC hepatitis B (93.33%) and 1 of 10 with mild chronic hepatitis B had detectable hfgl2 expression in PBMC (Figure 4C). There was no hfgl2 expression either in the liver tissue or in the PBMC from the normal donors.

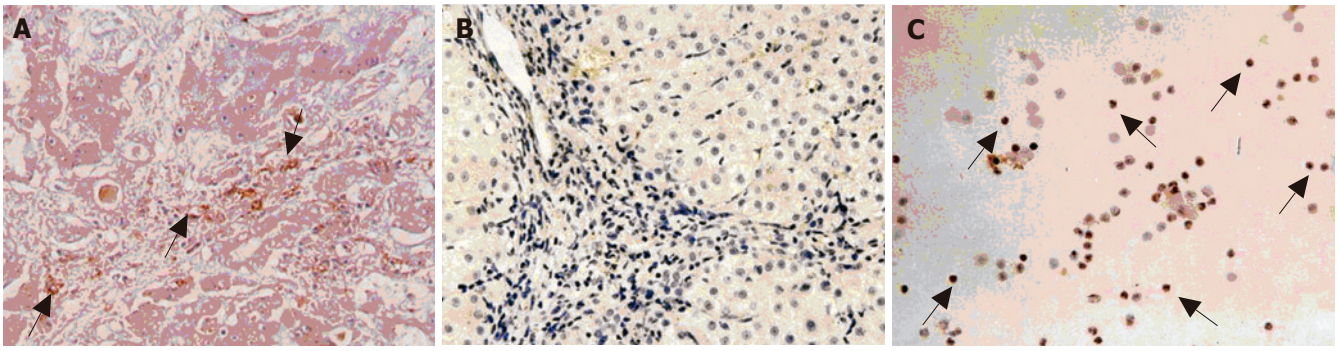

Figure 4 Immunohistochemical staining of hfgl2 in liver of patients with server AOC hepatitis B (**A**) and mild chronic hepatitis B (**B**) or in PBMC of patients with severe AOC hepatitis B (**C**). Arrows represent hfgl2 positive cells.

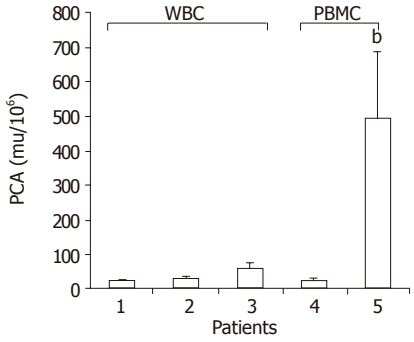

Figure 5 PCA levels in PBMC and WBC of patients.1. Healthy control; 2. patients with mild chronic hepatitis B; 3. patients with severe AOC hepatitis B; 4. healthy control; 5. patients with severe AOC hepatitis B. $^{b}P<0.01$ *vs* group 4

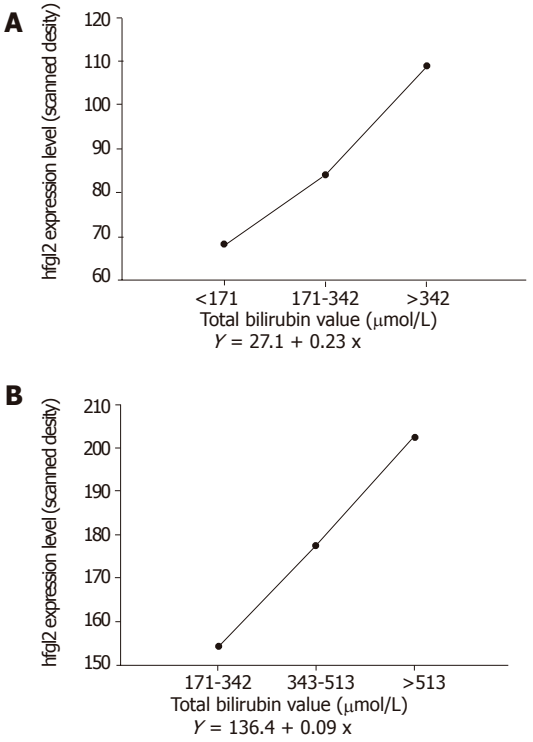

Figure 6 Correlation of hfgl2 expression in liver (**A**) and PBMC (**B**) with serum TBil level.

There was a significant increase in PCA activity in patients with serve AOC hepatitis B compared to patients with mild chronic hepatitis B, while there was no significant difference in PCA in various groups of patients (Figure 5).

Expression of hfgl2 prothrombinase correlates with the severity of hepatitis B

Hfgl2 expression both in liver and in PBMC was semi-quantified by a MPIAS-500 scanning analysis system. The data indicated that there was a close correlation between hfgl2 expression and the severity of the disease as shown in Figures 6A and 6B.

DISCUSSION

The inability to propagate human hepatitis viruses in culture and the lack of suitable animal models have impeded the determination of the pathological mechanisms of fulminant hepatic failure (FHF). However, animal models of FHF induced by murine hepatitis virus strain 3[4,7], transgenic models of hepatitis B virus infection[8,9] and clinical cases of FHF have provided insights into the pathogenesis of viral FHF[3,6]. MHV-3 produces a broad spectrum of diseases, including pneumonitis, encephalitis, enterocolitis, nephritis, and hepatitis[10,11]. This report demonstrated that Balb/cJ mice after MHV-3 infection developed fulminant viral hepatitis. HE staining showed infiltration of lymphocytes and massive hepatic necrosis in association with mfgl2 expression in the endothelial cells of hepatic sinusoids and in areas of focal necrosis. The serum ALT and bilirubin levels reflected the damage of liver tissue in MHV-3-induced FHF in Balb/cJ mice. In contrast, there was no or only minor hepatocyte injury with no mfgl2 in MHV-3-infected A/J mice. Therefore, these results further demonstrate that though MHV-3 replicates in tissues of both resistant and susceptible animals, suggesting that host factors may be more critical than viral replication in the pathogenesis of MHV-induced hepatitis. Our previous study have demonstrated that MHV-3 infection of macrophages results in transcription of host inflammatory cytokines, including TNF-α, IL-1, and superoxides[4]. Cytokines can play an important role in the course of inflammatory injury *in vivo*, and interference

with their action can alter the course of inflammatory diseases[12-15]. The importance of mfgl2 prothrombinase in the pathogenesis of MHV-3 infection is supported by the observation that a neutralizing antibody to this protein prevents fibrin deposition and protects mice from the lethality of MHV-3 infection. Furthermore, mfgl2 knockout mice lack fibrin deposition and liver necrosis and survival increased from 0% to 33%[3,16].

To address the relevance of hfgl2 in human chronic viral hepatitis, we studied patients with both minimal and severe AOC hepatitis B. We detected robust expression of hfgl2 near or within the areas of hepatic necrosis and elevated levels of hfgl2 were seen in PBMC isolated from patients with severe AOC hepatitis B. These findings are in contrast to the lack of expression of hfgl2 in the livers and PBMC of patients with minimal chronic hepatitis B. Functional assay of hfgl2 prothrombinase in PBMC showed a robust increase of PCA in patients with severe AOC hepatitis B compared to patients with minimal chronic hepatitis B. Semiquantitative analysis of hfgl2 expression both in liver tissue and PBMC showed a close correlation with the severity of the disease as indicated by elevations in serum bilirubin levels. There was no significant difference in terms of HBeAg level and HBV DNA level between different groups of patients, further supporting that host factors may be critical in the pathogenesis of severe hepatitis.

In conclusion, MHV-3-induced hfgl2 prothrombinase/fibroleukin expression and the potent function of the protein it encodes play a pivotal role in initiating both acute and fulminant hepatitis on chronic liver injury. The measurement of hfgl2 expression in PBMC may serve as a useful marker to monitor the severity of AOC hepatitis B and a target for therapeutic intervention.

REFERENCES

1 **Fattovich G.** Natural history and prognosis of hepatitis B. *Semin Liver Dis* 2003; **23:** 47-58

2 **Levy GA,** Liu M, Ding J, Yuwaraj S, Leibowitz J, Marsden PA, Ning Q, Kovalinka A, Phillips MJ. Molecular and functional analysis of the human prothrombinase gene (HFGL2) and its role in viral hepatitis. *Am J Pathol* 2000; **156:** 1217-1225

3 **Marsden PA,** Ning Q, Fung LS, Luo X, Chen Y, Mendicino M, Ghanekar A, Scott JA, Miller T, Chan CW, Chan MW, He W, Gorczynski RM, Grant DR, Clark DA, Phillips MJ, Levy GA. The Fgl2/fibroleukin prothrombinase contributes to immunologically mediated thrombosis in experimental and human viral hepatitis. *J Clin Invest* 2003; **112:** 58-66

4 **Ding JW,** Ning Q, Liu MF, Lai A, Leibowitz J, Peltekian KM, Cole EH, Fung LS, Holloway C, Marsden PA, Yeger H, Phillips MJ, Levy GA. Fulminant hepatic failure in murine hepatitis virus strain 3 infection: tissue-specific expression of a novel fgl2 prothrombinase. *J Virol* 1997; **71:** 9223-9230

5 **Ning Q,** Brown D, Parodo J, Cattral M, Gorczynski R, Cole E, Fung L, Ding JW, Liu MF, Rotstein O, Phillips MJ, Levy G. Ribavirin inhibits viral-induced macrophage production of TNF, IL-1, the procoagulant fgl2 prothrombinase and preserves Th1 cytokine production but inhibits Th2 cytokine response. *J Immunol* 1998; **160:** 3487-3493

6 **Chen Y,** Ning Q, Wang BJ, Zhang DS, Yan FM, Sun Y, Xi D, Yan WM, Hao LJ. Expression of human fibroleukin gene acute on chronic hepatitis B and its clinical significance. *Zhonghua Yi Xue Za Zhi* 2003; **83:** 446-450

7 **Ning Q,** Berger L, Luo X, Yan W, Gong F, Dennis J, Levy G. STAT1 and STAT3 alpha/beta splice form activation predicts host responses in mouse hepatitis virus type 3 infection. *J Med Virol* 2003; **69:** 306-312

8 **Guidotti LG,** Morris A, Mendez H, Koch R, Silverman RH, Williams BR, Chisari FV. Interferon-regulated pathways that control hepatitis B virus replication in transgenic mice. *J Virol* 2002; **76:** 2617-2621

9 **Guidotti LG,** McClary H, Loudis JM, Chisari FV. Nitric oxide inhibits hepatitis B virus replication in the livers of transgenic mice. *J Exp Med* 2000; **191:** 1247-1252

10 **Ning Q,** Luo XP, Wang ZM, Han MF, Yan WM, Liu MF, Levy G. The study of cis-element HNF4 in the regulation of mfg12 prothrombinase/fibroleukin gene expression in response to nucleocapsid protein of MHV-3. *Zhonghua Yi Xue Za Zhi* 2003; **83:** 678-683

11 **Lai MM.** RNA recombination in animal and plant viruses. *Microbiol Rev* 1992; **56:** 61-79

12 **Thimme R,** Wieland S, Steiger C, Ghrayeb J, Reimann KA, Purcell RH, Chisari FV. CD8(+) T cells mediate viral clearance and disease pathogenesis during acute hepatitis B virus infection. *J Virol* 2003; **77:** 68-76

13 **Major ME,** Dahari H, Mihalik K, Puig M, Rice CM, Neumann AU, Feinstone SM. Hepatitis C virus kinetics and host responses associated with disease and outcome of infection in chimpanzees. *Hepatology* 2004; **39:** 1709-1720

14 **McClary H,** Koch R, Chisari FV, Guidotti LG. Relative sensitivity of hepatitis B virus and other hepatotropic viruses to the antiviral effects of cytokines. *J Virol* 2000; **74:** 2255-2264

15 **Wieland SF,** Vega RG, Muller R, Evans CF, Hilbush B, Guidotti LG, Sutcliffe JG, Schultz PG, Chisari FV. Searching for interferon-induced genes that inhibit hepatitis B virus replication in transgenic mouse hepatocytes. *J Virol* 2003; **77:** 1227-1236

16 **Li C,** Fung LS, Chung S, Crow A, Myers-Mason N, Phillips MJ, Leibowitz JL, Cole E, Ottaway CA, Levy G. Monoclonal antiprothrombinase (3D4.3) prevents mortality from murine hepatitis virus (MHV-3) infection. *J Exp Med* 1992; **176:** 689-697

Science Editor Wang XL and Guo SY **Language Editor** Elsevier HK

PO Box 2345, Beijing 100023, China
www.wjgnet.com
wjg@wjgnet.com

ELSEVIER

World J Gastroenterol 2005;11(44):6941-6947
World Journal of Gastroenterology ISSN 1007-9327

• *BASIC RESEARCH* •

Clinical significance of telomerase and its associate genes expression in the maintenance of telomere length in squamous cell carcinoma of the esophagus

Chung-Ping Hsu, Li-Wen Lee, Sen-Ei Shai, Chih-Yi Chen

Chung-Ping Hsu, Li-Wen Lee, Sen-Ei Shai, Chih-Yi Chen, Division of Thoracic Surgery, Department of Surgery, Taichung Veterans General Hospital, Taichung, Taiwan, China
Chung-Ping Hsu, School of Medicine, National Yang-Ming University, Taipei, Taiwan, China
Supported by grant from NSC (NSC-92-2314-B-075A-011), Taipei, Taiwan, China
Correspondence to: Chung-Ping Hsu, MD, FCCP, Division of Thoracic Surgery, Taichung Veterans General Hospital, No. 160, Sec. 3, Taichung-Kang Road, Taichung, Taiwan, China. cliff@vghtc.gov.tw
Telephone: +886-4-23592525-2692 Fax:+886-4-23594065
Received: 2005-03-08 Accepted: 2005-07-08

Abstract

AIM: To observe the interaction between the expression of telomerase activity (TA) and its associate genes in regulation of the terminal restriction fragment length (TRFL) in esophageal squamous cell carcinoma (SCC).

METHODS: Seventy-four specimens of esophageal SCC were examined. The TA was measured by telomeric repeat amplification protocol (TRAP) assay, and the associated genes [human telomerase-specific reverse transcriptase (hTERT), hTERC, TP1, c-Myc, TRF1, and TRF2] were detected using RT-PCR method. The TRFL was measured by Telomere Length Assay Kit and Southern blotting. The correlations between the expression of telomerase and its associated genes with the TRFL and survivals were examined.

RESULTS: Expressions of the TA, hTERT, hTERC, TP1, c-Myc, TRF1, and TRF2 genes were observed in 85.1%, 64.9%, 79.7%, 100.0%, 94.6%, 82.4%, and 91.9% of the tumor tissues, respectively. The TRFL of the tumor and normal esophageal tissues were 2.70±1.42 and 4.93 ±1.74 kb, respectively (P<0.0001). The TRFL of the telomerase positive and telomerase negative tumor tissues were 2.72±1.44 and 2.58±1.32 kb, respectively (P = 0.767). The TRFL ratios (TRFLR) of the telomerase positive and telomerase negative tumor tissues were 0.55±0.22 and 0.59±0.41, respectively (P = 0.742). The expression rates of h-TERT (P = 0.0002), hTERC (P<0.0001), and TRF1 (P = 0.002) in the tumor tissues are higher than those of the normal paired tissues. Though TA is markedly activated in tumor tissues (P<0.0001), its expression is not related to clinicopathological parameters including gender, tumor differentiation, and TNM stages. The cumulative 4-year survival rates of telomerase positive and telomerase negative cases were 35.86% and 31.2%, respectively (P = 0.8442). The cumulative 4-year survival rates of patients with their TRFLR ≤85% and >85% were 38.7% and 15.7%, respectively (P = 0.1307).

CONCLUSION: Though telomerase expression is not related to tumor stages and prognosis, our data support that the TA increased as the TRFL decreased, probably under the control of hTERT, hTERC, and TRF1. When telomerase expression was activated, only TRF2 overexpression persisted to stabilize T-loop formation. Furthermore, as the TRFLR decreased to 85%, a trend of better prognosis was observed. Cox model analysis indicates a higher t/n TRFLR and distant metastasis are independent poorer prognostic factors (P = 0.035 and P = 0.042, respectively).

Key words: Telomere; Telomerase; hTERT; Terminal restriction fragment length; Esophageal cancer

Hsu CP, Lee LW, Shai SE, Chen CY. Clinical significance of telomerase and its associate genes expression in the maintenance of telomere length in squamous cell carcinoma of the esophagus. *World J Gastroenterol* 2005; 11(44): 6941-6947
http://www.wjgnet.com/1007-9327/11/6941.asp

INTRODUCTION

Telomerase is a ribonucleoprotein, which is responsible for the synthesis and maintenance of the telomeric repeats at the distal ends of human chromosomes. These end structures, named telomeres, serve as protective caps and consist of specific tandem repeats (5'-TTAGGG-3') with an average length of 5-20 kb[1-3]. Upon each cell division, the chromosomal ends shorten at a rate of 50-200 bp[4] This molecular erosion sets a physical limit to the potential number of cell divisions and serves as a "mitotic clock" defining the lifespan of somatic cells. Unlike somatic cells, new telomeric repeats are added to the chromosomal end of the germline cells to maintain their stability and also preserve their full genomic information for the next

generation[5]. Similarly, immortalized cell lines and more than 85% of the cancer cells can prevent the telomere from progressive shortening by telomerase activation. This phenomenon is regulated by a length-sensing feedback mechanism when the critical point is reached[6]. Telomerase contains a catalytic human telomerase-specific reverse transcriptase (hTERT) and a RNA template (hTERC) for the telomere, provides the cancer cells unlimited replicative capacity and prevents lethal chromosomal instability. Other telomerase-independent mechanism called as alternative lengthening of telomeres (ALT) may ensure the same chromosome ends replication functions.

Normally, the 3' DNA terminal protein-DNA complexes of the telomeres form capping structures to stabilize chromosomal ends and prevent them from being recognized as DNA double-strand breaks by the cells. The current model for chromosome capping is that telomeres form a higher-order chromatin structure that physically hides the 3'-chromosome end from cellular activities. This protective structure could be provided by the ability of the 3'-overhang to fold back and invade the double-strand region of the telomere forming the so-called T-loop and D-loop with the help of TRF1 and TRF2[7,8]. If these checkpoints fail, chromosomal instability may ensue leading to oncogenic mutations.

Since 1994, the telomeric repeat amplification protocol (TRAP) assay was extensively used for the detection of TA. Our previous report has demonstrated good correlations between the expressions of hTERT (not telomerase) and its associated genes such as c-Myc, TRF1 and TRF2[9]. We also found that the expression of the TA may indicate poorer prognosis[10]. A tumor-to-normal telomere restriction fragment length ratio (t/n TRFLR) $\leq$ 75% indicates a better prognosis[11]. In addition, we found a negative linear correlation between the t/n TRFLR and expression of TA, suggesting a negative feedback mechanism in the maintenance of TRFL[11]. In this study, we investigated for correlations between the changes of t/n TRFLR and expression of the telomerase associated genes including c-Myc, TRF1 and TRF2 in squamous cell carcinoma of the esophagus.

MATERIALS AND METHODS

Patients and follow-up

Between June 1999 and December 2003, we included 74 cases of squamous cell carcinoma of the esophagus who underwent surgical resection in this prospective study. Patients who received pre-operative chemotherapy or radiotherapy were excluded. Whole body bone scan and liver sonography were performed for all of the patients to rule out systemic metastasis. The tumor differentiation included well-differentiated carcinoma in none, moderately differentiated carcinoma in 49, and poorly differentiated carcinoma in 25. Tumor staging was performed according to the AJCC (6th edition) criteria[12]. The p-TNM stages included stage I in 2, stage II in 25, stage III in 33, and stage IV in 14. The clinicopathological characteristics of the patients are summarized in Table 1.

Table 1 Clinical characteristics of 74 patients with esophageal cancer

	Numbers of patients
Age (mean), years	36-79 (59.5)
Sex	
Male	71
Female	3
Differentiation	
Well	0
Moderate	49
Poor	25
Tumor site	
T1	3
T2	10
T3	50
T4	11
Lymph node	
N0	24
N1	50
Metastasis	
M0	60
M1	14
Stage	
I	2
II	25
III	33
IV	14

Preparation of cell extracts

Twenty milligrams of frozen tissue samples were lysed with 200 μL lysis buffer and homogenized by polytron. Samples were then incubated in ice for 30 min and the lysate was centrifuged at 16 000 g at 4 °C for 20 min. The supernatant was transferred to a fresh tube and the protein concentration was determined by the Bradford assay (Bio-Rad Protein Assay Kit, Bio-Rad Lab., Hercules, CA, USA).

DNA isolation from tissues

Twenty-five milligrams of fresh frozen tissue was lysed with 800 μL lysis buffer containing 0.5% sodium dodecyl sulfate (SDS), 2 mmol/L EDTA, 0.5 mol/L NaCl, 10 mmol/L $MgCl_2$, 10 mmol KCl and 10 mmol Tris-HCl (pH 76), and digested with proteinase K at 50 μg/mL at 50 °C for at least 2 h. High molecular weight DNA was extracted with phenol/chloroform.

Assay for telomerase activity

TA was measured twice in independent experiments using 1-3 μg of total protein. Assays were performed using Telomerase PCR ELISA Kit (Boehringer Mannheim GmbH, Mannheim, Germany) including TRAP assay and detection by ELISA in two steps. In the first step, using TRAP, cell extracts were incubated with biotinylated telomerase substrate oligonucleotide (P1-TS) at 25 °C for 30 min, followed by 94 °C for 10 min to inactivate the telomerase. The extended products were amplified by PCR using Taq polymerase, the P1-TS, P2 primers and nucleotides. The PCR conditions were 33 cycles of 94 °C for 30 s on a DNA thermocycler (GeneAmp PCR System 9700, Perkin Elmer, Norwalk, CT, USA). In the second step, using the ELISA method, the amplified products

were immobilized onto streptavidin-coated microtiter plates via biotin-streptavidin interaction, and then detected by anti-digoxigenin (DIG) antibody conjugated to peroxidase. After the addition of the peroxidase substrate (3,3',5,5'-tetramethyl benzidine), the amount of TRAP products were determined by measurement of their absorbance at 450 nm (with a reference wavelength of 690 nm). Negative control reactions were performed by incubating cell extracts with 1 μg/μL RNase for 20 min at 37 °C. The results were interpreted as negative, 1+, 2+, and 3+ when the optic density (OD) values were <0.2, 0.2-1, 1-2, and >2, respectively.

Moreover, to confirm the ELISA results, amplified products were systemically run on 15% non-denaturing polyacrylamide gel. After transferring the PCR products onto a positively charged nylon membrane, Southern blotting was performed by the semi-dry electrophoretic blotting instrument (Multiphore II NovaBlot Unit, Amersham Pharmacia Biotech, Buckinghamshire, UK). The membrane was then incubated with a streptavidin alkaline phosphatase conjugate (1:5 000 dilute in blocking solution), and after rinsing, blotted products were visualized by Biotin Luminescence Detection Kit (Boehringer Mannheim). In addition, all telomerase-negative tumor specimens were re-checked by additional TRAP assay using a 150 bp internal telomerase assay standard to exclude the possibility of Taq DNA polymerase inhibition in the tumor extracts[13].

Reverse transcription-polymerase chain reaction (RT-PCR) for telomerase-associated genes

Total RNA was isolated from tissue by SV Total RNA Isolation System (Promega Corporation, USA). First strand complementary DNA (cDNA) was synthesized using 5 mg of total cellular RNA with reverse transcriptase (Invitrogen Tech-Line SM, USA) and random primers (Protech Technology Enterprise Co. Ltd). PCR was performed using RT-MPCR* Kits for Human Telomerase Genes (Maxim Biotech, Inc., USA). RTMPCR* Kits included PCR primers for human 18S (hTELS-18S, 554 bp), PCR primers for human TRF-1 (hTELS-TRF1, 433 bp), PCR primers for human c-Myc (hTELS-MYC, 381 bp), PCR primers for human TRF-2 (hTELS-TRF2, 337 bp), PCR primers for human TP-1 (hTELS-TP1, 292 bp), PCR primers for hTERT (hTELS-TERT, 255 bp), and PCR primers for human TER (hTELS-TER, 191 bp). PCR reaction mixture contained RT-MPCR buffer, 200 mM each of dATP, dCTP, dTTP, and dGTP, 5U Taq DNA polymerase and 1 mL primers. The thermal cycles of PCR were performed as follows: 3 cycles at 95 °C for 1 min and 56 °C for 4 min followed by 30 cycles at 94 °C for 1 min and 55 °C for 2.5 min and then an extension of 1 cycle at 70 °C for 10 min. PCR products were subjected to electrophoresis through 3% agarose gel stained with ethidium bromide.

Terminal restriction fragment (TRF) length measurement and tumor-to-normal TRFL ratio (t/n TRFLR)

TRFL measurement was performed using TeloTAGGG Telomere Length Assay Kit (Roche, Mannheim, Germany). Eight micrograms of genomic DNA was digested with each 30U Hinf 1/Rsa l at 37 °C for 16 h. The resulting fragments were fractionated by electrophoresis on 0.8% agarose gel and transferred to nylon membrane using Southern blotting. After transfer, the transferred DNA was fixed on the membrane by UV-crosslinking (120 mJ). The membrane was first pre-hybridized at 42 °C for 30 min and then hybridized with telomere-specific DIG-labeled probe at 42 °C for 3 h. After washing the membrane in 2× SSC, the membrane was incubated with anti-DIG-alkaline phosphatase (1:5 000 dilute in blocking solution). Finally, the immobilized telomere probe was visualized by alkaline phosphatase metabolizing CDP-Star, a highly sensitive chemiluminescent substrate. The membrane was then exposed to X-ray film, and the average TRFL was determined by comparing the signals relative to a molecular weight standard (using BIO-PROFIL Bio-1D Software, Version 99, Vilber Lourmat, France), and the mean of three measured TRFLs deducted by 2.5 kb was used as the presented telomere length[14,15]. Furthermore, the TRFLR was defined as the ratio between the length of tumor tissue TRF (t-TRF) and their paired normal tissue TRF (n-TRF) from the same patient.

Statistical analysis

All probabilities were two-tailed, with a *P*-value less than 0.05 regarded as statistically significant. The statistical calculations were conducted with SPSS software (v10.5, SPSS Inc., Chicago, IL, USA).

RESULTS

Expression of telomerase activity and its associated genes

Positive TAs were observed in 63 of 74 (85.1%) tumor tissue samples, and 24 of 74 (32.4%) normal tissue samples, respectively. Expressions of hTERT, hTERC, TP1, c-Myc, TRF1 and TRF2 genes were observed in 64.9%, 79.7%, 100.0%, 94.6%, 82.4%, and 91.9% of the tumor tissues, respectively. Representative samples showing the expression of the TA by TRAP assay, and the associated genes in paired tumor (T) and normal (N) tissues are shown in Figure 1. Expression of TA according to the patient's clinicopathological characteristics are listed in Table 2. Expression of the telomerase associate genes in normal and tumor tissues are listed in Table 3. Expression of the telomerase associate genes in tumor tissues according to the TA are listed in Table 4.

Terminal restriction fragment (TRF) length and tumor-to-normal TRFL ratio (t/n TRFLR)

The mean TRFL of the tumor and normal esophageal tissues were 2.70±1.42 and 4.93±1.74 kb, respectively (P<0.0001). The mean TRFL of the telomerase positive and telomerase negative tumor tissues were 2.72±1.44 and 2.58±1.32 kb, respectively (P = 0.767). The TRFLR of the telomerase positive and telomerase negative tumor tissues were 0.55±0.22 and 0.59±0.41, respectively (P = 0.742). The mean TRFL were 3.04±0.42 kb in stage I tumor, 2.65±1.44 kb in stage II tumor, 2.83±1.44 kb in stage III

Table 2 Expression of telomerase activity according to the clinicopathological characteristics of 74 esophageal cancer patients

	Telomerase (+)	Telomerase (-)	*P* value[1]
Gender			1.0
Female	3	0	
Male	60	11	
Differentiation			0.492
Well to moderate	20	5	
Poor	43	6	
Tumor Size			1.0
T_1+T_2	11	2	
T_3+T_4	52	9	
Lymph node			0.321
N_0	19	5	
N_1	44	6	
Metastasis			0.110
M_0	49	11	
M_1	14	0	
Stage			0.194
I+II	21	6	
III+IV	42	5	

[1]Fisher's exact test (if expectation<5) or Yate's correction of contingency.

Table 3 Expression of telomerase associate genes of the tumor and normal tissues in 74 esophageal cancer patients

Expression	Positive	Negative	*P*-values[1]
TRF1			0.002
Tumor	61	13	
Normal	43	31	
TRF2			1.0
Tumor	68	6	
Normal	67	7	
c-Myc			0.160
Tumor	70	4	
Normal	64	10	
hTERT			0.0002
Tumor	48	26	
Normal	24	50	
hTERC			<0.0001
Tumor	59	14	
Normal	30	44	
TP1			N/A
Tumor	74	0	
Normal	74	0	
Tissue			0.288
Tumor	63	11	
Normal	24	50	<0.0001

[1]Pearson's χ^2-test.

Table 4 Expression of telomerase associate genes of the tumor tissues according to the telomerase activity in 74 esophageal cancer patients

	Telomerase (+)	Telomerase (-)	*P*-value[1]
hTERT			0.737
Positive	40	8	
Negative	23	3	
hTERC			0.684
Positive	51	8	
Negative	12	3	
c-Myc			0.103
Positive	61	9	
Negative	2	2	
TRF1			0.396
Positive	53	8	
Negative	10	3	
TRF2			0.039[1]
Positive	60	8	
Negative	3	3	
TP1			N/A
Positive	63	11	
Negative	0	0	

[1]Fisher's exact test (if expectation<5) or Yate's correction of contingency.

Table 5 TRFL and t/n TRFLR of the tumor tissues according to the telomerase expression and TNM stages

Variables	TRFL	*P*- values	t/n TRFLR	*P*- values
Tissues		<0.0001[1]		
Normal	4.93±1.74 kb			
Tumor	2.70±1.42 kb			
Telomerase		0.767[1]		0.742[2]
Positive	2.72±1.44 kb		0.55±0.22	
Negative	2.58±1.32 kb		0.59±0.41	
Tumor stages		0.936[2]		0.867[2]
Stage I	3.04±0.42 kb		0.818±0.019	
Stage II	2.65±1.44 kb		0.686±0.184	
Stage III	2.83±1.44 kb		0.729±0.265	
Stage IV	2.41±1.49 kb		0.649±0.185	
Total	2.70±1.42 kb		0.73±0.24	

P values: [1]Paired *t*-test, [2]Independent *t*-test.

tumor, and 2.41±1.49 kb in stage IV tumor, respectively (stage I+II *vs* stage III+IV, $P = 0.936$). The t/n TRFLR were 0.818±0.019 in stage I tumor, 0.686±0.184 in stage II tumor, 0.729±0.265 in stage III tumor, and 0.649±0.185 in stage IV tumor, respectively (stage I+II vs stage III+IV, $P = 0.867$). Table 5 lists the TRFL and t/n TRFLR data of our patients. The representative samples showing TRFL in paired T and N tissues are shown in Figure 2.

Survival analysis

The influence of TA expression was evaluated by cumulative survival period. The 5-year cumulative survival

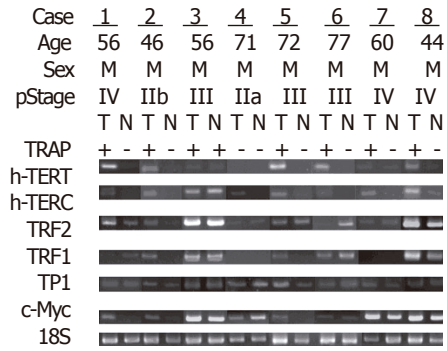

Figure 1 Representative samples showing expression of the telomerase activity by TRAP assay, and the associated genes in paired tumor (T) and normal (N) tissues.

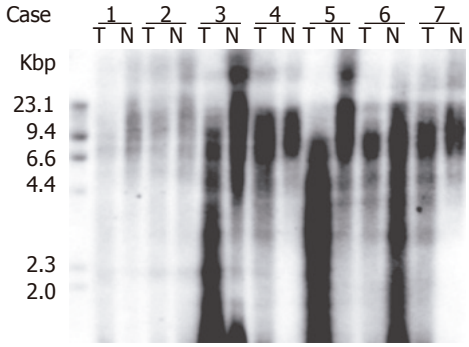

Figure 2 Representative samples showing TRFL by telomere length assay kit in paired tumor (T) and normal (N) tissues are shown.

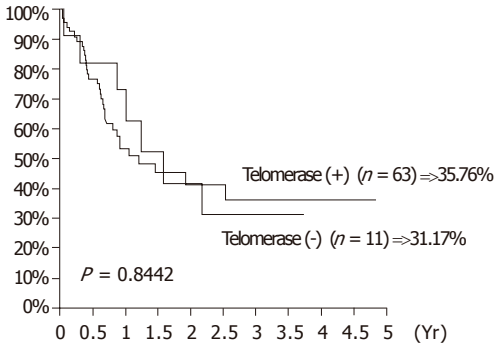

Figure 3 Cumulative survival rates according to the expression of telomerase activity in 74 SCC of esophagus.

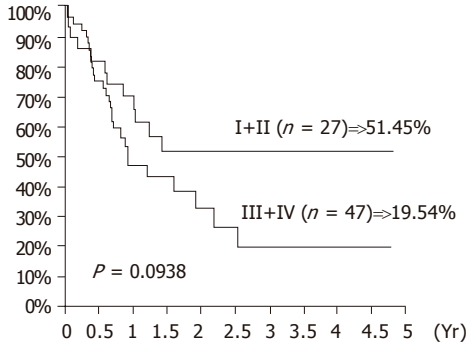

Figure 4 Cumulative survival rates according to the TNM stages in 74 SCC of esophagus.

rates of the patients by tumor stages and presence of distant metastasis are shown in Figures 3 and 4. As shown in Figure 5, the 4-year cumulative survival rates of telomerase-positive and telomerase-negative patients were 35.8, and 31.2%, respectively (P = 0.8442). When survival analyses were performed based on the change of TRFL in the tumor tissues, a cut-off value of 50% demonstrated a trend in survival difference. As shown in Figure 6, the 4-year cumulative survival rates of lower t/n TRFLR (≤85%) and higher t/n TRFLR (>85%) patients were 38.7, and 15.7%, respectively (P = 0.1307). Multivariate survival analysis using Cox proportional hazards model revealed

Table 6 Multivariate survival analysis for Cox proportional hazards model

Risk factors (# Patients)	Coefficients (SE)	Relative risk (95%CI)	*P*-values[1]
t/n TRFLR	0.78 (0.37)	(1.06-4.48)	0.035
≤85% (*n* = 57)		1	
>85% (*n* = 17)		2.18	
T-status	1.17 (0.78)	(0.70-15.06)	0.134
T1+T2 (*n* = 13)		1	
T3+T4 (*n* = 61)		3.24	
N-status	1.06 (0.66)	(0.79-10.48)	0.108
N0 (*n* = 24)		1	
N1+N2 (*n* = 50)		2.88	
M-status	0.87 (0.43)	(1.03-5.49)	0.042
M0 (*n* = 60)		1	
M1 (*n* = 14)		2.38	
Stage	-0.90 (0.78)	(0.09-1.89)	0.251
I+II (*n* = 27)		1	
III+IV (*n* = 47)		0.41	
Differentiation	0.33 (0.35)	(0.70-2.76)	0.352
W+M (*n* = 25)		1	
P (*n* = 49)		1.39	
Telomerase expression	-0.11 (0.46)	(0.36-2.22)	0.811
Negative (*n* = 11)		1	
Positive (*n* = 63)		0.90	

[1]Wald statistic

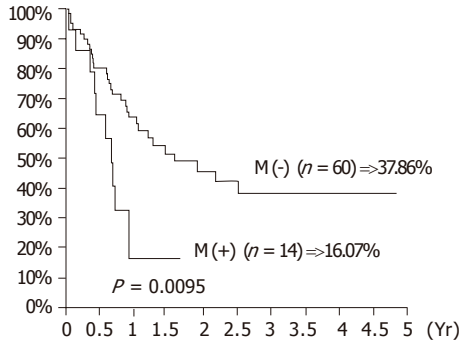

Figure 5 Cumulative survival rates according to the distant metastasis in 74 SCC of esophagus.

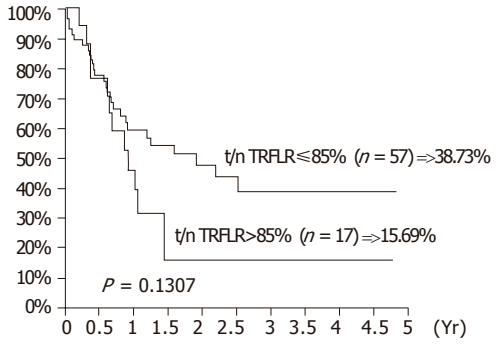

Figure 6 Cumulative survival rates according to the t/n TRFLR in 74 SCC of esophagus.

independent prognostic factors that includes t/n TRFLR (P = 0.035), and M-status (P = 0.042) of the tumor (Table 6).

DISCUSSION

Cell numbers are vigorously controlled within the body and, in human adults, only a few cell types are capable of continued division. Cultured cells *in vitro* can undergo only a limited number of cell divisions, known as the Hayflick limit, before entering a state of senescence where they remain metabolically active but have lost their capacity to replicate (M1 crisis). Reduction in telomere length could provide the signal to cause growth arrest. Cultured cells can be induced to continue to divide beyond the Hayflick limit by inactivation of p53 or p16INK4a genes. During this process of oncogenesis, their telomeres continue to shorten with each division and at a certain point cells enter a crisis where the majority will die (M2 crisis). Rare immortalized clones that emerge from crisis express the enzyme telomerase[16]. The regulation of TA is a complex issue, involving the transcriptional activity of the hTERC (telomerase RNA component gene), and the hTERT, as well as the interaction of telomerase with other telomerase-associated proteins, such as TP1/c-Myc/TRF1/TRF2/ Tankyrase. TP1, which is expressed ubiquitously, may play a role in coordinating telomerase holoenzyme tertiary or/and quaternary structures and/or serve as a docking/ scaffold protein in recruiting telomerase regulatory factors. The ability of c-Myc to function as a transcription factor has been shown to depend upon its dimerization with the protein Max[17]. In addition to the formation of stable complexes with c-Myc, Max also heterodimerizes with proteins of the Mad(Mxi1) family[18]. These Mad/Max complexes act in an antagonistic manner to c-Myc/Max-induced transactivation and result in potent repression of gene expression. Two proteins that bind to the double-stranded region of mammalian telomeres have been identified: TTAGGG repeat binding factor 1 (TRF1) and factor 2 (TRF2). These proteins are related and have a similar domain organization. Both proteins are associated with telomeres throughout the cell cycle and bind to the cognate telomeric sequence as homodimers using a carboxy-terminal myb-type DNA binding domain. TRF1 regulates telomere length and TRF2 protects chromosome ends. These two paralogs bind to double stranded telomeric DNA with high affinity, but no interaction between TRF1 and TRF2 has been observed so far[19,20]. However, TRF1 and TRF2 interact with other proteins in regulating telomeric repair. Together with tankyrase, TRF1 is involved in telomere length regulation via negative feedback mechanism; overexpression results in shortened telomeres, and mutation of telobox causes elongated telomeres[20,21]. Removal of TRF2 from the telomere results in the loss of the 3'-overhang, covalent fusion of telomeres, and the induction of ATM and p53 dependent apoptosis. Overexpression of TRF2 in telomerase negative cells prevents critically short telomeres from fusion and delays the onset of senescence[19] .

The expression rates of telomerase and hTERT were 85.1% and 64.9%, which were consistent with other reports. We also found telomerase expression in 32.4% of the paired normal esophageal mucosa. This had been attributed to actively dividing basal layer cells[22,23] or submucosal tumor infiltration[24]. A higher telomerase and hTERT expression rate in the normal esophageal mucosa makes it a distinct finding as compared with other digestive tract mucosa[25]. The telomerase expression of the tumor is not related to the clinicopathological parameters including gender, tumor differentiation, and TNM stages of the patients (see Table 2). Controversy in interpretation of the clinical significance of telomerase expression may be related to the presence of the alternative telomere lengthening (ATL) mechanism. ALT cells have long heterogeneous telomeres thought to be generated by a recombination-based mechanism[26]. Interestingly, tumor cells may simultaneously obtain both telomerase and ATL mechanisms in maintaining telomere length[27]. This will cause more complexity in analyzing the relation between the telomerase expression, telomere maintenance, and their impact on prognosis.

In a previous study in non-small cell lung cancers, we found that c-Myc, TRF1, and TRF2 expression was closely related to hTERT expression, although there was no association with telomerase expression[9]. We also found that when the TRFL decreased to a critical level, the TA could be elicited[11]. This hypothesis was further confirmed by the establishment of a negative linear association between the t/n TRFLR and the expression of TA in NSCLC tumor tissues[11] In the current study, we found a higher expression rate of the hTERT, hTERC, and TRF1 in the tumor tissues (Table 3). This suggests that hTERT, hTERC, and TRF1 are incorporated in the regulation of telomerase expression in the tumor tissues as the TRFL becomes progressively shortened. However, once the telomerase expression was activated, TRF1 expression becomes suppressed to prevent interference with telomerase binding. Instead, TRF2 overexpression persisted (see Table 4), which increases the number of TRF2 molecules binding on the telomeric DNA, and subsequently leads to more efficient and stable T-loop formation as described in the *in vitro* study[28]. Therefore, it is not only the telomere length, but also the TRF2 that determines whether senescence ensues or not.

Though a decreased TRFL was observed in the tumor tissues, there were no significant changes in TRFL between different tumor stages or different telomerase expression. Also, the t/n TRFLR did not change accordingly in different tumor stages. But when the t/n TRFLR decreased to a critical level ($\leqslant 85\%$), a better survival was observed (Figure 6). This may be due to the failure of the tumor cells to regain an adequate telomere length, which subsequently triggers the apoptosis pathway. Cox model analysis also confirmed t/n TRFLR as an independent prognostic factor in addition to distant metastasis.

In summary, our data suggest that telomerase expression in esophageal cancers is not related to tumor stages and patient's prognosis. This may be due to a high telomerase expression in the normal esophageal mucosa which makes telomerase not a reliable biomarker in esophageal tumors. However, TA can be elicited as the TRFL decreased in the tumor tissues, probably under the control of hTERT, hTERC, and TRF1 (but not TRF2).

Once the telomerase expression was elicited, TRF1 expression becomes suppressed to prevent interference with telomerase binding. Instead, TRF2 overexpression persisted, which increases the number of TRF2 molecules binding on the telomeric DNA, and subsequently leads to more efficient and stable T-loop formation. Moreover, as the t/n TRFLR decreased to 85%, a trend of poorer prognosis was observed. These findings further confirm our previous proposal using the t/n TRFLR as an indicator of chromosome ends replication ability[11]. The complex interweaving of the regulatory pathway for telomere maintenance and the mechanism involved in the detection of telomere loss by tumor cells, which subsequently activates telomerase expression require further study.

ACKNOWLEDGMENTS

The authors thank Ms SW Tang, and Ms HC Ho (Biostatistics Task Force of Taichung Veterans General Hospital) for their assistance in tissue preparation, data recording, and statistical analysis.

REFERENCES

1 **Allshire RC,** Dempster M, Hastie ND. Human telomeres contain at least three types of G-rich repeat distributed non-randomly. *Nucleic Acids Res* 1989; **17:** 4611-4627
2 **Moyzis RK,** Buckingham JM, Cram LS, Dani M, Deaven LL, Jones MD, Meyne J, Ratliff RL, Wu JR. A highly conserved repetitive DNA sequence, (TTAGGG)n, present at the telomeres of human chromosomes. *Proc Natl Acad Sci U S A* 1988; **85:** 6622-6626
3 **Cross SH,** Allshire RC, McKay SJ, McGill NI, Cooke HJ. Cloning of human telomeres by complementation in yeast. *Nature* 1989; **338:** 771-774
4 **Vaziri H,** Schachter F, Uchida I, Wei L, Zhu X, Effros R, Cohen D, Harley CB. Loss of telomeric DNA during aging of normal and trisomy 21 human lymphocytes. *Am J Hum Genet* 1993; **52:** 661-667
5 **Buchkovich KJ,** and Greider CW. Telomerase regulation during entry into the cell cycle in normal human T cells. *Mol Biol Cell* 1996; **7:** 1443-1454
6 **Harley CB.** Telomere loss: mitotic clock or genetic time bomb? *Mutat Res* 1991; **256:** 271-282
7 **Stansel RM,** de Lange T, Griffith JD. T-loop assembly in vitro involves binding of TRF2 near the 3' telomeric overhang. *EMBO J* 2001; **20:** 5532-5540
8 **Griffith JD,** Comeau L, Rosenfield S, Stansel RM, Bianchi A, Moss H, de Lange T. Mammalian telomeres end in a large duplex loop. *Cell* 1999; **97:** 503-514
9 **Hsu CP,** Miaw J, Hsia JY, Shai SE, Chen CY. Concordant expression of the telomerase-associated genes in non-small cell lung cancer. *Eur J Surg Oncol* 2003; **29:** 594-599
10 **Wu TC,** Lin P, Hsu CP, Huang YJ, Chen CY, Chung WC, Lee H, Ko JL. Loss of telomerase activity may be a potential favorable prognostic marker in lung carcinomas. *Lung Cancer* 2003; **41:** 163-169
11 **Hsu CP,** Miaw J, Shai SE, Chen CY. Correlation between telomerase expression and terminal restriction fragment length ratio in non-small cell lung cancer--an adjusted measurement and its clinical significance. *Eur J Cardiothorac* Surg 2004; **26:** 425-431
12 **Greene FL,** Page DL Fleming ID Fritz AG Balch CM Haller DG Morrow M. AJCC Cancer Staging Handbook. 6th ed. New York, Springer-Verlag Inc, 2002: 191-203
13 **Wright WE,** Shay JW, Piatyszek MA. Modifications of a telomeric repeat amplification protocol (TRAP) result in increased reliability, linearity and sensitivity. *Nucleic Acids Res* 1995; **23:** 3794-3795
14 **de Lange T,** Shiue L, Myers RM, Cox DR, Naylor SL, Killery AM, Varmus HE. Structure and variability of human chromosome ends. *Mol Cell Biol* 1990; **10:** 518-527
15 **Counter CM,** Avilion AA, LeFeuvre CE, Stewart NG, Greider CW, Harley CB, Bacchetti S. Telomere shortening associated with chromosome instability is arrested in immortal cells which express telomerase activity. *EMBO J* 1992; **11:** 1921-1929
16 **Wright WE,** Shay JW. Cellular senescence as a tumor-protection mechanism: the essential role of counting. *Curr Opin Genet Dev.* 2001; **11:** 98-103
17 **Schreiber-Agus N,** DePinho RA. Repression by the Mad(Mxi1)-Sin3 complex. *Bioessays* 1998; **20:** 808-818
18 **Ayer DE,** Kretzner L, Eisenman RN. Mad: a heterodimeric partner for Max that antagonizes Myc transcriptional activity. *Cell* 1993; **72:** 211-222
19 **van Steensel B,** Smogorzewska A, de Lange T. TRF2 protects human telomeres from end-to-end fusions. *Cell* 1998; **92:** 401-413
20 **van Steensel B,** de Lange T. Control of telomere length by the human telomeric protein TRF1. *Nature* 1997; **385:** 740-743
21 **Smith S,** Giriat I, Schmitt A, de Lange T. Tankyrase, a poly(ADP-ribose) polymerase at human telomeres. *Science* 1998; **282:** 1484-1487
23 **Ikeguchi M,** Unate H, Maeta M, Kaibara N. Detection of telomerase activity in esophageal squamous cell carcinoma and normal esophageal epithelium. *Langenbecks Arch Surg* 1999; **384:** 550-555
24 **Koyanagi K,** Ozawa S, Ando N, Kitagawa Y, Ueda M, and Kitajima M. Clinical significance of telomerase activity in peripheral blood of patients with esophageal squamous cell carcinoma. *Ann Thorac Surg* 2002; **73:** 927-932
25 **Koyanagi K,** Ozawa S, Ando N, Kitagawa Y, Ueda M, Kitajima M. Clinical significance of telomerase activity in peripheral blood of patients with esophageal squamous cell carcinoma. *Ann Thorac Surg* 2002; **73:** 927-932
26 **Bryan TM,** Englezou A, Gupta J, Bacchetti S, Reddel RR. Telomere elongation in immortal human cells without detectable telomerase activity. *EMBO J* 1995; **14:** 4240-4248
27 **Bryan TM,** Englezou A, Dalla-Pozza L, Dunham MA, Reddel RR. Evidence for an alternative mechanism for maintaining telomere length in human tumors and tumor-derived cell lines. *Nat Med* 1997; **3:** 1271-1274
28 **Karlseder J,** Smogorzewska A, de Lange T. Senescence induced by altered telomere state, not telomere loss. *Science* 2002; **295:** 2446-2449

Science Editor Guo SY **Language Editor** Elsevier HK

PO Box 2345, Beijing 100023, China
www.wjgnet.com
wjg@wjgnet.com

ELSEVIER

World J Gastroenterol 2005;11(44):6948-6953
World Journal of Gastroenterology ISSN 1007-9327

• *BASIC RESEARCH* •

Relationship between body surface area and ALT normalization after long-term lamivudine treatment

Makoto Nakamuta, Shusuke Morizono, Yuichi Tanabe, Eiji Kajiwara, Junya Shimono, Akihide Masumoto, Toshihiro Maruyama, Norihiro Furusyo, Hideyuki Nomura, Hironori Sakai, Kazuhiro Takahashi, Koichi Azuma, Shinji Shimoda, Kazuhiro Kotoh, Munechika Enjoji, Jun Hayashi: Kyushu University liver Disease Study Group

Makoto Nakamuta, Kazuhiro, Shusuke Morizono, Kotoh, Munechika Enjoji, Department of Medicine and Bioregulatory Science, Graduate School of Medical Sciences, Kyushu University, Japan
Norihiro Furusyo, Jun Hayashi, Department of Environmental Medicine and Infectious Diseases, Graduate School of Medical Sciences, Kyushu University, Japan
Shinji Shimoda, Department of Medicine and Biosystemic Science, Graduate School of Medical Sciences, Kyushu University, Japan
Koichi Azuma, Department of Medicine and Clinical Science, Graduate School of Medical Sciences, Kyushu University, Japan
Yuichi Tanabe, Department of Medicine, Fukuoka City Hospital, Fukuoka, Japan
Eiji Kajiwara, Department of Internal Medicine, Nippon Steel Yawata Memorial Hospital, Kitakyushu, Japan
Junya Shimono, Department of Medicine, Yahata Saiseikai Hospital, Kitakyushu, Japan
Akihide Masumoto, Department of Clinical Research, National Hospital Organization Kokura Hospital, Kitakyushu, Japan
Toshihiro Maruyama, Department of Medicine, Kitakyushu Municipal Medical Center, Kitakyushu, Japan
Hideaki Nomura, Department of Internal Medicine, Shin-Kokura Hospital, Kitakyushu, Japan
Hironori Sakai, Department of Gastroenterology, National Hospital Organization Kyushu Medical Center, Fukuoka, Japan
Kazuhiro Takahashi, Department of Medicine, Hamanomachi Hospital, Fukuoka, Japan
Correspondence to: Makoto Nakamuta, Department of Medicine and Bioregulatory Science, Graduate School of Medical Sciences, Kyushu University, 3-1-1 Maidashi, Higashi-ku, Fukuoka 812-5282, Japan. nakamuta@intmed3.med.kyushu-u.ac.jp
Telephone: +81-92-6425282 Fax: +81-92-6425287
Received: 2005-04-20 Accepted: 2005-05-12

Abstract

AIM: To further evaluate the relationship between BSA and the effects of lamivudine in a greater number of cases and over a longer period of observation than in our previous evaluation.

METHODS: We evaluated 249 patients with chronic hepatitis B. The effects of treatment for one year (n = 249), two years (n = 147), and three years (n = 72) were evaluated from the levels of serum ALT and HBV-DNA, as biological and virological effects (undetectable levels by PCR), respectively. Moreover, several variables that could influence the response to treatment, including ALT, albumin, bilirubin, platelet counts, BSA, HBV-DNA, and HBeAg were analyzed.

RESULTS: For 1-year treatment, multivariate analysis revealed that BSA (P = 0.0002) was the only factor for the biological effect, and that ALT (P = 0.0017), HBV-DNA (P = 0.0004), and HBeAg (P = 0.0021) were independent factors for the virological effect. For 2-year treatment, multivariate analysis again showed that BSA (P = 0.0147) was the only factor for the biological effect, and that ALT (P = 0.0192) and HBeAg (P = 0.0428) were independent factors for the virological effect. For 3-year treatment, multivariate analysis, however, could not reveal BSA (P = 0.0730) as a factor for the normalization of ALT levels.

CONCLUSION: BSA is a significant predictor for the normalizing the effect of lamivudine therapy on ALT for an initial 2-year period, suggesting that lamivudine dosage should be based on the individual BSA.

Key words: Lamivudine; Hepatitis B virus; Body surface area; Dose; Long-term treatment

Nakamuta M, Morizono S, Tanabe Y, Kajiwara E, Shimono J, Masumoto A, Maruyama T, Furusyo N, Nomura H, Sakai H, Takahashi K, Azuma K, Shinji S, Kotoh K, Enjoji M, Hayashi J. Kyushu University liver Disease Study Group. Relationship between body surface area and ALT normalization after long-term lamivudine treatment. *World J Gastroenterol* 2005; 11(44): 6948-6953
http://www.wjgnet.com/1007-9327/11/6948.asp

INTRODUCTION

Chronic hepatitis B is an important cause of morbidity and mortality resulting from cirrhosis-related liver failure and hepatocellular carcinoma (HCC)[1-3]. Lamivudine is an oral nucleoside analog approved for the treatment of chronic hepatitis B. It inhibits viral DNA replication by means of chain termination, and competitively inhibits viral polymerase. A daily dosage of lamivudine of 100 mg has been accepted worldwide for the treatment for chronic hepatitis B, since early studies showed that there was no

significant difference in the effect of lamivudine at doses of 100 and 300 mg[4,5]. However, to establish ideal dosages in those studies, efficacy was mainly evaluated by measuring hepatitis B virus (HBV)-DNA, and the assay used was much less sensitive than the polymerase chain reaction (PCR) assay. Studies in which HBV-DNA was measured by PCR assay reported an additional viral suppressive activity with high doses (300 mg) of lamivudine for 24 wk[6]. In addition to the limits imposed by the assay methods that were used, the observation periods in the studies on lamivudine doses of 100-300 mg were limited to a period of 12[4] or 24 wk[5]. Although the effect of doses greater than 100 mg on the emergence of YMDD mutants has not been evaluated, baseline body mass index has been reported to be significantly related to the emergence of HBV mutants during lamivudine treatment in patients co-infected with HBV and human immunodeficiency virus-1 (HIV-1)[7]. In a previous study of 134 patients treated for 23.1 mo(mean observation period), body surface area (BSA) was shown to be an independent factor contributing to the effects of lamivudine treatment[8]. In the present study, to further confirm these results, we evaluated the relationship between BSA and the effects of lamivudine effects in a greater number of patients and for longer observation periods than those in the previous report.

MATERIALS AND METHODS

Patients

Criteria for entry into this study were as follows: (a) the patients had not been treated with lamivudine previously; (b) they had chronic hepatitis caused by HBV, and persistent abnormal levels of alanine aminotransferase (ALT); and (c) patients with HCC were excluded. A total of 249 patients with chronic hepatitis B were evaluated. They had been treated with 100 mg of lamivudine for more than 1 year at Kyushu University Hospital and its affiliated hospitals (Table 1). For all the patients, the existence of serum HBV-DNA was confirmed by transcription-mediated nucleic acid amplification (TMA) assay ($10^{3.7}$-$10^{8.7}$ genome equivalents/mL; 3.7-8.7 log genome equivalents [LGE]/mL) (Chugai Diagnostic Science, Tokyo, Japan) or by a Roche Monitor kit ($10^{2.6}$-$10^{7.6}$ copies/mL; 2.6-7.6 log copies/mL) (Roche Diagnostics, Tokyo, Japan) before the treatment. None of the patients dropped out and all were treated with 100 mg/d lamivudine until the end of the observation period. After the start of medication, basic hepatic function and serum levels of HBV-DNA were measured at least every 3 mo for all the patients. The efficacy of lamivudine was evaluated from the serum levels of ALT and HBV-DNA, as biological and virological effects, respectively. The categories for the biological evaluation based on serum ALT were as follows: (1) sustained responder (SR) ALT: the serum levels of ALT decreased and remained at less than 30 U/L continuously during the observation period; and (2) non-responder (NR) ALT: the serum ALT was more than 30 U/L at the end of the observation. Similarly, the categories for the virological evaluation based on HBV-DNA were: (1) SR-HBV: serum HBV-DNA decreased to levels undetectable by PCR (<2.6 log copies/mL) and remained negative continuously during the observation period; and (2) NR-HBV: serum HBV-DNA was detectable at the end of the observation period (>2.6 log copies/mL). BSA was calculated using the method of DuBois.

Statistical analysis

The baseline characteristics of the patients prior to the beginning of the lamivudine therapy are expressed as mean±SD for the quantitative variables. In order to determine the contribution of these variables to the effect of the treatment, univariate and multivariate logistic analyses were performed. For multivariate logistic analysis, we analyzed BSA as an independent factor contributing to the effects of lamivudine treatment variables that showed χ^2 values of more than 1.0 in the univariate logistic

Table 1 Baseline characteristics of patients treated for 1 year[1]

	Total (range)	SR-ALT	NR-ALT	SR-DNA	NR-DNA
n	249	150	99	183	66
Male/female	180/67	99/51	82/17	127/54	53/13
ALT (U/L)	211.1±402.4 (16-4491)	242.1±424.2	163.6±363.6	240.3±462.2	128.8±88.1
Albumin (g/dL)	3.8±0.6 (2.2-4.9)	3.8±0.6	3.8±0.6	3.8±0.6	3.9±0.6
Bilirubin (mg/dL)	1.3±1.7 (0.1-12.9)	1.4±1.8	1.2±1.5	1.4±1.9	1.0±1.1
Platelet (10^4/mL)	14.1±6.1 (2.6-35.5)	14.2±5.8	14.0±6.5	13.9±6.2	14.9±5.6
BSA (m^2)	1.70±0.20 (1.25-2.17)	1.66±0.17	1.75±0.18	1.69±0.18	1.73±0.18
HBV-DNA					
≤5 (LEG/mL)	31	20	11	29	2
5< ≤6	33	18	15	27	6
6< ≤7	68	41	27	52	16
7<	117	71	46	75	42
HBeAg +/-	135/110	83/64	52/46	84/96	51/14
Age (yr)	48.6±11.6 (19-73)				
CH/LC [Child A/B/C]	162/87 [61/11/15]				

[1]Data are shown as mean±SD.

model. *P* value less than 0.05 was considered statistically significant.

RESULTS

The effects of lamivudine for 1 year were analyzed in a total of 249 patients (Table 1), of which 150 (60.2%) were identified as SR-ALT and 99 (39.8%) as NR-ALT, and 183 (73.5%) were identified as SR-DNA and 66 (26.5%) as NR-ALT (Table 1). To evaluate the contribution of the variables to the effect of treatment, univariate and multivariate logistic analyses were performed. In the univariate logistic analysis, BSA and ALT in the biological evaluation, and ALT, albumin, bilirubin, platelet count, BSA, HBV-DNA, and HBeAg in the virological evaluation, had χ^2 values of more than 1.0 (Table 2). Therefore, we used these factors as variables for multivariate logistic analysis. The results of multivariate analysis revealed that BSA was the only significant factor for the improvement of ALT levels (χ^2 = 14.3, P = 0.0002), and ALT, albumin, HBV-DNA and HBeAg were independent factors for the disappearance of serum HBV-DNA (ALT: χ^2 = 9.8, P = 0.0017; albumin: χ^2 = 5.1, P = 0.0238; HBV-DNA: χ^2 = 12.6, P = 0.0004; and HBeAg: χ^2 = 9.5, P = 0.0021) (Table3).

The effects of 2-year therapy were evaluated in 147 patients (Table 4). Of these patients, 75 (51.0%) were identified as SR-ALT and 72 (49.0%) as NR-ALT, while 85 (57.8%) were identified as SR-DNA and 62 (42.2%) as NR-ALT (Table 5). In the univariate logistic analysis, bilirubin, platelet count and BSA in the biological evaluation, and ALT, bilirubin, platelet, BSA and HBeAg in the virological evaluation, were selected (χ^2>1.0) (Table 5). Multivariate analysis revealed that BSA was the only significant factor in the biological effects (χ^2 = 5.6, P = 0.0147), and ALT and HBeAg were independent factors in the virological effects (ALT: χ^2 = 5.5, P = 0.0192; and HBeAg: χ^2 = 4.1, P = 0.0428) (Table 6).

Finally, the effects of 3-year therapy were evaluated in 72 patients (Table 7). Of these patients, 33 (45.8%) were identified as SR-ALT and 39 (54.2%) as NR-ALT, while

Table 2 Univariate analysis of the effects of lamivudine treatment for 1 year

Variables	χ^2	P
Biological effects		
ALT (U/L)	2.963405	0.0852
Albumin (g/dL)	0.230408	0.6312
Bilirubin (mg/dL)	0.934082	0.3338
Platelet count (10^4/mL)	0.097459	0.7549
BSA (m^2)	15.96269	<0.0001
HNV-DNA (LEG/mL)	0.000983	0.9750
HBeAg	0.275000	0.6000
Virological effects		
ALT (U/L)	8.293809	0.0040
Albumin (g/dL)	3.353949	0.0670
Bilirubin (mg/dL)	3.258437	0.0711
Platelet count (10^4/mL)	1.331910	0.2485
BSA (m^2)	2.586640	0.1078
HNV-DNA (LEG/mL)	14.38010	0.0001
HBeAg	19.51400	<0.0001

Table 3 Multivariate analysis on the effects of lamivudine treatment for 1 year

Variables	χ^2	P
Biological effects		
ALT (U/L)	1.921529	0.1657
BSA (m^2)	15.96269	0.0002
Virological effects		
ALT (U/L)	9.797455	0.0017
Albumin (g/dL)	5.106762	0.0238
Bilirubin (mg/dL)	0.450406	0.5021
Platelet count (10^4/mL)	0.009626	0.9218
BSA (m^2)	2.222164	0.1360
HNV-DNA (LEG/mL)	12.64904	0.0004
HBeAg	9.476967	0.0021

Table 4 Baseline characteristics of patients treated for 2 years[1]

	Total (range)	SR-ALT	NR-ALT	SR-DNA	NR-DNA
n	147	75	72	85	62
Male/female	112/35	52/23	60/12	62/23	50/12
ALT (U/L)	221.6±493.5 (17-4491)	258.9±548.5	182.3±428.2	291.3±626.3	122.2±132.0
Albumin (g/dL)	3.8±0.6 (2.2-4.9)	3.8±0.5	3.8±0.6	3.8±0.5	3.9±0.6
Bilirubin (mg/dL)	1.5±2.1 (0.3-12.9)	1.7±2.5	1.3±1.7	1.7±2.6	1.0±1.1
Platelet (10^4/mL)	13.8±6.2 (3.4-33.6)	12.9±5.4	14.6±6.8	13.1±5.5	14.9±5.6
BSA (m^2)	1.71±0.18 (1.30-2.17)	1.67±0.18	1.76±0.17	1.70±0.18	1.73±0.18
HBV-DNA					
≤5 (LEG/mL)	18	11	7	12	6
5< ≤6	20	7	13	11	9
6< ≤7	42	23	19	26	16
7<	69	35	34	38	31
HBeAg +/–	82/65	41/34	41/31	41/45	41/20
Age (yr)	48.9±11.4 (19-73)				
CH/LC [Child A/B/C]	95/54 [43/3/8]				

[1] Data are shown as mean±SD.

38 (52.8%) were identified as SR-DNA and 34 (47.2%) as NR-DNA (Table 8). In the univariate logistic analysis, albumin, platelet count, BSA, and HBeAg in the biological evaluation, and no variables in the virological evaluation, were selected (χ^2>1.0) (Table 8). Multivariate analysis did not reveal BSA as a factor for predicting the biological efficacy of lamivudine therapy $\chi^2 = 3.2$, $P = 0.0730$) (Table 9).

DISCUSSION

In this present study, we found that BSA was a significant factor that could contribute to the normalization of serum ALT (biological response) after the treatment with lamivudine for an initial 2-year period. Body weight was also a significant factor contributing to the effects of lamivudine treatment (data not shown). Because χ^2 values of BSA were higher than those of body weight and BSA is determined with body weight and height, we used BSA as a variable for statistical analysis. We initially reported that BSA was an independent factor contributing to both the biological and virological responses[8]. The difference in the contribution to the virological response between the present and the previous study might be attributed to the differences in the criteria used to evaluate treatment effects. In our previous study, we used a third category in addition to SR and NR transient responder (TR) which included patients with serum ALT levels that initially decreased to less than 30 U/L but increased to more than 30 U/L during the subsequent observation period (TR-ALT), and the patients in whom serum HBV-DNA initially decreased to undetectable levels (<2.6 log copies/mL) but became positive again during the subsequent observation period (TR-DNA). Regardless of the differences in evaluation criteria, both studies clearly demonstrated that BSA independently contributed to the normalization of ALT in the patients treated with lamivudine for an initial 2-year period. Because the pharmacokinetics of lamivudine correlate with body weight, as is the case with many other drugs[9], it is reasonable to conclude that patients with lower BSA would have achieved higher blood concentrations

Table 5 Univariate analysis of the effects of lamivudine treatment for 2 years

Variables	χ^2	*P* values
Biological effects		
ALT (U/L)	0.962196	0.3266
Albumin (g/dL)	0.279331	0.5971
Bilirubin (mg/dL)	1.384215	0.2394
Platelet count (10^4/mL)	2.943368	0.0862
BSA (m^2)	8.339371	0.0039
HNV-DNA (LEG/mL)	0.009964	0.9205
HBeAg	0.077000	0.7810
Virological effects		
ALT (U/L)	8.990505	0.0027
Albumin (g/dL)	0.643271	0.4225
Bilirubin (mg/dL)	3.176521	0.0747
Platelet count (10^4/mL)	2.064207	0.1508
BSA (m^2)	1.060739	0.3030
HNV-DNA (LEG/mL)	0.546020	0.4598
HBeAg	5.595000	0.0180

Table 6 Multivariate analysis of the effects of lamivudine treatment for 2 years

Variables	χ^2	*P* values
Biological effects		
Bilirubin (mg/dL)	0.496757	0.4809
Platelet count (10^4/mL)	0.572997	0.4491
BSA (m^2)	2.263849	0.0147
Virological effects		
ALT (U/L)	5.482584	0.0192
Bilirubin (mg/dL)	0.983777	0.3212
Platelet count (10^4/mL)	1.098891	0.2945
BSA (m^2)	0.714246	0.3980
HNV-DNA (LEG/mL)	0.592857	0.4413
HBeAg	4.101478	0.0428

Table 7 Baseline characteristics of patients treated for 3 years

	Total (range)	SR-ALT	NR-ALT	SR-DNA	NR-DNA
n	72	33	39	38	34
Male/female	53/19	21/12	32/7	27/11	26/8
ALT (U/L)	198.6±437.2 (18-3545)	200.0±229.0	197.5±562.1	191.2±218.0	207.2±602.6
Albumin (g/dL)	3.8±0.5 (2.5-4.9)	3.7±0.4	4.0±0.5	3.8±0.5	3.9±0.5
Bilirubin (mg/dL)	1.5±2.1 (0.3-12.9)	1.6±2.2	1.5±2.3	1.6±2.2	1.5±2.4
Platelet (10^4/mL)	13.8±6.2 (3.9-33.6)	11.6±4.6	15.1±6.9	13.3±5.8	13.8±6.5
BSA (m^2)	1.71±0.18 (1.30-2.17)	1.75±0.17	1.66±0.19	1.69±0.17	1.73±0.20
HBV-DNA					
≤5 (LEG/mL)	7	4	3	4	3
5< ≤6	15	4	11	6	9
6< ≤7	17	11	6	13	4
7<	33	14	19	15	18
HBeAg +/–	41/31	21/12	20/19	22/16	19/15
Age (yr)	49.5±11.1 (21-73)				
CH/LC [Child A/B/C]	43/29 [25/0/4]				

[1] Data are shown as mean±SD.

Table 8 Univariate analysis of the effects of lamivudine treatment for 3 years

Variables	χ^2	*P* values
Biological effects		
ALT (U/L)	0.000598	0.9805
Albumin (g/dL)	5.541899	0.0186
Bilirubin (mg/dL)	0.100733	0.7510
Platelet count (10^4/mL)	6.242535	0.0125
BSA (m^2)	4.393544	0.0361
HNV-DNA (LEG/mL)	0.001477	0.9693
HBeAg	1.113000	0.2915
Virological effects		
ALT (U/L)	0.023922	0.8771
Albumin (g/dL)	0.565446	0.4315
Bilirubin (mg/dL)	0.010128	0.9198
Platelet count (10^4/mL)	0.137799	0.7105
BSA (m^2)	0.805305	0.3695
HNV-DNA (LEG/mL)	0.065438	0.7981
HBeAg	0.030000	0.8633

Table 9 Multivariate analysis of the effects of lamivudine treatment for 3 years

Variables	χ^2	*P* values$_\chi$
Biological effects		
Albumin (g/dL)	0.865354	0.3522
Platelet count (10^4/mL)	2.391260	0.1220
BSA (m^2)	3.213451	0.0730
HBeAg	1.252959	0.2630

of lamivudine, although we did not actually monitor the concentration of lamivudine. Recent reports suggest that the baseline body mass index is significantly related to the emergence of HBV mutation during lamivudine treatment (300 mg/d, >6 mo) in patients co-infected with HBV and HIV-1[7]. Therefore, the results of our studies again question whether a lamivudine dosage of 100 mg/d is adequate, particularly for long-term treatment.

The standard lamivudine dose of 100 mg daily was based on early studies in which doses of 25, 100, and 300 mg were compared for 12[4] or 24 wk[5]. Because there were no significant differences reported in the rates of non-detection of HBV-DNA and normalization of ALT levels between the 100 and 300 mg doses, the dose of 100 mg has become a well-accepted therapeutic standard[4,5]. However, several factors should be considered when evaluating the results of these studies, including the number of patients, duration of treatment, emergence of lamivudine-resistant mutants over long-term treatment, and detection limits for HBV-DNA.

In the present study, we found that there was a significant difference in the contribution of BSA to the biological effect, although the differences in the mean values of BSA between SR-ALT and NR-ALT were relatively small. Therefore, it is possible that previous studies failed to detect a significant contribution of BSA to the effects of lamivudine because of the smaller number of patients examined. The major drawback of lamivudine monotherapy is the emergence of resistant HBV with mutations of the tyrosine-methionine-aspartate-aspartate (YMDD) motif. The incidence of these mutants rises from 15-20% in the first year of therapy to 40% by the second year, and to 67% by the fourth year[10]. In some cases, fatal liver failure subsequent to the emergence of the mutant was reported[11]. Therefore, observation periods of 24 wk may not be adequate for detecting the emergence of lamivudine-resistant mutants. In our evaluation of HBV-DNA, the rates of NR-DNA were found to be 26.5%, 42.2%, and 57.2% in patients who were positive for HBV-DNA (>2.6 log copies/mL) by the first, second, and third year, respectively. Although we did not confirm YMDD mutation in all cases of NR-DNA, the increase in NR-DNA ratio might be attributable to the emergence of mutants. Concomitant with the increases in HBV-DNA seen over the 3-year period, the NR-ALT ratio rose from 39.8% in the first year to 49.0% by the second year and to 54.8% by the third year in the present study, suggesting that the emergence of mutants could abolish the contribution of BSA to biological effects in the third year. Further studies will be needed to confirm whether BSA affects the incidence of YMDD mutants.

In previous studies that showed no difference in the effects of 100 and 300 mg lamivudine on HBV-DNA levels (as aforementioned)[4,5], HBV-DNA was measured quantitatively by liquid hybridization assay (Abbott Laboratories), which has a detection limit of 10^7 geq/mL[12]. Honkoop *et al*.[6] studied the efficacy of 100 and 300 mg lamivudine in viral suppression for 24 wk using a semi-quantitative PCR method with a detection limit of 10^2-10^3 geq/mL. In the present study, we used a Roche Monitor kit, which has detection limit of 2.6 log copies/mL, and could not find a significant relationship between BSA and the virological effect of lamivudine. Chun *et al*.[13], reported that there was no significant correlation between viral replication and liver damage in chronic hepatitis B. Hence, it seems reasonable that we did not find a contribution of BSA to the virological effects of treatment. Further study will be needed to evaluate dose-dependent lamivudine effects on viral suppression including the emergence of mutants which could directly affect the viral load.

In conclusion, we have shown that BSA is a statistically significant and potentially important factor for predicting the efficacy of lamivudine therapy for chronic hepatitis B. A noteworthy finding in our study was that small differences in BSA might significantly influence the effect of lamivudine treatment, suggesting that a small increase in lamivudine dose might markedly increase its therapeutic efficacy. We believe that a long-term clinical trial with higher-dose lamivudine treatment in a large number of cases is warranted, since lamivudine will continue to be a first-line treatment for HBV.

REFERENCES

1 **Ganem D,** Prince AM. Hepatitis B virus infection--natural history and clinical consequences. *N Engl J Med* 2004; **350:** 1118-1129

2 **Lai CL,** Ratziu V, Yuen MF, Poynard T. Viral hepatitis B.

Lancet 2003; **362:** 2089-2094
3 **Qin LX,** Tang ZY. Hepatocellular carcinoma with obstructive jaundice: diagnosis, treatment and prognosis. *World J Gastroenterol* 2003; **9:** 385-391
4 **Dienstag JL,** Perrillo RP, Schiff ER, Bartholomew M, Vicary C, Rubin M. A preliminary trial of lamivudine for chronic hepatitis B infection. *N Engl J Med* 1995; **333:** 1657-1661
5 **Nevens F,** Main J, Honkoop P, Tyrrell DL, Barber J, Sullivan MT, Fevery J, De Man RA, Thomas HC. Lamivudine therapy for chronic hepatitis B: a six-month randomized dose-ranging study. *Gastroenterology* 1997; **113:** 1258-1263
6 **Honkoop P,** de Man RA, Niesters HG, Main J, Nevens F, Thomas HC, Fevery J, Tyrrell DL, Schalm SW. Quantitative hepatitis B virus DNA assessment by the limiting-dilution polymerase chain reaction in chronic hepatitis B patients: evidence of continuing viral suppression with longer duration and higher dose of lamivudine therapy. *J Viral Hepat* 1998; **5:** 307-312
7 **Wolters LM,** Niesters HG, Hansen BE, van der Ende ME, Kroon FP, Richter C, Brinkman K, Meenhorst PL, de Man RA. Development of hepatitis B virus resistance for lamivudine in chronic hepatitis B patients co-infected with the human immunodeficiency virus in a Dutch cohort. *J Clin Virol* 2002; **24:** 173-181
8 **Nakamuta M,** Kotoh K, Tanabe Y, Kajiwara E, Shimono J, Masumoto A, Maruyama T, Furusyo N, Nomura H, Sakai H, Takahashi K, Azuma K, Shimoda S, Enjoji M, Hayashi J. Body surface area is an independent factor contributing to the effects of lamivudine treatment. *Hepatol Res* 2005; **31:** 13-17
9 **Johnson MA,** Moore KH, Yuen GJ, Bye A, Pakes GE. Clinical pharmacokinetics of lamivudine. *Clin Pharmacokinet* 1999; **36:** 41-66
10 **Liaw YF,** Leung NW, Chang TT, Guan R, Tai DI, Ng KY, Chien RN, Dent J, Roman L, Edmundson S, Lai CL. Effects of extended lamivudine therapy in Asian patients with chronic hepatitis B. Asia Hepatitis Lamivudine Study Group. *Gastroenterology* 2000; **119:** 172-180
11 **Kagawa T,** Watanabe N, Kanouda H, Takayama I, Shiba T, Kanai T, Kawazoe K, Takashimizu S, Kumaki N, Shimamura K, Matsuzaki S, Mine T. Fatal liver failure due to reactivation of lamivudine-resistant HBV mutant. *World J Gastroenterol* 2004; **10:** 1686-1687
12 **Zaaijer HL,** ter Borg F, Cuypers HT, Hermus MC, Lelie PN. Comparison of methods for detection of hepatitis B virus DNA. *J Clin Microbiol* 1994; **32:** 2088-2091
13 **Chun YK,** Kim JY, Woo HJ, Oh SM, Kang I, Ha J, Kim SS. No significant correlation exists between core promoter mutations, viral replication, and liver damage in chronic hepatitis B infection. *Hepatology* 2000; **32:** 1154-1162

Science Editor Wang XL and Guo SY **Language Editor** Elsevier HK

PO Box 2345, Beijing 100023, China
www.wjgnet.com
wjg@wjgnet.com

ELSEVIER

World J Gastroenterol 2005;11(44):6954-6959
World Journal of Gastroenterology ISSN 1007-9327

• *BASIC RESEARCH* •

Excessive portal flow causes graft failure in extremely small-for-size liver transplantation in pigs

Hong-Sheng Wang, Nobuhiro Ohkohchi, Yoshitaka Enomoto, Masahiro Usuda, Shigehito Miyagi, Takeshi Asakura, Hiroo Masuoka, Takashi Aiso, Keisuke Fukushima, Tomohiro Narita, Hideyuki Yamaya, Atsushi Nakamura, Satoshi Sekiguchi, Naoki Kawagishi, Akira Sato, Susumu Satomi

Hong-Sheng Wang, Yoshitaka Enomoto, Masahiro Usuda, Shigehito Miyagi, Takeshi Asakura, Hiroo Masuoka, Takashi Aiso, Keisuke Fukushima, Tomohiro Narita, Hideyuki Yamaya, Atsushi Nakamura, Satoshi Sekiguchi, Naoki Kawagishi, Akira Sato, Susumu Satomi, Division of Advanced Surgical Science and Technology, Graduate School of Medicine, Tohoku University, 1-1 Seiryo-machi, Aoba-ku, Sendai 980-8574, Japan

Nobuhiro Ohkohchi, Department of Surgery, Graduate School of Comprehensive Human Science, University of Tsukuba, 1-1-1 Tennoudai, Tsukuba 305-8577, Japan

Supported by Grants-in-Aid for Scientific Research from the Ministry of Education, Science, and Culture of Japan, the Ministry of Welfare of Japan, and by a grant from Graduate School of Medicine, Tohoku University

Co-correspondent: Hong-Sheng Wang

Correspondence to: Nobuhiro Ohkohchi, Department of Surgery, Graduate School of Comprehensive Human Science, University of Tsukuba, 1-1-1 Tennoudai, Tsukuba 305-8577, Japan. nokuchi3@md.tsukuba.ac.jp

Telephone: +81-29-8353221 Fax: +81-29-8353222

Received: 2005-04-28 Accepted: 2005-06-09

Abstract

AIM: To evaluate the effects of a portocaval shunt on the decrease of excessive portal flow for the prevention of sinusoidal microcirculatory injury in extremely small-for-size liver transplantation in pigs.

METHODS: The right lateral lobe of pigs, i.e. the 25% of the liver, was transplanted orthotopically. The pigs were divided into two groups: graft without portocaval shunt (n = 11) and graft with portocaval shunt (n = 11). Survival rate, portal flow, hepatic arterial flow, and histological findings were investigated.

RESULTS: In the group without portocaval shunt, all pigs except one died of liver dysfunction within 24 h after transplantation. In the group with portocaval shunt, eight pigs survived for more than 4 d. The portal flow volumes before and after transplantation in the group without portocaval shunt were 118.2±26.9 mL/min/100 g liver tissue and 270.5±72.9 mL/min/100 g liver tissue, respectively. On the other hand, in the group with portocaval shunt, those volumes were 124.2±27.8 mL/min/100 g liver tissue and 42.7±32.3 mL/min/100 g liver tissue, respectively (P<0.01). As for histological findings in the group without portocaval shunt, destruction of the sinusoidal lining and bleeding in the peri-portal areas were observed after reperfusion, but these findings were not recognized in the group with portocaval shunt.

CONCLUSION: These results suggest that excessive portal flow is attributed to post transplant liver dysfunction after extreme small-for-size liver transplantation caused by sinusoidal microcirculatory injury.

Key words: Hyperperfusion syndrome; Liver regeneration; Portocaval shunt; Postoperative liver dysfunction; Sinusoidal microcirculatory injury; Small-for-size liver transplantation

Wang HS, Ohkohchi N, Enomoto Y, Usuda M, Miyagi S, Asakura T, Masuoka H, Aiso T, Fukushima K, Narita T, Yamaya H, Nakamura A, Sekiguchi S, Kawagishi N, Sato A, Satomi S. Excessive portal flow causes graft failure in extremely small-for-size liver transplantation in pigs. *World J Gastroenterol* 2005; 11(44): 6954-6959
http://www.wjgnet.com/1007-9327/11/6954.asp

INTRODUCTION

Since the first successful living donor liver transplantation (LDLT) in a child[1] patient and an adult[2] patient, LDLT has become the established method to reduce the number of patients on the waiting list and is considered as an alternative to standard liver transplantation[3-7]. The survival rate of adults is significantly lower than that in children[8] and the key to a successful LDLT, especially in adult recipients, is the adequacy of the size of the graft that can be safely harvested from the donor[9-11]. In some cases, graft weight ratio of the recipient native liver weight (GWRLW) of 30% or less has been transplanted successfully, but in general, graft weight per recipient's body weight (GWBW) less than 0.8% or GWRLW less than 40% has been considered marginal or small-for-size. These small-for-size grafts are associated with an increased incidence of complications and graft failure[9-12]. A small-for-size graft cannot supply the metabolic demand of an adult recipient in the early posttransplant period. Poor early graft function is characterized by protracted

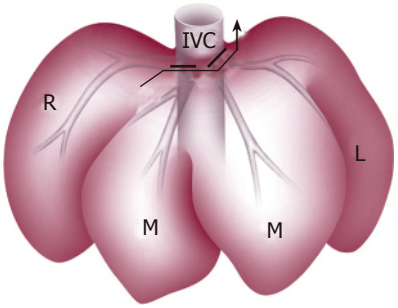

Figure 1 Anterior view of left tri-segmentectomy. Bold line indicates the left and middle hepatic veins ligated by transfixing suture; arrow indicates parenchymal transection of the left lobe and right paramedian lobe; L: left lateral lobe; M: median lobe; R: right lateral lobe; IVC: inferior vena cava.

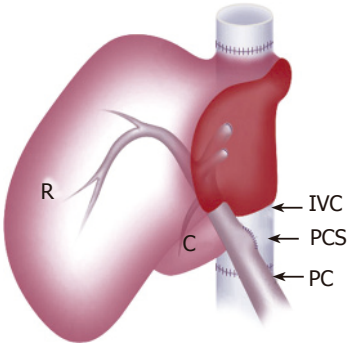

Figure 2 Schematic view of the liver graft with PCS placed by side-to-side anastomosis of PV and IVC. R: right lateral lobe; C: caudate lobe; PV: portal vein; IVC: inferior vena cava; PCS: portocaval shunt.

cholestasis, coagulopathy and ascites, and these findings are proposed to be the essential symptoms of small-for-size syndrome[13]. However, the precise mechanism for this dysfunction remains unclear.

Previously, we have reported that portal hypertension after reperfusion is one of the most important factors aggravating the microcirculatory injury of the graft[14]. In the present study, we hypothesized that the increment of portal flow played a major role in graft injury and poor function of small-for-size grafts, and investigated the effects of portocaval shunt (PCS) on the excessive portal flow for the prevention of the sinusoidal microcirculatory injury after extremely small-for-size liver transplantation using pigs.

MATERIALS AND METHODS

Animals

Landrace white pigs, weighing 18-28 kg, were used as donors and recipients. All experiments were conducted according to Principles of Laboratory Animal Care (NIH publication No. 86-23, revised in 1985). Food was withheld for 24 h before the operation. Anesthesia was induced by intramuscular administration of ketamine (5 mg/kg) and atropine sulfate (1.0 mg/body) followed by endotracheal intubation and maintenance with oxygen and isoflurane by positive pressure mechanical ventilation. A catheter was placed in the internal jugular vein for fluid administration and central venous pressure (CVP) monitoring and fixed at the back of the neck for postoperative venous sampling. A carotid arterial line was also placed for intraoperative blood sampling and monitoring mean arterial pressure (MAP). In recipients, an opposite internal jugular vein was used for the venovenous bypass from the portal vein and femoral vein. Eleven transplantations were carried out in each group.

Donor operation

After laparotomy, the left hepatic artery supplying the left lateral and left median lobes was ligated and divided. Glisson's sheaths of the left lobe and the right median lobe were identified and resected. After mobilization of the liver, by dissecting all ligamentous attachments, the left and middle hepatic veins were ligated with transfixing sutures (Figure 1). Parenchymal transection of the left lobe and the right median lobe was performed and finally left tri-segmentectomy of the liver was done.

Following intravenous administration of heparin, catheters were cannulated in the lower abdominal aorta and splenic vein. The diaphragm was widely opened and the supradiaphragmatic aorta was divided and encircled. Cold University of Wisconsin (UW) solution (4℃) was flushed in from both the aorta and the splenic vein after aortic clamp. The right lateral lobe was removed and preserved in UW solution.

Back table operation

In the group with shunt, the PCS was made on the back table and placed by means of side-to-side anastomosis between the portal vein and the infra-hepatic inferior vena cava (IVC) (Figure 2). The diameter of the PCS was 6 mm. The graft was weighed after the back table preparation.

Recipient operation

Total hepatectomy was performed under ilioportaljugular venovenous bypass[15]. The reduced-size graft with or without PCS was implanted orthotopically with end to end vascular anastomosis of the suprahepatic IVC, the portal vein, the infra-hepatic IVC, and the hepatic artery. Before anastomosis of the portal vein, rinse solution was perfused into the portal vein of the graft. Hepatic arterial reconstruction was performed under a microscope. A catheter was inserted into the common bile duct for bile drainage.

After transplantation, the pigs were placed in a warmed cage with free access to water and food. FK506 (0.1 mg/kg • d) was injected for immunosuppression from postoperative day (POD) 1-7. When recipients died, autopsy was performed to exclude the possibility of technical complications and to confirm the patency of all anastomoses. Liver grafts were also weighed.

Monitoring

Systemic hemodynamic monitoring of MAP and CVP was carried out continuously during the operation, as well as portal vein pressure was monitored. Portal flow

and hepatic arterial flow (HAF) were measured before hepatectomy in donors and after arterial reperfusion in recipients using ultrasound transit time flow probes and a flow meter (Transonic Systems Inc., Ithaca, NY, USA). The diameter of the probe was 8 mm for the portal vein and 3 mm for the artery. Total liver blood flow (TLBF) was calculated as the sum of portal flow and HAF. Liver biopsies were performed before hepatectomy, after reperfusion, and on every other day up to POD 7, and tissue specimens were examined under light microscope and Ki-67 staining was performed for the determination of proliferating hepatocytes. Transmission electron microscopical findings were also investigated in the specimen after reperfusion. Arterial blood samples were obtained hourly for gas analysis during the operation and determining alanine aminotransferase (ALT), aspartate aminotransferase (AST), total bilirubin (T-Bil), and anti-thrombin III (AT-III) before the operation, at 3 and 6 h after reperfusion and on every POD up to POD 7.

The graft weight at the time of transplantation expressed as a percentage of GWRLW and GWBW was calculated.

Statistical analysis

Values of parameters were expressed as mean±SD. Statistical significance was determined by Student's *t*-test. The survival rate was calculated by the Kaplan-Meier method. Values between the two groups were statistically analyzed by generalized Wilcoxon test. *P* values less than 0.05 were regarded as statistically significant.

RESULTS

Graft volume and operation time

Body weight, graft volume, and operation time are shown in Table 1. The graft volume was approximately 25% of the recipient native liver volume, and 0.6% of the recipient body weight in both groups. The cold ischemic time in the group with PCS was slightly longer than that in the group without PCS because of the time required for the PCS at the back table, but there was no statistical difference. There was no significant difference in MAP or CVP between the two groups (data not shown).

Table 1 Graft characteristics (mean±SD)

Parameters	Group without PCS (n = 11)	Group with PCS (n = 11)
DBW (kg)	21.8±2.7	20.8±1.1
RBW (kg)	22.8±1.2	22.1±2.6
GW (g)	131.8±18.3	139.3±32.0
RLW (g)	525.4±41.4	548.3±63.8
GWRLW (%)	25.1±2.7	25.4±3.4
GWBW (%)	0.58±0.09	0.63±0.13
Anhepatic time (min)	43±2	41±4
Operation time (min)	261±28	263±44
Total ischemic time (min)	151±51	161±20

DBW: donor body weight; RBW: recipient body weight; GW: liver graft weight at implantation; RLW: recipient native liver weight; GWRLW: percentage of GW to the recipient native liver weight; GWBW: percentage of GW to the recipient body weight.

Survival rate

In the group without PCS, all pigs except one died of liver dysfunction within 24 h after reperfusion. On the other hand, in the group with PCS, eight pigs survived for more than 4 d and the remaining three died of portal vein thrombosis at the anastomotic site of PCS or perforated gastric ulcer within 3 d. The PCS significantly improved the survival rate of the animals in comparison to the animals without the shunt after transplantation (P<0.05) (Figure 3).

Portal pressure

There were no significant differences in portal vein pressures at laparotomy in both groups. However, after reperfusion, portal vein pressures significantly increased up to 2.2±0.7 KPa in the group without PCS and 1.6±0.6 KPa in the group with PCS (Figure 4).

Hepatic hemodynamics

Hepatic hemodynamic parameters including portal flow, HAF and TLBF at laparotomy and after reperfusion in both groups are shown in Table 2. The portal flow after reperfusion in the group without PCS increased significantly more than that at laparotomy, whereas it decreased in the group with PCS (P<0.01). The HAF after reperfusion decreased compared to that at laparotomy in the group without PCS, while it increased more than that at laparotomy in the group with PCS (P<0.05).

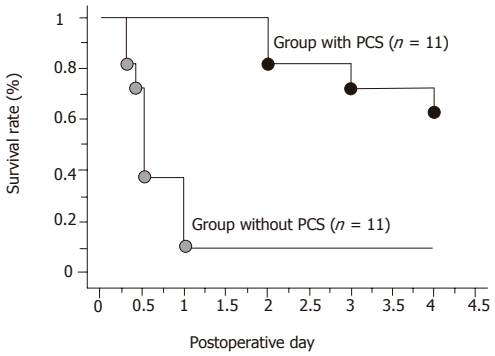

Figure 3 Survival rates. [b]P<0.01 *vs* the group without PCS.

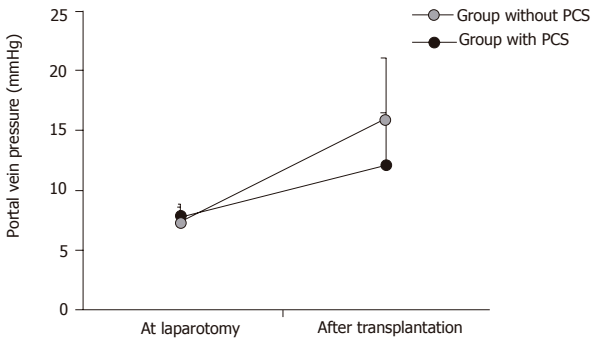

Figure 4 Changes of portal vein pressure (n = 11). [a]P<0.05 *vs* the group with PCS.

Table 2 Changes of hepatic hemodynamics (mean±SD)

Parameters	Group	At laparotomy	After transplantation
Portal flow	Group without PCS	118.2±26.9	270.5±72.9[b,a]
(mL/min/100 g liver tissue)	Group with PCS	124.2±27.8	42.7±32.3[a]
Hepatic arterial flow	Group without PCS	50.1±8.3	37.7±21.0[a]
(mL/min/100 g liver tissue)	Group with PCS	50.5±11.6	75.1±39.5
Total liver blood flow	Group without PCS	168.3±30.9	308.2±52.8[b,a]
(mL/min/100 g liver tissue)	Group with PCS	174.8±29.1	117.8±42.1[c]
Ratio of PF/TLBF (%)	Group without PCS	70.2±4.2	87.8±8.2[b,a]
	Group with PCS	71.1±4.9	36.3±19.5[a]

PF: portal flow; TLBF: total liver blood flow.

[b]P<0.01 *vs* the group with PCS; [a]P<0.01 *vs* at laparotomy; [a]P<0.05 *vs* the group with PCS; [c]P<0.05 *vs* at laparotomy.

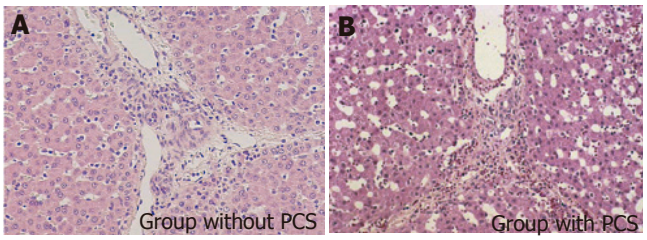

Figure 5 Histological findings of hepatic tissues after reperfusion (×100).

The TLBF after reperfusion increased significantly higher than that at laparotomy in the group without PCS, whereas the TLBF slightly decreased after reperfusion in the group with PCS. After reperfusion, the TLBF in the group without PCS was significantly greater than that in the group with PCS (P<0.01). In the group without PCS, the contribution of portal flow to TLBF increased from 70.2% to 87.8%, while in the group with PCS the contribution of the portal flow to TLBF decreased from 71.1% to 36.3%.

Histological findings

The light microscopical findings of the liver graft after reperfusion are shown in Figure 5. In the group without PCS, enlargement of the sinusoidal lumen and bleeding in the peri-portal triads were observed but these abnormal findings were not recognized in the group with PCS.

Transmission electron microscopic findings of the sinusoid after reperfusion are shown in Figure 6. In the group without PCS, the sinusoidal endothelial cells were destroyed and detached into the sinusoidal space with destruction of the Disse's spaces, while in the group with PCS the sinusoidal endothelial cells were well preserved, the Disse's spaces were intact, and the structure of endothelial lining was well preserved.

Liver regeneration in the group with PCS

The graft weight in the recipients who survived for more than 4 d (n = 8) increased to 87.3% of the recipient native liver. Ki-67 labeling index before and after transplantation is shown in Figure 7. The Ki-67 labeling index showed only 1.0% of hepatocytes at laparotomy. However, it increased abruptly after transplantation, reaching a peak value of approximately 60% at POD 2, and decreasing to 30% on POD 4.

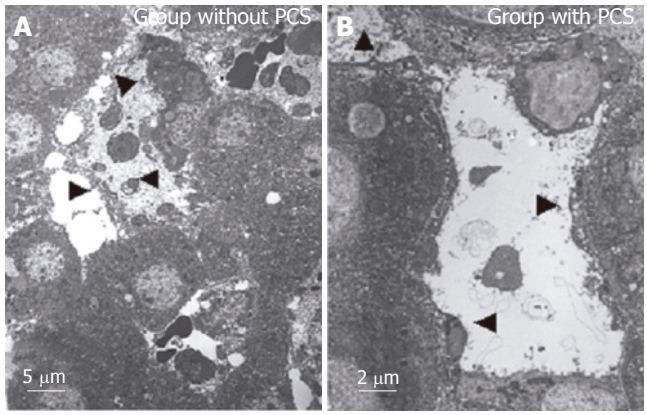

Figure 6 Transmission electron microscopical findings of the sinusoid after reperfusion. Arrowheads indicate the destroyed or preserved or detached sinusoidal endothelial cells into the sinusoidal space with destructed or intact Disse's spaces.

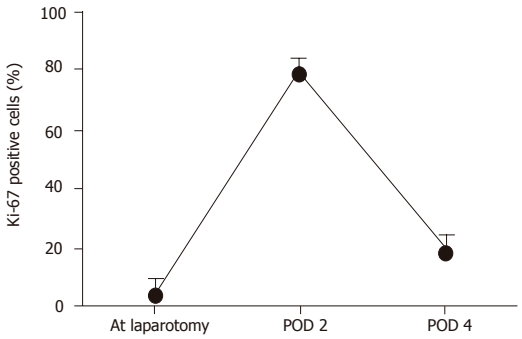

Figure 7 Ki-67 detection in the pigs that survived for more than 4 d in the group with PCS (n = 8).

Liver function

There were no significant differences in ALT, AST or T-Bil until POD 1 after reperfusion in either group (Table3). ALT and AST increased after reperfusion, taking a peak value on POD 2 and POD 1 and then decreased. However, T-Bil increased continuously until POD 4. AT-

Table 3 Changes of serum ALT, AST, T-Bil, and AT-III (mean±SD)

Parameters	Group	Preo	RP 3 h	RP 6 h	POD 1	POD 2	POD 3	POD 4
ALT (KU)	A	22±1	16±2	20±3	35±18	-	-	-
	B	25±7	18±5	25±9	33±13	38±15	30±11	27±10
AST (KU)	A	30±13	80±36	144±51	351±42	-	-	-
	B	32±19	78±38	172±37	306±36	293±46	217±21	152±48
T-Bil (mg/dL)	A	0.24±0.26	0.32±0.18	0.48±0.21	0.88±0.54	-	-	-
	B	0.10±0.07	0.27±0.16	0.48±0.31	0.83±0.24	1.39±0.37	1.75±0.71	1.79±0.86
AT-III (%)	A	122±26	69±19	57±23[a]	66±15a	-	-	-
	B	125±21	86±37	91±25	86±34	75±14	82±12	107±23

Preo: preoperation; RP 3 h: 3 h after reperfusion; RP 6 h: 6 h after reperfusion; POD: postoperative day; A: group without PCS; B: group with PCS; ALT: alanine aminotransferase; KU: karmen unit; AST: aspartate aminotransferase; T-Bil: total bilirubin; AT-III: anti-thrombin III. [a]$P<0.05$ *vs* the group with PCS.

III decreased after reperfusion in both groups. At 6 h after reperfusion and on POD 1, AT-III in the group with PCS was significantly higher than that in the group without PCS ($P<0.05$).

DISCUSSION

In clinical liver surgery, an extended hepatectomy of 80% or 85% of the whole liver can be tolerable in patients with a normal liver[16]. In previous reports, 70-75% hepatectomy in animals represents a model of critical residual liver volume and is used to study the mechanism of liver regeneration[17-19]. This means that 25-30% of the liver can sustain hepatic function. However, this cannot be translated directly into a minimum graft volume in small-for-size liver transplantation, in which grafts are subjected to cold and warm ischemia and subsequent reperfusion injury. This is why the minimum graft volume for successful liver transplantation is presumably higher than the residual liver volume in extended hepatectomy. Currently, experience with living-related and split-liver transplantation has demonstrated that the size of the graft required for a successful liver transplantation is at least 40% of the recipient's native liver volume and more than 0.8% of the recipient body weight[6,20]. This is associated with lack of portosystemic collateral circulation, which lessens the influence of a high portal flow on the grafts and prevents the development of severe portal hypertension[21]. The precise mechanism of graft injury in a small-for-size liver transplantation remains still unknown. But there is a case report of hemorrhagic necrosis secondary to excessive portal flow in an adult LDLT[22]. An adult LDLT with small-for-size graft has been successfully performed using a mesocaval shunt to avoid graft failure caused by portal hyperperfusion[23]. From these reports, we hypothesized that excessive portal flow could attribute to postoperative liver dysfunction caused by sinusoidal microcirculatory injury after small-for-size liver transplantation. In our experiment, we investigated the effect of PCS on excessive portal flow for the prevention of sinusoidal microcirculatory injury in extremely small-for-size liver transplantation in pigs, focusing on the prevention of primary graft dysfunction. We chose the pig model because the anatomy, metabolism, and physiology of the liver are similar to those in human beings. As a result, we clarified that PCS could prevent portal hypertension and excessive portal inflow in small-for-size liver transplantation.

The sinusoids are the principal vessels involved in the transvascular exchange between blood and the parenchymal cells and play an important role in hepatic microcirculation. In an experimental transplantation model using a small-for-size graft weighing less than 30% of the native liver, Asakura *et al*.[14] and Man *et al*.[24] demonstrated that portal hypertension is a determinant factor for the injury of sinusoidal endothelial cells and hepatic parenchyma. The portal flow through the reduced microvascular bed of the small-for-size graft after reperfusion is likely to induce injury of sinusoidal endothelial cells and activation of Kupffer's cells, which is similar to those after extended hepatectomy in rats reported by Panis *et al*.[19].

In this study, TLBF after reperfusion increased approximately twice in comparison to the flow at laparotomy in the group without PCS. The portal flow increased predominantly and HAF reduced. Histological findings clearly indicated disruption of the sinusoidal lining and disturbance of the sinusoidal microcirculation. Furthermore, the graft became swollen after reperfusion, progressing into severe bowel congestion and then blood oozing. These phenomena were associated with a poor survival rate in the group without PCS. On the other hand, in the group with PCS, graft inflow was modified by PCS which permitted a significantly lower portal flow and a higher HAF. The pathological findings of microcirculatory disturbance after reperfusion recognized in the group without PCS were not observed in the group with PCS. The results of our study strongly suggest that an excessive portal flow after reperfusion in small-for-size liver transplantation is one of the major factors that cause sinusoidal microcirculatory injury and result in graft failure.

With regard to the graft regeneration in the group with PCS, though the TLBF was low, the weight of the graft and Ki-67 index increased remarkably in the pigs that survived for more than 4 d. The decreased HAF subsequent to the excessive portal flow observed after reperfusion in the group without PCS was also believed to contribute to the poor regeneration of residual liver and the poor outcome. Sato *et al*.[25] reported that portal hypertension is a trigger of liver regeneration following partial hepatectomy. But surplus portal hypertension

induces liver dysfunction[25]. Results of our study support the hypothesis that portal flow controls liver regeneration in small-for-size liver transplantation and maintains liver function.

In conclusion, an extreme small-for-size graft weighing less than 25% of the native liver can be successfully transplanted with a PCS in pigs. Portal hyperperfusion in small-for-size liver transplantation appears to play a major role in aggravating microcirculatory injury of the graft and attenuation of portal hyperperfusion by PCS minimizes the injury and improves the survival. This study provides helpful information for transplant surgeons regarding the novel therapeutic strategies for the rescue of small-for-size liver grafts.

REFERENCES

1 **Strong RW,** Lynch SV, Ong TH, Matsunami H, Koido Y, Balderson GA. Successful liver transplantation from a living donor to her son. *N Engl J Med* 1990; **322:** 1505-1507

2 **Hashikura Y**, Makuuchi M, Kawasaki S, Matsunami H, Ikegami T, Nakazawa Y, Kiyosawa K, Ichida T. Successful living-related partial liver transplantation to an adult patient. *Lancet* 1994; **343:** 1233-1234

3 **Testa G,** Malago M, Broelsch CE. Living-donor liver transplantation in adults. Langenbecks *Arch Surg* 1999; **384:** 536-543

4 **Ito T,** Kiuchi T, Yamamoto H, Oike F, Ogura Y, Fujimoto Y, Hirohashi K, Tanaka AK. Changes in portal venous pressure in the early phase after living donor liver transplantation: pathogenesis and clinical implications. *Transplantation* 2003; **75:** 1313-1317

5 **Garcia-Valdecasas JC,** Fuster J, Charco R, Bombuy E, Fondevila C, Navasa M, Rodriguez-Laiz G, Ferrer J, Amador MA, Llovet JM, Forns X, Rimola A. Adult living donor liver transplantation. Analysis of the first 30 cases. *Gastroenterol Hepatol* 2003; **26:** 525-530

6 **Kawasaki S,** Makuuchi M, Matsunami H, Hashikura Y, Ikegami T, Nakazawa Y, Chisuwa H, Terada M, Miyagawa S. Living related liver transplantation in adults. *Ann Surg* 1998; **227:** 269-274

7 **Fan ST,** Lo CM, Liu CL. Technical refinement in adult-to-adult living donor liver transplantation using right lobe graft. *Ann Surg* 2000; **231:** 126-131

8 **Sugawara Y,** Makuuchi M. Small-for-size graft problems in adult-to-adult living-donor liver transplantation. *Transplantation* 2003; **75:** S20-22

9 **Emond JC, Renz JF,** Ferrell LD, Rosenthal P, Lim RC, Roberts JP, Lake JR, Ascher NL. Functional analysis of grafts from living donors. Implications for the treatment of older recipients. *Ann Surg* 1996; **224:** 544-52; discussion 552-554

10 **Nishizaki T,** Ikegami T, Hiroshige S, Hashimoto K, Uchiyama H, Yoshizumi T, Kishikawa K, Shimada M, Sugimachi K. Small graft for living donor liver transplantation. *Ann Surg* 2001; **233:** 575-580

11 **Kiuchi T,** Kasahara M, Uryuhara K, Inomata Y, Uemoto S, Asonuma K, Egawa H, Fujita S, Hayashi M, Tanaka K. Impact of graft size mismatching on graft prognosis in liver transplantation from living donors. *Transplantation* 1999; **67:** 321-327

12 **Lo CM,** Fan ST, Chan JK, Wei W, Lo RJ, Lai CL. Minimum graft volume for successful adult-to-adult living donor liver transplantation for fulminant hepatic failure. *Transplantation* 1996; **62:** 696-698

13 **Kelly DM,** Demetris AJ, Fung JJ, Marcos A, Zhu Y, Subbotin V, Yin L, Totsuka E, Ishii T, Lee MC, Gutierrez J, Costa G, Venkataraman R, Madariaga JR. Porcine partial liver transplantation: a novel model of the "small-for-size" liver graft. *Liver Transpl* 2004; **10:** 253-263

14 **Asakura T,** Ohkohchi N, Orii T, Koyamada N, Tsukamoto S, Sato M, Enomoto Y, Usuda M, Satomi S. Portal vein pressure is the key for successful liver transplantation of an extremely small graft in the pig model. *Transpl Int* 2003; **16:** 376-382

15 **Yanaga K,** Kishikawa K, Suehiro T, Nishizaki T, Shimada M, Itasaka H, Nomoto K, Kakizoe S, Sugimachi K. Partial hepatic grafting: porcine study on critical volume reduction. *Surgery* 1995; **118:** 486-492

16 **Starzl TE,** Putnam CW, Groth CG, Corman JL, Taubman J. Alopecia, ascites, and incomplete regeneration after 85 to 90 per cent liver resection. *Am J Surg* 1975; 129: 587-590

17 **Kahn D,** Hickman R, Terblanche J, von Sommoggy S. Partial hepatectomy and liver regeneration in pigs--the response to different resection sizes. *J Surg Res* 1988; **45:** 176-180

18 **Nagao M,** Isaji S, Iwata M, Kawarada Y. The remnant liver dysfunction after 84% hepatectomy in dogs. *Hepatogastroenterology* 2000; **47:** 1564-1569

19 **Panis Y,** McMullan DM, Emond JC. Progressive necrosis after hepatectomy and the pathophysiology of liver failure after massive resection. *Surgery* 1997; **121:** 142-149

20 **Garcia-Valdecasas JC,** Fuster J, Charco R, Bombuy E, Fondevila C, Ferrer J, Ayuso C, Taura P. Changes in portal vein flow after adult living-donor liver transplantation: does it influence postoperative liver function? *Liver Transpl* 2003; **9:** 564-569

21 **Smyrniotis V,** Kostopanagiotou G, Kondi A, Gamaletsos E, Theodoraki K, Kehagias D, Mystakidou K, Contis J. Hemodynamic interaction between portal vein and hepatic artery flow in small-for-size split liver transplantation. *Transpl Int* 2002; **15:** 355-360

22 **Ayata G,** Pomfret E, Pomposelli JJ, Gordon FD, Lewis WD, Jenkins RL, Khettry U. Adult-to-adult live donor liver transplantation: a short-term clinicopathologic study. *Hum Pathol* 2001; **32:** 814-822

23 **Boillot O,** Delafosse B, Mechet I, Boucaud C, Pouyet M. Small-for-size partial liver graft in an adult recipient; a new transplant technique. *Lancet* 2002; **359:** 406-407

24 **Man K,** Lo CM, Ng IO, Wong YC, Qin LF, Fan ST, Wong J. Liver transplantation in rats using small-for-size grafts: a study of hemodynamic and morphological changes. *Arch Surg* 2001; **136:** 280-285

25 **Sato Y,** Koyama S, Tsukada K, Hatakeyama K. Acute portal hypertension reflecting shear stress as a trigger of liver regeneration following partial hepatectomy. *Surg Today* 1997; **27:** 518-526

Science Editor Wang XL and Guo SY **Language Editor** Elsevier HK

PO Box 2345, Beijing 100023, China
www.wjgnet.com
wjg@wjgnet.com

ELSEVIER

World J Gastroenterol 2005;11(44):6960-6967
World Journal of Gastroenterology ISSN 1007-9327

• *BASIC RESEARCH* •

Nuclear factor-κB decoy oligodeoxynucleotides attenuates ischemia/reperfusion injury in rat liver graft

Ming-Qing Xu, Xiu-Rong Shuai, Mao-Lin Yan, Ming-Man Zhang, Lu-Nan Yan

Ming-Qing Xu, Mao-Lin Yan, Ming-Man Zhang, Lu-Nan Yan, Department of General Surgery, West China Hospital, Sichuan University, Chengdu 610041, Sichuan Province, China
Xiu-Rong Shuai, Department of General Surgery, Sichuan Provincial Hospital, Chinese People's Armed Police Forces, Leshan 640014, Sichuan Province, China
Supported by grants from China Postdoctoral Science Foundation, No. 2003033531
Correspondence to: Professor Lu-Nan Yan, Department of General Surgery, West China Hospital, Sichuan University, Chengdu 610041, Sichuan Province, China. xumingqing0018@163.com
Telephone: +86-28-85422476
Received: 2003-06-05 Accepted: 2003-08-16

Abstract

AIM: To evaluate the protective effect of NF-κB decoy oligodeoxynucleotides (ODNs) on ischemia/reperfusion (I/R) injury in rat liver graft.

METHODS: Orthotopic syngeneic rat liver transplantation was performed with 3 h of cold preservation of liver graft in University of Wisconsin solution containing phosphorothioated double-stranded NF-κB decoy ODNs or scrambled ODNs. NF-κB decoy ODNs or scrambled ODNs were injected intravenously into donor and recipient rats 6 and 1 h before operation, respectively. Recipients were killed 0 to 16 h after liver graft reperfusion. NF-κB activity in the liver graft was analyzed by electrophoretic mobility shift assay (EMSA). Hepatic mRNA expression of TNF-α, IFN-γ and intercellular adhesion molecule-1 (ICAM-1) were determined by semiquantitative RT-PCR. Serum levels of TNF-α and IFN-γ were measured by enzyme-linked immunosorbent assays (ELISA). Serum level of alanine transaminase (ALT) was measured using a diagnostic kit. Liver graft myeloperoxidase (MPO) content was assessed.

RESULTS: NF-κB activation in liver graft was induced in a time-dependent manner, and NF-κB remained activated for 16 h after graft reperfusion. NF-κB activation in liver graft was significant at 2 to 8 h and slightly decreased at 16 h after graft reperfusion. Administration of NF-κB decoy ODNs significantly suppressed NF-κB activation as well as mRNA expression of TNF-α, IFN-γ and ICAM-1 in the liver graft. The hepatic NF-κB DNA binding activity [presented as integral optical density (IOD) value] in the NF-κB decoy ODNs treatment group rat was significantly lower than that of the I/R group rat (2.16±0.78 *vs* 36.78 ±6.35 and 3.06±0.84 *vs* 47.62± 8.71 for IOD value after 4 and 8 h of reperfusion, respectively, $P<0.001$). The hepatic mRNA expression level of TNF-α, IFN-γ and ICAM-1 [presented as percent of β-actin mRNA (%)] in the NF-κB decoy ODNs treatment group rat was significantly lower than that of the I/R group rat (8.31 ±3.48 *vs* 46.37±10.65 and 7.46± 3.72 *vs* 74.82±12.25 for hepatic TNF-α mRNA, 5.58±2.16 *vs* 50.46±9.35 and 6.47±2.53 *vs* 69.72±13.41 for hepatic IFN-γ mRNA, 6.79 ±2.83 *vs* 46.23±8.74 and 5.28±2.46 *vs* 67.44±10.12 for hepatic ICAM-1 mRNA expression after 4 and 8 h of reperfusion, respectively, $P<0.001$). Administration of NF-κB decoy ODNs almost completely abolished the increase of serum level of TNF-α and IFN-γ induced by hepatic ischemia/reperfusion, the serum level (pg/mL) of TNF-α and IFN-γ in the NF-κB decoy ODNs treatment group rat was significantly lower than that of the I/R group rat (42.7±13.6 *vs* 176.7±15.8 and 48.4±15.1 *vs* 216.8±17.6 for TNF-α level, 31.5±12.1 *vs* 102.1±14.5 and 40.2±13.5 *vs* 118.6±16.7 for IFN-γ level after 4 and 8 h of reperfusion, respectively, $P<0.001$). Liver graft neutrophil recruitment indicated by MPO content and hepatocellular injury indicated by serum ALT level were significantly reduced by NF-κB decoy ODNs, the hepatic MPO content (A655) and serum ALT level (IU/L) in the NF-κB decoy ODNs treatment group rat was significantly lower than that of the I/R group rat (0.17±0.07 *vs* 1.12 ±0.25 and 0.46±0.17 *vs* 1.46±0.32 for hepatic MPO content, 71.7±33.2 *vs* 286.1±49.6 and 84.3±39.7 *vs* 467.8±62.3 for ALT level after 4 and 8 h of reperfusion, respectively, $P<0.001$).

CONCLUSION: The data suggest that NF-κB decoy ODNs protects against I/R injury in liver graft by suppressing NF-κB activation and subsequent expression of proinflammatory mediators.

Key words: Hepatic ischemia/reperfusion injury; NF-κB; Liver graft

Xu MQ, Shuai XR, Yan ML, Zhang MM, Yan LN. Nuclear factor-κB decoy oligodeoxynucleotides attenuates ischemia/reperfusion injury in rat liver graft. *World J Gastroenterol* 2005; 11(44): 6960-6967
http://www.wjgnet.com/1007-9327/11/6960.asp

INTRODUCTION

Liver transplantation is the only therapeutic strategy for many inherited and acquired disorders of the liver. The vulnerability of the transplantation liver to warm ischemia, cold preservation, and reperfusion injury is possibly associated with immediate posttransplant graft function loss, and graft damage caused by ischemia/reperfusion (I/R) is a serious problem after transplantation. Hepatic I/R injury still leads to primary graft nonfunction in about 4% of liver transplantation. Moreover, late consequences of ischemia injury include intrahepatic and extrahepatic biliary strictures, which further increase morbidity and jeopardize graft survival. Therefore, inhibition of I/R injury has become a more serious clinical interest.

Two distinct phases in the development of organ injury have been identified in experimental hepatic I/R injury animal models. During the initial phase of injury, Kupffer cells are activated and release reactive oxygen species and proinflammatory cytokines, including tumor necrosis factor (TNF)-α[1-4]. The enhanced production of TNF-α plays a more important role in the initiation of a cascade of events that causes significant liver injury mediated by neutrophils. One of the main functions of TNF-α is the up-regulation of adhesion molecules and neutrophil-attracting C-X-C chemokines[5,6]. The coordinated efforts of adhesion molecules and C-X-C chemokines mediate the recruitment of neutrophils into the liver. Sequestered neutrophils release protease and reactive oxygen intermediates (ROI), which directly damage hepatocytes and endothelial cells and also to capillary plugging causing hepatic hypoperfusion. The transcription factor nuclear factor (NF)-κB plays a key role in the regulation of genes that function in immune and inflammatory systems such as TNF-α, IFN-γ, chemokines and ICAM-1[7-15]. Previous studies suggested that NF-κB activation plays a deteriorative role during hepatic I/R injury[15-18]. In contrast to these studies, Bradham *et al.*[19] reported that NF-κB activation during orthotopic liver transplantation is protective.

In the present study, we have attempted to evaluate the exact effect of NF-κB activation on the I/R injury in liver graft after orthotopic liver transplantation in rats. For this aim, we used the recently developed technology of decoy ODNs. The original concept of using synthetic double-stranded ODN as "decoy" cis elements to block the binding of nuclear factors to promoter regions of target genes was introduced in 1990 by Sullenger *et al.* and Bielinska *et al.* In 1997, Morishita *et al.* reported the first *in vivo* application of this technology, they prevented myocardial infarction after reperfusion in rats by direct infusion of synthetic double-stranded 20-bp ODNs containing the NF-κB cis element into cannulated coronary arteries[20]. Subsequently, Kawamura *et al.* showed that the direct injection of NF-κB decoy ODNs into implanted tumors in mice inhibited cachexia, without affecting the tumor growth[21]. In 2000, Abeyama *et al.* reported that intraperitoneal and local administration of NF-κB decoy ODNs reduces the extent of UV-induced skin inflammation, and this is associated with NF-κB activation inhibition and decreased the transcription of inflammatory cytokines TNF-α and IL-1 and IL-6[22]. Here we report that the application of NF-κB decoy ODNs significantly attenuates the liver graft I/R injury in rats.

MATERIALS AND METHODS

NF-κB decoy ODNs and scrambled ODNs

Double-stranded NF-κB decoy ODNs were generated using equimolar amounts of single-stranded sense and antisense phosphorothioate-modified oligonucleotides containing two NF-κB binding sites(sense sequence 5' -AGGGACTTTCCGCTGGGGACTTTCC-3'; NF-κB binding sites bold and underlined)[23]. Scrambled ODNs (treatment control ODNs: 5'-TTGCCGTACCTGACTTAGCC-3')[22] were generated in the same way. Sense and antisense strands were mixed in the presence of 150 mmol PBS, heated to 100 ℃, and allowed to cool to room temperature to obtain double-stranded DNA .

Experimental design and liver transplantation

Male SD rats (220-250 g) were used for the liver graft I/R injury experiments. The animals were maintained with a 12-h light/dark cycle in a conventional animal facility with water and commercial chow provided *ad libitum*, with no fasting before the transplantation. The following experimental groups were compared: (1) the I/R group, in which orthotopic liver transplantation were performed with two-cuff method and liver graft reperfusion was initiated after 3 h of cold-preservation in chilled (4 ℃) University of Wisconsin (UW) solution containing NF-κB decoy ODNs or scrambled ODNs (5 μmol/L/mL); (2) the NF-κB decoy ODNs + I/R group, in which donor and recipient animals were injected intravenously through the penile vein with NF-κB decoy ODNs (1.0 mmol/L solution in PBS, 1 mL/rat) 6 and 1 h before liver harvesting or orthotopic liver transplantation; (3) the scrambled ODNs + I/R group in which donor and recipient animals were injected intravenously through the penile vein with scrambled ODNs (1.0 mmol/L solution in PBS, 1 mL/rat) 6 and 1 h before liver harvesting or orthotopic liver transplantation; (4) the sham control group in which rats only underwent a midline laparotomy. Orthotopic liver transplantation was performed according to the method described in our previous study[24]. All operations were performed under ether anesthesia in sterile conditions. The survival rate was >89% at 24 h after liver transplantation. Liver graft tissues and recipient blood samples (n = 5) were harvested at different time points (0, 0.5, 1, 2, 4, 8, and 16 h) after graft reperfusion and were immediately frozen in liquid nitrogen (only liver samples) and kept at -80 ℃ until use.

Myeloperoxidase assay

Liver myeloperoxidase (MPO) content was assessed by methods described elsewhere[15]. Briefly, liver tissue (50 mg) was homogenized in 2 mL of homogenization buffer (3.4 mmol/L KH_2HPO_4, 16 mmol/L Na_2HPO_4, pH 7.4).

After centrifugation for 20 min at 10 000 g, 10 volumes of resuspension buffer (43.2 mmol/L KH_2HPO_4, 6.5 mmol/L Na_2HPO_4, 10 mmol/L ethylenediaminetetraacetic acid, 0.5% hexadecyltrimethylammonium, pH 6.0) was added to the pellet and the samples were sonicated for 10 s. After heating for 2 h at 60 ℃, the supernatant was reacted with 3, 3', 3, 5'-tetramethylbenzidine (Sigma Chemicall Co.) and read at 655 nm.

Preparation of liver graft nuclear extract

Nuclear proteins from frozen liver graft tissue were extracted according to the method of Nanji[8]. One gram of liver tissue was homogenized in 5 mL buffer [0.32 mol/L sucrose, 50 mmol/L Tris-HCl (pH 7.5), 25 mmol/L KCl, 5 mmol/L $MgCl_2$, 0.5 mmol/L phenylmethylsulfonyl fluoride,10 μg/mL aprotinin, 10 μg/mL tosyllysylchloromethyl ketone(TLCK)] and centrifuged for 10 min at 600 r/min at 40 ℃. The pellet was resuspended in 2.5 mL of 2 mol/L sucrose-Tris HCl, KCl, and $MgCl_2$ (TKM) buffer and homogenized. The homogenate was centrifuged at 40 000 g at 4 ℃ for 2 h. The supernatant was carefully removed and the pellet containing the nuclear extract was resuspended in 40 μL of buffer A [10 mmol/L HEPES/KOH (pH 7.9), 2 mmol/L $MgCl_2$, 0.1 mmol/L ethylenediaminetetraacetic acid, 10 mmol/L KCl, 1 mmol/L dithiothreitol, 0.5 mmol/L phenylmethylsulfonyl fluoride] and left on ice for 10 min, mixed, and centrifuged at 15 000 g at 4 ℃ for 15 s. The pellet was then resuspended in 1.0 mL of buffer B [10 mmol/L HEPES/KOH (pH 7.9), 50 mmol/L KCl, 300 mmol/L NaCl, 0.1 mmol/L ethylenediaminetetraacetic acid, 10% (v/v) glycerol, 1 mmol/L dithiothreitol, 0.5 mmol/L phenylmethylsulfonyl fluoride, 10 μg/mL leupeptin, 10 μg/mL aprotinin, 10 μg/mL TPCK] and put on ice for 20 min. After centrifugation at 15 000 g at 4 ℃ for 5 min, the supernatant was stored at -80 ℃ as a nuclear extract. Before the experiments, the total protein concentration in the samples were determined according to the method of Bradford.

Electrophoretic mobility shift assay (EMSA) for hepatic NF-κB activity

NF-κB DNA binding activity was performed in a 10 μL binding reaction mixture containing 1×binding buffer [50 mg/L of double-stranded poly (dI-dC), 10 mmol/L Tris-HCl (pH 7.5), 50 mmol/L $NaCl_2$, 0.5 mmol/L EDTA, 0.5 mmol/L-1DTT, 1 mmol/L $MgCl_2$, and 100 mL/L glycerol], 5 μg of nuclear protein, and 35 fmol of double-stranded NF-κB consensus oligonucleotide (5' -AGTGAGGGGACTTTCCCAGGC -3') that was endly labeled with γ-^{32}P (111 TBq/mol/L at 370 GBq^{-1}) using T4 polynucleotide kinase. The binding reaction mixture was incubated at room temperature for 20 min and analyzed by electrophoresis on 7% nondenaturing polyacrylamide gels. After electrophoresis the gels were dried by Gel-Drier (Biol-Rad Laboratories, Hercules, CA, USA) and exposed to Kodak X-ray films at -70 ℃. NF-κB DNA binding activity was presented as integral optical density (OD) value.

Semiquantitative RT-PCR assay for hepatic expression of TNF-α, IFN-γ and ICAM-1 mRNA

Analysis of the expression of TNF-α, IFN-γ and ICAM-1 mRNA was determined by semiquantitative RT-PCR amplification in contrast with house-keeping gene β-actin. Total RNA from 10 mg liver graft tissue was extracted using Tripure™ reagent. First-strand cDNA was transcribed from 1 μg RNA using AMV and an oligo (dT15) primer. PCR was performed in a 25 μL reaction system. Specific primers used in PCR reaction were as follows: TNF-α, 5' primer 5'-AGCCCACGTAGCAAACCACCA-3' and 3' primer 5'-ACACCCATTCCCTTCACAGAGCAAT-3', to give a 446-bp product; $ICAM^{-1}$, 5' primer 5' -TGGAACTGCACGTGCTGTAT-3', 3' primer 5' -ACCATTCTGTTCAAAAGCAG-3', to give a 513-bp product; IFN-γ, 5' primer 5'-ACAATGAACGCTACACACTG-3', 3' primer 5'-TCAAACTTGGCAATACTCAT-3', to give a 362-bp product; β-actin, 5' primer 5' -ATGGATGATGATATCGCCGCG-3', 3' primer 5' -TGAAGGTAGTTTCGTGGATGC-3', to give a 813-bp product. PCR products of each sample were subjected to electrophoresis in a 15 g/L agarose gel containing 0.5 mg/L ethidium bromide. Densitometrical analysis using NIH image software was performed for semiquantification of PCR products, and mRNA expression was evaluated by the band-intensity ratio of TNF-α, IFN-γ and ICAM-1 to β-actin, and presented as percent of β-actin (%).

Blood assay for serum levels of TNF-α, IFN-γ and ALT

Blood was obtained by cardiac puncture at the time of killing. Serum samples were analyzed for TNF-α and IFN-γ by enzyme-linked immunosorbent assays (ELISA) according to the manufacturer's instructions. Serum samples were also analyzed for ALT level as indices of hepatocellular injury. Measurements of serum ALT level were made using a diagnostic kit from Sigma Chemical Co.

Statistical analysis

All data were expressed as mean±SE . Statistical analysis of data was performed using the Student's *t*-test; $P<0.05$ was considered statistically significant.

RESULTS

NF-κB activation in the liver graft

NF-κB activation in the liver graft at seven separate time points after reperfusion was determined by EMSA (as shown in Figure 1). NF-κB activation in the liver graft after reperfusion was induced in a time-dependent manner. Hepatic NF-κB activation was observed to start within 30 min after the initiation of reperfusion and continued for 16 h after liver graft reperfusion. NF-κB activation in the liver graft was significant at 2 to 8 h and slightly decreased at 16 h after graft reperfusion.

NF-κB decoy ODNs suppresses NF-κB activation in the liver graft

In the I/R + NF-κB decoy ODNs group rats, administration of NF-κB decoy ODNs group almost

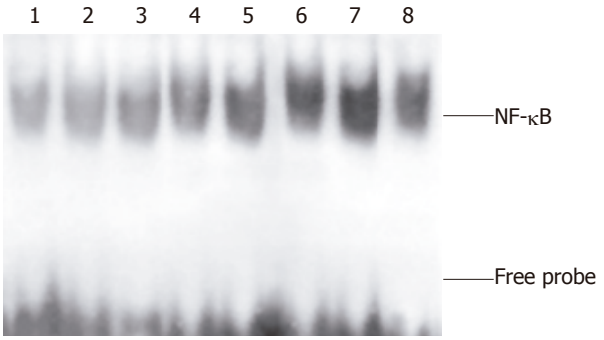

Figure 1 NF-κB activation in the liver graft. Lanes 1: Hepatic nuclear protein extracts from sham control rat; Lanes 2-8: Liver graft nuclear protein extracts on 0, 0.5, 1, 2, 4, 8 and 16 h after reperfusion.

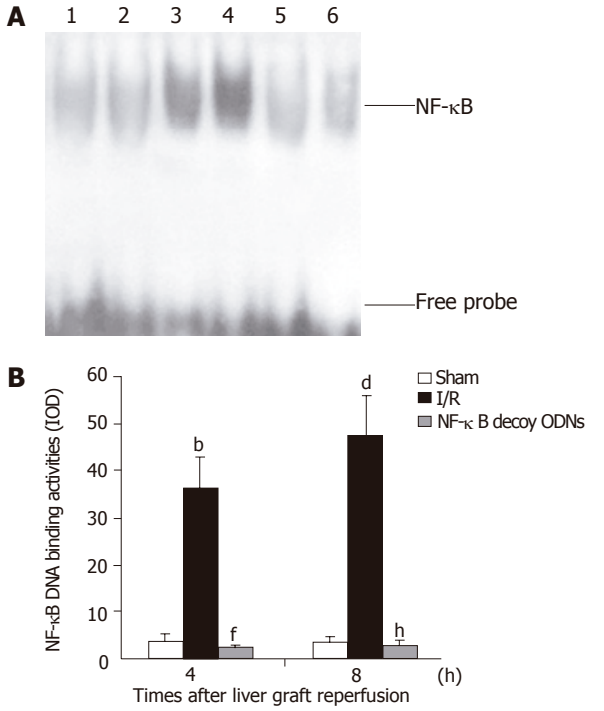

Figure 2 Hepatic NF-κB activation (**A**) and NF-κB DNA binding activities presented as IOD value (**B**). Lanes 1 and 2: Hepatic RNA extracts from sham control group. Lanes 3 and 4: Hepatic RNA extracts from I/R group. Lanes 5 and 6: Hepatic RNA extracts from I/R + NF-κB decoy ODNs group. [b, d]$P<0.001$ vs sham group, [f, h]$P<0.001$ *vs* I/R group.

completely abrogated NF-κB activation in the liver graft after 4 h and 8 h of reperfusion (as shown in Figure 2). Similar effects were observed at 0.5, 1, 2 or 16 h after hepatic reperfusion (data not shown). However, in the I/R + scrambled ODNs group rats, NF-κB activation in the liver graft were not significantly changed compared with the I/R group rats (data not shown).

NF-κB decoy ODNs suppresses hepatic mRNA expression of TNF-α, IFN-γ and ICAM-1

To investigate whether NF-κB decoy ODNs induced suppression of NF-κB was associated with reduced inflammatory mediator expression, mRNA expression of TNF-α, IFN-γ and ICAM-1 in the liver graft were assessed by RT-PCR. Hepatic ischemia/reperfusion increased hepatic mRNA expression of TNF-α, IFN-γ and ICAM-1. Administration of NF-κB decoy ODNs almost completely abrogated hepatic ischemia/reperfusion-induced increases of TNF-α, IFN-γ and ICAM-1 mRNA expression in the liver graft with reperfusion for 4 and 8 h (as shown in Figure 3). Similar effects were observed at 0.5, 1, 2 or 16 h after reperfusion (data not shown). However, administration of scrambled ODNs did not have any significant effect on the hepatic mRNA expression of these inflammatory mediators (data not shown). Thus, NF-κB decoy ODNs-mediated suppression of NF-κB activation in the liver graft is associated with the inhibited hepatic mRNA expression of these proinflammatory mediators.

NF-κB decoy ODNs reduces serum level of TNF- α and IFN-γ

To confirm the inhibitory effects of NF-κB decoy ODNs on the inflammatory mediator production, serum levels of TNF-α and IFN-γ were analyzed by ELISA. Serum levels of TNF-α and IFN-γ were significantly increased within 1 h and were maximal at 8 h after liver graft reperfusion. Administration of NF-κB decoy ODNs markedly reduced serum levels of TNF-α and IFN-γ ($P<0.001$) at every time point, respectively (Figure 4). However, administration of scrambled ODNs did not have any significant effect on the serum levels of TNF-α and IFN-γ (data not shown).

NF-κB decoy ODNs suppresses liver graft neutrophil recruitment and liver graft injury

Liver graft neutrophil recruitment was determined by liver MPO content and hepatocellular injury was assessed by serum level of ALT. Liver graft ischemia/reperfusion caused significant increases of liver MPO content and serum level of ALT compared with sham controls. In the presence of NF-κB decoy ODNs, the liver graft MPO content and the serum level of ALT were significantly reduced ($P<0.001$) (as shown in Figure 5), whereas administration of scrambled ODNs did not have any significant effect on the liver graft MPO content and serum level of ALT (data not shown).

DISCUSSION

Hepatic ischemia/reperfusion injury remains a significant problem and limitation of liver transplantation and may result in liver failure, remote organ failure, and death. Previous studies have identified many proinflammatory mediators (TNF-α, MIP-2, IFN-γ, KC, ENA-78, and ICAM-1) involved in the pathogenesis of hepatic ischemia/reperfusion injury, and production of TNF-α by activated Kupffer cells is central to this process[3,15, 6,25-27]. TNF-α enhances the inflammatory response in liver by inducing the expression of adhesion molecules on vascular endothelial cells and stimulating the production and release of neutrophil-attracting CXC chemokines[18,28]. TNF-α[29-33] and ICAM-1[15] also play significant roles in

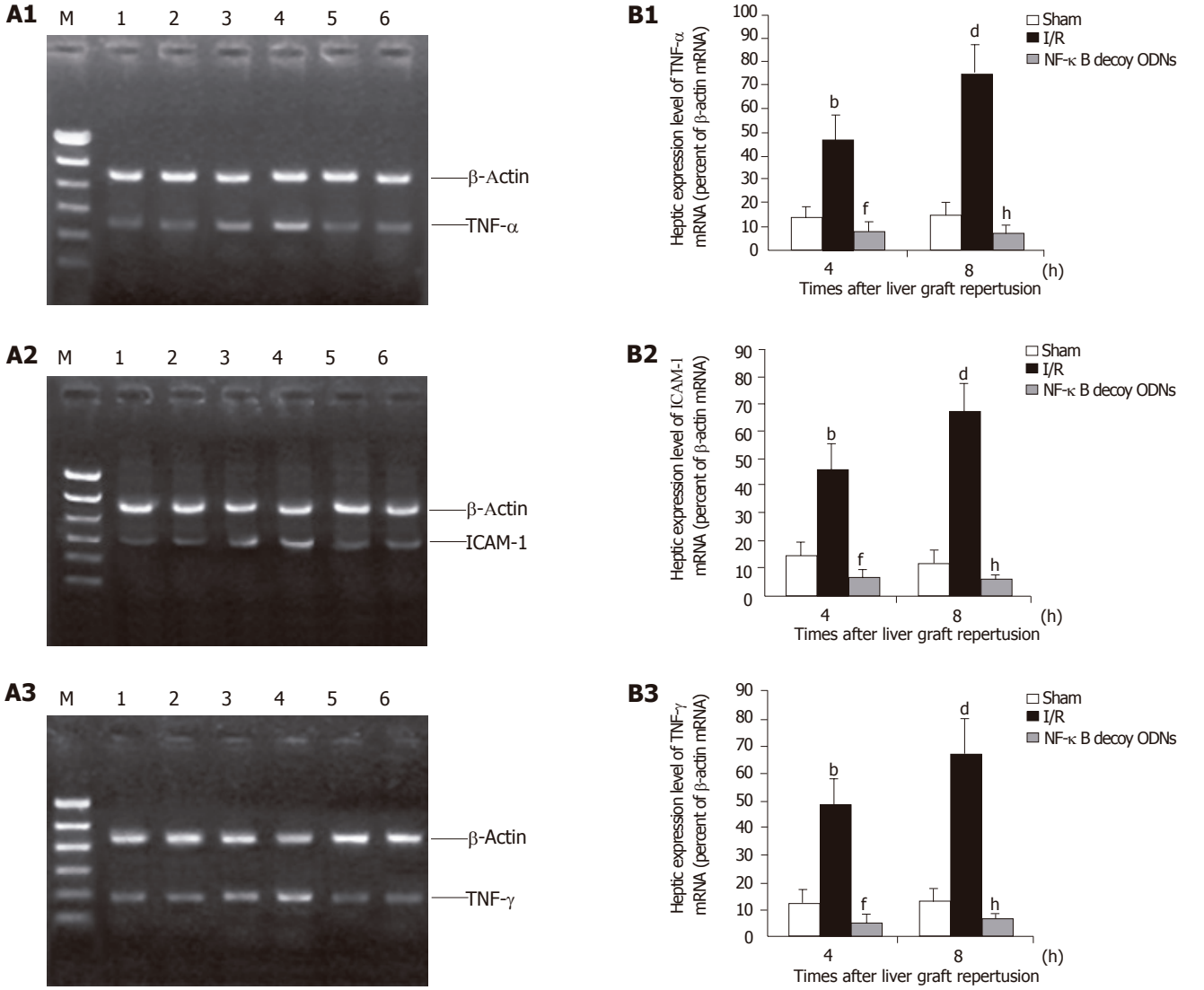

Figure 3 Hepatic expression (**A**) and the expression level (**B**) of cytokine mRNA after 4 and 8 h of reperfusion. Lanes 1 and 2: Hepatic RNA extracts from sham control group. Lanes 3 and 4: Hepatic RNA extracts from I/R group. Lanes 5 and 6: Hepatic RNA extracts from I/R + NF-κB decoy ODNs group. $^{b,d}P<0.001$ *vs* sham group; $^{f,h}P<0.001$ *vs* I/R group.

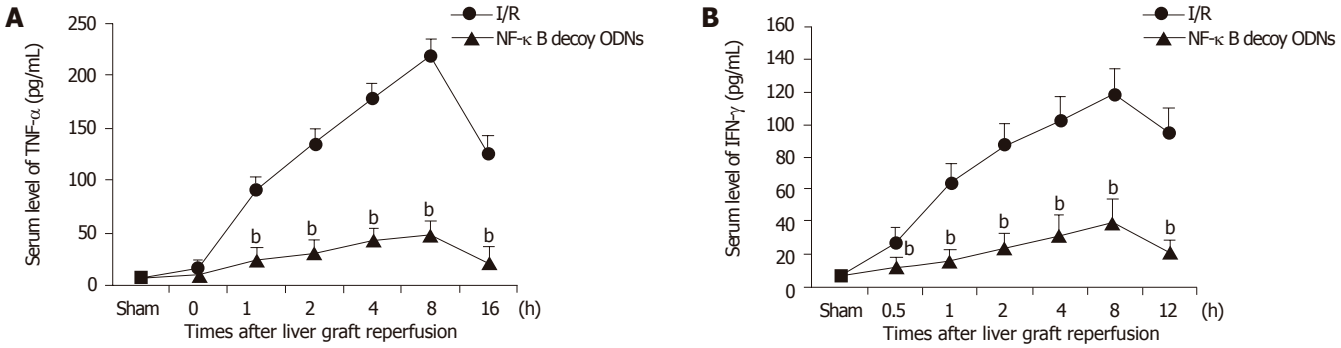

Figure 4 Serum levels of TNF-α (A) and IFN-γ (B) after hepatic ischemia/reperfusion. $^{b}P<0.001$ *vs* I/R group.

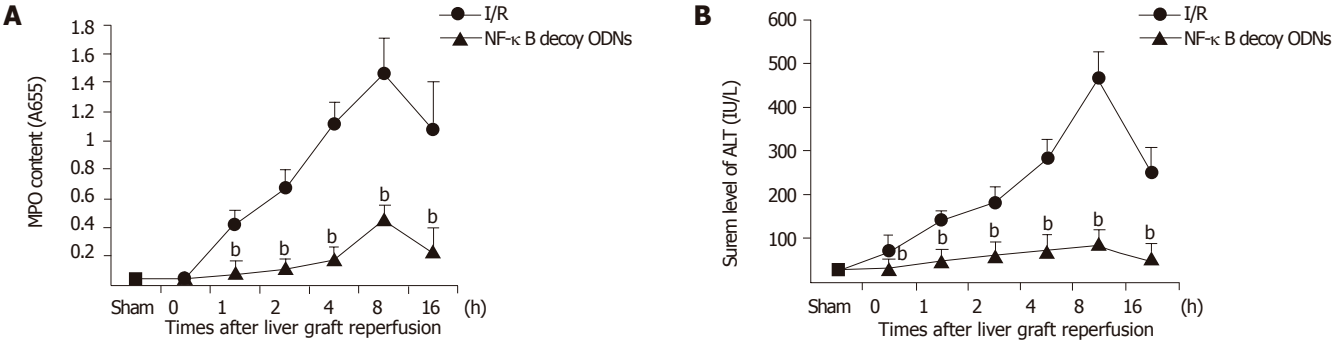

Figure 5 Hepatic MPO content (**A**) and serum level of ALT (**B**). $^{b}P<0.001$ *vs* I/R group.

the inflammatory and immune responses that mediate allograft rejection. Thus, they are important as they are against liver graft I/R injury and rejection to suppress the production of these proinflammatory mediators. Each of these mediators is controlled, at least in part, by the transcription factor, NF-κB. Yoshidome *et al.*[15] reported interleukin (IL)-10 protected against hepatic I/R injury by suppressing NF-κB activation and subsequent expression of proinflammatory mediators. Recent studies have confirmed that hepatic ischemic preconditioning (IPC) has protective effect on hepatic cold storage-reperfusion injury, including improved graft function, reduced graft circulatory impairment, enhanced bile production, augmented responses to a bile acid challenge, elevated O_2 consumption, improved hepatic tissue blood flow and decreased hepatic vascular resistance, reduced endothelial cell damage, suppressed Kupffer cell activation, decreased apoptosis of hepatocytes, and as a result, graft survival improves after liver transplantation[34-43]. The recent study have found out that attenuation of NF-κB activation and subsequent reduction in TNF-α production after sustained ischemia play important roles in the protective mechanism of IPC against hepatic I/R injury[16,44]. These data suggest a central role of NF-κB activation in the initiation of hepatic I/R injury, and NF-κB activation inhibition could protect against hepatic I/R injury. However, there are contrary reports about the role of NF-κB activation during I/R injury and liver transplantation. Maulik *et al.*[45] showed that IPC activated NF-κB, of which p38 mitogen-associated protein kinase (MAPK) might be upstream before sustained ischemia, and also that inhibitor of p38MAPK abolished preconditioning-induced cardioprotection. Teoh *et al.*[46] recently reported that the hepatoprotective effects of ischemic preconditioning are associated with the activation of NF-κB and SAPKs that are associated with entry of hepatocytes into the cell cycle, a critical biological effect that favors survival of the liver against ischemic and I/R injury. Bradham *et al.*[19] reported that the activation of NF-κB during orthotopic liver transplantation in rats is protective, inhibition of donor hepatic NF-κB activation by adenoviral-mediated IκB alpha superrepressor gene transfer resulted in increased serum ALT levels after 3 h of transplantation. In addition, the blockade of NF-κB resulted in increased histological tissue injury and increased hepatic terminal deoxyribonucleotide transferase-mediated deoxyuridine triphosphate nick end labeling (TUNEL) staining, indicating apoptosis.

To assess the role of NF-κB activation during liver transplantation, we examined the effect of NF-κB activation inhibition by NF-κB decoy ODNs containing two NF-κB binding sites on the liver graft I/R injury. We found that cold preservation-reperfusion of liver graft rapidly activated hepatic NF-κB and concomitantly elevated hepatic mRNA expression of TNF-α, INF-γ and ICAM-1 as well as serum levels of TNF-α and IFN-γ. Administration of NF-κB decoy ODNs almost completely abrogated the increased hepatic NF-κB activation, the up-regulated hepatic mRNA expression of the proinflammatory mediators, the elevated serum levels of TNF-α and IFN-γ as well as the increased hepatic neutrophil recruitment, and as a result, attenuated liver graft I/R injury. Liver I/R injury is considered to be primarily dependent on the activation of Kupffer cells, these cells are a major source of ROIs, proinflammatory cytokines or chemokines that promote neutrophils recruitment, adhesion, and activation eventually leading to organ injury. Bradham *et al.*[19] reported that the induction of TNF-α mRNA and serum protein during liver transplantation was unaffected by Kupffer cells depletion with $GdCl_3$. These results show that Kupffer cells are not the only major source of TNF-α production after liver transplantation and that stress-signaling protein activation occurs independently of Kupffer cells. A recent study reported that hepatic I/R injury critically depends on liver activated T cells[47,48]. Indeed, both cyclosporine and FK506, which are potent T cell-deactivating agents, were reported to decrease reperfusion injury after liver transplantation or warm ischemia compared with untreated controls. Besides the role of liver reside T cells, lymphocytes recruited from the circulatory cell pool within hours or days after reperfusion are also involved in the cascade of reperfusion in the kidney and in the liver[49, 50]. Circulating monocytes/macrophages are the primary systemic sources of TNF-α[51] in response to endotoxin stimulation. Previous studies showed that endotoxin in portal vein blood was significantly increased during portal vein occlusion and after liver transplantation, and the increased endotoxin could stimulat macrophages that reside in spleen, lung, and other organs, as well as circulating monocyte/

macrophage to produce TNF-α. Tsoulfas *et al*. have shown the LPS/CD14/LBP/NF-κB signaling pathway activation in hepatic transplantation preservation injury[52]. Thus, far besides Kupffer cells, T lymphocytes and monocytes/macrophages, either residing in the organ, or being recruited from the blood, should definitely be considered effector cells in I/R injury. IFN-γ released by activated T cells is able to prime macrophages/Kupffer cells for the production of proinflammatory cytokines like TNF, and to down-regulate the synthesis of IL-10, a protective cytokine which has been identified to protect against hepatic ischemia/reperfusion injury. Conversely, monomacrophages can also activate T cells and promote the synthesis of INF-γ through the release of cytokines like IL-12 and IL-18 and the engagement of costimulatory molecules[53]. In the present study, the administration of NF-κB decoy ODNs may attenuate not only donor hepatic Kupffer cells NF-κB activation, but also recipient monocytes/macrophages and T-cells NF-κB activation, and consequently decreases the hepatic mRNA expression of TNF-α and IFN-γ as well as the protein production of TNF-α and IFN-γ. Although blockade of NF-κB can result in increased hepatocytes apoptosis induced by TNF-α, the significantly decreased production of TNF-α by NF-κB decoy ODNs may attenuates the initiation of hepatocytes apoptosis. Thus, NF-κB decoy ODNs may protect against I/R injury in the transplanted liver graft by suppressing NF-κB activation and the subsequent production of TNF-α, ICAM-1 and IFN-γ.

REFERENCES

1 **Minor T,** Akbar S, Tolba R, Dombrowski F. Cold preservation of fatty liver grafts: prevention of functional and ultrastructural impairments by venous oxygen persufflation. *J Hepatol* 2000; **32:** 105-111

2 **Thurman RG,** Schemmer P, Zhong Z, Bunzendahl H, von Frankenberg M, Lemasters JJ. Kupffer cell-dependent reperfusion injury in liver transplantation: new clinically relevant use of glycine. *Langenbecks Arch Chir Suppl Kongressbd* 1998; **115**: 185-190

3 **Xu MQ,** Xue L, Gong JP. Significance of Kupffer cell NF-κB activation during hepatic ischemia-reperfusion in rats. *Shijie Huaren Xiaohua Zazhi* 2001; **9:** 1250-1253

4 **Iimuro Y,** Bradford BU, Yamashina S, Rusyn I, Nakagami M, Enomoto N, Kono H, Frey W, Forman D, Brenner D, Thurman RG. The glutathione precursor L-2-oxothiazolidine-4-carboxylic acid protects against liver injury due to chronic enteral ethanol exposure in the rat. *Hepatology* 2000; **31:** 391-398

5 **Colletti LM,** Cortis A, Lukacs N, Kunkel SL, Green M, Strieter RM. Tumor necrosis factor up-regulates intercellular adhesion molecule 1, which is important in the neutrophil-dependent lung and liver injury associated with hepatic ischemia and reperfusion in the rat. *Shock* 1998; **10:** 182-191

6 **Lentsch AB,** Yoshidome H, Cheadle WG, Miller FN, Edwards MJ. Chemokine involvement in hepatic ischemia/reperfusion injury in mice: roles for macrophage inflammatory protein-2 and KC. *Hepatology* 1998; **27:** 1172-1177

7 **Gong JP,** Liu CA, Wu CX, Li SW, Shi YJ, Li XH. Nuclear factor kB activity in patients with acute severe cholangitis. *World J Gastroenterol* 2002; **8:** 346-349

8 **Nanji AA,** Jokelainen K, Rahemtulla A, Miao L, Fogt F, Matsumoto H, Tahan SR, Su GL. Activation of nuclear factor kappa B and cytokine imbalance in experimental alcoholic liver disease in the rat. *Hepatology* 1999; **30:** 934-943

9 **Sakaguchi T,** Nakamura S, Suzuki S, Oda T, Ichiyama A, Baba S, Okamoto T. Participation of platelet-activating factor in the lipopolysaccharide-induced liver injury in partially hepatectomized rats. *Hepatology* 1999; **30:** 959-967

10 **Verhasselt V,** Vanden Berghe W, Vanderheyde N, Willems F, Haegeman G, Goldman M. N-acetyl-L-cysteine inhibits primary human T cell responses at the dendritic cell level: association with NF-kappaB inhibition. *J Immunol* 1999; **162:** 2569-2574

11 **Ouaaz F,** Arron J, Zheng Y, Choi Y, Beg AA. Dendritic cell development and survival require distinct NF-kappaB subunits. *Immunity* 2002; **16:** 257-270

12 **Grumont R,** Hochrein H, O'Keeffe M, Gugasyan R, White C, Caminschi I, Cook W, Gerondakis S. c-Rel regulates interleukin 12 p70 expression in CD8(+) dendritic cells by specifically inducing p35 gene transcription. *J Exp Med* 2001; **194:** 1021-1032

13 **Mann J,** Oakley F, Johnson PW, Mann DA. CD40 induces interleukin-6 gene transcription in dendritic cells: regulation by TRAF2, AP-1, NF-kappa B, AND CBF1. *J Biol Chem* 2002; **277:** 17125-17138

14 **Xu MQ,** Wang W, Xue L, Yan LN. NF-kappaB activation and zinc finger protein A20 expression in mature dendritic cells derived from liver allografts undergoing acute rejection. *World J Gastroenterol* 2003; **9:** 1296-1301

15 **Yoshidome H,** Kato A, Edwards MJ, Lentsch AB. Interleukin-10 suppresses hepatic ischemia/reperfusion injury in mice: implications of a central role for nuclear factor kappaB. *Hepatology* 1999; **30:** 203-208

16 **Funaki H,** Shimizu K, Harada S, Tsuyama H, Fushida S, Tani T, Miwa K. Essential role for nuclear factor kappaB in ischemic preconditioning for ischemia-reperfusion injury of the mouse liver. *Transplantation* 2002; **74:** 551-556

17 **Hiasa G,** Hamada M, Ikeda S, Hiwada K. Ischemic preconditioning and lipopolysaccharide attenuate nuclear factor-kappaB activation and gene expression of inflammatory cytokines in the ischemia-reperfused rat heart. *Jpn Circ J* 2001; **65:** 984-990

18 **Lentsch AB,** Kato A, Yoshidome H, McMasters KM, Edwards MJ. Inflammatory mechanisms and therapeutic strategies for warm hepatic ischemia/reperfusion injury. *Hepatology* 2000; **32:** 169-173

19 **Bradham CA,** Schemmer P, Stachlewitz RF, Thurman RG, Brenner DA. Activation of nuclear factor-kappaB during orthotopic liver transplantation in rats is protective and does not require Kupffer cells. *Liver Transpl Surg* 1999; **5:** 282-293

20 **Morishita R,** Sugimoto T, Aoki M, Kida I, Tomita N, Moriguchi A, Maeda K, Sawa Y, Kaneda Y, Higaki J, Ogihara T. In vivo transfection of cis element "decoy" against nuclear factor-kappaB binding site prevents myocardial infarction. *Nat Med* 1997; **3:** 894-899

21 **Kawamura I,** Morishita R, Tomita N, Lacey E, Aketa M, Tsujimoto S, Manda T, Tomoi M, Kida I, Higaki J, Kaneda Y, Shimomura K, Ogihara T. Intratumoral injection of oligonucleotides to the NF kappa B binding site inhibits cachexia in a mouse tumor model. *Gene Ther* 1999; **6:** 91-97

22 **Abeyama K,** Eng W, Jester JV, Vink AA, Edelbaum D, Cockerell CJ, Bergstresser PR, Takashima A. A role for NF-kappaB-dependent gene transactivation in sunburn. *J Clin Invest* 2000; **105:** 1751-1759

23 **Giannoukakis N,** Bonham CA, Qian S, Chen Z, Peng L, Harnaha J, Li W, Thomson AW, Fung JJ, Robbins PD, Lu L. Prolongation of cardiac allograft survival using dendritic cells treated with NF-kB decoy oligodeoxyribonucleotides. *Mol Ther* 2000; **1:** 430-437

24 **Xu MQ,** Yao ZX. Functional changes of dendritic cells derived from allogeneic partial liver graft undergoing acute rejection in rats. *World J Gastroenterol* 2003; **9:** 141-147

25 **Eckhoff DE,** Bilbao G, Frenette L, Thompson JA, Contreras JL. 17-Beta-estradiol protects the liver against warm ischemia/reperfusion injury and is associated with increased serum

nitric oxide and decreased tumor necrosis factor-alpha. *Surgery* 2002; **132:** 302-309
26 **Ben-Ari Z,** Hochhauser E, Burstein I, Papo O, Kaganovsky E, Krasnov T, Vamichkim A, Vidne BA. Role of anti-tumor necrosis factor-alpha in ischemia/reperfusion injury in isolated rat liver in a blood-free environment. *Transplantation* 2002; **73:** 1875-1880
27 **Zhu XH,** Qiu YD, Shen H, Shi MK, Ding YT. Effect of matrine on Kupffer cell activation in cold ischemia reperfusion injury of rat liver. *World J Gastroenterol* 2002; **8:** 1112-1116
28 **Kataoka M,** Shimizu H, Mitsuhashi N, Ohtsuka M, Wakabayashi Y, Ito H, Kimura F, Nakagawa K, Yoshidome H, Shimizu Y, Miyazaki M. Effect of cold-ischemia time on C-X-C chemokine expression and neutrophil accumulation in the graft liver after orthotopic liver transplantation in rats. *Transplantation* 2002; **73:** 1730-1735
29 **Fernandes H,** Koneru B, Fernandes N, Hameed M, Cohen MC, Raveche E, Cohen S. Investigation of promoter polymorphisms in the tumor necrosis factor-alpha and interleukin-10 genes in liver transplant patients. *Transplantation* 2002; **73:** 1886-1891
30 **Mazariegos GV,** Reyes J, Webber SA, Thomson AW, Ostrowski L, Abmed M, Pillage G, Martell J, Awad MR, Zeevi A.Cytokine gene polymorphisms in children successfully withdrawn from immunosuppression after liver transplantation. *Transplantation* 2002; **73:** 1342-1345
31 **Warle MC,** Farhan A, Metselaar HJ, Hop WC, van der Plas AJ, Kap M, de Rave S, Kwekkeboom J, Zondervan PE, IJzermans JN, Tilanus HW, Pravica V, Hutchinson IV, Bouma GJ. In vitro cytokine production of TNFalpha and IL-13 correlates with acute liver transplant rejection. *Hum Immunol* 2001; **62:** 1258-1265
32 **Grenz A,** Schenk M, Zipfel A, Viebahn R. TNF-alpha and its receptors mediate graft rejection and loss after liver transplantation. *Clin Chem Lab Med* 2000; **38:** 1183-1185
33 **Bathgate AJ,** Lee P, Hayes PC, Simpson KJ. Pretransplantation tumor necrosis factor-alpha production predicts acute rejection after liver transplantation. *Liver Transpl* 2000; **6:** 721-727
34 **Ricciardi R**, Schaffer BK, Kim RD, Shah SA, Donohue SE, Wheeler SM, Quarfordt SH, Callery MP, Meyers WC, Chari RS. Protective effects of ischemic preconditioning on the cold-preserved liver are tyrosine kinase dependent. *Transplantation* 2001; **72:** 406-412
35 **Peralta C,** Bartrons R, Serafin A, Blazquez C, Guzman M, Prats N, Xaus C, Cutillas B, Gelpi E, Rosello-Catafau J. Adenosine monophosphate-activated protein kinase mediates the protective effects of ischemic preconditioning on hepatic ischemia-reperfusion injury in the rat. *Hepatology* 2001; 34: 1164-1173
36 **Sindram D,** Rudiger HA, Upadhya AG, Strasberg SM, Clavien PA. Ischemic preconditioning protects against cold ischemic injury through an oxidative stress dependent mechanism. *J Hepatol* 2002; 36: 78-84
37 **Serafin A,** Rosello-Catafau J, Prats N, Xaus C, Gelpi E, Peralta C. Ischemic preconditioning increases the tolerance of Fatty liver to hepatic ischemia-reperfusion injury in the rat. *Am J Pathol* 2002; 161: 587-601
38 **Zhang X,** Cao H, Jiao Z, Ling W, Wu Z, Chen Z, Kuang Y. Effects of ischemic preconditioning on apoptosis of hepatocytes in liver transplantation in rats. *Zhonghua Gan Zang Bing Za Zhi* 2000; **8:** 221-213
39 **Arai M,** Thurman RG, Lemasters JJ. Contribution of adenosine A(2) receptors and cyclic adenosine monophosphate to protective ischemic preconditioning of sinusoidal endothelial cells against Storage/Reperfusion injury in rat livers. *Hepatology* 2000; **32:** 297-302
40 Totsuka E, Fung JJ, Urakami A, Moras N, Ishii T, Takahashi K, Narumi S, Hakamada K, Sasaki M. Influence of donor cardiopulmonary arrest in human liver transplantation: possible role of ischemic preconditioning. *Hepatology* 2000; **31:** 577-580
41 **Ricciardi R,** Meyers WC, Schaffer BK, Kim RD, Shah SA, Wheeler SM, Donohue SE, Sheth KR, Callery MP, Chari RS. Protein kinase C inhibition abrogates hepatic ischemic preconditioning responses. *J Surg Res* 2001; **97:** 144-149
42 **Fernandez L**, Heredia N, Grande L, Gomez G, Rimola A, Marco A, Gelpi E, Rosello-Catafau J, Peralta C. Preconditioning protects liver and lung damage in rat liver transplantation: role of xanthine/xanthine oxidase. *Hepatology* 2002; **36:** 562-572
43 **Yin DP,** Sankary HN, Chong AS, Ma LL, Shen J, Foster P, Williams JW. Protective effect of ischemic preconditioning on liver preservation-reperfusion injury in rats. *Transplantation* 1998; **66:** 152-157
44 **Ricciardi R,** Shah SA, Wheeler SM, Quarfordt SH, Callery MP, Meyers WC, Chari RS. Regulation of NFkappaB in hepatic ischemic preconditioning. *J Am Coll Surg* 2002; 195: 319-326
45 **Maulik N,** Sato M, Price BD, Das DK. An essential role of NFkappaB in tyrosine kinase signaling of p38 MAP kinase regulation of myocardial adaptation to ischemia. *FEBS Lett* 1998; **429:** 365-369
46 **Teoh N,** Dela Pena A, Farrell G. Hepatic ischemic preconditioning in mice is associated with activation of NF-kappaB, p38 kinase, and cell cycle entry. *Hepatology* 2002; **36:** 94-102
47 **Le Moine O,** Louis H, Demols A, Desalle F, Demoor F, Quertinmont E, Goldman M, Deviere J. Cold liver ischemia-reperfusion injury critically depends on liver T cells and is improved by donor pretreatment with interleukin 10 in mice. *Hepatology* 2000; 31: 1266-1274
48 **Shen XD,** Ke B, Zhai Y, Amersi F, Gao F, Anselmo DM, Busuttil RW, Kupiec-Weglinski JW. CD154-CD40 T-cell costimulation pathway is required in the mechanism of hepatic ischemia/reperfusion injury, and its blockade facilitates and depends on heme oxygenase-1 mediated cytoprotection. *Transplantation* 2002; **74:** 315-319
49 **Takada M,** Chandraker A, Nadeau KC, Sayegh MH, Tilney NL. The role of the B7 costimulatory pathway in experimental cold ischemia/reperfusion injury. *J Clin Invest* 1997; **100:** 1199-1203
50 **Zwacka RM,** Zhang Y, Halldorson J, Schlossberg H, Dudus L, Engelhardt JF. CD4(+) T-lymphocytes mediate ischemia/reperfusion-induced inflammatory responses in mouse liver. *J Clin Invest* 1997; **100:** 279-289
51 **Teramoto K,** Tanaka Y, Kusano F, Hara Y, Ishidate K, Iwai T, Sato C. Expression of tumor necrosis factor-alpha gene during allograft rejection following rat liver transplantation. *Liver* 1999; **19:** 19-24
52 **Tsoulfas G,** Takahashi Y, Ganster RW, Yagnik G, Guo Z, Fung JJ, Murase N, Geller DA. Activation of the lipopolysaccharide signaling pathway in hepatic transplantation preservation injury. *Transplantation* 2002; **74:** 7-13
53 **Okamura H,** Kashiwamura S, Tsutsui H, Yoshimoto T, Nakanishi K. Regulation of interferon-gamma production by IL-12 and IL-18. *Curr Opin Immunol* 1998; **10:** 259-264

Science Editor Ma JY **Language Editor** Elsevier HK

PO Box 2345, Beijing 100023, China
www.wjgnet.com
wjg@wjgnet.com

ELSEVIER

World J Gastroenterol 2005;11(44):6968-6974
World Journal of Gastroenterology ISSN 1007-9327

• *BASIC RESEARCH* •

Induction of pancreatic duct cells of neonatal rats into insulin-producing cells with fetal bovine serum: A natural protocol and its use for patch clamp experiments

San-Hua Leng, Fu-Er Lu

San-Hua Leng, Fu-Er Lu, Institute of Integrative Traditional Chinese and Western Medicine, Tongji Hospital, Tongji Medical College, Huazhong University of Science and Technology, Wuhan 430030, Hubei Province, China
Supported by the National Natural Science Foundation of China, No. 30472254
Correspondence to: Professor Fu-Er Lu, Institute of Integrative Traditional Chinese and Western Medicine, Tongji Hospital, Tongji Medical College, Huazhong University of Science and Technology, Wuhan 430030, Hubei Province, China. felu@tjh.tjmu.edu.cn
Telephone: +86-27-83662220 Fax: +86-27-83646605
Received: 2004-12-28 Accepted: 2005-03-24

Abstract

AIM: To induce the pancreatic duct cells into endocrine cells with a new natural protocol for electrophysiological study.

METHODS: The pancreatic duct cells of neonatal rats were isolated, cultured and induced into endocrine cells with 15% fetal bovine serum for a period of 20 d. During this period, insulin secretion, MTT value, and morphological change of neonatal and adult pancreatic islet cells were comparatively investigated. Pancreatic β-cells were identified by morphological and electrophysiological characteristics, while ATP sensitive potassium channels (K_{ATP}), voltage-dependent potassium channels (K_V), and voltage-dependent calcium channels (K_{CA}) in β-cells were identified by patch clamp technique.

RESULTS: After incubation with fetal bovine serum, the neonatal duct cells budded out, changed from duct-like cells into islet clusters. In the first 4 d, MTT value and insulin secretion increased slowly (MTT value from 0.024 ±0.003 to 0.028±0.003, insulin secretion from 2.6±0.6 to 3.1±0.8 mIU/L). Then MTT value and insulin secretion increased quickly from d 5 to d 10 (MTT value from 0.028 ±0.003 to 0.052±0.008, insulin secretion from 3.1±0.8 to 18.3±2.6 mIU/L), then reached high plateau (MTT value >0.052±0.008, insulin secretion >18.3±2.6 mIU/L). In contrast, for the isolated adult pancreatic islet cells, both insulin release and MTT value were stable in the first 4 d (MTT value from 0.029±0.01 to 0.031±0.011, insulin secretion from 13.9±3.1 to 14.3±3.3 mIU/L), but afterwards they reduced gradually (MTT value <0.031 ±0.011, insulin secretion <8.2±1.5 mIU/L), and the pancreatic islet cells became dispersed, broken or atrophied correspondingly. The differentiated neonatal cells were identified as pancreatic islet cells by dithizone staining method, and pancreatic β-cells were further identified by both morphological features and electrophysiological characteristics, i.e. the existence of recording currents from K_{ATP}, K_V, and K_{CA}.

CONCLUSION: Islet cells differentiated from neonatal pancreatic duct cells with the new natural protocol are more advantageous in performing patch clamp study over the isolated adult pancreatic islet cells.

Key words: Pancreatic duct cells; Pancreatic precursor cells; Insulin-producing cells; Patch clamp; Experimental protocol; ATP sensitive potassium channels; Voltage-dependent potassium channels; Voltage-dependent calcium channels

Leng SH, Lu FE. Induction of pancreatic duct cells of neonatal rats into insulin-producing cells with fetal bovine serum: A natural protocol and its use for patch clamp experiments. *World J Gastroenterol* 2005; 11(44): 6968-6974
http://www.wjgnet.com/1007-9327/11/6968.asp

INTRODUCTION

The pancreatic islets (containing α, β, and δ cells that produce glucagon, insulin, and somatostatin, respectively) are intensively involved in the regulation of physiological metabolic homeostasis[1]. Patch clamp technique is considered as a very important approach for studying the endocrine activities and mechanisms of these cells. The traditional method for the isolation of rat intact pancreatic islet cells[2] has been performed for almost 40 years, and is still the most widely acceptable method in electrophysiological study of pancreatic islet cells. Nevertheless, pancreatic islet cells usually survive poorly after isolation because the cells are fragile in the *in vitro* culture condition[3]. Thus, only the freshly isolated or shortly cultured islet cells can be introduced for patch clamp experiments. Furthermore, there are some disadvantages in performing patch clamp experiments with

isolated islet cells. The endocrine pancreas is considered as a slowly and continuously renewing tissue in the kinetic balance process of apoptosis and neogenesis[4]. Thus, pancreatic β cells isolated from adult rats are heterogeneous at different ages, including neonatal, adult, and senile cells. The isolated adult and senile β cells are more susceptible than neonatal β cells to the transition from the native living surroundings to the *in vitro* culture. Because the membrane of isolated adult β cells is fragile, it is difficult to manipulate gigaseal, a key step in patch clamp experiments.

Although there are other cell sources for performing patch clamp experiments without obvious problems mentioned above, such as β cell line and islet cells differentiated from marrow mesenchymal stem cells[5] or multipotent cells, and precursor cells of fetal pancreas, they still show considerable shortcomings. According to the reports, the β cell line only retains partial characteristics of primitive pancreatic islet cells, while the islet cells differentiated from marrow mesenchymal stem cells[6] and precursor cells of fetal pancreas[7-11] exhibit poor insulin secretory response to glucose. Therefore, it is essential to seek for more optimal cell sources and approaches suitable for patch clamp experiments.

Neonatal pancreatic duct cells are composed mainly of precursor cells[12,13] and can be induced into endocrine cells if appropriate morphogen stimuli are provided[10-13], and the induced endocrine cells are stable in culture condition[12,13], and their glucose-induced insulin secretion is evident[7-10]. Thus, we suppose that the neonatal pancreatic duct cells might be more suitable for patch clamp experiments.

Here the pancreatic duct cells were differentiated into endocrine islet cells with fetal bovine serum, a physiological nutrition[14]. The cell proliferation and insulin secretion of differentiated neonatal endocrine cells were compared to isolated adult endocrine islet cells. ATP sensitive potassium channels (K_{ATP}), voltage-dependent potassium channels (K_V) and voltage-dependent calcium channels (K_{CA}) of β cells were identified with patch clamp technique to prove the usefulness of this protocol.

MATERIALS AND METHODS

Reagents

Na_2-ATP, EGTA, HEPES, repaglinide, and diazoxide were purchased from Sigma Co. The other chemicals used were of analytical reagent grade.

Isolation and culture of pancreatic islet cells

Sprague-Dawley rats aged 1-3 and 50-60 d were obtained from Laboratory Animal Center, Tongji Medical College, Huazhong University of Science and Technology. Hubei Experimental Animal Association approved the experiments. The culture medium used for both neonatal and adult cells was RPMI 1640 medium (glucose 11.1 mmol/L) supplemented with 15% fetal bovine serum, 15 mmol/L HEPES buffer, pH 7.40, without any antibiotics (to eliminate its possible influence on the differentiation of precursor cells). The cells were cultured at 37 ℃ in the atmosphere containing 950 mL/L O_2+50 mL/L CO_2. The isolation of pancreatic islet cells from adult rats was performed as previously described[2]. The isolation and induction of duct cells were performed as follows: the pancreases were moved from 10 neonatal rats and thoroughly washed in KRBH solution containing (in mmol/L) 136 NaCl, 4.8 KCl, 1 $CaCl_2$, 1.2 $MgSO_4$, 1.2 KH_2PO_4, 5 $NaHCO_3$, 25 HEPES, 1% BSA, pH 7.40. The pancreases were minced into pieces of 1-2 mm in size. The minced pancreases were hand-shaken while being digested by 0.5 mg/mL type V collagenase in PBS (pH 7.40) for about 3-8 min in a 10-mL tube bathed in 37 ℃water. Then digestion was stopped by 4 ℃ KRBH. The production was centrifuged (50 r/min) thrice to eliminate collagenase and broken cells. Thereafter, the cells were suspended in the cell culture medium and seeded in plastic dishes (18 mm in diameter) with 2 mL culture medium in each dish. After being cultured for about 24 h, the culture medium was moved, and the duct cells were washed with KRBH solution five times to remove the floated cells thoroughly. Then the left cells were mostly duct cells (Figure 1). The cells were kept in the cell culture medium for 20 d, during which the dishes were replenished with a new medium every 2 d.

Morphology observation

The incubated cells were observed under inverted microscope each day. When the marked morphologic changes were observed, photograph of the cells was taken by phase difference microscopy.

Insulin measurement

All the isolated products from neonatal duct cells or adult pancreatic islet cells were equally seeded in gelatin-coated dishes (18 mm in diameter), and each dish contained 2 mL isolated products (about 10^4 cells). The supernatant of culture media in the five dishes was harvested every 2 d and kept at -20 ℃ for insulin determination by radioimmunoassay. The dishes were washed with KRBH solution twice, then 2 mL of the cell culture medium was added again for further culture.

MTT test

MTT assay was carried out as previously described[15]. The isolated products from neonatal or adult rats (about 10^5 cells) were equally seeded in 10 dishes (96 cells in each dish, and each cell containing 150 μL isolated products), one dish of cells was used every 2 d for MTT determination, and the remaining dishes were replenished with a new medium.

Identification of pancreatic islet cells

The pancreatic islet cells were identified by dithizone staining method[16]. The viable cells were determined by trypan blue exclusive test.

Identification of pancreatic β cells

Two steps were performed to identify pancreatic β cells from α and δ cells[17]. Therefore, only large cells with a capacitance of >5 pF were selected as β cells. Then

a depolarizing protocol was applied to the large cells to identify the properties of voltage-dependent Na^+ currents[18]. Thus, cells in which a Na^+ current could be activated by a small depolarizing pulse from a prolonged holding potential of -70 mV were discarded. By contrast, cells exhibiting a Na^+ current only after a hyperpolarizing pulse to -140 mV were considered to be β cells[19].

Patch clamp experiments

Patch clamp experiments were performed on β cells of isolated islet cells only in the first 4 d after the isolation, the β cells beyond this period of time could not be introduced into patch clamp experiments. The β cells differentiated from islet cells of neonatal rats were applied for patch clamp experiments from d 10 to d 16.

Rat pancreatic islet cells plated on the plastic dishes were placed in a recording chamber mounted on an inverted microscope (Olympus). Patch clamp recordings were done for cells that were not in contact with the other cells to avoid possible cell-cell coupling artifacts. For recording K_{ATP} currents, the solutions were as follows (in mmol/L): internal solution containing 140 KCl, 2 $CaCl_2$, 4 $MgCl_2$, 10 EGTA, 0.65 Na_2-ATP, and 20 HEPES (pH 7.15 with KOH); and external solution containing 140 NaCl, 5.6 KCl, 1.2 $MgCl_2$, 2.6 $CaCl_2$, 0.5 glucose and 10 HEPES (pH 7.4 with KOH). K_{ATP} currents were measured at a holding potential of -70 to -80 mV and -60 mV at 15-s intervals, and diazoxide (100 μmol/L) and repaglinide (100 μmol/L) were added respectively to further confirm whether it was K_{ATP} currents or not. For K_V currents recording, the solutions were the same as for recording K_{ATP} currents except that 100 μmol/L repaglinide was added into external solution to block K_{ATP} currents. The cells were held at -120 mV and depolarized at 15-s intervals to 30 mV to activate K_V currents. For K_{CA} recording, the solutions were as follows (in mmol/L): internal solution containing 70 CsCl, 1 $MgCl_2$, 4 ATP, 20 HEPES, 5 EGTA, pH 7.2; external solution containing 90 NaCl, 1 $MgCl_2$, 20 TEA-Cl, 10 HEPES, 20 $BaCl_2$, 5.6 KCl, 5 CsCl, pH 7.15. All cell membrane currents were measured using whole-cell mode of patch clamp technique at 22 ℃, using an EPC-9 patch clamp amplifier (Heka Electronics, Lambrecht/Pfalz, Germany) and the software Pulsefit. Patch clamp electrodes were made from borosilicate glass capillaries (Shanghai Physiology Institute, China) using a two-stage puller (PP-830, Narishige Co., Japan) to give a resistance of 4-5 MΩ.

RESULTS

Morphological evolvement and identification

The neonatal rat pancreatic duct cells were organized in duct-like cells when incubated for 3-4 d (Figure 1A). There were precursors of pancreatic islet cells among them. When cultured for 5-10 d, some duct cells changed into round cells organized as islet clusters, being similar to pancreatic islet cells *in vivo* (Figure 1B). Then the cells grew bigger and budded out (Figures 1C and 1D). The buds grew bigger and bigger and became new ground cells in clusters (Figure 1E), which were further identified as pancreatic islet cells by dithizone (Figure 1F), a chemical considered to selectively stain pancreatic islet cells[16].

In contrast, the freshly isolated pancreatic islet cells from adult rats were round, but gradually became dispersed, broken or atrophied. After being cultured for a week, the islet cells were dispersed to be single cells, and the cell number was greatly reduced (data not shown).

Insulin release

For neonatal pancreatic islet cells, the insulin concentration in

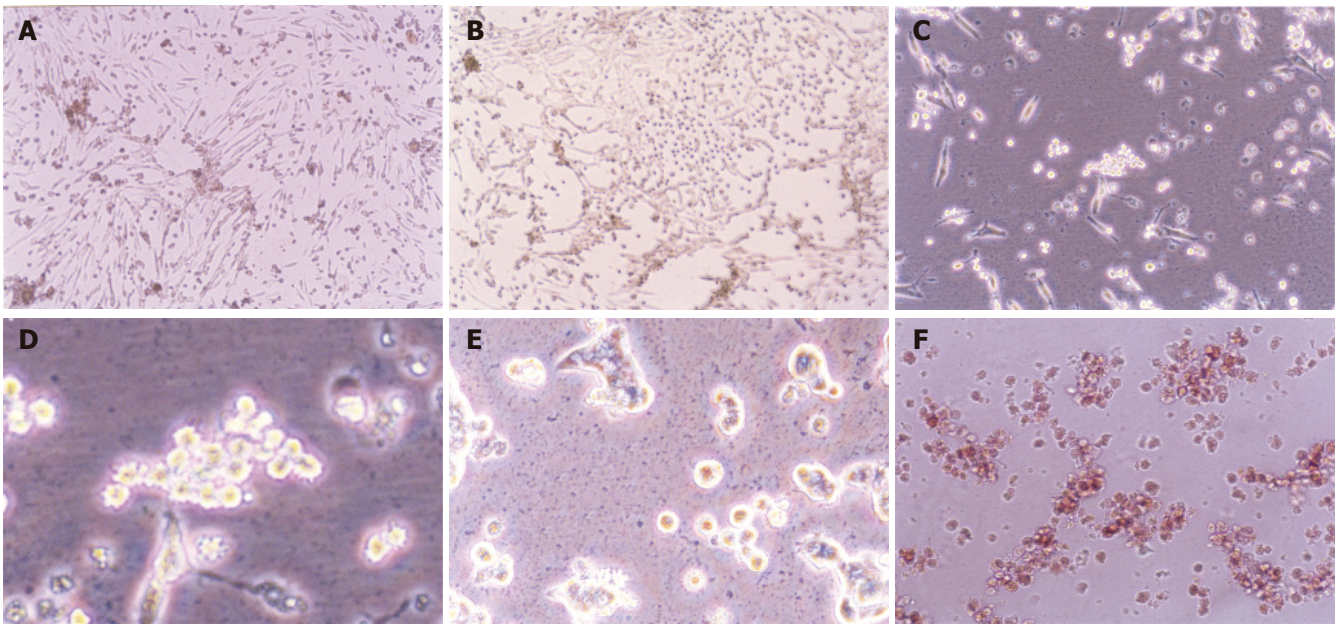

Figure 1 Morphological change of neonatal pancreatic duct cells cultured for 3-4 d (**A**), 5-7 d (**B**), 8-10 d (**C** and **D**) and more than 10 d (**E**), as well as identification of pancreatic islet cells by dithizone (**F**).

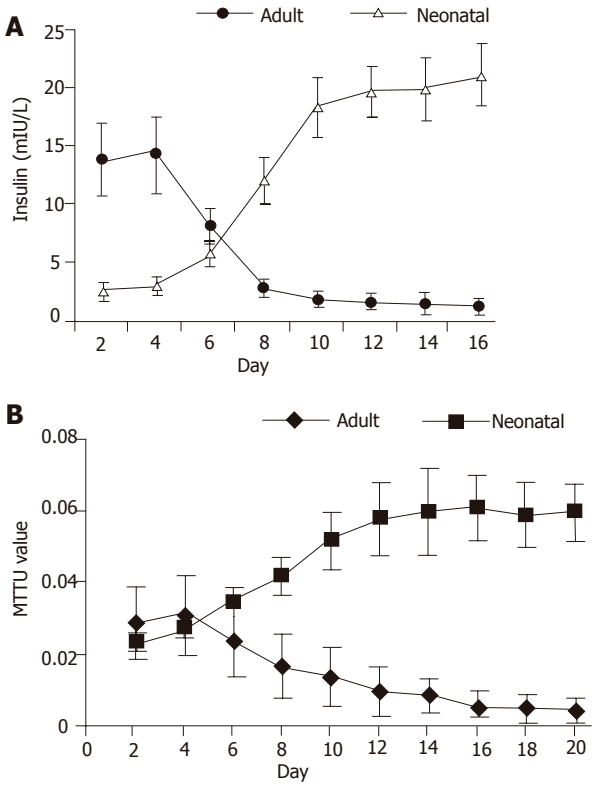

Figure 2 Insulin release curve (**A**) and MTT value curve (**B**) during the culture period of isolated adult islet cells and neonatal endocrine cells.

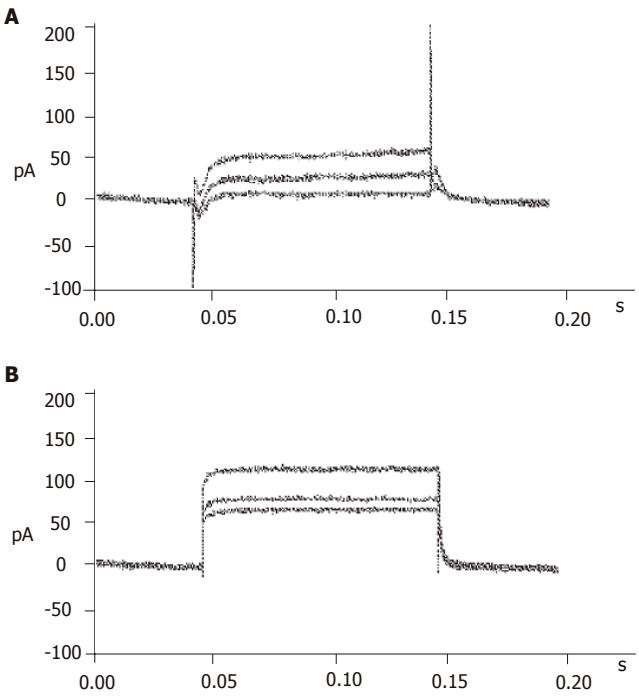

Figure 3 Identification of pancreatic β cells. **A:** Currents recorded from α or δ cells; **B:** currents recorded from β cells.

the cell culture medium was low (from 2.6±0.6 to 3.1±0.8 mIU/L) in the first 4 d, then quickly increased (from 3.1±0.8 to 12.1±2.1 mIU/L) from d 5 to d 10. Thereafter, the insulin release reached its high plateau (>18.3±2.6 mIU/L). For isolated pancreatic islet cells from adult rats, the insulin concentration was high (from 13.9±3.1 to 14.3±3.3 mIU/L) in the first 4 d, and gradually reduced (from 8.2±1.5 to 2.9 ±0.7 mIU/L) from d 5 to d 10. Then the insulin release was very low (<2.9±0.7 mIU/L) (Figure 2A).

MTT value

For neonatal pancreatic islet cells, the MTT value was low (0.024±0.003 to 0.028±0.003) in the first 4 d and gradually increased (0.028±0.003 to 0.052±0.008) from d 5 to d 10. Thereafter, the MTT value reached its high plateau (>0.052 ±0.008). For isolated pancreatic islet cells from adult rats, the MTT value was stable (from 0.029±0.01 to 0.031± 0.011) in the first 4 d and gradually reduced (0.031±0.01 to 0.014±0.008) from d 5 to d 10. Then the MTT value was very low (<0.014±0.008) (Figure 2B).

Identification of pancreatic islet cells and β cells

The big round cells (with a diameter >10 μm) were selected and their capacitance was determined (>5 pF). Then a depolarizing protocol was used to identify the properties of voltage-dependent Na^+ currents. The results showed that voltage-dependent Na^+ currents of selected cells could not be recorded at a holding potential of -70 mV (Figure 3B). On the contrary, the voltage-dependent Na^+ currents of small round cells (capacitance <5 pF) could be detected at a holding potential of -70 mV (Figure 3A). It was demonstrated that the big round cells were pancreatic β cells, while small round cells were not.

K_{ATP} current recording

With certain internal and external solutions and protocol, the currents recorded in pancreatic β cells were almost entirely K_{ATP} currents[19]. To verify this, 100 μmol/L diazoxide, a special opener of K_{ATP} channels, and 100 μmol/L repaglinide, a special antagonist of K_{ATP} channels, were added correspondingly. The results showed that diazoxide enhanced, while repaglinide reduced the currents greatly (Figure 4), suggesting that the detected currents were from K_{ATP} channels.

K_V current recording

Repaglinide was used in the external solution to block K_{ATP} currents. Then the currents recorded should be almost entirely K_V currents with the internal and external solutions and protocol. The recorded outward currents showed that the channels were inactive from -120 to -55 mV and active from -55 to 0 mV and the currents increased in proportion to voltage. When added with 100 μmol/L TEA, the currents could not be recorded, suggesting that the detected currents were from K_V channels (Figure 5).

K_{CA} current recording

To efficiently record K_{CA} currents, Cs^+ was added in the internal solution, while TEA and Ba^+ were added in the external solution to block voltage-dependent outward potassium currents. Meanwhile, Ba^+ enhanced

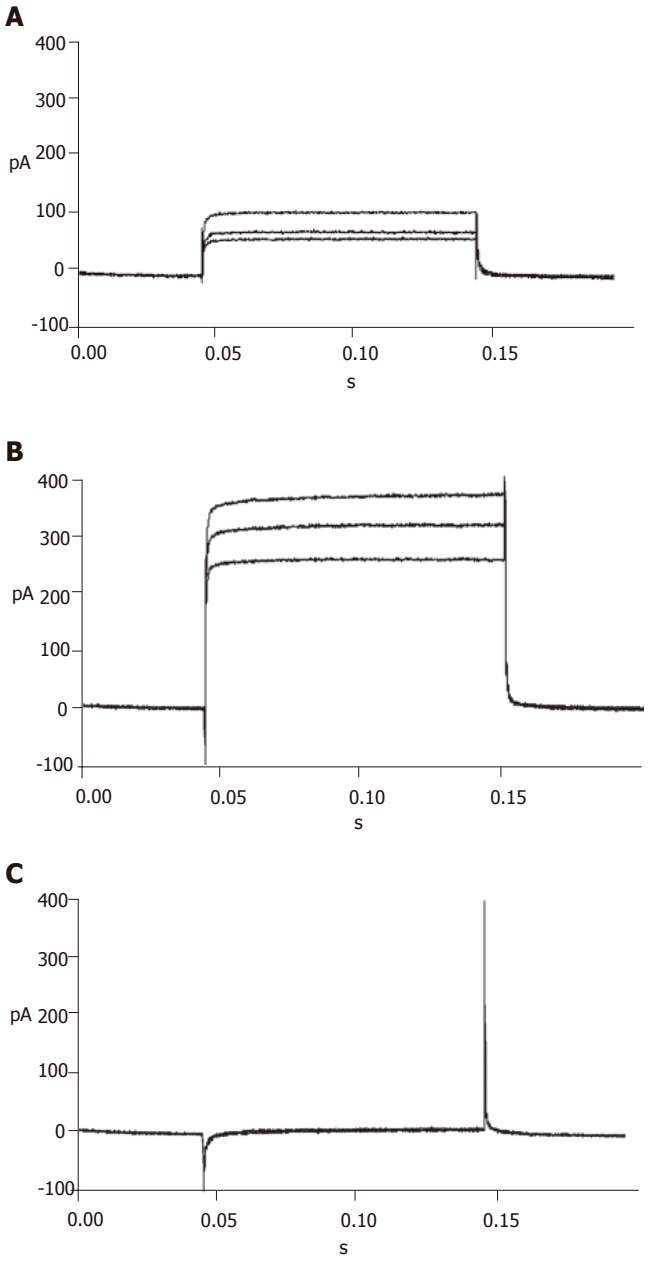

Figure 4 ATP sensitive potassium currents recorded in the absence (**A**), presence of diazoxide (**B**) and repaglinide (**C**).

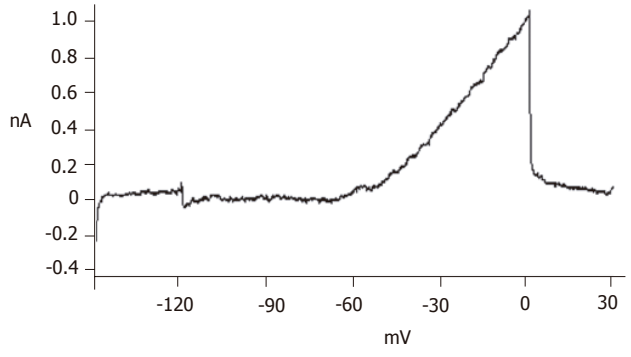

Figure 5 Voltage-dependent potassium currents recorded on neonatal pancreatic β cells.

K_{CA} currents. Inward currents were recorded at -40 mV and reached their peak at 0-10 mV, and then turned over at 50-60 mV. These dynamic electric patterns were characteristic of K_{CA} currents[20,21]. Furthermore, special opener and antagonist of K_{CA} channels were introduced to verify their existence. When added with 100 μmol/L Bay K8644, the currents enhanced greatly; while 100 μmol/L nifedipine was added, the currents reduced strikingly (Figure 6). These facts suggest that the detected currents were K_{CA} currents (mainly of L-type calcium currents).

DISCUSSION

It has been reported that pancreatic endocrine cells of neonatal rats can be used in long-term study of secretion and electrophysiology[22]. According to the experimental protocol, fibroblasts are cleared away by timerosal to enhance insulin release. However, the enhancing effect of

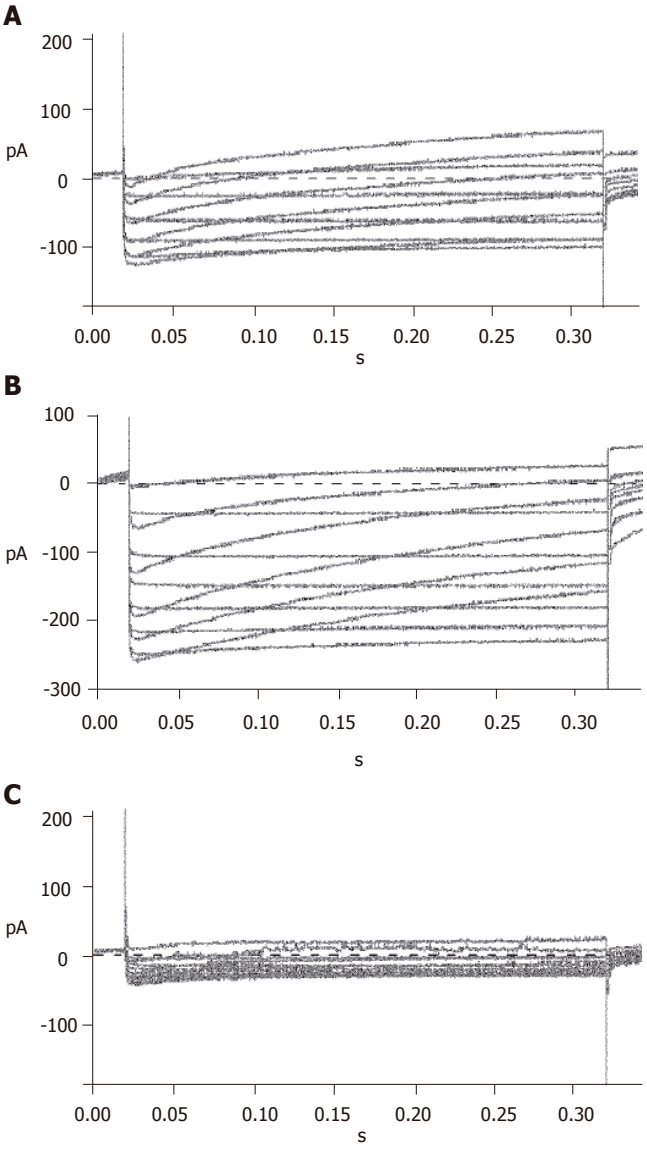

Figure 6 Voltage-dependent calcium currents recorded in the absence (**A**), presence of Bay K8644 (**B**) and nifedipine (**C**).

timerosal cannot be interpreted by the clearing away of fibroblasts, but might be produced due to the modified effects of timerosal on sulfonylurea receptor which regulates insulin release, because timerosal can modify mitochondrial sulfonylurea receptor[23]. Fibroblasts are present as the mesenchyme of islet cells, which may provide fibroblast growth factors and matrix to help the differentiation and replication of endocrine cells[24,25]. Therefore, alterations were made to optimize the experimental protocol correspondingly. Firstly, the fibroblasts in the pancreatic islet cells for the normal differentiation and replication of endocrine cells were retained. Secondly, timerosal was not introduced in our protocol to exclude its insulin regulating effect. Instead, fetal bovine serum, a physiological nutrition that does not intervene the normal neogenesis process, was administered in the cell incubation. With this natural protocol, the neonatal duct cells were successfully induced into endocrine cells.

It was reported that neonatal duct cells are composed mainly of precursor cells[12,13]. Thus, the harvested endocrine cells from neonatal rats should be mostly differentiated from precursor cells that lie in the pancreas duct tree. The harvested endocrine cells from the neonatal rats auto-organized as islet clusters (Figure 1B). Our observations that the islet cells changed from duct-like into round shape and that the round cells then budded outward *in vitro* culture, were in conformity with the report by Gershengorn *et al*.[26].

Gigaseal, the key step in patch clamp experiments, is difficult to perform on isolated islet cells because the membrane is fragile and easily gets broken by the electrode. Even when gigaseal was completed, the currents recorded may be deformed or lower than normal because there are tiny gaps between cell membrane and the electrode, through which the currents might leak out. However, we found that it was easy to manipulate gigaseal on islet cells differentiated with this natural protocol. To explain this phenomenon, we compared the morphological and functional characteristics of neonatal and adult pancreatic islet cells in culture condition. For differentiated neonatal islet cells, insulin release was low during the early phase, but increased rapidly from d 5 to d 10, and then kept in high plateau (Figure 2). Correspondingly, the cell mass grew much bigger. As for isolated islet cells from adult rats, insulin release was high in the first 4 d, but then reduced quickly (Figure 2). Correspondingly, the islet cells became dispersed, broken or atrophied. For neonatal endocrine islet cells, the MTT value increased quickly from d 5 to d 10 and then kept in high plateau. For isolated islet cells from adult rats, the MTT value was stable in the first 4 d and then reduced quickly (Figure 3). The data are in conformity with the idea that isolated islet cells survive poorly in culture condition[3] and support that neonatal pancreatic islet cells are more preferable for long-term and stable culture, thus more suitable for patch clamp experiments.

It was reported that the differentiated neonatal pancreatic islet cells have evident glucose-induced insulin secretion property[7-10]. To understand its mechanism, we investigated the electric activities of K_{ATP}, K_V, and K_{CA}, regulators of glucose-induced insulin secretion process. The role of K_{ATP} channels of β cells in glucose-induced insulinotropic process has been well demonstrated[27]; the K_{CA} and K_V channels are also suggested to couple with glucose-dependent insulinotropic effects[28-32]. Thus, the properties of these channels in differentiated islet cells were studied. The fact that K_{ATP}, K_V, and K_{CA} channels in differentiated islet β cells are sensitive to corresponding antagonist and/or opener (Figures 4-6) indicates that the differentiated islet cells have evident glucose-induced insulin secretion properties.

In conclusion, the natural protocol illustrated in this paper enables the long-term incubation of stable endocrine islet cells, which will greatly optimize and facilitate the performance of patch clamp experiments and other single cell studies.

ACKNOWLEDGMENTS

The authors thank Professor Yong-Jian Xu and technician Wang Ni (Respiratory Department of Tongji Hospital, Tongji Medical College, Huazhong University of Science and Technology) for their help in patch clamp technique.

REFERENCES

1 **Slack JM.** Developmental biology of the pancreas. *Development* 1995; **121:** 1569-1580
2 **Lacy PE,** Kostianovsky M. Method for the isolation of intact islets of Langerhans from the rat pancreas. *Diabetes* 1967; **16:** 35-39
3 **Brandhorst D,** Brandhorst H, Hering BJ, Bretzel RG. Long-term survival, morphology and in vitro function of isolated pig islets under different culture conditions. *Transplantation* 1999; **67:** 1533-1541
4 **Bonner-Weir S.** Perspective: Postnatal pancreatic beta cell growth. *Endocrinology* 2000; **141:** 1926-1929
5 **Lumelsky N,** Blondel O, Laeng P, Velasco I, Ravin R, McKay R. Differentiation of embryonic stem cells to insulin-secreting structures similar to pancreatic islets. *Science* 2001; **292:** 1389-1394
6 **Vogel G.** Developmental biology. Stem cells are coaxed to produce insulin. *Science* 2001; **292:** 615-617
7 **Asplund K,** Westman S, Hellerstrom C. Glucose stimulation of insulin secretion from the isolated pancreas of foetal and newborn rats. *Diabetologia* 1969; **5:** 260-262
8 **Asplund K.** Dynamics of insulin release from the foetal and neonatal rat pancreas. *Eur J Clin Invest* 1973; **3:** 338-344
9 **Rhoten WB**. Insulin secretory dynamics during development of rat pancreas. *Am J Physiol* 1980; **239:** E57-63
10 **Hole RL,** Pian-Smith MC, Sharp GW. Development of the biphasic response to glucose in fetal and neonatal rat pancreas. *Am J Physiol* 1988; **254:** E167-174
11 **Tuch BE,** Jones A, Turtle JR. Maturation of the response of human fetal pancreatic explants to glucose. *Diabetologia* 1985; **28:** 28-31
12 **Korbutt GS,** Elliott JF, Ao Z, Smith DK, Warnock GL, Rajotte RV. Large scale isolation, growth, and function of porcine neonatal islet cells. *J Clin Invest* 1996; **97:** 2119-2129
13 **Yoon KH,** Quickel RR, Tatarkiewicz K, Ulrich TR, Hollister-Lock J, Trivedi N, Bonner-Weir S, Weir GC. Differentiation and expansion of beta cell mass in porcine neonatal pancreatic cell clusters transplanted into nude mice. *Cell Transplant* 1999; **8:**

673-689
14 **Hulinsky I,** Hulinska H, Silink M. DNA synthesis in cultured neonatal rat islets--a comparison of two methods. *Diabetes Res Clin Prac*t 1995; **27:** 119-126
15 **Janjic D,** Wollheim CB. Islet cell metabolism is reflected by the MTT (tetrazolium) colorimetric assay. *Diabetologia* 1992; **35:** 482-485
16 **Fiedor P,** Rowinski W, Licinska I, Mazurek AP, Hardy MA. The survival identification of pancreatic islets of Langerhans. In vitro and in vivo effects of two dithizone preparations on staining of rat and human islets of Langerhans-preliminary study (Part I). *Acta Pol Pharm* 1995; **52:** 431-436
17 **Gopel SO,** Kanno T, Barg S, Rorsman P. Patch-clamp characterisation of somatostatin-secreting -cells in intact mouse pancreatic islets. *J Physiol* 2000; **528:** 497-507
18 **Plant TD.** Na+ currents in cultured mouse pancreatic B-cells. *Pflugers Arch* 1988; **411:** 429-435
19 **Jonas JC,** Plant TD, Henquin JC. Imidazoline antagonists of alpha 2-adrenoceptors increase insulin release in vitro by inhibiting ATP-sensitive K+ channels in pancreatic beta-cells. *Br J Pharmacol* 1992; **107:** 8-14
20 **Rorsman P,** Trube G. Calcium and delayed potassium currents in mouse pancreatic beta-cells under voltage-clamp conditions. *J Physiol* 1986; **374:** 531-550
21 **Satin LS,** Cook DL. Evidence for two calcium currents in insulin-secreting cells. *Pflugers Arch* 1988; **411:** 401-409
22 **Schwartz JL,** Mealing GA, Whitfield JF, Braaten JT. Long-term culture of neonatal rat pancreatic endocrine cells as model for insulin-secretion and ion-channel studies. *Diabetes* 1990; **39:** 1353-6130
23 **Szewczyk A,** Wojcik G, Lobanov NA, Nalecz MJ. Modification of the mitochondrial sulfonylurea receptor by thiol reagents. *Biochem Biophys Res Commun* 1999; **262:** 255-258
24 **Arany E, Hill DJ.** Ontogeny of fibroblast growth factors in the early development of the rat endocrine pancreas. *Pediatr Res* 2000; **48:** 389-403
25 **Hulinsky I,** Cooney S, Harrington J, Silink M. In vitro growth of neonatal rat islet cells is stimulated by adhesion to matrix. *Horm Metab Res* 1995; **27:** 209-215
26 **Gershengorn MC,** Hardikar AA, Wei C, Geras-Raaka E, Marcus-Samuels B, Raaka BM. Epithelial-to-mesenchymal transition generates proliferative human islet precursor cells. *Science* 2004; **306:** 2261-2264
27 **Schwanstecher C,** Schwanstecher M. Nucleotide sensitivity of pancreatic ATP-sensitive potassium channels and type 2 diabetes. *Diabetes* 2002; 51 Suppl **3:** S358-362
28 **Rorsman P.** The pancreatic beta-cell as a fuel sensor: an electrophysiologist's viewpoint. *Diabetologia* 1997; **40:** 487-495
29 **Lang J.** Molecular mechanisms and regulation of insulin exocytosis as a paradigm of endocrine secretion. *Eur J Biochem* 1999; **259:** 3-17
30 **MacDonald PE,** Sewing S, Wang J, Joseph JW, Smukler SR, Sakellaropoulos G, Wang J, Saleh MC, Chan CB, Tsushima RG, Salapatek AM, Wheeler MB. Inhibition of Kv2.1 voltage-dependent K+ channels in pancreatic beta-cells enhances glucose-dependent insulin secretion. *J Biol Chem* 2002; **277:** 44938-44945
31 **MacDonald PE,** Salapatek AM, Wheeler MB. Glucagon-like peptide-1 receptor activation antagonizes voltage-dependent repolarizing K(+) currents in beta-cells: a possible glucose-dependent insulinotropic mechanism. *Diabetes* 2002; 51 Suppl **3:** S443-447
32 **MacDonald PE,** Wang G, Tsuk S, Dodo C, Kang Y, Tang L, Wheeler MB, Cattral MS, Lakey JR, Salapatek AM, Lotan I, Gaisano HY. Synaptosome-associated protein of 25 kilodaltons modulates Kv2.1 voltage-dependent K(+) channels in neuroendocrine islet beta-cells through an interaction with the channel N terminus. *Mol Endocrinol* 2002; **16:** 2452-2461

Science Editor Wang XL **Language Editor** Elsevier HK

PO Box 2345, Beijing 100023, China
www.wjgnet.com
wjg@wjgnet.com

ELSEVIER

World J Gastroenterol 2005;11(44):6975-6980
World Journal of Gastroenterology ISSN 1007-9327

• *BASIC RESEARCH* •

Oral vaccination of mice against rodent malaria with recombinant *Lactococcus lactis* expressing MSP-1$_{19}$

Zhi-Hong Zhang, Pei-Hong Jiang, Ning-Jun Li, Mi Shi, Weida Huang

Zhi-Hong Zhang, Pei-Hong Jiang, Ning-Jun Li, Mi Shi, Weida Huang, Department of Biochemistry, School of Life Science, Fudan University, Shanghai 200433, China
Pei-hong Jiang, equal contribution as the first author
Supported by the UNDP/World Bank/WHO Special Programme for Research and Training in Tropical Diseases (TDR), No. 980198
Correspondence to: Weida Huang, Department of Biochemistry, Fudan University, 220 Han Dan Road, Shanghai 200433, China. whuang@fudan.edu.cn
Telephone: +86-21-65643446 Fax: +86-21-55522773
Received: 2004-09-18 Accepted: 2004-11-19

Abstract

AIM: To construct the recombinant *Lactococcus lactis* as oral delivery vaccination against malaria.

METHODS: The C-terminal 19-ku fragments of MSP1 (MSP-1$_{19}$) of *Plasmodium yoelii* 265-BY was expressed in *L. lactis* and the recombinant *L. lactis* was administered orally to BALB/c and C57BL/6 mice. After seven interval vaccinations within 4 wk, the mice were challenged with *P. yoelii* 265-BY parasites of erythrocytic stage. The protective efficacy of recombinant *L. lactis* was evaluated.

RESULTS: The peak parasitemias in average for the experiment groups of BALB/c and C57BL/6 mice were 0.8±0.4% and 20.8±26.5%, respectively, and those of their control groups were 12.0±0.8% and 60.8±9.6%, respectively. None of the BALB/c mice in both experimental group and control group died during the experiment. However, all the C57BL/6 mice in the control group died within 23 d and all the vaccinated mice survived well.

CONCLUSION: The results imply the potential of recombinant *L. lactis* as oral delivery vaccination against malaria.

Key words: Lactococcus lactis; Oral delivery vaccination; Malaria

Zhang ZH, Jiang PH, Li NJ, Shi M, Huang W. Oral vaccination of mice against rodent malaria with recombinant *Lactococcus lactis* expressing MSP-1$_{19}$. *World J Gastroenterol* 2005; 11(44): 6975-6980
http://www.wjgnet.com/1007-9327/11/6975.asp

INTRODUCTION

The development of efficacious vaccines against malaria is one of the greatest challenges for the application of current life sciences in infectious diseases. The easiness of administration of a vaccine provides an attractive alternative to continue drug treatments in a population exceeding hundreds of millions of people with limited health care resources. Merozoite surface protein 1 (MSP1) is present in all species of *Plasmodium*[1,2], and has been widely studied as the major candidate for vaccine against malaria[3-5]. The high level expression of MSP1 by *Plasmodium* in the asexual stage is closely related to its invasion into erythrocytes. MSP1 can be proteolytically cleaved into five fragments by two processing steps after the maturation of merozoite, with the carboxyl-terminal 19-ku fragment (MSP-1$_{19}$) remaining on the merozoite surface[6-8]. The MSP-1$_{19}$ comprises two epidermal growth factor (EGF)-like modules. Antibodies directed to this fragment have been shown to inhibit the invasion of *Plasmodium falciparum* into erythrocyte *in vitro*[9,10] and intranasal or subcutaneous immunization may protect mice against the challenge of *Plasmodium yoelii* asexual blood-stage parasite[11]. The recombinant MSP-1$_{19}$ has been expressed in several host organisms, such as *Escherichia coli*[12], *Saccharomyces cerivisae*[11], *Bacillus Calmette-Guerin* (BCG)[13], and Baculovirus[14]. It has also been proven to be immuno-effective against the challenge of parasite. In vaccination experiments with recombinant MPS-1$_{19}$ from *P. yoelii*, immunized mice were protected against challenge with blood-stage parasites, and the protection was confirmed to be largely mediated by antibodies[15-17].

The development of efficient mucosal vaccines is one of the hotspots in modern vaccinology. One approach to deliver the protective antigens to the mucosal surfaces is to use live bacteria carrying plasmids responsible for the expression of specific antigen. Until recently most of these are derived from attenuated pathogenic microorganisms, such as *Salmonella typhi*[18] and *chlorella*[19]. As an alternative to this strategy, non-pathogenic food grade bacteria such as lactic acid bacteria are being focused for their efficacy as live antigen carriers[20]. *Lactococcus lactis* has a long history of being used in food fermentations and has been, therefore, generally regarded as a safe (GRAS) status[21]. This food-grade lactic acid bacterium is able to survive through the gastrointestinal tract of human beings and other animals, with a retention time of 2-3 d, but it does not invade or colonize the mucous and does not evoke strong host im-

mune responses[21]. The availability of various food-grade genetic engineering systems for *L. lactis*[22] makes the bacteria a potentially functional food or medicines by expressing heterogeneous peptides. Recent report using *L. lactis* preloaded with a bacterial antigen, tetanus toxin fragment C of *Clostridium tetanus*, demonstrated the feasibility of this approach: a protective systemic antibody response was elicited after nasal or oral immunization of mice[21]. Similar study was carried out by Lee *et al*.[23], in which urease subunit B (UreB) gene of *Helicobacter pylori* was expressed in *L. lactis* MG1363 and the recombinant bacterium was used as an oral vaccine against *H pylori* infection in mice. However, in this case no protective effect was observed, which implied that the adjuvant effects of *L. lactis* are likely to be insufficient to produce an effective immune response to protect against *H pylori* challenge, when used to deliver a weak immunogen like UreB.

Since the use of oral (or other mucosal) routes for immunization against malaria is also desirable due to the easiness of administration, we attempted *L. lactis* as the live vehicle for vaccine development against malaria. In this work, we showed that the oral immunization, with recombinant *L. lactis* constitutively expressing MSP-1$_{19}$ antigen, could protect BALB/c and C57BL/6 mice against malaria parasites challenge.

MATERIALS AND METHODS

Genes, plasmids, bacteria, and malarial parasites

The DNA fragment encoding for MSP-1$_{19}$ domain was amplified from the genomic DNA of *P. yoelii*. Plasmid pTRKL2 was from Prof. Todd R. Klaenhammer at Food Science Center, North California University, USA[24]. Cloning vector pBluescriptSKII(+) was from Strategene (La Jolla, CA, USA), and fusion-protein expression vector pGEX-5X-3 was from Amersham Pharmacia. *L. lactis* LM2345 was from Prof. Keith Thompson at Agriculture and Food Science Center, Newforge Lane, Northern Ireland. *Lactobacillus brevis* (ATCC8287) and *Bacillus subtilis* BR151 (ATCC33677) were purchased from the American Type Culture Collection. *P. yoelii* 265-BY was by Professor Weibin Guan at Second Military Medical University, Shanghai, China.

Construction of expression vector

The plasmid for the expression of MSP-1$_{19}$ fragment was constructed by conventional DNA recombination manipulation. The promoter region and the first five amino acids of the signal peptide-coding region of S-layer protein A (*SlpA)* gene (nucleotides 1-282, GenBank Z14250) was amplified by polymerase chain reaction (PCR) from genomic DNA of *L. brevis* with forward primer GCTGAGCTCGATTACAAAGGCTTTAAGCAGGTTAGTGAC (with *Sac*I site) and reverse primer GTCGGATCCTAAACTTGATTGCATAATCTTTCTTCCTCC (with *Bam*HI site). The DNA fragment encoding MSP-1$_{19}$ (nucleotides 5 040-5 451, GenBank AF165928) was amplified from the genomic DNA of *P. yoelii* 265BY, with forward primer ACGGGATCCAA CACATAGCCTCAATAGCT (with *Bam*HI site) and reverse primer ACGGAATTCTAGCTGG AAGAACTACAGAA (with *Eco*RI site). The terminator of *N*-acetylmuramoyl-L-alanine amidase (*cwl*B) (nucleotides 2 187-2 471, GenBank M81324) was amplified from *Bacillus subtilis* BR151 by PCR with forward primer CTCGAGCTCCACAAGCTATTCATGAC (with *Xho*I site) and reverse primer GGTACCTCTCT GCACTCACTG ACACA (with *Kpn*I site). The PCR products were cloned on T-vector (Promega, USA) first, and then joined together in a tandem way on pBluescriptSKII(+) with restriction enzyme pairs of *Sac*I/BamHI, *Bam*HI/*Eco*RI, and *Xho*I/*Kpn*I respectively to obtain plasmid pSK-PSGT. For expression of MSP-1$_{19}$ in *L. lactis*, pSK-PSGT was then digested with *Pvu*II to release the 1.6-kb blunt-end fragment, which was then inserted into the *Eco*RV site of shuttle vector pTRKL2[24]. The final construct was referred as pL2-PSGT. For expression of fusion protein GST-MSP-1$_{19}$ in *E. coli*, the DNA fragment encoding MSP-1$_{19}$ was derived by PCR and joined to fusion protein expression vector pGEX-5X-3 with *Bam*HI and *Eco*RI sites. The derived plasmid was noted as pGEX-MSP-1$_{19}$.

Transformation

Electroporation[25] was used to transform *L. lactis* LM2345 with pL2-PSGT. $CaCl_2$ method was used to transform *E. coli* BL21 with plasmid pGEX-5X-3.

Preparation of antiserum against P. yoelii 265-BY

The antiserum against *P. yoelii* 265-BY was prepared from BALB/c mice infected with 10^4 asexual blood stage parasites. The serum was collected from the eye veins 4 d after burst with 10^4 parasites one month after infection, and stored at 4 ℃.

Expression and analysis of MSP-1$_{19}$ in E. coli and L. lactis

The BL21 transformant harboring plasmid pGEX-MSP-1$_{19}$ was cultured in L-broth to A_{600} around 1.0, and was treated with supplement containing 1.0 mmol/L of isopropylthio-β-galactoside (IPTG) for 3 h. The fusion protein GST-MSP-1$_{19}$ was purified from cell lysate by affinity chromatography of Glutathione Sepharose-4B according to manual instruction provided by the manufacturer. The purified fusion protein was used as positive control of immunoblotting. To express MSP-1$_{19}$ in *L. lactis*, the transformant harboring plasmid pL2-PSGT was cultured overnight in MRS medium[26] supplemented with 10 mg/L erythromycin. The cells were collected by centrifuge, and the lysates were analyzed by using SDS-polyacrylamide gel electrophoresis analysis followed with immunoblotting by using antiserum against *P. yoelii* 265-BY (1:500 dilution). All other operations were performed following standard protocols[27].

Oral immunization of BALB/c and C57BL/6 mice with recombinant L. lactis

Oral immunization experiments were performed according

to the protocol described by Robinson *et al*.[21]. The BALB/c and C57BL/6 mice were divided into groups of 10 mice and fed for 6-8 wk. The test group was administered with recombinant *L. lactis* constitutively expressing MSP-1$_{19}$, and the control groups were administered with free *L. lactis* bacteria or phosphate-buffered saline (PBS). For BALB/c mice, every dose containing 5×10^9 bacterial cells in the suspension buffer (0.2 mol/L sodium bicarbonate, 5% Casino acids, and 0.5% glucose); and for C57BL/6 mice (two dosage groups), every dose containing 5×10^9 or 1×10^8 cells were administered. All the groups were administered with recombinant *L. lactis* on d 1, 2, 3, 29, 30, 31, and 36, respectively.

Challenge infections and evaluation of protective efficacy

Mice in each group were challenged on d 49 with 1×10^5 asexual blood stage *P. yoelii* parasites obtained from a donor mouse. Parasitemia was monitored every two days after challenge using microscopic examination of blood film with Giemsa staining.

RESULTS

Expression of fusion protein GST-MSP-1$_{19}$ in E. coli

The fusion protein GST-MSP-1$_{19}$ was expressed in *E. coli* BL21 transformed with plasmid pGEX-MSP-1$_{19}$. The transformed BL21 cells were cultured in L-broth until the A_{600} reached 1.0, and then induced with 1.0 mmol/L IPTG for 3 h. Total proteins of BL 21 *E. coli* cells were analyzed by sodium dodecyl sulfate-polyacrylamide gel electrophoresis (SDS-PAGE). As shown in lane 4 of Figure 1, the thick band of the expressed protein showed a molecular weight of 45 ku, matching well with the theoretical value of fusion protein GST-MSP-1$_{19}$. The expressed fusion protein was about 40% of the total protein of *E. coli* cells. Most of the fusion protein was found in inclusion body, but a small fraction was soluble. Glutathione Sepharose-4B affinity chromatography was carried out with the soluble fraction of *E. coli* cell lysate, and the derived fusion protein was used as the positive control of immunoblotting.

Expression of MSP-1$_{19}$ in L. lactis

For the expression of MSP-1$_{19}$ in *L. lactis*, the transformant harboring plasmid pL2-PSGT was cultured overnight at 30 ℃ in MRS medium[26] supplemented with 10 mg/L erythromycin. The cells were collected by centrifuge, and the lysates were analyzed with SDS-PAGE. However, no obvious protein bands around 19 ku were detected. Immunoblotting with antiserum against *P. yoelii* 265-BY was applied to check if there was low-level expression of MSP-1$_{19}$. As a result, the presence of MSP-1$_{19}$ was confirmed by immunoblotting as shown in lane 3 of Figure 2. The stained protein band at 19 ku was a little bit broad. This might be the result of partial degradation of MSP-1$_{19}$ in *E coli* cells. At least part of the expressed MSP-1$_{19}$ was in its native structure, since the antiserum prepared by *P. yoelii* parasites infection is considered to preferentially recognize the MSP-1$_{19}$ fragment located on erythrocyte membrane with the native conformation.

In lane 2 of the positive control, two protein bands were stained: one was at 45 ku, and the other was slightly below 45 ku, but not detectable on SDS-PAGE with Coomassie brilliant blue staining. When fusion protein is isolated from inclusion body of corresponding *E. coli* and refolded by rapid dilution method, only one protein band could be stained (data not shown). Therefore, we concluded that the low molecular weight protein was the degraded fusion protein present in the soluble fraction of *E. coli*.

Evaluation of protective immunity induced by recombinant L. lactis

Previous work of Tian *et al*.[28] indicated that mice with different genetic backgrounds may have quite different responses to *P. yoelii* infection. C57BL/6 mice showed the highest level against challenge with infected erythrocytes after immunization with recombinant proteins consisting of the PyMSP-1 C terminus in adjuvants. In this work, two strains of mice, BALB/c and C57BL/6, were used for oral

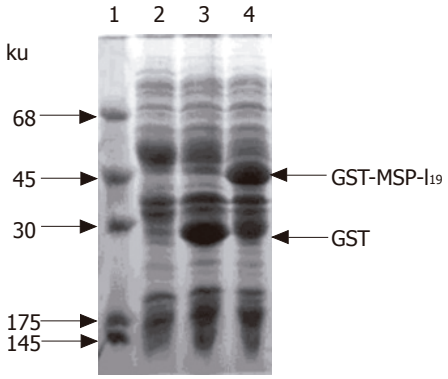

Figure 1 Expression of fusion protein in *E. coli* BL21 cells. Coomassie brilliant blue-stained 12% SDS-polyacrylamide gel. lane 1, protein markers; lane 2, total protein of BL21 cells; lane 3, total protein of *E. coli* BL21 transformed with plasmid pGEX-5X-3 with IPTG induction; lane 4, total protein of *E. coli* BL21 cells harboring plasmid pGEX-MSP-1$_{19}$ after with IPTG induction. The arrows indicate the positions of GST and fusion protein GST-MSP-1$_{19}$.

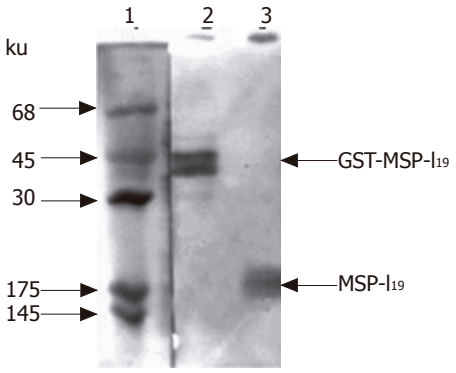

Figure 2 Immunoblotting analysis of MSP-1$_{19}$ expressed in *L. lactis*. Protein samples were first analyzed on 12% SDS-polyacrylamide gel and then transferred on nitrocellulose membrane followed by immunostaining with antiserum prepared by infecting mouse with *P. yoelii* parasites. lane 1, protein markers stained by amido black; lane 2, positive control of fusion protein GST-MSP-1$_{19}$ purified from *E. coli* cell lysate expressing the fusion protein by pGEX-MSP-1$_{19}$; lane 3, total protein of *L. lactis* cells harboring plasmid pL2-PSGT. The arrows indicate the position of fusion protein GST-MSP-1$_{19}$ and MSP-1$_{19}$.

immunization for comparison.

For BALB/c mice, two control groups were designed. Mice were administered with phosphate-buffered saline in control group 1, with 5×10^9 per dose of original *L. lactis* cells in control group 2, and with 5×10^9 per dose of *L. lactis* cells carrying pL2-PSGT construct in the test group, respectively. After seven doses of vaccination, each mouse was challenged with 1×10^5 asexual blood stage parasites. The parasitemias were measured from the next day of parasite challenging. The average and standard deviation of each group are shown in Figure 3. The peak p-arasitemias were 0.8±0.4% at d 4 for test group, 16.0±1.2% at d 8 for control group 1, and 12.0±0.8% at d 8 for control group 2, respectively. There was little difference between the peak parasitemias of the two control groups. Therefore, the non-specific immunity caused by the adjuvanticity of *L. lactis* was little. It should be noted that the appearance of parasitemia in the test group was one-day delayed compared with the control groups. None of the mice in any of the three groups died during the experiment. Overall, the BALB/c mice in all the three groups had the ability to scavenge *P. yoelii* parasites from their bodies by themselves.

For C57BL/6 mice, one control group and two test groups were designed. Mice were administered with 5×10^9 plasmid-harbored *L. lactis* cells per dose in test group 1, and 1×10^8 cells per dose in test group 2. Vaccination was performed by the same protocol for BALB/c mice, and the parasitemias were measured from the next day of parasite challenging. As shown in Figure 4A, the average peak parasitemias for the three groups were 60.8±9.6% for the control group, 41.6±8.8% for test group 1, and 20.8±26.5% for test group 2, respectively. Surprisingly, test group 2 administered with 1×10^8 bacterial cells per dose gained significantly stronger immune protection than test group 1, which was administered with 15 times more bacterial cells per dose. However, the standard deviation of test group 2 was remarkably bigger than the other two groups. This was largely due to the difference between individuals. Another important fact that should be noted was that all the mice in the control group died within 23 d after parasite infection, whereas all the vaccinated mice survived despite the high parasitemias (Figure 4B). After 30 d counting from the day of parasite challenging, malarial parasites were no more detectable in both of the two test groups (data not shown), implicating the complete elimination of the *P. yoelii* parasites.

We also checked the duration of recombinant bacteria in mice gut by investigation of the titers of recombinant bacterial cells in mice feces. After feeding of a single dose of 5×10^9 recombinant cells, the recombinant *L. lactis* reached a peak at 6 h with a density of 1×10^7 cells/g of feces, and then gradually decreased with time. The density of recombinant cells decreased to 1×10^4/g at 48 h, and 1×10^3/g at 72 h. Therefore, the interaction between the host and recombinant bacterial cell could be as long as 3 d per dose.

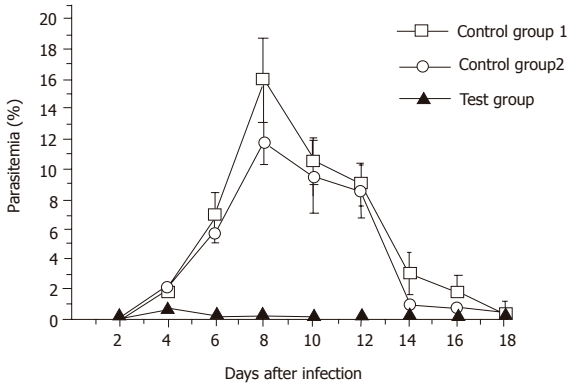

Figure 3 Blood-stage parasitemia of immunized BALB/c mice challenged with *P. yoelii* 265BY parasites. Mice were orally administered with PBS in the control group 1 (-□-), with 5×10^9 per dose of free *L. lactis* cells in the control group 2 (-○-), and with 5×10^9 per dose of *L. lactis* cells carrying pL2-PSGT construct in the test group (-▲-), respectively. Immunization procedure is described in Materials and Methods, and each mouse was challenged with 1×10^5 asexual blood-stage *P. yoelii* parasites.

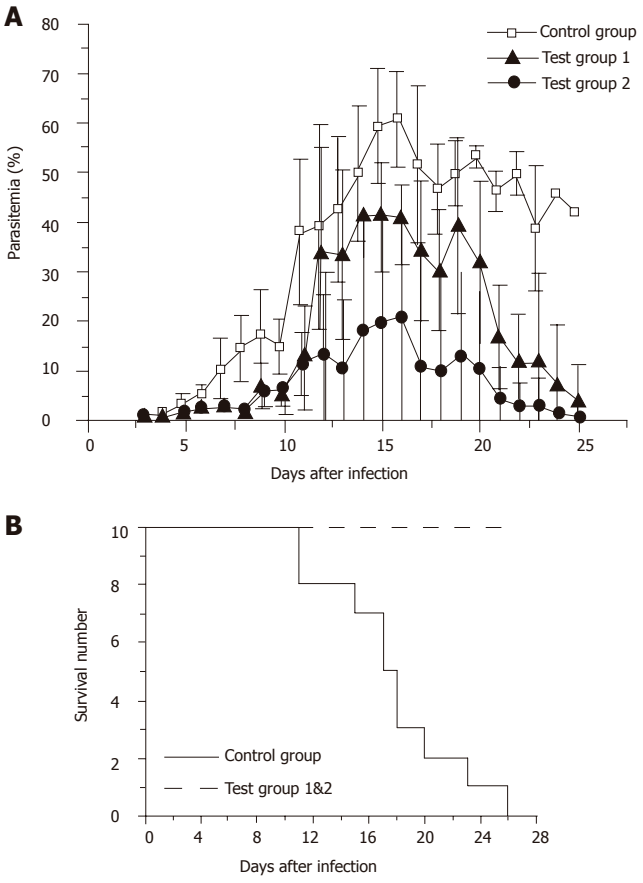

Figure 4 (**A**) Blood-stage parasitemia of immunized C57BL/6 mice challenged with *P. yoelii* 265BY parasites. Mice were orally administered with 5×10^9 per dose of free *L. lactis* cells in the control group (-□-), with 5×10^9 pL2-PSGT plasmid-harbored *L. lactis* cells per dose in the test group 1 (-▲-), and with 1×10^8 cells per dose of pL2-PSGT plasmid-harbored *L. lactis* cells in the test group 2 (-●-). Immunization procedure is described in Materials and Methods, and each mouse was challenged with 1×10^5 asexual blood-stage *P. yoelii* parasites. (**B**) Time course of survivals of the mice in the three groups is indicated in A.

DISCUSSION

It is known that the immunogenicity of soluble protein is low when administered orally but when expressed by genetically engineered bacteria and can be considerably enhanced. To achieve this goal, promoters that can drive the expression of a gene constitutively are essential. S-layer protein is a protein that forms regular crystalline arrays on prokaryotic cell surface. The *slp*A promoter can express the β-lactamase constitutively at a high level in *L. lactis*[27]. However, it failed to express MSP-1$_{19}$ with high efficiency in this study. The expression of MSP-1$_{19}$ in *L. lactis* could be detected only by immunoblotting; therefore, it was estimated at the level of several nanograms per 10^7 bacterial cells.

Unexpectedly, the low-level expression of MSP-1$_{19}$ in *L. lactis* was still able to elicit strong protection against *P. yoelii* infection on both BALB/c and C57BL/6 mice by oral administration. Although BALB/c mice seemed to be able to scavenge the malarial parasites by themselves, the parasitemia was reduced more than 10-folds (less than 1%) in the test group compared with the control groups. In the case of C57BL/6 strain, all the members in the control group died within 26 d after the infection, whereas all the members in the two test groups survived, and the parasites disappeared from both groups one month after the parasite challenging.

The different immune responses of the two C57BL/6 test groups also support the point of view that the expression level of MSP-1$_{19}$ is not critical for the elicitation of immune response, i.e., the group administered with a low dose of the recombinant bacterium gained stronger protection than the group administered with a high dose. The reason for the difference between the two groups is not clear at present; however, this might be partially due to immune tolerance caused by overdose. In the study by Robinson *et al*.[21], expression of tetanus toxin fragment C of *C. tetanus* in the intracellular accumulation of *L. lactis* was up to 3% of soluble cellular protein, and 5×10^9 cells were orally administered per dose to gain complete protection of mice from tetanus. Therefore, the optimal dose and the time schedule for oral administration should be carefully determined for each antigen.

It is striking to find the difference in immune response between the two strains of mice, BACL/c and C57BL/6. Our results partially support the report by Tian *et al*.[28] that C57BL/6 mice are most sensitive to *P. yoelii* infection. In most cases, BALB/c and C3H/He mice are used for protection test of a vaccine. Our results suggest that at least for protection experiments, C57BL/6 mice are better to be used in parallel.

In vaccination experiments with recombinant MPS-1$_{19}$ of *P. yoelii*, the protection effect has been found to be mediated by humoral immune response[15-17]. Robinson *et al*.[21] also reported high titers of IgG against tetanus toxin. We also tried immunoblotting and ELISA test with sera from the survivals of C57BL/6 mice in the test groups (data not shown). Nearly all the mice generated IgG against MSP-1$_{19}$, and there were no significant differences between the two test groups at the titers of IgG. In general, the titers were between 5×10^2 and 3×10^3, lower than the titers reported by Robinson *et al*. On the other hand, Lee *et al*.[23] measured the antigen-specific IgG titers in monkeys immunized with recombinant *L. lactis* bacterium expressing *H pylori UreB* gene, and titers as high as 1×10^5 were detected. However, despite the presence of high-titer antigen-specific IgG, all monkeys were infected after *H pylori* challenge, and there were no differences in the density of colonization. Taking our results obtained from low-dose test group of C57BL/6, we suggest that high-titer antigen-specific IgG should not be considered as the major indicator of the protective immune response. The role of cell-mediated immunity played in live bacteria vaccine should be focused.

ACKNOWLEDGMENTS

The authors thank Professor Weibin Guan of Second Military Medical University for his advices and kind instruction on *P. yoelii* culture. The authors are also grateful to Dr WeiQing Pan of Second Military Medical University for providing monoclonal antibody.

REFERENCES

1 **Cooper JA.** Merozoite surface antigen-1 of *Plasmodium*. Parasitol. *Today* 1993; **9:** 50-54
2 **Holder AA,** Blackman MJ. What is the function of MSP-1 on the malaria merozoite. Parasitol. *Today* 1994; **10:** 182-184
3 **Holder AA,** Freeman RR. Immunization against blood-stage rodent malaria using purified parasite antigens. *Nature* 1981; **294:** 361-364
4 **Siddiqui WA,** Tam LQ, Kramer KJ, Hui GS, Case SE, Yamaga KM, Chang SP, Chan EB, Kan SC. Merozoite surface coat precursor protein completely protects Aotus monkeys against Plasmodium falciparum malaria. *Proc Natl Acad Sci USA* 1987; **84:** 3014-3018
5 **Tian JH,** Kumar S, Kaslow DC, Miller LH. Comparison of protection induced by immunization with recombinant proteins from different regions of merozoite surface protein 1 of Plasmodium yoelii. *Infect Immun* 1997; **65:** 3032-3036
6 **Holder AA,** Sandhu JS, Hillman Y, Davey LS, Nicholls SC, Cooper H, Lockyer MJ. Processing of the precursor to the major merozoite surface antigens of Plasmodium falciparum. *Parasitology* 1987; **94**: 199-208
7 **Blackman MJ,** Ling IT, Nicholls SC, Holder AA. Proteolytic processing of the Plasmodium falciparum merozoite surface protein-1 produces a membrane-bound fragment containing two epidermal growth factor-like domains. *Mol Biochem Parasitol* 1991; **49:** 29-33
8 **Blackman MJ,** Heidrich HG, Donachie S, McBride JS, Holder AA. A single fragment of a malaria merozoite surface protein remains on the parasite during red cell invasion and is the target of invasion-inhibiting antibodies. *J Exp Med* 1990; **172:** 379-382
9 **Miller LH,** Roberts T, Shahabuddin M, McCutchan TF. Analysis of sequence diversity in the Plasmodium falciparum merozoite surface protein-1 (MSP-1). *Mol Biochem Parasitol* 1993; **59:** 1-14
10 **Kang Y,** Long CA. Sequence heterogeneity of the C-terminal, Cys-rich region of the merozoite surface protein-1 (MSP-1) in field samples of Plasmodium falciparum. *Mol Biochem Parasitol* 1995; **73:** 103-110
11 **Renia L,** Ling IT, Marussig M, Miltgen F, Holder AA, Mazier

D. Immunization with a recombinant C-terminal fragment of Plasmodium yoelii merozoite surface protein 1 protects mice against homologous but not heterologous P. yoelii sporozoite challenge. *Infect Immun* 1997; **65:** 4419-4423

12 **Matsumoto S,** Yukitake H, Kanbara H, Yamada T. Recombinant Mycobacterium bovis bacillus Calmette-Guerin secreting merozoite surface protein 1 (MSP1) induces protection against rodent malaria parasite infection depending on MSP1-stimulated interferon gamma and parasite-specific antibodies. *J Exp Med* 1998; **188:** 845-854

13 **Tian JH,** Kumar S, Kaslow DC, Miller LH. Comparison of protection induced by immunization with recombinant proteins from different regions of merozoite surface protein 1 of Plasmodium yoelii. *Infect Immun* 1997; **65:** 3032-3036

14 **Perera KL,** Handunnetti SM, Holm I, Longacre S, Mendis K. Baculovirus merozoite surface protein 1 C-terminal recombinant antigens are highly protective in a natural primate model for human Plasmodium vivax malaria. *Infect Immun* 1998; **66:** 1500-1506

15 **Calvo PA,** Daly TM, Long CA. *Plasmodium yoelii:* the role of the individual epidermal growth factor-like domains of the merozoite surface protein-1 in protection from malaria. *Exp. Parasitol* 1996; **82:** 54-64

16 **Daly TM,** Long CA. Humoral response to a carboxyl-terminal region of the merozoite surface protein-1 plays a predominant role in controlling blood-stage infection in rodent malaria. *J Immunol* 1995; **155:** 236-243

17 **Ling IT,** Ogun SA, Holder AA. The combined epidermal growth factor-like modules of Plasmodium yoelii Merozoite Surface Protein-1 are required for a protective immune response to the parasite. *Parasite Immunol* 1995; **17:** 425-433

18 **Hackett J.** Use of Salmonella for heterologous gene expression and vaccine delivery systems. *Curr Opin Biotechnol* 1993; **4:** 611-615

19 **Holmgren J,** Czerkinsky C. Cholera as a model for research on mucosal immunity and development of oral vaccines. *Curr Opin Immunol* 1992; **4:** 387-391

20 **Mercenier A,** Muller-Alouf H, Grangette C. Lactic acid bacteria as live vaccines. Curr Issues *Mol Biol* 2000; **2:** 17-25

21 **Robinson K,** Chamberlain LM, Schofield KM, Wells JM, Le Page RW. Oral vaccination of mice against tetanus with recombinant Lactococcus lactis. *Nat Biotechnol* 1997; **15:** 653-657

22 **de Vos WM.** Gene expression systems for lactic acid bacteria. *Curr Opin Microbiol* 1999; **2:** 289-295

23 **Lee MH,** Roussel Y, Wilks M, Tabaqchali S. Expression of Helicobacter pylori urease subunit B gene in Lactococcus lactis MG1363 and its use as a vaccine delivery system against H. pylori infection in mice. *Vaccine* 2001; **19:** 3927-3935

24 **O'Sullivan DJ,** Klaenhammer TR. High- and low-copy-number Lactococcus shuttle cloning vectors with features for clone screening. *Gene* 1993; **137:** 227-231

25 **Posno M,** Leer RJ, Luijk N, Giezen MJF, Heuvelmans PTH. M, Lokman BC, Pouwels PH. Incompatibility of *Lactobacillus* vectors with replicons derived from small cryptic lactobacillus plasmids and segregational instability of the introduced vectors. *Applied and Environmental Microbiology* 1991; **57**:1822-1828

26 **Harlow E,** Lane D. Antibodies: a laboratory manual. Cold Spring Harbor: Cold Spring Harbor Lab press 198827. Savijoki K, Kahala M, Palva A. High level heterologous protein production in Lactococcus and Lactobacillus using a new secretion system based on the Lactobacillus brevis S-layer signals. *Gene* 1997; **186:** 255-262

28 **Tian JH,** Miller LH, Kaslow DC, Ahlers J, Good MF, Alling DW, Berzofsky JA, Kumar S. Genetic regulation of protective immune response in congenic strains of mice vaccinated with a subunit malaria vaccine. *J Immunol* 1996; **157:** 1176-1183

Science Editor Wang XL and Li WZ **Language Editor** Elsevier HK

PO Box 2345, Beijing 100023, China
www.wjgnet.com
wjg@wjgnet.com

ELSEVIER

World J Gastroenterol 2005;11(44):6981-6987
World Journal of Gastroenterology ISSN 1007-9327

• *BASIC RESEARCH* •

Exogenous acid fibroblast growth factor inhibits ischemia-reperfusion-induced damage in intestinal epithelium via regulating P53 and P21WAF-1 expression

Wei Chen, Xiao-Bing Fu, Shi-Li Ge, Wen-Juan Li, Tong-Zhu Sun, Zhi-Yong Sheng

Wei Chen, Xiao-Bing Fu, Wen-Juan Li, Tong-Zhu Sun, Zhi-Yong Sheng, Key Research Laboratory of Wound Repair, Burns Institute, 304th Clinical Department, General Hospital of PLA, Beijing 100037, China
Shi-Li Ge, Institute of Radiation Medicine, Beijing 100850, China
Supported by the National Natural Science Foundation of China, No. 30400172, 30230370, and the National Basic Science and Development programme (973 programme, 2005 CB 522603)
Correspondence to: Professor Xiao-Bing Fu, MD, Key Research Laboratory of Wound Repair, Burns Institute, 304th Clinical Department, General Hospital of PLA, 51 Fu cheng Road, Beijing 100037, China. fuxb@cgw.net.cn
Telephone: +86-10-66867396 Fax: +86-10-88416390
Received: 2004-11-12 Accepted: 2005-02-18

Abstract

AIM: To detect the effect of acid fibroblast growth factor (aFGF) on P53 and P21WAF-1 expression in rat intestine after ischemia-reperfusion (I-R) injury in order to explore the protective mechanisms of aFGF.

METHODS: Male rats were randomly divided into four groups, namely intestinal ischemia-reperfusion group (R), aFGF treatment group (A), intestinal ischemia group (I), and sham-operated control group (C). In group I, the animals were killed after 45 min of superior mesenteric artery (SMA) occlusion. In groups R and A, the rats sustained for 45 min of SMA occlusion and were treated with normal saline (0.15 mL) and aFGF (20 μg/kg, 0.15 mL), then sustained at various times for up to 48 h after reperfusion. In group C, SMA was separated, but without occlusion. Apoptosis in intestinal villi was determined with terminal deoxynucleotidyl transferase-mediated dUTP-biotin nick-end labeling technique (TUNEL). Intestinal tissue samples were taken not only for RT-PCR to detect P53 and P21WAF-1 gene expression, but also for immunohistochemical analysis to detect P53 and P21WAF-1 protein expression and distribution.

RESULTS: In histopathological study, ameliorated intestinal structures were observed at 2, 6, and 12 h after reperfusion in A group compared to R group. The apoptotic rates were (41.17±3.49)%, (42.83±5.23)%, and (53.33±6.92)% at 2, 6, and 12 h after reperfusion, respectively in A group, which were apparently lower than those in R group at their matched time points (50.67±6.95)%, (54.17±7.86)%, and (64.33±6.47)%, respectively, (P<0.05)). The protein contents of P53 and P21WAF-1 were both significantly decreased in A group compared to R group (P<0.05) at 2-12 h after reperfusion, while the mRNA levels of P53 and P21WAF-1 in A group were obviously lower than those in R group at 6-12 h after reperfusion (P<0.05).

CONCLUSION: P53 and P21WAF-1 protein accumulations are associated with intestinal barrier injury induced by I-R insult, while intravenous aFGF can alleviate apoptosis of rat intestinal cells by inhibiting P53 and P21WAF-1 protein expression.

Key words: Acid fibroblast growth factor; Ischemia; Reperfusion; P53 gene; P21WAF-1 gene

Chen W, Fu XB, Ge SL, Li WJ, Sun TZ, Sheng ZY. Exogenous acid fibroblast growth factor inhibits ischemia-reperfusion-induced damage in intestinal epithelium via regulating P53 and P21WAF-1 expression. *World J Gastroenterol* 2005; 11(44): 6981-6987
http://www.wjgnet.com/1007-9327/11/6981.asp

INTRODUCTION

Intestinal ischemia-reperfusion (I-R) injury is characterized histologically by inflammation, villus abscission, and mucosal epithelial cell apoptosis[1]. Agents can modulate or prevent apoptosis after I-R[2-6]. Though the mechanisms of action are diverse, all these agents ultimately show their potent antiapoptotic properties that account, at least in part, for their protective effects. Accumulation of P53 protein, which is well known as a tumor suppressor gene product, plays a central role as the initiator of the intrinsic apoptotic cascade triggered by a wide variety of insults[7-10]. In addition, a role of P53 in regulating the extrinsic receptor-mediated apoptotic pathway has also been reported[11]. P21WAF-1, which is a downstream mediator of P53 function, plays a key role in determining the ultimate sensitivity of cells to myriad stimuli and insults that induce apoptosis[12-14]. Thus, P53 and P21WAF-1 are poised as the ideal candidates for mediating apoptosis after I-R, a setting

where many insults coexist.

Acid fibroblast growth factor (aFGF) is a mitogen *in vitro* for most of the ectoderm- and mesoderm-derived cell lines. In addition, this factor shows a wide range of endocrine-like activities[15,16]. As a multiple function growth factor, aFGF is involved in embryo development and tissue repair[17,18]. Previous studies have shown that intravenous administration of exogenous aFGF could improve the physiological functions of intestine after I-R injury[19,20]. Since the mechanism by which aFGF inhibits apoptosis is unknown, we investigated the effects of aFGF on gene expression and protein contents of P53 and P21WAF-1 underlying the protective mechanisms of aFGF against intestinal I-R injury.

MATERIALS AND METHODS

Animal model and experimental design

Healthy male Wistar rats weighing 220±20 g (Animal Centre, Academy of Military Medical Sciences, Beijing) were used in this study. Animals were housed in wire-bottomed cages placed in a room illuminated from 08:00 to 20:00 (12:12-h light-dark cycle) and maintained at 21±1 ℃. Rats were allowed free access to water and food. The animals were anesthetized with 3% sodium pentobarbital (40 mg/kg) and underwent laparotomy. The superior mesenteric artery (SMA) was identified and freed by blunt dissection. A micro-bulldog clamp was placed at the root of SMA to cause complete cessation of blood flow for 45 min, and thereafter the clamp was loosened to form reperfusion injury. The animals were randomly divided into four groups, namely intestinal ischemia-reperfusion group (R), intestinal ischemia group (I), reconstructive aFGF treatment group (A) and sham-operated control group (C). In group I, the animals were killed after 45 min of SMA occlusion. In groups R and A, the rats sustained for 45 min of SMA occlusion and were treated with 0.15 mL normal saline and 0.15 mL saline plus aFGF (20 μg/kg) injected from tail vein, then sustained for 15, 30 min, 1, 2, 6, 12, 24, and 48 h of reperfusion respectively. In C group, SMA was separated, but without occlusion, and samples were taken after exposure of SMA for 45 min. In groups R and A, rats were killed at different time points after reperfusion, and intestinal tissue biopsies were taken. Six specimens of the intestine were obtained at each time point from six rats. When any rat died during the study, additional rats were used until six specimens could be obtained from six rats at each time point. A small part of the intestine specimen was fixed with 10% neutral buffered formalin for immunohistochemical detections of intestinal epithelial apoptosis, and protein expression of P53 and P21WAF-1. The remaining tissue samples were placed in liquid nitrogen for RT-PCR to detect P53 and P21WAF-1 gene expression.

Histopathological study

Formalin-fixed, paraffin-embedded intestinal samples were cut into 5-μm-thick sections, deparaffinized in xylene, rehydrated in graded ethanol, and then stained with hematoxylin-eosin (HE) for histological observation under light microscope.

In situ detection of cell death

The apoptotic cells in intestinal tissues were detected by the terminal deoxynucleotidyl transferase (TdT)-mediated dUTP-biotin nick-end labeling (TUNEL) method. Specimens were dewaxed and immersed in phosphate-buffered saline containing 0.3% hydrogen peroxide for 10 min and then incubated with 20 μg/mL proteinase K for 15 min. Seventy-five microliters of equilibration buffer was applied directly onto the specimens for 10 min, followed by 55 μL of TdT enzyme and incubation, which were then incubated at 37 ℃ for 1 h. The reaction was terminated by transferring the slides to prewarmed stop/wash buffer for 30 min at 37 ℃. The specimens were covered with a few drops of rabbit serum and incubated for 20 min and then covered with 55 μL of anti-digoxigenin peroxidase and incubated for 30 min. Specimens were then soaked in Tris buffer containing 0.02% diaminobenzidine and 0.02% hydrogen peroxide for 1 min to achieve color development. Finally, the specimens were counterstained by immersion in hematoxylin. The cells with clear nuclear labeling were defined as TUNEL-positive cells. The results of positive cells and their distribution were observed under 400× microscope. Sixty intestinal villi per time point were required for counting, and then the apoptotic ratios were calculated and analyzed.

Immunohistochemistry

Immunostaining for proteins of P53 and P21WAF-1 was performed in paraffin sections with a high-temperature antigen-unmasking method in citrate buffer and ABC peroxidase, using P21WAF-1 monoclonal mouse antibody (Santa Cruz Cor, sc-6246) and P53 polyclonal rabbit antibody (Santa Cruz Cor, sc-6243) against antigens (1:100 in PBS). Tissues were fixed overnight in 4% paraformaldehyde, dehydrated, and embedded in paraffin. Five-micrometer thick sections were deparaffinized and rehydrated using graded alcohol concentrations. Antigen retrieval was performed by incubation in 100 mmol/L sodium citrate, pH 6.0, at 90 ℃for 20 min. Then, sections were blocked with 5% normal swine serum in PBS for 30 min at 25 ℃, followed by incubation with primary antibodies at a concentration of 5 μg/mL overnight at 4 ℃. Control slides were incubated with PBS without primary antibodies. Tissue sections were then incubated for 60 min with biotinylated secondary antibody. After being washed in PBS, the sections were exposed to acidin-biotin complex for 60 min, reacted with 0.05% (wt/vol) DAB in 50 mmol/L Tris-HCl (pH 7.4) with 0.1% (vol/vol) hydrogen peroxide for 5 min and counterstained with hematoxylin. The results of positive staining cells and their distribution were observed under 400× microscope. Sixty intestinal villi per time point were required for counting, and then the ratio of positive cells was calculated and analyzed.

RNA extraction and RT-PCR analysis

Tissue total RNA was extracted using TRIzol reagent

(Gibco BRL, USA). RNA was serially diluted with water containing 1 unit RNase inhibitor per μL and 3 mmol/L dithiothreitol (DTT). One microliter RNA, 1 μL oligo (dT12-18), 1 μL avian myeloblastosis virus reverse transcriptase (AMV-RT), 2 μL 10 mmol/L deoxynucleoside triphosphate (dNTP), 2 μL 0.1 mol/L DTT, 4 μL 5× buffer, and sterilized distilled water up to a total volume of 20 μL were incubated at 37 ℃ for 60 min. Subsequently, 2 μL of each reaction product was amplified in 50 μL of a PCR mixture. Then 29 cycles were performed with a Perkin-Elmer Cetus/DNA thermal cycler (Takara Shuzo Co., Tokyo, Japan) at 94 ℃ for 1 min, at 50 ℃ for 1 min, at 72 ℃for 1 min, and then at 72 ℃ for 10 min at the end of the procedure. In this study, β-actin, which is ubiquitously expressed, was used as a positive control in a pilot study before formal experimentation, and PCR reaction for each primer set was repeated four times to verify the reproducibility of results. After PCR, 5-μL sample aliquots was electrophoresed on a 2% agarose gel for 30 min, stained with ethidium bromide and photographed. Densitometry was done with a Bechman densitometer. The level of gene transcription was expressed as the ratio of gray density of the gene to β-actin.

Statistical analysis

All values were expressed as mean±SD. The statistical significance was determined by one-way analysis of variance (ANOVA) followed by the Student's and Newman-Keuls multiple comparison tests. $P<0.05$ was considered statistically significant.

RESULTS

Histopathological findings

After the SMA was clamped near its origin from the aorta, the entire small intestine showed a dark purple, cyanotic color within 45 min. The histological evaluation revealed that damage to the small intestine in I group was small, with slightly edematous villus tips and intact crypts just after the ischemic period. Two hours after reperfusion, partial loss of the mucosa could be observed. During 6-12 h after reperfusion, the damage of intestinal epithelial cells, hemorrhage and apoptosis could be found accompanied with inflammatory cells infiltrated into the intestinal wall, and the crypt-villus structure was seriously spoiled. In the period of 24-48 h after reperfusion, the mucosal integrity was partially restored. Histological structure of the intestinal mucosa was markedly improved after administration of aFGF. The protective function of aFGF on intestinal mucosa was very effective 2-12 h after reperfusion. The structures of crypt and villus were both guarded, with less damage of intestinal mucosa in A group compared to R group.

Change of cellular apoptotic rates

To quantify the extent of apoptosis after ischemia and reperfusion, TUNEL reaction was performed in serial sections prepared from the middle quarter of the small intestine (jejunum). The time, when the animals were killed after a 45-min SMA occlusion followed by reperfusion, varied to further define the apoptotic response. Statistically significant increase in TUNEL-positive cells was not detectable until 1 h after reperfusion and reached its peak at 12 h. The cellular apoptotic rate in intestinal mucosa at 12 h after reperfusion was 3.3 times of that in C group. After reperfusion for 24 and 48 h, the mucosal apoptotic rates were restored to the level of C group. Administration of aFGF resulted in statistically significant decrease of the apoptotic rates compared to R group 2-12 h after reperfusion ($P<0.05$). No statistically significant decrease of apoptotic rates was observed at 24 and 48 h after reperfusion (Table 1).

Table 1 Effect of aFGF on apoptotic rates in intestinal mucosa after ischemia-reperfusion insult (n = 6, mean±SD, %)

Groups	R group	A group
C group	19.67±3.50	19.67±3.50
I group	27.67±9.63	27.67±9.63
15 min after reperfusion	29.50±5.61	25.17±6.43
30 min after reperfusion	28.00±7.02	26.00±4.86
1 h after reperfusion	34.67±5.47[a]	29.83±7.08
2 h after reperfusion	50.67±6.95[a]	41.17±3.49[ac]
6 h after reperfusion	54.17±7.86[a]	42.83±5.23[ac]
12 h after reperfusion	64.33±6.47[a]	53.33±6.92[ac]
24 h after reperfusion	28.50±5.47	23.33±3.83
48 h after reperfusion	26.00±5.76	22.00±4.60

[a]$P<0.05$ *vs* C group; [c]$P<0.05$ *vs* R group at matched time point.

Expression characteristics of P53 and P21WAF-1 proteins

Quantitative immunohistochemical results for P53 and P21WAF-1 proteins are summarized in Table 2. Protein expression levels of P53 were weaker in the sham-operated intestinal and ischemic tissues, and positive particles were mainly located in the epithelial cells of the upper part of villi. However, the positive cellular rates elevated with the increment of duration after reperfusion injury. In the period of 1-12 h after reperfusion, P53 protein was expressed at a dramatically higher level in comparison to C group ($P<0.05$) and the maximum level was 2.1-fold of C group at 6 h after reperfusion. The positive signals of P53 were mostly distributed in the nuclei and cytoplasm of epithelial cells of villi and crypts. At 24-48 h after reperfusion, the positive cellular rates were not substantially changed compared to C group. Treatment with aFGF could apparently inhibit the protein contents of P53 in intestinal mucosal epithelial cells 2-12 h after reperfusion in comparison to R group at different matched time points ($P<0.05$, Figures 1A-1C). The levels of P21WAF-1 protein were also significantly increased 2-12 h after reperfusion with a peak at 12 h after reperfusion (1.5-fold of C group, $P<0.05$). The positive particles of P21WAF-1 were mainly localized in the cytoplasm and nuclei of intestinal epithelial cells (Figures 1D-1F). By 24-48 h after I-R, the P21WAF-1 levels tended to normalize back to baseline of C group ($P>0.05$). Compared to the saline-treated group, the positive cellular rates of P21WAF-1 were significantly

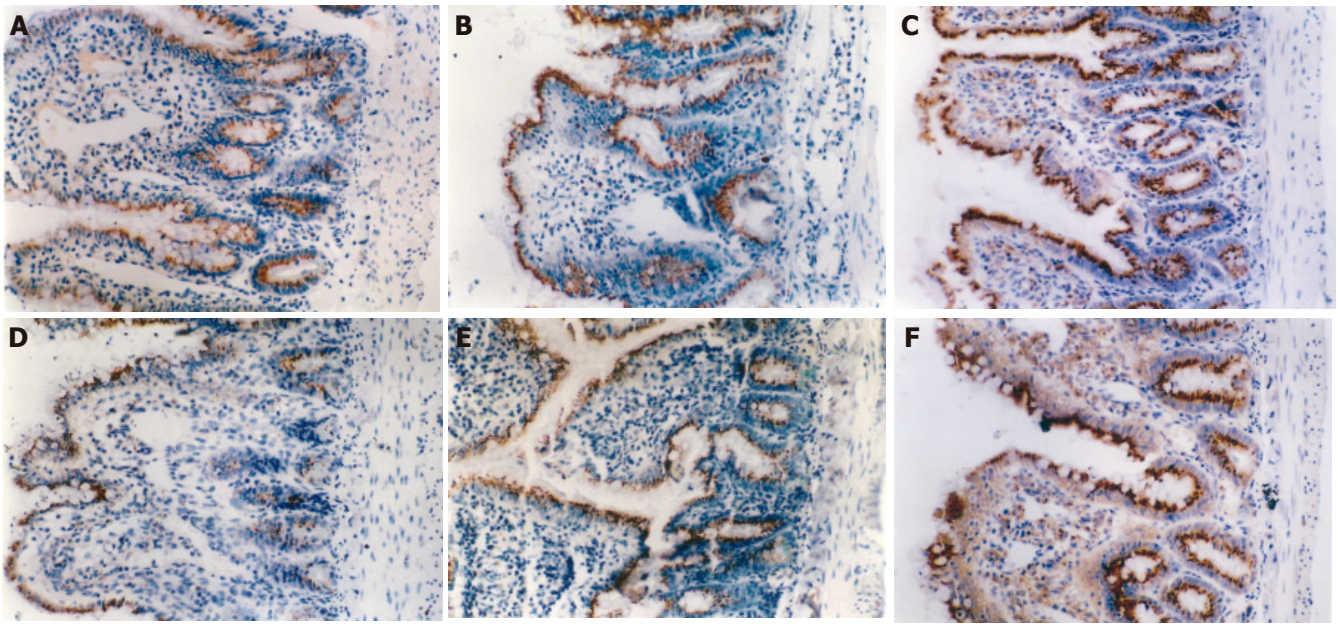

Figure 1 Expression of P53 and P21^{WAF-1} protein in C group (**A** and **D**, respectively), A group (**B** and **E**, respectively) and R group (**C** and **F**, respectively).

Table 2 Effect of aFGF on protein expression of P53 and P21WAF-1 in intestinal mucosa after ischemia-reperfusion (n = 6, mean±SD, %)

Groups	P53		P21WAF-1	
	R group	A group	R group	A group
C group	23.67±4.55	23.67±4.55	32.50±3.94	32.50±3.94
I group	29.17±4.45	29.17±4.45	35.83±4.83	35.83±4.83
15 min after reperfusion	27.00±3.90	23.83±5.08	34.67±4.76	31.50±4.37
30 min after reperfusion	30.67±3.98	26.67±3.78	36.17±3.31	37.00±4.86
1 h after reperfusion	33.17±3.19[a]	32.50±3.27[a]	39.83±4.58	37.83±4.36
2 h after reperfusion	40.33±3.50[a]	33.83±5.04[a,c]	49.33±4.18[a]	41.83±6.65[a,c]
6 h after reperfusion	50.50±4.23[a]	42.67±3.88[a,c]	53.00±4.39[a]	44.67±4.46[a,c]
12 h after reperfusion	45.67±5.65[a]	37.50±4.81[a,c]	57.50±3.62[a]	49.33±3.78[a,c]
24 h after reperfusion	30.00±6.13	25.33±3.33	34.50±6.02	30.00±3.79
48 h after reperfusion	28.17±8.89	25.67±4.32	33.83±7.31	30.67±4.18

[a]P<0.05 *vs* C group; [c]P<0.05 *vs* R group at matched time point.

Table 3 Effect of aFGF on mRNA contents of P53 and P21WAF-1 genes in intestinal mucosa after ischemia-reperfusion (n = 6, mean±SD, %)

Groups	P53		P21WAF-1	
	R group	A group	R group	A group
C group	23.5±6.0	22.4±2.5	26.7±2.0	24.6±4.1
I group	38.9±5.1[a]	34.8±4.2[a]	32.6±2.0[a]	31.7±2.0[a]
15 min after reperfusion	53.9±3.9[a]	45.8±10.7[a]	33.4±2.3[a]	24.0±3.4[c]
30 min after reperfusion	34.0±4.4[a]	41.9±5.2[a,c]	23.3±4.2	22.9±2.0
1 h after reperfusion	48.5±3.2[a]	44.7±5.4[a]	24.8±2.3	23.8±3.2
2 h after reperfusion	46.7±5.4[a]	41.3±6.3[a]	26.5±2.7	24.9±3.0
6 h after reperfusion	48.8±5.2[a]	38.3±4.7[a,c]	30.8±3.0[a]	20.9±2.6[c]
12 h after reperfusion	51.0±4.5[a]	34.1±4.8[a,c]	32.7±1.6[a]	21.9±2.8[c]
24 h after reperfusion	55.3±7.3[a]	56.9±5.3[a]	28.8±3.1	28.5±5.0
48 h after reperfusion	56.4±8.3[a]	61.0±4.0[a]	29.0±2.3	28.9±3.8

[a]P<0.05 *vs* C group; [c]P<0.05 *vs* R group at matched time point.

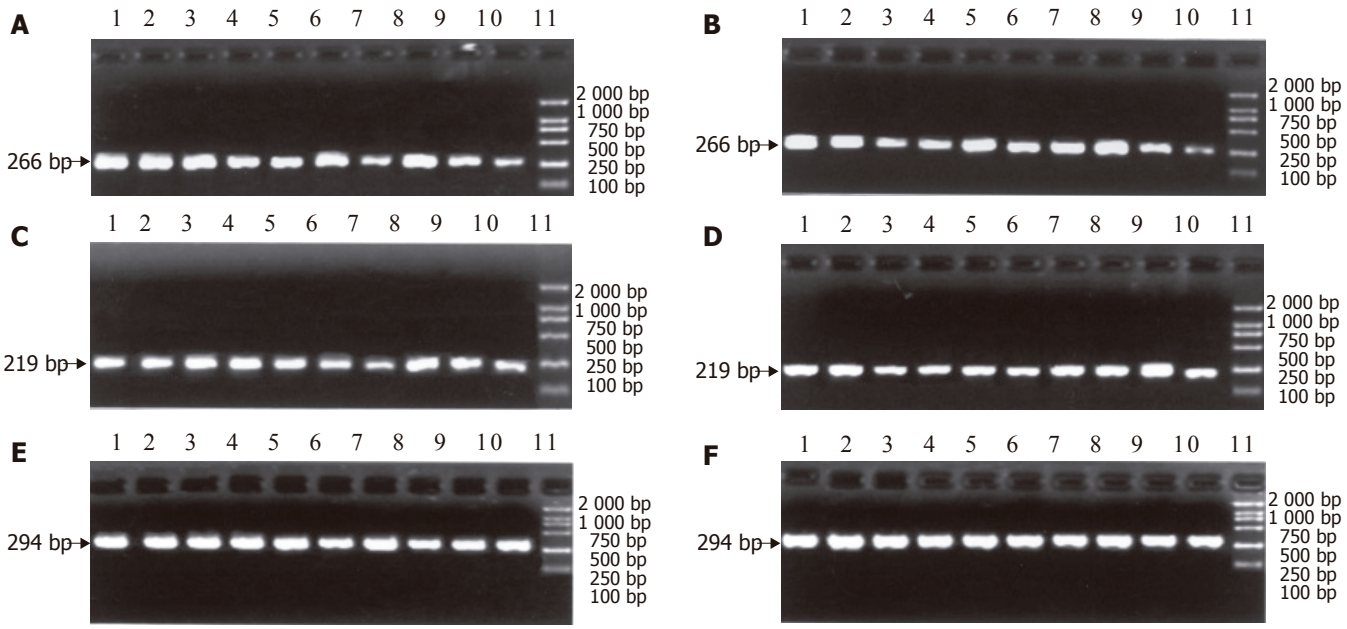

Figure 2 Expression of P53, $P21^{WAF-1}$, and β-actin genes in normal saline-treated (**A**, **C**, **E**, respectively) and aFGF treated (**B**, **D**, **F**, respectively) rat intestinal villi. Bar indicates the size of RT-PCR cDNA products. Lanes 1-8: 48, 24, 12, 6, 2, 1 h, and 30, 15 min after reperfusion; lane 9: ischemia group; lane 10: sham-operated control group; lane 11: DL 2000 marker.

lower 2 to 12 h after reperfusion in aFGF-treated group ($P<0.05$, Table 2).

Expression characteristics of P53 and P21WAF-1mRNA

We investigated the gene expression of P53 and P21WAF-1 in differentially treated intestinal villi through RT-PCR analysis (Table 3). The P53 gene amplification product was composed of 266 bp (Figures 2A-2C). Expression of this gene was remarkably and rapidly increased in intestinal mucosa after ischemia during the whole period of reperfusion. After aFGF administration, the mRNA level of P53 in villus cells was lower than that in normal saline-treated group. Especially at 30 min, 6 and 12 h after reperfusion, the discrepancy of P53 expression levels between the two groups was apparent ($P<0.05$, Table 3). Figures 2D-2F show that the length of RT-PCR products of P21WAF-1 was 219 bp. The P21WAF-1 gene was expressed at a pronounced high level in villi compared to sham-operated group at 15 min, 6 and 12 h after reperfusion ($P<0.05$). After treatment with aFGF, although P21WAF-1 gene expression was not substantially decreased after reperfusion in A group compared to C group, the content of P21WAF-1 gene transcript were markedly reduced at 15 min, 6 and 12 h after reperfusion in A group compared to R group ($P<0.05$, Table 3).

DISCUSSION

The major clinical disorders involving gastrointestinal circulation are hemorrhage and ischemia. It is well recognized that the small intestine is extremely sensitive to the deleterious effects of I-R, and it has been clearly demonstrated that I-R causes both mucosal and vascular injury within the small intestine[21,22]. Intestinal I-R injury may also cause release of bacteria and toxins from the gut into the host blood circulation and changes of inflammatory factors, cytokines, and growth factors, resulting in damage to the intestinal barrier. In the current study, we found that I-R, following occlusion of the SMA, induced apoptosis in the intestinal mucosal cells. Results of TUNEL method displayed that the apoptotic rate increased during ischemia and peaked at 12 h after reperfusion. The locations of apoptotic cells were extended from villus tip in sham-operated rats to the whole structure of mucosa in rats insulted by I-R. The quantification of apoptosis was corroborated with histological examination using HE staining. It was also found that administration of exogenous aFGF could reduce the intestinal injury caused by I-R insult. The antiapoptotic effect of aFGF was achieved by inhibiting the expression of some apoptosis-related genes. Previous experimental data showed that the change of expression of apoptosis-related genes played a pivotal role in alleviating cardiac, myocardial[23], cerebral[24,25], muscular[26], cutaneous[27], and adrenal cortex[28] apoptosis induced by I-R, which was in agreement with our results that I-R promoted P53 and P21WAF-1 expression.

After 45 min of ischemia, although gene expression of P53 was quickly increased, and lasted for the whole period after reperfusion, P21WAF-1 gene was only strongly expressed at 15 min, 6 h, and 12 h after reperfusion. The difference of time in the kinetics between these two genes may indicate that P21WAF-1 gene transcription might be activated in a P53-independent manner. Moreover, although protein levels of P53 and P21WAF-1 accumulated after reperfusion, there was a time lag in the

onset of elevation and the peak time point between these two proteins. These results indicate that the P21WAF-1 translation is activated by the elevated P53 protein contents. In this current study, we also found that the kinetics between the levels of P21WAF-1 and P53 protein expression and the apoptotic rate were similar, suggesting that protein levels of P21WAF-1 and P53 might be related to cell apoptosis. When severe histological damage of intestinal villi 2-12 h after reperfusion is considered, DNA damage in the intestinal cells cannot be repaired, resulting in cell apoptosis. Our study also found that the rate of apoptosis in intestinal villi insulted by I-R was significantly decreased by aFGF administration. aFGF could inhibit the increments of P21WAF-1 and P53 protein expression 2-12 h after reperfusion in comparison to normal saline treatment, suggesting that the decrement of P21WAF-1 and P53 protein contents caused by aFGF might be one of the mechanisms attenuating ischemia-reperfusion-induced apoptosis.

Studies have demonstrated that the activated neutrophils and oxygen free radicals produced in ischemic tissue during reperfusion play an important role in developing the injury of the intestine[26,28]. Free radicals are produced mainly by the activated neutrophils and xanthine dehydrogenase/xanthine oxidase enzyme system after reperfusion, but the free radicals produced from the neutrophils play a more important role than xanthine oxidase in mediating tissue-destroying events[29]. Our histopathological study showed that leukocyte sequestration into the villi was evident 6-12 h after reperfusion, and exogenous aFGF could alleviate leukocyte infiltration into intestinal villi. It is well known that free radicals cause DNA damage, and the series of cell reactions mediated by P53 might be investigated by free radicals produced during the reperfusion process. The protective mechanism of aFGF might inhibit P53 and P21WAF-1 protein translation by scavenging free radicals. The current study also demonstrated that apoptosis occurred 1 h after reperfusion and returned to baseline values after 24 h, suggesting that I-R-induced intestinal apoptosis and mucosal recovery is a rapid process. The mechanism underlying this interesting kinetics of induction of mucosal cell apoptosis and restoration is unclear. A time-dependent increment in protein expression of apoptosis-promoting factors including P53 and P21WAF-1 during ischemia and early phases of reperfusion, and decrement with prolonged reperfusion might be an alternative cause. Therefore, the protective effect of aFGF against intestinal I-R insult might be not only associated with inhibiting epithelial cell apoptosis but also related to inducing mucosal cell restoration.

In conclusion, the protective effects of aFGF against I-R in rat intestinal villi might be partially due to its ability to inhibit I-R-induced apoptosis. aFGF exerts its antiapoptotic effect via regulating P53 and P21WAF-1gene transcription and translation. The precise mechanisms of aFGF underlying the inhibition of intestinal I-R injury and attenuation of apoptosis need further investigation.

REFERENCES

1 **Fu XB,** Yang YH, Sun TZ, Chen W, Li JY, Sheng ZY. Rapid mitogen-activated protein kinase by basic fibroblast growth factor in rat intestine after ischemia/reperfusion injury. *World J Gastroenterol* 2003; **9:** 1312-1317

2 **Palmen M,** Daemen MJ, De Windt LJ, Willems J, Dassen WR, Heeneman S, Zimmermann R, Van Bilsen M, Doevendans PA. Fibroblast growth factor-1 improves cardiac functional recovery and enhances cell survival after ischemia and reperfusion: a fibroblast growth factor receptor, protein kinase C, and tyrosine kinase-dependent mechanism. *J Am Coll Cardiol* 2004; **44:** 1113-1123

3 **Kohda Y,** Chiao H, Star RA. alpha-Melanocyte-stimulating hormone and acute renal failure. *Curr Opin Nephrol Hypertens* 1998; **7:** 413-417

4 **Oskarsson HJ,** Coppey L, Weiss RM, Li WG. Antioxidants attenuate myocyte apoptosis in the remote non-infarcted myocardium following large myocardial infarction. *Cardiovasc Res* 2000; **45:** 679-687

5 **Schierle GS,** Hansson O, Leist M, Nicotera P, Widner H, Brundin P. Caspase inhibition reduces apoptosis and increases survival of nigral transplants. *Nat Med* 1999; **5:** 97-100

6 **Daemen MA,** de Vries B, Buurman WA. Apoptosis and inflammation in renal reperfusion injury. *Transplantation* 2002; **73:** 1693-1700

7 **Kelly KJ,** Plotkin Z, Vulgamott SL, Dagher PC. P53 mediates the apoptotic response to GTP depletion after renal ischemia-reperfusion: protective role of a p53 inhibitor. *J Am Soc Nephrol* 2003; **14:** 128-138

8 **Shirangi TR,** Zaika A, Moll UM. Nuclear degradation of p53 occurs during down-regulation of the p53 response after DNA damage. *FASEB J* 2002; **16:** 420-442

9 **Chen W,** Fu X, Sun TZ, Sun XQ, Zhao ZL, Sheng ZY. Different expression of p53 and c-myc in hypertrophic scars versus normal skins and their effects on apoptosis in scars. *Zhongguo Wei Zhong Bing Ji Jiu Yi Xue* 2002; **14:** 100-103

10 **Chen W,** Fu X, Sun TZ, Sun XQ, Zhao ZL, Sheng ZY. Characteristics of proliferating cell nuclear antigen and p53 expression in fetal and postnatal skins and their biological significance. *Zhongguo Wei Zhong Bing Ji Jiu Yi Xue* 2002; **14:** 654-657

11 **Ryan KM,** Ernst MK, Rice NR, Vousden KH. Role of NF-kappaB in p53-mediated programmed cell death. *Nature* 2000; **404:** 892-897

12 **Corbucci GG,** Perrino C, Donato G, Ricchi A, Lettieri B, Troncone G, Indolfi C, Chiariello M, Avvedimento EV. Transient and reversible deoxyribonucleic acid damage in human left ventricle under controlled ischemia and reperfusion. *J Am Coll Cardiol* 2004; **43:** 1992-1999

13 **Laubriet A,** Fantini E, Assem M, Cordelet C, Teyssier JR, Athias P, Rochette L. Changes in HSP70 and P53 expression are related to the pattern of electromechanical alterations in rat cardiomyocytes during simulated ischemia. *Mol Cell Biochem* 2001; **220:** 77-86

14 **Didenko VV,** Wang X, Yang L, Hornsby PJ. Expression of p21(WAF1/CIP1/SDI1) and p53 in apoptotic cells in the adrenal cortex and induction by ischemia/reperfusion injury. *J Clin Invest* 1996; **97:** 1723-1731

15 **Cuevas P,** Carceller F, Martinez-Coso V, Asin-Cardiel E, Gimenez-Gallego G. Fibroblast growth factor cardioprotection against ischemia-reperfusion injury may involve K+ ATP channels. *Eur J Med Res* 2000; **5:** 145-149

16 **Cuevas P,** Carceller F, Martinez-Coso V, Cuevas B, Fernandez-Ayerdi A, Reimers D, Asin-Cardiel E, Gimenez-Gallego G. Cardioprotection from ischemia by fibroblast growth factor: role of inducible nitric oxide synthase. *Eur J Med Res* 1999; **4:** 517-524

17 **Chen W,** Fu XB, Ge SL, Zhou G, Han B, Sun TZ, Sheng ZY. Gene expression of angiogenesis-related factors in fetal skin at

different developmental stages and childhood skin. *Zhongguo Wei Zhong Bing Ji Jiu Yi Xue* 2004; **16:** 85-89
18 **Cuevas P,** Martinez-Coso V, Fu X, Orte L, Reimers D, Gimenez-Gallego G, Forssmann WG, Saenz De Tejada I. Fibroblast growth factor protects the kidney against ischemia-reperfusion injury. *Eur J Med Res* 1999; **4:** 403-410
19 **Weng LX,** Fu XB, Li XX, Sun TZ, Zheng SY, Chen W. Effects of acidi fibroblast growth factor on hepatic and renal functions after intestinal ischemia/reperfusion injury. *Zhongguo Wei Zhong Bing Ji Jiu Yi Xue* 2004; **16:** 19-21
20 **Fu X,** Cuevas P, Gimenez-Gallego G, Wang Y, Sheng Z. The effects of fibroblast growth factors on ischemic kidney, liver and gut injuries. *Chin Med J (Engl)* 1998; **111:** 398-403
21 **Itoh H,** Yagi M, Hasebe K, Fushida S, Tani T, Hashimoto T, Shimizu K, Miwa K. Regeneration of small intestinal mucosa after acute ischemia-reperfusion injury. *Dig Dis Sci* 2002; **47:** 2704-2710
22 **Itoh H,** Yagi M, Fushida S, Tani T, Hashimoto T, Shimizu K, Miwa K. Activation of immediate early gene, c-fos, and c-jun in the rat small intestine after ischemia/reperfusion. *Transplantation* 2000; **69:** 598-604
23 **Chang TH,** Liu XY, Zhang XH, Wang HL. Effects of dl-praeruptorin A on interleukin-6 level and Fas, bax, bcl-2 protein expression in ischemia-reperfusion myocardium. *Acta Pharmacol Sin* 2002; **23:** 769-774
24 **Zhou H,** Ma Y, Zhou Y, Liu Z, Wang K, Chen G. Effects of magnesium sulfate on neuron apoptosis and expression of caspase-3, bax and bcl-2 after cerebral ischemia-reperfusion injury. *Chin Med J (Engl)* 2003; **116:** 1532-1534
25 **Wang Y,** Hayashi T, Chang CF, Chiang YH, Tsao LI, Su TP, Borlongan C, Lin SZ. Methamphetamine potentiates ischemia/reperfusion insults after transient middle cerebral artery ligation. *Stroke* 2001; **32:** 775-782
26 **Hatoko M,** Tanaka A, Kuwahara M, Yurugi S, Iioka H, Niitsuma K. Difference of molecular response to ischemia-reperfusion of rat skeletal muscle as a function of ischemic time: study of the expression of p53, p21(WAF-1), Bax protein, and apoptosis. *Ann Plast Surg* 2002; **48:** 68-74
27 **Hatoko M,** Tanaka A, Kuwahara M, Yurugi S. Molecular response to ischemia-reperfusion of rat skin: study of expression of p53, p21WAF-1, and Bax proteins, and apoptosis. *Ann Plast Surg* 2001; **47:** 425-430
28 **Baskin DS,** Ngo H, Didenko VV. Thimerosal induces DNA breaks, caspase-3 activation, membrane damage, and cell death in cultured human neurons and fibroblasts. *Toxicol Sci* 2003; **74:** 361-368
29 **Kerrigan CL,** Stotland MA. Ischemia reperfusion injury: a review. *Microsurgery* 1993; **14:** 165-175

Science Editor Wang XL, Li WZ and Guo SY **Language Editor** Elsevier HK

PO Box 2345, Beijing 100023, China
www.wjgnet.com
wjg@wjgnet.com

ELSEVIER

World J Gastroenterol 2005;11(44):6988-6994
World Journal of Gastroenterology ISSN 1007-9327

• *CLINICAL RESEARCH* •

Anti-*Saccharomyces cerevisiae* antibody titers are stable over time in Crohn's patients and are not inducible in murine models of colitis

Stefan Müller, Maya Styner, Beatrice Seibold-Schmid, Beatrice Flogerzi, Michael Mähler, Astrid Konrad, Frank Seibold

Stefan Müller, Maya Styner, Beatrice Seibold-Schmid, Beatrice Flogerzi, Astrid Konrad, Frank Seibold, Division of Gastroenterology, Department of Clinical Research, University Hospital Bern
Michael Mähler, Central Animal Facility and Institute for Laboratory Animal Science, Medical School Hannover, Germany
Supported by the Swiss National Science Foundation grant n° SNSF 31-59031.99 to F. Seibold
Co-first-authors: Stefan Müller and Maya Styner
Co-correspondence: Stefan Müller, stefan.mueller@dkf.unibe ch
Correspondence to: Professor Frank Seibold, University Hospital Bern, Department of Gastroenterology, Freiburgstr. 10, 3010 Bern, Switzerland. frank.seibold@insel.ch
Telephone: +41-31-6328025 Fax: +41-31-6323671
Received: 2005-03-11 Accepted: 2005-07-01

Abstract

AIM: To investigate ASCA production over time in CD and murine colitis in order to further our understanding of their etiology.

MATERIALS AND METHODS: Sixty-six CD patients were compared to ulcerative colitis (UC) and irritable bowel syndrome patients with respect to ASCA production as measured by ELISA. ASCA IgG or IgA positivity as well as change in titers over a period of up to 3 years ($\Delta_{IgG/A}$) was correlated with clinical parameters such as CD activity index (CDAI) and C-reactive protein levels (CRP). Moreover, two murine models of colitis (DSS and IL-10 knock out) were compared to control animals with respect to ASCA titers after oral yeast exposure.

RESULTS: ASCA IgG and IgA titers are stable over time in CD and non-CD patients. Fistular disease was associated with a higher rate of ASCA IgA positivity (P = 0.014). Ileal disease was found to have a significant influence on the Δ_{IgG} of ASCA (P = 0.032). There was no correlation found between ASCA positivity or $\Delta_{IgG/A}$ and clinical parameters of CD: CDAI and CRP. In mice, neither healthy animals nor animals with DSS-induced or spontaneous colitis exhibited a marked increase in ASCA titers after high-dose yeast exposure. On the other hand, mice immunized intraperitoneally with mannan plus adjuvant showed a marked and significant increase in ASCA titers compared to adjuvant-only immunized controls (P = 0.014).

CONCLUSION: The propensity to produce ASCA in a subgroup of CD patients is largely genetically predetermined as evidenced by their stability and lack of correlation with clinical disease activity parameters. Furthermore, in animal models of colitis, mere oral exposure of mice to yeast does not lead to the induction of marked ASCA titers irrespective of concomitant colonic inflammation. Hence, environment may play only a minor role in inducing ASCA.

Key words: Crohn's disease; Anti-*Saccharomyces cerevisiae* antibodies; Colitis

Müller S, Styner M, Seibold-Schmid B, Flogerzi B, Mähler M, Konrad A, Seibold F. Anti-*Saccharomyces cerevisiae* antibody titers are stable over time in Crohn's patients and are not inducible in murine models of colitis. *World J Gastroenterol* 2005; 11(44): 6988-6994
http://www.wjgnet.com/1007-9327/11/6988.asp

INTRODUCTION

Much attention has been focused on serologic markers in inflammatory bowel disease (IBD). The anti-*Saccharomyces cerevisiae* antibody (ASCA) is one such marker, which possesses an intermediate sensitivity and a high specificity for Crohn's disease (CD)[1-5]. Antibodies to *S cerevisiae* in CD were first described by Main *et al*.[6], using whole killed yeast cells as antigens. Sendid *et al*.[3] demonstrated greater diagnostic value for CD with *S cerevisiae* Su1, a strain of brewer's yeast, and identified the antigenic oligomannosidic epitopes of this organism. Subsequent work demonstrated that CD patients develop antibodies to a variety of baker's and brewer's yeast strains[4]. The antigen reacting with ASCA is a phosphopeptidomannan, a component of the *S. cerevisiae* cell wall[3].

Aside from the diagnostic role performed by ASCA, uncertainty remains as to whether they possess a pathophysiologic significance. One can argue for a genetic origin due to ASCA presence in 20-25% of unaffected first-degree family members[7-10]. Healthy monozygotic twins of CD patients also demonstrate increased IgA, IgG, and IgM ASCA levels[11]. In one study of non-IBD families,

ASCA were found to be familial with a vertical transmission pattern[12]. ASCA stability over time and independence from disease activity further indicate a genetic link[11,13]. Moreover, we have shown that T cells from ASCA-positive patients proliferated upon stimulation with mannan[14]. We were able to show that mannan binding lectin (MBL) deficient patients were significantly more frequently ASCA-positive and showed an enhanced T cell proliferation upon mannan stimulation compared to MBL wildtype patients[15]. These results further support the importance of genetic determination of ASCA.

Nevertheless, some of the familial studies have yielded conflicting data. For example, one group showed increased ASCA production in familial *vs* sporadic CD[7], but others have shown equal or increased ASCA prevalence for sporadic CD[9,16-18]. Thus, the case for an environmental etiology for ASCA has been articulated as well. For instance, a decline in ASCA levels has been observed post-surgically in a pediatric CD population[5]. Another group demonstrated lower ASCA titers in CD patients taking mesalazine than in CD patients not taking mesalazine[19]. Additionally, both brewing and baking strains of *S cerevisiae* provoke an antibody response in CD, implicating dietary antigens in disease pathogenesis[4]. One group has noted higher ASCA IgG antibody levels in patients with small bowel Crohn's disease *vs* those with colonic disease[18]. This same study found high levels of ASCA IgG but not IgA in celiac disease, indistinguishable from levels seen in CD. It was, thus, concluded that ASCA may result from a mucosal permeability defect. However, Vermeire *et al*.[20] were not able to show a correlation between ASCA and intestinal permeability.

In this study, our aim was to characterize ASCA over time in patients with IBD in order to further our understanding of their etiology. Furthermore, we assessed the possibility to induce an ASCA response in animal models.

MATERIALS AND METHODS

Patients

Sixty-six Crohn's disease (CD) patients, 29 ulcerative colitis (UC) patients, and 10 irritable bowel syndrome (IBS) patients with informed consent were enrolled in the study, and the study was approved by the ethical committee of the local authorities. Patient serum samples were drawn during routine outpatient visits (Gastroenterology clinic, University Hospital, Bern, Switzerland) for ASCA IgG and IgA analysis. Diagnosis of CD and UC was established by endoscopic, histological, and clinical criteria. Diagnosis of IBS was established by the Rome criteria[21].

A subgroup of CD (73 sera from 29 patients), UC (26 sera from 12 patients) and IBS (22 sera from 10 patients) patients, whose serum samples were drawn on at least 2 consecutive (maximally 4 consecutive) routine out-patient visits, were retrospectively selected for ASCA IgG and IgA titer analysis. An assessment of the Crohn's disease activity index (CDAI) was obtained at each CD patient's visit to the clinic[22]. The serum CRP levels were obtained at each clinic visit as well. Three patients with stoma were excluded from the CDAI analysis. One patient was excluded from the clinical analysis, since this patient's CDAI and CRP could not be obtained.

Mice

Four to six-weeks-old female interleukin-10 knockout mice (*Il10*^{tm1Cgn}; henceforth abbreviated as IL-10$^{0/0}$) on a C3H/HeJBir background were obtained from the University of Bern breeding facility (Bern, Switzerland) and housed under specified pathogen-free conditions. Four to six-week-old BALB/c mice were obtained from Harlan (Horst, The Netherlands). All procedures involving animals were performed in compliance with the local authorities on the use of animals in research.

ASCA ELISA for mouse and human sera

Investigators were blinded to disease status when performing the ELISA. Phosphopeptidomannans from baker's yeast (Hefe Vital Gold, Deutsche Hefewerke, Nürnberg, Germany) were extracted as previously described[8,23]. Ninety-six well ELISA plates (MaxiSorb, Nunc, Wiesbaden, Germany) were coated with 100 μL of 0.25 μg/mL phosphopeptidomannans in carbonate-bicarbonate buffer, pH 9.6 and incubated overnight at 4 °C. Serum diluted 1/1 000 was applied to the coated plates in triplicates. The plates were incubated for 1 h at 37 °C. Secondary antibody was added and plates were incubated for 1 h at RT. The secondary antibodies (Sigma, Buchs Switzerland) were as follows: goat anti-mouse polyvalent immunoglobulin peroxidase conjugate at 1/1 000; goat anti-human IgA (alpha-chain specific) peroxidase conjugate; and goat anti-human IgG (Fc specific) peroxidase conjugate, both at 1/5 000. The plates were developed using TMB substrate (Sigma) and the reaction was stopped with sulfuric acid. The absorbance at 450 nm (reference filter = 490 nm) was read by an EL 800 microplate reader (Bio-Tek Instruments, Winooski, Vermont). The mean absorbance value for the healthy control sera plus two standard deviations was used to discriminate between positive and negative subjects. Absorbance units equal to or above this value were considered positive for ASCA antibodies. A patient was considered ASCA$^+$, when positive for ASCA IgG, IgA or both.

For the human ELISA, one serum highly positive for ASCA was used to obtain a standard curve at dilutions ranging from 1/100 to 1/102 400. The curve was fitted using a four parameter logistic function to the logarithmically scaled dilutions. Human titers are expressed as dilution units from this curve. We computed the average change of IgG and IgA ($\Delta_{IgG/A}$) in human ASCA titer as our main variable of interest. An increase of $\Delta_{IgG/A}$ represents a decrease in ASCA levels and vice versa. Of the CD patients, two patient's IgG titer and one patient's IgA titer could not be reliably calculated from the standard curve after two repeated assays and thus were excluded from the IgG/A titer analysis. The murine ASCA titers are expressed as optical density (OD).

Preparation of yeast solution

Baker's yeast (Hefe Vital Gold, Deutsche Hefewerke, Nürnberg, Germany) was freshly grown in YPD broth

(Becton Dickinson, Le Pont de Claix, France) for 12 h at 30 ºC in a shaker at 200 r/min. The yeast solution was centrifuged at 2 000 r/min for 5 min. The cellular pellet was washed twice, resuspended in sterilized water and sonicated at 100 W for 2 min. Protein concentration was determined using the Bradford reagent (Sigma, Buchs, Switzerland).

Induction of chronic dextran sulfate sodium-induced (DSS) colitis, oral yeast administration and histological assessment

The previously described model of chronic DSS colitis was adapted from Mähler *et al*.[24]. Briefly, Balb/c mice were given three 5-day cycles of 3% DSS (DSS salt, MW= 36 000-50 000, ICN Biomedicals, Inc., Ohio), each interrupted by the 7th d without DSS. All mice received yeast *ad libitum* at a protein concentration of 100 or 500 μg/mL for the entire experiment. Murine serum samples were drawn on d 0 and the day of killing (d 36) for ASCA immunoglobulin analysis.

Mice were euthanized via CO_2 asphyxiation. Colons were harvested, fixed in 4% phosphate-buffered formaldehyde, embedded *in toto* and H&E-stained sections were examined by a pathologist (Mähler) blinded to the code. The sections were scored on a previously described[24] scale ranging from 0 (no inflammation) to 4 (severe inflammation). A total colonic inflammation score was obtained by averaging the individual scores of the proximal, middle, and distal colon.

Immunizations

Balb/c mice from our central animal facility were intraperitoneally injected with 50 μg phosphopeptidomannans or ovalbumin (Sigma, Gaithersburg, MD) mixed 1:1 (v/v) with GERBU adjuvant (GERBU, Gaiberg, Germany). Injection was repeated after two weeks and mice were killed for analysis one week later. Serum samples were obtained before primary immunization by tail tip bleeding and after euthanization by puncture of the caval vein.

Statistical analysis

We analyzed the CD population in regard to ASCA IgG and IgA positivity to test for a significant influence of the following patient variables: age, gender, anatomical location of disease, medication, fistulae, and extra-intestinal manifestations. Significance of each variable was computed via unpaired, two-tailed Student's *t*-test assuming equal variances if the additional *F*-test was non-significant. We analyzed the titer subgroup in respect to ASCA IgG and ASCA IgA positivity to test for a significant influence of the above-mentioned variables and additionally CD activity index (CDAI) and C-reactive protein (CRP) levels.

In order to qualitatively assess the amplitude and distribution of IgG and IgA, the respective $\Delta_{IgG/A}$ histograms for the CD, UC, and IBS titer subgroups were computed. The quantitative assessment is shown via the mean, SD and 95% confidence interval of each $\Delta_{IgG/A}$ distribution and via unpaired, two-tailed Student's *t*-tests. We also employed Student's *t*-tests for testing $\Delta_{IgG/A}$ differences with regard to gender, anatomical location of disease, fistulae, extra-intestinal manifestations, and medication. To assess the differences between the three patient groups with regard to IgG and IgA $\Delta_{IgG/A}$, we applied the one-way ANOVA test. The correlation coefficients between $\Delta_{IgG/A}$ and the two clinical parameters, change in CDAI (Δ_{CDAI}) and change in CRP (Δ_{CRP}), were also computed.

The differences between the mice groups on day 36 were statistically assessed using the unpaired, two-tailed Student's *t*-test. Significance level for all tests was 0.05.

RESULTS

ASCA positivity in the study population

Thirty-five of sixty-six CD patients, 4 of 29 UC patients and 3 of 10 IBS patients were ASCA positive. The sensitivity, specificity, and positive predictive value of the ASCA assay in distinguishing CD from UC are 53%, 86%, and 90%, respectively.

Fistular disease is associated with higher rate of ASCA IgA positivity

The baseline clinical characteristics of the patients and controls can be seen in Table 1. None of the following clinical characteristics had a significant effect on ASCA IgG and IgA positivity in the Crohn's disease patients: age, gender, anatomical locations of disease, medication, and extra-intestinal manifestations. Patients with fistular disease were significantly more likely to possess ASCA IgA positivity (P = 0.014, 71% *vs* 32%) than patients with non-fistular disease.

ASCA IgG and IgA titers are stable over time in CD and non-CD patients

ASCA IgG and IgA titers in the CD subgroup, expressed as logarithmically (ln) scaled dilutions of a high positive control, have been plotted over a time-period of up to 3 years (Figure 1). The change in titers did not vary significantly as can be seen in the Gaussian distribution in the histogram, which is centered close to zero for all patient groups with respect to both IgG and IgA titers (Figure 2). The means, standard deviations and 95% confidence intervals of $\Delta_{IgG/A}$ are shown in Table 2 and indicate stable titers over time. Nevertheless, the patient groups are significantly different in regard to Δ_{IgA} values (P<0.05, ANOVA), specifically between CD and UC patients (P<0.05, ANOVA *post hoc*). This suggests that patients with UC were more likely to experience a decrease in IgA ASCA levels over time than patients with CD. The patient groups are not significantly different with regard to Δ_{IgG} values.

Anatomic location of disease significantly influences the Δ_{IgG} of ASCA

Of the clinical parameters assessed upon entry, ileal disease was found to have a significant influence on the Δ_{IgG} of ASCA (Table 3). The mean Δ_{IgG} value for patients with ileal disease *vs* those without ileal disease was 0.13 and -0.34, respectively. This suggests that patients without ileal

Table 1 Baseline characteristics of the study populations tested for anti-*Saccharomyces cerevisiae* IgG and IgA antibodies. Unless otherwise indicated values are numbers of patients (%)

Study population	Crohn's disease (n = 66)	Ulcerative colitis (n = 29)	Healthy controls (n = 18)	IBS patients (n = 10)
Age, yr				
Mean±SD	38±16	37±15	40±13	57±13
Range	14-82	16-78	17-74	41-81
Male sex	32 (48)	15 (52)	10 (56)	6 (60)
Disease location				
Colonic	58 (88)	29 (100)		
Ileal	45 (68)			
Upper gastrointestinal involvement	3 (5)			
Presence of fistulae	15 (23)	1 (3)		
Extraintestinal manifestations	4 (6)	0 (0)		
Medical therapy				
Azathioprine	22 (33)	9 (31)		
Infliximab	5 (8)	3 (10)		
5-ASA compounds	4 (6)	11 (38)		
Methotrexate	4 (6)	0 (0)		
Oral steroids	29 (44)	15 (52)		
None of the above	19 (29)	7 (24)		

Table 2 Mean, standard deviation (SD) and the 95% confidence interval of the mean of the change in ASCA IgG and IgA titers

	Δ_{IgG}			Δ_{IgA}		
	Mean	SD	95%CI	Mean	SD	95%CI
CD	0.01	0.56	(-0.20, 0.22)	-0.04	0.25	(-0.13, 0.05)
UC	0.05	0.15	(-0.03, 0.14)	0.16	0.24	(0.02, 0.29)
IBS	0.05	0.08	(-0.003, 0.09)	-0.01	0.12	(-0.08, 0.06)

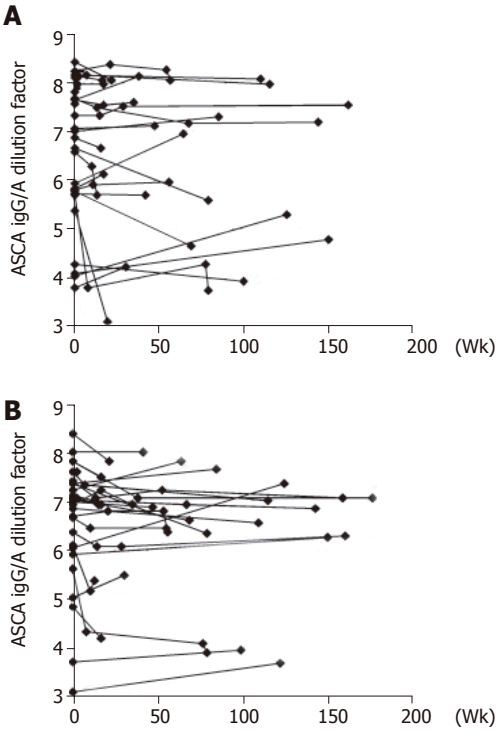

Figure 1 Anti-*Saccharomyces cerevisiae* (**A**) IgG and (**B**) IgA antibody titers in ASCA-positive patients with Crohn's disease expressed as a logarithmically (ln) scaled dilution unit of a highly positive control over a time-period of up to 3 years.

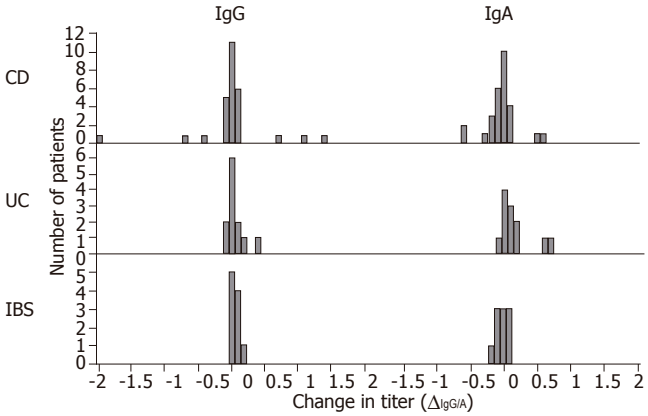

Figure 2 Histogram of change in ASCA IgA and IgG titers (ΔIgG/A) in patients with Crohn's disease (CD), ulcerative colitis (UC) and irritable bowel syndrome (IBS). CD patients demonstrate higher variability as compared to UC and IBS.

disease were more likely to experience an increase in ASCA level as opposed to patients with ileal disease. All other tested clinical parameters did not significantly influence the $\Delta_{IgG/A}$ of ASCA. Regarding the clinical parameters of disease, no strong corre=lation was found between the Δ_{CDAI} and Δ_{IgG} (c = -0.086) and Δ_{IgA} (c = -0.127). Moreover, no strong correlation was found between the Δ_{CRP} and Δ_{IgG} (c = 0.424) and Δ_{IgA} (c = -0.245).

Anti-S cerevisiae antibodies are not efficiently induced upon oral yeast administration, irrespective of concomitant induction of colitis in Balb/c or IL-10$^{0/0}$ mice

All mice given yeast lysate and unfed controls exhibited slightly increased ASCA titers at the end of the experimental period compared with values obtained at the beginning of the experiment. A slight increase in ASCA titers was observed in mice exposed to 500 μg/mL yeast lysate in their drinking water when compared with mice exposed to 100 μg/mL (Figure 3A). Concomitant DSS-

Table 3 Effect of the CD clinical characteristics on the following parameters: ASCA IgG and IgA positivity and change in IgG and IgA ASCA titers. Results are expressed as *P*-values of the mean-difference tests or as correlation coefficients (*c*)

Clinical characteristics	ASCA IgG	ASCA IgA	ΔIgG	ΔIgA
Correlation with age	*c* = –0.140	*c* = 0.198	*c* = –0.340	*c* = –0.197
Male *vs* female	0.881	0.881	0.089	0.571
Disease Location				
Colonic *vs* non-colonic	0.667	0.169	0.203	0.289
Ileal *vs* non-ileal	0.285	0.285	0.032[a]	0.395
Fistular *vs* Non-fistular disease	0.152	0.075	0.499	0.907
Medical therapy				
Azathioprine	0.881	0.881	0.749	0.375
Infliximab	0.233	0.233	0.870	0.844
5-ASA compounds	0.806	0.233	0.903	0.491
Oral steroids	0.512	0.385	0.475	0.531
None of the above medical therapy *vs* medical therapy	0.285	0.577	0.438	0.117

[a]*P*<0.05.

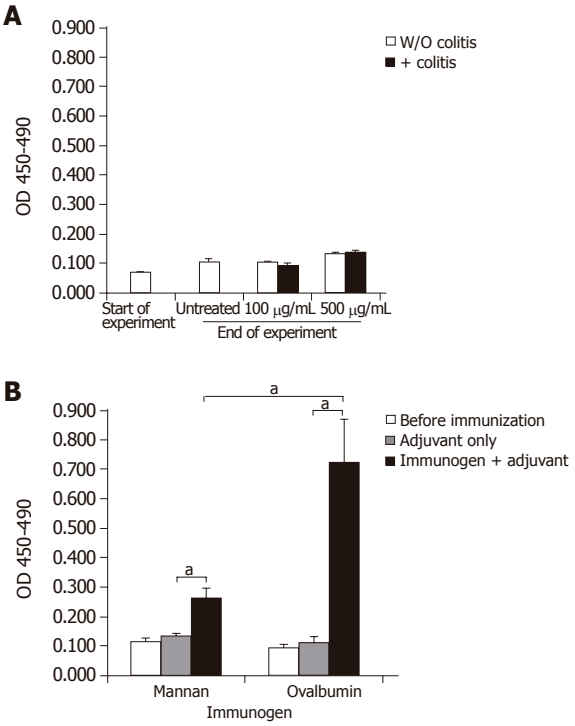

Figure 3 OD at 450 nm representing relative levels of polyclonal anti-*Saccharomyces cerevisiae* antibody (ASCA) (**A**) in control Balb/c mice (empty columns) or mice with DSS-induced experimental colitis (shaded columns). Basal ASCA titers were determined at the start of the experiment. During the experiment, mice received water containing 100 μg/mL or 500 μg/mL yeast solution *ad libitum*. (**B**) Balb/c mice were immunized with water or 50μg yeast mannan or ovalbumin mixed 1:1 (v:v) in GERBU adjuvant. After 2 wk, mice received a booster injection and ASCA or anti ovalbumin antibodies were determined 7 d later. [a]*P*<0.05.

treatment (Figure 3A) or onset of colitis in IL-10$^{0/0}$ mice (data not shown) did not lead to a further increase in ASCA titers. Development of colitis was evidenced by the observation of clinical signs such as soft stools and in some cases anal ulcerations and bloody stools. The average histological score±SD was as follows: 1.056±0.25 for the DSS-treated Balb/c group, 0±0 for the non-DSS-treated Balb/c group, and 1.5±0.19 for the IL-10$^{0/0}$ group.

ASCA titers are induced in mice after immunization with yeast mannan

Groups of Balb/c mice were immunized with adjuvant alone, or with adjuvant plus yeast mannan or, as a positive control, ovalbumin (Figure 3B). Mannan-immunized mice showed an average two-fold increase in ASCA titers when compared with mice receiving adjuvant only (P = 0.014). Mannan was poorly immunogenic compared to ovalbumin (P = 0.038) since specific serum antibody titers after ovalbumin plus adjuvant-immunization increased about seven-fold over adjuvant-only injected controls (P = 0.015).

DISCUSSION

Antibodies to the *S cerevisiae* cell wall mannans have been widely studied as a diagnostic tool to distinguish CD from UC. In this study, the rates of CD patient ASCA positivity correlate well with our previous results[8] as well as those cited in the literature[7,10,13]. Of all the clinical variables tested, fistular Crohn's disease was found to be associated with ASCA IgA positivity. This study is not the first to demonstrate such an association. Others have shown that the subgroup of CD patients with high levels of IgG and IgA ASCA has more aggressive, small-bowel fistulizing disease[25].

Our study was the first to assess time-period streamlined ASCA titers. We found no association between the change in ASCA titers and the following clinical characteristics: age, gender, presence of fistulae, medical therapy, CDAI or CRP levels. Of the clinical parameters tested, patients without ileal disease were more likely to encounter an increase in their ASCA titers over time as compared with CD patients with ileal disease. There is no good explanation why anatomic location of CD should provoke an increase or decrease in ASCA titers. It should be noted that Giaffer *et al.* noted increased ASCA IgG positivity association with small bowel disease as compared to

colonic disease[18]. Nevertheless, this study does not explain why these patient's titers were more likely to change over time. Also of special interest is the lack of association between Δ_{CDAI} and $\Delta_{IgG/A}$ and Δ_{CRP} and $\Delta_{IgG/A}$. ASCA stability over time in relation to the changes in CDAI was demonstrated by Landers *et al*.[13], utilizing a time period of at least 4 mo. Recently, Teml *et al*. established ASCA stability during a course of steroid or 5-ASA therapy[26]. Our data further strengthen this stability and lack of association with CDAI or medical therapy with the addition of CRP as a serologic marker of disease. This lack of association with clinical activity leads others and us away from thinking of ASCA as a subclinical marker of disease activity as it does not follow CD clinical status variations.

In line with the results obtained with human sera, the murine ASCA titers were rather stable, at least during the time of the experimental procedure (36 d). This is the first study to investigate murine ASCA production in the setting of DSS and IL-$10^{0/0}$ colitis. After oral treatment with a high antigen dose (500 μg/mL), we observed a slight increase of ASCA titers compared to untreated controls or mice treated with 100 μg/mL. Interestingly, we observed slightly lower ASCA titers in young untreated mice compared to untreated mice at the end of the experiment. It is very likely that ASCA titers in mice may slightly vary between the breeder company and our animal facility as a consequence of differential exposure to yeast-antigens depending on the hygiene status of the animal facility and/or the composition of food pellets. We did not, however, observe a further increase upon induction of colitis. Therefore, the impairment of mucosal barrier during inflammation and/or the enhanced presence of immune competent cells alone does not lead to markedly enhanced ASCA generation.

In contrast, systemic immunization of mice with phosphopeptidomannans in the context of appropriate adjuvant leads to a significant increase in ASCA titers. However, the increase of ASCA titers is much less pronounced than that of anti-ovalbumin antibodies after ovalbumin immunization. Thus, these data show that mannans are not very efficient antigens when used for immunization, further indicating that normally mice and human beings are tolerant to mannans. Local inflammation during colitis is not sufficient to break this tolerance. In our recent study we were able to show that ASCA positivity was associated with MBL deficiency[15]. Furthermore, family studies show an increased incidence of ASCA in healthy family members[7,8,20]. Thus, generation of ASCA in a subgroup of CD patients and healthy family members may be mainly a result of a genetic predisposition, although biochemical and genetic analyses supporting this notion are not currently available.

In conclusion, we have demonstrated the stability of the ASCA titers over time and their lack of association with clinical activity in the form of CDAI and CRP. These findings are in line with the observation that ASCA are only marginally inducible in mice via high dose oral exposure, and are not further influenced by concomitant induction of colitis. Hence, we speculate that the propensity to produce ASCA in a subgroup of CD patients is largely genetically predetermined and, thus, may reflect a predisposition of distinct genetic backgrounds to establish immune responses against normally tolerated antigens.

ACKNOWLEDGMENTS

We are grateful to Dr A Sergew and Dr M Weber for their editorial assistance. Dr MA Styner is acknowledged for insightful discussions regarding statistical analysis.

REFERENCES

1 **Quinton JF**, Sendid B, Reumaux D, Duthilleul P, Cortot A, Grandbastien B, Charrier G, Targan SR, Colombel JF, Poulain D. Anti-Saccharomyces cerevisiae mannan antibodies combined with antineutrophil cytoplasmic autoantibodies in inflammatory bowel disease: prevalence and diagnostic role. *Gut* 1998; **42**: 788-791

2 **Sandborn WJ**, Loftus EV Jr, Colombel JF, Fleming KA, Seibold F, Homburger HA, Sendid B, Chapman RW, Tremaine WJ, Kaul DK, Wallace J, Harmsen WS, Zinsmeister AR, Targan SR. Evaluation of serologic disease markers in a population-based cohort of patients with ulcerative colitis and Crohn's disease. *Inflamm Bowel Dis* 2001; **7**: 192-201

3 **Sendid B**, Colombel JF, Jacquinot PM, Faille C, Fruit J, Cortot A, Lucidarme D, Camus D, Poulain D. Specific antibody response to oligomannosidic epitopes in Crohn's disease. *Clin Diagn Lab Immunol* 1996; **3**: 219-226

4 **McKenzie H**, Main J, Pennington CR, Parratt D. Antibody to selected strains of Saccharomyces cerevisiae (baker's and brewer's yeast) and Candida albicans in Crohn's disease. *Gut* 1990; **31**: 536-538

5 **Ruemmele FM**, Targan SR, Levy G, Dubinsky M, Braun J, Seidman EG. Diagnostic accuracy of serological assays in pediatric inflammatory bowel disease. *Gastroenterology* 1998; **115**: 822-829

6 Main **J**, McKenzie H, Yeaman GR, Kerr MA, Robson D, Pennington CR, Parratt D. Antibody to Saccharomyces cerevisiae (bakers' yeast) in Crohn's disease. *BMJ* 1988; **297**: 1105-1106

7 **Annese V**, Andreoli A, Andriulli A, Dinca R, Gionchetti P, Latiano A, Lombardi G, Piepoli A, Poulain D, Sendid B, Colombel JF. Familial expression of anti-Saccharomyces cerevisiae Mannan antibodies in Crohn's disease and ulcerative colitis: a GISC study. *Am J Gastroenterol* 2001; **96**: 2407-2412

8 **Seibold F**, Stich O, Hufnagl R, Kamil S, Scheurlen M. Anti-Saccharomyces cerevisiae antibodies in inflammatory bowel disease: a family study. *Scand J Gastroenterol* 2001; **36**: 196-201

9 **Sendid B**, Quinton JF, Charrier G, Goulet O, Cortot A, Grandbastien B, Poulain D, Colombel JF. Anti-Saccharomyces cerevisiae mannan antibodies in familial Crohn's disease. *Am J Gastroenterol* 1998; **93**: 1306-1310

10 **Sutton CL**, Yang H, Li Z, Rotter JI, Targan SR, Braun J. Familial expression of anti-Saccharomyces cerevisiae mannan antibodies in affected and unaffected relatives of patients with Crohn's disease. *Gut* 2000; **46**: 58-63

11 **Lindberg E**, Magnusson KE, Tysk C, Jarnerot G. Antibody (IgG, IgA, and IgM) to baker's yeast (Saccharomyces cerevisiae), yeast mannan, gliadin, ovalbumin and betalactoglobulin in monozygotic twins with inflammatory bowel disease. *Gut* 1992; **33**: 909-913

12 **Poulain D**, Sendid B, Fajardy I, Danze PM, Colombel JF. Mother to child transmission of anti-S cerevisiae mannan antibodies (ASCA) in non-IBD families. *Gut* 2000; **47**: 870-871

13 **Landers CJ**, Cohavy O, Misra R, Yang H, Lin YC, Braun J, Targan SR. Selected loss of tolerance evidenced by Crohn's disease-associated immune responses to auto- and microbial antigens. *Gastroenterology* 2002; **123**: 689-699

14 **Konrad A**, Rutten C, Flogerzi B, Styner M, Goke B, Seibold F. Immune sensitization to yeast antigens in ASCA-positive patients with Crohn's disease. *Inflamm Bowel Dis* 2004; **10**: 97-105

15 **Seibold F**, Konrad A, Flogerzi B, Seibold-Schmid B, Arni S, Juliger S, Kun JF. Genetic variants of the mannan-binding lectin are associated with immune reactivity to mannans in Crohn's disease. *Gastroenterology* 2004; **127**: 1076-1084

16 **Halme L**, Turunen U, Helio T, Paavola P, Walle T, Miettinen A, Jarvinen H, Kontula K, Farkkila M. Familial and sporadic inflammatory bowel disease: comparison of clinical features and serological markers in a genetically homogeneous population. *Scand J Gastroenterol* 2002; **37**: 692-698

17 **Barnes RM**, Allan S, Taylor-Robinson CH, Finn R, Johnson PM. Serum antibodies reactive with Saccharomyces cerevisiae in inflammatory bowel disease: is IgA antibody a marker for Crohn's disease? *Int Arch Allergy Appl Immunol* 1990; **92**: 9-15

18 **Giaffer MH**, Clark A, Holdsworth CD. Antibodies to Saccharomyces cerevisiae in patients with Crohn's disease and their possible pathogenic importance. *Gut* 1992; **33**: 1071-1075

19 **Oshitani N**, Hato F, Matsumoto T, Jinno Y, Sawa Y, Hara J, Nakamura S, Seki S, Arakawa T, Kitano A, Kitagawa S, Kuroki T. Decreased anti-Saccharomyces cerevisiae antibody titer by mesalazine in patients with Crohn's disease. *J Gastroenterol Hepatol* 2000; **15**: 1400-1403

20 **Vermeire S**, Peeters M, Vlietinck R, Joossens S, Den Hond E, Bulteel V, Bossuyt X, Geypens B, Rutgeerts P. Anti-Saccharomyces cerevisiae antibodies (ASCA), phenotypes of IBD, and intestinal permeability: a study in IBD families. *Inflamm Bowel Dis* 2001; **7**: 8-15

21 **Thompson WG**. The road to Rome. i1999; **45** Suppl 2: II80

22 **Best WR**, Becktel JM, Singleton JW, Kern F Jr. Development of a Crohn's disease activity index. National Cooperative Crohn's Disease Study. *Gastroenterology* 1976; **70**: 439-444

23 **Kocourek J**, Ballou CE. Method for fingerprinting yeast cell wall mannans. *J Bacteriol* 1969; **100**: 1175-1181

24 **Mähler M**, Bristol IJ, Leiter EH, Workman AE, Birkenmeier EH, Elson CO, Sundberg JP. Differential susceptibility of inbred mouse strains to dextran sulfate sodium-induced colitis. *Am J Physiol* 1998; **274**: G544- G551

25 **Vasiliauskas EA**, Plevy SE, Landers CJ, Binder SW, Ferguson DM, Yang H, Rotter JI, Vidrich A, Targan SR. Perinuclear antineutrophil cytoplasmic antibodies in patients with Crohn's disease define a clinical subgroup. *Gastroenterology* 1996; **110**: 1810-1819

26 **Teml A**, Kratzer V, Schneider B, Lochs H, Norman GL, Gangl A, Vogelsang H, Reinisch W. Anti-Saccharomyces cerevisiae antibodies: a stable marker for Crohn's disease during steroid and 5-aminosalicylic acid treatment. *Am J Gastroenterol* 2003; **98**: 2226-2231

Science Editor Guo SY **Language Editor** Elsevier HK

PO Box 2345, Beijing 100023, China
www.wjgnet.com
wjg@wjgnet.com

ELSEVIER

World J Gastroenterol 2005;11(44):6995-7000
World Journal of Gastroenterology ISSN 1007-9327

• *CLINICAL RESEARCH* •

Computer-aided morphometry of liver inflammation in needle biopsies

N Dioguardi, B Franceschini, C Russo, F Grizzi

N Dioguardi, B Franceschini, C Russo, F Grizzi, Scientific Direction, Istituto Clinico Humanitas, Rozzano, Milan, Italy and "Michele Rodriguez" Foundation, Institute for Quantitative Measures in Medicine, Milan, Italy
Supported by the "Michele Rodriguez" Foundation, Institute for Quantitative Measures in Medicine, Milan, Italy
Correspondence to: Nicola Dioguardi, MD, Scientific Direction, Istituto Clinico Humanitas, Via Manzoni 56, 20089 Rozzano MI, Italy. nicola.dioguardi@humanitas.it
Telephone: +39-02-82244501 Fax: +39-02-82244590
Received: 2005-03-24 Accepted: 2005-04-18

Abstract

AIM: To introduce a computer-aided morphometric method for quantifying the necro-inflammatory phase in liver biopsy specimens using fractal geometry and Delaunay's triangulation.

METHODS: Two-micrometer thick biopsy sections taken from 78 chronic hepatitis C virus-infected patients were immunohistochemically treated to identify the inflammatory cells. An automatic computer-aided image analysis system was used to define the inflammatory cell network defined on the basis of Delaunay's triangulation, and the inflammatory cells were geometrically classified as forming a cluster (an aggregation of a minimum of three cells) or as being irregularly distributed within the tissue. The phase of inflammatory activity was estimated using Hurst's exponent.

RESULTS: The proposed automatic method was rapid and objective. It could not only provide rigorous results expressed by scalar numbers, but also allow the state of the whole organ to be represented by Hurst's exponent with an error of no more than 12%.

CONCLUSION: The availability of rigorous metrical measures and the reasonable representativeness of the status of the organ as a whole raise the question as to whether the indication for hepatic biopsy should be revised by establishing clear rules concerning the contraindications suggested by its invasiveness and subjective interpretation.

Key words: Biopsy; Grading; Image analysis; Fractal geometry; Topography; Delaunay

Dioguardi N, Franceschini B, Russo C, Grizzi F. Computer-aided morphometry of liver inflammation in needle biopsies. *World J Gastroenterol* 2005; 11(44): 6995-7000
http://www.wjgnet.com/1007-9327/11/6995.asp

INTRODUCTION

The antiviral treatment of chronic hepatitis C is expensive, efficacious in only 50% of cases, and has sometimes major undesired effects. The criteria for selecting the patients to treat are therefore a central problem and its solution is sought by evaluating the inflammatory lesions (grading) and fibrosis (staging) histologically observed in bioptic specimens.

A single bioptic sample is still the most effective means of obtaining the greatest amount of information for formulating a diagnosis of chronic hepatitis, excluding other diseases, hypothesizing the prognosis, and defining therapeutic indications[1-4]. However, taking a bioptic sample is expensive, carries a certain risk, and the results are not reliable insofar as they do not express real measures, but only semi-quantitative categories of severity, and its evaluation entirely depends on the subjective skill and experience of the pathologist[5-9]. It therefore follows that such semi-quantitative data cannot be used for statistical purposes[10,11].

The recently proposed alternative methods of estimating hepatic tissue inflammation by measuring the blood levels of molecules associated with the evolution of liver inflammation (including the extremely and widely used measurement of transaminase levels) have not shown any sure correspondence with actual tissue status[12-16].

It is therefore necessary to develop more rigorous and objective morphometric methods capable of providing scalars for the metrical quantification of inflammation structures within a liver biopsy sample. We have herein described the first results of our metrical measurements of the *fractal spaces* covered by necro-inflammatory lesions observed in the biopsies of consecutive chronic hepatitis C patients, and obtained by means of a totally computerized analysis that excludes any subjective influence.

The phase of inflammatory activity in the examined samples has been estimated using Hurst's exponent (*H*). *H* was first excogitated in the middle of the last century in order to study the local variations in water flow in the branches of the Nile delta during the construction of the Aswan dam[17]. Further refined in 1965 and 1969, it can

now be drawn from the fractal dimension (D)[18,19]. As it can describe even subtle quantitative differences in the smoothness of the configurations of natural objects with fractal properties, we used it to describe the phase of the inflammatory process on the basis of the fractal space occupied by inflammatory cells. In our case, a high H value indicates a small number of inflammatory cells within the tissue (i.e. the natural state), and a low value indicates the presence of many inflammatory cells (i.e. severe inflammatory states). H can be considered as a quantitative descriptor of the configuration pattern expressing the phase of the inflammatory process, and thus gives inflammatory cell density, the significance of a physical variable.

MATERIALS AND METHODS

Biopsy specimens

The study was conducted in accordance with the guidelines of the Ethics Committee of Istituto Clinico Humanitas, Rozzano, Milan, Italy.

The 72 liver specimens (>10 mm long) came from 43 male and 29 female chronic hepatitis C patients (mean age 50.3±14 years; range 25-77 years) admitted to our Hepato-gastroenterology Unit.

Histochemistry

Two consecutive 2-μm-thick sections were cut from the formalin-fixed and paraffin-embedded specimens. One was subsequently stained with hematoxylin-eosin (HE) solution, and the other was used for immunohistochemistry. HE stained sections were graded by two hepato-pathologists using a semi-quantitative scoring system.

Immunohistochemistry

In order to classify the inflammatory cells, the histological sections were treated with primary antibodies raised against human leukocyte common antigen (LCA, monoclonal mouse anti-LCA) for 1 h at room temperature, 1 mg/mL mouse IgG1 (Dako, Milan, Italy) was used as a negative control.

In order to distinguish settled macrophagic mesenchymal Kupffer cells from recruited inflammatory T cells, a further section was immersed in an antigen retrieval bath (Dako, Milan, Italy) for 30 min at 98 °C in 1 mmol/L of a freshly made EDTA solution. The inflammatory T cells were classified using primary antibodies raised against human CD3 (Dako, Milan, Italy), and the Kupffer cells by treatment with primary antibodies raised against human CD68 (Dako, Milan, Italy) at room temperature, or with 1 mg/mL mouse IgG1 (Dako, Milan, Italy) as a negative control.

The sections were then incubated with the DAKO Envision Doublestain System (Dako, Milan, Italy). Fast red was used as a chromogen to yield the red reaction products for CD68, and 3,3'-diaminobenzidine tetrahydrochloride (DAB, Sigma Ltd, MO, USA) to yield the brown reaction products for LCA and CD3.

The nuclei were lightly counterstained with Harris's hematoxylin solution (Medite, Bergamo, Italy).

Quantitative image analysis

The histological sections were digitized using an image analysis system consisting of a Leica DMLA microscope (Leica, Italy) equipped with an *x-y* translator table, a digital camera (Leica DC200, Leica, Italy), and an Intel dual Pentium IV, 660 MHz computer with incorporated *ad hoc* constructed image analysis software[20].

The computer program automatically selected the surface covered by the whole LCA-immunopositive inflammatory system. In this paper, the term *true area* indicates the surface of the liver tissue section without unfilled natural holes, vascular and biliary cavities, sinusoidal spaces or artificial spaces due to the needle excision and histological manipulations[20]. All the measurements were made at an objective magnification of ×20.

Determination of Hurst's exponent

This was obtained using the general relationship:

$$H=E+1-D \quad (1)$$

where E indicates the Euclidean topological dimension and D the fractal dimension of the surface covered by the whole LCA-immunopositive inflammatory system.

D was automatically estimated using the box-counting method and the formula:

$$D_B = \lim_{\varepsilon \to 0} \frac{\log N(\varepsilon)}{\log(1/\varepsilon)} \quad (2)$$

where D_B is the box-counting fractal dimension of the object, ε the side length of the box, and $N(\varepsilon)$ the smallest number of boxes of side ε required to cover the surface of the object completely, i.e. the whole LCA-immunopositive inflammatory system. As the zero limit cannot be applied to biological objects, the dimensions were calculated as $D=d$, where d is the slope of the graph of log $[N(\varepsilon)]$ against log $1/\varepsilon$. The log-log graphs were plotted and the linear segments were identified using least squares regression. Their gradients were calculated using an iterative resistant line method[20-28].

On the basis of the H value, two categories were considered. The first included all the samples characterized by $0.5<H<1.0$, and the second included all the samples verifying the relationship $0<H<0.5$.

Dynamic side of the shapes of chronic liver inflammation

The pictures indicating chronic liver inflammation appeared as portal, periportal, and perilobular aggregations of lymphocytes, plasma cells, and monocytes/macrophages (Figure 1). The extent of intralobular focal necro-inflammation varied with the severity of the disease, with confluent necrosis expressing its most severe clinical exacerbation[29-33].

These cell conglomerates arose when the viral etiological agent shaped critical points in the liver tissue consistent with hepatocyte necrosis. Each critical point acted as an attractor of the inflammatory cells naturally present within the liver tissue and recruited lymphocytes,

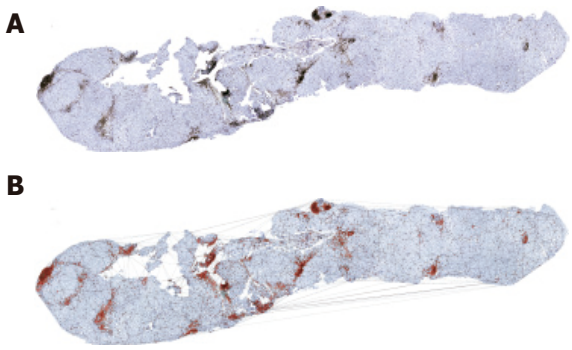

Figure 1 Liver biopsy section immunohistochemically treated with antibodies against LCA (**A**) and computer-aided recognition of the inflammatory cell network (**B**).

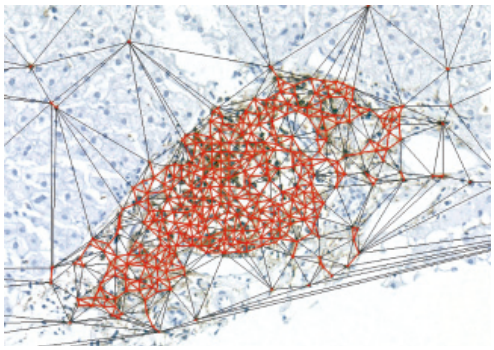

Figure 2 Border of clustered and non-clustered inflammatory cells.

plasma cells and other white blood cells. The trajectories of the inflammatory cells would die inside the attraction basin created by the necro-inflammatory process, where the motion of the recruited cells came to an end, and they formed a *cluster* marking the metrical space covered by the inflammation basin. The cell density of the cluster was transient and depended on the evolution of the inflammation connected to necrosis healing.

Definition of cluster outlines

As the cells of a cluster were not settled in tasseled forms, they were not bounded by a distinguishable contour. This meant that, in order to measure the fractal spaces they covered, the canonical step was to fix their bounds. To this end, we used a triangulation method based on the principles of Delaunay's tessellation[34-37], which can be very efficiently adapted to cluster geometry and involves the metrical measurement of the *distances* between the cells belonging to the whole inflammatory system.

Each inflammatory cell on the surface of the histological specimen was considered as a node of a continuous framework covering the entire section characterized by very irregular triangular windows in which any two triangles have one common side (Figure 1).

The border of the cluster (Figure 2) was arbitrarily fixed at the level of the continuous line formed by the set of the most external triangle sides with a length of ≤20 μm, corresponding to about twice the mean diameter of a lymphocyte (7-12 μm)[38]. All the points within this border were considered as belonging to the subset of cluster-resident cells, and those connected by longer segments as belonging to the non-clustered subset of inflammatory cells.

Geometrical structure of inflammatory clusters

The dynamics of the necro-inflammation shaping a cluster generate metrical spaces covered by two overlapping components. One belonged to the entire attraction basin of hepatocyte necrosis bounded by the cluster contour drawn by the triangulation, the other belonged to the sum of the surfaces of the inflammatory cells residing within the attraction (necro-inflammation) basin. The outline of the true area of the biopsy sample was indicated by the symbol A_B, the area of the triangulation-defined cluster (necrosis attraction zone) was indicated by the symbol A_C, and the sum of the areas of cluster-resident inflammatory cells was indicated by the symbol A_{CINF} (Figure 3). The dispersed cells were indicated by the symbol A_{PINF}, and their areas added to the area of resident inflammatory cells provided the area covered by the inflammation system as a whole, which was indicated by the symbol A_{TINF}

Physical parameters of inflammation

The physical parameters of inflammation were taken from analyses of the clusters consisting of at least three inflammatory cells. Smaller aggregates were considered as randomly united cells.

In the two dimensions of a histological section, we obtained the following physical parameters relating to the state of inflammation: (1) cluster extension: the area of the necro-inflammation basins identified by means of Delaunay's triangulation; (2) the area covered by the inflammatory cells resident within the cluster perimeter: i.e. the intracluster mass of inflammatory cells; (3) the whole area occupied by all the inflammatory parenchymal cells not residing inside the clusters; (4) the A_C/A_{CINF} ratio; (5) the extent of inflammatory tissue as a whole ($A_{CINF}+A_{PINF}$); (6) the discrimination of inflammatory T cells from Kupffer cells; (7) Hurst's exponent in order to evaluate the spatial heterogeneity of the chronic inflammatory process, i.e. the phase of the inflammatory process.

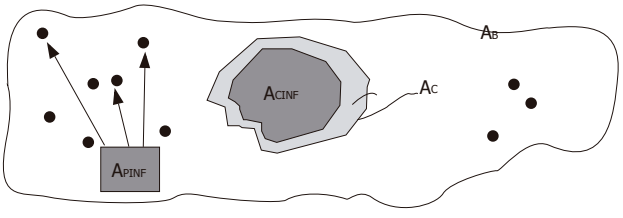

Figure 3 Geometrical structure of clustered inflammatory cells. A_B=true area of the biopsy sample; A_C=area of the triangulation-defined cluster (necrosis attraction zone); A_{CINF}=sum of the areas of cluster-resident inflammatory cells; A_{PINF}=dispersed non-clustered cells.

Statistical analysis

All the data were expressed as mean±SD.

RESULTS

Cluster extension

The area of the necro-inflammation basins obtained by Delaunay's triangulation ranged from 0.010% to 33.74% (mean 5.22±6.5%) of the area of the histological section. This area was a perceptible and measurable marker of the necrosis subtending each cluster. The sum of these areas could express the overall extension of the necrotic process in the evaluated section.

Area covered by clustered inflammatory cells

This area ranged from 0.021% to 15.36% (mean 2.22 ±2.9%) of the area of the histological section. As it represented effective inflammatory activity, its measure indicated the inflammatory potential of the set of clusters identified in the biopsy section.

Area of dispersed inflammatory cells

The area covered by the whole set of LCA-immunopositive inflammatory cells lying outside the clusters recognized in the histological sections ranged from 0.024% to 3.93% (mean 0.91±0.83%).

A_C/A_{CINF} ratio

This parameter, which expresses the density of the inflammatory cells lying within the clusters, ranged from 0.34 to 3.28 (mean 0.56±0.35).

Extension of inflammatory tissue

This area was drawn from the sum of the clustered and dispersed inflammatory cells immunopositive for LCA, and ranged from 0.045% to 18.58% (mean 3.13±3.30%).

Discrimination of recruited inflammatory T cells from resident macrophagic Kupffer cells

The whole LCA-immunopositive inflammatory area was shared by recruited blood cells (lymphocytes, monocytes, plasma cells, mast cells) and settled macrophagic Kupffer cells (Figure 4). The different range of the areas of Kupffer cells suggested that the number of Kupffer cells potentially capable of being activated might explain the distinction between fast and slow fibrosis. It is worth mentioning that this preliminary study found a high percentage of macrophages among the dispersed cells and a very low percentage in the clusters, which mainly consisted of lymphocytes and other recruited blood inflammation cells (Figure 4).

Quantification of spatial histological heterogeneity of chronic inflammatory process

This was evaluated using Hurst's exponent, the values of which range from 0 to 1 and indicate the actual phase of the inflammatory process. *H* coefficients of >0.5 were considered as belonging to tendentially less severe inflammatory pictures, and those of <0.5 as belonging to more severe pictures. The mean *H* value of all the cases was 0.67±0.14 (range 0.36-1).

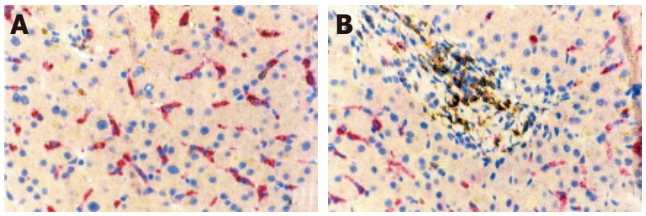

Figure 4 High percentage of macrophages among dispersed cells (**A**) and low percentage in clusters of lymphocytes and other inflammatory cells (**B**).

DISCUSSION

Given a hierarchy of logical concepts going from the purely qualitative or classificatory, to the semi-quantitative or ordering, and finally to the entirely quantitative or metrical (i.e. scientific variables), it is not a prejudice to consider that the maturity of a discipline is reflected by the number of quantitative concepts it adopts.

From this viewpoint, the phasing out of the clinical use of qualitative and semi-quantitative methods when evaluating the extension of chronic inflammatory lesions can be correlated with the maturity of hepatological disciplines. In this study, we used measurement theory, which forms the basis of our concrete knowledge of the real world and discriminates the specificity of its interrelationships, to construct a method of evaluating the different pictures of chronic liver inflammation.

Studying the measurement of inflammation (or the intensity of a process) obliged us to think in different terms from those that we were used to. In order to express new facts in intelligible terms, the confusion generated by the vague and emotive semi-quantitative definitions dictated by an observer's skill must be removed from every conceptual structure.

The method adopted by us is highly objective insofar as it is entirely computerized. Its foundations lie in the theory of measurement, a basic point of reference for all conceptual structures organizing knowledge[39].

The liver tissue lesions related to the inflammatory process at any given time caused variations in the concentrations of some specific blood molecules. These have been grouped and proposed as disease indices despite the fact that their concentrations depend not only on their production, but also on the rate of their metabolism in the bloodstream, thus depriving them of much of their significance as a quantitative index of the hepatic structure producing them. The changes in the concentrations of these blood indices over time can be described by the general equation:

$$dx_i/dt = f_i(x_1, x_2, \ldots, x_n) \quad (3)$$

where x_i denotes the blood concentration of the molecular species used, t is time, and the functions f_i are determined by the specific reactions of each x_i with the environmental factors in the bloodstream that affect their mean life (many

of which are unknown).

This makes these blood molecules independent variables that are incapable of expressing the state conditions of hepatic tissue even when the most sophisticated statistical methods are used. Similar conclusions can be made concerning the figured elements of blood (granulocytes, red cells, and platelets), and the characteristics of independent variables can also be found in the case of hepatofuge circulations (esophageal, gastric, hemorrhoidal, and umbilical varices). It therefore follows that the only variables describing the state of a chronic necro-inflammatory hepatic tissue lesion are those obtained by measuring their characteristics in the tissue in which they occur.

Since all theoretical hepatologists freely admit that the forms of chronic viral inflammation are so numerous and that they elude a complete verbal description, metrical measurements estimating the size of the true area covered by inflammatory cells and the density of the cells occupying it are the most real means of defining the stage of the process.

In practical terms, measuring chronic hepatitis B and C virus-related inflammation on the basis of a histological section of liver tissue is a problem of estimating the density of the points aggregated in clusters and those isolated in the interstitium of the hepatic parenchyma. As the points of the former (lymphocytes, monocytes, plasma cells) and the latter (which also include Kupffer cells) have the same mesenchymal nature and a similar capacity of activation during disease, it can be reasonably presumed that the degree of activity of the chronic viral process can be estimated by measuring the metrical spaces occupied by these cells and their density within them.

Whatever the method used, it is always difficult to determine the density of the punctiform particles representing the recruited inflammatory blood cells in a cluster because it depends on what is assumed to be the boundary of these basic elements of the chronic hepatitis virus-related process of liver tissue inflammation. After repeated tests (not described here), we decided to use cell sequences characterized by intercellular distances of $\leq$20 μm. Although this resolved our case, it certainly did not provide definitive solutions.

One basic question raised by our study is how much new knowledge of inflammation we have acquired after recognizing, measuring and classifying it. A first reply can be that we are able to acquire rigorous and repeatable metrical data concerning the anatomical (i.e. physical) state of the lesions induced by the etiological agent, which can be used as a reference point to give some significance to the hematological indices of disease whose uncertainty is always due to partially unknown factors. No other method of tissue or hematological analysis offers a result that is so near to reality.

Furthermore, using the same equation (4), we can now geometrically describe the morphometry of the histological picture offered by a liver biopsy. In this case, x_i represents the observable (i.e. measurable) quantities indicating the phase of the dynamic state of the inflammatory lesions that directly mark the evolution of the disease, t is time, and the functions f_i are determined by both viral and immune activity.

We included in x_i the observable, directly perceivable and metrically quantifiable measures that can change the blood concentrations of the individual molecules indicative of chronic liver disease.

Tissue and hematological indices can both be seen as dynamic variables and written using the same formula, but the hematological indices described by equation (3) are completely different functions (f_i) from those determining the dynamics of anatomical lesions. It therefore follows that blood indices cannot be used to validate the results of our method, and that the changes in hematological indices are due to the action of very different independent factors. At this point, it may be wondered what qualitative differences distinguish our method from previous recognition/classification and evaluation procedures. The most immediate reply is the rigorousness of the results expressed by scalar numbers, but it should also be added that our method allows the state of the whole organ to be represented by Hurst's exponent with an error of no more than 12% (manuscript in preparation).

The availability of rigorous metrical measures and the reasonable representativeness of the status of the organ as a whole raise the question as to whether the indication for hepatic biopsy should be reviewed by establishing clear rules in relation to the contraindications suggested by its invasiveness.

REFERENCES

1 **Kleiner DE**. The liver biopsy in chronic hepatitis C: a view from the other side of the microscope. *Semin Liver Dis* 2005; **25**: 52-64
2 **Desmet VJ**. Liver tissue examination. *J Hepatol* 2003; **39**: 43- 49
3 **Bravo AA**, Sheth SG, Chopra S. Liver biopsy. *N Engl J Med* 2001; **344**: 495-500
4 **Brunt EM**. Liver biopsy interpretation for the gastroenterologist. *Curr Gastroenterol Rep* 2000; **2**: 27-32
5 **Brunt EM**. Grading and staging the histopathological lesions of chronic hepatitis: the Knodell histology activity index and beyond. *Hepatology* 2000; **31**: 241-246
6 **Hubscher SG**. Histological grading and staging in chronic hepatitis: clinical applications and problems. *J Hepatol* 1998; **29**: 1015-1022
7 **Scheuer PJ**. Assessment of liver biopsies in chronic hepatitis: how is it best done? *J Hepatol* 2003; **38**: 240-242
8 **Rosenberg WM**. Rating fibrosis progression in chronic liver diseases. *J Hepatol* 2003; 38: 357-360
9 **Guido M**, Rugge M. Liver biopsy sampling in chronic viral hepatitis. *Semin Liver Dis* 2004; **24**: 89-97
10 **Lagging LM**, Westin J, Svensson E, Aires N, Dhillon AP, Lindh M, Wejstal R, Norkrans G. Progression of fibrosis in untreated patients with hepatitis C virus infection. *Liver* 2002; **22**: 136-144
11 **Svensson E**. Ordinal invariant measures for individual and group changes in ordered categorical data. *Stat Med* 1998; **17**: 2923-2936
12 **Poynard T**, Imbert-Bismut F, Munteanu M, Messous D, Myers RP, Thabut D, Ratziu V, Mercadier A, Benhamou Y, Hainque B. Overview of the diagnostic value of biochemical markers of liver fibrosis (FibroTest, HCV FibroSure) and necrosis (ActiTest) in patients with chronic hepatitis C. *Comp Hepatol* 2004; **3**: 8
13 **Silva IS**, Ferraz ML, Perez RM, Lanzoni VP, Figueiredo VM,

Silva AE. Role of gamma-glutamyl transferase activity in patients with chronic hepatitis C virus infection. *J Gastroenterol Hepatol* 2004; **19**: 314-318

14 **Myers RP**, Tainturier MH, Ratziu V, Piton A, Thibault V, Imbert-Bismut F, Messous D, Charlotte F, Di Martino V, Benhamou Y, Poynard T. Prediction of liver histological lesions with biochemical markers in patients with chronic hepatitis B. *J Hepatol* 2003; **39**: 222-230

15 **He QY**, Lau GK, Zhou Y, Yuen ST, Lin MC, Kung HF, Chiu JF. Serum biomarkers of hepatitis B virus infected liver inflammation: a proteomic study. *Proteomics* 2003; **3**: 666-674

16 **Lichtinghagen R**, Bahr MJ. Noninvasive diagnosis of fibrosis in chronic liver disease. *Expert Rev Mol Diagn* 2004; **4**: 715-726

17 **Hurst HE**. Long-term storage capacity of reservoirs. *Trans Amer Soc Civ Eng* 1951; **116**: 770-808

18 **Hurst HE**, Black RP, Simaiki YM. Long-term storage: an experimental study. London: Constable, 1965

19 **Bassingthwaighte JB**, Raymond GM. Evaluation of the dispersional analysis method for fractal time series. *Ann Biomed Eng* 1995; **23**: 491-505

20 **Bassingthwaighte JB**, Liebovitch LS, West BJ: Fractal physiology. New York: Oxford University Press, 1994

21 **Dioguardi N**, Franceschini B, Aletti G, Russo C, Grizzi F. A fractal dimension rectified meter for quantification of liver fibrosis and other irregular microscopy objects. *Anal Quant Cytol Histol* 2003; **25**: 312-320

22 **Dioguardi N**, Grizzi F, Bossi P, Roncalli M. Fractal and spectral dimension analysis of liver fibrosis in needle biopsy specimens. *Anal Quant Cytol Histol* 1999; **21**: 262-266

23 **Hastings HM**, Sugihara G. Fractals. A User's Guide for the Natural Sciences. Oxford: Oxford Science Publications, 1993.

24 **Nonnenmacher TF**, Baumann G, Barth A, Losa GA: Digital image analysis of self-similar cell profiles. *Int J Biomed Comput* 1994; **37**: 131-138

25 **Losa GA**, Nonnenmacher TF: Self-similarity and fractal irregularity in pathologic tissues. *Mod Pathol* 1996; **9**: 174-182

26 **Cross SS**: Fractals in pathology. *J Pathol* 1988; **182**: 1-8

27 **Grizzi F**, Dioguardi N. A fractal scoring system for quantifying active collagen synthesis during chronic liver disease. *Int J Chaos Theo Appl* 1999 **4**; 39-44,

28 **Dioguardi N**, Grizzi F. Fractal dimension exponent for quantitative evaluation of liver collagen in bioptic specimens. In "Mathematics and Biosciences in interaction" ,Basel, Boston, Berlin: Birkhauser Press, 2001: 113-120

29 **Ishak KG**. Pathologic features of chronic hepatitis. A review and update. *Am J Clin Pathol* 2000; **113**: 40-55. PMID: 10631857

30 **Nathan C**. Points of control in inflammation. *Nature* 2002; **420**: 846-852

31 **Baptista A**, Bianchi L, De Groote J, Desmet VJ, Ishak KG, Korb G, MacSween RN, Popper H, Poulsen H, Scheuer PJ, et al. The diagnostic significance of periportal hepatic necrosis and inflammation. *Histopathology* 1988; **12**: 569-579

32 **Ishak K**, Baptista A, Bianchi L, Callea F, De Groote J, Gudat F, Denk H, Desmet V, Korb G, MacSween RN, et al. Histological grading and staging of chronic hepatitis. *J Hepatol* 1995; **22**: 696-699

33 **Villari D**, Raimondo G, Brancatelli S, Longo G, Rodino G, Smedile V. Histological features in liver biopsy specimens of patients with acute reactivation of chronic type B hepatitis. *Histopathology* 1991; **18**: 73-77

34 **Wallet F**, Dussert C. Multifactorial comparative study of spatial point pattern analysis methods. *J Theor Biol* 1997; **187**: 437-447

35 **Fortune S**. A Sweepline Algorithm for Voronoi Diagrams. *Algorithmica* 1987; 2: 153-174

36 **Fitzsimons CJ**, Nikjoo H, Bolton CE, Goodhead DT. A novel algorithm for tracing the interaction of a track with molecular targets-use of Delaunay triangulation. *Math Biosci* 1998; **154**: 103-115

37 **Bostick D**, Vaisman II. A new topological method to measure protein structure similarity. *Biochem Biophys Res Commun* 2003; **304**: 320-325

38 **Weiler-Normann C**, Rehermann B. The liver as an immunological organ. *J Gastroent Hepatol* 2004; **19**: S279-S283

39 **Rosen R**. Fundamentals of measurements and representation of natural systems. Amsterdam: North-Holland, 1978

Science Editor Wang XL and Guo SY **Language Editor** Elsevier HK

PO Box 2345, Beijing 100023, China
www.wjgnet.com
wjg@wjgnet.com

ELSEVIER

World J Gastroenterol 2005;11(44):7001-7006
World Journal of Gastroenterology ISSN 1007-9327

• *CLINICAL RESEARCH* •

Open label trial of granulocyte apheresis suggests therapeutic efficacy in chronically active steroid refractory ulcerative colitis

Wolfgang Kruis, Axel Dignass, Elisabeth Steinhagen-Thiessen, Julia Morgenstern, Joachim Mössner, Stephan Schreiber, Maurizio Vecchi, Alberto Malesci, Max Reinshagen, Robert Löfberg

Wolfgang Kruis, Julia Morgenstern, Evangelisches Krankenhaus Kalk, Innere Abteilung, Universität zu Köln, Germany
Axel Dignass, Elisabeth Steinhagen-Thiessen, Medizinische Klinik für Hepatologie und Gastroenterologie, Campus Virchow-Klinikum, Universitätsklinikum, Charité, Berlin, Germany
Joachim Mössner, Medizinische Klinik und Poliklinik II, Universitätsklinikum Leipzig, Germany
Stephan Schreiber, Medizinische Klinik, Universität Kiel, Germany
Maurizio Vecchi, Dep of Int Medicine IRCCS Ospedale Policlinico, University of Milano, Italy
Alberto Malesci, Istituto Clinico Humanitas, Milano, Italy
Max Reinshagen, Innere Medizin, Universitätsklinikum Ulm, Germany
Robert Löfberg, Karolinska Institute at the IBD unit, Sophia Hemmet, Stockholm, Sweden
Correspondence to: Wolfgang Kruis, MD, Professor of Medicine, Evangelisches Krankenhaus Kalk. Buchforststr. 2, 51103 Cologne (Köln), Germany. ansorg@evkk.de
Telephone: +49-2-21-8289-5289 Fax: +49-2-21-8289-5291
Received: 2005-04-04 Accepted: 2005-04-18

Abstract

AIM: To study the efficacy, safety, and feasibility of a granulocyte adsorptive type apheresis system for the treatment of patients with chronically active ulcerative colitis despite standard therapy.

METHODS: An open label multicenter study was carried out in 39 patients with active ulcerative colitis (CAI 6-8) despite continuous use of steroids (a minimum total dose of 400 mg prednisone within the last 4 wk). Patients received a total of five aphereses using a granulocyte adsorptive technique (Adacolumn®, Otsuka Pharmaceutical Europe, UK). Assessments at wk 6 and during follow-up until 4 mo comprised clinical (CAI) and endoscopic (EI) activity index, histology, quality of life (IBDQ), and laboratory tests.

RESULTS: Thirty-five out of thirty-nine patients were qualified for intent-to-treat analysis. After the apheresis treatment at wk 6, 13/35 (37.1%) patients achieved clinical remission and 10/35 (28.6%) patients had endoscopic remission (CAI<4, EI<4). Quality of life (IBDQ) increased significantly (24 points, $P<0.01$) at wk 6. Apheresis could be performed in all but one patient. Aphereses were well tolerated, only one patient experienced anemia.

CONCLUSION: In patients with steroid refractory ulcerative colitis, five aphereses with a granulocyte/monocyte depleting filter show potential short-term efficacy. Tolerability and technical feasibility of the procedure are excellent.

Key words: Steroid; Refractory colitis; Ulcerative colitis; Granulocyte; Apheresis

Kruis W, Dignass A, Steinhagen-Thiessen E, Morgenstern J, Mössner J, Schreiber S, Vecchi M, Malesci A, Reinshagen M, Löfberg R. Open label trial of granulocyte apheresis suggests therapeutic efficacy in chronically active steroid refractory ulcerative colitis. *World J Gastroenterol* 2005; 11(44): 7001-7006
http://www.wjgnet.com/1007-9327/11/7001.asp

INTRODUCTION

Systemically acting corticosteroids are mainstay in the treatment of patients with severely active ulcerative colitis (UC). But steroid free remission cannot be achieved in up to 40% of these selected patients[1,2]. Thus, there is a need of alternative treatment options.

Etiology of inflammatory bowel disease (IBD) is still unknown, but the pathogenesis is thought to comprise interaction between genetic factors, intestinal flora, and immunomediated tissue injury[3] Extravasation of a large number of granulocytes and macrophages into the mucosa plays a major role in the release of proinflammatory cytokines[4,5], reactive oxygen derivatives[6-9], and degradative proteases[10]. Accordingly, immunosuppressive therapy has been introduced for refractory patients. Azathioprine/6-mercaptopurine, cyclosporin, and tacrolimus are widely used at present. But drawbacks such as delayed efficacy, adverse events, and costs are currently still limiting the clinical success in severely ill patients and proctocolectomy is necessary in about one-third of these patients. The search for a better treatment strategy has failed as yet. Trials with methotrexate, infliximab, and interferon have shown no convincing effects.

In view of the pathogenetic key role of granulocytes and macrophages, it makes sense to focus on therapeutic goals here. A recently developed adsorptive carrier-based granulocyte and monocyte apheresis device has demonstrated significant effects on inflammatory processes both *in vivo* and *in vitro*[11]. Preliminary data have shown promising therapeutic efficacy in IBD, rheumatoid arthritis, and other conditions[11]. Expanding on these findings, we have reported the results of an open label study on the efficacy of granulocyte apheresis treatment in severely ill patients with chronically active UC despite high doses of systemic corticosteroids.

MATERIALS AND METHODS

This was a prospective and open label trial investigating the efficacy, safety, and feasibility of therapeutic apheresis in patients with active UC despite chronic intake of high doses of systemic corticosteroids. The study was conducted in eight European gastrointestinal (GI) referral centers (Germany, Sweden, Italy, Spain) according to the Declaration of Helsinki (as amended in Edinburgh) and the good clinical practice (GCP) guidelines. The study was approved by the "Ethikkommission der Ärztekammer Nordrhein", Germany as well as local ethics committees of the participating centers. All patients received materials in their own language and gave written consent.

Patients were included if they were aged between 18 and 75 years and diagnosed with active disease (clinical activity index/CAI$\geqslant$6 and $\leqslant$8, and endoscopic index/EI>4)[12]. Additional inclusion criteria were as follows: patients who were dependent on steroids and relapsed despite continuous use of steroids (a minimum total dose of 400 mg prednisone or equivalent within the last 4 wk, dose of steroids was not changed 2 wk prior to the study), history of at least one previous attack with an unsuccessful attempt to taper corticosteroids, immunosuppressants, and aminosalicylates were constant, 3 mo and 4 wk prior to the study, respectively.

Exclusion criteria were patients with severe activity (CAI>8); pregnancy, nursing; arterial hypotension/systolic pressure <11.97 kPa and/or diastolic pressure <8.645 kPa or hypertension (systolic pressure >23.94 kPa or diastolic pressure >15.96 kPa); serious renal, hepatic or cardiovascular disease; laboratory abnormalities such as neutrophils $<1\times10^9$/L, platelets $<100\times10^9$/L, hemoglobin <10 g/L, aPT >1.25 times upper range, aPTT >1.66 times upper normal range, AST or ALT >3 times upper normal range, total bilirubin >2.5 times upper normal range, creatinine >1.8 mg/L; allergy to heparin; viral infection within 4 wk prior to the study; positive stool microbiology; major bowel resection.

Study treatment

Each patient was intended to receive a total of five apheresis sessions, each per week for 5 consecutive weeks. An apheresis session lasted for 60 min at a flow rate of 30 mL/min. Most treatments were performed in an outpatient clinic, partly in dialysis units and also in apheresis non-specialized settings.

The apheresis system used consists of a pump with an integrated monitor (Adamonitor®, manufactured by Otsuka Electronics, Japan) and a single use polycarbonate column (Adacolumn®, CE-Mark; EC certificate GI030136676005, TUV) with a capacity of about 335 mL, filled with 220 g cellulose acetate beads (about 35 000 pieces) of 2 mm in diameter (carriers) bathed in physiological saline and steam sterilized (manufactured by JIMRO, Japan).

Concomitant medication according to inclusion criteria was permitted.

Study design

The aim of this open label pilot study was to investigate the therapeutic effects of a granulocyte adsorptive type apheresis system in patients with chronically active UC despite high doses of corticosteroids. Clinical efficacy as well as feasibility and safety of the procedure were evaluated.

Clinical examination and laboratory tests

Assessments were performed at the beginning and end of the study as well as after 1, 2, 3, 4, and 5 wk of treatment. Clinical (clinical activity index, CAI) and endoscopic (endoscopic index, EI) findings were defined according to Rachmilewitz[12]. Endoscopies were performed at the beginning and the end of study. Histology was reviewed by pathologists who were blinded to the study. Clinical remission was defined by a score of CAI$\leqslant$4, while clinical response was defined as a drop of CAI$\geqslant$3. Endoscopic remission was defined by an EI$\leqslant$4, while endoscopic response was defined as a drop of EI$\geqslant$2. In addition, quality of life was assessed according to the IBDQ scoring system[13]. IBDQ was not assessed in Italian patients (n = 5). Physician's global assessment was asked for and the consumption of steroids was noted.

Laboratory tests included a differential blood count, hemoglobin, hematocrit, fibrinogen, aPT, aPTT, ESR, CRP, orosomucoid, calcium, sodium, potassium, phosphorus, creatinine, BUN/urea, uric acid, bilirubin, total protein albumin, alpha1-antitrypsin, haptoglobin, alkaline phosphatase, AST, ALT, GGT, LDH, and standard urine analyses.

Statistical analysis

The primary objective of this open multicenter study was to find the number of patients achieving clinical remission (CAI$\leqslant$4) at the end of the treatment (wk 6). Because of the uncontrolled pilot characteristics of the study, only descriptive statistical analyses were performed. Sample size was set at 35 patients. Two groups of patients were analyzed. The intent-to-treat (ITT) population consisted of all patients who experienced at least one complete (60 min) treatment of apheresis. Only patients who fulfilled the protocol without major violations were included into the per-protocol (PP) population. Comparisons were made using Wilcoxon signed rank test.

If not otherwise mentioned, data were expressed as mean$\pm$SE. P<0.05 was considered statistically significant.

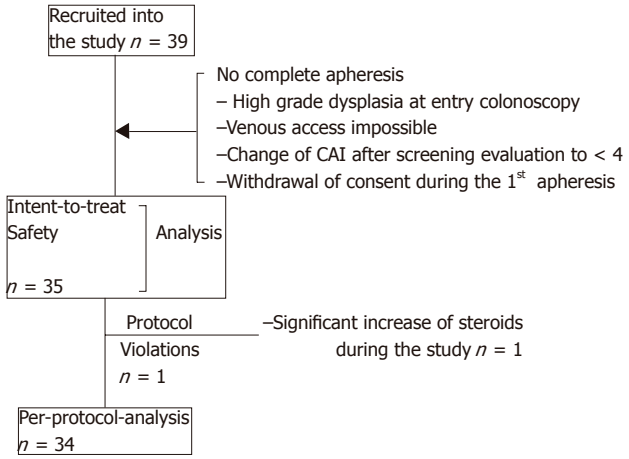

Figure 1 Patients: Analysis sets and drop outs.

Table 1 Biographical and clinical characteristics of the patients studied (intent-to-treat population[1])

Patients (ITT analysis)	*n* = 35	
Age: median/range (yr)	35	(20-72)
Female *n* (%)	10	(28.6)
Smoker *n* (%)	2	(5.7)
Ex-smoker *n* (%)	19	(54.3)
Disease: duration (mean+SE, yr) 7.2+0.8		
Site of disease: extent *n* (%):		
Proctosigmoiditis	3	(8.6)
Left sided	9	(25.7)
Pancolitis	23	(65.7)
Pretreatment (all patients had steroids)		
Aminosalicylates *n* (%)	25	(74.4%)
Immunosuppressants *n* (%)	13	(37.1%)

[1]Note: Per-protocol population comprised all but one ITT patient.

RESULTS

According to the inclusion criteria a total of 39 patients were recruited. Among the patients who underwent proctocolectomy, one patient received surgery before he started apheresis therapy because high grade dysplasia was found in the initial colonoscopy, the other two patients were operated upon because of refractory disease at wk 6 during the follow-up period. Figure 1 displays the different analysis sets and reasons for exclusion. Biographic and clinical characteristics are listed in Table 1. Suitable venous access could not be accomplished in one patient. All the other patients who started treatment received five treatments with apheresis. A total of 176 apheresis procedures could be performed without major technical difficulties. The majority of the patients (18/35) were treated in GI units, while 17/35 patients were treated in specialized dialysis units. Aphereses lasted for 60±3 min in 90.3% of the procedures and were prematurely stopped (50-55 min) in 1.7% procedures and the respective apheresis exceeded (65-91 min) in 8.0% procedures.

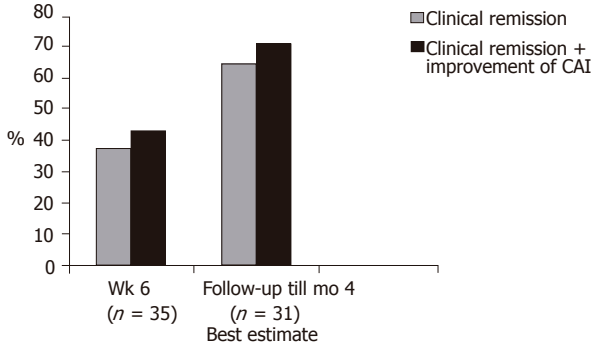

Figure 2 Patients (ITT analysis) in clinical remission or improved during a 4-mo follow-up period without additional apheresis therapy.

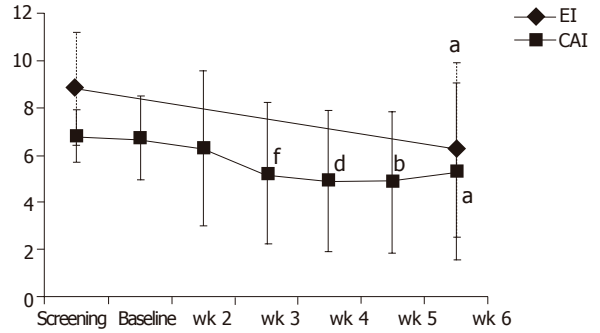

Figure 3 Course of clinical and endoscopic activity indices (CAI, EI) throughout the apheresis treatment. [a]*P*<0.05 *vs* Et at wk 6, [b]*P*<0.01 *vs* Et at wk 5, [d]*P*<0.01 *vs* Et at wk 4, [f]*P*<0.05 *vs* Et at wk 3.

Intent-to-treat analysis

At the end of the treatment period (at wk 6) 13/35 patients (37.1%) achieved clinical remission (CAI≤4). Remission or clinical improvement was observed in 15/35 (42.8%) of the patients. During a follow-up period (up to 4 mo), the number of patients achieving clinical remission increased to 20/31 patients (65%) (best estimate) (Figure 2). Except for doses of steroids no other relevant changes in medication occurred during the follow-up. Four patients lost the follow-up. The clinical remission rate of patients with concomitant immunosuppressants was 23% (3/13 patients) at wk 6 and 54.5% (6/11 patients) at the end of the follow-up. Figure 3 displays the course of clinical (CAI) and endoscopic (EI) activity. Both indices dropped significantly between the beginning and end (at wk 6) of the treatment period.

Endoscopic remission (EI<4) was observed at wk 6 in 10/35 (28.6%) patients. Mucosal healing (vulnerability of mucosa and mucosal damage scores) was improved in 19 patients, unchanged in 13 patients and deteriorated in 3 patients (P<0.001).

Between wk 0 and 6, changes in histology improved in 14 (44%) patients, no change in 16 (50%) and deteriorated in 2 (6%) patients (P<0.002).

Quality of life of the 30 non-Italian patients (IBDQ) improved rapidly by 17 points within 3 wk of treatment (P<0.01) and reached 162±6.4 points at wk 6 which was

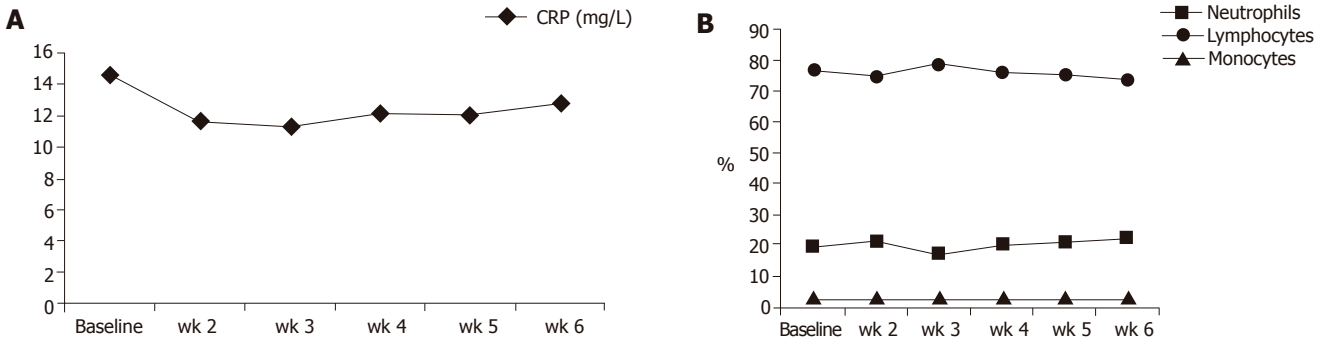

Figure 4 Course of neutrophil, lymphocyte, and monocyte counts as well as CRP between the beginning and wk 6 of the study (numbers are given as means; no significant differences).

significantly ($P<0.01$) better than that at the beginning of the study (138.1±4.8 points).

Physician's global assessment at wk 6 was 'very much improved' (11.4%), 'much improved' (37.1%), 'minimally improved' (25.7%), 'no change' (20.0%), 'minimally worse' (5.7%) and 'much worse' (0%).

Figure 4 displays the results of blood cell counts and CRP serum concentrations between the beginning and wk 6 of the study. With the exception of the lymphocyte count all other numbers dropped, but none of those changes reached statistical significance.

Consumption of systemic steroids decreased significantly ($P<0.05$) throughout the whole treatment period. The median total dose of systemic steroids was decreased from 20.0 mg/d at baseline to 15.0 mg/d at wk 6. The means were 26.1±18.04 mg/d and 16.5±15.56 mg/d, respectively. At the end of 4-mo follow-up period, the median daily dose of steroids was 6.5 mg (mean daily dose: 14.6±16.8 mg).

Per-protocol analysis

One patient of the ITT patient group experienced several changes of his dose of steroids (increase or decrease >10 mg) throughout the study. He was, therefore, excluded from the per-protocol analysis. The patient did not achieve clinical remission but had clinical improvement.

Safety analysis

No unexpected adverse events occurred. The 35 patients included experienced a total of 46 adverse events (AEs) in 65 episodes recorded. Three events were serious: thrombosis of the lower leg, worsening of UC, and a significant drop of hemoglobin which could not be explained despite extensive investigations (the patient recovered quickly). The causality was judged as unlikely, none and possible, respectively. All other AEs were judged as non-serious and mild or moderate. Ten had no causal relationship to the study treatment, 38 had a possible, and 3 had a probable relationship. The three AEs probably related to the therapy were finger edema, right arm phlebitis, and paresthesia of the left hand. All of them were classified as mild. The 38 events judged as possibly related were headache, abdominal disorder, dysesthesia, dizziness, nausea, flush, muscle cramps, fatigue, vegetative dystonia, mood alteration, prostate inflammation, and urinary tract infection. They were judged as mild (28) or moderate (10). Those events classified as unlikely related to the study treatment were oral aphthae, vertigo, headache, common cold, cramps, thrombosis, arthralgia, meralgia, ankle swelling, and bronchopneumonia. Laboratory testing as mentioned in Methods did not reveal any significant alterations.

DISCUSSION

Granulocyte apheresis application with five scheduled sessions strongly suggests efficacy in chronically active steroid refractory UC in the study reported here. A short treatment period of 5 wk resulted not only in significant clinical but also in significant endoscopic and histological improvements. Moreover, when aphereses were stopped, further beneficial effects could be observed. A follow-up period of 4 mo demonstrated carryover effects of the initial treatment leading to clinical remission in three out of four patients. Apheresis treatment was safe and well tolerated.

These very good results must be critically seen in the light of the open uncontrolled study design. Extracorporal treatment, apparently different from medicinal or surgical therapy, is a new method also for 'experienced' patients, a fact which may hold some placebo effects. Other studies demonstrated that the placebo effect is up to 30% in similar patient groups (e.g. 14) but to our knowledge, none of those trials allowed ongoing intensive treatment (dose of steroids, immunosuppressants) at entry to the study as in the present study. All patients kept on having their initial unsuccessful treatment with steroids and in part with immunosuppressants. Recent results of other studies support our findings. Yamamoto *et al*.[15] described 70% clinical remission in 30 patients with active distal UC and Naganuma *et al*.[16] found a remission rate of 55% in either steroid refractory or dependent patients. Both trials used a similar treatment protocol.

The apheresis system is used to remove excess and activated leukocytes from peripheral blood. The release of proinflammatory cytokines in the peripheral blood such as tumor necrosis factor-α (TNF-α), interleukin-1β (IL-

1β), IL-6, and IL-8 is suppressed as well as the leukocyte adhesion molecules (L-selectin) and neutrophil adhesion to IL-1β-activated endothelial cells are downregulated[17-20]. In addition, it exerts antioxidant effects[21] and the production of anti-inflammatory substances such as IL-1 receptor antagonist (IL-1ra), IL-10, and soluble TNF-α receptors I and II (sTNF-α RI and sTNF-α RII) is increased[22,23]. UC patients with high mucosal content of IL-8mRNA responding well to granulocyte apheresis and mucosal IL-8mRNA can be significantly reduced[24]. Granulocyte apheresis seems also to modulate apoptosis[17]. These far reaching interventions on inflammatory immune reactions may explain the carryover effects of granulocyte apheresis, when its application is stopped and standard treatment is continued.

Adsorption techniques may lead to a decrease of circulating blood cells. Indeed peripheral granulocytes decrease significantly by 22% after a 60-min apheresis application in UC patients, but no granulocytopenia occurs[18]. Measurements of pre- and post-column blood cell counts have demonstrated adsorption of 65% of granulocytes, 55% of monocytes, and 2% of lymphocytes, but the number of peripheral leukocytes does not fall below the normal level[19]. Flow cytometry has shown an increase in the number of immature circulating granulocytes (CD 10^- neutrophils) which should be less proinflammatory[17]. The modest effect of apheresis on blood cell counts may prevent dangerous immunosuppressive adverse events seen in systemically acting immunosuppressants.

The protocol of our study prescribed 5-wk apheresis sessions with a duration of 60 min and a flow rate of 30 mL/min, a procedure which is based on empiricism. Intensification of this low exchange technique might create more rapid and/or more favorable therapeutic results. In a large trial in patients with rheumatoid arthritis the protocol here was compared to apheresis twice per week and no therapeutic advantage of intense treatment could be observed[20]. In a small study in patients with UC, intensified apheresis revealed more rapid but not superior therapeutic effects[25]. As yet the most effective procedure remains unclear. Another way to intensify the effects of apheresis is to increase the exchange of blood per time by augmenting the flow rate during the procedure. This may create technical difficulties. The easy technical success of the protocol as it occurred in the present study is based on the low exchange protocol. Simple handling is a prerequisite of the method for its introduction to non specialized (apheresis) units.

In conclusion, granulocyte apheresis seems to be a very promising treatment, particularly in severely ill patients with UC. For patients refractory to standard therapies, it could offer an alternative which is safe and well tolerated. Controlled studies are urgently warranted.

REFERENCES

1 **Allison MC**, Dhillon AP, Lewis WG, Pounder RE (eds). Inflammatory Bowel Disease. London: Mosby, 1998

2 **Jarnerot G**, Rolny P, Sandberg-Gertzen H. Intensive intravenous treatment of ulcerative colitis. *Gastroenterology* 1985; **89:** 1005-1013

3 **Shanahan F**. Crohn's disease. *Lancet* 2002; **359:** 62-69

4 **van Dullemen HM**, van Deventer SJ, Hommes DW, Bijl HA, Jansen J, Tytgat GN, Woody J. Treatment of Crohn's disease with anti-tumor necrosis factor chimeric monoclonal antibody (cA2). *Gastroenterology* 1995; **109:** 129-135

5 **Lloyd AR**, Oppenheim JJ. Poly's lament: the neglected role of the polymorphonuclear neutrophil in the afferent limb of the immune response. *Immunol Today* 1992; **13:** 169-172

6 **Yamada T,** Volkmer C, Grisham MB. Antioxidant properties of 5-aminosalicylic acid: Potential mechanism for its anti-inflammatory activity. In: Trends in Inflammatory Bowel Disease Therapy. CN Williams (ed) Boston: *Kluwer Academic Publishers,* 1990: 73-84

7 **Yamada T,** Grisham MB. Role of neutrophil-derived oxidants in the pathogenesis of intestinal inflammation. *Klin Wochenschr* 1991; **69:** 988-994

8 **Grisham MB**, Yamada T. Neutrophils, nitrogen oxides, and inflammatory bowel disease. *Ann N Y Acad Sci* 1992; **664:** 103-115

9 **Kurtel H**, Granger DN, Tso P, Grisham MB. Vulnerability of intestinal interstitial fluid to oxidant stress. *Am J Physiol* 1992; **263:** G573-G578

10 **Grisham MB**, Granger N. Mechanisms of neutrophil-mediated tissue injury. In: Inflammatory Bowel Disease. RP MacDermott, WF Stenson (eds.) New York: *Elsevier*, 1992: 225-239

11 **Saniabadi AR,** Hanai H, Takeuchi K, Umemura K, Nakashima M, Adachi T, Shima C, Bjarnason I, Loefberg R. Adacolumn, an adsorptive carrier based granulocyte and monocyte apheresis device for the treatment of inflammatory and refractory diseases associated with leukocytes. *Ther Apher Dial* 2003; **7:** 48-59

12 **Rachmilewitz D.** Coated mesalazine (5-aminosalicylic acid) versus sulphasalazine in the treatment of active ulcerative colitis: a randomised trial. *BMJ* 1989; **298:** 82-86

13 **Irvine EJ**, Feagan B, Rochon J, Archambault A, Fedorak RN, Groll A, Kinnear D, Saibil F, McDonald JW. Quality of life: a valid and reliable measure of therapeutic efficacy in the treatment of inflammatory bowel disease. Canadian Crohn's Relapse Prevention Trial Study Group. *Gastroenterology* 1994; **106:** 287-296

14 **Probert CS**, Hearing SD, Schreiber S, Kuhbacher T, Ghosh S, Arnott ID, Forbes A. Infliximab in moderately severe glucocorticoid resistant ulcerative colitis: a randomised controlled trial. *Gut* 2003; **52:** 998-1002

15 **Yamamoto T**, Umegae S, Kitagawa T, Yasuda Y, Yamada Y, Takahashi D, Mukumoto M, Nishimura N, Yasue K, Matsumoto K. Granulocyte and monocyte adsorptive apheresis in the treatment of active distal ulcerative colitis: a prospective, pilot study. *Aliment Pharmacol Ther* 2004; **20:** 783-792

16 **Naganuma M**, Funakoshi S, Sakuraba A, Takagi H, Inoue N, Ogata H, Iwao Y, Ishi H, Hibi T. Granulocytapheresis is useful as an alternative therapy in patients with steroid-refractory or -dependent ulcerative colitis. *Inflamm Bowel Dis* 2004; **10:** 251-257

17 **Kashiwagi N,** Sugimura K, Koiwai H, Yamamoto H, Yoshikawa T, Saniabadi AR, Adachi M, Shimoyama T. Immunomodulatory effects of granulocyte and monocyte adsorption apheresis as a treatment for patients with ulcerative colitis. *Dig Dis Sci* 2002; **47:** 1334-1341

18 **Shimoyama T**, Sawada K, Hiwatashi N, Sawada T, Matsueda K, Munakata A, Asakura H, Tanaka T, Kasukawa R, Kimura K, Suzuki Y, Nagamachi Y, Muto T, Nagawa H, Iizuka B, Baba S, Nasu M, Kataoka T, Kashiwagi N, Saniabadi AR. Safety and efficacy of granulocyte and monocyte adsorption apheresis in patients with active ulcerative colitis: a multicenter study. *J Clin Apher* 2001; **16:** 1-9

19 **Ohara M,** Saniabadi AR, Kokuma S, Hirata I, Adachi M, Agishi T, Kasukawa R. Granulocytapheresis in the treatment of patients with rheumatoid arthritis. *Artif Organs* 1997; **21:** 989-994

20 **Kashiwagi N**, Hirata I, Kasukawa R. A role for granulocyte and monocyte apheresis in the treatment of rheumatoid arthritis. *Ther Apher* 1998; **2:** 134-141

21 **Hirayama A**, Nagase S, Ueda A, Ishizu T, Taru Y, Yoh K, Hirayama K, Kobayashi M, Koyama A. Oxidative stress during leukocyte absorption apheresis. *J Clin Apher* 2003; 18: 61-66

22 **Hanai H,** Takeuchi K, Iida T, Tanaka T, Tozawa K, Watanabe F, Maruyama Y, Yamada M, Iwaoka Y, Satou Y, Matsushita I, Saniabadi A. Release of IL-10, IL-1 receptor antagonist, soluble TNF-α receptors I and II during adsorptive granulocyte and monocyte/macrophage reduction therapy of patients with active ulcerative colitis. *Gastroenterology* 2004; **126 (Suppl 2):** A 567

23 **Takeda Y,** Hiraishi K, Takeda H, Shiobara H, Saniabadi AR, Adachi M, Kawata S. Cellulose acetate beads induce release of interleukin-1 receptor antagonist, but not tumour necrosis factor-α or interleukin-1β in human peripheral blood, *Inflamm Res* 2003; **52:** 287-290

24 **Tsukada Y,** Nakamura T, Iimura M, Iizuka BE, Hayashi N. Cytokine profile in colonic mucosa of ulcerative colitis correlates with disease activity and response to granulocytapheresis. *Am J Gastroenterol* 2002; **97:** 2820-2828

25 **Sakuraba A,** Naganuma M, Hibi T. Intensive therapy of granulocyte and adsorption apheresis induces rapid remission in patients with ulcerative colitis. *Gastroenterology* 2003; **124 (Suppl 1):** A 522

Science Editor Wang XL and Guo SY **Language Editor** Elsevier HK

PO Box 2345, Beijing 100023, China
www.wjgnet.com
wjg@wjgnet.com

ELSEVIER

World J Gastroenterol 2005;11(44):7007-7013
World Journal of Gastroenterology ISSN 1007-9327

• *CLINICAL RESEARCH* •

Appropriateness of indication and diagnostic yield of colonoscopy: First report based on the 2000 guidelines of the American Society for Gastrointestinal Endoscopy

Iqbal Siddique, Krishna Mohan, Fuad Hasan, Anjum Memon, Istvan Patty, Basil Al-Nakib

Iqbal Siddique, Fuad Hasan, Basil Al-Nakib, Department of Medicine, Faculty of Medicine, Kuwait University, Kuwait
Iqbal Siddique, Krishna Mohan, Fuad Hasan, Istvan Patty, Basil Al-Nakib, Thunayan Al-Ghanim Gastroenterology Center, Al-Amiri Hospital, Kuwait
Anjum Memon, Department of Public Health and Primary Care, Institute of Public Health, University of Cambridge, Cambridge, United Kingdom
Correspondence to: Dr Iqbal Siddique, Department of Medicine, Faculty of Medicine, Kuwait University, PO Box 24923, Safat 13110, Kuwait. isiddique@hsc.edu.kw
Telephone: +965-5319596 Fax: +965-5338907
Received: 2005-03-17 Accepted: 2005-06-09

Abstract

AIM: To assess the appropriateness of referrals and to determine the diagnostic yield of colonoscopy according to the 2000 guidelines of the American Society for Gastrointestinal Endoscopy (ASGE).

METHODS: A total of 736 consecutive patients (415 males, 321 females; mean age 43.6±16.6 years) undergoing colonoscopy during October 2001-March 2002 were prospectively enrolled in the study. The 2000 ASGE guidelines were used to assess the appropriateness of the indications for the procedure. Diagnostic yield was defined as the ratio between significant findings detected on colonoscopy and the total number of procedures performed for that indication.

RESULTS: The large majority (64%) of patients had colonoscopy for an indication that was considered "generally indicated", it was "generally not indicated" for 20%, and it was "not listed" for 16% in the guidelines. The diagnostic yield of colonoscopy was highest for the "generally indicated" (38%) followed by "not listed" (13%) and "generally not indicated" (5%) categories. In the multivariable analysis, the diagnostic yield was independently associated with the appropriateness of indication that was "generally indicated" (odds ratio=12.3) and referrals by gastroenterologist (odds ratio =1.9).

CONCLUSION: There is a high likelihood of inappropriate referrals for colonoscopy in an open-access endoscopy system. The diagnostic yield of the procedure is dependent on the appropriateness of indication and referring physician's specialty. Certain indications "not listed" in the guidelines have an intermediate diagnostic yield and further studies are required to evaluate whether they should be included in future revisions of the ASGE guidelines.

Key words: Colonoscopy; Indications; Diagnostic yield; Guidelines; Appropriateness

Siddique I, Mohan K, Hasan F, Memon A, Patty I, Al-Nakib B. Appropriateness of indication and diagnostic yield of colonoscopy: First report based on the 2000 guidelines of the American Society for Gastrointestinal Endoscopy. *World J Gastroenterol* 2005; 11(44): 7007-7013
http://www.wjgnet.com/1007-9327/11/7007.asp

INTRODUCTION

Over the last two decades, there has been a remarkable advancement in gastrointestinal endoscopy, and colonoscopy has become the most commonly performed procedure for the diagnosis and treatment of diseases of the large intestine as well as screening for colon cancer[1,2]. The increasing availability of colonoscopy, however, has also led to an inappropriate referral and overuse of this procedure, which is reported to range between 15% and 35% in different studies[3-6]. Consensus-based guidelines for appropriate referral of both upper and lower gastrointestinal endoscopic procedures have been developed by several expert panels[7,8]. The American Society for Gastrointestinal Endoscopy (ASGE) has also developed and periodically reviews the guidelines on the appropriate use of these procedures with the latest update made in the year 2000[9].

The diagnostic yield of an endoscopic procedure is defined as its capacity for identifying a lesion that is potentially important to patient care and has been reported for both upper and lower endoscopy in relation to the appropriateness of the indication[8]. For colonoscopy, it is reported to range 40-45% for procedures that are referred for appropriate indications, and 15-20% for those with inappropriate indications[3,6,8,10].

The objectives of this study were to evaluate the appropriateness of referrals for colonoscopy based on

the 2000 ASGE guidelines on the appropriate use of gastrointestinal endoscopy, and to assess the diagnostic yield of the procedure according to these guidelines.

MATERIALS AND METHODS

For administrative purposes, Kuwait with its population of about 2.2 million is divided into six districts, each with a well-defined area and population. Medical services in each district comprise a network of primary care clinics and a general public hospital. In addition, there are a number of centralized specialty hospitals. Our study was conducted at the Thunayan Al-Ghanim Gastroenterology Center, which offers modern facilities in gastrointestinal endoscopy, and treatment and follow-up of gastroenterology and hepatology patients. The center provides open access endoscopy services for five out of six general public hospitals in Kuwait. Primary care physicians and specialists working in hospitals can directly refer patients for endoscopy. The majority of endoscopies are performed without prior consultation with a gastroenterologist.

This study was carried out prospectively between October 2001 and March 2002. Demographic data, in/outpatient status, specialty of the referring physician, indications for the procedure, and results of colonoscopy (including histologic reports, if any) were recorded in a standardized form specifically developed for this study. The year 2000 ASGE guidelines were used to determine the appropriateness of indication(s) for the procedure. These guidelines were printed on the form used for data collection, but the headings "generally indicated" and "generally not indicated" were omitted to avoid bias. Before starting the colonoscopy, the endoscopist obtained a brief history from the patient to confirm the indications for the procedure and to exclude any contraindications. If the indications were not listed in the ASGE guidelines, the endoscopist was asked to record it separately on the form. If the patient had more than one indication for colonoscopy and at least one of these was "generally indicated" by the guidelines, then the procedure was considered appropriate.

Diagnostic yield in relation to each indication was defined as the ratio between significant findings detected on colonoscopy and the total number of procedures performed for that indication. Based on the criteria followed in previous studies[3,6,11], the presence of any of the following lesions was considered as a significant finding on colonoscopy: a pre-malignant or malignant lesion, inflammatory bowel disease (IBD) (either newly diagnosed or a more precise diagnosis or determination of the extent of the disease that influenced immediate management of the disease), angiodysplasia, stricture (benign or malignant), other colitides (infectious, ischemic, eosinophilic, microscopic), and diverticulosis (as a definite or presumptive cause of acute hematochezia)[12]. The following were not considered as significant findings: normal colonoscopy, hemorrhoids, anal fissures, previously established IBD, uncomplicated diverticulosis, and nonadenomatous polyps. The study was carried out in accordance with the ethical standards of our institution and the Helsinki Declaration as revised in 1989.

We used Student's *t*-test to compare the difference between two means and the normal *Z* test to assess the significant difference between two proportions. Multiple logistic regression analysis was performed to study the clinical parameters independently associated with diagnostic yield of colonoscopy. $P<0.05$ was considered statistically significant. All *P* values presented are two sided. The data were analyzed using SPSS 13.0 for Windows software (SPSS Inc., Chicago, IL, USA).

RESULTS

A total of 759 patients were referred for colonoscopy during the study period. Colonoscopy could not be performed in 23 of these patients because of inadequate bowel preparation. None of the patients had any contraindications for the procedure. Table 1 shows the demographic and clinical characteristics of the 736 patients (415 males, 321 females) who were prospectively enrolled in the study. The mean age of the patients was 43.6±16.6 years (range 1-90 years), and the large majority (82.3%) were outpatients. The majority of the patients were referred by general physicians (34.6%) and surgeons (33.4%).

Table 1 Demographic and clinical characteristic of 736 patients undergoing colonoscopy in Kuwait

Characteristic	*n* (%)
Gender	
Male	415 (56.4)
Female	321 (43.6)
Age (yr)	
Mean age (SD)	43.6 (16.6)
<15	31 (4.2)
15-49	441 (59.9)
⩾50	264 (35.9)
Referring clinician	
General physician	255 (34.6)
Surgeon	246 (33.4)
Gastroenterologist	205 (27.9)
Pediatric gastroenterologist	22 (3.0)
Other[1]	8 (1.1)
Clinical status	
Inpatient	130 (17.7)
Outpatient	606 (82.3)

[1]Oncologist (6), gynecologist (2).

Indications for colonoscopy

Of the 736 patients, 468 (63.6%) had colonoscopy for an indication that was considered appropriate according to the ASGE guidelines (Table 2). The two most common indications were "hematochezia" and "diarrhea of

Table 2 Indications for colonoscopy among 468 patients referred for reasons generally indicated according to the 2000 ASGE guidelines[1]

Indication	*n* (%)
1 Hematochezia	151 (20.5)
2 Clinically significant diarrhea of unexplained origin	65(8.8)
3 Irritable bowel syndrome or chronic abdominal pain: colonoscopy done once to rule out organic disease	48(6.5)
4 Chronic inflammatory bowel disease of the colon, if more precise diagnosis or determination of the extent of activity of disease will influence immediate management	34 (4.6)
5 Unexplained iron deficiency anemia	27 (3.7)
6 Following adequate clearance of neoplastic polyp(s) survey at 3-5 year intervals	24 (3.3)
7 Colonoscopy to remove synchronous neoplastic lesions at or around time of curative resection of cancer followed by colonoscopy at 3 years and 3-5 years thereafter to detect metachronous cancer	23 (3.1)
8 Evaluation of an abnormality on barium enema or other imaging study, which is likely to be clinically significant, such as a filling defect or stricture	19 (2.6)
9 Presence of fecal occult blood	12 (1.6)
10 Examination to evaluate the entire colon for synchronous cancer or neoplastic polyps in a patient with treatable cancer or neoplastic polyp	11 (1.5)
11 Excision of colonic polyp	9 (1.2)
12 Balloon dilation of stenotic lesions (e.g., anastomotic strictures)	9 (1.2)
13 Melena after an upper GI source has been excluded	8 (1.1)
14 In patients with ulcerative or Crohn's pancolitis eight or more years' duration or left sided colitis 15 or more years' duration every 1-2 years with systematic biopsies to detect dysplasia	8 (1.1)
15 Treatment of bleeding from such lesions as vascular malformation, ulceration, neoplasia, and polypectomy site (e.g., electrocoagulation, heater probe, laser or injection therapy)	7 (1.0)
16 Family history of sporadic colorectal cancer before the age of 60: colonoscopy every 5 years beginning at the age of 10 years earlier than the affected relative or every three years if adenoma is found	6 (0.8)
17 Intraoperative identification of a lesion not apparent at surgery (e.g., polypectomy site, location of a bleeding site)	3 (0.4)
18 Family history of hereditary non-polyposis colorectal cancer: colonoscopy every two years beginning at the age of 25, or five years younger than the earliest age of diagnosis of colorectal cancer. Annual colonoscopy beginning at the age of 40	2 (0.3)
19 Palliative treatment of stenosing or bleeding neoplasms (e.g., laser, electrocoagulation, stenting)	2 (0.3)

[1]According to 2000 American Society for Gastrointestinal Endoscopy (ASGE) guidelines on appropriate use of gastrointestinal endoscopy[9].

unexplained etiology". Whereas, 149 (20.2%) patients underwent colonoscopy for an indication, which was "generally not indicated" (Table 3), and for 119 (16.2%) patients the indication for colonoscopy was not listed in the guidelines (Table 4). The most common indications for patients in these two categories were "chronic, stable, irritable bowel syndrome or chronic abdominal pain", and "constipation", respectively.

Table 5 shows the appropriateness of indications for colonoscopy in relation to patients' gender, age, admission status, and specialty of the referring physician. There was no material difference in the appropriateness of indications between males and females or in- and out-patients. The mean age of patients who had colonoscopy for an indication that was "generally not indicated" was significantly lower than those who had the procedure for an indication that was "generally indicated" or "not listed" in the guidelines (38.2 *vs* 44.7 years, $P<0.0001$). Patients aged <15 years and those >50 years had a higher proportion of procedures for an indication that was considered "generally indicated" by the guidelines (77.4% and 74.6%, respectively). On the other hand, 29.5% of the patients aged 15-49 years had a significantly higher proportion of colonoscopies for an indication that was considered "generally not indicated" ($P<0.0001$). There was no real difference in the age groups when the procedure was performed for an indication that was "not listed" in the guidelines.

Pediatric gastroenterologists referred the highest proportion of patients (81.8%) for colonoscopy for an indication that was considered "generally indicated", followed by adult gastroenterologists (66.8%), surgeons (62.2%) and general physicians (60.4%). Among other specialists, general physicians referred the highest proportion of patients for colonoscopy for a reason that was considered "generally not indicated", while surgeons referred the highest proportion of patients for a "not listed" indication.

Diagnostic yield of colonoscopy

A total of 200 patients had one or more significant findings on colonoscopy giving an overall diagnostic yield of 27.2%. The most common significant findings were adenomatous polyps (29.5%), new diagnosis or more precise determination of the extent of IBD (23.5%) and colorectal cancer (12.0%). The yield of the procedures performed for "generally indicated" category was 37.8%, which was significantly higher than "generally not indicated" (4.7%, $P<0.0001$) and "not listed" (13.4%, $P<0.0001$) categories in the ASGE guidelines (Table 5). The yield of the procedures performed for "not listed" indications was also significantly higher than that for "generally not indicated" procedures (13.4% *vs* 4.7%, $P<0.05$). Inpatients had a higher diagnostic yield of

Table 3 Indications for colonoscopy among 149 patients referred for reasons generally not indicated according to the 2000 ASGE guidelines[1]

Indication	*n* (%)
1 Chronic, stable, irritable bowel syndrome or chronic abdominal pain	117 (15.9)
2 Routine follow-up of inflammatory bowel disease	15 (2.0)
3 Acute diarrhea	7 (1.0)
4 Metastatic adenocarcinoma of unknown primary site in the absence of colonic signs or symptoms when it will not influence management	6 (0.8)
5 Upper GI bleeding or melena with a demonstrated upper gastrointestinal source	4 (0.5)

[1]According to 2000 American Society for Gastrointestinal Endoscopy (ASGE) guidelines on appropriate use of gastrointestinal endoscopy[9].

Table 4 Indications for colonoscopy among 119 patients referred for reasons not listed in the 2000 ASGE guidelines[1]

Indication	*n* (%)
1 Constipation	71 (9.6)
2 Unexplained weight loss	14 (1.9)
3 Normochromic anemia	7 (1.0)
4 Perianal abscess or fistula	6 (0.8)
5 Abdominal mass of unknown origin	4 (0.5)
6 Periodic follow up of healed benign lesions	4 (0.5)
7 Surveillance after resection of colonic polyps or cancer, at different intervals from those recommended	3(0.4)
8 Intestinal obstruction	2 (0.3)
9 Routine examination of the colon in patients with no colon-related signs or symptoms about to have elective abdominal surgery for non-colonic disease	2 (0.3)
10 Others	6 (0.8)

[1]According to 2000 American Society for Gastrointestinal Endoscopy (ASGE) guidelines on appropriate use of gastrointestinal endoscopy[9].

Table 5 Appropriateness of indication and diagnostic yield of colonoscopy according to patients' characteristics

Characteristic (no. of patients)	Appropriateness of referral[1] *n* (%)			Diagnostic yield (%)
	Generally indicated	Generally not indicated	Not listed	
All patients (736)	468 (63.6)	149 (20.2)	119 (16.2)	27.2
Diagnostic yield	37.8%	4.7%	13.4%	-
Gender				
Male (415)	263(63.4)	87 (21.0)	65 (15.7)	28.0
Female (321)	205 (63.9)	62 (19.3)	54 (16.8)	26.2
Age (yr)				
Mean age (SD)	44.7 (17.3)	38.2 (12.1)	46.3 (17.3)	
<15 (31)	24 (77.4)	2 (6.5)	5 (16.1)	48.4
15-49 (441)	247 (56.0)	130 (29.5)	64 (14.5)	22.2
⩾50 (264)	197 (74.6)	17 (6.4)	50 (18.9)	33.0
Referring clinician				
General physician (255)	154 (60.4)	63 (24.7)	38 (14.9)	18.0
Surgeon (246)	153 (62.2)	34 (13.8)	59 (24.0)	27.6
Gastroenterologist (205)	137 (66.8)	49 (23.9)	19 (9.3)	36.6
Pediatric gastroenterologist (22)	18 (81.8)	1 (4.5)	3 (13.6)	50.0
Other[2] (8)	6 (75.0)	2 (25.0)	0	0
Clinical status				
Inpatient (130)	89 (68.5)	19 (14.6)	22 (16.9)	35.4
Outpatient (606)	379 (62.5)	130 (21.5)	97 (16.0)	25.4

[1]According to 2000 American Society for Gastrointestinal Endoscopy (ASGE) guidelines on appropriate use of gastrointestinal endoscopy[9]. [2]Oncologist (6), gynecologist (2).

Table 6 Clinical findings on colonoscopy by appropriateness of referral

	Appropriateness of referral[1] *n* (%)		
	Generally indicated	Generally not indicated	Not listed
Cancer	21 (4.5)	0[a]	3 (2.5)
Adenoma	54 (11.5)	1 (0.7)[c]	4 (3.4)[a]
IBD[2]	62 (13.2)	6 (4.0)[c]	8 (6.7)
Other colitides[3]	36 (1.3)	0	1 (0.8)
Angiodysplasia	5 (1.1)	0	0

[1]According to 2000 American Society for Gastrointestinal Endoscopy (ASGE) guidelines on appropriate use of gastrointestinal endoscopy[9].
[2]IBD, inflammatory bowel disease.
[3]Non-specific colitis (3), infectious colitis (3), eosinophilic colitis (1).
[a]$P<0.05$ compared to "Generally indicated".
[c]$P<0.005$ compared to "Generally indicated".

Table 7 Odds ratios (OR) and 95% confidence intervals (95% CI) for association between selected clinical parameters and diagnostic yield of colonoscopy

Parameter (*n*)	Diagnostic yield (%)	OR[1] (95% CI[2])	*P*
Gender			
Female (321)	26.2	1.0 -	
Male (415)	28.0	1.1 (0.8-1.5)	>0.50
Age (years)			
<50 (472)	23.9	1.0 -	
≥50 (264)	33.0	1.6 (1.1-2.2)	<0.05
Clinical status			
Outpatient (606)	25.4	1.0 -	
Inpatient (130)	35.4	1.6 (1.1-2.4)	<0.05
Referring clinician			
Other (531)	23.5	1.0 -	
Gastroenterologist (205)	36.6	1.9 (1.3-2.7)	<0.001
Appropriateness of indication[3]			
Generally not indicated (149)	4.7	1.0 -	
Not listed (119)	13.4	3.2 (1.3-7.9)	<0.05
Generally indicated (468)	37.8	12.3 (5.7-27.0)	<0.001

[1]OR, odds ratio.
[2]CI, confidence interval.
[3]According to 2000 American Society for Gastrointestinal Endoscopy (ASGE) guidelines on appropriate use of gastrointestinal endoscopy[9].

colonoscopy compared to outpatients (35.4% *vs* 25.4%, $P<0.05$). The highest diagnostic yield was obtained in those aged <15 years, and in those who were referred by a gastroenterologist.

Table 6 lists some of the significant findings on colonoscopy by appropriateness of referrals. Colorectal cancer, adenomatous polyps, and IBD were more likely to be detected, if the colonoscopy was performed for a "generally indicated" reason. The colon was reported as completely normal in 82.6% of the patients in the "generally not indicated" and 73.9% in "not listed" groups, compared to 51.7% in the "generally indicated" group.

Determinants of diagnostic yield

Table 7 shows the association between selected clinical parameters and diagnostic yield of colonoscopy. The probability of finding a clinically significant lesion was significantly higher in patients aged ⩾50 years (odds ratio = 1.6), inpatients (odds ratio = 1.6), those referred by gastroenterologists (odds ratio = 1.9), and those who had the colonoscopy for "generally indicated" (odds ratio = 12.3) or "not listed" (odds ratio = 3.2) categories. After adjustment for the other variables, appropriateness of indications for colonoscopy according to the ASGE guidelines and referrals by gastroenterologist were the two independent parameters associated with the diagnostic yield.

DISCUSSION

To our knowledge, this is the first study to assess the appropriateness of referrals for colonoscopy and to determine the diagnostic yield according to the year 2000 ASGE guidelines. About 64% of our patients had an indication for colonoscopy that was appropriate or

"generally indicated", according to the ASGE guidelines. This finding is similar to the 61-66% rate reported from open-access colonoscopy settings in the United States, Italy and Switzerland[3,5,6,8]. A higher rate (81%) has been reported in a study from the United States, where the referring physicians were instructed on the accepted indications for gastrointestinal endoscopy[4]. All these studies were based on the 1992 version of the ASGE guidelines. The year 2000 guidelines include several new conditions for which colonoscopy is now considered "generally indicated" such as all patients presenting with hematochezia, while the older guidelines only considered colonoscopy to be appropriate, if the hematochezia was not thought to be from the rectum or a perianal source. In addition, screening of asymptomatic, average risk patients for colonic neoplasia and seven new therapeutic indications have been included in the new guidelines. Inclusion of these additional indications means that a higher proportion of the patients referred for open-access colonoscopy should have an appropriate indication for the procedure. In our study, the overall rate of "generally indicated" colonoscopies was comparable to the studies based on the 1992 guidelines. It is noteworthy that our patients were relatively younger than those in other studies. Compared to an average age of 53-62 years in other studies, the average age of our patients was about 44 years and 60% were aged between 15 and 49 years. This may be the reason why we did not have a higher proportion of patients referred for appropriate indications even though we used more "liberal" ASGE guidelines. We did, however, observe a higher rate of "generally indicated" colonoscopy for patients aged <15 years (77%), which is not unexpected as colonoscopy is usually not performed in children unless an appropriate indication is present, and for those aged >50 years (75%).

We found no real difference between various specialties when patients were referred for a "generally indicated" colonoscopy. As for "generally not indicated" procedure, the rate was lowest for surgeons, while that for gastroenterologists was similar to general physicians. This finding is consistent with a study of open-access colonoscopy from Italy which reported similar rates of "generally not indicated" colonoscopy between gastroenterologists and family physicians[5], but is in contrast with studies of open access upper gastrointestinal endoscopy[13]. The majority (80%) of "generally not indicated" colonoscopies requested by gastroenterologists in our study were for chronic stable abdominal pain or irritable bowel syndrome (IBS), while the other 20% were for routine follow-up of IBD. This high referral rate of colonoscopy for chronic stable abdominal pain or IBS by gastroenterologists may be because in Kuwait many such patients after failing to respond to therapy are referred to the gastroenterology clinics by primary care physicians. When these patients were excluded from the analysis, the rate of "generally indicated" colonoscopy for gastroenterologists increased to about 83%, which was higher than that for all other specialties.

In our study, the definition of significant findings was based on certain positive results on colonoscopy. A normal colonoscopy was not considered significant, although this may be relevant to patient care as it may rule out a serious disease in the colon. Our results show that the diagnostic yield of colonoscopy was independently associated with appropriateness of indications and referrals by gastroenterologists. Our findings are consistent with studies conducted in Europe and the United States[3,6,11], but the difference between the yield of "generally indicated' and "generally not indicated' procedures (37.8% *vs* 4.7%) is much higher than reported in these studies. Charles *et al*.[3] reported that 40% of patients who have colonoscopy for an ASGE (1992 version) approved indication have a significant pathological finding compared to 22% of those who do not meet the guidelines. Similarly, Morini *et al*.[6] have reported a diagnostic yield of 43% for "generally indicated" and 16% for "generally not indicated" categories. De Bosset *et al*.[11], using the Swiss criteria developed by the Rand Corporation/University of California at Los Angeles (RAND/UCLA) panel, have reported a diagnostic yield of 26% for patients who have colonoscopy for an appropriate or uncertain indication and 17% for those with an inappropriate indication. The higher difference in the diagnostic yield of colonoscopy for a "generally indicated" and "generally not indicated" category seen in our study suggests that the 2000 ASGE guidelines for appropriate use of gastrointestinal endoscopy are more efficient in discriminating indications for colonoscopy than the earlier versions or the Swiss (RAND/UCLA) criteria.

The year 2000 ASGE guidelines clearly differentiate between the "generally indicated" and "generally not indicated" colonoscopies in terms of the diagnostic yield of the procedure. Clinicians can therefore predict the expected yield of colonoscopy as long as the indications for the procedure can clearly be classified as "generally indicated' or "generally not indicated". However, in clinical practice there are always some patients who undergo colonoscopy for indications that cannot be clearly classified into either of these two categories. It has been reported that about 12-28% of the patients undergoing colonoscopy have indications that are not listed in the ASGE guidelines[5,6,8]. In our study, the proportion of patients in "not listed' category was about 16% with a diagnostic yield of 13.4%, being about three times higher than the diagnostic yield of colonoscopy which is "generally not indicated". Among the patients in the "not listed' category, three were diagnosed with colorectal cancer compared to none in the "generally not indicated" group and the proportion of patients diagnosed with adenomatous polyps and IBD was also higher. The ASGE guidelines appear to be deficient with regard to these "not listed" indications, but it is acknowledged that clinical considerations may occasionally justify a course of action at variance with the recommendations of the ASGE. The two most frequent unlisted indications in our study were constipation and unexplained weight loss, and all three cases of colorectal cancer were found in patients who underwent colonoscopy for constipation. Clear recommendations are needed for such common unlisted

indications such as constipation as provided in the Swiss and American panel-based guidelines[8]. Further studies are needed to identify other common but unlisted indications that may be included in future versions of the ASGE guidelines.

In summary, the results of this prospective study demonstrate that a large proportion of colonoscopies performed in an open-access system in Kuwait is for the indications considered inappropriate by, or not listed in the 2000 guidelines of the ASGE on appropriate use of gastrointestinal endoscopy. The probability of identifying a significant finding on colonoscopy is particularly higher when the indications for the procedure are judged to be appropriate by the ASGE guidelines, but a proportion of patients who undergo colonoscopy for an unlisted indication also have significant findings. Further studies are required to evaluate these unlisted indications to determine whether they should be included in future revisions of the guidelines. General physicians need further edification for appropriate referrals of patients for colonoscopy.

REFERENCES

1 **Karasick S**, Ehrlich SM, Levin DC, Harford RJ, Rosetti EF, Ricci JA, Beam LM, Gigliotti JV. Trends in use of barium enema examination, colonoscopy, and sigmoidoscopy: is use commensurate with risk of disease? *Radiology* 1995; **195**: 777-784

2 **Scott B**. Endoscopic demands in the 90's. *Gut* 1990; **31**: 125-126

3 **Charles RJ**, Chak A, Cooper GS, Wong RC, Sivak MV Jr. Use of open access in GI endoscopy at an academic medical center. *Gastrointest Endosc* 1999; **50**: 480-485

4 **Mahajan RJ**, Barthel JS, Marshall JB. Appropriateness of referrals for open-access endoscopy. How do physicians in different medical specialties do? *Arch Intern Med* 1996; **156**: 2065-2069

5 **Minoli G**, Meucci G, Bortoli A, Garripoli A, Gullotta R, Leo P, Pera A, Prada A, Rocca F, Zambelli A. The ASGE guidelines for the appropriate use of colonoscopy in an open access system. *Gastrointest Endosc* 2000; **52**: 39-44

6 **Morini S**, Hassan C, Meucci G, Toldi A, Zullo A, Minoli G. Diagnostic yield of open access colonoscopy according to appropriateness. *Gastrointest Endosc* 2001; **54**: 175-179

7 **Burnand B**, Vader JP, Froehlich F, Dupriez K, Larequi-Lauber T, Pache I, Dubois RW, Brook RH, Gonvers JJ. Reliability of panel-based guidelines for colonoscopy: an international comparison. *Gastrointest Endosc* 1998; **47**: 162-166

8 **Froehlich F**, Pache I, Burnand B, Vader JP, Fried M, Beglinger C, Stalder G, Gyr K, Thorens J, Schneider C, Kosecoff J, Kolodny M, DuBois RW, Gonvers JJ, Brook RH. Performance of panel-based criteria to evaluate the appropriateness of colonoscopy: a prospective study. *Gastrointest Endosc* 1998; **48**: 128-136

9 Appropriate use of gastrointestinal endoscopy. American Society for Gastrointestinal Endoscopy. *Gastrointest Endosc* 2000; **52:** 831-837

10 **Berkowitz I**, Kaplan M. Indications for colonoscopy. An analysis based on indications and diagnostic yield. *S Afr Med J* 1993; **83**: 245-248

11 **De Bosset V**, Froehlich F, Rey JP, Thorens J, Schneider C, Wietlisbach V, Vader JP, Burnand B, Muhlhaupt B, Fried M, Gonvers JJ. Do explicit appropriateness criteria enhance the diagnostic yield of colonoscopy? *Endoscopy* 2002; **34**: 360-368

12 **Jensen DM**, Machicado GA, Jutabha R, Kovacs TO. Urgent colonoscopy for the diagnosis and treatment of severe diverticular hemorrhage. *N Engl J Med* 2000; **342**: 78-82

13 **Minoli G**, Prada A, Gambetta G, Formenti A, Schalling R, Lai L, Pera A. The ASGE guidelines for the appropriate use of upper gastrointestinal endoscopy in an open access system. *Gastrointest Endosc* 1995; **42**: 387-389

Science Editor Wang XL and Guo SY **Language Editor** Elsevier HK

PO Box 2345, Beijing 100023, China
www.wjgnet.com
wjg@wjgnet.com

ELSEVIER

World J Gastroenterol 2005;11(44):7014-7017
World Journal of Gastroenterology ISSN 1007-9327

• *RAPID COMMUNICATION* •

Treatment for isolated loco-regional recurrence of gastric adenocarcinoma: Does surgery play a role?

Fabio Carboni, Pasquale Lepiane, Roberto Santoro, Riccardo Lorusso, Pietro Mancini, Massimo Carlini, Eugenio Santoro

Fabio Carboni, Pasquale Lepiane, Roberto Santoro, Riccardo Lorusso, Pietro Mancini, Eugenio Santoro, Department of Digestive Surgery and Liver Transplantation, Regina Elena Cancer Institute, Rome, Italy
Massimo Carlini, Division of General A.T. Surgery, St. Eugenio Hospital, Rome, Italy
Correspondence to: Fabio Carboni, MD, PhD, Department of Digestive Surgery and Liver Transplantation, Regina Elena Cancer Institute, via Elio Chianesi 53, 00144, Rome, Italy. fabiocarb@tiscali.it
Telephone: +39-6-52666789 Fax: +39-6-52662338
Received: 2005-01-14 Accepted: 2005-04-26

Key words: Gastric adenocarcinoma; Recurrence; Diagnosis; Surgery

Carboni F, Lepiane P, Santoro R, Lorusso R, Mancini P, Carlini M, Santoro E. Treatment for isolated loco-regional recurrence of gastric adenocarcinoma: Does surgery play a role? *World J Gastroenterol* 2005; 11(44): 7014-7017
http://www.wjgnet.com/1007-9327/11/7014.asp

Abstract

AIM: To evaluate the role of surgical treatment for isolated loco-regional recurrences of operated gastric adenocarcinoma.

METHODS: Among the 837 patients operated for gastric adenocarcinoma between December 1979 and April 2004, 713 (85%) underwent resection with curative intent. A retrospective review of a prospectively collected gastric cancer database was carried out. Overall recurrence rate was 44% (315 cases), with 75% occurring within the first 2 years from the operation. Isolated L-R recurrences were observed in 38 (12%) patients. Symptomatic lesions were observed in 27 (71%).

RESULTS: Six (16%) patients were macroscopically resected with curative intent. The recurrence was located in the gastric stump after a STG in three patients, in the esophagojejunal anastomosis after a TG in two patients and in the gastric bed after a TG in one patient. Surgical procedures consisted of three secondary TG, two esophagojejunal resection and one excision of an extraluminal recurrence. Postoperative complications occurred in two patients (33%), including one anastomotic leakage and one hemorrhage. The latter patient died of sepsis 35 d after the surgery (mortality rate 17%). All patients died of recurrent gastric cancer: 2 within 1 year from surgery (8 and 11 mo, respectively), 2 after 16 and 17 mo respectively and 1 after 28 mo from the second operation.

CONCLUSION: Surgery plays a very limited role in the treatment for isolated loco-regional recurrence of gastric adenocarcinoma.

INTRODUCTION

Despite the decreasing overall incidence, gastric adenocarcinoma is still one of the most common causes of death for cancer worldwide. Even after curative gastrectomy, disease recurrence occurs in 22-50% of patients, mostly within two years from the operation[1-5].

Loco-regional (L-R) recurrence results from lymphatic spread or direct tumor propagation within the abdominal cavity[6]. Several series tried to clarify the relationship between clinicopathologic features of the primary tumor and failure patterns[1-5,7-11]. In any case, effective therapies are lacking and surgical resection is only rarely possible.

The aim of this study was to retrospectively analyze our experience with the surgical treatment of L-R recurrence in patients operated for gastric cancer.

MATERIALS AND METHODS

Out of the 905 patients submitted to gastric resections between December 1979 and April 2004, 837 with adenocarcinoma were entered and followed in a prospectively recorded database. Among these, 713 (85%) underwent resection with curative intent, consisting of 392 total gastrectomies (TG) and 321 proximal or subtotal distal gastrectomies (STG). Standard D2 lymph node dissection was performed in most patients, with D3 dissection performed for curative intent in selected cases. Pathologic stage distribution, according to the 1997 TNM classification[12], included stages IA (11%), IB (13%), II (14%), IIIA (15%), IIIB (16%), and IV (31%). All stages up to IV were due to N category or T4 classification in the presence of positive nodes. The most common histological type was intestinal (53%), according to Lauren's criteria.

All patients were included in a prospectively collected database. Follow-up examinations were performed 1 mo

Table 1 Resected patients' background at the time of the primary operation

Sex	Age	Staging	Operation	Adjuvant therapy	Histology	Tumor-free interval (mo)
1 M	72	T3N2M0	STG	CHT	Diffuse	9
2 F	60	T3N0M0	STG	–	Diffuse	21
3 M	49	T3N2M0	STG	CHT	Intestinal	12
4 M	63	T3N2M0	TG	CHT	Diffuse	16
5 M	66	T4N1M0	TG	CHT	Diffuse	24
6 F	58	T2N1M0	TG	–	Intestinal	50

after the surgery, once in every 3 mo during the first 2 years, every 6 mo for the first 5 years and yearly thereafter. Follow-up program included physical examination, laboratory analysis including serum tumor markers (CEA, CA 19-9, and CA 72-4) at each visit, abdominal ultrasound or computed tomography (CT) and chest radiograph every 6 mo and endoscopy once a year. Follow-up information was regularly obtained from outpatient clinical visits, from the time of surgery to May 2004 or until death. Median follow-up was 13 mo (range 1 mo to 163 mo).

Recurrences were classified according to the definition of Lenhert *et al*. as distant metastasis and L-R recurrences, including local lymph nodes metastasis, extraluminal recurrence, recurrence within the gastric remnant after STG and esophagojejunal anastomosis recurrence after TG[6].

Overall recurrence rate was 44% (315 cases), with 75% occurring within the first 2 years from the operation. Disease recurrence was rare after 5 years (5%). Isolated L-R recurrences were observed in 38 (12%) patients, while distant metastasis only in 167 (53%) and combined in the remaining 110 (35%). Symptomatic lesions were observed in 27 (71%), mostly including upper digestive obstruction and pain. In the asymptomatic patients, the recurrence was incidentally discovered during routine follow-up, most commonly by CT scan and occasionally by endoscopy or tumor markers elevation.

RESULTS

Six (16%) patients were macroscopically resected with curative intent, representing 4% only of all observed L-R recurrences. The other 32 patients underwent conservative treatment in 25 cases (66%), laparotomy only in five cases (13%) and by-pass procedure in two cases (5%). Resected patients' background at the time of the primary operation is shown in Table 1. Mean tumor-free interval was 22 mo.

The recurrence was located in the gastric stump after a STG in three patients, in the esophagojejunal anastomosis after a TG in two patients and in the gastric bed after a TG in one patient. Surgical procedures consisted of three secondary TG, two esophagojejunal resection and one excision of an extraluminal recurrence. Postoperative complications occurred in two patients (33%), including one anastomotic leakage and one hemorrhage. The latter patient died of sepsis 35 d after the surgery (mortality rate 17%). Three patients received adjuvant chemotherapy (CHT) after the second operation, in two combined with intraoperative radiation therapy (IORT). Clinical course of the resected cases is described in Table 2.

Table 2 Clinical course in resected cases

Case	Recurrent site	Operation	Adjuvant therapy	Survival (mon)	Recurrence
1	Gastric stump	TG-liver segmentectomy	–	16	Distant
2	Gastric stump	TG-splenectomy	CHT+IORT	28	Distant
3	Gastric stump	TG-liver segmentectomy	CHT+IORT	17	Combined
4	Esophagojejunal anastomosis	Resection	–	1	–
5	Esophagojejunal anastomosis	Resection	–	8	Combined
6	Gastric bed	Excision	CHT	11	Loco-regional

All patients died of recurrent gastric cancer: 2 within 1 year from surgery (8 and 11 mo, respectively), 2 after 16 and 17 mo respectively and 1 after 28 mo from the second operation (Table 2). Mean survival of the palliated or non-resected patients was 8 mo.

DISCUSSION

Despite considerable improvement in the surgical treatment of gastric adenocarcinoma, recurrences still constitute the main cause of death in operated patients. Recent series showed overall incidence rates of 22-50% after curative surgery, mostly (75-80%) occurring within 2 years[1-5,7-11]. Our 44% recurrence rate is probably due to the high incidence (62%) of advanced operated gastric cancer cases, as for most Western experience. Moreover, our results confirm that recurrences beyond 5 years are rare (3-9%)[1,4,5,10,13]. Median survival from the time of recurrence is approximately 6 mo[1,2,7,10,13].

Gastric cancer recurrence include: L-R recurrence (regional lymph nodes, perianastomotic region, gastric bed, and stump), peritoneal recurrence and hematogenous metastasis (liver, lungs, bones, brain, and skin)[2,3,5,7-11]. As confirmed by our experience, combined recurrences are frequently observed and hematogenous or lymphatic spread without intra-abdominal metastases occur rarely[2,6-8]. An isolated L-R recurrence is reported in 6-46% of patients[1-3,7,8,10,11,13] and they were 12% in our series. Such differences may be explained by variations in the presentation of data, the definition of recurrence, as well as the mode and timing of detection[6,7,10,11].

Clinicopathologic features of the primary tumor that predict L-R recurrences are: proximal location, older age and male gender, advanced stage of disease (T3-4, N+), infiltrative growth, diffuse type and stromal reaction[2-5,7-11]. Although not statistically significant, almost all our cases were males, with advanced age (median 61 years), T4 N+ and diffuse type. Even though advanced stage of the disease is a common risk factor, early gastric cancer (EGC) may relapse in 1.4-6.4% of patients, mostly being hematogenous metastasis, but in approximately 20% of cases, L-R recurrences[2,14].

Diagnosis is improved with modern imaging and

mainly suggested by tumor markers elevation, endoscopy, and CT scan. As occurred in our experience, most patients are symptomatic and diagnosis is earlier in such cases[10,13]. Since early detection of recurrence do not improve overall survival of patients; however, according to some authors, until the development of a more effective treatment, routine follow-up is not indicated and should be reserved for symptomatic patients and to provide psychological support[1,13,15].

Some retrospective and small series showed the usefulness of CEA, CA 19-9 and CA 72-4 monitoring in detecting the recurrence of operated gastric cancer[16,17]. However, their elevation is often seen much later than detection of recurrence by imaging, especially in patients with low preoperative levels.

Endoscopic surveillance is the most accurate method to identify anastomotic or gastric stump recurrences after STG, allowing early diagnosis and radical treatment in highly selected cases[18], as it occurred for one patient of our series. Helical CT scan is the most commonly employed diagnostic tool in such cases, but its sensitivity is very low because of the limit in differentiating recurrent tumor from postoperative fibrotic and inflammatory changes[1,19,20].

Once the diagnosis of L-R recurrence has been made, curative surgical resection is only rarely possible. Available data in the literature do not allow a valid interpretation with respect to the different types of recurrence[6]. Excluding anecdotal cases of local lymph nodes or extraluminal recurrence excision[21-23], it appears that a curative resection is possible when a partial gastrectomy was previously performed. Approximately 20% of patients undergo surgical resection but in 2-6% only it may be considered curative, with a mean survival lower than 2 years[1,2,6,13,17,21]. In our series, the resection rate was extremely low. In fact, considering the 38 patients with isolated L-R recurrence, only six (16%) were resected. The remaining group was excluded from surgery mostly because the recurrences were not considered amenable to a curative resection or to the poor general condition. According to some authors, adjuvant chemoradiotherapy has a potential effect on improving prognosis[6,21,23].

Palliative resections are indicated in highly selected symptomatic patient, mainly to restore the food passage, while tumor reduction is of minor importance[2,6]. In those with poor general conditions and a short life expectancy, placement of covered expandable metallic stents is technically feasible and clinically effective[24,25].

In conclusion, surgery plays a very limited role in the treatment for isolated L-R recurrences of gastric cancer. In low-risk patients, especially if symptomatic, an attempt at resection may be justified in specialized center with acceptable postoperative mortality and morbidity, as there are no effective alternative therapies. At present, however, prevention or reduction of the frequency of recurrence, with more extended lymph nodal resection and the combination of perioperative adjuvant treatment[2,4,6,7,10,11], seem more important than the early detection and surgical treatment.

REFERENCES

1 **Bohner H**, Zimmer T, Hopfenmuller W, Berger G, Buhr HJ. Detection and prognosis of recurrent gastric cancer. Is routine follow-up after gastrectomy worthwhile ? *Hepato-Gastroenterol* 2000; **47**: 1489-1494

2 **Yoo CH**, Noh SH, Shin DW, Choi SH, Min JS. Recurrence following curative resection for gastric carcinoma. *Br J Surg* 2000; **87**: 236-242

3 **Maehara Y**, Hasuda S, Koga T, Tokunaga E, Kakeji Y, Sugimachi K. Postoperative outcome and sites of recurrence in patients following curative resection of gastric cancer. *Br J Surg* 2000; **87**: 353-357

4 **Shiraishi N**, Inomata M, Osawa N, Yasuda K, Adachi Y, Kitano S. Early and late recurrence after gastrectomy for gastric carcinoma. Univariate and multivariate analyses. *Cancer* 2000; **89:** 255-261

5 **Marrelli D**, Roviello F, de Manzoni G, Morgagni P, Di Leo A, Saragoni L, De Stefano A, Folli S, Cordiano C, Pinto E. Different patterns of recurrence in gastric cancer depending on Lauren's histological type: longitudinal study. *World J Surg* 2002; **26:** 1160-1165

6 **Lehnert T**, Rudek B, Buhl K, Golling M. Surgical therapy for loco-regional recurrence and distant metastasis of gastric cancer. *Eur J Surg Oncol* 2002; **28:** 455-461

7 **Schwarz RE**, Zagala-Nevarez K. Recurrence patterns after radical gastrectomy for gastric cancer: prognostic factors and implications for postoperative adjuvant therapy. *Ann Surg Oncol* 2002; **9**: 394-400

8 **Wu CW**, Lo SS, Shen KH, Hsieh MC, Chen JH, Chiang JH, Lin HJ, Li AF, Lui WY. Incidence and factors associated with recurrence patterns after intended curative surgery for gastric cancer. *World J Surg* 2003; **27:** 153-158

9 **Otsuji E**, Kuriu Y, Ichikawa D, Okamoto K, Ochiai T, Hagiwara A, Yamagishi H. Time to death and pattern of death in recurrence following curative resection of gastric carcinoma: analysis based on depth of invasion. *World J Surg* 2004; **28**: 866-869

10 **D'Angelica M**, Gonen M, Brennan MF, Turnbull AD, Bains M, Karpeh MS. Patterns of initial recurrence in completely resected gastric adenocarcinoma. *Ann Surg* 2004; **240:** 808-816

11 **Lim DH**, Kim DY, Kang MK, Kim YI, Kang WK, Park CK, Kim S, Noh JH, Joh JW, Choi SH, Sohn TS, Heo JS, Park CH, Park JO, Lee JE, Park YJ, Nam HR, Park W, Ahn YC, Huh SJ. Patterns of failure in gastric carcinoma after D2 gastrectomy and chemoradiotherapy: a radiation oncologist's view. *Br J Cancer* 2004; **91:** 11-17

12 **Sobin LH**, Wittekind C. International Union Against Cancer (UICC) TNM Classification of Malignant Tumours. 5th ed. *New York: Wiley-Liss* 1997: 59-62

13 **Kodera Y**, Ito S, Yamamura Y, Mochizuki Y, Fujiwara M, Hibi K, Ito K, Akiyama S, Nakao A. Follow-up surveillance for recurrence after curative gastric cancer surgery lacks survival benefit. *Ann Surg Oncol* 2003; **10:** 898-902

14 **Lee HJ**, Kim YH, Kim WH, Lee KU, Choe KJ, Kim JP, Yang HK. Clinicopathological analysis for recurrence of early gastric cancer. *Jpn J Clin Oncol* 2003; **33**: 209-214

15 **Huguier M**, Houry S, Lacaine F. Is the follow-up of patients operated on for gastric carcinoma of benefit to the patient? *Hepatogastroenterology* 1992; **39:** 14-16

16 **Takahashi Y**, Takeuchi T, Sakamoto J, Touge T, Mai M, Ohkura H, Kodaira S, Okajima K, Nakazato H. The usefulness of CEA and/or CA19-9 in monitoring for recurrence in gastric cancer patients: a prospective clinical study. *Gastric Cancer* 2003; **6:** 142-145

17 **Marrelli D**, Pinto E, De Stefano A, Farnetani M, Garosi L, Roviello F. Clinical utility of CEA, CA 19-9, and CA 72-4 in the follow-up of patients with resectable gastric cancer. *Am J Surg* 2001; **181:** 16-19

18 **Hosokawa O**, Kaizaki Y, Watanabe K, Hattori M, Douden

K, Hayashi H, Maeda S. Endoscopic surveillance for gastric remnant cancer after early cancer surgery. *Endoscopy* 2002; **34:** 469-473

19 **Jadvar H**, Tatlidil R, Garcia AA, Conti PS. Evaluation of recurrent gastric malignancy with [F-18]-FDG positron emission tomography. *Clin Radiol* 2003; **58:** 215-221

20 **Kim KA**, Park CM, Park SW, Cha SH, Seol HY, Cha IH, Lee KY. CT findings in the abdomen and pelvis after gastric carcinoma resection. *AJR Am J Roentgenol* 2002; **179:** 1037-1041

21 **Takeyoshi I**, Ohwada S, Ogawa T, Kawashima Y, Ohya T, Kawate S, Nakasone Y, Arai K, Ikeya T, Morishita Y. The resection of non-hepatic intraabdominal recurrence of gastric cancer. *Hepatogastroenterology* 2000; **47:** 1479-1481

22 Nashimoto A, Sasaki J, Sano M, Tanaka O, Tsutsui M, Tsuchiya Y, Makino H. Disease-free survival for 6 years and 4 months after dissection of recurrent abdominal paraaortic nodes (no. 16) in gastric cancer: report of a case. *Surg Today* 1997; **27**: 169-173

23 **Inada T**, Ogata Y, Andoh J, Ozawa I, Matsui J, Hishinuma S, Shimizu H, Kotake K, Koyama Y. Significance of para-aortic lymph node dissection in patients with advanced and recurrent gastric cancer. *Anticancer Res* 1994; **14:** 677-682

24 **Jeong JY**, Kim YJ, Han JK, Lee JM, Lee KH, Choi BI, Yang HK, Lee KU. Palliation of anastomotic obstructions in recurrent gastric carcinoma with the use of covered metallic stents: clinical results in 25 patients. *Surgery* 2004; **135:** 171-177

25 Park KB, Do YS, Kang WK, Choo SW, Han YH, Suh SW, Lee SJ, Park KS, Choo IW. Malignant obstruction of gastric outlet and duodenum: palliation with flexible covered metallic stents. *Radiology* 2001; **219**: 679-683

Science Editor Guo SY **Language Editor** Elsevier HK

PO Box 2345, Beijing 100023, China
www.wjgnet.com
wjg@wjgnet.com

ELSEVIER

World J Gastroenterol 2005;11(44):7018-7023
World Journal of Gastroenterology ISSN 1007-9327

• *RAPID COMMUNICATION* •

Hemoconcentration is a poor predictor of severity in acute pancreatitis

José M. Remes-Troche, Andrés Duarte-Rojo, Gustavo Morales, Guillermo Robles-Díaz

José M. Remes-Troche, Andrés Duarte-Rojo, Gustavo Morales, Department of Gastroenterology, Instituto Nacional de Ciencias Médicas y Nutrición Salvador Zubirán, Vasco de Quiroga # 15, Colonia Seccion XVI, Tlalpan, CP 14000, Mexico City, Mexico
Guillermo Robles-Díaz, Department of Experimental Medicine, Facultad de Medicina, Universidad Nacional Autónoma de México, Hospital General de México, Dr Balmis # 148, Colonia de los Doctores, CP 06726, México City, Mexico
Co-first-authors: José M. Remes-Troche and Guillermo Robles-Díaz
Co-correspondent: José M. Remes-Troche
Correspondence to: Professor Guillermo Robles-Díaz, Department of Experimental Medicine, Facultad de Medicina, Universidad Nacional Autónoma de México, Hospital General de México, Dr Balmis # 148, Colonia de los Doctores, CP 06726, México City, Mexico. guiberodi@yahoo.com.mx
Telephone: +52-55-56232673 Fax: +52-55-56232673
Received: 2005-04-07 Accepted: 2005-04-26

Abstract

AIM: To determine whether the hematocrit (Hct) at admission or at 24 h after admission was associated with severe acute pancreatitis (AP), organ failure (OF), and pancreatic necrosis.

METHODS: A total of 336 consecutive patients with a first AP episode were studied. Etiology, Hct values at admission and at 24 h, development of severe AP according to Atlanta's criteria, pancreatic necrosis, OF and mortality were recorded. Hemoconcentration was defined as Hct level >44% for males and >40% for females. The *t*-test and χ^2 test were used to assess the association of hemoconcentration to the severity, necrosis and OF. Diagnostic accuracy was also determined.

RESULTS: Biliary disease was the most frequent etiology (n = 148). Mean Hct levels at admission were 41±6% for females and 46±7% for males (P<0.01). Seventy-eight (23%) patients had severe AP, and OF developed in 45 (13%) patients. According to contrast-enhanced computed tomography scan, 36% (54/150) patients showed pancreatic necrosis. Hct levels were elevated in 58% (55/96) and 61% (33/54) patients with interstitial and necrotizing pancreatitis, respectively. Neither Hct levels at admission nor hemoconcentration at 24 h were associated with the severity, necrosis or OF. Sensitivity, specificity and positive predictive values for both determinations were very low; and negative predictive values were between 61% and 86%, being the highest value for OF.

CONCLUSION: Hct is not a useful marker to predict a worse outcome in acute pancreatitis. In spite of the high negative predictive value of hemoconcentration, the prognosis gain is limited due to an already high incidence of mild disease.

Key words: Acute pancreatitis; Hematocrit; Hemoconcentration; Severity; Necrosis

Remes-Troche JM, Duarte-Rojo A, Morales G, Robles-Díaz G. Hemoconcentration is a poor predictor of severity in acute pancreatitis. *World J Gastroenterol* 2005; 11(44): 7018-7023
http://www.wjgnet.com/1007-9327/11/7018.asp

INTRODUCTION

Acute pancreatitis (AP) is an inflammatory process of the pancreas with variable involvement of peripancreatic tissues or remote organ systems. Mostly, it develops as a mild and auto-limited disease, but around 25% of patients present the severe form with an elevated mortality rate (30%), when compared with overall mortality (2-16%)[1,2]. This worrisome condition is due to the eventual development of organ failure (OF) and sepsis[3,4], both complications are associated with the concurrent development of necrotizing pancreatitis that occurs in 20-30% of the cases[2,5]. Severity is currently defined according to the Atlanta International Symposium on AP by the presence of local complications (pancreatic necrosis, pancreatic pseudocyst, and pancreatic abscess) and/or OF (cardiovascular, pulmonary or renal insufficiency, and gastrointestinal bleeding)[6]. Several efforts have been made to describe prognostic factors that could help for the identification of high risk patients in order to maintain a closer vigilance, thereby providing a more aggressive medical treatment and an earlier admittance to the intensive care unit[7].

The usefulness of multiple clinical and laboratory tests to predict severe and/or necrotizing pancreatitis has been studied[8]. Ranson's criteria are most widely accepted for the assessment of high risk patients; however numerous parameters need to be measured during the first 48 h after admission[9,10]. Other scales like Glasgow or APACHE II are commonly used, but these also require several measurements and have not been proven superior to Ranson's criteria[11,12]. More recently, biochemical

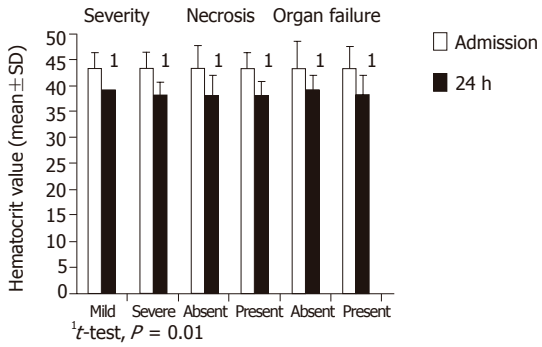

Figure 1 Mean hematocrit values at admission and 24 h later.

markers, such as C-reactive protein[13], polymorphonuclear elastase[14], interleukin-6 and trypsinogen activation peptide[15,16], have been used as predictors of severity in AP. C-reactive protein is a useful marker only 48 h after the onset of acute episodes[13,14] and overall usefulness of the remaining markers is restricted by their limited availability or elevated cost. Thus, so far, no early, accessible and economical predictive marker for severe AP has yet been described.

Hematocrit (Hct) is routinely assessed in every AP case at admission and is an accessible and low-cost test. Recent studies have proposed that hemoconcentration may constitute a good marker for severity of AP, but others were unable to find a significant correlation with the development of OF, pancreatic necrosis or death[17-20]. Thus, the value of hemoconcentration in the initial assessment of AP patients and its implications in prognosis remain controversial. We, therefore, aimed to determine whether hemoconcentration at admission and in the following 24 h was associated with the development of severe AP, pancreatic necrosis and/or OF.

MATERIALS AND METHODS

Patients with a first AP episode admitted consecutively to a tertiary medical center between June 1998 and December 2001 were included in this study. AP diagnosis was confirmed by typical clinical presentation and an increase in amylase or lipase concentration at least thrice the upper limit of normal, and/or evidence of pancreatic inflammation revealed by contrast-enhanced abdominal computed tomography[21]. Medical records of all the patients were reviewed retrospectively for the following variables: gender, age, etiology, Hct level at admission, Hct level at 24 h after admission, development of OF, and severity of AP (both defined according to Atlanta' s criteria)[6], evidence of necrosis in contrast-enhanced abdominal computed tomography, total hospital stay and mortality. Exclusion criteria included patients with previous AP episode(s) or with a first AP episode previously treated in other institutions.

Hematocrit levels at admission and 24 h later were compared with the severity of the pancreatitis, the presence of necrosis or OF. Categorical variables are expressed as absolute and relative frequencies and continuous variables as mean±SD. Receiver operator characteristic (ROC) curves were plotted for the range of Hct levels. Hemoconcentration was defined as an Hct level >44% for male and >40% for female patients[17-20]. The *t* test was used to analyze continuous variables, whereas the χ^2 or *F* tests were used on categorical variables, when appropriate. A *P* value <0.05 was considered statistically significant. Statistical analysis was performed using commercially statistical software SPSS 10 (SPSS, Chicago, IL, USA) and NCSS-2000 (NCSS, Kaysville, UT, USA).

RESULTS

Three hundred and thirty-six AP cases were included in the current study. Mean age was 45±17 (range, 15-90 years) years and 55% (*n* = 185) of patients were females. Sixteen patients (4.7%) were anemic according to reference values established for our population[22]. Mean Hct levels at admission were 41±6 for women and 46±7 for men (*P* = 0.00001). Biliary disease was the most common cause of the acute episode (*n* = 148, 44%), followed by alcohol abuse (*n* = 48, 14%). Other causes included: hypertriglyceridemia (9%), post endoscopic retrograde cholangiopancreatography (7%), drugs-induced (5%), post surgery (4%), obstructive disease (3%), hypercalcemia (1%), trauma (1%) and vasculitis (1%). Thirty-eight events were considered idiopathic (11%). When divided according to gender, biliary disease was more frequent in women and alcoholic pancreatitis was more frequent in men [odds ratio (OR) = 2.16; 95%CI 1.3-3.5 and OR = 40; 95%CI 9.7-243, respectively].

A mild AP episode was diagnosed in 258 (77%) patients, while the remaining 78 (23%) suffered from a severe attack. Organ failure developed in 45 (13%) patients. A contrast-enhanced abdominal computed tomography was performed during the first week after admission to assess the presence of necrosis in 150 cases. The Hct was determined in 233 (69%) patients 24 h after admission; of these, 183 patients (79%) presented with mild AP and 50 (21%) with severe AP. No differences were found in Hct levels at admission regardless of the presence of severe AP, necrosis or OF. A significant decrease in Hct levels was noted in all the patients at 24 h after admission, which was found to be independent of the severity status (Figure 1). There were no differences between the necrotizing and interstitial pancreatitis groups in terms of the fall in Hct levels after admission (7.5±4% *vs* 6.5±4%, respectively).

A ROC curve analysis for several cut offs of Hct levels at admission failed to show a single point combining good sensitivity, specificity, positive and negative predictive values for the detection of severe AP, necrotizing pancreatitis or OF (Figure 2).

However, the optimal cut-off values of Hct were similar to those used to define hemoconcentration (>44% for males and >40% for females). Neither the presence nor the absence of hemoconcentration at admission was associated to severity, necrosis or OF (Table 1). Hemoconcentration was present in 58% (55/96) and 61% (33/54) of patients with interstitial and necrotizing

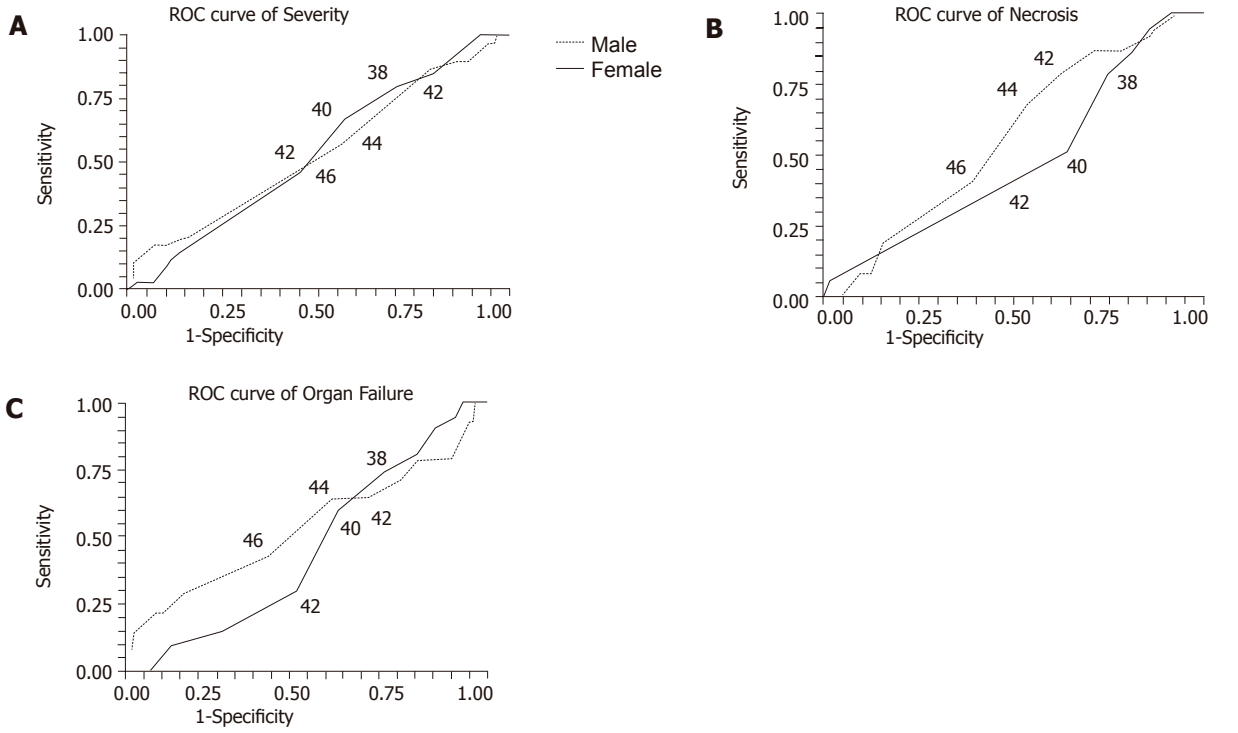

Figure 2 Receiver operating characteristic (ROC) curves for several hematocrit cut-off levels on admission as prognostic factors for severity (**A**), pancreatic necrosis (**B**) and organ failure (**C**).

Table 1 Hemoconcentration at admission as a marker for severe acute pancreatitis (AP), necrotizing AP and organ failure

	Hemoconcentration (Hct≥44% M, Hct≥40% F)[1]	No hemoconcentration (Hct <44% M, Hct <40% F)	Odds ratio (95%CI)	*P* value (χ^2)
Severe AP (*n* = 336)				
No	168	90	0.77	0.32
Yes	46	32	(0.4-1.3)	
Necrotizing AP (*n* = 150)				
No	55	41	1.17	0.64
Yes	33	21	(0.5-2.4)	
Organ failure (*n* = 336)				
No	187	104	0.83	0.58
Yes	27	18	(0.4-1.7)	

[1]Hct: hematocrit; M: male; F: female.

pancreatitis, respectively. Hemoconcentration at 24 h was not associated to severity, necrosis or OF (Table 2). Hemoconcentration at admission and 24 h later had very low sensitivity, specificity, and positive predictive values for severity, necrosis or OF. Better results were obtained for negative predictive values (Table 3).

Hospital and intensive care unit stays were higher in patients with severe AP than mild cases (18±15 and 8±3 d *vs* 10±7 and 0.5±0.1 d, $P<0.05$). Mortality was significantly higher in patients with severe AP (13% *vs* 0.03%, $P = 0.001$).

DISCUSSION

One of the most important actions to cope with patients suffering from AP is to quickly and accurately assess the severity of the attack. Earlier identification of patients at risk of developing pancreatic necrosis and OF potentially improves their care via prompt admission to intensive care unit[23-25].

Besides the development of several prognostic systems for severity in AP, there are multiple biochemical tests[13-16] and clinical parameters[8,9,26-29] proposed as single markers for severe or necrohemorrhagic pancreatitis. Most of the laboratory assays have significant limitations in clinical practice mainly because they are expensive and not widely available. The clinical features might be the most economical and easily available parameters because they result from routine patient assessment. Among them, the presence of older age[8], alcohol etiology[9], time interval between onset of symptoms and admission[26], rebound tenderness/guarding[27], obesity[28], and android fat distribution[29] have been associated with the subsequent development of severe AP. The identification of these parameters as risk factors for the development of severe AP contributed to the understanding of the disease, but their impause of several drawbacks, such as biased clinical

Table 2 Hemoconcentration at 24 h as a marker for severe acute pancreatitis (AP), necrotizing AP and organ failure

	Hemoconcentration (Hct≥44% M, Hct≥40% F)[1]	No hemoconcentration (Hct <44% M, Hct <40% F)	Odds ratio (95%CI)	*P* value(χ^2)
Severe AP (*n* = 233)				
No	125	58	0.64	0.23
Yes	29	21	(0.3–1.2)	
Necrotizing AP (*n* = 100)				
No	39	24	0.9	0.97
Yes	22	15	(0.4–2)	
Organ failure (*n* = 233)				
No	139	68	0.68	0.47
Yes	15	11	(0.3–1.5)	

[1]Hct: hematocrit; M: male; F: female.

Table 3 Accuracy of hemoconcentration at admission and at 24 h later as a marker for severe acute pancreatitis (AP), necrotizing AP and organ failure

Groups	Sensitivity (%)		Specificity (%)		PPV (%)		NPV(%)	
	Admission	24 h	Admission	24 h	Admission	24 h	Admission	24 h
Severe AP	59	58	35	31	21	18	74	73
Necrotizing AP	61	59	42	38	37	36	66	61
Organ failure	60	58	36	32	13	10	85	86

PPV: positive predictive value; NPV: negative predictive value.

Table 4 Prognostic values of hemoconcentration in previous studies

Studies	*n*	Prognostic criteria	sensitivy (%)	specificity (%)	PPV (%)	NPV (%)
		Necrosis				
Baillargeon *et al*.[17]	64	≥47% at admission	34	91	44	87
		Failure to decrease at 24 h	81	88		
		Necrosis				
Brown *et al*.[18]	128	>44% at admission	72	83	68	85
		Failure to decrease at 24 h	94	69	61	96
		Organ failure				
		>44% at admission	60	75	26	93
		Failure to decrease at 24 h	87	65	27	97
		Necrosis				
Goulis *et al*.[37]	63	>44% at admission	78	83	50	94
		Necrosis				
Lankisch *et al*.[20]	316	>43% for male and >39.6% for female at admission	74	45	24	88
		Necrosis				
Pezzilli *et al*.[36]	158	>43.8 at admission	52.3	74.6		
		Severity				
Khan *et al*. [16]	58	>47% at admission	0	92	0	65
		>44% at admission	32	82	46	71
		Hct not decreasing	21	66	24	63
Present study	336	Severity				
		>44% for male and 40% for female at admission	59	35	21	74
		Necrosis				
		>44% for male and 40% for female at admission	61	42	37	66
		Organ failure				
		>44% for male and 40% for female at admission	60	36	13	85

data obtainment, controversial results and low sensitivity and/or specificity, and the results have been controversial.

AP is considered as a consequence from an insult to the pancreatic parenchyma that generates a local inflammatory reaction which then propagates and gives place to a generalized inflammatory response. Multiple studies have underlined the role of cytokines (e.g., tumor necrosis factor-α and interleukin-1, -6, and -8) and other inflammatory response mediators (e.g., platelet activating factor) in this propagating process[30]. Interestingly, the inflammatory response is always accompanied by the increase in vascular permeability that produces extravasation of

intravascular fluid into the peritoneal cavity[31,32]. The fluid loss significantly decreases the perfusion pressure into the pancreas leading to microcirculatory changes that contribute to pancreatic necrosis[33]. Thus, it has been proposed that hemoconcentration resulting from this fluid loss might well be associated with AP severity.

Gray and Rosenman[34] in 1965 reported that hemoconcentration at admission was a poor prognostic sign in patients with AP, but Talamini *et al*.[35] did not find significant differences of Hct levels obtained within 24 h of admission in survivors and non-survivors of AP. On the other hand, the classic study of Ranson[10] found that a fall in Hct level by greater than 10% during the initial 48 h of therapy correlates with severity and mortality. Thereafter, Baillargeon *et al*.[17] in a retrospective study reported that an admission Hct ⩾47% or, opposed to Ranson's finding, a failure of Hct to decrease at 24 h were predictive of necrosis but not of OF. The same group of authors in a subsequent prospective study of 128 patients with AP established an admission Hct ⩾44% and a failure to decrease after 24 h as the best binary predictor for necrosis and OF[18]. Both studies may have a referral bias in patient selection because the included patients transferred from other hospitals may correspond to sicker cases with a delay or less vigorous hydration. In some of the subsequent studies[36,37], elevated values of admission Hct were reported in necrotizing pancreatitis and also associated with serious complications but in all the studies, neither hemoconcentration at admission nor an Hct not decreasing after 24 h were able to predict severity (Table 4). In the current study, we could not find differences in the admission Hct between severe and mild cases. In every case, independently of the presence or absence of necrosis and/or systemic complications, there was a significant decrease in Hct levels at 24 h after admission. This finding might be explained by the common practice of aggressive fluid resuscitation in most of our patients with AP. The mean Hct fall at 24 h was under 10%, being non-significantly lower in necrotizing pancreatitis as expected in agreement with Ranson. According to our results, the accuracy of hemoconcentration at admission and at 24 h later as a marker for severe AP, necrotizing pancreatitis or OF lies in its high negative predictive value, mainly for OF (85% and 86%, respectively), as has been found in the previous reports (Table 4).

We analyzed a series of consecutive patients, including 4.7% of them with anemia, in order to test the utility of the Hct in a realistic clinical setting as was done by Khan *et al*.[16]. Our results were similar to those found by them, unlike our higher mean Hct levels. Admission Hct was analyzed separately in males and females as done by Lankisch *et al*.[20], but in addition to their approach, we also analyzed the Hct at 24 h after admission. Since Hct levels may differ according to atmospheric oxygen pressure (higher in high altitudes) and to gender (lower in females)[22], we constructed ROC curves that displayed cut-off values of Hct to define hemoconcentration at risk for severity in agreement with those previously reported by others[17-20]. Thus, anemia does not seem to play a role in the poor predictive accuracy of Hct in our study.

Our study is the only one that proves that hemoconcentration analyzed according to gender at admission and at 24 h is not a good predictor for severity in AP. We consider that our findings of the poor prognostic value of Hct at admission in AP cannot be attributed to sample bias. However, this is a retrospective study and only 69% of the patients had Hct determination at 24 h after admission; thus the lack of utility of the Hct at this time cannot be established strongly.

In conclusion, the sole clinical application that follows from the current study and several previous reports could be that patients without hemoconcentration have a very low likelihood of developing pancreatic necrosis or organ failure. However, we consider that in spite of the consistent findings of high negative predictive value of hemoconcentration for necrosis and/or OF, there is no prognostic gain because of the pre-existing 75% prevalence of mild AP.

REFERENCES

1 **Halonen KI**, Leppaniemi AK, Puolakkainen PA, Lundin JE, Kemppainen EA, Hietaranta AJ, Haapiainen RK. Severe acute pancreatitis: prognostic factors in 270 consecutive patients. *Pancreas* 2000; **21:** 266-271

2 **Tenner S**, Sica G, Hughes M, Noordhoek E, Feng S, Zinner M, Banks PA. Relationship of necrosis to organ failure in severe acute pancreatitis. *Gastroenterology* 1997; **113**: 899-903

3 **Sakorafas GH**, Tsiotou AG. Etiology and pathogenesis of acute pancreatitis: current concepts. *J Clin Gastroenterol* 2000; **30:** 348-356

4 **Steinberg W**, Tenner S. Acute pancreatitis. *N Engl J Med* 1994; **330:** 1198-1210

5 **Baron TH,** Morgan DE. Acute necrotizing pancreatitis. *N Engl J Med* 1999; **340**: 1412-1417

6 **Bradley EL 3rd**. A clinically based classification system for acute pancreatitis. Summary of the International Symposium on Acute Pancreatitis, Atlanta, Ga, September 11 through 13, 1992. *Arch Surg* 1993; **128:** 586-590

7 **McKay CJ**, Imrie CW. Staging of acute pancreatitis. Is it important? *Surg Clin North Am* 1999; **79:** 733-743

8 **Lankisch PG**, Blum T, Maisonneuve P, Lowenfels AB. Severe acute pancreatitis: when to be concerned? *Pancreatology* 2003; **3:** 102-110

9 **Ranson JH,** Rifkind KM, Roses DF, Fink SD, Eng K, Spencer FC. Prognostic signs and the role of operative management in acute pancreatitis. *Surg Gynecol Obstet* 1974; **139**: 69-81

10 **Ranson JH**. Etiological and prognostic factors in human acute pancreatitis: a review. *Am J Gastroenterol* 1982; **77**: 633-638

11 **Blamey SL**, Imrie CW, O'Neill J, Gilmour WH, Carter DC. Prognostic factors in acute pancreatitis. *Gut* 1984; **25:** 1340-1346

12 **Wilson C,** Heath DI, Imrie CW. Prediction of outcome in acute pancreatitis: a comparative study of APACHE II, clinical assessment and multiple factor scoring systems. *Br J Surg* 1990; **77**: 1260-1264

13 **Chen CC**, Wang SS, Lee FY, Chang FY, Lee SD. Proinflammatory cytokines in early assessment of the prognosis of acute pancreatitis. *Am J Gastroenterol* 1999; **94**: 213-218

14 **Ikei S**, Ogawa M, Yamaguchi Y. Blood concentrations of polymorphonuclear leucocyte elastase and interleukin-6 are indicators for the occurrence of multiple organ failures at the early stage of acute pancreatitis. *J Gastroenterol Hepatol* 1998; **13:** 1274-1283

15 **Neoptolemos JP**, Kemppainen EA, Mayer JM, Fitzpatrick JM, Raraty MG, Slavin J, Beger HG, Hietaranta AJ, Puolakkainen PA. Early prediction of severity in acute pancreatitis by urinary trypsinogen activation peptide: a multicentre study. *Lan-*

cet 2000; **355:** 1955-1960
16 **Khan Z**, Vlodov J, Horovitz J, Jose RM, Iswara K, Smotkin J, Brown A, Tenner S. Urinary trypsinogen activation peptide is more accurate than hematocrit in determining severity in patients with acute pancreatitis: a prospective study. *Am J Gastroenterol* 2002; **97:** 1973-1977
17 **Baillargeon JD**, Orav J, Ramagopal V, Tenner SM, Banks PA. Hemoconcentration as an early risk factor for necrotizing pancreatitis. *Am J Gastroenterol* 1998; **93:** 2130-2134
18 **Brown A**, Orav J, Banks PA. Hemoconcentration is an early marker for organ failure and necrotizing pancreatitis. *Pancreas* 2000; **20**: 367-372
19 **Whitcomb DC,** Pedroso M, Oliva J, Venkatesan T,Ulrich C, Saul M. An admission hematocrit of 40 or less predicts a low risk of pancreatic necrosis and may reduce the need for diagnostic CT scan. *Gastroenterology* 1999; **116**: A1176, G 50967
20 **Lankisch PG**, Mahlke R, Blum T, Bruns A, Bruns D, Maisonneuve P, Lowenfels AB. Hemoconcentration: an early marker of severe and/or necrotizing pancreatitis? A critical appraisal. *Am J Gastroenterol* 2001; **96**: 2081-2085
21 **Balthazar EJ**, Ranson JH, Naidich DP, Megibow AJ, Caccavale R, Cooper MM. Acute pancreatitis: prognostic value of CT. *Radiology* 1985; **156:** 767-772
22 **Ruiz-Arguelles GJ**, Sanchez-Medal L, Loria A, Piedras J, Cordova MS. Red cell indices in normal adults residing at altitude from sea level to 2670 meters. *Am J Hematol* 1980; **8:** 265-271
23 **Klar E**, Foitzik T, Buhr H, Messmer K, Herfarth C. Isovolemic hemodilution with dextran 60 as treatment of pancreatic ischemia in acute pancreatitis. Clinical practicability of an experimental concept. *Ann Surg* 1993; **217:** 369-374
24 **Bassi C**, Falconi M, Talamini G, Uomo G, Papaccio G, Dervenis C, Salvia R, Minelli EB, Pederzoli P. Controlled clinical trial of pefloxacin versus imipenem in severe acute pancreatitis. *Gastroenterology* 1998; **115:** 1513-1517
25 **Pederzoli P**, Bassi C, Vesentini S, Campedelli A. A randomized multicenter clinical trial of antibiotic prophylaxis of septic complications in acute necrotizing pancreatitis with imipenem. *Surg Gynecol Obstet* 1993; **176**: 480-483
26 **McMahon MJ**, Playforth MJ, Pickford IR. A compaative study of methods for the prediction of severity of attacks of acute pancreatitis. *Br J Surg* 1980; **67:** 22-25
27 **Werner H-M,** Blum T, Haack U, Mahlke R, Lübbers H, Struckmann K, Brinkmann G, Maisonneuve P, Lowenfels AB, Lankisch PG. Acute pancreatitis: Limited value of physical examination for the prediction of pancreatic necrosis. *Pancreatology* 2002; **2**: 295-296
28 **Suazo-Barahona J**, Carmona-Sanchez R, Robles-Diaz G, Milke-Garcia P, Vargas-Vorackova F, Uscanga-Dominguez L, Pelaez-Luna M. Obesity: a risk factor for severe acute biliary and alcoholic pancreatitis. *Am J Gastroenterol* 1998; **93:** 1324-1328
29 **Mery CM,** Rubio V, Duarte-Rojo A, Suazo-Barahona J, Pelaez-Luna M, Milke P, Robles-Diaz G. Android fat distribution as predictor of severity in acute pancreatitis. *Pancreatology* 2002; **2**: 543-549
30 **Gomez-Cambronero LG,** Sabater L, Pereda J, Cassinello N, Camps B, Vina J, Sastre J. Role of cytokines and oxidative stress in the pathophysiology of acute pancreatitis: therapeutical implications. *Curr Drug Targets Inflamm Allergy* 2002; **1**: 393-403
31 **Eibl G**, Hotz HG, Faulhaber J, Kirchengast M, Buhr HJ, Foitzik T. Effect of endothelin and endothelin receptor blockade on capillary permeability in experimental pancreatitis. *Gut* 2000; **46:** 390-394
32 **Foitzik T**, Eibl G, Hotz HG, Faulhaber J, Kirchengast M, Buhr HJ. Endothelin receptor blockade in severe acute pancreatitis leads to systemic enhancement of microcirculation, stabilization of capillary permeability, and improved survival rates. *Surgery* 2000; **128:** 399-407
33 **Bassi D**, Kollias N, Fernandez-del Castillo C, Foitzik T, Warshaw AL, Rattner DW. Impairment of pancreatic microcirculation correlates with the severity of acute experimental pancreatitis. *J Am Coll Surg* 1994; **179:** 257-263
34 **Gray SH**, Rosenman LD. Acute pancreatitis. The significance of hemoconcentration at admission to the hospital. *Arch Surg* 1965; **91:** 485-489
35 **Talamini G**, Bassi C, Falconi M, Sartori N, Frulloni L, Di Francesco V, Vesentini S, Pederzoli P, Cavallini G. Risk of death from acute pancreatitis. Role of early, simple "routine" data. *Int J Pancreatol* 1996; **19:** 15-24
36 **Pezzilli R,** Morselli-Labate AM**.** Hematocrit determination (HCT) as an early marker associated with necrotizing pancreatitis and organ failure. *Pancreas* 2001; **4**: 433-435
37 **Goulis IG**, Koumpoudis P, Arvanitakis C. Hemoconcentration is an early marker of severe and/or necrotizing pancreatitis. *Gastroenterology* 2002; **122**: A366

Science Editor Kumar M and Guo SY **Language Editor** Elsevier HK

PO Box 2345, Beijing 100023, China
www.wjgnet.com
wjg@wjgnet.com

ELSEVIER

World J Gastroenterol 2005;11(44):7024-7027
World Journal of Gastroenterology ISSN 1007-9327

• *RAPID COMMUNICATION* •

Catheter tract implantation metastases associated with percutaneous biliary drainage for extrahepatic cholangiocarcinoma

Jun Sakata, Yoshio Shirai, Toshifumi Wakai, Tatsuya Nomura, Eiko Sakata, Katsuyoshi Hatakeyama

Jun Sakata, Yoshio Shirai, Toshifumi Wakai, Tatsuya Nomura, Eiko Sakata, Katsuyoshi Hatakeyama, Division of Digestive and General Surgery, Niigata University Graduate School of Medical and Dental Sciences, Niigata, Japan
Correspondence to: Yoshio Shirai, MD, PhD, Division of Digestive and General Surgery, Niigata University Graduate School of Medical and Dental Sciences, 1-757 Asahimachi-dori, Niigata City 951-8510, Japan. shiray@med.niigata-u.ac.jp
Telephone: +81-25-227-2228 Fax: +81-25-227-0779
Received: 2005-04-07 Accepted: 2005-07-15

Key words: Neoplasm seeding; Extrahepatic cholangiocarcinoma; Percutaneous transhepatic biliary drainage; Malignant biliary obstruction; Surgery; Prognosis

Sakata J, Shirai Y, Wakai T, Nomura T, Sakata E, Hatakeyama K. Catheter tract implantation metastases associated with percutaneous biliary drainage for extrahepatic cholangiocarcinoma. *World J Gastroenterol* 2005; 11(44): 7024-7027
http://www.wjgnet.com/1007-9327/11/7024.asp

Abstract

AIM: To estimate the incidence of catheter tract implantation metastasis among patients undergoing percutaneous transhepatic biliary drainage (PTBD) for extrahepatic cholangiocarcinoma, and to provide data regarding the management of this unusual complication of PTBD by reviewing cases reported in the literature.

METHODS: A retrospective analysis of 67 consecutive patients who underwent PTBD before the resection of extrahepatic cholangiocarcinoma was conducted. The median follow-up period after PTBD was 106 mo. The English language literature (PubMed, National Library of Medicine, Bethesda, MD, USA), from January 1966 through December 2004, was reviewed.

RESULTS: Catheter tract implantation metastasis developed in three patients. The cumulative incidence of implantation metastasis reached a plateau (6%) at 20 mo after PTBD. All of the three patients with implantation metastasis died of tumor progression at 3, 9, and 20 mo after the detection of this complication. Among the 10 reported patients with catheter tract implantation metastasis from extrahepatic cholangiocarcinoma (including our three patients), two survived for more than 5 years after the excision of isolated catheter tract metastases.

CONCLUSION: Catheter tract implantation metastasis is not a rare complication following PTBD for extrahepatic cholangiocarcinoma. Although the prognosis for patients with this complication is generally poor, the excision of the catheter tract may enable survival in selected patients with isolated metastases along the catheter tract.

INTRODUCTION

Percutaneous transhepatic biliary drainage (PTBD) has been widely employed as a biliary decompression procedure for malignant biliary obstruction[1-5]. It may cause implantation metastasis along the catheter tract, which has generally been considered as an unusual and lethal complication[6,7]. Although sporadic cases of such implantation metastasis have been reported[6-10], the incidence of this complication following PTBD is yet to be determined. Also, there is a paucity of data regarding the management of this complication. Taken together, these facts prompted us to conduct the current study.

The aims of this study were to estimate the incidence of catheter tract implantation metastasis among patients undergoing PTBD for extrahepatic cholangiocarcinoma, and to provide data regarding the management of this unusual complication by reviewing cases reported in the literature.

MATERIALS AND METHODS

Patient population

A total of 87 patients with carcinoma arising from the extrahepatic bile ducts (extrahepatic cholangiocarcinoma) underwent resection with curative intent at our department during the 15-year period between January 1988 and December 2002. Carcinoma arising from the cystic duct was categorized as extrahepatic cholangiocarcinoma according to the tumor-node-metastasis staging system[14]. Three patients who also had gallbladder carcinoma were excluded. Of the remaining 84 patients, 67 jaundiced patients underwent PTBD before the resection. They formed the basis of this retrospective study, and included 39 men and 28 women with a median age of 65 years (range: 35-88 years). All patients were Japanese.

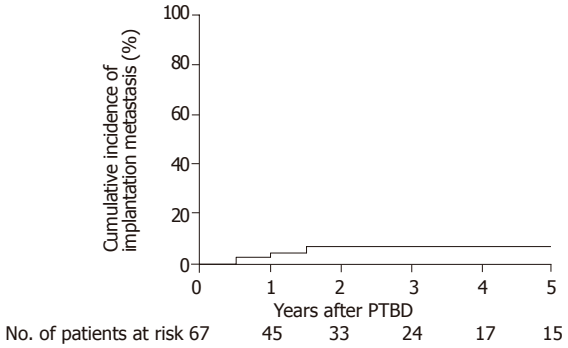

Figure 1 The cumulative incidence of catheter tract implantation metastasis after percutaneous transhepatic biliary drainage among 67 patients who underwent resection of extrahepatic cholangiocarcinoma.

Resectional procedure of the primary tumor

The resectional procedures were chosen according to the primary tumor location. Forty-one patients with hilar cholangiocarcinoma underwent a hepatectomy with bile duct resection, 12 with non-hilar tumor underwent a Whipple procedure or a pylorus-preserving pancreaticoduodenectomy, six underwent a bile duct resection, and eight underwent a combination of hepatectomy and pancreaticoduodenectomy. Regional lymphadenectomy was performed in all patients.

Pathologic examination

The resected specimens were submitted to the Department of Surgical Pathology at our hospital for histologic evaluation. The histologic findings were described according to the tumor-node-metastasis staging system[14]. The histologic grade was determined based on the areas of the tumor with the highest grade[14]. Adenocarcinoma was identified as the primary tumor in 64 patients and adenosquamous carcinoma was identified in three patients.

Patient follow-up

Patients were followed up regularly at outpatient clinics every 3 mo. The median follow-up period after PTBD was 106 mo (range: 4 to 186 mo). By the time of disease status assessment, 38 patients had died of tumor recurrence. Seven patients had died of other causes with no evidence of tumor recurrence. One patient was alive with recurrent disease, and the remaining 21 patients were alive without disease.

Review of the literature

The English language literature (PubMed, National Library of Medicine, Bethesda, MD, USA), from January 1966 through December 2004, was reviewed, and revealed that a total of seven patients undergoing resection of extrahepatic cholangiocarcinoma suffered from catheter tract implantation metastasis following PTBD[7-13].

Statistical analysis

Medical records and survival data were obtained for all the 67 patients. The causes of death were determined based on the medical records. The follow-up period was defined as the interval between the date of PTBD and that of the last follow-up. The Kaplan-Meier method was used to estimate both the cumulative incidence of catheter tract implantation metastasis and the cumulative patient survival rates. The differences in survival were evaluated using the log rank test. All statistical evaluations were performed using the SPSS 11.5J software package (SPSS Japan Inc., Tokyo, Japan). All tests were two-sided, and the differences with P values of <0.05 were considered statistically significant.

RESULTS

The incidence of catheter tract implantation metastasis after PTBD in the current series

Catheter tract implantation metastasis after PTBD presented as a subcutaneous nodule in 3 of the 67 patients during the follow-up period. The interval between PTBD and the detection of implantation metastases was 7, 14, and 20 mo for those 3 patients. The cumulative incidence of this complication reached a plateau (6%) at 20 mo after PTBD (Figure 1).

Of the three patients with implantation metastases, one underwent a resection of the catheter tract (patient 9 in Table 1), one underwent local radiation (patient 8), and the other received the best supportive care (patient 10). They died of disease at 3, 9, and 20 mo after the detection of this complication.

A review of the literature on catheter tract implantation metastasis from extrahepatic cholangiocarcinoma

An analysis of the 10 reported patients (including our three patients; Table 1) with catheter tract implantation metastasis revealed that the histologic grade of the primary tumor was well differentiated in four patients, moderately differentiated in three, poorly differentiated in one, and not documented in two. The median interval between PTBD and the detection of this complication was 14 mo (range: 3 to 45 mo).

Catheter tract implantation metastasis was isolated (without recurrences at other sites) in six patients, whereas it was non-isolated (with recurrences at other sites) in the other 4 patients (Table 1). Although the survival after the detection of implantation metastasis was generally poor, two patients who underwent excision of isolated implantation metastases survived for more than five years. Among the nine patients with documented outcomes, those with isolated implantation metastases survived longer than those with non-isolated implantation metastases ($P = 0.0457$; Figure 2).

DISCUSSION

The incidence of catheter tract implantation metastasis after PTBD has been reported to range from 0.6 to 6% in patients with malignant biliary obstruction due to tumors of various origins[7,11,15-17]. Nimura *et al*.[18] have reported

Table 1 Implantation metastases along the PTBD tract among patients who underwent a resection for extrahepatic cholangiocarcinoma

n	First author	Sex/age (yr)	Histology of the primary tumor		Detection of implantation metastases after PTBD (mo)	Sites of recurrences other than the PTBD tract	Management of implantation metastases	Outcome after the detection of implantation metastases (mo)
			Type	Grade				
1	Sano[7]	M/68	Adeno	G1	45	–	Hx	100; NED
2	Inagaki[8]	F/51	As	nd	6	–	Hx, EAW	65; NED
3	Matsumoto[9]	F/61	Adeno	G2	21	–	Hx	24; NED
4	Shimizu[10]	M/75	Adeno	G2	16	–	Hx	14; NED
5	Tersigni[11]	M/66	Adeno	G1	13	–	RTx, CTx	4; DOD
6	Omokawa[12]	M/45	Adeno	nd	3	-	Hx	nd; nd
7	Uenishi[13]	F/57	Adeno	G1	14	Pleura (right)	Pleuropneum-onectomy, ECW[2]	21; DOD
8	Sakata1	F/63	Adeno	G1	14	Bone, Local	RTx	20; DOD
9	Sakata1	M/70	Adeno	G2	20	Peritoneum	EAW	9; DO
10	Sakata1	M/76	Adeno	G3	7	Local	BSC	3; DOD

PTBD: percutaneous transhepatic biliary drainage; Adeno: adenocarcinoma; As: adenosquamous carcinoma; G1: well differentiated; G2: moderately differentiated; G3: poorly differentiated; Hx: hepatectomy; EAW: excision of the abdominal wall; RTx: radiotherapy; CTx: chemotherapy; ECW: excision of the chest wall, BSC: best supportive care; NED: (alive with) no evidence of disease; DOD: died of disease; nd: not documented. [1]Present case. [2]A PTBD catheter had been introduced transphrenically via the right pleural cavity in this patient.

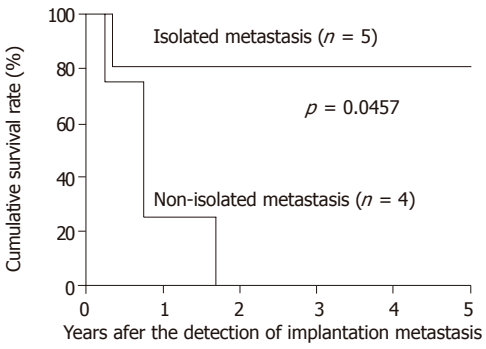

Figure 2 Kaplan-Meier estimates of survival after the detection of catheter tract implantation metastasis among nine patients with documented outcomes (Table 1). The median survival time was not reached with a cumulative 1-year survival rate of 80% in patients with isolated implantation metastasis, whereas it was 9 mo with that of 25% in patients with non-isolated metastasis. Patients with isolated implantation metastases survived longer than patients with non-isolated implantation metastases (P = 0.0457).

a 3% incidence of such implantation metastasis among 133 patients with hilar cholangiocarcinoma. In the current series, the cumulative incidence of this complication increased with time and reached a plateau (6%) 20 mo after PTBD (Figure 2). The above data suggests that catheter tract implantation is not a rare complication following PTBD for extrahepatic cholangiocarcinoma.

Uesaka *et al*.[19] have reported that catheter tract implantation metastasis from hilar cholangiocarcinoma occurred more frequently in patients with well differentiated tumors. Among the 10 reported patients with this complication (Table 1), only one had a poorly differentiated tumor, implying that differentiated tumors may be more related to the development of this complication than poorly differentiated ones. The association between implantation metastasis after PTBD and the histologic grade of extrahepatic cholangiocarcinoma warrants further investigation.

Although Sano *et al*.[7] have reported the occurrence of a late implantation metastasis arising 46 mo after PTBD for extrahepatic cholangiocarcinoma, most of our collected patients suffered from this complication within 21 mo after PTBD (Table 1). Thus, patients undergoing PTBD for extrahepatic cholangiocarcinoma should be monitored for catheter tract implantation for around 2 years.

The survival of patients with catheter tract implantation metastasis from extrahepatic cholangiocarcinoma was found to be generally poor (Table 1), as with our patients. Despite the metastatic nature of this condition, surprisingly, the outcome after the excision of the implantation metastasis was not so dismal in some patients with isolated implantation metastases (patients 1-4). The possibility that the course of deceased patients is unlikely to be reported (a publication bias) may, in part, explain this. In order to excise catheter tract metastases following PTBD, a hepatectomy is usually required, because the catheter tract runs through the liver parenchyma; in some patients, a local excision of the abdominal wall is also required. Two of the five patients who underwent a hepatectomy, with or without a local excision of the abdominal wall, for isolated implantation metastases (patients 1 and 2) survived for more than 5 years with no evidence of the disease. This clearly demonstrates that excision of the metastases offers the only chance for long-term survival.

The issue how to prevent catheter tract implantation metastasis following PTBD is yet to be resolved. Although excision of the catheter tract along with the resection of the primary tumor appears to be effective, it is practically difficult to excise the whole catheter tract between the surface of the skin and the punctured intrahepatic bile ducts. Some authors have advocated ethanol injection into the catheter tract to prevent cancer implantation[10,19,20]. However, Shimizu and colleagues have reported a case of implantation metastasis following ethanol injection[10]. Further investigation is warranted to conclude the effects of this procedure.

In conclusion, catheter tract implantation metastasis is not a rare complication following PTBD for extrahepatic

cholangiocarcinoma. Although the prognosis for patients with this complication is generally poor, excision of the catheter tract, which usually requires a hepatectomy, enables long-term survival in selected patients with isolated implantation metastases.

REFERENCES

1 **Takada T,** Hanyu F, Kobayashi S, Uchida Y. Percutaneous transhepatic cholangial drainage: direct approach under fluoroscopic control. *J Surg Oncol* 1976; **8**: 83-97

2 **Hatfield AR**, Tobias R, Terblanche J, Girdwood AH, Fataar S, Harries-Jones R, Kernoff L, Marks IN. Preoperative external biliary drainage in obstructive jaundice. A prospective controlled clinical trial. *Lancet* 1982; **2:** 896-899

3 **Nimura Y**, Hayakawa N, Kamiya J, Kondo S, Shionoya S. Hepatic segmentectomy with caudate lobe resection for bile duct carcinoma of the hepatic hilus. *World J Surg* 1990; **14:** 535-543; discussion 544

4 **Nagino M,** Hayakawa N, Nimura Y, Dohke M, Kitagawa S. Percutaneous transhepatic biliary drainage in patients with malignant biliary obstruction of the hepatic confluence. *Hepatogastroenterology* 1992; **39:** 296-300

5 **Wakai T**, Shirai Y, Moroda T, Yokoyama N, Hatakeyama K. Impact of ductal resection margin status on long-term survival in patients undergoing resection for extrahepatic cholangiocarcinoma. *Cancer* 2005; **103**: 1210-1216

6 **Chapman WC**, Sharp KW, Weaver F, Sawyers JL. Tumor seeding from percutaneous biliary catheters. *Ann Surg* 1989; **209:** 708-713; discussion 713-715

7 **Sano T,** Nimura Y, Hayakawa N, Kamiya J, Kondo S, Nagino M, Kanai M, Miyachi M, Uesaka K. Partial hepatectomy for metastatic seeding complicating pancreatoduodenectomy. *Hepatogastroenterology* 1997; **44**: 263-267

8 **Inagaki M,** Yabuki H, Hashimoto M, Maguchi M, Kino S, Sawa M, Ojima H, Tokusashi Y, Miyokawa N, Kusano M, Kasai S. Metastatic seeding of bile duct carcinoma in the transhepatic catheter tract: report of a case. *Surg Today* 1999; **29**: 1260-1263

9 **Matsumoto A,** Imamura M, Akagi Y, Kaibara A, Ohkita A, Mizobe T, Isomoto H, Aoyagi S. A case report of disseminated recurrence of inferior bile duct carcinoma in PTCD fistula. *Kurume Med* J 2002; **49**: 71-75

10 **Shimizu Y,** Yasui K, Kato T, Yamamura Y, Hirai T, Kodera Y, Kanemitsu Y, Ito S, Shibata N, Yamao K, Ohhashi K. Implantation metastasis along the percutaneous transhepatic biliary drainage sinus tract. *Hepatogastroenterology* 2004; **51**: 365-367

11 **Tersigni R,** Rossi P, Bochicchio O, Cavallini M, Ambrogi C, Bufalini G, Alessandroni L, Arena L, Armeni O, Miraglia F, Stipa S. Tumor extension along percutaneous transhepatic biliary drainage tracts. *Eur J Radiol* 1986; **6:** 280-282

12 **Omokawa S,** Hashizume T, Ohsato M, Nanjo H, Asanuma Y, Koyama K. Insemination of bile duct carcinoma to the liver after insertion of percutaneous biliary endoprosthesis. *Gastroenterol Jpn* 1991; **26**: 678-682

13 **Uenishi T,** Hirohashi K, Inoue K, Tanaka H, Kubo S, Shuto T, Yamamoto T, Kaneko M, Kinoshita H. Pleural dissemination as a complication of preoperative percutaneous transhepatic biliary drainage for hilar cholangiocarcinoma: report of a case. *Surg Today* 2001; **31**: 174-176

14 **Greene FL,** Page DL, Fleming ID, Fritz AG, Balch CM, Haller DG, Morrow M. American Joint Committee on Cancer (AJCC) Staging Manual. 6th ed. *New York: Springer-Verlag* 2002: 145-150

15 **Oleaga JA**, Ring EJ, Freiman DB, McLean GK, Rosen RJ. Extension of neoplasm along the tract of a transhepatic tube. *AJR Am J Roentgenol* 1980; **135:** 841-842

16 **Shorvon PJ**, Leung JW, Corcoran M, Mason RR, Cotton PB. Cutaneous seeding of malignant tumours after insertion of percutaneous prosthesis for obstructive jaundice. *Br J Surg* 1984; **71:** 694-695

17 **Kim WS,** Barth KH, Zinner M. Seeding of pancreatic carcinoma along the transhepatic catheter tract. *Radiology* 1982; **143**: 427-428

18 **Nimura Y,** Kamiya J, Kondo S, Nagino M, Uesaka K, Oda K, Sano T, Yamamoto H, Hayakawa N. Aggressive preoperative management and extended surgery for hilar cholangiocarcinoma: Nagoya experience. *J Hepatobiliary Pancreat Surg* 2000; **7**: 155-162

19 **Uesaka K**, Kamiya J, Nagino M, Yuasa N, Sano T, Oda K, Kanai M, Hayakawa N, Yamamoto H, Yokoi S, Nimura Y. [Treatment of recurrent cancer after surgery for biliary malignancies] *Nippon Geka Gakkai Zasshi* 1999; **100:** 195-199

20 **Kondo S,** Nimura Y, Hayakawa N, Kamiya J, Shionoya S. Ethanol injection for prevention of seeding metastasis along the tract after percutaneous transhepatic biliary drainage. *J Jpn Bil Assoc* 1989; **3:** 100-105 (in Japanese with English abstract)

Science Editor Guo SY **Language Editor** Elsevier HK

PO Box 2345, Beijing 100023, China
www.wjgnet.com
wjg@wjgnet.com

ELSEVIER

World J Gastroenterol 2005;11(44):7028-7032
World Journal of Gastroenterology ISSN 1007-9327

• *RAPID COMMUNICATION* •

Upper gastrointestinal carcinoid tumors incidentally found by endoscopic examinations

Seng-Kee Chuah, Tsung-Hui Hu, Chung-Mou Kuo, King-Wah Chiu, Chung-Huang Kuo, Keng-Liang Wu, Yeh-Pin Chou, Sheng-Nan Lu, Shue-Shian Chiou, Chi-Sin Changchien, Hock-Liew Eng

Seng-Kee Chuah, Tsung-Hui Hu, Chung-Mou Kuo, King-Wah Chiu, Chung-Huang Kuo, Keng-Liang Wu, Yeh-Pin Chou, Sheng-Nan Lu, Shue-Shian Chiou, Chi-Sin Changchien, Department of Hepato-Gastroenterology, Chang Gung Memorial Hospital, 123, Ta-Pei Road, Niao-sung Hsiang, Kaohsiung Hsien, Taiwan, China
Hock-Liew Eng, Department of Pathology, Chang Gung Memorial Hospital, 123, Ta-Pei Road, Niao-sung Hsiang, Kaohsiung Hsien, Taiwan, China
Co-first authors: Seng-Kee Chuah and Tsung-Hui Hu
Correspondence to: Shue-Shian Chiou, Department of Gastroenterology, Chang Gung Memorial Hospital, Kaohsiung Medical Center, 123, Ta-Pei Road, Niao-sung Hsiang, Kaohsiung Hsien, Taiwan, China. chuahsk@seed.net.tw
Telephone: +886-7-7317123 ext. 8301 Fax: +886-7-7322402
Received: 2005-03-27 Accepted: 2005-07-20

Abstract

AIM: This study shares Asian clinical experiences of carcinoid tumors that originated in the upper gastrointestinal tract.

METHODS: From May 1987 to June 2002, we had found only 13 cases of histologically confirmed carcinoid tumors in the upper gastrointestinal tract by endoscopic examinations. There were eight males and five females. The mean age was 53.16±20.51 years that ranged from 26 to 82 years. Each of their clinical presentations, locations, tumor morphology, and size and the treatment outcome were analyzed and discussed.

RESULTS: One patient had a polypoid lesion at the lower esophagus, nine were stomach lesions and three located at the duodenum. All patients with polypoid and submucosal tumor types were of small size (<1.7 cm) and all patients survived after simple excision or polypectomy. Four of the five patients in tumor mass forms died and the tumors were more than 2.0 cm in size.

CONCLUSION: Carcinoid tumors rarely originated from the upper gastrointestinal tract and are usually found accidentally after endoscopic study. Bigger size (more than 2 cm) tumor masses may indicate a more severe disease and poor prognosis.

Key words: Upper gastrointestinal carcinoid tumors; Tumor morphology; Sizes; Treatment courses; Prognosis

Chuah SK, Hu TH, Kuo CM, Chiu KW, Kuo CH, Wu KL, Chou YP, Lu SN, Chiou SS, Changchien CS, Eng HL. Upper gastrointestinal carcinoid tumors incidentally found by endoscopic examinations. *World J Gastroenterol* 2005; 11(44): 7028-7032
http://www.wjgnet.com/1007-9327/11/7028.asp

INTRODUCTION

Carcinoid tumors are a type of very slow-growing neuroendocrine tumors that originate from the embryonic neural crest. Their prominent feature is the production of multiple hormones[1]. The incidence is increasing at rates around 24.7-44.8 cases per million in the United States each year. Over 90% of all carcinoid tumors originate in the GI tract. Most carcinoid tumors are GI in origin, yet they only account for 1.5% of all gastrointestinal neoplasms. Most carcinoids are, in fact, found incidentally. Neither cytology nor histology can determine if the lesion is benign or malignant. Only the presence of distant metastases confirms malignancy.

However, all carcinoids must be considered malignant when found because of the high threat of metastasis. Although carcinoids <1 cm in diameter are unlikely to metastasize, a wide excision is recommended[1]. Five-year survival rates of patients with a local excision of carcinoid are >95%, metastases to the liver constitute a dismal 20% 5-year survival rate. Therefore, early detection as with most cancers is, desirable. In the past 15 years, we found only 13 cases of upper gastrointestinal tract carcinoid tumors by endoscopic examination. We tried to analyze and correlate the clinical settings, the sizes of tumors, their morphology, and the outcome of the disease.

MATERIALS AND METHODS

The medical records of these 13 patients who were diagnosed as upper GI carcinoid tumors at Chang Gung Memorial Hospital, Kaohsiung Center, Taiwan from May 1987 to June 2002 were reviewed. We excluded all the cases with an uncertain diagnosis, small-bowel cancers found in the GI tract but thought to have metastasized there from an extra-abdominal primary site, and patients were operated on for periampullary tumors. The final study population composed of 13 patients who were treated. There

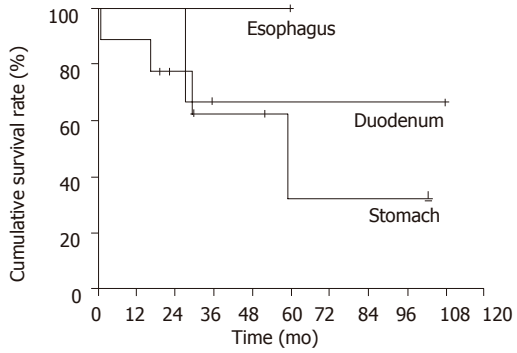

Figure 1 Cumulative survival of the upper gastrointestinal carcinoid tumors.

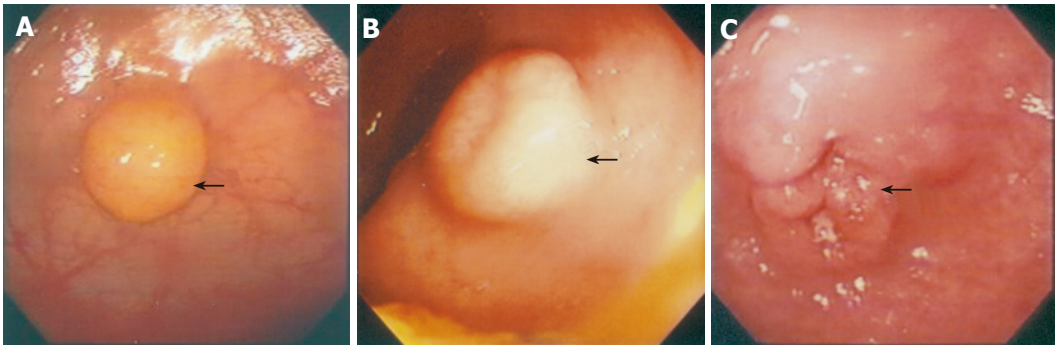

Figure 2 Subject **A:** A polypoid carcinoid lesion at the gastric fundus site about 0.8 cm with typical yellowish color of the lesion; **B:** A submucosal carcinoid lesion at the duodenal bulb about 1.7 cm; **C:** A carcinoid tumor with ulceration, at the antrum site, about 4.0 cm in size.

Table 1 Demographic data, morphology, sizes, treatment and outcome of patients with upper gastrointestinal carcinoid tumors

Patients	Age (yr)	Sex	Symptom	Location	Morphology	Size(cm)	Treatment	Outcome
1	26	Male	GI bleeding	Esophagus	Polyp	0.7	Polypectomy	(Survive)
2	81	Female	GI bleeding	Stomach	Polyp	0.4	Polypectomy	(Survive)
3	33	Female	Epigastralgia	Stomach	ST	0.9	Polypectomy	(Survive)
4	26	Female	Epigastralgia	Stomach	ST	1.0	Polypectomy	(Survive)
5	70	Female	Epigastralgia	Stomach	Polyp	0.5	Polypectomy	(Survive)
6	63	Male	Abdominal pain	Stomach	Tumor	10	Surgery	(Expired)
7	46	Male	GI bleeding	Stomach	ST	4.3	Surgery	(Survive)
8	62	Male	GI bleeding	Stomach	Tumor	4.0	Surgery	(Expired)
9	68	Male	Epigastralgia	Stomach	Tumor	1.5	Surgery	(Survive)
10	30	Male	Epigastralgia	Stomach	Tumor	>4.0	Supportive care	(Expired)
11	64	Female	Epigastralgia	Duodenum (bulb)	Polyp	0.9	Polypectomy	(Survive)
12	40	Male	Epigastralgia	Duodenum (bulb)	ST	1.7	Duodenectomy	(Survive)
13	82	Male	Jaundice	Duodenum (second portion)	Tumor	>2.0	Stenting	(Expired)

ST: submucosal tumor; All patients with polypoid and submucosal tumor types were of small size (<1.7 cm) and all survived. Four of the five patients in tumor mass form died and were more than 2.0 cm.

were eight males and five females. The mean age was 53.15 ±20.51 years ranging from 26 to 82 years (Figure 1).

The morphology of the tumors observed by endoscopic examinations was divided into three main categories: polypoid (Figure 2A), submucosal (Figure 2B), tumor-like (Figure 2C) lesions. A single surgical pathologist reviewed pathological specimens and histological features. Routine hematoxylin-eosin stains, immunohistochemistry, or elevated urinary 5-hydroxyindole acetic acid levels established the diagnosis of carcinoid tumor. Survival duration was measured from the time of diagnosis to the last follow-up evaluation or death. The follow-up observations were obtained from the medical records of the patients or direct contact with the patients, their relatives, or primary care physician. The endoscopic observations of the lesions such as the morphologic appearance and the sizes were analyzed in correlation to the treatment course and prognosis of each recorded patient (Table 1).

RESULTS

This study group included eight men and five women, with the median follow-up duration of 36 mo. The most common symptom was abdominal pain (53%), followed by weight loss (38.5%), GI tract bleeding (23%) and jaundice (7.7%). Some patients had more than one symptom or physical finding, though no combination of signs, symptoms, or acuity of presentation was thought to have any influence on the prognosis.

Only one 26-year-old male patient had a 0.7-cm esophageal carcinoid lesion, polypoid in appearance and located at the lower esophagus. Polypectomy was done for him and no signs of recurrence for more than 5 years. Nine patients suffered from gastric carcinoid tumors and three of them died. All these three patients had gastric tumor masses of at least 4 cm in size found by endoscope. One patient had tumor involving colon, spleen, and pancreas, while the other had metastatic mesenteric lymphnodes. Both underwent surgery but still failed to survive due to sepsis and organ failure.

A 30-year-old female had a huge mass over the pelvis extended to almost the whole of the left side abdomen. Endoscope showed a 4.0-cm ulcerated mass over the cardiac portion and fundus. Carcinoid tumor was proven by snare biopsy. She also suffered from a septic right knee. Due to the poor general condition, she received supportive treatment only. One 68-year-old male patient had a 1.5-cm tumor mass at gastric antrum who received complete resection already and survived for 6 years. One 46-year-old male patient had been suffering from repeated gastroduodenal ulcers bleeding. Scope reviewed a more than 4 cm slightly elevated submucosal lesion at the antrum. Computer tomography and angiography showed a tumor mass bulging out posterior to the stomach. He had been well after surgical resection of the antrum.

All four patients who had gastric carcinoid lesions smaller than 1.0 cm survived, and the morphology were polypoid (n = 2) and appearance of submucosa (n = 2). Two received polypectomies and two mucosectomies and there are no signs of recurrence so far.

Three patients had duodenal carcinoid lesions, two located in the duodenal bulb and one in the second portion of the duodenum. One 64-year-old female patient had a 0.9-cm polypoid lesion at the bulb portion, and polypectomy was performed. The other 40-year-old male patient who had a 1.7-cm submucosal lesion at bulb received duodenectomy. Both of them are still alive and disease-free at 4 and 6 years status post therapy. However, one 82-year-old female patient who suffered from obstructive jaundice by a carcinoid tumor mass at the duodenal second portion was not as fortunate. Stent was placed by using endoscope to relieve her obstructive jaundice but she still died because of sepsis shortly after.

The cumulative 5-year survival rate was 64% in the carcinoid tumor. Gastric carcinoid had the worse prognosis in this study with 5-year survival of less than 40%. Duodenal carcinoid tumor had a 5-year survival of about 60%. Only one case was found with a carcinoid in the esophagus and the patient is still surviving but the total number of patients is too small to come to any conclusion.

DISCUSSION

Carcinoid tumor of the esophagus is exceedingly rare, and the knowledge about this tumor is based primarily on case reports[2]. Several case reports have emphasized that esophageal carcinoid tumors are associated with a poor prognosis[2]. Primary endocrine tumors of the esophagus are rare tumors that include small cell carcinoma, large cell neuroendocrine carcinoma, atypical carcinoid tumor, classical carcinoid tumor, and combined endocrine tumor and adenocarcinoma[2]. Small cell carcinoma of the esophagus accounts for 1% of all esophageal tumors, and the overall median survival is 3.1 mo[3]. The only one case, who had a small polyp at distal esophagus, still survives, 50 mo after endoscopic polypectomy. Although only one case was treated, it supported that esophageal carcinoid tumors are not always associated with a poor prognosis probably as a non-small cell carcinoma.

Three types of gastric carcinoids have been described[4,5]. Type I is associated with chronic atrophic body-fundus gastritis type A. Type II is seen in Zollinger-Ellison syndrome/multiple endocrine neoplasia type I (MEN-1) syndrome. Type III is a sporadic tumor[6]. Gastric carcinoids arise from endocrine cells in gastric mucosa and recent reports indicate that 10-30% of all gastrointestinal carcinoids occur in the stomach[6].

Type I gastric carcinoids is the most frequent type encountered in about 65% of cases[7]. The tumors are usually small (<1 cm) polypoid lesions located in the gastric body or fundus[8]. Adjacent atrophic mucosa contains foci of precursor lesions, which are at different stages of ECL cell hyperplasia, dysplasia, and neoplasia. Hypergastrinemia is usually present[6]. Nodal metastasis is reported in up to 16% of cases and hepatic metastasis, in up to 4%[9]. Endocrine symptoms are rare; 5-year survival is high in our series, four gastric carcinoids were less than 1.0 cm in size, either in polypoid or submucosal in morphology endoscopically. Polypectomies and endoscopic mucosectomy were performed smoothly and they still survive.

One of our patients who belonged to type II gastric carcinoids suffered from repeated GI bleeding and hypergastrinemia. After receiving operation, he is still healthy. The adjacent mucosa is non-atrophic and entirely comprised precursor lesions[6]. Prognosis is intermediate, between types I and III[7].

Type III gastric lesions make about 20% of gastric carcinoids[6]. Forty percent occur in the antropyloric area[6] when discovered; they are usually single tumor more than 2 cm. They arise from ECL, EC, or X cells. There is no hypergastrinemia and no precursor lesions. They can cause either a classic syndrome of facial flushing, abdominal cramps, diarrhea, left-sided endocardial fibrosis, and 24 h urinary 5-HIAA more than 10 mg, or an atypical carcinoid syndrome associated with vasoactive substances and

polypeptide hormone production[6]. Nodal metastasis is reported in 55% of patients and liver metastases, in 25% of patients[5]. Five-year survival is only 50%[7]. All the four of our patients with gastric tumor masses of more than 4 cm in size were associated with adjacent and distant metastasis. Two had carcinoid syndrome. Three received surgical intervention and one had supportive care. Three of them expired.

Schneider *et al*.[10] showed that the patients with gastric carcinoids had an eight times higher risk of developing a secondary malignancy as compared with the normal population. None of our gastric carcinoids had secondary carcinomas so far.

The management of gastric carcinoids depends on the type; presence of symptoms, or metastases spread, size, and number of tumors[6]. Although multiple studies have been published, the treatment in many cases still remains controversial. Most agreed on the management of type III (or sporadic) carcinoids, which have the worst prognosis and the highest rate of metastasis and associated carcinoid syndrome[6]. The recommended therapy is *en bloc* surgical resection with regional lymph node dissection, especially for lesions of more than 2 cm[5,11,12]. If the tumor penetrated the serosa, gastrectomy is also recommended[13].

For the patients with liver metastasis, surgical resection of tumor foci or selective hepatic artery ligation or embolization may reduce the symptoms and improve survival[6]. Chemotherapy of disseminated disease with streptozocin, 5-FU, cyclophosphamide, and doxorubicin were reported to produce a 20-40% response rate[6]. Leukocyte interferon produced a temporary response in some patients[5]. Somatostatin analogs, octreotide, and lanreotide have been used successfully in recent years to relieve the symptoms of carcinoid syndrome[14]. Recently, the results of trials with long-acting formulations octreotide-LAR (10, 20, or 30 mg every 28 d) and lanreotide-PR (30 mg every 2 wk) were published and demonstrated effectiveness and convenience of the treatment[15-18].

The optimal management of the types I and II gastric carcinoids is less clear[6]. Many authors base their recommendations on the size and number of the tumors[6]. For lesions less than 1 cm in diameter and less than 3-5 in number, endoscopic removal and semiannual EGD surveillance is recommended[6]. If there is a recurrence, or if the lesions are larger than 1 cm or more than 3-5 in number, then antrectomy with endoscopic excision is recommended[5,13].

Type I is considered as the most benign type of gastric carcinoids, rarely affecting the 5-year survival[8]. There are strong arguments supporting surgery[6]. Although type I carcinoid is the most benign type, it is still associated with some incidence of lymph node and liver metastasis[7,8]. Most gastric carcinoids regress after antrectomy[12,19-21]. In contrast, improved overall survival for metastatic neuroendocrine tumors after the complete resection of primary and hepatic metastases is accomplished, with an actuarial 5-year survival rate of 70%.

Carcinoid tumor was the most common small bowel tumor. It occurred in 24% of patients. Forty-six percent of patients were asymptomatic during life, the tumors being found either at autopsy or during other surgical procedures. Of those that were symptomatic, half presented with intestinal obstruction and the rest with long-standing symptoms. An abdominal mass, which occurred in 14% of cases, is an uncommon physical finding since the majority present as small submucosal tumors. Fifty-eight percent overall and 72% of those having surgery had evidence of regional spread, either by local invasion or in the form of regional nodal involvement. Seven percent of patients have died because of their disease. Excision surgery should be performed for all cases where feasible, and repeated for recurrent symptoms[22].

Ampullary carcinoids are rare tumors. Like the 82-year-old male in our series, they most commonly present with obstructive symptoms like jaundice and nonspecific abdominal discomfort. They are difficult to diagnose preoperatively secondary to their relatively small size and submucosal location. Rarely, ulcerated duodenal carcinoids can present as a source of significant gastrointestinal bleeding. Overall, approximately 80-90% of all carcinoids secrete serotonin or its precursor 5-hydroxy tryptophan, and other tumors rarely do so. Measurements of serotonin and its metabolites like urinary 5-hydroxy indole acetic acid (5-HIAA) have been described to be very helpful in the diagnosis and postresection follow-up of carcinoids. In our patient, those levels were not obtained preoperatively as the patient did not have any signs, symptoms, or histologic evidence to suggest a diagnosis of carcinoid tumor[23].

In conclusion, carcinoid tumors rarely originated from the upper gastrointestinal tract in the eastern countries and are usually found incidentally after endoscopic study. Bigger size (more than 2 cm) tumor mass form may indicate a more severe disease and poor prognosis.

REFERENCES

1 **Onaitis MW**, Kirshbom PM, Hayward TZ, Quayle FJ, Feldman JM, Seigler HF, Tyler DS. Gastrointestinal carcinoids: characterization by site of origin and hormone production. *Ann Surg* 2000; **232:** 549-556

2 **Hoang MP**, Hobbs CM, Sobin LH, Albores-Saavedra J. Carcinoid tumor of the esophagus: a clinicopathologic study of four cases. *Am J Surg Pathol* 2002; **26:** 517-522

3 **Law SY**, Fok M, Lam KY, Loke SL, Ma LT, Wong J. Small cell carcinoma of the esophagus. *Cancer* 1994; **73:** 2894-2899

4 **Rindi G**, Luinetti O, Cornaggia M, Capella C, Solcia E. Three subtypes of gastric argyrophil carcinoid and the gastric neuroendocrine carcinoma: a clinicopathologic study. *Gastroenterology* 1993; **104:** 994-1006

5 **Creutzfeldt W**. The achlorhydria-carcinoid sequence: role of gastrin. *Digestion* 1988; **39**: 61-79

6 **Rybalov S**, Kotler DP. Gastric carcinoids in a patient with pernicious anemia and familial adenomatous polyposis. *J Clin Gastroenterol* 2002; **35:** 249-252

7 **Ahlman H**, Kolby L, Lundell L, Olbe L, Wangberg B, Granerus G, Grimelius L, Nilsson O. Clinical management of gastric carcinoid tumors. *Digestion* 1994; **55 Suppl 3:** 77-85

8 **Borch K**. Atrophic gastritis and gastric carcinoid tumours. *Ann Med* 1989; **21**: 291-297

9 **Higham AD**, Dimaline R, Varro A, Attwood S, Armstrong G, Dockray GJ, Thompson DG. Octreotide suppression test

predicts beneficial outcome from antrectomy in a patient with gastric carcinoid tumor. *Gastroenterology* 1998; **114:** 817-822
10 **Schneider C**, Wittekind C, Kockerling F. An unusual incidence of carcinoid tumors and secondary malignancies. *Chirurg* 1995; **66:** 607-611
11 **Modlin IM**, Gilligan CJ, Lawton GP, Tang LH, West AB, Darr U. Gastric carcinoids. The Yale Experience. *Arch Surg* 1995; **130:** 250-255; discussion 255-256
12 **Thirlby RC**. Management of patients with gastric carcinoid tumors. *Gastroenterology* 1995; **108**: 296-297
13 **Ahren B**, Borch K. Multiple gastric carcinoid tumours. *Eur J Surg* 1995; **161:** 375
14 **O'Toole D**, Ducreux M, Bommelaer G, Wemeau JL, Bouche O, Catus F, Blumberg J, Ruszniewski P. Treatment of carcinoid syndrome: a prospective crossover evaluation of lanreotide versus octreotide in terms of efficacy, patient acceptability, and tolerance. *Cancer* 2000; **88:** 770-776
15 **Bajetta E**, Bichisao E, Artale S, Celio L, Ferrari L, Di Bartolomeo M, Zilembo N, Stani SC, Buzzoni R. New clinical trials for the treatment of neuroendocrine tumors. *Q J Nucl Med* 2000; **44:** 96-101
16 **Ricci S**, Antonuzzo A, Galli L, Orlandini C, Ferdeghini M, Boni G, Roncella M, Mosca F, Conte PF. Long-acting depot lanreotide in the treatment of patients with advanced neuroendocrine tumors. *Am J Clin Oncol* 2000; **23:** 412-415
17 **Anthony LB**. Long-acting formulations of somatostatin analogues. *Ital J Gastroenterol Hepatol* 1999; **31 Suppl 2:** S216-S218
18 **Tomassetti P**, Migliori M, Corinaldesi R, Gullo L. Treatment of gastroenteropancreatic neuroendocrine tumours with octreotide LAR. *Aliment Pharmacol Ther* 2000; **14:** 557-560
19 **Hirschowitz BI**, Griffith J, Pellegrin D, Cummings OW. Rapid regression of enterochromaffinlike cell gastric carcinoids in pernicious anemia after antrectomy. *Gastroenterology* 1992; **102:** 1409-1418
20 **Richards AT**, Hinder RA, Harrison AC. Gastric carcinoid tumours associated with hypergastrinaemia and pernicious anaemia--regression of tumors by antrectomy. A case report. *S Afr Med J* 1987; **72:** 51-3
21 **Hirschowitz BI**, Griffith J, Pellegrin D, Cummings OW. Rapid regression of enterochromaffinlike cell gastric carcinoids in pernicious anemia after antrectomy. *Gastroenterology* 1992; **102:** 561-566
22 **O'Rourke MG**, Lancashire RP, Vattoune JR. Carcinoid of the small intestine. *Aust N Z J Surg* 1986; **56:** 405-8
23 **Singh VV**, Bhutani MS, Draganov P. Carcinoid of the minor papilla in incomplete pancreas divisum presenting as acute relapsing pancreatitis. *Pancreas* 2003; **27:** 96-97

Science Editor Guo SY **Language Editor** Elsevier HK

PO Box 2345, Beijing 100023, China
www.wjgnet.com
wjg@wjgnet.com

ELSEVIER

World J Gastroenterol 2005;11(44):7033-7035
World Journal of Gastroenterology ISSN 1007-9327

• *RAPID COMMUNICATION* •

Cell cycle and radiosensitivity of progeny of irradiated primary cultured human hepatocarcinoma cells

Zhi-Zhong Liu, Wen-Ying Huang, Ju-Sheng Lin, Xiao-Sheng Li, Kuo-Huan Liang, Jia-Long Huang

Zhi-Zhong Liu, Ju-Sheng Lin, Kuo-Huan Liang, Jia-Long Huang, Institute of Liver Diseases, Tongji Hospital, Tongji Medical College, Huazhong University of Science and Technology, Wuhan 430030, Hubei Province, China
Wen-Ying Huang, The People's Hospital of Chenzhou City, Chenzhou 423000, Hunan Province, China
Xiao-Sheng Li, Xiehe Hospital, Tongji Medical College, Huazhong University of Science and Technology, Wuhan 430030, Hubei Province, China
Correspondence to: Zhi-Zhong Liu, Institute of Liver Diseases, Tongji Hospital, Tongji Medical College, Huazhong University of Science and Technology, Wuhan 430030, Hubei Province, China. whzzl@163.net
Telephone: +86-27-13554460933
Received: 2004-06-18 Accepted: 2004-08-20

Abstract

AIM: To evaluate the change of growth characteristics and radiosensitivity of irradiated primary cultured human hepatocarcinoma cells.

METHODS: All tumor tissue samples were obtained from 39 hepatocarcinoma patients with a mean age of 49.6 years (range 22-76 years). We divided the samples into irradiated group and non-irradiated group and measured their plating efficiency (PE), population doubling time (PDT), radiosensitivity index SF2 and cell cycle.

RESULTS: The PDT of primary culture of hepatocarcinoma cells was 91.0±6.6 h, PE was 12.0±1.4%, SF2 was 0.41±0.05%. The PDT of their irradiated progeny was 124.8±5.8 h, PE was 5.0±0.7%, SF2 was 0.65±0.09%. The primary cultured human hepatocarcinoma cells showed significant S reduction and G^2 arrest in a dose-dependent manner. The progeny of irradiated primary cultured hepatocarcinoma cells grew more slowly and its radiosensitivity increased.

CONCLUSION: The progeny of irradiated primary cultured human hepatocarcinoma cells grows more slowly and its radiosensitivity increases.

Key words: Hepatocarcinoma; Cell cycle; Population doubling time; Radiosensitivity

Liu ZZ, Huang WY, Lin JS, Li XS, Liang KH, Huang JL. Cell cycle and radiosensitivity of progeny of irradiated primary cultured human hepatocarcinoma cells. *World J Gastroenterol* 2005; 11(44): 7033-7035
http://www.wjgnet.com/1007-9327/11/7033.asp

INTRODUCTION

Hepatocarcinoma cells have a better reaction to X-rays. The mechanism of radiosensitivity of hepatocarcinoma cells after radiotherapy is not very clear. In this study, we have used primary cultured human hepatocarcinoma cells *in vitro* to evaluate the change of growth characteristics and radiosensitivity of progeny of irradiated primary hepatocarcinoma cells.

MATERIALS AND METHODS

Specimens

All tumor tissue specimens were obtained from 39 hepatocarcinoma patients with a mean age of 49.6 years (range 22-76 years).

Cell culture

Primary hepatocarcinoma tissue specimens were obtained from hepatocarcinoma patients. The volume of the sample was 1.5 cm^3. Cells were grown in Dulbecco's minimal essential medium (DMEM) containing 25% fetal calf serum and incubated at 37 °C in 50 mL/L CO_2. Most cells were anchored after inoculation for 16 h and the cell growth could be seen after inoculation for 48 h. Then the primary cultured human hepatocarcinoma cells entered the experimental growth phase. The proliferation was very productive and ended 7-8 d after incubation. The density of cells was 50-95% in flask with a few fibroblasts. The time was the best opportunity for irradiation in flask.

Irradiation condition

The samples were divided into irradiated group and non-irradiated group. Cells in the experimental growth phase were irradiated with 2-8 Gy of X-ray at a dose rate of 200 cGy/min and divided into five groups (0-8 Gy). The lucite was placed in dishes.

Population doubling time (PDT)

Cells in the experimental growth phase were digested into single-cell suspension by 2.5 g/L trypsin. *In vitro* transduction was performed by plating 1×10^5 cells in 6-cm^2 flasks. Cells were digested after being irradiated for 48, 72, 96, 120, 144 h and counted. The experiment was repeated thrice. The cell growth curve was drawn and the cell PDT was calculated.

Table 1 PDT and PE between irradiated and non-irradiated human hepatocarcinoma cells (mean±SD)

Dose (Gy)	PDT (PDT) (t/h)	PE (%)
0	91.0±6.6	12.0±1.4
2	104.7±2.1	10.2±0.6
4	120.4±2.8	8.2±0.4
6	133.5±1.4	6.0±1.1
8	141.8±5.8[a]	5.0±0.7[b]

[a]P<0.05, [b]P<0.01 *vs* 0 Gy.

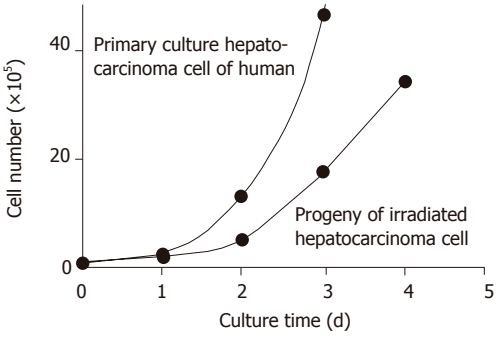

Figure 1 Cell growth curve and irradiated progeny of primary cultured human hepatocarcinoma cells.

Colony assay

Cells in the experimental growth phase were digested into single-cell suspension by 2.5 g/L trypsin. *In vitro* transduction was performed by plating 1×10^5 cells in 3-cm^2 flasks. Cells were irradiated with 2-8 Gy. After 12-15 d of plating, the culture was ended. Cells were fixed by formaldehyde and stained with Giemsa. The number of colonies exceeding 50 was defined as positive. The survival fraction rate was the colony rate. Three parallel samples were set in each dosage point and the experiment was repeated thrice. The formulations [SF2 = e-($aD+\beta D2$)] (the secondary equation) and [(S = 1-(1–e-KD)N)] (the multi-target click model) were used to simulate the cell survival curve of hepatocarcinoma cells. The radiosensitivity parameters such as SF2, α, D_0, and N were calculated.

Detection of cell cycle

Cells in the experimental growth phase were irradiated with 2-8 Gy (Linear Accelerator Saturn 43 type). Cells after being irradiated were retrieved at five time points (0, 6, 12, 24, 36 h) and centrifuged (800 r/min). Then the cells were washed twice with PBS. The single-cell suspension was fixed in 80% ethanol and then treated with RNase. At last, the cells were resuspended and incubated for 30 min at 4 ℃. Cellular fluorescence was measured by FASort flow cytometry (Becton Dickinson). The data were analyzed by CELLQuest software.

Statistical analysis

Using the SPSS 10.0 statistical analysis software, cell growth curve and cell survival curve were simulated by square regression. The cell cycle ratio and radiosensitivity parameters were expressed as mean±SD. Student's t-test was used to compare the difference between the two groups.

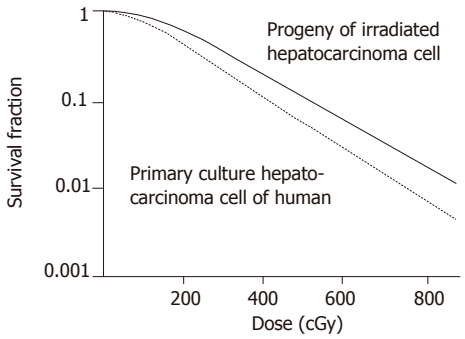

Figure 2 Cell survival curve of primary human hepatocarcinoma cells and irradiated progeny.

RESULTS

Plating efficiency (PE) and cell population doubling time of irradiated progeny

The plating efficiency (PE) of primary cultured human hepatocarcinoma cells was 12.0 ± 1.4%, the irradiated progeny was 5.0±0.7%, being significantly higher than that of non-irradiated cells (t = 8.547, P<0.01). The cell PDT of progeny of irradiated human hepatocarcinoma cells was longer than that of non-irradiated ones. The cell PDT of primary cultured human hepatocarcinoma cells was 91.0 ±6.6 h. The PDT difference between irradiated progeny and non-irradiated cells was significant (t = 3.672, P<0.05; Table 1 and Figure 1).

Radiosensitivity of irradiated progeny

The survival curve and irradiated progeny of human hepatocarcinoma cells are shown in Figure 2. SF2, α, D_0, and N of primary human hepatocarcinoma cells were 0.41±0.05, 0.37/Gy, 0.43 Gy, 2.52, respectively. SF2, α, D_0, and N of irradiated progeny were 0.65±0.09, 0.10/Gy, 0.61 Gy, 1.08, respectively (t = 3.863, P<0.05). The difference was significant. Both SF2 and radiosensitivity of hepatocarcinoma cells were increased in human hepatocarcinoma cells and irradiated progeny.

Detection of cell cycle

Cells in the experimental growth phase were irradiated with 2-8 Gy (Linear Accelerator Saturn 43 type). The cells decreased in S phase and increased in G_2/M phase in a dose-dependent manner (P<0.05). The DNA synthesis time was shorter and mitosis was delayed. The cells after mitosis entering G_0/G_1 phase decreased in a dose-dependent manner (Table 2).

DISCUSSION

The results of radiosensitivity *in vitro* of carcinoma cells are closely related with the clinical effect of carcinoma

Table 2 Cells in S and G2/M phase of irradiated progeny (mean±SD)

Dose (Gy)	SPF (%)	G2/M (%)
0	66.10±0.75	0.91±0.19
2	61.52±0.22	1.73±0.53
4	50.15±0.68	3.32±0.68
6	43.35±0.24	4.51±0.92
8	33.32±0.51[a]	6.48±0.57[a]

[a]$P<0.05$ *vs* oGy.

radiotherapy. But most studies showed that there have been great differences in radiosensitivity of identical carcinomas[1-2]. Studies indicate that radiation can lead to the instability of cell genes and survived progeny will occur[3]. It was reported that irradiated progeny produces resistance after radiation or DNA damage[4-5].

There is evidence that carcinoma is a cell cycle disease. The malignant level of carcinoma is closely related with cell cycle. The carcinoma cells in different cell cycle phases have different radiosensitivity to chemotherapy drugs. Proliferating cells have a good radiosensitivity. Radiotherapy can change the processes of cell cycle. It displays G_0, G_2/M, and S arrest. To study the alteration of cell cycle after radiation is of great significance in choosing suitable chemotherapy drugs after radiotherapy.

Our study indicated that the growth characteristics of progeny of human hepatocarcinoma cells were changed after being irradiated with 2-8 Gy. The growth speed was delayed, the PE was decreased and the radiosensitivity was increased. The radiosensitivity of irradiated progeny was related with G_2/M arrest and cells in S phase reduced in a dose-dependent manner. The radiosensitivity of cells in S phase was the highest due to decreased progeny of irradiated human hepatocarcinoma cells and PE as well as delayed PDT cell reaction in S phase and G_2/M arrest[6].

In conclusion, stereotactic radiotherapy can achieve better results in the treatment of hepatocarcinoma.

REFERENCES

1 **Xia YF**, Li MZ, Huang B, Chen JJ, Li ZQ, Wang HM, Brook WA. Cellular radiobiological characteristics of human nasopharyngeal carcinoma cell lines. *Ai Zheng* 2001; **20:** 683
2 **Hu B**, Zhou XY, Wang X, Zeng ZC, Iliakis G, Wang Y. The radioresistance to killing of A1-5 cells derives from activation of the Chk1 pathway. *J Biol Chem* 2001; **276:** 17693-17698
3 **Shi WM**, Fan YX, Chen LH. The study of radiosensitivity of two human being hepatocacinoma cell lines in vitro. *Zhongguo Xiandai Yixue* 2001; **11:** 6-7
4 **Pitot HC**, Hikita H, Dragan Y, Sargent L, Haas M. Review article: the stages of gastrointestinal carcinogenesis--application of rodent models to human disease. *Aliment Pharmacol Ther* 2000; **14 Suppl 1:** 153-160
5 **Zhang XW**, Zhang LZ, Zhou XM, Wu SY, Wang YP, Zhang W. The relationship between hydatidiform mole canceration and Y chromatosome. *Beijing Yixue* 2002; **24:** 82-83
6 **Ku JL**, Yoon KA, Kim IJ, Kim WH, Jang JY, Suh KS, Kim SW, Park YH, Hwang JH, Yoon YB, Park JG. Establishment and characterisation of six human biliary tract cancer cell lines. *Br J Cancer* 2002; **87:** 187-193

Science Editor Wang XL and Guo SY **Language Editor** Elsevier HK

PO Box 2345, Beijing 100023, China
www.wjgnet.com
wjg@wjgnet.com

ELSEVIER

World J Gastroenterol 2005;11(44):7036-7039
World Journal of Gastroenterology ISSN 1007-9327

• *RAPID COMMUNICATION* •

Prediction value of radiosensitivity of hepatocarcinoma cells for apoptosis and micronucleus assay

Zhi-Zhong Liu, Wen-Ying Huang, Xiao-Sheng Li, Ju-Sheng Lin, Xiao-Kun Cai, Kuo-Huang Lian, He-Jun Zhou

Zhi-Zhong Liu, Ju-Sheng Lin, Xiao-Kun Cai, Kuo-Huang Lian, He-Jun Zhou, Tongji Hospital, Tongji Medical College, Huazhong University of Science and Technology, Wuhan 430030, Hubei Province, China
Wen-Ying Huang, The People's Hospital of Chenzhou City, Chenzhou 423000, Hunan Province, China
Xiao-Sheng Li, Xiehe Hospital, Tongji Medical College, Huazhong University of Science and Technology, Wuhan 430030, Hubei Province, China
Correspondence to: Dr Zhi-Zhong Liu, Institute of Liver Diseases, Tongji Hospital, Tongji Medical College, Huazhong University of Science and Technology, Wuhan 430030, Hubei Province, China. whzzl@163.net
Telephone: +86-27-13554460433
Received: 2004-05-07 Accepted: 2004-08-18

Abstract

AIM: To investigate the prediction value of radiosensitivity of hepatocarcinoma cells for apoptosis and micronucleus assay.

METHODS: Clonogenic assay, flow cytometry, and CB micronuclei assay were used to survey the cell survival rate, radiation-induced apoptosis and micronucleus frequency of hepatocarcinoma cell lines SMMC-7721, HL-7702, and HepG2 after being irradiated by X-ray at the dosage ranging 0-8 Gy.

RESULTS: After irradiation, there was a dose-effect relationship between micronucleus frequency and radiation dosage among the three cell lines ($P<0.05$). A positive relationship was observed between apoptosis and radiation dosage among the three cell lines. The HepG2 cells had a significant correlation ($P<0.05$) but apoptosis incidence had a negative relationship with micronucleus frequency. There was a positive relationship between apoptosis and radiation dosage and the correlation between SMMC-7721 and HL-7702 cell lines had a significant difference ($P<0.01$). After irradiation, a negative relationship between cell survival rate and radiation dosages was found among the three cell lines ($P<0.01$). There was a positive relationship between cell survival rate and micronucleus frequency ($P<0.01$). No correlation was observed between apoptosis and cell survival rate.

CONCLUSION: The radiosensitivity of hepatocarcinoma cells can be reflected by apoptosis and micronuclei. Detection of apoptosis and micronuclei could enhance the accuracy for predicting radiosensitivity.

Key words: Hepatocarcinoma cell; Micronuclei; Apoptosis; Radiosensitivity

Liu ZZ, Huang WY, Li XS, Lin JS, Cai XK, Lian KH, Zhou HJ. Prediction value of radiosensitivity of hepatocarcinoma cells for apoptosis and micronucleus assay. *World J Gastroenterol* 2005; 11(44): 7036-7039
http://www.wjgnet.com/1007-9327/11/7036.asp

INTRODUCTION

The prediction of cell radiosensitivity is a main content in radiobiology and carcinoma treatment. Apoptosis of carcinoma cells can be induced by radiotherapy. Micronucleus is a product of abnormal mitosis. Studies have verified that micronucleus analysis can predict radiosensitivity of cells[1,2]. It was reported that apoptosis is correlated with cell survival[3,4]. Apoptosis and micronuclei occur after the first mitosis and are related with the damage in heredity substance. To investigate apoptosis and micronucleus assay is of significance in predicting radiosensitivity.

This study focused on the relationship among apoptosis, micronuclei, and cell survival rate of three hepatic cell lines (HL-7702, HepG2, SMMC-7721). The prediction value of radiosensitivity for apoptosis and micronucleus assay of hepatocarcinoma cells was investigated *in vitro*.

MATERIALS AND METHODS

Three hepatic carcinoma cell lines (HL-7702, HepG2, SMMC-7721) were cultured at 37 ℃ in RPMI 1640 medium supplemented with 10% fetal bovine serum and divided into irradiated group and non-irradiated group. Cells in experimental growth phase were irradiated by X-ray at a dose of 2-8 Gy (Linear Accelerator Saturn 43 type) with a dose rate of 200 cGy/min. The lucite was placed in dishes.

Cells in the experimental growth phase were digested by 2.5 g/L trypsin into a single-cell suspension. *In vitro* transduction was performed by plating 1×10^5 cells in 3-cm^2 flasks. Cells were irradiated with 2-8 Gy. After 12-15 d of plating, the culture was stopped. Cells were fixed by formaldehyde and stained with Giemsa. The number

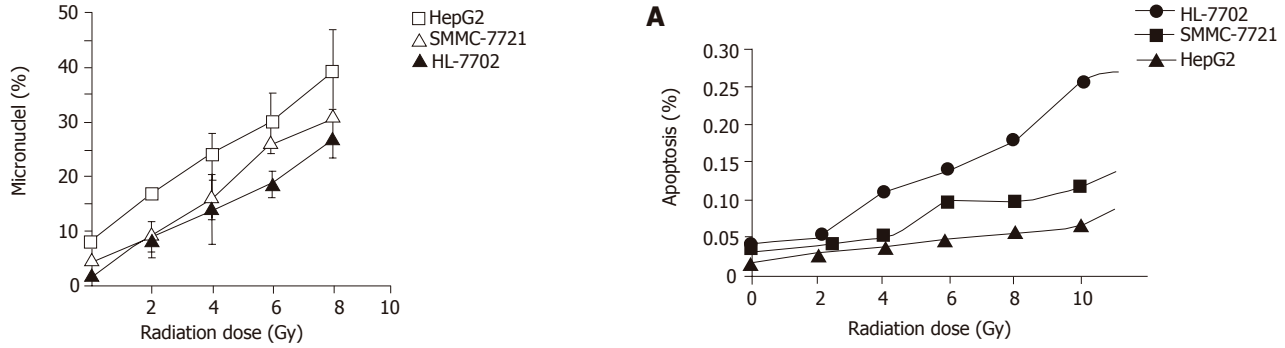

Figure 1 Micronucleus frequency of three cell lines.

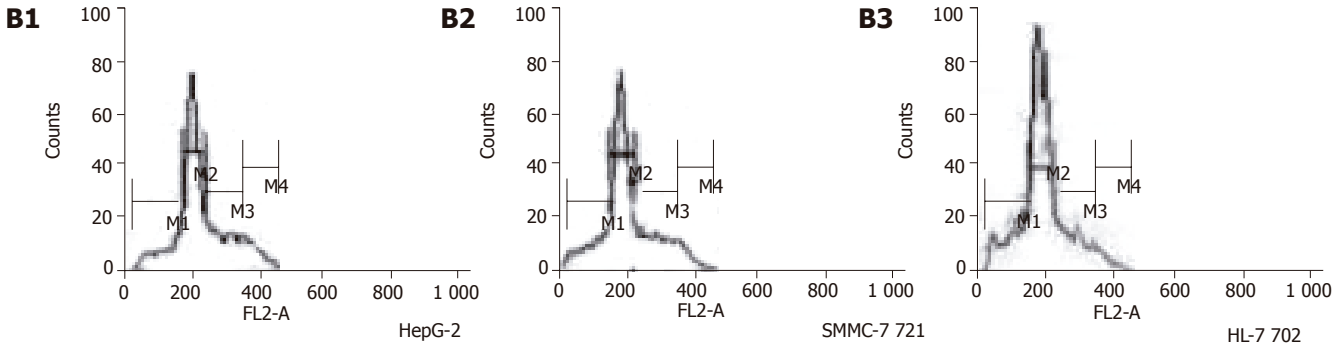

Figure 2 Apoptosis incidence (**A**) and DNA content (**B**) in three cell lines.

of colonies exceeding 50 was defined as positive. The survival fraction rate amounted to colony formation rate in irradiation group. Three parallel samples were set in each dosage point and repeated thrice.

Cells in the experimental growth phase were digested by 2.5 g/L trypsin into single-cell suspension at the concentration of 3×10^4 μg/mL and inoculated in petri dishes. When the cells were attached to the wall, they were cultured for 2 days and then irradiated with 2-8 Gy. After irradiation, samples were added in 2 μg/mL cytochalasin-B, and cultured for 48 h, and then stained *in situ*. The number of micronuclei in double nuclear cells was counted. At least 1 000 double nuclear cells were calculated. Each dosage had three parallel exponents and the experiment was repeated thrice.

Cells were centrifuged and washed 2-3 times with PBS and then fixed in 80% ethanol at -20 ℃. The samples were centrifuged for 5 min (800 r/min) and washed with PBS, mixed into mono cell suspension and diluted at 1:400 in PBS. The cells were treated with RNase for 30 min, resuspended in 10 μg/mL of PI and incubated overnight at 4 ℃. Cellular fluorescence was measured by FASort flow cytometry (Becton Dickinson, San Jose, CA, USA). We collected the data by CELLQuest software and analyzed the cell cycle by ModFit2.0.

Statistical analysis

Correlation analysis was made using the SPSS statistical analysis software.

RESULTS

After being irradiated with 2-8 Gy, the micronucleus frequency of HepG2, SMMC-7721, and HL-7702 was related with radiation dosage. The relationship between the micronucleus frequency of HepG2 and radiation dosage was significant ($P<0.05$, Figure 1).

After being irradiated with 2-8 Gy, a positive relationship was observed between apoptosis incidence and radiation dosages. The relationship between micronucleus frequency of HepG2, SMMC-7721 and radiation dosage was significant ($P<0.01$, Figure 2). But apoptosis incidence was negatively related with micronucleus frequency.

After being irradiated with 2-8 Gy, the cell survival rate of three cell lines was decreased ($P<0.05$, Tables 1 and 2).

After being irradiated with 2-8 Gy, a positive relationship was found between micronucleus frequency and cell survival rate ($P<0.01$, Figure 3) .

The relationship between micronucleus frequency and apoptosis of three cell lines was not significant ($P>0.05$).

DISCUSSION

Hepatocarcinoma is a common malignant tumor. Stereotactic radiotherapy of hepatocarcinoma can achieve better effects. Hepatocarcinoma cells may have corresponding radiosensitivity.

Micronucleus is a product of abnormal mitosis and consists of chromatosome fragments that cannot enter the

Table 1 Cell survival rate of three cell lines (mean±SD)

Cells	Radiation dose (Gy)			
	2	4	6	8
HepG2	0.45±0.08	0.22±0.02	0.06±0.02	0±0
SMMC-7721	0.72±0.05	0.29±0.05	0.08±0.05	0±0
HL-7702	0.79±0.02	0.31±0.09	0.11±0.06	0±0

Table 2 SF2 of three cell lines (mean±SD)

Cells	Do	Dq	*n*	SF_2
HepG2	1.5	0.8	1.7	0.45±0.08
SMMC-7721	1.8	1.5	2.5	0.72±0.05
HL-7702	2.0	1.8	3.0	0.79±0.02

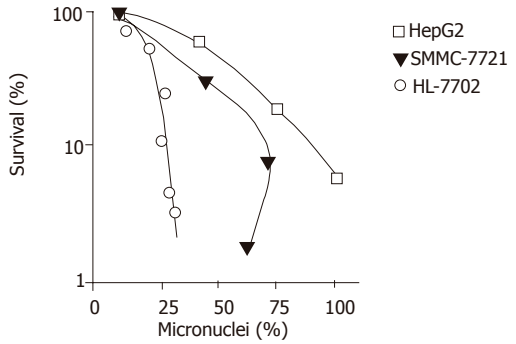

Figure 3 Relationship between micronucleus frequency and cell survival rate.

core nuclei when cells undergo mitosis. Micronucleus analysis is a method to detect cell radiosensitivity. Widel *et al*.[5] found that micronucleus frequency can be used as a marker to predict prognosis of hepatocarcinoma patients. Kolotas *et al*.[6] showed that the prognosis is better in patients with a higher micronucleus frequency than in those with a lower micronucleus frequency. But we found that micronucleus frequency of radiation-resistant cell lines was not related with cell survival rate. It is usually believed that micronuclei induced by X-ray express only in sensitive cells. Micronucleus frequency of sensitive cells is higher than that of radiation-resistant cells. Therefore, micronuclei as a marker to predict cell radiosensitivity of all cells needs to be studied further.

Apoptosis of carcinoma cells can be induced by radiotherapy. The sensitivity to apoptosis and X-ray of carcinoma cells is coincident. Studies showed that apoptosis index of carcinoma cells increases after radiation. The rate of apoptosis induced by radiotherapy increases after radiation, indicating that apoptosis can be used as a marker to predict radiosensitivity.

In this experiment, radiation dose was related with micronucleus frequency in three cell lines. There was a positive relationship between the micronucleus frequency and cell survival rate, suggesting that micronucleus frequency can be used as a marker to predict the radiosensitivity of hepatic carcinoma cells. Radiation dose was related with apoptosis incidence in three cell lines. The apoptosis incidence of HL-7702 and SMMC-7721 was higher than that of HepG2, suggesting that apoptosis incidence can be used as a marker to predict the radiosensitivity of hepatocarcinoma cells.

In this experiment, no significant difference was found between apoptosis incidence induced by radiotherapy and cell survival rate in three cell lines, indicating that the damage induced by radiotherapy is different from apoptosis of hepatic carcinoma cells and that response of radiation-resistant cells occurs due to apoptosis.

Masunaga *et al*.[10] showed that micronucleus frequency and apoptosis incidence can predict radiosensitivity of carcinoma cells. Our study confirmed that micronucleus frequency was negatively related with apoptosis incidence of three cell lines. Apoptosis resulted from cell damage. The impaired cells express apoptosis or micronuclei. This result supports that once apoptosis occurs, the cells lose the segregating opportunity, thus affecting micronucleus formation. Apoptosis may be an important factor affecting micronucleus frequency.

REFERENCES

1 **Vijayalaxmi**, Bisht KS, Pickard WF, Meltz ML, Roti Roti JL, Moros EG. Chromosome damage and micronucleus formation in human blood lymphocytes exposed in vitro to radiofrequency radiation at a cellular telephone frequency (847.74 MHz, CDMA). *Radiat Res* 2001; **156:** 430-432

2 **Bhattathiri VN**, Bindu L, Remani P, Chandralekha B, Davis CA, Nair MK. Serial cytological assay of micronucleus induction: a new tool to predict human cancer radiosensitivity. *Radiother Oncol* 1996; **41:** 139-142

3 **Kirsch-Volders M**, Elhajouji A, Cundari E, Van Hummelen P. The in vitro micronucleus test: a multi-endpoint assay to detect simultaneously mitotic delay, apoptosis, chromosome breakage, chromosome loss and non-disjunction. *Mutat Res* 1997; **392:** 19-30

4 **Levine EL**, Renehan A, Gossiel R, Davidson SE, Roberts SA, Chadwick C, Wilks DP, Potten CS, Hendry JH, Hunter RD. Apoptosis, intrinsic radiosensitivity and prediction of radiotherapy response in cervical carcinoma. *Radiother Oncol* 1995; **37:** 1-9

5 **Widel M**, Kolosza Z, Jedrus S, Lukaszczyk B, Raczek-Zwierzycka K, Swierniak A. Micronucleus assay in vivo provides significant prognostic information in human cervical carcinoma; the updated analysis. *Int J Radiat Biol* 2001; **77:** 631-636

6 **Kolotas C**, Tonus C, Baltas D, Cernea M, Vogt HG, Martin T, Strassmann G, Zamboglou N. Clinical relevance of tumor ploidy and micronucleus formation for oral cavity cancer. *Tumori* 1999; **85:** 253-258

7 **Guo GZ**, Sasai K, Oya N, Shibata T, Shibuya K, Hiraoka M. A significant correlation between clonogenic radiosensitivity and the simultaneous assessment of micronucleus and apoptotic cell frequencies. *Int J Radiat Biol* 1999; **75:** 857-864

8 **Pervan M**, Pajonk F, Sun JR, Withers HR, McBride WH. Molecular pathways that modify tumor radiation response. *Am J Clin Oncol* 2001; **24:** 481-485

9 **Kim JY**, Cho HY, Lee KC, Hwang YJ, Lee MH, Roberts SA, Kim CH. Tumor apoptosis in cervical cancer: its role as a prognostic factor in 42 radiotherapy patients. *Int J Cancer* 2001; **96:** 305-312

10 **Masunaga SI**, Ono K, Suzuki M, Nishimura Y, Kinashi Y, Takagaki M, Hori H, Nagasawa H, Uto Y, Tsuchiya I, Sadahiro S, Murayama C. Radiosensitization effect by combination with paclitaxel in vivo, including the effect on intratumor quiescent cells. *Int J Radiat Oncol Biol Phys* 2001; **50:** 1063-1072

11 **Kirsch-Volders M**, Elhajouji A, Cundari E, Van Hummelen

P. The in vitro micronucleus test: a multi-endpoint assay to detect simultaneously mitotic delay, apoptosis, chromosome breakage, chromosome loss and non-disjunction. *Mutat Res* 1997; **392:** 19-30

Science Editor Wang XL and Guo SY **Language Editor** Elsevier HK

PO Box 2345, Beijing 100023, China
www.wjgnet.com
wjg@wjgnet.com

ELSEVIER

World J Gastroenterol 2005;11(44):7040-7043
World Journal of Gastroenterology ISSN 1007-9327

• *RAPID COMMUNICATION* •

Cell survival curve for primary hepatic carcinoma cells and relationship between SF_2 of hepatic carcinoma cells and radiosensitivity

Zhi-Zhong Liu, Wen-Ying Huang, Ju-Sheng Lin, Xiao-Sheng Li, Xiao Lan, Xiao-Kun Cai, Kuo-Huan Liang, Hai-Jun Zhou

Zhi-Zhong Liu, Ju-Sheng Lin, Xiao-Kun Cai, Kuo-Huan Liang, Tongji Hospital, Tongji Medical College, Huazhong University of Science and Technology, Wuhan 430030, Hubei Province, China
Wen-Ying Huang, Hai-Jun Zhou, The People's Hospital of Chenzhou, Chenzhou 423000, Hunan Province, China
Xiao-Sheng Li, Xiao Lan, Xiehe Hospital, Tongji Medical College, Huazhong University of Science and Technology, Wuhan 430030, Hubei Province, China
Correspondence to: Dr Zhi-Zhong Liu, Institute of Liver Diseases, Tongji Hospital, Tongji Medical College, Huazhong University of Science and Technology, Wuhan 430030, Hubei Province, China. whzzl@163.net
Telephone: +86-27-13554460933
Received: 2004-06-18 Accepted: 2004-08-12

Abstract

AIM: To establish the cell survival curve for primary hepatic carcinoma cells and to study the relationship between SF_2 of primary hepatic carcinoma cells and radiosensitivity.

METHODS: Hepatic carcinoma cells were cultured *in vitro* using 39 samples of hepatic carcinoma at stages II-IV. Twenty-nine samples were cultured successfully in the fifth generation cells. After these cells were radiated with different dosages, the cell survival ratio and SF_2 were calculated by clonogenic assay and SF_2 model respectively. The relationship between SF_2 and the clinical pathological feature was analyzed.

RESULTS: Twenty-nine of thirty-nine samples were successfully cultured. After X-ray radiation of the fifth generation cells with 0, 2, 4, 6, 8 Gy, the cell survival rate was 41%, 36.5%, 31.0%, 26.8%, and 19%, respectively. There was a negative correlation between cell survival and irradiation dosage (r = -0.973, P<0.05). SF_2 ranged 0.28-0.78 and correlated with the clinical stage and pathological grade of hepatic carcinoma (P<0.05). There was a positive correlation between SF_2 and D0.5 (r = 0.773, P<0.05).

CONCLUSION: SF_2 correlates with the clinical stage and pathological grade of hepatic carcinoma and is a marker for predicting the radiosensitivity of hepatic carcinomas.

Key words: Hepatocarcinoma; SF_2; Radiosensitivity; D0.54

Liu ZZ, Huang WY, Lin JS, Li XS, Lan X, Cai XK, Liang KH, Zhou HJ. Cell survival curve for primary hepatic carcinoma cells and relationship between SF_2 of hepatic carcinoma cells and radiosensitivity. *World J Gastroenterol* 2005; 11(44): 7040-7043
http://www.wjgnet.com/1007-9327/11/7040.asp

INTRODUCTION

Hepatic carcinoma is the most common malignant tumors in China. Radiotherapy is its main therapy. But owing to the influence of radiosensitivity and other factors, the effect of radiotherapy on hepatic carcinoma is not obvious. About 40% of hepatic carcinoma patients do not respond to radiotherapy.

The cell survival curve is a curve that describes the relationship between radiation dose and survival cells.

In general, the proliferation ability of survival cells decreases with the increasing of radiation dose. Detecting the SF_2 is a reliable index to predict the radiosensitivity of tumors.

In this experiment, we used the primary cell culture and the clone-formation technique to establish the reliable cell survival curve for hepatic carcinoma. By application of the multi-target click model and calculation of SF_2, we studied the relationship between SF_2 and D0.5. The value of SF_2 for the prediction of the prognosis of hepatic carcinoma was evaluated.

MATERIALS AND METHODS

Source of samples

Thirty-nine fresh specimens were taken from hepatic carcinoma patients at stages II-IV. All the patients had their final diagnosis in Tongji Hospital and did not receive any therapy. Their average age was 49.6 years (22-76 years). All the cases were diagnosed by pathology. Twenty-four specimens of hepatocellular carcinoma and 15 samples of bile duct epithelial carcinoma were taken. Nine were in stage IIB (23%), 25 in stage IIIB (64.1%) and 5 in stage IV (12.9%). The maximum diameter of local carcinoma was <4 cm in 22 specimens (56.9%) and >4 cm

in 17 specimens (43.1%). The specimens were put into RPMI-1640 medium containing 25% fetal calf serum.

Reagents

RPMI-1640 medium, bovine trypsin (1:250), insulin, poly-lysine, and hydrocortisone were purchased from JingMei Company, Shenzhen, China. Agarose was purchased from DIFCO Company.

Irradiation condition

The specimens were irradiated by 6 MV X-ray at the doses of 0, 2, 4, 6, and 8 Gy. The irradiation field was 10 cm ×10 cm. The source skin distance (SSD) was 100 cm. The absorbed dose was 200 cGy/min. The culture bottle was covered with 1.5-cm lucite plate.

Primary culture of hepatic carcinoma cells

The specimens were rinsed 2-3 times with PBS containing streptomycin and penicillin. Blood, fibrous and necrosed tissue were removed. Then a small quantity of PBS was added and the tissue was cut into micro-blocks. The micro-blocks of tissue and PBS were left in the plate and incubated in a 50 mL/L CO_2 incubator. The plate was kept in inversion status for 4-6 h. The anchoring condition of cells was observed under a microscope. If the cells in the tissue were in good condition, RPMI-1640 medium containing 15-25% fetal calf serum was added. The anchoring condition of cells was observed under a microscope on the next day and poly-lysine was added. The poly-lysine promoted the anchoring of cells. In order to provide the cells a better growing condition, we could also add some stimulation factors such as hydrogenated cortadren (4 μg/mL) and insulin (4 μg/mL) on the third and fourth culture days. The culture medium was changed after 5 d, and then every 2-3 d. After incubation for about 14 d, the cultured cells were digested for future generation.

Clone formation rate of hepatic carcinoma cells detected by soft agarose cloning technique[1]

The fifth generation of hepatic carcinoma cells in logarithmic growth phase was digested by 0.25% trypsinogen and counted. Then the cells were inoculated into cell suspension containing 35% soft agarose. According to the irradiation dosage, the cell suspension was put into glass plates. The culture medium was changed after irradiation for about 12 h. The inoculated cells were divided into five groups and irradiated, and then cultured for 10-14 h. The surface culture medium of the plate was stained with hematoxylin and observed under invert microscope and the number of colonies was more than 50. The clone formation rate (SF) after irradiation was assayed thrice to obtain the mean value.

Drawing cell survival curve for hepatic carcinoma cells

Three petri dishes were selected from each dosage group to obtain the mean value. O Gy group was used in every experiment and the colony formation rate (SF) was calculated. On the basis of different dosage irradiation and different incubation time, the cell number was used as the ordinate and the irradiation dosage as the abscissa to draw the growth curve for hepatic carcinoma cells. SF_2 was calculated by the formula [$SF = 1-(1-e^{-D/D_0})^N$] (the multi-target click model)[2].

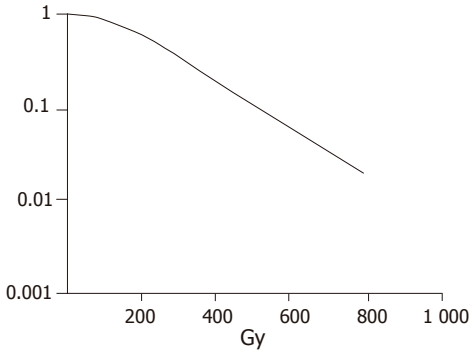

Figure 1 Survival curve of hepatic carcinoma cells.

Regression of hepatic carcinoma in vivo

The patients were examined once a week before and during radiotherapy. The stage plate was used to measure the size of carcinoma. The volume of tumor was calculated to describe the volume-dosage curve and the dosage decreasing tumor size of 50% (D0.5) was calculated.

Determination of colony formation

The fibroblasts were diffusely distributed in petri dishes after the culture medium was changed before one week. A small quantity of colony formation was also seen. The cell distribution in the center of colony was close. The surrounding cells were distributed outward. The cell density decreased. Different cell colonies had different sizes. Only a few cells could be seen in some new colonies. After 14 d, the fibroblasts in petri dishes increased and their diameter became bigger. The cell distribution in the center of the colony was dense. The diameter of the biggest colony was 8 mm.

Statistical analysis

Student's *t* test was used for the statistical analysis using SPSS 10.0.

RESULTS

After hepatic carcinoma tissue was primarily cultured for about 14-20 d, primary cell culture technique was established in 29 of 39 samples.

The survival curve was drawn after different dosage irradiation of hepatic carcinoma cells. The hepatic carcinoma cells were moderately radiosensitive cells (Figure 1).

The cell survival rate was 41%, 36.5%, 31.0%, 26.8%, and 19%, respectively, after irradiated at the dose of 0, 2, 4, 6, and 8 Gy, respectively. The survival rate of hepatic carcinoma cells had a significantly negative relationship with the irradiation dosage ($r = -0.973$, $P<0.05$, Figure 2).

SF_2 of hepatic carcinoma cells was 0.28-0.78, which

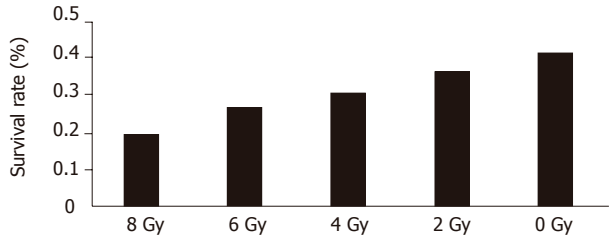

Figure 2 Relationship between survival rate of hepatic carcinoma cells and irradiation dosage.

Table 1 SF_2 of hepatic carcinoma in different clinical stages and pathological types

	Clinical stage		
	IIb	IIIb	IV
Pathology typing			
Hepatocellular carcinoma	0.28	0.47	0.61
Bile duct epithelial carcinoma	0.41	0.57	0.78

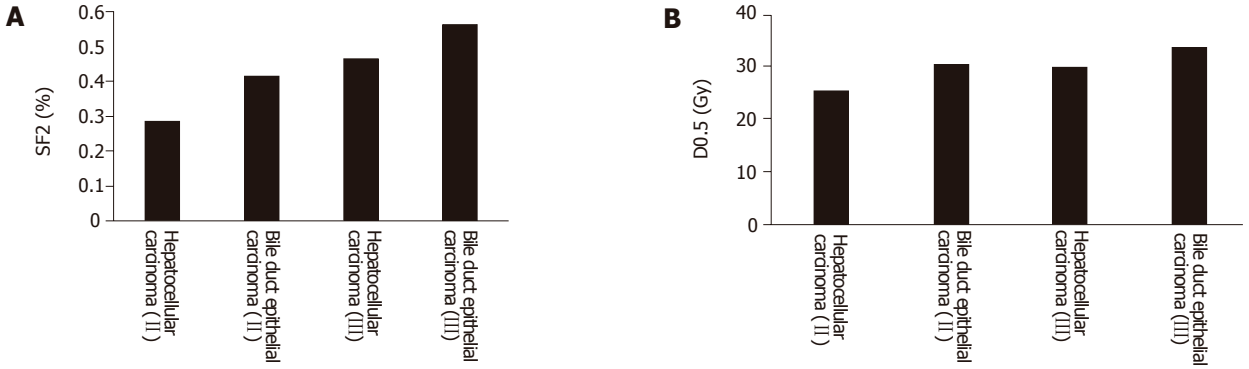

Figure 3 Relationship between the SF2 (**A**) and D0.5 (**B**) in different clinical stages and pathological typing.

was related with the clinical stage of hepatic carcinoma. The more advanced the clinical stage was, the higher the SF_2. SF_2 was also related with the pathological typing of hepatic carcinoma. SF_2 of bile duct epithelial carcinoma was higher than that of hepatocellular carcinoma (Table 1).

SF_2 had a positive relationship with D0.5 ($r = 0.773$, $P<0.05$). SF_2 in different clinical stages of hepatic carcinoma was also related with D0.5. SF_2 in different pathological types of hepatic carcinoma was correlated with D0.5 (Figures 3A and 3B).

DISCUSSION

The determination of radiosensitivity for tumor cells is an important component of tumor radiobiology. The final objective of tumor radiotherapy is to eradicate tumor. But the objective of clinical radiotherapy is to prevent tumor from growth and to eradicate the tumor. Based on the definition of cell survival, the judge of radiotherapy result is based on whether the cells proliferate or not. The survived cells are the main factor for the failure of radiotherapy[3].

Radiosensitivity of hepatic carcinoma cells is a main factor influencing the prognosis of radiotherapy for hepatic carcinoma. To predict the radiosensitivity of hepatic carcinoma cells before and during the therapy, individualization of reasonable and effective therapy is always the direction of tumor investigation.

Primary tumor cell culture *in vitro* has some difficulties such as longer time consumption, high cost, and easy contamination. Based on the past experience, the chief key point to the success of this technique is to draw the materials from tissue because it is closely related with the culture. Aseptic technique is one of the important factors for the success of culture.

It was reported that radiosensitivity is different in different hepatic carcinoma cells and that the local control rate of hepatic carcinoma with its SF_2 <0.55 is higher than that with its SF_2 >0.05[4,5]. SF_2 is related with the staging and pathological typing of tumor but not related with the age of patients and the diameter of tumor. SF_2 is also correlated with pathological typing and clinical stage of tumor. SF_2 for hepatic carcinoma cells in different clinical pathological typing and clinical stage has some differences. It is due to the necessity for individualized treatment of hepatic carcinoma in different clinical pathological typing and clinical stages.

The reports regarding the relationship between SF2 and radiosensitivity have different conclusions. But most experiments showed that SF_2 is negatively related with cell radiosensitivity[6]. SF_2 can be used as a marker for predicting the local control of head and neck tumor. It was reported that SF_2 can predict the reaction after radiotherapy[7]. SF_2 is related with the clinical prognosis of tumor[8]. In our study, SF_2 was significantly related with the radiosensitivity of hepatic carcinoma cells, suggesting that SF_2 can reflect the radiosensitivity of hepatic carcinoma cells.

In conclusion, SF_2 is a reliable marker for predicting the radiosensitivity of hepatic carcinoma cells before and during the therapy.

REFERENCES

1 **Tamamoto T**, Ohnishi K, Takahashi A, Wang X, Yosimura H, Ohishi H, Uchida H, Ohnishi T. Correlation between gamma-ray-induced G2 arrest and radioresistance in two human cancer cells. *Int J Radiat Oncol Biol Phys* 1999; **44**: 905-909

2 **Vral A**, Thierens H, Baeyens A, De Ridder L. Chromosomal aberrations and in vitro radiosensitivity: intra-individual versus inter-individual variability. *Toxicol Lett* 2004; **149:** 345-352

3 **Bedford JS**, Dewey WC. Radiation Research Society. 1952-2002. Historical and current highlights in radiation biology: has anything important been learned by irradiating cells? *Radiat Res* 2002; **158:** 251-291

4 **West CM**, Davidson SE, Roberts SA, Hunter RD. Intrinsic radiosensitivity and prediction of patient response to radiotherapy for carcinoma of the cervix. *Br J Cancer* 1993; ***68:*** 819-23

5 **West CM**, Davidson SE, Roberts SA, Hunter RD. The independence of intrinsic radiosensitivity as a prognostic factor for patient response to radiotherapy of carcinoma of the cervix. *Br J Cancer* 1997; **76:** 1184-1190

6 **Bjork-Eriksson T**, West C, Karlsson E, Mercke C. Tumor radiosensitivity (SF2) is a prognostic factor for local control in head and neck cancers. *Int J Radiat Oncol Biol Phys* 2000; **46:** 13-19

7 **Britten RA**, Evans AJ, Allalunis-Turner MJ, Franko AJ, Pearcey RG. Intratumoral heterogeneity as a confounding factor in clonogenic assays for tumour radioresponsiveness. *Radiother Oncol* 1996; **39:** 145-153

8 **Stausbol-Gron B**, Overgaard J. Relationship between tumour cell in vitro radiosensitivity and clinical outcome after curative radiotherapy for squamous cell carcinoma of the head and neck. *Radiother Oncol* 1999; **50:** 47-55

Science Editor Wang XL **Language Editor** Elsevier HK

PO Box 2345, Beijing 100023, China
www.wjgnet.com
wjg@wjgnet.com

ELSEVIER

World J Gastroenterol 2005;11(44):7044-7047
World Journal of Gastroenterology ISSN 1007-9327

• *CASE REPORT* •

A case of bowel schistosomiasis not adhering to endoscopic findings

Manfredi Rizzo, Pasquale Mansueto, Daniela Cabibi, Elisabetta Barresi, Kaspar Berneis, Mario Affronti, Gabriele Di Lorenzo, Sergio Vigneri, Giovam Battista Rini

Manfredi Rizzo, Pasquale Mansueto, Mario Affronti, Gabriele Di Lorenzo, Sergio Vigneri, Giovam Battista Rini, Department of Clinical Medicine and Emerging Diseases, University of Palermo, Italy
Daniela Cabibi, Elisabetta Barresi, Institute of Pathological Anatomy, University of Palermo, Italy
Kaspar Berneis, Medical University Clinic, Bruderholz, Switzerland
Correspondence to: Dr Manfredi Rizzo, Dipartimento di Medicina Clinica e delle Patologie Emergenti, Universita' di Palermo, Via del Vespro, 141, 90127 Palermo, Italy. mrizzo@unipa.it
Telephone: +39-091-6552945 Fax: +39-091-6552945
Received: 2005-04-03 Accepted: 2005-05-03

Abstract

Schistosomiasis is a chronic worm infection caused by a species of *trematodes,* the *Schistosomes*. We may distinguish a urinary form from *Schistosomes haematobium* and an intestinal-hepatosplenic form mainly from *Schistosomes mansoni* characterized by nausea, meteorism, abdominal pain, bloody diarrhea, rectal tenesmus, and hepatosplenomegaly. These infections represent a major health issue in Africa, Asia, and South America, but recently *S mansoni* has increased its prevalence in other continents, such as Europe and North America, due to international travelers and immigrants, with several diagnostic and prevention problems. We report a case of a 24-year-old patient without HIV infection, originated from Ghana, admitted for an afebrile dysenteric syndrome. All microbiologic studies were negative and colonoscopy revealed macroscopic lesions suggestive of a bowel inflammatory chronic disease. Since symptoms became worse, a therapy with mesalazine (2 g/d) was started, depending on the results of a bowel biopsy, but without any resolution. The therapy was stopped after 2 wk when the following result was available: a diagnosis of "intestinal schistosomiasis" was done (two *Schistosoma* eggs were detected in the colonic mucosa) and this was confirmed by the detection of *Schistosoma* eggs in the feces. Therapy was therefore changed to praziquantel (40 mg/kg, single dose), a specific anti-parasitic agent, with complete recovery. Schistosomiasis shows some peculiar difficulties in terms of differential diagnosis from the bowel inflammatory chronic disease, as the two disorders may show similar colonoscopic patterns. Since this infection has recently increased its prevalence worldwide, it has to be considered in the differential diagnosis of our patients with gastrointestinal symptoms.

Key words: Schistosomiasis; Chronic inflammatory bowel disease; Ulcerative colitis; Granuloma

Rizzo M, Mansueto P, Cabibi D, Barresi E, Berneis K, Affronti M, Di Lorenzo G, Vigneri S, Rini GB. A case of bowel schistosomiasis not adhering to endoscopic findings. *World J Gastroenterol* 2005; 11(44): 7044-7047
http://www.wjgnet.com/1007-9327/11/7044.asp

INTRODUCTION

Schistosomiasis or Bilharziasis is a chronic worm infection caused by a species of t*rematodes*, the *Schistosomes*, which are blood flukes that parasitize the venous channels of definitive human hosts. The infection is transmitted by fresh-water snails. Based on their organ localization, we may distinguish a urinary form from *Schistosomes haematobium*, and an intestinal or hepatosplenic form from *Schistosomes mansoni*, *Schistosomes japonicum*, *Schistosomes mekongi,* and *Schistosomes intercalatum*[1,2].

S mansoni, a main agent of the intestinal form, is a *trematode* which infects human beings more frequently and also infects other primates too. Adult females of *S mansoni* deposit the eggs in the small veins around the large intestine of infected individuals. Some of the eggs may be trapped in the gut wall or break loose into it and are then eliminated by defecation. The eggs trapped in the gut wall are responsible for inflammatory and immunopathologic responses, leading to erythema, edema, granulomas, ulcerations, hemorrhages, and fibrosis. The infection is characterized by nausea, meteorism, abdominal pain, bloody diarrhea, rectal tenesmus, and hepatosplenomegaly[3,5].

Infection with *S mansoni* is still a major health issue in Africa, Asia, and South America[6-10], but recent epidemiological studies showed that its prevalence increases in Europe[11-15] and USA[16,17], due to international travelers and immigrants. In our country, the presence of acute *S mansoni* infection with progression to chronic lesions has been reported in a group of Italian travelers returning from Africa, showing both diagnostic and preventive problems[18].

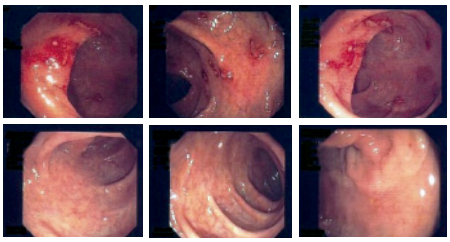

Figure 1 Colonoscopy before (**A**) and after (**B**) therapy.

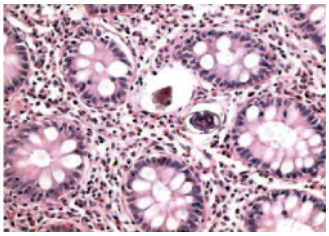

Figure 2 *Schistosoma* eggs detected in colonic mucosa.

Therefore, this infection was considered in the differential diagnosis of our patient with gastrointestinal symptoms. In particular, it is often hard to distinguish this infection from the bowel inflammatory chronic disease, since these two disorders may show similar colonoscopic patterns[19,20]. However, the contemporary presence of the two disorders (usually a chronic schistosomiasis precede the inflammatory disease in the same patient) represents a rare event[21,22].

We report a case of a 24-year-old patient without HIV infection, living in our region who immigrated from Ghana, and was admitted for an afebrile dysenteric syndrome. All microbiologic studies were negative and colonoscopy revealed macroscopic lesions suggestive of a bowel inflammatory chronic disease, and then treated with mesalazine, but without resolution. Further studies by bowel biopsy and feces examination revealed a *Schistosoma* infection, which was treated with praziquantel, a specific anti-parasitic agent and had a complete recovery.

CASE REPORT

A 24-year-old non-HIV patient immigrated from Ghana for economic reasons. He had pain in the left testicle 2 years ago and was hospitalized in his own country, where he was wrongly diagnosed and was given an unknown therapy. However, the pain occasionally recurred with exacerbation after the therapy. The patient was admitted to our hospital for diffuse abdominal pain with occasional bloody diarrhea and vomiting. Hematologic laboratory tests revealed no abnormalities; chest X-ray, and hepatosplenic ultrasonography were normal. The patient had no signs of distress but pain in epigastric and mesogastric regions. Small lymph nodes were observed in the latero-cervix area. All microbiologic studies were negative and colonoscopy revealed macroscopic lesions suggestive of a bowel inflammatory chronic disease reacutization (Figure 1A), like ulcerative colitis or a Crohn's disease. During the colonoscopy, a bowel biopsy was done. Since symptoms became worse, we started a therapy with mesalazine (2 g/d), pending the results of the intestinal biopsy. One week later, a second colonoscopy documented a minor improvement in the endoscopic pattern and the therapy with mesalazine was continued.

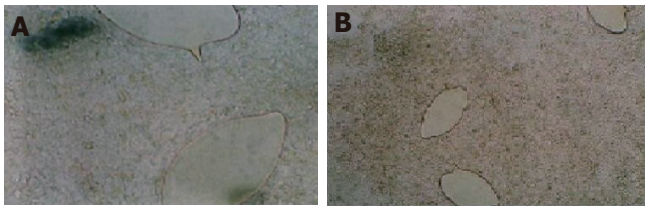

Figure 3 *Schistosoma mansoni* isolated in feces.

Two weeks later, the result of the bowel biopsy was available but did not support a diagnosis of a bowel inflammatory chronic disease, as suggested by the endoscopic patterns. The histopathological findings in colonic biopsies were negative for a bowel inflammatory chronic disease. Glands were regular in shape, with a normal amount of cytoplasmic mucous and without crypt abscesses. By contrast, the number of inflammatory cells increased in the *Lamina propria*, mostly eosinophils. These aspects, together with the clinical symptoms and the nationality of the patient, suggested that a searching for a parasitic infestation should be made. We were able to detect two *Schistosoma* eggs in the colonic mucosa, both of them were surrounded by a granuloma's reaction (Figure 2). Therefore, a diagnosis of "intestinal schistosomiasis" was made and was confirmed by the detection of *S mansoni* eggs in the feces (Figure 3).

On this basis, after two weeks, mesalazine was changed to praziquantel (40 mg/kg, single dose). Three weeks later, a third colonoscopy documented a significant improvement (data not shown). Therefore, the therapy with praziquantel was continued at the same dosage, and further improvement of the colonoscopy pattern was documented one month later (Figure 1B). Nothing was found in the other laboratory or radiographic tests, except of a weak plasma eosinophilia.

DISCUSSION

Schistosomiasis is an infectious disease, which affects more than 200 million people worldwide. Since it is endemic in at least three continents, Africa, Asia, and South America, it represents the most important public health problem of the tropical and sub-tropical areas[1,2]. In particular, Ghana is one of the African countries where schistosomiasis is more prevalent in both the urinary and intestinal forms[23,24].

Since the transmission of schistosomiasis is linked to the intermediate snail hosts, in the endemic countries the disease is more prevalent in subjects whose skin is more susceptible to contacts with water in rivers, lakes, swamps or artificial irrigation systems. This may occur frequently

in water-related activities of boatmen, fishermen, and rice workers. The infection is also promoted by unsanitary disposal of urine and feces and can occur in animals, such as dogs and cows[3,4,25].

S mansoni, a main agent of the intestinal form, together with *S japonicum*, *S mekongi,* and *S intercalatum*, is a trematode which parasitizes in human beings and also in other primates. *Schistosoma* eggs, upon deposition in the feces, mature in suitable environmental conditions (such as fresh water), giving rise to its larval forms (miracidia). These swimming forms reach and infect snails, species of the genus *Biomphalaria* (intermediate hosts), and mature in cercarie[26,27]. The cercarie are the infective forms for human beings and come out from the snails under specific conditions of light and temperature and infect men through the skin. During penetration, the cercarie shake off their tails and change into the next stage of the life cycle, the schistosomula, that reach the lungs and the liver. In the intrahepatic portal system, the worms complete the sexual stages of their development. Then, the adult females deposit the eggs in the small veins around the large intestine. Some of the eggs may be trapped in the gut wall or break loose into it and are then eliminated by feces. The eggs trapped in the gut wall are responsible for the inflammatory and immunopathologic responses, leading to erythema, edema, granulomas, ulcerations, hemorrhages, and fibrosis[28,29]. Regarding the pathogenesis of the disease, recent studies have dramatically changed the acknowledgment in this field. The T helper (Th) CD4+/CD8- cells, derived from hepatic granulomas of infected mice, may produce cytokines such as interleukin-2, interleukin-4, interferon-γ, with a type Th0 immunomediate response. After a longer period of infection, the murine models could show a type Th2 response[30-33].

The symptoms of our patient included nausea, meteorism, abdominal pain, bloody diarrhea, rectal tenesmus, and hepatosplenomegaly, which are consistent with those already reported[5]. The case showed some difficulties in terms of differential diagnosis of a chronic inflammatory bowel disease, since anatomical pathologic reports, in relation to the immediate endoscopic evidence, were not available.

Previous studies stated that colonoscopic findings are suggestive of schistosomiasis in about 45.3% of patients, but *S mansoni* eggs in feces are detectable in only 11.1% of the patients with colonic biopsies positive for *S mansoni*[34,35]. Endoscopic findings may not be typical and it is often hard to distinguish *Schistosoma* infection from a chronic inflammatory bowel disease, since these two disorders may show similar patterns, as shown in our patient[19,20].

Moreover, cystoscopy or rectosigmoidal endoscopy may be useful. In our case, the first probable diagnosis of bowel schistosomiasis was made by the detection of two *Schistosoma* eggs in the colonic mucosa, surrounded by a granuloma's reaction. During the disease's acute phase, the histological examination may show the presence of eggs on the ulcerated lesions as well as polyps-like forms on the bowel mucosa[36,37]. However, these aspects may be macroscopically and microscopically evocative of other disorders, such as chronic inflammatory bowel disease and infective colitis[38,39]. Therefore, diagnosis of schistosomiasis can be made by urine and feces examination and isolation of the agent.

When the correct diagnosis is made, the complete recovery of the patient can be achieved using a specific anti-parasitic therapy with praziquantel[40,41]. The intimate relationship between human beings and infected water leads to schistosomiasis elevated prevalence. Elimination of the intermediate hosts and avoiding the contact with infected water sources are the measures to prevent schistosomiasis[42]. For the treatment, current drugs include praziquantel, metriphonate[43], and oxamniquine[44].

We reported in this paper a case of an unsuspicious schistosomiasis, initially treated with mesalazine, for its peculiar difficulties in terms of differential diagnosis from a chronic inflammatory bowel disease. We suggest that the detection of the *Schistosoma* eggs in feces should always anticipate the colonoscopy examination. Since the prevalence of schistosomiasis has been increasing in Europe and USA, due to international travelers and immigrants[16-18,45], schistosomiasis should be considered in the differential diagnosis of patients with gastrointestinal symptoms.

REFERENCES

1 **Sturrock RF**. Schistosomiasis epidemiology and control: how did we get here and where should we go? *Mem Inst Oswaldo Cruz* 2001; **96 Suppl:** 17-27

2 **Goodburn EA**, Ross DA. Young people's health in developing countries: a neglected problem and opportunity. *Health Policy Plan* 2000; **15:** 137-144

3 **Ripert C**. [Schistosomiasis: diagnosis and treatment] *Presse Med* 2000; **29:** 1583-1585

4 **Ranque S**, Dessein A. [Schistosoma mansoni schistosomiasis] *Rev Prat* 2001; **51:** 2099-2103

5 **Schafer TW**, Hale BR. Gastrointestinal complications of schistosomiasis. *Curr Gastroenterol Rep* 2001; **3:** 293-303

6 **Erko B**, Medhin G, Berhe N, Abebe F, Gebre-Michael T, Gundersen SG. Epidemiological studies on intestinal schistosomiasis in Wondo Genet, southern Ethiopia. *Ethiop Med J* 2002; **40:** 29-39

7 **Lansdown R**, Ledward A, Hall A, Issae W, Yona E, Matulu J, Mweta M, Kihamia C, Nyandindi U, Bundy D. Schistosomiasis, helminth infection and health education in Tanzania: achieving behaviour change in primary schools. *Health Educ Res* 2002; **17:** 425-433

8 **Keiser J**, N'Goran EK, Traore M, Lohourignon KL, Singer BH, Lengeler C, Tanner M, Utzinger J. Polyparasitism with Schistosoma mansoni, geohelminths, and intestinal protozoa in rural Cote d'Ivoire. *J Parasitol* 2002; **88:** 461-466

9 **Zhou X**, Acosta L, Willingham AL 3rd, Leonardo LR, Minggang C, Aligui G, Zheng F, Olveda R. Regional Network for Research, Surveillance and Control of Asian Schistosomiasis (RNAS). *Acta Trop* 2002; **82:** 305-311

10 **Leonardo LR**, Acosta LP, Olveda RM, Aligui GD. Difficulties and strategies in the control of schistosomiasis in the Philippines. *Acta Trop* 2002; **82:** 295-299

11 **Roca C**, Balanzo X, Gascon J, Fernandez-Roure JL, Vinuesa T, Valls ME, Sauca G, Corachan M. Comparative, clinico-epidemiologic study of Schistosoma mansoni infections in travellers and immigrants in Spain. *Eur J Clin Microbiol Infect Dis* 2002; **21:** 219-223

12 **Kager PA**, Schipper HG. [Acute schistosomiasis: fever and eosinophilia, with or without urticaria, after a trip to Africa] *Ned Tijdschr Geneeskd* 2001; **145:** 220-225 (Dutch)
13 **Whitty CJ**, Mabey DC, Armstrong M, Wright SG, Chiodini PL. Presentation and outcome of 1107 cases of schistosomiasis from Africa diagnosed in a non-endemic country. *Trans R Soc Trop Med Hyg* 2000; **94:** 531-534
14 **Whitty CJ**, Carroll B, Armstrong M, Dow C, Snashall D, Marshall T, Chiodini PL. Utility of history, examination and laboratory tests in screening those returning to Europe from the tropics for parasitic infection. *Trop Med Int Health* 2000; **5:** 818-823
15 **Lademann M**, Burchard GD, Reisinger EC. Schistosomiasis and travel medicine. *Eur J Med Res* 2000; **5:** 405-410
16 **Adair R**, Nwaneri O. Communicable disease in African immigrants in Minneapolis. *Arch Intern Med* 1999; **159:** 83-85
17 **Ganem JP**, Marroum MC. Schistosomiasis of the urinary bladder in an African immigrant to North Carolina. *South Med J* 1998; **91:** 580-583
18 **Raglio A**, Russo V, Swierczynski G, Sonzogni A, Goglio A, Garcia LS. Acute Schistosoma mansoni infection with progression to chronic lesion in Italian travelers returning from Cameroon, West Africa: a diagnostic and prevention problem. *J Travel Med* 2002; **9:** 100-102
19 **Waye JD**, Hunt RH. Colonoscopic diagnosis of inflammatory bowel disease. *Surg Clin North Am* 1982; **62:** 905-913
20 **Tedesco FJ**, Moore S. Infectious diseases mimicking inflammatory bowel disease. *Am Surg* 1982; **48:** 243-249
21 **Torres EA**, Acosta H, Cruz M, Weinstock J, Hillyer GV. Seroprevalence of Schistosoma mansoni in Puerto Ricans with inflammatory bowel disease. *P R Health Sci J* 2001; **20:** 211-214
22 **Eaden JA**, Pararajasingam R, MacKay H, Thomas WM, Mayberry JF. Chronic schistosomiasis: an incidental finding in new onset ulcerative colitis. *Eur J Gastroenterol Hepatol* 1999; **11:** 443-445
23 **Brooker S**, Marriot H, Hall A, Adjei S, Allan E, Maier C, Bundy DA, Drake LJ, Coombes MD, Azene G, Lansdown RG, Wen ST, Dzodozmenyo M, Cobbinah J, Obro N, Kihamia CM, Issae W, Mwanri L, Mweta MR, Mwaikemwa A, Salimu M, Ntimbwa P, Kiwelu VM, Turuka A, Nkungu DR, Magingo J. Community perception of school-based delivery of anthelmintics in Ghana and Tanzania. *Trop Med Int Health* 2001; **6:** 1075-1083
24 The cost of large-scale school health programmes which deliver anthelmintics to children in Ghana and Tanzania. The Partnership for Child Development. *Acta Trop* 1999; **73:** 183-204
25 **Boisier P**, Ramarokoto CE, Ravoniarimbinina P, Rabarijaona L, Ravaoalimalala VE. Geographic differences in hepatosplenic complications of schistosomiasis mansoni and explanatory factors of morbidity. *Trop Med Int Health* 2001; **6:** 699-706
26 **Morgan JA**, Dejong RJ, Snyder SD, Mkoji GM, Loker ES. Schistosoma mansoni and Biomphalaria: past history and future trends. *Parasitology* 2001; 1**23 Suppl:** S211- S228
27 **Mavarez J**, Amarista M, Pointier JP, Jarne P. Fine-scale population structure and dispersal in Biomphalaria glabrata, the intermediate snail host of Schistosoma mansoni, in Venezuela. *Mol Ecol* 2002; **11:** 879-889
28 **Silva LM**, Fernandes AL, Barbosa A Jr, Oliveira IR, Andrade ZA. Significance of schistosomal granuloma modulation. *Mem Inst Oswaldo Cruz* 2000; **95:** 353-361
29 **Abdel-Hadi AM**, Talaat M. Histological assessment of tissue repair after treatment of human schistosomiasis. *Acta Trop* 2000; **77:** 91-96
30 **Yoshida A**, Maruyama H, Yabu Y, Amano T, Kobayakawa T, Ohta N. Immune response against protozoal and nematodal infection in mice with underlying Schistosoma mansoni infection. *Parasitol Int* 1999; **48:** 73-79
31 **Park MK**, Hoffmann KF, Cheever AW, Amichay D, Wynn TA, Farber JM. Patterns of chemokine expression in models of Schistosoma mansoni inflammation and infection reveal relationships between type 1 and type 2 responses and chemokines in vivo. *Infect Immun* 2001; **69:** 6755-6768
32 **Fallon PG**, Smith P, Richardson EJ, Jones FJ, Faulkner HC, Van Snick J, Renauld JC, Grencis RK, Dunne DW. Expression of interleukin-9 leads to Th2 cytokine-dominated responses and fatal enteropathy in mice with chronic Schistosoma mansoni infections. *Infect Immun* 2000; **68:** 6005-6011
33 **Almeida CA**, Leite MF, Goes AM. Signal transduction events in human peripheral blood mononuclear cells stimulated by Schistosoma mansoni antigens. *Hum Immunol* 2001; **62:** 1159-1166
34 **Yasawy MI**, El Shiekh Mohamed AR, Al Karawi MA. Comparison between stool examination, serology and large bowel biopsy in diagnosing Schistosoma mansoni. *Trop Doct* 1989; **19:** 132-134
35 **Mohamed AR**, al Karawi M, Yasawy MI. Schistosomal colonic disease. *Gut* 1990; **31:** 439-442
36 **Ricosse JH**, Emeric R, Courbil LJ. Anatomopathological aspects of schistosomiasis. A study of 286 pathological specimens. *Med Trop (Mars)* 1980; **40:** 77-94
37 **Geboes K**, el-Deeb G, el-Haddad S, Amer G, el-Zayadi AR. Vascular alterations of the colonic mucosa in schistosomiasis and portal colopathy. *Hepatogastroenterology* 1995; **42:** 343-347
38 **Sanguino J**. Schistosomiasis of the colon and rectum. *Hepatogastroenterology* 1994; **41:** 506
39 **Sanguino J**, Peixe R, Guerra J, Rocha C, Quina M. Schistosomiasis and vascular alterations of the colonic mucosa. *Hepatogastroenterology* 1993; **40:** 184-187
40 **Sturrock RF**, Davis A. Efficacy of praziquantel against Schistosoma mansoni in northern Senegal. *Trans R Soc Trop Med Hyg* 2002; **96:** 105; author reply 105-106
41 **Filho SB**, Gargioni C, Silva Pinto PL, Chiodelli SG, Gurgel Vellosa SA, da Silva RM, da Silveira MA. Synthesis and evaluation of new oxamniquine derivatives. *Int J Pharm* 2002; **233:** 461-471
42 **Lambertucci JR**, Serufo JC, Gerspacher-Lara R, Rayes AA, Teixeira R, Nobre V, Antunes CM. Schistosoma mansoni: assessment of morbidity before and after control. *Acta Trop* 2000; **77:** 101-109
43 **Stephenson I**, Wiselka M. Drug treatment of tropical parasitic infections: recent achievements and developments. *Drugs* 2000; **60:** 985-995
44 **Filho SB**, Gargioni C, Silva Pinto PL, Chiodelli SG, Gurgel Vellosa SA, da Silva RM, de Silveira MA. Synthesis and evaluation of new oxamniquine derivatives. *Int J Pharm* 2002; **233:** 35-41
45 **Grobusch MP**, Muhlberger N, Jelinek T, Bisoffi Z, Corachan M, Harms G, Matteelli A, Fry G, Hatz C, Gjorup I, Schmid ML, Knobloch J, Puente S, Bronner U, Kapaun A, Clerinx J, Nielsen LN, Fleischer K, Beran J, da Cunha S, Schulze M, Myrvang B, Hellgren U. Imported schistosomiasis in Europe: sentinel surveillance data from TropNetEurop. *J Travel Med* 2003; **10:** 164-169

Science Editor Wang XL and Guo SY **Language Editor** Elsevier HK

PO Box 2345, Beijing 100023, China
www.wjgnet.com
wjg@wjgnet.com

ELSEVIER

World J Gastroenterol 2005;11(44):7048-7050
World Journal of Gastroenterology ISSN 1007-9327

• *CASE REPORT* •

Gastric cancer occurring in a patient with Plummer-Vinson syndrome: A case report

Ki-Han Kim, Min-Chan Kim, Ghap-Joong Jung

Ki-Han Kim, Min-Chan Kim, Ghap-Joong Jung, Department of Surgery, Dong-A University College of Medicine, Busan, South Korea
Correspondence to: Ghap-Joong Jung, Department of Surgery, Dong-A University College of Medicine, 3-1 Dongdaeshin-Dong, Seo-Gu, Busan 602-715, South Korea. gjjung@donga.ac.kr
Telephone: +82-51-2405147 Fax: +82-51-2479316
Received: 2005-05-01 Accepted: 2005-06-09

Abstract

Plummer-Vinson syndrome (sideropenic dysphagia) is characterized by dysphagia due to an upper esophageal or hypopharyngeal web in patients with chronic iron deficiency anemia. The main cause of dysphagia is the presence of the web in the cervical esophagus, and abnormal motility of the pharynx or esophagus is also found to play a significant role in this condition. This syndrome is thought to be precancerous because squamous cell carcinoma of hypopharynx, oral cavity or esophagus takes place in 10% of those patients suffering from this malady, but it is even more unusual that Plummer-Vinson syndrome should be accompanied by gastric cancer. We have reported here a case of a 43-year-old woman with Plummer-Vinson syndrome who developed stomach cancer and recovered after a radical total gastrectomy with D2 nodal dissection.

Key words: Plummer-Vinson syndrome; Gastric cancer; Esophageal web

Kim KH, Kim MC, Jung GJ. Gastric cancer occurring in a patient with Plummer-Vinson syndrome: A case report. *World J Gastroenterol* 2005; 11(44): 7048-7050
http://www.wjgnet.com/1007-9327/11/7048.asp

INTRODUCTION

Plummer-Vinson syndrome is characterized by dysphagia due to upper esophageal or hypopharyngeal web in patients with chronic iron deficiency anemia[1,2]. It is also combined with iron deficiency anemia, mucosal lesion of oral cavity or pharynx. This syndrome has been reported since 1893 in various literatures describing its specific symptoms. In 1926, Sir Arthur Hurst designated this symptom complex as Plummer-Vinson syndrome[1]. This syndrome is also referred to as Paterson-Kelly syndrome or sideropenic dysphagia. The main cause of dysphagia is the presence of a web in the cervical esophagus, and the abnormal motility of pharynx or esophagus is also found to play a significant role in the above causes[1,2]. It is well known that this syndrome is associated with an increased incidence of hypopharyngeal or cervical esophageal cancer. However, it is even more unusual that this syndrome is combined with gastric cancer[3]. So, we have reported a case of a 43-year-old woman who was initially diagnosed as Plummer-Vinson syndrome 2 years ago, and recently developed stomach cancer, which was managed successfully by surgery.

CASE REPORT

A 43-year-old woman was admitted to our hospital with symptoms of nausea, dysphagia and general weakness. She was diagnosed as Plummer-Vinson syndrome in April 2002, and has been managed conservatively on routine follow-ups. In August 2003, her nausea and dysphagia were aggravated. Her past history and family history were not specific. On admission, she complained about general weakness, mild abdominal pain and vomiting. The blood pressure was 0.247 kPa, pulse rate 90 bpm and body temperature 36.4 °C. The laboratory findings were consistent with microcystic, hypochronic iron deficiency anemia with 62 g/L hemoglobin, 22.2% hematocrit, 76.8 fL MCV, 21.5 pg MCH, 279 g/L MCHC, 325 000/μL platelet, 46 μg/dL serum iron, 271 μg/dL total iron binding capacity (TIBC), and 11.33 ng/mL serum ferritin. Urine analysis, serum liver function test (LFT), and serum electrolytes were unremarkable.

A gastrointestinal radiographic series indicated a linear filling defect (1.5 cm length) in the upper esophagus, which suggested an esophageal web (Figure 1). Contrast-enhanced abdominal CT scan showed diffuse irregular wall thickening with multiple calcifications at the body and antrum of the stomach. The CT scan also showed lymph node enlargement in the perigastric area and a mild enlargement of the spleen (Figure 2).

Esophagogastroduodenoscopic findings showed a web at 16 cm from the incisors. Upon endoscopic procedure for esophageal bougienage, we found a lesion at the cardia suspecting gastric cancer involving the upper body and the esophagogastric junction. Endoscopic biopsy proved to be a poorly differentiated adenocarcinoma. On surgical exploration, the serosa of the stomach was not invaded

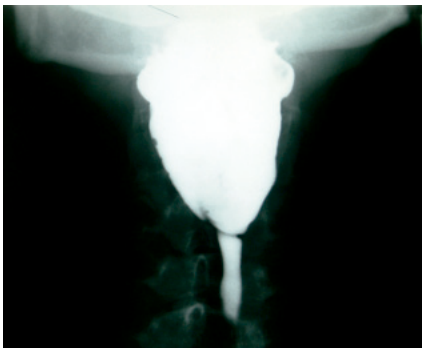

Figure 1 Esophagography showing a linear filling defect (1.5 cm length) at the upper esophagus, suggesting esophageal web.

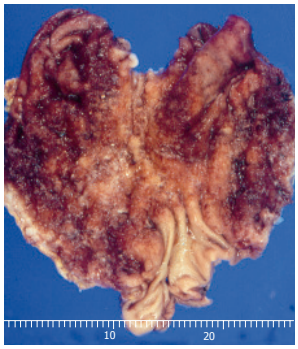

Figure 3 Macroscopic appearance of resected stomach showing a diffuse large Borrmann type 4 cancer in the whole body and cardia.

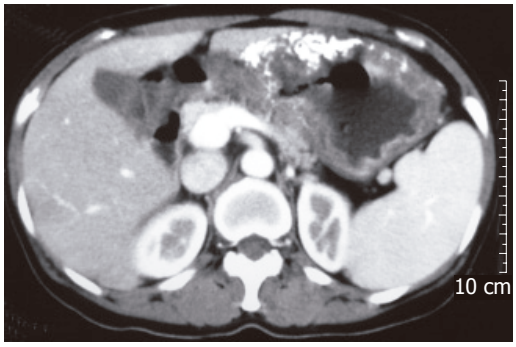

Figure 2 Contrast-enhanced abdominal CT scan showing diffuse irregular wall thickness with multiple calcifications at the body and antrum of the stomach.

macroscopically by cancer, but hilar lymph nodes of the spleen were grossly enlarged, suspecting tumor metastasis. The patient underwent a radical total gastrectomy with D2 nodal dissection. The spleen was taken out along with lymph node #10 and lymph node #11 d. No transfusion was required during and after the surgery. Excised surgical specimen demonstrated that the tumor size was 22 cm×18 cm, and both resection margins were tumor-free. The lesion was histologically confirmed as mucinous adenocarcinoma, Borrmann type IV, and it had infiltrated into the serosa with nodal metastasis of 33 out of 62 nodes. The TMN stage was T3N3M0 (Stage IV) (Figure 3). Iron supplemented soft diet was commenced on the 6th postoperative day. Peripheral blood findings improved within 2 wk after the surgery: 87 g/L hemoglobin, 28.5% hematocrit, 81.9 fL MCV, 25.0 pg MCH, 30.5 g/dL MCHC, and 1 186 000/μL platelets. The patient was discharged on the 19th postoperative day with no remarkable surgical complications except a mild nausea and surgical wound discomfort.

DISCUSSION

Plummer-Vinson syndrome, also known as Paterson-Kelly syndrome or sideropenic dysphagia[1], is characterized by dysphagia, iron deficiency anemia, and mucosal lesion of the oral cavity or pharynx. In 1893, Blackenstein reported a case with anemia, spasmodic stenosis of cervical esophagus and dysphagia[1]. The patient's symptoms were improved by endoscopic bougienage. In 1911, an another case with dysphagia due to upper esophageal web was reported, which was also alleviated by endoscopic bougienage. In 1912, Plummer[2] also reported cases with upper esophageal rigidity that the patients had iron deficiency anemia and splenomegaly. In 1922, Vinson named a series of patients with dysphagia, anemia, and splenomegaly as hysterical dysphagia[1]. In 1926, Sir Arthur Hurst designated similar cases of the syndrome as Plummer-Vinson syndrome[1].

The incidence of the Plummer-Vinson syndrome has recently decreased because of nutritional improvement, advanced health care, a decreased incidence of pregnancy and improved care programs for pregnant women. Moreover, this syndrome is now thought to be associated with the deficient intake of vitamins and iron[1,3,4]. Most patients are women aged over 40 years, and this group accounts for 75% in number[5,6]. The syndrome is usually asymptomatic, but the patients sometimes develop dysphagia, weight loss, and weakness. Other symptoms may include nail deformation of the hand and foot, cheilosis, atrophic glossitis, early loss of teeth, conjunctivitis, dermatitis seborrheica, hyperkeratosis, keratitis, blepharitis, visual disturbances and 30% of cases accompany splenomegaly[1]. The diagnosis of upper esophageal web is confirmed by radiologic methods or endoscopy. The radiologic method, however, is more suitable because endoscopy can sometimes miss the point of benign stricture, and does not verify most of the motility disorders[7]. On esophagography, the web is usually detected at the upper esophagus below the cricoid by showing a thin membrane across esophagus[8]. Pathologic finding of upper esophageal web shows hypertrophy or atrophy of squamous cells and it is sometimes combined with chronic inflammation[1].

Plummer-Vinson syndrome is known to be associated with an increased risk of upper alimentary tract cancers, and the incidence rate of upper esophageal cancer in this syndrome is 3-15%[6]. In Sweden, the incidence of upper alimentary tract cancer and hypopharyngeal cancer in Plummer-Vinson syndrome is decreasing along with that of the syndrome itself[3]. However, it is more unusual for

this syndrome to be accompanied by gastric cancer. Only two cases were reported in the literature, in which gastric cancer developed in the lower portion of the stomach[9,10]. In our case, the gastric cancer developed in the upper portion of the stomach involving esophagogastric junction.

It is not clear why Plummer-Vinson syndrome can exceptionally be associated with stomach cancer. However, it is widely accepted that atrophic mucosal change of alimentary tract due to iron deficiency anemia may lead to cancer development of the upper esophagus or hypopharynx. Therefore, careful examinations of hypopharynx, upper esophagus and stomach are of crucial importance for early detection of cancer development in this syndrome.

REFERENCES

1 **Lichtenstein GR**. Esophageal rings, webs, and diverticula. In: Haubrich WS, ed. Bockus gastroenterology. Volume 1.5th ed. *Philadelphia: WB Saunders Company*, 1994: 518-523

2 **Plummer HS**. Diffuse dilatation of the esophagus without anatomic stenosis (cardiospasm): Report of 91 cases. *JAMA* 1912; **58**: 2013-2015

3 **Larsson LG**, Sandstrom A, Westling P. Relationship of Plummer-Vinson disease to cancer of the upper alimentary tract in Sweden. *Cancer Res* 1975; **35**: 3308-3316

4 **Chen TS**, Chen PS. Rise and fall of the Plummer-Vinson syndrome. *J Gastroenterol Hepato*l 1994; **9:** 654-658

5 **Rosof BM**, Nagler RW. Plummer-Vinson syndrome. Revisited. *N Y State J Med* 1975; **75**: 414-415

6 **Chisholm M**. The association between webs, iron and post-cricoid carcinoma. *Postgrad Med J* 1974; **50**: 215-219

7 **Halpert RD**, Feczko PJ, Spickler EM, Ackerman LV. Radiological assessment of dysphagia with endoscopic correlation. *Radiology* 1985; **157**: 599-602

8 **SHAMMA'A MH**, BENEDICT EB. Esophageal webs; a report of 58 cases & an attempt at classification. *N Engl J Med* 1958; **259:** 378-384

9 **Nagai T**, Susami E, Ebihara T. Plummer-Vinson syndrome complicated by gastric cancer: a case report. *Keio J Med* 1990; **39**: 106-111

10 **Kitabayashi K**, Akiyama T, Tomita F, Saitoh H, Kosaka T, Kita I, Takashima S. Gastric cancer occurring in a patient with Plummer-Vinson syndrome: report of a case. *Surg Today* 1998; **28**: 1051-1055

Science Editor Kumar M and Guo SY **Language Editor** Elsevier HK

PO Box 2345, Beijing 100023, China
www.wjgnet.com
wjg@wjgnet.com

ELSEVIER

World J Gastroenterol 2005;11(44):7051-7053
World Journal of Gastroenterology ISSN 1007-9327

• *CASE REPORT* •

Very high alpha-fetoprotein in a young man due to concomitant presentation of hepatocellular carcinoma and Sertoli cell testis tumor

Ozdal Ersoy

Ozdal Ersoy, Sisili Etfal Education and Research Hospital, Kocamancur sok, Sisili
Correspondence to: Ozdal Ersoy, Sisili Etfal Education and Research Hospital, Kocamancur sok 16/6 80240, Sisili. ozdal@dr.com
Telephone: +90-2122413741
Received: 2004-12-16 Accepted: 2005-01-05

Abstract

Studies reported that there is a close relationship between hepatocellular carcinoma (HCC) and testis carcinoma. Both tumors can be presented as synchronal tumors, or as testicular metastases of HCC or as hepatic metastases of testicular tumor[7]. HCC is one of the most common malignancies worldwide and the incidence of HCC increases with age[8]. The relationship between hepatitis B incidence and HCC rates is also well recognized. Alpha fetoprotein (AFP) is produced by 70% of HCC. Though a level of AFP >400 ng/mL is diagnostic for HCC, in the presence of active hepatitis B infection, the cut-off level should be considered to be at least 1 000-4 000 ng/mL. Like HCC, germ cell tumors of the testis also release AFP; but it is shown that some of Sertoli cell tumors of testis can also release AFP[10]. Herein we have reported about the first case of HCC in the literature which is presented concomitantly with Sertoli-Leydig tumor of testis, leading to extremely high level of AFP in a 21-year-old man.

Key words: Hepatocellular carcinoma; Sertoli-Leydig cell tumor; AFP; Cirrhosis; Hypercholesterolemia

Ersoy O. Very high alpha-fetoprotein in a young man due to concomitant presentation of hepatocellular carcinoma and Sertoli cell testis tumor. *World J Gastroenterol* 2005; 11(44): 7051-7053
http://www.wjgnet.com/1007-9327/11/7051.asp

INTRODUCTION

Studies have reported that there is a close relationship between hepatocellular carcinoma (HCC) and testis carcinoma. Both tumors can be presented as synchronal tumors[1,2], or as testicular metastases of HCC[3-5] or as hepatic metastases of testicular tumor[6,7].

HCC is one of the most common malignancies worldwide and the incidence of HCC increases with age[8]. Alpha fetoprotein (AFP) is produced by 70% of HCC. Like HCC, germ cell tumors of the testis also release AFP[9]; but it is shown that some of Sertoli cell tumors of testis can also release AFP[10]. Herein we have reported the first case of HCC in the literature which is presented concomitantly with Sertoli-Leydig tumor of testis, leading to extremely high level of AFP in a 21-year-old man.

CASE REPORT

A 21-year-old man was admitted to our clinic in May 2002, with complaints of fatigue, nausea, vomiting, abdominal distention and weight loss. The patient was well before two months. His mother died of cirrhosis due to hepatitis B. His two sisters were HBsAg seropositive. On physical examination minimal ascites was detected and the abdomen was tender on palpation. The liver was palpated under the rib margin as 10 cm and was also tender. The spleen was palpated as 6 cm. Other systems were normal on examination. On admission, laboratory tests performed reported ALT: 64 IU/L (0-41), AST: 44 IU/L (0-37), fasting plasma glucose: 94 mg/dL, urea: 21 mg/dL, serum creatinine: 0.65 mg/dL, LDH: 500 IU/mL (240-480), GGT: 161 U/L (0-49), ALP: 372 U/L, T prot: 67 g/L, alb: 36 g/L, glob: 31 g/L, D bil: 0.76 mg/dL, I bil: 1.09 mg/dL, total cholesterol: 463 mg/dL, triglyceride: 130 mg/dL, LDL: 413 mg/dL, HDL: 24 mg/dL, VLDL: 38.2 mg/dL, Na: 138 mmol/L, K: 3.9 mmol/L, Ca: 9.4 mmol/L, Fe: 43 μg/dL, total iron binding capacity: 396 μg/dL, hemoglobin:11.5 g/dL, hematocrit: 34.8%, white blood cell: 2 700, platelet: 215 000, MCV: 83 fL, erythrocyte sedimentation rate: 12 mm/h. Markers of viral hepatitis were HBsAg (+), antiHBs (-), antiHCV -), HbeAg (-), antiHBe (-).

On ultrasonographic examination, the liver was heterogenous and there were multiple hypodense lesions in the right and left liver lobes. Thromboses were seen in both hepatic and portal veins in Doppler ultrasound. The AFP level was 5 181 000/mL (0-10) and beta-HCG was 0.5 mIU/mL (normal range: 5-10 mIU/mL). Computerized abdominal tomography showed that the craniocaudal sizes of the liver and spleen were 25 and 22 cm respectively. The liver margin was irregular, the right and

left lobes of the liver contained multiple hypodense lesions resembling metastasis or primary HCC. A liver biopsy was done to identify the hypodense lesions of the liver. Diffuse fibrosis and HCC were reported from the histopathological examination. Hepatocytes were positive for keratin and AFP, but negative for vimentin. Because of the young age of the patient, the presence of multiple hepatic hypodense lesions resembling metastasis and the extremely high AFP level, an examination of the testis was also done to exclude a testicular tumor. Physical examination of the testis revealed a painless mass on the left testis. Ultrasound sonography showed a hypoechoic lesion (19 mm× 18 mm×17 mm in size) in the left testis. High inguinal orchiectomy was performed. The tumor within the testis was histopathologically diagnosed as Sertoli cell testis tumor. Leydig cells were negative for keratin but positive for vimentin. Finally, the patient who had primary HCC and primary Sertoli cell tumor of the testis (two primary tumors concomitantly presented) was referred to the oncology clinic for further evaluation and therapy.

DISCUSSION

HCC is one of the commonest malignant diseases in the world and the majority of cases of HCC arise in individuals with chronic hepatitis B or C virus infections[11]. All ages can be affected by HCC. The mean age at diagnosis is 53 years in Asia and 62 years in the United States. Recently, an analysis of 76 HCC cases investigated by Butt *et al*.[8] showed that the mean age is 52.2±11.3 years and the mean AFP level is 142±155 ng/mL. In contrary, our patient was very young and the AFP level was very high. Transmission of hepatitis B virus from his mother at the very early time of his life might be the cause of HCC development at the very young age.

AFP continues to be the best marker for early diagnosis of HCC. In adults the value of AFP up to 20 ng/mL is considered to be normal. Patients with hepatitis B virus-related cirrhosis having AFP level greater than 100 ng/mL are in the very high risk group for HCC. The AFP level usually correlates with tumor size[12]. Thus, the very high level of AFP in our patient may be due to the large tumor size, which was multifocal in both lobes of the liver.

Extremely high AFP levels are found in endodermal sinus tumors (yolk sac tumors) also[13]. Such neoplasms occur in testis, ovary and extragonadal sites. Typically they occur in young subjects. Hence we also examined the testis in our patient and performed orchiectomy after we palpated a testicular mass. The histopathological result was a Sertoli cell tumor of the testis, which was a testicular gonadal stromal tumor. Sertoli cell tumor (SCT) is very rare among testis tumors accounting for lower than 1% of primary testicular neoplasms. It is subclassified into three groups: classic, large cell calcifying (LCCSCT), and sclerosing. Most SCTs are benign, metastases are the only reliable indicator of malignancy, occurring in lower than 10% of cases. The most common sites for metastatic spread are retroperitoneal lymph nodes, lungs, liver, and bone. LCCSCT and sclerosing SCT have minimal metastatic potential[14].

The risk for liver cancer is very high in cirrhotic liver. There is also evidence that the risk for extrahepatic cancers increases in patients with cirrhosis. The reason of the increased extrahepatic malignancy risk in cirrhosis is not clear but may be due to many abnormal and metabolic alterations in cirrhosis like hyperestrogenism, alterations in metabolism of lipid and water-soluble drugs and other chemicals, alterations in immune functions and risk of infections in cirrhosis[15]. In this cohort study, Sorensen *et al*.[15] also reported that the occurrence of liver cancer, tobacco- and alcohol-related cancers, testicular cancer, stomach and colon cancer is significantly higher in cirrhosis than expected. This study may explain two primary cancers in our young patient which were thought to be cirrhotic due to chronic hepatitis B infection.

Though our case was in a state of decompensated liver failure, he had hypercholesterolemia which was parallel to the change in serum AFP. Hwang *et al*.[16] also observed that HCC patients with hypercholesterolemia have significantly higher mean serum levels of albumin, triglyceride, and AFP compared with age-sex-tumor volume-matched HCC patients without hypercholesterolemia. It was reported that 11% of HCC patients have hypercholesterolemia, which can be explained by the possible result from the absence of dietary cholesterol suppression feedback regulation in the damaged liver[17].

In conclusion, this case is an example showing the increased risk of hepatic and extrahepatic tumors in cirrhosis. In the presence of HCC in a cirrhotic patient, there might be multiple primary cancers. The possibility of second primary malignancy in a patient with HCC should be kept in mind especially when a very high level of AFP is encountered and this second primary malignancy may be a kind of a very rare tumor. However, the co-existence of HCC and testis tumor is very rare. As far as we know, this is the first case report showing the co-existence of HCC and SCT in a young boy presented with an extremely high level of AFP.

REFERENCES

1 **Hiraki Y**, Nakajo M, Uchiyama N. [A case of multiple primary cancers, hepatoma and seminoma, detected by 67Ga citrate and 99mTc-HIDA scintigraphy] *Kaku Igaku* 1991; **28:** 1497-1502
2 **Yamauchi M**, Yoshigoe F, Mera F, Ogura K, Kameda H, Nakada J, Takasaka S, Machida T, Fukunaga M. An autopsy case of double cancer (Hepatocellular carcinoma and mixed germ cell tumor of the testis)--significance of alpha-fetoprotein and human chorionic gonadotropin as tumor markers. *Gan No Rinsho* 1983; **29:** A-22, 349-352
3 **Young RH**, Van Patter HT, Scully RE. Hepatocellular carcinoma metastatic to the testis. *Am J Clin Pathol* 1987; **87:** 117-120
4 **Fukuda T**, Ohnishi Y, Miyazaki Y, Ohnuki K, Tachikawa S. Clear cell hepatocellular carcinoma with abundant myxoid stroma. *Acta Pathol Jpn 1992*; **42:** 897-903
5 **Horie Y**, Kato M. Hepatoid variant of yolk sac tumor of the testis. *Pathol Int* 2000; **50:** 754-758
6 **de Boer HD**, Haerkens MH, van der Stappen W, van Ingen G, Wobbes T. Testicular carcinoma: postmortem diagnosis after a car accident. *Lancet* 2002; **359:** 1666

7 **Minowada S,** Okano Y, Miyazaki J, Homma Y, Kitamura T. Multidisciplinary treatment of advanced testicular tumor with bulky liver metastasis. *Urol Int* 2001; **67:** 178-180
8 **Butt AK,** Khan AA, Alam A, Ahmad S, Shah SW, Shafqat F, Naqvi AB. Hepatocellular carcinoma: analysis of 76 cases. *J Pak Med Assoc* 1998; **48:** 197-201
9 **Ganz M**, Joller-Jemelka HI, Grob PJ. [Severely increased alpha fetoprotein and associated diseases] *Schweiz Med Wochenschr* 1979; **109:** 1314-1322
10 **Taniyama K**, Suzuki H, Hara T, Yokoyama S, Tahara E. [An alpha-fetoprotein producing Sertoli-Leydig cell tumor--a case report] *Gan No Rinsho* 1989; **35:** 107-113
11 **Izzo F**, Cremona F, Delrio P, Leonardi E, Castello G, Pignata S, Daniele B, Curley SA. Soluble interleukin-2 receptor levels in hepatocellular cancer: a more sensitive marker than alfa fetoprotein. *Ann Surg Oncol* 1999; **6:** 178-185
12 **Sherlock S,** Dooley J.Hepatic tumours. Diseases of the liver and biliary system, 10th ed. *Massachusetts* 1997; 531-559
13 **Talerman A**, Haije WG, Baggerman L. Serum alphafetoprotein (AFP) in patients with germ cell tumors of the gonads and extragonadal sites: correlation between endodermal sinus (yolk sac) tumor and raised serum AFP. *Cancer* 1980; **46:** 380-385
14 **Rosl GJ**, Bajorin DF, Sheinfeld J, Motzer RJ, and Chaganti RSK. Cancer of the testis. In: DeVita VT, Hellman S and Rosenberg SA, eds. Cancer, 6th ed. Philadelphia: Lippincott Williams & Wilkins, 2001: 1491-1518
15 **Sorensen HT**, Friis S, Olsen JH, Thulstrup AM, Mellemkjaer L, Linet M, Trichopoulos D, Vilstrup H, Olsen J. Risk of liver and other types of cancer in patients with cirrhosis: a nationwide cohort study in Denmark. *Hepatology* 1998; **28:** 921-925
16 **Hwang SJ**, Lee SD, Chang CF, Wu JC, Tsay SH, Lui WY, Chiang JH, Lo KJ. Hypercholesterolaemia in patients with hepatocellular carcinoma. *J Gastroenterol Hepatol* 1992; **7:** 491-496
17 **Goldberg RB**, Bersohn I, Kew MC. Hypercholesterolaemia in primary cancer of the liver. *S Afr Med J* 1975; **49:** 1464-1466

Science Editor Wang XL and Guo SY **Language Editor** Elsevier HK

PO Box 2345, Beijing 100023, China
www.wjgnet.com
wjg@wjgnet.com

ELSEVIER

World J Gastroenterol 2005;11(44):7054-7056
World Journal of Gastroenterology ISSN 1007-9327

Immunosurveillance function of human mast cell?

Öner Özdemir

Öner Özdemir, Department of Pediatrics, Division of Allergy/Immunology, Louisiana State University Health Sciences Center, New Orleans, LA, United States
Correspondence to: Öner Özdemir, MD, Department of Pediatrics, Division of Allergy/Immunology, LSUHSC, New Orleans, LA, United States. ozdemir_oner@hotmail.com
Telephone: +1- 5045682578 Fax: +1- 504 5687598
Received: 2005-05-24 Accepted: 2005-07-08

Abstract

Mast cell (MC) is so widely recognized as a critical effector in allergic disorders that it can be difficult to think of MC in any other context. Indeed, MCs are multifunctional and recently shown that MCs can also act as antigen presenters as well as effector elements of human immune system. First observations of their possible role as anti-tumor cells in peri- or intra-tumoral tissue were mentioned five decades ago and a high content of MCs is considered as a favorable prognosis, consistent with this study. Believers of this hypothesis assumed them to be inhibitors of tumor development through their pro-apoptotic and -necrolytic granules e.g., granzymes and TNF-α. However, some still postulate them to be enhancers of tumor development through their effects on angiogenesis due to mostly tryptase. There are also some data suggesting increased MC density causes tumor development and indicates bad prognosis. Furthermore, since MC-associated mediators have shown to influence various aspects of tumor biology, the net effect of MCs on the development/progression of tumors has been difficult to evaluate. For instance, chymase induces apoptosis in targets; yet, tryptase, another MC protease, is a well-known mitogen. MCs with these various enzyme expression patterns may mediate different functions and the predominant MC type in tissues may be determined by the environmental needs. The coexistence of tryptase-expressing MCs (MC_T) and chymase and tryptase-expressing MCs (MC_{TC}) in physiological conditions reflects a naturally occurring balance that contributes to tissue homeostasis. We have recently discussed the role and relevance of MC serine proteases in different bone marrow diseases.

Key words: Mast cell; Immunosurveillance; Tryptase-chymase; Cytotoxicity; Tumors

Özdemir Ö. Immunosurveillance function of human mast cell? *World J Gastroenterol* 2005; 11(44): 7054-7056
http://www.wjgnet.com/1007-9327/11/7054.asp

LETTER TO THE EDITOR

I read the article by Tan *et al*.[1] describing `prognostic significance of cell infiltrations of immunosurveillance in colorectal cancer with great interest. My interest in this study is that we have recently demonstrated human mast cell (MC) mediated cytotoxicity against different human leukemia and lymphoma tumor cells *in vitro*[2-4]. Our *in vitro* results seem to support their study conclusion of MC cytotoxicity against tumor cells that might contribute to immunosurveillance *in vivo*. The genuine role of MC in tumor stroma has been a very controversial topic for the past five decades and needs still further clarification. Here, I have discussed further primarily the anti-tumor effects of MC in the light of recent literature and our findings.

MC is so widely recognized as a critical effector in allergic disorders that it can be difficult to think of MC in any other context. Indeed, MCs are multifunctional and recently shown that MCs can also act as antigen presenters as well as effector elements of human immune system. First observations of their possible role as anti-tumor cells in peri- or intra-tumoral tissue were mentioned five decades ago and a high content of MCs is considered as a favorable prognosis, consistent with this study[1,5,6]. Believers of this hypothesis assumed them to be inhibitors of tumor development through their pro-apoptotic and -necrolytic granules e.g. granzymes and TNF-α. However, some still postulate them to be enhancers of tumor development through their effects on angiogenesis due to mostly tryptase. There are also some data suggesting that increased MC density causes tumor development and indicates bad prognosis[7,8]. MCs with these various enzyme expression patterns may mediate different functions and the predominant MC type in tissues may be determined by the environmental needs. Furthermore, since MC-associated mediators have shown to influence various aspects of tumor biology, the net effect of MCs on the development/progression of tumors has been difficult to evaluate. For instance, chymase induces apoptosis in targets; yet, tryptase, another MC protease, is a well-known mitogen. We have recently discussed the role and relevance of MC serine proteases in different bone marrow diseases[9]. The coexistence of tryptase-expressing MCs (MC_T) and chymase and tryptase-expressing MCs (MC_{TC}) in physiological conditions reflects a naturally occurring balance that contributes to tissue homeostasis.

In the past two decades, it was believed that murine MC has natural cytotoxicity in the long term (>24 h) against murine tumor cells (WEHI-164, L929, etc.) by different mechanisms e.g. TNF-α dependent and non-TNF-α dependent[10]. Recent studies suggested that MC

can kill targets through degranulation of serine proteases, cathepsin G, leukotrienes and NO. Lately, MCs have been shown to contain granzyme B[11] and express Fas ligand[12], which are the most important components of cell mediated cytotoxicity. Chymase was also demonstrated to induce apoptosis in neonatal rat cardiomyocytes and human vascular smooth muscle cells[13]. Thus, MC mediated cytotoxicity seems to be operated by at least 2 pathways: by secretory pathways via exocytosis of granules containing serine proteases such as granzymes, chymase and soluble TNF-α; and nonsecretory (cell-to-cell contact) pathways via membranous TNF-α and FasL. We are the first to show human MC cytotoxicity against NK-sensitive/resistant human leukemia/lymphoma cells in short and long term by our established flow cytometric method[2-4]. Our studies suggested that increased chymase content of MCs in long-term culture could have played a role to mediate cytotoxicity.

Tan *et al.* demonstrated in this study that both MCT and MCTC may equally proliferate or infiltrate in colorectal cancer similar to hepatocellular carcinoma and intrahepatic cholangiocarcinoma, consistent with some earlier literature[14]. In contrast to these reports, in some malignant lesions, MCT`s were found to be concentrated at the tumor edge, i.e., the "invasion zone," whereas MCTCs were not increased in this area[15-17]. For instance, a significant increase of MCT phenotype was observed in the invasive carcinoma of the cervix throughout the different stages of malignant transformation. Furthermore, an abundant MCT (but not MCTC) increase was detected infiltrating the tumors in sections of invasive carcinoma although the number of MCT was shown to be similar to that of MCTC in benign lesions. Malignant tumors had 2 to 3 times more MCT than MCTC and the number of MCT was noted to be significantly higher in malignant than benign lesions.

Our studies and past literature review suggest that increase of MC density in tumor stroma is as important as the phenotypic change[18,19] causing predominance of one phenotype. Consistent with this study, if chymase containing MCs (MCTC/MCC) were dominant over MCT in tumor stroma, this would usually be predictor of good prognosis such as in localized bronchioloalveolar carcinoma[20] and human renal tumors[21]. In contrast to this opinion, there are a few data suggesting that MCTC/MCC are related to a bad prognosis e.g. lip and some gastrointestinal cancers[22,23]. Nevertheless, overall chymase content of granules in MCs as well as timing of biopsy and other factors could be also important in these exceptional cases. If MCT`s were dominant over MCCT/MCC, this would be a bad prognostic factor such as in cervix cancer, B-cell non-Hodgkin's lymphoma and others[24,25]. Mounting evidence certainly indicates that MCs accumulate around the tumors and could either promote or inhibit tumor growth depending on the local stromal conditions[26]. These findings overall emphasize the role of MCT type in the tumor development rather than chymase containing MCs (MCC and/or MCCT) but this requires further studies and clarification. My personal conclusion is that inhibitory or proliferative effects of MCs depend on multiple interactions among MC, tumor type and the environment.

REFERENCES

1 **Tan SY**, Fan Y, Luo HS, Shen ZX, Guo Y, Zhao LJ. Prognostic significance of cell infiltrations of immunosurveillance in colorectal cancer. *World J Gastroenterol* 2005; **11**: 1210-1214
2 **Özdemir Ö**, Ravindranath Y, Savasan S. Evaluation of long-term liquid culture grown human bone marrow mast cell cytotoxicity against human leukemia cells. *Blood* 2002; **100**, 45b, abstract # 3642
3 **Özdemir Ö**, Moore C, Ravindranath Y, Savasan S. Can Mast Cells Mediate Natural Cytotoxicity in Short Term Culture? *Ann Allergy Asthma Immunol* 2004; **94**: 185, abstract # 216
4 **Özdemir Ö**, Ravindranath Y, Savasan S. Short Term Mast Cell Natural Cell-Mediated Cytotoxicity. *Ann Allergy Asthma Immunol* 2004; **94**: 186-187, abstract # 220
5 **Aaltomaa S**, Lipponen P, Papinaho S, Kosma VM. Mast cells in breast cancer. *Anticancer Res* 1993; **13**: 785-788
6 **Ueda T**, Aozasa K, Tsujimoto M, Yoshikawa H, Kato T, Ono K, Matsumoto K. Prognostic significance of mast cells in soft tissue sarcoma. *Cancer* 1988; **62**: 2416-2419
7 **Grimbaldeston MA**, Skov L, Baadsgaard O, Skov BG, Marshman G, Finlay-Jones JJ, Hart PH. Communications: high dermal mast cell prevalence is a predisposing factor for basal cell carcinoma in humans. *J Invest Dermatol* 2000; **115:** 317–320
8 **Roche WR**. The nature and significance of tumour-associated mast cells. *J Pathol* 1986; **148**: 175-182
9 **Özdemir Ö**, Savaşan S. The role of mast cells in bone marrow diseases. *J Clin Path* 2004; **57**: 108-109
10 **Ghiara P**, Boraschi D, Villa L, Scapigliati G, Taddei C, Tagliabue A. In vitro generated mast cells express natural cytotoxicity against tumour cells. *Immunology* 1985; **55**: 317-324
11 **Kataoka TR**, Morii E, Oboki K, Kitamura Y. Strain-dependent inhibitory effect of mutant mi-MITF on cytotoxic activities of cultured mast cells and natural killer cells of mice. *Lab Invest* 2004; **84:** 376-384
12 **Wagelie-Steffen AL**, Hartmann K, Vliagoftis H, Metcalfe DD. Fas ligand (FasL, CD95L, APO-1L) expression in murine mast cells. *Immunology* 1998; **94:** 569-574
13 **Leskinen MJ**, Lindstedt KA, Wang Y, Kovanen PT. Mast cell chymase induces smooth muscle cell apoptosis by a mechanism involving fibronectin degradation and disruption of focal adhesions. *Arterioscler Thromb Vasc Biol* 2003; **23**: 238-243
14 **Terada T**, Matsunaga Y. Increased mast cells in hepatocellular carcinoma and intrahepatic cholangiocarcinoma. *J Hepatol* 2000; **33**: 961-966
15 **Kankkunen JP**, Harvima IT, Naukkarinen A. Quantitative analysis of tryptase and chymase containing mast cells in benign and malignant breast lesions. *Int J Cancer* 1997; **72**: 385-388
16 **Cabanillas-Saez A**, Schalper JA, Nicovani SM, Rudolph MI. Characterization of mast cells according to their content of tryptase and chymase in normal and neoplastic human uterine cervix. *Int J Gynecol Cancer* 2002; **12:** 92-98
17 **Benitez-Bribiesca L**, Wong A, Utrera D, Castellanos E. The role of mast cell tryptase in neoangiogenesis of premalignant and malignant lesions of the uterine cervix. *J Histochem Cytochem* 2001; **49:** 1061-1062
18 **de Rey BM**, Palmieri MA, Duran HA. Mast cell phenotypic changes in skin of mice during benzoyl peroxide-induced tumor promotion. *Tumour Biol* 1994; **15**: 166-174
19 **Yang M**, Zhang X, He A. [Mast cells in the labial cancer: histochemical and electron microscopical study] *Zhonghua Kouqiang Yixue Zazhi* 1997; **32:** 13-15
20 **Nagata M**, Shijubo N, Walls AF, Ichimiya S, Abe S, Sato N. Chymase-positive mast cells in small sized adenocarcinoma of

the lung. *Virchows Arch* 2003; **443**: 565-573

21 **Beil WJ**, Fureder W, Wiener H, Grossschmidt K, Maier U, Schedle A, Bankl HC, Lechner K, Valent P. Phenotypic and functional characterization of mast cells derived from renal tumor tissues. *Exp Hematol* 1998; **26**: 158-169

22 **Gulubova MV**. Structural examination of tryptase- and chymase-positive mast cells in livers, containing metastases from gastrointestinal cancers. *Clin Exp Metastasis* 2003; **20**: 611-620

23 **Rojas IG**, Spencer ML, Martinez A, Maurelia MA, Rudolph MI. Characterization of mast cell subpopulations in lip cancer. *J Oral Pathol Med* 2005; **34**: 268-273

24 **Welle M**. Development, significance, and heterogeneity of mast cells with particular regard to the mast cell-specific proteases chymase and tryptase. *J Leukoc Biol* 1997; **61:** 233–245

25 **Ribatti D**, Vacca A, Marzullo A, Nico B, Ria R, Roncali L, Dammacco F. Angiogenesis and mast cell density with tryptase activity increase simultaneously with pathological progression in B-cell non-Hodgkin's lymphomas. *Int J Cancer* 2000; **85**: 171–175

26 **Theoharides TC**, Conti P. Mast cells: the Jekyll and Hyde of tumor growth. *Trends Immunol* 2004; **25**: 235-241

Science Editor and Guo SY **Language Editor** Elsevier HK

PO Box 2345, Beijing 100023, China
www.wjgnet.com
wjg@wjgnet.com

ELSEVIER

World J Gastroenterol 2005;11(44):7057
World Journal of Gastroenterology ISSN 1007-9327

Hormone receptor status of primary tumor as a prognostic factor in patients with liver metastases from breast cancer treated with transcatheter arterial chemoembolization

Kadri Altundag, Ozden Altundag, Serdal Aktolga, Ozlem Yavas, Cem Boruban

Kadri Altundag, Department of Medical Oncology, Hacettepe University Faculty of Medicine, Ankara, Turkey
Ozden Altundag, 8181 Fannin Street No. 728 Houston, Texas, United States
Serdal Aktolga, Department of Internal Medicine, Marmara University School of Medicine, Istanbul, Turkey
Ozlem Yavas, Cem Boruban, Department of Medical Oncology, Selcuk University Faculty of Medicine, Konya, Turkey
Correspondence to: Kadri Altundag, 8181 Fannin Street No. 728, Houston, Texas 77054,
United States. altundag@sbcglobal.net
Telephone: +1-713-563-0909 Fax: +1-713-794-4385
Received: 2005-06-27 Accepted: 2005-07-20

TO THE EDITOR

We read with great interest the article by XP *et al*.[1] They reported the results of their experience with transcatheter arterial chemoembolization (TACE) and systemic chemotherapy for forty-five patients with liver metastases from breast cancer and evaluate the prognostic factors. In their study, the response and survival rates were significantly better in TACE group than in chemotherapy group. The lymph node status of the primary cancer, the clinical stage of liver metastases, the Child-Pugh grade, loss of weight were found to be significantly associated with survival in both univariate and multivariate and analyses. However, they did not mention hormone receptor status of the patients that might have an effect on the survival rate. Elias *et al*.[2] in their study evaluated 54 breast cancer patients with liver metastases as the sole site of metastatic disease (except for bone metastases in 3 patients) that underwent hepatectomy. They showed that the only factor influencing survival in both the univariate and multivariate analyses was the hormone receptor status ($P = 0.03$), and the relative risk of death increased by 3.5-fold when hormone receptor was negative. Moreover, Mack *et al* [3] reported excellent local tumor control and survival rates achieved by laser induced interstitial thermotherapy (LITT) in breast cancer patients with liver metastases. Regarding the prognostic and predictive factors related to primary tumor, they found no statistically significant difference in terms of mean survival between the patients with N0-N1 lymph nodes and N2-N3 lymph nodes. However, they found that the hormone receptor status is a significant ($P<0.05$) prognostic factor on both mean and median survival. The mean survival in patients with positive hormone receptor status was 5.5 years (95%CI: 4.8-6.3 years, median survival 4.7 years) starting the calculation at the date of diagnosis of the metastases treated with LITT. The mean survival in patients with negative hormone receptor status was 3.7 years (95%CI: 2.8-4.6 years, median survival 5.1 years)[4].

In the light of the above information, hormone receptor status of primary tumor should also be evaluated as a prognostic factor in patients with breast cancer and liver metastases treated with TACE and systemic chemotherapy.

REFERENCES

1 **Li XP**, Meng ZQ, Guo WJ, Li J. Treatment for liver metastases from breast cancer: results and prognostic factors. *World J Gastroenterol* 2005; **11**: 3782-3787
2 **Elias D**, Maisonnette F, Druet-Cabanac M, Ouellet JF, Guinebretiere JM, Spielmann M, Delaloge S. An attempt to clarify indications for hepatectomy for liver metastases from breast cancer. *Am J Surg* 2003; **185**: 158-164
3 **Mack MG**, Straub R, Eichler K, Sollner O, Lehnert T, Vogl TJ. Breast cancer metastases in liver: laser-induced interstitial thermotherapy--local tumor control rate and survival data. *Radiology* 2004; **233:** 400-409
4 **Altundag K**, Altundag O, Morandi P, Gunduz M. Hormone receptor status in patients with breast cancer and liver metastases treated with laser-induced intersititial thermotherapy. *Radiology* 2005; **235:** 339; author reply 339-340

Science Editor Guo SY **Language Editor** Elsevier HK

PO Box 2345, Beijing 100023, China
www.wjgnet.com
wjg@wjgnet.com

ELSEVIER

World J Gastroenterol 2005;11(44):7058
World Journal of Gastroenterology ISSN 1007-9327

Acknowledgments to Reviewers of World Journal of *Gastroenterology*

Many reviewers have contributed their expertise and time to the peer review, a critical process to ensure the quality of *World Journal of Gastroenterology*. The editors and authors of the articles submitted to the journal are grateful to the following reviewers for evaluating the articles (including those were published and those were rejected in this issue) during the last editing period of time.

Luigi Bonavina, Professor
Department of Surgery, Policlinico San Donato, University of Milano, via Morandi 30, Milano 20097, Italy

Yusuf Bayraktar, Professor
Department of Gastroenterology, School of Medicine, Hacettepe University, Ankara 06100, Turkey

David L Carr-Locke, M.D.
Director of Endoscopy, Brigham and Women's Hospital, Endoscopy Center, Brigham and Women's Hospital, 75 Francis St, Boston MA, 02115, United States

Da-Jun Deng, Professor
Department of Cancer Etiology, Peking University School of Oncology, 1 Da-Hong-Luo-Chang Street, Western District, Beijing 100034, China

Fabio Farinati, M.D.
Surgical And Gastroenterological Sciences, University of Padua, Via Giustiniani 2, Padua 35128, Italy

Burkhard Göke, Professor
Internal Medicine II, University of Munich, Marchioninistr. 15, Munich 81377, Germany

Edoardo G Giannini, Assistant Professor
Department of Internal Medicine, Gastroenterology Unit, Viale Benedetto XV, no. 6, Genoa, 16132, Italy

Fu-Lian Hu, Professor
Department of Gastroenterology, Peking University First Hospital, 8 Xishiku St, Xicheng District, Beijing 100034, China

Hiroyuki Hanai, Director
Director of Department of Endoscopic and Photodynamic Medicine,Hamamatsu University School of Medicine, 1-20-3 Izumi, Hamamatsu 433-8124, Japan

Robin G Lorenz, Associate Professor
Department of Pathology, University of Alabama at Birmingham, 845 19th Street South BBRB 730, Birmingham, AL 35294-2170, United States

Shou-Dong Lee, Professor
epartment of Medicine, Taipei Veterans General Hospital, 201 Shih-Pai Road, Sec. 2. Taipei 112, Taiwan, China

Hisataka S Moriwaki, Professor
Department Of Medicine, Gifu University, 1-1 Yanagido, Gifu 501-1194, Japan

Hisato Nakajima, M.D.
Department of Gastroenterology and Hepatology, The Jikei University School of Medicine, 3-25-8, Nishi-Shinbashi, Minato-ku, Tokyo 105-8461, Japan

James Neuberger, Professor
Liver Unit, Queen Elizabeth Hospital, Birmingham B15 2TH, United Kingdom

CS Pitchumoni, Professor
Robert Wood Johnson School of Medicine, Robert Wood Johnson School of Medicine, New Brunswiuc NJ D8903, United States

Gustav Paumgartner, Professor
University of Munich, Klinikum Grosshadern, Marchioninistr. 15, Munich, D-81377, Germany

Ian C Roberts-Thomson, Professor
Department of Gastroenterology and Hepatology, The Queen Elizabeth Hospital, 28 Woodville Road, Woodville South 5011, Australia

Chifumi Sato, Professor
Department of Analytical Health Science, Tokyo Medical and Dental University, Graduate School of Health Sciences, 1-5-45 Yushima, Bunkyoku, Tokyo 113-8519, Japan

Shingo Tsuji, Professor
Department of Internal Medicine and Therapeutics, Osaka University Graduate School of Medicine(A8), 2-2 Yamadaoka, Suita, Osaka 565-0871, Japan

Chun-Yang Wen, M.D.
Department of Molecular Pathology, Atomic Bomb Disease Institute, Nagasaki University Graduate School of Biomedical Sciences. 1-12-4 Sakamoto, Nagasaki 852-8523, Japan

Ming_shiang Wu, Dr, Associate Professor
Internal Medicine, National Taiwan University Hospital, No 7,Chung-Shan S. Rd., Taipei 100, Taiwan, China

Shinichi Wada, M.D.
Department of Gastroenterology, Jichi Medical School, Minamikawachimachi,Kwachi-gun, Tochigi-ken, Tochigi 329-0498, Japan

Masahide Yoshikawa, M.D.
Department of Parasitology, Nara Medical University, Shijo-cho 840, Kashihara 634-8521, Japan

Takayuki Yamamoto, M.D.
Inflammatory Bowel Disease Center, Yokkaichi Social Insurance Hospital, 10-8 Hazuyamacho, Yokkaichi 510-0016, Japan

PO Box 2345, Beijing 100023, China
www.wjgnet.com
wjg@wjgnet.com

ELSEVIER

World J Gastroenterol 2005;11(44):7059
World Journal of Gastroenterology ISSN 1007-9327

Meetings

MAJOR MEETINGS COMING UP

American College of Gastroenterology Annual Scientific Meeting
October 28 -November 2, 2005
annualmeeting@acg.gi.org
www.acg.gi.org

EVENTS AND MEETINGS IN THE UPCOMING 6 MONTHS

ISGCON2005
November 11-15, 2005
isgcon2005@yahoo.co.in
isgcon2005.com

II Latvian Gastroenterology Congress
November 29, 2005
gec@stradini.lv
www.gastroenterologs.lv

70th ACG Annual Scientific Meeting and Postgraduate Course
October 28-November 2, 2005

Advanced Capsule Endoscopy Users Course
November 18-19, 2005
www.asge.org/education

2005 CCFA National Research and Clinical Conference - 4th Annual Advances in the Inflammatory Bowel Diseases
December 1-3, 2005
c.chase@imedex.com
www.imedex.com/calendars/therapeutic.htm

EVENTS AND MEETINGS IN 2005

XIII Argentine Hepatology Congress
XIII Congreso Argentino de HepatologÃa
June 10-13, 2005
mci@mcimeetings.com
www.hepatologia.org

9th Annual Coolum Update in Gastroenterology & Hepatology
June 11-13, 2005
info@e-Kiddna.com.au

Canadian Digestive Disease Week Conference
February 26-March 6, 2005
www.cag-acg.org

2005 World Congress of Gastroenterology
September 12-14, 2005
wcog2005@congrex.nl

International Colorectal Disease Symposium 2005
February 3-5, 2005
info@icds-hk.org

15th World Congress of the International Association of Surgeons and Gastroenterologists
September 7-10, 2005
iasg2005@guarant.cz
www.iasg2005.cz

7th International Workshop on Therapeutic Endoscopy
September 10-12, 2005
alfa@alfamedical.com
www.alfamedical.com

EASL 2005 the 40th annual meeting
April 13-17, 2005
www.easl.ch/easl2005/

ISGCON2005
November 11-15, 2005
isgcon2005@yahoo.co.in
isgcon2005.com

Pediatric Gastroenterology, Hepatology and Nutrition
March 13, 2005

II Latvian Gastroenterology Congress
November 29, 2005
gec@stradini.lv
www.gastroenterologs.lv

21st annual international congress of Pakistan society of Gastroenterology & GI Endoscopy
March 25-27, 2005
psgc05@hotmail.com
www.psgc2005.com

8th Congress of the Asian Society of HepatoBiliary Pancreatic Surgery
February 10-13, 2005

1º Workshop de Gastrenterologia para Clínica Geral
April 29, 2005
luis.m.lopes@sapo.pt

APDW 2005 - Asia Pacific Digestive Week 2005
September 25-28, 2005
asiapdw@kornet.net
www.apdw2005.org

World Congress on Gastrointestinal Cancer
June 15-18, 2005
meetings@imedex.com

British Society of Gastroenterology Conference
March 14-17, 2005
www.bsg.org.uk

Training Director's Workshop:Developing and Teaching Principles in the New Era of GI Training
February 4-6, 2005
www.asge.org/education

The Pharmacological, Surgical and Endoscopic Management of GERD
April 8-9, 2005
www.asge.org/education

Digestive Disease Week
DDW 106th Annual Meeting
May 15-18, 2005
ddwadmin@gastr.org
www.ddw.org

ASGE Advanced Endscopy Skills Hands-on Sessions
May 15, 2005
www.asge.org/education

ASGE GERD Hands-on Session
May 17, 2005
www.asge.org/education

Annual Postgraduate Course
May 18-19, 2005
www.asge.org/education

Advanced Capsule Endoscopy Users Course
June 4-5, 2005
www.asge.org/education

Advanced Capsule Endoscopy Users Course
August 12-13, 2005
www.asge.org/education

GI Practice Management Symposium: Solutions for a Successful Practice
August 18, 2005
www.asge.org/education

70th ACG Annual Scientific Meeting and Postgraduate Course
October 28-November 2, 2005

Advanced Capsule Endoscopy Users Course
November 18-19, 2005
www.asge.org/education

2005 CCFA National Research and Clinical Conference - 4th Annual Advances in the Inflammatory Bowel Diseases
December 1-3, 2005
c.chase@imedex.com
www.imedex.com/calendars/therapeutic.htm

EVENTS AND MEETINGS IN 2006

10th World Congress of the International Society for Diseases of the Esophagus
February 22-25, 2006
isde@sapmea.asn.au
www.isde.net

Easl 2006 - The 41st Annual Meeting
April 26-30, 2006

Canadian Digestive Disease Week Conference
March 4-12, 2006
www.cag-acg.org

XXX pan-american congress of digestive diseases
XXX congreso panamericano de anfermedades digestivas
November 25-December 1, 2006
amg@gastro.org.mx
www.gastro.org.mx

World Congress on Gastrointestinal Cancer
June 14-17, 2006
c.chase@imedex.com

7th World Congress of the International Hepato-Pancreato-Biliary Association
September 3-7, 2006
convention@edinburgh.org
www.edinburgh.org/conference

Annual Postgraduate Course
May 25-26, 2006
www.asge.org/education

71st ACG Annual Scientific Meeting and Postgraduate Course
October 20-25, 2006

PO Box 2345, Beijing 100023, China
www.wjgnet.com
wjg@wjgnet.com

ELSEVIER

World J Gastroenterol 2005;11(44):7060-7061
World Journal of Gastroenterology ISSN 1007-9327

Instructions to authors

GENERAL INFORMATION

World Journal of Gastroenterology (*WJG,* ISSN 1007-9327 CN 14-1219/R) is a weekly journal of more than 48 000 circulation, published on the 7th, 14th, 21st and 28th of every month.

Original Research, Clinical Trials, Reviews, Comments, and Case Reports in esophageal cancer, gastric cancer, colon cancer, liver cancer, viral liver diseases, *etc*., from all over the world are welcome on the condition that they have not been published previously and have not been submitted simultaneously elsewhere.

Published jointly by
The WJG Press and Elsevier Inc.

SUBMISSION OF MANUSCRIPTS

Manuscripts should be typed double-spaced on A4 (297×210 mm) white paper with outer margins of 2.5 cm. Number all pages consecutively, and start each of the following sections on a new page: Title Page , Abstract, Introduction, Materials and Methods, Results, Discussion, Acknowledgements, References, Tables, Figures and Figure Legends. Neither the Editors nor the Publisher is responsible for the opinions expressed by contributors. Manuscripts formally accepted for publication become the permanent property of The WJG Press and Elsevier Inc., and may not be reproduced by any means, in whole or in part without the written permission of both the Authors and the Publisher. We reserve the right to put onto our website and copy-edit accepted manuscripts. Authors should also follow the guidelines for the care and use of laboratory animals of their institution or national animal welfare committee.

Authors should retain one copy of the text, tables, photographs and illustrations, as rejected manuscripts will not be returned to the author(s) and the editors will not be responsible for the loss or damage to photographs and illustrations.

Online submission
Online submission is strongly advised. Manuscripts should be submitted through the Online Submission System at: http://www.wjgnet.com/index.jsp. Authors are highly recommended to consult the ONLINE INSTRUCTIONS TO AUTHORS (http://www.wjgnet.com/wjg/help/instructions.jsp) before attempting to submit online. Authors encountering problems with the Online Submission System may send an email describing the problem to wjg@wjgnet.com for assistance. If you submit manuscript online, do not make a postal contribution. A repeated online submission for the same manuscript is strictly prohibited.

Postal submission
Send 3 duplicate hard copies of the full-text manuscript typed double-spaced on A4(297×210 mm) white paper together with any original photographs or illustrations and a 3.5 inch computer diskette or CD-ROM containing an electronic copy of the manuscript including all the figures, graphs and tables in native Microsoft Word format or *.rtf format to:

World Journal of Gastroenterology
Apartment 1066 Yishou Garden,
58 North Langxinzhuang Road,
PO Box 2345, Beijing 100023, China
E-mail: wjg@wjgnet.com
http: //www.wjgnet.com

MANUSCRIPT PREPARATION

All contributions should be written in English. All articles must be submitted using a word-processing software. All submissions must be typed in 1.5 line spacing and in word size 12 with ample margins. The letter font is Tahoma. For authors originating from China, one copy of the Chinese translation of the manuscript is also required (excluding references). Style should conform to our house format. Required information for each of the manuscript sections is as follows:

Title page
Full manuscript title, running title, all author(s) name(s), affiliations, institution(s) and/or department(s) where the work was accomplished, disclosure of any financial support for the research, and the name, full address, telephone and fax numbers and email address of the corresponding author should be involved. Titles should be concise and informative (removing all unnecessary words), emphasize what is NEW, and avoid abbreviations. A short running title of less than 40 letters should be provided. List the author(s)' name(s) as follows: initials and/or first name, middle name or initial(s) and full family name.

Abstract
An informative, structured abstract of no more than 250 words should accompany each manuscript. Abstracts for original contributions should be structured into the following sections: AIM: Only the purpose should be included. METHODS: The materials, techniques, instruments and equipments, and the experimental procedures should be included. RESULTS: The observatory and experimental results, including data, effects, outcome, *etc*. should be included. Authors should present *P* value where necessary, and the significant data should accompany. CONCLUSION: Accurate view and the value of the results should be included.

The format of structured abstracts is at: http://www.wjgnet.com/wjg/help/11.doc

Key words
Please list 3-10 key words that could reflect content of the study.

Text
For most article types, the main text should be structured into the following sections: INTRODUCTION, MATERIALS AND METHODS, RESULTS and DISCUSSION, and should include appropriate Figures and Tables. Data should be presented in the body text or Figures and Tables, not both.

Illustrations
Figures should be numbered as 1, 2, 3 and so on, and mentioned clearly in the main text. Provide a brief title for each figure on a separate page. No detailed legend should be involved under the figures. This part should add into the text where the figures are applicable. Digital images: black and white photographs should be scanned and saved in TIFF format at a resolution of 300 dpi; color images should be saved as CMYK (print files) and not RGB (screen-viewing files). Place each photograph in a separate file. Print images: supply images of size no smaller than 126× 76 mm printed on smooth surface paper; label the image by writing the Figure number and orientation using an arrow. Photomicrographs: indicate the original magnification and stain in the legend. Digital Drawings: supply files in EPS if created by Freehand and Illustrator, or TIFF from Photoshop. EPS files must be accompanied by a version in native file format for editing purposes. Scans of existing line drawings should be scanned at a resolution of 1200 dpi and as close as possible to the size at which they will appear when printed, not smaller. Please use uniform legends for the same subjects. For example: Figure 1 Pathological changes of atrophic gastritis after treatment. A: ...; B: ...;C: ...; D: ...; E: ...; F: ...; G: ...

Tables
Three-line tables should be numbered as 1, 2, 3 and so on, and mentioned clearly in the main text. Provide a brief title for each table. No detailed legend should be involved under the tables. This part should add into the text where the tables are applicable. The information should complement but not duplicate that contained in the text. Use one horizontal line under the title, a second under the column heads, and a third below the Table, above any footnotes. Vertical and italic lines should be omitted.

Notes in tables and illustrations
Data which is not statistically significant should not be noted. $^{a}P<0.05$, $^{b}P<0.01$ ($P>0.05$ should not be noted). If there are other series of *P* values, $^{c}P<0.05$ and $^{d}P<0.01$ are used; Third series of *P* values can be expressed as $^{e}P<0.05$ and $^{f}P<0.01$. Other notes in tables or under illustrations should be expressed as ^{1}F, ^{2}F, ^{3}F; or some other symbols with a superscript (Arabic

numerals) in the upper left corner. In a multi-curve illustration, each curve should be labeled with ●, ○, ■, □, ▲, △, *etc*. in a certain sequence.

Acknowledgments

Brief acknowledgments of persons who have made genuine contributions to the manuscripts and who endorse the data and conclusions are included. Authors are responsible for obtaining written permission to use any copyrighted text and/or illustrations.

References

Cited references should mainly be drawn from journals covered in the Science Citation Index (http://www.isinet.com) and/or Index Medicus (http://www.ncbi.nlm.nih.gov/PubMed) databases. Mention all references in the text, tables and figure legends, and set off by consecutive, superscripted Arabic numerals. References should be numbered consecutively in the order in which they appear in the text. Abbreviate journal title names according to the Index Medicus style (http://www.ncbi.nlm.nih.gov/entrez/query.fcgi?db=journals). Unpublished observations and personal communications are not listed as references. The style and punctuation of the references conform to ISO standard and the Vancouver style (5th edition); see examples below. Reference lists not conforming to this style could lead to delayed or even rejected publication status. Examples:

Standard jounal article (list all authors and include the PubMed ID [PMID] where applicable)

1 **Das KM,** Farag SA. Current medical therapy of inflammatory bowel disease. *World J Gastroenterol* 2000; 6: 483-489 [PMID: 11819634]

2 **Pan BR**, Hodgson HJF, Kalsi J. Hyperglobulinemia in chronic liver disease: Relationships between *in vitro* immunoglobulin synthesis, short lived suppressor cell activity and serum immunoglobulin levels. *Clin Exp Immunol* 1984; 55: 546-551 [PMID: 6231144]

3 **Lin GZ,** Wang XZ, Wang P, Lin J, Yang FD. Immunologic effect of Jianpi Yishen decoction in treatment of Pixu-diarrhoea. *Shijie Huaren Xiaohua Zazhi* 1999; 7: 285-287 [CMFAID:1082371101835979]

Books and other monographs (list all authors)

4 **Sherlock S,** Dooley J. Diseases of the liver and billiary system. 9th ed. Oxford: Blackwell Sci Pub, 1993: 258-296

Chapter in a book (list all authors)

5 **Lam SK.** Academic investigator's perspectives of medical treatment for peptic ulcer. In: Swabb EA, Azabo S. Ulcer disease: investigation and basis for therapy. New York: Marcel Dekker, 1991: 431-450

Electronic journal (list all authors)

6 **Morse SS.** Factors in the emergence of infectious diseases. Emerg Infect Dis serial online, 1995-01-03, cited 1996-06-05; 1(1):24 screens. Available from: URL: http//www.cdc.gov/ncidod/EID/eid.htm

PMID requirement

From the full reference list, please submit a separate list of those references embodied in PubMed, keeping the same order as in the full reference list, with the following information only: (1) abbreviated journal name and citation (e.g. *World J Gastroenterol* 2003;9(11):2400-2403; (2) article title (e.g. Epidemiology of gastroenterologic cancer in Henan Province, China; (3) full author list (e.g. Lu JB, Sun XB, Dai DX, Zhu SK, Chang QL, Liu SZ, Duan WJ; (4) PMID (e.g. 14606064). Provide the full abstracts of these references, as quoted from PubMed on a 3.5 inch disk or CD-ROM in Microsoft Word format and send by post to The *WJG* Press. For those references taken from journals not indexed by *Index Medicus*, a printed copy of the first page of the full reference should be submitted. Attach these references to the end of the manuscript in their order of appearance in the text.

Inappropriate references

Authors should always cite references that are relevant to their article, and avoid any inappropriate references. Inappropriate references include those that are linked with a hyphen and the difference between the two numbers at two sides of the hyphen is more than 5. For example, [1-6], [2-14] and [1, 3, 4-10, 22] are all considered as inappropriate references. Authors should not cite their own unrelated published articles.

Statistical data

Present as mean±SD and mean±SE.

Statistical expression

Express *t* test as *t*(in italics), *F* test as *F*(in italics), chi square test as χ^2(in Greek), related coefficient as *r*(in italics), degree of freedom as γ (in Greek), sample number as *n*(in italics), and probability as *P*(in italics).

Units

Use SI units. For example: body mass, m(B) = 78 kg; blood pressure, p(B)=16.2/12.3 kPa; incubation time, t(incubation)=96 h, blood glucose concentration, c(glucose) 6.4±2.1 mmol/L; blood CEA mass concentration, p(CEA) = 8.6 24.5 μg/L; CO_2 volume fraction, 50 mL/L CO_2 not 5% CO_2; likewise for 40 g/L formaldehyde, not 10% formalin; and mass fraction, 8 ng/g, *etc*. Arabic numerals such as 23,243,641 should be read 23 243 641.

The format about how to accurately write common units and quantum is at: http://www.wjgnet.com/wjg/help/15.doc

Abbreviations

Standard abbreviations should be defined in the abstract and on first mention in the text. In general, terms should not be abbreviated unless they are used repeatedly and the abbreviation is helpful to the reader. Permissible abbreviations are listed in Units, Symbols and Abbreviations: A Guide for Biological and Medical Editors and Authors (Ed. Baron DN, 1988) published by The Royal Society of Medicine, London. Certain commonly used abbreviations, such as DNA, RNA, HIV, LD50, PCR, HBV, ECG, WBC, RBC, CT, ESR, CSF, IgG, ELISA, PBS, ATP, EDTA, mAb, can be used directly without further mention.

Italicization

Quantities: *t* time or temperature, *c* concentration, *A* area, *l* length, *m* mass, *V* volume.

Genotypes: *gyr*A, *arg* 1, *c myc*, *c fos*, *etc*.

Restriction enzymes: *Eco*RI, *Hin*dI, *Bam*HI, *Kbo* I, *Kpn* I, *etc*.

Biology: *Helicobacter pylori, H pylori, E coli, etc*.

SUBMISSION OF THE REVISED MANUSCRIPTS AFTER ACCEPTED

Please revise your article according to the revision policies of *WJG*. The revised version including manuscript and high-resolution image figures (if any) should be copied on a floppy or compact disk. Author should send the revised manuscript, along with printed high-resolution color or black and white photos, copyright transfer letter, the final check list for authors, and responses to reviewers by a courier (such as EMS) (submission of revised manuscript by e-mail or on the WJG Editorial Office Online System is NOT available at present).

Language evaluation

The language of a manuscript will be graded before sending for revision. (1) Grade A: priority publishing; (2) Grade B: minor language polishing; (3) Grade C: a great deal of language polishing; (4) Grade D: rejected. The revised articles should be in grade B or grade A.

Copyright assignment form

It is the policy of WJG to acquire copyright in all contributions. Papers accepted for publication become the copyright of WJG and authors will be asked to sign a transfer of copyright form. All authors must read and agree to the conditions outlined in the Copyright Assignment Form (which can be downloaded from http://www.wjgnet.com/wjg/help/9.doc).

Final check list for authors

The format is at: http://www.wjgnet.com/wjg/help/13.doc

Responses to reviewers

Please revise your article according to the comments/suggestions of reviewers. The format for responses to the reviewers' comments is at: http://www.wjgnet.com/wjg/help/10.doc

Proof of financial support

For paper supported by a foundation, authors should provide a copy of the document and serial number of the foundation.

Publication fee

Authors of accepted articles must pay publication fee.

PO Box 2345, Beijing 100023, China
www.wjgnet.com
wjg@wjgnet.com

ELSEVIER

World J Gastroenterol 2005;11(44):7062
World Journal of Gastroenterology ISSN 1007-9327

World Journal of Gastroenterology standard of quantities and units

Number	Nonstandard	Standard	Notice
1	4 days	4 d	In figures, tables and numerical narration
2	4 days	four days	In text narration
3	day	d	After Arabic numerals
4	Four d	Four days	At the beginning of a sentence
5	2 hours	2 h	After Arabic numerals
6	2 hs	2 h	After Arabic numerals
7	hr, hrs,	h	After Arabic numerals
8	10 seconds	10 s	After Arabic numerals
9	10 year	10 years	In text narration
10	Ten yr	Ten years	At the beginning of a sentence
11	0,1,2 years	0,1,2 yr	In figures and tables
12	0,1,2 year	0,1,2 yr	In figures and tables
13	4 weeks	4 wk	
14	Four wk	Four weeks	At the beginning of a sentence
15	2 months	2 mo	In figures and tables
16	Two mo	Two months	At the beginning of a sentence
17	10 minutes	10 min	
18	Ten min	Ten minutes	At the beginning of a sentence
19	50% (*V/V*)	500 mL/L	
20	50% (m/*V*)	500 g/L	
21	1 M	1 mol/L	
22	10 μM	10 μmol/L	
23	1N HCl	1 mol/L HCl	
24	1N H_2SO_4	0.5 mol/L H_2SO_4	
25	4rd edition	4^{th} edition	
26	15 year experience	15- year experience	
27	18.5 kDa	18.5 ku,18 500u or M_r18 500	
28	25 $g.kg^{-1}/d^{-1}$	25 g/(kg·d) or 25 g/kg per day	
29	6900	6 900	
30	1000 rpm	1 000 r/min	
31	sec	s	After Arabic numerals
32	1 pg·L^{-1}	1 pg/L	
33	10 kilograms	10 kg	
34	13 000 rpm	13 000 *g*	High speed; *g* should be in italic and suitable conversion.
35	1000 *g*	1 000 r/min	Low speed. *g* cannot be used.
36	Gene bank	GenBank	International classified genetic materials collection bank
37	Ten L	Ten liters	At the beginning of a sentence
38	Ten mL	Ten milliliters	At the beginning of a sentence
39	umol	μmol	
40	30 sec	30 s	
41	1 g/dl	10 g/L	10-fold conversion
42	OD_{260}	A_{260}	"OD" has been abandoned.
43	One g/L	One microgram per liter	At the beginning of a sentence
44	*A*260 nm	A_{260} nm	*A* should be in italic.
	^{b}P<0.05	^{a}P<0.05	In Table, no note is needed if there is no significance in statistics: ^{a}P<0.05, ^{b}P<0.01 (no note if P>0.05). If there is a second set of P value in the same table, ^{c}P<0.05 and ^{d}P<0.01 are used for a third set: ^{e}P<0.05, ^{f}P<0.01.
45	**F*=9.87, $^{\S}F$=25.9, $^{\#}F$=67.4	^{1}F=9.87,^{2}F=25.9, ^{3}F=67.4	Notices in or under a table
46	KM	km	kilometer
47	CM	cm	centimeter
48	MM	mm	millimeter
49	Kg, KG	kg	kilogram
50	Gm, gr	g	gram
51	nt	N	newton
52	l	L	liter
53	db	dB	decibel
54	rpm	r/min	rotation per minute
55	bq	Bq	becquerel, a unit symbol
56	amp	A	ampere
57	coul	C	coulomb
58	HZ	Hz	
59	w	W	watt
60	KPa	kPa	kilo-pascal
61	p	Pa	pascal
62	ev	EV	volt (electronic unit)
63	Jonle	J	joule
64	J/mmol	kJ/mol	kilojoule per mole
65	10×10×$10cm^3$	10 cm×10 cm×10 cm	
66	N·km	KN·m	moment
67	$\bar{x}$±s	mean±SD	In figures, tables or text narration
68	Mean±SEM	mean±SE	In figures, tables or text narration
69	*im*	im	intramuscular injection
70	*iv*	iv	intravenous injection
71	Wang et al	Wang *et al.*	
72	EcoRI	*Eco*RI	*Eco* in italic and RI in positive. Restriction endonuclease has its prescript form of writing.
73	Ecoli	*E.coli*	Bacteria and other biologic terms have their specific ex pression.
74	Hp	*H pylori*	
75	Iga	*Iga*	writing form of genes
76	*igA*	IgA	writing form of proteins
77	-70 kDa	~70 ku	

PO Box 2345, Beijing 100023, China
www.wjgnet.com
wjg@wjgnet.com

ELSEVIER

World J Gastroenterol 2005;11(45):7063-7071
World Journal of Gastroenterology ISSN 1007-9327

• *REVIEW* •

Helicobacter pylori-infected animal models are extremely suitable for the investigation of gastric carcinogenesis

Masaaki Kodama, Kazunari Murakami, Ryugo Sato, Tadayoshi Okimoto, Akira Nishizono, Toshio Fujioka

Masaaki Kodama, Kazunari Murakami, Ryugo Sato, Tadayoshi Okimoto, Toshio Fujioka, Department of Gastroenterology, Faculty of Medicine, Oita University, Hasama-machi, Oita 879-5593, Japan
Akira Nishizono, Department of Infectious Diseases (Microbiology), Faculty of Medicine, Oita University, Hasama-machi, Oita 879-5593, Japan
Correspondence to: Masaaki Kodama, Department of Gastroenterology, Oita University, Faculty of Medicine, 1-1, Idaigaoka, Hasama-machi, Oita-gun, Oita 879-55, Japan. kodm@med.oita-u.ac.jp
Telephone: +81-975-86-6193 Fax: +81-975-86-6194
Received: 2005-06-06 Accepted: 2005-06-24

Abstract

Although various animal models have been developed to clarify gastric carcinogenesis, apparent mechanism of gastric cancer was not clarified in recent years. Since the recognition of the pathogenicity of *Helicobacter pylori* (*H pylori*), several animal models with *H pylori* infection have been developed to confirm the association between *H pylori* and gastric cancer. Nonhuman primate and rodent models were suitable for this study. Japanese monkey model revealed atrophic gastritis and p53 mutation after long-term infection of *H pylori*. Mongolian gerbil model showed the development of gastric carcinoma with *H pylori* infection alone, as well as with combination of chemical carcinogens, such as *N*-methyl-*N*-nitrosourea and *N*-methyl-*N*-nitro-*N*'-nitrosoguanidine. The histopathological changes of these animal models after *H pylori* inoculation are closely similar to those in human beings with *H pylori* infection. Eradication therapy attenuated the development of gastric cancer in *H pylori*-infected Mongolian gerbil. Although several features of animal models differ from those seen in human beings, these experimental models provide a starting point for further studies to clarify the mechanism of gastric carcinogenesis as a result of *H pylori* infection and assist the planning of eradication therapy to prevent gastric carcinoma.

Key words: *Helicobacter pylori*; Gastric carcinoma; Animal model; Japanese monkey; Mongolian gerbil

Kodama M, Murakami K, Sato R, Okimoto T, Nishizono A, Fujioka T. *Helicobacter pylori* infected animal models are extremely suitable for the investigation of gastric carcinogenesis. *World J Gastroenterol* 2005; 11(45): 7063-7071
http://www.wjgnet.com/1007-9327/11/7063.asp

INTRODUCTION

Gastric cancer is one of the main causes of cancer-related mortality, especially, in East Asia. To clarify the mechanism of gastric cancer development, many experimental models have been used. However, almost all experimental animals, that showed spontaneous gastric cancer were very rare[1]; therefore several animal models were established using chemical carcinogens, such as *N*-methyl-*N*-nitrosourea (MNU)[2,3] and *N*-methyl-*N*-nitro-*N'*-nitrosoguanidine (MNNG)[4,5], which showed a high rate of gastric cancer development, especially in the antrum.

Since Warren and Marshall[6] revealed the microorganism which inhabits the stomach, *Helicobacter pylori* (*H pylori*) was considered as the major factor of many kind of gastroduodenal diseases, such as acute gastritis[7-9], chronic atrophic gastritis[9,10], intestinal metaplasia[11], peptic ulcer[12,13], mucosal associated lymphoid tissue lymphoma[14], gastric cancer[15-18], and others[19,20].

Previously, a large number of epidemiological studies indicated that *H pylori* infection has a close relation with gastric cancer[15-18]. Therefore, the International Agency for Research on Cancer (IARC) conference of the World Health Organization (WHO) defined *H pylori* as a definite carcinogen (Group I) to the human stomach based on three prospective case-control studies[15-17] reported in 1991[21].

However, the mechanisms by which *H pylori* infection develop gastric cancer are not defined in detail. In further studies, attempts have been made to reveal the possible mechanisms by which *H pylori* contributes to the development of gastric carcinoma and many researchers have developed animal models of infection using *Helicobacter* species.

Previously, a large number of animal experimental models have been developed to define the association between *H pylori* infection and gastroduodenal disease, such as piglet[22], beagle dog[23], mice[24], rhesus monkey[25], Japanese monkey (*Macaca fuscata*)[9,26,27], Mongolian gerbil[28], and others. In the beginning of the development of experimental models, only a few models had long periods of infection.

We have reported the results of a 5-year study on *H pylori* infection using Japanese monkeys (*Macaca fuscata*)[27]

and have obtained the findings that advance gastric mucosal atrophy, increase proliferation and mutation of p53 in gastric epithelial cells[29,30].

Several experiments, which demonstrated that chronic *H pylori* infection models of Mongolian gerbils developed gastric carcinoma, were conducted[31-33]. In these experiments, the animals were mainly divided into two groups: one group was infected with *H pylori* alone and the group was given a known carcinogen such as MNU and MNNG in addition to persistent *H pylori* infection. The results of these experiments revealed that animals in different groups developed different histopathological types of gastric carcinoma. These results will be very useful to elucidate the mechanism of gastric carcinogenesis due to *H pylori* infection.

GASTRIC CANCER AND JAPANESE MONKEY

The nonhuman primate animals are useful to clarify the relationship between *H pylori* and gastric diseases. Their stomachs are similar to those of human beings anatomically, physiologically, and dietary, compared with rodent animals. They have 10-20 years of long life span, which enables long-term follow-up with endoscopy and repeated histological examinations of the stomach using biopsy or endoscopic resected specimens. Several primate animals have been reported to be successful in experimental transmission of *H pylori* in chimpanzees (*Pan troglodytes*)[34], and species of macaques: rhesus monkey (*M. mulatta*)[25], cynomolgus monkey (*M. fascicularis*)[25], and Japanese monkey (*M. fuscata*)[9,26,27]. In these animals, some kinds of *Macaque* species are available for a wide variety of research field. We have established the Japanese monkey model with *H pylori* infection. This experimental model is very useful and a promising nonhuman primate model[9,26,27].

The methods of development of this monkey model are described briefly. The bacterial strains used were *H pylori* MCO 88155, MCO 88099, MCO 88142, and MCO 88156, isolated from two patients with duodenal ulcers and two with gastric ulcers. The colonies were suspended in 5 mL of sterile saline, and the bacterial concentration was adjusted to 10^9 CFU/mL. These were resuspended in 8 mL of sterile saline, and 5 mL of the final resuspension was used in each monkey. The animals were given ampicillin orally to eradicate spiral bacteria other than *H pylori*. After treatment with ampicillin, spiral bacteria were not found in any of the stomachs. The monkeys were sprayed with 5 mL of a mixed suspension of four bacterial strains endoscopically around their antrum. The gastric mucosa was examined endoscopically, and endoscopic mucosal resection was performed repeatedly during 6 years of observation.

One week after inoculation, all infected monkeys showed endoscopic acute gastritis accompanied by marked erythema and edema. These findings were consistent with the acute gastric mucosal lesion observed in the human stomach. Infection of *H pylori* was recognized by culture, the rapid urease test, histology, and the elevation of *H pylori*-specific IgG in plasma. In the early phase of infection, infiltration of monocytes and polymorphonuclear leukocytes were marked in the edematous lamina propria and superficial erosions were evident. After 3 mo of inoculation, infiltration of mononuclear cells and plasma cells were predominant in the lamina propria layer. However, no superficial erosions and atrophic changes were observed.

In the infected group, the gastritis score which was evaluated by a scoring system based on the method of Rauws *et al*[35]. were markedly increased in the antral mucosa 1 wk after inoculation ($P<0.001$). The score then gradually decreased throughout the whole investigation period, but remained significantly higher ($P<0.01$) than that of the control group.

Six months after inoculation, the pyloric glandular height was apparently lower in the infected animals than in controls. Furthermore, the atrophic change advanced gradually throughout the 5-year observation period[27]. Endoscopically, according to the endoscopic-atrophic-border scale described by Kimura and Takemoto[36], gastric atrophy also gradually advanced for more than 3 years. These findings indicated evidently that *H pylori* infection caused atrophic gastritis in the Japanese monkey model. Cell proliferation activity, which was revealed with immunohistochemical detection of Ki-67 in the antral mucosa of infected animals, was significantly accelerated throughout the entire observation period (Figure 1). Immunohistochemical detection of p53 and point mutation of *p53* was exhibited in the gastric mucosa[29,30] of this model. Genetic alterations in exons 5-8 of the p53 gene were uncommon in the *H pylori*-uninfected monkeys, whereas a higher prevalence of missense mutations in the p53 gene appeared in association with *H pylori* infection (Table 1). The number of mutations in the p53 gene increased as the gastric atrophy score increased, which depends on the duration of *H pylori* infection[30]. These findings of Japanese monkey model may explain the potential mechanism for the causal role of *H pylori* in the chain of events leading to gastric carcinoma. This monkey model facilitates investigation of the correlation between the long-term sequence of *H pylori* infection and gradual gastric mucosal change. Although many pathophysiological changes were seen in *H pylori*-infected gastric mucosa, this Japanese monkey model did not show the development of gastric carcinoma. In their long life span, which is similar to human beings, further continuous infection may be needed to the more dramatic histological change.

DEVELOPMENT OF THE RODENT MODEL

Several rodent models were established for examining the etiological feature of *Helicobacter* species infection, such as mice[24,37], rat[38], and Mongolian gerbil[28]. Compared with nonhuman primate models, rodent models are treated easily, and are economical.

Marchetti *et al*[39]. reported the several clinical isolates colonized the stomach of SPF conditioned mice (CD1 mice) and Balb/c mice; however, colonization was very

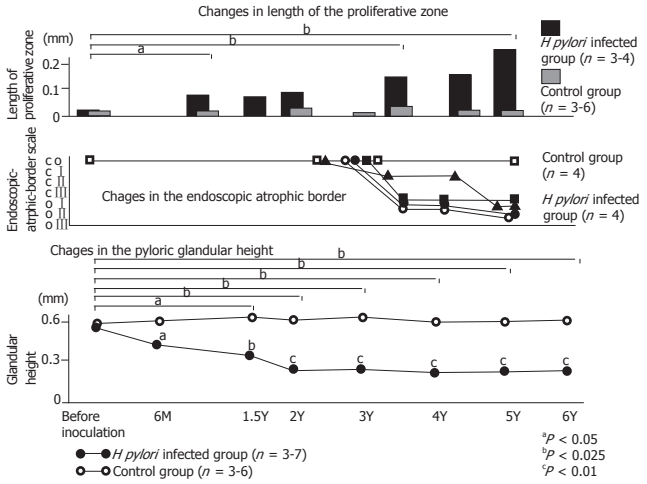

Figure 1 Gastric mucosal alteration of Japanese monkey model with *H pylori* infection. Upper graph showed the gradual increase of the proliferative zone of *H pylori*-infected Japanese monkey model. Middle graph showed the alteration of endoscopic-atrophic-border scale of this model. Macroscopically, gastric atrophy advanced for more than 3 yr. Lower graph showed the alteration of the pyloric glandular height. Six months after inoculation, the pyloric glandular height was apparently lower in the infected animals than in controls. Furthermore, the atrophic change advanced gradually throughout the 6-yr observation period.

Table 1 Duration of *H pylori* infection and number of point mutations in exon 5-8 of the p53 gene

Monkey	Duration of *H pylori* infection (yr)	Number of nucleotide (amino acid) substitutions in p53				Atrophy score[1]	Intensity of p53 immunostaining[2]
		Ex 5	Ex 6	Ex 7	Ex 8		
A	1.5	0 (0)	2 (1)	0 (0)	1 (1)	2	-
B	2	4 (0)	2 (2)	5 (4)	4 (3)	3	-
C	3	4 (2)	1 (0)	2 (2)	2 (2)	4	+
D	3	2 (1)	1 (0)	1 (1)	4 (2)	5	+
E	3.5	5 (2)	2 (1)	5 (4)	6 (4)	4	+
F	4.5	5 (1)	3 (1)	4 (3)	5 (4)	6	-
G	5	4 (1)	3 (1)	2 (1)	8 (6)	8	+
H	7.5	8 (5)	2 (1)	5 (4)	8 (4)	12	++

[1], The atrophy score was calculated as the sum of the histological evaluations of five gastric specimens according to Updated Sydney System. [2], The intensity of p53 immunostaining was classified into four grades: -, no staining; +, mild staining; ++, moderate staining; +++, intense staining.

low. Lee *et al*[40]. reported the quite good colonization by using the Sydney strain of *H pylori* (strain SS1), which is cagA and vacA positive.

These rodent models showed meager development of spontaneous gastric cancer. Cui *et al*[41]. reported the development of spontaneous gastric carcinoma, classified as malignant enterochromaffin-like (ECL) carcinomas in female cotton rats (*Sigmodon hispidus*). Previously, chemical carcinogens such as MNNG and MNU have been often used in the rodent species for the investigation of experimental gastric cancer[2-5].

From the recognition of *Helicobacter* species' pathogenicity, Fox *et al*[42]. reported a possible carcinogenic role for *Helicobacter* species in the gastric mucosa after oral administration of MNNG in ferrets infected with *Helicobacter mustelae*. Nine out of the ten ferrets, which were given a dose of 50 mg/kg MNNG orally, developed adenocarcinoma. This was the first experimental study using carcinogens combined with infection with a *Helicobacter* species. Although spontaneous gastric adenocarcinomas have been reported[43] in aged ferrets with *H mustelae* even in the absence of carcinogen exposure, an important additional problem is that the bacterium used was not *H pylori* but *H mustelae*. Fox *et al*[44]. also described the development of gastric adenocarcinoma, which was led from severe gastritis in C57BL/6 mice with *Helicobacter felis* inoculation. In their report, p53+/- mice showed significant low prevalence of fundic lymphoplasmacytic infiltration and submucosal lymphoid follicle formation than those in C57BL/6 mice. They indicated two distinct roles of p53, one of them displayed the gastric cancer risk. However, deletion of one *p53* allele results in a down-regulated Th1 response to *Helicobacter* infection, which may indirectly protect against the development of gastric cancer associated with chronic inflammation.

The differences between *H felis* in mice and *H pylori* in human beings are the lack of induction of neutrophil and cag pathogenicity island, which are recognized as main pathogens of *H pylori*. Kim *et al*[45]. reported that C57BL/6 mice infected with *H pylori* (SS1 strain) showed no evidence of gastric adenoma, dysplasia, and carcinoma during 80 wk of infection. They explained this result by the balance that exists between cell proliferation and apoptosis.

Transgenic hypergastrinemic (INS-GAS) mouse model have also been useful for the investigation of gastric carcinogenesis. Fox *et al*[46]. reported that male INS-GAS mice infected with *H pylori* developed atrophy, intestinal metaplasia, and dysplasia and adenocarcinoma. This murine model with *H pylori cagE* mutant showed the deletion of development of cancer. In contrast, none of the female mice with *H pylori* infection developed adenocarcinoma. However, IL-1 levels showed no significant difference between males and females. Fox *et al*. concluded that the INS-GAS model is effective for investigating discrete host-microbial interactions that culminate in gastric cancer within the context of biologic conditions induced by *H pylori*.

DEVELOPMENT OF MONGOLIAN GERBIL MODEL

Yokota *et al*[28]. developed the experimental Mongolian gerbil model with *H pylori* infection, in which only a mild inflammatory infiltration in the gastric mucosa was seen during two months of their observation. Hirayama *et al*[47]. described that ulcers and intestinal metaplasia were produced 6 mo after inoculation with *H pylori* in Mongolian gerbils.

In our laboratory, 5-wk-old male Mongolian gerbils weighing 30-40 g (Seiwa Experimental Animals Co. Ltd., Fukuoka, Japan) were used[48]. *H pylori* ATCC-43504 possessing the cagA gene and expressing vacuolating cytotoxin was used. A 4-d culture on blood agar at 37 ℃ under microaerophilic conditions was harvested and incubated in brucella broth (DIFCO Laboratories, Detroit,

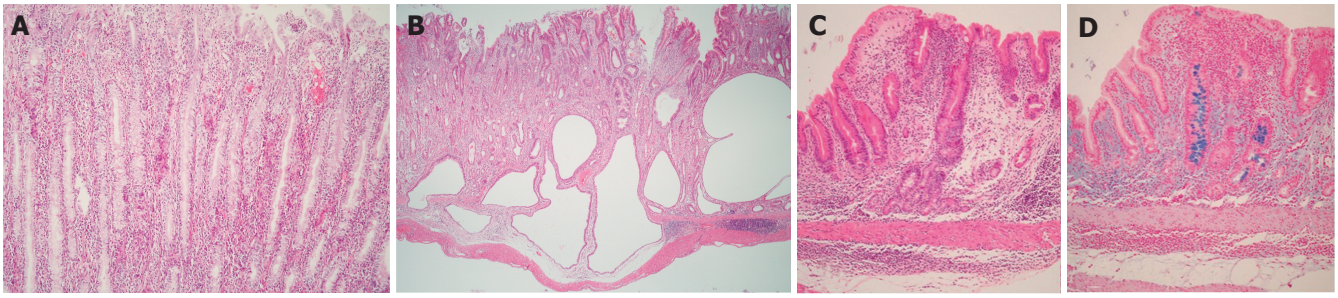

Figure 2 Microscopic views of the gastric body of Mongolian gerbils at 18 mo after *H pylori* inoculation. **A:** Severe infiltration of polymorphonuclear and mononuclear cells were seen in the lamina propria. (HE stain, x100); **B:** Some glands have extended into the submucosa but not into the proper muscularis layer. Severe infiltration of mononuclear cells in the submucosa (HE stain, x10); **C:** Intestinal metaplasia is seen scattering in gastric mucosa (HE stain, x10); **D:** Intestinal metaplasia (Alcian blue stain (pH 2.5); original magnification, x10).

MI, USA) with 10% horse serum for 24 h. Inoculum size was adjusted with sterile saline to produce the optical density of McFarland 4 at 540 nm. Mongolian gerbils were housed five per cage, starved for 24 h, and then fed with chow (Oriental Yeast Co., Tokyo, Japan) and water *ad libitum* beginning 12 h after *H pylori* inoculation. On the day of infection, the Mongolian gerbils were challenged orally with vehicle or 10^9 CFU *H pylori* in 1.0 mL of brucella broth with 10% horse serum. The spiral bacteria were observed in the mucus and gastric pits of all inoculated animals from 1 mo after inoculation throughout the whole observation period. However, nearly half of the animals had barely detectable *H pylori* in the stomach by bacterial culture. The bacterial counts from the stomachs of gerbils 1 and 6 mo after *H pylori* inoculation were 25 and 410 CFU/10 mg of gastric tissue, respectively[48]. These levels of colonized bacteria were nearly 1/10 to 1/100 than those of human being and monkey.

Mongolian gerbils with *H pylori* infection showed irregularly thickened gastric walls and spotty hemorrhages and erosions macroscopically, 1 year after inoculation. A severe infiltration of polymorphonuclear and mononuclear cells was seen in the lamina propria and mononuclear cells infiltration with lymphoid follicle in the submucosa, 1 mo after *H pylori* inoculation (Figure 2A). Erosion of the gastric mucosa appeared soon after inoculation, whereas gastric ulcers, gastritis cystica profunda (Figure 2B), and atrophy with goblet cell metaplasia (Figures 2C and D) occurred between 3 and 6 mo after inoculation[48,49]. Moreover, Suzuki *et al*[50]. reported that *H pylori* inoculation induced neutrophil followed by an increase in the level of lipid peroxidation and activated glutathione (antioxidant) turnover. These sequential changes of histological changes in gastric mucosa were quite similar to those observed in human beings. Therefore, Mongolian gerbil model may be useful to study the relationship between *H pylori* infection and gastric lesions, which include gastric malignancy.

GASTRIC CANCER AND MONGOLIAN GERBIL MODEL

Mongolian gerbils have also been induced by the development of gastric carcinoma with chemical carcinogen alone[51]. In addition, the results of several experimental studies have confirmed that administration of MNNG or MNU to Mongolian gerbils with chronic *H pylori* infection enhanced the development of different histopathological types of gastric carcinoma (Table 2)[31-33].

Sugiyama *et al*[31]. reported the development of carcinoma in the Mongolian gerbils evaluated at 40 wk after an experiment in which 7-wk-old animals were inoculated with *H pylori* (ATCC43504) and given 10 or 30 ppm MNU before or after inoculation. In this report, only the groups of the animals, which were administered with both *H pylori* and MNU, developed gastric cancers; more specifically, they developed different types of adenocarcinoma, such as well-differentiated, poorly differentiated, and signet ring cell carcinoma. These interesting experimental results support the results so far obtained in largescale epidemiological investigations[52].

The group inoculated with *H pylori* after being given MNU showed a distinctive initiation-promotion effect, whereas the group to which MNU was given after inoculation with *H pylori* appeared to demonstrate the simultaneous action of these two factors, with *H pylori* acting as a coinitiator. No gastric carcinoma was found within 40 wk of *H pylori* infection alone.

Tokieda *et al*[32]. conducted a study in which 5-wk-old Mongolian gerbils were inoculated with *H pylori* (ATCC43504) and orally given MNNG at 50 g/mL for 20 wk for comparison against animals administered with MNNG alone. At the 52nd wk after initiation, the group treated with MNNG and *H pylori* developed gastric carcinoma at a significantly higher frequency than the group treated with MNNG alone. In addition, cell proliferation was revealed to be markedly accelerated in those animals infected with *H pylori* with evaluation using a labeling index of 5-bromo-2'-deoxyuridine. This result suggests the possibility of explaining the link between *H pylori* infection and early events in gastric carcinogenesis. One of the interests in this study is that administration of MNNG reduced the infection rate of *H pylori* with the lapse of time, due to the likelihood of MNNG showing low-level (200 μg/mL) antibacterial activity against *H pylori*[32]. It is also of interest that *H pylori*-free animals did not develop gastric carcinoma even with

Table 2 Gastric carcinogenesis in *Helicobacter pylori*-infected Mongolian gerbils

Author	Year	Strain	Study design (ppm)	Incidence of cancer (%)	Duration of experiment (wk)
Sugiyama *et al*.	1998	ATCC43504	HP→MNU (10)	7/19 (36.8)	40
			HP alone	0/20 (0)	40
			MNU (30) → HP	6/18 (33.3)	40
			MNU alone	0/74 (0)	40
Tokieda *et al*.	1999	ATCC43504	HP → MNNG (50)	5/17 (29.4)	52
			persistent HP positive	5/8 (62.5)	52
			HP eradicated	0/9 (0)	52
			Br → MNNG (50)	3/22 (13.6)	50
Shimizu *et al*.	1999	ATCC43504	MNNG (300) → HP	12/27 (44.4)	50
			MNNG (300) → Br	1/19 (5.3)	50
			MNNG (60) → HP	6/25 (24.0)	50
			MNNG (60) → Br	0/20 (0)	50
			HP → MNNG (100)	4/27 (14.8)	50
			Br → MNNG (100)	3/18 (16.7)	50
			HP → MNNG (20)	15/25 (60)	50
			Br → MNNG (20)	1/20 (5)	50
			HP alone	0/20 (0)	50

HP, *Helicobacter pylori*; MNU, *N*-methyl-*N*-nitrosourea; MNNG, *N*-methyl-*N'*-nitroso-*N*-nitrosoguanidine; Br, Brucella broth.

Table 3 Gastric carcinogenesis in *Helicobacter pylori*-infected Mongolian gerbils

Author	Year	Strain	*cag*A gene	Vacuolating cytotoxin	Incidence of cancer (%)	Duration of experiment (wk)	Histological type of carcinoma
Watanabe *et al*.	1998	TN2GF4[1]	+	+	10/27 (37)	62	Well differentiated adenocarinoma
Honda *et al*.	1998	ATCC43504[2]	+	+	2/5 (40)	72	Well differentiated adenocarinoma
Hirayama *et al*.	1999	ATCC43504[2]	+	+	1/56 (1.8)	64	Poorly differentiated adenocarinoma
Ogura *et al*.	2000	TN2[2]	+	+	1/23 (4)	62	Well differentiated adenocarinoma
Zheng *et al*.	2004	ATCC43504[2]	+	+	3/17 (18)	84	Well differentiated adenocarinoma
		H pylori 161[3]	+	+			

[1]*H pylori* isolated from patient with gastric ulcer; [2]Type of strains; [3]*H pylori* isolated from patient with gastric adenocarcinoma.

MNNG administration. This result indicated a stronger carcinogenic role of *H pylori* infection. Although it has been reported by Sugiyama[31] that *H pylori* can persistently colonize the stomach of MNUtreated Mongolian gerbils, it is interesting that the two studies[32,33] report that MNNG administration eradicates *H pylori* infection, resulting in a reduction of its carcinogenic effects in the stomach. In *H pylori*-infected Mongolian gerbils with MNNG administration, duodenogastric reflux due to surgical procedure might attenuate the effect of *H pylori* on gastric tumorigenesis[53]. Because of our study, which indicated that bile reflux might lead to *H pylori* eradication[54], their results may probably depend on the *H pylori* eradication.

CARCINOGENICITY OF *H PYLORI* INFECTION ALONE

Although these studies showed marked increase of the chemical carcinogenic risk in the Mongolian gerbils, direct relationship between *H pylori* and gastric carcinogenesis was not indicated.

Two experimental studies attempted to confirm prior epidemiological studies that have demonstrated an association between *H pylori* infection and gastric carcinogenesis in human beings using Mongolian gerbils chronically infected with this bacterium (Table 3)[55,56]. Both studies confirmed gastric carcinogenesis resulting from *H pylori* infection alone, and were the first papers to fulfill Koch's postulates concerning *H pylori* infection and gastric carcinoma.

Watanabe *et al*[55]. used *H pylori* isolated from patients with gastric ulcer (TN2GF4), and Honda *et al*[56]. used ATCC43504 type strain, both of which were inoculated into 5-wk-old SPF Mongolian gerbils. The results showed that 37% (10 out of 27) of the animals in the former study developed well-differentiated adenocarcinoma at 62 wk after inoculation, whereas 40% (2 out of 5) of the animals in the latter study developed well-differentiated adenocarcinoma at 72 wk after inoculation (Figure 3). Both of these strains contained *cagA* and produced vacuolating cytotoxins. Sequential histopathological changes leading to carcinogenesis of the gastric mucosa were found to be common to the two studies, and very closely resembled the histopathological changes in human gastric mucosa caused by *H pylori* infection.

Hirayama *et al*[57]. reported that poorly differentiated adenocarcinoma and carcinoid were developed in

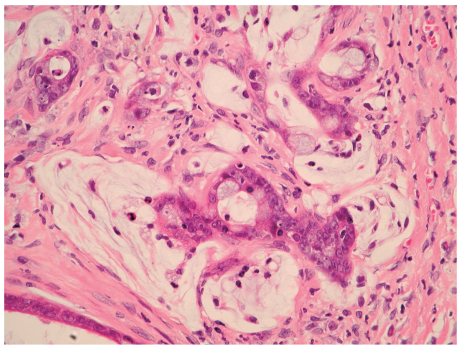

Figure 3 Microscopic views of the gastric mucosa of Mongolian gerbils at 18 mo after *H pylori* inoculation. Well-differentiated adenocarcinoma has extended into the muscular layer. Atypical glands and nuclei and abnormal mitosis are evident (HE stain, x40).

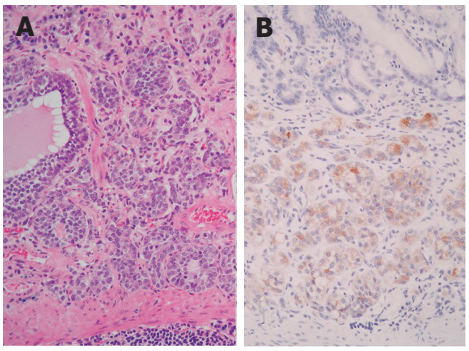

Figure 4 Gastric carcinoid in the stomach of a Mongolian gerbils colonized for 24 mo by *H pylori*. Microscopic view showing intramucosal carcinoid tumor (**A:** HE stain, x20; **B:** immunohistochemistry of chromogranin A, x20').

Mongolian gerbils model with *H pylori* (ATCC43504 type strain) infection alone. Zheng *et al*[58]. reported that Mongolian gerbils models, which were infected with *H pylori* (ATCC43504) and *H pylori* 161 (isolated from a Chinese patient with gastric adenocarcinoma) showed the development of well-differentiated adenocarcinoma (Table 3). Ogura *et al*[59]. reported the development of well-differentiated gastric cancer in wild type (TN2) and isogenic mutant of *vacA* (TN2Δ*vacA*) of Mongolian gerbil.

Mongolian gerbils' model also showed the development of gastric carcinoid[57,59,60]. In our laboratory, ECL cell tumors with marked atrophic gastritis and with hypergastrinemia were observed in the fundic gland area of infected Mongolian gerbils, 24 mo after inoculation (Figure 4); in contrast, adenocarcinoma developed in pyloric gland area. Histopathological findings of the entire observation period in Mongolian gerbils after *H pylori* inoculation are summarized in Table 4.

Ogura *et al*[59]. discussed the virulence factors of *H pylori* in Mongolian gerbils. Experimental gastric cancer derived in Mongolian gerbils with wild type of *H pylori* and *vacA* mutant infection, whereas *cagE* mutant induced far milder change of gastritis and induced no gastric cancer, which indicates the essential role of cagPAI in the gastric diseases with *H pylori* infection.

Table 4 Gastric carcinogenesis in *Helicobacter pylori*-infected Mongolian gerbils

Histropathological findings	Mo			
	6	12	18	24
Gastritis	5/5	4/4	5/5	10/10
Gastric ulcer	4/5	3/4	5/5	5/10
Atrophy	4/5	4/4	5/5	10/10
Intestinal metaplasia	2/5	3/4	5/5	10/10
Dysplasia	0/5	2/4	4/5	10/10
Gastric cancer	0/5	0/4	2/5	5/10
Gastric carcinoid	0/5	0/4	0/5	5/10

Data represent positive case/control Uninfected control. animals (n = 5 each) showed no abnormal findings.

Table 5 Relation between p53 and *H pylori* and gastric mucosal change (tentative opinion)

Condition	Human	Japanese monkey	Mongolian gerbil
H pylori and p53 overexpression (histology)	++	++	+[1]
H pylori and p53 point mutation	++	++	-
H pylori and atrophic gastritis	++	++	++
H pylori and intestinal metaplasia	++	-	++
H pylori and gastric cancer	+[2]	-	++

[1]The p53 overexpression was observed only in gastric cancer; [2]Not proven by interventional study; ++, strong evidence; +, weak evidence; -, no evidence

PREVENTION OF GASTRIC CARCINOMA BY ERADICATION OF *H PYLORI*

Shimizu *et al*[61]. reported that the incidence of adenocarcinomas in MNU-administered Mongolian gerbils with *H pylori* infection (15 out of 23) was significantly higher than in MNU-administered Mongolian gerbils that underwent *H pylori* eradication (5 out of 24). Their results suggest that *H pylori* eradication may prevent gastric carcinogenesis, and Mongolian gerbil's models have also been useful to study the prevention of gastric carcinogenesis in human beings.

DIFFERENCES BETWEEN ANIMAL MODELS AND HUMAN BEINGS

Although the Japanese monkey model and Mongolian gerbil model showed the similar change of human stomach that was infected with *H pylori*, several features of animal models differ from those seen in human beings. In Japanese monkey model intestinal metaplasia was not seen during the whole observation period. Severe gastritis and lymphoid follicular hyperplasia in the submucosal layer and gastritis cystica profunda, which are seen in Mongolian gerbils, are not observed in human gastric mucosa.

Table 5 shows our tentative opinion on p53 and *H pylori* infection in animal model and human beings. Although no gastric carcinoma developed in Japanese monkey model, Mongolian gerbil model showed gastric carcinoma resulting from *H pylori* infection alone. In human and Japanese monkey, both p53 immunostaining[29,62-64] and point mutations[30,65] were observed in *H pylori* infection. In

Mongolian gerbil, the p53 immunostaining was detected in gastric cancer but not in atrophic gastritis; moreover, there were no p53 mutations in exons 5 to 8 in infected gastric mucosa[66].

Suzuki *et al*[67]. reported that Mongolian gerbil model showed significant attenuation of apoptosis and promotion of cell proliferation than those seen in mice model with *H pylori* inoculation. Crabtree *et al*[68]. also described the differences of mucosal cytokine response between Mongolian gerbils and mice, and gender differences in the magnitude of cytokine response to *H pylori*. The differences of features between the species suggested that the pathogens of gastric diseases does not associate only with *H pylori* and may reflect in part other host factors.

Sonic hedgehog (Shh) is an important endometrial morphogenetic signal during the development of the vertebrate gut. Shh controls gastrointestinal patterning in general and gastric gland formation in particular. Suzuki *et al*[69]. reported that the long-term colonization of *H pylori* led to attenuation of Shh expression. Loss of Shh expression correlated with the loss of parietal cells, disturbed maturation of the mucous neck cell-zymogenic cell lineage. van den Brink *et al*[70]. described the loss of Shh expression in the intestinal metaplasia of the human stomach. Loss of Shh expression not only in intestinal metaplasia, but also in the tissue of *H pylori*-induced fundic gland atrophy is important for considering the possible link to preneoplastic lesion formation[69].

QUITE A NEW CONCEPT OF GASTRIC CANCER ORIGIN

In 2004, Houghton *et al*[71]. reported the innovative idea of gastric cancer origin with the usage of *H. felis*/C57BL/6 mouse model. Previously, tissue stem cells have been recognized as the origin of carcinoma. However, their study showed that bone marrow-derived cells (BMDCs) might also represent a potential source of malignancy. Female C57BL/6 mice after undergoing lethal irradiation were transplanted with bone marrow from male C57BL/*6JGtrosa26* (ROSA26), which was labeled with X-galactosidase or green fluorescent protein. In this model, gastric mucosal apoptosis increased at 6- 8 wk after *H. felis* inoculation. After 52 wk of inoculation, beta-galactosidase (gal) and trefoil factor2 (TFF2) positive cells increased gradually, then 90% of the gastric mucosa at the squamocolumnar junction was replaced with cells derived from the donor marrow. One year after infection, intramucosal carcinoma or high-grade gastrointestinal intraepithelial neoplasia were seen in these mice. No evidence of BMDC engraftment was seen in *H. felis* uninfected mice. Authors indicated that BMDC originated the epithelial cancer and the necessity of *Helicobacter* infection in this process.

CONCLUSION

In various experimental models, nonhuman primate and rodent models showed the variable evidences, which clarified the association between *H pylori* infection and gastric cancer.

Experiments developed using Mongolian gerbils have demonstrated that *H pylori* infection is clearly responsible for gastric carcinogenesis, and provide important confirmation of the statements issued by IARC/WHO. It will be of critical importance to extrapolate the sequential histopathological changes found in the Mongolian gerbil to lesions in the human gastric mucosa, since this model is proven to provide important pointers for the study of the mechanism of gastric carcinogenesis as a result of *H pylori* infection. While Koch's postulates for *H pylori* and gastric carcinoma have now been fulfilled, an important question to be addressed is why the Mongolian gerbil is the only species in which carcinogenesis has been experimentally induced by infection with *H pylori*.

REFERENCES

1 **Cui G**, Qvigstad G, Falkmer S, Sandvik AK, Kawase S, Waldum HL. Spontaneous ECLomas in cotton rats (Sigmodon hispidus): tumours occurring in hypoacidic/hypergastrinaemic animals with normal parietal cells. *Carcinogenesis* 2000; **21**: 23-27

2 **Fort L,** Taper HS, Brucher JM. Gastric carcinogenesis in rat induced by methylnitrosourea (MNU). Morphology, and histochemistry of nucleases. *Z Krebsforsch Klin Onkol Cancer Res Clin Oncol* 1974; **81:** 51-62

3 **Fujita M**, Taguchi T, Takami M, Usugane M, Takahashi A. Lung metastasis of canine gastric adenocarcinoma induced by N-methyl-N'-nitro-N-nitroguanidine. *Gan* 1975; **66**: 107-108

4 **Kartasheva LA**, Bykorez AI. Induction of stomach tumors in rats by N-methyl-N-nitroso-N1-nitroguanidine. *Vopr Onkol* 1975; **21:** 50-55

5 **Koestner AW**, Ruecker FA, Koestner A. Morphology and pathogenesis of tumors of the thymus and stomach in Sprague-Dawley rats following intragastric administration of methyl nitrosourea (MNU). *Int J Cancer* 1977; **20**: 418-426

6 **Marshall BJ**, Warren JR. Unidentified curved bacilli in the stomach of patients with gastritis and peptic ulceration. *Lancet* 1984; **1:** 1311-1315

7 **Marshall BJ,** Armstrong JA, McGechie DB, Glancy RJ**.** Attempt to fulfil Koch's postulates for pyloric Campylobacter. *Med J Aust* 1985; **142**: 436-439

8 **Morris A**, Nicholson G. Ingestion of *Campylobacter pylori*dis causes gastritis and raised fasting gastric pH. *Am J Gastroenterol* 1987; **82**: 192-199

9 **Fujioka T**, Shuto R, Kodama R, Fujiyama K, Kubota T, Murakami K, Perparim K, Nasu M. Experimental model for chronic gastritis with *Helicobacter pylori:* long term follow-up study in *H pylori*-infected Japanese macaques. *Eur J Gastroenterol Hepatol* 1993; **5** (supple 1)**:** S73-S78

10 **Kuipers EJ**, Uyterlinde AM, Peña AS, Roosendaal R, Pals G, Nelis GF, Festen HP, Meuwissen SG. Long-term sequelae of *Helicobacter pylori* gastritis. *Lancet* 1995; **345**: 1525-1528

11 **Sakaki N**, Momma K, Egawa N, Yamada Y, Kan T, Ishiwata J. The influence of *Helicobacter pylori* infection on the progression of gastric mucosal atrophy and occurrence of gastric cancer. *Eur J Gastroenterol Hepatol* 1995; **7** Suppl 1**:** S59- S62

12 **Schubert TT**, Bologna SD, Nensey Y, Schubert AB, Mascha EJ, Ma CK. Ulcer risk factors: interactions between *Helicobacter pylori* infection, nonsteroidal use, and age. *Am J Med* 1993; **94**: 413-418

13 **Maaroos HI**, Kekki M, Vorobjova T, Salupere V, Sipponen P. Risk of recurrence of gastric ulcer, chronic gastritis, and grade of *Helicobacter pylori* colonization. A long-term follow-up study

of 25 patients. *Scand J Gastroenterol* 1994; **29**: 532-536
14 **Wotherspoon AC**, Doglioni C, Diss TC, Pan L, Moschini A, de Boni M, Isaacson PG. Regression of primary low-grade B-cell gastric lymphoma of mucosa-associated lymphoid tissue type after eradication of *Helicobacter pylori*. *Lancet* 1993; **342:** 575-577
15 **Forman D**, Newell DG, Fullerton F, Yarnell JW, Stacey AR, Wald N, Sitas F. Association between infection with *Helicobacter pylori* and risk of gastric cancer: evidence from a prospective investigation. *BMJ* 1991; **302**: 1302-1305
16 **Parsonnet J**, Friedman GD, Vandersteen DP, Chang Y, Vogelman JH, Orentreich N, Sibley RK. *Helicobacter pylori* infection and the risk of gastric carcinoma. *N Engl J Med* 1991; **325**: 1127-1131
17 **Nomura A**, Stemmermann GN, Chyou PH, Kato I, Perez-Perez GI, Blaser MJ. *Helicobacter pylori* infection and gastric carcinoma among Japanese Americans in Hawaii. *N Engl J Med* 1991; **325**: 1132-1136
18 An international association between *Helicobacter pylori* infection and gastric cancer. The EUROGAST Study Group. *Lancet* 1993; **341:** 1359-1362
19 **Gasbarrini A**, Franceschi F, Tartaglione R, Landolfi R, Pola P, Gasbarrini G. Regression of autoimmune thrombocytopenia after eradication of *Helicobacter pylori*. *Lancet* 1998; **352**: 878
20 **Sato R**, Murakami K, Watanabe K, Okimoto T, Miyajima H, Ogata M, Ohtsuka E, Kodama M, Saburi Y, Fujioka T, Nasu M. Effect of *Helicobacter pylori* eradication on platelet recovery in patients with chronic idiopathic thrombocytopenic purpura. *Arch Intern Med* 2004; **164**: 1904-1907
21 **International Agency for Research on Cancer**: Infection with Schistosomes, Liver Flukes and *Helicobacter pylori* . IARC Monographs on the Evaluation of Carcinogenic Risks to Humans. 1994; **61**: 218-220
22 **Krakowka S,** Morgan DR, Kraft WG, Leunk RD**.** Establishment of gastric Campylobacter pylori infection in the neonatal gnotobiotic piglet. *Infect Immun* 1987; **55**: 2789-2796
23 **Radin MJ**, Eaton KA, Krakowka S, Morgan DR, Lee A, Otto G, Fox J. *Helicobacter pylori* gastric infection in gnotobiotic beagle dogs. *Infect Immun* 1990; **58**: 2606-2612
24 **Karita M,** Kouchiyama T, Okita K, Nakazawa T**.** New small animal model for human gastric *Helicobacter pylori* infection: success in both nude and euthymic mice. *Am J Gastroenterol* 1991; **86**: 1596-1603
25 **Euler AR**, Zurenko GE, Moe JB, Ulrich RG, Yagi Y. Evaluation of two monkey species (*Macaca mulatta* and *Macaca fascicularis*) as possible models for human *Helicobacter pylori* disease. *J Clin Microbiol* 1990; **28**: 2285-2290
26 **Shuto R**, Fujioka T, Kubota T, Nasu M. Experimental gastritis induced by *Helicobacter pylori* in Japanese monkeys. *Infect Immun* 1993; **61:** 933-939
27 **Fujioka T**, Kodama R, Honda S, Guei-Hua G, Nishizono A, Nasu M. Long-term sequelae of experimental gastritis with *Helicobacter pylori*: a 5-year follow-up study. *J Clin Gastroenterol* 1997; **25 Suppl 1:** S8- S12
28 **Yokota K**, Kurebayashi Y, Takayama Y, Hayashi S, Isogai H, Isogai E, Imai K, Yabana T, Yachi A, Oguma K. Colonization of *Helicobacter pylori* in the gastric mucosa of Mongolian gerbils. *Microbiol Immunol* 1991; **35**: 475-480
29 **Kodama M**, Fujioka T, Kodama R, Takahashi K, Kubota T, Murakami K, Nasu M. p53 expression in gastric mucosa with *Helicobacter pylori* infection. *J Gastroenterol Hepatol* 1998; **13**: 215-219
30 **Oda T**, Murakami K, Nishizono A, Kodama M, Nasu M, Fujioka T. Long-term *Helicobacter pylori* infection in Japanese monkeys induces atrophic gastritis and accumulation of mutations in the p53 tumor suppressor gene. *Helicobacter* 2002; **7**: 143-151
31 **Sugiyama A**, Maruta F, Ikeno T, Ishida K, Kawasaki S, Katsuyama T, Shimizu N, Tatematsu M. *Helicobacter pylori* infection enhances *N*-methyl-*N*-nitrosourea-induced stomach carcinogenesis in the Mongolian gerbil. *Cancer Res* 1998; **58**: 2067-2069
32 **Tokieda M**, Honda S, Fujioka T, Nasu M. Effect of *Helicobacter pylori* infection on the *N*-methyl-*N'*-nitro-*N*-nitrosoguanidine-induced gastric carcinogenesis in mongolian gerbils. *Carcinogenesis* 1999; **20**: 1261-1266
33 **Shimizu N**, Inada K, Nakanishi H, Tsukamoto T, Ikehara Y, Kaminishi M, Kuramoto S, Sugiyama A, Katsuyama T, Tatematsu M. *Helicobacter pylori* infection enhances glandular stomach carcinogenesis in Mongolian gerbils treated with chemical carcinogens. *Carcinogenesis* 1999; **20**: 669-676
34 **Hazell SL**, Eichberg JW, Lee DR, Alpert L, Evans DG, Evans DJ, Graham DY. Selection of the chimpanzee over the baboon as a model for *Helicobacter pylori* infection. *Gastroenterology* 1992; **103**: 848-854
35 **Rauws EA,** Langenberg W, Houthoff HJ, Zanen HC, Tytgat GN. Campylobacter pyloridis-associated chronic active antral gastritis. A prospective study of its prevalence and the effects of antibacterial and antiulcer treatment. *Gastroenterology* 1988; **94:** 33-40
36 **KimuraK**, Takemoto T. Endoscopic atrophy border. *Endoscopy* 1969; **1**: 1-3
37 **Lee A,** Fox JG, Otto G, Murphy J. A small animal model of human *Helicobacter pylori* active chronic gastritis. *Gastroenterology* 1990; **99**: 1315-1323
38 **Danon SJ**, Moss ND, Larsson H, Arvidsson S, Ottosson S, Dixon MF, Lee A. Gastrin release and gastric acid secretion in the rat infected with either *Helicobacter* felis or *Helicobacter heilmannii*. *J Gastroenterol Hepatol* 1998; **13**: 95-103
39 **Marchetti M**, Aricò B, Burroni D, Figura N, Rappuoli R, Ghiara P. Development of a mouse model of *Helicobacter pylori* infection that mimics human disease. *Science* 1995; **267**: 1655-1658
40 **Lee A,** O'Rourke J, De Ungria MC, Robertson B, Daskalopoulos G, Dixon MF. A standardized mouse model of *Helicobacter pylori* infection: introducing the Sydney strain. *Gastroenterology* 1997; **112**: 1386-1397
41 **Cui G**, Qvigstad G, Falkmer S, Sandvik AK, Kawase S, Waldum HL. Spontaneous ECLomas in cotton rats (Sigmodon hispidus): tumours occurring in hypoacidic/hypergastrinaemic animals with normal parietal cells. *Carcinogenesis* 2000; **21**: 23-27
42 **Fox JG**, Wishnok JS, Murphy JC, Tannenbaum SR, Correa P. MNNG-induced gastric carcinoma in ferrets infected with Helicobacter mustelae. *Carcinogenesis* 1993; **14:** 1957-1961
43 **Fox JG,** Dangler CA, Sager W, Borkowski R, Gliatto JM. Helicobacter mustelae-associated gastric adenocarcinoma in ferrets (Mustela putorius furo). *Vet Pathol* 1997; **34:** 225-229
44 **Fox JG,** Sheppard BJ, Dangler CA, Whary MT, Ihrig M, Wang TC. Germ-line p53-targeted disruption inhibits *helicobacter*-induced premalignant lesions and invasive gastric carcinoma through down-regulation of Th1 proinflammatory responses. *Cancer Res* 2002; **62**: 696-702
45 **Kim DH,** Kim SW, Song YJ, Oh TY, Han SU, Kim YB, Joo HJ, Cho YK, Kim DY, Cho SW, Kim MW, Kim JH, Hahm KB. Long-term evaluation of mice model infected with *Helicobacter pylori*: focus on gastric pathology including gastric cancer. *Aliment Pharmacol Ther* 2003; **18** Suppl 1: 14-23
46 **Fox JG,** Wang TC, Rogers AB, Poutahidis T, Ge Z, Taylor N, Dangler CA, Israel DA, Krishna U, Gaus K, Peek RM Jr. Host and microbial constituents influence *Helicobacter pylori*-induced cancer in a murine model of hypergastrinemia. *Gastroenterology* 2003; **124**: 1879-1890
47 **Hirayama F**, Takagi S, Kusuhara H, Iwao E, Yokoyama Y, Ikeda Y. Induction of gastric ulcer and intestinal metaplasia in mongolian gerbils infected with *Helicobacter pylori*. *J Gastroenterol* 1996; **31**: 755-757
48 **Honda S**, Fujioka T, Tokieda T, Gotoh T, Nishizono A, Nasu M. Gastric ulcer, atrophic gastritis, and intestinal metaplasia caused by *Helicobacter pylori* infection in Mongolian gerbils. *Scand J Gastroenterol* 1998; **33**: 454-60
49 **Ikeno T**, Ota H, Sugiyama A, Ishida K, Katsuyama T, Genta RM, Kawasaki S. *Helicobacter pylori*-induced chronic active

gastritis, intestinal metaplasia, and gastric ulcer in Mongolian gerbils. *Am J Pathol* 1999; **154:** 951-960

50 **Suzuki H**, Mori M, Seto K, Kai A, Kawaguchi C, Suzuki M, Suematsu M, Yoneta T, Miura S, Ishii H. *Helicobacter pylori*-associated gastric pro- and antioxidant formation in Mongolian gerbils. *Free Radic Biol Med* 1999; **26**: 679-684

51 **Tatematsu M**, Yamamoto M, Shimizu N, Yoshikawa A, Fukami H, Kaminishi M, Oohara T, Sugiyama A, Ikeno T. Induction of glandular stomach cancers in Helicobacter pylori-sensitive Mongolian gerbils treated with N-methyl-N-nitrosourea and N-methyl-N′-nitro-N-nitrosoguanidine in drinking water. *Jpn J Cancer Res* 1998; **89:** 97-104

52 **Huang JQ**, Sridhar S, Chen Y, Hunt RH. Meta-analysis of the relationship between *Helicobacter pylori* seropositivity and gastric cancer. *Gastroenterology* 1998; **114**: 1169-1179

53 **Tanaka Y**, Osugi H, Morimura K, Takemura M, Ueno M, Kaneko M, Fukushima S, Kinoshita H. Effect of duodenogastric reflux on N-methyl-N′-nitro-N-nitrosoguanidine-induced glandular stomach tumorigenesis in Helicobacter pylori-infected Mongolian gerbils. *Oncol Rep* 2004; **11:** 965-971

54 **Abe H**, Murakami K, Satoh S, Sato R, Kodama M, Arita T, Fujioka T. Influence of bile reflux and *Helicobacter pylori* infection on gastritis in the remnant gastric mucosa after distal gastrectomy. *J Gastroenterol* 2005; **40**: 563-569

55 **Watanabe T**, Tada M, Nagai H, Sasaki S, Nakao M. *Helicobacter pylori* infection induces gastric cancer in mongolian gerbils. *Gastroenterology* 1998; **115:** 642-648

56 **Honda S**, Fujioka T, Tokieda M, Satoh R, Nishizono A, Nasu M. Development of *Helicobacter pylori* induced gastric carcinoma in Mongolian gerbils. *Cancer Res* 1998; **58**: 4255-4259

57 **Hirayama F**, Takagi S, Iwao E, Yokoyama Y, Haga K, Hanada S. Development of poorly differentiated adenocarcinoma and carcinoid due to long-term *Helicobacter pylori* colonization in Mongolian gerbils. *J Gastroenterol* 1999; **34**: 450-454

58 **Zheng Q**, Chen XY, Shi Y, Xiao SD. Development of gastric adenocarcinoma in Mongolian gerbils after long-term infection with *Helicobacter pylori*. *J Gastroenterol Hepatol* 2004; **19**: 1192-1198

59 **Ogura K**, Maeda S, Nakao M, Watanabe T, Tada M, Kyutoku T, Yoshida H, Shiratori Y, Omata M. Virulence factors of *Helicobacter pylori* responsible for gastric diseases in Mongolian gerbil. *J Exp Med* 2000; **192:** 1601-1610

60 **Kagawa J**, Honda S, Kodama M, Sato R, Murakami K, Fujioka T. Enterocromaffin-like cell tumor induced by *Helicobacter pylori* infection in Mongolian gerbils. *Helicobacter* 2002; **7**: 390-397

61 **Shimizu N**, Ikehara Y, Inada K, Nakanishi H, Tsukamoto T, Nozaki K, Kaminishi M, Kuramoto S, Sugiyama A, Katsuyama T, Tatematsu M. Eradication diminishes enhancing effects of *Helicobacter pylori* infection on glandular stomach carcinogenesis in Mongolian gerbils. *Cancer Res* 2000; **60**: 1512-1514

62 **Hibi K**, Mitomi H, Koizumi W, Tanabe S, Saigenji K, Okayasu I. Enhanced cellular proliferation and p53 accumulation in gastric mucosa chronically infected with *Helicobacter pylori*. *Am J Clin Pathol* 1997; **108**: 26-34

63 **Satoh K**, Kihira K, Kawata H, Tokumaru K, Kumakura Y, Ishino Y, Kawakami S, Inoue K, Kojima T, Satoh Y, Mutoh H, Sugano K. p53 expression in the gastric mucosa before and after eradication of *Helicobacter pylori*. *Helicobacter* 2001; **6**: 31-36

64 **Kodama M**, Fujioka T, Murakami K, Okimoto T, Sato R, Watanabe K, Nasu M. Eradication of *Helicobacter pylori* reduced the immunohistochemical detection of p53 and MDM2 in gastric mucosa. *J Gastroenterol Hepatol* 2005; **20**: 941-946

65 **Murakami K**, Fujioka T, Okimoto T, Mitsuishi Y, Oda T, Nishizono A, Nasu M. Analysis of p53 gene mutations in *Helicobacter pylori*-associated gastritis mucosa in endoscopic biopsy specimens. *Scand J Gastroenterol* 1999; **34**: 474-477

66 **Murakami K**, Fujioka T, Kodama M, Honda S, Okimoto T, Oda T, Nishizono A, Sato R, Kubota T, Kagawa J, Nasu M. Analysis of p53 mutations and *Helicobacter pylori* infection in human and animal models. *J Gastroenterol* 2002; **37 Suppl 13:** 1-5

67 **Suzuki H**, Miyazawa M, Nagahashi S, Mori M, Seto K, Kai A, Suzuki M, Miura S, Ishii H. Attenuated apoptosis in *H pylori*-colonized gastric mucosa of Mongolian gerbils in comparison with mice. *Dig Dis Sci* 2002; **47:** 90-99

68 **Crabtree JE**, Court M, Aboshkiwa MA, Jeremy AH, Dixon MF, Robinson PA. Gastric mucosal cytokine and epithelial cell responses to *Helicobacter pylori* infection in Mongolian gerbils. *J Pathol* 2004; **202**: 197-207

69 **Suzuki H**, Minegishi Y, Nomoto Y, Ota T, Masaoka T, van den Brink GR, Hibi T. Down-regulation of a morphogen (sonic hedgehog) gradient in the gastric epithelium of *Helicobacter pylori*-infected Mongolian gerbils. *J Pathol* 2005; **206**: 186-197

70 **van den Brink GR**, Hardwick JC, Nielsen C, Xu C, ten Kate FJ, Glickman J, van Deventer SJ, Roberts DJ, Peppelenbosch MP. Sonic hedgehog expression correlates with fundic gland differentiation in the adult gastrointestinal tract. *Gut* 2002; **51**: 628-633

71 **Houghton J**, Stoicov C, Nomura S, Rogers AB, Carlson J, Li H, Cai X, Fox JG, Goldenring JR, Wang TC. Gastric cancer originating from bone marrow-derived cells. *Science* 2004; **306**: 1568-1571

Science Editor Xia HHX and Guo SY **Language Editor** ELsevier HK

PO Box 2345, Beijing 100023, China
www.wjgnet.com
wjg@wjgnet.com

ELSEVIER

World J Gastroenterol 2005;11(45): 7072-7077
World Journal of Gastroenterology ISSN 1007-9327

• *GASTRIC CANCER*•

Effect of p27^{KIP1} on cell cycle and apoptosis in gastric cancer cells

Jian-Yong Zheng, Wei-Zhong Wang, Kai-Zong Li, Wen-Xian Guan, Wei Yan

Jian-Yong Zheng, Wei-Zhong Wang, Wen-Xian Guan, Department of Gastrointestinal Surgery, Xijing Hospital, Fourth Military Medical University, Xi'an 710032, Shaanxi Province, China
Kai-Zong Li, Department of Hepatobiliary Surgery, Xijing Hospital, Fourth Military Medical University, Xi'an 710032, Shaanxi Province, China
Wei Yan, Department of Pathology, Fourth Military Medical University, Xi'an 710032, Shaanxi Province, China
Correspondence to: Jian-Yong Zheng, Department of Gastrointestinal Surgery, Xijing Hospital, Fourth Military Medical University, Xi'an 710032, Shaanxi Province, China. zhengjy2000@sohu.com
Telephone: +86-29-83375265
Received: 2004-11-16 Accepted: 2005-05-26

Abstract

AIM: To elucidate the effect of p27^{KIP1} on cell cycle and apoptosis regulation in gastric carcinoma cells.

METHODS: The whole length of p27^{KIP1} cDNA was transfected into human gastric cancer cell line SCG7901 by lipofectamine. Expression of p27^{KIP1} protein or mRNA was analyzed by Western blot and RNA dot blotting, respectively. Effect of p27^{KIP1} on cell growth was observed by MTT assay and anchorage-independent growth in soft agar. Tumorigenicity in nude mice was used to assess the *in vivo* biological effect of p27^{KIP1}. Flow cytometry, TUNEL, and electron microscopy were used to assess the effect of p27^{KIP1} on cell cycle and apoptosis.

RESULTS: Expression of p27^{KIP1} protein or mRNA increased evidently in SCG7901 cells transfected with p27^{KIP1}. The cell growth was reduced by 31% at 48 h after induction with zinc determined by cell viability assay. The alteration of cell malignant phenotype was evidently indicated by the loss of anchorage-independent growth ability in soft agar. The tumorigenicity in nude mice was reduced evidently (0.55±0.14 cm *vs* 1.36±0.13 cm, $P<0.01$). p27^{KIP1} overexpression caused cell arrest with 36% increase (from 33.7% to 69.3%, $P<0.01$) in G_1 population. Prolonged p27^{KIP1} expression induced apoptotic cell death reflected by pre-G1 peak in the histogram of FACS, which was also confirmed by TUNEL assay and electron microscopy.

CONCLUSION: p27^{KIP1} can prolong cell cycle in G1 phase and lead to apoptosis. p27^{KIP1} may be a good candidate for cancer gene therapy.

Key words: Cell cycle; Apoptosis; Gastric neoplasm; p27^{KIP1}

Zheng JY, Wang WZ , Li KZ, Guan WX, Yan W. Effect of p27^{KIP1} on cell cycle and apoptosis in gastric cancer cells. *World J Gastroenterol* 2005;11(45): 7072-7077
http://www.wjgnet.com/1007-9327/11/7072.asp

INTRODUCTION

The number of cells is regulated by a balance between proliferation, growth arrest and programmed cell death (apoptosis, PCD). Disorders of the cell cycle and apoptosis are closely related to the progression and aggressiveness of cancers[1]. p27^{KIP1}, a member of the Cip/Kip family of cyclin-dependent kinase inhibitors (CDKI), was first identified as a negative cell cycle regulator in transforming growth factor β-treated cells and in G_1 phase quiescent cells by cell contact inhibition[2,3]. p27^{KIP1} binds to a wide variety of cyclin/CDK complexes including CDK2 and CDK4[4], inhibits kinase activity[5] and blocks cell cycle[6-8]. The overexpression of p27^{KIP1} protein in mammalian cells induces G_1 arrest of the cell cycle and apoptosis[9,10]. Decreased p27^{KIP1}, which is positively correlated with a deceased rate of apoptosis, may be not only an indicator of tumor aggressiveness, but also an important prognostic marker in gastric carcinoma[11].

In this study, an inducible expression system was used to induce overexpression of p27^{KIP1} in human gastric cancer cells. Then whether transfection of SCG7901 with p27^{KIP1} gene could alter the cell and molecular biology as well as the spontaneous rate of apoptosis was studied.

MATERIALS AND METHODS

Cell culture

Human gastric cancer cell line SCG7901 was provided by the Department of Pathology, Fourth Military Medical University (Xi'an, China). SCG7901 cells were cultured in Eagle's medium containing phenol red supplemented with 50 mL/L fetal bovine serum (FBS) in a humidified atmosphere of 950 mL/L air and 50 mL/L CO_2 at 37℃. All the media were supplemented with 2 mmol/L L-glutamine, 100 mg/L penicillin and 100 kU/L streptomycin. Culture medium and supplements were obtained from Gibco BRL.

Plasmid construction and DNA transfection

pGEM T-Easy-KIP1 vector containing human full-length

cDNA of $p27^{KIP1}$ was used. Complementary DNA of $p27^{KIP1}$ cleaved from the pGEM T-Easy-KIP1 plasmid by EcoRI was subcloned into the inducible vector neo-control pMD-neo vector to generate pMD-KIP1 containing 0.6 kb $p27^{KIP1}$ cDNA and controlled expression of protein upon addition of 100 mmol/L zinc as an external inducer. Clonfectin (Clontech, USA) was used to transfect $p27^{KIP1}$ inducible expression vectors into SGC7901 cells. Logarithmically growing cells were transfected with 1 μg of plasmids and 2 μL of clonfectin reagent according to the manufacturer's instructions. For stable transfection, the transfected SGC7901 cells were selected in medium plus 0.5 g/L G418 (Life Technologies, USA) for 2 wk, then the G418 concentration was reduced to 0.2 g/L. Stable SGC7901 cell line transfected with pMD-KIP1 vector was treated by continuous exposure to 100 mmol/L $ZnSO_4$.

Western blot analysis of transgene expression

Monolayers of the cells were rinsed with PBS and lysed with SDS-PAGE loading buffer (50 mmol/L Tris-HCl pH 6.8, 100 mmol/L dithiothreitol, 2 g/L SDS). Mock and pMD-neo transfected cells served as controls. Samples were analyzed by SDS-PAGE and transferred into Hybond-C super membranes. The membranes were blocked with 50 mL/L skim-milk and 1 g/L Tween-20, then probed with primary antibody overnight according to the manufacturer's instructions, washed in PBS, 2g/L Tween-20 and then incubated with appropriate horseradish-peroxidase (HRP) conjugated second antibody. After being washed, the membranes were developed by DAB reagents according to the manufacturer's guide (Dako Co., USA). $p27^{KIP1}$ (Santa Cruz Biotechnology, USA) was detected after HRP-conjugated anti-rabbit IgG (Fc) was used. The level of β-actin was used as a control for equal loading of protein.

Total RNA extraction and RNA dot blotting

Total RNA was extracted from SGC7901 cells using TRIzol (Life Technologies, USA) following a standard acid-guanidium-phenolchloroform method. The digoxingenin-labeled specific DNA probe was obtained as follows. The plasmid containing $p27^{KIP1}$ cDNA was used as template, a pair of primers (-5 ℃-ggggtaccatgtcaaacgtgcgagt-3 ℃and -5 ℃-gctcaacgtttgacgtcttc-3 ℃) was used to amplify the sequence. The PCR system containing Dig-11-dUTP and four normal dNTPs and Taq polymerase were used. After a standard PCR procedure (94 ℃ to 30 s, 60 ℃ for 30 s, 72 ℃ for 1 min, 30 cycles), the PCR product was purified by 1% agarose electrophoresis and DNA extraction. The labeling efficiency was further determined by Dot blot of serially diluted plasmid. Finally, the digoxingenin-labeled DNA probe was used in the experiment. RNA Dot blot was performed according to the Dig system user's guide for filter hybridization (Boehringer Mannheim, Germany). Briefly, RNA sample was diluted in RNA dilution buffer (a mixture of DEPC-treated H_2O, 20×SSC, and formaldehyde at 5:3:2). The membrane was marked slightly with a pencil to identify each dilution before spotting. One microliter of the RNA sample was spotted onto a dry nylon membrane using a micropipettor. Then the RNA was fixed to the membrane by baking in an oven at 120 ℃ for 30 min. Hybridization and the following procedures were similar to *in situ* hybridization. Hybridization mixture contained 5×SSC, 500 g/L deionized formamide, 1 g/L sodium-lauroyl sarcosine, 0.2 g/L SDS, 20 g/L blocking reagent and a 25 ng/mL DNA probe. The level of GADPH mRNA was used as a control for equal loading of RNA.

MTT and colony assay

SGC7901/KIP1 and SGC7901/pMD cells (1×10^4) were seeded in 96-well plates and continuously exposed to 100 mmoL/L $ZnSO_4$. After treatment, 50 μL of 5 g/L 3-(4,4-dimethylthiazol-2-yl) 2,5-diphenyltetrazolium bromide (MTT) in PBS was added to each well, incubated for 4 h at 37 ℃ and the formed formazan crystals were dissolved in 50 μL of dimethyl sulfoxide. The absorbance was recorded at 490 nm on a microplate reader (BioRad). Cell proliferation was expressed as IC50 for cells. Soft agar was prepared with the 6 g/L bottom agar layer and the 4 g/L top agar layer. The number of cells plated for each clone was 2 000. Plates were incubated at 37 ℃ with 50 mL/L CO_2 for 2 wk and the colonies were counted and photographed under a phase contrast microscope (Nikon, Tokyo, Japan).

Tumorigenicity tests in nude mice

$p27^{KIP1}$-transfected SGC7901/KIP1 cells were injected into the right flank of a nude mouse at 2.5×10^6. pMD-neo-transfected SGC7901/pMD cells served as control. Each group had five nude mice. From the second day, each nude mouse received 100 mmol/L $ZnSO_4$ at a dose of 0.2 mL daily by subcutaneous injection for over 4 wk. The time of tumorigenicity and the tumor volume were measured.

Cell cycle analysis

SGC7901 cells including adherent cells (with trypsin-EDTA) and nonadherent cells were harvested. All cells were washed with PBS, resuspended and incubated in 700 mL/L ethanol for at least 12 h at 4 ℃ to permeabilize the plasma membrane. Cells were centrifuged at 1 000 r/min, resuspended in 100 mg/L RNase and 10 mg/L propidium iodide, incubated for 15 min at 25 ℃ in the dark. Single color fluorescent flow cytometry was performed with a FACScalibur flow cytometer (Becton Dickinson, USA). The histograms were analyzed with Multiplus Software Π.

Electron microscopy

SGC7901/pMD cells were gently washed with serum-free medium and fixed with 25 g/L glutaraldehyde in 0.1 mol/L sodium cacodylate buffer. These cells were scraped from the surface of the dishes and pelleted by spinning for 5 min at 10 000 *g*. The cells were osmicated with 10 g/L osmium tetroxide. The block was stained, dehydrated in graded ethanol, infiltrated with propylene oxide, embedded with EMBED overnight and cured in a 60 ℃ oven for 48 h. Silver sections were cut with an

Ultracut E microtome, collected on a formvar and carbon-coated grid, stained with uranyl acetate and Reynold's lead citrate, and viewed under a JEOL 100 CX electron microscope.

Apoptosis analyzed by TUNEL assay

SGC7901/KIP1 and SGC7901/pMD cells were harvested for TUNEL staining. The proportion of cells showing DNA fragmentation was measured by incorporation of fluorescein (FITC)-12-dUTP into DNA using terminal de oxynucleotidyltransferase (TdT). The kit was bought from Boehringer Mannheim (*In Situ Cell Death Detection*). Cells were fixed by 40 g/L paraformaldehyde in PBS overnight at 4 ℃. The samples were washed thrice with PBS and permeabilized by 2 g/L Triton X-100 in PBS for 15 min on ice. After being washed twice, cells were equilibrated at room temperature for 15-30 min in a equilibration buffer with 30 g/L BSA and 200 mL/L normal bovine serum in PBS at pH 7.4, then the slides were covered with the TUNEL mixture (calf thymus TdT, FITC-12-dUTP, and cobalt chloride in 1×reaction buffer) for 1-2 h at 37 ℃ in the dark. The tailing reaction was terminated by 2× standard saline citrate (SSC). The samples were washed thrice with PBS and analyzed by fluorescence microscopy. Routine HE staining was also conducted. Negative control was performed by omitting TdT. Quantitative analysis of apoptosis was represented by apoptotic index (AI) as described previously. AI referred to percentages from at least 1 000 counts apoptotic and non-apoptotic cells.

Statistical analysis

Fisher's exact test was performed. $P<0.05$ was considered statistically significant.

RESULTS

Inducible expression of p27^{KIP1} in SGC7901 cells

Western blot analysis demonstrated p27^{KIP1} expression 0, 4, 24, 48, and 72 h after the addition of $ZnSO_4$. Mock and pMD-neo vector-transfected cells as a control contained no detectable level of p27^{KIP1} in the presence of 100 mmol/L $ZnSO_4$. However, p27^{KIP1} expression was increased at 4 h and further increased to a steady level at 24 h after the addition of $ZnSO_4$ as determined by the Western blot analysis (Figure 1). In RNA dot blotting survey of the expression, p27^{KIP1} mRNA was very low in untransfected or noninduced SGC7901 cells. In contrast, mRNA for p27^{KIP1} was expressed at a high level 4 and 24 h after the addition of $ZnSO_4$ (Figure 2). This expression pattern was rather consistent with the expression of protein.

Inhibition of tumor cell growth by exogenous p27^{KIP1}

Exogenous p27^{KIP1} inhibited cell growth significantly. SGC7901 cell viability was determined by MTT assay (Figure 3). The cell viability rate decreased from 88% to 57% 48 h after p27^{KIP1} induction with zinc treatment ($P<0.01$). Another biological feature of malignant cells was anchorage-independent growth capability. The neo-

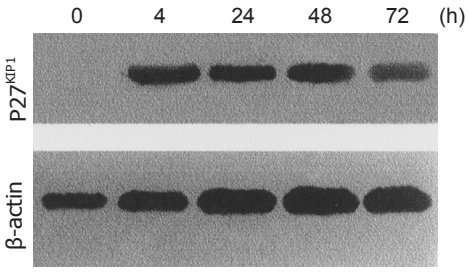

Figure 1 Induction of p27^{KIP1} expression by Western blotting analysis.

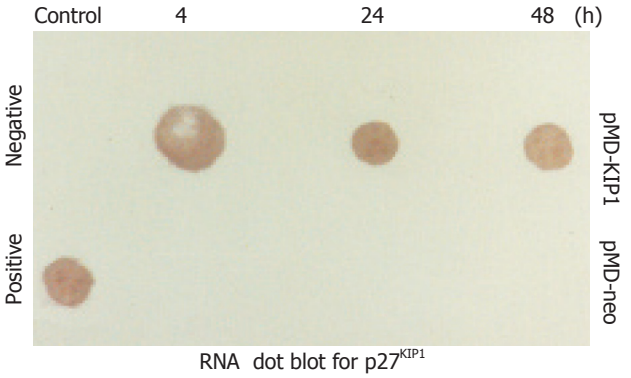

Figure 2 Expression of p27^{KIP1} in mRNA level by RNA dot blot analysis.

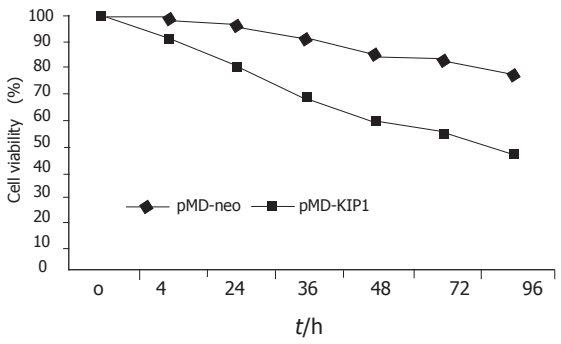

Figure 3 Growth course of SGC7901 cells.

control SGC7901/pMD and SGC7901 cells formed large colonies in each well after 2 wk, and the rate of colony formation was increased by 80% and 60%, respectively. SGC7901/KIP1 cells showed markedly lower ability to form colony with a rate of 30% ($P<0.01$). Moreover, tumors were generated in nude mice on the 7th d from SGC7901/pMD cells, but SGC7901/KIP1 cells generated tumor on the 12th d and grew slowly. The tumor diameter generated from SGC7901/KIP1 cells was smaller than that from SGC7901/pMD cells (0.55 ± 0.14 *vs* 1.36 ± 0.13 cm, $P<0.01$, Figure 4). These data indicated that the exogenous p27^{KIP1} had a cytostatic effect on cell growth.

Overexpression of p27^{KIP1} prolonged cell cycle in G$_1$ phase

p27^{KIP1} was identified as a negative cell cycle regulator

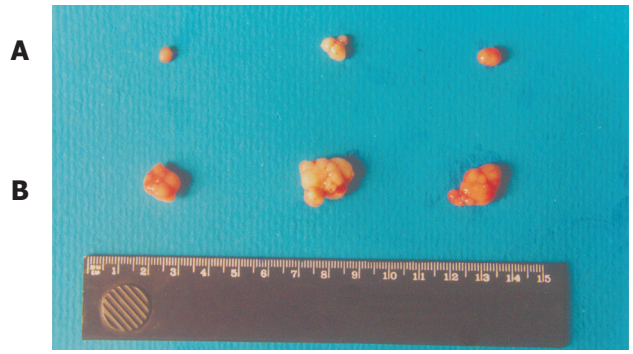

Figure 4 Tumorigenicity in nude mice. **A:** SGC7901/KIP1 group; **B:** SGC7901 group.

in transforming growth factor β-treated cells and in G_1 phase quiescent cells by cell contact inhibition. The overexpression of p27^{KIP1} protein in mammalian cells induced G_1 arrest of the cell cycle. In order to investigate whether p27^{KIP1} had the ability to induce G_1 arrest in SGC7901 cells, cell cycle analysis was performed on transfected SGC7901 cells. Flow cytometry analysis showed that overexpression of p27^{KIP1} increased remarkably the proportion of SGC7901 cells with G_1 phase DNA content increased from 33.7% to 69.3% ($P = 0.000$) and decreased with S phase DNA content at 48 h after induction (Figure 5). There was no significant change in the proportion of cells with G_2/M phase DNA content.

Overexpression of p27^{KIP1}-induced apoptosis in SGC7901 cells

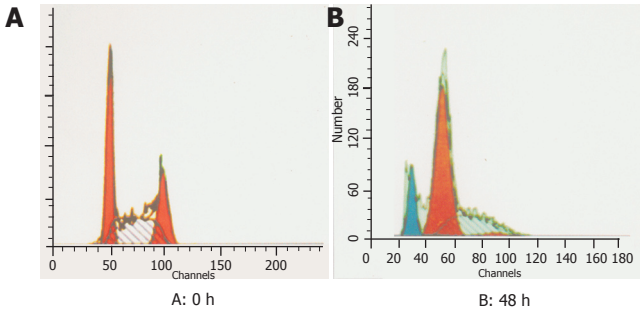

Figure 5 Flow cytometric analysis of SGC7901 cells at 0 h (**A**) and 48 h (**B**).

Morphological changes SGC7901/KIP1 cells-transfected p27^{KIP1} altered their morphology and induced DNA strand breaks in a manner consistent with apoptosis. The changes were indeed induced by apoptosis rather than necrosis, which was confirmed by electron microscopy. SGC7901/KIP1 cells showed compacted nuclear chromatin with fine granular masses marginated against the nuclear-enveloped and condensed cytoplasm, the nuclear outline was convoluted and the organelles were preserved (Figure 6).

TUNEL assay To determine whether overexpression of p27^{KIP1} was able to induce apoptosis in SGC7901 cells, TUNEL assay was performed. Compared to the pMD-neo-transfected SGC7901/pMD cells, p27^{KIP1}-overexpressed SGC7901/KIP1 cells showed obvious morphological changes. Some apoptotic cells appeared round and condensed cytoplasm as well as highly fragmented chromatin. TUNEL-positive cells were found with Kelly or green fluorescence in nucleoli. Cells without apoptosis observed by fluorescence microscopy had no fluorescence. Apoptotic index significantly increased in p27^{KIP1}-transfected SGC7901/KIP1 cells 24 and 48 h after being exposed to 100 mmol/L $ZnSO_4$ (3.0 *vs* 21.2, 3.6 *vs* 26.3, $P<0.05$).

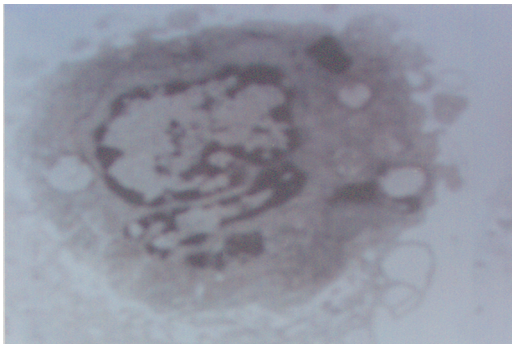

Figure 6 Ultrastructural changes associated with apoptosis in SGC7901/KIP1 cells (TEM×7 500).

Flow cytometry In order to determine the effect of p27^{KIP1} overexpression on apoptosis in SGC7901 cells, cells were exposed to 100 mmol/L $ZnSO_4$ for 48 h and apoptotic damage of DNA was detected according to the sub-G_1 peak on a flow cytometer. Overexpression of p27^{KIP1} showed significantly higher apoptotic peak than normal control as the sub-G_1 peak indicated. The apoptotic cells accounted for about 14.7% (Figure 5).

Taken together, p27^{KIP1} overexpression could inhibit proliferation of SGC7901 cells and subsequently induce apoptosis.

DISCUSSION

Gastric cancer is the second most common fatal malignancy in the world[12-14] and is still the leading cause of cancer-related deaths in China. The development of gastric cancer is a multi-factorial process[15]. A balance between proliferation and apoptosis of tumor cells is important for tumor growth. In gastric cancer, proliferative activity and apoptosis of cancer cells are associated with tumor growth[16]. Cyclins, cyclin-dependent kinase (CDK) and their inhibitors regulate cell growth, differentiation, survival and death. Cell cycle which progresses sequentially through G_1, DNA synthesis (S), G_2, and mitosis (M) phases, regulates DNA replication and chromosomal segregation into the daughter cells. Gene abnormalities and

aberrant expression of cell cycle regulators play a pivotal role in the pathogenesis of gastrointestinal tumors[17], of which CDKIs are major regulators.

$p27^{KIP1}$ is a member of the Cip/Kip family of CDKIs that regulate cell cycle progression, thus inhibiting various cycle-CDK complexes. Physiologically, $p27^{KIP1}$ is believed to primarily regulate progression of cells from late G_1 into S phase by interacting with cyclin E-CDK2 complexes[9]. $p27^{KIP1}$ has been implicated as a mediator of growth arrest due to TGF-β, cAMP and other extracellular factors. Moreover, elevated expression of $p27^{KIP1}$ protein leads to G_1 arrest in many cell types and promotes neuronal differentiation in mouse neuroblastoma cells, while inhibition of $p27^{KIP1}$ expression through the use of antisense technology prevents G_1 arrest and/or suppresses entry of fibroblasts into a state of quiescence in response to mitogen depletion.

Interestingly, in many types of tumors such as gastric[18,19], prostate[20,21] and breast carcinoma, the expression of $p27^{KIP1}$ gene is downregulated[22,23]. Loss of $p27^{KIP1}$ expression may result in tumor development and/or progression. However, this loss of expression does not appear from the result of gene mutations. It is believed that the aberrant expression of $p27^{KIP1}$ plays a pivotal role in the pathogenesis of carcinoma. Malignant human renal tumor cell transfection with $p27^{KIP1}$ gene leads to inhibition of proliferation and cell cycle arrest in G_1[24]. Ectopic overexpression of $p27^{KIP1}$ is associated with a striking decrease in aneuploid cells, loss of anchorage-independent growth in soft agar and failure to induce tumor development in a xenograft model[25]. In this report, we have also demonstrated that $p27^{KIP1}$ overexpression could inhibit proliferation of SGC7901 cells. The cell growth was reduced by 31% at 48 h, after the induction with zinc as determined by cell viability assay. The alteration of cell malignant phenotype was evidently indicated by the loss of anchorage-independent growth ability in soft agar. The tumorigenicity in nude mice was reduced evidently ($P<0.01$). $p27^{KIP1}$ overexpression increased cell arrest from 33.7% to 69.3% ($P<0.01$) in G_1 population.

Recent evidence demonstrated that high levels of $p27^{KIP1}$ protein induced by adenovirus vector leads to growth arrest as well as enhancement of apoptosis in several cell lines from different species and tissues of various origins[11,25]. Decreased $p27^{KIP1}$, which is positively correlated with a decreased rate of apoptosis, may be not only an indicator of tumor aggressiveness, but also an important prognostic marker in gastric carcinoma[16]. In this study, we have demonstrated that overexpression of $p27^{KIP1}$ not only prolonged cell cycle in G_1 phase of SGC7901 cells but also subsequently induced apoptosis as reflected by pre-G_1 peak in the histogram of FACS, TUNEL assay and electron microscopy. This is the first report in which a significant correlation between $p27^{KIP1}$ expression and cell cycle arrest and apoptosis has been demonstrated in SGC7901 cell line.

Mice lacking $p27^{KIP1}$ are abnormally large and display multiple organ hyperplasia indicative of tissue overgrowth[26,27]. Thus, it is possible that $p27^{KIP1}$ plays an important role in maintaining organ size through the induction of apoptosis. However, the mechanism of tumor growth suppression appears to include $p27^{KIP1}$ but also various other properties such as p53. p53 serves as a major G_1 checkpoint regulator through the induction of p21 but not of $p27^{KIP1}$ and p57, while it induces apoptosis. The p53-mediated CDK inhibitor p21 does not lead to significant apoptosis though both p21 and $p27^{KIP1}$ induce G_1 arrest through their potential abilities to inhibit CDK activity. These findings suggest that the inhibition of CDK activity may not be sufficient to induce apoptotic cell death. A possible explanation of these differences between $p27^{KIP1}$ and p53-mediated p21 function is that $p27^{KIP1}$ may have other functions in addition to its notable function as a CDKI. It can also be speculated that $p27^{KIP1}$, which has the potential to induce growth arrest and apoptosis, may play a more important role in tumor growth suppression than p53-mediated p21. Further understanding of the mechanism involved in this process can improve chemotherapeutic strategies aimed at achieving high level $p27^{KIP1}$ expression and gene therapy.

REFERENCES

1 **Krug U,** Ganser A, Koeffler HP. Tumor suppressor genes in normal and malignant hematopoiesis. *Oncogene* 2002; **21:** 3475-3495

2 **Nho RS,** Sheaff RJ. p27kip1 contributions to cancer. *Prog Cell Cycle Res* 2003; **5:** 249-259

3 **Hengst L,** Dulic V, Slingerland JM, Lees E, Reed SI. A cell cycle regulated inhibitor of cyclin-dependent kinases. *Proc Natl Acad Sci USA* 1994; **91:** 5291-5295

4 **Blain SW**, Scher HI, Cordon-Cardo C, Koff A. p27 as a target for cancer therapeutics. *Cancer Cell* 2003; **3:** 111-115

5 **Alkarain A,** Slingerland J. Deregulation of p27 by oncogenic signaling and its prognostic significance in breast cancer. *Breast Cancer Res* 2004; **6:** 13-21

6 **Chetty R.** p27 Protein and cancers of the gastrointestinal tract and liver: an overview. *J Clin Gastroenterol* 2003; **37:** 23-27

7 **Russo AA,** Jeffrey PD, Patten AK, Massagué J, Pavletich NP. Crystal structure of the p27Kip1 cyclin-dependent-kinase inhibitor bound to the cyclin A–Cdk2 complex. *Nature* 1996; **382:** 325-331

8 **Nakayama K,** Nagahama H, Minamishima YA, Matsumoto M, Nakamichi I, Kitagawa K, Shirane M, Tsunematsu R, Tsukiyama T, Ishida N, Kitagawa M, Nakayama K, Hatakeyama S. Targeted disruption of Skp2 results in accumulation of cyclin E and p27Kip1, polyploidy and centrosome overduplication. *EMBO J* 2000; **19:** 2069-2081

9 **Lloyd RV,** Erickson LA, JIN L, Kulig E, Qian X, Cheville JC, Scheithauer BW. p27KIP1: a multifunctional cyclin-dependent kinase inhibitor with prognostic significance in human cancers. *Am J Pathol* 1999, **154:** 313-323

10 **Davison EA,** Lee CS, Naylor MJ, Oakes SR, Sutherland RL, Hennighausen L, Ormandy CJ, Musgrove EA. The cyclin-dependent kinase inhibitor p27 (Kip1) regulates both DNA synthesis and apoptosis in mammary epithelium but is not required for its functional development during pregnancy. *Mol Endocrinol* 2003; **17:** 2436-2447

11 **Katayose Y,** Kim M, Rakkar AN, Li Z, Cowan KH, Seth P. Promoting apoptosis: a novel activity associated with the cyclin-dependent kinase inhibitor p27. *Cancer Res* 1997; **57:** 5441-5445

12 **Parkin DM,** Bray F, Ferlay J, Pisani P. Estimating the world cancer burden: Globocan 2000. *Int J Cancer* 2001; **94:** 153-156

13 **Bani-Hani KE,** Yaghan RJ, Heis HA, Shatnawi NJ, Matalka II, Bani-Hani AM, Gharaibeh KA. Gastric malignancies in Northern Jordan with special emphasis on descriptive epidemiology. *World J Gastroenterol* 2004; **10:** 2174-2178
14 **Wong JE,** Ito Y, Correa P, Peeters KC, van de Velde CJ, Sasako M, Macdonald J. Therapeutic strategies in gastric cancer. *J Clin Oncol* 2003; **21:** S267-269
15 **Oluwasola AO,** Ogunbiyi JO. Gastric cancer: aetiological, clinicopathological and management patterns in Nigeria. *Niger J Med* 2003; **12:** 177-186
16 **Ohtani M,** Isozaki H, Fujii K, Nomura E, Niki M, Mabuchi H, Nishiguchi K, Toyoda M, Ishibashi T, Tanigawa N. Impact of the expression of cyclin-dependent kinase inhibitor p27Kip1 and apoptosis in tumor cells on the overall survival of patients with non-early stage gastric carcinoma. *Cancer* 1999; **85:** 1711-1718
17 **Koide N,** Nishio A, Igarashi J, Kajikawa S, Adachi W, Amano J. Alpha-fetoprotein-producing gastric cancer: histochemical analysis of cell proliferation, apoptosis, and angiogenesis. *Am J Gastroenterol* 1999; **94:** 1658-1663
18 **Nitti D,** Belluco C, Mammano E, Marchet A, Ambrosi A, Mencarelli R, Segato P, Lise M. Low level of p27(Kip1) protein expression in gastric adenocarcinoma is associated with disease progression and poor outcome. *J Surg Oncol* 2002; **81:** 167-175; discussion 175-176
19 **Philipp-Staheli J,** Kim KH., Payne SR., Gurley KE, Liggitt D, Longto G, Kemp CJ. Pathway-specific tumor suppression. Reduction of p27 accelerates gastrointestinal tumorigenesis in Apc mutant mice, but not in Smad3 mutant mice. *Cancer Cell* 2002; **1:** 355-368
20 **Fernández PL,** Arce Y, Farré X, Martínez A, Nadal A, Rey MJ, Peiró N, Campo E, Cardesa A. Expression of p27/Kip1 is down-regulated in human prostate carcinoma progression. *J Pathol* 1999; **187:** 563-566
21 **Tsihlias J,** Kapusta LR, DeBoer G, Morava-Protzner I, Zbieranowski I, Bhattacharya N, Catzavelos GC, Klotz LH, Slingerland JM. Loss of cyclin-dependent kinase inhibitor p27Kip1 is a novel prognostic factor in localized human prostate adenocarcinoma. *Cancer Res* 1998; **58:** 542-548
22 **Slingerland J,** Pagano M. Regulation of the cdk inhibitor p27 and its deregulation in cancer. *J Cell Physiol* 2000; **183:** 10-17
23 **Tsihlias J,** Kapusta L , Slingerland J. The prognostic significance of altered cyclin-dependent kinase inhibitors in human cancer. *Annu Rev Med* 1999; **50:** 401-423
24 **Katner AL,** Gootam P, Hoang QB, Gnarra JR, Rayford W. A recombinant adenovirus expressing p7(Kip1) induces cell cycle arrest and apoptosis in human 786-0 renal carcinoma cells. *J Urol* 2002; **168:** 766-773
25 **Katner AL,** Hoang QB, Gootam P, Jaruga E, Ma Q, Gnarra J, Rayford W. Induction of cell cycle arrest and apoptosis in human prostate carcinoma cells by a recombinant adenovirus expressing p27(Kip1). *Prostate* 2002; **53:** 77-87 [PMID: 12210483]
26 **Cipriano SC,** Chen L, Burns KH, Koff A, Matzuk MM. Inhibin and p27 interact to regulate gonadal tumorigenesis. *Mol Endocrinol* 2001; **15:** 985-996
27 **Sotillo R,** Dubus P, Martín J, de la Cueva E, Ortega S, Malumbres M, Barbacid M. Wide spectrum of tumors in knock-in mice carrying a Cdk4 protein insensitive to INK4 inhibitors. *EMBO J* 2001; **20:** 6637-6647

Science Editor Wang XL and Li WZ **Language Editor** Elsevier HK

PO Box 2345, Beijing 100023, China
www.wjgnet.com
wjg@wjgnet.com

ELSEVIER

World J Gastroenterol 2005;11(45):7078-7083
World Journal of Gastroenterology ISSN 1007-9327

• *BASIC RESEARCH* •

Vitamin B12 deficiency and gastric histopathology in older patients

KR Dholakia, TS Dharmarajan, D Yadav, S Oiseth, EP Norkus, CS Pitchumoni

KR Dholakia, Department of Medicine, Our Lady of Mercy Medical Center, Bronx, NY; University Hospital of New York Medical College, Valhalla, NY, United States
TS Dharmarajan, Department of Medicine, Division of Geriatrics, Our Lady of Mercy Medical Center, Bronx, NY; University Hospital of New York Medical College, Valhalla, NY, United States
D Yadav, Department of Medicine, Division of Gastroenterology, Our Lady of Mercy Medical Center, Bronx, NY; University Hospital of New York Medical College, Valhalla, NY, United States
S Oiseth, Department of Pathology, Our Lady of Mercy Medical Center, Bronx, NY; University Hospital of New York Medical College, Valhalla, NY, United States
EP Norkus, Department of Medical Research, Our Lady of Mercy Medical Center, Bronx, NY; University Hospital of New York Medical College, Valhalla, NY, United States
CS Pitchumoni, Department of Medicine, Division of Gastroenterology, Hepatology and Clinical Nutrition, St. Peter's Medical Center, University of Medicine and Dentistry of New Jersey, New Brunswick, NJ, United States
Supported by the Fellowship Training Programs in Gastroenterology and Geriatric Medicine at Our Lady of Mercy Medical Center
Correspondence to: Dharmarajan TS, MD, 31 Pheasant Run, Scarsdale, New York 10583,
United States. dharmarajants@yahoo.com
Telephone: +1-718-920-9041 Fax: +1-914-723-4297
Received: 2005-03-18 Accepted: 2005-04-09

Abstract

AIM: To compare upper gastric endoscopic and histopathologic findings in older adults in the presence and absence of B12 deficiency.

METHODS: A prospective analysis of upper gastric endoscopic and gastric histopathologic findings from 30 newly identified B12-deficient patients (11 males, 19 females) and 16 controls with normal B12 status (6 males, 10 females) was performed. For all subjects, the indication for upper endoscopy and gastric biopsy were unrelated to B12 status. A single pathologist, blinded to B12 status, processed and interpreted the biopsy samples. Endoscopic and histopathologic findings were correlated with age, gender, hematocrit (Hct), MCV and B12 status.

RESULTS: The B12-deficient group had significantly lower mean serum B12 levels compared to the controls ($P<0.00005$) while their mean Hct, MCV and serum albumin levels were similar. Iron deficiency (ferritin-based) was present in 21% of B12-deficient patients and intrinsic factor antibodies were present in 29% (5/17) of B12-deficient patients. The endoscopic findings revealed significantly different rates of gastritis and atrophy between the B12-deficient and control groups ($P=0.017$). B12-deficient patients had significantly less superficial gastritis (62% *vs* 94%) and significantly more atrophic gastritis (28% *vs* 0%) as compared to the controls ($P=0.039$). Intestinal metaplasia was similar in both groups. *Helicobacter pylori* infection rates were similar in the B12-deficient patients and controls (40% *vs* 31%).

CONCLUSION: Significantly different endoscopic findings and types of gastritis could often be observed in the presence and absence of B12 deficiency. Atrophy, based on endoscopy, and atrophic gastritis, based on histopathology, suggest the presence of B12 deficiency. Gastric histopathology is not influenced by the age, gender, Hct or MCV of the patients.

Key words: Vitamin B12 deficiency; Gastric histopathology; Older adults

Dholakia KR, Dharmarajan TS, Yadav D, Oiseth S, Norkus EP, Pitchumoni CS. Vitamin B12 deficiency and gastric histopathology in older patients. *World J Gastroenterol* 2005; 11(45): 7078-7083
http://www.wjgnet.com/1007-9327/11/7078.asp

INTRODUCTION

Vitamin B12 deficiency is a common but under-recognized disorder with a prevalence ranging from 3% to 40% in the adult population[1-4]. In a previous study, we noted a prevalence of between 15% and 25% in the community and nursing home hospitalized older subjects[3]. B12 deficiency often goes undetected, with manifestations that range from asymptomatic to a wide spectrum of hematologic and/or neuropsychiatric features. For the purpose of this discussion, the term B12 will be used interchangeably with cobalamin.

B12 deficiency affects proliferating epithelium at all the sites[5]. Although the histopathological effects of B12 deficiency relating to the blood and nervous system are well described, histopathological changes in the stomach associated with cobalamin deficiency in older subjects have

received less emphasis in the literature. Presently, there exist some confusions whether gastric changes are a cause or an effect of deficiency[6]. It is worth stating that the stomach plays a major role both in the absorption of B12 and the pathogenesis of cobalamin deficiency[5,7]. Among the etiologies of cobalamin deficiency, pernicious anemia (PA), once believed to be the most common cause[6,9], actually accounts for only a small fraction of cases of B12 deficiency[2,3,8]. It is well recognized that PA, a type A gastritis, is characterized by fundic atrophic gastritis. There is a lack of knowledge about the examination of gastric endoscopic findings and histopathologic changes associated with vitamin B12 deficiency in older adults. We, therefore, have attempted to evaluate the endoscopic and histopathologic changes in older adults with newly diagnosed B12 deficiency and to compare the findings in adults of the same age group and normal B12 status.

MATERIALS AND METHODS

The study was performed by the staff from the divisions of geriatrics, gastroenterology, medicine, pathology and biomedical research at Our Lady of Mercy Medical Center, University Hospital of New York Medical College, Valhalla, NY, USA. A prospective analysis of upper gastric endoscopic and gastric histopathologic findings was performed on 30 adults who were above the age of 60 with newly diagnosed B12 deficiency. The subjects included men and women, ages ranging from 60 to 99 years. All patients required hospitalization for a cause other than B12 deficiency. The diagnosis of B12 deficiency was made following routine screening or during evaluation for hematological or neurological manifestations. A randomly selected group of 6 male and 10 female patients with normal B12 status, ages ranging from 63 to 93 years,served as controls. The male/female ratio in the B12-deficient group was 11/19, and 6/10 in the control group. Several indicators of nutritional status were assessed in the B12-deficient patients. We observed low folate status in 16%, low albumin status in 16% and low iron status (ferritin based) in 21% of the B12-deficient patients.

The primary indication for endoscopy was unrelated to cobalamin status and based on the usual indications for upper gastric endoscopy on both B12-deficient patients and controls. After obtaining informed consent, upper gastric endoscopy was performed and multiple endoscopic biopsies were obtained from several sites within the gastric fundus and antrum. Gastric biopsies were performed for reasons unrelated to cobalamin status and hence the sites examined and the number of biopsies taken varied between individuals. Endoscopic findings included a normal appearance of the stomach, atrophy and gastritis. Gastritis on endoscopy was defined as the presence of erosions or hemorrhage. Erosions were seen as breaks in the mucosa manifesting as multiple lesions with white bases that were commonly encircled by a halo of erythema. Atrophy on endoscopy was defined as the disappearance of gastric rugae and a thinning of the gastric mucosal folds with the prominence of the blood vessels seen through the thin mucosa (paper money appearance)[10]. Erosive gastritis and friable mucosa are suggestive findings of gastritis on endoscopy.

Gastric histopathology entailed the use of formalin-fixed and paraffin-embedded tissues, which were sectioned at five micrometer thickness, mounted on slides and stained with hematoxylin and eosin. All specimens (in both the B12-deficient group and controls) were reviewed by a single histopathologist who was unaware of the individual's B12 status. Biopsy findings were classified as normal (Figure 1A), inflammation (Figures 1B-D), atrophy and intestinal metaplasia (Figures 1B and C). Each specimen was also stained for the presence of *helicobacter*-like organisms using toluidine blue stain with Alcian yellow counterstain (Polyscientific, Bayshore, NY, USA) (Figure 1E). See Table 1 for definitions.

For the purpose of this study, B12 status was defined as normal, borderline and deficient as follows: normal >349 ng/L; borderline 100-349 ng/L; and deficient <100 ng/L. The reference range for cobalamin values in our laboratory is 157-1 059 ng/L. Endoscopic and histopathologic findings were correlated with age, gender, hematocrit

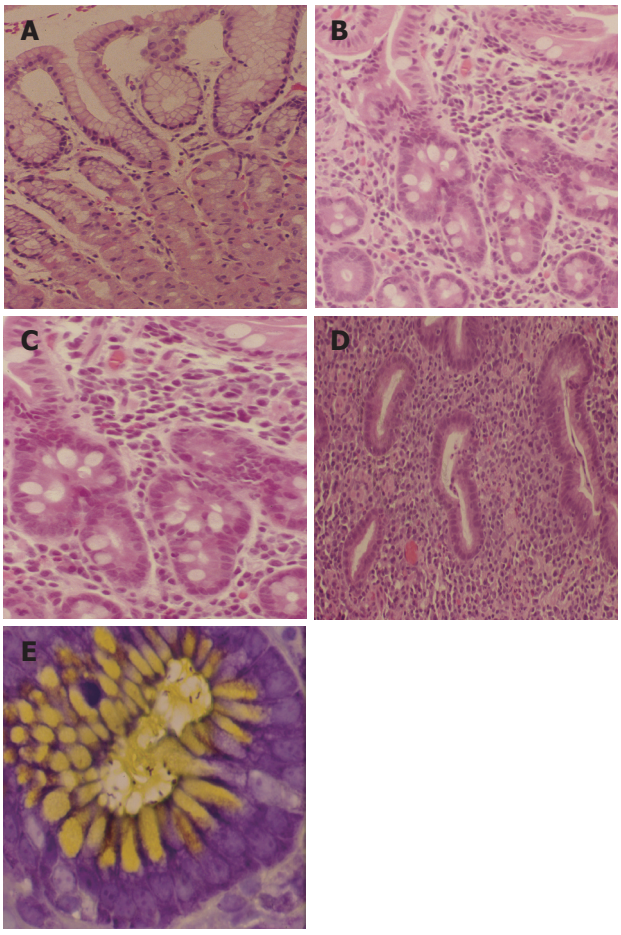

Figure 1 A: Normal histopathologic appearance of the gastric mucosa; **B:** Histopathology of the gastric mucosa, antral type, showing chronic inflammation with metaplasia (low power); **C:** Gastric mucosa, antral type (at higher power than in Figure 1B) showing chronic inflammation with intestinal metaplasia; **D:** Gastric biopsy showing presence of severe chronic active gastritis; **E:** Toluidine blue stain with alcian yellow counterstain of gastric mucosa revealing presence of *H pylori*.

Table 1 Histopathology: Definitions

- Chronic atrophic gastritis (CAG): more extensive inflammation accompanied by glandular atrophy. CAG further subdivided into mild, moderate and severe based on atrophy involving the upper one-third, upper two-thirds and full thickness of the mucosa respectively.
- Chronic superficial gastritis (CSG): inflammation limited to the foveolar region unaccompanied by glandular atrophy. (Figures 1B-1D).
- Gastric atrophy (GA): thinning of the mucosa with an absence of inflammatory changes.
- Hyperplasia: an increase in the number of mucosal epithelial cells.
- Metaplastic changes:
  Intestinal metaplasia characterized by goblet cells, brush border cells, Paneth cells and endocrine cells. (Figures 1B and 1C).
  Pyloric metaplasia of the fundus characterized by mucus secreting glands.

Table 3 Endoscopy findings

B12 deficient group (n=30) (%)		Control group (n=16) (%)	
Normal	11 (36.7)	Normal	5(31.3)
Gastritis	8 (26.7)	Gastritis	11(68.8)
Atrophy	8 (26.7)	Atrophy	0(0)
Polyps	1 (3.3)	Polyps	0(0)
Others [1]	2 (6.7)	Others	0(0)

[1] (includes 1 case of hiatal hernia and 1 case of candidiasis). Endoscopic findings between groups were compared using Fisher's exact test, (P=0.017).

Table 2 Baseline patient characteristics

Variable	B12 deficient (n = 30)	Controls (n = 16)	P-value
Age *(yr)*	78 ± 11	77 ± 8	0.9090 [1]
Gender *(M:F)*	11:19	6:10	1.0000 [2]
Serum B12 *(pg/L)*	183 ± 60	872 ± 459	<0.00005 [1]
Hematocrit *(%)*	34.9 ±4.8	33.4 ± 3.7	0.3010 [1]
MCV *(%)*	86.5 ± 7.6	87.4 ± 9.9	0.7321 [1]
Serum albumin *(g/dL)*	2.9 ± 0.5	2.9 ± 0.7	0.9692 [1]
H pylori infection *(+/-)*	12 / 18	5 / 11	1.000 [2]
Intrinsic factor Ab *(+/-)*	5/ 12	-	-

[1]Data presented as the means ± SD or actual numbers. Statistical comparisons used Student t-tests or χ^2-square analysis.

(Hct), MCV and B12 status. Additional tests, such as serum homocysteine and methylmalonic acid levels, which further delineate cobalamin status, were not performed in this study. Neither did we undertake to elucidate the etiology of B12 deficiency, barring tests for intrinsic factor antibodies in 23 patients in the B12-deficient group.

Statistical analysis

Statistical comparisons of sample means between patients and controls were performed using Student's t-tests while comparisons of proportions were carried out using Fisher' s exact test. Logistic regression analysis was used to examine the effect of aging, gender, and nutritional values on gastric histopathology.

RESULTS

Baseline characteristics of the study samples are shown in Table 2. The results of histopathological and endoscopic findings are shown in Tables 3-8. A statistically significant difference was observed for the endoscopic findings between the B12-deficient patients and controls (P=0.014). The prevalence of normal endoscopic appearance was similar in both groups. However, atrophy was noted only in patients with B12 deficiency, while gastritis was more common in patients with normal B12 status. Polyps, notably of the hyperplastic type, were more frequently detected in the presence of cobalamin deficiency (Table 3). We noted a statistically significant difference in the degree of gastritis between B12-deficient patients and controls (P=0.039). Atrophic gastritis was more common in individuals with B12 deficiency, while superficial gastritis was the most common finding in controls. The incidence of intestinal metaplasia (in the antrum) was similar in the individuals with or without B12 deficiency. None of the controls had features of atrophy on endoscopy or histopathology. In this study, age and gender had no influence on gastric histopathology. In addition, endoscopic findings and gastric histopathology were not related to Hct levels (Tables 4-7).

Our findings suggested that the rate of *H pylori* infection was similar in patients with B12 deficiency and controls (40% *vs* 31%; Table 8). Twenty-six percent of the B12-deficient patients had undiagnosed PA as demonstrated by the presence of intrinsic factor antibodies. Age appeared to have no effect on the presence or absence of intrinsic factor antibodies that is consistent with the literature. Parietal cell antibodies (not tested in our study), which are less specific, are known to increase with age[8]. The presence of intrinsic factor antibodies also was not related to *H pylori* infection (Table 8). Histopathological features also tended to overlap in both the groups.

DISCUSSION

Physiological changes accompanying the aging gut, in particular the stomach, may be difficult to differentiate from the disease[11]. Studies in older adults have suggested a high prevalence of subnormal cobalamin concentrations, and in some reports, an inverse relationship between age and serum cobalamin concentrations[12,13]. The most common etiology of vitamin B12 deficiency is food-cobalamin malabsorption resulting from gastric dysfunction. This entity is defined as the inability to absorb protein (or food) bound cobalamin, although the ability to absorb free cobalamin remains intact. Food cobalamin malabsorption may be a consequence of the use of acid-lowering agents, such as proton pump inhibitors (PPI) and histamine 2 receptor antagonists[2,14,15]. A small proportion of patients on continuous, long-term PPI therapy may manifest reduced cobalamin levels, however, a resultant distinct B12 deficiency is seldom reported[16]. Our earlier data suggested that the use of H2 antagonists and PPI

Table 4 Histopathology of the gastric fundic region

B12 deficient group (n = 27) (%)		Control group (n = 4) (%)	
Normal	3 (11.1)	Normal	0 (0)
Inflammation	16 (59.3)	Inflammation	4 (100)
Atrophy	8 (29.6)	Atrophy	0 (0)

Histopathology findings between groups were compared using Fisher's exact test, (P=0.541).

Table 5 Histopathology of the gastric antral region

B12 deficient group (n = 6) (%)		Control group (n = 12) (%)	
Normal	0 (0)	Normal	2 (14.3)
Inflammation	5 (83.3)	Inflammation	6 (42.9)
Hyperplasia	1 (16.7)	Hyperplasia	0 (0)
Intestinal metaplasia	0 (0)	Intestinal metaplasia	4 (28.6)

Histopathology findings between groups were compared using Fisher's exact test, (P=0.157).

Table 6 Gastritis types

B12 deficient group (n = 29) (%)		Control group (n = 16) (%)	
Normal	3 (10.3)	Normal	1 (6.3)
Superficial gastritis	18 (62.1)	Superficial gastritis	15 (93.7)
Atrophic gastritis	8 (27.6)	Atrophic gastritis	0 (0)

Gastritis types between groups were compared using Fisher's exact test, (P=0.039). The B12 deficient group is 29 in Table 6 *vs* 30 in Tables 7 and 8 because one biopsy sample could not be classified into a specific category.

Table 7 Metaplasia in B12 deficiency and controls

B12 deficient group (n = 30) (%)		Control group (n = 14) (%)	
No metaplasia	22 (73.3)	No metaplasia	10 (71.4)
Hyperplasia	1 (3.3)	Hyperplasia	0 (0)
Intestinal metaplasia	7 (23.3)	Intestinal metaplasia	4 (28.5)

Metaplasia between groups was compared using Fisher's exact test, (P=1.000).

Table 8 Frequency of *H pylori* infection

B12 deficient group (n = 30) (%)		Control group (n = 16) (%)	
H pylori positive	12 (40)	*H pylori* positive	5 (31.2)
H pylori negative	18 (60)	*H pylori* negative	11 (68.8)

Fisher's exact test determined that *H pylori* infection rates were similar in B12 deficient and control patients (P = 1.000) and that the presence of intrinsic factor antibodies was low and unrelated to *H.pylori* infection in the B12 deficient group (1/7 in *H pylori*+ *vs*. 0/10 in *H pylori*– patients, P = 0.338; data not presented).

over two years did not produce cobalamin deficiency[17]. As stated earlier, PA accounts only for a small number of cases of B12 deficiency. PA is characterized by an autoimmune gastric atrophy (GA) mediated by anti-intrinsic factor antibodies. Histomorphologically, PA is characterized by fundic atrophic gastritis (type A) leading to atrophy of the fundus and achlorhydria[18]. While the fundus and the body of the stomach contain acid-secreting gastric parietal cells and pepsinogen-secreting zymogenic cells, the antrum possesses gastrin-producing G cells. Chronic atrophic gastritis (CAG) is histopathologically classified into two types based on the presence or absence of antral involvement[8,19]. Strickland *et al*[19]. originally divided chronic nonspecific gastritis into type A (associated with PA) and type B (not associated with PA). Others have added type C (chemical gastritis, related to drug therapy or bile reflux)[20,21]. Though these concepts are still valid, the discovery of *H pylori* as an important cause of gastritis signifies that type B gastritis is now too broad a category and may not be as useful clinically. Hence, some authors suggest abandoning the alphabetic terminology[20]. Type A (autoimmune) gastritis involves the fundus and the body of the stomach and spares the antrum, whereas type B (non-autoimmune) gastritis involves the antrum as well as the fundus and body. Type A gastritis is associated with PA and the presence of auto-antibodies to gastric parietal cells and to intrinsic factor, achlorhydria, low serum pepsinogen 1 concentrations and high serum gastrin levels as a result of the lack of negative feedback inhibition by gastric acid and consequent hyperplasia of gastrin-producing cells. Type B gastritis, which is more common, is usually associated with *H pylori* infection, alcoholism and various medications, and is characterized by low serum gastrin concentrations because of the destruction of the gastrin-producing cells associated with antral gastritis[8,22]. Gastric biopsy specimens in PA demonstrate a mononuclear cellular infiltrate in the submucosa consisting of plasma cells, T cells and a large non-T cell population, extending into the lamina propria between the gastric glands[8,23]. The infiltrating plasma cells contain auto-antibodies to parietal cell antigen and to intrinsic factor[8,24]. Extension of the cellular infiltrate into the mucosa is accompanied by degenerative changes in parietal cells and zymogenic cells. With fully established lesions, there is a marked reduction in the number of gastric glands, parietal and zymogenic cells, with replacement by mucus containing cells[8]. More common than PA is a state, usually in the older patient, in which there is diffuse severe atrophic oxyntic gland gastritis with achlorhydria but the residual ability to absorb vitamin B12. To prove the existence of severe oxyntic gland gastritis, biopsy specimens are best taken from the midbody region on the greater curve since the mucosa on the lesser curve is thinner and can be falsely interpreted as atrophic. Severe oxyntic gland atrophy is commonly associated with only mild inflammatory cells infiltrate and a reduced prevalence of *H pylori*. The other features include varying amounts of metaplasia[10]. Hyperplastic or inflammatory polyps are the most common lesions found in endoscopic surveys in PA with a prevalence of 10-40%[10,25].

Characteristic gastric features, both gross and histopathologic, are not well described with B12 deficiency resulting from causes other than PA, particularly in older subjects. For this reason, we have attempted to relate gastric histopathology with B12 status in an attempt to examine whether gastric histopathology is a cause or an

effect of B12 deficiency. Furthermore, B12 deficiency can affect proliferating cells at all sites and so an association between B12 status and gastric histopathology would help in the development of strategies for screening and early diagnosis of B12 deficiency based on endoscopic and histopathologic findings.

Our study demonstrated that a normal endoscopic appearance was not correlated with B12 status but that endoscopic findings of atrophy and gastritis were significantly different between B12-deficient patients and controls (P = 0.017). Similar rates of normal and abnormal histopathologic findings were observed in older adults with and without B12 deficiency. Inflammation was the predominant histopathologic finding in older adults with and without B12 deficiency. Our findings suggested that histopathologic findings were variable and not correlated with B12 status, however, a statistically significant difference in the degree of gastritis was noted between the B12-deficient patients and controls (P=0.039). Atrophic gastritis was more common in the B12-deficient patients, while superficial gastritis was more common in the controls. It should also be noted that atrophy was not seen when B12 levels were normal. In these samples of older adults, neither increasing age nor gender influenced gastric histopathology result, while endoscopic findings and gastric histopathology bore no relationship to Hct. There is a strong evidence that *H pylori* infection is associated with cobalamin deficiency; this is true even with non-ulcer dyspepsia or the presence of minimal to no GA[26]. Whether this is merely an association or a cause and effect relationship is unclear. In an earlier study, two-thirds of the patients with atrophic gastritis of the body had *H pylori* infection[27]. Eradication of *H pylori* infection alone has been reported to correct B12 status and improve anemia in B12-deficient individuals[28]. Thus, the possible role of *H pylori* infection in cases of severe food cobalamin malabsorption suggests specific options to prevent and treat B12 deficiency when associated with *H pylori* infection[29].

We observed a 40% rate of *H pylori* infection in patients with cobalamin deficiency compared to a 31% rate in individuals with normal status. Though this finding was not statistically significant (Figure 1E), the comparative trend supported the belief that *H pylori* infection occurs more frequently in B12 deficiency and is consistent with recent studies that implicate *H pylori* as an etiological factor for B12 deficiency[28]. The data may not be uniform in all countries as concluded in a Japanese study that noted higher rates of both *H pylori* infection and atrophic gastritis in Japan where PA is uncommon[30]. The presence of intrinsic factor antibodies were not correlated with the presence or absence of *H pylori* in the present study. Moreover, intrinsic factor antibodies were present in 29% (5/17) of cobalamin-deficient patients, suggesting a higher prevalence of PA than the previously reported prevalence of less than 5% in B12 deficiency patients[31]. Also, age had no effect on the presence or absence of intrinsic factor.

We recognized that this study had some limitations. The total number of subjects was not large, and not every individual had biopsies from the gastric fundus, a site recognized for histopathologic changes in B12 deficiency[18]. In control subjects, although a small number of biopsies were obtained from the fundus, the reality was that a number of biopsies contained inadequate tissue for meaningful interpretation. In addition, intrinsic factor antibodies and ferro-kinetics were not obtained in all the patients. Iron deficiency is known to be associated with gastric histopathological changes and 4 of 19 patients tested with ferro-kinetics were noted to have iron deficiency as demonstrated by the ferritin assay. We also did not have precise data on the specifics of treatment for *H pylori* infection prior to endoscopy. Our aim was to evaluate endoscopic and histopathologic findings in B12 deficiency and controls irrespective of etiology and to attempt to decipher the changes related to cobalamin deficiency. This study made no attempt to delineate the etiology of B12 deficiency in our subjects. As stated, the indication for endoscopy was other than for an evaluation of B12 status. Thus, it is also possible that the primary disease process necessitating the endoscopy may have affected the gastric mucosa and influenced the histopathologic findings. Finally, the extent of injury from medications, bile reflux or infection also could not be assessed.

In conclusion, abnormal gastric endoscopic findings appear to be correlated with B12 levels, with GA being the predominant finding in cobalamin deficiency and gastritis being the common finding when B12 levels are normal. Normal en doscopic findings are also observed in B12-deficient as well as in control subjects. Histopathology results are variable, with a predominance of inflammation that lacks any correlation with B12 deficiency. However, gastritis type does correlate with B12 status in that atrophic gastritis is more prevalent in B12 deficiency and superficial gastritis is more common when B12 status is normal. GA is absent on both endoscopy and histopathology, when B12 levels are normal. Our findings are consistent with literature in that *H pylori* infection is associated with cobalamin deficiency, implicating *H pylori* as an etiological factor for B12 deficiency.

REFERENCES

1 **Herbert CP.** When things do not turn out the way we expect. *Patient Educ Couns* 1999;**37**:1-2

2 **Dharmarajan TS,** Norkus EP. Approaches to vitamin B12 deficiency: Early treatment may prevent devastating complications. *Postgrad Med* 2001; **110:** 99-106

3 **Dharmarajan TS,** Ugalino JT, Kanagala M, Pitchumoni S, Norkus EP. Vitamin B12 status in hospitalized elderly from nursing homes and the community. *J Am Med Dir Assoc* 2000; **1:** 21-24

4 **Dharmarajan TS,** Adiga GU, Norkus EP. Vitamin B12 deficiency: Recognizing subtle symptoms in older adults. *Geriatrics* 2003; **58:** 30-38

5 **Dharmarajan TS,** Adiga GU, Pitchumoni S, Norkus EP. Vitamin B12 deficiency. In: Dharmarajan TS, Norman RA. Clinical Geriatrics, 1st ed., Boca Raton: *CRC Press/Parthenon Publishing,* 2003: 625 - 634

6 **Dharmarajan TS,** Yadav D, Norkus EP, Pitchumoni CS. Vitamin B12 deficiency in older adults: Upper endoscopic and

fundic histopathologic findings in newly diagnosed patients. *J Am Geriatrics Soc* 2001; **49:** S119
7 **Pitchumoni S,** Dharmarajan TS. Vitamin B12, the gastrointestinal system and aging. *Pract Gastroenterol* 2001; **25:** 27- 40
8 **Toh BH,** van Driel IR, Gleeson PA. Pernicious anemia. *N Engl J Med* 1997; **337:** 1441-1448
9 **Pruthi RK,** Tefferi A. Pernicious anemia revisited. *Mayo Clin Proc* 1994; **69:** 144-150
10 **Weinstein WM.** Gastritis and gastropathies. In: Feldman M, Scharschmidt BF, Sleisenger MH. Gastrointestinal and Liver disease, Pathophysiology, *Diagnosis and Management. W. B. Saunders,* 1993: 711-732
11 **Pitchumoni CS,** Kokkat AJ, Dharmarajan TS. The gastrointestinal system. In: Dharmarajan TS, Norman RA. Clinical Geriatrics, 1st ed., Boca Raton: *CRC Press/Parthenon Publishing*, 2003: 416-428
12 **Boger WP,** Wright LD, Strickland SC, Gylfe JS, Ciminera JL, Vitamin B12: Correlation of serum concentrations and age. *Proc Soc Exp Biol Med* 1955; **89:** 375-378 .
13 **Chow BF,** Wood R, Horonick A, Okuda K. Agewise variation of vitamin B12 serum levels. *J Gerontol* 1956; **11:** 142-146
14 **Green R,** Kinsella LJ. Current concepts in the diagnosis of cobalamin deficiency. *Neurology* 1995; **45:** 1435-1440
15 **Marcuard SP,** Albernaz L, Khazanie PG. Omeprazole therapy causes malabsorption of cyanocobalamin (vitamin B12). *Ann Intern Med* 1994; **120:**211-215
16 **Richter JE.** Should patients receiving long-term gastric acid inhibition therapy be evaluated for vitamin B12 deficiency? *Cleve Clin J Med* 2000; **67:** 785-787
17 **Dharmarajan TS,** Patel B, Norkus EP. Do acid lowering agents lower vitamin B12 status in the community elderly? *J Am Coll Nutr* 1999; **18:** 546.
18 **Lehy T,** Roucayrol AM, Mignon M. Histomorphological characteristics of gastric mucosa in patients with Zollinger-Ellison syndrome or autoimmune gastric atrophy, role of gastrin and atrophying gastritis. *Microsc Res Tech* 2000; **48:** 327-338
19 **Strickland RG,** Mackay IR. A reappraisal of the nature and significance of chronic atrophic gastritis. *Am J Dig Dis* 1973; **18:** 426-440
20 **Owen DA.** The stomach. In: Sternberg SS. Diagnostic Surgical Pathology, 3rd ed., Philadelphia: *Lippincott Williams and Wilkins*, 1999: 1310-1327
21 **Wyatt JI,** Dixon MF. Chronic gastritis: a pathogenetic approach. *J Pathol* 1988; **154:** 113-124
22 **Fong TL,** Dooley CP, Dehesa M, Cohen H, Carmel R, Fitzgibbons PL, Perez-Perez GI, Blaser MJ. Helicobacter pylori infection in pernicious anemia: a prospective controlled study. *Gastroenterology* 1991; **100:** 328-332
23 **Kaye MD,** Whorwell PJ, Wright R. Gastric mucosal lymphocyte subpopulations in pernicious anemia and in normal stomach. *Clin Immunol Immunopathol* 1983; **28:** 431-440
24 **Baur S,** Fisher JM, Strickland RG, Taylor KB. Autoantibody containing cells in the gastric mucosa in pernicious anaemia. *Lancet* 1968; **2:** 887-894
25 **Loffeld BC,** van Spreeuwel JP. The gastrointestinal tract in pernicious anemia. *Dig Dis* 1991; **9:** 70-77
26 **Serin E,** Gümürdülü Y, Ozer B, Kayaselçuk F, Yilmaz U, Koçak R. Impact of Helicobacter pylori on the development of vitamin B12 deficiency in the absence of gastric atrophy. *Helicobacter* 2002; **7:** 337-341
27 **Annibale B,** Negrini R, Caruana P, Lahner E, Grossi C, Bordi C, Delle Fave G. Two-thirds of atrophic body gastritis patients have evidence of Helicobacter pylori infection. *Helicobacter* 2001; **6:** 225-233
28 **Kaptan K,** Beyan C, Ural AU, Cetin T, Avcu F, Gülşen M, Finci R, Yalçín A. Helicobacter pylori - is it a novel causative agent in Vitamin B12 deficiency? *Arch Intern Med* 2000; **160:** 1349-1353
29 **Carmel R,** Aurangzeb I, Qian D. Associations of food-cobalamin malabsorption with ethnic origin, age, Helicobacter pylori infection, and serum markers of gastritis. *Am J Gastroenterol* 2001; **96:** 63-70
30 **Haruma K,** Komoto K, Kawaguchi H, Okamoto S, Yoshihara M, Sumii K, Kajiyama G. Pernicious anemia and Helicobacter pylori infection in Japan: Evaluation in a country with a high prevalence of infection. *Am J Gastroenterol* 1995; **90:** 1107-1110
31 **Carmel R.** Cobalamin, the stomach, and aging. *Am J Clin Nutr* 1997; **66:** 750-759

Science Editor Guo SY **Language Editor** Elsevier HK

PO Box 2345, Beijing 100023, China
www.wjgnet.com
wjg@wjgnet.com

ELSEVIER

World J Gastroenterol 2005;11(45):7084-7090
World Journal of Gastroenterology ISSN 1007-9327

• *BASIC RESEARCH* •

Reperfusion injury after critical intestinal ischemia and its correction with perfluorochemical emulsion "perftoran"

Vyacheslav Leontjevich Kozhura, Dmitriy Alexeevich Basarab, Marina Innokentievna Timkina, Arkadiy Mikhailivich Golubev, Vasiliy Ivanovich Reshetnyak, Viktor Vasiljevich Moroz

Vyacheslav Leontjevich Kozhura, Dmitriy Alexeevich Basarab, Arkadiy Mikhailivich Golubev, Vasiliy Ivanovich Reshetnyak, Viktor Vasiljevich Moroz, Research Institute of General Reanimatology, Russian Academy of Medical Sciences, bd. 2, Petrovka str., 25, Moscow 107031, Russia Marina Innokentievna Timkina, Laboratory of Microcirculation and Haemolymphorheology of the Research Institute of General Pathology and Pathophysiology, Russian Academy of Medical Sciences, Baltiiskaya str., 8, Moscow 125315, Russia
Co-first-authors: Vyacheslav Leontjevich Kozhura and Dmitriy Alexeevich Basarab
Co-correspondent: Vasiliy Ivanovich Reshetnyak
Correspondence to: Dr Dmitriy Alexeevich Basarab, MD, Laboratory of Experimental Therapy, Research Institute of General Reanimatology, Russian Academy of Medical Sciences, bd. 2, Petrovka str., 25, Moscow 107031, Russia. basarab_da@pochta.ru
Telephone: +7-95-5200-27-08 Fax: +7-95-209-96-77
Received: 2005-01-12 Accepted: 2005-07-30

Abstract

AIM: To investigate the anti-ischemic properties of perfluorochemical emulsion "perftoran" in mesenteric region.

METHODS: Experiments were conducted on 146 nonlinear white male rats weighing 200-350 g. Partial critical intestinal ischemia was induced by thorough atraumatic strangulation of 5-6 cm jejunal loop with its mesentery for 90 min. Global critical intestinal ischemia was made by atraumatic occlusion of the cranial mesenteric artery (CMA) for 90 min also. Perftoran (PF, 0.8-1.0 mL per 100 g) in experimental groups or 0.9% sodium chloride in control groups was injected at 75 min of ischemic period. Mean systemic arterial blood pressure (BP_M) registration, intravital microscopy and morphological examination of ischemic intestine and its mesentery were performed in both groups.

RESULTS: During 90 min of reperfusion, BP_M progressively decreased to 27.3±7.4% after PF administration *vs* 38.6±8.0% in the control group of rats with partial intestinal ischemia (NS) and to 50.3±6.9% *vs* 53.1±5.8% in rats after global ischemia (NS). During the reperfusion period, full restoration of microcirculation was never registered; parts with restored blood flow had leukocyte and erythrocyte stasis and intra-vascular clotting, a typical "non-reflow" phenomenon. The reduction of mesenteric 50-400 μm feeding artery diameter was significantly less in the PF group than in the control group (24±5.5% *vs* 45.2±3.6%, $P<0.05$) 5 min after partial intestinal ischemia. This decrease progressed but differences between groups minimized at the 90th min of reperfusion (41.5±4.2% and 50.3±2.8%, respectively). In reperfusion of rat's intestine, a significant mucosal alteration was registered. Villous height decreased 2.5-3 times and the quantity of crypts decreased more than twice. In the group of rats administered PF, intestinal mucosal layer was protected from irreversible post-ischemic derangement during reperfusion. Saved cryptal epithelial cells were the source of regeneration of the epithelium, which began to cover renewing intestinal villi after 24 h of blood flow restoration. View of morphological alterations was more heterogeneous in CMA groups.

CONCLUSION: Systemic administration of perftoran promotes earlier and more complete structural regeneration during reperfusion in rats after partial and global critical intestinal ischemia.

Key words: Rats; Ischemia-reperfusion injury; Gut; Intestine; Perfluorocarbon emulsions

Kozhura VL, Basarab DA, Timkina MI, Golubev AM, Reshetnyak VI, Moroz VV. Reperfusion injury after critical intestinal ischemia and its correction with perfluorochemical emulsion "perftoran". *World J Gastroenterol* 2005; 11(45): 7084-7090
http://www.wjgnet.com/1007-9327/11/7084.asp

INTRODUCTION

Prophylaxis and treatment of ischemia-reperfusion injuries in common and especially in mesenteric circulation are the most actual problems of modern-day surgery, intensive care medicine and pathology, and still require improved understanding of the pathophysiology and mechanisms of the development of these disorders[1,2]. Pathophysiological derangement, which occurs after restoration of a blood flow known as the reperfusion syndrome, continues to be responsible for the very high mortality rate in the fields of surgery associated with acute mesenteric occlusion or

intestinal strangulation[3,4]. There is no generally accepted opinion about the critical terms of intestinal ischemia. During this time, the answer to this question has not only theoretical but also important practical significance. For example, this problem is one of the main aspects in the field of intestinal transplantation[5,6].

There has been extraordinary progress in the treatment of ischemia-reperfusion injuries over the past two decades. Though advances have been made in the management of acute vascular occlusion, the optimal treatment of a reperfusion injury is still not defined. Perfluorocarbon emulsion (PFCE) is among the medicines administered in different cases of ischemia-reperfusion injuries. Investigations in this field are one of the most priority branches of scientific researches in the world. Designation and intensive investigation of the effects of PFCE in different fields of biology and medicine have been conducted by a number of Russian scientists since 1979 under the general direction of the Institute of Biological Physics of the Acad. Sci. USSR. Perftoran (OAO NPF "Perftoran", Puschino Russia) is a well-known PFCE containing 20% of perfluorodecalin and perfluo romethylcyclohexylpiperidin stabilized by proxanol-168. The diameter of an average particle is about 0.07 μm. Local (intraluminal or intraperitoneal) administration of PFCE on intestinal ischemia-reperfusion injury has been extensively elucidated[7-13].

MATERIALS AND METHODS

Procedures

All animal procedures were performed in accordance with the recommendations for the proper use and care of laboratory animals. Experiments were performed on 146 white nonlinear adult male pathogen-free rats weighing 200-350 g. Before the surgery, they were anesthetized with pentobarbital sodium (CPF, Tallinn, Estonia) (5-7 mg per 100 g, i m). Except for chronic experiments, tracheostomy cannula was inserted and animals were supported by time-cycled, volume-limited ventilation with room air by mechanical respirator 4601-1 Advanced (Technical and Scientific Equipment, GmbH, Germany) at the frequency of 70 breaths/min and the tidal volume of 5 mL/kg.

Animal models

The rats were then randomized into two groups depending on the type of chosen critical intestinal ischemia. Each group was divided into two subgroups. In the subgroup A, perftoran was used as a protective remedy before reperfusion. In the subgroup B, the same volume of 0.9% sodium chloride was injected as a control.

In group 1 (n = 110), animals were exposed to a critical segmentary (local) tourniquet ischemia of the intestine. This model corresponded to incarcerated hernia or different types of bowel strangulation such as commissural ileus, volvulus, formation of knots and others. After a midline abdominal incision was made, intestinal ischemia was produced by atraumatic strangulation of the jejunal loop (5-6 cm in length) and its mesentery (15-30 cm distal after duodeno-jejunal flexion) with thick tourniquet until visual absence of regional artery pulsation for 90 min. In subgroup 1A (n = 48), perftoran (1 mL per 100 g) was injected slowly intra-arterially (i a) at 75 min of ischemic period. In subgroup IB (control group, n = 62), 0.9% sodium chloride solution was injected i.a. at the same time and volume.

In group 2 (n = 36), rats were exposed to a critical global (total) ischemia of the intestine. This model corresponded to acu 2A (n = 22), PF (1 mL per 100 g, 5-6% of circulating blood volume) was injected i a at 75 min of ischemic period. In subgroup 2B (control group, n = 14), 0.9% sodium chloride solution was injected i.a. at the same time and volume.

External hemoexfusion volume was thoroughly counted during the experiments and 0.95% sodium chloride (2:1) was injected i.a. in order to fill up the blood loss and maintain the volume of circulating plasma. In chronic experiments (n =17), gut contents were replaced in the abdominal cavity, the incision was closed with suture technique and animals were returned to the prone position.

Blood pressure registration

Caudal or femoral arteries were prepared and cannulated by polyethylene (PE)-10 or PE-50 catheters (Becton Dickinson, USA) after i.a. heparin administration (30 ME per 100 g). During the experiments, mean systemic arterial blood pressure (BPM) was monitored by pressure transducers of Bentley Trantec and Statham P231D (Cobe Laboratories, Inc., USA) or MPU-05-290-0-III (San-EI, Japan) connected to the polygraph Schwarzer (Picker International GmBH, Munchen, Germany) or the automatic recorder 142-8 (San-EI, Japan).

Intravital microscopical examination

After a midline abdominal incision was made, the chosen segment of the proximal jejunum with mesentery was extracted on a transparent table of the microscope and covered by a transparent film to prevent tissue withering. Rectal temperature of the animal and intestinal loop was kept at 36.5 ℃. Rat's mesenteric microcirculatory bed was observed under a through-passage light bio-microscope MBI-15 (LOMO, Russia) supplied with photo-camera Zenit-ET (Zenit, Russia), an original device for registration of micro-vessel diameters by the splitting image method[14]. An analogous signal with amplitude proportional to the external vessel diameter was registered simultaneously with BPM line on the automatic recorder 142-8. Diameters of the mesenteric micro-vessels were registered before ischemia and during 90 min of reperfusion.

Morphological examination

Tissue samples were harvested from ischemic zone in experiments with tourniquet intestinal loop strangulation. In experiments with mesenteric occlusion, a very heterogeneous view of the injured intestine was registered. Morphological examination of the different segments of the intestinal wall was performed. Morphological samples were harvested just before the end of 1.5 ischemic period

and after 1.5 and 24 h of reperfusion.

Tissue samples of the intestinal wall were prepared as rings, fixed in 10% neutral buffered formalin and embedded in paraffin. Four-to six-micrometer-thick sections were stained with hematoxylin and eosin and examined under light microscope. PAS-reaction was also conducted. Morphological examination was performed on 243 sections of the rat's intestine by the "blind" method. The numerical six-step scale proposed in 1970 by Chiu *et al*[15]. was used for qualitative evaluation of the degree of the mucosal layer alterations.

Statistical analysis

Data were analyzed with "Microsoft Excel 97 SR-2" statistical software. All values were expressed as mean±SD. Paired and unpaired *t*-criteria were used to test the differences within and between groups, respectively. $P<0.05$ was considered statistically significant.

RESULTS

Microcirculatory disorders

Tourniquet application on the intestinal loop (group I, $n = 42$) led to complete blood flow interruption in the mesenteric bed and intestinal wall. Erythrocyte diapedesis around the mesenteric micro-vessels increased with terms of ischemia. Capillary network structure underwent significant alterations. One minute after tourniquet removal, blood flow was registered visually as a rule, only in the large mesenteric vessels and their branches directly before the intestinal wall, the so-called "feeding" arteries and veins with a diameter from 100 to 400 μm (Figure 1). In smaller vessels, full restoration of microcirculation was never registered; parts with restored blood flow had leukocyte and erythrocyte stasis and intra-vascular clotting, a typical "no-reflow" phenomenon. Hemorrhages occupied considerable areas of intestinal mesentery. During the reperfusion period, decreased blood flow velocity, increased number of leukocytes with activated aggregation and leukocyte-endothelial wall interactions were also registered in the micro-vessels.

During the initial phase of global intestinal ischemia (group 2, $n = 9$) in some large mesenteric arteries, no total stasis but slow blood flow was registered in contrast with total mesenteric occlusion. Probably, total mesenteric occlusion activated the collateral circulation of ischemic intestine in the first few minutes. After 15-20 min of ischemia, full stasis came in the mesenteric bed. After the removal of occluder from CMA, blood flow was restored in large arteries and veins which divides mesentery on transparent "windows" and in branches near the intestinal wall, the "feeding" vessels. In smaller blood vessels of mesentery, the "no-reflow" phenomenon progressed within 90 min of reperfusion.

In general, reperfusion injuries of mesenteric microcirculation did not change either after partial tourniquet ischemia or CMA occlusion, but impairments were more heterogeneous in rats of group 2.

Blood pressure dynamics

Systemic BP_M level during 90 min of partial and global intestinal ischemia and reperfusion is shown in Figure 2A. BP_M level did not change during the ischemic period but abrupt decrease was significant at 5 min of reperfusion (about 40% in cases with CMA occlusion). This systemic BP_M level decrease continued till the end of the observation period (90 min of reperfusion).

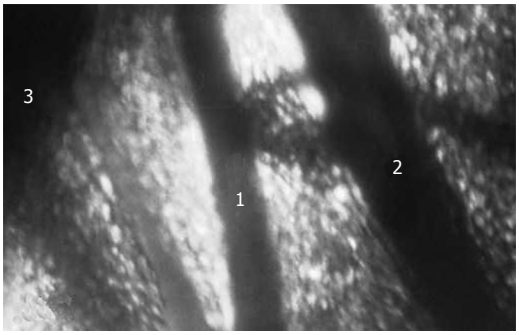

Figure 1 View of the "feeding" artery in rat's intestinal mesentery in light microscope. **1:** "feeding" vein; **2:** "feeding" arteries; **3:** mesenteric edge (wall) of intestine.

Effects of perftoran

Administration of PF in subgroups 1A and 2A (partial and global intestinal ischemia) had no impact on the general picture of microcirculatory alterations in the intestinal mesentery during reperfusion. As in the control group, the systemic BP_M level progressively decreased in the post-ischemic period (Figure 2B). As shown in Figures 2A and B, changes in the BP_M level during reperfusion had no differences after the administration of PF before the end of the ischemic period and in control rats. There were no significant differences between subgroups 1A and B or between subgroups 2A and B.

Though there were no post-ischemic significant changes in microcirculation of rat's intestinal mesenteric bed, intestinal blood supply was restored. During this time, blood flow restoration was not complete because the diameters of the "feeding" arteries in reperfusion period were significantly smaller. In eight rats of the subgroup 1A injected with PF before the end of ischemia, diameter of 19 "feeding" arteries at 5 min of reperfusion became smaller. At the same time, in six rats of subgroup 1B (15 arteries) this value differed ($P<0.05$, Figure 3). During this time, the diameter of mesenteric "feeding" arteries continued to decrease, but differences between groups became less visible after 90 min of reperfusion. In nine rats of subgroup 2A injected with PF before CMA occluding, micro-clamp removing vascular reaction was heterogeneous. The diameter of 15 "feeding" arteries at 5 min of reperfusion was decreased by 10% in comparison with the initial one. In contrast, this value in 10 arteries was increased by 23%. The increase of some feeding artery diameters in post-ischemic period was typically exact for global model of rat's intestinal ischemia.

Morphological examination

Morphological examination of the intestinal wall sections

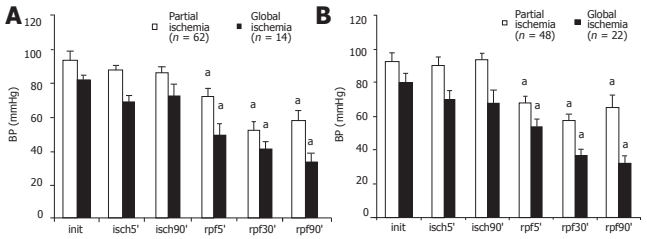

Figure 2 Systemic BP_M at 90 min of partial and global intestinal ischemia and during reperfusion after 0.9% sodium chloride injection (**A**) and perftoran administration (**B**). BP_M level decreased more significantly in groups after CMA occlusion. [a]*P*<0.05 *vs* initial values in each group.

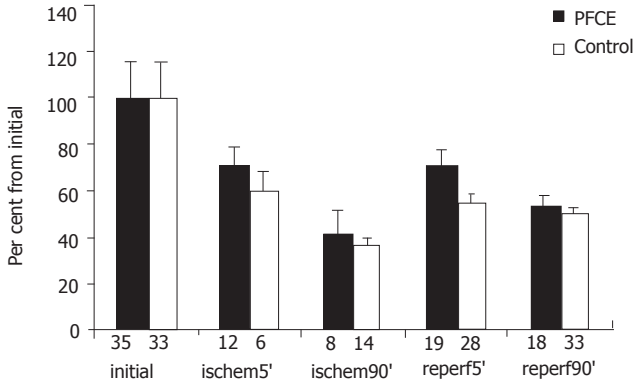

Figure 3 Diameter of "feeding" arteries at 90 min of partial intestinal ischemia and during reperfusion. The recovery of the diameter to initial value during reperfusion was more significant in the group administered PF in comparison with control group. [a]*P*<0.05 *vs* control group; initial – initial values, ischem-ischemic period, reperf-reperfusion.

harvested in group I (partial tourniquet ischemia) only revealed moderate alterations of mucosal layer such as slight apical swelling of intestinal villi with "lifting" of apical epithelium in the ischemic period. But within 90 min after tourniquet removal, degree of intestinal wall alteration progressively increased in comparison to the ischemic period. Therefore, impairment of crypts at 90 min of reperfusion was registered in rats of subgroup IB, spacious parts of intestinal luminal surface were completely denuded with marked villous architecture destruction (Figure 4A). At the same time, in rats of subgroup IA (administered PF) the intestinal wall structural safety was higher in the reperfusion period than in control rats (Figure 4B). Necrobiotic processes and structural changes in rats of subgroup IB progressed with the appearance of focal transmural necroses in the ischemic intestinal wall within 24 h after the end of ischemia (Figure 4C). In rats of subgroup IA (administered PF), alteration was not so significant and even reparative processes such as restoration of villous architecture and epithelial layer regeneration were also marked (Figures 4D and 5). Morphometric analysis data of intestinal wall sections in group I are presented in Table 1.

Morphological examination of intestinal tissue in group II (occlusion of CMA) revealed a number of characteristic

Table 1 Changes in the structure of rat's mucosal layer after 90 min of partial intestinal ischemia (mean±SD)

Groups	Subgroups (number of sections)	Morphometric indexes: Height of villi, μm	number of safety of crypts	degree by epithelium (%)	Chiu scale
Intact	(*n* = 13)	497±25	143±16	100	0
Ischemia (90 min)	(*n* = 8)	524±16	135±44	100	II–III
Ischemia (90 min)	IA (*n* = 5)	200±11[a]	66±16	63±18	III
Reperfusion (90 min)	IB (*n* = 5)	152±20	73±30	56±27	IV
Ischemia (90 min)	IA (*n* = 8)	304±8[a]	77±27[a]	70±19[a]	III
Reperfusion (24 h)	IB (*n* = 9)	168±28	27±33	17±20	IV–V

[a]*P*<0.05 *vs* subgroups IA (with PF) and IB (control).

peculiarities. As in a partial intestinal ischemia, moderate changes in the mucosa appeared only at the end of the ischemic period. Then, damage of mucosal and other layers of the intestinal wall progressively increased during 90 min of reperfusion. Destruction of superficial mucosal layer, erythrocyte diapedes, massive hemorrhages, and leukocyte infiltration of the intestinal wall and mesentery occurred in subgroups 2A and B. In general, view was more heterogeneous than in the intestine of group I rats. Moreover, a lot of rats died after 90 min of CMA occlusion in early reperfusion period because of intoxication and progressing circulatory failure. Results of intestinal wall section morphometric analysis in group II are presented in Table 2.

DISCUSSION

The problem of post-ischemic or reperfusion impairments of organ blood flow restoration arises acutely after pharmacological and surgical intervention. Therapeutic measures have been concentrated on a critical threshold, minimization of cell metabolism and degree of tissue microcirculation reperfusion injuries[16-20]. If significant success is achieved in ischemic disorders, the problem of

Table 2 Changes in the structure of rat's mucosal layer after 90 min of global intestinal ischemia (mean±SD)

Groups	Subgroups (number of sections)	Morphometric indexes: Height of villi, μm	number of safety of crypts	degree by epithelium (%)	Chiu scale
Intact	(*n* = 2)	525±19	125±24	100	0
Ischemia (90 min)	IIA (*n* = 3)	326±28	129±12	100	III
Reperfusion (90 min)	IIB (*n* = 7)	312±18	104±13	90±10	III
Ischemia (90 min)	IIA (*n* = 20)	296±9	118±9	97±3	III
Reperfusion (24 h)	IIB (*n* = 24)	285±9	107±6	91±4	III

There were no significant differences between subgroups 2A (with PF) and B (control).

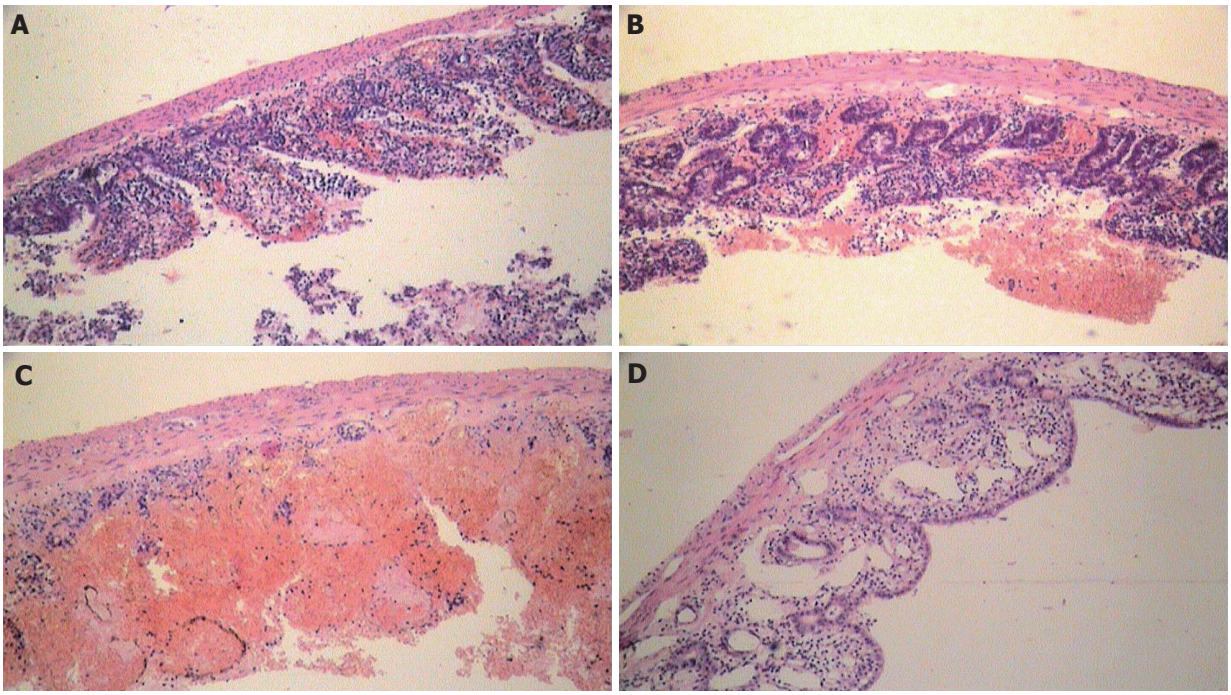

Figure 4 Changes during reperfusion following critical occlusive intestinal ischemia in rats. **A** almost complete denudation and insignificant destruction of villi; **B**: moderate changes after 90 min of reperfusion with perftoran; **C**: insignificant destruction, massive hemorrhages, and focal transmural necrosis formation after 24 h of reperfusion with 0.9% sodium chloride in the intestinal wall of controls; **D**: initial signs of the ischemic intestinal wall regeneration in rats after 24 h of reperfusion after perftoran injection.

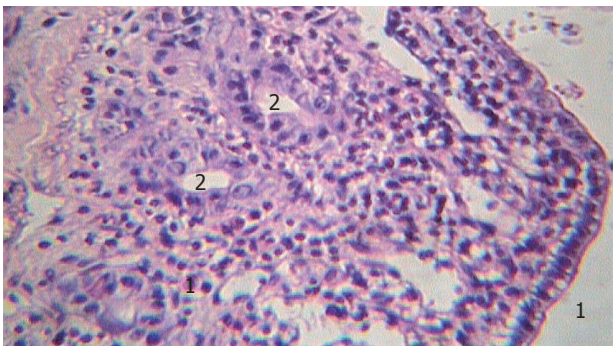

Figure 5 Villi of mucosal layer of the ischemic intestine covered by non-mature cubic epithelium after 24 h of reperfusion (**1**) and saved crypts in the post-ischemic period in rats administered perftoran (**2**).

reperfusion injury prophylaxis is far from its final solution and requires not only ways of correction but thorough investigation of its mechanisms. Investigation of the natural phenomena and main mechanisms of reperfusion injuries at "critical" terms of partial and global intestinal ischemia in rats was conducted in the current work.

The tourniquet partial intestinal ischemia model was chosen in the present work for more homogenous pathomorphological receipts. This model reproduces such disorders as incarcerated hernia and other types of bowel strangulation in clinical practice. The second model occluding CMA corresponds to global intestinal ischemia in consequence of arteriomesenteric thrombosis or embolism.

After significant and irreversible structural and functional changes occurred, the "critical term" (point-of-no-return) was about 90 min for tourniquet segmentary intestinal ischemia in rats. The distinct tendency to stable systemic BP_M level during ischemic period and its abrupt decrease in early reperfusion period were observed. This BP_M level falling was naturally more significant in experiments with CMA occlusion.

Anti-ischemic effect of PF was evaluated in intestinal wall sections from rats that received 0.9% sodium chloride solution. Morphometric analysis was used for quantitative evaluation of rats' intestinal wall alteration degree. A number of morphometric indexes such as the average villous height, number of crypts, epithelial layer safety, and degree of mucosal alteration were analyzed as previously described[15].

The destructive activity increased significantly during reperfusion of ischemic intestine. Mucosa was the most sensitive layer of the intestinal wall. Maximal degree in rat's ischemic intestine was noted at 1.5 h of reperfusion. At the same time, the reperfusion injury strength was significantly smaller in rats that received PF than in controls. In subgroup IA (PF), an explicit regenerative tendency was noted, while destructive process progressed in control rats. In general, luminal surface was covered by low non-mature cubic epithelium, suggesting that crypt's safety is a definitive factor in the viability of ischemic intestine.

It was reported that PFCE has multifunctional properties and is effective in preventing ischemic and reperfusion disorders[21-23]. At the same time, PFCE

administration is extremely limited and its mechanisms are poorly understood.

Differences in the intestinal morphologic structure of rats administered PF and control showed the protective role of PF in the reperfusion period. Though no significant destructive changes were found in mesenteric micro-vascular bed, intestinal circulation was restored during reperfusion period. Nevertheless, blood flow restoration during reperfusion was not complete because of "feeding" artery diameter and systemic BP_M were significantly smaller than before. At 5 min of reperfusion, feeding artery diameter was decreased by 45% in average compared to the control rats. At the same time, feeding artery diameter was decreased by 24% in rats after PF administration, while BP_M level was decreased in both groups (42%), suggesting that there are more feeding arteries after the "critical" ischemia in rats administered PF.

In the analysis of mechanisms of PF protective action on intestinal mucosa, polyfunctional properties of PFCE were taken into account. Therefore, some of them were protected from destruction and mucosal layer regeneration was maintained. Rheological and nitric oxide (NO) transporting properties of PF may take part in this phenomenon.

It is well known that powerful vasodilator NO can protect rat intestine against reperfusion injury[24]. Results of another investigation witness PFCE penetration from blood into endothelial cells of micro-vessels[25], suggesting that PFCE interacts directly with NO in tissues. PF in intestinal microvascular bed may play a role as a NO depot-regulator and protect intestinal wall tissues reperfusion against injury.

PF and NO interactions can be applied to vascular bed of the ischemic intestine. PF may support vasodilatatory potential of mesenteric feeding arteries as a NO depot-regulator during intestinal reperfusion.

In the present study, ischemia-reperfusion systemic and local pathological functional and structural changes were reproduced on experimental models of tourniquet segmentary intestinal loop strangulation and CMA occlusion in rats. "Critical" term (point-of-no-return) for normal thermic tourniquet segmentary intestinal ischemia in rats was about 90 min. Reperfusion could disregulate the systemic blood pressure support system and lead to its abrupt progressive decrease in the early reperfusion period.

In conclusion, the main pathophysiological reperfusion injury of rat's intestine is the significant mucosal alteration. The degree of intestinal changes is proportional to the duration of ischemia. Systemic administration of perftoran before the reperfusion promotes earlier and more complete structural regeneration in rats with critical partial intestinal ischemia.

REFERENCES

1 **Parks DA,** Grøgaard B, Granger DN. Comparison of partial and complete arterial occlusion models for studying intestinal ischemia. *Surgery* 1982; **92:** 896-901

2 **Granger DN.** Ischemia-reperfusion: mechanisms of microvascular dysfunction and the influence of risk factors for cardiovascular disease. *Microcirculation* 1999; **6:** 167-178

3 **Betzler M.** Surgical technical guidelines in intestinal ischemia. *Chirurg* 1998; **69:** 1-7

4 **Bjorck M.** Colonic ischemia after aortoiliac surgery. *Regionar Krovoobr i Microcirc* 2002; **1:** 10-16

5 **Grant D.** Intestinal transplantation: 1997 report of the international registry. Intestinal Transplant Registry. *Transplantation* 1999; **67:** 1061-1064

6 **Bauer R,** Kerschbaumer F. The results of Chiari's medial displacement osteotomy. *Arch Orthop Unfallchir* 1975; **81:** 301-314

7 **O'Donnell KA,** Caty MG, Zheng S, Rossman JE, Azizkhan RG. Oxygenated intraluminal perfluorocarbon protects intestinal muscosa from ischemia/reperfusion injury. *J Pediatr Surg* 1997; **32:** 361-365

8 **Kligunenko EN,** Kompaniets NG. Possibilities of Perftoran application in complex anti-paretic therapy after operations through laparotomy// Perfluorocarbons in Biology and Medicine: Proc. of Symp./Ed. by G.R. Ivanitsky, V.V.Moroz. *Puschino,* **2001:** 133-136, Russian

9 **Maltseva LA,** Mosentsev NF. Effects of Perftoran in patients with septic shock; block of cytokine chain as way of SIRS progression prophylaxis// Perfluorocarbons in Biology and Medicine: Proc. of Symp./Ed. by G.R. Ivanitsky, V.V.Moroz. *Puschino*, **2001:** 210-217, Russian

10 **Ohara M,** Unno N, Mitsuoka H, Kaneko H, Nakamura S. Peritoneal lavage with oxygenated perfluorochemical preserves intestinal mucosal barrier function after ischemia-reperfusion and ameliorates lung injury. *Crit Care Med* 2001; **29:** 782-788

11 **Vejchapipat P,** Proctor E, Ramsay A, Petros A, Gadian DG, Spitz L, Pierro A. Intestinal energy metabolism after ischemia-reperfusion: Effects of moderate hypothermia and perfluorocarbons. *J Pediatr Surg* 2002; **37:** 786-790

12 **Brown MF,** Ross AJ, Dasher J, Turley DL, Ziegler MM, O'Neill JA. The role of leukocytes in mediating mucosal injury of intestinal ischemia/reperfusion. *J Pediatr Surg* 1990; **25:** 214-216; discussion 216-217

13 **Bagnenko SF,** Korolkov SF, Dzhusoev IG. Effect of Perftoran on regeneration of intestinal anastomoses carried out during hemorrhagic shock experimental investigation// Perfluorocarbons in Medicine and Biology: Proc. of Symp./Ed. by G.R. Ivanitsky, E.B. Zhiburt, E.I. Maevsky. *Puschino,* **2003:** 151-154, Russian

14 **Aleksandrov PN,** Chernukh AM. Use of the method of image splitting for vital recording of the diameter of microvessels. *Patol Fiziol Eksp Ter* 1972; **16:** 83-85

15 **Chiu CJ,** McArdle AH, Brown R, Scott HJ, Gurd FN. Intestinal mucosal lesion in low-flow states. I. A morphological, hemodynamic, and metabolic reappraisal. *Arch Surg* 1970; **101:** 478-483

16 **Bilenko MV.** Ischemic and reperfusion injures of organs molecular mechanisms, ways of preventing and treatment. Moscow: *Medicine*, 1989.-368 p, Russian.

17 **Blaisdell FW.** The reperfusion syndrome. *Microcirc Endothelium Lymphatics* 1989; **5:** 127-141

18 **Ar'Rajab A,** Dawidson I, Fabia R. Reperfusion injury. *New Horiz* 1996; **4:** 224-234

19 **Lindsay TF,** Luo XP, Lehotay DC, Rubin BB, Anderson M, Walker PM, Romaschin AD. Ruptured abdominal aortic aneurysm, a "two-hit" ischemia/reperfusion injury: evidence from an analysis of oxidative products. *J Vasc Surg* 1999; **30:** 219-228

20 **Vlasov TD,** Smirnov DA, Nutfullina GM. [Adaptation of the rat small intestine to ischemia] *Ross Fiziol Zh Im I M Sechenova* 2001; **87:** 118-124

21 **Gennaro M,** Mohan C, Ascer E. Perfluorocarbon emulsion prevents eicoasanoid release in skeletal muscle ischemia and reperfusion. *Cardiovasc Surg* 1996; **4:** 399-404

22 **Memezawa H,** Katayama Y, Shimizu J, Suzuki S, Kashiwagi

F, Kamiya T, Terashi A. Effects of fluosol-DA on brain edema, energy metabolites, and tissue oxygen content in acute cerebral ischemia. *Adv Neuro*l 1990; **52:** 109-118

23 **Mosca RS,** Rohs TJ, Waterford RR, Childs KF, Brunsting LA, Bolling SF. Perfluorocarbon supplementation and postischemic cardiac function. *Surgery* 1996; **120:** 197-204

24 **Kubes P.** Ischemia-reperfusion in feline small intestine: a role for nitric oxide. *Am J Physiol* 1993; **264:** G143-G149

25 **Mathy-Hartert M,** Krafft MP, Deby C, Deby-Dupont G, Meurisse M, Lamy M, Riess JG. Effects of perfluorocarbon emulsions on cultured human endothelial cells. *Artif Cells Blood Substit Immobil Biotechnol* 1997; **25:** 563-575

Science Editor Wang XL and Guo SY **Language Editor** Elsevier HK

PO Box 2345, Beijing 100023, China
www.wjgnet.com
wjg@wjgnet.com

ELSEVIER

World J Gastroenterol 2005;11(45):7091-7096
World Journal of Gastroenterology ISSN 1007-9327

• *BASIC RESEARCH* •

Effects of arginine supplementation on splenocyte cytokine mRNA expression in rats with gut-derived sepsis

Huey-Fang Shang, Chun-Sen Hsu, Chiu-Li Yeh, Man-Hui Pai, Sung-Ling Yeh

Huey-Fang Shang, Department of Microbiology and Immunology, Taipei Medical University, Taipei, Taiwan, China
Chun-Sen Hsu, Department of Obstetrics and Gynecology, Taipei Medical University Municipal Wan Fang Hospital, Taipei, Taiwan, China
Man-Hui Pai, Department of Anatomy, Taipei Medical University, Taipei, Taiwan, China
Sung-Ling Yeh, Chiu-Li Yeh, School of Nutrition and Health Sciences, Taipei Medical University, Taipei, Taiwan, China
Supported by a research grant from the National Science Council, Taipei, Taiwan, China. No. NSC 92-2320-B-038-029
Correspondence to: Sung-Ling Yeh, PhD, School of Nutrition and Health Sciences Taipei Medical University, 250 Wu-Hsing Street, Taipei, Taiwan, China. sangling@tmu.edu.tw
Telephone: +8862-27361661
Received: 2005-02-15 Accepted: 2005-06-09

Abstract

AIM: To investigate the effects of arginine (Arg)-enriched diets before sepsis and/or Arg-containing total parenteral nutrition (TPN) after sepsis or both on cytokine mRNA expression levels in splenocytes of rats with gut-derived sepsis.

METHODS: Rats were assigned to four experimental groups. Groups 1 and 2 were fed with a semipurified diet, while groups 3 and 4 had part of the casein replaced by Arg which provided 2% of the total calories. After the rats were fed with these diets for 10 d, sepsis was induced by cecal ligation and puncture (CLP), at the same time an internal jugular vein was cannulated. All rats were maintained on TPN for 3 d. Groups 1 and 3 were infused with conventional TPN, while groups 2 and 4 were supplemented with Arg which provided 2% of the total calories in the TPN solution. All rats were killed 3 d after CLP to examine their splenocyte subpopulation distribution and cytokine expression levels.

RESULTS: Plasma interleukin (IL)-2, IL-4, tumor necrosis factor-α (TNF-α) and interferon (IFN-γ) were not detectable 3 d after CLP. There were no differences in the distributions of CD45Ra+, CD3+, CD4+, and CD8+ cells in whole blood and splenocytes among the four groups. The splenocyte IL-2 mRNA expression in the Arg-supplemented groups was significantly higher than that in group 1. IL-4 mRNA expression in groups 3 and 4 was significantly higher than that in groups 1 and 2. The mRNA expression of IL-10 and IFN-γ was significantly higher in group 4 than in the other three groups. There was no difference in TNF-α mRNA expression among the four groups.

CONCLUSION: The influence of Arg on the whole blood and splenic lymphocyte subpopulation distribution is not obvious. However, Arg administration, especially before and after CLP, significantly enhances the mRNA expression levels of Th1 and Th2 cytokines in the spleen of rats with gut-derived sepsis.

Key words: Arginine; Sepsis; Cytokine mRNA expression

Shang HF, Hsu CS, Yeh CL, Pai MH, Yeh SL. Effects of arginine supplementation on splenocyte cytokine mRNA expression in rats with gut-derived sepsis. *World J Gastroenterol* 2005;11(45): 7091-7096
http://www.wjgnet.com/1007-9327/11/7091.asp

INTRODUCTION

Sepsis is a major cause of death in critically ill patients. Under a condition of sepsis, different endogenous mediators are oversecreted, which may result in an imbalance of the metabolic pathway[1,2]. These metabolic abnormalities that occur during sepsis mainly result from the secretion of cytokines[3]. Cytokines belong to a superfamily of low molecular weight glycoproteins that act as important regulatory proteins, and play a key role in inflammatory responses either directly or by their ability to induce the synthesis of cellular adhesion molecules or other cytokines in numerous cell types[4-6]. Cytokines have beneficial properties in initiating immune responses and maintaining homeostasis in critically ill patients. However, exaggerated or prolonged secretion of cytokines may be detrimental for the host[4-6]. Modulation of cytokines is very important for patients under metabolic stress.

Arginine (Arg) is a semi-essential amino acid that possesses numerous useful physiologic properties[7]. Accumulating experimental and clinical evidence has suggested that Arg reduces protein catabolism and enhances immune function in severely injured animal models and critically ill patients[8–12]. Although a meta-analysis by Heyland *et al*[13]. suggested that immune-enhancing diets rich in Arg may be harmful in unstable critically ill patients, immunonutrition with Arg positively modulates postsurgical immunosuppressive and inflammatory responses[14]. Arg is considered to be an

essential amino acid for patients with catabolic diseases[7,15]. Previous reports by our laboratory showed that preventive use of a Arg-supplemented enteral diet or Arg administered both before and after cecal ligation and puncture (CLP) enhances peritoneal macrophage phagocytic activity and bacterial clearance[16]. Also, total lymphocyte yields in Peyer's patches and intestinal immunoglobin (Ig) A secretion are improved after Arg administration both before and after CLP[17]. In order to understand the protective mechanisms of Arg, the cytokine mRNA expression and protein secretion in septic hosts need to be investigated. However, cytokine protein detection is usually limited, due to lack of sensitive commercial ELISA kits and the short half-life of most cytokines in plasma. Wu *et al*[18]. have investigated the relation between cytokine mRNA expression and organ damage after sepsis. Cui *et al*[19]. reported that an Arg-supplemented diet decreases the expression of inflammatory cytokines in burn rats. As we know, there is no study investigating the effects of Arg on Th1 and Th2 cytokine mRNA expressions of splenocytes in septic rats. Therefore, the aim of this investigation was to study the effect of Arg-supplemented diets before sepsis and Arg-enriched total parenteral nutrition (TPN) after sepsis or both on plasma cytokine levels and splenic cytokine mRNA expression in gut-derived sepsis. Also, the lymphocyte subpopulations of whole blood and splenocytes were analyzed to understand the effects of Arg on the phenotype of lymphocytes in a septic condition.

MATERIALS AND METHODS

Animals

Male Wistar rats weighing 200-230 g were housed in stainless steel cages in a temperature- and humidity-controlled room with a 12:12 h light-dark cycle. Animals were allowed free access to standard rat chow for 3 d prior to the experiment. All procedures conducted in this study were approved by the Taipei Medical University Animal Care Committee.

Surgical procedure and grouping

All rats were divided into four groups. Groups 1 and 2 were fed a semipurified diet. Rats in groups 3 and 4 were fed an identical diet except that part of the casein was replaced by Arg, which provided 2% of the total energy intake (Table 1). After the rats were fed the experimental diets for 10 d, sepsis was induced by CLP according to the method of Wichterman *et al*[20]. Briefly, the rats were anesthetized with intraperitoneal pentobarbital (50 mg/kg), and the abdomen was opened through a midline incision. The cecum was isolated, and a 3-0 silk ligature was placed around it, ligating the cecum just below the ileocecal valve. The cecum was then punctured twice with an 18-gauge needle and placed back into the abdomen. The abdominal wound was closed in two layers.

Immediately after CLP, all rats underwent placement of a catheter for TPN infusion. A silicon catheter (Dow Corning, Midland, MI, USA) was inserted into the right internal jugular vein. The distal end of the catheter was tunneled subcutaneously to the back of the neck, and exited through a coiled spring which was attached to a swivel, allowing free mobility of animals inside individual metabolic cages. TPN at 2 mL/h was administered on the first day. Full-strength TPN (56-64 mL/d, according to body weight) was given thereafter for 3 d. The infusion speed was controlled by a Terufusion pump (Model STC-503, Terumo, Tokyo, Japan). The TPN solution without fat was prepared in a laminar flow hood. Sterilized fat emulsions were added to the TPN solution daily just before use. The TPN solution was infused for the entire day at room temperature. No enteral nutrition was administered during the period of TPN. Groups 1 and 3 were infused with conventional TPN. Groups 2 and 4 were supplemented with Arg, which replaced 10% of the total amino acids, and provided 2% of the total energy of the TPN solution. TPN provided 280 kcal/kg body weight, and the energy (kcal):nitrogen (g) ratio was 119:1. The calorie density was almost 1 kcal/mL. The TPN solutions were isonitrogenous and identical in nutrient composition except for the difference in the amino acid content (Table 2). There were four groups in this study: group 1, no Arg supplementation before or after CLP (–/–); group 2, a semipurified diet given before and Arg-enriched TPN after CLP (–/+); group 3, an Arg-supplemented diet before and conventional TPN after CLP (+/–); and group 4, Arg supplementation both before and after CLP (+/+). There were 10 rats in each group.

Table 1 Composition of the semipurified diet (g/kg)

Ingredients	Arg-supplemented	Non-supplemented
Casein	180	220
Arg	20	–
Total nitrogen	35.2	35.2
Corn starch	677	657
Soybean oi[1]	44	44
Vitamin[1]	10	10
Salt mixture[2]	35	35
Methyl-cellulose	30	30
Choline chloride	1	1
DL-methionine	3	3

[1]The vitamin mix contained 0.6 mg/g thiamine hydrochloride, 06 mg/g riboflavin, 0.7 mg/g pyridoxine hydrochloride, 3 mg/g nicotinic acid, 1.6 mg/g calcium pantothenate, 0.02 mg/g D-biotin, 0.001 mg/g cyanocobalamin, 1.6 mg/g retinyl palmitate, 20 mg/g DL-a-tocopherol acetate, 0.25 mg/g cholecalciferol, and 0.005 mg/g menaquinone. [2]The salt mixture contained 500 mg/g calcium phosphate diabasic, 74 mg/g sodium chloride, 52 mg/g potassium sulfate, 220 mg/g potassium citrate monohydrate, 24 mg/g magnesium oxide, 3.5 mg/g manganese carbonate, 6 mg/g ferric citrate, 1.6 mg/g zinc carbonate, 0.3 mg/g cupric carbonate, 0.01 mg/g potassium iodate, 0.01 mg/g sodium selenite, and 0.55 mg/g chromium potassium sulfate.

Lymphocyte subpopulation distribution in whole blood and spleen

On d 3 after CLP, all surviving rats were weighed and anesthetized with pentobarbital. The survival rates in groups 1-4 were 10/17, 10/19, 10/18, 10/15,

Table 2 Composition of the TPN solution (mL/L)

	Arg-supplemented	Non-supplemented
50% Glucose	412	400
20% Fat emulsion	50	50
10% Moriamin-SN[1]	450	556
Arg (g)	5	–
Infuvita[2]	8	8
3% NaCl	35	35
7% KCl	10	10
8.7%K_3PO_4	10	10
Ca-gluconate	10	10
$MgSO_4$	4	4
$ZnSO_4$	2	2
Choline chloride (g)	1	1

[1]From Chinese Pharmaceuticals, Taipei, Taiwan. Contents per deciliter: 1 250 mg Leu, 560 mg Ile, 1 240 mg Lys acetate, 350 mg Met, 935 mg Phe, 650mg Thr, 130 mg Trp, 450 mg Val, 620 mg Ala, 790 mg Arg, 380 mg Asp, 100 mg Cys, 650 mg Glu, 600 mg His, 330 mg Pro, 220 mg Ser, 35 mg Tyr, and 1 570 mg aminoacetic acid (Gly). [2]From Yu-Liang Pharmaceuticals, Taoyuan, Taiwan. Contents per milliliter: 20 mg ascorbic acid, 660 IU vitamin A, 40 IU ergocalciferol, 0.6 mg thiamine HCl, 0.72 mg riboflavin, 8 mg niacinamide, 0.8 mg pyridoxine HCl, 3 mg D-panthenol, 2 mg dl-a-tocopheryl acetate, 12 μg biotin, 80 μg folic acid, and 1 μg cyanocobalamin.

respectively. There were no differences in the survival rates among the groups as described previously[16]. A middle abdominal incision was made, and the spleen was aseptically removed and teased on a stainless mesh immersed in chilled RPMI-1640 (Gibco, BRL, Grand Island, NY, USA). After filtration through a sterile nylon mesh, cell suspensions were washed thrice in HBSS and resuspended in RPMI-1640. Flow cytometry was used to determine the proportions of CD45Ra, CD3, CD4, and CD8 from the whole blood or splenocytes. One hundred microliters of heparinized whole blood or 10^5 splenocytes suspended in 100 μL HBSS were stained with fluorescein-conjugated mouse anti-rat CD3 (Serotec, Oxford, UK) and phycoerythrin-conjugated mouse anti-rat CD45Ra (Serotec) to distinguish T cells from B cells, respectively. Fluorescein-conjugated mouse anti-rat CD8 and phycoerythrin-conjugated mouse anti-rat CD4 (Serotec) were used to identify T helper cells and cytotoxic T lymphocyte cells, respectively. After staining for 15 min, 1 mL red blood cell (RBC) lysing buffer (Serotec) was added to lyse the RBCs and to fix the stained lymphocytes. Fluorescence data were collected on 5×10^4 viable cells and analyzed by flow cytometry (Coulter, Miami, FL, USA).

Plasma cytokine immunoassay

Plasma interleukin (IL)-2, IL-4, IL-10, interferon (IFN-γ), and tumor necrosis factor (TNF-α) concentrations were determined by commercially available enzyme-linked immunosorbent assay (ELISA) kits (Amersham Pharmacia Biotech, Buckinghamshire, UK).

Primers of cytokines

The primers of IL-2, IL-4, IL-10, TNF-α, and IFN-γ, and the housekeeping gene (18S rRNA) of rats were purchased from PE Applied Biosystems (Foster City, CA, USA).

Real-time reverse-transcription polymerase chain reaction (RT-PCR) method

Total RNA from rat spleen was isolated using the TRIzol reagent according to the manufacturer's protocol. RNA was reverse-transcribed using the Reverse Transcript system (Frementas, Vilnins, Lithuania). Briefly, 20 μL water containing 2 μg RNA was mixed with 1 μL oligo (dT) primer (0.5 μg/μL) and incubated for 5 min at 70 ℃. To the mixture, 22 μL $MgCl_2$ (25 mmol/L), 10 μL 10× RT-buffer, 20 μL dNTP (10 mmol/L), 2 μL RNase inhibitor, and 2.5 μL MultiScribe-RT (50 U/μL) were added and incubated at 25 ℃ for 10 min, then at 42 ℃ for 30 min. The reaction was stopped by heating the samples for 5 min to 95 ℃. cDNA was used for the real-time PCR assay performed with an ABI 7700 Sequence Detection System (PE Applied Biosystems) according to the supplied guidelines. The PCR reaction for IL-2, IL-4, IL-10, IFN-γ and TNF-α was carried out using a TaqMan PCR kit (PE Applied Biosystems).

Statistical analysis

Data were expressed as mean±SD. Differences among the groups were analyzed by ANOVA using Duncan's test. $P<0.05$ was considered statistically significant.

RESULTS

There were no differences in initial body weights and body weights after feeding the experimental diets for 10 d and after TPN administration for 3 d (data not shown). In this study, we were unable to detect plasma IL-2, IL-4, TNF-α and IFN-γ 3 d after CLP. Plasma IL-10 levels could be detected, but there was no difference in IL-10 levels among the groups (data not shown).

No differences in the distribution of CD45Ra+, CD3+, CD4+, and CD8+ cells in blood and splenocytes were observed among the four groups (Figures 1A and 1B). The expression of IL-2 mRNA in splenocytes was significantly higher in the Arg-supplemented groups (groups 2, 3, and 4) than in group 1 (–/–) (Figure 2A). The mRNA expressions of IFN-γ and IL-10 in group 4 (+/+) were significantly higher than in the other three groups (Figures 2B and 2D). IL-4 mRNA expression in groups 3 and 4 was higher than that in groups 1 and 2 (Figure 2C). There were no differences in splenocyte TNF-α mRNA expression among the four groups (Figure 2E).

DISCUSSION

In this study, 2% of total energy was supplied in the diet by Arg. This amount of Arg has been proved to enhance immune functions in rodents with gut-derived sepsis[21]. We administered TPN for 3 d after CLP, because the severity of infection and mortality are the highest at this time point in an established septic animal model[20]. In this

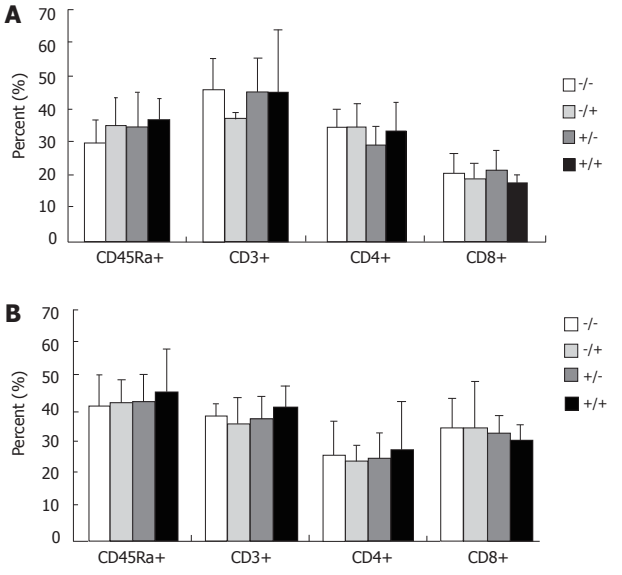

Figure 1 Distribution of CD45Ra+, CD3+, CD4+, and CD8+ lymphocytes in whole blood (**A**) and splenocytes (**B**) among the four groups 3 d after CLP (*n* = 10 in each group).

study, we did not include a sham-operation control (TPN without CLP) group; therefore, this study was not able to assess whether Arg supplementation could restore immune functions comparable to the control rats.

Circulating cytokine levels are usually used as a marker of injury or infection[3]. In order to understand the possible effects of Arg on the systemic cytokine expression in sepsis, IL-2, IL-4, IL-10, IFN-γ, and a pro-inflammatory cytokine TNF-α were measured. IL-2 and IFN-γ were produced by Th1 lymphocytes. Th1 cytokines enhance cell-mediated immunity. A predominant Th1 effect results in activation, growth, and differentiation of T and B lymphocytes as well as macrophages. Th2 cytokines, including IL-4 and IL-10, enhance humoral immunity. A predominant Th2 effect results in the activation of B lymphocytes, upregulation of antibody production, and mucosal immunity[22]. The effects of Th1 or Th2 lymphocytes were counter-regulatory.

In this study, we were unable to detect plasma IL-2, IL-4, TNF-α, and IFN-γ 3 d after CLP. Previous reports by our laboratory showed that IL-1β, IL-2, and IFN-γ were undetectable 24 h after CLP[23,24]. Cruickshank *et al*[25]. also reported that plasma IL-1, TNF, and IFN-γ are rarely detected in the plasma of injured patients. The inability to measure circulating cytokines may be due to a lack of highly sensitive assay kits and late assay times, or due to the fact that the quantities of cytokines do not enter the

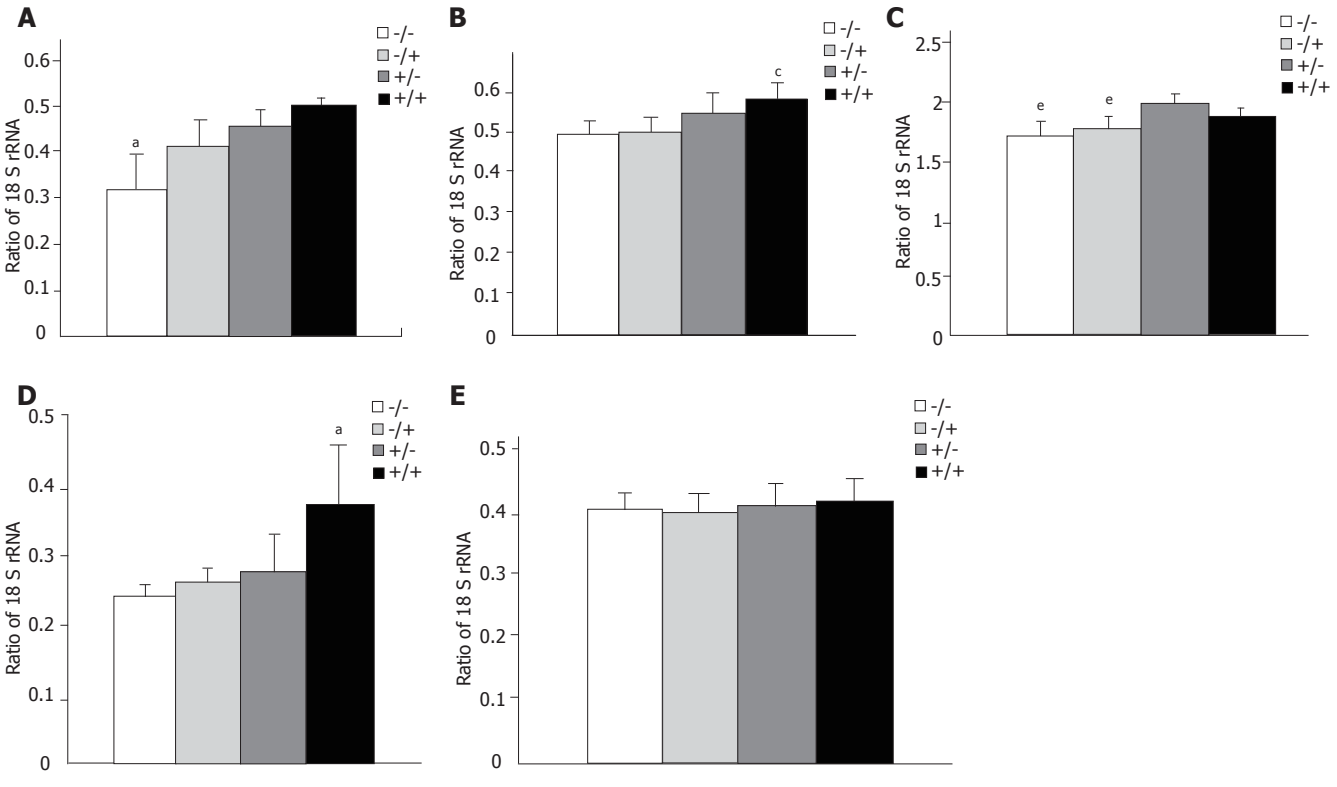

Figure 2 Expression of interleukin (IL)-2 (**A**), interferon (IFN-γ) (**B**), IL-4 (**C**), IL-10 (**D**) and tumor necrosis factor (TNF-**α**) (**E**) messenger RNA in the spleen as determined by real-time reverse-transcription polymerase chain reaction (*n* = 10 in each group). [a]*P*<0.05 *vs* other groups; [c]*P*<0.05 *vs* group 1 (–/–) and group 2 (–/+); [e]*P*<0.05 *vs* group 3 (+/–) and group 4 (+/+).

systemic circulation, even though the levels of cytokines in the tissues have increased[4]. Therefore, we used real-time RT-PCR to quantify splenic cytokine mRNA expression, this is a highly sensitive and reproducible tool to investigate the cytokine profiles at the mRNA level[26,27]. Our findings showed that Arg administration enhanced both Th1 (IL-2, IFN-γ) and Th2 (IL-4, IL-10) cytokine mRNA expression, and Arg given both before and after had a synergistic effect on enhancing cytokine mRNA expression in a septic condition. These results are consistent with our previous report that Arg supplementation promotes intestinal IgA secretion and enhances peritoneal macrophage phagocytic activity in septic rats[16,17]. Although Th1 type cytokines promote the differentiation of cytotoxic T cells, these cytokines usually respond to viral infection and intracellular pathogens. The secretion of IFN-γ may activate macrophages, promote microbicidal activity and stimulate expression of the secretory component for intestinal sIgA by epithelial cells[28]. IL-4 and IL-10 are anti-inflammatory cytokines released by Th2 cells. Furthermore, IL-10 induces the synthesis and secretion of sIgA[22,29,30].

In this study, Arg seemed to have no effect on splenocyte TNF-α mRNA expression. This result is inconsistent with a report by Cui *et al*[19]. who showed that dietary Arg supplementation decreases the mRNA expression of inflammatory cytokines in the spleen after thermal injury. Since the insults of scald burns and gut-derived sepsis differ, the inflammatory cytokine response may vary. Burn injury results in generalized inflammation in organs remote from the region of thermal injury due to activated neutrophil and reactive oxygen metabolites[31,32], whereas CLP causes peritoneal infection with mixed intestinal bacterial flora, which may result in a direct damage to the tissue and organs by circulating bacterial toxins.

In order to understand the effect of Arg on the distribution of lymphocyte subpopulations, the total B lymphocytes (CD45Ra+), total T cells (CD3+), helper T cells (CD4+), and cytotoxic T cells (CD8+) within the blood and splenocytes were evaluated. The results showed that there were no differences in the ratio of B cell and T cell subpopulations among the groups. This finding may indicate that the differences in cytokine mRNA expression after Arg supplementation do not influence the distribution of systemic and splenic lymphocyte subpopulations. Although the effects of Th1 and Th2 lymphocytes are counter-regulatory, cytokine mRNA expression and protein secretion may be regulated by different mechanisms in various tissues and organs, and the final performance of the immune response to specific tissues or organs may vary. Whether there are intracellular factors which regulate the post-transcriptional expression of these cytokines requires further investigation.

In conclusion, the influence of Arg supplementation on the distribution of whole blood and splenic lymphocyte subpopulations is not obvious. However, Arg supplementation, especially before and after CLP, significantly enhances the splenic mRNA expression of Th1 and Th2 cytokines in rats with gut-derived sepsis.

REFERENCES

1 **Souba WW,** Herskowitz K, Klimberg VS, Salloum RM, Plumley DA, Flynn TC, Copeland EM. The effects of sepsis and endotoxemia on gut glutamine metabolism. *Ann Surg* 1990; **211:** 543-9; discussion 549-551
2 **Zellweger R,** Ayala A, DeMaso CM, Chaudry IH. Trauma-hemorrhage causes prolonged depression in cellular immunity. *Shock* 1995; **4:** 149-153
3 **Ertel W,** Morrison MH, Wang P, Ba ZF, Ayala A, Chaudry IH. The complex pattern of cytokines in sepsis. Association between prostaglandins, cachectin, and interleukins. *Ann Surg* 1991; **214:** 141-148
4 **Fong Y,** Moldawer LL, Shires GT, Lowry SF. The biologic characteristics of cytokines and their implication in surgical injury. *Surg Gynecol Obstet* 1990; **170:** 363-378
5 **Baigrie RJ,** Lamont PM, Kwiatkowski D, Dallman MJ, Morris PJ. Systemic cytokine response after major surgery. *Br J Surg* 1992; **79:** 757-760
6 **Foëx BA,** Shelly MP. The cytokine response to critical illness. *J Accid Emerg Med* 1996; **13:** 154-162
7 **Evoy D,** Lieberman MD, Fahey TJ, Daly JM. Immunonutrition: the role of arginine. *Nutrition* 1998; **14:** 611-7
8 **Sitren HS,** Fisher H. Nitrogen retention in rats fed on diets enriched with arginine and glycine. 1. Improved N retention after trauma. *Br J Nutr* 1977; **37:** 195-208
9 **Seifter E,** Rettura G, Barbul A, Levenson SM. Arginine: an essential amino acid for injured rats. *Surgery* 1978; **84:** 224-30
10 **Barbul A,** Sisto DA, Wasserkrug HL, Efron G. Arginine stimulates lymphocyte immune response in healthy human beings. *Surgery* 1981; **90:** 244-251
11 **Barbul A,** Wasserkrug HL, Yoshimura N, Tao R, Efron G. High arginine levels in intravenous hyperalimentation abrogate post-traumatic immune suppression. *J Surg Res* 1984; **36:** 620-4
12 **Daly JM,** Reynolds J, Thom A, Kinsley L, Dietrick-Gallagher M, Shou J, Ruggieri B. Immune and metabolic effects of arginine in the surgical patient. *Ann Surg* 1988; **208:** 512-523
13 **Heyland DK,** Novak F, Drover JW, Jain M, Su X, Suchner U. Should immunonutrition become routine in critically ill patients? A systematic review of the evidence. *JAMA* 2001; **286:** 944-953
14 **Wu GH,** Zhang YW, Wu ZH. Modulation of postoperative immune and inflammatory response by immune-enhancing enteral diet in gastrointestinal cancer patients. *World J Gastroenterol* 2001; **7:** 357-362
15 **De-Souza DA,** Greene LJ. Pharmacological nutrition after burn injury. *J Nutr* 1998; **128:** 797-803
16 **Wang YY,** Shang HF, Lai YN, Yeh SL. Arginine supplementation enhances peritoneal macrophage phagocytic activity in rats with gut-derived sepsis. *JPEN J Parenter Enteral Nutr* 2003; **27:** 235-240
17 **Shang HF,** Wang YY, Lai YN, Chiu WC, Yeh SL. Effects of arginine supplementation on mucosal immunity in rats with septic peritonitis. *Clin Nutr* 2004; **23:** 561-569
18 **Wu RQ,** Xu YX, Song XH, Chen LJ, Meng XJ. Relationship between cytokine mRNA expression and organ damage following cecal ligation and puncture. *World J Gastroenterol* 2002; **8:** 131-134
19 **Cui XL,** Iwasa M, Iwasa Y, Ogoshi S. Arginine-supplemented diet decreases expression of inflammatory cytokines and improves survival in burned rats. *JPEN J Parenter Enteral Nutr* 2000; **24:** 89-96
20 **Wichterman KA,** Baue AE, Chaudry IH. Sepsis and septic shock--a review of laboratory models and a proposal. *J Surg Res* 1980; **29:** 189-201
21 **Gianotti L,** Alexander JW, Pyles T, Fukushima R. Arginine-supplemented diets improve survival in gut-derived sepsis and

peritonitis by modulating bacterial clearance. The role of nitric oxide. *Ann Surg* 1993; **217:** 644-53; discussion 653-654
22 **DiPiro JT.** Cytokine networks with infection: mycobacterial infections, leishmaniasis, human immunodeficiency virus infection, and sepsis. *Pharmacotherapy* 1997; **17:** 205-223
23 **Yeh SL,** Yeh CL, Lin MT, Lo PN, Chen WJ. Effects of glutamine-supplemented total parenteral nutrition on cytokine production and T cell population in septic rats. *JPEN J Parenter Enteral Nutr* 2001; **25:** 269-274
24 **Yeh CL,** Yeh SL, Lin MT, Chen WJ. Effects of arginine-enriched total parenteral nutrition on inflammatory-related mediator and T-cell population in septic rats. *Nutrition* 2002; **18:** 631-635
25 **Cruickshank AM,** Fraser WD, Burns HJ, Van Damme J, Shenkin A. Response of serum interleukin-6 in patients undergoing elective surgery of varying severity. *Clin Sci* (Lond) 1990; **79:** 161-165
26 **Blaschke V,** Reich K, Blaschke S, Zipprich S, Neumann C. Rapid quantitation of proinflammatory and chemoattractant cytokine expression in small tissue samples and monocyte-derived dendritic cells: validation of a new real-time RT-PCR technology. *J Immunol Methods* 2000; **246:** 79-90
27 **Giulietti A,** Overbergh L, Valckx D, Decallonne B, Bouillon R, Mathieu C. An overview of real-time quantitative PCR: applications to quantify cytokine gene expression. *Methods* 2001; **25:** 386-401
28 **Sollid LM,** Kvale D, Brandtzaeg P, Markussen G, Thorsby E. Interferon-gamma enhances expression of secretory component, the epithelial receptor for polymeric immunoglobulins. *J Immunol* 1987; **138:** 4303-4306
29 **Brière F,** Bridon JM, Chevet D, Souillet G, Bienvenu F, Guret C, Martinez-Valdez H, Banchereau J. Interleukin 10 induces B lymphocytes from IgA-deficient patients to secrete IgA. *J Clin Invest* 1994; **94:** 97-104
30 **Mocellin S,** Panelli MC, Wang E, Nagorsen D, Marincola FM. The dual role of IL-10. *Trends Immunol* 2003; **24:** 36-43
31 **Koksal C,** Bozkurt AK, Sirin G, Konukoglu D, Ustundag N. Aprotinin ameliorates ischemia/reperfusion injury in a rat hind limb model. *Vascul Pharmacol* 2004; **41:** 125-129
32 **Till GO,** Beauchamp C, Menapace D, Tourtellotte W, Kunkel R, Johnson KJ, Ward PA. Oxygen radical dependent lung damage following thermal injury of rat skin. *J Trauma* 1983; **23:** 269-277

Science Editor Wang XL and Guo SY **Language Editor** Elsevier HK

PO Box 2345, Beijing 100023, China
www.wjgnet.com
wjg@wjgnet.com

ELSEVIER

World J Gastroenterol 2005;11(45):7097-7103
World Journal of Gastroenterology ISSN 1007-9327

• *BASIC RESEARCH* •

Secretory expression and characterization of a recombinant-deleted variant of human hepatocyte growth factor in *Pichia pastoris*

Zhi-Min Liu, Hong-Liang Zhao, Chong Xue, Bing-Bing Deng, Wei Zhang, Xiang-Hua Xiong, Bing-Fen Yang, Xue-Qin Yao

Zhi-Min Liu, Hong-Liang Zhao, Chong Xue, Bing-Bing Deng, Wei Zhang, Xiang-Hua Xiong, Bing-Fen Yang, Xue-Qin Yao, Department of Microbiological Engineering, Beijing Institute of Biotechnology, 20 Dongdajie Street, Fengtai District, Beijing 100071, China
Supported by the grants from National High Technology Research and Development Program, No. 2002AA2Z345B and No. 2004AA2Z3803 of the Ministry of Science and Technology of China
Correspondence to: Dr Zhi-Min Liu, Department of Microbiological Engineering, Beijing Institute of Biotechnology, 20 Dongdajie Street, Fengtai District, Beijing 100071, China. liuzhm@vip.sina.com
Telephone: +86-10-66948825 Fax: +86-10-63833524
Received: 2005-04-14 Accepted: 2005-06-11

Abstract

AIM: To study the secretory expression of human hepatocyte growth factor (hdHGF) gene in *Pichia pastoris*.

METHODS: The full-length gene of human cDNA encoding the deleted variant of hdHGF was cloned by RT-PCR and overlapping-fragment PCR technique using mRNA of human placenta as a template. The cloned hdHGF cDNA was inserted into the *Escherichia coli-yeast* shuttle vector of pPIC9. The constructed plasmid, pPIC9-hdHGF, was transformed into the GS115 cells of the methylotrophic yeast, *P pastoris,* using a chemical method. The Mut$^+$ transformants were screened to obtain high-expression strains by the test and analysis of expressed products of shake-flask culture. A secretory form of rhdHGF was made with the aid of the leader peptide sequence of *Saccharomyces cerevisiae* α-factor.

RESULTS: The expressed products, which showed a band of molecular mass of about 80 ku, were observed on 15% SDS-PAGE and identified by Western blotting and N-terminal amino acid sequencing. In the high cell density culture of 5 L fermentor by fed-batch culture protocol, the cell biomass was reached at approximately 135 g (DCW)/L. The productivity of secreted total supernant protein concentration attained a high-level expression of more than 8.0 g/L and the ratio of rhdHGF band area was about 12.3% of the total band area scanned by SDS-PAGE analysis, which estimated that the product of rhdHGF was 500-900 mg/L.

CONCLUSION: The *P pastoris* system represents an attractive tool of generating large quantities of hdHGF for both research and industrial purposes.

Key words: Hepatocyte growth factor; *Pichia pastoris*; Secretory expressing

Liu ZM, Zhao HL, Xue C, Deng BB, Zhang W, Xiong XH, Yang BF, Yao XQ. Secretory expression and characterization of a recombinant-deleted variant of human hepatocyte growth factor in *Pichia pastoris*. *World J Gastroenterol;* 2005 11(45): 7097-7103
http://www.wjgnet.com/1007-9327/11/7097.asp

INTRODUCTION

Hepatocyte growth factor (HGF) was identified initially as a mitogen for hepatocytes, called as scatter factor (SF) and fibroblast-derived tumor cytotoxic factor (F-TCF) as well as fibroblast-derived growth factor called plasminogen-like growth factor (PLGF)[1-3]. Nakamura *et al*[16]. reported that HGF could be purified from the serum of partially hepatectomized rats. Subsequently, HGF has been purified from rat platelets and its subunit structure is determined. The purification of human HGF from human plasma is described by Godowski *et al*[5].

The gene locus of human HGF is assigned to chromosome 7q21.1. The genomic gene consists of 18 exons and 17 introns, and spans about 70 kb. The whole length form of human hepatocyte growth factor (preproHGF) consists of 727 amino acids and the mature form of hHGF is composed of 674 amino acids, corresponding to the major form purified from human serum[5]. HGF is a disulfide-linked heterodimer derived by proteolytic cleavage of the human pro-hormone between amino acids R494 and V495. This cleavage process generates a molecule composed of an alpha-subunit of 440 amino acids (MW 69 ku) and a beta-subunit of 234 amino acids (MW 34 ku). The nucleotide sequence of hHGF cDNA reveals that both the alpha-and the beta-chains are contained in a single open reading frame coding for a pre-pro precursor protein. In the predicted primary structure of mature hHGF, an interchain S-S bridge is formed between Cys 487 of the alpha-chain and Cys 604 in the beta-chain. The N-terminus of the alpha-chain is preceded by 54 amino acids, starting with a methionine

group. This segment includes a characteristic hydrophobic leader (signal) sequence of 31 residues and the prosequence. The alpha-chain starts at amino acid (aa) 55 and contains four Kringle domains. The Kringle 1 domain extends from about aa 128 to about aa 206, the Kringle 2 domain is between about aa 211 and about aa 288, the Kringle 3 domain extends from about aa 303 to about aa 383, the Kringle 4 domain extends from about aa 391 to about aa 464 of the alpha-chain. It will be understood that the definition of the various Kringle domains is based on their homology with Kringle-like domains of other proteins (prothrombin, plasminogen). Therefore, the above limits are only approximate. Until now, the function of these Kringles has not been determined. The beta-chain of hHGF shows high homology to the catalytic domain of serine proteases (38% homology to the plasminogen serine protease domain). However, two of the three residues, which form the catalytic triad of serine proteases, are not conserved in hHGF. Therefore, despite its serine protease-like domain, hHGF appears to have no proteolytic activity and the precise role of the beta-chain remains unknown. HGF contains four putative glycosylation sites, which are located at positions 294 and 402 of the alpha-chain and at positions 566 and 653 of the beta-chain. Wild-type human HGF gene *in vivo* exists in the polymorphism. It has been observed that human HGF has a few natural variants. For example, hdHGF-encoded HGF molecule lacking five amino acids in the Kringle 1 domain (FLPSS) is fully functional[6-8].

HGF biological activity refers to any mitogenic, motogenic or morphogenic activities exhibited by wild-type human HGF or hdHGF, which have a broad spectrum of mitogenic cell specificity that can promote the proliferation of hepatocytes, endothelial cells, fibroblasts, melanocytes, and epithelial cells etc.[1,4], inhibit the growth of some tumor cell lines such as $HepG_2$, B6/F1, and KB from tumorigenic target cell lines[9]. Recent studies displayed that hdHGF can exert many important biological effects mediated via their specific tyrosine kinase receptor, C-met. Even to the extent, hdHGF has more significant biological effects on promoting the regeneration of hepatocytes and kidney epithelial cells compared to wild-type human HGF, suggesting that hdHGF has the therapeutic effect *in vivo* on liver injury[2].

Recently, methylotrophic yeast *Pichia pastoris* has become a dominant tool in molecular biology for the production of recombinant proteins. *P pastoris* is known for its high-level expression of heterologous proteins and its tightly regulated alcohol oxidase 1 (AOX1) gene promoter[10]. *P pastoris* can be easily grown to high cell densities using defined minimal media and is able to introduce eukaryotic post-translational modifications[11,12]. The techniques for molecular genetic manipulation are similar to those well established for *Saccharomyces cerevisiae*. At present, *P pastoris* as an efficient protein expression system can be fermented routinely in large scale to meet the industrial demands of interest proteins[13-15]. In the present report, we have described the recombinant production of hdHGF in *P pastoris* and its characterization.

MATERIALS AND METHODS

Strain, vector, reagents, and enzymes

P pastoris host strain GS115 (His^+Mut^+) and secretion expression vector pPIC9 were purchased from Invitrogen (San Diego, CA, USA). *E coli* DH5α was used for routine plasmid amplification and the cloned vector of pUC19 was maintained in our laboratory. Superscript™ II RNase H⁻Reverse transcriptase was purchased from GibcoBRL. Human placenta mRNA was obtained from Clontech Co. Expand™ High Fidelity PCR System was purchased from Boehringer Mannheim Co. Yeast nitrogen base, D-biotin, yeast extract and tryptone were obtained from Sangon (Shanghai, China). *EcoRI*, *NotI, SalI, XbaI, SphI,* T4 DNA ligase, and *Taq* DNA polymerase were obtained from TaKaRa Biotechnology (Dalian, China). Anti-hHGF antibody was purchased from Santa Cruz Biotechnology Co.

Molecular cloning of hdHGF

The whole length gene of human cDNA encoding the deleted variant of hdHGF was amplified by RT-PCR and overlapping fragments were amplified by PCR technique using mRNA of human placenta as the template. Three pairs of PCR primers for amplified hdHGF fragments were designed as follows.

In primer M1, single bottom line stands for SphI and two lines for SalI. Oblique boldface capital letters (included 8 codons) represent the frequently used codons in the highly expressed *P pastoris* genes. In primer M2, single bottom line stands for *XbaI* and two lines for *NotI*. Its complementary chain encodes the sequence for *TACAAGGTTCCACAGTCTTAA* (included 6 codons) and the oblique boldface capital letters represent the bias of codons in the highly expressed *P pastoris* genes. Therefore, the codons encoding N-and C-terminal amino acids of the deleted variant of hdHGF were amplified by RT-PCR and overlapping-fragment PCR technique, using mRNA of human placenta as the template, which has the advantage to acquire high-level expression of foreign genes in *P pastoris*.

A forward primer(P1: 5'TTCTTTCACCCAGGCATCTC3') and a reverse primer (P2: 5'CTATGTTTGTTCGTGTTGG AATCC3') as well as another forward primer (P3: 5'GTGG GACAAAGAACATGGAAGACTTAC3') and its reverse primer (P4: 5'GCTTCAGACACACTTACTT CAGCTA3') were designed to synthesize the two cDNA fragments based on the hdHGF sequence reported by Nakamura *et al*[16], namely one fragment (F1, about 1.6 kb) was amplified using a pair of primers P1 and P2 and the other fragment (F2, approximately 1.0 kb) was amplified using a pair of primers P3 and P4. Overlapping-fragment amplification using F1 and F2 fragments as templates was performed by routine PCR procedure using a pair of primers M1 and M2 (Figure 3). The cDNA product obtained from RT-PCR was modified by introducing *SphI* and *SalI* sites at the 5'end and *XbaI* and *NotI* sites as well as a TAA stop codon at the 3'end. Thirty-five cycles of PCR were performed: denaturation at 94 ℃ for 60 s, annealing at 55 ℃ for 60 s,

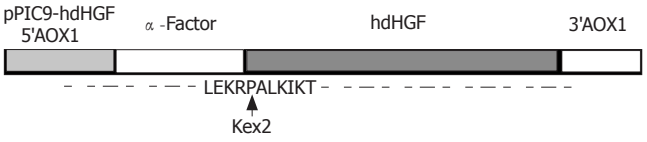

Figure 1 Schematic representation of hdHGF expression cassettes used. Arrowhead indicates the cleavage site of Kex2 protease.

extension at 72 ℃ for 90 s, and then a further extension at 72 ℃ for 10 min. The PCR procedures were carried out according to the standard procedures published earlier[17].

Construction of expression plasmid

The PCR products were digested with *SphI* and *XbaI*, and cloned into the same enzyme digested vector pUC19. The recombinant vectors were transformed into *E coli* DH5 α . The recombinant transformants were acquired via the blue-white colony screening in the agar medium containing X-gal and characterized using restriction endonucleases *SphI* and *XbaI*. The gene sequence analysis of the recombinant pUC-hdHGF was carried out by Sanger's dideoxynucleotide DNA sequencing. The verified hdHGF cDNA fragment with *SalI* and *NotI* was cloned into the site of expression vector pPIC9 digested with *XhoI* and *NotI* enzymes. The recombinant plasmids were transformed into *E coli* strains of JM109. Screening and selection of expression plasmid clones containing hdHGF cDNA fragments through the identification with restriction endonucleases *Bam*HI and *NotI*, resulted in the plasmid pPIC9-hdHGF containing hdHGF gene under the control of AOX1 promoter and in-frame with α -factor signal sequence (Figure 1).

Yeast transformation

Plasmids used for transformation were linearized with *SalI*. The *SalI*-linearized pPIC9-hdHGF or parent pPIC9 was transformed into *his4* competent *P pastoris* GS115 cells by a chemical method. After the growth on minimal dextrose medium (MD) plates at 30 ℃ for 3 d, several colonies containing the linearized pPIC9-hdHGF fragment were selected for PCR confirmation by colony PCR, which was designed to amplify the 200-bp special sequence of pPIC9-hdHGF using a pair of primers, namely P5 (sense, 5'GTGGGACAAGAACATGGAAGA CTTA3') and P6 (antisense, 5'CTATGTTTGTTCGTGTTGGAATCC3').

Expression of hdHGF by recombinant Pichia in shake flask

Ten colonies were used to inoculate 10 mL buffered minimal glycerol-complex medium (BMGY) in a 50 mL shake flask, respectively. After being shook at 250 r/min for 2 d at 30 ℃, the cells were pelleted and resuspended in a 2 mL buffered minimal methanol-complex medium (BMMY). Following the additional 2 d of induction at 30 ℃, the samples of expressed hdHGF in culture supernatants were determined and hdHGF in culture supernatants was also analyzed by SDS-PAGE.

Fed-batch cultivation of P pastoris in a 5-L bioreactor

The clones exhibiting the highest level expression of hdHGF were selected for fed-batch fermentations which were carried out in a 5-L working volume bioreactor using a BIOFLO 3000 (New Brunswick Scientific) interfaced with AFS-Biocommand Bioprocessing software version 2.6 (New Brunswick Scientific) for data acquisition and supervisory control.

Seed culture for the bioreactor was started from the fresh glycerol stock and inoculated directly into 500-mL shake flasks (50-mL working volume) containing a minimum glycerol medium (1.34% YNB, 1% glycerol, and 1.61 μmol/L biotin). After 24 h of growth, seed culture was inoculated with 1% inoculum. After 16-20 h of growth, seed culture was used to inoculate the bioreactor. Ten percentage of the inoculum was used for the inoculation of a 5-L bioreactor containing 2.-L medium of high-cell density fermentation, comprising of 10× basal salts (42 mL/L 85% H_3PO_4, 1.8 g/L $CaSO_4{\cdot}2H_2O$, 28.6 g/L K_2SO_4, 50 g/L glycerol, 23.4 g/L $MgSO_4{\cdot}7H_2O$, 6.5 g/L KOH, and 4.35 mL/L 10·PTM_1 salts, 6.0 g/L $CuSO_4 \cdot 5H_2O$, 0.08 g/L KI, 3.0 g/L $MnSO_4{\cdot}H_2O$, 200 g/L $ZnCl_2$, 0.02 g/L HBO_4, 65 g/L $FeSO_4{\cdot}7H_2O$, 0.2 g/L $Na_2MoO_4{\cdot}2H_2O$, 0.5 g/L $CoCl_2$, 0.2 g/L biotin, and 5 mL/L H_2SO_4, buffered to pH 5.5 using 2 mol/L NH_4OH). Dissolved oxygen was maintained at over 20% air saturation at 30 ℃ and aeration was maintained at 2 vvm. pH was maintained at 5.5 and fermentation was carried out in two phases. Growth phase consisted of a glycerol batch phase and cells were grown batch-wise until glycerol in the medium was utilized. To achieve a high cell density, the glycerol (50% glycerol, 4.3 mL/L PTM_1, feeding rate: 18 mL/h·L) fed-batch phase was initiated and lasted for 6-10 h. Production phase consisted of a methanol fed-batch phase when cells were induced by methanol (100% methanol plus 12 mL/L PTM_1 salts). The methanol feed rate was gradually increased over a period of 6 h-6 mL/h and the fermentation continued for an additional 46-92 h. Expressed hdHGF in culture supernatants was analyzed by SDS-PAGE and the concentration of secreted total supernant proteins was also determined at different intervals of induction phase using the standard curve analysis of human serum albumin (HSA).

Western blotting of rhdHGF

The purified recombinant hdHGF was run in 15% Tris-tricine electrophoresis[20] and then transferred onto a polyvinylidene difluoride (PVDF) membrane and probed with rabbit anti-hdHGF antibody as described previously[19].

RESULTS

Molecular cloning of hdHGF fragments

Based on the hdHGF sequence reported by Nakamura *et al*[16], we designed three pairs of PCR primers for amplified hdHGF fragments. A forward primer P1 and a reverse primer P2 and another forward primer P3 and

its reverse primer P4 were designed to synthesize the two fragments. The two fragments of hdHGF PCR products about 1 570 (F1) and 970 bp (F2), respectively, were also clearly seen in 1% agarose gel electrophoresis stained with 5 mg/mL ethidium bromide amplified with P1-P2 and P3-P4 primer pairs (Figure 2A). Overlapping-fragment PCR amplification using F1 and F2 fragments as templates was performed by routine PCR procedure using a pair of primers M1 and M2 and the PCR product of full-length gene of hdHGF was revealed (Figure 2B).

Construction of the expression plasmid

A cDNA encoding the mature form of hdHGF was used in these experiments. This cDNA consisted of 2.1 kb (Figure 2B) with an open-reading frame encoding a 669 amino acid peptide. The DNA fragment encoding the mature hdHGF was digested with *XhoI* and *NotI* from pUC19 vector and cloned into the same enzyme digested vector pPIC9 downstream of the alcohol oxidase I (AOXI) promoter (Figures 1 and 3). The resultant

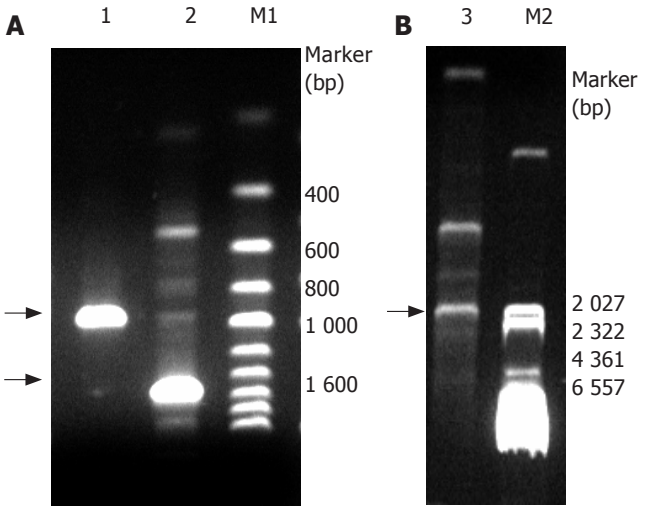

Figure 2 Analysis of PCR products by 1% agarose electrophoresis (**A** and **B**). Lane 1: fragment (F2) amplified with P3-P4 primer pair; lane 2: fragment (F1) amplified with P1-P2 primer pair; lane 3: fragment (whole length) amplified with M1-M2 primer pair; M1: 200-bp ladder marker; M2: λ+*Hind*III marker. The arrowheads show the bands of the interesting fragments

construct harbored a single open reading frame encoding a 85 amino acid translation product consisting of the α-factor secretion leader peptide (Figures 1 and 3). Prior to the secretion of the peptide into the culture medium, the signal peptide should be cleaved off by the *KEX2* gene products at the site (Glu-Lys-Arg-X) (Figure 1). The integrity of the recombinant plasmid was confirmed by direct DNA sequencing. Enzyme identification of the recombinant plasmids of pPIC9-hdHGF digested by *BamHI* and *NotI* is shown in Figure 4. This constructed vector was linearized with *SalI* and transformed into the competent cells of *P pastoris* GS115. The transformants were selected on MD plates and confirmed by colony PCR. Forty-one colonies presenting strong amplification

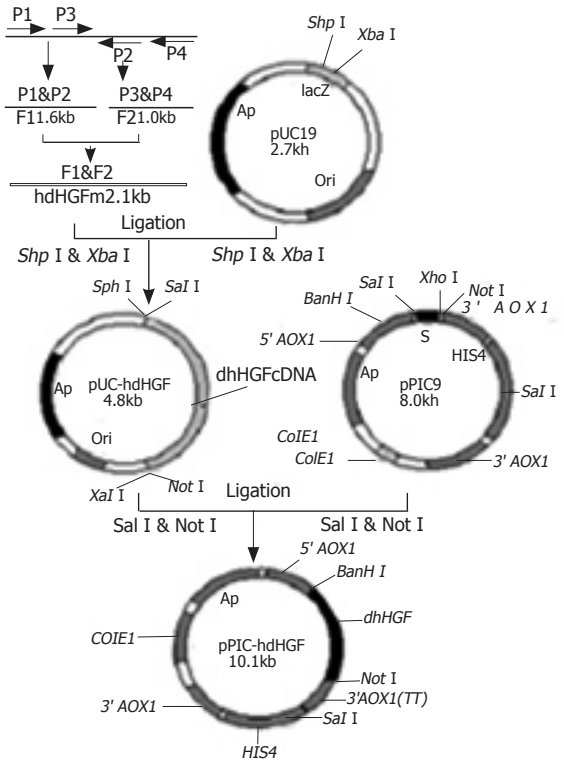

Figure 3 Cloning of hdHGF cDNA and construction of expression vectors pUC-hdHGF and pPIC9-hdHGF.

products were used for small-scale expression trials and the amount of the recombinant peptide was determined by SDS-PAGE.

Expression of recombinant hdHGF in shake flask

We investigated the expression of recombinant hdHGF by both Mut^s and Mut^+ (GS115) strains in shake flasks. Since SDS-PAGE analysis revealed that the hdHGF level expressed by Mut^s strain was much higher than that of Mut^+ (data not shown), Mut^s was chosen for the expression of th e growth factor. In addition, Mut^s phenotype was selected over the Mut^+ phenotype because

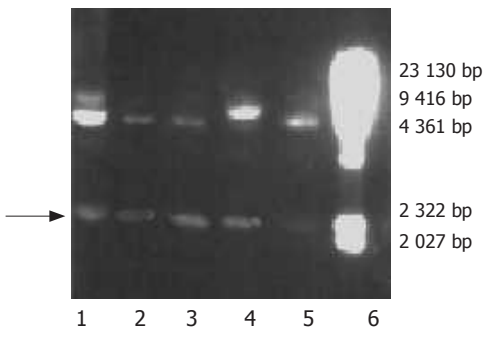

Figure 4 Agarose electrophoresis analysis of restriction enzyme mapping of recombinant plasmids of pPIC9-hdHGF. Lanes 1-5: recombinant plasmids of pPIC9-hdHGF digested by *Bam*HI and *Not*I; lane 6: λ-DNA/*Hind*III marker. The arrowhead reveals bands of the interesting fragment.

of the latter's higher oxygen requirement that could result in oxygen-deficient conditions within the bioreactor. Fifty transformants (Mut^s) were used for the expression studies in shake flask experiments and secretion of the recombinant hdHGF into the culture medium was determined by SDS-PAGE analysis. The expression experiments were performed to screen out four high-level expression strains of hdHGF, which were named as HG209, HG211, HG305, and HG309 (Figure 5).

Expression of recombinant hdHGF in fermenter cultures

The selected clones with the highest expression level were chosen for fed-batch cultivation. A time-course study of

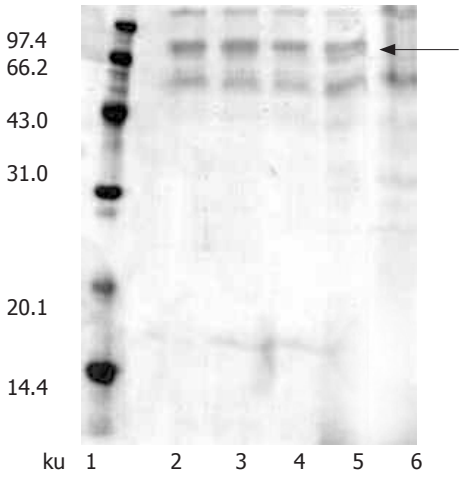

Figure 5 Fifteen percentage SDS-PAGE analysis of high expression strains in shake-flask culture.Lane 1: LMW marker; lane 2: GH209; lane 3: HG211; lane 4: HG305; lane 5:HG309; lane 6: GS115. The arrowhead shows bands of the interesting protein.

secretion of hdHGF revealed a gradual accumulation of recombinant cytokines. The effect of induction pH on the production of recombinant cytokines was investigated. *P pastoris* is known to grow over a wide pH range from 3 to 7, with a minimal effect of pH on the growth rate. However, pH could significantly affect the productivity of secreted recombinant proteins in the fermentation broth. To find out the optimal pH for the expression of recombinant hdHGF, we conducted experiments with pH between 3.5 and 6.5 during the fed-batch production phase. The highest yield of recombinant hdHGF was observed at pH 5.5 (Figure 6).

Protein expression was initiated by changing carbon source from glycerol to methanol. At first, we attempted to express hdHGF in baffled shake flasks and obtained about 50 mg/L of hdHGF secreted into the medium after 72-h induction. For more systematic production of hdHGF, we expressed the protein using fermenter cultures. Figure 6 shows the secretion level of hdHGF using 5 L fermenter. Upon depletion of glycerol, the dry cell weight reached 45.6 g/L. A glycerol fed-batch phase was performed for an additional 6-12 h and the cell biomass reached at

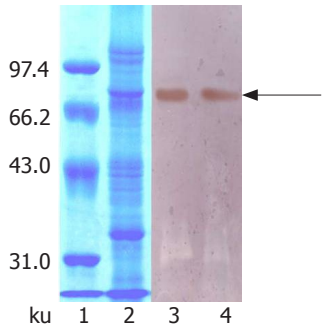

Figure 6 Fifteen percentage SDS-PAGE and Western blotting analysis of the 5-L fed-batch high cell density fermentation of GH209. Lane 1: LMW marker; lane 2: 10% SDS-PAGE result; lanes 3 and 4: Western blotting result. The arrowhead shows bands of the interesting protein.

approximately 135 g (DCW)/L. Induction of hdHGF was initiated by the addition of 100% methanol containing 12 mL of PTM1 trace salts/L. Sample analysis at different intervals was also performed to show the increasing amounts of recombinant hdHGF presented in the culture medium with increasing induction time until 96 h. Dissolved oxygen (DO) was monitored by DO sensor and the oxygen transfer rate 1 min after turning off the carbon source feed. Dissolved oxygen was maintained between 20% and 30% air saturation in the two-phase fermentation. The secreted total supernant protein concentration in the induction phase was traced and observed to attain the high-level expression of more than 8.0 g/L after 84-96 h of induction cultivation, which was determined using the standard curve analysis of human serum albumin (HSA). The scanning result showed that the secreted rhdHGF protein band (in lane 3 of Figure 6) achieved about 12.3% of the total supernatant proteins. By comparison with the standard protein markers, the estimated product of rhdHGF was 500-900 mg/L. The maximum secretion yield was approximately 980 mg/L (Figure 6). Upon induction by methanol, four clones secreted a specific 80-ku protein with the same size as the standard HGF. The productivity varied among the four high-level expression strains of hdHGF.

These clones indicated that the highest product of rhdHGF was named HG209 (GS115/pPIC9-hdHGF) and selected for further analysis. Western blotting analysis showed that the 80-ku protein band from HG209 (GS115/pPIC9-hdHGF) reacted specifically with the rabbit anti-hHGF antiserum (Figure 6). The N-terminal sequence of the recombinant hdHGF was determined to be PALKI, which was identical to the N-terminal sequence of native hdHGF (Figure 1).

DISCUSSION

hdHGF is a large complex protein comprising of 669 amino acids. It is the most potent multifunctional cytokine on the regeneration of hepatocytes and kidney epithelial cells compared to wild-type human HGF[20]. It can promote cell division, migration, and differentiation.

Its receptor is the product of oncogene c-met. Besides being a nutritional factor of liver and kidney, hdHGF also promotes angiogenesis for peripheral artery disease and myocardial ischemia[20] and can affect synthesis of extracellular matrix and matrix metalloproteinases and tissue inhibitor of metalloproteinases in autosomal dominant polycystic kidney disease cyst-lining epithelial cells[21].

Since the concentration of native HGF in plasma is very low, purification of HGF from plasma is very difficult. It was reported that HGF is expressed in foreign gene expression systems such as mammalian cells, CHO cells[22,23], insect cells[24], and gene therapy[25]. Dang *et al*[26] and Li *et al*[27]. reported that the HGF gene is expressed in *E coli* and *P pastoris*. However, the expression of recombinant-deleted variants of human hepatocyte growth factor (hdHGF) has not been reported in yeast expression system. Therefore, in this investigation, we used the methylotrophic yeast *P pastoris* as the host for the high-level expression and secretion of recombinant hdHGF. Recombinant hdHGF was successfully secreted by *P pastoris* and the productivity of secreted total supernatant protein concentration attained high-level expression of more than 8.0 g/L and the ratio of rhdHGF band area was about 12.3% of the total band area scanned by SDS-PAGE analysis, which estimated the product of rhdHGF to be 500-900 mg/L. It had an approximately fivefold increase in productivity compared to that of HGF expressed in *P pastoris*[27]. Western blot analysis showed that the 80-ku protein band of GS115 (pPIC9-hdHGF) reacted specifically with the rabbit anti-hHGF antibody. N-terminal sequencing revealed that recombinant rhdHGF had the correct N-terminal amino acid sequence. These results suggest that the optimization of bias codons of *P pastoris* encoding N-and C-terminal amino acids of hdHGF via PCR-mediated codon replacement can acquire high-level expression of foreign genes in *P pastoris*. Nakamura *et al*[16]. reported that native hdHGF is composed of an alpha-subunit of 440 amino acids (MW 69 ku) and a beta-subunit of 234 amino acids (MW 34 ku). However, we found that the recombinant hdHGF produced by *P pastoris* was translated as a single-chain polypeptide comprising of 669aa, which was not cut by the proteolytic cleavage of the human pro-hormone between amino acids R494 and V495 in host cells of *P pastoris*.

In conclusion, though further characterization, bioassay, and optimization of the expression and cultivation of recombinant hdHGF by *P pastoris* are required, this expression system of hdHGF is expected to be a powerful tool in the industrial production of this foreign protein.

REFERENCES

1 **Kataoka H,** Miyata S, Uchinokura S, Itoh H. Roles of hepatocyte growth factor (HGF) activator and HGF activator inhibitor in the pericellular activation of HGF/scatter factor. *Cancer Metastasis Rev* 2003; **22:** 223-236

2 **Kinosaki M,** Yamaguchi K, Murakami A, Morinaga T, Ueda M, Higashio K. Analysis of deleted variant of hepatocyte growth factor by alanine scanning mutagenesis: identification of residues essential for its biological function and generation of mutants with enhanced mitogenic activity on rat hepatocytes. *FEBS Lett* 1998; **434:** 165-170

3 **Weidner KM,** Arakaki N, Hartmann G, Vandekerckhove J, Weingart S, Rieder H, Fonatsch C, Tsubouchi H, Hishida T, Daikuhara Y. Evidence for the identity of human scatter factor and human hepatocyte growth factor. *Proc Natl Acad Sci U S A* 1991; **88:** 7001-7005

4 **Matsumoto K,** Nakamura T. Emerging multipotent aspects of hepatocyte growth factor. *J Biochem* (Tokyo) 1996; **119:** 591-600

5 **Godowski PJ,** Lokker NA, Mark MR. Single-chain hepatocyte growth factor variants. *United States Patent* 5580963, 1996

6 **Shima N,** Tsuda E, Goto M, Yano K, Hayasaka H, Ueda M, Higashio K. Hepatocyte growth factor and its variant with a deletion of five amino acids are distinguishable in their biological activity and tertiary structure. *Biochem Biophys Res Commun* 1994; **200:** 808-815

7 **Kinosaki M,** Yamaguchi K, Murakami A, Ueda M, Morinaga T, Higashio K. Identification of heparin-binding stretches of a naturally occurring deleted variant of hepatocyte growth factor (dHGF). *Biochim Biophys Acta* 1998; **1384:** 93-102

8 **Yasuda H,** Imai E, Shiota A, Fujise N, Morinaga T, Higashio K. Antifibrogenic effect of a deletion variant of hepatocyte growth factor on liver fibrosis in rats. *Hepatology* 1996; **24:** 636-642

9 **Shiota G,** Rhoads DB, Wang TC, Nakamura T, Schmidt EV. Hepatocyte growth factor inhibits growth of hepatocellular carcinoma cells. 1992; **89:** 373-377

10 **Cregg JM,** Vedvick TS, Raschke WC. Recent advances in the expression of foreign genes in Pichia pastoris. *Biotechnology* (N Y) 1993; **11:** 905-910

11 **Brierley RA,** Bussineau C, Kosson R, Melton A, Siegel RS. Fermentation development of recombinant Pichia pastoris expressing the heterologous gene: bovine lysozyme. *Ann N Y Acad Sci* 1990; **589:** 350-362

12 **O'Leary JM,** Radcliffe CM, Willis AC, Dwek RA, Rudd PM, Downing AK. Identification and removal of O-linked and non-covalently linked sugars from recombinant protein produced using Pichia pastoris. *Protein Expr Purif* 2004; **38:** 217-227

13 **Zhang W,** Li ZJ, and Foster A Agblevor. Microbubble fermentation of recombinant Pichia pastoris for human serum albumin production. *Process Biochemistry* 2005; **40:** 2073-2078

14 **Werten MW,** van den Bosch TJ, Wind RD, Mooibroek H, de Wolf FA. High-yield secretion of recombinant gelatins by Pichia pastoris. *Yeast* 1999; **15:** 1087-1096

15 **Cregg JM,** Cereghino JL, Shi J, Higgins DR. Recombinant protein expression in Pichia pastoris. *Mol Biotechnol* 2000; **16:** 23-52

16 **Nakamura T,** Nishizawa T, Hagiya M, Seki T, Shimonishi M, Sugimura A, Tashiro K, Shimizu S. Molecular cloning and expression of human hepatocyte growth factor. *Nature* 1989; **342:** 440-443

17 **Sambrook J and Russell DW.** Molecular cloning: A Laboratory Manual. Cold Spring Harbor Laboratory Press, Third Edition, *New York*, 2001

18 **Schägger H,** von Jagow G. Tricine-sodium dodecyl sulfate-polyacrylamide gel electrophoresis for the separation of proteins in the range from 1 to 100 kDa. *Anal Biochem* 1987; **166:** 368-379

19 **Sanchez JC,** Wirth P, Jaccoud S, Appel RD, Sarto C, Wilkins MR, Hochstrasser DF. Simultaneous analysis of cyclin and oncogene expression using multiple monoclonal antibody immunoblots. *Electrophoresis* 1997; **18:** 638-641

20 **Jin H,** Wyss JM, Yang R, Schwall R. The therapeutic potential of hepatocyte growth factor for myocardial infarction and heart failure. *Curr Pharm Des* 2004; **10:** 2525-2533

21 **Yuan AH and Mei CL.** effects of hepatocyte growth factor on synthesis of extracellular matrix and matrix metalloproteinases and tissue inhibitor of metalloproteinases in autosomal dominant polycystic kidney disease cyst-lining epithelial cells. *Dier Junyi Daxue Xuebao* 2003; **24:** 11-17

22 **Wu SG,** Yu CL, Xu W, Guo YJ, and Ce XY. Expression and

biological activity of human hepatocyte growth factor (HGF) by Chinese hamster ovary (CHO) cells. *Diyi Junyi Daxue Xuebao* 1995; **15:** 321-324

23 **Qiu YC,** Zhu ZG, Xu JH, Xu W, Wu SG. Purification and identification of human recombinant hepatocyte growth factor expressed by CHO cells. *Acad J First Mil Med Univ* 2001; **21**: 332-333

24 **Wang MY,** Yang YH, Lee HS, Lai SY. Production of functional hepatocyte growth factor (HGF) in insect cells infected with an HGF-recombinant baculovirus in a serum-free medium. *Biotechnol Prog* 2000; **16:** 146-151

25 **Bosch A,** McCray PB, Walters KS, Bodner M, Jolly DJ, van Es HH, Nakamura T, Matsumoto K, Davidson BL. Effects of keratinocyte and hepatocyte growth factor in vivo: implications for retrovirus-mediated gene transfer to liver. *Hum Gene Ther* 1998; **9:** 1747-1754

26 **Dang SY,** Cheng NL, Niu B, Wang HZ, Zhao JB. Expression of human recombinant hepatocyte growth factor heavy chain in Escherichia coli. *J Shanxi Med Univ* 2000; **31**: 481-483

27 **Li XG,** Gu YL, Zhu YS, Song HY. Molecular cloning of cDNA gene encoding human hepatocyte growth factor and its expression with Pichia. *Pharmaceutical Biotechnology* 1997; **4**: 193-197

Science Editor Wang XL and Guo SY **Language Editor** Elsevier HK

PO Box 2345, Beijing 100023, China
www.wjgnet.com
wjg@wjgnet.com

ELSEVIER

World J Gastroenterol 2005;11(45):7104-7108
World Journal of Gastroenterology ISSN 1007-9327

• *BASIC RESEARCH* •

A novel gain of function mutant in C-kit gene and its tumorigenesis in nude mice

Chen-Guang Bai, Xiao-Hong Liu, Qiang Xie, Fei Feng, Da-Lie Ma

Chen-Guang Bai, Qiang Xie, Fei Feng, Da-lie Ma, Department of Pathology, Changhai Hospital, Second Military Medical University, Shanghai 200433, China
Xiao-Hong Liu, Institute of Thoracic Cardiac Surgery, Changhai Hospital, Second Military Medical University, Shanghai 200433, China
Supported by the National Natural Science Foundation of China, No. 30070743 and No. 30471702
Co-first-authors: Chen-Guang Bai and Xiao-Hong Liu
Correspondence to: Da-Lie Ma, Professor of Department of Pathology, Changhai Hospital, Second Military Medical University, Changhai Road, Shanghai 200433, China. madalie@126.com
Telephone: +86-21-25074851 Fax: +86-21-25070660
Received: 2005-04-15 Accepted: 2005-06-06

Abstract

AIM: To transfect mutant C-kit cDNA at codon 579 into human embryonic kidney cell line to observe its role in the pathogenesis of gastrointestinal stromal tumor (GIST).

METHODS: Eukaryotic expression vectors of pcDNA3-Kit-NW and pcDNA3-Kit-W were constructed. Then pcDNA3-Kit-NW and pcDNA3-Kit-W plasmids were transfected into human embryonic kidney cell line by Lipofectamine. The resistant clone was screened by G418 filtration and identified by sequencing, Western blotting, and immunocytochemical staining. Human embryonic kidney cells were divided into three groups including pcDNA3-Kit-NW, pcDNA3-Kit-W, and vector control groups. Absorbency value with a wavelength of 574 nm was detected by MTT analysis. Mice were injected with three groups of cells. Volume, mass, and histological examinations of the tumors in different groups were measured and compared.

RESULTS: The C-kit gene and mutant C-kit gene were successfully cloned into the eukaryotic expression vector pcDNA3. pcDNA3-Kit-NW and pcDNA3-Kit-W were successfully transfected into human embryonic kidney cell line and showed stable expression in this cell line. Cell proliferating activity had significant differences between pcDNA3-Kit-NW and pcDNA3, pcDNA3-Kit-NW and pcDNA3-Kit-W ($P<0.05$), respectively. Tumors were only observed in nude mice implanted with cells transfected with pcDNA3-Kit-NW.

CONCLUSION: Mutation of C-kit gene increases the proliferation activity of human cells and plays an important role in the malignant transformation of GIST.

Key words: Gastrointestinal stromal tumors; Protooncogene C-kit; Gene mutation; Malignant transformation

Bai CG, Liu XH, Xie Q, Feng F, Ma DL. A novel gain of function mutant in C-kit gene and its tumorigenesis in nude mice. *World J Gastroenterol* 2005; 11(45): 7104-7108
http://www.wjgnet.com/1007-9327/11/7104.asp

INTRODUCTION

Gastrointestinal stromal tumor (GIST) is a designation for a major subset of mesenchymal tumors of the gastrointestinal tract. Their line of differentiation or cell of origin and clinical behavior are a persistent source of controversy[1-5]. Recently, specific mutations between transmembrane and tyrosine kinase domains in exon 11 at codon 550-560 of C-kit have been found in GISTs, which can lead to ligand-independent activation of the tyrosine kinase of C-kit and have a tumor promoting effect *in vitro*[4,6-10]. We studied the C-kit mutation type of exon 11 by PCR-SSCP and DNA sequencing in a series of Chinese GIST[11]. The results showed that C-kit mutations existed among GISTs. Compared to the reports in the published data, an insertion of 12 bp at codon 579 lies outside the hot spot area[12]. In order to fully characterize the activation of the insert mutation at codon 579 of C-kit gene, we constructed an expression vector containing mutant C-kit and evaluated its effect on implanted tumor in nude mice.

MATERIALS AND METHODS

Main reagents

Fetal bovine serum was produced by Hyclone and 96-well plates by Costa. Dimethyl sulfoxide (DMSO), ethylened iaminetetraacetic acid (EDTA), 3-(4,5-dimethy1-thiazol-2-yl), 2,5-diphenyl tetrazolium bromide (MTT), *N*-2-hydroxyethyl piperazine-*N*'-2-ethanesulfonic acid (HEPES) and trypsin were the products of Sigma. Rabbit polyclonal antibody against C-kit was obtained from DAKO. Envision two-step and DAB test kits were obtained from Beijing Zhongshan Biotechnology Inc.

Human embryonic kidney cell line

Human embryonic kidney cell (HEKC) line was established in our laboratory and prepared after long-term generation.

Construction of plasmids

Eukaryotic expression vector of pcDNA3 (Invitrogen, USA), plasmid pMD18-T-KIT-NW containing full-length of C-kit gene (C-kit cDNA was conducted in our laboratory) and plasmid pMD18-T-Kit-NW containing mutant-type C-kit cDNA with insertion of 12 bp at codon 579 (mutant C-kit cDNA was conducted in our laboratory) were digested by restriction enzymes *Xba*I *and Hind*III. The digested vector and plasmid cDNA fragment were ligated. Recombinant clones were identified by *Xba*I *and Hind*III double digestion. Positive clones named pcDNA3-Kit-W and pcDNA3-Kit-NW were further confirmed by sequencing.

Transfection of recombinant plasmid into HEKCs and grouping

Cultured HEKCs were divided into three groups, which were transfected with pcDNA3 vector, recombinant pcDNA3-Kit-W, and recombinant pcDNA3-Kit-NW, respectively. Transfection was performed according to the instructions of Lipofectamine TM2000 reagent kit (Gibco). Cells were cultured in RPMI 1640 medium containing 200 mL/L fetal calf serum and 350 mg/L G418. Resistant clones could be detected 2 wk later.

Cell culture

HEKCs were inoculated in RPMI 1640 with 100 g/L fetal bovine serum and incubated at 37 ℃ in an incubator containing 50 mL/L CO_2 to measure the logarithmic growth phase. After the treatment with digestive fluid, HEKCs were suspended by adding D-Hank's fluid, deposited by centrifugation at 190 r/min for 5 min and then counted. Using RPMI 1640 containing 100 g/L fetal bovine serum, HEKCs were adjusted to a density of 5×10^4/mL and added to a 24-well plate containing flying sheets, 0.2 mL/well. Flying sheets were taken out respectively at 24, 48, and 72 h, fixed with cold acetone for 10 min, dried and preserved at -60 ℃.

Cell fixation and immunocytochemical staining

Preserved cell flying sheets were immersed in PBS for 5 min, blocked with 10 mL/L H_2O_2 for 10 min, washed thrice with PBS (5 min each time) and then incubated with 10% goat serum for 30 min. C-kit antibody was diluted at a concentration of 1:50 and added as the first antibodies, staying 1 h at 37 ℃. After being washed thrice with PBS (5 min each time), horseradish peroxidase-conjugated goat anti-rabbit secondary antibody was added, staying 30 min at 37 ℃, washed thrice with PBS (5 min each time) and stained with DAB. Counterstaining with hematoxylin was performed before the final analysis. The first antibody was replaced with fetal bovine serum as a negative control.

Western blot analysis

Cell lysates were prepared in extraction buffer containing 50 mmol/L Tris-HCl (pH 7.4), 150 mmol/L NaCl, 10 g/L Triton-100, 1 g/L SDS, 1 mmol/L EDTA, 1 mmol/L AEBSF, 20 g/mL aprotinin, and 20 g/mL leupeptin. After centrifugation at 12 000 *g* for 10 min at 4 ℃, the supernatant was collected. Equal amounts of total protein (10 g) from each sample were loaded and separated by 120 g/L SDS-polyacrylamide gel electrophoresis and then transferred to Hybond-P polyvinylidene difluoride (PVDF) membrane (Amersham Pharmacia Biotech, Piscataway, NJ, USA). After being blocked with 50 g/L nonfat dry milk in PBS (pH 7.4) with 1 g/L Tween-20, membranes were probed with a rabbit anti-C-kit polyclonal antibody (1:500 dilution) followed by subsequent incubation with horseradish peroxidase-conjugated goat anti-rabbit secondary antibody (1:1 000 dilution).

MTT assay

HEKCs with a density of approximately 2.5×10^5/mL were seeded into each well of the 96-well plate (0.2 mL/well). Each group contained 12 wells. After 4 d of incubation at 37 ℃ in an incubator containing 50 mL/L CO_2, 50 mL of MTT (50 mg MTT) was added and the culture was continued for 4 h at 37 ℃. After the fluid at the top was removed, 150 mL DMSO was added to each well. After being concussed and dissolved, absorbency value with a wavelength of 574 nm was detected by enzyme-labeled instrument (BioRad 2250, Japan).

Animal experiment

Nine Balb/c male mice aged 4-6 wk (body mass 18-20 g) were purchased from Experimental Animal Center of Second Military Medical University, Shanghai and randomly divided into three groups, three mice in each group. The mice in vector-treated control group were injected with HEKCs transfected with pcDNA3 vector, the mice in Kit-W group received an injection of HEKCs transfected with recombinant pcDNA3-Kit-W, the mice in Kit-NW group received an injection of HEKCs transfected with recombinant pcDNA3-Kit-NW. After the cancer cells were cultured into the stage of logarithmic growth phase, they were digested with trypsin to make cancer cell suspension of 2.5×10^7/L. Then, 0.2 mL of each suspension was subcutaneously injected into the right back of the nude mice.

Tumor volume measurement

The survival of nude mice was observed every day. After tumor cell injection, the nude mice were killed after 6 wk. The surrounding fatty tissues were dissected and the tumors were weighed. Tumors were fixed in 10% buffered formalin and processed in paraffin wax. Five-micrometer thick sections were stained with hematoxylin and eosin.

Statistical analysis

Data were treated with SPSS for LSD and one-way ANOVA test. $P<0.05$ was considered statistically significant.

RESULTS

Identification of recombinant plasmids pcDNA3-Kit-W and pcDNA3-Kit-NW

After digestion by *Xba*I *and Hind*III, bands at 3 kD could be detected for positive clones (Figure 1), suggesting

that Kit-W and Kit-NW fragments were inserted into the pcDNA3 vector, named as recombinant plasmids pcDNA3-Kit-W and pcDNA3-Kit-NW, respectively.

pcDNA3-Kit-W and pcDNA3-Kit-NW DNA were prepared for sequencing. The sequence obtained was the same as the reported sequence of C-kit cDNA and mutant

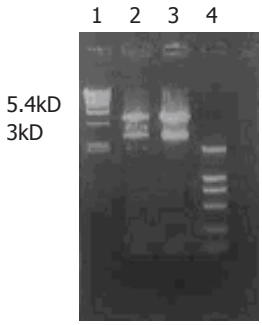

Figure 1 Restriction enzyme digestion of recombinant plasmids pcDNA3-Kit-W and pcDNA3-Kit-NW at *Xba*I and *Hind*III. Lane 1: DNA/*EcoR*I+*Hind*III marker; lane 2: pcDNA3-Kit-W clone; lane 3: pcDNA3-Kit-NW clone; lane 4: DL-2000 marker.

C-kit cDNA, indicating that the C-kit gene and mutant C-kit gene were successfully cloned into the eukaryotic expression vector pcDNA3.

Screening of C-kit gene-transfected cells

No significant differences were observed between the morphological characteristics of transfected cells and normal HEKCs.

Expression of C-kit protein

Supernatants of cultured cells in three groups were collected and analyzed by immunocytochemistry. The cells transfected with pcDNA3-Kit-W and pcDNA3-Kit-NW were positively stained for C-kit protein (Figure 2). However, the cells in vector control group were negatively stained for C-kit. In accordance with the findings on immunocytochemical staining, a band in a molecular mass of 145 ku was detected with rabbit anti-C-kit antibody from the cells transfected with pcDNA3-Kit-W and pcDNA3-Kit-NW, but no bands were detected in the vector control group. There was no significant difference in the protein level of C-kit between pcDNA3-Kit-W and pcDNA3-Kit-NW groups (Figure 3).

MTT assay

Absorbance values of the three groups were 0.1340±2.353×10^{-3}, 0.1830±3.888×10^{-3}, and 0.1274±3.537×10^{-3}, respectively. LSD analysis and one-way ANOVA analysis with SPSS10.0 software were used to compare the difference of absorbance in each group at 574 nm. Statistical analysis indicated that significant differences were detected between pcDNA3-Kit-NW and pcDNA3, pcDNA3-Kit-NW and pcDNA3-Kit-W ($P<0.05$), respectively. The results implied that the cell proliferating activity in pcDNA3-Kit-NW group was higher than that in control group.

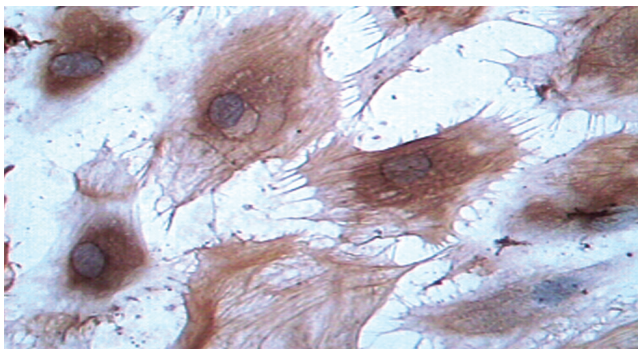

Figure 2 Positive immunocytochemical staining of C-kit transfected with pcDNA3-Kit-NW (×400).

Figure 3 Western blotting of pcDNA3-Kit-W, pcDNA3-Kit-NW, and pcDNA3 on HEKC line. Lanes 1-3: pcDNA3-Kit-NW; lanes 4-6: pcDNA3-Kit-W; lanes 7 and 8: pcDNA3.

Tumor growth in nude mice

Tumors were observed in the nude mice 3 wk after being implanted with cells transfected with pcDNA3-Kit-NW (Figure 4). Mice had no visible tumor after cell injection in pcDNA3-Kit-W transfection group and vector control group after 6 wk. Tumor volumes in pcDNA3-Kit-NW transfection group were approximately similar and no significant difference was observed between the three tumors ($t = 13.07$ $P>0.05$). Many areas of hemorrhage and necrosis were present, residual tumor cells were frequently found to have giant, bizarre-shaped pyknotic nucleoli, or prominent pathologic mitosis in the tumors (Figure 5).

DISCUSSION

GIST is the most common mesenchymal tumor in human gastrointestinal tract and is enigmatic in terms of its differentiation or cell origin and clinical behavior. In recent years, C-kit protein expression and activated gene mutation have been found in GIST[13-17]. C-kit encodes a growth factor receptor with ligand-dependent tyrosine kinase activity[18,19]. Kit ligand-stem cell factor (SCF) is the only known ligand of the Kit receptor[20]. SCF binding to the receptor mediates receptor dimerization, activation of kinase activity, and autophosphorylation. Subsequently, Kit activates several signaling cascades, leading to cell proliferation, cell survival, and other cellular responses. Kit and SCF are encoded at the white spotting (W) and steel (Sl) loci in mice, respectively[20-22]. Mutation at the murine W and Sl loci generates deficiencies in several major cell systems during embryogenesis and in postnatal animals. In hematopoiesis Kit receptor signaling is critical in the stem cell hierarchy, erythropoiesis, mast cell development and

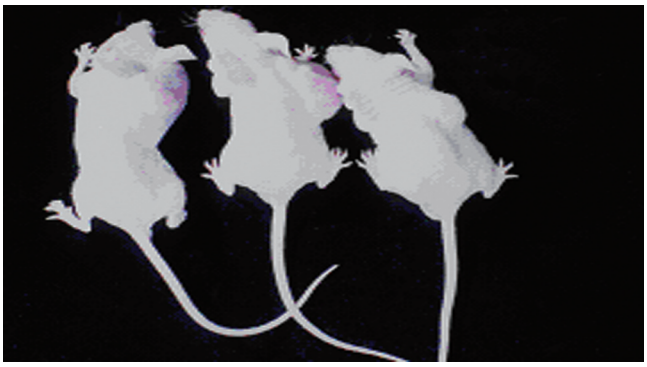

Figure 4 Tumor growth in nude mice 6 wk after being implanted with cells transfected with pcDNA3-Kit-NW.

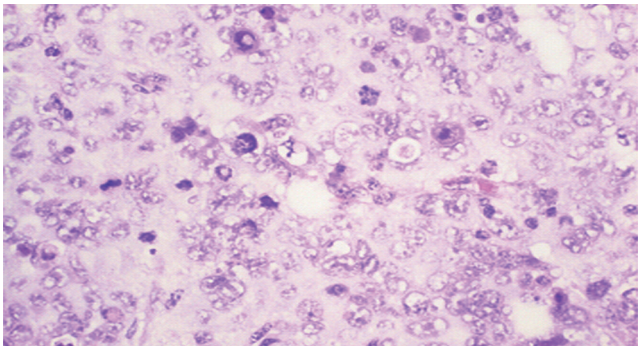

Figure 5 Giant, bizarre-shaped pyknotic nucleoli, or prominent pathologic mitosis in tumor (HE ×200).

function, megakaryopoiesis, and lymphopoiesis[23-26].

GISTs most often harbor mutations at exon 11 codon 550-560 of C-kit cDNA, while the mutations in human mastocytosis predominantly involve the activation loop of the Kit kinase[27,28]. The C-kit mutations in this domain can lead to spontaneous ligand-independent activation of the tyrosine kinase of C-kit and was called "gain-of-function mutation". Development of GIST is highly associated with Kit-activating mutations, suggesting that the activated Kit receptor plays a critical role in tumor development[29]. In addition, gene mutation has shown a good correlation with biologic behavior in such tumors. For instance, it can provide valuable adjunctive prognostic information. In agreement with this notion, familial cases of GIST have been reported with Kit-activating mutations in the germ line[30]. We have found a mutation at codon 579 in malignant GIST, which lies outside the hot spot area[12]. In order to fully characterize the activation of the insert mutation at codon 579 of C-kit gene, we studied the expression of mutant C-kit gene in human embryonic kidney cell line and its effect on implanted carcinoma in the nude mice.

In the present study, we constructed a target fragment containing mutant-type C-kit cDNA with insertion of 12 bp at codon 579 and full-length of C-kit gene. The target gene fragment of 5.4 kD in length was cloned into *Xba*I *and Hind*III restriction sites of eukaryotic expression vector pcDNA3. Restriction digestion and sequence analysis for positive clones indicated that the two recombinant eukaryotic expression vectors containing the gene were successfully constructed. These recombinant vectors were then transfected into HEKCs and screened by G418. The result of direct sequencing showed that the recombinant plasmids were stably integrated into the cells. Immunocytochemical staining revealed that HEKCs transfected with pcDNA3-Kit-W and pcDNA3-Kit-NW were stained positively for C-kit, indicating that C-kit protein is expressed in transfected HEKCs. Furthermore, a protein (145 kD) was detected by Western blotting and there was no significant difference in the expression level of C-kit protein between transfected pcDNA3-Kit-W and pcDNA3-Kit-NW HEKCs, indicating that the insert mutation at codon 579 of C-kit gene has no effect on protein expression of HEKCs.

In vitro characterization of the Kit V558 mutation in BaF/3 cells indicates that the Kit V558 mutation promotes cell proliferation and abolishes the growth factor dependence of BaF/3 cells[30]. Sommer *et al*[31]. showed that young bone marrow-derived mast cell cultures are refractory to growth factor deprivation-induced apoptosis. However, these cultures do not promote cell cycle progression. There is evidence that short kit protein product is more active than long Kit protein product. Therefore, it may be possible that the long-Kit variant is expressed predominantly in the young mutant bone marrow-derived mast cells, while the older cultures express the short-Kit variant, which may explain the progression from partial to complete growth factor independently of these cultures. Our results showed that the insert mutation at codon 579 of C-kit gene promoted HEKC proliferation. In addition, no significant differences between the morphological characteristics of transfected cells and normal HEKCs were observed, suggesting that mutant C-kit has no effect on the morphology of HEKCs.

In this experiment, HEKCs transfected with recombinant pcDNA3-Kit-NW and pcDNA3 vector were subcutaneously implanted into the nude mice. The implanted tumors appeared later in the pcDNA3-Kit-NW transfection group. Mice had no visible tumor after cell injection in pcDNA3-Kit-W transfection group and vector control group after 6 wk. These results suggest that the insert mutation at codon 579 of C-kit gene can significantly induce the growth of tumors and constitutive Kit signaling is critical and sufficient for the induction of neoplasia in the mice.

REFERENCES

1 **Wong NA,** Young R, Malcomson RD, Nayar AG, Jamieson LA, Save VE, Carey FA, Brewster DH, Han C, Al-Nafussi A. Prognostic indicators for gastrointestinal stromal tumours: a clinicopathological and immunohistochemical study of 108 resected cases of the stomach. *Histopathology* 2003; **43:** 118-126

2 **Nagasako Y,** Misawa K, Kohashi S, Hasegawa K, Okawa Y, Sano H, Takada A, Sato H. Evaluation of malignancy using Ki-67 labeling index for gastric stromal tumor. *Gastric Cancer* 2003; **6:** 168-172

3 **Lin SC,** Huang MJ, Zeng CY, Wang TI, Liu ZL, Shiay RK.

Clinical manifestations and prognostic factors in patients with gastrointestinal stromal tumors. *World J Gastroenterol* 2003; **9:** 2809-2812

4 **Miettinen M,** Sobin LH, Lasota J. Gastrointestinal stromal tumors of the stomach: a clinicopathologic, immunohistochemical, and molecular genetic study of 1765 cases with long-term follow-up. *Am J Surg Pathol* 2005; **29:** 52-68

5 **Kim MK,** Lee JK, Park ET, Lee SH, Seol SY, Chung JM, Kang MS, Yoon HK. [Gastrointestinal stromal tumors: clinical, pathologic features and effectiveness of new diagnostic criteria] *Korean J Gastroenterol* 2004; **43:** 341-348

6 **Taniguchi M,** Nishida T, Hirota S, Isozaki K, Ito T, Nomura T, Matsuda H, Kitamura Y. Effect of c-kit mutation on prognosis of gastrointestinal stromal tumors. *Cancer Res* 1999; **59:** 4297-4300

7 **Berman J,** O'Leary TJ. Gastrointestinal stromal tumor workshop. *Hum Pathol* 2001; **32:** 578-582

8 **Lasota J,** Jasinski M, Sarlomo-Rikala M, Miettinen M. Mutations in exon 11 of c-Kit occur preferentially in malignant versus benign gastrointestinal stromal tumors and do not occur in leiomyomas or leiomyosarcomas. *Am J Pathol* 1999; **154:** 53-60

9 **Lasota J,** Wozniak A, Sarlomo-Rikala M, Rys J, Kordek R, Nassar A, Sobin LH, Miettinen M. Mutations in exons 9 and 13 of KIT gene are rare events in gastrointestinal stromal tumors. A study of 200 cases. *Am J Pathol* 2000; **157:** 1091-1095

10 **Hirota S,** Isozaki K, Moriyama Y, Hashimoto K, Nishida T, Ishiguro S, Kawano K, Hanada M, Kurata A, Takeda M, Muhammad Tunio G, Matsuzawa Y, Kanakura Y, Shinomura Y, Kitamura Y. Gain-of-function mutations of c-kit in human gastrointestinal stromal tumors. *Science* 1998; **279:** 577-580

11 **Ma D,** Liu X, Cai Z, Xie Q. Expression and mutation of c-kit gene in gastrointestinal stromal tumor. *Zhonghua Zhong Liu Za Zhi* 2002; **24:** 461-464

12 **Feng F,** Liu XH, Xie Q, Liu WQ, Bai CG, Ma DL. Expression and mutation of c-kit gene in gastrointestinal stromal tumors. *World J Gastroenterol* 2003; **9:** 2548-2551

13 **Hou Y,** Wang J , Zhu X, Du X , Sun M, Zheng A. A clinicopathologic and immunohistochemical study on 76 cases of gastrointestinal stromal tumor. *Zhonghua Binglixue Zazhi* 2002; **31:** 20-25

14 **Liu XH,** Ma DL, Xie Q, Wu LL. Stromal tumors of the duodenum: a clinicopathological and immunohistochemical study of 18 cases. *Linchuang Yu Shiyan Binglixue Zazhi* 2002; **18:** 122-126.

15 **Ma DL,** Liu XH, Bai CG, Xie Q, Feng F. Effect of c-kit gene on prognosis of gastrointestinal stromal tumor. *Zhonghua Waikexue Zazhi* 2004; **42:** 140-144.

16 **Ma DL,** Liu XH, Bai CG, Wu LL, Xie Q. Stromal tumors of the esophagus: a clinicopathological and immunohistochemical study. *Zhonghua Waikexue Zazhi* 2002; **40:** 237

17 **Liu XH,** Ma DL, Bai CG, Wu LL, Xie Q. Gastrointestinal primary stromal tumor in omentum and mesentery: a clinicopathological and immunohistochemical study. *Jiefangjun Yixue Zazhi* 2002; **5:** 401-402.

18 **Besmer P,** Murphy JE, George PC, Qiu FH, Bergold PJ, Lederman L, Snyder HW, Brodeur D, Zuckerman EE, Hardy WD. A new acute transforming feline retrovirus and relationship of its oncogene v-kit with the protein kinase gene family. *Nature* 1986; **320:** 415-421

19 **Qiu FH,** Ray P, Brown K, Barker PE, Jhanwar S, Ruddle FH , Besmer P. Primary structure of c-kit: relationship with the CSF-1/PDGF receptor kinase family--oncogenic activation of v-kit involves deletion of extracellular domain and C terminus. *EMBO J* 1988; **7:** 1003-1011

20 **Besmer P.** The kit ligand encoded at the murine Steel locus: a pleiotropic growth and differentiation factor. *Curr Opin Cell Biol* 1991; **3:** 939-946

21 **Chabot B,** Stephenson DA, Chapman VM, Besmer P, Bernstein A. The proto-oncogene c-kit encoding a transmembrane tyrosine kinase receptor maps to the mouse W locus. *Nature* 1988; **335:** 88-89

22 **Geissler EN,** Cheng SV, Gusella JF, Housman DE. Genetic Analysis of the Dominant White-Spotting (W) Region on Mouse Chromosome 5: Identification of Cloned DNA Markers near W. *Proc Natl Acad Sci USA* 1988; **85:** 9635-9639

23 **Russell ES.** Hereditary anemias of the mouse: a review for geneticists. *Adv Genet* 1979; **20:** 357-459

24 **Besmer P,** Manova K, Duttlinger R, Huang EJ, Packer A, Gyssler C, Bachvarova RF. The kit-ligand (steel factor) and its receptor c-kit/W: pleiotropic roles in gametogenesis and melanogenesis. *Dev Suppl* 1993; 125-137

25 **Galli SJ,** Zsebo KM, Geissler EN. The kit ligand, stem cell factor. *Adv Immunol* 1994; **55:** 1-96

26 **Besmer P.** Kit-ligand-Stem Cell Factor. In: Garland JM, Quesenbery P, Hilton D,eds. Colony Stimulating Factors, Molecular& Cell Biology, Second Edition. New York: *Marcel Dekker* 1997, 369-404.

27 **Nagata H,** Worobec AS, Oh CK, Chowdhury BA, Tannenbaum S, Suzuki Y, Metcalfe DD. Identification of a point mutation in the catalytic domain of the protooncogene c-kit in peripheral blood mononuclear cells of patients who have mastocytosis with an associated hematologic disorder. *Proc Natl Acad Sci USA* 1995; **92:** 10560-10564

28 **Brockow K,** Metcalfe DD. Mastocytosis. Curr Opin Allergy Clin Immunol 2001; **1:** 449-454

29 **Kissel H,** Timokhina I, Hardy MP, Rothschild G, Tajima Y, Soares V, Angeles M, Whitlow SR, Manova K, Besmer P. Point mutation in kit receptor tyrosine kinase reveals essential roles for kit signaling in spermatogenesis and oogenesis without affecting other kit responses. *EMBO J* 2000; **19:** 1312-1326

30 **Nishida T,** Hirota S, Taniguchi M, Hashimoto K, Isozaki K, Nakamura H, Kanakura Y, Tanaka T, Takabayashi A, Matsuda H, Kitamura Y. Familial gastrointestinal stromal tumours with germline mutation of the KIT gene. *Nat Genet* 1998; **19:** 323-324

31 **Sommer G,** Agosti V, Ehlers I, Rossi F, Corbacioglu S, Farkas J, Moore M, Manova K, Antonescu CR, Besmer P. Gastrointestinal stromal tumors in a mouse model by targeted mutation of the Kit receptor tyrosine kinase. *Proc Natl Acad Sci USA* 2003; **100:** 6706-6711

Science Editor Wang XL and Guo SY **Language Editor** Elsevier HK

PO Box 2345, Beijing 100023, China
www.wjgnet.com
wjg@wjgnet.com

ELSEVIER

World J Gastroenterol 2005;11(45):7109-7117
World Journal of Gastroenterology ISSN 1007-9327

• *CLINICAL RESEARCH* •

Associations between γ-glutamyl transferase, metabolic abnormalities and inflammation in healthy subjects from a population-based cohort: A possible implication for oxidative stress

Simona Bo, Roberto Gambino, Marilena Durazzo, Sabrina Guidi, Elisa Tiozzo, Federica Ghione, Luigi Gentile, Maurizio Cassader, Gian Franco Pagano

Simona Bo, Roberto Gambino, Marilena Durazzo, Sabrina Guidi, Elisa Tiozzo, Federica Ghione, Maurizio Cassader, Gian Franco Pagano, Department of Internal Medicine, University of Turin, Italy
Luigi Gentile, Diabetic Clinic, Hospital of Asti, Italy
Supported by a grant: "Progetto di Ricerca Sanitaria Finalizzata, Regione Piemonte, 2003"
Correspondence to: Simona Bo, Dipartimento di Medicina Interna, Universita' di Torino, Corso Dogliotti 14, 10126 Torino, Italy. sbo@molinette.piemonte.it
Telephone: +39-11-6967864 Fax: +39-11-6634751
Received: 2005-03-31 Accepted: 2005-04-18

Abstract

AIM: To examine the relationships between γ-glutamyl-transferase (GGT), alanine-aminotransferase (ALT), aspartate-aminotransferase (AST) and various metabolic parameters, C-reactive protein (CRP) and an oxidative stress marker (nitrotyrosine, NT) in subjects without any metabolic abnormalities from a population-based sample.

METHODS: Two hundred and five subjects with normal body mass index (BMI), glucose tolerance, and without any metabolic abnormality were studied out of 1 339 subjects, without known liver diseases, alcohol abuse or use of hepatotoxic drugs, who are representative of the 45-64 aged population of Asti (north-western Italy).

RESULTS: In all patients metabolic parameters and hs-CRP levels linearly increase from the lowest to the highest ALT and GGT tertiles, while in subjects without metabolic abnormalities, there is a significant association between fasting glucose, uric acid, waist circumference, hs-CRP, triglyceride values, and GGT levels. In these subjects, male sex, higher hs-CRP and glucose levels are associated with GGT levels in a multiple regression model, after adjustments for multiple confounders. In the same model, median NT levels are significantly associated with the increasing GGT tertile (β = 1.06; 95%CI 0.67-1.45), but not with the AST and ALT tertiles. In a multiple regression model, after adjusting for age, sex, BMI, waist, smoking, and alcohol consumption, both NT (β = 0.05; 95%CI 0.02-0.08) and hs-CRP levels (β = 0.09; 95%CI 0.03-0.15) are significantly associated with fasting glycemia.

CONCLUSION: GGT, an easy, universally standardized and available measurement, could represent an early marker of sub-clinical inflammation and oxidative stress in otherwise healthy individuals. Prospective studies are needed to establish if GGT could predict future diabetes in these subjects.

Key words: Alanine aminotransferase; Aspartate aminotransferase; Body mass index; C-reactive protein; γ-Glutamyl transferase; Metabolic syndrome; Nitrotyrosine

Bo S, Gambino R, Durazzo M, Guidi S, Tiozzo E, Ghione F, Gentile L, Cassader M, Pagano GF. Associations between γ-glutamyl transferase, metabolic abnormalities and inflammation in healthy subjects from a population-based cohort: A possible implication for oxidative stress. *World J Gastroenterol* 2005; 11(45): 7109-7117
http://www.wjgnet.com/1007-9327/11/7109.asp

INTRODUCTION

Increased levels of the liver enzymes, γ-glutamyl transferase (GGT), alanine aminotransferase (ALT) and aspartate aminotransferase (AST) have been found to be associated with diabetes, cardiovascular risk factors and components of the insulin resistance syndrome, even within normal reference intervals[1-12]. In many prospective studies, strong relationships between GGT or ALT concentrations and incident diabetes have also been observed in non-drinkers, in individuals with normal levels of liver enzymes, independently of classical cardiovascular risk factors[2-10]. However, a strong interaction between body mass index (BMI) and GGT has been described, suggesting that this enzyme acts as an intervening factor in the association between obesity and diabetes[1,4,5,7,9]. Some authors have speculated that visceral fat could play a role in the association of GGT with metabolic abnormalities, or that this enzyme could be considered as a reliable marker of visceral fat[1,2,13]. Furthermore, GGT and ALT might be interpreted as markers of hepatic steatosis,

a condition well known to be associated with insulin resistance, type 2 diabetes and the metabolic syndrome[14,15]. Thus, the associations recently found between the levels of liver enzymes and insulin resistance might be mediated by a fatty liver, which is accompanied by higher GGT and aminotransferase concentrations.

Increasing data are available about the associations between GGT levels and markers of oxidative stress (directly with F2-isoprostanes, an oxidative damage product of arachidonic acid; inversely with serum and dietary antioxidant vitamins), suggesting that the strong associations between cardiovascular risk factors might be explained by some oxidative mechanism[4,16-18]. Indeed, oxidative processes are key components of chronic inflammation, acting on multiple pathways and amplifying inflammatory reactions[19]. Recent reports have found associations between elevated liver enzymes and several inflammatory parameters[3,4,9,10,20,21].

However, previous studies have always included a group of overweight, or obese subjects, or did not take into account the deposition of body fat; thus adiposity might be a confounding factor. Two recent papers suggested that a non-alcoholic fatty liver could be considered as an early predictor of metabolic disorders also in non-obese non-diabetic Asiatic cohorts; however, in these studies, the control group included individuals with other components of the metabolic syndrome and Asians have a higher proportion of visceral fat and a lower lean body mass than white subjects with the same BMI[22,23]. It seems thus interesting to evaluate the associations between the liver enzyme levels and metabolic and inflammatory parameters in a cohort of Caucasian subjects without any metabolic abnormalities, which could potentially influence this association.

Therefore, the aims of the present study are to examine the relationships between liver enzyme concentrations and various metabolic parameters, a marker of inflammation (C-reactive protein, CRP) and a marker of oxidative stress (nitrotyrosine, NT) in subjects without any metabolic abnormalities from a population-based cohort of middle-aged individuals, recognizing that the cross-sectional design of the study does not definitively establish causal or temporal relationships, and should be considered hypothesis-generating only.

MATERIALS AND METHODS

All the patients aged between 45 and 64 years under the practice of six family physicians from the province of Asti (north-western Italy), whose patients are representative of the local health districts, were enrolled for a metabolic screening. Of these 1 877 subjects, 1 658 (88.3%) accepted to be interviewed on personal habits, and to be tested for several clinical and laboratory measurements, giving written consent, while 219 refused. The resident population of corresponding age, in the same area, and missing patients show the same percentage of males, level of education, known diabetes, and subjects living in a rural area than participating patients.

All procedures were in accordance with the Declaration of Helsinki.

Subjects with >30 g/d alcohol consumption, with known liver or gastrointestinal diseases, as recorded by the family physicians, with liver enzyme concentrations higher than three times the upper limit of the sex-related reference range, or on corticosteroids, methotrexate, amiodarone, tamoxifen or other hepatotoxic drugs were excluded. Estrogen users (both on contraceptive medications or estrogen replacement therapy) were included, all being on low-dose estrogen drugs.

One thousand and three hundred and thirty-nine subjects (80.8%) were evaluated.

In the morning, a fasting venous blood sample was drawn to measure glucose, total and HDL-cholesterol, uric acid, triglyceride, insulin, liver enzymes, and hs-CRP levels.

Weight and height were measured after an overnight fast. Overweight and obese subjects were those with BMI respectively, $\geqslant$25, <30, and $\geqslant$30 kg/m^2. Waist circumference was measured with a plastic tape meter at the level of the umbilicus. Systolic and diastolic blood pressures were measured twice with a standard mercury sphygmomanometer in a sitting position, after at least 10 min of rest. Values reported are the mean of the two determinations. A resting electrocardiogram (ECG) was performed in all the subjects, and interpreted according to the Minnesota Code criteria. If fasting serum glucose value was $\geqslant$6.1 mmol/L, a second fasting glucose determination was then performed. Diabetes and impaired fasting glucose (IFG) were diagnosed according to published recommendations[24].

The metabolic syndrome (MS) was defined as the presence of at least three of the following five criteria: fasting serum glucose $\geqslant$6.1 mmol/L; arterial blood pressure $\geqslant$130/85 mmHg; plasma triglycerides $\geqslant$1.69 mmol/L; HDL-cholesterol <1.29 mmol/L (females) and <1.04 mmol/L (males); waist >88 cm (females) and >102 cm (males), in line with the National Cholesterol Education Program (Adult Treatment Panel III) (NCEP-ATP III) criteria[25].

Insulin resistance was calculated from the homeostasis model assessment (HOMA-IR), according to published algorithm[26].

Vascular disease was assessed on the basis of the Rose questionnaire, ECG evidence of ischemic heart disease, and history of documented events, recorded by the family physician (angina, previous myocardial infarction, coronary artery by-pass graft or other invasive procedures to treat coronary artery disease, transient ischemic attacks, strokes, gangrene, amputation, vascular surgery, intermittent claudication, absence of foot pulses, and abnormal brachial and posterior tibial blood pressure using Doppler techniques).

Former or present smokers were defined as ever smokers. Alcohol intake was assessed by multiplying the mean daily consumption for each beverage by the ethanol content, to give grams of alcohol/d (one can/bottle/glass of beer = 13 g, one glass of wine = 12 g, one standard drink of spirit = 14 g).

Later, we identified 205 subjects with normal BMI (<25 kg/m^2) and without any component of the MS. To avoid considering as normoglycemic individuals who could be classified as hyperglycemic after the stimulatory test, these subjects were submitted to the 75 g oral glucose tolerance test (OGTT), performed and interpreted in accordance to the guidelines[24]. All of the subjects showed normal glucose tolerance at the OGTT. NT levels were measured in all these subjects.

Serum glucose was measured by the glucose oxidase method (HITACHI 911 Analyzer, Sentinel Ch., Milan, Italy), and serum insulin by immunoradiometric assay (Radim SpA, Pomezia, Italy; intra-assay CV: 1.6-2.2%, inter-assay CV: 6.1-6.5%). Plasma triglycerides and HDL-cholesterol were measured by enzymatic colorimetric assay (HITACHI 911 Analyzer), the latter after precipitation of LDL and VLDL fractions using heparin-$MnCl_2$ solution (Mn^{2+} concentration: 0.092 mol/L) and centrifugation at 4 °C.

AST was evaluated by a kinetic determination. Malate dehydrogenase catalyzes the reaction of oxalacetic acid with β-NADH2 by forming lactic acid and β-NAD (HITACHI 911 Analyzer). ALT was evaluated by a kinetic determination. Lactate dehydrogenase catalyzes the reaction of pyruvic acid with β-NADH2 by forming lactic acid and β-NAD (HITACHI 911 Analyzer). GGT was evaluated by an enzymatic colorimetric method (HITACHI 911 Analyzer).

Uric acid was evaluated by an enzymatic colorimetric method with uricase (HITACHI 911 Analyzer). Serum hs-CRP levels were determined via a high-sensitivity latex agglutination method on the HITACHI 911 Analyzer. The kit had a minimum detection of less than 0.05 mg/L and a measurable concentration range of up to 160 mg/L. The intra-assay and inter-assay CVs were respectively 0.8-1.3% and 1.0-1.5%. Plasma NT values were determined by an ELISA kit (HyCult Biotechnology b.v., sold in Italy by Pantec, Turin; inter-assay and intra-assay CV respectively: 7 ±4% and 5±2%). All samples were run in blind.

Statistical analysis

Since the distribution of GGT, hs-CRP, insulin, HOMA, triglyceride, and NT values were highly skewed, the levels of these variables were log-transformed, in order to obtain a normal distribution. In all the analyses, the log-transformed values of these variables were used. For an easy interpretation, median (and range) of not transformed values are reported.

Linear (unadjusted) and multiple regression analyses were performed to evaluate the associations between liver enzyme levels with metabolic, inflammatory, and oxidative parameters, after adjustments for multiple confounders.

RESULTS

BMI, waist, blood pressure, fasting glucose, and insulin, HOMA-IR, triglyceride, low HDL-cholesterol, uric acid, and hs-CRP levels, percentages of males and prevalence of the metabolic syndrome increase from the lowest to the highest tertiles of ALT and GGT, and their values are significantly associated with these enzyme levels (Table 1). This trend is less evident within AST tertiles.

In subjects with normal BMI and without any component of the MS, there is a significant association of percentage of males, waist circumference, glucose, uric acid, hs-CRP, and triglyceride values with increasing GGT levels (Table 2). Waist, uric acid levels and percentages of males are significantly associated with ALT levels, while there is no significant association with AST values.

Table 3 describes the associations between the levels of each liver enzyme and age, gender, BMI, waist circumference, alcohol consumption, smoking habits, hs-CRP, HOMA-IR, and triglyceride uric acid levels (and hypertension in all the cohort) in a multiple regression model, after introducing all these as independent variables into the model. In all patients: waist levels are significantly associated with AST levels; male sex, waist, and higher levels of HOMA-IR, triglycerides, uric acid with ALT levels; male sex, alcohol and higher levels of hs-CRP, triglycerides, uric acid with GGT values.

In the subgroup of subjects with normal BMI, without any component of the MS, male sex and higher hs-CRP levels are associated with GGT levels, while no significant association is evident for the other liver enzymes. Fasting glucose is significantly associated with GGT levels in the same model, after adjusting for all previous variables, but insulin instead of HOMA-IR levels (β = 0.23; 95%CI 0.07-0.39); fasting glucose is not significantly associated with AST or ALT values.

In the subgroup of normal BMI subjects, the median NT levels are significantly associated with the increasing GGT tertile (β = 1.07; 95%CI 0.70-1.44), but not with the AST and ALT tertiles in a simple regression (Figure 1). After adjustments for age, sex, BMI, waist, smoking, and alcohol consumption, this association remains significant (β = 1.06; 95%CI 0.67-1.45).

Median NT levels are significantly correlated with: fasting glucose (β = 1.00; 95%CI 0.45-1.55) and waist circumference (β = 0.04; 95%CI 0.002-0.08). In a multiple regression model, after adjustments for age, sex, BMI, waist, smoking, and alcohol consumption, both NT (β = 0.05; 95%CI 0.02-0.08) and hs-CRP levels (β = 0.09; 95%CI 0.03-0.15) are significantly associated with fasting glycemia.

Correlations are similar also in non-drinkers, and after adjusting for AST or ALT levels (data not shown). Data do not change after excluding the subjects with CRP>10 (respectively n = 48 in the entire cohort and n = 2 in the subgroup of normal BMI), those with cardiovascular diseases (respectively n = 50 and n = 3) or those subjects on estrogen therapy (respectively n = 73 and n = 12).

DISCUSSION

Prospective studies have described that high levels of ALT and GGT[2-10] are associated with subsequent development of diabetes, while the association between AST levels and metabolic abnormalities is weaker and often attenuated or

Table 1 Clinical and laboratory characteristics of all the patients, according to liver enzyme tertiles (left); associations of the variables listed with liver enzyme levels, as a continuous variable, by unadjusted linear regression analyses (right)

	AST	1st tertile (≤14 U/L)	2nd tertile (>14≤19 U/L)	3rd tertile (>19 U/L)	β; 95%CI	
Number		452	440	447		
Age (yr)		54.0±5.8	54.7±5.8	55.0±5.5	0.08; 0.002	0.15
Male (%)		31.9	34.1	47.2	1.88; 1.00	2.76
Alcoholics (%)		41.6	45.0	51.8	1.28; 0.42	2.14
Alcohol (g/day within drinkers)		14.4±8.7	15.8±8.9	16.3±8.5	0.03; -0.05	0.11
Ever smokers (%)		48.3	40.2	41.4	-0.41; -1.27	0.45
BMI (kg/m^2)		26.3±5.1	26.1±4.4	27.1±4.9	0.13; 0.04	0.22
Waist (cm)		88.6±13.4	89.3±12.4	92.5±13.0	0.09; 0.06	0.12
Systolic blood pressure (mmHg)		132.1±15.3	132.8±16.2	134.8±16.3	0.034; 0.007	0.06
Diastolic blood pressure (mmHg)		82.3±8.7	82.9±9.5	83.7±9.6	0.05;-0.02	0.078
Uric acid (mmol/L)		178.4±53.5	190.3±59.5	208.2±59.5	0.04;-0.007	0.087
Insulin (pmol/L)		10.2 (0.6-259.8)	10.8 (1.2-137.4)	11.4 (0.6-409.8)	0.74; 0.26	1.22
HOMA insulin resistance (mU/mL×mmol/L)		0.40 (0.02-31.8)	0.44 (0.05-16.6)	0.47 (0.02-25.9)	0.74; 0.30	1.18
Fasting glucose (mmol/L)		5.8±1.9	5.6±1.2	5.9±1.7	0.27; 0.0	0.54
HDL-cholesterol (mmol/L)		1.6±0.4	1.6±0.4	1.6±0.4	-0.46;-1.69	0.77
Triglycerides (mmol/L)		1.2 (0.5-5.2)	1.3 (0.6-8.7)	1.4 (0.4-5.4)	1.45; 0.5	2.5
Hs-CRP (mg/L)		1.40 (0.20-50.8)	1.30 (0.20-49.5)	1.60 (0.10-130.9)	0.33;-0.07	0.73
Metabolic syndrome (%)		20.1	19.3	26.4	1.54; 0.5	2.6
	ALT	1st tertile (≤14 U/L)	2nd tertile(>14≤22 U/L)	3rd tertile(>22 U/L)	β; 95%CI	
Number		444	459	436		
Age (yr)		53.8±5.9	55.2±5.7	54.6±5.4	0.03; -0.09	0.16
Male (%)		23.4	35.1	55.0	5.1; 3.7	6.6
Alcoholics (%)		45.5	44.2	48.7	0.97; -0.46	2.4
Alcohol (g/day within drinkers)		15.2±8.4	16.0±9.0	15.5±8.8	0.03; -0.10	0.17
Ever smokers (%)		42.9	42.3	44.9	-0.07; -1.5	1.4
BMI (kg/m^2)		25.0±4.5	26.6±4.6	28.0±4.9	0.69; 0.55	0.83
Waist (cm)		85.4±12.9	89.7±12.1	95.3±12.3	0.29; 0.23	0.35
Systolic blood pressure (mmHg)		131.1±16.0	133.0±15.3	135.5±16.3	0.09; 0.05	0.13
Diastolic blood pressure (mmHg)		81.7±9.3	82.8±8.8	84.4±9.5	0.15; 0.07	0.23
Uric acid (mmol/L)		172.5±53.5	190.3±53.5	214.1±59.5	0.05; 0.04	0.06
Insulin (pmol/L)		10.2 (0.6-151.2)	10.8 (0.6-409.8)	15.0 (0.6-244.2)	3.4; 2.6	4.2
HOMA insulin resistance (mU/mL×mmol/L)		0.38 (0.02-14.3)	0.43 (0.02-31.8)	0.63 (0.02-19.9)	3.5; 2.8	4.2
Fasting glucose (mmol/L)		5.5±1.4	5.6±1.2	6.1±2.1	1.5; 1.1	1.9
HDL-cholesterol (mmol/L)		1.6±0.4	1.6±0.3	1.5±0.3	-6.8; -8.8	-4.8
Triglycerides (mmol/L)		1.2 (0.5-8.0)	1.3 (0.4-8.7)	1.5 (0.5-5.4)	5.8; 4.2	7.4
Hs-CRP (mg/L)		1.10 (0.10-50.8)	1.40 (0.20-49.5)	1.60 (0.10-130.9)	1.4; 0.8	2.1
Metabolic syndrome (%)		12.8	21.1	32.1	5.5; 3.8	7.2
	GGT	1st tertile (≤12 U/L)	2nd tertile (>12≤20 U/L)	3rd tertile(>20 U/L)	β; 95%CI	
Number		412	460	467		
Age (yr)		53.6±5.5	54.8±5.8	55.1±5.7	0.009; 0.003	0.015
Male (%)		15.5	38.9	56.1	0.43; 0.37	0.50
Alcoholics (%)		36.6	47.9	52.7	0.15; 0.08	0.22
Alcohol (g/day within drinkers)		14.1±7.9	15.0±9.0	16.9±8.8	0.013; 0.007	0.019
Ever smokers (%)		36.9	43.6	48.8	0.13; 0.06	0.20
BMI (kg/m^2)		24.9±4.2	26.7±4.7	27.7±5.0	0.03; 0.02	0.04
Waist (cm)		84.4±12.5	90.4±12.4	94.8±12.2	0.016; 0.014	0.018
Systolic blood pressure (mmHg)		129.7±15.0	133.4±15.4	136.1±16.8	0.006; 0.004	0.008
Diastolic blood pressure (mmHg)		81.5±8.7	82.8±9.3	84.4±9.6	0.009; 0.005	0.013
Uric acid (mmol/L)		166.5±47.6	190.3±59.5	214.1±59.5	0.0037;0.003	0.004
Insulin (pmol/L)		10.2 (0.6-120.0)	10.8 (1.2-409.8)	13.8 (0.6-396.0)	0.13; 0.09	0.17
HOMA insulin resistance (mU/mL´mmol/L)		0.37 (0.02-5.13)	0.43 (0.04-25.9)	0.60 (0.02-31.8)	0.14; 0.10	0.18
Fasting glucose (mmol/L)		5.4±1.1	5.7±1.4	6.1±2.1	0.09; 0.07	0.11
HDL-cholesterol (mmol/L)		1.7±0.3	1.6±0.3	1.5±0.3	-0.32;-0.22	-0.42
Triglycerides (mmol/L)		1.1 (0.4-4.4)	1.3 (0.4-8.7)	1.5 (0.6-8.0)	0.44; 0.36	0.52
Hs-CRP (mg/L)		1.00 (0.10-20.0)	1.40 (0.20-50.8)	1.80 (0.20-130.9)	0.12; 0.09	0.15
Metabolic syndrome (%)		11.6	20.2	32.8	0.35; 0.27	0.43

Median (range) is reported for not-normally distributed variables; their log-transformed values and log-GGT values are used in the analyses.

abolished after adjustment for adiposity[2-6,8-10].

Accordingly, we have found in all our patients a worse metabolic pattern in subjects within the highest ALT and GGT tertiles than those within the highest AST tertile. Increased ALT and GGT levels are associated with hepatic insulin resistance and a subsequent decline in hepatic insulin sensitivity[1-5] and GGT seems implicated in oxidative stress[4,16-18].

Excess deposition of fat in the liver, the non-alcoholic fatty liver disease, shows strong cross-sectional associations with obesity, insulin resistance and type 2 diabetes[14,15] and is associated with liver enzyme elevation.

Table 2 Clinical and laboratory characteristics of the subjects with normal BMI and without any component of the metabolic syndrome, according to the tertile of liver enzyme concentrations (left); associations of the variables listed with liver enzyme levels, as a continuous variable, by unadjusted linear regression analyses (right)

	AST	1st tertile (≤13 U/L)	2nd tertile (>13≤17 U/L)	3rd tertile (>17 U/L)	β; 95%CI	
Number		67	69	69		
Age (yr)		52.2±5.5	52.5±5.7	52.1±5.1	0.001;-0.16	0.16
Male (%)		22.4	34.8	42.0	0.8; -1.0	2.6
Alcoholics (%)		47.8	47.8	56.5	1.2; -0.5	2.9
Alcohol (g/day within drinkers)		15.5±9.1	13.8±9.0	18.5±9.1	0.05; -0.07	0.18
Ever smokers (%)		47.8	39.1	44.9	-0.63;-2.35	1.09
BMI (kg/m^2)		21.8±2.0	22.1±1.9	22.1±2.1	0.07;-0.35	0.49
Waist (cm)		76.3±8.1	78.4±7.8	75.3±5.6	0.08;-0.02	0.18
Systolic blood pressure (mmHg)		117.4±7.7	116.7±7.4	116.6±9.1	-0.05;-0.15	0.05
Diastolic blood pressure (mmHg)		74.9±6.0	75.1±5.8	75.3±5.6	-0.01;-0.16	0.14
Uric acid (mmol/L)		154.6±47.6	160.6±41.6	172.5±53.5	0.014;-0.004	0.03
Insulin (pmol/L)		6.0 (0.6-49.2)	9.6 (1.2-108.6)	9.0 (3.0-72.0)	0.41;-0.90	1.72
HOMA insulin resistance (mU/mL´mmol/L)		0.25 (0.02-2.08)	0.34 (0.05-5.40)	0.30 (0.10-2.28)	0.48;-0.85	1.81
Fasting glucose (mmol/L)		5.1±0.4	5.1±0.5	5.2±0.7	0.84;-0.68	2.36
HDL-cholesterol (mmol/L)		1.8±0.3	1.7±0.4	1.8±0.3	1.73;-0.73	4.19
Triglycerides (mmol/L)		1.0 (0.5-1.7)	1.1 (0.6-1.7)	1.0 (0.4-1.7)	-0.48;-3.65	2.69
Hs-CRP (mg/L)		0.80 (0.10-20.0)	0.60 (0.20-12.6)	0.70 (0.20-8.90)	-0.16;-0.96	0.64
	ALT	1st tertile (≤12 U/L)	2nd tertile (>12≤17 U/L)	3rd tertile (>17 U/L)	β; 95%CI	
Number		66	67	72		
Age (yr)		51.9±5.5	52.3±5.4	52.6±5.5	-0.04; -0.29	0.21
Male (%)		15.1	35.8	47.2	4.43; 1.57	7.29
Alcoholics (%)		45.4	50.7	55.6	2.02; -0.72	4.76
Alcohol (g/day within drinkers)		14.8±9.3	16.7±9.1	16.6±9.4	0.03; -0.2	0.26
Ever smokers (%)		47.0	46.3	38.9	-1.10; -3.86	1.66
BMI (kg/m^2)		21.8±2.1	21.5±2.1	22.6±1.7	0.55; -0.13	1.23
Waist (cm)		76.8±7.2	75.4±8.8	81.2±7.3	0.23; 0.07	0.39
Systolic blood pressure (mmHg)		115.2±9.0	117.4±6.3	117.9±8.4	0.09; -0.08	0.26
Diastolic blood pressure (mmHg)		75.3±6.3	74.0±5.3	75.9±5.7	0.15; -0.08	0.38
Uric acid (mmol/L)		154.6±41.6	160.6±53.5	172.5±47.6	0.035; 0.008	0.06
Insulin (pmol/l)		7.5 (0.6-108.6)	9.6 (2.4-49.2)	8.4 (1.2-72.0)	1.24; -0.88	3.36
HOMA insulin resistance (mU/mL×mmol/L)		0.29 (0.02-5.40)	0.34 (0.09-2.08)	0.30 (0.05-2.56)	1.41; -0.73	3.54
Fasting glucose (mmol/L)		5.2±0.6	5.0±0.5	5.2±0.6	1.43; -1.02	3.88
HDL-cholesterol (mmol/L)		1.8±0.3	1.7±0.4	1.7±0.4	-2.07; -6.05	1.91
Triglycerides (mmol/L)		0.9 (0.5-1.7)	1.0 (0.4-1.5)	1.0 (0.4-1.7)	0.91; -4.22	6.04
Hs-CRP (mg/L)		0.80 (0.10-20.0)	0.50 (0.20-17.8)	0.95 (0.20-12.6)	1.15; -0.12	2.42
	GGT	1st tertile (≤10 U/L)	2nd tertile (>10≤16 U/L)	3rd tertile (>16 U/L)	β; 95%CI	
Number		68	71	66		
Age (year)		51.7±5.2	52.3±5.6	52.8±5.5	0.009; -0.008	0.026
Male (%)		17.6	29.6	53.0	0.48; 0.29	0.66
Alcoholics (%)		36.8	54.9	60.6	0.24; 0.06	0.42
Alcohol (g/day within drinkers)		11.2±7.9	16.6±8.6	18.6±9.6	0.012; -0.002	0.026
Ever smokers (%)		35.3	45.1	51.5	0.14; -0.05	0.33
BMI (kg/m^2)		21.7±1.9	22.0±2.0	22.3±2.1	0.034; -0.012	0.08
Waist (cm)		76.4±7.2	76.4±8.6	81.1±7.7	0.19; 0.18	0.20
Systolic blood pressure (mmHg)		116.0±9.0	117.3±6.3	117.4±8.7	0.008;-0.004	0.02
Diastolic blood pressure (mmHg)		74.6±6.3	74.9±5.7	75.8±5.4	-0.012;-0.004	0.03
Uric acid (mmmol/L)		148.7±35.7	166.5±41.6	178.4±59.5	0.004; 0.002	0.006
Insulin (pmol/L)		9.6 (3.0-72.0)	9.0 (0.6-63.6)	8.4 (1.2-108.6)	0.004;-0.14	0.14
HOMA insulin resistance (mU/mL×mmol/L)		0.34 (0.10-2.28)	0.30 (0.02-2.56)	0.30 (0.04-5.40)	0.047; -0.09	0.18
Fasting glucose (mmol/L)		4.8±0.4	5.1±0.5	5.5±0.5	0.35; 0.19	0.51
HDL-cholesterol (mmol/L)		1.8±0.3	1.7±0.3	1.7±0.4	-0.12; -0.39	0.15
Triglycerides (mmol/L)		0.9 (0.4-1.5)	1.0 (0.4-1.7)	1.1 (0.7-1.7)	0.52; 0.19	0.85
Hs-CRP (mg/L)		0.50 (0.20-8.30)	0.80 (0.10-8.90)	0.95 (0.20-20.0)	0.21; 0.13	0.29

Median (range) is reported for not-normally distributed variables; their log-transformed values and log-GGT values are used in the analyses.

Thus, the relationships previously found might reflect associations between ALT or GGT levels and obesity or insulin resistance. Accordingly, authors have found that the associations between GGT levels and diabetes or blood pressure have been attenuated on adjustment for known risk factors for diabetes or for plasma insulin levels and have speculated that visceral fat could play a role in the association of GGT with type 2 diabetes[2,4,27].

The subgroup of subjects free from abnormal glucose, lipid, pressure values and with normal BMI and waist circumference avoids these possible interference from confounding factors. Within this group, increased GGT levels are significantly associated with hs-CRP and fasting glucose values, after multiple adjustments.

Table 3 Associations of different clinical and laboratory variables with liver enzyme levels in all the patients (left) and in subjects with normal BMI and without any component of the metabolic syndrome (right) in a multiple regression model

	ALL			Normal	BMI and no component of the MS	
	β	95%CI		β	95%CI	
	AST					
Age	0.02	-0.06	0.10	-0.015	-0.17	0.14
Male	0.58	-0.54	1.70	-0.70	-3.05	1.65
Ever smoking	-1.06	-2.16	0.04	-0.54	-2.34	1.26
BMI	-0.13	-0.29	0.03	-0.25	-0.83	0.33
Waist	0.09	0.03	0.15	0.12	-0.04	0.28
G/day alcohol	0.04	0.0	0.08	0.07	-0.02	0.16
Hs-CRP	-0.015	-0.06	0.03	-0.29	-0.55	1.13
HOMA-IR	0.25	-0.28	0.77	0.26	-1.11	1.63
Triglycerides	0.17	-0.91	1.25	-1.39	-4.76	1.98
Uric acid	0.01	0.0	0.02	0.01	-0.009	0.03
	ALT					
Age	-0.09	-0.21	0.02	-0.12	-0.37	0.13
Male	3.32	1.58	5.06	3.36	-0.32	7.04
Ever smoking	1.13	-0.30	2.56	-2.27	-5.11	0.57
BMI	0.22	-0.01	0.45	0.07	-0.83	0.97
Waist	0.10	0.01	0.19	0.11	-0.14	0.36
G/day alcohol	0.015	-0.05	0.08	0.03	-0.11	0.17
Hs-CRP	-0.04	-0.74	0.66	1.16	-0.15	2.47
HOMA-IR	1.85	1.03	2.67	0.91	-1.25	3.07
Triglycerides	2.07	0.37	3.77	-0.88	-6.15	4.39
Uric acid	0.015	0.001	0.03	0.01	-0.02	0.04
	GGT					
Age	-0.0004	-0.006	0.006	-0.003	-0.019	0.013
Male	0.29	0.21	0.37	0.31	0.10	0.52
Ever smoking	0.02	-0.04	0.07	0.025	-0.16	0.20
BMI	-0.0003	-0.012	0.012	-0.02	-0.07	0.04
Waist	0.004	0.0	0.008	0.0035	-0.012	0.019
G/day alcohol	0.006	0.002	0.010	0.005	-0.003	0.014
Hs-CRP	0.09	0.05	0.12	0.19	0.11	0.27
HOMA-IR	0.03	-0.01	0.07	-0.05	-0.19	0.09
Triglycerides	0.21	0.13	0.29	0.26	-0.05	0.57
Uric acid	0.0012	0.0006	0.0018	0.002	0.0	0.004

Multiple regression analyses with adjustments for all the variables listed.

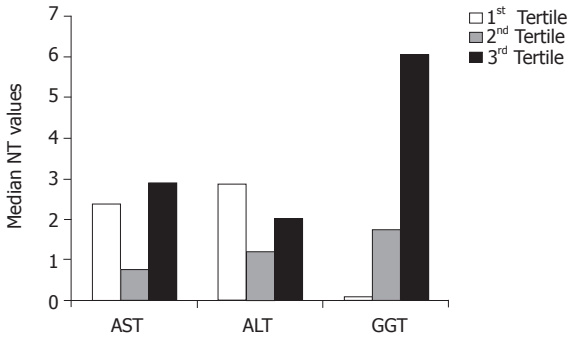

Figure 1 Median NT values for tertile of liver enzyme levels in subjects with normal BMI and without any component of the metabolic syndrome. At simple and multiple regression analyses NT values are associated with increasing GGT tertiles (P<0.001), but not with ALT or AST tertiles.

There is a progressive and significant increment of NT levels with increasing GGT tertile, not evident within the tertiles of the other liver enzymes that were tested (Figure 1). Furthermore, NT levels are significantly associated to fasting glucose values.

NT, generated from the oxidation of tyrosine, has been considered as a measure of oxidative injury from peroxynitrite (deriving from the reaction of nitric oxide with superoxide anion radicals), and reported to be elevated in diabetes, a condition associated with oxidative stress[28,29].

It could be speculated that the association between GGT levels and fasting glucose, not confounded by other metabolic abnormalities in the subgroup of "metabolically" healthy individuals, could be due to the adverse oxidative pattern of these subjects, suggested by the sharp increase of NT levels in the individuals within the highest GGT tertile.

In line with this, previous studies have reported a primary role for GGT in metabolizing extracellular reduced glutathione, a cellular antioxidant, allowing for precursor amino acids to be reutilized for the intracellular synthesis of glutathione[4,5,18]. Furthermore, dietary and serum antioxidants inversely predicted future GGT levels, while these latter are associated to F2-isoprostanes, a marker of oxidative damage[4,16-18]. It has been speculated that elevated GGT levels might be a defensive response to oxidative stress or, otherwise a marker of oxidative stress, being involved directly in the generation of reactive oxygen species, especially in the presence of iron or other transition metals, inducing lipid peroxidation in

human biological membranes[17,18,30,31]. Whether GGT is a causative factor for oxidative stress or a marker is currently unknown.

Aminotransferases were not associated with NT levels (Figure 1), in agreement with studies that showed lower associations between ALT levels and antioxidant vitamins and micronutrients, at least in individuals with normal BMI or fat distribution[18,32].

Thus, in subjects without other metabolic abnormalities, serum GGT might represent a marker of oxidative stress, and justify the associations found with higher fasting glucose values in these healthy individuals.

We cannot exclude the possibility that abnormal GGT values reflect fatty liver deposition, predating the development of subsequent diabetes; furthermore, hepatic ultrasonography or more invasive instrumental methods have not been performed in our subjects. Otherwise, they could be considered as "metabolically obese, normal weight" individuals, in consideration of their higher, though within the normal range, waist values[33]. Indeed our subjects with elevated GGT levels do not show higher insulin levels or insulin resistance (Table 2) and fatty liver has been associated with hyperinsulinemia and insulin resistance[14,15], and associations remain significant, after adjustments for waist circumference and BMI. Accordingly, abnormal liver enzymes have been found in a proportion of normal BMI individuals without fatty liver by ultrasound[34].

Furthermore, the correlations found are independent by adjustment for aminotransferase levels, which are better indicators of hepatocellular statuses and these latter are not associated with glycemia in the subgroup of normal BMI individuals.

Finally, increased GGT levels are conventionally considered as a marker of alcoholic abuse; however, only moderate drinkers have been included in the study, adjustments for alcohol intake have been performed, and correlations do not change after including only non-drinkers.

Another possible mechanism implicated is chronic inflammation: hs-CRP, an acute-phase reactant of hepatic origin and a sensitive marker for systemic inflammation, predicts the occurrence of diabetes, the metabolic syndrome and atherosclerotic diseases in healthy subjects[35]. Previous studies have found associations between GGT and CRP or other inflammatory parameters, suggesting that this enzyme represents the expression of sub-clinical inflammation, and has a role in cellular stress[3,4,9,10,20,21]. In our healthy cohort, hs-CRP levels are significantly associated either with highest GGT values or with fasting glucose. Oxidative processes might have an implication in chronic inflammation[19]; it has been hypothesized that elevation in GGT might occur before an elevation in CRP, and the related oxidative stress would give rise to a subsequent inflammatory response[21].

Again, aminotransferases are not associated with hs-CRP in normal BMI individuals, in line with previous reports, which did not find such an association[6,8,21].

Another explanation might be related to the liver response to pro-inflammatory cytokine tumor necrosis factor-α, giving fatty hepatic changes, or to the inflammatory processes accompanying non-alcoholic fatty liver and contributing to the systemic inflammation observed in these subjects, frequently affected by the MS[20,36]. However, the lack of a significant association between hs-CRP and ALT (a better marker for liver fat accumulation) levels in our normal BMI individuals is against this pathogenetic hypothesis at least in this subgroup. Accordingly, other authors demonstrated that CRP and aminotransferases predicted diabetes independent of each other, with similar magnitude associations[8].

Since the majority of healthy subjects within the highest GGT tertile show enzyme levels within targets of normality (89%), it could be suggested that variations within the normal ranges of GGT are associated with a worse oxidative or inflammatory pattern.

A single measurement of glucose, insulin, hs-CRP or liver enzyme levels represents a limitation of the present study, although common to most epidemiological studies. However, random errors due to the fluctuations of laboratory measurements usually lead to a reduced estimate of the associated strength. Serum oxidative markers could not directly reflect hepatocellular levels, and the existence of oxidative stress depends on the relative balance of reactive oxygen species and all the microenvironment antioxidant defenses, that could not be evaluated in such an observational study.

Whether elevated GGT levels should be added to the cluster of cardiovascular risk factors that form the metabolic syndrome and link insulin resistance to cardiovascular disease, as supported by literature[37,38] or if elevated GGT levels represent a marker of oxidative stress or inflammation could not be established by a cross-sectional study. Nevertheless, the hypothesis that elevated GGT levels may represent an early, easy, and inexpensive marker for a higher subsequent metabolic risk in apparently healthy subjects seems intriguing and worthy of future investigation.

In conclusion, in adult healthy subjects without any measurable metabolic abnormality, those with the highest GGT levels present with either higher fasting glucose values (even within the range of normality) and evidence of some oxidative stress or inflammation; aminotransferase levels do not show these correlations. The follow-up of these individuals would determine if GGT values might be considered as an early predictor of subsequent diabetes occurrence.

ACKNOWLEDGMENTS

We are indebted to Dr Carla Baldi, Dr Lorenzo Benini, Dr Ferruccio Dusio, Dr Giuseppe Forastiere, Dr Claudio Lucia, Dr Claudio Nuti, for their precious assistance in performing the study.

REFERENCES

1 **Nilssen O**, Førde OH. Seven-year longitudinal population

study of change in gamma-glutamyltransferase: the Tromsø Study. *Am J Epidemiol* 1994; **139:** 787-792
2 **Perry IJ**, Wannamethee SG, Shaper AG. Prospective study of serum gamma-glutamyltransferase and risk of NIDDM. *Diabetes Care* 1998; **21:** 732-737
3 **Vozarova B**, Stefan N, Lindsay RS, Saremi A, Pratley RE, Bogardus C, Tataranni PA. High alanine aminotransferase is associated with decreased hepatic insulin sensitivity and predicts the development of type 2 diabetes. *Diabetes* 2002; **51:** 1889-1895
4 **Lee DH**, Jacobs DR, Gross M, Kiefe CI, Roseman J, Lewis CE, Steffes M. Gamma-glutamyltransferase is a predictor of incident diabetes and hypertension: the Coronary Artery Risk Development in Young Adults (CARDIA) Study. *Clin Chem* 2003; **49:** 1358-1366
5 **Lee DH**, Ha MH, Kim JH, Christiani DC, Gross MD, Steffes M, Blomhoff R, Jacobs DR. Gamma-glutamyltransferase and diabetes--a 4 year follow-up study. *Diabetologia* 2003; **46:** 359-364
6 **Sattar N**, Scherbakova O, Ford I, O'Reilly DS, Stanley A, Forrest E, Macfarlane PW, Packard CJ, Cobbe SM, Shepherd J. Elevated alanine aminotransferase predicts new-onset type 2 diabetes independently of classical risk factors, metabolic syndrome, and C-reactive protein in the west of Scotland coronary prevention study. *Diabetes* 2004; **53:** 2855-2860
7 **Lee DH**, Silventoinen K, Jacobs DR, Jousilahti P, Tuomileto J. gamma-Glutamyltransferase, obesity, and the risk of type 2 diabetes: observational cohort study among 20,158 middle-aged men and women. *J Clin Endocrinol Metab* 2004; **89:** 5410-5414
8 **Hanley AJ**, Williams K, Festa A, Wagenknecht LE, D'Agostino RB, Kempf J, Zinman B, Haffner SM. Elevations in markers of liver injury and risk of type 2 diabetes: the insulin resistance atherosclerosis study. *Diabetes* 2004; **53:** 2623-2632
9 **Nakanishi N**, Nishina K, Li W, Sato M, Suzuki K, Tatara K. Serum gamma-glutamyltransferase and development of impaired fasting glucose or type 2 diabetes in middle-aged Japanese men. *J Intern Med* 2003; **254:** 287-295
10 **Nakanishi N**, Suzuki K, Tatara K. Serum gamma-glutamyltransferase and risk of metabolic syndrome and type 2 diabetes in middle-aged Japanese men. *Diabetes Care* 2004; **27:** 1427-1432
11 **Sakugawa H**, Nakayoshi T, Kobashigawa K, Nakasone H, Kawakami Y, Yamashiro T, Maeshiro T, Tomimori K, Miyagi S, Kinjo F, Saito A. Metabolic syndrome is directly associated with gamma glutamyl transpeptidase elevation in Japanese women. *World J Gastroenterol* 2004; **10:** 1052-1055
12 **Liu CM**, Tung TH, Liu JH, Chen VT, Lin CH, Hsu CT, Chou P. A community-based epidemiological study of elevated serum alanine aminotransferase levels in Kinmen, Taiwan. *World J Gastroenterol* 2005; **11:** 1616-1622
13 **van Barneveld T**, Seidell JC, Traag N, Hautvast JG. Fat distribution and gamma-glutamyl transferase in relation to serum lipids and blood pressure in 38-year old Dutch males. *Eur J Clin Nutr* 1989; **43:** 809-818
14 **Marchesini G**, Brizi M, Bianchi G, Tomassetti S, Bugianesi E, Lenzi M, McCullough AJ, Natale S, Forlani G, Melchionda N. Nonalcoholic fatty liver disease: a feature of the metabolic syndrome. *Diabetes* 2001; **50:** 1844-1850
15 **Pagano G**, Pacini G, Musso G, Gambino R, Mecca F, Depetris N, Cassader M, David E, Cavallo-Perin P, Rizzetto M. Nonalcoholic steatohepatitis, insulin resistance, and metabolic syndrome: further evidence for an etiologic association. *Hepatology* 2002; **35:** 367-372
16 **Lee DH**, Gross MD, Jacobs DR. Association of serum carotenoids and tocopherols with gamma-glutamyltransferase: the Cardiovascular Risk Development in Young Adults (CARDIA) Study. *Clin Chem* 2004; **50:** 582-588
17 **Lee DH**, Steffen LM, Jacobs DR. Association between serum gamma-glutamyltransferase and dietary factors: the Coronary Artery Risk Development in Young Adults (CARDIA) Study. *Am J Clin Nutr* 2004; **79:** 600-605
18 **Lim JS**, Yang JH, Chun BY, Kam S, Jacobs DR, Lee DH. Is serum gamma-glutamyltransferase inversely associated with serum antioxidants as a marker of oxidative stress? *Free Radic Biol Med* 2004; **37:** 1018-1023
19 **Pleiner J**, Mittermayer F, Schaller G, Marsik C, MacAllister RJ, Wolzt M. Inflammation-induced vasoconstrictor hyporeactivity is caused by oxidative stress. *J Am Coll Cardiol* 2003; **42:** 1656-1662
20 **Kerner A**, Avizohar O, Sella R, Bartha P, Zinder O, Markiewicz W, Levy Y, Brook GJ, Aronson D. Association between elevated liver enzymes and C-reactive protein. possible hepatic contribution to systemic inflammation in the metabolic syndrome. *Arterioscler Thromb Vasc Biol* 2005; **25:** 193-197
21 **Lee DH**, Jacobs DR. Association between serum gamma-glutamyltransferase and C-reactive protein. *Atherosclerosis* 2005; **178:** 327-330
22 **Kim HJ**, Kim HJ, Lee KE, Kim DJ, Kim SK, Ahn CW, Lim SK, Kim KR, Lee HC, Huh KB, Cha BS. Metabolic significance of nonalcoholic fatty liver disease in nonobese, nondiabetic adults. *Arch Intern Med* 2004; **164:** 2169-2175
23 **Suzuki A**, Angulo P, Lymp J, St Sauver J, Muto A, Okada T, Lindor K. Chronological development of elevated aminotransferases in a nonalcoholic population. *Hepatology* 2005; **41:** 64-71
24 The Expert Committee on the Diagnosis and Classification of Diabetes Mellitus. Report of the Expert Committee on the Diagnosis and Classification of Diabetes Mellitus. *Diabetes Care* 2003; **26:** S5-S20
25 Executive Summary of The Third Report of The National Cholesterol Education Program (NCEP) Expert Panel on Detection, Evaluation, And Treatment of High Blood Cholesterol In Adults (Adult Treatment Panel III). *JAMA* 2001; **285:** 2486-2497
26 **Matthews DR**, Hosker JP, Rudenski AS, Naylor BA, Treacher DF, Turner RC. Homeostasis model assessment: insulin resistance and beta-cell function from fasting plasma glucose and insulin concentrations in man. *Diabetologia* 1985; **28:** 412-419
27 **Ikai E**, Ishizaki M, Suzuki Y, Ishida M, Noborizaka Y, Yamada Y. Association between hepatic steatosis, insulin resistance and hyperinsulinaemia as related to hypertension in alcohol consumers and obese people. *J Hum Hypertens* 1995; **9:** 101-105
28 **Ceriello A**, Mercuri F, Quagliaro L, Assaloni R, Motz E, Tonutti L, Taboga C. Detection of nitrotyrosine in the diabetic plasma: evidence of oxidative stress. *Diabetologia* 2001; **44:** 834-838
29 **Ceriello A**, Quagliaro L, Catone B, Pascon R, Piazzola M, Bais B, Marra G, Tonutti L, Taboga C, Motz E. Role of hyperglycemia in nitrotyrosine postprandial generation. *Diabetes Care* 2002; **25:** 1439-1443
30 **Drozdz R**, Parmentier C, Hachad H, Leroy P, Siest G, Wellman M. gamma-Glutamyltransferase dependent generation of reactive oxygen species from a glutathione/transferrin system. *Free Radic Biol Med* 1998; **25:** 786-792
31 **Paolicchi A**, Minotti G, Tonarelli P, Tongiani R, De Cesare D, Mezzetti A, Dominici S, Comporti M, Pompella A. Gamma-glutamyl transpeptidase-dependent iron reduction and LDL oxidation--a potential mechanism in atherosclerosis. *J Investig Med* 1999; **47:** 151-160
32 **Ruhl CE**, Everhart JE. Relation of elevated serum alanine aminotransferase activity with iron and antioxidant levels in the United States. *Gastroenterology* 2003; **124:** 1821-1829
33 **Ruderman N**, Chisholm D, Pi-Sunyer X, Schneider S. The metabolically obese, normal-weight individual revisited. *Diabetes* 1998; **47:** 699-713
34 **Sakugawa H**, Nakayoshi T, Kobashigawa K, Nakasone H, Kawakami Y, Yamashiro T, Maeshiro T, Tomimori K, Miyagi S, Kinjo F, Saito A. Alanine aminotransferase elevation not associated with fatty liver is frequently seen in obese Japanese women. *Eur J Clin Nutr* 2004; **58:** 1248-1252
35 **Ridker PM**, Wilson PW, Grundy SM. Should C-reactive protein be added to metabolic syndrome and to assessment of

global cardiovascular risk? *Circulation* 2004; **109:** 2818-2825
36 **Yin M**, Wheeler MD, Kono H, Bradford BU, Gallucci RM, Luster MI, Thurman RG. Essential role of tumor necrosis factor alpha in alcohol-induced liver injury in mice. *Gastroenterology* 1999; **117:** 942-952
37 **Wannamethee G**, Ebrahim S, Shaper AG. Gamma-glutamyltransferase: determinants and association with mortality from ischemic heart disease and all causes. *Am J Epidemiol* 1995; **142:** 699-708
38 **Jousilahti P**, Rastenyte D, Tuomilehto J. Serum gamma-glutamyl transferase, self-reported alcohol drinking, and the risk of stroke. *Stroke* 2000; **31:** 1851-1855

Science Editor Guo SY **Language Editor** ELsevier HK

PO Box 2345, Beijing 100023, China
www.wjgnet.com
wjg@wjgnet.com

ELSEVIER

World J Gastroenterol 2005;11(45):7118-7121
World Journal of Gastroenterology ISSN 1007-9327

• *CLINICAL RESEARCH* •

Usefulness of ω-3 fatty acid supplementation in addition to mesalazine in maintaining remission in pediatric Crohn's disease: A double-blind, randomized, placebo-controlled study

C Romano, S Cucchiara, A Barabino, V Annese, C Sferlazzas, SIGENP Italian Study Group of Pediatric Inflammatory Bowel Diseases

C Romano, Pediatric Department, University of Messina, Italy
S Cucchiara, University "La Sapienza", Roma, Italy
A Barabino, IRCCS G. Gaslini, Genova, Italy
V Annese, IRCCS, S. Giovanni Rotondo, Italy
C Sferlazzas, University of Messina, Italy
Correspondence to: Claudio Romano, MD, Pediatric Department, University of Messina, Italy. romanoc@unime.it
Telephone: +39-0902212918 Fax: +39-0902213788
Received: 2005-02-15 Accepted: 2005-04-02

Abstract

AIM: To assess the value of long-chain ω-3 fatty acids (FAs) supplementation in addition to amino-salicylic-acid (5-ASA) in pediatric patients with Crohn's disease (CD).

METHODS: Thirty-eight patients (20 males and 18 females, mean age 10.13 years, range 5-16 years) with CD in remission were randomized into two groups and treated for 12 mo. Group I (18 patients) received 5-ASA (50 mg/kg/d)+ω-3 FAs as triglycerides in gastro-resistant capsules, 3 g/d (eicosapentanoic acid, EPA, 400 mg/g, docosahexaenoic acid, DHA, 200 mg/g). Group II (20 patients) received 5-ASA (50 mg/kg/d)+olive oil placebo capsules. Patients were evaluated for fatty acid incorporation in red blood cell membranes by gas chromatography at baseline 6 and 12 mo after the treatment.

RESULTS: The number of patients who relapsed at 1 year was significantly lower in group I than in group II ($P<0.001$). Patients in group I had a significant increase in the incorporation of EPA and DHA ($P<0.001$) and a decrease in the presence of arachidonic acids.

CONCLUSION: Enteric-coated ω-3 FAs in addition to treatment with 5-ASA are effective in maintaining remission of pediatric CD.

Key words: Crohn's disease; ω-3 fatty acids; Remission maintenance; Treatment
Romano C, Cucchiara S, Barabino A, Annese V, Sferlazzas C. Usefulness of ω-3 fatty acid supplementation in addition to mesalazine in maintaining remission in pediatric Crohn's disease: A double-blind, randomized, placebo-controlled study. *World J Gastroenterol*; 2005 11(45): 7118-7121

http://www.wjgnet.com/1007-9327/11/7118.asp

INTRODUCTION

The etiology and pathogenesis of CD are still unknown[1]. First-line therapy is still based on the combinations of glucocorticoids and amino-salicylic acid (5-ASA) derivatives. Knowledge of inflammatory mechanisms and the high incidence of side effects with steroids have induced researchers to look for valid alternatives, especially in maintaining remission secondary to steroid treatment[2]. The rationale for the use of ω-3 FAs in uncomplicated CD is that metabolites of the arachidonic acid (AA), which are considered as primarily responsible for inflammatory process and intestinal inflammation in CD, are produced from fatty acids[3]. Administration of EPA and DHA, the predominant fatty acids in fish oil, causes competition with AA for the utilization of 5-lipoxygenase enzyme cascade, thus inhibiting the production of inflammatory metabolites such as LTB4[4].

Data in literature on the use of ω-3 fatty acids are controversial. Belluzzi *et al*[5]. claimed that ω-3 FAs seem prudent to promote a diet rich in fish oil in patients with CD, while Lorenz-Meyer *et al*[6]. did not demonstrate any effect of ω-3 FA supplementation on the remission of CD in adults.

Since the use of fish oil has not yet been intensively studied in children with CD, we carried out a placebo-controlled clinical trial in children with CD by administering either ω-3 fatty acid or olive oil capsules used as a placebo in addition to 5-ASA.

MATERIALS AND METHODS

A double-blind, randomized study was carried out in 38 patients with CD (20 males and 18 females, mean age 10.13 years, range 5-16 years) recruited from eight Italian Pediatric Gastroenterology Centers. All of them had a definite diagnosis of CD based on accepted endoscopic and histological criteria if available (27 patients)[7].

Inclusion criteria were pediatric Crohn's disease activity index (PCDAI) score <20 for at least 2 mo obtained by an 8-wk course of corticosteroid treatment (1 mg/kg/d), no extraintestinal involvement of the disease, no previous intestinal resection (apart from appendectomy), no previous immunosuppressant treatment and a wash-out

period of at least 3 mo from corticosteroids.

All patients were non-smokers. After enrollment, patients were randomized into two groups according to the intestinal localization of the disease (Table 1) and treated for 12 mo as follows. Eighteen patients (9 males and 9 females) in group 1 were treated with time-dependant 5-ASA (50 mg/kg/d)+ω-3 FAs as triglycerides in gastro-resistant capsules, 3 g/d (TRIOLIP - SOFAR, Italy). Each capsule contained 400 mg/g EPA and 200 mg/g DHA. Eighteen patients (11 males and 9 females) in group 2 were treated with time-dependant 5-ASA (50 mg/kg/d)+olive oil placebo capsules. Patients who had a relapse were excluded from the study.

Clinical evaluations and several laboratory tests [assessment of blood cell count, erythrocyte sedimentation rate (ESR), C-reactive protein (PCR) and electrophoresis] were carried out at enrollment (T0) and after 6 (T1) and then 12 (T2) months of treatment. Fatty acids in the red blood cell membranes were also evaluated with gas chromatography on capillar column (SP 2340 Supelco). Analysis temperature was set at 160 ℃ and 210 ℃ with a gradient of 8 ℃/min, while the gas carrier (He) flow was 2 mL/min. The percentage (% mol) of each single fatty acid was compared to an external standard.

Statistical analysis

Data were analyzed by the statistical program 7.0 for Windows. The significance of the differences between averages and proportions was calculated by bivariate analysis (χ^2 square). $P<0.005$ was considered statistically significant.

Table 1 Characteristics of patients at the beginning of the study

	Group 1 (5-ASA+ω-3)	Group 2 (5-ASA+placebo)
Number of patients	18	20
Mean age (yr)	9.33	10.85
Sex (M/F)	9/9	11/9
Disease localization		
Ileal	10	7
Ileo-colic	6	8
Colic	2	5

RESULTS

Relapse (PCDAI score >20) after 1 year occurred in 11 patients (61%) of group 1 and 19 patients (95%) of group 2 (Figure 1A) with a statistically significant difference ($P = 0.0016$). However, no relapse occurred after 6 mo of follow-up in patients of group 1 who received capsules of EPA and DHA. The disease relapse occurred 8 mo after the treatment in group 1 and 1 mo in group 2 (Figure1B) with a statistically significant difference ($P<0.001$). Patients in group 2 and those with ileo-colonic localization presented a greater number of relapses (Figure 1C)

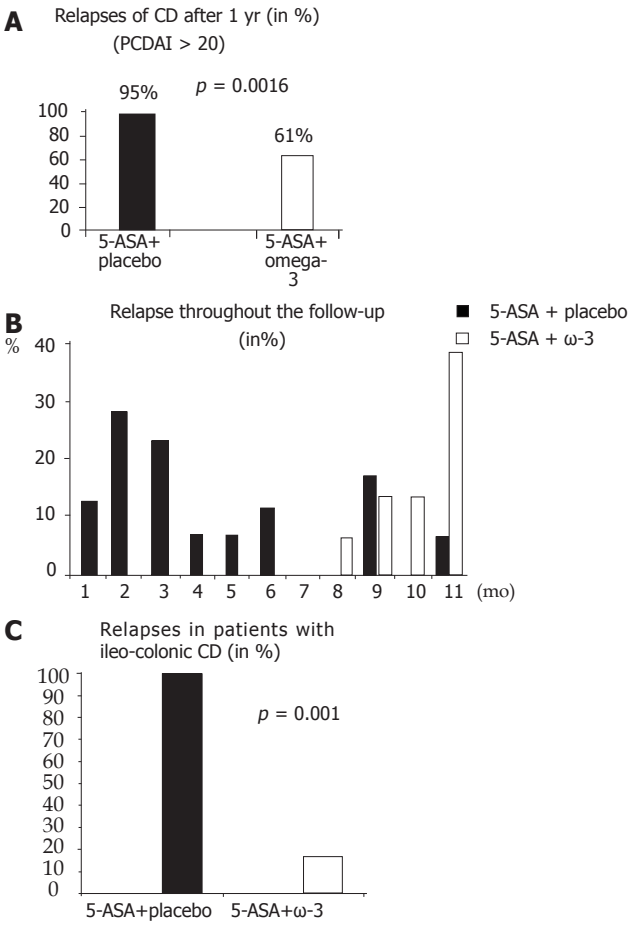

Figure 1 Relapses of CD after 1 yr (**A**), throughout the follow-up (**B**) and in those with ileo-colonic CD (**C**) (%).Characteristics of patients at the beginning of the study

compared to those under treatment (group 1) who had the same initial localization of the disease ($P = 0.001$). Compliance to the assumption of the capsules was optimal in all the patients and no side effects were reported in patients of either group.

All subjects in group 1 showed a significant increase in the range of incorporation of EPA (%/mol): 1.1±1, 2.48±1.83, 2.07±0.5 ($P<0.005$) and DHA (% mol): 1.81±0.68, 2.55±0.97, 3.54±0.85 ($P<0.001$) and a decrease in the presence of AA (% mol): 6.17±2.63, 5.5±2.33, 5.56±2.05 between T0 and T2.

DISCUSSION

Since no definite treatment for CD is available and the precise mechanism which triggers and maintains the intestinal inflammation is not yet well known, the aim of the treatment is to induce and maintain clinical remission[8]. There are several therapeutic options for the treatment of CD. Mild-to-moderate disease has been managed with nutritional support, 5-ASA and antibiotics[9], while the mainstay therapy for severe or complicated disease includes steroids, immunosuppressants and biological therapy[10].

Drugs most commonly used in the treatment of

inflammatory bowel disease (IBD) act by interfering with the AA metabolic pathway. Glucocorticoids prevent the formation of free AA through the inhibition of the activity of phospholipases A2 and C on the membrane phospholipids, while mesalazine acts with its N-acetyl-5-ASA metabolite through the inhibition of 5-lipoxygenase in the colonic mucosa. However, both drugs have not proved to be effective in maintaining the remission of CD[11] and many relapses of the disease can occur[12]. Biological agents introduced in recent years seem to be effective in inducing remission of active disease resistant to standard treatment but not in maintaining the remission[13].

The most prolonged remission has been obtained with 6-mercaptopurine and its pro-drug azathioprine[14]. Their efficacy in maintaining remission is widely accepted, but toxicity and possible side-effects have been reported[15]. Another therapeutic option to maintain CD remission is represented by w-FAs. In 1986, Lee *et al*[16]. reported that fatty acids contained in fish oil can limit the AA pathway. Kim[17] reported that patients with active CD have increased levels of LTB4 in the colic mucosa associated with the severity of the disease. The anti-inflammatory effect of fish oil has been tested on animals (rats with induced colitis) and ω-3 FAs are observed to determine other biochemical effects such as reduction of mucosal and circulating levels of the main powerful pro-inflammatory cytokines (IL-1, TNF-α) and reduction of synthesis of the platelet activating factor (PAF), which has a strong pro-inflammatory activity. In addition, it has even been demonstrated that it acts as a free radical scavenger[18]. Fish oil reduces the inflammatory process competing with the AA. In fact, EPA, a polinsaturi fatty acid of 20 carbon atoms produced by the metabolism of α-linoleic acids, is different from the AA only for the presence of various double bonds in position-17. It is a good substratum for 5-lipoxygenase and competes with the AA for the utilization of this enzyme together with its corresponding DHA. The incorporation of EPA and DHA into the erythrocyte membranes is necessary to stimulate a competitive action on the AA. This effect involves a reduced LTB4 production and synthesis of a new leukotriene, LTB5, which has no inflammatory effects[19]. In 1990 Mc Call *et al*[20]. and Salomon *et al*[21]. carried out the preliminary clinical studies, showing that administration of fish oil in patients with IBD causes a significant reduction of the disease activity score (CDAI score). Hawthorne *et al*[22]. have verified how fish oil supplementation in patients with IBD in the active phase significantly reduces steroid consumption and results in a longer clinical remission. Confirmation of the usefulness of EPA in IBD is demonstrated by the significant decrease in the production of LTB4[23]. Since there are no adequate formulations of fish oil which could be used as a drug without side-effects, its widespread use in the treatment of IBD is limited. Belluzzi *et al*[5]. showed that capsules of EPA and DHA, a free fatty acid mixture, are well tolerated and can be used to treat patients for long periods instead of administering pure fish oil. Other reports are controversial, showing contrasting results in maintaining the remission of CD[24,25].

All these experiences reported in literature are referred to adult CD, but ω-3 FAs have not yet been evaluated in children with CD. Our study is the first placebo-controlled clinical trial in pediatric CD and has achieved several interesting results though the number of patients enrolled was less. In fact, the addition of enteric-coated capsules to a conventional therapy with 5-ASA in pediatric CD delayed the relapse of the disease even if it could not prevent it. This association seems that the addition of enteric-coated capsules is more effective than 5-ASA alone probably due to the synergistic effect of the drugs used. 5-ASA can inhibit some key factors of the inflammatory cascade (cyclooxygenase, thromboxane-synthetase and PAF-synthetase) as well as production of interleukin 1 and free radicals[26-28] and has an intrinsic anti-oxidant activity[29]. Furthermore, ω-3 FAs inhibit PAF-synthetase and thromboxane-synthetase acts as a free radical scavenger decreasing mucosal and circulating levels of some powerful pro-inflammatory cytokines (such as IL-1 and TNF-α)[18]. In light of these biochemical characteristics, it is clear that the association of these two anti-inflammatory compounds may strengthen their single anti-inflammatory role and explain the better results obtained with 5-ASA alone in maintaining the remission of pediatric CD. 5-ASA/ω-3 FAs seem to play the same role in pediatric CD as the balsalazide/VSL#3 in the treatment of adult ulcerative colitis. 5-ASA plus a probiotic mixture can obtain significantly better results than balsalazide alone or mesalazine alone in maintaining remission of mild-to-moderate ulcerative colitis due to the synergistic effect of the two powerful anti-inflammatory compounds[30].

In conclusion, supplementation of ω-3 fatty acids to a standard treatment with 5-ASA is a good choice for maintaining remission of pediatric CD.

ACKNOWLEDGMENTS

This study was carried out by the authors on behalf of the other members of the Italian Society of Paediatric Gastroenterology and Hepatology: Paola Roggero, University of Milan, Milano; Irene Papadatou, IRCCS Bambino Gesu', Roma; Sergio Amarri, University of Modena; Manila Candusso, IRCCS Burlo Garofalo, Trieste; Paolo Lionetti, University of Firenze.

The authors thank Dr Antonio Tursi for his constructive criticisms in preparing the manuscript.

REFERENCES

1 **Rampton DS.** Management of Crohn's disease. *BMJ* 1999; **319:** 1480-1485

2 **Beattie RM.** Therapy of Crohn's disease in childhood. *Paediatr Drugs* 2000; **2:** 193-203

3 **Kremer JM,** Jubiz W, Michalek A, Rynes RI, Bartholomew LE, Bigaouette J, Timchalk M, Beeler D, Lininger L. Fish-oil fatty acid supplementation in active rheumatoid arthritis. A double-blinded, controlled, crossover study. *Ann Intern Med* 1987; **106:** 497-503

4 **Lawson LD,** Hughes BG. Human absorption of fish oil fatty acids as triacylglycerols, free acids, or ethyl esters. *Biochem*

Biophys Res Commun 1988; **152:** 328-335
5 **Belluzzi A,** Brignola C, Campieri M, Pera A, Boschi S, Miglioli M. Effect of an enteric-coated fish-oil preparation on relapses in Crohn's disease. *N Engl J Med* 1996; **334:** 1557-1560
6 **Lorenz-Meyer H,** Bauer P, Nicolay C, Schulz B, Purrmann J, Fleig WE, Scheurlen C, Koop I, Pudel V, Carr L. Omega-3 fatty acids and low carbohydrate diet for maintenance of remission in Crohn's disease. A randomized controlled multicenter trial. Study Group Members (German Crohn's Disease Study Group). *Scand J Gastroenterol* 1996; **31:** 778-785
7 **Kornbluth A,** Salomon P, Sachard DB. Crohn's Disease. In: Sleisenger MH, Fordtrand JS, eds. Gastrointestinal Disease, 5th ed. Philadelphia: *WB Saunders*, **1993:** 1270-1304
8 **Seegers D,** Bouma G, Peña AS. Review article: a critical approach to new forms of treatment of Crohn's disease and ulcerative colitis. *Aliment Pharmacol Ther* 2002; **16** Suppl 4**:** 53-58
9 **Farrell RJ,** Banerjee S, Peppercorn MA et al. Recent advances in inflammatory bowel disease. *Crit Rev Clin Lab Sci* 2001; **38:** 33-108
10 **van Dullemen HM,** van Deventer SJ, Hommes DW, Bijl HA, Jansen J, Tytgat GN, Woody J. Treatment of Crohn's disease with anti-tumor necrosis factor chimeric monoclonal antibody (cA2). *Gastroenterology* 1995; **109:** 129-135
11 **Pestell K.** New targets for Crohn's disease. *Trends Pharmacol Sci* 2001; **22:** 342
12 **Markowitz J,** Grancher K, Kohn N, Daum F. Immunomodulatory therapy for pediatric inflammatory bowel disease: changing patterns of use, 1990-2000. *Am J Gastroenterol* 2002; **97:** 928-932
13 **Stephens MC,** Shepanski MA, Mamula P, Markowitz JE, Brown KA, Baldassano RN. Safety and steroid-sparing experience using infliximab for Crohn's disease at a pediatric inflammatory bowel disease center. *Am J Gastroenterol* 2003; **98:** 104-111
14 **Barabino A,** Torrente F, Ventura A, Cucchiara S, Castro M, Barbera C. Azathioprine in paediatric inflammatory bowel disease: an Italian multicentre survey. *Aliment Pharmacol Ther* 2002; **16:** 1125-1130
15 **Fefferman DS,** Alsahli M, Lodhavia PJ, Shah SA, Farrell RJ. Re: Triantafillidis. -Acute idiopathic pancreatitis complicating active Crohn's disease: favorable response to infliximab treatment. *Am J Gastroenterol* 2001; **96:** 2510-2511
16 **Lee TH.** Hoover RL, Williams JD, Sperling RI, Ravalese J, Spur BW, Robinson DR, Corey EJ, Lewis RA, Austen KF. Effect of dietary enrichment with eicosapentaenoic and docosahexaenoic acids on in vitro neutrophil and monocytes leukotrienes generation and monocyte leukotriene. *N Engl J Med* 1985; **312:** 1217-1224
17 **Kim YI.** Can fish oil maintain Crohn's disease in remission ? *Nutr Rev* 1996; **54:** 248-252
18 **von Schacky C,** Fischer S, Weber PC. Long-term effects of dietary marine omega-3 fatty acids upon plasma and cellular lipids, platelet function and eicosanoid formation in humans. *J Clin Invest* 1985; **76:** 1626-1631
19 **Weber PC.** Iatrogenic complications from chronic ear surgery. *Otolaryngol Clin North Am* 2005; **38:** 711-722
20 **McCall TB,** O'Learly D, Bloomfield J, O'Moráin CA. Therapeutic potential fish oil in the treatment of ulcerative colitis. *Aliment Pharmacol Ther* 1989; **3:** 415-424
21 **Salomon P,** Kornbluth AA, Janowitz HD. Treatment of ulcerative colitis with fish oil n-3-omega-fatty acid: an open trial. *J Clin Gastroenterol* 1990; **12:** 157-161
22 **Hawthorne AB,** Daneshmend TK, Hawkey CJ, Belluzzi A, Everitt SJ, Holmes GK, Malkinson C, Shaheen MZ, Willars JE. Treatment of ulcerative colitis with fish oil supplementation: a prospective 12 month randomised controlled trial. *Gut* 1992; **33:** 922-928
23 **Strasser T,** Fischer S, Weber PC . Leukotriene B5 is formed in human neutrophils after dietary supplementation with icosapentaenoic acid. *Proc Natl Acad Sci USA* 1985; **82:** 1540-1543
24 **Lorenz R,** Weber PC, Szimnau P, Heldwein W, Strasser T, Loeschke K. Supplementation with n-3 fatty acids from fish oil in chronic inflammatory bowel disease-a randomized, placebo-controlled, double-blind cross-over trial. *J Intern Med* Suppl 1989; **731:** 225-2322
25 **Geerling BJ,** Badart-Smook A, van Deursen C, van Houwelingen AC, Russel MG, Stockbrügger RW, Brummer RJ. Nutritional supplementation with N-3 fatty acids and antioxidants in patients with Crohn's disease in remission: effects on antioxidant status and fatty acid profile. *Inflamm Bowel Dis* 2000; **6:** 77-84
26 **Eliakim R,** Rachmilewitz D. Gastric lymphoma--an infectious disease? *Harefuah* 1994; **127:** 541-543
27 **Grisham MB.** Oxidants and free radicals in inflammatory bowel disease. *Lancet* 1994; **344:** 859-861
28 **Hanauer SB.** Inflammatory bowel disease. *N Engl J Med* 1996; **334:** 841-848
29 **Gonçalves E,** Almeida LM, Dinis TC. Antioxidant activity of 5-aminosalicylic acid against peroxidation of phosphatidylcholine liposomes in the presence of alpha-tocopherol: a synergistic interaction? *Free Radic Res* 1998; **29:** 53-66
30 **Tursi A,** Brandimarte G, Giorgetti GM, Forti G, Modeo ME, Gigliobianco A. Low-dose balsalazide plus a high-potency probiotic preparation is more effective than balsalazide alone or mesalazine in the treatment of acute mild-to-moderate ulcerative colitis. *Med Sci Monit* 2004; **10:** PI126-PI131

Science Editor Wang XL and Guo SY **Language Editor** Elsevier HK

PO Box 2345, Beijing 100023, China
www.wjgnet.com
wjg@wjgnet.com

ELSEVIER

World J Gastroenterol 2005;11(45):7122-7130
World Journal of Gastroenterology ISSN 1007-9327

• *CLINICAL RESEARCH* •

Outcome of non-variceal acute upper gastrointestinal bleeding in relation to the time of endoscopy and the experience of the endoscopist: A two-year survey

Fabrizio Parente, Andrea Anderloni, Stefano Bargiggia, Venerina Imbesi, Emilio Trabucchi, Cinzia Baratti, Silvano Gallus, Gabriele Bianchi Porro

Fabrizio Parente, Gastroenterology Unit, A. Manzoni Hospital, Lecco, Italy
Andrea Anderloni, Gastrointestinal Unit, Ospedale Maggiore della Carità, Novara, Italy
Stefano Bargiggia, Venerina Imbesi, Gabriele Bianchi Porro, Academic Department of Gastroenterology, L. Sacco University Hospital, Milan, Italy
Emilio Trabucchi, Cinzia Baratti, Department of Accident and Emergency and Postgraduate School of General Surgery, L. Sacco University Hospital, Milan, Italy
Silvano Gallus, Mario Negri Pharmacological Institute, Section of Medical Epidemiology, Milan, Italy
Correspondence to: Dr Fabrizio Parente, Gastroenterology Unit, A. Manzoni Hospital, Via dell'Eremo 9-11, 23900 Lecco, Italy. fabrizio. parente@tiscalinet.it
Fax: +39-0341-489966
Received: 2005-03-25 Accepted: 2005-05-12

Abstract

AIM: To prospectively assess the impact of time of endoscopy and endoscopist's experience on the outcome of non-variceal acute upper gastrointestinal (GI) bleeding patients in a large teaching hospital.

METHODS: All patients admitted for non-variceal acute upper GI bleeding for over a 2-year period were potentially eligible for this study. They were managed by a team of seven endoscopists on 24-h call whose experience was categorized into two levels (high and low) according to the number of endoscopic hemostatic procedures undertaken before the study. Endoscopic treatment was standardized according to Forrest classification of lesions as well as the subsequent medical therapy. Time of endoscopy was subdivided into two time periods: routine (8 a.m.-5 p.m.) and on-call (5 p.m.-8 a.m.). For each category of experience and time periods rebleeding rate, transfusion requirement, need for surgery, length of hospital stay and mortality we compared. Multivariate analysis was used to discriminate the impact of different variables on the outcomes that were considered.

RESULTS: Study population consisted of 272 patients (mean age 67.3 years) with endoscopic stigmata of hemorrhage. The patients were equally distributed among the endoscopists, whereas only 19% of procedures were done out of working hours. Rockall score and Forrest classification at admission did not differ between time periods and degree of experience. Univariate analysis showed that higher endoscopist's experience was associated with significant reduction in rebleeding rate (14% *vs* 37%), transfusion requirements (1.8±0.6 *vs* 3.0±1.7 units) as well as surgery (4% *vs* 10%), but not associated with the length of hospital stay nor mortality. By contrast, outcomes did not significantly differ between the two time periods of endoscopy. On multivariate analysis, endoscopist's experience was independently associated with rebleeding rate and transfusion requirements. Odds ratios for low experienced endoscopist were 4.47 for rebleeding and 6.90 for need of transfusion after the endoscopy.

CONCLUSION: Endoscopist's experience is an important independent prognostic factor for non-variceal acute upper GI bleeding. Urgent endoscopy should be undertaken preferentially by a skilled endoscopist as less expert staff tends to underestimate some risk lesions with a negative influence on hemostasis.

Key words: Non-variceal acute GI bleeding; Time of endoscopy; Surgeon's experience; Endoscopic hemostasis

Parente F, Anderloni A, Bargiggia S, Imbesi V, Trabucchi E, Baratti C, Gallus S, Porro GB. Outcome of non-variceal acute upper gastrointestinal bleeding in relation to the time of endoscopy and the experience of the endoscopist: A two-year survey. *World J Gastroenterol*; 2005 11(45): 7122-7130
http://www.wjgnet.com/1007-9327/11/7122.asp

INTRODUCTION

Acute upper gastrointestinal bleeding (AUGB) is the most common emergency managed by gastroenterologists, with an incidence ranging from approximately 50 to 150 per 100 000 per year in the Western population[1,2]. The treatment of this condition has made important progress since the introduction of emergency endoscopy and endoscopic techniques for hemostasis along with

the application of specific post-endoscopic protocols, significantly decreases rebleeding and the need for surgery[3-7], whereas mortality rates associated with AUGB still range as 5-15%[8,9].

Several clinical and endoscopic score systems have been proposed to risk-stratify patients with AUGB in order to predict outcome and several factors such as age, shock and tachycardia at presentation, the presence of severe medical comorbidity and the lesion's appearance at endoscopy have been shown to be associated with adverse prognosis[10 -13]. In particular, Forrest's classification of endoscopic findings closely associated with peptic ulcer disease but sometimes seen with other causes of AUGB is associated with specific recurrent bleeding rates and is commonly used to assess the need for endoscopic therapy[14].

As far as the effectiveness of various endoscopic therapies for AUGB is concerned, a recent review indicates that differences in terms of hemostatic results using the same treatment modality, exist between research studies and clinical practice as well as among various randomized clinical trials and are probably related to surgeon-dependent factors[15]. Surprisingly, the experience of surgeons in achieving endoscopic hemostasis has not yet been examined, whereas the time of endoscopy has received so far little attention as a possible variable influencing the outcome of AUGB[16-19].

We therefore undertook a 2-year survey in order to assess prospectively the impact of surgeon's experience and time of endoscopy on the outcome of acute non-variceal upper gastrointestinal (GI) bleeding patients in a large tertiary referral center of western Milan.

MATERIALS AND METHODS

Patients

Two hundred and seventy-two (mean age 67.3 years) patients who presented with AUGB to L. Sacco University Hospital, Milan, between June 2001 and July 2003 were included in this study. L. Sacco Hospital is a large teaching hospital located in western Milan with a catchment area of nearly 250.000 inhabitants and provides 24 h emergency endoscopy for two district neighboring hospitals serving an additional population of approximately 200 000 inhabitants.

The treatment protocol for patients with AUGB did not change during the study period and could be summarized in short as follows. All patients who arrived or were referred from a district hospital to the Accident and Emergency Department of our hospital with clinical manifestations of AUGB were managed according to a three-stage scheme: stage I: initial clinical and laboratory evaluation in the Emergency Department including placement of a double-bore nasogastric tube; stage II: hemodynamic stabilization including infusion of crystalloid fluids to maintain adequate blood pressure; stage III: urgent endoscopy within 12 h from presentation in patients who had at least one of the following presenting features: hematemesis with red blood or coffee grounds, passage of melena and a hematocrit below the normal range with a nasogastric aspirate demonstrating red blood or coffee ground material. Recommendations regarding admission to the various hospital departments were made to the attending physicians by the endoscopist mainly based on the assessment of clinical and endoscopic criteria.

We used the Forrest's classification[14] for endoscopic grading of bleeding lesions as follows: class 1A: active ulcer bleeding presenting as arterial spurting or pulsatile bleeding from the ulcer base; class 1B: milder forms present as continuous oozing either from a visible vessel or from underneath an adherent clot; class 2A: in the absence of active bleeding, the stigmata of recent hemorrhage including a non-bleeding visible vessel seen as a red or whitish-gray elevated lesion at the base of the ulcer; class 2B: an adherent clot covering the base of an ulcer; class 2C: a flat pigmented spot or a black membrane covering the ulcer base; class 3: a clean ulcer bottom (i.e, without vessel nor clot).

Patients with endoscopic stigmata of recent hemorrhage, regardless of whether they received endoscopic hemostasis or not were usually admitted to the surgical or gastroenterological ward. The allocation choice was mainly based on the presence of additional medical comorbidity (such as diabetes mellitus, renal failure, etc.) and available space at the different services. Patients with hemodynamic instability after the endoscopic procedure were usually admitted to the intensive care unit (ICU).

Study population

All patients aged 16-95 years undergoing urgent endoscopy (within 12 h after admission) for non-variceal AUBG and those who presented endoscopic stigmata of recent hemorrhage were potentially eligible for this study. Patients were excluded if they had variceal bleeding (both from esophagus and stomach), those who bled from an evident digestive tumor and other non-ulcer lesions such as Dieulafoy's lesions and Mallory-Weiss tears. In particular, Mallory-Weiss tears could not enrolled be since they have a low risk of recurrent bleeding[20]. Dieulafoy's lesions were excluded since we preferred to treat these lesionsby mechanical methods (such as banding or clipping) or APC rather than by epinephrine injection plus heat probe as in this study. Even patients with clearly malignant ulcers at endoscopy (i.e, patients with large flat, plaque-like, ulcerated tumors) were excluded due to the difficulty of standardizing the endoscopic hemostatic maneuvers under these circumstances. Finally, patients with ASA grade 5 were not enrolled in the study due to their severe clinical conditions as defined in this category.

Patients were evaluated at the time of admission using an extensive standardized-item list. The medical history (including concomitant disease, smoking habit, previous peptic disorders) and complaints (melena, hematemesis, hematochezia, dyspeptic complaints, syncope) were recorded. Concomitant diseases were categorized into six main classes (Table 1). The findings on physical examination were also recorded. Hemodynamic instability

Table 1 Distribution of 272 patients with acute non-variceal upper GI bleeding according to age, sex, and other selected covariates

Covariates		*n* (%)
Sex, male		186 (68.4)
Mean age (yr)		67.4±15.8
<40		19 (7.0)
40–49		24 (8.8)
50–59		26 (9.6)
60–69		51 (18.8)
70–79		88 (32.4)
⩾ 80		64 (23.5)
Shock grade[1]: 0		213 (78.3)
1		35 (12.8)
2		24 (8.8)
Comorbidities: cardiovascular		73 (26.8)
Neoplastic		30 (11.0)
Hepatic		26 (9.5)
Nephropathic		17 (6.2)
Multiple		48 (17.6)
Others		37 (13.3)
Main symptom at presentation[2]: hematemesis		114 (42.0)
	Melena	89 (33.0)
	Anemia	69 (25.0)
	Epigastric pain	19 (7.0)
Time of endoscopy: 8.00 a.m.–5.00 a.m.		221 (81.0)
5.00 p.m.–8.00 a.m.		51 (19.0)
Rockall score: 1–3		58 (21.3)
4–6		146 (53.7)
>6		68 (25.0)
Ulcer location: esophagus		21 (7.7)
Stomach		121 (44.5)
Duodenum		130 (47.8)
Ulcer size[3]: <20 mm		152 (68.5)
⩾20 mm		70 (31.5)
Forrest classification: 1A		6 (2.2)
1B		59 (21.7)
2A		19 (7.0)
2B		63 (23.2)
2C		125 (45.9)
Transfusion requirements before endoscopy: (number of blood units)	0	229 (84.2)
	1–4	37 (13.6)
	⩾5	6 (2.2)

[1]Shock grade: grade 0 = no shock signs (systolic BP >100, pulse <100), grade 1 = tachycardia (systolic BP >100, pulse >100), grade 2 = hypotension (systolic BP <100, pulse >100). [2]The sum of main symptoms is higher than the number of patients as some patients had more than one main symptom at presentation. [3]The sum does not add up to the total because of some missing values.

was defined as a systolic blood pressure <100×0.133 kpa or a heart rate >100 r/mm.

The Rockall score was calculated from age, hemodynamic characteristics, endoscopic findings, and comorbidity as previously described[21].

Medications before and during the hospital stay [apart from intravenous proton pump inhibitors (PPIs) used for the bleeding episode] as well as the number of units of blood transfused before and after endoscopy were specifically noted.

Endoscopists and endoscopic procedures

We limited the endoscopists to seven gastroenterologists who were on a 24-h call for emergency endoscopy and whose experience was arbitrarily categorized into two levels according to the number of hemostatic endoscopic procedures done at the time of study. Five endoscopists (three consultant gastroenterologists and two senior registrars) had high experience (each one had performed more than 3 000 upper GI endoscopies and more than 100 emergency procedures). The three consultants had been in practice for more than 8 years, whereas the two senior registrars had completed 6 years of training in general gastroenterology and gastrointestinal endoscopy. The other endoscopists (young senior registrars in gastroenterology) had less experience as they had just completed only 4 years of training in general gastroenterology and had performed less than 1 000 upper GI endoscopies and 40–70 emergency procedures, as a principal surgeon before participating in this study. All emergency endoscopies were undertaken by the gastroenterologists on call in a separate endoscopic suite. Endoscopies performed between 8 am and 5 pm from Monday to Friday were defined as done within working hours (routine), whereas those performed at other time points were classified as done out of working hours (on call).

The endoscope employed was a Pentax EG 3440 video endoscope with a large operative channel (3.5 mm, Pentax, GmbH, Hamburg, Germany).

To improve the visual field, gastric lavage with a broad double-bore nasogastric tube was used and continuous normal saline infusion was carried out before endoscopy. Ulcers with bleeding stigmata were cleaned by water irrigation through the biopsy channel. Adherent clots were washed with a jet of water delivered through a catheter passed through the endoscope.

Only ulcerative lesions with endoscopic stigmata of acute bleeding, visible vessels or adherent clot (Forrest Ia–IIc) were included in the present study. Since previous studies have shown medium to poor inter observer variability in assessing endoscopic stigmata of bleeding[21],we attempted at reducing interobserver bias onthe grading of endoscopic stigmata by reviewing the video records of 20 explicative cases at a pre-study meeting.

Endoscopic therapy was standardized as follows: initial injection of 1:10 000 adrenaline around the bleeding lesion (up to a maximum of 20 mL) to achieve a tamponade effect, followed by application of a 3.2-mm heater probe

(Olympus, CD-120 U, Tokyo, Japan) at settings of 30 J per goal until the achievement of a coaptive effect[22]. This method was used whenever endoscopic stigmata of hemorrhage such as acute spurting, oozing, visible vessel or adherent clots were present. Written guidelines containing the above mentioned recommendations concerning the hemostatic maneuvers to be undertaken were circulated among the endoscopists participating in this survey before the study.

The success of endoscopic hemostasis was defined as the cessation of bleeding together with the achievement of cavitation over the lesion after the application of the heater probe.

After endoscopy, the surgeon filled in a specific form with all the details concerning the procedure with specific reference to the appearance of bleeding lesions (according to the Forrest's classification) and the hemostatic maneuvers that were undertaken. Epinephrine solution injected and the number of pulses with the heater probe whenever employed were recorded. The time of endoscopy after admission was also recorded.

No patient was initially treated either with endoscopic band ligation or with hemoclipping, whereas these therapies were occasionally used by a senior endoscopist to obtain hemostasis in case of recurrent bleeding.

All patients received high dose intravenous PPIs: omeprazole or pantoprazole, 80 mg bolus within 12 h of endoscopy followed by 8 mg/h for 3 d [23] and then an oral PPI, 40 mg once daily for the remainder of their hospital stay. Patients were closely monitored and underwent clinical reviews with their blood pressure, pulse, respiratory rate, and urine output measured hourly for the first 24 h followed by close observation for symptoms and signs of recurrent bleeding throughout their stay in the hospital. Subsequent management decision was made by the attending physician. No attempt was made to persuade the attending physician to follow a specific course of action beyond the recommendations quoted above and to determine the length of hospital stay.

Outcome measures

The major outcome parameters were rebleeding, surgical intervention, and mortality. Rebleeding was defined as repeated melena, hematemesis or a drop in hemoglobin concentration (>2 g/dL in 24 h) after a period of stabilization and unexplained by fluid replacement within 28 d of the initial bleeding episode. We performed a second endoscopy to confirm clinical recurrent bleeding which was defined as persistent endoscopic stigmata of acute spurting or oozing, visible vessels or adherent clots with the appearance of blood clots or coffee ground material in the stomach or duodenum. Our study had a result greater than 95% to reject the null hypothesis that the proportion of rebleeding patients was the same in endoscopists with high and low experience.

Surgery was performed in those patients whose bleeding could not be stopped by primary endoscopic hemostasis or by a second or third endoscopic therapy. Interventional radiology was not available for patients who did not respond to endoscopic therapy when the study started. The choice of surgery was left to the individual surgeon though gastrectomy was the most preferred operation for the control of ulcer bleeding. The mortality was defined as death within 28 d of the bleeding episode.

Secondary outcome measures included the number of packed red cell units transfused after endoscopy and the length of hospital stay.

Appropriateness of endoscopic hemostatic maneuvers

The appropriateness of each endoscopic procedure was evaluated jointly by the two consultant gastroenterologists who did not participate in the procedures and were blinded to the outcome of patients and name of the endoscopist. Treatment in accordance with the implemented guidelines[6] was classified as appropriate, treatment in disagreement as inappropriate. In many instances video taping of the cases was also used with regard to the appropriateness.

Statistical analysis

Univariate analysis was performed by the χ^2 test for frequencies and by the Man-Whitney rank sum test for means.

Odds ratios (OR) and corresponding 95% confidence intervals (CI) were estimated by unconditional multiple logistic regression models[24] after adjustment for age (<40 /40-49/50-59/60-69/70-79/≥80 years), sex, Rockall (<6/ ≥6) and Forrest's score (IA,IB/2A-2C), blood transfusion (no/yes), endoscopist's experience (high/low), and time of endoscopy (routine/on-call). Moreover, we estimated ORs after a further adjustment for appropriateness of treatment (appropriate/inappropriate).

The significance of OR estimates was represented by the corresponding 95%CI. If OR did not include unity, the estimate was statistically significant.

RESULTS

Overall results

Between June 2001 and July 2003, we recruited 272 patients (mean age 67.3 years, 186 males, 94% Caucasians) who presented to the A&E, Department of Luigi, Sacco University Hospital for non-variceal AUGB and underwent upper GI endoscopy within 12 h after admission with the presence of endoscopic stigmata of hemorrhage. They satisfied all the inclusion criteria of the study. Table 1 describes the distribution of these patients according to sex, age, and other selected covariates.

Overall, the rebleeding, surgical intervention, and mortality rates were 18.7%, 5.5%, and 13.2%, respectively. Initial endoscopic hemostasis was achieved in 268 of the 272 patients (98.5%) and four patients required immediate surgery for failure of primary endoscopic hemostasis. Fifty-one patients had at least a rebleeding episode after initial hemostasis (Figure 1). Thirty-six patients died within 28 d from the initial episode of bleeding. Their ultimate causes of death were cardiac failure (15), pulmonary failure (9), liver failure (4), multi organ failure (2), renal failure (4), and cerebral edema (2).

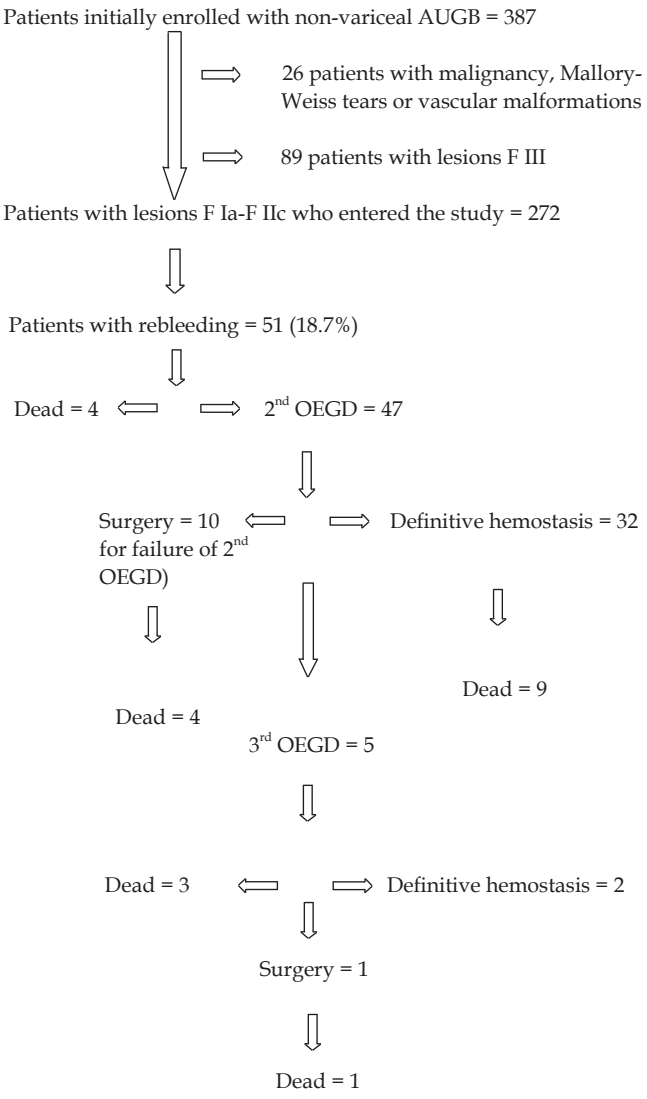

Figure 1 Flow chart illustrates the study design and how the 51 patients who had at least one rebleeding episode were managed and their clinical outcomes.

Outcome of patients

Eighty-one percent of the emergency procedures were performed between 8 a.m. and 5 p.m. whereas only 19% were done out of working hours.

Forrest's classification of lesions at admission did not significantly differ between the two endoscopist categories, though no significant trend towards a higher mean Rockall' s score was found in patients undergoing endoscopy out of working hours.

Univariate analysis showed that higher endoscopist's experience was associated with significant reduction in rebleeding rate (14% *vs* 37%), transfusion requirements (1.8 ± 0.6 *vs* 3.0 ± 1.7 units) as well as the need for surgery (4% *vs* 10%), but not associated with the length of hospital stay and mortality (Table 2). In contrast, outcomes did not significantly differ between the two time periods of endoscopy.

Table 3 shows the distribution of patients according to the experience of endoscopists and the time of endoscopy. Univariate (Table 3) and multivariate (Table 4) analyses showed that low endoscopist's experience was associated with the higher rebleeding rate and transfusion requirements, but not significantly associated with the need for surgery, the length of hospital stay, and higher mortality rate. After adjustment for age, sex, and other selected covariates, the OR of low experienced endoscopist was 4.47 for rebleeding, 6.90 for need of transfusion after endoscopy, 2.36 for need of surgery, 0.47 for mortality, and 0.88 for length of hospital stay, respectively (Table 4). The estimates were statistically significant for rebleeding and need of blood transfusions. However, after further adjustment for appropriateness, the association with rebleeding disappeared (OR = 1.33), whereas it was still significant with the need of transfusion (OR = 5.07). The OR of making endoscopy in non-ordinary time period was 0.94 for rebleeding, 0.89 for need of transfusion after endoscopy, 1.85 for need of surgery, 1.96 for mortality, and 1.51 for length of hospital stay, respectively. None of the estimates were statistically significant even after further adjustment for appropriateness.

Table 5 shows the effect of an inappropriate endoscopic treatment on the occurrence of events of interest. A direct association was found between inappropriateness of treatment and risk of subsequent rebleeding (OR = 43.49),

Table 2 Rebleeding rate according to age, sex, Rockall score, Forrest's classification, ulcer size, operator's experience, and time of endoscopy

	Total NO. of patients	Rebleeding rate		*P*	
Age (yr)					
<65	88	8	9.1% (A)	0.046	A *vs* B
65-74	75	15	20.0% (B)	0.370	B *vs* C
> 74	109	28	25.7% (C)	0.003	A *vs* C
Sex					
Males	186	36	19.4%	0.707	
Females	86	15	17.4%		
Rockall score					
1–4	92	6	6.5% (A)	0.016	A *vs* B
5–6	112	20	17.8% (B)	0.005	B *vs* C
>6	68	25	36.7% (C)	<0.001	A *vs* C
Forrest's classification					
Ⅰ A– Ⅰ B	65	9	13.8% (A)	0.001	A *vs* B
Ⅱ A– Ⅱ B	82	33	40.2% (B)	<0.001	B *vs* C
ⅢC	125	9	7.2% (C)	0.138	A *vs* C
Ulcer size[a]					
< 20 mm	152	24	15.8%	0.079	
⩾ 20 mm	70	18	25.7%		
Surgeon's experience					
High	214	29	13.6%	< 0.001	
Low	58	22	37.9%		
Time of endoscopy					
Working hours	221	41	18.5 %	0.862	
Out of working hours	51	10	19.6%		

[1] The sum does not add up to the total because of some missing values.

Table 3 Distribution of patients by experience of endoscopists and time period of treatment, according to selected outcomes. Univariate analysis.

	Experience of endoscopist			Time period		
	High *n* (%)	Low *n* (%)	*P*	8AM-5PM *n* (%)	5PM-8AM *n* (%)	*P*
				n	*n*	
Rebleeding						
Yes	29 (58.9)	22 (43.1)	< 0.001	41 (80.4)	10 (19.6)	0.862
No	185 (83.7)	36 (16.3)		180 (81.5)	41 (18.6)	
N. of blood units transfused after endoscopy						
⩾ 3	14 (48.3)	15 (51.7)	< 0.001	23 (79.3)	6 (20.7)	0.777
< 3	200 (82.3)	43 (17.7)		198 (81.5)	45 (18.5)	
Need for Surgery						
Yes	9 (60.0)	6 (40.0)	0.069	10 (66.7)	5 (33.3)	0.137
No	205 (79.8)	52 (20.2)		211 (82.1)	46 (17.9)	
Mortality						
Death	31 (86.1)	5 (13.9)	0.242	26 (72.2)	10 (27.8)	0.136
Alive	183 (77.5)	53 (22.5)		195 (82.6)	41 (17.4)	
Length of hospital staying						
⩾ 13 d	107 (75.9)	34 (24.1)	0.244	120 (85.1)	21 (14.9)	0.091
< 13 d	107 (81.7)	24 (18.3)		101 (77.1)	30 (22.9)	
Rockall score						
< 6	111 (83.5)	22 (16.5)	0.06	108 (81.2)	25 (18.8)	0.985
⩾ 6	103 (74.1)	36 (25.9)		113 (81.3)	26 (18.7)	
Forrest's classification						

Table 4 OR and corresponding 95%CI for patients treated by less *vs* well experienced endoscopists and for patients treated between 5 p.m. and 8 a.m. compared to those treated between 8 a.m. and 5 p.m. according to selected outcomes

	Low *vs* high experience of endoscopist		8 a.m.-5 p.m. *vs* 5 p.m.-8 a.m. time period	
	OR[1] (95%CI)	OR[2] (95%CI)	OR[3] (95%CI)	OR[4] (95%CI)
Rebleeding				
Yes	4.47	1.33	0.94	1.40
No	(2.11-9.47)	(0.46-3.83)	(0.38-2.30)	(0.51-3.83)
Number of blood units transfused after endoscopy				
⩾3	6.90	5.07	0.89	0.92
<3	(2.80-16.98)	(1.89-13.61)	(0.31-2.56)	(0.32-2.70)
Need for surgery				
Yes	2.36	1.67	1.85	1.99
No	(0.74-7.50)	(0.43-6.41)	(0.54-6.37)	(0.56-7.04)
Mortality				
Dead	0.47	0.64	1.96	1.92
Alive	(0.17-1.34)	(0.20-2.11)	(0.80-4.78)	(0.79-4.69)
Length of hospital stay				
⩾13 d	0.88	1.66	1.51	0.52
<13 d	(0.51-1.53)	(0.85-3.28)	(0.84-2.72)	(0.27-1.01)

[1]Estimates from multiple logistic regression after adjustment for age, sex, Rockall and Forrest score, blood transfusion, and time period. Reference category is highly experienced endoscopists. [2]As in 1 after further adjustment for appropriateness. Reference category is highly experienced endoscopists [3]Estimates from multiple logistic regression after adjustment for age, sex, Rockall and Forrest score, blood transfusion,and experience of endoscopists. Reference category is 5 p.m.-8 a.m. [4]As in 3 after further adjustment for appropriateness. Reference category is 5 p.m.-8 a.m.

whereas no significant association was found between inappropriateness and need of transfusion after endoscopy (OR = 2.98), need of surgery (OR = 2.62), mortality (OR = 0.47), and length of hospital stay (OR = 0.60). The latter findings showed that appropriateness of endoscopic therapy rather than the endoscopist experience was the main variable associated with rebleeding. Of course, the lower the endoscopist's experience, the higher the inappropriateness in hemostatic maneuvers. Again, the two time periods of endoscopy were not associated with any of the variables evaluated.

When considering subjects with lesions 2A and 2B of the Forrest's classification, we found a stronger association between low endoscopist's experience and rebleeding, the

Table 5 OR and corresponding 95%CI for patients cured with inappropriate and appropriate treatment according to selected outcomes

	Treatment used		
	Appropriate	Inappropriate	
	n (%)	*n* (%)	OR[1] (95%CI)
Rebleeding			
Yes	27 (52.9)	24 (47.1)	43.49
No	216 (97.7)	5 (2.3)	(11.29-167.60)
Number of blood units transfused after endoscopy			
⩾3	21 (72.4)	8 (27.6)	2.98
<3	222 (91.4)	21 (8.6)	(0.82-10.78)
Need for surgery			
Yes	11 (73.3)	4 (26.7)	2.62
No	232 (90.3)	25 (9.7)	(0.46-14.94)
Mortality			
Dead	33 (91.7)	3 (8.3)	0.47
Alive	210 (88.9)	26 (11.0)	(0.10-2.25)
Length of hospital stay			
⩾13 d	125 (88.7)	16 (11.4)	0.60
<13 d	118 (90.1)	13 (9.9)	(0.24-1.54)

[1]Estimates from multiple logistic regression after adjustment for age, sex, Rockall and Forrest score, blood transfusion, time period, and experience of endoscopists. Reference category is appropriate endoscopic treatment.

multivariate OR being 9.82 (95%CI: 2.62-36.89).

Finally, there was a trend towards more adrenaline injected and a significant difference in the number of heater probe pulses used by endoscopists with high and low experience, respectively. The mean adrenaline injected was 9.4 and 8.6 mL, whereas the median number of heater probe pulses was 7 (range 0-15) *vs* 4 (range 0-10) for high- and low-experienced endoscopists, respectively.

DISCUSSION

Over the past two decades, advances have been made in the management of non-variceal AUGB[5]. Various endoscopic single-modality treatments including epinephrine injection, thermal therapy (heater probe, electrocoagulation, laser, etc.) and their combination are efficacious in achieving hemostasis in clinical trials[7]. These endoscopic procedures can control active bleeding in 85-90% of patients with a significant decrease in the rate of recurrent bleeding and need for surgery[6,7,25]. Therefore, the management decision for preventing recurrent bleeding is a rapid endoscopic diagnosis with adequate hemostasis. Recent data demonstrate that the best predictor of recurrent bleeding is the endoscopic finding of ulcer since the presence of a visible vessel or sentinel clot in the ulcer base indicates a high likelihood of rebleeding (43% and 22%, respectively), whereas ulcers with a clean base have a recurrent bleeding risk that is negligible[25]. The above rebleeding rates can be lowered by 60-80% by the application of aggressive endoscopic therapeutic modalities (such as a combined injection/thermal therapy[26]). However, one should keep in mind that these results are obtained in centers of excellence, often known internationally for their expertise in the treatment of peptic ulcer bleeding. Whether the aforementioned results are reproducible in centers with less endoscopic expertise is currently a matter of debate[15].

The influence of endoscopy time on the outcome of patients with non-variceal AUGB remains a subject of debate as very few studies have addressed the question so far. Adler *et al*[17] showed that complications are significantly more frequent after emergency endoscopy between 7 p.m. and 11 p.m. as compared to regular working hours, which may be due to the fact that during non-working hours endoscopy is performed by more fatigued personnel. Choudari *et al*[16] and Ramage *et al*[18] found that there is no difference in the outcome of patients with non-variceal AUGB who had undergone endoscopy during working or non-working hours and weekdays *vs* weekends, respectively.

The present survey aimed at evaluating the impact of these two single factors (endoscopist's experience and time of endoscopy) on the outcome of patients with non-variceal AUGB presenting at a single large tertiary referral center. We did not include in our study inpatient referrals in order to deal with similar patients and to reduce as much as possible the severe comorbidities usually present in patients during their hospital stay. upper GI haemorrhage while hospitalized for another reason (so-called secondary bleeding) has been associated with an increased risk of rebleeding and death[26].

Findings from our study showed that the endoscopist' s experience was an important independent prognostic factor for the outcome of non-variceal AUGB. Indeed, less experienced surgeon resulted in a significantly higher recurrent bleeding rate and transfusion requirement than highly experienced endoscopists, whereas mortality was not influenced probably due to comorbidities.

We found a direct significant association between low experience endoscopists and risk of rebleeding (multivariate OR = 4.47). After a further adjustment for appropriateness, the association disappeared (OR = 1.33), suggesting that if surgeons with lower experience have a rate of appropriateness of treatment similar to that of high experience endoscopists, we could not obtain any significant difference in terms of rebleeding rate between low and high experience endoscopists.

Moreover, the recurrent bleeding of F2A and F2B ulcers was significantly higher among the less experienced endoscopists as compared to the rate of highly skilled surgeons as well as the value reported in the literature[27]. The evaluation of appropriateness of endoscopic therapy by the two consultants who blindly examined the endoscopic reports might help understand the discrepancy. Planned guidelines of hemostasis were not followed entirely by less experienced staff in 36% of cases, particularly in patients with F2B ulcers, where the most frequent protocol violation was the non removal of an adherent clot. The fear of removing an apparently stable clot adherent to the ulcer base as well as the hypothetical difficulties in managing the subsequent hemorrhage under unfavorable circumstances (i.e, without any supervision) is the most frequently reported explanation by the youngest

endoscopists to justify guideline violations. Independently by the experience of endoscopists, fewer protocol violations have been done for patients with lesions classified as both F1A, F1B, and F2C, which might explain at least in part the lower rebleeding rate in these subjects (13.8% and 7.2%, respectively) as compared to those classified as F2A and F2B (40.2%).

Our findings also add some useful information to a still intricate problem that is the optimum treatment for ulcers with no hemorrhage at the time of endoscopy but present with the stigmata of hemorrhage. While there is no doubt that ulcers with actively bleeding vessels are treated immediately with injection and thermocoagulation by both highly experienced and less expert endoscopists, is the management strategy for intermediate findings (Forrest IIa & IIb) which remains less certain, especially when considering the great benefit of acid suppression in this group[28]. If aggressive endoscopic therapy (clot removal^{+}epinephrine injection and thermal therapy) is superior to non endoscopic intervention in patients with adherent clots receiving oral PPI[29], profound in acid suppression without clot removal is more effective than endoscopic intervention alone[30]. A supplemental jog to this matter was provided by our current survey during which all bleeding patients received the same PPI scheme after endoscopy. We adjusted the paradigm to study the value of high dose in PPI alone over endoscopic therapy^{+} of PPI in F2A and 2B ulcers, showing that combination of appropriate endoscopic therapy with profound acid suppression is better than PPI alone (or PPI plus endoscopic under treatment)[31].

As far as the time of endoscopy is concerned, our findings suggest that emergency endoscopy out of working hours is as safe and effective as endoscopy performed during working hours provided that it is done under optimal conditions as during working hours. The success of procedures out of hours in this study may be related to the existence of a specific bleeding team composed of the endoscopist and two well-trained specialized nurses. It is conceivable that the same results cannot be obtained in other institutions with less endoscopic facilities and untrained assistants (i.e, non-specialized nurses), where examinations may perhaps be delayed by a few hours in order to perform endoscopy more safely during working hours.

In conclusion, endoscopist's experience is an important independent predicting variable for the outcome of non-variceal AUGB, whereas time of endoscopy (working *vs* non working hours) does not make any difference in terms of patients' prognosis. Urgent endoscopy for AUGB should be undertaken by experienced endoscopists because less experienced staff may not achieve hemostasis.

REFERENCES

1 **Non-variceal upper gastrointestinal haemorrhage:** guidelines. *Gut* 2002; 51 Suppl **4:** iv1-iv6

2 **Longstreth GF Epidemiology of hospitalization for acute upper gastrointestinal hemorrhage:** a population-based study. *Am J Gastroenterol* 1995; **90:** 206-210

3 **Sacks HS,** Chalmers TC, Blum AL, Berrier J,Pagano D. Endoscopic hemostasis. An effective therapy for bleeding peptic ulcers. *JAMA* 1990; **264:** 494-499

4 **Sanderson JD,** Taylor RF, Pugh S, Vicary FR. Specialized gastrointestinal units for the management of upper gastrointestinal haemorrhage. *Postgrad Med J* 1990; **66:** 654-656

5 **Cook DJ,** Guyatt GH, Salena BJ, Laine LA. Endoscopic therapy for acute nonvariceal upper gastrointestinal hemorrhage: a meta-analysis. *Gastroenterology* 1992; **102**: 139-148

6 **Adler DG,** Leighton JA, Davila RE, Hirota WK, Jacobson BC, Qureshi WA, Rajan E, Zuckerman MJ, Fanelli RD, Hambrick RD, Baron T, Faigel DO. ASGE guideline: The role of endoscopy in acute non-variceal upper-GI hemorrhage. *Gastrointest Endosc* 2004; **60:** 497-504

7 **Rollhauser C,** Fleischer DE. Nonvariceal upper gastrointestinal bleeding: *an update*. *Endoscopy* 1997; **29:** 91-105

8 **Rockall TA,** Logan RF, Devlin HB, Northfield TC. Incidence of and mortality from acute upper gastrointestinal haemorrhage in the United Kingdom. Steering Committee and members of the National Audit of Acute Upper Gastrointestinal Haemorrhage. *BMJ* 1995; **311:** 222-226

9 **Skok P.** Does endoscopic hemostasis effect the reduction of mortality in patients with hemorrhage from the digestive tract? *Hepatogastroenterology* 1998; **45:** 123-127

10 **Brullet E,** Calvet X, Campo R, Rue M, Catot L, Donoso L Factors predicting failure of endoscopic injection therapy in bleeding duodenal ulcer. *Gastrointest Endosc* 1996; **43:** 111-116

11 **Brullet E,** Campo R, Calvet X, Coroleu D, Rivero E, Simó Deu J .Factors related to the failure of endoscopic injection therapy for bleeding gastric ulcer. *Gut* 1996; **39:** 155-158

12 **Saeed ZA,** Ramirez FC, Hepps KS, Cole RA, Graham DY. Prospective validation of the Baylor bleeding score for predicting the likelihood of rebleeding after endoscopic hemostasis of peptic ulcers. *Gastrointest Endosc* 1995; **41:** 561-565

13 **Saeed ZA,** Ramirez FC, Hepps KS, Cole RA, Graham DY Prospective validation of the Baylor bleeding score for predicting the likelihood of rebleeding after endoscopic hemostasis of peptic ulcers. *Gastrointest Endosc* 1995; **41:** 561-565

14 **Forrest JA,** Finlayson ND, Shearman DJ. Endoscopy in gastrointestinal bleeding. *Lancet* 1974; **2:** 394-397

15 **Rollhauser C,** Fleischer DE. Current status of endoscopic therapy for ulcer bleeding. *Baillieres Best Pract Res Clin Gastroenterol* 2000; **14:** 391-410

16 **Choudari CP,** Rajgopal C, Elton RA, Palmer KR. Failures of endoscopic therapy for bleeding peptic ulcer: an analysis of risk factors. *Am J Gastroenterol* 1994; **89:** 1968-1972

17 **Adler DG,** Adler AL, Nolte T, Hermans J, Gostout CJ, Baron TH. Complications of urgent and emergency endoscopy in patients with GI bleeding as a function of time. *Am J Gastroenterol* 2001; **96:** 3452-3454

18 **Ramage J,** Harewood G, Gostout C Effect of a dedicated GI bleed team on emergent upper endoscopy outcome: weekday versus weekend. *Gastrointest Endosc* 2003; **57:** AB148

19 **Bjorkman DJ,** Zaman A, Fennerty MB, Lieberman D, Disario JA, Guest-Warnick G. Urgent vs. elective endoscopy for acute non-variceal upper-GI bleeding: an effectiveness study. *Gastrointest Endosc* 2004; **60:** 1-8

20 **Laine L,** Cohen H, Brodhead J, Cantor D, Garcia F, Mosquera M. Prospective evaluation of immediate versus delayed refeeding and prognostic value of endoscopy in patients with upper gastrointestinal hemorrhage. *Gastroenterology* 1992; **102:** 314-316

21 **Rockall TA,** Logan RF, Devlin HB, Northfield TC Risk assessment after acute upper gastrointestinal haemorrhage. *Gut* 1996; **38:** 316-321

22 **Fullarton GM,** Birnie GG, Macdonald A, Murray WR. Controlled trial of heater probe treatment in bleeding peptic ulcers. *Br J Surg* 1989; **76**: 541-544

23 **Lau JY,** Sung JJ, Lee KK, Yung MY, Wong SK, Wu JC, Chan FK, Ng EK, You JH, Lee CW, Chan AC, Chung SC. Effect of intravenous omeprazole on recurrent bleeding after endoscopic

treatment of bleeding peptic ulcers. *N Engl J Med* 2000; **343:** 310-316
24 Breslow NE, Day NE. Statistical methods in cancer research. Volume I - The analysis of case-control studies. *IARC Sci Publ* 1980; 5-338
25 **Laine L,** Peterson WL Bleeding peptic ulcer. *N Engl J Med* 1994; **331:** 717-727
26 **Lau JY,** Sung JJ, Lam YH, Chan AC, Ng EK, Lee DW, Chan FK, Suen RC, Chung SC. Endoscopic retreatment compared with surgery in patients with recurrent bleeding after initial endoscopic control of bleeding ulcers. *N Engl J Med* 1999; **340:** 751-756
27 **Das A,** Wong RC Prediction of outcome of acute GI hemorrhage:a review of risk scores and predictive models. *Gastrointest Endosc* 2004; **60:** 85-93
28 **Khuroo MS,** Yattoo GN, Javid G, Khan BA, Shah AA, Gulzar GM, Sodi JS. A comparison of omeprazole and placebo for bleeding peptic ulcer. *N Engl J Med* 1997; **336:** 1054-1058
29 **Bleau BL,** Gostout MJ, Shaw RF Final results : rebleeding from peptic ulcers associated with adherent clots : a prospective randomized controlled study comparing endoscopic therapy with medical therapy. *Gastrointest Endosc* 1997; **45:** AB87
30 **Jensen DM,** Kovacs T, Jutabha GM Final results and cost assessment of endoscopic vs medical therapies for prevention of recurrent ulcer hemorrhage from adherent clots in a randomized controlled trial. *Gastrointest Endosc* 1995; **41:** AB365
31 **Sung JJ,** Chan FK, Lau JY, Yung MY, Leung WK, Wu JC, Ng EK, Chung SC The effect of endoscopic therapy in patients receiving omeprazole for bleeding ulcers with nonbleeding visible vessels or adherent clots: a randomized comparison, Ann Intern Med 2003; **139:** 237-243

Science Editor Wang XL and Guo SY **Language Editor** Elsevier HK

PO Box 2345, Beijing 100023, China
www.wjgnet.com
wjg@wjgnet.com

ELSEVIER

World J Gastroenterol 2005;11(45):7131-7135
World Journal of Gastroenterology ISSN 1007-9327

• *RAPID COMMUNICATION* •

Prevalence of *Helicobacter pylori* infection and intestinal metaplasia in subjects who had undergone surgery for gastric adenocarcinoma in Northwest Italy

Giorgio Palestro, Rinaldo Pellicano, Gian Ruggero Fronda, Guido Valente, Marco De Giuli, Tito Soldati, Agostino Pugliese, Stefano Taraglio, Mauro Garino, Donata Campra, Miguel Angel Cutufia, Elena Margaria, Giancarlo Spinzi, Aldo Ferrara, Giorgio Marenco, Mario Rizzetto, Antonio Ponzetto

Giorgio Palestro, Department of Oncology, University of Torino, Italy
Rinaldo Pellicano, Mario Rizzetto, Antonio Ponzetto, Department of Gastro-Hepatology, Ospedale S. Giovanni Battista (Molinette), Torino, Italy
Gian Ruggero Fronda, Mauro Garino, Donata Campra, Department of Surgery, Ospedale S. Giovanni Battista (Molinette), Torino, Italy
Guido Valente, Department of Pathology, University of Piemonte Orientale, Novara, Italy
Marco De Giuli, Department of Surgery, Ospedale S. Giovanni Antica Sede, Torino, Italy
Tito Soldati, Department of Surgery, Ospedale degli Infermi, Biella, Italy
Agostino Pugliese, Department of Infectious Diseases, University of Torino, Italy
Stefano Taraglio, Department of Pathology, Ospedale Maria Vittoria, Torino, Italy
Miguel Angel Cutufia, Department of Biology, Biochemistry and Genetics, University of Torino, Italy
Elena Margaria, Department of Pathology, Ospedale S. Giovanni Antica Sede, Torino, Italy
Giancarlo Spinzi, Gastroenterology Unit, Ospedale Valduce, Como, Italy
Aldo Ferrara, Gastroenterology Unit, Ospedale di Legnano, Legnano, Italy
Giorgio Marenco, General Medicine Unit, Ospedale Santa Corona, Pietra Ligure, Italy
Supported by the grants from Regione Piemonte, Ministry of Instruction, University and Research, University of Torino, AIRC, Stola AutoSpA
Correspondence to: Professor Antonio Ponzetto, Department of Internal Medicine, University of Torino and Ambulatorio di Gastroenterologia, Ospedale S Giovanni Battista, Via Chiabrera 34, III piano, 10126 Torino, Italy. ponzetto@inwind.it
Telephone: +39-11-6336033 Fax: +39-11-6336033
Received: 2004-08-13 Accepted: 2004-10-06

Abstract

AIM: To investigate the seroprevalence of *Helicobacter pylori* (*H pylori*) infection and its more virulent strains as well as the correlation with the histologic features among patients who had undergone surgery for gastric cancer (GC).

METHODS: Samples from 317 (184 males, 133 females, mean age 69±3.4 years) consecutive patients who had undergone surgery for gastric non-cardia adenocarcinoma were included in the study. Five hundred and fifty-five (294 males, 261 females, mean age 57.3±4.1 years) patients consecutively admitted to the Emergency Care Unit served as control. Histological examination of tumor, lymph nodes and other tissues obtained at the time of surgery represented the diagnostic "gold standard". An enzyme immunosorbent assay was used to detect serum anti-*H pylori* (IgG) antibodies and Western blotting technique was utilized to search for anti-CagA protein (IgG).

RESULTS: Two hundred and sixty-one of three hundred and seventeen (82.3%) GC patients and 314/555 (56.5%) controls were seropositive for anti-*H pylori* ($P<0.0001$; OR, 3.58; 95%CI, 2.53-5.07). Out of the 317 cases, 267 (84.2%) were seropositive for anti-CagA antibody *vs* 100 out of 555 (18%) controls ($P<0.0001$; OR, 24.30; 95%CI, 16.5-35.9). There was no difference between the frequency of *H pylori* in intestinal type carcinoma (76.2%) and diffuse type cancer (78.8%). Intestinal metaplasia (IM) was more frequent but not significant in the intestinal type cancer (83.4% *vs* 75.2% in diffuse type and 72.5% in mixed type). Among the patients examined for IM, 39.8% had IM type I, 8.3% type II and 51.9% type III (type III *vs* others, $P = 0.4$).

CONCLUSION: This study confirms a high seroprevalence of *H pylori* infection in patients suffering from gastric adenocarcinoma and provides further evidence that searching for CagA status over *H pylori* infection might confer additional benefit in identifying populations at greater risk for this tumor.

Key words: *H pylori* infection; Gastric cancer; Intestinal metaplasia; Italy

Palestro G, Pellicano R, Fronda GR, Valente G, De Giuli M, Soldati T, Pugliese A, Taraglio S, Garino M, Campra D, Cutufia MA, Margaria E, Spinzi G, Ferrara A, Marenco G, Rizzetto M, Ponzetto A. Prevalence of *Helicobacter pylori* infection and intestinal metaplasia in subjects who had undergone surgery for gastric adenocarcinoma in Northwest Italy. *World J Gastroenterol* 2005; 11(45): 7131-7135
http://www.wjgnet.com/1007-9327/11/7131.asp

INTRODUCTION

Gastric cancer (GC) is the world's second leading cause of cancer-related mortality[1] but in some countries it represents the most common malignancy in males[2].

GC occurrence in many Italian regions is similar to that in Japan. In Italy, GC is usually discovered at a later stage and therapeutic approaches cannot save a majority of patients. As a consequence, mortality parallels incidence[3].

The most frequent histologic type of GC is adenocarcinoma, which is thought to originate from a continuing and active proliferation of gastric pits following the destruction of glands due to active inflammatory infiltration. The process that has been described by Correa[4] from an inflammatory setting (gastritis) through intestinal metaplasia (IM) and dysplasia, evolves to adenocarcinoma.

In 1994, the International Agency for Research on Cancer defined *H pylori* as a class I gastric carcinogen[5]. Evidence supporting a causal association has been demonstrated by epidemiological data[6], ecologic studies[1] and in experimental animal models[7]. Regarding the first aspect, in a prospective study including 1 526 Japanese subjects during a mean follow-up of 7.8 years (range 1.0-10.6 years), 2.9% of infected persons developed GC *vs* none among uninfected subjects[8]. A combined analysis of 12 case-control studies (with 1 228 GC cases considered) nested within prospective cohorts has found an association between non-cardia GC and *H pylori* infection of 5.9 (95% confidence interval [CI] 3.4-10.3)[9]. A meta-analysis of 21 case-control studies suggested that the risk of GC is increased by threefold in those chronically infected with *H pylori*[10]. More recently, another meta-analysis of case-control studies with age- and sex-matched controls was published by Huang *et al*[11]. In this work, a comprehensive literature search identified 16 qualified studies with 2 284 cases and 2 770 controls. The authors found that *H pylori* and CagA (cytotoxin-associated gene A) protein seropositivity significantly increases the risk for GC by 2.28- and 2.87-fold, respectively.

There is still no final conclusion regarding the association between the infection and the malignancy due to marked geographic variations. Some studies have not found any correlation between seropositivity for *H pylori* antibodies (as an indicator of *H pylori* infection) and GC[12-14]. For example, in the study performed by Rudi *et al*[12] in Germany, 58.6% of patients suffering from GC and 50.6% of control subjects have IgG antibodies against *H pylori*. In Gambia, though more virulent strains of *H pylori* are present, gastric atrophy and IM are rare[15]. Seropositivity for *H pylori* and the CagA antigen cannot explain the differences in the prevalence of precancerous gastric lesions in two Chinese populations with contrasting GC rates[16]. Recently, Wong *et al*[17] found that the incidence in GC development is similar between the subjects receiving *H pylori* eradication treatment and those receiving placebo during a period of 7.5 years in a high-risk region of China. Furthermore, not all the stomach tumors are *H pylori* positive.

In previous local pilot studies in North Italy, a high prevalence of *H pylori* infection has been associated to the presence of GC[18,19]. To investigate the correlation in a vast area of Northwest Italy in more detail, we started a research network on gastric cancer and precursor lesions in 1993, which we named Metaplasia *H pylori* Histology (MHEPHISTO). In this multicenter survey, a prospective case-control study of patients who had undergone surgery for GC in Northwestern Italy was performed. The aim was to ascertain the seroprevalence of *H pylori* infection and its more virulent strains by searching for antibodies against the CagA protein and to establish the correlation with the subtypes of IM.

MATERIALS AND METHODS

Study population

Specimens from 317 (184 males, 133 females, mean age 69±3.4 years) consecutive patients who had undergone surgery for gastric non-cardia adenocarcinoma were included in the study. Five hundred and fifty-five patients (294 males, 261 females) consecutively admitted to the Emergency Care Unit of S. Giovanni Battista (Molinette) Hospital of Torino served as control with a mean age 57.3 ±4.1 years. Cases and controls came from the geographical area of Northwestern Italy.

Methods

Clinical diagnosis of malignancy was established by standard medical examinations including upper GI endoscopy, diagnostic ultrasound and computed tomography (CT) scan. Endoscopic ultrasound (EUS) served as a part of the routine examination.

Histological examination of tumor, lymph nodes and other tissues obtained at the time of surgery represented the diagnostic "gold standard". Pathologists with special interest and experience in GI pathology reviewed the histological sections. Appropriate forms were used to record the pathological findings. All the diagnostic criteria used for our survey were discussed and sample slides were reviewed by the pathologists before the study to minimize interobserver variations as far as possible.

Surgical specimens were immersed in paraffin for routine pathological examination. Microtome sections (7-8 μm thick) were stained with hematoxylin and eosin as well as high iron diamine/alcian blue to identify sialo-and sulfomucins. Adenocarcinoma was diagnosed when the malignant cells invaded the lamina propria in single cells, glandular or solid nest arrangements, usually accompanied with fibrosis of the surrounding tissue. Carcinomas were classified histologically as either intestinal or diffuse type in accordance with Lauren's classification[20]. Intestinal metaplasia classified according to Filipe *et al*[21] was defined as metaplastic transformation of gastric glandular and surface epithelium towards intestinal mucosal elements including goblet, absorptive, and Paneth cells.

Personnel not aware of the histological diagnoses performed serological testing. A commercial enzyme

Table 1 Seroprevalence of anti-*H pylori* antibodies among patients with gastric cancer and controls

Parameters	Gastric cancer (%)	Controls (%)
H pylori positive	261 (82.3)	314 (56.5)
H pylori negative	56	241
Anti-CagA positive	267 (84.2)	100 (18)
Anti-CagA negative	50	455

Table 2 Features of patients suffering from gastric cancer based on tumor subtype

Parameters	Intestinal type carcinoma (%)	Diffuse type carcinoma (%)
H pylori positive	138/181 (76.2%)	67/85 (78.8%)
Intestinal metaplasia	151/181 (83.4%)	64/85 (75.2%)

immunosorbent assay (ELISA, Helori-test® Eurospital, Trieste, Italy) was used to detect serum anti-*H pylori* (IgG) antibodies. The assay sensitivity and specificity were 94% and 87%[22]. Briefly, calibrators, positive and negative controls and diluted (1:200) serum samples were added to the wells coated with purified *H pylori* group-specific antigens. Plates were incubated for 60 min at 37 ℃, and then the liquid was removed completely and washed thrice with 200 μL/well of washing solution. One hundred microliters of anti-IgG conjugate was pipetted into each well. The wells were incubated for 60 min at 37 ℃, washed thrice with 200 μL/well of washing solution and 100 μL of chromogenic substrate was added to each well. The wells were again incubated for 30 min at 37 ℃, the reaction was stopped by adding 25 μL of the stopping solution. Reading was performed at 405 nm and the mean optical density was expressed as a percentage of the optical density of positive control serum assayed on the same plate. To detect the presence of serum IgG against *H pylori* CagA protein, Western blotting technique was used. *H pylori* CCUG 17874 (type strain, CagA positive, CagA mass = 128 ku) was cultured in *Brucella* broth containing 0.2% cyclodextrin at 37 ℃ in a microaerobic environment for 48 h. At the end of incubation, to exclude the presence of contaminants, the broth culture was subcultured onto plain blood agar plates and examined under optical microscope after staining with carbol fuchsin. The broth culture was centrifuged and the pellet was washed twice with phosphate buffered saline (PBS, pH 7.4) at 4 ℃. A whole cell suspension containing approximately 10^{10} bacteria was lysed and denatured in Laemmli buffer at 95 ℃ for 5 min, then run electrophoretically on 10% polyacrylamide gel with sodium dodecyl sulfate. Proteins were transferred onto nitrocellulose sheets saturated with 3% defatted milk in PBS with 0.1% Triton X (PBSMT). Strips were cut and serum samples were assayed at the dilution of 1:100 in PBSMT. After overnight incubation with constant agitation at room temperature, strips were washed with PBSMT and then incubated with an anti-human IgG serum conjugated with peroxidase at room temperature for 90 min. After the washings, the reaction was visualized by adding the substrate (H_2O_2 in a solution of 4-chloro-1-naphthol in Tris buffer 0.05 mol/L, pH 6.8). We used serum samples from patients infected respectively with CagA positive and negative *H pylori* strains as positive and negative controls with or without antibodies to CagA. Specific polyclonal antisera against CagA (kindly donated by Biocine-Chiron, Siena) was used as further controls.

The seroprevalence of anti-*H pylori* as well as the distribution of anti-CagA seropositivity in cases and controls were compared using the χ^2 test. Odds ratio (OR) and 95%CI assessing the risk of GC associated with *H pylori* infection were calculated using the Mantel-Haenszel method. $P<0.05$ was considered statistically significant.

RESULTS

All patients selected were suffering from gastric non-cardia adenocarcinoma (intestinal type in 181, diffuse type in 85 and mixed type in 51). Among these, 261 out of 317 (82.3%) were seropositive for IgG anti-*H pylori* compared to 314 out of 555 (56.5%) controls ($P<0.0001$; OR, 3.58; 95%CI, 2.53-5.07) (Table 1). Moreover, out of the 317 cases, 267 (84.2%) were seropositive for anti-CagA antibody *vs* 100 out of 555 (18%) controls ($P<0.0001$; OR, 24.30; 95%CI, 16.5-35.9) (Table 1).

There was no difference between the frequency of *H pylori* in intestinal type and diffuse type carcinoma. Overall, *H pylori* occurred in 138 out of 181 patients (76.2%) suffering from the former compared to 67 out of 85 (78.8%) suffering from the latter (P = NS) (Table 2). Intestinal metaplasia was more frequently seen in the intestinal type cancer (151/181, 83.4% *vs* 64/85, 75.2% in diffuse type and 37/51, 72.5% in mixed type) but the difference was not statistically significant (P = NS, Table 2). Among the patients examined for IM, 72 out of 181 (39.8%) had IM type I, 15 out of 181 (8.3%) type II, and 94 out of 181 (51.9%) type III, (type III *vs* others $P = 0.4$). Furthermore, among the patients with IM of either body or antral mucosa, 117 out of 151 (77.4%) with intestinal type carcinoma were positive for *H pylori* compared to 59 out of 85 (69.4%) with diffuse type carcinoma ($P = 0.17$).

DISCUSSION

Gastric carcinogenesis involves a slow but continuous stepwise evolution from superficial gastritis and glandular atrophy to metaplasia and dysplasia and finally to adenocarcinoma[23]. The process of carcinogenesis which may well extend over decades provides an excellent opportunity for early detection and intervention to prevent further progression of the sequence of events preceding the development of the neoplasma. This is especially true because *H pylori* (which can be readily treated) is known to be the main factor though not the only[24] etiological agent

and initiating carcinogen.

On the other hand, the prognosis of GC is poor. In most industrialized countries, only around 10% subjects survive for 5 years. The sole exception is Japan where this malignancy is often identified at an early stage and in younger and fitter patients[26]. In Italy, 10-year survival is 12.1% in all GC patients and 20.8% in resected cases. However, though the survival is good when the diagnosis is performed at an early stage, only a few cases are diagnosed at stages when cure by radical surgery is more probable[3].

Regarding the biological plausibility for a causal role, a higher intragastric pH after the development of atrophic gastritis provoked by *H pylori* may favor the production of carcinogens[26]. The generation of reactive oxygen species and increased level of inducible nitric oxide synthase may in turn cause genetic alterations leading to cancer[27]. Nardone *et al*[28] demonstrated by morphometric and immunohistochemical techniques that *H pylori* infection seems to be responsible for genomic instability in patients with chronic atrophic gastritis and eradication of *H pylori* can reverse inflammation, atrophy, metaplasia, and genomic instability.

CagA gene is situated at the end of the large region of the genome identified to be a pathogenicity island (PAI). The strains of *H pylori* expressing CagA protein are considered more virulent, being linked with an increased risk of duodenal ulcer and GC[23]. Moreover, CagA status is associated with a higher prevalence of p53 mutation in gastric adenocarcinoma[29].

This multicenter study showed a significant association between *H pylori* infection in particular by its more virulent strains and the presence of GC. In addition, the results confirmed that type III IM was most frequently associated with *H pylori* infection. These data suggest that CagA status is a helpful parameter in defining a subgroup of *H pylori*-infected patients at increased risk of developing gastric adenocarcinoma. The difference between the rate of *H pylori* infection and more virulent strains can be explained by the fact that CagA antibodies persist for a longer time than *H pylori* IgG surface antibodies. Hence, relying on *H pylori* IgG antibodies alone might misclassify a significant proportion of patients who once had the infection[11].

The established epidemiological association does not prove that there is a direct causal relationship. Therefore, to further confirm a causal role, we are going to evaluate the effect of *H pylori* on the morphological changes of gastric mucosa in patients with precancerous gastric lesions.

In conclusion, seroprevalence of *H pylori* infection is high in patients suffering from gastric adenocarcinoma, which provides further evidence that searching for CagA status over *H pylori* infection might confer additional benefit for identifying populations at greater risk for this tumor.

REFERENCES

1 **Kelley JR**, Duggan JM. Gastric cancer epidemiology and risk factors. *J Clin Epidemiol* 2003; **56**: 1-9

2 **El-Helal TA**, Bener A, Galadari I. Pattern of cancer in the United Arab Emirates referred to Al-Ain Hospital. *Ann Saudi Med* 1997; **17**: 506-509

3 **Barchielli A,** Amorosi A, Balzi D, Crocetti E, Nesi G. Long-term prognosis of gastric cancer in a European country: a population-based study in Florence (Italy). 10-year survival of cases diagnosed in 1985-1987. *Eur J Cancer* 2001; **37:** 1674-1680

4 **Correa P.** A human model of gastric carcinogenesis. *Cancer Res* 1988; **48**: 3554-3560

5 Infection with Helicobacter pylori. *IARC Monogr Eval Carcinog Risks Hum* 1994;**61**:177-240

6 **Wang KX**, Wang XF, Peng JL, Cui YB, Wang J, Li CP. Detection of serum anti-*Helicobacter pylori* immunoglobulin G in patients with different digestive malignant tumors. *World J Gastroenterol* 2003; **9**: 2501-2504

7 **Han SU**, Kim YB, Joo HJ, Hahm KB, Lee WH, Cho YK, Kim DY, Kim MW. *Helicobacter pylori* infection promotes gastric carcinogenesis in a mice model. *J Gastroenterol Hepatol* 2002; **17**: 253-261

8 **Uemura N**, Okamoto S, Yamamoto S, Matsumura N, Yamaguchi S, Yamakido M**, Taniyama K, Sasaki N, Schlemper RJ.** *Helicobacter pylori* infection and the development of gastric cancer. *N Engl J Med* 2001; **345:** 784-789

9 **.** Gastric cancer and *Helicobacter pylori:* a combined analysis of 12 case **control studies nested within prospective cohorts.** *Gut* 2001; **49**: 347-353

10 **Xue FB,** Xu YY, Wan Y, Pan BR, Ren J, Fan DM. Association of *H pylori* infection with gastric carcinoma: a Meta **analysis.** *World J Gastroenterol* 2001; **7**: 801-804

11 **Huang JQ,** Zheng GF, Sumanac K, Irvine EJ, Hunt RH. Meta-analysis of the relationship between *cagA* seropositivity and gastric cancer. *Gastroenterology* 2003; **125**: 1636-1644

12 **Rudi J**, Müller M, **von Herbay A, Zuna I, Raedsch R, Stremmel** W, Räth U. Lack of association of *Helicobacter pylori* seroprevalence and gastric cancer in a population with low gastric cancer incidence. *Scand J Gastroenterol* 1995; **30**: 958-963

13 **Kuipers EJ**, Gracia-Casanova M, Peña AS, Pals G, **Van Kamp** G, Kok A, Kurz-Pohlmann E, Pels NF, Meuwissen SG**.** *Helicobacter pylori* serology in patients with gastric carcinoma. *Scand J Gastroenterol* 1993; **28**: 433-437

14 **Holcombe C**. *Helicobacter pylori:* the African enigma. *Gut* 1992; **33**: 429-431

15 **Campbell DI,** Warren BF, Thomas JE, Figura N, Telford JL, Sullivan PB. The African enigma: low prevalence of gastric atrophy, high prevalence of chronic inflammation in West African adults and children. *Helicobacter* 2001; **6**: 263-267

16 **Groves FD**, Perez-Perez G, Zhang L, You WC, Lipsitz SR, Gail MH, Fraumeni JF, Blaser MJ. Serum antibodies to *Helicobacter pylori* and the CagA antigen do not explain differences in the prevalence of precancerous gastric lesions in two Chinese populations with contrasting gastric cancer rates. *Cancer Epidemiol. Biomarkers. Prev* 2002; **11**: 1091-1094

17 **Wong BC,** Lam SK, Wong WM, Chen JS, Zheng TT, Feng RE, Lai KC, Hu WH, Yuen ST, Leung SY, Fong DY, Ho J, Ching CK, Chen JS. *Helicobacter pylori* eradication to prevent gastric cancer in a high-risk region of China: **a randomized controlled** trial. *JAMA* 2004; **291**: 187-194

18 **Ponzetto A**, Soldati T, DeGiuli M. *Helicobacter pylori* screening and gastric cancer. *Lancet* 1996; **348**: 758

19 **Ponzetto A,** De Giuli M, Sanseverino P, Soldati T, Bazzoli F Re: *Helicobacter pylori* and atrophic gastritis : importance of the cagA status. *J Natl Cancer Inst* 1996; **88**: 465-466

20 **Laurén P.** Histogenesis of intestinal and diffuse types of gastric carcinoma. *Scand J Gastroenterol* 1991; **180** Suppl**:** 160-164

21 **Filipe MI,** Muñoz N, Matko I, Kato I, Pompe-Kirn V, Jutersek A, Teuchmann S, Benz M, Prijon T. Intestinal metaplasia types and the risk of gastric cancer: a cohort study in Slovenia. *Int J Cancer* 1994; **57**: 324-329

22 **Danielli E.** A fluorometric enzyme-linked immunosorbent

assay for serological diagnosis of *Helicobacter pylori* infection. *Eur J Gastroenterol Hepatol* 1993; **5(suppl 2):** S57-S59
23 **Sepulveda AR**, Coelho LG. *Helicobacter pylori* and gastric malignancies. *Helicobacter* 2002; **7 Suppl 1**: 37-42
24 **Mladenova I**, Pellicano R. Infectious agents and gastric tumours. An increasing role for Epstein-Barr virus. *Panminerva Med* 2003; **45**: 183-188
25 **Axon A.** Review article: gastric cancer and *Helicobacter pylori*. *Aliment Pharmacol Ther* 2002; **16** Suppl 4**:** 83-88
26 **Calam J**, Baron JH. **ABC of the upper gastrointestinal tract:** Pathophysiology of duodenal and gastric ulcer and gastric cancer. *BMJ* 2001; **323:** 980-982
27 **Choi J**, Yoon SH, Kim JE, Rhee KH, Youn HS, Chung MH. Gene-specific oxidative DNA damage in *Helicobacter pylori*-infected human gastric mucosa. *Int J Cancer* 2002; **99**: 485-490
28 **Nardone G**, Staibano S, Rocco A, Mezza E, D'**armiento FP, In**-sabato L, Coppola A, Salvatore G, Lucariello A, Figura N, De Rosa G, Budillon G. Effect of *Helicobacter pylori* infection and its eradication on cell proliferation, DNA status, and oncogene expression in patients with chronic gastritis. *Gut* 1999; **44**: 789-799
29 **Shibata A**, Parsonnet J, Longacre TA, Garcia MI, Puligandla B, Davis RE, Vogelman JH, Orentreich N, Habel LA. CagA status of *Helicobacter pylori* infection and *p53* gene mutations in gastric adenocarcinoma. *Carcinogenesis* 2002; **23**: 419-424

Science Editor Wang XL and Guo SY **Language Editor** Elsevier HK

PO Box 2345, Beijing 100023, China
www.wjgnet.com
wjg@wjgnet.com

ELSEVIER

World J Gastroenterol 2005;11(45):7136-7141
World Journal of Gastroenterology ISSN 1007-9327

• *RAPID COMMUNICATION* •

Upregulation of 25-hydroxyvitamin D_3-1α-hydroxylase by butyrate in Caco-2 cells

Oliver Schröder, Sinan Turak, Carolin Daniel, Tanja Gaschott, Jürgen Stein

Oliver Schröder, Sinan Turak, Carolin Daniel, Tanja Gaschott, Jürgen Stein, I[st] Department of Internal Medicine, Division of Gastroenterology and Clinical Nutrition, ZAFES, Johann Wolfgang Goethe-University, Frankfurt, Germany
Supported by the Else Kröner-Fresenius Foundation, Bad Homburg, Germany
Correspondence to: Dr Oliver Schröder, I[st] Department of Internal Medicine, Division of Gastroenterology and Clinical Nutrition, ZAFES, Johann Wolfgang Goethe-University, Theodor-Stern-Kai 7, 60590 Frankfurt,
Germany. o.schroeder@em.uni-frankfurt.de
Telephone: +49-69-6301-6204 Fax: +49-69-6301-83112
Received: 2005-01-12 Accepted: 2005-04-02

Abstract

AIM: To investigate the possible involvement of 25-hydroxyvitamin D_3-1α-hydroxylase [1α-25$(OH)_2D_3$] in butyrate-induced differentiation in human intestinal cell line Caco-2 cells.

METHODS: Caco-2 cells were incubated either with 3 mmol/L butyrate and 1 μmol/L 25$(OH)_2D_3$ or with 1 μmol/L 1α-25$(OH)_2D_3$ for various time intervals ranging from 0 to 72 h. Additionally, cells were co-incubated with butyrate and either 25$(OH)_2D_3$ or 1α-25$(OH)_2D_3$. 1α-25$(OH)_2D_3$ mRNA was determined semi-quantitatively using the fluorescent dye PicoGreen. Immunoblotting was used for the detection of 1α-25$(OH)_2D_3$ protein. Finally, enzymatic activity was measured by ELISA.

RESULTS: Both butyrate and 1α-25$(OH)_2D_3$ stimulated differentiation of Caco-2 cells after a 48 h incubation period, while 25$(OH)_2D_3$ had no impact on cell differentiation. Synergistic effects on differentiation were observed when cells were co-incubated with butyrate and vitamin D metabolite. Butyrate transiently upregulated 1α-25$(OH)_2D_3$ mRNA followed by a timely delayed protein upregulation. Coincidently, enzymatic activity was enhanced significantly. The induction of the enzyme allowed for comparable differentiating effects of both vitamin D metabolites.

CONCLUSION: Our experimental data provide a further mechanism for the involvement of the vitamin D signaling pathway in colonic epithelial cell differentiation by butyrate. The enhancement of 1α-25$(OH)_2D_3$ followed by antiproliferative effects of the vitamin D prohormone in the Caco-2 cell line suggest that 25$(OH)_2D_3$ in combination with butyrate may offer a new therapeutic approach for the treatment of colon cancer.

Key words: 25-Hydroxyvitamin D_3-1α-hydroxylase; Butyrate; Caco-2 cells; Colon cancer; Differentiation; Vitamin D

Schröder O, Turak S, Daniel C, Gaschott T, Stein J. Upregulation of 25-hydroxyvitamin D_3-1α-hydroxylase by butyrate in Caco-2 cells. *World J Gastroenterol* 2005; 11(45): 7136-7141
http://www.wjgnet.com/1007-9327/11/7136.asp

INTRODUCTION

In addition to its well-known role in mineral and skeletal homeostasis, it is widely recognized that the physiologically most active molecular form of vitamin D_3, 1α-25$(OH)_2D_3$, also re-strains cell proliferation, induces differentiation, and apoptosis in a large variety of normal and tumor cells, including cells of the large intestine[1-3]. Most of the long-term pleiotropic actions of 1α-25$(OH)_2D_3$ are mediated by binding to a high-affinity vitamin D receptor (VDR)[3-5], which is a member of the nuclear hormone-receptor superfamily. The growth-restraining anticancer effects of vitamin D on colon cells are conveyed through genomic and post-genomic pathways involving a crosstalk with mediator synthesis and signaling, the mediation of a cell-cycle arrest, and finally the induction of apoptosis[6].

1α-25$(OH)_2D_3$, the active form of vitamin D, is enzymatically formed from its precursor 25$(OH)_2D_3$. The enzyme was thought to exist only in the kidney, until recently it has been identified in other non-renal tissues including the large intestine[7,8]. Further studies demonstrated that in colorectal cancer expression of 1α-25$(OH)_2D_3$ and VDR increases in parallel with ongoing proliferation in the early phase of tumorigenesis, whereas in poorly differentiated late-stage carcinomas only low levels of both genes can be detected[9-11]. It is postulated that through this upregulation, colorectal cancer cells become able to increase their potential for an autocrine counter-regulatory response to neoplastic cell growth in the early stages of malignancy. Thus, 1α-25$(OH)_2D_3$ theoretically represents a suitable target for the prevention of colorectal carcinogenesis.

Short-chain fatty acids, in particular butyrate, have been shown to inhibit growth in colon cancer cell lines. We

have previously shown that butyrate and 1α-25(OH)$_2$D$_3$ act synergistically in inducing differentiation of Caco-2 cells[12,13]. Furthermore, at least some of the anti-proliferative and pro-differentiating effects of butyrate are mediated via an upregulation of VDR with subsequent p21$^{Waf1/Cip1}$ expression[14]. These data prompted us to investigate a possible effect of butyrate on the expression of 1α-25(OH)$_2$D$_3$ in Caco-2 cells.

MATERIALS AND METHODS

Chemicals and supplies

Disposable cell culture was purchased from Nalge Nunc International (Wiesbaden, Germany). Dulbecco's modified Eagle's medium (DMEM), fetal calf serum (FCS), sodium pyruvate, nonessential amino acids, and PBS were obtained from GIBCO BRL (Eggenstein, Germany). Penicillin and streptomycin were obtained from Biochrom (Berlin, Germany). Butyric acid (sodium salt) was purchased from Merck-Schuchardt (Munich, Germany).

25(OH)$_2$D$_3$ and 1α-25(OH)$_2$D$_3$ were dissolved in ethanol (final maximal concentration of ethanol in medium was 1 mL/L to yield a 10 mmol/L stock solution, which was stored at -20 ℃). Butyric acid was dissolved in PBS (final maximal concentration of PBS in medium was 1 mL/L). Control experiments with either 0.1% ethanol or 0.1% PBS were performed to exclude effects of the solvents on the results of our investigations.

Cell culture

Caco-2 cells were obtained from the German Cancer Research Center (Heidelberg, Germany). The stock was maintained in 175-cm^2 flasks in a humidified incubator at 37 ℃ in an atmosphere of 95% air and 50 mL/L CO_2. The medium consisted of DMEM supplemented with 10% FCS, 1% penicillin/streptomycin, 1% sodium pyruvate, and 1% nonessential amino acids. The cells were passaged weekly using Dulbecco's PBS containing 0.25% trypsin and 1% EDTA. The medium was changed thrice per week. Passages 30-38 were used in all the experiments. Cells were screened routinely for possible contamination with mycoplasma by PCR at monthly intervals using the VenorGem mycoplasma detection kit (Minerva Biolabs, Berlin, Germany). For the experiments, the cells were seeded onto plastic cell culture wells in serum-containing medium and allowed to attach for 24 h. Before the treatment, the cells were synchronized in a medium containing 1% FCS. Cells were treated with 3 mmol/L butyrate, 1 μmol/L 25(OH)D$_3$, or 1 μmol/L 1α-25(OH)$_2$D$_3$ for various time intervals ranging from 0 to 72 h. Additionally, cells were co-incubated with butyrate and either 25(OH)$_2$D$_3$ or 1α-25(OH)$_2$D$_3$ or solvent.

Cytotoxicity

Cytotoxicity was assayed by measuring lactate dehydrogenase activity in a cell culture medium using a commercially available kit (LDH kit, Merck, Darmstadt, Germany).

Cell differentiation

Alkaline phosphatase activity was used to assess the differentiation of Caco-2 cells. Enzymatic activity was determined as previously described[12] using the Ecoline alkaline phosphatase assay kit (Merck, Darmstadt, Germany). Cellular protein was determined by Coomassie blue assay using a commercial kit (Bio-Rad Laboratories GmbH, Munich, Germany).

Analysis of 1α-25(OH)$_2$D$_3$ mRNA by semi-quantitative RT-PCR

RT-PCR was conducted with the Gene Amp/Perkin Elmer RNA PCR kit according to the manufacturer's protocol, starting from 2 μg total RNA. Amplification of glyceraldehyde-3-phosphate dehydrogenase (GAPDH) served as control. From the results of preliminary experiments, 20 PCR cycles for GAPDH and 30 cycles for 1α-25(OH)$_2$D$_3$ were selected as optimal amplification conditions to produce a log-linear relationship between the amount of each mRNA and intensity of PCR product. The PCR reaction contained 0.2 mmol/L dNTP and 2.5 U AmpliTaqGold DNA polymerase (Applied Biosystems, NJ, USA) and either 0.1 μmol/L primers for 1α-25(OH)$_2$D$_3$ or 0.2 μmol/L primers for GAPDH. The conditions of the reaction for 1α-25(OH)$_2$D$_3$ were: initial denaturation at 94 ℃ for 15 s followed by annealing at 59 ℃ for 30 s, extension at 72 ℃ for 60 s and a final extension at 72 ℃ for 7 min after the last cycle. The respective annealing temperature for GAPDH was 45 ℃. Primers for amplification were as follows: 1α-25(OH)$_2$D$_3$ sense 5' -CAGAGGCAGCCATGAGGAAC-3', 1α-25(OH)$_2$D$_3$ antisense 5'-GGGTCCCTTGAAGTGGCATAG-3; GAPDH sense 5'-GCACCGTCAAGGCTGAGAAC-3', GAPDH antisense 5'-CCACCACCCTGTTGCTGTAG-3'. The expected sizes of 1α-25(OH)$_2$D$_3$ and GAPDH were 440 and 803 base pairs (bp), respectively. Aliquots of the PCR mixtures (10 μL) were analyzed by electrophoresis using a 1% agarose gel containing 0.5 μg/mL ethidium bromide.

For semi-quantitative analysis of amplified PCR products, the fluorescent dye PicoGreen (Molecular Probes, Goettingen, Germany) was used according to the manufacturer's instructions[15,16]. Two microliters of amplified dsDNA in 100 μL TE buffer was mixed with an equal volume of diluted PicoGreen reagent (5 mL/L in TE buffer). Samples were incubated for 5 min at room temperature and protected from light in a microtiter plate. The fluorescence was measured (λ_{ex} = 485 nm; λ_{em} = 538 nm) in a Spectra Fluor Plus fluorometer from Tecan (Crailsheim, Germany). The standard curve for the quantitative analysis was obtained with λ DNA standard in TE buffer, being linear from 1 to 128 ng/well.

Immunoblot analysis of 1α-25(OH)$_2$D$_3$

For the analysis of 1α-25(OH)$_2$D$_3$ protein expression levels, an equal number of cells was directly lysed in cell lysis buffer (Cell Signaling Technology, Beverly, MA, USA) and aliquots of 5 μg protein in the loading buffer were separated by SDS/PAGE through a 12.5% Tris-HCl-precasted linear gradient gel (Bio-Rad GmbH, Munich,

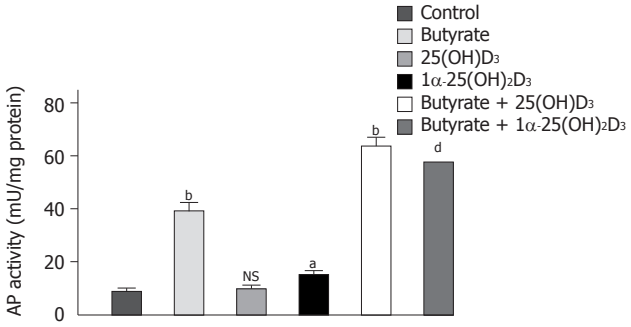

Figure 1 Effects of 1α-25(OH)$_2$D$_3$, 25(OH)$_2$D$_3$ and butyrate on differentiation of Caco-2 cells as assessed by AP activity. Cells were treated for 48 h with a medium supplemented with 10^{-6} mol/L 1α-25(OH)$_2$D$_3$, 10^{-6} mol/L 25(OH)$_2$D$_3$, 3 mmol/L butyrate, or with one of the combinations of butyrate (3 mmol/L) and 1α-25(OH)$_2$D$_3$ (10^{-6} mol/L) or butyrate (3 mmol/L) and 25(OH)$_2$D$_3$, (10^{-6} mol/L). Values are expressed as milliunits of AP activity per milligram cellular protein. ^{a}P<0.05; ^{b}P<0.01; ^{d}P<0.001; NS: non significant.

Germany) and electroblotted onto protran nitrocellulose transfer membranes (Schleicher & Schuell Bioscience, Dassel, Germany). The transfer efficiency was visualized using prestained molecular weight protein standards (Bio-Rad GmbH, Munich, Germany). Membranes were then soaked for 1 h at 25 ℃ in Tris-buffered saline (100 mmol/L Tris-HCl, pH 7.5, 150 mmol/L NaCl) containing 1 mL/L Tween 20 (0.1% TTBS) and 50 g/L dried nonfat milk. The membranes were subsequently washed (2×5 min) in 0.1% TTBS followed by an incubation for 90 min at 25 ℃ with a commercial sheep anti-murine 1α-25(OH)$_2$D$_3$ antibody (Binding Site Limited, Birmingham, UK) at a dilution of 1:500. After washing, the blot was incubated for 1 h at 25 ℃ with a horseradish peroxidase-linked donkey anti-rabbit antibody (Santa Cruz Biotechnology Inc., Santa Cruz, CA, USA) at a dilution of 1:1 000 in 0.1% TTBS and 20 g/L dried nonfat milk. The washing steps were repeated and subsequently enhanced chemiluminescence detection was performed according to the manufacturer's instructions (ECL Plus, Amersham Biosciences, UK). SDS-PAGE immunoblots were quantitated using a luminescent image scanner Desaga CabUVIS and ProViDoc software (Desaga, Wiesloch, Germany).

1α-25(OH)$_2$D$_3$ activity

Cells were seeded (10^6 cells/well/mL) in RPMI medium in a six-well plate. After incubation for 24 h with 5×10^{-8} mol/L 25(OH)$_2$D$_3$, the supernatant and cells were harvested. 1α-25(OH)$_2$D$_3$ was separated from other vitamin D metabolites by extraction columns (J.T. Baker, Phillipsburg, NJ, USA) and determined with a commercially available enzyme-linked immunosorbent assay (Immundiagnostik, Bensheim, Germany), being specific for 1α-25(OH)$_2$D$_3$ and unable to recognize other vitamin D metabolites.

Statistical analysis

All data were expressed as mean±SD. One-way ANOVA was used to compare means. P<0.05 was considered statistically significant.

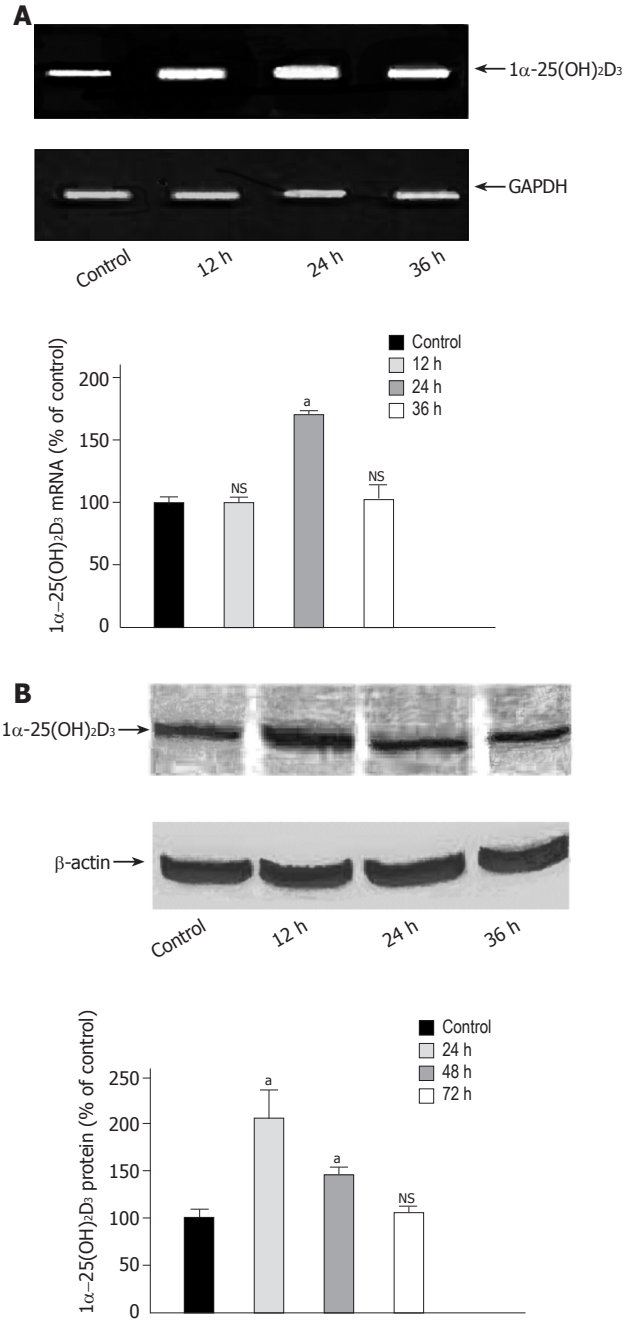

Figure 2 Time-dependent effect of butyrate on 1α-25(OH)$_2$D$_3$ expression. **A**: Caco-2 cells were grown for 36 h in serum-free medium in the absence (lane 1) or presence of butyrate (3 mmol/L) (lanes 2-4). 1α-25(OH)$_2$D$_3$ mRNA was analyzed by semiquantitative RT-PCR with the fluorescent dye PicoGreen. **B**: Caco-2 cells were treated for 72 h in the absence (lane 1) or presence of butyrate (3 mmol/L) (lanes 2-4) and then harvested for immunoblot analysis. The band at approximately 55 ku corresponds to 1α-25(OH)$_2$D$_3$ protein. Quantitation of protein was performed using a luminescent image scanner. ^{a}P<0,05 *vs* control; NS: non significant.

RESULTS

Influence of active vitamin D forms on butyrate-induced cell differentiation

After any cytotoxicity of either substrate was ruled out (data not shown), the influence of the two active vitamin D forms, 25(OH)$_2$D$_3$ and 1α-25(OH)$_2$D$_3$, on butyrate-induced

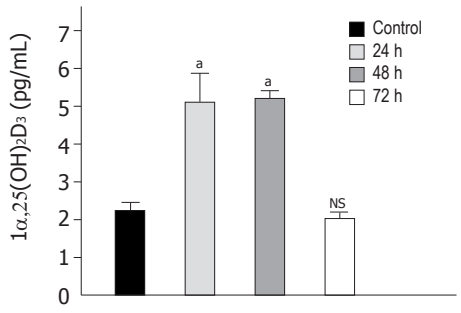

Figure 3 Time-dependent effect of butyrate on 1α-25(OH)$_2$D$_3$ activity. Caco-2 cells were treated for 72 h in the absence (lane 1) or presence of butyrate (3 mmol/L) (lanes 2-4) and then harvested for ELISA. Values are expressed as pg/mL of 1α-25(OH)2D3. [a]*P*<0,05 *vs* control; NS, non significant.

cell differentiation was determined. Figure 1 displays the individual and combined effect of butyrate, 25(OH)$_2$D$_3$ and 1α-25(OH)$_2$D$_3$ on AP activity. As compared to control, butyrate and 1α-25(OH)$_2$D$_3$ significantly stimulated differentiation of Caco-2 cells after a 48-h incubation period, the effect of butyrate being much more prominent (436±27% *vs* 70±7%, respectively). In contrast, 25(OH)$_2$D$_3$ had no impact on cell differentiation. Synergistic effects on differentiation were observed when Caco-2 cells were co-incubated with butyrate and either vitamin D metabolite. In this case, AP activity increased to 633± 7% (butyrate+25(OH)$_2$D$_3$) and 702±107% (butyrate+1α-25(OH)$_2$D$_3$) as compared to control.

Effect of butyrate on 1α-25(OH)$_2$D$_3$ expression

The above mentioned data suggested a possible impact of 1α-25(OH)$_2$D$_3$ mRNA on the synergistic potential of butyrate and vitamin D forms in inducing colonic epithelial cell differentiation. We therefore investigated 1α-25(OH)$_2$D$_3$ mRNA expression in Caco-2 cells treated with butyrate. As shown in Figure 2A, butyrate led to a transient increase of 1α-25(OH)$_2$D$_3$ mRNA by 67.3± 27% as compared to control after 24 h, which returned to basal values after 36 h. Induction of gene expression was increased after 24 h and gradually decreased thereafter (Figure 2B).

Effect of butyrate on 1α-25(OH)$_2$D$_3$ enzymatic activity

We finally assessed whether induction of 1α-25(OH)$_2$D$_3$ mRNA and protein was accompanied with an increased enzymatic capacity of Caco-2 cells. Enzymatic conversion into the active metabolite 1α-25(OH)$_2$D$_3$ was enhanced by a factor of 2.3±0.6 after 24 and 48 h of treatment with 3 mmol/L butyrate as compared to control (Figure 3).

DISCUSSION

The present report provides further experimental evidence that butyrate-induced colonic epithelial cell differentiation at least in part is mediated by the vitamin D signaling pathway. Our data demonstrate that butyrate treatment of the Caco-2 cell line results in an upregulation of gene and protein expression of 1α-25(OH)$_2$D$_3$, followed by an increased enzymatic activity with conversion of 25(OH)$_2$D$_3$ to 1α-25(OH)$_2$D$_3$. The induction of this enzyme then allowed for the matchable differentiating effects of 25(OH)$_2$D$_3$ in comparison to 1α-25(OH)$_2$D$_3$, thereby presenting a possible new chemopreventive mechanism in colon cancer.

We and others have previously shown that some of the antineoplastic effects of the short-chain fatty acid butyrate in colonic epithelial cells are operated by synergistic actions with 1α-25(OH)$_2$D$_3$. It has been demonstrated in various colonic cancer cell lines that butyrate and 1α-25(OH)$_2$D$_3$ act synergistically in reducing proliferation and enhancing differentiation[13,14,17,18]. One molecular mechanism participating in this interplay represents the upregulation of VDR expression, followed by a stimulation of the negative cell cycle regulator p21$^{Waf1/Cip1}$ and a downregulation of cyclins and cdks[12]. The alteration of the expression of a variety of genes as well as by inhibiting histone acetylase[19,20] and phosphorylation by enhancing nonhistone protein phosphorylation[21] and causing hypo- or hypermethylation of DNA[22,23] is the other known molecular mechanism by which butyrate mediates its antitumor effects. Similar additive antiproliferative effects of vitamin D with other histone deacetylation inhibitors such as TSA have also been described in a non-malignant epithelial breast cell line[24].

Evidence from a variety of experimental studies, epidemiological findings and a few human clinical trials indicate that vitamin D can modulate and inhibit carcinogenesis[6]. Vitamin D activity in epithelial cells involves the conversion of 25(OH)$_2$D$_3$ to 1α-25(OH)$_2$D$_3$ during the interaction of 1α-25(OH)$_2$D$_3$ with VDR. Subsequently, activation of VDR leads to repression or activation of specific proto-oncogenes or tumor-suppressor genes that are related to proliferation and differentiation in a large variety of normal and tumor tissues including the small and large intestine[1–5,25]. In addition, post-genomic pathways also seem to be involved in growth regulation. VDR seems to undergo specific alterations in expression during the development and progression of colon cancer. Compared to normal colon mucosa, VDR density is increased in hyperplastic polyps and in early stages of tumorigenesis, but declines in late-stage neoplasia[9-11]. As a further support to this stage-dependent expression, Belleli *et al*[26] found that the number of 1α-25(OH)$_2$D$_3$-binding sites is significantly decreased in the colon of carcinogen-treated rats.

1α-25(OH)$_2$D$_3$ is believed to exist solely in the kidney and it has also been identified in other non-renal tissues including the large intestine[7,8].

Due to its higher affinity to VDR, 1α-25(OH)$_2$D$_3$, the active form of vitamin D, is about 500-1 000-fold more active than its precursor 25(OH)$_2$D$_3$. Though there exists a large body of evidence, that 1α-25(OH)$_2$D$_3$ exerts pleiotropic antitumor effects against several malignancies *in vitro*, its clinical use as a chemopreventive agent is limited by hypercalcemia. For example, the concentrations of

1α-25(OH)$_2$D$_3$ required to inhibit colon cancer in tissue culture are in the range of 10^{-6}-10^{-9} mol/L[27-29]. Therefore, several groups have searched for other vitamin D-related anti-neoplastic therapeutic strategies. Recently, Schwartz *et al*[30] have demonstrated not only the expression of 1α-25(OH)$_2$D$_3$ and VDR in normal and malignant pancreatic tissue but also antiproliferative effects of the prohormone 25(OH)D$_3$[30]. Furthermore, prostatic 1α-25(OH)$_2$D$_3$ has been found to be largely unregulated by serum levels of parathyroid hormone and calcium[31]. Due to the large therapeutic window of 25(OH)$_2$D$_3$ compared to 1α-25(OH)$_2$D$_3$, the authors concluded that 25(OH)$_2$D$_3$ could play a role in the prevention of both pancreatic and prostate cancers. In our experimental setting, 25(OH)$_2$D$_3$ was not able to exert antiproliferative effects in Caco-2 cells as a result of the weak expression of 1α-25(OH)$_2$D$_3$. However, the induction of this enzyme by butyrate provoked the same impact on the differentiation of this colon cancer cell line as 1α-25(OH)$_2$D$_3$. Whether these activities are specific for Caco-2 cells or represent tissue-specific peculiarities of colonic epithelium has to be determined.

REFERENCES

1 **Lamprecht SA**, Lipkin M. Cellular mechanisms of calcium and vitamin D in the inhibition of colorectal carcinogenesis. *Ann N Y Acad Sci* 2001; **952**: 73-87
2 **Studzinski GP**, McLane JA, Uskoković MR. Signaling pathways for vitamin-D-induced differentiation: implications for therapy of proliferative and neoplastic diseases. *Crit Rev Eukaryot Gene Expr* 1993; **3**: 279-312
3 **Ylikomi T**, Laaksi I, Lou YR, Martikainen P, Miettinen S, Pennanen P, Purmonen S, Syvälä H, Vienonen A, Tuohimaa P. Antiproliferative action of vitamin D. *Vitam Horm* 2002; **64**: 357-406
4 **Haussler MR**, Whitfield GK, Haussler CA, Hsieh JC, Thompson PD, Selznick SH, Dominguez CE, Jurutka PW. The nuclear vitamin D receptor: biological and molecular regulatory properties revealed. *J Bone Miner Res* 1998; **13**: 325-349
5 **Sutton AL**, MacDonald PN. Vitamin D: more than a "bone-a-fide" hormone. *Mol Endocrinol* 2003; **17**: 777-791
6 **Lamprecht SA**, Lipkin M. Chemoprevention of colon cancer by calcium, vitamin D and folate: molecular mechanisms. *Nat Rev Cancer* 2003; **3**: 601-614
7 **Tangpricha V**, Flanagan JN, Whitlatch LW, Tseng CC, Chen TC, Holt PR, Lipkin MS, Holick MF. 25-hydroxyvitamin D-1alpha-hydroxylase in normal and malignant colon tissue. *Lancet* 2001; **357**: 1673-1674
8 **Ogunkolade BW**, Boucher BJ, Fairclough PD, Hitman GA, Dorudi S, Jenkins PJ, Bustin SA. Expression of 25-hydroxyvitamin D-1-alpha-hydroxylase mRNA in individuals with colorectal cancer. *Lancet* 2002; **359**: 1831-1832
9 **Shabahang M**, Buras RR, Davoodi F, Schumaker LM, Nauta RJ, Evans SR. 1,25-Dihydroxyvitamin D3 receptor as a marker of human colon carcinoma cell line differentiation and growth inhibition. *Cancer Res* 1993; **53**: 3712-3718
10 **Sheinin Y**, Kaserer K, Wrba F, Wenzl E, Kriwanek S, Peterlik M, Cross HS. In situ mRNA hybridization analysis and immunolocalization of the vitamin D receptor in normal and carcinomatous human colonic mucosa: relation to epidermal growth factor receptor expression. *Virchows Arch* 2000; **437**: 501-507
11 **Cross HS,** Bareis P, Hofer H, Bischof MG, Bajna E, Kriwanek S, Bonner E, Peterlik M. 25-Hydroxyvitamin D(3)-1alpha-hydroxylase and vitamin D receptor gene expression in human colonic mucosa is elevated during early cancerogenesis. *Steroids* 2001; **66**: 287-292
12 **Gaschott T**, Wächtershäuser A, Steinhilber D, Stein J. 1,25-Dihydroxycholecalciferol enhances butyrate-induced p21$^{(Waf1/Cip1)}$ expression. *Biochem Biophys Res Commun* 2001; **283**: 80-85
13 **Gaschott T**, Steinhilber D, Milovic V, Stein J. Tributyrin, a stable and rapidly absorbed prodrug of butyric acid, enhances antiproliferative effects of dihydroxycholecalciferol in human colon cancer cells. *J Nutr* 2001; **131**: 1839-1843
14 **Gaschott T**, Werz O, Steinmeyer A, Steinhilber D, Stein J. Butyrate-induced differentiation of Caco-2 cells is mediated by vitamin D receptor. *Biochem Biophys Res Commun* 2001; **288**: 690-696
15 **Singer VL**, Jones LJ, Yue ST, Haugland RP. Characterization of PicoGreen reagent and development of a fluorescence-based solution assay for double-stranded DNA quantitation. *Anal Biochem* 1997; **249**: 228-238
16 **Romppanen EL**, Savolainen K, Mononen I. Optimal use of the fluorescent PicoGreen dye for quantitative analysis of amplified polymerase chain reaction products on microplate. *Anal Biochem* 2000; **279**: 111-114
17 **Yoneda T**, Aya S, Sakuda M. Sodium butyrate (SB) augments the effects of 1,25 dihydroxyvitamin D$_3$ (1,25(OH)2D3) on neoplastic and osteoblastic phenotype in clonal rat osteosarcoma cells. *Biochem Biophys Res Commun* 1984; **121**: 796-801
18 **Tanaka Y**, Bush KK, Eguchi T, Ikekawa N, Taguchi T, Kobayashi Y, Higgins PJ. Effects of 1,25-dihydroxyvitamin D$_3$ and its analogs on butyrate-induced differentiation of HT-29 human colonic carcinoma cells and on the reversal of the differentiated phenotype. *Arch Biochem Biophys* 1990; **276**: 415-423
19 **Archer SY**, Meng S, Shei A, Hodin RA. p21(WAF1) is required for butyrate-mediated growth inhibition of human colon cancer cells. *Proc Natl Acad Sci U S A* 1998; **95**: 6791-6796
20 **Wu JT,** Archer SY, Hinnebusch B, Meng S, Hodin RA. Transient vs. prolonged histone hyperacetylation: effects on colon cancer cell growth, differentiation, and apoptosis. *Am J Physiol Gastrointest Liver Physiol* 2001; **280**: G482-G490
21 **Archer SY**, Johnson JJ, Kim HJ, Hodin RA. p21 gene regulation during enterocyte differentiation. *J Surg Res* 2001; **98**: 4-8
22 **Christman JK**, Weich N, Schoenbrun B, Schneiderman N, Acs G. Hypomethylation of DNA during differentiation of Friend erythroleukemia cells. *J Cell Biol* 1980; **86**: 366-370
23 **Parker MI**, de Haan JB, Gevers W. DNA hypermethylation in sodium butyrate-treated WI-38 fibroblasts. *J Biol Chem* 1986; **261**: 2786-2790
24 **Banwell CM,** O'Neill LP, Uskokovic MR, Campbell MJ. Targeting 1alpha,25-dihydroxyvitamin D3 antiproliferative insensitivity in breast cancer cells by co-treatment with histone deacetylation inhibitors. *J Steroid Biochem Mol Biol* 2004; **89-90**: 245-249
25 **Minghetti PP**, Norman AW. 1,25(OH)$_2$-vitamin D$_3$ receptors: gene regulation and genetic circuitry. *FASEB J* 1988; **2**: 3043-3053
26 **Belleli A,** Shany S, Levy J, Guberman R, Lamprecht SA. A protective role of 1,25-dihydroxyvitamin D$_3$ in chemically induced rat colon carcinogenesis. *Carcinogenesis* 1992; **13**: 2293-2298
27 **Thomas MG**, Tebbutt S, Williamson RC. Vitamin D and its metabolites inhibit cell proliferation in human rectal mucosa and a colon cancer cell line. *Gut* 1992; **33**: 1660-1663
28 **Cross HS**, Pavelka M, Slavik J, Peterlik M. Growth control of human colon cancer cells by vitamin D and calcium in vitro. *J Natl Cancer Inst* 1992; **84**: 1355-1357
29 **Gaschott T**, Steinmeyer A, Steinhilber D, Stein J. ZK 156718, a low calcemic, antiproliferative, and prodifferentiating vitamin D analog. *Biochem Biophys Res Commun* 2002; **290**: 504-509
30 **Schwartz GG**, Eads D, Rao A, Cramer SD, Willingham MC, Chen TC, Jamieson DP, Wang L, Burnstein KL,

Holick MF, Koumenis C. Pancreatic cancer cells express 25-hydroxyvitamin D-1 alpha-hydroxylase and their proliferation is inhibited by the prohormone 25-hydroxyvitamin D3. *Carcinogenesis* 2004; **25**: 1015-1026

31 **Young MV**, Schwartz GG, Wang L, Jamieson DP, Whitlatch LW, Flanagan JN, Lokeshwar BL, Holick MF, Chen TC. The prostate 25-hydroxyvitamin D-1 alpha-hydroxylase is not influenced by parathyroid hormone and calcium: implications for prostate cancer chemoprevention by vitamin D. *Carcinogenesis* 2004; **25**: 967-971

Science Editor Wang XL and Guo SY **Language Editor** Elsevier HK

PO Box 2345, Beijing 100023, China
www.wjgnet.com
wjg@wjgnet.com

ELSEVIER

World J Gastroenterol 2005;11(45):7142-7147
World Journal of Gastroenterology ISSN 1007-9327

• *RAPID COMMUNICATION* •

Using the polymerase chain reaction coupled with denaturing gradient gel electrophoresis to investigate the association between bacterial translocation and systemic inflammatory response syndrome in predicted acute severe pancreatitis

Callum B Pearce, Vitaly Zinkevich, Iwona Beech, Viera Funjika, Ana Garcia Ruiz, Afraa Aladawi, Hamish D Duncan

Callum B Pearce, Hamish D Duncan, Queen Alexandra Hospital, Portsmouth, United Kingdom
Vitaly Zinkevich, Iwona Beech, Viera Funjika, Ana Garcia Ruiz, Afraa Aladawi, Microbiology Research Laboratory, School of Pharmacy and Biomedical Sciences, University of Portsmouth, United Kingdom
Supported by a grant from Fresenius-Kabi Ltd
Correspondence to: Callum B Pearce, Senior Registrar in Gastroenterology, Diagnostic Procedures Unit, Fremantle Hospital, Fremantle, Western Australia, WA 6011, Australia. pearcey@screaming.net
Telephone: +61-415-668-466 Fax: +61-894-312-340
Received: 2004-11-09 Accepted: 2005-02-21

Abstract

AIM: To investigate the use of PCR and DGGE to investigate the association between bacterial translocation and systemic inflammatory response syndrome in predicted severe AP.

METHODS: Patients with biochemical and clinical evidence of acute pancreatitis and an APACHE II score ≥ 8 were enrolled. PCR and DGGE were employed to detect bacterial translocation in blood samples collected on d 1, 3, and 8 after the admission. Standard microbial blood cultures were taken when there was clinical evidence of sepsis or when felt to be clinically indicated by the supervising team.

RESULTS: Six patients were included. Of all the patients investigated, only one developed septic complications; the others had uneventful illness. Bacteria were detected using PCR in 4 of the 17 collected blood samples. The patient with sepsis was PCR-positive in two samples (taken on d 1 and 3), despite three negative blood cultures. Using DGGE and specific primers, the bacteria in all blood specimens which tested positive for the presence of bacterial DNA were identified as *E coli.*

CONCLUSION: Our study confirmed that unlike traditional microbiological techniques, PCR can detect the presence of bacteria in the blood of patients with severe AP. Therefore, this latter method in conjunction with DGGE is potentially an extremely useful tool in predicting septic morbidity and evaluating patients with the disease. Further research using increased numbers of patients, in particular those patients with necrosis and sepsis, is required to assess the reliability of PCR and DGGE in the rapid diagnosis of infection in AP.

Key words: Polymerase chain reaction; Acute pancreatitis; Bacterial translocation

Pearce CB, Zinkevich V, Beech I, Funjika V, Ruiz AG, Aladawi A, Duncan HD. Using the polymerase chain reaction coupled with denaturing gradient gel electrophoresis to investigate the association between bacterial translocation and systemic inflammatory response syndrome in predicted acute severe pancreatitis. *World J Gastroenterol* 2005; 11(45): 7142-7147 http://www.wjgnet.com/1007-9327/11/7142.asp

INTRODUCTION

Infection and septic complications are the major factors contributing to the poor outcome in acute severe pancreatitis. They cause up to 80% of deaths and occur in 5-10% of patients[1-3]. It is thought that in the majority of cases infection is caused by bacterial translocation from the gut lumen[4-7], a hypothesis which animal experiments have generally supported[8-10]. Unfortunately attempts to confirm the link between bacterial translocation and morbidity and mortality in acute pancreatitis in human beings have been largely unsuccessful[11,12].

Conventional microbiological blood culture methods are currently used widely[13-15], but may fail to yield positive results, if the causative organism is fastidious in nature, cell dependent or has a fungal etiology. It is thought that 60-70% of the bacteria in the human intestinal tract cannot be cultured[16,17]. Molecular-based diagnostic approaches are therefore being increasingly employed, especially when a quick diagnosis is required[18-21].

The use of the polymerase chain reaction (PCR) to identify microbial DNA in clinical specimens has been described by many investigators[22-25]. PCR using 16S rRNA-specific primers has identified bacterial DNA in blood after the surgery[26]. 16S rRNA is a highly conserved region of bacterial DNA, found in all Gram-positive and Gram-negative bacteria[27]; if these primers are used, the majority of pathogenic bacteria can theoretically

Table 1 Oligonucleotide primers used for amplification of total DNA extracted from human blood samples and total chromosomal DNA recovered from selected bacterial strains

Primer designate	Sequences of (+) and (-) primers (nucleotide)	Gene target	Size of amplicon (bp)
BG-1 (+ strand)	5′CTT TGC CTG GTT TCC GGC ACC AGA A- 3′ (201-225)	b-Galactosidase gene of *E coli*	762
BG-4 (- strand)	5′AAC CAC CGC ACG ATA GAG ATT CGG G- 3′ (983-939)		
BD-1 (+ strand)	5′AGT TTG ATC CTG GCT GAG- 3′ (8-27)	DNA coding for 16S rRNA	798
BD-2 (- strand)	5′GGA CTA CCA GGG TAT CTA AT- 3′ (805-787)		
BFR-1 (+ strand)	5′ACT CTT TGT ATC CCG ACG ATT-3′ (484-504)	Glutamine synthase gene of *Bacteroides* spp.	581
BFR-2 (- strand)	5′GAG GTT GAT GCC TGT ATC GGT-3′ (1 065-1 045)		
F3 (+ strand)	5′CGCCCGCCGCGCGCGGCGGGCGGGGCGGGGGCAC-GGGGGGCCTACGGGAGGCAGCAG-3′	Variable V3 region of 16S rRNA	233
Rev-2 (- strand)	5′ATTACCGCGGCTGCTGG-3′		

be detected and identified by subsequent cloning and sequencing. From a practical point of view blood cultures can take days to yield a result, whereas PCR can produce results within hours.

PCR without subsequent cloning can identify the bacterial genus leaving the species undefined, which may cause difficulties, for instance, if the therapeutic guidelines for the species are different. Polymicrobial infections can also be problematic due to the inability of PCR to identify several microorganisms in a single specimen[28]. These problems can be solved by denaturing gradient gel electrophoresis (DGGE)[27], which uses the presence of unique heterodiplexes in DNA affecting migration to separate different DNA fragments[29].

Our investigation was carried out to assess the potential of PCR and DGGE as rapid tools for the detection and identification of systemic bacterial translocation in blood samples of patients with acute severe pancreatitis. The study also aimed to elucidate the relationship between the presence or absence of clinical infection; manifested as either sepsis or infected necrosis, and the detection of translocated bacterial DNA.

MATERIALS AND METHODS

Sample collection and subjects

Patients who were admitted with a diagnosis of acute pancreatitis predicted to have severe disease during the study period were enrolled. Patients were only considered if their duration of symptoms was 48 h or less on admission. Pancreatitis was defined as appropriate clinical signs and symptoms with hyperamylasemia of more than three times the upper limit of normal. Patients predicted to have severe disease were identified by an APACHE II score of eight or more on admission[30].

Blood samples were taken on d 1, 3, and 8 of admission for examination by PCR and DGGE techniques. Standard microbial blood cultures were taken only when there was a clinical evidence of sepsis or when felt to be clinically indicated by the supervising team to limit the number of venesections patients enrolled in the study would need to volunteer. The supervising teams were not aware of the PCR results.

Blood samples

Blood was transferred from Na_2 EDTA tubes (Sigma, UK) to sterile 1.5 mL Eppendorf tubes (Sigma, UK), and purified using the QIAamp DNA Blood Mini Kit (Qiagen, Hilden, Germany), according to the manufacturer' s instructions. Whole blood samples were processed in aliquots of 400 μL for DNA extraction.

DNA extraction

The DNA from human blood samples and from different bacterial strains was purified, and bacterial DNA was amplified using PCR with primers specific for (i) the bacterial 16S rRNA region, (ii) *E coli,* and (iii) *Bacteroides* spp., as outlined below. Enzymatic amplification for DGGE was performed on human blood samples tested PCR positive for the presence of bacterial DNA.

Bacterial cells

Prior to DNA extraction, bacterial cells were cultured in LB medium (10 mL) overnight at +37 ℃ inside an incubator shaker (New Brunswick Scientific). Chromosomal DNA was extracted using the QIAGEN Genomic DNA Purification Kit (QIAGEN, Hilden, Germany), according to the manufacturer's instructions.

Oligonucleotide primers for PCR

The oligonucleotide primers were synthesized by Sigma Aldrich Co. The primer pairs, sequences, gene targets and size of the product amplified after PCR are listed in Table 1. The primer pair designated BD-1 and BD-2 is specific for a highly conserved region of different bacterial DNA coding for 16S ribosomal RNA. The second primer pair BG-1 and BG-4 was derived from the β-galactosidase gene of *E coli*, which is found in most *E coli* strains. The third primer pair used BFR-1 and BFR-2 targets specifically for the ubiquitous glutamine synthase gene found in many *Bacteroides* spp[26]. The fourth primer pair F3 and Rev 2 was used for amplification of variable V3 region of 16S rDNA gene[29].

Microbial DNA amplification by PCR

PCR was performed with minor modification following the protocol of Kane *et al*[26]. Extracted DNA (20-30 μL) was placed in 0.5 mL sterile Eppendorf tube to which the

Table 2 A summary of the results obtained from testing of blood samples from six patients; CRP and SIRS evaluation, blood culture testing using selective growth media and PCR analysis

Patient no.	Day	1	2	3	4	8	Complications
1	CRP	135	158	91	70	40	None
	SIRS	Y	Y	N	N	N	
	PCR	Negative		Negative		Positive	
2	CRP	55	83	108	105	94	None
	SIRS	N	N	N	N	N	
	PCR	Negative		Negative		Negative	
3	CRP	345	301	289	234	142	None
	SIRS	Y	Y	Y	N	N	
	PCR	Negative		Negative		Negative	
4	CRP	301	284	248	169	122	None
	SIRS	Y	Y	Y	Y	N	
	PCR	Positive		Negative		Negative	
5	CRP	59	201	193	155	114	Pneumonia, sepsis
	SIRS	Y	Y	Y	Y	N	(-ve blood culture)
	PCR	Positive		Positive		Negative	
6	CRP	326	209	150	128		None
	SIRS	Y	Y	Y	Y		
	PCR	Negative		Negative			

NB: patient no. 6 was discharged before d 8. Patient no. 5 was treated with antibiotics on d 2.

PCR reaction mixture was added to make a final volume of 50 μL per tube. The mixture consisted of the following: 5 μL of 10× PCR reaction buffer, 1 μL each of (10 μmol/L) designated primers, 1 μL of a mixture of 10 mmol/L deoxynucleotide triphosphate (dNTP), 0.2 μL of 1 unit/μL Super Taq DNA polymerase (HT Biotechnology Ltd) and nuclease free dH_2O (Sigma Chemical Ltd) up to the final volume.

PCR amplification was carried out using a Techne (Progene) machine through the cycles as follows: an initial cycle of 95 ℃/3 min, 60 ℃/45 s, and 72 ℃/10 min was followed by 35 cycles of 95 ℃/45 s, 60 ℃/45 s, and 72 ℃/1 min; an extension period of 72 ℃/10 min completed the cycling sequence.

PCR amplification of 16S rDNA fragments for DGGE

Enzymatic amplification for DGGE was performed on samples positive for bacterial DNA. PCR reaction quantifications were outlined as above. The amplification was performed as follows: an initial cycle of 95 ℃ for 15 min was followed by 35 cycles each of 1 min at 94, 60, and 70 ℃, respectively; an extension period of 72 ℃ for 5 min completed the cycling sequence.

Agarose gel electrophoresis

All PCR products were separated by electrophoresis on 1% agarose gel in 1× TAE buffer (0.04 mol/L Tris-acetate, 0.002 mol/L EDTA). The gels were stained with ethidium bromide (0.5 μg/mL) for 30 min, washed twice with distilled H_2O and photographed under UV light using a UVP gel documentation system. A 1-kbp DNA ladder (Sigma) was used as a molecular weight marker. All reagents were purchased from Sigma, UK.

DGGE analysis

DGGE was performed using Ingeny Phos system (Leiden, The Netherlands). A 10 μL volume of each PCR product was applied directly onto 9% (wt/vol) polyacrylamide gels in 0.5× TAE (20 mmol/L Tris-acetate, 10 mmol/L sodium acetate, 0.5 mmol/L Na_2-EDTA) with gradients which were formed with 9% (wt/vol) acrylamide, 37:1) and which contained 0 and 100% denaturant [7 mol/L urea (GIBCO BRL)] and 40% (wt/vol) formamide. The gel was subjected to 200 V for 10 min at 60 ℃ and 85 V for 16 h. After electrophoresis, the gel was stained in ethidium bromide solution (0.5 μg/mL) for 30 min, washed twice by distilled H_2O and analyzed under UV light using UVP gel documentation system.

Blood cultures

Conventional blood cultures were processed using the BacT/ALERT® system manufactured by BioMerieux©. BacT/ALERT® aerobic (SA) and anaerobic (SN) culture media bottles were taken peripherally from patients under aseptic conditions and a BacT/ALERT® 3D analyzer was used to process the samples. Positive samples were Gram stained, and subcultured onto appropriate solid culture media, which was examined at 24 and 48 h.

Ethics

The study was performed as part of a larger study into enteral nutrition in acute pancreatitis. Written informed consent was a condition of entry into the study. The local ethics committee (Portsmouth, Hampshire, UK) approved the study.

RESULTS

Of the six patients tested one developed septic complications; pneumonia, respiratory failure and severe systemic inflammatory response syndrome, although this patient subsequently made a full recovery (patient

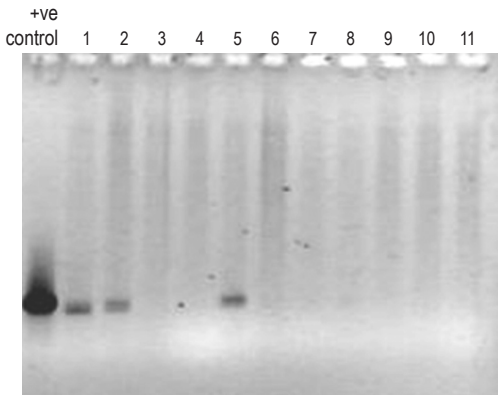

Figure 1 PCR profiles of total DNA recovered from human blood samples and of *E coli* DNA (control) obtained using primers BD1 and BD2 specific for bacterial 16S rRNA region. Positive control: Chromosomal DNA from *E coli*. Lanes 1-11: total DNA extracted from human blood samples.

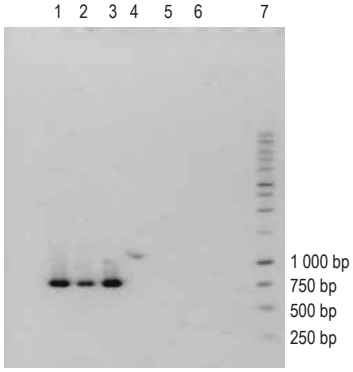

Figure 2 PCR profile of *E coli* chromosomal DNA. Lanes 1-3: DNA amplified using primers BG1 and BG4 specific for *E coli*. Lanes 4-6: DNA amplified using primers BFR1 and BFR2 specific for *Bacteroides* spp. Lane 7: 1 kb standard DNA ladder.

no. 5, Table 2). This was the only patient in the group that retrospectively developed severe acute pancreatitis according to the Santorini Consensus definitions[31]. This patient did not, however, require ventilatory support, and did not develop necrosis, infected or otherwise. The other patients had uneventful illness.

PCR detected the presence of bacteria in 4 of the 17 samples (23.6%). The blood samples from the patient with sepsis tested PCR-positive for bacterial DNA in specimens collected on d 1 and 3. This patient had three sets of standard blood cultures taken on d 1, 3, and 5, all of which were negative; he/she was the only patient in our study in whom standard blood cultures were taken.

When the incidence of the systemic inflammatory response syndrome (SIRS), C-reactive protein (CRP) levels and septic complications were compared with the PCR results there was no observed correlation between the presence of bacterial DNA in the blood, as confirmed by PCR, and SIRS or CRP data (Table 2).

The PCR profiles of DNA recovered from human blood samples and of *E coli* DNA (positive control), treated with general bacterial primers (Table 1) are depicted in Figure 1 (lanes 1 and 2-13, respectively). The appearance

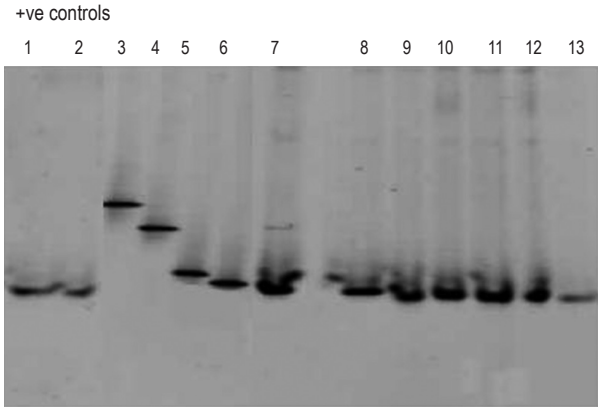

Figure 3 DGGE profiles of the amplified region of bacterial DNA coding for 16S rRNA using primers F3 and Rev 2. Positive controls: Lane 3. *Staphylococcus aureus*; Lane 4. *Pseudomonas aeruginosa*; Lane 5. *Bacillus cereus*; *Lane* 6. *E coli*; Lanes 1-2 and 7-13: bacterial DNA present in human blood samples.

of characteristic bands indicative of the presence of bacterial DNA (lane marked positive control) can be seen in human blood samples (lanes 1-11). Figure 2 (lanes 1-6) illustrates the profile of *E coli* DNA obtained using two different pairs of primers (Table 1); one pair specific only for *E coli* (lanes 1-3) and another pair for *Bacteroides* spp. (lanes 4-6, negative control). The treatment of *E coli* DNA with *Bacteroides* specific primers resulted in a blank PCR profile (i.e. no bands were observed in lanes 4-6), while the use of *E coli* specific primers resulted in the appearance of characteristic PCR product (lanes 1-3).

Human blood samples treated with *Bacteroides* specific primers did not reveal any bands when subjected to PCR (data not shown).

Subsequent analysis employing DGGE (Figure 3, lanes 1-13) revealed that the blood samples which tested PCR positive for bacterial DNA (lanes 1-2 and 7-13) contained DNA fragments of the identical size as the one characteristic for *E coli* DNA (lane 6). DGGE profiles of DNA from bacterial strains, such as *Staphylococcus aureus* (lane 3), *Pseudomonas aeruginosa* (lane 4) and *Bacillus cereus* (lane 5) served as negative controls.

DISCUSSION

These results from our preliminary investigation reveal that although conventional blood cultures techniques fail to demonstrate bacterial infection, using PCR and DGGE it is possible to detect bacterial DNA in the blood in patients with acute severe pancreatitis and also to identify the species present. The number of patients tested in the study is inadequate to make inferences regarding the connection between the presence of bacteria, systemic inflammatory response syndrome and morbidity.

Based on the obtained results it seems plausible to propose that the bacteria detected on d 1 and 3 in patient no. 5 were related to the infectious complications and sepsis. It is unlikely that the pneumonia was caused by *E coli* (sputum cultures were negative). The detection of bacterial DNA was probably indicative of a higher degree

of bacterial translocation, which led to other infections as well as the possible *E coli* sepsis. The positive PCR profile of blood samples taken on admission from patient no. 4 is also not surprising. This patient represented a case of relatively severe disease with a high CRP and probably also had bacterial translocation.

The DGGE profile of the samples from all the patients was exactly the same, i.e. positive exclusively for *E coli*. Interpretation of these results in view of the low numbers of subjects has to be treated with great caution, and it is not until more samples are taken from a larger cohort of patients that statistically valid interpretations can be offered.

To the best of our knowledge, prior to our study, reports on PCR detection of bacterial DNA in patients with acute pancreatitis are limited to two publications[11,12]; neither of these investigations used DGGE as a method of identifying bacteria.

Zhang *et al*[12] performed a PCR on blood specimens on patients only with acute necrotizing pancreatitis. They reported a PCR detection of bacterial DNA in 8 out of 22 tested samples (33.35%), but the samples were taken exclusively during periods of likely sepsis. The lower PCR positive rate of 23.6% in our study probably reflects the fact that blood specimens from patients were collected in a sequential fashion i.e. from the time of admission onwards, and from patients with predicted severe pancreatitis, rather than diagnosed necrotizing disease. Similarly to our study all of the positive blood samples tested were found to contain *E coli*.

Ammori *et al*[11] failed to find any bacterial DNA by performing PCR on blood samples from 26 patients with acute pancreatitis. Blood cultures that tested positive for bacterial infection revealed the presence of *E coli* and *Enterococcus* in blood of one patient, and coagulase negative *Staphylococcus* in the blood of another. The reasons for the negative PCR results reported by Ammori *et al*. are not clear, but may include contamination by substances which inhibit the polymerase reaction.

In acute pancreatitis it is perhaps what separates necrotizing from non-necrotizing disease and what differentiates infected necrosis from sterile necrosis which is of most interest. The controversy surrounding when to operate on necrotizing pancreatitis illustrates this[32-34]; a debate which centers on whether it is necessary to prove infection before operative therapy. The diagnosis of infection is not straightforward, and the currently recommended method of diagnosis, i.e. needle aspiration[34], carries its own risk due to the inherent interventional nature of the procedure. It is possible that more sensitive non-invasive methods of detecting infection such as PCR could improve diagnostic accuracy.

The presence of *E coli* DNA in blood specimens does not necessarily mean that the intestine is the source of infection. It is conceivable that these organisms arose from, for example, the biliary tract due to cholangitis. Moreover, the PCR detection method simply demonstrates the presence of bacterial DNA, and does not specify genera and species. DNA extraction methods provide total DNA that could originate from dead or living microorganisms in the blood or microbes that have been engulfed, or subsequently released by the phagocytes. This approach cannot differentiate between controlled and invasive infections.

The importance of PCR techniques with respect to clinical application will depend on establishing a relationship between the presence or absence of clinical infection and the presence of bacterial DNA in the blood. The PCR detection of bacterial DNA may provide information about the nature of the inflammatory response in acute pancreatitis when traditional methods fail to detect bacteria, even in the absence of culture-positive complications. This type of research may also reveal more about the nature of susceptibility towards infective complications in pancreatitis. In addition, the sensitivity and accuracy of PCR could help target antibiotic therapy in the future.

It is anticipated that in a cohort study including patients with sepsis or septic necrosis, and with the development of more sophisticated quantitative PCR techniques, the proposed approach could offer considerable diagnostic potential.

REFERENCES

1 **Howard TJ**, Wiebke EA, Mogavero G, Kopecky K, Baer JC, Sherman S, Hawes RH, Lehman GA, Goulet RJ, Madura JA. Classification and treatment of local septic complications in acute pancreatitis. *Am J Surg* 1995; **170**: 44-50

2 **Runkel NS**, Rodriguez LF, Moody FG. Mechanisms of sepsis in acute pancreatitis in opossums. *Am J Surg* 1995; **169**: 227-232

3 **Bassi C,** Larvin M, Villatoro E. Antibiotic therapy for prophylaxis against infection of pancreatic necrosis in acute pancreatitis. *Cochrane Database Syst Rev* 2003; **4**: CD002941

4 **Danner RL**, Elin RJ, Hosseini JM, Wesley RA, Reilly JM, Parillo JE. Endotoxemia in human septic shock. *Chest* 1991; **99**: 169-175

5 **Brisson-Noël A**, Gicquel B, Lecossier D, Lévy-Frébault V, Nassif X, Hance AJ. Rapid diagnosis of tuberculosis by amplification of mycobacterial DNA in clinical samples. *Lancet* 1989; **2**: 1069-1071

6 **Rush BF,** Sori AJ, Murphy TF, Smith S, Flanagan JJ, Machiedo GW. Endotoxemia and bacteremia during hemorrhagic shock. The link between trauma and sepsis? *Ann Surg* 1988; **207**: 549-54

7 **Sibbald WJ**, Vincent JL. Round table conference on clinical trials for the treatment of sepsis. *Crit Care Med* 1995; **23**: 394-399

8 **Cicalese L**, Sahai A, Sileri P, Rastellini C, Subbotin V, Ford H, Lee K. Acute pancreatitis and bacterial translocation. *Dig Dis Sci* 2001; **46**: 1127-1132

9 **Gianotti L**, Munda R, Alexander JW, Tchervenkov JI, Babcock GF. Bacterial translocation: a potential source for infection in acute pancreatitis. *Pancreas* 1993; **8**: 551-558

10 **Tarpila E**, Nyström PO, Franzén L, Ihse I. Bacterial translocation during acute pancreatitis in rats. *Eur J Surg* 1993; **159**: 109-113

11 **Ammori BJ**, Fitzgerald P, Hawkey P, McMahon MJ. The early increase in intestinal permeability and systemic endotoxin exposure in patients with severe acute pancreatitis is not associated with systemic bacterial translocation: molecular investigation of microbial DNA in the blood. *Pancreas* 2003; **26**: 18-22

12 **Zhang WZ**, Han TQ, Tang YQ, Zhang SD. Rapid detection

of sepsis complicating acute necrotizing pancreatitis using polymerase chain reaction. *World J Gastroenterol* 2001; **7**: 289-292

13 **Schwabe LD**, Thomson RB, Flint KK, Koontz FP. Evaluation of BACTEC 9240 blood culture system by using high-volume aerobic resin media. *J Clin Microbiol* 1995; **33**: 2451-2453

14 **Alfa MJ**, Degagne P, Olson N, Harding GK. Improved detection of bacterial growth in continuous ambulatory peritoneal dialysis effluent by use of BacT/Alert FAN bottles. *J Clin Microbiol* 1997; **35**: 862-866

15 **Viganò EF**, Vasconi E, Agrappi C, Clerici P. Use of simulated blood cultures for time to detection comparison between BacT/ALERT and BACTEC 9240 blood culture systems. *Diagn Microbiol Infect Dis* 2002; **44**: 235-240

16 **Badillo AT**, Sarani B, Evans SR. Optimizing the use of blood cultures in the febrile postoperative patient. *J Am Coll Surg* 2002; **194**: 477-487; quiz 554-546

17 **Mylotte JM**, Tayara A. Blood cultures: clinical aspects and controversies. *Eur J Clin Microbiol Infect Dis* 2000; **19**: 157-163

18 **Murray PR**, Traynor P, Hopson D. Critical assessment of blood culture techniques: analysis of recovery of obligate and facultative anaerobes, strict aerobic bacteria, and fungi in aerobic and anaerobic blood culture bottles. *J Clin Microbiol* 1992; **30**: 1462-1468

19 **Weinstein MP**, Mirrett S, Wilson ML, Reimer LG, Reller LB. Controlled evaluation of 5 versus 10 milliliters of blood cultured in aerobic BacT/Alert blood culture bottles. *J Clin Microbiol* 1994; **32**: 2103-2106

20 **Wilson ML**, Weinstein MP, Mirrett S, Reimer LG, Feldman RJ, Chuard CR, Reller LB. Controlled evaluation of BacT/alert standard anaerobic and FAN anaerobic blood culture bottles for the detection of bacteremia and fungemia. *J Clin Microbiol* 1995; **33**: 2265-2270

21 **McDonald LC**, Fune J, Gaido LB, Weinstein MP, Reimer LG, Flynn TM, Wilson ML, Mirrett S, Reller LB. Clinical importance of increased sensitivity of BacT/Alert FAN aerobic and anaerobic blood culture bottles. *J Clin Microbiol* 1996; **34**: 2180-2184

22 **Bernet C**, Garret M, de Barbeyrac B, Bebear C, Bonnet J. Detection of Mycoplasma pneumoniae by using the polymerase chain reaction. *J Clin Microbiol* 1989; **27**: 2492-2496

23 **Relman DA**, Schmidt TM, MacDermott RP, Falkow S. Identification of the uncultured bacillus of Whipple's disease. *N Engl J Med* 1992; **327**: 293-301

24 **Kane TD**, Johnson SR, Alexander JW, Babcock GF, Ogle CK. Detection of intestinal bacterial translocation using PCR. *J Surg Res* 1996; **63**: 59-63

25 **Yamashita Y**, Kohno S, Koga H, Tomono K, Kaku M. Detection of Bacteroides fragilis in clinical specimens by PCR. *J Clin Microbiol* 1994; **32**: 679-683

26 **Kane TD**, Alexander JW, Johannigman JA. The detection of microbial DNA in the blood: a sensitive method for diagnosing bacteremia and/or bacterial translocation in surgical patients. *Ann Surg* 1998; **227**: 1-9

27 **Mai V**, Morris JG. Colonic bacterial flora: changing understandings in the molecular age. *J Nutr* 2004; **134**: 459-464

28 **Rantakokko-Jalava K**, Nikkari S, Jalava J, Eerola E, Skurnik M, Meurman O, Ruuskanen O, Alanen A, Kotilainen E, Toivanen P, Kotilainen P. Direct amplification of rRNA genes in diagnosis of bacterial infections. *J Clin Microbiol* 2000; **38:** 32-39

29 **Muyzer G**, de Waal EC, Uitterlinden AG. Profiling of complex microbial populations by denaturing gradient gel electrophoresis analysis of polymerase chain reaction-amplified genes coding for 16S rRNA. *Appl Environ Microbiol* 1993; **59**: 695-700

30 **Larvin M,** McMahon MJ. APACHE-II score for assessment and monitoring of acute pancreatitis. *Lancet* 1989; **2**: 201-205

31 **Dervenis C**, Johnson CD, Bassi C, Bradley E, Imrie CW, McMahon MJ, Modlin I. Diagnosis, objective assessment of severity, and management of acute pancreatitis. Santorini consensus conference. *Int J Pancreatol* 1999; **25**: 195-210

32 **Ramesh H**, Prakash K, Lekha V, Jacob G, Venugopal A. Are some cases of infected pancreatic necrosis treatable without intervention? *Dig Surg* 2003; **20**: 296-299; discussion 300

33 **Bradley EL**. Necrotizing pancreatitis. *Br J Surg* 1999; **86**: 147-148

34 **Uhl W**, Warshaw A, Imrie C, Bassi C, McKay CJ, Lankisch PG, Carter R, Di Magno E, Banks PA, Whitcomb DC, Dervenis C, Ulrich CD, Satake K, Ghaneh P, Hartwig W, Werner J, McEntee G, Neoptolemos JP, Büchler MW. IAP Guidelines for the Surgical Management of Acute Pancreatitis. *Pancreatology* 2002; **2**: 565-573

Science Editor Li WZ **Language Editor** Elsevier HK

PO Box 2345, Beijing 100023, China
www.wjgnet.com
wjg@wjgnet.com

ELSEVIER

World J Gastroenterol 2005;11(45):7148-7151
World Journal of Gastroenterology ISSN 1007-9327

• *RAPID COMMUNICATION* •

Gastro esophageal reflux disease is associated with absence from work: Results from a prospective cohort study

Andreas Leodolter, Marc Nocon, Michael Kulig, Stefan N Willich, Peter Malfertheiner, Joachim Labenz

Andreas Leodolter, Peter Malfertheiner, Department of Gastroenterology, Hepatology and Infectious Diseases, Otto-von-Guericke University, Magdeburg, Germany
Marc Nocon, Michael Kulig, Stefan N Willich, Institute of Social Medicine, Epidemiology and Health Economics, Charité Hospital, Humboldt University, Berlin, Germany
Joachim Labenz, Ev. Jung-Stilling-Krankenhaus, Siegen, Germany
Supported by a grant from AstraZeneca, Germany
Correspondence to: Professor Andreas Leodolter, Klinik für Gastroenterologie und Hepatologie, Otto-von-Guericke Universität, Leipziger Str. 44, D-39120 Magdeburg, Germany. andreas@leodolter.de
Telephone: +49-391-6713100 Fax: +49-391-6713105
Received: 2005-04-20 Accepted: 2005-06-18

Abstract

AIM: To study the association of gastro-esophageal reflux disease (GERD) with the absence from work and to estimate the extent of loss in gross domestic product due to inability to work.

METHODS: Analysis was based on the prospectively gathered data of a large European cohort study involving 6 215 symptomatic GERD patients (ProGERD). Among these patients, 2 871 were initially employed. The calculation of the loss of gross domestic product was based on the assumption that the prevalence of GERD was about 15% in Germany. According to the German Federal Statistical Office, the mean gross wage of employees was 150 €/d in 2002.

RESULTS: The data of 2 078 employed patients who were prospectively followed up for over 2 years were analyzed. At study entry, the patients reported a mean of 1.8 d per year of inability to work. During the prospective follow-up under routine clinical care, the proportion of patients reporting days with inability to work decreased from 14% to 6% and the mean number of days per year with inability to work decreased to 0.9 d. Assuming a prevalence of troublesome GERD of 15% in the employed German population, the loss of gross domestic product amounted to 668 million €/year in Germany.

CONCLUSION: GERD causes a relevant impairment on the national economics by absence from work. The presented data demonstrate the importance of GERD, not only for patients and health insurance companies, but also for the community at large.

Key words: Gastro-esophageal reflux; Sick leave; Medical economics

Leodolter A, Nocon M, Kulig M, Willich SN, Malfertheiner P, Labenz J. Gastro esophageal reflux disease is associated with absence from work: Results from a prospective cohort study. *World J Gastroenterol* 2005; 11(45): 7148-7151
http://www.wjgnet.com/1007-9327/11/7148.asp

INTRODUCTION

With a prevalence of 15-40%, gastro-esophageal reflux disease (GERD) is a common adult condition in Western countries[1-3]. GERD may be associated with a marked decrease in quality of life, a loss of productivity and impairment of daily activities[4]. In some patients symptoms may be severe enough to prevent the patient from going to work. The resulting decrease in working time is associated with a significant loss in productivity. In North America, up to 10% of GERD patients have to be absent from work[5,6] and the indirect costs in the USA caused only by time away from paid labor resulting from consumption of health care were 470 million US$ in 1998[7]. The complete costs of labor lost have to be borne by employers and/or health insurance companies, and there is an accompanying decrease in the gross domestic product. The aim of the present investigation was to estimate the extent of such losses on the basis of the data of a large prospective European trial in patients with symptomatic GERD.

MATERIALS AND METHODS

The ProGERD study is an ongoing prospective, multicenter cohort study comprising an initial treatment phase and a 5-year follow-up phase. Patients (n = 6 215) were recruited from centers (n = 1 253) in Germany (more than 90%), Austria and Switzerland. The majority of these patients were recruited by gastrointestinal specialists in private practice. The protocol of the study was designed to include half of the patients with erosive reflux disease (ERD) and half with non-erosive reflux disease (NERD). Barrett's esophagus was not an exclusion criterion and in 702 patients this condition was diagnosed. The patients were treated with esomeprazole for up to 8 wk, and in

the follow-up period at the discretion of their physicians. After 2 years of follow-up, 64% of the patients were still on proton pump inhibitor (PPI) medication (continuous PPI or on demand treatment).

At study entry and every year, the patients completed a standardized questionnaire that assessed demographic, medical, and social characteristics and quality of life. One section of the questionnaires dealt with the patient' s inability to work (IW) caused by reflux symptoms in the year prior to inclusion in the study and to the last year before the study visit. The patients were carefully instructed about the aims and the methods of the study, including repetition of the initial questionnaire. Further details of the ProGERD trial have been published elsewhere[8].

The most reliable assumption of the frequency of GERD in Europe was available from a large population-based telephone survey performed in 5 046 randomly chosen persons[1]. More than 1 000 persons per country (Germany, France, Italy, Sweden, and UK) were interviewed. Reflux symptoms occurred in 28% of German adults with about 58% of them claiming impaired quality of life. This means that the overall frequency of GERD is 16% in the entire adult population of Germany[9].

The number of overall IW days reported in the ProGERD trial was projected on the overall German employed population, based on the data from the German Federal Statistical Office. Germany has 82.5 million inhabitants and the labor force is composed of 36.5 millions, of whom some 33 millions are compulsorily insured. The mean gross wage of employees was 150 €/d in 2002.

In this study, the human capital method was used to calculate the indirect costs of GERD, a method that uses the full replacement costs independent of whether the worker is replaced or not[10]. We assumed a loss of the gross domestic product in the same amount of the whole mean gross wage of employees. The basis for the calculation of the decrease of gross domestic product was the number of IW days caused by GERD symptoms reported in the ProGERD trial.

We conducted an explorative analysis of potential patient-associated predictors (gender, age, BMI, consumption of alcohol, smoking, and severity of the GERD disease) of IW days using univariate statistics as appropriate. The level of significance was 5%.

RESULTS

Data about employment were available from 5 965 out of 6 215 patients (96.0%). At the beginning of the trial, 2 871 out of 5 965 (48.1%) patients were gainfully employed, 2 103 retired (35.3%), and 991 without employment (16.6%). After a 2-year follow-up period, the data about employment of 5 286 patients were available (2 312 employed, 2 097 retired, 877 without employment). We included the data of 2 078 patients who were gainfully employed and answered the respective questions about inability to work due to GERD at the initial visit and during the 2-year follow-up period. This excluded the data of those who lost their work or retired in the follow-up period or did not answer the questions at both time points of investigation.

Initially 14% of the employed patients were admitted retrospectively to IW due to reflux symptoms during the past year. During the 2-year follow-up period, the percentage decreased to 6% under routine clinical care. The mean number of IW days was 2.5/yr prior to inclusion in the study (mean value 2.5 d in 12 mo and adjusted with the exclusion of the weekend period: 1.8 d), and decreased to 1.2/yr during the prospective follow-up period (mean value 1.2 d in 12 mo and adjusted with the exclusion of the weekend period: 0.9 d). There was no significant relationship between IW and gender, age, BMI, consumption of alcohol, smoking, and severity of GERD. In Germany, the labor force is composed of 36.5 millions, of whom some 33 millions are compulsorily insured. The mean gross wage of employees is 150 €/d (source: German Federal Statistical Office 2002). Based on the human capital method for calculating costs of illness, the total loss of gross domestic product is shown in Tables 1 and 2 assuming different frequencies of GERD in the labor force. Table 1 shows the retrospective data before entering into the follow-up period, and Table 2 lists the prospective data after the 2-year follow-up period.

Table 1 Loss of gross domestic product due to inability to work (IW) in patients with untreated GERD in Germany on the basis of three different frequency assumptions

Prevalence of GERD in the adult population	10%	15%	20 %
Total days of inability to work	5.9 million	8.9 million	11.9 million
Loss of gross domestic product	891 million €	1.34 billion €	1.78 billion €

Table 2 Loss of gross domestic product due to inability to work (IW) in patients with GERD under routine clinical care in Germany on the basis of three different frequency assumptions

Prevalence of GERD in the adult population	10%	15%	20 %
Total days of inability to work	2.97 million	4.46 million	5.94 million
Loss of gross domestic product	446 million €	668 million €	891 million €

DISCUSSION

ProGERD is a large prospective cohort study designed to examine the endoscopic and symptomatic progression of GERD in routine care as well as the economic burden of the disease. With more than 6 000 included patients, the study is the largest prospective clinical trial in this field and could answer several questions on a high level of confidence. The influence of GERD on the gross

domestic product, being part of the indirect costs of the disease, was estimated in this analysis. On the basis of these data, the total costs of the economy of GERD, due to loss of gross domestic product were reliably assessable. Assuming a prevalence of 15% of the disease in the employed German population, costs amounted to 668 million €/yr under routine clinical care. The costs in the same population were twice as high in the year before entering the trial. These calculations highlight the great economic importance of GERD, which is not only a problem for patients and health insurance companies, but also has a major impact on the community at large. The total loss of gross domestic product estimated by our analysis was, for example, close to the total yearly PPI sales of 842 million € in Germany in 2003[11].

Our calculation was based on the human capital method for calculating the costs of illness. Another approach to calculating indirect costs is the friction cost method, which measures the amount of production lost due to the disease based on the time span organizations needed to restore the initial production, so that production losses are assumed to be confined to the period needed to replace a sick worker[10]. A stated advantage of the friction cost method is that, unlike the human capital method, it takes into account the fact that employees with long-term illness or disabilities can be replaced in markets with less than full employment. There is no general agreement on whether the human capital or friction cost method is more valid for measuring the productivity costs of illness. Long-term sick leave due to GERD symptoms is probably rare-none of the patients included in the ProGERD study reported long-term sick leave because of GERD symptoms during the prospective follow-up period-and replacement of the worker is an exceptional event. Therefore, the human capital method might be the more reliable approach. Even assuming more conservative estimates of indirect costs based on the friction cost method, GERD is certainly still associated with a considerable social and economic burden.

As expected, only a limited portion of about 14% of the GERD patients even got admitted to IW caused by reflux symptoms. The symptoms are mostly mild to moderate, though the quality of life in patients with GERD is markedly decreased[12], the level is comparable to other chronic or even life-threatening diseases[13]. In the follow-up period, the portion of patients with IW declined to 6%. Other trials from the USA have reported partially a lower portion of 2-10%[5,6], suggesting that socioethical factors might influence the willingness to be absent from work.

The follow-up data indicated the effectiveness of the treatment of GERD in reducing the IW days. The mean number of IW days decreased from 2.5 to 1.2 in the 2-year observation period. The patients were treated in the follow-up period at the discretion of their physicians, and around two out of the three patients were still on PPI treatment after the 2-year follow-up period.

GERD is nowadays the disease with the highest direct costs in the USA (9.3 billion US$)[7]. European data are available from Sweden that includes the costs for dyspepsia and peptic ulcer disease. Therefore, it is difficult to compare them with our findings[14].

Our calculation of the loss of gross domestic product was based on the statement of the patients using a long recall period of one year, and it might result in an underestimation of disease-related absence from work. A recall bias on self-reported work productivity occurs more often already after a 4-wk recall period compared with a 2- or 1-wk recall period[15]. Therefore, our calculation can be considered as conservative, and the loss might be significantly higher. A recent study showed that the impact of GERD on the costs of reduced productivity is even higher compared to that on the costs of absence from work[16]. Therefore, it is highly possible that our calculation might further underestimate the overall loss of gross domestic product due to GERD, because we only referred to the IW days instead of estimating the reduced productivity.

The exact calculation of the indirect costs is somehow difficult. Typically indirect costs include costs associated with the lost or impaired ability to work or to enjoy leisure activities because of morbidity, the time required by the patient's family to receive medical care, and loss of future earning potential owing to premature death. Data about impaired ability to work due to GERD are insufficient. In a small cross-sectional study from the USA, about 41% of GERD patients reported that they have lost some work productivity[6]. The authors have reported here in addition that the time off for physician visits and reduced productivity are the most costly losses from GERD. Our main focus was on the additional part of costs due to absence from work.

The impact of GERD on the economy differs widely between different countries depending on several factors (like cultural, socioeconomic, and economical status). Nevertheless, our data clearly suggest that the loss of gross domestic product due to GERD-related IW days might be higher compared to the total sale volume of PPI in Western countries in general. Definite data on this topic are lacking. It would, therefore, be interesting to study the impact of effective pharmacotherapy not only on clinical symptoms and healing of lesions but also on the loss of productivity.

REFERENCES

1 **Armstrong,** D and Jones, R. Gastroesophageal reflux disease (GERD) symptoms (GS) in 5 European countries: a common and poorly understood condition. *Gastroenterology* 2001; **120:** 2180 [A]

2 **Locke GR,** Talley NJ, Fett SL, Zinsmeister AR, Melton LJ. Prevalence and clinical spectrum of gastroesophageal reflux: a population-based study in Olmsted County, Minnesota. *Gastroenterology* 1997; **112:** 1448-1456

3 **Valle C,** Broglia F, Pistorio A, Tinelli C, Perego M. Prevalence and impact of symptoms suggestive of gastroesophageal reflux disease. *Dig Dis Sci* 1999; **44:** 1848-1852

4 **Wahlqvist P.** Symptoms of gastroesophageal reflux disease, perceived productivity, and health-related quality of life. *Am J Gastroenterol* 2001; **96:** S57-S61

5 **Frank L,** Kleinman L, Ganoczy D, McQuaid K, Sloan S, Eggleston A, Tougas G, Farup C. Upper gastrointestinal symptoms in North America: prevalence and relationship to healthcare utilization and quality of life. *Dig Dis Sci* 2000; **45:** 809-818
6 **Henke CJ,** Levin TR, Henning JM, Potter LP. Work loss costs due to peptic ulcer disease and gastroesophageal reflux disease in a health maintenance organization. *Am J Gastroenterol* 2000; **95:** 788-792
7 **Sandler RS,** Everhart JE, Donowitz M, Adams E, Cronin K, Goodman C, Gemmen E, Shah S, Avdic A, Rubin R. The burden of selected digestive diseases in the United States. *Gastroenterology* 2002; **122:** 1500-1511
8 **Kulig M,** Nocon M, Vieth M, Leodolter A, Jaspersen D, Labenz J, Meyer-Sabellek W, Stolte M, Lind T, Malfertheiner P, Willich SN. Risk factors of gastroesophageal reflux disease: methodology and first epidemiological results of the ProGERD study. *J Clin Epidemiol* 2004; **57:** 580-589
9 An evidence-based appraisal of reflux disease management-the Genval Workshop Report. *Gut* 1999; 44 Suppl **2:** S1-16
10 **Koopmanschap MA,** Rutten FF. A practical guide for calculating indirect costs of disease. *Pharmacoeconomics* 1996; **10:** 460-466
11 **Schwabe U,** Paffrath D. *Arzneiverordnungs-Report* 2003. Springer: Berlin, 2004
12 **Kulig M,** Leodolter A, Vieth M, Schulte E, Jaspersen D, Labenz J, Lind T, Meyer-Sabellek W, Malfertheiner P, Stolte M, Willich SN. Quality of life in relation to symptoms in patients with gastro-oesophageal reflux disease-- an analysis based on the ProGERD initiative. *Aliment Pharmacol Ther* 2003; **18:** 767-776
13 **Farup C,** Kleinman L, Sloan S, Ganoczy D, Chee E, Lee C, Revicki D. The impact of nocturnal symptoms associated with gastroesophageal reflux disease on health-related quality of life. *Arch Intern Med 2001*; **161:** 45-52
14 **Agréus L,** Borgquist L. The cost of gastro-oesophageal reflux disease, dyspepsia and peptic ulcer disease in Sweden. *Pharmacoeconomics* 2002; **20:** 347-355
15 **Stewart WF,** Ricci JA, Leotta C. Health-related lost productive time (LPT): recall interval and bias in LPT estimates. J Occup Environ *Med* 2004; **46:** S12-S22
16 **Dean BB,** Crawley JA, Reeves JD, Aguilar D, Sullivan S, Berglund R, Dubois R. The costs of gastroesophageal reflux disease: It's what you don't see that counts. *J Managed Care Medicine* 2003; **7:** 6-13

Science Editor Wang XL and Guo SY **Language Editor** Elsevier HK

PO Box 2345, Beijing 100023, China
www.wjgnet.com
wjg@wjgnet.com

ELSEVIER

World J Gastroenterol 2005;11(45):7152-7158
World Journal of Gastroenterology ISSN 1007-9327

• *RAPID COMMUNICATION* •

Internet-based data inclusion in a population-based European collaborative follow-up study of inflammatory bowel disease patients: Description of methods used and analysis of factors influencing response rates

Frank L Wolters, Gilbert van Zeijl, Jildou Sijbrandij, Frederik Wessels, Colm O'Morain, Charles Limonard, Maurice G Russel, Reinhold W Stockbrügger

Frank L Wolters, Reinhold W Stockbrügger, Department of Gastroenterology and Hepatology, University Hospital Maastricht, P. Debyeplein 25, 6202 AZ Maastricht, The Netherlands
Gilbert van Zeijl, Jildou Sijbrandij, Charles Limonard, MEMIC, Centre for Data and Information Management, P. Debyeplein 1, 6229 HA Maastricht, The Netherlands
Frederik Wessels, Global Vitis, Wattstraat 52, 2171 TR Sassenheim, The Netherlands
Colm O'Morain, Adelaide and Meath Hospital, Department of Gastroenterology, Trinity College, Tallaght, SE-41345 Dublin 24, Ireland
Maurice G Russel, Department of Gastroenterology and Hepatology, Medisch Spectrum Twente, Haaksbergerstraat 55, 7513 ER Enschede, The Netherlands
Supported by the European Commission as a fifth framework shared cost action (QLG4-CT-2000-01414)
Correspondence to: Dr FL Wolters, Department of Gastroenterology and Hepatology, PO box 5800, 6202 AZ Maastricht, The Netherlands. frankwolters@ace-on-air.nl
Telephone: +31-43-3875021
Received: 2005-01-13 Accepted: 2005-02-18

Abstract

AIM: To describe an Internet-based data acquisition facility for a European 10-year clinical follow-up study project of a population-based cohort of inflammatory bowel disease (IBD) patients and to investigate the influence of demographic and disease related patient characteristics on response rates.

METHODS: Thirteen years ago, the European Collaborative study group of IBD (EC-IBD) initiated a population-based prospective inception cohort of 2 201 uniformly diagnosed IBD patients within 20 well-described geographical areas in 11 European countries and Israel. For the 10-year follow-up of this cohort, an electronic patient questionnaire (ePQ) and electronic physician per patient follow-up form (ePpPFU) were designed as two separate data collecting instruments and made available through an Internet-based website. Independent demographic and clinical determinants of ePQ participation were analyzed using multivariate logistic regression.

RESULTS: In 958 (316 CD and 642 UC) out of a total number of 1 505 (64%) available IBD patients, originating from 13 participating centers from nine different countries, both ePQ and ePpPFU were completed. Patients older than 40 years at ePQ completion (OR: 1.53 (95%CI: 1.14-2.05)) and those with active disease during the 3 mo previous to ePQ completion (OR: 3.32 (95%CI: 1.57-7.03)) were significantly more likely to respond.

CONCLUSION: An Internet-based data acquisition tool appeared successful in sustaining a unique Western-European and Israelian multi-center 10-year clinical follow-up study project in patients afflicted with IBD.

Key words: Internet; Questionnaire; IBD; Cohort study; Population-based

Wolters FL, van Zeijl G, Sijbrandij J, Wessels F, O'Morain C, Limonard C, Russel MG, Stockbrügger RW. Internet-based data inclusion in a population-based European collaborative follow-up study of inflammatory bowel disease patients: Description of methods used and analysis of factors influencing response rates. *World J Gastroenterol* 2005; 11(45): 7152-7158
http://www.wjgnet.com/1007-9327/11/7152.asp

INTRODUCTION

Data acquisition in multi-center epidemiological follow-up studies traditionally has been dependent on postal paper form questionnaires filled out by study subjects and on paper form extraction files for relevant medical information completed by physicians and/or research assistants. Great advantages of the use of the Internet as a platform for health status measurements have been reported since the mid-1990s[1]. Internet-based facilities supporting data acquisition in studies concerning patients with inflammatory bowel disease (IBD) have been performed from then onwards[2-4]. Traditionally, in multi-center studies, questionnaires in paper format are forwarded from patients and centers to central database-hosting facilities, where data are manually transformed

into electronic databases. This multi-step process is time- and labor-consuming and prone to errors. Paper form data acquisition utilities normally contain question flow instructions for study subjects and for physicians that can easily be misinterpreted resulting in missing or wrong answers. Furthermore, the physical transformation of large numbers of paper format data into an electronic database adds to the risk of human errors.

For the purpose of a large multi-center follow-up study of a European population-based cohort of patients with IBD[5], we created an Internet-based data acquisition facility, in order to avoid the above-mentioned methodological imperfections and to assure data quality. The design of the mentioned study as well as practical and technical details and implications of the new electronic instrument are described and discussed. The influence of demographic and disease-related patient characteristics on the patient questionnaire response rates is also analyzed.

History of the cohort

After 3 years of preparation, between October 1991 and September 1993, the European Collaborative study group of IBD (EC-IBD) gathered a population-based prospective inception cohort of 2 201 uniformly diagnosed IBD patients within 20 well-described geographical areas in 12 European countries[6]. Initially it was hypothesized that a North-South incidence gradient in IBD existed, which could be proved[5]. Later, in the context of this registry, a 1- and 4-year clinical follow-up[7,8] were studied, as well as the occurrence of rheumatologic manifestations[9] and the relationship between quality of care and quality of life[10].

The currently executed 10-year clinical follow-up study project was planned since 1998, granted by the European Commission, and was started in 2001.

MATERIALS AND METHODS

Materials

In order to optimize data acquisition in this European multi-center study project, electronic data acquisition tools were designed for Internet-based access. The development of the tools and the subsequent data management leading to an analyzable dataset involved a five-step process; (1) a "patient questionnaire" (PQ) and "physician per patient follow-up form" (PpPFU) were prepared as two separate data collecting instruments and originally constructed for the purpose of this study. The information obtained by the PQ was derived from direct questioning of the patients, whereas physicians and research assistants extracted data from patient files into the PpPFU. PQ items were demographics, life style factors, disease activity and use of medication, family history, data on pregnancy and fertility, health care consumption, disability, and quality of life (SF-36 was used). PpPFU items, as observed during the 10-year follow-up period, were vital status, cause of death, disease activity (change of immunosuppressive medication and surgical events were used as indicators due to the retrospective nature of data acquisition), disease location and behavior, use of medication, surgery, health care consumption, colorectal cancer, and dysplasia. Members of the original study group and additional investigators formed "working groups" to deal with various research topics of the follow-up, including genotype-phenotype, course of disease, pregnancy and fertility, cancer, health care consumption and costs, and dissemination of messages to the medical and lay public. A central body of senior representatives from the EC-IBD group constructed final comprehensive versions of both instruments based on the input of all the members of the working groups. The electronic patient questionnaire (ePQ) questions were translated into the nine languages of the participating countries by a professional translation agency and subsequently checked for correctness by a representative from every participating country from within the EC-IBD study group. For the PpPFU, the language used was English; (2) a tailor-made innovative high performance data entry application was designed, assuring maximum flexibility for programmers and users. The ePQ was designed by the construction of a questionnaire design module, where questions and answers could be directly introduced in different languages with needed routings. The final ePQ contained 747 questions and could be used in nine different languages including Hebrew. The electronic physician per patient follow-up form (ePpPFU) was designed to receive an unlimited number of entries on multiple topics on a 10-year time scale. Graphic design using simple colors in order to visually discriminate users' choices improved user friendliness; (3) the PQ questions and the PpPFU items, originally constructed on paper, were introduced into the electronic facilities. A pre-designed compulsive question flow was implemented in the ePQ. This implicated that patients filling in the ePQ were automatically guided towards a subsequent question, based on a given previous answer thus skipping irrelevant questions. Electronic guidance facilities concerning mandatory and optional fields were embedded in the ePpPFU. In this way, physicians and/or research assistants completing the ePpPFU of a particular patient were not allowed to close and finalize the document concerning an individual patient before having collected all the minimally required information; (4) the electronic data acquisition facilities were made available to all data collecting centers through a username-password secured and firewall protected Internet-based website. Links to ePQ statistics and ePpPFU statistic pages displayed real time counts of both instruments for all centers together showing instantaneous, comparative and cumulative progress of data inclusion, accessible to every member involved in the data inclusion of this project; (5) after completion of the data acquisition phase, export files from the Internet questionnaire program were imported into the database environment. The database was situated in Maastricht. Database validation took place at this center before the distribution of the final database to all working groups. The validation was done by logical comparison of the crude database with existing databases of previous EC-

Table 1 Cumulative number of IBD (CD+UC) patients per center followed-up or lost to follow-up for ePQ and ePpPFU. Centers indicated in gray had not reached the 60% response rate threshold

Center	Total number of CD+ CU patients	EPQ response (%)	EPQ response without deaths and No IBD %	Reason for non response EPQ					PpPFU response (%)	PpPFU response without No IBD %	Reason for non response PpPFU				EPQ ànd PpPFU (%)
				Not willing	Untrace-able	No IBD	Death	Not started			Not willing	Untrace-able	No IBD	Not started	
Beer Sheeva	60	41 (68)	76	5	8	3	3	0	46 (77)	77	3	11	0	0	42 (70)
Copenhagen	147	103 (70)	84	12	7	0	25	0	132 (90)	90	6	9	0	0	120 (82)
Cremona	51	35 (68)	76	4	7	0	5	0	43 (84)	84	1	7	0	0	40 (78)
Heraklion	62	38 (61)	68	2	13	0	5	4	49 (79)	79	3	17	0	0	40 (65)
Ioannina	43	36 (84)	88	2	3	0	2	0	39 (91)	91	0	4	0	0	38 (88)
Oslo	378	226 (60)	69	65	34	6	45	2	332 (88)	89	21	25	1	0	271 (72)
Reggio Emilia	84	61 (73)	79	4	12	0	7	0	69 (82)	82	5	11	0	0	68 (81)
S-Limburg	216	156 (72)	76	28	20	0	11	1	194 (90)	90	0	23	0	0	159 (74)
Vigo	100	73 (73)	77	4	18	0	5	0	81 (81)	81	3	16	0	0	77 (77)
SUBTOTAL	1 141	769 (67)	75	126	122	9	108	7	985 (86)	86	42	123	1	0	855 (75)
Almada	21	11 (52)	58	1	7	0	2	0	12 (57)	57	0	9	0	0	11 (52)
Dublin	186	57 (30)	34	10	58	3	17	41	80 (43)	43	1	26	2	78	56 (30)
Firenze	115	48 (42)	42	0	0	0	0	67	39 (34)	34	0	4	0	72	36 (31)
Milano	42	19 (45)	58	1	6	0	9	7	0 (0)	0	0	0	0	42	0 (0)
SUBTOTAL	364	135 (37)	41	12	71	3	28	115	131 (36)	36	1	39	2	192	103 (28)
Total	1 505	904 (60)	67	138	193	12	136	122	1 116 (74)	74	43	162	3	192	958 (64)

IBD projects in terms of numbers of patients per center with known diagnosis, sex, age, and disease behavioral characteristics. The results of this data validation effort were summarized in a logbook that was distributed to all the project members for possible revisions that subsequently were implemented as changes in the database. Final data sets were available for analysis promptly after closing the data acquisition phase.

Methods

Before the start of the data collection, a minimally required response rate per center was set at 60% identification of the patients to have both ePQ and ePpPFU completed. Centers that did not comply with this minimum response rate were analyzed separately from those that did.

UC patients were grouped for disease location at diagnosis as: (1) rectum only; (2) rectum and sigmoid and/or descending colon; and (3) disease location beyond the splenic flexure. The CD patients were classified for disease location at diagnosis, according to the Vienna classification[11], into: (1) upper gastrointestinal (esophagus and/or stomach and/or duodenum and/or jejunum); (2) (terminal) ileum; (3) ileocolonic; and (4) colon only.

Independently, both demographic and clinical determinants of ePQ participation (diagnosis, gender, center, disease location at diagnosis, age at ePQ completion, and disease activity during 3 mo period previous of ePQ completion) were analyzed using univariate and multivariate logistic regression models. All potential predictors were included in both models. A $P \leqslant 0.05$ was considered to be statistically significant in the multivariate analysis. The statistical package for the social sciences (SPSS 11.5.1 for Windows; SPSS Inc., Chicago, IL, USA) was used for the analysis.

The Ethics Committees of all the participating centers approved the study protocol, and all subjects gave their informed consent before the start of the study.

RESULTS

During the data collection period from August 1st 2002 to January 1st 2004, the electronic data entry facilities appeared to be well-equipped and flexible tools for data entry and storage. However, the data export facility used in order to enable fast provision of stored data into formats prepared for analysis showed some initial deficiencies. Questions, answer categories and formal control rules, used for feedback during insertion, were not always automatically incorporated in the export process. This could, however, be repaired by the information management team.

All centers that originally participated in the EC-IBD cohort had been approached to take part in the follow-up study. Thirteen out of the original twenty centers distributed over nine countries participated. In 958 (316 CD and 642 UC) out of a total number of 1 505 IBD patients eligible for follow-up (64%), both ePQ and ePpPFU were completed (Table 1). When considering the entire cohort of both CD and UC patients, nine centers complied with the minimal 60% response threshold rendering 855 out of 1 141 patients (75%). Table 1 summarizes the details of the total number of IBD (both CD and UC) patients in the cohort. In the CD category, 10 of the participating 13 centers complied with the minimal 60% response threshold leaving 378 patients of whom 288 (76%)had completed both ePQ and ePpPFU (Table 2). In the UC category, nine centers complied leaving 776 patients of whom 575 (74%) had completed both instruments (Table 3).

Table 2 shows two Beer Sheeva patients indicated as "no IBD" in the ePQ, who were not classified as such in the ePpPFU. Review of available clinical data revealed that both patients have CD. An identical discrepancy concerning one Dublin patient in the "no IBD" category could not be clarified. This patient was considered to have CD. In the UC category (Table 3) divergences between ePQ and ePpPFU for patients indicated as "no IBD"

Table 2 Number of CD patients per center followed-up or lost to follow-up for ePQ and ePpPFU. Centers indicated in gray had not reached the 60% response rate threshold

Center	Total number of CD patients	EPQ response (%)	EPQ response without deaths and No IBD %	Reason for non response EPQ					PpPFU response (%)	PpPFU response without No IBD %	Reason for non response PpPFU				EPQ ànd PpPFU (%)
				Not willing	Untrace-able	No IBD	Death	Not started			Not willing	Untrace-able	No IBD	Not started	
Almada	13	8 (62)	67	0	4	0	1	0	8 (62)	62	0	5	0	0	8 (62)
Beer Sheeva	21	13 (62)	72	2	3	2	1	0	15 (71)	71	1	5	0	0	14 (67)
Copenhagen	58	41 (71)	85	5	2	0	10	0	52 (90)	90	6	0	0	0	47 (81)
Cremona	10	7 (70)	78	2	0	0	1	0	9 (90)	90	1	0	0	0	8 (80)
Heraklion	14	7 (50)	70	0	3	0	3	1	11 (79)	79	0	5	0	0	9 (64)
Ioannina	6	4 (67)	80	0	1	0	1	0	5 (83)	83	0	1	0	0	5 (83)
Oslo	110	69 (63)	70	15	13	1	11	1	97 (88)	89	4	8	1	0	79 (73)
Reggio Emilia	34	24 (71)	77	0	7	0	3	0	27 (79)	79	1	6	0	0	27 (79)
S-Limburg	77	60 (78)	82	8	5	0	4	0	69 (90)	90	0	8	0	0	61 (79)
Vigo	35	27 (77)	84	1	4	0	3	0	30 (86)	86	1	4	0	0	30 (86)
SUBTOTAL	378	260 (69)	77	33	42	3	38	2	323 (85)	85	14	42	1	0	288 (76)
Dublin	63	17 (27)	30	2	25	2	5	12	25 (40)	40	0	6	1	31	17 (27)
Firenze	29	13 (45)	45	0	0	0	0	16	13 (45)	45	0	1	0	15	11 (38)
Milano	13	4 (31)	50	0	2	0	5	2	0 (0)	0	0	0	0	13	0 (0)
SUBTOTAL	105	34 (32)	36	2	27	2	10	30	38 (36)	37	0	7	1	59	28 (27)
TOTAL	483	294 (61)	69	35	69	5	48	32	361 (75)	75	14	49	2	59	316 (65)

Table 3 Number of UC patients per center followed-up or lost to follow-up for ePQ and ePpPFU. Centers indicated in gray had not reached the 60% response rate threshold

Center	Total number of CU patients	EPQ Response (%)	EPQ response without deaths and No IBD %	Reason for non response EPQ					PpPFU response (%)	PpPFU response without No IBD %	Reason for non response PpPFU				EPQ ànd PpPFU (%)
				Not willing	Untrace-able	No IBD	Death	Not started			Not willing	Untrace-able	No IBD	Not started	
Beer Sheeva	39	28 (72)	78	3	5	1	2	0	31 (79)	79	2	6	0	0	28 (72)
Copenhagen	89	62 (70)	84	7	5	0	15	0	80 (90)	90	0	9	0	0	73 (82)
Cremona	41	28 (68)	76	2	7	0	4	0	34 (83)	83	0	7	0	0	32 (78)
Heraklion	48	31 (65)	67	2	10	0	2	3	38 (79)	79	3	12	0	0	31 (65)
Ioannina	37	32 (86)	89	2	2	0	1	0	34 (92)	92	0	3	0	0	33 (89)
Oslo	268	157 (59)	69	50	21	5	34	1	235 (88)	88	17	17	0	0	192 (72)
Reggio Emilia	50	37 (74)	80	4	5	0	4	0	42 (84)	84	4	5	0	0	41 (82)
S-Limburg	139	96 (69)	72	20	15	0	7	1	125 (90)	90	0	15	0	0	98 (71)
Vigo	65	46 (70)	73	3	14	0	2	0	51 (78)	78	2	12	0	0	47 (72)
SUBTOTAL	776	517 (67)	74	93	84	6	71	5	670 (86)	86	28	86	0	0	575 (74)
Almada	8	3 (38)	50	1	3	0	1	0	4 (50)	50	0	4	0	0	3 (38)
Dublin	123	40 (33)	36	8	33	1	12	29	55 (45)	45	1	20	1	47	39 (32)
Firenze	86	35 (41)	41	0	0	0	0	51	26 (30)	30	0	3	0	57	25 (29)
Milano	29	15 (51)	60	1	4	0	4	5	0 (0)	0	0	0	0	29	0 (0)
SUBTOTAL	246	93 (38)	41	10	40	1	17	85	85 (35)	35	1	27	1	133	67 (27)
TOTAL	1 022	610 (60)	67	103	124	7	88	90	755 (74)	74	29	113	1	133	642 (63)

regarding one patient from Beer Sheeva and five patients from Oslo could not be clarified. These six patients were considered to have UC. Discrepancies between total numbers of patients for ePQ and ePpPFU also occurred because of Internet disruptions during the insertion process in the CD category regarding two patients from Heraklion (Table 2), and in the UC category regarding five patients from Heraklion, one from Oslo, one from Reggio Emilia, one from South-Limburg and one from Dublin (Table 4). The answers given by these patients were lost and these patients were excluded from the database. Disease location at diagnosis was known for 739 of 766 UC patients and 363 of 378 CD patients.

In the 60% of complying centers, 126 of 1 141 patients [11%] refused to participate without a large difference between the age groups (79/707 [11.2%] in patients older than 40 years at ePQ completion and 47/434 [10.8%] in patients equal to or younger than 40 years at ePQ completion). 10.7% of the patients lost to follow-up for the ePQ were indicated as untraceable. Of patients aged >40 years at ePQ completion, 56/707 [7.9%] could not be traced. In those ⩽40 years at ePQ completion, 66/434 [15.2%] of patients could not be traced.

In the UC patient group, age >40 years and in the combined CD and UC patient groups active disease recorded within 3 mo previous to ePQ completion were significant positive predictors of ePQ response. Gender, center, diagnosis, age at diagnosis and disease location showed no significant differences in ePQ response in centers that had complied with the 60% minimal ePQ

Table 4 Results of univariate and multivariate logistic regression analyses for identification of predictors of ePQ completion in the entire cohort

CD+UC *N* total = 1 141	*n*	Response (%)	Unadjusted Odds Ratio (95%CI)	Adjusted Odds Ratio (95%CI)	*P*
CD/UC	365/776	289 (79)/588 (76)	1.22 (0.90-1.64)	1.24 (0.91-1.70)	0.171
Female/male	552/589	429 (77)/448 (76)	1.10 (0.84-1.44)	1.09 (0.82-1.44)	0.564
Age at ePQ completion >40/≤40 yr	707/434	559 (79)/318 (73)	1.38 (1.04-1.82)	1.53 (1.14-2.05)	0.004
Flare/no flare[1]	88/1 053	80 (91)/797 (76)	3.21 (1.53-6.73)	3.32 (1.57- 7.03)	0.002

[1]Flare within 3 mo period previous of the moment of ePQ completion. *N*: number of patients; CI: confidence interval.

Table 5 Results of univariate and multivariate logistic regression analyses for identification of predictors of ePQ completion in the UC population separately

UC *N* total = 776	*n*	Response (%)	Unadjusted Odds Ratio (95%CI)	Adjusted Odds Ratio (95%CI)	*P*
Female/male	370/406	280 (76)/308 (76)	0.99 (0.71-1.38)	1.01 (0.72-1.42)	0.956
Age at ePQ completion >40/≤40 yr	520/256	409 (78)/179 (70)	1.59 (1.13-2. 23)	1.70 (1.19-2.41)	0.003
Flare/no flare[1]	55/721	48 (87)/540 (75)	2.30 (1.02-5.17)	2.35 (1.03-5.37)	0.043
Left sided/rectum	333/221	252 (76)/169 (77)	0.96 (0.64-1.43)	0.99 (0.65-1.51)	0.965
Pancolitis/rectum	185/221	140 (76)/169 (77)	0.96 (0.61-1.51)	1.04 (0.65- 1.67)	0.875
Unknown/rectum	37/221	27 (73)/169 (77)	0.83 (0.38-1.83)	0.71 (0.31-1.64)	0.426

[1]Flare within 3 mo period previous of the moment of ePQ completion. N: number of patients; CI: confidence interval; Left sided: rectum and sigmoid and/or descending colon; Unknown: unknown disease location.

Table 6 Results of univariate and multivariate logistic regression analyses for identification of predictors of ePQ completion in the CD population separately

CD *N* total = 378	*n*	Response (%)	Unadjusted Odds Ratio (95%CI)	Adjusted Odds Ratio (95%CI)	*P*
Female/male	190/188	154 (81)/144 (77)	1.31 (0.80-2.15)	1.35 (0.79-2.30)	0.270
Age at ePQ completion >40/≤40 yr	196/182	156 (80)/142 (78)	1.10 (0.67-1.80)	1.34 (0.79-2.30)	0.281
Flare/no flare[1]	34/344	33 (97)/265 (77)	9.84 (1.32-73.1)	10.9 (1.43-82.4)	0.021
Ileo colon/upper	136/20	110 (81)/16 (80)	1.06 (0.33-3.42)	0.91 (0.26-3.19)	0.879
Ileum/upper	54/20	41 (76)/16 (80)	0.79 (0.22-2.78)	0.95 (0.27-3.35)	0.631
Colon/upper	153/20	122 (80)/16 (80)	0.98 (0.31-3.15)	0.71 (0.18-2.77)	0.622
Unknown/upper	15/20	9 (60)/16 (80)	0.38 (0.083-1.69)	0.38 (0.075-1.90)	0.237

[1]Flare within 3 mo period previous of the moment of ePQ completion. *n*: number of patients; CI: confidence interval; Upper: esophagus and/or stomach and/or duodenum and/or jejunum; Unknown: unknown disease location.

response in neither the uni- nor multivariate analyses. Details of the results of these analyses are displayed in Tables 4, 5, and 6.

Results of identical analyses performed in the patients of non-complying centers revealed no different viewpoints.

DISCUSSION

An Internet-based data acquisition tool sustaining a unique European multinational multi-center 10-year clinical follow-up study in patients afflicted with IBD appeared successful. User-friendly tailor-made software applications facilitated remote data inclusion, making it a one-step process, thereby minimizing the risk of human error, optimizing efficiency and convenience of the study effort and rendering continuous transparency of the project progress. The data management procedure made a reliable analyzable data set available promptly after the completion of the data acquisition phase. Overall 67% and 74% follow-up rates were observed for ePQ and ePpPFU, respectively. UC patients older than 40 years at the moment of ePQ completion and UC and CD patients with active disease in the 3 mo period previous to ePQ completion were significantly more likely to respond.

Does the use of Internet-based data acquisition instruments compare to or even outweigh the traditionally available methods? Some comparative studies are available in this field. In one study comprising UC patients, it appeared possible to use direct electronic mail contact to conduct follow-up research; response rates appeared to be related to the number of messages sent, the age of the recipients and the time since the initial contact[12]. The use of Internet tools in psychological research and Web-based assessments of personality constructs have proven to render outcome scores comparable to those of traditional

methods[13,14]. In one study the traditional paper-and-pencil questionnaire resulted in a higher number of errors compared with the Web-based questionnaire[15]. Two other studies compared several student populations that were similar in terms of age, gender, and racial backgrounds with regard to differences in outcome for Web-based and traditional questionnaires[16,17]. In these studies outcome scores of the Internet-based questionnaire and the traditional paper-and-pencil based questionnaires were not different. The time- and cost-effectiveness, convenience for both patients and researchers, the possibilities of immediate availability of data for analysis, and the structural prevention of missing data and incomplete responses by a priori programmed configuration, are important advantages related to the use of Internet-based data inclusion instruments as already discussed elsewhere[18,19].

The type of survey population addressed is of importance in this context. In open Web-based surveys, selection bias occurs due to the non-representative nature of the Internet population, and - more importantly - through self-selection of participants, also called as the 'volunteer effect'[18]. Furthermore, exact measurement of response rates is not possible, because the original size of the patient population is unknown. In quantitative epidemiological research, averages are measured of pre-defined patient populations, and therefore representative patient samples and adequate response rates are needed[20]. In the present study a finite 'closed' patient sample with known socio-demographic details was approached for follow-up for the fourth time in its disease history. In this way the exact response rate could easily be calculated. The patients could not log on to the username-password secured web site by themselves, but were guided by a project representative who assisted with the insertion procedure according to the patients' individual needs.

The patient group under study, being a population-based cohort, was representative by its nature. High follow-up rates were observed in the majority of the centers complying with the minimally required 60% response rate. This reduced selection bias. Thirteen of the original twenty EC-IBD centers participated in this FU study. The remaining seven had to refrain because of technical and/or logistic reasons. This did not jeopardize the population-based character of the study, since all participating centers had individually met the criteria for population based patient inclusion when the cohort was formed in the period of 1991-1993. In the present study, centers not reaching the minimally required 60% follow-up rate were analyzed separately acknowledging their effort and also securing the intent of overall population based methodology. The original population size of almost 930 000 inhabitants negatively influenced the follow-up rates in Dublin. The magnitude of the Irish project covering six university and six private hospitals made sufficient follow-up percentages, 10 years after the diagnosis, unrealistic. Most areas that reached the 60% follow-up rate threshold had original population sizes between 300 000 and 500 000 inhabitants, suggesting that this size enables successful long-term follow-up. Considering the broad European multi-center nature of this study and the fact that the entire patient population had been diagnosed 10 years earlier, the high response rates must be regarded as excellent.

UC patients who responded to the ePQ were significantly older than those who did not. This reflects most probably the higher dedication and availability of this age group compared to the younger patients. In the CD group, there was no difference between the age groups. The expected drop of response of the elderly because of supposed computer anxiety could not be confirmed in this study. Eleven percent of the patients indicated to have been lost to follow-up for the ePQ were in fact traced, but refused to participate without a difference between the age groups. The need of physical presence to complete the ePQ could explain at least part of the observed refusal rate. Furthermore, active disease within 3 mo period from ePQ completion was shown to be a clear positive predictor of ePQ participation in both UC and CD, and the majority of patients (1 073/1 162 [92.3%]) were in clinical remission during this period. Most probably, disease activity accompanies increased concern and increases motivation to participate. This observation could be an important factor of bias that has to be controlled for in the quality of life analyses planned in this project. 10.7% of the patients lost to follow-up for the ePQ were indicated to be untraceable. Patients equal to or younger than 40 years at ePQ completion were less likely to be traced, compared to those patients being older than 40 years at ePQ completion. This difference could be explained by the high mobility characteristic of younger people.

Apart from 11 occasions of system failure and some initial inconsistencies of the data export facility, this electronic facility appeared to be a well-equipped flexible tool for data entry and storage. Possibilities for an efficiency gain in terms of a better fit between Internet questionnaire application and the data management process had been described before[21] and could be confirmed in this study.

In conclusion, an Internet-based electronic data acquisition application successfully sustained a unique multinational multi-center study project in patients afflicted with IBD. The application has high potential for future use in follow-up studies of this cohort and could serve as a template for other multi-national follow-up studies.

ACKNOWLEDGMENTS

This study was initiated and carried out by all members of the European Collaborative study Group of IBD (EC-IBD).

REFERENCES

1 **Bell DS**, Kahn CE. Health status assessment via the World Wide Web. *Proc AMIA Annu Fall Symp* 1996: 338-342
2 **Soetikno RM**, Mrad R, Pao V, Lenert LA. Quality-of-life

research on the Internet: feasibility and potential biases in patients with ulcerative colitis. *J Am Med Inform Assoc* 1997; **4**: 426-435

3 **Hilsden RJ**, Meddings JB, Verhoef MJ. Complementary and alternative medicine use by patients with inflammatory bowel disease: An Internet survey. *Can J Gastroenterol* 1999; **13:** 327-32

4 **Soetikno RM**, Provenzale D, Lenert LA. Studying ulcerative colitis over the World Wide Web. *Am J Gastroenterol* 1997; **92:** 457-460

5 **Shivananda S**, Lennard-Jones J, Logan R, Fear N, Price A, Carpenter L, van Blankenstein M. Incidence of inflammatory bowel disease across Europe: is there a difference between north and south? Results of the European Collaborative Study on Inflammatory Bowel Disease (EC-IBD). *Gut* 1996; **39:** 690-697

6 **Stockbrügger RW**, Russel MG, van Blankenstein M S. EC-IBD: a European effort in inflammatory bowel disease. *Eur J Intern Med* 2000; **11:** 187-190

7 **Lennard Jones JE**, Shivananda S. Clinical uniformity of inflammatory bowel disease a presentation and during the first year of disease in the north and south of Europe. EC-IBD Study Group. *Eur J Gastroenterol Hepatol* 1997; **9:** 53-59

8 **Witte J**, Shivananda S, Lennard-Jones JE, Beltrami M, Politi P, Bonanomi A, Tsianos EV, Mouzas I, Schulz TB, Monteiro E, Clofent J, Odes S, Limonard CB, Stockbrügger RW, Russel MG. Disease outcome in inflammatory bowel disease: mortality, morbidity and therapeutic management of a 796-person inception cohort in the European Collaborative Study on Inflammatory Bowel Disease (EC-IBD). *Scand J Gastroenterol* 2000; **35:** 1272-1277

9 **Salvarani C**, Vlachonikolis IG, van der Heijde DM, Fornaciari G, Macchioni P, Beltrami M, Olivieri I, Di Gennaro F, Politi P, Stockbrügger RW, Russel MG. Musculoskeletal manifestations in a population-based cohort of inflammatory bowel disease patients. *Scand J Gastroenterol* 2001; **36:** 1307-1313

10 **van der Eijk I R,** Russel M. Influence of quality of care on quality of life in inflammatory bowel disease (IBD): literature review and studies planned. *Eur J Intern Med* 2000;**11**:228-234

11 **Gasche C**, Scholmerich J, Brynskov J, D'Haens G, Hanauer SB, Irvine EJ, Jewell DP, Rachmilewitz D, Sachar DB, Sandborn WJ, Sutherland LR. A simple classification of Crohn's disease: report of the Working Party for the World Congresses of Gastroenterology, Vienna 1998. *Inflamm Bowel Dis* 2000; **6:** 8-15

12 **Treadwell JR**, Soetikno RM, Lenert LA. Feasibility of quality-of-life research on the Internet: a follow-up study. *Qual Life Res* 1999; **8:** 743-747

13 **Riva G**, Teruzzi T, Anolli L. The use of the internet in psychological research: comparison of online and offline questionnaires. *Cyberpsychol Behav* 2003; **6:** 73-80

14 **Cronk BC**, West JL. Personality research on the Internet: a comparison of Web-based and traditional instruments in take-home and in-class settings. *Behav Res Methods Instrum Comput* 2002; **34:** 177-180

15 ***Pettit FA***. A comparison of World-Wide Web and paper-and-pencil personality questionnaires. *Behav Res Methods Instrum Comput* 2002; **34:** 50-54

16 **Fouladi RT**, McCarthy CJ, Moller NP. Paper-and-pencil or online? Evaluating mode effects on measures of emotional functioning and attachment. *Assessment* 2002; **9:** 204-215

17 **Davis RN**. Web-based administration of a personality questionnaire: comparison with traditional methods. *Behav Res Methods Instrum Comput* 1999; **31:** 572-577

18 **Eysenbach G**, Wyatt J. Using the Internet for surveys and health research. *J Med Internet Res* 2002; **4:** E13

19 **Schleyer TK**, Forrest JL. Methods for the design and administration of web-based surveys. *J Am Med Inform Assoc* 2000; **7:** 416-425

20 **Braithwaite D**, Emery J, De Lusignan S, Sutton S. Using the Internet to conduct surveys of health professionals: a valid alternative? *Fam Pract* 2003; **20:** 545-551

21 **Wright G**. The triple-s standard. Presented at the Association for Survey Computing conference "Open Standards: Breaking down the barriers" at Imperial College 2002

Science Editor Guo SY **Language Editor** ELsevier HK

PO Box 2345, Beijing 100023, China
www.wjgnet.com
wjg@wjgnet.com

ELSEVIER

World J Gastroenterol 2005;11(45):7159-7164
World Journal of Gastroenterology ISSN 1007-9327

• RAPID COMMUNICATION •

Serum insulin, insulin resistance, β-cell dysfunction, and gallstone disease among type 2 diabetics in Chinese population: A community-based study in Kinmen, Taiwan

Chi-Ming Liu, Tao-Hsin Tung, Shih-Tzer Tsai, Jorn-Hon Liu, Yeh-Kuang Tsai, Victor Tze-Kai Chen, Tseng-Nip Tam, Hsu-Feng Lu, Kuang-Kuo Wang, Chung-Te Hsu, Hui-Chuan Shih, De-Chuan Chan, Pesus Chou

Chi-Ming Liu, Tao-Hsin Tung, Community Medicine Research Center and Institute of Public Health, National Yang-Ming University, Cheng Hsin General Hospital, Taipei, Taiwan, China
Shih-Tzer Tsai, Department of medicine, Veterans General Hospital, Taipei, Taiwan, China
Jorn-Hon Liu, Cheng Hsin General Hospital, Faculty of Medicine, School of Medicine, National Yang-Ming University, Taipei, Taiwan, China
Yeh-Kuang Tsai, University of California San Francisco, San Francisco, CA, United States
Victor Tze-Kai Chen, Cardinal Tien Hospital, College of Medicine, Fu-Jen Catholic University, National Defence Medicine Center, Taipei, Taiwan, China
Tseng-Nip Tam, Hsu-Feng Lu, Kuang-Kuo Wang, Chung-Te Hsu, Cheng Hsin General Hospital, Taipei, Taiwan, China
Hui-Chuan Shih, Department of Nursing, Kaohsiung Military General Hospital, Kaohsing, Taiwan, China
De-Chuan Chan, Division of General Surgery, Tri-Service General Hospital, National Defence Medical Center, Taipei, Taiwan, China
Pesus Chou, Community Medicine Research Center and Institute of Public Health, National Yang-Ming University, Taipei, Taiwan, China
Supported by the grants from the National Science Council, Nos. NSC-91-2320-B-010-102 and NSC-92-2320-B-010-102
Co-first-author: Tao-Hsin Tung
Co-correspondent: Jorn-Hon Liu
Correspondence to: Dr Pesus Chou, Community Medicine Research Center, National Yang-Ming University, Shih-Pai, 112, Taipei, Taiwan, China. pschou@ym.edu.tw
Telephone: +886-2-28267050 Fax: +886-2-28201461
Received: 2005-04-28 Accepted: 2005-05-12

Abstract

AIM: To explore the association of serum insulin, insulin resistance, and β-cell dysfunction with gallstone disease (GSD) in type 2 diabetics.

METHODS: We used a community-based study conducted between 1991 and 1993 in Kinmen, Taiwan to identify type 2 diabetics. A screening program for GSD was performed in 2001 by a panel of specialists who employed real-time ultrasound sonography to examine the abdominal region after the patient had fasted for at least 8 h. Screening was conducted in 2001 on 848 patients diagnosed with type 2 diabetes. The HOMA method was used to compare the profile differences for insulin resistance (HOMA IR) and β-cell dysfunction (HOMA β-cell).

RESULTS: We studied 440 type 2 diabetics who attended sonography check-ups. After excluding eight insulin-treated diabetics, the prevalence of GSD among the remaining 432 was 13.9% (26/187) among males and 14.7% (36/245) among females. After adjustment for other GSD-associated risk factors in addition to age and obesity, GSD risk increased among females with levels of serum insulin [4th *vs* 1st quartile odds ratios (OR) = 4.46 (95%CI: 1.71-11.66)] and HOMA IR [4th *vs* 1st quartile OR = 4.46 (95%CI: 1.71-11.66)]. Better HOMA β-cell function was significantly related to decreased risk of GSD [4th *vs* 1st quartile OR = 0.16 (95%CI: 0.03-1.70)]. Among males, age and central obesity were the most significant risk factors for GSD. No association of GSD with serum insulin, HOMA IR, and HOMA β-cell was observed among males.

CONCLUSION: Serum insulin, insulin resistance, and β-cell dysfunction are risk factors for GSD in females, but not males with type 2 diabetes.

Key words: Type 2 diabetes; Gallstone disease; Insulin resistance; β-cell dysfunction; Community-based study

Liu CM, Tung TH, Tsai ST, Liu JH, Tsai YK, Chen VTK, Tam TN, Lu HF, Wang KK, Hsu CT, Shih HC, Chan DC, Chou P. Serum insulin, insulin resistance, β-cell dysfunction and gallstone disease among type 2 diabetics in Chinese population: A community-based study in Kinmen, Taiwan. *World J Gastroenterol* 2005; 11(45): 7159-7164
http://www.wjgnet.com/1007-9327/11/7159.asp

INTRODUCTION

Clinically, type 2 diabetes with concomitant gallstone disease (GSD) increases the incidence of acute cholecystitis and has a higher probability for progression to septicemia. It is generally believed that subjects with diabetes secrete more lithogenic bile than non-diabetics; i.e., diabetes and GSD might be viewed as closely linked diseases[1]. Indeed, several community-based epidemiologic studies have demonstrated that not only diabetics have an increase in GSD-related morbidity[2-4], but also, our previous report showed that the prevalence of overall GSD among type 2 diabetics was higher as compared with

other general Chinese populations when using the same methods of GSD assessment[5]. In order to reduce health-care expenditures caused by GSD, organized preventive strategies are recommended.

Insulin resistance syndrome, initially described by Reaven[6], is a cluster of risk factors for coronary artery disease. This pathological condition is characterized by an inadequate physiological response of peripheral tissues to circulating insulin, and results in metabolic and hemodynamic disturbances[7]. Hyperinsulinemia has also characteristically been found in subjects with type 2 diabetes as a result of insulin resistance, which is considered to be of primary importance in the pathogenesis of diabetes. In addition, impairment of β-cell function, which becomes most evident during insulin resistance due to increased demands for insulin, is also well known now as a major factor influencing the progression from normal glucose tolerance, through impaired glucose tolerance to frank type 2 diabetes[8,9]. Results of the epidemiological studies have shown that increased insulin resistance and decreased insulin secretion are strongly related to the risk of developing type 2 diabetes[10-12].

The insulin-related factors responsible for the development of GSD remain to be clarified. Although it has been suggested that serum insulin affects the development of this co-disease in the general population[13,14], few community-based studies have been conducted to explore the direct effect of serum insulin, insulin resistance, and β-cell dysfunction to GSD among the diabetics. Additionally, other factors, including diabetic duration and glucose toxicity, have been proposed to affect the development of GSD in type 2 diabetics[3]. Using the community-based study in Kinmen, Taiwan, we aimed to determine whether serum insulin, insulin resistance, and β-cell dysfunction, were independently related to GSD among type 2 diabetics.

MATERIALS AND METHODS

Organization of community-based gallstone disease screening for type 2 diabetes

We used baseline data from a community-based screening for type 2 diabetes targeted to subjects aged 30 years or more in Kinmen, Taiwan, between January 1991 and December 1993. The details of the study design and execution have been described in detail elsewhere[15]. The identification of type 2 diabetes was based on the WHO definition in 1985[16]: subjects with fasting plasma glucose (FPG) ≥7.8 mmol/L (≥140 mg/dL) or 2 h postload ≥ 11.1 mmol/L (≥200 mg/dL) were defined as individuals with type 2 diabetes. Subjects with a history of type 2 diabetes and who received medication were defined as known cases. However, in the GSD screening done in 2001, the patients that fulfilled the criteria of the revised WHO criteria (revised in 1999) were enrolled. Patients with FPG ≥7.0 and <7.8 mmol/L in 1991 to 1993 were also recruited[17]. A total of 1 123 type 2 diabetics aged 30 and above were identified based on the population survey carried out by the Yang-Ming Crusade in Kinmen. After excluding those who migrated or died, the remaining 858 type 2 diabetics formed a cohort who were eligible for abdominal ultrasound sonography. These 858 subjects were invited by telephone calls or invitation letters in 2001 to be screened for GSD. Informed consent was obtained from all participants before the survey[5].

Information concerning biochemical markers and diagnosis of gallstone disease

The details of the data collection have also been described in detail elsewhere[5]. In brief, baseline information including demographic and biochemical variables was collected in the period 1991-93. Face to face interviews were conducted by the Yang-Ming Crusade, a volunteer organization of well-trained medical students of National Yang-Ming University. Fasting blood samples were drawn by public health nurses. Overnight fasting serum and plasma samples (preserved with EDTA and NaF) were collected and kept frozen (-20 ℃) until analysis. FPG concentrations were determined using the hexokinase-glucose-6-phosphate dehydrogenase method with a glucose (HK) reagent ldt (Gilford, Oberlin, OH, USA). Higher systolic blood pressure (SBP) was defined as SBP ≥140 mmHg, and higher diastolic blood pressure (DBP) was defined as DBP ≥90 mmHg. Obesity was defined by a body mass index (BMI) ≥25 kg/m^2, an abnormal total cholesterol was defined as ≥5.17 mmol/L (≥200 mg/dL), a raised triglyceride as ≥2.24 mmol/L (≥200 mg/dL), a raised blood urea nitrogen (BUN) as ≥7.14 mmol/L (≥20 mg/dL), a high level of uric acid was defined for males as ≥0.42 mmol/L (≥7 mg/dL) and for females as ≥0.36 mmol/L (≥6 mg/dL), and central obesity as a waist circumference ≥90 cm in males or ≥80 cm in females[18].

The follow-up screening regime for GSD was performed in 2001. GSD was diagnosed by a panel of specialists using real-time ultrasound sonography to examine the abdominal region, after fasting for at least 8 h, for the presence of "movable hyperechoic material with acoustic shadow". Cases of GSD were classified as follows: single gallbladder stone; multiple gallbladder stones; and cholecystectomy, excluding gallbladder polyps. Cases were identified as any type of GSD among type 2 diabetics. Furthermore, in order to ensure consistency of GSD diagnosis among the specialists, the Kappa statistic was used to assess the agreement of interobserver reliability among study specialists. A pilot study was performed with 50 randomly selected type 2 diabetics who were not study subjects. For interobserver reliability, the Kappa value for diagnosis of GSD was 0.77 (95%CI: 0.50-0.96).

Assessment of insulin resistance and β-cell dysfunction

The HOMA method was used to compare differences in the profiles for insulin resistance (HOMA IR) and for β-cell dysfunction (HOMA β-cell) in subjects with and without GSD[19]. The HOMA model assumes that the control of FPG and fasting insulin (FI) is governed by a self-contained feedback loop between the pancreas, liver, and insulin-sensitive and insulin-insensitive glucose

Table 1 Crude and age-adjusted odds ratios of baseline-associated factors of GSD among type 2 diabetics in Kinmen

	GSD (yes *vs* no)							
	Male				Female			
	Crude OR (95%CI)		Age-adjusted OR (95%CI)		Crude OR (95%CI)		Age-adjusted OR (95%CI)	
Age (≥65 *vs* <65 yr)	3.14	(1.32-7.47)[a]	-	-	2.25	(1.04-4.90)[a]	-	-
Type 2 diabetes (known *vs* new cases)	0.90	(0.34-2.39)	0.87	(0.32-2.34)	1.44	(0.68-3.02)	1.46	(0.68-3.13)
FPG (≥11.1 *vs* <11.1 mmol/L)	2.12	(0.70-6.37)	1.95	(0.64-5.94)	1.24	(0.50-3.07)	1.49	(0.59-3.79)
SBP (≥140 *vs* <140 mmHg)	1.70	(0.73-3.97)	1.50	(0.63-3.56)	2.59	(1.23-5.46)[a]	1.99	(0.92-4.31)
DBP (≥90 *vs* <90 mmHg)	1.44	(0.62-3.35)	1.57	(0.67-3.73)	1.12	(0.52-2.42)	1.21	(0.55-2.67)
Obesity (yes *vs* no)	2.04	(0.85-4.88)	2.00	(0.83-4.83)	2.97	(1.30-6.83)[a]	2.88	(1.24-6.70)[a]
Central obesity (yes *vs* no)	2.76	(1.13-6.77)[a]	2.36	(1.01-5.97)	1.85	(0.68-5.02)	1.47	(0.53-4.09)
Cholesterol (≥5.17 *vs* <5.17 mmol/L)	1.02	(0.19-1.91)	0.88	(0.18-1.09)	0.92	(0.45-1.88)	0.85	(0.41-1.77)
Triglyceride (≥2.24 *vs* <2.24 mmol/L)	1.92	(0.12-2.36)	1.61	(0.13-2.84)	1.43	(0.20-2.46)	1.35	(0.15-1.96)
BUN (≥7.14 *vs* <7.14 mmol/L)	0.44	(0.16-1.25)	0.38	(0.13-1.09)	1.65	(0.75-3.61)	1.30	(0.58-2.93)
Uric acid (high *vs* normal)	0.30	(0.09-1.06)	0.29	(0.08-1.03)	1.61	(0.77-3.38)	1.12	(0.51-2.48)
AST (≥40 *vs* <40 U/L)	1.05	(0.08-5.72)	0.60	(0.07-5.31)	3.68	(1.01-9.32)[a]	3.93	(1.04-10.89)[a]
ALT (≥40 *vs* <40 U/L)	1.09	(0.19-4.33)	1.09	(0.21-5.61)	2.00	(0.67-6.02)	2.20	(0.71-6.85)
Serum insulin (2^{nd} *vs* 1^{st} quartile)	0.29	(0.06-1.33)	0.30	(0.06-1.39)	1.39	(0.44-4.40)	1.68	(0.52-5.45)
(μU/mL) (3^{rd} *vs* 1^{st} quartile)	0.61	(0.19-2.00)	0.56	(0.17-1.86)	2.05	(0.71-5.88)	2.20	(0.75-6.45)
(4^{th} *vs* 1^{st} quartile)	0.61	(0.18-2.03)	0.65	(0.20-2.17)	5.38	(2.14-13.48)[a]	5.32	(2.08-13.64)[a]
Log HOMA IR (2^{nd} *vs* 1^{st} quartile)	0.61	(0.19-2.00)	0.60	(0.18-1.99)	1.17	(0.38-3.57)	1.65	(0.52-5.29)
(3^{rd} *vs* 1^{st} quartile)	0.58	(0.06-1.29)	0.49	(0.06-1.36)	2.60	(1.02-6.64)[a]	2.66	(1.02-6.94)[a]
(4^{th} *vs* 1^{st} quartile)	0.63	(0.19-2.08)	0.60	(0.18-2.01)	2.60	(1.01-6.66)[a]	2.59	(1.01-6.76)[a]
Log HOMA β-cell (2^{nd} *vs* 1^{st} quartile)	1.16	(0.35-3.80)	1.27	(0.38-4.25)	0.35	(0.08-1.55)	0.45	(0.10-2.03)
(3^{rd} *vs* 1^{st} quartile)	0.52	(0.11-2.43)	0.51	(0.11-2.39)	0.16	(0.02-1.23)	0.17	(0.02-1.35)
(4^{th} *vs* 1^{st} quartile)	0.25	(0.03-2.97)	0.22	(0.03-1.73)	0.17	(0.02-1.28)	0.16	(0.02-1.21)

[a]$P<0.05$.

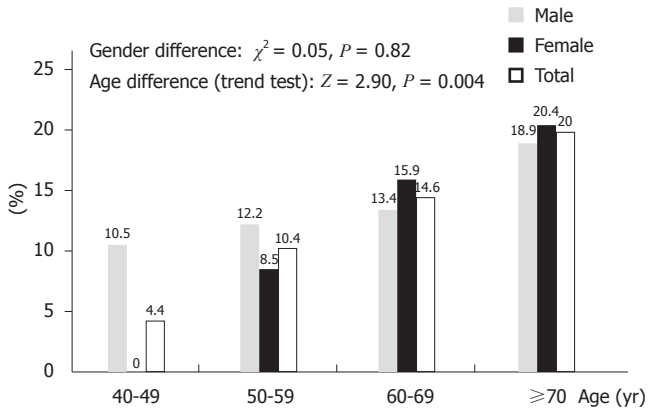

Figure 1 Sex and age-specific prevalence of gallstone diseases among type 2 diabetics in Kinmen.

metabolizing tissues[19]. The formulas were developed and validated against the hyperinsulinemic-euglycemic clamp for insulin resistance and the hyperglycemic clamp for insulin secretion[19]. The details are as follows:

$$\text{Insulin resistance(HOMA IR)} = \frac{\text{FI}\times\text{FPG}}{22.5}$$

$$\beta\text{-cell function(HOMA }\beta\text{-cell)} = \frac{20\text{-FI}}{\text{FPG-3.5}}$$

Because the HOMA model is not applicable to type 2 diabetics treated with insulin, eight insulin-treated subjects were excluded from the HOMA analysis. In addition, due to skewed distributions, the values of the HOMA model were subjected to log transformation in further analysis and re-transformed for tabulations.

Statistical analysis

Statistical analysis was performed using SAS version 9.0 (SAS Institute Inc., Cary, NC, USA). In the univariate analysis, crude and adjusted OR (adjustment for sex and age) were estimated and 95% confidence intervals (CI) were used. Multiple logistic regression was used to investigate whether insulin resistance and β-cell dysfunction were independently associated with GSD after adjustment for confounding factors. A P value <0.05 was considered statistically significant. In addition, HOMA IR, and HOMA β-cell scores were divided into quartiles after log transformation.

RESULTS

In our earlier study in 2001, 440 of 858 type 2 diabetic subjects (51.3%) had received real-time ultrasound sonography of the abdomen[5]. Using this cohort in the present study, and after excluding eight type 2 diabetics who had been treated with insulin, we determined the distribution of GSD among the remaining 432 participants. Figure 1 shows the sex- and age-specific prevalence of all types of GSD among type 2 diabetics. The sex-specific prevalence values [male: 13.9% (26/187); female: 14.7% (36/245)] were not significantly different (χ^2 = 0.05, P = 0.82). The prevalence of all types of GSD was significantly increased with age [Z (trend) = 2.90, P = 0.004]. Among the subjects aged 40-59 years, males had a higher prevalence of GSD than females. Conversely, among subjects aged 60 and above, females had a higher prevalence of GSD than males.

Table 1 presents the crude and age-adjusted OR for the association between certain relevant baseline-associated risk factors and GSD. Among males, baseline factors that were significantly related to GSD included age (≥65 *vs* <65 years, crude OR = 3.14, 95%CI: 1.32-7.47) and central obesity (yes *vs* no, age-adjusted OR = 2.36, 95%CI:

Table 2 Multiple logistic regression of association between baseline serum insulin, insulin resistance, β-cell dysfunction and GSD among type 2 diabetics in Kinmen

	GSD (yes *vs* no)					
	Male			Female		
Variables	OR	(95%CI)	*P* for trend test	OR	(95%CI)	*P* for trend test
Model I						
Age (≥65 *vs* <65 years)	1.04	(1.00-1.09)	-	1.05	(1.02-1.09)	-
Obesity (yes *vs* no)	-	-	-	2.35	(1.04-5.62)	-
Central obesity(yes *vs* no)	2.66	(1.01-6.99)	-	-	-	-
Serum insulin (μU/mL)						
2nd *vs* 1st quartile	0.39	(0.08-1.99)		1.47	(0.44-4.87)	
3rd *vs* 1st quartile	0.52	(0.14-1.95)	0.51	2.01	(0.68-5.96)	<0.0001
4th *vs* 1st quartile	0.56	(0.16-2.04)		4.46	(1.71-11.66)	
Model II						
Age (≥65 vs <65 years)	1.04	(1.02-1.09)	-	1.06	(1.02-1.10)	-
Obesity (yes *vs* no)	-	-	-	2.25	(1.02-5.52)	-
Central obesity(yes *vs* no)	2.68	(1.03-6.97)	-	-	-	-
Log HOMA IR						
2nd *vs* 1st quartile	0.79	(0.22-2.78)		1.63	(0.49-5.43)	
3rd *vs* 1st quartile	0.53	(0.07-1.51)	0.18	1.63	(0.55-4.82)	0.02
4th *vs* 1st quartile	0.68	(0.20-2.36)		2.81	(1.03-7.91)	
Model III						
Age (≥65 *vs* <65 years)	1.05	(1.00-1.10)	-	1.05	(1.01-1.09)	-
Obesity (yes *vs* no)	-	-	-	2.58	(1.09-6.13)	-
Central obesity(yes *vs* no)	2.82	(1.03-7.69)	-	-	-	-
Log HOMA β-cell						
2nd *vs* 1st quartile	0.94	(0.60-9.97)		0.45	(0.10-2.09)	
3rd *vs* 1st quartile	0.78	(0.15-4.09)	0.14	0.17	(0.02-1.31)	0.01
4th *vs* 1 quartile	0.32	(0.04-2.89)		0.16	(0.03-1.70)	

Other independent variables controlled in model included age, type of cases, SBP, DBP, cholesterol, triglyceride, BUN, uric acid, AST, and ALT.

1.01-5.97). According to univariate analysis in which the highest quartile was compared with the lowest, the female diabetics with GSD (compared to those without GSD) were older (≥65 *vs* <65 years, crude OR = 2.25, 95%CI: 1.04-4.90), were more obese (yes *vs* no, age-adjusted OR = 2.88, 95%CI: 1.24-6.70), had higher AST values (≥40 *vs* <40 U/L, age-adjusted OR = 3.93, 95%CI: 1.04-10.89), had greater serum insulin values (4th *vs* 1st quartile, age-adjusted OR = 5.32, 95%CI: 2.08-13.64) and had higher log HOMA IR values (4th *vs* 1st quartile, age-adjusted OR = 2.59, 95%CI: 1.01-6.76).

Associations between baseline serum insulin, insulin resistance, β-cell dysfunction, and GSD in each gender after adjustment for confounding factors were examined using a multiple logistic regression model. Fasting insulin was correlated with HOMA IR and HOMA β-cell dysfunction. These correlations were shown to be independent through the use of separate models. Furthermore, because the level of significance was very similar for raw (non-transformed) and log transformed data, in order to interpret the results more easily, the results for serum insulin were calculated for raw values. As shown in Table 2, older age was significantly associated with GSD in both males and females. Among males, there was a statistically significant association of GSD with central obesity, but no association of GSD with serum insulin, log HOMA IR, or log HOMA β-cell. Among females, not only obesity, but also serum insulin ($P<0.0001$ for trend test) and log HOMA IR ($P = 0.02$ for trend test) were significantly related to GSD (after adjustment for confounding variables). The association of GSD with serum insulin (4th *vs* 1st quartile, OR = 4.46, 95%CI: 1.71-11.66) and log HOMA IR (4th *vs* 1st quartile, OR = 2.81, 95%CI: 1.03-7.91) was revealed when the highest quartile was compared with the lowest. Although an association between log HOMA β-cell dysfunction and GSD was not found in the multivariate model, the test for trend was still strongly significant ($P = 0.01$).

DISCUSSION

Consistent with other epidemiologic studies[3,5], our study also revealed that age is a significant risk factor for GSD among type 2 diabetics (after adjustment for confounding factors). Larger amounts of cholesterol secreted by the liver and a decrease in the catabolism of cholesterol to bile acid were observed in the elderly population[20]. Long-term exposure, such as longer duration of type 2 diabetes, also might account for the increased risk of developing GSD among the elderly population[21]. In addition, the present study also showed the interaction between sex and age to prevalence of GSD. Further epidemiological and etiological investigations are clearly needed in order to clarify the pathophysiological mechanisms of interactive effects between sex, age, and GSD among type 2 diabetics.

Obesity might raise the saturation of bile by increasing biliary secretion of cholesterol, with the latter probably depending on a higher synthesis of cholesterol in obese subjects[5,22]. Our data demonstrated a significant association between obesity and GSD among females.

As in other studies, both univariate and multivariate analyses showed significantly higher BMI among females when compared to controls[23,24]. However, among males, the present study failed to find a positive association between higher BMI and GSD, whereas central obesity was significantly associated with GSD. These results are consistent with those of other population-based studies[25,26]. It has been suggested that BMI might not be as good an indictor of obesity among males as among females[27]. Some studies have also suggested that failing to find a relationship between BMI and GSD among males reveals a tendency for a positive association with other indices of obesity, such as slimming treatment and skinfold thickness[27,28]. Another possible reason is that loss of muscle bulk might be associated with GSD among males, i.e., males with GSD had gained less weight during adult life than non-GSD males despite having more abdominal fat, suggesting that they had lost more lean body mass[26]. Because central obesity was shown to be an important predictor of type 2 diabetes and various metabolic abnormalities, further study is needed to determine the contribution to and pathophysiological mechanisms of the formation of GSD in type 2 diabetics.

The results of this community-based study provide further support for an association between hyperinsulinemia and insulin resistance with GSD among females. Female diabetics with GSD had significantly higher baseline serum insulin, higher HOMA IR and lower HOMA β-cell function in comparison to controls without GSD pathology. This relationship persisted even after controlling the most common confounding factor of the association, such as central obesity, which was related to GSD and serum insulin[3]. Males showed no significant differences from controls regarding insulin resistance or its surrogates, lending support to a proposed interaction of these factors and sex with regard to lithogenesis. Previous clinical case-control studies and epidemiologic studies also showed similar results in the general population and in the diabetic population[3,13,29]. The mechanism underlying the interaction between insulin and gallstone formation is undetermined, though it has been speculated that decreased GSD motility and increased cholesterol saturation of bile are involved[29]. Gallstone motility had been demonstrated to be impaired in diabetics, favoring cholesterol gallstone crystal formation and growth[30]. Insulin may inhibit basal and cholecystokinin-stimulated gallbladder motility[31]. Another possible reason for the lack of an association between serum insulin and GSD among males is abdominal adiposity, which probably explains the hyperinsulinemia as the association of serum insulin with the disappearance of GSD. In addition, the fact that the HOMA model was used to estimate insulin resistance could be viewed as showing an interaction between serum insulin and FPG. The higher insulin levels mean the greater insulin resistance. Insulin resistance related to GSD with response to the duration of type 2 diabetes would also increase the risk of prevalent GSD[3].

Among females, a positive relationship between serum C-peptide and GSD was obtained in previous studies[13]. Measurement of C-peptide under standardized conditions provides a sensitive, well accepted and clinically validated assessment of β-cell function[32]. The intravenous glucose tolerance test (IVGTT) is widely used to test pancreatic β-cell function. Plasma C-peptide concentration is measured and used to infer insulin secretion since it is secreted in equimolar amounts with insulin, and its extraction by the liver is negligible[33]. In the present study, HOMA β-cell dysfunction was strongly related to GSD among females but not among males, implying that insulin secretion might act differently in relation to GSD formation in males and females, even among those with type 2 diabetes.

The present study took advantage of several important and valuable methods. First, most previous studies were hospital-based, and Berkson's bias (selection bias) was inevitable. A community-based study design, such as the one we used, could diminish this kind of selection bias. Second, potential information bias was reduced because GSD screening for type 2 diabetics in 2001 was collected without the knowledge by the specialists of results of the baseline biochemical factors in 1991-1993. Third, we used ultrasound examination instead of clinical history of GSD as used in the previous study[3]. Because of this, we should have improved diagnostic accuracy and diminished underestimation and misclassification of GSD. Nevertheless, associated biochemical markers of GSD were obtained retrospectively, and the causal relationship between serum insulin, insulin resistance, β-cell dysfunction and GSD could not be clarified in our study. Baseline characteristics pertinent to the risk of type 2 diabetes for attendants were not significantly different from those for non-attendants except for age, which means that the 51.3% who participated may also be representative of those refusing to join our study (after adjustment for age)[5]. But the relatively lower response rate still might be caused by decreased statistical power. In addition, due to the complications and expense associated with the clamp technique (which prohibited its use in our community-based epidemiologic studies that had substantial sample sizes), the measurements of insulin resistance and β-cell dysfunction were based on an indirect method (the HOMA model). However, previous studies confirmed that the HOMA method and clamp-measured insulin resistance were highly correlated, implying that we could also obtain unbiased results using less sophisticated methods[34,35].

In conclusion, the present study shows that there are gender differences with regard to the relationships between serum insulin, insulin resistance, β-cell dysfunction and GSD among type 2 diabetics (after adjustment for confounding factors). These observations suggest that factors related to type 2 diabetes might need to be considered separately in male and female diabetic patients in the pathogenic mechanism of increased risk of GSD.

REFERENCES

1 **de Leon MP**, Ferenderes R, Carulli N. Bile lipid composition and bile acid pool size in diabetes. *Am J Dig Dis* 1978; **23**: 710-716

2 **Shaw SJ**, Hajnal F, Lebovitz Y, Ralls P, Bauer M, Valenzuela J, Zeidler A. Gallbladder dysfunction in diabetes mellitus. *Dig Dis Sci* 1993; **38**: 490-496

3 **Haffner SM**, Diehl AK, Valdez R, Mitchell BD, Hazuda HP, Morales P, Stern MP. Clinical gallbladder disease in NIDDM subjects. Relationship to duration of diabetes and severity of glycemia. *Diabetes Care* 1993; **16**: 1276-1284

4 **De Santis A**, Attili AF, Ginanni Corradini S, Scafato E, Cantagalli A, De Luca C, Pinto G, Lisi D, Capocaccia L. Gallstones and diabetes: A case-control study in a free-living population sample. *Hepatology* 1997; **25**: 787-790

5 **Liu CM**, Tung TH, Liu JH, Lee WL, Chou P. A community-based epidemiologic study on gallstone disease among type 2 diabetics in Kinmen, Taiwan. *Dig Dis* 2004; **22**: 87-91

6 **Reaven GM**. Banting lecture-1988. Role of insulin resistance in human disease. *Diabetes* 1988; **37**: 1595-1607

7 **Ascaso JF**, Pardo S, Real JT, Lorente RI, Priego A, Carmena R. Diagnosing insulin resistance by simple quantitative methods in subjects with normal glucose metabolism. *Diabetes Care* 2003; **26**: 3320-3325

8 **Rojo-Martínez G**, Esteva I, de Adana SR, Catalá M, Merelo MJ, Tinahones F, Gómez-Zumaquero JM, Cuesta AL, Cardona F, Soriguer F. Patterns of insulin resistance in the general population of southeast Spain. *Diabetes Res Clin Pract* 2004; **65**: 247-256

9 **Kahn SE**. The importance of the beta-cell in the pathogenesis of type 2 diabetes mellitus. *Am J Med* 2000; **108 Suppl 6a**: 2S-8S

10 **Ferrannini E**. Insulin resistance versus insulin deficiency in non-insulin-dependent diabetes mellitus: problems and prospects. *Endocr Rev* 1998; **19**: 477-490

11 **Haffner SM**, D'Agostino R, Saad MF, Rewers M, Mykkänen L, Selby J, Howard G, Savage PJ, Hamman RF, Wagenknecht LE. Increased insulin resistance and insulin secretion in nondiabetic African-Americans and Hispanics compared with non-Hispanic whites. The Insulin Resistance Atherosclerosis Study. *Diabetes* 1996; **45**: 742-748

12 **Li CL**, Tsai ST, Chou P. Relative role of insulin resistance and beta-cell dysfunction in the progression to type 2 diabetes—The Kinmen Study. *Diabetes Res Clin Pract* 2003; **59**: 225-232

13 **Ruhl CE**, Everhart JE. Association of diabetes, serum insulin, and C-peptide with gallbladder disease. *Hepatology* 2000; **31**: 299-303

14 **Méndez-Sánchez N**, Chavez-Tapia NC, Motola-Kuba D, Sanchez-Lara K, Ponciano-Rodríguez G, Baptista H, Ramos MH, Uribe M. Metabolic syndrome as a risk factor for gallstone disease. *World J Gastroenterol* 2005; **11**: 1653-1657

15 **Chou P**, Liao MJ, Kuo HS, Hsiao KJ, Tsai ST. A population survey on the prevalence of diabetes in Kin-Hu, Kinmen. *Diabetes Care* 1994; **17**: 1055-1058

16 **Diabetes mellitus.** Report of a WHO Study Group. *World Health Organ Tech Rep Ser* 1985;**727**:1-113

17 **World Health Organization**. Definition, diagnosis and classification of diabetes mellitus and its complications: Report of a WHO Consultation. Part 1 Diagnosis and classification of diabetes mellitus. Geneva, *World Health Organization* 1999

18 **Liu CM,** Tung TH, Liu JH, Chen VT, Lin CH, Hsu CT, Chou P. A community-based epidemiological study of elevated serum alanine aminotransferase levels in Kinmen, Taiwan. *World J Gastroenterol* 2005; **11: 1616-1622**

19 **Matthews DR**, Hosker JP, Rudenski AS, Naylor BA, Treacher DF, Turner RC. Homeostasis model assessment: insulin resistance and beta-cell function from fasting plasma glucose and insulin concentrations in man. *Diabetologia* 1985; **28**: 412-419

20 **Méndez-Sánchez N**, Cárdenas-Vázquez R, Ponciano-Rodríguez G, Uribe M. Pathophysiology of cholesterol gallstone disease. *Arch Med Res* 1996; **27**: 433-441

21 **Chen CY**, Lu CL, Lee PC, Wang SS, Chang FY, Lee SD. The risk factors for gallstone disease among senior citizens: an Oriental study. *Hepatogastroenterology* 1999; **46**: 1607-1612

22 **Bouchier IAD**. Gallstones: formation and epidemiology. In: Blumgart LH ed. Surgery of the liver and biliary tract. *Edinburgh: Churchill linvingstone*, 1998: pp503-516.

23 **Pacchioni M**, Nicoletti C, Caminiti M, Calori G, Curci V, Camisasca R, Pontiroli AE. Association of obesity and type II diabetes mellitus as a risk factor for gallstones. *Dig Dis Sci* 2000; **45**: 2002-2006

24 **Kodama H**, Kono S, Todoroki I, Honjo S, Sakurai Y, Wakabayashi K, Nishiwaki M, Hamada H, Nishikawa H, Koga H, Ogawa S, Nakagawa K. Gallstone disease risk in relation to body mass index and waist-to-hip ration in Japanese men. *Int J Obes Relat Metab Disord* 1999; **23**: 211-216

25 **Kono S**, Shinchi K, Todoroki I, Honjo S, Sakurai Y, Wakabayashi K, Imanishi K, Nishikawa H, Ogawa S, Katsurada M. Gallstone disease among Japanese men in relation to obesity, glucose intolerance, exercise, alcohol use, and smoking. *Scand J Gastroenterol* 1995; **30**: 372-376

26 **Heaton KW,** Braddon FE, Emmett PM, Mountford RA, Hughes AP, Bolton CH. Why do men get gallstones? Roles of abdominal fat and hyperinsulinemia. *Eur J Gastroenterol Hepatol* 1991; **3**: 745-751

27 **Jørgensen T**. Gall stones in a Danish population. Relation to weight, physical activity, smoking, coffee consumption, and diabetes mellitus. *Gut* 1989; **30**: 528-534

28 **Maurer KR**, Everhart JE, Knowler WC, Shawker TH, Roth HP. Risk factors for gallstone disease in the Hispanic populations of the United States. *Am J Epidemiol* 1990; **131**: 836-844

29 **Misciagna G**, Guerra V, Di Leo A, Correale M, Trevisan M. Insulin and gall stones: a population case control study in southern Italy. *Gut* 2000; **47**: 144-147

30 **Hahm JS**, Park JY, Park KG, Ahn YH, Lee MH, Park KN. Gallbladder motility in diabetes mellitus using real time ultrasonography. *Am J Gastroenterol* 1996; **91**: 2391-2394

31 **Gielkens HA**, Lam WF, Coenraad M, Frolich M, van Oostayen JA, Lamers CB , Masclee AA. Effect of insulin on basal and cholecystokinin-stimulated gallbladder motility in humans. *J Hepatol* 1998; **28**: 595-602

32 **Palmer JP**, Fleming GA, Greenbaum CJ, Herold KC, Jansa LD, Kolb H, Lachin JM, Polonsky KS, Pozzilli P, Skyler JS, Steffes MW. C-peptide is the appropriate outcome measure for type 1 diabetes clinical trials to preserve beta-cell function: report of an ADA workshop , 21-22 October 2001. *Diabetes* 2004; **53**: 250-64

33 **Toffolo G**, De Grandi F, Cobelli C. Estimation of beta-cell sensitivity from intravenous glucose tolerance test C-peptide data. Knowledge of the kinetics avoids errors in modeling the secretion. *Diabetes* 1995; **44**: 845-854

34 **Emoto M**, Nishizawa Y, Maekawa K, Hiura Y, Kanda H, Kawagishi T, Shoji T, Okuno Y, Morii H. Homeostasis model assessment as a clinical index of insulin resistance in type 2 diabetic patients treated with sulfonylureas. *Diabetes Care* 1999; 22: 818-822

35 **Bonora E**, Targher G, Alberiche M, Bonadonna RC, Saggiani F, Zenere MB, Monauni T, Muggeo M. Homeostasis model assessment closely mirrors the glucose clamp technique in the assessment of insulin sensitivity: studies in subjects with various degrees of glucose tolerance and insulin sensitivity. *Diabetes Care* 2000; **23**: 57-63

Science Editor Wang XL and Guo SY **Language Editor** Elsevier HK

PO Box 2345, Beijing 100023, China
www.wjgnet.com
wjg@wjgnet.com

ELSEVIER

World J Gastroenterol 2005;11(45):7165-7168
World Journal of Gastroenterology ISSN 1007-9327

• *RAPID COMMUNICATION* •

Evaluation of immunogenicity and reactogenicity of recombinant DNA hepatitis B vaccine produced in India

Zahid Hussain, Syed S Ali, Syed A Husain, Mohammad Raish, Deepika R Sharma, Premashis Kar

Zahid Hussain, Premashis Kar, PCR Hepatitis Laboratory, Department of Medicine, Maulana Azad Medical College, New Delhi 110002, India
Syed S Ali, Deepika R Sharma, Panacea Biotec Ltd, Industrial Estate, Mathura Road, New Delhi 110044, India
Zahid Hussain, Syed A Husain, Mohammad Raish, Human Genetics Laboratory, Department of Biosciences, Jamia Millia Islamia, New Delhi 110025, India
Supported by the Panacea Biotec Limited, New Delhi 110044, India
Co-first author: Zahid Hussain
Correspondence to: Dr Premashis Kar, Department of Medicine, Maulana Azad Medical College, New Delhi 110002, India. pkar@vsnl.com
Telephone: +91-11-23230132 Fax: +91-11-23230132
Received: 2004-11-23 Accepted: 2005-01-26

Abstract

AIM: (1) To gain information on immune responses to an accelerated schedule of 0, 1, and 2 mo in paramedical staff and BDS students who are at an increased risk of getting hepatitis B infection and come under high risk groups. (2) To assess the efficacy and safety of *Enivac-HB* in different age groups, using genetically modified yeast strain *Pichia pastoris,* a new recombinant hepatitis B vaccine developed and manufactured in India.

METHODS: A prospective, comparative, and single blinded trial of rapid (0, 1, and 2 mo) hepatitis B immunization schedulewas reported. A total of three hundred and seven (212 females and 95 males) healthy volunteers divided into three age groups (18-29, 30-39, and 40-49) were enrolled after screening for markers of hepatitis B. All the volunteers received 20 mg of the vaccine intramuscularly at 0, 1, and 2 mo.

RESULTS: Geometric mean titers were calculated pre and post vaccination. Before immunization the GMT was 0.0124 mIU/mL. One month after the administration of the third dose of recombinant vaccine 296/307 (96.5%) subjects achieved seroprotective levels of anti-HBs. The geometric mean anti-HBs titers achieved after one month of the third dose was 2 560.0 mIU/mL. The geometric mean anti-HBs titer of males was 2 029.0 mIU/mL, while that of the females was 2 759.0 mIU/mL. In the age group of 18-29 years, anti-HBs titer was 3 025.0 mIU/mL, while that in the age group of 30-39 years was 2 096.0 mIU/mL. In third age group of 40-49 years, anti-HBs titer was 1 592.0 mIU/mL. Hyper-responses (anti-HBs$\geqslant$100 mIU/mL) were shown in 88.0% (271/307) of subjects. Eleven (3.5%) subjects responded poorly to the vaccine in the age group of 40-49 years. There was only mild pain at the site of injection otherwise there were no other adverse drug reactions (ADRs).

CONCLUSION: This vaccine (*Enivac-HB*) is safe and efficacious, providing significant protection after the third dose and rapid hepatitis B immunization schedule of 0, 1, and 2 mo can be recommended whenever rapid protection is the goal.

Key words: *Enivac-HB*; *Pichia pastoris*; Anti-HBs antibody; Hepatitis B vaccine

Hussain Z, Ali SS, Husain SA, Raish M, Sharma DR, Kar P. Evaluation of immunogenicity and reactogenicity of recombinant DNA hepatitis B vaccine produced in India. *World J Gastroenterol* 2005; 11(45): 7165-7168
http://www.wjgnet.com/1007-9327/11/7165.asp

INTRODUCTION

Hepatitis B virus (HBV) infection is responsible for a high proportion of the worlds cases of cirrhosis, and is the cause of up to 80% of all cases of hepatocellular carcinoma (HCC)[1,2]. The situation is grim in developing countries like India, where blood bank infrastructure is non-existent outside the major metropolitan cities and safe blood handling practice standards are low[3]. The weighed prevalence of hepatitis B in India has been estimated to be 4.7%[4,5], which makes this an intermediate prevalence country.

Hepatitis B vaccination has been one of the success stories of the 20th century and has been extensively used in a wide range of groups throughout the world. Hepatitis B vaccination program have successfully reduced the prevalence of hepatitis B, in Taiwan[6] where universal HBV vaccination has led to a significant reduction of hepatitis B prevalence and incidence of hepatocellular carcinoma in children. The immunogenicity, efficiency, and safety profile of hepatitis B vaccine has been well established. More than 90% seroconversion has been achieved in adult populations consistently[7-10]. The safety profile of the recombinant hepatitis B vaccine has been very good[11].

Numerous genetically engineered hepatitis B vaccines are available in India today. However, vaccines do differ in terms of latency (time taken for the production of effective antibodies), reactogenicity and price. Newer technologies involving more advanced yeast strains like *Pichia pastoris*[12] used for manufacturing the vaccines are today revolutionizing genetically engineered hepatitis B vaccines.

The aim of the study was (1) to gain information on immune responses to an accelerated schedule of 0, 1, and 2 mo in paramedical staff and BDS students who are at an increased risk of getting hepatitis B infection and come under high risk groups. (2) To assess the efficacy and safety of *Enivac-HB* in different age groups, using genetically modified yeast strain *P pastoris,* a new recombinant hepatitis B vaccine developed and manufactured in India.

MATERIALS AND METHODS

Blood samples

The study was conducted in Maulana Azad Medical College, New Delhi for over the period of 6 mo (October 2002-April 2003). Five milliliters of blood sample was taken by venipuncture with the informed consent of all the 317 volunteers. Serum sample was separated and stored at -20 ℃ to perform various serological tests.

Clinical protocol

Permission to conduct this study on adult human volunteers was obtained from Drugs Controller of India. The Institute Ethics Committee approved the study protocol. The study population consisted of 317 volunteers. The following inclusion criteria had to be met. The subjects had to be tested negative for hepatitis B surface antigen (HBsAg), anti-hepatitis B surface antibody (anti-HBs), and anti-hepatitis B core antibody, IgM anti-HBe, IgG anti-HBe and subjects had to be at least 18 years of age and had to sign an informed consent. Subjects were excluded from the study if they had been previously vaccinated with HBV vaccine; or if they were presently taking immunosuppressive drugs; or had a history of hypersensitivity to yeast; or had to receive immunoglobulins, blood or blood products within the previous 6 mo. Subjects who were pregnant, who had significant hematological, hepatic, renal, cardiac or respiratory diseases or who had participated in any other trial 30 d before or during the present study were excluded. Physical examination such as pulse, blood pressure, temperature, and edema were checked. All the 307 healthy seronegative volunteers of the age ranging between 18 and 49 years were recruited for participating in the vaccination schedule of 0, 1, and 2 mo.

HBV vaccination

Of the 317 volunteers, 307 volunteers, who were negative for all the serological markers of hepatitis B infection, completed the hepatitis B vaccination program. Seven were positive for HBV markers and three volunteers had high anti-HBs titers. All the 307 volunteers received the three doses of HBV vaccination. The subjects were administered 1 mL (20 mg of recombinant DNA) of hepatitis B (*Enivac-HB*) vaccine intramuscularly in the deltoid muscle according to the following schedule: 1st dose-0 d, 2nd dose -30 d after the 1stdose, 3rddose-60 d after the 1stdose. Vaccinees were monitored for adverse events closely for 3 d after each dose, i.e. fever, pain at the site of injection, erythema, and swelling, nausea, rash, fatigue, bodyache, and scored as absent, mild, moderate or severe. Samples for anti-HBs antibody titers were determined at 0 and 90 d. Anti-HBs antibodies were done using a commercially available quantitative ELISA kit (AUSAB-EIA, Abbot Labs, USA). Protection with hepatitis B vaccination was considered to be achieved when the concentration of anti-HBs antibody titers was $\geqslant$10 mIU/mL. A non-response was defined as anti-HBs antibody titers $\leqslant$10 mIU/mL[13], responders were those with titer levels $\geqslant$10 mIU/mL and $\leqslant$100 mIU/mL, high responders were those with anti-HBs titers $\geqslant$100 mIU/mL, and those with titers $\geqslant$1 000 mIU/mL was hyper-responder[13].

Vaccine

A new recombinant DNA hepatitis B vaccine (*Enivac-HB*, Panacea Biotec, India) containing hepatitis B surface antigen (s-gene) produced in genetically engineered yeast *P pastoris* cells[12] was evaluated. A derivative of the plasmid V322 carrying hepatitis B viral DNA was used to amplify the HBsAg. The s-gene isolated from hepatitis B was placed in *P pastoris* cell. The HBsAg nucleotide sequence[14] was purified to >95% by adsorption by the antigen in the cellular extract to colloidal silica, followed by its desorption, ion exchange chromatography and ultracentrifugation. The vaccine was prepared by adsorbing the purified HBsAg onto aluminum hydroxide gel (0.5 mg aluminum per dose) and thiomersal was added as a preservative to a final concentration of 0.05 mg/dL. *P pastoris* is the most advance second generation yeast strain with proven advantages over other yeast strains like *Saccharomyces cerevisiae*[12] which is used in the manufacturing process of many commercially available genetically engineered hepatitis B vaccines in India. The yeast strain *P pastoris* can grow at a highly acidic pH that becomes a barrier for growth of many contaminating microbes during the process of fermentation[12]. In short, the manufacturing process itself is a purification procedure. The yield of hepatitis B surface antigen obtained with this strain of *P pastoris* is higher and it means per liter more surface antigen is obtained with *P pastoris* than with many other strains[12]. *Enivac-HB* is manufactured using a technology that is free from toxic substances like cesium chloride[12]. Some commercially available vaccines in India are known to use technology that involves the usage of cesium chloride[12]. This advantage automatically translates into lesser contamination and hence, lesser chances of reactogenicity[12].

Statistical analysis

Seroconversion and seroprotection were compared by

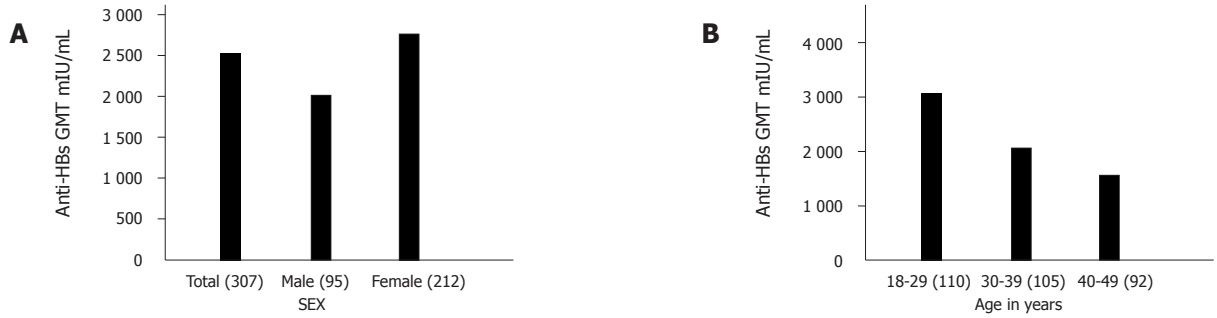

Figure 1 Efficacy of *Enivac-HB* in study participants by gender variation (**A**) and age (**B**) on the 90th d evaluation after the initial vaccination. The anti-HBs titer is expressed in milli-international unit per milliliter.

descriptive statistics. Geometric mean titers (GMTs) pre and post-vaccinations were compared by Student's *t* test. $P<0.05$ was compared as statistically significant (95%CI).

RESULTS

A total of 317 subjects were screened, 307 subjects negative for all the serological markers of hepatitis B were enrolled in the study. The mean age of the study group was 33.5±9.4 years, with 95 male subjects and 212 female subjects. Dose schedules were 0, 1, and 2 mo. Adverse events were recorded by specifically interviewing each subject during the entire duration of the study. The adverse drug reactions (ADRs) were assessed closely for 3 d after each dose and that no vaccinee had fever or any other designated systemic complaint with only mild pain at the site in 79%, 84.9%, and 75.4% of the vaccinees following doses 1, 2, and 3, respectively. Hematological and biochemical parameters were normal in all the subjects at the end of the study compared to the baseline value. None of the patients became HBsAg and/or anti HBe positive during the follow-up period. "The geometric mean anti-HBs titer" at the initiation of the vaccination program was 0.124 mIU/mL. One month after the administration of the third dose of recombinant vaccine, 296/307 (96.5%) subjects achieved seroprotective levels of anti-HBs antibodies. "The geometric mean anti-HBs titer" achieved after one month of the third dose was 2 560.0 mIU/mL geometric mean titers. "The geometric mean anti-HBs titer" of males was 2 029.0 mIU/mL, while that of females was 2 759.0 mIU/mL as shown in Figure 1A. In the age group of 18-29 years, anti-HBs titer was 3 025.0 mIU/mL, while that of 30-39 years was 2 096.0 mIU/mL. In 40-49 years of age, anti-HBs titer was 1 592.0 as shown in Figure 1B. The above value is statistically significant with $P<0.05$, and had 95%CI. Hyper-responses (anti-HBs ≥100 mIU/mL) was shown by 88.0% (271/307; $P<0.05$) of subjects. Twenty subjects all in the age group of 40-49 were (11/307; 3.5%) non-responders, with the geometric mean anti-HBs titers 8.60 mIU/mL. The mean age of the 11 non-responders was 46.4±6.9 years, 1.3% (4) males and 2.2% (7) females were non-responders but the difference was not statistically significant.

DISCUSSION

Accelerating the vaccination schedule against hepatitis B is appealing because it may increase patient compliance and provide earlier protection for the people who are already in a high risk group or environment. A comparative Indian study of HBV vaccine in three age groups, 18-29, 30-39, and 40-49 years, was done. The experimental data obtained during the course of the trial indicated that seroprotection one month[15] after the third dose was (96.5%) with mean geometric anti-HBs titers 2 560.0 mIU/mL. Twenty subjects all in the age group of 40-49 years (11/307; 3.5%) showed low response to the vaccine and demonstrated an antibody titer of 8.60 mIU/mL. While all the subjects in rest of the age group achieved 100% seroconversion. Risk factors that have been associated with non-response to hepatitis B vaccine include increasing age, male gender, obesity, history of smoking, administration of vaccine in buttock rather than deltoid[5]. The relationship of hepatitis B vaccination response with age is controversial. Our study suggests that seroconversion in age group >40 years is 79% which is considered high compared to most other studies[16,17] where seroconversion rate of 60% has been reported. However, as all the above studies, we too found a decreasing seroconversion rate with increasing age. These findings favor the hypothesis that increasing age decreases seroprotective antibody formation after vaccination.

In the present clinical study, it was observed that female volunteers showed a better response in comparison to male volunteers ($P<0.001$). Jilg *et al*[18] reported a slightly lower response in males and Dentico *et al*[19] also reported that the sex factor is one of the parameters influencing the response following vaccination. Whether or not there exists a sex related variation of the immunogenic response is still controversial.

The vaccination schedule (0, 1, and 2 mo) employed in the present study has been well studied in the other trials[15-19]. Marsano *et al*[20] have established that the 0, 1, and 2 mo schedule of vaccination gives a rate that is quicker than and identical to the rate of seroprotection of the standard schedule of vaccination of 0, 1, and 6 mo and is much quicker. The recombinant yeast-derived vaccine evaluated did not produce any severe adverse reactions. There was only mild pain at the site of injection otherwise

it was completely safe with no adverse drug reactions.

From the present data, we can confirm that the *Enivac-HB* is highly immunogenic. This new indigenously manufactured vaccine using *P pastoris* as yeast strain is safe and provides effective titers against hepatitis B. In a country with an estimated 40 million or more carriers of the hepatitis B virus and an estimated 18 million newborns each year, the availability of an indigenously manufactured vaccine would probably make it easier to include the vaccine in a community-based program.

The study conclusively proves that the recombinant DNA hepatitis B vaccine (*Enivac-HB*) produced using genetically engineered yeast cell *P pastoris* appears to be highly immunogenic and safe and confers a seroprotection of 96.5% of the subjects with 88.0% showing hyper-response. The study suggests that the vaccine appears to be well tolerated and the rapid vaccination schedule of 0, 1, and 2 mo can be recommended whenever rapid protection is the goal.

ACKNOWLEDGMENTS

The vaccines and finance for the clinical study were provided by Panacea Biotec Limited, New Delhi, India. The authors are grateful to Mrs Alice Jacob, a member of PCR Hepatitis Laboratory, New Delhi, India for helping us during the study.

REFERENCES

1 Report of a WHO meeting: prevention of liver cancer, technical report no. 691,World Health Organization, Geneva, 1983: 8-9
2 **Ghendon Y.** WHO strategy for the global elimination of new cases of hepatitis B. *Vaccine* 1990; **8** Suppl: S129-S133; discussion S134-S138
3 **Das K,** Gupta RK, Kumar V, Kar P. Immunogenicity and reactogenicity of a recombinant hepatitis B vaccine in subjects over age of forty years and response of a booster dose among nonresponders. *World J Gastroenterol* 2003; **9**: 1132-1134
4 **Thyagarajan SP,** Jayararn S, Mohanvalli B. Prevalence of HBV in the general population of India. In: Sarin SK, Singhal AK, editors. Hepatitis B in India: problems and prevention. New Delhi: CBS Publishers, 1996: 5-16
5 **Tandon BN.** Dimension and issues of HBV control in India ' Hepatitis B in India: problems and prevention' (ed) Sarin SK and Singal AK 1996
6 **Chen CJ**, You SL, Lin LH, Hsu WL, Yang YW. Cancer epidemiology and control in Taiwan: a brief review. *Jpn J Clin Oncol* 2002; **32 Suppl**: S66-S81
7 **Arslanoğlu I,** Cetin B, Işgüven P, Karavuş M. Anti-HBs response to standard hepatitis B vaccination in children and adolescents with diabetes mellitus. *J Pediatr Endocrinol Metab* 2002; **15**: 389-395
8 **Cook IF**, Murtagh J. Comparative immunogenicity of hepatitis B vaccine administered into the ventrogluteal area and anterolateral thigh in infants.*J Paediatr Child Health* 2002; **38**: 393-396
9 **Abraham B,** Baine Y, De-Clercq N, Tordeur E, Gerard PP, Manouvriez PL, Parenti DL. Magnitude and quality of antibody response to a combination hepatitis A and **hepatitis** B vaccine. *Antiviral Res* 2002; **53**: 63-73
10 **Cassidy WM.** Adolescent hepatitis B vaccination. A review. *Minerva Pediatr* 2001; **53**: 559-566
11 **Elkayam O**, Yaron M, Caspi D. Safety and efficacy of vaccination against hepatitis B in patients with rheumatoid arthritis. *Ann Rheum Dis* 2002; **61**: 623-625
12 **Cregg JM,** Vedvick TS, Raschke WC. Recent advances in the expression of foreign genes in *Pichia pastoris*. *Biotechnology* (N Y) 1993; **11:** 905-910
13 **Belloni C,** Pistorio A, Tinelli C, Komakec J, Chirico G, Rovelli D, Gulminetti R, Comolli G, Orsolini P, Rondini G. Early immunisation with hepatitis B vaccine: a five-year study. *Vaccine* 2000; **18**: 1307-1311
14 **Valenzuela P,** Gray P, Quiroga M, Zaldivar J, Goodman HM, Rutter WJ. Nucleotide sequence of the gene coding for the major protein of hepatitis B virus surface antigen. *Nature* 1979; **280**: 815-819
15 **Elavia AJ,** Marfatia SP, Banker DD. Immunization of hospital personnel with low-dose intradermal hepatitis B vaccine. *Vaccine* 1994; **12**: 87-90
16 **Looney RJ,** Hasan MS, Coffin D, Campbell D, Falsey AR, Kolassa J, Agosti JM, Abraham GN, Evans TG. Hepatitis B immunization of healthy elderly adults: relationship between naive CD4+ T cells and primary immune response and evaluation of GM-CSF as an adjuvant. *J Clin Immunol* 2001; **21**: 30-**36**
17 **Bennett RG,** Powers DC, Remsburg RE, Scheve A, Clements ML. Hepatitis B virus vaccination for older adults. *J Am Geriatr Soc* 1996; **44**: 699-703
18 **Jilg W,** Lorbeer B, Schmidt M, Wilske B, Zoulek G, Deinhardt F. Clinical evaluation of a recombinant hepatitis B vaccine. *Lancet* 1984; **2**: 1174-1175
19 **Dentico P,** Buongiorno R, Volpe A, Zavoianni A, Pastore G, Schiraldi O. Long-**term immunogenicity safety and efficacy** of a recombinant hepatitis B vaccine in healthy adults. *Eur J Epidemiol* 1992; **8**: 650-655
20 **Marsano LS,** Greenberg RN, Kirkpatrick RB, Zetterman RK, Christiansen A, Smith DJ, DeMedina MD, Schiff ER. Comparison of a rapid hepatitis B immunization schedule to the standard schedule for adults. *Am J Gastroenterol* 1996; **91**: 111-115

Science Editor Wang XL and Guo SY **Language Editor** Elsevier HK

PO Box 2345, Beijing 100023, China
www.wjgnet.com
wjg@wjgnet.com

ELSEVIER

World J Gastroenterol 2005;11(45):7169-7173
World Journal of Gastroenterology ISSN 1007-9327

• *RAPID COMMUNICATION* •

Bone disorders in experimentally induced liver disease in growing rats

Viktória Ferencz, Csaba Horváth, Béla Kári, János Gaál, Szilvia Mészáros, Zsuzsanna Wolf, Dalma Hegedűs, Andrea Horváth, Anikó Folhoffer, Ferenc Szalay

Viktória Ferencz, Csaba Horváth, Szilvia Mészáros, Zsuzsanna Wolf, Dalma Hegedűs, Andrea Horváth, Anikó Folhoffer, Ferenc Szalay, 1st Department of Internal Medicine, Semmelweis University, Budapest, Hungary
Béla Kári, Department of Diagnostic Radiology and Oncotherapy, Semmelweis University, Budapest, Hungary
János Gaál, Department of Polymer Engineering and Textile Technology, Budapest University of Technology and Economics, Hungary
Supported by The Medical Research Council of Hungary, ETT 226/2003, 232/2003, and The Hungarian Scientific Research Fund, OTKA T038067, T038154
Correspondence to: Professor Ferenc Szalay, MD, PhD, 1st Department of Internal Medicine, Semmelweis University, Korányi S. 2/A, H-1083 Budapest, Hungary. szalay@bel1.sote.hu
Telephone: +36-1-210-1007 Fax: +36-1-210-1007
Received: 2005-01-05 Accepted: 2005-04-30

Abstract

AIM: To investigate the change of bone parameters in a new model of experimentally induced liver cirrhosis and hepatocellular carcinoma (HCC) in growing rats.

METHODS: Fischer-344 rats (n = 55) were used. Carbon tetrachloride (CCl_4), phenobarbital (PB), and a single diethylnitrosamine (DEN) injection were used. Animals were killed at wk 8 and 16. Bone mineral content, femoral length, cortical index (quotient of cortical thickness and whole diameter) and ultimate bending load (F_{max}) of the femora were determined. The results in animals treated with DEN+PB+CCl_4 (DPC, n = 21) were compared to those in untreated animals (UNT, n = 14) and in control group treated only with DEN+PB (DP, n = 20).

RESULTS: Fatty liver and cirrhosis developed in each DPC-treated rat at wk 8 and HCC was presented at wk 16. No skeletal changes were found in this group at wk 8, but each parameter was lower (P<0.05 for each) at wk 16 in comparison to the control group. Neither fatty liver nor cirrhosis was observed in DP-treated animals at any time point. Femoral length and F_{max} values were higher (P<0.05 for both) in DP-treated animals at wk 8 compared to the UNT controls. However, no difference was found at wk 16.

CONCLUSION: Experimental liver cirrhosis and HCC are accompanied with inhibited skeletal growth, reduced bone mass, and decreased mechanical resistance in growing rats. Our results are in concordance with the data of other studies using different animal models. A novel finding is the transiently accelerated skeletal growth and bone strength after a 8-wk long phenobarbital treatment following diethylnitrosamine injection.

Key words: Bone disorder; Bone mineral content; Mechanical resistance; Experimental liver cirrhosis; Growing rat

Ferencz V, Horváth C, Kári B, Gaál J, Mészáros S, Wolf Z, Hegedűs D, Horváth A, Folhoffer A, Szalay F. Bone disorders in experimentally induced liver disease in growing rats. *World J Gastroenterol* 2005; 11(45): 7169-7173
http://www.wjgnet.com/1007-9327/11/7169.asp

INTRODUCTION

Metabolic bone disease is a common complication of chronic liver diseases[1-4]. However, the pathogenesis is not fully understood and is scarcely investigated in an animal model. Both increased bone resorption[5-7] and decreased bone formation[8-11] have been described in chronic liver diseases. Decreased bone density[10] and impaired microarchitecture[12] are associated with increased fracture risk[13]. Though several methods are available to examine different aspects of bone metabolism, there is not a single test to define the quality of bones. We have investigated how the bone mineral content (BMC), cortical thickness, bone length, and mechanical loading capacity of femora were changed during the development of experimentally induced fatty liver, liver cirrhosis, and HCC in growing rats. No published data are available on simultaneous measurements of these parameters in growing rats. We used a new cirrhosis model in this study. Our results are in concordance with those of other studies. Novel finding is the transiently accelerated skeletal growth and bone strength after a 8-wk long phenobarbital treatment following diethylnitrosamine injection.

MATERIALS AND METHODS

Animals and induction of liver diseases

A total of 60 male Fisher-344 rats, weighing 273.3±38.7 g, were included and 55 rats survived the study protocol.

Table 1 Serum parameters and body weight in UNT, DP-treated control and DPC-treated rats at wk 8 and 16 (mean±SD)

Parameter	UNT control (wk 8) $n = 8$	UNT control (wk 16) $n = 6$	DP control (wk 8) $n = 10$	DP control (wk 16) $n = 10$	DPC (wk 8) $n = 10$	DPC (wk 16) $n = 11$
Bilirubin (mmol/L)	1.8±1.2	2.1±1.3	1.85±0.9	0.88±0.3	48.14±66[a]	1.31±0.5
ALP (U/L)	735.7±89.3	619.5±96.3	493.9±52.3	402.8±80.2	1 354±1 108[a]	437.8±116.2
AST (U/L)	112.7±13.3	158.8±40.9	157.3±52.9	127.5±43.3	7 095±5 483[a]	115.8±15
ALT (U/L)	69.42±8.9	107.8±12.1	158.5±78.4	93.1±71.1	5 175±3 675[a]	81.54±17.9
Albumin (g/L)	32.85±0.4	34.66±1	33.6±2.2	37.4±1.2	27.8±3[a]	35.36±1.6
Body weight (g)	240.1±14.3	321.8±48.9	269.4±12.1	307.7±11.3	227.4±16.4	284.2±25.2

[a]$P<0.05$ *vs* for comparison between DPC and both UNT and DP controls at wk 8.

The animals were housed in steel cages (5 rats/cage) in an air-conditioned room with a relative humidity of 55%. Tap water and pelleted rodent chow (CRLT/N, Farmer Product Ltd, Hungary) were available *ad libitum*. The Animal Care and Use Committee of Semmelweis University, Faculty of Medicine approved all the animal procedures.

Fatty liver and liver cirrhosis were induced by the administration of CCl_4 (0.5 mL/kg body weight, dissolved in sunflower oil, administered thrice a week by intragastric tube) and phenobarbital (PB, phenobarbital-Na; Sigma, St. Louis, MO, USA, tap water was replaced by 0.05% of PB-solution after a 12-h fasting, daily) throughout the 8-wk treatment following a single injection of diethylnitrosamine (DEN; Serva, Heidelberg, at a dose of 200 mg/kg body weight, dissolved in 0.9% NaCl solution). HCC developed at wk 16 as described earlier[14]. Animals were killed at wk 8 and 16 under light ether-anesthesia (all animals were fasted for 24 h prior to killing).

Results in animals treated with DEN+PB+CCl_4 (group DPC, $n = 21$) were compared to those in untreated animals (group UNT, $n = 14$) and in control group treated only with DEN+PB (group DP, $n = 20$).

Biochemical tests

Serum bilirubin, alkaline phosphatase (ALP), aspartate aminotransferase (AST), and alanine aminotransferase (ALT) as well as albumin were measured using the Olympus AU600 autoanalyzer (Olympus Ltd, Japan).

Pathological investigation of liver

Livers were macroscopically and histologically investigated. Slices from the removed liver were fixed in 8% buffered formalin and embedded in paraplast. Picrosirius red, H&E, and PAS staining were used for histological examination[14]. Hepatic fibrosis, cirrhosis[15], and lesions[16] were classified according to the international recommendations.

Bone investigation

Partial carcass preparation was performed. The left rear limb was carefully dissected free from the iliac acetabulum with the head of the femur preserved. Then, the isolated femur was prepared by dissecting from the tibia along with the remaining muscles and ligaments and stored in saline-soaked gauze at -20 ℃ until further testing.

Radiological studies

Soft radiographs were performed using an X-ray imaging system (Siemens Mammomat 3000, Germany) with exposure at 25 kVp, 10 mAs on the femur. Femora were carefully positioned anteroposteriorly. Exposure period was 0.3 s. Exposed plates (Agfa, Germany) were analyzed using OSIRIS imaging software. Femoral length (mm) was measured and the values were validated by an aluminum phantom (1 mm in diameter). Each exposure included both the phantoms and the investigated bone. Cortical index was calculated: cortical thickness divided by the whole diameter at the mid-point of medial diaphysis.

Bone densitometry

Using an I-125 source (1 000 MBq initial activity from Nordion), a water-bath system (single photon absorption, SPA) device (NK364/A, Gamma Technical Corporation, Budapest, Hungary) was used to determine the BMC in mg/cm. A precise, replaceable and narrow collimator was made for the source holder for the *in vitro* animal experiments. Aluminum phantoms (Gamma Technical Corporation, Budapest, Hungary) were used for the calibration. The femora were fixed by sellotape on a water equivalent plastic sheet and then placed on the attenuation block. The attenuation block was 2 cm wide. BMC value was measured at the mid-point of the medial diaphysis.

Biomechanical testing

Biomechanical tests were carried out by a computer-controlled testing device (Zwick-020, Zwick, Ulm, Germany) using the whole bone specimens. The anteroposterior three-point bending test of the femoral shaft was performed as previously described[17]. The femur was placed on a testing bearer, and the distance between the supporting rods was fixed at 15.7 mm. Force was elicited by a rod at a constant deformation rate of 2 mm/min at a right angle to the anterior midpoint of the femoral midshaft. We determined the ultimate bending load of the whole bone specimen (F_{max}, N). The F_{max} was corrected by BMC (load/density, N/mg/cm) and cortical index (described above, load/cortical index, N/mm/mm) of femoral midshafts avoiding the impact of BMC and cortical index on bone strength.

Statistical analysis

Mann-Whitney test was used for intergroup comparisons.

Table 2 Femur length, cortical index, BMC, and ultimate bending load of femoral mid-diaphysis and corrected loading data for cortical index and BMC in UNT, DP-treated control and DPC-treated rats at wk 8 and 16 (mean±SD)

Parameter	UNT control (wk 8) $n = 8$	UNT control (wk 16) $n = 6$	DP control (wk 8) $n = 10$	DP control (wk 16) $n = 10$	DPC (wk 8) $n = 10$	DPC (wk 16) $n = 11$
Femur length(mm)	34.8±1.0	40.1±1.2	37.9±0.6	40.2±0.8	36.8±0.8	38.6±0.9
Cortical index (mm/mm)	0.277±0.026	0.325±0.029	0.287±0.015	0.33±0.018	0.285±0.021	0.286±0.036
BMC (mg/cm)	0.049±0.005	0.06±0.008	0.056±0.003	0.057±0.002	0.047±0.006	0.049±0.004
Femur F_{max} (N)	88.3±14.3	123.2±13.0	111.8±7.9	118.5±6.02	93.8±5.41	96.5±12.6
F_{max}/Cortical index (N/mm/mm)	328.7±53.4	382.6±62.5	390.4±32.4	359.8±24.25	331.1±35.4	339.9±46.5
F_{max}/BMC (N/mg/cm)	1 796±239	2 049±95.2	2 000±124	2 075±114.6	2 019±195	1 961±115.9

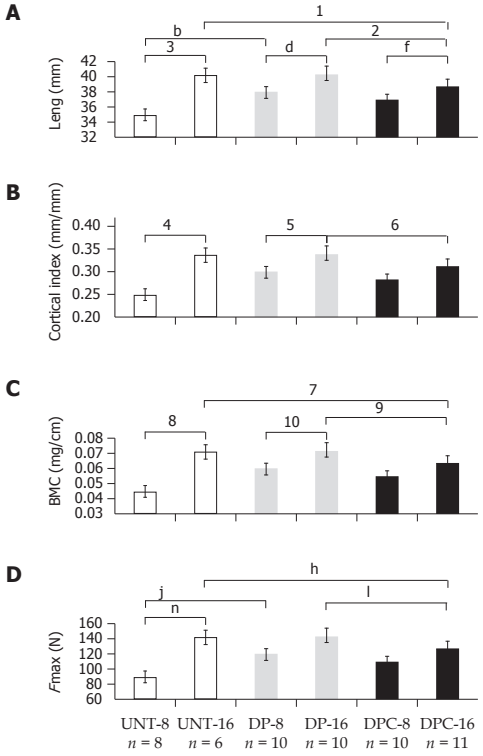

Figure 1 Mean±SD of femur length (**A**), cortical index of femoral midshaft (**B**), BMC of femur in mid-point of medial diaphysis (**C**), and ultimate bending load of femoral midshaft (**D**) in UNT, DP-treated control and DPC-treated rats at wk 8 and 16. A: [1]$P = 0.020$, [2]$P = 0.002$ *vs* DPC-16, [3]$P = 0.001$ *vs* UNT-8, [b]$P<0.001$ *vs* UNT-8, [d]$P<0.001$ *vs* DP-8, [f]$P<0.001$ *vs* DPC-8; B: [4]$P = 0.018$ *vs* UNT-8,[5]$P = 0.013$ *vs* DP-8, [6]$P = 0.004$ *vs* DPC-16; C:[7]$P = 0.001$ *vs* DPC-16, [8]$P = 0.002$ *vs* UNT-8, [9]$P = 0.016$ *vs* DPC-16, [10]$P = 0.003$ *vs* DP-8; D: [h]$P<0.001$ *vs* DPC-16, [j]$P<0.001$ *vs* UNT-8, [l]P<0.001 *vs* DPC-16, [n]$P<0.001$ *vs* UNT-8.

Pearson's parametric correlation test was applied for measuring the strength of a relationship between the two variables. $P<0.05$ was considered statistically significant. All statistical analyses were performed using SPSS version 10.0 for Windows (Chicago, IL, USA). Results were expressed as mean±SD.

RESULTS

Biochemical results, body weight, and liver histology

Serum parameters and body weight of UNT, DP- and DPC-treated rats are shown in Table 1. DPC-treated rats had elevated bilirubin, ALP, AST, and ALT ($P<0.001$ for each parameter) compared to UNT and DP-treated rats at wk 8. Serum albumin was decreased in DPC-treated animals at wk 8 compared to the other two groups ($P<0.001$). There were no differences in the laboratory values between the study groups at wk 16. No differences were found between DP-treated and UNT groups neither at wk 8 nor at wk 16.

Increased body weight was observed in UNT and DP-treated controls and DPC-treated rats from wk 8 to 16 ($P<0.001$). However, weight was reduced in DPC-treated in comparison to DP-treated group at wk 8 ($P<0.001$) and 16 ($P = 0.016$). DP-treated group had significantly higher body weight at wk 8 than UNT controls ($P<0.001$).

Liver histology showed inflammatory cell infiltrates, necrosis, fatty changes, regenerating nodules and cirrhosis in DPC-treated rats at wk 8 (10 out of 10 rats). Neoplastic nodules were found in five samples. Cirrhosis and HCC (11 out of 11) developed in DPC-treated group at wk 16. Normal hepatic histology was found in all UNT and DP-treated control rats.

Bone length, cortical index, bone mineral content and ultimate bending load of the femora

The femoral length increased in each group from wk 8 to 16 (Table 2, Figure 1A). However, animals treated with DPC had shorter femora than controls at wk 16. Femora were longer in DP-treated rats than in UNT controls at wk 8. Femoral length correlated with body weight ($r = 0.824$, $P<0.001$).

Significant increases of cortical index were seen in both UNT and DP-treated control rats (Table 2, Figure 1B). At wk 16, cortical index was smaller in DPC-treated animals than in DP-treated rats. Poor but significant correlation was measured between cortical index and BMC ($r = 0.362$, $P = 0.008$).

BMC increased only in UNT control rats from wk 8 to 16, indicating the physiological bone mineralization (Table 2, Figure 1C). DPC-treated rats had lower BMC than DP-treated rats at wk 8. BMC was lower in DPC-treated animals than in UNT and DP-treated control rats at wk 16. Body weight strongly correlated with BMC ($r = 0.748$, $P<0.001$).

Ultimate bending load increased from wk 8 to 16 in UNT controls (Table 2, Figure 1D). F_{max} in DP-treated rats was greater than that in UNT rats at wk 8. At wk 16,

F_{max} was smaller in DPC-treated rats than in both UNT and DP-treated controls. However, when we corrected the ultimate bending load by BMC or cortical index, no differences were found between the groups. Strong correlation was found between BMC and ultimate bending load ($r = 0.842$, $P<0.001$). Relationship was also found between F_{max} and cortical index ($r = 0.548$, $P<0.001$). F_{max} correlated with body weight ($r = 0.758$, $P<0.001$) and femoral length ($r = 0.751$, $P<0.001$).

DISCUSSION

Using a new model, we have found that bone disorders due to diethylnitrosamine, phenobarbital, and CCl_4 administration were characterized by decreased femoral length, reduced bone mass, and increased fragility after 16-wk long treatment in growing rats. Our findings on cortical bone mass are in concordance with other studies using different models of experimentally induced liver cirrhosis[18-21]. van der Merwe *et al*[22] found that the femoral length, the bone mass and the midshaft thickness were lower in CCl_4-treated rats after portosystemic shunting. Muguerza *et al*[23] found that the femoral density, the anteroposterior and lateromedial diameters and the ultimate bending load decreased in CCl_4-induced cirrhotic rats, but no significant differences were observed in the bone length. In our experiment, the age-dependent growth of femoral length, BMC and ultimate bending load were arrested as cirrhosis progressed and HCC developed. Tanaka *et al*[24] also found that longitudinal bone growth is reduced on the femora of rats with CCl_4-induced liver cirrhosis. Decreased bone mineral density has been observed in growing rats with liver cirrhosis induced by the administration of CCl_4 and phenobarbital[20].

In our study, DP-treated rats had longer femora and increased ultimate bending load than untreated control rats at wk 8, nevertheless BMC and cortical index did not differ from untreated controls. The stimulating skeletal effect of DP treatment at wk 8 might be caused by the enzyme inductor effect of phenobarbital. It is well known that phenobarbital induces not only xenobiotic-metabolizing cytochrome P450 (e.g. CYP2B1)[25] but also estrogen and vitamin D_3 synthesizer cytochrome P450 enzymes (CYP19A1, CYP27A1 CYP27B1, CYP3A4, CYP2D)[26-28]. Therefore, the increased longitudinal bone growth and ultimate bending load in DP-treated rats may be the consequence of enhanced estrogen and vitamin D activation. However, the increase in ultimate bending load was stunted after 8 wk in DP-treated rats. It is possible that bone maturation has become adapted to the accelerated skeletal growth and mineralization after 8 wk. In DPC-treated rats, only a tendency towards both longitudinal bone growth and ultimate bending load was observed in comparison to untreated controls at wk 8, suggesting that the adverse skeletal effect of CCl_4 does not allow to reveal stimulating effect of phenobarbital.

The biochemical parameters of liver function showed serious inflammation in DPC-treated rats at wk 8 corresponding to the histology showing fatty liver and inflammatory cell accumulation beyond the regenerating nodules. The decrease in serum albumin level at wk 8 in DPC-treated rats indicates the reduced synthetic capacity of the liver. Though biochemical and histological symptoms of steatohepatitis were present, it had no detectable negative effect on bone mass, bone length, cortical index and ultimate bending load at this time point, which is in concordance with results of van der Merwe *et al*[22] who did not find detectable bone disease in early stage liver dysfunction. Similar to human liver diseases, longer time is needed for the development of metabolic bone disease. Biochemical and histological signs of inflammation ceased in DPC-treated rats at wk 16, while fibrosis, cirrhosis with regenerative nodules and HCC foci dominated the histological picture. However, femoral length, BMC and ultimate bending load were stunted at this time point, which is in concordance with results of Figueiredo *et al*[29]. The mechanism is complex. The high level of hyperbilirubinemia detected at wk 8 could be one of the factors, since bilirubin has a direct inhibitory effect on osteoblast proliferation[30].

Bone fractures depend not only on BMC but also on bone quality, size and shape[31-33]. The decrease of F_{max} at wk 16 clearly showed the altered bone metabolism. Since correlation was found between F_{max} and cortical index, femoral length and BMC and there was no difference in F_{max}/cortical index and F_{max}/BMC ratios between the different groups, the increased fragility should be the consequence of stunted longitudinal and cortical growth and arrested mineralization in growing rats with liver cirrhosis and HCC.

The mechanism by which liver cirrhosis arrests skeletal growth and influences other features of bone metabolism is not fully understood. Whether the bone alteration is caused by a direct toxic effect of the applied agents on bones or it is a secondary consequence of the experimentally induced liver cirrhosis remains unknown.

In conclusion, experimentally induced liver cirrhosis and HCC are accompanied with inhibited growth, reduced BMC and cortical index and decreased mechanical resistance in growing rats. Our results are in concordance with the data of other studies using different animal models. A novel finding is the transiently accelerated skeletal growth and bone strength after a 8-wk long phenobarbital treatment following diethylnitrosamine injection.

REFERENCES

1 **Diamond T,** Stiel D, Lunzer M, Wilkinson M, Roche J, Posen S. Osteoporosis and skeletal fractures in chronic liver disease. *Gut* 1990; **31**: 82-87
2 **Heathcote J.** Osteoporosis in chronic liver disease. *Curr Gastroenterol Rep* 1999; **1**: 455-458
3 **McCaughan GW,** Feller RB. Osteoporosis in chronic liver disease: pathogenesis, risk factors, and management. *Dig Dis* 1994; **12**: 223-231
4 **Monegal A,** Navasa M, Guanabens N, Peris P, Pons F, Martinez de Osaba MJ, Rimola A, Rodes J, Munoz-Gomez J. Osteoporosis and bone mineral metabolism disorders in

cirrhotic patients referred for orthotopic liver transplantation. *Calcif Tissue Int* 1997; **60**: 148-154

5 **Corazza GR,** Trevisani F, Di Stefano M, De Notariis S, Veneto G, Cecchetti L, Minguzzi L, Gasbarrini G, Bernardi M. Early increase of bone resorption in patients with liver cirrhosis secondary to viral hepatitis. *Dig Dis Sci* 2000; **45**: 1392-1399

6 **Moller S,** Hansen M, Hillingso J, Jensen JE, Henriksen JH. Elevated carboxy terminal cross linked telopeptide of type I collagen in alcoholic cirrhosis: relation to liver and kidney function and bone metabolism. *Gut* 1999; **44**: 417-423

7 **Chappard D,** Plantard B, Fraisse H, Palle S, Alexandre C, Riffat G. Bone changes in alcoholic cirrhosis of the liver. A histomorphometric study. *Pathol Res Pract* 1989; **184**: 480-485

8 **Diamond TH,** Stiel D, Lunzer M, McDowall D, Eckstein RP, Posen S. Hepatic osteodystrophy. Static and dynamic bone histomorphometry and serum bone Gla-protein in 80 patients with chronic liver disease. *Gastroenterology* 1989; **96**: 213-221

9 **Capra F,** Casaril M, Gabrielli GB, Stanzial A, Ferrari S, Gandini G, Falezza G, Corrocher R. Plasma osteocalcin levels in liver cirrhosis. *Ital J Gastroenterol* 1991; **23**: 124-127

10 **Pietschmann P,** Resch H, Müller C, Woloszczuk W, Willvonseder R. Decreased serum osteocalcin levels in patients with liver cirrhosis. *Bone Miner* 1990; **8**: 103-108

11 **Tsuneoka K,** Tameda Y, Takase K, Nakano T. Osteodystrophy in patients with chronic hepatitis and liver cirrhosis. *J Gastroenterol* 1996; **31**: 669-678

12 **Kalef-Ezra JA,** Merkouropoulos MH, Challa A, Hatzikonstantinou J, Karantanas AH, Tsianos EV. Amount and composition of bone minerals in chronic liver disease. *Dig Dis Sci* 1996; **41**: 1008-1013

13 **Stellon AJ,** Davies A, Compston J, Williams R. Osteoporosis in chronic cholestatic liver disease. *Q J Med* 1985; **57**: 783-790

14 **Zalatnai A,** Lapis K. Simultaneous induction of liver cirrhosis and hepatocellular carcinomas in F-344 rats: establishment of a short hepatocarcinogenesis model. *Exp Toxic Pathol* 1994; **46**: 215-222

15 **Pilette C,** Rousselet MC, Bedossa P, Chappard D, Oberti F, Rifflet H, Maiga MY, Gallois Y, Cales P. Histopathological evaluation of liver fibrosis: quantitative image analysis vs Semi-quantitative scores. Comparison with serum markers. *J Hepatol* 1998; **28**: 439-446

16 **Stewart HL,** williams G, Keysser CH, Lombard LS,Montaly RJ. Histologic typing of liver tumors of the rat. Institute of Laboratory Animal Resources, National Research Council, National Academy of Sciences, Washington, D.C. *J Natl Cancer Inst* 1980; **64**: 177-206

17 **Mosekilde L,** Thomsen JS, Orhii PB, McCarter RJ, Mejia W, Kalu DN. Additive effect of voluntary exercise and growth hormone treatment on bone strength assessed at four different skeletal sites in an aged rat model. *Bone* 1999; **24**: 71-80

18 **Cemborain A,** Castilla-Cortázar I, García M, Quiroga J, Muguerza B, Picardi A, Santidrián S, Prieto J. Osteopenia in rats with liver cirrhosis: beneficial effects of IGF-I treatment. *J Hepatol* 1998; **28**: 122-131

19 **Nakano A,** Kanda T, Abe H. Bone changes and mineral metabolism disorders in rats with experimental liver cirrhosis. *J Gastroenterol Hepatol* 1996; **11**: 1143-1154

20 **Cemborain A,** Castilla-Cortázar I, García M, Muguerza B, Delgado G, Díaz-Sánchez M, Picardi A. Effects of IGF-I treatment on osteopenia in rats with advanced liver cirrhosis. *J Physiol Biochem* 2000; **56**: 91-99

21 **Mabuchi M,** Kawamura I, Fushimi M, Inoue T, Takeshita S, Takakura S, Matsuo M, Tomoi M, Goto T. Induction of bone loss by bile duct ligation in rats. *In Vivo* 2001; **15**: 281-287

22 **van der Merwe SW,** van den Bogaerde JB, Goosen C, Maree FF, Milner RJ, Schnitzler CM, Biscardi A, Mesquita JM, Engelbrecht G, Kahn D, Fevery J. Hepatic osteodystrophy in rats results mainly from portasystemic shunting. *Gut* 2003; **52**: 580-585

23 **Muguerza B,** Lecároz C, Picardi A, Castilla-Cortázar I, Quiroga J, Cemborain A, Prieto J, Santidrián S. A potential experimental model for the study of osteopenia in CCl4 liver cirrhotic rats. *Rev Esp Fisiol* 1996; **52**: 113-119

24 **Tanaka S,** Tsurukami H, Sakai A, Okimoto N, Ikeda S, Otomo H, Nakamura T. Effects of 1,25(OH)2D3 on turnover, mineralization, and strength of bone in growing rats with liver cirrhosis induced by administration of carbon tetrachloride. *Bone* 2003; **32**: 275-283

25 **Bauer D,** Wolfram N, Kahl GF, Hirsch-Ernst KI. Transcriptional regulation of CYP2B1 induction in primary rat hepatocyte cultures: repression by epidermal growth factor is mediated via a distal enhancer region. *Mol Pharmacol* 2004; **65**: 172-180

26 **Nebert DW,** Russell DW. Clinical importance of the cytochromes P450. *Lancet* 2002; **360**: 1155-1162

27 **Wikvall K.** Cytochrome P450 enzymes in the bioactivation of vitamin D to its hormonal form (review). *Int J Mol Med* 2001; **7**: 201-209

28 **Wyde ME,** Bartolucci E, Ueda A, Zhang H, Yan B, Negishi M, You L. The environmental pollutant 1,1-dichloro-2,2-bis (p-chlorophenyl)ethylene induces rat hepatic cytochrome P450 2B and 3A expression through the constitutive androstane receptor and pregnane X receptor. *Mol Pharmacol* 2003; **64**: 474-481

29 **Figueiredo FA,** Brandão C, Perez Rde M, Barbosa WF, Kondo M. Low bone mineral density in noncholestatic liver cirrhosis: prevalence, severity and prediction. *Arq Gastroenterol* 2003; **40**: 152-158

30 **Janes CH,** Dickson ER, Okazaki R, Bonde S, McDonagh AF, Riggs BL. Role of hyperbilirubinemia in the impairment of osteoblast proliferation associated with cholestatic jaundice. *J Clin Invest* 1995; **95**: 2581-2586

31 **Volkman SK,** Galecki AT, Burke DT, Paczas MR, Moalli MR, Miller RA, Goldstein SA. Quantitative trait loci for femoral size and shape in a genetically heterogeneous mouse population. *J Bone Miner Res* 2003; **18**: 1497-1505

32 **Stenstrom M,** Olander B, Lehto-Axtelius D, Madsen JE, Nordsletten L, Carlsson GA. Bone mineral density and bone structure parameters as predictors of bone strength: an analysis using computerized microtomography and gastrectomy-induced osteopenia in the rat. *J Biomech* 2000; **33**: 289-297

33 **Nordsletten L,** Kaastad TS, Madsen JE, Reikerås O, Ovstebø R, Strømme JH, Falch J. The development of femoral osteopenia in ovariectomized rats is not reduced by high intensity treadmill training: a mechanical and densitometric study. *Calcif Tissue Int* 1994; **55**: 436-442

Science Editor Wang XL and Guo SY **Language Editor** Elsevier HK

PO Box 2345, Beijing 100023, China
www.wjgnet.com
wjg@wjgnet.com

ELSEVIER

World J Gastroenterol 2005;11(45):7174-7178
World Journal of Gastroenterology ISSN 1007-9327

• *RAPID COMMUNICATION* •

Retinol-binding protein, acute phase reactants and *Helicobacter pylori* infection in patients with gastric adenocarcinoma

Nicolas Tsavaris, Christos Kosmas, Petros Kopterides, Dimitrios Tsikalakis, Hlias Skopelitis, Fotini Sakelaridi, Nikitas Papadoniou, Michalis Tzivras, Vasilios Balatsos, Christos Koufos, Athanasios Archimandritis

Nicolas Tsavaris, Petros Kopterides, Hlias Skopelitis, Christos Koufos, Department of Pathophysiology, Oncology Unit, "Laiko" University Hospital, University of Athens, School of Medicine, Athens 11527, Greece
Fotini Sakelaridi, Department of Pathophysiology, Biochemistry Laboratory, "Laiko" University Hospital, University of Athens, School of Medicine, Athens 11527, Greece
Michalis Tzivras, Athanasios Archimandritis, Department of Pathophysiology, Gastroenterology Unit, "Laiko" University Hospital, University of Athens, School of Medicine, Athens 11527, Greece
Christos Kosmas, 2nd Department of Oncology, "Metaxa" Hospital, Piraeus 185 37, Greece
Dimitrios Tsikalakis, Biochemistry Laboratory, "Metaxa" Hospital, Piraeus 185 37, Greece
Nikitas Papadoniou, Department of Gastroenterology, "A. Papandreou" General Hospital of Rhodes, Rhodes 85100, Greece
Vasilios Balatsos, Department of Gastroenterology, "A. Papandreou" General Hospital of Athens, Mesogion 154, Athens 11527, Greece
Correspondence to: Dr Petros Kopterides, 28-30 Korai Street, Nea Ionia - Athens 14233, Greece. petkop@ath.forthnet.gr
Telephone: +30-210-2759863 Fax: +30-210-2855476
Received: 2005-03-01 Accepted: 2005-04-02

Abstract

AIM: To determine the serum levels of c-reactive protein (CRP), transferrin (TRF), a2-macroglobulin (A2M), ceruloplasmin (CER), a1-acid glycoprotein (AAG), pre-albumin (P-ALB) and retinol-binding protein (RBP) in gastric carcinoma patients and to explore their possible correlation with underlying *Helicobacter pylori* (*H pylori*) infection.

METHODS: We measured the serum levels of CRP, TRF, A2M, CER, AAG, P-ALB, and RBP in 153 preoperative patients (93 males; mean age: 63.1±11.3 years) with non-cardia gastric adenocarcinoma and 19 healthy subjects.

RESULTS: The levels of CRP, CER, RBP, and AAG in cancer patients were significantly higher than those in healthy controls (P<0.0001), while no difference was found regarding the TRF, P-ALB, and A2M levels. Cancer patients with *H pylori* infection had significantly lower RBP values compared to non-infected ones (P<0.0001) and also higher values of CRP and AAG (P = 0.09 and P = 0.08, respectively).

CONCLUSION: High serum levels of CRP, CER and AAG in cancer patients do not seem to be related to *H pylori* infection. Retinol-binding protein seems to discriminate between infected and non-infected patients with gastric carcinoma. Further studies are needed to explore if it is directly involved in the pathogenesis of the disease or is merely an epiphenomenon.

Key words: Gastric cancer; *Helicobacter pylori*; Acute phase reactants; A1-acid glycoprotein; Transferrin; A2-macroglobulin; Ceruloplasmin; Retinol-binding protein; Pre-albumin; c-reactive protein

Tsavaris N, Kosmas C, Kopterides P, Tsikalakis D, Skopelitis H, Sakelaridi F, Papadoniou N, Tzivras M, Balatsos V, Koufos C, Archimandritis A. Retinol-binding protein, acute phase reactants, and *Helicobacter pylori* infection in patients with gastric adenocarcinoma. *World J Gastroenterol* 2005; 11(45): 7174-7178
http://www.wjgnet.com/1007-9327/11/7174.asp

INTRODUCTION

Though the incidence of gastric adenocarcinoma has decreased during the last 50 years, it still remains one of the most common cancers worldwide. Even though the exact molecular mechanisms leading to gastric carcinogenesis are incompletely understood, the current school of thought accepts a multifactorial model in which various dietary and non-dietary factors (i.e. *Helicobacter pylori* infection) operate at different steps in the process.

Epidemiological studies in the early 1990s demonstrated an up to sixfold increased risk of developing gastric adenocarcinoma in patients infected with *H pylori*[1-4]. More than 10 years ago, *H pylori* was classified as a type I carcinogen for human beings by the World Health Organization, being recognized in this way as a crucial player in the gastric carcinogenesis. Increased epithelial cell proliferation and oxidative damage of the gastric mucosa are the two main mechanisms that seem to operate as a result of *H pylori* infection[5].

Table 1 Characteristics of studied populations and demographic data

Group	Number of subjects	Sex (M/F)	Mean age(yr)	Tumor location (antrum/body)
Gastric cancer	153	93/60	63.1	125/28
Infected	82	46/36	64.2	64/18
Non-infected	71	42/29	62.4	56/15
Healthy controls	19	10/9	62.2	

M, male; F, female.

The other environmental factor that has been shown to play a significant role in gastric carcinogenesis is diet. Diets with low intake of fruits, vegetables and milk and high intake of smoked or salted foods, dried fish, cooking oil, and complex carbohydrates have been shown to increase the risk for gastric cancer[6,7]. Contrary to that, intake of antioxidants has been associated with decreased risk of gastric cancer[8].

The search for useful biomarkers that can help in the diagnosis of cancer and add prognostic information to that already provided by the tumor staging is a field of active research. Even though numerous studies have been published, no single substance has been found to be clinically useful in the management of patients with gastric carcinoma. Immunohistochemical analysis of gastric tumors has shown that they contain protease inhibitors such as a2-macroglobulin[9,10] or a1-acid glycoprotein[11-13] and suggests that they may serve as markers of tumor aggressiveness. Some data also suggest that the acute phase reactants CRP and AAG may have prognostic value[13,14]. Stored sera from patients that later develop gastric cancer contain lower values of ferritin, while transferrin values were not different[15]. Ceruloplasmin has been shown to be useful in some studies[16] but not in others[15-17]. Serum interleukin-6 (IL-6) level correlates with the disease status of gastric cancer, suggesting that it may be used as a new tumor marker for monitoring the response to treatment[18]. Other studies even suggested that IL-6 might have a direct role in the pathogenesis[19,20]. A recent study[21] confirmed that IL-6 is a useful parameter for the diagnosis and grading of gastric cancer, but also suggested a role for malonyldialdehyde (MDA), nitric oxide (NO) and, especially vascular endothelial growth factor (VEGF). Finally, inconclusive data surround the usefulness of the so-called negative acute phase reactants, pre-albumin, and retinol-binding protein, in the assessment of cancer patients[22-26]. Retinol-binding protein was also included in our analysis because retinol and its ligand has been associated with lower risk of gastric cancer in some studies[27] but not in others[28].

The aim of this prospective, observational study was to measure the serum levels of the acute phase reactants a1-acid glycoprotein, transferrin, a2-macroglobulin, ceruloplasmin, retinol-binding protein, pre-albumin, and c-reactive protein in patients with gastric adenocarcinoma and to explore their correlation with *H pylori* infection.

MATERIALS AND METHODS

Patients

One hundred and fifty-three patients (93 men, 60 women) with a mean age of 63.1±11.3 years and histologically confirmed non-cardia gastric cancer were included in the study. In each case we recorded the location of the tumor, the histological type and the lymph node involvement. One hundred and twenty-five malignant tumors were located in the antrum and 28 in the body of the stomach. None of the patients had any gross metastatic disease as determined by chest and abdomen CT scans and received chemotherapy or radiation therapy prior to surgery. The histological diagnosis was based on morphologic examination of hematoxylin/eosin-stained specimens. Table 1 summarizes the demographic data and characteristics of the studied populations. Nineteen healthy volunteers (10 men, 9 women) with a mean age of 62.2±13.1 years were used as controls. We defined "healthy" status as the absence of a cardiovascular disorder, malignancy, gastrointestinal pathology, and *H pylori* infection. Neither patients nor controls had any evidence of infection or received antibiotics for at least 2 mo prior to serum collection with only the use of antacids. Sera from 48 patients were prospectively collected, the rest of the sera were collected in the previous 17 mo and kept frozen at -70 ℃.

The study was approved by the Institutional Review Boards of the participating hospitals and all study individuals gave their informed consent.

Determination of H pylori serology

All enrolled subjects (cancer patients and controls) underwent an enzyme-linked immunosorbent assay (ELISA) IgG serologic test for *H pylori* (Allergy Immunotechnologies Inc., Newport Beach, CA, USA) in accordance with the manufacturer's instructions. The specificity and sensitivity of the serology test validated in our local population were 95% and 90%, respectively. *H pylori* antibody titers higher than 155 mU/L were considered positive and lower than 155 mU/L negative.

Determination of acute phase proteins

Concentrations of the specific acute-phase proteins (c-reactive protein, a1-acid glycoprotein, ceruloplasmin, transferrin, a2-macroglobulin, prealbumin, and retinol-binding protein) were measured by nephelometric method on a Dade Behring nephelometer BNII (Dade Behring, USA), using Dade Behring antibodies and standard reagents. The intra- and inter-assay coefficients of variation were in the range of 2% and 5%, respectively.

Examined parameters

Serum levels of the acute phase reactants were recorded from healthy controls and patients suffering from gastric cancer. These patients were grouped according to whether they were infected with *H pylori* or not. Normal values for the examined parameters were as follows: c-reactive protein (CRP) <50 mg/L, A1-acid glycoprotein (AAG) <1

Table 2 Mean levels of TRF, A2M, AAG, CER, RBP, P-ALB, and CRP in cancer patients and controls

Parameter (mg/dL)	Cancer patients (n = 153)	Controls (n = 19)	P
TRF	265,43	274,95	NS
A2M	263,25	233,11	NS
AAG	245,48	94,79b	<0.001
CER	53,26	41,74b	<0.001
RBP	23,78	3,77b	<0.001
P-ALB	23,04	17,74	NS
CRP	9,32	2,92b	<0.001

[b]P<0.001 *vs* controls, NS: not significant.

Table 3 Mean levels of TRF, A2M, AAG, CER, RBP, P-ALB, and CRP between infected and non-infected cancer patients

Parameter (mg/dL)	Non-infected (n = 71)	Infected (n = 82)	P
TRF	276.46	255.88	NS
A2M	281.49	247.46	NS
AAG	238.21	251.77	NS
CER	52.03	54.32	NS
RBP	31.89	16.75[b]	<0.001
P-ALB	22.35	23.64	NS
CRP	7.99	10.47	NS

[b]P<0.001 *vs* infected, NS: not significant.

200 mg/L, ceruloplasmin (CER) <550 mg/L, transferrin (TRF) <4 300 mg/L, A2-macroglobulin (A2M) <3 200 mg/L, pre-albumin (P-ALB) <450 mg/L and retinol-binding protein (RBP) <60 mg/L.

Statistical analysis

The nonparametric Mann-Whitney *U*-test was employed to study the differences in values between cancer patients and controls and to compare the significance of values' differences between infected and non-infected patients. P<0.05 was considered statistically significant. All analyses were completed using the Statistical Package for Social Sciences (SPSS 11.5).

RESULTS

The assessed parameters found between cancer patients and healthy controls and between infection and non-infection groups of cancer patients are shown in Tables 2 and 3, respectively. Out of a total of 153 cancer patients participating in the study, 82 (53.6%) were infected with *H pylori*. The levels of CRP, CER, RBP, and AAG in cancer patients were significantly higher than those in healthy controls (P<0.0001), while no difference was found regarding the TRF, P-ALB, and A2M levels. Cancer patients with *H pylori* infection had significantly lower RBP (P<0.0001) and higher CRP and AAG (P = 0.09 and P = 0.08, respectively) than those without *H pylori* infection.

DISCUSSION

In the current study, we have measured the serum levels of a group of acute phase reactants in patients with adenocarcinoma localized in the non-cardia part of the stomach. We separated these patients to either antibody-positive or antibody-negative to *H pylori*. From the examined acute phase reactants, we found that the levels of c-reactive protein, ceruloplasmin, a1-acid glycoprotein and retinol-binding protein in cancer patients were significantly higher than those in healthy controls, while no difference was found regarding the transferrin, prealbumin and a2-macroglobulin levels. However, only retinol-binding protein was significantly related to *H pylori* infection as its values were significantly lower in infected patients than in non-infected ones. The etiology of these biochemical aberrations is probably multifactorial.

Numerous studies have shown that gastric cancer patients have significantly higher levels of CRP[14,21] than healthy controls. A previous study[13] has even showed that elevated CRP levels have a prognostic significance and a recent study suggested that CRP levels contribute to the diagnosis of infection in cancer patients[21]. Our data confirm that CRP is elevated in cancer patients, but we cannot comment on its usefulness in the diagnosis of infection in cancer patients, as this was not the aim of our study. Though it was not different between infected and non-infected patients with *H pylori* (P = 0.09), one possible explanation is that chronic *H pylori* infection did not cause the elevation of CRP with acute infections as pneumonia or bacteremia. The other explanation is that our study did not have the statistical power to detect any difference.

Immunohistochemical analysis of the tumor epithelium showed that the protease inhibitor a2-macroglobulin is related to the invasive growth of gastric cancers[9,10]. Similar preliminary data exist for a1-acid glycoprotein[11-13]. Our data do not support routine measurement of A2M, but confirmed that AAG is a potentially useful marker as it was consistently higher in cancer patients and showed a trend to reach statistical significance in *H pylori*-infected patients (P = 0.08).

The role of iron-carrying protein transferrin is undetermined. Studies showed that there is no difference in the mean TRF values between controls and patients while ferritin values are significantly different[15,29], suggesting that TRF may not be a prognostic factor for future gastric carcinogenesis but its role remains uncertain. In accordance with previous studies, our data did not require measuring transferrin in gastric cancer patients whether they were infected with *H pylori* or not.

Finally, we decided to include the so-called nutritional indices (prealbumin and retinol-binding protein) in our analysis to explore their relation to cancer or *H pylori* infection. In patients with colon cancer, the levels of serum prealbumin, retinol-binding protein, transferrin, and albumin were interrelated and tended to show a similar pattern of change. More specifically, in metastatic colon cancer, prealbumin was the most sensitive indicator of nutritional status and its levels and rates of change

had a prognostic significance. A rapid fall of prealbumin often occurs 2-3 mo prior to death of the patients and this preterminal phase is also frequently heralded by a progressive rise in the CRP level in the absence of any obvious infection[30]. Prealbumin concentration has a prognostic importance in women with epithelial ovarian carcinoma[24] and a general cancer population as well[23]. We cannot confirm the data on the usefulness of prealbumin testing because we did not perform any formal assessment of nutritional status in our study population.

Serum ceruloplasmin levels are higher in gastric and lung cancer[16] and our data have confirmed this finding. We did not find any correlation of *H pylori* infection with ceruloplasmin levels and cannot suggest a pathogenetic role for this copper-chelating protein apart from being a marker of systemic inflammation.

The most interesting findings of our study are the significantly higher levels of retinol-binding protein in gastric cancer patients than healthy controls, the only marker being statistically different between infected and non-infected patients with *H pylori* (it was lower in *H pylori*-infected patients). Our findings are novel and in contrast with previous studies showing decreased RBP levels in the lung[25] and colorectal cancer[17]. Retinol, the ligand of retinol-binding protein, is required to maintain immunity and epithelial turnover and is a key micronutrient needed for combating infection. Studies have shown a good correlation between RBP and retinol even in the context of infection and protein malnutrition[31]. Retinol deficiency could either directly disrupt epithelial integrity or indirectly increase susceptibility to the damaging factors contained in either tobacco smoke (in the case of lung cancer) or diet (in the case of gastric and colorectal cancer). One would expect a lower and not a higher retinol-binding protein value in gastric cancer patients.

A fundamental difference between stomach cancer and other types of cancer is the involvement of *H pylori* in the former. There is evidence that *H pylori* infection *per se* is associated with the abnormalities of the nutritional markers even in the absence of malignancy. Aguilera *et al*[32] studied the relationship between *H pylori* infection, anorexia and malnutrition in 48 peritoneal dialysis patients and found that infected patients with anorexia have lower lymphocyte counts, pre-albumin, transferrin, serum albumin, normalized equivalent of protein-nitrogen appearance and residual renal function. Eradication of *H pylori* could significantly improve the clinical syndrome and the biochemical abnormalities implying a causative role, but unfortunately retinol-binding protein was not measured in that study. The significant decrease in the activity of class IV alcohol dehydrogenase (ADH) in the antrum and corpus of stomachs of men and women infected with *H pylori* may be one of the underlying mechanisms as class IV ADH is the major isoenzyme controlling the production of retinoic acid from retinol and its supply to the human gastric mucosa[33,34]. It has been shown in animal models that the inflammatory response to infection and tissue injury is associated with low concentrations of plasma retinol and its specific transport proteins, retinol-binding protein and pre-albumin[35], suggesting that inflammation-induced hyporetinemia is attributed to a reduction in the hepatic synthesis of RBP and secretion of the retinol-RBP complex. The marked depressing effect of infections on serum retinol and retinol-binding protein has also been shown in human beings[36,37]. We speculate that *H pylori* infection in gastric carcinoma patients can lead to a decrease of retinol-binding protein by one of the above mechanisms but it remains unclear why uninfected patients with gastric cancer still have higher RBP levels than healthy controls.

The role of retinoids in gastric carcinogenesis has been studied in epidemiologic studies with conflicting results[27,28], but the molecular mechanisms that operate at either healthy or disease states have begun to be elucidated. Retinol has been shown to enhance differentiation of the gastric cell lineage in developing rabbits[38] and the reduction of retinoic acid signal has been implicated in the development and evolution of pre-malignant lesions of the human gastric mucosa[39]. The activation of the retinoic acid receptor induces cell differentiation and may antagonize cancer progression. Cellular retinol-binding protein I (CRBP-I) functions in retinol storage and its expression is lower in human cancers than in normal cells. A very recent study[40] showed that CRBP-I downregulation in human mammary epithelial cells chronically compromises retinoic acid receptor activity, leading to the loss of cell differentiation and tumor progression. The fact that class IV ADH is the major isoenzyme responsible for retinoic acid production from retinol and the more significantly decreased enzyme in the presence of *H pylori* infection associated with morphologic changes in the human gastric mucosa is intriguing. The retinoic acid pathway may be one of the missing links in the interplay of *H pylori* infection with gastric carcinogenesis.

In conclusion, gastric cancer patients with *H pylori* infection have significantly lower retinol-binding protein values than non-infected ones and both infected and non-infected groups have higher retinol-binding protein values than healthy controls. This finding may add to our understanding and management of this dreadful disease.

REFERENCES

1 **Parsonnet J,** Hansen S, Rodriguez L, Gelb AB, Warnke RA, Jellum E, Orentreich N, Vogelman JH, Friedman GD. Helicobacter pylori infection and gastric lymphoma. *N Engl J Med* 1994; **330**: 1267-1271

2 An international association between Helicobacter pylori infection and gastric cancer. The EUROGAST Study Group. *Lancet* 1993; **341**: 1359-1362

3 **Nomura A,** Stemmermann GN, Chyou PH, Kato I, Perez-Perez GI, Blaser MJ. Helicobacter pylori infection and gastric carcinoma among Japanese Americans in Hawaii. *N Engl J Med* 1991; **325**: 1132-1136

4 **Forman D,** Newell DG, Fullerton F, Yarnell JW, Stacey AR, Wald N, Sitas F. Association between infection with Helicobacter pylori and risk of gastric cancer: evidence from a prospective investigation. *BMJ* 1991; **302**: 1302-1305

5 **De Luca A,** Iaquinto G. Helicobacter pylori and gastric diseases: a dangerous association. *Cancer Lett* 2004; **213**: 1-10

6 **Ngoan LT,** Mizoue T, Fujino Y, Tokui N, Yoshimura T. Dietary

factors and stomach cancer mortality. *Br J Cancer* 2002; **87**: 37-42

7 **Kobayashi M,** Tsubono Y, Sasazuki S, Sasaki S, Tsugane S. Vegetables, fruit and risk of gastric cancer in Japan: a 10-year follow-up of the JPHC Study Cohort I. *Int J Cancer* 2002; **102**: 39-44

8 **Serafini M,** Bellocco R, Wolk A, Ekström AM. Total antioxidant potential of fruit and vegetables and risk of gastric cancer. *Gastroenterology* 2002; **123**: 985-991

9 **Tahara E,** Ito H, Taniyama K, Yokozaki H, Hata J. Alpha 1-antitrypsin, alpha 1-antichymotrypsin, and alpha 2-macroglobulin in human gastric carcinomas: a retrospective immunohistochemical study. *Hum Pathol* 1984; **15**: 957-964

10 **Allgayer H,** Babic R, Grützner KU, Beyer BC, Tarabichi A, Schildberg FW, Heiss MM. Tumor-associated proteases and inhibitors in gastric cancer: analysis of prognostic impact and individual risk protease patterns. *Clin Exp Metastasis* 1998; **16**: 62-73

11 **Saito T,** Kuwahara A, Shimoda K, Kinoshita T, Sato K, Miyahara M, Kobayashi M. Factors influencing the acute phase protein levels in patients with esophageal cancer. *Jpn J Surg* 1991; **21**: 402-411

12 **Möschl P,** Lubec G, Keiler A, Kreuzer W. [Significance of alpha 1-acid glycoprotein for the diagnosis of stomach cancer (author's transl)]. *Wien Med Wochenschr* 1979; **129**: 24-26

13 **Rashid SA,** O'Quigley J, Axon AT, Cooper EH. Plasma protein profiles and prognosis in gastric cancer. *Br J Cancer* 1982; **45**: 390-394

14 **Wu CW,** Lui WY, P'eng FK, Wang SR. Alterations of humoral immunity in patients with gastric cancer. *Asian Pac J Allergy Immunol* 1988; **6**: 7-10

15 **Nomura A,** Chyou PH, Stemmermann GN. Association of serum ferritin levels with the risk of stomach cancer. *Cancer Epidemiol Biomarkers Prev* 1992; **1**: 547-550

16 **Scanni A,** Licciardello L, Trovato M, Tomirotti M, Biraghi M. Serum copper and ceruloplasmin levels in patients with neoplasias localized in the stomach, large intestine or lung. *Tumori* 1977; **63**: 175-180

17 **Putzki H,** Reichert B, Hinz M. Retinol-binding protein, haptoglobin and ceruloplasmin--tumor markers in colorectal cancer? *Z Gesamte Inn Med* 1990; **45**: 50-52

18 **Wu CW,** Wang SR, Chao MF, Wu TC, Lui WY, P'eng FK, Chi CW. Serum interleukin-6 levels reflect disease status of gastric cancer. *Am J Gastroenterol* 1996; **91**: 1417-1422

19 **Ito R,** Yasui W, Kuniyasu H, Yokozaki H, Tahara E. Expression of interleukin6 and its effect on the cell growth of gastric carcinoma cell lines. *Jpn J Cancer Res* 1997; **88**: 953-958

20 **Tanahashi T,** Kita M, Kodama T, Yamaoka Y, Sawai N, Ohno T, Mitsufuji S, Wei YP, Kashima K, Imanishi J. Cytokine expression and production by purified *Helicobacter pylori* urease in human gastric epithelial cells. *Infect Immun* 2000; **68**: 664-671

21 **Ilhan N,** Ilhan N, Ilhan Y, Akbulut H, Kucuksu M. C-reactive protein, procalcitonin, interleukin-6, vascular endothelial growth factor and oxidative metabolites in diagnosis of infection and staging in patients with gastric cancer. *World J Gastroenterol* 2004; **10**: 1115-1120

22 **Tsuburaya A,** Noguchi Y, Yoshikawa T, Nomura K, Fukuzawa K, Makino T, Imada T, Matsumoto A. Long-term effect of radical gastrectomy on nutrition and immunity. *Surg Today* 1993; **23**: 320-324

23 **Ho SY,** Guo HR, Chen HH, Peng CJ. Nutritional predictors of survival in terminally ill cancer patients. *J Formos Med Assoc* 2003; **102**: 544-550

24 **Mählck CG,** Grankvist K. Plasma prealbumin in women with epithelial ovarian carcinoma. *Gynecol Obstet Invest* 1994; **37**: 135-140

25 **Edes TE,** McDonald PS. Retinol and retinol-binding protein in lung cancer screening. *Cancer Detect Prev* 1991; **15**: 341-344

26 **Criqui MH,** Bangdiwala S, Goodman DS, Blaner WS, Morris JS, Kritchevsky S, Lippel K, Mebane I, Tyroler HA. Selenium, retinol, retinol-binding protein, and uric acid. Associations with cancer mortality in a population-based prospective case-control study. *Ann Epidemiol* 1991; **1**: 385-393

27 **Zheng W**, Sellers TA, Doyle TJ, Kushi LH, Potter JD, Folsom AR. Retinol, antioxidant vitamins, and cancers of the upper digestive tract in a prospective cohort study of postmenopausal women. *Am J Epidemiol* 1995; **142**: 955-960

28 **Zhang L**, Blot WJ, You WC, Chang YS, Liu XQ, Kneller RW, Zhao L, Liu WD, Li JY, Jin ML. Serum micronutrients in relation to pre-cancerous gastric lesions. *Int J Cancer* 1994; **56**: 650-654

29 **Akiba S,** Neriishi K, Blot WJ, Kabuto M, Stevens RG, Kato H, Land CE. Serum ferritin and stomach cancer risk among a Japanese population. *Cancer* 1991; **67**: 1707-1712

30 **Milano G,** Cooper EH, Goligher JC, Giles GR, Neville AM. Serum prealbumin, retinol-binding protein, transferrin, and albumin levels in patients with large bowel cancer. *J Natl Cancer Inst* 1978; **61**: 687-691

31 **Baeten JM,** Richardson BA, Bankson DD, Wener MH, Kreiss JK, Lavreys L, Mandaliya K, Bwayo JJ, McClelland RS. Use of serum retinol-binding protein for prediction of vitamin A deficiency: effects of HIV-1 infection, protein malnutrition, and the acute phase response. *Am J Clin Nutr* 2004; **79**: 218-225

32 **Aguilera A,** Codoceo R, Bajo MA, Diéz JJ, del Peso G, Pavone M, Ortiz J, Valdez J, Cirugeda A, Fernández-Perpén A, Sánchez-Tomero JA, Selgas R. Helicobacter pylori infection: a new cause of anorexia in peritoneal dialysis patients. *Perit Dial Int* 2001; **21 Suppl 3**: S152- S156

33 **Chrostek L,** Jelski W, Szmitkowski M, Laszewicz W. Effect of Helicobacter pylori infection on the activity of class I, III and IV alcohol dehydrogenase in the human stomach. *Digestion* 2002; **66**: 14-18

34 **Matsumoto M**, Yokoyama H, Suzuki H, Shiraishi-Yokoyama H, Hibi T. Retinoic acid formation from retinol in the human gastric mucosa: role of class IV alcohol dehydrogenase and its relevance to morphological changes. *Am J Physiol Gastrointest Liver Physiol* 2005; **289**: G429-G433

35 **Rosales FJ,** Ritter SJ, Zolfaghari R, Smith JE, Ross AC. Effects of acute inflammation on plasma retinol, retinol-binding protein, and its mRNA in the liver and kidneys of vitamin A-sufficient rats. *J Lipid Res* 1996; **37**: 962-971

36 **Arroyave G,** Calcaño M. Decrease in serum levels of retinol and its binding protein (RBP) in infection. *Arch Latinoam Nutr* 1979; **29**: 233-260

37 **Cser MA,** Majchrzak D, Rust P, Sziklai-László I, Kovács I, Bocskai E, Elmadfa I. Serum carotenoid and retinol levels during childhood infections. *Ann Nutr Metab* 2004; **48**: 156-162

38 **Karam SM,** Ansari HR, Al-Dhaheri WS, Alexander G. Retinol enhances differentiation of the gastric parietal cell lineage in developing rabbits. *Cell Physiol Biochem* 2004; **14**: 333-342

39 **Jiang SY,** Shen SR, Shyu RY, Yu JC, Harn HJ, Yeh MY, Lee MM, Chang YC. Expression of nuclear retinoid receptors in normal, premalignant and malignant gastric tissues determined by in situ hybridization. *Br J Cancer 1999;* **80**: 206-214

40 **Farias EF,** Ong DE, Ghyselinck NB, Nakajo S, Kuppumbatti YS, Mira y Lopez R. Cellular retinol-binding protein I, a regulator of breast epithelial retinoic acid receptor activity, cell differentiation, and tumorigenicity. *J Natl Cancer Inst* 2005; **97**: 21-29

Science Editor Wang XL and Guo SY **Language Editor** Elsevier HK

PO Box 2345, Beijing 100023, China
www.wjgnet.com
wjg@wjgnet.com

ELSEVIER

World J Gastroenterol 2005;11(45):7179-7182
World Journal of Gastroenterology ISSN 1007-9327

• *RAPID COMMUNICATION* •

Histological outcome of chronic hepatitis B in children treated with interferon alpha

Sobaniec-Lotowska Maria Elzbieta, Lebensztejn Dariusz Marek

Sobaniec-Lotowska Maria Elzbieta, Department of Clinical Pathomorphology, Medical University of Bialystok, Poland
Lebensztejn Dariusz Marek, III[rd] Department of Pediatrics, Medical University of Bialystok, Poland
Correspondence to: Maria Sobaniec-Lotowska, MD, PhD, Assistant Professor, Department of Clinical Pathomorphology, Medical University of Bialystok, 13 Waszyngtona Str., 15-269 Bialystok, Poland. mariasl@zeus.amb.edu.pl
Telephone: +48-85-7485940 Fax: +48-85-7485990
Received: 2005-02-15 Accepted: 2005-03-09

Abstract

AIM: To evaluate the effect of interferon alpha (IFN-α) treatment on the liver histology in children with chronic hepatitis B and to evaluate the usefulness of various histological scoring systems of liver histology in this group of patients.

METHODS: Fibrosis stage and inflammation grade were assessed according to Batts and Ludwig, Ishak *et al*, and METAVIR (only fibrosis stage) before and 12 mo after IFN-α treatment termination in 93 children aged 2-16 years with chronic hepatitis B.

RESULTS: None of the three numerical scoring systems for liver fibrosis showed statistically significant differences in liver fibrosis, while evolution of inflammatory activity revealed statistically significant improvement in the whole group of children with chronic hepatitis B treated with IFN-α and in responders. Significantly positive correlations were found between fibrosis stage and inflammation grade in the respective scoring systems.

CONCLUSION: Treatment with IFN-α did not improve histological fibrosis but decreased inflammatory activity in children with chronic hepatitis B. The three semiquantitative scoring systems seem to be comparable in the estimation of the inflammation grade and fibrosis stage in this group of children.

Key words: Children; Chronic hepatitis B; Interferon alpha; Fibrosis stage, Inflammation grade; Semiquantitative scoring systems

Maria Elzbieta SL, Marek LD. Histological outcome of chronic hepatitis B in children treated with interferon alpha. *World J Gastroenterol* 2005; 11(45): 7179-7182

http://www.wjgnet.com/1007-9327/11/7179.asp

INTRODUCTION

Interferon alpha (IFN-α) is currently used as a standard treatment for chronic hepatitis B in children. According to Bortolotti[1], the clearance of HBeAg and HBV DNA from serum, normalization of serum ALT activity and improvement of liver histology within 12 mo after treatment discontinuation are considered as the most important endpoints in therapy efficacy evaluation.

Several semiquantitative histological scoring systems have been used in the morphological evaluation of chronic viral hepatitis. The most widely used are the scoring systems according to Ishak *et al*[2], Batts and Ludwig[3], Desmet *et al*[4] and METAVIR[5], which is contrary to the scale proposed by Knodell *et al*[6], definitely separate inflammation grade from fibrosis stage.

The aim of the study was to evaluate the effect of IFN-α treatment on liver histology in children with chronic hepatitis B and to assess the usefulness of different scoring systems of liver histology in pediatric patients. This is the first morphological analysis using different histological semiquantitative scoring systems performed on such a large material obtained from children.

MATERIALS AND METHODS

Patients

The study was carried out prospectively on 93 consecutive children (range 2-16 years, mean age 7.1 years; 69 boys and 24 girls) with biopsy-verified chronic hepatitis B (HBs/+/, HBe/+/, DNA/+/ for at least 12 mo; mean 39±27 mo). Mean ALT activity was 95±79 IU/L. Patients with diagnosed autoimmune hepatitis, liver cirrhosis or HCV coinfection were excluded from the study. None of the children were treated with antiviral or immunomodulating drugs during the 12-mo period before entering the study. IFN-α was applied in the dose of 3 MU thrice a week subcutaneously for 20 wk (this schedule is accepted for children in Poland by Polish Interferon Study Group[7]). The presence of HBeAg/antiHBe seroconversion 1 year after therapy discontinuation was considered to be the criterion of treatment efficacy. Informed consent was obtained from all parents of the patients. The study protocol was approved by the local ethical committee.

Table 1 Morphological evaluation of liver biopsies in children with chronic hepatitis B treated with IFN-α (*n* = 93)

Scoring system	Baseline biopsy	Final biopsy
Batts grade	1.516±0.619	1.312±0.51[a]
Batts stage	1.892±0.598	1.839±0.631
Ishak grade	4.054±1.683	3.344±1.514[b]
Ishak stage	2.462±1.006	2.398±1.034
METAVIR stage	1.667±0.712	1.645±0.702

[a]$P<0.05$ *vs* baseline biopsy; [b]$P<0.01$ *vs* baseline biopsy.

Table 2 Morphological evaluation of liver biopsies in children with chronic hepatitis B treated with IFN-α in the subgroups of responders (*n* = 35) and nonresponders (*n* = 58)

Scoring system	Subgroups	Baseline biopsy	Final biopsy
Batts grade	Nonresponders	1.431±0.596	1.379±0.524
	Responders	1.657±0.639	1.2±0.473[b]
Batts stage	Nonresponders	1.793±0.554	1.81±0.606
	Responders	2.057±0.639	1.886±0.676
Ishak grade	Nonresponders	3.81±1.503	3.43±1.403
	Responders	4.457±1.899	3.2±1.694[b]
Ishak stage	Nonresponders	2.293±0.878	2.431±0.901
	Responders	2.743±1.146	2.343±1.255
METAVIR stage	Nonresponders	1.62±0.644	1.638±0.667
	Responders	1.743±0.816	1.657±0.764

[b]$P<0.01$ *vs* baseline biopsy.

Table 3 Correlations between staging and grading according different histological scoring systems

Scoring system	Batts grade	Batts stage	Ishak grade	Ishak stage	METAVIR stage
Batts grade	-	$r = 0.385$ $P = 0.00014$	$r = 0.825$ $P = 0.0000001$	$r = 0.392$ $P = 0.0001$	$r = 0.405$ $P = 0.00005$
Batts stage	$r = 0.385$ $P = 0.00014$	-	$r = 0.522$ $P = 0.0000001$	$r = 0.713$ $P = 0.0000001$	$r = 0.713$ $P = 0.0000001$
Ishak grade	$r = 0.825$ $P = 0.0000001$	$r = 0.522$ $P = 0.0000001$	-	$r = 0.409$ $P = 0.000045$	$r = 0.41$ $P = 0.000045$
Ishak stage	$r = 0.392$ $P = 0.0001$	$r = 0.713$ $P = 0.0000001$	$r = 0.409$ $P = 0.000045$	-	$r = 0.758$ $P = 0.0000001$
METAVIR stage	$r = 0.405$ $P = 0.00005$	$r = 0.713$ $P = 0.0000001$	$r = 0.41$ $P = 0.000045$	$r = 0.758$ $P = 0.0000001$	-

Histological analysis

The percutaneous liver biopsies were obtained immediately before the treatment and 12 mo after the end of the IFN-α treatment. The liver biopsies were fixed in 10% buffered formalin and embedded in paraffin. Four-micrometer histological sections were prepared and stained with hematoxylin and eosin, Masson's trichrome, Masson's-Goldner and reticulin stain. Fibrosis stage and inflammation grade were assessed in a blinded fashion by a single pathologist according to Batts and Ludwig[3] and Ishak *et al*[2]; METAVIR scoring system[5] was additionally used for assessing only fibrosis.

Statistical analysis

The results were expressed as mean±SD. Differences in the respective groups were analyzed using Wilcoxon's test for pairs. Spearman's correlation coefficient was used to define correlations between the examined scoring systems. Differences were considered statistically significant at $P<0.05$.

RESULTS

Table 1 shows the results of morphological evaluation of hepatic inflammation and fibrosis in children with chronic hepatitis B prior to the IFN-α treatment (baseline biopsy) and 12 mo after IFN-α therapy discontinuation (final biopsy).

There was a significant improvement of histological inflammation both in the system of Batts and Ludwig ($P = 0.039$) and Ishak *et al* ($P = 0.0019$). However, there were no significant differences in liver fibrosis of the three semiquantitative scoring systems used.

HBeAg/antiHBe seroconversion 12 mo after therapy termination was observed in 38% of treated children. Therefore, two subgroups were distinguished: responders (35 children) and nonresponders (58 children).

The results of morphological examinations of liver biopsy before the treatment in both subgroups showed more severe intensification (although statistically insignificant) of the inflammation grade and the stage of fibrosis in the subgroup of responders. There was significant improvement of histological inflammation only in the subgroup of responders ($P = 0.0058$ according to Batts and Ludwig; $P = 0.0039$ according to Ishak *et al*), but there were no significant changes in liver fibrosis in either subgroup according to the three respective scoring systems (Table 2).

Significantly positive correlations were found between fibrosis stage and inflammation grade in the respective systems (Table 3).

DISCUSSION

The improvement of liver morphology evaluated not earlier than 12 mo after treatment discontinuation in

comparison to the baseline biopsy is one of the criteria of IFN-α therapy efficacy.

The comparison of three histological scoring systems used to evaluate chronic hepatitis in children with HBV infection revealed a high coefficient of positive correlation between the respective scales. Thus, the systems seem comparable in the estimation of the inflammation grade and stage of fibrosis in children and therefore they can be used according to the preferences of a hepatological center. In adults, Rozario and Ramakrishna[8] were in agreement with our results; they concluded that concordance between Ishak and METAVIR scoring systems was good for necroinflammatory change and excellent for fibrotic change. We also showed a close correlation between liver fibrosis and inflammatory activity, which is in agreement with Lu *et al*[9]. Assy and Minuk[10] also confirmed good correlation between the previously and currently used histological assessment of chronic hepatitis, according to the International Group[11] and Desmet *et al*[4]. As no comparative analysis of the above systems in children have been known to the authors, the current study may inspire further analysis performed on a large group of patients in order to make up the standard morphological estimation of liver biopsy in childhood.

We found no significant changes in the stage of liver fibrosis in children with chronic hepatitis B, neither in responders nor in nonresponders to IFN-α, while a statistically significant decrease was noted in the intensification of necrotic-inflammatory process in the whole group and in the subgroup of responders.

The inhibition of HBV replication was most widely discussed in the previous reports on the treatment of HBV infections in children[12,13]. Considerably less attention was paid to the changes in the morphological picture of liver biopsy after antiviral therapy (changes in necrotic-inflammatory process intensification were mainly evaluated); single reports discuss the changes of liver fibrosis. So far, a statistically significant decrease has been reported in the inflammation grade[14-20], which is in agreement with our analysis. In literature, the reduction in inflammatory activity in IFN-α treated children is estimated at 80%[16,17].

Only a few studies in the world literature analyze the effect of IFN-α therapy on the stage of fibrosis in children with chronic hepatitis B. Most authors did not show improvement of the stage of liver fibrosis caused by antiviral treatment[14,20,21]. Gregorio *et al*[15] found significant improvement only in staging in the responders. But these trials included a relatively small number of liver biopsies. Further studies by Ruiz Moreno *et al*[19] were conducted on a representative group of 60 children with chronic hepatitis B treated with IFN-α, who underwent two liver biopsies (baseline and final). They found that when biopsies were obtained within 12 mo after HBeAg clearance, the degree of histological fibrosis was significantly higher than that seen in biopsies taken after 12 mo. These data seem to indicate that in order to achieve a reliable evaluation of final hepatic fibrosis, histological examination should be performed not earlier than 12 mo after HBeAg/antiHBe seroconversion. In the present study, the liver biopsies were taken not earlier than after 12 mo of IFN-α therapy discontinuation, as this length of time seems sufficient to evaluate the therapy efficacy determined by histopathological analyses.

Studies conducted on the population of adults with chronic hepatitis B and C also do not provide a satisfactory answer to the question whether IFN-α treatment reduces the stage of liver fibrosis. Many authors have shown no significant changes of liver fibrosis due to this cytokine[22-24]; others, however, have proved a beneficial effect of IFN-α therapy on the reduction of the stage of fibrosis[25-29], particularly in responders[30-32]. Yet, they all underline the effect of IFN-α on the reduction of inflammation grade. The analysis of natural history of HBV infection shows that the inflammatory process in the liver is a triggering mechanism preceding fibrosis. It also seems that the IFN-α-induced reduction in fibrosis is preceded by the regression of inflammatory activity. Considerable divergence in the evaluation of the effect of IFN-α on fibrotic lesions in the liver of patients with chronic viral hepatitis seems to suggest that longer observation period (a few years) prior to the final biopsy is necessary to properly evaluate therapy-induced changes in fibrotic processes.

In conclusion, the treatment with IFN-α did not improve histological fibrosis but decreased inflammatory activity in children with chronic hepatitis B. The various semiquantitative histological scoring systems seem to be comparable in the estimation of the inflammation grade and fibrosis stage in this group of children.

REFERENCES

1 **Bortolotti F.** Treatment of chronic hepatitis B in children. *J Hepatol* 2003; **39** Suppl 1: S200-S205

2 **Ishak K,** Baptista A, Bianchi L, Callea F, De Groote J, Gudat F, Denk H, Desmet V, Korb G, MacSween RN. Histological grading and staging of chronic hepatitis. *J Hepatol* 1995; **22**: 696- 699

3 **Batts KP,** Ludwig J. Chronic hepatitis. An update on terminology and reporting. *Am J Surg Pathol* 1995; **19**: 1409-1417

4 **Desmet VJ,** Gerber M, Hoofnagle JH, Manns M, Scheuer PJ. Classification of chronic hepatitis: diagnosis, *grading and staging*. *Hepatology* 1994; **19**: 1513-1520

5 . Intraobserver and interobserver variations in liver biopsy interpretation in patients with chronic hepatitis C. The French METAVIR Cooperative Study Group. *Hepatology* 1994; **20**: 15-20

6 **Desmet VJ**, Knodell RG**,** Ishak KG, Black WC, Chen TS, Craig R, Kaplowitz N, Kiernan TW, Wollman J. Formulation and application of a numerical scoring system for assessing histological activity in asymptomatic chronic active hepatitis. *Hepatology* 1981; **1**: 431-435

7 **Woynarowski M,** Socha J, Słuzewski J, Chmurska-Motyka T, Mizerski J, Czerwionka-Szaflarska M, Mikina M, Karczewska K, Lebensztejn D, Zaleska I, Chlebcewicz-Szuba W, Smukalska E, Korzon M, Wysocki J, Strawinska E, Kowalik-Mikolajewska B, Kuydowicz J, Kownacka M, Kowalczyk J, Mierzejewska-Rudnicka A, Trocha H, Planeta-Malecka I, Wozniakowska-Gesicka T, Wozniak M. HBeAg clearance rate and interferon alfa dose. *Pediatric Gastroenterology* 2004: 253 - 256.

8 **Rozario R,** Ramakrishna B. Histopathological study of chronic

hepatitis B and C: a comparison of two scoring systems. *J Hepatol* 2003; **38**: 223-229

9 **Lu LG,** Zeng MD, Wan MB, Li CZ, Mao YM, Li JQ, Qiu DK, Cao AP, Ye J, Cai X, Chen CW, Wang JY, Wu SM, Zhu JS, Zhou XQ. Grading and staging of hepatic fibrosis, and its relationship with noninvasive diagnostic parameters. *World J Gastroenterol* 2003; **9**: 2574-2578

10 **Assy N,** Minuk G. A comparison between previous and present histologic assessments of chronic hepatitis C viral infections in humans. *World J Gastroenterol* 1999; **5**: 107-110

11 Acute and chronic hepatitis revisited. Review by an international group. *Lancet* 1977; **2**: 914-919

12 **Vajro P,** Migliaro F, Fontanella A, Orso G. Interferon: a meta-analysis of published studies in pediatric chronic hepatitis B. *Acta Gastroenterol Belg* 1998; **61**: 219-223

13 **Torre D,** Tambini R. Interferon-alpha therapy for chronic hepatitis B in children: a meta-analysis. *Clin Infect Dis* 1996; **23**: 131 - 137

14 **Ruiz-Moreno M,** Rua MJ, Molina J, Moraleda G, Moreno A, García-Aguado J, Carreño V. Prospective, randomized controlled trial of interferon-alpha in children with chronic hepatitis B. *Hepatology* 1991; **13**: 1035-1039

15 **Gregorio GV,** Jara P, Hierro L, Diaz C, de la Vega A, Vegnente A, Iorio R, Bortolotti F, Crivellaro C, Zancan L, Daniels H, Portmann B, Mieli-Vergani G. Lymphoblastoid interferon alfa with or without steroid pretreatment in children with chronic hepatitis B: a multicenter controlled trial. *Hepatology* 1996; **23**: 700-707

16 **Cullu F,** Tümay GT, Kutlu T, Erkan T, Ozbay G, Badur S. Treatment of chronic viral hepatits B in children with moderate doses of alpha interferon. *Gastroenterol Clin Biol* 1995; **19**: 53-57

17 **Sokal EM,** Conjeevaram HS, Roberts EA, Alvarez F, Bern EM, Goyens P, Rosenthal P, Lachaux A, Shelton M, Sarles J, Hoofnagle J. Interferon alfa therapy for chronic hepatitis B in children: a multinational randomized controlled trial. *Gastroenterology* 1998; **114**: 988-995

18 **Bortolotti F,** Jara P, Crivellaro C, Hierro L, Cadrobbi P, Frauca E, Camarena C, De La Vega A, Diaz C, De Moliner L, Noventa F. Outcome of chronic hepatitis B in Caucasian children during a 20-year observation period. *J Hepatol* 1998; **29**: 184-190

19 **Ruiz-Moreno M,** Otero M, Millán A, Castillo I, Cabrerizo M, Jiménez FJ, Oliva H, Ramon y Cajal S, Carreño V. Clinical and histological outcome after hepatitis B e antigen to antibody seroconversion in children with chronic hepatitis B. *Hepatology* 1999; **29**: 572-575

20 **Ozer E, Ozer E,** Helvaci M, Yaprak I. Hepatic expression of viral antigens, hepatocytic proliferative activity and histologic changes in liver biopsies of children with chronic hepatitis B after interferon-alpha therapy. *Liver* 1999; **19**: 369-374

21 **Fujisawa T,** Komatsu H, Inui A, Sogo T, Miyagawa Y, Fujitsuka S, Sekine I, Kosugi T, Inui M. Long-term outcome of chronic hepatitis B in adolescents or young adults in follow-up from childhood. *J Pediatr Gastroenterol Nutr* 2000; **30**: 201-206

22 **Capra F,** Casaril M, Gabrielli GB, Tognella P, Rizzi A, Dolci L, Colombari R, Mezzelani P, Corrocher R, De Sandre G. alpha-Interferon in the treatment of chronic viral hepatitis: effects on fibrogenesis serum markers. *J Hepatol* 1993; **18**: 112-118

23 **Nakano Y,** Kiyosawa K, Sodeyama T, Tanaka E. Comparative study of clinical, histological, and immunological responses to interferon therapy in type non-A, non-B, and type B chronic hepatitis. *Am J Gastroenterol* 1990; **85**: 24-29

24 **Okuno T,** Shindo M, Arai K, Matsumoto M, Takeda M. Histological improvement of chronic hepatitis B, and non-A, non-B with interferon treatment: application of a numerical scoring system for evaluating sequential morphologic changes. *Gastroenterol Jpn* 1990; **25**: 70-77

25 **Shiffman ML,** Hofmann CM, Contos MJ, Luketic VA, Sanyal AJ, Sterling RK, Ferreira-Gonzalez A, Mills AS, Garret C. A randomized, controlled trial of maintenance interferon therapy for patients with chronic hepatitis C virus and persistent viremia. *Gastroenterology* 1999; **117**: 1164-1172

26 **Sobesky R,** Mathurin P, Charlotte F, Moussalli J, Olivi M, Vidaud M, Ratziu V, Opolon P, Poynard T. Modeling the impact of interferon alfa treatment on liver fibrosis progression in chronic hepatitis C: a dynamic view. The Multivirc Group. *Gastroenterology* 1999; **116**: 378-386

27 **Tsubota A,** Kumada H, Chayama K, Arase Y, Saitoh S, Koida I, Suzuki Y, Kobayashi M, Murashima N, Ikeda K. Time course of histological changes in patients with a sustained biochemical and virological response to interferon-alpha therapy for chronic hepatitis C virus infection. *J Hepatol* 1997; **27**: 49-55

28 **Dufour JF,** DeLellis R, Kaplan MM. Regression of hepatic fibrosis in hepatitis C with long-term interferon treatment. *Dig Dis Sci* 1998; **43**: 2573-2576

29 **Han HL,** Lang ZW. Changes in serum and histology of patients with chronic hepatitis B after interferon alpha-2b treatment. *World J Gastroenterol* 2003; **9**: 117-121

30 **Williams SJ,** Craig PI, Cooksley WG, Bye WA, Bilous M, Grierson JM, Nightingale BN, Burnett L, Hensley WJ, Batey RG. Randomised controlled trial of recombinant human interferon alpha A for chronic active hepatitis B. *Aust N Z J Med* 1990; **20**: 9-19

31 **Caballero T,** Perez-Milena A, Masseroli M, O'Valle F, Salmeron FJ, Del Moral RM, Sanchez-Salgado G. Liver fibrosis assessment with semiquantitative indexes and image analysis quantification in sustained-responders and non-responder interferon-treated patients with chronic hepatitis C. *J Hepatol* 2001; **34**: 740- 747

32 **Bruno S,** Battezzati PM, Bellati G, Manzin A, Maggioni M, Crosignani A, Borzio M, Solforosi L, Morabito A, Ideo G, Podda M. Long-term beneficial effects in sustained responders to interferon-alfa therapy for chronic hepatitis C. *J Hepatol* 2001; **34**: 748-755

Science Editor Guo SY **Language Editor** Elsevier HK

PO Box 2345, Beijing 100023, China
www.wjgnet.com
wjg@wjgnet.com

ELSEVIER

World J Gastroenterol 2005;11(45):7183-7187
World Journal of Gastroenterology ISSN 1007-9327

• *RAPID COMMUNICATION* •

Effects of *Helicobacter pylori* infection on gastric epithelial cell kinetics in patients with chronic renal failure

Selim Aydemir, Binnaz Handan Ozdemir, Gurden Gur, Ibrahim Dogan, Ugur Yilmaz, Sedat Boyacioglu

Selim Aydemir, Department of Gastroenterology, Zonguldak Karaelmas University Faculty of Medicine, Zonguldak 67800, Turkey
Binnaz Handan Ozdemir, Department of Pathology, Baskent University Faculty of Medicine, Ankara 06000, Turkey
Gurden Gur, Ugur Yilmaz, Sedat Boyacioglu, Department of Gastroenterology, Baskent University Faculty of Medicine, Ankara 06000, Turkey
Ibrahim Dogan, Department of Gastroenterology, Gazi University Faculty of Medicine, Ankara 06000, Turkey
Co-first-authors: Selim Aydemir and Binnaz Handan Ozdemir
Co-correspondent: Ibrahim Dogan
Correspondence to: Dr. Selim Aydemir, Department of Gastroenterology, Zonguldak Karaelmas University Faculty of Medicine, Zonguldak 67800, Turkey. selimaydemir@hotmail.com
Telephone: +90-372-2576169 Fax: +90-372-2610155
Received: 2005-03-15 Accepted: 2005-04-18

Abstract

AIM: To evaluate the effects of *Helicobacter pylori* infection on gastric epithelial cell kinetics in patients with chronic renal failure (CRF).

METHODS: Forty-four patients were enrolled in this study and divided into four groups with respect to their *Helicobacter pylori (H pylori)* and CRF status. Groups were labeled as follows: 1a: normal renal function, *H pylori* negative (n = 12), 1b: normal renal function, *H pylori* positive (n = 11), 2a: CRF, *H pylori* negative (n = 10), 2b: CRF, *H pylori* positive (n = 11). Upper gastrointestinal endoscopy was done in all the patients involved in the study. During endoscopical investigation, antral biopsy specimens were taken from each patient. In order to evaluate the cell apoptosis and proliferation in gastric epithelial cells, Bax and proliferating cell nuclear antigen (PCNA) labeling indexes (LI) were assessed with immunohistochemical staining method.

RESULTS: For groups 1a, 1b, 2a, and 2b, mean Bax LI was identified as 34.4±13.7, 44.1±16.5, 46.3±20.5, 60.7±13.8, respectively and mean PCNA LI was identified as 36.2±17.2, 53.6±25.6, 59.5±25.6, 67.2±22, respectively. When the one-way ANOVA test was applied, statistically significant differences were detected between the groups for both Bax LI (P = 0.004 <0.01) and PCNA LI (P = 0.009 <0.01). When groups were compared further in terms of Bax LI and PCNA LI with Tukey's HSD test for multiple pairwise comparisons, statistically significant difference was observed only between groups 1a and 2b (P = 0.006 <0.01).

CONCLUSION: In gastric epithelial cells, expression of both the pre-apoptotic protein Bax and the proliferation marker PCNA increase with *H pylori* infection. This increase is more evident in patients with uremia. These findings suggest that uremia accelerates apoptosis and proliferation in gastric epithelial cells.

Key words: *Helicobacter pylori*; Chronic renal failure; Bax; Proliferating cell nuclear antigen

Aydemir S, Ozdemir BH, Gur G, Dogan I, Yilmaz U, Boyacioglu S. Effects of *Helicobacter pylori* infection on gastric epithelial cell kinetics in patients with chronic renal failure. *World J Gastroenterol* 2005;11(45): 7183-7187
http://www.wjgnet.com/1007-9327/11/7183.asp

INTRODUCTION

Helicobacter pylori (H pylori) is the most common chronic infection in human beings. *H pylori* infection has been related to peptic ulcer disease, gastric lymphoma and stomach cancers[1,2]. It is an important problem for public health as it can cause several diseases.

Gastrointestinal mucosa is characterized with rapid epithelial cell turnover and homeostasis that is mainly provided by apoptosis[3]. Therefore, it can be considered that the impaired apoptosis may have a role in the pathogenesis of many gastrointestinal system diseases.

In many studies, it has been shown that apoptotic cells are increased after colonization of *H pylori* in the stomach[4-7], and those increased apoptotic cell levels decrease to normal levels after *H pylori* eradication[5,8,9]. Increase in apoptotic cell rates causes compensatory hyperproliferative response in order to maintain gastric mucosal tissue mass[10-12].

The mechanisms by which *H pylori* induces apoptosis of gastric epithelial cells have remained unclear. It has been suggested that many bacterial products might be inducing apoptosis[5,13-15]. One of the factors that has been responsible for apoptosis of gastric epithelial cells is ammonia, which is produced via the degradation of urea by the urease enzyme of *H pylori*[5,16]. Because of high intragastric urea concentrations in patients with chronic renal failure (CRF), levels of ammonia produced by *H pylori* are significantly high[16]. Therefore, disorders associated with excessive ammonia production are more

prevalent[17,18].

Although the relationship of *H pylori* with apoptosis and proliferation in gastric epithelial cells has been mostly studied in cases with normal renal functions, gastric epithelial cell kinetics in patients with CRF still remains unknown. This study aims to investigate the effect of *H pylori* on gastric epithelial cell kinetics in patients with CRF.

MATERIALS AND METHODS

Subjects

The study included 44 patients, of whom 23 with normal renal function and 21 with CRF who were on hemodialysis treatment.

Those with gastric and/or duodenal ulcers as confirmed by upper gastrointestinal endoscopy were excluded from the study. None of the patients included had a history of gastric surgery. Patients who had been treated for *H pylori* or who had used any antibiotics, proton-pump inhibitor, H_2 receptor blocker or any compound that includes bismuth during the last one month were also excluded from the study.

The CRF patients were on a thrice-weekly hemodialysis program. The dialysis prescription included 4-5 h of bicarbonate hemodialysis with standard cuprophane membranes (hollow fiber 1-1.2 m2 surface area, Gambro, Sweden).

We divided the patients into four groups based on their *H pylori* and renal function status:

Group 1a: normal renal function, *H pylori* negative (12 patients)
Group 1b: normal renal function, *H pylori* positive (11 patients)
Group 2a: CFR, *H pylori* negative (10 patients)
Group 2b: CRF, *H pylori* positive (11 patients)

Endoscopy method

All patients were examined by using the upper gastrointestinal endoscopy (video-endoscope Olympus GIP Q240) after premedication with intravenous midazolam (2.5-7.5 mg), after an overnight fast.

During upper gastrointestinal endoscopy, multiple biopsy materials were taken from the antral region of the stomach. The biopsy specimens were transferred to the pathology laboratory in 10% buffered formalin. This study was conducted after getting permission from the local ethics committee of the Baskent University School of Medicine, Ankara, Turkey.

Identification of H pylori infection

H pylori was detected under microscopy on the histological sections stained with Giemsa staining method.

Laboratory methods

After a 12-h fasting period, venous blood samples were taken from the forearm-superficial veins of the patients in the morning. In the HD patients, the blood samples were taken before HD session. Serum levels of creatinine (normal <1.2 mg/dL) and blood urea nitrogen (BUN, normal <20 mg/dL) were measured in the central laboratory of our hospital by using routine automated techniques.

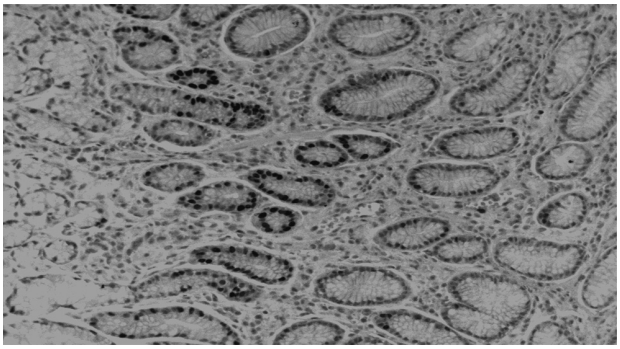

Figure 1 Proliferating cell nuclear antigen (PCNA) immunostaining of the gastric mucosa, original magnification ×250.

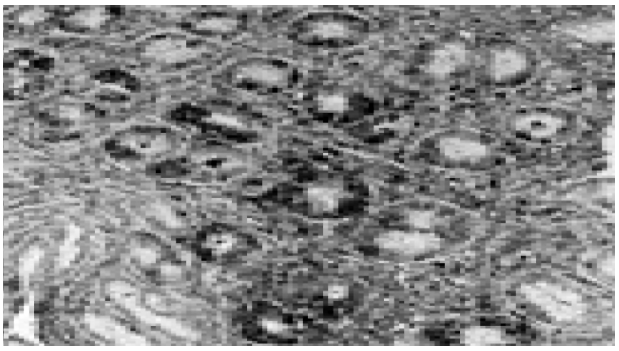

Figure 2 Bax immunostaining of the gastric mucosa, original magnification ×400.

Immunohistochemical staining for proliferating cell nuclear antigen and Bax

All biopsies were fixed in formalin, embedded in paraffin and processed routinely. Briefly, 4-mm-thick sections were deparaffinized and mounted on poly-L-lysine-coated slides. The sections in a citrate buffer (0.01 mol/L, pH 6) were heated in a microwave oven for 15 min at a maximum power (700 W), and then cooled at room temperature for 20 min. A standard three-step immunoperoxidase avidin-biotin peroxidase complex (ABC) technique was used to identify the proliferating cell nuclear antige (PCNA) (PC10, Neomarkers, CA, USA) (Figure 1). A catalyzed signal amplification (CSA) system was used to detect the polyclonal antibody Bax (K1500, Dako, Denmark) (Figure 2). PCNA and Bax positive cells were counted in the glandular neck region, which corresponds to the area of cell proliferation[19,20]. The field to be counted was chosen under ×400 magnification from the well-labeled area. About 1 000 cells were counted in each case to determine the PCNA and Bax labeling indexes (LI). The percentage of positively stained cells over total cells counted was then calculated and used as a labeling index for PCNA and Bax expression[21,22]. All histological slides were reviewed by the same experienced pathologist. The pathologist who rated the PCNA and Bax LI was unaware of the *H pylori* and renal function status of the patients.

Statistical analysis

Statistical analyses were carried out using the program SPSS 9.0 for Windows. To compare the groups, we used Student's *t*-test, Mann-Whitney *U* test, one-way ANOVA and Tukey's HSD test when appropriate. *P* values <0.05 were considered statistically significant.

RESULTS

The number of patients, their mean ages and HD duration are shown in Table 1 for each group separately. There were no statistically significant differences between the groups with regard to mean ages, gender, and HD duration ($P>0.05$).

Creatinine levels were 0.7±02, 0.8±0.2, 7.3±1.1, 7.1±1.3 mg/dL, and BUN levels were 13.8±3.5, 15.4±4.1, 98.7±12.2, 96.1±11.5 mg/dL in groups 1a, 1b, 2a, 2b, respectively (Table 2). Considering the creatinine and BUN levels, there were no statistically significant differences between the groups 1a and 1b ($P>0.05$), and between the groups 2a and 2b ($P>0.05$) but levels were higher in groups 2a and 2b than 1a and 1b ($P<0.001$).

Table 1 Number, gender, mean age, and hemodialysis duration of patient groups

	Group 1a	Group 1b	Group 2a	Group 2b
Patients (*n*)	12	11	10	11
Sex (M/F)	7/5	6/5	5/5	6/5
Mean age (yr)	37±7	39±7	35±8	36±11
Hemodialysis duration (mo)	–	–	10.4±4.5	9.3±4.4

Group 1a: normal renal function, *H pylori* negative; group 1b: normal renal function, *H pylori* positive; group 2a: CRF, *H pylori* negative; group 2b: CRF, *H pylori* positive.

For groups 1a, 1b, 2a, 2b, mean Bax LI was identified as 34.4±13.7, 44.1±16.5, 46.3±20.5, 60.7±13.8, respectively, and mean PCNA LI was identified as 36.2±17.2, 53.6±25.6, 59.5±25.6, 67.2±22, respectively.

When the one-way ANOVA test was applied, statistically significant differences were detected between the groups for both Bax LI ($P = 0.004 <0.01$) and PCNA LI ($P = 0.009 <0.01$). When groups were compared further in terms of Bax LI and PCNA LI with Tukey's HSD test for multiple pairwise comparisons, statistically significant difference was observed only between groups 1a and 2b ($P = 0.006 <0.01$).

In patients with *H pylori* infection and CRF, Bax LI and PCNA LI were found to be increased. However, the increase was more prominent in patients with CRF compared to patients with *H pylori* infection.

Table 2 Creatinine, BUN, Bax, and PCNA LI in different patient groups

	Group 1a	Group 1b	Group 2a	Group 2b
Creatinine	0.7±0.2	0.8±0.2	7.3±1.1[a,b]	7.1±1.3[c,d]
BUN	13.8±3.5	15.4±4.1	98.7±12.2[a,b]	96.1±11.5[c,d]
Bax labeling index	34.4±13.7	44.1±16.5	46.3±20.5	60.7±13.8[e]
PCNA labeling index	36.2±17.2	53.6±25.6	59.5±25.6	67.2±22.1[e]

Group 1a: normal renal function, *H pylori* negative; group 1b: normal renal function, *H pylori* positive; group 2a: CRF, *H pylori* negative; group 2b: CRF, *H pylori* positive. [a]$P<0.001$ group 1a *vs* 2a; [b]$P<0.001$ group 1b *vs* 2a; [c]$P<0.001$ group 1a *vs* 2b; [d]$P<0.001$ group 1b *vs* 2b; [e]$P<0.01$ group 1a *vs* 2b.

DISCUSSION

This is the first study where cell turnover of gastric epithelial cells is investigated in patients with CRF. We have shown that both *H pylori* infection and uremia cause increases in Bax and PCNA LI in gastric epithelial cells. Other studies in the literature that show *H pylori* increases the proliferation and apoptosis in gastric epithelial cells in cases with normal renal function support the results of our study. In addition, we also noted that both apoptosis and proliferation in gastric epithelial cells are more increased in patients with CRF.

Maintaining gastric mucosal integrity is a complex biological process[23]. This subject is provided with the balance between programmed cell death, which is also called apoptosis, and epithelial cell proliferation[23–26]. Apoptosis has been accepted as a physiological form of death and is a genetically programmed process where the cell commits suicide[27,28]. Unlike necrosis, dead cells do not cause inflammatory response in apoptosis[28]. Deranged apoptosis has been implicated in carcinogenesis, autoimmune diseases, and various infectious diseases including *H pylori* infection[5,23,28,29]. Regulation of apoptosis is a complex process. This process includes the activation of various apoptosis-related proteins such as the Bcl-2 family, p53, Fas and its ligand (FasL), and the interleukin-1b-related concerning enzyme (ICE) family[23,30].

There are several methods for evaluating cell division[31]. PCNA is a co-factor of DNA polymerase and mainly determined in late G_1 or S phase. There are several evidences that PCNA assessment is a useful tool to evaluate cell proliferation and previous studies have shown that PCNA index correlates with S phase fraction of tumor cells determined by DNA flow cytometry[32-35]. Furthermore, it has been found that PCNA immunostaining correlates with Ki67, the latter marking cells in G_1 and G_2 phases in addition to those in S phase and also with tymidine labeling index[36] and with bromodeoxyuridine uptake in cancer cell lines[20,37].

Many genes regulate the balance between apoptosis and cell proliferation. The pro-apoptotic protein, Bax, is a member of Bcl-2 gene family and is one of the genes that regulate apoptosis. Bax gene is a tumor suppressor gene and induces apoptosis via encoding Bax protein. It has been suggested that proliferation and apoptosis in the antral mucosa caused by *H pylori* is associated with the alterations in genes that regulate the process[8,22,38,39]. Konturek *et al*[23] showed that apoptosis induced by *H pylori* in gastric epithelial cells is associated with the upregulation

of proapoptotic Bax.

In many studies, it has been shown that the number of apoptotic cells in the stomach increase after *H pylori* colonization[4-6]. In addition, it has also been shown that the apoptotic cell number in stomach decreases to normal after *H pylori* eradication[5,8,9]. This increase in apoptotic rate causes compensatory hyperproliferative response in order to maintain gastric mucosa tissue mass[11].

In the literature, there are some data which suggest that apoptosis is associated with both bacterial and host factors[13-15,23]. However, the mechanism of apoptosis in *H pylori* infection is still not clear.

Some of the factors accused within the apoptosis are lipopolysaccharides, ammonia, and monochloramine (NH_2Cl), which is a highly toxic substance generated as a result of the reaction of ammonia with neutrophil-derived free radicals[13-15]. There are still debates on the role of cytotoxic agents such as *H pylori*-CagA and *H pylori*-VacA in apoptosis. In recent *in vivo* and *in vitro* studies, it has been found that *H pylori* strains can induce apoptosis without any dependency on Cag-A and Vac-A genotype[23]. In addition to the bacterial factors in infections of *H pylori*, characteristics of the host can also play important roles. Evidences are increasing about the inflammatory reactions that are induced by *H pylori* in gastric mucosa, especially cytokines such as nitric oxide and TNFα might assist to induce apoptosis[6].

One of the major factors that are responsible for *H pylori* derived apoptosis is ammonia. *H pylori* has a strong urease activity and the hydrolysis of urea causes production of high level of ammonia concentration in mucous gel layer[40]. *In vitro* studies have shown that *H pylori* derived ammonia causes lesions in insulated gastric epithelial cells. Ammonia concentrations, determined in *H pylori* infected subjects, cause gastric mucosal lesions[40-42], delay in mucosal improvement[43], and induce apoptosis in gastric epithelial cells[13,44].

Ammonia level, which is produced by *H pylori*, is controlled by the existence of urea in gastric juice. Patients with CRF have high intragastric urea concentrations and levels of ammonia produced by *H pylori* are significantly high[16]. Therefore, disorders associated with excessive ammonia production may be more prevalent in patients with uremia. In our cases, increased apoptosis and proliferation rate that are observed in uremia patients can be associated with excessive ammonia production by *H pylori* infection in uremia patients compared with cases that have normal renal functions.

In conclusion, in gastric epithelial cells, expression of both the pre-apoptotic protein Bax and the proliferation marker PCNA increase with *H pylori* infection. This increase is more evident in patients with uremia. These findings suggest that uremia accelerates apoptosis and proliferation in gastric epithelial cells.

REFERENCES

1 **NIH Consensus Conference.** Helicobacter pylori in peptic ulcer disease. NIH Consensus Development Panel on *Helicobacter pylori* in Peptic Ulcer Disease. *JAMA* 1994; **272:** 65-69

2 **Malaty HM,** Nyren O. Epidemiology of Helicobacter pylori infection. *Helicobacter* 2003; 8 Suppl **1:** 8-12

3 **Brenes F,** Ruiz B, Correa P, Hunter F, Rhamakrishnan T, Fontham E, Shi TY. Helicobacter pylori causes hyperproliferation of the gastric epithelium: pre- and post-eradication indices of proliferating cell nuclear antigen. *Am J Gastroenterol* 1993; **88:** 1870-1875

4 **Jones NL,** Shannon PT, Cutz E, Yeger H, Sherman PM. Increase in proliferation and apoptosis of gastric epithelial cells early in the natural history of Helicobacter pylori infection. *Am J Pathol* 1997; **151:** 1695-1703

5 **Moss SF,** Calam J, Agarwal B, Wang S, Holt PR. Induction of gastric epithelial apoptosis by Helicobacter pylori. *Gut* 1996; **38:** 498-501

6 **Mannick EE,** Bravo LE, Zarama G, Realpe JL, Zhang XJ, Ruiz B, Fontham ET, Mera R, Miller MJ, Correa P. Inducible nitric oxide synthase, nitrotyrosine, and apoptosis in Helicobacter pylori gastritis: effect of antibiotics and antioxidants. *Cancer Res* 1996; **56:** 3238-3243

7 **Martin JH,** Potthoff A, Ledig S, Cornberg M, Jandl O, Manns MP, Kubicka S, Flemming P, Athmann C, Beil W, Wagner S. Effect of H pylori on the expression of TRAIL, FasL and their receptor subtypes in human gastric epithelial cells and their role in apoptosis. *Helicobacter* 2004; **9:** 371-386

8 **Xia HH,** Talley NJ. Apoptosis in gastric epithelium induced by Helicobacter pylori infection: implications in gastric carcinogenesis. *Am J Gastroenterol* 2001; **96:** 16-26

9 **Nardone G,** Staibano S, Rocco A, Mezza E, D'armiento FP, Insabato L, Coppola A, Salvatore G, Lucariello A, Figura N, De Rosa G, Budillon G. Effect of Helicobacter pylori infection and its eradication on cell proliferation, DNA status, and oncogene expression in patients with chronic gastritis. *Gut* 1999; **44:** 789-799

10 **Beales IL.** Effect of interlukin-1beta on proliferation of gastric epithelial cells in culture. *BMC Gastroenterol* 2002; **2:** 7

11 **Anti M,** Armuzzi A, Gasbarrini A, Gasbarrini G. Importance of changes in epithelial cell turnover during Helicobacter pylori infection in gastric carcinogenesis. *Gut* 1998; 43 Suppl **1:** S27-S32

12 **Suzuki H,** Ishii H. Role of apoptosis in Helicobacter pylori-associated gastric mucosal injury. *J Gastroenterol Hepatol* 2000; **15** Suppl: D46-D54

13 **Hagen SJ,** Takahashi S, Jansons R. Role of vacuolation in the death of gastric epithelial cells. *Am J Physiol* 1997; **272: C**48-C58

14 **Kamada S,** Shimono A, Shinto Y, Tsujimura T, Takahashi T, Noda T, Kitamura Y, Kondoh H, Tsujimoto Y. bcl-2 deficiency in mice leads to pleiotropic abnormalities: accelerated lymphoid cell death in thymus and spleen, polycystic kidney, hair hypopigmentation, and distorted small intestine. *Cancer Res* 1995; **55:** 354-359

15 **Piotrowski J,** Piotrowski E, Skrodzka D, Slomiany A, Slomiany BL. Induction of acute gastritis and epithelial apoptosis by Helicobacter pylori lipopolysaccharide. *Scand J Gastroenterol* 1997; **32:** 203-211

16 **el Nujumi AM,** Rowe PA, Dahill S, Dorrian CA, Neithercut WD, McColl KE. Role of ammonia in the pathogenesis of the gastritis, hypergastrinaemia, and hyperpepsinogenaemia I caused by Helicobacter pylori infection. *Gut* 1992; **33:** 1612-1616

17 **Lieber CS,** Lefevre A. Ammonia as a source of gastric hypoacidity in patients with uremia. *J Clin Invest* 1959; **38:** 1271-1277

18 **Suzuki H,** Yanaka A, Shibahara T, Matsui H, Nakahara A, Tanaka N, Muto H, Momoi T, Uchiyama Y. Ammonia-induced apoptosis is accelerated at higher pH in gastric surface mucous cells. *Am J Physiol Gastrointest Liver Physiol* 2002; **283:** G986-G995

19 **Correa P,** Ruiz B, Shi TY, Janney A, Sobhan M, Torrado J, Hunter F. Helicobacter pylori and nucleolar organizer regions in the gastric antral mucosa. *Am J Clin Pathol* 1994; **101:** 656-660

20 **Rokkas T,** Liatsos C, Karameris A, Petridou E, Lazaris A, Antoniades D, Kalafatis E. Proliferating cell nuclear antigen (PCNA) immunostaining in Helicobacter pylori infection:

impact of eradication. *Pathol Oncol Res* 1999; **5:** 304-308
21 **Havard TJ,** Sarsfield P, Wotherspoon AC, Steer HW. Increased gastric epithelial cell proliferation in Helicobacter pylori associated follicular gastritis. *J Clin Pathol* 1996; **49:** 68-71
22 **Xia HH,** Zhang GS, Talley NJ, Wong BC, Yang Y, Henwood C, Wyatt JM, Adams S, Cheung K, Xia B, Zhu YQ, Lam SK. Topographic association of gastric epithelial expression of Ki-67, Bax, and Bcl-2 with antralization in the gastric incisura, body, and fundus. *Am J Gastroenterol* 2002; **97:** 3023-3031
23 **Konturek PC,** Pierzchalski P, Konturek SJ, Meixner H, Faller G, Kirchner T, Hahn EG. Helicobacter pylori induces apoptosis in gastric mucosa through an upregulation of Bax expression in humans. *Scand J Gastroenterol* 1999; **34:** 375-383
24 **Hall PA,** Coates PJ, Ansari B, Hopwood D. Regulation of cell number in the mammalian gastrointestinal tract: the importance of apoptosis. *J Cell Sci* 1994; **107** (Pt 12)**:** 3569-3577
25 **Watson AJ.** Necrosis and apoptosis in the gastrointestinal tract. *Gut* 1995; **37:** 165-167
26 **Han SU,** Kim YB, Joo HJ, Hahm KB, Lee WH, Cho YK, Kim DY, Kim MW. Helicobacter pylori infection promotes gastric carcinogenesis in a mice model. *J Gastroenterol Hepatol* 2002; **17:** 253-261
27 **Kerr JF,** Wyllie AH, Currie AR. Apoptosis: a basic biological phenomenon with wide-ranging implications in tissue kinetics. *Br J Cancer* 1972; **26:** 239-257
28 **Que FG,** Gores GJ. Cell death by apoptosis: basic concepts and disease relevance for the gastroenterologist. *Gastroenterology* 1996; **110:** 1238-1243
29 **Thompson CB.** Apoptosis in the pathogenesis and treatment of disease. *Science* 1995; **267:** 1456-1462
30 **Rudin CM,** Thompson CB. Apoptosis and disease: regulation and clinical relevance of programmed cell death. *Annu Rev Med* 1997; **48:** 267-281
31 **Unger Z,** Molnár B, Szaleczky E, Törgyekes E, Müller F, Zágoni T, Tulassay Z, Prónai L. Effect of *Helicobacter pylori* infection and eradication on gastric epithelial cell proliferation and apoptosis. *J Physiol Paris* 2001; **95:** 355-360
32 **Liu WZ,** Zheng X, Shi Y, Dong QJ, Xiao SD. Effect of Helicobacter pylori infection on gastric epithelial proliferation in progression from normal mucosa to gastriccarcinoma. *World J Gastroenterol* 1998; **4:** 246-248
33 **Zhang Z,** Yuan Y, Gao H, Dong M, Wang L, Gong YH. Apoptosis, proliferation and p53 gene expression of *H pylori* associated gastric epithelial lesions. *World J Gastroenterol* 2001; **7:** 779-782
34 **Garcia RL,** Coltrera MD, Gown AM. Analysis of proliferative grade using anti-PCNA/cyclin monoclonal antibodies in fixed, embedded tissues. Comparison with flow cytometric analysis. *Am J Pathol* 1989; **134:** 733-739
35 **Hall PA,** Levison DA, Woods AL, Yu CC, Kellock DB, Watkins JA, Barnes DM, Gillett CE, Camplejohn R, Dover R, . Proliferating cell nuclear antigen (PCNA) immunolocalization in paraffin sections: an index of cell proliferation with evidence of deregulated expression in some neoplasms. *J Pathol* 1990; **162:** 285-294
36 **Battersby S,** Anderson TJ. Correlation of proliferative activity in breast tissue using PCNA/cyclin. *Hum Pathol* 1990; **21:** 781
37 **Coltrera MD,** Gown AM. PCNA/cyclin expression and BrdU uptake define different subpopulations in different cell lines. *J Histochem Cytochem* 1991; **39:** 23-30
38 **Chen G,** Sordillo EM, Ramey WG, Reidy J, Holt PR, Krajewski S, Reed JC, Blaser MJ, Moss SF. Apoptosis in gastric epithelial cells is induced by Helicobacter pylori and accompanied by increased expression of BAK. *Biochem Biophys Res Commun* 1997; **239:** 626-632
39 **Liu HF,** Liu WW, Fang DC, Men RP. Expression and significance of proapoptotic gene Bax in gastric carcinoma. *World J Gastroenterol* 1999; **5:** 15-17
40 **Graham DY,** Go MF, Evans DJ. Review article: urease, gastric ammonium/ammonia, and Helicobacter pylori--the past, the present, and recommendations for future research. *Aliment Pharmacol Ther* 1992; **6:** 659-669
41 **Murakami M,** Saita H, Teramura S, Dekigai H, Asagoe K, Kusaka S, Kita T. Gastric ammonia has a potent ulcerogenic action on the rat stomach. *Gastroenterology* 1993; **105:** 1710-1715
42 **Takeuchi K,** Ohuchi T, Harada H, Okabe S. Irritant and protective action of urea-urease ammonia in rat gastric mucosa. Different effects of ammonia and ammonium ion. *Dig Dis Sci* 1995; **40:** 274-281
43 **Suzuki H,** Yanaka A, Muto H. Luminal ammonia retards restitution of guinea pig injured gastric mucosa in vitro. *Am J Physiol Gastrointest Liver Physiol* 2000; **279**: G107-G117
44 **Smoot DT,** Mobley HL, Chippendale GR, Lewison JF, Resau JH. *Helicobacter pylori* urease activity is toxic to human gastric epithelial cells. *Infect Immun* 1990; **58:** 1992-1994

Science Editor Wang XL and Guo SY **Language Editor** Elsevier HK

PO Box 2345, Beijing 100023, China
www.wjgnet.com
wjg@wjgnet.com

ELSEVIER

World J Gastroenterol 2005;11(45):7188-7191
World Journal of Gastroenterology ISSN 1007-9327

• *RAPID COMMUNICATION* •

Intrahepatic and peripheral T-cell responses in genotype 1b hepatitis C virus-infected patients with persistently normal and elevated aminotransferase levels

Filiz Akyüz, Nuray Polat, Sabahattin Kaymakoglu, Nevzat Aksoy, Kadir Demir, Fatih Beşışık, Selim Badur, Yilmaz Çakaloglu, Atilla Ökten

Filiz Akyüz, Sabahattin Kaymakoglu, Nevzat Aksoy, Kadir Demir, Fatih Beşışık, Yilmaz Çakaloglu, Atilla Ökten, Department of Gastroenterohepatology, Istanbul Medical Faculty, Istanbul University, Capa 34590, Istanbul, Turkey
Nuray Polat, Selim Badur, Department of Microbiology, Istanbul Medical Faculty, Istanbul University, Capa 34590, Istanbul, Turkey
Correspondence to: Filiz Akyüz, MD, Şakacı sok. Birlik apt. No 43/6 Kazasker, 81090 Istanbul, Turkey. filizakyuz@hotmail.com
Telephone: +90-212-4142000/31140 Fax: +90-212-6319743
Received: 2005-04-28 Accepted: 2005-05-24

Abstract

AIM: To evaluate whether the cytokine responses in liver and serum differ in chronic hepatitis C patients with normal and high alanine aminotransferase (ALT) levels.

METHODS: Thirty-three (16 with normal ALT level as group 1 and 17 with elevated ALT level as group 2) patients infected with genotype 1b hepatitis C virus (HCV) were examined. Liver infiltrating lymphomononuclear cells (LILMCs) were isolated from liver biopsy by collagenase type 1 and stimulated with phytohemagglutinin and interleukin 2 (IL-2). IL-10, IL-12, interferon gamma (IFN-γ) and tumor necrosis factor alpha (TNF-α) were determined in serum and LILMCs by ELISA.

RESULTS: Serum cytokine levels were similar in both groups (P>0.05). Stimulated IFN-γ and TNF-α levels in LILMCs were increased in both groups. IL-12 and IL-10 levels stimulated with IL-2 were higher in group 1 than in group 2 (P = 0.023). Histological activity index (HAI) and stage had a negative correlation with TNF-α and IFN-γ levels in group 2.

CONCLUSION: Increased T-helper type 2 (Th2) cytokine response may regress inflammatory and biochemical activity. Progression of histological abnormalities in persons with elevated ALT probably depends on insufficient Th2 cytokine response, which does not balance Th1 cytokine response.

Key words: Liver cytokines; HCV; ALT

Akyüz F, Polat N, Kaymakoglu S, Aksoy N, Demir K, Beşışık F, Badur S, Çakaloglu Y, Ökten A. Intrahepatic and peripheral T cell responses in genotype 1b hepatitis C virus infected-patients with persistently normal and elevated aminotransferase levels. *World J Gastroenterol*; 2005 11(45): 7188-7191
http://www.wjgnet.com/1007-9327/11/7188.asp

INTRODUCTION

The liver is the primary site of hepatitis C virus (HCV) replication[1]. Clearance and control of HCV infection depend on immune responses. T lymphocytes and immunoregulatory cytokines play an important role in the host response to HCV infection[2]. Intrahepatic T-cell response to HCV may determine the hepatic injury of HCV infection[3,4]. T cells also play a role in HCV clearance[5]. Th1 cytokines such as IL-2 and IFN-γ are required for host antiviral immune response, while Th2 cytokine (IL-10) can inhibit the development of these responses[2]. TNF-α also triggers a partially overlapping set of antiviral defense mechanisms and serum level of TNF-α reflects the progression of inflammation[6,7].

The natural course of HCV infection is not clear. Also, the behavior of HCV infection cannot be estimated. Different immune responses in each patient may determine the clinical course. Approximately 30% of patients with chronic HCV infection show persistently normal ALT levels that are positive for HCV-RNA. Only a small number of these patients (0-20%) have normal histology. These people are referred as healthy HCV carriers[8]. Immunological differences between patients with normal and elevated ALT levels are not well known. Most patients with normal ALT levels have a certain degree of liver damage and show a slow progression[9].

This study aimed to evaluate whether the cytokine responses in liver and serum differ in chronic hepatitis C patients with normal and high ALT levels.

MATERIALS AND METHODS

Thirty-three patients infected with genotype 1b HCV were studied. Sixteen of them had persistently normal ALT levels (group 1), while 17 had high ALT levels (group 2) by at least four analyses in a year. Anti-HCV was determined by UBI EIA 4.0 (Organon Teknika, Holland). HCV-RNA was determined by polymerase chain reaction (COBAS Amplicor 2, Roche Diagnostics, Germany)

and HCV genotyping was carried out with INNO-LiPA HCV assay (Innogenetics NV, Belgium). Hepatitis B surface antigen (HBsAg) and anti-HIV were negative in all patients. HBsAg was detected by immunoenzymatic assay [Hepanostika HBsAg Uni-Form II (Organon Teknika, Holland)]. All patients were also negative for any other etiology of liver diseases. Blood was drawn from all patients and centrifuged at 2 500 r/min for 5 min and separated serum samples were stored at -85 ℃. Liver biopsy was performed in all the patients before the treatment. Histological changes (HAI and extent of fibrosis) were assessed according to the Knodell's scoring system[10].

LILMCs were isolated from liver biopsies as previously described by Bertoletti *et al*[11]. Biopsies were washed twice in RPMI 1640 medium to remove contaminated blood and digested with collagenase type-I (1 mg/mL CO130, Sigma Chemical Co., USA) and deoxyribonuclease I (25 mg/mL D4263, Sigma Chemical Co., USA) for 1 h at 37 ℃ on a shaking device. The liver specimen was then pipetted vigorously to disrupt the hepatic tissue and to release infiltrating lymphomononuclear cells. The mononuclear cell suspension was washed twice and the cells were recovered by centrifugation over a Ficoll-hypaque density gradient. Cells were then suspended in RPMI 1640 (GIBCO Lab) containing 10% heat inactivated fetal calf serum, 25 mmol/L HEPES, 2 mmol/L L-glutamine and 50μg/mL gentamycin. Viability was >95% by the trypan blue dye exclusion test. Cells were cultured in duplicate (1.0×10^5 viable cells/100 μL) in flat-bottomed 96-well plates at 37 ℃ in an atmosphere containing 50 mL/L CO_2 with medium alone (unstimulated culture) and stimulated with 10 μg/mL phytohemagglutinin (1:100 PHA, Sigma Chemical Co., USA) and recombinant IL-12 (20 U/mL, R&D Systems, USA). Restimulation was performed every 10 d. Supernatants were collected at the end of the proliferation assay and kept frozen at -70 ℃ for later analyses. Culture supernatants and sera were thawed and the serum level of cytokines was measured by ELISA.

The local ethic committee approved this study. Informed consent was obtained from each patient included in this study. Data were presented as mean±SD. Data analysis was made by the χ^2, Fisher's exact, Mann-Whitney *U* and Pearson's correlation tests using SPSS for Windows (Chicago, IL, USA) when appropriate. $P<0.05$ was considered statistically significant.

RESULTS

Age, gender and viral load were similar in groups 1 and 2 (Table 1). The results of biochemical analyses except for aspartate aminotransferase (AST) and ALT were also similar in both the groups. In group 1, five patients underwent liver biopsy before being enrolled in the study. Though liver histology was similar in three patients, histological progression from stage 1 to stage 3 was observed in two of them.

Serum levels of IFN-γ (1.2±1.8; 1.1±0.9 pg/mL), IL-12 (0.2±0.4; 0.11±0.26 pg/mL), IL-10 (17.7±55.6; 18.2±47.8 pg/mL) and TNF-α (0.9±1.2; 0.4±0.25 pg/mL) were similar in groups 1 and 2 ($P>0.05$). Both stimulated IFN-γ and TNF-α levels in LILMCs were increased in comparison to their serum levels in both groups.

In ALT normal patients, there was a positive correlation between TNF-α and IFN-γ levels (both serum and liver) ($P<0.05$, $r = 0.5$). IL-12 and IL-10 levels stimulated by IL-2

Table 1 Demographic and biochemical features of patients (mean±SD)

	Normal ALT	Elevated ALT	*P*
n	16	17	
Age	51.4±10	47±10.7	>0.05
Female/male	10/6	8/9	>0.05
Duration of infection (mo)	33±32 (12-108)	21±22 (6-72)	>0.05
ALT (IU/L)	36±6	115±60	<0.05
AST (IU/L)	32±7.8	70±21	<0.05
ALP (IU/L)	187.9±95	219.8±104.5	>0.05
GGT (IU/L)	50.2±92.7	102.5±81.6	>0.05
Total bilirubin (mg/dL)	0.7±0.5	0.6±0.2	>0.05
Albumin (g/dL)	4.1±0.2	4±0.3	>0.05
Globulin (g/dL)	1.2±0.2	1.4±0.4	>0.05
Histology			
Minimal abnormalities	3	0	
Stage (1/2/3/4)	9/1/3/0	010/5/0/2	
HAI	4.4±2.8	6.1±3.5	>0.05
HCV-RNA (copies/mL)	456 532±277 761	461 710±324 860	>0.05

ALT: alanine aminotransferase; AST: aspartate aminotransferase; ALP: alkaline phosphatase; GGT: gamma-glutamyl transpeptidase, HAI: histological activity index.

Table 2 Cytokine levels stimulated by IL-2 and phytohemagglutinin in LILMCs (mean±SD)

pg/mL	Normal ALT	Elevated ALT	*P*
IFN-γ			
IL-2	1.8±2.3	2.2±3.4	>0.05
PHA	2.1±2.7	2.8±3.7	>0.05
IL-12			
IL-2	0.6±0.5	0.24±0.5	0.027
PHA	0.9±0.6	0.7±0.7	>0.05
IL-10			
IL-2	12.2±23.8	4.1±5.3	0.023
PHA	15.9±30.6	9.2±7.1	>0.05
TNF-α			
IL-2	2.5±1.06	2.5±2.9	>0.05
PHA	3.3±1.4	3.8±3.2	>0.05

ALT: alanine aminotransferase; PHA: phytohemagglutinin; LILMCs: liver infiltrating lymphomononuclear cells.

were higher in group 1 than in group 2 ($P<0.05$, Table 2).

In elevated ALT patients, there was a negative correlation between serum IL-12 and IFN-γ levels ($P = 0.01$, $r = –0.6$). HAI and stage had a negative correlation with TNF-α ($P<0.05$, $r = –0.8$; $P<0.05$, $r = –0.6$, respectively) and IFN-γ ($P<0.05$, $r = –0.5$; $P<0.05$, $r = –0.4$, respectively) levels (Figure 1). IL-10 stimulated by IL-2 had a positive correlation with HAI ($P<0.05$, $r = 0.49$) and stage ($P<0.05$, $r = 0.59$) (Figure 2). TNF-α and IFN-γ levels in LILMCs were positively correlated ($P<0.05$, $r = 0.8$). Cytokine levels in serum and LILMCs were not correlated with serum HCV-RNA loads in both groups.

DISCUSSION

Factors involved in the progression to end-stage liver disease in HCV-infected patients are not well characterized. It is thought that cytotoxic T lymphocyte (CTL) response early in infection may be important for viral clearance, while continuous low-level anti-HCV CTL-dependent immune response may be responsible for accumulated liver damage[12]. Prezzi *et al*[13] showed that LILMCs have phenotypic and functional characteristics distinct from peripheral blood lymphocytes. All these immunological processes define natural progress of HCV infection. Patients with normal and elevated ALT levels show different clinical patterns[14]. Generally, HCV carriers with normal ALT have mild and stable diseases with a favorable prognosis[8]. Liver histology was normal in 20% of our cases with persistently normal ALT. Progression of liver fibrosis was observed in two of five patients (40%) who had a second liver biopsy in a period of 41.5±22.1 months.

Immunological studies concerning HCV infection generally focus on T lymphocytes. However, the serum cytokine levels have been found to be different in chronic hepatitis C patients[2,15,16]. Rico *et al*[1] showed that HCV specific CD4+ T-cell proliferation responses do not parallel in LILMCs and peripheral blood mononuclear cells. The magnitude of T-cell response is higher in the liver than in peripheral blood. In our study, serum levels of cytokines were similar in patients with persistently normal and elevated ALT, suggesting that liver cytokine levels are more important than serum levels in mediating T-cell responses.

IL-10 and IL-12 levels stimulated with IL-2 were higher in patients with normal ALT than in those with elevated ALT ($P<0.05$). While IL-10 showed Th2 response, IL-12 promoted Th1 cell induction and cell-mediated immunity. Interestingly both of them were high in patients with normal ALT, suggesting that strong Th2 response may be the cause of the mild biochemical and histological activity in patients with normal ALT.

Sobue *et al*[4] revealed that disease activity and progression correlate with dominant Th1 response in chronic hepatitis C patients. On the other hand, Tsai *et al*[17] showed that predominant Th1 response is stronger in patients with resolved infection than in those with chronic diseases. In our study, while histological stage and HAI were increased, TNF-α and IFN-γ levels were decreased in patients with elevated ALT (Figure 1). TNF-α and IFN-γ trigger antiviral defense mechanisms and have a principal effect on inflammation[6,7]. This means that the magnitude of antiviral immune response is decreased, while the histological activity and stage are increased. Though Th1 and Th2 responses were both strong in patients with normal ALT, Th1 response was not as high as that

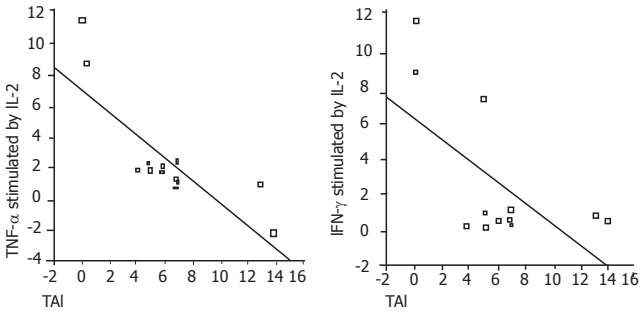

Figure 1 Negative correlations between histological activity index (HAI) and TNF-α and IFN-γ levels in LILMCs of patients with elevated ALT.

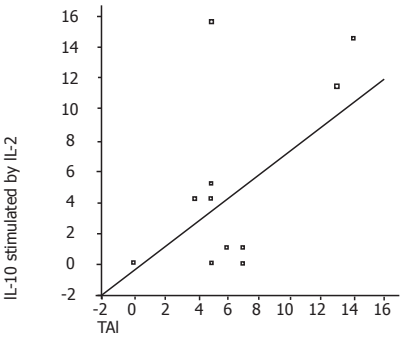

Figure 2 Positive correlation between IL-10 stimulated by IL-2 and HAI in patients with elevated ALT.

in patients with elevated ALT, suggesting that strong antiviral defense against HCV infection can normalize liver enzymes. On the other hand, histological abnormalities might be impaired by the increased Th2 response.

In conclusion, both Th1 and Th2 responses in liver are elevated in patients with normal ALT. Increased Th2 response may regress inflammatory activity. In patients with normal ALT, progression of histological findings may probably depend on insufficient Th2 response, which does not balance Th1 response. A differentiation between virus-specific and non-specific T-cell populations is the greatest challenge in future studies.

REFERENCES

1 **Rico MA,** Quiroga JA, Subira D, Garcia E, Castanon S, Sallberg M, Leroux-Roels G, Weiland O, Pardo M, Carreno V. Features of the CD4+ T-cell response in liver and peripheral blood of hepatitis C virus-infected patients with persistently normal and abnormal alanine aminotransferase levels. *J Hepatol* 2002; **36: 408-416**

2 **Cacciarelli TV,** Martinez OM, Gish RG, Villanueva JC, Krams SM. Immunoregulatory cytokines in chronic hepatitis C virus infection: pre-and posttreatment with interferon alfa. *Hepatology* 1996; **24:** 6-9

3 **Koziel MJ.** Cytokines in viral hepatitis. *Semin Liver Dis* 1999; **19:** 157-169

4 **Sobue S,** Nomura T, Ishikawa T, Ito S, Saso K, Ohara H, Joh T, Itoh M, Kakumu S. Th1/Th2 cytokine profiles and their relationship to clinical features in patients with chronic hepatitis C virus infection. *J Gastroenterol* 2001; **36:** 544-551

5 **Diepolder HM,** Zachoval R, Hoffmann RM, Wierenga EA, Santantonio T, Jung MC, Eichenlaub D, Pape GR. Possible mechanism involving T-lymphocyte response to non-structural protein 3 in viral clearance in acute hepatitis C virus infection. *Lancet* 1995; **346:** 1006-1007

6 **Neuman MG,** Benhamou JP, Malkiewicz IM, Ibrahim A, Valla DC, Martinot-Peignoux M, Asselah T, Bourliere M, Katz GG, Shear NH, Marcellin P. Kinetics of serum cytokines reflect changes in the severity of chronic hepatitis C presenting minimal fibrosis. *J Viral Hepat* 2002; **9:** 134-140

7 **Frese M,** Barth K, Kaul A, Lohmann V, Schwärzle V, Bartenschlager R. Hepatitis C virus RNA replication is resistant to tumour necrosis factor-alpha. *J Gen Virol* 2003; **84:** 1253-1259

8 **Puoti C.** HCV carriers with persistently normal aminotransferase levels: normal does not always mean healthy. *J Hepatol* 2003; **38:** 529-532

9 **Mathurin P,** Moussalli J, Cadranel JF, Thibault V, Charlotte F, Dumouchel P, Cazier A, Huraux JM, Devergie B, Vidaud M, Opolon P, Poynard T. Slow progression rate of fibrosis in hepatitis C virus patients with persistently normal alanine transaminase activity. *Hepatology* 1998; **27:** 868-872

10 **Knodell RG,** Ishak KG, Black WC, Chen TS, Craig R, Kaplowitz N, Kiernan TW, Wollman J. Formulation and application of a numerical scoring system for assessing histological activity in asymptomatic chronic active hepatitis. *Hepatology* 1981; **1:** 431-435

11 **Bertoletti A,** D'Elios MM, Boni C, De Carli M, Zignego AL, Durazzo M, Missale G, Penna A, Fiaccadori F, Del Prete G, Ferrari C. Different cytokine profiles of intraphepatic T cells in chronic hepatitis B and hepatitis C virus infections. *Gastroenterology* 1997; **112:** 193-199

12 **Boisvert J,** Kunkel EJ, Campbell JJ, Keeffe EB, Butcher EC, Greenberg HB. Liver-infiltrating lymphocytes in end-stage hepatitis C virus: subsetes, activation status, and chemokine receptor phenotypes. *J Hepatol* 2003; **38:** 67-75

13 **Prezzi C,** Casciaro MA, Francavilla V, Schiaffella E, Finocchi L, Chircu LV, Bruno G, Sette A, Abrignani S, Barnaba V. Virus-specific CD8(+) T cells with type 1 or type 2 cytokine profile are related to different disease activity in chronic hepatitis C virus infection. *Eur J Immunol* 2001; **31:** 894-906

14 **Jamal MM,** Soni A, Quinn PG, Wheeler DE, Arora S, Johnston DE. Clinical features of hepatitis C-infected patients with persistently normal alanine transaminase levels in the Southwestern United States. *Hepatology* 1999; **30:** 1307-1311

15 **Osna N,** Silonova G, Vilgert N, Hagina E, Kuse V, Giedraitis V, Zvirbliene A, Mauricas M, Sochnev A. Chronic hepatitis C: T-helper1/T-helper2 imbalance could cause virus persistence in peripheral blood. *Scand J Clin Lab Invest* 1997; **57:** 703-710

16 **Kallinowski B,** Haseroth K, Marinos G, Hanck C, Stremmel W, Theilmann L, Singer MV, Rossol S. Induction of tumour necrosis factor (TNF) receptor type p55 and p75 in patients with chronic hepatitis C virus (HCV) infection. *Clin Exp Immunol* 1998; **111:** 269-277

17 **Tsai SL,** Liaw YF, Chen MH, Huang CY, Kuo GC. Detection of type 2-like T-helper cells in hepatitis C virus infection: implications for hepatitis C virus chronicity. *Hepatology* 1997; **25:** 449-458

Science Editor Wang XL and Guo SY **Language Editor** Elsevier HK

PO Box 2345, Beijing 100023, China
www.wjgnet.com
wjg@wjgnet.com

ELSEVIER

World J Gastroenterol 2005;11(45):7192-7196
World Journal of Gastroenterology ISSN 1007-9327

• *RAPID COMMUNICATION* •

Diagnostic accuracy of serum biochemical fibrosis markers in children with chronic hepatitis B evaluated by receiver operating characteristics analysis

Dariusz Marek Lebensztejn, Elżbieta Skiba, Jolanta Tobolczyk, Maria Elżbieta Sobaniec-Lotowska, Maciej Kaczmarski

Dariusz Marek Lebensztejn, Elżbieta Skiba, Maciej Kaczmarski, III[rd] Department of Pediatrics, Medical University of Bialystok, Poland
Jolanta Tobolczyk, Department of Children Allergology, Medical University of Bialystok, Poland
Maria Elżbieta Sobaniec-Lotowska, Department of Clinical Pathomorphology, Medical University of Bialystok, Poland
Correspondence to: Assistant Professor Dariusz Marek Lebensztejn, MD, III[rd] Department of Pediatrics, Medical University of Bialystok, 17 Waszyngtona Str., 15-274 Bialystok, Poland. dariuszmar. 8810735@pharmanet.com.pl
Telephone: +48-85-7450539 Fax: +48-85-7423841
Received: 2005-04-12 Accepted: 2005-04-30

Abstract

AIM: To investigate the diagnostic accuracy of potent serum biochemical fibrosis markers in children with chronic hepatitis B evaluated by receiver operating characteristics (ROC) analysis.

METHODS: We determined the serum level of apolipoprotein A-I (APO A-I), haptoglobin (HPT) and a-2 macroglobulin (A2M) with an automatic nephelometer in 63 children (age range 4-17 years, mean 10 years) with biopsy-verified chronic HBeAg-positive hepatitis B. Fibrosis stage and inflammation grade were assessed in a blinded fashion according to Batts and Ludwig. We defined mild liver fibrosis as a score $\leqslant$2 and advanced fibrosis as a score equal to 3. ROC analysis was used to calculate the power of the assays to detect advanced liver fibrosis (AccuROC, Canada).

RESULTS: Serum concentrations of APO A-I, HPT and A2M were not significantly different in patients with chronic hepatitis B compared to controls. However, APO A-I level of 1.19 ng/L had a sensitivity of 85.7% and a specificity of 60.7% (AUC = 0.7117, P = 0.035) to predict advanced fibrosis. All other serum biochemical markers and their combination did not allow a useful prediction. None of these markers was a good predictor of histologic inflammation.

CONCLUSION: Apolipoprotein A-I may be a suitable serum marker to predict advanced liver fibrosis in children with chronic hepatitis B.

Key words: Chronic hepatitis B; Liver fibrosis; Children; Apolipoprotein A-I; Haptoglobin; a-2 macroglobulin

Lebensztejn DM, Skiba E, Tobolczyk J, Sobaniec-Lotowska ME, Kaczmarski M. Diagnostic accuracy of serum biochemical fibrosis markers in children with chronic hepatitis B evaluated by receiver operating characteristics analysis. *World J Gastroenterol* 2005; 11(45): 7192-7196
http://www.wjgnet.com/1007-9327/11/7192.asp

INTRODUCTION

Liver biopsy is regarded as the gold standard for the determination of the stage of liver fibrosis. However, in clinical practice, the use of invasive liver biopsy has several limitations such as complications, sampling variability, low reproducibility and it only provides static information about the fibrotic process[1-3]. There is a clinical need for noninvasive measurement of liver fibrosis both to diagnose significant hepatic fibrosis and to monitor the effects of antiviral or antifibrotic therapy.

Several matrix-derived surrogate markers of extracellular matrix (ECM) turnover have been studied in adults so far and some were found to be correlated with matrix deposition, while their role as predictors of ECM turnover remains unclear[4-6]. This applies particularly for children whose serum levels of ECM-derived parameters are usually influenced by body growth[7,8]. Therefore, there is an urgent need for noninvasive parameters that better define those children who should undergo liver biopsy in order to assess fibrosis stage, to decide whether they should receive antiviral therapy or not, to predict fibrosis progression or to monitor potential antifibrotic treatment. Serum levels of type IV collagen[9,10], hyaluronic acid[10-13], laminin[14], collagen VI[15], transforming growth factor beta 1 (TGF beta 1)[16] and metalloproteinases (MMPs) or tissue inhibitors of metalloproteinases (TIMPs)[10,17] have recently been studied in children, but almost exclusively in patients with secondary biliary fibrosis due to biliary atresia and cystic fibrosis.

To our knowledge, serum fibrosis markers predicting liver fibrosis have not been assessed before in children with chronic hepatitis B (HBV) except our previous studies[18-20]. From a broad panel of matrix-derived serum markers (collagen IV, collagen VI, PIIINP, laminin-2, hyaluronan, MMP-2, TIMP-1, MMP-9/TIMP1 complex, tenascin-C), the combination of serum hyaluronan and laminin-2 can accurately predict significant liver fibrosis[18].

In our previous studies, we have reported that serum TGF beta 1 and cystatin C level did not predict advanced liver fibrosis in children with chronic hepatitis B[19,20].

In the present study, the serum levels of apolipoprotein A-I (APO A-I), haptoglobin (HPT) and a-2 macroglobulin (A2M) were measured in children with chronic hepatitis B and compared to liver histological features to determine whether the measurement of these biochemical tests have any clinical usefulness as markers of liver fibrosis. Receiver operating characteristics (ROC) analysis was used to determine the sensitivity and specificity of the assays in detecting advanced liver fibrosis.

MATERIALS AND METHODS

Patients

The study was carried out in 63 children, including 41 boys and 22 girls (range 4-17 years, mean age 10 years) with biopsy-verified chronic HBeAg-positive hepatitis B prior to antiviral therapy. Other causes of chronic liver diseases, such as HCV coinfection, autoimmune hepatitis and metabolic liver disorders, were excluded. Children with diagnosed liver cirrhosis and evidence of other acute or chronic infections were also excluded from this study. Informed consent was obtained from all the parents of patients and the protocol used was approved by the Ethics Committee of the Medical University of Bialystok, Poland. As a control group, 16 children (mean age 10 years) were included without anamnestical, clinical or laboratory signs of liver or other systemic diseases.

Measurement of serum level of biochemical markers

APO A-I, HPT and A2M were measured in serum samples (obtained after an overnight fast) with an automatic nephelometer (BNII, Dade Behring; Marburg, Germany).

Histological analysis

All children underwent liver biopsy on the day after serum sampling. Liver specimens were fixed in buffered formalin and embedded in paraffin. Histological sections were stained using hematoxylin-eosin, Masson's-Goldner, Masson's trichrome and reticulin. Fibrosis stage and inflammation grade were assessed in a blinded fashion by a single pathologist who was without the knowledge of the patients' laboratory or clinical data. In order to determine specificity and sensitivity of the assay, we arbitrarily defined mild liver fibrosis or inflammation as a score $\leqslant$ 2 and advanced liver disease as fibrosis or inflammation score equal to 3 according to Batts and Ludwig[21].

Statistical analysis

Serum concentrations of biochemical tests were expressed as mean±SD. Statistical analysis was performed using the Mann-Whitney two-sample test for nonparametric data. The relationship between the enzymes and liver histology scores was analyzed by the Spearman's rank-correlation test for nonparametric data. Tests were considered statistically significant at $P<0.05$. Receiver operating characteristics (ROC) analysis (AccuROC, Montreal, Canada) was used to calculate the power of the assays to detect advanced liver fibrosis. The best cut-off points for the diagnosis of advanced fibrosis are those which maximize the sum of sensitivity and specificity. Sensitivity of the assays was plotted against the false positivity (1-specificity). Comparison of the area under the curve (AUC) was performed using a *P*-test, which compares the AUC to the diagonal line of no information (AUC 0.5)[22].

RESULTS

Characteristics of the patients

Selected biochemical and histological data are presented in Table 1.

Table 1 Initial characteristics of children with chronic hepatitis B

Parameters	Mean	SD	Minimum	Maximum
Age (yr)	10	3.41	4	17
ALT (IU/L)	84	57	12	312
AST (IU/L)	68	37	27	264
GGT (IU/L)	15	9	3	69
Bilirubin (μmol/L)	10.26	4.45	2.74	32.83
APO A-I (g/L)	1.14	0.3	0.5	1.77
HPT (g/L)	0.58	0.36	0.31	1.69
A2M (g/L)	2.27	0.57	1.0	3.59
Staging	1.9	0.56	1	3
Grading	1.49	0.56	1	3

Serum concentration of APO, HPT and A2M

Serum concentrations of APO A-I, HPT and A2M were not significantly different in patients with chronic hepatitis B as compared with the controls (1.14±0.3 *vs* 1.13±0.2; 0.58±0.36 *vs* 0.71±0.62, 2.27±0.57 *vs* 2.53±0.3, respectively). There were no significant correlations of examined markers with liver fibrosis and inflammation according to Batts and Ludwig[21].

Diagnostic value of biochemical markers for identification of patients with advanced liver fibrosis and inflammation

Seven children (11.1%) had advanced liver fibrosis. The ability of examined biochemical markers to differentiate the children with advanced liver fibrosis from those with mild fibrosis was not significant except APO A-I (Table 2 and Figure 1). Using the APO A-I and the Batts and Ludwig score, 34 and 6 out of 63 children could be correctly allocated either to the group with mild or advanced fibrosis, respectively, potentially avoiding biopsy in 40 (63.5%) of the examined children. HPT and A2M did not reach the predictive power of APO A-I (Table 2). None of the combination of examined markers resulted in a significant increase in sensitivity and specificity for the identification of patients with advanced liver fibrosis. None of these markers was a good predictor of histologic inflammation (Table 3).

Table 2 Diagnostic value of serum markers for predicting advanced fibrosis

Markers	Cut-off (g/L)	Se (%)	Sp (%)	PPV (%)	NPV (%)	AUC	*P* values
APO A-I	1.19	85.7	60.7	21.4	97.1	0.7117	0.035
HPT	1.01	14.3	87.5	12.5	89.1	0.3878	NS
A2M	1.79	100.0	23.2	14.0	100.0	0.5268	NS

Se: sensitivity; Sp: specificity; PPV: positive predictive value; NPV: negative predictive value; AUC: area under curve; NS: no statistical significance.

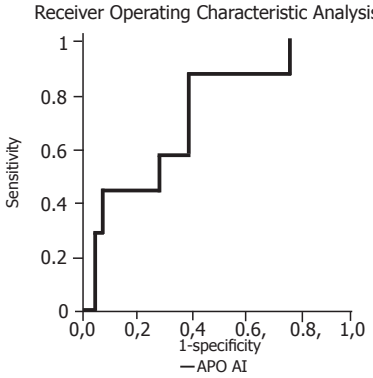

Figure 1 ROC curve of ability of serum APO A-I to detect advanced liver fibrosis according to Batts and Ludwig in children with chronic hepatitis B.

Table 3 Diagnostic values of serum markers for predicting advanced inflammation

Markers	Cut-off (g/L)	Se (%)	Sp (%)	PPV (%)	NPV (%)	AUC	P values
APO A-I	0.87	89.7	20.6	49.1	70.0	0.3803	NS
HPT	0.59	34.5	70.6	50.0	55.8	0.4701	NS
A2M	1.6	96.6	14.7	49.1	83.3	0.3813	NS

Se: sensitivity; Sp: specificity; PPV: positive predictive value; NPV: negative predictive value; AUC: area under curve; NS: no statistical significance.

DISCUSSION

Infection with the hepatitis B virus remains one of the most important epidemiological problems all over the world. It was estimated that chronic HBV infection, which is the single most common cause of cirrhosis and hepatocellular carcinoma (HCC), affects more than 400 million people worldwide[23,24].

During the early phase of chronic hepatitis B, the underlying disease is usually subclinical and can be quite mild, particularly in children[25]. This is referred to as the immune-tolerant phase of infection[26]. While the natural history of chronic hepatitis B in children is usually marked by an indolent course, advanced disease with significant fibrosis can be found in up to one-third of the children, and decompensated cirrhosis and even HCC have been reported[27,28]. For this reason, noninvasive diagnosis and monitoring of liver fibrosis in children are urgently needed.

There are several features required for an ideal serum fibrosis marker. It should be liver-specific, independent of metabolic alterations, minimally influenced by impaired urinary and biliary excretion, easy to perform and it should measure either the dynamic processes of fibrogenesis or fibrolysis and reflect the degree of fibrosis. Unfortunately, no current assay fulfills enough of these criteria[5].

Recently, algorithms of non-ECM-derived serum markers have been proposed as the predictors of fibrosis stage in adult patients with chronic hepatitis C[29-31]. APO A-I, HPT and A2M are the components of FibroTest[32] and APO A-I and A2M are the components of PGAA index[33,34]; they have also been validated as single serum fibrosis markers[6,35-38].

In the present study, we did not find significantly different levels of examined serum fibrosis markers in children with chronic hepatitis B as compared with the controls. There were also no significant correlation of APO A-I, HPT, and A2M levels with histologically assessed stage of liver fibrosis and inflammation grade. Because liver biopsy is not necessarily a gold standard for assessing liver histology, noninvasive markers will not have complete concordance with histological staging. Only 11.1% children had advanced fibrosis according to Batts and Ludwig[21] and probably for this reason, we also did not observe statistically significant correlation between the examined markers and fibrosis stage.

These findings confirmed previous observation in children by Selimoglu *et al*[35,37] who also demonstrated that mean APO A-I level of the patients with chronic hepatitis B was not different from controls and did not correlate with fibrosis and inflammation scores. To our knowledge, A2M and HPT as potent serum fibrosis markers have not been assessed in children yet.

In adults with chronic hepatitis B, Oberti *et al*[6] and Huang and Gong[36] observed that APO A-I and A2M were significantly correlated with the staging of liver fibrosis. Lu *et al*[34] confirmed that A2M but not APO A-I was significantly correlated with fibrosis stage. However, HPT was negatively associated with fibrosis[38]. These opposing correlation of A2M and HPT with fibrosis staging could be explained by the different roles of hepatocyte growth factor (HGF) and TGF beta 1 in fibrogenesis and acute phase response[39-41]. As seen in experimental fibrosis, transduction with HGF gene suppresses increase of TGF beta 1[39] and the factor stimulates synthesis of A2M[40] and reduces synthesis of haptoglobin[40,41].

Recently, ROC analysis has been recommended to calculate the power of the assays to detect advanced liver fibrosis[42-46]. In this study, the ability of examined biochemical markers to differentiate children with advanced liver fibrosis from those with mild fibrosis was not significant except APO A-I. The high negative predictive value of this marker could potentially be useful in the selection of patients without significant fibrosis and in avoiding invasive liver biopsy in this group of children. Our study is not consistent with the findings of Selimoglu *et al*[35], because they did not find diagnostic performance of APO A-I for discriminating patients with advanced liver

disease. Usefulness of APO A-I as well as HPT and A2M as potent serum fibrosis markers in patients with chronic liver disease needs to be evaluated in large controlled studies.

REFERENCES

1 **Kirchner GI,** Wagner S, Flemming P, Bleck JS, Gebel M, Schedel I, Schüler A, Galanski M, Manns MP. COACH syndrome associated with multifocal liver tumors. *Am J Gastroenterol* 2002; **97:** 2664-2669
2 **Bedossa P,** Dargère D, Paradis V. Sampling variability of liver fibrosis in chronic hepatitis C. *Hepatology* 2003; **38:** 1449-1457
3 **Piccinino F,** Sagnelli E, Pasquale G, Giusti G. Complications following percutaneous liver biopsy: a multicentre retrospective study on 68,276 biopsies. *J Hepatol* 1986; **2:** 165-173
4 **Plebani M,** Burlina A. Biochemical markers of hepatic fibrosis. *Clin Biochem* 1991; **24:** 219-239
5 **Schuppan D,** Stölzel U, Oesterling C, Somasundaram R. Serum assays for liver fibrosis. *J Hepatol* 1995; **22:** 82-88
6 **Oberti F, Valsesia E,** Pilette C, Rousselet MC, Bedossa P, Aubé C, Gallois Y, Rifflet H, Maïga MY, Penneau-Fontbonne D, Calès P. Noninvasive diagnosis of hepatic fibrosis or cirrhosis. *Gastroenterology* 1997; **113:** 1609-1616
7 **Trivedi P,** Risteli J, Risteli L, Tanner MS, Bhave S, Pandit AN, Mowat AP. Serum type III procollagen and basement membrane proteins as noninvasive markers of hepatic pathology in Indian childhood cirrhosis. *Hepatology* 1987; **7:** 1249-1253
8 **Danne T,** Grüters A, Schuppan D, Quantas N, Enders I, Weber B. Relationship of procollagen type III propeptide-related antigens in serum to somatic growth in healthy children and patients with growth disorders. *J Pediatr* 1989; **114:** 257-260
9 **Kobayashi H,** Miyano T, Horikoshi K, Tokita A. Prognostic value of serum procollagen III peptide and type IV collagen in patients with biliary atresia. *J Pediatr Surg* 1998; **33:** 112-114
10 **Pereira TN,** Lewindon PJ, Smith JL, Murphy TL, Lincoln DJ, Shepherd RW, Ramm GA. Serum markers of hepatic fibrogenesis in cystic fibrosis liver disease. *J Hepatol* 2004; **41:** 576-583
11 **Kobayashi H,** Horikoshi K, Yamataka A, Yamataka T, Okazaki T, Lane GJ, Miyano T. Hyaluronic acid: a specific prognostic indicator of hepatic damage in biliary atresia. *J Pediatr Surg* 1999; **34:** 1791-1794
12 **Hasegawa T,** Sasaki T, Hoki M, Okada A, Mushiake S, Yagi M, Imura K. Measurement of serum hyaluronic acid as a sensitive marker of liver fibrosis in biliary atresia. *J Pediatr Surg* 2000; **35:** 1643-1646
13 **Wyatt HA,** Dhawan A, Cheeseman P, Mieli-Vergani G, Price JF. Serum hyaluronic acid concentrations are increased in cystic fibrosis patients with liver disease. *Arch Dis Child* 2002; **86:** 190 -193
14 **Sasaki F,** Hata Y, Hamada H, Takahashi H, Uchino J. Laminin and procollagen-III-peptide as a serum marker for hepatic fibrosis in congenital biliary atresia. *J Pediatr Surg* 1992; **27:** 700 -703
15 **Gerling B,** Becker M, Staab D, Schuppan D. Prediction of liver fibrosis according to serum collagen VI level in children with cystic fibrosis. *N Engl J Med* 1997; **336:** 1611-1612
16 **Rosensweig JN,** Omori M, Page K, Potter CJ, Perlman EJ, Thorgeirsson SS, Schwarz KB. Transforming growth factor beta 1 in plasma and liver of children with liver disease. *Pediatr Res* 1998; **44:** 402-409
17 **Kobayashi H,** Li ZX, Yamataka A, Lane GJ, Miyano T. Clinical evaluation of serum levels of matrix metalloproteinases and tissue inhibitors of metalloproteinases as predictors of progressive fibrosis in postoperative biliary atresia patients. *J Pediatr Surg* 2002; **37:** 1030-1033
18 **Lebensztejn DM,** Kaczmarski M, Sobaniec-Łotowska M, Bauer **M, Voelker M,** Schuppan D. Serum laminin-2 and hyaluronan predict severe liver fibrosis in children with chronic hepatitis B. *Hepatology* 2004; **39:** 868-869
19 **Lebensztejn DM,** Sobaniec-Lotowska M, Kaczmarski M, Werpachowska I, Sienkiewicz J. Serum concentration of transforming growth factor (TGF) beta 1 does not predict advanced liver fibrosis in children with chronic hepatitis B. *Hepatogastroenterology* 2004; **51:** 229-233
20 **Lebensztejn DM,** Skiba E, Kaczmarski M, Tobolczyk J, Koput A, Sobaniec-Łotowska ME. Serum cystatin C concentration does not predict advanced liver disease in children with chronic hepatitis B. *Clin Chim Acta* 2004; **347:** 227-228
21 **Batts KP, Ludwig J.** Chronic hepatitis. An update on terminology and reporting. *Am J Surg Pathol* 1995; 19: 1409-1417
22 **Vida S.** A computer program for non-parametric receiver operating characteristic analysis. *Comput Methods Programs Biomed* 1993; **40:** 95-101
23 **Lee WM.** Hepatitis B virus infection. *N Engl J Med* 1997; **337:** 1733-1745
24 **Lok AS,** Heathcote EJ, Hoofnagle JH. Management of hepatitis B: 2000--summary of a workshop. *Gastroenterology* 2001; **120:** 1828-1853
25 **Tang JR,** Hsu HY, Lin HH, Ni YH, Chang MH. Hepatitis B surface antigenemia at birth: a long term follow up study. *J Pediatr* 1998; **133:** 374-377
26 **Lok AS,** Lai CL. A longitudinal follow-up of asymptomatic hepatitis B surface antigen positive Chinese children. *Hepatology* 1988; **8:** 1130-1133
27 **Bortolotti F,** Jara P, Crivellaro C, Hierro L, Cadrobbi P, Frauca E, Camarena C, de La Vega A, Diaz C, De Moliner L, Noventa F. Outcome of chronic hepatitis B in Caucasian children during a 20-year observation period. *J Hepatol* 1998; **29:** 184-190
28 **Fujisawa T,** Komatsu H, Inui A, Sogo T, Miyagawa Y, Fujitsuka S, Sekine I, Kosugi T, Inui M. Long-term outcome of chronic hepatitis B in adolescent or young adults in follow-up from childhood. *J Pediatr Gastroenterol Nutr* 2000; **30:** 201-206
29 **Imbert-Bismut F,** Ratziu V, Pieroni L, Charlotte F, Benhamou Y, Poynard T. Biochemical markers of liver fibrosis in patients with hepatitis C virus infection: a prospective study. *Lancet* 2001; **357:** 1069-1075
30 **Forns X,** Ampurdanès S, Llovet JM, Aponte J, Quintó L, Martíne-Bauer E, Bruguera M, Sánchez-Tapias JM, Rodés J. Identification of chronic hepatitis C patients without hepatic fibrosis by a simple predictive model. *Hepatology* 2002; **36:** 986-992
31 **Wai CT,** Greenson JK, Fontana RJ, Kalbfleisch JD, Marrero JA, Conjeevaram HS, Lok AS. A simple noninvasive index can predict both significant fibrosis and cirrhosis in patients with chronic hepatitis C. *Hepatology* 2003; **38:** 518-526
32 **Halfon P,** Imbert-Bismut F, Messous D, Antoniotti G, Benchetrit D, Cart-Lamy P, Delaporte G, Doutheau D, Klump T, Sala M, Thibaud D, Trepo E, Thabut D, Myers RP, Poynard T. A prospective assessment of the inter-laboratory variability of biochemical markers of fibrosis (FibroTest) and activity (ActiTest) in patients with chronic liver disease. *Comp Hepatol* 2002; **1:** 3
33 **Naveau S,** Poynard T, Benattar C, Bedossa P, Chaput JC. Alpha-2-macroglobulin and hepatic fibrosis. Diagnostic interest. *Dig Dis Sci* 1994; **39:** 2426-2432
34 **Lu LG,** Zeng MD, Mao YM, Li JQ, Qiu DK, Fang JY, Cao AP, Wan MB, Li CZ, Ye J, Cai X, Chen CW, Wang JY, Wu SM, Zhu JS, Zhou XQ. Relationship between clinical and pathologic findings in patients with chronic liver diseases. *World J Gastroenterol* 2003; **9:** 2796-2800
35 **Selimoglu MA,** Yagcl RV, Yüce G. Low plasma apolipoprotein A-I level is not a reliable marker of fibrosis in children with chronic hepatitis B. *World J Gastroenterol* 2004; **10:** 2864 - 2866
36 **Huang W,** Gong FY. [Diagnostic value of serum biochemical markers for liver fibrosis in patients with hepatitis B virus.]*Di Yi Jun Yi Da Xue Xue Bao* 2002; **22:** 1034-1036

37 **Selimoğlu MA,** Aydoğdu S, Yağci RV. Low plasma apolipoprotein A-I level: new prognostic criterion in childhood cirrhosis? *Turk J Pediatr* 2001; **43:** 307-311
38 **Bacq Y,** Schillio Y, Brechot JF, De Muret A, Dubois F, Metman EH. [Decrease of haptoglobin serum level in patients with chronic viral hepatitis C] *Gastroenterol Clin Biol* 1993; **17:** 364-369
39 **Ueki T,** Kaneda Y, Tsutsui H, Nakanishi K, Sawa Y, Morishita R, Matsumoto K, Nakamura T, Takahashi H, Okamoto E, Fujimoto J. Hepatocyte growth factor gene therapy of liver cirrhosis in rats. *Nat Med* 1999; **5:** 226-230
40 **Guillén MI,** Gómez-Lechón MJ, Nakamura T, Castell JV. The hepatocyte growth factor regulates the synthesis of acute-phase proteins in human hepatocytes: divergent effect on interleukin-6-stimulated genes. *Hepatology* 1996; **23:** 1345-1352
41 **Moshage H.** Cytokines and the hepatic acute phase response. *J Pathol* 1997; **181:** 257-266
42 **Zheng M,** Cai WM, Weng HL, Liu RH. ROC curves in evaluation of serum fibrosis indices for hepatic fibrosis. *World J Gastroenterol* 2002; **8:** 1073-1076
43 **Lu LG,** Zeng MD, Wan MB, Li CZ, Mao YM, Li JQ, Qiu DK, Cao AP, Ye J, Cai X, Chen CW, Wang JY, Wu SM, Zhu JS, Zhou XQ. Grading and staging of hepatic fibrosis, and its relationship with noninvasive diagnostic parameters. *World J Gastroenterol* 2003; **9:** 2574-2578
44 **Zhang BB,** Cai WM, Weng HL, Hu ZR, Lu J, Zheng M, Liu RH. Diagnostic value of platelet derived growth factor-BB, transforming growth factor beta 1, matrix metalloproteinase-1, and tissue inhibitor of matrix metalloproteinase-1 in serum and peripheral blood mononuclear cells for hepatic fibrosis. *World J Gastroenterol* 2003; **9:** 2490-2496
45 **Patel K,** Gordon SC, Jacobson I, Hézode C, Oh E, Smith KM, Pawlotsky JM, McHutchison JG. Evaluation of a panel of non-invasive serum markers to differentiate mild from moderate-to-advanced liver fibrosis in chronic hepatitis C patients. *J Hepatol* 2004; **41:** 935 - 942
46 **Rosenberg WM,** Voelker M, Thiel R, Becka M, Burt A, Schuppan D, Hubscher S, Roskams T, Pinzani M, Arthur MJ. Serum markers detect the presence of liver fibrosis: A cohort study. *Gastroenterology* 2004; **127:** 1704 - 1713

Science Editor Kumar M and Guo SY **Language Editor** Elsevier HK

PO Box 2345, Beijing 100023, China
www.wjgnet.com
wjg@wjgnet.com

ELSEVIER

World J Gastroenterol 2005;11(45):7197-7202
World Journal of Gastroenterology ISSN 1007-9327

• RAPID COMMUNICATION •

Effects of L-carnitine in patients with hepatic encephalopathy

Mariano Malaguarnera, Giovanni Pistone, Rampello Elvira, Carmelo Leotta, Linda Scarpello, Rampello Liborio

Mariano Malaguarnera, Giovanni Pistone, Rampello Elvira, Carmelo Leotta, Linda Scarpello, Department of Senescence, Urological e Neurological, University of Catania, Cannizzaro Hospital, Catania, Italy
Rampello Liborio, Department of Neurosciences, University of Catania, Italy
Correspondence to: Professor Mariano Malaguarnera, Ospedale Cannizzaro, via Messina, 829 95125 Catania, Italy. malaguar@unict.it
Telephone: +39-95-7262008 Fax: +39-95-7262011
Received: 2005-04-19 Accepted: 2005-05-24

Abstract

AIM: To evaluate the influence of L-carnitine on mental conditions and ammonia effects on patients with hepatic encephalopathy (HE).

METHODS: One hundred and fifty patients (10 patients with alcoholism, 41 patients with hepatitis virus B infection, 78 patients with hepatitis C virus infection, 21 patients with cryptogenetic cirrhosis) meeting the inclusion criteria were randomized into group A receiving a 90-d treatment with L-carnitine (2 g twice a day) or into group B receiving placebo in double blind.

RESULTS: At the end of the study period, a significant decrease in NH4 fasting serum levels was found in patients with hepatic encephalopathy ($P<0.05$) after the treatment with levocarnitine (LC). Significant differences were also found between symbol digit modalities test and block design in patients with hepatic encephalopathy ($P<0.05$).

CONCLUSION: Results of our study suggest an important protective effect of L-carnitine against ammonia-precipitated encephalopathy in cirrhotic patients.

Key words: Hepatic encephalopathy; Carnitine; Cirrhosis; Ammonia; Treatment

Malaguarnera M, Pistone G, Elvira R, Leotta C, Scarpello L, Rampello L. Effects of L-carnitine in patients with hepatic encephalopathy. *World J Gastroenterol* 2005; 11(45): 7197-7202
http://www.wjgnet.com/1007-9327/11/7197.asp

INTRODUCTION

Hepatic encephalopathy (HE) commonly occurs in patients with liver cirrhosis and is characterized by impaired mental function, neuromuscular disorders and altered states of consciousness. The pathogenesis of HE is controversial although ammonia has been found to induce alterations of cerebral neurotransmitter balance especially at the astrocyte-neuron interface.

Hyperammonemia induces abnormalities such as brain edema and intracranial hypertension in cirrhotic patients. In cirrhotic patients, the relation between blood levels of ammonia and brain events is also influenced by the changes in the permeability-surface area of the blood-brain barrier[1].

In hepatic encephalopathy, the Alzheimer type II astrocytes are the main neuropathological alteration, characterized by swollen cellular nuclei, with their chromatin displaced to the periphery.

The accumulation of glutamine, a product of ammonia detoxification generated within astrocytes expressing activity of glutamine synthetase, is a major factor for the swelling of astrocytes[2].

Previous studies have reported a significant protective effect of L-carnitine in mice, rats, and human beings. In fact L-carnitine treatment is associated with a significant reduction of blood and brain ammonia concentration[3-6]. Carnitine is a natural substance involved in regulating substrate flux and energy balance across cell membranes.

The pharmacological activity of L-carnitine presents various aspects. The carnitine acts by shuttling acetyl-CoA into mitochondria, enhances the metabolic flux in the tricarboxylic acid cycle by sparing free CoA and activating the transport of adenine nucleotides across the inner mitochondrial membrane and prevents adenylate translocase inhibition of the activity of pyruvate dehydrogenase by decreasing the acetyl-CoA/CoA ratio, thus enhancing the oxidative utilization of glucose.

Increased extra-intestinal ammonia production and reduced ammonia detoxification capacity in patients with cirrhosis[7-9] and HE, have not been studied[10].

L-carnitine, inducing ureagenesis, may decrease blood and brain ammonia levels[4,5]. In order to assess the clinical efficacy of L-carnitine in the treatment of HE, a randomized, double-blind, placebo-controlled study with oral administration in cirrhotic patients with hyperammonemia was carried out.

MATERIALS AND METHODS

Patients

One hundred and fifty patients (10 with alcoholism, 41 with hepatitis B virus infection, 78 with hepatitis C virus infection, 21 with cryptogenetic cirrhosis) meeting

the following inclusion criteria were enrolled in the study: chronic hepatitis with spontaneous manifest HE (mental state grade 1 or 2 according to the West Haven criteria) minimal HE (MHE) (mental status grade 0) and a number connection test performance time >30 s[11-13]; hyperammonemia (venous ammonia concentration >50 mmol/L); cooperative, hospitalized, adult patients with liver cirrhosis diagnosed by clinical, histological, and ultrasonographic findings.

Exclusion criteria included: major complications of portal hypertension, such as gastrointestinal blood loss, hepatorenal syndrome or bacterial peritonitis; acute superimposed liver injury; patients with other neurological disease and metabolic disorders, diabetes mellitus, unbalanced heart failure and/or respiratory failure or end-stage renal disease; severe HE (mental state grade 3-4); administration of anti-HE medications such as neomycin, lactulose, lactitol, branched-chain aminoacids; any additional precipitating factors such as high protein intake (additional high-protein meals), constipation or intake of psychostimulants, sedatives, antidepressants, benzodiazepines, or benzodiazepines-antagonists (flumazenil); patients with fever, sepsis or shock were also excluded to avoid variations caused by body temperature.

Study design

Patients meeting the inclusion criteria were randomized either into group receiving a 90-d treatment with L-carnitine (2 g twice daily) or into group receiving placebo in double-blind. Concomitant medications throughout the study included diuretics and beta-blockers.

Patients were visited weekly throughout the treatment period for the assessment of adherence to the study protocol, blood pressure and cognitive functions, as well as recording of adverse events. Throughout the trial, levo-carnitine was supplied as 2 g vials for oral use.

All administered drugs were identical in appearance, and neither investigators nor patients were informed of the selected agents at the end of the study. Administration instructions were provided with each patient pack. All patients were instructed to take the trial medication as prescribed. Patients were considered compliant, if the number of returned vials was between 80% and 120% of the planned treatment regimen. For the duration of the trial, concomitant drugs were administered at the lowest possible therapeutic dosage, and unchanged as far as possible.

Study series

A total of 150 cirrhotic hepatopathic patients met the criteria for inclusion in this study performed between January 2000 and December 2001. They were randomly assigned to receive placebo (75 patients) or L-carnitine (75 patients). The two groups had similar demographic characteristics, etiology, course of disease and Child-Pugh grade. All study series were subdivided into groups of MHE or HE 1 or HE 2 according to the initial HE grade (West-Haven criteria). Group A consisted of patients with MHE (21 patients receiving LC, 19 patients receiving placebo). Group B consisted of patients with initial HE 1 (30 patients receiving LC, 30 patients receiving placebo). Group C consisted of patients with initial HE 2 (25 patients receiving LC, 25 patients receiving placebo). The effectiveness of therapy was compared and evaluated separately in the different subgroups.

The groups were homogeneous with regard to anamnestic and diagnostic criteria. Differences in composition of the two groups with respect to precipitant factors might be minimized, because the patient population was well defined by inclusion and exclusion criteria.

Diagnosis of minimal hepatic encephalopathy

Psychometric tests and automated EEG analysis were performed for all the patients.

Minimal hepatic encephalopathy was defined as the presence of at least one of the abnormal psychometric tests.

Trail making test: The trail making test was used to evaluate abstract reasoning, tactile performance, tactile-visual and spatial memory, rhythm perception and memory, speech-sound perception, primary motor speed, intelligence, psychomotor speed, sequencing abilities, language function, sensory function, grip strength, and personality functioning.

Time was recorded in seconds. This test included part A and B.

In part A, patients were asked to serially connect digits that were scattered on a page as quickly as possible. In part B, patients were asked to sequentially alternate numbers and letters (i.e. 1-A-2-B-3-C) as quickly as possible. A decrease in the time indicated an improvement in neuropsycological function.

Wechsler adult intelligence scale-revised: Block design test and symbol digit modalities test. The Wechsler adult intelligence scale-revised (WAIS-R) could provide information on global intellectual functioning.

Cognitive functions assessed in the block design test (BDT) were construction, praxis, spatial reasoning motor function, and processing speed. The symbol digit modalities test (SDMT) was used to assess attention, concentration executive function, motor function, and processing speed.

An increase in the number of points in the BDT and SDMT indicated an improvement in neurological function.

Diagnosis of hepatic encephalopathy

Hepatic encephalopathy grade was diagnosed on the basis of the evaluation of consciousness, intellectual functions, behavior and neuromuscular functions according to West Haven criteria introduced by Conn and Liebertahl[11].

Neurophysiological assessment

The EEG was recorded using standardized techniques. Five electrodes were attached to the skin at the positions T3, T4, O1, O2, and Cz according to the international "10-20 system". Electrode impedance was kept lower than 5 KQ. After applying the usual handpass filters (0.53-35 Hz), 2 runs of 100 s each were recorded and

compared for reproducibility. Artefact-free recordings were selected and fed into a computer after digital conversion (sample frequency 102.4 Hz). Ten epochs of 10 s each were analyzed by applying fast Fourier transformation, and the mean power spectrum was calculated.

Patients were graded into different studies of hepatic encephalopathy according to their mean dominant frequency (MDF) and the relative powers of delta and theta activity[14].

Liver function assessment

The Child-Pugh[15] score was determined to assess the severity of cirrhosis, including three biochemical variables (serum albumin, bilirubin, and prothrombin time) and two clinical characteristics (presence or absence of ascites and clinical hepatic encephalopathy).

A patient had a Child-Pugh score A cirrhosis if the score was ≤6 points, a Child-Pugh B cirrhosis if the score was 7-9 points and a Child-Pugh C cirrhosis if the score was >9 points. Patients without signs of ascites were scored as two points for ascites[15].

Venous ammonia concentration

The ammonia was determined according to the enzymatic determination of ammonia with glutamate dehydrogenase in a rapid and interference-free photometric determination (340 nm) of NH4+ in native blood plasma as previously described[16].

Due to reasons of safety, blood was immediately sent to the laboratory for determination of NH4+.

Safety parameters

Safety parameters included blood tests (hemoglobin, hematocritus, white blood cell count, and thrombocytes) and liver function tests (alanine amino transferase, aspartate amino transferase, gamma glutamyl-transpeptidase, cholinesterase activity, serum bilirubin concentrations, prothrombin time and partial thromboplastin time) on d 0, 30, 60 and 90.

Statistical analysis

Descriptive statistics was proposed from the study sample and results were expressed as mean±SD.

Statistical analyses were performed by two-way analysis of variance (ANOVA), as well as by controlling for multiple correction of Bonferroni.

All *P* values were two-sided, using $\alpha = 0.05$ as the reference standard for determining the significance of the principal outcomes.

Statistical Analysis System (Cari, NC, USA) software version 6.11 was used for all analyses.

The primary population for statistical analysis was to intent to treat population of all randomized patients (I.T.T.).

RESULTS

Baseline values

The two groups had similar general characteristics. Serum NH4+ fasting concentrations were not significantly different before the treatment.

Comparison with baseline

In MHE, ammonia serum levels were significantly decreased to 13.10 μmol/L (CI-24.3 to-1.8; $P<0.05$), to 19.10 μmol/L (CI-30.2 to-8.0; $P<0.001$), to 28.1 μmol/L (CI-38.5 to 17.6; $P<0.001$) after 30, 60, and 90 d of treatment, respectively.

The trial making test-A and trial making test-B were significantly decreased to 13.80 s (CI-19.87 to-7.73; $P<0.05$), to 25.00 s (CI-29.09 to –20.91; $P<0.05$), to 18.00 s (CI-23.50 to-12.50; $P<0.05$) and to 26.00 s (CI-29.61 to-22.39; $P<0.05$), to 21.50 s (CI-26.62 to-16.38; $P<0.05$), and to 28.9 (CI-32 to-25; $P<0.05$) respectively, after 30, 60 and 90 d of treatment.

The symbol digit modalities test was significantly increased from 4.00 points (CI 3.51 to 4.49; $P<0.05$), after 30 d of treatment, to 8.00 points (CI 7.56 to 8.44; $P<0.05$), and 8.00 points (CI 7.53 to 8.47; $P<0.05$) after 60 and 90 d of treatment, respectively.

The block design in MHE were significantly increased from 4.10 points (CI 3.59 to 4.61; $P<0.05$), to 7.90 points (CI 7.35 to 8.45; $P<0.05$), and to 12.90 points (CI 12.53 to 13.27; $P<0.05$) respectively after 30, 60, and 90 d of treatment.

In HE1, ammonia serum levels were significantly decreased to 12.0 μmol/L (CI-22.57 to-3.65; $P<0.05$), to 23.90 μmol/L (CI-33.23 to-14.57; $P<0.05$) and to 41.00 (CI -50.23 to 31.77; $P<0.05$) respectively after 30, 60, 90 d of treatment.

The TMT A and B were significantly decreased to 11.60 s (CI-18.08 to-5.12; $P<0.05$) and to 9.20 s (CI-12.62 to-5.78; $P<0.05$), to 21.60 s (-27.73 to-15.47; $P<0.05$) and to 19.10 s (CI-22.70 to-15.50; $P<0.05$), to 28.80 s (CI-34.87 to-22.73; $P<0.05$) and to 23.80 s (CI-27.06 to 20.54; $P<0.05$) respectively after 30, 60, 90 d of treatment.

The SDMT were significantly increased from 5.10 (CI 4.45 to 5.75; $P<0.05$) to 8.00 (CI 7.30 to 8.70; $P<0.05$) and to 14.00 (CI 13.39 to 14.10; $P<0.05$) respectively after 30, 60, 90 d of treatment.

The BDT were significantly increased from 3.00 points (CI 2.40 to 3.60; $P<0.05$) from 6.10 points (CI 5.47 to 6.73; $P<0.05$) and from 12.10 points (CI 11.62 to 12.58; $P<0.05$) respectively after 30, 60 and 90 d of treatment.

In HE2, ammonia serum levels were significantly decreased to 15.10 μmol/L (CI-23.44 to-6.76; $P<0.05$) and to 36.00 μmol/L (CI-44.84 to-27.16; $P<0.05$) respectively after 60 and 90 d of treatment.

The TMT A and B were significantly decreased to 10.50 s (CI-16.97 to-4.03; $P<0.05$) and to 9.50 s (CI-13.31 to-5.60; $P<0.05$), to 26.20 s (CI 32.97 to-22.39; $P<0.05$) and 21.79 s (CI-25.70 to 17.88; $P<0.05$), to 30.20 s (CI-36.48 to 23.92; $P<0.05$) and 35.00 s (CI 39.13 to 30.87; $P<0.05$) respectively after 30, 60, and 90 d of treatment.

The SDMT were significantly increased to 3.10 points (CI 2.56 to 3.64; $P<0.05$), to 7.00 points (CI 4.15 to 9.85; $P<0.05$) and to 12.90 points (CI 12.27 to 13.53; $P<0.05$) respectively after 30, 60, and 90 d of treatment.

The BDT were significantly increased from 4.10 points (CI 3.5 to 4.7; $P<0.05$) to 8.10 points (CI 7.60 to 8.60; $P<0.05$) and to 13.00 points (CI 12.40 to 13.60; $P<0.05$) respectively after 30, 60, and 90 d of treatment.

No significant differences were observed in the patients treated with placebo compared to baseline (Table1).

Table 1 Baseline data of patients

Parameter	Carnitine group, *n* = 75	Placebo group, *n* = 75
Male/female	50/25	45/30
Age (yr)	51.7 ± 9.6	53.2 ± 9.2
Cirrhosis etiology		
Alcohol	7	5
Post-hepatitis B	20	22
Post-hepatitis C	38	38
Cryptogenetic	10	10
Child–Pugh class		
A	30	31
B	34	34
C	11	10
Prothrombin time (%)	62.8 ± 6.9	63.1 ± 6.8
Serum albumin level (g/dL)	2.9 ± 0.7	2.8 ± 0.9
Serum bilirubin level (mg/dL)	3.1 ± 1.2	3.2 ± 1.4
Serum alanine aminotransferase level (IU/L)	119 ± 74	116 ± 77
Blood urea nitrogen (mg/dL)	40 ± 9	39 ± 11
Serum creatinine level (mg/dL)	0.88 ± 0.21	0.82 ± 0.30
Natriemia (mEq/L)	136 ± 3.4	138 ± 4.7
Kaliemia (mEq/L)	4.1 ± 1.2	4.2 ± 0.9

Comparison between treatments

At the end of the study period, fasting serum levels of NH4, TMT-A, TMT-B were significantly decreased in patients with hepatic encephalopathy compared to controls ($P<0.05$) after treatment with LC and placebo respectively. MHE-28.10 *vs* -2.00, $P < 0.05$; HE1-41.00 *vs* -1.50, $P<0.05$; HE2-36.00 *vs* 3.90, $P < 0.05$; TMT-A MHE -21.50 *vs* -7.30, $P < 0.05$, HE1 -28.8 *vs*-7.30, $P<0.05$; HE2 -30.20 *vs* -2.90, $P < 0.05$; TMT-B MHE-28.9 *vs* 1.0, $P < 0.05$; HE1-23.8 *vs*-4.00, $P < 0.05$; HE2-12.29 *vs* 0.90, $P < 0.05$.

Significant differences were also found between symbol digit modalities test and block design.

The SDMT was increased to 4.00 *vs* 0.20, 2.90 *vs* 0.80, 3.90 *vs* 0.20, respectively in MHE, HE1, and HE2 ($P<0.05$). The block design was increased to 3.80 *vs* 0.40, 3.10 *vs* 0.40, 4.00 *vs* 1.00, respectively in MHE, HE1, and HE2 ($P<0.05$) (Table 2).

DISCUSSION

The pathogenetic mechanisms underlying the development of hepatic encephalopathy are complex.

Symptoms of hepatic encephalopathy are generally reversible, suggesting a metabolic cause. Among the possible neurotoxins implicated in hepatic encephalopathy, ammonia is considered as a leading candidate[17,18].

The majority of blood ammonia results from muscle protein catabolism at the intestinal level. The remnant is produced by the action of colic bacteria on the nitrium present in digested foods. Ammonia is vehicled to the liver throughout the portal flux and normally eliminated as urea. The liver damage or the presence of porto-systemic shunts increases its serum levels[19-21]. The excess ammonia is eliminated from the blood by transforming glutamate into glutamine in skeletal muscle and central nervous system. Neurotoxicity of ammonia is probably due to a direct action on neurons, because the reduction of glutamate and the increase of glutamine may induce swelling of the astrocytes[22,23].

O'Connor *et al*[19] observed that mice treated with L-carnitine experience a continuous rise in blood urea N until a plateau is reached 1 h after injection, whereas mice not treated with L-carnitine experience a rise in blood urea N, but one died within 15 min after ammonium acetate administration.

Intravenous L-carnitine significantly can lower plasma ammonia N levels in ewes after an oral urea challenge even though the concentration of ruminal free, non-ionized ammonia N is similar to those in ewes treated only with the urea solution, suggesting that L-carnitine administration may prevent hyperammonemia in ruminants[24].

Carnitine has been shown to be efficacious in valproic acid hyperammonemia[25]. Preventive supplementations with L-carnitine might afford some benefits. Ohtani *et al*[26] have showed that oral administration of carnitine for 4 wk corrects hyperammonemia in patients treated with valproic acid. Studies in valproate-treated rats indicate that L-carnitine supplementation can correct hyperammonemia, hypocarnitinemia and protect rat liver against mitochondrial swelling[27].

Results of our study showed a protective effect of L-carnitine against ammonia-precipitated encephalopathy in cirrhotic patients[6].

In patients with MHE, HE 1, or 2, we observed a significant reduction of ammonia serum levels after 30 d of treatment. After 60 and 90 d of treatment, we observed a persistent trend of decreased ammonia serum levels.

A significant therapeutic effect of carnitine was also observed in the NCT-A, which is an accepted and reliable psychometric test for the assessment of mental function in cirrhotic patients with HE[12,28]. L-carnitine crosses the hemato-encephalic barrier slowly (brain uptake index 5.5%) but its amount in brain is relatively large[29]. The protective effect of L-carnitine is accompanied with a significant attenuation of the increased cerebrospinal fluid and brain alanine as well as cerebrospinal fluid lactate content, caused by ammonium acetate administration[30], suggesting that mitochondrial respiration is at least partially restored in L-carnitine-treated animals. The possible beneficial effect of carnitine may be related to an improved pyruvate oxidation, Krebs cycle and flux through

Table 2 Comparison between evaluated parameters of the two groups (mean+SD)

		Carnitine group (A)				Placebo group (B)			
Duration of treatment (days)		0	30	60	90	0	30	60	90
NH_4 fasting	MHE	68.2±38.2	55.1±31.4	49.1±30.1	40.1±25.1	69.1±39.2	68.2±38.2	68.2±33.6	67.1±34.1
	HE1	82.1±29.1	69.2±28.2	58.2±28.7	41.4±28.1	80.1±30.1	78.7±36.2	77.2±33.4	76.2±31.8
	HE2	89.2±34.2	80.1±28.1	74.1±12.9	53.2±18.2	88.2±34.1	87.1±35.2	86.1±38.1	85.4±39.2
Trail making test-A	MHE	48.9±18.7	35.1±18.9	30.9±15.2	274±12.4	51.4±19.2	50.2±18.9	52.1±20.1	50.4±20.2
	HE1	62.4±21.2	50.8±18.9	40.8±16.5	33.6±16.1	60.9±19.9	59.9±19.8	58.4±20.1	53.6±19.8
	HE2	69.3±21.8	58.8±18.1	43.1±20.1	39.1±16.8	64.3±22.4	65.6±20.4	64.9±21.9	61.4±22.9
Trail making test-B	MHE	66.1±12.1	41.1±13.2	40.1±10.2	37.2±12.1	65.2±13.1	61.1±14.1	60.1±13.2	59±14.1
	HE1	74.2±10.1	65±11.1	55.1±12.1	50.4±10.1	75.8±11.9	74.2±12.1	70.11±12.8	71.4±13.2
	HE2	96.9±12.4	87.4±11.2	75.11±11.8	61.9±13.2	91.4±12.1	90.6±10.8	91.5±10.6	93.4±11.8
Symbol digit modalities test	MHE	36±1.2	40±1.8	44±1.5	44±1.7	35±1.9	36±2.1	36.2±11.8	36.4±22.2
	HE1	30±1.9	35.1±2.1	38±2.4	44±1.9	31.2±1.8	32.4±1.9	33.2±1.8	34.1±1.9
	HE2	25.1±1.4	28.2±1.9	32.1±12.4	38±2.4	26.1±2.1	27.2±2.4	28.1±1.9	27.9±1.8
Block design test	MHE	31.1±1.2	35.2±1.9	39±2.1	44±1.1	30.1±2.8	32±2.6	32.4±2.9	32.7±1.8
	HE1	27±1.8	30±1.9	33.1±2.1	39.1±1.1	26±2.9	28±1.9	28.4±2.1	27.1±2.2
	HE2	22±1.9	26.1±1.8	30.1±1.1	35±1.8	22.6±21	23.2±1.4	24.2±1.9	24.8±2.1

glutamate dehydrogenase. The latter could then explain the lowering of blood ammonia levels that follows L-carnitine administration .

The best-known function on L-carnitine is the facilitation of b-oxidation by transforming activated long-chain fatty acids into mitochondria. High concentration of fatty acids has numerous deleterious effects upon mitochondrial metabolism.

Acyl-CoA derivates competitively inhibit the activation of the gluconeogenetic enzyme pyruvate carboxylase with acetyl-CoA[31]. Thus when mitochondrial b-oxidation is inhibited, not only is acetyl-CoA, but also the activating effect of acetyl-CoA is further inhibited by non-esterified acyl-CoA esters, an effect that further decreases gluconeogenesis.

High levels of acyl-CoA derivates also may inhibit ureagenesis (resulting in hyperammonemia and the tricarboxylic acid cycle)[32].

Treatment with levocarnitine decreases the serum levels of ammonia and improves the mental functions in cirrhotic patients, and has been proven effective with small adverse events.

REFERENCES

1 **Lockwood AH,** Yap EW, Wong WH Cerebral ammonia metabolism in patients with severe liver disease and minimal hepatic encephalopathy. *J Cereb Blood Flow Metab* 1991; **11:** 337-341

2 **Blei AT.** Brain edema and portal-systemic encephalopathy. *Liver Transpl*. 2000; **6:** S14-20

3 **O'Connor JE,** Costell M, Grisolia S. Prevention of ammonia toxicity by L-carnitine: metabolic changes in brain. *Neurochem Res* 1984; **9:** 563-570

4 **Therrien G,** Rose C, Butterworth J, Butterworth RF. Protective effect of L-carnitine in ammonia-precipitated encephalopathy in the portacaval shunted rat. *Hepatology* 1997; **25:** 551-556

5 **Matsuoka M,** Igisu H, Kohriyama K, Inoue N. Suppression of neurotoxicity of ammonia by L-carnitine. *Brain Res*. 1991; **567:** 328-331

6 **Malaguarnera M,** Pistone G, Astuto M, Dell'Arte S, Finocchiaro G, Lo Giudice E, Pennisi G. L-Carnitine in the treatment of mild or moderate hepatic encephalopathy. *Dig Dis* 2003; **21:** 271-275

7 **Bremer J.** The role of carnitine in cell metabolism. In: De Simone C, Famularo G. (eds). Carnitine Today. Springer-Verlag, *Heidelberg*, 1997; pp. 1-37

8 **Kaiser S,** Gerok W, Häussinger D. Ammonia and glutamine metabolism in human liver slices: new aspects on the pathogenesis of hyperammonaemia in chronic liver disease. *Eur J Clin Invest* 1988; **18:** 535-542

9 **Gebhardt R,** Reichen J. Changes in distribution and activity of glutamine synthetase in carbon tetrachloride-induced cirrhosis in the rat: potential role in hyperammonemia. *Hepatology* 1994; **20:** 684-691

10 **Kircheis G,** Nilius R, Held C, Berndt H, Buchner M,

Görtelmeyer R, Hendricks R, Krüger B, Kuklinski B, Meister H, Otto HJ, Rink C, Rösch W, Stauch S. Therapeutic efficacy of L-ornithine-L-aspartate infusions in patients with cirrhosis and hepatic encephalopathy: results of a placebo-controlled, double-blind study. *Hepatology* 1997; **25:** 1351-1360

11 **Conn HO,** Liebertahl MM. The hepatic coma syndromes and lactulose. Baltimore: *Williams and Wilkins*, 1979: 1-121

12 **Conn HO.** Trailmaking and number connection tests in the assessment of mental state in portal systemic encephalopathy. *Am J Dig Dis* 1977; **22:** 541-550

13 **Atterbury CE,** Maddrey WC, Conn HO. Neomycin-sorbitol and lactulose in the treatment of acute portal-systemic encephalopathy. A controlled, double-blind clinical trial. *Am J Dig Dis* 1978; **23:** 398-406

14 **Van der Rijt CC,** Schalm SW, De Groot GH, De Vlieger M. Objective measurement of hepatic encephalopathy by means of automated EEG analysis. *Electroencephalogr Clin Neurophysiol* 1984; **57:** 423-426

15 **Pugh RN,** Murray-Lyon IM, Dawson JL, Pietroni MC, Williams R. Transection of the oesophagus for bleeding oesophageal varices. *Br J Surg* 1973; **60:** 646-649

16 **Da Fonseca-Wollheim F.** Direct determination of plasma ammonia without deproteinization. An improved enzymic determination of ammonia, II (author's transl). *Z Klin Chem Klin Biochem* 1973; **11:** 426-431

17 **Butterworth RF,** Giguère JF, Michaud J, Lavoie J, Layrargues GP. Ammonia: key factor in the pathogenesis of hepatic encephalopathy. *Neurochem Pathol* 1987; **6:** 1-12

18 **Lockwood AH,** Yap EW, Wong WH. Cerebral ammonia metabolism in patients with severe liver disease and minimal hepatic encephalopathy. *J Cereb Blood Flow Metab* 1991; **11:** 337-341

19 **O'Connor JE,** Costell M, Míguez MP, Portolés M, Grisolía S. Effect of L-carnitine on ketone bodies, redox state and free amino acids in the liver of hyperammonemic mice. *Biochem Pharmacol* 1987; **36:** 3169-3173

20 **Michalak A,** Qureshi IA. Plasma and urinary levels of carnitine in different experimental models of hyperammonemia and the effect of sodium benzoate treatment. *Biochem Med Metab Biol* 1990; **43:** 163-174

21 **Ratnakumari L,** Qureshi IA, Butterworth RF. Effect of L-carnitine on cerebral and hepatic energy metabolites in congenitally hyperammonemic sparse-fur mice and its role during benzoate therapy *Metabolism* 1993; **42:** 1039-1046

22 **Basile AS,** Jones EA. Ammonia and GABA-ergic neurotransmission: interrelated factors in the pathogenesis of hepatic encephalopathy. *Hepatology* 1997; **25:** 1303-1305

23 **Norenberg MD.** Astrocytic-ammonia interactions in hepatic encephalopathy. *Semin Liver Dis* 1996; **16:** 245-253

24 **Chapa AM,** Fernandez JM, White TW, Bunting LD, Gentry LR, Ward TL, Blum SA. Influence of intravenous L-carnitine administration in sheep preceding an oral urea drench. *J Anim Sci* 1998; **76:** 2930-2937

25 **Raskind JY,** El-Chaar GM. The role of carnitine supplementation during valproic acid therapy. *Ann Pharmacother* 2000; **34:** 630-638

26 **Ohtani Y,** Endo F, Matsuda I. Carnitine deficiency and hyperammonemia associated with valproic acid therapy. *J Pediatr* 1982; **101:** 782-785

27 **Sugimoto T,** Araki A, Nishida N, Sakane Y, Woo M, Takeuchi T, Kobayashi Y. Hepatotoxicity in rat following administration of valproic acid: effect of L-carnitine supplementation. *Epilepsia*. 1987; **28:** 373-377

28 **Reitan RM,** Wolfson D. The Halstead-Reitan. Neuropsychological test battery: theory and clinical interpretation. Tucson, AZ: *Neuropsychology Press*; 1993

29 **Hearn TJ,** Coleman AE, Lai JC, Griffith OW, Cooper AJ. Effect of orally administered L-carnitine on blood ammonia and L-carnitine concentrations in portacaval-shunted rats. *Hepatology* 1989; **10:** 822-828

30 **Therrien G,** Giguere JF, Butterworth RF. Increased cerebrospinal fluid lactate reflects deterioration of neurological status in experimental portal-systemic encephalopathy. *Metab Brain Dis* 1991; **6:** 231-238

31 **Sherratt HS.** Acyl-CoA esters of xenobiotic carboxylic acids as biochemically active intermediates. *Biochem Soc Trans* 1985; **13:** 856-858

32 **Corkey BE,** Hale DE, Glennon MC, Kelley RI, Coates PM, Kilpatrick L, Stanley CA. Relationship between unusual hepatic acyl coenzyme A profiles and the pathogenesis of Reye syndrome. *J Clin Invest* 1988; **82:** 782-788

Science Editor Wang XL and Guo SY **Language Editor** Elsevier HK

PO Box 2345, Beijing 100023, China
www.wjgnet.com
wjg@wjgnet.com

ELSEVIER

World J Gastroenterol 2005;11(45):7203-7207
World Journal of Gastroenterology ISSN 1007-9327

• *RAPID COMMUNICATION* •

Synergistic action of famotidine and chlorpheniramine on acetic acid-induced chronic gastric ulcer in rats

Zhen Qin, Chao Chen

Zhen Qin, Chao Chen, Laboratory of natural drugs of Medical College, China Three Gorges University, Yichang 443002, Hubei Province, China
Supported by Scientific and Technological Offices of Yichang Municipality, No A03210
Correspondence to: Professor Chao Chen, Laboratory of Natural Drugs of Medical College, China Three Gorges University, Yichang 443002, Hubei Province, China. chaochen1954@163.com
Telephone: +0717-6397466
Received: 2005-04-15 Accepted: 2005-05-25

Abstract

AIM: To assess the synergistic action of famotidine (FMD) and chlorpheniramine (CPA) on acetic acid-induced chronic gastric ulcer in rats.

METHODS: Chronic gastric lesions were induced in male Sprague-Dawley (SD) rats by serosal application of the acetic acid. Forty SD rats were randomly divided into blank group (n = 8), control group (n = 8), FMD group (n = 8), CPA group (n = 8), and FMD+CPA group (n = 8). Each group was given intraperitoneally (i.p.) 0.5 mL/100 g distilled water, 9 g/L NaCl saline, 4 mg/kg FMD, 10 mg/kg CPA, 4 mg/kg FMD+10 mg/kg CPA, respectively, daily for 10 d. On d 10, ulcer area was determined by planimetry. The level of myeloperoxidase (MPO) in the liver homogenation was determined by biochemical methods and the plasma levels of 6-ketoprostaglandin F1 alpha (6-keto-PGF_{1a}) and IL-8 were determined by radioimmunoassay.

RESULTS: The synergistic effects of FMD+CPA group on the lesion, IL-8, 6-keto-PGF_{1a} and MPO were confirmed. The effect of FMD+CPA group was significantly different as compared to the control and FMD groups. The lesion (mm^2) was reduced from 40.18±2.6 in control group to 6.83±2.97 in PMD+CPA group, P<0.01, and from 32.9 ±3.27 in FMD group to 6.83±2.97 in PMD+CPA group, P<0.01. The plasma levels of IL-8 decreased from 0.69± 0.11 ng/L in control group to 0.4±0.04 ng/L in PMD+CPA group, P<0.01, and from 0.51±0.08 ng/L in FMD group to 0.4±0.04 ng/L in PMD+CPA group, P<0.05. The level of 6-keto-PGF_{1a} increased from 7.55±1.65 ng/L in control group to 16.62±0.97 ng/L in PMD+CPA group, P<0.01, and from 13.15±1.48 ng/L in FMD group to 16.62±0.97 ng/L in PMD+CPA group, P<0.05. The levels of MPO in the liver homogenate decreased from 9.12±2.05 u/L in control group to 4.33±0.95 u/L in PMD+CPA group, P<0.01, and from 8.3±1.29 u/L in FMD group to 4.33± 0.95 u/L, P<0.01.

CONCLUSION: The synergistic action of FMD and CPA on acetic acid-induced chronic gastric ulcer in rats decreases the incidence of ulcer and also enhances the healing of ulcer.

Key words: Gastric ulcer; Acetic acid; Famotidine; Chlorpheniramine; Interleukin-8; 6-Ketoprostaglandin F1 alpha; Myeloperoxidase

Qin Z, Chen C. Synergistic action of famotidine and chlorpheniramine on acetic acid-induced chronic gastric ulcer in rats. *World J Gastroenterol* 2005; 11(45): 7203-7207

http://www.wjgnet.com/1007-9327/11/7203.asp

INTRODUCTION

Peptic ulcer is a common disorder of the gastrointestinal system and the pathogenesis of peptic ulcer disease is multifactorial, including *Helicobacter pylori*, gastric acid, pepsin, gastroduodenal motility, smoking, use of nicotine, and complex interaction between so-called aggressive and protective factors[1]. Mast cells are initiators and regulators of inflammation. After mast cell degranulation, histamine causes the secretion of gastric acid by triggering H_2-receptors, marked infiltration of inflammatory cells into the gastric mucosa, and expression of cytokines by triggering the H_1-receptors. Consequently, mast cells are considered as important effector cells in the pathogenesis of gastritis, especially in *H pylori*-associated peptic ulcer[2]. Histamine H_2-receptor antagonists that possess a potent antisecretory activity can greatly enhance the healing rate of peptic ulcers. However, after H_2-receptor antagonist therapy peptic ulcer recurs rapidly and frequently. The possible reasons why the recurrence rate is high after H_2-antagonist therapy are acid rebound after the cessation of treatment, deficiency in gastric defensive factors such as gastric prostaglandin levels, and low maturity of regenerated mucosa. Recently, H_1-receptor antagonists are potent anti-inflammatory compounds. Erwin[3] reported that H_1-receptor antagonists have anti-inflammatory activity, including their effects on eicosanoid production

and cytokine release and their influence on the release rate of proinflammatory mediators. Cetirizine reduces the attraction of inflammatory cells to the inflammatory focus after the antigen challenge and inhibits the expression of the intercellular adhesion molecule 1 (ICAM-1) on the surface of epithelial cells[4]. It also might be able to block the antigen-induced production of leukotrienes (LTC4)[5]. Loratadine and its metabolite decarboethoxyloratadine inhibit the release of tryptase and amacroglobulin[6], interleukins (IL) 6 and 8[7], leukotrienes and prostaglandin D2 (PGD2)[8], and suppress the expression of ICAM-1 and of HLA-II antigens on the surface of epithelial cells[9]. Therefore, H_1 and H_2 blockers have not only antisecretory activity but also anti-inflammatory activity when they are used in the treatment of gastric ulcer. The aim of the present study was to assess the synergistic action of famotidine (FMD) and chlorpheniramine (CPA) on acetic acid-induced chronic gastric ulcer in rats.

MATERIALS AND METHODS

Materials

IL-8 and 6-ketoprostaglandin F1 alpha (6-keto-PGF_{1a}) kits were obtained from Beijing North Institute of Biological Technology. Myeloperoxidase (MPO) kit was obtained from Nanjing Jiancheng Bioengineering Institute.

Animals

Male Sprague-Dawley (SD) rats (180-220 g) were provided by the Medical Experimental Animal Center, Tongji Medical College, Huazhong University of Science and Technology (No: TJLA-2004-159). Animals were fed with standard laboratory chow and tap water, and kept in a room with constant humidity and temperature (25 °C) in a 12-h light-dark cycle for 1 wk before the experiments.

Induction of gastric ulcer

Gastric ulcers were induced using the method described by Takagi *et al*[10] with some modifications. Gastric ulcers were produced by the application of round filter paper (diameter: 5 mm) immersed in a 100% acetic acid on the serosal surface of anterior wall of the stomach approximately at the center of the corpus for 30 s and the process was repeated twice. This produced an immediate necrosis of the entire mucosa and submucosa (but not serosa) within the area (20 mm^2), where the acetic acid was applied. The excess of acetic acid was then removed and the serosa was gently washed with saline. Control animals received no surgery. The abdomen was then sutured, and the animals were allowed to recover and returned to their cages with free access to food and water.

Experimental groups

Two days after the ulcer induction, 40 male SD rats, weighing 180-220 g, were randomly divided into blank group (n = 8), control group (n = 8), FMD group (n = 8), CPA group (n = 8), FMD+CPA group (n = 8). Rats were given intraperitoneally (i.p.) 0.5 mL/100 g distilled water, 0.5 mL/100 g, 9 g/L NaCl saline, 4 mg/kg FMD, 10 mg/kg CPA, 4 mg/kg FMD+10 mg/kg CPA for 10 d. On d 8, the rats were deprived of food for 48 h prior to the experiment but allowed free access to water. After the last dose, each animal was anesthetized with 10 g/L sodium thiopental. Five milliliters of blood was collected by intracardiac puncture. Each sample contained 0.22 mL 6-keto EDTA, and was centrifuged for 15 min at 5 500 r/min. The plasma from each sample was stored at -80 °C for the determination of the level of interleukin IL-8 and 6-keto-PGF1a by RIA using IL-8 and 6-keto PGF1a kits, respectively. Subsequently, the abdomen was opened and the stomach was exposed after the esophagus and pyloric were ligated, and then 5 mL 40 g/L neutral buffered formalin was instilled into the stomach via the incision for pathological examination.

Ulcerated area (mm^2) determination

After being fixed in formalin overnight, the stomach was opened along the greater curvature and spread out with pins on a cork board, and then photographed. The ulcerated area (mm^2)[11] was computed using the following equation: $S = \pi(d_1/2)\times(d_2/2)$, where S represents the ulcerated area (mm^2), d_1 and d_2 represent the longest longitudinal and transverse diameters of the ulcer respectively.

Light microscopy

After fixation, the stomach was divided into two parts and each part was subdivided into four tissue strips by cutting along the whole width of the half stomach. The blocks were embedded in paraffin wax. Five micrometer thick sections were cut in a standard fashion and stained with hematoxylin and eosin.

Radioimmunoassay (RIA) for IL-8 and 6-keto-PGF1a

All the blood samples for IL-8 and 6-keto-PGF_{1a} determination were stored in the tubes. Serum level of IL-8 and 6-keto-PGF_{1a} was determined by RIA with the IL-8 and 6-keto-PGF_{1a} RIA kits according to their manufacturer's instructions.

MPO activity

The level of MPO in the liver homogenate was determined by biochemical methods with the MPO kits according to its manufacturer's instructions.

Statistical analysis

All the values were expressed as mean±SD. One-way ANOVA was used to analyze the differences among them. Student's t-test was applied to comparisons between the two groups. $P<0.05$ was considered statistically significant. Software SPSS10.0 was used in all statistical analyses.

RESULTS

Ulcerated area (mm^2)

The lesion (mm^2) decreased from 40.18±2.6 in control

Table 1 Effects of combined famotidine (FMD) and chlorpheniramine (CPA) on the ulcerated area in different groups (mean±SD)

Group	Dose (mg/kg)	Area of ulcer (mm^2)	6-keto-PGF_{1a} (ng/L)	IL-8 (ng/L)	MPO (μ/L)
Blank		0	22.74±5.03	0.3±0.09	3.13±0.39
Control		40.18±2.6[b]	7.55±1.65[b]	0.69±0.11[b]	9.12±2.05[b]
FMD	4	32.9±3.27[d]	13.15±1.48[d]	0.51±0.08[d]	8.3±1.29
CPA	10	35.15±3.0[d]	10.79±1.48[c]	0.41±0.07[d]	5.7±1.00[d]
FMD+CPA	4+10	6.83±2.97[d,f]	16.62±0.97[d,e]	0.4±0.04 [d,e]	4.33±0.95[d,f]

[a]P<0.05; [b]P<0.01 *vs* blank; [c]P<0.05; [d]P<0.01 *vs* control; [e]P<0.05; [f]P<0.01 *vs* FMD.

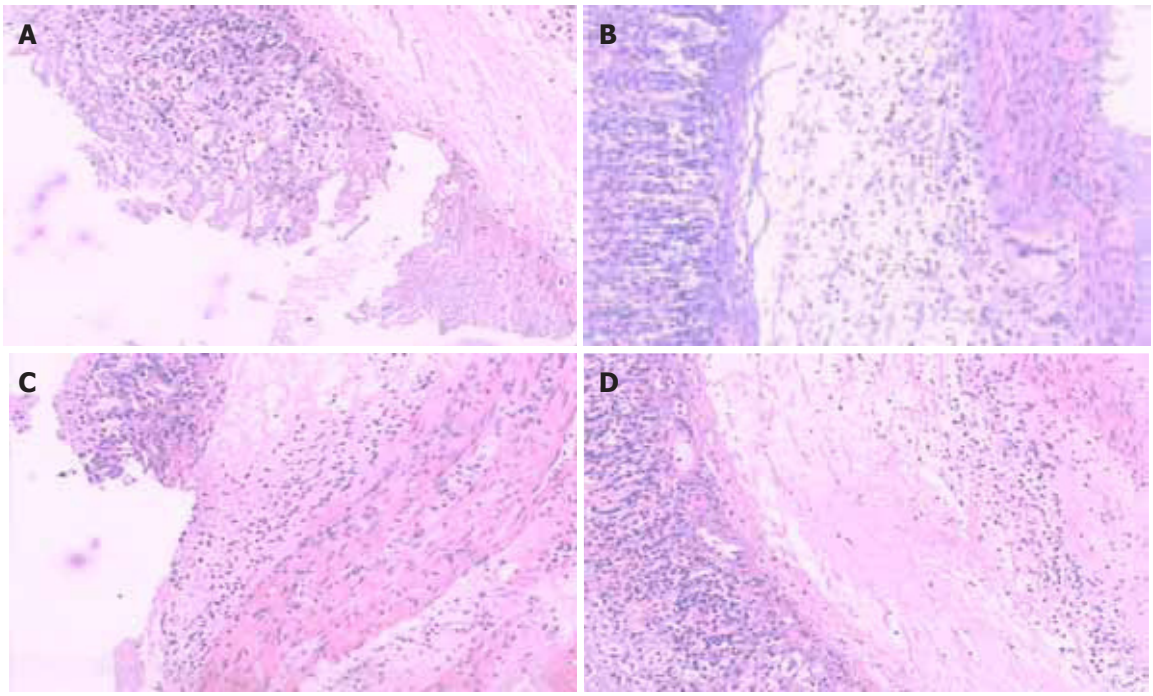

Figure 1 Pathological feature of gastric mucosa in the control group (**A**), FMD group (**B**), CPA group (**C**), and FMD+CPA group (**D**) under light microscope, HE ×200.

group to 0 in the blank group. The lesion (mm^2) was reduced from 40.18±2.6 in the control group to 6.83±2.97 in the PMD+CPA group (P<0. 01), and from 32.9 ±3.27 in FMD group to 6.83±2.97 in PMD+CPA group (P<0.01) (Table 1).

Light microscopy

Microscopic findings on the gastric mucosal scar showed that the mucosal architecture of the scar healed by FMD+CPA group (Figure 1D) was better restored than that of the scar in the control group or in the case of treatment with FMD alone which exhibited much lymphocyte infiltration, and surface epithelial lesions (Figures 1A and B).

Plasma level of 6-keto-PGF_{1a}

The level of 6-keto-PGF_{1a} in the FMD+CPA group was significantly different from that in the control and the FMD groups, which increased from 7.55±1.65 ng/L in the control group to 16.62±0.97 ng/L in the PMD+CPA group (P<0.01) ng/L, and from 13.15±1.48 ng/L in the FMD group to 16.62±0.97 ng/L in the PMD+CPA group, P<0.05 (Table 1).

MPO level in liver homogenate

In the liver homogenate, the level of MPO activity decreased from 9.12±2.05 μ/L in the control group to 4.33 ±0.95 μ/L in the PMD+CPA group, P<0.01, and from 8.3 ±1.29 μ/L in the FMD group to 4.33±0.95 μ/L (P<0.01) (Table 1).

The plasma levels of IL-8

The plasma level of IL-8 decreased from 0.69±0.11 ng/L in the control group to 0.4±0.04 ng/L, P<0.01, and from 0.51±0.08 ng/L in the FMD group to 0.4±0.04 ng/L in the PMD+CPA group (P<0.05) (Table 1).

DISCUSSION

The acetic acid injection-induced ulcer model is a mature classical model. The drawback of the model is that the dose of injection is not rigorous. We used a round filter paper (diameter: 5 mm) immersed in a 100% acetic acid

on the serosal surface to establish the model, which is characterized by high success rate, small coefficient of variation, low rate of perforation.

Prostaglandins (PGs) are well-known mucosal defense factors, protecting the gastric mucosa against injury caused by a variety of toxic stimuli[12,13]. PGE2 stimulates the secretion of gastric mucus and bicarbonate, increases mucosal blood flow, inhibits acid secretion, and reduces gastric motility. In addition, downregulation of proinflammatory cytokine expression by PGs is also likely to be important for mucosal protection against *H pylori* infection. 6-Keto PGF_{1a} is a PGI2 metabolite, and PGI2 plays an important role in gastric cytoprotection. This study also approved that the ulcerated area decreased with the increase in the level of 6-Keto PGF_{1a} and this supports that prostaglandins possess gastric cytoprotection function.

Gastric mucosal integrity is maintained by an interplay of some aggressive and defensive factors controlling cell apoptosis and proliferation. Disturbing this balance leads to ulcer. Proinflammatory cytokines play an important role. IL-8 is an important cytokine in the host inflammatory response to *H pylori*[14-16], which correlates with its induction in gastric epithelial cells co-cultured with *H pylori in vitro*[17-19]. Upregulation of IL-8 by *H pylori* may lead to free radical generation and the release of proteolytic enzymes from activated neutrophils, affecting mucosal integrity[20]. Eradication of *H pylori* in ulcer patients results in a reduction in antral IL-8 mRNA expression, neutrophil infiltration, and surface epithelial lesions[16], suggesting that inflammatory cytokines may play an important role in mucosal damage due to *H pylori* infection. Leukocyte infiltration in gastric mucosa is assessed by determining tissue activity of MPO[21], an enzyme used as a marker for leukocyte infiltration in a variety of tissues including the rat gastric mucosa. Recently, experimental data on H_1 receptor antagonists demonstrate potentially anti-inflammatory effects in addition to their anti-allergic effects on histamine production, the histamine-induced response. Cook *et al*[22] reported that human conjunctival mast cells can be purified (>95%) from cadaveric tissues and that olopatadine inhibits anti-IgE antibody-mediated release of TNF-α from human conjunctival mast cells. Bakker[23] showed that the histamine H_1 receptor, which is also an important player in allergic and inflammatory conditions, activates NF-κB in a constitutive- and agonist-dependent manner and that the observed constitutive NF-κB activation is inhibited by various H_1-receptor antagonists, suggesting that inverse agonism may account, at least in part, for their ascribed antiallergic properties. Miki *et al*[24] showed that histamine concentration-dependently enhances the TNF-α-induced expression of E-selectin and intercellular adhesion molecule-1 (ICAM-1) in vascular endothelial cells. Arnold[25] suggested that cetirizine reduced the release of IL-8 from A549 cells stimulated with PMA and TNF-α, by lowering IL-8 gene expression. Modlin *et al*[26] reported that histamine may also act as an autocrine growth factor for ECL hyperplasia via H_1 receptors. Therefore, histamine may be an important regulator of all gastric endocrine cells. It was reported that a high dose FMD administration significantly increases serum gastrin concentration and proliferates G and ECL cells[27] indicating that the synergistic action of histamine H_1 receptor antagonists and histamine H_2 receptor antagonists may reduce the incidence rate of carcinoids.

The present experimental study demonstrated that FMD, a H_2 receptor antagonist, afforded against gastric ulcers. Chlorpheniramine, a H_1 receptor antagonist could give partial protection. When both H_1 and H_2 blockers were given, they decreased the incidence of ulcer and also enhanced the healing of ulcers. At the same time, this study showed that H_1-antagonists reduced the release of proinflammatory mediators (IL-8 and MPO) from mast cells in comparison with the controls. The synergistic effect indicates that H_1 receptors play a role in gastric ulceration as the H_2 receptors.

REFERENCES

1 **Eastwood GL.** Is smoking still important in the pathogenesis of peptic ulcer disease? *J Clin Gastroenterol* 1997; **25 Suppl 1**: S1- S7

2 **Nakajima S,** Krishnan B, Ota H, Segura AM, Hattori T, Graham DY, Genta RM. Mast cell involvement in gastritis with or without Helicobacter pylori infection. *Gastroenterology* 1997; **113**: 746-754

3 **Sneddon P,** Machaly M. Regional variation in purinergic and adrenergic responses in isolated vas deferens of rat, rabbit and guinea-pig. *J Auton Pharmacol* 1992; **12**: 421-428

4 **Ciprandi G,** Buscaglia S, Pesce G, Passalacqua G, Rihoux JP, Bagnasco M, Canonica GW. Cetirizine reduces inflammatory cell recruitment and ICAM-1 (or CD54) expression on conjunctival epithelium in both early- and late-phase reactions after allergenspecific challenge. *J Allergy Clin Immunol* 1995; **95**: 612-621

5 **Du Buske LM.** Clinical comparison of histamine H_1-receptor antagonist drugs. *J Allergy Clin Immunol* 1996; **98**: S307-S318

6 **Greiff L,** Persson CG, Svensson C, Enander I, Andersson M. Loratadine reduces allergen-induced mucosal output of alpha 2-macroglobulin and tryptase in allergic rhinitis. *J Allergy Clin Immunol* 1995; **96**: 97-103

7 **Lippert U,** Kruger-Krasagakes S, Moller A, Kiessling U, Czarnetzki BM. Pharmacological modulation of IL-6 and IL-8 secretion by the H1-antagonist decarboethoxy-loratadine and dexamethasone by human mast and basophilic cell lines. *Exp Dermatol* 1995; **4**: 272-276

8 **Bousquet J,** Lebel B, Chanal I, Morel A, Michel FB. Antiallergic activity of H_1-receptor antagonists assessed by nasal challenge. *J Allergy Clin Immunol* 1988; **82**: 881-887

9 **Vignola AM,** Crampette L, Mondain M, Sauvère G, Czarlewski W, Bousquet J, Campbell AM. Inhibitory activity of loratadine and descarboethoxyloratadine on expression of ICAM-1 and HLA-DR by nasal epithelial cells. *Allergy* 1995; **50**: 200-203

10 **Takagi K,** Okabe S, Saziki R. A new method for the production of chronic gastric ulcer in rats and the effect of several drugs on its healing. *Jpn J Pharmacol* 1969; **19**: 418-426

11 Drug administration of Ministry of Health,the People's Republic of China.Collection of guilding principle of new drug (Western medicine) research before clinic(pharmacy,pharmacology and toxicology). Beijing, 1993: 88–89

12 **Eberhart CE,** Dubois RN. Eicosanoids and the gastrointestinal tract. *Gastroenterology* 1995; **109**: 285-301

13 **Robert A,** Nezamis JE, Lancaster C, Hanchar AJ. Cytoprotection by prostaglandins in rats. Prevention of gastric necrosis produced by alcohol, HCl, NaOH, hypertonic NaCl, and thermal injury. *Gastroenterology* 1979; **77**: 433-443

14 **Peek RM Jr,** Miller GG, Tham KT, Perez-Perez GI, Zhao X, Atherton JC, Blaser MJ. Heightened inflammatory response and cytokine expression in vivo to cagA+ Helicobacter pylori strains. *Lab Invest* 1995; **73**: 760-770
15 **Moss SF,** Legon S, Davies J, Calam J. Cytokine gene expression in Helicobacter pylori associated antral gastritis. *Gut* 1994; **35**: 1567-1570
16 **Crabtree JE,** Wyatt JI, Trejdosiewicz LK, Peichl P, Nichols PH, Ramsay N, Primrose JN, Lindley IJ. Interleukin-8 expression in Helicobacter pylori infected, normal, and neoplastic gastroduodenal mucosa. *J Clin Pathol* 1994; **47**: 61-66
17 **Crabtree JE.,** Farmery SM, Lindley IJ, Figura N, Peichl P, Tompkins DS. CagA/cytotoxic strains of Helicobacter pylori and interleukin-8 in gastric epithelial cell lines. *J Clin Pathol* 1994; **47**:945-950
18 **Sharma SA,** Tummuru MK, Miller GG, Blaser MJ. Interleukin-8 response of gastric epithelial cell lines to Helicobacter pylori stimulation in vitro. *Infect. Immun* 1995; **63**:1681-1687
19 **Crowe SE,** Alvarez L,Dytoc M, Hunt RH, Muller M, Sherman P, Patel J, Jin Y, Ernst PB. Expression of interleukin-8 and CD54 by human gastric epithelium after Helicobacter pylori infection in vitro. *Gastroenterology* 1995; **108**: 65-74
20 **Yoshida N,** Granger DN, Evans DJ, Evans DG, Graham DY, Anderson DC, Wolf RE, Kvietys PR. Mechanisms involved in Helicobacter pylori-induced inflammation. *Gastroenterology* 1993;**105**:1431-1440
21 **Cooper LC,** Dial EJ, Lichtenberger LM. Effects of milk, prostaglandin, and antacid on experimentally induced duodenitis in the rat. Use of myeloperoxidase as an index of inflammation. *Dig Dis Sci* 1990; **35**: 1211-1216
22 **Cook EB,** Stahl JL, Barney NP, Graziano FM. Olopatadine inhibits TNFalpha release from human conjunctival mast cells. *Ann Allergy Asthma Immunol* 2000; **84**: 504-508
23 **Bakker RA,** Schoonus SB, Smit MJ, Timmerman H, Leurs R. Histamine H(1)-receptor activation of nuclear factor-kappa B: roles for G beta gamma- and G alpha(q/11)-subunits in constitutive and agonist-mediated signaling. *Mol Pharmacol* 2001; **60**: 1133-1142
24 **Miki I,** Kusano A, Ohta S, Hanai N, Otoshi M, Masaki S, Sato S, Ohmori K. Histamine enhanced the TNF-alpha-induced expression of E-selectin and ICAM-1 on vascular endothelial cells. *Cell Immunol* 1996; **171**: 285-288
25 **Arnold R,** Rihoux J, König W. Cetirizine counter-regulates interleukin-8 release from human epithelial cells (A549) *Clin Exp Allergy* 1999; **29**: 1681-1691
26 **Modlin IM,** Kumar RR, Soroka CJ, Ahlman H, Nilsson O, Goldenring JR. Histamine as an intermediate growth factor in genesis of gastric ECLomas associated with hypergastrinemia in mastomys. *Dig Dis Sci* 1994; **39**: 1446-1453
27 **Chen G,** Kashiwagi H, Omura N, Aoki T. Effect of a histamine H1 receptor antagonist on gastric endocrine cell proliferation induced by chronic acid suppression in rats. *J Gastroenterol* 2000; **35**: 742-747

Science Editor Wang XL and Guo SY **Language Editor** Elsevier HK

PO Box 2345, Beijing 100023, China
www.wjgnet.com
wjg@wjgnet.com

ELSEVIER

World J Gastroenterol 2005;11(45):7208-7210
World Journal of Gastroenterology ISSN 1007-9327

• RAPID COMMUNICATION •

Effect of liniment levamisole on cellular immune functions of patients with chronic hepatitis B

Ke-Xia Wang, Li-Hua Zhang, Jiang-Long Peng, Yong Liang, Xue-Feng Wang, Hui Zhi, Xiang-Xia Wang, Huan-Xiong Geng

Ke-Xia Wang, Li-Hua Zhang, Jiang-Long Peng, Yong Liang, Xue-Feng Wang, Hui Zhi, Department of Pathogenic Biology, School of Medicine, Anhui University of Science and Technology, Huainan 232001, Anhui Province, China
Xiang-Xia Wang, Huan-Xiong Geng, Huainan Railway Central Hospital, Huainan 232001, Anhui Province, China
Correspondence to: Dr. Ke-Xia Wang, Department of Pathogenic Biology, School of Medicine, Anhui University of Science and Technology, Huainan 232001, Anhui Province, China. cpli@aust.edu.cn
Telephone: +86-554-6658770 Fax: +86-554-6662469
Received: 2004-09-08 Accepted: 2004-10-26

Abstract

AIM: To explore the effects of liniment levamisole on cellular immune functions of patients with chronic hepatitis B.

METHODS: The levels of T lymphocyte subsets and mIL-2R in peripheral blood mononuclear cells (PBMCs) were measured by biotin-streptavidin (BSA) technique in patients with chronic hepatitis B before and after the treatment with liniment levamisole.

RESULTS: After one course of treatment with liniment levamisole, the levels of $CD3^+$, $CD4^+$, and the ratio of $CD4^+/CD8^+$ increased as compared to those before the treatment but the level of $CD8^+$ decreased. The total expression level of mIL-2R in PBMCs increased before and after the treatment with liniment levamisole.

CONCLUSION: Liniment levamisole may reinforce cellular immune functions of patients with chronic hepatitis B.

Key words: Liniment levamisole; Chronic hepatitis B; Cellular immune function; T lymphocyte subsets; mIL-2R

Wang KX, Zhang LH, Peng JL, Liang Y, Wang XF, Zhi H, Wang XX, Geng HX. Effect of liniment levamisole on cellular immune functions of patients with chronic hepatitis B. *World J Gastroenterol* 2005; 11(45): 7208-7210
http://www.wjgnet.com/1007-9327/11/7208.asp

INTRODUCTION

It has been reported that cellular immune functions are abnormal in patients with hepatitis B[1]. To explore the effects of liniment levamisole on cellular immune functions of patients with chronic hepatitis B, we measured the levels of $CD3^+$, $CD4^+$, $CD8^+$ and the ratio of $CD4^+/CD8^+$ cells as well as the expression level of mIL-2R in PBMC in patients with chronic hepatitis B before and after the treatment with liniment levamisole. The results support that levamisole can improve cellular immune functions of patients with chronic hepatitis B.

MATERIALS AND METHODS

Patients

According to the diagnostic criteria modified during the 10th National Conference on Viral Hepatitis and Hepatopathy 2 000, 76 patients with chronic hepatitis B (45 males and 21 females) aged 25-64 years (average 48.25 years) were enrolled in this study and randomly divided into treatment group (n = 38, 27 males and 11 females, aged 32-64 years and averaged 51.8 years) and control group (n = 38, 18 males and 10 females, aged 25-58 years and averaged 44.7 years).

Treatment methods

Vitamins B and C, silymarin compound and other liver-protecting drugs were used in the 76 patients. The treatment group was primed with liniment levamisole at a dose of 500 mg twice a week for 3 mo (a course of treatment). Five milliliters of liniment levamisole was smeared on the surface of skin inside the four limbs near the body. The area of the skin should be as large as possible and the smeared skin was washed within 24 h to assure absorption of the drug. No antiviral agent or immunomodulator was used in the two groups.

Samples

Five milliliters of peripheral vein blood was collected at 8:00 a.m. from each patient with hepatitis B and 2.5 mL was put into a sterile test tube and 2.5 mL into an anticoagulant test tube with heparin.

Separation of PBMC and detection of T cell subsets, mIL-2R

After the heparinized blood was mixed with an equal

volume of Hanks' liquid without Ca^{2+} and Mg^{2+}, PBMCs were harvested from heparinized whole blood by centrifugation on Ficoll-Hypaque sedimentation gradient and diluted to (1-3)×10^6/L cell suspension with RPMI 1 640 culture liquid. Ten microliter suspension of PBMCs was smeared on sheet glass pores so that the cells with $CD3^+$, $CD4^+$, $CD8^+$ and the rest phrase of mIL-2R could be detected. Of the PBMC suspension, 0.5 mL was mixed with RPMI 1640 culture liquid. The cells were grown in continuous culture (37 ℃, 50 mL/L CO_2 in atmosphere) for 72 h and mIL-2R could be measured by antibodies against the membrane of T cells[1].

Immunocytochemical BSA technique

Different monoclonal antibodies (mAb) against $CD3^+$, $CD4^+$, $CD8^+$ and Tac with biotin and SA-HRP were smeared on different sheet glasses. The smears were left to dry naturally and fixed with acetone for 15-20 min. The cells were incubated in continuous culture (37 ℃, 50 mL/L CO_2 in atmosphere) for 30 min. The immune sheet glass pores were measured after being stained with color-developing agents and washed with Tris buffer solution (TBS). The total number of PBMCs was counted and the positive cells were analyzed with the help of high power lens.

Reagents and instruments

Antibodies against T-lymphocyte subsets were provided by Shanghai Jing'an Medical Institute; Ficoll-Hypaque sedimentation gradients were offered by Shanghai Second Reagent Factory. Carbon dioxide incubator (MDF-135) was from Japan.

Statistical analysis

Statistical analysis was performed using *t* test to determine the difference between the two groups.

RESULTS

Before the treatment, there was no significant difference in the levels of $CD3^+$, $CD4^+$, $CD8^+$, mIL-2R and the ratio of $CD4^+/CD8^+$ between the two groups. After one course of treatment, the levels of $CD3^+$, $CD4^+$ and the ratio of $CD4^+/CD8^+$ increased, while the level of $CD8^+$ decreased. The total expression level of mIL-2R in PBMCs increased before and after the treatment with liniment levamisole.

DISCUSSION

This study demonstrated that levamisole could exert its immunopotentiating activity in patients with chronic hepatitis B. As an immune stimulant, levamisole could be connected with receptors of thymopentin on the surfaces of immunologic cells and induces inhibited T lymphocytes into immunologically competent cells, which take part in cell-mediated immune, induce interferon production and prime the lymphocytes and macrophages[2-11]. According to clinical experiments, levamisole has therapeutic effectiveness and boosts immunity in a variety of infectious diseases and some cancers[11-24]. Krastev *et al*[25] treated 25 viremic patients with chronic HBV infection with LMS and found that LMS may benefit some patients with chronic ongoing viral replication including patients who are contraindicated for TNF-α. It was reported that LMS acts by resetting the immune balance toward a type 1 response via the induction of IL-18[26].

We have previously shown that decreased $CD3^+$ and $CD4^+$ levels and $CD4^+/CD8^+$ ratio as well as increased $CD8^+$ level occur in patients with chronic hepatitis B[1]. We have also shown that the level of mIL-2R in PBMCs is lower than that in normal controls[1]. In the present study, all these parameters including the levels of $CD3^+$, $CD4^+$, $CD8^+$, mIL-2R and the $CD4^+/CD8^+$ ratio became normal in the levamisole-treated patients. This reversion of aberrant cellular immunity may improve symptoms of chronic hepatitis B patients.

Liniment levamisole is made from levamisole, which is applied on the surface of skin and can penetrate into the liver, spleen, lungs, kidneys and other internal organs through the skin. We suggest that liniment levamisole should be used in the treatment of patients with chronic hepatitis B.

REFERENCES

1 **Wang KX,** Peng JL, Wang XF, Tian Y, Wang J, Li CP. Detection of T lymphocyte subsets and mIL-2R on surface of PBMC in patients with hepatitis B. *World J Gastroenterol* 2003; **9:** 2017-2020

2 **Johnkoski JA,** Peterson SM, Doerr RJ, Cohen SA. Levamisole regulates the proliferation of murine liver T cells through Kupffer-cell-derived cytokines. *Cancer Immunol Immunother* 1996; **43:** 299-306

3 **Daniluk J,** Kandefer-Szerszeń M. Isoprinosine and levamisole as stimulators of interferon production in blood leukocytes of patients with alcoholic liver cirrhosis. *Arch Immunol Ther Exp (Warsz)* 1997; **45:** 183-187

4 **Prakash MS,** Rao VM, Reddy V. Effect of levamisole on the immune status of malnourished children. *J Trop Pediatr* 1998; **44:** 165-166

5 **Hajnzić TF,** Kastelan M, Lukac J, Hajnzić T. Immunocompetent cells and lymphocyte reactivity to mitogens in levamisole-treated brain tumor children. *Pediatr Hematol Oncol* 1999; **16:** 335-340

6 **Martel F,** Ribeiro L, Calhau C, Azevedo I. Inhibition by levamisole of the organic cation transporter rOCT1 in cultured rat hepatocytes. *Pharmacol Res* 1999; **40:** 275-279

7 **Artwohl M,** Hölzenbein T, Wagner L, Freudenthaler A, Waldhäusl W, Baumgartner-Parzer SM. Levamisole induced apoptosis in cultured vascular endothelial cells. *Br J Pharmacol* 2000; **131:** 1577-1583

8 **Kayataş M.** Levamisole treatment enhances protective antibody response to hepatitis B vaccination in hemodialysis patients. *Artif Organs* 2002; **26:** 492-496

9 **Cuesta A,** Esteban MA, Meseguer J. Levamisole is a potent enhancer of gilthead seabream natural cytotoxic activity. *Vet Immunol Immunopathol* 2002; **89:** 169-174

10 **Bozić F,** Bilić V, Valpotić I. Levamisole mucosal adjuvant activity for a live attenuated Escherichia coli oral vaccine in weaned pigs. *J Vet Pharmacol Ther* 2003; **26:** 225-231

11 **Kimball ES,** Fisher MC. Levamisole effects on major histocompatibility complex and adhesion molecule expression and on myeloid cell adhesion to human colon tumor cell lines.

J Natl Cancer Inst 1996; **88:** 109-116

12 **Sun A,** Chia JS, Chang YF, Chiang CP. Levamisole and Chinese medicinal herbs can modulate the serum interleukin-6 level in patients with recurrent aphthous ulcerations. *J Oral Pathol Med* 2003; **32:** 206-214

13 **Holcombe RF,** Milovanovic T, Stewart RM, Brodhag TM. Investigating the role of immunomodulation for colon cancer prevention: results of an in vivo dose escalation trial of levamisole with immunologic endpoints. *Cancer Detect Prev* 2001; **25:** 183-191

14 **Creagan ET,** Rowland KM, Suman VJ, Kardinal CG, Marschke RF, Marks RS, Maples WJ. Phase II study of combined levamisole with recombinant interleukin-2 in patients with advanced malignant melanoma. *Am J Clin Oncol* 1997; **20:** 490-492

15 **Lai WH,** Lu SY, Eng HL. Levamisole aids in treatment of refractory oral candidiasis in two patients with thymoma associated with myasthenia gravis: report of two cases. *Chang Gung Med J* 2002; **25:** 606-611

16 **Aksoy H,** Baltaci S, Türkölmez K, Seçkiner I, Bedük Y. Combined interferon alpha with levamisole in patients with metastatic renal cell carcinoma. *Int Urol Nephrol* 2001; **33:** 457-459

17 **Lam P,** Yuen AP, Ho CM, Ho WK, Wei WI. Prospective randomized study of post-operative chemotherapy with levamisole and UFT for head and neck carcinoma. *Eur J Surg Oncol* 2001; **27:** 750-753

18 **Cafiero F,** Gipponi M, Peressini A, Bertoglio S, Lionetto R. Preliminary analysis of a randomized clinical trial of adjuvant postoperative RT vs. postoperative RT plus 5-FU and levamisole in patients with TNM stage II-III resectable rectal cancer. *J Surg Oncol* 2000; **75:** 80-88

19 **Fu LS,** Chi CS. Levamisole in steroid-sensitive nephrotic syndrome children with steroid-dependency and/or frequent relapses. *Acta Paediatr Taiwan* 2000; **41:** 80-84

20 **Sun A,** Chia JS, Chang YF, Chiang CP. Serum interleukin-6 level is a useful marker in evaluating therapeutic effects of levamisole and Chinese medicinal herbs on patients with oral lichen planus. *J Oral Pathol Med* 2002; **31:** 196-203

21 **Donia AF,** Amer GM, Ahmed HA, Gazareen SH, Moustafa FE, Shoeib AA, Ismail AM, Khamis S, Sobh MA. Levamisole: adjunctive therapy in steroid dependent minimal change nephrotic children. *Pediatr Nephrol* 2002; **17:** 355-358

22 **Sun A,** Chiang CP. Levamisole and/or Chinese medicinal herbs can modulate the serum level of squamous cell carcinoma associated antigen in patients with erosive oral lichen planus. *J Oral Pathol Med* 2001; **30:** 542-548

23 **Wolmark N,** Rockette H, Mamounas E, Jones J, Wieand S, Wickerham DL, Bear HD, Atkins JN, Dimitrov NV, Glass AG, Fisher ER, Fisher B. Clinical trial to assess the relative efficacy of fluorouracil and leucovorin, fluorouracil and levamisole, and fluorouracil, leucovorin, and levamisole in patients with Dukes' B and C carcinoma of the colon: results from National Surgical Adjuvant Breast and Bowel Project C-04. *J Clin Oncol* 1999; **17:** 3553-3559

24 **Burch PA,** Keppen MD, Schroeder G, Rubin J, Krook JE, Dalton RJ, Gerstner JB, Jancewicz MT, Ebbert LP. North Central Cancer Treatment Group Phase II study of 5-fluorouracil and high-dose levamisole for gastric and gastroesophageal cancer using survival as the primary endpoint of efficacy. *Am J Clin Oncol* 1999; **22:** 505-508

25 **Krastev Z,** Jelev D, Antonov K, Alagozian V, Kotzev I. Chronic HBV infection. Immunomodulation with levamisole in viremic HBeAg positive or anti-HBe positive patients--a pilot study. *Hepatogastroenterology* 1999; **46:** 3184-3188

26 **Szeto C,** Gillespie KM, Mathieson PW. Levamisole induces interleukin-18 and shifts type 1/type 2 cytokine balance. *Immunology* 2000; **100:** 217-224

Science Editor Wang XL and Li WZ **Language Editor** Elsevier HK

PO Box 2345, Beijing 100023, China
www.wjgnet.com
wjg@wjgnet.com

ELSEVIER

World J Gastroenterol 2005;11(45):7211-7217
World Journal of Gastroenterology ISSN 1007-9327

• *RAPID COMMUNICATION* •

Correlation between the expressions of gastrin, somatostatin and cyclin and cyclin-depend kinase in colorectal cancer

Pei Wu, Jia-Ding Mao, Jing-Yi Yan, Jing Rui, You-Cai Zhao, Xian-Hai Li, Guo-Qiang Xu

Pei Wu, Jia-Ding Mao, Jing-Yi Yan, Jing Rui, You-Cai Zhao, Xian-Hai Li, Guo-Qiang Xu, Department of General Surgery, The First Affiliated Yijishan Hospital of Wannan Medical College, Wuhu 241001, Anhui Province, China

You-Cai Zhao, Guo-Qiang Xu, Department of Pathology, The First Affiliated Yijishan Hospital of Wannan Medical College, Wuhu 241001, Anhui Province, China

Supported by the Natural Science Foundation of Anhui Province, No.03043704

Co-first-authors: Pei Wu and Jia-Ding Mao
Co-correspondent: Pei Wu
Correspondence to: Professor Pei Wu, Department of General Surgery, The First Affiliated Yijishan Hospital of Wannan Medical College, Wuhu 241001, Anhui Province, China. wp5708@sina.com
Telephone: +86-0553-5739343

Received: 2005-03-04 Accepted: 2005-04-11

Abstract

AIM: To explore the correlation between the expressions of gastrin (GAS), somatostatin (SS) and cyclin, cyclin-dependent kinase (CDK) in colorectal cancer, and to detect the specific regulatory sites where gastrointestinal hormone regulates cell proliferation.

METHODS: Seventy-nine resected large intestine carcinomatous specimens were randomly selected. Immunohistochemical staining for GAS, SS, cyclin D1, cyclin E, cyclin A, cyclin B1, CDK2 and CDK4 was performed according to the standard streptavidin-biotin-peroxidase (S-P) method. According to the semi-quantitative integral evaluation, SS and GAS were divided into high, middle and low groups. Cyclin D1, cyclin E, cyclin A, cyclin B1, CDK2, CDK4 expressions in the three GAS and SS groups were assessed.

RESULTS: The positive expression rate of cyclin D1 was significantly higher in high (78.6%, 11/14) and middle GAS groups (73.9%, 17/23) than in low GAS group (45.2%, 19/42) ($P<0.05$, $\chi^2_{\text{high } vs \text{ low}} = 4.691$; $P<0.05$, $\chi^2_{\text{middle } vs \text{ low}} = 4.945$). The positive expression rate of cyclin A was significantly higher in high (100%, 14/14) and middle GAS groups (82.6%, 19/23) than in low GAS group (54.8%, 23/42) ($P<0.01$, $\chi^2_{\text{high } vs \text{ low}} = 9.586$; $P<0.05$, $\chi^2_{\text{middle } vs \text{ low}} = 5.040$). The positive expression rate of CDK2 was significantly higher in high (92.9%, 13/14) and middle GAS groups (87.0%, 20/23) than in low GAS group (50.0%, 21/42) ($P<0.01$, $\chi^2_{\text{high } vs \text{ low}} = 8.086$; $P<0.01$, $\chi^2_{\text{middle } vs \text{ low}} = 8.715$). The positive expression rate of CDK4 was significantly higher in high (78.6%, 11/14) and middle GAS groups (78.3%, 18/23) than in low GAS group (42.9%, 18/42) ($P<0.05$, $\chi^2_{\text{high } vs \text{ low}} = 5.364$; $P<0.01$, $\chi^2_{\text{middle } vs \text{ low}} = 7.539$). The positive expression rate of cyclin E was prominently higher in low SS group (53.3%, 24/45) than in high (9.1%, 1/11) and middle (21.7%, 5/23) SS groups ($P<0.05$, $\chi^2_{\text{high } vs \text{ low}} = 5.325$; $P<0.05$, $\chi^2_{\text{middle } vs \text{ low}} = 6.212$). The positive expression rate of CDK2 was significantly higher in low SS group (77.8%, 35/45) than in high SS group (27.3%, 3/11) ($P<0.01$, $\chi^2_{\text{high } vs \text{ low}} = 8.151$). There was a significant positive correlation between the integral ratio of GAS to SS and the semi-quantitative integral of cyclin D1, cyclin E, cyclin A, CDK2, CDK4 ($P<0.05$, ${}^{D1}r_s = 0.252$; $P<0.01$, ${}^{E}r_s = 0.387$; $P<0.01$, ${}^{A}r_s = 0.466$; $P<0.01$, ${}^{K2}r_s = 0.519$; $P<0.01$, ${}^{K4}r_s = 0.434$).

CONCLUSION: The regulation and control of gastrin, SS in colorectal cancer cell growth may be directly related to the abnormal expressions of cyclins D1, A, E, and CDK2, CDK4. The regulatory site of GAS in the cell cycle of colorectal carcinoma may be at the G_1, S and G_2 phases. The regulatory site of SS may be at the entrance of S phase.

Key words: Colorectal cancer; Gastrin; Somatostatin; Cyclin; CDK

Wu P, Mao JD, Yan JY, Rui J, Zhao YC, Li XH, Xu GQ. Correlation between the expressions of gastrin, somatostatin and cyclin and cyclin-depend kinase in colorectal cancer. *World J Gastroenterol* 2005; 11(45): 7211-7217
http://www.wjgnet.com/1007-9327/11/7211.asp

INTRODUCTION

Colorectal cancer is one of the most common human malignant tumors in the world, with a high incidence rate in North America, Western Europe, Australia, New Zealand and France, and is the second leading cause of gastrointestinal cancer-related mortality worldwide[1–3]. Although great progress has been made in understanding the molecular aspects of colorectal cancer and several therapeutic agents have been developed, it still poses a serious threat to public health and remains as the major killer among the Chinese. The general survival rate of colorectal cancer patients does not exceed

40%[4,5]. Studies demonstrate that the occurrence of colorectal cancer is directly related to the abnormal expression of gastrointestinal hormones such as gastrin, somatostatin, etc[6]. At the same time, some studies found that somatostatin is able to induce apoptosis of large intestinal cancer cells and inhibit cell proliferation, but the role of GAS (gastrin) is opposite[7-9]. However, the detailed molecule mechanism by which gastrin and somatostatin regulate and control the growth of large intestinal carcinoma is not fully known. We have used immunohistochemical staining standard streptavidin-biotin-peroxidase (S-P) method to detect the expressions of GAS, somatostatin (SS), cyclin D1, cyclin E, cyclin A, cyclin B1, CDK2, CDK4 proteins in large intestinal cancer tissue. The aim of our study was to explore the correlation between the expressions of SS, GAS and cyclins, cyclin-dependent kinase (CDKs) and to further confirm whether GAS, SS could regulate and control large intestinal cancer cell growth by affecting the expression of cyclins and CDKs.

MATERIALS AND METHODS

Seventy-nine cancer tissue samples were randomly selected from patients with large intestinal carcinoma hospitalized in the Department of Pathology of the First Affiliated Yijishan Hospital of Wannan Medical College from June 2001 to June 2003. All patients were confirmed to have colorectal carcinoma by clinical pathology. Among them, 37 were cases of rectum cancer, 42 were cases of colorectal carcinoma. Thirty-five were females and 44 were males. The median age was 52.9±14.3 years, with a range of 27-78 years. Ulcerative type was found in 44 patients, protruded type in 33, infiltrating type in 2, papillary adenocarcinoma in 7, glandular adenocarcinoma in 40, mucoid carcinoma in 14, signet-ring cell carcinoma in 11, and undifferentiated carcinoma in 7. The clinical stage was determined according to the Dukes' stage. Dukes' stages A and B were found in 38 patients, Dukes' stages C and D in 41 patients.

The polyclonal rabbit antibodies against human SS and GAS, monoclonal mouse antibodies against human cyclins D1, E, A, B1, and CDK2, CDK4, and immunohistochemical staining kits were all purchased from Beijing Zhongshan Biological Technology Co., Ltd.

Specimens obtained during surgery were routinely fixed in 10% neutral formalin and embedded in paraffin. Serial 4-μm-thick sections were cut. Immunohistochemical staining for cyclins D1, E, A, B1, and CDK2, CDK4, GAS, SS was performed according to the S-P method. The detailed manipulation was conducted according to the introduction for users. Positive pancreatic tissue, stomach antrum mucous membrane, healthy amygdalae tissue, breast cancer tissue, reactive lymph node tissue, healthy skin tissue were used as a positive control for GAS, SS, cyclins A, B1, D1, E, and CDK2, CDK4, respectively. PBS (0.01mol/L) as a negative control replaced the primary antibody.

Positive SS and GAS were stained brown-yellow mainly in cell plasma, partly in cell membranes. When SS and GAS protein expression were scored, both the extent and intensity of immunopositivity were considered. The intensity of staining was scored as follows: 0 as no staining, 1 as weak-yellow, 2 as brown-yellow, and 3 as brown-black. The extent of positive cells was scored as follows (100 cells were counted by two independent observers, who did not know the clinicopathological features of these large intestinal cancers): 1 = positively stained cells <5%, 2 = positively stained cells being 5-10%, 3 = positively stained cells being 10-20%, 4 = positively stained cells >20%. The final score was determined by multiplying the intensity and extent of positivity scores, yielding a range from 1 to 12. According to the semi-quantitative integral evaluation, SS and GAS were divided into three groups as follows: scores 1-3 were defined as the low group, 4-6 as the middle group, and 7-12 as the high group.

Positive cyclin B1 was stained brown-yellow mainly in the cell plasma. Positive cyclins D1, E, A, and CDK2, CDK4 were stained brown-yellow mainly in karyons. The degree of their staining was estimated by semiquantitative evaluation and categorized by the extent and intensity of staining as follows[10]. The intensity of staining was scored as follows: 0 as negative, 1 as weak-yellow, 2 as brown-yellow, and 3 as brown-black. The extent of positively stained cells was scored as follows: 0=positively stained cells being 0-5%, 1 = positively stained cells being 6-25%, 2 = positively stained cells being 26-50%, 3 = positively stained cells being 51-75%, 4 = positively stained cells>75%. Combined staining score was used to evaluate the staining of cyclins D1, E, A, B1, and CDK2, CDK4. The final score was determined by adding the intensity and extent of staining scores, yielding a range from 0 to 7. Scores1-2 were defined as negative staining (-), 3 as weak staining (+), 4 as moderate staining (++), ⩾5 as strong staining (+++).

Statistical analysis was performed using chi-square test to differentiate the positive rates of different groups and using Spearman's test to analyze the correlation between the ratio of GAS to SS and the integral of cyclins D1, E, A, B1, and CDK2, CDK4. All data were analyzed with SPSS version 10.0. $P<0.05$ was considered statistically significant.

RESULTS

The positive expression rate of cyclin D1 was significantly higher in high (78.6%, 11/14) and middle GAS groups (73.9%, 17/23) than in low GAS group (45.2%, 19/42) ($P<0.05$, $\chi^2_{\text{high } vs \text{ low}} = 4.691$; $P<0.05$, $\chi^2_{\text{middle } vs \text{ low}} = 4.945$). The positive expression rate of cyclin A was significantly higher in high (100%, 14/14) and middle GAS groups (82.6%, 19/23) than in low GAS group (54.8%, 23/42) ($P<0.01$, $\chi^2_{\text{high } vs \text{ low}} = 9.586$; $P<0.05$, $\chi^2_{\text{middle } vs \text{ low}} = 5.040$). The positive expression rate of CDK2 was significantly higher in high (92.9%, 13/14) and middle GAS groups (87.0%, 20/23) than in low group (50.0%, 21/42) ($P<0.01$, $\chi^2_{\text{high } vs \text{ low}} = 8.086$; $P<0.01$, $\chi^2_{\text{middle } vs \text{ low}} = 8.715$). The positive

Table 1 CDK2, CDK4, cyclins D1, E, A, and B1 expressions in high, middle, and low SS and GAS groups of colorectal carcinoma

Groups	*n*	Cyclin D1 -	Cyclin D1 + (%)	Cyclin E -	Cyclin E + (%)	Cyclin A -	Cyclin A + (%)	CyclinB1 -	CyclinB1 +(%)	CDK2 -	CDK2 + (%)	CDK4 -	CDK4 + (%)
GAS													
High	14	3	11 (78.6)[a]	6	8	0	14 (100)[b]	1	13(92.9)	1	13 (92.9)[b]	3	11 (78.6)[a]
Middle	23	6	17 (73.9)[a]	12	11	4	19 (82.6)[a]	6	17	3	20 (87.0)[b]	5	18 (78.3)[b]
Low	42	23	19	31	11	19	23	14	28	21	21	24	18
SS													
High	11	6	5	10	1 (9.1)[c]	3	8	2	9	8	3 (27.3)[d]	7	4
Middle	23	9	14	18	5 (21.7)[c]	7	16	6	17	7	16	9	14
Low	45	17	28	21	24	13	32	13	32	10	35	16	29

[a]P<0.05, [b]P<0.01 *vs* low GAS group; [c]P<0.05, [d]P<0.01 *vs* low SS group.

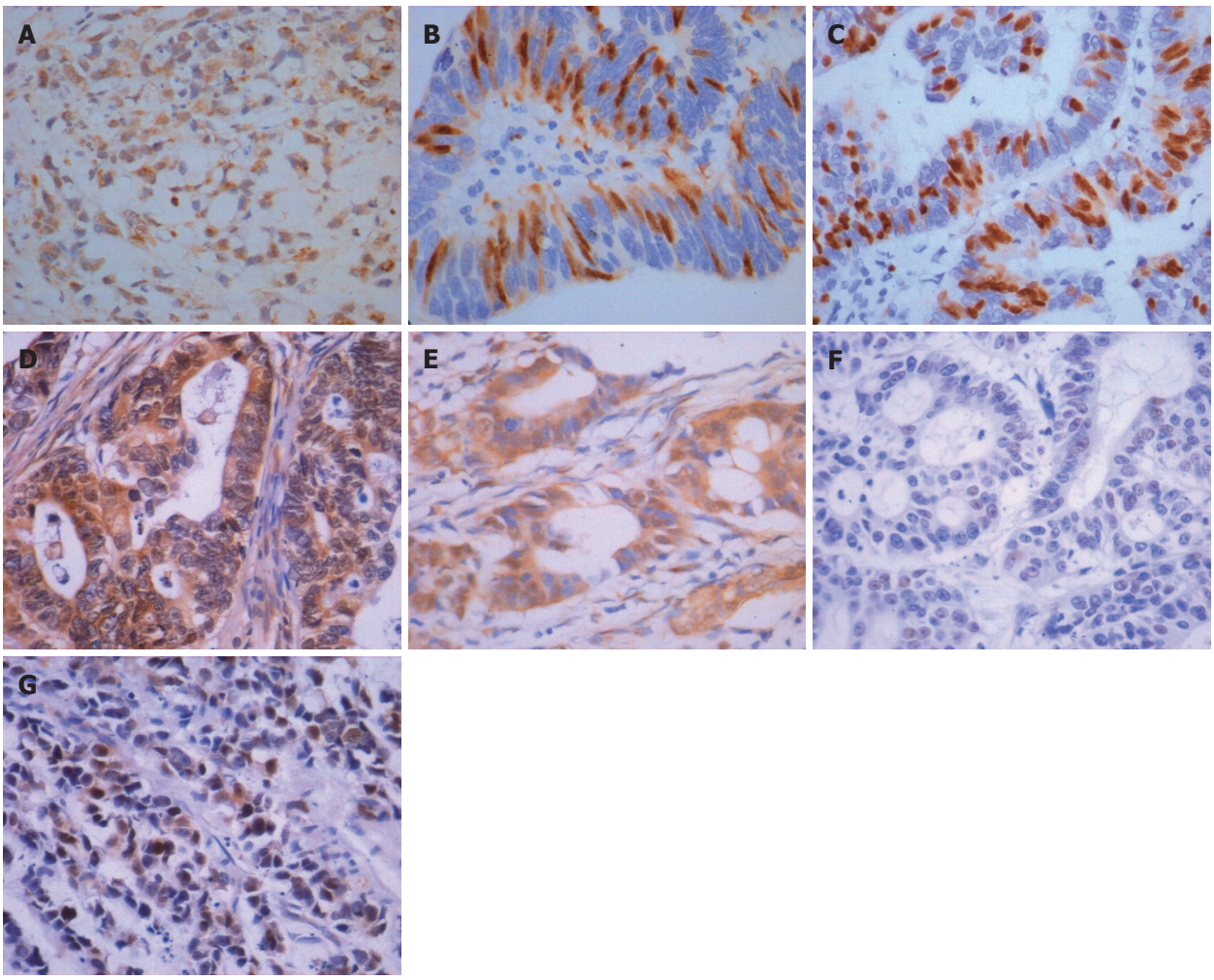

Figure 1 Strong expressions of GAS (**A**), cyclin D1 (**B**), cyclin A (**C**), CDK4 (**D**), SS (**E**), cyclin E (**F**) and CDK2 (**G**) in colorectal carcinoma tissue, S-P×400.

expression rate of CDK4 was significantly higher in high (78.6%, 11/14) and middle GAS groups (78.3%, 18/23) than in low group (42.9%, 18/42) (P<0.05, $\chi^2_{\text{high vs. low}}$ = 5.364; P<0.01, $\chi^2_{\text{middle vs. low}}$ = 7.539). However, the positive expression rate of cyclins E and B1 was significantly higher in high (57.1%, 8/14; 92.9%, 13/14) and middle GAS groups (47.8%, 11/23; 73.9%, 17/23) than in low GAS group (26.2%, 11/42; 66.9%, 28/42), but there was no statistically significant difference among the three groups when compared to three groups to each other (P>0.05, χ^2 = 5.608; P>0.05, χ^2 = 4.417) (Table 1, Figure 1 A-D).

The positive expression rate of cyclin E was prominently higher in low SS group (53.3%, 24/45) than in high (9.1%, 1/11) and middle (21.7%, 5/23) SS groups (P<0.05, $\chi^2_{\text{high vs low}}$ = 5.325; P<0.05, $\chi^2_{\text{middle vs low}}$ = 6.212). The positive expression rate of CDK2 was significantly higher in low SS group (77.8%, 35/45) than in high SS

group (27.3%, 3/11) ($P<0.01$, $\chi^2_{\text{high vs low}} = 8.151$). However, the positive expression rate of CDK4, cyclin D1 was significantly higher in low SS group (64.4%, 29/45; 62.2%, 28/45) than in high SS group (36.4%, 4/11; 45.5%, 5/11), it was not statistically significant ($P>0.05$, $\chi^2 = 2.868$; $P>0.05$, $\chi^2 = 1.038$). There was no statistically significant difference in the positive expression rate of cyclins A and B1 in high (72.2%, 8/11; 81.8%, 9/11), middle (69.6%, 16/23; 73.9%, 17/23) and low SS groups (71.0%, 32/45; 71.1%, 32/45) when compared to each other ($P>0.05$, $\chi^2 = 0.039$; $P>0.05$, $\chi^2 = 0.554$) (Table 1, Figure 1 E-G).

There was a significant positive correlation between the integral ratio of GAS to SS and the semiquantitative integral of cyclins D1, E, A, and CDK2, CDK4 ($P<0.05$, ${}^{D1}r_s = 0.252$; $P<0.01$, ${}^{E}r_s = 0.387$; $P<0.01$, ${}^{A}r_s = 0.466$; $P<0.01$, ${}^{K2}r_s = 0.519$; $P<0.01$, ${}^{K4}r_s = 0.434$). But there was no correlation between the integral ratio of GAS to SS and cyclin B1 integral ($P>0.05$, $r = -0.108$).

DISCUSSION

Cancer arises mainly from mutations in the somatic cells. However, conversion of normal cells to cancer cells is not the result of a single mutation; it is achieved through a multi-step process that is closely associated with the accumulation of multiple gene changes including both oncogenes and tumor suppressor genes[11-13]. Uncontrolled cell proliferation is one of the main hallmarks of cancer, and tumor cells have acquired damage to genes that are directly involved in regulating the cell cycle. The cell cycling process is carefully regulated. The switch or transition between phases is a hallmark of the cell cycle, with an extremely accurate timing and order of molecular events. However, if something goes wrong, the cells have several systems for interrupting the cell cycle[12,14,15].

In order to ensure the cell cycling process, CDK timing-activity is a critical step in the regulation and control mechanism of cell cycle. At least nine different CDKs are known today. However, only some of them seem to be involved in cell cycle regulation. CDKs that are required for cell cycle regulation contain an active kinase subunit in complex with a regulatory subunit, or activator, commonly called cyclin[16,17]. Cyclins are important mediators of CDKs activity, and their level fluctuates throughout the cell cycle, some being more abundant in specific cell phases than others[18]. These cyclins have been divided into three classes: G_1-S cyclin, S cyclin, and M cyclin. Cyclins response to mitogenic signals and unscheduled expression, leading to uncontrolled proliferation, has been implicated in different human cancers[19], such as colon cancer[20] and breast cancer[21]. The CDK/cyclin complex is subjected to several kinds of regulation factors, both positive and negative.

Cell cycle progression is positively regulated by multiple cyclins and CDKs and cyclin/CDK complexes are negatively regulated by a number of CDK inhibitors including p27[22,23]. P27 is a CDK inhibitor and plays an important role in the negative regulation of the cell cycle during G_0 and G_1 phases[12,13,24,25]. Proliferating cells pass through several cell cycle checkpoints, mainly the G_1 to S and G_2 to M transitions. The former checkpoint is considered as the most important one in the replication of DNA and mitosis. The G_1-S transition is a highly regulated and important transition in the cell cycle. At this stage, the cell cycle passes a point between G_1 and S phases (restriction point) with an irreversible commitment to a new cycle. The underlying molecular mechanisms are the induced expression of CDKs and cyclins required for the cells to progress from early G_1 phase into late G_1 phase of the cell cycle, reaching the restriction point. This is a critical point in the late G_1 phase where the mammalian cells become committed to entering the S phase and to complete the cell cycle, even in the absence of growth factors[23,26,27]. The main CDKs involved in the progression from mid- to late G_1 are CDK4 and CDK6, driven by three G_1-specific cyclins, D1, D2 and D3[15]. Cycle progression from G_1 to S phase is usually accompanied with Rb phosphorylation induced by cyclin D_1-CDK_4 and cyclin E-CDK_2 complexes in the late G_1 phase[28]. Cyclin-dependent kinase 2 (CDK2) activity is critical for S phase entry. CDK2 activation is apparently cyclin E-dependent. Late G_1 phase CDK2/cyclin E activity depends on early G_1 phase CDK2/cyclin E function[29,30].

Previous studies have shown that some tissue growth is regulated by hormones, and these tissues that have turned into tumors are still controlled by hormones[31]. Gastrointestinal hormones such as gastrin and somatostatin regulate the secretion, motility, absorption, blood flow and cell nutrition of the digestive tract. Abnormality of their secretion often affects the normal functions of the digestive tract, even causes clinical symptoms or syndromes[32,33]. Some studies demonstrated that there is a high correlation between the abnormal expressions of GAS, SS and the occurrence and development of colorectal cancer[34-36]. Recently, great progress has been made in understanding the cell cycle mechanisms of GAS and SS. Some studies showed that the abnormal expressions of GAS and SS are closely related to cell apoptosis and proliferation of colorectal cancer, and that the expression of gastrin protein and the proliferation index are higher in colorectal cancer tissue, while the action of somatostatin is opposite in colorectal carcinoma[9,37,38]. Though there is abundant evidence that gastrin plays an important role in promoting tumor growth in the stomach, as well as malignancies in the GI tract, the precise mechanisms governing the gastrin-induced and somatostatin-restrained proliferation are still largely unknown. To elucidate the mechanisms of gastrin and somatostatin in regulating mitogenesis, we have analyzed their effects on the expression of cyclins and CDKs in human colorectal cancer tissue.

Gastrin is a gastrointestinal (GI) peptide that possesses potent trophic effects on most normal and neoplastic mucosae of the GI tract. Gastrin is mainly secreted from gastrin secreting cells (G cells) in the antrum mucosa or upper small intestine, large intestine. Medulla oblongata and dorsal nuclei of vagus nerves in central nervous system also secrete gastrin[39,40]. Studies indicate that

chronic hypergastrinemia increases the risk of colorectal cancer and cancer growth, and that interruption of the effects of gastrin may be a potential target in the treatment of colorectal cancer[41]. Shen *et al*[42] showed that gastrin is able to promote DNA and protein synthesis in colorectal cancer tissue. However, gastrin-released peptide receptor antagonist proglumide could block these effects of gastrin, and restrain colorectal cancer cells from G_0/G_1 phase into S and G_2, M phase transitions. It was recently reported that gastrin (G-17) is able to induce a significant increase in G_1-specific marker cyclin D1 transcripts, protein, and promoter activity via the activation of beta-catenin and CRE-binding protein pathways in gastric adenocarcinoma cells, which promote transition of tumor cells from G_1 phase into S phase, and lead to uncontrolled proliferation of tumor cells[43]. Lefranc *et al*[44] studies found that gastrin is able to significantly modify the growth of a number of experimental gliomas. This effect seems to occur via a cytostatic effect, that is, an accumulation of tumor astrocytes occurs in the G_1 cell cycle phase. The cytostatic effect relates to a gastrin-induced decrease in the level of cyclin D3-CDK4 complex. In this study, we have found that the level of gastrin protein expression was higher and the positive expression rate of cyclins D1, A, and CDK2, CDK4 was higher in large intestinal carcinoma tissue, indicating that mechanism of gastrin in promoting colorectal cancer cell proliferation is via inducing the overexpression of cyclins D1, A, and CDK2, CDK4, thus leading to the rise of the level of cyclin D1-CDK4 and cyclin A-CDK2 complexes, which influence cell cycle progress and promote cell proliferation.

Somatostatin is a widely distributed inhibitory hormone that plays an important role in several biological processes including neurotransmission, inhibition of exocrine and endocrine secretions, and cell proliferation. Somatostatin acts as an inhibitory peptide of various secretory and proliferative responses. Somatostatin is secreted from somatostatin secreting cells (D cells). D cells are distributed mainly in intestinal nerve plexus, stomach and pancreas. The diverse biological effects of somatostatin are mediated by a family of five somatostatin receptors (sst1-sst5) that belong to the family of G-protein-coupled receptors and regulate diverse signal transduction pathways including adenylate cyclase, phospholipase C-β phospholipase A_2, guanylate cyclase, ionic conductance channels, and tyrosine phosphatase[45-48]. The mechanisms underlying the inhibition are the combined interaction of somtostatin and its analogs to SST1-5R in tumor tissues, either directly inhibiting division and proliferation of tumor cells or the activities of growth factors such as vascular endothelial growth factor, insulin-like growth factor, etc[49-51], thus counteracting tumorigenesis and tumor cell proliferation[52]. The ability of somatostatin and its stable analogs to inhibit normal and tumor cell growth has been demonstrated in various cell types including mammary, prostatic, gastric, pancreatic, colorectal, and small cell lung cancer cells. However, the mechanisms of somatostatin underlying cell growth arrest are still poorly understood. Pages *et al*[53] showed that activation of sst2 promotes cell growth arrest through the ability of somatostatin to maintain high levels of $p27^{Kip1}$ and inactivates cyclin E-CDK2 complexes, leading to hypophosphorylation of pRb, restraining transition of tumor cells from G_1 phase into S phase. Charland *et al*[54] reported that somatostatin is able to inhibit cyclin E expression in pancreatic cells and cyclin E-associated CDK2 activity, as well as pRb phosphorylation, and to restrain transition of cells from G_1 phase into S phase, thus inhibiting cell proliferation. Zhao *et al*[55] demonstrated that somatostatin analog, octreotide, inhibits the proliferation of cholangiocarcinoma cells through G_0/G_1 cell cycle arrest rather than through the process of apoptosis. These effects are partially mediated by enhancing the expression of p27kipl, and decreasing the level of cyclin E-CDK2 complex. In this study, the higher the integral of SS, the lower the positive expression rate of cyclin E and CDK2. Our data indicate that the mechanism of somatostatin in inhibiting colorectal cancer cell proliferation is via restraining the expression of cyclin E and CDK2, and decreasing the level of cyclin E-CDK2 complex, which inhibits transition of cells from G_1 phase into S phase and induces cell cycle arrest, thus restraining cell proliferation.

In the present study, we have found that the ratio of GAS to SS had an effect on the biological characteristics of large intestinal cancer[56]. The increased ratio of GAS to SS is an event of significance in large intestinal cancer occurrence and development[31]. Our results indicate that there is a positive correlation between the ratio of GAS to SS and the semi-quantitative integral expression of cyclins D1, A, E, and CDK2, CDK4. Furthermore, the expression of GAS and SS has a direct relation with the expression of cyclins D1, A, E, and CDK2, CDK4 in colorectal cancer.

In conclusion, the regulation and control of gastrin, somatostatin in colorectal cancer cell growth may be directly related to the abnormal expressions of cyclins D1, A, E, and CDK2, CDK4. The regulatory site of GAS in the cell cycle of colorectal carcinoma may be at the G_1, S and G_2 phases. The regulatory site of SS may be at the entrance of S phase.

REFERENCES

1 **Zhang ZS**, Zhang YL. Progress in research of colorectal cancer in China. *Shijie Huaren Xiaohua Zazhi* 2001; **9**: 489-494

2 **Colonna M,** Grosclaude P, Launoy G, Tretarre B, Arveux P, Raverdy N, Benhamiche AM, Herbert C, Faivre J. Estimation of colorectal cancer prevalence in France. *Eur J Cancer* 2001; **37**: 93-96

3 **Greenlee RT**, Murray T, Bolden S, Wingo PA. Cancer statistics, 2000. *CA Cancer J Clin* 2000; **50**: 7-33

4 **Greenlee RT**, Hill-Harmon MB, Murray T, Thun M. *Cancer statistics*, 2001. CA Cancer J Clin 2001; **51**: 15-36

5 **Konturek PC**, Bielanski W, Konturek SJ, Hartwich A, Pierzchalski P, Gonciarz M, Marlicz K, Starzynska T, Zuchowicz M, Darasz Z, Götze JP, Rehfeld JF, Hahn EG. Progastrin and cyclooxygenase-2 in colorectal cancer. *Dig Dis Sci* 2002; **47**: 1984-1991

6 **Saga T**, Tamaki N, Itoi K, Yamazaki T, Endo K, Watanabe G, Maruno H, Machinami R, Koizumi K, Ichikawa T, Takami H, Ishibashi M, Kubo A, Kusakabe K, Hirata Y, Murata Y, Miyachi Y, Tsubuku M, Sakahara H, Katada K, Tonami N,

Yamamoto K, Konishi J, Imamura M, Doi R, Shimatsu A, Noguchi S, Hasegawa Y, Ishikawa O, Watanabe Y, Nakajo M. Phase III additional clinical study of 111In-pentetreotide (MP-1727): diagnosis of gastrointestinal hormone producing tumors based on the presence of somatostatin receptors. *Kaku Igaku* 2003; **40**: 185-203

7 **Sadji-Ouatas Z**, Lasfer M, Julien S, Feldmann G, Reyl-Desmars F. Doxorubicin and octreotide induce a 40 kDa breakdown product of p53 in human hepatoma and tumoral colon cell lines. *Biochem J* 2002; **364**: 881-885

8 **Watson SA**, Morris TM, McWilliams DF, Harris J, Evans S, Smith A, Clarke PA. Potential role of endocrine gastrin in the colonic adenoma carcinoma sequence. *Br J Cancer* 2002; **87**: 567-573

9 **Wu P**, Tu JS, Riu J, Hang H, Hang WB, Yuan P. To study the correlation between expression of gastrin, somatostatin and cell proliferation, apoptosis in colorectal carcinoma. *Zhonghua Shiyan Waike Zaizhi* 2003; **20**: 947

10 **Fromowitz FB**, Viola MV, Chao S, Oravez S, Mishriki Y, Finkel G, Grimson R, Lundy J. ras p21 expression in the progression of breast cancer. *Hum Pathol* 1987; **18**: 1268-1275

11 **Hartwell LH,** Kastan MB. Cell cycle control and cancer. *Science* 1994; **266**: 1821-1828

12 **Arisi E,** Pruneri G, Carboni N, Sambataro G, Pignataro L. Prognostic significance of P27 and cyclin D1 co-expression in laryngeal squamous cell carcinoma: possible target for novel therapeutic strategies. *J Chemother* 2004; **16 Suppl 5**: 3-6

13 **Kudo Y,** Kitajima S, Ogawa I, Miyauchi M, Takata T. Down-regulation of Cdk inhibitor p27 in oral squamous cell carcinoma. *Oral Oncol* 2005; **41**: 105-116

14 **Hanahan D,** Weinberg RA. The hallmarks of cancer. *Cell* 2000; **100**: 57-70

15 **Sandal T.** Molecular aspects of the mammalian cell cycle and cancer. *Oncologist* 2002; **7**: 73-81

16 **Elledge SJ**. Cell cycle checkpoints: preventing an identity crisis. *Science* 1996; **274**: 1664-1672

17 **Morgan DO**. Principles of CDK regulation. *Nature* 1995; **374**:131-134

18 **Sherr CJ.** Cancer cell cycles. *Science* 1996; **274**: 1672-1677

19 **Sherr CJ**. The Pezcoller lecture: cancer cell cycles revisited. *Cancer Res* 2000; **60**: 3689-3695

20 **Tetsu O,** McCormick F. Proliferation of cancer cells despite CDK2 inhibition. Cancer Cell 2003; **3**: 233-245

21 **Yu Q**, Geng Y, Sicinski P. Specific protection against breast cancers by cyclin D1 ablation. *Nature* 2001; **411**: 1017-1021

22 **Managlia EZ**, Landay A, Al-Harthi L. Interleukin-7 signalling is sufficient to phenotypically and functionally prime human CD4 naive T cells. *Immunology* 2005; **114:** 322-335

23 **Yang M,** Huang HL, Zhu BY, Tuo QH, Liao DF. Onychin inhibits proliferation of vascular smooth muscle cells by regulating cell cycle. *Acta Pharmacol Sin* 2005; **26:** 205-211

24 **Li B,** DiCicco-Bloom E. Basic fibroblast growth factor exhibits dual and rapid regulation of cyclin D1 and p27 to stimulate proliferation of rat cerebral cortical precursors. *Dev Neurosci* 2004;26:197-207

25 **Zhang W,** Bergamaschi D, Jin B, Lu X. Posttranslational modifications of p27kip1 determine its binding specificity to different cyclins and cyclin-dependent kinases in vivo. *Blood* 2005; **105**: 3691-3698

26 **Planas-Silva MD**, Weinberg RA. The restriction point and control of cell proliferation. *Curr Opin Cell Biol* 1997; **9**: 768-772

27 **Huang X,** Di Liberto M, Cunningham AF, Kang L, Cheng S, Ely S, Liou HC, Maclennan IC, Chen-Kiang S. Homeostatic cell-cycle control by BLyS: Induction of cell-cycle entry but not G1/S transition in opposition to p18INK4c and p27Kip1. *Proc Natl Acad Sci USA* 2004; **101**: 17789-17794

28 **King KL,** Cidlowski JA. Cell cycle regulation and apoptosis. *Annu Rev Physiol* 1998; **60**: 601-617

29 **Senderowicz AM.** Small molecule modulators of cyclin-dependent kinases for cancer therapy. *Oncogene* 2000; **19**: 6600-6606

30 **Owa T**, Yoshino H, Yoshimatsu K, Nagasu T. Cell cycle regulation in the G_1 phase: a promising target for the development of new chemotherapeutic anticancer agents. *Curr Med Chem* 2001; **8**: 1487-1503

31 **Sereti E**, Gavriil A, Agnantis N, Golematis VC, Voloudakis-Baltatzis IE. Immunoelectron study of somatostatin, gastrin and glucagon in human colorectal adenocarcinomas and liver metastases. *Anticancer Res* 2002; **22**: 2117-2123

32 **Larsson LI**. Developmental biology of gastrin and somatostatin cells in the antropyloric mucosa of the stomach. *Microsc Res Tech* 2000; **48**: 272-281

33 **Portela-Gomes GM**, Albuquerque JP, Ferra MA. Serotonin and gastrin cells in rat gastrointestinal tract after thyroparathyroidectomy and induced hyperthyroidism. *Dig Dis Sci* 2000; **45**: 730-735

34 **Glover SC**, Tretiakova MS, Carroll RE, Benya RV. Increased frequency of gastrin-releasing peptide receptor gene mutations during colon-adenocarcinoma progression. *Mol Carcinog* 2003; **37**: 5-15

35 **Carroll RE,** Matkowskyj KA, Tretiakova MS, Battey JF, Benya RV. Gastrin-releasing peptide is a mitogen and a morphogen in murine colon cancer. *Cell Growth Differ* 2000; **11**: 385-393

36 **Tejeda M**, Gaal D, Barna K, Csuka O, Kéri G. The antitumor activity of the somatostatin structural derivative (TT-232) on different human tumor xenografts. *Anticancer Res* 2003; **23**: 4061-4066

37 **Yu HG**, Schrader H, Otte JM, Schmidt WE, Schmitz F. Rapid tyrosine phosphorylation of focal adhesion kinase, paxillin, and p130Cas by gastrin in human colon cancer cells. *Biochem Pharmacol* 2004; **67**: 135-146

38 **Wu H**, Rao GN, Dai B, Singh P. Autocrine gastrins in colon cancer cells Up-regulate cytochrome c oxidase Vb and down-regulate efflux of cytochrome c and activation of caspase-3. *J Biol Chem* 2000; **275**: 32491-32498

39 **Swatek J**, Chibowski D. Endocrine cells in colorectal carcinomas. Immunohistochemical study. *Pol J Pathol* 2000; **51**: 127-136

40 **Song DH,** Rana B, Wolfe JR, Crimmins G, Choi C, Albanese C, Wang TC, Pestell RG, Wolfe MM. Gastrin-induced gastric adenocarcinoma growth is mediated through cyclin D1. *Am J Physiol Gastrointest Liver Physiol* 2003: **285**: G217- G 222

41 **Yao M,** Song DH, Rana B, Wolfe MM. COX-2 selective inhibition reverses the trophic properties of gastrin in colorectal cancer. *Br J Cancer* 2002; **87**: 574-579

42 **Shen K,** He S, He Y. Effects of proglumide, a gastrin receptor antagonist, on human large intestine carcinoma SW480 cell line. *Chin Med J (Engl)* 1998; **111**: 1075-1078

43 **Pradeep A,** Sharma C, Sathyanarayana P, Albanese C, Fleming JV, Wang TC, Wolfe MM, Baker KM, Pestell RG, Rana B. Gastrin-mediated activation of cyclin D1 transcription involves beta-catenin and CREB pathways in gastric cancer cells. *Oncogene* 2004; **23**: 3689-3699

44 **Lefranc F,** Sadeghi N, Metens T, Brotchi J, Salmon I, Kiss R. Characterization of gastrin-induced cytostatic effect on cell proliferation in experimental malignant gliomas. *Neurosurgery* 2003; **52**: 881-890; discussion 890-891

45 **Zatelli MC**, Piccin D, Tagliati F, Ambrosio MR, Margutti A, Padovani R, Scanarini M, Culler MD, degli Uberti EC. Somatostatin receptor subtype 1 selective activation in human growth hormone (GH)- and prolactin (PRL)-secreting pituitary adenomas: effects on cell viability, GH, and PRL secretion. *J Clin Endocrinol Metab* 2003; **88**: 2797-2802

46 **Guillermet J,** Saint-Laurent N, Rochaix P, Cuvillier O, Levade T, Schally AV, Pradayrol L, Buscail L, Susini C, Bousquet C. Somatostatin receptor subtype 2 sensitizes human pancreatic cancer cells to death ligand-induced apoptosis. *Proc Natl Acad Sci USA* 2003; **100:** 155-160

47 **Faiss S,** Pape UF, Böhmig M, Dörffel Y, Mansmann U, Golder W, Riecken EO, Wiedenmann B.Prospective, randomized, multicenter trial on the antiproliferative effect of lanreotide, interferon alfa, and their combination for therapy of

metastatic neuroendocrine gastroenteropancreatic tumors--the International Lanreotide and Interferon Alfa Study Group. *J Clin Oncol* 2003; **21**: 2689-2696

48 **Benali N,** Ferjoux G, Puente E, Buscail L, Susini C. Somatostatin receptors. *Digestion* 2000; **62 Suppl 1**: 27-32

49 **Hortala M,** Ferjoux G, Estival A, Bertrand C, Schulz S, Pradayrol L, Susini C, Clemente F. Inhibitory role of the somatostatin receptor SST2 on the intracrine-regulated cell proliferation induced by the 210-amino acid fibroblast growth factor-2 isoform: implication of JAK2. *J Biol Chem* 2003; **278**: 20574-20581

50 **Buscail L,** Vernejoul F, Faure P, Torrisani J, Susini C. Regulation of cell proliferation by somatostatin. *Ann Endocrinol (Paris)* 2002; **63(2 Pt 3)**: 2S13-2S18

51 **Puente E,** Saint-Laurent N, Torrisani J, Furet C, Schally AV, Vaysse N, Buscail L, Susini C. Transcriptional activation of mouse sst2 somatostatin receptor promoter by transforming growth factor-beta. Involvement of Smad4. *J Biol Chem* 2001; **276**: 13461-13468

52 **Ferjoux G,** Bousquet C, Cordelier P, Benali N, Lopez F, Rochaix P, Buscail L, Susini C. Signal transduction of somatostatin receptors negatively controlling cell proliferation. *J Physiol Paris* 2000; **94**: 205-210

53 **Pagès P,** Benali N, Saint-Laurent N, Estève JP, Schally AV, Tkaczuk J, Vaysse N, Susini C, Buscail L.sst2 somatostatin receptor mediates cell cycle arrest and induction of p27(Kip1). Evidence for the role of SHP-1. *J Biol Chem* 1999; **274**: 15186-15193

54 **Charland S,** Boucher MJ, Houde M, Rivard N. Somatostatin inhibits Akt phosphorylation and cell cycle entry, but not p42/p44 mitogen-activated protein (MAP) kinase activation in normal and tumoral pancreatic acinar cells. *Endocrinology* 2001; **142**: 121-128

55 **Zhao B,** Zhao H, Zhao N, Zhu XG. Cholangiocarcinoma cells express somatostatin receptor subtype 2 and respond to octreotide treatment. *J Hepatobiliary Pancreat Surg* 2002; **9**: 497-502

56 **Wu P,** Rui J, Xia XH, Yuan P, Ma Y, Zhou G. Expression of Gastrin, somatostatin and their specific power in colorectal carcinoma. *Zhonghua Shiyan Waike Zaizhi* 1998; **11**: 520-521

Science Editor Wang XL and Guo SY **Language Editor** Elsevier HK

PO Box 2345, Beijing 100023, China
www.wjgnet.com
wjg@wjgnet.com

ELSEVIER

World J Gastroenterol 2005;11(45):7218-7221
World Journal of Gastroenterology ISSN 1007-9327

• *CASE REPORTS* •

Delayed development of hepatocellular carcinoma during long-term follow-up after eradication of hepatitis C virus by interferon therapy

Yukiko Ito, Natsuyo Yamamoto, Ryo Nakata, Yoshihisa Kato, Masashi Iori, Keisuke Sakai, Tamiko Takemura, Ryosuke Tateishi, Haruhiko Yoshida, Takao Kawabe, Masao Omata

Yukiko Ito, Natsuyo Yamamoto, Ryo Nakata, Yoshihisa Kato, Masashi Iori, Keisuke Sakai, Tamiko Takemura, Ryosuke Tateishi, Haruhiko Yoshida, Takao Kawabe, Masao Omata, Department of Gastroenterology, Department of Pathology, Department of Surgery, Japanese Red Cross Medical Center, Department of Gastroenterology, Department of Endoscopy and Endoscopic Surgery, University of Tokyo, Japan

Correspondence to: Takao Kawabe, MD, Department of Endoscopy, University of Tokyo, 7-3-1, Hongo, Bunkyo-ku, Tokyo 113-8655, Japan. kawabet-tky@umin.ac.jp
Telephone: +81-3-3815-5411 Fax: +81-3-3814-0021
Received: 2005-06-18 Accepted: 2005-08-27

Abstract

A 42-year-old Japanese man with liver cirrhosis by hepatitis C virus (HCV) had successful interferon therapy in May 1991. Since then, serum HCV-RNA and liver function tests had been negative. He had continued to drink more than 100 g/d of alcohol as before. In June 2003, a 5-cm tumor was found in the posterior segment of the liver. The tumor was curatively resected and the surgical specimen showed a well-differentiated hepatocellular carcinoma (HCC). Non-cancerous lesions of the liver revealed fibrosis at stage F3 with minimal to mild inflammation of grade A1. Heavy drinking may retard the dissolution of fibrosis and accelerate HCC development in patients with sustained virological response.

Key words: Hepatocellular carcinoma; Interferon; HCV; Eradication

Ito Y, Yamamoto N, Nakata R, Kato Y, Iori M, Sakai K, Takemura T, Tateishi R, Yoshida H, Kawabe T, Omata M. Delayed development of hepatocellular carcinoma during long-term follow-up after eradication of hepatitis C virus by interferon therapy. *World J Gastroenterol* 2005; 11(45): 7218-7221
http://www.wjgnet.com/1007-9327/11/7218.asp

INTRODUCTION

Hepatocellular carcinoma (HCC) is the third leading cause of death in Japan. Hepatitis C virus (HCV) infection is apparently a major cause of HCC[1-6]. Patients with chronic HCV infection seem destined for progression from milder forms of hepatitis to cirrhosis and, eventually, to HCC. The more advanced is the fibrosis of the liver, the higher is the risk of HCC development. This risk is surprisingly high in cirrhotic patients, the incident rate being about 7% per year[7]. Previously, those patients had no choice but to pass uneasy days in fear of HCC development. It was believed that liver fibrosis is an irreversible change and liver cirrhosis is an incurable disease. Recently, however, it has been shown that the risk of HCC is reduced in HCV-infected patients by interferon therapy, even in cirrhotic patients[8-13]. Interferon therapy can not only improve inflammation, but also ameliorate fibrosis and reduce the risk of HCC. More recently, it has been considered that HCC rarely develops long after HCV eradication[14,15].

Although interferon therapy has been employed for more than a decade, it is not clear how long the risk of HCC lasts among patients who have achieved sustained virological response (SVR). Recently, we had a case with HCC developing 12 years after HCV eradication. This case seems worthy of noting the details, and the data might be helpful for managing patients after HCV eradication.

CASE REPORT

A 42-year-old Japanese man had abnormal liver function tests at a health check-up in 1987. Serum ALT and AST were moderately elevated, 80 and 79 IU/L, respectively. He had no history of blood transfusion or drug abuse, but had been consuming more than 100 g/d of alcohol for 20 years. The liver biopsy specimen showed liver cirrhosis, diagnosed later as A1F4 according to the Classification by Desmet[17]. Alcohol hyaline was not found in the specimen (Figure 1).

In May 1991, he underwent successful interferon therapy after a diagnosis of HCV infection using a total dose of 390 MU of natural interferon-alpha (Sumiferon®, Sumitomo Pharmaceuticals Co., Ltd., Osaka, Japan). Serum HCV-RNA had been negative ever since, and liver function tests, including ALT and AST, had also been normalized. He had continued to drink alcohol heavily as before.

His follow-up had included blood tests and ultrasound examinations every 4-6 mo. In June 2003, ultrasonography

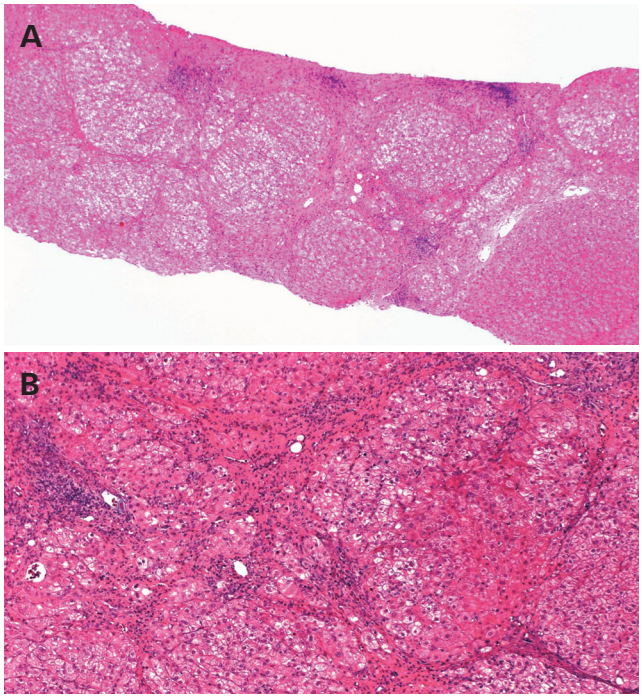

Figure 1 (**A** and **B**) Liver biopsy specimen before interferon therapy revealed liver cirrhosis with mild inflammation. It was graded as A1F4 according to the Classification by Desmet. Alcohol hyaline was not found (H&E stain, original magnifications A: ×4, B: ×200).

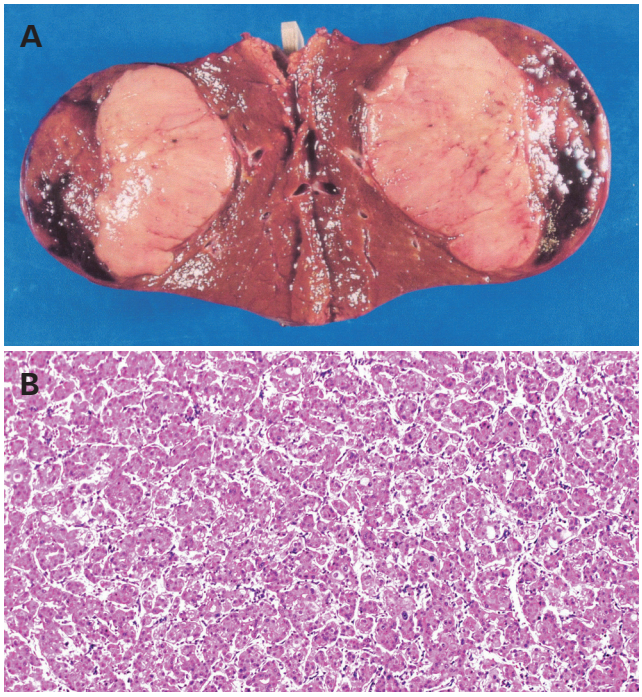

Figure 3 (**A**) Surgical specimen showing an 8-cm tumor. (**B**) Histological examination revealing a well-differentiated hepatocellular carcinoma (H&E stain, original magnification ×200).

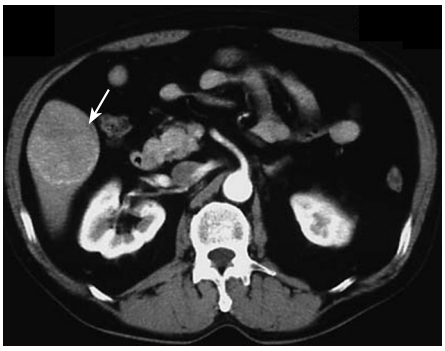

Figure 2 Contrast medium-enhanced CT image of the liver tumor of the right inferior segment (a white arrow).

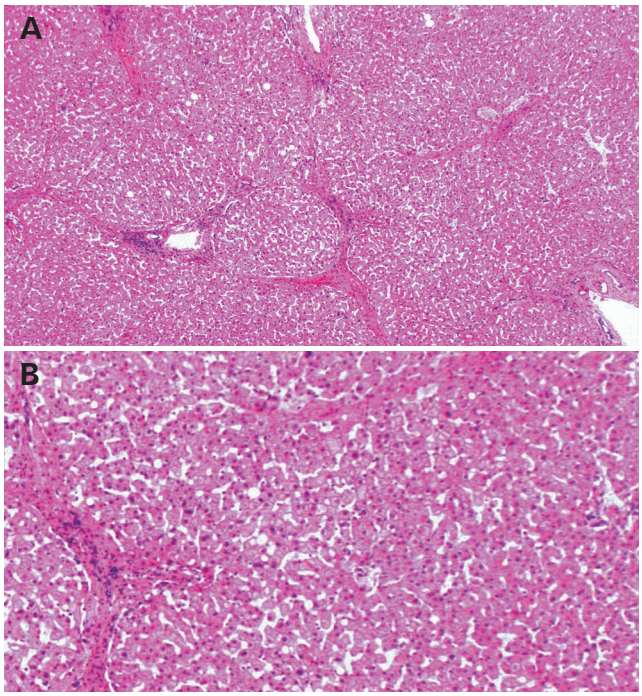

Figure 4 (**A** and **B**) Surgical specimen of non-cancerous lesion showing improvement of fibrosis and inflammation. However, great amounts of septa were observed, although fibrous bundles apparently decreased. Fibrosis resolved, revealing liver cirrhosis with mild inflammation. It was graded as A1F3 (H&E stain, original magnifications A: ×4, B: ×200).

and CT scan demonstrated a tumor of 5 cm in diameter in the posterior segment of the liver (Figure 2). Blood tests were normal except for elevated desgamma carboxy prothrombin (DCP, 44 mAu/mL, normal <40 mAu/mL). Angiography confirmed a hypervascular nodule, suggesting HCC.

The tumor was curatively resected and the surgical specimen showed a well-differentiated HCC (Figure 3). Non-cancerous lesions revealed minimal to mild inflammation and severe fibrosis of A1F3 (Figure 4).

The patient had recurrence of multiple HCCs, 12 mo after the surgery. Chemoembolization was performed repeatedly, and he was in remission up to September 2004.

DISCUSSION

Interferon therapy has been shown to reduce the risk of HCC development among the patients with chronic HCV infection. Their risk is decreased to one-third and their

survival is also significantly improved when they obtain SVR[17,18].

In patients achieving SVR, fibrosis is gradually dissolved and the risk for HCC development is reduced. Our concern is how long their risk of HCC lasts. There have been few documented cases of HCC development for more than 10 years after the interferon therapy, with more than 10 years having passed since its introduction. At that point, the possibility of HCC development is also believed to be notably decreased.

The present case developed HCC, 12 years after HCV eradication, perhaps the latest developed HCC case on record. It may be helpful for the management of post-eradication patients to review the details of this case in terms of the potential of HCC development.

The present patient had been showing normal aminotransferase values, including ALT and AST, and negative results for serum HVC RNA for 12 years after receiving interferon treatment. Although the histological findings of the liver were improved, great amounts of septa were still observed in the surgical specimen, suggesting F3. In patients with this status, the HCC risk is appraised at 5% per year. The dissolution of fibrosis may have been retarded in the present case. Shiratori *et al*[19] reported that the *F* values regress at a rate of -0.282/year among patients with SVR that is based on the method of Poynard[20]. The regression rate in the present case was from F4 to F3 for over the course of 12 years, a meager -0.083/year compared to the reported rate.

The patient had been consuming alcohol since the successful interferon therapy, perhaps accounting for the fact that the hepatic fibrosis had not been dissolved as expected. Alternatively, a long time after eradication, the regression rate in patients may not be as high as in those previously reported. As little data is available regarding regression or HCC development in patients with more than 10 years of follow-up, further studies will be needed.

In addition, alcohol itself may accelerate HCC development. Alcohol intake of 41-80 g/d and over 80 g/d is reported to increase the risk of HCC in HCV-infected patients by two- and four-fold, respectively[21]. Alcohol may also facilitate the growth of HCC, as the doubling time of tumor volume was reported as 148 d in abstemious patients and 78 d in imbibing patients[22].

The degree of liver fibrosis, male gender, higher age, and alcohol intake are well-known risk factors for HCC in chronic HCV-infected patients. The present patient met all these conditions, although little is known as to whether they serve as risk factors in patients with SVR. However, alcohol may have played a role in the development of HCC in this case. If he had stopped consuming alcohol, his liver fibrosis would likely have been improved to a greater extent, and he might have escaped from HCC entirely.

In conclusion, heavy drinking may retard the dissolution of fibrosis and accelerate HCC development in patients with SVR. A larger population of similar cases needs to be studied.

REFERENCES

1 **Ikeda K,** Saitoh S, Koida I, Arase Y, Tsubota A, Chayama K, Kumada H, Kawanishi M. **A multivariate analysis of risk factors for hepatocellular carcinogenesis: a prospective** observation of 795 **patients with viral and alcoholic cirrhosis.** *Hepatology* 1993; **18**: 47-53

2 **Takano S,** Yokosuka O, Imazeki F, **Tagawa M, Omata M.** Incidence of **hepatocellular carcinoma in chronic hepatitis B** and C: a **prospective study of 251 patients.** *Hepatology* 1995; **21**: 650-655

3 **Bruix J,** Barrera JM, Calvet X, Ercilla G, Costa J, Sanchez-Tapias JM, Ventura M, Vall M, Bruguera M, Bru C. Prevalence of antibodies to hepatitis C virus in Spanish patients with hepatocellular carcinoma and hepatic cirrhosis. *Lancet* 1989; **2**: 1004-1006

4 **Colombo M,** Kuo G, Choo QL, Donato MF, Del Ninno E, Tommasini MA, Dioguardi N, Houghton M. Prevalence of antibodies to hepatitis C virus in Italian patients with hepatocellular carcinoma. Lancet 1989; **2**: 1006-1008

5 **Di Bisceglie AM,** Order SE, Klein JL, Waggoner JG, Sjogren MH, Kuo G, Houghton M, Choo QL, Hoofnagle JH. **The role** of chronic viral hepatitis in hepatocellular carcinoma in the United States. *Am J Gastroenterol* 1991; **86**: 335-338

6 **Wietzkebetaraun P**, Meier V, Braun F, Ramadori G. Combination of "low-dose" ribavirin and interferon alfa-2a therapy followed by interferon alfa-2a monotherapy in chronic HCV-infected non-responders and relapsers after interferon alfa-2a monotherapy. *World J Gastroenterol* 2001; **7**: 222-227

7 **Shiratori Y,** Omata M. Predictors of the efficacy of interferon therapy for patients with chronic hepatitis C before and during therapy: how does this modify the treatment course? *J Gastroenterol Hepatol* 2000; **15 Suppl**: E141- E151

8 **Chemello L**, Cavalletto L, Casarin C, Bonetti P, Bernardinello E, Pontisso P, Donada C, Belussi F, Martinelli S, Alberti A. Persistent hepatitis C viremia predicts late relapse after sustained response to interferon-alpha in chronic hepatitis C. TriVeneto Viral Hepatitis Group. *Ann Intern Med* 1996; **124**: 1058-1060

9 **Hoofnagle JH,** Mullen KD, Jones DB, Rustgi V, Di Bisceglie A, Peters M, Waggoner JG, Park Y, Jones EA. Treatment of chronic non-A,non-B hepatitis with recombinant human alpha interferon. A preliminary report. *N Engl J Med* 1986; **315**: 1575-1578

10 **Davis GL,** Balart LA, Schiff ER, Lindsay K, Bodenheimer HC, Perrillo RP, Carey W, Jacobson IM, Payne J, Dienstag JL. **Treat**ment of chronic hepatitis C with recombinant interferon alpha. A multicenter randomized, controlled trial. Hepatitis Interventional Therapy Group. *N Engl J Med* 1989; **321**: 1501-1506

11 **Di Bisceglie AM,** Martin P, Kassianides C, Lisker-Melman M, Murray L, Waggoner J, Goodman Z, Banks SM, Hoofnagle JH. Recombinant interferon al**fa therapy for chronic hepatitis C. A** randomized, double-blind, placebo-controlled trial. *N Engl J Med* 1989; **321**: 1506-1510

12 **Wietzkebetaraun P,** Meier V, **Braun F, Ramadori G. Combi**nation of "low-dose" ribavirin and interferon alfa-2a therapy followed by interferon alfa-2a monotherapy in chronic HCV-infected non-responders and relapsers after interferon alfa-2a monotherapy. *World J Gastroenterol* 2001; **7**: 222-227

13 **Azzaroli F,** Accogli E, Nigro G, Trere D, Giovanelli S, Miracolo A, Lodato F, Montagnani M, Tamé M, Colecchia A, Mwangemi C, Festi D, Roda E, Derenzini M, Mazzella G. **Interferon** plus ribavirin and interferon alone in preventing hepatocellular carcinoma: a prospective study on patients with HCV related cirrhosis. *World J Gastroenterol* 2004; **10**: 3099-3102

14 **Yamaura T,** Matsumoto A, Rokuhara A, Ichijo T, Tanaka E, Hanazaki K, Kajikawa S, Kiyosawa K. Development of small hepatocellular carcinoma in a patient with chronic hepatitis C after 77 months of a sustained and complete response to interferon therapy. *J Gastroenterol Hepatol* 2002; **17**: 1229-1235

15 **Toyoda H,** Kumada T, Tokuda A, Horiguchi Y, Nakano H, Honda T, Nakano S, Hayashi K, Katano Y, Nakano I, Hay-

akawa T, Nishimura D, Kato K, Imada K, Imoto M, Fukuda Y. Long-term follow-up of sustained responders to interferon therapy, in patients with chronic hepatitis C. *J Viral Hepat* 2000; **7**: 414-**419**

16 **Yoshida H,** Shiratori Y, Moriyama M, Arakawa Y, Ide T, Sata M, Inoue O, Yano M, Tanaka M, Fujiyama S, Nishiguchi S, Kuroki T, Imazeki F, Yokosuka O, Kinoyama S, Yamada G, Omata M. Interferon **therapy reduces the risk for hepatocellular** carcinoma: **national surveillance program of cirrhotic and** noncirrhotic **patients with chronic hepatitis C in Japan. IHIT** Study Group. *Inhibition of Hepatocarcinogenesis by Interferon Therapy. Ann Intern Med* 1999; **131**: 174-181

17 **Desmet VJ,** Gerber M, **Hoofnagle JH, Manns M, Scheuer PJ.** Classification of chronic hepatitis: diagnosis, **grading and stag**ing. *Hepatology* 1994; **19**: 1513-**1520**

18 **Yoshida H,** Arakawa Y, Sata M, Nishiguchi S, Yano M, Fujiyama S, Yamada G, Yokosuka O, Shiratori Y, Omata M. Interferon **therapy prolonged life expectancy among chronic** hepatitis **C patients.** *Gastroenterology* 2002**; 123**: **483-491**

19 **Shiratori Y,** Imazeki F, Moriyama M, Yano M, Arakawa Y, Yokosuka O, Kuroki T, Nishiguchi S, Sata M, Yamada G, Fujiyama S, Yoshida H, Omata M. Histologic improvement of fibrosis in patients with hepatitis C who have sustained response to interferon therapy. *Ann Intern Med* 2000; **132**: 517-**524**

20 **Poynard T,** Bedossa P, Opolon P. Natural history of liver fibrosis progression in patients with chronic hepatitis **C. The** OBSVIRC, METAVIR, CLINIVIR, and DOSVIRC groups. *Lancet* 1997; **349**: 825-**832**

21 **Tagger A,** Donato F, Ribero ML, Chiesa R, Portera G, Gelatti U, Albertini A, Fasola M, Boffetta P, Nardi G. Case-control study on hepatitis C virus (HCV) as a risk factor for hepatocellular carcinoma: the role of HCV genotypes and the synergism with hepatitis B virus and alcohol. Brescia HCC Study. *Int J Cancer* 1999; **81**: 695-**699**

22 **Matsuhashi T,** Yamada N, Shinzawa H, Takahashi T. Effect of alcohol on tumor growth of hepatocellular carcinoma with type C cirrhosis. *Intern Med* 1996; **35**: 443-**448**

Science Editor Wang XL and Guo SY **Language Editor** Elsevier HK

PO Box 2345, Beijing 100023, China
www.wjgnet.com
wjg@wjgnet.com

ELSEVIER

World J Gastroenterol 2005;11(46):7227-7236
World Journal of Gastroenterology ISSN 1007-9327

• *REVIEW* •

Extraintestinal manifestations in inflammatory bowel disease

Silvio Danese, Stefano Semeraro, Alfredo Papa, Italia Roberto, Franco Scaldaferri, Giuseppe Fedeli, Giovanni Gasbarrini, Antonio Gasbarrini

Silvio Danese, Stefano Semeraro, Alfredo Papa, Italia Roberto, Franco Scaldaferri, Giuseppe Fedeli, Giovanni Gasbarrini, Antonio Gasbarrini, Department of Internal Medicine, Catholic University School of Medicine, L.go Vito 1, Rome 00168, Italy
Supported by an unrestricted grant from Fondazione Ricerca in Medicina
Correspondence to: Silvio Danese, MD, Department of Internal Medicine, Catholic University School of Medicine, L.go Vito 1, Rome 00168, Italy. sdanese@hotmail.com
Telephone: -39-3392318230 Fax: +39-06-97606741
Received: 2005-04-25 Accepted: 2005-06-18

Abstract

Inflammatory bowel diseases (IBD) can be really considered to be systemic diseases since they are often associated with extraintestinal manifestations, complications, and other autoimmune disorders. Indeed, physicians who care for patients with ulcerative colitis and Crohn's disease, the two major forms of IBD, face a new clinical challenge every day, worsened by the very frequent rate of extraintestinal complications. The goal of this review is to provide an overview and an update on the extraintestinal complications occurring in IBD. Indeed, this paper highlights how virtually almost every organ system can be involved, principally eyes, skin, joints, kidneys, liver and biliary tracts, and vasculature (or vascular system) are the most common sites of systemic IBD and their involvement is dependent on different mechanisms.

Key words: Crohn's disease; Ulcerative colitis; Inflammatory bowel disease

Danese S, Semeraro S, Papa A, Roberto I, Scaldaferri F, Fedeli G, Gasbarrini G, Gasbarrini A. Extraintestinal manifestations in inflammatory Bowel disease. *World J Gastroenterol* 2005; 11(46): 7227-7236
http://www.wjgnet.com/1007-9327/11/7227.asp

INTRODUCTION

Inflammatory bowel diseases (IBD) can be really considered to be systemic diseases since they are often associated with extraintestinal manifestations, complications, and other autoimmune disorders. Indeed, physicians who care for patients with ulcerative colitis (UC) and Crohn's disease (CD), the two major forms of IBD, face a new clinical challenge every day, worsened by the very frequent rate of extraintestinal complications. Virtually almost every system can be involved, principally eyes, skin, joints, kidneys, liver and biliary tracts, and vasculature (or vascular system) are the most common sites of systemic IBD and their involvement is dependent on different mechanisms.

Extraintestinal IBD-related immune disease can be classified into two major groups: the first one includes reactive manifestations often associated with intestinal inflammatory activity and therefore reflecting a pathogenic mechanism common with intestinal disease (arthritis, erythema nodosum, pyoderma gangrenosum, aphthous stomatitis, iritis/uveitis)[1,2] (Table 1); the second one includes many autoimmune diseases independent of the bowel disease that reflect only a major susceptibility to autoimmunity. They are not considered (apart for primary sclerosing cholangitis) as specific IBD features but only as autoimmune associated diseases such as ankylosing spondilitis, primary biliary cirrhosis, alopecia areata, and thyroid autoimmune disease and others[1] (Table 2).

Moreover, many extraintestinal complications due to metabolic or anatomical abnormalities caused directly by

Table 1 Major extraintestinal immune-related manifestations of IBD

Arthritis
Erythema nodosum
Pyoderma gangrenosum
Aphthous stomatitis
Iritis/uveitis

Table 2 Autoimmune disorders associated to IBD

Alopecia areata
Ankylosing spondylitis
Bronchiolitis obliterans
Cold urticaria
Hemolytic anemia
Henoch-Schoenlein purpura
Insulin-dependent diabetes mellitus
Pancreatitis
Primary biliary cirrhosis
Primary sclerosing cholangitis
Polymyositis
Raynaud phenomenon
Seropositive rheumatoid arthritis
Sjogren syndrome
Thyroid disease
Vitiligo
Wegener's granulomatosis
Takayasu's arteritis

Table 3 Extraintestinal complications in IBD and principal pathogenetic mechanisms of arthritis

Extraintestinal complications in IBD	Principal pathogenetic mechanisms of arthritis
Anemia	Iron deficiency, inflammation
Thromboembolic events	Hypercoagulopathies, platelet activation
Osteopathy	Steroid therapy, vitamin D deficiency inflammation
Growth failure	Malnutrition
Nephrolithiasis	Dehydration, hyperoxaluria, low urinary PH
Cholelithiasis	Intestinal loss of bile acids
Amyloidosis	Acute phase reaction, chronic inflammation
Fatty liver	Malnutrition

IBD have been reported frequently and include osteoporosis, biliary and urinary lithiasis, and anemia (Table 3).

Aim of this paper is to review the pathogenic mechanisms, frequency, features, and therapy of the major IBD-associated extraintestinal manifestations.

Pathogenesis of immune-related extraintestinal manifestation in IBD

Extraintestinal immune-related manifestations in IBD are directly dependent on intestinal disease, often coexist in the same patients and have probably the same, even if not completely clarified, pathogenesis[2]. Evidence coming from many studies in genetically susceptible animal models of colitis suggests the crucial role of enteric flora in activating the immune system against bacterial antigens and contemporary against colonic mucosa on the basis of an antigenic cross-reactivity ("antigen mimicry")[3]. The sharing of these colonic antigens by extraintestinal organs, associated with a genetic susceptibility, would finally lead to an immune attack to these organs[2]. One of the best example is represented by primary sclerosing cholangitis occurring in UC: in a subset of patients, the presence (in sera and colonic mucosa) of anti-colonic mucosa auto-antibodies that cross react with biliary epithelium has been identified[4]. Furthermore, recently a colonic epithelial protein (CEP) and the human tropomyosin isoform 5 (hTM5), which are not only expressed in the colon but also in the biliary tract, skin, eyes, and joints, have been suspected to be the major common targets of autoimmune attack in extraintestinal organs of IBD patients being IgG1 specific auto-antibodies identified in UC patients presenting multiple extraintestinal manifestations[5].

It remains unclear why the extraintestinal organs are not always involved at the same time and why these auto-antibodies are absent in colonic CD. A partial explanation is that genetic factors or local co-existent damage factors (infections, trauma) could regulate the display of cryptic antigens and the susceptibility to autoimmune attack[2].

According to the previously explained mechanism, we can identify an immune induction site, where T cells are primed, represented by the colon and the effectors sites that are the extraintestinal organs. Immune cells infiltrate the effectors sites (where they will proliferate) with the help of adhesion molecules (α4β7 integrin, vascular adhesion protein 1) that have a cytokine-mediated overexpression in specific tissues[6].

It is interesting how autoimmune attack can happen many years after the removal of the colon. In the case of primary sclerosing cholangitis (PSC), probably memory lymphocytes that have been primed in the bowel can recirculate for many years also even after the removal of the colon without causing damage until the occurrence of a stimulus in the liver that activates inflammation with the overexpression of adhesion molecules (MAdCAM and CCL 25) and consequent persistent lymphocytes recruitment[7]. Interference with adhesion molecules could be useful in the treatment of extraintestinal manifestation as it has already been shown for the intestinal inflammatory activity[8].

Genetic susceptibility

Extraintestinal manifestations have certainly a familial predisposition (83% of concordance between siblings)[9] and this suggests the existence of a strong genetic influence leading to the identification of many suspected predisposal genes.

HLA system is considered as one of the major genetic markers associated with IBD and extraintestinal manifestations, probably a specific and appropriate antigen presentation that leads to autoimmune reaction in particular predisposing conditions.

It has been reported that UC patients who display HLA-B8, DR3 phenotype have a 10-fold higher risk of primary sclerosing cholangitis[10].

Moreover, UC patients who have HLA DRB1*0103 (DR103) have a higher risk of ocular and articular manifestations[11] and patients with HLA-B*27 and B*58 have a higher risk of uveitis (Orchard TR 2002). HLA-B*27 is strongly associated with ankylosing spondylitis (AS) being present in 90% of these patients but it seems not to be significantly associated with IBD; anyway IBD patients with HLA-B*27 positiveness have a higher risk to develop AS and IBD patients with axial articular involvement are HLA-B*27 positive from 25% to 75%[12]. The polymorphism -1031 C TNF-α has been associated with erythema nodosum in IBD patients[13]. It is possible that HLA genes interfere actively in the pathogenesis of IBD-extraintestinal manifestations or that are in linkage disequilibrium with other really responsible unknown genes. Moreover, caspase-activation recruitment domain containing protein 15 (CARD15), a gene found in association with ileocecal CD with a potential role in the bacterial handling, has been recently associated with sacroiliitis even if previous results did not agree[14].

Joint involvement in IBD

Inflammatory arthropathies are the most common extraintestinal manifestations in IBD patients with a prevalence ranging between 7% and 25%[1,12]. Articular and musculoskeletal manifestations are included in the spondyloarthropathies (SpAs) that are a group of seronegative autoimmune related disorders with common characteristics including: ankylosing spondylitis, reactive arthritis, psoriatic arthritis, inflammatory bowel disease,

some forms of juvenile arthritis and acute anterior uveitis[15].

Articular involvement (peripheral or axial) can precede, be synchronous or begin afterward the diagnosis of IBD, it is characteristically pauciarticular, asymmetrical, transitory, migrating, prevalently non deforming. The axial involvement can vary from asymptomatic sacroiliitis to inflammatory lower back pain to ankylosing spondylitis (that occurs in 3% of IBD patients)[1].

It is interesting that the high incidence of asymptomatic sacroiliitis (varying from 10% to 52%)[16,17,18] and on the other hand the equally high incidence (about 50%) of characteristic inflammatory low back pain in the absence of radiological findings in IBD patients[12] indicating how history and physical examination should be the diagnostic tools. Peripheral arthritis, different from axial involvement, has a significant positive association with the skin, mouth, and ocular manifestation; it happens more frequently in CD (and particularly in colonic localization), often accompanies intestinal activity ameliorating with IBD pharmacological or surgical treatment[1]. In some patients, despite the amelioration of gut inflammatory activity, articular disease persists[19].

Arthritis is often associated with enthesitis, tenosynovitis, dactylitis that can also appear in the absence of arthritis[20]; typically they do not alter inflammatory markers and can compromise deeply the quality of life.

Conventional treatment of inflamed joints include nonsteroidal anti-inflammatory drugs and cyclooxygenase-2-inhibitor that should be used for short-term period because of gastrointestinal side effect and IBD reactivation risk[21,22] nevertheless at drug suspension articular relapse can occur. Also local intra-articular steroid treatment can be useful.

The majority of interventional studies included undifferentiated spondyloarthropathies- or ankylosing spondilytis patients and no IBD patients, so that the results can only be extrapolated. Sulfasalazine has been shown to be effective in peripheral joint disease in SpAs patients[23,24] and positive but limited results have been obtained with methotrexate[25].

Interesting results have been obtained with anti TNF-α inhibitors in resistant SpAs with IBD. In uncontrolled studies, infliximab has shown efficacy in the treatment of SpAs in CD patients as induction and maintenance therapy[26-28], also in the absence of acute phase reactants and intestinal activity; there is also a reported case of positive results in SpA associated with ulcerative colitis[29]. In limited reports (two cases) etanercept, that is ineffective in IBD treatment[30], has given good results in the treatment of SpAs associated to CD[31]. It is not clear at the moment the effect of anti TNF-α therapies on articular damage evolution, certainly the early recognition and appropriate treatment can help to limit the patient's inability.

Hepatobiliary disease

Hepatobiliary diseases are common in IBD patients; they can or cannot be immuno-mediated and can also depend on side effects of medications (see Table 4). Elevation of liver function tests have been observed from 11% to 49% in IBD patients in observational studies[32-34]. The most common immuno-mediated hepatobiliary disease is primary sclerosing cholangitis (PSC) that is a chronic cholestatic disorder characterized by inflammation and fibrosis of the intrahepatic and extrahepatic bile ducts. It is more frequent in male individuals, and the prevalence of IBD (mostly UC) in PSC is about 70-80%[35]. Conversely about 2-7% of UC patients[35,1] and 0.7-3.4% of MC patients have a diagnosis of PSC[36,1]. Suggestive symptoms of PSC are fatigue, pruritus, jaundice, and abdominal discomfort but it is not rare that the isolate finding of abnormalities in liver biochemical markers (first of all alkaline phosphatase); in fact 15-70% of PSC patients are asymptomatic[37,1]. There are no specific auto-antibodies and so biopsy or cholangiography is often necessary for the diagnosis. In PSC patients, IBD frequently present some specific features: pancolonic extension with rectal sparing, backwash ileitis, low intestinal activity, and high pouchitis incidence after colectomy. These distinguishing features have suggested the existence of an IBD-PSC specific clinical phenotype[38]. It is well-known that the increased risk of colonic dysplasia/carcinoma in PSC patients compared to the general population (10-fold risk)[39] and to other UC patients[35] it could depend on the long-lasting and asymptomatic colitis (consequently often underestimated) and by alterations in bile salts pool or folate deficiency. Similarly it has significantly increased the risk of bile duct cancer[40] and metabolic bone disease[41,38]. PSC has a median survival time of 9-12 years from the time of diagnosis; it seems that neither concomitant IBD presence nor colectomy (in UC patients) alter its natural history. Moreover, the colorectal cancer risk does not seem to be decreased after liver transplantation[42].

The therapeutic possibilities in PSC are limited; the best results have been obtained with UDCA at a high dose (until 20 mg/kg)[43-45] and the combined use of corticosteroids showed only a little additive benefit[46,47].

The best clinical approaches to PSC include colonoscopic examination with a biopsy to identify a possible asymptomatic UC and/or cancer and a prevention colonoscopy program in patients identified to have had UC. Association between primary biliary cirrhosis (PBC) and UC is rare but possible and it has been reported in 15 cases; similarly to the CSP it seems that colectomy does not alter the progression of the hepatic disease[48].

Apart from classical immunological liver diseases in IBD patients, they are often observed for other abnormalities. Liver enlargement is the most common reported finding and is strictly related to steatosis grade. Steatosis has been described in more than 30% of patients and it does not seem to be related to the kind of IBD and sex. Data about the influence of disease activity and pharmacological treatment on steatosis are contradictory[49].

Also cholelithiasis is more frequent in IBD patients (about 10%) than in the general population (7%) and mainly in CD (first of all in ileal localization); it seems

to correlate with female sex, previous surgery (mainly ileal resection), and old age. In limited series, it has been shown to be less often symptomatic than in the general population[49]. Probably cholelithiasis is caused by bile salt pool alteration for malabsorption.

Rare complications reported in literature are liver abscesses; it is thought that in most cases portal bacteremia, favorite by mucosal barrier alterations, can be the principal mechanism; rarely an ascending acute cholangitis in PSC has been suspected to be the cause[50]. Portal vein thrombosis and suppurative pylephlebitis has also been described in rare cases[49].

Cutaneous manifestations

Cutaneous manifestations of IBD are relatively common. The incidence varies from about 10% at the time of IBD diagnosis to more than 20% in the course of the disease[1]. Skin lesions can be classified into three principal classes: granulomatous, reactive, and secondary to nutritional deficiency.

Granulomatous cutaneous lesions have the same histological features of the bowel disease and include: perianal and peristomal ulcers and fistulas, metastatic CD, oral granulomatous ulcers.

Perianal disease is very frequent occurring in about 50% of CD patients during their clinical history, and it varies from perianal erythema to abscesses and perianal complex fistulae[51].

Other fistulae can be internal or entero-cutaneous; rarely develop on the abdominal scar of laparotomy or at the umbilicus. Many efforts have been made to treat fistulizing disease, and the classical surgical approach has been supported recently by a larger use of drugs. Antibiotics, azathioprine/mercaptopurine, tacrolimus, thalidomide showed efficacy in uncontrolled studies[52] but at the moment only infliximab showed effectiveness as induction[53] and maintenance therapy[54] in phase III controlled trials; consequently it has been approved as first line therapy in perianal and enterocutaneous fistulizing CD by the United States Food and Drug Administration (FDA) and the European Agency for the Evaluation of Medicinal Products in Europe. Surgical procedures as colostomy in the more severe cases of perianal fistulas, fistulotomy, abscesses drainage, and non-cutting setons placement seem to be very useful, and the combined medical and surgical approach is probably the best one[55].

Metastatic CD is a rare complication defined as the occurrence of specific granulomatous cutaneous lesions remote from the intestinal disease[56]. It manifests as subcutaneous nodules or ulcers mainly at the lower extremities with rare case of genital (testicular and vulvar) localizations. It seems unrelated to the bowel activity. Corticosteroids, antibiotics, azathioprine, methotrexate[57], and more recently infliximab[58,59] have been used successfully.

The group of reactive skin manifestations of IBD includes aphthous stomatitis, erythema nodosum, pyoderma gangrenosum, and the rare Sweet's syndrome.

Aphthous stomatitis is observed in about 10% of patients: it occurs generally during active intestinal disease, often recurs and shows a good response to intestinal treatment.

The prevalence of erythema nodosum in IBD is 3-8%. It appears more often in women, in the colonic localization, in concomitance with arthritis and active intestinal disease[1]; furthermore, there is a positive response to proctocolectomy[42].

Histological examination shows lympho-histiocytic infiltrate of the lower derma. On the basis of uncontrolled data, corticosteroids are generally an effective therapy; also immunosuppressive therapy is used[56]. Resistant cases have been treated effectively with infliximab[60].

Pyoderma gangrenosum is a very debilitating ulcerating chronic skin disorder occurring in about 1-2% of IBD patients. It occurs often on the extensor surface of the legs, particularly in coincidence with exacerbation of intestinal disease and in association with other extraintestinal manifestations (arthritis and erythema nodosum)[1,61]. Moreover, it is often associated with colonic involvement and in UC patients it seems to benefit lesser than erythema nodosum from colectomy[42].

According to disease severity, the treatment (based on non-controlled evidence) can be local or systemic and includes a high dose of oral or intralesional corticosteroids, immunosuppressive/immunomodulatory therapy (cyclosporine, tacrolimus, mycophenolate mofetil, azathioprine, dapsone)[61]. Infliximab has shown to be very effective in the refractory disease and can be used as first choice therapy[59,62,63]; also etanercept has been reported to be effective in a refractory case of pyoderma gangrenosum[64].

Another rare cutaneous manifestation associated with IBD is the Sweet's syndrome. It is a neutrophilic dermatosis probably related to pyoderma gangrenosum consistent with painful erythematous plaques or nodules often associated with fever and leukocytosis that usually responds to corticosteroids[65].

The more frequent nutritional-deficient cutaneous manifestation is the acrodermatitis enteropathica; it is caused by zinc deficiency and manifests as a psoriasis form erythema[61].

Furthermore, an association between autoimmune cutaneous disease and IBD has been reported. The most frequent disease is psoriasis (7-11% of IBD population *vs* 1-2% of general population) than vitiligo and more rarely are polimyositis, lupus erythematosus and scleroderma[66].

Ocular manifestations of IBD

Ocular manifestations occur in about 10% of IBD patients. They can be immune-related (episcleritis, scleritis, uveitis, corneal disease) or related to drug exposure (cataract, glaucoma).

Episcleritis manifests as acute redness, irritation, burning, tender to palpation; if there is also an impairment of vision, the presence of a scleritis is possible. In this case, a referral to an ophthalmologist is mandatory for risk of vision loss. Uveitis can be anterior and posterior and is often associated with joints and skin manifestations.

Anterior uveitis is the most common and presents painful eye, visual blurring, and photophobia but can be also asymptomatic and sometimes precedes the diagnosis of IBD. Concomitance with IBD activity is typical for episcleritis and uveitis[1,67].

Corneal disease (potential cause of perforation) has also been reported; conjunctivitis is frequent in IBD population but probably does not differ in frequency and etiologic factors from the general population. Anyway it is important that the clinician is aware that serious ocular disease can mimic conjunctivitis in IBD patients[67].

Ocular manifestations can benefit first of all by the treatment of the underlying IBD (particularly for anterior uveitis and episcleritis).

Treatment of ocular disease can prevent complications such as retinal detachment or optic nerve swelling in scleritis and secondary glaucoma and cataracts in uveitis.

Cycloplegics, NSAIDs, topical and systemic steroids are useful. Immunosuppression can be necessary in case of scleritis; sulfasalazine/mesalazine seems to prevent anterior uveitis recurrence[67]. Recently infliximab has shown efficacy in acute uveitis, in episcleritis, and scleritis[68,69]. Other rare reported ocular manifestations of IBD are: retinitis, orbital IBD, retinal arterial and venal occlusion, optic neuritis, retinal vasculitis, marginal corneal disease, lid margin ulcers[70,67].

Metabolic osteopathy

IBD is also associated with an increased risk of osteoporosis and osteopenia. The prevalence rates ranges from 2% to 30% for osteoporosis and from 40% to 50% for osteopenia[71]. The risk of fractures in IBD patients varies widely in different studies[72-74] (from an OR of 1.41 to 2.5) the real impact being completely clear on the IBD population; because of contrasting results, it is also uncertain if the risk is comparable for UC and MC and for men and women.

Osteoporosis occurrence is often underestimated as shown in an observational study conducted in the UK[74] in which women aged 65 years with severe IBD have shown a 10-years probability of hip fracture of 7%; nevertheless only 13% of patients who had already sustained a fracture were in bone-sparing therapy.

Furthermore, a significant number of fractures in IBD patients (as in the general osteoporotic population) are asymptomatic (14.2% in a study of Stockbrugger) and many fractures will be underreported[75].

Bone loss and consequent fractures are certainly multifactorial processes. They are significantly dependent on the age (above 60 years), the use of corticosteroids[74-76] and the grade of systemic inflammation (intestinal disease activity correlates with the risk of fracture)[74].

Recently the role of the inflammatory-induced osteopenia has been revaluated and a surface receptor (RANK) localized on osteoclasts that induces osteoclastogenesis has been identified. Its ligand (RANKL) is induced by proinflammatory cytokines; its decoy receptor that prevents ligation of RANKL to RANK is called osteoprotegerin (OPG), and is produced by osteoblasts and prevents bone loss. Its production is inhibited by corticosteroids and increased by bisphosphonates. So OPG-RANKL-RANK system is certainly a pivot in inflammatory-induced bone loss[77,78]. Initial therapeutical use of recombinant OPG in inflammation-induced osteoporosis seems to be promising[79].

On the basis of these findings, the role of nutritional deficiency could be smaller than previously thought, as also shown in a preliminary recent observational study that found low intake of calcium (<1 000 mg/die) and vitamin D (<200 IU/die) in premenopausal IBD women not to be a predictor of bone loss[80].

Other factors that could favor osteoporosis are the use of corticosteroids, the hypogonadism, and the immobility. Also genetic markers have been proposed as determinants of bone loss in IBD patients. In the future, they could contribute to identify high-risk patients and support clinical behavior[81].

Definition of a correct clinical approach is difficult because therapeutic trials on IBD patients with the specific end-point of fractures prevention are lacking and an extrapolation by the major clinical trials on osteoporosis is difficult, since these studies involve postmenopausal patients, certainly older than IBD patients with osteoporosis.

A small randomized, placebo-controlled trial showed that alendronate significantly ameliorates spine bone density compared with the control group after 1-year-long therapy in IBD patients[82]. Also azathioprine, effective on intestinal activity, seems to have positive effect on bone loss retardation[83].

The expert recommendations on therapy, in the absence of more specific evidence, do not significantly differ from that of the general population. Supplementation of vitamin D for patients above 60 years, therapy with bisphosphonates in case of osteoporosis (identified with densitometry), osteoporotic fractures and chronically steroid treatment, use of minimum dosage of corticosteroids (preferentially non-systemic), correction of early menopause or male hypogonadism by hormone therapy have also been reported[84,85]. Recently apart from OPG use, another osteoanabolic substance, the parathyroid hormone 1-34, is under evaluation for the steroid-induced osteoporosis[86]; in the future they could show effectiveness in IBD osteoporosis. More efforts are yet to be taken in the identification of high-risk patients and in the definition of the most cost-effective clinical behavior in IBD patients.

Thromboembolism and IBD

Patients with IBD have a well-known increased risk (threefold higher than in controls) of thromboembolism (TE), which is an important cause of morbidity and mortality. The incidence ranges from 1.2% to 6.1% according to different studies and in necropsy studies it reaches 39%[87].

Thrombosis accidents occur prevalently as deep vein thrombosis and pulmonary thromboembolism; they happen in earlier age than in non-IBD patients and are more frequent in active or complicated IBD; the type of

IBD and the sex seems not to influence thromboembolic risk[87,88]. Using the logistic regression model, it has been found that IBD is an independent risk factor for thrombosis that is a specific IBD feature. In fact, other inflammatory chronic condition as rheumatoid arthritis or chronic intestinal malabsorptive conditions as celiac disease do not show an increased risk of TE[87].

IBD patients have a frequent exposure to classical thrombosis risk factors: immobility, surgery, steroid therapy, central venous catheter, contraceptives/hormone substitution, smoke; nevertheless, these risk factors do not explain the TE risk increase completely[87].

It is well-known that in IBD patients there is not a completely explained imbalance between coagulation and fibrinolysis in favor of coagulation.

Active intestinal inflammation is not probably the unique risk determinant since about 30-40%[87,89] of thrombosis occurs during quiescence of the IBD and proctocolectomy has not shown a very clear protective effect on recurrent venous thrombosis[90].

Also other factors have been claimed; hyperhomocysteinemia, a well-known risk factor for venous and arterial thrombosis, occurs more often in IBD patients than in the general population and seems to be directly dependent by folate and vitamin B12 deficiency even if there is not a complete concordance in literature[91-93].

The role of the inherited thrombophilia has been recently reviewed[94]. The analysis has shown that the most frequent prothrombotic genetic mutations (factor V Leiden mutation, G20210A mutation in the gene of prothrombin, homozygous in the gene of methylenetetrahydrofolate reductase) are not significantly associated with IBD.

At the same time with the limit of a small number of subjects participating in the studies, it seems that there is no difference in the prevalence of genetic mutations in IBD patients with thrombosis compared with non-IBD subjects with thrombosis. Anyway a recent study comparing IBD patients with thrombosis and IBD controls has revaluated the role of genetic factors finding a significant higher prevalence of factor V Leiden in the thrombosis group (20% *vs* 0%)[95].

The data regarding the prevalence of antiphospholipid antibodies in IBD are conflicting, but seem to suggest an increase frequency in IBD. In limited series, the level of lipoprotein (A) has been found to be higher than in controls[87]. No evidence exists about treating thrombotic events differently than in non-IBD patients[87].

Conclusively many factors are suspected to play a role in the thromboembolic increased risk of IBD patients but further studies are necessary to identify their specific contribution.

At the moment in IBD patients the elimination of removable risk factors is recommendable; in case of thrombosis probably is useful to evaluate the thrombotic risk performing coagulation laboratory parameters and genetic tests.

Anemia

Anemia is a frequent extraintestinal manifestation in IBD; about one-third of IBD patients have hemoglobin levels below 12 g/dL[96]. The anemic state correlates strictly with the quality of life and so is certainly an important problem in the therapeutic management of chronic patients[97]. Multiple pathogenic mechanisms often coexist in anemic patients leading to mixed features anemia. Chronic intestinal bleeding with iron loss (due to bowel inflammation) causes a hypochromic and microcytic anemia with associated hypoferremia and hypoferritinemia; the chronic inflammatory disease (typically characterized by hyperferritinemia) can cause anemia through the proinflammatory cytokine-dependent diversion of iron traffic to reticuloendothelial system and erythroid progenitor cell development interference[98]. The same inflammatory cytokines are able to inhibit erythropoietin production[99]. Recently, *in vitro* anti-TNF-α factors showed positive effects in preventing apoptosis of erythroid cells[100]. Other mechanisms implied in anemia are iron malabsorption (in duodenum or upper jejunum disease CD), vitamin B12 malabsorption (in terminal ileum and gastric CD), and folate deficiency (malabsorption, inadequate diet, and side effects of sulfasalazine and methotrexate). Vitamin B12 and folate deficient anemia is characteristically macrocytic. Myelosuppressive direct effects have been reported frequently for azathioprine/6-mercaptopurine and sometimes also for sulfasalazine and 5-aminosalycilic acid[101]. Correction of the anemic state is useful also in low-grade anemia. It is important to prevent and treat intestinal flares that are often the cause of anemia and to reintegrate the lacking of iron, B12, and folate.

In low-ferritin patients, prevention therapy with oral iron can be sufficient; in overt anemia iron intravenous (preferentially iron sucrose) supplementation should be preferred to oral route because of major efficacy and no collateral intestinal side effect. Epo therapy is useful in patients with no satisfactory response to iron therapy alone[101]. Low levels of Epo, soluble transferring receptors or transferrin have shown to predict iron sucrose resistance[102].

Urinary system manifestations

IBD is a risk factor for renal immune and non-immune mediated diseases.

The prevalence of nephrolithiasis in IBD varies from 2% to 6% and is more frequent in CD than in UC[103]. Calcium-oxalate stones are the most common and are caused by hyperoxaluria due to increased intestinal absorption of oxalate. In fact in the bowel that does not absorb fatty acids link calcium preventing calcium-oxalate precipitation with the consequent increased absorbable oxalate fraction. More than one lithogenic factors are often present in the same patient, more frequently during active disease. The main lithogenic risk factors are: low urinary volume, low urinary PH, increased excretion of lithogenic substances as oxalate, phosphate, uric acid, and decreased concentration of anti-lithogenic substances as citrate and magnesium. Colectomy in UC and ileo-colonic resection in CD seems to further increase the risk of lithiasis and oxalate stone formation occurs mainly in ileal CD[104].

Table 4 Drugs and their possible adverse side effects

Drugs	Possible adverse side effects
Corticosteroids	Acne, fluid retention, fat redistribution, hypertension, hyperglycemia, psycho-neurological disturbances, cataracts, growth failure in children, osteonecrosis[115]
Mesalazine	Nausea, dyspepsia, rare nephritis, rare idiosyncratic worsening of IBD[116]
Sulfapyridine	Headache, nausea, anorexia, rare hypersensibility hepatitis, hemolytic anemia, pancreatitis, reversible sperm abnormalities, worsening of IBD[116]
Azathioprine/mercaptopurine	Pancreatitis, bone marrow suppression, hepatotoxicity[115]
Methotrexate	Nausea, leucopenia, hepatic fibrosis, hypersensibility pneumonia[117]
Cyclosporin	Nephrotoxicity, hypertension, headache, gingival hyperplasia, paresthesias[115]
Tacrolimus	Nephrotoxicity[115]
Infliximab	Infusion reactions, delayed hypersensitivity-like reactions, drug-induced lupus, tuberculosis reactivation[118]
Metronidazole	Nausea, metallic taste, peripheral neuropathy[115]

Periodic sonographic examination is recommended for early diagnosis and for the prevention of complications. Furthermore, minimal signs of tubular damage have been found in about 20% of IBD patients but rarely they are clinically relevant[105].

A calculus uretheral obstruction, prevalently localized on the right, is also possible and is related to the mechanisms of adherence and compression by inflamed bowel (prevalently terminal ileum)[103]. Urinary tract fistulas occur in about 1.7-7.7% of patients. They can cause pneumaturia, dysuria, recurrent infections, and fecaluria. At the moment in most cases, the non-satisfactory response to medical therapy makes surgery the best option[106].

Clinical relevant renal amyloidosis has been reported in about 1% of IBD patients (more frequently in ileal CD). It is probably related to acute phase reaction proteins[107]. In IBD patients, cases of glomerulonephritis causing nephrotic syndrome and renal failure have also been reported. They are related to intestinal disease activity, are quite responsive to IBD therapy and can present many patterns at histology[108]. Moreover, it seems that mi nimal, clinically non significant, glomerular inflammatory changes are quite frequent in IBD patients as shown in a post mortem study (70% of subtle renal lesions *vs* 8% of controls)[109] but following data do not exploit this aspect.

Other rare extraintestinal manifestations

It has been reported in literature about the occurrence of other rare extraintestinal manifestations of IBD, such as, chronic recurrent multifocal osteomyelitis (CRMO), myositis[110], polyneuropathy, Guillain-Barre syndrome[111], lymphocytic encephalomyeloneuritis[112], myocarditis[113], and pleuropericarditis[114].

Drug-induced side effects

Many drugs used in IBD treatment can cause side effects involving various organs (Table 4). These effects that often need drug interruption enter in differential diagnosis with extraintestinal manifestations/complications of IBD; their early diagnosis is facilitated by periodical serum analysis exploring liver, pancreatic, renal, and hematological system integrity as for example is recommended in methotrexate and azathioprine use[115]. Furthermore, the limited use to short period of other drugs can prevent their effect as for example as it often happens for corticosteroids (Table 4).

CONCLUSION

IBD is a systemic disease, since its clinical manifestations can affect not only the bowel but also practically any other organ (eyes, liver, osteoarticular system, kidneys, and so on) through different (often not completely cleared) mechanisms. At the moment, awareness of the high incidence of extraintestinal manifestations is often inadequate. Therefore, prevention, early diagnosis, and adequate treatment of these pathological conditions, sometimes more dramatic than the intestinal disease, are necessary to increase patients' health. Clinical interventional trials in IBD patients should consider these conditions with more attention to indicate the best cost-effective method for clinicians.

REFERENCES

1 **Veloso FT, Carvalho J, Magro F.** Immune-related systemic manifestations of inflammatory bowel disease. A prospective study of 792 patients. *J Clin Gastroenterol* 1996; **23**: 29-34

2 **Das KM**. Relationship of extraintestinal involvements in inflammatory bowel disease: new insights into autoimmune pathogenesis. *Dig Dis Sci* 1999; **44**: 1-13

3 **Taurog JD**, Richardson JA, Croft JT, Simmons WA, Zhou M, Fernandez-Sueiro JL, Balish E, Hammer RE. The germfree state prevents development of gut and joint inflammatory disease in HLA-B27 transgenic rats. *J Exp Med* 1994; *180*: 2359-2364

4 **Chapman RW**, Cottone M, Selby WS, Shepherd HA, Sherlock S, Jewell DP. Serum autoantibodies, ulcerative colitis and primary sclerosing cholangitis. *Gut* 1986; **27**: 86-91

5 **Geng X**, Biancone L, Dai HH, Lin JJ, Yoshizaki N, Dasgupta A, Pallone F, Das KM. Tropomyosin isoforms in intestinal mucosa: production of autoantibodies to tropomyosin isoforms in ulcerative colitis. *Gastroenterology* 1998; **114**: 912-922

6 **Salmi M,** Alanen K, Grenman S, Briskin M, Butcher EC, Jalkanen S. Immune cell trafficking in uterus and early life is dominated by the mucosal addressin MAdCAM-1 in humans. *Gastroenterology* 2001; **121**: 853-864

7 **Eksteen B**, Grant AJ, Miles A, Curbishley SM, Lalor PF, Hubscher SG, Briskin M, Salmon M, Adams DH. Hepatic endothelial CCL25 mediates the recruitment of CCR9+ gut-homing lymphocytes to the liver in primary sclerosing cholangitis. *J Exp Med* 2004; **200**: 1511-1517

8 **Rutgeers P**. ColombelJ, Enns R, et al. Subanalyses from a phase 3 study on the evaluation of natalizumab in active Crohn's disease therapy-1(ENACT-1). *Gut* 2003; **52**: A239

9 **Satsangi J**, Grootscholten C, Holt H, Jewell DP Clinical patterns of familial inflammatory bowel disease. *Gut* 1996; **38**: 738-741

10 **Chapman RW**, Varghese Z, Gaul R, Patel G, Kokinon N, Sherlock S. Association of primary sclerosing cholangitis with HLA-B8. *Gut* 1983; **24**: 38-41

11 **Roussomoustakaki M**, Satsangi J, Welsh K, Louis E, Fanning G, Targan S, Landers C, Jewell DP. Genetic markers may predict disease behavior in patients with ulcerative colitis. *Gastroenterology* 1997; **112**:1845-1853

12 **De Vos M**. Review article: joint involvement in inflammatory bowel disease. *Aliment Pharmacol Ther* 2004; **20**: 36-42

13 **Orchard TR**, Chua CN, Ahmad T, Cheng H, Welsh KI, Jewell DP. Uveitis and erythema nodosum in inflammatory bowel disease: clinical features and the role of HLA genes. *Gastroenterology* 2002; **123**: 714-718

14 **Peeters H,** Vander Cruyssen B, Laukens D, Coucke P, Marichal D, Van Den Berghe M, Cuvelier C, Remaut E, Mielants H, De Keyser F, Vos MD. Radiological sacroiliitis, a hallmark of spondylitis, is linked with CARD15 gene polymorphisms in patients with Crohn's disease. *Ann Rheum Dis* 2004; **63**: 1131-1134

15 **Dougados M**, van der Linden S, Juhlin R, Huitfeldt B, Amor B, Calin A, Cats A, Dijkmans B, Olivieri I, Pasero G.The European Spondylarthropathy Study Group preliminary criteria for the classification of spondylarthropathy. *Arthritis Rheum* 1991; **34**: 1218-1227

16 **Dekker-Saeys BJ**, Meuwissen SG, Van Den Berg-Loonen EM, De Haas WH, Agenant D, Tytgat GN. Ankylosing spondylitis and inflammatory bowel disease. Prevalence of peripheral arthritis, sacroiliitis, and ankylosing spondylitis in patients suffering from inflammatory bowel disease. *Ann Rheum Dis* 1978; **37**: 33-35

17 **de Vlam K**, Van de Wiele C, Mielants H, Dierckx RA, Veys EM. Is 99mTc human immunoglobulin G scintigraphy (HIG-scan) useful for the detection of spinal inflammation in ankylosing spondylitis? *Clin Exp Rheumatol* 2000; **18**: 379-382

18 *Davis P*, Thomson AB, Lentle BC. Quantitative sacroiliac scintigraphy in patients with Crohn's disease. *Arthritis Rheum* 1978; **21**: 234-237

19 **Orchard TR**, Wordsworth BP, Jewell DP. Peripheral arthropathies in inflammatory bowel disease: their articular distribution and natural history. *Gut* 1998; **42**: 387-391

20 **Salvarani C**, Fornaciari G, Beltrami M, Macchioni PL. Musculoskeletal manifestations in inflammatory bowel disease. *Eur J Intern Med* 2000; **11**: 210-214

21 **Felder JB**, Korelitz BI, Rajapakse R, Schwarz S, Horatagis AP, Gleim G. Effects of nonsteroidal antiinflammatory drugs on inflammatory bowel disease: a case-control study. *Am J Gastroenterol* 2000; **95**: 1949-54

22 **Mahadevan U**, Loftus EV Jr, Tremaine WJ, Sandborn WJ. Safety of selective cyclooxygenase-2 inhibitors in inflammatory bowel disease. *Am J Gastroenterol* 2002; **97**: 910-914

23 **Clegg DO**, Reda DJ, Weisman MH, Cush JJ, Vasey FB, Schumacher HR Jr, Budiman-Mak E, Balestra DJ, Blackburn WD, Cannon GW, Inman RD, Alepa FP, Mejias E, Cohen MR, Makkena R, Mahowald ML, Higashida J, Silverman SL, Parhami N, Buxbaum J, Haakenson CM, Ward RH, Manaster BJ, Anderson RJ, Henderson WG. Comparison of sulfasalazine and placebo in the treatment of reactive arthritis (Reiter's syndrome). A Department of Veterans Affairs Cooperative Study. *Arthritis Rheum* 1996; **39**: 2021-2027

24 **Dougados M**, vam der Linden S, Leirisalo-Repo M, Huitfeldt B, Juhlin R, Veys E, Zeidler H, Kvien TK, Olivieri I, Dijkmans B. Sulfasalazine in the treatment of spondylarthropathy. A randomized, multicenter, double-blind, placebo-controlled study. *Arthritis Rheum* 1995; **38**: 618-627

25 **Altan L, Bingol U**, Karakoc Y, Aydiner S, Yurtkuran M, Yurtkuran M. Clinical investigation of methotrexate in the treatment of ankylosing spondylitis. *Scand J Rheumato*l 2001; **30**: 255-259

26 **Generini S**, Giacomelli R, Fedi R, Fulminis A, Pignone A, Frieri G, Del Rosso A, Viscido A, Galletti B, Fazzi M, Tonelli F, Matucci-Cerinic M. Infliximab in spondyloarthropathy associated with Crohn's disease: an open study on the efficacy of inducing and maintaining remission of musculoskeletal and gut manifestations. *Ann Rheum Dis* 2004; **63**: 1664-1669

27 **Van den Bosch F**, Kruithof E, De Vos M, De Keyser F, Mielants H. Crohn's disease associated with spondyloarthropathy: effect of TNF-alpha blockade with infliximab on articular symptoms. *Lancet* 2000; **356**: 1821-1822

28 **Herfarth H**, Obermeier F, Andus T, Rogler G, Nikolaus S, Kuehbacher T, Schreiber S. Improvement of arthritis and arthralgia after treatment with infliximab (Remicade) in a German prospective, open-label, multicenter trial in refractory Crohn's disease. *Am J Gastroenterol* 2002; **97**: 2688-2690

29 **Gamian A**, Romanowska A, Romanowska E. Immunochemical studies on sialic acid-containing lipopolysaccharides from enterobacterial species. *FEMS Microbiol Immunol* 1992; 4: 323-328

30 **Sandborn WJ,** Hanauer SB, Katz S, Safdi M, Wolf DG, Baerg RD, Tremaine WJ, Johnson T, Diehl NN, Zinsmeister AR. Etanercept for active Crohn's disease: a randomized, double-blind, placebo-controlled trial. *Gastroenterology* 2001; **121**: 1088-1094

31 **Marzo-Ortega H**, McGonagle D, Emery P. Etanercept treatment in resistant spondyloarthropathy: imaging, duration of effect and efficacy on reintroduction. *Clin Exp Rheumatol* 2002; **20**: S175-177

32 **Broome U, Hauzenberger D**, Klominek J. Adhesion molecules in primary biliary cirrhosis and primary sclerosing cholangitis. *Hepatogastroenterology* 1996; **43**: 1109-1112

33 **Okolicsanyi L**, Fabris L, Viaggi S, Carulli N, Podda M, Ricci G. Primary sclerosing cholangitis: clinical presentation, natural history and prognostic variables: an Italian multicentre study. The Italian PSC Study Group. *Eur J Gastroenterol Hepato*l 1996; **8**: 685-691

34 **Talwalkar JA**, Lindor KD. Primary sclerosing cholangitis. *Inflamm Bowel Dis* 2005; **11**: 62-72

35 **Loftus EV Jr**, Sandborn WJ, Tremaine WJ, Mahoney DW, Zinsmeister AR, Offord KP, Melton LJ 3rd. Risk of colorectal neoplasia in patients with primary sclerosing cholangitis. *Gastroenterology* 1996; **110**: 432-440

36 **Rasmussen HH**, Fallingborg JF, Mortensen PB, Vyberg M, Tage-Jensen U, Rasmussen SN. Hepatobiliary dysfunction and primary sclerosing cholangitis in patients with Crohn's disease. *Scand J Gastroenterol* 1997; **32**: 604-610

37 **Wiesner RH**, Grambsch PM, Dickson ER, Ludwig J, MacCarty RL, Hunter EB, Fleming TR, Fisher LD, Beaver SJ, LaRusso NF. Primary sclerosing cholangitis: natural history, prognostic factors and survival analysis. *Hepatology* 1989; **10**: 430-436

38 **Loftus EV Jr**, Harewood GC, Loftus CG, Tremaine WJ, Harmsen WS, Zinsmeister AR, Jewell DA, Sandborn WJ. PSC-IBD: a unique form of inflammatory bowel disease associated with primary sclerosing cholangitis. *Gut* 2005; **54**: 91-96

39 **Bergquist A**, Ekbom A, Olsson R, Kornfeldt D, Loof L, Danielsson A, Hultcrantz R, Lindgren S, Prytz H, Sandberg-Gertzen H, Almer S, Granath F, Broome U. Hepatic and extrahepatic malignancies in primary sclerosing cholangitis. *J Hepatol* 2002; **36**: 321-327

40 **Boberg KM**, Bergquist A, Mitchell S, Pares A, Rosina F, Broome U, Chapman R, Fausa O, Egeland T, Rocca G, Schrumpf E. Cholangiocarcinoma in primary sclerosing cholangitis: risk factors and clinical presentation. *Scand J Gastroenterol* 2002; **37**: 1205-1211

41 **Angulo P**, Therneau TM, Jorgensen A, DeSotel CK, Egan KS, Dickson ER, Hay JE, Lindor KD. Bone disease in patients with primary sclerosing cholangitis: prevalence, severity and prediction of progression. *J Hepatol* 1998; **29**: 729-735

42 **Goudet P**, Dozois RR, Kelly KA, Ilstrup DM, Phillips SF. Characteristics and evolution of extraintestinal manifestations associated with ulcerative colitis after proctocolectomy. *Dig Surg* 2001; **18**: 51-55

43 **Harnois DM**, Angulo P, Jorgensen RA, Larusso NF, Lindor KD. High-dose ursodeoxycholic acid as a therapy for patients with primary sclerosing cholangitis. *Am J Gastroenterol* 2001;

96: 1558-1562
44 **Mitchell SA**, Bansi DS, Hunt N, Von Bergmann K, Fleming KA, Chapman RW. A preliminary trial of high-dose ursodeoxycholic acid in primary sclerosing cholangitis. *Gastroenterology* 2001; **121**: 900-907
45 **Rost D, Rudolph G**, Kloeters-Plachky P, Stiehl A. Effect of high-dose ursodeoxycholic acid on its biliary enrichment in primary sclerosing cholangitis. *Hepatology* 2004; **40**: 693-698
46 **Boberg KM**, Egeland T, Schrumpf E. Long-term effect of corticosteroid treatment in primary sclerosing cholangitis patients. *Scand J Gastroenterol* 2003; **38**: 991-995
47 **van Hoogstraten HJ**, Vleggaar FP, Boland GJ, van Steenbergen W, Griffioen P, Hop WC, van Hattum J, van Berge Henegouwen GP, Schalm SW, van Buuren HR. Budesonide or prednisone in combination with ursodeoxycholic acid in primary sclerosing cholangitis: a randomized double-blind pilot study. Belgian-Dutch PSC Study Group. *Am J Gastroenterol* 2000; **95**: 2015-2022
48 **Ohge H**, Takesue Y, Yokoyama T, Hiyama E, Murakami Y, Imamura Y, Shimamoto F, Matsuura Y Progression of primary biliary cirrhosis after proctocolectomy for ulcerative colitis. *J Gastroenterol* 2000; **35**: 870-2
49 **Bargiggia S**, Maconi G, Elli M, Molteni P, Ardizzone S, Parente F, Todaro I, Greco S, Manzionna G, Porro GB. Sonographic prevalence of liver steatosis and biliary tract stones in patients with inflammatory bowel disease: study of 511 subjects at a single center. *J Clin Gastroenterol* 2003; **36**: 417-420
50 **Margalit M**, Elinav H, Ilan Y, Shalit M. Liver abscess in inflammatory bowel disease: report of two cases and review of the literature. *J Gastroenterol Hepatol* 2004; **19**: 1338-1342
51 **Schwartz DA**, Loftus EV Jr, Tremaine WJ, Panaccione R, Harmsen WS, Zinsmeister AR, Sandborn WJ. The natural history of fistulizing Crohn's disease in Olmsted County, Minnesota. *Gastroenterology* 2002; **122**: 875-80
52 **Sandborn WJ**. Evidence-based treatment algorithm for mild to moderate Crohn's disease. *Am J Gastroenterol* 2003; **98**: S1-5
53 **Hanauer SB,** Feagan BG, Lichtenstein GR, Mayer LF, Schreiber S, Colombel JF, Rachmilewitz D, Wolf DC, Olson A, Bao W, Rutgeerts P. Maintenance infliximab for Crohn's disease: the ACCENT I randomised trial. *Lancet* 2002; 359: 1541-1549
54 **Sands BE**, Anderson FH, Bernstein CN, Chey WY, Feagan BG, Fedorak RN, Kamm MA, Korzenik JR, Lashner BA, Onken JE, Rachmilewitz D, Rutgeerts P, Wild G, Wolf DC, Marsters PA, Travers SB, Blank MA, van Deventer SJ. Infliximab maintenance therapy for fistulizing Crohn's disease. *N Engl J Med* 2004; **350**: 876-885
55 **Regueiro M**, Mardini H. Treatment of perianal fistulizing Crohn's disease with infliximab alone or as an adjunct to exam under anesthesia with seton placement. *Inflamm Bowel Dis* 2003; **9**: 98-103
56 **Tavarela Veloso F**. Review article: skin complications associated with inflammatory bowel disease. *Aliment Pharmacol Ther* 2004; **20** Suppl 4: 50-53
57 **Guest GD**, Fink RL. Metastatic Crohn's disease: case report of an unusual variant and review of the literature. *Dis Colon Rectum* 2000; **43**: 1764-1766
58 **Konrad A**, Seibold F. Response of cutaneous Crohn's disease to infliximab and methotrexate. *Dig Liver Dis* 2003; **35**: 351-6
59 **Kugathasan S**, Miranda A, Nocton J, Drolet BA, Raasch C, Binion DG Dermatologic manifestations of Crohn disease in children: response to infliximab. *J Pediatr Gastroenterol Nut*r 2003; **37**: 150-154
60 **Kaufman I**, Caspi D, Yeshurun D, Dotan I, Yaron M, Elkayam O. The effect of infliximab on extraintestinal manifestations of Crohn's disease. *Rheumatol Int* 2005; 25: 406-410
61 **Menachem Y**, Gotsman I. Clinical manifestations of pyoderma gangrenosum associated with inflammatory bowel disease. *Isr Med Assoc J* 2004; **6**: 88-90
62 **Regueiro M**, Valentine J, Plevy S, Fleisher MR, Lichtenstein GR. Infliximab for treatment of pyoderma gangrenosum associated with inflammatory bowel disease. *Am J Gastroenterol* 2003; **98**: 1821-1826
63 **Gupta AK**, Skinner AR. A review of the use of infliximab to manage cutaneous dermatoses. *J Cutan Med Surg*. 2004; **8**: 77-89
64 **McGowan JW 4th**, Johnson CA, Lynn A. Treatment of pyoderma gangrenosum with etanercept. *J Drugs Dermatol* 2004; **3**: 441-444
65 **Gibson LE**. Sweet syndrome. *Mayo Clin Proc* 2005; **80**: 549
66 **Hoffmann RM**, Kruis W. Rare extraintestinal manifestations of inflammatory bowel disease. *Inflamm Bowel Dis* 2004; **10**: 140-147
67 **Mintz R**, Feller ER, Bahr RL, Shah SA. Ocular manifestations of inflammatory bowel disease. *Inflamm Bowel Dis* 2004; **10**: 135-139
68 **Diaz-Valle D**, Miguelez Sanchez R, Fernandez Espartero MC, Pascual Allen D. Treatment of refractory anterior diffuse scleritis with infliximab. *Arch Soc Esp Oftalmol* 2004; **79**: 405-408
69 **Fries W**, Giofre MR, Catanoso M, Lo Gullo R. Treatment of acute uveitis associated with Crohn's disease and sacroileitis with infliximab. *Am J Gastroenterol* 2002; **97**: 499-500
70 **DiSilvestro RA,** Greenson JK, Liao Z. Effects of low copper intake on dimethylhydrazine-induced colon cancer in rats. Proc Soc Exp Biol Med 1992; 201: 94-97
71 **Papaioannou A**, Giangregorio L, Kvern B, Boulos P, Ioannidis G, Adachi JD. The osteoporosis care gap in Canada. *BMC Musculoskelet Disord* 2004; **5**: 11
72 **Bernstein CN**, Blanchard JF, Leslie W, Wajda A, Yu BN. The incidence of fracture among patients with inflammatory bowel disease. A population-based cohort study. *Ann Intern Med* 2000; **133**: 795-799
73 **Vestergaard P**, Krogh K, Rejnmark L, Laurberg S, Mosekilde L. Fracture risk is increased in Crohn's disease, but not in ulcerative colitis. *Gut* 2000; **46**: 176-181
74 **van Staa TP**, Cooper C, Brusse LS, Leufkens H, Javaid MK, Arden NK. Inflammatory bowel disease and the risk of fracture. *Gastroenterology* 2003; **125**: 1591-1597
75 **Stockbrugger RW**, Schoon EJ, Bollani S, Mills PR, Israeli E, Landgraf L, Felsenberg D, Ljunghall S, Nygard G, Persson T, Graffner H, Bianchi Porro G, Ferguson A. Discordance between the degree of osteopenia and the prevalence of spontaneous vertebral fractures in Crohn's disease. *Aliment Pharmacol Ther* 2002; **16**: 1519-1527.
76 **Bernstein CN**, Blanchard JF, Metge C, Yogendran M. The association between corticosteroid use and development of fractures among IBD patients in a population-based database. *Am J Gastroenterol* 2003; **98**: 1797-1801
77 **Viereck V**, Emons G, Lauck V, Frosch KH, Blaschke S, Grundker C, Hofbauer LC. Bisphosphonates pamidronate and zoledronic acid stimulate osteoprotegerin production by primary human osteoblasts. *Biochem Biophys Res Commun* 2002; **291**: 680-686
78 **Vidal NO**, Brandstrom H, Jonsson KB, Ohlsson C. Osteoprotegerin mRNA is expressed in primary human osteoblast-like cells: down-regulation by glucocorticoids. *J Endocrinol* 1998; **159**: 191-195
79 **Redlich K**, Hayer S, Maier A, Dunstan CR, Tohidast-Akrad M, Lang S, Turk B, Pietschmann P, Woloszczuk W, Haralambous S, Kollias G, Steiner G, Smolen JS, Schett G. Tumor necrosis factor alpha-mediated joint destruction is inhibited by targeting osteoclasts with osteoprotegerin. *Arthritis Rheum* 2002; **46**: 785-792
80 **Bernstein CN**, Bector S, Leslie WD. Lack of relationship of calcium and vitamin D intake to bone mineral density in premenopausal women with inflammatory bowel disease. *Am J Gastroenterol* 2003; **98**: 2468-2473
81 **Schulte CM**, Dignass AU, Goebell H, Roher HD, Schulte KM. Genetic factors determine extent of bone loss in inflammatory bowel disease. *Gastroenterology* 2000; **119**: 909-920
82 **Haderslev KV**, Tjellesen L, Sorensen HA, Staun M. Alendronate increases lumbar spine bone mineral density in patients with Crohn's disease. *Gastroenterology* 2000; **119**: 639-646

83 **Reffitt DM**, Meenan J, Sanderson JD, Jugdaohsingh R, Powell JJ, Thompson RP. Bone density improves with disease remission in patients with inflammatory bowel disease. *Eur J Gastroenterol Hepatol* 2003; **15**: 1267-1273

84 American Gastroenterological Association medical position statement: guidelines on osteoporosis in gastrointestinal diseases. Gastroenterology 2003; 124: 791-794

85 **Schulte CM**. Review article: bone disease in inflammatory bowel disease. *Aliment Pharmacol Ther* 2004; **20** Suppl 4: 43-49

86 **Buxton EC**, Yao W, Lane NE. Changes in serum receptor activator of nuclear factor-kappaB ligand, osteoprotegerin, and interleukin-6 levels in patients with glucocorticoid-induced osteoporosis treated with human parathyroid hormone (1-34). *J Clin Endocrinol Metab* 2004; **89**: 3332-3336

87 **Miehsler W,** Reinisch W, Valic E, Osterode W, Tillinger W, Feichtenschlager T, Grisar J, Machold K, Scholz S, Vogelsang H, Novacek G. Is inflammatory bowel disease an independent and disease specific risk factor for thromboembolism? *Gut* 2004; **53**: 542-548

88 **Grip O**, Svensson PJ, Lindgren S. Inflammatory bowel disease promotes venous thrombosis earlier in life. *Scand J Gastroenterol* 2000; **35**: 619-623

89 **Talbot RW**, Heppell J, Dozois RR, Beart RW Jr. Vascular complications of inflammatory bowel disease. *Mayo Clin Proc* 1986; **61**: 140-145

90 **Solem CA**, Loftus EV, Tremaine WJ, Sandborn WJ. Venous thromboembolism in inflammatory bowel disease. *Am J Gastroenterol* 2004; **99**: 97-101

91 **Papa A**, De Stefano V, Danese S, Gasbarrini A, Gasbarrini G. Thrombotic complications in inflammatory bowel disease: a multifactorial etiology. *Am J Gastroenterol* 2001; **96**: 1301-1302

92 **Cattaneo M**, Vecchi M, Zighetti ML, Saibeni S, Martinelli I, Omodei P, Mannucci PM, de Franchis R. High prevalence of hyperchomocysteinemia in patients with inflammatory bowel disease: a pathogenic link with thromboembolic complications? *Thromb Haemost* 1998; **80**: 542-545

93 **Oldenburg B**, Fijnheer R, van der Griend R, vanBerge-Henegouwen GP, Koningsberger JC. Homocysteine in inflammatory bowel disease: a risk factor for thromboembolic complications? *Am J Gastroenterol* 2000; **95**: 2825-2830

94 **Papa A**, Danese S, Grillo A, Gasbarrini G, Gasbarrini A. Review article: inherited thrombophilia in inflammatory bowel disease. *Am J Gastroenterol* 2003; **98**: 1247-1251

95 **Oldenburg B**, Van Tuyl BA, van der Griend R, Fijnheer R, van Berge Henegouwen GP. Risk factors for thromboembolic complications in inflammatory bowel disease: the role of hyperhomocysteinaemia. *Dig Dis Sci* 2005; **50**: 235-240

96 **Oldenburg B**, Koningsberger JC, Van Berge Henegouwen GP, Van Asbeck BS, Marx JJ. Iron and inflammatory bowel disease. *Aliment Pharmacol Ther* 2001; **15**: 429-438

97 **Crawford J**. Anemia and lung cancer. *Lung Cancer* 2002; **38**: S75-S78

98 **Wang CQ**, Udupa KB, Lipschitz DA. Interferon-gamma exerts its negative regulatory effect primarily on the earliest stages of murine erythroid progenitor cell development. *J Cell Physiol* 1995; **162**: 134-138

99 **Faquin WC**, Schneider TJ, Goldberg MA. Effect of inflammatory cytokines on hypoxia-induced erythropoietin production. *Blood* 1992; **79**: 1987-1994

100 **Papadaki HA**, Kritikos HD, Valatas V, Boumpas DT, Eliopoulos GD. Anemia of chronic disease in rheumatoid arthritis is associated with increased apoptosis of bone marrow erythroid cells: improvement following anti-tumor necrosis factor-alpha antibody therapy. *Blood* 2002; **100**: 474-482

101 **Gasche C**, Lomer MC, Cavill I, Weiss G. Iron, anaemia, and inflammatory bowel diseases. *Gut* 2004; **53**: 1190-1197

102 **Gasche C,** Waldhoer T, Feichtenschlager T, Male C, Mayer A, Mittermaier C, Petritsch W. Prediction of response to iron sucrose in inflammatory bowel disease-associated anemia. *Am J Gastroenterol* 2001; 96: 2382-2387

103 **Gasche C**. Complications of inflammatory bowel disease. *Hepatogastroenterology* 2000; **47**: 49-56

104 **Caudarella R**, Rizzoli E, Pironi L, Malavolta N, Martelli G, Poggioli G, Gozzetti G, Miglioli M. Renal stone formation in patients with inflammatory bowel disease. *Scanning Micros*c 1993; 7: 371-379

105 **Kreisel W**, Wolf LM, Grotz W, Grieshaber M. Renal tubular damage: an extraintestinal manifestation of chronic inflammatory bowel disease. *Eur J Gastroenterol Hepatol* 1996; **8:** 461-468

106 **Solem CA**, Loftus EV Jr, Tremaine WJ, Pemberton JH, Wolff BG, Sandborn WJ. Fistulas to the urinary system in Crohn's disease: clinical features and outcomes. *Am J Gastroenterol* 2002; **97**: 2300-2305

107 **Fernandez-Castroagudin J**, Brage Varela A, Lens Neo XM, Martinez Castro J, Abdulkader I. Renal amyloidosis as initial clinical manifestation of Crohn's disease. *Gastroenterol Hepatol* 2002; **25**: 395-397

108 **Shaer AJ**, Stewart LR, Cheek DE, Hurray D, Self SE. IgA antiglomerular basement membrane nephritis associated with Crohn's disease: a case report and review of glomerulonephritis in inflammatory bowel disease. *Am J Kidney Dis* 2003; **41**: 1097-1109

109 **Jensen EJ**, Baggenstoss AH, Bargen JA. Renal lesions associated with chronic ulcerative colitis. *Am J Med Sci* 1950; **219**: 281-290

110 **Druschky A**, Heckmann J, Engelhardt A, Neundorfer. Myositis--a rare complication of Crohn disease. *Fortschr Neurol Psychiatr 1996;* **64**: 422-424

111 **Moormann B**, Herath H, Mann O, Ferbert A. Involvement of the peripheral nervous system in Crohn disease. *Nervenarzt* 1999; **70**: 1107-1111

112 **Kraus JA**, Nahser HC, Berlit P. Lymphocytic encephalomyeloneuritis as a neurologic complication of ulcerative colitis. *J Neurol Sci* 1996; **141**: 117-119

113 **Nash CL**, Panaccione R, Sutherland LR, Meddings JB. Giant cell myocarditis, in a patient with Crohn's disease, treated with etanercept--a tumour necrosis factor-alpha antagonist. *Can J Gastroenterol* 2001; **15**: 607-611

114 **Orii S,** Chiba T, Nakadate I, Fujiwara T, Ito N, Ishii M, Oana S, Chida T, Kudara N, Terui T, Yamaguchi T, Suzuki K. Pleuropericarditis and disseminated intravascular coagulation in ulcerative colitis. *J Clin Gastroenterol* 2001; **32 :**251-254

115 **Stein RB,** Hanauer SB. Comparative tolerability of treatments for inflammatory bowel disease. *Drug Saf* 2000; **23:** 429-448

116 **Baker DE,** Kane S. The short- and long-term safety of 5-aminosalicylate products in the treatment of ulcerative colitis. *Rev Gastroenterol Disord* 2004; **4:** 86-91

117 **Lemann M,** Zenjari T, Bouhnik Y, Cosnes J, Mesnard B, Rambaud JC, Modigliani R, Cortot A, Colombel JF. Methotrexate in Crohn's disease: long-term efficacy and toxicity. *Am J Gastroenterol* 2000; **95:** 1730-1734

118 **Sandborn WJ,** Hanauer SB. Infliximab in the treatment of Crohn's disease: a user's guide for clinicians. *Am J Gastroenterol* 2002; **97:** 2962-2972

Science Editor Guo SY **Language Editor** Elsevier HK

PO Box 2345, Beijing 100023, China
www.wjgnet.com
wjg@wjgnet.com

ELSEVIER

World J Gastroenterol 2005;11(46):7237-7241
World Journal of Gastroenterology ISSN 1007-9327

Radiation therapy for portal venous invasion by hepatocellular carcinoma

Keiichi Nakagawa, Hideomi Yamashita, Kenshiro Shiraishi, Naoki Nakamura, Masao Tago, Hiroshi Igaki, Yoshio Hosoi, Shuichiro Shiina, Masao Omata, Masatoshi Makuuchi, Kuni Ohtomo

Keiichi Nakagawa, Hideomi Yamashita, Kenshiro Shiraishi, Naoki Nakamura, Masao Tago, Hiroshi Igaki, Yoshio Hosoi, Kuni Ohtomo, Department of Radiology, University of Tokyo 7-3-1 Hongo, Bunkyo-ku, Tokyo 113-8865, Japan
Shuichiro Shiina, Masao Omata, Department of Gastroenterology, University of Tokyo 7-3-1 Hongo, Bunkyo-ku, Tokyo 113-8865, Japan
Masatoshi Makuuchi, Department of Hepatobiliary Surgery, University of Tokyo 7-3-1 Hongo, Bunkyo-ku, Tokyo 113-8865, Japan
Correspondence to: Keiichi Nakagawa, Department of Radiology, Faculty of Medicine, University of Tokyo 7-3-1 Hongo, Bunkyo-ku, Tokyo 113, Japan. nakagawa-rad@umin.ac.jp
Telephone: +81-3-58008667 Fax: +81-3-58008935
Received: 2005-02-17 Accepted: 2005-07-01

Abstract

AIM: To clarify the efficacy and safety of three-dimensional conformal radiotherapy (3-D CRT) for this disease and to specify patient subgroups suitable for this treatment.

METHODS: Fifty-two patients with HCC received PVI-targeted radiation therapy from January 1995 through December 2003. Portal venous invasion (PVI) was found in the second or lower order branches of the portal vein in 6 patients, in the first branch in 24 patients and in the main trunk in 22 patients. Child classifications of liver function before radiation therapy were A, B, and C for 19, 24 and 2 patients, respectively. All patients received three-dimensional conformal radiotherapy with a total dose ranging from 39 to 60 Gy (57.0 Gy in average).

RESULTS: Overall survival rates at 1, 2, 3, 4, and 5 years were 45.1%, 25.3%, 15.2%, 10.1%, and 5.1%, respectively. Univariate analysis revealed that Child status, the number of tumor foci, tumor type, transcatheter arterial embolization (TAE) after radiation therapy were statistically significant prognostic factors. Multivariate analysis showed that the number of tumor foci and TAE after radiation therapy were statistically significant.

CONCLUSION: The results of this study strongly suggest the efficacy of 3-D CRT as treatment for PVI in HCC. 3-D CRT is recommended in combination with post-radiation TAE for PVI of HCC with 5 tumor foci or less in the liver and with Child A liver function.

Key words: Hepatocellular carcinoma; Portal venous invasion; Radiation therapy

Nakagawa K, Yamashita H, Shiraishi K, Nakamura N, Tago M, Igaki H, Hosoi Y, Shiina S, Omata M, Makuuchi M, Ohtomo K. Radiation therapy for portal venous invasion by hepatocellular carcinoma. *World J Gastroenterol* 2005; 11(46): 7237-7241
http://www.wjgnet.com/1007-9327/11/ 7237.asp

INTRODUCTION

Patients with primary hepatocellular carcinoma (HCC) often develop portal venous invasion (PVI)[1-6]. PVI is associated with a high probability of extensive tumor spread and an elevation of portal vein pressure, which subsequently may cause esophageal varices and liver dysfunction. Transcatheter arterial embolization (TAE) which is performed frequently for advanced HCC is not indicated when portal blood flow decreases due to PVI. It is, therefore, associated with a poor prognosis[2-3]. No treatment strategy for PVI has been established, and the median survival has been reported to range only from 5 to 11 mo[7-12]. Notably, the 1-year survival rate is less than 50% and there are only a few 3-year survivors of PVI affecting the first branch and/or the main trunk of the portal vein[3, 13].

Few articles on the radiation therapy have been reported for the disease. The aim of the study is to clarify the efficacy and safety of three-dimensional conformal radiotherapy (3-D CRT) for PVI from HCC and to specify patient subgroups who are best benefited by this treatment strategy.

MATERIALS AND METHODS

Fifty-two patients with HCC received PVI-targeted radiation therapy from January 1995 through December 2003. The aim of the treatment was to prevent and/or improve liver dysfunction caused by PVI and re-actualize transcatheter arterial embolization (TAE) for intrahepatic tumors as well as to control PVI itself. All patients but one were male. A diagnosis of HCC was made using ultrasonography (US), computed tomography (CT), angiography, and liver biopsy, as previously reported. Histopathological diagnosis was confirmed in all the patients. Criteria of diagnostic imaging of PVT is a low-attenuation intraluminal mass that expanded the portal vein on enhanced CT or conventional US[14-16] and/or the detection of pulsatile flow in portal vein thrombi by Doppler US[17].

Table 1 List of size of intrahepatic tumor

Size of intrahepatic tumor (cm)	No. of patients
No HCC	1
1-1.99	2
2-2.99	21
3-3.99	11
4-4.99	7
5-5.99	3
6-6.99	2
⩾7	5

The observation period ranged between 17.4 mo and 123.6 mo (average, 60.4 mo; median, 58.4 mo). These patients ranged in age from 43 years to 82 years (average, 63.1 years; median, 64.0 years) when radiation therapy was started. Eight patients were hepatitis B virus (HBV) related, 40 patients were hepatitis C virus (HCV) related, and 45 had pathologically proven liver cirrhosis. Child classifications of liver function before radiation therapy were A, B, and C for 19, 24 and 2 patients, respectively. Values of the Karnofsky index ranged from 70 to 100 (average, 90.8; median 90). PVI was found in the second or lower order branches of the portal vein in 6 patients, in the first branch in 24 patients and in the main trunk in 22 patients. HCCs were classified as nodular, massive, and diffuse, according to the criteria of the Liver Cancer Study Group of Japan[18]. Thirty-six patients had nodular, 9 had massive, and 6 had diffuse HCCs. The size of the intrahepatic tumors varied patient to patient and no intrahepatic tumor was detected in one patient as summarized in Table 1. Thirteen patients had a single focus for the intrahepatic tumor, 7 had 2 to 5 foci, and 31 patients had 6 or more.

Regarding treatment for HCC before the detection of PVI, 31 patients had undergone percutaneous tumor ablation (PTA) such as percutaneous ethanol injection (PEIT) and percutaneous microwave coagulation therapy (PMCT), 40 patients had undergone TAE, and 22 patients had both procedures. Tumors were surgically resected in 7 patients.

All patients received 3-D CRT with a multi-leaf collimator (MLC) using 6 MV X-ray. Figure 1 is an example of dose distributions in one patient. Our goal to give a total dose of 60 Gy to each patient was achieved in 38 cases (mean total dose, 57.0 Gy, range: 39-60 Gy). A daily dose of 2 Gy was delivered 5 times a wk. Clinical tumor volume (CTV) was the tumor itself which was depicted on CT and/or US. Planning target volume (PTV) was defined as 1.5 to 2.0 cm beyond the enhanced lesion on CT scan. Radiation was performed while the patient was breathing shallowly without the use of breath control or respiratory gating. Initial effects of radiation therapy on PVI was evaluated 8 to 12 wk after the completion of radiation and expressed according to the WHO criteria[19].

After the completion of radiation therapy for PVI, 10 underwent PTA, 25 underwent TAE, and 8 patients had both procedures. No surgical operation was performed following radiotherapy for PVI.

The survival period was measured from first day of irradiation and the Kaplan-Meier technique was used to calculate the survival rate. The differences in survival rates were analyzed using the log rank test. Uni and multivariate analyses were performed by Cox's proportional hazard model. Statistical analyses were considered significant if the *P*-value was 0.05 or less.

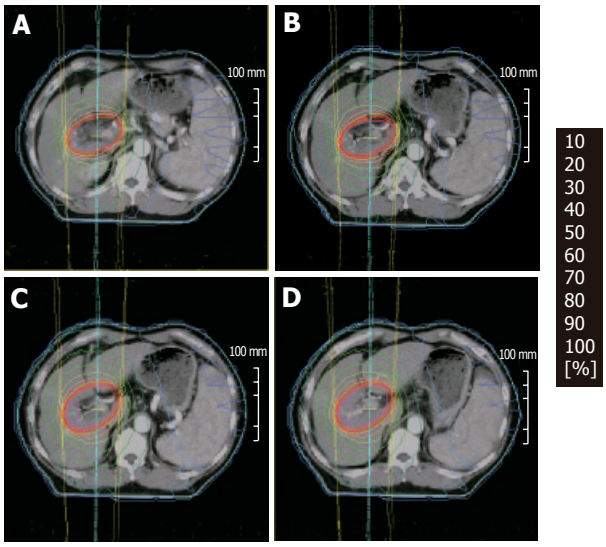

Figure 1 An example of dose distributions (**A, B, C, D**) in 3D-CRT.

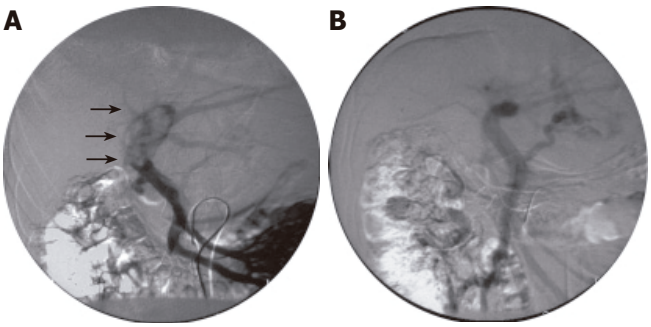

Figure 2 Angiographs of the portal vein showing disappearance of a tumoral embolus after irradiation therapy. Angiographs taken before and after treatment are shown to the left (**A**) and right (**B**), respectively.

Written informed consent was obtained in all the patients in this study.

RESULTS

The initial effects of radiation therapy on PVI were complete regression (CR) in 2 patients, partial regression (PR) in 24 patients, stable disease (SD) in 18 patients and progressive disease (PD) in 8 patients. Figure 2 shows angiographs of the portal vein before (A) and after irradiation (B). Defect of the portal blood flow which was marked with arrows (A) disappeared after the treatment (B). Intrahepatic tumors increased in 31 patients (59.6%).

Overall survival rates at 1, 2, 3, 4, and 5 years were 45.1%, 25.3%, 15.2%, 10.1%, and 5.1%, respectively (Figure 3). Neither age, nor Karnofsky performance index was related to the survival rate. Survival time greatly depended on

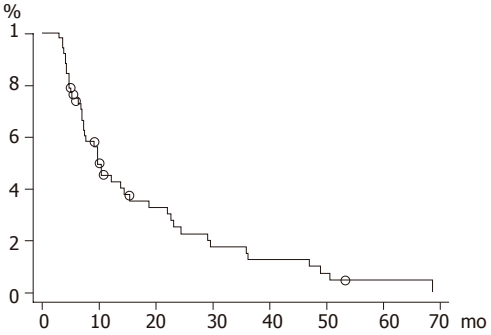

Figure 3 Overall survival curve.

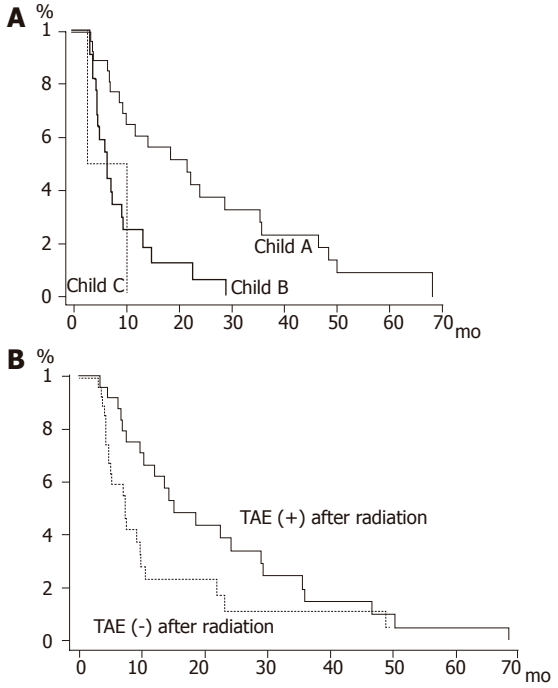

Figure 4 A: Survival curves according to Child classification. Solid line: Child A; bold line: Child B; dashed line: Child C; **B:** Survival curves for the patient group with and without post-radiation TAE. Solid line: post-radiation TAE (+); dashed line: post-radiation TAE (–).

the Child status as shown in Figure 4A (P = 0.0007). Diffuse type HCC showed a significant lower survival rate compared with nodular or massive type HCC (P = 0.0389). We also noted a higher survival rate in cases with 5 foci or less in the liver (P = 0.01). The spread of PVI (invasion of the main trunk, first branch, and second or lower order branches) was not relevant to the survival rate at all (P = 0.7679) (Figure 4B).

Treatment preceding irradiation, namely, surgical resection, PTA and TAE, was irrelevant to the prognosis as well. We noted a significant longer survival periods in cases with favorable primary effects following radiation therapy (P = 0.0419). Regarding the effect of treatments given after radiation therapy, PTA had no influence on the survival rate (P = 0.3987). On the other hand, the survival rate was higher, *albeit* marginally, in the TAE-treated group

Table 2 Univariate analysis

	Hazard ratio	95%CI	*P* value
Child classification (A)	0.217	0.048-0.978	0.0015
No. of HCC (≤5)	0.411	0.204-0.828	0.0129
Tumor type (diffuse)	2.897	1.147-7.313	0.0244
No TAE after RT	2.406	1.001-5.786	0.0498
Initial effect (CR)	0.194	0.043-0.878	0.0625
No surgery before RT	0.6	0.247-1.456	0.2589
No PTA before RT	1.373	0.741-2.544	0.3136
No TAE before RT	0.718	0.358-1.438	0.3494
No PTA after RT	1.372	0.654-2.880	0.4026
KPS (<90)	1.252	0.483-0.262	0.6457
age	1.008	0.971-1.046	0.681
Main trunk invasion	1.049	0.573-1.920	0.8772

CR: complete regression; PR: partial regression; SD: stable disease; PD: progressive disease; TAE: transcatheter arterial embolization; RT: radiation therapy; HCC: hepatocellular carcinoma; PTA: percutaneous tumor ablation; CI: confidence interval.

Table 3 Multivariate analysis

	Hazard ratio	95%CI	*P* value
No. of HCC (≤5)	0.414	0.188-0.912	0.0285
No TAE after RT	3.206	1.463-7.024	0.0364
Child classification A	0.729	0.111-4.667	0.0864
Initial effect (CR)	0.314	0.059-1.664	0.5783
Tumor type (diffuse)	1.309	0.190-9.011	0.7019

CR: complete regression; PR: partial regression; SD: stable disease; PD: progressive disease; TAE: transcatheter arterial embolization; RT: radiation therapy; HCC: hepatocellular carcinoma; CI: confidence interval.

than in the TAE-untreated group (P = 0.0465).

Univariate analysis by the Cox proportional hazard model revealed that Child status, the number of tumor foci, tumor type, TAE after radiation therapy were statistically significant prognostic factors (Table 2). Multivariate analysis by Cox's proportional hazard model using five variables, namely, Child status, the number of tumor foci, tumor type, TAE after radiation therapy, initial effect showed that the number of tumor foci in the liver (P = 0.0285) were the most important factors contributing to the eligible prognosis of patients with HCC invading the portal vein, followed by TAE after radiation therapy (P = 0.0364) (Table 3).

Hepatic function, expressed using the Child classification, remained unaltered in 34 cases after radiation therapy. In the remaining 18 patients the classification changed from Child A to B in 13 cases, from Child B to C in two cases, and from Child B to A in three cases. A patient whose liver function deteriorated from Child B to C lapsed into a hepatic coma after radiation therapy. No other serious side effects of irradiation were observed.

DISCUSSION

PVI has been considered to be an important contributor to a poor prognosis in primary HCC, and no definitive treatment strategy has been established to it. The results of the present study demonstrated a relatively favorable survival following radiation therapy for PVI. The 3-year survival rate of 15.2 % among the present study patients

is excellent in comparison with survival rates reported previously[8-9]. In contrast to the surgical series[3,13], in the present study, 3-year survival did not depend on whether PVI invaded the first branch and/or the main trunk of the portal vein. The authors consider, therefore, that radiation therapy seems to be superior to surgical intervention for the patients who developed PVI in the proximal portal vein.

Survival rates did not differ significantly among groups of patients who received one of three different treatments prior to radiation therapy, namely surgical resection, PTA and TAE. On the other hand, a significantly favorable outcome of TAE after radiation therapy was found. The TAE was performed preferentially in patients whose PVI was controlled sufficiently and whose liver function was kept relatively normal; thus, this bias in selecting patients for TAE was probably the main reason for the favorable outcome. However, 6 of 7 patients who survived for more than 2 years had undergone TAE after radiation therapy. Therefore, it appears beneficial to perform TAE in cases in which PVI is under sufficient control.

Radiation therapy for hepatic carcinoma is not performed widely, and reports of such treatment are infrequent[20-23]. Reports of radiotherapy for PVI from HCC is even rare[24-26] Radiation therapy markedly damages normal hepatic cells when used with conventional large fields. According to the experience in the present paper, however, decreases in liver function were within the acceptable range if only PVIs of the patients classified into Child A and B were treated with 3-D CRT. With 3-D CRT, high doses of radiation are confined to the target region while surrounding areas of the liver are exposed only to lower doses. Although clinical data have accumulated concerning hepatic dysfunction after whole or partial irradiation of the liver, those data are not directly applicable to predict hepatic dysfunction after conformal radiotherapy. The biological effect on the liver of such inhomogenous irradiation has not been elucidated fully. Further accumulation of clinical experience is required to determine the most appropriate method of irradiation for this disease.

The results of this study strongly suggest the efficacy of 3-D CRT as treatment for PVI in HCC. From the present analyses, the authors will recommend 3-D CRT in combination with post-radiation TAE for HCCs with 5 tumor foci or less in the liver and with Child A liver function.

Needless to say, because this study was retrospective, the presence of bias in the selection of treatments for individual patients cannot be excluded completely. To more fully clarify the significance of this therapy, a prospective randomized trial should be performed. We hope that the outcomes reported here may contribute to designing future clinical trials and optimizing treatment for this disease.

REFERENCES

1 **Albacete RA,** Matthews MJ, Saini N. Portal vein thromboses in malignant hepatoma. *Ann Intern Med* 1967; **67:** 337-348

2 **Adachi E,** Maeda T, Kajiyama K, Kinukawa N, Matsumata T, Sugimachi K, Tsuneyoshi M. Factors correlated with portal venous invasion by hepatocellular carcinoma: univariate and multivariate analyses of 232 resected cases without preoperative treatments. *Cancer* 1996; **77:** 2022-2031

3 **Tobe T,** Takayasu K, Kasugai F, Ikeya S, Muramatsu Y, Moriyama N. Primary liver cancer in Japan. Clinicopathologic features and results of surgical treatment. Liver Cancer Study Group of Japan. *Ann Surg* 1990; **211:** 277-287

4 **Koike Y,** Shiratori Y, Sato S, Obi S, Teratani T, Imamura M, Yoshida H, Shiina S, Omata M. Des-gamma-carboxy prothrombin as a useful predisposing factor for the development of portal venous invasion in patients with hepatocellular carcinoma: a prospective analysis of 227 patients. *Cancer* 2001; **91:** 561-569

5 **Stuart KE,** Anand AJ, Jenkins RL. Hepatocellular carcinoma in the United States. Prognostic features, treatment outcome, and survival. *Cancer* 1996; **77:** 2217-2222

6 **Fong Y,** Sun RL, Jarnagin W, Blumgart LH. An analysis of 412 cases of hepatocellular carcinoma at a Western center. *Ann Surg* 1999; **229:** 790-9; discussion 799-800

7 **Kumada K,** Ozawa K, Okamoto R, Takayasu T, Yamaguchi M, Yamamoto Y, Higashiyama H, Morikawa S, Sasaki H, Shimahara Y. Hepatic resection for advanced hepatocellular carcinoma with removal of portal vein tumor thrombi. *Surgery* 1990; **108:** 821-827

8 **Chen SC,** Lian SL, Chang WY. The effect of external radiotherapy in treatment of portal vein invasion in hepatocellular carcinoma. *Cancer Chemother Pharmacol* 1994; **33 Suppl:** S124-127

9 **Chung JW,** Park JH, Han JK, Choi BI, Han MC. Hepatocellular carcinoma and portal vein invasion: results of treatment with transcatheter oily chemoembolization. *AJR Am J Roentgenol* 1995; **165:** 315-321

10 **Ando E,** Yamashita F, Tanaka M, Tanikawa K. A novel chemotherapy for advanced hepatocellular carcinoma with tumor thrombosis of the main trunk of the portal vein. *Cancer* 1997; **79:** 1890-1896

11 **Lee HS,** Kim JS, Choi IJ, Chung JW, Park JH, Kim CY. The safety and efficacy of transcatheter arterial chemoembolization in the treatment of patients with hepatocellular carcinoma and main portal vein obstruction. A prospective controlled study. *Cancer* 1997; **79:** 2087-2094

12 **Yamakado K,** Tanaka N, Nakatsuka A, Matsumura K, Takase K, Takeda K. Clinical efficacy of portal vein stent placement in patients with hepatocellular carcinoma invading the main portal vein. *J Hepatol* 1999; **30:** 660-668

13 **Yamanaka N,** Okamoto E, Toyosaka A, Mitunobu M, Fujihara S, Kato T, Fujimoto J, Oriyama T, Furukawa K, Kawamura E. Prognostic factors after hepatectomy for hepatocellular carcinomas. A univariate and multivariate analysis. *Cancer* 1990; **65:** 1104-1110

14 **Inamoto K,** Sugiki K, Yamasaki H, Miura T. CT of hepatoma: effects of portal vein obstruction. *AJR Am J Roentgenol* 1981; **136:** 349-353

15 **Mathieu D,** Grenier P, Larde D, Vasile N. Portal vein involvement in hepatocellular carcinoma: dynamic CT features. *Radiology* 1984; **152:** 127-132

16 **Van Gansbeke D,** Avni EF, Delcour C, Engelholm L, Struyven J. Sonographic features of portal vein thrombosis. *AJR Am J Roentgenol* 1985; **144:** 749-752

17 **Dodd GD 3rd,** Memel DS, Baron RL, Eichner L, Santiguida LA. Portal vein thrombosis in patients with cirrhosis: does sonographic detection of intrathrombus flow allow differentiation of benign and malignant thrombus? *AJR Am J Roentgenol* 1995; **165:** 573-577

18 The general rules for the clinical and pathological study of primary liver cancer. Liver Cancer Study Group of Japan. *Jpn J Surg* 1989; **19:** 98-129

19 **Miller AB,** Hoogstraten B, Staquet M, Winkler A. Reporting results of cancer treatment. *Cancer* 1981; **47:** 207-214

20 **Matsuzaki Y,** Osuga T, Saito Y, Chuganji Y, Tanaka N, Shoda J,

Tsuji H, Tsujii H. A new, effective, and safe therapeutic option using proton irradiation for hepatocellular carcinoma. *Gastroenterology* 1994; **106:** 1032-1041

21 **Thorn K,** Williams J. Solitary osseus plasmacytoma as a cause of back pain in a young patient. *Am J Emerg Med* 1999; **17:** 615-617

22 **Cheng JC,** Chuang VP, Cheng SH, Huang AT, Lin YM, Cheng TI, Yang PS, You DL, Jian JJ, Tsai SY, Sung JL, Horng CF. Local radiotherapy with or without transcatheter arterial chemoembolization for patients with unresectable hepatocellular carcinoma. *Int J Radiat Oncol Biol Phys* 2000; **47:** 435-442

23 **Seong J,** Park HC, Han KH, Lee DY, Lee JT, Chon CY, Moon YM, Suh CO. Local radiotherapy for unresectable hepatocellular carcinoma patients who failed with transcatheter arterial chemoembolization. *Int J Radiat Oncol Biol Phys* 2000; **47:** 1331-1335

24 **Fan J,** Zhou J, Wu ZQ, Qiu SJ, Wang XY, Shi YH, Tang ZY. Efficacy of different treatment strategies for hepatocellular carcinoma with portal vein tumor thrombosis. *World J Gastroenterol* 2005; **11:** 1215-1219

25 **Yamada K,** Izaki K, Sugimoto K, Mayahara H, Morita Y, Yoden E, Matsumoto S, Soejima T, Sugimura K. Prospective trial of combined transcatheter arterial chemoembolization and three-dimensional conformal radiotherapy for portal vein tumor thrombus in patients with unresectable hepatocellular carcinoma. *Int J Radiat Oncol Biol Phys* 2003; **57:** 113-119

26 **Ishikura S,** Ogino T, Furuse J, Satake M, Baba S, Kawashima M, Nihei K, Ito Y, Maru Y, Ikeda H. Radiotherapy after transcatheter arterial chemoembolization for patients with hepatocellular carcinoma and portal vein tumor thrombus. *Am J Clin Oncol* 2002; **25:** 189-193

Science Editor Guo SY **Language Editor** Elsevier HK

PO Box 2345, Beijing 100023, China
www.wjgnet.com
wjg@wjgnet.com

ELSEVIER

World J Gastroenterol 2005;11(46):7242-7247
World Journal of Gastroenterology ISSN 1007-9327

Effect of oral *Lactococcus lactis* containing endostatin on 1, 2-dimethylhydrazine-induced colon tumor in rats

Wei Li, Chong-Bi Li

Wei Li, Department of Obstetrics and Gynecology, First People's Hospital of Hangzhou, Hangzhou 310006, Zhejiang Province, China
Chong-Bi Li, Department of Biology, Zhaoqing College, Zhaoqing 526000, Guangdong Province, China
Correspondence to: Dr. Chong-Bi Li, Department of Biology, Zhaoqing College, Zhaoqing 526000, Guangdong Province, China. lchongbi@yahoo.com
Telephone: +86-758-2716359 Fax: +86-758-2776882
Received: 2005-02-17 Accepted: 2005-07-04

Abstract

AIM: To investigate the effects of oral *Lactococcus lactis* (*L lactis*) containing endostatin on 1, 2-dimethylhydrazine (DMH)-induced rat colorectal cancer.

METHODS: Recombinant endostatin was produced by the expression of *L lactis* NZ9000. Sixty male Wistar rats were injected with DMH (40 mg/kg body weight) subcutaneously once a week for 10 wk to induce colorectal cancer. The rats were gavaged with 1 mL of endostatin at a dose of 1×10^8/d and fed with the basal diet. The animals were killed after 22 wk for histopathological examination. The total time of experimental observation was 58 wk.

RESULTS: Rat endostatin protein was expressed in *L lactis*. Recombinant endostatin exhibited a significant effect on colorectal cancer ($P<0.05$). Furthermore, the mean survival time of the rats treated with endostatin was longer than that of the animals treated with DMH. There was no statistically significant difference between the rats treated with endostatin and those treated with DMH. The results showed that endostatin could not result in complete cure.

CONCLUSION: Oral endostatin exerts an influence on the progression of chemically induced colon tumors.

Key words: Endostatin; DMH; Tumors

Li W, Li CB. Effect of oral *Lactococcus lactis* containing endostatin on 1, 2-dimethylhydrazine-induced colon tumor in rats. *World J Gastroenterol* 2005; 11(46):7242-7247
http://www.wjgnet.com/1007-9327/11/7242.asp

INTRODUCTION

There are lines of evidence that angiogenesis is essential for the growth and persistence of solid tumors and their metastases[1,2]. Tumor angiogenesis is regulated by the balance between proangiogenesis and antiangiogenesis factors, and this balance varies in different organ environments[3]. Systemic administration of recombinant endostatin potently inhibits angiogenesis and maintains metastases at a microscopic size, resulting in a strong anti-tumor activity[4-6]. Endostatin has been shown in some studies to inhibit the formation or growth of lung and liver metastases[7,8]. Endostatin, an angiogenesis inhibitor produced by hemangioendothelioma, is a 20 kDa carboxy-terminal fragment of collagen XVIII[5]. The efficacy of endostatin in colon environment is not well established. To our knowledge, there are no published reports on the efficacy of endostatin against chemically induced colon tumor progression.

An autochthonous colon cancer model is useful to evaluate the clinical therapeutic efficacy of drugs for colorectal cancer[9,10]. As DMH model is known to closely parallel the human disease in terms of disease presentation, gross and microscopic pathology[11], it is anticipated that DMH-induced colon tumors respond to chemotherapeutic drugs. Drugs such as 5-fluorouracil (5-FU) can inhibit the growth of DMH-induced colon tumors and prolong the survival of their rodent hosts[12]. Therefore, DMH-induced colon tumors at present are the most popular models to study the morphology, pathogenesis, prevention, and treatment of colorectal cancer[11,13]. Though 5-FU derivatives have been tested in the DMH model, whether this colon cancer model of rats can be applied to the evaluation of the effect of endostatin on colon tumors remains unknown. The aim of the present study was to investigate the effects of recombinant endostatin on the progression of DMH-induced colon tumors in rats.

MATERIALS AND METHODS

Animals and chemicals

Five-week-old male Wistar rats were provided by the Laboratory Animal Center, Chinese Academy of Medical Sciences, Beijing, China, and housed in plastic cages in a 12-h light/dark cycle at 22±2 ℃ and 44±5% relative humidity. Rats were fed with the basal diet with free access to water. Body weight and food consumption were measured weekly during the experiments. DMH was purchased from Tokyo Kasei Co. (Tokyo, Japan).

Preparation of recombinant endostatin

Endostatin expression experiments were performed with *L lactis* NZ9000 (donated by Institute National de la Research Agromique, France). All cloning steps were done with *E coli* Top 10. *E coli* (stored in our laboratory, China) was grown on Luria-Bertani (LB) medium and incubated at 37 ℃. *L lactis* was grown on M17 medium containing 0.5% (wt/vol) glucose and incubated at 30 ℃. When appropriate, chloramphenicol was added at a final concentration of 10 μg/mL and ampicillin was supplied at a concentration of 100 μg/mL. Expression of the endostatin gene was induced by nisin promotor. *L lactis* was cultured overnight and then transferred into a fresh medium at a dilution of 1:50. After 3-4 h of incubation, 1 μg/mL of nisin (Sigma) was added to the culture and incubated for 3-4 h.

Cloning and expression of rat endostatin in L lactis

Total RNA was extracted from rat kidney tissue using the SV total RNA isolation systems kit (Promega) and reverse-transcribed by reverse transcription system kit (Promega). The mixture was incubated at 25 ℃ for 10 min, at 42 ℃ for 60 min, at 95 ℃ for 5 min, and at 4 ℃ for 5 min. The two gene-specific primers were designed by the sequence encoding the carboxy terminal portion of rat collagen XVIII. The primer sequences were 5'-TTT GAA TTC GCC CAC ACC CAC CGC GAC TTC CAG CCG-3' and 5'-AAA AGC GGC CGC CTA CTT GGA GGC GGC AGT CAT GAA GCT-3'. PCR was performed in a total volume of 50 μL of reaction solution and 2 μL of RT template. The PCR conditions were as follows: denaturation at 94 ℃ for 5 min, then 25-35 cycles at 94 ℃ for 0.5 min, at 56 ℃ for 0.5 min, at 72 ℃ for 1 min, a final extension at 72 ℃ for 5 min and a DNA fragment was obtained. The amplified fragment was purified using the QIAquick PCR purification kit (QIAGEN Inc.) and digested with *EcoRI* and *Not*I. The resulting fragment was respectively ligated to nisin promotor plasmids pLA141 and pLA151 digested with *EcoRI* and *Not*I. The pLA141 plasmid carried a signal peptide Usp45. The recombinant plasmid DNA was transferred into *L lactis* NZ9000 by electroporation and transformants were plated on GM17 agar plates containing chloramphenicol according to the method of Wells *et al*.[15]. The recombinant plasmid DNA was isolated from *L lactis* as described previously[15,16] and the nucleotide sequence was further determined.

Western blotting

Total protein was prepared from exponentially growing cultures. The bacteria were harvested by centrifugation at 3 000 r/min for 10 min at 4 ℃, washed with PBS, resuspended in 1 mL of 10 mmol/L Tris-HCl (pH 7.5) and disrupted with a French press (Bioritech). The cell suspension was centrifuged at 10 000 g for 10 min at 4 ℃ to remove cell debris. The samples were mixed in *Laemmli* buffer and subjected to SDS-12% polyacrylamide gel electrophoresis. The protein was transferred onto nitrocellulose membranes with a Bio-Rad electroblotter. The blots were developed with BCIP/NBT developing buffer (Sigma).

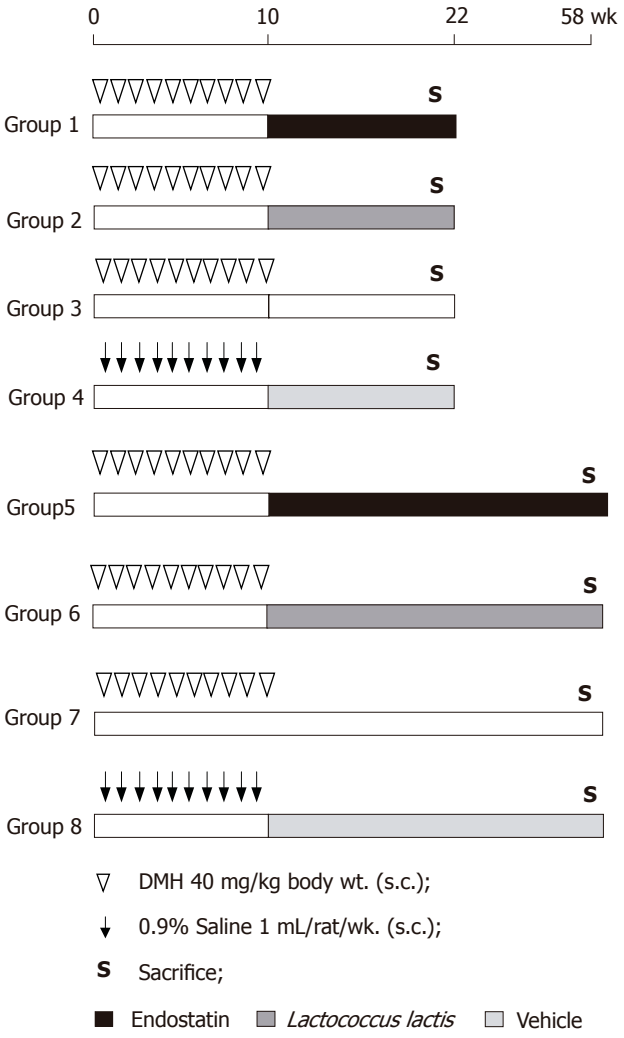

Figure 1 Experimental design.

Treatment protocol

The experimental design is shown in Figure 1. After 1 wk of acclimatization, 80 six-week-old rats were randomly divided into 8 groups (10 rats/group). Animals in groups 1-3 and 5-7 received subcutaneous injections of DMH dissolved in normal saline solution (40 mg/kg body weight) once a week for 10 wk. Rats in groups 4 and 8 were injected with 0.9% normal saline (vehicle) at the same time. After the last DMH treatment, the animals were additionally gavaged with 1 mL of *L lactis*-secreted endostatin protein (groups 1 and 5) and *L lactis* without endostatin gene but containing plasmids (groups 2 and 6) once a day for 12 wk or until they were killed after 58 wk. The dose of endostatin and *L lactis* was 1×10^8 daily. Groups 4 and 8 were gavaged with 1 mL of the solutions not containing *L lactis* (the vehicle control). Groups 3 and 7 served as a carcinogen control. The time of treatment differed slightly in each experiment. All animals that survived were killed under either anesthesia at wk 22 (groups 1-4) or to end of the experiment. The total time of experimental observation was 58 wk.

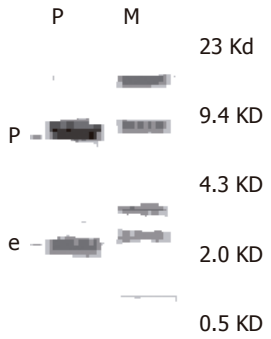

Figure 2 Expression plasmid obtained by restriction enzyme analysis. P: expression plasmid cut by *Eco*RI and *Not* I; e: endostatin gene; M: molecular weight marker.

Autopsy

The colons were removed, flushed with saline and opened along the longitudinal median axis. Tumor width (*W*) and length (*L*) were measured with calipers. The tumor volume (TV) was determined by the following formula: $TV = (L \times W^2)/2$[8]. After the gross pathologic changes (number, dimensions, and distribution of the tumors) were recorded, the colons were fixed flat in 10% phosphate-buffered formalin. The liver and kidneys were removed and weighed. Other major organs (stomach, small intestine, spleen, lungs, and lymph nodes) were also excised and fixed in 10% phosphate-buffered formalin. All tissues were embedded in paraffin, cut into sections and stained with hematoxylin and eosin. The proximal, intermediate and distal segments of the colon were examined for histopathological analysis.

Tumor staging

Animals with DMH-induced colon cancer developed multiple tumors and each tumor had a different histological stage[14]. Consequently, the animals were staged (Duke's stage) with reference to a single index tumor, defined as the largest macroscopically and histologically identifiable colon tumor.

Statistical analysis

Statistical analyses were completed with SPSS 9.0 software. The significance of differences between the average values of the groups was analyzed using Cochran's two-tailed Student's *t*-test. The significance of differences in lesion incidence between the groups was assessed by χ^2 test. Rat mortality was analyzed by the log-rank method of Peto *et al*.[17].

RESULTS

Construction of expression plasmid

The plasmid containing the endostatin gene was pla148, identified as the expression plasmid I. Recombinant *L lactis* was obtained by PCR and restriction enzyme analysis when the recombinant plasmid was transformed into *L lactis* by electroporation (Figure 2).

Expression of rat endostatin gene in L lactis

Recombinant lactic acid bacteria were incubated and induced by *nisin* in M17-Glu for 6 h. Endostatin protein was identified by SDS-PAGE and Western blot with the antibody prepared from rabbits immuned with human endostatin protein. Rat endostatin protein was expressed in *L lactis* (Figures 3A and 3B).

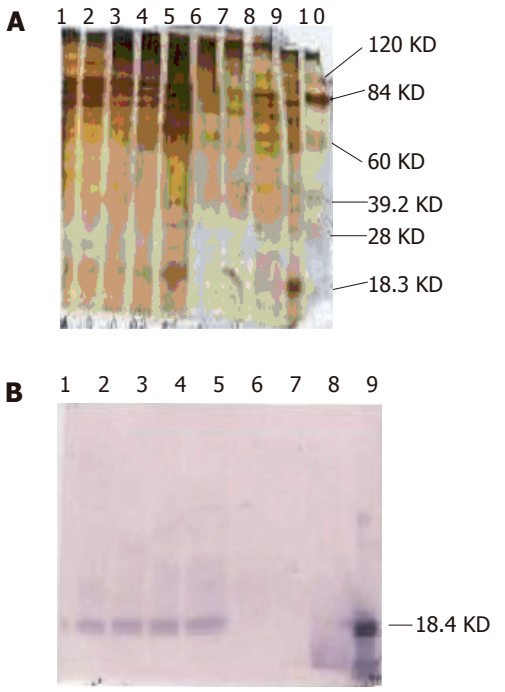

Figure 3 Expression of rat endostatin gene in *L lactis*. **A:** Silver-strained SDS-PAGE of expressed endostatin in L lactis; **B:** Western blot. Lanes 1-6: engineered *L lactis* 1-6 h after induction; lane 7: *L lactis* without endostatin gene; lane 8: rat sera from groups after oral recombinant *L lactis*; lane 9: endostatin protein expression in *E coli* cells.

Animal experiment

All rats in groups 1-4 and 8 survived until the final termination and were relatively healthy throughout the experiment. No signs of severe toxicity were observed in all the animals that were given endostatin. No tumor was found in vehicle-treated animals. By the end of wk 22, the average body weights of the rats treated with DMH or endostatin or *L lactis* were significantly decreased compared to the vehicle control ($P<0.05$). Relative liver and kidney weights and food consumption did not significantly differ among the groups (Table 1). Macroscopically, the distribution of colon tumors in the proximal and middle colon at the end of wk 22 had no significant difference among the groups (data not shown).

Histopathological findings are summarized in Table 2. Colon epithelial lesions were divided into adenomas and carcinomas. At the end of wk 22, the incidence of colon tumors was not significantly affected by endostatin. The mean tumor incidence in a single tumor-bearing rat was 2.50 in group 1 and 4.00 in group 3. Tumor volume was decreased in rats receiving endostatin. However, it did not differ from that in DMH-treated group. In addition, there was a significant difference in Duke's stage between the animals treated with DMH and those treated with

Table 1 Average final body weight, relative liver and kidney weights, and food consumption data (mean±SD)

Group	Treatment	*n*	Final body Weight, g	Relative liver Weight, g	Relative kidney Weight, g	Food consumption (g/rat/d)
1	DMH+endostatin	10	379.0±24.9[a]	2.94±0.26	0.56±0.12	18.02
2	DMH+*L lactis*	10	395.0±36.5[a]	3.05±0.25	0.56±0.08	18.00
3	DMH	10	383.5±19.2[a]	3.10±0.40	0.55±0.07	18.48
4	Saline+vehicle	10	439.5±39.3	3.09±0.35	0.56±0.12	20.07

[a]$P<0.05$ *vs* group 4.

Table 2 Colon tumor incidence, classification, multiplicity, tumor volume, and stage in rats treated with DMH with or without endostatin (mean±SD)

Treatment		Incidence	Adenoma	Carcinoma	Multiplicity	Tumor volume	Duke's stage		
	n	*n* (%)	*n* (%)	*n* (%)	number	mm^3	A	B	C
DMH+endostatin	10	10(100)	5 (50)	5 (50)	2.50±1.80	2.35±1.84	1	4	-a
DMH+*L lactis*	10	9(90)	2 (22)	7 (78)	2.67±1.47	2.54±2.00	4	6	-a
DMH	10	10 (100)	5 (50)	5 (50)	4.00±2.96	4.31±4.56	2	-	3

[a]$P<0.05$ *vs* DMH-treated rats.

Table 3 Tumor classification, distribution, and differentiation in rats treated with DMH with or without endostatin

Treatment	Tumor	Classification (%)		Distribution in colon (%)			Differentiated carcinoma (%)		
	number	Adenoma	Carcinoma	Proximal	Middle	Distal	Well	Moderately	Poorly
DMH+endostatin	25	16 (64)	9 (36)	12 (48)	9 (36)	4 (16)	6 (66.7)	3 (33.3)[a]	0
DMH+ *L lactis*	24	15 (62.5)	9 (37.5)	10 (41.7)	12 (50)	2 (8.3)	6 (66.7)	3 (33.3)[a]	0
DMH	40	27 (67.5)	13 (32.5)	15 (37.5)	19 (47.5)	6 (15)	3 (23.1)	10 (76.9)	0

[a]$P<0.05$ *vs* DMH-treated rats.

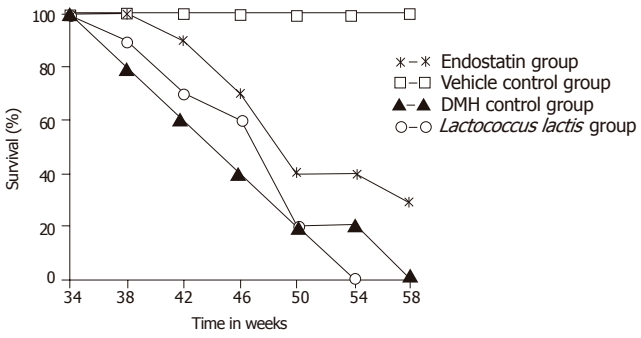

Figure 4 Survival rate of rats injected with DMH with or without endostatin and normal saline.

endostatin ($P<0.05$). Liver lesions and lymph node metastases were observed in about 30% of the animals in group 3.

The survival rates of rats in groups 5-8 are shown in Figure 4. The group that received endostatin had a survival rate of 30%. The survived rats were killed and metastases were found in their lungs and livers. All the saline-injected rats were alive at the end of the experiment. However, none of the DMH-treated rats survived the full duration of the experiment. The mean survival time of endostatin-treated animals was longer than that of DMH-treated rats. The range of ages at death in DMH-treated animals was 38-57 wk (Table 3).

DISCUSSION

Studies using preclinical models of nonhematologic malignancies indicate that antiangiogenic therapies may delay or even abrogate tumor growth[5,18,19]. Endostatin is one of the antiangiogenic drugs and our data indicate that the administration of endostatin after DMH treatment could prolong the survival time of rats. The Duke's staging system for human colorectal cancer provides accurate prognostic information. In other words, animals with less advanced disease (stage A) survive significantly longer than those with advanced disease (stages B and C) irrespective of the treatment. In our study, there was a significant difference in the levels of differentiation and metastases (Duke's stage) between the animals treated with DMH and those treated with endostatin. Endostatin-treated rats had an improved survival compared to untreated rats, indicating that the survival time of rats with colon cancer parallels to that of human beings with this disease. These results can at least in part explain the mechanism of the potent antiangiogenic and antitumor activities of endostatin. Furthermore, the improved survival is directly attributable to the effective induction of tumor stabilization and its ability to inhibit specifically endothelial proliferation in endostatin-treated animals. However, oral administration of endostatin could only prolong the survival time of tumor-bearing rats but not result in complete cure.

There are reports on endostatin against metastases in lung, stomach, and liver[7,8,20]. Recent studies showed that endostatin has an antiangiogenic action[21-24] and can

induce apoptosis in colon cancer cells by inhibiting tumor angiogenesis and inhibit tumor growth and metastases of human colon cancer xenograft in nude mice[24]. Some other mechanisms may be involved in endostatin stabilizing and maturating newly formed blood vessels[21]. Jia *et al*.[22] reported that endostatin could inhibit tumor growth and angiogenesis by blocking Vegf/Flk-1 pathway. In addition to its antiangiogenic activity, endostatin exerts a direct anticancer action that appears to be restricted to some tumor cell lines[25]. At the same time, endostatin has been demonstrated to induce regression of tumors in mice[7,26], but actual regression as opposed to growth inhibition has not been demonstrated in the colon environment. Though our study demonstrated that endostatin could influence rat colon tumor progression, the precise mechanisms by which endostatin exerts effects on colon carcinoma are not well understood.

Long-term administration of endostatin is needed because the inhibition of tumor metastases has not been observed after a shorter endostatin-treated period. The ultimate goal of antiangiogenic therapy is to induce long-term tumor stabilization[27] because data from studies in nonhuman primates indicate that endostatin may be administered for a long time without toxicity[28]. Furthermore, studies *in vitro* and *in vivo* suggest that endostatin gene therapy can effectively suppress angiogenic processes in model systems[29,30]. It was reported that endostatin treatment is not associated with any recognizable vascular changes in tumor samples[31].

Certain strains of lactic acid bacteria have been found to prevent putative preneoplastic lesions induced by carcinogens[32,33]. The antimutagenic activity of lactic acid bacteria is suspected to reside in the cell wall[34] as lactic acid itself has no antimutagenic effect[35]. The findings of the current study do not support the suggestion that the addition of *L lactis* may also prolong the survival time of DMH-treated rats. The reason for this is unclear, but might be explained by the differences in bacterial strains. The antitumor effect of lactic acid bacteria is still controversial[36]. Further study is needed to identify the antitumor effect of endostatin and the precise mechanisms by which these effects are mediated.

In conclusion, long-term administration of endostatin can inhibit the progression of chemically-induced colon tumors and prolong the survival time of rats.

ACKNOWLEDGMENTS

The authors thank Professor Shoji Fukushima, Department of Pathology, Osaka City Medical School (Japan) for valuable discussion and comments, and Professor Yanfeng Zhong, Department of Pathology, Beijing University Medical School for histopathological examination.

REFERENCES

1 **Kim KJ,** Li B, Winer J, Armanini M, Gillett N, Phillips HS, Ferrara N. Inhibition of vascular endothelial growth factor-induced angiogenesis suppresses tumur growth in vivo. *Nature* 1993; **362:** 841-844
2 **Millauer B,** Shawver LK, Plate KH, Risau W, Ullrich A. Glioblastoma growth inhibited in vivo by a dominant-negative Flk-1 mutant. *Nature* 1994; **367:** 576-579
3 **Hanahan D,** Folkman J. Patterns and emerging mechanisms of the angiogenic switch during tumorigenesis. *Cell* 1996; **86:** 353-364
4 **Shi W,** Teschendorf C, Muzyczka N, Siemann DW. Adeno-associated virus-mediated gene transfer of endostatin inhibits angiogenesis and tumor growth in vivo. *Cancer Gene Ther* 2002; **9:** 513-521
5 **O'Reilly MS,** Boehm T, Shing Y, Fukai N, Vasios G, Lane WS, Flynn E, Birkhead JR, Olsen BR, Folkman J. Endostatin: an endogenous inhibitor of angiogenesis and tumor growth. *Cell* 1997; **88:** 277-285
6 **Ye C,** Feng C, Wang S, Liu X, Lin Y, Li M. Antiangiogenic and antitumor effects of endostatin on follicular thyroid carcinoma. *Endocrinology* 2002; **143:** 3522-3528
7 **Blezinger P,** Wang J, Gondo M, Quezada A, Mehrens D, French M, Singhal A, Sullivan S, Rolland A, Ralston R, Min W. Systemic inhibition of tumor growth and tumor metastases by intramuscular administration of the endostatin gene. *Nat Biotechnol* 1999; **17:** 343-348
8 **Yoon SS,** Eto H, Lin CM, Nakamura H, Pawlik TM, Song SU, Tanabe KK. Mouse endostatin inhibits the formation of lung and liver metastases. *Cancer Res* 1999; **59:** 6251-6256
9 **Tsunoda A,** Shibusawa M, Tsunoda Y, Yasuda N, Nakao K, Kusano M. A model for sensitivity determination of anticancer agents against chemically-induced colon cancer in rats. *Anticancer Res* 1994; **14:** 2637-2642
10 **Tsunoda A,** Shibusawa M, Tsunoda Y, Yokoyama N, Nakao K, Kusano M, Nomura N, Nagayama S, Takechi T. Antitumor effect of S-1 on DMH induced colon cancer in rats. *Anticancer Res* 1998; **18:** 1137-1141
11 **LaMont JT,** O'Gorman TA. Experimental colon cancer. *Gastroenterology* 1978; **75:** 1157-1169
12 **Danzi M,** Lewin MR, Cruse JP, Clark CG. Combination chemotherapy with 5-fluorouracil (5FU) and 1, 3-bis (2-chloro-ethyl)-1-nitrosourea (BCNU) prolongs survival of rats with dimethylhydrazine-induced colon cancer. *Gut* 1983; **24:** 1041-1047
13 **Li W,** Wanibuchi H, Salim EI, Wei M, Yamamoto S, Nishino H, Fukushima S. Inhibition by ginseng of 1, 2- dimethylhydrazine induction of aberrant crypt foci in the rat colon. *Nutr Cancer* 2000; **36:** 66-73
14 **Pozharisski KM.** Morphology and morphogenesis of experimental epithelial tumors of the intestine. *J Natl Cancer Inst* 1975; **54:** 1115-1135
15 **Wells JM,** Wilson PW, Le Page RW. Improved cloning vectors and transformation procedure for Lactococcus lactis. *J Appl Bacter* 1993; **74:** 629-636
16 **Hols P,** Slos P, Dutot P, Reymund J, Chabot P, Delplace B, Delcour J, Mercenier A. Efficient secretion of the model antigen M6-gp41E in Lactobacillus plantarum NCIMB8826. *Microbiology* 1997; **143 (Pt 8):** 2733-2741
17 **Peto R,** Pike MC, Armitage P. Design and analysis of randomized clinical trials requiring prolonged observation of each patient. *Br J Cancer* 1977; **35:** 1-39
18 **Scappaticci FA,** Contreras A, Smith R, Bonhoure L, Lum B, Cao Y, Engleman EG, Nolan GP. Statin-AE: a novel angiostatin-endostatin fusion protein with enhanced antiangiogenic and antitumor activity. *Angiogenesis* 2001; **4:** 263-268
19 **Boehm T,** Folkman J, Browder T, O'Reilly MS. Antiangiogenic therapy of experimental cancer does not induce acquired drug resistance. *Nature* 1997; **390:** 404-407
20 **Zhang G,** Wang Y, Zhang M, Wang Q, Luo Y, Han C, Lu Y, Rao Y. Inhibition of growth and metastasis of human gastric cancer implanted in nude mice by the angiogenesis inhibitor endostatin. *Zhonghua Waike Zazhi* 2002; **40:** 59-61
21 **Ergun S,** Kilic N, Wurmbach JH, Ebrahimnejad A, Fernando M,

Sevinc S, Kilic E, Chalajour F, Fiedler W, Lauke H, Lamszus K, Hammerer P, Weil J, Herbst H, Folkman J. Endostatin inhibits angiogenesis by stabilization of newly formed endothelial tubes. *Angiogenesis* 2001; **4:** 193-206

22 **Jia YH,** Dong XS, Wang XS. ffects of endostatin on expression of vascular endothelial growth factor and its receptors and neovascularization in colonic carcinoma implanted in nude mice. *World J Gastroenterol* 2004; **10:** 3361-3364

23 ***Chen W,*** Fu J, Liu Q, Ruan C, Xiao S. Retroviral endostatin gene transfer inhibits human colon cancer cell growth in vivo. *Chin Med J (Engl)* 2003; **116:** 1582-1584

24 **Zhang GF,** Wang YH, Zhang MA, Wang Q, Luo YB, Wang DS, Han CR. Inhibition of growth and metastases of human colon cancer xenograft in nude mice by angiogenesis inhibitor endostatin. *Ai Zheng* 2002; **21:** 50-53

25 **Dkhissi F,** Lu H, Soria C, Opolon P, Griscelli F, Liu H, Khattar P, Mishal Z, Perricaudet M, Li H. Endostatin exhibits a direct antitumor effect in addition to its antiangiogenic activity in colon cancer cells. *Hum Gene Ther* 2003; **14:** 997-1008

26 **Harris AL.** Antiangiogenesis for cancer therapy. *Lancet* 1997; **349 Suppl 2:** 13-15

27 **Dixelius J,** Cross M, Matsumoto T, Sasaki T, Timpl R, Claesson-Welsh L. Endostatin regulates endothelial cell adhesion and cytoskeletal organization. *Cancer Res* 2002; **62:** 1944-1947

28 **Dhanabal M,** Ramchandran R, Volk R, Stillman IE, Lombardo M, Iruela-Arispe ML, Simons M, Sukhatme VP. Endostatin: yeast production, mutants, and antitumor effect in renal cell carcinoma. *Cancer Res* 1999; **59:** 189-197

29 **Jin X,** Bookstein R, Wills K, Avanzini J, Tsai V, LaFace D, Terracina G, Shi B, Nielsen LL. Evaluation of endostatin antiangiogenesis gene therapy in vitro and in vivo. *Cancer Gene Ther* 2001; **8:** 982-989

30 **Hampl M,** Tanaka T, Albert PS, Lee J, Ferrari N, Fine HA. Therapeutic effects of viral vector-mediated antiangiogenic gene transfer in malignant ascites. *Human Gene Ther* 2001; **12:** 1713-1729

31 **Mundhenke C,** Thomas JP, Wilding G, Lee FT, Kelzc F, Chappell R, Neider R, Sebree LA, Friedl A. Tissue examination to monitor antiangiogenic therapy: a phase I clinical trial with endostatin. *Clinl Cancer Res* 2001; **7:** 3366-3374

32 **Kelkar SM,** Shenoy MA, Kaklij GS. Antitumor activity of lactic acid bacteria on a solid fibrosarcoma, sarcoma-180 and Ehrlich ascites carcinoma. *Cancer Lett* 1988; **42:** 73-77

33 **Goldin BR,** Gualtieri LJ, Moore RP. The effect of Lactobacillus GG on the initiation and promotion of DMH-induced intestinal tumors in the rat. *Nutr Cancer* 1996; **25:** 197-204

34 **Tejada-Simon MV,** Pestka JJ. Proinflammatory cytokine and nitric oxide induction in murine macrophages by cell wall and cytoplasmic extracts of lactic acid bacteria. *J Food Prot* 1999; **62:** 1435-1444

35 **Morita T,** Takeda K, Okumura K. Evaluation of clastogenicity of formic acid, acetic acid and lactic acid on cultured mammalian cells. *Mutat Res* 1990; **240:** 195-202

36 **Drouault S,** Corthier G. Health effects of lactic acid bacteria ingested in fermented milk. *Vet Res* 2001; **32:** 101-117

Science Editor Wang XL and Guo SY **Language Editor** Elsevier HK

PO Box 2345, Beijing 100023, China
www.wjgnet.com
wjg@wjgnet.com

ELSEVIER

World J Gastroenterol 2005;11(46):7248-7253
World Journal of Gastroenterology ISSN 1007-9327

• *BASIC RESEARCH* •

MORT1/FADD is involved in liver regeneration

Marcus Schuchmann, Felix Rückert, Jose F Garcia-Lazaro, Andrea Karg, Jürgen Burg, Natalia Knorr, Jürgen Siebler, Eugene E Varfolomeev, David Wallach, Wolfgang Schreiber, Ansgar W Lohse, Peter R Galle

Marcus Schuchmann, Felix Rückert, Jose F Garcia-Lazaro, Natalia Knorr, Jürgen Siebler, Ansgar W Lohse, Peter R Galle, I. Department of Medicine, University of Mainz, Langenbeckstr. 1, Mainz 55101, Germany
Andrea Karg, Wolfgang Schreiber, Institute of Radiology, University of Mainz, Langenbeckstr. 1, Mainz 55101, Germany
Jürgen Burg, Institute of Pathology, University of Mainz, Langenbeckstr. 1, Mainz 55101, Germany
Eugene E Varfolomeev, Genentech, South San Francisco, CA, United States
David Wallach, The Weizmann Institute of Science, Rehovot, Israel
Supported by the Intramural grant (MAIFOR) to M.S.
Correspondence to: Marcus Schuchmann, MD, I. Department of Medicine University of Mainz, Langenbeckstr. 1, Mainz 55101, Germany. schuchm@mail.uni-mainz.de
Telephone: +49-6131170 Fax: + 49-6131176-621
Received: 2005-03-18 Accepted: 2005-07-01

Abstract

AIM: To explore the role of the adaptor molecule in liver regeneration after partial hepatectomy (PH).

METHODS: We used transgenic mice expressing an N-terminal truncated form of MORT1/FADD under the control of the albumin promoter. As previously shown, this transgenic protein abrogated CD95- and CD120a-mediated apoptosis in the liver. Cyclin A expression was detected using Western blotting. ELISA and RT-PCR were used to detect IL-6 and IL-6 mRNA, respectively. DNA synthesis in liver tissue was measured by BrdU staining.

RESULTS: Resection of 70% of the liver was followed by a reduced early regenerative response in the transgenic group at 36 h. Accordingly, 36 h after hepatectomy, cyclin A expression was only detectable in wild-type animals. Consequently, the onset of liver mass restoration was retarded as measured by MRI volumetry and mortality was significantly higher in the transgenic group.

CONCLUSION: Our data demonstrate for the first time an involvement of the death receptor molecule MORT1/FADD in liver regeneration, beyond its well described role as part of the intracellular death signaling pathway.

Key words: MORT1/FADD; CD95; TNF; Apoptosis; Liver regeneration

Schuchmann M, Rückert F, Garcia-Lazaro JF, Karg A, Burg J, Knorr N, Siebler J, Varfolomeev EE, Wallach D, Schreiber W, Lohse AW, Galle PR. MORT1/FADD is involved in liver regeneration. *World J Gastroenterol* 2005; 11(46):7248-7253
http://www.wjgnet.com/1007-9327/11/7248.asp

INTRODUCTION

Liver regeneration upon extensive liver damage is critical to survive diseases, such as fulminant hepatitis without liver transplantation. Beyond the cause of the underlying liver disease, it is well accepted that death receptor-mediated hepatocyte apoptosis is an important mechanism for liver damage[1,2]. The cascade of intracellular signaling events during apoptosis is reasonably well understood. Of critical importance is the activation of caspases, the subsequent cleavage of different death substrates and finally the disintegration of the cell. In this setting, MORT1/FADD is a central adaptor molecule for a number of death receptors to recruit and activate the initiator caspase-8 upon ligand-mediated aggregation[3,4]. Gene targeting of MORT1/FADD[5,6] or expression of a dominant negative mutant[7,8] confers resistance to CD95-mediated apoptosis in T cells. Recently, we have demonstrated that MORT1/FADD is also pivotal for CD95- and TNF-mediated apoptosis in hepatocytes *in vivo*[9]. In addition, emerging evidence suggests that death receptors and their intracellular signaling proteins have a dual role and may also be involved in the regeneration and repair mechanisms. TNF receptor I (CD120a) has been found to induce proliferation in a number of cells[10] and is involved in the initiation of liver regeneration[11]. Even the prototypical death receptor CD95 was described to exert non-apoptotic functions[12], e.g., stimulation of liver regeneration after partial hepatectomy (PH)[13]. In line with this observation, mice with the */pr* genotype and decreased expression of CD95 showed a delayed regenerative response after PH[13]. In addition, the most upstream signaling molecules of the intracellular death pathway MORT1/FADD and caspase-8 have been described to be critical for T-cell proliferation[5,6,14]. To our knowledge, the mechanism by which MORT1/FADD contributes to T-cell proliferation is not completely elucidated yet. The regulatory function of MORT1/FADD seems to be structurally independent of the death domain and its role in apoptosis, but to rely on phosphorylation at serine residue S191, which has been shown to be critical for the regulative role of MORT1/FADD in cell proliferation[15].

The role of MORT1/FADD in liver regeneration has not been described so far. We used transgenic mice expressing a dominant negative mutant of MORT1/FADD in a liver-specific manner to investigate a possible role of the adaptor molecule in liver regeneration. We observed a delayed onset of liver proliferation upon PH compared to wild-type littermates and found a higher early postoperative mortality in dnMORT1/FADD transgenic mice. The increased rate of mortality might be due to initially retarded liver regeneration and underlines the critical role of MORT1/FADD in the complex network of signaling proteins which orchestrate liver regeneration.

MATERIALS AND METHODS

Animal model of liver regeneration

Heterozygous transgenic mice (strain CB6F1) expressing liver-specific dominant negative mutant of the adaptor protein MORT1/FADD under the control of the albumin promoter were generated as previously described[9]. All animals were bred at the animal facility of the University of Mainz, had *ad libitum* access to water and food under standard conditions with 12-h dark/light cycle. All experiments were done in accordance with the Federal law and were approved by the Local Committee for Experimental Animal Research.

Partial hepatectomy

Male transgenic and wild-type animals at 6-8 wk of age were fasted overnight and operated in the morning. Mice were anaesthetized with subcutaneous injection of a solution containing 0.16% xylazinum and 1.2 mg ketamin (200 μL/20 g body weight). A 70% PH was performed by ligating and removing the left and median lobe at its root. The mice were killed at different time points and livers were harvested. The livers were either shock-frozen in liquid nitrogen and stored at -80 ℃ or fixed at 4 ℃ in 40 g/L paraformaldehyde overnight for further use. Serum was obtained by heart puncture.

DNA-synthesis measurement of BrdU incorporation and mitosis

After PH, the mice were treated at different time points with 1 mmol/L BrdU (10 g/kg body weight) 3 h prior to killing. The livers were harvested and shock-frozen. The livers were cut into 5-μm-thick slides with a microtome. BrdU incorporation was measured using the *In situ* Cell Proliferation Kit (Roche Diagnostics GmbH, 82372 Penzberg, Germany) according to the manufacturer's instructions. Results were presented as an average percentage of BrdU-positive cells counted in at least two fields of each slide under 10× high power field. Mitosis of the was counted by two independent observers in a blinded fashion.

Cytokine assays

Cytokine concentrations were assessed using ELISA, OptEIA Mouse IL-6 Set (Pharmingen, BD Biosciences, 69126 Heidelberg, Germany) following manufacturer's instructions. Samples were analyzed with an Elisa reader (MRX TC II, Dynex Technologies Lim., West Sussex BN).

Western blotting for cyclin A

Western blot analysis was performed with whole liver extract lysed in a lysis buffer. Protein concentration was equilibrated using Bradford assay reagent. The samples were boiled with sodium dodecyl sulfate sample buffer and electrophoresed on a 100 g/L sodium dodecyl sulfate-polyacrylamide gel. Following electrophoresis, the samples were blotted onto a PVDF-membrane (Pall, Germany), and the membrane was blocked with 20 g/L milk powder for 30 min, followed by an overnight incubation with a rabbit anti-cyclin A serum (Anti-rabbit polyclonal Cyc A C-19, # sc596, Santa Cruz) at 4 ℃ with phosphate-buffered saline/Tween (0.1%) with 20 g/L milk powder (PBSTM). After washing, the membranes were incubated for 45 min with horseradish peroxidase-conjugated goat-anti-rabbit serum (dilution 1:3 000) in PBSTM. Blots were developed using the Western Lightning Chemiluminescence Reagent (PerkinElmer Life Sciences, Boston, MA, USA).

Magnetic resonance imaging

Magnetic resonance imaging (MRI) was performed on a Magnetom Vision whole body scanner (Siemens Medical Solutions, Germany) at 1.5 T. The scanner was equipped with an experimental gradient system with maximum gradient field strength of 50 mT/m and a slew-rate of 160 mT/m/ms. A circular polarized small loop coil with 4 cm as diameter was used for imaging the mice.

For the imaging of the liver, a T1-weighed spinecho sequence with fat saturation and TR/TE/α = 640 ms/14 ms/90 ℃ was used. The experimental gradient system allowed a high resolution of 0.39 mm×0.39 mm with a slice thickness of 1 mm at a 50 mm×100 mm field of view. The gap between the slices was 0.8 mm.

Post processing was done using the Java-based free software ImageJ (National Institutes of Health, USA, download at http://rsb.info.nih.gov/ij). After drawing a region of interest (ROI) following the borders of the liver in every slice, the liver volume was calculated from the sum of pixels in each ROI over all slices with respect to the pixel size, the slice thickness and the slice gap is as follows:

$$\text{Volume}_{\text{liver}} = \sum_{\text{slice}} \sum_{\text{pixels}} \text{size}_{\text{pixel}}(\text{thickness}_{\text{slice}} + \text{gap}_{\text{slice}})$$

RT-PCR and light cycler

RNA was isolated from the cells using the First Strand cDNA Synthesis Kit for RT-PCR (Roche Diagnostics GmbH, 68305 Mannheim) according to the manufacturer's instructions. Primers for IL-6 were purchased from Metabion GmbH, D-82152 Planegg-Martinsried, Germany.

Duplicate PCR amplifications were carried out in a Light Cycler Fast Start DNA Master Green I™ (Roche Diagnostics GmbH, 68305 Mannheim) using Fast Start Light Cycler™ DNA Master containing Taq-polymerase, reaction buffer, and dNTPs (Roche). All reactions

were performed in 10 μL volumes and fluorescence quantification was calculated with the aid of built-in Light Cycler software, version 3.01 (Roche).

For quantification of the mRNA, we chose the method of relative quantification with external standards (HPRT-specific primers).

Liver enzymes

Liver enzymes in serum were measured with a Roche Hitachi 917.

Hematoxylin-eosin staining

Liver samples were fixed overnight at 4 ℃ with 40 g/L paraformaldehyde. The tissue was then dehydrated, embedded in paraffin, and 5-μm sections were stained with HE. Mitosis of the cells was counted by two independent observers in blinded fashion under 10×high power fields (about 50 cells/field).

RESULTS

A delayed proliferative response in dnMORT1/FADD mice after partial hepatectomy

As previously described, PH was performed by resection of around 70% of the total liver volume. DNA synthesis as a marker of the regenerative response was measured by BrdU staining. Kinetics of BrdU staining after PH obviously differed between transgenic and wild-type animals (Figure 1A). We observed a significantly more BrdU-positive cells in wild-type animals after 36 h, which was attenuated after 48 h (Figure 1A). In line with this observation, the number of mitoses differed in regenerating liver 48 h after PH (Figure 1B). Differences were also observed in expression levels of cyclin A at 36 h after hepatectomy (Figure 1C), when the expression was detected only in wild-type mice. These observations were further substantiated by MRI technique (Figure 1E), which allowed to follow closely the kinetic of liver mass restoration after hepatectomy. Here we could demonstrate that the delayed onset of liver regeneration was paralleled by a retarded gain of liver volume (Figure 1D). After all, surviving transgenic animals finally also reached complete volume restoration around at d 10 after PH, as did wild-type animals.

IL-6 levels after partial hepatectomy

IL-6 has been shown to be an essential factor during initial liver regeneration[16]. Wuestefeld *et al.*[17] specified the effect of IL-6 and demonstrated an important hepatoprotective role of IL-6 during the early phase of liver regeneration. We therefore investigated possible differences in IL-6 levels after PH. Serum IL-6 levels peaked around 24 h after PH (Figure 2A), however, did not significantly differ between wild-type and transgenic animals. Interestingly, a significantly higher IL-6 mRNA expression was detected in transgenic livers 36 h after hepatectomy (Figure 2B). This observation demonstrated a functional IL-6 deficiency to be unlikely and rather pointed to a compensatory reaction towards delayed

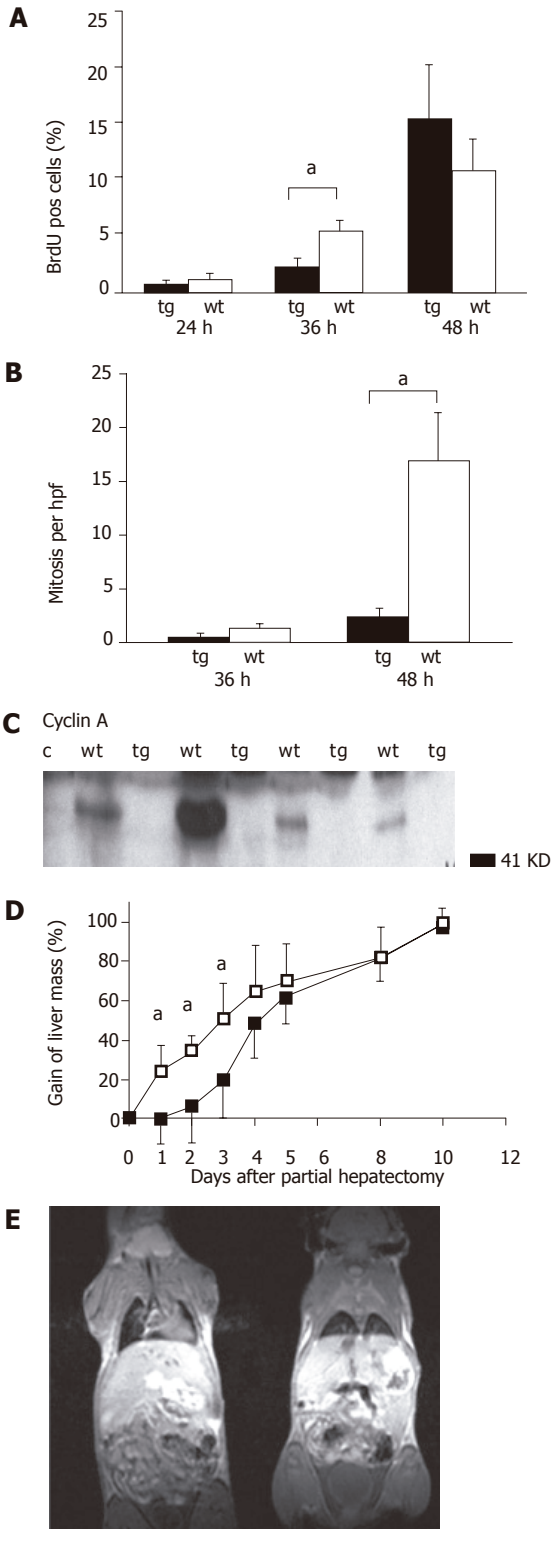

Figure 1 Retarded liver regeneration in dnFADD mice. **A:** Onset of DNA synthesis was delayed in transgenic animals; after 36 h of PH, the amount of BrdU-positive cells was significantly smaller compared to wild-type animals, while the numbers did not differ significantly later on; **B:** Showing a markedly higher number of mitosis per high power field in wild-type animals after 48 h ($^aP<0.05$); **C:** Cyclin A protein expression was not detectable in transgenic animals whereas, detectable in wild-type animals at 36 h after hepatectomy. **D:** Onset of liver mass restoration was retarded in transgenic animals ($^aP<0.05$) but surviving mice reached around 90% of the pre-operative volume as did wild-type animals. The average immediate postoperative liver volumes in the wild-type and transgenic group were 49% and 48% of the preoperative liver volume, respectively. **E:** MRI scans were used to determine liver mass during regeneration.

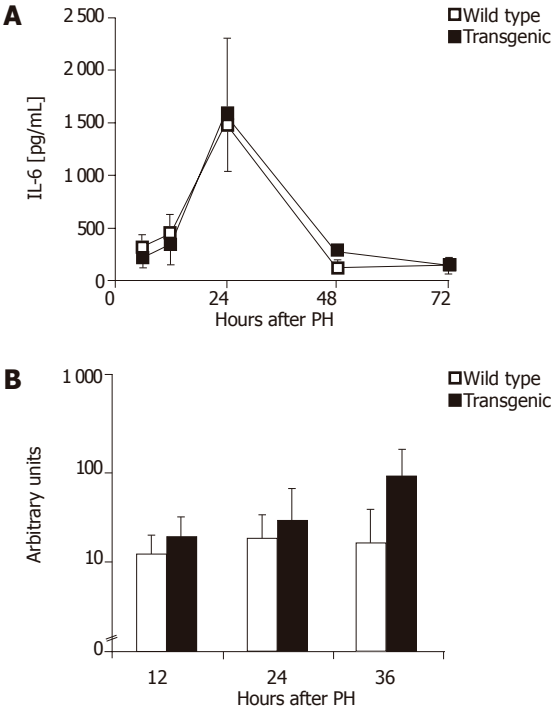

Figure 2 Expression of IL-6 in transgenic hepatocytes. **A:** Serum IL-6 levels peaked around 24 h after partial hepatectomy. There was no difference between wild-type and transgenic animals; **B:** After 36 h of PH, transgenic animals showed significant higher IL-6 mRNA expression in whole liver lysate as compared to wild-type animals, measured by Light Cycler analysis.

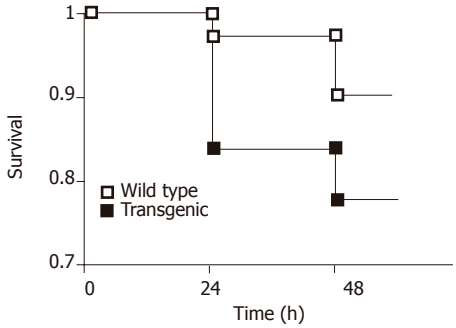

Figure 3 Differences in postoperative mortality. Within the first 24 h after PH, transgenic mice expressing the dominant negative FADD mutant showed a significant higher postoperative mortality (P<0.01). Within the first 24 h, 13 out of 81 transgenic mice died whereas only 2 out of 72 wild-type mice died. At later time points, no difference in postoperative mortality was detected.

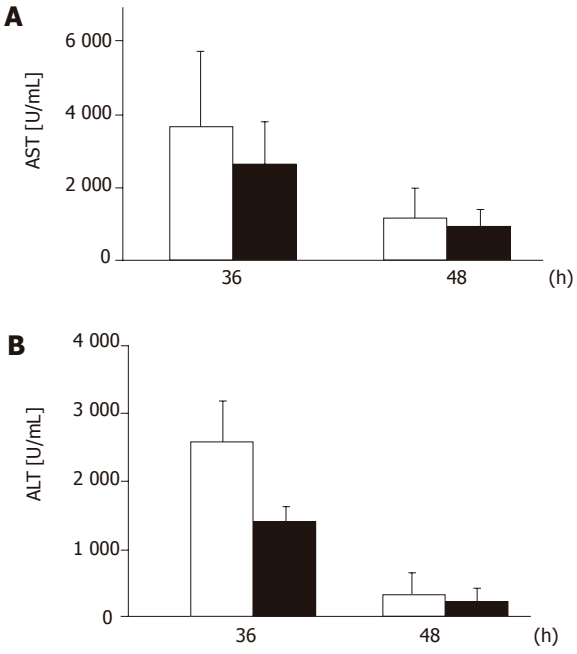

Figure 4 Liver enzymes test. Serum AST (left panel) and ALT (right) levels in wild-type and transgenic mice were not significantly different at 36 or 48 h after PH.

regeneration.

High mortality after partial hepatectomy in dnMORT1/FADD mice

Surprisingly, we observed significantly higher early postoperative mortality after resection of 70% of the liver mass among the transgenic mice expressing the dominant negative MORT1/FADD mutant (Figure 3) compared to the wild-type littermates. We found a significant difference in postoperative mortality during the first 24 h, when 16.49% (13/81) of transgenic animals whereas, only 2.77% (2/72) of wild-type mice died (P<0.01, Fisher's exact test). However, the mortality did not significantly differ later on. In order to elucidate the cause of different mortality rate, we measured liver enzymes during the early phase of regeneration. However, we did neither detect significant differences in liver function tests (Figure 4) nor differences in the degree of steatosis in liver sections at 36 or 48 h after PH (data not shown).

DISCUSSION

In the present study, we could show for the first time that MORT1/FADD acts as a multi-functional adaptor protein in the liver *in vivo*. In addition to its critical role in CD95- and CD120a-mediated liver failure[9], MORT1/FADD is involved in initiating liver regeneration upon PH. These results underline the dual role of MORT1/FADD, i.e., it was originally identified as an adaptor protein which is pivotal to convey death signals of the death receptors CD95 and CD120a[3,4] and the TRAIL receptors DR4 and DR5[18]. Initial evidence that the axis MORT1/FADD-caspase-8 has an additional role beside mediating apoptotic cell death revealed in the experiments with MORT1/FADD and caspase-8 knock out animals, showing that both genetic defects lead to embryonic lethality around d 11 *in utero* with similar pathology of cardiac malformation[5,6,19]. Interestingly, mice lacking functional flip/cash gene, a caspase-8 homolog without enzymatic activity, also died[20] *in utero* with a similarly impaired cardiac development. Later on, experiments with T-cells lacking MORT1/FADD or expressing a dominant negative mutant indicated an additional role of MORT1/FADD in

the regulation of cell proliferation[5-8,21].

The exact mechanism by which MORT1/FADD contributes to cell proliferation is still enigmatic, especially when the involved downstream molecules are not identified. Phosphorylation of MORT1/FADD at position serine 191 in mouse (corresponding to serine 194 in human beings) seems to be of crucial importance[15,22]. Current data have substantiated the idea of a bifurcation of the signal pathway at the level of MORT1/FADD by either sending a death signal via activation of caspase-8 or signaling towards cell proliferation. FLIP, which is also recruited to the receptor complex, has been reported to modulate caspase-8-mediated cell death and is a good candidate for further delivering a proliferation signal[23]. Indeed, FLIP has been shown to be involved in T-cell proliferation[23]. However, it has not been completely understood how FLIP further mediates the proliferation signal leading to the activation of ERK[23]. The molecular architecture of the intracellular bifurcation is complex, since the lack of caspase-8 does not only provide deficiency in death receptor apoptosis signaling but also confers an impaired T-cells proliferation[14]. According to data of Iimuro *et al*.[24] and Chaisson *et al*.[25], NF-κB is not involved in the orchestration of the initial DNA synthesis after PH.

A regenerating liver is protected against CD95-induced cell death[26]. This might partially be attributed to the downregulation of CD95 but resetting the function of proapoptotic molecules, such as MORT1/FADD during the initial proliferative response might also contribute. It is not obvious which receptor engages MORT1/FADD to contribute to liver regeneration. CD120a (TNF-receptor 1) and CD95 are both candidates since TNF-R1 knock-out mice[27] as well as mice with the decreased hepatic CD95 expression (*lpr*-genotype)[13] showed a pronounced delay of liver regeneration after PH. In our study, the cause of a high postoperative mortality in transgenic mice remains unclear. We could not find signs of liver dysfunction in the early postoperative phase and there was also presence of IL-6 expression. We even detected higher intrahepatic IL-6 mRNA levels in the transgenic mice. A previous study also reported no difference between wild-type and transgenic animals upon LPS or CpG-DNA challenge[28].

In conclusion, we provide further evidence for a complex role of the adaptor molecule MORT1/FADD which is also involved in death and proliferation pathways in hepatocytes. This observation should be taken into consideration while targeting anti-apoptotic as well as anti-proliferative therapies.

ACKNOWLEDGMENTS

The authors thank Sonja Bamberger, Sonja Klein and Nicole Voltz for expert technical assistance, Dr. Kurt Reifenberg for support in the animal facility and Regine Weisbrod M.A. for critically reading the manuscript. The data presented are part of the MD thesis of F.R.

REFERENCES

1 **Galle PR,** Hofmann WJ, Walczak H, Schaller H, Otto G, Stremmel W, Krammer PH, Runkel L. Involvement of the CD95 (APO-1/Fas) receptor and ligand in liver damage. *J Exp Med* 1995; **182:** 1223-1230

2 **Streetz K,** Leifeld L, Grundmann D, Ramakers J, Eckert K, Spengler U, Brenner D, Manns M, Trautwein C. Tumor necrosis factor alpha in the pathogenesis of human and murine fulminant hepatic failure. *Gastroenterology* 2000; **119:** 446-460

3 **Boldin MP**, Varfolomeev EE, Pancer Z, Mett IL, Camonis JH, Wallach D. A novel protein that interacts with the death domain of Fas/APO1 contains a sequence motif related to the death domain. *J Biol Chem* 1995; **270:** 7795-7798

4 **Chinnaiyan AM,** O'Rourke K, Tewari M, Dixit VM. FADD, a novel death domain-containing protein, interacts with the death domain of Fas and initiates apoptosis. *Cell* 1995; **81:** 505-512

5 **Zhang J,** Cado D, Chen A, Kabra NH, Winoto A. Fas-mediated apoptosis and activation-induced T-cell proliferation are defective in mice lacking FADD/Mort1. *Nature* 1998; **392:** 296-300

6 **Yeh WC,** Pompa JL, McCurrach ME, Shu HB, Elia AJ, Shahinian A, Ng M, Wakeham A, Khoo W, Mitchell K, El-Deiry WS, Lowe SW, Goeddel DV, Mak TW. FADD: essential for embryo development and signaling from some, but not all, inducers of apoptosis. *Science* 1998; **279:** 1954-1958

7 **Newton K,** Harris AW, Bath ML, Smith KGC, and Strasser A. A dominant interfering mutant of FADD/MORT1 enhances deletion of autoreactive thymocytes and inhibits proliferation of mature T lymphocytes. *EMBO-J* 1998; **17:** 706-718

8 **Walsh CM,** Wen BG, Chinnaiyan AM, O'Rourke K, Dixit VM, Hedrick SM. A role for FADD in T cell activation and development. *Immunity* 1998; **8:** 439-449

9 **Schuchmann M,** Varfolomeev EE, Hermann F, Rueckert F, Strand D, Koehler H, Strand S, Lohse AW, Wallach D, Galle PR. Dominant negative MORT1/FADD rescues mice from CD95 and TNF-induced liver failure. *Hepatology* 2003; **37:** 129-135

10 **Chen G,** Goeddel DV. TNF-R1 signaling: a beautiful pathway. *Science* 2002; **296:** 1634-1635

11 **Yamada Y,** Kirillova I, Peschon JJ, Fausto N. Initiation of liver growth by tumor necrosis factor: deficient liver regeneration in mice lacking type I tumor necrosis factor receptor. *Proc Natl Acad Sci USA* 1997; **94:** 1441-1446

12 **Wajant H.** The Fas signaling pathway: more than a paradigm. *Science* 2002; **296:** 1635-1636

13 **Desbarats J,** Newell MK. Fas engagement accelerates liver regeneration after partial hepatectomy. *Nat Med* 2000; **6:** 920-923

14 **Salmena L,** Lemmers B, Hakem A, Matysiak-Zablocki E, Murakami K, Au PY, Berry DM, Tamblyn L, Shehabeldin A, Migon E, Wakeham A, Bouchard D, Yeh WC, McGlade JC, Ohashi PS, Hakem R. Essential role for caspase 8 in T-cell homeostasis and T-cell-mediated immunity. *Genes Dev* 2003; **17:** 883-895

15 **Hua ZC,** Sohn SJ, Kang C, Cado D, Winoto A. A function of Fas-associated death domain protein in cell cycle progression localized to a single amino acid at its C-terminal region. *Immunity* 2003; **18:** 513-521

16 **Cressman DE,** Greenbaum LE, DeAngelis RA, Ciliberto G, Furth EE, Poli V, Taub R. Liver failure and defective hepatocyte regeneration in interleukin-6-deficient mice. *Science* 1996; **274:** 1379-1383

17 **Wuestefeld T,** Klein C, Streetz KL, Betz U, Lauber J, Buer J, Manns MP, Muller W, Trautwein C. Interleukin-6/glycoprotein 130-dependent pathways are protective during liver regeneration. *J Biol Chem* 2003; **278:** 11281-1128

18 **Kuang AA,** Diehl GE, Zhang J, Winoto A. FADD is required for DR4- and DR5-mediated apoptosis: lack of trail-induced

apoptosis in FADD-deficient mouse embryonic fibroblasts. *J Biol Chem* 2000; **275:** 25065-25068

19 **Varfolomeev EE,** Schuchmann M, Luria V, Chiannilkulchai N, Beckmann JS, Mett IL, Rebrikov D, Brodianski VM, Kemper OC, Kollet O, Lapidot T, Soffer D, Sobe T, Avraham KB, Goncharov T, Holtmann H, Lonai P, Wallach D. Targeted disruption of the mouse Caspase 8 gene ablates cell death induction by the TNF receptors, Fas/Apo1, and DR3 and is lethal prenatally. *Immunity* 1998; **9:** 267-276

20 **Yeh WC,** Itie A, Elia AJ, Ng M, Shu HB, Wakeham A, Mirtsos C, Suzuki N, Bonnard M, Goeddel DV, Mak TW. Requirement for Casper (c-FLIP) in regulation of death receptor-induced apoptosis and embryonic development. *Immunity* 2000; **12:** 633-642

21 **Zornig M,** Hueber AO, Evan G. p53-dependent impairment of T-cell proliferation in FADD dominant-negative transgenic mice. *Curr Biol* 1998; **8:** 467-470

22 **Alappat EC,** Volkland J, Peter ME. Cell cycle effects by C-FADD depend on its C-terminal phosphorylation site. *J Biol Chem* 2003; **278:** 41585-41588

23 **Kataoka T,** Budd RC, Holler N, Thome M, Martinon F, Irmler M, Burns K, Hahne M, Kennedy N, Kovacsovics M, Tschopp J. The caspase-8 inhibitor FLIP promotes activation of NF-kappaB and Erk signaling pathways. *Curr Biol* 2000; **10:** 640-648

24 **Iimuro Y,** Nishiura T, Hellerbrand C, Behrns KE, Schoonhoven R, Grisham JW, Brenner DA. NFkappaB prevents apoptosis and liver dysfunction during liver regeneration. *J Clin Invest* 1998; **101:** 802-811

25 **Chaisson ML,** Brooling JT, Ladiges W, Tsai S, Fausto N. Hepatocyte-specific inhibition of NF-kappaB leads to apoptosis after TNF treatment, but not after partial hepatectomy. *J Clin Invest* 2002; **110:** 193-202

26 **Takehara T,** Hayashi N, Mita E, Kanto T, Tatsumi T, Sasaki Y, Kasahara A, Hori M. Delayed Fas-mediated hepatocyte apoptosis during liver regeneration in mice: hepatoprotective role of TNF alpha. *Hepatology* 1998; **27:** 1643-1651

27 **Yamada Y,** Kirillova I, Peschon JJ, Fausto N. Initiation of liver growth by tumor necrosis factor: deficient liver regeneration in mice lacking type I tumor necrosis factor receptor. *Proc Natl Acad Sci U S A* 1997; **94:** 1441-1446

28 **Schuchmann M,** Hermann F, Herkel J, van der Zee R, Galle PR, Lohse AW. HSP60 and CpG-DNA-oligonucleotides differentially regulate LPS-tolerance of hepatic Kupffer cells. *Immunol Lett* 2004; **93:** 199-204

Science Editor Guo SY **Language Editor** Elsevier HK

PO Box 2345, Beijing 100023, China
www.wjgnet.com
wjg@wjgnet.com

ELSEVIER

World J Gastroenterol 2005;11(46):7254-7260
World Journal of Gastroenterology ISSN 1007-9327

• *BASIC RESEARCH* •

Vascular endothelial growth factor and angiopoietins regulate sinusoidal regeneration and remodeling after partial hepatectomy in rats

Hiroaki Shimizu, Noboru Mitsuhashi, Masayuki Ohtsuka, Hiroshi Ito, Fumio Kimura, Satoshi Ambiru, Akira Togawa, Hiroyuki Yoshidome, Atsushi Kato, Masaru Miyazaki

Hiroaki Shimizu, Noboru Mitsuhashi, Masayuki Ohtsuka, Hiroshi Ito, Fumio Kimura, Satoshi Ambiru, Akira Togawa, Hiroyuki Yoshidome, Atsushi Kato, Masaru Miyazaki, Department of General Surgery, Graduate School of Medicine, Chiba University, Chiba 260-0856, Japan
Correspondence to: Hiroaki Shimizu, Department of General Surgery, Graduate School of Medicine, Chiba University, 1-8-1 Inohana, Chuo-ku, Chiba 260-0856, Japan. h-shimizu@umin.ac.jp
Telephone: +81-43-2262103 Fax: +81-43-226-269
Received: 2005-03-11 Accepted: 2005-06-09

Abstract

AIM: To study the regulatory mechanisms of sinusoidal regeneration after partial hepatectomy.

METHODS: We investigated the expression of angiopoietin (Ang)-1, Ang-2, Tie-2, and vascular endothelial growth factor (VEGF) in regenerating liver tissue by quantitative reverse-transcription polymerase chain reaction (RT-PCR) using a LightCycler (Roche Diagnostics) and also immunohistochemical staining after 70% hepatectomy in rats. In the next step, we isolated liver cells (hepatocytes, sinusoidal endothelial cell (SEC), Kupffer cell, and hepatic stellate cells (HSC)) from regenerating liver tissue by *in situ* collagenase perfusion and counterflow elutriation, to determine potential cellular sources of these angiogenic factors after hepatectomy. Proliferation and apoptosis of SECs were also evaluated by proliferating cell nuclear antigen (PCNA) staining and the terminal deoxynucleotidyl transferase d-uridine triphosphate nick end labeling (TUNEL) assay, respectively.

RESULTS: VEGF mRNA expression increased with a peak at 72 h after hepatectomy, decreasing thereafter. The expression of Ang-1 mRNA was present at detectable levels before hepatectomy and increased slowly with a peak at 96 h. Meanwhile, Ang-2 mRNA was hardly detected before hepatectomy, but was remarkably induced at 120 and 144 h. In isolated cells, VEGF mRNA expression was found mainly in the hepatocyte fraction. Meanwhile, mRNA for Ang-1 and Ang-2 was found in the SEC and HSC fractions, but was more prominent in the latter. The PCNA labeling index of SECs increased slowly, reaching a peak at 72 h, whereas apoptotic SECs were detected between 120 h and 144 h.

CONCLUSION: Ang-Tie system, together with VEGF, plays a critical role in regulating balance between SEC proliferation and apoptosis during sinusoidal regeneration after hepatectomy. However, the VEGF system plays a more important role in the early phase of sinusoidal regeneration than angiopoietin/Tie system.

Key words: Vascular endothelial cell growth factor; Angiopoietin; Sinusoidal endothelial cell; Hepatectomy; Liver regeneration

Shimizu H, Mitsuhashi N, Ohtsuka M, Ito H, Kimura F, Ambiru S, Togawa A, Yoshidome H, Kato A, Miyazaki M. Vascular endothelial growth factor and angiopoietins regulate sinusoidal regeneration and remodeling after partial hepatectomy in rats. *World J Gastroenterol* 2005; 11(46):7254-7260
http://www.wjgnet.com/1007-9327/11/7254.asp

INTRODUCTION

The regenerative capacity of the liver is typically triggered by hepatic injuries, including partial hepatectomy or hepatocyte loss caused by viral or chemical injury[1-3]. Liver regeneration is a highly complex and organized process, but extensive studies have revealed that a number of cytokines and growth factors are involved in the regulation of hepatocyte proliferation[4-6]. Nonparenchymal cells (Kupffer cells, sinusoidal endothelial cells (SECs)) have both stimulatory and inhibitory influences on hepatocyte replication though a paracrine manner after hepatectomy[7]. As a consequence of hepatocyte proliferation, remodeling of the sinusoids has to be carried out for the supply of blood flow to the newly replicating hepatocytes in the process of liver regeneration, most probably with penetration of SECs into hepatocyte clusters. Presumably, SECs proliferate and assemble into tubes with cell-cell connections, followed by recruitment of hepatic stellate cells (HSCs) and Kupffer cells, to restore normal sinusoidal architecture. Lindahl *et al*.[8] reported that during vascular development and remodeling, endothelial cells initially proliferate, and recruit mural cell (pericytes or smooth muscle cells) precursors via secretion of platelet-derived growth factor-BB, and endothelial cell-mural cell contact is essential for vessel stabilization[9]. On the other hand, Martinez-Hernandez *et al*.[10] suggested that during liver regeneration, the laminin-containing Ito cells initially extend cell processes into the

hepatocyte clusters, followed by SECs, to form new sinusoids after hepatectomy, but at present the precise steps involved in sinusoidal regeneration remain poorly understood. However, recent studies including ours showed that vascular endothelial growth factor (VEGF) greatly contributes to the proliferation of SECs via up-regulated VEGF receptors during liver regeneration[11-15]. Moreover, we have clearly shown that newly replicated hepatocytes that are devoid of sinusoids are the major source of VEGF after hepatectomy[13]. However, the detail mechanisms of sinusoidal regeneration and remodeling are still open to discussion.

Recently, the angiopoietin (Ang)-Tie system has been identified as a second family of endothelial cell-specific growth factors[16-18], and has been reported to act in a complementary and coordinated fashion with VEGF, thus playing an important role in vascular maturation and remodeling[17,18]. The modulatory effect of angiopoietins on VEGF-induced angiogenesis is distinct[19-21], although angiopoietins alone are not mitogenic for endothelial cells *in vitro*[18], and do not promote neovascularization *in vivo*[19]. Angiopoietins include both receptor activators (Ang-1) and receptor antagonists (Ang-2)[18]. Binding of Ang-1 causes auto-phosphorylation of tyrosine kinase Tie-2 receptor, whereas Ang-2 binding conversely suppresses auto-phosphorylation of Tie-2. The Tie-2 signal is, therefore, defined by quantitative balance between Ang-1 and Ang-2 activities[19,20]. The Ang-1/Tie-2 pathway in the presence of VEGF is thought to mediate the vital functions of vascular stabilization and vascular maturation, via integration of peri-endothelial cells into the vascular wall. In contrast to Ang-1, Ang-2 induces vascular regression in the absence of VEGF but increases vascular sprouting in its presence[19-21]. Accordingly, it seems to be reasonable to assume that the Ang-Tie system and the VEGF system, participate in the process of sinusoidal regeneration and remodeling after partial hepatectomy.

In this study, we investigated the expression of Ang-1, Ang-2, Tie-2, and VEGF in regenerating liver tissue by quantitative reverse-transcription polymerase chain reaction (RT-PCR) using a LightCycler (Roche Diagnostics, Mannheim, Germany) and immunohistochemical staining after 70% hepatectomy in rats. In the next step, we isolated liver cells (hepatocyte, SEC, Kupffer cell, and HSC) from regenerating liver tissue by *in situ* collagenase perfusion and counterflow elutriation, to determine potential cellular sources of these angiogenic factors after hepatectomy. Proliferation and apoptosis of SECs were also evaluated by proliferating cell nuclear antigen (PCNA) staining and the terminal deoxynucleotidyl transferase d-uridine triphoshate nick end labeling (TUNEL) assay, respectively, to determine the putative role of VEGF and angiopoietins, especially their complementary and coordinated effects during sinusoidal regeneration after hepatectomy.

MATERIALS AND METHODS

Animals

Male Wistar rats, weighing 250 to 300 g, were used with the approval of the Chiba Animal Care Committee. The animals were housed in a temperature- and humidity-controlled environment with a 12-h light dark cycle. The study followed our institution's criteria for care and use of laboratory animals in research, which conform to the National Institutes of Health guidelines. Under ether anesthesia, 70% of the liver was resected as previously described[22]. The operative procedure was carried out by means of a clean, but not sterile technique. For the assessment of the Ang-1, Ang-2, Tie-2, and VEGF expressions, the right inferior lobe of the liver was carefully excised before and 12, 24, 48, 72, 96, 120, 144, and 240 h (n = 6 at each time point) after hepatectomy.

Table 1 Primer sequences

Gene		Primer sequence	T (℃)
VEGF	Sense	GCA CTG GAC CCT GGC TTT AC	56
	Antisense	CTG CAG GAA GCT CAT CTC TC	
Ang-1	Sense	GTG GCT GGA AAA ACT TGA GA	52
	Antisense	TGG ATT TCA AGA CGG GAT GT	
Ang-2	Sense	GAC CAG TGG GCA TCG CTA CG	56
	Antisense	CTG GTT GGC TGA TGC TAC TG	
Tie-2	Sense	TGC CAC CAT CAC TCA ATA CC	54
	Antisense	AAA CGC CAA TAG CAC GGT GA	
GAPDH	Sense	GGC ATG GAC TGT GGT CAT GAG	56
	Antisense	TGC ACC ACC AAC TGC TTA GC	

T : annealing temperature.

Quantitative RT-PCR analysis of VEGF, angiopoietins, and Tie-2 mRNA expressions

Total RNA was extracted from liver tissues or freshly isolated liver cells by the acid guanidium-thiocyanate/phenol/chloroform method, and 1 mg of extracted total RNA was subjected to a reverse transcription reaction, using Ready To Go™ T-primed 1st strand cDNA synthesis kit (Amersham Pharmacia Biotech, Buckinghamshire, England). The cDNA from 33 ng of total RNA was used as a template. VEGF, Ang-1, Ang-2, and Tie-2 mRNA levels were quantified by a LightCycler (Roche Diagnostics, Mannheim, Germany), using the double-strand-specific dye SYBE Green I. Details of the primers used in this study are summarized in Table 1. The PCR conditions were as follows: initial denaturation at 95 ℃ for 10 min, followed by 45 cycles of denaturation at 95 ℃ for 15 s, annealing for 10 s, and extension at 72 ℃ for 20 s. The expression level of each angiogenic factor was adjusted by the level of glyceraldehydes-3-phosphate dehydrogenase (GAPDH) mRNA, and expressed as a ratio to GAPDH mRNA. To confirm the specific amplification from the target mRNAs, some of the PCR products of each primer set were directly sequenced.

Liver cell isolation from regenerating liver tissue

In the next step, liver cells were isolated from the regenerating liver tissue at the peak periods of each angiogenic factor expression (at 48 and 72 h for VEGF, at 72 and 96 h for Ang-1, at 120 and 144 h for Ang-2, and at 72 and 96 h for Tie-2) after hepatectomy, to determine potential cellular sources of VEGF, Ang-1, Ang-2, and

Tie-2 mRNA. Rat hepatocytes were isolated according to the methods of Gumucio *et al*.[23] Briefly, the rat liver was portally perfused first with Mg^{2+}/Ca^{2+}-free Hanks' buffer at 37 ℃, and then with Eagle's minimal essential medium (EMEM) containing 0.05% collagenase (Type I, Sigma, St Louis, MO, USA). The liver was excised and placed in a petri dish containing fresh EMEM with 0.05% collagenase. Glisson's capsule was stripped, and cells were released by gentle manipulation. The resulting crude preparation was filtered though 250-mm and 100-μm nylon meshes. Hepatocytes were then separated by differential centrifugation. Cell viability and purity were >95%. The SECs, Kupffer cells, HSCs were also isolated by *in situ* collagenase perfusion and counterflow elutriation, as described by Knook *et al*.[24] with minor modifications. A JE-5.0 elutriator rotor (Beckman Instruments, Palo Alto, CA, USA) was used in a J6-MI Beckman centrifuge. The separation process was started by adding the nonparenchymal cell suspension to a sample-mixing chamber. The HSCs were eluted at a flow rate of 16 to 18 mL/min, and at a speed of 3 200 r/min. The SECs were then eluted at a flow rate of 23 to 26 mL/min, and Kupffer cells at a flow rate of 36 to 39 mL/min, and at a speed of 2 500 r/min. The purity of HSCs was >92%, as assessed 24 h after seeding by their typical light-microscopic appearance and their positive immunofluorescent staining for desmin[25]. The purity of SECs and Kupffer cells was >95%, >90%, respectively, as assessed 24 h after seeding by diacetyl-low-density lipoprotein incorporation[26], and positive immunofluorescent staining for ED-1[27]. To evaluate the expression of Ang-1, Ang-2, Tie-2, and VEGF mRNA in each cell fraction, freshly isolated cells were used for total RNA extraction.

Immunohistochemical examination of Ang-1, Ang-2 and Tie-2

For immunohistochemical examination of Ang-1, Ang-2, and Tie-2, the liver tissues excised after hepatectomy were fixed overnight in 2% paraformaldehyde solution at 4 ℃, embedded in tissue-tek compound (Miles Laboratories, Elkhart, IN, USA), and frozen in liquid nitrogen for preparation of cryostat sections. Sections (6 μm) were stained with Ang-1, Ang-2, and Tie-2 antibodies (dilution: 1:100, respectively, Santa Cruz Biotechnology Inc. Delaware, CA, USA) and incubated overnight at 4 ℃. Immunostained cells were detected out using LSAB kit (Dako, Copenhagen, Denmark) according to the manufacturer' s instructions. All sections were then lightly counterstained with 0.1% hematoxylin.

PCNA labeling index

Immunohistochemical staining for PCNA was performed on formalin-fixed and paraffin-embedded liver tissue with anti-PCNA antibody as previously described[28, 29]. The three-step immunoperoxidase method using streptavidin biotin complex (Dako, Copenhagen, Denmark) was performed, according to the procedure described by Hall *et al*.[29]. PC-10 monoclonal antibody (Dako, Copenhagen, Denmark) was used at a dilution of 1:100 and incubated overnight at 4 ℃. PC-10 immunostaining was evaluated based on the percentage of positive nuclei of 100 SECs at high power (400x), and expressed as a PCNA labeling index. In this study, the spindle-shaped sinusoid-lining cells in the open sinusoids at high power (400x) were regarded as SECs[30].

TUNEL assay

Regenerating liver tissue was evaluated using the TUNEL assay to identify SECs undergoing apoptosis. Portions of the liver were fixed with 4% paraformaldehyde and embedded in paraffin. Six micrometer thick sections were prepared, and stained by the TUNEL method using an *in situ* apoptosis detection kit (Takara Biomedicals Co., Osaka, Japan) according to the manufacturer' s instructions. Each stained section was examined at high power fields (200 x), and TUNNEL-positive cells in sinusoids were evaluated.

Statistical analysis

The results were expressed as mean±SD. Statistical analysis was made by the Mann-Whitney test for unpaired data. $P<0.05$ was considered significant.

RESULTS

Changes expression of VEGF, angiopoietin, and Tie-2 mRNA in regenerating liver tissue

The expression of VEGF mRNA was at very low levels before hepatectomy. However, VEGF mRNA in the regenerating liver tissue started to increase 24 h after hepatectomy, with a peak at 72 h. A significant increase was found at 48 and 72 h when compared to the prehepatectomy value ($P<0.05$, respectively). Thereafter, VEGF mRNA returned to baseline levels at 120 h (Figure 1A). The changes in Ang-1, Ang-2, and Tie-2 mRNA expressions are shown in Figure 1B. Ang-1 mRNA was present at detectable levels even before hepatectomy, and increased after 48 h of hepatectomy, with a peak at 96 h. A significant increase was seen at 72 and 96 h ($P<0.05$ *vs* 0 h, respectively). Meanwhile, Ang-2 mRNA was hardly detectable before hepatectomy, but was significantly up-regulated at 120 and 144 h ($P<0.03$ *vs* 0 h, respectively). The expression of Tie-2 mRNA was low before hepatectomy, but tended to increase between 72 h and 120 h after hepatectomy.

VEGF, angiopoietin, and Tie-2 mRNA in specific cell populations isolated from regenerating liver tissue

To determine the cellular sources of VEGF, Ang-1, Ang-2, and Tie-2 mRNA in the regenerating liver tissue, four types of liver cells were isolated at key time points: at 48 and 72 h for VEGF, at 72 and 96 h for Ang-1, at 120 and 144 h for Ang-2, at 72 and 96 h for Tie-2, because the expression of each was strongly induced at the indicated time points after hepatectomy (Figure 1). The results are shown in Figure 2. In cell isolates, the mRNA for VEGF was found mainly in the hepatocyte fraction, but in other

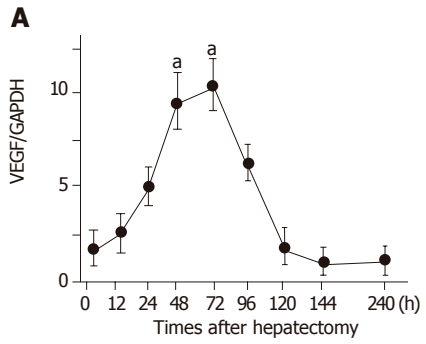

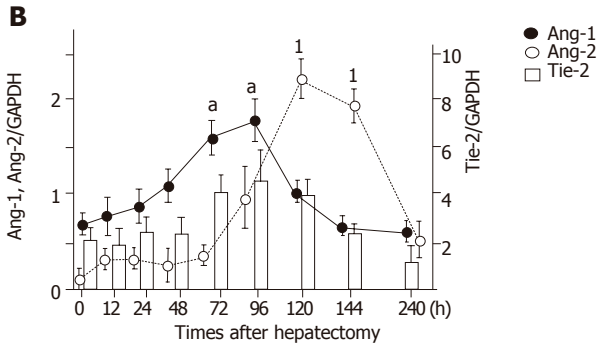

Figure 1 Changes in vascular endothelial growth factor (VEGF), angiopoietin (Ang) and Tie-2 mRNA expressions after 70% hepatectomy. **A:** Quantification of VEGF mRNA levels after hepatectomy by RT-PCR using a LightCycler (Roche Diagnostics). [a]*P*<0.05 *vs* 0 h; **B:** quantification of Ang-1 (closed circle), Ang-2 (open circle), and Tie-2 (open bar) mRNA levels after hepatectomy by RT-PCR using a LightCycler. [a]*P*<0.05 *vs* 0 h, [1]*P*<0.03 *vs* 0 h, respectively.

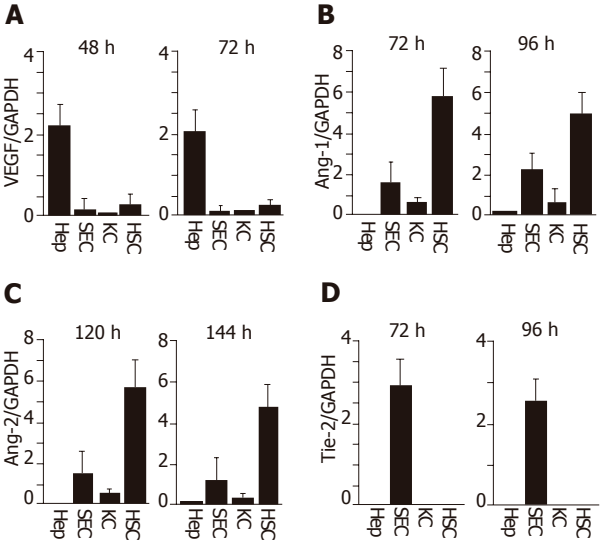

Figure 2 Expressions of VEGF (**A**), Ang-1 (**B**), Ang-2 (**C**) and Tie-2 mRNA (**D**) in isolated liver cells at different time points.

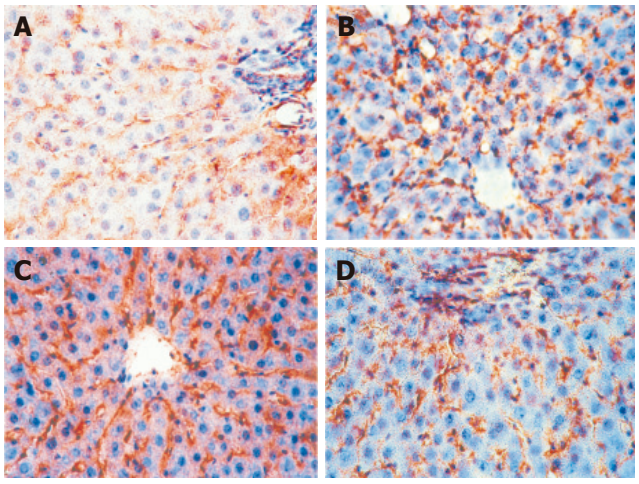

Figure 3 Immunohistochemical staining for angiopoietins (Ang) and Tie-2 protein. Ang-1 protein before hepatectomy (**A**), 96 h after hepatectomy (**B**), Ang-2 protein induction 120 h after hepatectomy (**C**), Tie-2 protein before hepatectomy (**D**) (original magnification x 200).

cell fractions, VEGF mRNA was hardly expressed. On the other hand, the mRNA for Ang-1 and Ang-2 was found mainly in the SEC and HSC fractions, but Ang-2 mRNA expression was more prominent in the latter. The mRNA for Tie-2 was found to be in the SEC fraction alone.

Immunohistochemical staining for angiopoietins and Tie-2

Ang-1 protein was detectable along sinusoids even before hepatectomy (Figure 3A), and was upregulated at 96 h after hepatectomy (Figure 3B). Meanwhile, Ang-2 protein was not detected before hepatectomy, but was remarkably up-regulated along sinusoids at 120 h after hepatectomy (Figure 3C). The Tie-2 protein was observed along sinusoids even before hepatectomy (Figure 3D).

PCNA labeling index and TUNEL staining

The PCNA labeling index was less than 5% in SECs before hepatectomy. However, a slow increase in the PCNA labeling index of SECs was observed after 24 h

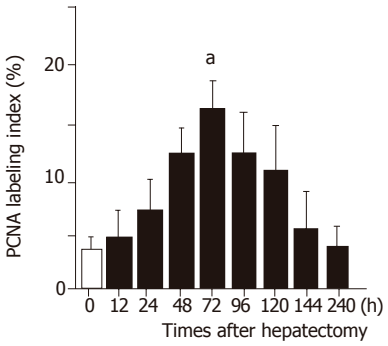

Figure 4 PCNA labeling index of sinusoidal endothelial cells (SECs) after 70 % hepatectomy in rats. [a]*P*<0.05 *vs* 0 h.

of hepatectomy, reaching a peak of 16 % at 72 h ($P< 0.05$ *vs* 0 h) after hepatectomy (Figure 4). Figure 5 shows TUNEL staining of the regenerating liver at 120 h after hepatectomy. Before hepatectomy, apoptotic cells in

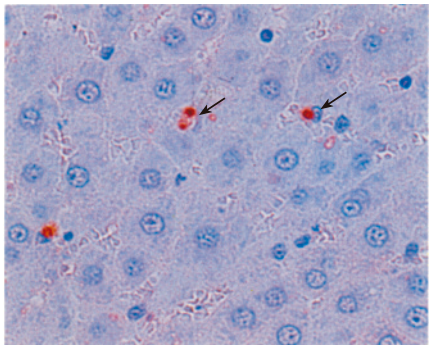

Figure 5 TUNEL staining of regenerating liver tissue at 120 h after hepatectomy. Arrows indicate TUNEL stained-positive sinusoidal cells.

sinusoids were uncommon in the liver, and even fewer such cells were detected within 72 h of hepatectomy. However, a few sinusoidal cells were found to be TUNEL stain-positive between 120 h and 144 h after hepatectomy.

DISCUSSION

In the present study, we showed that VEGF expression in the remnant liver started to increase 24 h after hepatectomy, with a peak at 72 h, which coincided with SEC proliferation, as assessed by PCNA staining. Moreover, in cell isolates from the regenerating liver tissue, VEGF mRNA expression was found mainly in the hepatocyte fraction, suggesting that VEGF secreted from hepatocytes may greatly contribute to SEC proliferation in a paracrine manner. Thereafter, Ang-1 and Ang-2 mRNA expression in the remnant liver increased, but the Ang-2 peak was much later than the Ang-1 peak. In isolated cells, both Ang-1 mRNA and Ang-2 mRNA were found to be abundant in nonparenchymal cells, especially in HSCs. Furthermore, apoptosis of SECs was only detected at 120 and 144 h after hepatectomy, which overlapped with elevated levels of Ang-2. Viewed from the standpoint of Ang-1 function as previously reported in angiogenesis, increased expression of Ang-1 might be related with maturation of sinusoids, presumably characterized by cell-cell contact between SECs and surrounding cells. Meanwhile, elevated Ang-2 in the absence of VEGF induction might be associated with the apoptotic changes in superfluous SECs for cessation of the regenerative process. On the other hand, their receptor, Tie-2 was constitutively expressed on SECs, and tended to increase in the later phase of regeneration, synchronized with up-regulation of Ang-1 and Ang-2. Altogether, these results strongly suggest that angiopoietins released from nonparenchymal cells may largely contribute to the later phase of sinusoidal regeneration and remodeling via Tie-2 receptor after hepatectomy.

In the present study, Ang-1 was constitutively expressed in the liver at the mRNA level and also at the protein level, but VEGF mRNA and Ang-2 mRNA were hardly detectable before hepatectomy. These results might be associated with the maintenance of stability and the maturation of existing sinusoids in the steady state of the liver. Meanwhile, Ang-2 mRNA expression was largely induced in the late phase of regeneration after hepatectomy. Furthermore, apoptotic SECs were detected between 120 h and 144 h, suggesting that SEC apoptosis might be associated with elevated levels of Ang-2 in the absence of VEGF induction. Since apoptosis is known to be a strategic biologic process of eliminating unnecessary cells under certain physiological conditions[31], the SEC apoptosis observed in this study might be related to the presence of superfluous SECs in the late phase of regeneration. Greene *et al.*[32] recently demonstrated that SECs play an important role in the regulation of regenerating hepatic mass by means of proliferation and apoptosis. Therefore, apoptosis of SECs in the late phase of regeneration in this study might be associated with cessation of the regenerative process of the liver.

In cell isolates from the regenerating liver tissue, Ang-2-produced cells were found to be nonparenchymal cells, mainly HSCs. HSCs are known to be located in the space of Disse, below the sinusoidal endothelial cell lining, in close to and partially intercalated between hepatocytes, with their long processes extending along sinusoids [33]. Under physiological conditions, HSCs embrace the sinusoids as "liver-specific pericytes"[34]. At present, the factors that initiate HSC activation are not yet fully understood, although platelet-derived growth factor and transforming growth factor-b (TGF-b) may play a key role in HSC activation and proliferation[35]. On the other hand, TGF-b, a potent inhibitor of hepatocyte proliferation has been reported to increase significantly in the later phase of regeneration, and is known to be mainly released from sinusoidal cells after 70% hepatectomy in rats[36-38]. That is, it would be reasonable to expect activation and proliferation of HSCs in a late phase of regeneration, and subsequent release of several growth factors, including angiopoietins, as well as induction of extracellular matrix, after hepatectomy.

In this study, we focused on the role of angiopoietins and VEGF, especially their complementary and coordinated role in the process of sinusoidal regeneration after hepatectomy, and clearly demonstrated that the Ang-Tie system, together with VEGF, played a critical role in regulating the balance between SEC proliferation and apoptosis during sinusoidal regeneration and remodeling after partial hepatectomy. Accordingly, it is clear that production of VEGF and angiopoietins in the liver must be coordinated both quantitatively and temporally to ensure appropriate sinusoidal regeneration after hepatectomy. However, the VEGF system plays a more important role in the early phase of sinusoidal regeneration than the angiopoietin/Tie system. In addition, close communications between different types of liver cells are clearly important in proceeding through these complex steps of regeneration. However, more detail studies are required to elucidate the regulatory mechanisms of sinusoidal regeneration and remodeling, which are only understood at a descriptive level at present, and

also to provide clues for treatment of impaired hepatic regeneration after major hepatectomy, from this point of view.

REFERENCES

1 **Bucher NLR.** Regeneration of mammalian liver. *Int Rev Cytol* 1963; **15:** 245-300
2 **Bucher NLR,** McGowan JA, Wright R, Alberti K, Karran S, Millward-Sadler H. Liver and biliary disease: A pathophysiological approach. London: WB Saunders Co., 1984
3 **Nagasue N,** Yukaya H, Ogawa Y, Kohno H, Nakamura T. Human liver regeneration after major hepatic resection. A study of normal liver and livers with chronic hepatitis and cirrhosis. *Ann Surg* 1987; **206:** 30-39
4 **Leffert HL,** Koch KS, Lad PJ, Shapiro IP, Skelly H, deHemptinne B. Hepatocyte regeneration, replication and differentiation. In: Arias IM, Jacoby WB, Popper H, ed. The liver: Biology and Pathobiology. New York: *Raven Press* 1988: 833-850
5 **Bucher NL.** Liver regeneration: an overview. *J Gastroenterol Hepatol* 1991; **6:** 615-624
6 **Fausto N,** Laird AD, Webber EM. Liver regeneration. 2. Role of growth factors and cytokines in hepatic regeneration. *FASEB J* 1995; **9:** 1527-1536
7 **Fausto N.** Growth factors in liver development, regeneration and carcinogenesis. *Prog Growth Factor Res* 1991; **3:** 219-234
8 **Lindahl P,** Johansson BR, Leveen P, Betsholtz C. Pericyte loss and microaneurysm formation in PDGF-B-deficient mice. *Science* 1997; **277:** 242-245
9 **Hirschi KK,** Rohovsky SA, Beck LH, Smith SR, D'Amore PA. Endothelial cells modulate the proliferation of mural cell precursors via platelet-derived growth factor-BB and heterotypic cell contact. *Circ Res* 1999; **84:** 298-305
10 **Martinez-Hernandez A,** Amenta PS. The extracellular matrix in hepatic regeneration. *FASEB J* 1995; **9:** 1401-1410
11 **Mochida S,** Ishikawa K, Inao M, Shibuya M, Fujiwara K. Increased expressions of vascular endothelial growth factor and its receptors, flt-1 and KDR/flk-1, in regenerating rat liver. *Biochem Biophys Res Commun* 1996; **226:** 176-179
12 **Assy N,** Spira G, Paizi M, Shenkar L, Kraizer Y, Cohen T, Neufeld G, Dabbah B, Enat R, Baruch Y. Effect of vascular endothelial growth factor on hepatic regenerative activity following partial hepatectomy in rats. *J Hepatol* 1999; **30:** 911-915
13 **Shimizu H,** Miyazaki M, Wakabayashi Y, Mitsuhashi N, Kato A, Ito H, Nakagawa K, Yoshidome H, Kataoka M, Nakajima N. Vascular endothelial growth factor secreted by replicating hepatocytes induces sinusoidal endothelial cell proliferation during regeneration after partial hepatectomy in rats. *J Hepatol* 2001; **34:** 683-689
14 **Sato T,** El-Assal ON, Ono T, Yamanoi A, Dhar DK, Nagasue N. Sinusoidal endothelial cell proliferation and expression of angiopoietin/Tie family in regenerating rat liver. *J Hepatol* 2001; **34:** 690-698
15 **Ross MA,** Sander CM, Kleeb TB, Watkins SC, Stolz DB. Spatiotemporal expression of angiogenesis growth factor receptors during the revascularization of regenerating rat liver. *Hepatology* 2001; **34:** 1135-1148
16 **Davis S,** Aldrich TH, Jones PF, Acheson A, Compton DL, Jain V, Ryan TE, Bruno J, Radziejewski C, Maisonpierre PC, Yancopoulos GD. Isolation of angiopoietin-1, a ligand for the TIE2 receptor, by secretion-trap expression cloning. *Cell* 1996; **87:** 1161-1169
17 **Suri C,** Jones PF, Patan S, Bartunkova S, Maisonpierre PC, Davis S, Sato TN, Yancopoulos GD. Requisite role of angiopoietin-1, a ligand for the TIE2 receptor, during embryonic angiogenesis. *Cell* 1996; **87:** 1171-1180
18 **Maisonpierre PC,** Suri C, Jones PF, Bartunkova S, Wiegand SJ, Radziejewski C, Compton D, McClain J, Aldrich TH, Papadopoulos N, Daly TJ, Davis S, Sato TN, Yancopoulos GD. Angiopoietin-2, a natural antagonist for Tie2 that disrupts in vivo angiogenesis. *Science* 1997; **277:** 55-60
19 **Asahara T,** Chen D, Takahashi T, Fujikawa K, Kearney M, Magner M, Yancopoulos GD, Isner JM. Tie2 receptor ligands, angiopoietin-1 and angiopoietin-2, modulate VEGF-induced postnatal neovascularization. *Circ Res* 1998; **83:** 233-240
20 **Holash J,** Maisonpierre PC, Compton D, Boland P, Alexander CR, Zagzag D, Yancopoulos GD, Wiegand SJ. Vessel cooption, regression, and growth in tumors mediated by angiopoietins and VEGF. *Science* 1999; **284:** 1994-1998
21 **Holash J,** Wiegand SJ, Yancopoulos GD. New model of tumor angiogenesis: dynamic balance between vessel regression and growth mediated by angiopoietins and VEGF. *Oncogene* 1999; **18:** 5356-5362
22 **Higgins GM,** Anderson RM. Experimental pathology of the liver. *Arch Pathol* 1931; **12:** 186-202
23 **Gumucio JJ,** May M, Dvorak C, Chianale J, Massey V. The isolation of functionally heterogeneous hepatocytes of the proximal and distal half of the liver acinus in the rat. *Hepatology* 1986; **6:** 932-944
24 **Knook DL,** Sleyster EC. Separation of Kupffer and endothelial cells of the rat liver by centrifugal elutriation. *Exp Cell Res* 1976; **99:** 444-449
25 **Tsutsumi M,** Takada A, Takase S. Characterization of desmin-positive rat liver sinusoidal cells. *Hepatology* 1987; **7:** 277-284
26 **Irving MG,** Roll FJ, Huang S, Bissell DM. Characterization and culture of sinusoidal endothelium from normal rat liver: lipoprotein uptake and collagen phenotype. *Gastroenterology* 1984; **87:** 1233-1247
27 **Kaplow LS.** Manual of macrophage methodology. Herscowitz HB, Holden HT, Bellanti JA, Ghaffar A, Eds. 1981, 199-227. Marcel Dekker, New York
28 **Chijiiwa K,** Nakano K, Kameoka N, Nagai E, Tanaka M. Proliferating cell nuclear antigen, plasma fibronectin, and liver regeneration rate after seventy percent hepatectomy in normal and cirrhotic rats. *Surgery* 1994; **116:** 544-549
29 **Hall PA,** Levison DA, Woods AL, Yu CC, Kellock DB, Watkins JA, Barnes DM, Gillett CE, Camplejohn R, Dover R. Proliferating cell nuclear antigen (PCNA) immunolocalization in paraffin sections: an index of cell proliferation with evidence of deregulated expression in some neoplasms. *J Pathol* 1990; **162:** 285-294
30 **Takebayashi J,** Kamatani M, Katagami Y, Hayashi K, Yanagi Z. A comparative study on the patency of crimped and noncrimped vascular prostheses, with emphasis on the earliest morphological changes. *J Surg Res* 1975; **19:** 209-218
31 **Kerr JF,** Wyllie AH, Currie AR. Apoptosis: a basic biological phenomenon with wide-ranging implications in tissue kinetics. *Br J Cancer* 1972; **26:** 239-257
32 **Greene AK,** Wiener S, Puder M, Yoshida A, Shi B, Perez-Atayde AR, Efstathiou JA, Holmgren L, Adamis AP, Rupnick M, Folkman J, O'Reilly MS. Endothelial-directed hepatic regeneration after partial hepatectomy. *Ann Surg* 2003; **237:** 530-535
33 **Geerts A.** History, heterogeneity, developmental biology, and functions of quiescent hepatic stellate cells. *Semin Liver Dis* 2001; **21:** 311-335
34 **Pinzani M,** Failli P, Ruocco C, Casini A, Milani S, Baldi E, Giotti A, Gentilini P. Fat-storing cells as liver-specific pericytes. Spatial dynamics of agonist-stimulated intracellular calcium transients. *J Clin Invest* 1992; **90:** 642-646
35 **Matsuoka M,** Tsukamoto H. Stimulation of hepatic lipocyte collagen production by Kupffer cell-derived transforming growth factor beta: implication for a pathogenetic role in alcoholic liver fibrogenesis. *Hepatology* 1990; **11:** 599-605
36 **Nakamura T,** Tomita Y, Hirai R, Yamaoka K, Kaji K, Ichihara A. Inhibitory effect of transforming growth factor-beta on DNA synthesis of adult rat hepatocytes in primary culture. *Biochem*

Biophys Res Commun 1985; **133:** 1042-1050

37 **Masuhara M,** Katyal SL, Nakamura T, Shinozuka H. Differential expression of hepatocyte growth factor, transforming growth factor-alpha and transforming growth factor-beta 1 messenger RNAs in two experimental models of liver cell proliferation. *Hepatology* 1992; **16:** 1241-1249

38 **Braun L,** Mead JE, Panzica M, Mikumo R, Bell GI, Fausto N. Transforming growth factor beta mRNA increases during liver regeneration: a possible paracrine mechanism of growth regulation. *Proc Natl Acad Sci USA* 1988; **85:** 1539-1543

Science Editor Wang XL Guo SY **Language Editor** Elsevier HK

PO Box 2345, Beijing 100023, China
www.wjgnet.com
wjg@wjgnet.com

ELSEVIER

World J Gastroenterol 2005;11(46):7261-7265
World Journal of Gastroenterology ISSN 1007-9327

• *BASIC RESEARCH* •

Clinical value of rapid urine trypsinogen-2 test strip, urinary trypsinogen activation peptide, and serum and urinary activation peptide of carboxypeptidase B in acute pancreatitis

Jesús Sáez, Juan Martínez, Celia Trigo, José Sánchez-Payá, Luis Compañy, Raquel Laveda, Pilar Griñó, Cristina García, Miguel Pérez-Mateo

Jesús Sáez, Juan Martínez, Luis Compañy, Pilar Griñó, Raquel Laveda, Cristina García, Miguel Pérez-Mateo, Section of Gastroenterology and Department of Internal Medicine, Hospital General Universitario de Alicante, Alicante, Spain
Celia Trigo, Service of Clinical Laboratory, Hospital General Universitario de Alicante, Alicante, Spain
José Sánchez-Payá, Service of Preventive Medicine, Hospital General Universitario de Alicante, Alicante, Spain
Supported by grants from the Instituto de Salud Carlos III No. C03/02, No. G03/156
Correspondence to: Dr Miguel Pérez-Mateo, Department of Internal Medicine, Hospital General Universitario de Alicante, Pintor Baeza s/n, E-03010 Alicante, Spain. perzmato_mig@gva.es
Telephone: +34-96-5938345 Fax: +34-96-5938355
Received: 2005-02-24 Accepted: 2005-07-08

Abstract

AIM: To assess the usefulness of urinary trypsinogen-2 test strip, urinary trypsinogen activation peptide (TAP), and serum and urine concentrations of the activation peptide of carboxypeptidase B (CAPAP) in the diagnosis of acute pancreatitis.

METHODS: Patients with acute abdominal pain and hospitalized within 24 h after the onset of symptoms were prospectively studied. Urinary trypsinogen-2 was considered positive when a clear blue line was observed (detection limit 50 μg/L). Urinary TAP was measured using a quantitative solid-phase ELISA, and serum and urinary CAPAP by a radioimmunoassay method.

RESULTS: Acute abdominal pain was due to acute pancreatitis in 50 patients and turned out to be extrapancreatic in origin in 22 patients. Patients with acute pancreatitis showed significantly higher median levels of serum and urinary CAPAP levels, as well as amylase and lipase than extrapancreatic controls. Median TAP levels were similar in both groups. The urinary trypsinogen-2 test strip was positive in 68% of patients with acute pancreatitis and 13.6% in extrapancreatic controls ($P<0.01$). Urinary CAPAP was the most reliable test for the diagnosis of acute pancreatitis (sensitivity 66.7%, specificity 95.5%, positive and negative predictive values 96.6% and 56.7%, respectively), with a 14.6 positive likelihood ratio for a cut-off value of 2.32 nmol/L.

CONCLUSION: In patients with acute abdominal pain, hospitalized within 24 h of symptom onset, CAPAP in serum and urine was a reliable diagnostic marker of acute pancreatitis. Urinary trypsinogen-2 test strip showed a clinical value similar to amylase and lipase. Urinary TAP was not a useful screening test for the diagnosis of acute pancreatitis.

Key words: Acute pancreatitis; Urinary trypsinogen-2; Urinary trypsinogen activation peptide; Activation peptide of carboxypeptidase B; Acute abdominal pain

Sáez J, Martínez J, Trigo C, Sánchez-Payá J, Compañy L, Laveda R, Griñó P, García C, Pérez-Mateo M. Clinical value of rapid urine trypsinogen-2 test strip, urinary trypsinogen activation peptide, and serum and urinary activation peptide of carboxypeptidase B in acute pancreatitis. *World J Gastroenterol* 2005; 11(46): 7261-7265
http://www.wjgnet.com/1007-9327/11/7261.asp

INTRODUCTION

Most patients with acute pancreatitis have mild and self-limited disease that resolves spontaneously, but about 20% of attacks are severe, with a mortality of about 10-25%[1]. Early diagnosis of acute pancreatitis is crucial to ensure rapid and appropriate treatment. However, the clinical features of acute pancreatitis can be difficult to distinguish from those of other acute abdominal conditions, and the diagnosis may be overlooked at first. Determination of amylase in serum or urine is the principal laboratory method for diagnosing acute pancreatitis. However, hyperamylasemia may be absent in 19% of cases[2], and increases in pancreatic enzyme levels can occur in patients with acute abdominal pain of extrapancreatic in origin[3-5]. The pathophysiology of acute pancreatitis involves the activation of the pancreatic proenzymes. The activation of trypsinogen followed by the activation of other pancreatic zymogens occurs early in the course of pancreatitis, in proportion to the extent of pancreatic injury[6]. Concentrations of the activation peptide of trypsinogen (TAP) in urine and of the activation peptide

of procarboxypeptidase B (CAPAP) in urine and serum have shown to be promise predictors of severity in acute pancreatitis[7,8]. However, the clinical value of these markers for the early diagnosis of acute pancreatitis is unclear. Until now, a previous study of urinary TAP levels[7] and three other studies of serum and urine CAPAP[9-11] have shown significantly higher concentrations of these peptides in acute pancreatitis compared to non-pancreatic abdominal pain, therefore, suggesting the usefulness of these assays for diagnosing acute pancreatitis. On the other hand, qualitative rapid urine trypsinogen-2 test strip is easy to perform and has been shown to be a reliable and useful screening test for acute pancreatitis in daily practice[12-16], particularly in healthcare units lacking laboratory facilities. This study was conducted to assess the usefulness of urinary trypsinogen-2 test strip, urinary TAP, and serum and urine CAPAP levels compared with conventional enzymes (serum amylase and lipase) for diagnosing acute pancreatitis.

MATERIALS AND METHODS

Patients

All consecutive patients with acute abdominal pain admitted to the Section of Gastroenterology of an Acute-care University Hospital in Alicante, Spain, in an 8-month period, participated in an observational, prospective, cohort study. Admission to the hospital within 24 h of symptom onset was the criterion for inclusion. The diagnosis of acute pancreatitis was based on (1) typical clinical symptoms and at least a threefold increase of serum amylase, once other causes of abdominal pain had been excluded, and (2) evidence of pancreatic inflammation by imaging studies and/or surgery. The severity of acute pancreatitis was assessed according to the criteria established at the International Symposium on Acute Pancreatitis in Atlanta in 1992[17]. According to our protocol, a CT scan was performed in patients with severe acute pancreatitis, with unknown etiology and whenever it was necessary to establish the diagnosis of acute pancreatitis. In all the patients, blood and urine samples were collected within the first 24 h of hospitalization. The Hospital General Universitario Ethic's Committee approved the protocol, and all patients gave their informed consent for the inclusion in the study. Patients were divided into two groups according to the origin of acute abdominal disease. There were 50 patients with acute pancreatitis (25 men, 25 women, mean age 62.5 ±16.5 years) and 22 patients (11 men, 11 women, mean age 50.8±22.4 years) whose acute abdominal pain turned out to be extrapancreatic in origin. A CT scan was performed in all the 22 patients with non-pancreatic abdominal pain to rule out the possibility of acute pancreatitis.

Laboratory tests

Serum amylase and lipase concentrations were measured by routine methods of our laboratory and for the remaining diagnostic markers, urine and serum samples were frozen immediately after collection and stored at (-20 °C) until analysis.

Serum amylase concentrations were measured using an enzymatic assay (Amyl, Boehringer Mannheim Systems, Mannheim, Germany). For this assay the limit of detection is 3 U/L and the range of the standard curve was comprised between 3 and 1 200 U/L. The reference range of serum amylase, previously established in our laboratory, was 26-100 U/L. Serum lipase was measured using a colorimetric enzymatic technique (Lip, Boehringer Mannheim Systems, Mannheim, Germany). For this assay the limit of detection was 3 U/L and the range of the standard curve was comprised between 3 and 300 U/L. The reference range of serum lipase, previously established in our laboratory, was 13-60 U/L.

Serum and urine CAPAP concentrations were measured using a radioimmunoassay method (CAPAP RIA kit, Euro-Diagnostica, Malmö, Sweden). The kit is based on a competitive radioimmunoassay using antibodies against human CAPAP. CAPAP both in standards and samples compete with ^{125}I-labeled CAPAP in binding to the antibodies. The ^{125}I-CAPAP binds to the antibodies in an inverse proportion to the concentrations of CAPAP both in standards and samples. Antibody-bound ^{125}I-CAPAP is separated from the unbound fraction using the double antibody solid-phase technique. The radioactivity of the pellets was then measured. For this assay, the lower limit of detection was about 0.4 nmol/L and the range of the standard curve was comprised between 0 and 20 nmol/L. When the results above this limit were obtained, serum samples were diluted at 1:5 and urine samples at 1:10 were processed again.

Urinary TAP was measured using a quantitative solid-phase ELISA based on the competition between free and immobilized peptide binding to an antibody to TAP (TAPKIT, Biotrin International Ltd, Dublin, Ireland). Urine samples were collected in sterile containers with EDTA (at final concentration 5-10 nmol/L) and diluted to a ratio of 1:4 in the assay buffer according to the manufacturer's instructions. TAP linked to a carrier protein is immobilized on the solid phase to which the peptide calibrator or diluted (1:4) urine sample, plus the TAP antibody, was added. After the reaction, the amount of antibody bound to the solid phase was measured spectrophotometrically (450 nm) after sequential addition of rabbit antibody to IgG-biotin conjugate, streptavidin-horseradish peroxidase, and tetramethyl-benzidine. The lower detection limit was 0.2 nmol/L (0.8 nmol/L in the 1:4 diluted samples) and the range of the standard curve was comprised between 0.14 and 200 nm.

The Actim Pancreatitis test strip (Medix Biochemica, Finland) for urinary trypsinogen-2 is an immunochromatographic test. After the test strip has been dipped into the urine sample, trypsinogen-2 is bound to monoclonal antibody-labeled blue latex particles, which migrate across a nitrocellulose membrane with a zone containing another antibody specific for another epitope on trypsinogen-2. At trypsinogen-2 concentrations higher than 50 μg/L, a blue line develops

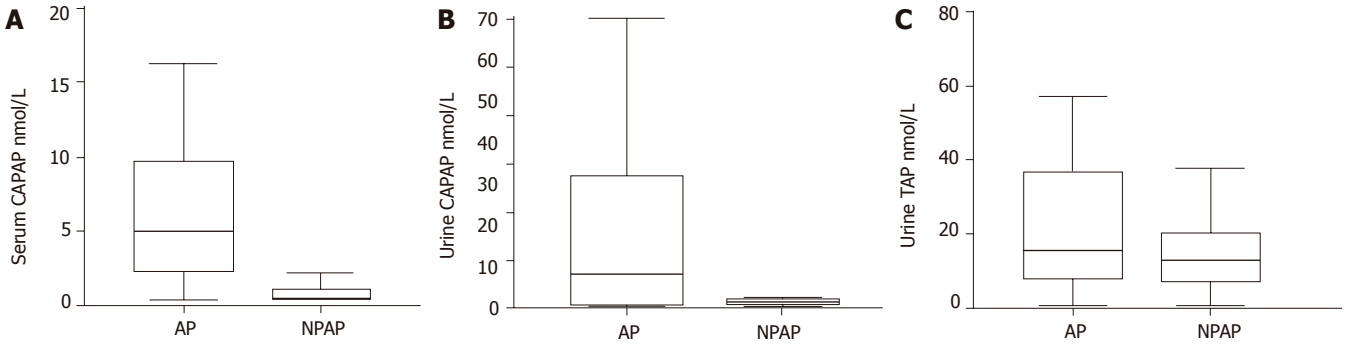

Figure 1 A: CAPAP concentration in serum within 24 h of hospital admission in patients with acute pancreatitis and in extrapancreatic controls. Data as median and interquartile range (AP, acute pancreatitis; NPAP, non-pancreatic abdominal pain); **B:** CAPAP concentration in urine within 24 h of hospital admission in patients with acute pancreatitis and in extrapancreatic controls. Data as median and interquartile range (AP: acute pancreatitis; NPAP, non-pancreatic abdominal pain); **C:** Urinary TAP levels within 24 h of hospital admission in patients with acute pancreatitis and in extrapancreatic controls. Data as median and interquartile range (AP: acute pancreatitis; NPAP, non-pancreatic abdominal pain).

Table 1 Clinical and outcome data in 50 patients with acute pancreatitis

	Number of patients	Percentage
Male/female	25/25	
Age, yr, mean (SD)	62.5 (16.5)	
Etiology		
Gallstones	30	60
Idiopathic	12	24
Alcohol	3	6
Post-ERCP	3	6
Hypertriglyceridemia	2	4
Severity		
Severe	15	30
Mild	35	70
Complications		
Local	12	24
Systemic	17	34
Death	5	10

ERCP, endoscopic retrograde cholangiopancreatography.

Table 2 Etiology in 22 controls with non-pancreatic acute abdomen

Etiology	Number of patients	Percentage
Acute cholecystitis	5	22.7
Acute appendicitis	3	13.6
Coliky pain	3	13.6
Intestinal obstruction	2	9.1
Active Crohn's disease	2	9.1
Acute cholangitis	1	4.5
Perforated peptic ulcer	1	4.5
Gastric carcinoma	1	4.5
Epiploic appendicitis	1	4.5
Abdominal abscess	1	4.5
Bleeding peptic ulcer	1	4.5
Mesenteric lymphadenitis	1	4.5

in this zone. The test was considered positive when a clear blue line was detected within 5 min. A control line was used to indicate proper functioning of the strip. If the control line was undetectable the assay was repeated.

Statistical analysis

Descriptive data were given as median with interquartile range (25th and 75th percentiles). The Mann-Whitney *U* test was used to compare the results between patients with acute pancreatitis and extrapancreatic controls. Statistical significance was set at $P<0.05$. Receiver operating characteristics (ROC) curves of serum and urine CAPAP levels and urinary TAP concentrations were used to determine the optimal cut-off levels. For serum concentrations of amylase and lipase, threefold increases in the reference values recommended by our laboratory were selected as cut-off values. Using these cut-off points, the sensitivity, specificity, positive and negative predictive values and positive likelihood ratio in establishing the diagnosis of acute pancreatitis were calculated. Comparison of different prognostic markers was made using the positive likelihood ratio for the different cut-off values that were selected. The SPSS/PC+10 statistical package on a personal computer was used for the analysis of data.

RESULTS

Of the 50 patients with acute pancreatitis, 15 (10 men and 5 women, mean age 66±16 years) had severe disease and 35 (17 men and 18 women, mean age 61±17 years) had mild disease. Etiology of pancreatitis and outcome are shown in Table 1. Local pancreatic complications included necrosis in 7 patients, pseudocyst in 4 and abscess in 1. Systemic complications consisted of renal failure in 6 patients, respiratory insufficiency in 6 and gastrointestinal hemorrhage in 5. Death occurred in 5 of 15 patients with severe pancreatitis. Diagnoses established in controls with non-pancreatic acute abdomen are shown in Table 2.

As compared with extrapancreatic controls, patients with acute pancreatitis had significantly higher values of amylase [942.20 (316.25-1 333.42) U/L *vs* 52 (29.50-91.20) U/L, $P<0.001$] and lipase [1 084 (228.75-2 133.75) U/L *vs* 22 (15.50-39) U/L, $P<0.001$] in serum. On the other hand, patients with acute pancreatitis showed significantly higher values of CAPAP in the serum and urine than controls with non-pancreatic acute abdomen, i.e., CAPAP in serum 5.05 (2.23-10.04) nmol/L *vs* 0.40 (0.40-1.14) nmol/L, $P<0.001$;

Table 3 Diagnostic accuracy of cut-off values of CAPAP in serum and urine and urinary TAP to distinguish severe acute pancreatitis from the mild form of the disease

Proenzyme, cut-off value within 24 h of admission	Pre-test probability %	Sensitivity %	Specificity %	PPV %	NPV %	Positive likelihood ratio	Post-test probability %
Amylase serum, >330 U/L	69.4	74	86.4	92.5	59.3	5.4	92.4
Lipase serum, >180 U/L	69.4	84	85.7	93.4	72	5.87	93
CAPAP serum, >1.53 nmol/L	69.4	85	90.9	95.2	74	9.3	95
CAPAP urine, >2.32 nmol/L	69.4	66.7	95.5	96.9	56.7	14.6	97
TAP urine, >10.01 nmol/L	69.4	68.8	40	73.3	34.7	1.13	71.9
Trypsinogen-2 urine, positive	69.4	68	86.4	91.9	54.3	5	91.9

PPV, positive predictive value; NPV, negative predictive value.

CAPAP in urine 7.05 (0.93-29.5) nmol/L *vs* 1.36 (0.80-1.85) nmol/L, $P<0.01$) (Figures 1A and B). However, there were no statistically significant differences in urinary TAP between patients and controls [15.45 (7.79-37.05) nmol/L *vs* 12.70 (7.03-20.27) nmol/L] (Figure 1C). The urinary trypsinogen-2 test strip was positive in 68% of patients with acute pancreatitis and 13.6% in extrapancreatic controls ($P<0.01$).

Sensitivity, specificity, predictive values, pre-test probability, post-test probability and positive likelihood ratio for the different cut-off values of CAPAP in serum and urine, urinary TAP and trypsinogen-2 test are shown in Table 3. Urinary CAPAP was the most reliable test for the diagnosis of acute pancreatitis (sensitivity 66.7%, specificity 95.5%, positive predictive value 96.6%, negative predictive value 56.7% and post-test probability 97%), with a 14.6 positive likelihood ratio for a cut-off value of 2.32 nmol/L.

DISCUSSION

This study demonstrates that CAPAP in serum and urine (especially urinary CAPAP) was a reliable diagnostic marker of acute pancreatitis providing slightly better results than serum amylase and lipase. Urinary trypsinogen-2 test strip showed a clinical value similar to amylase and lipase. Urinary TAP was not a useful screening test for the diagnosis of acute pancreatitis. In agreement with previous studies[18,19], we also found that serum amylase and lipase were adequate diagnostic markers of acute pancreatitis.

In respect to urinary TAP concentrations, the present results are consistent with other studies[20,21] in which this marker was not useful for diagnosing acute pancreatitis. However, in the study of Neoptolemos *et al*.[7], there were statistically significant differences in urinary TAP levels between patients with acute pancreatitis and controls both at 24-48 h of hospital admission and 24-48 h after the onset of symptoms. It may be possible that the increase in urinary TAP levels at 48 h compared to 24 h and the high rate of alcoholic pancreatitis included in the study of Neoptolemos *et al*.[7] may account for the differences observed with the present findings.

With regard to clinical value of serum and urine CAPAP concentrations, both assays were reliable early markers for diagnosing acute abdominal pain of pancreatic origin. These results are similar to previous findings by our group in a series of 22 patients[22] and confirm that this marker of acute pancreatitis is capable of both simultaneously diagnosing and assessing severity of disease at the time of admission to the hospital[8-11]. Certainly, we do not know why urinary TAP was not a useful screening test for the diagnosis of acute pancreatitis whereas urinary CAPAP levels were a reliable test, since both assays indicate an activation of pancreatic zymogens. Probably, the different kinetics of release and techniques of determination of both markers could explain this point. More studies are necessary to assess it. On the other hand, laborious and time consuming work are pitfalls of current CAPAP assays for rapid screening in a routine diagnostic setting. Moreover, it hardly improves the diagnostic accuracy of the routine markers (amylase and lipase).

Rapid urine trypsinogen-2 strip test has been introduced in an effort to decrease the number of misdiagnosed cases of acute pancreatitis in an emergency setting. In the present study, the test was positive in 68% of patients with acute pancreatitis and 13.6% in extrapancreatic controls, with a sensitivity of 68% and specificity of 86.4%. These results are slightly less favorable than those reported in other series[12-16], in which 90% sensitivity was almost reached. However, it should be noted that a high percentage of patients with non-pancreatic acute abdominal pain with a clinical profile similar to acute pancreatitis (cholecystitis five cases, biliary colic three cases) were included in our study. Therefore, the present results far from decreasing the clinical usefulness of urinary trypsinogen-2 test strip, contribute to delimit the true value of this rapid screening test in clinical practice. On the other hand, it has to be considered that the inclusion process of patients with abdominal pain in this investigation may be biased, since patients admitted to our department have been pre-selected by the emergency department, and this likely justifies the high proportion of patients with AP in our series (50/72).

In summary, in patients with acute abdominal pain, hospitalized within 24 h of symptom onset, CAPAP in serum and urine was a reliable diagnostic marker of acute pancreatitis, but it provided only slightly better results than serum amylase and lipase and, although we have not made a detailed economical analysis, it seems not to be cost-effective to use it as a routine diagnostic marker. On the other hand, urinary trypsinogen-2 test strip showed a clinical value similar to amylase and lipase. Urinary TAP was not a useful screening test for the diagnosis of acute pancreatitis.

ACKNOWLEDGMENTS

We thank Marta Pulido, MD, for editing the manuscript and editorial assistance.

REFERENCES

1 **Dervenis C**, Johnson CD, Bassi C, Bradley E, Imrie CW, McMahon MJ, Modlin I. Diagnosis, objective assessment of severity, and management of acute pancreatitis. Santorini consensus conference. *Int J Pancreatol* 1999; **25:** 195-210
2 **Clavien PA**, Robert J, Meyer P, Borst F, Hauser H, Herrmann F, Dunand V, Rohner A. Acute pancreatitis and normoamylasemia. Not an uncommon combination. *Ann Surg* 1989; **210:** 614-620
3 **Dutta SK**, Douglass W, Smalls UA, Nipper HC, Levitt MD. Prevalence and nature of hyperamylasemia in acute alcoholism. *Dig Dis Sci* 1981; **26:** 136-141
4 **Yadav D**, Nair S, Norkus EP, Pitchumoni CS. Nonspecific hyperamylasemia and hyperlipasemia in diabetic ketoacidosis: incidence and correlation with biochemical abnormalities. *Am J Gastroenterol* 2000; **95:** 3123-3128
5 **Terada T**, Nakanuma Y. Immunohistochemical demonstration of pancreatic alpha-amylase and trypsin in intrahepatic bile ducts and peribiliary glands. *Hepatology* 1991; **14:** 1129-1135
6 **Borgström A,** Appelros S. Activation peptides in acute pancreatitis. In: Büchler MW, Uhl W, Friess H, Malfertheiner P, ed. Acute pancreatitis. Novel concepts in biology and therapy. Blackwell Wissenschafts-Verlag, Berlin-Viena 1999: 219-223
7 **Neoptolemos JP**, Kemppainen EA, Mayer JM, Fitzpatrick JM, Raraty MG, Slavin J, Beger HG, Hietaranta AJ, Puolakkainen PA. Early prediction of severity in acute pancreatitis by urinary trypsinogen activation peptide: a multicentre study. *Lancet* 2000; **355:** 1955-1960
8 **Appelros S**, Petersson U, Toh S, Johnson C, Borgstrom A. Activation peptide of carboxypeptidase B and anionic trypsinogen as early predictors of the severity of acute pancreatitis. *Br J Surg* 2001; **88:** 216-221
9 **Pezzilli R**, Morselli-Labate AM, Barbieri AR, Plate L. Clinical usefulness of the serum carboxypeptidase B activation peptide in acute pancreatitis. *JOP* 2000; **1:** 58-68
10 **Ung CT**, Westlake S, Brennan H, Johnson CD. Activation peptide of carboxy peptidase B (CAPAP) for prediction of complicated acute pancreatitis (abstract). *Digestion* 2000; **61**: 289
11 **Muller CA,** Appelros S, Uhl W, Buchler MW, Borgstrom A. Serum levels of procarboxypeptidase B and its activation peptide in patients with acute pancreatitis and non-pancreatic diseases. *Gut* 2002; **51:** 229-235
12 **Hedstrom J,** Korvuo A, Kenkimaki P, Tikanoja S, Haapiainen R, Kivilaakso E, Stenman UH. Urinary trypsinogen-2 test strip for acute pancreatitis. *Lancet* 1996; **347:** 729-730
13 **Kemppainen EA**, Hedstrom JI, Puolakkainen PA, Sainio VS, Haapiainen RK, Perhoniemi V, Osman S, Kivilaakso EO, Stenman UH. Rapid measurement of urinary trypsinogen-2 as a screening test for acute pancreatitis. *N Engl J Med* 1997; **336:** 1788-1793
14 **Kylänpäa-Bäck ML**, Kemppainen E, Puolakkainen P, Hedstrom J, Haapiainen R, Perhoniemi V, Kivilaakso E, Korvuo A, Stenman U. Reliable screening for acute pancreatitis with rapid urine trypsinogen-2 test strip. *Br J Surg* 2000; **87:** 49-52
15 **Pezzilli R**, Morselli-Labate AM, d'Alessandro A, Barakat B. Time-course and clinical value of the urine trypsinogen-2 dipstick test in acute pancreatitis. *Eur J Gastroenterol Hepatol* 2001; **13:** 269-274
16 **Kemppainen E,** Hedstrom J, Puolakkainen P, Halttunen J, Sainio V, Haapiainen R, Stenman UH. Urinary trypsinogen-2 test strip in detecting ERCP-induced pancreatitis. *Endoscopy* 1997; **29:** 247-251
17 **Bradley EL 3rd.** A clinically based classification system for acute pancreatitis. Summary of the International Symposium on Acute Pancreatitis, Atlanta, Ga, September 11 through 13, 1992. *Arch Surg* 1993; **128:** 586-590
18 **Gumaste VV**, Roditis N, Mehta D, Dave PB. Serum lipase levels in nonpancreatic abdominal pain versus acute pancreatitis. *Am J Gastroenterol* 1993; **88:** 2051-2055
19 **Steinberg WM**, Goldstein SS, Davis ND, Shamma'a J, Anderson K. Diagnostic assays in acute pancreatitis. A study of sensitivity and specificity. *Ann Intern Med* 1985; **102:** 576-580
20 **Fernandez-del Castillo C,** Harringer W, Warshaw AL, Vlahakes GJ, Koski G, Zaslavsky AM, Rattner DW. Risk factors for pancreatic cellular injury after cardiopulmonary bypass. *N Engl J Med* 1991; **325:** 382-387
21 **Banks PA**, Carr-Locke DL, Slivka A, Van Dam J, Lichtenstein DR, Hughes M. Urinary trypsinogen activation peptides (TAP) are not increased in mild ERCP-induced pancreatitis. *Pancreas* 1996; **12**: 294-297
22 **Sáez J**, Martínez J, Trigo C, Griño P, Garcia C, Laveda R, Compañy L, Perez-Mateo M. CAPAP as diagnostic and prognostic factor in acute pancreatitis (abstract). *Digestion* 2000; **61**: 289

Science Editor Guo SY **Language Editor** Elsevier HK

PO Box 2345, Beijing 100023, China
www.wjgnet.com
wjg@wjgnet.com

ELSEVIER

World J Gastroenterol 2005;11(46):7266-7271
World Journal of Gastroenterology ISSN 1007-9327

• *BASIC RESEARCH* •

Lymphocytic colitis: A clue to bacterial etiology

Thanaa EA Helal, Naglaa S Ahmed, Osama Abo El Fotoh

Thanaa EA Helal, Naglaa S Ahmed, Department of Pathology, Faculty of Medicine, Ain Shams University, Egypt
Osama Abo El Fotoh, Department of Internal Medicine, Faculty of Medicine, Ain Shams University, Egypt
Correspondence to: Professor Thanaa EA Helal, Department of Pathology, Faculty of Medicine, Ain Shams University, Cairo, Egypt. thanaahelal@hotmail.com
Telephone: +202-4534449 Fax: +202-6859928
Received: 2004-02-27 Accepted: 2004-05-18

Abstract

AIM: To find out the role of bacteria as a possible etiological factor in lymphocytic colitis.

METHODS: Twenty patients with histopathological diagnosis of lymphocytic colitis and 10 normal controls were included in this study. Colonoscopic biopsies were obtained from three sites (hepatic and splenic flexures and rectosigmoid region). Each biopsy was divided into two parts. A fresh part was incubated on special cultures for bacterial growth. The other part was used for the preparation of histologic tissue sections that were examined for the presence of bacteria with the help of Giemsa stain.

RESULTS: Culture of tissue biopsies revealed bacterial growth in 18 out of 20 patients with lymphocytic colitis mostly *Escherichia coli* (14/18), which was found in all rectosigmoid specimens (14/14), but only in 8/14 and 6/14 of splenic and hepatic flexure specimens respectively. In two of these cases, *E coli* was associated with proteus. Proteus was found only in one case, Klebsiella in two cases, and *Staphylococcus aureus* in one case. In the control group, only 2 out of 10 controls showed the growth of *E coli* in their biopsy cultures. Histopathology showed rod-shaped bacilli in the tissue sections of 12 out of 14 cases with positive *E coli* in their specimen's culture. None of the controls showed these bacteria in histopathological sections.

CONCLUSION: This preliminary study reports an association between *E coli* and lymphocytic colitis, based on histological and culture observations. Serotyping and molecular studies are in process to assess the role of *E coli* in the pathogenesis of lymphocytic colitis.

Key words: Lymphocytic colitis; *E coli*; Histopathology; Culture

Helal TEA, Ahmed NS, Fotoh OAE. Lymphocytic colitis: A clue to bacterial etiology. *World J Gastroenterol* 2005; 11(46):7266-7271
http://www.wjgnet.com/1007-9327/11/7266.asp

INTRODUCTION

Microscopic colitis is a syndrome consisting of chronic watery diarrhea, a normal or near normal gross appearance of the colonic mucosa, and a specific histological picture described as either lymphocytic or collagenous colitis[1]. The term microscopic colitis was first introduced by Read *et al*.[2] that was found in eight patients who were having idiopathic chronic diarrhea and normal colonoscopic findings. The diagnosis of microscopic colitis in such patients was based on the presence of excess amount of chronic inflammatory cells in the lamina propria of colorectal mucosa. A closely related term "lymphocytic colitis" was introduced by Lazenby *et al*.[3], who reported that the most distinctive histological feature of microscopic colitis is the presence of an excess amount of intraepithelial lymphocytes, and renamed microscopic colitis as "lymphocytic colitis". Recently, the histopathology of lymphocytic colitis has been more specified by Lamps and Lazenby[4].

The etiology of lymphocytic colitis is still unclear, and several factors have been claimed. First, it is induced by drugs especially non-steroidal-anti-inflammatory drugs (NSAIDs)[5]. However, subsequent studies found that there is no association between NSAID consumption and microscopic colitis[6]. Vascular tonics have also been suspected to play a part in the pathogenesis of lymphocytic colitis via chronic activation of the mucosal immune system by one or several components of such drugs[7]. Other drugs that claimed to be a cause of lymphocytic colitis include Lansoprazole[8] and Modopar[9]. The second concept is the reported association of microscopic colitis with celiac disease, which may indicate a common pathogenesis[1,10,11]. Nevertheless, many patients with celiac disease do not show colonic lymphocytosis[12]. Lastly it is the possible role of pathogenic organisms. Some investigators have found spirochetes in some patients with microscopic colitis, and suggested that these microorganisms are capable of inducing the disease[13]. Conversely, earlier studies reported that spirochetes have no clinical significance[14]. In a search for infectious causes, Afzalpurkar *et al*.[15] investigated 14 patients with chronic idiopathic diarrhea by stool examination and stool culture as well as a culture of the jejunal fluid. Although stool examination and culture were negative, abnormal growth

of bacteria in the jejunal fluid was noted in four patients. Similarly, the culture of the jejunal aspirate in 14 patients having chronic idiopathic diarrhea has revealed bacterial growth in one patient who was successfully treated with antibiotics[2].

The aim of the current preliminary study was to search for a possible role of the pathogenic bacteria in lymphocytic colitis. This has been achieved by thorough histologic examination as well as culture of the colonic tissue specimens, which is to the best of our knowledge not previously reported in the literature.

MATERIALS AND METHODS

Patients

The present study consisted of 20 patients fulfilling the classic definition of lymphocytic colitis, which is described as a triad of idiopathic chronic, watery diarrhea, normal or nearly normal colonoscopic findings, and colonic epithelial lymphocytosis without a thickened subepithelial collagen band[16]. The patients were chosen from the in- and outpatients of Ain-Shams University Hospital during the period between 1999 and 2001, after excluding all other causes of diarrhea by a thorough clinical examination, radiologic, endoscopic, and laboratory investigations. The exclusion criteria were autoimmune diseases, any systemic disease that could cause diarrhea as diabetes, history of food sensitivity, use of laxatives or other drugs that could cause diarrhea, presence of ova and parasites or occult blood in stools.

Ten age- and sex-matched healthy volunteers with no diarrhea or any other gastrointestinal diseases were used as negative controls. The endoscopic and histologic pictures of their colonic mucosae were normal. All patients and controls were not allowed to take antibiotics for 3 wk before the biopsy, since antibiotic treatment may affect the bowel microbial flora. Informed written consent was obtained from all the patients and volunteers.

Stool analysis

Microscopic examination of fresh unstained smears was done to exclude parasitic infestation.

Colonoscopic examination and biopsy

Using lower CF 100 L video colonoscope (Olympus), the whole colon was examined for any pathological lesions including the inspection of the terminal ileum if possible. Patients were selected on the basis of having normal or nearly normal colonoscopic findings. From each patient and control, four tissue samples were taken from each of the following sites: hepatic flexure (HF), splenic flexure (SF), and rectosigmoid region (RS). These biopsy specimens were collected separately, then each specimen was divided into two parts, the first part was put in normal saline and sent for culture, the other part was fixed in 10% buffered formalin and sent for histopathology.

Culture studies of biopsy samples

For all subjects, fresh colonic tissue specimens obtained from HF, SF, and RS regions were incubated separately on the media listed in Table 1 to detect bacterial flora. Specimens were crushed before incubation. The isolated intestinal bacteria were identified by colony morphology, microscopic examination of gram stained smears, conventional biochemical reactions and API20 E identification system (BioMerieux) for the identification of Gram-negative bacteria.

Histopathology

Formalin-fixed colonic tissue specimens obtained from the 20 patients and 10 controls (3 specimens from each subject) were processed separately for the preparation of paraffin blocks. The latter were sectioned at 5 μm and stained with hematoxylin and eosin (H&E) for routine examination, Masson trichrome for the demonstration of subepithelial collagen band, and modified Giemsa stain to search for bacteria (as followed in the cases of chronic gastritis) to detect *Helicobacter pylori*[17]. One pathologist (T.E.H.) examined all the tissue sections without the knowledge of the clinical or endoscopic findings. All 60 specimens were examined for the histologic criteria of lymphocytic colitis, which were modified by Lazenby *et al*.[3]. These criteria were simplified as follows. (1) Surface epithelial damage, which was seen as flattened or syncytial appearance of surface cells instead of the tall columnar cells that are normally observed. (2) Crypt distortion. Each of these two findings was graded according to severity into 1-3 scales (1+: mild, 2+: moderate, and 3+: marked). (3) Mononuclear cellular infiltrate in the lamina propria. This was graded into 1-4 scales (1+: normal, 2+: mild, 3+: moderate, and 4+: marked). (4) Intraepithelial lymphocytes. It was scored as the number of lymphocytes per 100 surface epithelial cells. It is worth mentioning that any case showing histologic features other than lymphocytic colitis was excluded from the study. These histologic exclusion criteria included features suggestive of inflammatory bowel disease[18], features of collagenous colitis[19], presence of ova or parasites, presence of viral inclusions, and melanosis coli.

Statistical analysis

Fisher's exact test was used to compare the patients and controls regarding the frequency of the bacterial growth.

Chi-square test was used to assess the association between the presence of bacteria and the severity of the histopathological features.

RESULTS

Clinical data

Patients with lymphocytic colitis included in the study consisted of 15 males and 5 females with a male to female ratio of 3:1. Ages ranged 20-67 years, with a mean of 36 ±10.3 years. All patients presented with chronic watery diarrhea of unknown cause for a period of 1-4.5 years with a mean of 2.5±0.76 years. The daily motions ranged 3-7 times (mean 4.5±1.3 times). All patients had associated mild to moderate abdominal discomfort. Five patients

Table 1 Culture media used for the detection of bacterial flora in colonic biopsies

Medium	Temperature	Incubation time (h)	Organism
MacConkey's agar	37 ℃	48-72	Coliform bacilli (*E coli* and Klebsiella) and Proteus
Aerobic blood agar	37 ℃	24-48	*Staphylococcus aureus*
Anaerobic blood agar	37 ℃	24-48	Anaerobic bacteria as Bacteroides spp.
Microaerophilic Campy-blood agar	42 ℃	24-48	*Campylobacter jejuni*
MacConkey's selective medium	25 ℃	24-48	*Yersinia Enterocolitica*
Selenite broth enrichment medium and Salmonella-Shigella agar	37 ℃	24	*Salmonella* and *Shigella*

Table 2 Culture results of 60 colonic tissue specimens from 20 patients with lymphocytic colitis

Organism	Patients (n = 20)	RS specimens (n = 20)	SF specimens (n = 20)	HF specimens (n = 20)
E coli	12	12	8	6
E coli + Proteus	2	2	0	0
Proteus	1	1	1	0
Klebsiella	2	2	2	1
Staphylococcus aureus	1	1	1	1
Total number	18	18	12	20

RS: rectosigmoid, SF: splenic flexure, HF: hepatic flexure.

Table 3 Histopathologic data of 60 colonic biopsies from 20 patients with lymphocytic colitis

Feature	RS	SF	HF
1 Surface epithelial damage			
1+	8	10	8
2+	6	6	6
3+	6	4	6
2 Crypt distortion			
1+	17	16	17
2+	3	4	3
3+	0	0	0
3 LP Inflammation			
2+	5	6	2
3+	11	10	12
4+	4	4	6
4 Mean % of IEL	23	22	28

RS: rectosigmoid, SF: splenic flexure, HF: hepatic flexure, LP: lamina propria, IEL: intraepithelial lymphocytes.

had significant weight loss. No other gastrointestinal manifestations were found.

Culture results

Bacterial growth was observed in the colonic tissue specimens of 18 out of the 20 patients (90%). The most frequent isolated organism was *E coli*, which was demonstrated in 14 out of 18 culture positive cases (77.8%). These organisms were seen in the rectosigmoid specimens in all the 14 cases, splenic flexure growth was found in 8 of them, and hepatic flexure growth in 6 cases only. In 2 out of the 14 cases, *E coli* was associated with the growth of Proteus. Other isolated bacteria were Klebsiella (two cases) and *Staphylococcus* aureus (one case). Other organisms such as *Shigella, Salmonella, Campylobacter, Yersinia* did not grow on their specific media. In the controls, *E coli* was obtained from the rectosigmoid samples of two cases (20%). The frequency of the bacterial growth was significantly higher in the patients than in the controls (P = 0.0003) (Table 2).

Histopathological results

The most prominent feature in all 60 colonic biopsies obtained from the 20 patients was the increased number of mononuclear cells in the lamina propria (Figure 1A) observed in all the three regions examined (rectosigmoid, splenic, and hepatic flexures), indicating total colitis. The inflammatory cells were mainly lymphocytes with less number of plasma cells and histiocytes; few polymorphonuclear cells were present in two cases with no crypt abscess formation. A small number of eosinophils were seen in three patients. Epithelial damage was mild to moderate in the majority of colonic biopsies (Figure 1A). The average crypt distortion was mild to moderate in all colonic biopsies. Few lymphocytes could be seen between the crypt epithelial cells, but not in the crypt lumen (Figure 1B). No other inflammatory cells were present in the lumen or epithelial cells of the crypts.

The percentage of the inflammatory cells in the surface epithelium ranged 15-50% with a mean of 23%, 22%, and 28% in the rectosigmoid, splenic flexure and hepatic flexure, respectively. The intraepithelial inflammatory cells were lymphocytes only (Table 3 and Figure 1C).

In 12 out of 18 patients with bacterial overgrowth in their colonic tissue specimens, rod-shaped bacilli were seen in the histologic tissue sections obtained from various colonic sites. These bacilli were visible on H&E-stained sections, but were more easily demonstrated by Giemsa stain. They were closely applied to the surface epithelium (Figure 1D), or within the lumen of the crypts which showed destruction of their lining cells (Figure 1E). It is important to note that the intercellular and intracellular localization of the organisms could not be assessed because these modes of colonization could not be definitely identified by light microscopy alone. The presence of bacteria was significantly associated with the degree of epithelial damage (χ^2 = 9.9, P = 0.007) and the degree of the cellular infiltrate in the lamina propria

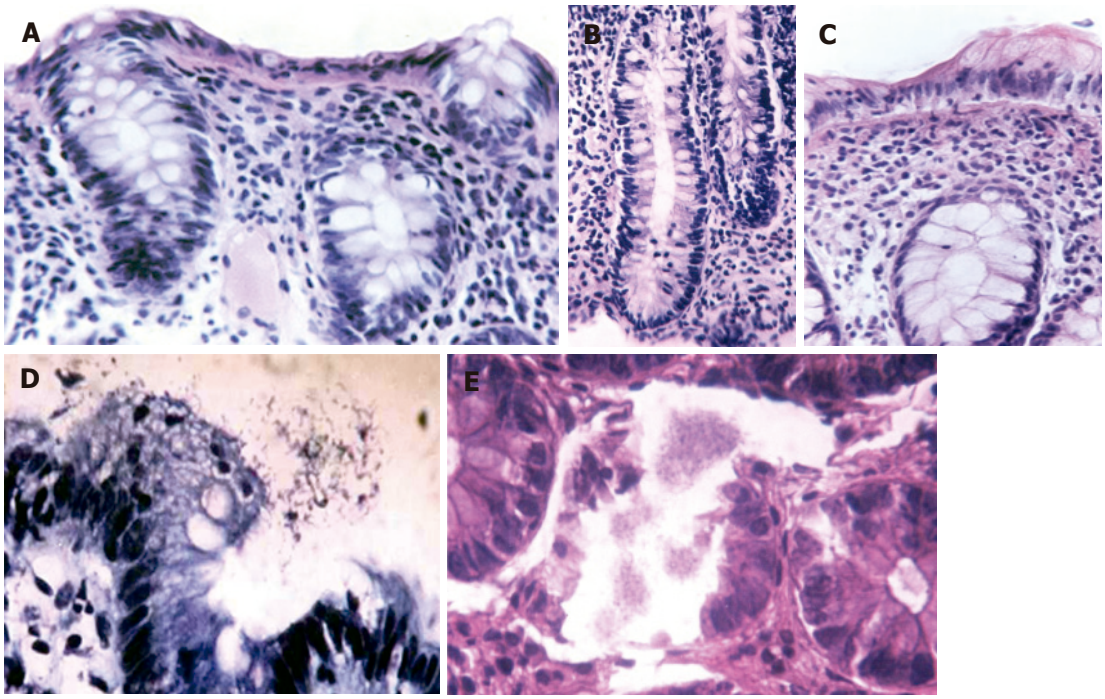

Figure 1 Cases of lymphocytic colitis showing respectively the damage of surface epithelium and increased mononuclear cells in lamina propria (H&E ×250) (**A**), few lymphocytes between crypt epithelial cells (H&E ×250) (**B**), intraepithelial lymphocytes (H&E ×250) (**C**), rod-shaped bacilli adherent to the surface epithelium (Giemsa stain ×400) (**D**), and bacilli within the lumen of transverse section of crypt (H&E ×400) (**E**).

(χ^2 = 6.0, P = 0.05). No significant relationship could be obtained between the presence of bacteria and the degree of crypt distortion (Table 4).

In all 30 colonic biopsies obtained from the 10 healthy controls, the colonic mucosa was nearly normal with no visible bacilli by H&E and Giemsa staining.

Table 4 Correlation between bacteria in tissue sections and histopathologic features in 60 colonic biopsies from 20 patients with lymphocytic colitis

Feature	Bacteria		χ^2	P
	+	−		
1 Epithelial damage				
1+	1	25	9.9	0.007
2+	4	14		
3+	7	9		
2 Crypt distortion				
1+	10	40	0.4	NS
2+	2	8		
3+	0	0		
3 LP Inflammation				
2+	2	11	6.0	0.05
3+	4	29		
4+	6	8		

LP: lamina propria, NS: not significant.

DISCUSSION

The main purpose of the present preliminary study was to investigate the possible role of bacteria in the pathogenesis of lymphocytic colitis. To achieve this aim, patients with definite diagnosis of lymphocytic colitis and normal controls were subjected to colonoscopy and biopsy. Specimens were examined in two ways. First, histopathological examination, including a thorough search for bacteria, similar to that for *H pylori* in gastric biopsies. Second, culture of colonic tissue specimens on specific media to isolate bacterial growth. Although some authors have investigated the possible role of infection in lymphocytic colitis or chronic idiopathic diarrhea, their methodology is limited to stool culture and/or culture of the jejunal fluid[2,15,19,20]. To the best of our knowledge, this is the first study, which attempted to search for bacteria in the colonic biopsies in cases of lymphocytic colitis by histologic examination of tissue sections as well as culture of the colonic tissue.

Microscopically, we could identify small or large number of rod-shaped bacilli closely related to the surface of the colonic mucosa and within the lumen of the crypts in 12 out of 14 patients with positive *E coli* in biopsy culture. It seems that *E coli* was most likely seen in the histologic sections of our tissue specimens, because these bacilli were seen in patients with positive *E coli* in biopsy culture.

The demonstration of these bacilli in the colonic mucosa of our patients with lymphocytic colitis raises several questions. The first question is why they have not been seen before in colonic tissue sections of such cases? We think that these bacteria have not been previously demonstrated because Giemsa stain is not routinely applied for colonic mucosal biopsy specimens and bacteria are easily overlooked on H&E-stained sections. The second question to be raised is whether these bacteria

are pathogenic or merely commensals in the colonic mucosa. From our point of view, we suggest that these bacilli, which have been demonstrated histologically, are pathogenic rather than commensals, since they are closely related to the mucosal surface and within the lumen of crypts, and not within the tissue debris. Moreover, they are always associated with prominent colonic pathology. It is worthy of notion that we could not demonstrate such bacteria in all colonic biopsies obtained from the healthy controls.

The relation between lymphocytic colitis and bacterial infection is still controversial. Gebbers and Laissue[13] reported the presence of spirochetes in some patients with microscopic colitis, and suggested that these microorganisms are capable of inducing the disease. On the other hand, earlier studies reported that spirochetes have no clinical significance[14]. Perk *et al*.[21] presented a patient who had chronic watery diarrhea and showed stool culture positive for *Campylobacter jejuni*. Examination of her colonic biopsies led to the diagnosis of lymphocytic colitis. The authors believed that the patient's disease is due to an infectious process. Also, Tremaine[22] reported that bismuth subsalicylate is effective in the treatment of some patients with lymphocytic colitis, a finding that supports the concept of infectious etiology in such disease.

It is interesting to note that the search for bacterial etiology in cases of chronic watery diarrhea has been expanded to include the type of bacteria responsible for this disease. The most common organism investigated in this regard is *E coli*[23-25].

Diarrheagenic *E coli* (*E coli* causing diarrhea) is divided into four groups: enteropathogenic (causing acute diarrhea in infants and children), enteroinvasive (causing Shigella-like dysentery), enterohemorrhagic (causing hemorrhagic colitis and bloody diarrhea) and enterotoxigenic (causing travelers' diarrhea)[26]. In addition to these groups, two other types, which were previously classified as enteropathogenic, have been recently identified. The first is enteroaggregative *E coli* (EaggEC), which is now considered as a cause of prolonged diarrhea[27]. Another recently described type of *E coli* is the diffusely adherent type which has been found to be significantly associated with chronic diarrhea[28]. It is important to note that many strains of *E coli* belonging to the classic enteropathogenic type are now found to be enteroaggregative by DNA hybridization or PCR. This indicates that routine culture studies and even serotyping are of limited value for the identification of various groups of diarrheagenic *E coli*[29].

These new types of *E coli* may be more likely the types seen in the tissue sections and biopsy culture of our patients, being associated with chronic diarrhea as mentioned above, and may be related to the pathogenesis of lymphocytic colitis, since it can colonize both in large and in small intestines. In a study by Kang *et al*.[30], strains of enteroaggregative *E coli* isolated from patients with diarrhea resulted in the colonization of both small and large intestines. In support to this suggestion is the study of Afzalpurkar *et al*.[15], who found that 4 out of 14 patients with chronic idiopathic diarrhea have abnormal growth of bacteria in aspirated jejunal fluid and the results of quantitative cultures are consistent with contamination. In addition, one of the four patients had steatorrhea, which is one of the hallmarks of bacterial overgrowth syndrome. These data have led the authors to speculate that *E coli* or other bacteria not identified by routine culture methods are involved in the etiology of chronic idiopathic diarrhea. It is worth mentioning that the lack of response to antibiotics in the four patients with bacterial overgrowth reported in the previous study should not be considered as evidence against bacterial etiology, since multiple drug resistance in EaggEC has been reported by some studies recommending quinolone treatment for EaggEC-associated diarrhea[31].

In conclusion, bacteria play a possible role in lymphocytic colitis in which rod-shaped bacilli adherent to the colonic mucosa can be seen as in cases of *Helicobacter* gastritis. Further studies are now in process to investigate the pathogenicity of these organisms in case of lymphocytic colitis.

REFERENCES

1 **Schiller LR**. Microscopic colitis syndrome: lymphocytic colitis and collagenous colitis. *Semin Gastrointest Dis* 1999; **10**: 145-155
2 **Read NW,** Krejs GJ, Read MG, Santa Ana CA, Morawski SG, Fordtran JS. Chronic diarrhea of unknown origin. *Gastroenterology* 1980; **78**: 264-271
3 **Lazenby AJ,** Yardley JH, Giardiello FM, Jessurun J, Bayless TM. Lymphocytic ("microscopic") colitis: a comparative histopathologic study with particular reference to collagenous colitis. *Hum Pathol* 1989; **20**: 18-28
4 **Lamps LW,** Lazenby AJ. Colonic epithelial lymphocytosis and lymphocytic colitis: descriptive histopathology versus distinct clinicopathologic entities. *Adv Anat Pathol* 2000; **7**: 210-213
5 **Riddell RH,** Tanaka M, Mazzoleni G. Non-steroidal anti-inflammatory drugs as a possible cause of collagenous colitis: a case-control study. *Gut* 1992; **33**: 683-686
6 **Veress B,** Lofberg R, Bergman L. Microscopic colitis syndrome. *Gut* 1995; **36**: 880-886
7 **Beaugerie L,** Luboinski J, Brousse N, Cosnes J, Chatelet FP, Gendre JP, LeQuintrec Y. Drug induced lymphocytic colitis. *Gut* 1994; **35**: 426-428
8 Ghilain JM, Schapira M, Maisin JM, De Maeght S, Piron A, Gerard R, Henrion J . lymphocytic colitis associated with lansoprazole treatment. *Gastroenterol Clin Biol* 2000; 24: 960-962
9 **Rassiat E,** Michiels C, Sgro C, Yaziji N, Piard F, Faivre J. Lymphocytic colitis due to Modopar. *Gastroenterol Clin Biol* 2000; **24**: 852-853
10 **Fine KD,** Do K, Schulte K, Ogunji F, Guerra R, Osowski L, McCormack J. High prevalence of celiac sprue-like HLA-DQ genes and enteropathy in patients with the microscopic colitis syndrome *Am J Gastroenterol* 2000; **95**: 1974-1982
11 **Gillett HR,** Freeman HJ. Prevalence of celiac disease in collagenous and lymphocytic colitis. *Can J Gastroenterol* 2000; **14**: 919-921
12 **Yardley JH,** Lazenby AJ, Giardiello FM, Bayless TM. Collagenous, "microscopic," lymphocytic, and other gentler and more subtle forms of colitis. (editorial) *Hum Pathol* 1990; **21**: 1089-1091
13 **Gebbers JO,** Laissue JA. Diarrhea due to rare forms of colitis: microscopic (lymphocytic, collagenous) colitis and spirochetosis. *Schweiz Med Wochchenschr* 1994; **124**: 1852-1861
14 **Nielsen RH,** Orholm M, Pedersen JO, Hovind-Hougen K, Teglbjaerg PS, Thaysen EH. Colorectal spirochetosis: clinical significance of the infestation. *Gastroenterology* 1983; **85**: 62-67

15 **Afzalpurkar RG,** Schiller LR, Little KH, Santangelo WC, Fordtran JS. The self-limited nature of chronic idiopathic diarrhea. *N Engl J Med* 1992; **327**: 1849-1852
16 **Wang N,** Dumot JA, Achkar E, Easley KA, Petras RE, Goldblum JR. Colonic epithelial lymphocytosis without a thickened subepithelial collagen table: a clinicopathologic study of 40 cases supporting a heterogeneous entity. *Am J Surg Pathol* 1999; **23**: 1068-1074
17 **Gray SF,** Wyatt JI, Rathbone BJ. Simplified techniques for identifying Campylobacter pyloridis. *J Clin Pathol* 1986; **39**: 1279
18 **Jones JH,** Lennard-Jones JE, Morson BC, Chapman M, Sackin MJ, Sneath PH, Spicer CC, Card WI. Numerical taxonomy and discriminant analysis applied to non-specific colitis. *Q J Med* 1973; **42**: 715-732
19 **Sylwestrowicz T,** Kelly JK, Hwang WS, Shaffer EA. Collagenous colitis and microscopic colitis: the watery diarrhea-colitis syndrome. *Am J Gastroenterol* 1989; **84**: 763-768
20 **Giardiello FM,** Lazenby AJ, Bayless TM, Levine EJ, Bias WB, Ladenson PW, Hutcheon DF, Derevjanik NL, Yardley JH. Lymphocytic (microscopic) colitis. Clinicopathologic study of 18 patients and comparison to collagenous colitis. *Dig Dis Sci* 1989; **34**: 1730-1738
21 **Perk G,** Ackerman Z, Cohen P, Eliakim R. Lymphocytic colitis: a clue to an infectious trigger. *Scand J Gastroenterol* 1999; **34**: 110-112
22 **Tremaine WJ**. Collagenous colitis and lymphocytic colitis. *J Clin Gastroenterol* 2000; **30**: 245-249
23 **Goosney DL,** Gruenheid S, Finlay BB. Gut feelings: enteropathogenic E. coli (EPEC) interactions with the host. *Annu Rev Cell Dev Biol* 2000: 173-189
24 **Goosney DL,** DeVinney R, Finlay BB. Recruitment of cytoskeletal and signaling proteins to enteropathogenic and enterohemorrhagic Escherichia coli pedestals. *Infect Immun* 2001; **69**: 3315-3322
25 **Mishra OP,** Dhawan T, Singla PN, Dixit VK, Arya NC, Nath G. Endoscopic and histopathological evaluation of preschool children with chronic diarrhoea. *J Trop Pediatr* 2001; **47**: 77-80
26 **Raj P**. Pathogenesis and laboratory diagnosis of Escherichia coli-associated enteritis. *Clinical microbiology Newsletter* 1993, **15**: 89-93
27 **Law D**. Adhesion and its role in the virulence of enteropathogenic Escherichia coli. *Clin Microbiol Rev* 1994; **7**: 152-173
28 **Benz I,** Schmidt MA. Isolation and serologic characterization of AIDA-I, the adhesin mediating the diffuse adherence phenotype of the diarrhea-associated Escherichia coli strain 2787 (O126:H27). *Infect Immun* 1992; **60**: 13-18
29 **Collier L,** Balows A, Duerden BI: Topley and Wilson's Microbiology and Microbial Infections. 9th ed., Arnold, London, 1998: 935-967
30 **Kang G,** Pulimood AB, Mathan MM, Mathan VI. Enteroaggregative Escherichia coli infection in a rabbit model. *Pathology* 2001; **33**: 341-346
31 Wood MJ The use of antibiotics in infections due to Escherichia coli: 0157-H7. *PHLS Microbiol Dig* 1990; **8**: 18-22

Science Editor Wang XL Language **Editor Elsevier** HK

PO Box 2345, Beijing 100023, China
www.wjgnet.com
wjg@wjgnet.com

ELSEVIER

World J Gastroenterol 2005;11(46):7272-7276
World Journal of Gastroenterology ISSN 1007-9327

• *BASIC RESEARCH* •

Effects of ethanol on antioxidant capacity in isolated rat hepatocytes

Sien-Sing Yang, Chi-Chang Huang, Jiun-Rong Chen, Che-Lin Chiu, Ming-Jer Shieh, Su-Jiun Lin, Suh-Ching Yang

Sien-Sing Yang, Liver Unit, Cathay General Hospital, Taipei 106, Taiwan, China
Chi-Chang Huang, Graduate Institute of Pharmacy, School of Pharmacy, Taipei Medical University, Taipei 110, Taiwan, China
Jiun-Rong Chen, Che-Lin Chiu, Ming-Jer Shieh, Suh-Ching Yang, School of Nutrition and Health Sciences, Taipei Medical University, Taipei 110, Taiwan, China
Su-Jiun Lin, Graduate Institute of Biology and Environment Science, School of Cellular and Molecular Biology, University of New Haven, CT 06516, United States
Supported by the Research Fund from Cathay General Hospital in Taiwan, 93CGH-TMU-15
Co-first-authors: Sien-Sing Yang and Chi-Chang Huang
Correspondence to: Dr Suh-Ching Yang, School of Nutrition and Health Sciences, Taipei Medical University, Taipei 110, 250 Wu-Hsing Street, Taipei 110, Taiwan, China. sokei@tmu.edu.tw
Telephone: +886-2-27361661 Fax: +886-2-27373112
Received: 2005-03-18 Accepted: 2005-09-12

Abstract

AIM: To investigate dose-response and time-course of the effects of ethanol on the cell viability and antioxidant capacity in isolated rat hepatocytes.

METHODS: Hepatocytes were isolated from male adult Wistar rats and seeded into 100-mm dishes. Hepatocytes were treated with ethanol at concentrations between 0 (C), 10 (E10), 50 (E50), and 100 (E100) mmol/L (dose response) for 12, 24, and 36 h (time course). Then, lactate dehydrogenase (LDH) leakage, malondialdehyde (MDA) concentration, glutathione (GSH) level, and activities of glutathione peroxidase (GPX), glutathione reductase (GRD), superoxide dismutase (SOD), and catalase (CAT) were measured.

RESULTS: Our data revealed that LDH leakage was significantly increased by about 30% in group E100 over those in groups C and E10 at 24 and 36 h, The MDA concentration in groups C, E10 and E50 were significantly lower than that in group E100 at 36 h. Furthermore, the concentration of MDA in group E100 at 36 h was significantly higher by 4.5- and 1.7-fold, respectively, than that at 12 and 24 h. On the other hand, the GSH level in group E100 at 24 and 36 h was significantly decreased, by 32% and 28%, respectively, compared to that at 12 h. The activities of GRD and CAT in group E100 at 36 h were significantly less than those in groups C and E10. However, The GPX and SOD activities showed no significant change in each group.

CONCLUSION: These results suggest that long-time incubation with higher concentration of ethanol (100 mmol/L) decreased the cell viability by means of reducing GRD and CAT activities and increasing lipid peroxidation.

Key words: Hepatocyte; Ethanol; Lipid peroxidation; Antioxidant capacity

Yang SS, Huang CC, Chen JR, Chiu CL, Shieh MJ, Lin SJ, Yang SC. Effects of ethanol on antioxidant capacity in isolated rat hepatocytes. *World J Gastroenterol* 2005; 11(46): 7272-7276
http://www.wjgnet.com/1007-9327/11/7272.asp

INTRODUCTION

Ethanol is metabolized to acetaldehyde by some enzymes in the body, including alcohol dehydrogenase (ADH), cytochrome P450 2E1 (CYP 2E1), catalase (CAT), xanthine oxidase (XO), etc. Then acetaldehyde is decomposed to acetic acid by acetaldehyde dehydrogenase (ALDH) in mitochondria. Several studies have provided evidences for reactive oxygen species (ROS) generation during ethanol metabolism, including superoxide radical[1], hydrogen peroxide[2], hydroxyl radical[3], and 1-hydroxyethyl radical[4]. Numerous studies have indicated that excessive ethanol intake induces the mass production of free radicals in the body, which are considered to be associated with alcoholic liver disease[5]. Furthermore, a number of experimental studies demonstrated that either acute or chronic alcohol administration to experimental animals increases the formation of lipid peroxidation products, such as malondialdehyde (MDA), and decreases tissue levels of antioxidants, such as glutathione (GSH), in the liver[6]. Bailey and Cunningham also indicated that the exposure of hepatocytes to ethanol resulted in increased production of ROS, which correlated with decreased cell viability[7]. The impairment of cellular antioxidant defenses along with the formation of oxygen-derived radicals has been proposed to play a role in causing oxidative damage associated with alcoholic liver disease. Moreover, the individual differences in animals always makes the results inconsistent; therefore, the purpose of this study was to investigate and clarify the influences of different concentrations of ethanol on the

cell viability, antioxidant capacity, and antioxidant enzymes activities in the isolated liver parenchymal cells during different incubation times.

MATERIALS AND METHODS

Preparation of isolated rat hepatocytes

Hepatocytes were isolated from rats according to the two-step collagenase perfusion technique described by Berry and Friend[8]. Isolated cells were cultured as monolayers in William's medium E with 5% fetal bovine serum and 1 μmol/L dexamethasone at a density of 1×10^5 cells/mL. After 24 h of incubation at 37 ℃ in 50 mL/L CO_2, hepatocytes were treated with ethanol at concentrations between 0 (C), 10 (E10), 50 (E50), and 100 (E100) mmol/L (dose response) for 12, 24, and 36 h (time course). Then, the cells were collected using a scraper and resuspended in Tris buffer (50 mmol/L Tris-HCl, 5 mmol/L EDTA, and 1 mmol/L DTT, pH 7.5) for analysis as follows.

Lactate dehydrogenase (LDH) leakage

The viability of hepatocytes was expressed as the percentage of LDH leakage, which was the LDH activity in the culture medium relative to the total LDH activity including the culture medium and cytosolic fraction. The LDH level was determined using the method described by a previous study[9].

Lipid peroxidation of hepatocytes

The MDA concentration of hepatocytes was assessed colorimetrically at 586 nm using a commercial kit (Calbiochem 437634; Calbiochem-Novabiochem, La Jolla, CA, USA). The concentration was expressed as nmol/mg protein in hepatocytes.

Glutathione (GSH) concentration of hepatocytes

The concentration of reduced GSH in hepatocytes was measured spectrophotometrically at 400 nm using a commercial kit (Calbiochem 354102; Calbiochem-Novabiochem). The concentration was expressed as nmol/mg protein in hepatocytes.

Glutathione peroxidase (GPX) activity of hepatocytes

GPX activity of hepatocytes was determined with a commercial kit (RS 504; Randox Laboratories, Antrim, UK). Twenty microliters of the diluted sample was added to 1 mL of mixed substrate (4 mmol/L GSH, 0.5 U/L GRD and 0.34 mmol/L NADPH dissolved in 50 mmol/L phosphate buffer, pH 7.2, 4.3 mmol/L EDTA). Forty microliters of cumene hydroperoxide (diluted in deionized water) was added to the mixture and GPX activity was measured at 37 ℃ on a Hitachi U-2000 Spectrophotometer at 340 nm for 3 min. The activity was expressed as mU/mg protein in hepatocytes.

Glutathione reductase (GRD) activity of hepatocytes

GRD activity of hepatocytes was measured with a commercial kit (Calbiochem 359962; Calbiochem-Novabiochem). Two hundred microliters of the diluted sample was added to 400 μL of 2.4 mmol/L GSSG buffer (dissolved in 125 mmol/L potassium phosphate buffer, pH 7.5, 2.5 mmol/L EDTA). Four hundred microliters of 0.55 mmol/L NADPH (dissolved in deionized water) was added to the mixture and GRD activity was measured at 340 nm for 5 min on a Hitachi U-2000 Spectrophotometer. The activity was expressed as mU/mg protein in hepatocytes.

Superoxide dismutase (SOD) activity of hepatocytes

SOD activity of hepatocytes was measured with a commercial kit (SD 125; Randox Laboratories). Fifty microliters of the diluted sample was added to 1.7 mL of mixed substrate (50 μmol/L xanthine and 25 μmol/L 2-(4-iodophenyl)-3-(4-nitrophenyl)-5-phenyl tetrazolium chloride, INT). Two hundred and fifty microliters of XO was added to the mixture and SOD activity was measured at 37 ℃ on a Hitachi U-2000 Spectrophotometer at 505 nm for 3 min. The activity was expressed as U/mg protein in hepatocytes.

Catalase (CAT) activity of hepatocytes

CAT activity of hepatocytes was determined at 25 ℃ with Hitachi U-2000 Spectrophotometer UV-VIS Spectrophotometer according to the previous study[10]. Diluted sample was added to 59 mmol/L H_2O_2 (dissolved in 50 mmol/L potassium phosphate buffer, pH 7.0) and CAT activity was measured at 240 nm for 3 min. One unit of CAT activity was defined as the mmol of H_2O_2 degraded/min/mg protein. The activity was expressed as U/mg protein in hepatocytes.

Total protein concentration

In order to express the antioxidant enzymes activities per gram of protein, total protein concentration of hepatocytes was determined colorimetrically by using a Bio-Rad DC protein assay kit (Cat. No. 500-0116; Bio-Rad Laboratories, Hercules, CA, USA).

Statistical analysis

Values were expressed as mean±SD. To evaluate the differences between the groups studied, two-way analysis of variance (ANOVA) with Fisher's *post hoc* test was used. The SAS software (Vers. 8.2, SAS Institute Inc., Cary, NC, USA) was used to analyze all the data. Differences were considered statistically significant when $P<0.05$.

RESULTS

Effect of ethanol on LDH leakage

LDH leakage into the culture media of hepatocyte was used to assess the hepatotoxicity of ethanol (Figure 1). LDH leakage in group E10 was nearly the same as that in group C at 12, 24, and 36 h. In contrast, LDH leakage in group E100 was significantly increased by about 30% more than that in groups C and E10 at 24 and 36 h ($P<0.05$). Furthermore, the LDH leakage showed dose-dependent correlation with the ethanol concentrations ($P = 0.0026$). However, there was no significant correlation between LDH leakage and incubation time of ethanol ($P>0.05$).

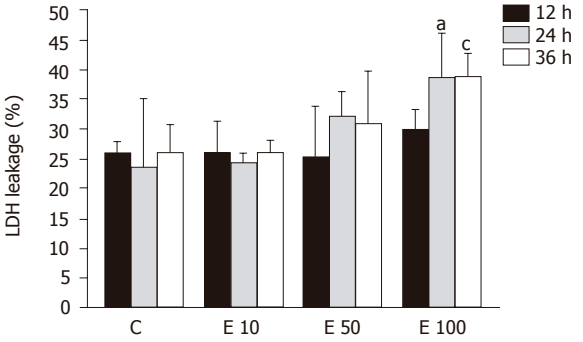

Figure 1 Lactate dehydrogenase (LDH) leakage of primary rat hepatocytes in each group. Data are mean±SD for 3 hepatocyte preparations. Cultures were incubated without ethanol (C), with 10 mmol/L ethanol (E 10), with 50 mmol/L ethanol (E 50), and with 100 mmol/L ethanol (E 100) for 12, 24, and 36 h, respectively. [a]*P*<0.05 *vs* 24 h of group C and E 10; [c]*P*<0.05 *vs* 36 h of groups C and E 10.

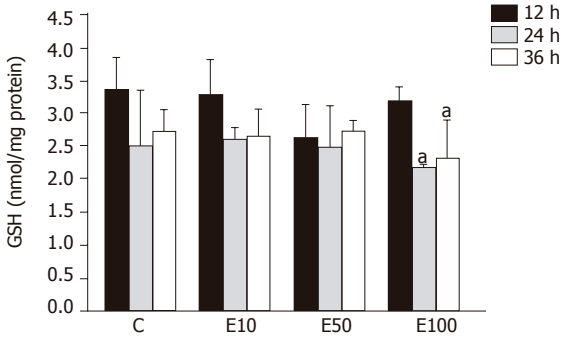

Figure 3 Glutathione (GSH) concentrations of primary rat hepatocytes in each group. Data are mean±SD for 3 hepatocyte preparations. Cultures were incubated without ethanol (C), with 10 mmol/L ethanol (E 10), with 50 mmol/L ethanol (E 50), and with 100 mmol/L ethanol (E 100) for 12, 24, and 36 h, respectively. [a]*P*<0.05 *vs* 12 h of group E 100.

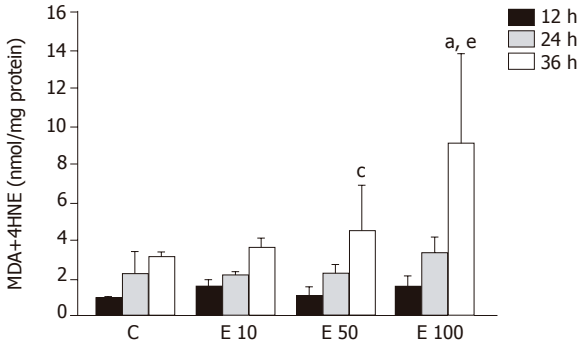

Figure 2 Lipid peroxidation of primary rat hepatocytes in each group. Lipid peroxidation was estimated by the measurement of MDA. Data are mean±SD for 3 hepatocyte preparations. Cultures were incubated without ethanol (C), with 10 mmol/L ethanol (E 10), with 50 mmol/L ethanol (E 50), and with 100 mmol/L ethanol (E 100) for 12, 24, and 36 h, respectively. [a]*P*<0.05 *vs* 36 h of groups C, E 10 and E 50; [c]*P*<0.05 *vs* 12 h of group E 50; [e]*P*<0.05 *vs* 12 h and 24 h of group E 100.

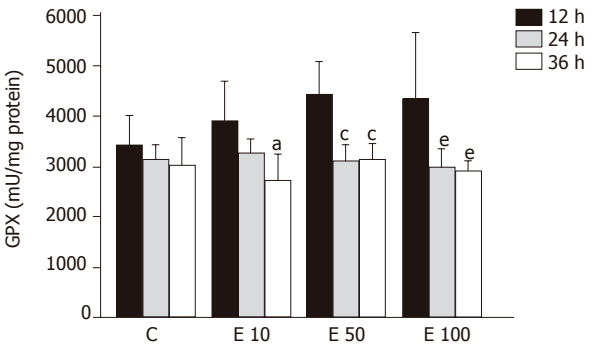

Figure 4 Glutathione peroxidase (GPX) activities of primary rat hepatocytes in each group. Data are mean±SD for 3 hepatocyte preparations. Cultures were incubated without ethanol (C), with 10 mmol/L ethanol (E 10), with 50 mmol/L ethanol (E 50), and with 100 mmol/L ethanol (E 100) for 12, 24, and 36 h, respectively. [a]*P*<0.05 *vs* 12 h of group E10; [c]*P*<0.05 *vs* 12 h of group E 50; [e]*P*<0.05 *vs* 12 h of group E 100.

Effect of ethanol on lipid peroxidation

The level of MDA in group E100 at 36 h was significantly increased by 1.9-, 1.5-, and 1.0-fold, respectively, over that in groups C, E10, and E50 ($P<0.05$, Figure 2). In group E50 and group E100, the lipid peroxidation product was significantly elevated at 36 h ($P<0.05$), by 2.9- and 4.5-fold, respectively, when compared to that at 12 h. In addition, there was no significant difference in group C and group E10. The level of MDA also showed significant correlation with the incubation concentration and time of ethanol ($P = 0.0105$ and $P = 0.0001$, respectively).

Effect of ethanol on antioxidant level

There was no significant difference across the groups at different times (Figure 3). However, in group E100, the GSH level was significantly decreased at 24 and 36 h, by 32% and 28%, respectively, over that at 12 h ($P<0.05$).

Effect of ethanol on antioxidant enzymes activities

There was no significant difference in GPX activity in each group at different times (Figure 4). However, in group E10, the GPX activity was significantly decreased at 36 h from that at 12 h ($P<0.05$). Furthermore, both in groups E50 and E100, GPX activities were significantly lowered at 24 and 36 h from those at 12 h ($P<0.05$). As a result, the activity of GPX was significantly correlated with the incubation time course ($P = 0.0004$).

After 36-h incubation, there were significantly fewer GRD activities in groups E50 and E100 than in groups C and E10 ($P<0.05$, Figure 5). However, both in group C and group E10 at 36 h, the activities of GRD were significantly increased over those at 12 and 24 h ($P<0.05$). On the other hand, the relation of GRD activity and the incubation time showed positive correlation ($P = 0.0002$).

There were no significant differences among the groups at different times in SOD activity (Figure 6). SOD activity of group E50 was significantly decreased at 36 h, by 45%, from that at 12 h ($P<0.05$). Furthermore, in group E100, the SOD activities were significantly decreased at 24 and 36 h, by 40% and 38%, respectively, from that at 12 h ($P<0.05$). In addition, the activity of SOD exhibited the reverse correlation with the incubation time ($P = 0.0018$).

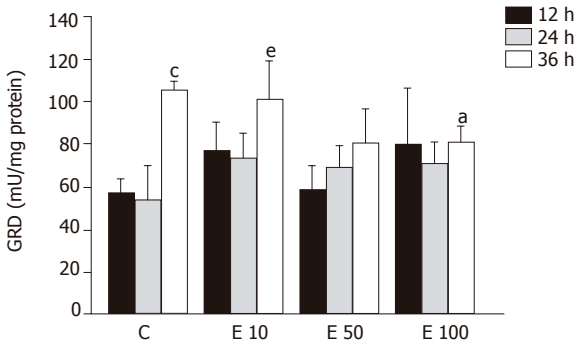

Figure 5 Glutathione reductase (GRD) activities of primary rat hepatocytes in each group. Data are mean±SD for 3 hepatocyte preparations. Cultures were incubated without ethanol (C), with 10 mmol/L ethanol (E 10), with 50 mmol/L ethanol (E 50), and with 100 mmol/L ethanol (E 100) for 12, 24, and 36 h, respectively. $^{a}P<0.05$ *vs* 36 h of groups C and E 10; $^{c}P<0.05$ *vs* 12 h and 24 h of groups C; $^{e}P<0.05$ *vs* 12 h and 24 h of group E 10.

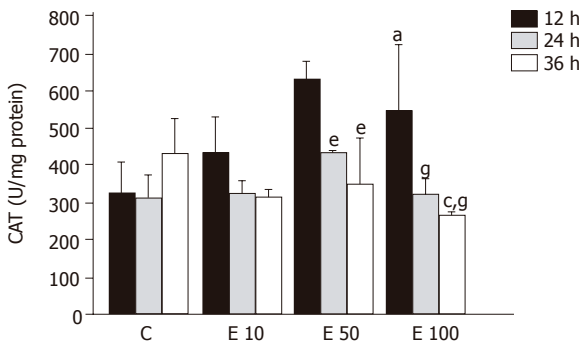

Figure 7 Catalase (CAT) activities of primary rat hepatocytes in each group. Data are mean±SD for 3 hepatocyte preparations. Cultures were incubated without ethanol (C), with 10 mmol/L ethanol (E 10), with 50 mmol/L ethanol (E 50), and with 100 mmol/L ethanol (E 100) for 12, 24, and 36 h, respectively. $^{a}P<0.05$ *vs* 12 h of groups C; $^{c}P<0.05$ *vs* 36 h of groups C and E 50; $^{e}P<0.05$ *vs* 12 h of group E 50; $^{g}P<0.05$ *vs* 12 h of group E 100.

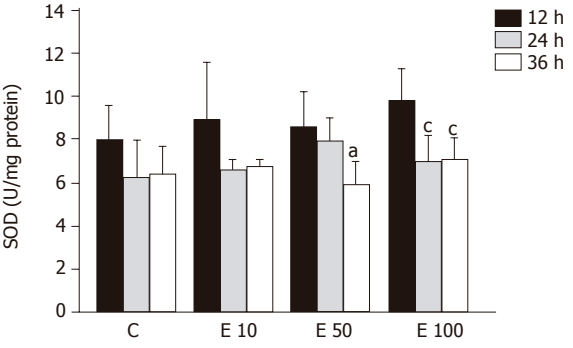

Figure 6 Superoxide dismutase (SOD) activities of primary rat hepatocytes in each group. Data are mean±SD for 3 hepatocyte preparations. Cultures were incubated without ethanol (C), with 10 mmol/L ethanol (E 10), with 50 mmol/L ethanol (E 50), and with 100 mmol/L ethanol (E 100) for 12, 24, and 36 h, respectively. $^{a}P<0.05$ *vs* 12 h of group E50; $^{c}P<0.05$ *vs* 12 h of group E 100.

After 12-h incubation, CAT activities in groups E50 and E100 were significantly increased, by 94% and 68%, respectively, over those in group C ($P<0.05$, Figure 7). On the contrary, CAT activity in group E100 at 36 h was significantly decreased from that in groups C and E50 ($P<0.05$). Moreover, both in groups E50 and E100, CAT activities were significantly lowered at 24 and 36 h from those at 12 h ($P<0.05$). There was a significant increase in correlation between CAT activity and incubation time ($P = 0.0003$).

DISCUSSION

LDH is an enzyme that exists in many tissues and organs, such as the heart, muscle, kidney, liver, etc. When those tissues or organs are damaged, LDH is released into the blood from the cells. Therefore, LDH leakage can be used to indicate cell viability. In this study, the viability of hepatocytes was monitored by the release of LDH into the medium. That is to say, higher LDH leakage was interpreted as lower viability of hepatocytes. The previous study has shown that ethanol increased the production of ROS and resulted in a decrease in hepatocyte viability[7]. Results in this study also suggest that high concentration of ethanol (100 mmol/L) may decrease cell viability of hepatocytes.

MDA was one of the main lipid peroxidation products, its elevated levels could reflect the degrees of lipid peroxidation induced injury in hepatocytes[11]. Many reports have demonstrated that ethanol exposure promotes the accumulation of lipid peroxidation *in vivo*[12] and *in vitro*[13]. Lipid peroxidation induced by ethanol administration results from not only increasing ROS production but also the mass generation of acetaldehyde[14]. Our data also indicated that the MDA concentration showed significant correlation with the incubation concentration and time of ethanol in isolated rat hepatocytes.

It has been reported that chronic ethanol feeding results in increased[15], decreased[16], or unchanged hepatic GSH contents[17] *in vivo*. The discrepancies in the total GSH levels in the livers of rats chronically fed with ethanol might have originated from the differences in the strains of rats used and the dose, duration, and route of ethanol administration among the different studies. On the other hand, the previous study has demonstrated that acute ethanol administration neither decreases nor increases the GSH level in hepatocytes, at least within 4 h after treating with 50 mmol/L ethanol *in vitro*[18]. Our results also showed that there was no significant difference in GSH content after 50 mmol/L ethanol treatment in hepatocytes. But the GSH concentration in hepatocytes significantly declined after 100 mmol/L ethanol treatment at 24 and 36 h. In this study, the reduction of GSH and the elevation of lipid peroxidation were simultaneously observed in the 100 mmol/L ethanol exposure. Thus, it could be speculated that ethanol-induced lipid peroxidation might contribute to decreased GSH contents in this study as previously shown by others[18].

Metabolism of ethanol is believed to result in the increased production of ROS, especially superoxide and

H_2O_2, and the removal of these toxic species is thought to be a vital initial step in ensuring cell survival during ethanol intoxication[6]. Four major antioxidant enzymes available to the cell during ethanol-induced oxidant stress include GPX, GRD, SOD, and CAT. The previous study has shown that GPX, CAT, and SOD activities showed an inverse correlation with the severity of pathological injury in rats fed with ethanol[12]. In contrast, Oh *et al.* reported that chronic ethanol feeding resulted in the lower activity of GPX with significantly higher activities of GRD and CAT[15]. However, there have been a few reports about the effects of ethanol on antioxidant enzymes activities in hepatocytes *in vitro*. Our data suggest that higher concentration of ethanol may reduce antioxidant enzymes activities of GRD and CAT after long-time incubation and contribute to decreased cell viability and increased lipid peroxidation.

In conclusion, this study indicates the direct relatedness between ethanol and hepatocytes and excludes the factor of gastrointestinal absorption. It was demonstrated that 100 mmol/L ethanol exposure diminished the cell viability because the lipid peroxidative product accumulated, which was caused by the decreased antioxidative status, including the reduction of GSH contents, GRD and CAT activities.

REFERENCES

1 **Boveris A,** Fraga CG, Varsavsky AI, Koch OR. Increased chemiluminescence and superoxide production in the liver of chronically ethanol-treated rats. *Arch Biochem Biophys* 1983; **227:** 534-541

2 **Ekstrom G,** Ingelman-Sundberg M. Rat liver microsomal NADPH-supported oxidase activity and lipid peroxidation dependent on ethanol-inducible cytochrome P-450 (P-450IIE1). *Biochem Pharmacol* 1989; **38:** 1313-1319

3 **Ingelman-Sundberg M**, Johansson I. Mechanisms of hydroxyl radical formation and ethanol oxidation by ethanol-inducible and other forms of rabbit liver microsomal cytochromes P-450. *J Biol Chem* 1984; **259:** 6447-6457

4 **Rashba-Step J,** Turro NJ, Cederbaum AI. Increased NADPH- and NADH-dependent production of superoxide and hydroxyl radical by microsomes after chronic ethanol treatment. *Arch Biochem Biophys* 1993; **300:** 401-408

5 **Ishii H,** Kurose I, Kato S. Pathogenesis of alcoholic liver disease with particular emphasis on oxidative stress. *J Gastroenterol Hepatol* 1997; **12:** S272-S282

6 **Nordmann R,** Ribiere C, Rouach H. Implication of free radical mechanisms in ethanol-induced cellular injury. *Free Radic Biol Med* 1992; **12:** 219-240

7 **Bailey SM**, Cunningham CC. Effect of dietary fat on chronic ethanol-induced oxidative stress in hepatocytes. *Alcohol Clin Exp Res* 1999; **23:** 1210-1218

8 **Berry MN**, Friend DS. High-yield preparation of isolated rat liver parenchymal cells: a biochemical and fine structural study. *J Cell Biol* 1969; **43:** 506-520

9 **Moldeus P,** Hogberg J, Orrenius S. Isolation and use of liver cells. *Methods Enzymol* 1978; **52:** 60-71

10 **BEERS RF Jr,** SIZER IW. A spectrophotometric method for measuring the breakdown of hydrogen peroxide by catalase. *J Biol Chem* 1952; **195:** 133-140

11 **Hu YY**, Liu CH, Wang RP, Liu C, Liu P, Zhu DY. Protective actions of salvianolic acid A on hepatocyte injured by peroxidation in vitro. *World J Gastroenterol* 2000; **6:** 402-404

12 **Polavarapu R,** Spitz DR, Sim JE, Follansbee MH, Oberley LW, Rahemtulla A, and Nanji AA. Increased lipid peroxidation and impaired antioxidant enzyme function is associated with pathological liver injury in experimental alcoholic liver disease in rats fed diets high in corn oil and fish oil. *Hepatology* 1998; **27:** 1317-1323

13 **Sergent O,** Morel I, Cogrel P, Chevanne M, Pasdeloup N, Brissot P, Lescoat G, Cillard P, and Cillard J. Increase in cellular pool of low-molecular-weight iron during ethanol metabolism in rat hepatocyte cultures. Relationship with lipid peroxidation. *Biol Trace Elem Res* 1995; **47:** 185-192

14 **Muller A**, Sies H. Role of alcohol dehydrogenase activity and the acetaldehyde in ethanol- induced ethane and pentane production by isolated perfused rat liver. *Biochem J* 1982; **206:** 153-156

15 **Oh SI,** Kim CI, Chun HJ, Park SC. Chronic ethanol consumption affects glutathione status in rat liver. *J Nutr* 1998; **128:** 758-763

16 **Rouach H,** Fataccioli V, Gentil M, French SW, Morimoto M, Nordmann R. Effect of chronic ethanol feeding on lipid peroxidation and protein oxidation in relation to liver pathology. *Hepatology* 1997; **25:** 351-355

17 **Shaw S,** Jayatilleke E, Ross WA, Gordon ER, Leiber CS. Ethanol-induced lipid peroxidation: potentiation by long-term alcohol feeding and attenuation by methionine. *J Lab Clin Med* 1981; **98:** 417-422

18 **Higuchi H,** Kurose I, Kato S, Miura S, Ishii H. Ethanol-induced apoptosis and oxidative stress in hepatocytes. *Alcohol Clin Exp Res* 1996; **20:** 340A-346A

Science Editor Guo SY and Xu XQ **Language Editor** Elsevier HK

PO Box 2345, Beijing 100023, China
www.wjgnet.com
wjg@wjgnet.com

ELSEVIER

World J Gastroenterol 2005;11(46):7277-7283
World Journal of Gastroenterology ISSN 1007-9327

• *CLINICAL RESEARCH* •

Bacterial biota in reflux esophagitis and Barrett's esophagus

Zhiheng Pei, Liying Yang, Richard M Peek, Jr Steven M Levine, David T Pride, Martin J Blaser

Zhiheng Pei, Departments of Pathology and Medicine, New York University School of Medicine, New York, NY 10016, the United States of America, and Department of Veterans Affairs New York Harbor Health System, New York, NY 10010, United States
Liying Yang, Department of Pathology, New York University School of Medicine, New York, NY 10016, United States
Richard M Peek, Jr, Department of Medicine, Vanderbilt University School of Medicine, Nashville, TN 37212, United States
Steven M Levine, Department of Medicine, New York University School of Medicine, New York, NY 10016, United States
David T Pride, Departments of Medicine and Microbiology, New York University School of Medicine, New York, NY 10016, United States
Martin J Blaser, Departments of Medicine and Microbiology, New York University School of Medicine, New York, NY 10016, the United States of America, and Department of Veterans Affairs New York Harbor Health System, New York, NY 10010, United States
Supported by R01CA97946, R21DK57941, R01GM63270, R01 DK58587, and R01CA77955, and by the General Clinical Research Center core grant to New York University School of Medicine (NIH/NCRR M01 RR00096) from the National Institutes of Health, by the Medical Research Service of the Department of Veterans Affairs, and by the Ellison Medical Foundation
Correspondence to: Zhi-Heng Pei, MD, PhD, Department of Pathology and Laboratory Services (113), Department of Veterans Affairs New York Harbor Health System , 423 E 23rd Street, New York, NY 10010, United States. zhiheng.pei@med.nyu.edu.
Telephone: +1-2129515492 Fax: +1-2122527167
Received: 2005-04-01 Accepted: 2005-04-30

Abstract

AIM: To identify the bacterial flora in conditions such as Barrett's esophagus and reflux esophagitis to determine if they are similar to normal esophageal flora.

METHODS: Using broad-range 16S rDNA PCR, esophageal biopsies were examined from 24 patients [9 with normal esophageal mucosa, 12 with gastroesophageal reflux disease (GERD), and 3 with Barrett's esophagus]. Two separate broad-range PCR reactions were performed for each patient, and the resulting products were cloned. In one patient with Barrett's esophagus, 99 PCR clones were analyzed.

RESULTS: Two separate clones were recovered from each patient (total = 48), representing 24 different species, with 14 species homologous to known bacteria, 5 homologous to unidentified bacteria, and 5 were not homologous (<97% identity) to any known bacterial 16S rDNA sequences. Seventeen species were found in the reflux esophagitis patients, 5 in the Barrett's esophagus patients, and 10 in normal esophagus patients. Further analysis concentrating on a single biopsy from an individual with Barrett's esophagus revealed the presence of 21 distinct bacterial species. Members of four phyla were represented, including *Bacteroidetes, Firmicutes, Proteobacteria, and Actinobacteria.* Microscopic examination of each biopsy demonstrated bacteria in intimate association with the distal esophageal epithelium, suggesting that the presence of these bacteria is not transitory.

CONCLUSION: These findings provide evidence for a complex, residential bacterial population in esophageal reflux-related disorders. While much of this biota is present in the normal esophagus, more detailed comparisons may help identify potential disease associations.

Key words: Bacterial biota; Esophagus; 16S rDNA PCR

Pei ZH, Yang LY, Peek RM, Jr Levine SM, Pride DT, Blaser MJ. Bacterial biota in reflux esophagitis and Barrett's esophagus. *World J Gastroenterol* 2005; 11(46): 7277-7283
http://www.wjgnet.com/1007-9327/11/7277.asp

INTRODUCTION

Colonizing bacteria exist in each portion of the human digestive tract, from the oral cavity to the anus. Colonizing bacterial populations are essential for the development of the gastrointestinal mucosal immune system, for the maintenance of a normal physiological environment, and for the provision of essential nutrients[1,2]. Colonizing bacteria also play a role in a variety of disease conditions, as exemplified by the gastric colonizer *Helicobacter pylori* in relation to gastric cancer[3]. Conversely, loss of normal biota is responsible for the overgrowth of opportunistic pathogens that normally are inhibited, such as that occurs in antibiotic-associated colitis[4,5], or in candida vaginitis[6]. Microenvironment alterations may favor overgrowth of bacteria that produce carcinogenic metabolites[7-11], promoting tumorigenesis in inflammation-induced cancers, such as adenocarcinoma in experimental colitis mouse models[12].

A complex bacterial biota has been defined recently in the normal distal esophagus, estimated to be composed of approximately 140 species, of which 95 are identified[13].

Members of six phyla, *Firmicutes, Bacteroides, Actinobacteria, Proteobacteria, Fusobacteria,* and *TM7* are represented. *Firmicutes* represent the most commonly identified phylum in the distal esophagus, followed by phylum *Bacteroidetes*. Some of the phyla, including Spirochaetes and *Deferribacteres* that are commonly represented in the oral cavity, are not identified as esophageal flora, indicating that conditions in the distal esophagus are not ideal for the colonization of all oral flora. These are 14 species identified in the distal esophagus in all four persons studied[13], indicating that the esophageal biota are unique residents, and not identified simply as organisms transiting from the oral to the gastric cavity. Thus, although the esophagus is generally viewed as a conduit for food passage, the environment in which the bacteria reside is relatively stable.

The distal esophagus may be distinguished from other portions of the esophagus by the changes induced by the reflux of gastric and duodenal contents. Persistent untreated gastroesophageal reflux disease (GERD) can lead to a metaplastic and premalignant condition known as Barrett's esophagus, which carries an increased risk of esophageal adenocarcinoma. Repeated exposure of the distal esophagus to gastric acid and duodenal bile salts likely alters the biota present in the distal esophagus; as has been previously demonstrated in the stomach, changes in the microenvironment lead to alterations in colonizing bacterial populations[15]. One possibility is that perturbation of the normal esophageal biota could contribute to the progression from GERD to Barrett's esophagus towards the development of adenocarcinoma. Because little is known about the nature of bacterial biota in reflux esophagitis-related diseases, we sought to identify whether there exists a population of bacteria in patients with GERD and Barrett's esophagus. Our specific goal in this pilot study was to use broad-range 16S rDNA PCR to identify the presence of colonizing bacteria in patients with reflux esophagitis or Barrett's esophagus.

MATERIALS AND METHODS

Subjects

Patients presenting to the Department of Veterans Affair Medical Center, Nashville, TN, USA with gastrointestinal symptoms requiring upper gastrointestinal endoscopy were eligible for this study. Those who were willing to participate in the studies of upper gastrointestinal microbiology and who signed an informed consent form were recruited for this study[16]. Exclusion criteria included recent use of antibiotics, previous gastric/esophageal surgery, and active infection of the oral cavity[17]. Esophagogastroduodenoscopy was performed and endoscopic findings were recorded for 24 consecutive patients who met the above criteria. Esophageal biopsies were obtained 2 cm above the squamocolumnar junction or in the case of Barrett's esophagus, 2 cm above the gastroesophageal junction. Each biopsy was examined microscopically for morphological features of GERD and intestinal metaplasia (Barrett's esophagus). As described, features consistent with GERD included mucosal erosions/superficial ulcerations, epithelial hyperplasia, and inflammatory infiltrate of polymorphonuclear cells or eosinophils in the mucosal layer. Features of Barrett's esophagus included the presence of intestinal-type epithelium in the esophagus[18]. Tissue sections of esophageal biopsies from representative patients with normal esophagus, esophagitis, or Barrett's esophagus were examined by microscopy using Gram-Twort stain[19].

Specimen processing for molecular biological studies

Biopsies of 2 mm×2 mm×2 mm obtained for this study were placed in a 1.5-mL screw-top test tube and stored at -70 ℃. The specimens were coded so that the laboratorian performing the studies was blinded to the clinical information. DNA was extracted from the biopsy using a tissue DNA extraction kit (Qiagen) in a PCR-free clean-room and the DNA-enriched fractions were eluted in 200 microliters of buffer, as described by the manufacturer.

PCR

For each PCR amplification, 5 microliters of the DNA extracted from each biopsy was added to 45 μL of PCR reaction mixture containing 5 μL of 10× PCR buffer (Qiagen), 1.5 mmol/L $MgCl_2$, 200 μmol/L each dNTP, 50 pmol of each primer, and 5 units of Taq DNA polymerase. Reactions were run at 94 ℃ for 2 min, followed by 30 cycles of amplification at 94 ℃ for 30 s, 55 ℃ for 30 s, and 72 ℃ for 30 s and a 10-min extension at 72 ℃. Primers used were fPB7I (forward): 5' -GGIACTGAGACACIGICCIIACTCCT-3' and rPB10I (reverse): 5'-CGTATTACCGCIGCTGCTGGCAC-3', where I represents inosine, which was used at positions of nucleotide ambiguity, since it forms stable base pairs with A, G, T, and C. Use of inosine-containing primers significantly reduces the complexity accompanying the use of conventional degenerate primers[20-22]. As such, both inosine-containing primers perfectly match the consensus sequence-derived 16S rDNA pools composed of 21 evolutionarily-well diversified eubacterial groups including *Agrobacterium, Aquifex, Arthrobacter, Bacillus, Chlamydia, Chlorobium, Chloroflexus, Chloroplast, Clostridium, Desulfovibrio, Escherichia, Flavobacterium, Flexibacter, Gloeobacter, Heliobacterium, Leptonema, Planctomyces, Rhodocyclus, Synechococcus, Thermotoga,* and *Thermus*[23], but do not have significant 3' homology with human 18S rDNA, and human mitochondrial small subunit rDNA sequences. The expected PCR products are approximately 210 bp, depending on the species. In a study to determine the sensitivity, the above primer pair was able to amplify as little as one copy of an *Escherichia coli* genome (data not shown). An amplification control was designed to assess whether DNA extracted from the esophageal biopsy is of sufficient quality and quantity to be amplified by PCR. A primer pair specific for human 18S rDNA

was designed to serve this purpose: PBH (forward), 5' -TTGCCAAGAATGTTTTC-3' and rPBH (reverse), 5' -CGCGTAACTAGTTAGCA-3'.

Cloning and sequencing

The PCR products were separated from free PCR primers using a PCR purification kit (Qiagen), then ligated with the pGEM® T Easy (Promega) vector, and used to transform into *E coli* DH5α competent cells. The cloned inserts underwent sequence analysis using vector-based primers.

Phylogenetic analysis

Primer sequences were removed from all sequence files, and only inter-primer sequences were used in subsequent analyses. The sequences were analyzed using standard nucleotide BLAST (Blastn) search of GenBank for homology with known bacterial 16S rDNA sequences. In this study, 16S rDNA sequences with >97% identity with known sequences were considered as homologous with known bacterial species, as described[24]. 16S rDNA sequences were aligned using ClustalW[25] and phylograms of nucleotide alignments generated using Paup 4.0b10 (Paup 4.0b2. Phylogenetic Analysis Using Parsimony and Other Methods, Version 4, Sinauer Associates, Sunderland, MA, USA) neighbor-joining method based on HKY85 distance matrices[26]. All novel sequences were deposited in GenBank (accession numbers: AY212255-21225564).

RESULTS

Microscopic examination of bacterial flora in the distal esophagus

The 24 patients examined included 9 with normal esophagus, 12 with esophagitis, and 3 with Barrett's esophagus (Table 1). Because chronic gastritis is generally associated with the presence of overlaying *H pylori* in the lumen[27], we examined the inflamed distal esophagus to determine whether bacterial cells might be visible. Such a study, if positive, can provide morphological evidence for an indigenous esophageal biota, and provide a rationale for its further characterization. Of the 24 biopsies, 21 had sufficient tissue materials remaining for Gram-Twort stain, including 6 from patients with normal esophagus, 12 with esophagitis, and 3 with Barrett's esophagus. Bacteria were observed in 52% of the biopsies (from 4 of 6 with normal esophagus, 5 of 12 with esophagitis, and 2 of 3 with Barrett's esophagus). Bacteria appeared to be closely associated with the epithelial cell surfaces (Figure 1). All bacteria observed in the two biopsies with Barrett's esophagus were Gram-positive cocci, while in the 9 non-Barrett's biopsies, all were Gram-negative cocci or bacilli.

Bacterial 16S rDNA in esophageal biopsy specimens

To examine the nature of the bacterial populations present in the distal esophagus and to define their ancestry, we performed universal bacterial 16S PCR on biopsies

Table 1 Clinical and pathological features of 24 patients included in this study[1]

Case#	Age[2]	Symptoms of heartburn		Esophageal features	
		Frequency (time/week)	Duration[3]	Endoscopic diagnosis	Histopathology[4]
Normal esophagus (*n* = 9)					
248	73	0	NA	Normal	NP
251	66	0	NA	Normal	NP
256	66	0	NA	Normal	NP
259	75	3	1 Y	Hiatal hernia	NP
261	81	3	>1 Y	Esophageal ring	NP
262	65	0	NA	Esophagitis	NP
263	51	3	1 Y	Gastric erosions	NP
264	72	0	NA	Esophageal ring	NP
265	71	0	NA	Hiatal hernia	NP
Esophagitis (*n* = 12)					
247	63	3	>1 Y	Esophagitis	AI, CI, EO
252	51	0	NA	Normal	AI, CI, EO
254	57	3	1 Y	Esophageal ring	AI, CI, EO
257	52	3	1 M	Esophagitis	AI, CI, EO
249	34	0	NA	Esophagitis	AI, CI
243	53	3	>1 Y	Esophagitis	CI, EO
255	66	3	>1 Y	Esophagitis	CI, EO
258	52	3	2–3 Y	Barrett's esophagus	CI, EO
244	74	3	2 M	Esophagitis	CI
250	68	0	NA	Esophageal ring	CI
260	75	3	2–3 M	Esophagitis	CI
253	71	5	4 Y	Esophagitis	CI
Barrett's esophagus (*n* = 3)					
242	69	0	NA	BE	BE
245	70	0	NA	BE	BE
246	66	3	>1 Y	BE	BE, CI, EO

[1]None of the 24 patients had a history of recent use of antibiotics, previous gastric/esophageal surgery, active infection of the oral cavity[17].
[2]All 24 patients are males, reflecting the veterans population.
[3]NA, not available; Y, year; M, month.
[4]NP: no pathologic changes; BE: Barrett's esophagus; EO: eosinophils; CI: chronic inflammation; AI: acute inflammation.

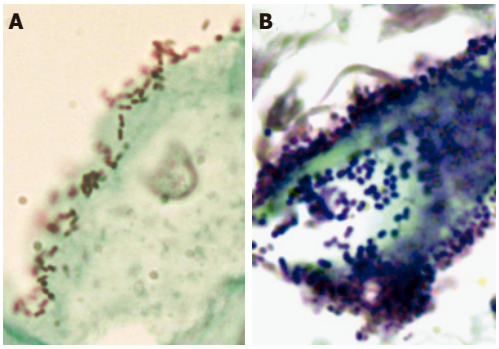

Figure 1 Microscopic examination of bacterial cells in the esophagus. Esophageal biopsies were fixed in formalin, paraffin-embedded, sectioned, and examined by using Gram-Twort stain. **A:** In the biopsy from patient #265 with a normal esophagus, Gram-negative cocci and coccobacilli were tightly associated with the surface of squamous epithelial cells. **B:** In the biopsy from patient #246 with Barrett's esophagus, Gram-positive cocci were highly concentrated within the lumen of an intestinal-type gland.

from each of the 24 studied patients. From each of the 24 biopsies, 2 clones of PCR products were randomly picked and sequenced. The 48 samples yielded 36 unique sequences belonging to 24 different species (97% identical), as established through GenBank BLAST searches. Of the 24 species identified, 14 represented known cultivation-defined bacterial species by sharing 97% identity, 5 shared 97% identity to 5 noncultured/unidentified bacterial species, and 5 did not share significant homology (<97% identity) with any existing bacterial 16S rDNA sequences in the GenBank (Table 2).

Of the 48 clones sampled, unidentified oral bacterium SH66 was the most prevalent species amplified, accounting for 22.9% (11 clones from 9 patients), followed by *Prevotella veroralis* (10.4%, 5 clones from 5 patients), members of the *Streptococcus genus* (10.4%, 5 clones from 5 patients), and *H pylori* (6.3%, 3 clones from 2 patients) (Table 2). None of the remaining species constituted more than 5% of

Table 2 Analysis of 48 bacterial 16S rDNA sequences detected in the esophageal biopsies from 24 patients

Best matched bacterial 16S rDNA	% Identity[1]	Number of sequences detected			
		Normal esophagus	Esophageal disease		All patients (n = 24)
		(n = 9)[2]	Esophagitis (n = 12)	Barrett's (n = 3)	
Cultivation-defined species[3] (n = 14)					
Prevotella veroralis	98.2	4	1		5
Streptococcal species	100	1	2		3
Pseudomonas species	100		2	1	3
Helicobacter pylori	100, 99.3, 98.6		3		3
Prevotella pallens	100	1		1	2
Streptococcus salivarius	100, 99.4	1		1	2
Actinobacillus pleuropneumoniae	99.4, 98.8	1	1		2
Acinetobacter sp. OM-E81	100			1	1
Citrobacter amalonaticus	100		1		1
Haemophilus influenzae	100		1		1
Haemophilus parainfluenzae	99.4		1		1
Veillonella atypica	99.4	1			1
Campylobacter fetus	97.9	1			1
Prevotella oulora	97		1		1
Subtotal		**10**	**13**	**4**	**27**
Unidentified species[4] (n = 5)					
Oral bacterium SH66	100, 99.4, 98.8	6	3	2	11
Oral bacterium RP55-18	100, 99.4		2		2
Oral bacterium SH13	100	1			1
Oral bacterium SH64	99.4	1			1
Oral bacterium AP60-12	98.3		1		1
Subtotal		**8**	**6**	**2**	**16**
Unknown[5] (n = 5)					
(Bacterium CEC2)	96.5		1		1
(Veillonella ratti)	93		1		1
(Cytophagales)	92.1		1		1
(Marine bacterium SS1)	89.9		1		1
(Rumen bacterium RFN91)	89.2		1		1
Subtotal			**5**		**5**

[1]Multiple numbers indicate that sequences were obtained from more than one clone, and that the identity to the specified best matching bacteria varied between clones.
[2]n indicates number of patients in each group.
[3]Cultivation-defined species: 16S rDNA sequence with equal or greater than 97% identity with 16S rDNA of cultivation-defined bacterial species[24].
[4]Unidentified species: 16S rDNA sequence with equal or greater than 97% identity with PCR-derived 16S rDNA sequence[24].
[5]Unknown: 16S rDNA sequence with <97% identity with any known 16S rDNA sequences.

the sequenced pool. Cultivation-defined and unidentified species were distributed to nearly the same extent between specimens from normal or diseased esophagus. Of the 27 clones of cultivation-defined bacterial species, 10 were from patients with normal esophagus and 17 were from the 15 patients with esophageal diseases. Of the 16 clones of unidentified/noncultured species, 8 were from the 15 patients with normal esophagus and 8 were from the 9 patients with esophageal disease. In contrast, the 5 clones of novel species were all from the 15 patients with esophageal diseases. In total, 17 species were found in reflux esophagitis, 5 in Barrett's esophagus, and 10 in the normal esophagus.

Table 3 Prevalence of specific 16S rDNA in 99 subclones from a single biopsy from patient #242 with Barrett's esophagus

Best matched bacterial 16S rDNA	% Identity[1]	Number of sequences
Cultivation-defined species[2] (n = 10)		
Neisseria flavescens	98.8, 98.2	11
Prevotella pallens	100	6
Porphyromonas sp oral clone CW034	100, 99.4, 97.6	3
Gemella morbillorum	100	2
Prevotella sp oral clone BI027	100	1
Campylobacter fetus	99.4	1
Rothia mucilaginosa	99.4	1
Veillonella sp oral clone AA050	98.8	1
Veillonella parvula	98.2	1
Catonella morbi	98.1	1
Subtotal		**28**
Unidentified species[3] (n = 5)		
Oral bacterium SH66	100, 99.4	50
Oral bacterium SH25	99.4	4
Oral bacterium SH13	100	1
Oral bacterium AP60-12	98.7	1
Oral bacterium AP60-35	98.2, 97.6	2
Subtotal		**58**
Unknown[4] (n = 7)		
(*Prevotella* sp oral clone FO45)	95	3
(Rumen bacterium JW17)	93.9	3
(Rumen bacterium RFN91)	88.4, 89	3
(Rumen bacterium 30-15)	94.5, 93.9	2
(Rumen bacterium JW17)	96.3	1
(*Prevotella* sp oral clone AH125)	93.9	1
Subtotal		**13**

[1]Multiple numbers indicate that sequences were obtained from more than one clone, and that the identity to the specified best matching bacteria varied between clones.
[2]Cultivation-defined species: 16S rDNA sequence with equal or greater than 97% identity with 16S rDNA of cultivation-defined bacterial species[24].
[3]Unidentified species: 16S rDNA sequence with equal or greater than 97% identity with PCR-derived 16S rDNA sequence[24].
[4]Unknown: 16S rDNA sequence with <97% identity with any known 16S rDNA sequences.

Colonization of the bacterial populations within a single esophageal biopsy

To characterize the bacterial populations within a single esophageal biopsy in the presence of esophageal disease, we further analyzed the biota from a patient with Barrett's esophagus (case 242; Table 3). From this biopsy, 99 clones were randomly picked and sequenced to allow a more in-depth analysis of the bacterial population in this biopsy. The 99 clones contained 36 unique 16S rDNA sequences comprising 21 species, including 10 homologous to cultivation-defined bacterial species, 5 homologous to unidentified/noncultured species, and 6 without significant homology (<97% identity) to any known 16S sequences at the species level (Table 4). Unidentified oral bacterium SH66 represented the most prevalent bacterial species (50.5% of the clones sequenced), followed by *Neisseria flavescens* (11.1%) and *Prevotella pallens* (6%).

Through combining the preliminary examination of the 24 patients, and the in-depth examination of a single patient with Barrett's esophagus, 147 sequences were obtained, belonging to 39 different species (Figure 2). Twenty-two of the sequences were homologous with cultivation-defined bacterial species, 7 with uncultivated species, and 10 were not homologous with any known bacterial species. The clones belonged to four phyla: *Bacteroidetes, Firmicutes, Proteobacteria,* and *Actinobacteria* (Figure 2).

DISCUSSION

Although 147 sequences from the biopsy specimens were analyzed, this study must be considered preliminary. Our strategy was to sample small populations of patients with reflux-related esophageal diseases to determine whether bacterial biota exist and ascertain any outstanding

Table 4 Comparison of representation of bacterial phyla observed in studies of the esophagus and subgingival crevice

Phylum	Subgingival crevice			Esophagus			
	Number of clones	Number of species		Number of clones	Number of species	Number of clones	Number of species
	Paster[1]	Paster[1]	Kroes[2]	Pei[3]		Present study	
Clostridium group	0	0	13	0	0	0	0
Obsidian pool OB11	6	1	0	0	0	0	0
Deferribacteres	86	8	8	0	0	0	0
Spirochaetes	537	58	0	0	0	0	0
TM7	34	5	0	13	3	0	0
Fusobacteria	353	19	2	20	6	0	0
Actinobacteria	275	32	15	39	8	2	2
Firmicutes	659	113	15	626	41	18	11
Proteobacteria	338	51	14	20	14	31	11
Bacteroidetes	234	58	8	182	23	96	15
Total	2522	347	75	900	95	147	39

[1]From Paster *et al.*[14] ; [2]from Kroes *et al.*[28] ; [3]from Pei *et al.*[13].

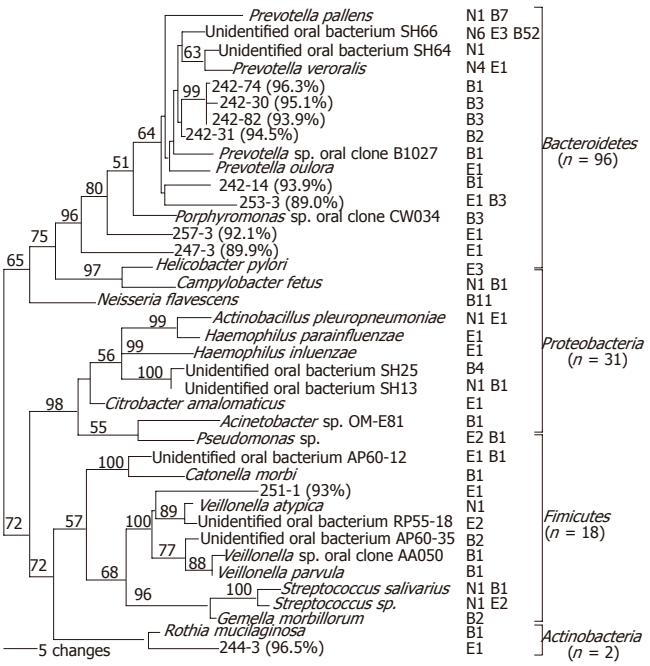

Figure 2 Phylogenetic analysis of bacterial 16S rDNA detected in the distal esophagus. Sequences were aligned using ClustalW, and subjected to phylogenetic analysis using Paup 4.0b10 neighbor-joining analysis, based on HKY85 distance matrices. Bootstrap values (based on 500 replicates) are represented at each node when >50%, and the branch length index is represented below the phylogram. Names of bacterial species closest in homology with the detected 16S rDNA are located at the termination of each branch. "Unidentified" oral bacterial clones are potential bacterial species whose phylogenetic positions were designated by PCR-amplified 16S sequences only, rather than based on cultured organisms. The serial number of a clone followed by percentage of homology with the closest DNA sequence in GenBank is used as the species name for 16S rDNA sequence with <97% identity with all known DNA sequences. The frequency that a species was detected and its sources are shown following the species name. 'N' represents normal esophagus, 'E' represents esophagitis, and 'B' represents Barrett's esophagus. The 39 species belong to four phyla, as shown at the right.

associations. The aim of these studies was thus hypothesis-generating, to establish parameters for more definitive studies. This approach was necessary because when this study was begun there was no prior information relating to bacterial populations in reflux-related disorders. We recognize the preliminary nature of this inquiry, but believe it can serve as a first approximation that can help guide future work.

Our findings suggest the existence of highly complex bacterial populations in the distal esophagus of patients with GERD-related disorders. Because many bacteria are fastidious, slow growing, or even uncultivable, simple culture methods often overlook a large number of bacteria, such as has been documented in the oral cavity and colon[14,28-30]. These drawbacks can be overcome by universal bacterial 16S rDNA PCR, since PCR does not discriminate bacteria based on their culture properties. However, PCR cannot distinguish living bacteria from naked bacterial genomes. In organs in which major digestive activities occur, such as the stomach and small intestine, bacteria brought downstream by peristaltic movement may be lysed and genomes released. Such DNA can be falsely interpreted by PCR as representing colonizing bacteria. Using microscopy in the present study, we observed a polymorphic population of bacteria in association with the epithelium of esophageal biopsies from patients with reflux-related diseases that included Gram-positive and Gram-negative bacilli, cocci, and coccobacilli. The variety of morphologically diversified esophageal bacteria is consistent with the highly diversified bacterial constituents identified using molecular techniques. The presence of intact bacteria closely associated with epithelial cells of the distal esophagus suggests that the 16S rDNA detected was from viable bacteria rather than from bacterial DNA only.

Because only a few PCR clones were sampled from each biopsy specimen, this study is not a quantitative comparison of the bacteria found in GERD-related disorders with those from normal esophagus or oral cavity[13,14,28-30], as the species identified may reflect chance rather than prevalence. However, the majority of bacterial species found in GERD-related disorders are shared with the previously identified bacteria in the normal esophagus[13], suggesting that certain bacterial species in the normal esophagus are resistant to the substantial environmental changes due to reflux. Finding *H pylori* 16S rDNA in the esophagus of two patients with GERD indicates that gastric bacteria can be brought into the distal esophagus by reflux, consistent with the previous detection of *H pylori* in Barrett's esophagus[31,32]. These observations suggest that the detected organisms (or DNA) may be transiently present, rather than persistent in the distal esophagus. Longitudinal studies of individual patients would help to address this question. Conversely, the microenvironment in the distal esophagus likely does not include all oral bacteria. Similar to our previous study of the normal esophageal biota[13], the most prevalent of the nine phyla identified in the subgingival crevice[14,28], *Spirochaetes*, was not found in the esophagus, consistent with the presence of endogenous bacterial populations unique to the distal esophagus.

In-depth study of a Barrett's esophagus case (Biopsy 242) revealed a single predominant species (unidentified oral bacterium SH66), representing 50.5% of the 99 clones sampled. SH66 was found in patients with or without the disease of the distal esophagus; whether there is overgrowth in Barrett's esophagus cannot be addressed without quantitative comparisons. SH66 was originally identified in the saliva by its 16S sequence, but never has been cultured[33]. Phylogenetic analysis indicates that SH66 resembles several members of the genus *Provotella* and belongs in the phylum *Bacteriodetes* (Figure 2).

Identifying complex bacterial populations in GERD-related disorders offers a new approach to understand bacterial roles as markers or as pathogenic factors in esophageal diseases. Bacterial populations in other portions of the digestive system, such as the oral cavity and colon, play important roles in the maintenance of local physiology as well as in disease pathogenesis[1-5,6-10,11-13]. The composition, transience, or stability of this complex bacterial biota in the distal esophagus and associations

with the disease remain to be determined. The results from this study justify large-scale comparisons of bacterial biota between normal and pathological conditions in the distal esophagus.

ACKNOWLEDGMENTS

We thank Dr. Kyi T. Tham for processing the specimens for histological examination and Mr. Joseph Szmulewicz for performing Gram-Twort stains.

REFERENCES

1 **Gustafsson BE.** The physiological importance of the colonic microflora. *Scand J Gastroenterol Suppl* 1982; **77:** 117-131
2 **Cunningham-Rundles S,** Ahrn S, Abuav-Nussbaum R, Dnistrian A. Development of immunocompetence: role of micronutrients and microorganisms. *Nutr Rev* 2002; **60:** S68-72
3 **Peek RM Jr,** Blaser MJ. Helicobacter pylori and gastrointestinal tract adenocarcinomas. *Nat Rev Cancer* 2002; **2:** 28-37
4 **Gerding DN,** Gebhard RL, Sumner HW, Peterson LR. Pathology and diagnosis of Clostridium difficile disease. In: Rolfe R, Finegold SM (eds) Clostridium difficile: its role in intestinal disease. *San Diego, Academic Press* 1988: 259-286
5 **Hopkins MJ,** Macfarlane GT. Changes in predominant bacterial populations in human faeces with age and with Clostridium difficile infection. *J Med Microbiol* 2002; **51:** 448-454
6 **Hill LV,** Embil JA. Vaginitis: current microbiologic and clinical concepts. *CMAJ* 1986; **134:** 321-331
7 **Roediger WE,** Lawson MJ, Radcliffe BC. Nitrite from inflammatory cells--a cancer risk factor in ulcerative colitis? *Dis Colon Rectum* 1990; **33:** 1034-1036
8 **Mueller RL,** Hagel HJ, Greim G, Ruppin H, Domschke W. Endogenous synthesis of carcinogenic N-nitroso compounds: bacterial flora and nitrite formation in the healthy human stomach. *Zentralbl Bakteriol Mikrobiol Hyg [B]* 1983; **178:** 297-315
9 **Mowat C,** Williams C, Gillen D, Hossack M, Gilmour D, Carswell A, Wirz A, Preston T, McColl KE. Omeprazole, Helicobacter pylori status, and alterations in the intragastric milieu facilitating bacterial N-nitrosation. *Gastroenterology* 2000; **119:** 339-347
10 **Calmels S,** Ohshima H, Henry Y, Bartsch H. Characterization of bacterial cytochrome cd(1)-nitrite reductase as one enzyme responsible for catalysis of nitrosation of secondary amines. *Carcinogenesis* 1996; **17:** 533-536
11 **Charriere M,** Poirier S, Calmels S, De Montclos H, Dubreuil C, Poizat R, Hamdi Cherif M, de The G. Microflora of the nasopharynx in Caucasian and Maghrebian subjects with and without nasopharyngeal carcinoma. *IARC Sci Publ* 1991; **105:** 158-161
12 **Kado S,** Uchida K, Funabashi H, Iwata S, Nagata Y, Ando M, Onoue M, Matsuoka Y, Ohwaki M, Morotomi M. Intestinal microflora are necessary for development of spontaneous adenocarcinoma of the large intestine in T-cell receptor beta chain and p53 double-knockout mice. *Cancer Res* 2001; **61:** 2395-2398
13 **Pei Z,** Bini EJ, Yang L, Zhou M, Francois F, Blaser MJ. Bacterial biota in the human distal esophagus. *Proc Natl Acad Sci USA* 2004; **101:** 4250-4255
14 **Paster BJ,** Boches SK, Galvin JL, Ericson RE, Lau CN, Levanos VA, Sahasrabudhe A, Dewhirst FE. Bacterial diversity in human subgingival plaque. *J Bacteriol* 2001; **183:** 3770-3783
15 **Donowitz LG,** Page MC, Mileur BL, Guenthner SH. Alteration of normal gastric flora in critical care patients receiving antacid and cimetidine therapy. *Infect Control* 1986; **7:** 23-26
16 **Peek RM Jr,** van Doorn LJ, Donahue JP, Tham KT, Figueiredo C, Blaser MJ, Miller GG. Quantitative detection of Helicobacter pylori gene expression in vivo and relationship to gastric pathology. *Infect Immun* 2000; **68:** 5488-5495
17 **Peek RM Jr,** Thompson SA, Donahue JP, Tham KT, Atherton JC, Blaser MJ, Miller GG. Adherence to gastric epithelial cells induces expression of a Helicobacter pylori gene, iceA, that is associated with clinical outcome. *Proc Assoc Am Physicians* 1998; **110:** 531-544
18 **Riddell RH.** The biopsy diagnosis of gastroesophageal reflux disease, "carditis," and Barrett's esophagus, and sequelae of therapy. *Am J Surg Pathol* 1996; **20 Suppl 1:** S31-50
19 **Ollett WS.** A method for staining both Gram positive and Gram negative bacteria in sections. *J Pathol Bacteriol* 1947; **59:** 357
20 **Novelli G,** Gennarelli M, De Santis L, Angeloni P, Dallapiccola B. Inosine-containing primers in human papillomavirus detection by polymerase chain reaction. *Biomed Pharmacother* 1992; **46:** 167-169
21 **Ehlen T,** Dubeau L. Detection of ras point mutations by polymerase chain reaction using mutation-specific, inosine-containing oligonucleotide primers. *Biochem Biophys Res Commun* 1989; **160:** 441-447
22 **Knoth K,** Roberds S, Poteet C, Tamkun M. Highly degenerate, inosine-containing primers specifically amplify rare cDNA using the polymerase chain reaction. *Nucleic Acids Res* 1988; **16:** 10932
23 **Pace NR.** A molecular view of microbial diversity and the biosphere. *Science* 1997; **276:** 734-740
24 **Stackebrandt E,** Goebel BM. Taxonomic note: a place for DNA-DNA reassociation and 16S rRNA sequence analysis in the present species definition in bacteriology. *Int J Syst Bacteriol* 1994; **44:** 846-849
25 **Thompson JD,** Higgins DG, Gibson TJ. CLUSTAL W: improving the sensitivity of progressive multiple sequence alignment through sequence weighting, position-specific gap penalties and weight matrix choice. *Nucleic Acids Res* 1994; **22:** 4673-4680
26 **Hasegawa M,** Kishino H, Yano T. Dating of the human-ape splitting by a molecular clock of mitochondrial DNA. *J Mol Evol* 1985; **22:** 160-174
27 **Dooley CP,** Cohen H, Fitzgibbons PL, Bauer M, Appleman MD, Perez-Perez GI, Blaser MJ. Prevalence of Helicobacter pylori infection and histologic gastritis in asymptomatic persons. *N Engl J Med* 1989; **321:** 1562-1566
28 **Kroes I,** Lepp PW, Relman DA. Bacterial diversity within the human subgingival crevice. *Proc Natl Acad Sci USA* 1999; **96:** 14547-1452
29 **Paster BJ,** Boches SK, Galvin JL, Ericson RE, Lau CN, Levanos VA, Sahasrabudhe A, Dewhirst FE. Bacterial diversity in human subgingival plaque. *J Bacteriol* 2001; **183:** 3770-3783
30 **Suau A,** Bonnet R, Sutren M, Godon JJ, Gibson GR, Collins MD, Dore J. Direct analysis of genes encoding 16S rRNA from complex communities reveals many novel molecular species within the human gut. *Appl Environ Microbiol* 1999; **65:** 4799-4807
31 **Wright TA,** Myskow M, Kingsnorth AN. Helicobacter pylori colonization of Barrett's esophagus and its progression to cancer. *Dis Esophagus* 1997; **10:** 196-200
32 **Henihan RD,** Stuart RC, Nolan N, Gorey TF, Hennessy TP, O'Morain CA. Barrett's esophagus and the presence of Helicobacter pylori. **Am J Gastroenterol** 1998; **93:** 542-546
33 **Sakamoto M,** Umeda M, Ishikawa I, Benno Y. Comparison of the oral bacterial flora in saliva from a healthy subject and two periodontitis patients by sequence analysis of 16S rDNA libraries. *Microbiol Immunol* 2000; **44:** 643-652

Science Editor Guo SY **Language Editor** Elsevier HK

PO Box 2345, Beijing 100023, China
www.wjgnet.com
wjg@wjgnet.com

ELSEVIER

World J Gastroenterol 2005;11(46):7284-7289
World Journal of Gastroenterology ISSN 1007-9327

• *CLINICAL RESEARCH* •

Lymphomatous involvement of gastrointestinal tract: Evaluation by positron emission tomography with ^{18}F-fluorodeoxyglucose

Sith Phongkitkarun, Vithya Varavithya, Toshiki Kazama, Silvana C Faria, Martha V Mar, Donald A Podoloff, Homer A Macapinlac

Sith Phongkitkarun, Vithya Varavithya, Toshiki Kazama, Silvana C Faria, Martha V Mar, Donald A Podoloff, Homer A Macapinlac, Departments of Diagnostic Radiology and Nuclear Medicine, Box 057, The University of Texas MD, Anderson Cancer Center, 1515 Holcombe Blvd., Houston, TX, United States
Correspondence to: Sith Phongkitkarun, MD, Department of Radiology, Faculty of Medicine, Ramathibodi Hospital, Rama VI Road, Rajchathewi, Bangkok 10400, Thailand. rasih@mahidol.ac.th
Telephone: +66-02-2011260 Fax: +66-02-2011297
Received: 2005-04-03 Accepted: 2005-04-09

Abstract

AIM: To demonstrate the ^{18}F-fluorodeoxyglucose positron emission tomography (^{18}F-FDG PET) findings in patients with non-Hodgkin's lymphoma (NHL) involving the gastrointestinal (GI) tract and the clinical utility of modality despite of the known normal uptake of FDG in the GI tract.

METHODS: Thirty-three patients with biopsy-proven gastrointestinal NHL who had undergone FDG-PET scan were included. All the patients were injected with 10-15 mCi FDG and scanned approximately 60 min later with a CTI/Siemens HR (+) PET scanner. PET scans were reviewed and the maximum standard uptake value (SUV_{max}) of the lesions was measured before and after the treatment, if data were available and compared with histologic diagnoses.

RESULTS: Twenty-five patients had a high-grade lymphoma and eight had a low-grade lymphoma. The stomach was the most common site of the involvement (20 patients). In high-grade lymphoma, PET showed focal nodular or diffuse hypermetabolic activity. The average SUV_{max}±SD was 11.58±5.83. After the therapy, the patients whose biopsies showed no evidence of lymphoma had a lower uptake without focal lesions. The SUV_{max}±SD decreased from 11.58±5.83 to 2.21±0.78. In patients whose post-treatment biopsies showed lymphoma, the SUV_{max}±SD was 9.42±6.27. Low-grade follicular lymphomas of the colon and stomach showed diffuse hypermetabolic activity in the bowel wall (SUV_{max} 8.2 and 10.3, respectively). The SUV_{max} was 2.02-3.8 (mean 3.02) in the stomach lesions of patients with MALT lymphoma.

CONCLUSION: ^{18}F-FDG PET contributes to the diagnosis of high-grade gastrointestinal non-Hodgkin's lymphoma, even when there is the normal background FDG activity. Furthermore, the SUV plays a role in evaluating treatment response. Low-grade NHL demonstrates FDG uptake but at a lesser intensity than seen in high-grade NHL.

Key words: Positron emission tomography; Non-Hodgkin's lymphoma; Gastrointestinal neoplasm

Phongkitkarun S, Varavithya V, Kazama T, Faria SC, Mar MV, Podoloff DA, Macapinlac HA. Lymphomatous involvement of gastrointestinal tract: Evaluation by positron emission tomography with ^{18}F-fluorodeoxyglucose. *World J Gastroenterol* 2005; 11(46): 7284-7289
http://www.wjgnet.com/1007-9327/11/7284.asp

INTRODUCTION

Non-Hodgkin's lymphoma (NHL) is known to arise from extranodal sites in 10-30% of cases[1,2]. Among the extranodal sites, the gastrointestinal tract is most frequently affected by NHL. It can involve the gastrointestinal tract partly or entirely[3]. Generally, the diagnosis of lymphomatous involvement of the gastrointestinal tract is based on clinical symptoms and imaging studies, such as double-contrast barium study, computed tomography (CT) and is confirmed by endoscopy with biopsy. CT has been widely used as the imaging modality for staging and restaging of lymphoma[4]. However, in evaluating lymphomatous involvement of the gastrointestinal tract, CT has some limitations. Examples are non-specific imaging patterns and findings that may be difficult to interpret such as wall thickening in a non-distended stomach or unopacified small bowel loops[5-7]. Gallium-67 citrate scintigraphy also plays an important role in patients with NHL for the detection of lesions, initial staging and assessment of therapeutic responses[8,9]. Gallium-67 citrate scintigraphy is known to be more sensitive for the detection of lesions in thoracic locations, but it is much less sensitive in the identification of infradiaphragmatic sites owing to physiologic hepatic and splenic uptake and excretion into the bowel[10]. Since Paul[11] first reported ^{18}F-FDG PET imaging in lymphoma, this modality has been increasingly used to examine patients with lymphomas. Many published articles have shown that ^{18}F-FDG PET is more sensitive in detect-

ing disease sites than gallium-67 scintigraphy. ^{18}F-FDG PET is at least as sensitive as CT, but more specific than CT, especially in patients undergoing restaging[12-15]. In addition, many studies have demonstrated that persistent FDG uptake after therapy may predict treatment failure or a high recurrence rate[16,17]. Most reported studies have assessed primarily patients with nodal NHL. A few studies have used ^{18}F-FDG PET to assess NHL in the gastrointestinal tract[18-21]. Rodriguez *et al.*[18] demonstrated that ^{18}F-FDG PET may have a novel application in the evaluation of gastric NHL and may complement endoscopy and CT in selected patients. However, in a study by Hoffmann *et al.*[19] in patients with mucosa-associated lymphoid tissue (MALT)-type lymphoma, no focal tracer uptake was demonstrated with ^{18}F-FDG PET in either gastric or extragastric lesions. In addition, there is concern that normal FDG accumulation in the gastrointestinal tract or abnormal uptake in patients with inflammatory bowel disease could cause confusion in the interpretation of ^{18}F-FDG PET images in patients with lymphoma[22-25]. Thus the clinical utility of ^{18}F-FDG PET imaging in the evaluation of lymphomatous involvement of the gastrointestinal tract has not been clearly established. This study aimed to demonstrate the ^{18}F-FDG PET findings in patients with NHL (high-grade *vs* low-grade) involving the gastrointestinal tract and the clinical utility of this modality through the normal uptake of FDG in the gastrointestinal tract was known.

MATERIALS AND METHODS

In this study, the electronic database of 907 consecutive patients with lymphoma who underwent PET imaging from October 2000 to June 2002 was retrospectively reviewed. Thirty-three patients with biopsy-proven NHL involving the gastrointestinal tract who underwent a ^{18}F-FDG PET scan were included in this study. There were 24 men and 9 women aged 34-80 years (mean 58 years). For scanning, all patients were injected with 10-15 mCi FDG and scanned approximately 60 min later with a CTI/Siemens HR (+) PET scanner (Siemens, Knoxville, TN, USA). Each scan was performed from the head to the pelvic floor with the total time of about 60 min for image acquisition. The acquired data were reconstructed using standard vendor-provided iterative reconstruction with segmented attenuation correction. Additional transmission scanning for attenuation correction was performed.

The PET scans obtained were reviewed by an experienced nuclear physician and a radiologist who together provided the consensus reading. Reviewing was done without patient's clinical data and the status of lymphoma. The SUV_{max} of the lesions was measured before and after the treatment in case the data were available. The SUV_{max} was measured in at least two orthogonal planes to demonstrate the best lesion appreciation. The CT scan obtained on the corresponding data was used as the guideline for demarcating those lesions when their boundaries were difficult to define. The highest SUV_{max} was used for each lesion. The ^{18}F-FDG PET results and the SUV measurements at each time point were compared with the histologic data from the corresponding data. The SUV_{max} was compared before and after the treatment using Student's *t*-test. $P<0.05$ was considered statistically significant.

Table 1 Sites of gastrointestinal involvement of NHL in 33 patients

Sites of GI involvement	Number of patients (%)
Stomach	21 (64)
Colon and rectum	12 (36)
Terminal ileum and cecum	9 (27)
Duodenum	8 (24)
Small bowel	6 (18)
Esophagus	2 (6)

RESULTS

Of the 33 patients with NHL involving the gastrointestinal tract, 25 had a high-grade lymphoma and 8 had a low-grade lymphoma as determined using the revised European-American classification of lymphoid neoplasm (REAL classification). The histologic subtypes included diffuse large cell lymphoma (n = 16), mantle cell lymphoma (n = 6), MALT-type lymphoma (n = 5), peripheral T-cell lymphoma (n = 3), follicular lymphoma (n = 2) and B-cell small lymphocytic lymphoma (n = 1). The stomach was the most common site of the involvement, followed (in order of decreasing prevalence) by the colon and rectum, cecum and terminal ileum, duodenum, small bowel, and esophagus (Table 1).

In high-grade NHL, ^{18}F-FDG PET showed focal nodular or diffuse hypermetabolic activity, which involved mainly the wall of the gastrointestinal tract. This activity's appearance was different from that of the normal activity in the bowel wall, which was less intense and uniform. Fifteen patients received ^{18}F-FDG PET for staging before the treatment. In these patients, ^{18}F-FDG PET identified 30 (100%) of 30 intestinal locations that had biopsy-proven lymphomatous involvement. These locations were the esophagus (n = 2), stomach (n = 11), duodenum (n = 5), small bowel (n = 6), cecum/terminal ileum (n = 3), and colon (n = 3). The SUV_{max} ranged from 3.64 to 25.10 (11.22±5.79). The SUV_{max}±SD in non-involved intestine was 3.09±2.34. After the therapy, uptake was absent or reduced without focal lesions in 14 patients who had complete responses and whose biopsies showed benign inflammation without evidence of lymphoma (Figure 1). The post- treatment SUV_{max} values were significantly lower ($P<0.05$), ranging from 0.89 to 4.30 (2.21±0.78). In three patients, the post-treatment biopsies still showed lymphoma (Figure 2) and the post-treatment SUV_{max} ranged from 3.44 to 21.90 (9.42 ±6.27).

In low-grade NHL, ^{18}F-FDG PET showed diffuse hypermetabolic activity in the bowel wall in two patients with follicular lymphoma of the colon and stomach (SUV_{max} 8.20 and 10.30, respectively). In one patient with follicular lymphoma of the stomach, the SUV_{max} after 5 wk of therapy decreased from 10.30 to 2.40. In four patients with

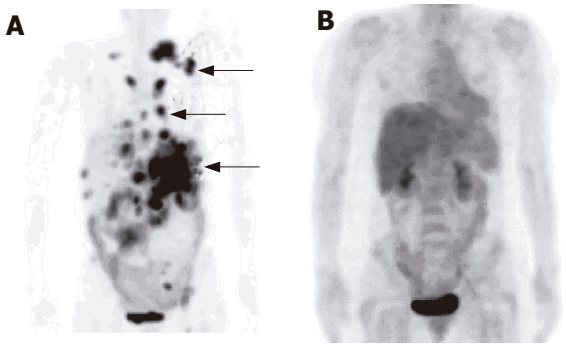

Figure 1 A 61-year-old woman with large cell lymphoma. **A:** Pre-treatment ^{18}F-FDG PET scan revealed multifocal hypermetabolic activity involving the neck, chest, and abdomen (arrow). The highest SUV_{max} was 20.3 in the left upper abdominal area, corresponding to a positive result of a gastric biopsy; **B:** Follow-up ^{18}F-FDG PET scan 5 mo later showed no evidence of residual FDG disease.

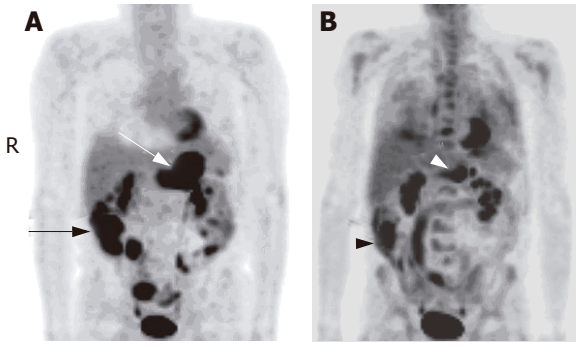

Figure 2 A 68-year-old man with large cell lymphoma. **A:** Base line ^{18}F-FDG PET scan showed hypermetabolic foci in the stomach (white arrow), cecum and terminal ileum (black arrow), and bowel loops (SUV_{max} = 12.7); **B:** ^{18}F-FDG PET scan obtained after therapy showed partial metabolic response of the activity in the stomach (white arrowhead) and cecum (black arrowhead, SUV_{max} = 10.7).

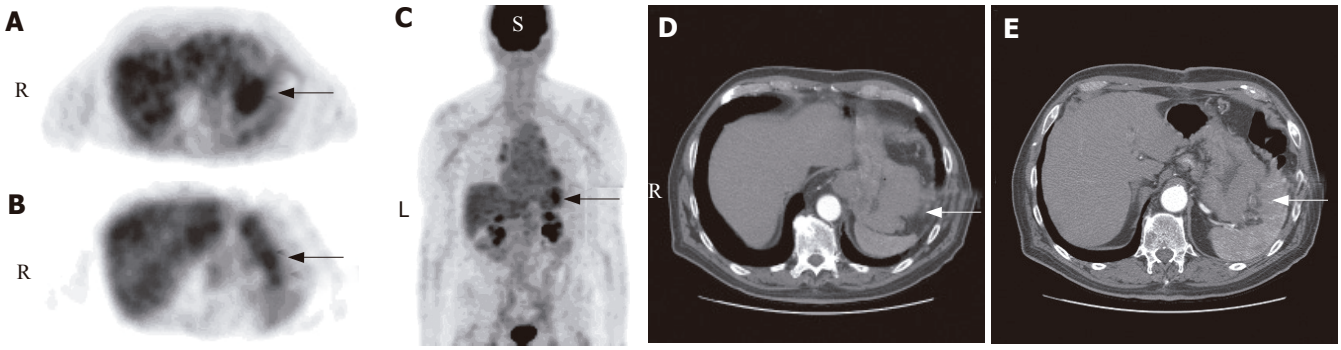

Figure 3 An 80-year-old man with MALT-type lymphoma. **A-C:** ^{18}F-FDG PET scans in transaxial and projection images showed a focal mild hypermetabolic activity (SUV_{max} = 3.8) in the region of stomach (black arrow); **D** and **E:** CT scans showed a bulky mass in the wall of gastric fundus and body (white arrow).

MALT-type lymphoma (Figure 3), lesions in the stomach and duodenum showed diffuse and low metabolic activity similar to that in the liver, and the SUV_{max} was 2.02-3.8 (average 3.02) at the time of the positive biopsy results. In another patient with MALT-type lymphoma involving the colon, the SUV_{max} was 6.82. However, follow-up biopsy in this patient showed high-grade transformation. The mean SUV_{max} in high-grade and low-grade NHL before and after the treatment is shown in Table 2. Negative post-treatment biopsy results corresponded to significantly decreased SUV_{max} in high-grade NHL (P<0.05). However, the SUV_{max} before and after the treatment was not significantly lower in low-grade NHL.

Table 2 SUV_{max} in high- and low-grade NHL before and after treatment (mean±SD)

NHL grade	SUV_{max} before treatment	SUV_{max} after treatment	
		Biopsy positive	Biopsy negative
High grade	11.22±5.79 (n = 15)	9.42±6.27 (n = 14)	2.21±0.78[a,c] (n = 3)
Low grade	8.57±2.47 (n = 2)	3.76±2.08 (n = 5)	3.03±0.89 (n = 2)

n, number of patients.
[a]P<0.05 *vs* SUV_{max} in high grade NHL before treatment; [c]P<0.05 *vs* SUV_{max} with biopsy positive after treatment.

DISCUSSION

The gastrointestinal tract is the most common extranodal site of NHL[1,3]. The stomach is most frequently involved (60-74% of cases), followed by the duodenum and small bowel (10-20%), ileocecal region (7-10%) and large bowel (<10%)[26,27]. Our results are consistent with these reports, except that the large bowel was involved in a greater percentage of patients in our study than the previous studies. Lymphomatous involvement of the gastrointestinal tract may be primary or secondary. The gastrointestinal tract is involved at autopsy in as many as 50% of patients with secondary lymphoma. However, most of these patients have subclinical disease while patients who have gastrointestinal symptoms are found to have primary gastrointestinal lymphoma[6,28].

Diagnostic imaging studies play an important role in documenting lymphoma, staging and re-staging the disease, evaluating treatment response and performing follow-up evaluations. Anatomical imaging modalities including computed tomography (CT) and magnetic resonance (MR) imaging have some limitations, especially when defining the viability of the residual mass, treatment

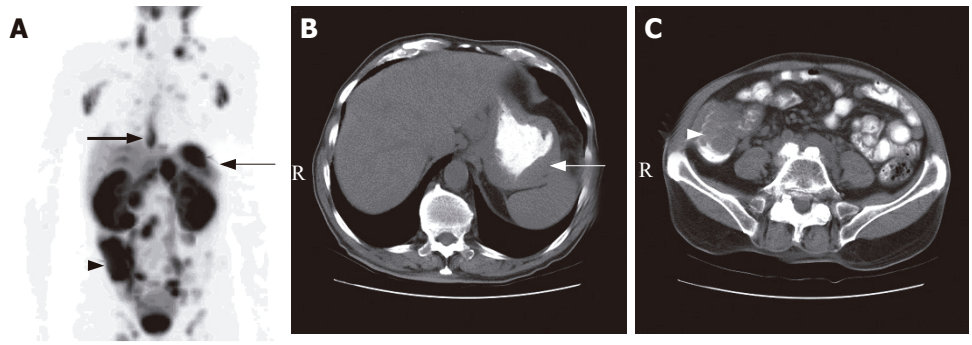

Figure 4 A 78-year-old man with mantle cell lymphoma. **A:** ^{18}F-FDG PET scan revealed multiple hypermetabolic foci involving the lower esophagus (thick arrow), gastric fundus (thin arrow), cecum and terminal ileum (arrow head); **B** and **C:** The corresponding CT scans of the abdomen showed wall thickening at the gastric fundus (white arrow) and the cecum and terminal ileum (white arrow head)

response or both[4,29]. Gallium-67 scintigraphy has been proposed as a functional imaging modality to assess remission and to evaluate the nature of residual masses in patients with lymphoma. However, gallium-67 scintigraphy is of little use in the abdomen because of the high hepatic uptake and excretion into the bowel and should be performed before treatment to determine whether the patient has a gallium-fixing tumor and whether the absence of fixation after treatment corresponds to a residual mass[8,9,30]. ^{18}F-FDG PET imaging has shown its clinical usefulness in patients with lymphoma. Several articles have reported that ^{18}F-FDG PET has a higher sensitivity in detecting disease sites than gallium-67 scintigraphy[11-13]. ^{18}F-FDG PET can also be used to assess the response after the therapy[16,17,31]. However, a limited number of studies have shown the utility of ^{18}F-FDG PET imaging for the evaluation of lymphomatous involvement of the gastrointestinal tract[18-21,32,33].

In our study, ^{18}F-FDG PET showed fixed focal nodular or diffuse hypermetabolic activity of all lesions in patients with high-grade non-Hodgkin's lymphoma, which was confirmed by histopathologic analysis. The appearance of focal intense hypermetabolic activity of the lesions was different from that of the normal activity in the bowel wall. Rodriguez *et al.*[4,18] evaluated CT, MRI, and PET in eight patients with primary gastric lymphoma and showed that ^{18}F-FDG PET can demonstrate both the presence and the extent of gastric NHL and is more accurate than endoscopy and CT for evaluating the extent of NHL in the gastric wall. In our study, ^{18}F-FDG PET clearly demonstrated the involvement of specific sites, particularly in the stomach (e.g. the fundus, body, antrum, lesser and greater curvature of the stomach), corresponding to endoscopic biopsy sites. However, extension outside the bowel wall was better appreciated when interpreted with the guidance of a CT scan. It should be noted that an evaluation of the extent of NHL in the gastric wall and careful assessment of multiplicities affect the selection of therapy, since radical surgery with lymph node dissection seems to be needed for most patients with high-grade and even low-grade NHL[34].

Ullerich *et al.*[20] and Sam *et al.*[21] showed that ^{18}F-FDG PET could find lesions in patients with small bowel lymphoma. Najjar *et al.*[32] also reported that ^{18}F-FDG PET could identify lymphoma of the colon. These results are consistent with the results in our study, in which pre-treatment ^{18}F-FDG PET showed pertinently high metabolic activity in the small bowel and colon in patients with high-grade NHL (Figure 4). It is difficult to differentiate high-grade non-Hodgkin's lymphoma from other neoplastic or inflammatory diseases. However, interpreting the results in the light of a careful clinical history, the extent of the disease and corresponding CT images, can contribute to the correct diagnosis. Moog *et al.*[33] showed that ^{18}F-FDG PET imaging could achieve 100% correct diagnoses of malignant lymphoma. In almost all cases of high-grade NHL in our study, CT scans also demonstrated the abnormal wall thickening or mass lesions. However, the results did not reveal the sensitivity of ^{18}F-FDG PET *vs* that of CT, because both modalities were interpreted together as complementary studies.

^{18}F-FDG PET can demonstrate diffuse hypermetabolic activity in patients with low-grade follicular NHL in the colon and stomach. The ability of gallium-67 scintigraphy and ^{18}F-FDG PET to detect MALT-type lymphoma of the gastrointestinal tract is controversial. Hsu *et al.*[35] showed that gallium-67 scintigraphy could not show abnormal uptake of radioactivity in patients with low-grade gastric MALT-type lymphoma. Hoffmann *et al.*[19] studied ^{18}F-FDG PET imaging in patients with MALT-type lymphoma and found that PET scans do not show focal tracer uptake in either gastric or extragastric lesions. Our study showed similar results of low activity in the stomach and duodenum. Even though it has been reported that CT scans may demonstrate gastric MALT-type lymphoma either as an infiltrative form or as a polypoid pattern[36,37], CT is limited in its ability to monitor the treatment response. Taken together, ^{18}F-FDG PET imaging in low-grade NHL seems to be able to monitor the treatment response and determine high-grade transformation.

Generally, in patients with NHL, histologic grade and disease stage are clearly identified as the two major prognostic factors and therapeutic determinants. Endoscopy with biopsy and histopathologic examination

are the gold standard for grading malignancies[38]. However, there have been attempts to differentiate high-grade from low-grade NHL by different methods (e.g. double-contrast radiography, CT scan and gallium-67 scintigraphy)[35,39]. ^{18}F-FDG PET imaging in our study showed that high-grade NHL of the gastrointestinal tract had high FDG activity in the lesions as was confirmed by high SUV measurements. Though the normal background FDG activity in the gastrointestinal tract was known, abnormalities were identified in this study. In low-grade NHL of the gastrointestinal tract, it was difficult to document existing disease, especially in patients with MALT-type lymphoma. However, there was a significant difference in the SUV_{max} measurement between high-grade and low-grade NHL.

This study also demonstrated the clinical utility of ^{18}F-FDG PET imaging for monitoring patients with NHL of the gastrointestinal tract especially those with high-grade lymphoma. The SUV_{max} measurements were significantly decreased after therapy and post-treatment biopsies were negative for lymphoma. In addition, benign inflammatory conditions such as gastritis showed significantly lower FDG activity. In patients whose post-treatment biopsies were positive for lymphoma, the SUV_{max} measurements were persistently high and even higher in patients with disease progression. Many studies have demonstrated that persistent FDG uptake after therapy may help to predict treatment failure or a high risk of recurrence[16,17].

In conclusion, ^{18}F-FDG PET contributes to the diagnosis of high-grade lymphoma involving the gastrointestinal tract, even when there is the normal background FDG activity. Furthermore, the SUV plays a role in evaluating treatment response especially when the PET images are interpreted with CT scans. Low-grade lymphoma demonstrates FDG uptake, but the intensity of the uptake is lower than that in high-grade lymphoma.

ACKNOWLEDGMENTS

The authors thank Beth Wagner for manuscript preparation and literature search and Mariann Crapanzano for editorial review.

REFERENCES

1 **Banfi A,** Bonadonna G, Carnevali G, Oldini C, Salvini E. Preferential sites of involvement and spread in maignant lymphomas. *Eur J Cancer* 1968; **4:** 319-324
2 **Gospodarowicz MK,** Sutcliffe SB, Brown TC, Chua T, Bush RS. Patterns of disease in localized extranodal lymphomas. *J Clin Oncol* 1987; **5:** 875-880
3 **Amer MH,** el-Akkad S. Gastrointestinal lymphoma in adults: clinical features and management of 300 cases. *Gastroenterology* 1994; **106:** 846-858
4 **Rodriguez M.** Computed tomography, magnetic resonance imaging and positron emission tomography in non-Hodgkin's lymphoma. *Acta Radiol Suppl* 1998; **417:** 1-36
5 **Kaye MD,** Young SW, Hayward R, Castellino RA. Gastric pseudotumor on CT scanning. *AJR Am J Roentgenol* 1980; **135:** 190-193
6 **Levine MS,** Rubesin SE, Pantongrag-Brown L, Buck JL, Herlinger H. Non-Hodgkin's lymphoma of the gastrointestinal tract: radiographic findings. *AJR Am J Roentgenol* 1997; **168:** 165-172
7 **Komaki S.** Normal or benign gastric wall thickening demonstrated by computed tomography. *J Comput Assist Tomogr* 1982; **6:** 1103-1107
8 **Adler S,** Parthasarathy KL, Bakshi SP, Stutzman L. Gallium-67-citrate scanning for the localization and staging of lymphomas. *J Nucl Med* 1975; **16:** 255-260
9 **Brown ML,** O'Donnell JB, Thrall JH, Votaw ML, Keyes JW Jr. Gallium-67 scintigraphy in untreated and treated non-hodgkin lymphomas. *J Nucl Med* 1978; **19:** 875-879
10 **Coiffier B.** Positron emission tomography and gallium metabolic imaging in lymphoma. *Curr Oncol Rep* 2001; **3:** 266-270
11 **Paul R.** Comparison of fluorine-18-2-fluorodeoxyglucose and gallium-67 citrate imaging for detection of lymphoma. *J Nucl Med* 1987; **28:** 288-292
12 **Shen YY,** Kao A, Yen RF. Comparison of ^{18}F-fluoro-2-deoxyglucose positron emission tomography and gallium-67 citrate scintigraphy for detecting malignant lymphoma. *Oncol Rep* 2002; **9:** 321-325
13 **Kostakoglu L,** Leonard JP, Kuji I, Coleman M, Vallabhajosula S, Goldsmith SJ. Comparison of fluorine-18 fluorodeoxyglucose positron emission tomography and Ga-67 scintigraphy in evaluation of lymphoma. *Cancer* 2002; **94**: 879-888
14 **Jerusalem G,** Beguin Y, Fassotte MF, Najjar F, Paulus P, Rigo P, Fillet G. Whole-body positron emission tomography using ^{18}F-fluorodeoxyglucose for posttreatment evaluation in Hodgkin's disease and non-Hodgkin's lymphoma has higher diagnostic and prognostic value than classical computed tomography scan imaging. *Blood* 1999; **94:** 429-433
15 **Stumpe KD,** Urbinelli M, Steinert HC, Glanzmann C, Buck A, von Schulthess GK. Whole-body positron emission tomography using fluorodeoxyglucose for staging of lymphoma: effectiveness and comparison with computed tomography. *Eur J Nucl Med* 1998; **25:** 721-728
16 **Jerusalem G,** Beguin Y, Fassotte MF, Najjar F, Paulus P, Rigo P, Fillet G. Persistent tumor ^{18}F-FDG uptake after a few cycles of polychemotherapy is predictive of treatment failure in non-Hodgkin's lymphoma. *Haematologica* 2000; **85:** 613-618
17 **Spaepen K,** Stroobants S, Dupont P, Van Steenweghen S, Thomas J, Vandenberghe P, Vanuytsel L, Bormans G, Balzarini J, De Wolf-Peeters C, Mortelmans L, Verhoef G. Prognostic value of positron emission tomography (PET) with fluorine-18 fluorodeoxyglucose ([^{18}F]FDG) after first-line chemotherapy in non-Hodgkin's lymphoma: is [^{18}F]FDG-PET a valid alternative to conventional diagnostic methods? *J Clin Oncol* 2001; **19:** 414-419
18 **Rodriguez M,** Ahlstrom H, Sundin A, Rehn S, Sundstrom C, Hagberg H, Glimelius B. [^{18}F] FDG PET in gastric non-Hodgkin's lymphoma. *Acta Oncol* 1997; **36:** 577-584
19 **Hoffmann M,** Kletter K, Diemling M, Becherer A, Pfeffel F, Petkov V, Chott A, Raderer M. Positron emission tomography with fluorine-18-2-fluoro-2-deoxy-D-glucose (F18-FDG) does not visualize extranodal B-cell lymphoma of the mucosa-associated lymphoid tissue (MALT)-type. *Ann Oncol* 1999; **10:** 1185-1189
20 **Ullerich H,** Franzius CH, Domagk D, Seidel M, Sciuk J, Schober, Domschke W. ^{18}F-Fluorodeoxyglucose PET in a patient with primary small bowel lymphoma: the only sensitive method of imaging. *Am J Gastroenterol* 2001; **96:** 2497-2499
21 **Sam JW,** Levine MS, Farner MC, Schuster SJ, Alavi A. Detection of small bowel involvement by mantle cell lymphoma on F-18 FDG positron emission tomography. *Clin Nucl Med* 2002; **27:** 330-333
22 **Cook GJ,** Maisey MN, Fogelman I. Normal variants, artefacts and interpretative pitfalls in PET imaging with 18-fluoro-2-deoxyglucose and carbon-11 methionine. *Eur J Nucl Med* 1999;

26: 1363-1378
23 **Shreve PD,** Anzai Y, Wahl RL. Pitfalls in oncologic diagnosis with FDG PET imaging: physiologic and benign variants. *Radiographics* 1999; **19:** 61-77; quiz 150-151
24 **Meyer MA.** Diffusely increased colonic F-18 FDG uptake in acute enterocolitis. *Clin Nucl Med* 1995; **20:** 434-435
25 **Kresnik E,** Mikosch P, Gallowitsch HJ, Heinisch M, Lind P. F-18 fluorodeoxyglucose positron emission tomography in the diagnosis of inflammatory bowel disease. *Clin Nucl Med* 2001; **26:** 867
26 **Kolve ME,** Fischbach W, Wilhelm M. Primary gastric non-Hodgkin's lymphoma: requirements for diagnosis and staging. *Recent Results Cancer Res* 2000; **156:** 63-68
27 **Koch P,** Grothaus-Pinke B, Hiddemann W, Willich N, Reers B, del Valle F, Bodenstein H, Pfreundschuh M, Moller E, Kocik J, Parwaresch R, Tiemann M. Primary lymphoma of the stomach: three-year results of a prospective multicenter study. The German Multicenter Study Group on GI-NHL. *Ann Oncol* 1997; **8 Suppl 1:** 85-88
28 **Ehrlich AN,** Stalder G, Geller W, Sherlock P. Gastrointestinal manifestations of malignant lymphoma. *Gastroenterology* 1968; **54:** 1115-1121
29 **Coiffier B.** How to interpret the radiological abnormalities that persist after treatment in non-Hodgkin's lymphoma patients? *Ann Oncol* 1999; **10:** 1141-1143
30 **Kaplan WD,** Jochelson MS, Herman TS, Nadler LM, Stomper PC, Takvorian T, Andersen JW, Canellos GP. Gallium-67 imaging: a predictor of residual tumor viability and clinical outcome in patients with diffuse large-cell lymphoma. *J Clin Oncol* 1990; **8:** 1966-1970
31 **Zinzani PL,** Magagnoli M, Chierichetti F, Zompatori M, Garraffa G, Bendandi M, Gherlinzoni F, Cellini C, Stefoni V, Ferlin G, Tura S. The role of positron emission tomography (PET) in the management of lymphoma patients. *Ann Oncol* 1999; **10:** 1181-1184
32 **Najjar F,** Hustinx R, Jerusalem G, Fillet G, Rigo P. Positron emission tomography (PET) for staging low-grade non-Hodgkin's lymphomas (NHL). *Cancer Biother Radiopharm* 2001; **16:** 297-304
33 **Moog F,** Bangerter M, Diederichs CG, Guhlmann A, Merkle E, Frickhofen N, Reske SN. Extranodal malignant lymphoma: detection with FDG PET versus CT. *Radiology* 1998; **206:** 475-481
34 **Kong SH,** Kim MA, Park DJ, Lee HJ, Lee HS, Kim CW, Yang HK, Heo DS, Lee KU, Choe KJ. Clinicopathologic features of surgically resected primary gastric lymphoma. *World J Gastroenterol* 2004; **10:** 1103-1109
35 **Hsu CH,** Sun SS, Kao CH, Lin CC, Lee CC. Differentiation of low-grade gastric MALT lymphoma and high-grade gastric MALT lymphoma: the clinical value of Ga-67 citrate scintigraphy--a pilot study. *Cancer Invest* 2002; **20:** 939-943
36 **Brown JA,** Carson BW, Gascoyne RD, Cooperberg PL, Connors JM, Mason AC. Low grade gastric MALT Lymphoma: radiographic findings. *Clin Radiol* 2000; **55:** 384-389
37 **Kessar P,** Norton A, Rohatiner AZ, Lister TA, Reznek RH. CT appearances of mucosa-associated lymphoid tissue (MALT) lymphoma. *Eur Radiol* 1999; **9:** 693-696
38 **Skarin AT,** Dorfman DM. Non-Hodgkin's lymphomas: current classification and management. *CA Cancer J Clin* 1997; **47:** 351-372
39 **Park MS,** Kim KW, Yu JS, Park C, Kim JK, Yoon SW, Lee KH, Ryu YH, Kim H, Kim MJ, Lee JT, Yoo HS. Radiographic findings of primary B-cell lymphoma of the stomach: low-grade versus high-grade malignancy in relation to the mucosa-associated lymphoid tissue concept. *AJR Am J Roentgenol* 2002; **179:** 1297-1304

Science Editor Guo SY **Language Editor** Elsevier HK

PO Box 2345, Beijing 100023, China
www.wjgnet.com
wjg@wjgnet.com

ELSEVIER

World J Gastroenterol 2005;11(46):7290-7295
World Journal of Gastroenterology ISSN 1007-9327

• *CLINICAL RESEARCH* •

Have patients with esophagitis got an increased risk of adenocarcinoma? Results from a population-based study

Seamus J Murphy, Lesley A Anderson, Brian T Johnston, Deirdre A Fitzpatrick, Peter RG Watson, Pauline Monaghan, Liam J Murray

Seamus J Murphy, BSc MB BCh MRCP, Research Registrar in Gastroenterology, Northern Ireland Cancer Registry (NICR), Northern Ireland
Lesley A Anderson, PhD, Research assistant, NICR, Northern Ireland
Brian T Johnston, MD MRCP, Royal Victoria Hospital, Grosvenor Road, Belfast BT12 6BA, Northern Ireland
Peter RG Watson, MD FRCP, Consultant Gastroenterologists, Royal Victoria Hospital, Grosvenor Road, Belfast BT12 6BA, Northern Ireland
Deirdre A Fitzpatrick, Pauline Monaghan, Biostatisticians, NICR, Northern Ireland
Liam J Murray, MB, MFPHM, Consultant/Senior lecturer in Epidemiology, Department of Epidemiology and Public Health, Mulhouse Building, Grosvenor Road, Belfast BT12 6BJ, Northern Ireland
Supported by The establishment of the NI Barrett's Register was assisted by a grant from the Ulster Cancer Foundation
Correspondence to: Dr Seamus J Murphy, Northern Ireland Cancer Registry, Department of Epidemiology and Public Health, Mulhouse Building, Grosvenor Road, Belfast BT12 6BJ, Northern Ireland. s.murphy@qub.ac.uk
Telephone: +28-90240503 Fax: +28-90248017
Received: 2005-01-15 Accepted: 2005-01-26

Abstract

AIM: To examine an increased risk of esophageal adenocarcinoma is restricted to patients who develop Barrett's esophagus or whether esophagitis *per se* is a risk factor for adenocarcinoma.

METHODS: A population-based cohort of patients with histological evidence of esophagitis without Barrett's esophagus was constructed using electronic pathology reports relating to all esophageal biopsies in Northern Ireland between 1993 and 1996. Person-years of follow-up and incident cases of esophageal cancer were calculated by linking the cohort to death files and the Northern Ireland Cancer Registry records. Standardized incidence ratios (SIR) were calculated for esophageal cancers (adenocarcinoma, squamous cell carcinoma (SCC), and histologically unspecified cancers).

RESULTS: A total of 2 013 patients in the cohort provided 13 559 patient-years of follow-up (mean follow-up 6.7 years). None of the patients developed adenocarcinoma. Three patients developed SCC, and six developed histologically unspecified cancers. The SIR for all esophageal cancers and for SCC were 2.73 (95%CI 1.25-5.19) and 2.93 (95%CI 0.61-8.59), respectively. In a sensitivity analysis in which all unspecified esophageal cancers were treated as adenocarcinomas, the SIR for adenocarcinoma was 2.64 (0.97-5.75).

CONCLUSION: The risk of adenocarcinoma is not elevated in patients with histological evidence of esophagitis without Barrett's esophagus; however, these patients may have a moderately increased risk of SCC. Further studies are required to confirm these findings, which suggest that Barrett's esophagus, not esophagitis, is the key precursor lesion in the development of adenocarcinoma.

Key words: Barrett's esophagus; Esophageal adenocarcinoma; Esophageal squamous cell carcinoma; Esophagitis; Population-based study

Murphy SJ, Anderson LA, Johnston BT, Fitzpatrick DA, Watson PRG, Monaghan P, Murray LJ. Have patients with esophagitis got an increased risk of adenocarcinoma? Results from a population-based study. *World J Gastroenterol* 2005; 11(46): 7290-7295
http://www.wjgnet.com/1007-9327/11/7290.asp

INTRODUCTION

The incidence of esophageal adenocarcinoma (OAC) is increasing at a rate faster than any other cancer in the Western world[1]. The most important risk factor for its development is Barrett's esophagus (BO), a metaplastic condition in which the native squamous epithelium of the esophagus is replaced by columnar epithelium, in response to chronic gastro-esophageal reflux[2]. OAC appears to result from a sequence of changes from esophagitis to non-dysplastic BO, to dysplastic BO, and finally to adenocarcinoma[3,4]. It is generally accepted that most, if not allpatients who develop OAC, pass through this sequence. It is on this basis that endoscopic surveillance of BO is recommended, in an attempt to reduce mortality from OAC[5]. However, some aspects of the relationship between BO and OAC remain unclear. While BO is the only known precursor to this tumor, there is a huge variation in the proportion of cases of OAC in which it is detectable, ranging from 23% to 100% of cases in different studies[6-12]. The difficulty in

identifying BO in patients with OAC is thought to result from tumor overgrowth of the Barrett's segment. However, in a large prospective case-control study in Sweden, Lagergren *et al.*[13] found that in patients with OAC, only 62% had evidence of BO identified by biopsy, despite extensive sampling by a rigorous protocol. They also found that symptoms of gastro-esophageal reflux *per se* were strongly associated with adenocarcinoma, and that the presence or absence of BO in cancer cases had no effect on the strength of this association. These findings have led to the speculation that gastro-esophageal reflux, rather than BO, is the crucial factor in the development of OAC. If that is the case, then esophagitis may be an important risk factor for its development. To our knowledge, there are no studies assessing the risk of OAC in patients with biopsy-proven esophagitis. We undertook a study to examine the incidence of OAC in a population-based cohort of patients who had histological evidence of esophagitis without BO.

MATERIALS AND METHODS

Patients and biopsies

This study is a follow-up study of a population-based cohort of patients with esophagitis. The cohort comprised every adult within Northern Ireland (NI), population 1.7 million, with histological evidence of inflammation of the esophagus that was not due to infection or radiation. The cohort was constructed by examining pathological reports relating to all esophageal biopsies undertaken within all the hospitals in NI between January 1993 and December 1996. Data were available for biopsies taken between 1993 and 1999, but only the first 4 years were used in order to maximize the period of follow-up. These reports were made available to the NI Cancer Registry (NICR) in an electronic format during the construction of the NI Barrett's Register[14]. The reports contained information on the nature and site of the submitted biopsy specimen, the clinical summary recorded by the endoscopist on the request form, the full text of the pathologist's report on the specimen, and the pathologist's diagnosis. The clinical summaries contained information relating to the site at which the biopsies were taken. All pathological reports in which the summary stated that the biopsies were taken from the esophagus, including the esophago-gastric junction (OGJ), were examined. A list of SNOMED (Systematized nomenclature of medicine)[15] codes indicating inflammation in the esophagus was compiled and biopsies were included in the study, if any of these codes appeared on the biopsy report (Table 1). The report which included more than one diagnostic code was considered if at least one of the codes indicated inflammation .

Exclusion criteria for biopsy reports

Biopsy reports were excluded, if patients were less than 16 years of age, or if the diagnostic codes included malignancy, fungal or viral infection, or radiation injury. The bodies of the reports were then examined and any reports in which the pathologist recorded the presence of columnar epithelium were excluded.

Table 1 SNOMED diagnostic codes used in study

Code	Diagnostic term	Number of patients
M40000	Inflammation	777
MZ0005	Non-specific inflammation	9
M40005	Active inflammation	88
M41000	Acute inflammation	31
M42100	Active chronic inflammation	62
M43000	Chronic inflammation	279
M76820	Inflammatory polyp	2
M36500	Edema	2
M36100	Congestion	52
M45020	Granulation tissue	11
M14110	Erosion	6
M38000	Ulcer/ulceration	570
MY0102	Reflux esophagitis	125

Identification and classification of individual patients

A substantial number of patients in the cohort had esophageal biopsies taken on more than one occasion. Individual patients were identified within the dataset by matching on surname, forename(s), and date of birth (and hospital numbers when they were available). The date of the earliest biopsy showing the inflammation was taken as the date of entry into the cohort.

Further exclusion criteria for patients with columnar epithelium

Some patients had an esophageal biopsy that contained columnar epithelium prior to their first biopsy showing inflammation (NB data only available from January 1993). These patients were excluded from the cohort. Other patients had an esophageal biopsy subsequent to their first biopsy showing inflammation that showed columnar epithelium. These patients were not excluded, unless the biopsy showing columnar epithelium occurred within 3 mo of the initial biopsy. These steps were taken to exclude prevalent cases of BO but to include incident cases in the cohort, the rationale being that if esophagitis leads to malignancy through the development of BO, excluding incident BO would potentially miss these patients.

Follow-up of patients

Members of the cohort were followed up for deaths and incident esophageal cancer OAC, squamous cell carcinoma (SCC), and histologically unspecified cancers and lung cancer till the end of December 2002. Lung cancer incidence within the cohort was determined as a proxy for smoking exposure. Deaths among the cohort were identified by matching with the death files from the Registrar General's Office (NI) using the patient's surname, forename(s), and date of birth. These files contained information on all the deaths that occurred within NI.

Incident cases of esophageal cancer with a date of diagnosis at least 6 mo after the date of entry into the cohort were identified by matching the cohort with the NICR database (using the patient's surname, forename(s), date of birth, and hospital numbers where available). This

population-based cancer registry had collected data on all cancers occurring in NI residents, since the beginning of 1993. When assessing lung cancer incidence, a threshold of 3 mo after the date of entry into the cohort was used.

Statistical methods

Person-years of follow-up were calculated for each member of the cohort with censoring either on the date of diagnosis of the esophageal or lung cancer, on the date of death, or on 31st December 2002. Incidences of OAC, SCC, histologically unspecified esophageal cancers, and lung cancer were calculated as the number of events divided by the person-years of follow-up. These incidences were expressed as events per hundred person-years of follow-up, which is equivalent to percentage incidence per year. The standardized incidence ratio (SIR) for these cancers was calculated by comparing the observed number of cancers in the cohort with the expected number, and by applying the relevant age-specific cancer incidence rates in the NI population to the cohort. Exact confidence intervals (CI) of rates and ratios were estimated using the Poisson distribution. Sensitivity analyses were performed in which histologically unspecified esophageal cancers were reclassified as OACs and then as SCCs and the corresponding SIRs were recalculated. This was done to illustrate the most extreme case scenarios, by assuming that all unspecified cancers were one or the other histological type of cancer. These analyses are secondary analyses of data collected during the construction of the NI Barrett's Register. Establishment of this Register received ethical approval from the Research Ethics Committee of the Queen's University, Belfast.

RESULTS

Figure 1 shows how the cohort was constructed and the effect of exclusion criteria. There were 2 013 patients in the cohort, comprising 996 (49.5%) men and 1 017 (50.5%) women. The mean age was 59.8 years, range 16.2-95.6 years. Men were substantially younger than women (56.6± 17.0 *vs* 63.0±16.2 years). The age and sex distributions of patients are shown in Figure 2. In 90 (4.5%) patients, the biopsies had been taken at the OGJ.

Members of the cohort were followed up for a mean of 6.7 years for a total of 13 559 person-years of follow-up. Nine patients developed esophageal cancer (4 men and 5 women), a mean of 3.1 years (range, 1.0-6.8 years) after the initial biopsy showing esophagitis. Mean age at diagnosis was 75.1 years (range, 60.8-86.3 years). None of the incident esophageal cancers were adenocarcinomas; three were SCCs and six were histologically unspecified. Two of the three patients who developed SCC were women. Histological confirmation of cancer was not possible in five of the six unspecified tumors, as biopsies were not taken. These diagnoses were based on the clinical opinion and in one case the registered causes of death did not include esophageal cancer. The pathological diagnosis in the single unspecified cancer case in whom biopsies had been taken was recorded as anaplastic carcinoma but in the body of the report the pathologist stated that it was 'probably squamous in type'.

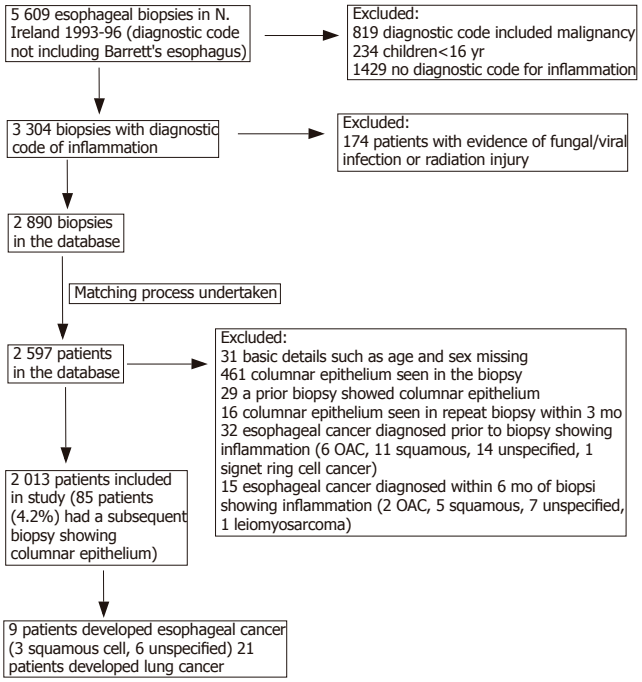

Figure 1 Flow diagram showing how cohort of patients with esophagitis was constructed.

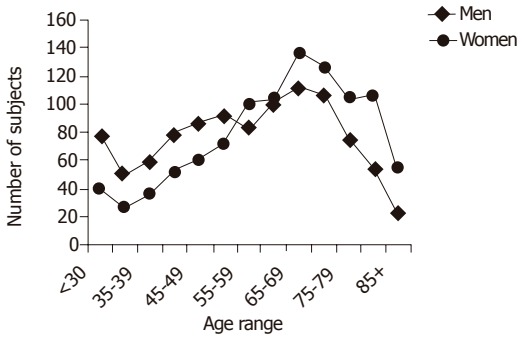

Figure 2 Age and sex distribution of patients with esophagitis.

The incidences and SIRs of esophageal cancers are shown in Table 2. The SIR (95%CI) for all esophageal cancers in the cohort was 2.73 (1.25-5.19), with a higher risk in women than men. The SIR (95%CI) for SCC was also raised at 2.93 (0.61-8.59) but this did not reach conventional statistical significance. The SIR for adenocarcinoma was 0 with an upper 97.5%CI of 2.73. None of the esophageal cancers occurred in patients whose biopsies were taken at the OGJ and exclusion of these patients had little effect on observed SIRs (data not shown). In the sensitivity analyses in which histologically unspecified cancers were reclassified as OACs and then as SCCs, the SIRs (95%CI) for OAC and SCC were 2.64 (0.97-5.75) and 4.64 (2.12-8.81), respectively. Dysplasia was noted in 20 (1%) patients; none of these patients

Table 2 Risk of esophageal and lung cancer in patients with histologically confirmed esophagitis and without Barrett's esophagus

		Number of cases	Incidence per 100 person-years of follow-up (95%CI)	Expected number of cases	Standardized incidence ratio (95%CI)
OAC	All patients	0	-	1.35	0 (-, 2.73)[1]
All esophageal	All patients	9	0.07 (0.04, 0.14)	3.29	2.73 (1.25-5.19)
cancers	Men	4	0.06 (0.02, 0.16)	1.8	2.22 (0.61-5.69)
	Women	5	0.07 (0.02, 0.17)	1.43	3.49 (1.14-8.16)
Esophageal	All patients	3	0.02 (0.01, 0.07)	1.02	2.93 (0.61-8.59)
SCC					
	Men	1	0.02 (0, 0.10)	0.44	2.28 (0.06-12.6)
	Women	2	0.03 (0, 0.12)	0.59	3.40 (0.41-12.2)
Lung cancer	All patients	21	0.16 (0.10, 0.24)	19.71	1.07 (0.66-1.63)
	Men	16	0.25 (0.14, 0.40)	11.36	1.41 (0.81-2.29)
	Women	5	0.07 (0.02, 0.17)	7.63	0.66 (0.21-1.53)
Sensitivity analyses					
Reclassified	All patients	6	0.04 (0.01, 0.13)	2.27	2.64 (0.97-5.75)
OAC[2]	Men	3	0.05 (0.02, 0.11)	1.36	2.20 (0.45-6.45)
	Women	3	0.04 (0.01, 0.13)	0.85	3.54 (0.73-10.31)
Reclassified	All patients	9	0.07 (0.02, 0.17)	1.94	4.64 (2.12-8.81)
esophageal	Men	4	0.06 (0.02, 0.16)	0.91	4.39 (1.20-11.25)
SCC[3]	Women	5	0.07 (0.02, 0.17)	1.02	4.92 (1.59-11.44)

[1]One-sided 97.5%CI; [2]OAC+histologically unspecified cancers; [3]SCC+histologically unspecified cancers.

developed esophageal cancer.

Eighty-five (4.2%) patients in the cohort had a subsequent esophageal biopsy (after a minimum of 3 mo and before December 1999) showing columnar epithelium. None of the patients developed esophageal cancers in this group.

Twenty-one patients developed lung cancer, including 16 men and 5 women. Mean age at diagnosis of lung cancer was 71.3 years (range, 32.7-80.6 years). Overall, the SIR for lung cancer was not raised although a modest increase in risk was seen in men, which was not statistically significant (SIR 1.41, 95%CI 0.81-2.29).

DISCUSSION

This is the first population-based study to assess the risk of esophageal cancer in patients with histologically proven esophagitis that is not complicated by BO. We found that none of the 2 013 patients with esophagitis developed OAC after an average follow-up of 6.7 years. However, some of the six histologically unspecified tumors that occurred within the cohort might be adenocarcinomas.

This study has got many advantages. All patients had histologically confirmed esophagitis, and every patient in whom this diagnosis was made in NI between 1993 and 1996 was included in the study. The population-based nature of this study avoids selection biases that may operate when only patients attending specific centers are investigated. Also, patients who showed evidence of BO were excluded from the cohort, which allowed us to examine the risk of esophageal cancer in esophagitis uncomplicated by BO. Finally, follow-up of patients is likely to be near-completion for two reasons: firstly, population-based cancer and death registers were used to determine deaths and cancer incidence among the cohort; and secondly, emigration from NI is uncommon, averaging 1.1% of the population per year in the period 1991-2003[16].

This study also has limitations. A diagnosis of 'reflux esophagitis' was made in only a small proportion of cases because scant clinical details were provided on the pathology request forms. However, reflux of gastric contents was the most likely cause of esophagitis that was not due to infection or radiation. Also, patients with esophagitis were not routinely biopsied, so patients included in this cohort may represent a subset of patients with esophagitis who had suspicious features at endoscopy. Risk of esophageal cancer may, therefore, be exaggerated in this cohort but exclusion of prevalent cancers and cancers occurring within the first 6 mo reduces the effect of this problem. Accurate histological classification of the incident esophageal tumors occurring in the cohort was not available for 60% of tumors. Some of the unclassified tumors may be adenocarcinomas rendering the absolute incidence of OAC, an underestimate. However, classification of esophageal cancer incidence in the general population is subject to the same limitations, meaning that the SIRs presented for all cancers and for cancer subgroups should be valid comparisons between the cohort and the general population. Furthermore, we performed sensitivity analyses to estimate the maximum incidence of OAC and SCC, by assuming that all the histologically unspecified cancers were actually OACs or SCCs, respectively. Lastly, the modest size of the cohort and the period of follow-up have resulted in small numbers of incident cancers, which may render some of the estimates of cancer risk unstable. Another effect of the relatively short period of follow-up is that a late increase in the risk of OAC associated with esophagitis cannot be discounted.

When all histologically unspecified cancers were treated as OACs, giving a maximal possible risk of OAC, the risk in the cohort was approximately 2.5 times than that of the general population. This is undoubtedly an overestimate but the extent cannot be ascertained. We have previously demonstrated a 17-fold increase in risk of OAC in a cohort

of patients with BO (histologically confirmed specialized intestinal metaplasia) drawn from the same population and followed up in the same manner as in this study[14]. These data suggest that, unlike BO, esophagitis without BO is not an important risk factor for OAC.

The literatures regarding the risk of adenocarcinoma in esophagitis are conflicting. Previous case-control studies have shown that esophagitis or esophageal ulcer is associated with a two- to fivefold increased risk of OAC[17-19]. However, the diagnosis of esophagitis was obtained from case-note review or questionnaire and was not histologically confirmed. Also, it was not possible to identify and exclude patients with BO in these studies. Ye *et al*.[20] reported a sixfold increase in the incidence of OAC in a large population-based cohort study of patients with a hospital diagnosis of gastro-esophageal reflux disease (GORD), but patients with BO were not excluded. A recent study utilizing data from the United Kingdom General Practice Research Database estimated that patients with esophagitis had a 4.5-fold increased risk of OAC compared to the normal population, whereas the risk in BO patients was increased 30-fold[21]. Moreover, following long-term follow-up of patients with GORD, Spechler *et al*.[22] found that patients with BO at baseline developed OAC at an annual rate of 0.4%, whereas the rate in patients without BO was only 0.07%. These data from patients with clinical diagnoses of esophagitis and BO appear to be in agreement with our findings from patients with histological confirmation of their diagnoses.

Only 4.5% of patients in our cohort had a subsequent esophageal biopsy showing columnar epithelium, suggesting that progression from esophagitis to BO may be uncommon. However, it must be borne in mind that there was no systematic recall of patients for endoscopy, so the incidence of BO in the cohort may be underestimated. Also, a systematic biopsy protocol was not employed, so columnar epithelium may have been missed in some patients, either in their initial biopsy or subsequent biopsies.

The low incidence of OAC in our cohort suggests that progression along a path from esophagitis to BO and to OAC may not be the normal sequence of events. Rather, an individual's response to reflux of gastric contents may result in either esophagitis or BO, with a future risk of OAC being confined to those who develop BO. Cameron and Arora[23] carried out a detailed study in which they mapped areas of damage seen at endoscopy in patients with esophagitis and in patients with BO. Their findings suggest that BO is unlikely to develop directly from areas of esophagitis, adding plausibility to the proposed pathway in Figure 3.

The incidence of SCC within the cohort was almost three times than that of the general population. There is limited evidence in the literature supporting a link between esophagitis and SCC. Munoz *et al*.[24] showed a very high prevalence of esophagitis (84%) in people living in the Linxian region of China, where there is a very high incidence of esophageal SCC. However, the authors stated that this esophagitis affected the middle and lower thirds of the esophagus as opposed to the distal esophagus; also, it was not accompanied by erosions or ulcers, features characteristic of esophagitis secondary to gastro-esophageal reflux. These patients are very different from the cohort that we had examined, particularly in terms of lifestyle and nutritional status and gastro-esophageal reflux may not be important in the etiology of esophagitis in China. Ribet *et al*.[25] found evidence of an association between reflux symptoms and SCC in the patients who underwent resection of esophageal cancers, but this was a small study involving a highly selected group. Ye *et al*.[20] found a moderately raised risk of SCC in a Swedish cohort of hospital patients with GERD. On the other hand, in a large Swedish case-control study, Lagergren *et al*.[13] found no association between symptoms of reflux and risk of SCC of the esophagus.

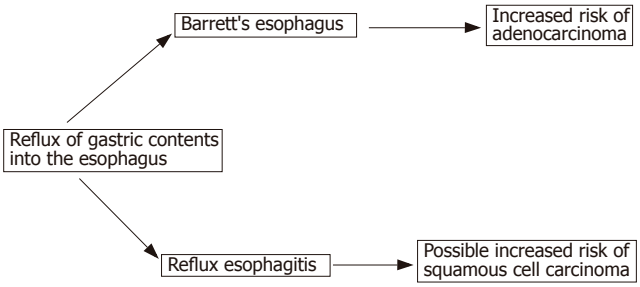

Figure 3 Potential pathways of cancer causation in the esophagus.

Our finding of increased SCC risk in patients with esophagitis could result from over-representation of smokers within the cohort, since smoking is associated with reflux symptoms[26,27]. However, this was unlikely because the risk of lung cancer was not raised in the cohort. It may also result from inclusion of patients with suspicious lesions seen at endoscopy, which might include dysplastic squamous epithelium; however, less than 1% of patients had evidence of dysplasia, and none of these developed SCC. Further research is required to examine the association we have seen between esophagitis and SCC.

In summary, our study shows that esophagitis that is not complicated by BO is not associated with an increased risk of OAC. This finding supports the view that BO, not esophagitis, is the key precursor of OAC. Further studies are required to see if these findings can be replicated. Determination of the relative importance of esophagitis in esophageal cancer causation is important because this has implications for the management of patients with gastro-esophageal reflux and for the prevention of OAC.

ACKNOWLEDGMENT

The authors thank Dr. Dermot Hughes, Consultant Pathologist at Altnagelvin Area Hospital, for advice relating to SNOMED codes used in the study. Thanks are also due to Mr. Colin Fox, Mr. Richard Middleton, and the Tumor Verification Officers of the NICR for their assistance with the processing of pathological records. We are also grateful to Dr. Anna Gavin, Director of the NICR

and to the administrative, medical and pathology staff of local Health Care Trusts and the staff of the Directorate of Information Services DHSSPS (NI) for assistance in the construction of the NI Barrett's Register.

REFERENCES

1 **Devesa SS,** Blot WJ, Fraumeni JF Jr. Changing patterns in the incidence of esophageal and gastric carcinoma in the United States. *Cancer* 1998; **83:** 2049-2053
2 **Spechler SJ,** Goyal RK. Barrett's esophagus. *N Engl J Med* 1986; **315:** 362-371
3 **Reid BJ,** Sanchez CA, Blount PL, Levine DS. Barrett's esophagus: cell cycle abnormalities in advancing stages of neoplastic progression. *Gastroenterology* 1993; **105:** 119-129
4 **Altorki NK,** Oliveria S, Schrump DS. Epidemiology and molecular biology of Barrett's adenocarcinoma. *Semin Surg Oncol* 1997; **13:** 270-280
5 **Sampliner RE.** Practice guidelines on the diagnosis, surveillance, and therapy of Barrett's esophagus. The Practice Parameters Committee of the American College of Gastroenterology. *Am J Gastroenterol* 1998; **93:** 1028-1032
6 **Haggitt RC,** Tryzelaar J, Ellis FH, Colcher H. Adenocarcinoma complicating columnar epithelium-lined (Barrett's) esophagus. *Am J Clin Pathol* 1978; **70:** 1-5
7 **Hamilton SR,** Smith RR, Cameron JL. Prevalence and characteristics of Barrett esophagus in patients with adenocarcinoma of the esophagus or esophagogastric junction. *Hum Pathol* 1988; **19:** 942-948
8 **Duhaylongsod FG,** Wolfe WG. Barrett's esophagus and adenocarcinoma of the esophagus and gastroesophageal junction. *J Thorac Cardiovasc Surg* 1991; **102:** 36-41; discussion 41-42
9 **Streitz JM Jr,** Ellis FH Jr, Gibb SP, Balogh K, Watkins E Jr. Adenocarcinoma in Barrett's esophagus. A clinicopathologic study of 65 cases. *Ann Surg* 1991; **213:** 122-125
10 **Li H,** Walsh TN, Hennessy TP. Carcinoma arising in Barrett's esophagus. *Surg Gynecol Obstet* 1992; **175:** 167-172
11 **Clark GW,** Smyrk TC, Burdiles P, Hoeft SF, Peters JH, Kiyabu M, Hinder RA, Bremner CG, DeMeester TR. Is Barrett's metaplasia the source of adenocarcinomas of the cardia? *Arch Surg* 1994; **129:** 609-614
12 **Cameron AJ,** Lomboy CT, Pera M, Carpenter HA. Adenocarcinoma of the esophagogastric junction and Barrett's esophagus. *Gastroenterology* 1995; **109:** 1541-1546
13 **Lagergren J,** Bergstrom R, Lindgren A, Nyren O. Symptomatic gastroesophageal reflux as a risk factor for esophageal adenocarcinoma. *N Engl J Med* 1999; **340:** 825-831
14 **Murray L,** Watson P, Johnston B, Sloan J, Mainie IM, Gavin A. Risk of adenocarcinoma in Barrett's oesophagus: population based study. *BMJ* 2003; **327:** 534-535
15 **Spackman KA,** Campbell KE, Cote RA. SNOMED RT: a reference terminology for Health Care. *Northfield , IL, College of Pathologists,* 2000
16 Northern Ireland Migration Flows 1991-2003. Available from URL: http://www.nisra.gov.uk/statistics/financeandpersonnel/dmb/datavault.ht
17 **Chow WH,** Finkle WD, McLaughlin JK, Frankl H, Ziel HK, Fraumeni JF Jr. The relation of gastroesophageal reflux disease and its treatment to adenocarcinomas of the esophagus and gastric cardia. *JAMA* 1995; **274:** 474-477
18 **Farrow DC,** Vaughan TL, Sweeney C, Gammon MD, Chow WH, Risch HA, Stanford JL, Hansten PD, Mayne ST, Schoenberg JB, Rotterdam H, Ahsan H, West AB, Dubrow R, Fraumeni JF Jr, Blot WJ. Gastroesophageal reflux disease, use of H2 receptor antagonists, and risk of esophageal and gastric cancer. *Cancer Causes Control* 2000; **11:** 231-238
19 **Wu AH,** Tseng CC, Bernstein L. Hiatal hernia, reflux symptoms, body size, and risk of esophageal and gastric adenocarcinoma. *Cancer* 2003; **98:** 940-948
20 **Ye W,** Chow WH, Lagergren J, Yin L, Nyren O. Risk of adenocarcinomas of the esophagus and gastric cardia in patients with gastroesophageal reflux diseases and after antireflux surgery. *Gastroenterology* 2001; **121:** 1286-1293
21 **Solaymani-Dodaran M,** Logan RF, West J, Card T, Coupland C. Risk of oesophageal cancer in Barrett's oesophagus and gastro-oesophageal reflux. *Gut* 2004; **53:** 1070-1074
22 **Spechler SJ,** Lee E, Ahnen D, Goyal RK, Hirano I, Ramirez F, Raufman JP, Sampliner R, Schnell T, Sontag S, Vlahcevic ZR, Young R, Williford W. Long-term outcome of medical and surgical therapies for gastroesophageal reflux disease: follow-up of a randomized controlled trial. *JAMA* 2001; **285:** 2331-2338
23 **Cameron AJ,** Arora AS. Barrett's esophagus and reflux esophagitis: is there a missing link? *Am J Gastroenterol* 2002; **97:** 273-278
24 **Munoz N,** Crespi M, Grassi A, Qing WG, Qiong S, Cai LZ. Precursor lesions of oesophageal cancer in high-risk populations in Iran and China. *Lancet* 1982; **1:** 876-879
25 **Ribet ME,** Mensier EA. Reflux esophagitis and carcinoma. *Surg Gynecol Obstet* 1992; **175:** 121-125
26 **Murray L,** Johnston B, Lane A, Harvey I, Donovan J, Nair P, Harvey R. Relationship between body mass and gastro-oesophageal reflux symptoms: The Bristol Helicobacter Project. *Int J Epidemiol* 2003; **32:** 645-650
27 **Locke GR 3rd,** Talley NJ, Fett SL, Zinsmeister AR, Melton LJ 3rd. Risk factors associated with symptoms of gastroesophageal reflux. *Am J Med* 1999; **106:** 642-649

Science Editor Kumar M and Guo SY **Language Editor** Elsevier HK

PO Box 2345, Beijing 100023, China
www.wjgnet.com
wjg@wjgnet.com

ELSEVIER

World J Gastroenterol 2005;11(46):7296-7301
World Journal of Gastroenterology ISSN 1007-9327

• *CLINICAL RESEARCH* •

Ultrasonographic study of postcibal gastro-esophageal reflux and gastric emptying in infants with recurrent respiratory disease

Agostino Di Ciaula, Piero Portincasa, Leonardo Di Terlizzi, Domenico Paternostro, Giuseppe Palasciano

Agostino Di Ciaula, Division of Internal Medicine, Hospital of Bisceglie, Italy
Piero Portincasa, Giuseppe Palasciano, Section of Internal Medicine, Department of Internal Medicine and Public Medicine (DIMIMP), University Medical School, Bari, Italy
Leonardo Di Terlizzi, Domenico Paternostro, Division of Pediatrics, Hospital of Bisceglie, Italy
Correspondence to: Agostino Di Ciaula, MD, Division of Internal Medicine, P.O. Bisceglie, 70052 Bisceglie (BA), Italy. agostinodiciaula@tiscali.it
Telephone: +39-80-3357271
Received: 2005-04-30 Accepted: 2004-05-18

Abstract

AIM: To check the utility of postcibal ultrasonography for the evaluation of reflux in relation to gastric emptying in infants with recurrent respiratory symptoms and to link imaging with clinical data.

METHODS: Esophageal reflux (hyperechoic retrograde filling) and gastric emptying (antral areas) were quantified before and after ingestion of a standard formula in 35 untreated infants (13 with chronic cough, 22 with recurrent bronchitis) and in 31 controls.

RESULTS: The prevalence of abnormal (≥8 episodes) postcibal refluxes was 74% in patients and 3% in controls. Number, duration of the longest episode and extent of refluxes were significantly higher in patients compared to controls. Number of refluxes was higher in patients with symptomatic refluxes than in those without. Infants with recurrent bronchitis had more refluxes than those with chronic cough and controls. Extent and timing of gastric emptying were similar in patients and controls.

CONCLUSION: Esophageal ultrasonography is a useful and physiological test in infants with recurrent respiratory diseases, which have a high prevalence of abnormal postcibal esophageal reflux and a gastric emptying similar to that of normal controls. Esophageal reflux is more severe in subjects with recurrent bronchitis than in those with chronic cough.

Key words: Ultrasonography; Gastro-esophageal reflux; Gastric emptying; Recurrent respiratory disease

Di Ciaula A, Portincasa P, Di Terlizzi L, Paternostro D, Palasciano G. Ultrasonographic study of postcibal gastro-esophageal reflux and gastric emptying in infants with recurrent respiratory disease. *World J Gastroenterol* 2005; 11(46): 7296-7301
http://www.wjgnet.com/1007-9327/11/7296.asp

INTRODUCTION

Gastro-esophageal reflux has been frequently linked to several acute and chronic respiratory diseases in infants[1-4]. As ultrasonography may allow direct visualization of gastro-esophageal junction and of retrograde reflux episodes[5,6], it has been used as an alternative to invasive techniques in pediatric age[5-9]. Validation studies reported high sensitivity and specificity for ultrasonography in diagnosing gastro-esophageal reflux, as compared to standard barium swallow examination[6], esophageal pH monitoring[8,10], and esophagomanometry[10]. The application of ultrasonography in pediatric age has major advantages due to its non-invasiveness, wide availability, and optimal compliance. Thus, in the present study, we aimed to: (1) employ ultrasound for the evaluation of gastro-esophageal reflux in relation to postprandial gastric emptying in infants with or without recurrent respiratory diseases; and (2) relate the gastro-esophageal imaging with clinical data in the postcibal period.

MATERIALS AND METHODS

Subjects

The ultrasonographic test was part of a routine work-up abdominal assessment. Informed consent was obtained from parents for each infant participating in the study and the study protocol was approved by an institutional review board. The study comprised 66 non-preterm infants (age range, 1-12 mo). Characteristics of the subjects are summarized in Table 1. Thirty-five inpatient or outpatient infants with a recent history of recurrent respiratory diseases were recruited. Patients had at least two episodes of asthmatic bronchitis requiring hospital admission (group A, $n = 22$) or unexplained chronic cough (group B, $n = 13$). Patients, who were referred only for respiratory problems, underwent *de novo* evaluation without prior investigations or therapies. Parents denied, in all cases, the consent to

invasive techniques. In all patients, immune deficiencies, cystic fibrosis, and allergopathies were excluded by clinical and biohumoral assessment. Parents were asked for the presence of daily regurgitation in all the patients.

Additionally, 31 inpatient or outpatient infants, who never experienced respiratory or gastrointestinal diseases, were considered as controls. Patients were not examined during acute respiratory disease. Neither patients nor controls were under medications able to influence gastrointestinal motility or secretion and were not affected by conditions known to alter gastrointestinal tract functions.

Study design

Each subject underwent a simultaneous ultrasonographic study of the esophagus and of the antrum with a Toshiba Capasee scanner and a 3.5-MHz convex probe. Ultrasonography was performed in a sitting position before and after the ingestion of a low volume liquid standard meal (10 mL/kg standard infant formula). Subjects were fed in the upright position. The observation was carried out continuously for at least 20 min and in all cases until complete antral evacuation was recorded. All tests started in the morning, in the fasting state (at least 4 h) and were performed by a single examiner who was unaware of patient's history and clinical examination. Ultrasonographic findings were analyzed while being done and events were recorded on a specific form. The infants were not burped after the feeding and pacifiers were not employed. All infants were awake during the examination. Subjects with excessive gas in the stomach or excessive crying time (able to interrupt the continuity of observation) were excluded by analysis due to technical limitations.

Gastro-esophageal reflux study

The employment of ultrasound in the diagnosis of gastro-esophageal reflux disease has previously been validated against other techniques[6,8,10]. The esophagus and the gastro-esophageal junction were studied by transverse and longitudinal scans at the epigastrium[5,6,11] at the level of the left lobe of the liver, slightly rotating up the probe. In all the subjects, this allowed the visualization of the esophagus like a three-layer canalicular structure posterior to the left lobe of the liver and anterior to the aorta, which were used as landmark points[11]. Immediately after the ingestion of the standard liquid meal, the esophageal lumen appeared dilated by hyperechoic content flowing towards the gastric lumen. First, a longitudinal scan was performed to show the emptying of the distal esophagus. Subsequently, a *"real time"* observation of the esophagus and the gastro-esophageal junction was performed[11] by splitting the image on the ultrasound monitor. In particular, the esophagus and the gastro-esophageal junction were imaged on one half of the monitor continuously during 20 min. At regular intervals (mentioned below), the observation was stopped shortly for 2-3 s to catch antral sections on the second half of the screen for subsequent antral area measurement.

Gastro-esophageal reflux, when present, was visible like a flow of hyperechoic material directed from gastric lumen to distal esophagus through gastro-esophageal junction.

In the present series, gastro-esophageal reflux was defined as abnormal when the total number of episodes lasting for more than 2 s was $\geqslant$8 (upper limit derived from mean+2SD in normal control group = 7.5). The presence/absence and the number of gastro-esophageal reflux episodes during 20 min were recorded and the frequency of gastro-esophageal reflux episodes (i.e., no. of episodes/time unit) was therefore calculated.

Immediately after the retrograde flow of hyperechoic material from gastric lumen to distal esophagus, the ultrasonographic image was frozen on one half of the monitor and the amount of gastro-esophageal reflux was subsequently quantified by measuring maximal esophageal lumen enlargement (distance between external esophageal layers). On the second half of the monitor (set as "real time" imaging), the duration of the reflux episode was counted by a timer. Maximal esophageal lumen enlargement and duration of the longest reflux episode for each examination were noted.

During the real-time continuous monitoring, all cough episodes were counted in both patients and controls. Cough episodes starting within 2 s from hyperechoic retrograde filling of esophageal lumen were therefore marked on a specific form and were considered related to reflux.

Gastric emptying study

Postprandial evacuation of the stomach was assessed by functional ultrasonography by monitoring antral areas, a well standardized technique in adults[11-15] and in infants[16-20]. Antral area was quantified in fasting infants and subsequently monitored at regular time intervals postprandially by longitudinal scans at the epigastrium at the level of antral-body connection in a single section. The superior mesenteric vein and the aorta were used as landmark points. Antral emptying was described by the following indices: (1) antral (basal) area (mean of two measurements between -5 and 0 min before meal, in cm^2); (2) maximal postprandial antral area, measured 2 min after meal ingestion; (3) postprandial antral areas each taken at 5-min intervals from meal ingestion; (4) minimal postprandial antral area observed throughout the emptying curve; and (5) half-emptying time.

Antral emptying curves were obtained by plotting antral areas *vs* time. In order to obviate interindividual variability of antrum size[13], postprandial areas were normalized to maximal areas after subtracting basal areas: $100\times(A_t\text{-}a)/(A_2\text{-}a)$, where A_t = postprandial area at any given time; a = basal area; A_2 = maximal antral area (measured at 2 min postprandially)[21]. Half-emptying time was the time at which 50% decrease of antral area occurred ($T_{1/2}$, min), and was calculated by linear regression analysis from the linear part of antral emptying curve. This index closely correlates with the scintigraphic half-emptying time[14].

Statistical analysis

All calculations were performed with the NCSS2001

Table 1 Characteristics of enrolled subjects

	Patients	Controls	*P*
N	35	31	
Age (mo)	5.6±2.9	4.5±3.6	NS
Weight (kg)	7.4±2.0	6.7±1.7	NS
Height (m)	0.7±0.07	0.6±0.01	NS

Data are expressed as mean±SD. NS: not significantly different.

Table 2 Ultrasonographic characteristics of gastro-esophageal reflux in infants with recurrent respiratory diseases and in healthy controls

	Patients	Controls	*P*
Number of reflux episodes	10 (2-21)	3 (1-9)	<0.01
Reflux frequency (reflux episodes/min)	0.5 (0.1-1.05)	0.15 (0.05-0.45)	<0.01
Maximal esophageal lumen enlargement (mm)	5 (1-17)	1.5 (1-9)	<0.01
Duration of the longest reflux episode (s)	11 (2-18)	4 (2-12)	<0.01

Results are expressed as median (range). Differences between groups were tested using Mann-Whitney *U* test.

software (Kaysville, UT, USA). Results were expressed as mean±SE or mean±SD or median and range, where appropriate. Data were statistically compared using two-tailed Student's t-test for unpaired data or by non-parametric Mann-Whitney *U* test, where appropriate. Analysis of variance followed by Fisher's LSD multiple comparison test was utilized to compare the differences among the groups. The χ^2 test was used to compare proportions of categorical data. Two-tailed *P* values less than 0.05 were considered statistically significant[22].

RESULTS

Patients and controls were similar in age-weight and height distribution (Table 1) and all subjects were below the 95th percentile for body weight. Overall, patients had significantly greater prevalence of abnormal postcibal reflux (74% in patients *vs* 3% in controls, $P<0.05$), number and frequency of reflux episodes, extent of refluxes and duration of the longest reflux episode as compared to controls (Table 2). Stratification of patients by age (0-6 mo, $n = 22$ and 7-12 mo, $n = 13$) showed similar results in the two age groups that were examined (Table 3).

The total number of cough episodes was significantly greater in patients than in controls (2.7±0.5 *vs* 0.03±0.03; $P<0.01$). Symptomatic reflux episodes (i.e., cough observed within 2 s from hyperechoic retrograde filling of esophageal lumen) were documented in 57% of patients (2.0±0.4 symptomatic refluxes in the observation period) and in none of the controls. Cough episodes not preceded by reflux were 0.5±0.3 in patients without symptomatic reflux episodes and 0.8±0.2 in patients with symptomatic refluxes.

The median number and frequency of gastro-esophageal reflux episodes were obviously higher in patients with symptomatic reflux episodes than in those without (Table 4).

Table 3 Ultrasonographic characteristics of gastro-esophageal reflux in patients with recurrent respiratory diseases in two age groups

	0-6 mo	7-12 mo	*P*
Number of reflux episodes	9.5 (3-21)	11 (2-18)	NS
Reflux frequency (reflux episodes/min)	0.5 (0.15-1.05)	0.6 (0.1-0.9)	NS
Maximal esophageal lumen enlargement (mm)	5.5 (1-17)	4 (1.6-11.5)	NS
Duration of the longest reflux episode (s)	11 (2-17)	7 (4-18)	NS

Results are expressed as median (range). Differences between groups were tested by Mann-Whitney *U* test; NS: not significantly different.

Table 4 Ultrasonographic characteristics of gastro-esophageal reflux in patients with or without symptomatic reflux episodes

	With symptomatic reflux	Without symptomatic reflux	*P*
Subjects	20	15	
Number of reflux episodes	11.5 (4-21)	7 (2-18)	<0.02
Reflux frequency (reflux episodes/min)	0.58 (0.2-1.05)	0.4 (0.1-0.9)	<0.05
Maximal esophageal lumen enlargement (mm)	5.5 (1.7-13.5)	3.0 (1-17)	NS
Duration of the longest reflux episode (s)	11 (6-18)	8 (2-17)	NS

Results are expressed as median (range). Differences between groups were tested using Mann-Whitney *U* test. NS: not significantly different.

The prevalence of abnormal refluxes was higher in patients with recurrent bronchitis (group A) and in patients with chronic cough (group B) as compared to controls (Table 5). Both subgroups of patients had more reflux episodes, higher reflux frequency, higher esophageal lumen enlargement and duration of the longest reflux episode as compared to controls ($P<0.01$, ANOVA, Figure 1 and Table 5). Patients with recurrent bronchitis also showed more reflux episodes, higher reflux frequency and higher duration of the longest reflux episode as compared to infants with chronic cough (Table 5). The number of symptomatic reflux episodes was similar in patients with recurrent bronchitis (2.6±0.6) and in those with chronic cough (1.2±0.4).

Daily regurgitation was present in 57% of patients with recurrent respiratory diseases, who showed a higher number, frequency, and duration of the longest reflux episode compared to patients without this symptom (Table 6). The number of symptomatic refluxes was similar in patients with (2.4±0.6) and without (1.7±0.6) daily regurgitation.

The study of gastric emptying showed a rapid and continuous decrement of the antral areas starting immediately after meal ingestion in both patients and controls (Figure 2). Patients and controls showed comparable fasting (1.3±0.01 and 1.2±0.1 cm^2, respectively) and maximal postprandial areas (5.7±0.3 *vs* 5.6±0.4 cm^2), and similar postprandial emptying indices, in terms of both minimal postprandial areas (1.4±0.1 *vs* 1.3±0.2 cm2; 4.6±1.9% *vs* 3.5±1.4%) and half-emptying time (9±0.6 *vs* 9±0.5 min, respectively). No significant difference was observed in time to maximal emptying between patients

Table 5 Ultrasonographic characteristics of gastro-esophageal reflux in patients with recurrent episodes of bronchitis (group A), chronic cough (group B), and in healthy controls

	Group A	Group B	Controls	ANOVA
Reflux prevalence (%)	82[a]	54[a]	3	
Number of reflux episodes (*N*)	12.0 (2-21)[a,c]	8.0 (2-12)[a]	3.0 (1-9)	<0.00001
Reflux frequency (*N*/min)	0.6 (0.1-1.05)[a,c]	0.4 (0.1-0.6)[a]	0.15 (0.05-0.45)	<0.00001
Maximal esophageal lumen enlargement (mm)	5 (1-17)[a]	4 (1.5-11.8)[a]	1.5 (1-9)	<0.0001
Duration of the longest reflux episode (s)	11.5 (2-18)[a,c]	7 (3-12)[a]	4 (2-12)	<0.00001

Results are expressed as median (range). Differences between percentage reflux prevalence were tested by χ^2 test. Differences between groups were examined by using ANOVA, followed by Fisher's LSD multiple comparison test. [a]$P<0.05$ *vs* controls; [c]$P<0.05$ *vs* group B.

Table 6 Ultrasonographic characteristics of gastro-esophageal reflux in infants with recurrent respiratory diseases, with or without daily regurgitation

	With daily regurgitation	Without daily regurgitation	*P*
Subjects	20 (57%)	15 (43%)	NS
Number of reflux episodes (*N*)	10.5 (5-21)	8 (2-18)	<0.03
Reflux frequency (*N*/min)	0.5 (0.25-1.05)	0.4 (0.1-0.9)	<0.03
Maximal esophageal lumen enlargement (mm)	5 (1.5-17)	4 (1.0-11.5)	NS
Duration of the longest reflux episode (s)	11.5 (3-17)	7 (2-18)	<0.01

Results are expressed as median (range). Differences between groups were tested by using Mann–Whitney *U* test. NS: not significantly different.

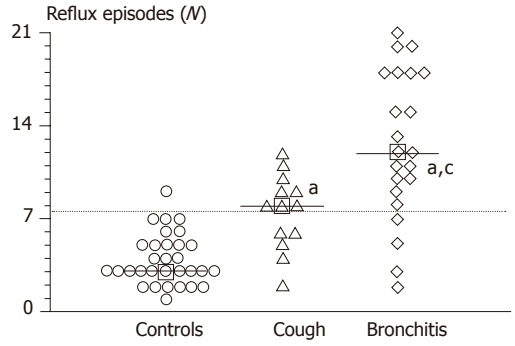

Figure 1 Number of postcibal gastro-esophageal reflux episodes, as determined by ultrasound, in controls (n = 31) and in infants with recurrent respiratory diseases (n = 35). Horizontal dotted line indicates the mean+2SD in the normal control group. Squares and continuous horizontal lines indicate medians. Differences between the groups were tested by using ANOVA, followed by Fisher's LSD multiple comparison test. [a]$P<0.05$ *vs* controls; [c]$P<0.05$ *vs* chronic cough.

(20±1 min) and controls (19±1 min). Invariably, gastric emptying was complete after 30 min in all cases. Gastric emptying speed was also similar in patients with and without symptomatic reflux episodes (half-emptying time 9±1 and 10±1 min, respectively) and in patients with and without daily regurgitation (half-emptying time 9±1 and 9±1 min, respectively).

DISCUSSION

The present study shows that ultrasonography is useful in providing important information about the presence, extent, and duration of postcibal gastro-esophageal reflux

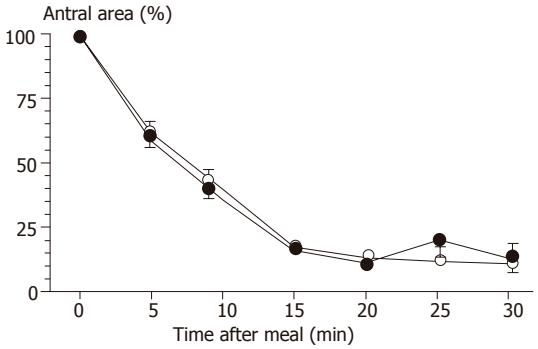

Figure 2 Postcibal gastric emptying curves, determined by ultrasound, in controls (n = 31) and in infants with recurrent respiratory diseases (n = 35). Symbols indicate means (○: controls; ●: patients), and vertical lines indicate SE. Differences between groups were tested by using ANOVA.

in infants with recurrent respiratory diseases.

Gastro-esophageal reflux is the effortless retrograde flow of gastric content in the esophageal lumen and, when abnormal, it is a recognized clinical problem in infancy, where it has been frequently associated with respiratory diseases[1-4,23].

Respiratory diseases and gastro-esophageal reflux disease have long been linked in childhood by both physiopathological and epidemiological studies, and the complex interplay between these two frequent clinical conditions is still under debate[24,25].

By prolonged pH-metry, a high prevalence of abnormal esophageal pH was reported in infants with recurrent bronchopulmonary infections, suggesting that this technique may be useful for diagnosing gastro-esophageal reflux and its association with recurrent bronchopulmonary diseases[26]. pH-metry, however, has several pitfalls, since it does not help with alkaline gastric content as seen in a number of conditions, namely after the ingestion of normal infant formula, achlorhydria or duodenogastric reflux[27,28], and alkaline reflux episodes[29,30]. In a recent study, intraluminal impedance has been used in infants with respiratory phenomena and it has been shown that gastro-esophageal refluxes accompanied by respiratory symptoms can be detected only in a minority of cases by pH-metry[29]. Similar findings were also evident in a large ultrasonographic study in symptomatic infants undergoing pH-metry[7].

Impedance monitoring is a pH-independent method for detecting bolus movement within the esophagus.

It might provide a valid alternative to esophageal pH-metry because it evaluates reflux occurring both in the interprandial and postprandial period, and it is sensitive to very small volumes of refluxate[29-33].

On the other hand, functional ultrasonography of the gastro-esophageal junction may allow direct visualization of lower esophageal sphincter relaxation and reflux episodes. The technique offers several advantages in that it has low costs, it is simple, non-invasive and is a more physiological alternative to invasive techniques[5,6,8-10]. In this respect, our results suggest that ultrasonography might represent a useful and physiological screening test in infants with recurrent respiratory diseases.

The importance of meal volume also needs to be addressed. We used a relatively low-volume liquid standard meal (i.e. of lower volume compared to that currently used during a physiological feeding). Such low volume would not affect the observed results, since in early studies, gastro-esophageal reflux was either unrelated to feed volume[17] or it was worsened by a high volume meal, through significant changes in lower esophageal sphincter pressure[20]. Here, we have observed several postcibal refluxes with a low-volume meal, suggesting that meal volume *per se* may not be a determinant in postcibal reflux occurrence.

The short postprandial observation period might be considered as a major pitfall of the ultrasonographic study. However, by using a 20-min postprandial time-window to check for persistence of intragastric content, we found significant differences for extent and timing of gastro-esophageal reflux between patients with recurrent respiratory diseases and controls, and an event/symptom relationship. Indeed, patients with recurrent involvement of lower respiratory tract (i.e. bronchitis) showed a higher number of postcibal reflux episodes compared to both patients with chronic cough and controls.

While interprandial refluxes could not be documented at ultrasonography, we underlined the importance of postcibal reflux in the pathogenesis of recurrent respiratory diseases in infants. Transient lower esophageal sphincter relaxation is the predominant mechanism of gastro-esophageal reflux[34] and postprandial reflux has been suggested to be a dynamic indicator of sphincter competency[20,35]; in this respect, postcibal ultrasonography allows direct visualization of both gastro-esophageal reflux and sphincter incompetency.

It has been reported that delayed clearance of refluxed material and clustering of reflux events may precipitate respiratory symptoms in infants[36,37]. Indeed, we found that amount, extent and number of postcibal gastro-esophageal reflux episodes were higher in subjects with symptomatic refluxes than in those without.

Although ultrasound visualization of reflux is limited to the distal esophagus, our results suggest the possibility that the involvement of the respiratory tract might be partly due to a greater chance for microaspiration of refluxed materials reaching the proximal esophagus. This possibility is more likely in subjects with a great amount and timing of gastro-esophageal reflux episodes. Interestingly, a recent study found a direct relation between incidence and duration of refluxes in the proximal and in the distal esophagus[38]. However, other mechanisms responsible for respiratory tract involvement secondary to gastro-esophageal reflux, particularly vagally mediated reflexes, may be taken into account[39].

The association of gastro-esophageal reflux disease and chronic cough in infants has been well demonstrated[2,23,40], and our results suggest that postcibal ultrasonography might be employed as a useful diagnostic approach also in patients with chronic cough.

Delayed gastric emptying has been frequently linked to gastro-esophageal reflux both in adults[41-43] and in pediatric age[16,44]. In a scintigraphic study in pediatric patients, it was found that delayed gastric emptying increased postprandial reflux by increasing the refluxate volume per episode of reflux through an underlying incompetent lower esophageal sphincter[44]. By using ultrasonography, we also performed the measurement of gastric emptying by a well standardized and validated procedure[11,16-20]. Our data demonstrated a similar extent and timing of postprandial gastric emptying in patients and controls. This is in accordance with a previous ultrasonographic study in infants with reflux disease, in which the speed of gastric emptying was unrelated to any interprandial or postprandial indices of gastro-esophageal reflux by a 24-h pH-metry[17]. Similar conclusions were also depicted by another recent study by (13)C-octanoic acid breath test, showing that gastric emptying was not delayed in infants with gastro-esophageal reflux[34].

In conclusion, postcibal esophageal ultrasonography is a useful and physiological screening test in patients with recurrent respiratory diseases, who show lower esophageal sphincter incompetence and high postprandial gastro-esophageal reflux prevalence, with a postprandial gastric emptying similar to controls. Subjects with recurrent bronchitis seem to have a greater amount of gastro-esophageal reflux episodes compared to those with chronic cough.

REFERENCES

1 **Andze GO,** Brandt ML, St Vil D, Bensoussan AL, Blanchard H. Diagnosis and treatment of gastroesophageal reflux in 500 children with respiratory symptoms: the value of pH monitoring. *J Pediatr Surg* 1991; **26:** 295-299; discussion 299-300

2 **Burton DM,** Pransky SM, Katz RM, Kearns DB, Seid AB. Pediatric airway manifestations of gastroesophageal reflux. *Ann Otol Rhinol Laryngol* 1992; **101:** 742-749

3 **Orenstein SR,** Shalaby TM, Cohn JF. Reflux symptoms in 100 normal infants: diagnostic validity of the infant gastroesophageal reflux questionnaire. *Clin Pediatr (Phila)* 1996; **35:** 607-614

4 **Shepherd RW,** Wren J, Evans S, Lander M, Ong TH. Gastroesophageal reflux in children. Clinical profile, course and outcome with active therapy in 126 cases. *Clin Pediatr (Phila)* 1987; **26:** 55-60

5 **Naik DR,** Moore DJ. Ultrasound diagnosis of gastro-oesophageal reflux. *Arch Dis Child* 1984; **59:** 366-367

6 **Naik DR,** Bolia A, Moore DJ. Comparison of barium swallow and ultrasound in diagnosis of gastro-oesophageal reflux in

children. *Br Med J (Clin Res Ed)* 1985; **290:** 1943-1945
7 **Gomes H.** Gastroesophageal reflux in infants: ultrasonographic reading of pHmetry. *Arch Pediatr* 1994; **1:** 639-645
8 **Westra SJ,** Wolf BH, Staalman CR. Ultrasound diagnosis of gastroesophageal reflux and hiatal hernia in infants and young children. *J Clin Ultrasound* 1990; **18:** 477-485
9 **Westra SJ,** Derkx HH, Taminiau JA. Symptomatic gastroesophageal reflux: diagnosis with ultrasound. *J Pediatr Gastroenterol Nutr* 1994; **19:** 58-64
10 **Riccabona M,** Maurer U, Lackner H, Uray E, Ring E. The role of sonography in the evaluation of gastro-oesophageal reflux--correlation to pH-metry. *Eur J Pediatr* 1992; **151:** 655-657
11 **Portincasa P,** Colecchia A, Di Ciaula A, Larocca A, Muraca M, Palasciano G, Roda E, Festi D. Standards for diagnosis of gastrointestinal motility disorders. Section: ultrasonography. A position statement from the Gruppo Italiano di Studio Motilita Apparato Digerente. *Dig Liver Dis* 2000; **32:** 160-172
12 **Bergmann JF,** Chassany O, Petit A, Triki R, Caulin C, Segrestaa JM. Correlation between echographic gastric emptying and appetite: influence of psyllium. *Gut* 1992; **33:** 1042-1043
13 **Bolondi L,** Bortolotti M, Santi V, Calletti T, Gaiani S, Labo G. Measurement of gastric emptying time by real-time ultrasonography. *Gastroenterology* 1985; **89:** 752-759
14 **Hveem K,** Jones KL, Chatterton BE, Horowitz M. Scintigraphic measurement of gastric emptying and ultrasonographic assessment of antral area: relation to appetite. *Gut* 1996; **38:** 816-821
15 **Ricci R,** Bontempo I, Corazziari E, La Bella A, Torsoli A. Real time ultrasonography of the gastric antrum. *Gut* 1993; **34:** 173-176
16 **Carroccio A,** Iacono G, Li Voti G, Montalto G, Cavataio F, Tulone V, Lorello D, Kazmierska I, Acierno C, Notarbartolo A. Gastric emptying in infants with gastroesophageal reflux. Ultrasound evaluation before and after cisapride administration. *Scand J Gastroenterol* 1992; **27:** 799-804
17 **Ewer AK,** Durbin GM, Morgan ME, Booth IW. Gastric emptying and gastro-oesophageal reflux in preterm infants. *Arch Dis Child Fetal Neonatal Ed* 1996; **75:** F117-F121
18 **Fabiani E,** Bolli V, Pieroni G, Corrado G, Carlucci A, De Giacomo C, Catassi C. Effect of a water-soluble fiber (galactomannans)-enriched formula on gastric emptying time of regurgitating infants evaluated using an ultrasound technique. *J Pediatr Gastroenterol Nutr* 2000; **31:** 248-250
19 **LiVoti G,** Tulone V, Bruno R, Cataliotti F, Iacono G, Cavataio F, Balsamo V. Ultrasonography and gastric emptying: evaluation in infants with gastroesophageal reflux. *J Pediatr Gastroenterol Nutr* 1992; **14:** 397-399
20 **Salvia G,** De Vizia B, Manguso F, Iula VD, Terrin G, Spadaro R, Russo G, Cucchiara S. Effect of intragastric volume and osmolality on mechanisms of gastroesophageal reflux in children with gastroesophageal reflux disease. *Am J Gastroenterol* 2001; **96:** 1725-1732
21 **Wedmann B,** Schmidt G, Wegener M, Coenen C, Ricken D, Althoff J. Effects of age and gender on fat-induced gallbladder contraction and gastric emptying of a caloric liquid meal: a sonographic study. *Am J Gastroenterol* 1991; **86:** 1765-1770
22 **Armitage P,** Berry G. Statistical methods in medical research. Oxford: Blackwell Science Ltd, 1994
23 **Megale SR,** Scanavini AB, Andrade EC, Fernandes MI, Anselmo-Lima WT. Gastroesophageal reflux disease: Its importance in ear, nose, and throat practice. *Int J Pediatr Otorhinolaryngol* 2005; :
24 **Gold BD.** Asthma and gastroesophageal reflux disease in children: exploring the relationship. *J Pediatr* 2005; **146:** S13-S20
25 **Scarupa MD,** Mori N, Canning BJ. Gastroesophageal reflux disease in children with asthma: treatment implications. *Paediatr Drugs* 2005; **7:** 177-186
26 **Chen PH,** Chang MH, Hsu SC. Gastroesophageal reflux in children with chronic recurrent bronchopulmonary infection. *J Pediatr Gastroenterol Nutr* 1991; **13:** 16-22
27 **Sutphen JL,** Dillard VL. pH-adjusted formula and gastroesophageal reflux. *J Pediatr Gastroenterol Nutr* 1991; **12:** 48-51
28 **Tolia V,** Kuhns L, Kauffman RE. Comparison of simultaneous esophageal pH monitoring and scintigraphy in infants with gastroesophageal reflux. *Am J Gastroenterol* 1993; **88:** 661-664
29 **Wenzl TG,** Silny J, Schenke S, Peschgens T, Heimann G, Skopnik H. Gastroesophageal reflux and respiratory phenomena in infants: status of the intraluminal impedance technique. *J Pediatr Gastroenterol Nutr* 1999; **28:** 423-428
30 **Wenzl TG,** Moroder C, Trachterna M, Thomson M, Silny J, Heimann G, Skopnik H. Esophageal pH monitoring and impedance measurement: a comparison of two diagnostic tests for gastroesophageal reflux. *J Pediatr Gastroenterol Nutr* 2002; **34:** 519-523
31 **Peter CS,** Wiechers C, Bohnhorst B, Silny J, Poets CF. Detection of small bolus volumes using multiple intraluminal impedance in preterm infants. *J Pediatr Gastroenterol Nutr* 2003; **36:** 381-384
32 **Skopnik H,** Silny J, Heiber O, Schulz J, Rau G, Heimann G. Gastroesophageal reflux in infants: evaluation of a new intraluminal impedance technique. *J Pediatr Gastroenterol Nutr* 1996; **23:** 591-598
33 **Wenzl TG,** Skopnik H. Intraluminal impedance: an ideal technique for evaluation of pediatric gastroesophageal reflux disease. *Curr Gastroenterol Rep* 2000; **2:** 259-264
34 **Omari TI,** Barnett CP, Benninga MA, Lontis R, Goodchild L, Haslam RR, Dent J, Davidson GP. Mechanisms of gastro-oesophageal reflux in preterm and term infants with reflux disease. *Gut* 2002; **51:** 475-479
35 **Mason RJ,** Oberg S, Bremner CG, Peters JH, Gadenstatter M, Ritter M, DeMeester TR. Postprandial gastroesophageal reflux in normal volunteers and symptomatic patients. *J Gastrointest Surg* 1998; **2:** 342-349
36 **Gustafsson PM,** Kjellman NI, Tibbling L. Bronchial asthma and acid reflux into the distal and proximal oesophagus. *Arch Dis Child* 1990; **65:** 1255-1258
37 **Jolley SG,** Herbst JJ, Johnson DG, Matlak ME, Book LS. Esophageal pH monitoring during sleep identifies children with respiratory symptoms from gastroesophageal reflux. *Gastroenterology* 1981; **80:** 1501-1506
38 **Bagucka B,** Badriul H, Vandemaele K, Troch E, Vandenplas Y. Normal ranges of continuous pH monitoring in the proximal esophagus. *J Pediatr Gastroenterol Nutr* 2000; **31:** 244-247
39 **Ricciardolo FL,** Gaston B, Hunt J. Acid stress in the pathology of asthma. *J Allergy Clin Immunol* 2004; **113:** 610-619
40 **Contencin P,** Narcy P. Gastropharyngeal reflux in infants and children. A pharyngeal pH monitoring study. *Arch Otolaryngol Head Neck Surg* 1992; **118:** 1028-1030
41 **Baldi F,** Corinaldesi R, Ferrarini F, Stanghellini V, Miglioli M, Barbara L. Gastric secretion and emptying of liquids in reflex esophagitis. *Dig Dis Sci* 1981; **26:** 886-889
42 **McCallum RW,** Berkowitz DM, Lerner E. Gastric emptying in patients with gastroesophageal reflux. *Gastroenterology* 1981; **80:** 285-291
43 **Shay SS,** Eggli D, McDonald C, Johnson LF. Gastric emptying of solid food in patients with gastroesophageal reflux. *Gastroenterology* 1987; **92:** 459-465
44 **Estevao-Costa J,** Campos M, Dias JA, Trindade E, Medina AM, Carvalho JL. Delayed gastric emptying and gastroesophageal reflux: a pathophysiologic relationship. *J Pediatr Gastroenterol Nutr* 2001; **32:** 471-474

Science Editor Guo SY **Language Editor** Elsevier HK

PO Box 2345, Beijing 100023, China
www.wjgnet.com
wjg@wjgnet.com

ELSEVIER

World J Gastroenterol 2005;11(46):7302-7307
World Journal of Gastroenterology ISSN 1007-9327

Human leukocyte antigen class II DQB1*0301, DRB1*1101 alleles and spontaneous clearance of hepatitis C virus infection: A meta-analysis

Xin Hong, Rong-Bin Yu, Nan-Xiong Sun, Bin Wang, Yao-Chu Xu, Guan-Ling Wu

Xin Hong, Yao-Chu Xu, Rong-Bin Yu, Department of Epidemiology and Biostatistics, School of Public Health, Nanjing Medical University, Nanjing 210029, Jiangsu Province, China
Nan-Xiong Sun, Research Laboratory for infectious Diseases, The First Affiliated Hospital, Nanjing Medical University, Nanjing 210029, Jiangsu Province, China
Bin Wang, Department of Pharmacology, Nanjing Medical University, Nanjing 210029, Jiangsu Province, China
Guan-Ling Wu, Department of Microbiology, Nanjing Medical University, Nanjing 210029, Jiangsu Province, China
Supported by the National Natural Science Foundation of China, No. 30200232
Correspondence to: Rong-Bin Yu, Department of Epidemiology and Biostatistics, School of Public Health, Nanjing Medical University, Nanjing 210029, Jiangsu Province, China. rongbinyu@njmu.edu.cn
Telephone: +86-25-86862815 Fax: +86-25-86527613
Received: 2005-04-15 Accepted: 2005-07-15

Abstract

AIM: To assess the associations of human leukocyte antigen (HLA) class II DQB1*0301 and/or DRB1*1101 allele with spontaneous hepatitis C virus (HCV) clearance by meta-analysis of individual dataset from all studies published till date.

METHODS: To clarify the impact of HLA class II polymorphisms on viral clearance, we performed a meta-analysis of the published data from 11 studies comparing the frequencies of DQB1*0301 and DRB1*1101 alleles in individuals with spontaneous resolution to those with persistent infection. As we identified the heterogeneity between studies, summary statistical data were calculated based on a random-effect model.

RESULTS: Meta-analyses yielded summary estimates-odds ratio (OR) of 2.36 [95%CI (1.62, 3.43), $P<0.00001$] and 2.02 [95%CI (1.56, 2.62), $P<0.00001$] for the effects of DQB1*0301 and DRB1*1101 alleles on spontaneous clearance of HCV, respectively.

CONCLUSION: These results support the hypothesis that specific HLA class II alleles might influence the susceptibility or resistance to persistent HCV infection. Both DQB1*0301 and DRB1*1101 are protective alleles and present HCV epitopes more effectively to $CD4^+$T lymphocytes than others, and subjects with these two alleles are at a lower risk of developing chronic HCV infection. Large, multi-ethnic confirmatory and well-designed studies are needed to determine the host genetic determinants of HCV infection.

Key words: Human leukocyte antigen; Genetic polymorphism; DQB1*0301; DRB1*1101; Hepatitis C virus; Spontaneous clearance; Meta-analysis

Hong X, Yu RB, Sun NX, Wang B, Xu YC, Wu GL. Human leukocyte antigen class II DQB1*0301, DRB1*1101 alleles and spontaneous clearance of hepatitis C virus infection: A meta-analysis. *World J Gastroenterol* 2005; 11(46): 7302-7307
http://www.wjgnet.com/1007-9327/11/7302.asp

INTRODUCTION

HCV infection presents with diverse clinical manifestations. Approximately 20% of infected patients successfully eliminate the virus, whereas the majority of patients develop chronic infection with a wide spectrum of liver lesions, ranging from minimal inflammation to cirrhosis and hepatocelluar carcinoma (HCC)[1]. The mechanisms underlying the spontaneous viral clearance or development of chronic HCV infection have not yet been identified[2]. Apart from viral characteristics (viral genotype, quasi-species distribution and viral load), it is generally accepted that cellular immune responses play an important role in viral clearance and disease resolution[3]. Clearance of the virus during acute infection has been shown to be associated with strong and sustained HCV-specific $CD4^+$ and $CD8^+$ T-cell responses[4-8]. Though $CD8^+$ T cells are primary effector cells directly eliminating HCV-infected cells, $CD4^+$ T cells play a central regulatory role, which modulates the $CD8^+$ T-cell responses and is crucial for the production of neutralizing antibodies. A number of recent studies have suggested that early sustaining vigorous and multi-specific $CD4^+$ T-cell responses might be a critical determinant for the primary HCV infection[9,10]. The importance to $CD4^+$ T-cell response is the presentation of HCV antigens in the context of HLA class II molecules. Therefore, the differences in HLA class II alleles may strongly influence the clinical course of hepatitis C.

HLA genes located on chromosome 6 encode peptides

Table 1 Characteristics of studies included in the meta-analysis

First author (year) [reference]	Country (ethnicity)	Spontaneous resolution	Persistent infection	Matching	Anti-HCV tests	HLA typing
Alric (1997) [21]	France (European)	25, M/F: 9/16 Age: 40.6±15.7 yr	103, M/F: 58/45 Age: 45.4±12.4 yr	Sex, age, source of HCV infection, HCV-serotype	2G EIA and RIBA	PCR-SSOP
Cramp (1998) [22]	UK (European)	49, M/F: 30/19 Duration: 15.5 (3-42) yr	55, M/F: 31/24 Duration: 14.2 (2-40) yr	Sex, age, source of HCV infection and duration	2G line immunoassay	PCR-SSOP
Minton (1998) [23]	UK (European)	35, M/F: 19/16 Age: 37.9±10.8 yr	138, M/F: 87/51 Age: 37.2±10.1 yr	Sex, age, source of HCV infection	2G ELISA and RIBA	PCR-SSOP
Mangia (1999) [24]	Italy (European)	35	149	Sex, HCV-serotype, not age, not duration	RIBA and 3G EIA	PCR-SSP
Thursz (1999) [25]	European	85, M/F: 37/48 Age: 45±14 yr	170, M/F: 74/96 Age: 50±16 yr	Sex, center, not age	ELISA and RIBA	PCR-SSP
Vejbaesya (2000) [26]	Thailand (Asian)	43 Blood donor M/F: 25/18	57 M/F: 31/18	Sex	2G EIA and RIBA	PCR-SSOP
Alric (2000) [27]	France (European)	63, M/F: 21/42 Age: 42.1±15.4 yr	282, M/F: 150/132 Age: 46±12.3 yr	Age, source of HCV infection and duration, not sex	2G EIA and RIBA	PCR-SSOP
Fanning (2000) [13]	Irish (European)	85 Female	72 Female	From single source	RIBA	Reverse line probe hybridization
Thio (2001) [28]	North America	200, M/F: 166/34 Age: 25.7 yr	374, M/F: 310/64 Age: 27.8 yr	Age, sex, race	2G EIA and RIBA	PCR-SSP PCR-SSCP
Azocar (2003) [29]	Hispanic (European)	40,M/F: 33/7 Age: 37.9 yr	72, M/F: 54/18 Age: 39.2 yr	Age, sex	EIA and RIBA	PCR-SSOP PCR-SSP
Spada (2004) [30]	Italy (European)	10, M/F: 5/5 Age: 40.5 (20-61) yr	24,M/F:22/2 Age: 29 (20-56) yr	Not sex, age, source of HCV infection, HCV-serotype	3G ELISA and RIBA	PCR-SSP

EIA: enzyme-immunoassay; RIBA: recombinant immunoblot assay; ELISA: enzyme-linked-immunosorbent assay; 2G: second generation; 3G: third generation; SSOP: sequence-specific oligonucleotide probes; SSP: sequence specific primers; SSCP: single stranded conformational polymorphisms.

involved in host immune response. Moreover, the HLA loci display an unprecedented degree of diversity in human genome, presumably an evolutionary adoption to immune pressure from various infectious agents. Polymorphisms in HLA class II molecules can give rise to amino acid substitutions with different peptide-binding characteristics and determine antigenic specificities, the strength of immune response to HCV[11,12]. Consequently, distinct HLA class II alleles may be expected to exert an impact on the development of host immune responses against HCV infection. However, few studies have demonstrated consistency in different populations. In several Irish studies performed in women exposed to HCV genotype 1b from a single inoculum, DRB1*0101 and DQB1*0501 alleles are found to be associated with viral elimination[13–17]. One German study suggests that HLA-DR15 (B1*15011) might constitute an important genetic factor for the clearance of HCV[18]. Thio *et al*.[19] reported that HLA-A*1101, HLA-B*57, and HLA-Cw*0102 contribute to the spontaneous resolution of primary HCV infection. It was reported that the DQA1*03 and DQB1*0302 alleles promote viral clearance and confer protection against chronic HCV infection in Caucasians[20]. A number of studies have been conducted in different ethnic populations to investigate the associations of DQB1*0301 or DRB1*1101 allele with spontaneous HCV clearance[13,21-30]. However, the results from these molecular epidemiological studies are confusing rather than being conclusive. Single study might be underpowered to detect the association between DQB1*0301 and/or DRB1*1101 allele and HCV infection because of the limited sample size. The aim of this study was to assess the associations of HLA class II DQB1*0301 and/or DRB1*1101 allele(s) with spontaneous HCV clearance by meta-analysis of individual dataset from all studies published till date.

MATERIALS AND METHODS

Identification and eligibility of studies

PubMed was used to search for relevant reports published between 1997 and 2004 (using the key words: human leukocyte antigen, genetic polymorphism, hepatitis C virus, spontaneous clearance). The inclusion criteria for our analysis were as follows: studies reporting odds ratio (OR) or risk ratio (RR) calculated by comparing those with self-limiting infection to those with chronic infection as a measure of association; study designs such as cohort study, population-based case control study, hospital-based case-control study; studies using HLA class II molecular genotyping technique; studies including DQB1*0301 and DRB1*1101 alleles. A total of 11 candidate papers were identified.

Data extraction

Data were collected on the DQB1*0301 and DRB1*1101 allele frequencies, authors, journals, years of publication, country of origin, demographics, selection, definition of spontaneous viral clearance (anti-HCV positive and HCV-RNA negative at least for 6 mo), chronically persistent infection (anti-HCV positive and HCV-RNA positive for more than 1 year) and racial descents (categorized as Asian, European, and North American descents).

Table 2 Effect of DRB1*1101 allele on self-limiting HCV infection

Study	Spontaneous resolution *n/N*	Persistent infection *n/N*	OR (random) 95%CI
Alric	10/25	10/102	6.13 (2.18, 17.22)
Minton	11/35	11/135	5.17 (2.01, 13.27)
Cramp	9/49	6/55	1.84 (0.60, 5.60)
Mangia	7/35	24/149	1.30 (0.51, 3.32)
Thursz 1	26/85	29/170	2.14 (1.16, 3.94)
Thursz 2	14/57	15/152	2.97 (1.33, 6.65)
Fanning	4/68	4/64	0.94 (0.22, 3.92)
Alric	20/59	25/170	2.97 (1.50, 5.91)
Vejbaesya	2/43	3/57	0.88 (0.14, 5.50)
Thio	15/200	24/374	1.18 (0.61, 2.31)
Azocar	4/40	11/72	0.62 (0.18, 2.08)
Spada	2/10	2/24	2.75 (0.33, 22.92)
Total (95%CI)	124/706	164/1 524	2.02 (1.56, 2.62)

Test for heterogeneity: χ^2 = 19.38, df = 11 (P<0.05), I^2 = 43.2%. Test for overall effect: Z = 5.30 (P<0.00001).

Table 3 Effect of DQB1*0301 allele on self-limiting HCV infection

Study	Spontaneous resolution *n/N*	Persistent infection *n/N*	OR (random) 95%CI
Alric	21/25	28/91	11.81 (3.71, 37.61)
Minton	18/35	33/135	3.27 (1.51, 7.07)
Cramp	26/49	10/55	5.09 (2.10, 12.33)
Mangia	17/33	42/143	2.56 (1.18, 5.53)
Thursz 1	39/85	47/170	2.22 (1.29, 3.82)
Thursz 2	25/57	37/152	2.43 (1.28, 4.61)
Fanning	25/78	18/67	1.28 (0.63, 2.64)
Alric	38/59	45/157	4.50 (2.39, 8.50)
Vejbaesya	24/43	18/57	2.74 (1.20, 6.22)
Thio	49/200	71/374	1.38 (0.92, 2.09)
Azocar	6/40	13/72	0.80 (0.28, 2.30)
Spada	4/10	15/24	0.40 (0.09, 1.81)
Total (95%CI)	292/714	377/1 497	2.36 (1.62, 3.43)

Test for heterogeneity: χ^2 = 33.33, df = 11 (P = 0.0005), I^2 = 67.0%. Test for overall effect: Z = 4.48 (P<0.00001).

Furthermore, we examined whether matching was used and HLA class II molecular-typing assay was validated.

Statistical analysis

The OR of sustained HCV clearance associated with HLA class II polymorphisms (DQB1*0301 and DRB1*1101 alleles) was estimated for each study. The primary analysis was to estimate the allele frequencies between the groups with viral elimination and chronic infection. For each genetic group, we estimated the heterogeneity between the studies[31]. Data were combined using both fixed effect (Mantel-Haenszel) and random effect (DerSimonian and Laird) models[32]. In the absence of heterogeneity, the two methods provided identical results. Random effects were more appropriate, when heterogeneity was present. Analyses were performed by the software of SAS 8.0 (SAS Institute, Cary, NC, USA) and Review Manager 4.2 (Cochrance Collaboration, Oxford, UK). All P values were two-sided.

RESULTS

Characteristics of the studies are shown in Table 1. Multiple studies were conducted in the European population (n = 9). The number of individuals with spontaneous resolution and persistent infection in DRB1*1101 and DQB1*0301 studies was 706 and 1 524, 714 and 1 497, respectively. All the subjects of these studies were selected based on a histological diagnosis of strict criteria. With two exceptions[24,25] where the mean age of two groups differed and one where the age status was not stated[26], all other studies were matched for age. Most studies also stated the use of matching on sex status except for two[27,30]. Compared to other studies, only one was homogenous in terms of gender, source of HCV infection, HCV-serotype and ethnicity[13]. This subject population was derived from a cohort of females inoculated with anti-D immunoglobulin in 1977 that was contaminated with HCV from a single source.

With regard to the anti-HCV antibody testing, most studies used a combination of two tests, while only one used a single test[13]. Five studies used low resolution molecular typing (PCR-SSOP) for HLA, while others used high resolution molecular typing (PCR-SSP) for HLA[33]. Low resolution molecular typing methods for HLA could not identify the specific alleles. Accurate methods for HLA class II typing should involve the combination of PCR-SSOP, PCR-SSP, and PCR-SSCP[12].

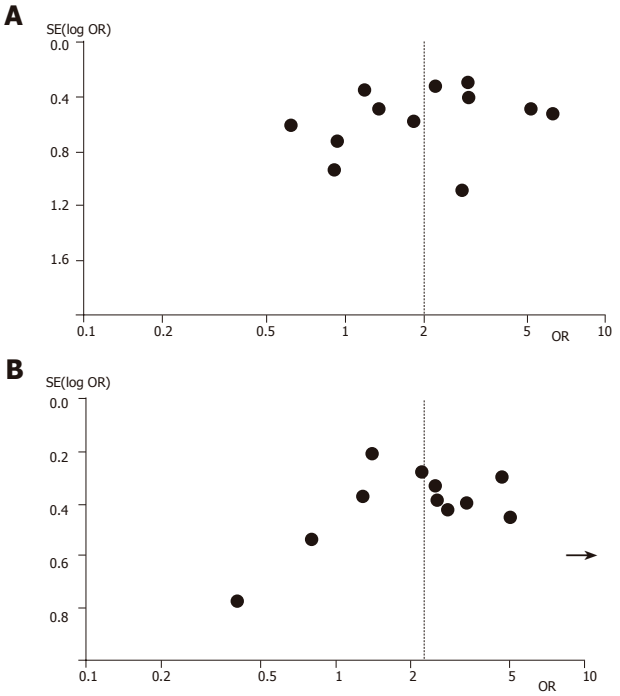

Figure 1 Funnel plot analysis of publication bias for DRB1*1101 allele (**A**) and DQB1*0301 allele (**B**). Each data point represents a separate study for the indicated association.

Table 2 shows the OR on HCV spontaneous clearance associated with DRB1*1101 allele. Overall, individuals with DRB1*1101 allele had a significantly reduced risk for chronic hepatitis C compared to individuals without it [OR = 2.02, 95%CI (1.56, 2.62) (P<0.00001)]. Similarly, subjects with DQB1*0301 allele appeared to be more

likely to clear the virus, while those lacking it were more prone to develop chronic infections [OR = 2.36, 95%CI (1.62, 3.43), $P<0.00001$] (Table 3). These analyses were based on the data from 11 studies regardless of ethnics.

We performed tests for homogeneity with respect to the studies of DRB1*1101 and DQB1*0301 alleles and viral clearance and obtained statistically significant results (DRB1*1101: $\chi^2 = 19.38$, $P<0.05$; DQB1*0301: $\chi^2 = 33.33$, $P = 0.0005$). Therefore, summary statistics were calculated based on a random-effect model.

Figure 1 shows the funnel plot analysis to detect publication bias of each study for DRB1*1101 and DQB1*0301, respectively. The shape of the funnel plot seemed to be asymmetrical, suggesting that publication bias might affect the findings of our meta-analysis. Furthermore, an Egger's test was used to provide statistical evidence for funnel plot symmetry[45]. In the linear regression analysis, the intercept value provided a measure of asymmetry, the larger the deviation the more pronounced the asymmetry. The intercept value in our study was 2.33 for DQB1*0301 and 2.03 for DRB1*1101, respectively, both of them were significantly deviated from zero ($P<0.0001$ for DQB1*0301 and $P<0.0022$ for DRB1*1101).

DISCUSSION

DQB1*0301 allele is reproducibly involved in spontaneous viral clearance of HCV in different populations[21-26,28,34-36]. Studies conducted in patients from France[21], Britain[22], Italy[24,35] with different genetic backgrounds have identified significant genetic associations with different DQB1*0301-bearing haplotypes, suggesting that DQB1*0301 might be one of the most prominent factors in HCV clearance[37,38].

Another allele correlated with self-limiting HCV is DRB 1*1101[21,23,25,27,34,39]. But disagreement exists over the allele. In Italy[24,35] BRB1*1104 correlates with HCV clearance, while in Japan[40] DR13 is linked to self-limiting infection.

It is difficult to determine whether HLA-DRB1*1101 or DQB1*0301 allele is the more relevant factor as HLA-DRB1*11 is associated with DQB1*0301. Some studies found that DRB1*1101 rather than DQB1*0301 is closely associated with viral elimination[23,30,41,42]. While some findings suggest that DQB1*0301 is dominant in determining the outcome of HCV infection[21,22,27,43,44]. In our meta-analysis, the OR for the two alleles was virtually identical, but which one is responsible for the viral elimination is not clear.

The outcome of HCV infection varies substantially among the individuals. Though the exact mechanisms involved in viral clearance have not been fully elucidated, there is evidence that cellular immune response, especially T-helper lymphocyte responses to HCV, plays an important role in the control of persistent HCV infection. DQB1*0301, DRB1*1101 alleles are closely associated with self-limiting HCV infection. Our meta-analysis demonstrated that subjects with HLA-DRB1*1101 allele reduced 102% risk of developing chronic HCV infection and those carrying HLA-DQB1*0301 allele reduced 136% risk of persistent infection. HLA-DQB1*0301 and DRB1*1101 alleles might act as the most prominent factors favoring the elimination of HCV and conferring protection against chronic evolution.

There are two possible explanations for these observations. (1) Because HCV is not cytopathic for infected cells, the immune response may play an important role in HCV infection. Binding to HCV peptides of HLA molecules is the first step for the initiation of this immune response. Due to the extensive polymorphisms of HLA, the strength of the response may vary among the individuals. It is assumed that DQB1*0301 and DRB1*1101 alleles may present HCV epitopes more effectively to $CD4^+$ Th cells than others, resulting in vigorous proliferative response to HCV and probably disease recovery[37,43,46-47]. $CD4^+$ Th responses have been characterized in patients with self-limiting infection and most immunodominant epitopes are present in the context of DQB1*0301 and DRB1*1101 molecules[48]. Therefore, individuals with these two alleles may present peptides derived from HCV in a more efficient manner than those without, thus clearing the infection spontaneously. (2) Another explanation for the association between the two alleles and viral elimination may be due to the other protective HLA loci[22,36]. Interpreting results of genetic studies can be complicated by linkage disequilibrium of the implicated gene linked to the true gene of interest[12]. Other candidate susceptible genes located in the HLA class II region also require antigen presentation. An excess of DQB1*0301 and DRB1*1101-restricted peptide-specific responses in individuals, who clear the virus, needs to be shown in order to prove conclusively whether the mechanism of the gene effect is direct or indirect.

While there are some consistent observations on DQB1*0301 and DRB1*1101 with self-limiting infection, many results are not uniform. These inconsistencies may be due to ethnic differences, patient selection, sample size, HCV-serotype, and HLA typing technique. Firstly, a primary cause for the difference in results by different authors may be related to the great variability of the frequency of HLA alleles in different populations. It is quite possible that one ethnic group may have the preferential use of different allele(s) in viral eradication compared to other ethnic groups. This DRB1*1101 association with viral clearance was not observed in the Irish anti-D population, which might be explained by the lower frequency of DRB1*1101 in Irish[16] (6.4%) than in French[21] control populations (25.2%). The association of DRB1*0101 and DQB1*0501 alleles with viral clearance has been documented in Caucasian Americans, whereas in African–American patients viral clearance is mainly associated with DQB1*0301[28]. Another study showed that there are marked differences in the frequency of viral clearance in Caucasians and African-Americans[49]. Racial heterogeneity has to be taken into account in the future studies[50,51]. Secondly, many studies were conducted on relatively smaller samples. Insufficient number of

individuals might decrease the power to detect a difference in the distribution of DQB1*0301 and DRB1*1101 alleles between patients with resolving infection and those with chronic evolution, though a true difference exists[52]. Lack of an association may not mean that associations do not exist. Thirdly, a number of HLA studies concerning the association between HLA class II and outcome of infection have compared allele frequency in HCV patients to that in healthy controls[20,53,54]. Studies including both HCV RNA positive and negative patients have failed to discover particular genetic associations[20]. Fourthly, effects of interactions in other environmental/behavioral and/or viral factors may be inevitable. There is a clear correlation between the HLA haplotype of individuals and outcome of HCV infection[55]. A complex interplay between various genes is likely to modulate the anti-HCV response rather than a single allele. Moreover, several variables including young age at infection and female sex have been suggested to determine HCV clearance[17,30,56]. Another possible reason for the discrepancy between these studies lies in the viral genotype.

In conclusion, large and well-designed studies should be carried out to investigate the host genetic determinants for HCV infection. Finding an association between specific alleles and favorable clinical outcomes in HCV patients might open new avenues to explore and understand the pathogenesis of HCV.

REFERENCES

1 **Seeff LB.** Natural history of chronic hepatitis C. *Hepatology* 2002; **36:** S35-46
2 **Sun J,** Li K, Shata MT, Chan TS. The immunologic basis for hepatitis C infection. *Curr Opin Gastroenterol* 2004; **20:** 598-602
3 **Neumann-Haefelin C,** Blum HE, Chisari FV, Thimme R. T cell response in hepatitis C virus infection. *J Clin Virol* 2005; **32:** 75-85
4 **Gruner NH,** Gerlach TJ, Jung MC, Diepolder HM, Schirren CA, Schraut WW, Hoffmann R, Zachoval R, Santantonio T, Cucchiarini M, Cerny A, Pape GR. Association of hepatitis C virus-specific CD8+ T cells with viral clearance in acute hepatitis C. *J Infect Dis* 2000; **181:** 1528-1536
5 **Thimme R,** Oldach D, Chang KM, Steiger C, Ray SC, Chisari FV. Determinants of viral clearance and persistence during acute hepatitis C virus infection. *J Exp Med* 2001; **194:** 1395-1406
6 **Lechner F,** Wong DK, Dunbar PR, Chapman R, Chung RT, Dohrenwend P, Robbins G, Phillips R, Klenerman P, Walker BD. Analysis of successful immune responses in persons infected with hepatitis C virus. *J Exp Med* 2000; **191:** 1499-1512
7 **Thimme R,** Bukh J, Spangenberg HC, Wieland S, Pemberton J, Steiger C, Govindarajan S, Purcell RH, Chisari FV. Viral and immunological determinants of hepatitis C virus clearance, persistence, and disease. *Proc Natl Acad Sci USA* 2002; **99:** 15661-1568
8 **Cooper S,** Erickson AL, Adams EJ, Kansopon J, Weiner AJ, Chien DY, Houghton M, Parham P, Walker CM. Analysis of a successful immune response against hepatitis C virus. *Immunity* 1999; **10:** 439-449
9 **Eckels DD,** Wang H, Bian TH, Tabatabai N, Gill JC. Immunobiology of hepatitis C virus (HCV) infection: the role of CD4 T cells in HCV infection. *Immunol Rev* 2000; **174:** 90-97
10 **Wertheimer AM,** Miner C, Lewinsohn DM, Sasaki AW, Kaufman E, Rosen HR. Novel $CD4^+$ and $CD8^+$ T-cell determinants within the NS3 protein in subjects with spontaneously resolved HCV infection. **Hepatology** 2003; **37:** 577-589
11. **Andrade DR Jr,** de Andrade DR. The influence of the human genome on chronic viral hepatitis outcome. *Rev Inst Med Trop Sao Paulo* 2004; **46:** 119-126
12. **Thio CL,** Thomas DL, Carrington M. Chronic viral hepatitis and the human genome. *Hepatology* 2000; **31:** 819-827
13 **Fanning LJ,** Levis J, Kenny-Walsh E, Wynne F, Whelton M, Shanahan F. Viral clearance in hepatitis C (1b) infection: relationship with human leukocyte antigen class II in a homogeneous population. *Hepatology* 2000; **31:** 1334-1337
14 **McKiernan SM,** Hagan R, Curry M, McDonald GS, Kelly A, Nolan N, Walsh A, Hegarty J, Lawlor E, Kelleher D. Distinct MHC class I and II alleles are associated with hepatitis C viral clearance, originating from a single source. *Hepatology* 2004; **40:** 108-114
15 **McKiernan SM,** Hagan R, Curry M, McDonald GS, Nolan N, Crowley J, Hegarty J, Lawlor E, Kelleher D. The MHC is a major determinant of viral status, but not fibrotic stage, in individuals infected with hepatitis C. *Gastroenterology* 2000; **118:** 1124-1130
16 **Barrett S,** Ryan E, Crowe J. Association of the HLA-DRB1*01 allele with spontaneous viral clearance in an Irish cohort infected with hepatitis C virus via contaminated anti-D immunoglobulin. *J Hepatol* 1999; **30:** 979-983
17 **Barrett S,** Goh J, Coughlan B, Ryan E, Stewart S, Cockram A, O'Keane JC, Crowe J. The natural course of hepatitis C virus infection after 22 years in a unique homogenous cohort: spontaneous viral clearance and chronic HCV infection. *Gut* 2001; ***49:*** 423-430
18 **Lechmann M,** Schneider EM, Giers G, Kaiser R, Dumoulin FL, Sauerbruch T, Spengler U. Increased frequency of the HLA-DR15 (B1*15011) allele in German patients with self-limited hepatitis C virus infection. Eur J Clin Invest 1999; **29:** 337-343
19 Thio CL, Gao X, Goedert JJ, Vlahov D, Nelson KE, Hilgartner MW, O'Brien SJ, Karacki P, Astemborski J, Carrington M, Thomas DL. HLA-Cw*04 and hepatitis C virus persistence. *J Virol* 2002; **76:** 4792-4797
20 **Tibbs C,** Donaldson P, Underhill J, Thomson L, Manabe K, Williams R. Evidence that the HLA DQA1*03 allele confers protection from chronic HCV-infection in Northern European Caucasoids. *Hepatology* 1996; **24:** 1342-1345
21 **Alric L,** Fort M, Izopet J, Vinel JP, Charlet JP, Selves J, Puel J, Pascal JP, Duffaut M, Abbal M. Genes of the major histocompatibility complex class II influence the outcome of hepatitis C virus infection. *Gastroenterology* 1997; **113:** 1675-1681
22 **Cramp ME,** Carucci P, Underhill J, Naoumov NV, Williams R, Donaldson PT. Association between HLA class II genotype and spontaneous clearance of hepatitis C viraemia. *J Hepatol* 1998; **29:** 207-213
23 **Minton EJ,** Smillie D, Neal KR, Irving WL, Underwood JC, James V. Association between MHC class II alleles and clearance of circulating hepatitis C virus. Members of the Trent Hepatitis C Virus Study Group. *J Infect Dis* 1998; **178:** 39-44
24 **Mangia A,** Gentile R, Cascavilla I, Margaglione M, Villani MR, Stella F, Modola G, Agostiano V, Gaudiano C, Andriulli A. HLA class II favors clearance of HCV infection and progression of the chronic liver damage. *J Hepatol* 1999; **30:** 984-989
25 **Thursz M,** Yallop R, Goldin R, Trepo C, Thomas HC. Influence of MHC class II genotype on outcome of infection with hepatitis C virus. The HENCORE group. Hepatitis C European Network for Cooperative Research. *Lancet* 1999; **354:** 2119-2124
26 **Vejbaesya S,** Songsivilai S, Tanwandee T, Rachaibun S, Chantangpol R, Dharakul T. HLA association with hepatitis C virus infection. *Hum Immunol* 2000; **61:** 348-353
27 **Alric L,** Fort M, Izopet J, Vinel JP, Bureau C, Sandre K, Charlet JP, Beraud M, Abbal M, Duffaut M. Study of host- and virus-related factors associated with spontaneous hepatitis C virus

clearance. *Tissue Antigens* 2000; **56:** 154-158
28 **Thio CL,** Thomas DL, Goedert JJ, Vlahov D, Nelson KE, Hilgartner MW, O'Brien SJ, Karacki P, Marti D, Astemborski J, Carrington M. Racial differences in HLA class II associations with hepatitis C virus outcomes. *J Infect Dis* 2001; **184:** 16-21
29 **Azocar J,** Clavijo OP, Yunis EJ. MHC class II genes in HCV viral clearance of hepatitis C infected Hispanic patients. *Hum Immunol* 2003; **64:** 99-102
30 **Spada E,** Mele A, Berton A, Ruggeri L, Ferrigno L, Garbuglia AR, Perrone MP, Girelli G, Del Porto P, Piccolella E, Mondelli MU, Amoroso P, Cortese R, Nicosia A, Vitelli A, Folgori A. Multispecific T cell response and negative HCV RNA tests during acute HCV infection are early prognostic factors of spontaneous clearance. *Gut* 2004; **53:** 1673-1681
31 **Lau J,** Ioannidis JP, Schmid CH. Quantitative synthesis in systematic reviews. *Ann Intern Med* 1997; **127:** 820-826
32 **Petitti D.B.** Meta-analysis, decision analysis, and cost-effectiveness analysis. New York: Oxford University Press, 1994
33 **Welsh K,** Bunce M. Molecular typing for the MHC with PCR-SSP. *Rev Immunogenet* 1999; **1:** 157-176
34 **Yenigun A,** Durupinar B. Decreased frequency of the HLA-DRB1*11 allele in patients with chronic hepatitis C virus infection. *J Virol* 2002; **76:** 1787-1789
35 **Zavaglia C,** Martinetti M, Silini E, Bottelli R, Daielli C, Asti M, Airoldi A, Salvaneschi L, Mondelli MU, Ideo G. Association between HLA class II alleles and protection from or susceptibility to chronic hepatitis C. *J Hepatol* 1998; **28:** 1-7
36 **Wawrzynowicz-Syczewska M,** Underhill JA, Clare MA, Boron-Kaczmarska A, McFarlane IG, Donaldson PT. HLA class II genotypes associated with chronic hepatitis C virus infection and response to alpha-interferon treatment in Poland. *Liver* 2000; **20:** 234-239
37 **Donaldson PT.** The interrelationship between hepatitis C virus and HLA. *Eur J Clin Invest* 1999; **29:** 280-283
38 **Thursz M.** MHC and the viral hepatitides. *QJM* 2001; **94:** 287-291
39 **Tillmann HL,** Chen DF, Trautwein C, Kliem V, Grundey A, Berning-Haag A, Boker K, Kubicka S, Pastucha L, Stangel W, Manns MP. Low frequency of HLA-DRB1*11 in hepatitis C virus induced end stage liver disease. *Gut* 2001; **48:** 714-718
40 **Kuzushita N,** Hayashi N, Moribe T, Katayama K, Kanto T, Nakatani S, Kaneshige T, Tatsumi T, Ito A, Mochizuki K, Sasaki Y, Kasahara A, Hori M. Influence of HLA haplotypes on the clinical courses of individuals infected with hepatitis C virus. *Hepatology* 1998; **27:** 240-244
41 **Amoroso A,** Berrino M, Canale L, Cornaglia M, Guarrera S, Mazzola G, Savoldi S, Scolari F, Sallberg M, Clementi M, Gabrielli A. Are HLA class II and immunoglobulin constant region genes involved in the pathogenesis of mixed cryoglobulinemia type II after hepatitis C virus infection? *J Hepatol* 1998; **29:** 36-44
42 **Harcourt GC,** Lucas M, Sheridan I, Barnes E, Phillips R, Klenerman P. Longitudinal mapping of protective CD4+ T cell responses against HCV: analysis of fluctuating dominant and subdominant HLA-DR11 restricted epitopes. *J Viral Hepat* 2004; **11:** 324-331
43 **Harcourt G,** Hellier S, Bunce M, Satsangi J, Collier J, Chapman R, Phillips R, Klenerman P. Effect of HLA class II genotype on T helper lymphocyte responses and viral control in hepatitis C virus infection. *J Viral Hepat* 2001; **8:** 174-179
44 **De Re V,** Caggiari L, Talamini R, Crovatto M, De Vita S, Mazzaro C, Cannizzaro R, Dolcetti R, Boiocchi M. Hepatitis C virus-related hepatocellular carcinoma and B-cell lymphoma patients show a different profile of major histocompatibility complex class II alleles. *Hum Immunol* 2004; **65:** 1397-1404
45 **Egger M,** Davey Smith G, Schneider M, Minder C. Bias in meta-analysis detected by a simple, graphical test. *BMJ* 1997; **315:** 629-634
46 Hue S, Cacoub P, Renou C, Halfon P, Thibault V, Charlotte F, Picon M, Rifflet H, Piette JC, Pol S, Caillat-Zucman S. Human leukocyte antigen class II alleles may contribute to the severity of hepatitis C virus-related liver disease. *J Infect Dis* 2002; **186:** 106-109
47 **Hamed NA,** Hano AF, Raouf HA, Gamal M, Eissa M. Relationship between HLA-DRB1*0101, DRB1*0301 alleles and interleukin-12 in haemophilic patients and hepatitis C virus positive hepatocellular carcinoma patients. *Egypt J Immunol* 2003; **10:** 17-26
48 ***Lamonaca V,*** Missale G, Urbani S, Pilli M, Boni C, Mori C, Sette A, Massari M, Southwood S, Bertoni R, Valli A, Fiaccadori F, Ferrari C. Conserved hepatitis C virus sequences are highly immunogenic for CD4(+) T cells: implications for vaccine development. *Hepatology* 1999; **30:** 1088-1098
49 **Thomas DL,** Astemborski J, Rai RM, Anania FA, Schaeffer M, Galai N, Nolt K, Nelson KE, Strathdee SA, Johnson L, Laeyendecker O, Boitnott J, Wilson LE, Vlahov D. The natural history of hepatitis C virus infection: host, viral, and environmental factors. *JAMA* 2000; **284:** 450-456
50 **Sarmiento OL,** Ford CL, Newbern EC, Miller WC, Poole C, Kaufman JS. The importance of assessing effect modification when asserting racial differences in associations between human leukocyte antigen class II alleles and hepatitis C virus outcomes. *J Infect Dis* 2002; **185:** 266-268
51 **Hoggart CJ,** Parra EJ, Shriver MD, Bonilla C, Kittles RA, Clayton DG, McKeigue PM. Control of confounding of genetic associations in stratified populations. *Am J Hum Genet* 2003; **72:** 1492-1504
52 **Rothman KJ,** Greenland S. Modern Epidemiology. Lippincott-Raven Publishers: Philadelphia, 1998
53 **Higashi Y,** Kamikawaji N, Suko H, Ando M. Analysis of HLA alleles in Japanese patients with cirrhosis due to chronic hepatitis C. *J Gastroenterol Hepatol* 1996; **11:** 241-246
54 **Hohler T,** Gerken G, Notghi A, Knolle P, Lubjuhn R, Taheri H, Schneider PM, Meyer zum Buschenfelde KH, Rittner C. MHC class II genes influence the susceptibility to chronic active hepatitis C. *J Hepatol* 1997; **27:** 259-264
55 **McKiernan S,** Kelleher D. Immunogenetics of hepatitis C virus. *J Viral Hepat* 2000; **7 Suppl 1:** 13-14
56 **Renou C,** Halfon P, Pol S, Cacoub P, Jouve E, Bronowicki JP, Arpurt JP, Rifflet H, Picon M, Causse X, Canva V, Denis J, Tran A, Bourliere M, Ouzan D, Pariente A, Dantin S, Alric L, Cartier V, Reville M, Caillat-Zucman S. Histological features and HLA class II alleles in hepatitis C virus chronically infected patients with persistently normal alanine aminotransferase levels. *Gut* 2002; **51:** 585-590

Science Editor Wang XL and Guo SY **Language Editor** Elsevier HK

PO Box 2345, Beijing 100023, China
www.wjgnet.com
wjg@wjgnet.com

ELSEVIER

World J Gastroenterol 2005;11(46):7308-7313
World Journal of Gastroenterology ISSN 1007-9327

• *RAPID COMMUNICATION* •

Pyrrolidine dithiocarbamate reduces ischemia-reperfusion injury of the small intestine

Ismail H Mallick, Wen-Xuan Yang, Marc C Winslet, Alexander M Seifalian

Ismail H Mallick, Wen-Xuan Yang, Marc C Winslet, Alexander M Seifalian, GI and Hepatobiliary Research Unit, University Department of Surgery, Royal Free and University College Medical School, University College London, London, United Kingdom
Ismail H Mallick, Marc C Winslet, Department of Surgery, Royal Free Hospital Hampstead NHS Trust, London, United Kingdom
Correspondence to: Professor Alexander M Seifalian, University Department of Surgery, Royal Free and University College Medical School, University College London, Rowland Hill Street, London NW3 2PF, United Kingdom. a.seifalian@medsch.ucl.ac.uk
Telephone: +44-20-78302901 Fax: +44-20-74726444
Received: 2005-02-13 Accepted: 2005-04-26

Abstract

AIM: To evaluate whether pyrrolidine dithiocarbamate (PDTC), an enhancer of HO production, attenuates intestinal IR injury.

METHODS: Eighteen male rats were randomly allocated into three groups: (a) sham; (b) IR, consisting of 30 min of intestinal ischemia, followed by 2-h period of reperfusion; and (c) PDTC treatment before IR. Intestinal microvascular perfusion (IMP) was monitored continuously by laser Doppler flowmetry. At the end of the reperfusion, serum samples for lactate dehydrogenase (LDH) levels and biopsies of ileum were obtained. HO activity in the ileum was assessed at the end of the reperfusion period.

RESULTS: At the end of the reperfusion in the IR group, IMP recovered partially to 42.5% of baseline ($P<0.05$ *vs* sham), whereas PDTC improved IMP to 67.3% of baseline ($P<0.01$ *vs* IR). There was a twofold increase in HO activity in PDTC group (2 062.66±106.11) as compared to IR (842.3±85.12) ($P<0.001$). LDH was significantly reduced ($P<0.001$) in PDTC group (585.6±102.4) as compared to IR group (1 973.8±306.5). Histological examination showed that the ileal mucosa was significantly less injured in PDTC group as compared with IR group.

CONCLUSION: Our study demonstrates that PDTC improves the IMP and attenuates IR injury of the intestine possibly via HO production. Additional studies are warranted to evaluate the clinical efficacy of PDTC in the prevention of IR injury of the small intestine.

Key words: Intestine; Ischemia-reperfusion injury; Heme oxygenase; Pyrrolidine

Mallick IH, Yang WX, Winslet MC, Seifalian AM. Pyrrolidine dithiocarbamate reduces ischemia-reperfusion injury of the small intestine. *World J Gastroenterol* 2005; 11(46): 7308-7313
http://www.wjgnet.com/1007-9327/11/7308.asp

INTRODUCTION

Intestinal ischemia and subsequent reperfusion (IR) injury is encountered in a variety of clinical conditions, including hypovolemic shock[1], strangulation obstruction[2], cardiovascular surgery[3], abdominal aortic surgery[4], and small bowel transplantation[5]. The attenuation of IR injury is vital for intestinal graft function and survival after small bowel transplantation[6]. IR injury is associated with the breakdown of microvascular perfusion with subsequent impairment of tissue oxygenation[7]. The maintenance of microvascular perfusion is the ultimate determinant of viability of an organ[8]. IR injury of the intestine is a systemic phenomenon resulting in bacterial translocation[9], endotoxemia[10], acute respiratory distress syndrome[11], acute hepatic injury[12], which may eventually lead to multiple organ dysfunction syndrome[13].

Therapeutic strategies aimed at ameliorating IR injury have focused both on preventing the effects of reactive oxygen species and on downregulating the signal transduction cascades related to the expression of pro-inflammatory genes. Pharmacologic preconditioning based on enhancing the production or activity of endogenous protective molecules has also been proposed as an alternative therapeutic intervention. Among such agents, pyrrolidine dithiocarbamate (PDTC) has a variety of biochemical activities, such as redox state alternation, chelation of heavy metals, and enzyme inhibition[14]. PDTC was initially regarded as a potent inhibitor of nuclear factor-kappa B (NF-$\varkappa$B) and used as an antioxidant compound to counteract the toxic effects of free radicals[15]. PDTC is one of the most effective inducers of heme oxygenase-1 (HO-1), which also confers cytoprotection against oxidative stress[16]. HO is the rate-limiting enzyme in the conversion of heme into carbon monoxide (CO), biliverdin (which is rapidly converted to bilirubin) and free iron (Fe^{2+})[17]. Three isoforms of HO have so far been identified: inducible HO-1; constitutively expressed HO-2; and HO-3 which is related to HO-2, but is less well characterized[17]. The HO system is thought to

play a pivotal role in the maintenance of antioxidant and oxidant homeostasis during cellular injury. The HO system exerts four major beneficial effects broadly: (a) antioxidant function; (b) maintenance of the microcirculation; (c) anti-apoptosis; and (d) anti-inflammatory function[17]. The antioxidant function relies on heme degradation, production of bilirubin[18], and the formation of ferritin via Fe^{2+}[19]. The production of CO with its vasodilatory and anti-platelet properties maintains the microcirculation and may be involved in anti-apoptotic and cell arrest mechanisms. The HO system exerts anti-inflammatory effects via the modulation of endothelial adhesion molecules.

To the best of our knowledge, there are no previous studies exploring the effect of PDTC on IR injury of the intestine. Therefore, we have designed the present study to examine whether PDTC preconditioning induces HO expression in the small intestine and reduces the inflammatory response during reperfusion by focusing on the intestinal microvascular perfusion.

MATERIALS AND METHODS

Animals

Male Sprague-Dawley rats, weighing 250-300 g, were used in this study. Rats were kept in a temperature-controlled environment with 12-h light-dark cycle and allowed tap water and standard rat chow pellets *ad libitum*. Animal care and experimental protocols were performed in accordance with the UK Government Guidance in the Operation of the Animals (Scientific Procedures) Act 1986.

Surgical procedures

Animals were anaesthetized using isoflurane (Baxter, Norfolk, UK) and allowed to breathe spontaneously via concentric mask connected to an oxygen regulator. The animal's body temperature was maintained at 36-38 °C using a heating pad (Harvard Apparatus Ltd, Kent, UK) and monitored with a rectal temperature probe. The arterial oxygen saturation (SaO_2) and heart rate (HR) were continuously monitored with a pulse oximeter (Ohmeda Biox 3740 pulse oximeter, Ohmeda Louisville Co., USA). The left carotid artery was cannulated with a polyethylene catheter (0.76 mm inner diameter, Portex, Kent, UK) and connected to a pressure transducer for the monitoring of mean arterial blood pressure (MABP). The right jugular vein was cannulated with a smaller polyethylene catheter (0.40 mm inner diameter, Portex, Kent, UK) for the administration of normal saline (1 mL/100 g body weight/h) to compensate for intra-operative fluid evaporation. All animals had an intravenous bolus of heparin (20 U/kg) to prevent potential thrombus formation in the ischemic segment of the intestine due to hemostasis.

Laparotomy was carried out through a midline incision. The superior mesenteric artery (SMA) was identified and dissected out from the mesentery to enable the passage of a 4/0 vicryl (Ethicon, Edinburgh, UK) suture loop. The SMA was occluded according to the method described by Arumugam *et al.*[20]. The free ends of the vicryl suture were then passed through a 5-cm segment of polyethylene tube (1.4 mm inner diameter). The tube was then gently advanced over the suture onto the mesentery and fixed in place with a hemostat. Reperfusion started when the hemostat was released. The animal's abdomen was covered with a plastic wrap (Saran wrap) to prevent fluid evaporation. At the end of the experiment, the animals were killed by exsanguination.

Experimental design

Rats were randomly allocated to three study groups ($n = 6$/group). Group 1: sham laparotomy, the SMA was identified and passage of vicryl suture was performed, but without vascular occlusion. Group 2: IR, the SMA was clamped for 30 min, followed by a 2-h period of reperfusion. Group 3: PDTC+IR, the animals received intramuscularly a single dose of 100 mg/kg of PDTC (Sigma Chemical Co., St. Louis, MO, USA) 30 min before IR.

Measurement of intestinal microvascular perfusion

Intestinal microvascular perfusion was measured by a surface laser Doppler flowmeter (LDF, DRT4, Moor Instruments Limited, Axminster, UK) in flux units. The Doppler signal varies linearly with the product of the total number of moving red blood cells in the measured volume of a few cubic millimeter multiplied by the mean velocity of these red blood cells. The numeric product is termed as perfusion units or blood cell flux units. LDF has been validated as a method for measuring gastrointestinal microvascular blood flow in animal models[21] and in clinical studies[22]. The LDF probe was placed on a fixed site on the serosa of the ileum and was held in place by a probe holder. Serosal blood flow has previously been shown to correlate well with mucosal flow[23].

Heme oxygenase assay

HO activity in ileal microsomal fractions was measured using a spectrophotometric assay of bilirubin production according to the method previously described by Motterlini *et al.*[24]. Briefly, tissue microsomes were added to the following mixture: $MgCl_2$ (2 mmol/L), phosphate-buffered saline (100 mmol/L, pH 7.4; Sigma, UK), rat liver cytosol as a source of biliverdin reductase (3 mg of total protein), hemin (10 μmol/L; Sigma, UK), glucose-6-phosphate (2 mmol/L; Sigma, UK), glucose-6-phosphate dehydrogenase (0.2 U; Sigma, UK) and NADPH (0.8 mmol/L; Sigma, UK). The reaction was conducted in the dark for 30 min at 37 ℃ and terminated by the addition of chloroform (Sigma, UK). The amount of the extracted bilirubin was calculated by the difference in absorption between 464 and 530 nm and an extinction coefficient of 40 mmol/L/cm was used for bilirubin. The total protein content of the samples was determined using a colorimetric assay according to the manufacturer's instructions (Bio-Rad, UK), and bovine gamma globulin was used as a standard.

Biochemical assays

Blood samples were taken at the end of the experiments from the carotid artery. The blood samples were

Table 1 Systemic hemodynamic parameters in three experimental groups at baseline, 5 min before, at the end of 30 min ischemia and at 1 and 2 h post-reperfusion

Hemodynamic parameters	Baseline	End of ischemia	1 h of reperfusion	2 h of reperfusion	*P* values
Heart rate (BPM)					
Sham	250±5	252±3	240±8	230±10	>0.05
IR	251±2	252±2	220±4	227±12	>0.05
PDTC	252±3	251±3	240±10	232±7	>0.05
SaO_2 (%)					
Sham	98±2	95±2	94±3	95±2	>0.05
IR	98±1	95±2	97±2	95±3	>0.05
PDTC	98±1	96±3	93±1	96±3	>0.05
MABP (mmHg)					
Sham	83±6	76± 5	74±6	78±8	>0.05
IR	90±3	108±5[b]	81±3	72±5	<0.01
PDTC	87±5	107±5[b]	79±4	73±6	<0.01

Values are expressed as mean±SE of six animals in each group. SaO_2: arterial oxygen saturation; MABP: mean arterial blood pressure. [b]P<0.01 *vs* baseline.

centrifuged at 2 000 g for 10 min at room temperature to sediment the erythrocytes. The serum was removed and analyzed on a Hitachi 747 auto-analyzer (Hitachi Ltd, Tokyo, Japan) by using commercially available enzymatic kits (Boehringer Mannheim Ltd, East Sussex, UK) for lactate dehydrogenase (LDH), aspartate aminotransferase (AST) and alanine aminotransferase (ALT).

Histological investigation

At the end of the experiment, tissue samples of ileum were taken, fixed in 10% neutral buffered formalin and embedded in paraffin, and 4-μm-thick sections were cut using a microtome and mounted on slides for hematoxylin and eosin staining. Ileal injury was assessed using a scoring system devised by Chiu *et al*.[25] under light microscopy without the knowledge of study groups.

Data collection and statistical analysis

Data from the pulse oximeter, pressure transducer and LDF were fed into a laptop computer and collected continuously at a sampling rate of 2 Hz. The data were calculated as 1-min averages at baseline and every 30 min till the end of the experiment. All values are expressed as mean±SE. ANOVA and Bonferroni adjustment for multiple comparisons were used unless otherwise stated, where unpaired Student's *t*-test was used for statistical analysis between groups. $P<0.05$ was considered statistically significant.

RESULTS

Systemic hemodynamic parameters

In all the animals in the experimental groups, the HR and the SaO_2 did not change significantly throughout the experiment (Table 1). In the sham group, MABP did not change significantly throughout the experiment. However, during ischemia, there was a transient increase in MABP from the baseline values in both IR (11.97±0.53 to 14.50 ±0.67 KPa, $P<0.01$) and PDTC groups (11.70±0.67 to 14.23±1.33 KPa, $P<0.01$). However, the MABP did not change significantly during the reperfusion period between the three groups (Table 1).

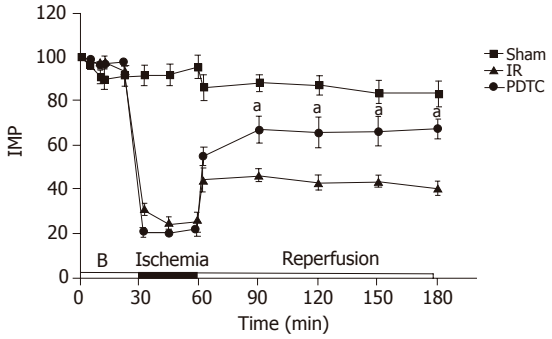

Figure 1 Intestinal microvascular perfusion in (% of baseline) during 30 min of ischemia and 2 h of reperfusion measured by L-DF. Values are expressed as mean±SE of six animals in each group ([a]$P<0.05$ *vs* IR). B: Baseline.

Intestinal microvascular perfusion

IMP did not alter significantly during the course of the experiment in the sham group. There were significant differences between IR and PDTC groups in IMP at 30 min of reperfusion (46.7±2.8% in IR *vs* 67.3±6.2% in PDTC, $P<0.01$). The increase in IMP persisted till the end of the 2-h reperfusion period (42.5±2.8% in IR *vs* 69.1± 4.5% in PDTC, $P<0.01$) (Figure 1).

HO activity assay

The mean HO activity in the sham group was 409.66±62.95 pmol bilirubin/(mg protein·h). PDTC led to a twofold increase in HO activity (2 085.83±158.65) as compared to IR (768.66±103.82) ($P<0.001$, Figure 2).

Biochemical analysis

LDH was significantly reduced in PDTC group (576.3± 98.7) as compared to IR group (1 866.0±267.5) ($P<0.001$, Figure 3). The LDH value in sham group at the end of the reperfusion was 335.23±77.7. Significant changes were not detected in serum indicators of liver function (AST and ALT) in any of the groups (data not shown).

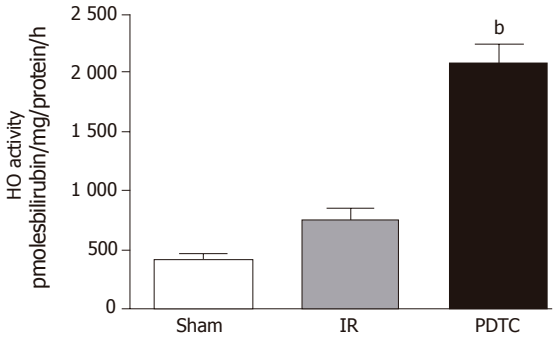

Figure 2 Ileal HO activity in all three experimental groups at the end of 2 h of reperfusion (^bP<0.01 *vs* IR).

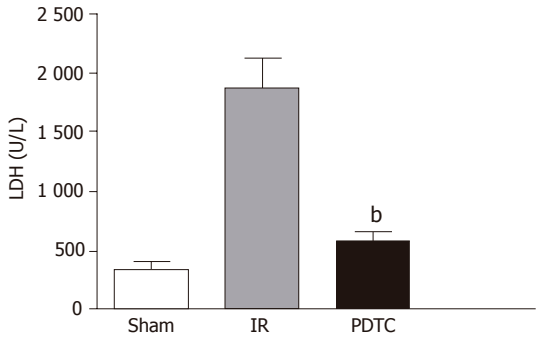

Figure 3 Serum LDH levels (U/L) at the end of 2 h reperfusion period. Values are expressed as mean±SE of six animals in each group. In PDTC group, LDH was significantly lower compared to the IR group (^bP<0.001 *vs* IR).

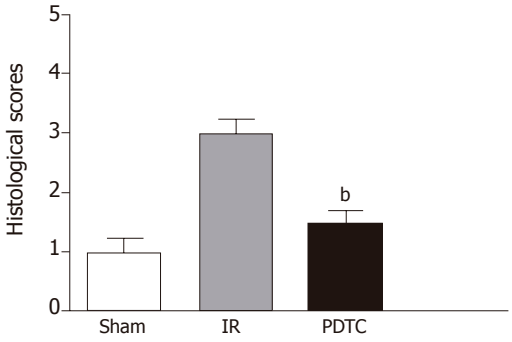

Figure 4 Comparison of histological scores of ileal mucosa between three experimental groups (^bP<0.01 *vs* IR).

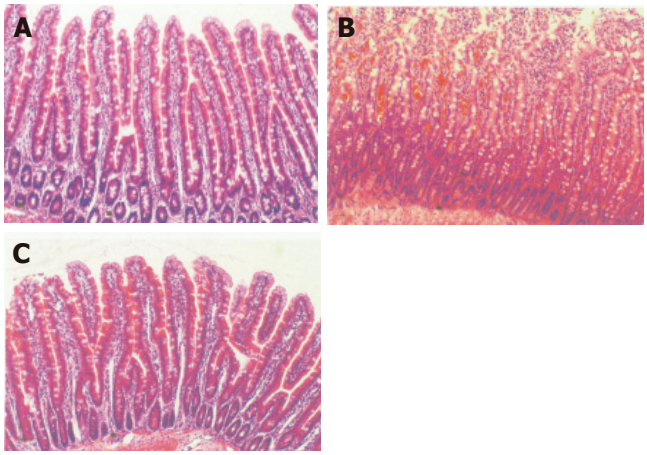

Figure 5 Representative photomicrographs of histological sections of ileum (a) in sham operated animals, (b) subjected to 30-min period of ischemia and 2-h period of reperfusion (IR) and (c) subjected to PDTC+IR (H&E, original magnification ×100).

Histological analysis

IR resulted in an increase in the histological score from a mean of 1.0±0.2 in sham-operated animals to 3±0.2. PDTC treatment improved the histological score significantly to 1.5±0.5 (P<0.01, Figures 4 and 5).

DISCUSSION

The present study clearly showed that PDTC improved the small bowel microvascular perfusion and increased HO activity, while ameliorating IR injury. Serum LDH levels, which is used as a marker for intestinal injury[6], reflected intestinal damage in IR group, whereas PDTC decreased these levels. IR injury resulted in villous and crypt damage, which attributed to hemorrhage and necrosis, whereas PDTC ameliorated this effect. These results suggest that PDTC protects small bowel from IR injury possibly via HO production.

The model of 30-min period of SMA occlusion with 2-h reperfusion was reliable with no procedure-related mortality, suggesting that 30 min of intestinal ischemia is non-lethal but induces substantial intestinal injury. A considerable number of experimental studies have indicated that IR injury of the intestine occurs in a biphasic manner characterized by different time frames and mechanisms: (a) an early phase that immediately follows the ischemia and lasts for 2-3 h; and (b) a late phase which begins 12-24 h from the ischemia and lasts for about 3-4 d[13]. Hence, a period of 2 h of reperfusion following ischemia was chosen to assess the changes in the early phase of reperfusion injury. One of the effective approaches for attenuating IR injury is to induce endogenous antioxidant genes, such as HO-1.

PDTC has been shown to be a potent inducer of HO-1 in many experimental models[16,14]. Whereas increasing evidences suggest that HO-1 induction may mediate cellular protection against oxidant injury in both *in vitro* and *in vivo* models, the role of HO in the intestinal microcirculation is poorly understood. In this study, the effects of PDTC on IR-induced intestinal microcirculatory changes were studied by continuously measuring intestinal blood flow with LDF, which has been used extensively in both animals and human beings[22]. It is non-invasive, safe, and easy to use[23]. This technique allows repeated measurements of blood flow without access to venous or arterial blood. In our study, the comparison of IMP between the groups at different time points showed that PDTC increased the IMP in the initial

30 min of reperfusion, suggesting that the mechanism of pharmacologic preconditioning by PDTC modulating flow in the microcirculation is an immediate phenomenon. Therefore, the effect of PDTC is likely to involve modulation of immediate microcirculatory events at the level of capillaries and postcapillary venules, because these are the primary sites of microcirculatory failure induced by IR injury.

The results of the present study clearly demonstrated that PDTC induced maintenance of adequate microvascular perfusion *in vivo*, and indicated that this protective effect might be mediated through the action of HO, which catalyzes the conversion of heme to CO, biliverdin and free iron. CO and its action on capillary pericytes may play a major role in this protection. It is well known that capillaries are associated abluminally with pericytes which protrude primary cytoplasmic processes running along the axes of the capillaries[26]. From these primary processes, lateral processes arise, which completely encircle the capillaries and form tight connections to the endothelial cells[26]. These pericytes contain muscle cytoskeletal proteins, in particular alpha-smooth muscle actin, which regulate microvascular blood flow[27]. In the liver, Ito cells, which are the sinusoids-associated pericytes, are primarily responsible for CO-mediated regulation in sinusoidal blood flow[28]. In addition, there is an increasing evidence that CO inhibits the aggregation of platelets[29], which could result in highly improved microvascular perfusion because of unhindered flow. Hence, tissue viability increases because of improved nutritional supply and better elimination of toxic residues of oxidative stress. Recently, Nakao *et al*.[30] demonstrated that inhalation of CO ameliorates IR injury in a model of bowel transplantation.

Biliverdin is subjected to further degradation to bilirubin by the cytosolic enzyme biliverdin reductase[31]. It acts as an antioxidant and is capable of scavenging oxygen free radicals that are thought to be primarily responsible for the tissue injury[18]. Iron, the last product of heme breakdown, acts as an oxidant like other transition metals and catalyzes the formation of reactive hydroxyl radicals (OH) by the Haber-Weiss reaction. Typically, the OH · causes biological damage by stimulating the free chain reaction known as lipid peroxidation, in which OH · attacks the fatty acid side chains of the membrane phospholipids and causes organelle and cell disruption[32]. Therefore, it seems to be of paramount importance to eliminate free iron from the tissue in order to maintain the cellular integrity after the stress event. To enable this process, an additional expression of ferritin, the iron-binding protein, is induced simultaneously by HO[33].

In summary, this study has demonstrated that intestinal IR injury induces rapid microcirculatory breakdown with tissue damage. Administration of PDTC maintains the intestinal microvascular blood flow and markedly attenuates the IR injury. PDTC may be of particular value in preventing IR injury to the small intestine and might help to improve the results of small bowel transplantation. Intestinal IR injury is also an obligatory component of numerous surgical procedures. The results of the present study may, therefore, prove beneficial in many areas of clinical research. Further studies are clearly warranted to evaluate the clinical efficacy of PDTC in the prevention of IR injury of the small intestine.

REFERENCES

1 **Kong SE**, Blennerhassett LR, Heel KA, McCauley RD, Hall JC. Ischaemia-reperfusion injury to the intestine. *Aust N Z J Surg* 1998; **68:** 554-561

2 **Akcakaya A,** Alimoglu O, Sahin M, Abbasoglu SD. Ischemia-reperfusion injury following superior mesenteric artery occlusion and strangulation obstruction. *J Surg Res* 2002; **108:** 39-43

3 **Ghosh S,** Roberts N, Firmin RK, Jameson J, Spyt TJ. Risk factors for intestinal ischaemia in cardiac surgical patients. *Eur J Cardiothorac Surg* 2002; **21:** 411-416

4 **Reber PU,** Peter M, Patel AG, Stauffer E, Printzen G, Mettler D, Hakki H, Kniemeyer HW. Ischaemia/reperfusion contributes to colonic injury following experimental aortic surgery. *Eur J Vasc Endovasc Surg* 2001; **21:** 35-39

5 **Kimizuka K,** Nakao A, Nalesnik MA, Demetris AJ, Uchiyama T, Ruppert K, Fink MP, Stolz DB, Murase N. Exogenous IL-6 inhibits acute inflammatory responses and prevents ischemia/reperfusion injury after intestinal transplantation. *Am J Transplant* 2004; **4:** 482-494

6 **Sola A,** De Oca J, Gonzalez R, Prats N, Rosello-Catafau J, Gelpi E, Jaurrieta E, Hotter G. Protective effect of ischemic preconditioning on cold preservation and reperfusion injury associated with rat intestinal transplantation. *Ann Surg* 2001; **234:** 98-106

7 **Turnage RH,** Kadesky KM, Bartula L, Guice KS, Oldham KT, Myers SI. Splanchnic PGI2 release and "no reflow" following intestinal reperfusion. *J Surg Res* 1995; **58:** 558-564

8 **Kaminski PM**, Proctor KG. Attenuation of no-reflow phenomenon, neutrophil activation, and reperfusion injury in intestinal microcirculation by topical adenosine. *Circ Res* 1989; **65:** 426-435

9 **Fujino Y,** Suzuki Y, Kakinoki K, Tanioka Y, Ku Y, Kuroda Y. Protection against experimental small intestinal ischaemia-reperfusion injury with oxygenated perfluorochemical. *Br J Surg* 2003; **90:** 1015-1020

10 **Deitch EA.** The role of intestinal barrier failure and bacterial translocation in the development of systemic infection and multiple organ failure. *Arch Surg* 1990; **125:** 403-404

11 **Turnage RH,** Guice KS, Oldham KT. Pulmonary microvascular injury following intestinal reperfusion. *New Horiz* 1994; **2:** 463-475

12 **Turnage RH,** Kadesky KM, Myers SI, Guice KS, Oldham KT. Hepatic hypoperfusion after intestinal reperfusion. *Surgery* 1996; **119:** 151-160

13 **Mallick IH,** Yang W, Winslet MC, Seifalian AM. Ischemia-reperfusion injury of the intestine and protective strategies against injury. *Dig Dis Sci* 2004; **49:** 1359-1377

14 **Tsuchihashi S,** Tamaki T, Tanaka M, Kawamura A, Kaizu T, Ikeda A, Kakita A. Pyrrolidine dithiocarbamate provides protection against hypothermic preservation and transplantation injury in the rat liver: the role of heme oxygenase-1. *Surgery* 2003; **133:** 556-567

15 **Liu SF,** Ye X, Malik AB. Inhibition of NF-kappaB activation by pyrrolidine dithiocarbamate prevents In vivo expression of proinflammatory genes. *Circulation* 1999; **100:** 1330-1337

16 **Hartsfield CL,** Alam J, Choi AM. Transcriptional regulation of the heme oxygenase 1 gene by pyrrolidine dithiocarbamate. *FASEB J* 1998; **12:** 1675-1682

17 **Katori M,** Anselmo DM, Busuttil RW, Kupiec-Weglinski JW. A novel strategy against ischemia and reperfusion injury: cytoprotection with heme oxygenase system. *Transpl Immunol* 2002; **9:** 227-233

18 **Stocker R,** Yamamoto Y, McDonagh AF, Glazer AN, Ames

BN. Bilirubin is an antioxidant of possible physiological importance. *Science* 1987; **235:** 1043-1046
19 **Balla G,** Jacob HS, Balla J, Rosenberg M, Nath K, Apple F, Eaton JW, Vercellotti GM. Ferritin: a cytoprotective antioxidant strategem of endothelium. *J Biol Chem* 1992; **267:** 18148-18153
20 **Arumugam TV,** Shiels IA, Woodruff TM, Reid RC, Fairlie DP, Taylor SM. Protective effect of a new C5a receptor antagonist against ischemia-reperfusion injury in the rat small intestine. *J Surg Res* 2002; **103:** 260-267
21 **Shepherd AP,** Riedel GL. Continuous measurement of intestinal mucosal blood flow by laser-Doppler velocimetry. *Am J Physiol* 1982; **242:** G668-672
22 **Thollander M,** Hellstrom PM, Gazelius B. Semi-invasive laser-Doppler flowmetry technique. New application for recordings of hemodynamics in combination with manometry of human small intestine. *Int J Microcirc Clin Exp* 1997; **17:** 15-21
23 **Corbett EJ,** Barry BN, Pollard SG, Lodge JP, Bellamy MC. Laser Doppler flowmetry is useful in the clinical management of small bowel transplantation. *The Liver Transplant Group. Gut* 2000; **47:** 580-583
24 **Motterlini R,** Foresti R, Intaglietta M, Winslow RM. NO-mediated activation of heme oxygenase: endogenous cytoprotection against oxidative stress to endothelium. *Am J Physiol* 1996; **270:** H107-H114
25 **Chiu CJ,** McArdle AH, Brown R, Scott HJ, Gurd FN. Intestinal mucosal lesion in low-flow states. I. A morphological, hemodynamic, and metabolic reappraisal. *Arch Surg* 1970; **101:** 478-483
26 **Hirschi KK,** D'Amore PA. Pericytes in the microvasculature. *Cardiovasc Res* 1996; **32:** 687-698
27 **Skalli O,** Pelte MF, Peclet MC, Gabbiani G, Gugliotta P, Bussolati G, Ravazzola M, Orci L. Alpha-smooth muscle actin, a differentiation marker of smooth muscle cells, is present in microfilamentous bundles of pericytes. *J Histochem Cytochem* 1989; **37:** 315-321
28 **Suematsu M,** Wakabayashi Y, Ishimura Y. Gaseous monoxides: a new class of microvascular regulator in the liver. *Cardiovasc Res* 1996; **32**: 679-686
29 **Brune B,** Ullrich V. Inhibition of platelet aggregation by carbon monoxide is mediated by activation of guanylate cyclase. *Mol Pharmacol* 1987; **32:** 497-504
30 **Nakao A,** Kimizuka K, Stolz DB, Neto JS, Kaizu T, Choi AM, Uchiyama T, Zuckerbraun BS, Nalesnik MA, Otterbein LE, Murase N. Carbon monoxide inhalation protects rat intestinal grafts from ischemia/reperfusion injury. *Am J Pathol* 2003; **163:** 1587-1598
31 **Maines MD.** Heme oxygenase: function, multiplicity, regulatory mechanisms, and clinical applications. *FASEB J* 1988; **2:** 2557-2568
32 **Halliwell B.** Antioxidant defence mechanisms: from the beginning to the end (of the beginning). *Free Radic Res* 1999; **31:** 261-272
33 **Bauer M,** Bauer I. Heme oxygenase-1: redox regulation and role in the hepatic response to oxidative stress. *Antioxid Redox Signal* 2002; **4:** 749-758

Science Editor Kumar M and Guo SY **Language Editor** Elsevier HK

PO Box 2345, Beijing 100023, China
www.wjgnet.com
wjg@wjgnet.com

ELSEVIER

World J Gastroenterol 2005;11(46):7314-7317
World Journal of Gastroenterology ISSN 1007-9327

• *RAPID COMMUNICATION* •

Plasma leptin and ghrelin concentrations in patients with Crohn's disease

Yoshito Nishi, Hajime Isomoto, Hiroaki Ueno, Ken Ohnita, Chun Yang Wen, Fuminao Takeshima, Ryosuke Mishima, Masamitsu Nakazato, Shigeru Kohno

Yoshito Nishi, Hajime Isomoto, Ken Ohnita, Fuminao Takeshima, Ryosuke Mishima, Shigeru Kohno, Second Department of Internal Medicine, Nagasaki University School of Medicine, Sakamoto 1-7-1, Nagasaki, Japan
Hajime Isomoto, Shigeru Kohno, Department of Endoscopy, Nagasaki University School of Medicine, Sakamoto 1-7-1, Nagasaki, Japan
Chun Yang Wen, Department of Molecular Pathology, Atomic Bomb Disease Institute, Nagasaki University School of Medicine, Sakamoto 12-4, Nagasaki, Japan
Hiroaki Ueno, Masamitsu Nakazato, Third Department of Internal Medicine, Miyazaki Medical College, Kiyotake, Miyazaki, Japan
Correspondence to: Dr Hajime Isomoto, Division of Gastroenterology and Hepatology, Mayo Clinic and Foundation, 200 First Street SW, Rochester, MN 55905, United States. hajimei2002@yahoo.co.jp
Telephone: +1-507-284-0690 Fax: +1-507-284-0762
Received: 2005-07-11 Accepted: 2005-09-09

Abstract

AIM: To determine the concentrations of leptin and ghrelin, which have opposite effects on appetite, energy expenditure, and weight control, in the plasma of patients with Crohn's disease (CD), which is often associated with weight loss and malnutrition.

METHODS: Plasma leptin and ghrelin concentrations were determined in 28 outpatients with CD by radioimmunoassay. Age- and sex-matched controls with and without *Helicobacter pylori* (*H pylori*) infection (28 for each) were enrolled in the study. Circulating levels of these hormones were assessed with respect to CD activity, disease localization and medical treatment.

RESULTS: There were no significant differences in ghrelin levels between CD patients and *H pylori*-negative controls. However, circulating ghrelin levels were significantly lower in *H pylori*-infected subjects than in CD patients and uninfected controls. Plasma leptin levels were comparable among the groups. Localization and medication profile had no significant impact on circulating ghrelin and leptin levels.

CONCLUSION: Apart from *H pylori* infection, CD itself has no significant influence on circulating ghrelin and leptin levels in the outpatients who were mostly in inactive state.

Key words: Crohn's disease; Ghrelin; Leptin; *Helicobacter pylori*

Nishi Y, Isomoto H, Ueno H, Ohnita K, Wen CY, Takeshima F, Mishima R, Nakazato M, Kohno S. Plasma leptin and ghrelin concentrations in patients with Crohn's disease. *World J Gastroenterol* 2005; 11(46): 7314-7317
http://www.wjgnet.com/1007-9327/11/7314.asp

INTRODUCTION

Crohn's disease (CD) is characterized by a relapsing inflammatory process throughout the digestive tract[1,2]. CD is frequently accompanied with malnutrition and weight loss[1,2]. Possible explanations for these complications include malabsorption of nutrients, intestinal losses during inflammatory process, and anorexia[3]. However, the exact etiology is not completely understood.

Leptin is mainly synthesized by the adipose tissue and plays a crucial role in the homeostasis of the body weight by reducing appetite and increasing energy expenditure[4,5]. Contrary to the initial reports, leptin production is not restricted to adipocytes. It is also detected in the human placenta, muscles, and gastric chief cells[6-10].

Ghrelin is a novel endogenous ligand for growth hormone secretagogue receptor[11,12]. It was originally isolated from the stomach and has been subsequently identified in various tissues including the small and large intestine[11,12]. In addition to its potent growth hormone-releasing activity, ghrelin displays metabolic effects opposed to those of leptin[11-13]. It stimulates food intake, enhances the use of carbohydrates and reduces fat utilization. In fact, circulating ghrelin levels are decreased in obesity and increased in anorexia nervosa or cachexia[11-14].

At present, no data on the interplay of ghrelin and leptin in CD are available. This is the first report to assess the circulating ghrelin and leptin concentrations in patients with CD simultaneously.

MATERIALS AND METHODS

Patients

Twenty-eight consecutive outpatients with CD were enrolled in the study between October 2002 and

Table 1 Plasma leptin and ghrelin levels in patients with CD and controls with or without *H pylori* infection (mean±SD)

	CD	Controls	
		H pylori-infected	*H pylori*-uninfected
Body mass index (kg/m^2)	20.5±0.4 (16.2-29.9)[1]	21.3±0.8 (16.4-28.5)	20.8±0.5 (16.4-26.7)
Plasma ghrelin levels (fmol/mL)	195.7±1.5 (45.7-368.7)	143.4±7.1 (53.2-481.0)	182.4±1.4 (75.7-322.2)
Plasma leptin levels (ng/mL)	3.8±0.4 (0.0-15.0)	4.3±0.6 (0.8-8.4)	3.8±0.6 (0.0-10.8)

[1]Mean±SD (range).

Table 2 Plasma leptin and ghrelin levels in terms of various parameters (mean±SD)

	Ghrelin (fmol/mL)	Leptin (ng/mL)	Body mass index
Disease activity			
Active (*n* = 5)	220.6±98.8	4.7±4.1	19.9±4.5
Inactive (*n* = 23)	202.3±86.4	3.6±2.4	20.6±2.7
Disease location			
Small intestine (*n* = 3)	186.3±68.6	2.8±2.3	18.5±1.6
Large intestine (*n* = 10)	246.8±83.3	4.2±3.3	20.9±2.4
Small and large intestine (*n* = 15)	186.8±92.4	4.1±3.1	20.5±4.0
Anal lesion			
Present (*n* = 7)	213.4±85.1	3.4±2.5	20.1±4.8
Absent (*n* = 21)	206.5±92.4	4.1±3.2	20.5±2.6
Medical treatment			
5-Aminosalicylates (*n* = 16)	185.5±86.5	2.8±1.5	20.1±2.4
5-Aminosalicylates and elementary diet (*n* = 7)	229.5±98.9	4.8±3.6	20.1±5.2
No medications (*n* = 5)	243.4±76.8	5.7±4.8	21.8±3.1
Helicobacter pylori status			
Positive (*n* = 5)	265.8±109.8	3.5±2.6	20.2±3.4
Negative (*n* = 23)	195.7±81.5	5.5±3.9	21.8±0.1

December 2004. The study was approved by Nagasaki University Human Ethics Committee. All samples were obtained with written informed consent of the patients prior to their inclusion, in accordance with the Helsinki Declaration. A diagnosis of CD is based on the generally accepted clinical, radiographic, endoscopic and histologic criteria[1,2]. The exclusion criteria were age <18 or >80 years, pregnancy, body mass index (BMI) >30 kg/m^2, diabetes mellitus, systemic infection, thyroid and liver diseases, renal impairment, use of medications against *H pylori* during the preceding 3 mo, alcohol abuse, drug addiction, and long-term corticosteroid or nonsteroidal anti-inflammatory drug use. None underwent gastrointestinal surgery. They included 16 men and 12 women, aged between 18 and 56 years (mean, 32 years). According to the CD activity index (>150), 5 patients suffered from active CD. As for disease localization, the disease process was limited to the small bowel in 3 patients, to the colon in 10 and affected both regions in 15. Seven had anal lesions and none had upper gastrointestinal involvement. Of those, 16 were treated with 5-aminosalicylates, 7 with 5-aminosalicylates and elementary diet, and 5 received no medications.

Since ghrelin is primarily produced by X/A-like cells in the gastric fundus[11,12], its production and release may be affected by inflammatory and atrophic events associated with *H pylori* infection[15,16]. Thus, *H pylori* status was assessed, as described below.

Age- and sex-matched 23 *H pylori*-negative healthy subjects served as controls. Moreover, age- and sex-matched 23 *H pylori*-infected patients with non-ulcer dyspepsia were enrolled in the study.

Plasma leptin and ghrelin concentrations

Blood samples were taken between 9 and 11 a.m. after an overnight fast, transferred into chilled tubes containing eth ylenediaminetetraacetic acid-2Na and aprotinin, stored on ice during collection and centrifuged. Then, the plasma was separated, and stored at -80 ℃ until assay. Plasma ghrelin concentrations were measured in-house in duplicate by radioimmunoassay (RIA), as described previously[17]. This assay system employs a rabbit polyclonal antibody against the C-terminal fragment of human ghrelin. Plasma leptin concentrations were measured in duplicate by commercial RIA kit (Linco Research Co., St. Charles, USA), based on the protocol provided by the manufacturer.

Detection of H pylori infection

H pylori status was assessed by anti-*H pylori* immunoglobulin G antibody (HELp TEST, an enzyme linked immunosorbent assay kit, AMRAD Co., Melbourne, Australia) using the stored plasma and ^{13}C-urea breath test (UBiT, Otsuka Pharmaceutical Co., Tokyo, Japan).

Statistical analysis

Statistical analyses were performed using Fisher's exact, χ^2, Student's *t*, Mann-Whitney *U*, Kruskal-Wallis, Spearman's rank, and Wilcoxon signed ranks tests, as appropriate. $P<0.05$ was considered statistically significant. Data were expressed as mean±SD.

RESULTS

There were no significant differences in ghrelin levels between CD patients and *H pylori*-negative controls (Table 1). However, circulating ghrelin levels were significantly lower in *H pylori*-infected subjects than in CD patients ($P<0.01$, Table 1) and controls negative for the infection ($P<0.05$, Table 1). On the other hand, circulating leptin levels were comparable between the groups (Table 1).

Other parameters such as disease activity, localization and medication profile and *H pylori* status had no significant impact on circulating ghrelin and leptin levels (Table 2).

There was a significant positive correlation between plasma leptin levels and BMI ($r = 0.61$, $P<0.005$). Plasma ghrelin concentrations tended to decrease with increase in BMI, *albeit* insignificantly. There was no significant correlation between circulating ghrelin and leptin levels.

DISCUSSION

Our results suggest that circulating ghrelin levels are not altered in CD patients who mainly consisted of those with the inactive disease. In our study, plasma concentrations of leptin, the opposing metabolic counterpart of ghrelin[10-13], were not affected by the disease. In addition, there were no significant association of such factors as localization and medication profile with circulating ghrelin and leptin. These findings suggest that alterations in these hormones involved in appetite and energy metabolism are unlikely to mediate nutrition state in CD. However, these results must be interpreted within the context of the limitations in our study. First, the sample size was relatively small. Second, severe patients with wasting symptoms or malnutrition were not enrolled in this study, as it was in the outpatient-based setting. Although our series were not associated with upper gastrointestinal lesions, where ghrelin is primarily produced[10,17], such involvement might have an impact on the circulating ghrelin levels.

Murch *et al*.[18] demonstrated that suppression of growth velocity in children with CD correlates with circulating tumor necrosis factor (TNF) alpha concentrations. In cachectic state, a positive correlation has been found between ghrelin and TNF alpha circulating levels[19]. On the other hand, there is a significant association between serum levels of leptin and TNF receptor 1[20]. We did not measure TNF alpha and TNF receptor 1 levels in the present series of CD, but accumulating evidence indicates that the TNF system is activated in CD[1,2].

Recently, Suzuki *et al*.[15] demonstrated that *H pylori* infection modifies gastric and plasma ghrelin dynamics in Mongolian gerbils. There are contradictory reports on the relationship between *H pylori* and ghrelin. A Turkish study reported that *H pylori* has no effect on plasma ghrelin levels[21], whereas a British study demonstrated that circulating ghrelin increases following the cure of *H pylori* infection[16]. In our series, the principal determinant of circulating ghrelin might be the *H pylori* status. The exact reason for such a discrepancy is not clear, but the following factors should be considered: differences in the study populations of diverse races, nutrient status and dietary habits, small sample size and inadequate assessment of *H pylori* status, i.e., only by histology, leading to underestimation of infection in their series[21]. In turn, circulating leptin concentrations are not associated with *H pylori* status, consistent with previous reports[22,23]. On the other hand, plasma leptin concentrations significantly correlate with BMI, as the primary contributor of circulating leptin is exclusively the adipose tissue[4,5].

In conclusion, CD itself has no significant influence on the circulating levels of leptin and ghrelin. Further evaluation of a larger population with the active disease or response to medical treatment including parenteral and enteric nutrition and infliximab is warranted. Plasma ghrelin dynamics may be affected by *H pylori* status in human beings.

REFERENCES

1 **Forbes A.** Review article: Crohn's disease--the role of nutritional therapy. *Aliment Pharmacol Ther* 2002; **16 Suppl 4:** 48-52

2 **Goh J,** O'Morain CA. Review article: nutrition and adult inflammatory bowel disease. *Aliment Pharmacol Ther* 2003; **17:** 307-320

3 **Schneeweiss B,** Lochs H, Zauner C, Fischer M, Wyatt J, Maier-Dobersberger T, Schneider B. Energy and substrate metabolism in patients with active Crohn's disease. *J Nutr* 1999; **129:** 844-848

4 **Zhang Y,** Proenca R, Maffei M, Barone M, Leopold L, Friedman JM. Positional cloning of the mouse obese gene and its human homologue. *Nature* 1994; **372:** 425-432

5 **Coleman DL.** Obese and diabetes: two mutant genes causing diabetes-obesity syndromes in mice. *Diabetologia* 1978; **14:** 141-148

6 **Faggioni R,** Feingold KR, Grunfeld C. Leptin regulation of the immune response and the immunodeficiency of malnutrition. *FASEB J* 2001; **15:** 2565-2571

7 **Bado A,** Levasseur S, Attoub S, Kermorgant S, Laigneau JP, Bortoluzzi MN, Moizo L, Lehy T, Guerre-Millo M, Le Marchand-Brustel Y, Lewin MJ. The stomach is a source of leptin. *Nature* 1998; **394:** 790-793

8 **Azuma T**, Suto H, Ito Y, Ohtani M, Dojo M, Kuriyama M, Kato T. Gastric leptin and Helicobacter pylori infection. *Gut* 2001; **49:** 324-329

9 **Sobhani I,** Bado A, Vissuzaine C, Buyse M, Kermorgant S, Laigneau JP, Attoub S, Lehy T, Henin D, Mignon M, Lewin MJ. Leptin secretion and leptin receptor in the human stomach. *Gut* 2000; **47:** 178-183

10 **Blaser MJ,** Atherton JC. Helicobacter pylori persistence: biology and disease. *J Clin Invest* 2004; **113:** 321-333

11 **Murray CD,** Kamm MA, Bloom SR, Emmanuel AV. Ghrelin for the gastroenterologist: history and potential. *Gastroenterology* 2003; **125**: 1492-1502

12 **Selva S,** Scaltrini S, Bordoni M, Lubatti L, Cristofori GB, Trazzi R, Meloni G. Methods for protecting the spinal cord in surgery of the thoraco-abdominal aorta. *Minerva Anestesiol* 1992; **58:** 1123-1125

13 **Gale SM,** Castracane VD, Mantzoros CS. Energy homeostasis, obesity and eating disorders: recent advances in endocrinology. *J Nutr* 2004; **134:** 295-298

14 **Beales IL,** Calam J. Interleukin 1 beta and tumour necrosis factor alpha inhibit acid secretion in cultured rabbit parietal

cells by multiple pathways. *Gut* 1998; **42:** 227-234
15 **Suzuki H,** Masaoka T, Hosoda H, Ota T, Minegishi Y, Nomura S, Kangawa K, Ishii H. Helicobacter pylori infection modifies gastric and plasma ghrelin dynamics in Mongolian gerbils. *Gut* 2004; **53:** 187-194
16 **Nwokolo CU,** Freshwater DA, O'Hare P, Randeva HS. Plasma ghrelin following cure of Helicobacter pylori. *Gut* 2003; **52:** 637-640
17 **Date Y,** Kojima M, Hosoda H, Sawaguchi A, Mondal MS, Suganuma T, Matsukura S, Kangawa K, Nakazato M. Ghrelin, a novel growth hormone-releasing acylated peptide, is synthesized in a distinct endocrine cell type in the gastrointestinal tracts of rats and humans. *Endocrinology* 2000; **141:** 4255-4261
18 **Murch SH,** Lamkin VA, Savage MO, Walker-Smith JA, MacDonald TT. Serum concentrations of tumour necrosis factor alpha in childhood chronic inflammatory bowel disease. *Gut* 1991; **32:** 913-7
19 **Nagaya N,** Uematsu M, Kojima M, Date Y, Nakazato M, Okumura H, Hosoda H, Shimizu W, Yamagishi M, Oya H, Koh H, Yutani C, Kangawa K. Elevated circulating level of ghrelin in cachexia associated with chronic heart failure: relationships between ghrelin and anabolic/catabolic factors. *Circulation* 2001; **104:** 2034-2038
20 **Blanco Quiros A,** Arranz Sanz E, Garrote Adrados JA, Oyaguez Ugidos P, Calvo Romero C, Alonso Franch M. The tumor necrosis factor system and leptin in coeliac disease. *An Esp Pediatr* 2001; **55:** 198-204
21 **Gokcel A,** Gumurdulu Y, Kayaselcuk F, Serin E, Ozer B, Ozsahin AK, Guvener N. Helicobacter pylori has no effect on plasma ghrelin levels. Eur J Endocrinol 2003; **148:** 423-426
22 **Azuma T,** Suto H, Ito Y, Ohtani M, Dojo M, Kuriyama M, Kato T. Gastric leptin and Helicobacter pylori infection. *Gut* 2001; **49:** 324-329
23 **Shimzu T,** Satoh Y, Yamashiro Y. Serum leptin and body mass index in children with H pylori infection. *Gut* 2002; **51:** 142

Science Editor Wang XL **Language Editor** Elsevier HK

PO Box 2345, Beijing 100023, China
www.wjgnet.com
wjg@wjgnet.com

ELSEVIER

World J Gastroenterol 2005;11(46):7318-7322
World Journal of Gastroenterology ISSN 1007-9327

• *RAPID COMMUNICATION* •

Accuracy of a predictive model for severe hepatic fibrosis or cirrhosis in chronic hepatitis C

Agostino Colli, Alice Colucci, Silvia Paggi, Mirella Fraquelli, Sara Massironi, Marco Andreoletti, Vittorio Michela, Dario Conte

Agostino Colli, Sara Massironi , Marco Andreoletti, Vittorio Michela, Department of Internal Medicine, Ospedale "A. Manzoni", 23900 Lecco, Italy
Alice Colucci, Silvia Paggi, Mirella Fraquelli, Dario Conte, Postgraduate School of Gastroenterology, IRCCS Ospedale Maggiore, 20122 Milan, Italy
Supported by the "Research Competition Award 2002" from IRCCS Ospedale Maggiore, Milan, and "Associazione Amici della Gastroenterologia del Granelli", Milan, Italy
Correspondence to: Dario Conte, MD, Postgraduate School of Gastroenterology, Padiglione Granelli 3° piano, IRCCS -Ospedale Maggiore, Via F. Sforza 35, 20122 Milan, Italy. dario.conte@unimi.it
Telephone: +39-02-55033418 Fax: +39-02-55033644
Received: 2005-03-26 Accepted: 2005-07-20

Abstract

AIM: To assess the accuracy of a model in diagnosing severe fibrosis/cirrhosis in chronic hepatitis C virus (HCV) infection.

METHODS: The model, based on the sequential combination of the Bonacini score (BS: ALT/AST ratio, platelet count and INR) and ultrasonography liver surface characteristics, was applied to 176 patients with chronic HCV infection. Assuming a pre-test probability of 35%, the model defined four levels of post-test probability of severe fibrosis/cirrhosis: <10% (low), 10-74% (not diagnostic), 75-90% (high) and >90% (almost absolute). The predicted probabilities were compared with the observed patients' distribution according to the histology (METAVIR).

RESULTS: Severe fibrosis/cirrhosis was found in 67 patients (38%). The model discriminated patients in three comparable groups: 34% with a very high (>90%) or low (<10%) probability of severe fibrosis, 33% with a probability ranging from 75% to 90%, and 33% with an uncertain diagnosis (i.e., a probability ranging from 10% to 74%). The observed frequency of severe fibrosis/cirrhosis was within the predefined ranges.

CONCLUSION: The model can correctly identify 67% of patients with a high (>75%) or low (<10%) probability of cirrhosis, leaving only 33% of the patients still requiring liver biopsy.

Key words: Liver fibrosis; Ultrasonography; Bonacini score; Liver biopsy; Hepatitis C

Colli A, Colucci A, Paggi S, Fraquelli M, Massironi S, Andreoletti M, Michela V, Conte D. Accuracy of a predictive model for severe hepatic fibrosis or cirrhosis in chronic hepatitis C. *World J Gastroenterol* 2005; 11(46): 7318-7322
http://www.wjgnet.com/1007-9327/11/7318.asp

INTRODUCTION

Hepatitis C virus (HCV) infection is a major cause of chronic liver disease worldwide: nearly 80% of HCV-infected patients develop chronic infection, and about 20% progress to cirrhosis[1]. Liver histology is currently considered as the "reference standard" for evaluating hepatic damage on the basis of the degree of necrotic inflammatory activity and fibrosis, with the latter having prognostic significance and playing a major role in therapeutic decision making[2,3].

However, liver biopsy is an invasive procedure with mild and severe complications of 20% and 0.5%, respectively[4,5]. Furthermore, its sensitivity in diagnosing liver cirrhosis is not absolute and the rate of false negative results is approximately 30%[6]. In addition, as it has been well evidenced by the recent studies, an adequate liver specimen should be at least 2.5 cm long[7] and 1.4 mm wide[8] including at least 6-8 portal tracts[9]. This has recently led various groups to investigate the non-invasive methods of detecting severe fibrosis/cirrhosis, including only biochemical (ALT, AST, GGT) tests[10-14] or in combination with hematological (platelet count) tests[15], test panels[16-25], serum "markers" of fibrosis (such as hyaluronic acid or procollagen peptides)[26-30] and ultrasonographic parameters (e.g., liver surface nodularity (LSN), portal blood flow)[31-34], but none of which have proved to be capable of avoiding liver biopsy.

The aim of this prospective study was to evaluate the accuracy of a model based on the sequential combination of a set of simple biochemical tests (Bonacini score, BS)[19,20] and liver surface ultrasound (US) examination[32] in diagnosing severe fibrosis/cirrhosis in a large series of consecutive patients with chronic HCV infection undergoing liver biopsy.

MATERIALS AND METHODS

All anti-HCV positive patients (EIA III, Abbott Laboratories, Chicago, IL, USA) with detectable HCV-RNA serum levels (Amplicor HCV kit, Roche, Molecular Systems, Basel, Switzerland) were evaluated for enrollment between September 2001 and June 2004.

The presence of decompensated liver disease (i.e., portosystemic encephalopathy, jaundice or ascites detected by means of US) and or an absolute contraindication to liver biopsy (PLT <60 000/mm^3, PT <60%) excluded patients from the study, whereas patients with an increase of ≥1.5 UNL in the serum alanine-aminotransferase (ALT) levels recorded twice in the previous 6 months, were included in the study, whose protocol was approved by the pertinent ethics committee after having obtained their written informed consent. Socio-demographic and clinical data were recorded as those on past and/or current alcohol intake for which a semi-quantitative questionnaire with three pre-defined levels of daily consumption (<30, 30-80 and >80 g) was used. At the time of liver biopsy, the laboratory data included AST, ALT (IU/L r.v. <40), platelet count (10^6/μL r.v. 130 000-400 000), the international normalized ratio (INR 0.8-1.2), level of albumin (g/dL r.v. 3.5-5.0), total bilirubin (mg/dL r.v. 0.3-1.0) and hemoglobin (g/dL r.v. 14-18 for men and 12-16 for women), as well as HCV genotyping by means of restriction fragment length polymorphism after amplification of the 5' non-coding region of the HCV genome[35]. As detailed in Table 1, the "cirrhosis discriminant score" (range 0-11) of each patient was calculated according to the method of Bonacini *et al.*[19], based on ALT/AST ratio, platelet count and INR. After an overnight fast, a US liver scan was performed using an ATL HDI 5000 equipment (Advanced Technology Laboratories, Bothell, WA, USA) and both 3.5 and a 5-12 MHz transducer by one of three gastroenterologists (AC, SM or MA) blinded to the clinical, biochemical and histologic data. A 5-12 MHz transducer was used to obtain multiple scans of the outer 2-3 cm of the liver parenchyma and of both lobes. LSN was considered positive when the liver surface appeared as a dotted or an irregular line and/or the liver parenchyma was not homogeneous, with areas of different echogenicity, reflecting an underlying nodularity. The interobserver agreement for this sign was calculated according to K statistics.

A US-guided transcostal or subcostal liver biopsy was performed (by AC or MF) using an 18-gauge needle (Biomol Hospital Service, Pomezia, Rome, Italy). We considered acceptable only specimens ⩾2.0 cm long including >12 portal tracts, that were fixed in formalin and stained with hematoxylin-eosin, silver impregnation for reticulin, and Masson's trichrome or picrosirius red for collagen. In case of inadequacy of the sample, a second biopsy was obtained.

The specimens evaluated by the same pathologist (VM) unaware of the patients' characteristics were staged according to METAVIR scoring system[36], where F0 indicates the lack of fibrosis, F1 corresponds to portal fibrosis without septa, F2 to the presence of few septa, F3 and F4 to the finding of numerous septa without or with cirrhosis, respectively. Histologic findings were considered as the reference standard for the presence and degree of fibrosis.

Table 1 Determinants of Bonacini score

Laboratory	Score						
parameters	0	1	2	3	4	5	6
INR	<1.1	1.1-1.4	>1.4				
ALT/AST ratio	>1.7	1.7-1.2	1.19-0.6	<0.6			
PLT ×1 000 /mm^3	>340	340-280	279-220	219-160	159-100	99-40	<40

Statistical analysis

The pre-test probability of severe fibrosis/cirrhosis (i.e., a staging score 3-4) was estimated to be about 35% on the basis of recent data from comparable series[2,32,37-39]. A predictive model was obtained by the sequential application of the BS and US liver surface examination, which could obtain the post-test probability of severe fibrosis/cirrhosis. As the BS and US signs of LSN could be considered conditionally independent, the probability of severe fibrosis/cirrhosis obtained by calculating the BS has been considered as the pre-test probability before the US examination. The post-test probabilities were calculated on the basis of post-test odds as previously described[40,41]. The values of sensitivity, specificity, positive and negative likelihood ratios (LR+ and LR-) of both BS and US in diagnosing severe fibrosis have been previously defined[19,32].

In detail, three possibilities had to be taken into account. Firstly, for a staging score 0-2, a BS ⩽3 had a sensitivity of 58% and a specificity of 85%, accounting for a LR+ of 4. Accordingly, in our model in the presence of a BS ⩽3, the probability of stage 0-2 increased from a pre-test one of 65% to 88%. Secondly, the sensitivity and specificity for severe fibrosis in the presence of a BS of 4-7 were 50%, making it impossible to modify the 35% pre-test probability of severe fibrosis/cirrhosis on the basis of a LR+ and a LR- of about one. Thirdly, the specificity of 100% for a BS >7 led to an almost absolute post-test probability of staging score 3-4, with a LR+ higher than 100. As far as the US finding of LSN was concerned, an inter-observer variability of 0.80 was reported. Our own previous data[32] demonstrated a sensitivity of 54% and a specificity of 95% for a staging score 3-4, with a LR+ and a LR- of 11.6 and 0.5, respectively. By combining the BS and the US signs of LSN, five groups of patients (I-V) were defined (Figure 1) with different post-test probability of severe fibrosis/cirrhosis. In the last group, with BS ≥7 the post-test probability of a staging score of 3-4 was close to 100% regardless of the US results. Finally, as detailed in Figure 1, to test the predictive accuracy and clinical usefulness of the model, four *clinically acceptable* ranges of post-test probability of severe fibrosis/cirrhosis were predefined based on BS and US findings*: low probability* (<10%), *not diagnostic* (10-74%), *high probability* (75-90%) and *almost absolute probability* (>90%).

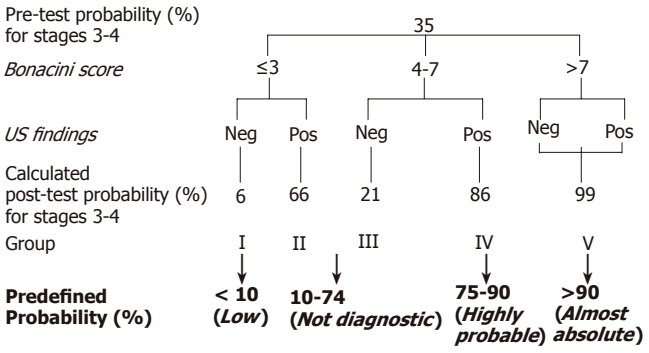

Figure 1 Post-test probability of severe fibrosis/cirrhosis calculated on the basis of both BS and US findings (starting from the pre-test value of 35%), and ranges of post-test probability for severe fibrosis/cirrhosis predefined as "clinically relevant" (in bold).

Table 2 Clinical and biochemical characteristics of 176 consecutive patients with chronic hepatitis C included in

	#	%	Mean±SD
Age (yr)			53.5±21.2
Sex: Male	96	55	
Female	80	45	
BMI (kg/m^2)			25.9±2.9
<25	90	51	
⩾25	86	49	
Alcohol intake (g/d)			
⩽30	142	80	
31-80	24	14	
>80	10	6	
HCV genotype			
1	92	52	
2	60	34	
3	19	11	
4	5	3	
Platelet count			181±128
AST (IU/L)			78.5±101
ALT (IU/L)			125±178
AST/ALT			1.6±1.1
INR			1.05±0.1
Hemoglobin (g/dL)			14.5±2.1
Albumin (g/dL)			4.5±0.6
Bilirubin (mg/dL)			0.9±0.2

RESULTS

During the recruitment period, 1 089 patients were investigated for liver disease, and 363 were chronically infected with HCV. Of them, 184 were excluded for the refusal of liver biopsy (#11) because of already established cirrhosis with Child-Pugh score >5 (#67), or because of normal or slightly elevated ALT levels (<1.5 times the upper normal limit) or uncompleted ALT data (less than six distinct determinations) (#106). The remaining 179 fulfilled the inclusion criteria. Based on the inadequate US findings, three were excluded accounting for an overall recruitment of 176 patients, whose characteristics are detailed in Table 2. The inter-observer agreement for the detection of the LSN sign was 0.77. The average length of liver specimens was 4.1±0.4 cm and in 18 cases a second liver sample was obtained because of the inadequacy of the first one. At liver biopsy, well tolerated in all the cases, 67 patients (38%) had severe fibrosis (#52) or cirrhosis (#15, all in Child's A class). Of the remaining 109 (62%), fibrosis was absent in 6, mild (score 1) in 40 and moderate (score 2) in 63. LSN was present in 9 out of the 109 (8%) patients with a fibrosis score of 0-2 and in 40 out of 67 (60%) with F 3-4 with a sensitivity, specificity, LR+ and LR- of 60%, 92% and 7.5 and 0.5, respectively. Patients' distribution according to the BS and LSN, and corresponding observed frequency (%) of severe fibrosis/cirrhosis (stage 3-4) *vs* expected post-test probability calculated by the model, are shown in Table 3. Overall, the diagnostic accuracy of the model was 86.5% in groups I, IV, and V, accounting for 67% of the patients. Sixteen of one hundred and nineteen patients were incorrectly defined (1 in group I with fibrosis stage ⩾3, 15 in group IV with fibrosis stage <3). In groups II and III (33% of the total), the model did not show any predictive role and did not significantly modify the pre-test probability of severe fibrosis/cirrhosis.

Table 3 Distribution of 176 patients according to Bonacini score and pre-defined grouping

Bonacini score	⩽3	4-7	>7
LSN	-ve	-ve	-ve
	+ve	+ve	+ve
Patients (#)	56	49	0
	8	59	4
Pre-defined	I	III	V
group[1]	II	IV	
F 3-4	1/56	14/49	0
Patients (#)	4/8	44/59	4/4
Observed (%)	2	29	100
Expected[2] (%)	50	76	99
	6	21	
	66	86	

[1]See text and Figure 1; [2]As from Table 1.

DISCUSSION

In this prospective study, we have evaluated the accuracy of a non-invasive predictive model, consisting of the sequential combination of laboratory data score (BS) and US finding of a nodular liver surface, in detecting severe liver fibrosis or cirrhosis in patients with chronic hepatitis C. In clinical practice, it is easy to use the two elements with their operative characteristics individually validated in previous studies[19,20,32]. The BS is based on simple and widely available laboratory tests (ALT, AST, INR and platelet count) that assure its repeatability, and LSN can be easily detected using commercially available US equipment. Previous series using platelet count or ALT and AST level or BS or US can precisely predict the presence or absence of fibrosis but with a low discriminating power; thus, few patients have a very low or high probability of fibrosis, and most of them are in the gray zone of uncertainty[19,20,32]. On the contrary, the sequential model, which is applicable to the vast majority of enrolled patients (98%, because the US examination was technically inadequate in three cases), has been proved to have an adequate discriminating power and an accurate calibration. Its discriminating power is demonstrated by the fact that we were able to divide the patients into three comparable groups: 34% with a very

high (>90%) or low (<10%) probability of severe fibrosis, 33% with a probability ranging between 75% and 90%, and 33% with an uncertain diagnosis (i.e., with a fibrosis score 3-4 probability between 10% and 74%). The precise calibration of the model is demonstrated by the fact that the observed frequency of severe fibrosis/cirrhosis was within the predefined ranges for each group (Table 3).

The validity of the model is further supported by the finding that the 38% frequency of severe fibrosis/cirrhosis in the study population was similar to the theoretical value of 35% assumed by considering series of patients with comparable characteristics, represented by a $\geqslant$1.5 times increase in ALT levels recorded twice during a period of 6 months or more[2,32,37-39].

The operative characteristics of US are slightly different from those indicated by our own recent data[32], which were used for the model. However, the variations in LR+ and LR- remained within the broad confidence intervals of the original estimates and did not critically challenge the calibration of the model. Further studies are needed to assess the generalizability of the model, i.e. its reproducibility and transportability, for which independent validations are advisable.

Although our simple model could detect the presence or absence of severe fibrosis in nearly two-thirds of the patients, thus avoiding the need for liver biopsy, some limitations of the study require further discussion. Because of its intrinsic characteristics, the model was unable to detect moderate (stage 2) fibrosis, which together with grading is relevant in therapeutic decision making. Furthermore, the study seemed to underestimate the diagnostic role of liver biopsy, which was used not only to define staging and grading, but also to detect concomitant pathologies. However, the latter role which is already questionable in patients with liver disease of uncertain etiology[42] was irrelevant in our series of patients with chronic HCV infection. Conversely, liver biopsy still has some limitations in clinical practice, such as the difficulty in obtaining a liver sample of adequate size, as recently reported by some studies[7,8], and which can be considered as representative of the whole liver, given the patchy distribution of liver fibrosis in chronic hepatitis C. The above limitations in our opinion are a major issue in evaluating the diagnostic accuracy of non invasive diagnostic tests compared to liver biopsy. In fact in these types of studies, the major drawback is the imperfection of the reference standard itself, which can significantly affect the estimates of the operative characteristics of the test under investigation. To reduce the possible sample size effect, in the present study we obtained all the liver specimens >3 cm with >12 portal tracts from patients.

Previous studies assessing the individual role of BS and US findings of LSN in detecting severe fibrosis have found that they are inaccurate because their low power of discrimination means that a large proportion of patients still require liver biopsy[19,20,32]. It has recently been shown that the use of laboratory tests[10-16] and specific fibrosis markers, such as hyaluronic acid[26-30], is highly accurate in diagnosing cirrhosis. However, the considerable differences in the study design and the particularly high prevalence of symptomatic cirrhosis sometimes make it difficult to compare these data to our own. It has also recently been shown that relatively complex laboratory scores are accurate in discriminating stage 0-1 from stage 2-4, but fail to confirm severe fibrosis[17-25] although the aim of these studies was to detect patients with minimal or absent fibrosis with stage 3-4 found in only 15% (*vs* 37% in our series), possibly because they included patients with normal ALT levels and a younger age.

Recently, preliminary data from patients with chronic HCV liver disease[43] suggest a promising role of fibroscan [one-dimensional (1-D) transient elastography] in predicting the degree of liver fibrosis with a good accuracy in discriminating stage 0-2 from 3-4, and a LR+ and LR- of 5.7 and 0.16, respectively, similar to those observed in the present series for the US sign of LSN (LR+ and LR- of 7.5 and 0.5, respectively).

In conclusion, our data suggest that the use of liver biopsy to detect severe fibrosis can be avoided in about two-thirds of patients. Furthermore, the model can also be used in patients aged more than 65 years for whom liver biopsy could be questioned.

REFERENCES

1 **Seeff LB,** Hoofnagle JH. National Institutes of Health Consensus Development Conference: management of hepatitis C: 2002. *Hepatology* 2002; **36:** S1-2

2 **Khan MH,** Farrell GC, Byth K, Lin R, Weltman M, George J, Samarasinghe D, Kench J, Kaba S, Crewe E, Liddle C. Which patients with hepatitis C develop liver complications? *Hepatology* 2000; **31:** 513-520

3 **Poynard T,** Ratziu V, Benmanov Y, Di Martino V, Bedossa P, Opolon P. Fibrosis in patients with chronic hepatitis C: detection and significance. *Semin Liver* Dis 2000; **20:** 47-55

4 **Cadranel JF,** Rufat P, Degos F. Practices of liver biopsy in France: results of a prospective nationwide survey. For the Group of Epidemiology of the French Association for the Study of the Liver (AFEF). *Hepatology* 2000; **32:** 477-481

5 **Piccinino F,** Sagnelli E, Pasquale G, Giusti G. Complications following percutaneous liver biopsy. A multicentre retrospective study on 68,276 biopsies. *J Hepatol* 1986; **2:** 165-173

6 **Poniachik J,** Bernstein DE, Reddy KR, Jeffers LJ, Coelho-Little ME, Civantos F, Schiff ER. The role of laparoscopy in the diagnosis of cirrhosis. *Gastrointest Endosc* 1996; **43:** 568-571

7 **Bedossa P,** Dargere D, Paradis V. Sampling variability of liver fibrosis in chronic hepatitis C. *Hepatology* 2003; **38:** 1449-1457

8 **Colloredo G,** Guido M, Sonzogni A, Leandro G. Impact of liver biopsy siza on the histological evaluation of chronic hepatitis: the smaller the sample the milder the disease. *J Hepatol* 2003; **39:** 239-244

9 **Scheuer PG.** Liver biopsy size matter in chronic hepatitis: bigger is better. *Hepatology* 2003; **38:** 1356-1358

10 **Giannini E,** Botta F, Fasoli A, Ceppa P, Risso D, Lantieri PB, Celle G, Testa R. Progressive liver functional impairment is associated with an increase in AST/ALT ratio. *Dig Dis Sci* 1999; **44:** 1249-1253

11 **Sheth SG,** Flamm SL, Gordon FD, Chopra S. AST/ALT ratio predicts cirrhosis in patients with chronic hepatitis C virus infection. *Am J Gastroenterol* 1998; **93:** 44-48

12 **Haber MM,** West AB, Haber AD, Reuben A. Relationship of aminotransferases to liver histological status in chronic hepatitis C. *Am J Gastroenterol* 1995; **90:** 1250-1257

13 **Assy N,** Minuk GY. Serum aspartate but not alanine aminotransferase levels help to predict the histological

features of chronic hepatitis C viral infections in adults. *Am J Gastroenterol* 2000; **95:** 1545-1550

14 **Park GJ,** Lin BP, Ngu MC, Jones DB, Katelaris PH. Aspartate aminotransferase: alanine aminotransferase ratio in chronic hepatitis C infection: is it a useful predictor of cirrhosis? *J Gastroenterol Hepatol* 2000; **15:** 386-390

15 **Pohl A,** Behling C, Oliver D, Kilani M, Monson P, Hassanein T. Serum aminotransferase levels and platelet counts as predictors of degree of fibrosis in chronic hepatitis C virus infection. *Am J Gastroenterol* 2001; **96:** 3142-3146

16 **Myers RP,** De Torres M, Imbert-Bismut F, Ratziu V, Charlotte F, Poynard T. Biochemical markers of fibrosis in patients with chronic hepatitis C: a comparison with prothrombin time, platelet count, and age-platelet index. *Dig Dis Sci* 2003; **48:** 146-153

17 **Imbert-Bismut F,** Ratziu V, Pieroni L, Charlotte F, Benhamou Y, Poynard T. Biochemical markers of liver fibrosis in patients with hepatitis C virus infection: a prospective study. *Lancet* 2001; **357:** 1069-1075

18 **Forns X,** Ampurdanes S, Llovet JM, Aponte J, Quinto L, Martinez-Bauer E, Bruguera M, Sanchez-Tapias JM, Rodes J. Identification of chronic hepatitis C patients without hepatic fibrosis by a simple predictive model. *Hepatology* 2002; **36**: 986-992

19 **Bonacini M,** Hadi G, Govindarajan S, Lindsay KL. Utility of a discriminant score for diagnosing advanced fibrosis or cirrhosis in patients with chronic hepatitis C virus infection. *Am J Gastroenterol* 1997; **92:** 1302-1304

20 **Saadeh S,** Cammell G, Carey WD, Younossi Z, Barnes D, Easley K. The role of liver biopsy in chronic hepatitis C. *Hepatology* 2001; **33:** 196-200

21 **Poynard T,** Munteanu M, Imbert-Bismut F, Charlotte F, Thabut D, Le Calvez S, Messous D, Thibault V, Benhamou Y, Moussalli J, Ratziu V. Prospective analysis of discordant results between biochemical markers and biopsy in patients with chronic hepatitis C. *Clin Chem* 2004; **50:** 1344-1355

22 **Le Calvez S,** Thabut D, Messous D, Munteanu M, Ratziu V, Imbert-Bismut F, Poynard T. The predictive value of Fibrotest vs. APRI for the diagnosis of fibrosis in chronic hepatitis C. *Hepatology* 2004; **39:** 862-863; author reply 863

23 **Wai CT,** Greenson JK, Fontana RJ, Kalbfleisch JD, Marrero JA, Conjeevaram HS, Lok AS. A simple noninvasive index can predict both significant fibrosis and cirrhosis in patients with chronic hepatitis C. *Hepatology* 2003; **38:** 518-526

24 **Sud A,** Hui JM, Farrell GC, Bandara P, Kench JG, Fung C, Lin R, Samarasinghe D, Liddle C, McCaughan GW, George J. Improved prediction of fibrosis in chronic hepatitis C using measures of insulin resistance in a probability index. *Hepatology* 2004; **39:** 1239-1247

25 **Rossi E,** Adams L, Prins A, Bulsara M, de Boer B, Garas G, MacQuillan G, Speers D, Jeffrey G. Validation of the FibroTest biochemical markers score in assessing liver fibrosis in hepatitis C patients. *Clin Chem* 2003; **49:** 450-454

26 **Oberti F,** Valsesia E, Pilette C, Rousselet MC, Bedossa P, Aube C, Gallois Y, Rifflet H, Maiga MY, Penneau-Fontbonne D, Cales P. Noninvasive diagnosis of hepatic fibrosis or cirrhosis. *Gastroenterology* 1997; **113:** 1609-1616

27 **Murawaki Y,** Ikuta Y, Okamoto K, Koda M, Kawasaki H. Diagnostic value of serum markers of connective tissue turnover for predicting histological staging and grading in patients with chronic hepatitis C. *J Gastroenterol* 2001; **36:** 399-406

28 **Murawaki Y,** Koda M, Okamoto K, Mimura K, Kawasaki H. Diagnostic value of serum type IV collagen test in comparison with platelet count for predicting the fibrotic stage in patients with chronic hepatitis C. *J Gastroenterol Hepatol* 2001; **16:** 777-781

29 **McHutchison JG,** Blatt LM, de Medina M, Craig JR, Conrad A, Schiff ER, Tong MJ. Measurement of serum hyaluronic acid in patients with chronic hepatitis C and its relationship to liver histology. Consensus Interferon Study Group. *J Gastroenterol Hepatol* 2000; **15:** 945-951

30 **Xie SB,** Yao JL, Zheng RQ, Peng XM, Gao ZL. Serum hyaluronic acid, procollagen type III and IV in histological diagnosis of liver fibrosis. *Hepatobiliary Pancreat Dis Int* 2003; **2:** 69-72

31 **Gaiani S,** Gramantieri L, Venturoli N, Piscaglia F, Siringo S, D'Errico A, Zironi G, Grigioni W, Bolondi L. What is the criterion for differentiating chronic hepatitis from compensated cirrhosis? A prospective study comparing ultrasonography and percutaneous liver biopsy. *J Hepatol* 1997; **27:** 979-985

32 **Colli A,** Fraquelli M, Andreoletti M, Marino B, Zuccoli E, Conte D. Severe liver fibrosis or cirrhosis: accuracy of US for detection--analysis of 300 cases. *Radiology* 2003; **227:** 89-94

33 **Hirata M,** Akbar SM, Horiike N, Onji M. Noninvasive diagnosis of the degree of hepatic fibrosis using ultrasonography in patients with chronic liver disease due to hepatitis C virus. *Eur J Clin Invest* 2001; **31:** 528-535

34 **Xu Y,** Wang B, Cao H. An ultrasound scoring system for the diagnosis of liver fibrosis and cirrhosis. *Chin Med J (Engl)* 1999; **112:** 1125-1128

35 **Lopez-Labrador FX,** Ampurdanes S, Forns X, Castells A, Saiz JC, Costa J, Bruix J, Sanchez Tapias JM, Jimenez de Anta MT, Rodes J. Hepatitis C virus (HCV) genotypes in Spanish patients with HCV infection: relationship between HCV genotype 1b, cirrhosis and hepatocellular carcinoma. *J Hepatol* 1997; **27:** 959-965

36 **Poynard T,** Bedossa P, Opolon P. Natural history of liver fibrosis progression in patients with chronic hepatitis C. The OBSVIRC, METAVIR, CLINIVIR, and DOSVIRC groups. *Lancet* 1997; **349:** 825-832

37 **Niederau C,** Lange S, Heintges T, Erhardt A, Buschkamp M, Hurter D, Nawrocki M, Kruska L, Hensel F, Petry W, Haussinger D. Prognosis of chronic hepatitis C: results of a large, prospective cohort study. *Hepatology* 1998; **28:** 1687-1695

38 **Patel K,** Gordon SC, Jacobson I, Hezode C, Oh E, Smith KM, Pawlotsky JM, McHutchison JG. Evaluation of a panel of non-invasive serum markers to differentiate mild from moderate-to-advanced liver fibrosis in chronic hepatitis C patients. *J Hepatol* 2004; **41:** 935-942

39 **Camma C,** Di Bona D, Schepis F, Heathcote EJ, Zeuzem S, Pockros PJ, Marcellin P, Balart L, Alberti A, Craxi A. Effect of peginterferon alfa-2a on liver histology in chronic hepatitis C: a meta-analysis of individual patient data. *Hepatology* 2004; **39:** 333-342

40 **Black ER,** Panzer RJ, Mayewski RJ, Griner PF. Characteristics of diagnostic tests and principles for their use in quantitative decision making in diagnostic strategies for common medical problems. In: Black ER., Bordley DR., Tape TG., Panzer RJ eds. Diagnostic strategies for common medical problems. 2nd ed. Philadelphia: *American College of Physicians*, 1999:1-17

41 **Suchman AL,** Dolan JG. Odds and likelihood ratios. In: Black ER., Bordley DR., Tape TG., Panzer RJ. Eds. 2nd ed. Diagnostic strategies for common medical problems. Philadelphia: *American College of Physicians* 1999: 31-36

42 **Sorbi D,** McGill DB, Thistle JL, Therneau TM, Henry J, Lindor KD. An assessment of the role of liver biopsies in asymptomatic patients with chronic liver test abnormalities. *Am J Gastroenterol* 2000; **95:** 3206-3210

43 **Ziol M,** Handra-Luca A, Kettaneh A, Christidis C, Mal F, Kazemi F, de Ledinghen V, Marcellin P, Dhumeaux D, Trinchet JC, Beaugrand M. Noninvasive assessment of liver fibrosis by measurement of stiffness in patients with chronic hepatitis C. *Hepatology* 2005; **41:** 48-54

Science Editor Guo SY **Language Editor** Elsevier HK

PO Box 2345, Beijing 100023, China
www.wjgnet.com
wjg@wjgnet.com

ELSEVIER

World J Gastroenterol 2005;11(46):7323-7329
World Journal of Gastroenterology ISSN 1007-9327

• *RAPID COMMUNICATION* •

Combined carriership of *TLR9* -1237C and *CD14* -260T alleles enhances the risk of developing chronic relapsing pouchitis

KM Lammers, S Ouburg, SA Morré, JBA Crusius, P Gionchetti, F Rizzello, C Morselli, E Caramelli, R Conte, G Poggioli, M Campieri, AS Peña

KM Lammers, P Gionchetti, F Rizzello, C Morselli, M Campieri, Department of Internal Medicine and Gastroenterology, Policlinico S. Orsola, University of Bologna, Bologna, Italy
S Ouburg, SA Morré, JBA Crusius, AS Peña, Laboratory of Immunogenetics, VU University Medical Center, Amsterdam, The Netherlands
E Caramelli, Institute of Histology and General Embryology, University of Bologna, Bologna, Italy
R Conte, Department of Immunohaematology and Blood Transfusion, Policlinico S. Orsola, University of Bologna, Bologna, Italy
AS Peña, Laboratory of Immunogenetics and Department of Gastroenterology, VU University Medical Center, Amsterdam, The Netherlands
G Poggioli, Department of Surgery and Organ Transplantation, Policlinic S. Orsola, University of Bologna, Bologna, Italy
Correspondence to: KM Lammers, Department Internal Medicine and Gastroenterology, Policlinic S. Orsola, University of Bologna, Nuove patologie-Pad. 5, Via Massarenti 9, 40138 Bologna, Italy. kmlammers@hotmail.com
Telephone: +39-51-6364122 Fax: +39-51-392538
Received: 2005-05-02 Accepted: 2005-06-09

CONCLUSION: There is no evidence that the SNPs predispose to the need for IPAA surgery. The significant increase of the combined carriership of the *CD14* -260T and *TLR9* -1237C alleles in the chronic relapsing pouchitis group suggests that these markers identify a subgroup of IPAA patients with a risk of developing chronic or refractory pouchitis.

Key words: Pouchitis; Innate immunity; Single nucleotide polymorphisms; *CD14*; *TLR9*

Lammers KM, Ouburg S, Morré SA, Crusius JBA, Gionchetti P, Rizzello F, Morselli C, Caramelli E, Conte R, Poggioli G, Campieri M, Peña AS. Combined carriership of *TLR9*-1237C and *CD14*-260T alleles enhances the risk of developing chronic relapsing pouchitis. *World J Gastroenterol* 2005; 11(46): 7323-7329
http://www.wjgnet.com/1007-9327/11/7323.asp

Abstract

AIM: To investigate the single nucleotide polymorphisms (SNPs) in genes involved in bacterial recognition and the susceptibility to pouchitis or pouchitis severity.

METHODS: Analyses of *CD14* -260C>T, *CARD15/NOD2* 3020insC, Toll-like receptor (*TLR*)4 +896A>G, *TLR9* -1237T>C, *TLR9*+2848G>A, and *IRAKM* + 22148G>A SNPs were performed in 157 ileal-pouch anal anastomosis (IPAA) patients (79 patients who did not develop pouchitis, 43 infrequent pouchitis patients, 35 chronic relapsing pouchitis patients) and 224 Italian Caucasian healthy controls.

RESULTS: No significant differences were found in SNP frequencies between controls and IPAA patients. However, a significant difference in carriership frequency of the *TLR9*-1237C allele was found between the infrequent pouchitis and chronic relapsing pouchitis groups [$P = 0.028$, odd's ratio (OR) = 3.2, 95%CI = 1.2-8.6]. This allele uniquely represented a 4-locus *TLR9* haplotype comprising both studied *TLR9* SNPs in Caucasians. Carrier trait analysis revealed an enhanced combined carriership of the alleles *TLR9* -1237C and *CD14* -260T in the chronic relapsing pouchitis and infrequent pouchitis group ($P = 0.018$, OR = 4.1, 95%CI = 1.4 -12.3).

INTRODUCTION

Patients with ulcerative colitis may need surgery for their disease and proctocolectomy with ileal-pouch anal anastomosis (IPAA) is the surgical procedure of choice for the management of these patients[1,2]. Most patients undergoing IPAA for severe colitis or chronic continuous disease achieve good functional results, but some patients develop pouchitis, a non-specific idiopathic inflammation of the ileal reservoir. Frequency rates of pouchitis are highly variable, ranging 10-59% depending on the length of follow-up and the diagnostic criteria used[3]. Though the origin of pouchitis remains unknown, genetic and immunological factors are likely to be involved in addition to ileal mucosa that needs to adapt to its new role as a reservoir[4]. This is illustrated by the fact that pouchitis occurs almost exclusively in patients with IPAA for ulcerative colitis and not in patients with IPAA for familial adenomatous polyposis, a hereditary non-inflammatory disease of the colon with high risk of developing colon cancer. An important role of luminal bacteria in the development of pouchitis is underscored by various reports on bacterial overgrowth and dysbiosis in pouchitis[5] and is further confirmed by the efficacy of antibiotic and probiotic therapy[6,7].

Pattern recognition receptors (PRRs), including Toll-like receptors (TLRs), are essential components of the innate

immune system as recognition of microbial products occurs via PRRs that are expressed by innate effector cells. Microbial recognition results in a rapid and efficient immune response against invading microorganisms[8].

Given the role of luminal bacteria in driving the inflammatory response in pouchitis, identification and functional characterization of polymorphisms in innate immunity genes may provide insight in a possible genetically determined susceptibility to pouchitis and/or chronic relapsing pouchitis[9].

CD14 is part of the endotoxin/lipopolysaccharide (LPS) receptor complex[8] and is important in conjunction with TLR4 and with TLR2[10] in the recognition of LPS, a membrane glycolipid on Gram-negative bacteria. CD14 may also recognize cell membrane components of Gram-positive mycobacteria and viruses[11-15]. CD14 exists in a membrane form on monocytes and neutrophils and in a soluble form in serum[16-18]. The SNP at position -260C>T (also known as *CD14*-159C>T) in the promoter region of the *CD14* gene (located on chromosome 5q31) is associated with enhanced transcriptional activity[19] and significantly higher CD14 serum levels[20]. Increased expression of CD14 in macrophages has been found in inflammatory bowel disease (IBD)[21]. An association of the *CD14*-260C>T gene polymorphism with IBD[22,23] and atherosclerosis[24] has been described. Genetically determined variation in CD14 serum levels may have functional consequences given the ability of soluble CD14 to confer pathogen responsiveness to cells such as intestinal, epithelial and endothelial cells that do not express CD14 on their membranes[25].

The *TLR4* gene is located on chromosome 9q32-q33. The *TLR4*+896A>G SNP affects the leucine-rich repeat domain of TLR4 and is associated with hyporesponsiveness to LPS[26] with increased susceptibility to severe bacterial infections and IBD[27] and may predispose to septic shock with Gram-negative microorganisms[28,29].

TLR9 is required for the recognition of CpG motifs, short sequences of unmethylated DNA predominantly present in bacterial DNA. CpG motifs have immunostimulatory activity by inducing dendritic cell maturation, B-cell proliferation and production of cytokines, including interleukin-6 (IL-6) and interleukin-12 (IL-12)[30,31]. TLR9 signaling has been shown to mediate the resolution of intestinal inflammation in experimental colitis[32], suggesting that the release of bacterial DNA from the microflora might favor immune homeostasis. The promoter *TLR9* -1237T>C SNP located on chromosome 3p21.3 is associated with susceptibility to asthma in European Americans, but not in Hispanic or African Americans[33] and the marker D3S1076 in this region shows association with IBD in a classical TDT test[42]. Török and colleagues[34] studied the *TLR9* -1237T>C and *TLR9*+2848 G>A SNPs in German patients with Crohn's disease, ulcerative colitis and healthy blood controls and found that the allele *TLR9* -1237C carrier status is associated with Crohn's disease compared to controls. *TLR9* +2848 G>A allele frequencies are not different between the study groups.

CARD15/NOD2 is a cytoplasmatic bacterial PRR expressed in monocytes and intestinal epithelial cells and mediates response against muramyl dipeptide derived from peptidoglycan[35,36]. The *CARD15/NOD2* gene is located on chromosome 16q12. Three major polymorphisms in this gene (R702W, G908R, and L1007 frameshift mutation) are associated with susceptibility to Crohn's disease, possibly as a result of a defective response against muramyl dipeptide derived from peptidoglycan[37]. Recently, an increased frequency of the L1007 frameshift mutation has been observed in Italian patients with ulcerative colitis when compared to controls[38].

The intracellular domains of TLRs are homologous to the interleukin-1 receptor (IL-1R) type I intracellular domain and use a common pathway of intracellular signaling with shared components including the protein kinase IL-1R-associated kinase1 (IRAK1) and IRAK-M, as a negative regulator of TLR signaling. Cytokine production increases in IRAK-M-/- macrophages after TLR/IL-1 stimulation and bacterial challenge, while endotoxin tolerance reduces in these cells. Furthermore, IRAK-M-/- mice have increased inflammatory responses to bacterial infection and develop intestinal inflammation. These data suggest that IRAK-M has a regulatory function in TLR/IL-1R signaling and innate immune homeostasis[39]. The *IRAKM* (or *IRAK3*) gene is located at chromosome 12q14.2 within the IBD2 region associated with ulcerative colitis[40,41]. Genetic variation in the *IRAKM* gene may be involved in the development of chronic intestinal inflammation. For this reason, we chose to analyze a non-synonymous SNP in exon 5 resulting in an Ile/Val substitution.

A candidate gene approach, based on the determination of frequencies of functional SNPs, can be used to investigate the relevance of genes to the disease susceptibility and severity. Carrier trait analysis investigates combinations of SNPs and allows studying the implication of different SNPs in disease susceptibility and severity as a result of their synergistic action.

The aim of this study was whether SNPs in innate immunity genes could contribute to the susceptibility to pouchitis and/or severity of pouchitis. We chose candidate genes of *CD14, TLR4, TLR9, NOD2/CARD15*, and *IRAKM* for their involvement in bacterial recognition and intracellular signaling pathways.

MATERIALS AND METHODS

Patients

One hundred and fifty-seven unrelated patients with IPAA for ulcerative colitis and 224 healthy blood donors were studied. All individuals were Italian Caucasians. Consent was obtained and the local ethics committee approved the protocol. Their demographic and clinical information is described in Table 1. IPAA patients were subdivided into three test groups according to the pouchitis pattern. One group consisted of IPAA patients who had never developed pouchitis, another group consisted of IPAA patients who had up to two episodes of pouchitis during IPAA (infrequent pouchitis) and third group consisted of IPAA patients who developed three or more episodes of

pouchitis (chronic relapsing pouchitis).

DNA isolation

Venous blood (5-10 mL) was drawn and genomic DNA was isolated using standard protocols. Polymorphisms of the *CD14, TLR4, TLR9, CARD15/NOD2*, and *IRAKM* genes in these three groups were analyzed. Genomic DNA (5-100 ng) was used for each genotyping.

Analysis of gene polymorphisms

Polymerase chain reaction (PCR) for RFLP analyses was performed on a thermal cycler GeneAmp 9700 (Perkin-Elmer Cetus, Norwalk, CT, USA). Digested fragments were analyzed on a 4% agarose gel except for the *IRAKM* SNP analyzed on a 2% agarose gel and visualized with an UV-illuminator after ethidium bromide staining. SNPs were analyzed with the TaqMan assay (Applied Biosystems, Foster City, CA, USA). MGB TaqMan probes and primer pairs were designed with Primer Express software (version 2.0). TaqMan thermocycling consisted of an initial step at 50 ℃ for 2 min and denaturation at 95 ℃ for 10 min followed by 40 cycles of denaturation at 95 ℃ for 15 s and annealing/extension at 60 ℃ for 1 min. We used the ABI Prism 7000 sequence detector (Applied Biosystems) for data acquisition.

Genotyping

CD14-260C>T genotyping (NCBI SNP CLUSTER ID: rs2569190) was performed by PCR. Primers used were: forward primer 5'-TCA CCT CCC CAC CTC TCT T-3' and reverse primer 5'-CCT GCA GAA TCC TTC CTG TT-3'. The PCR conditions were initial denaturation at 95 ℃ for 5 min, followed by 35 cycles of denaturation at 95 ℃ for 30 s, annealing at 59 ℃ for 30 s, extension at 72 ℃ for 1 min and a final extension at 72 ℃ for 5 min followed by cooling to 4 ℃. The 107-bp amplicons were digested overnight with *HaeIII* (New England Biolabs, UK). Digestion resulted in two fragments of 83 and 24 bp (C allele) or 107 bp (T allele), respectively.

Genotyping of the *TLR4*+896 A>G SNP (NCBI SNP CLUSTER ID: rs4986790) was performed with forward primer 5'-TTT ACC CTT TCA ATA GTC ACA CTC A-3' and reverse primer 5'-AGC ATA CTT AGA CTA CTA CCT CCA TG-3'. PCR conditions were: initial denaturation at 94 ℃ for 5 min followed by 35 cycles of denaturation at 94 ℃ for 30 s, annealing at 55 ℃ for 30 s, extension at 72 ℃ for 30 s and a final extension at 72 ℃ for 5 min followed by cooling to 4 ℃. The 102-bp amplicons were digested overnight with *NcoI* (New England Biolabs, UK). Digestion resulted in two fragments of 80 and 22 bp (G allele) or 102 bp (A allele), respectively.

CARD15/NOD2 3020InsC (*CARD15 L1007fs*) (NCBI SNP CLUSTER ID: rs2066847) genotyping was performed with forward primer 5'-GGC AGA AGC CCT CCT GCA GGG CC-3' and reverse primer 5'-CCT CAA AAT TCT GCC ATT CC-3'. PCR conditions were: initial denaturation at 94 ℃ for 5 min followed by 35 cycles of denaturation at 94 ℃ for 30 s, annealing at 59 ℃ for 30 s, extension at 72 ℃ for 45 s and a final extension at 72 ℃ for 5 min followed by cooling to 4 ℃. The 150-bp amplicons were digested overnight with *ApaI*. Digestion resulted in a fragment of 150 bp (no insertion) or 128 bp and 22 bp (insertion C), respectively.

TLR9-1237T>C (NCBI SNP CLUSTER ID: rs5743836) genotyping was performed with TaqMan method. Primers used were: forward primer 5'-GGC CTT GGG ATG TGC TGT T-3' and reverse primer 5'-GGT GAC ATG GGA GCA GAG ACA-3'. Dual-labeled fluorogenic hybridization MGB-probes used were: CTGCCTGAAAACT 5' Fluor Label (FAM, 6-carboxyfluorescein) and CTGGAAACTCCCC 5' Fluor Label (VIC).

TLR9+2848G>A genotyping (NCBI SNP CLUSTER ID: rs352140) was performed with TaqMan method. Primers used were: forward primer 5'-CCG GTC TGC AGG TGC TAG AC-3' and reverse primer 5'-CCA AAG GGC TGG CTG TTG TA-3'. Dual-labeled fluorogenic hybridization MGB probes used were: AGCTACCGCGACTGG 5' Fluor Label (FAM) and AGCTACCACGACTGGA 5' Fluor Label (VIC).

Genotyping of the *IRAKM*+22148G>A exon 5 SNP (NCBI SNP CLUSTER ID: rs1152888) was performed by PCR with forward primer 5´-AGT GGA AC T GAT GTC CTG TGA CAG-3´ and reverse primer 5´-GCA ACA CAT TGA CCT AAT GAC CAG-3´.

The PCR conditions were: initial denaturation at 95 ℃ for 5 min, followed by 35 cycles of denaturation at 95 ℃ for 50 s, at 60 ℃ for 50 s, at 72 ℃ for 150 s and a final extension at 72 ℃ for 5 min followed by cooling to 4 ℃. Digestion overnight with RsaI (Invitrogen Life Technologies) of the 505-bp amplicons resulted in two fragments of 188+317 bp (allele G) or 505 bp (allele A).

Statistical analysis

Hardy-Weinberg equilibrium was determined in healthy controls to assess the Mendelian inheritance. Comparisons of the genotypes between control and different groups of IPAA patients were performed by Fisher's exact or χ^2 two-tailed tests where appropriate. Carrier trait analysis was performed to determine whether combinations of SNPs were acting synergistically on the risk of developing pouchitis or of predisposing to chronic relapsing pouchitis. Adjusted odd's ratio (OR) and 95% confidence intervals (95%CI) were calculated. $P<0.05$ was considered statistically significant.

Table 1 Demographic features of IPAA patients and healthy controls

	IPAA patients	Healthy controls
Total number (*n*)	157	224
Gender M/F	88/69	118/106
Mean age in yr (SD)	42.9 (11.8)	45.8 (12.8)
Range	17-73	21-77
Median	41	45.5

RESULTS

Characteristics of patients and control groups

The demographic features of IPAA patients and healthy

Table 2 Clinical data obtained from IPAA patients

IPAA patients	Mean (SD)	Median	Range
Age (yr) at diagnosis of ulcerative colitis	29.7 (11.7)	27	8-61
Time (yr) from diagnosis of ulcerative colitis to IPAA surgery	6.3 (5.5)	5	0-34
Time from IPAA surgery to first episode of pouchitis			
Total pouchitis group (n = 78)	2.8 (3.1)	2	0-12
Infrequent pouchitis (≤2 episodes, n = 43)	3.7 (3.3)	3	0-12
Chronic relapsing pouchitis (≥3 episodes, n = 35)	2 (2.6)	1	0-12
Pattern of pouchitis			
Duration of pouch (yr)			
No episodes of pouchitis (n = 79)	6.3 (4.1)	5	0-14
Infrequent pouchitis (≤2 episodes, n = 43)	7.6 (3.8)	7	1-16
Chronic relapsing pouchitis (≥3 episodes, n = 35)	7.9 (3.6)	7	2–14

Table 3 Genotypes of the *CD14, CARD15, TLR4, TLR9*, and *IRAKM* gene polymorphisms in subgroups of patients with IPAA and controls

Polymorphisms	Genotype	Controls n = 224 (%)	No pouchitis n = 79 (%)	Infrequent pouchitis n = 43 (%)	Chronic relapsing pouchitis n = 35 (%)
CD14 –260 C>T	CC	55 (24.6)	24 (30.4)	11 (25.6)	7 (20)
	CT	102 (45.5)	34 (43)	21 (48.8)	22 (62.9)
	TT	67 (29.9)	21 (26.6)	11 (25.6)	6 (17.1)
CARD15 3020InsC	WT/WT	218 (97.3)	77 (97.5)	43 (100)	34 (97.1)
	WT/InsC	6 (2.7)	2 (2.5)	0 (0)	1 (2.9)
	InsC/InsC	0 (0)	0 (0)	0 (0)	0 (0)
TLR4 +896 A>G	AA	208 (92.9)	73 (92.4)	38 (88.4)	33 (94.3)
	AG	16 (7.1)	5 (6.3)	5 (11.6)	2 (5.7)
	GG	0 (0)	1 (1.3)	0 (0)	0 (0)
TLR9 –1237 T>C	TT	158 (70.5)	52 (65.8)	34 (79.1)	19 (54.3)
	TC	60 (26.8)	24 (30.4)	9 (20.9)	14 (40)
	CC	6 (2.7)	3 (3.8)	0 (0)	2 (5.7)
TLR9 +2848 G>A	GG	40 (17.9)	20 (25.3)	9 (20.9)	6 (17.1)
	GA	104 (46.4)	38 (48.1)	22 (51.2)	16 (45.7)
	AA	80 (35.7)	21 (26.6)	12 (27.9)	13 (37.2)
IRAKM +22148G>A	GG	181 (80.8)	64 (81)	33 (76.7)	28 (80)
	GA	42 (18.8)	14 (17.7)	7 (16.3)	7 (20)
	AA	1 (0.4)	1 (1.3)	3 (7)	0 (0)

controls are shown in Table 1. No statistical differences were found in the variables including gender and age between the IPAA group and healthy controls.

The clinical characteristics of patients with IPAA for ulcerative colitis were summarized. Information on the pattern of pouchitis within the group of IPAA patients for ulcerative colitis (patients who did not develop a pouchitis, patients who had infrequent pouchitis and patients who suffered from chronic relapsing pouchitis, respectively) is shown in Table 2. No statistically significant differences were found in gender and age between controls and IPAA patients as well as in the duration of pouch and the first episode of pouchitis after IPAA, respectively and among IPAA groups and between infrequent pouchitis and chronic relapsing pouchitis groups.

Genotyping

The genotype frequencies in the control group were in Hardy-Weinberg equilibrium for the *CD14, TLR4, TLR9, CARD15/NOD2,* and *IRAKM* gene polymorphisms. The genotype frequencies of these polymorphisms are described in Table 3. No significant differences in allele-, genotype- or carrier frequencies of the gene polymorphisms were found between the healthy controls and IPAA patients.

No significant differences in allele-, genotype- or carrier frequencies of the gene polymorphisms were found between the three subgroups of IPAA patients except that the carriership of allele *TLR9* -1237 C was more frequent in patients with chronic relapsing pouchitis (45.7%) as compared to those with infrequent pouchitis (20.9%) (P =0.028, OR = 3.2, 95%CI = 1.2-8.6). When the combined groups of infrequent pouchitis and chronic relapsing pouchitis (i.e. total pouchitis group) were compared to the patients without pouchitis, carriership of this allele was not significantly different (P = 0.87, OR = 1.1, 95%CI = 0.6-2.1).

TLR9 haplotype

The two analyzed *TLR9* SNPs were chosen based on the study of Lazarus *et al*.[33] in which a set of four frequent *TLR9* SNPs designated as *TLR9* -1486, *TLR9* -1237, *TLR9* +1174, and *TLR9* +2848, were described. Genotyping of both *TLR9* -1237 and *TLR9* +2848 could distinguish all four-locus haplotypes commonly present in the European American population. We therefore calculated the haplotypic genotypes in Italian Caucasians (Table 4). The haplotype frequencies in the healthy controls were identical to the European-Americans as reported by Lazarus *et al*.[33].

Table 4 Frequencies of *TLR9* haplotypes formed by -1237 T>C and +2848 G>A SNPs

TLR9 -1237	TLR9 +2848	Haplotype	Controls	No pouchitis	Infrequent pouchitis	Chronic relapsing pouchitis
			2*n* = 448	2*n* = 158	2*n* = 86	2*n* = 70
T	G	I	181 (40)	51 (32)	40 (47)	28 (40)
T	A	II	195 (44)	77 (49)	37 (43)	24 (34)
C	A	III	69 (15)	29 (18)	9 (10)[1]	18 (26)[1]
C	G	IV	3 (1)	1 (1)	0	0

[1]*P* = 0.018, OR = 3.0, 95%CI = 1.2-7.1.

Haplotype III was more frequent in chronic relapsing pouchitis as compared to infrequent pouchitis (*P* = 0.018; OR = 3.0, 95%CI = 1.2-7.1). This haplotype, however, did not show nucleotides uniquely present (tag SNPs) on position -1486 (allele T present in haplotypes I and III) or on position +1174 (allele G present in haplotypes II and III), indicating that allele *TLR9*-1237C could provide the strongest association.

Carrier trait analysis

To investigate if SNPs in different genes could act synergistically on disease susceptibility and/or severity, carrier trait analysis with the associated *TLR9* allele was performed. Simultaneous carriership of alleles *TLR9* -1237C and *CD14* -260T was more frequent in patients with chronic relapsing pouchitis as compared to those with infrequent pouchitis (*P* = 0.018, OR = 4.1, 95%CI = 1.4-12.3), which was more significant as compared to the analysis of allele *TLR9* -1237C alone (*P* = 0.028, OR = 3.2, 95%CI = 1.2-8.6). No other significant carrier traits were observed.

DISCUSSION

There is convincing evidence that enteric bacteria play a role in driving the inflammatory response in IBD and that genetic factors contribute not only to the pathogenesis but also to the course and extent of these disorders. Given these processes, we investigated whether polymorphisms in the following genes encoding for proteins involved in innate immunity, *TLR4* +896 A>G, *TLR9* +2848 G>A, *TLR9* -1237T>C, *CD14* -260C>T, *CARD15/NOD2* 3020insC, and *IRAKM* +22148 G>A, were associated with the development of pouchitis, disease frequency or severity.

Analysis of the three subgroups of IPAA patients (i.e. patients who never developed pouchitis, patients with infrequent pouchitis and patients with a chronic refractory form of pouchitis) revealed a positive association of allele *TLR9* -1237C with the risk of developing chronic refractory pouchitis, once these patients developed pouchitis. Haplotype analysis showed that out of the four SNPs defining *TLR9* haplotypes, this allele was uniquely responsible for this finding. Subsequently, we investigated whether interactions of allele *TLR9* -1237C with SNPs in the other candidate genes might strengthen this association. Carrier trait analysis revealed that an even stronger association was apparent with the combination of alleles *TLR9* -1237C and *CD14* -260T. These data suggest that this combination of alleles might be a valuable genetic marker to identify a clinical subgroup of IPAA patients with an enhanced risk of developing chronic pouchitis, compared to alleles of the SNPs *TLR4* +896 A>G, *TLR9* +2848 G>A, *CARD15/NOD2* 3020insC, and *IRAKM* +22148 G>A.

It cannot be excluded that the group of patients who did not develop pouchitis consisted of a mixture of patients who never developed pouchitis on the one hand and patients who proceeded to the infrequent or chronic relapsing pouchitis group on the other hand. This could explain why we did not detect an association of allele *TLR9* -1237C between the no-pouchitis and the chronic relapsing pouchitis groups. It should be noted that no significant differences were found in the mean duration of IPAA between the three groups.

At present it is unknown as to what effect of the *TLR9*-1237 T>C SNP exerts on the expression of *TLR9* given its location in the far promoter region where no DNA-binding site for known transcription factors is apparent. The association observed might therefore result from linkage disequilibrium with another polymorphism(s) in a nearby gene.

The mechanism underlying increased risk of developing chronic relapsing pouchitis by a combined carriership of alleles *TLR9* -1237C and *CD14* -260T might be a dysfunction in bacterial recognition or a lack of an adequate immune response to bacterial challenge. This could start at the level of the plasmacytoid dendritic cells, which play a central role in bacterial recognition, selectively express *TLR9* and have soluble *CD14* facilitating reactivity to a broad array of bacterial components[43] or at the level of the intestinal epithelium. Soluble *CD14* might confer epithelial cell responsiveness[25].

The regulatory role of dendritic cells is of particular importance in the intestine where the mucosal immune system is closely associated with the external environment[44]. Dendritic cells sample bacterial products either indirectly via M cells or directly by reaching between epithelial cells into the gut lumen[45]. In this perspective, it is noteworthy to mention a recent article that reported a lack of immature blood dendritic cells, which possibly migrate to the gut in IBD patients with active disease[46].

Recently, carriership of the *TLR9* -1237C allele has been associated with Crohn's disease[34]. Ileal involvement is present in about 60% of patients with Crohn's disease. Since the pouch is an ileal reservoir that is more vulnerable to the continuous contact with high bacterial titers, it could

be hypothesized that carriership of the allele *TLR9* -1237C (with or without *CD14* -260T) is associated with an impaired immune response at the level of the ileal tissue. Paneth cells are located in the crypts and are central in host defense to luminal bacteria by releasing antimicrobial substances[47,48].

If this is true, carriership of allele *TLR9* -1237C may become an important predictive marker to the enhanced risk of developing refractory chronic pouchitis and eventually pouch failure.

SNPs in different genes might work synergistically and constitute a small to moderate relative risk of developing diseases. Though the observations we described in this article were based on a relatively less number of patients, it should be realized that this study might represent one of the largest series available.

In conclusion, our data suggest that the alleles *TLR9*-1237C and *CD14*-260T synergistically enhance the risk of developing chronic relapsing pouchitis and eventually pouch failure in ulcerative colitis patients who need surgical intervention. Larger studies are required to determine whether this allelic combination becomes a valuable predictive marker and functional studies on the biological role of TLR9 and CD14 in pouchitis.

ACKNOWLEDGMENTS

We are indebted to Italian patients and healthy controls for their participation in this study. S.A. Morré was supported by Tramedico BV, the Netherlands, the Falk Foundation, Germany; the Foundation of Immunogenetics, The Netherlands; the Department of Internal Medicine of the VU University Medical Centre, the Netherlands. We thank Jolein Pleijster and Roel Heijmans for excellent technical assistance in the genotyping.

REFERENCES

1 **Pemberton JH,** Kelly KA, Beart RW Jr, Dozois RR, Wolff BG, Ilstrup DM. Ileal pouch-anal anastomosis for chronic ulcerative colitis. Long-term results. *Ann Surg* 1987; **206:** 504-513
2 **Nicholls RJ,** Moskowitz RL, Shepherd NA. Restorative proctocolectomy with ileal reservoir. *Br J Surg* 1985; **72 Suppl:** S76-579
3 **Gionchetti P,** Amadini C, Rizzello F, Venturi A, Poggioli G, Campieri M. Probiotics for the treatment of postoperative complications following intestinal surgery. *Best Pract Res Clin Gastroenterol* 2003; **17:** 821-831
4 **Sandborn WJ,** Tremaine WJ, Batts KP, Pemberton JH, Phillips SF. Pouchitis after ileal pouch-anal anastomosis: a Pouchitis Disease Activity Index. *Mayo Clin Proc* 1994; **69:** 409-415
5 **Ruseler-van Embden JG,** Schouten WR, van Lieshout LM. Pouchitis: result of microbial imbalance? *Gut* 1994; **35:** 658-664
6 **Gionchetti P,** Rizzello F, Venturi A, Brigidi P, Matteuzzi D, Bazzocchi G, Poggioli G, Miglioli M, Campieri M. Oral bacteriotherapy as maintenance treatment in patients with chronic pouchitis: a double-blind, placebo-controlled trial. *Gastroenterology* 2000; **119:** 305-309
7 **Mimura T,** Rizzello F, Helwig U, Poggioli G, Schreiber S, Talbot IC, Nicholls RJ, Gionchetti P, Campieri M, Kamm MA. Once daily high dose probiotic therapy (VSL#3) for maintaining remission in recurrent or refractory pouchitis. *Gut* 2004; **53:** 108-114
8 **Wright SD,** Ramos RA, Tobias PS, Ulevitch RJ, Mathison JC. CD14, a receptor for complexes of lipopolysaccharide (LPS) and LPS binding protein. *Science* 1990; **249:** 1431-1433
9 **Shen B,** Lashner B. Can we immunogenotypically and immunophenotypically profile patients who are at risk for pouchitis? *Am J Gastroenterol* 2004; **99:** 442-444
10 **Medzhitov R,** Preston-Hurlburt P, Janeway CA Jr. A human homologue of the Drosophila Toll protein signals activation of adaptive immunity. *Nature* 1997; **388:** 394-397
11 **Cleveland MG,** Gorham JD, Murphy TL, Tuomanen E, Murphy KM. Lipoteichoic acid preparations of gram-positive bacteria induce interleukin-12 through a CD14-dependent pathway. I*nfect Immun* 1996; ***64:*** 1906-1912
12 **Dobrovolskaia MA,** Vogel SN. Toll receptors, CD14, and macrophage activation and deactivation by LPS. *Microbes Infect* 2002; **4:** 903-914
13 **Kurt-Jones EA,** Popova L, Kwinn L, Haynes LM, Jones LP, Tripp RA, Walsh EE, Freeman MW, Golenbock DT, Anderson LJ, Finberg RW. Pattern recognition receptors TLR4 and CD14 mediate response to respiratory syncytial virus. *Nat Immunol* 2000; **1:** 398-401
14 **Vignal C,** Guerardel Y, Kremer L, Masson M, Legrand D, Mazurier J, Elass E. Lipomannans, but not lipoarabinomannans, purified from Mycobacterium chelonae and Mycobacterium kansasii induce TNF-alpha and IL-8 secretion by a *CD14*-toll-like receptor 2-dependent mechanism. *J Immunol* 2003; **171:** 2014-2023
15 **Compton T,** Kurt-Jones EA, Boehme KW, Belko J, Latz E, Golenbock DT, Finberg RW. Human cytomegalovirus activates inflammatory cytokine responses via CD14 and Toll-like receptor 2. *J Virol* 2003; **77:** 4588-4596
16 **Frey EA,** Miller DS, Jahr TG, Sundan A, Bazil V, Espevik T, Finlay BB, Wright SD. Soluble CD14 participates in the response of cells to lipopolysaccharide. *J Exp Med* 1992; **176:** 1665-1671
17 **Hailman E,** Vasselon T, Kelley M, Busse LA, Hu MC, Lichenstein HS, Detmers PA, Wright SD. Stimulation of macrophages and neutrophils by complexes of lipopolysaccharide and soluble CD14. *J Immunol* 1996; **156:** 4384-4390
18 **Landmann R,** Knopf HP, Link S, Sansano S, Schumann R, Zimmerli W. Human monocyte CD14 is upregulated by lipopolysaccharide. *Infect Immun* 1996; **64:** 1762-1769
19 **LeVan TD,** Bloom JW, Bailey TJ, Karp CL, Halonen M, Martinez FD, Vercelli D. A common single nucleotide polymorphism in the CD14 promoter decreases the affinity of Sp protein binding and enhances transcriptional activity. *J Immunol* 2001; **167:** 5838-5844
20 **Baldini M,** Lohman IC, Halonen M, Erickson RP, Holt PG, Martinez FD. A Polymorphism* in the 5' flanking region of the CD14 gene is associated with circulating soluble CD14 levels and with total serum immunoglobulin E. *Am J Respir Cell Mol Biol* 1999; **20:** 976-983
21 ***Grimm MC,*** Pavli P, Van de Pol E, Doe WF. Evidence for a CD14+ population of monocytes in inflammatory bowel disease mucosa--implications for pathogenesis. *Clin Exp Immunol* 1995; **100:** 291-297
22 **Obana N,** Takahashi S, Kinouchi Y, Negoro K, Takagi S, Hiwatashi N, Shimosegawa T. Ulcerative colitis is associated with a promoter polymorphism of lipopolysaccharide receptor gene, CD14. *Scand J Gastroenterol* 2002; **37:** 699-704
23 **Klein W,** Tromm A, Griga T, Fricke H, Folwaczny C, Hocke M, Eitner K, Marx M, Duerig N, Epplen JT. A polymorphism in the CD14 gene is associated with Crohn disease. *Scand J Gastroenterol* 2002; **37:** 189-191
24 **Hubacek JA,** Rothe G, Pit'ha J, Skodova Z, Stanek V, Poledne R, Schmitz G. C(-260)-->T polymorphism in the promoter of the CD14 monocyte receptor gene as a risk factor for myocardial infarction. *Circulation* 1999; **99:** 3218-3220

25 **Vercelli D.** Learning from discrepancies: CD14 polymorphisms, atopy and the endotoxin switch. *Clin Exp Allergy* 2003; **33:** 153-155

26 **Arbour NC,** Lorenz E, Schutte BC, Zabner J, Kline JN, Jones M, Frees K, Watt JL, Schwartz DA. TLR4 mutations are associated with endotoxin hyporesponsiveness in humans. *Nat Genet* 2000; **25:** 187-191

27 **Franchimont D,** Vermeire S, El Housni H, Pierik M, Van Steen K, Gustot T, Quertinmont E, Abramowicz M, Van Gossum A, Deviere J, Rutgeerts P. Deficient host-bacteria interactions in inflammatory bowel disease? The toll-like receptor (TLR)-4 Asp299gly polymorphism is associated with Crohn's disease and ulcerative colitis. *Gut* 2004; **53:** 987-992

28 **Agnese DM,** Calvano JE, Hahm SJ, Coyle SM, Corbett SA, Calvano SE, Lowry SF. Human toll-like receptor 4 mutations but not CD14 polymorphisms are associated with an increased risk of gram-negative infections. *J Infect Dis* 2002; **186:** 1522-1525

29 **Lorenz E,** Mira JP, Frees KL, Schwartz DA. Relevance of mutations in the TLR4 receptor in patients with gram-negative septic shock. *Arch Intern Med* 2002; ***162:*** 1028-1032

30 **Krieg AM,** Yi AK, Matson S, Waldschmidt TJ, Bishop GA, Teasdale R, Koretzky GA, Klinman DM. CpG motifs in bacterial DNA trigger direct B-cell activation. *Nature* 1995; **374:** 546-549

31 **Klinman DM,** Yi AK, Beaucage SL, Conover J, Krieg AM. CpG motifs present in bacteria DNA rapidly induce lymphocytes to secrete interleukin 6, interleukin 12, and interferon gamma. *Proc Natl Acad Sci USA* 1996; **93:** 2879-8283

32 **Rachmilewitz D,** Katakura K, Karmeli F, Hayashi T, Reinus C, Rudensky B, Akira S, Takeda K, Lee J, Takabayashi K, Raz E. Toll-like receptor 9 signaling mediates the anti-inflammatory effects of probiotics in murine experimental colitis. *Gastroenterology* 2004; **126:** 520-528

33 **Lazarus R,** Klimecki WT, Raby BA, Vercelli D, Palmer LJ, Kwiatkowski DJ, Silverman EK, Martinez F, Weiss ST. Single-nucleotide polymorphisms in the Toll-like receptor 9 gene (*TLR9*): frequencies, pairwise linkage disequilibrium, and haplotypes in three U.S. ethnic groups and exploratory case-control disease association studies. *Genomics* 2003; **81:** 85-91

34 **Torok HP,** Glas J, Tonenchi L, Bruennler G, Folwaczny M, Folwaczny C. Crohn's disease is associated with a toll-like receptor-9 polymorphism. *Gastroenterology* 2004; **127:** 365-366

35 **Inohara N,** Ogura Y, Fontalba A, Gutierrez O, Pons F, Crespo J, Fukase K, Inamura S, Kusumoto S, Hashimoto M, Foster SJ, Moran AP, Fernandez-Luna JL, Nunez G. Host recognition of bacterial muramyl dipeptide mediated through NOD2. Implications for Crohn's disease. *J Biol Chem* 2003; **278:** 5509-5512

36 **Girardin SE,** Boneca IG, Viala J, Chamaillard M, Labigne A, Thomas G, Philpott DJ, Sansonetti PJ. Nod2 is a general sensor of peptidoglycan through muramyl dipeptide (MDP) detection. *J Biol Chem* 2003; **278**: 8869-8872

37 **Bonen DK,** Cho JH. The genetics of inflammatory bowel disease. *Gastroenterology* 2003; **124:** 521-536

38 **Andriulli A**, Annese V, Latiano A, Palmieri O, Fortina P, Ardizzone S, Cottone M, D'Inca R, Riegler G. The frame-shift mutation of the NOD2/CARD15 gene is significantly increased in ulcerative colitis: an *IG-IBD study. *Gastroenterology* 2004; **126:** 625-627

39 **Kobayashi K,** Hernandez LD, Galan JE, Janeway CA Jr, Medzhitov R, Flavell RA. IRAK-M is a negative regulator of Toll-like receptor signaling. *Cell* 2002; **110:** 191-202

40 **Hampe J,** Schreiber S, Shaw SH, Lau KF, Bridger S, Macpherson AJ, Cardon LR, Sakul H, Harris TJ, Buckler A, Hall J, Stokkers P, van Deventer SJ, Nurnberg P, Mirza MM, Lee JC, Lennard-Jones JE, Mathew CG, Curran ME. A genomewide analysis provides evidence for novel linkages in inflammatory bowel disease in a large European cohort. *Am J Hum Genet* 1999; **64:** 808-816

41 **Duerr RH,** Barmada MM, Zhang L, Davis S, Preston RA, Chensny LJ, Brown JL, Ehrlich GD, Weeks DE, Aston CE. Linkage and association between inflammatory bowel disease and a locus on chromosome 12. *Am J Hum Genet* 1998; **63:** 95-100

42 **Hampe J,** Lynch NJ, Daniels S, Bridger S, Macpherson AJ, Stokkers P, Forbes A, Lennard-Jones JE, Mathew CG, Curran ME, Schreiber S. Fine mapping of the chromosome 3p susceptibility locus in inflammatory bowel disease. *Gut* 2001; **48:** 191-197

43 **Rothenfusser S,** Tuma E, Endres S, Hartmann G. Plasmacytoid dendritic cells: the key to CpG. *Hum Immunol* 2002; **63:** 1111-1119

44 **Stagg AJ,** Hart AL, Knight SC, Kamm MA. The dendritic cell: its role in intestinal inflammation and relationship with gut bacteria. *Gut* 2003; **52:** 1522-1529

45 **Rescigno M,** Urbano M, Valzasina B, Francolini M, Rotta G, Bonasio R, Granucci F, Kraehenbuhl JP, Ricciardi-Castagnoli P. Dendritic cells express tight junction proteins and penetrate gut epithelial m`onolayers to sample bacteria. *Nat Immunol* 2001; **2:** 361-367

46 **Baumgart DC,** Metzke D, Schmitz J, Scheffold A, Sturm A, Wiedenmann B, Dignass AU. Patients with active inflammatory bowel disease lack immature peripheral blood plasmacytoid and myeloid dendritic cells. *Gut* 2005; **54:** 228-236

47 **Rumio C, Besusso D,** Palazzo M, Selleri S, Sfondrini L, Dubini F, Menard S, Balsari A. Degranulation of paneth cells via toll-like receptor 9. *Am J Pathol* 2004; **165:** 373-381

48 **Ogura Y,** Lala S, Xin W, Smith E, Dowds TA, Chen FF, Zimmermann E, Tretiakova M, Cho JH, Hart J, Greenson JK, Keshav S, Nunez G. Expression of NOD2 in Paneth cells: a possible link to Crohn's ileitis. *Gut* 2003; **52:** 1591-1597

Science Editor Wang XL **Language Editor** Elsevier HK

PO Box 2345, Beijing 100023, China
www.wjgnet.com
wjg@wjgnet.com

ELSEVIER

World J Gastroenterol 2005;11(46):7330-7334
World Journal of Gastroenterology ISSN 1007-9327

• *RAPID COMMUNICATION* •

Impairment of IFN-α production capacity in patients with hepatitis C virus and the risk of the development of hepatocellular carcinoma

Kazuko Uno, Yoshiki Suginoshita, Kazuhiro Kakimi, Fuminori Moriyasu, Mayumi Hirosaki, Taro Shirakawa, Tsunataro Kishida

Kazuko Uno, Tsunataro Kishida, Louis Pasteur Center for Medical Research, Kyoto, Japan
Yoshiki Suginoshita, Kazuhiro Kakimi, Fuminori Moriyasu, Department of Gastroenterology and Hepatology, Faculty of Medicine, Kyoto University, Kyoto, Japan
Mayumi Hirosaki, Taro Shirakawa, Department of Health Promotion and Human Behavior, Kyoto University Graduate School of Public Health, Kyoto, Japan
Supported by a grant-in-aid for Scientific Research from the Ministry of Education, Science, Sports and Culture of Japan (No.17606005 and 16201041), and a Research Grant for Allergic Disease and Immunology from the Ministry of Health, Labour and Welfare of Japan (H16-Immunology-002)
Correspondence to: Kazuko Uno, Louis Pasteur Center for Medical Research, 103-5, Tanaka-monzen-cho, Sakyo-ku, Kyoto, 606, Japan. kazukouno@louis-pasteur.or.jp
Telephone: +81-75-7917726 Fax: +81-75-7151071
Received: 2005-03-17 Accepted: 2005-07-15

Abstract

AIM: To determine the utility of interferon (IFN) -α production capacity in patients with hepatitis C virus (HCV) infection for the measurement of immuno-surveillance potential and for the early detection of hepatocellular carcinoma (HCC) by investigating the Sendai virus (HVJ) stimulated IFN-α production capacity of patients with HCV infection.

METHODS: HVJ stimulated IFN-α production was determined in a large number of patients with HCV infection and the development of HCC was monitored for 3 years in patients with liver cirrhosis (LC).

RESULTS: IFN-α production capacity decreases gradually with the progression of liver disease from chronic hepatitis (CH) to HCC. A significant correlation between the duration of HCV infection and impaired IFN-α production capacity was observed. IFN-α production in patients who developed HCC within 3 years was significantly lower than that of patients who remained in LC without developing HCC.

CONCLUSION: Measurement of IFN-α production in LC patients may be useful for the early detection of HCC.

Key words: IFN-α production capacity; Hepatitis C virus; Hepatocellular carcinoma

Uno K, Suginoshita Y, Kakimi K, Moriyasu F, Hirosaki M, Shirakawa T, Kishida T. Impairment of IFN-α production capacity in patients with hepatitis C virus and the risk of the development of hepatocellular carcinoma. *World J Gastroenterol* 2005; 11(46): 7330-7334
http://www.wjgnet.com/1007-9327/11/7330.asp

INTRODUCTION

The natural history of chronic hepatitis C virus (HCV) infection entails a gradual progression from chronic hepatitis (CH) to liver cirrhosis (LC) over 10-20 years leading to hepatocellular carcinoma (HCC) within 30 years[1-3]. Some common factors influencing the development of HCC include the degree of liver fibrosis, old age, sex (male), high alanine aminotransferase (ALT) level and a history of diabetes and alcohol consumption[4,5]. In addition, the development of HCC is affected by viral factors[6] and host immune factors[7]. Although recent progress in hepatitis research has illustrated the role of viral factors, analysis of the role if any played by immune factors has been insufficient. Several investigators have discussed the impairment of NK cell function, cytotoxic T lymphocyte (CTL) function and dendritic cell (DC) function in hepatitis C patients[8-11].

In previous papers, we have reported about the impairment of HVJ induced IFN-α production in whole blood cultures of patients with lung cancer, mylodysplastic syndrome, pulmonary tuberculosis, HIV, diabetes mellitus and IgA nephritis[12,13]. Additionally, we mentioned that IFN-α production in patients with lung cancer gradually decreases with the progress of cancer[12]. In the present study, we examined the IFN-α production in a large number of patients with HCV infection and LC who were monitored for more than 3 years for the development of HCC. IFN-α production in patients who developed HCC within 3 years was significantly lower than that of patients who remained in LC without developing HCC. These results suggest that IFN-α production could be a parameter with promising anti-tumor immuno-surveillance potential, i.e., measurement of IFN-α production in patients with HCV infection may be useful for the early detection of HCC.

MATERIALS AND METHODS

Subjects

IFN-α production in whole blood cultures was measured

in 155 healthy individuals and 82 patients with chronic HCV infection including CH, LC and HCC. Blood was drawn after receiving informed consent.

The patients with HCV infection were all outpatients at Kyoto University Hospital, and were followed up at least once a month from 1994. All patients tested positive for anti-HCV (Abbot Japan, Tokyo) and/or HCV RNA by RT-PCR. The diagnoses of CH, LC and HCC were made by conducting a comprehensive analysis of liver histology, image analysis and blood tests. Patients underwent abdominal ultrasonography every 3-6 mo and/or contrast enhanced computed tomography every 6-12 mo. The CH group included 27 men and 12 women (age, 48.9±12.2 years). The LC group included 11 men and 10 women (age, 64.0±7.5 yeas). The HCC group included 13 men and 9 women (age, 64.1±5.4 years). Patients with HCV infection had not received interferon therapy for at least 3 mo prior to the measurement of IFN production capacity. In the case of patients with HCC, the IFN production capacity values of patients used were those determined at the point of first diagnosis of HCC.

We selected age-matched healthy persons as controls for comparison with the patients with HCV infection. Healthy subjects, 30 men (age, 53.6±8.9 years) and 95 women (age, 53.2±7.6 years), were selected from the people receiving medical examinations at the clinic of the Louis Pasteur Center for Medical Research who were over 40 years of age and had no acute and/or chronic disease and no abnormal values in blood tests.

Measurement of IFN-α production capacity in human whole blood

Two milliliters of heparinized blood was cultured with 500 HA U/mL Sendai virus (HVJ) within 5 h after the withdrawal of blood. The blood-virus mixture was incubated at 37 ℃ for 20 h. Supernatants were harvested by centrifugation at 3 000 r/min for 10 min. IFN-α activity in the supernatants was determined by bioassay as mentioned in a previous paper[12].

Statistical analysis

Results were expressed as mean±SD. Statistical significance was tested by Student's *t*-test. For multiple comparisons, one-way analysis of variance (ANOVA) or the χ^2 test was used, when appropriate.

RESULTS

IFN-α production capacity in patients with chronic HCV infection in the various stages

A previous study has reported that there was a significant difference in IFN-α production between men and women, but that the IFN-α production capacity per 1 000 leukocytes (WBC) did not differ significantly between men and women throughout various groups[12]. In this study, IFN-α production capacity in various stages is expressed as IFN-α production per 1 000 WBC for comparing each stage, normalized for any difference between men and women. We found that IFN-α production capacity per 1 000 WBC decreased with the progression of the disease (healthy control: 1.54±0.57, CH: 1.41±1.01; LC: 0.89±0.49; HCC: 0.87±0.45 IU/1 000 WBC) (Figure 1). Using ANOVA,we found that HCV groups showed a significantly lower IFN-α titer as compared with the control group.

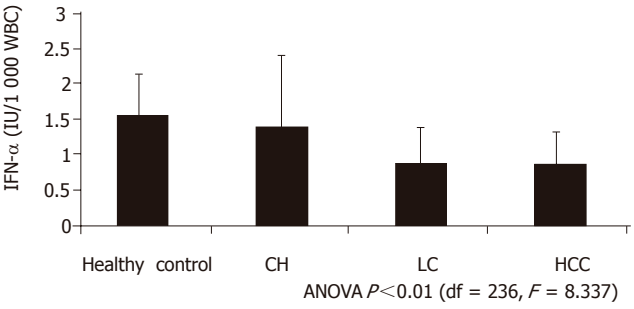

Figure 1 IFN-α production capacity per 1 000 WBC in patients with persistent HCV infection in various stages.

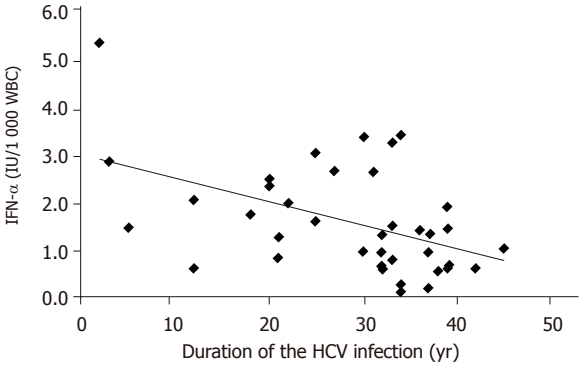

Figure 2 IFN-α production capacity per 1 000 WBC and duration of HCV infection.

IFN-α production capacity per 1 000 WBC and the duration from HCV infection by blood transfusion

It has been reported that a significant correlation exists between the incidence of HCC and the duration of HCV infection[1-3]. As the time of initial infection is precisely known for patients who were infected while undergoing transfusion, we chose HCV patients infected in this manner. We then looked at the relationship between the patient's IFN-α production capacity and the duration of the HCV infection (Figure 2). A significant correlation between the duration of HCV infection and impaired IFN-α production capacity per 1 000 WBC was observed (n = 39, r = 0.48, P = 0.0019). We could not find any significant correlation between platelet number, which was a surrogate marker for liver fibrosis, and ALT and AST levels, which were markers for the activity grade.

Table 1a IFN-α production capacity and the risk of HCC development within 3 years of LC

		Group A	Group B
n		11	10
Age	(yr)	63.6 ± 8.3	64.6 ± 6.7
IFN-α	(IU/mL	2 406 ± 1 239	3 936 ± 2 284
IFN-α/WBC	(IU/1 000 WBC)	0.66 ± 0.32	1.14 ± 0.53[a]
AST(GOT)	(IU/mL)	97.0 ± 52.7	55.9 ± 21.3[a]
ALT(GPT)	(IU/mL)	99.2 ± 47.0	54.8 ± 22.4[b]
Plt	(x103/μL)	79.8 ± 44.8	93.6 ± 39.2

[a]$P<0.05$, [b]$P<0.01$

IFN-α production capacity and the risk of HCC development within 3 years of LC

We measured IFN-α production capacity in the LC group. After 3 years, we divided the original group into two, according to whether each patient developed HCC or not. We observed a significant difference ($P<0.05$) in the initial IFN-α production capacity per 1 000 WBC between the patients who developed HCC (Group A, $n = 11$) and those who remained in LC without developing HCC (Group B, $n = 10$). In addition, we observed significant differences in AST and ALT levels as well as IFN-α production capacity per 1 000 WBC between the two groups (Table 1a).

Since the mean IFN-α production value of the HCC patients was 0.87±0.45 IU/1 000 WBC, we divided the LC group into two sub-groups: patients with IFN-α production value greater or less than the mean value (0.87 IU/1 000 WBC) (Table 1b). After 3 years, we determined whether each patient had developed HCC or not. Compared to the 22% of patients in the high titer group, 75% of patients in the low titer group developed HCC. The c2 test showed significant differences between the two groups ($P<0.05$). These results indicated that LC patients with a low IFN-α production capacity (<0.87 IU/1 000 WBC) had a high risk of developing HCC within 3 years. Although low IFN-α production and high AST and ALT values, HCV copies and genotypes were demonstrated as risk factors of HCC development, no correlations were found between IFN-α production and these factors.

DISCUSSION

In this study, we have demonstrated that (1) HVJ-stimulated IFN-α production capacity decreased gradually with the progression of HCV infection from CH to LC to HCC; (2) the longer the duration of HCV infection was, the lower was the patient's IFN-α production capacity; and (3) IFN-α production capacity was lower in patients who developed HCC within 3 years as compared to those who did not develop HCC. Based on these results, a patient with lower IFN-α production capacity might be considered to be at a high risk for the development of HCC.

The progress of chronic HCV infection is one of slow progression from the early stages of CH without fibrosis to LC and HCC[1-3]. The disease progresses to its advanced stages over a period of 10-30 years, unless the viral infection is terminated by antiviral therapy[14]. In this study, we have demonstrated that the IFN-α production capacity of patients with HCV infection gradually decreased as the disease progressed, resulting in the development of HCC, suggesting that extended dysfunction of the type I IFN system may lead to an increased risk of HCC development.

Table 1b Relationship between IFN-α production capacity and incidence of HCC development of patients within 3 years

IFN-α IU/1 000 WBC	No of patients	No of patients who developed HCC within 3 yr	%
≥0.87	9	2	22.2
<0.87	12	9	75[a]

[a]$P<0.05$

In our previous studies, we have reported that IFN-α production was somehow decreased in patients with lung cancer, MDS, pulmonary tuberculosis, HIV infection, diabetes mellitus and IgA nephritis[12,13], suggesting that IFN-α production capacity is impaired by various diseases, including cancer, infections, and metabolic disorder. In addition, periodic measurements of IFN-α production revealed decreased IFN-α production capacities in patients with lung[12]. Consistent with these results, we demonstrated that LC patients who developed HCC within 3 years possessed a decreased capacity to produce IFN-α, suggesting that a low level of IFN-α production is associated with a higher incidence of HCC development in LC patients. In this study, 75% of LC patients with IFN-α production less than 0.87 IU/1 000 WBC developed HCC within 3 years. In the previous study, we have reported the mean values of IFN-α production in lung cancer and MDS to be 0.88±0.80 and 0.35±0.28 IU/1 000 WBC, respectively. These results suggest that patients with IFN-α production less than 0.87 IU/1 000 WBC need to be cautioned that they are at particularly high risk of cancer development. Consistently, MDS patients with low IFN-α production capacity developed cancer within several years[12,15,16]. Moreover, DM patients with low IFN-α production had a higher risk of developing cancer[6]. To clarify the utility of this IFN-α production capacity in the early detection of various types of cancers, further large scale clinical surveys are needed.

Why is impaired IFN-α production a risk factor for developing HCC? In our previous study, we have demonstrated that impairment of IFN-α production capacity in whole blood mainly depends not only on a defect in the number of mononuclear lymphocytes but also on the lower capacity of HVJ-stimulated IFN-α production from mononuclear lymphocytes. Mononuclear lymphocytes included monocytes, B cells, NK cells and plasmacytoid dendritic cells, all of which were producers of IFN-α[17,18]. Recently, there has been a new interest in type I IFN as a "bridge system" linking innate and adaptive immunity stemming from the identification of natural IFN producing cells, characterized as plasmacytoid dendritic cells[19,20]. Since IFN-α/β participate in cancer

immunosurveillance[21], IFN-α production capacity is considered to reflect a facet of individual cancer immunosurveillance potential. In fact, some studies have clearly demonstrated that metastatic tumor cells grow progressively in mice pre-treated with neutralizing antibodies to murine IFN-α/β, demonstrating the critical role of endogenous IFN-α/β in the inhibition of anti-tumor immune responses[20,22,23]. Furthermore, type I IFN is involved in the anti-tumor activation of NK cells and macrophages as well as the induction of anti-tumor CTLs[24-27].

IFN-α production capacity is determined by both the genetic background and by the physical condition of each individual, such as the presence/absence of infection, metabolic disorder and cancer[28]. It is therefore anticipated that periodic measurements of IFN-α production and the early detection of reduced IFN-α production capacity will contribute to the early detection of HCC as well as the early detection of cancer and infectious disease. Furthermore, intervention to increase and/or maintain IFN-α production capacity may be useful for the prevention of HCC development.

REFERENCES

1 **Kiyosawa K,** Sodeyama T, Tanaka E, Gibo Y, Yoshizawa K, Nakano Y, Furuta S, Akahane Y, Nishioka K, Purcell RH. Interrelationship of blood transfusion, non-A, non-B hepatitis and hepatocellular carcinoma: analysis by detection of antibody to hepatitis C virus. *Hepatology* 1990; **12:** 671-675

2 **Seeff LB.** Natural history of hepatitis C. *Hepatology* 1997; **26:** 21S-28S

3 **Di Bisceglie AM,** Goodman ZD, Ishak KG, Hoofnagle JH, Melpolder JJ, Alter HJ. Long-term clinical and histopathological follow-up of chronic posttransfusion hepatitis. *Hepatology* 1991; **14:** 969-974

4 **Ikeda K,** Saitoh S, Suzuki Y, Kobayashi M, Tsubota A, Koida I, Arase Y, Fukuda M, Chayama K, Murashima N, Kumada H. Disease progression and hepatocellular carcinogenesis in patients with chronic viral hepatitis: a prospective observation of 2215 patients. *J Hepatol* 1998; **28:** 930-938

5 **Kiyosawa K,** Umemura T, Ichijo T, Matsumoto A, Yoshizawa K, Gad A, Tanaka E. Hepatocellular carcinoma: recent trends in Japan. *Gastroenterology* 2004; **127:** S17-2

6 **Huo TI,** Lui WY, Huang YH, Chau GY, Wu JC, Lee PC, Chang FY, Lee SD. Diabetes mellitus is a risk factor for hepatic decompensation in patients with hepatocellular carcinoma undergoing resection: a longitudinal study. *Am J Gastroenterol* 2003; **98:** 2293-2298

7 **Nakajima T,** Mizushima N, Kanai K. Relationship between natural killer activity and development of hepatocellular carcinoma in patients with cirrhosis of the liver. *Jpn J Clin Oncol* 1987; **17:** 327-332

8 **Kanto T,** Hayashi N, Takehara T, Tatsumi T, Kuzushita N, Ito A, Sasaki Y, Kasahara A, Hori M. Impaired allostimulatory capacity of peripheral blood dendritic cells recovered from hepatitis C virus-infected individuals. *J Immunol* 1999; **162:** 5584-5591

9 **Jinushi M,** Takehara T, Tatsumi T, Kanto T, Groh V, Spies T, Suzuki T, Miyagi T, Hayashi N. Autocrine/paracrine IL-15 that is required for type I IFN-mediated dendritic cell expression of MHC class I-related chain A and B is impaired in hepatitis C virus infection. *J Immunol* 2003; **171:** 5423-5429

10 **Jinushi M,** Takehara T, Kanto T, Tatsumi T, Groh V, Spies T, Miyagi T, Suzuki T, Sasaki Y, Hayashi N. Critical role of MHC class I-related chain A and B expression on IFN-alpha-stimulated dendritic cells in NK cell activation: impairment in chronic hepatitis C virus infection. *J Immunol* 2003; **170:** 1249-1256

11 **Jinushi M,** Takehara T, Tatsumi T, Kanto T, Miyagi T, Suzuki T, Kanazawa Y, Hiramatsu N, Hayashi N. Negative regulation of NK cell activities by inhibitory receptor CD94/NKG2A leads to altered NK cell-induced modulation of dendritic cell functions in chronic hepatitis C virus infection. *J Immunol* 2004; **173:** 6072-6081

12 **Uno K,** Nakano K, Maruo N, Onodera H, Mata H, Kurosu I, Akatani K, Ikegami N, Kishi A, Yasuda Y, Tanaka K, Setoguchi J, Kondo M, Muramatsu S, Kishida T. Determination of interferon-alpha-producing capacity in whole blood cultures from patients with various diseases and from healthy persons. *J Interferon Cytokine Res* 1996; **16:** 911-918

13 **Shirakawa K,** Muso E, Nogaki F, Maeda M, Kawamura T, Ono T, Yoshimoto M, Uno K, Kishida T, Sasayama S. Correlation between the severity of clinicopathological parameters and whole blood interferon-alpha production capacity in active phase IgA nephropathy patients. *Nephron* 2002; **90:** 24-30

14 **Yoshida H,** Tateishi R, Arakawa Y, Sata M, Fujiyama S, Nishiguchi S, Ishibashi H, Yamada G, Yokosuka O, Shiratori Y, Omata M. Benefit of interferon therapy in hepatocellular carcinoma prevention for individual patients with chronic hepatitis C. *Gut* 2004; **53:** 425-430

15 **Mufti G,** List AF, Gore SD, Ho AY. Myelodysplastic syndrome. Hematology (Am Soc Hematol Educ Program) 2003: 176-199

16 **Germing U,** Kundgen A, Gattermann N. Risk assessment in chronic myelomonocytic leukemia (CMML). *Leuk Lymphoma* 2004; **45:** 1311-1318

17 **Gobl AE,** Funa K, Alm GV. Different induction patterns of mRNA for IFN-alpha and -beta in human mononuclear leukocytes after in vitro stimulation with herpes simplex virus-infected fibroblasts and Sendai virus. *J Immunol* 1988; **140:** 3605-3609

18 **Gary-Gouy H,** Lebon P, Dalloul AH. Type I interferon production by plasmacytoid dendritic cells and monocytes is triggered by viruses, but the level of production is controlled by distinct cytokines. *J Interferon Cytokine Res* 2002; **22:** 653-659

19 **Belardelli F,** Ferrantini M, Proietti E, Kirkwood JM. Interferon-alpha in tumor immunity and immunotherapy. *Cytokine Growth Factor Rev* 2002; **13:** 119-134

20 **Gresser I,** Belardelli F. Endogenous type I interferons as a defense against tumors. *Cytokine Growth Factor Rev* 2002; **13:** 111-118

21 **Dunn GP,** Old LJ, Schreiber RD. The immunobiology of cancer immunosurveillance and immunoediting. *Immunity* 2004; **21:** 137-148

22 **Reid LM,** Minato N, Gresser I, Holland J, Kadish A, Bloom BR. Influence of anti-mouse interferon serum on the growth and metastasis of tumor cells persistently infected with virus and of human prostatic tumors in athymic nude mice. *Proc Natl Acad Sci USA* 1981; **78:** 1171-1175

23 **Gresser I,** Maury C, Kaido T, Bandu MT, Tovey MG, Maunoury MT, Fantuzzi L, Gessani S, Greco G, Belardelli F. The essential role of endogenous IFN alpha/beta in the anti-metastatic action of sensitized T lymphocytes in mice injected with Friend erythroleukemia cells. *Int J Cancer* 1995; **63:** 726-731

24 **Ramani P,** Balkwill FR. Action of recombinant alpha interferon against experimental and spontaneous metastases in a murine model. *Int J Cancer* 1989; **43:** 140-146

25 **Ferrantini M,** Giovarelli M, Modesti A, Musiani P, Modica A, Venditti M, Peretti E, Lollini PL, Nanni P, Forni G. IFN-alpha 1 gene expression into a metastatic murine adenocarcinoma (TS/A) results in CD8+ T cell-mediated tumor rejection and development of antitumor immunity. Comparative studies with IFN-gamma-producing TS/A cells. *J Immunol* 1994; **153:** 4604-4615

26 **Kaido TJ,** Maury C, Gresser I. Host CD4+ T lymphocytes are

required for the synergistic action of interferon-alpha/beta and adoptively transferred immune cells in the inhibition of visceral ESb metastases. *Cancer Res* 1995; **55:** 6133-6139

27 **Uno K,** Shimizu S, Inaba K, Kitaura M, Nakahira K, Kato T, Yamaguchi Y, Muramatsu S. Effect of recombinant human interferon-alpha A/D on in vivo murine tumor cell growth. *Cancer Res* 1988; **48:** 2366-2371

28 **Akahoshi M,** Ishihara M, Remus N, Uno K, Miyake K, Hirota T, Nakashima K, Matsuda A, Kanda M, Enomoto T, Ohno S, Nakashima H, Casanova JL, Hopkin JM, Tamari M, Mao XQ, Shirakawa T. Association between IFNA genotype and the risk of sarcoidosis. *Hum Genet* 2004; **114:** 503-509

Science Editor Kumar M and Guo SY **Language Editor** Elsevier HK

PO Box 2345, Beijing 100023, China
www.wjgnet.com
wjg@wjgnet.com

ELSEVIER

World J Gastroenterol 2005;11(46):7335-7339
World Journal of Gastroenterology ISSN 1007-9327

• *RAPID COMMUNICATION* •

Risk factors for bleeding after endoscopic mucosal resection

Masatsugu Shiba, Kazuhide Higuchi, Kaori Kadouchi, Ai Montani, Kazuki Yamamori, Hirotoshi Okazaki, Makiko Taguchi, Tomoko Wada, Atsushi Itani, Toshio Watanabe, Kazunari Tominaga, Yoshihiro Fujiwara, Tomoshige Hayashi, Kei Tsumura, Tetsuo Arakawa

Masatsugu Shiba, Kazuhide Higuchi, Kaori Kadouchi, Ai Montani, Kazuki Yamamori, Hirotoshi Okazaki, Makiko Taguchi, Tomoko Wada, Atsushi Itani, Toshio Watanabe, Kazunari Tominaga, Yoshihiro Fujiwara, Tomoshige Hayashi, Kei Tsumura, Tetsuo Arakawa, Department of Gastroenterology, Osaka City University Medical School, Osaka, Japan
Tomoshige Hayashi, Department of Preventive Medicine and Environmental Health, Osaka City University Medical School, Osaka, Japan
Kei Tsumura, Department of Cardiology, Osaka City University Medical School, Osaka, Japan
Correspondence to: Kazuhide Higuchi, MD, Department of Gastroenterology, Osaka City University Medical School, 1-4-3, Asahi-machi, Abeno-ku, Osaka 545-8585, Japan. khiguchi@med.osaka-cu.ac.jp
Telephone:+81-6-66452341 Fax: +81-6-66452341
Received: 2005-04-01 Accepted: 2005-04-30

Abstract

AIM: To clarify the risk factors for bleeding after endoscopic mucosal resection (EMR).

METHODS: A total of 297 consecutive patients who underwent EMR were enrolled. Some of the patients had multiple lesions. Bleeding requiring endoscopic treatment was defined as bleeding after EMR. Odds ratios (OR) with 95% confidence intervals (CI), calculated by logistic regression with multivariate adjustments for covariates, were the measures of association.

RESULTS: Of the 297 patients, 57 (19.2%) patients with bleeding after EMR were confirmed. With multivariate adjustment, the cutting method of EMR, diameter, and endoscopic pattern of the tumor were associated with the risk of bleeding after EMR. The multivariate-adjusted OR for bleeding after EMR using endoscopic aspiration mucosectomy was 3.07 (95%CI, 1.59-5.92) compared with strip biopsy. The multiple-adjusted OR for bleeding after EMR for the highest quartile (16-50 mm) of tumor diameter was 5.63 (95%CI, 1.84-17.23) compared with that for the lowest (4-7 mm). The multiple-adjusted OR for bleeding after EMR for depressed type of tumor was 4.21 (95%CI, 1.75-10.10) compared with elevated type.

CONCLUSION: It is important to take tumor characteristics (tumor size and endoscopic pattern) and cutting method of EMR into consideration in predicting bleeding after EMR.

Key words: Endoscopic mucosal resection; Bleeding; Tumor characteristics; Cutting method

Shiba M, Higuchi K, Kadouchi K, Montani I, Yamamori K, Okazaki H, Taguchi M, Wada T, Itani A, Watanabe T, Tominaga K, Fujiwara Y, Hayashi T, Tsumura K, Arakawa T. Risk factors for bleeding after endoscopic mucosal resection. *World J Gastroenterol* 2005; 11(46): 7335-7339
http://www.wjgnet.com/1007-9327/11/7335.asp

INTRODUCTION

Endoscopic mucosal resection (EMR) of early gastric cancers has been widely accepted as a standard procedure because of its low degree of invasiveness and the excellent quality of life in patients[1-3]. Bleeding is one of the major complications of EMR for gastric lesions. The reported bleeding rate after EMR for early gastric cancers is between 1.4% and 20%[4-8]. As indications for EMR expands, more complications such as bleeding may occur with it. It is reported that patients who required blood transfusion after EMR due to severe bleeding account for 4-14% of all patients undergoing EMR[7,13]. Several factors related to bleeding after EMR, such as tumor diameter, have been reported[9]. Our aim is to clarify the risk factors for bleeding after EMR in 297 patients with gastric lesions.

MATERIALS AND METHODS

Study population

A total of 297 consecutive patients who underwent EMR between April 1991 and December 1997 in the Department of Gastroenterology of Osaka City University Medical School were enrolled. Inclusion criteria were all gastric lesions confined to the lamina propria. The depth of tumor invasion was determined by endoscopic ultrasound. There was no bleeding tendency in any of the studied patient, and no patients used drugs such as anticoagulants.

Methods and measurements

The gastric lesions were removed by strip biopsy or endoscopic aspiration mucosectomy. We defined early gastric cancer using the Japanese Classification of Gastric Carcinoma[9,10], and we have defined the absolute indication

for endoscopic treatment as follows: elevated type mucosal cancer less than 2 cm or depressed type mucosal cancer without ulceration less than 1 cm in size. We have also carried out endoscopic treatment in cases extending beyond these criteria as a relative indication, when we could not perform surgery due to patient's refusal or due to significant heart, lung or kidney failure. Strip biopsy was performed with a two-channel scope (GIF2T-200; Olympus Optical Co., Tokyo, Japan), as described by Tanabe *et al*.[11]. Physiologic saline was injected locally to elevate the lesion. Endoscopic aspiration mucosectomy was performed as described by Torii[10]. A snare was introduced through a Teflon tube and tightened around the outer circumference of a transparent plastic cylinder cap (Olympus Optical Co., Tokyo, Japan). The Teflon tube, used as a snare introducer, was taped along the external axis of the endoscope. The snare was tightened by manipulating the handle, just as in polypectomy, and was fixed by taping it to the endoscope so that the snare loop remained at the tip of the cylinder cap. Physiologic saline was injected via an injection needle at the lesion to elevate the lesion. The snare was pushed over the tumor, while the lesion was aspirated along with the surrounding normal mucosa, and resection was performed by electrocauterization. A transparent cap was attached to the tip of an endoscope (GIFQ-200, GIFQ-230, GIFXQ-200, GIFXQ-230; Olympus Optical Co., Tokyo, Japan). The outer diameter of the transparent cap was 14.8 mm (MH-589) or 12.6 mm (MH-587).

Patients with a gastric lesion that required endoscopic treatment for bleeding after EMR were considered to have bleeding after EMR. We examined the patients with bleeding immediately after EMR, because they were treated with anti-ulcer drugs after EMR. Some of the patients had multiple lesions in our study in which the largest lesion per patient was selected as a representative lesion. Furthermore, when a patient had multiple tumors with the same largest diameter, we excluded the patient from analysis. We analyzed the data according to this rule.

The location of the lesion, tumor diameter, endoscopic pattern, histological findings for the tumor and cutting method were examined for their relationship to bleeding after EMR. After EMR, the removed mucosa was semifixed in formalin, and the lesion diameter was measured with a stereoscopic microscope (SZH-ILLB, Olympus Optical Co. Ltd., Tokyo, Japan). Based on the location, gastric lesions of the stomach was classified into an antrum group including the antrum and angle of the stomach, and a corpus group including the lower, middle, and upper body of the stomach. There were 158 lesions in the antrum group and 139 in the corpus group. By endoscopic pattern, lesions were classified into two types: elevated type and depressed type. There were 253 lesions of elevated type and 44 of depressed type. Histological examination revealed 139 early gastric cancers and 158 gastric adenomas[8]. We removed 177 lesions by the strip biopsy method and 144 lesions by endoscopic aspiration mucosectomy. Informed consent for EMR was obtained from all the patients.

Table 1 Baseline characteristics of study patients

	No bleeding after EMR (n = 240)	Bleeding after EMR (n = 57)	P
Age (yr)	65.3±9.3	66.0±8.4	0.582
Sex (M:F)	170:70	41:16:00	0.998
Tumor factors			
Location			
Antrum group	135 (85.4%)	23 (14.6%)	0.044
Corpus group	105 (75.5%)	34 (24.5%)	
Tumor diameter (mm)	12.4±6.7	13.9±7.1	0.152
Endoscopic pattern of lesion			
Elevated type	211 (83.4%)	42 (16.6%)	0.012
Depressed type	29 (65.9%)	15 (34.1%)	
Histological type			
Borderline adenoma	115 (82.7%)	24 (17.3%)	0.52
Cancer	125 (79.1%)	33 (20.9%)	
Cutting method			
Strip biopsy	156 (88.1%)	21 (11.9%)	0.001
Endoscopic aspiration mucosectomy	84 (70.0%)	36 (30.0%)	

Values are mean±SE or no. of gastric lesions.

Statistical analysis

Values were expressed as mean±SD. Categorical variables were compared using the χ^2 test. Differences in mean values between the two groups were compared using the unpaired t test. $P<0.05$ were considered significant. Multiple logistic regression analysis was used to evaluate the simultaneous effects of age, location of lesion, diameter, endoscopic pattern, histology of the tumor and the cutting method of EMR. Linear trends in risk associated with the tumor diameter were evaluated by indicators for each categorical level of tumor diameter using the median value for each category. The 95%CI for each odds ratio (OR) was calculated, and all P values are two-tailed. Statistical analyses were made using the SPSS 10.0 software package.

RESULTS

Of the 297 patients, 57 patients (19.2%) were confirmed to have bleeding after EMR. Baseline characteristics of the patients are summarized in Table 1. There was no significant difference in age and gender of patients, tumor diameter or histological type of tumor between the groups. The bleeding incidence after EMR in the corpus group was significantly higher than that in the antrum group (P = 0.038). The bleeding rate for depressed type lesions was significantly higher than that for elevated type lesions (P = 0.012). The bleeding rate with endoscopic aspiration mucosectomy was much higher than that with strip biopsy ($P<0.001$).

Of the 57 patients with bleeding, 18 (31.6%) patients had spurting bleeding (12 patients underwent EMR by endoscopic aspiration mucosectomy, and 6 underwent EMR by strip biopsy). Of these 57 patients, 39 (68.4%) had oozing bleeding (28 patients underwent EMR by endoscopic aspiration mucosectomy, and 11 underwent EMR by strip biopsy). All bleeding, except in one case, was controlled by endoscopic treatment with endoscopic clipping (HX5LR-1, Olympus, Japan), ethanol injection,

Table 2 Odds ratio of bleeding after endoscopic mucosal resection

	n	Cases	%	Crude-OR (95%CI)	Multiple-adjusted OR[1] (95% CI)	Multiple-adjusted OR[2] (95% CI)
Age (each additional year of age)	297	57	19.2	1.01 (0.98-1.05)	1.00 (0.97-1.04)	1.01 (0.97-1.04)
Tumor factors						
Location of gastric lesions						
Antrum group	158	23	14.6	1	1	1
Corpus group	139	34	24.5	2.24 (1.20-4.18)	2.24 (1.20-4.18)	1.69 (0.88-3.26)
Tumor diameter						
Quartile 1 (4-7)	58	5	8.6	1	1	1
Quartile 2 (8-11)	89	18	20.2	3.15 (1.06-9.38)	3.15 (1.06-9.38)	3.01 (0.99-9.07)
Quartile 3 (12-15)	76	13	17.1	2.53 (0.81-7.87)	2.53 (0.81-7.87)	2.90 (0.91-9.20)
Quartile 4 (16-50)	74	21	28.4	5.35 (1.78-16.10)	5.35 (1.78-16.10)	5.63 (1.84-17.23)
P for trend				0.048	0.022	0.022
Endoscopic pattern of lesion						
Elevated type	253	42	16.6	1	1	1
Depressed type	44	15	34.1	2.60 (1.28-5.26)	3.95 (1.69-9.24)	4.21 (1.75-10.10)
Histological type						
Adenoma	139	24	17.3	1	1	1
Cancer	158	33	20.9	1.27 (0.71-2.27)	0.67 (0.33-1.35)	0.56 (0.27-1.16)
Cutting method						
Strip biopsy	177	17	9.6	1		1
Endoscopic aspiration mucosectomy	120	40	33.3	3.18 (1.75-5.80)		3.07(1.59-5.92)

[1]Adjusted for age, tumor factors, location of gastric lesions, tumor diameter, endoscopic pattern of lesion, histological type. AT indicates antrum of stomach; [2]Adjusted for age, tumor factors, location of gastric lesions, tumor diameter, endoscopic pattern of lesion, histological type, and cutting method.

and injection of hypertonic saline-epinephrine solution. No patient required blood transfusion in our study, only one patient underwent open emergency surgery because of severe bleeding after EMR.

Multivariate analysis of bleeding risk after EMR

The multivariate analysis of bleeding after EMR is summarized in Table 2. Cutting method of EMR was the strongest factor identified in this analysis. Location of gastric lesion, tumor diameter, and endoscopic pattern of the lesion were associated with an increased risk of bleeding after EMR, when the multivariate analysis was adjusted for age, location of gastric lesions, tumor diameter, endoscopic pattern of lesion and histological type. However, when cutting method of EMR was added to these factors in the multivariate analysis, location of the gastric lesion was no longer a significant factor. The multiple-adjusted OR excluding the factor of the cutting method for bleeding after EMR in the corpus group was 2.24 (95%CI, 1.20-4.18) compared with that in the antrum group. However, the multiple-adjusted OR including the factor of cutting method for bleeding after EMR in the corpus group was 1.69 (95%CI, 0.88-3.26) compared with that in the antrum group.

Tumor diameter and endoscopic pattern of the lesion were not significant factors in the multiple-adjusted analysis, either including or excluding the factor of cutting method. To examine in detail the risk of tumor diameter, tumor diameter was divided into four categories. The multiple-adjusted OR including the factor of cutting method for the highest quartile of diameter was 5.63 (95%CI, 1.84-17.23) compared with that for the lowest.

Concerning endoscopic pattern of lesions, the multiple-adjusted OR for depressed type lesions with the inclusion of the factor of cutting method was 4.21 (95%CI, 1.75-10.10) compared with that for elevated type lesions. The multiple-adjusted OR for bleeding after EMR with endoscopic aspiration mucosectomy was 3.07 (95%CI, 1.59-5.92) compared with that for strip biopsy.

On crude analysis, the histology of the lesion was also associated with the risk of bleeding after EMR, but in the multiple-adjusted analyses this association was not significant.

DISCUSSION

EMR is an established treatment for early-stage gastric cancers, and is an alternative to surgery for patients with superficial neoplastic lesions of the digestive tract. EMR can achieve a complete resection in a majority of patients, but is associated with a higher risk of bleeding than standard polypectomy[4-7,13,14]. Bleeding incidence, however, appears to vary according to how bleeding is defined. Bleeding during EMR of colorectal polyp is common, occurring in 24% of polypectomy of large colorectal polyps[15]. Morales *et al.*[15] defined procedural bleeding as a complication. Various forms of endoscopic treatment, such as multipolar electrocoagulation, use of heat probe, and injection therapy, are usually highly effective in stopping acute upper gastrointestinal ulcer bleeding[16-18]. Similarly, bleeding during the performance of EMR can almost always be controlled by the injection of saline epinephrine solution, thermal coagulation, or endoscopic clipping[25]. Endoscopic clipping is believed to be the safest therapeutic modality for controlling spurting bleeding after EMR[19,20,23]. However, it is reported that patients who required blood transfusion after EMR due to large bleeding accounted for 4-14% of patients undergoing EMR[7,13].

We came across one patient who underwent open emergency surgery because of severe bleeding after EMR.

Most bleeding occurs during the procedure, although delayed bleeding (up to 3 d in 10% of patients) has been reported[15]. In our study, patients with a gastric lesion that required endoscopic treatment for bleeding after EMR were considered to be cases to have bleeding after EMR.

The association of various factors with bleeding rates, such as tumor diameter[13], diameter of the removed mucosa, cutting method[6,12,13,21], location of gastric lesions, endoscopic pattern of lesions[13], and histological type of gastric tumor has been reported[6]. Those studies examined not only the risk of bleeding but also the rate of bleeding.

We found that tumor diameter, endoscopic pattern of lesions, and cutting method were associated with the increased risk of bleeding after EMR. These associations existed even on multivariate analysis.

It has been reported that larger diameter tumors bled readily after EMR[13]. We evaluated linear trends in risks of tumor diameter by indicators for each categorical level, and found that the findings were consistent with our results from the previous reports. We used tumor diameter determined by postfixation measurement as a predictor of post-EMR bleeding, because formalin fixation did not cause shrinkage of the specimens[22-23].

No significant relationship was found between bleeding incidence and the cutting diameter[12], and large cutting diameter was easy to bleed, because bleeding incidence may depend on the size of the cutting diameter[24]. We did not evaluate the diameter of the removed mucosa because this factor could not be measured before EMR was undertaken, and therefore could not be a predictor of bleeding.

Submucosal injection is an important part of the EMR procedure. Injection of fluid into the submucosa beneath a gastric lesion increases the distance between the base of the polyp and the deeper tissues of the gastric wall. It has been reported that a large submucosal cushion of saline solution increases the safety of polypectomy by preventing thermal injury to these deeper tissues[26,27]. Therefore, submucosal injection may influence bleeding after EMR. However, effects of the volume of physiologic saline solution injected were not investigated in our study, because the administration volume of physiologic saline solution was not routinely recorded. The endoscopic pattern of the lesion influences the risk of bleeding after EMR has not been reported. Depressed type lesion was a risk factor for bleeding after EMR in our study. However, the volume of submucosal injection used may have affected this result.

There is one report that bleeding incidence is higher with strip biopsy than with endoscopic aspiration mucosectomy, a finding inconsistent with our results[21]. It was reported that the size of resected specimens was significantly larger with endoscopic aspiration mucosectomy than with strip biopsy[11]. We did not evaluate the diameter of the removed mucosa in our study, though it might influence the bleeding rate associated with the cutting method.

Blood vessel diameter in the antral region of the stomach is smaller than that in the gastric corpus, and the number of blood vessels in the antral region is low[27]. In our study, no significant relationship was found between the locations of the lesion and cutting method in multivariate analysis. However, the bleeding incidence in the corpus group [24.5% (34/139)] was higher than that in the antrum group [14.6% (23/158)]. Therefore, if the sample size of our study was enlarged, a significant difference might be found.

Of the 297 patients, 64 (21.5%) patients underwent EMR by piecemeal resection, with a bleeding incidence of 15.6% (10/64). A total of 233 (78.5%) patients underwent EMR by en-bloc resection, with a bleeding incidence of 20.2% (47/233). There was no significant relationship between *en-bloc* resection or piecemeal resections and bleeding incidence after EMR.

In our study, ten endoscopists performed EMR for patients with bleeding after EMR. Categorical variables, such as location of the lesion, tumor diameter (four categories), endoscopic pattern, histology of the tumor and cutting method were compared among the 10 endoscopists using the χ^2 test. There was no significant difference among the endoscopists in the location of lesion ($P = 0.618$), tumor diameter ($P = 0.182$), endoscopic pattern ($P = 0.374$), histology of the tumor ($P = 0.395$) or cutting method ($P = 0.138$). Therefore, the particular endoscopist performing the procedure did not influence the risk of bleeding.

Conio *et al.* divided the definition of "bleeding after EMR" into three categories, i.e., intraprocedure (occurring during EMR), early (within 24 h), and delayed (≧24 h). In our study, "bleeding after EMR" was defined as intraprocedure.

In conclusion, our study indicated that tumor diameter, endoscopic pattern of lesions, and cutting method are risk factors for bleeding after EMR. It is important to consider these three factors in predicting bleeding after EMR.

REFERENCES

1 **Inoue H,** Takeshita K, Hori H, Muraoka Y, Yoneshima H, Endo M. Endoscopic mucosal resection with a cap-fitted panendoscope for esophagus, stomach, and colon mucosal lesions. *Gastrointest Endosc* 1993; **39:** 58-62

2 **Ono H,** Kondo H, Gotoda T, Shirao K, Yamaguchi H, Saito D, Hosokawa K, Shimoda T, Yoshida S. Endoscopic mucosal resection for treatment of early gastric cancer. *Gut* 2001; **48:** 225-229

3 **Takeshita K,** Tani M, Inoue H, Saeki I, Hayashi S, Honda T, Kando F, Saito N, Endo M. Endoscopic treatment of early oesophageal or gastric cancer. *Gut* 1997; **40:** 123-127

4 **Yokota K,** Tanabe Y, Komatsu H, Watari J, Ohta T, Tniguchi M et al: Safety and risk in the endoscopic mucosal resection of gastric disease. The Strip Biopsy Method. *Endoscopia Digestiva* 1996; **8:** 465-471

5 **Shuuji I,** Michio T: Safer and More Reliable Endoscopic Mucosal Resection By the Four Point Fixation Method in the Treatment of Early Gastric Cancer. *Endoscopia Digestiva* 1996; **8:** 499-507

6 **Nelson DB,** Block KP, Bosco JJ, Burdick JS, Curtis WD, Faigel DO, Greenwald DA, Kelsey PB, Rajan E, Slivka A, Smith P, Wassef W, Vandam J, Wang KK. Endoscopic mucosal resection: May 2000. *Gastrointest Endosc* 2000; **52:** 860-863

7 **Kojima T,** Parra-Blanco A, Takahashi H, Fujita R. Outcome of endoscopic mucosal resection for early gastric cancer: review of the Japanese literature. *Gastrointest Endosc* 1998; **48:** 550-555

8 **Yamaguchi Y,** Katsumi N, Tauchi M, Toki M, Nakamura K, Aoki K, Morita Y, Miura M, Morozumi K, Ishida H, Takahashi S. A prospective randomized trial of either famotidine or omeprazole for the prevention of bleeding after endoscopic mucosal resection and the healing of endoscopic mucosal resection-induced ulceration. *Aliment Pharmacol Ther* 2005; **21 (Suppl 2):** 111-115

9 **Okano A,** Hajiro K, Takakuwa H, Nishio A, Matsushita M. Predictors of bleeding after endoscopic mucosal resection of gastric tumors. *Gastrointest Endosc* 2003; **57:** 687-690

10 **Torii A,** Sakai M, Kajiyama T, Kishimoto H, Kin G, Inoue K, Koizumi T, Ueda S, Okuma M. Endoscopic aspiration mucosectomy as curative endoscopic surgery; analysis of 24 cases of early gastric cancer. *Gastrointest Endosc* 1995; **42:** 475-479

11 **Tanabe S,** Koizumi W, Kokutou M, Imaizumi H, Ishii K, Kida M, Yokoyama Y, Ohida M, Saigenji K, Shimao H, Mitomi H. Usefulness of endoscopic aspiration mucosectomy as compared with strip biopsy for the treatment of gastric mucosal cancer. *Gastrointest Endosc* 1999; **50:** 819-822

12 **Kamiya R**, Terui T, Ikeda S, Suzuki A, Seki H, Oikawa M.: The new technique of closing mucosal defects to prevents bleeding by endoscopic removal of large gastric polyp. *Morioka Sekijyuuji Byouin Kiyou* 1999; **8:** 13-22

13 **Ahmad NA,** Kochman ML, Long WB, Furth EE, Ginsberg GG.: Efficacy, safety, and clinical outcomes of endoscopic mucosal resection: a study of 101 cases. *Gastrointest Endosc* 2002 Mar; **55**(3): 390-396

14 **Schoen RE,** Gerber LD, Margulies C. The pathologic measurement of polyp size is preferable to the endoscopic estimate. Gastrointest Endosc 1997; **46:** 492-496

15 **Morales TG,** Sampliner RE, Garewal HS, Fennerty MB, Aickin M. The difference in colon polyp size before and after removal. Gastrointest Endosc 1996; **43:** 25-28

16 **Sasako M,** Aiko T. Reply to Professor Hermanek's comments on the new Japanese classification of gastric carcinoma. *Gastric Cancer* 1999; **2:** 83-85

17 **Japanese Gastric Cancer Association.** Japanese Classification of Gastric Carcinoma - 2nd English Edition - *Gastric Cancer* 1998; **1:** 10-24

18 **Van Gossum A,** Cozzoli A, Adler M, Taton G, Cremer M. Colonoscopic snare polypectomy: analysis of 1485 resections comparing two types of current. *Gastrointest Endosc* 1992; **38:** 472-475

19 **Muhldorfer SM,** Kekos G, Hahn EG, Ell C. Complications of therapeutic gastrointestinal endoscopy. *Endoscopy* 1992; **24:** 276-283

20 **Chung SC,** Leung JW, Sung JY, Lo KK, Li AK. Injection or heat probe for bleeding ulcer. *Gastroenterology* 1991; **100:** 33-37

21 **Waring JP,** Sanowski RA, Sawyer RL, Woods CA, Foutch PG. A randomized comparison of multipolar electrocoagulation and injection sclerosis for the treatment of bleeding peptic ulcer. *Gastrointest Endosc* 1991; **37:** 295-298

22 **Laine L.** Multipolar electrocoagulation versus injection therapy in the treatment of bleeding peptic ulcers. A prospective, randomized trial. *Gastroenterology* 1990; **99:** 1303-1306

23 **Binmoeller KF,** Bohnacker S, Seifert H, Thonke F, Valdeyar H, Soehendra N. Endoscopic snare excision of "giant" colorectal polyps. *Gastrointest Endosc* 1996; **43:** 183-188

24 **Inoue H,** Tani M, Nagai K, Kawano T, Takeshita K, Endo M, Iwai T. Treatment of esophageal and gastric tumors. *Endoscopy* 1999; **31:** 47-55

25 **Parra-Blanco A,** Kaminaga N, Kojima T, Endo Y, Uragami N, Okawa N, Hattori T, Takahashi H, Fujita R. Hemoclipping for postpolypectomy and postbiopsy colonic bleeding. *Gastrointest Endosc* 2000; **51:** 37-41

26 **Waye JD.** Techniques of colonoscopy, hot biopsy forceps, and snare polypectomy. *Prog Clin Biol Res* 1988; **279:** 61-69

27 **Waye JD,** Ramaiah C, Hipona J. Saline assisted polypectomy: risk and balances [abstract]. Gastrointest Endosc 1994; **40:** 38

28 **Conio M,** Repici A, Demarquay JF, Blanchi S, Dumas R, Filiberti R. EMR of large sessile colorectal polyps. *Gastrointest Endosc* 2004; **60:** 234-241

Science Editor Ma JY and Guo SY **Language Editor** Elsevier HK

PO Box 2345, Beijing 100023, China
www.wjgnet.com
wjg@wjgnet.com

ELSEVIER

World J Gastroenterol 2005;11(46):7340-7344
World Journal of Gastroenterology ISSN 1007-9327

• *RAPID COMMUNICATION* •

Stool antigen tests in the diagnosis of *Helicobacter pylori* infection before and after eradication therapy

Lea Veijola, Eveliina Myllyluoma, Riitta Korpela, Hilpi Rautelin

Lea Veijola, Department of Bacteriology and Immunology, Haartman Institute, University of Helsinki, and Malmi Hospital, Helsinki, Finland
Eveliina Myllyluoma, Institute of Biomedicine, Pharmacology, University of Helsinki, and Foundation for Nutrition Research, Helsinki, Finland
Riitta Korpela, Institute of Biomedicine, Pharmacology, University of Helsinki, and Valio Ltd. Research Centre, Helsinki, Finland
Hilpi Rautelin, Department of Bacteriology and Immunology, Haartman Institute, University of Helsinki, and HUSLAB, Helsinki University Central Hospital Laboratory, Helsinki, Finland
Supported by the Valio Research Centre and by grants from City of Helsinki, Terke 2004-368 (Lea Veijola) and Foundation for Nutrition Research, No. 0116610-9 (Eveliina Myllyluoma)
Correspondence to: Dr. Lea Veijola, Department of Bacteriology and Immunology, Haartman Institute, University of Helsinki, PO Box 21, Fin-00014 Helsinki, Finland. lea.veijola@helsinki.fi.
Telephone: +358-9-19126716 Fax: +358-9-19126382
Received: 2005-02-25 Accepted: 2005-04-18

Abstract

AIM: To evaluate two enzyme immunoassay-based stool antigen tests, Premier Platinum HpSA and Amplified IDEIA HpStAR, and one rapid test, ImmunoCard STAT! HpSA, in the primary diagnosis of *Helicobacter pylori (H pylori)* infection and after eradication therapy.

METHODS: Altogether 1 574 adult subjects were screened with a whole-blood *H pylori* antibody test and positive results were confirmed with locally validated serology and ^{13}C-urea breath test. All 185 subjects, confirmed to be *H pylori* positive, and 97 *H pylori*-negative individuals, randomly selected from the screened study population and with negative results in serology and UBT, were enrolled. After eradication therapy the results of 182 subjects were assessed.

RESULTS: At baseline, the sensitivity of HpSA and HpStAR was 91.9% and 96.2%, respectively, and specificity was 95.9% for both tests. ImmunoCard had sensitivity of 93.0% but specificity of only 88.7%. After eradication therapy, HpSA and HpStAR had sensitivity of 81.3% and 100%, and specificity of 97.0% and 97.6%, respectively. ImmunoCard had sensitivity of 93.8% and specificity of 97.0%. HpSA, HpStAR, and ImmunoCard had PPV 77%, 80%, and 75%, and NPV 98%, 100%, and 99%, respectively.

CONCLUSION: In primary diagnosis, the EIA-based tests performed well. After eradication therapy, negative results were highly accurate for all the three tests. HpStAR had the best overall performance.

Key words: Diagnosis; Feces; *Helicobacter pylori*; Therapy

Veijola L, Myllyluoma E, Korpela R, Rautelin H. Stool antigen tests in the diagnosis of *Helicobacter pylori* infection before and after eradication therapy. *World J Gastroenterol* 2005; 11(46): 7340-7344
http://www.wjgnet.com/1007-9327/11/7340.asp

INTRODUCTION

H pylori infection is one of the most common infections in human beings worldwide, strongly associated with peptic ulcer disease and gastric cancer[1,2]. There are several methods available to detect *H pylori* infection including invasive methods based on gastric biopsies and non-invasive methods like serology, urea breath tests (UBTs), and stool antigen tests[3,4]. Stool antigen tests have recently been welcomed with great expectations as they are convenient to the patients and can be easily performed even in small laboratories[5,6]. However, the accuracy of stool antigen tests in different clinical situations and outside of controlled studies is a matter of concern[7-9].

Several commercial stool antigen tests are available: enzyme immunoassays (EIAs) based on either polyclonal (Premier Platinum HpSA, Meridian Inc., Cincinnati, OH, USA) or mAbs (Amplified IDEIA HpStAR, also known as Femtolab, Dako, Glostrup, Denmark) and rapid bed-side tests like ImmunoCard STAT! HpSA (Meridian Bioscience Europe, Milan, Italy). HpSA is the most widely studied of these tests and it has shown acceptable performance in the primary diagnosis of *H pylori* infection but the accuracy in post-treatment setting and in special clinical situations (e.g. upper gastrointestinal hemorrhage, gastric surgery, PPI therapy) has been controversial[5,7,8]. The three stool antigen tests have rarely been compared in parallel in the same study. The differences in patient characteristics (e.g. peptic ulcer *vs* gastritis) and widely variable prevalence of *H pylori* in different studies make the comparisons between the tests difficult as the statistical parameters of the performance of the tests are often dependent on the prevalence of the infection.

Recently, we evaluated the three stool antigen tests in *H pylori*-positive patients before and after eradication therapy[10]. In the present study we also included *H pylori*-negative individuals. *H pylori* infection in all the subjects was verified by serology and ^{13}C-UBT.

MATERIALS AND METHODS

Subjects

Adults were invited with a newspaper announcement to participate in the study. Exclusion criteria were antibiotic treatment during previous 2 mo; use of H_2-receptor antagonists, bismuth or proton pump inhibitor therapy during previous 2 wk; *H pylori* eradication therapy during previous 5 years; gastric surgery; chronic gastrointestinal diseases; contraindications to drugs used in the study; pregnancy or lactation. Study subjects were screened for *H pylori* infection with rapid whole-blood antibody tests (Pyloriset Screen II, Orion Diagnostica, Espoo, Finland, or Biocard *Helicobacter pylori* IgG, AniBiotech Ltd, Vantaa, Finland). The present study was subsidiary to another study investigating the efficacy of probiotics in the eradication therapy of *H pylori*. Therefore, allergy to fruit juice containing the probiotics also belonged to the exclusion criteria.

The population screened comprised 1 574 subjects. Positive results in screening were confirmed with UBT and an in-house EIA-based serologic method. Of the 300 *H pylori*-positive subjects in screening, 196 were positive in both of the confirmatory tests, but 11 subjects met one of the exclusion criteria; thus 185 *H pylori*-positive subjects were included in the study (of the remaining 104 subjects positive in screening, 49 were negative in both of the confirmatory tests and for the rest either no confirmatory tests were performed or the results were discordant). From the subjects with *H pylori*-negative test result in screening, 114 (randomly selected by a computer program SPSS 12.0) were invited to bring the specimens for the confirmatory tests and 97 subjects followed this invitation. For these *H pylori*-negative study subjects, the infection was excluded with both of the confirmatory tests. Thus, the final study population consisted of 282 subjects: 185 were *H pylori* positive and 97 negative. The median age of the subjects was 52 years, range 23-71 years. The median age of *H pylori*-positive subjects was 55 years (range 25-71 years) and of *H pylori*-negative subjects 43 years (range 23-64 years). In total there were 186 females and 96 males.

H pylori eradication therapy

A total of 185 *H pylori*-positive subjects received the same eradication therapy: amoxicillin 1 g b.i.d., clarithromycin 500 mg b.i.d. and lanzoprazole 30 mg b.i.d. for 1 wk. Exclusion criteria for the therapy were penicillin allergy, prolonged QT-interval, and antifungal therapy for dermatophyte infection.

Serology

At baseline and 4 mo after the end of eradication therapy the subjects gave serum samples for locally validated in-house EIA[11]. At baseline, serum samples had been investigated in order to confirm the infection, and they were stored at -20 ℃ until further used. Serum samples before and after eradication therapy were analyzed in parallel for both immunoglobulin G (IgG) and IgA antibodies as described earlier[12]. *H pylori* eradication therapy was considered successful when antibody titers of at least IgG class had fallen 40% or more from the pre-treatment level[11].

UBT

UBT was performed at baseline and 4 wk after the end of eradication therapy. Diabact tablets were used (Diabact UBT, Diabact AB, Uppsala, Sweden) [13,14]. After overnight fast the subjects swallowed either one or two 50 mg Diabact tablets and blew into the test tube before and 10 min after ingesting the tablet(s). Results were analyzed by isotope ratio mass spectrometry (BreathMATPlus, Finnigan MAT GmbH, Bremen, Germany) and expressed as delta over baseline (DOB). Cut-off point for positive test result was DOB 2.2‰.

Stool antigen tests

All subjects gave stool specimens at baseline and those treated 4 wk after the end of eradication therapy. Stool specimens were stored at -20 ℃ before analysis and were thawed twice at most. Stool samples before and after therapy were always run in parallel in all three antigen tests.

The polyclonal antibody-based Premier Platinum HpSA test, later HpSA (Meridian Inc., Cincinnati, USA) was performed according to manufacturer's instructions. Diluted stool specimens were added to the microtiter wells with a peroxidase-conjugated polyclonal antibody. After washing, substrate was added. The results were read at 450 nm by a spectrophotometry (Titertek Multiskan analyzer, Eflab Oy, Helsinki, Finland). Optical density (OD) values <0.140 were negative, 0.140-0.159 equivocal (gray zone) and ⩾0.160 positive, as suggested by the manufacturer. In cases with gray zone values, the same stool samples stored at -20 ℃ were retested as recommended.

For the mAb-based Amplified IDEIA HpStAR test, later HpStAR (also known by name FemtoLab, Dako), the supernatant of stool suspension and peroxidase-conjugated mAbs were pipetted into the wells. After washing substrate was added, and the results were read by spectrophotometry. According to manufacturer's instructions, OD values ⩾0.190 (450 nm) were assessed as positive and <0.190 as negative.

ImmunoCard STAT! HpSA-test, later ImmunoCard (Meridian Bioscience Europe) is based on monoclonal *H pylori* antibodies and a lateral flow chromatography technique. The diluted stool sample was dispensed to the sample port of the test cassette, and after incubation of 5 min at room temperature, the appearance of a pink-red line in the reading window indicated a positive result.

The Ethics Committee of the Hospital District of Helsinki and Uusimaa approved the studies and all subjects

Table 1 Performance of the three stool antigen tests as compared with UBT and serology in 282 subjects at baseline

UBT, serology	HpSA		HpStAR	ImmunoCard
Positive 185	Positive	170[1]	178	172
	Negative	13[1]	7	13
	2 gray zone[2]			
Negative 97	Negative	93	93	86
	Positive	4[3]	4	11

[1]One subject originally had gray zone result.
[2]Gray zone result even in re-examination.
[3]Three subjects originally had gray zone results.

Table 2 Performance of the three stool antigen tests as compared with UBT and serology in 182 subjects after eradication therapy

UBT, serology	HpSA	HpStAR	ImmunoCard
Negative 166	Negative 161[1]	162	161
	Positive 4	4	5
	1 gray zone[2]		
Positive 16	Positive 13	16	15
	Negative 3[3]	0	1

[1]Six subjects originally had gray zone result.
[2]Gray zone result even in re-examination.
[3]One subject originally had gray zone result.

gave their written informed consent.

RESULTS

The performance of the stool antigen tests at baseline is shown in Table 1 and after eradication therapy in Table 2. Four patients were treated with antimicrobials after eradication therapy before the 4 wk had elapsed and thus, stool specimens and UBTs of these particular patients were not collected until they gave the serum sample for serology 4 mo after the therapy. For all the other subjects, UBT was performed and stool specimens were collected 4 wk after therapy according to the study protocol.

The results after eradication therapy are presented for 182 subjects; 3 subjects had the results only at baseline. One patient died before the follow-up. Serum sample was collected and another subject discontinued the study during antimicrobial therapy because of severe headache, which later turned out to be viral meningitis as examined by a neurologist. After eradication therapy, the confirmatory tests (UBT and serology) showed concordant results in all but one subject, who had eradication failure according to the UBT and all three stool antigen tests but successful eradication according to the serology: his results after eradication therapy were excluded from the analysis.

The performance of the tests at baseline is presented in Table 3 and after eradication therapy in Table 4. The adjusting of the cut-off points would not have had any beneficial effect to the results either before or after eradication treatment (data not shown). The false-positive test results in stool antigen tests were randomly distributed between the individual tests. However, half of the false-negative HpSA test results at baseline were also negative with the other two stool tests.

The HpSA tests with gray zone values were re-examined using the same stool specimens according to manufacturer's recommendations. However, no new stool specimen was collected (although recommended by the manufacturer) if the result was in gray zone even in re-examination. Out of the 464 samples analyzed, 15 (3.2%) fell into the gray zone but only three were equivocal when re-tested. Gray zone results obtained after re-examination were considered neither true positive nor true negative in statistical calculations.

Table 3 Performance of the three stool antigen tests at baseline

	Sensitivity	Specificity	PPV	NPV	Accuracy
	(%)	(%)	(%)	(%)	(%)
HpSA	91.9	95.9	97.7	87.7	93.3
HpStAR	96.2	95.9	97.8	93.0	96.1
ImmunoCard	93.0	88.7	94.0	86.9	91.5

PPV, positive predictive value; NPV, negative predictive value.

Table 4 Performance of the three stool antigen tests after eradication therapy

	Sensitivity	Specificity	PPV	NPV	Accuracy
	(%)	(%)	(%)	(%)	(%)
HpSA	81.3	97.0	76.5	98.2	95.6
HpStAR	100	97.6	80.0	100	97.8
ImmunoCard	93.8	97.0	75.0	99.4	96.7

PPV, positive predictive value; NPV, negative predictive value.

DISCUSSION

In the primary diagnosis of *H pylori* infection, the EIA-based HpSA and HpStAR tests had high sensitivities in accordance with our previous study[10] and those of others[6,8]. Earlier the specificities of these tests have varied between 63% and 100% for HpSA and 87% and 100% for HpStAR in studies with high prevalence of *H pylori* infection[6,8,15-19] and are in line with the specificity of 96% in our present study population. ImmunoCard had a good sensitivity, 93.0%, but a low specificity, 88.7%, at baseline, leading to a high number of false-positive test results. In previous studies, ImmunoCard has shown variable results in the primary diagnosis with sensitivities between 83% and 96% and specificities between 82% and 94%[8,10,20-25].

The positive predictive values (PPVs) for all the three stool antigen tests were very high (94.0-97.8%) at baseline in our study population with a high prevalence (65.6%) of *H pylori*. However, if these stool antigen tests had been used to detect the infection in the original group of 1 574 screened study subjects with the prevalence of *H pylori* being 12% (in assuming that all the screened but not confirmed *H pylori*-negative subjects would have been negative also in the both confirmatory tests), the PPVs for these tests would have been only as follows: HpSA 76.6%, HpStAR 77.5%, and ImmunoCard 54.8%. It has been earlier suggested that at an *H pylori* prevalence of lower than 30%, the most cost effective diagnostic strategy would be to use stool antigen test and confirm positive results with UBT[4]. In our study, the ImmunoCard test had the lowest specificity and thus a high number of false-positive test results emphasizing the need for a confirmation of a

positive test result by UBT or serology.

In post-eradication setting, the position of these stool antigen tests is most controversial[7,8]. This is true especially for the most widely studied HpSA test, which also in our study showed a low sensitivity after eradication therapy. We had an exceptionally low eradication failure rate in this study, only 8.8%, and HpSA test was unable to find 19% of our eradication failures, which is in accordance with our previous endoscopy-based study, in which 25% of eradication failures were unidentified with this test[10]. For the HpStAR test, the sensitivity has varied after eradication therapy between 86% and 100%, specificity 95% and 100%, PPV 83% and 100%, and NPV 96% and 100%[8,18,19]. Our results fell well into this range. The performance of ImmunoCard after eradication therapy in the few published studies available has varied widely. In a study in adults ImmunoCard showed very low sensitivity both before (83%) and after (73%) eradication therapy but high specificity 98%[23] whereas in the study of Gatta *et al*.[21] the sensitivity was 92% and specificity 100%. In our study all the three stool antigen tests had false-positive results in 2.5%-3.1% of successfully eradicated subjects, figures comparable with UBT[3,26,27].

All patients except three in our study brought the follow-up UBT and stool specimens 4 wk after finishing the eradication therapy. In some previous studies using the HpSA test, it has been shown that the time elapsed after eradication therapy should not be less than 4 wk but extending the time beyond that would not clearly improve the results[8,10,19,28,29]. A positive HpSA test as early as 3 d after finishing eradication therapy has been highly predictive of eradication failure but a negative test result was reliable only after 3 wk[29]. Therefore, it is unlikely that after treatment a longer time before the collection of stool samples would have improved the results in our study.

In conclusion, in the primary diagnosis of *H pylori* infection, the EIA-based HpSA and HpStAR stool antigen tests performed well. However, in a population with a lower prevalence of *H pylori* infection, positive results even in these tests may be reasonable to confirm with UBT or serology. After eradication therapy, negative results were highly accurate for all the three tests and HpStAR even found all the subjects with an unsuccessful eradication. HpStAR had the best overall performance before and after eradication therapy.

ACKNOWLEDGMENTS

This study was in part presented at the XVI[th] International Workshop, European Helicobacter Study Group, Vienna, Austria 24th September 2004. Our deepest appreciation goes to Pirjo Kosonen, Leena Seppo, Anu Kosonen, Minna Hietala, and Tiina Vikstedt for their skillful and assiduous assistance.

REFERENCES

1 International Agency for Research on Cancer. Schistosomes, liver flukes and Helicobacter pylori. IARC Working Group on the Evaluation of Carcinogenic Risks to Humans. Lyon, 7-14 June 1994. *IARC Monogr Eval Carcinog Risks Hum* 1994; **61:** 1-241

2 **Fox JG**, Wang TC. *Helicobacter pylori*--not a good bug after all! *N Engl J Med* 2001; **345:** 829-32

3 **Nakamura R**. Laboratory tests for the evaluation of Helicobacter pylori infections. *J Clin Lab Anal* 2001; **15:** 301-307

4 **Vakil N**. Review article: the cost of diagnosing Helicobacter pylori infection. *Aliment Pharmacol Ther* 2001; **15 (Suppl 1):** 10-15

5 **Malfertheiner P,** Megraud F, O'Morain C, Hungin AP, Jones R, Axon A, Graham DY, Tytgat G. Current concepts in the management of Helicobacter pylori infection--the Maastricht 2-2000 Consensus Report. *Aliment Pharmacol Ther* 2002; **16:** 167-180

6 **Vaira D**, Ricci C, Menegatti M, Gatta L, Berardi S, Tampieri A, Miglioli M. Stool test for Helicobacter pylori. *Am J Gastroenterol* 2001; **96:** 1935-1938

7 **Parente F**, Maconi G, Porro GB, Caselli M. Stool test with polyclonal antibodies for monitoring Helicobacter pylori eradication in adults: a critical reappraisal. *Scand J Gastroenterol* 2002; **37:** 747-749

8 **Gisbert JP**, Pajares JM. Stool antigen test for the diagnosis of Helicobacter pylori infection: a systematic review. *Helicobacter* 2004; **9:** 347-368

9 **Hunt R**, Fallone C, Veldhuyzan van Zanten S, Sherman P, Smaill F, Flook N, Thomson A. Canadian Helicobacter Study Group Consensus Conference: Update on the management of Helicobacter pylori--an evidence-based evaluation of six topics relevant to clinical outcomes in patients evaluated for H pylori infection. *Can J Gastroenterol* 2004; **18:** 547-554

10 **Veijola L**, Oksanen A, Löfgren T, Sipponen P, Karvonen AL, Rautelin H. Comparison of three stool antigen tests in confirming *Helicobacter pylori* eradication in adults. *Scand J Gastroenterol* 2005; **40**: 395-401

11 **Rautelin H**, Kosunen TU. *Helicobacter pylori* infection in Finland. *Ann Med* 2004; **36**: 82-88

12 **Oksanen A**, Veijola L, Sipponen P, Schauman KO, Rautelin H. Evaluation of Pyloriset Screen, a rapid whole-blood diagnostic test for *Helicobacter pylori* infection. *J Clin Microbiol* 1998; **36**: 955-957

13 **Pettersson A**, Rasmussen M, Kyrönpalo S, Sipponen P, Rautelin H, Färkkilä M, Oksanen A. A 10 minutes tablet based 13C-Urea breath test for the diagnosis of *Helicobacter pylori*. *Gastroenterology* 2001; **120 (Suppl 1):** A579

14 **Gatta L**, Vakil N, Ricci C, Osborn JF, Tampieri A, Perna F, Miglioli M, Vaira D. A rapid, low-dose, 13C-urea tablet for the detection of Helicobacter pylori infection before and after treatment. *Aliment Pharmacol Ther* 2003; **17:** 793-798

15 **Agha-Amiri K**, Peitz U, Mainz D, Kahl S, Leodolter A, Malfertheiner P. A novel immunoassay based on monoclonal antibodies for the detection of *Helicobacter pylori* antigens in human stool. *Z Gastroenterol* 2001; **39**: 555-560

16 **Andrews J**, Marsden B, Brown D, Wong VS, Wood E, Kelsey M. Comparison of three stool antigen tests for *Helicobacter pylori* detection. *J Clin Pathol* 2003; **56**: 769-771

17 **Koletzko S**, Konstantopoulos N, Bosman D, Feydt-Schmidt A, van der Ende A, Kalach N, Raymond J, Russmann H. Evaluation of a novel monoclonal enzyme immunoassay for detection of Helicobacter pylori antigen in stool from children. *Gut* 2003; **52:** 804-806

18 **Leodolter A**, Peitz U, Ebert MP, Agha-Amiri K, Malfertheiner P. Comparison of two enzyme immunoassays for the assessment of Helicobacter pylori status in stool specimens after eradication therapy. *Am J Gastroenterol* 2002; **97:** 1682-1686

19 **Makristathis A**, Barousch W, Pasching E, Binder C, Kuderna C, Apfalter P, Rotter ML, Hirschl AM. Two enzyme immunoassays and PCR for detection of Helicobacter pylori in stool specimens from pediatric patients before and after eradication therapy. *J Clin Microbiol* 2000; **38:** 3710-3714

20 **Chisholm SA**, Watson CL, Teare EL, Saverymuttu S, Owen RJ. Non-invasive diagnosis of Helicobacter pylori infection in

adult dyspeptic patients by stool antigen detection: does the rapid immunochromatography test provide a reliable alternative to conventional ELISA kits? *J Med Microbiol* 2004; **53:** 623-627

21 **Gatta L**, Perna F, Ricci C, Osborn JF, Tampieri A, Bernabucci V, Miglioli M, Vaira D. A rapid immunochromatographic assay for *Helicobacter pylori* in stool before and after treatment. *Aliment Pharmacol Ther* 2004; **20**: 469-474

22 **Wu IC**, Ke HL, Lo YC, Yang YC, Chuang CH, Yu FJ, Lee YC, Jan CM, Wang WM, Wu DC. Evaluation of a newly developed office-based stool test for detecting Helicobacter pylori: an extensive pilot study. *Hepatogastroenterology* 2003; **50:** 1761-1765

23 **Leodolter A**, Wolle K, Peitz U, Schaffranke A, Wex T, Malfertheiner P. Evaluation of a near-patient fecal antigen test for the assessment of *Helicobacter pylori* status. *Diagn Microbiol Infect Dis* 2004; **48**: 145-147

24 **Li YH**, Guo H, Zhang PB, Zhao XY, Da SP. Clinical value of Helicobacter pylori stool antigen test, ImmunoCard STAT HpSA, for detecting H pylori infection. *World J Gastroenterol* 2004; **10:** 913-914

25 **Makristathis A**, Hirschl AM, Lehours P, Megraud F. Diagnosis of *Helicobacter pylori* infection. *Helicobacter* 2004; **9 (Suppl 1):** 7-14

26 **Vaira D**, Vakil N. Blood, urine, stool, breath, money, and *Helicobacter pylori*. *Gut* 2001; **48**: 287-289

27 **Lerang F**, Haug JB, Moum B, Mowinckel P, Berge T, Ragnhildstveit E, Bjorneklett A. Accuracy of IgG serology and other tests in confirming Helicobacter pylori eradication. *Scand J Gastroenterol* 1998; **33:** 710-715

28 **Odaka T**, Yamaguchi T, Koyama H, Saisho H, Nomura F. Evaluation of the Helicobacter pylori stool antigen test for monitoring eradication therapy. *Am J Gastroenterol* 2002; **97**: 594-599

29 **Vaira D,** Vakil N, Menegatti M, van't Hoff B, Ricci C, Gatta L, Gasbarrini G, Quina M, Pajares Garcia JM, van Der Ende A, van Der Hulst R, Anti M, Duarte C, Gisbert JP, Miglioli M, Tytgat G. The stool antigen test for detection of Helicobacter pylori after eradication therapy. *Ann Intern Med* 2002; **136:** 280-287

Science Editor Guo SY **Language Editor** Elsevier HK

PO Box 2345, Beijing 100023, China
www.wjgnet.com
wjg@wjgnet.com

ELSEVIER

World J Gastroenterol 2005;11(46):7345-7350
World Journal of Gastroenterology ISSN 1007-9327

• *RAPID COMMUNICATION* •

Disrupted NF-κB activation after partial hepatectomy does not impair hepatocyte proliferation in rats

Stéphanie Laurent, Yves Horsmans, Peter Stärkel, Isabelle Leclercq, Christine Sempoux, Luc Lambotte

Stéphanie Laurent, Yves Horsmans, Peter Stärkel, Isabelle Leclercq, Christine Sempoux, Luc Lambotte, Gastroenterology, Pathology and Experimental Surgery Laboratories, Université catholique de Louvain, 1200 Brussels, Belgium
Supported by a grant from Glaxo-Smithkline, Belgium, a grant from Astra Zeneca, Belgium, and a grant (3-4598) of FRSM, Belgium
Correspondence to: Professor Yves Horsmans, Department of Gastroenterology, St. Luc University Hospital, Av. Hippocrate 10, 1200 Brussels, Belgium. horsmans@gaen.ucl.ac.be
Telephone: +32-27642822
Received: 2005-02-18 Accepted: 2005-09-16

Abstract

AIM: To analyze the effects of NF-κB inhibition by antioxidant pyrrolidine dithiocarbamate (PDTC) or TNF inhibitor pentoxifylline (PTX) on liver regeneration after partial hepatectomy (PH).

METHODS: Saline, PDTC or PTX were injected 1 h before PH and rats were killed at 0.5 and 24 h after PH. Several control groups were used for comparison (injection control groups).

RESULTS: Compared to saline injected controls, NF-κB activation was absent 0.5 h after PH in rats treated with PDTC or PTX. At 24 h after PH, DNA synthesis and PCNA expression were identical in treated and control rats and thus occurred irrespectively of the status of NF-κB activation at 0.5 h. Signal transducer and activator of transcription 3 (Stat3) activation was observed already 0.5 h after PH in saline, PDTC or PTX group and was similar to Stat3 activation in response to injection without PH.

CONCLUSION: These data strongly suggest that (1) NF-κB p65/p50 DNA binding produced in response to PH is not a signal necessary to initiate the liver regeneration, (2) Stat3 activation is a stress response unrelated to the activation of NF-κB. In conclusion, NF-κB activation is not critically required for the process of liver regeneration after PH.

Key words: Partial hepatectomy; Nuclear factor kappa B; Signal transducer and activator of transcription 3; Hepatocyte proliferation; Antioxidant

Laurent S, Horsmans Y, Stärkel P, Leclercq I, Sempoux C, Lambotte L. Disrupted NF-κB activation after partial hepatectomy does not impair hepatocyte proliferation in rats. *World J Gastroenterol* 2005; 11(46): 7345-7350
http://www.wjgnet.com/1007-9327/11/7345.asp

INTRODUCTION

The mechanisms initiating the regenerative response after partial hepatectomy (PH) remain controversial. Several lines of evidence point to the critical role of the activation of nuclear factor kappa B (NF-κB)[1,2]. This is one of the earliest events constantly detectable in the liver after PH and the previous findings have advocated NF-κB being a critical effector of the cascade initiating the regenerative process[3,4]. Some authors also emphasize an anti-apoptotic role of NF-κB during the regenerative process[5]. Mice lacking TNF receptor type 1 (TNF-R1) showed deficient NF-κB binding, low interleukin-6 (IL-6) production, decreased signal transducer and activator of transcription 3 (Stat3) activation and low levels of hepatocyte DNA replication after PH[6-8]. Based on this and similar observations, it has been proposed that activation of the NF-κB pathway is a critical step to usher cells into the cell cycle in response to PH. This process might also require the sequential activation of TNF/NF-κB/IL-6 and Stat3. However, recent studies using mice lacking the common signal transducer of all IL-6 family members gp130 showed only minor effects on the cell cycle and on the peak of DNA synthesis after PH despite an abolished acute phase response and inhibition of Stat3[9]. Moreover, recent studies in a model of transgenic mice, with specific inhibition of NF-κB at the hepatocyte level, did not impair DNA synthesis and did not increase liver apoptosis[10]. In order to clarify the importance of the activation of NF-κB in the liver regeneration process, we have evaluated the consequences of NF-κB inhibition on downstream activation of Stat3 and DNA synthesis after PH. Numerous exogenous and endogenous stimuli are capable of inducing NF-κB activity[11], but the pathways leading to NF-κB activation are complex. One of them involves oxidative stress with elevated level of reactive oxygen species[12,13]. We have therefore administered the anti-oxidant pyrrolidine dithiocarbamate (PDTC), a compound with metal chelator properties that has been used as a reversible inhibitor of NF-κB *in vitro* and *in vivo*[14-17]. Increased production of TNF-α is a potential activator of NF-κB after PH[4], although the source of TNF-α after

PH has not been entirely elucidated. To reduce TNF-α production, we administered pentoxifylline (PTX), a methylxanthine derivative, which has been demonstrated to suppress LPS-induced TNF-α production[18-20]. It may also modulate the expression of other cytokines like IL-6 and IL-1[21,22].

MATERIALS AND METHODS

Animals

Male Wistar rats (220-270 g body weight) were obtained from the Rat Breeding Facilities of the Catholic University of Louvain Medical School, Brussels, Belgium. All animals were kept in a temperature- and humidity-controlled environment in a 12 h light-dark cycle. At all times, they were allowed free access to water and standard food pellet diet (Usine d'Alimentation Rationnelle, Villemoisson-sur-Orges, France). The animals were handled according to the guidelines established by the Catholic University of Louvain.

Surgical procedures and experimental design

All animal manipulations were carried out under light ether anesthesia at room air between 9:00 a.m. and 12:00 noon with the use of a clean, but non-sterile technique. PH consisted in mid-ventral laparotomy and resection of the left lateral and median lobes (70% of the liver), according to Higgins and Anderson[23]. Saline, PDTC (100 mg/kg) and PTX (100 mg/kg) were injected intraperitoneally (i.p.) to the rats 1 h before PH. The rats were killed under ether anesthesia by exsanguination after the puncture of the abdominal aorta and transection of the inferior vena cava in the thoracic cavity, at 0.5 h after PH, i.e. 1 h 30 min after the initial injection of saline or the active compound, and 24 h after PH. Several additional control groups were used for comparison: (1) rats administered saline, PDTC or PTX without PH and killed 1 h after the injection (injection control group), (2) naïve rats that received neither injection not PH (true controls). The livers were removed, lobes were rapidly weighed, snap frozen in liquid nitrogen and stored at -80 ℃. A minimum of three rats was killed in each group at each of the indicated time points.

Preparation of nuclear extracts and electrophoretic mobility shift assays (EMSA)

Nuclear extracts were prepared as previously described[24]. Protein content was determined using a bicinchoninic acid (BCA) protein assay with serum albumin as a standard (Pierce Chemical, Rockford, IL, USA).

Six to ten micrograms of nuclear proteins were pre-incubated for 10 min at room temperature with 2 μg poly (dI-dC) in the following binding buffers: NF-κB (20 mmol/L Hepes, 60 mmol/L KCl, 5 mmol/L $MgCl_2$, 0.2 mmol/L EDTA, 0.5 mmol/L PMSF, 0.5 mmol/L DTT, glycerol 10%, Nonidet P40 1%); Stat3 (10 mmol/L Hepes, 50 mmol/L NaCl, 1 mmol/L EDTA, glycerol 10%). Double stranded oligonucleotides were ^{32}P end-labeled with γ-^{32}P ATP and added to the extracts (10^5 cpm). The mixtures were incubated for 30 min at room temperature and then electrophoresed (200 V, 2 h) on a 5% polyacrylamide gel in a 1× TBE buffer (25 mmol/L Tris-HCl, 25 mmol/L boric acid, 0.5 mmol/L EDTA). To confirm the identity of the protein/DNA complex, supershift analysis was performed: 4 μL of specific antibody (1 μg/μL) was added to the samples after 30 min of incubation with the labeled probe and incubated for a further 30 min. Polyclonal antibodies against NF-κB components p50 and p65, but also p52, c-rel, and rel-B, and anti-Stat3 were purchased from Santa Cruz (CA, USA). The following probes were used: chromatography-purified double stranded oligonucleotides from the class I major histocompatibility complex enhancer element H2κB; TCGAGGGCTGGGGATTCCC CATCTC (NF-κB) and from the serum-inducible factor binding element in the c-fos promoter; CCAGCATTTCCCGTAAATCCTCCAG; (Stat3). A rabbit reticulocyte (Promega Benelux, Leiden, Netherlands) and an EGF-stimulated A431 cell nuclear extract (Santa Cruz Biotechnology) were used as standards for NF-κB and Stat3, respectively. Gels were dried and exposed to a Kodak Biomax MS film (NEN™ Life Science Products, Inc., Boston, MA, USA) for 16 to 24 h.

Thymidine incorporation

One hour before being killed, 50 μCi of [^{3}H]-Thymidine (Amersham, Buckinghamshire, UK) was administrated into the femoral vein under light ether anesthesia. At the time of killing (24 h after PH), livers were removed, weighed and rapidly snap frozen in liquid nitrogen and stored at -80 ℃. Hepatic DNA synthesis was evaluated by measuring the incorporation of [^{3}H]-Thymidine into the DNA. Total hepatic DNA was extracted as previously described[25], and incorporation of radioactive nucleotide was measured in a liquid scintillation counter (Wallac 1409, Turku, Finland). Its value is expressed as disintegrations per minute (dpm) per μg of DNA. All samples were analyzed in duplicate.

PCNA labeling index

Sections from formalin fixed liver tissue (5 μm thick) were air-dried at 37 ℃ overnight and dewaxed. Slides were incubated for 30 min in H_2O_2 0.3% to inhibit endogenous peroxidases, then in TBS containing 10% normal goat serum (NGS, APP Products Ltd, West Midlands, UK) to block non-specific binding sites. Slides were incubated in a monoclonal primary anti-PCNA mouse antibody (PC10, Dako, Denmark; 1:100; overnight), and after washing, with the secondary antibody (anti-mouse antibody; Boehringer, Mannheim, Germany; 1:500; 30 min) followed by streptavidin peroxidase (Boehringer, Mannheim, Germany; 1:1 000; 30 min). Peroxidase activity was revealed by immersion of the slides for 10 min in a 3,3-diaminobenzidine hypochloride solution (DAB 50 mg/100 mL, pH 7.4, Amersham, Cardiff, UK) supplemented with 0.02% H_2O_2. All slides were treated simultaneously to ensure homogeneity of the technique. PCNA labeling index was obtained by examining 3-5 high-power fields in three rats per group. Each field was divided into four zones,

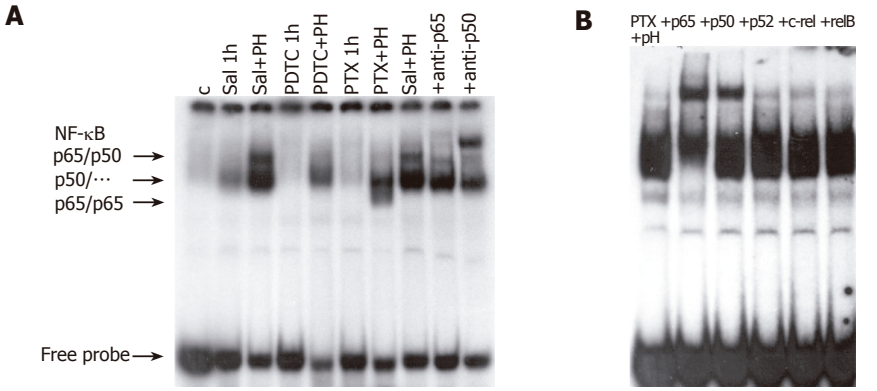

Figure 1 Effect of saline, PDTC, and PTX on NF-κB binding activity. **A:** Nuclear extracts were prepared from non-treated rats (control), from rats injected with saline, PDTC or PTX subjected or not to partial hepatectomy (PH). No NF-κB DNA binding activity was observed in the liver nuclear extracts of non-treated rats (controls) nor 1 h after injection of PDTC or PTX. Faint DNA binding was noticed 1 h after the injection of saline which mainly corresponds to NF-κB p50. Thirty minutes after PH, strong DNA binding was observed in saline-treated groups and two complexes were identified. Supershift experiments identified the upper complex in saline +PH as p65/p50. In the PTX group, a third complex was present 0.5 h after PH, which migrated faster than the dose obtained after saline; **B:** Detailed supershift experiments showed that this faster migrating complex in the PTX+PH group was completely supershifted with the p65 antibody. p52, c-rel and rel-B had no influence on the NF-κB DNA binding activity.

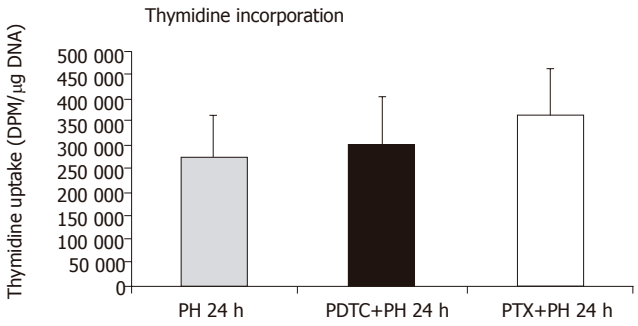

Figure 2 Thymidine incorporation. Similar thymidine incorporation was obtained 24 h after PH in rats pre-treated with an injection of PDTC or PTX compared to non-treated partial hepatectomized rats.

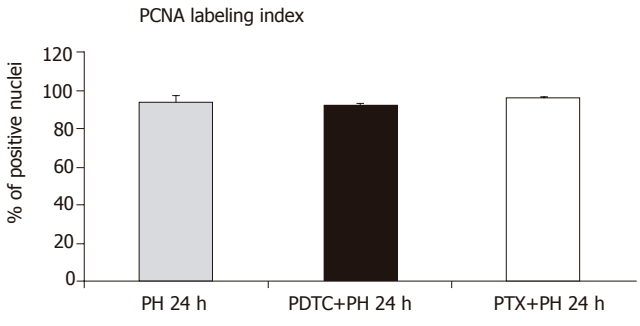

Figure 3 PCNA labeling index. Similar PCNA labeling index was obtained 24 h after PH in rats pre-treated with an injection of PDTC, or PTX compared to non-treated partial hepatectomized rats.

zone 1 being closest to the centrolobular vein and zone 4 corresponding to the periportal areas. Labeling index was defined as the ratio between marked cells and total counted cells.

The same experimented pathologist examined all the slides carefully to detect evidence of necrosis or apoptosis.

Statistical analysis

Results were expressed as mean±SE. The statistical differences between the groups were tested using the one-way analysis of variance (ANOVA), followed by Student-Newman-Keuls multiple comparison tests. Statistical significance was admitted for a P value of <0.05.

RESULTS

Effect of saline, PDTC, and PTX on NF-κB binding activity (Figure 1A)

NF-κB p65/p50 DNA binding activity was not detected in the liver of untreated rats (lane 1) nor in the livers from non-hepatectomized rats 1 h after i.p. injection of saline (lane 2), PDTC (lane 4) or PTX (lane 6). NF-κB was strongly activated 0.5 h after PH preceded by saline injection (lane 3), similarly to activation observed 0.5 h after PH alone[24]. Supershift analysis confirmed the binding of the heterodimer p65/p50 NF-κB complex (lanes 8-10). Injection of PDTC or PTX 1 h before PH prevented the occurrence of the expected p65/p50 DNA binding complex at 0.5 h after PH, since the upper complex was not observed on EMSA (lanes 5 and 7). However, two distinct faster-migrating complexes have been found after PTX (lane 7). The first one, also present after saline or PDTC injection, was partially supershifted by p50 antibody; the second one totally disappeared with p65 antibody. Supershift assays performed with p52, rel B, and c-rel had no influence on this lower complex (Figure 1B).

Effect of PDTC and PTX on hepatocyte proliferation 24 h after PH (Figures 2 and 3)

Hepatocyte proliferation was followed by PH peaks at 24 h. Pretreatment of rats with PDTC or PTX 1 h prior to PH had no effect on liver regeneration. Thymidine incorporation was indeed similarly elevated in all the groups (Figure 2). In untreated rats, 90% of hepatocytes

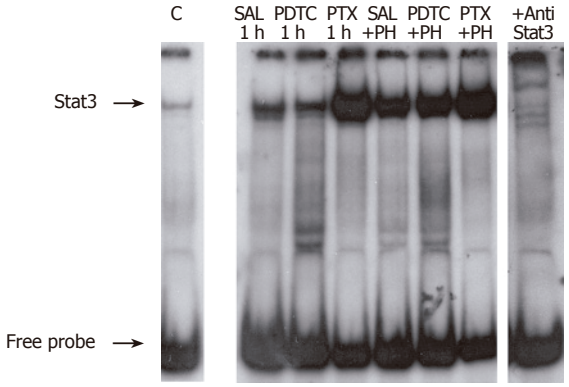

Figure 4 Effect of saline, PDTC and PTX on Stat3 DNA binding activity. No Stat3 DNA binding activity was identified in controls (C). Injection of saline, PDTC or PTX enhanced the binding at 1 h. At 0.5 h after PH, strong Stat3 DNA binding was observed in rats injected with saline, PDTC or PTX. Supershift experiments with a Stat3 specific antibody confirmed that Stat3 is the principal compound of these DNA-binding complexes.

nuclei expressed PCNA 24 h after HP. Pretreatment with PDTC or PTX did not modify the proportion of PCNA positive nuclei in agreement with the thymidine incorporation (Figure 3). No evidence of liver necrosis or massive apoptosis was observed by histological examination.

Effect of injection of saline, PDTC and PTX on Stat3 binding activity (Figure 4)

Stat3 DNA binding activity was not detected in the liver of untreated rats (lane 1), but a Stat3 DNA binding complex was present in the livers from non-hepatectomized rats receiving saline 1 h before being killed (lane 2), PDTC (lane 3) or PTX (lane 4). PH was associated with high Stat3 activity at 0.5 h in animals pretreated with saline (lane 5), PDTC (lane 6) or PTX (lane 7), contrasting with very low Stat3 activation after PH in non-injected rats at this time point. Indeed, as already reported by us and others, PH in non-injected rats was followed by slight Stat3 activation at 0.5 h after PH, peaked at 3 h and was still detected till 8 h[24,26]. Identity of Stat3 was confirmed by supershift analysis with a specific Stat3 antibody (lane 8).

DISCUSSION

PH induces an early cellular response involving pro-inflammatory cytokines like TNF-α or IL-6[27-29] and transcription factors molecules such as NF-κB and Stat3[3,4,30]. In the initiation of proliferating response following hepatic cell mass reduction, a key role seems to be attributed to the activation of the transcription factor NF-κB. The inducible NF-κB factor regulates the expression of numerous genes involved in immune, inflammatory and cellular growth control[11,31,32]. Migrating to the nucleus as soon as 0.5 h after PH[3], it induces the transcription of a large set of immediate-early genes[33]. The NF-κB p65 subunit, important for liver development[34], is responsible for the transcriptional activity of NF-κB[35] and also for its anti-apoptotic effects, preventing the cytotoxic effect of TNF-α and cell death[36,37]. Convergent data suggest that this mediator collaborates with other acute phase gene products in order to protect the cells during the regenerative process[5,38-40]. The most active form of NF-κB is a heterodimer consisting of subunits p50 or NF-κB1 and p65 also called RelA, which contains the transactivation domain necessary for the induction of target genes[41,43]. This active form has been identified after PH as the post-hepatectomy factor[3,30]. Although not consistently reported, the activation of NF-κB after PH has been supposed to be related to an increased expression of TNF-α, although not consistently reported, and/or to oxidative stress[2]. However, various other non specific stimuli are able to induce this activation[44]. Although the importance of the TNF-α pathway has been outlined[6-8], recent studies analyzing liver regeneration in different types of knockout mice suggest that a complete regenerative response may occur in the absence of early factors such as TNF-α, IL-6 or Stat3[43,45]. In order to investigate the role of NF-κB activation in determining the progression into the cell cycle and liver regeneration, we analyzed the effect of NF-κB inhibition on hepatocyte proliferation after PH in normal rat with otherwise normal cytokine expression, regulation and signaling capabilities. Two strategies have been used to prevent NF-κB activation. First, we administered an antioxidant molecule (PDTC) to reduce the oxidative stress, a known stimulus of NF-κB activation. Second, we aimed at decreasing the influence of TNF-α by reducing its production by the use of PTX. PTX and PDTC effectively prevented the activation of NF-κB p65/p50 complex observed 0.5 h after PH in non-treated and saline-treated animals. Despite this absence of NF-κB activation, the hepatocytes responded to the proliferation stimulus: PCNA expression as well as DNA synthesis analyzed 24 h post-PH were normal compared to a classical PH. At that time we did not observe any evidence of liver necrosis or massive apoptosis compared to livers from untreated animals (data not shown). This last observation is in contrast with the results obtained when NF-κB is inhibited by an adenoviral vector expressing a mutated form of IκB-α[5]. The inhibition of NF-κB using this adenoviral vector led to massive apoptosis but also failed to interfere with hepatocyte proliferation. This massive apoptosis could be induced by the adenovirus itself which causes increase of TNF levels and apoptosis before PH. More recently, it has been advocated that the activation of NF-κB in hepatocytes is not needed to induce liver regeneration after PH[10]. The authors also postulated that a preserved activation in non-parenchymal cells could be sufficient to drive both proliferative and anti-apoptotic effects of NF-κB during liver regeneration. This last assumption cannot be found in our experiments, since the inhibition of NF-κB was not targeted to a specific cell type in the liver and, in principal, the substances used in our experiments do act on all liver cell types including the non-parenchymal cells.

We observed that PTX induced another DNA binding

complex after PH, migrating faster, and partially supershifted by the p65 antibody. The functional role of such a complex is not elucidated but may constitute a compensatory response of the Rel family of transcription factors to substitute the usual factor. In a recent study using $p50^{-/-}$ mice[46], PH was associated with a normal regenerative response. P65 protein expression was elevated but without p65/p50 DNA binding activity suggesting that p65 could be part of other complexes, allowing normal regeneration. Considering our data and those obtained in p50 knockout mice, the p65/p50 DNA binding after PH does not seem to be absolutely required for proper liver regeneration. PTX is a potent inhibitor of TNF production which inhibited NF-κB activation but without reducing liver regeneration. These data further reinforce the absence of a link between NF-κB activation and hepatocyte proliferation. However, they do not bring any information concerning a role for TNF-α in the initiation of liver regeneration, since the expression of this factor was not investigated in the study. In contrast to the data demonstrating the quasi absence of Stat3 activation during the first hour after PH[24,26], an early activation of Stat3 was observed as soon as 0.5 h after PH preceded by saline, PDTC and PTX. This suggested that Stat3 was already induced in our model by the first stimulus, i.e. the injection and the required animal handling. This hypothesis was confirmed by the increased Stat3 DNA binding obtained after a single injection of saline, PDTC and PTX. It seems therefore that Stat3 is a component of the acute-phase response induced by stress procedures as minimal as the i.p. injection. This rather non-specific origin for Stat3 activation does not exclude that this factor may play an important role in liver regeneration as documented in studies conducted in IL-6 and TNFR-1 knockout mice in which the restoration of the Stat3 DNA binding following IL-6 supplementation corrected the impaired liver regeneration process[6,47]. It seems thus that Stat3 activation, which is a part of the priming process as described by Bucher *et al.*[48], can be produced by a great variety of stimuli and not necessarily by the PH itself.

As demonstrated previously, sham operation also induced activation of NF-κB and Stat3[24]. PH preceded by a sham operation was associated with a second activation of these transcription factors[49]. In this work, the i.p. injection is a minor stress compared to a sham operation. However, the i.p. injection procedure produced by itself an activation of Stat3 that persisted at the time of PH and probably for a longer period, possibly masking the effects induced by this second intervention. By contrast, a NF-κB response was clearly observed after PH when only saline was injected. When drugs able to inhibit NF-κB activation were injected, this response was indeed suppressed but the proliferation indices were not affected. An activation of liver NF-κB seems thus unnecessary to initiate liver regeneration in those conditions. In conclusion, and in complement to those of others using a transgenic model, our data strongly suggest that an increase of liver NF-κB p65/p50 DNA binding as an immediate response to PH is not essential for inducing liver cell proliferation.

ACKNOWLEDGMENTS

We thank Valérie Lebrun and Véronique Van Den Berge for expert technical assistance and Alain Saliez for carrying out the surgical procedures.

REFERENCES

1 **Akerman P**, Cote P, Yang SQ, McClain C, Nelson S, Bagby GJ, Diehl AM. Antibodies to tumor necrosis factor-alpha inhibit liver regeneration after partial hepatectomy. *Am J Physiol* 1992; **263**: G579-G585
2 **Kirillova I**, Chaisson M, Fausto N. Tumor necrosis factor induces DNA replication in hepatic cells through nuclear factor kappaB activation. *Cell Growth Differ* 1999; **10**: 819-828
3 **Cressman DE**, Greenbaum LE, Haber BA, Taub R. Rapid activation of post-hepatectomy factor/nuclear factor kappa B in hepatocytes, a primary response in the regenerating liver. *J Biol Chem* 1994; **269**: 30429-30435
4 **FitzGerald MJ**, Webber EM, Donovan JR, Fausto N. Rapid DNA binding by nuclear factor kappa B in hepatocytes at the start of liver regeneration. *Cell Growth Differ* 1995; **6**: 417-427
5 **Iimuro Y**, Nishiura T, Hellerbrand C, Behrns KE, Schoonhoven R, Grisham JW, Brenner DA. NFkappaB prevents apoptosis and liver dysfunction during liver regeneration. *J Clin Invest* 1998; **101**: 802-811
6 **Yamada Y**, Kirillova I, Peschon JJ, Fausto N. Initiation of liver growth by tumor necrosis factor: deficient liver regeneration in mice lacking type I tumor necrosis factor receptor. *Proc Natl Acad Sci USA* 1997; **94**: 1441-1446
7 **Yamada Y**, Fausto N. Deficient liver regeneration after carbon tetrachloride injury in mice lacking type 1 but not type 2 tumor necrosis factor receptor. *Am J Pathol* 1998; **152**: 1577-1589
8 **Yamada Y**, Webber EM, Kirillova I, Peschon JJ, Fausto N. Analysis of liver regeneration in mice lacking type 1 or type 2 tumor necrosis factor receptor: requirement for type 1 but not type 2 receptor. *Hepatology* 1998; **28**: 959-970
9 **Wuestefeld T**, Klein C, Streetz KL, Betz U, Lauber J, Buer J, Manns MP, Muller W, Trautwein C. Interleukin-6/glycoprotein 130-dependent pathways are protective during liver regeneration. *J Biol Chem* 2003; **278**: 11281-11288
10 **Chaisson ML**, Brooling JT, Ladiges W, Tsai S, Fausto N. Hepatocyte-specific inhibition of NF-kappaB leads to apoptosis after TNF treatment, but not after partial hepatectomy. *J Clin Invest* 2002; **110**: 193-202
11 **Baldwin AS JR**. The NF-kappa B and I kappa B proteins: new discoveries and insights. *Annu Rev Immunol* 1996; **14**: 649-683
12 **Schreck R**, Rieber P, Baeuerle PA. Reactive oxygen intermediates as apparently widely used messengers in the activation of the NF-kappa B transcription factor and HIV-1. *EMBO J* 1991; **10**: 2247-2258
13 **Bowie A,** O'Neill LA. Oxidative stress and nuclear factor-kappaB activation: a reassessment of the evidence in the light of recent discoveries. *Biochem Pharmacol* 2000; **59:** 13-23
14 **Brennan P**, O'Neill LA. Effects of oxidants and antioxidants on nuclear factor kappa B activation in three different cell lines: evidence against a universal hypothesis involving oxygen radicals. *Biochem Biophys Acta* 1995; **1260**: 167-175
15 **Schreck R**, Meier B, Mannel DN, Droge W, Baeuerle PA. Dithiocarbamates as potent inhibitors of nuclear factor kappa B activation in intact cells. *J Exp Med* 1992; **175**: 1181-1194
16 **Pinkus R**, Weiner LM, Daniel V. Role of oxidants and antioxidants in the induction of AP-1, NF-kappaB, and glutathione S-transferase gene expression. *J Biol Chem* 1996; **271**: 13422-13429
17 **Lauzurica P**, Martinez-Martinez S, Marazuela M, Gomez del Arco P, Martinez C, Sanchez-Madrid F, Redondo JM. Pyrrolidine dithiocarbamate protects mice from lethal shock induced by LPS or TNF-alpha. *Eur J Immunol* 1999; **29**:

1890-1900
18 **LeMay LG**, Vander AJ, Kluger MJ. The effects of pentoxifylline on lipopolysaccharide (LPS) fever, plasma interleukin 6 (IL 6), and tumor necrosis factor (TNF) in the rat. *Cytokine* 1990; **2**: 300-306
19 **Doherty GM**, Jensen JC, Alexander HR, Buresh CM, Norton JA. Pentoxifylline suppression of tumor necrosis factor gene transcription. *Surgery* 1991; **110**: 192-198
20 **Refsum SE**, Halliday MI, Campbell G, McCaigue M, Rowlands BJ, Boston VE. Modulation of TNF alpha and IL-6 in a peritonitis model using pentoxifylline. *J Pediatr Surg* 1996; **31**: 928-930
21 **Voisin L**, Breuille D, Ruot B, Ralliere C, Rambourdin F, Dalle M, Obled C. Cytokine modulation by PX differently affects specific acute phase proteins during sepsis in rats. *Am J Physiol* 1998; **275**: R1412-R1419
22 **Nelson JL**, Alexander JW, Mao JX, Vohs T, Ogle CK. Effect of pentoxifylline on survival and intestinal cytokine messenger RNA transcription in a rat model of ongoing peritoneal sepsis. *Crit Care Med* 1999; **27**: 113-119
23 **Higgins GM**, Anderson RM. Restoration of the liver of the white rat following partial surgical removal. *Arch Pathol* 1931; **12**: 186-202
24 **Laurent S**, Otsuka M, De Saeger C, Maiter D, Lambotte L, Horsmans Y. Expression of presumed specific early and late factors associated with liver regeneration in different rat surgical models. *Lab Invest* 2001; **81**: 1299-1307
25 **Vander Borght TM**, Lambotte LE, Pauwels SA, Dive CC. Uptake of thymidine labeled on carbon 2: a potential index of liver regeneration by positron emission tomography. *Hepatology* 1990; **12**: 113-118
26 **Cressman DE**, Diamond RH, Taub R. Rapid activation of the Stat3 transcription complex in liver regeneration. *Hepatology* 1995; **21**: 1443-1449
27 **Fausto N**, Laird AD, Webber EM. Liver regeneration. 2. Role of growth factors and cytokines in hepatic regeneration. *FASEB J* 1995; **9:** 1527-1536
28 **Diehl AM**, Rai R. Review: regulation of liver regeneration by pro-inflammatory cytokines.. *FASEB J* 1996; **11**: 466-470
29 **Trautwein C**, Rakemann T, Niehof M, Rose-John S, Manns MP. Acute-phase response factor, increased binding, and target gene transcription during liver regeneration. *Gastroenterology* 1996; **110**: 1854-1862
30 **Tewari M**, Dobrzanski P, Mohn KL, Cressman DE, Hsu JC, Bravo R, Taub R. Rapid induction in regenerating liver of RL/IF-1 (an I kappa B that inhibits NF-kappa B, RelB-p50, and c-Rel-p50) and PHF, a novel kappa B site-binding complex. *Mol Cell Biol* 1992; **12**, 2898-2908
31 **Sha WC**. Regulation of immune responses by NF-kappa B/Rel transcription factor. *J Exp Med* 1998; **187**: 143-146
32 **Mercurio F**, Manning AM. NF-kappaB as a primary regulator of the stress response. *Oncogene* 1999; **18**: 6163-6171
33 **Pahl HL**. Activators and target genes of Rel/NF-kappaB transcription factors. *Oncogene* 1999; **18**: 6853-6866
34 **Beg AA**, Sha WC, Bronson RT, Ghosh S, Baltimore D. Embryonic lethality and liver degeneration in mice lacking the RelA component of NF-kappa B. *Nature* 1995; **376**: 167-170
35 **Schmitz ML**, Baeuerle PA. The p65 subunit is responsible for the strong transcription activating potential of NF-kappa B. *EMBO J* 1991; **10**: 3805-3817
36 **Beg AA**, Baltimore D. An essential role for NF-kappaB in preventing TNF-alpha-induced cell death. *Science* 1996; **274**: 782-784
37 **Van Antwerp DJ**, Martin SJ, Verma IM, Green DR. Inhibition of TNF-induced apoptosis by NF-kappa B. *Cell Biol* 1998; **8**: 107-111
38 **Xu Y**, Bialik S, Jones BE, Iimuro Y, Kitsis RN, Srinivasan A, Brenner DA, Czaja MJ. NF-kappaB inactivation converts a hepatocyte cell line TNF-alpha response from proliferation to apoptosis. *Am J Physiol* 1998; **275**: C1058-C1066
39 **Plumpe J**, Malek NP, Bock CT, Rakemann T, Manns MP, Trautwein C. NF-kappaB determines between apoptosis and proliferation in hepatocytes during liver regeneration. *Am J Physiol Gastrointest Liver Physiol* 2000; **278**: G173-G183
40 **Leu JI**, Crissey MA, Leu JP, Ciliberto G, Taub R. Interleukin-6-induced STAT3 and AP-1 amplify hepatocyte nuclear factor 1-mediated transactivation of hepatic genes, an adaptive response to liver injury. *Mol Cell Biol* 2001; **21**: 414-424
41 **Grilli M**, Chiu JJ, Lenardo MJ. NF-kappa B and Rel: participants in a multiform transcriptional regulatory system. *Int Rev Cytol* 1993; **143**: 1-62
42 **Ghosh S**, May MJ, Kopp EB. NF-kappa B and Rel proteins: evolutionarily conserved mediators of immune responses. *Annu Rev Immunol* 1998; **16**: 225-260
43 **Sakamoto T**, Liu Z, Murase N, Ezure T, Yokomuro S, Poli V, Demetris AJ. Mitosis and apoptosis in the liver of interleukin-6-deficient mice after partial hepatectomy. *Hepatology* 1999; **29**: 403-411
44 **Baeuerle PA, Henkel T.** Function and activation of NF-kappa B in the immune system. *Annu Rev Immunol* 1994; **12**: 141-179
45 **Fujita J**, Marino MW, Wada H, Jungbluth AA, Mackrell PJ, Rivadeneira DE, Stapleton PP, Daly JM. Effect of TNF gene depletion on liver regeneration after partial hepatectomy in mice. *Surgery* 2001; **129**: 48-54
46 **DeAngelis RA**, Kovalovich K, Cressman DE, Taub R. Normal liver regeneration in p50/nuclear factor kappaB1 knockout mice. *Hepatology* 2001; **33**: 915-924
47 **Cressman DE**, Greenbaum LE, DeAngelis RA, Ciliberto G, Furth EE, Poli V, Taub R. Liver failure and defective hepatocyte regeneration in interleukin-6-deficient mice. *Science* 1996; **274**: 1379-1383
48 **Bucher NL**, Schrock TR, Moolten FL. An experimental view of hepatic regeneration. *Johns Hopkins Med J* 1969; **125**: 250-257
49 **Laurent S**, Stärkel P, Starkel P, Leclercq IA, Lambotte L, Maiter D, Horsmans Y. Molecular events associated with accelerated proliferative response in rat livers when partial hepatectomy is preceded by a sham operation. *Eur J Clin Invest* 2005; **35**: 140-147

Science Editor Guo SY and Xu XQ **Language Editor** Elsevier HK

PO Box 2345, Beijing 100023, China
www.wjgnet.com
wjg@wjgnet.com

ELSEVIER

World J Gastroenterol 2005;11(46):7351-7354
World Journal of Gastroenterology ISSN 1007-9327

• RAPID COMMUNICATION •

Serum arylesterase and paraoxonase activity in patients with chronic hepatitis

Suleyman Sirri Kilic, Suleyman Aydin, Nermin Kilic, Fazilet Erman, Suna Aydin, İlhami Celik

Suleyman Sirri Kilic, İlhami Celik, Department of Infection and Clinical Microbiology, Medical School (Firat Medical Center), Firat University, Elazig 23119, Turkey
Suleyman Aydin, Nermin Kilic, Fazilet Erman, Department of Biochemistry and Clinical Biochemistry, Medical School (Firat Medical Center), Firat University, Elazig 23119, Turkey
Suna Aydin, Department of Medical Education, Medical School (Firat Medical Center), Elazig 23119, Turkey
Correspondence to: Dr Suleyman Aydin, Department of Biochemistry and Clinical Biochemistry, Medical School (Firat Medical Center), Firat University, Elazig 23119, Turkey. saydinl@hotmail.com
Telephone: +90-533-4934643 Fax: +90-424-2379138
Received: 2005-01-19 Accepted: 2005-04-18

Abstract

AIM: To investigate the relationship between serum paraoxonase (PON1), AST, ALT, GGT, and arylesterase (AE) activity alterations and the degree of liver damage in patients with chronic hepatitis.

METHODS: We studied 34 chronic hepatitis patients and 32 control subjects, aged between 35 and 65 years, in the Department of Infection and Clinical Microbiology at the Firat University School of Medicine. Blood samples were collected from subjects between 8:00 and 10:00 a.m. following a 12-h fast. Baseline and salt-stimulated PON1 activities were measured by the hydrolysis of paraoxon. Phenyl acetate was used as the substrate and formed phenol was measured spectrophotometrically at 270 nm after the addition of a 10-fold diluted serum sample in AE activity measurements.

RESULTS: The results of this investigation revealed that the levels of AE activity decreased from 132±52 to 94±36 (29%), baseline PON1 activity from 452±112 to 164±67 (64%), salt-stimulated PON1 activity from 746±394 to 294±220 (61%), HDL from 58.4±5.1 to 47.2±5.6 (20%), triglyceride from 133±51.2 to 86±34.0 (35%), while a slight increase in the level of LDL (from 163±54.1 to 177.3±56.0; 9%) and significant increases in the levels of AST (from 29±9.3 to 98±44), ALP (from 57.2±13.1 to 91±38.1), ALT (from 27.9±3.32 to 89±19.1), GGT (from 24.3±2.10 to 94±48.2), total bilirubin (from 0.74±0.02 to 1.36±0.06; 84%) and direct bilirubin (from 0.18±0.01 to 0.42±0.04; 133%) were detected. However, the levels of albumin, total protein, cholesterol, and uric acid were almost the same in chronic hepatitis and the control subjects.

CONCLUSION: Low PON1 and AE activity may contribute to the increased liver dysfunction in chronic hepatitis patients by reducing the ability of HDL to retard LDL oxidation and might be clinically useful for monitoring the disease of chronic hepatitis.

Key words: Paraoxonase; Arylesterase; Chronic hepatitis; Lipoproteins

Kilic SS, Aydin S, Kilic N, Erman F, Aydin S, Celik I. Serum arylesterase and paraoxonase activity in patients with chronic hepatitis. *World J Gastroenterol* 2005; 11(46): 7351-7354
http://www.wjgnet.com/1007-9327/11/7351.asp

INTRODUCTION

The paraoxonase (PON1), a 44-ku glycoprotein, is synthesized mainly in the liver, which hydrolyzes organophosphates like pesticides, neurotoxins, and arylesters[1-4]. PON1 activity exhibits a substrate-dependent activity polymorphism in human beings[4-6]. This polymorphism is related to two polymorphic sites at amino acid positions. One at position 192, which is a glutamine→arginine substitution, hydrolyzes paraoxon with a high enzyme activity, and the other at position 55, which is a leucine→methione substitution causes a low enzyme activity[7]. The activity of PON1 shows great inter-ethnic variability[8-11]. The gene frequency for $PON1_{R192}$ allele is 0.31 in Turkish population[11] and in Caucasian population[8], 0.41 in Hispanic populations, 0.66 in a Japanese population[8]. Three different phenotypes are reported based on the responses of the two isoenzymes to salt concentrations[6,12]. The ratio of salt-stimulated PON1 activity to arylesterase (AE) activity is used for the definition of phenotypes[6,12,13].

Environmental factors that change PON1 activity include tobacco consumption, which has been reported to depress PON1 activity and concentration[14]. Also, several studies have shown that PON1 level is tightly linked with HDL in the serum and contributes to the protection conferred by HDL against LDL oxidation. Human paraoxonase (PON), an HDL-associated enzyme carried on apo A-I, is believed to protect lipoproteins against oxidative modification[15,16].

As mentioned above, the role of PON1 and AE activity may be particularly meaningful as an index of liver func-

tion status because preliminary studies have revealed a remarkable decrease of serum AE activity in patients with liver cirrhosis[17,18], and AE and PON1 activities have been demonstrated to be a function of a single enzyme[19].

To the best of our knowledge, although AE and PON1 activities have been demonstrated to be a function of a single enzyme[19], both PON1 (only studied by Ferre *et al*.[20]), and AE activity (only studied partly[17,18]) in chronic HBV have not been studied together, as yet. The paucity of data on serum PON1 and AE does not allow for a conclusion about its role in chronic HBV. Therefore, we carried out this study aiming to compare PON1 and AE activities and traditional standard biochemical test of liver function parameters (such as, ALT, AST, and so on), and whether there were changes due to chronic hepatitis.

MATERIALS AND METHODS

We studied 34 chronic hepatitis patients and 32 control subjects, aged between 35 and 65 years, in the Department of Infection and Clinical Microbiology at the Firat University School of Medicine. Control subjects were healthy and evaluated for any symptoms of clinical or analytical evidence of diabetes, renal disease, cardiovascular disease, neoplasia, or hepatic damage and were matched for age and body mass index. Cirrhosis was graded according to Child-Pugh criteria[21]. Blood samples were collected from subjects between 8:00 and 10:00 a.m. following a 12-h fast. The extracted blood samples were then centrifuged at 4 000 r/min for 10 min and stored at -70 ℃ until the assay was performed. This study was performed with the approval of the ethics committee and all subjects volunteered for the study with informed consent.

Assay of paraoxonase activity

PON1 assays were done without additional NaCl (baseline activity) and with 1 mol/L NaCl included in the assay buffer (salt-stimulated activity), following the formation of *p*-nitrophenol by its absorbance at 405 nm for 5 min. Assay buffer contained 0.125 mol/L Tris-HCl (pH 8.5), 1.25 mmol/L $CaCl_2$, and 1 mol/L NaCl (pH 8.5)[4,12]. For each set of assays, 6 mmol/L freshly prepared paraoxon (*O,O*-diethyl-*O*-*p*-nitrophenylphosphate; Sigma Chemical Co.) substrate solution of 120 mmol/L paraoxon in acetone diluted with 0.125 mmol/L Tris-HCl was used. Paraoxon stock solution was handled very cautiously with protective measures. The assay tube contained 750 μL of Tris buffer, 50 μL of serum (1:2 diluted with water) and 200 μL of 6 mmol/L paraoxon. The reaction was initiated at 37 ℃ by the addition of the substrate solution, and using a Techcomp 8500 II Spectrophotometer, absorbance was continuously monitored at 405 nm and 25 ℃. The PON1 unit was defined as the enzyme quantity that disintegrates 1 μmol paraoxon substrate in one minute[4,12]. The percent stimulation of PON1 was calculated as follows[6]: [(PON1 activity with 1 mol/L NaCl)-(basal activity)/basal PON1 activity]×100.

Assay of arylesterase activity

AE activity was measured with phenylacetate as a substrate as previously described[17,18,22]. AE activity was affected with salt. The assay tube contained 750 μL of 0.1 mol/L Tris-HCl (pH 8.5), 1 mmol/L $CaCl_2$, 125 μL of 12 mmol/L phenylacetate and 125 μL of serum (1:10 diluted with water). The absorbance was continuously monitored at 270 nm and 37 ℃. The units were expressed as millimoles of phenylacetate hydrolyzed per minute.

Biochemical parameters of liver function

Serum AST, ALT, ALP, GGT, albumin, total protein, indirect bilirubin, total bilirubin and other biochemical parameters were analyzed with an auto analyzer (Olympus 600).

Statistical analysis

Statistical analysis was performed using Student's *t* test for group comparisons and data for biochemical analyses were expressed as mean±SD. Pearson's correlation coefficients were used to test the correlation between each of the two biochemical variables. Multiple linear regression analysis was used between PON1 and AE activity and possible determinants, such as AST, ALT, ALP, and GGT. A *P* value less than 0.05 was considered statistically significant.

RESULTS

Laboratory results of the standard liver functions tests are documented in Table 1, and provide evidence of the spectrum of disease. As expected, the levels of AST, ALT, ALP, and GGT in the chronic hepatitis patients were significantly increased as compared to the controls. Increased values of transaminase were also matched by a corresponding rise in serum bilirubin. The serum PON1 and AE were obviously correlated with each HDL parameter and triglyceride (TG) in chronic hepatitis patients compared to the controls.

In the present study, we also observed markedly elevated LDL (9%) and decreased HDL (20%) in chronic hepatitis patients as compared to the controls (Table 1). The activities of AE were significantly reduced (by 29%) in the chronic hepatitis group (94±36 U/mL) compared with the control group (132±52 U/mL, $P<0.001$, Table 1). Furthermore, PON1 baseline activity was significantly decreased (by 64%) in the chronic hepatitis group (164±98 U/mL) as compared with the control group (452±138 U/mL, $P<0.001$, Table 1). Also, salt-stimulated serum PON1 activity was decreased (by 61%) in chronic hepatitis group (294±220 U/mL) as compared with the control group (746 ±394 U/mL, $P<0.001$, Table 1).

Comparison of serum PON1/AE activity and traditional standard biochemical test of liver function

We observed negative correlations between ALT and AE activities ($r = -0.112$, $P<0.11$), as well as between the percent stimulation of PON1 and ALT ($r = -0.412$, $P<0.05$) in the chronic hepatitis patients, but not in the controls ($r = 0.142$). In addition, we found obvious negative

Table 1 Traditional standard biochemical test of liver function and some other parameters (mean±SD)

Parameters	Control (n = 32)	Chronic hepatitis (n = 34)
ALT (U/L)	27.9±3.12	89±19.1[b]
AST (U/L)	8±44	29±9.3
GGT (U/L)	24.3±2.10	94±48.2[b]
ALP (U/L)	57.2±13.1	91±38.1[b]
Albumin (mg/dL)	4.83±0.28	4.62±0.17
Total bilirubin (mg/dL)	0.74±0.02	1.36±0.06[b]
Direct bilirubin (mg/dL)	0.18±0.01	0.42±0.03[b]
Total protein (mg/dL)	7.3±0.18	7.3±0.42[a]
Cholesterol (mg/dL)	196±23.3	187±23.2[a]
Uric acid (mg/dL)	4.9±0.33	5.2±0.29[a]
HDL (mg/dL)	58.4±5.4	47.1±5.6[a]
LDL (mg/dL)	163±54.1	177.3±56.0[b]
TG (mg/dL)	133±51.2	86±34.0[b]
[1]Salt-stimulated PON1 (U/mL)	746±364	294±220[a]
Baseline PON1 (U/mL)	452±112	164±67[b]
AE (U/mL)	132±52	94±36[b]

[a]P<0.05, [b]P<0.001 *vs* control subjects; [1]salt stimulated activity.

correlations between GGT and AE activities (r = -0.901, P<0.01), as well as between the percent stimulation of PON1 and ALT (r = -0.412, P<0.05), but not such correlation in the controls (r = -0.122, not significant). We also previously reported similar correlations between AE and PON levels in severe pre-eclamptic women[23].

ALP activity was also correlated with PON1 (r = -0.41, P<0.05) and AE (r = -0.44, P<0.03) activities in the chronic hepatitis group, but not in the controls (r = 0.102). This moderate correlation might be a result of ALP demonstration in different tissues such as bone and small bowel when compared with ALT, which is demonstrated only in the liver.

DISCUSSION

Chronic HBV infection is one of the most important diseases leading to a high morbidity and mortality due to the development of liver failure, liver cirrhosis (LC), and liver cancer[24,25]. There are over 300 million people suffering from HBV infection worldwide[26]. The destruction of liver cells can be extensive, and death follows from liver failure in about 1% of cases. Many of those recover progress to shed the virus for years, while some develop a progressive degenerative liver disease called chronic active hepatitis[24,25,27]. Dramatic alterations in chronic hepatitis remain within laboratory values until gross disease becomes evident. To diagnose such a slow progressive liver disease (chronic hepatitis) before advancing hepatocellular necrosis and fibrosis, beside traditional biochemical tests needs alternative parameters to evaluate liver damage[20].

PON1 and AE activities have been demonstrated in different tissues, such as liver (including microsomes), kidney[28,29], brain[30,31] and lung[30], and it has been studied extensively in relation to cardiovascular diseases[2,3,5,16], whereas there are scarce data available on the hepatic enzyme. Some of these enzymes are released into the circulation and some portions are stored in the liver. Serum PON1, which is carried in circulation bound to HDL particles, protects LDL from peroxidation[2,3,10,14-16,32]. The putative function of PON1 in the liver is to provide hepatic protection against oxidative stress[33].

In the present study, the relation between serum PON1 and AE activity levels and chronic hepatitis was examined. We observed that PON1 and AE activities were obviously lower in the chronic hepatitis patients compared with the control subjects, and were significantly correlated with each HDL parameter, and consistent with reports that this enzyme is bound to a large apo A-I containing HDL subspecies and also confirmed previously reported results[10,15,34-36]. The decrease in PON1/AE activity in the serum was also correlated with serum AST, ALT, GGT, albumin, and bilirubin concentrations. It has been reported that the diagnostic accuracy of PON1 is equivalent to that of ALT in patients with chronic hepatitis and far superior to that of the other tests in patients with cirrhosis[20]. Our results are in agreement with some recent studies in cirrhotic patients[20], rats[33], and chronic hepatitis patients[17,18].

Serum PON1 and AE are mainly the result of liver activity[17]. We have some possible explanations for decreased PON1 and AE activities with chronic hepatitis. One is that even though hepatic PON1 and AE levels may be normal, serum PON1 and AE activity would be lowered as a result of changes in synthesis or secretion of the HDL secondary. This assumption is supported by other researchers[20,37-39]. Alterations in HDL structure and levels related to decreased serum PON1 activities in mice with LCAT deficiency are the consequence of LCAT gene-targeted disruptions. PON1 and AE have also been reported to play a role in the lipid transfer and assembly of VLDL particles in liver microsomes[39]. The other is that liver cells damaged via chronic hepatitis do not express the protein PON1 and AE. Both have been shown to be functions of single enzymes. Supporting this putative function is the report of inhibition of microsomal PON1 activity in rats with chronically administered CCl_4[32]. So, elevated LDL and decreased HDL might have a causal role in the pathogenesis of chronic hepatitis. It is known that PON1 is bound to HDL and acts as an antioxidant that protects LDL from oxidative modifications and can reduce oxidized lipids in oxidized lipoproteins[23].

In conclusion, a significant decrement in PON1 and AE is probably the consequence of liver dysfunction. For this reason, serum PON1 and AE activities could be a beneficial tool for chronic hepatitis patients. However, further research is needed to elucidate the mechanism leading to decreased serum PON1 and AE activities in liver diseases and potential pathophysiologic implications.

ACKNOWLEDGMENTS

We thank Dr. Mehmet Ozdin for help in the initial experimental stage.

REFERENCES

1 **Aldridge WN.** Serum esterases. II. An enzyme hydrolysing diethyl p-nitrophenyl phosphate (E600) and its identity with the A-esterase of mammalian sera. *Biochem J* 1953; **53:** 117-124
2 **Mackness MI**, Arrol S, Abbott C, Durrington PN. Protection of low-density lipoprotein against oxidative modification by high-density lipoprotein associated paraoxonase. *Atherosclerosis* 1993; **104:** 129-135
3 **Nevin DN**, Zambon A, Seidel SL, Motulsky AG. Role of genetic polymorphism of human plasma paraoxonase/arylesterase in hydrolysis of the insecticide metabolites chlorpyrifos oxon and paraoxon. *Am J Hum Genet* 1988; **43:** 230-238
4 **Furlong CE**, Richter RJ, Min WK, Kim JQ. Genetic variations of the paraoxonase gene in patients with coronary artery disease. *Clin Biochem* 2001; **34:** 475-481
5 **Hong SH**, Song J, Min WK, Kim JQ. Genetic variations of the paraoxonase gene in patients with coronary artery disease. *Clin Biochem* 2001; **34:** 475-481
6 **Eckerson HW**, Wyte CM, La Du BN. The human serum paraoxonase/arylesterase polymorphism. *Am J Hum Genet* 1983; **35:** 1126-1138
7 **Playfer JR**, Eze LC, Bullen MF, Evans DA. Genetic polymorphism and interethnic variability of plasma paroxonase activity. *J Med Genet* 1976; **13:** 337-42
8 **Furlong CE,** Li WF, Richter RJ, Shih DM, Lusis AJ, Alleva E, Costa LG. Genetic and temporal determinants of pesticide sensitivity: role of paraoxonase (PON1). *Neurotoxicology* 2000; **21:** 91-100
9 **Geldmacher V**, Mallinckrodt M, Diepgen TL. The human paraoxonase-polymorphism and specifity. *Toxicol Env Chem* 1988; **35**: 214–227
10 **Mackness MI**, Harty D, Bhatnagar D, Winocour PH, Arrol S, Ishola M, Durrington PN. Serum paraoxonase activity in familial hypercholesterolaemia and insulin-dependent diabetes mellitus. *Atherosclerosis* 1991; **86:** 193-199
11 **Karakaya A**, Suzen S, Sardas S, Karakaya AE, Vural N. Analysis of the serum paraoxonase/arylesterase polymorphism in a Turkish population. *Pharmacogenetics* 1991; **1:** 58-61
12 **Eckerson HW**, Romson J, Wyte C, La Du BN. The human serum paraoxonase polymorphism: identification of phenotypes by their response to salts. *Am J Hum Genet* 1983; **35**: 214-227
13 **Serhatlioglu S**, Gursu MF, Gulcu F, Canatan H, Godekmerdan A. Levels of paraoxonase and arylesterase activities and malondialdehyde in workers exposed to ionizing radiation. *Cell Biochem Funct* 2003; **21**: 371-375
14 **Mackness MI,** Mackness B, Durrington PN, Connelly PW, Hegele RA. Paraoxonase: biochemistry, genetics and relationship to plasma lipoproteins. *Curr Opin Lipidol* 1996; **7:** 69-76
15 **Gowri MS**, Van der Westhuyzen DR, Bridges SR, Anderson JW. Decreased protection by HDL from poorly controlled type 2 diabetic subjects against LDL oxidation may Be due to the abnormal composition of HDL. *Arterioscler Thromb Vasc Biol* 1999; **19:** 2226-2233
16 **Sanghera DK**, Saha N, Kamboh MI. DNA polymorphisms in two paraoxonase genes (PON1 and PON2) are associated with the risk of coronary heart disease. *Am J Hum Genet* 1998; **62:** 36-44
17 **Burlina A**, Galzigna L. Serum arylesterase isoenzymes in chronic hepatitis. *Clin Biochem* 1974; **7**: 202-205
18 **Burlina A**, Michielin E, Galzigna L. Characteristics and behaviour of arylesterase in human serum and liver. *Eur J Clin Invest* 1977; **7:** 17-20
19 **Primo-Parmo SL**, Sorenson RC, Teiber J, La Du BN. The human serum paraoxonase/arylesterase gene (PON1) is one member of a multigene family. *Genomics* 1996; **33:** 498-507
20 **Ferre N**, Camps J, Prats E, Vilella E, Paul A, Figuera L, Joven J. Serum paraoxonase activity: a new additional test for the improved evaluation of chronic liver damage. *Clin Chem* 2002; **48**: 261-268
21 **Infante-Rivard C,** Esnaola S, Villeneuve JP. Clinical and statistical validity of conventional prognostic factors in predicting short-term survival among cirrhotics. *Hepatology* 1987; **7:** 660-664
22 **Drevenkar V,** Radic Z, Vasilic Z, Reiner E. Dialkylphosphorus metabolites in the urine and activities of esterases in the serum as biochemical indices for human absorption of organophosphorus pesticides. *Arch Environ Contam Toxicol* 1991; **20:** 417-422
23 **Kumru S**, Aydin S, Gursu MF, Ozcan Z. Changes of serum paraoxonase (an HDL-cholesterol-associated lipophilic antioxidant) and arylesterase activities in severe preeclamptic women. *Eur J Obstet Gynecol Reprod Biol* 2004; **114**: 177-181
24 **Wang FS**. Current status and prospects of studies on human genetic alleles associated with hepatitis B virus infection. *World J Gastroenterol* 2003; **9**: 641-644
25 **Cicognani C**, Malavolti M, Morselli-Labate AM, Zamboni L, Sama C, Barbara L. Serum lipid and lipoprotein patterns in patients with liver cirrhosis and chronic active hepatitis. *Arch Intern Med* 1997; **157**: 792-796
26 **Berger G.** Theoretical aspects of signal processing. *Rev Fr Gynecol Obstet* 1989; **84:** 152-7
27 **Stanier RY**, Ingraham JL, Wheelis Mark L, Painter PR. The Microbial World. 5th ed. New Jersey, 1986: 652-623
28 **Chemnitius JM**, Losch H, Losch K, Zech R. Organophosphate detoxicating hydrolases in different vertebrate species. *Comp Biochem Physiol C* 1983; **76:** 85-93
29 **Pla A**, Johnson MK. Degradation by rat tissues in vitro of organophosphorus esters which inhibit cholinesterase. *Biochem Pharmacol* 1989; **38:** 1527-1533
30 **Pond AL,** Coyne CP, Chambers HW, Chambers JE. Identification and isolation of two rat serum proteins with A-esterase activity toward paraoxon and chlorpyrifos-oxon. *Biochem Pharmacol* 1996; **52:** 363-369
31 **Tanimoto N**, Kumon Y, Suehiro T, Ohkubo S, Ikeda Y, Nishiya K, Hashimoto K. Serum paraoxonase activity decreases in rheumatoid arthritis. *Life Sci* 2003; **72**: 2877-2885
32 **Aviram M,** Rosenblat M, Billecke S, Erogul J, Sorenson R, Bisgaier CL, Newton RS, La Du B. Human serum paraoxonase (PON 1) is inactivated by oxidized low density lipoprotein and preserved by antioxidants. *Free Radic Biol Med* 1999; **26:** 892-904
33 **Ferre N**, Camps J, Cabre M, Paul A, Joven J. Hepatic paraoxonase activity alterations and free radical production in rats with experimental cirrhosis. *Metabolism* 2001; **50**: 997-1000
34 **Kono Y**, Hayashida K, Tanaka H, Ishibashi H, Harada M. High-density lipoprotein binding rate differs greatly between genotypes 1b and 2a/2b of hepatitis C virus. *J Med Virol* 2003; **70**: 42-48
35 **Selimoglu MA**, Aydogdu S, Yagci RV. Lipid parameters in childhood cirrhosis and chronic liver disease. *Pediatr Int* 2002; **44**: 400-403
36 **Tacikowski T**, Milewski B, Dzieniszewski J, Nowicka G, Walewska-Zielecka B. Comparative analysis of plasma lipoprotein components assessed by ultracentrifugation in primary biliary cirrhosis and chronic hepatitis. *Med Sci Monit* 2000; **6**: 325-329
37 **Sabesin SM**, Hawkins HL, Kuiken L, Ragland JB. Abnormal plasma lipoproteins and lecithin-cholesterol acyltransferase deficiency in alcoholic liver disease. *Gastroenterology* 1977; **72**: 510-518
38 **Forte TM,** Oda MN, Knoff L, Frei B, Suh J, Harmony JA, Stuart WD, Rubin EM, Ng DS. Targeted disruption of the murine lecithin:cholesterol acyltransferase gene is associated with reductions in plasma paraoxonase and platelet-activating factor acetylhydrolase activities but not in apolipoprotein J concentration. *J Lipid Res* 1999; **40:** 1276-1283
39 Neimark II. Experience in the diagnosis and treatment of cancer of the rectum. *Vopr Onkol* 1976; **22:** 85-91

Science Editor Kumar M and Guo SY **Language Editor** Elsevier HK

PO Box 2345, Beijing 100023, China
www.wjgnet.com
wjg@wjgnet.com

ELSEVIER

World J Gastroenterol 2005;11(46):7355-7358
World Journal of Gastroenterology ISSN 1007-9327

• *RAPID COMMUNICATION* •

Effects of fermented soy milk on the liver lipids under oxidative stress

Ching-Yi Lin, Zheng-Yu Tsai, I-Chi Cheng, Shyh-Hsiang Lin

Ching-Yi Lin, Zheng-Yu Tsai, I-Chi Cheng, Shyh-Hsiang Lin, Graduate Institute of Nutrition and Health Sciences, Taipei Medical University, Taipei, Taiwan, China
Supported by the fund from Taiwan Tobacco & Liquor Company (TTL) for the financial support on this project
Correspondence to: Shyh-Hsiang Lin, Graduate Institute of Nutrition and Health Sciences, Taipei Medical University, (110) 250 Wu-Hsing Street, Taipei, Taiwan, China. lin5611@tmu.edu.tw
Telephone: +886-2-27361661 Fax: +886-2-27373112
Received: 2005-03-22 Accepted: 2005-08-26

Abstract

AIM: To investigate the effects of fermented soy milk powder on the antioxidative status and lipid metabolism in the livers of CCl_4-injected rats.

METHODS: Forty-five healthy male Sprague-Dawley rats were randomly assigned to five groups according to five different diets: control (AIN-76), AIN-76+high-dose fermented soy milk powder, AIN-76+low-dose fermented soy milk powder, AIN-76+high-dose milk yogurt powder and AIN-76+low-dose milk yogurt powder. The experiment lasted for 8 wk. After 4 wk, all the rats received intraperitoneal administration of CCl_4 (0.2 mL/100 g body weight) every week. Total cholesterol (TC), triglyceride (TG), TBARS, ALP, and antioxidative enzymes in the liver were evaluated.

RESULTS: There was also no significant difference in TBARS and antioxidative enzymes in the liver. TC and TG in the groups fed with fermented soy milk powder were generally lower than those fed with casein powder.

CONCLUSION: Consumption of fermented soy milk was positive in lowering total cholesterol and TG accumulation in the liver under CCl_4-induced oxidative stress.

Key words: Soy; Fermented soy milk; Antioxidative; Liver protection

Lin CH, Tsai ZY, Cheng IC, Lin SH. Effects of fermented soy milk on the liver lipids under oxidative stress. *World J Gastroenterol* 2005; 11(46): 7355-7358
http://www.wjgnet.com/1007-9327/11/7355.asp

INTRODUCTION

Soybeans contain valuable nutritional attributes. It has been found that the intake of soy foods is closely related to lowering the occurrences of chronic diseases[1]. There are many functional ingredients contained in soy foods such as soy protein, isoflavones, saponins, phytic acid, phytosterol, and phenolic acid[2-4]. Compared to casein, soy protein showed a greater antioxidative ability in preventing lipid oxidation[5]. Isoflavones have been found to increase the activities of some antioxidative enzymes in the liver[6]. Soy foods in Oriental countries can be divided into two categories: unfermented and fermented products. Fermented soy products have been greatly researched recently because their nutritional attributes may be changed due to the metabolism of microorganisms. Fermented soy milk, unlike fermented milk or yogurt drinks, contains no lactose or cholesterol and may have the health benefits from both soy itself and the fermentation. Cheng *et al*.[7] suggested that consumption of fermented soy milk was beneficial to human intestinal health. Our purpose was to investigate the effect of fermented soy milk on liver protection under induced oxidative stress.

MATERIALS AND METHODS

Fermented soy milk

Fermented soy milk was provided by Taiwan Tobacco & Liquor Cooperation (TTL, Taipei, Taiwan, China) Spray drying was applied to produce fermented soy milk powder.

Animals

Forty-five 6-wk-old healthy male Sprague-Dawley (SD) rats (National Laboratory Animal Center, Taiwan, China) were randomly assigned to five groups according to different diets. Guidelines for the ethical care and treatment of animals from the Animal Care Committee at Taipei Medical University were strictly followed. Rats were individually housed and maintained in a temperature-controlled (23±2 ℃) room with a 12-h light/dark cycle. They were fed a chow diet for 1 wk before switching to the experimental diet. Five rats were killed to acquire the baseline biological values of liver. Water and food were available *ad libitum*.

Treatment and sample collection

Fasting blood samples from the tail vein were collected in tubes containing heparin on the last day of wk 0, 2, 4, and 6.

Table 1 Composition of different diets (g/25 g)[1]

	CC[2]	HCS	LCS	HCM	LCM
Corn starch	13.2	4.8	9.0	6.7	9.8
Casein	5.0	4.4	4.7	2.1	4.0
Cellulose	1.6	1.1	1.4	1.1	1.4
Soybean oil	1.5	1.5	1.5	1.5	1.5
Mineral mixture	1.5	0.9	1.2	0.9	1.2
Sucrose	1.5	0.9	1.2	0.9	1.2
Vitamin mixture	0.5	0.3	0.4	0.3	0.4
Methionine	0.1	0.1	0.1	0.1	0.1
Fermented soy milk		10.0	5.0		
Milk yogurt				10.0	5.0

[1]Diets were iso-caloric; [2]CC, control group; HCS, high-dose fermented soy milk powder; LCS, low-dose fermented soy milk powder; HCM, high-dose fermented milk powder; LCM, low-dose fermented milk powder.

The blood was then centrifuged for 15 min at 1 400 r/min to separate the plasma and erythrocytes and stored at -80 ℃. Starting from the 4th wk, rats received an abdominal injection of CCl_4 (0.2 mL/100 g body weight) once a week until the end of the experiment. The body weight of each rat was recorded every 2 d. At the end of wk 8, rats were killed, and liver samples were collected, weighed, and stored at -80 ℃.

Diets

The diets were iso-energetically formulated (Table 1). The control diet was AIN76 (CC). Four experimental diets were prepared by mixing 10 g (HCS), 5 g of fermented soy milk powder (LCS), 10 g (HCM), and 5 g of milk yogurt powder (LCM).

Preparation of liver homogenates and lipid extraction

For preparing liver homogenate, 1.5 g of liver samples was mixed with 2.5 mL of buffer (0.25 mol/L sucrose, 1 mmol/L EDTA, and 10 mmol/L Tris-HCl, pH 7.4) and blended at 4 ℃ (avoiding light), followed by centrifugation at 4 500 r/min for 6 min. The isolated liver cells were stored at -80 ℃.

For extracting liver lipid, 1 g of the liver samples was mixed well with 12 mL of chloroform/methanol (2:1) and then filtered. The filtrate was evenly distributed into two test tubes and chloroform/methanol/H_2O (3:48:47) was added to each tube to 10 mL. Then 2 mL of 0.05% $CaCl_2$ was added to each tube, followed by degassing for 15 min and centrifugation at 2 500 r/min and 4 ℃ for 3 min. The supernatant was removed and methanol was added to the sample to 10 mL. The sample in each tube was then mixed together, to which chloroform/methanol (2:1) was added to 25 mL.

Alkaline phosphatase (ALP) determinations

ALP was evaluated using commercial kits (ALP reagent L-type, Wako).

Activities of antioxidant enzymes in the liver

The activities of antioxidative enzymes were determined using commercial kits: superoxide dismutase (SOD, Calbiochem), glutathione peroxidase (GPx, Randox), and glutathione reductase (GR, Randox).

Table 2 Body weights of each group fed with different diets (mean±SD, g)

	Wk 0	Wk 2	Wk 4	Wk 6	Wk 8
	(Before injection of CCl_4)			(After injection of CCl_4)	
CC[1]	223.6±13.61	267.4±16.51	317.0±30.2	371.9±36.5	402.1±25.2
HCS	237.7±11.81	276.5±11.11	338.7±14.11	395.3±17.91	429.0±27.01
LCS	231.4±14.31	272.1±11.01	329.2±9.41	395.0±17.91	435.4±26.71
HCM	231.6±9.71	264.7±9.41	314.3±11.0	367.4±12.82	403.1±10.3
LCM	225.2±10.8	260.6±14.3	309.9±19.9	364.5±17.02	405.3±17.4

[1]CC, HCS, LCS, HCM, LCM, as in Table 1. n = 7-9.

Table 3 Plasma ALP concentration (IU/dL) of each group fed with different diets[1]

	Wk 0	Wk 2	Wk 4	Wk 6	Wk 8
	(Before injection of CCl_4)			(After injection of CCl_4)	
CC	33.8±0.0	51.3±9.5	43.8±14.0	194.4±65.6	303.7±119.9
HCS	50.2±11.1	70.5±8.9	57.8±6.6	472.6±235.1	338.6±130.3
LCS	49.9±21.3	64.2±4.4	47.1±3.6	278.6±205.7	360.7±206.1
HCM	35.1±6.9	56.4±4.9	39.2±6.7	577.8±74.2	548.0±150.8
LCM	37.7±6.8	57.3±8.0	43.0±3.5	255.1±170.3	592.8±115.6

Thiobarbituric acid reactive substances (TBARS)

A blank (0.1 mL of water), a standard (0.1 mL of 4.2 μmol/L malonaldehyde), or 0.1 mL of the sample was mixed well with the reagent (a mixture of 4 mL of 22% sulfuric acid, 0.5 mL of 10% phosphotungstic acid, and 1 mL of 0.67% 2-thiobarbituric acid). Then the mixture was heated in a water bath to 95 ℃ for 1 h. After being cooled with ice water, 2 mL of butanol was added to the sample, followed by centrifugation at 3 000 r/min for 15 min. The optical density of the pinkish upper part was determined using a fluorescence spectrometer with excitation at 515 nm and emission at 555 nm.

Statistical analysis

All the results were presented as mean±SD. Two-way analysis of variance (ANOVA) and the least significant difference test were performed using SAS® 6.13 to analyze the time and diet effects.

RESULTS

Body weights of the animals

During the feeding period, body weights in each group of all the rats increased (Table 2). At the end of the feeding period, the body weights of rats fed with fermented soy milk powder (HCS and LCS) were significantly higher than those in the other groups (P<0.05). None of the rats showed any abnormal condition.

Alkaline phosphatase (ALP) determinations

ALP activity in the plasma was used to evaluate the liver function. Before injection (i.e. before wk 4) of CCl_4, the ALP (Table 3) in any group did not significantly differ. After injecting CCl_4, ALP activities in all the groups increased (P<0.05). HCS and HCM had higher ALP activities than did the other groups. After wk 6, the ALP activities in the HCS and HCM groups had significantly decreased (P<0.05). In wk 8, the ALP activity in the HCS

Table 4 Activities of antioxidative enzymes and concentrations of TBARS, TC, and TG of the liver in CCl_4-treated rats[1] (mean±SD)

	Baseline	CC[1]	HCS	LCS	HCM	LCM
CAT[2]	0.92±0.19	0.25±0.14	0.30±0.123	0.45±0.25	0.47±0.16	0.44±0.27
GPx	703±154	615±166	680±141	857±179	734±94	762±120
GR	613±288	591±160	768±94	906.4±158	772±283	668±125
SOD	0.118±0.035	0.094±0.015	0.082±0.007	0.088±0.026	0.111±0.035	0.084±0.024
TBARS	6.32±0.71	5.53±1.00	6.08±0.77	4.79±0.67	6.24±0.97	5.92±0.97
TC	5.54±0.73	6.69±2.77	5.37±2.71	4.16±1.55	7.07±2.83	7.06±2.85
TG	12.82±0.69	15.86±3.93	18.633±5.62	16.76±0.067	19.60±0.79	20.62±5.21

group had decreased even lower than those in the HCM group ($P<0.05$).

Antioxidative enzymes, TBARS, TC, and TG in the liver (Table 4)

Results showed that at the end of the feeding period, the catalase activity in the liver in all the groups decreased ($P<0.05$), while the activities in CC and HCS rats were significantly lower than those in the other groups ($P<0.05$). The activity of GPx in all the groups did not significantly change through the experiment. The activity of GR in the LCS group significantly increased at the end and was higher than those in the other groups ($P<0.05$), while those in the other groups did not differ from each other and from the baseline. The activities of SOD in all the groups decreased at the end but only those in the HCS and LCS groups were significantly lower than that in the baseline ($P<0.05$).

At the end of feeding period, the TABRS in all the groups did not differ from each other but tended to be lower or significantly lower (CC, LCS, and LCM; $P<0.05$) than that in the baseline. Rats in the LCS and HCS groups had lower TC value than did those in the HCM, LCM, and control groups ($P<0.05$). Rats in the LCS and HCS groups tended to have lower TG than did those in the HCM and LCM groups.

DISCUSSION

The isoflavone contents of HCS and LCS groups were 0.97 and 0.47 mg/d, respectively in our experiment. Converting the amounts for rats to that for a 70-kg adult, values were about 54 and 27 mg of isoflavones daily although the isoflavone contents in the plasma were either trace or undetectable. It has been pointed out that a daily intake of 50 mg of isoflavones is beneficial to health[8]. The reason why the isoflavones were not detected was due to that all rats were fasted for 8 h before their blood samples were collected. It was found that daidzein and genistein in the plasma were undetectable in rats after 8 h of ingestion[9-11]. The time might have been too long for the isoflavones to be detected.

We found that under such doses of CCl_4, all rats in this experiment had similar activities of GPx and GR in the liver no matter if they had consumed fermented soy milk powder or not. This could be due to a relatively high dose of CCl_4. Zavate[12] pointed out that injecting a dose of 0.2 g/100 g BW of CCl_4 in rats resulted in decreases or deactivation in the activities of catalase, SOD, and GPx, and increases in lipid oxidation in the liver. In addition, the CCl_4 injection produced acute damage to the liver. Protection of the liver through food consumption may not be effective enough in a short period.

In the diets of HCS and LCS groups, we found 3-hydroxyanthranilic acid (3-HAA; data not shown). 3-HAA is a by-product of soy fermentation[13]. It has been found as effective as α-tocopherol and was more effective than genistein[14,15] in inhibiting lipid oxidation *in vivo*. The effect of 3-HAA on protecting liver lipids from oxidation needs further research. Other than 3-HAA, many components in soy are antioxidative. Soy isoflavones, soy protein, and saponins all possess antioxidative abilities[16]. Our data did not clearly suggest that consumption of fermented soy powder was effective in reducing TBARS. This could be due to the limitation when applying TBARS to evaluate lipid oxidation in the liver. Massie *et al.*[17] pointed out that the storage time of liver samples before measuring TBARS affected the results. In addition, the antioxidants such as BHT and EDTA added to the test tubes during the preparation of the liver homogenate also affected the outcomes[18]. In our experiment, addition of EDTA was included in the procedure. In addition, Morrow *et al.*[19] found that under high oxidative stress, the oxidative damages to the liver resulted in an increase in F2-isoprostane (F2-IsoPs) which could not be evaluated with TBARS method.

Our result suggested that consumption of fermented soy milk powder slightly reduced the accumulation of TG in the liver caused by CCl_4. Pencil *et al.*[20] indicated that CCl_4 inhibited the secretion of lipoproteins in the liver and altered the metabolism of fatty acids and resulted in fatty livers.

In conclusion, consumption of fermented soy milk was positive in lowering total cholesterol and TG accumulation in the liver under oxidative stress. Fermented soy milk drink is relatively new to the market. The results open an opportunity to further research on the amount and formula of fermented soy milk needed to achieve health benefits.

REFERENCES

1 **Adlercreutz CH,** Goldin BR, Gorbach SL, Hockerstedt KA, Watanabe S, Hamalainen EK, Markkanen MH, Makela TH, Wahala KT, Adlercreutz T. Soybean phytoestrogen intake and cancer risk. *J Nutr* 1995; **125**: 757S-770S

2 **Anderson RL,** Wolf WJ. Compositional changes in trypsin inhibitors, phytic acid, saponins and isoflavones related to soybean processing. *J Nutr* 1995; **125**: 581S-588S

3 **Wang C,** Wixon R. Phytochemicals in soybeans: their potential

health benefits. *Iform* 1999; **10**: 315-321
4 **Yamauchi N,** Yokoo Y, Fujimaki M. Studies on antioxidative activities of amino compounds on fats and oils part III; antioxidative activities of soybean protein hydrolysates and synergistic effect of hydrolysate on tocopherol. *Nippon Shokiuhin Kogyo Gakkaishi* 1975; **22**: 431-421
5 **Sekizaki H,** Yokosawa R, Chinen C, Adachi H, Yamane Y. Synthesis is isoflsvones and their attracting activity to *Aphanomyces euteiches* zoospore. *Biol Pharm Bull* 1993; **16**: 698-701
6 Wei H, Wei L, Frenkel K, Bowen R, Barnes S. Inhibition of tumor promoter-induced hydrogen peroxide formation in vitro and in vivo by genistein. *Nutr Cancer* 1993; **20:** 1-12
7 **Cheng IC,** Shang HF, Lin TF, Wang TH, Lin HS, Lin SH. Effect of fermented soy milk on the intestinal bacterial ecosystem. *World J Gastroenterol* 2005; **11:** 1225-1227
8 **Setchell KD.** Absorption and metabolism of soy isoflavones-from food to dietary supplements and adults to infants. *J Nutr* 2000; **130:** 654S-655S
9 **Uehara M,** Ohta A, Sakai K, Suzuki K, Watanabe S, Adlercreutz H. Dietary fructooligosaccharides modify intestinal bioavailability of a single dose of genistein and daidzein and affect their urinary excretion and kinetics in blood of rats. *J Nutr* 2001; **131:** 787-795
10 **Setchell KDR,** Brown NM, Desai P, Zimmer-Nechemias L, Wolfe BE, Brashear WT, Kirschner AS, Cassidy A, Heubi JE. Bioavailability of pure isoflavones in healthy humans and analysis of commercial soy isoflavone supplements. *J Nutr* 2001; **131**: 1362S-1375S
11 **Watanabe S,** Yamaguchi M, Sobue T, Takahashi T, Miura T, Arai Y, Mazur W, Wahala K, Adlercreutz H. Pharmacokinetics of soybean isoflavones in plasma, urine and feces of men after ingestion of 60 g baked soybean powder (kinako). *J Nutr* 1998; **128**: 1710-1715
12 **Zavate O,** Ivan A, Irinescu A, Barzu A, Lupascu G, Niculescu N, Lungu I, Capsa O, Apostol S, Mereuta M. Sources of hepatitis B virus infection in hospital environment. *Virologie* 1975; **26:** 63-69
13 **Matsuo M.** In vivo antioxidant activity of okara koji, a fermented okara, by Aspergillus oryzae. *Biosci biotecnol biochem* 1997; **61**: 1968-1972
14 **Esaki H,** Onozaki H, Kawakishi S, Osawa T. New antioxidant isolated from tempeh. *J Agric Food Chem* 1996; **44**: 696-700
15 **Thomas SR,** Witting PK, Stocker R. 3-Hydroxyanthranilic acid is an efficient, cell-derived co-antioxidant for alpha-tocopherol, inhibiting human low density lipoprotein and plasma lipid peroxidation. *J Biol Chem* 1996; **271**: 32714-32721
16 **Esaki H,** Onozaki H, Kawakishi S, Osawa T. Potent antioxidative isoflavones isolated from soybeans fermented with *Aspergillus saitoi. Biosci Biotechnol Biochem* 1998; **62**: 740-746
17 **Massie HR,** Aiello VR, Banziger V. Iron accumulation and lipid peroxidation in aging C57BL/6J mice. *Exp Gerontol* 1983; **18**: 277-285
18 **Gutteridge JM,** Halliwell B. The measurement and mechanism of lipid peroxidation in biological systems. *Trends Biochem Sci* 1990; **15:** 129-135
19 **Morrow JD,** Roberts LJ, Daniel VC, Awad JA, Mirochnitchenko O, Swift LL, Burk RF. Comparison of formation of D2/E2-isoprostanes and F2-isoprostanes in vitro and in vivo--effects of oxygen tension and glutathione. *Arch Biochem Biophys* 1998; **353:** 160-171
20 **Pencil SD,** Brattin WJ Jr, Glende EA Jr, Recknagel RO. Carbon tetrachloride-dependent inhibition of lipid secretion by isolated hepatocytes. Characterization and requirement for bioactivation. *Biochem Pharmacol* 1984; **33:** 2419-2423

Science Editor Guo SY **Language Editor** Elsevier HK

PO Box 2345, Beijing 100023, China
www.wjgnet.com
wjg@wjgnet.com

ELSEVIER

World J Gastroenterol 2005;11(46):7359-7363
World Journal of Gastroenterology ISSN 1007-9327

• *RAPID COMMUNICATION* •

Alteration of chaperonin60 and pancreatic enzyme in pancreatic acinar cell under pathological condition

Yong-Yu Li, Moise Bendayan

Yong-Yu Li, Department of Pathophysiology, Medical College of Tongji University, Shanghai 200092, China
Moise Bendayan, Department of Pathology and Cell Biology, University of Montreal, Montreal, QC, Canada H3C 3J7
Supported by the National Natural Science Foundation of China, No. 30370643, and Shanghai Municipal Health Bureau, China, No. 034111
Correspondence to: Dr. Yong-Yu Li, Department of Pathophysiology, Medical College of Tongji University, Shanghai 200092, China. liyongyu@mail.tongji.edu.cn
Telephone: +86-21-65985447 **Fax:** +86-21-65984556
Received: 2005-03-01 **Accepted:** 2005-04-30

Abstract

AIM: To investigate the changes of chaperonin60 (Cpn60) and pancreatic enzymes in pancreatic acinar cells, and to explore their roles in the development of experimental diabetes and acute pancreatitis (AP).

METHODS: Two different pathological models were replicated in Sprague-Dawley rats: streptozotocin-induced diabetes and sodium deoxycholate-induced AP. The contents of Cpn60 and pancreatic enzymes in different compartments of the acinar cells were measured by quantitative immunocytochemistry.

RESULTS: The levels of Cpn60 significantly increased in diabetes, but decreased in AP, especially in the zymogen granules of the pancreatic acinar cells. The elevation of Cpn60 was accompanied with the increased levels of pancreatic lipase and chymotrypsinogen in diabetes. However, a decreased Cpn60 level was accompanied by high levels of lipase and chymotrypsinogen in AP. The amylase level was markedly reduced in both the pathological conditions.

CONCLUSION: The equilibrium between Cpn60 and pancreatic enzymes in the acinar cells breaks in AP, and Cpn60 content decreases, suggesting an insufficient chaperone capacity. This may promote the aggregation and autoactivation of the premature enzymes in the pancreatic acinar cells and play roles in the development of AP.

Key words: Chaperonin60; Pancreatic enzymes; Immunocytochemistry; Diabetes; Acute pancreatitis

Li YY, Bendayan M. Alteration of chaperonin60 and pancreatic enzyme in pancreatic acinar cell under pathological condition. *World J Gastroenterol* 2005; 11(46): 7359-7363
http://www.wjgnet.com/1007-9327/11/7359.asp

INTRODUCTION

Recently, a great deal of work has focused on a family of specific factors known as molecular chaperones. It has been established that molecular chaperones are involved in protein folding, assembly, disassembly, and degradation under normal conditions. It has also been established that molecular chaperones respond to stress states and certain disorders[1-4]. Previous studies demonstrated that Cpn60 was co-distributed with various secretory proteins in acinar cells of the mammalian exocrine pancreas and associated with pancreatic secretory proteins in the intracellular compartments involved in the secretion, such as the rough endoplasmic reticulum (RER), the Golgi (G), and the zymogen secretory granules (ZG). Cpn60 follows the RER →G→ZG pathway in an increasing gradient as pancreatic enzymes[1,5,6]. The association of Cpn60 and pancreatic enzymes along the secretory pathway was confirmed by immunoprecipitation assay on isolated zymogen granule extracts, where amylase and lipase co-precipitated with Cpn60[5]. However, to our knowledge, there is little information available in literature about the relationship between Cpn60 and the enzymes change and also their significance in pancreatic pathogenesis. Therefore, streptozotocin-induced diabetes and deoxycholate-induced acute pancreatitis (AP) models in the Sprague-Dawley (SD) rats were replicated in order to explore the possible alterations of Cpn60 and pancreatic enzymes in the pancreatic acinar cells under the two experimental pathological conditions.

MATERIALS AND METHODS

Chemicals

Rabbit anti-Cpn60 was purchased from Stressgen, Victoria, BC, Canada. Rabbit anti-lipase, rabbit anti-chymotrypsinogen and protein A-gold complex were prepared in the laboratory as previously described[7,8]. Rabbit anti-amylase, sodium deoxycholate (NaDc), urethane and some other chemical reagents were purchased from Sigma Chemical Co., St. Louis, USA.

Animals and preparation of pathological models

SD male rats (n = 15, part from St. Charles River, Quebec, Canada and part from the Animal Center, Shanghai Medical College of Fudan University, China) were randomly divided into three groups: normal control group (n = 4), AP group (n = 6) and diabetes group (n = 5). (1) AP model: Six rats (each weighing 250 g) were fasted overnight with free access to water. They were anesthetized by an intraperitoneal injection of urethane at 1 g/kg body weight. AP was induced by a retrograde injection of 4% NaDc into the biliopancreatic duct (BPD) using a modified method of Zhang *et al*.[9,10]. After a small median laparotomy, the BPD was temporarily closed at the liver hilum with a soft microvascular clamp to prevent reflux of the infused material into the liver. A retrograde injection of 4% NaDc into the distal BPD was performed (40 mg/kg body weight). The clamp was removed 5 min after the injection. The abdomen was closed and the rats were then kept for 5 h. (2) Diabetes model: Five rats were administered with a single intraperitoneal injection of streptozotocin dissolved in 10 mmol/L citrate buffer (pH 4.5), at 70 mg/kg body weight. The hyperglycemic state developed in the first 72 h after injection and remained throughout the 3 mo of the experiment.

Tissue processing

At the end of the experiments, all the rats were anesthetized with urethane and the splenic parts of the pancreases were removed and fixed by immersion with 10 g/L glutaraldehyde in 0.1 mol/L phosphate buffer (pH 7.4) for 2 h at 4 ℃. The tissue samples were washed with the phosphate buffer, dehydrated in a series of graded ethanol solutions, and embedded in Lowicryl K4M at -20 ℃ as described previously[7]. Ultrathin sections were cut, mounted on Parlodion-carbon-coated nickel grids, and processed for immunocytochemistry.

Immunocytochemistry

The ultrathin sections mounted on nickel grids were incubated by floating them on a drop of 1% ovalbumin in PBS (pH 7.2) for 10 min at room temperature (RT). They were then transferred separately to a drop of differently diluted primary antibodies for 2 h at RT (except 4 h for anti-amylase). The antibodies used here included rabbit anti-Cpn60 (1:10), rabbit anti-lipase (1:10), rabbit anti-chymotrypsinogen (1:10), and rabbit anti-amylase (1:500). The grids were rinsed with PBS, transferred to the ovalbumin solution for 10 min, and then incubated on a drop of the protein A-gold complex (10 nm in diameter)[6] for 30 min. They were then thoroughly washed with PBS and rinsed with distilled water. After staining with uranyl acetate, the sections were examined under a Philips 410 electron microscope. The specificity of each immunolabeling was tested effectively by two control experiments described previously[7].

Evaluation

Morphometrical evaluation of the labeling densities, as a reflection of the quantity, was performed using a Videoplan 2 image processing system. At least 30 micrographs, recorded at 28 000× final magnification, were analyzed for each animal tissue. Labeling densities were evaluated as described previously[6] and were reported as the mean of gold particles/μm^2±SE to the mean. Statistical analyses of the results were carried out using the Student's t-test. P<0.05 was considered statistically significant.

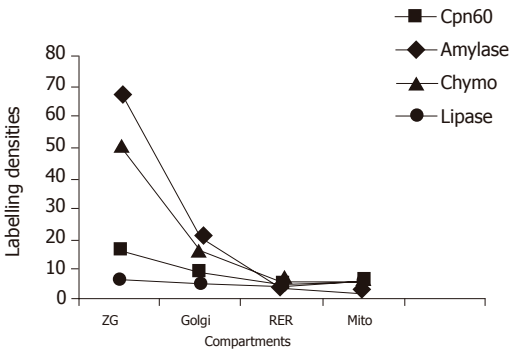

Figure 1 Distribution of Cpn60 and pancreatic enzymes in the compartments of the pancreatic acinar cells in normal rats. Labeling densities (gold particles/μm^2) were measured by immunocytochemistry. ZG: zymogen granules; RER: rough endoplasmic reticulum; Mito: mitochondria; Chymo: chymotrypsinogen.

RESULTS

Distribution of Cpn60 and pancreatic enzymes in the pancreatic acinar cells of rats

Immunocytochemistry labeling study on the sections of the pancreatic tissue revealed that in the acinar cells, both Cpn60 and the pancreatic enzymes, such as lipase, chymotrypsinogen, and amylase, co-existed in the RER, Golgi, and ZG. Increasing gradients of the labeling densities for both Cpn60 and the enzymes were present along the RER-G-ZG secretory pathway, with very low labeling in the mitochondria, in the normal rats and also in the experimental groups. (Figure 1).

Changes of Cpn60 and pancreatic enzymes in the pancreatic acinar cells of diabetic rats

Compared with the normal group, the sections from the diabetic rats showed a significant increase in the Cpn60 labeling density, and also in the lipase and chymotrypsinogen labeling densities, especially in the zymogen granules of the pancreatic acinar cells (Figures 2 and 3). In addition, the immunolabelings of Cpn60 increased nearly 3-fold, lipase 2.5-fold, and chymotrypsinogen was twice as high as the normal group (P<0.05), but amylase level decreased drastically to a very low level (P<0.01 *vs* normal group, Figure 3).

Changes of Cpn60 and pancreatic enzymes in the pancreatic acinar cells of AP rats

In AP, however, the labeling densities of Cpn60 declined through the secretory pathway (RER-G-ZG) of the

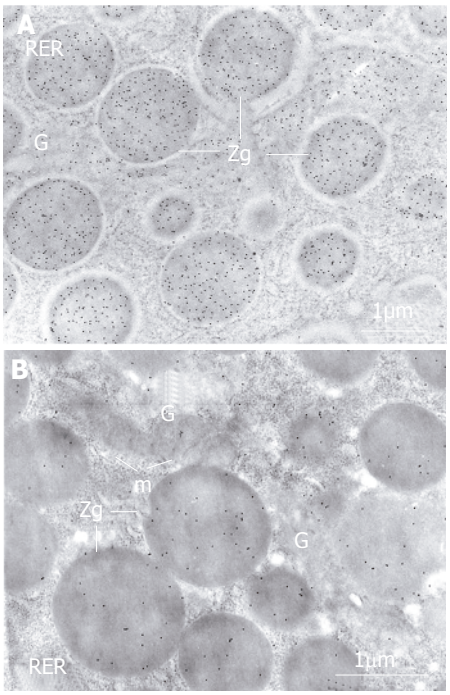

Figure 2 Changes of Cpn60 and pancreatic enzymes in the acinar cells of diabetic rats. The labeling by gold particles (black particles), reflecting Cpn60 antigenic sites, is more intense over the zymogen granules (ZG) in the pancreatic acinar cell in diabetic rat (**A**) compared with that in normal rat (**B**). RER: rough endoplasmic reticulum; G: Golgi; m: mitochondria.

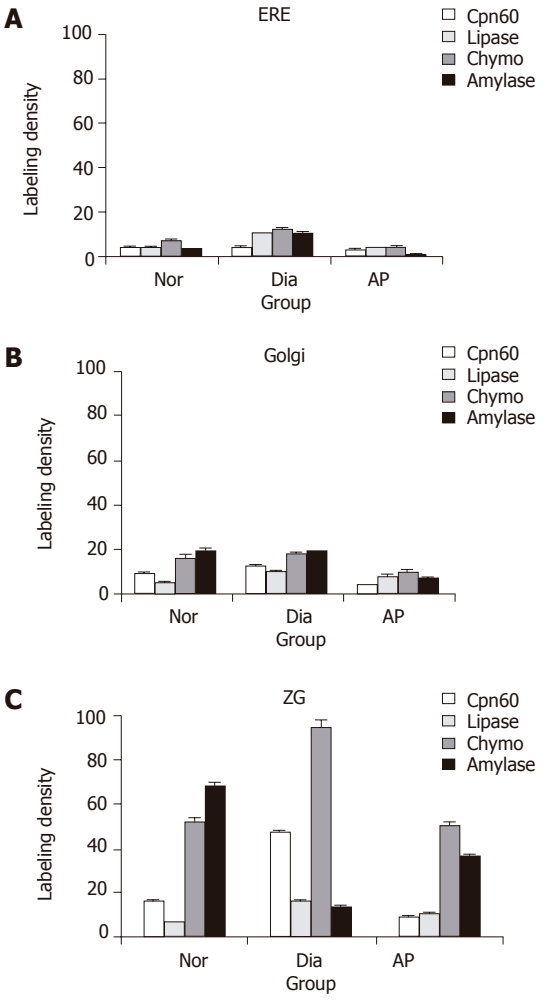

Figure 3 Immunolabeling densities of Cpn60 and the pancreatic enzymes in pancreatic acinar cells rats (particles/μm^2, mean± SE). **A:** Rough endoplasmic reticulum; **B:** Golgi; and **C:** zymogen granules. Nor: normal group; Dia: diabetic group; Chymo: chymotrypsinogen.

pancreatic acinar cells (Figure 3), more significant in the zymogen granules where Cpn60 content decreased about 40% as compared with the normal group (P<0.05). However, lipase markedly increased and chymotrypsinogen was kept at a high level in the compartment, suggesting a nonparallel change with Cpn60 (Figure 3).

DISCUSSION

Molecular chaperones, including chaperonins (Cpn60 and Cpn10), heat shock proteins (Hsps) and other components are a large family of specialized proteins present in various cellular compartments. Some of them play important roles in enabling polypeptides to reach biologically active forms by serving as "detergents" and "proofreading apparatus" during protein synthesis and secretion[11]. In pancreatic acinar cells, like pancreatic enzymes, Cpn60 follows the well-characterized secretory pathway, sequentially increasing along the RER-G-ZG secretory pathway, and finally being discharged into the pancreatic juice[12-14]. In our former work, we have explored and analyzed the characteristic distribution of Cpn60 in the pancreatic acinar cells of rats, and an association of Cpn60 with lipase, amylase, and trypsinogen in the secretory pathway of normal rats[1,5,6].

The interesting finding, in this study, was that lipase and chymotrypsinogen increased to almost two to three times their normal levels in the acinar cells of the diabetic rats. However, the increased enzymes were not aggregated and autoactivated within the acinar cells like what happened in AP. The acinar cells and the pancreatic tissues were not damaged in this situation. The important protective mechanism may be associated with enough chaperon capacity where Cpn60 content increased significantly (nearly threefold) in the pathological condition. In this regard, it has been reported that Cpn60 is involved in successful folding, sorting, and assembly of pancreatic oligomeric polypeptides, and prevents aggregation of the premature polypeptides[15-17]. In addition, the increase of lipase and chymotrypsinogen and the decrease of amylase in diabetes may represent an adaptive process in which the diabetic body reduced starch digestion and then glucose absorption, and exhausted the fat and protein as the energy sources. In this regard, Nagy *et al.*[18] found a temporarily increased lipase content, when plasma free fatty acid concentration was elevated. The present results demonstrated that the pancreatic lipase and chymotrypsinogen were affected by the body metabolism, and confirmed the complicated correlation between the hormones, enzymes, and the metabolic situation of glucose, fat, and proteins in the body.

AP is caused by different etiologic factors, and each of them affects firstly the pancreatic acinar cells, resulting

in the intracellular activation of trypsinogen, and then the lipolytic enzymes which, in turn, injure the acinar cells and the whole pancreas[19,20]. The autodigestion of the pancreas by its own prematurely activated digestive proteases has been considered as an important event in the occurrence of AP[21,22], but the mechanism is under elucidation. Recently, Lee *et al*.[23] found that water immersion stress induced Hsp60 expression, prevented intrapancreatic trypsinogen activation, and then protected against cerulein-induced rat pancreatitis. Other reports also demonstrated that stresses, such as heat, acid, and osmotic shock, induced an increased transcription and production of Cpn60, and showed a protection for the pancreas, which was considered as an "adaptive cytoprotection"[24–26]. It is well known that in the early stage of AP, progressive increases of amylase, trypsin, and lipase levels are found in the ascites and the plasma (hyperenzymemia), and there is also an increase of enzyme content in the individual acinar cells[27,28].

In the present study, increased labeling densities of lipase and chymotrypsinogen were displayed in the AP sections. As an adaptive cytoprotection, the level of Cpn60 should increase; however, the data showed a decreased Cpn60 level and implied an insufficient chaperone capacity. This could in fact alter the steady-state equilibrium between some pancreatic secretory enzymes and chaperones, thus initiating premature enzyme aggregation and autoactivation in acinar cells. In this regard, Strowski *et al*.[29] found that the pancreas reacted to various kinds of stresses with different inductions of Hsp mRNAs during cerulein-induced AP, and they hypothesized that failure to appropriately increase Hsp levels in response to high doses of cerulein might be a factor involved in the development of pancreatitis. The results of our present study also support this hypothesis.

In summary, the changes in Cpn60 levels coincide with the changes of pancreatic enzyme levels, mostly with lipase, chymotrypsinogen in the pancreatic acinar cells. The equilibrium between Cpn60 and the pancreatic enzymes in the acinar cells breaks in AP, and Cpn60 content decreases, thereby suggesting an insufficient chaperone capacity. This may promote pancreatic premature enzyme autoactivation and play a role in the AP pathogenesis. The findings suggest that replenishing Cpn60 and increasing chaperone capacity may be a new therapeutic clue of AP.

ACKNOWLEDGMENTS

We are grateful to Dr. Irene Londono and Ms. Diane Gingras for their competent help with skilled technical assistance.

REFERENCES

1 **Velez-Granell CS,** Arias AE, Torres-Ruiz JA, Bendayan M. Molecular chaperones in pancreatic tissue: the presence of cpn10, cpn60 and hsp70 in distinct compartments along the secretory pathway of the acinar cells. *J Cell Sci* 1994; **107** (Pt 3): 539-549

2 **Bruneau N**, Lombardo D. Chaperone function of a Grp 94-related protein for folding and transport of the pancreatic bile salt-dependent lipase. *J Biol Chem* 1995; **270**: 13524-13533

3 **Rakonczay Z Jr,** Takacs T, Ivanyi B, Mandi Y, Papai G, Boros I, Varga IS, Jost K, Lonovics J. The effects of hypo- and hyperthermic pretreatment on sodium taurocholate-induced acute pancreatitis in rats. *Pancreas* 2002; **24:** 83-89

4 **Keskin O,** Bahar I, Flatow D, Covell DG, Jernigan RL. Molecular mechanisms of chaperonin GroEL-GroES function. *Biochemistry* 2002; **41**: 491-501

5 **Le Gall IM,** Bendayan M. Possible association of chaperonin 60 with secretory proteins in pancreatic acinar cells. *J Histochem Cytochem* 1996; **44**: 1-159

6 **Bendayan M.** Colloidal gold post-embedding immunocytochemistry. *Prog Histochem Cytochem* 1995; **29**: 1-163

7 **Li YY,** Gingras D, Londono I, Bendayan M. Expression differences in mitochondrial and secretory chaperonin 60 (Cpn60) in pancreatic acinar cells. *Cell Stress Chaperones* 2003; **8:** 287-294

8 **Bendayan M,** IIto S. Immunohistochemical localization of exocrine enzymes in normal rat pancreas. *J Histochem Cytochem* 1979; **27:** 1029-1034

9 **Zhang H**, Li YY, Li LJ, Li YS, Wei Y. Therapeutic effect of tetrandrine on experimental acute pancreatitis. *Zunyi Yi Xue Yuan Xue Bao* 2000; **23**: 91-95

10 **Robinson AS,** Bockhaus JA, Voegler AC, Wittrup KD. Reduction of BiP levels decreases heterologous protein secretion in Saccharomyces cerevisiae. *J Biol Chem* 1996; **271**: 10017-10022

11 **Li YY,** Li XL, Yang CX, Zhong H, Yao H, Zhu L. Effects of Tetrandrine and QYT on ICAM-1 and SOD gene expression in pancreas and liver of rats with acute pancreatitis. *World J Gastroenterol* 2003; **9:** 155-159

12 **Arias AE,** Velez-Granell CS, Torres-Ruiz JA, Bendayan M. Involvement of molecular chaperones in the aberrant aggregation of secretory proteins in pancreatic acinar cells. *Exp Cell Res* 1994; **215:** 1-8

13 **Velez-Granell CS**, Arias AE, Torres-Ruiz JA, Bendayan M. Molecular chaperones in pancreatic tissue: the presence of cpn10, cpn60 and hsp70 in distinct compartments along the secretory pathway of the acinar cells. *J Cell Sci* 1994; **107** (Pt 3): 539-549

14 **Bruneau N,** Lombardo D, Levy E, Bendayan M. Roles of molecular chaperones in pancreatic secretion and their involvement in intestinal absorption. *Microsc Res Tech* 2000; **49**: 329-345

15 **Hendrick JP**, Hartl FU. Molecular chaperone functions of heat-shock proteins. *Annu Rev Biochem* 1993; **62**: 349-384

16 **Archibald JM,** Blouin C, Doolittle WF. Gene duplication and the evolution of group II chaperonins: implications for structure and function. *J Struct Biol* 2001; **135:** 157-169

17 **Tabeta K,** Yoshie H, Yamazaki K. Characterization of serum antibody to Actinobacillus actinomycetemcomitans GroEL-like protein in periodontitis patients and healthy subjects. *Oral Microbiol Immunol* 2001; **16**: 290-295

18 **Nagy I,** Nemeth J, Laszik Z. Effect of L-aminocarnitine, an inhibitor of mitochondrial fatty acid oxidation, on the exocrine pancreas and liver in fasted rats. *Pharmacol Res* 2000; **41**: 9-17

19 **Michael L Steer**. Etiology and pathophysiology of acute pancreatitis in Vay Liang W. Go, Emanuel Lebenthal, Eugene P. DiMagno, eds. The Pancreas - Biology, Pathobiology and Disease. *New York: Raven Press* 1993; 581-592

20 **Qiu Y**, Li YY, Li SG, Song BG, Zhao GF. Effect of Qingyitang on activity of intracellular Ca2+-Mg2+-ATPase in rats with acute pancreatitis. *World J Gastroenterol* 2004; **10:** 100-104

21 **Mayer JM,** Rau B, Siech M, Beger HG. Local and systemic zymogen activation in human acute pancreatitis. *Digestion* 2000; **62**: 164-170

22 **Lerch MM,** Gorelick FS. Early trypsinogen activation in acute pancreatitis. *Med Clin North Am* 2000; **84:** 549-563

23 **Lee HS,** Bhagat L, Frossard JL, Hietaranta A, Singh VP, Steer ML, Saluja AK. Water immersion stress induces heat shock protein 60 expression and protects against pancreatitis in rats. *Gastroenterology* 2000; **119**: 220-229

24 **Hennequin C,** Collignon A, Karjalainen T. Analysis of expres-

sion of GroEL (Hsp60) of Clostridium difficile in response to stress. *Microb Pathog* 2001; **31:** 255-260

25 **Otaka M,** Okuyama A, Otani S, Jin M, Itoh S, Itoh H, Iwabuchi A, Sasahara H, Odashima M, Tashima Y, Masamune O. Differential induction of HSP60 and HSP72 by different stress situations in rats. Correlation with cerulein-induced pancreatitis. *Dig Dis Sci* 1997; **42:** 1473-1479

26 **Tashiro M,** Schafer C, Yao H, Ernst SA, Williams JA. Arginine induced acute pancreatitis alters the actin cytoskeleton and increases heat shock protein expression in rat pancreatic acinar cells. *Gut* 2001; **49**: 241-250

27 **Manso MA,** Orfao A, Tabernero MD, Vicente S, de Dios I. Changes in both the membrane and the enzyme content of individual zymogen granules are associated with sodium taurocholate-induced pancreatitis in rats. *Clin Sci (Lond)* 1998; **94:** 293-301

28 **Urunuela A,** Manso MA, Ma Pinto R, Orfao A, De Dios I. Enzyme load in pancreatic acinar cells is increased in the early stages of acute pancreatitis induced by duct obstruction in rats. *Clin Sci* (Lond) 2000; **98:** 143-150

29 **Strowski MZ,** Sparmann G, Weber H, Fiedler F, Printz H, Jonas L, Goke B, Wagner AC. Caerulein pancreatitis increases mRNA but reduces protein levels of rat pancreatic heat shock proteins. *Am J Physiol* 1997; **273:** G937-G945

Science Editor Kumar M and Guo SY **Language Editor** Elsevier HK

PO Box 2345, Beijing 100023, China
www.wjgnet.com
wjg@wjgnet.com

ELSEVIER

World J Gastroenterol 2005;11(46):7364-7367
World Journal of Gastroenterology ISSN 1007-9327

• *RAPID COMMUNICATION* •

Determination of platelet-activating factor by reverse phase high-performance liquid chromatography and its application in viral hepatitis

Hong-Cui Cao, Xiao-Ming Chen, Wei Xu

Hong-Cui Cao, Xiao-Ming Chen, Wei Xu, Department of Infectious Diseases, First Affiliated Hospital, Medical School of Zhejiang University; Key Laboratory of Infectious Diseases of Ministry of Public Health, Hangzhou 310003, Zhejiang Province, China
Supported by a Health Foundation of Zhejiang Province, No. 2004C083, 2004B068
Co-first-authors: Hong-Cui Cao and Xiao-Ming Chen
Correspondence to: Xiao-Ming Chen, Department of Infectious Disease, First Affiliated Hospital, Medical School of Zhejiang University; Key Laboratory of Infectious Disease of Ministry of Public Health, Hangzhou 310003, Zhejiang Province, China. shi9876@hzcnc.com
Telephone: +86-571-87236759
Received: 2005-04-21 Accepted: 2005-07-21

Abstract

AIM: To detect the platelet-activating factor (PAF) and the plasma or serum levels of tumor necrosis factor-α (TNF-α) malondialdehyde (MDA), endotoxin (ET) and to discuss their significance in various types of viral hepatitis.

METHODS: PAF, TNF-α, MDA, and ET levels in 60 controls, 16 cases of acute viral hepatitis, 71 cases of chronic viral hepatitis, 19 cases of severe viral hepatitis were detected by reverse phase high-performance liquid chromatography (rHPLC), bio-assay, ELISA, thiobarbituric acid (TBA), and limulus lysate test (LLT), respectively.

RESULTS: The rHPLC was more sensitive and specific than bio-assay (r = 0.912, P<0.01). The plasma levels of PAF, TNF-α, MDA, and ET in patients with viral hepatitis were higher than those in controls (P<0.01).

CONCLUSION: rHPLC is more reliable and accurate for the detection of PAF.

Key words: Platelet-activating factor; Malondialdehyde; Endotoxin; rHPLC; Viral hepatitis

Cao HC, Chen XM, Xu W. Determination of platelet-activating factor by reverse phase high-performance liquid chromatography and its application in viral hepatitis. *World J Gastroenterol* 2005; 11(46): 7364-7367
http://www.wjgnet.com/1007-9327/11/7364.asp

INTRODUCTION

Platelet-activating factor (PAF) is an autocoid mediator which controls intra- and extra-cellular signal transduction[1]. PAF is produced by a variety of cells including platelets, macrophages, neutrophils, and endothelial cells. Intrahepatic PAF is mainly secreted from Kupffer cells and hepatic sinusoidal endothelial cells. It activates platelets, leukocytes, and smooth muscle contraction. It was reported that PAF, as a mediator of lipid, plays an important role in the occurrence of hepatocyte injuries[2]. Direct infusion of PAF into the liver can result in the rapid release of superoxide and direct damage to liver cells[3,4]. PAF is also a mediator necessary for the development of endotoxin (ET) damage[5]. In endotoxic shock, the production of PAF in tissues is significantly increased. When the concentration of PAF is extremely low in the body, PAF manifests a short half-life of only 30 s and is then transformed rapidly into lyso-PAF without biological activity. PAF is hard to link to the carriers of protein due to its low immunogenicity, which makes the explanation difficult in the antibody preparation. Consequently, the current biological and immunological techniques cannot meet the clinical requirements[6]. Based on the biological determination, we used reverse phase high-performance liquid chromatography (rHPLC) to determine plasma PAF, tumor necrosis factor-α (TNF-α), malondialdehyde (MDA), and ET in patients with viral hepatitis and further clarified their effect and significance in all types of viral hepatitis in order to study the mechanism of viral hepatitis.

MATERIALS AND METHODS

Study population

Between January 2001 and June 2002, 106 patients of both sexes diagnosed as viral hepatitis at the Department of Infectious Diseases of our hospital were recruited in the study. The patients consisted of 16 cases of acute hepatitis, 26 cases of chronic light hepatitis, 20 cases of chronic moderate hepatitis, 25 cases of chronic severe hepatitis (n = 25) and 19 cases of severe hepatitis, ranging in age from 40 to 61 years, with a mean age of 49.5±10.4 years. All the patients were diagnosed by the specialists of the Department of Infectious Diseases in accordance with the diagnostic criteria for viral hepatitis recommended on the 10th National Viral Hepatitis and Hepatopathy Conference in Xi'an 2000. All the patients did not receive

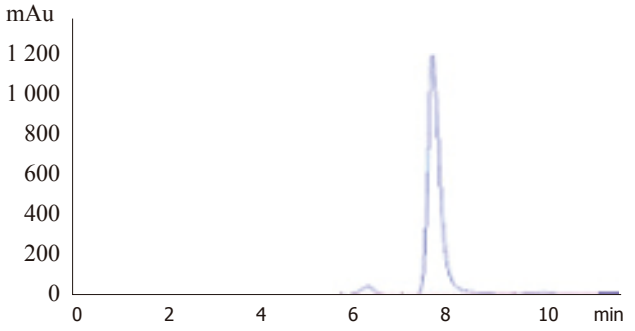

Figure 1 Standard C18 PAF. The horizontal and vertical axes represent the retention time (min) and milli-absorption unit (mAu) respectively, by which the peak area was calculated.

any immunomodulators and any drugs within 2 wk prior to this study.

Healthy control subjects (n = 60) without any thrombotic or communicable diseases were recruited from the blood center.

Blood PAF levels were measured in patients and normal volunteers. We also measured the plasma or serum levels of TNF-α, ET, and MDA.

Agents and devices for PAF analysis by rHPLC

Agilent 1100 series HPLC, water chromatographic column (3.9 mm×150 mm), Lab-line® Aquawave™ ultrasonic cleaner, standard lyso-PAF-C16 and PAF-C18 (chromatographic grade) were from Sigma Company.

Assay of ET, MDA and TNF-α

TNF-α was assayed with ELISA. The testing kits were from Jingmei Biological Engineering Co., Ltd.

ET was determined by limulus lysate test (LLT). The testing kits were from Shanghai Yi-Hua Clinical Medicine Technology Co., Ltd.

MDA was determined by thiobarbituric acid (TBA). The testing kits were from Nanjing Jian-Cheng Biological Engineering Research Institute.

PAF assay

Plasma was separated from whole blood by centrifugation at 3 000 r/min for 10 min and then stored at -70 ℃ until assay. PAF was assayed as previously described[7]. The mobile phase was required according to chromatographic condition, the velocity of flow was 1.0 mL/min, the column temperature was at 25 ℃ (Figure 1) and the determination wave was 208 nm. The PAF values of 20 randomly selected samples were determined by the biological technique established in our laboratory.

Statistical analysis

The descriptive values of variables were expressed as mean±SD. Categorical data were compared between the two groups with the Cochran's Q test. The correlations between laboratory results were evaluated by Pearson's correlation test. P<0.05 was considered statistically significant. All statistical analyses were performed by SPSS for Windows.

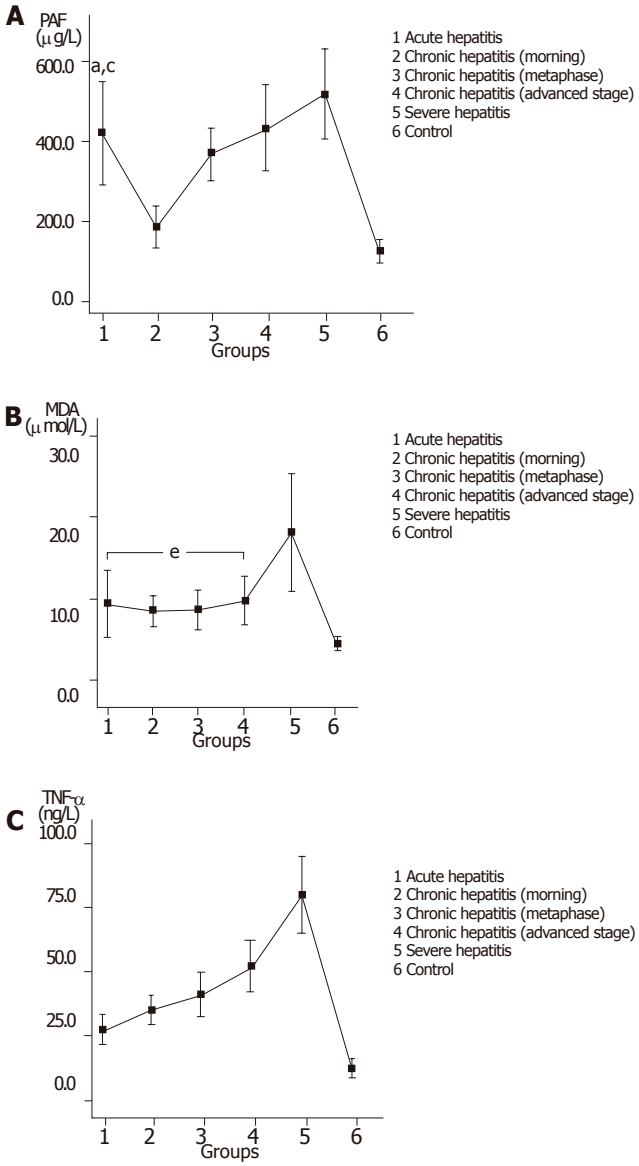

Figure 2 Plasma or serum levels of PAF (**A**), MDA (**B**) and TNF-α (**C**) in patients and controls. The values of PAF, TNF-α and MDA in patients with hepatitis were significantly higher than those in controls (P<0.01). [a]P<0.05 *vs* group 3, [c]P>0.05 *vs* group 4, [e]P>0.05 *vs* every two groups in groups 1-4.

RESULTS

In the assay of PAF by rHPLC, the retention times of lyso-PAF and C18 PAF were 6.2 and 7.8 min, respectively. The correlation analysis was performed for the results in the chromatography group and the biological technique group (r = 0.912, P<0.01).

The ET value of over 50 ng/L represented the positive finding in endotoxemia detection[6]. The detection rate of endotoxemia was 51.9%, 55.9%, 67.8%, and 0% in the patients with acute hepatitis, chronic hepatitis, severe hepatitis, and in the controls, respectively. The positive detection rate in the patients was significantly higher than that in the controls (P<0.01).

The values of PAF, MDA and TNF-α in the patients and controls are shown in Figures 2A-C.

DISCUSSION

The biological assay or radio immunoassay of PAF fails to manifest satisfactory specificity and sensitivity, because PAF in the body is rapidly transformed into lyso-PAF without biological activity[8]. In addition, the procedure is complicated and the results may be influenced by the individual difference of rabbit thrombocytes as well as the surgeon's skill in plate preparation and sample application[9]. The immunoassay may also be limited by antibody preparation that is actually difficult to complete. A desirable correlation is indicated between rHPLC and biological assay. The assay of PAF by rHPLC can lead to the effective separation and then the assay of PAF components (including C16 and C18) with different structures in the assayed sample not related to the biological activity of PAF. Thus, the reference values obtained are notably higher than those obtained by biological assay, contributing to a great increase in accuracy.

The liver plays an important role in removing ET by Kupffer cells and macrophages[10]. In our study, the detection rate of endotoxemia was 52.80%, 56.41%, and 69.57% in acute, chronic and severe hepatitis, respectively. Besides direct damage to the liver, ET is able to induce and release a large amount of inflammatory mediators including PAF and TNF-α by activating Kupffer cells, macrophages and hepatic sinusoidal endothelial cells. These mediators are not only involved in various biological effects of ET, but also exhibit their own biological effects by inducing generation of other inflammatory mediators, resulting in inflammation and tissue injuries in the body by various mechanisms[11,12]. PAF may cause many symptoms of endotoxic shock, including hypotension, cardiac function inhibition, and blood plasma exudation. The specific receptor antagonist of PAF has preventive and therapeutic effects on endotoxic shock. ET also has certain synergistic effect on PAF. Animal experiments showed that simultaneous use of ET and PAF could lead to severe endotoxic shock, granulopenia, and bowel necrosis. The TNF-α gene expression induced by ET is also related to PAF. The PAF antagonist can be used to effectively reduce the level of TNF in blood plasma and partially inhibit intrahepatic synthesis of TNF mRNA, indicating that TNF mRNA may be synthesized in a PAF-dependent manner or in a PAF-independent manner[13].

MDA is generated through lipid peroxidation. It can damage the complete membrane structure of hepatocytes and organelles, activate Kupffer cells, lead to endotoxemia and is closely correlated with the occurrence of hepatopathy[14]. In this study, PAF in patients with acute hepatitis was notably higher than that in patients with early- or medium-phase chronic hepatitis, suggesting that ET, PAF, TNF, and MDA may result in the aggravation of liver injury[15]. The PAF antagonist perfusion into the liver in advance can increase bile production in the affected liver, decrease the production of lipid peroxides (including MDA) and prevent energy damage by PAF. The value of blood MDA is remarkably increased in the early stage of severe hepatitis and returns to the normal levels during convalescence (data not shown)[16]. Therefore, MDA can be used as one of the indicators of diagnosis and prognosis of severe hepatitis.

REFERENCES

1 **Cuschieri J,** Bulger E, Garcia I, Jelacic S, Maier RV. Calcium/calmodulin-dependent kinase II is required for platelet-activating factor priming. *Shock* 2005; **23:** 99-106

2 **Grypioti AD,** Theocharis SE, Papadimas GK, Demopoulos CA, Papadopoulou-Daifoti Z, Basayiannis AC, Mykoniatis MG. Platelet-activating factor (PAF) involvement in acetaminophen-induced liver toxicity and regeneration. *Arch Toxicol* 2005; **79:** 466-474

3 **Moy JA,** Bates JN, Fisher RA. Effects of nitric oxide on platelet-activating factor- and alpha-adrenergic-stimulated vasoconstriction and glycogenolysis in the perfused rat liver. *J Biol Chem* 1991; **266:** 8092-8096

4 **Murohisa G,** Kobayashi Y, Kawasaki T, Nakamura S, Nakamura H. Involvement of platelet-activating factor in hepatic apoptosis and necrosis in chronic ethanol-fed rats given endotoxin. *Liver* 2002; **22:** 394-403

5 **Watanabe J,** Marathe GK, Neilsen PO, Weyrich AS, Harrison KA, Murphy RC, Zimmerman GA, McIntyre TM. Endotoxins stimulate neutrophil adhesion followed by synthesis and release of platelet-activating factor in microparticles. *J Biol Chem* 2003; **278:** 33161-33168

6 **Ammit AJ,** O'Neill C. Studies of the nature of the binding by albumin of platelet-activating factor released from cells. *J Biol Chem* 1997; **272:** 18772-18778

7 **Cao HC,** Xu WR, Zhu W, Chen XM, Li LJ. Determination of platelet-activating factor (PAF) by reversed phase high-performance liquid chromatographic technique (rHPLC) and its application in some elderly diseases, *Linchuang Jianyan Zazhi* 2003; **21:** 129-131

8 **Owen JS,** Wykle RL, Samuel MP, Thomas MJ. An improved assay for platelet-activating factor using HPLC-tandem mass spectrometry. *J Lipid Res* 2005; 46: 373-382

9 Kita Y, Takahashi T, Uozumi N, Shimizu T. A multiplex quantitation method for eicosanoids and platelet-activating factor using column-switching reversed-phase liquid chromatography-tandem mass spectrometry. *Anal Biochem* 2005; **342:** 134-143

10 **Hiraoka A,** Horiike N, Akbar SM, Michitaka K, Matsuyama T, Onji M. Expression of CD163 in the liver of patients with viral hepatitis. *Pathol Res Pract* 2005; **201:** 379-384

11 **Zhou F,** Ajuebor MN, Beck PL, Le T, Hogaboam CM, Swain MG. CD154-CD40 interactions drive hepatocyte apoptosis in murine fulminant hepatitis. *Hepatology* 2005; **42:** 372-380

12 **Cao Q,** Mak KM, Lieber CS. Cytochrome P4502E1 primes macrophages to increase TNF-alpha production in response to lipopolysaccharide. *Am J Physiol Gastrointest Liver Physiol* 2005; **289:** G95-107

13 **Souza DG,** Teixeira MM. The balance between the production of tumor necrosis factor-alpha and interleukin-10 determines tissue injury and lethality during intestinal ischemia and reperfusion. *Mem Inst Oswaldo Cruz* 2005; **100 Suppl 1:** 59-66

14 **Liu LG,** Yan H, Yao P, Zhang W, Zou LJ, Song FF, Li K, Sun XF. CYP2E1-dependent hepatotoxicity and oxidative damage after ethanol administration in human primary hepatocytes. *World J Gastroenterol* 2005; **11:** 4530-4535

15 **Buke AC,** Buke M, Altuglu IE, Cicekliogl M, Kamcioglu S, Karakartal G, Huseyinov A. Tumor necrosis factor alpha and interleukin 6 productions in response to platelet-activating factor in chronic hepatitis B virus infection. *Med Princ Pract* 2004; **13:** 273-276

16 **Eboumbou C,** Steghens JP, Abdallahi OM, Mirghani A,

Gallian P, van Kappel A, Qurashi A, Gharib B, De Reggi M. Circulating markers of oxidative stress and liver fibrosis in Sudanese subjects at risk of schistosomiasis and hepatitis. *Acta Trop* 2005; **94:** 99-106

Science Editor Wang XL and Guo SY **Language Editor** Elsevier HK

PO Box 2345, Beijing 100023, China
www.wjgnet.com
wjg@wjgnet.com

ELSEVIER

World J Gastroenterol 2005;11(46):7368-7373
World Journal of Gastroenterology ISSN 1007-9327

• *RAPID COMMUNICATION* •

Chloromycetin resistance of clinically isolated *E coli* is conversed by using EGS technique to repress the chloromycetin acetyl transferase

Mei-Ying Gao, Chuan-Rui Xu, Ru Chen, Shou-Gui Liu, Jiang-Nan Feng

Mei-Ying Gao, Ru Chen, Shou-Gui Liu, Department of Infectious Diseases, Tongji Hospital, Tongji Medical College, Huazhong University of Science and Technology, Wuhan 430030, Hubei Province, China
Chuan-Rui Xu, School of Pharmacy, Tongji Medical College, Huazhong University of Science and Technology, Wuhan 430030, Hubei Province, China
Jiang-Nan Feng, Laboratory of Immunology, Wuhan Bioproduct Institute of Ministry of Public Health, Wuhan 430060, Hubei Province, China
Supported by the National Natural Science Foundation of China, No. 39570846
Co-first authors: Mei-Ying Gao and Chuan-Rui Xu
Co-correspondent: Mei-Ying Gao
Correspondence to: Jiang-Nan Feng, Wuhan Bioproduct Institute of Ministry of Public Health, 9 Linjiang Dadao, Wuhan, 430030, Hubei Province, China. bruck02@sina.com
Telephone: +86-27-87531783 Fax: +86-27-87531782
Received: 2005-03-11 Accepted: 2005-04-26

Abstract

AIM: To explore the possibility of repression of chloromycetin (Cm) acyl transferase by using external guided sequence (EGS) in order to converse the clinical *E coli* isolates from Cm- resistant to Cm- sensitive.

METHODS: EGS directed against chloromycetin acetyl transferase gene (*cat*) was cloned to vector pEGFP-C1 which contains the kanamycin (Km) resistance gene. The recombinant plasmid pEGFP-C1+EGScat1+cat2 was constructed and the blank vector without EGS fragment was used as control plasmids. By using the $CaCl_2$ transformation method, the recombinant plasmids were introduced into the clinically isolated Cm resistant but Km sensitive *E coli* strains. Transformants were screened on LB agar plates containing Km. Extraction of plasmids and PCR were applied to identify the positive clones. The growth curve of EGS transformed bacteria cultured in broth with Cm resistance was determined by using spectrophotometer at A_{600}. Drug sensitivity was tested in solid culture containing Cm by using KB method.

RESULTS: Transformation studies were carried out on 16 clinically isolated Cm-resistant (250 μg/mL of Cm) *E coli* strains by using pEGFP-C1-EGScat1cat2 recombinant plasmid. Transformants were screened on LB-agar plates containing Km after the transformation using EGS. Of the 16 tested strains, 4 strains were transformed successfully. Transformants with EGS plasmid showed growth inhibition when grown in liquid broth culture containing 200 μg/mL of Cm. In drug sensitivity test, these strains were sensitive to Cm on LB-agar plates containing 200 μg/mL of Cm. Extraction of plasmids and PCR amplification showed the existence of EGS plasmids in these four transformed strains. These results indicated that the Cat of the four clinical isolates had been suppressed and the four strains were converted to Cm sensitive ones.

CONCLUSION: The EGS directed against Cat is able to inhibit the expression of Cat, and hence convert Cm-resistant bacteria to Cm-sensitive ones. Thus, the EGS has the capability of converting the phenotype of clinical drug-resistant isolates strains to drug-sensitive ones.

Key words: External guide sequence; Drug-resistant bacteria; Conversion of drug resistance

Gao MY, Xu CR, Chen R, Liu SG, Feng JN. Chloromycetin resistance of clinically isolated *E coli* is conversed by using EGS technique to repress the chloromycetin acetyl transferase. *World J Gastroenterol* 2005; 11(46): 7368-7373
http://www.wjgnet.com/1007-9327/11/7368.asp

INTRODUCTION

Drug resistance in pathogenic bacteria is a problem of major clinical importance, which has not been effectively solved yet. The traditional approach to this problem is searching for novel antibiotics. However, this is expensive and time consuming, and the bacteria can quickly develop drug resistance to these novel antibiotics. With advances in gene therapy, ribozyme technology[1,2] appeared following antisense RNA technique[3-6], which though is abstract of the activity of catalysis and cleavage. Then, external guide sequence (EGS) technique[7] was found, with the advantages of both ribozyme and antisense RNA. EGS, a synthetic gene coding for small oligoribonucleotides, is able to form complexes with the mRNA encoded by target gene. The complexes are recognized as substrates of RNase P[8-11]. Then, EGS directs RNase P to cleave and inactivate the target mRNA. Therefore, the EGS technique is a method to block a particular gene by inhibiting the translation of its mRNA[12-14]. In 1997, by designing EGS directed against chloromycetin (Cm) acyl transferase (*cat*), Sidney Altman successfully applied EGS technique in engineered bacteria to convert the Cm-resistant bacteria into Cm-sensitive

ones, and hence paved a new way to solve the drug resistance problem[15]. In this study, we investigated the feasibility of applying EGS technique in converting the phenotype of clinically isolated *E coli* from Cm-resistant to Cm-sensitive.

MATERIALS AND METHODS

Materials

The *E coli* samples were clinically isolated from Affiliated Tongji Hospital of Huazhong University of Science and Technology between 2001 and 2002, from which 16 strains resistant to Cm 250 μg/mL and sensitive to kanamycin (Km) 50 μg/mL were selected as test strains. Plasmid pEGFP-C1 and pKB EGS cat1+cat2 were kindly provided by Dr. Sidney Altman (Yale University, USA). The plasmid pKB EGS cat1+cat2 was constructed according to the method in the literature[15].

Methods

Construction of pEGFP-C1-EGS cat1+cat2 recombinant plasmids A 510-bp EGS fragment directed against Cm acetyl transferase gene (*cat*) was cloned into pEGFP-C1 plasmid containing kanamycin-resistant gene between EcoRI and I sites. The EGS includes: M1RNA promoter, EGScat1, hammerhead sequence (HH1, HH2), EGScat2, HH3, and M1 terminator. The recombinant pEGFP-C1 plasmid containing EGScat1+cat2 was named K_3 plasmid, while pEGFP-C1 plasmid that had Km resistance gene but without EGS fragment was named as K plasmid.

Identification of partial phenotypes of clinically isolated *E coli*: (1) *Purification of the test bacteria* The clinically isolated bacterial strains were streaked on the LB plates and cultured for 6-8 h. A single colony on the plates was selected for Gram staining and its cellular configuration was checked under the microscope. Other single colony was then taken and diluted to 10^{-8}. The clone grown on plates with 30-300 colonies was taken for tests of Cm drug resistance and Km drug sensitivity again, and then Gram stained for morphology check. These steps were repeated until pure bacterium strains were obtained[16]; (2) *Extraction of plasmids of the test bacteria and determination of plasmid incompatibility* The methods for plasmid extraction and incompatibility determination were described by Huang[17]; (3) *Determination of spontaneous mutation rate of the test bacteria* The spontaneous mutation rate of testing bacteria to Km was determined for colonies grown on LB and LB+Km plates by using dilution plate counting method[18]; (4) *Determination of logarithmic growth stage of test* bacteria *Bacterial* growth curve were plotted based on bacterial optical density (A_{600})[19].

Transformation of test bacteria by pEGFP-C1-EGScat1+cat2 recombinant plasmids and identification: (1) *Transforming test* The competent cells of testing bacteria were prepared by using $CaCl_2$ method, and were transformed respectively with plasmids K3 and K[20]. The transformants that received K3 plasmid were designated as testing bacteria, and those transformed with K plasmid without EGS were used as plasmid controls. The competent cells from original testing bacteria were mock-transformed (without plasmid) and served as strain controls. Competent cells were inoculated on LB plates containing 50 μg/mL of Km after transformation, followed by incubation at 37 ℃ for 12-16 h; (2) *Extraction of plasmids and total DNA* Plasmid was extracted by using alkaline cleavage method[17] and total DNA was extracted by using the boiling method[21]. Positive clones were selected and transferred into Eppendorf tubes containing 20 μL sterilized water and boiled for 10 min. The supernatant was collected after centrifugation; (3) *PCR amplification* The primers were designed specifically for the inserted EGS on the vector. The amplified fragment containing EGScat1 and cat2 was 391 bp. The primer pairs used for PCR amplification were 5'-AGCCTGACCGATGATGTTG-3' and 5' -TCCTCACGGACTCATC AGAC-3'. The PCR reactions were performed at 94 ℃ for 1 min, 57 ℃ for 1 min, and 72 ℃ for 1.5 min, total 30 cycles. The PCR products were electrophoresed on a 1.5% agarose gel; (4) *Cm sensitivity test of the transformants* After transformation, the colonies grown on plates and the original colonies were re-inoculated on the LB plates containing 200 μg/mL of Cm and plates containing 50 μg/mL of Km, and incubated at 37 ℃ for 8-12 h. Then, their growth conditions on these two plates were checked and recorded; (5) *Growth determination of transformants in liquid broth* The colonies (K3, K plasmid transformants and original bacteria) were separately inoculated into 200 mL of broth culture containing Cm (200 μg/mL) with the inoculating concentration A_{600} = 0.05, and incubated in an orbital shaker at 37 ℃ and 200 r/min. A 0.5 mL bacterial suspension was sampled hourly and its A value was determined. Growth curve was plotted according to the constantly collected A values. The transformants were also incubated at the same concentrations into PA bottles at 37 ℃ and the bacterial growth was observed hourly as well.

RESULTS

Study of the partial phenotypes of the clinically isolated E coli strains' rates of spontaneous mutation

Sixty-one Cm-resistant but Km-sensitive *E coli* strains were clinically isolated. Of them, 16 strains were selected as test strains for their comparatively low simultaneous mutation rate. However, the test strains sensitive to Km were still suitable to present the spontaneous mutation and hence obtain Km resistance after culturing in a big scale. Among them, strains 16, 20, 3 900, and 6 470 showed the lowest mutation rate of Km drug resistance, being 8.85×10^{-6}, 3.36×10^{-6}, 6.57×10^{-7}, and 2.96×10^{-7}, respectively. The data of others were little higher than 10^{-5}.

Plasmids' profile of the test bacteria The plasmid profile of the test strains showed that each contained 2-3 plasmid bands. Introducing the plasmids extracted from test bacteria into *E coli* DH5α (no indigenous plasmids) indicated that Cm-resistant gene was located in the plasmids. The existence of resistance plasmids in the test strains may account for the difficulty of introducing EGS

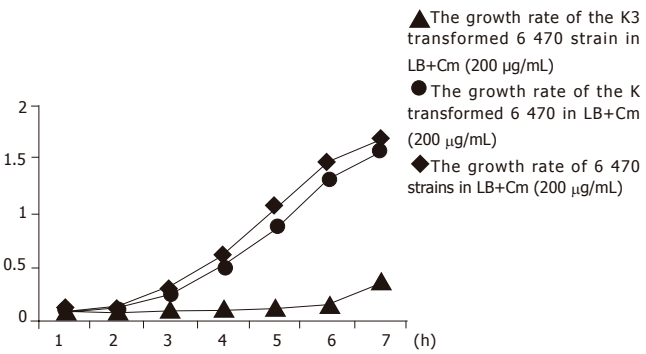

Figure 1 Growth curve of the transformants in the broth containing Cm after K3 plasmid and K plasmid were introduced into 6 470 strains of Cm-resistant *E coli*.

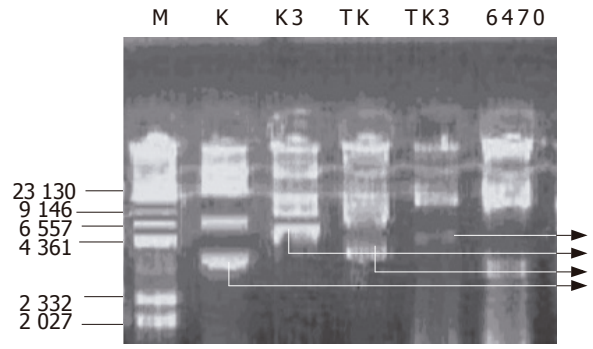

Figure 3 Results of rapid plasmid extraction after K3 plasmid and K plasmid were introduced into 6 470, K and TK, K3 and TK3 can be detected in similar bands.

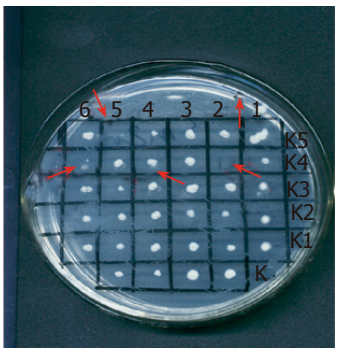

In the grids (red arrows), the K3 transformed 6 470 became sensitive to Cm in the LB-+Cm (200 μg/mL) plates. Up to low, the lines of 4 and 5 showed that the K transformed bacteria grew well in LB+Cm (200 μg/mL) plates. The last line showed the growth of the original 6 470 strains

Figure 2 Susceptibility test of the transformed bacteria in solid culture containing Cm (200 μg/mL) after K3 plasmids and K plasmids were introduced into 6 470

plasmid into the cells. Furthermore, the DH5α derivatives transformed with the plasmids extracted from test bacteria were hard to be transformed again with K3 and K. This suggested the plasmid incompatibility between original plasmids and K or K3 plasmids.

Determination of logarithmic phase The bacterial growth curve revealed that the logarithmic growth stage was from 4 to 8 h after being inoculated in the broth. In this study, the fresh culture of test strains was harvested in this period to prepare competitive cells.

Growth rate of the transformed bacteria in liquid broth culture

Four strains, 16, 20, 3 900, and 6 470 were transformed with K3 successfully. Kinetic growth study demonstrated that these four strains transformed with K3 plasmid exhibited growth inhibition in the broth containing 200 μg/mL of Cm (Figure 1). The growth inhibition became apparent at 2 h and peaked at 3 and 4 h, but active growth resumed at 5 h. In contrast, neither bacteria transformed with K plasmid nor original bacteria with mock-transformation showed any growth inhibition in the incubation condition described above. Their concentrations increased steadily as demonstrated by A_{600} values. Although the number of bacteria transformed with EGS began to elevate at 5 h, the degree of growth was much lower than that of the original bacteria. In PA bottles, the K3 plasmid transformed bacterial culture was still clear at 6 h to the naked eye and started to be turbid at 8 h, while the culture for K plasmid transformed bacteria or mock-transformed original bacteria started to be turbid at 3 h and was highly turbid at 6 h. The above findings demonstrated that EGS gene was able to convert bacteria from Cm-resistant to Cm-sensitive phenotype. All of the four strains that obtained their phenotypic conversion of drug resistance showed a lower spontaneous mutation rate, which may contribute to their easy transformation because of their stability. They exhibited very few variant strains when cultured on Km plates, and thus the transformants could be easily identified and collected.

Drug sensitivity test of transformed bacteria

Drug sensitivity test showed that the four strains transformed with K3 plasmid not only obtained sensitivity to Cm in liquid broth culture but also became sensitive to Cm in LB+Cm (200 μg/mL) solid culture (as indicated in Figure 2). The bacteria transformed with K plasmid and the original isolates grew well in LB+Cm (200 μg/mL) solid culture.

Determination of plasmid extraction from testing bacteria transformed by pEGFP-C1-EGS cat1+cat2 and identification of clones by PCR

Determination of the plasmids in transformed bacteria Four strains of transformed bacteria were subjected to the determination of the plasmid extraction. Figure 3 is the map of rapid extraction of plasmid and Figure 4 is the map of plasmid extraction after the transformants were cultured for 2 d. Figure 3 shows that the K and K3 can be detected in the strains transformed with K and K3, respectively. This indicated that K3 and K plasmids had been introduced into the cells successfully. In Figure 4, TK had the same bands as K, while TK3 had no similar bands as K3, indicating that the K3 plasmid was lost or had been degraded after 2 d of culturing. This may explain why the transformant retained its growing capacity gradually after several hours of culturing in the broth medium.

Identification of EGS gene by PCR The colonies transformed with K3, which did not grow on LB+Cm (200 μg/mL) plate (restoration of Cm sensitivity) but grew well in the corresponding LB+Km (50 μg/mL) plate, were

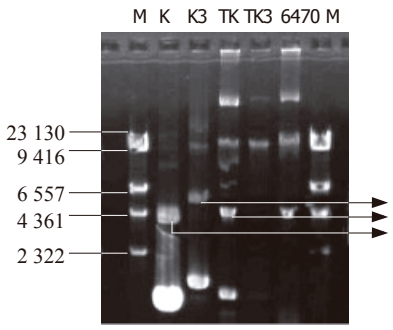

Figure 4 The map of plasmid extraction after the transformants were cultured for 2 d, K and TK can be detected in similar bands, while TK3 had no similar bands as K3, indicating the K3 plasmid was lost or had been degraded. M: Marker; lane K: control plasmid; K3; EGS plasmid; TK, 6 470 transformed with K plasmid; TK3, 6 470 transformed with K3; 6 470, original Cm-resistant 6 470.

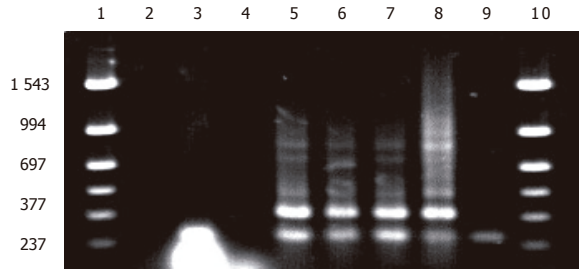

Figure 5 Electrophoresis of PCR amplification of EGS genes in the transformed bacteria after K plasmid and K3 plasmid introduced into 6 470. Lanes 1 and 10 Mmarker; Llane 2, blank control; lane 3, transformants cultured 2 d more; lane 4, original 6 470 strains; lanes 5, 6 and 7: 6 470 derivatives transformed with K3; lane 8: plasmid K3 (positive control); lane 9: K plasmid transformants (negative control).

used for PCR amplification of EGS fragments. K3 plasmid was used as positive control and clones transformed with K plasmid, original testing bacteria and DNA-free distilled water were used as negative controls. As shown in Figure 5, lanes 5, 6, and 7 were clones transformed with K3 plasmid that did not grow on LB+Cm plate, showing that these clones contained the EGS gene fragment (391 bp, lane 8). Lanes 4 and 9 were original test bacteria and K plasmid transformed bacteria, showing no EGS gene fragment in these strains. Lane 3 was the clone that initially resumed Cm sensitivity but lost the sensitivity 2 d later on LB+Cm plate. PCR amplification failed to detect any EGS band, suggesting the loss of EGS plasmid in this clone.

DISCUSSION

The problem of microbial drug resistance is growing severely year after year clinically. To cope with this problem, destroying the drug resistance gene is an effective and potential approach, in which no effective method has so far been achieved[22-24]. In 1997, Sidney Altman introduced EGS technique, which conversed the Cm resistance successfully. On the basis of the study on engineered bacteria by Altman, this study further introduced the EGS gene into the clinically isolated bacterial strains. Our study demonstrated EGS-mediated conversion of a Cm-resistant to a Cm-sensitive phenotype, and further showed the successful conversion of drug resistance by the introduction of EGS gene not only in laboratory bacteria but also in clinically isolated bacteria. This indicates a potential clinical utilization.

Mutation is a common phenomenon present in microorganisms. The clinically isolated bacterial strains are characterized with even higher spontaneous mutation rate than lab strains. In the early period of our experiments, it was found that the competent cells of the control bacteria sensitive to Km not transformed with plasmids and originally sensitive to Km still grew on the Km plates. At first, it was mistakenly rendered as the result of impurity of test strain. After further purification and spontaneous mutation study, we understood that it has resulted from high mutation rate of the clinically isolated bacteria. Mutated test strains obtained Km resistance, lost Km-sensitiveness, and therefore made selecting transformants difficult. To solve this problem, our efforts focused on selecting stable strains with low spontaneous mutation rate. At the end of the procedure, 16 comparatively stable strains were screened from the clinically isolated bacterial strains.

In this study, only 4 of 16 test strains were converted from drug-resistant to drug-sensitive phenotype. The low efficiency of conversion may be ascribed to the low transformation efficiency. Firstly, as *Enterobacteriaceae*, test strains were hard to be transformed for their native low transformation frequency[25]. Secondly, the low transformation rate can be contributed to the existence of host plasmids in test strain which may result in plasmid incompatibility. Thirdly, although the criteria for screening positive transformants in the culture medium containing Km were set up, not all of the transformed bacteria were desired transformants due to the spontaneous mutation of the testing bacteria. We believe that even if we select other sensitive antibiotics to testing bacterial strains, spontaneous mutation would also happen. So suitable methods to screen positive transformants were abstract. Km resistance in this study did not function as an effective selection marker due to the spontaneous mutation of the test strains. To increase the efficiency of conversion, we tried to apply one-step method[26] and electroporation transformation method, but the results were also not satisfactory. Although we can construct recombinant plasmids and insert a fluorescence enzyme's gene into the vector (EGFP site at pEGFP-C1 vector) to aid in screening, it may increase the transforming difficulty or render the transformed bacteria. In order to reduce the false positive clone in transformation assay, the original bacteria with high spontaneous mutation rate were excluded. At the same time, we found that the efficiency of transformation could be enhanced by using SOC medium and by collecting cell culture at early logarithmic phase. Transformation could be facilitated by washing cell culture with $CaCl_2$ solution for 2-3 times instead of once as well. This might be contributed to the increased permeability of the *E coli* wall.

PCR amplification was used to identify positive clones. In contrast to the spontaneously mutated bacterial strains, the transformants obtained through transformation grew slowly on the Km plates. On the other hand, long time culturing resulted in the loss of plasmids. Thus, it was difficult to identify the EGS transformants by plasmid extraction. In this study, PCR was applied to identify the presence of EGS in the EGS transformed bacteria and it worked effectively. Certainly, further study is to perform Northern blot to know the attenuation of mRNA transcribed from cat gene, which could further definitely verify the roles of EGS. As our conditions are limited, the experiment was not done.

EGS as a sort of synthesized oligonucleotides can combine the target RNA to form the substrate similar to pre-tRNA, which can be cleaved by RNase P and lose the ability of further gene expression. The targeted mRNA is cleaved but EGS itself is not cleaved[7]. EGS can function continuously. In this study, however, we found that the positive clones regained the Cm resistance after being cultured in broth containing Cm for 8 h and then on solid culture for 2 d. No EGS was detected and no plasmid could be extracted in clones that regained Cm resistance. This demonstrated that EGS plasmid had been lost in the host because of continuous culture. The reason might be due to an incompatibility between indigenous and exogenous plasmids.

Our experiments demonstrated that culturing on Km plates facilitated EGS plasmid inheritance, while culturing on the Cm plates was prone to result in the loss of EGS plasmid. This study also suggested the need for more effective methods to introduce EGS into the bacterial cells and to maintain its stability. Though a lot of challenges were involved in this study, transformants were still obtained. The results reflected the effectiveness of the EGS transforming drug-resistant bacteria, and provided a foundation for the clinical application of EGS.

In recent years, although RNA interference technique has been developed, no RNA interference phenomenon was observed in prokaryotes[27-30]. Thus, the EGS technique still is the most prospective way to solve bacterial drug resistance. As to the development of EGS technique, Sidney Altman put forward that enhancing the promoter, increasing the copy of EGS, augmenting the binding sites of EGS and stabling the EGS-mRNA complex are the potential methods. Furthermore, combined with nanotechnology, the EGS technology could be more promising. Conclusively, to improve this study, more measures should be explored for further investigation.

ACKNOWLEDGMENTS

We are deeply indebted to Professor Altman for kindly providing the plasmid and for his abundant help in this study.

REFERENCES

1 **Akashi H,** Matsumoto S, Taira K. Gene discovery by ribozyme and siRNA libraries. *Nat Rev Mol Cell Biol* 2005; **6:** 413-422
2 **Lilley DM.** Structure, folding and mechanisms of ribozymes. *Curr Opin Struct Biol* 2005; **15:** 313-323
3 **Chan MW,** Chan VY, Leung WK, Chan KK, To KF, Sung JJ, Chan FK. Anti-sense trefoil factor family-3 (intestinal trefoil factor) inhibits cell growth and induces chemosensitivity to adriamycin in human gastric cancer cells. *Life Sci* 2005; **76:** 2581-2592
4 **Jhaveri MS,** Rait AS, Chung KN, Trepel JB, Chang EH. Antisense oligonucleotides targeted to the human alpha folate receptor inhibit breast cancer cell growth and sensitize the cells to doxorubicin treatment. *Mol Cancer Ther* 2004; **3:** 1505-1512
5 **Sarno R,** Ha H, Weinsetel N, Tolmasky ME. Inhibition of aminoglycoside 6'-N-acetyltransferase type Ib-mediated amikacin resistance by antisense oligodeoxynucleotides. *Antimicrob Agents Chemother* 2003; **47:** 3296-3304
6 **Delihas N,** Rokita SE, Zheng P. Natural antisense RNA/target RNA interactions: possible models for antisense oligonucleotide drug design. *Nat Biotechnol* 1997; **15:** 751-753
7 **Forster AC,** Altman S. External guide sequences for an RNA enzyme. *Science* 1990; **249:** 783-786
8 **Yuan Y**, Altman S. Selection of guide sequences that direct efficient cleavage of mRNA by human ribonuclease P. *Science* 1994; **263:** 1269-1273
9 **Li Y,** Guerrier-Takada C, Altman S. Targeted cleavage of mRNA in vitro by RNase P from Escherichia coli. *Proc Natl Acad Sci USA* 1992; **89:** 3185-3189
10 **Yuan Y,** Hwang ES, Altman S. Targeted cleavage of mRNA by human RNase P. *Proc Natl Acad Sci U S A* 1992; **89:** 8006-8010
11 **Werner M,** Rosa E, Nordstrom JL, Goldberg AR, George ST. Short oligonucleotides as external guide sequences for site-specific cleavage of RNA molecules with human RNase P. *RNA* 1998; **4:** 847-855
12 **Zhang H,** Altman S. Inhibition of the expression of the human RNase P protein subunits Rpp21, Rpp25, Rpp29 by external guide sequences (EGSs) and siRNA. *J Mol Biol* 2004; **342:** 1077-1083
13 **Guerrier-Takada C,** Li Y, Altman S. Artificial regulation of gene expression in Escherichia coli by RNase P. *Proc Natl Acad Sci U S A* 1995; **92:** 11115-11119
14 **Li Y,** Altman S. A specific endoribonuclease, RNase P, affects gene expression of polycistronic operon mRNAs. *Proc Natl Acad Sci USA* 2003; **100:** 13213-13218
15 **Guerrier-Takada C,** Salavati R, Altman S. Phenotypic conversion of drug-resistant bacteria to drug sensitivity. *Proc Natl Acad Sci USA* 1997; **94:** 8468-8472
16 **Zhao B, He SJ.** Microbiology Lab Manual. First Edition. Beijing: *Science press* 2002: 121-123
17 **Huang PT**. Molecular Cloning: A Laboratory Manual (Translation). Third Edition. Beijing: *Science press* 2002: 29-30
18 **Zhao B,** He SJ. Microbiology Lab Manual. First Edition. Beijing: *Science press* 2002: 187-189
19 **Zhao B,** He SJ. Microbiology Lab Manual. First Edition. Beijing: *Science press* 2002: 75-76
20 **Huang PT.** Molecular Cloning: A Laboratory Manual(Translation). Third Edition. Beijing: *Science press* 2002: 96
21 **Huang PT.** Translation. Molecular Cloning: A Laboratory Manual. Third Edition. Beijing: *Science press* 2002: 41-43
22 **Tekos A,** Stathopoulos C, Tsambaos D, Drainas D. RNase P: a promising molecular target for the development of new drugs. Curr Med Chem 2004; **11:** 2979-2989
23 **Altman S.** RNA enzyme-directed gene therapy. *Proc Natl Acad Sci U S A* 1993; **90:** 10898-10900
24 **Gopalan V,** Vioque A, Altman S. RNase P: variations and uses. *J Biol Chem* 2002; **277:** 6759-6762
25 **Zheng SL.** Basis to Microbiology. First Edition. Beijing: *Chemistry industry press* 1992: 322-325
26 **Chung CT,** Niemela SL, Miller RH. One-step preparation of competent Escherichia coli: transformation and storage of bacterial cells in the same solution. *Proc Natl Acad Sci USA*

1989; **86:** 2172-2175
27 **Hannon G J.** RNAi: A Guide to Gene silencing. First Edition. Photolithograph book. Beijing: *Chemistry industry press* 2004: 23-24
28 **Hannon G J.** RNAi: A Guide to Gene silencing. First Edition. Photolithograph book. Beijing: *Chemistry industry press* 2004: 243-246
29 **Hannon G J.** RNAi: A Guide to Gene silencing. First Edition. Photolithograph book. Beijing: *Chemistry industry press* 2004: 361-364
30 **Hannon G J.** RNAi: A Guide to Gene silencing. First Edition. Photolithograph book. Beijing: *Chemistry industry press* 2004: 265-267

Science Editor Guo SY **Language Editor** Elsevier HK

PO Box 2345, Beijing 100023, China
www.wjgnet.com
wjg@wjgnet.com

ELSEVIER

World J Gastroenterol 2005;11(46):7374-7377
World Journal of Gastroenterology ISSN 1007-9327

• *RAPID COMMUNICATION* •

Peritoneal lavage cytology and carcinoembryonic antigen determination in predicting peritoneal metastasis and prognosis of gastric cancer

Ji-Kun Li, Miao Zheng, Chuan-Wen Miao, Jian-Hai Zhang, Guang-Han Ding, Wen-Shen Wu

Ji-Kun Li, Miao Zheng, Chuan-Wen Miao, Jian-Hai Zhang, Guang-Han Ding, Department of General Surgery, First Affiliated People's Hospital of Shanghai Jiaotong University, Shanghai 200080, China
Wen-Shen Wu, Department of Pathology, First Affiliated First People's Hospital of Shanghai Jiaotong University, Shanghai 200080, China
Correspondence to: Ji-Kun Li, PhD, Department of General Surgery, First Affiliated People's Hospital of Shanghai Jiaotong University, Shanghai 200080, China. jkli2000@citiz.net
Telephone: +86-21-63240090 Fax: +86-21-63240825
Received: 2004-11-02 Accepted: 2004-12-28

Abstract

AIM: To evaluate the role of peritoneal lavage cytology (PLC) and carcinoembryonic antigen (CEA) determination of peritoneal washes (pCEA) in predicting the peritoneal metastasis and prognosis after curative resection of gastric cancer.

METHODS: PLC and radioimmunoassay of CEA were performed in peritoneal washes from 64 patients with gastric cancer and 8 patients with benign diseases.

RESULTS: The positive rate of pCEA (40.6%) was significantly higher than that of PLC (23.4%) (P<0.05). The positive rates of PLC and pCEA correlated with the depth of tumor invasion and lymph node metastasis (P<0.05). pCEA was found to have a higher sensitivity and a lower false-positive rate in predicting peritoneal metastasis after curative resection of gastric cancer as compared to PLC. The 1-, 3-, and 5-year survival rates of patients with positive cytologic findings or positive pCEA results were significantly lower than those of patients with negative cytologic findings or negative pCEA results (P<0.05). Multivariate analysis indicated that pCEA was an independent prognostic factor for the survival of patients with gastric cancer.

CONCLUSION: Intraoperative pCEA is a more sensitive and reliable predictor of peritoneal metastasis as well as prognosis in patients with gastric cancer as compared to PLC method.

Key words: Stomach neoplasm; CEA protein; Peritoneal metastasis; Prognosis

Li JK, Zheng M, Miao CW, Zhang JH, Ding GH, Wu WS. Peritoneal lavage cytology and carcinoembryonic antigen determination in predicting peritoneal metastasis and prognosis of gastric cancer. *World J Gastroenterol* 2005; 11(46): 7374-7377
http://www.wjgnet.com/1007-9327/11/7374.asp

INTRODUCTION

Peritoneal metastasis is the most common mode of relapse of gastric cancer after surgery and is the most frequent cause of death in patients with gastric cancer[1-3]. Peritoneal recurrence develops from micrometastasis originating from peritoneal free cancer cells. Therefore, it is very important to examine the presence or absence of free cancer cells in the peritoneal cavity at the time of surgery[4,5]. PLC is the gold standard for assessing the presence of peritoneal dissemination of gastric cancer, but its sensitivity is relatively low, ranging 14-21% in gastric cancer involving the serosa[6-8]. Recently, several new methods for detecting micrometastasis, including immunohistochemical and biological methods have been developed[9-11]. However, these diagnostic techniques are time-consuming and laborious compared to conventional cytological method. Therefore, a new and more sensitive method for the early detection of peritoneal metastasis is required.

In this paper, we have reported the clinical significance of a new method to detect peritoneal micrometastasis in combination with cytological method and measurement of pCEA level in peritoneal washes.

MATERIALS AND METHODS

Patients

Between December 1995 and December 1997, 64 patients with histologically confirmed gastric cancer underwent surgery at the Department of General Surgery of First Affiliated People's Hospital of Shanghai Jiaotong University. All patients underwent either a total or a partial gastrectomy with lymph node dissection and received no preoperative chemotherapy or radiotherapy before the surgery. These 64 cases included 42 male and 22 female patients with an average age of 59 (range 34-84 years) years. All specimens were histologically examined by HE staining according to the general rules of the Japanese Classification of Gastric Carcinoma[12]. Seven patients with

the maximum depth of tumor invasion at mucosal or submucosal level, were diagnosed as early gastric cancer. The other 57 cases were diagnosed as advanced gastric cancer with invasion deep into the gastric wall. In this study, eight patients with benign diseases such as peptic ulcer or cholecystolithiasis served as controls. The follow-up period ranged 9-74 mo and the median follow-up period was 39 mo.

Examination of peritoneal washes

The study consisted of 64 patients with gastric cancer and 8 patients with benign disease. After laparotomy, 50 mL physiological saline was introduced into the right upper quadrant or the Douglas pouch immediately and then 20 mL fluid was collected. The fluid sample was immediately centrifuged for 5 min at 1 500 r/min. The sediment of each fluid sample was smeared on a glass slide. The slide was fixed in 99% alcohol, stained with HE and examined for the presence of cancer cells by an experienced pathologist. The supernatant of each sample was concentrated by ultrafiltration. CEA levels of the concentrated supernatant (pCEA) were measured with a radiometric immunoassay kit (Delfia CEA kit, Wallac Oy, Turku, Finland) and expressed as ng/g of protein. The cut-off level was set according to Takayuki method (pCEA level ≥100 ng/g of protein was defined as positive)[13].

Statistical analysis

All the statistical analyses were done with SPSS statistical software. The χ^2 test was used to compare the positive results in CEA level and cytological examination. The survival rate was calculated by the Kaplan-Meier method and statistical difference was evaluated by the long-rank test. A Cox proportional hazard model was established to identify the independent prognostic factors.

RESULTS

Correlation between PLC or pCEA and clinicopathologic parameters

All the eight patients with benign diseases had a negative PLC finding or a pCEA level below the positive standard. Fifteen of sixty-four patients with gastric cancer had a positive PLC finding and an elevated pCEA level. Among the 49 patients with negative PLC findings, 11 had an elevated pCEA level. The overall pCEA positive rate in 64 patients with gastric cancer was 40.6% (26/64), which was significantly higher than that of PLC [23.4% (15/64), $P<0.05$]. We analyzed the correlation between PLC or pCEA positive rate and various clinicopathologic factors. The PLC and pCEA positive rates were significantly associated with the depth of tumor invasion and lymph node involvement. The patients with serosal invasion had a significantly higher PLC or pCEA positive rate than those without serosal invasion ($P<0.01$). The pCEA positive rate in patients with lymph node involvement was significantly higher than that in patients without lymph node involvement ($P<0.05$). Though the PLC positive rate in patients with lymph node involvement was also higher than that in patients without lymph node involvement, the difference did not reach statistical significance ($P>0.05$, Table 1).

Predicting values of PLC and pCEA for postoperative peritoneal recurrence of gastric cancer

Thirty-seven of sixty-four patients with gastric cancer had various postoperative recurrences (57.8%). Among the 37 patients with recurrence, 19 had peritoneal recurrence within 2 years after the surgery. The peritoneal recurrence rate was 29.7%. The accuracy, sensitivity, specificity, positive and negative predictive values, false negative and positive rates of PLC or pCEA in predicting peritoneal recurrence are shown in Table 2.

Correlation between PLC or pCEA and prognosis

The 1-, 3-, and 5-year survival rates were 53.3%, 13.3%, and 0.0%, respectively in patients with positive PLC findings, which were significantly lower than 87.8%, 71.4%, and 55.1% in those with negative PLC findings ($P<0.05$). Similarly, a significant difference in survival rates between pCEA-positive group and pCEA-negative group was observed. The 1-, 3-, and 5-year survival rates were 46.2%, 23.1%, and 15.4% in pCEA positive group and 89.5%, 73.7%, and 60.5% in pCEA negative group ($P<0.05$). Multivariate Cox survival analysis showed that PLC was not an independent prognostic factor, but pCEA was an independent prognostic factor with a relative risk rate of 9.046 ($P = 0.0092$).

Table 1 Correlation between the results of peritoneal washes and clinicopathological factors

Clinicopathological factors	*N*	PLC(+)		*P*	pCEA(+)		*P*
		n	%		*n*	%	
Tumor size							
≤4 cm	28	4	14.3	>0.05	9	32.1	>0.05
>4 cm	36	11	30.6		17	47.2	
Histological type							
Differentiated	30	5	16.7	>0.05	10	33.3	>0.05
Undifferentiated	34	10	29.4		16	47.1	
Serosal invasion							
Negative	27	2	7.4	<0.01	5	18.5	<0.01
Positive	37	13	35.1		21	56.8	
Lymph node involvement							
Negative	16	1	6.3	>0.05	3	18.8	<0.05
Positive	48	14	29.2		23	47.9	

Table 2 Results of PLC and pCEA in predicting peritoneal recurrence of gastric cancer after surgery (%)

	Accuracy	Sensitivity	Specificity	Positive predictive value	Negative predictive value	False negative rate	False positive rate
PLC	90.6	73.7	97.8	93.3	89.8	26.3	2.2
pCEA	85.9	94.7	82.2	69.2	97.4	5.3	17.8

DISCUSSION

Though radical surgery is routinely practised, tumor recurrence is frequent in patients with gastric cancer. Peritoneal recurrence of gastric cancer is one of the most common patterns of recurrence and predicts a very poor prognosis for patients with gastric cancer[2,3,14,15]. Peritoneal dissemination was also prevalent in our current prospective study, which was observed in 19 of 64 patients (29.7%) following a potentially curative surgery. Peritoneal recurrence develops from peritoneal free cancer cells originating from primary lesion or metastatic lymph nodes[6,14,15]. However, it is difficult to identify these free cancer cells in the peritoneal cavity before or during the surgery[16]. In order to prevent postoperative peritoneal recurrence and increase the survival rate, it is important to find a more sensitive, accurate, and convenient method to detect the presence of free cancer cells in the peritoneal cavity and to eliminate these cells with effective measures such as adjuvant intra-peritoneal chemotherapy[17,18].

PLC is the gold standard for assessing the presence of free gastric cancer cells in the peritoneal cavity[6-8,19]. Cytology-positive patients are classified as stage IV of Union International Contrele Cancer (UICC) gastric cancer classification and curative surgery is impossible in such cases. The present study revealed that the PLC positive rate in patients with serosal invasion (35.1%) was significantly higher than that in patients without serosal invasion (7.4%), indicating that the PLC positive rate increases with the invasion of gastric serosa and the chance of peritoneal dissemination increases in case, the gastric serosa is infiltrated. However, 14 of 19 patients with postoperative peritoneal recurrence had a positive PLC finding and the other five cases were PLC negative. PLC showed an accuracy of 90.6%, a sensitivity of 73.7%, and a specificity of 97.8% in predicting peritoneal recurrence of gastric cancer. The positive and negative predicting value, the false negative and positive rates of PLC were 93.3%, 89.8%, 26.3%, and 2.2%, respectively, suggesting that PLC is a very useful method for predicting peritoneal recurrence of gastric cancer with a high accuracy and a high specificity. However, PLC lacks sensitivity and has a relatively high false negative rate. Some patients with negative PLC results may have recurrence in the form of peritoneal dissemination.

CEA is generally accepted as a specific marker of gastrointestinal tumor[20,21]. Recently, measurement of CEA level and CEA RT-PCR assay in peritoneal washes have been used to detect the existence of free cancer cells in the peritoneal cavity[10,22,23]. It was reported that RT-PCR based assay has a relatively high sensitivity but is time-consuming, relatively laborious and less practical[10,22]. In the present study, pCEA levels in peritoneal washes were measured in order to detect the presence of free cancer cells in 64 patients with gastric cancer. The results showed that all the 15 patients with PLC positive findings were pCEA positive. However, 11 of 49 patients with PLC negative findings were also pCEA positive. The total pCEA positive rate was 40.6%, which was significantly correlated with the presence of serosal invasion and lymph node metastasis. Thus, as a useful method for detecting the presence of free cancer cells in the peritoneal cavity and for clinical staging of gastric cancer, pCEA level determination is considered to be superior to PLC. In our study, 18 of 19 patients with postoperative peritoneal recurrence of gastric cancer were pCEA positive and only one patient who died of postoperative peritoneal recurrence was pCEA negative, suggesting that pCEA assay is a highly sensitive method to predict postoperative peritoneal recurrence with a relatively high accuracy and specificity as compared to conventional PLC method.

In addition, our results showed that the positive rates of PLC and pCEA assay were significantly correlated with survival. Patients with negative results in PLC or pCEA assay survived significantly longer than those with positive findings in PLC or pCEA assay. In a multivariate analysis, pCEA level was found to be an independent prognostic factor even when all the clinicopathological variables were considered.

In conclusion, pCEA is a potential predictor of peritoneal recurrence as well as poor prognosis in patients with gastric cancer. Intra-operative pCEA assay can be considered as a reliable method for patients with gastric cancer.

REFERENCES

1 **Boku T,** Nakane Y, Minoura T, Takada H, Yamamura M, Hioki K, Yamamoto M. Prognostic significance of serosal invasion and free intraperitoneal cancer cells in gastric cancer. *Br J Surg* 1990; **77:** 436-439

2 **Nakamura K,** Ueyama T, Yao T, Xuan ZX, Ambe K, Adachi Y, Yakeishi Y, Matsukuma A, Enjoji M. Pathology and prognosis of gastric carcinoma. Findings in 10,000 patients who underwent primary gastrectomy. *Cancer* 1992; **70:** 1030-1037

3 **Kodera Y,** Yamamura Y, Torii A, Uesaka K, Hirai T, Yasui K, Morimoto T, Kato T, Kito T. Postoperative staging of gastric carcinoma. A comparison between the UICC stage classification and the 12th edition of the Japanese General Rules for Gastric Cancer Study. *Scand J Gastroenterol* 1996; **31:** 476-480

4 **Bando E,** Yonemura Y, Takeshita Y, Taniguchi K, Yasui T, Yoshimitsu Y, Fushida S, Fujimura T, Nishimura G, Miwa K. Intraoperative lavage for cytological examination in 1,297 patients with gastric carcinoma. *Am J Surg* 1999; **178:** 256-262

5 **Kodera Y,** Yamamura Y, Shimizu Y, Torii A, Hirai T, Yasui K, Morimoto T, Kato T. Peritoneal washing cytology: prognostic value of positive findings in patients with gastric carcinoma undergoing a potentially curative resection. *J Surg Oncol* 1999; **72:** 60-64; discussion 64-65

6 **Juhl H,** Stritzel M, Wroblewski A, Henne-Bruns D, Kremer B, Schmiegel W, Neumaier M, Wagener C, Schreiber HW, Kalthoff H. Immunocytological detection of micrometastatic cells: comparative evaluation of findings in the peritoneal cavity and the bone marrow of gastric, colorectal and pancreatic cancer patients. *Int J Cancer* 1994; **57:** 330-335

7 **Wu CC,** Chen JT, Chang MC, Ho WL, Chen CY, Yeh DC, Liu TJ, P'eng FK. Optimal surgical strategy for potentially curable serosa-involved gastric carcinoma with intraperitoneal free cancer cells. *J Am Coll Surg* 1997; **184:** 611-617

8 **Benevolo M,** Mottolese M, Cosimelli M, Tedesco M, Giannarelli D, Vasselli S, Carlini M, Garofalo A, Natali PG. Diagnostic and prognostic value of peritoneal immunocytology in gastric

cancer. *J Clin Oncol* 1998; **16:** 3406-3411
9 **Nekarda H,** Gess C, Stark M, Mueller JD, Fink U, Schenck U, Siewert JR. Immunocytochemically detected free peritoneal tumour cells (FPTC) are a strong prognostic factor in gastric carcinoma. *Br J Cancer* 1999; **79:** 611-619
10 **Kodera Y,** Nakanishi H, Ito S, Yamamura Y, Kanemitsu Y, Shimizu Y, Hirai T, Yasui K, Kato T, Tatematsu M. Quantitative detection of disseminated free cancer cells in peritoneal washes with real-time reverse transcriptase-polymerase chain reaction: a sensitive predictor of outcome for patients with gastric carcinoma. *Ann Surg* 2002; **235:** 499-506
11 **Sakakura C,** Takemura M, Hagiwara A, Shimomura K, Miyagawa K, Nakashima S, Yoshikawa T, Takagi T, Kin S, Nakase Y, Fujiyama J, Hayasizaki Y, Okazaki Y, Yamagishi H. Overexpression of dopa decarboxylase in peritoneal dissemination of gastric cancer and its potential as a novel marker for the detection of peritoneal micrometastases with real-time RT-PCR. *Br J Cancer* 2004; **90:** 665-671
12 **Japanese Gastric Cancer Association.** Japanese Classification of Gastric Carcinoma - 2nd English Edition - *Gastric Cancer* 1998; **1:** 10-24
13 **Asao T,** Fukuda T, Yazawa S, Nagamachi Y. Carcinoembryonic antigen levels in peritoneal washings can predict peritoneal recurrence after curative resection of gastric cancer. *Cancer* 1991; **68:** 44-47
14 **Yoo CH,** Noh SH, Shin DW, Choi SH, Min JS. Recurrence following curative resection for gastric carcinoma. Br J Surg 2000; **87:** 236-242
15 **Sakakura C,** Hagiwara A, Nakanishi M, Shimomura K, Takagi T, Yasuoka R, Fujita Y, Abe T, Ichikawa Y, Takahashi S, Ishikawa T, Nishizuka I, Morita T, Shimada H, Okazaki Y, Hayashizaki Y, Yamagishi H. Differential gene expression profiles of gastric cancer cells established from primary tumour and malignant ascites. *Br J Cancer* 2002; **87:** 1153-1161
16 **Fujimura T,** Kinami S, Ninomiya I, Kitagawa H, Fushida S, Nishimura G, Kayahara M, Shimizu K, Ohta T, Miwa K. Diagnostic laparoscopy, serum CA125, and peritoneal metastasis in gastric cancer. *Endoscopy* 2002; **34:** 569-574
17 **Fujimoto S,** Takahashi M, Mutou T, Kobayashi K, Toyosawa T. Successful intraperitoneal hyperthermic chemoperfusion for the prevention of postoperative peritoneal recurrence in patients with advanced gastric carcinoma. *Cancer* 1999; **85:** 529-534
18 **Ceelen WP,** Hesse U, de Hemptinne B, Pattyn P. Hyperthermic intraperitoneal chemoperfusion in the treatment of locally advanced intra-abdominal cancer. *Br J Surg* 2000; **87:** 1006-1015
19 **Hayes N,** Wayman J, Wadehra V, Scott DJ, Raimes SA, Griffin SM. Peritoneal cytology in the surgical evaluation of gastric carcinoma. *Br J Cancer* 1999; **79:** 520-524
20 **Holyoke ED,** Chu TM, Murphy GP. CEA as a monitor of gastrointestinal malignancy. *Cancer* 1975; **35:** 830-836
21 **Korenaga D,** Funahashi S, Yano K, Maekawa S, Ikeda T, Sugimachi K. Relationship between peritoneal collagen type IV concentrations and the presence of disseminated metastases in gastric cancer. *Arch Surg* 1995; **130:** 769-773
22 **Abe N,** Watanabe T, Toda H, Machida H, Suzuki K, Masaki T, Mori T, Sugiyama M, Atomi Y, Nakaya Y. Prognostic significance of carcinoembryonic antigen levels in peritoneal washes in patients with gastric cancer. *Am J Surg* 2001; **181:** 356-361
23 **To EM,** Chan WY, Chow C, Ng EK, Chung SC. Gastric cancer cell detection in peritoneal washing: cytology versus RT-PCR for CEA transcripts. *Diagn Mol Pathol* 2003; **12:** 88-95

Science Editor Wang XL, Guo SY and Li WZ **Language Editor** Elsevier HK

PO Box 2345, Beijing 100023, China
www.wjgnet.com
wjg@wjgnet.com

ELSEVIER

World J Gastroenterol 2005;11(46):7378-7383
World Journal of Gastroenterology ISSN 1007-9327

• *RAPID COMMUNICATION* •

Small intestinal submucosa improves islet survival and function during *in vitro* culture

Xiao-Hui Tian, Wu-Jun Xue, Xiao-Ming Ding, Xin-Lu Pang, Yan Teng, Pu-Xun Tian, Xin-Shun Feng

Xiao-Hui Tian, Wu-Jun Xue, Xiao-Ming Ding, Xin-Lu Pang, Yan Teng, Pu-Xun Tian, Xin-Shun Feng, Center of Renal Transplantation, The First Hospital of Xi'an Jiaotong University, Xi'an 710061, Shaanxi Province, China
Supported by the Key Program of Science and Technique of Ministry of Education of the People's Republic of China, No. 104169
Correspondence to: Dr Wu-Jun Xue, Center of Renal Transplantation, The First Hospital of Xi'an Jiaotong University, Xi'an 710061, Shaanxi Province, China. drtxh@yahoo.com.cn
Telephone: +86-29-85324033 Fax: +86-29-85324133
Received: 2005-05-25 Accepted: 2005-06-11

Abstract

AIM: To evaluate the recovery and function of isolated rat pancreatic islets during *in vitro* culture with small intestinal submucosa (SIS).

METHODS: Pancreatic islets were isolated from Wistar rats by standard surgical procurement followed by intraductal collagenase distension, mechanical dissociation and Euroficoll purification. Purified islets were cultured in plates coated with multilayer SIS (SIS-treated group) or without multilayer SIS (standard cultured group) for 7 and 14 d in standard islet culture media of RPMI 1640. After isolation and culture, islets from both experimental groups were stained with dithizone and counted. Recovery of islets was determined by the ratio of counts after the culture to the yield of islets immediately following islet isolation. Viability of islets after the culture was assessed by the glucose challenge test with low (2.7 mmol/L) and high glucose (16.7 mmol/L) solution supplemented with 50 mmol/L 3-isobutyl-1-methylxanthine (IBMX) solution. Apoptosis of islet cells after the culture was measured by relative quantification of histone-complexed DNA fragments using ELISA.

RESULTS: After 7 or 14 d of *in vitro* tissue culture, the recovery of islets in SIS-treated group was significantly higher than that cultured in plates without SIS coating. The recovery of islets in SIS-treated group was about twice more than that of in the control group. In SIS-treated group, there was no significant difference in the recovery of islets between short- and long-term periods of culture (95.8±1.0% *vs* 90.8±1.5%, $P>0.05$). When incubated with high glucose (16.7 mmol/L) solution, insulin secretion in SIS-treated group showed a higher increase than that in control group after 14 d of culture (20.7±1.1 mU/L *vs* 11.8±1.1 mU/L, $P<0.05$). When islets were placed in high glucose solution containing IBMX, stimulated insulin secretion was higher in SIS-treated group than in control group. Calculated stimulation index of SIS-treated group was about 23 times of control group. In addition, the stimulation index of SIS-treated group remained constant regardless of short- and long-term periods of culture (9.5±0.2 *vs* 10.2±1.2, $P>0.05$). Much less apoptosis of islet cells occurred in SIS-treated group than in control group after the culture.

CONCLUSION: Co-culture of isolated rat islets with native sheet-like SIS might build an extracellular matrix for islets and provide possible biotrophic and growth factors that promote the recovery and subsequent function of islets.

Key words: Islet culture; Islet survival; Islet function; Small intestinal submucosa

Tian XH, Xue WJ, Ding XM, Pang XL, Teng Y, Tian PX, Feng XS. Small intestinal submucosa improves islet survival and function during *in vitro* culture. *World J Gastroenterol* 2005; 11(46): 7378-7383
http://www.wjgnet.com/1007-9327/11/7378.asp

INTRODUCTION

In the last 10 years, both the prevalence and incidence of diabetes have increased sharply all over the world and this disease has already become one of the global health care problems. For example, there are 14 000 000 patients suffering from diabetes in USA and 1 000 000 of them suffer from type I diabetes mellitus[1]. Islet transplantation can control blood sugar effectively, reduce complications of diabetes and prevent hypoglycemia and insulin resistance caused by ectogenic insulin. Therefore, pancreatic islet cell transplantation may be an effective means for treating type I diabetes mellitus.

Human islet transplantation has been demonstrated to be a viable option for the treatment of type I diabetes mellitus[2]. However, there are still many difficulties hindering the transplantation alleviating complications of the disease. A major limitation for its use as a standard treatment is the lack of available viable islets for transplantation.

To maintain islets of Langerhans in tissue culture provides a chance for islet storage after being isolated from pan-

creas before clinical transplantation. The storage period can be utilized to assess the function of the islets and to confirm microbiologic sterility of the preparation. In addition, it can increase purity of the islet preparation and to reduce the immunogenicity of islets[3]. However, islet culture loses tissue mass over culturing time, which is one of its disadvantages[4]. Given the importance of transplanting sufficient islets to increase the chance of successful graft[5], any loss of islet tissue mass jeopardizes this possibility.

Both morphology and metabolic activities of cultured cells are affected by the composition of substrates on which they grow. Cultured cells may proliferate and/or perform their *in vivo* functions when cultured on substrates that closely mimic their natural environments. In fact, many commercially available matrices such as human extracellular matrix (ECM) derived from human placentas and matrigel (a soluble basement membrane extract from the Engelbreth-Holm-Swarm tumor) can be used in cell culture, which supports cell growth. Previous studies have showed that human islets cultured with bovine corneal endothelial cell matrix increase their ability to secrete insulin[6].

SIS is a relatively acellular collagen-based matrix derived from porcine small intestine by mechanical removal of the mucosal and smooth muscle layers[7]. The resulting cell-free translucent sheets are about 100 mm thick. The collagen-based matrix comprised highly conserved collagen, glycoprotein, proteoglycan, and glycoaminoglycan in their native configuration and concentration. In addition, SIS includes various growth factors such as fibroblast growth factor-2 (FGF-2), TGF-β and vascular endothelial cell growth factor (VEGF), which promote cell growth[8].

In 1966, Matsumoto *et al*.[9] reported that inverted small intestine could replace large veins in dogs. Improved processing of this biomaterial (SIS) has made it readily available for tissue engineering studies. Extensive *in situ* tissue remodeling from SIS has been shown in both rat and canine models. SIS has been used as a scaffold for proliferation, remodeling, and regeneration of a variety of host tissues including blood vessels[10], dura mater[11], urinary bladder[12], abdominal wall[13], and tendons[14]. Grossly and microscopically the remodeled tissue resembles the native tissue. Recently, SIS has been evaluated for its potential *in vivo* use in hepatocyte transplantation[15]. For these reasons, in this study we have investigated whether the use of SIS in co-culture with rat islets could improve islet survival and their *in vitro* function.

MATERIALS AND METHODS

Animals

Male Wistar rats (250-400 g body weight, Animal Laboratory of Xi'an Jiaotong University, China) were used for islet isolation. All animals received care in compliance with the guidelines of the local Animal Care and Use Committee following National Institutes of Health guidelines.

Design of study

Islets were isolated using a collagenase and purified by discontinuous Euroficoll gradient. The purified islets were separated into study group and control group. In study group, islets were cultured in plates coated with SIS. In control group, islets were cultured in plates not coated with SIS. The number of islets was counted after isolation and culture. Recovery of islets was determined by the ratio of counts after the culture to the yield of islets immediately following islet isolation. Islet function was determined by a static glucose challenge test after a short period of culture for 7 d and a long period of culture for 14 d. Glucose challenge test was performed in the absence and presence of IBMX. Apoptosis of islet cells following culture was measured by relative quantification of histone-complexed DNA fragments (mono- and oligonucleosomes) out of the cytoplasm of cells by ELISA.

Preparation of soluble SIS supplement

SIS was prepared as previously described[10]. In brief, freshly harvested porcine jejunum was obtained from a local slaughterhouse. The tube of intestinal material was rinsed, until it was free of contents and inverted. Superficial layers of the tunica mucosa were removed by scraping with a knife handle. The tissue was then reverted to its original direction, serosa and tunica muscularis were removed. The resulting membrane was approximately 80-100 μm thick consisting of tunica submucosa and basilar portion of the tunica mucosa. The prepared intestinal submucosa tube was split open longitudinally and rinsed extensively in water to get rid of any of the cells associated with the matrix to eliminate cell degradation products. The sheets of SIS were sterilized by exposure to 1 g/L per acetic acid. To make multilayered SIS, five sheets of SIS were mechanically compressed by vacuum pressing and dried. The multilayered SIS was then terminally sterilized with ethylene oxide and kept until ready to use. Re-soaking in saline prior to use made the SIS sheets pliable and soft.

Islet isolation and culture

Islets were isolated and purified from the rat pancreas as previously described[16]. Briefly, rats were anesthetized with intraperitoneal pentobarbital. Pancreas was infused via the common bile duct with Hanks' balanced salt solution, set apart, and minced on ice. Digestion was performed with type V collagenase (7.5 g/L; Sigma) for 25 min at 37 ℃. Islets were purified on a discontinuous Euroficoll gradient (Sigma), handpicked under an inverted light microscope, pooled and then separated into study group and control group. In study group, islets were cultured in plates coated with suitable size multilayer SIS. In control group, islets were cultured in plates not coated with SIS. Islets were cultured in RPMI 1640 medium (Gibco) supplemented with 100 mL/L fetal calf serum (Gibco), 200 kU/L penicillin, 100 mg/L streptomycin, and 2 mmol/L L-glutamine (Gibco) at 37 ℃ in a humidified 50 mL/L CO_2 atmosphere for a period of 7 or 14 d.

Islet quantification and recovery

Islets from both groups were stained with dithizone and counted in accordance with the criteria established at

the 1989 International Workshop on Islet Assessment after isolation and culture. The number of islets was determined using an optical graticule attached to the eyepiece of a dissecting microscope and converted to the standard of islet equivalent (IE). Recovery of islets following culture was determined by the ratio of counts after the culture to the yield of islets immediately following islet isolation.

Islet viability

For each group, 6 separate samples of 20 islets each were tested simultaneously for their stimulated insulin secretion. Islets (150±50 μm in diameter) were first pre-incubated for 45-50 min in 2 mL RPMI 1640 solution containing 2.7 mmol/L glucose. Insulin secretion was then assessed by three consecutive incubations with RPMI 1640 solution containing 2.7, 16.7, and 16.7 mmol/L glucose with 1 g/L IBMX (Sigma), each for 45 min. At the end of incubation with each solution, the supernatant was completely removed and used to test the insulin secretion level by radioimmunoassay (Department of Isotope, China Institute of Atomic Energy). Insulin secretory responses of 20 islets to glucose stimulation were expressed as milliunit per liter. To eliminate variation of islet size causing differences of insulin response, the stimulation index for each group of islets was determined by the ratio of insulin secretion stimulated by high glucose solution containing IBMX to the basal insulin secretion stimulated by low glucose solution.

Evaluation of apoptosis of islet cells

Apoptosis of islet cells was measured by relative quantification of DNA/histone fragmentation (mono- and oligonucleosomes) in culture supernatants. After 7-14 d of incubation, culture medium was collected from each well of two groups. The supernatants were analyzed to measure cytoplasmic histone-associated DNA fragments generated by cell death based on mouse monoclonal antibodies against DNA and histones, respectively. The cultured supernatant sample (20 μL) was mixed with 80 μL of immunoreagent containing two monoclonal antibodies, antihistone (biotin-labeled) and anti-DNA (peroxidase-conjugated) in the well coated with streptavidin of a 96-well plate. Antibody–nucleosome complexes were bound to the microplate by streptavidin. The solution mixture was incubated by gently shaking (300 r/min) for 2 h at room temperature. The solution was then collected and the well was completely rinsed thrice with 150 μL of an incubation buffer and 100 μL of premixed 2, 2'-azino-di-3-ethylbenzthiazoline sulfonate (ABTS) substrate solution was added to each well. The mixed solution was agitated on a plate shaker for 20 min at room temperature and the solution absorbance was measured at a wavelength of 405 nm. The enrichment of nucleosomes due to apoptosis of islet cells was calculated from these absorbance values by the following formula: enrichment factor of nucleosomes=(values of the sample-the background values)/values of the negative control. The assay was done independently thrice for each experimental group. This method could permit us to specifically determine mono- and oligonucleosomes released into culture supernatants accompanying apoptosis and necrosis of islet cells. Accumulation of mono- and oligonucleosomes in the cytoplasm of apoptotic and necrotic cells caused DNA degradation, occurring several hours before the breakdown of plasma membrane.

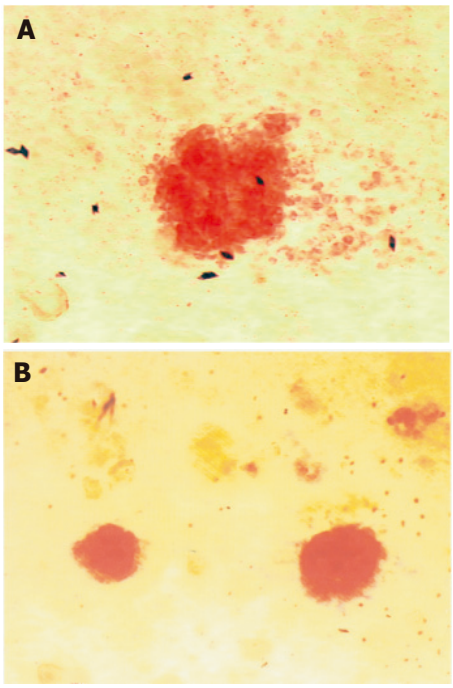

Figure 1 Morphology of islets after culture. **A:** Loose appearance of islets after 14 d of culture under standard condition; **B:** excellent morphology of islets after 14 d of culture on SIS (×400).

Statistical analysis

Results were expressed as mean±SE. Differences between the two groups were analyzed by *t*-test using SPSS10.0. $P<0.05$ was considered statistically significant.

RESULTS

After 7 and 14 d of *in vitro* tissue culture, SIS-treated group indicated a significantly higher ($P<0.05$) recovery of islets than control group (Table 1). The recovery in SIS-treated group was about twice more than that in control group. In SIS-treated group, there was no statistical difference in the recovery between the short and the long periods of culture (95.8±1.0% *vs* 90.8±1.5%, $P<0.05$). Most islets cultured in control group lost their initial morphology, becoming "loose" in appearance at the end of culture. Islets cultured with SIS exhibited excellent morphology (Figure 1).

In vitro viability of the islets was assessed using the glucose challenge test. There was no statistical difference in the basal level of insulin secretion between SIS treated group and control group (9.1±0.3 mU/L *vs* 7.8±0.6 mU/L after 7 d of culture, 5.9±0.4 mU/L *vs* 7.1±0.4 mU/L after

Table 1 Recovery of rat islets and enrichment factor of nucleosomes after being cultured for 7 and 14 d (n = 6, mean±SE)

Parameter	Group	7 d (%)	14 d (%)
Recovery			
	Standard culture	67.1±2.6	42.2±1.5
	SIS culture	95.8±1.0[a]	90.8±1.5[a]
Enrichment factor			
	Standard culture	1.98±0.06	2.90±0.23
	SIS culture	1.08±0.02[a]	1.12±0.09[a]

[a]P<0.05 *vs* standard culture.

Table 2 Stimulated insulin secretion of rat islets cultured for 7 and 14 d during static incubation assay (n = 6, mean±SD)

Group	T (d)	Low glucose solution (2.7 mmol/L)	High glucose solution (16.7 mmol/L)	High glucose solution +50 μmol/L IBMX	SI[1]
Standard culture	7	9.1±0.3	18.3±1.1	51.3±3.4	5.7±0.4
SIS culture	7	7.8±0.6	21.8±1.9	75.8±2.1[a]	10.2±1.2[a]
Standard culture	14	5.9±0.4	11.8±1.1	20.5±1.8	3.6±0.4
SIS culture	14	7.1±0.4	20.7±1.1[a]	66.9±3.7[a]	9.5±0.2[a]

[1]SI (stimulation index)=insulin secretion during incubation with 16.7 mmol/L high glucose solution+50 μmol/L IBMX/insulin secretion during incubation with 2.7 mmol/L low glucose solution. [a]P<0.05 *vs* standard culture.

14 d of culture, P>0.05). There was a two- to threefold increase in insulin secretion in both groups upon stimulation by high glucose solution (16.7 mmol/L). After 14 d of culture, SIS-treated group showed a significantly higher increase in insulin secretion than control group (20.7±1.1 mU/L *vs* 11.8±1.1 mU/L, P<0.05). When islets were placed in the high glucose solution containing IBMX, the stimulated insulin secretion was significantly higher in SIS-treated group than in control group. Similar results occurred when the stimulation index was used as a reference (a ratio of insulin secreted upon stimulation by high glucose solution plus IBMX to basal insulin secreted). The stimulation index of SIS-treated group was about 2-3 times than that of the control group. In addition, the stimulation index of SIS-treated group were statistically equivalent to that of the group cultured for 7 and 14 d group (9.5±0.2 *vs* 10.2±1.2, P>0.05) (Table 2).

Apoptosis of islet cells was measured by relative quantification of DNA/histone fragmentation (mono- and oligonucleosomes) in culture supernatants using ELISA. The enrichment factor of nucleosomes was significantly lower in SIS-treated group than in control group, suggesting that much less apoptosis of islet cells occurred in SIS-treated group (Table 1).

DISCUSSION

Islet transplantation is a viable option of treatment for insulin-dependent diabetes mellitus. Maintaining islets in culture is important to increase the safety, practicality and efficacy of successful clinical results. In addition to reducing the immunogenicity of islets[3,17], islet culture simplifies the procedure of transplantation, which can be scheduled during regular hospital hours, and the patient is not necessary to move from a distant location to the transplantation center before a donor is available. Culture may facilitate novel immunosuppressive techniques[18]. Moreover, improved methods and supplementation of islet culture provide a unique opportunity to optimize recovery of islet mass for transplantation. Islets do not form monolayers, fail to replicate and contain multiple cell types, making them similar to a tiny organ. All these are the unique challenges for maintaining islets in culture. Procedures related to isolation and *in vitro* culture can lead to a considerable loss of islet tissue. Apoptosis and anoikis may be the mechanisms involved in tissue loss[19,20].

It has been reported that binding of ECM to integrin, a protein located on cell membrane, stimulates intracellular signaling pathways to prevent cells from their entry into the cascade of apoptosis[21], suggesting that interaction between cells and ECM plays an important role in the subsequent cell behaviors. It is possible that cell–ECM interaction is disrupted by the procedures related to islet isolation and purification. As a consequence, functions of isolated islets could be damaged. A recent study showed that the viability of porcine islet cells embedded in fibrous skeleton of pancreas is higher viability which may be due to cellular adhesion and ligation of ECM to integrins as opposed to their isolated counterparts. Further studies of these embedded cells demonstrated that the viability of the cells is sustained for 30 days or more and islet function is excellent 30 days after the isolation[22].

Frisch *et al.*[23] and Thomas *et al.*[22] have shown that anoikis resulted from a death signal induced by MEKK-1 group of caspases[23,24]. As a critical safeguard of nature, anoikis can prevent cells from taking up residence and growth in ectopic positions as in tumor metastases. Thomas *et al.*[22] reported that the apoptotic rate is markedly reduced when cells are attached to ECM, suggesting that ECM plays an essential role in the maintenance of differentiated cells. Preparation of islet isolation especially enzymatic digestion of pancreas can result in the loss of peripheral basement membrane or interstitial membrane of islets, suggesting that purity is not essential to achieve engraftment. The presence of other cellular elements may be critical for engraftment and long-term maintenance of graft function and survival[25]. The fact that transplantation of purified preparations of autologous islets loses islet function in early periods also supports this hypothesis[26].

A number of novel approaches have been developed to create a favorable physiological microenvironment for islets in culture to limit anoikis. The major method is to use ECM. Studies indicate that ECM can increase islet survival time and/or insulin secretion[21,27,28]. As a natural ECM, SIS is obtained from the intestine using a process that retains the natural composition and configuration of matrix molecules such as collagen (Types I, III and VI), glycosaminoglycans (hyaluronic acid, chondroitin sulfate A and B, heparin and heparin sulfate), proteoglycans,

glycoproteins (fibronectin), and growth factors (FGF-2, TGF-β, and VEGF), which play an important role in host tissue repair, remodel, and cell growth[8]. Mapping of the distribution of significant proteins and proteoglycans in small intestinal submucosa by fluorescence microscopy indicates that heparan sulfate proteoglycans (HSPG) is extensively distributed but concentrated in vessels. FGF-2 is diffusely distributed and associated with fibrous structures. VEGF is distributed mainly around the vessels. Collagen fibrils are distinctly present in the background. This anatomic structure of SIS is likely to play an important role in the regeneration of tissues and factors in remnant vessels may facilitate penetration of the matrix along these avenues[29].

SIS has excellent mechanical properties (high compliance, a high burst pressure point, and an effective porosity index), satisfactory histocompatibility, non-immunogenicity and safety for human use, allowing it to be used for vascular and connective tissue graft construct[7,10-14]. The porous nature and three-dimensional microarchitecture of SIS allow diffusion of cell nutrients and induce proliferation, remodeling and regeneration of host tissues when implanted in microenvironments *in vivo* (e.g. artery, tendon, bone, and articular cartilage)[10,14,30,31]. The same situation occurs in the cells during in vitro culture. In a recent study, several cell lines, including NIH Swiss mouse 3T3 fibroblasts, NIH 3T3/J2 fibroblasts, primary human fibroblasts, primary human keratinocytes, human microvascular endothelial cells (HMECs) and rat osteosarcoma (ROS) cells were cultured in the presence of sheet form SIS. All cell types showed the ability to attach and proliferate. All fibroblast cell lines and keratinocytes proliferated and/or migrated into the three-dimensional scaffold of SIS matrix. Co-culturing of NIH 3T3/J2 fibroblasts and primary human keratinocytes with SIS resulted in a distinctive spatial orientation of the two cell types. Fibroblasts populated the mid-substance of the three-dimensional matrix and keratinocytes formed an epidermal structure with rete ridge-like formation and stratification, when the composite was lifted to an air liquid interface in culture[32]. For these reasons, we hypothesize that SIS with native sheet-like configuration can imitate the natural growth environments of islets and improve islet survival and function *in vitro*, thus decreasing loss of tissue mass during culture.

We observed a higher recovery and stimulation index of islets and a lower enrichment factor of nucleosomes in SIS-treated group than in control group. These results may prove our hypothesis and are comparable to previous studies in different cell lines[32] and islets[6]. In pancreas, ECM is composed of interstitial matrix and basement membrane, the latter is composed of fibronectin, laminin and collagens IV and V[33]. These submucosal cell growth substrates provide islet cells with a collagenous matrix environment *in vitro*, resembling that in *in vivo*. We think that the unique configuration and composition of SIS may contribute to such improvements for islet culture. Firstly, the porous nature of SIS allows diffusion of cell nutrients, thus decreasing the central cell damage of isolated islets of Langerhans[34]. Secondly, SIS provides a substratum with a three-dimensional scaffold allowing for cell migration and spatial organization[35]. Thirdly, abundant collagen and various growth factors activate the signaling pathways, which induce attachment, proliferation, and differentiation of the cells[36].

In conclusion, co-culture of isolated rat islets with native sheet-like SIS can provide an ECM and possible biotrophic and growth factors, which promote the recovery and subsequent function of islets during *in vitro* tissue culture. In view of the rapid degradation of SIS *in vivo*[37], whether SIS improves the recovery and subsequent function of islets *in vitro* and the effect of SIS on islets *in vivo* needs to be further studied.

REFERENCES

1 **Xu G,** Yuan MS. Current situation and prospect of the islet transplantation. *Zhongguo Tangniaobing zhazi* 2001; **9:** 49-51

2 **Shapiro AM,** Lakey JR, Ryan EA, Korbutt GS, Toth E, Warnock GL, Kneteman NM, Rajotte RV. Islet transplantation in seven patients with type 1 diabetes mellitus using a glucocorticoid-free immunosuppressive regimen. *N Engl J Med* 2000; **343:** 230-238

3 **Kneteman NM,** Halloran PF, Sanden WD, Wang T, Seelis RE. Major histocompatibility complex antigens and murine islet allograft survival. *Transplantation* 1991; **51:** 247-251

4 **Fraga DW,** Sabek O, Hathaway DK, Gaber AO. A comparison of media supplement methods for the extended culture of human islet tissue. *Transplantation* 1998; **65:** 1060-1066

5 **Markmann JF,** Deng S, Huang X, Desai NM, Velidedeoglu EH, Lui C, Frank A, Markmann E, Palanjian M, Brayman K, Wolf B, Bell E, Vitamaniuk M, Doliba N, Matschinsky F, Barker CF, Naji A. Insulin independence following isolated islet transplantation and single islet infusions. *Ann Surg* 2003; **237:** 741-749; discussion 749-750

6 **Beattie GM,** Lappi DA, Baird A, Hayek A. Functional impact of attachment and purification in the short term culture of human pancreatic islets. *J Clin Endocrinol Metab* 1991; **73:** 93-98

7 **Roeder R,** Wolfe J, Lianakis N, Hinson T, Geddes LA, Obermiller J. Compliance, elastic modulus, and burst pressure of small-intestine submucosa (SIS), small-diameter vascular grafts. *J Biomed Mater Res* 1999; **47:** 65-70

8 **Luo JC,** Yang ZM. Preparation and characteristics of small intestinal submucosa. *Zhongguo Xiufu Chongjian Waike Zazhi* 2003; **17:** 425-428

9 **Matsumoto T,** Holmes RH, Burdick CO, Heisterkamp CA 3rd, O'Connell TJ Jr. Replacement of large veins with free inverted segments of small bowel: autografts of submucosal membrane in dogs and clinical use. *Ann Surg* 1966; **164:** 845-848

10 **Badylak SF,** Lantz GC, Coffey A, Geddes LA. Small intestinal submucosa as a large diameter vascular graft in the dog. *J Surg Res* 1989; **47:** 74-80

11 **Cobb MA,** Badylak SF, Janas W, Boop FA. Histology after dural grafting with small intestinal submucosa. *Surg Neurol* 1996; **46:** 389-393; discussion 393-394

12 **Kropp BP,** Eppley BL, Prevel CD, Rippy MK, Harruff RC, Badylak SF, Adams MC, Rink RC, Keating MA. Experimental assessment of small intestinal submucosa as a bladder wall substitute. *Urology* 1995; **46:** 396-400

13 **Clarke KM,** Lantz GC, Salisbury SK, Badylak SF, Hiles MC, Voytik SL. Intestine submucosa and polypropylene mesh for abdominal wall repair in dogs. *J Surg Res* 1996; **60:** 107-114

14 **Badylak SF,** Tullius R, Kokini K, Shelbourne KD, Klootwyk T, Voytik SL, Kraine MR, Simmons C. The use of xenogeneic

small intestinal submucosa as a biomaterial for Achilles tendon repair in a dog model. *J Biomed Mater Res* 1995; **29:** 977-985

15 **Kim SS,** Kaihara S, Benvenuto MS, Kim BS, Mooney DJ, Kim SS, Kaihara S, Benvenuto MS, Kim BS, Mooney DJ, Vacanti JP. Small intestinal submucosa as a small-caliber venous graft: a novel model for hepatocyte transplantation on synthetic biodegradable polymer scaffolds with direct access to the portal venous system. *J Pediatr Surg* 1999; **34:** 124-128

16 **Lacy PE,** Kostianovsky M. Method for the isolation of intact islets of Langerhans from the rat pancreas. *Diabetes* 1967; **16:** 35-39

17 **Kuttler B,** Hartmann A, Wanka H. Long-term culture of islets abrogates cytokine-induced or lymphocyte-induced increase of antigen expression on beta cells. *Transplantation* 2002; **74:** 440-445

18 **Ricordi C.** Islet transplantation: a brave new world. *Diabetes* 2003; **52:** 1595-1603

19 **Paraskevas S,** Duguid WP, Maysinger D, Feldman L, Agapitos D, Rosenberg L. Apoptosis occurs in freshly isolated human islets under standard culture conditions. *Transplant Proc* 1997; **29:** 750-752

20 **Thomas FT,** Contreras JL, Bilbao G, Ricordi C, Curiel D, Thomas JM. Anoikis, extracellular matrix, and apoptosis factors in isolated cell transplantation. *Surgery* 1999; **126:** 299-304

21 **Ris F,** Hammar E, Bosco D, Pilloud C, Maedler K, Donath MY, Oberholzer J, Zeender E, Morel P, Rouiller D, Halban PA. Impact of integrin-matrix matching and inhibition of apoptosis on the survival of purified human beta-cells in vitro. *Diabetologia* 2002; **45:** 841-850

22 **Thomas F,** Contreras J, Bilbao G, Invarardi L, Thomas J. An improved technique for isolating pig islets: the importance of tensegrity in islet long-term culture viability. *Transplant Proc* 1999; **31:** 633-634

23 **Frisch SM,** Vuori K, Kelaita D, Sicks S. A role for Jun-N-terminal kinase in anoikis; suppression by bcl-2 and crmA. *J Cell Biol* 1996; **135:** 1377-1382

24 **Cardone MH,** Salvesen GS, Widmann C, Johnson G, Frisch SM. The regulation of anoikis: MEKK-1 activation requires cleavage by caspases. *Cell* 1997; **90:** 315-323

25 **Metrakos P,** Yuan S, Agapitos D, Rosenberg L. Intercellular communication and maintenance of islet cell mass--implications for islet transplantation. *Surgery* 1993; **114:** 423-427; discussion 427-428

26 **Kneteman NM,** Warnock GL, Evans MG, Nason RW, Rajotte RV. Prolonged function of canine pancreatic fragments autotransplanted to the spleen by venous reflux. *Transplantation* 1990; **49:** 679-681

27 **Beattie GM,** Montgomery AM, Lopez AD, Hao E, Perez B, Just ML, Lakey JR, Hart ME, Hayek A. A novel approach to increase human islet cell mass while preserving beta-cell function. *Diabetes* 2002; **51:** 3435-3439

28 **Oberg-Welsh C.** Long-term culture in matrigel enhances the insulin secretion of fetal porcine islet-like cell clusters in vitro. *Pancreas* 2001; **22:** 157-163

29 **Hurst RE,** Bonner RB. Mapping of the distribution of significant proteins and proteoglycans in small intestinal submucosa by fluorescence microscopy. *J Biomater Sci Polym Ed* 2001; **12:** 1267-1279

30 **Suckow MA,** Voytik-Harbin SL, Terril LA, Badylak SF. Enhanced bone regeneration using porcine small intestinal submucosa. *J Invest Surg* 1999; **12:** 277-287

31 **Fox DB,** Cook JL, Arnoczky SP, Tomlinson JL, Kuroki K, Kreeger JM, Malaviya P. Fibrochondrogenesis of free intraarticular small intestinal submucosa scaffolds. *Tissue Eng* 2004; **10:** 129-137

32 **Badylak SF,** Record R, Lindberg K, Hodde J, Park K. Small intestinal submucosa: a substrate for in vitro cell growth. *J Biomater Sci Polym Ed* 1998; **9:** 863-878

33 **Geutskens SB,** Homo-Delarche F, Pleau JM, Durant S, Drexhage HA, Savino W. Extracellular matrix distribution and islet morphology in the early postnatal pancreas: anomalies in the non-obese diabetic mouse. *Cell Tissue Res* 2004; **318:** 579-589

34 **Ilieva A,** Yuan S, Wang RN, Agapitos D, Hill DJ, Rosenberg L. Pancreatic islet cell survival following islet isolation: the role of cellular interactions in the pancreas. *J Endocrinol* 1999; **161**: 357-364

35 **Falorni A,** Basta G, Santeusanio F, Brunetti P, Calafiore R. Culture maintenance of isolated adult porcine pancreatic islets in three-dimensional gel matrices: morphologic and functional results. *Pancreas* 1996; **12:** 221-229

36 **Wang RN,** Paraskevas S, Rosenberg L. Characterization of integrin expression in islets isolated from hamster, canine, porcine, and human pancreas. *J Histochem Cytochem* 1999; **47:** 499-506

37 **Badylak SF,** Kropp B, McPherson T, Liang H, Snyder PW. Small intestional submucosa: a rapidly resorbed bioscaffold for augmentation cystoplasty in a dog model. *Tissue Eng* 1998; **4:** 379-387

Science Editor Wang XL and Guo SY **Language Editor** Elsevier HK

PO Box 2345, Beijing 100023, China
www.wjgnet.com
wjg@wjgnet.com

ELSEVIER

World J Gastroenterol 2005;11(46):7384-7385
World Journal of Gastroenterology ISSN 1007-9327

Complete or partial trisomy 3 in gastro-intestinal MALT lymphomas co-occurs with aberrations at 18q21 and correlates with advanced disease stage: A study on 25 cases

Jens Krugmann, Alexandar Tzankov, Stephan Dirnhofer, Falko Fend, Dominik Wolf, Reiner Siebert, Pensiri Probst, Martin Erdel

Jens Krugmann, Alexandar Tzankov, Institute of Pathology, Medical University of Innsbruck, Austria
Stephan Dirnhofer, Institute of Pathology, University of Basel, Switzerland
Falko Fend, Institute of Pathology, Technical University of Munich, Germany
Dominik Wolf, Department of Internal Medicine, Division of Hematology/Oncology, Medical University of Innsbruck, Austria
Reiner Siebert, Institute of Human Genetics, University Hospital Schleswig-Holstein Campus Kiel, Germany
Jens Krugmann, Pensiri Probst, Martin Erdel, Department of Medical Genetics, Molecular and Clinical Pharmacology, Medical University of Innsbruck, Austria
Correspondence to: Jens Krugmann, MD, Institute of Pathology, Medical University of Innsbruck, Müllerstraße 44, A-6020 Innsbruck, Austria. jens.krugmann@uibk.ac.at
Telephone: +43-512-507-3659 Fax: +43-512-582088
Received: 2005-03-21 Accepted: 2005-08-25

Key words: MALT lymphoma; Trisomy 3; Trisomy 18

Krugmann J, Tzankov A, Dirnhofer S, Fend F, Wolf D, Siebert R, Probst P, Erdel M. Complete or partial trisomy 3 in gastro-intestinal MALT lymphomas co-occurs with aberrations at 18q21 and correlates with advanced disease stage: A study on 25 cases. *World J Gastroenterol* 2005; 11(46): 7384-7385
http://www.wjgnet.com/1007-9327/11/7384.asp

TO THE EDITOR

Taji *et al*.[1] have reported in their study on 13 patients with gastric mucosa-associated lymphoid tissue (MALT) lymphomas an aggressive tumor course in trisomy 3 positive cases. The authors analyzed only stage I patients with classical low-grade marginal zone lymphoma of the MALT type and detected the trisomy 3 using an alpha-satellite DNA probe directed to the centromere. Their data support the observation that trisomy 3 is the most frequent cytogenetic aberration in MALT lymphomas[2,3].

In our previous published series[4] of 29 surgically resected gastrointestinal (GI) *t*(11;18) negative MALT lymphomas, we have described an adverse prognostic impact of trisomy 18q21 detected by a *MALT1*-specific fluorescence *in situ* hybridization (FISH) probe, especially in the lymphomas with high grade component. We have additionally studied 25 of the previously reported GI lymphomas including 7 low grade marginal zone lymphomas and 18 GI diffuse large B-cell lymphomas (DLBCL, including 3 cases with low grade lymphoma component) diagnosed in stage I (n = 8) and in stage >II (n = 17) for complete and partial trisomies 3 using FISH probes for the centromere of chromosome 3 (Vysis, Downer's Groove, IL, USA) as well as for the BCL6 gene at 3q27 (flanking BAC clones RP11- 528E8 and 690C8)[5]. The latter double-color assay was selected because it targets the critically gained band of chromosome 3 in MALT lymphomas and can detect breakpoints affecting the BCL6 locus, which are recurrent in extranodal DLBCL. For each hybridization, we evaluated 100 cell nuclei. The cut-off level, defined as mean false positive rate (determined in normal gastric mucosa and samples from *Helicobacter pylori* gastritis) plus three standard deviations, was 5.4% for the centromere 3 probe (trisomy). For the BCL6 probe mix no split or gain of signals was observed in the control samples, but according to the literature, the cut-off level for the detection of trisomy 3q27 or BCL6 breaks was set to 3%[5].

In agreement with the previously published studies, we detected trisomy 3q27 as the most frequent aberration in GI MALT lymphomas, occurring in 9/25 (36%) of the cases. In three of these nine cases, trisomy 3 was indicated by the presence of supernumerary signals for both the centromeric region and the *BCL6* locus, whereas in the remaining six cases, a gain of 3q27/*BCL6* was detected without a change in the number of centromere signals (partial trisomy 3q27). The only positive stage I lymphoma showed a partial trisomy 3q27. In three cases of the DLBCL subset, one with trisomy 3 and two with partial trisomy 3q27, a separation of the *BCL6* signal pair was additionally detected indicating both a *BCL6* translocation (two cases potentially with *BCL6*/IGH rearrangement) and overrepresentation of proximal/distal 3q27.

Trisomies 3q27 were present in 1/8 (13%) stage I and 8/17 (47%) stage >II diseases indicating a significant ($P<0.01$; χ^2 test) association of trisomy 3q27 with

lymphoma dissemination. There was a strong correlation between the occurrence of trisomies 18q21/*MALT1* and 3q27/*BCL6* in the present series of GI MALT lymphomas with 5/6 (83%) 18q21 positive tumors carrying both aberration and only 1/6 (17%) case showing trisomy 18q21 without trisomy 3q27 ($P<0.05$). We have previously reported that trisomy 18q21/*MALT1* to be associated with an unfavorable prognosis in the same series of surgically resected GI MALT lymphomas, which was particularly pronounced in the DLBCL subset[4]. With regard to trisomy 3q27, we observed a trend towards an inferior survival too, $P = 0.0727$.

Our data highlight that partial trisomies of chromosomes 3 and 18 have to be taken into account when evaluating the course of GI MALT lymphomas. Roughly two-thirds of the gains on the respective chromosomes might not include the centromeric region. Moreover, the co-occurrence of trisomies 3q27 and 18q21 in our group of surgically resected GI MALT lymphomas points to a possible interaction of both loci, especially in patients with an advanced stage disease.

REFERENCES

1 **Taji S,** Nomura K, Matsumoto Y, Sakabe H, Yoshida N, Mitsufuji S, Nishida K, Horiike S, Nakamura S, Morita M, Taniwaki M. Trisomy 3 may predict a poor response of gastric MALT lymphoma to Helicobacter pylori eradication therapy. *World J Gastroenterol* 2005; **11:** 89-93

2 **Wotherspoon AC**, Finn TM, Isaacson PG. Trisomy 3 in low-grade B-cell lymphomas of mucosa-associated lymphoid tissue. *Blood* 1995; **85:** 2000-2004

3 **Ott G,** Kalla J, Steinhoff A, Rosenwald A, Katzenberger T, Roblick U, Ott MM, Muller-Hermelink HK. Trisomy 3 is not a common feature in malignant lymphomas of mucosa-associated lymphoid tissue type. *Am J Pathol* 1998; **153:** 689-694

4 **Krugmann J,** Tzankov A, Dirnhofer S, Fend F, Greil R, Siebert R, Erdel M. Unfavourable prognosis of patients with trisomy 18q21 detected by fluorescence in situ hybridisation in t(11;18) negative, surgically resected, gastrointestinal B cell lymphomas. *J Clin Pathol* 2004; **57:** 360-364

5 **Sanchez-Izquierdo D,** Siebert R, Harder L, Marugan I, Gozzetti A, Price HP, Gesk S, Hernandez-Rivas JM, Benet I, Sole F, Sonoki T, Le Beau MM, Schlegelberger B, Dyer MJ, Garcia-Conde J, Martinez-Climent JA. Detection of translocations affecting the BCL6 locus in B cell non-Hodgkin's lymphoma by interphase fluorescence in situ hybridization. *Leukemia* 2001; **15:** 1475-1484

Science Editor Guo SY **Language Editor** Elsevier HK

PO Box 2345, Beijing 100023, China
www.wjgnet.com
wjg@wjgnet.com

ELSEVIER

World J Gastroenterol 2005;11(46):7386
World Journal of Gastroenterology ISSN 1007-9327

Acknowledgments to Reviewers of World Journal of *Gastroenterology*

Many reviewers have contributed their expertise and time to the peer review, a critical process to ensure the quality of *World Journal of Gastroenterology*. The editors and authors of the articles submitted to the journal are grateful to the following reviewers for evaluating the articles (including those were published and those were rejected in this issue) during the last editing period of time.

Anthony Thomas Roger Axon, Professor
Department of Gastroenterology, Infirmary At Leeds, Room 190a, Clarendon Wingthe General Infirmary At Leedsgreat George Stree, Leeds Ls1 3ex, United Kingdom

Giovanni Addolorato, M.D.
Institute of Internal medicinie, L.go Gemelli 8, Rome 00168, Italy

Fernando Azpiroz, M.D.
Digestive System Research Unit, University Hospital Vall d' Hebron, Paseo Vall d'Hebron, 119-129, Barcelona 08035, Spain

Yasuji Arase, M.D.
Department of Gastroenterology, Toranomon Hospital, 2-2-2Toranomonminato-ku, Tokyo 105-8470, Japan

Giovanni Cammarota, M.D.
Department of Internal Medicine and Gastroent, Catholic University of Medicine and Surgery, Rome, Policlinico A. Gemelli; Istituto di Medicina Interna; Largo A. Gemlli, 8, Roma 00168, Italy

Jun Cheng, Professor, Dean Assistant
Beijing Earth Altar Hospital Dean 13 Earth Altar Park, Anwai Avenue, East District, Beijing 100011, China

Kiron M Das, MD, PhD, FACP, FRCP
Chief of Gastroenterology and Hepatology,
Professor of Medicine, Director of Crohn's and Colitis Center of NJ, 1 Robert Wood Johnson Place, MEB Rm. 478, New Brunswick, NJ 08903, United States

Ulrich Robert Fölsch, Professor
1st Department of Medicine,
Christian-Albrechts-University of Kiel, Schittenhelmstrasse 12, Kiel 24105, Germany

David Y Graham, Professor
Department of Medicine, Michael E. DeBakey VAMC, Rm 3A-320 (111D), 2002 Holcombe Blvd, Houston, TX 77030, United States

Shinn-Jang Hwang, Professor
Department of Family Medicine, Taipei Veterans General Hospital, VGH, 201, Shih-Pai Road, Section 2, 11217, Taiwan, China

Vladimir T Ivashkin, M.D.
Director of The Clinic of Internal Diseases, Gastroenterology And Hepatology Named After V.Vasilenko of The Moscow Sechenov Medical Academy, 119992 Pogodinskaya 1, Moscow, Russian

Tsuneo Kitamura, Associate Professor
Department of Gastroenterology, Juntendo University Urayasu Hospital, Juntendo University School of Medicine, 2-1-1 Tomioka, Urayasu-shi, Chiba 279-0021, Japan

Zahariy Krastev, Professor
Department of Gastroneterology, Universiti Hospital "St. Ivan Rilski",#15, blvd "Acad. Ivan Geshov", Sofia 1431, Bulgaria

Reza Malekzadeh, Professor, Director
Digestive Disease Research Center, Tehran University of Medical Sciences, Shariati Hospital, Kargar Shomali Avenue, 19119 Tehran, Ira

Stephan Miehlke, PhD
Medical Department I, Technical University Hospital, Fetscher Str. 74, Dresden 01307, Germany

Yoshiharu Motoo, Professor
Department of Medical Oncology, Kanazawa Medical University, 1-1 Daigaku, Uchinada, Ishikawa 920-0293, Japan

Yuji Naito, Professor
Kyoto Prefectural University of Medicine, Kamigyo-ku, Kyoto 602-8566, Japan

Kazuichi Okazaki, Professor
Third Department of Internal Medicine, Kansai Medical University, 10-15 Fumizono-cho, Moriguchi City, Osaka, 570-8506, Japan

Lun-Xiu Qin, Professor
Liver Cancer Institute and Zhongshan Hospital, Fudan University, 180 Feng Lin Road, Shanghai 200032, China

Bruno Stieger, Professor
Department of Medicine, Division of Clinical Pharmacology and Toxicology,University Hospital, Zurich 8091, Switzerland

Ken Shirabe, M.D.
Department of sugery, Aso Iizuka Hospital, 3-83 Yoshio Machi, Iizuka City 820-8205, Japan

Simon D Taylor-Robinson, M.D.
Department of Medicine A, Imperial College London, Hammersmith Hospital, Du Cane Road, London W12 0HS, United Kingdom

Yuan Wang, Professor
Institute of Biochemistry and Cell Biology, Shanghai Institutes for Biological Sciences, Chinese Academy of Sciences, Shanghai 200031, China

Jia-Yu Xu, Professor
Shanghai Second Medical University, Rui Jin Hospital, 197 Rui Jin Er Road, Shanghai 200025, China

Koji Yamaguchi, Associate Professor
Department of Surgery and Oncology, Kyushu University, Graduate School of Medical Sciences, 3-1-1 Maidashi, Higashi-Ku, Fukuoka 812-8582, Japan

Takayuki Yamamoto, M.D.
Inflammatory Bowel Disease Center, Yokkaichi Social Insurance Hospital, 10-8 Hazuyamacho, Yokkaichi 510-0016, Japan

PO Box 2345, Beijing 100023, China
www.wjgnet.com
wjg@wjgnet.com

ELSEVIER

World J Gastroenterol 2005;11(46):7387
World Journal of Gastroenterology ISSN 1007-9327

Meetings

MAJOR MEETINGS COMING UP

American College of Gastroenterology Annual Scientific Meeting
October 28 -November 2, 2005
annualmeeting@acg.gi.org
www.acg.gi.org

EVENTS AND MEETINGS IN THE UPCOMING 6 MONTHS

ISGCON2005
November 11-15, 2005
isgcon2005@yahoo.co.in
isgcon2005.com

II Latvian Gastroenterology Congress
November 29, 2005
gec@stradini.lv
www.gastroenterologs.lv

70th ACG Annual Scientific Meeting and Postgraduate Course
October 28-November 2, 2005

Advanced Capsule Endoscopy Users Course
November 18-19, 2005
www.asge.org/education

2005 CCFA National Research and Clinical Conference - 4th Annual Advances in the Inflammatory Bowel Diseases
December 1-3, 2005
c.chase@imedex.com
www.imedex.com/calendars/therapeutic.htm

EVENTS AND MEETINGS IN 2005

XIII Argentine Hepatology Congress
XIII Congreso Argentino de HepatologÃa
June 10-13, 2005
mci@mcimeetings.com
www.hepatologia.org

9th Annual Coolum Update in Gastroenterology & Hepatology
June 11-13, 2005
info@e-Kiddna.com.au

Canadian Digestive Disease Week Conference
February 26-March 6, 2005
www.cag-acg.org

2005 World Congress of Gastroenterology
September 12-14, 2005
wcog2005@congrex.nl

International Colorectal Disease Symposium 2005
February 3-5, 2005
info@icds-hk.org

15th World Congress of the International Association of Surgeons and Gastroenterologists
September 7-10, 2005
iasg2005@guarant.cz
www.iasg2005.cz

7th International Workshop on Therapeutic Endoscopy
September 10-12, 2005
alfa@alfamedical.com
www.alfamedical.com

EASL 2005 the 40th annual meeting
April 13-17, 2005
www.easl.ch/easl2005/

ISGCON2005
November 11-15, 2005
isgcon2005@yahoo.co.in
isgcon2005.com

Pediatric Gastroenterology, Hepatology and Nutrition
March 13, 2005

II Latvian Gastroenterology Congress
November 29, 2005
gec@stradini.lv
www.gastroenterologs.lv

21st annual international congress of Pakistan society of Gastroenterology & GI Endoscopy
March 25-27, 2005
psgc05@hotmail.com
www.psgc2005.com

8th Congress of the Asian Society of HepatoBiliary Pancreatic Surgery
February 10-13, 2005

1º Workshop de Gastrenterologia para Clínica Geral
April 29, 2005
luis.m.lopes@sapo.pt

APDW 2005 - Asia Pacific Digestive Week 2005
September 25-28, 2005
asiapdw@kornet.net
www.apdw2005.org

World Congress on Gastrointestinal Cancer
June 15-18, 2005
meetings@imedex.com

British Society of Gastroenterology Conference
March 14-17, 2005
www.bsg.org.uk

Training Director's Workshop:Developing and Teaching Principles in the New Era of GI Training
February 4-6, 2005
www.asge.org/education

The Pharmacological, Surgical and Endoscopic Management of GERD
April 8-9, 2005
www.asge.org/education

Digestive Disease Week
DDW 106th Annual Meeting
May 15-18, 2005
ddwadmin@gastr.org
www.ddw.org

ASGE Advanced Endscopy Skills Hands-on Sessions
May 15, 2005
www.asge.org/education

ASGE GERD Hands-on Session
May 17, 2005
www.asge.org/education

Annual Postgraduate Course
May 18-19, 2005
www.asge.org/education

Advanced Capsule Endoscopy Users Course
June 4-5, 2005
www.asge.org/education

Advanced Capsule Endoscopy Users Course
August 12-13, 2005
www.asge.org/education

GI Practice Management Symposium: Solutions for a Successful Practice
August 18, 2005
www.asge.org/education

70th ACG Annual Scientific Meeting and Postgraduate Course
October 28-November 2, 2005

Advanced Capsule Endoscopy Users Course
November 18-19, 2005
www.asge.org/education

2005 CCFA National Research and Clinical Conference - 4th Annual Advances in the Inflammatory Bowel Diseases
December 1-3, 2005
c.chase@imedex.com
www.imedex.com/calendars/therapeutic.htm

EVENTS AND MEETINGS IN 2006

10th World Congress of the International Society for Diseases of the Esophagus
February 22-25, 2006
isde@sapmea.asn.au
www.isde.net

Easl 2006 - The 41st Annual Meeting
April 26-30, 2006

Canadian Digestive Disease Week Conference
March 4-12, 2006
www.cag-acg.org

XXX pan-american congress of digestive diseases
XXX congreso panamericano de anfermedades digestivas
November 25-December 1, 2006
amg@gastro.org.mx
www.gastro.org.mx

World Congress on Gastrointestinal Cancer
June 14-17, 2006
c.chase@imedex.com

7th World Congress of the International Hepato-Pancreato-Biliary Association
September 3-7, 2006
convention@edinburgh.org
www.edinburgh.org/conference

Annual Postgraduate Course
May 25-26, 2006
www.asge.org/education

71st ACG Annual Scientific Meeting and Postgraduate Course
October 20-25, 2006

PO Box 2345, Beijing 100023, China
www.wjgnet.com
wjg@wjgnet.com

ELSEVIER

World J Gastroenterol 2005;11(46):7388-7389
World Journal of Gastroenterology ISSN 1007-9327

Instructions to authors

GENERAL INFORMATION

World Journal of Gastroenterology (*WJG,* ISSN 1007-9327 CN 14-1219/R) is a weekly journal of more than 48 000 circulation, published on the 7th, 14th, 21st and 28th of every month.

Original Research, Clinical Trials, Reviews, Comments, and Case Reports in esophageal cancer, gastric cancer, colon cancer, liver cancer, viral liver diseases, *etc*., from all over the world are welcome on the condition that they have not been published previously and have not been submitted simultaneously elsewhere.

Published jointly by
The WJG Press and Elsevier Inc.

SUBMISSION OF MANUSCRIPTS

Manuscripts should be typed double-spaced on A4 (297×210 mm) white paper with outer margins of 2.5 cm. Number all pages consecutively, and start each of the following sections on a new page: Title Page , Abstract, Introduction, Materials and Methods, Results, Discussion, Acknowledgements, References, Tables, Figures and Figure Legends. Neither the Editors nor the Publisher is responsible for the opinions expressed by contributors. Manuscripts formally accepted for publication become the permanent property of The WJG Press and Elsevier Inc., and may not be reproduced by any means, in whole or in part without the written permission of both the Authors and the Publisher. We reserve the right to put onto our website and copy-edit accepted manuscripts. Authors should also follow the guidelines for the care and use of laboratory animals of their institution or national animal welfare committee.

Authors should retain one copy of the text, tables, photographs and illustrations, as rejected manuscripts will not be returned to the author(s) and the editors will not be responsible for the loss or damage to photographs and illustrations.

Online submission
Online submission is strongly advised. Manuscripts should be submitted through the Online Submission System at: http://www.wjgnet.com/index.jsp. Authors are highly recommended to consult the ONLINE INSTRUCTIONS TO AUTHORS (http://www.wjgnet.com/wjg/help/instructions.jsp) before attempting to submit online. Authors encountering problems with the Online Submission System may send an email describing the problem to wjg@wjgnet.com for assistance. If you submit manuscript online, do not make a postal contribution. A repeated online submission for the same manuscript is strictly prohibited.

Postal submission
Send 3 duplicate hard copies of the full-text manuscript typed double-spaced on A4(297×210 mm) white paper together with any original photographs or illustrations and a 3.5 inch computer diskette or CD-ROM containing an electronic copy of the manuscript including all the figures, graphs and tables in native Microsoft Word format or *.rtf format to:

World Journal of Gastroenterology
Apartment 1066 Yishou Garden,
58 North Langxinzhuang Road,
PO Box 2345, Beijing 100023, China
E-mail: wjg@wjgnet.com
http: //www.wjgnet.com

MANUSCRIPT PREPARATION

All contributions should be written in English. All articles must be submitted using a word-processing software. All submissions must be typed in 1.5 line spacing and in word size 12 with ample margins. The letter font is Tahoma. For authors originating from China, one copy of the Chinese translation of the manuscript is also required (excluding references). Style should conform to our house format. Required information for each of the manuscript sections is as follows:

Title page
Full manuscript title, running title, all author(s) name(s), affiliations, institution(s) and/or department(s) where the work was accomplished, disclosure of any financial support for the research, and the name, full address, telephone and fax numbers and email address of the corresponding author should be involved. Titles should be concise and informative (removing all unnecessary words), emphasize what is NEW, and avoid abbreviations. A short running title of less than 40 letters should be provided. List the author(s)' name(s) as follows: initials and/or first name, middle name or initial(s) and full family name.

Abstract
An informative, structured abstract of no more than 250 words should accompany each manuscript. Abstracts for original contributions should be structured into the following sections: AIM: Only the purpose should be included. METHODS: The materials, techniques, instruments and equipments, and the experimental procedures should be included. RESULTS: The observatory and experimental results, including data, effects, outcome, *etc*. should be included. Authors should present *P* value where necessary, and the significant data should accompany. CONCLUSION: Accurate view and the value of the results should be included.

The format of structured abstracts is at: http://www.wjgnet.com/wjg/help/11.doc

Key words
Please list 3-10 key words that could reflect content of the study.

Text
For most article types, the main text should be structured into the following sections: INTRODUCTION, MATERIALS AND METHODS, RESULTS and DISCUSSION, and should include appropriate Figures and Tables. Data should be presented in the body text or Figures and Tables, not both.

Illustrations
Figures should be numbered as 1, 2, 3 and so on, and mentioned clearly in the main text. Provide a brief title for each figure on a separate page. No detailed legend should be involved under the figures. This part should add into the text where the figures are applicable. Digital images: black and white photographs should be scanned and saved in TIFF format at a resolution of 300 dpi; color images should be saved as CMYK (print files) and not RGB (screen-viewing files). Place each photograph in a separate file. Print images: supply images of size no smaller than 126× 76 mm printed on smooth surface paper; label the image by writing the Figure number and orientation using an arrow. Photomicrographs: indicate the original magnification and stain in the legend. Digital Drawings: supply files in EPS if created by Freehand and Illustrator, or TIFF from Photoshop. EPS files must be accompanied by a version in native file format for editing purposes. Scans of existing line drawings should be scanned at a resolution of 1200 dpi and as close as possible to the size at which they will appear when printed, not smaller. Please use uniform legends for the same subjects. For example: Figure 1 Pathological changes of atrophic gastritis after treatment. A: ...; B: ...;C: ...; D: ...; E: ...; F: ...; G: ...

Tables
Three-line tables should be numbered as 1, 2, 3 and so on, and mentioned clearly in the main text. Provide a brief title for each table. No detailed legend should be involved under the tables. This part should add into the text where the tables are applicable. The information should complement but not duplicate that contained in the text. Use one horizontal line under the title, a second under the column heads, and a third below the Table, above any footnotes. Vertical and italic lines should be omitted.

Notes in tables and illustrations
Data which is not statistically significant should not be noted. $^{a}P<0.05$, $^{b}P<0.01$ ($P>0.05$ should not be noted). If there are other series of *P* values, $^{c}P<0.05$ and $^{d}P<0.01$ are used; Third series of *P* values can be expressed as $^{e}P<0.05$ and $^{f}P<0.01$. Other notes in tables or under illustrations should be expressed as ^{1}F, ^{2}F, ^{3}F; or some other symbols with a superscript (Arabic

numerals) in the upper left corner. In a multi-curve illustration, each curve should be labeled with ●, ○, ■, □, ▲, △, *etc*. in a certain sequence.

Acknowledgments

Brief acknowledgments of persons who have made genuine contributions to the manuscripts and who endorse the data and conclusions are included. Authors are responsible for obtaining written permission to use any copyrighted text and/or illustrations.

References

Cited references should mainly be drawn from journals covered in the Science Citation Index (http://www.isinet.com) and/or Index Medicus (http://www.ncbi.nlm.nih.gov/PubMed) databases. Mention all references in the text, tables and figure legends, and set off by consecutive, superscripted Arabic numerals. References should be numbered consecutively in the order in which they appear in the text. Abbreviate journal title names according to the Index Medicus style (http://www.ncbi.nlm.nih.gov/entrez/query.fcgi?db=journals). Unpublished observations and personal communications are not listed as references. The style and punctuation of the references conform to ISO standard and the Vancouver style (5th edition); see examples below. Reference lists not conforming to this style could lead to delayed or even rejected publication status. Examples:

Standard jounal article (list all authors and include the PubMed ID [PMID] where applicable)

1 **Das KM,** Farag SA. Current medical therapy of inflammatory bowel disease. *World J Gastroenterol* 2000; 6: 483-489 [PMID: 11819634]

2 **Pan BR**, Hodgson HJF, Kalsi J. Hyperglobulinemia in chronic liver disease: Relationships between *in vitro* immunoglobulin synthesis, short lived suppressor cell activity and serum immunoglobulin levels. *Clin Exp Immunol* 1984; 55: 546-551 [PMID: 6231144]

3 **Lin GZ,** Wang XZ, Wang P, Lin J, Yang FD. Immunologic effect of Jianpi Yishen decoction in treatment of Pixu-diarrhoea. *Shijie Huaren Xiaohua Zazhi* 1999; 7: 285-287 [CMFAID:1082371101835979]

Books and other monographs (list all authors)

4 **Sherlock S,** Dooley J. Diseases of the liver and billiary system. 9th ed. Oxford: Blackwell Sci Pub, 1993: 258-296

Chapter in a book (list all authors)

5 **Lam SK.** Academic investigator's perspectives of medical treatment for peptic ulcer. In: Swabb EA, Azabo S. Ulcer disease: investigation and basis for therapy. New York: Marcel Dekker, 1991: 431-450

Electronic journal (list all authors)

6 **Morse SS.** Factors in the emergence of infectious diseases. Emerg Infect Dis serial online, 1995-01-03, cited 1996-06-05; 1(1):24 screens. Available from: URL: http//www.cdc.gov/ncidod/EID/eid.htm

PMID requirement

From the full reference list, please submit a separate list of those references embodied in PubMed, keeping the same order as in the full reference list, with the following information only: (1) abbreviated journal name and citation (e.g. *World J Gastroenterol* 2003;9(11):2400-2403; (2) article title (e.g. Epidemiology of gastroenterologic cancer in Henan Province, China; (3) full author list (e.g. Lu JB, Sun XB, Dai DX, Zhu SK, Chang QL, Liu SZ, Duan WJ; (4) PMID (e.g. 14606064). Provide the full abstracts of these references, as quoted from PubMed on a 3.5 inch disk or CD-ROM in Microsoft Word format and send by post to The *WJG* Press. For those references taken from journals not indexed by *Index Medicus*, a printed copy of the first page of the full reference should be submitted. Attach these references to the end of the manuscript in their order of appearance in the text.

Inappropriate references

Authors should always cite references that are relevant to their article, and avoid any inappropriate references. Inappropriate references include those that are linked with a hyphen and the difference between the two numbers at two sides of the hyphen is more than 5. For example, [1-6], [2-14] and [1, 3, 4-10, 22] are all considered as inappropriate references. Authors should not cite their own unrelated published articles.

Statistical data

Present as mean±SD and mean±SE.

Statistical expression

Express *t* test as *t*(in italics), *F* test as *F*(in italics), chi square test as χ^2(in Greek), related coefficient as *r*(in italics), degree of freedom as γ (in Greek), sample number as *n*(in italics), and probability as *P*(in italics).

Units

Use SI units. For example: body mass, m(B) = 78 kg; blood pressure, p(B)=16.2/12.3 kPa; incubation time, t(incubation)=96 h, blood glucose concentration, c(glucose) 6.4±2.1 mmol/L; blood CEA mass concentration, p(CEA) = 8.6 24.5 μg/L; CO_2 volume fraction, 50 mL/L CO_2 not 5% CO_2; likewise for 40 g/L formaldehyde, not 10% formalin; and mass fraction, 8 ng/g, *etc*. Arabic numerals such as 23,243,641 should be read 23 243 641.

The format about how to accurately write common units and quantum is at: http://www.wjgnet.com/wjg/help/15.doc

Abbreviations

Standard abbreviations should be defined in the abstract and on first mention in the text. In general, terms should not be abbreviated unless they are used repeatedly and the abbreviation is helpful to the reader. Permissible abbreviations are listed in Units, Symbols and Abbreviations: A Guide for Biological and Medical Editors and Authors (Ed. Baron DN, 1988) published by The Royal Society of Medicine, London. Certain commonly used abbreviations, such as DNA, RNA, HIV, LD50, PCR, HBV, ECG, WBC, RBC, CT, ESR, CSF, IgG, ELISA, PBS, ATP, EDTA, mAb, can be used directly without further mention.

Italicization

Quantities: *t* time or temperature, *c* concentration, *A* area, *l* length, *m* mass, *V* volume.

Genotypes: *gyr*A, *arg* 1, *c myc*, *c fos*, *etc*.

Restriction enzymes: *Eco*RI, *Hin*dI, *Bam*HI, *Kbo* I, *Kpn* I, *etc*.

Biology: *Helicobacter pylori, H pylori, E coli, etc*.

SUBMISSION OF THE REVISED MANUSCRIPTS AFTER ACCEPTED

Please revise your article according to the revision policies of *WJG*. The revised version including manuscript and high-resolution image figures (if any) should be copied on a floppy or compact disk. Author should send the revised manuscript, along with printed high-resolution color or black and white photos, copyright transfer letter, the final check list for authors, and responses to reviewers by a courier (such as EMS) (submission of revised manuscript by e-mail or on the WJG Editorial Office Online System is NOT available at present).

Language evaluation

The language of a manuscript will be graded before sending for revision. (1) Grade A: priority publishing; (2) Grade B: minor language polishing; (3) Grade C: a great deal of language polishing; (4) Grade D: rejected. The revised articles should be in grade B or grade A.

Copyright assignment form

It is the policy of WJG to acquire copyright in all contributions. Papers accepted for publication become the copyright of WJG and authors will be asked to sign a transfer of copyright form. All authors must read and agree to the conditions outlined in the Copyright Assignment Form (which can be downloaded from http://www.wjgnet.com/wjg/help/9.doc).

Final check list for authors

The format is at: http://www.wjgnet.com/wjg/help/13.doc

Responses to reviewers

Please revise your article according to the comments/suggestions of reviewers. The format for responses to the reviewers' comments is at: http://www.wjgnet.com/wjg/help/10.doc

Proof of financial support

For paper supported by a foundation, authors should provide a copy of the document and serial number of the foundation.

Publication fee

Authors of accepted articles must pay publication fee.

PO Box 2345, Beijing 100023, China
www.wjgnet.com
wjg@wjgnet.com

ELSEVIER

World J Gastroenterol 2005;11(46):7390
World Journal of Gastroenterology ISSN 1007-9327

World Journal of Gastroenterology standard of quantities and units

Number	Nonstandard	Standard	Notice
1	4 days	4 d	In figures, tables and numerical narration
2	4 days	four days	In text narration
3	day	d	After Arabic numerals
4	Four d	Four days	At the beginning of a sentence
5	2 hours	2 h	After Arabic numerals
6	2 hs	2 h	After Arabic numerals
7	hr, hrs,	h	After Arabic numerals
8	10 seconds	10 s	After Arabic numerals
9	10 year	10 years	In text narration
10	Ten yr	Ten years	At the beginning of a sentence
11	0,1,2 years	0,1,2 yr	In figures and tables
12	0,1,2 year	0,1,2 yr	In figures and tables
13	4 weeks	4 wk	
14	Four wk	Four weeks	At the beginning of a sentence
15	2 months	2 mo	In figures and tables
16	Two mo	Two months	At the beginning of a sentence
17	10 minutes	10 min	
18	Ten min	Ten minutes	At the beginning of a sentence
19	50% (*V/V*)	500 mL/L	
20	50% (m/*V*)	500 g/L	
21	1 M	1 mol/L	
22	10 μM	10 μmol/L	
23	1N HCl	1 mol/L HCl	
24	1N H_2SO_4	0.5 mol/L H_2SO_4	
25	4rd edition	4^{th} edition	
26	15 year experience	15- year experience	
27	18.5 kDa	18.5 ku,18 500u or M_r18 500	
28	25 $g.kg^{-1}/d^{-1}$	25 g/(kg·d) or 25 g/kg per day	
29	6900	6 900	
30	1000 rpm	1 000 r/min	
31	sec	s	After Arabic numerals
32	1 pg·L^{-1}	1 pg/L	
33	10 kilograms	10 kg	
34	13 000 rpm	13 000 *g*	High speed; *g* should be in italic and suitable conversion.
35	1000 *g*	1 000 r/min	Low speed. *g* cannot be used.
36	Gene bank	GenBank	International classified genetic materials collection bank
37	Ten L	Ten liters	At the beginning of a sentence
38	Ten mL	Ten milliliters	At the beginning of a sentence
39	umol	μmol	
40	30 sec	30 s	
41	1 g/dl	10 g/L	10-fold conversion
42	OD_{260}	A_{260}	"OD" has been abandoned.
43	One g/L	One microgram per liter	At the beginning of a sentence
44	*A*260 nm	A_{260} nm	*A* should be in italic.
	$^bP<0.05$	$^aP<0.05$	In Table, no note is needed if there is no significance in statistics: $^aP<0.05$, $^bP<0.01$ (no note if $P>0.05$). If there is a second set of *P* value in the same table, $^cP<0.05$ and $^dP<0.01$ are used for a third set: $^eP<0.05$, $^fP<0.01$.
45	**F*=9.87, §*F*=25.9, #*F*=67.4	^1F=9.87,^2F=25.9, ^3F=67.4	Notices in or under a table
46	KM	km	kilometer
47	CM	cm	centimeter
48	MM	mm	millimeter
49	Kg, KG	kg	kilogram
50	Gm, gr	g	gram
51	nt	N	newton
52	l	L	liter
53	db	dB	decibel
54	rpm	r/min	rotation per minute
55	bq	Bq	becquerel, a unit symbol
56	amp	A	ampere
57	coul	C	coulomb
58	HZ	Hz	
59	w	W	watt
60	KPa	kPa	kilo-pascal
61	p	Pa	pascal
62	ev	EV	volt (electronic unit)
63	Jonle	J	joule
64	J/mmol	kJ/mol	kilojoule per mole
65	10×10×$10cm^3$	10 cm×10 cm×10 cm	
66	N·km	KN·m	moment
67	$\bar{x}\pm s$	mean±SD	In figures, tables or text narration
68	Mean±SEM	mean±SE	In figures, tables or text narration
69	*im*	im	intramuscular injection
70	*iv*	iv	intravenous injection
71	Wang et al	Wang *et al.*	
72	EcoRI	*Eco*RI	*Eco* in italic and RI in positive. Restriction endonuclease has its prescript form of writing.
73	Ecoli	*E.coli*	Bacteria and other biologic terms have their specific ex pression.
74	Hp	*H pylori*	
75	Iga	*Iga*	writing form of genes
76	*igA*	IgA	writing form of proteins
77	-70 kDa	~70 ku	

PO Box 2345, Beijing 100023, China
www.wjgnet.com
wjg@wjgnet.com

ELSEVIER

World J Gastroenterol 2005;11(47):7391-7400
World Journal of Gastroenterology ISSN 1007-9327

• *REVIEW* •

Hepatocellular carcinoma: Therapy and prevention

Hubert E Blum

Hubert E Blum, Department of Medicine II, University of Freiburg, D-79106 Freiburg, Germany
Correspondence to: Hubert E Blum, MD, Department of Medicine II, University of Freiburg, Hugstetter Strasse 55, D-79106 Freiburg, Germany. hubert.blum@uniklinik-freiburg.de
Telephone: +49-761-270-3404 Fax: +49-761-270-3610
Received: 2004-12-22 Accepted: 2005-03-10

Abstract

Hepatocellular carcinoma (HCC) is one of the most common malignant tumors worldwide. The major etiologies and risk factors for the development of HCC are well defined and some of the multiple steps involved in hepatocarcinogenesis have been elucidated in recent years. Despite these scientific advances and the implementation of measures for the early detection of HCC in patients at risk, patient survival has not improved during the last three decades. This is due to the advanced stage of the disease at the time of clinical presentation and limited therapeutic options. The therapeutic options fall into five main categories: surgical interventions including tumor resection and liver transplantation, percutaneous interventions including ethanol injection and radiofrequency thermal ablation, transarterial interventions including embolization and chemoembolization, radiation therapy and drugs as well as gene and immune therapies. These therapeutic strategies have been evaluated in part in randomized controlled clinical trials that are the basis for therapeutic recommendations. Though surgery, percutaneous and transarterial interventions are effective in patients with limited disease (1-3 lesions, <5 cm in diameter) and compensated underlying liver disease (cirrhosis Child A), at the time of diagnosis more than 80% patients present with multicentric HCC and advanced liver disease or comorbidities that restrict the therapeutic measures to best supportive care. In order to reduce the morbidity and mortality of HCC, early diagnosis and the development of novel systemic therapies for advanced disease, including drugs, gene and immune therapies as well as primary HCC prevention are of paramount importance. Furthermore, secondary HCC prevention after successful therapeutic interventions needs to be improved in order to make an impact on the survival of patients with HCC. New technologies, including gene expression profiling and proteomic analyses, should allow to further elucidate the molecular events underlying HCC development and to identify novel diagnostic markers as well as therapeutic and preventive targets.

Key words: HCC resection; Liver transplantation; Percutaneous ethanol injection; Radiofrequency thermal ablation; Transarterial embolization or chemoembolization; Chemotherapy; Gene therapy; Immune therapy; Prevention

Blum HE. Hepatocellular carcinoma: Therapy and prevention. *World J Gastroenterol* 2005; 11(47): 7391-7400
http://www.wignet.com/1007-9327/11/7391.asp

INTRODUCTION

Hepatocellular carcinoma (HCC) is one of the most common malignant tumors worldwide[1-10]. The incidence ranges from <10 cases per 100 000 persons in North America and Western Europe to 50-150 cases per 100 000 persons in parts of Africa and Asia, where HCC is responsible for a large number of cancer deaths. However, a rise in the incidence and mortality of HCC, most likely reflecting the increased prevalence of hepatitis C virus (HCV) infection, has recently been observed in most industrialized countries[11-14].

The major etiologies of HCC are well defined (Table 1). An elevated body mass index, especially in men[15], and diabetes mellitus[9] are included among the well-known factors. Some of the steps involved in the molecular pathogenesis of HCC have been elucidated in the recent years. As for most types of cancer, hepatocarcinogenesis is a multistep process involving different genetic alterations that ultimately lead to the malignant transformation of hepatocytes. While significant progress has been made in recognizing the sequence of events involved in other forms of cancer, most notably in colorectal cancer and certain hematopoietic malignancies, the molecular contribution of the multiple factors and their interactions in hepatocarcinogenesis are still poorly understood. HCCs are phenotypically (morphology and microscopy) and genetically heterogenous tumors, possibly reflecting in part the heterogeneity of etiologic factors implicated in HCC development, the complexity of hepatocyte functions and the late stage at which HCCs usually become clinically symptomatic and detectable. Malignant transformation of hepatocytes may occur regardless of the etiologic agent through a pathway of increased liver cell turnover, induced by chronic liver injury and regeneration in a context of inflammation, immune response, and oxidative DNA damage. This may result in genetic alterations, such as activation of cellular oncogenes, inactivation of tumor suppressor genes, possibly in cooperation with genomic instability, including

Table 1 Major etiologies of HCC

Chronic viral hepatitis B, C, D
Toxins (e.g., alcohol, aflatoxins)
Hereditary metabolic liver diseases (e.g., hereditary hemochromatosis, α-1-antitrypsin deficiency)
Autoimmune hepatitis
Overweight, especially in males, and diabetes mellitus; nonalcoholic steatohepatitis (NASH) or nonalcoholic fatty liver disease (NAFLD)

Table 2 Okuda stages I-III of HCC

Tumor mass	<50% of liver	⩾50% of liver
Ascites	No	Yes
Albumin (g/L)	>3	⩽3
Bilirubin (mg/dL)	<3	⩾3
Points	0	1
Stage I	0 points	
Stage II	1-2 points	
Stage III	3-4 points	

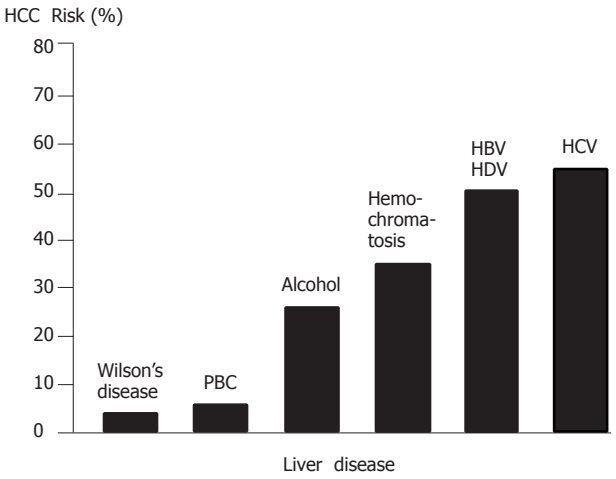

Figure 1 HCC Risk in Liver Cirrhosis

DNA mismatch repair defects and impaired chromosomal segregation, overexpression of growth and angiogenic factors, and telomerase activation[16-23]. Chronic viral hepatitis B, C, and D, alcohol, metabolic liver diseases such as hemochromatosis and α-1-antitrypsin deficiency as well as non-alcoholic fatty liver disease may act predominantly through this pathway of chronic liver injury, regeneration and cirrhosis. Accordingly, the major clinical risk factor for the development of HCC is liver cirrhosis since 70-90% of HCCs develop into a cirrhotic liver. Most HCCs occur after many years of chronic hepatitis that provides the mitogenic and mutagenic environments to precipitate random genetic alterations resulting in the malignant transformation of hepatocytes and HCC development.

The HCC risk in patients with liver cirrhosis depends on the activity, duration and etiology of the underlying liver disease (Figure 1). Clinical and biological variables (age, anti-HCV positivity, PTT and platelet count) allow to further identify a subset of cirrhotic patients with the highest risk of HCC development[24]. Coexistence of etiologies, such as hepatitis B virus (HBV) and HCV infection, HBV infection and aflatoxin B1[23,25], HBV/HCV infection and alcohol or diabetes mellitus[26], or HCV infection and liver steatosis[27], increases the relative risk of HCC development. Also, occult HBV infection (anti-HBc positive only) carries a significant HCC risk[28,29]. In general, HCCs are more frequent in males than in females and the incidence increases with age. On the other hand, there is evidence that HBV and possibly HCV under certain circumstances play an additional direct role in the molecular pathogenesis of HCC. Finally, aflatoxins can induce mutations of the p53 tumor suppressor gene, thus pointing to the contribution of an environmental factor to tumor development at the molecular level. Furthermore, in a transgenic mouse model it has been shown that chronic immune-mediated liver cell injury without environmental or infectious agents is sufficient to cause HCC[30] and that inhibition of cytotoxic T lymphocyte-induced apoptosis and chronic inflammation by neutralization of the Fas ligand and prevents HCC development in this model[31]. In addition, in a transgenic mouse model it has been demonstrated that NF-κB may be the link between inflammation and HCC development[32,33]. Finally, individual polymorphisms of drug-metabolizing enzymes, such as cytochrome P450 oxidases, N-acetyltransferases and glutathione-*S*-transferase, may contribute to the genetic susceptibility to HCC development[34].

HCC screening, staging, and natural course

For the staging of HCCs, five systems have been proposed for the assessment of the extent and prognosis of the disease[35,36]: the Okuda staging system (Table 2)[37], the TNM classification and its modification by the Union International Contre Cancer (UICC), the Barcelona Clinic Liver Cancer (BCLC) classification[38] and the Cancer of the Liver Italian Program (CLIP) score[39]. The Okuda staging system is very effective for the identification of a subgroup of patients (Okuda III) with a very good prognosis of patients who should be treated with best supportive care (BSC) only. The BCLC classification appears especially useful for the selection of treatment but has not been independently validated. The CLIP score is superior to the Okuda staging system but has not been systematically assessed in patients undergoing resection or liver transplantation. Thus, one staging system is not clearly superior to the others. The natural course of the disease and the median survival of patients with HCC depend on the stage of the disease at the time of diagnosis. In patients with CLIP score 0 or Okuda stage I, the median survival is in the range of 23-69 mo, while in patients with CLIP score 3-5 or Okuda stage III, the median survival is only 1-14 mo[4]. The staging system is clinically most important for the appropriate choice of therapeutic strategy for individual patients.

Treatment of HCC

Therapies for HCC can be divided into four categories: surgical interventions (tumor resection and liver

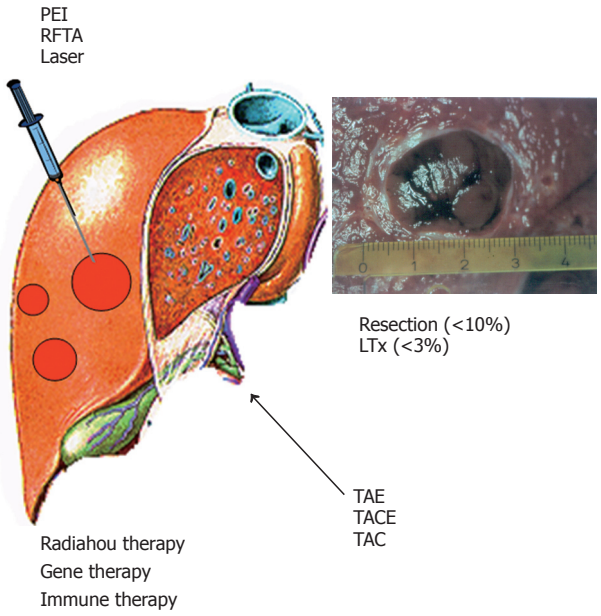

Figure 2 HCC treatment.

transplantation), percutaneous interventions (ethanol injection, radiofrequency thermal ablation), transarterial interventions (embolization, chemoperfusion, or chemoembolization) and drugs including gene and immune therapy (Figure 2). Potentially curative therapies are tumor resection, liver transplantation, and percutaneous interventions that can result in complete responses and improved survival in a large number of patients. In selected cases, transarterial interventions result in palliation with good response rates and improved survival in some cases. Drugs as well as conventional radiotherapy have no proven efficacy.

Till date, surgical, percutaneous and transarterial interventions have not been compared in randomized controlled trials. Tumor resection and transplantation can achieve a 5-year survival rate of 60-70% in selected patients transplantation is the best treatment for patients with single lesions and advanced liver diseases, such as decompensated cirrhosis and multicentric small tumors. Percutaneous interventions, again in selected patients, result in a 5-year survival rate of 40-50%. The following different therapeutic options as well as primary and secondary HCC prevention are discussed in detail.

Surgical interventions

Resection in patients without concomitant liver cirrhosis (5% in Western countries, 40% in Sub-Sahara Africa and Asia), HCC resection is the treatment of choice with a low rate of life-threatening complications. By comparison, in the majority of patients with cirrhosis, strict selection is required to avoid resection-related complications, especially postoperative liver failure[40]. Apart from bilirubin and albumin concentration as well as platelet count and indocyanine green clearance[14,42], a recent study has identified an elevated serum concentration of 7s-collagen as an independent risk factor for postoperative liver failure[43].

Resection-related mortality should be <1-3%, and the 5-year survival rate should be >50%. In patients with normal liver function (normal indocyanine green retention rate and bilirubin level), absence of clinically relevant portal hypertension (hepatic venous pressure gradient <1.33 kpa, no esophageal varices, no splenomegaly, platelet count $>100\times10^9$/L) and one asymptomatic HCC lesion only, the 5-year survival rate of 70% can be achieved. By comparison in patients with clinically relevant portal hypertension, the 5-year survival rate is about 50% only and in patients with portal hypertension and evidence of impaired liver function, the 5-year survival rate is even lower.

After successful HCC resection, tumor recurrence in the cirrhotic liver (local recurrence as well as *de novo* tumors) in about 70% of patients after 5 years is a major clinical problem. The risk of recurrence is especially high in patients with microvascular invasion and/or additional tumor nodules[41,44]. Therefore, strategies aimed at secondary HCC prevention are of paramount importance.

Liver transplantation Liver transplantation is in principle the optimal therapeutic option for HCCs, because it simultaneously removes the tumor and the underlying cirrhosis, including the risk of HCC recurrence[40,45-47]. While broad selection criteria applied previously led to poor results with the recurrence rate of about 50% and the 5-year survival rate <40%, the current criteria for liver transplantation in patients with HCC (1 lesion <5 cm in diameter or maximum 3 lesions <3 cm in diameter) result in the 5-year survival rate of 70% or more and the recurrence rate <15%[48-50]. Possibly these criteria can be extended in future, depending on more experiences based on the stage of the disease, macrovascular invasion, histopathological characteristics (histopathology, aneuploidy, microvascular invasion) as well as DNA and RNA chip data (molecular signature, proteomic signature and others)[51,52].

Clinically, it is most important to shorten the waiting time for transplantation to <6 mo. This is difficult to achieve with cadaveric liver transplantation due to the shortage of donors. With a waiting time of >12 mo in some Western countries, the drop-out rate of patients is 20-50%. To bridge the time to transplantation and to prevent tumor progression, neoadjuvant treatments, such as percutaneous and transarterial interventions may lead to an improved outcome[53]. While marginal livers, domino donors, and split liver transplantation have no major impact, living donor liver transplantation has been shown to be an alternative to cadaveric liver transplantation. Around 3 000 interventions have been done worldwide. However, living donor liver transplantation is a complex procedure with a morbidity of 20-40% and a donor mortality of 0.3-0.5%[50,54,55]. Therefore, a very careful selection of patients and donors, including consideration of ethical, societal and legal issues is central to the successful implementation of living donor liver transplantation for the treatment of HCC patients[56].

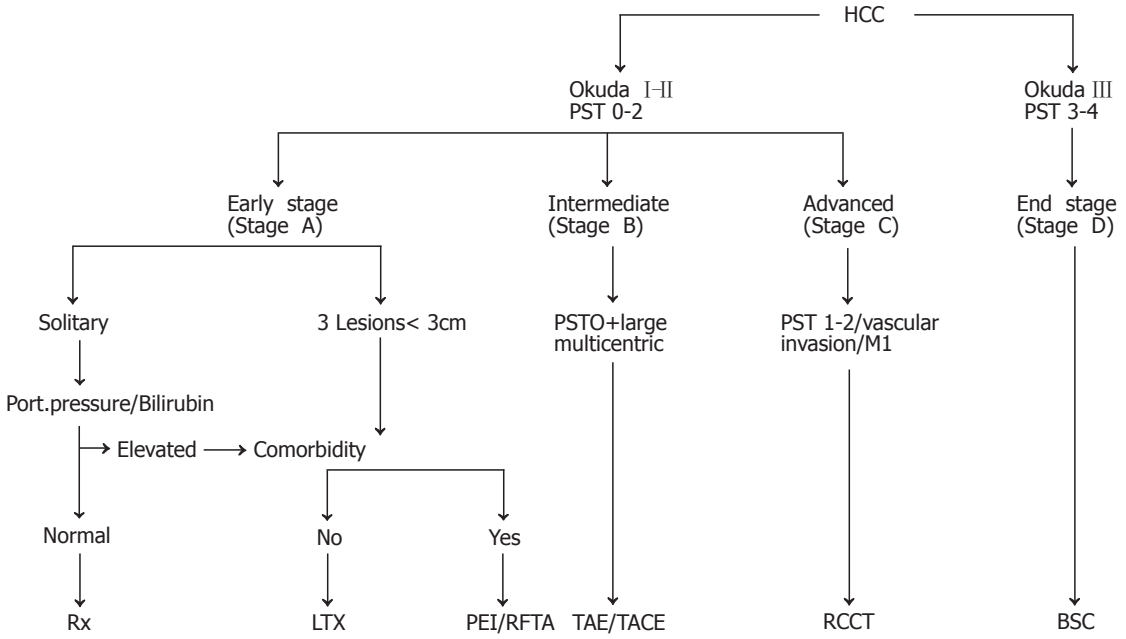

Figure 3 Stage-Dependent HCC Treatment.

Percutaneous interventions

Percutaneous intervention is the best option for small unresectable HCCs[57-59]. Tumor ablation can be achieved chemically by percutaneous ethanol injection (PEI) or acetic acid injection (PAI) or thermally by radiofrequency thermal ablation (RFTA), microwave heat-induced thermotherapy (HiTT), laser-induced thermotherapy (LiTT), or cryoablation. Apart from percutaneous interventions, these techniques can be applied also laparoscopically or after laparotomy.

Percutaneous ethanol injection PEI is the most widely used technique[60,61]. It is safe, easy to perform, inexpensive and can achieve complete tumor response rate of 90-100% in HCCs smaller than 2 cm in diameter, 70% in HCCs (3 cm in diameter) and 50% in HCCs (5 cm in diameter). Patients with liver cirrhosis Child A with complete responses can achieve a 5-year survival rate of 50% or more. Therefore, PEI is the procedure of choice for patients with a single HCC lesion smaller than 5 cm in diameter or with up to three lesions smaller than 3 cm in diameter (Figure 3).

Radiofrequency thermal ablation RFTA is an alternative to PEI[58,59,62,63]. Several devices are available that can be applied percutaneously, laparoscopically, or during laparotomy. The efficacy of RFTA is similar to that of PEI but requires generally only a single session. While being more expensive than PEI, RFTA offers a better local tumor control and a potential advantage of allowing the ablation of tumors larger than 5 cm in diameter especially when newer generation devices are used. However, the 5-year survival rate after complete response to RFTA is currently similar to that of PEI (around 30-40%) depending on the child stage of the underlying liver cirrhosis. In a review of 3 670 patients treated with RFTA, the mortality is 0-5% and the complication rate is 8-9%[64]. Predictors of treatment response are tumor size and morphology (well encapsulated *vs* invasive).

Percutaneous HCC ablation by PEI and/or RFTA when considered together is an effective treatment for patients with HCCs that prolongs the tumor-free and overall survival time, especially if surgery is not feasible. This strategy has been evaluated also for the treatment of liver metastases[65].

Transarterial interventions

Transarterial embolization and chemoembolization are the most widely used treatments for HCCs which are unresectable or cannot be effectively treated with percutaneous interventions[66-69]. Embolization agents may be administered alone (embolization) or after selective intra-arterial chemotherapy (generally doxorubicin, mitomycin or cisplatin) or in combination with lipiodol (chemoembolization). Transarterial embolization or chemoembolization results in partial responses in 15-55% of patients, delays tumor progression and vascular invasion, and prolongs the survival time compared to conservative management. The most important aspect is the selection of patients, i.e., patients should have preserved liver function (Child A) and asymptomatic multinodular tumors without vascular invasion or extrahepatic spread[67,69]. In patients with advanced liver disease (Child B or C), treatment-induced liver failure may offset the antitumor effect or survival benefit of the intervention. As has been shown recently, postoperative adjuvant TACE may improve survival in patients with risk factors for residual tumor[70].

Radiation therapy

While radiotherapy plays only a minor role in the treatment of primary HCC, selective intra-arterial

Table 3 Drugs evaluated in clinical trials for the treatment of patients with HCC

5-Fluorouracil
Capecitabine
Doxorubicin
Epirubicin
Etoposide
Cisplatin
Gemcitabine
Mitoxantrone
Interferon alpha
Megestrol acetate
Tamoxifen
Octreotide
Thalidomide
Thymophysin
α-1-thymosin

injection of ^{131}iodine-labeled lipiodol has been performed in some patients[71] but needs further clinical evaluation before a recommendation can be made. Furthermore, high dose proton beam radiotherapy and external beam radiation as well as Yttrium-90 microsphere treatment have been recently explored in clinical trials in patients with unresectable HCC[72-74]. These strategies will certainly be further explored in clinical studies and may become a treatment option in future.

Drugs

A number of chemotherapeutic, hormonal and other drugs (Table 3) have been evaluated in clinical trials[75-77]. While most chemotherapeutic agents, such as tamoxifen[78], octreotide[79] and interferon[66], have not been shown to be effective in randomized controlled clinical trials, there are a number of substances that may deserve further clinical evaluation, such as gemcitabine[80,81], thymostimulin[82], α-1-thymosin[83], pravastatin[84], thalidomide[85] and megestrol acetate[86], antiangiogenic small molecules, Cox-2 inhibitors in combination with capecitabine and possibly others. Till date, however, none of these drugs can be recommended outside clinical studies.

Experimental strategies

In view of the limited therapeutic options for advanced HCCs, a number of experimental strategies are being evaluated (Figure 4), including gene and immune therapies based on suicide, cytokine and antiangiogenic genes or DNA vaccination with tumor-specific genes[87-90], oncolytic viruses[91] as well as novel drugs such as 3-bromopyruvate[92].

HCC prevention

HCC prevention falls into two categories. Primary prevention that is aimed at the prevention of HCC development in patients with chronic liver diseases of different etiologies and secondary prevention that is aimed at preventing the recurrence and/or the development of new HCC lesions after successful surgical or non-surgical HCC treatment[93,94].

Primary HCC prevention Primary prevention is aimed at the interference with HCC development at four stages (Figure 5).

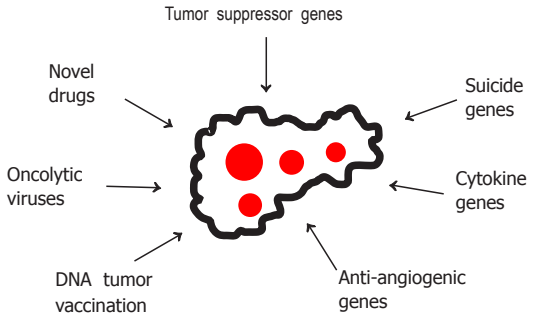

Figure 4 HCC Experimental Therapeutic Strategies

Stage 1: Interventions at this step are aimed at the prevention of acquired liver diseases. Apart from avoiding liver toxins, including alcohol and certain drugs, or infections with HBV or HCV by hygienic measures, avoiding parenteral exposure to blood, blood products or contaminated needles etc., a prime example is vaccination against HBV infection using commercially available active and passive vaccines. Several HBV vaccines using natural or recombinant hepatitis B surface antigen (HBsAg) from different sources are well introduced in clinical practice and universal vaccination in Taiwan has indeed already resulted in a decline of the incidence of HCCs[95]. In addition, novel HBV vaccination strategies are being explored, including a novel triple HBsAg recombinant vaccine[96], epidermal HBsAg powder immunization[97] as well as oral immunization using HBsAg transgenic plants[98-100]. Furthermore, DNA vaccination has been shown in animal models to induce antibodies against HBsAg/anti-HBs[101,102] even after topical application to the skin. For the prevention of HCV infection, however no effective vaccine is available till date. While several HCV vaccination concepts are being evaluated, including HCV proteins[103], HCV-like particles[104] as well as intravenous, intrahepatic, intraepidermal, intramuscular or oral cDNA immunization[105-109], it is not expected that a vaccine against HCV infection will become commercially available within the next few years.

Stage 2: Interventions at this step are aimed at the early treatment of acute liver diseases, thereby blocking their transition into chronic hepatitis that carries the risk of developing liver cirrhosis and its sequelae, including HCC development. While the principles mentioned above regarding liver toxins can also be applied here, the early diagnosis and treatment of inherited liver diseases, such as Wilson's disease and hemochromatosis, are of paramount importance. Furthermore, recent studies suggest that early treatment of acute HCV infection prevents its progression to chronic hepatitis C[110-112].

Stage 3: Interventions at this step are aimed at the prevention of the progression of chronic hepatitis to liver cirrhosis that carries a high risk of HCC development. Apart from avoiding liver toxins and long-term use of high dose androgens or other anabolic steroids, the treatment

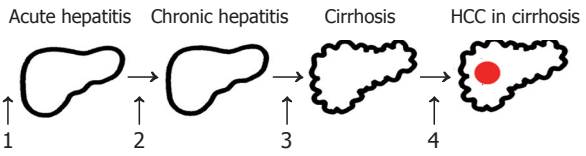

Figure 5 Primary HCC Prevention.

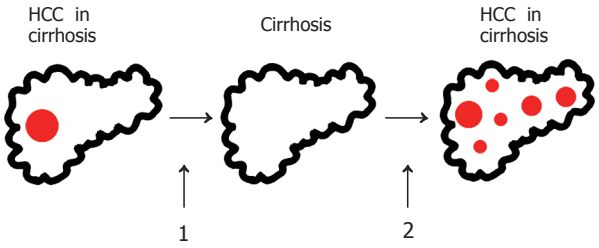

Figure 6 Secondary HCC Prevention.

of chronic hepatitis is of paramount importance. This includes the treatment of inherited, cholestatic or autoimmune liver diseases as well as the treatment of chronic viral hepatitis B or C. Reduction of iron overload by phlebotomy, for example, has been shown to stop the progression of hemochromatosis to liver cirrhosis and HCC. Treatment of chronic hepatitis B with interferon alpha or nucleoside analogs[113-118] and chronic hepatitis C with interferon alpha and now the combination of interferon alpha and ribavirin has demonstrated biochemical, virological, and histopathological improvements[119-123] and a lower incidence of HCC development[124-126].

Stage 4: Interventions at this step are aimed at interfering with the molecular events leading to HCC development, usually in a cirrhotic liver. These strategies include all treatment modalities detailed above (stage 3) as far as they can be implemented in patients with compensated or decompensated liver cirrhosis. In addition, some of the measures to prevent HCC recurrence after successful HCC treatment (secondary prevention) should in principle be useful for HCC prevention at this stage of the disease. Furthermore, some concepts of molecular therapy of HCCs should be applicable also in the prevention of HCCs. Without experimental pre-clinical data on these issues, it would be premature to discuss their potential clinical impact.

Secondary HCC prevention The prevention of a local recurrence and/or the development of new HCC lesions in patients after successful surgical or non-surgical HCC treatment (Figure 6) is of paramount importance and can significantly improve disease-free and overall patient survival.

After successful HCC resection or non-surgical ablation, HCC recurrence in the remaining cirrhotic liver is the major limitation of life expectancy of these patients. The probability of recurrence is about 50% within 3 years after successful treatment[38,127]. Strategies to prevent HCC recurrence are therefore central to the improvement of survival of HCC patients after initial cure. Apart from liver transplantation after successful resection[44], the strategies explored to date include administration of polyprenoic acid (an acyclic retinoid)[128] interferon alpha[129] and interferon beta[130]. Furthermore, adoptive immunotherapy[131] and intra-arterial injection of ^{131}iodine-labeled lipiodol[132,133] have been evaluated in clinical studies. All these interventions can result in lower HCC recurrence rates. These findings have to be confirmed in larger randomized controlled studies, demonstrating that a clear clinical benefit before secondary prevention with one of the strategies mentioned above should enter clinical practice.

Summary and perspectives

HCC is one of the most common malignant tumors in some areas of the world with an extremely poor prognosis HCC treatment is based on randomized controlled trials and many observational studies. Treatment options fall into four main categories: surgical interventions including tumor resection and liver transplantation, percutaneous interventions including ethanol injection and RFTA, transarterial interventions including embolization and chemoembolization, and drugs as well as gene and immune therapies. Though surgery as well as percutaneous and transarterial interventions are effective in patients with limited disease (up to three lesions smaller than 3 cm in diameter or one lesion smaller than 5 cm in diameter) and compensated underlying liver disease (cirrhosis Child A), at the time of diagnosis more than 80% patients present with multicentric HCC and advanced liver disease or co-morbidities that restrict the therapeutic measures to BSC.

In order to reduce the morbidity and mortality of HCC, early diagnosis and the development of novel systemic therapies for advanced disease, including drugs, gene and immune therapies as well as primary HCC prevention are of paramount importance. Furthermore, secondary HCC prevention after successful therapeutic interventions needs to be improved in order to achieve better survival of patients with HCC. New technologies, including gene expression profiling and proteomic analyses, should allow to further elucidate the molecular events underlying HCC development and to identify novel diagnostic markers as well as therapeutic and preventive targets.

REFERENCES

1 **Okuda K.** Hepatocellular carcinoma. *J Hepatol* 2000; **32**: 225-237
2 **Bruix J,** Sherman M, Llovet JM, Beaugrand M, Lencioni R, Burroughs AK, Christensen E, Pagliaro L, Colombo M, Rodes J. Clinical management of hepatocellular carcinoma. Conclusions of the Barcelona-2000 EASL conference. European Association for the Study of the Liver. *J Hepatol* 2001; **35**: 421-430
3 **Bruix J,** Llovet JM. Prognostic prediction and treatment strategy in hepatocellular carcinoma. *Hepatology* 2002; **35**: 519-524
4 **Befeler AS,** Di Bisceglie AM. Hepatocellular carcinoma: diagnosis and treatment. *Gastroenterology* 2002; **122**: 1609-1619
5 **Llovet JM,** Burroughs A, Bruix J. Hepatocellular carcinoma. *Lancet* 2003; **362**: 1907-1917
6 **Llovet JM,** Fuster J, Bruix J. The Barcelona approach: diagnosis, staging and treatment of hepatocellular carcinoma. *Liver Transpl* 2004; **10**: S115-S120

7 **Bruix J,** Sala M, Llovet JM. Chemoembolization for hepatocellular carcinoma. *Gastroenterology* 2004; **127**: S179-S188
8 **Kiyosawa K,** Umemura T, Ichijo T, Matsumoto A, Yoshizawa K, Gad A, Tanaka E. Hepatocellular carcinoma: recent trends in Japan. *Gastroenterology* 2004; **127**: S17-S26
9 **El-Serag HB.** Hepatocellular carcinoma: recent trends in the United States. *Gastroenterology* 2004; **127**: S27-S34
10 **Fattovich G,** Stroffolini T, Zagni I, Donato F. Hepatocellular carcinoma in cirrhosis: incidence and risk factors. *Gastroenterology* 2004; **127**: S35-S50
11 **Taylor-Robinson SD,** Foster GR, Arora S, Hargreaves S, Thomas HC. Increase in primary liver cancer in the UK, 1979-1994. Lancet 1997; 350: 1142-1143
12 **Deuffic S,** Poynard T, Buffat L, Valleron AJ. Trends in primary liver cancer. *Lancet* 1998; **351**: 214-215
13 **El-Serag HB,** Mason AC. Rising incidence of hepatocellular carcinoma in the United States. *N Engl J Med* 1999; **340**: 745-750
14 **El-Serag HB,** Davila JA, Petersen NJ, McGlynn KA. The continuing increase in the incidence of hepatocellular carcinoma in the United States: an update. *Ann Intern Med* 2003; **139**: 817-823
15 **Calle EE,** Rodriguez C, Walker-Thurmond K, Thun MJ. Overweight, obesity, and mortality from cancer in a prospectively studied cohort of U.S. adults. N Engl J Med 2003; 348: 1625-1638
16 **Ozturk M.** Genetic aspects of hepatocellular carcinogenesis. *Semin Liver Dis* 1999; 19: 235-242
17 **Bergsland EK.** Molecular mechanisms underlying the development of hepatocellular carcinoma. *Semin Oncol* 2001; 28: 521-531
18 **Thorgeirsson SS,** Grisham JW. Molecular pathogenesis of human hepatocellular carcinoma. *Nat Genet* 2002; **31**: 339-346
19 **Block TM,** Mehta AS, Fimmel CJ, Jordan R. Molecular viral oncology of hepatocellular carcinoma. *Oncogene* 2003; **22**: 5093-5107
20 **Suriawinata A,** Xu R. An update on the molecular genetics of hepatocellular carcinoma. *Semin Liver Dis* 2004; **24**: 77-88
21 **Satyanarayana A,** Manns MP, Rudolph KL. Telomeres and telomerase: a dual role in hepatocarcinogenesis. *Hepatology* 2004; **40**: 276-283
22 **Bréchot C.** Pathogenesis of hepatitis B virus-related hepatocellular carcinoma: old and new paradigms. *Gastroenterology* 2004; **127**: S56-S61
23 **Yu MC,** Yuan JM. Environmental factors and risk for hepatocellular carcinoma. *Gastroenterology* 2004; **127**: S72-78
24 **Velázquez RF,** Rodríguez M, Navascués CA, Linares A, Pérez R, Sotorríos NG, Martínez I, Rodrigo L. Prospective analysis of risk factors for hepatocellular carcinoma in patients with liver cirrhosis. *Hepatology* 2003; **37**: 520-527
25 **Ming L,** Thorgeirsson SS, Gail MH, Lu P, Harris CC, Wang N, Shao Y, Wu Z, Liu G, Wang X, Sun Z. Dominant role of hepatitis B virus and cofactor role of aflatoxin in hepatocarcinogenesis in Qidong, China. *Hepatology* 2002; **36**: 1214-1220
26 **Hassan MM,** Hwang LY, Hatten CJ, Swaim M, Li D, Abbruzzese JL, Beasley P, Patt YZ. Risk factors for hepatocellular carcinoma: synergism of alcohol with viral hepatitis and diabetes mellitus. *Hepatology* 2002; **36**: 1206-1213
27 **Ohata K,** Hamasaki K, Toriyama K, Matsumoto K, Saeki A, Yanagi K, Abiru S, Nakagawa Y, Shigeno M, Miyazoe S, Ichikawa T, Ishikawa H, Nakao K, Eguchi K. Hepatic steatosis is a risk factor for hepatocellular carcinoma in patients with chronic hepatitis C virus infection. *Cancer* 2003; **97**: 3036-3043
28 **Yano Y,** Yamashita F, Sumie S, Ando E, Fukumori K, Kiyama M, Oyama T, Kuroki S, Kato O, Yamamoto H, Tanaka M, Sata M. Clinical features of hepatocellular carcinoma seronegative for both HBsAg and anti-HCV antibody but positive for anti-HBc antibody in Japan. *Am J Gastroenterol* 2002; **97**: 156-161
29 **Pollicino T,** Squadrito G, Cerenzia G, Cacciola I, Raffa G, Craxi A, Farinati F, Missale G, Smedile A, Tiribelli C, Villa E, Raimondo G. Hepatitis B virus maintains its pro-oncogenic properties in the case of occult HBV infection. *Gastroenterology* 2004; **126**: 102-110
30 **Nakamoto Y,** Guidotti LG, Kuhlen CV, Fowler P, Chisari FV. Immune pathogenesis of hepatocellular carcinoma. *J Exp Med* 1998; **188**: 341-350
31 **Nakamoto Y,** Kaneko S, Fan H, Momoi T, Tsutsui H, Nakanishi K, Kobayashi K, Suda T. Prevention of hepatocellular carcinoma development associated with chronic hepatitis by anti-fas ligand antibody therapy. *J Exp Med* 2002; **196**: 1105-1111
32 **Pikarsky E,** Porat RM, Stein I, Abramovitch R, Amit S, Kasem S, Gutkovich-Pyest E, Urieli-Shoval S, Galun E, Ben-Neriah Y. NF-kappaB functions as a tumour promoter in inflammation-associated cancer. *Nature* 2004; **431**: 461-466
33 **Balkwill F,** Coussens LM. Cancer: an inflammatory link. *Nature* 2004; **431**: 405-406
34 **Chen CJ,** Chen DS. Interaction of hepatitis B virus, chemical carcinogen, and genetic susceptibility: multistage hepatocarcinogenesis with multifactorial etiology. *Hepatology* 2002; **36**: 1046-1049
35 **Di Bisceglie AM.** Screening for hepatocellular carcinoma: being old is not all bad. *Am J Gastroenterol* 2004; 99: 1477-1478
36 **Talwalkar JA,** Gores GJ. Diagnosis and staging of hepatocellular carcinoma. *Gastroenterology* 2004; **127**: S126-S132
37 **Okuda K,** Ohtsuki T, Obata H, Tomimatsu M, Okazaki N, Hasegawa H, Nakajima Y, Ohnishi K. Natural history of hepatocellular carcinoma and prognosis in relation to treatment. Study of 850 patients. *Cancer* 1985; **56**: 918-928
38 **Llovet JM,** Brú C, Bruix J. Prognosis of hepatocellular carcinoma: the BCLC staging classification. *Semin Liver Dis* 1999; **19**: 329-338
39 **Farinati F,** Rinaldi M, Gianni S, Naccarato R. How should patients with hepatocellular carcinoma be staged? Validation of a new prognostic system. *Cancer* 2000; **89**: 2266-2273
40 **Song TJ,** Ip EW, Fong Y. Hepatocellular carcinoma: current surgical management. *Gastroenterology* 2004; **127**: S248-S260
41 **Llovet JM,** Fuster J, Bruix J. Intention-to-treat analysis of surgical treatment for early hepatocellular carcinoma: resection versus transplantation. *Hepatology* 1999; **30**: 1434-1440
42 **Arii S,** Yamaoka Y, Futagawa S, Inoue K, Kobayashi K, Kojiro M, Makuuchi M, Nakamura Y, Okita K, Yamada R. Results of surgical and nonsurgical treatment for small-sized hepatocellular carcinomas: a retrospective and nationwide survey in Japan. The Liver Cancer Study Group of Japan. *Hepatology* 2000; **32**: 1224-1229
43 **Kubo S.** Neuer Marker für Leberversagen nach Resektion. *Ann Surg* 2004; **239**: 186-193
44 **Sala M,** Fuster J, Llovet JM, Navasa M, Solé M, Varela M, Pons F, Rimola A, García-Valdecasas JC, Brú C, Bruix J. High pathological risk of recurrence after surgical resection for hepatocellular carcinoma: an indication for salvage liver transplantation. *Liver Transpl* 2004; **10**: 1294-1300
45 **Wiesner RH,** Freeman RB, Mulligan DC. Liver transplantation for hepatocellular cancer: the impact of the MELD allocation policy. *Gastroenterology* 2004; **127**: S261-S267
46 **Schwartz M.** Liver transplantation for hepatocellular carcinoma. *Gastroenterology* 2004; **127**: S268-S276
47 **Kulik L,** Abecassis M. Living donor liver transplantation for hepatocellular carcinoma. Gastroenterology 2004;127: S277-S282
48 Mazzaferro V, Regalia E, Doci R, Andreola S, Pulvirenti A, Bozzetti F, Montalto F, Ammatuna M, Morabito A, Gennari L. Liver transplantation for the treatment of small hepatocellular carcinomas in patients with cirrhosis. *N Engl J Med* 1996; **334**: 693-699
49 **Shetty K,** Timmins K, Brensinger C, Furth EE, Rattan S, Sun W, Rosen M, Soulen M, Shaked A, Reddy KR, Olthoff KM. Liver transplantation for hepatocellular carcinoma validation of present selection criteria in predicting outcome. *Liver Transpl*

2004; **10**: 911-918
50 **Sala M,** Varela M, Bruix J. Selection of candidates with HCC for transplantation in the MELD era. *Liver Transpl* 2004; **10**: S4-S9
51 **Lee JS,** Chu IS, Heo J, Calvisi DF, Sun Z, Roskams T, Durnez A, Demetris AJ, Thorgeirsson SS. Classification and prediction of survival in hepatocellular carcinoma by gene expression profiling. *Hepatology* 2004; **40**: 667-676
52 **Locker J.** A new way to look at liver cancer. *Hepatology* 2004; **40**: 521-523
53 **Graziadei IW,** Sandmueller H, Waldenberger P, Koenigsrainer A, Nachbaur K, Jaschke W, Margreiter R, Vogel W. Chemoembolization followed by liver transplantation for hepatocellular carcinoma impedes tumor progression while on the waiting list and leads to excellent outcome. *Liver Transpl* 2003; **9**: 557-563
54 **Cronin DC**, Millis JM, Siegler M. Transplantation of liver grafts from living donors into adults--too much, too soon. *N Engl J Med* 2001; **344**: 1633-1637
55 **Trotter JF,** Wachs M, Everson GT, Kam I. Adult-to-adult transplantation of the right hepatic lobe from a living donor. *N Engl J Med* 2002; **346**: 1074-1082
56 **Lo CM,** Fan ST, Liu CL, Chan SC, Wong J. The role and limitation of living donor liver transplantation for hepatocellular carcinoma. *Liver Transpl* 2004; **10**: 440-744
57 **Livraghi T,** Meloni F, Morabito A, Vettori C. Multimodal image-guided tailored therapy of early and intermediate hepatocellular carcinoma: long-term survival in the experience of a single radiologic referral center. *Liver Transpl* 2004; **10**: S98-106.
58 **Omata M,** Tateishi R, Yoshida H, Shiina S. Treatment of hepatocellular carcinoma by percutaneous tumor ablation methods: Ethanol injection therapy and radiofrequency ablation. *Gastroenterology* 2004; **127**: S159-166
59 **Head HW,** Dodd GD. Thermal ablation for hepatocellular carcinoma. *Gastroenterology* 2004; **127**: S167-S178
60 **Livraghi T,** Giorgio A, Marin G, Salmi A, de Sio I, Bolondi L, Pompili M, Brunello F, Lazzaroni S, Torzilli G. Hepatocellular carcinoma and cirrhosis in 746 patients: long-term results of percutaneous ethanol injection. *Radiology* 1995; **197**: 101-108
61 **Lencioni R,** Pinto F, Armillotta N, Bassi AM, Moretti M, Di Giulio M, Marchi S, Uliana M, Della Capanna S, Lencioni M, Bartolozzi C. Long-term results of percutaneous ethanol injection therapy for hepatocellular carcinoma in cirrhosis: a European experience. *Eur Radiol* 1997; **7**: 514-519
62 **Buscarini L,** Buscarini E, Di Stasi M, Vallisa D, Quaretti P, Rocca A. Percutaneous radiofrequency ablation of small hepatocellular carcinoma: long-term results. *Eur Radiol* 2001; **11**: 914-921
63 **Lencioni RA,** Allgaier HP, Cioni D, Olschewski M, Deibert P, Crocetti L, Frings H, Laubenberger J, Zuber I, Blum HE, Bartolozzi C. Small hepatocellular carcinoma in cirrhosis: randomized comparison of radio-frequency thermal ablation versus percutaneous ethanol injection. *Radiology* 2003; **228**: 235-240
64 **Mulier S,** Mulier P, Ni Y, Miao Y, Dupas B, Marchal G, De Wever I, Michel L. Complications of radiofrequency coagulation of liver tumours. *Br J Surg* 2002; **89**: 1206-1222
65 **Livraghi T,** Solbiati L, Meloni F, Ierace T, Goldberg SN, Gazelle GS. Percutaneous radiofrequency ablation of liver metastases in potential candidates for resection: the "test-of-time approach". *Cancer* 2003; 97: 3027-3035
66 **Lo CM,** Ngan H, Tso WK, Liu CL, Lam CM, Poon RT, Fan ST, Wong J. Randomized controlled trial of transarterial lipiodol chemoembolization for unresectable hepatocellular carcinoma. *Hepatology* 2002; **35**: 1164-1171
67 **Llovet JM,** Real MI, Montaña X, Planas R, Coll S, Aponte J, Ayuso C, Sala M, Muchart J, Solà R, Rodés J, Bruix J. Arterial embolisation or chemoembolisation versus symptomatic treatment in patients with unresectable hepatocellular carcinoma: a randomised controlled trial. *Lancet* 2002; **359**: 1734-1739
68 **Llovet JM,** Bruix J. Systematic review of randomized trials for unresectable hepatocellular carcinoma: Chemoembolization improves survival. *Hepatology* 2003; **37**: 429-442
69 **Llovet JM,** Bruix J. Unresectable hepatocellular carcinoma: meta-analysis of arterial embolization. *Radiology* 2004; **230**: 300-301
70 **Ren ZG,** Lin ZY, Xia JL, Ye SL, Ma ZC, Ye QH, Qin LX, Wu ZQ, Fan J, Tang ZY. Postoperative adjuvant arterial chemoembolization improves survival of hepatocellular carcinoma patients with risk factors for residual tumor: a retrospective control study. *World J Gastroenterol* 2004; **10**: 2791-2794
71 **Risse JH,** Grünwald F, Kersjes W, Strunk H, Caselmann WH, Palmedo H, Bender H, Biersack HJ. Intraarterial HCC therapy with 1-131-Lipiodol, *Cancer Biother Radiopharm* 2000; **15**: 65-70
72 **Bush DA,** Hillebrand DJ, Slater JM, Slater JD. High-dose proton beam radiotherapy of hepatocellular carcinoma: preliminary results of a phase Ⅱ trial. *Gastroenterology* 2004; **127**: S189-193
73 **Fuss M,** Salter BJ, Herman TS, Thomas CR. External beam radiation therapy for hepatocellular carcinoma: potential of intensity-modulated and image-guided radiation therapy. *Gastroenterology* 2004; **127**: S206-217
74 **Geschwind JF,** Salem R, Carr BI, Soulen MC, Thurston KG, Goin KA, Van Buskirk M, Roberts CA, Goin JE. Yttrium-90 microspheres for the treatment of hepatocellular carcinoma. *Gastroenterology* 2004; **127**: S194-205
75 **Simonetti RG,** Liberati A, Angiolini C, Pagliaro L, Treatment of hepatocellular carcinoma: a systematic review of randomized controlled trials. *Ann Oncol* 1997; **8**: 117-136
76 **Mathurin P,** Rixe O, Carbonell N, Bernard B, Cluzel P, Bellin MF, Khayat D, Opolon P, Poynard T. Review article: Overview of medical treatments in unresectable hepatocellular carcinoma--an impossible meta-analysis? *Aliment Pharmacol Ther* 1998; **12**: 111-126
77 **Schwartz JD,** Schwartz M, Mandeli J, Sung M. Neoadjuvant and adjuvant therapy for resectable hepatocellular carcinoma: review of the randomised clinical trials. *Lancet Oncol* 2002; **3**: 593-603
78 **Chow PK,** Tai BC, Tan CK, Machin D, Win KM, Johnson PJ, Soo KC. High-dose tamoxifen in the treatment of inoperable hepatocellular carcinoma: A multicenter randomized controlled trial. *Hepatology* 2002; **36**: 1221-1226
79 **Yuen MF,** Poon RT, Lai CL, Fan ST, Lo CM, Wong KW, Wong WM, Wong BC. A randomized placebo-controlled study of long-acting octreotide for the treatment of advanced hepatocellular carcinoma. *Hepatology* 2002; **36**: 687-691
80 **Yang TS,** Lin YC, Chen JS, Wang HM, Wang CH. Phase Ⅱ study of gemcitabine in patients with advanced hepatocellular carcinoma. *Cancer* 2000; **89**: 750-756
81 **Kubicka S,** Rudolph KL, Tietze MK, Lorenz M, Manns M. Phase Ⅱ study of systemic gemcitabine chemotherapy for advanced unresectable hepatobiliary carcinomas. *Hepatogastroenterology* 2001; **48**: 783-789
82 **Palmieri G,** Biondi E, Morabito A, Rea A, Gravina A, Bianco A. Thymostimulin treatment of hepatocellular carcinoma on liver cirrhosis. *Int J Oncol* 1996; **8**: 827-832
83 **Stefanini GF,** Foschi FG, Castelli E, Marsigli L, Biselli M, Mucci F, Bernardi M, Van Thiel DH, Gasbarrini G. Alpha-1-thymosin and transcatheter arterial chemoembolization in hepatocellular carcinoma patients: a preliminary experience. *Hepatogastroenterology* 1998; **45**: 209-215
84 **Kawata S,** Yamasaki E, Nagase T, Inui Y, Ito N, Matsuda Y, Inada M, Tamura S, Noda S, Imai Y, Matsuzawa Y. Effect of pravastatin on survival in patients with advanced hepatocellular carcinoma. A randomized controlled trial. *Br J Cancer* 2001; **84**: 886-891
85 **Hsu C,** Chen CN, Chen LT, Wu CY, Yang PM, Lai MY, Lee

PH, Cheng AL. Low-dose thalidomide treatment for advanced hepatocellular carcinoma. *Oncology* 2003; **65**: 242-249
86 **Villa E,** Ferretti I, Grottola A, Buttafoco P, Buono MG, Giannini F, Manno M, Bertani H, Dugani A, Manenti F. Hormonal therapy with megestrol in inoperable hepatocellular carcinoma characterized by variant oestrogen receptors. *Br J Cancer* 2001; **84**: 881-885
87 **Mohr L,** Geissler M, Blum HE. Gene therapy for malignant liver disease. *Expert Opin Biol Ther* 2002; **2**: 163-175
88 **Geissler M,** Mohr L, Ali MY, Grimm CF, Ritter M, Blum HE. Immunobiology and gene-based immunotherapy of hepatocellular carcinoma. *Z Gastroenterol* 2003; **41**: 1101-1110
89 **Mohr L,** Yeung A, Aloman C, Wittrup D, Wands JR. Antibody-directed therapy for human hepatocellular carcinoma. *Gastroenterology* 2004; **127**: S225-231
90 **Butterfield LH.** Immunotherapeutic strategies for hepatocellular carcinoma. *Gastroenterology* 2004; **127**: S232-S241
91 **Pei Z,** Chu L, Zou W, Zhang Z, Qiu S, Qi R, Gu J, Qian C, Liu X. An oncolytic adenoviral vector of Smac increases antitumor activity of TRAIL against HCC in human cells and in mice. *Hepatology* 2004; **39**: 1371-1381
92 **Geschwind JF,** Ko YH, Torbenson MS, Magee C, Pedersen PL. Novel therapy for liver cancer: direct intraarterial injection of a potent inhibitor of ATP production. *Cancer Res* 2002; **62**: 3909-3913
93 **Heathcote EJ.** Prevention of hepatitis C virus-related hepatocellular carcinoma. *Gastroenterology* 2004; **127**: S294-S302
94 **Lok AS.** Prevention of hepatitis B virus-related hepatocellular carcinoma. *Gastroenterology* 2004; **127**: S303-S309
95 **Chang MH,** Chen CJ, Lai MS, Hsu HM, Wu TC, Kong MS, Liang DC, Shau WY, Chen DS. Universal hepatitis B vaccination in Taiwan and the incidence of hepatocellular carcinoma in children. Taiwan Childhood Hepatoma Study Group. *N Engl J Med* 1997; **336**: 1855-1859
96 **Young MD,** Schneider DL, Zuckerman AJ, Du W, Dickson B, Maddrey WC. Adult hepatitis B vaccination using a novel triple antigen recombinant vaccine. *Hepatology* 2001; **34**: 372-376
97 **Chen D,** Weis KF, Chu Q, Erickson C, Endres R, Lively CR, Osorio J, Payne LG. Epidermal powder immunization induces both cytotoxic T-lymphocyte and antibody responses to protein antigens of influenza and hepatitis B viruses. *J Virol* 2001; **75**: 11630-11640
98 **Arntzen CJ.** Pharmaceutical foodstuffs-oral immunization with transgenic plants. *Nat Med* 1998; **4**: 502-503
99 **Kapusta J,** Modelska A, Figlerowicz M, Pniewski T, Letellier M, Lisowa O, Yusibov V, Koprowski H, Plucienniczak A, Legocki AB. A plant-derived edible vaccine against hepatitis B virus. *FASEB J* 1999; **13**: 1796-1799
100 **Richter LJ,** Thanavala Y, Arntzen CJ, Mason HS. Production of hepatitis B surface antigen in transgenic plants for oral immunization. *Nat Biotechnol* 2000; **18**: 1167-1171
101 **Davis HL,** Mancini M, Michel ML, Whalen RG. DNA-mediated immunization to hepatitis B surface antigen-longevity of primary response and effect of boost. *Vaccine* 1996; **14**: 910-915
102 **Prince AM,** Whalen R, Brotman B. Successful nucleic acid based immunization of newborn chimpanzees against hepatitis B virus. *Vaccine* 1997; **15**: 916-919
103 **Choo QL,** Kuo G, Ralston R, Weiner A, Chien D, Van Nest G, Han J, Berger K, Thudium K, Kuo C. Vaccination of chimpanzees against infection by the hepatitis C virus. *Proc Natl Acad Sci USA* 1994; **91**: 1294-1298
104 **Lechmann M,** Murata K, Satoi J, Vergalla J, Baumert TF, Liang TJ. Hepatitis C virus-like particles induce virus-specific humoral and cellular immune responses in mice. *Hepatology* 2001; **34**: 417-423
105 **Lee AY,** Manning WC, Arian CL, Polakos NK, Barajas JL, Ulmer JB, Houghton M, Paliard X. Priming of hepatitis C virus-specific cytotoxic T lymphocytes in mice following portal vein injection of a liver-specific plasmid DNA. *Hepatology* 2000; **31**: 1327-1333
106 **Weiner AJ,** Paliard X, Selby MJ, Medina-Selby A, Coit D, Nguyen S, Kansopon J, Arian CL, Ng P, Tucker J, Lee CT, Polakos NK, Han J, Wong S, Lu HH, Rosenberg S, Brasky KM, Chien D, Kuo G, Houghton M. Intrahepatic genetic inoculation of hepatitis C virus RNA confers cross-protective immunity. *J Virol* 2001; **75**: 7142-7148
107 **Brinster C,** Muguet S, Lone YC, Boucreux D, Renard N, Fournillier A, Lemonnier F, Inchauspé G. Different hepatitis C virus nonstructural protein 3 (Ns3)-DNA-expressing vaccines induce in HLA-A2.1 transgenic mice stable cytotoxic T lymphocytes that target one major epitope. *Hepatology* 2001; **34**: 1206-1217
108 **Forns X,** Payette PJ, Ma X, Satterfield W, Eder G, Mushahwar IK, Govindarajan S, Davis HL, Emerson SU, Purcell RH, Bukh J. Vaccination of chimpanzees with plasmid DNA encoding the hepatitis C virus (HCV) envelope E2 protein modified the infection after challenge with homologous monoclonal HCV. *Hepatology* 2000; **32**: 618-625
109 **Wedemeyer H,** Gagneten S, Davis A, Bartenschlager R, Feinstone S, Rehermann B. Oral immunization with HCV-NS3-transformed Salmonella: induction of HCV-specific CTL in a transgenic mouse model. *Gastroenterology* 2001; **121**: 1158-1166
110 **Jaeckel E,** Cornberg M, Wedemeyer H, Santantonio T, Mayer J, Zankel M, Pastore G, Dietrich M, Trautwein C, Manns MP. Treatment of acute hepatitis C with interferon alfa-2b. *N Engl J Med* 2001; **345**: 1452-1457
111 **Gerlach JT,** Diepolder HM, Zachoval R, Gruener NH, Jung MC, Ulsenheimer A, Schraut WW, Schirren CA, Waechtler M, Backmund M, Pape GR. Acute hepatitis C: high rate of both spontaneous and treatment-induced viral clearance. *Gastroenterology* 2003; **125**: 80-88
112 **Nomura H,** Sou S, Tanimoto H, Nagahama T, Kimura Y, Hayashi J, Ishibashi H, Kashiwagi S. Short-term interferon-alfa therapy for acute hepatitis C: a randomized controlled trial. *Hepatology* 2004; **39**: 1213-1219
113 **Malik AH,** Lee WM. Chronic hepatitis B virus infection: treatment strategies for the next millennium. *Ann Intern Med* 2001; **132**: 723-731
114 **Torresi J,** Locarnini S. Antiviral chemotherapy for the treatment of hepatitis B virus infections. *Gastroenterology* 2000; **118**: S83-103
115 **Lok AS,** Heathcote EJ, Hoofnagle JH. Management of hepatitis B: 2000--summary of a workshop. *Gastroenterology*2001; **120**: 1828-1853
116 **Liaw YF,** Sung JJ, Chow WC, Farrell G, Lee CZ, Yuen H, Tanwandee T, Tao QM, Shue K, Keene ON, Dixon JS, Gray DF, Sabbat J. Lamivudine for patients with chronic hepatitis B and advanced liver disease. *N Engl J Med* 2004; **351**: 1521-1531
117 **Wands JR.** Prevention of hepatocellular carcinoma. *N Engl J Med* 2004; **351**: 1567-1570
118 **Marcellin P,** Lau GK, Bonino F, Farci P, Hadziyannis S, Jin R, Lu ZM, Piratvisuth T, Germanidis G, Yurdaydin C, Diago M, Gurel S, Lai MY, Button P, Pluck N. Peginterferon alfa-2a alone, lamivudine alone, and the two in combination in patients with HBeAg-negative chronic hepatitis B. *N Engl J Med* 2004; **351**: 1206-1217
119 **EASL** International Consensus Conference on Hepatitis C. Paris, 26-28, February 1999, Consensus Statement. European Association for the Study of the Liver. *J Hepatol* 1999; **30**: 956-961
120 **Davis GL.** Current therapy for chronic hepatitis C. *Gastroenterology* 2000; **118**: S104-S114
121 **Manns MP,** McHutchison JG, Gordon SC, Rustgi VK, Shiffman M, Reindollar R, Goodman ZD, Koury K, Ling M, Albrecht JK. Peginterferon alfa-2b plus ribavirin compared with interferon alfa-2b plus ribavirin for initial treatment of chronic hepatitis C: a randomized trial. *Lancet* 2001; **358**: 958-965
122 **Di Bisceglie AM,** Hoofnagle JH. Optimal therapy of hepatitis C. *Hepatology* 2002; 36: S121-S127

123 **Hadziyannis SJ,** Sette H, Jr., Morgan TR, Balan V, Diago M, Marcellin P, Ramadori G, Bodenheimer H, Jr., Bernstein D, Rizzetto M, Zeuzem S, Pockros PJ, Lin A, Ackrill AM. Peginterferon-alpha2a and ribavirin combination therapy in chronic hepatitis C: a randomized study of treatment duration and ribavirin dose. *Ann Intern Med* 2004; **140**: 346-355

124 **Yoshida H,** Shiratori Y, Moriyama M, Arakawa Y, Ide T, Sata M, Inoue O, Yano M, Tanaka M, Fujiyama S, Nishiguchi S, Kuroki T, Imazeki F, Yokosuka O, Kinoyama S, Yamada G, Omata M. Interferon therapy reduces the risk for hepatocellular carcinoma: national surveillance program of cirrhotic and noncirrhotic patients with chronic hepatitis C in Japan. IHIT Study Group. Inhibition of Hepatocarcinogenesis by Interferon Therapy. *Ann Intern Med* 1999; **131**: 174-181

125 **Nishiguchi S,** Shiomi S, Nakatani S, Takeda T, Fukuda K, Tamori A, Habu D, Tanaka T. Prevention of hepatocellular carcinoma in patients with chronic active hepatitis C and cirrhosis. *Lancet* 2001; **357**: 196-197

126 **Toyoda H,** Kumada T, Nakano S, Takeda I, Sugiyama K, Kiriyama S, Sone Y, Tanikawa M, Hisanaga Y, Hayashi K, Honda T. Effect of the dose and duration of interferon-alpha therapy on the incidence of hepatocellular carcinoma in noncirrhotic patients with a nonsustained response to interferon for chronic hepatitis C. *Oncology* 2001; **61**: 134-142

127 **Koike Y, Shiratori Y**, Sato S, Obi S, Teratani T, Imamura M, Hamamura K, Imai Y, Yoshida H, Shiina S, Omata M. Risk factors for recurring hepatocellular carcinoma differ according to infected hepatitis virus-an analysis of 236 consecutive patients with a single lesion. *Hepatology* 2000; **32**: 1216-1223

128 **Muto Y,** Moriwaki H, Ninomiya M, Adachi S, Saito A, Takasaki KT, Tanaka T, Tsurumi K, Okuno M, Tomita E, Nakamura T, Kojima T. Prevention of second primary tumors by an acyclic retinoid, polyprenoic acid, in patients with hepatocellular carcinoma. Hepatoma Prevention Study Group. *N Engl J Med* 1996; **334**: 1561-1567

129 **Kubo S,** Nishiguchi S, Hirohashi K, Tanaka H, Shuto T, Yamazaki O, Shiomi S, Tamori A, Oka H, Igawa S, Kuroki T, Kinoshita H. Effects of long-term postoperative interferon-alpha therapy on intrahepatic recurrence after resection of hepatitis C virus-related hepatocellular carcinoma. A randomized, controlled trial. *Ann Intern Med* 2001; **134**: 963-967

130 **Ikeda K,** Arase Y, Saitoh S, Kobayashi M, Suzuki Y, Suzuki F, Tsubota A, Chayama K, Murashima N, Kumada H. Interferon beta prevents recurrence of hepatocellular carcinoma after complete resection or ablation of the primary tumor-A prospective randomized study of hepatitis C virus-related liver cancer. *Hepatology* 2000; **32**: 228-232

131 **Takayama T,** Sekine T, Makuuchi M, Yamasaki S, Kosuge T, Yamamoto J, Shimada K, Sakamoto M, Hirohashi S, Ohashi Y, Kakizoe T. Adoptive immunotherapy to lower postsurgical recurrence rates of hepatocellular carcinoma: a randomized trial. *Lancet* 2000; **356**: 802-807

132 **Lau WY,** Leung TW, Ho SK, Chan M, Machin D, Lau J, Chan AT, Yeo W, Mok TS, Yu SC, Leung NW, Johnson PJ. Adjuvant intra-arterial iodine-131-labelled lipiodol for resectable hepatocellular carcinoma: a prospective randomised trial. *Lancet* 1999; **353**: 797-801

133 **Boucher E,** Corbinais S, Rolland Y, Bourguet P, Guyader D, Boudjema K, Meunier B, Raoul JL. Adjuvant intra-arterial injection of iodine-131-labeled lipiodol after resection of hepatocellular carcinoma. *Hepatology* 2003; **38**: 1237-1241

Science Editor Wang XL and Guo SY **Language Editor** Elsevier HK

PO Box 2345, Beijing 100023, China
www.wjgnet.com
wjg@wjgnet.com

ELSEVIER

World J Gastroenterol 2005;11(47):7401-7404
World Journal of Gastroenterology ISSN 1007-9327

Expression of human chorionic gonadotropin, CD44v6 and CD44v4/5 in esophageal squamous cell carcinoma

Dao-Ming Li, Shan-Shan Li, Yun-Han Zhang, Hui-Juan Zhang, Dong-Ling Gao, Yong-Xia Wang

Dao-Ming Li, Shan-Shan Li, Yun-Han Zhang, Dong-Ling Gao, Yong-Xia Wang, Henan Key Laboratory of Tumor Pathology, Department of Pathology, the First Affiliated Hospital, Zhengzhou University, Zhengzhou 450052, Henan Province, China
Hui-Juan Zhang, Department of Endocrinology, the First Affiliated Hospital, Zhengzhou University, Zhengzhou 450052, Henan Province, China
Correspondence to: Dao-Ming Li, Henan Key Laboratory of Tumor Pathology, Department of Pathology, the First Affiliated Hospital, Zhengzhou University, 40 Daxue Road, Zhengzhou 450052, Henan Province, China. rjmli@163.com
Telephone: +86-371-65163867
Received: 2004-11-15 Accepted: 2004-12-03

Abstract

AIM: To study the relationship between the expression of human chorionic gonadotropin (HCG), CD44v6, CD44v4/5 and the infiltration, metastasis of esophageal squamous cell carcinoma.

METHODS: By labeled streptavidin-biotin technique, the expressions of HCG, CD44v6, and CD44v4/5 in 42 patients with esophageal squamous cell carcinoma were examined.

RESULTS: The positive rate of HCG expression in patients with lymph node metastasis was 85.71% (18/21), higher than that (57.14%, 12/21) in those without lymph node metastasis (P<0.05). The positive rate of CD44v6 expression was 71.43% (15/21) in lymph node metastasis group, and 38.09% (8/21) in non-metastasis group; there was a significant difference between the two groups (P<0.05). The positive rate of CD44v4/5 expression was 76.19% (16/21) in lymph node metastasis group, and 42.86% (9/21) in non-metastasis group; there was also a significant difference between them (P<0.05). From grade Ⅰ to grade Ⅲ in differentiation, the positive rate of HCG expression was 84.62% (11/13), 70.59% (12/17) and 58.33% (7/12), respectively; there was no significant difference among them (P>0.05). The positive rate of CD44v6 expression in grades Ⅰ-Ⅲ of cancer tissues was 76.92% (10/13), 52.94% (9/17), and 33.33% (4/12) respectively; there was no significant difference among them. The positive rate of CD44v4/5 expression in grades Ⅰ-Ⅲ of cancer tissues was 69.23% (9/13), 64.71% (11/17), and 41.67% (5/12) respectively; there was no significant difference among the three groups. There was no correlation between the positive rates of HCG and CD44v6, CD44v4/5 expression. Cancer cells in carcinomatous emboli and those infiltrating into vascular wall strongly expressed HCG, CD44v6, and CD44v4/5.

CONCLUSION: Expression of HCG, CD44v6, and CD44v4/5 in esophageal squamous cell carcinoma is related to its infiltration and metastasis. HCG, CD44v6, and CD44v4/5 have different effects on the infiltration and metastasis of esophageal squamous cell carcinoma.

Key words: Esophageal tumor; Squamous cell carcinomas; HCG; CD44v6; CD44v4/5; Immunohistochemistry; Infiltration; Metastasis

Li DM, Li SS, Zhang YH, Zhang HJ, Gao DL, Wang YX. Expression of human chorionic gonadotropin, CD44v6 and CD44V4/5 in esophageal squamous cell carcinoma. *World J Gastroenterol* 2005; 11(47): 7401-7404
http://www.wjgnet.com/1007-9327/11/7401.asp

INTRODUCTION

Human chorionic gonadotropin (HCG) is a glycoprotein molecule. Ectopic HCG produced by malignant tumors is one of the indexes of early diagnosis[1]. Researchers have studied the expression of HCG in malignant tumors, such as tumor of lung, bladder, breast[1-4], and found that HCG expression has a close correlation with the differentiation, infiltration, and metastasis of tumors. Expression of CD44 gene and its relation with metastasis of tumors are the hotspots of tumor study in recent years[5]. It has been found that expressions of mutant CD44 molecules exist in many tumors, such as stomach, lung, and cervix tumors, and have an obvious relation with metastasis of tumors[6-8]. In order to explore the relationship between the expression of HCG, CD44v6, and CD44v4/5 and the infiltration and metastasis of esophageal carcinoma, labeled streptavidin-biotin (LSAB) was used to detect the expression of these three proteins in 42 patients with esophageal squamous cell carcinoma.

MATERIALS AND METHODS

Selection of cases

Specimens were excised from 42 esophageal carcinoma patients in Tumour Hospital of Anyang city. There

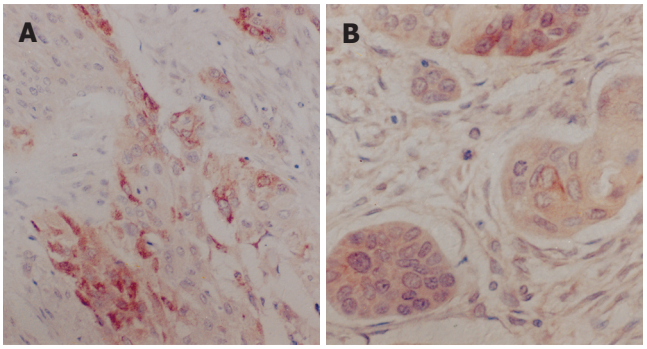

Figure 1 Spot or focus (**A**) and diffuse (**B**) distribution of HCG positive cells.

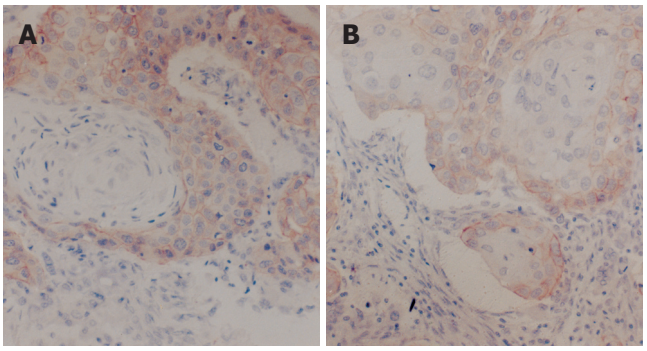

Figure 2 Diffuse distribution of CD44v6 (**A**) and CD44v4/5 (**B**) positive cells.

were 23 male patients and 19 female patients. Their age range was 33-73 years, averaged 55.7 years. None of the patients received chemotherapy, radiation therapy, or immunotherapy before surgery. All the formalin-fixed and paraffin-embedded specimens were sectioned and stained with hematoxylin-eosin. The sections were carefully diagnosed under light microscope. All the specimens excised from the patients proved to be squamous cell carcinoma by histopathology and 13 cases were grade Ⅰ, 17 cases were grade Ⅱ, and 12 cases were grade Ⅲ. Lymph node metastasis was found in 21 cases.

Detection of HCG, CD44v6, and CD44v4/5 proteins

Immunohistochemical LSAB technique was applied. Rabbit anti-human HCG antibody was purchased from DAKO (Denmark), mouse anti-human CD44v6 and CD44v4/5 mAb was the product of R&D (USA). LSAB immunohistochemical reagent kit was purchased from Zymed (USA). Human placental chorion was taken from pregnant women as HCG positive control. Squamous basal cells were taken from normal people as CD44v6 and CD44v4/5 positive control. Antibody I was replaced with normal goat serum as negative control group. Antibody I was replaced with PBS as blank negative control group.

The criteria were established as previously described[9]. The positive cells were stained brown-yellow. The positive expression of HCG mainly displayed on cytoplasm, while CD44v6 and CD44v4/5 mainly appeared on cell membrane. The positive cells of 10 high power fields were counted and the positive expression was categorized as follows: weakly positive (+), with positive cells less than 10%; moderately positive (++), with positive cells 10-50%; strongly positive (+++), with positive cells more than 50%.

Table 1 Correlation between expression of HCG and differentiation degree, lymph node metastasis of esophageal squamous cell carcinoma

Pathologic characteristics	*n*	Positive expression				Positive rates (%)	χ^2	*P*
		-	+	++	+++			
Differentiation Degree								
Ⅰ	13	2	3	3	5	84.62		
Ⅱ	17	5	4	2	6	70.59	2.122	>0.05
Ⅲ	12	5	2	3	2	58.33		
Lymph node metastasis								
Positive	21	3	5	4	9	85.71		
Negative	21	9	4	4	4	57.14	4.2	<0.05
Tumor focus								
Primary	21	3	5	5	8	85.71		
Metastasis	21	4	7	6	4	80.95	0.171	>0.05

Statistical analysis

Microsoft SPSS10.0 was applied. Comparison between two and multiple specimens was made by χ^2 test. Difference and correlation were analyzed by coupled χ^2 test and Spearman's correlation test.

RESULTS

Distribution features of HCG and CD44v6, CD44v4/5 positive cells

There were three patterns in the distribution of HCG and CD44v6, CD44v4/5 positive cells, namely spot, focal and diffuse distribution. In squamous cell carcinoma tissues of grade I, the distribution of HCG and CD44v6 was focal and diffuse (Figures 1A, 1B and 2A), while that of CD44v4/5 was spot, focal or diffuse. In grade II, the distribution of HCG, CD44v6, and CD44v4/5 was focal and diffuse (Figure 2B). In grade III, staining of HCG was focal or diffuse, while CD44v6 was multi-focal, CD44v4/5 was focal or spot. In carcinoma tissues with lymph node metastasis, the distribution of HCG and CD44v6, CD44v4/5 was multi-focal. The expression of keratinous pearl in grade I was negative. Tumor cells in emboli or tumor cells invading the vascular wall were frequently stained and highly positive for HCG, CD44v6, and CD44v4/5. The tumor cells at periphery of carcinoma nests with interstitial or intermuscular infiltration and mitosis were highly positive for CD44v6, CD44v4/5.

Correlation between expression of HCG, CD44v6, CD44v4/5, and differentiation degree, lymph node metastasis of esophageal squamous cell carcinoma

The correlations between expressions of HCG, CD44v6,

Table 2 Correlation between expression of CD44v6 and differentiation degree, lymph node metastasis of esophageal squamous cell carcinoma

Pathologic characteristics	*n*	Positive expression				Positive rates (%)	χ^2	*P*
		-	+	++	+++			
Differentiation Degree								
I	13	3	3	4	3	76.92		
II	17	8	5	1	3	52.94	4.788	>0.05
III	12	8	2	2	0	33.33		
Lymph node metastasis								
Positive	21	6	7	3	5	71.43		
Negative	21	13	5	3	0	38.09	4.709	<0.05
Tumor focus								
Primary	21	6	7	2	6	71.43		
Metastasis	21	8	7	4	2	61.9	0.429	>0.05

Table 3 Correlation between expression of CD44v4/5 and differentiation degree, lymph node metastasis of esophageal squamous cell carcinoma

Pathologic characteristics	*n*	Positive expression				Positive rates (%)	χ^2	*P*
		-	+	++	+++			
Differentiation Degree								
I	13	4	5	3	1	69.23		
II	17	6	7	3	1	64.71	2.286	>0.25
III	12	7	4	1	0	41.67		
Lymph node metastasis								
Positive	21	5	10	4	2	76.19		
Negative	21	12	6	3	0	42.86	4.842	<0.05
Tumor focus								
Primary	21	5	10	4	2	76.19		
Metastasis	21	6	12	3	0	71.43	0.123	>0.5

CD44v4/5 and differentiation degree, lymph node metastasis of esophageal squamous cell carcinoma are listed in Tables 1-3.

Expression of HCG, CD44v6, and CD44v4/5 in primary and metastatic carcinoma

According to Tables 1-3, if the expression of HCG, CD44v6, and CD44v4/5 was positive in primary tumor, it could be negative in metastasis tumor. If both of them were positive, the expression was similar or lower in metastasis tumor compared to primary tumor, but there was no statistically significant difference.

Positive rate of HCG, CD44v6, and CD44v4/5 expressions in esophageal squamous cell carcinoma

The positive rate of HCG, CD44v6, and CD44v4/5 expression was 71.43%, 54.76%, and 59.52% respectively. There was no significant difference among them ($P>0.05$), nor was there any correlation ($P>0.05$).

DISCUSSION

HCG is a glycoprotein hormone. Recent studies found that HCG can be expressed in many tumors, such as the tumor of lung[2], bladder[3], breast[4], HCG is related with tumor differentiation degree, infiltration and metastasis. According to our study, there is a significant difference between lymph node metastasis and non-metastasis groups in terms of the positive expression of HCG, indicating that HCG plays an important role in lymphatic metastasis of esophageal squamous cell carcinoma. The stained tumor cells in emboli or invading the vascular wall were highly positive for HCG, suggesting that HCG also has a relationship with hematogenous metastasis of esophageal squamous cell carcinoma. Most tumor cells with positive expression of HCG in esophageal squamous cell carcinoma were well differentiated and had plenty of cytoplasm. The expression of HCG was mainly in central tumor cells of carcinoma nests, and in peripheral cells. But the keratinous pearls were not stained. All of these are in accordance with the study of Li[2] on lung squamous cell carcinoma. The expression of HCG was mainly in cytoplasm, and the amount of cytoplasm of the central tumor cells was more than that in periphery of carcinoma nests, suggesting that the different expression levels of HCG of these two types of carcinoma cells result from different amounts of cytoplasm. The tumor cells with positive expression of HCG infiltrated the vascular wall, suggesting that the expression of HCG has some relationship with infiltration and metastasis of esophageal squamous cell carcinoma.

Previously it was found that the expression of HCG is negatively related with the differentiation degree of carcinoma of bladder[3] and squamous cell carcinoma of lung[2]. These discrepancies may be due to the following reasons. Types of the tumor tissues are different (the difference between squamous cell carcinoma and transitional cell carcinoma). The expression of HCG is mainly in cytoplasm, while the quantity of cytoplasm is correlated with the differentiation degree of tumor cells (there is more cytoplasm in squamous cell carcinoma of grade I, less in grade II, and the least in grade III). The positive rate of HCG in the 42 cases of esophageal squamous cell carcinoma (71.42%) was much higher than that in carcinoma of bladder[3], and also higher than that in squamous cell carcinoma of the lung (60%)[2]. All of these indicate that HCG may become a new and more sensitive biological marker.

There was a close correlation between the expression of CD44v6, CD44v4/5, and the infiltration and metastasis of tumors. The study showed that the tumor cells at the periphery of carcinoma nest with interstitial or intermuscular infiltration and the stained tumor cells with mitosis were highly positive for CD44v6 and CD44v4/5, suggesting that CD44v6 and CD44v4/5 play a role in the infiltration of esophageal squamous cell carcinoma. The results are consistent with other studies[6-8]. There was a significant difference in the positive rate of CD44v6, CD44v4/5 expression between lymph node metastasis group and non-metastasis group, indicating a correlation

between the positive expression of CD44v6, CD44v4/5, and lymph node metastasis of esophageal squamous cell carcinoma. The stained tumor cells in the emboli or invading the vascular wall were highly positive for CD44v6 and CD44v4/5, suggesting that there is some relationship between the expression and risk of hematogenous metastasis of human esophageal squamous cell carcinoma.

The correlation between CD44v and metastasis of tumors was identified, while studies on relationship between CD44v and differentiation are few. This study showed that the expression rate of CD44v6, CD44v4/5 reduced with decline of the differentiation degree of esophageal squamous cell carcinoma. Yokozaki *et al*.[10] reported that if the differentiation of carcinoma is poor, the expression of CD44v is much lower.

There was no significant difference or any correlation among HCG, CD44v6, and CD44v4/5 in the 42 cases of esophageal squamous cell carcinoma. All these indicate that although HCG, CD44v6 and CD44v4/5 are related with the infiltration and metastasis of esophageal squamous cell carcinoma, their pathogenesis may be different.

REFERENCES

1 **Regelson W.** Have we found the "definitive cancer biomarker"? The diagnostic and therapeutic implications of human chorionic gonadotropin-beta expression as a key to malignancy. *Cancer* 1995; **76**: 1299-1301
2 **Li DC,** Zhou XL, Cao GQ, Li BQ. Carcinoma of lung and human chorionic gonadotropin. *Zhonghua Binglixue Zazhi* 1993; **22**: 181
3 **Huang JX**, Zhang YH, Lin Y, Qiu QC. The expression and significance of HCG in transitional-cell carcinoma of bladder. *Shantou Daxue Yixueyuan Xuebao* 2001; **14**: 20-21
4 **Chi F**, Sun BC, Zhao XL, Yan YH. The expression of ectopic HCG in breast cancer and its significance. *Aizheng* 2000; **19**: 493,503
5 **Guo LX**, Xie H. CD44 and the metastasis of tumor. *Shengming Kexue* 2001; **13**: 60-63
6 **Zhou Y**, Zong H, Xu H. Expression of CD44v6 in gastric cancer and its adjacent cancer tissues .*Zhengzhou Daxue Xuebao* 2002; **37**: 593-595
7 **Qiu XF**, Wang XY, Zhang ZF, Zhang CP. CD44v6 expression in non-small cell lung carcinomas. *Linchuang Yu Shiyan Binglixue Zazhi* 2003; **19**: 413-415
8 **Chen YQ**, Zheng AW, Zhang G. Expression and clinical significance of CD44v6 in cervical carcinoma. *Zhongguo Zhongliu* 2002; **11**: 485-486
9 **Fan ZW**, Wan YX, An ZG, Zhang ZX. Study on expression of Bcl-2 and CD44 in human lung cancer. *Zhongliu Fangzhi Yanjiu* 2002; **29**: 373-375
10 **Yokozaki H,** Ito R, Nakayama H, Kuniyasu H, Taniyama K, Tahara E. Expression of CD44 abnormal transcripts in human gastric carcinomas. *Cancer Lett* 1994; **83**: 229-234

Science Editor Zhu LH and Li WZ **Language Editor** Elsevier HK

PO Box 2345, Beijing 100023, China
www.wjgnet.com
wjg@wjgnet.com

ELSEVIER

World J Gastroenterol 2005;11(47):7405-7412
World Journal of Gastroenterology ISSN 1007-9327

• *GASTRIC CANCER* •

Gene expression profiling of gastric cancer by microarray combined with laser capture microdissection

Ming-Shiang Wu, Yi-Shing Lin, Yu-Ting Chang, Chia-Tung Shun, Ming-Tsan Lin, Jaw-Town Lin

Ming-Shiang Wu, Yu-Ting Chang, Jaw-Town Lin, Department of Internal Medicine and Primary Care Medicine, College of Medicine, National Taiwan University, Taipei, Taiwan, China
Yi-Shing Lin, Genasia Biotechnology, Ltd., Taipei, Taiwan, China
Chia-Tung Shun, Department of Pathology, National Taiwan University Hospital, Taipei, Taiwan, China
Ming-Tsan Lin, Department of Surgery, National Taiwan University Hospital, Taipei, Taiwan, China
Supported by National Science Council, NSC-91-3112-B002-007, Taipei, Taiwan, China
Correspondence to: Jaw-Town Lin, Department of Internal Medicine, National Taiwan University Hospital, No. 1, Chung-Shan S. Rd., Taipei, Taiwan, China. jawtown@ha.mc.ntu.edu.tw
Telephone: +886-2-23123456
Received: 2005-03-31 Accepted: 2005-07-20

Abstract

AIM: To examine the gene expression profile of gastric cancer (GC) by combination of laser capture microdissection (LCM) and microarray and to correlate the profiling with histological subtypes.

METHODS: Using LCM, pure cancer cells were procured from 45 cancerous tissues. After procurement of about 5 000 cells, total RNA was extracted and the quality of RNA was determined before further amplification and hybridization. One microgram of amplified RNA was converted to cDNA and hybridized to cDNA microarray.

RESULTS: Among 45 cases, only 21 were qualified for their RNAs. A total of 62 arrays were performed. These included 42 arrays for cancer (21 cases with dye-swab duplication) and 20 arrays for non-tumorous cells (10 cases with dye-swab duplication) with universal reference. Analyzed data showed 504 genes were differentially expressed and could distinguish cancerous and non-cancerous groups with more than 99% accuracy. Of the 504 genes, trefoil factors 1, 2, and 3 were in the list and their expression patterns were consistent with previous reports. Immunohistochemical staining of trefoil factor 1 was also consistent with the array data. Analyses of the tumor group with these 504 genes showed that there were 3 subgroups of GC that did not correspond to any current classification system, including Lauren's classification.

CONCLUSION: By using LCM, linear amplification of RNA, and cDNA microarray, we have identified a panel of genes that have the power to discriminate between GC and non-cancer groups. The new molecular classification and the identified novel genes in gastric carcinogenesis deserve further investigations to elucidate their clinicopathological significance.

Key words: Gastric cancer; Microarray; Laser capture microdissection

Wu MS, Lin YS, Chang YT, Shun CT, Lin MT, Lin JT. Gene expression profiling of gastric cancer by microarray combined with laser capture microdissection. *World J Gastroenterol* 2005; 11(47): 7405-7412
http://www.wjgnet.com/1007-9327/11/7405.asp

INTRODUCTION

Gastric cancer (GC) is the second most common cause of cancer-related deaths in the world[1]. In Taiwan, GC ranks the fourth cancer-related death and caused more than 2 000 deaths annually[2]. The prognosis of GC depends mainly on early detection and adequate surgical resection. Although endoscopy with biopsy has been effectively used since 1980s for early diagnosis, the proportion of early to advanced GC being found through this method has not appreciably increased in recent years[3]. In spite of the current surgical techniques and chemotherapy that have made significant improvements, the cure rate for advanced GC remains low and the morbidity remains high[4]. Thus, to improve its detection and therapy, understanding of the pathogenesis and biologic features of GC is crucial.

Gastric carcinogenesis is a multi-factorial and multi-step process accompanied by accumulation of alterations of critical growth regulatory genes[5]. Delineating these genes involved may lead to important new insights into carcinogenesis[6]. Despite the fact that some interesting and promising genetic alterations have been elucidated[7], previous studies of gastric carcinogenesis were incomprehensive and inconclusive. The overall information of the genetic alterations is scanty due to technical problems of analyses. Firstly, the value of even the most sophisticated genetic testing methods will be limited if the inputs of genetic materials are not derived from pure populations or are contaminated by the wrong cells. In solid neoplasm such as GC, stromal and inflammatory cells usually intermingled with cancer cells. Therefore, special procedures to isolate cancer cells from heterogeneous tissues are mandatory. Secondly,

most of previous studies on genetic alterations of GC have focused on selected genes or chromosomal regions known in other cancers. These obstacles may be overcome using the recently developed techniques of laser capture microdissection (LCM) and microarray. LCM allows for the rapid, reliable, and accurate procurement of cells from specific microscopic regions of tissue sections under direct visualization[8]. It affords the opportunity to perform molecular genetic analysis of pure populations of malignant cells in their native tissue environment. On the other hand, the advent of high-density cDNA microarray technology with its capacity for simultaneous monitoring of thousands of genes, provides a unique opportunity for high-throughput genetic analysis of cancer[9]. For GC, several investigators have demonstrated the use of DNA microarray is beneficial for elucidation of gastric carcinogenesis[10-24]. However, to our knowledge, combined analyses of LCM and microarray in GC remain scanty[22-24]. Therefore, we aimed to examine gene expression profiles of GC by these two techniques.

MATERIALS AND METHODS

Tissues samples for LCM and RNA isolation

A total of 45 cancerous tissues and their respective non-cancerous tissues obtained at operation from patients with GC were collected and immediately frozen in liquid nitrogen. Gastric cancer and normal cells were stained by HistoGene LCM Frozen Section Staining Kit and laser capture microdissected by using a Pix Cell II LCM system (Arturus, USA). Malignant and normal cells were captured in a number of about 5 000 cells and their total RNAs were isolated by using PicoPure RNA extraction kit (Arturus, USA). The quality of RNA was determined by Bioprocessor before further amplification and hybridization.

RNA amplification, probe labeling, and hybridization

Linear RNA amplification was performed by using the RiboAmp kit (Arturus, USA). Two rounds of RNA amplification were performed to obtain enough amplified RNA (aRNA) for a microarray experiment. To serve as reference in cDNA microarray comparison, a human reference RNA pooled from 9 cell lines (Stratagene, USA) was amplified identically. cDNA was transcribed from aRNA at a quantity of 1.5 μg per channel in the presence Cy3- or Cy5-dUTP by using Cyscribe First-Strand cDNA Labelling kit (Amersham Biosciences, USA). Free conjugated dUTP was removed by Millipore Microcon YM-30 column. Cy3-labeled cDNA was pooled with Cy5-labeled reference probe in 30 μL of hybridization solution and hybridized to an Agilent human 1 cDNA microarray (Agilent Technology, USA). Hybridization was carried out at 65 ℃ for 17 h in a humidified dark chamber (Genetix, UK). After hybridization, slides were washed at the following condition: 2 X SSC/0.1 g/L SDS at 60 ℃ for 10 min, 2X SSC at room temperature for 10 min, and 0.2X SSC at room temperature for 10 min.

Scanning, image analysis, and data processing

Washed microarrays were scanned with a Virtek fluorescence reader (Virtek, CA, USA) at 535 nm for Cy3 and 625 nm for Cy5. Scanned images were analyzed by using Array-Pro image acquisition software (Media Cybernetics, USA), an image analysis algorithm was used to quantify the signal and background intensity for each target element. Data normalization was performed by Iowess method using R package (written by Terry Speeds Microarray Data Analysis Group, University of Berkerley, USA). Measurements from dye-swap replicates were average after normalization. A software developed by researchers in Stanford University-Prediction Analysis of Microarray (PAM) and Spotfire software was utilized to analyze the data.

Immunohistochemistry

Immunostaining for trefoil factor 3 protein was performed by using a standard avidin-biotin-peroxidase complex detection system[25]. The monoclonal antibody used for this study was purchased from Signet Laboratory (Bedham, MA, USA). In brief, 5-μm sections were dewaxed, microwaved, and rehydrated. Endogenous peroxidase activity and non-specific bindings were blocked by incubation with 30 mL/L hydrogen peroxide (H_2O_2) and non-immune serum, respectively. The slides were then incubated sequentially at 4 ℃ with the primary mouse monoclonal antibody overnight, a biotinylated goat anti-mouse secondary antibody for 30 min, peroxidase-conjugated streptavidin for 10 min and finally diaminobenzidine tetrachloride/H_2O_2 chromogen substrate for 10 min. Slides were then counterstained with Mayer's hematoxylin. Negative control sections were prepared by substituting the primary antibody with buffered saline. The percentage of positively stained cells was determined for each tumor section as well as its adjacent intestinal metaplasia and non-metaplastic epithelium. The immunostaining for trefoil factor 3 was registered as negative only if less than 5% of the cells showed a positive staining.

RESULTS

Among the 45 subjects with GC, only 21 (12 intestinal and 9 diffuse subtypes by Lauren classification; 19 advanced and 2 early gastric cancer by depth of invasion) of their respective RNAs were qualified for further analyses after capture of malignant cells by LCM. Figure 1 shows a representative example of LCM. A total of 62 arrays were then performed, including 42 arrays for cancer (21 cases with dye-swap duplication) and 20 arrays for non-tumorous cells (10 cases with day-swap duplication) with universal reference. PAM analyses showed differential expression of 504 genes (Tables 1 and 2) could distinguish the cancerous and non-cancerous groups with more than 99% accuracy. Of the 504 genes, trefoil factors 1, 2, and 3 were in the list and their expression patterns (down-regulation of trefoil factors 1 and 2, and up-regulation of trefoil factor 3 in cancer cases) were consistent with

Table 1 Up-regulated genes noted in gastric cancer

Biosynthesis

Argininosuccinate synthetase [BC009243], hydroxymethylbilane synthase [BC000520], hypothetical protein CL640 [BC008804], methylenetetrahydrofolate dehydrogenase ($NADP^+$-dependent), methenyltetrahydrofolate cyclohydrolase, formyltetrahydrofolate synthetase [BC001014]

Cell adhesion

Collagen, type XVIII, alpha 1 [AF01808], mesothelin [U40434], CD9 antigen (p24) (X60111), collagen, type VI, alpha 3 [X52022], thrombospondin 2 [L12350], immunoglobulin superfamily containing leucine-rich repeat [AB003184]

Cell death

Nerve growth factor receptor (TNFR superfamily, member 16) [M14764], phosphoprotein enriched in astrocytes 15 [AF153274], programmed cell death 5 [AF014955]

Cell growth and/or maintenance

Cell division cycle 25B [S78187], cyclin D2 [D13639], hippocalcin [BC001777], anillin, actin binding protein (scraps homolog, Drosophila) [AF273437], afamin [L32140], chromosome 14 open reading frame 58 [AK000378], C1q and tumor necrosis factor related protein 1 [AF32984], low density lipoprotein receptor-related protein 8, apolipoprotein e receptor [D86407], enhancer of rudimentary homolog (Drosophila) [U66871], tissue inhibitor of metalloproteinase 1 (erythroid potentiating activity, collagenase inhibitor) [D11139], insulin receptor substrate 2 [AF073310], low density lipoprotein receptor-related protein 8, apolipoprotein e receptor [D50678], thyroid hormone receptor interactor 10 [AJ000414], collagen, type I, alpha 1 [Z74615], ATPase, Na^+/K^+ transporting, beta 3 polypeptide [AF005896], T-LAK cell-originated protein kinase [AB027249], platelet-derived growth factor receptor, beta polypeptide [J03278], nucleolar protein 1 120 ku [BC000656], keratin 7 [BC002700], oncostatin M receptor [BC010943], tissue inhibitor of metalloproteinase 1 (erythroid potentiating activity, collagenase inhibitor) [BC000866], insulin-like growth factor 2 (somatomedin A) [S77035], karyopherin (importin) beta 1 [L38951], nuclear transport factor 2 (NTF-2) (Placental protein 15) (PP15) [X07315], nucleolar protein 1 120ku [X55504], thymosin beta-10 [S54005]

Cell motility

Hyaluronan-mediated motility receptor (RHAMM) [AF03286], sorcin [M32886], troponin T1, skeletal, slow [BC010963]

Cell-cell signaling

Ephrin-A2 [U92896], midkine (neurite growth-promoting factor 2) [X55110], prostaglandin I2 (prostacyclin) receptor (IP) [D25418]

Immune response

Carcinoembryonic antigen-related cell adhesion molecule 1 (biliary glycoprotein) [X14831], Human 1-8D gene from interferon-inducible gene family [X57351], GTP binding protein over-expressed in skeletal muscle [U10550], indoleamine-pyrrole 2,3 dioxygenase [M34455], interferon induced transmembrane protein 1 (9-27) [J04164]

Macromolecule metabolism

Cathepsin L2 [AB001928], PAK2 [AF09213], ribosomal protein, large P2 [M17887], hypothetical protein FLJ22761 [AK026414], KIAA0205 [D86960], proteasome (prosome, macropain) subunit, alpha type, 1 [D00759], protein tyrosine phosphatase type IVA, member 1 [U48296], peptidylprolyl isomerase (cyclophilin)-like 1 [BC003048], ribosomal protein L14 [BC009294], pyruvate kinase, muscle [BC007952], proteasome (prosome, macropain) subunit, alpha type, 7 [BC001895], isocitrate dehydrogenase 3 (NAD+) alpha [U07681], transglutaminase 4 (prostate) [U31905]

Organogenesis

Secreted protein, acidic, cysteine-rich (osteonectin) [M25743], caudal type homeo box transcription factor 2(CDX2) [AJ278434], transcription factor AP-2 alpha (activating enhancer binding protein 2 alpha) [M36711]

Regulation of metabolism

Homeo box B7 [BC015345], B-cell receptor-associated protein 37 [AF126021], Mediterranean fever [AJ003147], homeo box B7 [M16937], homeo box D4 [X17360], TIP49 [AB012122], sin3-associated polypeptide, 18 ku [AF153608]

Response to stress

Complement component 2 [X04481], complement component 3 [K02765], inhibin, beta A (activin A, activin AB alpha polypeptide) [X57579], serine (or cysteine) proteinase inhibitor, clade A (alpha-1 antiproteinase, antitrypsin), member 1 [K02212], serine (or cysteine) proteinase inhibitor, clade H (heat shock protein 47), member 1, (collagen binding protein 1) [D83174], meiotic recombination (*S. cerevisiae*) 11 homolog A [AF073362], RecQ protein-like 4 [BC013277]

Signal transduction

Secreted frizzled-related protein 4 [AF026692], lymphocyte antigen 6 complex, locus E(RIG-E) [Z68179], dimethylarginine dimethylaminohydrolase 2 [BC001435]

Unclassified

Angiotensin I converting enzyme (peptidyl-dipeptidase A) 1 [BI826471], apolipoprotein C-I [AV709433], argininosuccinate synthetase [BF305206], ATPase, Ca^{++} transporting, plasma membrane 4 [AI885833], ATPase, Na^+/K^+ transporting, beta 3 polypeptide [AU151263], B-cell associated protein [BG771222], BTG family, member 2 [BG750101], cadherin 3, type 1, P-cadherin (placental) [NM001793], calcium modulating ligand [AW474551], carbonyl reductase 3 [AI658832], cathepsin Z [AI913006], CDC-like kinase 2 [BG286233], cell division cycle 25B [BF976307], CGI-01 protein [AK027886], chloride intracellular channel 1 [AA291390], claudin 4 [BI760179], claudin 7 [AI279608], collagen, type I, alpha 1 [AW577407], collagen, type X, alpha 1 (Schmid metaphyseal chondrodysplasia) [NM000493], core-binding factor, beta subunit [NM001755], D123 gene product [BE792735], deoxythymidylate kinase (thymidylate kinase) [BF312526], diubiquitin [AW270961], DKFZP566C134 protein [BG621382], E2F transcription factor 3 [AU153511], epithelial protein lost in neoplasm alpha [AAF23756], exostoses (multiple) 1 [BF057267], FK506-binding protein 4 (59 ku) [NM002014], follistatin-like 3 (secreted glycoprotein) [NM005860], forkhead box M1 [AL525810], glutamine-fructose-6-phosphate transaminase 2 [AK001242], GTP-binding protein over-expressed in skeletal muscle [AW297828], guanylate cyclase 2C (heat stable enterotoxin receptor) [NM004963], heme oxygenase (decycling) 1 [BI596354], HMT1 (hnRNP methyltransferase, *S. cerevisiae*)-like 2 [BG167159], Homo sapiens cDNA FLJ11796 fis, clone HEMBA1006158, highly similar to Homo sapiens transcription factor forkhead-like 7 [FKHL7] gene [BI914918], homo sapiens mRNA for short form of beta II spectrin, partial [AA131993], human cDNA: FLJ22528 fis, clone HRC12825 [AK026181], human cDNA: FLJ22998 fis, clone KAT11985, highly similar to AB000712 Human hCPE-R mRNA for CPE-receptor [AK026651], human chromosome 20 clone h119, complete sequence [AF312913], human claudin 3 [CLDN3] gene, [AF007189], regenerating islet-derived family, member 4 [AF254415], human genomic DNA, chromosome 22q11.2, clone KB1125A3 [AP000350], likely ortholog of mouse membrane bound C2 domain containing protein [AB018290], KIAA0930 protein [AB02314], hypothetical protein LOC90499 [AL137712], fuse-binding protein-interacting repressor [AF190744], Thy-1 cell surface antigen [M11749], biglycan [BC002416], CK2 interacting protein 1; HQ0024c protein [BC010149], hypothetical protein FLJ12436 [BC011993], tissue inhibitor of metalloprotease 1 (erythroid potentiating activity, collagenase inhibitor) [BC000866], hypothetical protein FLJ20277 [M11749], hypothetical protein FLJ22393 [H45848],hypothetical protein PRO1489 [AI536671], interferon induced transmembrane protein 1 (9-27) [BG506643], interferon induced transmembrane protein 3 (1-8U) [BE886918], interleukin 13 [NM002188], interleukin 8 [BG777366], JM4 protein [BI818455], keratin 7 [BI094014], keratin 7 [AA307373], KIAA0747 protein [BG744628], low density lipoprotein receptor-related protein 8, apolipoprotein e receptor [BF110337], lymphocyte antigen 6 complex, locus E [BM101706], matrix metalloproteinase 7 (matrilysin, uterine) [NM002423], membrane protein of cholingeric synaptic vesicles [BG760616], mesothelin [AI813749], midkine (neurite growth-promoting factor) [AI784469], msh (Drosophila) homeo box homolog 1 [AI912103], MyoD family inhibitor [BG675569], neural precursor cell expressed, developmentally down-regulated 5 [AU131176], neuromedin U [BG661038], NIPSNAP, C. elegans, homolog 1 [BC006473], nucleolar and coiled-body phosphoprotein [AL553791], platelet-derived growth factor receptor, beta polypeptide [BI755841], procollagen-lysine, 2-oxogutarate 5-dioxygenase 3 [AL544817], proliferating cell nuclear antigen [AA523378], proliferation-associated 2G4, 38KD [BI088072], protein C receptor, endothelial (EPCR) [BG831881], pyruvate kinase, muscle [BF690275], rhoG [BG338917], regulatory factor X, 5 [AW027312], ribosomal protein L23 [AI349581], ribosomal protein L35 [BF310946], ribosomal protein L37 [BG032793], ribosomal protein S16 [BG765030], ribosomal protein S3 [AA593872], S100 calcium-binding protein A4 [AV713821], serine (or cysteine) proteinase inhibitor, clade A (alpha-1 antiproteinase, antitrypsin) [BG567810], sigma receptor (SR31747 binding protein 1) [AL571572], small inducible cytokine subfamily A (Cys-Cys), member 19 [W07401], superoxide dismutase 2, mitochondrial [BG773219], survival of motor neuron 1, telomeric [AA029190], thymosin, beta 10 [AV707021], thyroid hormone receptor interactor 10 [N98668], transKetolase [BI195990], translocase of outer mitochondrial membrane 34 [BE798732], trefoil factor 3 (intestinal) [AA633399], tumor suppressing subtransferable candidate 3 [BE670374], zinc finger protein 267 [AU128446]

[ ]: GeneBank accession number

Table 2 Down-regulated genes noted in gastric cancer

Biosynthesis

5-aminoimidazole-4-carboxamide ribonucleotide formyltransferase/IMP cyclohydrolase [D89976], adenosine monophosphate deaminase 1 (isoform M) [M60092], histidine decarboxylase [D16583], Human histidine decarboxylase (HDC) [M60445]

Catabolism

Human bilirubin UDP-glucuronosyltransferase isozyme 1 [M57899], Human placental cDNA coding for 5'nucleotidase (EC 3.1.3.5) [X55740]

Cell adhesion

Collagen, type IV, alpha 6 [D21337], collagen, type XVII, alpha 1[U76585], tenascin C (hexabrachion) [X78565], dermatopontin [AL049455], Human pancreatitis associated protein [M84337], sialic acid binding Ig-like lectin 11 [AF337818], Macaque brain cDNA clone:QflA-14173, full insert sequence [AB062939]

Cell death

Baculoviral IAP repeat-containing 1 [U80017], CD3E antigen, epsilon polypeptide (TiT3 complex) [X03884], programmed cell death 4 (neoplastic transformation inhibitor) [U96628]

Cell growth and/or maintenance

Core-binding factor, runt domain, alpha subunit 2; translocated to, 1; cyclin D-related [S69002], ATPase, Ca++ transporting, ubiquitous [Z69881], ATP-binding cassette, sub-family C (CFTR/MRP), member 5 [AB005659], B-cell CLL/lymphoma 3 [M31732], CDC7 (cell division cycle 7, S. cerevisiae, homolog)-like 1 [AF015592], gastrokine 1 [AB039886], Human chondroadherin mRNA, complete cds [AF371328], CDC28 protein kinase regulatory subunit 2 [X54942], solute carrier family 39 (zinc transporter), member 6 [U41060], ATPase, H^+/K^+ exchanging, alpha polypeptide [M63962], golgi autoantigen, golgin subfamily a, 4 [U31906], ATPase, H^+/K^+ exchanging, beta polypeptide [M75110], solute carrier family 7 (cationic amino acid transporter, y+ system), member 8 [AB037669], transcription factor-like 5 (basic helix-loop-helix) [AF070992], kinesin family member 11 [U37426], cholecystokinin B receptor [D13305], choline kinase alpha [D10704], sodium channel, nonvoltage-gated 1, gamma [X87160], MCM7 minichromosome maintenance deficient 7 (S. cerevisiae) [D28480], sodium channel, nonvoltage-gated 1 alpha [X76180], oxysterol binding protein-like 7 [AF323729], zinc finger protein 145 (Kruppel-like, expressed in promyelocytic leukemia) [AF060568], solute carrier organic anion transporter family, member 2A1 [U70867], aurora kinase B [AF004022], CDC-like kinase 1 [M59287], trefoil factor 1 [X52003], quiescin (Q6) [U97276], signal recognition particle receptor ('docking protein'), clone MGC:1609 IMAGE:3528505, mRNA, complete cds [BC001162], villin-like, clone MGC:656 IMAGE:3356294, mRNA, complete cds. [BC000243], inhibitor of DNA binding 1, dominant negative helix-loop-helix protein [S78825], insulin-like growth factor binding protein 2 36 ku [S37730], Macaque somatostatin I mRNA, complete cds. solute carrier family 9 (sodium/hydrogen exchanger), isoform 1 (antiporter, Na^+/H^+, amiloride sensitive) [S68616], platelet-derived growth factor receptor, alpha polypeptide [M21574], SH3-domain GRB2-like 2 [AF036268], solute carrier family 9 (sodium/hydrogen exchanger), isoform 1 (antiporter, Na^+/H^+, amiloride sensitive) [M96067], thiosulfate sulfurtransferase (rhodanese) [BI820468], thrombomodulin [M16552]

Cell-cell signaling

NAD(P)H dehydrogenase, quinone 1 [J03934], dopamine receptor D5 [BC009748], monoamine oxidase A [M69226]

Digestion

Japanese Macaque (Macaca fuscata) mRNA for pepsinogen A-2/3. [X59755]

Electron transport

Cytochrome P450, family 4, subfamily F, polypeptide 12 [AY008841], cytochrome P450, family 2, subfamily C, polypeptide 18 [M61853], cytochrome P450, family 4, subfamily F, polypeptide 11 [AF23608], cytochrome P450, family 2, subfamily S, polypeptide 1 [AF33527], dual oxidase 1 [AF21346], cytochrome c oxidase subunit Vic [BC000187]

Immune response

Diacylglycerol kinase, delta 130 ku [D63479], Fc fragment of IgG, high affinity Ia, receptor for (CD64) [X14356], beta-site APP-cleaving enzyme 2 [AL163285], X-box binding protein 1 [L13850]

Macromolecule metabolism

Sphingomyelin phosphodiesterase, acid-like 3A [Y08136], calpain 9 (nCL-4) [AB038463], carboxypeptidase A2 (pancreatic) [BC007009], 2,4-dienoyl CoA reductase 2, peroxisomal [AE006463], protein kinase (cAMP-dependent, catalytic) inhibitor beta [AF225513], calpain 13 [AK027176], calpain 9 (nCL-4) [AF022799], fructose-1,6-bisphosphatase 1 [L10320], fructose-1,6-bisphosphatase [Y10812], gastric lipase [X05997], heat shock 10 ku protein [AJ250915], progastricsin (pepsinogen C) [M23077], protein tyrosine phosphatase, receptor type, N polypeptide 2 [U66702], carboxypeptidase A2 (pancreatic) [U19977], prostaglandin-endoperoxide synthase 1 (prostaglandin G/H synthase and cyclooxygenase) [M59979], hyaluronoglucosaminidase 1 [U03056], galactose-4-epimerase, UDP-[L41668], chaperonin containing TCP1, subunit 3 (gamma)[BC008019], proprotein convertase subtilisin/kexin type 7 [BC010696], ubiquitin specific protease 14 (tRNA-guanine transglycosylase), [BC003556], Kallikrein 11 [AB013730], KIAA0089 protein [BC006168], prostaglandin-endoperoxide synthase 1 (prostaglandin G/H synthase and cyclooxygenase) [S36219], prostaglandin-endoperoxide synthase 1 (prostaglandin G/H synthase and cyclooxygenase) [U63846]

Metabolism

Aldo-keto reductase family 1, member C1 (dihydrodiol dehydrogenase 1; 20-alpha (3-alpha)-hydroxysteroid dehydrogenase) [AB032150], alcohol dehydrogenase 7 (class IV), mu or sigma polypeptide [X76342], carbonic anhydrase II [J03037], carbonic anhydrase IX [Z54349], transcription termination factor, mitochondrial [Y09615], hydroxyprostaglandin dehydrogenase 15-(NAD) [L76465], dehydrogenase/reductase (SDR family) member 9 [AY017349], sulfotransferase family, cytosolic, 1C, member 1 [AF186261], ribonuclease, RNase A family, 4 [BC015520]

Organogenesis

GATA binding protein 4 [L34357], aldehyde dehydrogenase 3 family, member A2 [U46689], tropomyosin 4 [BC002827]

Regulation of blood pressure

Chromogranin A (parathyroid secretory protein 1) [BC009384]

Regulation of coagulation

Annexin A10 [AJ238979]

Regulation of metabolism

Estrogen-related receptor gamma [AB020639], zinc finger protein 345 [X78933], Kruppel-like factor 2 (lung) [AF134053], RAR-related orphan receptor C [U16997], PEPP subfamily gene 2 [AL590526]

Response to stress

Checkpoint suppressor 1 [BC007506], CHK1 (checkpoint, S.pombe) homolog [AF016582], for protein disulfide isomerase-related [D49490], glutathione S-transferase A3 [BG573805], glutathione synthetase [AK000947], glutathione S-transferase A4-4 (GSTA4) [AF025887], cathepsin E (CatE gene), [AJ250716], glutathione peroxidase 3 (plasma) [D00632], RAD51 homolog (RecA homolog, *E. coli*) (*S. cerevisiae*) [D14134], RAD51 (*S. cerevisiae*) homolog C [BC000667]

Signal transduction

G protein-coupled receptor 30[U63917], hypothetical protein FLJ22595[AK026248], G protein-coupled receptor 30[AF015257], RAP1, GTPase activating protein 1[M64788], active BCR-related gene[U01147], G protein-coupled receptor, family C, group 5, member B[AL137684], G protein-coupled receptor, family C, group 5, member C[AF207989], RAS protein activator like 1 (GAP1 like)[AF086713], regulator of G-protein signaling 17 [RGS17] mRNA, complete cds. [AF202257], histidine triad nucleotide-binding protein, [BC007090], RAB26, member RAS oncogene family, [BC007681]

Unclassified

Actin binding LIM protein 1 [NM006719], activated leucocyte cell adhesion molecule [AI050952], adrenergic, beta-2-, receptor, surface [NM000024], alcohol dehydrogenase 1C (class I), gamma polypeptide[NM000669], aldehyde dehydrogenase 1 family, member A1 [AV649527], aldehyde dehydrogenase 3 family, member A2 (BF679509), aldo-keto reductase family 1, member C1 (dihydrodiol dehydrogenase 1; 20-alpha (3-alpha)-hydroxysteroid dehydrogenase)

[BI759009], annexin A7 [NM004034], arylacetamide deacetylase (esterase) [L32179], ATPase, H+ transporting, lysosomal (vacuolar proton pump) 42 ku [N75606], ATPase, H+/K+ exchanging, beta polypeptide [BI760752], ATP-binding cassette, sub-family C (CFTR/MRP), member 5 [NM005688], bA438B23.1 (neuronal leucine-rich repeat protein) [CAC22713], bB379O24.1 (novel protein similar to transcription factor GATA-5) [CAC36001], beta-1,3-glucuronyltransferase 1 (glucuronosyltransferase P) [BE550952], calpain 2, (m/II) large subunit [BI771158], cathepsin E [AI598121], CDC28 protein kinase 2 [BG618998], chaperonin containing TCP1, subunit 2 (beta) [N98764], chromosome 1 open reading frame 8[BG476131], clathrin, light polypeptide (Lcb) (BE791502), cleavage and polyadenylation specific factor 5 25 ku subunit [AA738354], contactin 2 (axonal) [AI366526], cytochrome P450 isoform 4F12 [NM023944], cytochrome P450, subfamily IIC (mephenytoin 4-hydroxylase), polypeptide 9[BG567504], keratin 20 [X73501], delta sleep inducing peptide, immunoreactor [AL525317], DNA segment, numerous copies, expressed probes (GS1 gene) [AL570791], ESTs [AW960145], ESTs[N24233], ESTs, Highly similar to A32915 nucleophosmin [BG033160], ESTs, highly similar to AF078844 1 hqp0376 protein [BG165945], ESTs, Weakly similar to CA18 MOUSE COLLAGEN ALPHA 1(VIII) CHAIN PRECURSOR [M. musculus] [AW275800], ESTs, weakly similar to JC5314 CDC28/cdc2-like kinase associating arginine-serine cyclophilin [*H. sapiens*] [R85437], Fc fragment of IgG binding protein [D84239], flap structure-specific endonuclease 1 [BG773959], forkhead box O3A [AU134033], Friedreich ataxia region gene X123 [BI771919], galactose-4-epimerase, UDP-[BE388744], GATA-binding protein 6 [NM005257], glucosaminyl (N-acetyl) transferase 2, I-branching enzyme [NM001491], glutamic-pyruvate transaminase (alanine aminotransferase) [NM005309], glutathione S-transferase A4 [BI597618], granuphilin-a [BAA84656], hepatocyte nuclear factor 3, gamma [NM004497], highly expressed in cancer, rich in leucine heptad repeats [AA878068], holocytochrome c synthase (cytochrome c heme-lyase) [AL561481], Homer, neuronal immediate early gene, 2(BG742654), Homo sapiens clone 23763 unknown mRNA, partial cds [BG743005], homo sapiens SNC73 protein [SNC73] mRNA, complete cds[BF663123], homolog of yeast long chain polyunsaturated fatty acid elongation enzyme 2 [BF966630], human (clone HUAB2-3) Ig mRNA, variable region, partial cds. [L19893], human [JER47] MUC5AC mRNA for mucin (partial). [Z34277], peroxisomal membrane protein 2 22 ku (AIBC1) [AF250136], breast carcinoma amplified sequence 1 (AIBC1) [AF041260], Human cDNA FLJ11341 fis, clone PLACE1010786. [AK002203], human cDNA: FLJ20990 fis, clone CAE01666.[AK024463], cell-type T-cell Ig gamma-chain, V region (IGHV@) [L03144], KFAL6 lambda 1 Ig light chain variable region [AF124182], hypothetical protein FLJ22795 [AF316855], defensin, theta 1 [U10267], immunoglobulin heavy diversity 2-21 [AB019441], Human gastric H,K-ATPase catalytic subunit gene, complete cds. [M63962], genomic DNA of 21q22.2 Down Syndrome region, segment 11/13. [AP000020], BIC transcript [AP001693], immunoglobulin kappa variable 1-8 [AP001209], genomic DNA, chromosome 8q23, clone:KB1747F8. [AP003113], glucocorticoid receptor alpha mRNA, variant 3′ UTR [U25029], immunoglobulin lambda constant 1 (Mcg marker) [D87023], Ig lambda light chain variable region gene (24-12ITIIIE213) rearranged; Ig-Light-Lambda; VLambda. [Z85038], Ig rearranged gamma chain mRNA, V-J-C region and complete cds. [M63438], Ig rearranged gamma chain mRNA, V-J-C region and complete cds. [M63438], metallothionein 1F (functional) [M13003], metallothionein 1A (functional) [K01383], mRNA for anti-Sm antibody VL chain (V kappa 4/J kappa 3). [Z46347], heat shock 70 ku protein 4 [AB023420], Ig heavy chain variable region, clone ToPA214. [Z98733], Ig kappa light chain, anti-RhD, therad 7. [AJ010422], Ig lambda light chain. [Y14738], sterile alpha and TIR motif containing 1 [AJ290445], KIAA0832 protein, complete cds.[AB020639], synaptotagmin-like 2 [AB046817], metallothionein 1L [X97261], NPC-related protein NAG73 [AF280797], prion protein (p27-30) (Creutzfeld-Jakob disease, Gerstmann-Strausler-Scheinker syndrome, fatal familial insomnia) [AY008282], Human promyelocytic leukemia zinc finger protein (PLZF) gene, complete cds. [AF060568], cystatin A (stefin A) [X05978], sema domain, immunoglobulin domain (Ig), short basic domain, secreted, (semaphorin) 3F [U38276], serine protease inhibitor, Kazal type 1 [AF286028], SM22 alpha gene, 5′ flanking region. [D84344], hypothetical protein MGC27165 [AF067420], activating transcription factor 4 pseudogene (tax-responsive enhancer element B67 pseudogene) [U03712], chromosome 7 open reading frame 28B [BC010130], Human, clone MGC:2392 IMAGE:2961444, [BC001646], Human, LIM domain only 4, clone MGC:872 IMAGE:3355972, [BC003600], S100 calcium binding protein P [BC006819], Similar to Ig kappa constant, clone MGC:12418 IMAGE:3934658, [BC005332], hyaluronoglucosaminidase 1 [AL578077], hypothetical protein [AI202106], immunoglobulin heavy constant mu [BM008087], immunoglobulin heavy constant mu [AI634950], immunoglobulin lambda joining 3 [BF338816], immunoglobulin lambda locus [M87790], IMP (inosine monophosphate) dehydrogenase 1[AL518727], interleukin 1, beta [AA577318], karyopherin alpha 2 (RAG cohort 1, importin alpha 1) [BE889289], KIAA0008 gene product [BI087140], KARP-1-binding protein [AB022659], KIAA0657 protein [BC007201], family with sequence similarity 13, member A1 [AF009202], glutamate receptor interacting protein 2 [AF052177], KIAA1727 protein [AB051514], Kruppel-like factor 4 (gut)[AI568487], lactotransferrin [BI021407], lamin B receptor [L25931], lethal giant larvae homolog 2 (Drosophila) [AK025401], leukemia inhibitory factor receptor [NM002310], lipase, gastric [NM004190], Macaque dd-4 gene for 3(20)alpha-hydroxysteroid/dihydrodiol dehydrogenase, complete cds. [AB020711], Macaque testis cDNA clone:QtsA-14970, full insert sequence. [AB070147], mammaglobin 2 [NM002407], membrane-bound transcription factor protease, site 2 [AU099021], metallothionein 1E (functional) [H72532], metallothionein 1X[BF130769], methylmalonate-semialdehyde dehydrogenase [BG743099], minichromosome maintenance deficient (S. cerevisiae) 2 (mitotin) [BG491883], mucin 5, subtypes A and C, tracheobronchial/gastric [AW867962], myeloid differentiation primary response gene (88) [AW965179], myosin X [AU151619], non-metastatic cells 1, protein [NM23A] expressed in [BG753664], osteoblast specific factor 2 (fasciclin I-like) [N71912], pancreatitis-associated protein [NM002580], peptidylprolyl isomerase F (cyclophilin F) [AL531948], period (Drosophila) homolog 1 [BE615751], phosphatidic acid phosphatase type 2B [AW131816], phosphoinositide-3-kinase, class 2, gamma polypeptide [BG196286], phosphorylase, glycogen; liver (Hers disease, glycogen storage disease type VI) [BE884737], pituitary tumor-transforming 1 [AW957275], platelet-derived growth factor receptor, alpha polypeptide [AW887370], plexin B2 [BC004542], potassium inwardly-rectifying channel, subfamily J, member 15 [BG288548], predicted using Genefinder~contains similarity to Pfam domain: PF00465 (Iron-containing alcohol dehydrogenases), Score=177.7, E-value=1.9e-50, N=2~cDNA EST EMBL:Z14517 comes from this gene; cDNA EST yk18d4.3 comes from this gene~c [CAA21631], proprotein convertase subtilisin/kexin type 7 [BG820292], prostate stem cell antigen (AJ297436), protein disulfide isomerase [NM006849], protein tyrosine phosphatase, receptor-type, Z polypeptide 1 [BI488535], patative [BAB32258], RAB27A, member SAS oncogene family [AL120794] RAD21 (S. pombe) homolog [BF696386], RAP1, GTPase activating protein 1 [M64788], Ras homolog enriched in brain 2 [AW519065], RecQ protein-like 5 [AI123482], regenerating islet-derived 1 alpha (pancreatic stone protein, pancreatic thread protein) [BI713022], replication factor C (activator 1) 2 (40 ku) [BE295474], replication factor C (activator 1) 5 (36.5 ku) [AL525427], ribonuclease, RNase A family, 1 (pancreatic) [BI596306], ribosomal protein L12 [BG471683], ribosomal protein S10 [BC004334], ribosomal protein S12 [AA314429], ribosomal protein S15a [BG285655], ribosomal protein S20 [BG684583], S100 calcium-binding protein P [AI148603], pleckstrin homology domain containing, family E (with leucine rich repeats) member 1 [AB011178], selenium binding protein 1 [BC009084], serine/threonine kinase 15 [AI038260], Sjogren syndrome antigen B (autoantigen La) [AA479280], small nuclear ribonucleoprotein D2 polypeptide (16.5 ku) [BM015197], sodium channel, nonvoltage-gated 1 alpha [BI160595], sodium channel, nonvoltage-gated 1, beta (Liddle syndrome) [BI763841], sodium channel, nonvoltage-gated 1, beta (Liddle syndrome) [AI683977], somatostatin [BI713744], stem-loop (histone) binding protein [AW150631], trefoil factor 2 (spasmolytic protein 1) [BI517365], tumor necrosis factor (ligand) superfamily, member 13BG [272792], UDP-glucose ceramide glucosyltransferase [AI609116], vaccinia related kinase 1 [AA312869], v-akt murine thymoma viral oncogene homolog 2 [AU130605], vascular cell adhesion molecule 1 [AL037837]

[ ]: GeneBank accession number

previous reports. In addition, we verified expression status of trefoil factor 3 in GC by immunohistochemical staining (Figure 2). Comparison of the tumor group and non-cancerous group with these 504 genes showed that there were 3 subgroups of GC (Figure 3) that did not correspond to any current classification system, including Lauren's classification.

DISCUSSION

The completion of human genome sequencing has facilitated high-throughput quantitative analysis of gene expression alterations. Such transcriptome analyses utilizing DNA microarray offer a new avenue to understand the biological diversity of human cells and

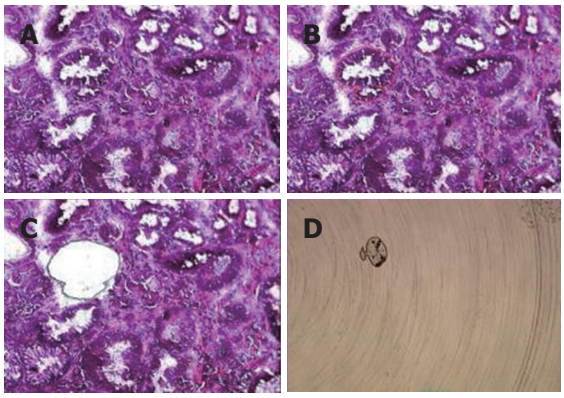

Figure 1 A representative example demonstrating precisely procurement of target cells from admixture of different cells by laser capture microdissection (Hematoxylin & eosin staining, X 100) (**A, B, C, D**).

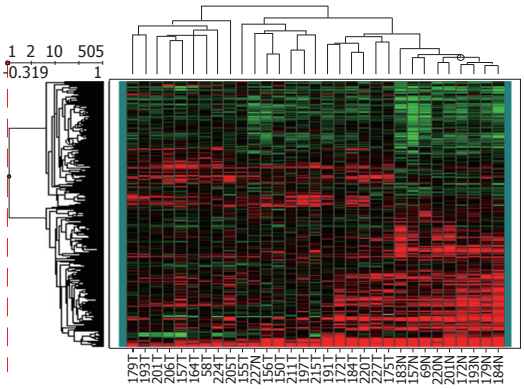

Figure 3 Molecular classification of gastric cancer into 3 subgroups by 504 differentially expressed genes found by microarray.

tumors. Microarray analysis of malignancies from other organ sites has revealed molecular subtypes of tumors that are histologically indistinguishable and clinically informative[26-29]. To elucidate the molecular portrait of GC, we extracted RNA from microdissected normal gastric epithelium and corresponding tumor cells for examining gene expression profiles in the cells as they exist *in vivo*. Coupling with common "reference" sample as an internal standard, we found this strategy is a rapid and efficient way to identify differentially expressed genes and can readily distinguish GC into 3 molecular subtypes.

Most previous gene expression studies on GCs have used whole tumor tissues[10-21]. The overall information of genetic alterations with this approach was comprehensive but might be hampered by the fact that stromal and inflammatory cells usually intermingled with cancer cells. Therefore, special procedures to isolate cancer cells from heterogeneous tissues are mandatory. To overcome the obstacles of the contamination of cancer cells with wrong cells, we adopted LCM. LCM allows for the rapid, reliable and accurate procurement of cells from the specific microscopic regions of tissue sections under direct visualization. The proportion of contaminated cells with this method is estimated to the less than 0.3%[30]. It thus affords the opportunity to perform molecular genetic

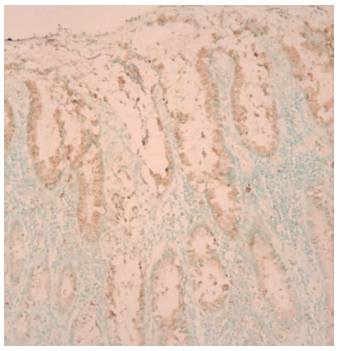

Figure 2 A representative example of increased expression of trefoil factor 1 in a patient with intestinal type gastric cancer (immunohistochemical staining, X 100).

analysis of pure populations of malignant cells in their native tissue environment.

However, the RNAs obtained from procured cancer cells were not sufficient to hybridize with cDNA microarray. The recent advances of amplification techniques have provided the key to resolve this problem[31]. In particular, linear RNA amplification could not only provide sufficient RNAs for further analyses but also preserve the overall genetic information.

By the successfully developed techniques of LCM, linear amplification of RNA and cDNA microarray, we found that 504 genes could distinguish cancerous and non-cancerous groups with more than 99% accuracy. Of the genes discovered, some have known association with gastrointestinal cancers. Among them, trefoil factors 1, 2, and 3 were in the list. Furthermore, the expression patterns of these 3 genes were in agreement with previous reports in GCs[32]. These results confirmed our microarray data indirectly. Moreover, we selected trefoil factor 1 for further verification by immunohistochemical staining and the data were also consistent. The remaining novel genes differentially expressed in cancerous and non-cancerous tissues provided a starting point for identification of new biomarkers in GC and are worthy of future in-depth studies to elucidate their roles in GCs.

By comparing expression patterns of the identified 504 genes in individual tissues, we noticed a phylogenetic tree that not only showed clear segregation between normal and cancerous gastric tissues but also assorted GC into 3 subtypes. Although most previous studies suggested classification of GC based on gene expression largely recapitulate that based on histology[33], we did not find such correlation in our system. This discrepancy may be, in part, due to methodological differences and small case numbers in our study. In addition, one intriguing possibility is that tumors sharing similar genes expression profile arise from a common molecular genetic lesion but present with different histological appearances[16,18]. Enrollment of a larger number of tumor samples with well-documented information is under way to further clarify the clinicopathological significance of this molecular classification.

Another unique feature distinct from previous

microarray studies of GC is that we hybridized each tumor or normal mRNA against a "universal reference" of mRNA. This concept was advocated by investigators from Stanford University, who prepared cDNA for microarray experiments from a pool of mRNA isolated from 11 different cells lines[29]. Although normal epithelium from a spectrum of histological changes from atrophy to metaplasia could be easily microdissected by LCM, the so-called normal epithelium adjacent to tumor may not be similar to epithelium distant from the tumor at the molecular level. Therefore, the definition of control normal tissue will need to be carefully assessed in future global analysis of gene expression.

In conclusion, combined LCM and cDNA microarray is a rapid and efficient way to identify differentially expressed genes and can readily distinguish GCs by their molecular portraits. Further characterization of the genes identified in this study and prospective translational studies to determine their potential clinical value may lead to a deeper insight into the pathogenesis of GCs and facilitate the development of novel biomarkers for diagnostic and therapeutic applications.

REFERENCES

1 **Parkin DM**, Bray FI, Devesa SS. Cancer burden in the year 2000. The global picture. *Eur J Cancer* 2001; **37** Suppl 8: S4-S66
2 **Wu MS**, Lin JT, Lee WJ, Yu SC, Wang TH. Gastric cancer in Taiwan *J Formos Med Assoc* 1994; **93** Suppl 2: S77-S89
3 **Lin JT**, Wu MS, Wang JT, Shun CT, Chen CJ, Wang TH. Clinicopathologic study of 208 patients with early gastric cancer in Taiwan: a comparison between Eastern and Western countries. *J Gastroenterol Hepatol* 1994; **9**: 344-349
4 **Fuchs CS**, Mayer RJ. Gastric carcinoma. *N Engl J Med* 1995; **333**: 32-41
5 **Wright PA**, Quirke P, Attanoos R, Williams GT. Molecular pathology of gastric carcinoma: progress and prospects. *Hum Pathol* 1992; **23**: 848-859
6 **Stemmermann G**, Heffelfinger SC, Noffsinger A, Hui YZ, Miller MA, Fenoglio-Preiser CM. The molecular biology of esophageal and gastric cancer and their precursors: oncogenes, tumor suppressor genes, and growth factors. *Hum Pathol* 1994; **25**: 968-981
7 **Tahara E**, Semba S, Tahara H. Molecular biological observations in gastric cancer. *Semin Oncol* 1996; **23**: 307-315
8 **Emmert-Buck MR**, Bonner RF, Smith PD, Chuaqui RF, Zhuang Z, Goldstein SR, Weiss RA, Liotta LA. Laser capture microdissection. *Science* 1996; **274**: 998-1001
9 **Alizadeh AA**, Ross DT, Perou CM, van de Rijn M. Towards a novel classification of human malignancies based on gene expression patterns. *J Pathol* 2001; **195**: 41-52
10 **Hippo Y**, Taniguchi H, Tsutsumi S, Machida N, Chong JM, Fukayama M, Kodama T, Aburatani H. Global gene expression analysis of gastric cancer by oligonucleotide microarrays. *Cancer Res* 2002; **62**: 233-240
11 **Ji J**, Chen X, Leung SY, Chi JT, Chu KM, Yuen ST, Li R, Chan AS, Li J, Dunphy N, So S. Comprehensive analysis of the gene expression profiles in human gastric cancer cell lines. *Oncogene* 2002; **21**: 6549-6556
12 **Sakakura C**, Hagiwara A, Nakanishi M, Shimomura K, Takagi T, Yasuoka R, Fujita Y, Abe T, Ichikawa Y, Takahashi S, Ishikawa T, Nishizuka I, Morita T, Shimada H, Okazaki Y, Hayashizaki Y, Yamagishi H. Differential gene expression profiles established from primary tumor and malignant ascites. *Br J Cancer* 2002; **87**: 1153-1161
13 **Inoue H**, Matsuyama A, Mimori K, Ueo H, Mori M. Prognostic score of gastric cancer determined by cDNA microarray. *Clin Cancer Res* 2002; **8**: 3475-3479
14 **Weiss MM**, Kuipers EJ, Postma C, Snijders AM, Siccama I, Pinkel D, Westerga J, Meuwissen SG, Albertson DG, Meijer GA. Genomic profiling of gastric cancer predicts lymph node status and survival. *Oncogene* 2003; **22**: 1872-1879
15 **Boussioutas A**, Li H, Liu J, Waring P, Lade S, Holloway AJ, Taupin D, Gorringe K, Haviv I, Desmond PV, Bowtell DD. Distinctive patterns of gene expression in premalignant gastric mucosa and gastric cancer. *Cancer Res* 2003; **63**: 2569-2577
16 **Tay ST**, Leong SH, Yu K, Aggarwal A, Tan SY, Lee CH, Wong K, Visvanathan J, Lim D, Wong WK, Soo KC, Kon OL, Tan P. A combined comparative genomic hybridization and expression microarray analysis of gastric cancer reveals novel molecular subtypes. *Cancer Res* 2003; **63**: 3309-3316
17 **Suganuma K**, Kubota T, Saikawa Y, Abe S, Otani Y, Furukawa T, Kumai K, Hasegawa H, Watanabe M, Kitajima M, Nakayama H, Okabe H. Possible chemoresistance related genes for gastric cancer detected by cDNA microarray. *Cancer Sci* 2003; **94**: 355-359
18 **Kim B**, Bang S, Lee S, Kim S, Jung Y, Lee C, Choi K, Lee SG, Lee K, Lee Y, Kim SS, Yeom YI, Kim YS, Yoo HS, Song K, Lee I. Expression profiling and subtype-specific expression of stomach cancer. *Cancer Res* 2003; **63**: 8248-8255
19 **Kang HC**, Kim IJ, Park JH, Shin Y, Ku JL, Jung MS, Yoo BC, Kim HK, Park JG. Identification of genes with differential expression in acquired drug-resistant gastric cancer cells using high-density oligonucleotide microarrays. *Clin Cancer Res* 2004; **10**: 272-284
20 **Kim HK**, Choi IJ, Kim HS, Kim JH, Kim E, Park IS, Chun JH, Kim IH, Kim IJ, Kang HC, Park JH, Bae JM, Lee JS, Park JG. DNA microarray analysis of the correlation between gene expression patterns and acquired resistance to 5-FU/cisplatin in gastric cancer. *Biochem Biophys Res Commun* 2004; **316**:781-789
21 **Nørsett KG**, Laegreid A, Midelfart H, Yadetie F, Erlandsen SE, Falkmer S, Grønbech JE, Waldum HL, Komorowski J, Sandvik AK. Gene expression based classification of gastric carcinoma. *Cancer Lett* 2004; **210**: 227-237
22 **Hasegawa S**, Furukawa Y, Li M, Satoh S, Kato T, Watanabe T, Katagiri T, Tsunoda T, Yamaoka Y, Nakamura Y. Genome-wide analysis of gene expression in intestinal-type gastric cancers using a complementary DNA microarray representing 23,040 genes. *Cancer Res* 2002; **62**: 7012-7017
23 **Mori M**, Mimori K, Yoshikawa Y, Shibuta K, Utsunomiya T, Sadanaga N, Tanaka F, Matsuyama A, Inoue H, Sugimachi K. Analysis of the gene-expression profile regarding the progression of human gastric carcinoma. *Surgery* 2002; **131**: S39-S47
24 **Haraguchi N**, Inoue H, Mimori K, Tanaka F, Utsunomiya T, Yoshikawa K, Mori M. Analysis of gastric cancer with cDNA microarray. *Cancer Chemother Pharmacol* 2004; **54 Suppl 1**: S21-S24
25 **Wu MS**, Shun CT, Wang HP, Lee WJ, Wang TH, Lin JT. Loss of pS2 protein expression is an early event of intestinal-type gastric cancer. *Jpn J Cancer Res* 1998; **89**: 278-282
26 **Hedenfalk I**, Duggan D, Chen Y, Radmacher M, Bittner M, Simon R, Meltzer P, Gusterson B, Esteller M, Kallioniemi OP, Wilfond B, Borg A, Trent J, Raffeld M, Yakhini Z, Ben-Dor A, Dougherty E, Kononen J, Bubendorf L, Fehrle W, Pittaluga S, Gruvberger S, Loman N, Johannsson O, Olsson H, Sauter G. Gene-expression profiles in hereditary breast cancer. *N Engl J Med* 2001; **344**: 539-548
27 **Alizadeh AA**, Eisen MB, Davis RE, Ma C, Lossos IS, Rosenwald A, Boldrick JC, Sabet H, Tran T, Yu X, Powell JI, Yang L, Marti GE, Moore T, Hudson J, Lu L, Lewis DB, Tibshirani R, Sherlock G, Chan WC, Greiner TC, Weisenburger DD, Armitage JO, Warnke R, Levy R, Wilson W, Grever MR, Byrd JC, Botstein D, Brown PO, Staudt LM. Distinct types of diffuse large B-cell lymphoma identified by gene expression profiling. *Nature* 2000; **403**: 503-511
28 **Bittner M**, Meltzer P, Chen Y, Jiang Y, Seftor E, Hendrix M,

Radmacher M, Simon R, Yakhini Z, Ben-Dor A, Sampas N, Dougherty E, Wang E, Marincola F, Gooden C, Lu**eders J,** Glatfelter A, Pollock P, Carpten J, Gillanders E, Leja D, Dietrich K, Beaudry C, Berens M, Alberts D, Sondak V. Molecular classification of cutaneous malignant melanoma by gene expression profiling. *Nature* 2000; **406**: 536-540

29 **Perou CM,** Sørlie T, Eisen MB, van de Rijn M, Jeffrey SS, Rees CA, Pollack JR, Ross DT, Johnsen H, Akslen LA, Fluge O, Pergamenschikov A, Williams C, Zhu SX, Lønning PE, Børresen-Dale AL, Brown PO, Botstein D. Molecular portraits of human breast tumours. *Nature* 2000; **406**: 747-752

30 **Nakamura T**, Furukawa Y, Nakagawa H, Tsunoda T, Ohigashi H, Murata K, Ishikawa O, Ohgaki K, Kashimura N, Miyamoto M, Hirano S, Kondo S, Katoh H, Nakamura Y, Katagiri T. Genome-wide cDNA microarray analysis of gene expression profiles in pancreatic cancers using populations of tumor cells and normal ductal epithelial cells selected for purity by laser microdissection. *Oncogene* 2004; **23**: 2385-2400

31 **Aoyagi K**, Tatsuta T, Nishigaki M, Akimoto Si, Tanabe C, Omoto Y, Hayashi S, Sakamoto H, Sakamoto M, Yoshida T, Terada M, Sasaki H. A faithful method for PCR-mediated global mRNA amplification and its integration into microarray analysis on laser-captured cells. *Biochem Biophys Res Commun* 2003; **300**: 915-920

32 **Katoh M**. Trefoil factors and human gastric cancer (review). *Int J Mol Med* 2003; **12**: 3-9

33 **Jinawath N**, Furukawa Y, Hasegawa S, Li M, Tsunoda T, Satoh S, Yamaguchi T, Imamura H, Inoue M, Shiozaki H, Nakamura Y. Comparison of gene-expression profiles between diffuse- and intestinal-type gastric cancers using a genome-wide cDNA microarray. *Oncogene* 2004; **23**: 6830-6844

Science Editor Guo SY **Language Editor** Elsevier HK

PO Box 2345, Beijing 100023, China
www.wjgnet.com
wjg@wjgnet.com

ELSEVIER

World J Gastroenterol 2005;11(47):7413-7417
World Journal of Gastroenterology ISSN 1007-9327

• *BASIC RESEARCH* •

Effect of synbiotics on intestinal microflora and digestive enzyme activities in rats

Suh-Ching Yang, Ju-Yen Chen, Huey-Fang Shang, Ting-Ying Cheng, Su Chen Tsou, Jiun-Rong Chen

Suh-Ching Yang, Ju-Yen Chen, Jiun-Rong Chen, School of Nutrition and Health Sciences, College of Public Health and Nutrition, Taipei Medical University, Taipei, Taiwan, China
Ju-Yen Chen, Department of Microbiology and Immunology, School of Medicine, Taipei Medical University, Taipei, Taiwan, China
Ting-Ying Cheng, Su Chen Tsou, Viva Life Science/Westar Nutrition, Costa Mesa, CA, United States
Supported by Viva Life Science/Westar Nutrition, Costa Mesa, CA, United States
Correspondence to: Jiun-Rong Chen, School of Nutrition and Health Sciences, College of Public Health and Nutrition, Taipei Medical University, 250 Wu-Hsing Street, Taipei 110, Taiwan, China. sokei@tmu.edu.tw
Telephone: +886-2-2736-1661 Fax: +886-2-2737-3112
Received: 2005-03-31 Accepted: 2005-05-12

Abstract

AIM: To investigate the effect of synbiotics, i.e. probiotics and prebiotics mixture, on the gut microbial ecology and digestive enzyme activities in rats.

METHODS: Forty-eight SD rats weighing about 280 g were used in this study. Rats were divided into three groups according to the contents of probiotics and prebiotics mixture in the feed as control, low and high dose groups. The duration of the experiment was 8 wk.

RESULTS: Compared with the control group, the fecal *Lactobacillus* and *Bifidobacterium* counts were significantly increased and the fecal Coliform organism counts were markedly reduced in the low and high dose groups. Concerning the digestive enzyme activity of jejunum, only lactase activity increased in low dose group. However, significant increase of lipase, lactase, sucrase, and isomaltase activities were observed in high dose group.

CONCLUSION: Intake of low and high dosages of probiotics and prebiotics mixture significantly improved the ecosystem of the intestinal tract by increasing the probiotics population and digestive enzyme activities in rats.

Key words: Synbiotics; Intestinal microflora; Digestive enzyme activity

Yang SC, Chen JY, Shang HF, Cheng TY, Tsou SC, Chen JR. Effect of synbiotics on intestinal microflora and digestive enzyme activities in rats. *World J Gastroenterol* 2005; 11(47): 7413-7417
http://www.wjgnet.com/1007-9327/11/7413.asp

INTRODUCTION

Gastrointestinal microfloras contain hundred different types of microorganisms and are a biologically important component of the body. According to the effect of microbial ecosystem of the human gastrointestinal tract on health, they are divided into two groups: one is probiotics and the other is harmful bacteria. Probiotics, defined as a live microbial food supplement, benefits the host by improving its intestinal microbial balance[1]. Modern perspectives on consumption of probiotics supplements are aimed at consumer well-being, using products enriched with acid bacteria (*Lactobacilli*), particularly *Bifidobacteria*, *Lactobacillus acidophilus* and *Lactobacillus bulgaricus,* and *Streptococcus thermophilus*. Through a process of fermentation, the metabolites of these complex microbes produce varying consequences on host health[2,3]. Health claims associated with probiotics supplements include prevention of diarrhea and colitis, antitumorigenic effects, and cholesterol reduction[4-8].

In contrast, prebiotics is a nondigestible nutritional compound (e.g. inulin, oligosaccharide, dietary fiber) that selectively stimulates the growth of endogenous lactic acid bacteria and *Bifidobacteria* to improve the health of the host[9]. The fermentability and bifidogenic effect of prebiotics have been confirmed with *in vitro* and *in vivo* studies[10-13].

The concept of synbiotics has been proposed recently to characterize colonic food with probiotics and prebiotics properties as health enhancing functional food[14]. Research and development of synbiotic products have been increasingly focusing on evidence of functional benefits including resistance to infection, antibacterial activity, and improved immune status[14].

Although there are numerous researches of biotic products focusing on balanced colonic microflora, few reports investigated into the intestinal digestive enzyme activities. Therefore, the role of enteric feeding and the microenvironment in host defense, the effect of synbiotics, i.e. probiotics and prebiotics mixture, on the gut microbial ecology and digestive enzyme activities in rats were investigated in this study.

Table 1 The composition of synbiotics powder[1]

	Amount/7.5 g
Thiamin (as thiamin hydrochloride)	0.375 mg
Riboflavin	0.425 mg
Niacin (as niacinamide)	5 mg
Vitamin B_6 (as pyridoxine hydrochloride)	0.5 mg
Folate (as folic acid)	100 μg
Vitamin B_{12} (as cyanocobalamin)	1.5 7 μg
Biotin	75 μg
Pantothenic acid (as d-calcium pantothenate)	2.5 mg
Inulin from chicory, powdered extract (root)	250 mg
Proprietary blend culture count	10 billion[2]
Lactobacillus acidophilus and *Lactobacillus bulgaricus*	2.7 billion
Bifidobacterium bifidum and *Bifidobacterium longum*	6.7 billion
Streptococcus thermophilus	0.6 billion

[1] FloraGuard®, Viva Life Science, Costa Mesa, CA, USA. [2] The viable count of each bacterium in powder was checked once a week.

MATERIALS AND METHODS

Animals and experimental diets

Forty-eight male SD rats (6 wk old) were purchased from the laboratory animal sources of the National Taiwan University College of Medicine. Rats were fed with a standard laboratory diet and distilled water *ad libitum*, and housed in an air-conditioned room at 23±2 °C with 12 h of light per day. Experiments were started after the rats reached a weight of about 280 g each and adapted to the individual stainless-steel cages. Rats were randomly divided into three groups of 16 animals: control, low dose and high dose groups. The control group was given 20 g laboratory rodent diet 5001 (PMI Feeds, St. Louis, MO, USA) per day. The low and high dose groups were fed with the synbiotics-containing diets, which contained 20 g/d laboratory rodent diet 5001 and low (1.5 g/kg body weight/day) or high (7.5 g/kg body weight/day) dosages of synbiotics powder (FloraGuard®, Viva Life Science, Costa Mesa, CA, USA). The composition of synbiotics powder is described in Table 1. The duration of the experiment was 8 wk.

Assessment of fecal weights and moisture

Before the rats were killed, feces were collected from each rat on the final 7 d of the experimental period. The feces were freeze-dried and weighed. The wet weight, dry weight, moisture content, and physical appearance of the feces were recorded.

Analysis of microbial ecosystem in the intestine

At 10:00 a.m., the day before the end of the experiment, all rats were anesthetized by ethyl ether inhalation and fecal samples were collected in sterile centrifuged tubes containing 9 mL of anaerobic dilution buffer (0.2% gelatin, 0.05% cysteine, and 0.0002% resazurin). Samples were brought to the laboratory within 2 h after defecation. Additionally, each sample was duplicated and inoculated onto the agar by the spread plate method for plate count determination. Ten-fold serial dilutions of the fecal samples (10^{-1}-10^{-6}) were m-ade in sterile physiological saline (9 g/L) and 50 μL was inoculated onto the following agar plates.

Total anaerobic bacteria counts

CDC anaerobe blood agar plates (Oxoid CM271, Basingstoke, Hants., UK) was used for the detection of total aerobic bacterial flora. Blood agar plates were incubated aerobically at 37 °C for 24 h.

Probiotics

Detection of *Lactobacillus* *Lactobacillus* anaerobic MRS with vancomycin and bromocresol green (LAMVAB) was used for the detection of *lactobacilli*. LAMVAB (pH 5) was prepared with MRS broth (104.4 g/L), cysteine-HCl (0.5 g/L), bromocresol green (0.05 g/L), agar (40 g/L) and vancomycin hydrochloride (>95% purity, 2 mg/mL) according to the method described previously[15]. LAMVAB agar plates were pre-reduced in the anaerobic cabinet for 24 h before the inoculation and were incubated in the anaerobic cabinet at 37 °C for 48 h after inoculation.

Plate count of viable *Bifidobacteria* Modified *Bifidobacterium* iodoacetate medium-25 (BIM-25) was used for the enumeration of bifidobacteria. All plates were incubated for 72 h at 37 °C.

Harmful bacteria

Detection of Coliform organisms Detection of Coliform organisms in fecal samples collected from rats were directly inoculated onto the Endo agar plates and incubated anaerobically in McIntosh Fildes jar at 37 °C for 48 h. Fourteen grams of dehydrated Endo agar media was dissolved in 500 mL of water and brought to a rolling boil. The media were then autoclaved at 121 °C for 15 min. Twenty milliliters of the agar was poured into the Petri plates that were sterilized under UV light and allowed to cool. The Endo agar plates were capped and stored upside down in the refrigerator for future use.

Analyses of digestive enzymes activities

Preparation of tissues After 8 wk, all rats were anesthetized by ethyl ether inhalation and killed. Blood was collected via the abdominal aorta. The small intestine was immediately removed, and then washed in ice-cold physiological saline (9 g/L NaCl). The length of the small intestine was measured. The mucosal cells of the jejunums (about 10 cm), where sucrase activity is most highly concentrated, were scraped off with a piece of glass and homogenized in ice-cold distilled water. The homogenates were centrifuged at 7 000×*g* for 10 min at 4 °C. Supernatants were transferred into new Eppendorf tubes and stored at -80 °C for further analysis.

Measurement of lipase and disaccharidase activities Lipase activity was measured with a commercial kit (lipase assay kit, LI-186, Randox Laboratories Ltd, Co.).

Sucrase, isomaltase and lactase activities from mucosal extracts were measured according to the modified method of Dahlqvist with some modifications[16]. Substrate

Table 2 Effect of synbiotics on feed intake in rats[1]

Wk	Control (g)	Low dose (g)	High dose (g)
1	19.9±0.6	19.4±1.7	19.8±0.7
2	20.0±0.1	19.6±1.4	19.9±0.2
3	19.9±0.4	19.9±0.2	19.9±0.2
4	18.5±1.5	18.1±0.1	18.9±0.2
5	19.9±0.3	19.9±0.3	20.0±0.4
6	19.9±0.1	19.8±0.4	19.8±0.5
7	20.0±0.1	20.0±0.1	19.8±0.8
8	19.9±0.3	20.0±0.3	19.4±0.3

[1]Mean±SD of 16 rats for each group. Mean in a horizontal row with a same superscript letter is not significantly different by one way ANOVA.

Table 3 Effect of synbiotics on intestinal microorganisms in rats[1]

	Control	Low dose	High dose
Total anaerobic bacteria counts (log CFU/g)	9.26±0.30	8.95±0.37	8.95±0.18
Lactobacillus (log CFU[2] /g)	7.42±0.44	9.35±0.64[a]	9.41±0.55[c]
Bifidobacteria (log CFU/g)	8.52±0.59	9.60±0.26[e]	9.40±0.39[g]
Coliform organisms (log CFU/g)	8.44±0.74	6.70±0.57	7.13±0.51

[1]Mean±SD of 16 rats for each group. [a]P<0.05 *vs* control, [c]P<0.05 *vs* control, [e]P<0.05 *vs* control, [g]P<0.05 *vs* control. [2]CFU: colony forming unit.

buffer solution containing maltose, sucrose, or lactose was incubated with a diluted sample for 60 min at 37 °C. The reaction was terminated by adding *O*-dianisidine, and released glucose was determined by means of a Tris glucose-oxidase (TGO) procedure (Tris-HCl, 100 mL, 0.5 mol/L, pH 7.0; glucose oxidase, 1.7 mg; peroxidase, 0.5 mg and Triton X-100, 1 mL) and the samples were analyzed by spectrophotometry at 420 nm. One unit of disaccharidase activity was defined as the amount of the enzyme that can hydrolyze 1 μmol/L of substrate equivalent per minute under the assay conditions. The specific disaccharidase activities were expressed as units/g protein.

Total protein concentrations Total protein concentrations of samples were spectrophotometrically estimated by the method of Biuret with bovine serum albumin as a standard.

Statistical analysis

All data were expressed as the mean±SD. One-way analysis of variance and Fisher's least significant difference test were used to compare the differences of means using the SAS software (version 8.2, SAS Institute, Cary, NC, USA). Statistical significance was assigned at the 0.05 level.

RESULTS

Feed intake and body weight changes

There was no difference in the feed intake in each group (Table 2). Body weight changes are shown in Figure 1. There were no changes in body weight among the three groups until 5 wk. However, the rats of high dose group showed significantly decreased body weights, as compared with the rats of control or low dose groups at the 6th, 7th and 8th wk.

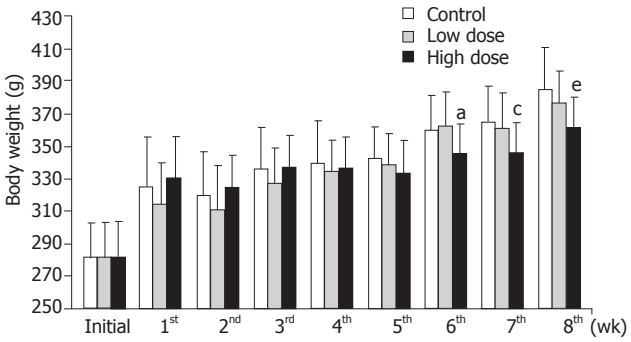

Figure 1 Effect of synbiotics on body weight changes in rats. All results are expressed as mean and standard errors of 16 rats. [a]P<0.05 *vs* control, [c]P<0.05 *vs* control, [e]P<0.05 *vs* control.

Fecal weight and moisture

The fecal weight and moisture in the low dose group did not differ at the 4th and 8th wk, in contrast to those of the control group (Figure 2). Although, the fecal weight and moisture in high dose group did not change at the 4th wk, they significantly increased at the 8th wk (Figure 2).

Microbial ecosystem in the intestine

Table 3 presents the intestinal microorganisms in each group. There was no change in anaerobic bacteria counts in each group. In addition, the *Lactobacillus* and *Bifidobacteria* counts were significantly increased in low and high dose groups as compared with the control group. On the contrary, the count of Coliform organisms was significantly decreased in low and high groups.

Digestive enzymes activities in jejunum

As shown in Figure 3, lipase, sucrase and isomaltase activities did not change, but lactase was significantly higher in low dose group, than in control group. On the other hand, not only lipase but also disaccharidase activities significantly increased in high dose group as compared with control group (Figure 3).

DISCUSSION

In this study, the effect of synbiotics containing probiotics and prebiotics on gut microbial ecology and digestive enzyme activities were investigated.

Many researches proved that consumption of prebiotics, such as inulin, could stimulate intestinal peristalsis by means of increasing fecal bulk and moisture[9,17]. The mechanism of action has been observed that indigestible water-soluble dietary fiber may incorporate a lot of water in the intestine[9]. Inulin consists of 2-60 fructose units linked by a β-(2→1)-glycosidic linkage often with a terminal glucose unit[9]. These fructans are not hydrolyzed by the digestive enzymes in the small intestine; they reach the colon unabsorbed and are utilized selectively

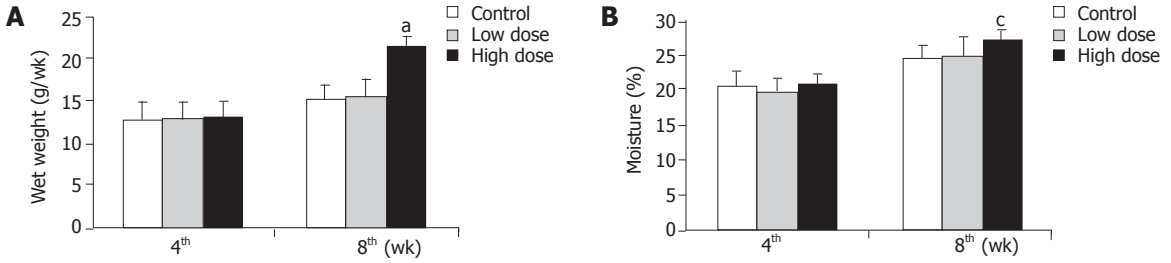

Figure 2 Effect of synbiotics on fecal weight and moisture in rats. All results are expressed as mean and standard errors of 16 rats. Feces were collected at the last one week of the experimental period. $^{a}P<0.05$ *vs* control, $^{c}P<0.05$ *vs* control (**A** and **B**).

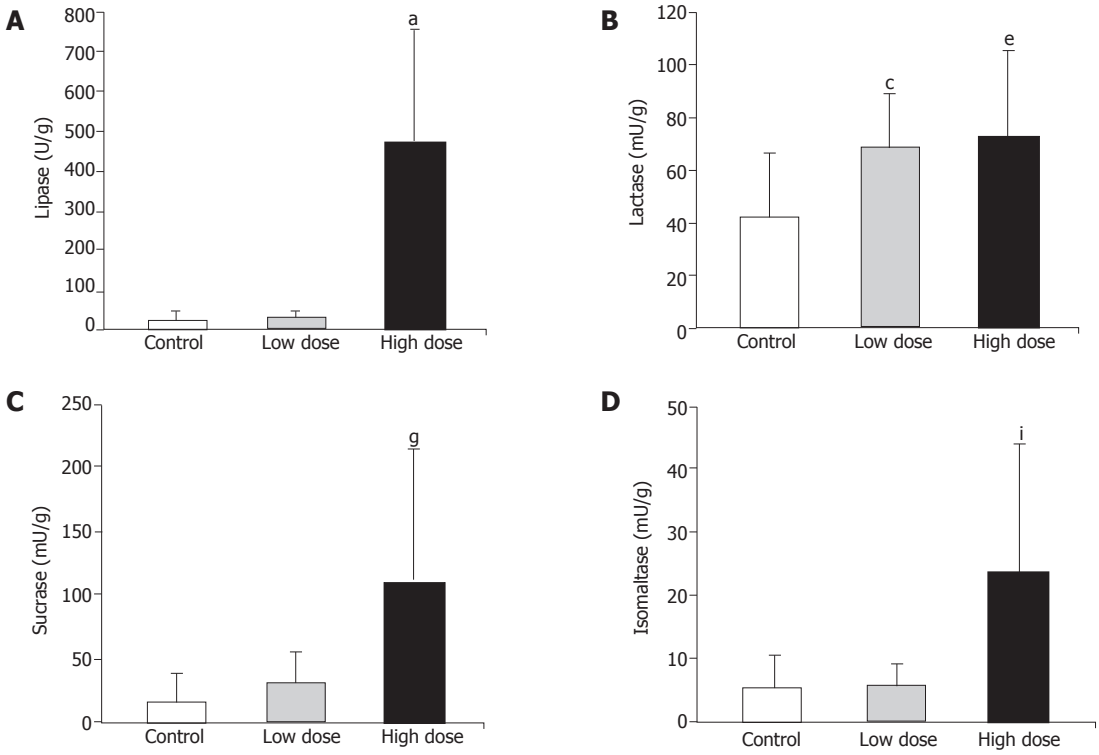

Figure 3 Effect of synbiotics on jejunal digestive enzyme activities in rats. All results are expressed as mean and standard errors of 16 rats. $^{a}P<0.05$ *vs* control, $^{c}P<0.05$ *vs* control, $^{e}P<0.05$ *vs* control, $^{g}P<0.05$ *vs* control, $^{i}P<0.05$ *vs* control (**A, B, C, D**).

as a substrate for the growth of *bifidobacteria*. The most widely accepted effect of inulin is to enlarge both the number and the proportion of fecal *bifidobacteria*[18]. These bacteria are recognized for creating conditions unfavorable for the growth of potentially pathogenic organisms, such as Coliform organism[19,20]. However, there seems to be no increase in the total bacteria number or a change in the anaerobe number[21].

In this study, rats that ingested high dose synbiotics showed lower body weight after 6 wk and higher fecal weight after 8 wk (Figures 1 and 2). Thus, it was speculated that consumption of synbiotics containing inulin may reduce body weight by means of improving the fecal bulk and moisture. Furthermore, the intestinal side-effect of synbiotics powder consumption, including diarrhea or constipation, was not observed in rats during the experimental period. This result may support the clinical application of synbiotics to weight management. In addition, it was also observed that the *Lactobacillus* and *Bifidobacteria* counts were significantly increased, but there was no change in the anaerobic bacteria counts in rats fed with low and high dose synbiotics, while the count of Coliform organisms, the harmful bacteria, were significantly reduced in rats fed with low and high dose synbiotics in this study (Table 3). These results were similar to our previous researches. There are two possibilities to explain the results. The first is the fermentation of inulin that provided short-chain fatty acids, stimulating the proliferation of *Lactobacillus* and *Bifidobacteria* and suppressing potential pathogenic organisms in the gut; and the second was the supplement of probiotics, including *Bifidobacteria*, *Lactobacillus acidophilus*, that directly improved the total number of these bacteria.

Some reported advantages of bifidobacterial proli-

feration in the human gut included the production of digestive enzymes. However, these reports were limited in *in vitro* testing[2]. Jiang *et al*[22]. proved that *Bifidobacterium longum* improved the lactose intolerance in human beings by secreting the lactase to the gut. In this study, jejunal lactase activity was improved in both low dose and high dose intake of synbiotics, and furthermore, lipase, sucrase and isomaltase activities were also increased in rats fed with high dose synbiotics (Figure 3). The causes for the improvement of digestive enzyme activity possibly are that synbiotics created the healthy gastrointestinal microbial ecology or modified the secretion of bacterial enzyme. Delzenne *et al*[23]. also suggested that polyamines may be synthesized from dietary fermentable substrates such as inulin or guar gum by bacteria. The exogenous sources of polyamines seemed to be essential for small intestinal and colonic mucosal growth and development[23]. Thus, the high digestive enzyme activities in rats fed with synbiotics powder were possibly caused by the well growth and high turnover rate of intestinal mucosa.

In conclusion, intake of low and high dose of synbiotics, which was the combination of probiotics and prebiotics, significantly improved the ecosystem of intestinal tract by increasing the probiotics population and jejunal digestive enzyme activities in rats. Based on this study, another possibility in the benefits of synbiotics is the weight management, and the clinical trial is still necessary in future.

REFERENCES

1 **Djouzi Z,** Andrieux C, Degivry MC, Bouley C, Szylit O. The association of yogurt starters with *Lactobacillus casei* DN 114.001 in fermented milk alters the composition and metabolism of intestinal microflora in germ-free rats and in human flora-associated rats. *J Nutr* 1997; **127:** 2260-2266

2 **Collins MD,** Gibson GR. Probiotics, prebiotics, and synbiotics: approaches for modulating the microbial ecology of the gut. *Am J Clin Nutr* 1999; **69:** S1052-S1057

3 **Cui HH,** Chen CL, Wang JD, Yang YJ, Sun Y, Wang YD, Lai ZS. The effects of bifidobacterium on the intestinal mucosa of the patients with ulcerative colitis. *Zhonghua Neike Zazhi* 2004; **10:** 1521-1525

4 **Duffy LC,** Zielezny MA, Riepenhoff-Talty M, Dryja D, Sayahtaheri-Altaie S, Griffiths E, Ruffin D, Barrett H, Rossman J, Ogra PL. Effectiveness of *Bifidobacterium bifidum* in mediating the clinical course of murine rotavirus diarrhea. *Pediatr Res* 1994; **35:** 690-695

5 **Yolken RH,** Ojeh C, Khatri IA, Sajjan U, Forstner JF. Intestinal mucins inhibit rotavirus replication in an oligosaccharide-dependent manner. *J Infect Dis* 1994; **169:** 1002-1006

6 **Favier C,** Neut C, Mizon C, Cortot A, Colombel JF, Mizon J. Fecal beta-D-galactosidase production and Bifidobacteria are decreased in Crohn's disease. *Dig Dis Sci* 1997; **42:** 817-822

7 **Wollowski I,** Rechkemmer G, Pool-Zobel BL. Protective role of probiotics and prebiotics in colon cancer. *Am J Clin Nutr* 2001; **73:** S451-S455

8 **Tahri K,** Crociani J, Ballongue J, Schneider F. Effects of three strains of *bifidobacteria* on cholesterol. *Lett Appl Microbiol* 1995; **21:** 149-151

9 **Gibson GR,** Beatty ER, Wang X, Cummings JH. Selective stimulation of *bifidobacteria* in the human colon by oligofructose and inulin. *Gastroenterology* 1995; **108:** 975-982

10 **Wang X,** Gibson GR. Effects of the in vitro fermentation of oligofructose and inulin by bacteria growing in the human large intestine. *J Appl Bacteriol* 1993; **75:** 373-380

11 **Fuller R,** Gibson GR. Modification of the intestinal microflora using probiotics and prebiotics. *Scand J Gastroenterol Suppl* 1997; **222:** 28-31

12 **Gallaher DD,** Stallings WH, Blessing LL, Busta FF, Brady LJ. Probiotics, cecal microflora, and aberrant crypts in the rat colon. *J Nutr* 1996; **126:** 1362-1371

13 **Campbell JM,** Fahey GC, Wolf BW. Selected indigestible oligosaccharides affect large bowel mass, cecal and fecal short-chain fatty acids, pH and microflora in rats. *J Nutr* 1997; **127:** 130-136

14 **Gibson GR,** Roberfroid MB. Dietary modulation of the human colonic microbiota: introducing the concept of prebiotics. *J Nutr* 1995; **125:** 1401-1412

15 **Hartemink R,** Rombouts FM. Comparison of media for the detection of bifidobacteria, lactobacilli and total anaerobes from faecal samples. *J Microbiol Methods* 1999; **36:** 181-192

16 **Dahlqvist A.** Assay of intestinal disaccharidases. *Enzymol Biol Clin (Basel)* 1970; **11:** 52-66

17 **Bouhnik Y,** Flourié B, Riottot M, Bisetti N, Gailing MF, Guibert A, Bornet F, Rambaud JC. Effects of fructo-oligosaccharides ingestion on fecal bifidobacteria and selected metabolic indexes of colon carcinogenesis in healthy humans. *Nutr Cancer* 1996; **26:** 21-29

18 **Roberfroid MB,** Van Loo JA, Gibson GR. The bifidogenic nature of chicory inulin and its hydrolysis products. *J Nutr* 1998; **128:** 11-19

19 **Gibson GR,** Wang X. Regulatory effects of bifidobacteria on the growth of other colonic bacteria. *J Appl Bacteriol* 1994; **77:** 412-420

20 **Roberfroid MB.** Health benefits of non-digestible oligosaccharides. *Adv Exp Med Biol* 1997; **427:** 211-219

21 **Roberfroid MB.** Prebiotics and probiotics: are they functional foods? *Am J Clin Nutr* 2000; **71:** 1682S-1687S; discussion S1688-1690

22 **Jiang T,** Mustapha A, Savaiano DA. Improvement of lactose digestion in humans by ingestion of unfermented milk containing Bifidobacterium longum. *J Dairy Sci* 1996; **79:** 750-757

23 **Delzenne NM,** Kok N, Deloyer P, Dandrifosse G. Dietary fructans modulate polyamine concentration in the cecum of rats. *J Nutr* 2000; **130:** 2456-2460

Science Editor Ma JY and Guo SY **Language Editor** Elsevier HK

PO Box 2345, Beijing 100023, China
www.wjgnet.com
wjg@wjgnet.com

ELSEVIER

World J Gastroenterol 2005;11(47):7418-7429
World Journal of Gastroenterology ISSN 1007-9327

• *BASIC RESEARCH* •

Hepatocyte cytoskeleton during ischemia and reperfusion - influence of ANP-mediated p38 MAPK activation

Melanie Keller, Alexander L Gerbes, Stefanie Kulhanek-Heinze, Tobias Gerwig, Uwe Grützner, Nico van Rooijen, Angelika M Vollmar, Alexandra K Kiemer

Melanie Keller, Stefanie Kulhanek-Heinze, Tobias Gerwig, Angelika M Vollmar, Alexandra K Kiemer, Department of Pharmacy, Centre of Drug Research, University of Munich, Butenandtstr. 5-13, 81377 Munich, Germany
Alexander L Gerbes, Tobias Gerwig, Alexandra K Kiemer, Department of Medicine II, Klinikum Großhadern, University of Munich, Marchionistr. 17, 81377 Munich, Germany
Uwe Grützner, Institute for Surgical Research, Klinikum Großhadern, University of Munich, Marchionistr. 17, 81377 Munich, Germany
Nico van Rooijen, Vrije Universiteit, VUMC, Department of Molecular Cell Biology, Faculty of Medicine, 1081 BT Amsterdam, The Netherlands
Supported by the Deutsche Forschungsgemeinschaft, DFG-FOR 440/1. M.K. was supported by the LMU Munich, grant GVBI. S.527
Correspondence to: Alexandra K Kiemer, PhD, Professor of Pharmaceutical Biology, Saarland University, P.O. Box 15 11 50, D-66041 Saarbrücken,
Germany. pharm.bio.kiemer@mx.uni-saarland.de
Telephone: +49-681-302-57301 Fax: +49-681-302-57302
Received: 2005-01-31 Accepted: 2005-04-18

Abstract

AIM: To determine functional consequences of this activation, whereby we focused on a potential regulation of the hepatocyte cytoskeleton during ischemia and reperfusion.

METHODS: For *in vivo* experiments, animals received ANP (5 μg/kg) intravenously. In a different experimental setting, isolated rat livers were perfused with KH-buffer ±ANP (200 nmol/L)±SB203580 (2 μmol/L). Livers were then kept under ischemic conditions for 24 h, and either transplanted or reperfused. Actin, Hsp27, and phosphorylated Hsp27 were determined by Western blotting, p38 MAPK activity by *in vitro* phosphorylation assay. F-actin distribution was determined by confocal microscopy.

RESULTS: We first confirmed that ANP preconditioning leads to an activation of p38 MAPK and observed alterations of the cytoskeleton in hepatocytes of ANP-preconditioned organs. ANP induced an increase of hepatic F-actin after ischemia, which could be prevented by the p38 MAPK inhibitor SB203580 but had no effect on bile flow. After ischemia untreated livers showed a translocation of Hsp27 towards the cytoskeleton and an increase in total Hsp27, whereas ANP preconditioning prohibited translocation but caused an augmentation of Hsp27 phosphorylation. This effect is also mediated via p38 MAPK, since it was abrogated by the p38 MAPK inhibitor SB203580.

CONCLUSION: This study reveals that ANP-mediated p38 MAPK activation leads to changes in hepatocyte cytoskeleton involving an elevation of phosphorylated Hsp27 and thereby for the first time shows functional consequences of ANP-induced hepatic p38 MAPK activation.

Key words: Hormonal preconditioning; Atrial natriuretic peptide; Hsp 27; Actin; Polymerization

Keller M, Gerbes AL, Kulhanek-Heinze S, Gerwig T, Grützner U, van Rooijen N, Vollmar AM, Kiemer AK. Hepatocyte cytoskeleton during ischemia and reperfusion – influence of ANP-mediated p38 MAPK activation. *World J Gastroenterol* 2005; 11(47): 7418-7429
http://www.wjgnet.com/1007-9327/11/7418.asp

INTRODUCTION

Ischemia/reperfusion injury (IRI) remains a serious problem after liver surgery or liver transplantation, as it is a major cause of primary nonfunction or dysfunction of the graft[1-3]. In previous studies, we could demonstrate that atrial natriuretic peptide (ANP) has protective effects on the liver *ex vivo,* as reperfusion damage in ANP-preconditioned organs after cold and warm ischemia was significantly reduced[4-6]. Recently, Cottart *et al*[7]. also demonstrated beneficial properties of the peptide on the liver after ischemia *in vivo*. We have previously shown that preconditioning with ANP increases p38 mitogen activated kinase (MAPK) activity in the liver[8]. Enhanced p38 MAPK activity was reported to contribute to the protection against hepatic IRI in models of ischemic preconditioning (IPC)[9,10]. Furthermore, other groups assigned an important role to p38 MAPK in protection against IRI in the heart[11,12].

In contrast, ANP's cytoprotective effects in post-ischemic livers are independent of an activation of the p38 MAPK but are mediated via an activation of protein kinase A[13]. Accordingly, the functional significance of an ANP-

mediated p38 MAPK activation in the liver after ischemia/reperfusion (I/R) remains unknown. We therefore studied a potential functional role of p38 MAPK in the regulation of the hepatocyte cytoskeleton following I/R.

Structural alterations of the cytoskeleton, such as changes of cell shape of hepatocytes, sinusoidal endothelial cells (SEC), and platelets have been reported to cause disturbances of intracellular transport processes, cell motility, and microcirculation following I/R leading to dysfunction of the organ (for review see Refs.[14-16]). The subcellular distribution of filamentous actin (F-actin), being an important component of the cytoskeleton, as well as the balance between F-actin and monomeric G-actin seem to largely determine the functional outcome[17-19]. In liver cells F-actin forms microfilaments, which are involved in intracellular transport processes, exo- and endocytosis, maintenance of cell shape, and canalicular motility responsible for bile flow[14,18,19]. They are located particularly around the bile canaliculi exhibiting regulatory functions on bile secretion[17,20], but also in the apical membrane region of hepatocytes ensuring stability and mobility[21]. In hepatocytes, a decrease in hepatic F-actin content determines inhibition of store-operated calcium-channels (SOCs), disruption of the organization of the endoplasmic reticulum, and functional disturbances of tight junctions[19,22,23]. Cytoskeletal disruption caused by the administration of phalloidin or by chemical hypoxia results in decreased bile flow and plasma membrane breakdown in liver cells[15,24]. Shinohara *et al*[25]. proved that after warm ischemia *in vivo*, F-actin is reduced in rabbit livers resulting in the loss of cell-integrity and cytoplasmic transport in the liver causing damage to organelles and changes in cell morphology. The small heat shock protein Hsp27, which corresponds to Hsp25 in rodents and is able to interact with the cytoskeleton, plays an important role in the regulation of actin dynamics in other cell types[26-30]: Its phosphorylation leads to an increased conversion of monomeric G-actin into actin filaments (F-actin)[31], while unphosphorylated Hsp27 inhibits the polymerization of actin by binding to the capping end of actin filaments[32,33]. Its functions have been thoroughly investigated in the heart, suggesting an involvement of the heat shock protein in cardioprotection after IPC *in vitro* and *in vivo*[12,34].

The phosphorylation of Hsp27 is exhibited by the p38 MAPK/MAPKAPK2 pathway in different cells and organ systems, but has as yet been unknown in the liver[35-38]. As mentioned above, ANP activates the p38 MAPK in the liver. Due to the lack of knowledge about the downstream targets and functional consequences of this hepatic p38 MAPK activation by ANP, we aimed to determine a potential link to cytoskeletal alterations during I/R. Since the reported activation of p38 MAPK by ANP was detected as an early signaling event after preconditioning[8], we focused on early pre- and post-ischemic events.

MATERIALS AND METHODS

Materials

Rat ANP and SB203580-HCl were purchased from Calbiochem/Novabiochem (Bad Soden, Germany). Complete® was from Roche Diagnostics GmbH (Mannheim, Germany), recombinant murine Hsp25 and rabbit anti-Hsp25 polyclonal antibody from StressGen Biotechnologies (Victoria, Canada), rabbit anti-phospho-Hsp27 polyclonal antibody from New England Biolabs GmbH (Frankfurt, Germany), mouse anti-actin monoclonal antibody from Chemicon International (Hofheim, Germany), rabbit anti-p38 polyclonal antibody from Calbiochem-Novabiochem (Bad Soden, Germany), peroxidase conjugated goat anti-rabbit-IgG antibody from Dianova (Hamburg, Germany), and goat anti-mouse-IgG1 antibody conjugated to horseradish peroxidase from BIOZOL (Eching, Germany).

All other materials were purchased from either Sigma (Deisenhofen, Germany), or VWR international™ (Munich, Germany).

Animals

Male Sprague-Dawley rats weighing 200-300 g or male Lewis rats (donors: 207±12 g; recipients: 276±18 g body mass) were purchased from Charles River Wiga GmbH (Sulzfeld, Germany) and housed in a climatized room with a 12-h light-dark cycle. The animals had free access to chow (Sniff, Soest, Germany) and water up to the time of experiments. All animals received humane care according to the guidelines for care and use of laboratory animals. The study was registered with the local animal welfare committee.

ANP treatment

Under anesthesia Lewis rats received an intravenous infusion of ANP (5 μg/kg) or NaCl for 20 min. Thereafter, livers were excised, kept in cold UW solution (4 °C) for 24 h, transplanted into the recipient animal and reperfused for up to 2 h. At the indicated times (after 20-min perfusion, 24-h ischemia, 2-h reperfusion), livers were frozen in liquid nitrogen. Bile was collected during perfusion and reperfusion and quantified volumetrically. The bile flow was calculated per minute and gram liver tissue.

For isolated perfused rat liver experiments, Sprague-Dawley rats were anesthetized with Narcoren® (Merial, Hallbergmoos, Germany, 50 mg/kg body weight, intraperitoneally), 250 IU heparin were administered, the portal vein was cannulated, and the liver was perfused *in situ* with hemoglobin-free and albumin-free bicarbonate buffered Krebs-Henseleit (KH) solution (pH 7.4, 37 °C) gassed with 95% O_2 and 50 mL/L CO_2. The perfusion medium was pumped through the liver with a membrane pump at a constant flow rate in a non-recirculating fashion[5]. After 10 min of perfusion, ANP (200 nmol/L) was added to the perfusion buffer (depending on the treatment group), followed by an additional perfusion for 20 min. In some groups, SB203580 was added to the perfusion buffer from the beginning of perfusion followed by 30 min of perfusion. After these pretreatment procedures, livers were perfused with 30 mL of cold (4 °C) University of Wisconsin (UW) solution (DuPont Pharma

GmbH, Bad Homburg, Germany) for 1 min and stored in UW solution (4 °C) for 24 h. After this period of ischemia, the liver was reperfused with KH solution for up to 45 min. At the indicated times (after 30-min perfusion, 24 h ischemia, 45-min reperfusion), livers were frozen in liquid nitrogen.

Homogenization and fractionation of liver tissue for Western blot analysis

A fractionation protocol was employed according to published methods with minor modifications[39,40]. Briefly, 50 mg of liver tissue were homogenized in 1.5 mL of lysis buffer (50 mmol/L Tris-HCl pH 7.0, 5 mmol/L EGTA, 1 mmol/L PMSF, 1 mmol/L sodium vanadate, 40 μL Complete®) containing 1% Triton® X-100 (Roth, Karlsruhe, Germany) with a dounce homogenizer. Centrifugation at 15 000×*g* (15 min, 4 °C) delivered the cytoskeletal fraction in the pellet; supernatants representing the cytosolic fraction were cleared by ultracentrifugation (100 000×*g*, 2.5 h, 4 °C). The pellet was resuspended in SDS-containing sample buffer and the cytosolic fraction was diluted with the same sample buffer. Samples were stored at -20 °C until use for Western blot analysis.

Immunoprecipitation

Liver tissue was homogenized as described above, but not fractionated. Protein concentration was determined by the bicinchoninic acid assay method[41]. Five hundred micrograms of protein in 500 μL lysis buffer was incubated with 5 μL of primary antibody (rabbit anti-Hsp25) with shaking overnight at 4 °C. The antibody-antigen complex was precipitated by incubation with 50 μL of washed agarose-A-beads (Sigma, Deisenhofen, Germany) for 2 h, followed by centrifugation. The beads were washed thrice with cold lysis buffer and resuspended in 25 μL of 3× SDS-containing sample buffer. After addition of 25 μL 1× sample buffer, samples were boiled for 5 min at 95 °C followed by centrifugation to remove the beads. Thirty-five microliters of the supernatant for phosphorylated Hsp27 and 10 μL for total Hsp27 were used for protein detection by Western blot analysis.

Western blot analysis

Livers were homogenized, fractionated, and treated as described above. Proteins in total liver homogenates, fractionated liver samples, or immunoprecipitates were separated by SDS-PAGE[42] and, after electrophoretical transfer, visualized via binding of specific first and HRP-conjugated secondary antibodies followed by chemoluminescent detection (NEN, Cologne, Germany). Detection and quantification was performed with a Kodak image station (NEN, Cologne, Germany).

Quantification of actin content in liver fractions

After detection of either F- or G-actin in liver samples via Western blot analysis, the densitometric intensity of the corresponding bands was used to evaluate the ratio of F-resp. G-actin referred to total actin signal (F- + G-actin) in the respective sample.

Staining of tissue sections

At the indicated times, livers were snap-frozen in liquid nitrogen and cut into 6-μm sections. Slices were dried overnight at room temperature. Before staining, samples were fixed in 3% formaldehyde for 15 min, rinsed thrice with PBS (phosphate buffered saline, pH 7.4, with calcium and magnesium), and stained with 1 U of rhodamine-conjugated phalloidin (stock solution: 200 U/mL; MoBiTec, Göttingen, Germany) and Hoechst 33342. Staining was performed for 1 h by gentle shaking in a dark room (room temperature). After two more washing steps, stained liver sections were covered with Mounting Medium (DakoCytomation GmbH, Hamburg, Germany), dried overnight, and observed by confocal laser microscopy (LSM 510 Meta, Zeiss, Jena, Germany).

Kupffer cell depletion

For Kupffer cell (KC) depletion, male Sprague-Dawley rats weighing 200-300 g were anesthetized with diethyl ether. Then 900 μL of a solution containing liposome-encapsulated Cl_2MBP were administered 48 h before perfusion experiments via a single intravenous injection into the tail vein. Animals of the control group received 900 μL NaCl instead. After injection, Cl_2MBP accumulates and induces KC apoptosis. Free Cl_2MBP released from dead macrophages has an extremely short half life in the circulation and is removed by the renal system. After 2 d, the livers of Cl_2MBP- and NaCl-pretreated rats were perfused for 30 min±ANP (200 nmol/L; 20 min), snap-frozen, and stored at -85 °C until further analysis.

Immunohistological analysis

Liver slices were fixed for 24 h in buffered formalin solution, embedded in paraffin and cut into 2 μm sections. Paraffin was removed and samples were pretreated by boiling in TRS 6 (Dako, Hamburg, Germany) in the microwave. Endogenous peroxidase was blocked by treatment with aqueous H_2O_2 solution. To verify KC depletion, ED2 as KC marker (antibody from Serotec, Oxford, England) was used. Blue staining of ED2-positive cells was realized with the ChemMate™ APAAP Kit (Dako, Hamburg, Germany) based on the alkaline phosphatase-anti-alkaline phosphatase method. The Alkaline Phosphatase Substrate Kit III (Linaris, Wertheim, Germany) served as a substrate for the alkaline phosphatase. Samples were counterstained in hematoxylin solution.

In vitro phosphorylation assay

Tissue samples (100 μg) were homogenized in ice-cold lysis buffer (containing 2 mmol/L EDTA, 137 mmol/L NaCl, 10% glycerol, 2 mmol/L tetrasodium pyrophosphate, 20 mmol/L Tris, 1 % Triton® X-100, 20 mmol/L sodium glycerophosphate, 10 mmol/L sodium fluoride, 2 mmol/L sodium vanadate, 1 mmol/L PMSF, 1× Complete). Samples were centrifuged at 11 180r/min and 4 °C for 10 min and aliquots of the supernatant were used for the determination of protein concentration by the bicinchoninic acid assay method[41]. Equal amounts

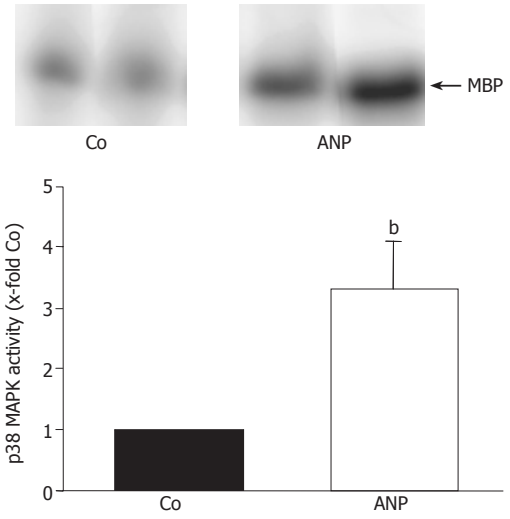

Figure 1 Effect of ANP pretreatment on p38 MAPK activity. After intravenous infusion of ANP (5 μg/kg) or NaCl (Co) for 20 min livers were snap-frozen and homogenized in lysis buffer. Following immunoprecipitation, the assay was performed as described in "Materials and methods", and samples were separated by SDS-PAGE. One representative kinase activity assay specific for p38 MAPK is shown with $n = 2$ (out of $n = 4$) for each treatment group. p38 MAPK activity in the liver homogenates is presented as 10-fold control (30-min perfusion), and is expressed as mean±SE of $n = 4$ experiments in each treatment group. $^{b}P<0.01$ *vs* control.

of protein were incubated with 1.5 μL of anti-p38 antibody shaking for 2 h. Afterwards immunoprecipitation was performed with 15 μL protein A agarose shaking overnight at 4 °C. Samples were centrifuged at 11 180×*g* (4 °C, 10 min) and pellets were washed thrice with lysis buffer and once with kinase buffer (20 mmol/L Hepes pH 7.5, 20 mmol/L $MgCl_2$, 25 mmol/L sodium glycerophosphate, 100 μmol/L sodium vanadate, 2 mmol/L DTT). Precipitates were resuspended in 20 μL kinase buffer, before 3 μL substrate solution (1 mg/mL of recombinant MBP, Sigma, Deisenhofen, Germany) and 10 μL of an ATP mix were added, the latter containing kinase buffer with 10 mCi/mL [γ^{32}P]-ATP, (3 000 Ci/mmol, Amersham, Braunschweig, Germany), 5 mmol/L ATP and 2 mol/L $MgCl_2$. The reaction mixture was then incubated for 20 min at 30 °C shaking. Phosphorylation was stopped by adding 6 μL 5× Laemmli buffer and heating for 3 min at 90 °C. Samples were separated by SDS-PAGE and band intensities quantified by phosphor-imaging (Packard, Meriden, USA). The ratio of digital light units (DLU) of respective values *vs* controls was determined.

Statistical analysis

All experiments were performed at least thrice per treatment group (5 animals per treatment). Results were expressed as mean±SE (n = number of organs). Statistical significance between the groups was determined with one sample or Student's t-test using GraphPad Prism® Version 3.02 for Windows (GraphPad Software Inc., San Diego, USA). $P<0.05$ were considered statistically significant.

RESULTS

ANP pretreatment causes increased p38 MAPK activity

In order to confirm our previous findings that preconditioning with ANP increases p38 MAPK activity in the liver[8], rats were treated intravenously with 200 nmol/L ANP or NaCl and livers were excised and homogenized in lysis buffer. Homogenates were analyzed by *in vitro* phosphorylation assay to determine the activity of p38 MAPK. As shown in Figure 1, hepatic p38 MAPK activity in livers of ANP-preconditioned rats was significantly increased compared to NaCl treated animals. These data confirm the stimulatory effect of ANP on p38 MAPK *in vivo,* with increased p38 MAPK activity after 20 min perfusion representing an early signaling event in ANP preconditioning.

ANP preconditioning leads to increased F-actin content after ischemia

As an activation of p38 MAPK has been shown to be connected with alterations of the cytoskeleton in other cells and organ systems, we investigated the polymerization state of actin in untreated *vs* ANP-perfused livers. Liver tissue was fractionated into a cytosolic (G-actin) and a cytoskeletal (F-actin) fraction in order to discriminate between the hepatic content of G- and F-actin, respectively. In untreated livers, F-actin content did not change during ischemia and reperfusion (Figures 2A and B). In contrast, ANP-preconditioned livers exhibited an obvious augmentation of F-actin after 24 h ischemia accompanied by a decrease in hepatic G-actin, which prolonged during reperfusion (Figures 2A and B). Neither I/R nor ANP preconditioning altered total hepatic actin content. This was examined by homogenizing liver tissue and analyzing samples by Western blotting without prior fractionation (Figures 2C and D).

Perfusion with SB203580 abrogates ANP-mediated increase of hepatocyte F-actin

In order to study the correlation between activation of p38 MAPK and cytoskeletal changes in untreated and ANP-preconditioned livers, we used the specific p38 MAPK inhibitor SB203580. Perfusion with 2 μmol/L SB203580 together with ANP completely abolished the enhanced hepatic F-actin content after ANP preconditioning (Figure 3A). Similarly, inhibition of p38 MAPK by SB203580 abrogated the decrease of G-actin in ANP pretreated liver homogenates, so that G-actin content in these samples resembled untreated controls (Figure 3B). Perfusion with the inhibitor alone did not affect the distribution of cytosolic G- and cytoskeletal F-actin in the liver (Figures 3A and B).

Changes in F-actin by ANP detected by Western blot analysis were confirmed by staining of tissue sections. Staining with rhodamine-conjugated phalloidin, which specifically binds to F-actin, showed a low fluorescence in tissue sections of untreated livers, which correlated with a marginal F-actin content (Figure 4A). Pretreatment

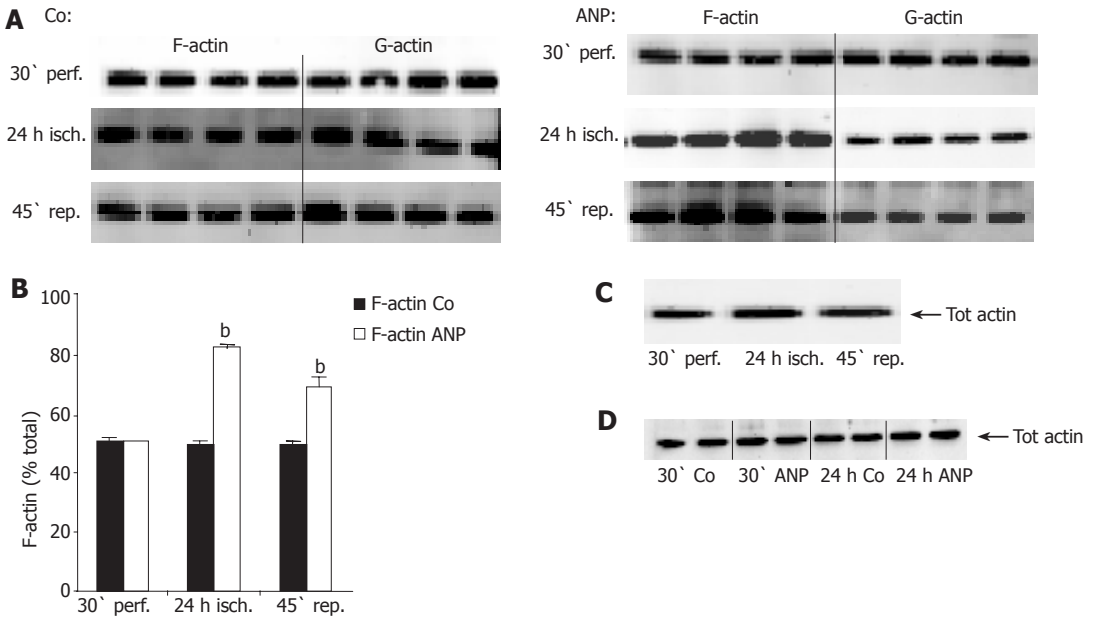

Figure 2 Influence of ANP preconditioning and ischemia on total actin and F-actin content. Livers were perfused for 30 min in the absence or presence of 200 nmol/L ANP, which was added 20 min prior to ischemia. Afterwards, livers were kept under ischemic conditions for 24 h (4 °C) in UW solution. At the indicated times, livers were snap-frozen, homogenized, and analyzed by Western blot using an anti-actin antibody. For differentiation between F- and G-actin (cytoskeleton and cytosol, respectively), liver homogenates were fractionated before Western blot analysis according to "Materials and methods" (**A** and **B**). One representative Western blot is imaged for each experimental setting. (**A**) Western blots representing hepatic F- and G-actin content during IR in untreated (Co) and ANP-preconditioned livers after 30-min perfusion (30' perf.), 24-h ischemia (24-h isch.), and 45-min reperfusion (45' rep.). (**B**) Quantitative/densitometric analysis of F- and G-actin content during IR in untreated (Co) or ANP-preconditioned livers. Data are expressed as percent of total actin content (F-actin+G-actin=100%) as mean±SE of n = 4 experiments in each treatment group. $^{b}P<0.001$ *vs* appropriate control. (**C**) Western blot showing total actin in untreated liver homogenates after 30-min perfusion, 24-h ischemia, and 45-min reperfusion. (**D**) Total hepatic actin content after perfusion (30') and ischemia (24-h) in ANP treated or untreated (Co) livers detected by Western blot analysis.

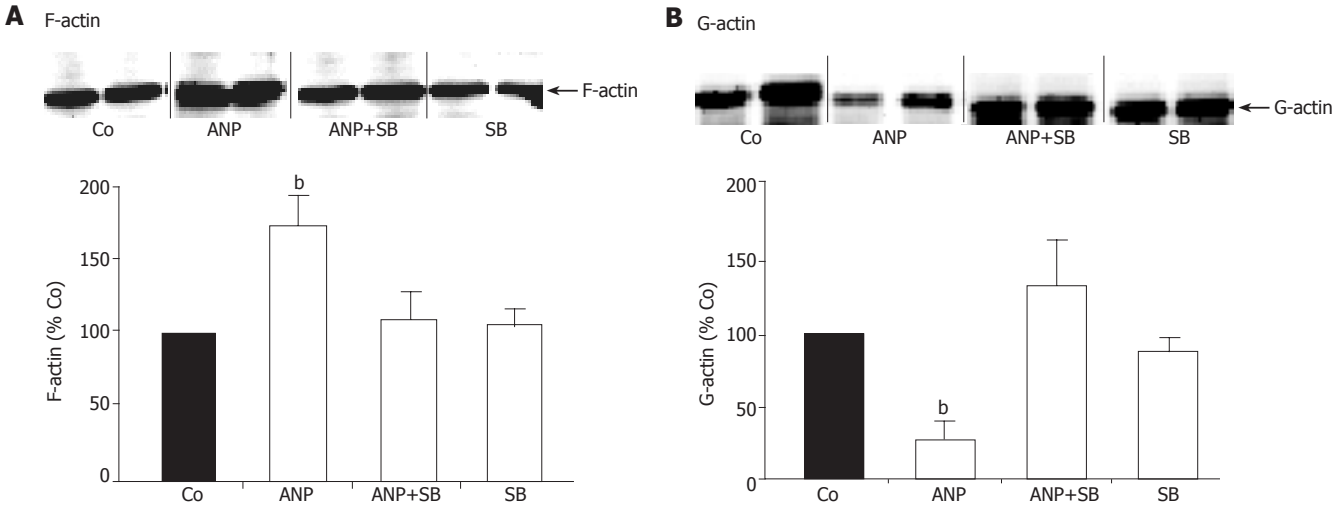

Figure 3 Effect of p38 MAPK inhibition on distribution of F- and G-actin. 20 min prior to ischemia livers were preconditioned with 200 nmol/L ANP or left untreated (Co) followed by 24-h ischemia at 4 °C. In different experiments, livers were perfused with SB203580 (2 μmol/L) or with a combination of SB203580 (2 μmol/L) and ANP (200 nmol/L). After ischemia livers were snap-frozen, homogenized and divided into cytoskeletal (**A**) and cytosolic (**B**) fraction by fractionation as described above. Samples were analyzed by Western blotting using an anti-actin antibody for detection of F-actin (**A**) in the cytoskeletal fraction and G-actin (**B**) in the cytosolic fraction. One representative Western blot is shown for each fraction. Bars show percentage of hepatic F-actin (**A**) or G-actin (**B**) in ANP, ANP+SB203580 and SB203580 treated livers referring to untreated control livers. Results are expressed as mean±SE of n = 4 experiments in each treatment group. $^{b}P<0.01$ *vs* control after 24-h ischemia.

with ANP caused very intensive staining of liver slices, representing an obvious increase in hepatic F-actin content (Figure 4B).

When stained with rhodamine-conjugated phalloidin, slices of ANP pretreated livers showed very intensive staining, representing an obvious increase in hepatic F-actin content especially at apical membranes of hepatocytes (Figure 4B) confirming the results obtained by Western blot analysis. Again, perfusion of the livers with SB203580 abolished the effect of ANP preconditioning on

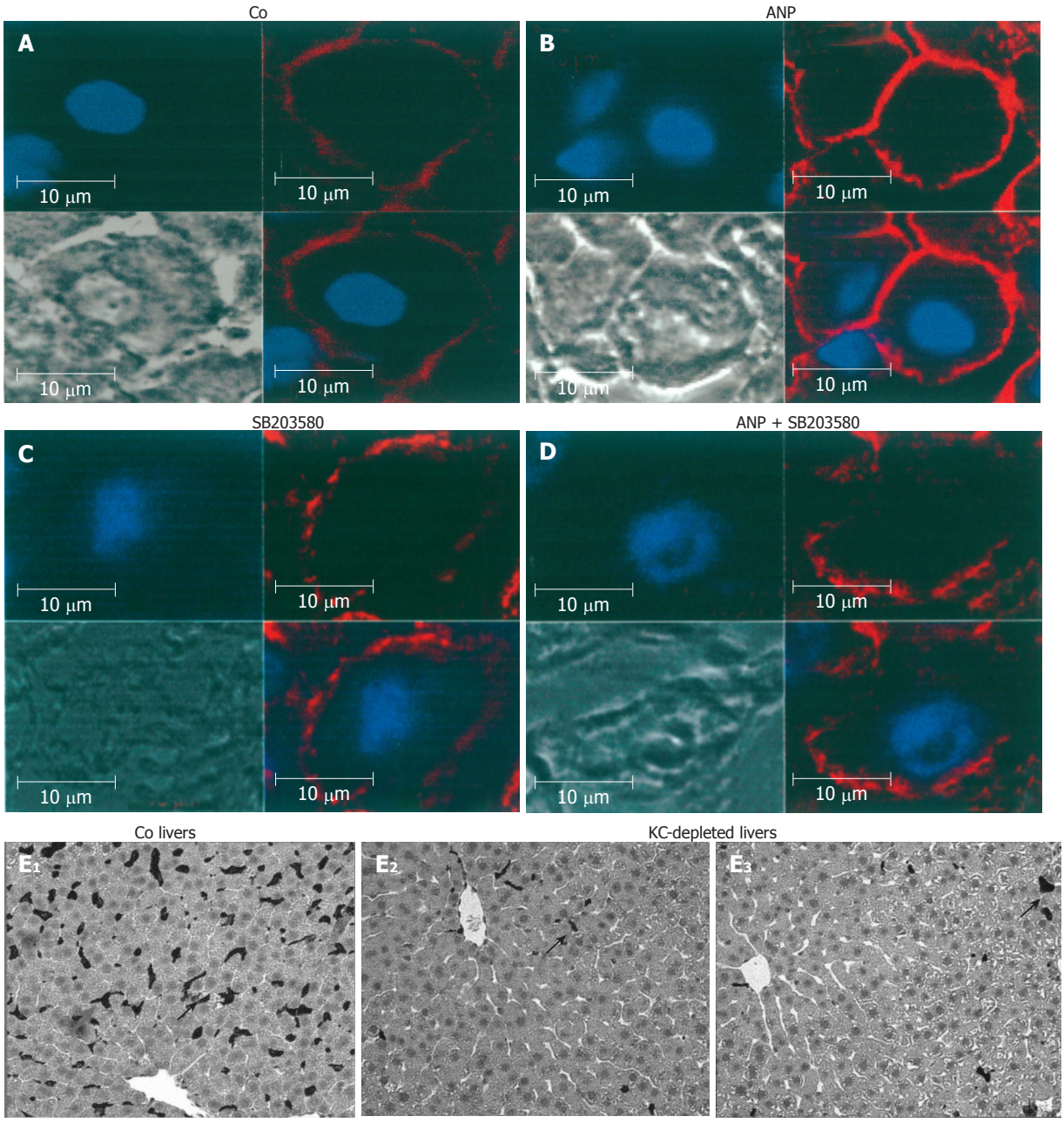

Figure 4 Analysis of the influence of ANP preconditioning on localization of F-actin in the liver by confocal microscopy. Livers were left untreated (**A**): preconditioned with 200 nmol/L ANP (**B**): 2 μmol/L SB203580 (**C**): or perfused with a combination of ANP (200 nmol/L) and SB203580 (2 μmol/L) (**D**): After ischemia (24 h, 4 °C), livers were snap-frozen, cut into 6-μm slices and stained with rhodamine-conjugated phalloidin (red, F-actin) and Hoechst 33342 (blue, nuclei) as described in "Materials and methods". Liver sections were observed by confocal laser microscopy (63-fold amplification). Immunohistological staining of KCs in untreated (Co) and KC-depleted livers (**E**): rats received an intravenous injection of 900 μL NaCl (Co) or 900 μL liposomes (12 mmol/L Cl_2MBP) into the tail vein. After 48 h rat livers were perfused, snap-frozen and liver slices were stained with an antibody against the KC-specific surface marker ED2 (see "Methods") to verify the Cl_2MBP-dependent depletion of the KCs. Dark staining represents KC (hallmarked with arrows). (**F**): KCs were depleted with Cl_2MBP as described under "Methods". After 48 h control organs (Co) or KC-depleted livers (12 mmol/L Cl_2MBP) were perfused ±ANP (200 nmol/L) for 20 min. Then p38 MAPK activity was investigated by *in vitro* phosphorylation assay (see "Methods"). Determination of density light units was performed by phosphorimaging and values of ANP-pretreated cells were divided by mean values of the respective control group. Columns show mean±SE of 4-5 independent perfusion experiments with $^bP<0.01$ being statistically different from the respective control group.

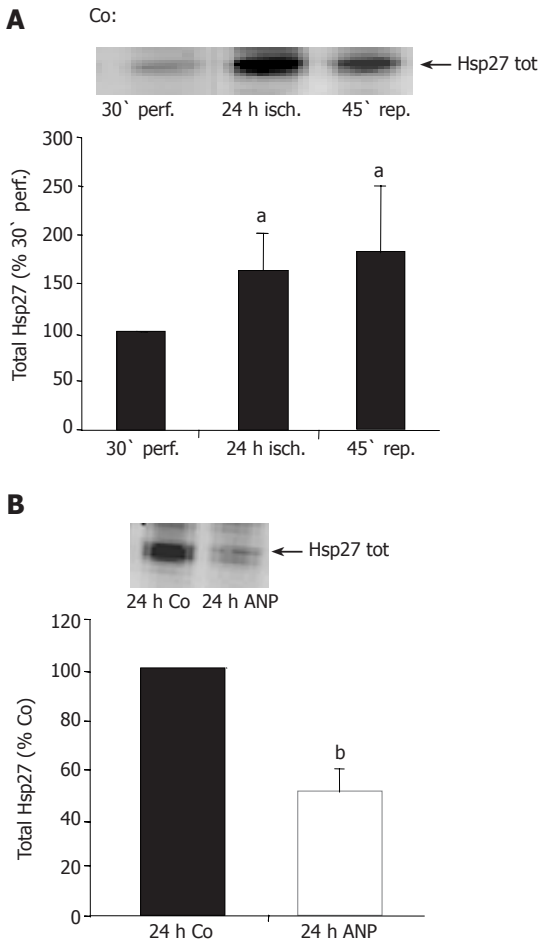

Figure 5 Changes in hepatic total Hsp27 during ischemia – influence of ANP pretreatment. Livers were perfused for 30 min in the presence or absence of ANP followed by 24-h ischemia at 4 °C in UW solution and reperfusion for 45 min. Afterwards, livers were snap-frozen at the indicated times, homogenized and analyzed via Western blot using an anti-Hsp27 antibody for detection of total Hsp27. One representative Western blot is shown for each experimental setting (untreated controls: (**A**), ANP pretreated livers: (**B**)). (**A**) Effect of IR on total Hsp27 in the liver. The graph shows percentage of values for untreated livers (Co) after 30-min perfusion (30' perf.) as means±SE of $n = 4$ experiments in each group. [a]$P<0.05$ *vs* untreated control after 30-min perfusion. (**B**) Influence of ANP preconditioning on total Hsp 27 after 24-h ischemia. Bars represent total Hsp27 as % Co after 24-h ischemia. Data are expressed as means±SE of $n = 4$ experiments in each treatment group. [b]$P<0.01$ *vs* control after 24-h ischemia.

F-actin, as it yielded a marginal staining intensity matching the intensity of untreated livers (Figure 4D), linking the effect to an activation of p38 MAPK.

Confocal data showed that changes in hepatic cytoskeleton occurred in parenchymal cells. The localization of p38 MAPK activation, however, has yet to be determined. We, therefore, measured p38 MAPK activation in both isolated Kupffer cells as well as in isolated hepatocytes. This experiment revealed no activation of p38 MAPK upon ANP treatment in KC, but a significant activation in hepatocytes (data not shown). Since the extent of activation was lower than that observed in whole livers[8] and since ANP has been reported as a regulator of Kupffer cell functions[43], we hypothesized that activation might occur in whole livers as a paracrine effect of Kupffer cells on hepatocytes.

To verify this potential cell interaction, we investigated the ANP-mediated effect on p38 MAPK in KC-depleted livers. For this purpose, we first audited the Cl_2MBP-dependent KC depletion via immunohistological staining of the macrophages with ED2 antibody (Figure 4E). In fact, Cl_2MBP led to a depletion of the KCs compared to NaCl-treated livers (Figure 4F). Furthermore, LDH efflux into the perfusate was determined to exclude Cl_2MBP-induced liver damage. The measurement indicated no increase in LDH-activity and thus no liver toxicity of Cl_2MBP (data not shown).

Subsequently, ANP-induced p38 MAPK activity was measured by determination of the radioactive labeled kinase substrate MBP. Surprisingly, liver perfusion with ANP exhibited no differences in kinase activity in KC-depleted or non-depleted livers (Figure 4F). Due to this observation we suggest that ANP mediates p38 MAPK activation not via hepatocyte-KC interaction.

Changes of total Hsp27 content and translocation of the heat shock protein

As the small heat shock protein Hsp27 has been demonstrated to be an important downstream target of p38 MAPK, which plays a critical role in the regulation of F-actin polymerization in different systems, we focused on a possible influence of ischemia on the expression of Hsp27 in the liver. Liver homogenates were analyzed by Western blot analysis without prior fractionation in order to investigate the hepatic content of total Hsp27. At the end of ischemia, Hsp27 levels in untreated livers were significantly higher than after 30-min perfusion (Figure 5A). This increase persisted during 45 min reperfusion.

To prove whether changes in total Hsp27 content are accompanied by a translocation of the heat shock protein towards the cytoskeleton, as described in previous studies[31,32], we investigated its subcellular distribution in liver tissue after ischemia. Liver tissue was fractionated, Hsp27 content in the cytosolic and cytoskeletal fraction was determined by Western blot analysis, and band intensity was considered proportional to the content of Hsp27 in the respective fraction. We were able to demonstrate that ischemia caused a translocation of the heat shock protein towards the cytoskeleton, as the content of total Hsp27 in cytoskeletal fractions accelerated after 24 h ischemia (Figure 6A). At this time more than 80% of the heat shock protein was localized in the cytoskeletal fraction of untreated liver homogenates (Figures 6A and B). This translocation seemed to decline during reperfusion (Figure 6A).

Interestingly, Western blot analysis of the whole tissue samples revealed that after 24 h ischemia ANP-pretreated livers showed significantly lower levels of total Hsp27 compared to untreated samples (Figure 5B). Surprisingly, the translocation of the heat shock protein detected in control livers was completely missing, so that the content of total Hsp27 in cytoskeletal and cytosolic fraction after ischemia was very similar (Figure 6B). Thus, pretreatment with ANP apparently both attenuates Hsp27 protein rise induced by I/R and prevents the translocation of Hsp27 to the cytoskeleton after ischemia.

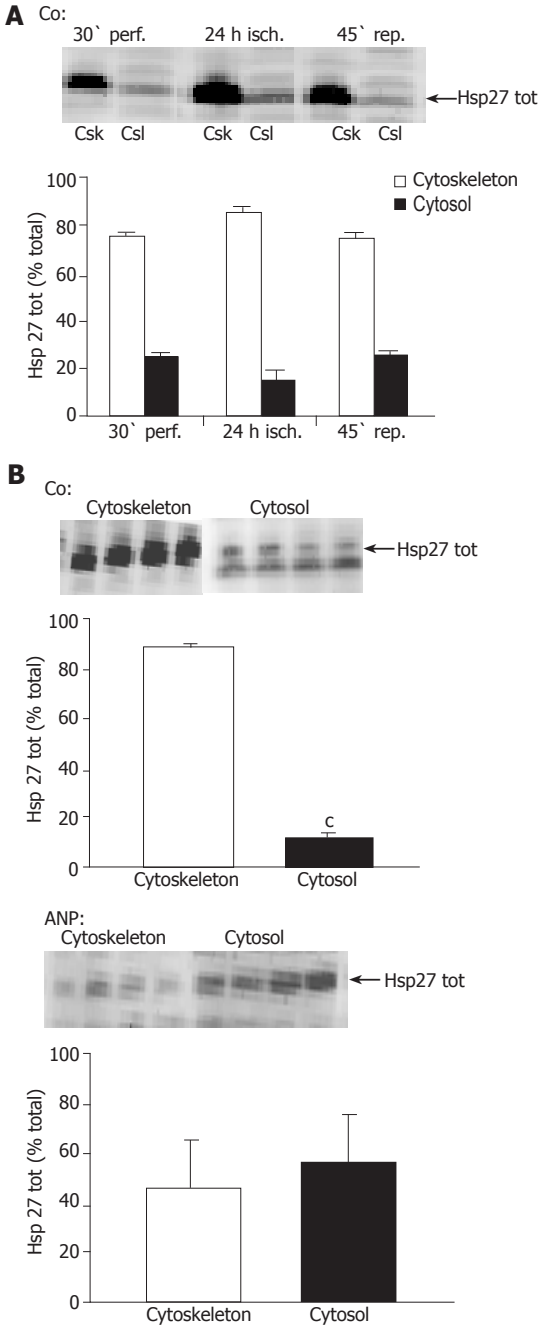

Figure 6 Influence of ischemia and ANP pretreatment on Hsp27 distribution. After perfusion for 30 min in the absence (**A** and **B**) or presence (**B**) of ANP, 24-h ischemia in cold UW solution, and reperfusion for 45 min, livers were snap-frozen, homogenized and fractionated as described in "Materials and methods". Samples were taken at indicated times and total Hsp27 in cytoskeletal (Csk) and cytosolic (Csl) fraction was detected via Western blot analysis using an anti-Hsp27 antibody. One representative Western blot is shown for each treatment group. (**A**) Effect of ischemia and reperfusion on the distribution of total Hsp27 in the liver. Quantification of total Hsp27 in the liver samples was verified via densitometric analysis of the corresponding bands, which was used to evaluate the ratio of Hsp27 in the cytoskeletal fraction (Csk) resp. cytosolic fraction (Csl) referring to total Hsp27 signal (cytoskeleton+cytosol) in the respective sample. Data are expressed as percent of total Hsp27 in cytoskeletal (F-actin) and cytosolic (G-actin) fraction as mean±SE of n=4 experiments in each treatment group. [a]P<0.05, *vs* Hsp27 content in cytoskeletal fraction in untreated livers after 30-min perfusion. (**B**) Distribution of total Hsp27 in untreated (control) and ANP-preconditioned livers after 24-h ischemia. Results are shown as percent of total Hsp27 in cytosolic and cytoskeletal fraction. Data are presented as mean±SE of n=4 experiments in each treatment group. [c]P<0.001 *vs* Hsp27 content in cytoskeletal fraction of untreated livers after 24-h ischemia. In ANP treated livers the differences in the values were not significant.

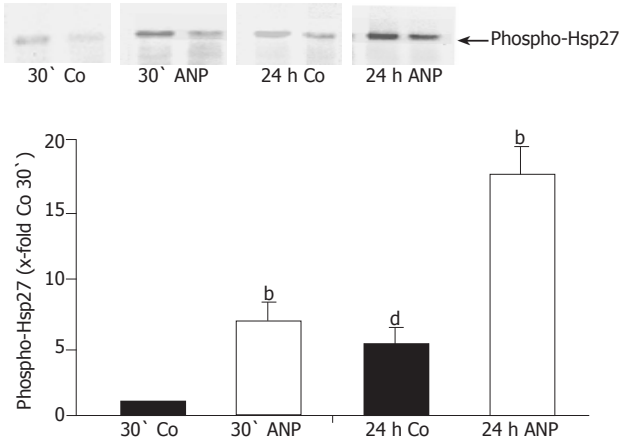

Figure 7 Influence of pretreatment with ANP on phosphorylation status of Hsp27. After perfusion for 10 min with KH-buffer livers were preconditioned with ANP for 20 min or left untreated, followed by 24-h ischemia (4 °C) according to the study protocol. Samples were taken after 30-min perfusion and 24-h ischemia. Livers were snap-frozen and homogenized, followed by immunoprecipitation with an anti-Hsp27 antibody and Western blot analysis using an anti-phospho-Hsp27 antibody. One representative Western blot is shown. Content of phospho-Hsp27 in the liver homogenates is presented as 10-fold control after 30-min perfusion, using the respective control as reference value and expressed as mean±SE of n = 4 experiments in each treatment group. Statistical analysis of ANP pretreated samples: [b]P<0.001 *vs* phospho-Hsp27 in respective control (after 30-min perfusion or 24-h ischemia). Statistical analysis of untreated control samples: [d]P<0.01 *vs* phospho-Hsp27 in control after 30-min perfusion.

ANP preconditioning causes increased phosphorylation of Hsp27

The influence of Hsp27 on actin polymerization depends on its phosphorylation status. Hence it was important to analyze the effect of ischemia and ANP preconditioning on the phosphorylation status of Hsp27. Detecting phospho-Hsp27 by Western blot analysis we obtained a significant increase of phosphorylation of the heat shock protein after ischemia in homogenates of untreated livers (Figure 7). In ANP-preconditioned samples phosphorylation seen after 30-min perfusion was already more intense than in untreated livers but increased even more after 24 h ischemia. Resuming these results, ANP seems to enhance the phosphorylation status of Hsp27 after 30-min perfusion and 24-h ischemia (Figure 7).

Inhibition of p38 MAPK prevents phosphorylation of Hsp27 in ANP pretreated livers

Pretreatment with ANP leads to an enhanced activation of p38 MAPK both in the isolated perfused liver as well as *in vivo* (Ref.[8] and Figure 1). We, therefore, investigated a possible connection between p38 MAPK activation and phosphorylation of its downstream target Hsp27 by using the specific p38 MAPK inhibitor SB203580. This treatment in fact completely abrogated the increase of Hsp27 phosphorylation induced by ANP (Figure 8). Pretreatment with SB203580 alone exerted no significant effect on phosphorylation of Hsp27 (Figure 8). Thus, activation of p38 MAPK is essential for the phosphorylation of the heat shock protein.

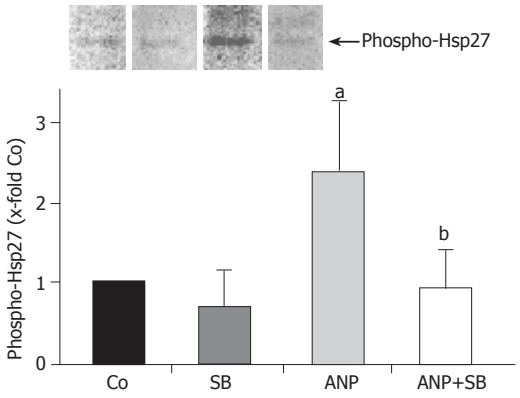

Figure 8 Effect of p38 MAPK inhibition on phosphorylation status of Hsp27. Livers were perfused for 30 min in the absence (Co) or presence of 200 nmol/L ANP, which was added 20 min prior to 24-h ischemia (4 °C). In different experiments, livers were perfused for 20 min with SB203580 (2 μmol/L) or with a combination of SB203580 (2 μmol/L) and ANP (200 nmol/L). After ischemia, livers were snap-frozen and homogenized. Total Hsp27 was precipitated as described and the content of phosphorylated Hsp27 was determined by Western blotting and detection with anti-phospho-Hsp27 primary antibody. One representative Western blot is shown. In the graph hepatic content of phospho-Hsp27 is expressed as percent of control samples after 24-h ischemia as mean±SE of n = 4 experiments in each treatment group. [a]P<0.05 *vs* control after 24-h ischemia, [b]P<0.01 *vs* phospho-Hsp27 content in ANP pretreated livers.

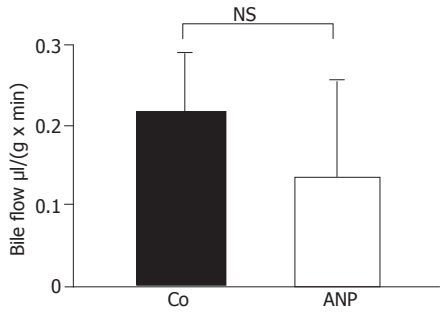

Figure 9 Effect of ANP preconditioning on bile flow. Bile was collected during perfusion and reperfusion and quantified volumetrically. Bile flow is expressed as μL per min and g liver tissue. Results show mean±SE of n = 4 experiments in each treatment group. The differences between untreated (Co) and ANP-preconditioned group were not significant.

ANP preconditioning shows no effect on bile flow

The cytoskeleton, more precisely F-actin, plays an important role in the maintenance of liver function[14,18,19]. In order to investigate a functional significance of an increase in F-actin after treatment with ANP, we studied the bile flow in transplanted organs of ANP- and NaCl-treated rats. Bile was collected as described during infusion and reperfusion. As shown in Figure 9, no significant differences between livers from NaCl-treated and from ANP-preconditioned rats could be detected. Thus, ANP-mediated increase of hepatic F-actin content does not cause an improvement of bile flow after ischemia.

DISCUSSION

This paper provides an important insight into the changes in hepatic cytoskeletal structures during I/R, signaling mechanisms in their modulation, and the interference of ANP preconditioning with these mechanisms.

Besides its vasodilating, hypotensive, and natriuretic activities[44], ANP has been described to protect against IRI *ex vivo* in the liver and *in vivo* in the heart[7,5,8,45], and to strongly activate p38 MAPK[8]. Interestingly, this activation has no influence on ANP's potential to protect from hepatic cell death, as previously shown by Kulhanek-Heinze *et al*[13]. In the present work, we therefore aimed to elucidate other potential functional consequences of ANP-induced p38 MAPK activity. In this context, we were able to demonstrate a clear coherence between ANP-mediated activation of p38 MAPK in the liver after ischemia and structural changes of the hepatocyte cytoskeleton. Interestingly, however, no functional correlation to improved bile flow could be established.

Cytoskeleton of hepatocytes during IR

Due to the evidence that activation of p38 MAPK leads to cytoskeletal changes in other systems[46] and the lack of knowledge about similar pathways in the liver, we investigated cytoskeletal changes during IR. We were able to show that hepatic content of total actin was affected neither by IR alone nor in combination with preconditioning of livers with ANP. Surprisingly, F-actin levels were not impaired by ischemia in control tissue after I/R. This result does not correspond to the findings of Cutrin *et al*[47]. who demonstrated structural changes of actin filaments after cold ischemia (120 min) and particularly after reperfusion (60-90 min) in transplanted human livers. Besides different species that were investigated, especially the much longer ischemic period employed in our model might account for these differences. In the kidney, Schwartz *et al*[30]. found a distinct increase of G-actin, paralleled by apical actin disruption after 30 min of warm ischemia. Again, the length, and also the temperature of ischemia cannot be compared to our experimental settings. Moreover, mechanisms in the kidney might differ from that in the livers. To the best of our knowledge, our data for the first time describe no significant cytoskeletal alterations in rat livers after prolonged hypothermic storage.

Cytoskeletal changes in ANP pretreated livers

Recently Gomes *et al*[28]. proved that IPC preserves rat kidneys from IRI by upregulation of genes coding for cytoskeletal proteins. The demonstrated increase in mRNA of these proteins, which have an F-actin-stabilizing function, is discussed to contribute to the tolerance of preconditioned tissue to ischemia. This effect, which was observed already after 30 min of preconditioning, goes along with our findings of an augmentation of F-actin in ANP-preconditioned livers confirming the influence of protective preconditioning (IPC or ANP pretreatment) on F-actin content of the affected tissue. Based on the findings that ANP preconditioning as well as IPC protects against IRI and due to the importance of F-actin for regulating cell morphology, intracellular processes, and bile secretion in liver cells, we hypothesized

that an augmentation of hepatic F-actin after ischemia might be a feature of the cytoprotective activities of ANP. Interestingly, however, although F-actin content increased in pretreated organs, we found no improvement of bile flow. Therefore, other functional parameters depending on the demonstrated F-actin formation in ANP pretreated livers need to be further investigated.

Involvement of p38 MAPK

As there are no data concerning a possible connection between p38 MAPK activation and cytoskeletal changes in liver tissue, we focused on the effect of p38 MAPK inhibition on hepatic F-actin content after ANP pretreatment. We applied the p38 MAPK inhibitor SB203580 at a concentration of 2 μmol/L to assure its specificity[48]. We demonstrated that perfusion with the inhibitor alone does not cause any cytoskeletal changes in liver tissue, but completely abolishes the ANP-induced effect of increased F-actin content in pretreated livers. Thus, we showed for the first time that ANP-mediated p38 MAPK activation leads to hepatic cytoskeletal changes by increasing the hepatocyte F-actin content in rat livers. To investigate a possible paracrine effect of KC on hepatocytes, p38 MAPK activity was determined in KC-depleted livers. Since KC depletion did not alter the activation of p38 MAPK, we suggest that an interaction between hepatocytes and KCs is not involved in ANP-mediated p38 MAPK activation.

Changes in total Hsp27

Analyzing total Hsp27 protein levels, we were able to show that the hepatic content of total Hsp27 increases during ischemia. It is a known fact that Hsp27 accumulates after cellular stress like hyperthermia[36], but also bacterial lipopolysaccharide (LPS) and Cyclosporine A enhance Hsp27 levels[49,50]. Thus, cellular stress can lead to an increase of Hsp27 content in the affected tissue elucidating the augmentation of the heat shock protein in the liver, which we observed during ischemia in untreated livers. This increased expression of the heat shock protein has been discussed to be a protective response, as it provides prevention from simulated IRI in canine myocytes[51]. Although our results of an augmentation of Hsp27 expression during ischemia, representing a situation of cellular stress, confirm these published data, our findings are surprising, as energy-dependent processes such as protein synthesis seem rather unlikely at 4 °C during a period of 24 h. Interestingly, however, such incidents have been observed before: Gerwig *et al*[6]. demonstrated an increase of caspase-3 precursor CPP 32 during an ischemic period and Wilhelm *et al*[52]. proved that cold ischemia induces upregulation of endothelin-1 in the kidney.

Detection of total Hsp27 in ANP-pretreated livers, however, yielded a rather astonishing result, as these organs showed markedly decreased levels of the heat shock protein. Interestingly, an increase of Hsp27 after cellular stress and decrease of the heat shock protein after treatment with a substance possessing protective properties has been described before for the kidney by Stacchiotti *et al*[50]. Hsp27 overexpression was seen after oxidative stress but disappeared after administration of an antioxidant[50]. This effect was ascribed to the cytoprotective effect of the antioxidant, which made additional protective Hsp27 response unnecessary. As ANP has been shown to protect against IRI[7,5], the effects seen in pretreated livers could be similar to the results of Stacchiotti *et al*. Thus, ANP might contribute to a protection of the liver tissue, so that higher levels of total Hsp27 as an additional protective response are no longer necessary.

It has to be noted that the functional consequences of changes in Hsp27 expression largely depend on its phosphorylation status and on its subcellular distribution, which will be subsequently discussed.

Translocation of total Hsp27

Sakamoto *et al*[34]. demonstrated that in rat hearts ischemia induces translocation of Hsp27 to the cytoskeleton and Aufricht *et al*[26]. showed the same effect in rat kidneys. Therefore, we investigated the subcellular distribution of the heat shock protein in isolated perfused rat livers after ischemia. In fact, significant augmentation of total Hsp27 in the cytoskeletal liver fraction could be detected after 24 h ischemia, suggesting a translocation of the heat shock protein towards the cytoskeleton. Pretreatment with ANP, however, completely abolished translocation of Hsp27 after ischemia. This observation enforces the assumption that ANP radically alters the response of liver cells to ischemia in isolated rat livers.

Phosphorylation status of Hsp27

As functional consequences of changes in Hsp27 protein expression and subcellular distribution largely depend on the phosphorylation status of the heat shock protein, we focused on this parameter next.

We proved that ischemic conditions cause phosphorylation of Hsp27 in isolated perfused rat liver, confirming the results of Huot *et al*[53]. who demonstrated an increased content of phosphorylated Hsp27 in vascular endothelial cells after oxidative stress. As the heat shock protein in its phosphorylated form is able to enhance F-actin formation, we expected a higher F-actin content in livers after ischemia. Interestingly, we could not detect an increase in hepatic F-actin in these organs. Since the augmentation of phosphorylation in untreated livers was not excessively high, the resulting effect on the cytoskeleton might not be sufficient to induce F-actin formation in liver tissue after ischemia.

In contrast, pretreatment with ANP resulted in a much stronger increase of the phosphorylation of the heat shock protein, which could be seen already after perfusion and obviously accelerated during ischemia (up to almost 20-fold of untreated controls). These findings correlate with data presented by Sanada *et al*[12]. showing changes in the phosphorylation status of Hsp27 after protective pretreatment of organs before ischemia *in vivo* in terms of an increased phosphorylation of the heat shock protein

after IPC. As Sanada *et al*. furthermore demonstrated coherence between Hsp27 phosphorylation and activation of p38 MAPK, we investigated this possible connection by perfusion of the livers with SB203580 in combination with ANP. An inhibition of p38 MAPK reduced the phosphorylation status of Hsp27 to basal levels. Thus, our results clearly prove the dependency of Hsp27-phosphorylation in the liver on prior activation of p38 MAPK.

Alterations of the cytoskeleton, particularly of F-actin content, are often discussed as a consequence of changes in the phosphorylation status of Hsp27 in other cell/organ systems[54]. We were able to confirm for the first time this correlation in the liver by showing an ANP-mediated increase of Hsp27 phosphorylation, which results in an accumulation of hepatic F-actin after ischemia. This effect is mediated via p38 MAPK, as an increase of F-actin in the liver after ANP preconditioning was abrogated by the p38 MAPK inhibitor SB203580.

Higher hepatic F-actin levels are thought to stabilize the cytoskeleton and to improve contractility resulting in improved bile flow after ischemia[15]. Our own data, however, do not show improved bile flow upon ANP pretreatment. Functional parameters other than improved bile flow are therefore hypothesized to be mediated by cytoskeletal changes, which need further investigation.

In summary, we were able to show for the first time the dependency of F-actin content in the liver on activation of p38 MAPK and that ANP preconditioning mediates changes in the cytoskeleton via an activation of p38 MAPK and phosphorylation of Hsp27 in the liver.

ACKNOWLEDGMENTS

We thank Dr. Stefan Zahler for his excellent support in confocal microscopy and processing of images, Kathrin Ladezki-Baehs for determination of p38 MAPK activity, and Dr. H. Meißner and Andrea Sendelhofert (both Institute of Pathology, University of Munich, Germany) for performing immunostaining. Clodronate was a gift of Roche Diagnostics GmbH, Mannheim, Germany.

REFERENCES

1 **Bilzer M,** Gerbes AL. Preservation injury of the liver: mechanisms and novel therapeutic strategies. *J Hepatol* 2000; **32**: 508-515
2 **Jaeschke H**. Molecular mechanisms of hepatic ischemia-reperfusion injury and preconditioning. *Am J Physiol Gastrointest Liver Physiol* 2003; **284**: G15-G26
3 **Kang KJ**. Mechanism of hepatic ischemia/reperfusion injury and protection against reperfusion injury. *Transplant Proc* 2002; **34**: 2659-2661
4 **Bilzer M,** Witthaut R, Paumgartner G, Gerbes A**L**. Prevention of ischemia/reperfusion injury in the rat liver by atrial natriuretic peptide. *Gastroenterology* 1994; **106**: 143-151
5 **Gerbes AL,** Vollmar AM, Kiemer AK, Bilzer M. The guanylate cyclase-coupled natriuretic peptide receptor: a new target for prevention of cold ischemia-reperfusion damage of the rat liver. *Hepatology* 1998; **28**: 1309-1317
6 **Gerwig T,** Meissner H, Bilzer M, Kiemer AK, Arnholdt H, Vollmar AM, Gerbes AL. Atrial natriuretic peptide preconditioning protects against hepatic preservation injury by attenuating necrotic and apoptotic cell death. *J Hepatol* 2003; **39**: 341-348
7 **Cottart CH,** Nivet-Antoine V, Do L, Al-Massarani G, Descamps G, Xavier-Galen F, Clot JP. Hepatic cytoprotection by nitric oxide and the cGMP pathway after ischaemia-reperfusion in the rat. *Nitric Oxide* 2003; **9**: 57-63
8 **Kiemer AK,** Kulhanek-Heinze S, Gerwig T, Gerbes AL, Vollmar AM. Stimulation of p38 MAPK by hormonal preconditioning with atrial natriuretic peptide. *World J Gastroenterol* 2002; **8**: 707-711
9 **Schauer RJ,** Gerbes AL, Vonier D, op den Winkel M, Fraunberger P, Bilzer M. Induction of cellular resistance against Kupffer cell-derived oxidant stress: a novel concept of hepatoprotection by ischemic preconditioning. *Hepatology* 2003; **37**: 286-295
10 **Teoh N,** Dela Pena A, Farrell G. Hepatic ischemic preconditioning in mice is associated with activation of NF-kappaB, p38 kinase, and cell cycle entry. *Hepatology* 2002; **36**: 94-102
11 **Nakano A,** Baines CP, Kim SO, Pelech SL, Downey JM, Cohen MV, Critz SD. Ischemic preconditioning activates MAPKAPK2 in the isolated rabbit heart: evidence for involvement of p38 MAPK. *Circ Res* 2000; **86**: 144-151
12 **Sanada S,** Kitakaze M, Papst PJ, Hatanaka K, Asanuma H, Aki T, Shinozaki Y, Ogita H, Node K, Takashima S, Asakura M, Yamada J, Fukushima T, Ogai A, Kuzuya T, Mori H, Terada N, Yoshida K, Hori M. Role of phasic dynamism of p38 mitogen-activated protein kinase activation in ischemic preconditioning of the canine heart. *Circ Res* 2001; **88**: 175-180
13 **Kulhanek-Heinze S,** Gerbes AL, Gerwig T, Vollmar AM, Kiemer AK. Protein kinase A dependent signalling mediates anti-apoptotic effects of the atrial natriuretic peptide in ischemic livers. *J Hepatol* 2004; **41**: 414-420
14 **Denk H,** Lackinger E, Vennigerholz F. Pathology of the cytoskeleton of hepatocytes. *Prog Liver Dis* 1986; **8**: 237-251
15 **Rungger-Brändle E, Gabbiani G**. The role of cytoskeletal and cytocontractile elements in pathologic processes. *Am J Pathol* 1983; **110**: 361-392 [PMID: 6219586]
16 **Selzner N,** Rüdiger H, Graf R, Clavien PA. Protective strategies against ischemic injury of the liver. *Gastroenterology* 2003; **125**: 917-936
17 **Feldmann G**. The cytoskeleton of the hepatocyte. Structure and functions. *J Hepatol* 1989; **8**: 380-386
18 **Fisher MM,** Phillips MJ. Cytoskeleton of the hepatocyte. *Prog Liver Dis* 1979; **6**: 105-121
19 **Marceau N,** Loranger A, Gilbert S, Daigle N, Champetier S. Keratin-mediated resistance to stress and apoptosis in simple epithelial cells in relation to health and disease. *Biochem Cell Biol* 2001; **79**: 543-555
20 **Ohashi M,** Sano N, Takikawa H. Effects of phalloidin on the biliary excretion of cholephilic compounds in rats. *Pharmacology* 2002; **66**: 31-35
21 **Arias I.M.** The Liver: Biology and Pathobiology. Raven Press, Ltd, New York 2001; Book Chapter
22 **Song JY,** Van Marle J, Van Noorden CJ, Frederiks WM. Disturbed structural interactions between microfilaments and tight junctions in rat hepatocytes during extrahepatic cholestasis induced by common bile duct ligation. *Histochem. Cell Biol* 1996; **106**: 573-580
23 **Wang YJ,** Gregory RB, Barritt GJ. Maintenance of the filamentous actin cytoskeleton is necessary for the activation of store-operated Ca2+ channels, but not other types of plasma-membrane Ca2+ channels, in rat hepatocytes. *Biochem J* 2002; **363**: 117-126
24 **Nishimura Y,** Romer LH, Lemasters JJ. Mitochondrial dysfunction and cytoskeletal disruption during chemical hypoxia to cultured rat hepatic sinusoidal endothelial cells: the pH paradox and cytoprotection by glucose, acidotic pH, and glycine. *Hepatology* 1998; **27**: 1039-1049

25 **Shinohara H,** Tanaka A, Fujimoto T, Hatano E, Satoh S, Fujimoto K, Noda T, Ide C, Yamaoka Y. Disorganization of microtubular network in postischemic liver dysfunction: its functional and morphological changes. *Biochim.Biophys.Acta* 1996; **1317**: 27-35

26 **Aufricht C,** Ardito T, Thulin G, Kashgarian M, Siegel NJ, Van Why SK. Heat-shock protein 25 induction and redistribution during actin reorganization after renal ischemia. *Am J Physiol* 1998; **274**: F215-F222

27 **Dalle-Donne I,** Rossi R, Milzani A, Di Simplicio P, Colombo R. The actin cytoskeleton response to oxidants: from small heat shock protein phosphorylation to changes in the redox state of actin itself. *Free Radic Biol Med* 2001; **31**: 1624-1632

28 **Gomes MD,** Cancherini DV, Moreira MA, Rebouças NA. Ischemic preconditioning of renal tissue: identification of early up-regulated genes. *Nephron Exp Nephrol* 2003; **93**: e107-e116

29 **Panasenko OO,** Kim MV, Marston SB, Gusev NB. Interaction of the small heat shock protein with molecular mass 25 kDa (hsp25) with actin. *Eur J Biochem* 2003; **270**: 892-901

30 **Schwartz N,** Hosford M, Sandoval RM, Wagner MC, Atkinson SJ, Bamburg J, Molitoris BA. Ischemia activates actin depolymerizing factor: role in proximal tubule microvillar actin alterations. *Am J Physiol Renal Physiol* 1999; **276**: F544-F551

31 **Arrigo AP,** Landry J. Expression and function of the low-molecular weight heat shock proteins.1994; 335-373

32 **Benndorf R,** Hayess K, Ryazantsev S, Wieske M, Behlke J, Lutsch G. Phosphorylation and supramolecular organization of murine small heat shock protein HSP25 abolish its actin polymerization-inhibiting activity. *J Biol Chem* 1994; **269**: 20780-20784

33 **Wieske M,** Benndorf R, Behlke J, Dolling R, Grelle G, Bielka H, Lutsch G. Defined sequence segments of the small heat shock proteins HSP25 and alphaB-crystallin inhibit actin polymerization. *Eur J Biochem.* 2001; **268**: 2083-2090

34 **Sakamoto K,** Urushidani T, Nagao T. Translocation of HSP27 to sarcomere induced by ischemic preconditioning in isolated rat hearts. *Biochem Biophys Res Commun* 2000; **269**: 137-142

35 **Freshney NW,** Rawlinson L, Guesdon F, Jones E, Cowley S, Hsuan J, Saklatvala J. Interleukin-1 activates a novel protein kinase cascade that results in the phosphorylation of Hsp27. *Cell* 1994; **78**: 1039-1049

36 **Landry J,** Huot J. Modulation of actin dynamics during stress and physiological stimulation by a signaling pathway involving p38 MAP kinase and heat- shock protein 27. *Biochem Cell Biol* 1995; **73**: 703-707

37 **Murashov AK,** Haq IU, Hill C, Park E, Smith M, Wang X, Wang X, Goldberg DJ, Wolgemuth DJ. Crosstalk between p38, Hsp25 and Akt in spinal motor neurons after sciatic nerve injury. *Brain Res Mol Brain Res* 2001; **93**: 199-208

38 **Nakano A,** Cohen MV, Downey JM. Ischemic preconditioning: from basic mechanisms to clinical applications. *Pharmacol Ther* 2000; **86**: 263-275

39 **Carey DJ,** Rafferty CM, Schramm MM. Association of heparan sulfate proteoglycan and laminin with the cytoskeleton in rat liver. *J Biol Chem* 1987; **262**: 3376-3381

40 **Fox JE,** Reynolds CC, Boyles JK. Studying the platelet cytoskeleton in Triton X-100 lysates. *Methods Enzymol* 1992; **215**: 42-58

41 **Smith PK,** Krohn RI, Hermanson GT, Mallia AK, Gartner FH, Provenzano MD, Fujimoto EK, Goeke NM, Olson BJ, Klenk DC. Measurement of protein using bicinchoninic acid. *Anal Biochem* 1985; **150**: 76-85

42 **Laemmli UK**. Cleavage of structural proteins during the assembly of the head of bacteriophage T4. *Nature* 1970; **227**: 680-685

43 **Kiemer AK**, Baron A, Gerbes AL, Bilzer M, Vollmar AM. The atrial natriuretic peptide as a regulator of Kupffer cell functions. *Shock* 2002; **17**: 365-371

44 **Vesely DL**. Atrial natriuretic peptides in pathophysiological diseases. *Cardiovasc Res* 2001; **51**: 647-658

45 **Sangawa K,** Nakanishi K, Ishino K, Inoue M, Kawada M, Sano S. Atrial natriuretic peptide protects against ischemia-reperfusion injury in the isolated rat heart. *Ann Thorac Surg* 2004; **77**: 233-237

46 **Guay J,** Lambert H, Gingras-Breton G, Lavoie JN, Huot J, Landry J. Regulation of actin filament dynamics by p38 map kinase-mediated phosphorylation of heat shock protein 27. *J Cell Sci* 1997; **110**: 357-368

47 **Cutrin JC,** Cantino D, Biasi F, Chiarpotto E, Salizzoni M, Andorno E, Massano G, Lanfranco G, Rizzetto M, Boveris A, Poli G. Reperfusion damage to the bile canaliculi in transplanted human liver. *Hepatology* 1996; **24**: 1053-1057

48 **McGovern SL,** Shoichet BK. Kinase inhibitors: not just for kinases anymore. *J Med Chem* 2003; **46**: 1478-1483

49 **Kojima K,** Musch MW, Ropeleski MJ, Boone DL, Ma A, Chang EB. Escherichia coli LPS induces heat shock protein 25 in intestinal epithelial cells through MAP kinase activation. *Am J Physiol Gastrointest Liver Physiol* 2003; **286**: G645-G652

50 **Stacchiotti A,** Rezzani R, Angoscini P, Rodella L, Bianchi R. Small heat shock proteins expression in rat kidneys treated with cyclosporine A alone and combined with melatonin. *Histochem J* 2002; **34**: 305-312

51 **Vander Heide RS**. Increased expression of HSP27 protects canine myocytes from simulated ischemia-reperfusion injury. *Am J Physiol Heart Circ Physiol* 2002; **282**: H935-H941

52 **Wilhelm SM,** Simonson MS, Robinson AV, Stowe NT, Schulak JA. Cold ischemia induces endothelin gene upregulation in the preserved kidney. *J Surg Res* 1999; **85**: 101-108

53 **Huot J,** Houle F, Marceau F, Landry J. Oxidative stress-induced actin reorganization mediated by the p38 mitogen-activated protein kinase/heat shock protein 27 pathway in vascular endothelial cells. *Circ Res* 1997; **80**: 383-392

54 **Mounier N,** Arrigo AP. Actin cytoskeleton and small heat shock proteins: how do they interact? *Cell Stress Chaperones* 2002; **7**: 167-176

Science Editor Guo SY **Language Editor** Elsevier HK

PO Box 2345, Beijing 100023, China
www.wjgnet.com
wjg@wjgnet.com

ELSEVIER

World J Gastroenterol 2005;11(47):7430-7435
World Journal of Gastroenterology ISSN 1007-9327

• *BASIC RESEARCH* •

Therapeutic effect of DA-9601 on chronic reflux gastritis induced by sodium taurocholate in rats

Tae Young Oh, Chang Yell Shin, Yong Sung Sohn, Dong Hwan Kim, Byoung Ok Ahn, Eun Bang Lee, Cho Hyun Park

Tae Young Oh, Chang Yell Shin, Yong Sung Sohn, Dong Hwan Kim, Byoung Ok Ahn, Eun Bang Lee, Dong-A Pharmaceutical Research Institute, Yongin, Korea
Cho Hyun Park, Department of General Surgery, Catholic University of Medicine, Seoul, Korea
Supported by the grant from Korean Ministry of Health and Welfare, HMP-98-D-1-0007
Correspondence to: Tae Young Oh, Dong-A Pharmaceutical Research Institute, 47-5, Sanggal-ri, Kiheung-up, Yongin-shi, Kyunggi-do 449-905, Korea. solemiooh@donga.co.kr
Telephone: +82-31-280-1389 Fax: +82-31-282-8564
Received: 2005-03-31 Accepted: 2005-08-09

Abstract

AIM: To investigate the therapeutic effects of DA-9601 on sodium taurocholate (TCA)-induced chronic reflux gastritis in SD rats.

METHODS: In this study, we have investigated the therapeutic effects of DA-9601 on chronic erosive and atrophic gastritis induced by 6 mo of TCA administration (5 mmol/L in drinking water) in SD rats.

RESULTS: Four weeks of DA-9601 administration (0.065%, 0.216% in rat chow), following the withdrawal of TCA treatment, resulted in a significant decrease in total length of erosions in rats in a dose-dependent manner. Furthermore, the indicators of atrophic gastritis, such as reduced mucosal thickness and reduction in the number of parietal cells, were improved by the administration of DA-9601 in a dose-related manner. DA-9601 also attenuated inflammatory cell infiltration and the proliferation of collagenous fiber in the gastric mucosa. The improvement in the reduction of the gastric mucus was observed in the rats receiving a high dose of DA-9601 (0.216%). The therapeutic effect of DA-9601 on experimental chronic erosive gastritis was superior to that of rebamipide (1.08% in rat chow). Biochemical analyses showed increased mucosal prostaglandin E_2 and reduced glutathione levels by DA-9601 treatment.

CONCLUSION: We suggest that DA-9601 is a promising agent for the treatment of chronic erosive and atrophic gastritis with an etiological factor of bile reflux. Increased mucosal prostaglandin E_2 and reduced glutathione by DA-9601 treatment may be therapeutic mechanisms for chronic erosive and atrophic gastritis.

Key words: DA-9601; Reflux gastritis; Erosive gastritis; Atrophic gastritis; Sodium taurocholate

Oh TY, Shin CY, Sohn YS, Kim DH, Ahn BO, Lee EB, Park CH. Therapeutic effect of DA-9601 on chronic reflux gastritis induced by sodium taurocholate in rats. *World J Gastroenterol* 2005; 11(47): 7430-7435
http://www.wjgnet.com/1007-9327/11/7430.asp

INTRODUCTION

Reflux gastritis is a chronic disease in which the duodenal contents, particularly bile acid, are flown back into the stomach. It is associated with various symptoms, such as epigastric pain, dyspepsia, loss of appetite, nausea or vomiting[1,2]. While reflux gastritis is an occasional occurrence, it is primarily found in patients with pyloric insufficiency or delayed gastric emptying. It can also be found in patients who have previously undergone cholecystectomy or gastrectomy[3]. The reflux of intestinal fluid containing bile juice to the residual stomach has been considered as a primary pathogenic factor in this type of gastritis[4].

Although a number of treatments, such as improved gastric emptying, reduction of hydrochloric acid secretion and bile salt binding are available, a considerable portion of patients do not achieve the complete mucosal healing or suffer from sustained symptoms. Some studies have suggested the possible participation of bile acid in the development of erosive and atrophic gastritis[1,2]. Sodium taurocholate (TCA), a component of bile acid, induces erosive and atrophic gastritis, and is increasingly utilized in animal models for the study of bile reflux gastritis because of its simplicity and reproducibility[5]. Chronic exposure of the gastric mucosa of rats to TCA induces chronic erosive gastritis characterized by mucosal erosions, inflammatory cell infiltration, decreases in the number of parietal cells and mucosal thickness, and interstitial fibrosis. These characterizations are similar to those observed in human chronic erosive and reflux gastritis[6].

DA-9601 was developed for the treatment of gastritis[7-9]. DA-9601 was demonstrated to possess cytoprotective actions in various experimental models, including ethanol-induced gastric mucosal damage, and trinitrobenzene sulfonic acid (TNBS)-induced colitis[10]. Recently, DA-9601 has been reported to be effective in reflux esophagitis[11,12]. Although the mechanism via which DA-9601 exerts its mucosal protective effect has

not been fully elucidated, stimulation of the mucus, mucosal prostaglandins (PG), and reduced glutathione (GSH) are thought to play crucial roles in producing the gastric mucosal protective effect. The present study was undertaken to evaluate the effects of DA-9601 on TCA-induced chronic and atrophic gastritis in rats.

MATERIALS AND METHODS

Animals

Male Sprague-Dawley rats (weighing 210-230 g, aged 7 wk) were purchased from Charles River Japan (Kanagawa, Japan). Experimental procedures were performed in conformity with the Institutional Standard Procedure for Animal Care and Experiment (SOP-ANC) of Dong-A Pharmaceutical Company. The animals were kept under standard laboratory conditions and allowed free access to rodent chow (Cheil, Korea) and UV-sterilized tap water *ad libitum* in standard wire cage under a 12:12-h light-dark (LD) cycle. After a 5 d acclimation period, rats were treated according to the experimental protocols. Each group contained 20 rats, of them 10 rats were used for histological evaluation and the other rats were used for molecular assay.

Materials

DA-9601 was produced by Dong-A Pharmaceutical Co. Ltd. (Yongin, Korea). TCA was purchased from Sigma (St. Louis, USA), and rebamipide was obtained from Korea Otsuka (Seoul, Korea). DA-9601 (0.065% and 0.0216%) and rebamipide (1.08%) were mixed with rodent chow and then administered to the rats.

Sodium taurocholate (TCA)-induced gastritis and administration of DA-9601

Chronic gastritis was induced in rats by the administration of 5 mmol/L TCA dissolved in distilled water for 6 mo[13,14]. After discontinuation of TCA treatment, rats were allowed to drink plain tap water. To investigate the effects of the treatment, rats were divided into five groups, each consisting of 10 rats. In group 1, rats were fed a standard pellet meal and tap water for 7 mo. In group 2, rats were treated with TCA for 6 mo and then given the same standard pellet meals as used in the previous 6 mo and tap water alone for 1 mo. In groups 3, 4, and 5, rats were treated with TCA for 6 mo and then fed a standard pellet meal which was formulated to contain 0.065%, 0.216% of DA-9601 and 1.08% of rebamipide, respectively for 1 mo. Group 3 (0.065% of DA-9601), group 4 (0.216% of DA-9601), and group 5 (1.08% of rebamipide) all received tap water, following discontinuation of TCA treatment.

Histological evaluation

Rats were fasted for 24 h prior to the experiment and killed by decapitation under light ether anesthesia. The abdomen was opened and the stomach was then excised, opened along the greater curvature, laid flat so as not to cause any damage, and examined carefully for any evidence of macroscopic damage. The flattened stomach was divided into five parts, and each part was rolled in a Swiss manner for observation from the cardiac to the pyloric region. The Swiss-rolled tissue specimens were fixed in Bouin's solution for 6 h at 4 °C, and paraffin-embedded blocks were prepared by the routine method. After sectioning, each specimen was stained with H&E and Masson's trichrome and examined under a light microscope (BH-2, Olympus, Japan) by a pathologist who was blinded to the study. The length of mucosal surface injury was measured on the entire length of each tissue section in a visual field of 100-fold magnification. The total length of mucosal surface injury for the five parts per stomach was expressed as a measured length. The mucosal thickness was measured in a visual field of 100-fold magnification. The number of parietal cells per unit area (mm^2) in a visual field of 400-fold magnification was counted. The extents of inflammatory cell infiltration, the proliferation of collagenous fiber and stained gastric mucosa were evaluated in a visual field of 100-fold magnification.

Tissue malondialdehyde (MDA) and reduced glutathione (GSH)

The content of hepatic MDA was determined using the method described by Ohkawa *et al*[15]. In brief, after mincing and trimming, the pieces of liver were homogenized with four volumes of an ice-cold 0.1 mol/L potassium phosphate buffer (pH 7.4) solution. Then, the reaction mixture containing 0.2 mL of the homogenate, 81 g/L sodium dodecyl sulfate, 200 g/L acetate buffer (pH 3.5), and 8 g/L thiobarbituric acid (TBA) solution was mixed well for 3 min and incubated at 95 °C for 60 min. TBA reactive substance, MDA, was extracted with a butanol-pyrimidine mixture solution. The absorbance measured at 532 nm was expressed as nmol/mg protein. The content of hepatic glutathione (GSH) was determined by the spectrophotometric method of Griffith and expressed as nmol/mg protein[16]. Protein content was determined by the method described by Lowry *et al*[17]. using BSA as the standard.

Level of prostaglandin E_2

Using a commercially available EIA kits (Amersham, UK), gastric mucosal PGE_2 levels were measured. Immediately after biopsy and gross observation, mucosal specimens were frozen in liquid nitrogen and stored at -70 °C until the measurement of PGE_2. Tissue specimens were processed for the assay according to the method described previously by Lipscomb and Rees[18]. The final PGE_2 level was expressed in pg/mg of wet biopsy weight.

Statistical analysis

All data were expressed as mean±SE. Scheffe's *t*-test was used for comparing body weight, tissue MDA, tissue GSH, and endoscopic scores between the control group and experimental groups. Rank transformation and Kruskal-Wallis test were performed to determine the inter-group difference of non-parametric data, and Bonferroni's test was used for multiple pair-wise comparison. A $P<0.05$ was considered statistically significant.

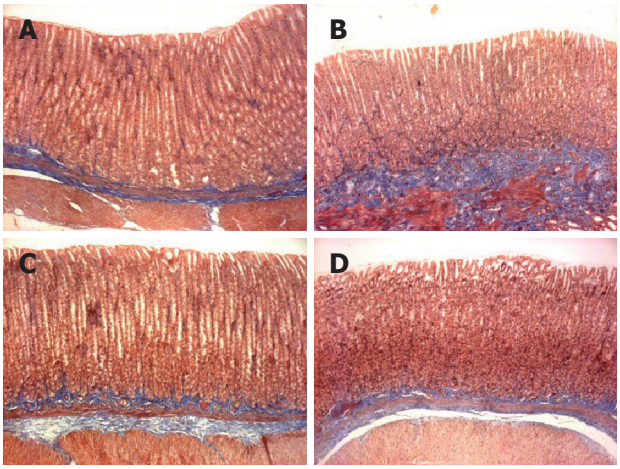

Figure 1 Microscopic appearance of gastric mucosa showing the effect of DA-9601 and rebamipide on sodium taurocholate (TCA)-induced erosive and atrophic gastritis in rats (×100). Rats were administered with 5 mmol/L TCA for 6 mo (given along with drinking water). **A:** Normal; **B:** control; **C:** 0.216% DA-9601; **D:** 1.08% rebamipide.

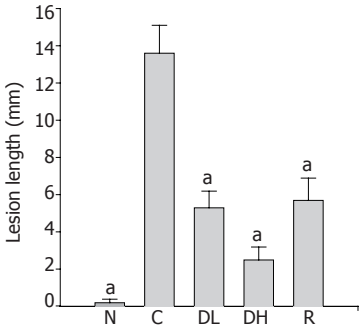

Figure 2 Inhibitory effects of DA-9601 and rebamipide on the length of mucosal lesion of TCA-induced erosive and atrophic gastritis in rats. DA-9601 (0.065% and 0.0.216%) and rebamipide (1.08%) were mixed with rodent chow and then administered to the rats. N: Normal; C: control; DL: 0.065% DA-9601; DH: 0.216% DA-9601; R: 1.08% rebamipide. Data are expressed as mean±SE. $^{a}P<0.05$ *vs* controls.

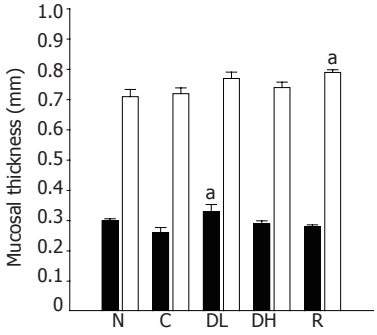

Figure 3 Effects of DA-9601 and rebamipide on the mucosal thickness of TCA-induced erosive and atrophic gastritis in rats. N: Normal; C: control; DL: 0.065% DA-9601; DH: 0.216% DA-9601; R: 1.08% rebamipide. Data are expressed as mean±SE. $^{a}P<0.05$ *vs* controls.

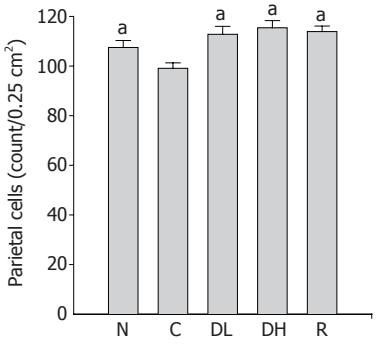

Figure 4 Effects of DA-9601 and rebamipide on the number of parietal cells in TCA-induced erosive and atrophic gastritis in rats. N: Normal; C: control; DL: 0.065% DA-9601; DH: 0.216% DA-9601; R: 1.08% rebamipide. Data are expressed as mean±SE. $^{a}P<0.05$ *vs* controls.

RESULTS

Inhibitory effect of DA-9601 on chronic gastritis

Macroscopic lesions were not observed on the surface of mucosa in any of the groups, while marked changes were observed microscopically in the gastric mucosa of the rats treated with TCA for 6 mo (Figure 1). A significant increase in the length of erosion was observed in the control animals as compared to normal level (Figure 2). However, the microscopic appearance of the gastric mucosa taken from group 3 or 4, treated with 0.065% and 0.216% DA-9601, respectively, showed a significant decrease in the length of erosion. DA-9601 significantly decreased the length of erosion in a dose-dependent manner. Although treatment with rebamipide also caused a significant decrease of erosive lesion, this protective effect by rebamipide was not as prominent as observed in group 4 (treated with 0.216% DA-9601). To explore the mechanism underlying DA-9601-induced protection against gastric lesions, the thickness of the gastric mucus layer was measured (Figure 3). We observed that 0.065% DA-9601 ameliorated the TCA-induced reduction of mucosal thickness in the antrum, while 1.08% rebamipide significantly thickened the mucus layer in the fundus.

Effect of DA-9601 on parietal cells, infiltration of inflammatory cells and intestinal fibrosis

The number of parietal cells in the controls (99.1±2.2 cells/0.25 cm^2) was significantly lower than that of the normal level (107.5±2.8 cells/0.25 cm^2). Furthermore, 0.065% DA-9601 (112.8±3.2 cells/0.25 cm^2), 0.216% DA-9601 (115.4±2.9 cm^2) and 1.08% rebamipide (113.9 ±2.9 cm^2) significantly increased the number of parietal cells in TCA-induced chronic gastritis as compared to the control (Figure 4).

The number of infiltrating inflammatory cells in the gastric mucosa of animals in the control group (4.7±0.86) was compared to the normal level (0.9±0.11). We observed significantly decreased number of infiltrating inflammatory cells in the gastric mucosa of the animals treated with 0.065% DA-9601 (1.4±0.27), 0.216% DA-9601 (2.0± 0.35) and 1.08% rebamipide (3.0±0.37) as compared to the controls ($P<0.05$) (Figure 5).

In addition, 0.065% DA-9601 (0.4±0.1) significantly

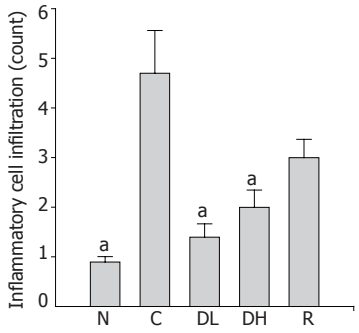

Figure 5 Effects of DA-9601 and rebamipide on the infiltration of inflammatory cells induced by TCA. N: Normal; C: control; DL: 0.065% DA-9601; DH: 0.216% DA-9601; R: 1.08% rebamipide. Data are expressed as mean±SE. [a]*P*<0.05 *vs* controls.

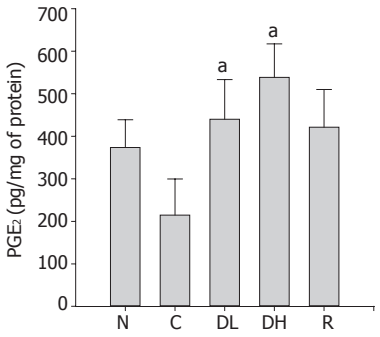

Figure 8 Effects of DA-9601 and rebamipide on PGE_2 induced by TCA in rat gastric mucosa. N: normal; C: control; DL: 0.065% DA-9601; DH: 0.216% DA-9601; R: 1.08% rebamipide. Data are expressed as mean±SE. [a]*P*<0.05 *vs* controls.

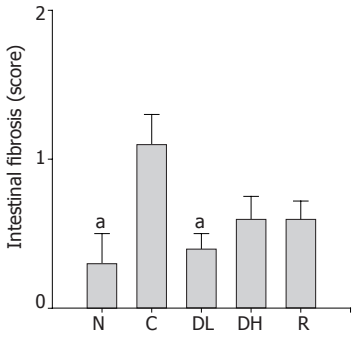

Figure 6 Effects of DA-9601 and rebamipide on the proliferation of collagenous fiber induced by TCA in rats. N: Normal; C: control; DL: 0.065% DA-9601; DH: 0.216% DA-9601; R: 1.08% rebamipide. Data are expressed as mean±SE. [a]*P*<0.05 *vs* controls.

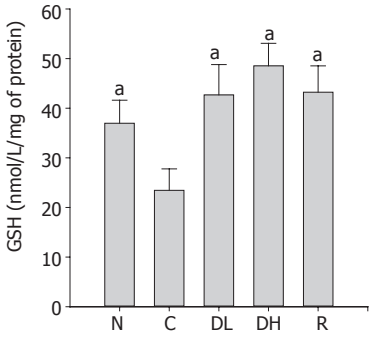

Figure 9 Effects of DA-9601 and rebamipide on glutathione (GSH) induced by TCA in rat gastric mucosa. N: Normal; C: control; DL: 0.065% DA-9601; DH: 0.216% DA-9601; R: 1.08% rebamipide. Data are expressed as mean±SE. [a]*P*<0.05 *vs* controls.

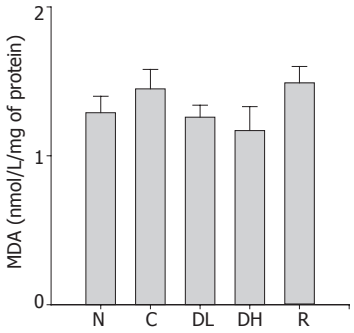

Figure 7 Effects of DA-9601 and rebamipide on malondialdehyde (MDA) induced by TCA in rat gastric mucosa. N: Normal; C: control; DL: 0.065% DA-9601; DH: 0.216% DA-9601; R: 1.08% rebamipide. Data are expressed as mean±SE. [a]*P*<0.05 *vs* controls.

reduced TCA-induced intestinal fibrosis (Figure 6). We found an obvious increase in the score of intestinal fibrosis in controls (1.1±0.2) as compared to normal level (0.3±0.2). On contrary, 0.216% DA-9601 (0.6±0.1) and 1.08% rebamipide (0.6±0.1) showed a decreasing tendency in the score of intestinal fibrosis (Figure 6).

Effects of DA-9601 on gastric mucosal MDA, PGE_2, and GSH

Lipid peroxidation is a well-established mechanism of cellular injury, and the accumulation of MDA is used as an indicator of oxidative stress in cells and tissues. The mean level of MDA in animals treated with DA-9601 and rebamipide was not significantly different from that of controls (Figure 7).

PGE_2 plays an important role in the regulation of gastric mucus secretion. As shown in Figure 8, we detected a significant decrease in PGE_2 contents in the controls (215.2±84.4 pg/mg of protein) as compared to the normal level (374.0±64.9 pg/mg of protein). The treatment with 0.065% DA-9601 (440.3±93.0 pg/mg of protein) and 0.216% DA-9601 (538.7±78.5 pg/mg of protein) could significantly increase the PGE_2 contents in a dose-dependent manner, and 1.08% rebamipide (421.6±88.4 pg/mg of protein) could significantly ameliorate the PGE_2 production (Figure 8).

As shown in Figure 9, we found a significant decrease in the GSH contents in the controls (23.5±4.3 nmol/mg of protein) as compared to normal level (37.0±4.6 nmol/mg of protein). We observed that the treatment with 0.065% DA-9601 (42.7±6.1 nmol/mg of protein) and 0.216% DA-9601 (48.5±4.5 nmol/mg of protein) significantly increased the GSH contents in a dose-dependent manner, and 1.08% rebamipide (43.2±5.3 nmol/mg of protein) significantly ameliorated the GSH production.

DISCUSSION

In the present study, 6 mo of DA-9601 administration resulted in a significant improvement of the experimental chronic erosive and atrophic gastritis induced by 6 mo of TCA treatment. The therapeutic effects of DA-9601 on experimental gastritis were superior to those of rebamipide observed in clinical practice for the treatment of gastritis. Six months of oral administration of TCA solution as drinking water induced the mucosal surface erosions and gastric mucosal thinning, and decreased parietal cell numbers, inflammatory cell infiltration in the lamina propria of the mucosa and mucosal fibrosis in rats. These characterizations were similar to those observed in chronic gastritis caused by bile reflux in human beings[19,20]. DA-9601 ameliorated the reduction in mucosal thickness and the decrease in the number of parietal cells induced by TCA treatment. Furthermore, DA-9601 increased the stimulation of PGE_2 and GSH in the gastric mucosa. These results suggest that DA-9601 promotes the healing of TCA-induced chronic erosive and atrophic gastritis with an etiological factor of the bile reflux.

The TCA-induced infiltration of inflammatory cells in the gastric mucosa was ameliorated by the administration of DA-9601. Tissue damage causes the infiltration of inflammatory cells that have migrated from the capillary vessels. Therefore, this amelioration of inflammatory cell infiltration by DA-9601 may be due to a decreased inflammatory response against damaging tissues through the healing of gastric surface injury. The interstitial space in the gastric mucosa may play an important role as a regulative factor in local microcirculation, and changes in this area may influence the gastric gland, particularly the glandular portion and the cell proliferative zone. Mizumachi *et al*[21]. reported that interstitial fibrosis was associated with decreased gastric mucosal blood flow. In this study, DA-9601 markedly ameliorated the TCA-induced proliferation of collagenous fiber. This change appears to be associated with the improvements in microcirculation via DA-9601-induced increased PGE_2 level.

In fact, reactive oxygen species has been suggested to be involved in the pathogenesis of gastric lesion caused by indomethacin[22,23]. In addition, previous studies have reported that the levels of scavengers and mucosal SOD activity were decreased and the lipid peroxide concentration was increased in the gastric mucosa before the sign of tissue injury appeared[24,25]. Some drugs that are capable of scavenging or inhibiting the generation of ROS have been introduced as effective agents to prevent the gastric mucosal injuries induced by various agents[26,27]. Recently, DA-9601 has been demonstrated to inhibit xanthine oxidase, a major source of ROS generation[28].

One of the causes of TCA-induced gastric lesions is that taurocholate selectively inhibits the synthesis of the vasodilator, PGI_2, an endogenous gastroprotector[29]. The suppression of PGI_2 production decreases the PGI_2/TXA_2 ratio, suggesting that the action of TXA_2 overcomes the action of PGI_2. This decreased ratio may reflect the pathogenesis of gastric ischemia due to vasoconstriction[30,31].

The mechanism by which DA-9601 produces such a therapeutic effect is possibly through its actions that elevate mucosal concentrations of PGE_2, increase the gastric mucosal blood flow, and stimulate re-epithelization and the formation of glandular tissue. PGE_2 has been reported to exert its cytoprotective effect on gastric mucosal epithelial cells by increasing gastric mucus secretion and stimulating cell proliferation in pyloric glands in rats[32]. It has been suggested that DA-9601 promotes the compensatory elevation in proliferative activity of generative cells through the possible increase in PG, which would be available to repair the gastric mucosa in erosive and atrophic gastritis. Gastric mucosal blood flow is essential for the homeostasis of the mucosal structure and function[33]. Whittle *et al*[30]. reported that the administration of (15s)-15-methyl PGE_2 decreased acid back diffusion, increased mucosal blood flow, and significantly reduced the lesions formed by topical TCA plus HCl and indomethacin administration. Kishimoto *et al*[5]. reported that mucosal blood flow was decreased by the administration of TCA. DA-9601 may improve the decreased mucosal blood flow induced by TCA administration although the mucosal blood flow was not measured in this study.

Another possible mechanism is that DA-9601, an antioxidant, neutralizes reactive free oxygen metabolites in the mucosa and attenuates the inflammation. Our results demonstrated that gastric mucosal GSH concentrations were depleted in TCA-induced chronic erosive and atrophic gastritis. The depletion of gastric mucosal GSH in rats with chronic gastritis is likely to render the gastric mucosa more susceptible to oxidative damages and the injurious effects of reactive oxygen species. GSH acts as a scavenger of free radicals and toxic substances ingested with foods or produced directly in the gastrointestinal tract[34].

Reflux gastritis, which occasionally occurs after gastrectomy, is associated with various symptoms, such as abdominal pain, nausea, emesis, and loss of appetite. However, the pathogenic mechanism responsible for the development of gastritis due to bile regurgitation in the stomach has not been fully elucidated. Treating patients exhibiting alkaline reflux symptoms with bile acid binding agents, such as cholestyramine or sucralfate, has been reported to be successful in some cases, but not uniformly successful. It is possible that the presence of lysolecithin, pancreatic enzymes, and cholic acids is responsible for causing erosive changes in the stomach wall[11]. A study has suggested that these factors destroy the mucosal barrier and increase its permeability to hydrogen ions, which can initiate inflammation through a mechanism similar to the one attributed to the erosive effects of salicylates[12].

In conclusion, DA-9601 is a promising agent for the treatment of chronic erosive and atrophic gastritis with an etiological factor of bile reflux. Increased mucosal PGE_2 and reduced glutathione levels by DA-9601 may be its therapeutic mechanisms for chronic erosive and atrophic gastritis.

REFERENCES

1 **van Heerden JA,** Phillips SF, Adson MA, McIlrath DC. Postoperative reflux gastritis. *Am J Surg* 1975; **129:** 82-88
2 **Mackman S,** Lemmer KE, Morrissey JF. Postoperative reflux alkali gastritis and esophagitis. *Am J Surg* 1971; **121:** 694-697
3 **Madura JA.** Primary bile reflux gastritis: diagnosis and surgical treatment. *Am J Surg* 2003; **186:** 269-273
4 **Ritchie WP.** Alkaline reflux gastritis: a critical reappraisal. *Gut* 1984; **25:** 975-987
5 **Kishimoto S,** Ogawa M, Takaba N, Kambara A, Okamoto K, Shimizu S, Kunita T, Daitoku K, Kajiyama G. Experimental model of gastritis induced by sodium taurocholate in rats. *Hiroshima J Med Sci* 1986; **35:** 143-147
6 **Kishimoto S,** Kobuke H, Kobayashi H, Kajiyama G, Miyoshi A. Treatment of established taurocholate-induced chronic erosive gastritis in rats with cimetidine. *Res Commun Chem Pathol Pharmacol* 1991; **71:** 273-292
7 **Oh TY,** Ryu BK, Park JB, Lee SD, Kim WB, Yang J, Lee EB. Studies on antiulcer effects of DA-9601, an *Artemisia Herba* extract against experimental gastric ulcers and its mechanism. *Korean J Appl Pharmacol* 1996; **4:** 111-121
8 **Ahn BO,** Ryu BK, Ko JI, Oh TY, Kim SH, Kim WB, Yang J, Lee EB, Hahm KB. Beneficial effect of DA-9601, an extract of *Artemisiae Herba*, on animal models of inflammatory bowel disease. *Korean J Appl Pharmacol* 1997; **5:** 165-173
9 **Ahn BO,** Oh TY, Ryu BK, Kim SH, Kim WB, Kang SH, Chun MS, Yoon JH. Protective effect of DA-9601, an *Artemisia Herba* extract, on radiation-induced colitis in wistar rats. *Korean J Appl Pharmacol* 1998; **6:** 37-44
10 **Oh TY,** Ryu BK, Ko JI, Ahn BO, Kim SH, Kim WB, Lee EB, Jin JH, Hahm KB. Protective effect of DA-9601, gastric damage in arthritic rats. *Arch Res* 1997; **20:** 414-419
11 **Oh TY,** Lee JS, Ahn BO, Cho H, Kim WB, Kim YB, Surh YJ, Cho SW, Lee KM, Hahm KB. Oxidative stress is more important than acid in the pathogenesis of reflux oesophagitis in rats. *Gut* 2001; **49:** 364-371
12 **Lee JS,** Oh TY, Ahn BO, Cho H, Kim WB, Kim YB, Surh YJ, Kim HJ, Hahm KB. Involvement of oxidative stress in experimentally induced reflux esophagitis and Barrett's esophagus: clue for the chemoprevention of esophageal carcinoma by antioxidants. *Mutat Res* 2001; **480-481:** 189-200
13 **Kishimoto S,** Konemori R, Kambara A, Okamoto K, Shimizu S, Koh H, Kunita T, Daitoku K, Kajiyama G. Endocrine profile in rats with postgastrectomy malabsorption: a pilot study. *Hiroshima J Med Sci* 1985; **34:** 209-213
14 **Kishimoto S,** Kato R, Mukai T, Kanbara A, Okamoto K, Shimizu S, Daitoku K, Kajiyama G. Distribution and endocrine morphology of polypeptide YY (PYY) containing cells in the human gut. *Hiroshima J Med Sci* 1985; **34:** 155-160
15 **Ohkawa H,** Ohishi N, Yagi K. Assay for lipid peroxides in animal tissues by thiobarbituric acid reaction. *Anal Biochem* 1979; **95:** 351-358
16 **Griffith OW.** Determination of glutathione and glutathione disulfide using glutathione reductase and 2-vinylpyridine. *Anal Biochem* 1980; **106:** 207-212
17 **Lowry OH,** Rosebrough NJ, Farr AL, Randall RJ. Protein measurement with the Folin phenol reagent. *J Biol Chem* 1951; **193:** 265-275
18 **Lipscomb GR,** Rees WD. Gastric mucosal injury and adaptation to oral and rectal administration of naproxen. *Aliment Pharmacol Ther* 1996; **10:** 133-138
19 **Jerzy Glass GB,** Pitchumoni CS. Structural and ultrastructural alterations, exfoliative cytology and enzyme cytochemistry and histochemistry, proliferation kinetics, immunological derangements and other causes, and clinical associations and sequallae. *Hum Pathol* 1975; **6:** 219-250
20 **Morson BC,** Dawson IMP. Chronic atrophic gastritis. In: Morson BC Gastrointestinal pathology. Oxford: Blackwell Sci Pub, 1979: 99-101
21 **Mizumachi S,** Takeuchi K, Matsuda K, Harada H, Shimata M, Tada M, Saito M, Sakaki N, Iida Y, Okazaki Y. The histological and functional studies of experimental gastritis in rats. *Nippon Shokakibyo Gakkai Zasshi* 1986; **83:** 7-16
22 **Vaananen PM,** Meddings JB, Wallace JL. Role of oxygen-derived free radicals in indomethacin-induced gastric injury. *Am J Physiol* 1991; **261:** G470-G475
23 **Yoshikawa T,** Naito Y, Kishi A, Tomii T, Kaneko T, Iinuma S, Ichikawa H, Yasuda M, Takahashi S, Kondo M. Role of active oxygen, lipid peroxidation, and antioxidants in the pathogenesis of gastric mucosal injury induced by indomethacin in rats. *Gut* 1993; **34:** 732-737
24 **Oka S,** Ogino K, Hobara T, Yoshimura S, Yanai H, Okazaki Y, Takemoto T, Ishiyama H, Imaizumi T, Yamasaki K. Role of active oxygen species in diethyldithiocarbamate-induced gastric ulcer in the rat. *Experientia* 1990; **46:** 281-287
25 **Ogino K,** Hobara T, Kawamoto T, Kobayashi H, Iwamoto S, Oka S, Okazaki Y. Mechanism of diethyldithiocarbamate-induced gastric ulcer formation in the rat. *Pharmacol Toxicol* 1990; **66:** 133-137
26 **Cho CH,** Pfeiffer CJ, Misra HP. Ulcerogenic mechanism of ethanol and the action of sulphanilyl fluoride on the rat stomach *in-vivo*. *J Pharm Pharmacol* 1991; **43:** 495-498
27 **Hearse DJ,** Manning AS, Downey JM, Yellon DM. Xanthine oxidase: a critical mediator of myocardial injury during ischemia and reperfusion ? *Acta Physiol Scand* Suppl 1986; **548:** 65-78
28 **Huh K,** Kwon TH, Shin US, Kim WB, Ahn BO, Oh TY, Kim JA. Inhibitory effects of DA-9601 on ethanol-induced gastrohemorrhagic lesions and gastric xanthine oxidase activity in rats. *J Ethnopharmacol* 2003; **88:** 269-273
29 **Calcamuggi G,** Lanzio M, Babini G, Martini S, Anfossi G, Emanuelli G. Sodium taurocholate affects prostacyclin constitutive production by cultured human vascular endothelial cells. *J Lab Clin Med* 1990; **115:** 756-760
30 **Whittle BJ,** Kauffman GL, Moncada S. Vasoconstriction with thromboxane A_2 induces ulceration of the gastric mucosa. *Nature* 1981; **292:** 472-474
31 **Esplugues JV,** Whittle BJ. Gastric mucosal damage induced by local intra-arterial administration of Paf in the rat. *Br J Pharmacol* 1988; **93:** 222-228
32 **Sasaki Z,** Murakami M, Misaki F, Kawai K. Turnover of the superficial epithelial cells of the gastric mucosa. *Nihon Rinsho* 1984; **42:** 95-102
33 **Gannon B,** Browning J, O'Brien P, Rogers P. Mucosal microvascular architecture of the fundus and body of human stomach. *Gastroenterology* 1984; **86:** 866-875
34 **Shirin H,** Pinto JT, Liu LU, Merzianu M, Sordillo EM, Moss SF. *Helicobacter pylori* decreases gastric mucosal glutathione. *Cancer Lett* 2001; **164:** 127-133

Science Editor Kumar M and Guo SY **Language Editor** Elsevier HK

PO Box 2345, Beijing 100023, China
www.wjgnet.com
wjg@wjgnet.com

ELSEVIER

World J Gastroenterol 2005;11(47):7436-7443
World Journal of Gastroenterology ISSN 1007-9327

• *BASIC RESEARCH* •

Superoxide dismutase prevents development of adenocarcinoma in a rat model of Barrett's esophagus

Elena Piazuelo, Carmelo Cebrián, Alfredo Escartín, Pilar Jiménez, Fernando Soteras, Javier Ortego, Angel Lanas

Elena Piazuelo, Pilar Jiménez, Instituto Aragonés de Ciencias de la Salud, Unidad Mixta de Investigación, C/Domingo Miral s/n 50009 Zaragoza, Spain
Javier Ortego, Carmelo Cebrián, Service of Pathology, Hospital Clínico Universitario "Lozano Blesa", Avenida San Juan Bosco, 15 50009 Zaragoza, Spain
Fernando Soteras, Alfredo Escartín, Unidad Mixta de Investigación, University of Zaragoza, Domingo Miral s/n 50009 Zaragoza, Spain
Angel Lanas, Service of Gastroenterology, Hospital Clínico Universitario "Lozano Blesa", Avenida San Juan Bosco, 15 50009 Zaragoza, Spain
Supported by grants from CICYT (SAF2000-0123) and Instituto de Salud Carlos III (C03/02). Elena Piazuelo is supported by Instituto de Salud Carlos III and Instituto Aragonés de Ciencias de la Salud
Correspondence to: Elena Piazuelo Ortega, Unidad Mixta de Investigación, Servicio de Biomedicina y Biomateriales, Universidad de Zaragoza, C/Domingo Miral, s/n. 50009 Zaragoza, Spain. epiazor@unizar.es
Telephone: +34-976-762538 Fax: +34-976-762539
Received: 2004-12-16 Accepted: 2005-02-18

Abstract

AIM: To test whether antioxidant treatment could prevent the progression of Barrett's esophagus to adenocarcinoma.

METHODS: In a rat model of gastroduodenoesophageal reflux by esophagojejunal anastomosis with gastric preservation, groups of 6-10 rats were randomized to receive treatment with superoxide dismutase (SOD) or vehicle and followed up for 4 mo. Rat's esophagus was assessed by histological analysis, superoxide anion and peroxinitrite generation, SOD levels and DNA oxidative damage.

RESULTS: All rats undergoing esophagojejunostomy developed extensive esophageal mucosal ulceration and inflammation by mo 4. The process was associated with a progressive presence of intestinal metaplasia beyond the anastomotic area (9% 1st mo and 50% 4th mo) (94% at the anastomotic level) and adenocarcinoma (11% 1st mo and 60% 4th mo). These changes were associated with superoxide anion and peroxinitrite mucosal generation, an early and significant increase of DNA oxidative damage and a significant decrease in SOD levels (P<0.05). Exogenous administration of SOD decreased mucosal superoxide levels, increased mucosal SOD levels and reduced the risk of developing intestinal metaplasia beyond the anastomotic area (odds ratio = 0.326; 95%CI: 0.108-0.981; P = 0.046), and esophageal adenocarcinoma (odds ratio = 0.243; 95%CI: 0.073-0.804; P = 0.021).

CONCLUSION: Superoxide dismutase prevents the progression of esophagitis to Barrett's esophagus and adenocarcinoma in this rat model of gastrointestinal reflux, supporting a role of antioxidants in the chemoprevention of esophageal adenocarcinoma.

Key words: Barrett's esophagus; Esophageal adenocarcinoma; Free radicals; Oxidative damage; Superoxide dismutase

Piazuelo E, Cebrián C, Escartín A, Jiménez P, Soteras F, Ortego J, Lanas A. Superoxide dismutase prevents development of adenocarcinoma in a rat model of Barrett's esophagus. *World J Gastroenterol* 2005; 11(47): 7436-7443
http://www.wjgnet.com/1007-9327/11/7436.asp

INTRODUCTION

The incidence of esophageal adenocarcinoma (EAC) has increased dramatically in Western countries in recent years[1]. Today, the existence of a cause-effect relationship between gastroesophageal reflux disease (GERD) and EAC is firmly accepted. In order to design preventive strategies that might stop/delay the malignant transformation of the esophageal epithelium under the impact of chronic gastroesophageal reflux, it is important to define the mechanisms and mediators of the inflammatory process driving the esophageal mucosa from chronic inflammation to adenocarcinoma. Recent studies have implicated reactive oxygen species (ROS) in the pathogenesis of GERD, Barrett's esophagus (BE) and esophageal cancer. Increased levels of ROS have been found in esophageal tissues of patients with esophagitis and Barrett's epithelium[2]. Furthermore, a positive correlation between the severity of esophagitis and ROS levels has been demonstrated, with the highest levels in patients with BE. At the same time, the free-radical scavenger superoxide dismutase (SOD) level is decreased in esophageal tissue of patients with gastroesophageal reflux, being lowest in patients with severe esophagitis and BE[3,4]. Studies performed in animal models of both acute and chronic reflux esophagitis have

suggested a pathogenic role of ROS, especially superoxide anion, in the development of esophageal mucosal damage. Moreover, administration of SOD has been shown to either prevent or reduce mucosal damage[5-8]. However, it is not known whether SOD is effective in preventing the development of BE and EAC. In order to answer this question, we used an experimental model of gastroenteroesophageal reflux in rats that could lead to the development of EAC, to determine the temporal sequence of development of intestinal metaplasia (IM) and EAC and to assess the involvement of superoxide anion as a mechanism of damage. Finally, we tested whether administration of SOD was able to prevent the development of BE and/or EAC.

MATERIALS AND METHODS

Rat experimental model

All animal studies were carried out in the Service of Biomedicine and Biomaterials of the University of Zaragoza, officially inscribed as a "Research Establishment" for the adequate husbandry and use of all research animals under the "Good Laboratory Practices" norms and Spanish laws (RD 223/1988). The Ethics Committee approved all the procedures. Wistar rats weighing 250-300 g were studied. Rats underwent esophagojejunostomy with gastric preservation, allowing the gastroduodenal content to flow back into the esophagus. In a clean operating field, a midline abdominal incision was made and the liver was retracted to expose the stomach and intra-abdominal portion of the esophagus. Bilateral vagus nerves were preserved and the abdominal esophagus was transected proximal to the cardia and the distal cut end was closed with sutures. The esophagus was anastomosed end-to-side to an enterostomy performed in a jejunum loop distal to Treitz's ligament with 12 interrupted stitches of all layers using 7/0 silk sutures. Sham operation consisted of laparotomy and blunt manipulation of abdominal contents. After the operation, rats were housed in hanging cages to prevent bed ingestion and fasted until d 3 with free access to drinking water. Buprenorphine was used as an analgesic.

Study design and drug administration

For the first purpose of the study, groups of animals (6-10 rats/group) were killed at 1 mo intervals up to 8 mo after esophagojejunostomy or sham operation. Since a high incidence of EAC and IM was found 4 mo after surgery, this follow-up was considered for the second part of the study, where the effect of SOD administration on the development of BE and EAC was tested. SOD (Orgotein-Ontosein®, Tedec-Zambaletti, Madrid, Spain) was administered at a dose of 3 mg/kg (10 000 U/kg) every 3 d subcutaneously. The SOD used was a liver bovine metalloprotein which has been shown to be highly effective in the treatment of secondary effects of radiotherapy on human head and neck tumors[9] and in reducing acid and pepsin-induced esophagitis in rabbits[5,6]. Previously, we have confirmed that the dose of SOD administered to rats increased blood levels of SOD activity for several hours, which returned to basal levels approximately 24 h after SOD administration. However, given the duration of the study and the need for long-term parenteral treatment, we decided to administer SOD to rats once in every 72 h, mimicking the dosage used in patients receiving radiotherapy. Groups of rats (6-10 rats/group) with esophagojejunostomy receiving SOD treatment were killed at 1 mo intervals. Control rats with esophagojejunostomy were administered vehicle following the same pattern as that of SOD treatment.

Rats were killed by CO_2 inhalation. The esophagus was removed and opened longitudinally. More than half of the esophageal specimen was prepared for pathological study. The rest of the esophagus was cut into two slices: the lower and the upper half of the esophagus. For superoxide anion measurements, samples were processed immediately. For the rest of the determinations, samples were frozen immediately in liquid nitrogen and then kept at -70 °C until biochemical studies were performed.

Macroscopic and microscopic evaluation

The tissues were examined by two independent pathologists who were unaware of the experimental conditions. Changes of the squamous epithelium were classified into the following four categories. *Reactive changes*: characterized by the presence of basal cell hyperplasia, papillomatosis and hyperqueratosis with areas of inflammation and ulceration; *Barrett's esophagus*: squamous epithelium was replaced with columnar-lined epithelium comprising occasional and incomplete differentiation of goblet cells, the length must be superior to 3 mm from the anastomosis site or intercalated with squamous epithelium and metaplasia of cells beyond the anastomosis or containing areas of dysplasia; *Dysplasia*: characterized by nuclear atypia, partial loss of mucosecretory function and cell polarity, and an increase in mitotic figures; *Adenocarcinoma*: glandular structures of epithelial cells with architectural dysplasia and cytologic atypia with stromal invasion and deep infiltration. In general, the two pathologists showed a high concordance (kappa coefficient >0.8). However, in case of disagreement, a third pathologist was required to resolve the diagnosis.

Measurement of superoxide anion, peroxynitrite, and SOD activity

The presence of superoxide anion was determined by chemiluminescence using lucigenin (*N*-methyl-acridinium nitrate) as previously described[10]. Results were expressed as counts per minute per milligram of fresh tissue (CPM/mg). Total SOD activity was measured according to a previously described method[10] based on the inhibition of nitro blue tetrazolium (NBT) mediated by superoxide anion. Results were expressed as units of SOD per gram of fresh tissue (U/g). The presence of peroxynitrites was indirectly measured by nitrotyrosine immunohistochemistry using a monoclonal anti-

nitrotyrosine antibody (Chemicon, Temecula, CA, USA). Slides were examined microscopically and scored for relative staining intensity of nitrotyrosine: 0 (negative), 1+ (weak), 2+ (medium), 3+ (strong).

Nitrotyrosine immunoprecipitation

In order to purify the proteins containing tyrosine-nitrated residues, immunoprecipitation was performed using a monoclonal anti-nitrotyrosine antibody as previously described[11,12]. For this purpose, total protein was extracted from rat's esophagus and protein concentrations were measured by Bradford assay (Bio-Rad, Hercules, CA, USA). Extracted proteins (500 μg) were precleared (3 h at room temperature) with 25 μL of protein G-agarose (Roche Applied Science, Mannheim, Germany). After a brief centrifugation, the supernatants were collected and incubated (2 h at room temperature) with 20 μL of anti-nitrotyrosine agarose conjugate (Alexis Biochemicals, Lausen, Switzerland). After the incubation, beads were collected, resuspended in 25 μL of 1× Laemmli sample buffer and boiled for 5 min. Then, the supernatants were immediately subjected to electrophoresis in 12% SDS polyacrylamide gels.

Western blot analysis

For analysis of Cu, Zn-SOD and Mn-SOD expression and detection of nitrated Mn-SOD, Western blot analysis was performed in both total protein extracts (60 μg of total protein) and immunoprecipitated fractions, respectively. After separation by SDS/PAGE, proteins were transferred electrophoretically to PDVF membranes, which were blocked (4 °C, overnight) with 5% non-fat dry milk in 50 mmol/L Tris-HCl, pH 7.4/150 mmol/L NaCl/0.05% Tween 20 (TBST). For detection of Mn-SOD, blots were incubated (1 h, room temperature) with a rabbit polyclonal anti-MnSOD antibody (1:1 000 dilution, Upstate, Charlottesville, VA, USA). For the detection of Cu, Zn-SOD, blots were incubated (1 h, room temperature) with a rabbit polyclonal anti-Cu, Zn-SOD antibody (1:1 000 dilution, Santa Cruz Biotechnology Inc., Santa Cruz, CA, USA). After incubation with primary antibodies, membranes were probed (1 h, room temperature) with 1:3 000 dilution of peroxidase-conjugated secondary antibody in TBS with 0.1% of blocking agent. Immunoreactive proteins were detected using enhanced chemiluminescence (ECL Western blotting analysis system, Amersham Biosciences, Buckinghamshire, UK).

Measurement of 8-hydroxy-2'-deoxyguanosine levels in esophagus

Genomic DNA was extracted from the lower half of the esophagus and digested with DNAse I, alkaline phosphatase, nuclease P1 and phosphodiesterases I and II (Roche Molecular Bio-Chemicals, Indianapolis, IN, USA), in order to obtain free nucleosides according to previously described methods[13]. The nucleoside samples were used for the determination of the amount of 8-hydroxy-2' -deoxyguanosine, which was measured using a competitive enzyme-linked immunosorbent assay kit (Bioxytech 8-OHdG-EIA kit, OXIS Health Products, Portland, USA). Thirty micrograms of digested DNA was added to each well. Each sample was performed in triplicate. Results were expressed as nanograms of 8-OHdG per milligram of total DNA.

Statistical analysis

Data management and statistical analysis were performed using the SPSS software v.10.1. Results from biochemical assays were expressed as mean±SE. Data were compared between groups by non-parametric tests (Kruskall-Wallis and Mann-Whitney). $P<0.05$ was considered statistically significant.

Covariance analysis was used for the analysis of the drug on the quantitative variables, introducing the number of months as covariant. Multiple comparisons were corrected by means of the Bonferroni method. Logistic models were adjusted for the qualitative variables, evaluating in turn the effect of the drug and the months passed.

RESULTS

Pathological findings

Macroscopically, all rats with esophagojejunostomy showed dilatation and thickening of middle and lower esophagus. The inner surface of the esophagus showed ulcerations, which were larger the closer they were to the distal esophagus. Macroscopically, no esophageal tumors were identified. Microscopically, in most animals, the upper and the middle parts of the esophagus showed squamous hyperplasia. Squamous epithelium also showed extensive defects, in the form of erosions in the upper third or ulcers in the proximity of the anastomosis. In all rats with esophagojejunostomy, columnar-lined metaplasia was found in the area of anastomosis, in continuity with the jejunal epithelium (Figures 1A and 1B) after 5 mo. A second type of metaplasia was found far above the anastomosis in some animals. This metaplasia consists of isolated or grouped goblet cells, which formed authentic mucus glands in some cases (Figures 1C and 1D). In all cases an important inflammatory infiltrate was present. Neoplastic transformation of the epithelium was always found near the anastomosis, surrounded by columnar epithelium. Histologically, all tumors were adenocarcinomas, most of them mucinous (70.37%) (Figure 1E).

Incidence of lesions over time

Only rats that were killed in the protocol time were included in the study of the sequence esophagitis-BE-dysplasia-adenocarcinoma. The outcome of the rats included in different groups is shown in Table 1. Sham-operated rats did not show any esophageal change after 8 mo of follow-up. Inflammation, basal cell hyperplasia, hyperqueratosis and ulceration were present in mo 1. Columnar metaplasia was present in the first month,

Table 1 Histological findings after surgery

Mo	1 (n = 11) (%)	2 (n = 11) (%)	3 (n = 8) (%)	4 (n = 16) (%)	5 (n = 11) (%)	6 (n = 8) (%)	7 (n = 11) (%)	8 (n = 8) (%)
Reactive epithelium, ulceration, inflammation	100	100	100	100	100	100	100	100
Intestinal metaplasia in continuity to anastomosis	66.6	100	100	93.75	100	100	100	100
Intestinal metaplasia beyond the anastomosis	9.09	70	62.5	50	63.63	75	40	70
Dysplasia	36.36	85.12	100	93.75	100	100	100	75
Adenocarcinoma	11.11	54.54	87.5	60	90.9	75	80	75

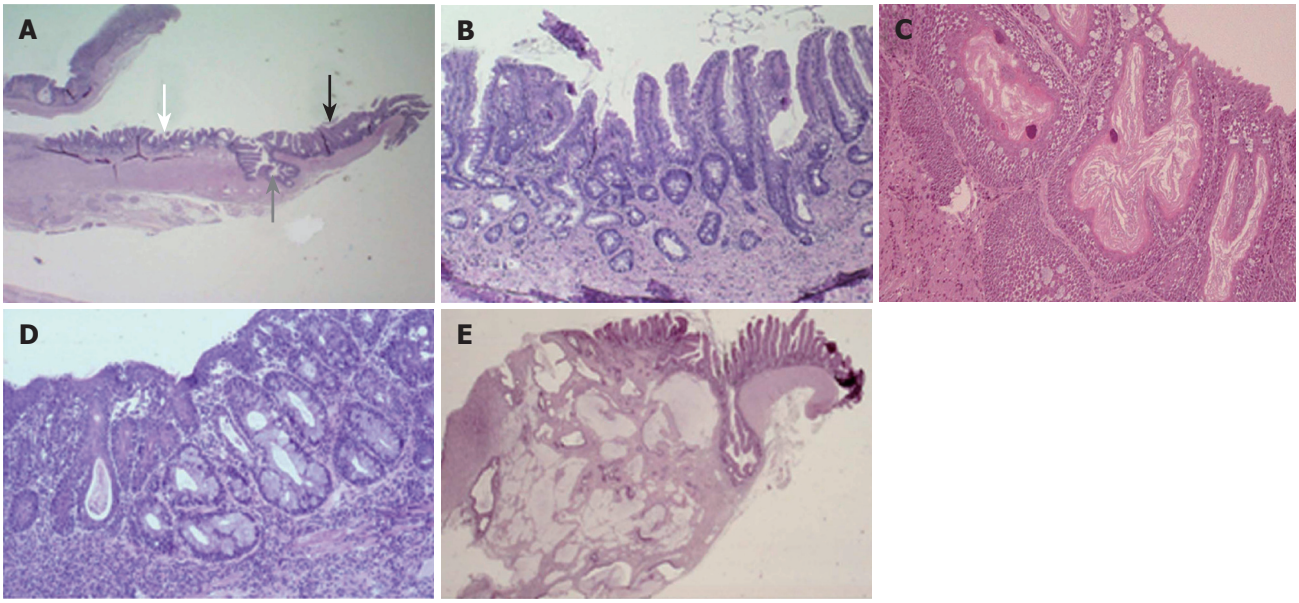

Figure 1 Pathological findings in the esophagus of rats with esophagojejunostomy. (**A**) Development of intestinal metaplasia in the area of anastomosis contiguous to the jejunal epithelium. Characteristic jejunal epithelial villi (white arrow) contrast with blunt villi of metaplastic areas (black arrow). The gray arrow shows the site of anastomosis (H&E staining, ×12.5); (**B**) A higher magnification of (**A**) shows the metaplastic epithelium in detail, with incomplete development of villi and crypts lined by absorptive cells with brush borders and goblet cells (H&E, ×100); (**C**) Intestinal metaplasia developed distant from the anastomosis, consisting of isolated goblet cells immersed within squamous epithelium (H&E, ×100); (**D**) Formation of mucus glands in squamous epithelium; (**E**) Development of mucinous adenocarcinoma from metaplasia in continuity, infiltrating the esophageal wall in depth. The site of anastomosis is shown by the gray arrow (H&E, ×12.5).

reaching an incidence of 100% in mo 2. The length of metaplasia increased progressively over time, with an average length of 1.61 mm in the first month to 6.75 mm in mo 8. Metaplasia also showed a progressive differentiation over time. Metaplasia beyond the anastomosis was identified in the first month, but increased substantially after 2 mo. Dysplasia and adenocarcinoma rates increased dramatically in the second month.

Superoxide anion generation, SOD activity and nitrotyrosine immunohistochemistry

An early and significant increase in superoxide anion generation and a significant decrease in SOD activity were evident in the second month after esophagojejunostomy (Figures 2A and 3A). When grouping the animals according to the highest lesion found in the sequence BE-dysplasia-adenocarcinoma, all groups showed higher superoxide anion levels than control rats (P<0.05), reaching the highest level in those rats with BE (Figure 2B). In parallel to these changes, a significant decrease in SOD activity was observed in all groups of rats with mucosal lesions when compared to control rats (Figure 3B).

In sham-operated rats, nitrotyrosine staining was absent or weak in the esophagus (Figure 4A). In contrast, in rats with esophagojejunostomy, a positive nitrotyrosine staining was found in all rats (55% grade 2, 45% grade 1). Interestingly, the intensity of staining was stronger in squamous epithelium, while weaker positive staining was seen in columnar epithelium (Figure 4B).

SOD expression

The expression of MnSOD and Cu, Zn-SOD was analyzed in total protein extracts. Immunoblot analysis of anti-Cu, Zn-SOD antibody revealed a unique immunoreactive band at 16 ku, corresponding to the molecular mass of monomeric Cu, Zn-SOD. This band was present in rats performed either with sham operation or with esophagojejunostomy and no significant differences were observed among them (Figure 5A). When blots were probed with an anti-MnSOD antibody, the band of 24 ku corresponding to monomeric MnSOD was detected in all cases, though the intensity was progressively increased

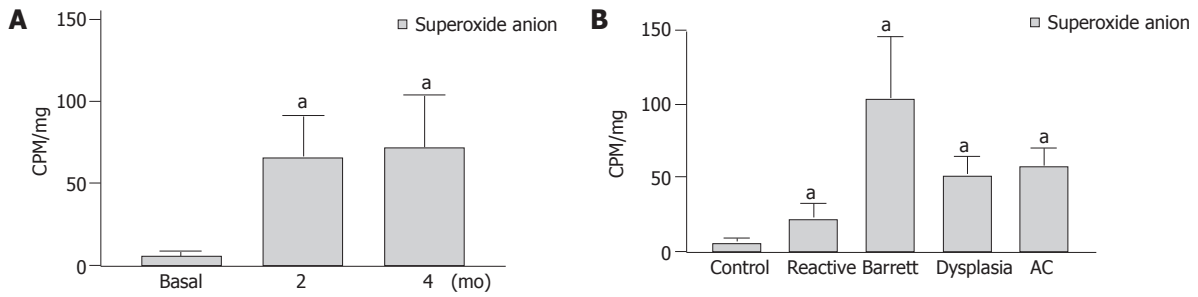

Figure 2 Superoxide anion levels in distal esophagus at different time points (**A**) and in different types of lesion (**B**) after esophagojejunostomy. $^{a}P<0.05$ *vs* control group (sham-operated rats) (n = 6-10).

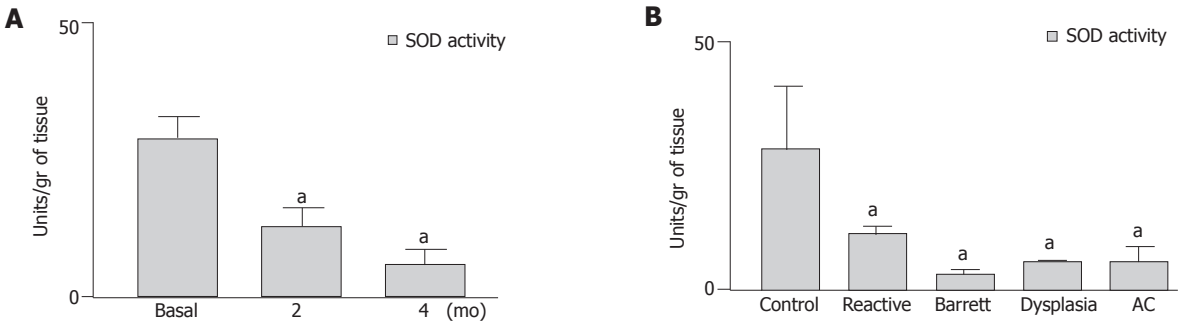

Figure 3 Superoxide dismutase levels in distal esophagus at different time points (**A**) and in different types of lesion (**B**) after surgery. $^{a}P<0.05$ *vs* control group (sham-operated rats) (n = 6-10).

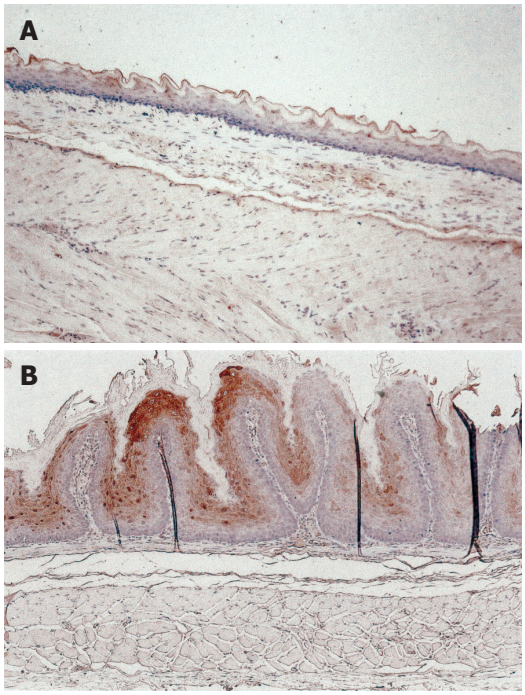

Figure 4 Representative nitrotyrosine immunohistochemical staining in the distal esophagus of rats without reflux (sham operation), showing weak and superficial staining (**A**) and stronger staining (**B**) in the cytoplasm of squamous epithelial cells of rats after 8 weeks of reflux (esophagojejunostomy).

in the esophagus of rats with esophagojejunostomy when compared to sham-operated rats (Figure 5B). Western blot analysis of MnSOD was also performed for nitrotyrosine immunoprecipitates from the rat's esophagus. Immunoblots demonstrated very low but detectable levels of tyrosine-nitrated MnSOD in some of the control tissues. In contrast, the intensity of the band was increased in the esophagus of rats with esophagojejunostomy, especially 4 mo after surgery (Figure 5C).

8-OHdG contents in rat esophagus

When compared to the sham-operated controls, rats with esophagojejunostomy had significantly higher levels of 8-OHdG (8.07±1.08 ng/mg of DNA in sham-operated rats *vs* 15.86±2.34 1st mo, $P<0.05$; 14.4±1.07 2nd mo, $P<0.01$; 14.63±0.63 4th mo, $P<0.01$). However, we did not find a time-dependent increase of 8-OH-dG content in rats with esophagojejunostomy.

Effect of SOD treatment

The exogenous administration of SOD did not significantly affect the development of inflammation, erosions, ulcers or metaplasia in continuity. However, SOD significantly reduced the risk of IM beyond the anastomotic level (odds ratio = 0.326, 95%CI = 0.108-0.981, P = 0.046) (Figure 6A). SOD also significantly decreased the risk of EAC (odds ratio = 0.243, 95%CI = 0.073-0.804, P = 0.021) (Figure 6B). In addition, esophageal mucosal levels of superoxide anion and SOD activity in rats with and without treatment were determined, confirming that administration of SOD significantly decreased superoxide anion production (53.7±10.11 cpm/mg *vs* 22±5.67 cpm/mg protein, $P<0.01$) and significantly increased SOD

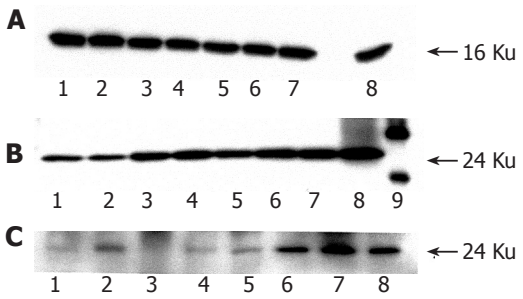

Figure 5 Cu, Zn-SOD and MnSOD expression in total protein extracts from sham-operated rats and rats with esophagojejunostomy. (**A**) A band of 16 ku corresponding to Cu, Zn-SOD observed in both normal rats and rats with enteroesophageal reflux; (**B**) Esophagojejunostomy-induced progressive increase of MnSOD expression; (**C**) Absent or weak nitrated MnSOD in control esophagus and its increase after esophagojejunostomy. Lanes 1-3: sham-operated rats; lanes 4-6: esophagojejunostomy 2 mo of evolution; lanes 7-8: esophagojejunostomy 4 mo of evolution; lane 9: molecular weight marker.

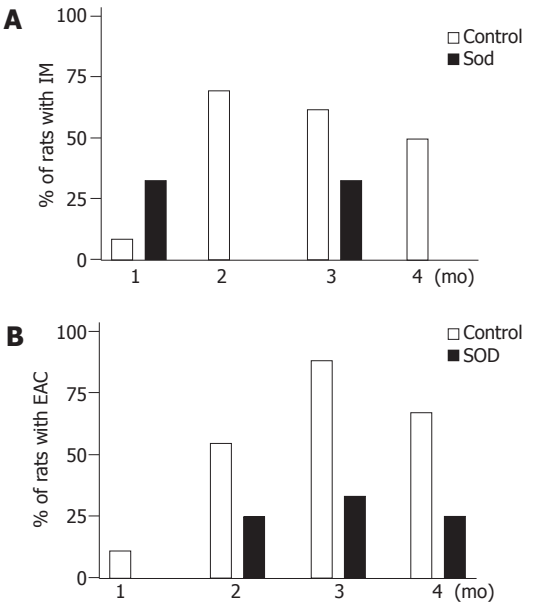

Figure 6 Incidence of intestinal metaplasia distant from the anastomosis site (**A**) and esophageal adenocarcinoma (**B**). The risk of both intestinal metaplasia and adenocarcinoma was significantly lower in the SOD-treated group than in the control group ($P = 0.046$ and $P = 0.021$, respectively) ($n = 6$-10).

activity in rats that received treatment when compared to non-treated rats (28.2±4.72 U/g *vs* 13.4±1.82 U/g tissue, $P<0.05$).

DISCUSSION

Surgical models allowing gastro-duodeno-esophageal reflux or duodeno-esophageal reflux in rats are commonly used to produce experimental BE and EAC[14-17]. Most studies using these models analyzed the prevalence of BE and AC only at one point, but the sequence esophagitis-BE-dysplasia-AC has not been analyzed. The present study established the chronology of this sequence, which is especially useful for analyzing the effect of treatments. Thus, reactive changes and intestinal metaplasia in continuity to the anastomotic site appeared at high rates in the first month, while the prevalence of metaplasia distant from the anastomosis increased considerably in mo 2. High rates of AC were found in mo 4, so we considered this time of follow-up to be sufficient for the second part of the study, which evaluated the efficacy of exogenous administration of SOD in preventing different lesions. The next step of the study was to evaluate the involvement of free radicals, especially superoxide anion as a mechanism of damage in this model. Thus, we showed that the progression of normal mucosa to AC in the esophagus was associated with a parallel increase in superoxide anion mucosal levels. Superoxide anion remained increased until the end of the follow-up, suggesting that superoxide anion plays a pathogenic role in the development of EAC. Furthermore, in the present study we avoided administration of iron, since it has been shown to promote oxidative stress in similar models[18-20]. Therefore, our results provide evidence that gastroduodenal reflux *per se* induces oxidative stress and the development of EAC. Apart from superoxide anion, the involvement of other ROS in this model cannot be excluded. Superoxide anion is scavenged by SOD, generating hydrogen peroxide and oxygen. In this experimental study, a significant and progressive decrease of SOD activity was found, which was parallel to the increase of superoxide anion levels. When SOD activity was analyzed by different degrees of lesion, all groups showed a significantly lower SOD activity than control rats. These data suggest that the decrease of SOD activity may be in part responsible for the accumulation of superoxide anion observed and makes unlikely the generation of hydrogen peroxide in substantial amounts. Since nitric oxide is a natural scavenger of superoxide anion and overexpression of the inducible nitric oxide synthase has been reported in a similar model of EAC in rats[20], the search for generation of the $ONOO^-$ radicals in the mucosa is the next logical step. In the current study, substantial amounts of peroxynitrites analyzed by nitrotyrosine immunostaining were found in the esophagus of rats with esophagojejunostomy, suggesting that peroxynitrite formation is a common event in the presence of excess superoxide anion radicals in this model.

DNA damage resulting from exposure to ROS is believed to play a significant role in carcinogenesis. Though the spectrum of ROS-induced DNA lesions is quite extensive, the modified base 8-hydroxy-2'-deoxyguanosine (8-OHdG) is the most abundant and extensively studied because it can be easily measured[21]. In the present study, 8-OHdG levels were significantly increased at all the time points (1, 2, and 4 mo after esophagojejunostomy), though there were no differences between the different periods. These data indicate that oxidative DNA damage is a very early event and may explain why AC appears so fast in this model. Our results agree with previous studies showing an early increase of oxidative damage to DNA both in an EDA model in rats[22] and in the human esophagitis-metaplasia-dysplasia-AC sequence[23].

The progressive decrease of SOD activity may be due to two main causes: decrease in SOD expression and/or enzyme inactivation. Therefore, we investigated SOD expression by Western blot at different time points of follow-up. Blots revealed that Cu, Zn-SOD expression remained unchanged after esophagojejunostomy, while a progressive increase of MnSOD expression was found, which agrees with previous reports showing higher levels of MnSOD in esophageal carcinomas in comparison to normal tissue[24,25]. The observed increase in MnSOD expression may reflect a compensatory mechanism against the decrease of activity[11]. Therefore, enzyme inactivation is the more plausible mechanism underlying the low SOD activity found in this model. Since tyrosine nitration by peroxynitrite has been shown to inhibit the activity of MnSOD[11], we studied this possibility. We showed that MnSOD was partially tyrosine-nitrated in esophagi exposed to chronic reflux and the amount of nitrated MnSOD increased with time. The low level of nitrated MnSOD observed in some of the control esophagi may reflect the post-mortem ischemia or the basal tyrosine nitration levels under normal physiological conditions. Therefore, we suggest that nitration of MnSOD contributes to partially decrease the SOD activity, but other mechanisms known to inactivate SOD isoforms[26] such as oxidation are likely to be involved in this model.

Administration of various free-radical scavengers can prevent esophageal mucosal damage in different animal models of reflux esophagitis[5-8,27,28], where the most pronounced scavenging effect can be achieved with SOD. However, there is no information about the effect of SOD on the progression of esophageal mucosal damage to BE and EAC. In the present study, administration of SOD significantly reduced the risk of developing IM beyond the anastomotic level and also decreased the risk of EAC, being associated with a relative risk reduction of 68% and 76% respectively. The fact that SOD had no effect on inflammation is in discordance with previous studies demonstrating its effectiveness in preventing esophageal damage in experimental models of esophagitis. However, these studies evaluated the effect of SOD for a short period of time, just hours or at most a few days. Thus, it is possible that the scavenging effect of SOD might be sufficient to decrease mucosal damage in the short term but the magnitude of injury induced by continuous reflux extending over a much longer period of time overwhelms the ability of SOD to avoid mucosal inflammation and ulceration. However, the reduction of IM and AC achieved with the administration of SOD in this study suggests that SOD might be a therapeutic tool for preventing the development of BE and AC in patients with esophagitis. Though administration of SOD in such basis could not completely eliminate the generation of superoxide anion, treatment with SOD significantly lowered superoxide anion levels and increased SOD activity in rat esophagi, indicating that ontosein thus administrated can reach the esophageal mucosa and effectively scavenge superoxide anion at this level.

In conclusion, gastrointestinal reflux induces esophageal IM and AC in most animals undergoing esophagojejunostomy in mo 4. The development of these lesions is associated with esophageal superoxide anion and peroxynitrite generation, reduction of endogenous SOD activity due in part to MnSOD inactivation by nitration and early oxidative damage to DNA. Exogenous administration of SOD reduces the risk of IM and AC in this rat model of gastrointestinal reflux, which constitutes the first evidence showing that antioxidant treatment is effective in preventing BE and EAC.

ACKNOWLEDGMENTS

The authors thank Sara Serrano, Pilar Pina and Lidia Floría from the Service of Pathology for their invaluable technical assistance.

REFERENCES

1 **Blot WJ**, Devesa SS, Fraumeni JF. Continuing climb in rates of esophageal adenocarcinoma: an update. *JAMA* 1993; **270:** 1320
2 **Olyaee M**, Sontag S, Salman W, Schnell T, Mobarhan S, Eiznhamer D, Keshavarzian A. Mucosal reactive oxygen species production in oesophagitis and Barrett's oesophagus. *Gut* 1995; **37**: 168-173
3 **Wetscher GJ,** Hinder RA, Klingler P, Gadenstätter M, Perdikis G, Hinder PR. Reflux esophagitis in humans is a free radical event. *Dis Esophagus* 1997; **10:** 29-32; discussion 33
4 **Wetscher GJ**, Hinder RA, Bagchi D, Hinder PR, Bagchi M, Perdikis G, McGinn T. Reflux esophagitis in humans is mediated by oxygen-derived free radicals. *Am J Surg* 1995; 170: 552-556; discussion 556-557
5 **Naya MJ**, Pereboom D, Ortego J, Alda JO, Lanas A. Superoxide anions produced by inflammatory cells play an important part in the pathogenesis of acid and pepsin induced oesophagitis in rabbits. *Gut* 1997; **40**: 175-181
6 **Lanas A**, Soteras F, Jimenez P, Fiteni I, Piazuelo E, Royo Y, Ortego J, Iñarrea P, Esteva F. Superoxide anion and nitric oxide in high-grade esophagitis induced by acid and pepsin in rabbits. *Dig Dis Sci* 2001; **46**: 2733-2743
7 **Wetscher GJ**, Hinder PR, Bagchi D, Perdikis G, Redmond EJ, Glaser K, Adrian TE, Hinder RA. Free radical scavengers prevent reflux esophagitis in rats. *Dig Dis Sci* 1995; **40**: 1292-1296
8 **Wetscher GJ**, Perdikis G, Kretchmar DH, Stinson RG, Bagchi D, Redmond EJ, Adrian TE, Hinder RA. Esophagitis in Sprague-Dawley rats is mediated by free radicals. *Dig Dis Sci* 1995; **40**: 1297-1305
9 **Valencia J**, Velilla C, Urpegui A, Alvarez I, Llorens MA, Coronel P, Polo S, Bascón N, Escó R. The efficacy of orgotein in the treatment of acute toxicity due to radiotherapy on head and neck tumors. *Tumori* 2002; **88**: 385-389
10 **Soteras F**, Lanas A, Fiteni I, Royo Y, Jimenez P, Iñarrea P, Ortego J, Esteva F. Nitric oxide and superoxide anion in low-grade esophagitis induced by acid and pepsin in rabbits. *Dig Dis Sci* 2000; **45**: 1802-1809
11 **MacMillan-Crow LA**, Crow JP, Kerby JD, Beckman JS, Thompson JA. Nitration and inactivation of manganese superoxide dismutase in chronic rejection of human renal allografts. *Proc Natl Acad Sci USA* 1996; **93**: 11853-11858
12 **Pittman KM,** MacMillan-Crow LA, Peters BP, Allen JB. Nitration of manganese superoxide dismutase during ocular inflammation. *Exp Eye Res* 2002; **74:** 463-471
13 **Huang X,** Powell J, Mooney LA, Li C, Frenkel K. Importance of complete DNA digestion in minimizing variability of 8-oxo-dG analyses. *Free Radic Biol Med* 2001; **31:** 1341-1351

14 **Fein M**, Ireland AP, Ritter MP, Peters JH, Hagen JA, Bremner CG, DeMeester TR. Duodenogastric reflux potentiates the injurious effects of gastroesophageal reflux. *J Gastrointest Surg* 1997; **1**: 27-33
15 **Fein M**, Peters JH, Chandrasoma P, Ireland AP, Oberg S, Ritter MP, Bremner CG, Hagen JA, DeMeester TR. Duodenoesophageal reflux induces esophageal adenocarcinoma without exogenous carcinogen. *J Gastrointest Surg* 1998; **2**: 260-268
16 **Miwa K**, Sahara H, Segawa M, Kinami S, Sato T, Miyazaki I, Hattori T. Reflux of duodenal or gastro-duodenal contents induces esophageal carcinoma in rats. *Int J Cancer* 1996; **67**: 269-274
17 **Seto Y**, Kobori O. Role of reflux oesophagitis and acid in the development of columnar epithelium in the rat oesophagus. *Br J Surg* 1993; **80**: 467-470
18 **Chen X**, Yang Gy, Ding WY, Bondoc F, Curtis SK, Yang CS. An esophagogastroduodenal anastomosis model for esophageal adenocarcinogenesis in rats and enhancement by iron overload. *Carcinogenesis* 1999; **20**: 1801-1808
19 **Goldstein SR**, Yang GY, Curtis SK, Reuhl KR, Liu BC, Mirvish SS, Newmark HL, Yang CS. Development of esophageal metaplasia and adenocarcinoma in a rat surgical model without the use of a carcinogen. *Carcinogenesis* 1997; **18**: 2265-2270
20 **Goldstein SR**, Yang GY, Chen X, Curtis SK, Yang CS. Studies of iron deposits, inducible nitric oxide synthase and nitrotyrosine in a rat model for esophageal adenocarcinoma. *Carcinogenesis* 1998; **19**: 1445-1449
21 **Marnett LJ**. Oxyradicals and DNA damage. *Carcinogenesis* 2000; **21**: 361-370
22 **Chen X**, Ding YW, Yang Gy, Bondoc F, Lee MJ, Yang CS. Oxidative damage in an esophageal adenocarcinoma model with rats. *Carcinogenesis* 2000; **21**: 257-263
23 **Sihvo EI**, Salminen JT, Rantanen TK, Rämö OJ, Ahotupa M, Färkkilä M, Auvinen MI, Salo JA. Oxidative stress has a role in malignant transformation in Barrett's oesophagus. *Int J Cancer* 2002; **102**: 551-555
24 **Janssen AM**, Bosman CB, van Duijn W, Oostendorp-van de Ruit MM, Kubben FJ, Griffioen G, Lamers CB, van Krieken JH, van de Velde CJ, Verspaget HW. Superoxide dismutases in gastric and esophageal cancer and the prognostic impact in gastric cancer. *Clin Cancer Res* 2000; **6**: 3183-3192
25 **Izutani R**, Asano S, Imano M, Kuroda D, Kato M, Ohyanagi H. Expression of manganese superoxide dismutase in esophageal and gastric cancers. *J Gastroenterol* 1998; **33**: 816-822
26 **MacMillan-Crow LA**, Crow JP, Thompson JA. Peroxynitrite-mediated inactivation of manganese superoxide dismutase involves nitration and oxidation of critical tyrosine residues. *Biochemistry* 1998; **37**: 1613-1622
27 **Lee JS**, Oh TY, Ahn BO, Cho H, Kim WB, Kim YB, Surh YJ, Kim HJ, Hahm KB. Involvement of oxidative stress in experimentally induced reflux esophagitis and Barrett's esophagus: clue for the chemoprevention of esophageal carcinoma by antioxidants. *Mutat Res* 2001; **480-481**: 189-200
28 **Oh TY**, Lee JS, Ahn BO, Cho H, Kim WB, Kim YB, Surh YJ, Cho SW, Hahm KB. Oxidative damages are critical in pathogenesis of reflux esophagitis: implication of antioxidants in its treatment. *Free Radic Biol Med* 2001; **30**: 905-915

Science Editor Wang XL and Guo SY **Language Editor** Elsevier HK

PO Box 2345, Beijing 100023, China
www.wjgnet.com
wjg@wjgnet.com

ELSEVIER

World J Gastroenterol 2005;11(47):7444-7449
World Journal of Gastroenterology ISSN 1007-9327

• *BASIC RESEARCH* •

Overexpression of NK2 inhibits liver regeneration after partial hepatectomy in mice

Toshiyuki Otsuka, Norio Horiguchi, Daisuke Kanda, Takashi Kosone, Yuichi Yamazaki, Kazuhisa Yuasa, Naondo Sohara, Satoru Kakizaki, Ken Sato, Hitoshi Takagi, Glenn Merlino, Masatomo Mori

Toshiyuki Otsuka, Norio Horiguchi, Daisuke Kanda, Takashi Kosone, Yuichi Yamazaki, Kazuhisa Yuasa, Naondo Sohara, Satoru Kakizaki, Ken Sato, Hitoshi Takagi, Masatomo Mori, Department of Medicine and Molecular Science, Gunma University Graduate School of Medicine, 3-39-15 Showa, Maebashi, Gunma 371-8511, Japan
Glenn Merlino, Laboratory of Cell Regulation and Carcinogenesis, National Cancer Institute, Building 37, Room 5002, Bethesda, MD 20892-4264, United States
Correspondence to: Hitoshi Takagi, Department of Medicine and Molecular Science, Gunma University Graduate School of Medicine, 3-39-15 Showa, Maebashi, Gunma 371-8511, Japan. htakagi@med.gunma-u.ac.jp
Telephone: +81-27-220-8127 Fax: +81-27-220-8136
Received: 2005-03-28 Accepted: 2005-05-03

Abstract

AIM: To investigate the *in vivo* effects of NK2 on liver regeneration after partial hepatectomy (PH).

METHODS: Survival after PH was observed with 21 NK2 transgenic mice and 23 wild-type (WT) mice over 10 d. Liver regeneration was analyzed using histology and immunohistochemistry. Expressions of genes were analyzed using Northern blot analysis, immunoprecipitation and immunoblotting, and reverse transcriptase polymerase chain reaction assay. Kaplan-Meier method and the log-rank test were used for analyzing the survival after PH. Differences in the results of immunohistochemistry and percentage of liver regeneration was determined by the Student's *t*-test.

RESULTS: More than half of NK2 transgenic mice died within 48 h after PH. After PH, increased deposition of small lipid droplets in hepatocytes was evident and hepatic proliferation was inhibited in NK2 transgenic mice. The hepatic expression and kinase activity of HGF receptor, c-Met, were unchanged among WT mice and NK2 transgenic mice after PH. The expression of tumor necrosis factor-α (TNF-α) and interleukin-6 (IL-6) in liver tissues were prolonged in NK2 transgenic mice that died after PH.

CONCLUSION: Our findings indicate that overexpression of NK2 inhibits liver regeneration after PH.

Key words: Hepatocyte growth factor; NK2; Transgenic mice; Partial hepatectomy; Liver regeneration

Otsuka T, Horiguchi N, Kanda D, Kosone T, Yamazaki Y, Yuasa K, Sohara N, Kakizaki S, Sato K, Takagi H, Merlino G, Mori M. Overexpression of NK2 inhibits liver regeneration after partial hepatectomy in mice. *World J Gastroenterol* 2005; 11(47): 7444-7449
http://www.wjgnet.com/1007-9327/11/7444.asp

INTRODUCTION

Hepatocyte growth factor (HGF) is a multifunctional cytokine involved in proliferation, motility, and morphogenesis[1]. The effects of HGF are mediated through the tyrosine kinase receptor, c-Met[2]. HGF is reportedly the most potent mitogen for hepatocytes and acts as a trigger for liver regeneration[3,4]. Indeed, HGF knockout mice died *in utero* and the embryonic liver was reduced in size and had extensive loss of parenchymal cells[5]. In c-Met conditional knockout mice produced by using the Mx-cre transgene to introduce the mutation in the adult, liver regeneration after PH was impaired[6,7]. In c-Met conditional knockout mice produced by Cre/loxP-mediated gene targeting, recovery from necrosis induced by carbon tetrachloride (CCl_4) was impaired[8]. These data indicate that the HGF/c-Met signaling pathway plays an important role in liver regeneration and repair.

HGF is a heterodimeric glycoprotein consisting of an α chain of 60 ku and a β chain of 30 ku[9]. The α chain has an N domain and four kringle domains. HGF mRNA can undergo alternative splicing to create a truncated isoform, NK2, which consists of an N domain and the first two kringle domains of HGF[10]. NK2 is also able to bind to c-Met with relatively high affinity and is thought to be an HGF antagonist of a variety of biological activities *in vitro*[1,11-13]. *In vivo*, it has been reported that NK2 acts as an antagonist of HGF in cellular proliferation and protective effect on CCl_4 induced hepatotoxicity[14,15].

Here we have reported that NK2 inhibits hepatocyte proliferation and impairs liver regeneration after PH in our transgenic model.

MATERIALS AND METHODS

Animals

NK2 transgenic mice were generated on an albino FVB

genetic background as previously described[14]. Expressions of human NK2 cDNA was under the control of the mouse metallothionein-1 (MT-1) promoter and associated locus control regions as previously described[16]. Wild-type (WT) mice were littermates of NK2 transgenic mice. All studies were performed using 6-wk-old female mice. PH, consisting of removal of the median and left lateral hepatic lobes, was performed as previously described[17]. Survival was observed with 21 NK2 transgenic mice and 23 WT mice over 10 d. Percentage of liver regeneration was defined as follows: [wet weight of regenerating liver/body weight (g/g mouse)]/[wet weight of original liver/body weight (g/g mouse)]×100%[18]. The animal experiments were conducted in compliance with the guidelines for animal care and use established by Gunma University Graduate School of Medicine.

Histology

Mice were injected with 50 μg/g of 5-bromo-2' -deoxyuridine (BrdU, Becton Dickinson, San Jose, CA, USA) 1 h before being killed. Livers were removed before and 48 h after PH. The tissues were fixed in 10% formalin, embedded in paraffin and stained with hematoxylin-eosin (H-E) and Oil-red-O. For immunohistochemistry, slides were stained with monoclonal antibody to BrdU. At 48 h after PH, the labeled hepatocyte nuclei were scored by counting 30 high-power light microscope fields (×1 000) for each animal.

Northern blot analysis

Total RNAs from liver tissues were prepared using TRIzol (Gibco BRL, Gaithersburg, MD, USA) according to the instructions provided by the manufacturer, and 20 μg of total RNA was loaded per lane onto a 1% agarose-formaldehyde gel and transferred to a nylon membrane (Amersham Pharmacia Biotech, Piscataway, NJ, USA). As described previously, transcripts of the NK2 transgene and endogenous c-Met were detected with a 2.2-kbp mouse HGF cDNA probe and a 1.5-kbp mouse c-Met cDNA probe, respectively[15]. The membrane was rehybridized with a mouse β-actin probe (generously provided by Kojima I) to control for RNA loading and transfer variation.

Immunoprecipitation (IP) and immunoblotting (IB)

Quantification of c-Met and c-Met tyrosine phosphorylation was performed as described previously[19]. Briefly, frozen liver tissues were solubilized in RIPA buffer consisting of 50 mmol/L Tris (pH 7.4), 50 mmol/L NaCl, 1% Triton X-100, 5 mmol/L ethylenediaminetetraacetic acid, 10 mmol/L sodium PPi (Sigma, St. Louis, MO, USA), 50 mmol/L sodium fluoride (Sigma), 1 mmol/L sodium orthovanadate (Sigma), 1 mmol/L phenylmethylsulfonyl fluoride (Boehringer Mannheim, Mannheim, Germany), 10 μg/mL leupeptin (Boehringer Mannheim), 10 μg/mL pepstatin (Boehringer Mannheim, Tokyo, Japan) and 10 μg/mL aprotinin (Boehringer Mannheim). Protein concentration in the resulting lysates was determined using Albumin Standard (Pierce, Rockford, IL, USA) and equivalent amounts of lysate (200 μg) were incubated with anti c-Met antibody (Santa Cruz Biotechnology, Santa Cruz, CA, USA) for 2 h on ice. After the addition of GammaBind G Sepharose (Boehringer Mannheim) and washing in RIPA buffer, samples were fractionated on 10% polyacrylamide gels (Biocraft). After electrophoretic transfer to nitrocellulose membranes (Bio-Rad, Richmond, CA, USA), filters were blocked and then incubated with anti c-Met antibody overnight. c-Met was visualized by incubation with anti-goat antibody conjugated to horseradish peroxidase (Santa Cruz Biotechnology, CA, USA) by using enhanced chemiluminescence (Santa Cruz Biotechnology, CA, USA) according to the instructions supplied by the manufacturer. Subsequently, filters were stripped with buffer consisting of 100 mmol/L 2-mercaptoethanol (Sigma), 2% sodium dodecyl sulfate, and 62.5 mmol/L Tris-HCl (pH 6.7) at 50 ℃ for 30 min. Filters were reblocked and incubated overnight with anti-phosphotyrosine (PY) antibody (Transduction Laboratories, Lexington, KY, USA) overnight. PY was visualized using an anti-rabbit antibody conjugated to horseradish peroxidase (Santa Cruz Biotechnology, CA, USA) and enhanced chemiluminescence (Santa Cruz Biotechnology, CA, USA) according to the instructions obtained from the manufacturer.

Reverse transcriptase polymerase chain reaction (RT-PCR) assay

RT-PCR was used to measure the expression of liver TNF-α mRNA and liver IL-6 mRNA. Total RNAs from liver tissues were prepared using TRIzol as previously described[15]. cDNA was prepared from 1 μg of total RNA from each liver sample by the SuperScript Preamplification System for First Strand cDNA Synthesis kit (GIBCO BRL) according to the manufacturer's instructions. The PCR reaction contained, in the same buffer as the reverse transcriptase reaction, cDNA corresponding to 50 ng of input RNA and 2.5 U AmpliTaq DNA polymerase. It was performed at 94 ℃ for 1 min, 55 ℃ for 1 min, 72 ℃ for 1.5 min for 35 cycles. Amplified products were electrophoresed in 2% agarose gels and stained with ethidium bromide. The primer pairs used were as follows[20]. TNF-α sense, 5'-AGCCCACGTCGTAGCA AACCACCAA-3'; antisense, 5'-ACACCCATTCCCTT CACAGAGCAAT-3' (448-bp product size), IL-6 sense, 5'-TATGAAGTTCCTCTCTGCAA-3'; antisense, 5' -CTTTGTATCTCTGGAAGTTT-3' (285-bp product size), β-actin sense, 5'-GCACCACACCTTCTACAATGA G-3'; antisense, 5'-AAATAGCACAGCCTGGATAGCAA C-3' (150-bp product size).

Statistical analysis

All experimental data are shown as mean±SD. Cumulative survival was plotted by the Kaplan-Meier method, and the significance of differences was examined by the log-rank test. Differences in the index of BrdU-labeled hepatocytes and percentage of liver regeneration were determined by

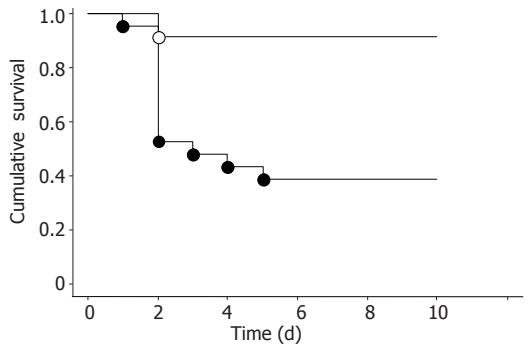

Figure 1 Cumulative survival after PH.Survival of WT mice (n = 23, open circles) and NK2 transgenic mice (n = 21, closed circles) after PH. The survival rate was significantly low in NK2 transgenic mice (^bP<0.01 *vs* WT mice).

the Student's t-test for each group. The level of significance for all statistical analyses was set at P<0.01.

RESULTS

Survival after PH

We examined the effect of NK2 on mortality of mice after PH (Figure 1). Ten of 21 NK2 transgenic mice (47.6%) died within 2 d. In contrast, 2 of 23 WT mice (8.7%) died within 2 d. Survival of NK2 transgenic mice after PH was significantly decreased compared with that of WT mice (P<0.01). Sham operation was performed using four mice per group. All four NK2 transgenic mice and all four WT mice survived until experiments were terminated after 10 d (data not shown).

Morphological alteration in liver and hepatocyte proliferation after PH

The liver structure of regenerating livers of WT mice after PH was normal (Figure 2A). NK2 transgenic mice that died during the first 48 h after PH had smooth and yellow livers. Histological examination revealed that livers of the dying NK2 transgenic mice contained a very large amount of intracellular small droplets at 48 h after PH (Figure 2B). These vesicles were readily identifiable as lipid by Oil-red-O stain (Figure 2C). BrdU staining was performed to analyze hepatocyte proliferation of each mouse at 48 h after PH (Figures 2D and E). The labeling index of the dying NK2 transgenic hepatocytes was significantly decreased relative to that of WT at 48 h after PH (WT, 18.0±6.6; dying NK2, 0.8±1.0, P<0.01) (Figure 2F). On the other hand, the percentage of liver regeneration of healthy NK2 transgenic mice and that of WT mice at 48 h after PH were 69.0±8.6% (n = 5) and 66.1±5.0% (n = 4), respectively (P = 0.59).

Expression of the transgene, endogenous c-Met and activation of c-Met in the liver after PH

High expression of transgene was detected at each time point in NK2 transgenic livers (Figure 3A). There was no difference of endogenous c-Met expression among WT mice, dying NK2 transgenic mice and healthy NK2 transgenic mice (Figure 3A). We next investigated the expression and phosphorylation of c-Met protein. The levels of c-Met protein were in accordance with the c-Met transcription findings and there was no difference of tyrosine phosphorylation of c-Met among the WT mice, dying NK2 transgenic mice and healthy NK2 transgenic mice (Figure 3B).

Hepatic expression of TNF-α and IL-6 after PH

We next examined the expressions of TNF-α and IL-6 mRNAs before PH and 48 h after PH in the livers of WT mice, dying NK2 transgenic mice and healthy NK2 transgenic mice by RT-PCR (Figure 4). TNF-α mRNA was increased in the livers of the dying NK2 at 48 h after PH. In contrast, the level of TNF-α mRNA expression at that point was similar to that before PH in WT mice and healthy NK2 transgenic mice. IL-6 mRNA was detected in the livers of the dying NK2 at 48 h after PH but not detected in WT mice and healthy NK2 transgenic mice at that point.

DISCUSSION

HGF is a potent mitogen for hepatocytes and appears to act on hepatocytes during liver regeneration after PH[3]. Indeed, HGF stimulates liver regeneration after PH in HGF transgenic mice[18,21]. NK2 is a naturally occurring HGF alternative splice variant and acts as an antagonist of HGF *in vitro*[1]. However, very little is known about the *in vivo* role of NK2 in the modulation of HGF activity. When NK2 transgenic mice, created using a mouse MT-1 promoter and associated locus control regions, were treated with zinc sulfate in water, a small reduction in liver size was observed[14]. This finding indicated that NK2 was able to inhibit endogenous HGF-mediated hepatocyte proliferation *in vivo*. Recently, we have demonstrated that overexpression of NK2 does not inhibit hepatocyte proliferation after liver damage induced by CCl_4 administration using NK2 transgenic mice[15]. In this study, we have investigated the effects of NK2 on liver regeneration after PH using NK2 transgenic mice. After PH, about half of the NK2 transgenic mice died within 2 d, whereas almost all WT mice survived that period. NK2 transgenic mice did not exhibit overt abnormal phenotypes, including the liver[15]. However, the NK2 transgenic mice that died after PH showed massive intracellular accumulation of lipid in hepatocytes at 48 h after PH. Moreover, the BrdU leveling index of hepatocytes in NK2 transgenic mice at 48 h after PH demonstrated their poor capacity to enter the S phase. Because DNA replication after PH starts at 20 to 34 h and reaches a peak at 36 to 44 h in mice[22,23], these results indicate that overexpression of NK2 inhibited DNA replication of hepatocytes after PH. The plasma HGF level was reported to peak at 48 h after PH[24]. Hepatic expression of the NK2 transgene transcript was very high at each time point after PH. This suggested that overexpression of NK2 inhibited the proliferative effect of endogeneous HGF after PH. On the other hand, the

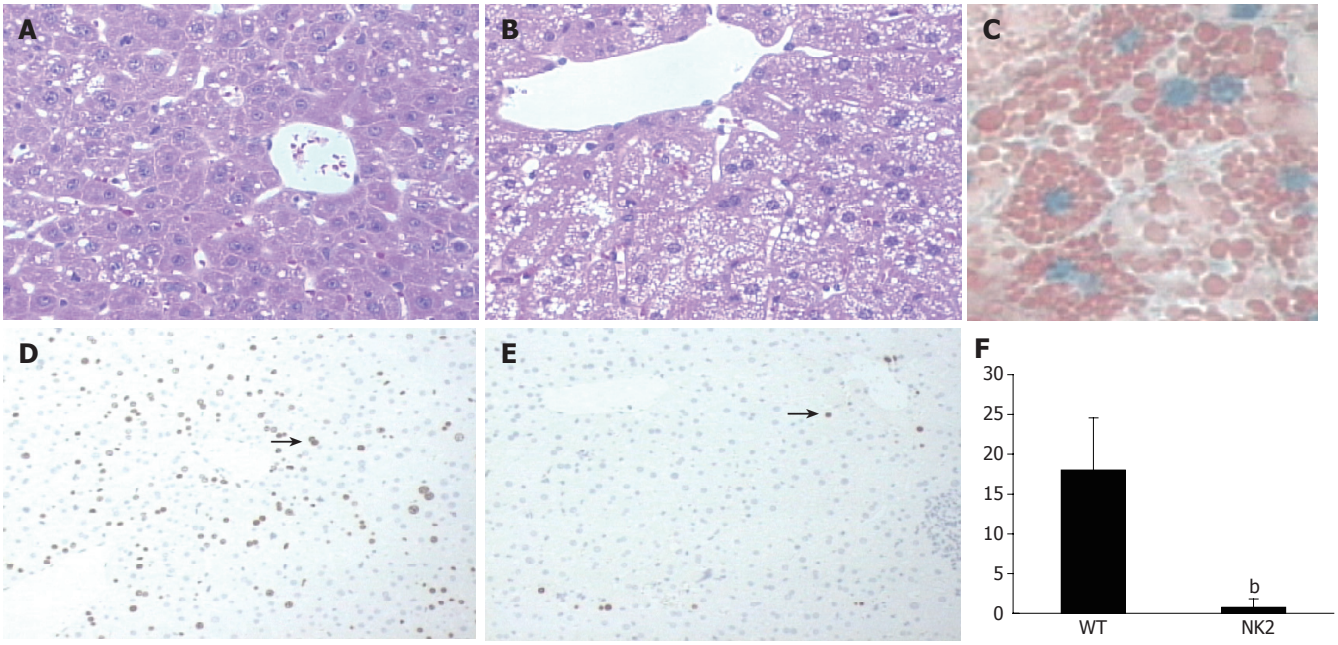

Figure 2 Liver regeneration and proliferation of hepatocytes after PH. H-E stain of WT mouse liver (**A**) and NK2 transgenic mouse liver (**B**) at 48 h after PH. NK2 transgenic mouse liver contained a large amount of intracellular small droplets. Magnification, ×200. Oil-red-O stain of NK2 transgenic mouse liver (**C**) at 48 h after PH. Note the presence of many small lipid droplets in hepatocytes. Magnification, ×400. BrdU stain of WT mouse liver (**D**) and NK2 transgenic mouse liver (**E**) at 48 h after PH. The arrows show hepatocytes undergoing DNA synthesis. Magnification, ×100. The BrdU labeling index of WT mice and NK2 transgenic mice at 48 h after PH (n = 30 per group). (**F**) Data are mean±SD of the mean. Hepatocyte proliferation was significantly reduced in NK2 transgenic mouse liver ($^bP<0.01$ *vs* WT mouse liver).

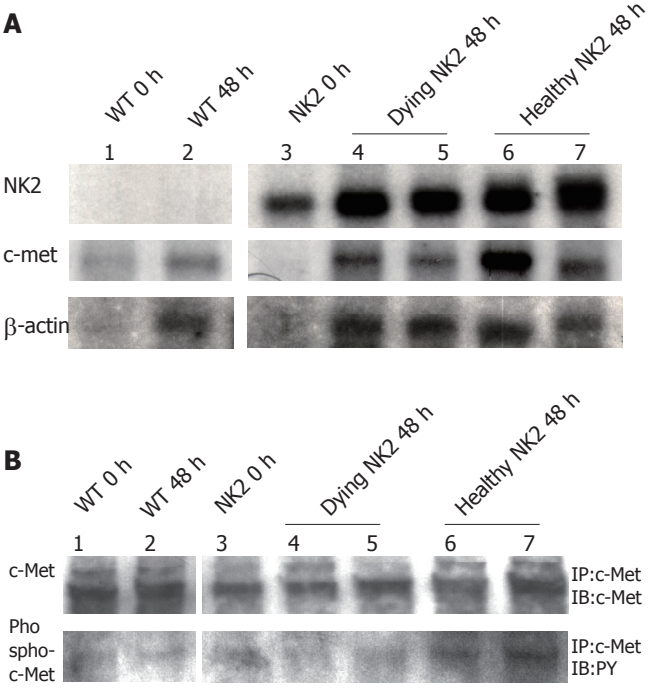

Figure 3 Expressions of RNAs and proteins of transgene and c-Met after PH. RNA expression of transgenic NK2 and c-Met, and c-Met protein levels and activity in livers from WT and NK2 transgenic mice after PH. Lane 1, WT mouse before PH; lane 2, WT mouse at 48 h after PH; lane 3, NK2 transgenic mouse before PH; lanes 4 and 5, dying NK2 transgenic mice at 48 h after PH; lanes 6 and 7, healthy NK2 transgenic mice at 48 h after PH. (**A**) Each RNA sample was subjected to Northern blot analysis. Expression levels of all transgenes were high at each time point and endogeneous c-Met expression was unaltered in each group. β-actin RNA expression was also examined as a control. (**B**) Each protein sample was subjected to IP and then IB with an anti c-Met antibody or an anti PY antibody. c-Met expression and the kinase activity were unaltered in each group.

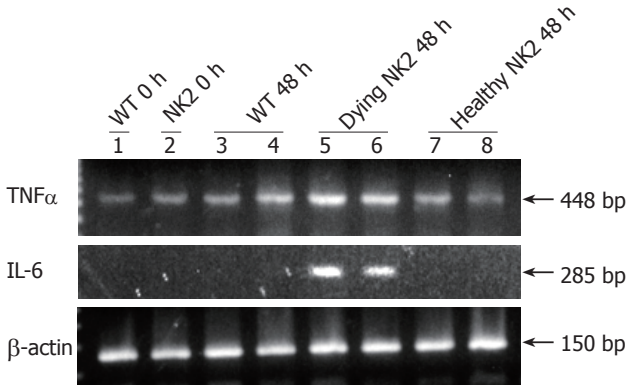

Figure 4 RNA expression of TNF-α and IL-6 after PH. TNF-α mRNA and IL-6 mRNA expression in livers of WT mice and NK2 transgenic mice. Lane 1, WT mouse before PH; lane 2, NK2 transgenic mouse before PH; lanes 3 and 4, WT mice at 48 h after PH; lanes 5 and 6, dying NK2 transgenic mice at 48 h after PH; lanes 7 and 8, healthy NK2 transgenic mice at 48 h after PH. The expression of TNF-α mRNA was increased in NK2 transgenic mice that died at 48 h after PH. IL-6 mRNA expression was detected in NK2 transgenic mice that died at 48 h after PH. β-actin mRNA expression was also examined as a control.

expression of endogenous c-Met RNA and c-Met protein, and phosphorylation of c-Met in the livers of WT and NK2 transgenic mice was unchanged at each time point after PH. Although we did not understand why only half of NK2 transgenic mice died, there could be differences in circulating levels of NK2 or critical local changes in the transgene expression[25].

Hepatocyte proliferation after PH occurs first in periportal cells, and then in perivenous cells[26]. This indicates that HGF is produced from endothelial and

Kupffer cells, and stimulates hepatocyte proliferation via a paracrine mechanism. In addition, HGF acts on hepatocytes located around the central vein by an endocrine mechanism. On the other hand, after CCl_4 administration, hepatocyte proliferation occurs randomly in the lobulus[27]. This indicates that HGF is produced by a paracrine mechanism. HGF may therefore have a differential role in hepatocyte proliferation in the PH and CCl_4 administration models. That is, NK2 overexpression might be inhibitory to hepatocyte proliferation after PH but not after CCl_4-induced acute liver injury.

TNF-α and IL-6 are known to be initiators of liver regeneration after PH[22]. Studies in TNF receptor 1 and IL-6 knock out mice demonstrated the sequence in which TNF-α is induced first after PH, followed by induction of IL-6[22]. Hepatic IL-6 mRNA expression peaked at 4 h after PH in WT mice[28]. TNF receptor 1 knock out mice showed massive lipid accumulation in hepatocytes at 40 h after PH[29] and IL-6 knock out mice showed poor hepatocyte DNA synthesis at 36 h after PH[30]. The observations in these mice are similar to those in NK2 transgenic mice after PH. We have investigated hepatic expression of TNF-α and IL-6 mRNA in NK2 transgenic mice after PH. TNF-α mRNA was increased and IL-6 mRNA was detected in the dying NK2 at 48 h after PH. This result indicates that liver regeneration was impaired in NK2 transgenic mice.

In conclusion, our study demonstrates that overexpression of NK2 prevents liver regeneration after PH.

REFERENCES

1 **Montesano R,** Soriano JV, Malinda KM, Ponce ML, Bafico A, Kleinman HK, Bottaro DP, Aaronson SA. Differential effects of hepatocyte growth factor isoforms on epithelial and endothelial tubulogenesis. *Cell Growth Differ* 1998; **9:** 355-365

2 **Bottaro DP,** Rubin JS, Faletto DL, Chan AM, Kmiecik TE, Vande Woude GF, Aaronson SA. Identification of the hepatocyte growth factor receptor as the c-met proto-oncogene product. *Science* 1991; **251:** 802-804

3 **Fausto N,** Laird AD, Webber EM. Liver regeneration. 2. Role of growth factors and cytokines in hepatic regeneration. *FASEB J* 1995; **9:** 1527-1536

4 **Phaneuf D,** Moscioni AD, LeClair C, Raper SE, Wilson JM. Generation of a mouse expressing a conditional knockout of the hepatocyte growth factor gene: demonstration of impaired liver regeneration. *DNA Cell Biol* 2004; **23:** 592-603

5 **Schmidt C,** Bladt F, Goedecke S, Brinkmann V, Zschiesche W, Sharpe M, Gherardi E, Birchmeier C. Scatter factor/hepatocyte growth factor is essential for liver development. *Nature* 1995; **373:** 699-702

6 **Borowiak M,** Garratt AN, Wustefeld T, Strehle M, Trautwein C, Birchmeier C. Met provides essential signals for liver regeneration. *Proc Natl Acad Sci USA* 2004; **101:** 10608-10613

7 **Hodgson H**. c-met-there when it's needed? *J Hepatol* 2005; **43:** 544-546

8 **Huh CG,** Factor VM, Sanchez A, Uchida K, Conner EA, Thorgeirsson SS. Hepatocyte growth factor/c-met signaling pathway is required for efficient liver regeneration and repair. *Proc Natl Acad Sci USA* 2004; **101:** 4477-4482

9 **Nakamura T,** Nishizawa T, Hagiya M, Seki T, Shimonishi M, Sugimura A, Tashiro K, Shimizu S. Molecular cloning and expression of human hepatocyte growth factor. *Nature* 1989; **342:** 440-443

10 **Chan AM,** Rubin JS, Bottaro DP, Hirschfield DW, Chedid M, Aaronson SA. Identification of a competitive HGF antagonist encoded by an alternative transcript. *Science* 1991; **254:** 1382-1385

11 **Recio JA,** Merlino G. Hepatocyte growth factor/scatter factor induces feedback up-regulation of CD44v6 in melanoma cells through Egr-1. *Cancer Res* 2003; **63:** 1576-1582

12 **Liang H**, O'Reilly S, Liu Y, Abounader R, Laterra J, Maher VM, McCormick JJ. Sp1 regulates expression of MET, and ribozyme-induced down-regulation of MET in fibrosarcoma-derived human cells reduces or eliminates their tumorigenicity. *Int J Oncol* 2004; **24:** 1057-1067

13 **Guerin C,** Luddy C, Abounader R, Lal B, Laterra J. Glioma inhibition by HGF/NK2, an antagonist of scatter factor/hepatocyte growth factor. *Biochem Biophys Res Commun* 2000; **273:** 287-293

14 **Otsuka T,** Jakubczak J, Vieira W, Bottaro DP, Breckenridge D, Larochelle WJ, Merlino G. Disassociation of met-mediated biological responses in vivo: the natural hepatocyte growth factor/scatter factor splice variant NK2 antagonizes growth but facilitates metastasis. *Mol Cell Biol* 2000; **20:** 2055-2065

15 **Otsuka T,** Takagi H, Horiguchi N, Toyoda M, Sato K, Takayama H, Mori M. CCl4-induced acute liver injury in mice is inhibited by hepatocyte growth factor overexpression but stimulated by NK2 overexpression. *FEBS Lett* 2002; **532:** 391-395

16 **Palmiter RD,** Sandgren EP, Koeller DM, Brinster RL. Distal regulatory elements from the mouse metallothionein locus stimulate gene expression in transgenic mice. *Mol Cell Biol* 1993; **13:** 5266-5275

17 **Webber EM,** Wu JC, Wang L, Merlino G, Fausto N. Overexpression of transforming growth factor-alpha causes liver enlargement and increased hepatocyte proliferation in transgenic mice. *Am J Pathol* 1994; **145:** 398-408

18 **Sakata H,** Takayama H, Sharp R, Rubin JS, Merlino G, LaRochelle WJ. Hepatocyte growth factor/scatter factor overexpression induces growth, abnormal development, and tumor formation in transgenic mouse livers. *Cell Growth Differ* 1996; **7:** 1513-1523

19 **Horiguchi N**, Takayama H, Toyoda M, Otsuka T, Fukusato T, Merlino G, Takagi H, Mori M. Hepatocyte growth factor promotes hepatocarcinogenesis through c-Met autocrine activation and enhanced angiogenesis in transgenic mice treated with diethylnitrosamine. *Oncogene* 2002; **21:** 1791-1799

20 **Tozawa K,** Hanai H, Sugimoto K, Baba S, Sugimura H, Aoshi T, Uchijima M, Nagata T, Koide Y. Evidence for the critical role of interleukin-12 but not interferon- gamma in the pathogenesis of experimental colitis in mice. *J Gastroenterol Hepatol* 2003; **18:** 578-587

21 **Shiota G,** Wang TC, Nakamura T, Schmidt EV. Hepatocyte growth factor in transgenic mice: effects on hepatocyte growth, liver regeneration and gene expression. *Hepatology* 1994; **19:** 962-972

22 **Fausto N.** Liver regeneration. *J Hepatol* 2000; **32:** 19-31

23 **Tzung SP,** Fausto N, Hockenbery DM. Expression of Bcl-2 family during liver regeneration and identification of Bcl-x as a delayed early response gene. *Am J Pathol* 1997; **150:** 1985-1995

24 **Pediaditakis P,** Lopez-Talavera JC, Petersen B, Monga SP, Michalopoulos GK. The processing and utilization of hepatocyte growth factor/scatter factor following partial hepatectomy in the rat. *Hepatology* 2001; **34:** 688-693

25 **Yu Y,** Merlino G. Constitutive c-Met signaling through a nonautocrine mechanism promotes metastasis in a transgenic transplantation model. *Cancer Res* 2002; **62:** 2951-2956

26 **Sakai H,** Tsukamoto T, Yamamoto M, Shirai N, Iidaka T, Yanai T, Masegi T, Tatematsu M. Differential effects of partial hepatectomy and carbon tetrachloride administration on induction of liver cell foci in a model for detection of initiation activity. *Jpn J Cancer Res* 2001; **92:** 1018-1025

27 **Ishiki Y,** Ohnishi H, Muto Y, Matsumoto K, Nakamura T. Di-

rect evidence that hepatocyte growth factor is a hepatotrophic factor for liver regeneration and has a potent antihepatitis effect in vivo. *Hepatology* 1992; **16:** 1227-1235

28 **Yamada Y,** Kirillova I, Peschon JJ, Fausto N. Initiation of liver growth by tumor necrosis factor: deficient liver regeneration in mice lacking type I tumor necrosis factor receptor. *Proc Natl Acad Sci USA* 1997; **94:** 1441-1446

29 **Yamada Y,** Webber EM, Kirillova I, Peschon JJ, Fausto N. Analysis of liver regeneration in mice lacking type 1 or type 2 tumor necrosis factor receptor: requirement for type 1 but not type 2 receptor. *Hepatology* 1998; **28:** 959-970

30 **Aldeguer X,** Debonera F, Shaked A, Krasinkas AM, Gelman AE, Que X, Zamir GA, Hiroyasu S, Kovalovich KK, Taub R, Olthoff KM. Interleukin-6 from intrahepatic cells of bone marrow origin is required for normal murine liver regeneration. *Hepatology* 2002; **35:** 40-48

Science Editor Guo SY **Language Editor** Elsevier HK

PO Box 2345, Beijing 100023, China
www.wjgnet.com
wjg@wjgnet.com

ELSEVIER

World J Gastroenterol 2005;11(47):7450-7456
World Journal of Gastroenterology ISSN 1007-9327

• *BASIC RESEARCH* •

Increased susceptibility of ethanol-treated gastric mucosa to naproxen and its inhibition by DA-9601, an *Artemisia asiatica* extract

Tae Young Oh, Gook Jun Ahn, Seul Min Choi, Byoung Ok Ahn, Won Bae Kim

Tae Young Oh, Gook Jun Ahn, Seul Min Choi, Byoung Ok Ahn, Won Bae Kim, Research Laboratories, Dong-A Pharm. Co., Ltd., 47-5, Sanggal, Kiheung, Yongin, Kyunggi, 449-905, South Korea
Supported by the National Ministry of Health and Welfare
Co-first-authors: Tae Young Oh and Gook Jun Ahn
Correspondence to: Gook Jun Ahn, Research Laboratories, Dong-A Pharm. Co., Ltd., 47-5, Sanggal, Kiheung, Yongin, Kyunggi, 449-905, South Korea. ahnsnu2@donga.co.kr
Telephone: +82-31-280-1359 Fax: +82-31-282-8564
Received: 2005-04-07 Accepted: 2005-07-05

Abstract

AIM: To examine the effect of DA-9601, a new gastroprotective agent, on the vulnerability of ethanol-treated rat's stomach to naproxen (NAP).

METHODS: Male Sprague-Dawley rats were pretreated with 1 mL of 50% ethanol twice a day for 5 d and then NAP (50 mg/kg) was administered. DA-9601 was administered 1 h before NAP. Four hours after NAP, the rats were killed to examine gross injury index (mm^2), histologic change and to determine mucosal levels of malondialdehyde (MDA), prostaglandin E_2 (PGE_2), glutathione (GSH) and myeloperoxidase (MPO).

RESULTS: Pretreatment of ethanol significantly increased NAP-induced gastric lesions, as well as an increase in MDA and MPO. On the contrary, mucosal PGE_2 and GSH contents were decreased dramatically by ethanol pretreatment, which were aggravated by NAP. DA-9601 significantly reduced NAP-induced gastric injury grossly and microscopically, regardless of pretreatment with ethanol. DA-9601 preserved, or rather, increased mucosal PGE_2 and GSH in NAP-treated rats ($P<0.05$), with reduction in mucosal MDA and MPO levels.

CONCLUSION: These results suggest that repeated alcohol consumption renders gastric mucosa more susceptible to NSAIDs though, at least in part, reduction of endogenous cytoprotectants including PGE_2 and GSH, and increase in MPO activation, and that DA-9601, a new gastroprotectant, can reduce the increased vulnerability of ethanol consumers to NSAIDs-induced gastric damage via the mechanism in which PGE_2 and GSH are involved.

Key words: DA-9601; Alcohol; Naproxen; Gastric damage; Malondialdehyde; Prostaglandin E_2; Glutathione; Myeloperoxidase; NSAIDs

Oh TY, Ahn GJ, Choi SM, Ahn BO, Kim WB. Increased susceptibility of ethanol-treated gastric mucosa to naproxen and its inhibition by DA-9601, an *Artemisia asiatica* extract. *World J Gastroenterol* 2005; 11(47): 7450-7456
http://www.wjgnet.com/1007-9327/11/7450.asp

INTRODUCTION

The prevalence of gastrointestinal (GI) disease is increasing in subjects aged 65 years and above. Among them, gastroesophageal reflux disease (GERD) and peptic ulcer are the most important and common GI disorders[1]. Peptic ulcer is one of the most common gastrointestinal diseases with 4-5% prevalence in the human society. Although it was speculated that food or stress was a main causative factor in the early 20th century, genetic and environmental factors are considered most relevant and it is generally accepted that their complicated correlation has a great role in the occurrence of peptic ulcer at present[2].

The number of patients with peptic ulcer is increasing as a result of complicated social activity and the continued advance of civilization. Whereas people over the middle age were predisposed to have peptic ulcer in the past, even teenaged group is also susceptible recently. Major etiologic factors of peptic ulcer include *Helicobacter pylori* (*H pylori*) infection, excessive use of drugs such as non steroidal anti-inflammatory drugs (NSAIDs), irregular eating habits, food containing causative materials such as linoleic acid, smoking, alcohol consumption, psychological, and physiological stress[3]. Chronic medication of NSAIDs often evokes dyspepsia, ulcer, hemorrhage, and perforation of upper gastrointestinal tract[4].

These side effects that arise from NSAIDs are augmented by the suppression of prostaglandin (PG) synthesis and neutrophil-mediated injury secondary to the production of inflammatory mediators such as tumor necrosis factor alpha (TNF-α) and leukotrienes (LTs)[5,6]. The risk factors responsible for the aggravation of gastrointestinal lesion by NSAIDs are believed to be age[7], gender[8], dyspepsia[9], clinical history ulcer and complicated ulcer disease[10] as well as heavy usage of alcohol and smoking[11] and *H pylori* infection[12].

Especially, NSAIDs and alcohol consumption increase the risk for major upper GI bleeding. Alcohol-induced disorders of the GI tract are very common[13]. Alcoholic gastritis subsequently leads to the impairment of the integrity of gastric mucosal barrier, contributing to acid reflux into the subluminal layers of the mucosa and submucosa. The underlying mechanism of mucosal lesions such as petechiae, hemorrhage, and erosion elicited by alcohol is similar to various NSAIDs[14].

In this connection, this study was carried out to investigate the effect of NSAIDs on the susceptibility of gastric lesion sensitized by serial administration of alcohol and preventative effect of DA-9601 (Stillen™), *Artemisia asiatica* extract, on the progression of gastric lesion and finally to reveal the underlying mechanism of action. DA-9601 is now on the market in South Korea and will be on sale in other Asian countries in the near future. It is reported to be effective to erosive gastritis[15] and to possess antioxidative and cytoprotective actions in models of gastric mucosal damage[16,17]. The active ingredient of DA-9601 is eupatilin, which is reported to prevent experimental gastric damage induced by a variety of noxious agents.

MATERIALS AND METHODS

Test materials and experimental animals

DA-9601 (Lot No. DA-9601-L-07) with 0.42% of active ingredient, eupatilin, was extracted from *Artemisiae herba* and supplied to this study after HPLC analysis in Dong-A pharmaceutical institute. (*S*)-6-methoxy-α-methyl-2-napthaleneacetic acid (Naproxen), 10% neutral formalin, sodium phosphate monobasic, sodium phosphate dibasic, ferric chloride ($FeCl_3$), thiobarbituric acid (TBA), trichloroacetic acid (TCA), malondialdehyde (MDA), sulfosalicylic acid, DTNB, β-nicotineamide adenine dinucleotide phosphate reduced form (β-NADPH), glutathione reductase, hexadecyltrimethylammonium bromide (HTAB), *O*-dianisidine dihydrochloride, bovine serum albumin (BSA) were obtained from Sigma (USA). Prostaglandin (PG) E_2 [^{125}I] radioimmunoassay kit (NEN) was obtained by DuPont (USA) and *p*-nitrothiophenol was obtained from TCI (Japan). Absolute ethanol, ether, and hydrochloric acid were purchased from Duksan (Korea). DA-9601 was suspended in 5% hydroxypropylmethylcell ulose (HPMC) dissolved in sterilized saline (v/v). Seven-week-old SPF male Sprague-Dawley rats were obtained from Charles River (Kanagawa, Japan) and acclimatized at least 1 wk under standard laboratory conditions [temperature: 23±2 ℃, humidity range: 40-70%, ventilation: 15-20/h, luminous intensity: 150-300 lux, 12 h light/dark cycle (lighting: 7:00 to 19:00)]. The rats were given regular chow and UV-sterilized tap water *ad libitum*.

Preventative effect of DA-9601 on ethanol-induced acute experimental gastric lesion

Rats fasted for 24 h were given 50% ETOH orally twice a day (8:00 a.m. and 4:00 p.m.) for 5 d. After body weight changes and clinical signs such as diarrhea and mortality were carefully examined, DA-9601 and naproxen (NAP) were administered orally after the last administration of ethanol and fasting animals. Rats were assigned to one of six experimental groups; group Ⅰ: normal age-matched control, group Ⅱ: alcohol administration, group Ⅲ: NAP 50 mg/kg without alcohol administration, group Ⅳ: alcohol+NAP, group Ⅴ: DA-9601 100 mg/kg pretreatment+NAP without alcohol administration, group Ⅵ: alcohol administration+DA-9601 100 mg/kg+NAP. Four hours after NAP administration, rats were anesthetized with ether and total extirpation of the stomach was performed. Thirteen milliliters of 4 ℃ saline was injected into the lumen of isolated stomach and maintained for 30 min. Surface area (mm^2) of gastric lesion was measured using optical microscope (Olympus ×10) following gastrotomy along with greater curvature. Small portion of tissue was fixed in 10% formalin solution and mucosal fluid collected from gastric mucosa stored at -74 ℃ refrigerator.

Homogenization of gastric mucosal fluid

Frozen mucosal fluid was thawed at room temperature and diluted with 1 mL Tris-HCl buffer (pH 7.4) per 100 mg and homogenized at 3 000 r/min for 10 min. Supernatant was stored at -20 ℃.

Measurement of the level of malondialdehyde in gastric mucosal fluid

TBA method was applied to accomplish MDA measurement. Two millimole per liter of $FeCl_3$ was added to 100 μL supernatant, which was agitated and incubated in 37 ℃ water bath for 30 min. Then 30% TCA, 0.75% TBA and 5 mol/L HCl were added as well and boiled for reaction in water bath for 15 min. Reacted mixture was cooled down to room temperature and centrifuged at 3 000 r/min for 10 min. Supernatant was assigned to measure absorbance at 550 nm thereby the amount of MDA (nmol/L/mg protein) was generated from standard curve of MDA.

Measurement of PGE_2 in gastric mucosal fluid

The amount of PGE_2 was measured with [^{125}I] RIA kit. After sample and tracer were added to the assay buffer, they were mixed with anti-serum and incubated at 2-8 ℃ for 24 h. Precipitating reagent was added to the sample, agitated well and then incubated for 30 min at 2-8 ℃. The amount of PGE_2 (pg/mg protein) was measured with gamma counter using pellet obtained from centrifugation at 3 000 r/min for 30 min.

Measurement of the amount of glutathione in gastric mucosal fluid

Sample added to 4% sulfosalicylic acid was centrifuged at 3 000 r/min for the elimination of protein and reacted with 0.1 mol/L sodium phosphate buffer (pH 7.5) containing 6 mmol/L DTNB, 0.3 mmol/L NADPH,

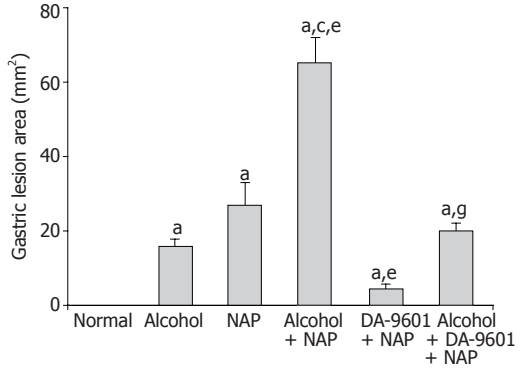

Figure 1 The effect of DA-9601 on the area of gastric lesion induced by alcohol and NAP. Data are expressed as mean±SD. [a]*P*<0.05 *vs* normal control, [c]*P*<0.05 *vs* alcohol group, [e]*P*<0.05 *vs* NAP, [g]*P*<0.05 *vs* alcohol + NAP.

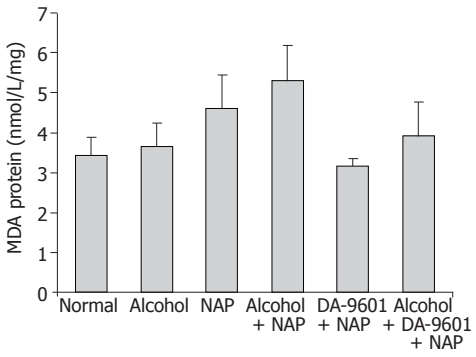

Figure 2 The effect of DA-9601 on MDA levels in gastric mucosal fluid. There were no statistical significances among all groups.

50 unit glutathione reductase at room temperature. The amount of GSH (nmol/L/mg protein) was generated by the absorbance of *p*-nitrophenol measured at 412 nm using the supernatant from centrifugation at 3 000 r/min for 10 min.

Measurement of the amount of myeloperoxidase in gastric mucosal fluid

The amount of myeloperoxidase (mU/mg protein) was measured at gastric mucosa modifying the method of previous reports. After gastric mucosa was homogenized in 0.5% HTAB solution containing 50 mmol/L potassium phosphate (pH 6.5), homogenized samples were freezed and thawed thrice and homogenized. Supernatant was added to the reaction buffer containing *O*-dianisidine dihydrochloride and H_2O_2 and the amount of myeloperoxidase was calculated from the absorbance of the reaction buffer at 460 nm at every 1 min.

Protein assay

Protein assay was performed by means of measuring absorbance at 535 nm compared using standard curve of BSA.

Statistical analysis

Data were expressed as the mean±SD and all statistical analyses were performed using SigmaStat® for Windows 2.0 software (Jandel Corporation, USA). Statistical significance was evaluated by one-way analysis of variance (ANOVA) followed by Bonferroni *post hoc* test or Dunnett's test for a multiple comparison. $P<0.05$ were considered significant.

RESULTS

Preventative effect of DA-9601 on ethanol-induced acute experimental gastric lesion

There was an apparent linear lesion on gastric mucosa of group Ⅱ (alcohol) with area of gross lesion (mm^2) of 16.0±1.8 (Figure 1). Group Ⅲ (NAP) had a petechial lesion on gastric mucosa and area of gross lesion was 27.0±6.0. Group Ⅳ (alcohol+NAP) exhibited hemorrhage on gastric mucosa with a significantly different area of hemorrhagic lesion (65.3±6.7, $P<0.05$), which was more severe than groups Ⅱ and Ⅲ. Group Ⅴ (DA-9601+NAP) significantly inhibited gross gastric lesion in comparison to group Ⅲ (4.5±1.2, $P<0.05$). The area of gross gastric lesion of group Ⅵ (alcohol+DA-9601+NAP) was 20.0±2.1 which was significantly different from group Ⅳ ($P<0.05$).

MDA level in gastric mucosal fluid

MDA levels (Figure 2) of groups Ⅰ (normal control) and Ⅱ (alcohol) indicating lipid peroxidation were 3.43±0.44 (nmol/L/mg protein) and 3.66±0.58 with no significant difference between them. It was found that groups Ⅲ (NAP) and Ⅳ (alcohol+NAP) had 4.61±0.83 and 5.30±0.89, respectively. There was a tendency to increase MDA levels of groups Ⅲ and Ⅳ without statistical significance. Group Ⅴ (DA-9601+NAP) exhibited MDA level of 3.16±0.18 which was reduced by 31.5% compared with group Ⅲ (NAP), but there was no significant difference between them. In case of group Ⅵ (alcohol+DA-9601+NAP), MDA level was 3.92±0.84 (nmol/L/mg protein) with 15.0% reduction compared to group Ⅳ, but no significance was found.

Prostaglandin E2 level in gastric mucosal fluid

PGE_2 level as a cytoprotection marker in group Ⅰ (normal control) was determined to be 194.5±21.5 (pg/mg protein) (Figure 3), group Ⅱ (alcohol) showed 159.5±30.2 which was reduced to the extent of 18.0% compared to group Ⅰ (normal control) but did not produce significance. Group Ⅲ (NAP) represented 62.0±13.8 indicating significant difference due to 68.1% reduction ($P<0.05$). PGE_2 level of group Ⅳ (alcohol+NAP) was 47.1±11.9 which produced 70.5% reduction which was significantly different ($P<0.05$) from group Ⅱ (alcohol) and 24.0% reduction without significance compared to group Ⅲ (NAP). 307.2±27.3 was determined as the PGE_2 level of group Ⅴ (DA-9601+NAP) and it was 57.9% higher than normal ($P<0.05$) and 395.5% higher than group Ⅲ (NAP) ($P<0.05$). Group Ⅵ (alcohol+DA-9601+NAP) showed 180.3±18.3 similar to group Ⅰ (normal control) normal control but 282.8%

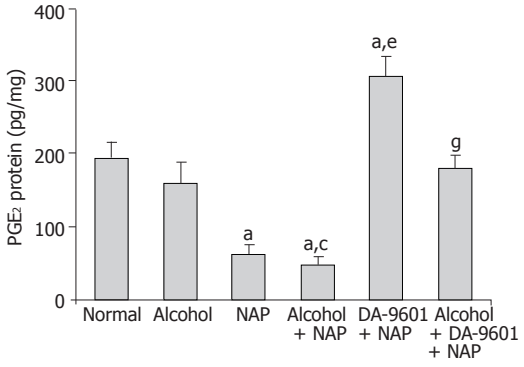

Figure 3 The effect of DA-9601 on PGE_2 levels in gastric mucosal fluid. Data are expressed as mean±SD. [a]*P*<0.05 *vs* normal control, [c]*P*<0.05 *vs* alcohol group, [e]*P*<0.05 *vs* NAP, [g]*P*<0.05 *vs* alcohol + NAP.

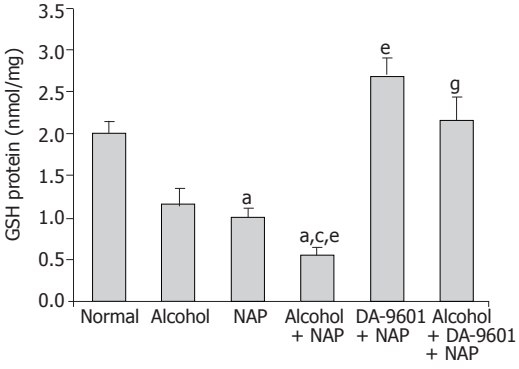

Figure 4 The effect of DA-9601 on GSH levels in gastric mucosal fluid. Data are expressed as mean±SD. [a]*P*<0.05 *vs* normal control, [c]*P*<0.05 *vs* alcohol group, [e]*P*<0.05 *vs* NAP, [g]*P*<0.05 *vs* alcohol + NAP.

increase with a significant difference (*P*<0.05) compared to group Ⅳ (alcohol+NAP).

Glutathione level

The levels of GSH in gastric mucosa (Figure 4) were 2.01±0.14 (nmol/L/mg protein) in group Ⅰ (normal control) and 1.18±0.17 in group Ⅱ (alcohol) and there was no significant difference between them. 1.01±0.21 of group Ⅲ (NAP) produced 49.8% reduction with significant difference (*P*<0.05). GSH level of group Ⅳ (alcohol+NAP) was 0.55±0.10 which generated 53.4% and 45.5% reduction and was significantly different (*P*<0.05) from group Ⅱ (alcohol) and group Ⅲ (NAP), respectively. Group Ⅴ (DA-9601+NAP) exhibited 2.68±0.22 with significant increase compared with group Ⅲ, and that was even higher than group Ⅰ (normal control). The level of GSH in group Ⅵ was 2.16±0.28 which was significantly higher than group Ⅳ (*P*<0.05).

Myeloperoxidase level

The level of MPO in group Ⅰ (normal control) was 0.78±0.11 (mU/protein) (Figure 5). Whereas group Ⅱ (alcohol) exhibited significant increase of MPO (1.19±0.27) compared to normal (*P*<0.05), there was an increase of MPO in group Ⅲ (NAP) without significance.

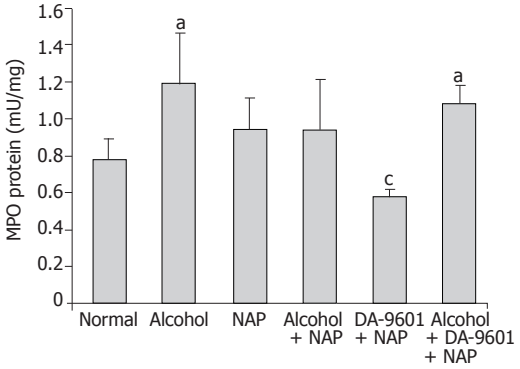

Figure 5 The effect of DA-9601 on MPO levels in gastric mucosal fluid. Data are expressed as mean±SD. [a]*P*<0.05 *vs* normal control, [c]*P*<0.05 *vs* NAP group.

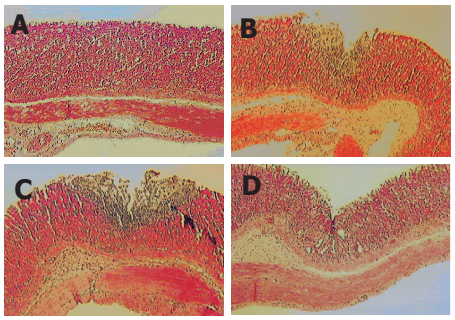

Figure 6 Histopathological changes induced either by alcohol, NAP and alcohol + NAP administration and its inhibition by DA-9601. **A:** Minimal inflammatory change in gastric mucosa in group Ⅱ (alcohol); **B:** Focal epithelial erosion and inflammatory cell infiltration in gastric mucosa and submucosa of group Ⅲ (NAP); **C:** Multifocal and diffuse epithelial erosion and severe inflammatory change in gastric mucosa and submucosa of Group Ⅳ (alcohol + NAP); **D:** DA-9601 treatment ameliorates the pathological changes of gastric mucosa and submucosa induced by NAP in alcohol pre-treated group Ⅵ (alcohol + DA-9601+NAP).

0.94±0.27 of group Ⅳ (alcohol+NAP) generated 21.1% reduction compared to group Ⅱ, but was similar to group Ⅲ. Group Ⅴ (DA-9601+NAP) showed 0.58±0.04 which produced 25.6% reduction in comparison to group Ⅰ (normal control) and was significantly decreased compared to group Ⅱ (alcohol) and group Ⅲ (NAP) (*P*<0.05). The level of MPO in group Ⅵ (alcohol+DA-9601+NAP) was 1.08±0.10 similarly to group Ⅱ (alcohol) and group Ⅲ (NAP).

Histopathological examination

Histopathological changes are depicted in Figure 6. In group Ⅱ (alcohol), there was a minimal inflammatory change in gastric mucosa; however, it was found that group Ⅲ (NAP) had focal epithelial erosion and inflammatory cell infiltration in gastric mucosa and submucosa. Whereas group Ⅳ (alcohol+NAP) aggravated the gastric lesion by forming multifocal and diffuse epithelial erosion and severe inflammatory change in gastric mucosa and submucosa, DA-9601 treatment ameliorates the pathological changes of gastric mucosa and submucosa induced by NAP in alcohol pre-treated group (group Ⅵ).

DISCUSSION

Considering the outcomes from this experiment, it was demonstrated that co-administration of alcohol and naproxen, one of the currently available NSAIDs, augmented the gastric mucosal lesion in comparison to the administration of alcohol or naproxen alone. Subsequently, treatment of DA-9601 that is being developed for targeting a new gastric mucoprotectant was shown to account for the preventative effects on gastric mucosa effectively against the lesion caused by alcohol and naproxen. Besides the effects on quantified gastric lesion, the level of MDA and MPO in DA-9601 treated group exhibited similar level to that in normal control and it was also revealed that DA-9601 contributed to intact maintenance of the gastric mucosa at the extent of normal control on histopathological examination.

The well-known etiologies for peptic ulcer can be categorized as follows: eating habits, environmental factors, stress by social life, drinking behavior, smoking, and drugs. Among these causative factors, drug-induced peptic ulcer is increasing dramatically with respect to the overuse of NSAIDs and increased susceptibility of gastric mucosa by single or co-administration of oral anti-coagulants (warfarin, phenindione, phenprocoumon, acenocoumarol, anisindione, diphenadione, *etc*.) and corticosteroid hormones (triamcinolone, dexamethasone, cortisone, hydrocortisone, prednisolone, prednisone)[18]. It is reported that alcohol is responsible for the hemorrhage of gastric mucosa and edema in submucosal muscle layer by means of direct irritation[19] and also leads to acute gastritis associated with microcirculer stasis[20]. Once gastric mucosa is injured, thereby ischemia and decreased level of ATP in gastric mucosa and intervention of microcirculation occurs[21]. Gastric mucosal damage due to chronic ingestion of low concentration of alcohol is generally not discernible on gross examination; however, if gastric mucosa is exposed to an external mucosal irritant, gastric lesion becomes more extensive and consistent with increased susceptibility as well as persistent submucosal microcircular stasis[22]. It was demonstrated that DA-9601 100 mg/kg treatment exerted excellent preventative or therapeutic effects on gastric mucosal lesion with action of duration being effective for more than 2 h. It was also well documented that these effects were in accordance with the facilitation of the synthesis of PG by DA-9601.

Since aspirin was first synthesized in the year of 1899, a variety of NSAIDs has emerged so far and they are being used as antipyretic analgesics and anti-inflammatory drugs. Nowadays, the market size of NSAIDs is more than 60 billion/year, in addition, more extended indications are making the need for NSAIDs to increase[23]. Despite these facts, NSAIDs were reported to cause gastric lesion since 1930s and underlying mechanism was related to the fact that NSAIDs inhibit cyclooxygenase (COX) thereby block the synthesis of PG[24]. More specifically, NSAIDs elicit gastromucosal lesion not only by reducing the physiological role of PG, but also by directly inducing neutrophilic infiltration in gastric capillaries causing subsequent stasis and free radical formation by extravasated neutrophil[25]. Several methods are suggested to alleviate the adverse effects of NSAIDs until recently. First of all, aspirin is administered in the form of enteric-coated tablet or direct irritation to gastric mucosa is prevented by administration of prodrug[26]. Secondly, NSAIDs are administered to patients being chemically modified with nitric oxide that is known to act as a gastric mucosal protectant similarly to PG[27,28]. Lastly, NSAIDs with high sensitivity to COX Ⅱ are designed[29,30]. Despite these efforts, 62.2% of patients treated with NSAIDs on a long-term basis complained of upper gastrointestinal clinical signs of which gastritis (38.5%), gastric ulcer (15.5%), duodenal ulcer (1.9%) were most prevalent; however, it appears that more patients suffered from these adverse effects due to complicated drug administration or eating habits. The underlying mechanisms that result in gastrointestinal symptoms can be classified as follows: firstly, it is generally accepted that NSAIDs inhibit COX responsible for the synthesis of PG. Secondly, NSAIDs have a direct effect on gastric mucosa and lastly it is also proposed that overproduction of LTs, especially for LTB4, by 5-lipoxygenase (5-LO) resulting from compensation for the inhibition of COX is a causative factor[31,32]. LTs are known to be mediators that induce inflammatory process and take part in the formation and infiltration of neutrophils[33]. The most commonly prescribed formula considering NSAIDs treatment is the co-administration of extrinsic or intrinsic PG. Whereas Misoprostol, one of the extrinsic PG synthetics, has the advantage in the aspect of potency, and it exhibits adverse effect such as diarrhea. The intrinsic PG derivative, ornoprostil, is known to be not effective in the patients with gastric ulcer or gastritis because of the fact that NSAIDs inhibit COX[34]. It was revealed that DA-9601 increased the level of PGE_2 and GSH dose-dependently in normal state as well as alcohol or ammonia-induced gastric lesion. Moreover, DA-9601 elevated the level of PGE_2 protecting gastric mucosa without affecting the efficacy of NSAIDs, when DA-9601 was co-administered with NSAIDs in arthritis-induced rats. Oxygen free radical and lipid peroxidation are regarded as the crucial etiologies leading to gastric mucosal lesion by oxidative stress[35]. Once oxygen free radical triggers and maintains ischemic status in gastric mucosa, hydroxyl radical generated from superoxide anion results in gastric lesion by virtue of decreasing the velocity of blood flow subsequently[36].

In this present study, we measured not only the level of MDA and MPO in order to quantify the materials contributing to gastric mucosal lesion but also the level of PGE_2 and GSH that are produced as protective markers. As a whole, it was demonstrated that the level of MDA and MPO were decreased similarly to the level of normal control, whereas PGE_2 and GSH were increased in DA-9601 treated group. In the previous report, DA-9601 treatment alone had the ability to facilitate the production of mucosal PGE_2[17]. From the findings of this study, DA-9601 treatment was proven to protect effectively against the NSAIDs-induced lesion of gastric

mucosa which was more susceptible to NSAIDs by the administration of alcohol in rats. On closer inspection of results, the underlying mechanism of the action of DA-9601 can be centered on the cytoprotective effect by normalizing the production of PG, additional improvement of gastric mucosal function by elevating GSH content, alleviation of inflammation by decreasing the level of MDA and MPO. Bearing all these in mind, it is worth making a conclusion that DA-9601 treatment has a protective effect on gastric mucosa of patients who are accustomed to drinking alcohol regularly and will be of great value in human clinical study.

REFERENCES

1 **Pilotto A.** Aging and upper gastrointestinal disorders. *Best Pract Res Clin Gastroenterol* 2004; **18** (Suppl): 73-81
2 **Aihara T,** Nakamura E, Amagase K, Tomita K, Fujishita T, Furutani K, Okabe S. Pharmacological control of gastric acid secretion for the treatment of acid-related peptic disease: past, present, and future. *Pharmacol Ther* 2003; **98:** 109-127
3 **Behrman SW.** Management of complicated peptic ulcer disease. *Arch Surg* 2005; **140:** 201-208
4 **Roth SH.** From peptic ulcer disease to NSAID gastropathy. An evolving nosology. *Drugs Aging* 1995; **6:** 358-367
5 **Appleyard CB,** McCafferty DM, Tigley AW, Swain MG, Wallace JL. Tumor necrosis factor mediation of NSAID-induced gastric damage: role of leukocyte adherence. *Am J Physiol* 1996; **270:** G42-G48
6 **Andrews FJ,** Malcontenti-Wilson C, O'Brien PE. Effect of nonsteroidal anti-inflammatory drugs on LFA-1 and ICAM-1 expression in gastric mucosa. *Am J Physiol* 1994; **266:** G657-G664
7 **Gutthann SP,** García Rodríguez LA, Raiford DS. Individual nonsteroidal antiinflammatory drugs and other risk factors for upper gastrointestinal bleeding and perforation. *Epidemiology* 1997; **8:** 18-24
8 **Hernández-Díaz S,** Rodríguez LA. Association between nonsteroidal anti-inflammatory drugs and upper gastrointestinal tract bleeding/perforation: an overview of epidemiologic studies published in the 1990s. *Arch Intern Med* 2000; **160:** 2093-2099
9 **Weil J,** Langman MJ, Wainwright P, Lawson DH, Rawlins M, Logan RF, Brown TP, Vessey MP, Murphy M, Colin-Jones DG. Peptic ulcer bleeding: accessory risk factors and interactions with non-steroidal anti-inflammatory drugs. *Gut* 2000; **46:** 27-31
10 **García Rodríguez LA,** Cattaruzzi C, Troncon MG, Agostinis L. Risk of hospitalization for upper gastrointestinal tract bleeding associated with ketorolac, other nonsteroidal anti-inflammatory drugs, calcium antagonists, and other antihypertensive drugs. *Arch Intern Med* 1998; **158:** 33-39
11 **Kaufman DW,** Kelly JP, Wiholm BE, Laszlo A, Sheehan JE, Koff RS, Shapiro S. The risk of acute major upper gastrointestinal bleeding among users of aspirin and ibuprofen at various levels of alcohol consumption. *Am J Gastroenterol* 1999; **94:** 3189-3196
12 **Chan FK.** NSAID-induced peptic ulcers and Helicobacter pylori infection: implications for patient management. *Drug Saf* 2005; **28:** 287-300
13 **Riezzo G,** Chiloiro M, Montanaro S. Protective effect of amtolmetin guacyl versus placebo diclofenac and misoprostol in healthy volunteers evaluated as gastric electrical activity in alcohol-induced stomach damage. *Dig Dis Sci* 2001; **46:** 1797-1804
14 **Stern AI,** Hogan DL, Isenberg JI. A new method for quantitation of ion fluxes across in vivo human gastric mucosa: effect of aspirin, acetaminophen, ethanol, and hyperosmolar solutions. *Gastroenterology* 1984; **86:** 60-70
15 **Seol SY,** Kim MH, Ryu JS, Choi MG, Shin DW, Ahn BO. DA-9601 for erosive gastritis: results of a double-blind placebo-controlled phase III clinical trial. *World J Gastroenterol* 2004; **10:** 2379-2382
16 **Oh TY,** Ryu BK, Yang JI, Kim WB, Park JB, Lee SD, Lee EB. Studies on antiulcer effects of DA-9601, an *Artemisia Herba* extract, against experimental gastric ulcers and its mechanism. *J Appl Pharmacol* 1996; **4:** 111-121
17 **Oh TY,** Ahn BO, Ko JI, Ryu BK, Son MW, Kim SH, Kim WB, Lee WB. Studies on protective effect of DA-9601, an Artemisiae herba extract, against ethanol-induced gastric mucosal damage and its mechanism. *J Appl Pharmacol* 1997; **5:** 202-210
18 **Griffin MR,** Smalley WE. Drugs and ulcers: clues about mucosal protection from epidemiologic studies. *J Clin Gastroenterol* 1995; **21** Suppl 1: S113-S119
19 **Oates PJ,** Hakkinen JP. Studies on the mechanism of ethanol-induced gastric damage in rats. *Gastroenterology* 1988; **94:** 10-21
20 **Nakagawa S.** Relationship between histological gastritis and mucosal microvascular observations using magnifying endoscopy. *Hokkaido Igaku Zasshi* 2003; **78:** 349-356
21 **Silen W.** Experimental models of gastric ulceration and injury. *Am J Physiol* 1988; **255:** G395-G402
22 **Miller DA,** Chernin VV, Tkachev VA, Matiash BL. Microcirculation in patients with chronic gastritis depending on its exacerbation severity and morphological type. *Eksp Klin Gastroenterol* 2002; **4:** 14-17
23 **Garner A.** Adaptation in the pharmaceutical industry, with particular reference to gastrointestinal drugs and diseases. *Scand J Gastroenterol* Suppl 1992; **193:** 83-89
24 **Peng S,** Duggan A. Gastrointestinal adverse effects of non-steroidal anti-inflammatory drugs. *Expert Opin Drug Saf* 2005; **4:** 157-169
25 **McCafferty DM,** Granger DN, Wallace JL. Indomethacin-induced gastric injury and leukocyte adherence in arthritic versus healthy rats. *Gastroenterology* 1995; **109:** 1173-1180
26 **Miedzybrodzki R.** Trends in nonsteroidal anti-inflammatory drug development and application. *Postepy Hig Med Dosw(Online)* 2004; **58:** 438-448
27 **Cuzzolin L,** Conforti A, Adami A, Lussignoli S, Menestrina F, Del Soldato P, Benoni G. Anti-inflammatory potency and gastrointestinal toxicity of a new compound, nitronaproxen. *Pharmacol Res* 1995; **31:** 61-65
28 **Reuter BK,** Cirino G, Wallace JL. Markedly reduced intestinal toxicity of a diclofenac derivative. *Life Sci* 1994; **55:** PL1-PL8
29 **Onoe Y,** Miyaura C, Kaminakayashiki T, Nagai Y, Noguchi K, Chen QR, Seo H, Ohta H, Nozawa S, Kudo I, Suda T. IL-13 and IL-4 inhibit bone resorption by suppressing cyclooxygenase-2-dependent prostaglandin synthesis in osteoblasts. *J Immunol* 1996; **156:** 758-764
30 **Slater DM,** Berger LC, Newton R, Moore GE, Bennett PR. Expression of cyclooxygenase types 1 and 2 in human fetal membranes at term. *Am J Obstet Gynecol* 1995; **172:** 77-82
31 **Hudson N,** Balsitis M, Everitt S, Hawkey CJ. Enhanced gastric mucosal leukotriene B4 synthesis in patients taking non-steroidal anti-inflammatory drugs. *Gut* 1993; **34:** 742-747
32 **Wallace JL,** McCafferty DM, Carter L, McKnight W, Argentieri D. Tissue-selective inhibition of prostaglandin synthesis in rat by tepoxalin: anti-inflammatory without gastropathy? *Gastroenterology* 1993; **105:** 1630-1636
33 **Vaananen PM,** Keenan CM, Grisham MB, Wallace JL. Pharmacological investigation of the role of leukotrienes in the pathogenesis of experimental NSAID gastropathy. *Inflammation* 1992; **16:** 227-240
34 **Lanas A.** Prevention and treatment of non-steroidal anti-inflammatory drug gastroenteropathy. *Rev Gastroenterol Mex* 2004; **69:** 251-260

35 **Demir S,** Yilmaz M, Köseoğlu M, Akalin N, Aslan D, Aydin A. Role of free radicals in peptic ulcer and gastritis. *Turk J Gastroenterol* 2003; **14:** 39-43

36 **Perry MA,** Wadhwa S, Parks DA, Pickard W, Granger DN. Role of oxygen radicals in ischemia-induced lesions in the cat stomach. *Gastroenterology* 1986; **90:** 362-267

Science Editor Wang XL and Guo SY **Language Editor** Elsevier HK

PO Box 2345, Beijing 100023, China
www.wjgnet.com
wjg@wjgnet.com

ELSEVIER

World J Gastroenterol 2005;11(47):7457-7460
World Journal of Gastroenterology ISSN 1007-9327

• *BASIC RESEARCH* •

Colon-specific drug delivery systems based on cyclodextrin prodrugs: *In vivo* evaluation of 5-aminosalicylic acid from its cyclodextrin conjugates

Mei-Juan Zou, Gang Cheng, Hirokazu Okamoto, Xiu-Hua Hao, Feng An, Fu-De Cui, Kazumi Danjo

Mei-Juan Zou, Gang Cheng, Xiu-Hua Hao, Feng An, Fu-De Cui, School of Pharmacy, Shenyang Pharmaceutical University, Shenyang 110016, Liaoning Province, China
Hirokazu Okamoto, Kazumi Danjo, Faculty of Pharmacy, Meijo University, 150 Yagotoyama, Tempaku-ku, Nagoya 468-8503, Japan
Co-first-authors: Mei-Juan Zou and Gang Cheng
Correspondence to: Gang Cheng, School of Pharmacy, Shenyang Pharmaceutical University, PO Box 32, 103 Wenhua Road, Shenhe District, Shenyang 110016, Liaoning Province, China. chenggang1963@hotmail.com
Telephone: +86-24-23986326 Fax: +86-24-23903547
Received: 2004-05-25 Accepted: 2004-08-17

Abstract

AIM: To investigate the release of cyclodextrin-5-aminosalicylic acid (CyD-5-ASA) in cecum and colon.

METHODS: An anti-inflammatory drug 5-ASA was conjugated onto the hydroxyl groups of α-, β- and γ-cyclodextrins (CyDs) through an ester linkage, and the *in vivo* drug release behavior of these prodrugs in rat's gastrointestinal tract after the oral administration was investigated.

RESULTS: The 5-ASA concentration in the rat's stomach and small intestine after the oral administration of CyD-5-ASA conjugate was much lower than that after the oral administration of 5-ASA alone. The lower concentration was attributable to the passage of the conjugate through the stomach and small intestine without significant degradation or absorption, followed by the degradation of the conjugate site-specific in the cecum and colon. The oral administration of CyD-5-ASA resulted in lower plasma and urine concentration of 5-ASA than that of 5-ASA alone.

CONCLUSION: CyD-5-ASA conjugates may be used as prodrugs for colon-specific drug delivery system.

Key words: Cyclodextrin; 5-Aminosalicylic acid; *In vivo*; Colon-specific

Zou MJ, Cheng G, Okamoto H, Hao XH, An F, Cui FD, Danjo K. Colon-specific drug delivery systems based on cyclodextrin prodrugs: *In vivo* evaluation of 5-aminosalicylic acid from its cyclodextrin conjugates. *World J Gastroenterol* 2005; 11(47): 7457-7460
http://www.wjgnet.com/1007-9327/11/7457.asp

INTRODUCTION

Ulcerative colitis and Crohn's disease are recurrent disorders chronically involving the mucosa and submucosa of the colon. 5-Aminosalicylic acid (5-ASA) is an active ingredient of agents used for the long-term maintenance therapy to prevent relapses of Crohn's disease and ulcerative colitis[1-3]. However, when 5-ASA is administered orally, a large amount of the drug is absorbed from the upper gastrointestinal tract (GIT), and causes systemic side effects. Therefore, it is preferable to deliver the drug site-specifically to the colon. Various approaches have been developed, including coating with biodegradable polymers[4,5], coating with pH-sensitive polymers[6,7], time-dependent formulations[8,9], forming biodegradable matrices[10,11], and forming prodrugs.

Azo prodrugs of 5-ASA are the most effective prodrugs used for the treatment of inflammatory bowel disease (IBD). Polymeric prodrugs of 5-ASA have not been used in clinics[12,13]. Natural polysaccharides have been used as tools to deliver the drugs to the colon. These polysaccharides remain intact in the physiological environment of the stomach and small intestine, but once the dosage form enters into the colon, it is acted upon by polysaccharides, which release the drug into the colon[14-16]. Cyclodextrins are cyclic oligosaccharides that consists of 6-8 glucose units. They are known to be barely capable of being hydrolyzed and only slightly absorbed in the passage through the stomach and small intestine, and are fermented by colonic microflora into small saccharides. The present study aimed to clarify the *in vivo* release behavior of 5-ASA from its CyD ester prodrugs in rat's intestines.

MATERIALS AND METHODS

Materials

α-, β-, γ-CyDs and carbonyldiimidazole (CDI) were obtained from Sigma Chemical Co (St. Louis, USA). 5-ASA was purchased from Acros Organics Ltd (NJ, USA). CyD-5-ASA and Ac-5-ASA were prepared according to the method reported in a previous paper[17].

All other chemicals and solvents were of analytical reagent grade, and deionized double-distilled water was used throughout the study.

Analytical methods

The HPLC system that consisted of LC-10ADvp pumps, SPD-10ADvp detector, and SIL-10ADvp autoinjector was purchased from Shimadzu. Reversed-phase HPLC conditions[18,19] for the determination of 5-ASA and its metabolites were as follows: a mobile phase of 5.0 mmol/L pH 6.0 phosphate buffer/acetonitrile/ 0.1 mol/L tetrabutyl-ammonium chloride (90:10:0.5 v/v/v), a flow rate of 1.0 mL/min, and a detection of wavelength 330 nm for 0-9 min, 240 nm after 9 min.

Release of 5-ASA in rat's gastrointestinal tract and tissues

Male SD rats, weighing about 200 g, were fasted for 8 h prior to drug administration while water was allowed *ad libitum*. 5-ASA or CyD-5-ASA (equivalent to 50 mg of 5-ASA) was orally administered to the rats and then the rats were placed in metabolic cages. At appropriate intervals (4, 8, 12, and 24 h), blood samples (about 3 mL) were taken from the jugular vein, and the rats were killed by ether anesthesia, followed by thoracotomy. The blood was centrifuged at 10 000 *g* for 5 min, and serum was frozen at -20 °C and stored until analysis. The GIT was isolated and divided into stomach, small intestine, cecum, and colon. The intestinal contents were removed by gently squeezing the gastrointestinal segments, which were then rinsed with a small amount of phosphate buffer (about 10 mL) to remove the adherent materials. The separated contents and tissues were quickly frozen at -20 °C and stored until analysis. Urine and feces samples were collected and frozen at -20 °C.

The frozen intestinal contents were thawed, weighed, and diluted with 1.5 mL of 0.1 mol/L HCl. They were vortexed for 3 min, centrifuged at 5 000 r/min for 5 min, then 2.5 mL of methanol was added to 0.8 mL of the supernatant, vortexed for 2 min. The mixture was centrifuged for 10 min at 5 000 r/min. The supernatant of 3.0 mL was transferred into another cleaning tube and evaporated under N_2 at 40 °C. The remaining supernatant was dissolved in mobile phase and filtered through 0.2-mL membrane. The frozen tissues were thawed, weighed, cut into small pieces and homogenized with five volumes of cold 0.1 mol/L HCl using a tissue homogenizer (Polytron PT-MR3100, Kinematica, Switzerland) at 0 °C.

RESULTS

Recovery of CyD-5-ASA, 5-ASA and its metabolite

In a previous paper[17], we have reported that the hydroxyl propyl cellulose/5-ASA (HPC-5-ASA), chitosan/5-ASA (ChT-5-ASA) conjugate are stable in rat's GIT, where CyD-5-ASA liberates 5-ASA site-specifically in rat's cecum and colon. In this study, the distribution of CyD-5-ASA prodrugs, 5-ASA and its metabolites were investigated.

Tables 1-3 show the recovery percentage of the intact prodrugs, 5-ASA and *N*-acetyl-5-ASA (Ac-5-ASA), a metabolite of 5-ASA in GIT, blood, liver, feces, and urine after the oral administration of CyD-5-ASA to rats. The sampling time was chosen on the basis of the time necessary for CyD-5-ASA to reach the cecum after oral administration. The total recovery was defined as the sum of the intact prodrugs, 5-ASA and Ac-5-ASA in the entire GIT and tissues, blood (assuming that the blood volume is 6.5% of body weight), urine and feces, and expressed as a percentage of the dose administered. The recovery from the stomach, small intestine, cecum, colon, blood, urine, feces, and liver was expressed as a percentage of the total recovery described above.

Four hours after dosing, about 60% of 5-ASA and Ac-5-ASA were recovered in intact form from the stomach and small intestine and about 40% in the cecum and colon. Eight hours after dosing, 20% of the prodrugs were located in the stomach and small intestine and a large portion (>70%) was recovered from cecum and colon. After 12 h, the major portion of the prodrugs was recovered from the cecum, colon, and feces. There was only a negligible amount of 5-ASA and Ac-5-ASA in blood and urine. These results indicated that the CyD prodrugs survived passage through the rat's stomach and small intestine and were subjected to the ring-opening process in the cecum and colon.

Release behavior in rat's gastrointestinal tract and tissues

In this study, 5-ASA, α-CyD-5-ASA, β-CyD-5-ASA and γ-CyD-5-ASA (equivalent to 50 mg/kg 5-ASA) were administered to the rats. There was no or a very small amount of 5-ASA detected in the tissues after the oral administration. The results of β-CyD-5-ASA and γ-CyD-5-ASA were similar to those of α-CyD-5-ASA.

Figure 1 shows the concentrations of 5-ASA and Ac-5-ASA in rat's blood, urine, feces, liver homogenates after the oral administration of 5-ASA (50 mg/kg) and α-CyD-5-ASA (equivalent to 50 mg/kg 5-ASA). With the oral administration of 5-ASA, 5-ASA being absorbed in the upper GIT, the concentration in cecum and colon was very low. Whereas during the oral administration of α-CyD-5-ASA, the levels of 5-ASA and Ac-5-ASA in the plasma and urine were very low in the whole experimental period, which might indicate the limited oral absorption of α-CyD-5-ASA. α-CyD-5-ASA was not degraded to release 5-ASA in the GIT, and 5-ASA was detected in the cecum and colon. A portion of the released 5-ASA might be absorbed in the large intestine and appeared in the plasma concentration of Ac-5-ASA.

DISCUSSION

In this study, formation of prodrugs has improved the delivery properties of the parent drug molecule. Activated by the microbial enzymes in the large intestine, CyD-5-ASA released 5-ASA at a controlled rate. These results suggest that after the oral administration of prodrugs there is no or a very small amount of 5-ASA in the tissues of rats. Oral administration of 5-ASA gives much higher

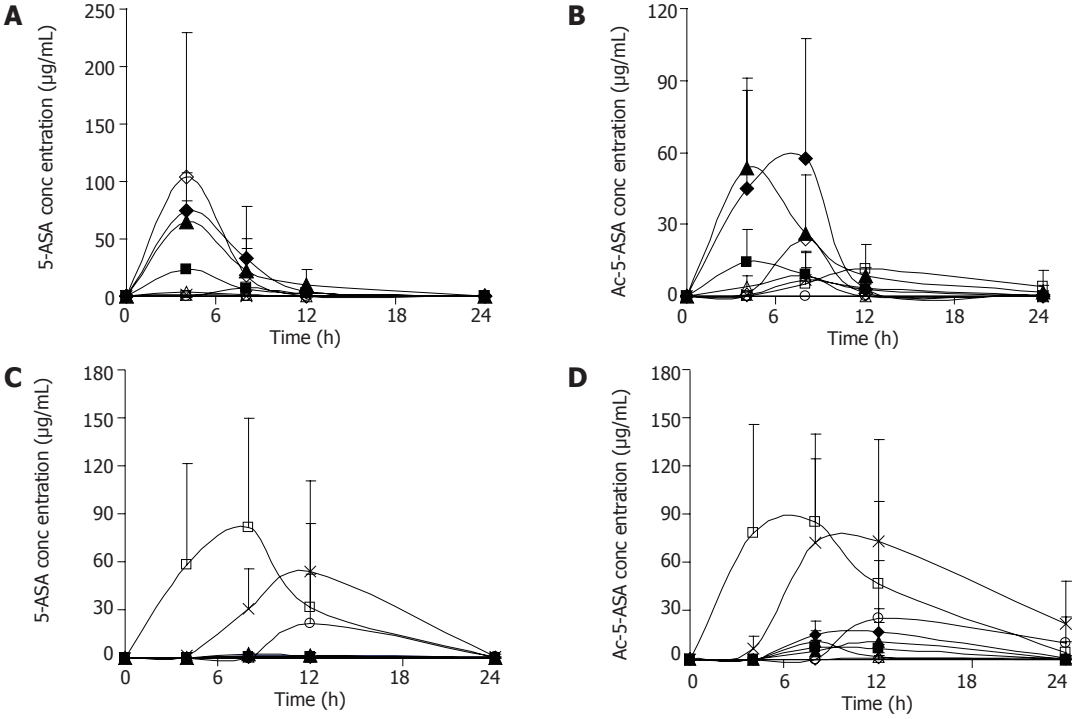

Figure 1 Concentration of 5-ASA and Ac-5-ASA in serum (◆), urine (■), feces (○), liver homogenates (△), stomach contents (◇), small intestinal contents (▲), cecal contents (□), colonic contents (×) after the oral administration of 50 mg/kg 5-ASA or α-CyD-5-ASA (equivalent to 50 mg/kg 5-ASA) to rats. **A:** Concentration of 5-ASA after oral administration of 5-ASA; **B:** concentration of Ac-5-ASA after oral administration of 5-ASA; **C:** concentration of 5-ASA after oral administration of 10 α-CyD-5-ASA; **D:** concentration of Ac-5-ASA after oral administration of α-CyD-5-ASA.

Table 1 Recovery (%) of α-CyD-5-ASA, 5-ASA and Ac-5-ASA in the GIT, plasma, urine, feces, and liver after oral administration of α-CyD-5-ASA to rats (mean±SD)

Time	Stomach			Small intestine			Cecum			Colon			
(h)	Prodrug	5-ASA	AC-5-ASA	Prodrug	5-ASA	AC-5-ASA	Prodrug	5-ASA	AC-5-ASA	Prodrug	5-ASA	AC-5-ASA	
4	19.8±4.8	0.0±0.0	0.0±0.0	41.6±30.8	0.0±0.0	0.0±0.0	7.7±7.6	14.7±17.3	7.3±12.6	6.3±11.0	0.8±1.0	1.8±1.6	
8	2.8±4.3	0.0±0.0	0.0±0.0	14.3±6.5	0.7±0.4	0.0±0.0	11.3±14.0	20.2±22.4	6.1±5.8	7.2±9.9	9.1±7.7	18.4±13.6	
12	0.0±0.0	0.1±0.1	0.4±0.5	1.7±0.4	0.5±0.7	2.5±3.9	9.4±11.8	4.7±7.4	6.2±6.4	17.2±24.0	17.3±23.7	16.6±17.9	
24	0.0±0.0	0.0±0.0	0.0±0.0	0.0±0.0	0.0±0.0	22.8±24.2	9.2±9.0	0.3±0.5	7.9±13.6	13.3±15.6	1.4±1.1	23.4±15.6	
	Plasma			Urine			Feces			Liver			Total
	Prodrug	5-ASA	AC-5-ASA	Prodrug	5-ASA	AC-5-ASA	Prodrug	5-ASA	AC-5-ASA	Prodrug	5-ASA	AC-5-ASA	recovery
4	0.0±0.0	0.0±0.0	0.0±0.0	0.0±0.0	0.0±0.0	0.0±0.0	0.0±0.0	0.0±0.0	0.0±0.0	0.0±0.0	0.0±0.0	0.0±0.0	69.3±29.0
8	0.0±0.0	0.5±0.3	4.0±2.6	0.0±0.0	0.2±0.1	2.0±1.3	0.0±0.0	0.0±0.0	0.0±0.0	0.0±0.0	0.3±0.1	3.0±2.2	65.0±11.9
12	0.0±0.0	0.4±0.5	4.7±4.0	0.0±0.0	0.3±0.4	2.8±2.4	0.3±0.5	7.1±8.2	7.1±8.0	0.0±0.0	0.2±0.3	0.4±0.8	50.5±20.0
24	0.0±0.0	1.4±1.2	1.9±1.9	0.0±0.0	0.0±0.0	0.0±0.0	4.3±7.4	1.3±1.3	9.3±11.8	0.0±0.0	1.4±1.3	2.1±2.5	12.6±7.6

Total recovery=100×(amount of the intact prodrugs, 5-ASA and Ac-5-ASA recovered from stomach, small intestine, cecum, colon, blood, urine, liver, and feces)/dose.

Table 2 Recovery (%) of β-CyD-5-ASA, 5-ASA, and Ac-5-ASA in GIT, plasma, urine, feces, and liver after oral administration of 9 9 β-CyD-5-ASA to rats (mean±SD)

Time	Stomach			Small intestine			Cecum			Colon			
(h)	Prodrug	5-ASA	AC-5-ASA	Prodrug	5-ASA	AC-5-ASA	Prodrug	5-ASA	AC-5-ASA	Prodrug	5-ASA	AC-5-ASA	
4	26.7±3.2	0.0±0.0	0.0±0.0	47.0±27.6	0.0±0.0	0.0±0.0	13.2±13.7	1.0±0.6	0.3±0.3	9.7±16.9	1.2±1.4	0.9±1.4	
8	8.5±12.9	0.0±0.0	0.0±0.0	14.9±6.6	2.4±3.4	0.0±0.0	30.6±35.8	7.5±11.6	3.8±3.8	12.3±17.0	9.1±4.4	4.3±2.9	
12	0.0±0.0	0.0±0.0	0.7±1.2	6.6±7.9	0.4±0.3	3.0±0.8	8.4±7.4	18.7±13.1	11.7±12.8	16.1±12.6	13.5±12.4	7.9±7.3	
24	0.0±0.0	0.0±0.0	0.0±0.0	0.0±0.0	0.0±0.0	2.9±4.4	16.6±16.1	10.3±16.7	17.4±15.2	27.2±45.2	11.0±12.9	5.3±5.9	
	Plasma			Urine			Feces			Liver			Total
	Prodrug	5-ASA	AC-5-ASA	Prodrug	5-ASA	AC-5-ASA	Prodrug	5-ASA	AC-5-ASA	Prodrug	5-ASA	AC-5-ASA	recovery
4	0.0±0.0	0.0±0.0	0.0±0.0	0.0±0.0	0.0±0.0	0.0±0.0	0.0±0.0	0.0±0.0	0.0±0.0	0.0±0.0	0.0±0.0	0.0±0.0	64.0±14.3
8	0.0±0.0	0.7±0.7	2.4±3.0	0.0±0.0	0.1±0.0	0.4±0.4	0.0±0.0	0.1±0.0	0.1±0.1	0.0±0.0	1.9±2.5	1.1±1.6	40.6±14.7
12	0.0±0.0	1.2±0.5	4.1±4.6	0.0±0.0	2.4±3.5	2.3±2.2	0.3±0.9	0.0±0.0	1.1±1.8	0.0±0.0	0.5±0.7	0.8±1.2	35.6±10.7
24	0.0±0.0	2.3±2.6	1.7±2.2	0.0±0.0	0.0±0.0	0.0±0.0	4.6±7.9	0.2±0.2	0.7±0.9	0.0±0.0	0.0±0.0	0.0±0.0	14.8±6.5

Total recovery=100×(amount of the intact prodrugs, 5-ASA, and Ac-5-ASA recovered from stomach, small intestine, cecum, colon, blood, urine, liver, and feces)/dose.

Table 3 Recovery (%) of γ-CyD-5-ASA, 5-ASA, and Ac-5-ASA in GIT, plasma, urine, feces, and liver after oral administration of γ-CyD-5-ASA to rats (mean±SD)

Time	Stomach			Small intestine			Cecum			Colon			
(h)	Prodrug	5-ASA	AC-5-ASA	Prodrug	5-ASA	AC-5-ASA	Prodrug	5-ASA	AC-5-ASA	Prodrug	5-ASA	AC-5-ASA	
4	19.8±9.4	0.0±0.0	0.0±0.0	46.4±28.7	0.2±0.3	0.0±0.0	10.0±10.1	0.9±0.3	5.4±4.8	8.4±14.6	6.4±5.4	2.2±1.8	
8	3.2±5.0	0.0±0.0	0.0±0.0	16.2±3.3	2.4±1.5	0.0±0.0	18.2±24.8	15.7±9.4	2.2±2.7	4.0±4.2	20.2±8.2	7.7±4.2	
12	0.0±0.0	0.2±0.0	0.6±0.6	2.1±1.2	0.8±0.3	0.0±0.0	7.6±7.0	4.9±2.5	14.1±12.2	7.9±5.2	7.2±1.5	34.6±20.8	
24	0.0±0.0	0.0±0.0	0.0±0.0	0.0±0.0	0.0±0.0	0.8±0.7	5.3±5.8	2.1±1.8	40.5±35.4	15.0±22.3	19.4±15.6	5.1±4.0	
	Plasma			Urine			Feces			Liver			Total
	Prodrug	5-ASA	AC-5-ASA	Prodrug	5-ASA	AC-5-ASA	Prodrug	5-ASA	AC-5-ASA	Prodrug	5-ASA	AC-5-ASA	recovery
4	0.0±0.0	0.0±0.0	0.2±0.2	0.0±0.0	0.0±0.0	0.0±0.0	0.0±0.0	0.0±0.0	0.0±0.0	0.0±0.0	0.0±0.0	0.0±0.0	76.8±12.2
8	0.0±0.0	0.2±0.1	2.5±2.4	0.0±0.0	1.1±0.2	1.8±1.8	0.0±0.0	0.0±0.0	0.0±0.0	0.0±0.0	2.9±2.2	1.7±1.8	61.9±22.0
12	0.0±0.0	1.8±1.7	3.8±3.5	0.0±0.0	0.1±0.0	6.4±6.6	0.5±0.8	2.2±0.8	0.0±0.0	0.0±0.0	0.9±0.6	4.3±0.2	48.5±6.8
24	0.0±0.0	1.3±1.4	0.6±0.1	0.0±0.0	0.1±0.0	2.5±2.4	3.7±4.1	0.3±0.0	3.4±1.3	0.0±0.0	0.0±0.0	0.0±0.0	17.2±2.4

Total recovery=100×(amount of the intact prodrugs, 5-ASA, and Ac-5-ASA recovered from stomach, small intestine, cecum, colon, blood, urine, liver, and feces)/dose.

plasma and urine concentrations of 5-ASA than CyD-5-ASA and the conjugate can lower the plasma concentration of 5-ASA. The lower concentration is attributable to the passage of the conjugate through the stomach and small intestine without significant degradation or absorption, followed by the degradation of the conjugate site-specifically in the cecum and colon. Therefore, CyD-5-ASA conjugates may be useful as prodrugs for colon-specific delivery system.

REFERENCES

1 **Schacht E,** Gevaert A, Kenawy ER, Molly K, Verstraete W, Adriaensens P, Caleer R, Gelan J. Polymers for colon specific drug delivery. *J Control Release* 1996; **39:** 327-338

2 **Carceller E,** Salas J, Merlos M, Giral M, Ferrando R, Escamilla I, Ramis J, García-Rafanell J, Forn J. Novel azo derivatives as prodrugs of 5-aminosalicylic acid and amino derivatives with potent platelet activating factor antagonist activity. *J Med Chem* 2001; **44:** 3001-3013

3 **Brown JP,** McGarraugh GV, Parkinson TM, Wingard RE, Onderdonk AB. A polymeric drug for treatment of inflammatory bowel disease. *J Med Chem* 1983; **26:** 1300-1307

4 **Milojevic S,** Newton JM, Cummings JH, Gibson GR, Botham RL, Ring SG, Stockham M, Allwood MC. Amylose as a coating for drug delivery to the colon: Preparation and *in vitro* evaluation using glucose pellets. *J Control Release* 1996; **38:** 85-94

5 **Van den Mooter G,** Maris B, Samyn C, Augustijns P, Kinget R. Use of azo polymers for colon-specific drug delivery. *J Pharm Sci* 1997; **86:** 1321-1327

6 **Khan MZ,** Stedul HP, Kurjaković N. A pH-dependent colon-targeted oral drug delivery system using methacrylic acid copolymers. II. Manipulation of drug release using Eudragit L100 and Eudragit S100 combinations. *Drug Dev Ind Pharm* 2000; **26:** 549-554

7 **Wilding IR,** Hardy JG, Sparrow RA, Davis SS, Daly PB, English JR. *In vivo* evaluation of enteric-coated naproxen tablets using gamma scintigraphy. *Pharm Res* 1992; **9:** 1436-1441

8 **Fukui E,** Miyamura N, Uemura K, Kobayashi M. Preparation of enteric coated timed-release press-coated tablets and evaluation of their function by *in vitro* and *in vivo* tests for colon targeting. *Int J Pharm* 2000; **204:** 7-15

9 **Gupta VK,** Beckert TE, Price JC. **A novel pH- and time-based** multi-unit potential colonic drug delivery system. I. Development. *Int J Pharm* 2001; **213:** 83–91

10 **Siew LF,** Man SM, Newton JM, Basit AW. Amylose formulations for drug delivery to the colon: a comparison of two fermentation models to assess colonic targeting performance *in vitro*. *Int J Pharm* 2004; **273:** 129-134

11 **Zambito Y,** Di Colo G. Preparation and *in vitro* evaluation of chitosan matrices for colonic controlled drug delivery. *J Pharm Pharm Sci* 2003; **6:** 274-281

12 **Sinha VR,** Kumria R. Polysaccharide matrices for microbially triggered drug delivery to the colon. *Drug Dev Ind Pharm* 2004; **30:** 143-150

13 **Jung YJ,** Lee JS, Kim YM. Colon-specific prodrugs of 5-aminosalicylic acid: synthesis and *in vitro*/*in vivo* properties of acidic amino acid derivatives of 5-aminosalicylic acid. *J Pharm Sci* 2001; **90:** 1767-1775

14 **Sinha VR,** Kumria R. Polysaccharides in colon-specific drug delivery. *Int J Pharm* 2001; **224:** 19-38

15 **Watts PJ**, Illum L. Colonic drug delivery. *Drug Dev Ind Pharm* 1997; **23:** 893-913

16 **Chourasia MK**, Jain SK. Pharmaceutical approaches to colon targeted drug delivery systems. *J Pharm Pharm Sci* 2003; **6:** 33-66

17 **Zou M,** Okamoto H, Cheng G, Hao X, Sun J, Cui F, Danjo K. Synthesis and properties of polysaccharide prodrugs of 5-aminosalicylic acid as potential colon-specific delivery systems. *Eur J Pharm Biopharm* 2005; **59:** 155-160

18 **Chungi VS,** Rekhi GS, Shargel L. A simple and rapid liquid chromatographic method for the determination of major metabolites of sulfasalazine in biological fluids. *J Pharm Sci* 1989; **78:** 235-238

19 **Hussain FN,** Ajjan RA, Moustafa M, Anderson JC, Riley SA. Simple method for the determination of 5-aminosalicylic and N-acetyl-5-aminosalicylic acid in rectal tissue biopsies. *J Chromatogr B Biomed Sci Appl* 1998; **716:** 257-266

Science Editor Wang XL **Language Editor** Elsevier HK

PO Box 2345, Beijing 100023, China
www.wjgnet.com
wjg@wjgnet.com

ELSEVIER

World J Gastroenterol 2005;11(47):7461-7465
World Journal of Gastroenterology ISSN 1007-9327

• *BASIC RESEARCH* •

Fibroblast growth factor-4 and hepatocyte growth factor induce differentiation of human umbilical cord blood-derived mesenchymal stem cells into hepatocytes

Xin-Qin Kang, Wei-Jin Zang, Li-Jun Bao, Dong-Ling Li，Tu-Sheng Song, Xiao-Li Xu, Xiao-Jiang Yu

Xin-Qin Kang,Tu-Sheng Song, Department of Genetics and Molecular Biology, Medical School of Xi'an Jiaotong University, Xi'an 710061, Shaanxi Province, China
Wei-Jin Zang, Dong-Ling Li, Xiao-Li Xu, Xiao-Jiang Yu, Department of Pharmacology, Key Laboratory of Environment and Genes Related to Diseases of Ministry of Education, School of Medicine, Xi'an Jiaotong University, Xi'an 710061, Shaanxi Province, China
Li-Jun Bao, Department of Obstetrics and Gynecology, First Hospital of Xi'an Jiaotong University, Xi'an 710061, Shaanxi Province, China
Supported by National Natural Science Foundation of China, No. 30470633 and Doctoral Foundation of Xi'an Jiaotong University, No.DFXJTU2002-16
Correspondence to: Wei-Jin Zang, Box 77, Department of Pharmacology, Key Laboratory of Environment and Genes Related to Diseases of Ministry of Education, School of Medicine, Xi'an Jiaotong University, Xi'an 710061, Shaanxi Province, China. zwj@mail.xjtu.edu.cn
Telephone: +86-29-82655003 Fax: +86-29-82655003
Received: 2005-06-13 Accepted: 2005-07-04

Abstract

AIM: To investigate the differentiation of human umbilical cord blood (HUCB)-derived mesenchymal stem cells (MSCs) into hepatocytes by induction of fibroblast growth factor-4 (FGF-4) and hepatocyte growth factor (HGF), and to find a new source of cell types for therapies of hepatic diseases.

METHODS: MSCs were isolated by combining gradient density centrifugation with plastic adherence. When HUCB-derived MSCs reached 70% confluence, they were cultured in Iscove modified Dulbecco medium (IMDM) supplemented with 10 mL/L FBS, 20 ng/mL HGF and 10 ng/mL FGF-4. The medium was changed every 4 d and stored for albumin, alpha-fetoprotein (AFP) and urea assay. Expression of CK-18 was detected by immunocytochemistry. Glycogen storage in hepatocytes was determined by PAS staining.

RESULTS: By combining gradient density centrifugation with plastic adherence, we could isolate MSCs from 25.6% of human umbilical cord blood. When MSCs were cultured with FGF-4 and HGF, approximately 63.6% of cells became small, round and epithelioid on d 28 by morphology. Compared with the control, the level of AFP increased significantly from d 12 to 18.20±1.16 μg/L (t = 2.884, P<0.05) in MSCs cultured with FGF-4 and HGF, and was higher (54.28±3.11 μg/L) on d 28 (t = 13.493, P<0.01). Albumin increased significantly on d 16 (t = 6.68, P<0.01) to 1.02±0.15 μg/mL, and to 3.63±0.30 μg/mL on d 28 (t = 11.748, P<0.01). Urea (4.72±1.03 μmol/L) was detected on d 20 (t = 4.272, P<0.01), and continued to increase to 10.28±1.06 μmol/L on d 28 (t = 9.276, P<0.01). Cells expressed CK-18 on d 16. Glycogen storage was observed on d 24.

CONCLUSION: HUCB-derived MSCs can differentiate into hepatocytes by induction of FGF-4 and HGF. HUCB-derived MSCs are a new source of cell types for cell transplantation therapy of hepatic diseases.

Key words: Mesenchymal stem cell; Differentiation; Hepatocyte

Kang XQ, Zang WJ, Bao LJ, Li DL，Song TS, Xu XL, Yu XJ. Fibroblast growth factor-4 and hepatocyte growth factor induce differentiation of human umbilical cord blood-derived mesenchymal stem cells into hepatocytes. *World J Gastroenterol* 2005; 11(47): 7461-7465
http://www.wjgnet.com/1007-9327/11/7461.asp

INTRODUCTION

Cell transplantation therapy is an alternative to the treatment of liver conditions that sustain significant liver injury. It has been reported that bone marrow-derived MSCs can differentiate into mesoderm cells such as osteoblasts[1-3], adipocytes[4-6], neural and brain cells[7-10],cardiomyocytes[11-13] and hepatocytes[14,15] *in vivo* or *in vitro*. However, it has been demonstrated that the number and the differentiating potential of bone marrow MSCs decrease with age [16]. Therefore, search for alternative sources of MSCs is of significant value.

Studies have shown that human umbilical cord blood (HUCB) contains hematopoietic stem cells and MSCs, both of them can be used as alternative sources to bone marrow for cell transplantation therapy. Hematopoietic stem cells of HUCB have already been proven to be useful for the treatment of various hematological disorders. On the other hand, identification of the MSCs remained elusive until they were recently isolated as a homogeneous cell population by a number of different laboratories[17,18]. The extensive characterization of these cells has revealed

that they are similar to bone marrow-derived MSCs not only with respect to cellular properties and multi-lineage differentiation potential, but also with respect to their molecular context[19,20]. It was reported that HUCB-derived MSCs could differentiate into mesoderm cells such as osteoblasts, adipocytes[21], neuron-like cells[19, 22], and cardiomyocytes[23, 24]. Schwartz *et al*[14]. and Kang *et al*[15]. reported that FGF-4 and HGF could induce differentiation of bone marrow MSCs into functional hepatocyte-like cells. We hypothesized that FGF-4 and HGF could also induce differentiation of HUCB-derived MSCs into functional hepatocyte-like cells.

Using a relatively simple method, namely gradient density centrifugation in combination with adherence, we isolated HUCB-derived MSCs and cultured them in plastic culture flasks by induction of FGF-4 and HGF.The results showed that HUCB-derived MSCs could differentiate into hepatocytes *in vitro*.

MATERIALS AND METHODS

Materials and reagents

Human cord blood was obtained from Department of Obstetrics and Gynecology, First Hospital of Xi' an Jiaotong University. Fetal bovine serum (FBS) was purchased from Hangzhou Sijiqing Biological Engineering Material Co.Ltd. Albumin RIA kit and alpha-fetoprotein RIA kit were purchased from Beijing Atom High-tech Co.Ltd. Mouse anti-human monoclonal antibody cytokeratin 18(CK-18) was purchased from Chemicon Company. Iscove modified Dulbecco medium (IMDM) was purchased from GIBCO. Acid fibroblast growth factor-4 (FGF-4) and hepatocyte growth factor (HGF) were purchased from R&D Systems, Inc. Ficoll-Paque (1.077 g/mL) was pursed from Amersham-Pharmacia.

Isolation and culture of MSCs from HUCB

Ten mL of umbilical cord blood was taken from each patient (n = 49).The blood sample was diluted with an equal volume of D-Hanks. The diluted umbilical cord blood was layered over an equal volume of Ficoll-Paque (1.077g/mL). Mononuclear cells (MNCs) were recovered from the gradient interface and washed twice with D-Hanks after centrifugation at 800r/min for 20 min. The MNCs were suspended in 5 mL IMDM supplemented with 100 mL/L FBS, 100 U/mL penicillin, 100 U/mL streptomycin, at last plated in 25 cm^2 plastic cell culture flasks at the density of 10^6 /mL. The cells were maintained at 37 ℃ in 50 mL/L CO_2 in fully humidified air. The medium was changed for the first time on d 5 and then changed every 4 d. Because of limited time, 27 blood samples were treated within 3 h, 22 samples within 3-6 h, 8 samples within 6-12 h, and 2 samples after 12 h.

Hepatocyte differentiation

The cultured cells were harvested from the culture bottles with 0.25g/L trypsin. Cultured cells at passage 3 were seeded in six- well cell culture clusters. When the cells grew at 70% confluence, the control group was continuously cultured in IMDM supplemented with 10 mL/L FBS, 100 U/mL penicillin, 100 U/mL streptomycin. The hepatocyte differentiation group was cultured in IMDM supplemented with 10 ml/L FBS, 20 ng/mL HGF, 10 ng/mL FGF-4,100 U/mL penicillin and 100 U/mL streptomycin. Each well was added 2 mL of the medium, and changed every 4 d. The medium was stored at -20 ℃ for albumin, alpha-fetoprotein (AFP) and urea assay.

Radioimmunoassay

Concentrations of AFP and albumin in the changed medium were determined by radioimmunoassay on d 4, 8, 12, 16, 20, 24, and 28. Since there might be a very small amount of AFP and albumin in the changed medium, the medium was condensed 5 times by freeze drying before radioimmunoassay.

Urea assay

Cell culture media at the indicated time points after the induction of hepatogenic differentiation were collected, analyzed for urea as previously described by Buga *et al*[25]. and optical densities were measured at 492 nm using a spectrophotometer. The control group was used as a negative control, which was cultured in IMDM supplemented with 10 mL/L FBS, 100 U/mL penicillin and 100 U/mL streptomycin.

Immunocytochemistry

A slide was put in each well. Cells on the slides were fixed with 4% paraformaldehyde at 20 ℃ for 10 min and permeabilized with 0.3% Triton X-100 in PBS for 10 min. Cells were incubated with 3 mL/L hydrogen peroxide in methanol for 10 min to block endogeneous peroxidase activity and then washed twice in PBS for 5 min. Nonspecific binding sites were blocked with 3 mL/L normal goat serum. Cells were incubated overnight at 4 ℃ with primary antibody (mouse anti-human monoclonal antibody of CK-18, 1:200). After washed twice for 15 min in PBS, slides were incubated at 37 ℃ for 30 min with secondary antibody (goat anti -mouse IgG marked by biotin), with streptoavidin marked by horseradish peroxidase, and then developed color with DAB, 0.01 mol/L PBS was substituted for primary antibody as the negative control. The positive cells presented as brownish yellow.

Periodic acid-Schiff treatment for glycogen

In the hepatocyte differentiation group, on d 16, 20, 24, and 28, we took out the medium from the flasks, rinsed cells 3 times with PBS , fixed them with 100 mL/L formaldehyde for 30 min. The cells were oxidized in 10 g/L periodic acid for 10 min and rinsed three times in dH_2O. Then, the cells were treated with Schiff's reagent for 10 min, rinsed in dH_2O for 10 min, stained with hematoxylin for 2 min, differentiated by 1% alcohol/ HCL, rinsed in dH_2O again and observed under an invert

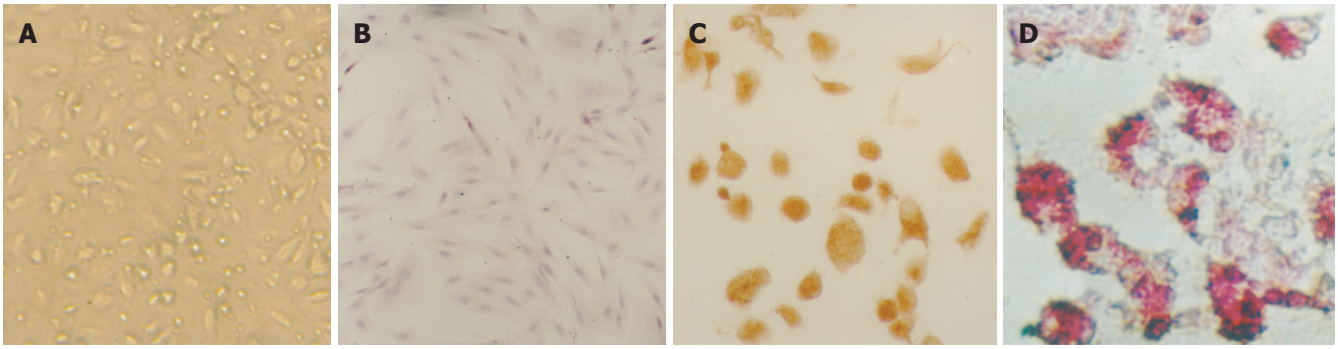

Figure 1 Different morphology and differentiation of HUCB-derived MSCs. **A**: morphology of primary cultured HUCB-derived MSCs. MSCs are spindle-like and osteroclasts are big and round; **B**: morphology of sub-cultured HUCB-derived MSCs stained with HE. The fibroblast-like cells are growing as a whirlpool (×100); **C**: representative immuocytochemistry showing expression of CK-18 on HUCB-derived MSCs on d 28 (SABC×200); **D**: cells stained by PAS. Glycogen storage is seen as accumulated magenta staining, the round and epithelioid cells show magenta staining in the region (×400).

Table1 Concentrations of AFP, albumin and urea in the medium at different time points (mean±SE)

Group	4 d	8 d	12 d	16 d	20 d	24 d	28 d
				AFP (μg/L)			
Differentiation	15.92±0.76	15.72±1.06	18.20±1.16[a]	20.57±1.98[a]	38.53±6.07[a]	39.47±4.06[b]	54.28±3.11[b]
Control	15.77±0.72	14.30±0.69	14.67±1.10	13.72±0.40	16.57±1.03	14.13±1.11	15.67±0.93
				Albumin (μg/mL)			
Differentiation	–	–	0.63±0.07	1.02±0.15[b]	1.45±0.21[b]	3.08±0.35[b]	3.63±0.30[b]
Control	–	–	0.40±0.12	0.20±0.06	0.15±0.06	0.22±0.07	0.25±0.10
				Urea (μmol/L)			
Differentiation	–	–	–	–	4.72±1.03[b]	7.27±0.89[b]	10.28±1.06[b]
Control	–	–	–	–	0.47±0.30	0.87±0.43	0.55±0.26

[a]P<0.05 *vs* control, [b]P<0.01 *vs* control, – stands for what could not detected. n = 6

microscope.

Statistical analysis

The data of AFP, albumin and urea were expressed as mean±SE. The statistical software SPSS12.0 was used. The results were analyzed by t-test. P<0.05 was considered statistically significant.

RESULTS

Isolation and culture of MSCs from HUCB

The cells isolated by gradient density centrifugation showed heterogeneity during the first five days. Adherent cells were observed on d 9-12. Spindle-shape cells appeared at the bottom of culture flasks. In addition, some big and round osteroclasts were observed among the spindle-like cells. Many round cells were suspended in the medium (Figure 1A). By changing the medium, the suspending cells became less and less. After the medium was changed twice, the suspending cells were completely removed from the medium, but osteroclasts still existed in the cells. The adhered cells were fibroblast-like and grew as a whirlpool. The sub-cultured cells were much pure and fibroblast-like, the osteroclasts disappeared (Figure 1B). The primary culture cells reached confluence 10-12 d later, the cells sub-cultured at a ratio of 1:3 reached confluence 8-10 d later. Using the method, we isolated HUCB-derived MSCs from 10 samples of 39, which were isolated within 6 h. The rate of separation was 25.6%. MSCs could not be isolated from the other sample.

MSCs became small, round and epithelioid cells after cultured with FGF-4 and HGF

When the cultured cells reached 70% confluence, they were treated with hepatocyte differentiation medium, containing IMDM supplemented with 10 mL/L FBS, 20 ng/mL HGF, 10 ng/mL FGF-4, 100 U/mL penicillin and 100 U/mL streptomycin. Before the 8-d treatment they did not show any change compared to the controls. After treatment, small round cells appeared in the treatment group, epithelioid cells were also observed. The diameter of the cells was 12-16 μm. On d 28, approximately 63.6% of the cells were small, round and epithelioid. The control cells were still fibroblast-like, the density of the cells increased. The cells were overlapped in some regions.

Radioimmunoassay

By radioimmunoassay, albumin and AFP production was measured at various time points throughout the differentiating process. We could detect low levels of AFP on undifferentiated HUCB-derived MSCs, but not of albumin. However, there was a small amount of albumin in the medium, which was hardly detected by

albumin RIA. Compared to controls, the levels of AFP increased significantly from d 12 with a concentration of 18.20±1.16 μg/L ($P<0.05$) in MSCs cultured with FGF-4, and HGF continued to increase and was higher on d 28 ($P<0.01$) with a concentration of 54.28±3.11 μg/L. The level of albumin could not be detected by radioimmunoassay before d 12, albumin increased significantly on d 16 with a concentration of 1.02±0.15 μg/mL ($P<0.01$), and to 3.63±0.30 μg/mL on d 28 ($P<0.01$). According to the data, increasing time points were different between AFP and albumin (Table 1).

Urea assay

Urea production and secretion by hepatocytes were detected at various time points throughout the differentiating process. Following treatment with FGF-4 and HGF, urea produced by MSCs was detected with a concentration of 4.72±1.03 μmol/L on d 20, and increased to 10.28±1.06 μmol/L on d 28 (Table 1).

Immunocytochemistry

On d 8, 16, 24, and 28, we took out the cells on the slides respectively. The cells expressed CK-18 on d 16 (Figure 1C). The control group was negative.

Periodic acid-Schiff treatment for glycogen

We analyzed the levels of glycogen storage by periodic acid-Schiff (PAS) staining of FGF-4 and HGF-induced MSCs on d 20, 24, and 28. Glycogen storage was seen on d 24, being positively stained for PAS (Figure 1D).

DISCUSSION

There are many hematopoietic stem cells and MSCs in HUCB. Many methods can isolate MSCs from HUCB[26-28]. In this study, we used the Ficoll (1.077 g/mL) to isolate MSCs from HUCB, we combined the gradient density centrifugation with plastic adherence and changed the medium many times to purify MSCs after gradient density centrifugation. This method is relatively simply, and can easily get pure MSCs. We isolated MSCs from 10 of 39 samples, which is in accordance with the previous study[28]. MSCs should be isolated from the sample as soon as possible. Our results showed that it was difficult to isolate MSCs from the samples, because the activity of MSCs is low, even loses with time prolonged.

During the 28 d of differentiation, FGF-4 and HGF induced MSCs into cells with morphological and functional characteristics of hepatocytes. In our study, the cells that differentiated into hepatocyte-like cells could produce urea, secrete albumin, AFP and Ck-18, and store glycogens. Urea production was characterized by hepatocyte activity, although kidney tubular epithelium also produced urea. In contrast, albumin, AFP and Ck-18 production is a specific test for the presence and metabolic activity of hepatocytes. Only hepatocytes can generate and store glycogens. In our research, we found that AFP could be detected throughout the differentiating process because the medium contained a low level of AFP. From d 12, the level of AFP increased significantly compared to controls, suggesting that MSCs can secrete AFP. It was reported that AFP is produced by immature hepatocytes. That is to say, hepatocytes are immature on d 12. Before d 12, the concentration of albumin could not be measured by radioimmunoassay because the amount of albumin was small in the medium. When MSCs differentiated, albumin was significantly secreted by MSCs from d 16, CK-18 was expressed by cells from d 16, and urea was significantly secreted from d 20. By periodic acid-Schiff (PAS) staining, the differentiated cells could store glycogens. The data suggest that HUCB-derived MSCs can differentiate into hepatocytes by induction of FGF-4 and HGF.

HGF was first identified as a blood-derived mitogen for hepatocytes. HGF and its receptor c-Met are the key factors for liver growth and function. After cultured with only HGF, adult human bone marrow MSCs could also differentiate into hepatocytes *in vitro*[29]. FGF-4 is mitogenic for fibroblasts and endothelial cells. Mouse embryonic stem cells grown in medium supplemented with FGF-4 could differentiate into cells expressing hepatocyte-specific genes and antigens[30]. By cooperation of HGF and FGF, the differentiation of MSCs could be triggered and MSCs could develop into hepatocytes.

Our experimental data showed the hepatic differentiation potential of HUCB-derived MSCs. HUCB-derived MSCs have more advantages over bone marrow MSCs. It is suggested that HUCB-derived MSCs are a source of cell types for cell transplantation therapy of liver diseases.

REFERENCES

1 **Chen TL,** Shen WJ, Kraemer FB. **Human BMP-7/OP-1 induces** the growth and differentiation of adipocytes and osteoblasts in bone marrow stromal cell cultures. *J Cell Biochem* 2001; **82**: 187-199

2 **Ahdjoudj S,** Lasmoles F, Oyajobi BO, Lomri A, Delannoy P, Marie PJ. Reciprocal control of osteoblast/chondroblast and osteoblast/adipocyte differentiation of multipotential clonal human marrow stromal F/STRO-1(+) cells. *J Cell Biochem* 2001; **81**: 23-38

3 **Atmani H,** Chappard D, Basle MF. Proliferation and differentiation of osteoblasts and adipocytes in rat bone marrow stromal cell cultures: effects of dexamethasone and calcitriol. *J Cell Biochem* 2003; **89**: 364-372

4 **Allan EH,** Ho PW, Umezawa A, Hata J, Makishima F, Gillespie MT, Martin TJ. Differentiation potential of a mouse bone marrow stromal cell line. *J Cell Biochem* 2003; **90**: 158-169

5 **Atmani H,** Audrain C, Mercier L, Chappard D, Basle MF. Phenotypic effects of continuous or discontinuous treatment with dexamethasone and/or calcitriol on osteoblasts differentiated from rat bone marrow stromal cells. *J Cell Biochem* 2002; **85**: 640-650

6 **Porter RM,** Huckle WR, Goldstein AS. Effect of dexamethasone withdrawal on osteoblastic differentiation of bone marrow stromal cells. *J Cell Biochem* 2003; **90**: 13-22

7 **Wislet-Gendebien S,** Leprince P, Moonen G, Rogister B. Regulation of neural markers nestin and GFAP expression by cultivated bone marrow stromal cells. *J Cell Sci* 2003; **116**: 3295-3302

8 **Song S,** Kamath S, Mosquera D, Zigova T, Sanberg P, Vesely DL, Sanchez-Ramos J. Expression of brain natriuretic peptide by human bone marrow stromal cells. *Exp Neurol* 2004; **185**:

191-197
9 **Rismanchi N,** Floyd CL, Berman RF, Lyeth BG. Cell death and long-term maintenance of neuron-like state after differentiation of rat bone marrow stromal cells: a comparison of protocols. *Brain Res* 2003; **991**: 46-55
10 **Lou Sj,** Gu P, Chen F, He C, Wang Mw, Lu CI. The effect of bone marrow stromal cells on neuronal differentiation of mesencephalic neural stem cells in Sprague-Dawley rats. *Brain Res* 2003; **968**: 114-121
11 **Orlic D,** Kajstura J, Chimenti S, Jakoniuk I, Anderson SM, Li B, Pickel J, McKay R, Nadal-Ginard B, Bodine DM, Leri A, Anversa P. Bone marrow cells regenerate infarcted myocardium. *Nature* 2001; **410**: 701-705
12 **Orlic D.** Adult bone marrow stem cells regenerate myocardium in ischemic heart disease. *Ann N Y Acad Sci* 2003; **996**: 152-157
13 **Jackson KA**, Majka SM, Wang H, Pocius J, Hartley CJ, Majesky MW, Entman ML, Michael LH, Hirschi KK, Goodell MA. Regeneration of ischemic cardiac muscle and vascular endothelium by adult stem cells. *J Clin Invest* 2001; **107:** 1395-1402
14 **Schwartz RE**, Reyes M, Koodie L, Jiang Y, Blackstad M, Lund T, Lenvik T, Johnson S, Hu WS, Verfaillie CM. Multipotent adult progenitor cells from bone marrow differentiate into functional hepatocyte-like cells. *J Clin Invest* 2002; **109**: 1291-1302
15 **Kang XQ**, Zang WJ, Song TS, Xu XL, Yu XJ, Li DL, Meng KW, Wu SL, Zhao ZY. Rat bone marrow mesenchymal stem cells differentiate into hepatocytes in vitro. *World J Gastroenterol* 2005; **11**: 3479-3484
16 **D'Ippolito G,** Schiller PC, Ricordi C, Roos BA,Howard GA. Age-related osteogenic potential of mesenchymal stromal stem cells from human vertebral bone marrow. *J Bone Miner Res* 1999; **14**: 1115-1122
17 **Lee MW,** Choi J, Yang MS, Moon YJ, Park JS, Kim HC, Kim YJ. Mesenchymal stem cells from cryopreserved human umbilical cord blood. *Biochem Biophys Res Commun* 2004; **320**: 273-278
18 **Bieback K,** Kern S, Klüter H, Eichler H. Critical parameters for the isolation of mesenchymal stem cells from umbilical cord blood. *Stem Cells* 2004; **22**: 625-634
19 **Panepucci RA**, Siufi JL, Silva WA, Proto-Siquiera R, Neder L, Orellana M, Rocha V, Covas DT, Zago MA. Comparison of gene expression of umbilical cord vein and bone marrow-derived mesenchymal stem cells. *Stem Cells* 2004; **22**: 1263-1278
20 **Jeong JA**, Hong SH, Gang EJ, Ahn C, Hwang SH, Yang IH, Han H, Kim H. Differential gene expression profiling of human umbilical cord blood-derived mesenchymal stem cells by DNA microarray. *Stem Cells* 2005; **23**: 584-593
21 **Lee OK**, Kuo TK, Chen WM, Lee KD, Hsieh SL, Chen TH. Isolation of multipotent mesenchymal stem cells from umbilical cord blood. *Blood* 2004; **103**: 1669-1675
22 **Hou L,** Cao H, Wang D, Wei G, Bai C, Zhang Y, Pei X. Induction of umbilical cord blood mesenchymal stem cells into neuron-like cells in vitro. *Int J Hematol* 2003; **78**: 256-261
23 **Ma N,** Stamm C, Kaminski A, Li W, Kleine HD, Müller-Hilke B, Zhang L, Ladilov Y, Egger D, Steinhoff G. Human cord blood cells induce angiogenesis following myocardial infarction in NOD/scid-mice. *Cardiovasc Res* 2005; **66**: 45-54
24 **Henning RJ,** Abu-Ali H, Balis JU, Morgan MB, Willing AE, Sanberg PR. Human umbilical cord blood mononuclear cells for the treatment of acute myocardial infarction. *Cell Transplant* 2004; **13**: 729-739
25 Buga GM, Singh R, Pervin S, Rogers NE, Schmitz DA, Jenkinson CP, Cederbaum SD, Ignarro LJ. Arginase activity in endothelial cells: inhibition by NG-hydroxy-L-arginine during high-output NO production. *Am J Physiol* 1996; 271: H1988-H1998
26 **Bornstein R**, Flores AI, Montalbán MA, del Rey MJ, de la Serna J, Gilsanz F. A modified cord blood collection method achieves sufficient cell levels for transplantation in most adult patients. *Stem Cells* 2005; **23**: 324-334
27 **Schwinger W**, Benesch M, Lackner H, Kerbl R, Walcher M, Urban C. Comparison of different methods for separation and ex vivo expansion of cord blood progenitor cells. *Ann Hematol* 1999; **78**: 364-370
28 **Yang SE,** Ha CW, Jung M, Jin HJ, Lee M, Song H, Choi S, Oh W, Yang YS. Mesenchymal stem/progenitor cells developed in cultures from UC blood. *Cytotherapy* 2004; **6**: 476-486
29 **Fiegel HC,** Lioznov MV, Cortes-Dericks L, Lange C, Kluth D, Fehse B, Zander AR. Liver-specific gene expression in cultured human hematopoietic stem cells. *Stem Cells* 2003; **21**: 98-104
30 **Ruhnke M,** Ungefroren H, Zehle G, Bader M, Kremer B, Fändrich F. Long-term culture and differentiation of rat embryonic stem cell-like cells into neuronal, glial, endothelial, and hepatic lineages. *Stem Cells* 2003; **21**: 428-436

Science Editor Wang XL and Guo SY **Language Editor** Elsevier HK

PO Box 2345, Beijing 100023, China
www.wjgnet.com
wjg@wjgnet.com

ELSEVIER

World J Gastroenterol 2005;11(47):7466-7472
World Journal of Gastroenterology ISSN 1007-9327

• *CLINICAL RESEARCH* •

Effect of fish oil enriched enteral diet on inflammatory bowel disease tissues in organ culture: Differential effects on ulcerative colitis and Crohn's disease

Doris Meister, Subrata Ghosh

Doris Meister, Subrata Ghosh, Gastrointestinal Unit, University of Edinburgh, Western General Hospital, Edinburgh EH4 2XU, United Kingdom
Correspondence to: Professor Subrata Ghosh, MD (Edin.), FRCP, FRCP(E), Imperial College London, Hammersmith Campus, Du Cane Road, London W12 0NN, United Kingdom. s.ghosh@imperial.ac.uk
Telephone: +44-20-8383-3266 Fax: +44-20-8749-3436
Received: 2005-03-29 Accepted: 2005-06-02

Abstract

AIM: To investigate the influence of fish oil enriched enteral diet on intestinal tissues taken from Crohn's disease (CD), ulcerative colitis (UC) and non-inflamed non-IBD control patients *in vitro*.

METHODS: Colonoscopic biopsies from patients with active CD (n = 4), active UC (n = 7), and non-inflamed non-IBD control patients (n = 4) were incubated (three dilutions of 1:20, 1:10, and 1:5) with Waymouth's culture medium and enteral elemental diet (EO28, SHS, Liverpool, UK) modified in the fatty acid composition with fish oil (EF) in an organ culture system for 24 h. In each experimental set-up, incubation with Waymouth's medium alone as control was included. Tissue viability was assessed by adding bromodeoxyuridine (BrdU) to the culture fluid and immunohistochemically staining for BrdU uptake. Cytokine ratio of IL-1ra/IL-1β (low ratio indicative of inflammation) and production of those cytokines as a percentage of medium control were assayed in the culture supernatant.

RESULTS: Incubation of CD-affected tissue with EF (1:20, 1:10, and 1:5) modestly and non-significantly increased IL-1ra/IL-1β ratio as compared with medium control (CD 39.1±16.1; 26.5±7.8, 47.1±16.8 *vs* control 13.0±2.2), but incubation of UC-affected tissues increased IL-1ra/IL-1β ratio significantly in all three dilutions (UC 69.1±32.2, P<0.05; 76.1±36.4, P = 0.05; 84.5±37.3, P<0.02; *vs* control 10.2±3.7). Incubation of non-inflamed non-IBD control tissue did not increase the IL-1ra/IL-1β ratio in any dilution compared to medium control (69.3±47.0, 54.1±30.6, 79.4±34.0 *vs* control 76.1±37.3). Average percentage production of IL-1β indexed against medium control was significantly less in UC after EF incubation as compared with CD (UC 24.0±4.8 *vs* CD 51.8±8.1; P<0.05). Average percentage production of IL-1ra was markedly higher in UC (135.9±3.4) than that in control patients (36.5±4.3) (P<0.0001).

CONCLUSION: IBD tissues, after incubation with elemental diet modified in its fatty acid composition with fish oil, show an increase in IL-1ra /IL-1β cytokine ratio. This effect of ω-3 fatty acid modulation is significantly more marked in UC compared with CD and is accompanied by both a reduction of IL-1β and increase of IL-1ra. The positive direct anti-inflammatory effect of elemental diet with fish oil in tissue affected with UC suggests dietary treatment of UC may be possible.

Key words: Inflammatory bowel disease; ω-3 fatty acids; Cytokine ratio; IL-1ra/IL-1β; *In vitro*

Meister D, Ghosh S. Effect of fish oil enriched enteral diet on inflammatory bowel disease tissues in organ culture: Differential effects on ulcerative colitis and Crohn's disease. *World J Gastroenterol* 2005; 11(47): 7466-7472
http://www.wjgnet.com/1007-9327/11/7466.asp

INTRODUCTION

Enteral defined formula nutritional therapy is currently an option only in Crohn's disease (CD), and this may result in an improvement in clinical inflammatory parameters[1], histological appearance[2], and disease activity[3]. Hypotheses about how elemental diet might work include withdrawal of food antigens, decrease and alteration in luminal bacteria, reduction in pancreatic and biliary secretion, bowel rest (or medical bypass), alteration of dietary lipids and improvement in nutritional status[3]. Increased production of IL-1β during active inflammatory bowel disease (IBD)[4] and an imbalance of IL-1β and its receptor antagonist (IL-1ra) are now well-known features of IBD[5-7], and ratio of anti-inflammatory to pro-inflammatory cytokines IL-1ra/IL-1β may be used as an index of inflammatory status. The possible influence and modulation of cytokine balance by dietary fatty acids are of interest and might have clinical implication[8,9].

The main fatty acids of fish oil are the long-chain-polyunsaturated fatty acids (FA) of eicosapentaenoic acid

(EPA, C20:5 ω-3) and docosahexaenoic acid (DHA, C20:6 ω-3). The use of these FA in inflammatory conditions has been explored in other inflammatory disorders, such as rheumatoid arthritis[10,11] and inflammatory skin disorders[12,13]. In IBD, especially in ulcerative colitis (UC), treatment with fish oil preparations may have a better impact than in CD, though this is still controversial. Studies have shown a decrease in clinical activity and some morphological improvements in UC but no change was observed in CD after 7-mo treatment with 3.2 g of ω-3 FA per day in active IBD[14]. Stenson *et al*[15]. reported the effect of oral fish oil treatment in UC in a double-blind placebo controlled crossover trial of 18 patients. Fish oil supplementation resulted in a significant decrease in rectal dialysate of LTB_4, and significant improvement in the histological appearance of the colon. Furthermore, they reported a significant increase in body weight, averaging 1.74 kg, as compared to controls who had no change in body weight[15]. Clinical improvement in 11 patients with mild to moderate UC after ingestion of ω-3 FA was reported by Aslan and Triadafilopoulos[16]. Six months of supplementation with ω-3 FA in patients with proctocolitis resulted in a significant improvement in sigmoidoscopic and histologic appearance in the distal colon. Blood analysis showed a decreased natural killer (NK) cell activity and markedly reduced LTB_4 serum levels, which correlated with a decrease in IL-2[17,18]. In contrast, Hawthorne *et al*[19]. reported only limited clinical benefit despite increased synthesis of LTB_5 and suppression of LTB_4 in ω-3-supplemented UC patients.

These studies, although controversial and differing in the delivery system and dose, demonstrate that dietary modulation via FA, especially of ω-3 and ω-6, can modulate and influence the inflammatory mediator production and response in IBD.

A theoretical advantage of dietary intake of ω-3 FA is that these FA do not have to go through the processes of elongation and saturation, and can therefore be immediately incorporated into the plasma membrane.

The aim of this study was to investigate the direct effect of fish oil containing enteral diet *in vitro* on cytokine response of IL-1ra/IL-1β ratio and on cytokine production as a percentage of medium control in tissue affected with CD, UC, and non-inflamed non-IBD control patients. Such *in vitro* experiments, though reductionist may provide indirect evidence of the alteration in inflammatory profile after the ingestion of defined formulae diet, which rapidly changes tissue levels of nutrients. In CD, it is clear that local effect cannot explain the benefit of such therapy in distal ileum and colon as most of elemental diet is absorbed in proximal small intestine. We specifically aimed to explore whether such modification of enteral diet used in CD might show evidence of efficacy in UC.

MATERIALS AND METHODS

Subjects

Fifteen patients were included in this study. Four patients with CD (mean age 41±14 years), seven patients with UC (mean age 56±6 years) and four patients as non-inflamed non-IBD control group (mean age 36±9 years). The latter group included patients with a final diagnosis of irritable bowel syndrome. The patients attended routine colonoscopy and gave consent to obtain additional biopsies along with the biopsies taken for clinical management. Ethical approval was obtained from Research Ethics Committee.

Biopsies were taken from the following anatomic areas: in CD (2 sigmoid, 1 rectum, 1 ileocolonic anastomosis), UC (5 sigmoid, 2 rectum) and control group (4 sigmoid). Disease duration for IBD patients was as follows: (1) 1-3 years (1 CD, 2 UC); (2) 4-6 years (1 CD, 1 UC); and (3) >6 years (2 CD, 4 UC). Medications at the time of biopsy were (1) in CD with azathioprine (n = 2), steroids and azathioprine (n = 1), steroids and 5-ASA (n = 1) and (2) in UC with steroids (n = 1), azathioprine (n = 1), 5-ASA (n = 3).

The biopsies in IBD patients were taken from macroscopically affected areas but avoiding frankly ulcerated areas, and histologically confirmed active inflammation and the diagnosis of IBD. The biopsies in control patients showed no evidence of inflammation. All biopsies were taken with identical biopsy forceps by the same surgeon (SG) to ensure uniform size of the biopsies.

Methods

Biopsies obtained from endoscopy were incubated for 24 h with elemental diet EO28 (SHS, Liverpool, UK), specially modified in its FA composition for fish oil (EF), as previously described[20]. Tables 1 and 2 show the details of diet composition regarding general composition of diet and FA profile, respectively. Briefly, enteral diet was diluted in distilled water in three dilutions of 1:5, 1:10, and 1:20 with Waymouth's medium (MB752/1, Flow-labs 12-52-54). The medium was supplemented with 100 mL/L heat-inactivated fetal calf serum (Ako Tech), 200 mmol/mL L-glutamine (Gibco 43-8030), 300 μg/mL ascorbic acid (Sigma A 4544), 0.45 μg/mL ferrous sulfate (Sigma F 8633), 50 μg/mL gentamycin (Flow-labs 16-760-45), 5 000 IU/mL penicillin and 5 000 μg/mL streptomycin (Flow-labs 16-700-49).

From each patient, one biopsy was always incubated with only medium as control. Tissue viability over culture period was confirmed by adding 10 μL/mL BrdU (Sigma B5002) to the culture fluid. After the culture period, supernatant was stored and frozen at -70 °C for immunoassay and tissue was processed for BrdU immunohistochemistry and validated as described previously[20,21]. All explants were examined in a blinded fashion under a light microscope (100× and 250×). The explants were considered viable only if the morphology of the tissue was considered intact with well-defined crypts, epithelial surface and adequate and strong uptake of BrdU with labeled cells in horizontal and vertical crypts. Formal scoring to determine labeling index was not performed as the focus of this study was not on colonic epithelial proliferation.

Table 1 Composition of enteral diet (EO28, SHS, Liverpool, UK)

Nutrient	Per 100 g powder
Energy (kcal)	443
Protein equivalent (g)	12.5
Carbohydrate (g)	60
Fat (g)	17.45
Sodium (mg)	305
Potassium (mg)	466
Chloride (mg)	333
Calcium (mg)	187.5
Phosphorus (mg)	200
Magnesium (mg)	81.6
Iron (mg)	4.2
Zinc (mg)	4.2
Iodine (μg)	33.3
Manganese (mg)	0.6
Copper (mg)	0.4
Molybdenum (μg)	33.3
Selenium (μg)	15
Chromium (μg)	15
Vitamin A (μg)	330
Vitamin E (mg)	8.3
Vitamin C (mg)	28.3
Thiamine (mg)	0.6
Riboflavin (mg)	0.6
Pyridoxine (mg)	0.8
Niacin (mg)	4.2
Pantothenic acid (mg)	2
Inositol (mg)	9.2
Choline (mg)	91.6
Vitamin D (μg)	1.9
Vitamin B12 (μg)	1.8
Biotin (μg)	58.3
Vitamin K (μg)	25

Table 2 Modified FA profile for fish oil

Fatty acid g/100 g fat	Theoretical FA profilein % for fish oil (total 17.65 g)
C14:0	6.6
C16:0	13.67
C16:1	8.32
C18:0	2.58
C18:1	10.33
C18:2	3.44
C18:3	0.57
C20:1	1.34
C20:4	1.62
C20:5 ω-3	18
C22:5 ω-3	17.3
C22:5 ω-6	1.91
C22:6 ω-3	7.27

Cytokine assay for IL-1ra and IL-1β

After 24 h incubation, IL-1ra and IL-1β were measured in culture supernatants by ELISA using matched antibody pairs (R&D Systems, UK) as previously described[20]. Capture antibody was supplied by R&D Systems (IL-1ra MAB280, IL-1β MAB601, R&D Systems). Standard proteins for IL-1ra (280-RA-010) and for IL-1β (201-LB-005) were also supplied by R&D Systems. Biotinylated detection antibodies, IL-1ra (BAF280) and IL-1β (BAF201), were purchased from R&D Systems. Streptavidin-horse-radish peroxidase conjugate (Zymed Laboratories, UK) and substrate TMB (R&D Systems) were used for IL-1ra and OPD substrate for IL-1β. Plates were read at 450 nm for IL-1ra, and at 490 nm for IL-1β.

Preliminary experiments showed that cytokine recoveries after incubation in defined formula diet for both IL-1ra and IL-1β were satisfactory. Formula diet spiked at low concentration (100 pg/mL) showed that more than 50% of IL-1ra cytokine was detected over the entire 24-h incubation period and that in diet spiked with IL-1ra at high concentration (1 000 pg/mL), a steady decrease of detectable cytokine was measured from 100% recovery at 0 h to 52% after 24 h.

Defined formula diet spiked with IL-1β at low concentration (10 pg/mL) showed that IL-1β was 100% detectable at all time points (0, 3, 6, and 24 h), and at a high concentration (100 pg/mL), 100% recovery at time points 0, 3, and 6 h but only 60% at 24 h.

As IL-1ra and IL-1β were continually secreted into the supernatant, the actual recovery in these experiments is likely to be higher than the recovery 24 h after spiking with cytokines. Standard curves in EF diet for IL-1ra and IL-1β showed no evidence of interference with the ELISA as compared with curves performed with medium alone, which again confirmed the reproducibility of the obtained data.

Statistical analysis

Statistics was performed using the Minitab 10 program. Mann-Whitney test and one-way analysis of variance (ANOVA) were performed to detect differences between diet incubations. Differences were considered significant at $P<0.05$. Data for IL-1ra/IL-1β ratio were compared with medium control, if not otherwise stated and presented as mean values and standard error of the mean (SEM). The numbers were too low to perform any subgroup analysis depending on the duration of disease or concurrent medications.

RESULTS

A total of 59 biopsies were included in the final analysis as follows: (1) CD medium ($n = 4$), EF diet ($n = 12$); (2) UC medium ($n = 6$), EF diet ($n = 21$); and (3) control patients' medium ($n = 4$), EF diets ($n = 12$). All the explants fulfilled the criteria of intact morphology and BrdU uptake in order to be included in this final analysis. BrdU-labeled cells occurred in vertical crypts at the base of the crypts and along the sides of the crypts and intact epithelium.

Cytokine response determined by IL-1ra/IL-1β ratio

IL-1ra/IL-1β ratio is indicative of the inflammatory status of the tissue and is independent of the tissue weight. We have reported this ratio previously in organ culture of

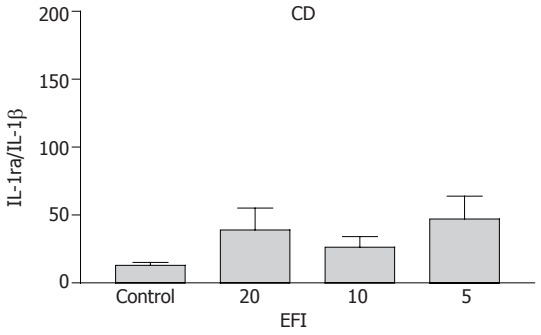

Figure 1 IL-1ra/IL-1β ratio in CD patients after incubation with elemental diet fish oil (EFI).

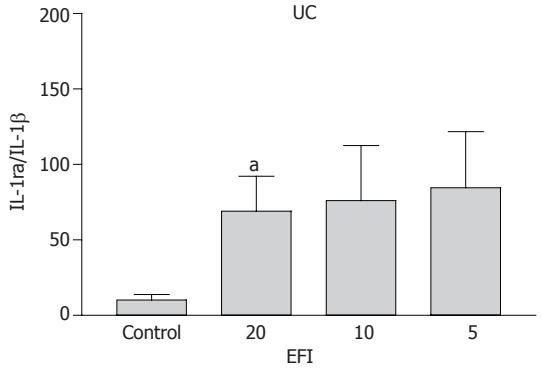

Figure 2 IL-1ra/IL-1β ratio in UC patients after incubation with elemental diet fish oil (EFI). [a]*P*<0.05 *vs* control; *P* = 0.05 (1:10 dilutions of EFI); *P*<0.02 (1:5 dilutions of EFI).

IBD-affected tissue as sensitive to changes after incubation with defined formula diets of different compositions[20]. As the tissue is inflamed, the ratio tends to decrease and vice versa.

Crohn's disease A trend towards an increase in IL-1ra/IL-1β ratio was observed for 1:20, 1:10, and 1:5 dilutions of EFI (39.1±16.1; 26.5±7.8; 47.1±16.8 *vs* medium control 13.0±2.2), respectively, but this did not reach statistical significance (Figure 1).

Ulcerative colitis A significant increase in IL-1ra/IL-1β ratio for 1:20, 1:10, and 1:5 dilutions of EFI (69.1±32.2, *P*<0.05; 76.1±36.4, *P* = 0.05; 84.5±37.3, *P*<0.02 *vs* medium control 10.2±3.7) was noted (Figure 2). The ratio was similar in CD and UC patients for medium control alone and significantly lower than non-inflamed non-IBD control patients (shown below), confirming the inflammatory status of these tissues.

Control patients No increase in the IL-1ra/IL-1β ratio was detectable for 1:20, 1:10, 1:5 dilutions of EFI (69.3±47.0; 54.1±30.6; 79.4±34.0 *vs* 76.1±37.3). This is mainly due to the fact that the ratio in the medium control was high (as expected in non-inflamed tissues) and this did not increase any further with EF incubation.

Cytokine response of IL-1β and IL-1ra as percentage of medium control

Interleukin-1β Percentage production of IL-1β in UC (as a proportion of medium control) was lower at all the three dilutions as compared with CD and this reached statistical significance for 1:20 dilution (UC 32.6±9.8% *vs* CD 62.1±19.1%; *P* = 0.02). The average production (in all three dilutions of EF) of IL-1β was significantly more suppressed in UC than that in CD (24.0±4.8% *vs* 51.8±8.1%; *P*<0.05). In UC patients, the decrease in production of IL-1β was also significant as compared with control patients at 1:20 dilution (32.6±9.8% *vs* 117.3±87.3%; *P* = 0.02). In control patients, there was a little suppression of IL-1β after incubation with EF except at the highest concentration of 1:5 (Figure 3).

Interleukin1-receptor antagonist In UC patients, secretion of IL-1ra (as percentage of medium control) tends to be higher when compared with CD patients at 1:10 and 1:5 dilutions (UC 142.3±33.2% and 130.5±50.3% *vs* CD 104.9±13.2% and 70.1±35.9%), respectively. Compared with control patient, secretion of IL-1ra was increased for 1:20, 1:10, and 1:5 dilutions of EF [UC (134.9±66.1%; 142.3±33.2%; 130.5±50.3%) *vs* control (44.1±16.2%; 29.4±13.2%; 35.9±10.1%)], respectively, and average production of IL-1ra for all dilutions was significantly increased (UC 135.9±3.4% *vs* controls 36.5±4.3%; *P*<0.0001).

In CD patients, there was an increase in IL-1ra secretion (as percentage of medium control) at all three dilutions as compared with control patients (in whom IL-1ra decreased) (CD 146.3±45.6%; 104.9±13.2%; 70.1±35.9%; control 44.1±16.2%; 29.4±13.2%; 35.9±10.1%), reaching significance at 1:10 dilution (*P* = 0.03). The average increase in IL-1ra in CD patients for all three dilutions was significant *vs* control patients (CD 107.1±22.0% *vs* 36.5±4.3%; *P* = 0.03).

In control patients, IL-1ra production tends to decrease after incubation with EF as a proportion of medium control, unlike CD and UC (Figure 4).

DISCUSSION

Fish oil preparations in the form of gelatin-coated fish oil capsules have been used to treat UC in several studies. Hawthorne *et al*[16,19]. Stenson *et al*[15]. and Loeschke *et al*[22]. investigated (in placebo-controlled trials) the influence of ω-3 FA, EPA and DHA derived from fish oil on prostaglandin and leukotriene synthesis in patients with UC. These studies illustrated that treatment with fish oil led to a corticosteroid sparing effect and a reduction in LTB_4 measured in colonic mucosa, rectal dialysate and suppression in synthesis of LTB_4 in peripheral blood neutrophils[15,16,19]. Contrary to these studies, we investigated, in the *in vitro* organ culture model, the direct influence of fish oil containing enteral diet (EFI) on pro- and anti-inflammatory cytokine production assayed in the culture supernatant. We found a significant increase in IL-1ra/IL-1β ratio in UC patients as compared with medium control as a result of enteral diet-fish oil incubation. This increase was not found in non-inflamed non-IBD control patients and was less marked in CD patients. This might be as a result of an increased production of IL-1ra and decreased pro-

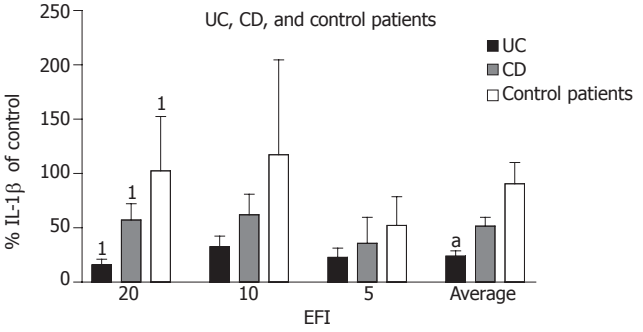

Figure 3 Percentage production of IL-1β of medium control in UC, CD, and non-inflamed non-IBD patients after incubation with EFI. [1]*P* = 0.02, UC *vs* CD and UC *vs* control patients (1:20 dilution of EFI); [a]*P*<0.05, UC *vs* CD (average of all dilutions).

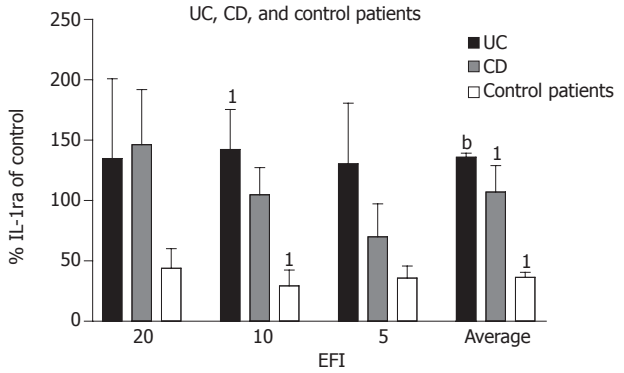

Figure 4 Percentage production IL-1ra of medium control in UC, CD, and controls (non-inflamed non-IBD patients) after incubation with EFI. [1]*P* = 0.03, CD *vs* control patients (1:10) and CD *vs* control patients (average of three dilutions); [b]*P*<0.0001, UC *vs* control patients (average of all dilutions).

duction of IL-1β. Average percentage of IL-1ra release in UC patients was higher than in CD and significantly higher compared with control patients after the incubation with EF. The percentage of IL-1β production of medium control showed, in all three dilutions of EF, a more marked decrease in UC compared with CD and control patients. In this model of intestinal tissue incubation for 24 h period, it would appear that enteral diets containing ω-3 FA have a direct *in vivo* anti-inflammatory and immunomodulatory impact, especially in UC. It seems that fish oil not only increases IL-1ra production, but also inhibits the production of IL-1β. This modulation of cytokine response by fish oil containing defined formula diet EF in UC patients is possibly due to the modified fatty acid profile with increased ω-3 FA. This preferentially favors the production of prostaglandins and thromboxanes of series 3 and leukotrienes of series 5, with decreased pro-inflammatory properties.

Mahida *et al*[23]. also used a similar organ culture model similar to that used by us in their study. Colonic biopsies of patients with UC were incubated with and without 5-aminosalicylic acid (5-ASA). Significantly higher IL-1β was detected in inflamed colonic biopsies compared to normal controls. After the incubation with 5-ASA, there was a significant dose-dependent decrease of IL-1β production as a percentage of controls. It also showed a significant correlation of IL-1β and TXB_2 synthesis in culture medium of inflamed tissue as compared with controls. A significant decrease in LTB_4 was found in inflamed tissue treated with 5-ASA. It is known that 5-ASA can inhibit the synthesis of PGE_2, LTB_4 and their products of the 5-lipoxygenase pathway. It is likely that these ω-3 FA affect the IL-1β synthesis either by altering the eicosanoid synthesis or by having a direct influence of FA on gene expression. The two major polyunsaturated fatty acids (PUFAs) in fish oil are EPA and DHA, which are also major PUFAs incorporated into the cell membrane. EPA is a substrate for eicosanoid production via cyclooxygenase pathway for PG_3 and lipoxygenase pathway for TX_3, both known as having less inflammatory properties. Watanabe *et al*[24]. showed that in LPS stimulated mice lymphocytes, where mice had been fed with beef tallow, the two fish oil FA, DHA and EPA, produced different IL-1β mRNA expression. Decreased production of IL-1β mRNA after EPA and DHA was significant in DHA *vs* tallow and slightly lower in EPA as compared with DHA. Production of PGE_2 was significantly decreased in EPA and DHA, though DHA is not a precursor for eicosanoids[25]. As IL-1β mRNA response differed between EPA and DHA, though the PGE_2 production was similar, it seems that the balance of EPA/DHA in cellular lipids might be important in affecting intracellular signaling through modifications of specific gene transcription[24]. FA in the cell are bound on fatty acid binding proteins (FABP), which exist in the cytosol and nucleus, in the form of fatty acid acyl-CoA (FA-CoA). The nuclear receptors peroxisome proliferator-activated receptors (PPARs) occur in three identified subtypes of α, β, and γ, which are regulated by FA. It is likely that some FA or their metabolites may act as hormones to control specific transcription factors. For example, PPARα is required for fish oil-mediated induction of $mRNA_{AOX}$ (mRNA - acyl-CoA oxidase). Nuclear transcription factor, NFκB, is required in genes, which are involved in pro-inflammatory responses, such as cyclooxygenase 2 and cytokines IL-1β and TNF-α. The effect of ω-3 FA might be attributed to the PPARα activation and the regulation of NFκB-mediated transcription[26]. As incubation with fish oil resulted in marked and divergent anti- and pro-inflammatory cytokine response, it is possible that ω-3 PUFA result in different cytokine production in various cell types[24]. It may also reflect a different response in IBD subtypes, as IL-1ra/IL-1β was not significantly increased in CD after incubation with EF. Furthermore, as EPA and DHA act differently in eicosanoid and IL-1β production, both of these ω-3 FA in fish oil may contribute to the anti-inflammatory effect of fish oil.

Biopsies incubated with EF, as a major source of ω-3 FA in the present study, have shown a significant positive response towards an anti-inflammatory effect only in UC. In the current literature, the immunomodulatory properties of fish oil manifests as a decrease of LTB_4 or increased synthesis of LTB_5[16,27]; however, a change in IL-1β mRNA expression after LPS stimulation in mouse spleen lymphocytes has also been reported[24]. The actual increase

in IL-1ra/IL-1β ratio could be interpreted as a reaction of eicosanoid-modulated cytokine production through G proteins and/or FA-modulated gene transcription via transcription factor. Which of these factors may have the predominant impact on immunomodulatory properties of fish oil is not defined as yet. Several studies have demonstrated that DHA might be superior as compared with EPA in immunomodulatory activity[24,28]. This suggests that the effects of fish oil might be a response of FA-induced gene transcription, as eicosanoids are derivatives of dihomo-γ-linolenic acid (DLGA, 20:3 ω-6), arachidonic acid (AA C20:4 ω-6) and eicosapentaenoic acid (EPA C20:5 ω-3)[25] and not of docosahexaenoic acid (DHA C22:6 ω-3).

In this study, the results of the supernatant cytokine concentration were presented predominantly as a ratio of anti-inflammatory to pro-inflammatory cytokine (IL-1ra:IL-1β) as this was independent of the weights of the biopsies. The cytokine concentrations were not indexed against the protein or DNA content of the biopsies as the biopsies were processed for the uptake of BrdU and determination of tissue viability after 24 h incubation. The ratio of cytokines, which is independent of the explant weights, has been used in our previous publication on the effect of elemental diet alone[20]. Each individual set of biopsies from one patient was simultaneously put in organ culture at the different dilutions of EI as well as a medium control, within 10 min of collection of the biopsies. All biopsies in this study were taken with identical biopsy forceps by the same surgeon, and therefore were uniform in size. This enabled representation of the results of EF incubation as a proportion of the cytokine concentration produced by incubation in medium control alone without any added defined formula diet. The results of the changes in cytokine ratios were consistent with the changes in individual cytokines indexed as a proportion of the medium control incubation. All explants included in the analysis were considered viable by morphology and BrdU uptake.

We have previously reported on the results of incubation of IBD (CD and UC) affected explants with elemental diet (EO-28) as well as modified elemental diet with altered nitrogen source (casein and whey). These experiments were identical in design to the present study and showed direct anti-inflammatory effect of elemental diet on CD but not UC-affected tissues. This anti-inflammatory effect was manifested by a rise in IL-1ra/IL-1β ratio, and persisted when elemental diet was modified with casein and whey. In this study, we have showed that when elemental diet was modified by fish oil, but the rest of its composition including amino acids were kept unaltered, the anti-inflammatory effect could be observed on UC-affected tissues. It is striking that by modifying the composition of elemental diet, the anti-inflammatory effect could be made to be more pronounced in CD (conventional EO-28) or in UC patients (fish oil modified EO-28). This raises the possibility that such modifications could provide the option of nutritional therapy for UC patients, and again illustrates the difference between CD and UC patients in nutritional modulation and immunology.

The *in vitro* model is reductionist and local delivery of fish oil could be a problem by the oral delivery of fish oil modified enteral diet. Rectal delivery or enteric coated preparations would be necessary. Systemic effects of oral delivery are also possible and almost certainly mediate part of the beneficial effects of elemental diet especially on terminal ileum and colon. Nevertheless, these experiments suggest that enteral defined formula diet may have direct anti-inflammatory effects, and the composition may determine whether it is effective in CD or UC patients. Absorption after oral administration will alter the nutrient milieu of cells and possibly their inflammatory response.

In conclusion, we have shown a positive anti-inflammatory effect on tissues incubated with enteral diets modified with fish oil, which is significant only in UC, but much more modest in CD. This study provides a rationale for exploring dietary therapies for UC patients.

ACKNOWLEDGMENTS

We thank SHS, Liverpool UK for supplying us with the specially prepared enteral diet modification and MC Aldhous for technical assistance.

REFERENCES

1 **Rigaud D,** Cosnes J, Le Quintrec Y, René E, Gendre JP, Mignon M. Controlled trial comparing two types of enteral nutrition in treatment of active Crohn's disease: elemental versus polymeric diet. *Gut* 1991; **32:** 1492-1497
2 **Fell JM,** Paintin M, Arnaud-Battandier F, Beattie RM, Hollis A, Kitching P, Donnet-Hughes A, MacDonald TT, Walker-Smith JA. Mucosal healing and a fall in mucosal pro-inflammatory cytokine mRNA induced by a specific oral polymeric diet in paediatric Crohn's disease. *Aliment Pharmacol Ther* 2000; **14:** 281-289
3 **Teahon K,** Pearson M, Smith T, Bjarnason I. Alterations in nutritional status and disease activity during treatment of Crohn' s disease with elemental diet. *Scand J Gastroenterol* 1995; **30:** 54-60
4 **Ligumsky M,** Simon PL, Karmeli F, Rachmilewitz D. Role of interleukin 1 in inflammatory bowel disease-enhanced production during active disease. *Gut* 1990; **31:** 686-689
5 **Dionne S,** D'Agata ID, Hiscott J, Vanounou T, Seidman EG. Colonic explant production of IL-1and its receptor antagonist is imbalanced in inflammatory bowel disease (IBD). *Clin Exp Immunol* 1998; **112:** 435-442
6 **Andus T,** Daig R, Vogl D, Aschenbrenner E, Lock G, Hollerbach S, Köllinger M, Schölmerich J, Gross V. Imbalance of the interleukin 1 system in colonic mucosa-association with intestinal inflammation and interleukin 1 receptor antagonist [corrected] genotype 2. *Gut* 1997; **41:** 651-657
7 **Casini-Raggi V,** Kam L, Chong YJ, Fiocchi C, Pizarro TT, Cominelli F. Mucosal imbalance of IL-1 and IL-1 receptor antagonist in inflammatory bowel disease. A novel mechanism of chronic intestinal inflammation. *J Immunol* 1995; **154:** 2434-2440
8 **Grimble RF,** Tappia PS. Modulation of pro-inflammatory cytokine biology by unsaturated fatty acids. *Zeitschrift fur Ernaehrungswissenschaft* 1998; **37:** 57-65
9 **Meydani SN,** Dinarello CA. Influence of dietary fatty acids on cytokine production and its clinical implications. *Nutr Clin Pract* 1993; **8:** 65-72
10 **Kremer JM**. n-3 fatty acid supplements in rheumatoid arthritis. *Am J Clin Nutr* 2000; **71:** 349S-351S
11 **Belch JJ,** Hill A. Evening primrose oil and borage oil in rheumatologic conditions. *Am J Clin Nutr* 2000; **71:** 352S-356S

12 **Ziboh VA,** Miller CC, Cho Y. Metabolism of polyunsaturated fatty acids by skin epidermal enzymes: generation of antiinflammatory and antiproliferative metabolites. *Am J Clin Nutr* 2000; **71:** 361S-366S
13 **Burton JL.** Dietary fatty acids and inflammatory skin disease. *Lancet* 1989; **1:** 27-31
14 **Lorenz R,** Weber PC, Szimnau P, Heldwein W, Strasser T, Loeschke K. Supplementation with n-3 fatty acids from fish oil in chronic inflammatory bowel disease-a randomized, placebo-controlled, double-blind cross-over trial. *J Intern Med Suppl* 1989; **731:** 225-232
15 **Stenson WF,** Cort D, Rodgers J, Burakoff R, DeSchryver-Kecskemeti K, Gramlich TL, **Beeken W. Dietary supplementa**tion with fish oil in ulcerative colitis. *Ann Intern Med* 1992; **116:** 609-614
16 **Aslan A,** Triadafilopoulos G. Fish oil fatty acid supplementation in active ulcerative colitis: a double-blind, placebo-controlled, crossover study. *Am J Gastroenterol* 1992; **87:** 432-437
17 **Almallah YZ,** Richardson S, O'Hanrahan T, Mowat NA, Brunt PW, Sinclair TS, Ewen S, Heys SD, Eremin O. Distal proctocolitis, natural cytotoxicity, and essential fatty acids. *Am J Gastroenterol* 1998; **93:** 804-809
18 **Almallah YZ,** El-Tahir A, Heys SD, Richardson S, Eremin O. Distal procto-colitis and n-3 polyunsaturated fatty acids: the mechanism(s) of natural cytotoxicity inhibition. *Eur J Clin Invest* 2000; **30:** 58-65
19 **Hawthorne AB,** Daneshmend TK, Hawkey CJ, Belluzzi A, Everitt SJ, Holmes GK, Malkinson C, Shaheen MZ, Willars JE. Treatment of ulcerative colitis with fish oil supplementation: a prospective 12 month randomised controlled trial. *Gut* 1992; **33:** 922-928
20 **Meister D,** Bode J, Shand A, Ghosh S. Anti-inflammatory effects of enteral diet components on Crohn's disease-affected tissues in-vitro. *Dig Liver Dis* 2002; **34:** 430-438
21 **Wilson RG,** Smith AN, Bird CC. Immunohistochemical detection of abnormal cell proliferation in colonic mucosa of subjects with polyps. *J Clin Pathol* 1990; **43:** 744-747
22 **Loeschke K,** Ueberschaer B, Pietsch A, Gruber E, Ewe K, Wiebecke B, Heldwein W, Lorenz R. n-3 fatty acids only delay early relapse of ulcerative colitis in remission. *Dig Dis Sci* 1996; **41:** 2087-2094
23 **Mahida YR,** Lamming CE, Gallagher A, Hawthorne AB, Hawkey CJ. 5-Aminosalicylic acid is a potent inhibitor of interleukin 1 beta production in organ culture of colonic biopsy specimens from patients with inflammatory bowel disease. *Gut* 1991; **32:** 50-54
24 **Watanabe S,** Katagiri K, Onozaki K, Hata N, Misawa Y, Hamazaki T, Okuyama H. Dietary docosahexaenoic acid but not eicosapentaenoic acid suppresses lipopolysaccharide-induced interleukin-1 beta mRNA induction in mouse spleen leukocytes. *Prostaglandins, Leukot Essent Fatty Acids* 2000; **62:** 147-152
25 **Calder PC.** Dietary fatty acids and the immune system. *Nutr Rev* 1998; **56:** S70-S83
26 **Jump DB,** Clarke SD. Regulation of gene expression by dietary fat. *Annu Rev Nutr* 1999; **19:** 63-90
27 **Hillier K,** Jewell R, Dorrell L, Smith CL. Incorporation of fatty acids from fish oil and olive oil into colonic mucosal lipids and effects upon eicosanoid synthesis in inflammatory bowel disease. *Gut* 1991; **32:** 1151-1155
28 **Løchsen T,** Ormstad H, Braud H, Brodal B, Christiansen EN, Osmundsen H. Effects of fish oil and n-3 fatty acids on the regulation of delta9-fatty acid desaturase mRNA and -activity in rat liver. *Lipids* 1999; **34** Suppl: S221-S222

Science Editor Wang XL and Guo SY **Language Editor** Elsevier HK

PO Box 2345, Beijing 100023, China
www.wjgnet.com
wjg@wjgnet.com

ELSEVIER

World J Gastroenterol 2005;11(47):7473-7479
World Journal of Gastroenterology ISSN 1007-9327

• *CLINICAL RESEARCH* •

Expression of triggering receptor on myeloid cell 1 and histocompatibility complex molecules in sepsis and major abdominal surgery

Nestor González-Roldán, Eduardo Ferat-Osorio, Rosalía Aduna-Vicente, Isabel Wong-Baeza, Noemí Esquivel-Callejas, Horacio Astudillo-de la Vega, Patricio Sánchez-Fernández, Lourdes Arriaga-Pizano, Miguel Angel Villasís-Keever, Constantino López-Macías, Armando Isibasi

Nestor González-Roldán, Eduardo Ferat-Osorio, Rosalía Aduna-Vicente, Isabel Wong-Baeza, Noemí Esquivel-Callejas, Lourdes Arriaga-Pizano, Constantino López-Macías, Armando Isibasi, Unidad de Investigación Médica en Inmunoquímica, Hospital de Especialidades, Centro Médico Nacional Siglo XXI, Instituto Mexicano del Seguro Social (IMSS), México

Horacio Astudillo-de la Vega, Laboratorio de Oncología Molecular, Unidad de Investigación Médica en Enfermedades Oncológicas, Hospital de Oncología, Centro Médico Nacional Siglo XXI, IMSS, México

Patricio Sánchez-Fernández, Servicio de Gastrocirugía, Hospital de Especialidades, Centro Médico Nacional Siglo XXI, IMSS, México

Miguel Angel Villasís Keever, Unidad de Investigación en Epidemiología Clínica, Hospital de Pediatría, Centro Médico Nacional Siglo XXI, IMSS, México

Supported by Fondo para el Fomento de la Investigación Médica (FOFOI), Instituto Mexicano del Seguro Social No. IMSS-2004/045

Correspondence to: Dr Armando Isibasi, Coordinación de Investigación en Salud, Unidad de Investigación Médica en Inmunoquímica, Hospital de Especialidades, Centro Médico Nacional Siglo XXI, IMSS, P.O. Box A047, 06703, México. isibasi@prodigy.net.mx
Telephone: +52-55-56-27-69-15 Fax: +52-55-57-61-09-52
Received: 2005-04-30 Accepted: 2005-07-08

Abstract

AIM: To evaluate the surface expression of triggering receptor on myeloid cell 1 (TREM-1), class II major histocompatibility complex molecules (HLA-DR), and the expression of the splicing variant (svTREM-1) of TREM-1 in septic patients and those subjected to major abdominal surgery.

METHODS: Using flow cytometry, we examined the surface expression of TREM-1 and HLA-DR in peripheral blood monocytes from 11 septic patients, 7 elective gastrointestinal surgical patients, and 10 healthy volunteers. svTREM-1 levels were analyzed by RT-PCR.

RESULTS: Basal expression of TREM-1 and HLA-DR in healthy volunteers was 35.91±14.75 MFI and 75.8±18.3%, respectively. In septic patients, TREM-1 expression was 59.9±23.9 MFI and HLA-DR expression was 44.39±20.25%, with a significant difference between healthy and septic groups (P<0.05) for both molecules. In the surgical patients, TREM-1 and HLA-DR expressions were 56.8±20.85 MFI and 71±13.8% before surgery and 72.65±29.92 MFI and 72.82±22.55% after surgery. TREM-1 expression was significantly different (P = 0.0087) between the samples before and after surgery and svTREM-1 expression was 0.8590± 0.1451 MF1, 0.8820±0.1460 MF1, and 2.210±0.7873 MF1 in the healthy, surgical (after surgery) and septic groups, respectively. There was a significant difference (P = 0.048) in svTREM-1 expression between the healthy and surgical groups and the septic group.

CONCLUSION: TREM-1 expression is increased during systemic inflammatory conditions such as sepsis and the postoperative phase. Simultaneous low expression of HLA-DR molecules correlates with the severity of illness and increases susceptibility to infection. Additionally, TREM-1 expression is distinctly different in surgical patients at different stages of the inflammatory response before and after surgery. Thus, surface TREM-1 appears to be an endogenous signal during the course of the inflammatory response. svTREM-1 expression is significantly increased during sepsis, appearing to be an indicator of severity of illness. Together, these data indicate that TREM-1 may play an important role in establishing and amplifying the systemic inflammatory response. TREM-1, HLA-DR, and svTREM-1 expression analysis can provide useful diagnostic and prognostic indicators during SIRS, CARS, and sepsis.

Key words: TREM-1; HLA-DR; SIRS; CARS; Sepsis

González-Roldán N, Ferat-Osorio E, Aduna-Vicente R, Wong-Baeza I, Esquivel-Callejas N, Astudillo-de la Vega H, Sánchez-Fernández P, Arriaga-Pizano L, Villasís-Keever MA, López-Macías C, Isibasi A. Expression of triggering receptor on myeloid cell 1 and histocompatibility complex molecules in sepsis and major abdominal surgery. *World J Gastroenterol* 2005; 11(47): 7473-7479
http://www.wjgnet.com/1007-9327/11/7473.asp

INTRODUCTION

Inflammation constitutes the initial and essential response of the host against infection and injury. In the presence of infection, inflammation is triggered through the recognition of microorganism-associated molecular structures by Toll-like receptors (TLRs)[1,2], which are expressed in a nonclonal manner on the surface of innate immune cells such as monocytes, macrophages, and dendritic cells[3,4]. This interaction leads to the activation of nuclear factor κB (NF-κB) and to the release of pro-inflammatory (tumor necrosis factor α (TNF-α), interleukin (IL-12, IL-1, IL-6, IL-8, *etc.*) and anti-inflammatory (IL-10 and TGF-β) cytokines[3,5-7]. In the absence of infection, injuries such as trauma, burns, pancreatitis, and major surgery also induce an inflammatory response. In most cases, inflammation is a local response, but in some situations, it becomes a systemic phenomenon and leads to the development of systemic inflammatory response syndrome (SIRS), characterized by the massive release of pro-inflammatory mediators in the absence of infection[8-10]. On the other hand, the excessive release of anti-inflammatory mediators leads to the development of compensatory anti-inflammatory response syndrome (CARS)[8,11]. During this phase, patients frequently suffer from temporary impairment of immunological functions, which in its most severe form is referred to as immunoparalysis[8-10]. This diminished the ability to respond to stimuli is paralleled by a strong downregulation of MHC class II (mainly HLA-DR, invariant chain) expression on the surface of monocytes. Such monocytes produce only minor amounts of pro-inflammatory cytokines, as well as NO[12,13]. Very similar alterations of monocyte function exist with experimental endotoxin tolerance and in patients after trauma, burns, pancreatitis, and major surgery[10,14-17]. These alterations often predispose patients to life-threatening infections and to the development of sepsis. Furthermore, it has been reported that immunoparalysis correlates with the severity of sepsis and injury as well as the postoperative course[15,17-19].

However, progress has been made in sepsis research improving the knowledge of the basic pathophysiological processes of sepsis, in daily intensive care unit (ICU) practice, it remains difficult to adequately identify and treat sepsis and its related conditions[20]. In some cases, measurement of serum proteins such as interleukin 6 (IL-6) has been demonstrated to be useful in evaluating the severity and in predicting the outcome for patients with SIRS/sepsis, but not in CARS and susceptibility to infection[21,22]. Therefore, it is essential to search for and identify endogenous mediators of inflammatory response suitable for use as early indicators of infection in cases of sepsis and as prognostic indicators during SIRS and CARS[20,23-27].

TREM-1 is an activating receptor of the Ig superfamily exclusively expressed on blood neutrophils and monocytes[28]. Expression of TREM-1 on these cells is induced by TLR ligands such as lipopolysaccharide and lipoteichoic acid[29]. Though its natural ligand has not been identified, engagement of TREM-1 on monocytes with agonist monoclonal antibodies results in the production of pro-inflammatory cytokines (TNF-α and IL-1β) as well as chemokines such as IL-8 and monocyte chemoattractant protein-1. When monocytes are stimulated with lipopolysaccharide, leading to a pro-inflammatory response, engagement of TREM-1 dramatically enhances this effect when used as a costimulus, showing that TREM-1 can amplify inflammatory responses initiated by TLRs[28-30].

TREM-1 surface expression is greatly increased on infiltrating neutrophils isolated from the peritoneal cavity of patients with septic shock due to bacterial peritonitis. In contrast, peritoneal lavage cells of patients with SIRS caused by nonmicrobial peritoneal inflammation show normal levels of TREM-1, and it has been proposed that TREM-1 is upregulated in the presence of infection[30]. At the mRNA level, an alternative splicing variant of TREM-1 (svTREM-1) has been described, which might encode a soluble form[31], as it has been detected in patients receiving mechanical ventilation. Rapid detection of soluble TREM-1 in bronchoalveolar lavage fluid has been proposed for establishing or excluding a diagnosis of bacterial or fungal pneumonia[32,33], and TREM-1 mRNA upregulation correlates with the severity of acute pancreatitis[34].

In this study, we aimed to explore the expression of TREM-1, svTREM-1, and HLA-DR as early indicators of infection or as prognostic indicators during systemic inflammation, using surgical and septic patients as models of the inflammatory response.

MATERIALS AND METHODS

Patients

Samples were obtained from 11 septic patients, 7 elective gastrointestinal surgical patients (pre- and post-surgery) and 10 healthy volunteers who gave their informed consent, according to the protocol approved by the Institute Ethics Committee (reference number 034/2004, IMSS 2004-3601-0064). Sepsis diagnosis was determined by the presence of at least two of the following signs: hypothermia or hyperthermia, tachycardia, tachypnea or hyperventilation as defined by $PaCO_2$ of 4.256 Kpa and leukocytosis, bandemia or leukopenia.

Blood samples

Blood (15 mL) was collected from healthy volunteers, septic patients (at their admission to gastro surgery service with sepsis diagnosis) and surgical patients (first sample 30 min before surgery and second sample 12-24 h after surgical procedure ended) and heparinized (10 U/mL).

Flow cytometry

Peripheral blood mononuclear cells were obtained from the heparinized samples by centrifuging at 800 r/min for 30 min over a Ficoll-Hypaque gradient. Cells were washed thrice with isotonic solution at 150 r/min for 10 min, the

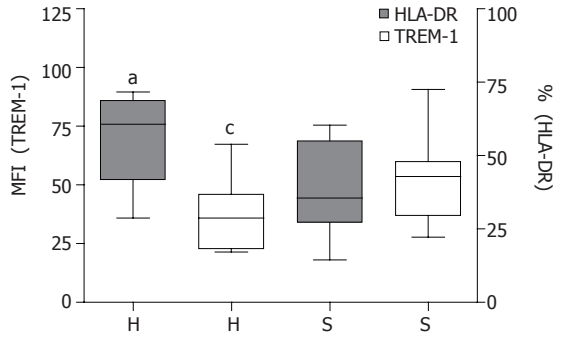

Figure 1 TREM-1 and HLA-DR expression in healthy volunteers and septic patients. Comparison of expression levels of TREM-1 (mean of fluorescence intensity) and HLA-DR (percentage of CD14+HLA-DR+cells) between healthy volunteers (H) and septic patients (S). [a]*P*<0.05 healthy *vs* septic for HLA-DR expression, [c]*P*<0.05 healthy *vs* septic for TREM-1 expression.

supernatant was discarded, and the pellet was resuspended in an isotonic solution. Trypan blue staining was done on an aliquot of the cell suspension to determine cell numbers and to assess their viability. Cells were transferred to a 96-well conical well plate (1×10^6 cells/well). Cells were blocked with a 20 g/L human gamma globulin solution (Beriglobina®, Aventis) for 1 h at 4 °C and washed by centrifuging at 800 r/min for 3 min at 4 °C. The supernatant was discarded and the pellet was resuspended. Cell staining for flow cytometry was done by adding anti-CD14/FITC, anti-HLA-DR/PE (BD Biosciences), anti-TREM-1/PE (R&D Systems) and an isotype control. The contents in each well were transferred to flow cytometry tubes in 400 μL of sheath fluid. Finally, samples were analyzed in a BD FACScalibur flow cytometer.

Total RNA extraction, RT-PCR and semiquantitative analysis

Total RNA was extracted from peripheral blood mononuclear cells using TRIzol reagent (Invitrogen). The concentrations and purity of the extracted RNA were determined spectrophotometrically at 260 and 280 nm (Beckman DU640, USA). Single-stranded cDNA was synthesized by mixing 1 μg RNA with 1 μL oligo-dT (0.5 g/L, Promega), 1 μL dNTP mix (10 mmol/L, Promega), 4 μL reaction buffer (Promega), 2 μL DTT (0.1 mol/L, Promega), 1 μL SuperScript II RNase H reverse transcriptase (200 U/μL, Promega) and DEPC-treated water to 20 μL. The reaction mixture was incubated at 42 °C for 50 min, followed by 70 °C for 15 min to inactivate the reverse transcriptase. cDNA (1 μg) was used as the template for PCR amplification of TREM-1. The mixture consisted of 0.5 μL dNTP mix (10 mmol/L, Promega), 1.5 μL $MgCl_2$ (25 mmol/L, Promega), 5 μL primers (5'-GGACGGAGAGATGCCCAAGACC-3' and 5'-ACCAGCCAGGAGAATGACAATG-3' for TREM-1 or 5'-GTGGGGCGCCCCAGGCACCA-3' and 5'-CTCCTTAATGTCACGCACGATTTC-3' for β-actin)[31], 0.25 μL DMSO, 0.25 μL Taq DNA polymerase (5 U/μL, Promega), 2.5 μL PCR buffer (Promega) and DEPC-treated water to 25 μL. The reaction was performed using a programmable thermocycler (Techne, Progene). The DNA was predenatured at 94 °C for 15 s, followed by 32 cycles of denaturation (94 °C for 15 s), annealing (60 °C for 15 s), and extension (72 °C for 20 s). The mixture was finally extended for 5 min at 72 °C. β-Actin served as an internal control in each experiment. PCR products (10 μL) were electrophoresed using 20 g/L agarose gels in TAE at 70 V for 60 min. The samples were stained with ethidium bromide (0.1 mg/L) and observed by ultraviolet illumination. The images were photographed and analyzed with an IS-1000 digital imaging system (Alpha Innotech Corporation). The pixel densities of TREM-1 and β-actin bands were determined and the ratios of TREM-1/β-actin were calculated. These ratios were represented as the relative expression levels (expression index) of TREM-1 mRNA and were used for semiquantitative analysis.

ELISA

Sera levels of IL-6 were measured using a commercial kit (BD-Pharmingen) according to the manufacturer's instructions.

Statistical analysis

Due to the sample size, we performed qualitative analysis with the data expressed as medians and quartiles. For comparison between each group, the nonparametric Mann-Whitney *U*-test was used. $P\leqslant0.05$ was considered statistically significant.

RESULTS

Twenty-eight subjects were included: 11 septic patients, 7 elective gastrointestinal surgical patients (pre- and post-surgery) and 10 healthy volunteers. The age range was 20-83 years and the average age over each group was 52.7, 52.25, and 35.4 years for the surgical, septic and healthy groups, respectively. Demographic data for all the subjects included in this study, as well as diagnostic and disease evolution data, are shown in Table 1.

Expression levels of TREM-1 and HLA-DR

Surface expression levels of TREM-1 and HLA-DR were measured by flow cytometry. Results were expressed as mean fluorescence intensity (MFI) related to the entire monocyte population for TREM-1 and as the percentage of HLA-DR-positive monocytes in the total monocyte population[35].

The expression of TREM-1 and HLA-DR in healthy volunteers was 35.91±14.75 MFI and 75.8±18.3%, respectively. We considered this group as showing the basal level of expression of both molecules. In septic patients, the TREM-1 expression level was 59.9±23.9 MFI and HLA-DR expression was 44.39±20.25%. There was a significant difference between healthy and septic groups ($P<0.05$) for both molecules (Figure 1).

In the surgical patients, TREM-1 and HLA-DR expressions were 56.8±20.85 MFI and 71±13.8% before

Table 1 Patients' data

Group	Sex	Age	Diagnosis	Procedure	Survival	HLA-DR (%)		TREM-1 (MFI)	
						pre-s	post-s	pre-s	post-s
Surgery	M	52	Diverticulitis	Hemicolectomy	L	N	82	56.8	46.5
Surgery	F	43	Portal hypertension	Gastro-gastro[2]	L	64.18	87.56	50.8	82.9
Surgery	F	76	GRD	ARS[4]	D	49.8	82.19	73.4	102.6
Surgery	F	50	GRD	Nissen funduplication	L	77.9	63.45	39.1	44.1
Surgery	M	52	GRD	Nissen funduplication	L	83.82		94	
Surgery	F	39	Choledocal cyst	H-J[3]	L	59.8	53.07	32.8	62.4
Surgery	M	62	Cholangiocarcinoma	H-J	L	82.38		63.7	
Septic	M	48	AP	NA	D	52.88		36.9	
Septic	M	53	Acute abdominal pain	Splenectomy	D	22		59.9	
Septic	M	73	Gastric cancer	Total Gastrectomy	D	44.3		48.3	
Septic	M	58	AP	Laparotomy	L	33.98		29.1	
Septic	F	33	Pancreatic neoplasm[1]	Laparotomy	L	67.28		50.06	
Septic	F	83	Obstructive jaundice	Cholecystectomy	D	70.97		54.7	
Septic	M	50	AP	Pseudocyst drainage	D	68.82		90.7	
Septic	F	58	Bile duct injury	H-J[3]	L	37.63		27.8	
Septic	M	24	Pancreatic fistulae	NA	L	75.4		54.8	
Septic	M	50	EC[5]	NA	D	18.6		53.6	
Septic	M	46	AP	Laparotomy	D	38.12		63.1	
Healthy	M	67	NA	None	L	81.37		47.6	
Healthy	M	42	NA	None	L	53.37		35.2	
Healthy	M	55	NA	None	L	87.5		83	
Healthy	M	24	NA	None	L	82.4		37.8	
Healthy	M	50	NA	None	L	70.31		44.3	
Healthy	M	29	NA	None	L	89.66		67.3	
Healthy	F	24	NA	None	L	50.92		21.4	
Healthy	M	20	NA	None	L	84.43		35.9	
Healthy	F	23	NA	None	L	35.87		24.1	
Healthy	M	20	NA	None	L	63.16		21.4	

A = years; M = masculine; F = feminine; AP = acute pancreatitis; GRD = gastroesophageal reflux disease; L=live; D=death; [1]mixed papillary neoplasm of the pancreas; [2]gastro-gastro-anastomosis; [3]H-J = hepatico-jejunostomy; [4]ARS = anti-reflux surgery; [5]EC = emphysematous cholecystitis; NA = not applicable; pre-s = pre-operative; post-s = post-operative.

surgery and 72.65±29.92 MFI and 72.82±22.55% after surgery, respectively. There was a significant difference ($P<0.05$) in TREM-1 expression between the samples before and after surgery (Figure 2).

svTREM-1 expression levels

svTREM-1 expression was 0.8590±0.1451 in the healthy group, 0.8820±0.1460 in the surgical group (after surgery; pre-surgical value was 0.377±3.7) and 2.210±0.7873 in the septic group. There was a significant difference ($P<0.05$) when svTREM-1 in both the healthy and surgical groups was compared to the septic group (Figure 3).

Serum interleukin-6 levels

Serum level of IL-6 was 0.0±28.49, 0.1320±1.547, 24.53±51.94, and 155.5±124.5 (pg/mL) in the healthy surgical (before and after surgery) and septic groups, respectively. There was a significant difference ($P<0.05$) when the serum IL-6 levels in the healthy and surgical groups were compared to the septic group. There was also a significant difference between the surgical patients before and after surgery (Figure 4).

DISCUSSION

The SIRS concept is valid to the extent that a systemic inflammatory response can be triggered by a variety of infectious and noninfectious conditions. Sepsis is a clinical syndrome defined by the presence of both infection and a systemic inflammatory response. However, these definitions are also considered nonspecific in clinical diagnosis or prognosis[9,20,36,37]. Here we have demonstrated that both low levels of HLA-DR and high levels of TREM-1 expression were related with sepsis and its resolution.

Major injuries such as extensive abdominal surgery, which involves stress and tissue necrosis, could lead to immunoparalysis as a consequence of CARS and get infected independent of their surgical and medical treatment, developing sepsis[15,38]. In addition to the massive release of pro- and anti-inflammatory mediators such as cytokines, acute phase proteins, heat shock proteins, and intracellular molecules such as HMGB1[19,24,25,39-43] there is a modification of expression of surface receptors such as TLRs, TREM-1 and HLA-DR in monocytes during the evolution of inflammatory response (SIRS, CARS, and sepsis)[15,30,35,38,44,45].

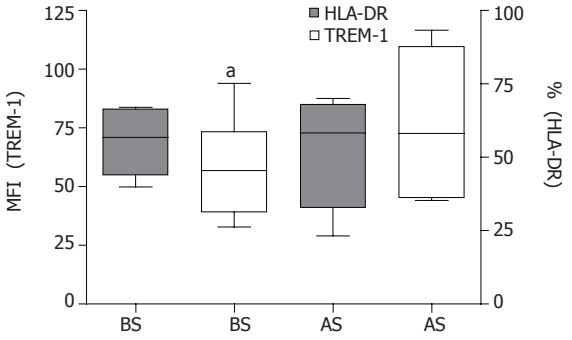

Figure 2 TREM-1 and HLA-DR expression in surgical patients. Comparison of expression levels of TREM-1 (mean of fluorescence intensity) and HLA-DR (percentage of CD14+HLA-DR+cells) in surgical patients before (BS) and after surgery (AS). [a]*P*<0.05 before surgery *vs* after surgery for TREM-1.

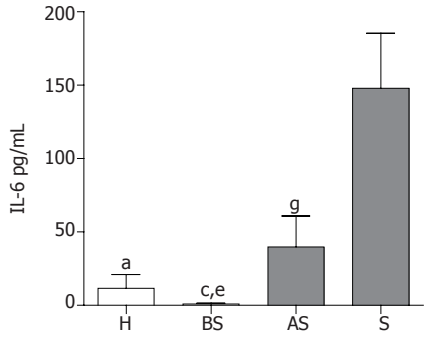

Figure 4 Serum interleukin-6 levels. Serum levels of IL-6 in healthy volunteers (H), surgical patients before surgery (BS) and after surgery (AS), and septic patients (S). [a]*P*<0.05 healthy *vs* septic groups; [c]*P*<0.05 surgical groups before *vs* after surgery; [e]*P*<0.05 before surgery *vs* septic groups; [g]*P*<0.05 after surgery *vs* septic groups.

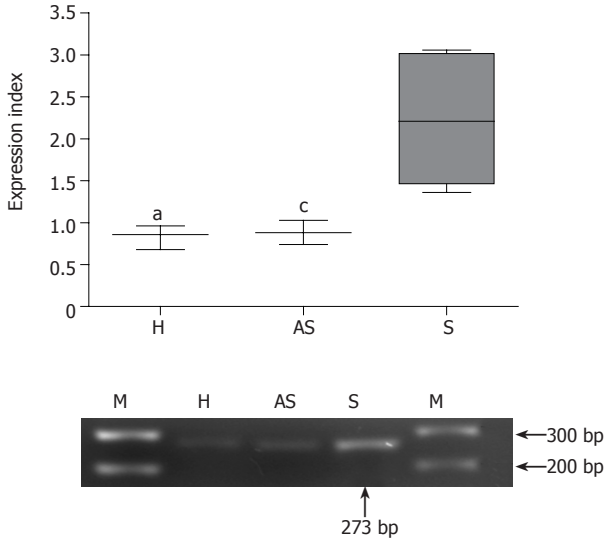

Figure 3 mRNA expression of svTREM-1. **A:** Expression index of svTREM-1/β-actin in each group. [a]*P*<0.05 healthy *vs* septic groups, [c]*P*<0.05 surgical (after surgery) *vs* septic groups; **B:** Representative svTREM-1 PCR products from healthy volunteers (H), surgical patients after surgery (AS) and septic patients (S).

HLA-DR expression level in septic patients was strongly diminished compared to pre-surgical patients and healthy volunteers. This correlates with studies in which low expression of HLA-DR is considered as a sign of immunoparalysis and is related to the presence of infection in septic patients[12,13,35]. The relationship between high levels of TREM-1 and low HLA-DR expression correlates with the severity of illness. On the other hand, healthy volunteers showed low levels of TREM-1 and high levels of HLA-DR, as the surgical patients did before and after surgery, indicating that the immunocompetence of these subjects correlates with their optimal outcome and recovery.

During the onset of an infection, monocytes and neutrophils trigger inflammation in response to the recognition of microorganism-associated molecular structure by pattern recognition receptors, which may lead to the upregulation of surface TREM-1 expression[29]. Subsequently, stimuli through TREM-1 may amplify the inflammatory response by the release of TNFα, IL-1β, and IL-8, as well as the upregulation of co-stimulatory molecules[28,30].

In our study, the TREM-1 expression level in septic patients was significantly higher than in healthy volunteers. This correlates with previous reports where TREM-1 surface expression is strongly increased in infiltrating neutrophils isolated from the peritoneal cavity of patients with septic shock due to bacterial peritonitis[30].

Among the surgical patients, TREM-1 expression before surgery increased when compared to healthy volunteers, while after surgery there was a statistically significant upregulation as compared to the pre-surgical and healthy volunteer groups. This increase without clinical signs of infection might be the result of the inflammatory status due to the disease that led to operation and/or to surgical stress, instead of other factors such as age or gender. Thus, TREM-1 appears to be an endogenous signal reflecting the course of the inflammatory response.

We also measured the svTREM-1 mRNA level in mononuclear cells of each group, since this molecule might encode soluble TREM-1, which has been proposed as a marker for establishing the diagnosis of bacterial or fungal pneumonia[33]. svTREM-1 could serve as a soluble receptor for a yet unknown ligand, and its upregulation at the transcriptional, translation and secretion level may be a negative regulation mechanism by preventing surface TREM-1 engagement and pro-inflammatory activity during severe inflammatory processes such as SIRS and sepsis. We speculate that the increased svTREM-1 expression observed in septic patients compared to both healthy and surgical groups may correlate with the presence of pathogens that activate the immune response leading to complications such as sepsis.

We measured serum IL-6 in each group as an indicator of disease severity and for prediction of patient outcomes. IL-6 increased as previously described[21,46].

We found a correlation between the upregulation of surface TREM-1 and svTREM-1 and the downregulation of surface HLA-DR in critically ill patients.

In conclusion, TREM-1 may play an important role in establishing and amplifying the systemic inflammatory response. In the future, with the support of epidemiological data, TREM-1, HLA-DR and svTREM-1

expression may be used as diagnostic and prognostic indicators to identify different phases of the inflammatory response, such as in SIRS, CARS and sepsis.

ACKNOWLEDGMENTS

Nestor González-Roldán, Eduardo Ferat-Osorio, and Isabel Wong-Baeza are recipients of a scholarship from the National Council of Science and Technology, Mexico (CONACYT).

The authors thank Dr. Martha Moreno from Escuela Nacional de Ciencias Biologicas, Instituto Politecnico Nacional for her valuable comments and assistance in the study.

REFERENCES

1 **Kaisho T,** Akira S. Pleiotropic function of Toll-like receptors. *Microbes Infect* 2004; **6:** 1388-1394
2 **Medzhitov R,** Janeway C. Innate immunity. *N Engl J Med* 2000; **343:** 338-344
3 **Janeway CA,** Medzhitov R. Innate immune recognition. *Annu Rev Immunol* 2002; **20:** 197-216
4 **Ozinsky A,** Underhill DM, Fontenot JD, Hajjar AM, Smith KD, Wilson CB, Schroeder L, Aderem A. The repertoire for pattern recognition of pathogens by the innate immune system is defined by cooperation between toll-like receptors. *Proc Natl Acad Sci USA* 2000; **97:** 13766-13771
5 **Akira S,** Hemmi H. Recognition of pathogen-associated molecular patterns by TLR family. *Immunol Lett* 2003; **85:** 85-95
6 **Donnelly RP,** Dickensheets H, Finbloom DS. The interleukin-10 signal transduction pathway and regulation of gene expression in mononuclear phagocytes. *J Interferon Cytokine Res* 1999; **19:** 563-573
7 **Kopp E,** Medzhitov R. Recognition of microbial infection by Toll-like receptors. *Curr Opin Immunol* 2003; **15:** 396-401
8 **Bone RC.** Sir Isaac Newton, sepsis, SIRS, and CARS. *Crit Care Med* 1996; **24:** 1125-1128
9 **Bone RC,** Grodzin CJ, Balk RA. Sepsis: a new hypothesis for pathogenesis of the disease process. *Chest* 1997; **112:** 235-243
10 **Davies MG,** Hagen PO. Systemic inflammatory response syndrome. *Br J Surg* 1997; **84:** 920-935
11 **Bone RC.** The pathogenesis of sepsis. *Ann Intern Med* 1991; **115:** 457-469
12 **Wolk K,** Döcke W, von Baehr V, Volk H, Sabat R. Comparison of monocyte functions after LPS- or IL-10-induced reorientation: importance in clinical immunoparalysis. *Pathobiology* 1999; **67:** 253-256
13 **Wolk K,** Kunz S, Crompton NE, Volk HD, Sabat R. Multiple mechanisms of reduced major histocompatibility complex class II expression in endotoxin tolerance. *J Biol Chem* 2003; **278:** 18030-18036
14 **Hensler T,** Heidecke CD, Hecker H, Heeg K, Bartels H, Zantl N, Wagner H, Siewert JR, Holzmann B. Increased susceptibility to postoperative sepsis in patients with impaired monocyte IL-12 production. *J Immunol* 1998; **161:** 2655-2659
15 **Lemaire LC,** van der Poll T, van Lanschot JJ, Endert E, Buurman WA, van Deventer SJ, Gouma DJ. Minimally invasive surgery induces endotoxin-tolerance in the absence of detectable endotoxemia. *J Clin Immunol* 1998; **18:** 414-420
16 **Saluja AK**. Pathophysiology of pancreatitis. Role of cytokines and other mediators of inflammation. *Digestion* 1999; **60** Suppl 1: 27-33
17 **Karima R,** Matsumoto S, Higashi H, Matsushima K. The molecular pathogenesis of endotoxic shock and organ failure. *Mol Med Today* 1999; **5:** 123-132
18 **Lin E,** Calvano SE, Lowry SF. Inflammatory cytokines and cell response in surgery. *Surgery* 2000; **127:** 117-126
19 **McKay CJ,** Buter A. Natural history of organ failure in acute pancreatitis. *Pancreatology* 2003; **3:** 111-114
20 **Weigand MA,** Hörner C, Bardenheuer HJ, Bouchon A. The systemic inflammatory response syndrome. *Best Pract Res Clin Anaesthesiol* 2004; **18:** 455-475
21 **Harbarth S,** Holeckova K, Froidevaux C, Pittet D, Ricou B, Grau GE, Vadas L, Pugin J. Diagnostic value of procalcitonin, interleukin-6, and interleukin-8 in critically ill patients admitted with suspected sepsis. *Am J Respir Crit Care Med* 2001; **164:** 396-402
22 **Oda S,** Hirasawa H, Shiga H, Nakanishi K, Matsuda K, Nakamua M. Sequential measurement of IL-6 blood levels in patients with systemic inflammatory response syndrome (SIRS)/sepsis. *Cytokine* 2005; **29:** 169-175
23 **Ohashi K,** Burkart V, Flohé S, Kolb H. Cutting edge: heat shock protein 60 is a putative endogenous ligand of the toll-like receptor-4 complex. *J Immunol* 2000; **164:** 558-561
24 **Tsan MF,** Gao B. Endogenous ligands of Toll-like receptors. *J Leukoc Biol* 2004; **76:** 514-519
25 **Wallin RP,** Lundqvist A, Moré SH, von Bonin A, Kiessling R, Ljunggren HG. Heat-shock proteins as activators of the innate immune system. *Trends Immunol* 2002; **23:** 130-135
26 **Vabulas RM,** Ahmad-Nejad P, Ghose S, Kirschning CJ, Issels RD, Wagner H. HSP70 as endogenous stimulus of the Toll/interleukin-1 receptor signal pathway. *J Biol Chem* 2002; **277:** 15107-15112
27 **Asea A,** Rehli M, Kabingu E, Boch JA, Bare O, Auron PE, Stevenson MA, Calderwood SK. Novel signal transduction pathway utilized by extracellular HSP70: role of toll-like receptor (TLR) 2 and TLR4. *J Biol Chem* 2002; **277:** 15028-15034
28 **Bouchon A,** Dietrich J, Colonna M. Cutting edge: inflammatory responses can be triggered by TREM-1, a novel receptor expressed on neutrophils and monocytes. *J Immunol* 2000; **164:** 4991-4995
29 **Bleharski JR,** Kiessler V, Buonsanti C, Sieling PA, Stenger S, Colonna M, Modlin RL. A role for triggering receptor expressed on myeloid cells-1 in host defense during the early-induced and adaptive phases of the immune response. *J Immunol* 2003; **170:** 3812-3818
30 **Bouchon A,** Facchetti F, Weigand MA, Colonna M. TREM-1 amplifies inflammation and is a crucial mediator of septic shock. *Nature* 2001; **410:** 1103-1107
31 **Gingras MC,** Lapillonne H, Margolin JF. TREM-1, MDL-1, and DAP12 expression is associated with a mature stage of myeloid development. *Mol Immunol* 2002; **38:** 817-824
32 **Gibot S,** Kolopp-Sarda MN, Béné MC, Cravoisy A, Levy B, Faure GC, Bollaert PE. Plasma level of a triggering receptor expressed on myeloid cells-1: its diagnostic accuracy in patients with suspected sepsis. *Ann Intern Med* 2004; **141:** 9-15
33 **Gibot S,** Cravoisy A, Levy B, Bene MC, Faure G, Bollaert PE. Soluble triggering receptor expressed on myeloid cells and the diagnosis of pneumonia. *N Engl J Med* 2004; **350:** 451-458
34 **Wang DY,** Qin RY, Liu ZR, Gupta MK, Chang Q. Expression of TREM-1 mRNA in acute pancreatitis. *World J Gastroenterol* 2004; **10:** 2744-2746
35 **Monneret G,** Elmenkouri N, Bohe J, Debard AL, Gutowski MC, Bienvenu J, Lepape A. Analytical requirements for measuring monocytic human lymphocyte antigen DR by flow cytometry: application to the monitoring of patients with septic shock. *Clin Chem* 2002; **48:** 1589-1592
36 **Levy MM,** Fink MP, Marshall JC, Abraham E, Angus D, Cook D, Cohen J, Opal SM, Vincent JL, Ramsay G. 2001 SCCM/ESICM/ACCP/ATS/SIS International Sepsis Definitions Conference. *Intensive Care Med* 2003; **29:** 530-538
37 **Matot I,** Sprung CL. Definition of sepsis. *Intensive Care Med* 2001; **27** Suppl 1: S3-S9
38 **Kawasaki T,** Ogata M, Kawasaki C, Tomihisa T, Okamoto K, Shigematsu A. Surgical stress induces endotoxin hyporesponsiveness and an early decrease of monocyte

mCD14 and HLA-DR expression during surgery. *Anesth Analg* 2001; **92:** 1322-1326
39 **Pepys MB,** Hirschfield GM. C-reactive protein: a critical update. *J Clin Invest* 2003; **111:** 1805-1812
40 **Wang H,** Yang H, Tracey KJ. Extracellular role of HMGB1 in inflammation and sepsis. *J Intern Med* 2004; **255:** 320-331
41 **Dinarello CA.** Proinflammatory and anti-inflammatory cytokines as mediators in the pathogenesis of septic shock. *Chest* 1997; **112:** 321S-329S
42 **Mortensen RF,** Zhong W. Regulation of phagocytic leukocyte activities by C-reactive protein. *J Leukoc Biol* 2000; **67:** 495-500
43 **Scaffidi P,** Misteli T, Bianchi ME. Release of chromatin protein HMGB1 by necrotic cells triggers inflammation. *Nature* 2002; **418:** 191-195
44 **Fumeaux T,** Pugin J. Role of interleukin-10 in the intracellular sequestration of human leukocyte antigen-DR in monocytes during septic shock. *Am J Respir Crit Care Med* 2002; **166:** 1475-1482
45 **Ramírez Cruz NE,** Maldonado Bernal C, Cuevas Urióstegui ML, Castañoń J, López Macías C, Isibasi A. Toll-like receptors: dysregulation in vivo in patients with acute respiratory distress syndrome. *Rev Alerg Mex* 2004; **51:** 210-217
46 **Riché FC,** Cholley BP, Laisné MJ, Vicaut E, Panis YH, Lajeunie EJ, Boudiaf M, Valleur PD. Inflammatory cytokines, C reactive protein, and procalcitonin as early predictors of necrosis infection in acute necrotizing pancreatitis. *Surgery* 2003; **133:** 257-262

Science Editor Wang XL and Guo SY **Language Editor** Elsevier HK

PO Box 2345, Beijing 100023, China
www.wjgnet.com
wjg@wjgnet.com

ELSEVIER

World J Gastroenterol 2005;11(47):7480-7485
World Journal of Gastroenterology ISSN 1007-9327

• *CLINICAL RESEARCH* •

Steatosis recovery after treatment with a balanced sunflower or olive oil-based diet: Involvement of perisinusoidal stellate cells

Raquel Hernández, Esther Martínez-Lara, Ana Cañuelo, Mª Luisa del Moral, Santos Blanco, Eva Siles, Ana Jiménez, Juan Ángel Pedrosa, Mª Ángeles Peinado

Raquel Hernández, Esther Martínez-Lara, Ana Cañuelo, Mª Luisa del Moral, Santos Blanco, Eva Siles, Ana Jiménez, Juan Ángel Pedrosa, Mª Ángeles Peinado, Department of Experimental Biology, University of Jaén, Paraje Las Lagunillas s/n, E-23071 Jaén, Spain
Supported by Dirección General de Investigación Científica y Técnica, SAF 2003 04398-C02-02, and Junta de Andalucía, CVI-0184
Co-first-authors: Raquel Hernández and Mª Ángeles Peinado
Co-correspondent: Mª Ángeles Peinado
Correspondence to: Mª Ángeles Peinado, Department of Experimental Biology, University of Jaén, Paraje Las Lagunillas s/n, E-23071 Jaén, Spain. apeinado@ujaen.es
Telephone: +34-953-012303 Fax: +34-953-012141
Received: 2005-01-18 Accepted: 2005-04-08

Abstract

AIM: To analyze the relationship between perisinusoidal stellate cell (PSC) activation and the dietary fat quantity and composition in the treatment of hepatic steatosis.

METHODS: Using an experimental rat model of steatosis based on the intake of a hyperlipidic diet (14% fat as olive oil or sunflower oil, HL-O and HL-S, respectively), we analyzed the liver's capability of recovery after the treatment with a normal-lipidic diet (5% fat as olive oil or sunflower oil, NL-O and NL-S, respectively) by immunocytochemical and Western blot analysis of glial fibrillary acidic protein (GFAP) expression in PSCs, collagen quantification and serum aminotransferase determination.

RESULTS: The fatty infiltration in the steatotic livers decreased after the treatment with both NL diets, indicating liver recovery. This decrease was accompanied with a lower collagen deposition and aminotransferase level as well as changes in the PSC population that increased the GFAP expression. The above-mentioned effects were more pronounced in animals fed on NL-O based diet.

CONCLUSION: Treatment with a balanced diet enriched in olive oil contributes to the liver recovery from a steatotic process. The PSC phenotype is a marker of this hepatic-recovery model.

Key words: PSCs; GFAP; Steatosis; Collagen; Hyperlipidic diet; Liver recovery; Olive oil

Hernández R, Martínez-Lara E, Cañuelo A, Del Moral ML, Blanco S, Siles E, Jiménez A, Pedrosa JA, Peinado MA. Steatosis recovery after treatment with a balanced sunflower or olive oil-based diet: Involvement of perisinusoidal stellate cells. *World J Gastroenterol* 2005; 11(47): 7480-7485
http://www.wjgnet.com/1007-9327/11/7480.asp

INTRODUCTION

Hepatic steatosis is associated with obesity[1,2], toxic injury by toxins such as alcohol[3] or thioacetamide[4], and intake of high quantities of dietary fat[1,4]. Particularly, high-fat diets lead to biochemical and morphological hepatic changes, including steatosis and collagen deposition as well as alterations in the levels of plasma lipoproteins and serum aminotransferases (ALT, AST)[1,4,5]. These features are affected not only by the quantity but also by the composition of the dietary fat [1,5,6].

Perisinusoidal stellate cells (PSCs), also known as Ito cells or fat-storing cells, are liver pericytes that are involved in the hepatic metabolism of lipoproteins[7], synthesis of extracellular matrix proteins[8] and release of some hepatocyte growth factors[9], thus playing a key role in different pathologies such as hepatic fibrosis[10] and non-alcoholic steatohepatitis[11]. In addition, these cells due to their privileged location among hepatocytes, endothelial cells and nerve endings, have been proposed to be the main cell type responsible for the microcirculation control at the sinusoidal level[12].

In the normal liver, PSCs show a quiescent phenotype characterized by the presence of numerous intracytoplasmic fat droplets[13]. Nevertheless, in different hepatic pathologies, these cells are detected without lipid droplets showing an activated phenotype that implies changes in their antigenic composition[14,15] as well as in their morphology and functions[15,16].

PSCs share several features with astrocytes[16,19] and contain the glial fibrillary acidic protein (GFAP), a type of intermediate filament protein like these glial cells[20]. The plasticity in the expression of this cytoskeletal protein in PSCs has been proposed to be an instrument

to discriminate between quiescent and activated phenotypes[20].

The aim of the present study was to analyze the relationship between PSC activation and dietary fat quantity and composition in the treatment of hepatic steatosis. For this, an evaluation of the expression and distribution of the liver glial fibrillary acidic protein was made, and the liver collagen and the aminotransferase serum level were quantified in a rat model. These diets were prepared with olive or sunflower oils to compare the efficacy of the two fats on steatosis recovery.

MATERIALS AND METHODS

Animal diet and experimental design

Semipurified and balanced high-lipidic (HL; 14% fat) and normal-lipidic (NL; 5% fat) sunflower oil and olive oil diets were prepared as previously described[1,4]. The only difference between HL and NL diets was that the fat energy content was reduced from 14% to 5%, with a corresponding increase in the carbohydrate energy content. To avoid auto-oxidation, the oils were added to the diets on a daily basis immediately before feeding. All the animals had free access to the diet and water.

A total of 32 weaned Wistar rats were divided into two groups of 16 rats each and fed *ad libitum* on high-lipidic olive (HL-O) or high-lipidic sunflower (HL-S) oil diets for 1 mo. This time period was long enough to induce steatotic pathology[1,4]. Half of the rats of each HL oil group (n = 8 olive, n = 8 sunflower) were killed, and the other half were fed on a normal-lipidic (NL-O, NL-S) diet without changing the type of oil for an additional month.

The experiments followed the European Union guidelines on the use of animals for biomedical research (86/609/EU).

Histopathological examination

Four rats from each group were intraperitoneally anaesthetized with Ketolar (15 mg/100 mg body weight), and heparin was injected through the penis dorsal vein (500 IU/kg body weight) to avoid blood coagulation. The livers were perfused with 20-30 mL of carbogenated 0.01 mol/L phosphate buffer saline (PBS), and then with 100-120 mL of 4% paraformaldehyde-0.1 mol/L phosphate buffer (PB). After this, the organ was dissected out, cut into small blocks and immersed in the same fixative for 3 h at 4 ºC, and then immersed in 30% sucrose-0.1 mol/L phosphate buffer overnight at 4 ºC. The blocks were covered with OCT compound and frozen with 2-methylbutane at liquid-nitrogen temperature.

Histological study for the analysis of fatty infiltration was performed on 20-μm-thick sections stained with 1% OsO_4 0.1 mol/L phosphate buffer for 1 h at 4 ºC and mounted in PBS:glycerol (1:1).

Free-floating sections (40-μm thick) were obtained for collagen quantification by the colorimetric method described elsewhere[21].

Immunohistochemistry

For immunohistochemical analysis, free-floating (40-μm thick) sections were incubated overnight with a rabbit polyclonal anti-bovine GFAP (1:100; DAKO A/S, Z334) antiserum diluted in PBS containing 0.2% Triton X-100 at 4 °C. After several washes in PBS, the sections were incubated with biotinylated goat anti-rabbit IgG (Vector Laboratories Ltd) followed by peroxidase-linked ABC. The peroxidase activity was demonstrated following the nickel-enhanced diamino-benzidine procedure[24]. The sections were then mounted on slides, dehydrated in ascending grades of ethanol series, and covered using DPX. Controls for background staining, which was usually negligible, were performed by replacing the primary antiserum with normal rabbit serum.

Western blotting

Four rats from each group were killed by cervical dislocation and the livers were individually triturated with liquid nitrogen. The resulting powder was kept at -80 ºC and used for the preparation of crude extracts. Frozen liver powder (0.3 g) was homogenized (Polytron, PT 1200) in 30 mmol/L Tris-HCl buffer, pH 7.4, containing 0.5 mmol/L DTT, 1% SDS, 1 mmol/L EDTA and 1 mmol/L PMSF (1:3 w/v). The resulting homogenates were centrifuged for 60 min at 100 000 *g*. All the procedures were performed at 0-4 ºC. Protein concentrations in the supernatants were determined by the Bradford method[23].

For Western blot analysis, equal amount of the denatured proteins per lane (30 μg) were loaded and separated on an 8% SDS-polyacrylamide gel (Mini Protean II, BioRad), and transferred to a PVDF membrane (Hybond-P, Amersham). The membrane was blocked with 5% defatted milk powder in Tris-buffered saline buffer (25 mmol/L Tris-HCl, pH 7.6, 137 mmol/L NaCl, 2.6 mmol/L KCl, 0.2% Tween-20) and incubated at room temperature with diluted rabbit polyclonal anti-cow GFAP antibody (1/1 000) in a blocking buffer. Bound antibodies were revealed with an enhanced chemiluminescence kit (ECL, Amersham) according to the manufacturer's instructions. After immunodetection, membranes were probed with anti α-tubulin (Sigma) as a loading control. The relative expression of GFAP in each sample was quantified by densitometric scanning.

Serum aminotransferase levels

Blood samples were taken from the mesenteric vein of the same animals used for Western blot analysis. Serum alanine aminotransferase (ALT) and aspartate aminotransferase (AST) activities were automatically analyzed with a multifunctional biochemistry analyzer (Autoanalyzer Hitachi 917, Roche).

Statistical analysis

Data were expressed as mean±SD. Student's t-test was performed to evaluate significant differences between groups. $P<0.05$ was considered statistically significant.

Table 1 Body weight and liver weight (mean±SD)

	Body weight (g)	Liver weight (g)
HL-O	307.44±18.61	14.66±0.36
NL-O	255.33±23.58	12.05±0.87[a]
HL-S	310.55±16.48	
NL-S	207.16±32.83[a]	14.85±0.41

HL-O, high-lipidic olive oil; NL-O, normal-lipidic olive oil; HL-S, high-lipidic sunflower oil; NL-S, normal-lipidic sunflower oil. [a]P<0.05 *vs* HL-S, P<0.02 *vs* NL-O.

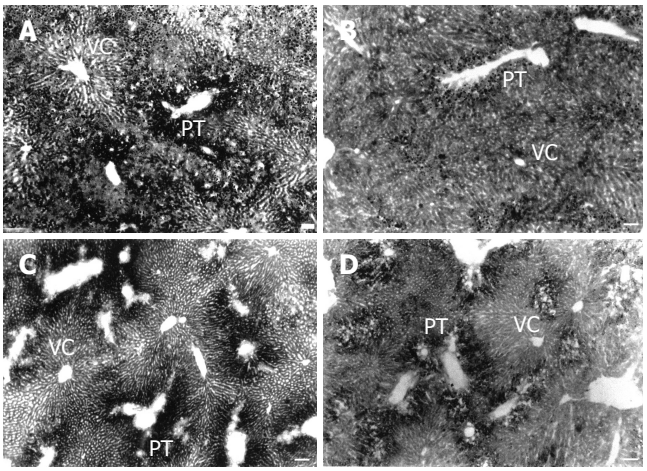

Figure 1 Light micrographs of representative liver sections from rats of each dietary group stained for fat with OsO_4. **A:** High-lipidic olive oil; **B:** normal-lipidic olive oil; **C:** high-lipidic sunflower oil; **D:** normal-lipidic sunflower oil. PT: portal triad; CV: central vein. Scale bar, 100 μm.

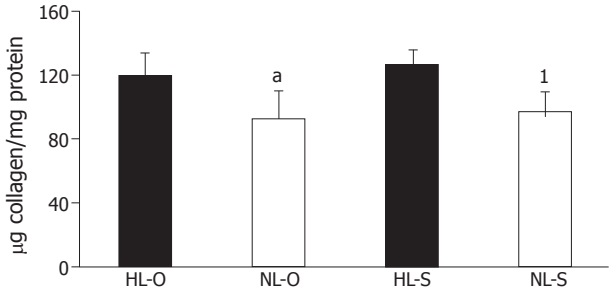

Figure 2 Collagen quantification in the high fat-induced steatotic liver (HL-O, HL-S) after its treatment with a normal-lipidic diet (NL-O, NL-S). Data are mean ±SD of four determinations. HL-O, high-lipidic olive oil; NL-O normal-lipidic olive oil; HL-S, high-lipidic sunflower oil; NL-S normal-lipidic sunflower oil. Significantly greater than in corresponding HL group: [a]P<0.05 *vs* HL-S, [1]P<0.02 *vs* NL-O.

RESULTS

Body and liver weights

Table 1 lists the body weight and liver weight before and after hyperlipidic and normal-lipidic diets.

Histopathological manifestations

Sections stained with OsO_4 revealed steatosis in the HL groups[4], characterized by the accumulation of many fat droplets inside the hepatocytes, mainly in those from the portal zone. After treatment with NL diets, steatosis was reduced principally in the NL-O group (Figure 1).

Regardless of the type of diet, the collagen quantification significantly decreased in rats after treatment with NL diets (Figure 2).

Table 2 Serum alanine aminotransferase (ALT) and aspartate aminotransferase (AST) levels (mean±SD)

	ALT (IU/L)	AST (IU/L)
HL-O	39±1.41	83.50±12.02
NL-O	27±5.66[1]	60±2.83[a]
HL-S	52±1.41	75±4.24
NL-S	26±14.14[b]	57.50±16.26

HL-O, high-lipidic olive oil; NL-O, normal-lipidic olive oil; HL-S, high-lipidic sunflower oil; NL-S, normal-lipidic sunflower oil. [a]P<0.05, [1]P<0.02 *vs* HL-S, [b]P<0.01 *vs* HL-O.

Distribution of GFAP immunoreactive PSCs

In all experimental groups, glial fibrillary acidic protein immunoreactive (GFAP-IR) cells were uniformly distributed in the liver parenchyma throughout the hepatic lobule (Figure 3A). These cells had a stellate shape with a large nucleus surrounded by a cytoplasm that exhibited many long processes (Figures 3B-D). Most of the cells contained numerous lipid droplets in their cytoplasm (Figure 3C), though some cells lacked fat droplets (Figure 3B).

The GFAP-IR cells had their cytoplasmic processes preferentially circumscribed to the Disse's space, running along or encircling the hepatic sinusoids (Figure 3B). Nevertheless, some cells, probably those called the "second layer cells"[24] located near the vascular network of the liver, sent out some processes towards the wall vessel, where they formed structures resembling the end-feed of astrocytes (Figures 3B and 3D).

When different dietary groups were compared, a lower frequency of GFAP-IR cells was found in the steatotic liver of animals fed on HL diets (sunflower or olive oil) in relation to the group receiving NL balanced diets (sunflower or olive oil) (Figure 4). No differences were found when diets with the same lipid content but with a different oil were compared.

Semiquantification of GFAP expression

Western blot analysis of denatured hepatic homogenates from HL and NL groups revealed a 51-ku protein detected by the GFAP antibody (Figure 5). The densitometric semiquantification showed that, after the normalization of the fat level in the diets (5%), GFAP expression was significantly increased but only in the olive oil diet (P<0.001).

Changes of aminotransferase levels

Serum ALT and AST levels are shown in Table 2. Compared with the HL groups, serum ALT activity significantly decreased after the treatment with NL diets. This decrease was more significant in the sunflower oil group (P<0.01). AST activity decreased only in the olive oil group after the treatment with NL diet (P<0.05).

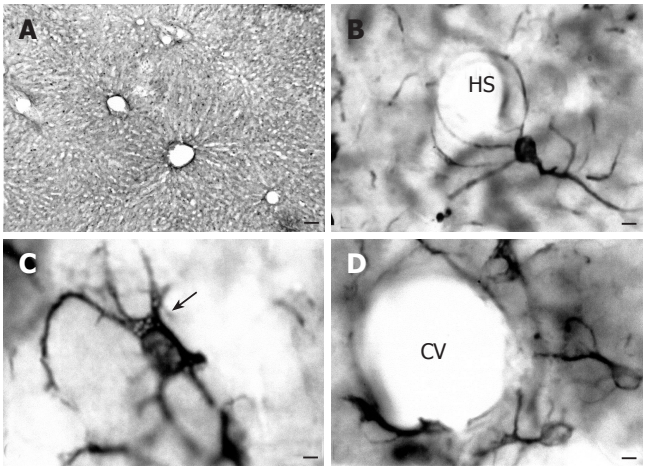

Figure 3 Distribution and location of GFAP immunoreactivity. **A:** GFAP-positive cells were distributed evenly in the lobule; **B:** GFAP-IR cells with processes circumscribing a hepatic sinusoid; **C:** GFAP-IR cell showing lipid droplets in its cytoplasm; **D:** GFAP-IR cell sending processes towards the vascular vessel. HS, hepatic sinusoid. CV, central vein; black arrow, lipid droplets; scale bar A: 100 mm; scale bars **B-D:** 10 μm.

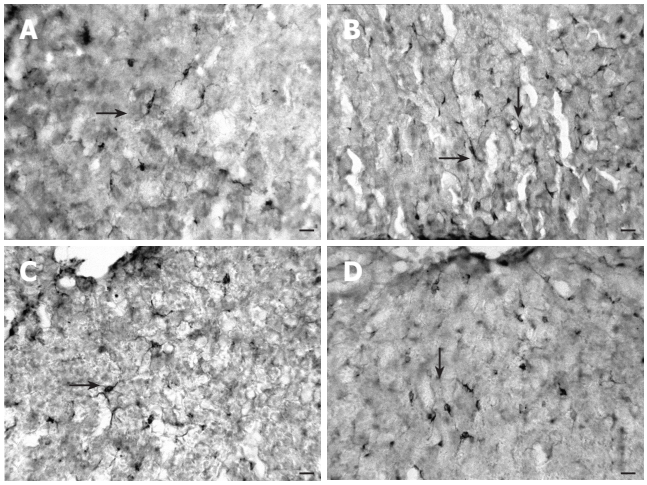

Figure 4 Light micrographs of representative liver sections from rats of each dietary group immunostained with GFAP antiserum. **A:** High-lipidic olive oil; **B:** normal-lipidic olive oil; **C:** high-lipidic sunflower oil; **D:** normal-lipidic sunflower oil. Scale bar, 10 μm.

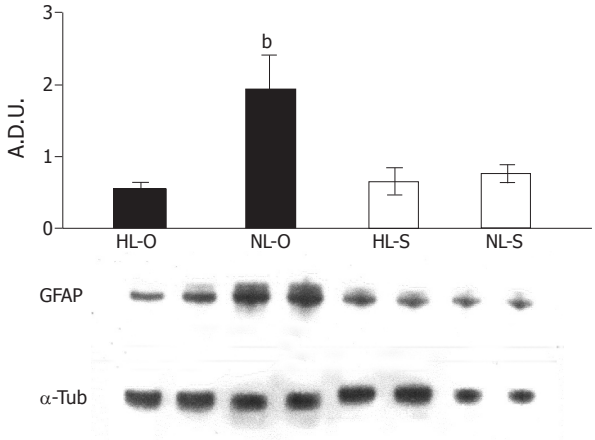

Figure 5 Western blot analysis of GFAP expression. Top panel: densitometric quantification of GFAP in the high-fat-induced steatotic liver (HL-O and HL-S), and after its treatment with a normal-lipidic diet (NL-O, NL-S). Results were average values of four experimental animals in each group. HL-O, high-lipidic olive oil; NL-O, normal-lipidic olive oil; HL-S, high-lipidic sunflower oil; NL-S, normal-lipidic sunflower oil. Bottom panel: representative autoradiography of the corresponding GFAP band. α-Tubulin immunodetection was also included as a protein-loading control. Protein expression is significantly greater than in HL-O group ($^bP<0.001$).

DISCUSSION

Several studies have emphasized the importance of dietary composition in the treatment of fatty liver[5,24]. Our results based on the induction of a steatotic process by diets of 14% fat and its recovery by diets of 5% fat demonstrated that these NL diets could reduce the collagen deposition and aminotransferase serum level as well as changes in the PSC population that increased the GFAP expression. In addition, taking into account that both HL and NL diets were prepared with sunflower or olive oils, we found that the above-mentioned effects were more pronounced in animals fed on NL olive oil-based diet.

No information is available on the involvement of PSCs in the regenerative potential of steatotic liver induced by high-lipidic diets, even though it is well known in other models of liver injuries. GFAP is the most reliable marker for testing the functional status of these liver cells[20]. In this sense, we used the immunohistochemical study of GFAP as well as its expression by Western blot to evaluate the dynamics of the PSC changes. Our results showed a significant increase in the GFAP expression after the treatment of steatotic animals with a NL-O diet.

The GFAP is an essential molecule for the formation and maintenance of the characteristic cytoplasmic processes[12]. Moreover, the role of PSCs in lipid storage and metabolism[7,17], synthesis of growth factors, and particularly in regulation of the hepatic microcirculation[10] is crucial in the development of and recovery from steatosis. In fact, the location of GFAP-IR cells surrounding the hepatic sinusoids, and also forming a peculiar barrier with their processes ending in the vascular wall of the periportal and pericentral vessels, allows us to suggest the participation of PSCs not only in the lipoprotein metabolism but also in the lipoprotein exchange between the Disse's space and the blood stream. Indeed, it has been reported that during hepatocyte proliferation after partial hepatectomy, PSCs send out their processes between hepatocytes and in vascular spaces, allowing the restoration of hepatic vascularization[25]. Thus, the present results showing GFAP increases in the PSCs population after the treatment with NL-O may be correlated with the recovery from the steatotic process.

It was reported that the type of fat in the diet affects serum lipid levels[1,4], as well as the quantity and spatial distribution pattern of the fat stored in hepatocytes[4]. It is noteworthy that, under our experimental conditions, both the doses and the type of dietary fat effectively influenced GFAP expression and the activation degree of PSCs. It has been shown that activation of PSCs by peroxidation

reactions is induced by free radicals[26,27]. In this sense, polyunsaturated fatty acids (PUFAs) from sunflower oils can be more easily affected by oxidative stress. Consequently, given that NL-S diet does not significantly augment GFAP expression in the liver, we might conclude that PSCs from animals fed on the sunflower-oil diet are more strongly activated than those from animals fed with olive oil containing mainly monounsaturated fatty acids (MUFAs), which are less sensitive to peroxidation.

Hepatic steatosis due to excessive dietary fat contents is characterized by an increased collagen deposition, like other hepatic pathologies such as cirrhosis and fibrosis[28,29]. Previous studies carried out in fibrotic rats showed that olive oil, in contrast to polyunsaturated oils, could protect against the development of fibrosis[30] though this depends on the experimentally induced fibrotic model that was employed[4]. It is therefore interesting to determine how the quality of fat in the diet affects this parameter. The present study showed that the restoration to a NL diet in animals previously fed on the HL diet significantly reduced hepatic collagen, this reduction being greater in the olive oil group (with a diet rich in MUFAs) than in the sunflower oil group (with a diet rich in PUFAs). These results agree with the observations of Fernandez *et al*[31].

It is well known that hepatic steatosis raises the serum aminotransferase level[28,32,33], which is decreased after the treatment with hypocaloric diets[5,32]. Our results showed that treatment with a NL diet (olive or sunflower oil) could reduce the aminotransferase level. However, the decrease was more significant in the olive oil group. Since sunflower oil is more susceptible to oxidative stress due to its PUFA content, its hepatic recovery ability is presumably lower. Polavarapu *et al*[34]. and Grattagliano *et al*[35]. found that ALT activity increases in alcoholic subjects fed on high PUFAs diets, which also supports our results.

In short, the results of the present work indicate that a balanced diet enriched in olive oil contributes to the recovery from hepatic steatosis.

ACKNOWLEDGMENTS

The authors thank Mr. David Nesbitt for his editorial help.

REFERENCES

1 **Del Moral ML**, Esteban FJ, Torres MI, Camacho MV, Hernandez R, Jimenez A, Aránega A, Pedrosa JA, Peinado MA. High-fat sunflower and olive oil diets affect serum lipid levels in steatotic rat liver differently. *J Nutr Sci Vitaminol (Tokyo)* 1997; **43**: 155-160

2 **Scheen AJ,** Luyckx FH. Metabolic syndrome: definitions and epidemiological data. *Rev Med Liege* 2002; **58:**479-484

3 **Keegan A,** Martini R, Batey R. Ethanol-related liver injury in the rat: a model of steatosis, inflammation and pericentral fibrosis. *J Hepatol* 1995; **23:** 591-600

4 **Esteban FJ,** Sánchez-López AM, Del Moral ML, Camacho MV, Hernández R, Jiménez A, Pedrosa JA, Peinado MA. Effect of thioacetamide and dexamethasone on serum lipids in rats fed on high-fat sunflower or olive oil diets. *J Nutr Sci Vitaminol (Tokyo)* 1999; **45:** 231-238

5 **Fan JG,** Zhong L, Xu ZJ, Tia LY, Ding XD, Li MS, Wang GL. Effects of low-calorie diet on steatohepatitis in rats with obesity and hyperlipidemia. *World J Gastroenterol* 2003; **9**: 2045-2049

6 **Cha YS,** Sachan DS. Opposite effects of dietary saturated and unsaturated fatty acids on ethanol-pharmacokinetics, triglycerides and carnitines. *J Am Coll Nutr* 1994; **13:** 338-343

7 **Ramadori G,** Rieder H, Theiss F, Meyer zum Büschenfelde KH. Fat-storing (Ito) cells of rat liver synthesize and secrete apolipoproteins: comparison with hepatocytes. *Gastroenterology* 1989; **1:** 163-172

8 **Burt AD,** Le Bail B, Balabaud C, Bioulac-Sage P. Morphologic investigation of sinusoidal cells. *Semin Liver Dis* 1993; **13:** 21-38

9 **Ramadori G.** Pathogenesis of liver fibrosis. Synthesis of collagen and non-collagen proteins in cell culture and in vivo. *Z Gastroenterol* 1992; **30** Suppl 1: 17-20

10 **Gressner AM.** Transdifferentiation of hepatic stellate cells (Ito cells) to myofibroblasts: a key event in hepatic fibrogenesis. *Kidney-Int-Suppl* 1996; **54:** S39-S45

11 **Higuchi H**, Gores GJ. Mechanisms of liver injury: an overview. *Curr Mol Med* 2003; **3**: 483-490

12 **Niki T,** De Bleser PJ, Xu G, Van Den Berg K, Wisse E, Geerts A. Comparison of glial fibrillary acidic protein and desmin staining in normal and CCl4-induced fibrotic rat livers. *Hepatology* 1996; **23:** 1538-1545

13 **Geerts A,** Bouwens L, Wisse E. Ultrastructure and function of hepatic fat-storing and pit cells. *J Electron Microsc Tech* 1990; **14:** 247-256

14 **Rockey DC,** Boyles JK, Gabbiani G, Friedman SL. Rat hepatic lipocytes express smooth muscle actin upon activation in vivo and in culture. *J Submicrosc Cytol Pathol* 1992; **24:** 193-203

15 **Friedman SL,** Rockey DC, McGuire RF, Maher JJ, Boyles JK, Yamasaki G. Isolated hepatic lipocytes and Kupffer cells from normal human liver: morphological and functional characteristics in primary culture. *Hepatology* 1992; **15:** 234-243

16 **Akiyoshi H,** Terada T. Centrilobular and perisinusoidal fibrosis in experimental congestive liver in the rat. *J Hepatol* 1999; **30:** 433-439

17 **Wake K.** Perisinusoidal stellate cells (fat-storing cells, interstitial cells, lipocytes), their related structure in and around the liver sinusoids, and vitamin A-storing cells in extrahepatic organs. *Int Rev Cytol* 1980; **66:** 303-353

18 **Blomhoff R,** Wake K. Perisinusoidal stellate cells of the liver: important roles in retinol metabolism and fibrosis. *FASEB J* 1991; **5:** 271-277

19 **Burt AD,** Robertson JL, Heir J, MacSween RN. Desmin-containing stellate cells in rat liver; distribution in normal animals and response to experimental acute liver injury. *J Pathol* 1986; **150:** 29-35

20 **Buniatian G,** Hamprecht B, Gebhardt R. Glial fibrillary acidic protein as a marker of perisinusoidal stellate cells that can distinguish between the normal and myofibroblast-like phenotypes. *Biol Cell* 1996; **87:** 65-73

21 **Jimenez W,** Parés A, Caballería J, Heredia D, Bruguera M, Torres M, Rojkind M, Rodés J. Measurement of fibrosis in needle liver biopsies: evaluation of a colorimetric method. *Hepatology* 1985; **5:** 815-818

22 **Shu SY,** Ju G, Fan LZ. The glucose oxidase-DAB-nickel method in peroxidase histochemistry of the nervous system. *Neurosci Lett* 1988; **85:** 169-171

23 **Bradford MM.** A rapid and sensitive method for the quantitation of microgram quantities of protein utilizing the principle of protein-dye binding. *Anal Biochem* 1976; **72:** 248-254

24 **Tsukamoto H,** Cheng S, Blaner WS. Effects of dietary polyunsaturated fat on ethanol-induced Ito cell activation. *Am J Physiol* 1996; **270:** G581-G586

25 **Martinez-Hernandez A,** Amenta PS. The extracellular matrix in hepatic regeneration. *FASEB J* 1995; **9:** 1401-1410

26 **Lee KS,** Buck M, Houglum K, Chojkier M. Activation of hepatic stellate cells by TGF alpha and collagen type I is mediated by oxidative stress through c-myb expression. *J Clin*

Invest 1995; **96:** 2461-2468
27 **Parola M,** Leonarduzzi G, Robino G, Albano E, Poli G, Dianzani MU. On the role of lipid peroxidation in the pathogenesis of liver damage induced by long-standing cholestasis. *Free Radic Biol Med* 1996; **20:** 351-359
28 **Ueno T,** Sugawara H, Sujaku K, Hashimoto O, Tsuji R, Tamaki S, Torimura T, Inuzuka S, Sata M, Tanikawa K. Therapeutic effects of restricted diet and exercise in obese patients with fatty liver. *J Hepatol* 1997; **27:** 103-107
29 **Alcolado R,** Arthur MJ, Iredale JP. Pathogenesis of liver fibrosis. *Clin Sci (Lond)* 1997; **92:** 103-112
30 **Szende B,** Timár F, Hargitai B. Olive oil decreases liver damage in rats caused by carbon tetrachloride (CCl4). *Exp Toxicol Pathol* 1994; **46:** 355-359
31 **Fernández I,** Torres I, Moreira E, Fontana L, Gil A, Rios A. Influence of administration of long-chain polyunsaturated fatty acids on process of histological recovery in liver cirrhosis produced by oral intake of thioacetamide. *Dig Dis Sci* 1996; **41:** 197-207
32 **Foster KJ,** Griffith AH, Dewbury K, Price CP, Wright R. Liver disease in patients with diabetes mellitus. *Postgrad Med J* 1980; **56:** 767-772
33 **Nomura F,** Ohnishi K, Ochiai T, Okuda K. Obesity-related nonalcoholic fatty liver: CT features and follow-up studies after low-calorie diet. *Radiology* 1987; **162:** 845-847
34 **Polavarapu R,** Spitz DR, Sim JE, Follansbee MH, Oberley LW, Rahemtulla A, Nanji AA. Increased lipid peroxidation and impaired antioxidant enzyme function is associated with pathological liver injury in experimental alcoholic liver disease in rats fed diets high in corn oil and fish oil. *Hepatology* 1998; **27:** 1317-1323
35 **Grattagliano I**, Palmieri VO, Palasciano G.Hepatotoxicity of polyunsaturated fatty acids in alcohol abuser. *J Hepatol* 2002; **37:** 291-292

Science Editor Wang XL and Guo SY **Language Editor** Elsevier HK

PO Box 2345, Beijing 100023, China
www.wjgnet.com
wjg@wjgnet.com

ELSEVIER

World J Gastroenterol 2005;11(47):7486-7493
World Journal of Gastroenterology ISSN 1007-9327

• *CLINICAL RESEARCH* •

Prospective randomized comparison of oral sodium phosphate and polyethylene glycol lavage for colonoscopy preparation

Kai-Lin Hwang, William Tzu-Liang Chen, Koung-Hong Hsiao, Hong-Chang Chen, Ting-Ming Huang, Chien-Ming Chiu, Ger-Haur Hsu

Kai-Lin Hwang, Department of Public Health, Chung-Shan Medical University, Taichung 402, Taiwan; Center for Clinical Trials, ChangHua Christian Hospital, Changhua 500, Taiwan, China
William Tzu-Liang Chen, Koung-Hong Hsiao, Hong-Chang Chen, Ting-Ming Huang, Chien-Ming Chiu, Ger-Haur Hsu, Division of Colorectal Surgery at ChangHua Christian Hospital, Changhua 500, Taiwan, China
This study was conducted at the Division of Colorectal Surgery at ChangHua Christian Hospital, Changhua 500, Taiwan, China
Correspondence to: Dr. William Tzu-Liang Chen, Division of Colorectal Surgery, ChangHua Christian Hospital, 135 Nanhsiao Street, Changhua, 500, Taiwan, China. 37599@cch.org.tw
Telephone: +886-4-7238595 Fax: +886-4-7227945
Received: 2005-04-07 Accepted: 2005-07-08

Abstract

AIM: To compare the effectiveness, patient acceptability, and physical tolerability of two oral lavage solutions prior to colonoscopy in a Taiwanese population.

METHODS: Eighty consecutive patients were randomized to receive either standard 4 L of polyethylene glycol (PEG) or 90 mL of sodium phosphate (NaP) in a split regimen of two 45 mL doses separated by 12 h, prior to colonoscopic evaluation. The primary endpoint was the percent of subjects who had completed the preparation. Secondary endpoints included colonic cleansing evaluated with an overall assessment and segmental evaluation, the tolerance and acceptability assessed by a self-administered structured questionnaire, and a safety profile such as any unexpected adverse events, electrolyte tests, physical exams, vital signs, and body weights.

RESULTS: A significantly higher completion rate was found in the NaP group compared to the PEG group (84.2% *vs* 27.5%, $P<0.001$). The amount of fluid suctioned was significantly less in patients taking NaP *vs* PEG (50.13±54.8 cc *vs* 121.13±115.4 cc, $P<0.001$), even after controlling for completion of the oral solution ($P = 0.031$). The two groups showed a comparable overall assessment of bowel preparation with a rate of "good" or "excellent" in 78.9% of patients in the NaP group and 82.5% in PEG group ($P = 0.778$). Patients taking NaP tended to have significantly better colonic segmental cleansing relative to stool amount observed in the descending (94.7% *vs* 70%, $P = 0.007$) and transverse (94.6% *vs* 74.4%, $P = 0.025$) colon. Slightly more patients graded the taste of NaP as "good" or "very good" compared to the PEG patients (32.5% *vs* 12.5%; $P = 0.059$). Patients' willingness to take the same preparation in the future was 68.4% in the NaP compared to 75% in the PEG group ($P = 0.617$). There was a significant increase in serum sodium and a significant decrease in phosphate and chloride levels in NaP group on the day following the colonoscopy without any clinical sequelae. Prolonged (>24 h) hemodynamic changes were also observed in 20-35% subjects of either group.

CONCLUSION: Both bowel cleansing agents proved to be similar in safety and effectiveness, while NaP appeared to be more cost-effective. After identifying and excluding patients with potential risk factors, sodium phosphate should become an alternative preparation for patients undergoing elective colonoscopy in the Taiwanese population.

Key words: Colonoscopy; Bowel preparation; Sodium phosphate; Polyethylene glycol

Hwang KL, Chen WTL, Hsiao KH, Chen HC, Huang TM, Chiu CM, Hsu GH. A prospective randomized comparison of oral sodium phosphate and polyethylene glycol lavage for colonoscopy preparation. *World J Gastroenterol* 2005; 11(47): 7486-7493
http://www.wjgnet.com/1007-9327/11/7486.asp

INTRODUCTION

Colonoscopy has become an essential procedure for the detection and treatment of colonic lesions; therefore, cleansing the bowel for adequate visualization of the colonic mucosa during colonoscopic examination is important. In the past two decades, various bowel preparation methods have been proposed including castor oil, anthroquinones, diphenylmethanes, phenolphthalein, and magnesium citrate, in combination with a low residue diet[1-5]. Along with these bowel-cleansing agents, cleansing enemas formed the "traditional" bowel preparation[6-10]. The introduction of polyethylene glycol (PEG) in 1980, an osmotically balanced solution, gradually replaced the

rigorous traditional 2 d preparation of enemas, a clear liquid diet, and laxatives in various combinations[11-15]. Although PEG provided safe and effective bowel cleansing, the patient was required to take 3-4 L of a salty tasting solution within a short period of time[16-19]. As reported, 5-15% of patients were unable to finish the prescribed dosage[8,16], potentially resulting in a poorly cleansed colon and inadequate colonoscopic assessment[17,19].

Oral sodium phosphate (NaP), a highly osmotic cathartic containing monobasic and dibasic sodium phosphate, was first evaluated by Vanner *et al*[19]. in 1990 by comparing it with PEG solutions. The mechanism of NaP is through the osmotic effect of phosphate. This draws large amounts of water into the bowel, creating a flushing action and a laxative effect within 30 min after ingestion and lasting an average of 2-3 h[19,20]. Several studies have been conducted to compare both NaP and PEG solutions, the majority of which have suggested a superiority or equivalence of NaP for adequate mechanical bowel preparation and safety[16-18,21,22]. Moreover, NaP was proven more cost-effective and has since been used worldwide[18,21,23]. With few studies being conducted in Singapore and Hong Kong[24-26], the effectiveness and safety of NaP for bowel preparation has not been prospectively assessed within the confines of a trial in the Taiwanese population. Due to the National Health Insurance (NHI) policy in Taiwan, only one bottle of magnesium citrate solution (MagVac, Pfizer Inc., USA) combined with six tablets of Bisacodyl (Durolax®, Boehringer-ingelheim GmbH, Ingelheim, Germany) are covered by NHI for bowel preparation; however, the results of bowel cleansing are often unsatisfactory. Other agents such as Klean Prep (Helsinn Birex Pharmaceuticals Ltd, UK), a PEG solution, and Fleet® Phospho-soda® (C.B. Fleet Company, Inc., Lynchburg, VA, USA), a NaP solution licensed after this trial, may be available at patients' own expense, if the hospitals carry such products. Most of the elective colonoscopic evaluations were performed at outpatient practice in Taiwan. Patients were scheduled for the examination on the day of consent, and bowel preparation agents were dispensed off on the same day along with both written and oral instructions. Patients were advised to start the preparation at home on the evening before the day of colonoscopy and only clear liquids were allowed after the procedure. The price of regular use of Klean Prep is NT$800 (about US$25) for four sachets (to be diluted to 4 L solution for use), while a 90 mL Fleet® Phospho-soda® costs NT$380 (about US$12). Since Fleet® Phospho-soda® had not been licensed by the Department of Health (DOH), Taiwan, until the results of this bridging study were available, and most of the doctors here do not have much experience with it, it becomes essential to provide effectiveness and safety data in this population along with cost-effective concerns. This study was undertaken to prospectively compare the effectiveness, patients' acceptability, and physical tolerability between the NaP and PEG in the Taiwanese population.

MATERIALS AND METHODS

Patients and methods

From August 2003 to December 2003, 80 consecutive patients who underwent elective colonoscopy were enrolled in this study. Eligible patients who had given written informed consent were randomized to receive either the standard 4 L of PEG (Klean Prep solution; Helsinn Birex Pharmaceuticals Ltd, UK) or 90 mL of NaP (Fleet® Phospho-soda®; C.B. Fleet Company, Inc., USA), in a split regimen of two 45 mL doses separated by 12 h, prior to the colonoscopic evaluation. Colonoscopy was scheduled after 8:00 a.m. for all the subjects, and study subjects were asked to report to the endoscopy room by 8:00 a.m. on the day of examination. Both groups were instructed to start the preparation around 6:00-7:00 p.m. the day before the colonoscopy. One sachet of Klean Prep should be diluted in 1 L of water (repeat for all four sachets) and one glassful (250 mL) of the solution would be taken every 10-15 min until the entire solution was consumed. The first 45 mL dose of Fleet® Phospho-soda® (diluted with a cold clear liquid or water by 1:16) was taken at 6:00-7:00 p.m. on the previous evening, and the second dose was taken at 6:00-7:00 a.m. on the day of the colonoscopy. A clear liquid diet was allowed during the bowel preparation. This study was approved by both the Health Department of Taiwan and the Institutional Review Board of ChangHua Christian Hospital, Taiwan. Exclusion criteria included symptomatic congestive heart failure, myocardial infarction, serum creatinine greater than 1.5 mg/dL, abnormal liver function defined as glutamic-oxaloacetic transaminase (GOT)/glutamic-pyruvic transaminase (GPT) greater than 120 U/L, ascites, electrolyte abnormalities, gastrointestinal obstruction, gastric retention, bowel perforation, obstructive or paralytic ileus, uncontrolled hypertension, unstable angina pectoris, pregnancy or breast feeding, and severe chronic constipation.

Demographic characteristics such as age, gender, prior bowel preparation experience, indication for colonoscopy, and medical history were obtained for all the patients. Laboratory assessment including blood urea nitrogen (BUN), GOT, GPT, sodium (Na), potassium (K), chloride (Cl), calcium (Ca), and phosphate (P), were done for all patients at baseline (the day of screening and consent, within 15 d prior to colonoscopy) and on the day following colonoscopy. In addition, a pregnancy test was performed on all the female patients and an electrocardiogram was performed on all the patients if no data were available within the prior 6 mo, during the initial screening visit. Body weight and routine vital signs, including pulse rate, blood pressure, and temperature were obtained at baseline, on the day of colonoscopy, and on the following day. Blood pressure and pulse rate were measured with the patient in both the supine (after resting for 5 min) and standing (after standing for 1 min) positions.

A self-administered structured questionnaire was completed by the patients to assess the tolerance, acceptability, and palatability of the bowel preparation

Table 1 Grades of bowel cleansing

Score	Stool amount	Stool consistency	Percent wall visualized	Overall assessment
0	None	None	⩾90%	
1	Small	Clear lavage	75-89%	Excellent (small volume of clear liquid)
2	Moderate	Liquid stool	50-74%	Good (large volume of clear liquid)
3	Large	Particulate stool	⩽49%	Fair (some semi-solid stool that could be suctioned or washed away)
4		Semi-solid stool		Poor (semi-solid stool that could not be suctioned or washed away)
5		Solid stool		

Table 2 Demographic characteristics and prior bowel preparation experience

Variables	NaP (n = 40)		PEG (n = 40)		
	N	%	*N*	%	P^1
Gender					0.178
Male	18	45.0	25	62.5	
Female	22	55.0	15	37.5	
Age					0.948
Mean±SD[2]	52.2±13.6		52.4±12.6		
Median (range)	51.9 (25.6-75.6)		54.2 (23.1-77.3)		
Frame size					0.571
Small (BMI<21)	6	15.0	6	15.0	
Medium (BMI:21–24)	30	75.0	26	65.0	
Large (BMI>24)	4	10.0	8	20.0	
Concomitant edication	4	10.0	5	12.5	1.000
Anti-hypertensive	1	2.5	4	10.0	
Others	3	7.5	4	10.0	
Previous bowel preparation					1.000
	13	32.5	14	35.0	

[1]Fisher's exact test or 2-sample Student's *t*-test, when appropriate. [2]SD: standard deviation.

method. The taste of the oral solutions was graded as very poor, poor, fair, good, and excellent. The ease of taking or swallowing, convenience, and the entire preparation process were graded as very difficult, difficult, tolerable, easy, and very easy. The occurrence and severity of several adverse events commonly associated with bowel preparation, the percentage of the solution ingested, and willingness to repeat the assigned preparation in the future were also addressed in the questionnaire. Patients were instructed to complete and return the questionnaire prior to the colonoscopy.

A single surgeon who was blinded to the type of preparation performed all of the colonoscopies. The time to reach the cecum, the scope of insertion and removal time, the volume of fluid irrigated and suctioned, and the level of the colon reached were recorded. Colonic cleansing was evaluated as to the amount and consistency of stool and the estimated percentage of the bowel wall visualized at the level of the rectum, descending colon, transverse colon, ascending colon, and cecum, as well as the overall assessment rated by the colonoscopist and scored according to the scale shown in Table 1.

Table 3 Consumption rate of oral solution

Variables	NaP (n = 38)		PEG (n = 40)		
	N	%	*N*	%	P^1
Consumption rate (%)					
100%	32	84.2	11	27.5	<0.001
75-99%	6	15.8	15	37.5	
<75%	0	0	14	35.0	
Mean±SD[2]	97.2±6.9		73.4±21.1		<0.001
Median (range)	100 (75–100)		75 (25–100)		

[1]Mantel–Haenszel χ^2 test and *t*-test when appropriate. [2]SD: standard deviation.

Statistical analysis

The Mantel-Haenszel χ^2 test and Fisher's exact test were used to compare the ordinal scores of the global and segmental assessment of bowel cleansing and patient index of experience, preference, and acceptability between the two groups. The Cochran-Mantel-Haenszel χ^2 was used to compare these categorical variables between the two groups, controlling for the completion of oral solution. General linear regression analysis was conducted by SAS Proc GLM procedure (SAS v.8.12, SAS Institute Inc., Cary, NC, USA) for the comparison of continuous variables between the two groups, controlling for the completion of oral solution. Changes from baseline of the laboratory tests and vital signs were analyzed across the treatment groups by the paired *t*-test. With a one-sided test, type I error rate of 0.05, power of 80% and a drop out rate of 7.5%, 40 patients for each group are needed to distinguish the difference of completion rate between a 62% for Klean Prep and 87% for Fleet® Phospho-soda® Solution.

RESULTS

Among the 80 patients who were prospectively randomized and completed the study, two NaP subjects were excluded from effectiveness analysis due to invalid laboratory tests at screening visit. The demographic characteristics and prior bowel preparation experience of all the 80 patients are summarized in Table 2. No significant differences in any of these variables were observed between the two groups. The major indications for colonoscopic evaluation were change in bowel habits (34/80; 42.5%), history of polyps (11/80; 13.8%), bleeding (11/80; 13.8%), family history of colorectal cancer (10/80; 12.5%), and cancer surveillance (9/80; 11.3%). There were four patients (three from NaP, and one from PEG group) in whom the cecum was not reached due to a surgical history of colorectal cancer. None of the baseline variables for the laboratory assessment/vital sign measurements were significantly different between the two groups. However, the NaP group had a significantly higher preparation completion rate than the PEG group (84.2% *vs* 27.5%, respectively; P<0.001) (Table 3).

Assessment of bowel cleansing

The amount of fluid suctioned was significantly less in patients taking NaP than those taking PEG (50.13±

Table 4 Overall assessment of preparation by the colonoscopist and stratified by completion of solution

Group	Excellent (%)	Good (%)	Fair (%)	Poor (%)	χ^2_{M-H} *P*	Good/excellent (%)	*P*
Overall							
NaP (*n* = 38)	22 (57.9)	8 (21.1)	8 (21.1)	0 (0.0)	0.648	30 (78.9)	0.778[1]
PEG (*n* = 40)	22 (55.0)	11 (27.5)	3 (7.5)	4 (10.0)		33 (82.5)	
Complete	100				0.584[2]		0.321[2]
NaP (*n* = 32)	19 (59.4)	7 (21.9)	6 (18.8)	0 (0.0)		26 (81.3)	
PEG (*n* = 11)	8 (72.7)	2 (18.2)	1 (9.1)	0 (0.0)		10 (90.9)	
Incomplete	0-99						
NaP (*n* = 6)	3 (50.0)	1 (16.7)	2 (33.3)	0 (0.0)		4 (66.7)	
PEG (*n* = 29)	14 (48.3)	9 (31.0)	2 (6.9)	4 (13.8)		23 (79.3)	

[1]Fisher's exact test. [2]Cochran-Mantel-Haenszel χ^2 test controlling for completion of oral solution.

Table 5 Colonic segmental assessment of preparation

	Stool amount (none/small) *N* (%)			Stool consistency (none/clear lavage) *N* (%)			% Colonic wall visualized (≥75%) *N* (%)		
	NaP (*N* = 38)	PEG (*N* = 40)	*P*	NaP (*N* = 38)	PEG (*N* = 40)	*P*	NaP (*N* = 38)	PEG (*N* = 40)	*P*
Rectum	37 (97.4)	33 (82.5)	0.057	31 (81.6)	32 (80.0)	1.000	37 (97.4)	37 (92.5)	0.616
Descending	36 (94.7)	28 (70.0)	0.007	32 (84.2)	33 (82.5)	1.000	38 (100)	35 (87.5)	0.055
Transverse[1]	35 (94.6)	29 (74.4)	0.025	31 (83.8)	34 (87.2)	0.752	37 (100)	37 (94.9)	0.494
Ascending[2]	35 (100)	35 (89.7)	0.117	24 (68.6)	31 (79.5)	0.302	35 (100)	38 (97.4)	1.000
Cecum[2]	35 (100)	35 (89.7)	0.117	23 (65.7)	31 (79.5)	0.202	35 (100)	37 (94.9)	0.495

[1]One patient in NaP group and 1 in PEG group did not have this data. [2]Three patients in NaP group and 1 in PEG group did not have this data.

54.8 cm^3 *vs* 121.13±115.4 cm^3, respectively; $P<0.001$), even after controlling for the completion of oral solution ($P = 0.031$). The two groups showed a comparable overall assessment of bowel preparation with a grade of "good" or "excellent" in 78.9% in the NaP and 82.5% in the PEG group ($P = 0.778$) (Table 4). Patients taking NaP tended to have significantly better colonic segmental cleansing as assessed by the colonoscopist in the amount of stool observed in the descending ($P = 0.007$) and transverse ($P = 0.025$) colon, even after controlling for the completion of oral solution ($P = 0.006$ for descending and $P = 0.048$ for transverse colon). Twenty-two (57.9%) patients in the NaP group had the stool amount graded as "none" for the descending and 22 (59.5%) for the transverse colon, while only 11 (27.5%) and 16 (41%) patients in the PEG group had perfect visibility in the descending and transverse colon, respectively. Furthermore, more patients in the NaP group had a grade of "none" in terms of stool consistency and ≥90% of the colonic wall visualized throughout the entire colon, although this difference was not statistically significant. A slightly better grade in the rectum ($P = 0.057$) relative to stool amount and in the descending colon for percent of wall visualized ($P = 0.055$) was also observed in the NaP group (Table 5).

Patient acceptability and preference

When assessing for the taste of the bowel preparation, four patients disliked the NaP and did not wish to have this preparation again, while slightly more patients enjoyed the taste and rated it as "good" or "very good" compared to patients taking PEG (13/40, 32.5% *vs* 5/40, 12.5%, respectively; $P = 0.059$). No differences were observed relative to ease of taking or swallowing, convenience, and ease of the entire preparation process, although slightly more patients in our study taking PEG rated these variables as "good/easy" or "very good/easy". When asked whether the patient would take the same preparation in the future, 26 (68.4%) in the NaP group and 30 (75%) in the PEG group replied "yes" ($P = 0.617$). Among the patients who had previous experience with bowel preparation, 8 (66.7%) of the 12 receiving NaP and 11 (78.6%) of the 14 receiving PEG would have the same preparation in the future ($P = 0.665$).

Adverse events

A total of 33 patients had 117 adverse events in the NaP group and 33 had 91 adverse events in the PEG group. These are summarized in Table 6. Although patients who received NaP had a slightly higher incidence than those who received PEG, no significant differences between the two groups were observed. One 32-year-old female patient in the NaP group who had a history of allergies to seafood was taking Lorazepan (Ativan, Wyeth, USA) for insomnia during the study period. Consequently, the patient experienced severe nausea, dizziness, and chills after taking the entire NaP solution. The patient's follow-up electrolytes were normal and all the symptoms subsided on the day following the colonoscopy.

Serum electrolyte changes

Comparison of baseline and post colonoscopy laboratory assessment revealed a significantly elevated Na, while Cl

Table 6 Occurrence and severity of anticipated adverse events

	NaP (n = 40)				PEG (n = 40)				
	Mild	Moderate	Severe	Occurrence (%)[1]	Mild	Moderate	Severe	Occurrence (%)[1]	P[2]
Nausea	17	0	1	18 (45)	14	4	0	18 (45)	1.000
Vomiting	9	1	0	10 (25)	5	4	0	9 (22.5)	1.000
Abdominal bloating	16	2	0	18 (45)	12	0	0	12 (30)	0.248
Abdominal pain	14	1	1	16 (40)	11	0	0	11 (27.5)	0.344
Anal irritation	13	3	0	16 (40)	10	1	1	12 (30)	0.482
Dizziness	13	2	1	16 (40)	10	1	0	11 (27.5)	0.344
Chills	3	0	1	4 (10)	3	0	0	3 (7.5)	1.000
Hunger pains	7	0	0	7 (17.5)	7	0	0	7 (17.5)	1.000
Headache	6	1	0	7 (17.5)	6	0	0	6 (15)	1.000
Insomnia[3]	4	1	0	5 (12.8)	2	0	0	2 (5)	0.263
Total	11	4	117	11	80	10	1	91	

[1]Occurrence rate was calculated by "frequency of occurrence/total number of subject". [2]Fisher's exact test for occurrence frequency of adverse events. [3]One patient in NaP group was taking Lorazepan (Ativan, Wyeth, USA) for insomnia during the bowel preparation, therefore this event was not assessable for this patient.

Table 7 Electrolytes

	NaP (n = 40)			PEG (n = 40)			Overall			2-Sample
	Baseline	Follow-up	Change[1]	Baseline	Follow-up	Change[1]	Baseline	Follow-up	Change[1]	t-test
	Mean±SD[2]	Mean±SD[2]	Mean±SD[2]	Mean±SD[2]	Mean±SD[2]	Mean±SD[2]	Mean±SD[2]	Mean±SD[2]	Mean±SD[2]	P[3]
Na (meq/L)	138.83±2.15	140.40±2.42	1.58±2.57[b]	138.85±2.15	140.88±2.37	2.03±1.83[b]	138.84±2.14	140.64±2.39	1.80±2.23[b]	0.370
K (meq/L)	3.99±0.34	3.86±0.39	-0.13±0.43	4.02±0.40	4.10±0.50	0.09±0.40	4.00±0.37	3.98±0.46	-0.02±0.43	0.022[a]
Cl (meq/L)	104.93±2.75	101.48±2.77	-3.45±2.84[b]	105.20±2.85	101.43±2.38	-3.78±2.71[b]	105.06±2.78	101.45±2.57	-3.61±2.76[b]	0.602
Ca (mg/dL)	9.17±0.35	9.17±0.39	-0.01±0.49	9.14±0.36	9.29±0.34	0.15±0.40[a]	9.16±0.35	9.23±0.37	0.07±0.46	0.129
P (mg/dL)	3.42±0.83	2.71±0.50	-0.71±0.76[b]	3.25±0.57	3.10±0.51	-0.16±0.57	3.34±0.71	2.90±0.54	-0.43±0.73[b]	<0.001[b]

[a]P<0.05; [b]P<0.01. [1]Change: value obtained at follow-up visit – value obtained at baseline visit. [2]SD: standard deviation. [3]The change from baseline (change) was compared between the two groups by independent 2-sample t-test.

Table 8 Hemodynamic profile

	Baseline		Day of colonoscopy change[1] from baseline		Follow-up visit change[1] from baseline	
	NaP	PEG	NaP	PEG	NaP	PEG
Pulse (beats/min) mean±SD[2]	76.4±11.2	72.9±12.4	5.4±13.6	6.7±12.6	1.7±10.9	0.6±13.0
Elevation in pulse rate ±10 beats/min (n %)			13 (32.5%)	13 (32.5%)	8 (20%)	9 (22.5%)
Elevation in pulse rate ±20 beats/min (n %)			5 (12.5%)	4 (10%)	3 (7.5%)	3 (7.5%)
SBP[3] (mmHg) mean±SD[2]	128.0±16.4	130.4±16.0	-6.8±12.5	-1.7±10.8	-4.3±10.7	-1.4±13.6
Drop in SBP ≥10 mmHg (n %)			13 (32.5%)	11 (27.5%)	14 (35%)	7 (17.5%)
Drop in SBP ≥20 mmHg (n %)			3 (7.5%)	0 (0.0%)	2 (5%)	4 (10%)

[1]Change: value obtained at the visit – value obtained at baseline visit. [2]SD: standard deviation. [3]SBP: systolic blood pressure.

and P were decreased in both groups (P<0.001; Table 7). The changes from baseline for both K and P were significantly different (P<0.05), while the changes of Na, Cl, and Ca were comparable between the two groups. Most of the laboratory values remained within the normal range and none of the patients complained of any discomfort during the follow-up period.

Hemodynamic profile and body weight

Hemodynamic profile is summarized in Table 8. Change from baseline in pulse rate (≥10 beats/min) and systolic blood pressure (SBP≥10 mmHg) were observed in 27.5-32.5% subjects from each group on the day of colonoscopy after the preparation, and were seen in 17.5-35% subjects on the day following the colonoscopic evaluation, though only <10% of the subjects had a change of >20 beats/min (mmHg) at the follow-up visit. Following the colonoscopy, after rest and resumption of a normal diet, most of the average values of vital signs, including body temperature, body weight, and pulse rate returned to baseline level except blood pressure (change from baseline of SBP for all subjects: -2.8±12.3, P = 0.042; diastolic BP: -3.5±7.9, P<0.001). None of these hemodynamic fluctuations were clinically significant

and no patients reported a syncopal episode or postural dizziness.

DISCUSSION

A "clean" colon is essential in colonoscopic examination for the early diagnosis of colonic neoplasia. A higher compliance rate for a bowel preparation agent will help to achieve this goal. In this study, 84% of the patients who received NaP completed the entire bowel preparation regimen compared with only 27.5% of the PEG group ($P<0.001$). All four patients in the PEG group who reported a "poor" grade for overall assessment were associated with poor compliance. Consistently more patients in the NaP group had perfect cleanliness in terms of the stool amount, stool consistency, and percent of colonic wall visualized in the majority of the colonic segments compared to those patients in the PEG group. In our study, although significantly better performance was found in some of the colonic segmental evaluations, NaP did not demonstrate a dramatic superiority over PEG in terms of the overall assessment. Our results differ from those of previous studies that have reported a 10-40% difference in favor of NaP[16,17,19,21,22]. In addition to these studies, two Asian studies conducted in Singapore and Hong Kong[24,25] also indicated a significantly higher proportion of patients reporting good or excellent grades with the NaP compared to the PEG solutions (22% and 20% difference, respectively for each study; $P<0.05$). However, this study did not demonstrate any statistically significant difference between patients receiving PEG who were graded as "good" or "excellent" in terms of overall assessment by the physician, compared to those who took NaP (82.5% *vs* 78.9%, respectively; $P = 0.78$). Although some of the studies used less amount, i.e., 3 or 2 L, instead of 4 L for PEG preparation[18,27-29], most of the trials adopted a standard amount of 4 L recommended by the manufacturer for a better cleansing result. The Hintertux study group even demonstrated that the 4 L PEG group was significantly superior to the 3 L PEG group[28]. However, a remarkably low completion rate of PEG solution (27.5%) was observed in this study. Using 75% as the cut-off for the completion rate, i.e., 3 L of PEG solution, there were still 14 (35%) subjects who failed to complete the PEG preparation in this study, which indicated a cultural difference in terms of the practice of bowel preparation. Instead of getting admitted to the hospital the day prior to the colonoscopic evaluation as did in some other trials[19,30], all of our subjects initiated the preparation at home without assistance. With the large amount (4 L) of the solution, some subjects tended to stop drinking PEG when they felt that they were already clean. Others stated that they were afraid of having the needs to go to the restroom on a bus or a train to the hospital and therefore stopped taking the rest of the solution after going to bed in the night before the colonoscopy. This kind of stress and inconvenience are less likely to happen to inpatients, subjects who have their own vehicles or those who live close to the hospital. Contrary to the results reported by Cohen *et al*[17]. in which significantly more fluid was suctioned from the colon after NaP, while more irrigation was necessary to cleanse the bowel after PEG, our data show that significantly more fluid was suctioned in patients who took PEG than those taking NaP, while the amount of irrigation did not differ between the two groups. More fluid in the colon may result in missed colonic lesions or tumors while the use of suction may cause more mucosal injury.

There were four patients who disliked the NaP and did not wish to have this preparation again. The same situation was mentioned by some studies[22,24,31], although some patients reported discomfort with the NaP solution due to its salty and unpalatable taste, still found it easier to complete than the PEG solution due to the smaller volumes. Although the 4 L required for the PEG solution is much greater than that required for NaP, none of the patients in the PEG group complained about taking or swallowing the large amount of solution. Furthermore, none of them rated the convenience of taking or ease of the entire preparation as "very poor", though the completion rate was also much lower than expected. In contrast to most of the other studies, slightly more patients in our study taking PEG rated the ease of taking or swallowing, convenience of taking, and ease of the preparation as "good/easy" or "very good/easy", and answered "yes" to the question "would you take the same preparation in the future" compared with the NaP group, although these differences were not statistically significant. The majority of our patient population lived in rural areas and tended to unquestionably follow physician's instructions more than their urban counterparts, which may explain the high satisfaction rates with the PEG preparation.

The patients in our study reported a consistently higher incidence of several anticipated adverse events than cited by other studies[17,18,24,25], although there was no significant difference between the two groups. Nevertheless, the NaP group had a slightly higher overall occurrence of these symptoms than did the PEG group. The majority of the adverse events were graded as mild-to-moderate and had subsided by the day following the colonoscopy. One patient in the NaP group who suffered from severe nausea, dizziness, and chills was taking Lorazepan (Ativan, Wyeth, USA) for insomnia during the bowel preparation. This observation might be just a coincidence or a result from multiple factors, i.e., the concomitant use of NaP and Lorazepan along with the patient's history of allergy, which will need further investigations. A transient hypophosphatemia was observed in the NaP group the day following the colonoscopy, compared to baseline. Hyperphosphatemia is a recognized consequence of sodium phosphate. According to the reports by Kolts *et al*[22]. and Huynh *et al*[30]. serum phosphate rose significantly 2 h after NaP consumption, but subsequently returned to normal within 26 h. Since the preparation was done at the subjects' residence, instead of continuous monitoring the electrolytes during the preparation, only the value on the day after the colonoscopy was obtained to compare the baseline level, and therefore we failed to observe the elevation phase of serum phosphate but observed only the decrease phase at more than 24 h after the preparation. The same pattern was also observed by Vanner *et al*[19]. in which serum phosphate of seven patients in NaP group elevated from 3.7±0.2 mg/dL on the day of admission to 7.2±0.6 mg/dL at 8:00 a.m. on the

day of colonoscopy, then dropped to 3.7±0.3 mg/dL at 4:00 p.m. in the evening and to 3.1±0.3 mg/dL at 8:00 a.m. on the following day. Consistent with known effect of oral sodium phosphate solution, serum sodium levels remained higher and potassium levels were lower than baseline on the day following the colonoscopy. Although different from baseline, most of the values were still within normal ranges and none of the subjects developed any clinically relevant adverse events that accompanied these metabolic changes after the cessation of the preparation.

Contraindications to the use of NaP have been emphasized, and serious electrolyte disturbances have been reported in individual patients taking oral sodium phosphate[20,32,33]. Some studies have indicated that NaP should not be used in women who are pregnant or breast-feeding, or patients with renal failure, congestive heart failure, ascites, or congenital megacolon[34,35]. Furthermore, hypokalemia resulting from the ingestion of NaP can increase the risk of cardiac arrhythmias in patients who are taking diuretics or digitalis[30,36]. The proportion of subjects (27.5-32.5%) with a hemodynamic change greater than 10 beats/min in pulse rate or 10 mmHg in systolic blood pressure on the morning of colonoscopy compared to baseline levels are slightly higher than reported studies, i.e., 14-28% of oral sodium phosphate solution recipients with decreases in SBP >1.33 Kpa and 15-30% with changes in postural pulse $\geqslant$10 beats/min from baseline[19,30,34]. Without taking any solid food since the previous afternoon, suffering from the preparation process and insufficient sleep, along with an early commute to the hospital (some had a commute longer than 30 min), most of the subjects appeared weak on arrival at the endoscopic station. It might explain why the outpatient subjects had a larger hemodynamic change on the day of colonoscopy compared with those who were admitted to the hospital on the previous day[19]. One study reported that 12% NaP patients had changes in SBP>20 mmHg[34], which was higher than what we observed (7.5%). Hemodynamic changes suggest that intravascular volume decreases during the bowel preparation, and it is considered to be transient unless contraindications are encountered. Patients in both the groups were instructed to take adequate amounts of fluid during the preparation, therefore, no significant body weight changes were observed in either group.

CONCLUSION

Both bowel cleansing agents were found to be equally safe and effective for bowel preparation prior to colonoscopy. Although NaP was more effective in some of the colonic segmental cleansing, both solutions were found to be equally acceptable and had the same overall assessment. However, the high completion rate related to NaP may prevent inadequate bowel preparation and facilitate colonoscopic evaluation. Taking its more affordable price into consideration (about half price of PEG), NaP demonstrates its cost effectiveness. Severe adverse events were observed in only one patient who was taking medication for insomnia during the NaP preparation, which implies that caution should be taken relative to concomitant medications. Although not clinically significant, some hemodynamic and electrolyte changes were prolonged more than 24 h. After identifying and excluding patients with potential risk factors, NaP should become an alternative bowel preparation for patients undergoing colonoscopy in the Taiwanese population.

REFERENCES

1 **Yang HC,** Sheu MH, Wang JH, Chang CY. **Bowel preparation** of outpatients for intravenous urography: efficacy of castor oil versus bisacodyl. *Kaohsiung J Med Sci* 2005; **21:** 153-158
2 **Chen CC,** Ng WW, Chang FY, Lee SD. Magnesium citrate-bisacodyl regimen proves better than castor oil for colonoscopic preparation. *J Gastroenterol Hepatol* 1999; **14:** 1219-1222
3 **Strates BS,** Hofmann LM. A randomized study of two preparations for large bowel radiology. *Pharmatherapeutica* 1987; **5:** 57-61
4 **Delegge M,** Kaplan R. Efficacy of bowel preparation with the use of a prepackaged, low fibre diet with a low sodium, magnesium citrate cathartic vs. a clear liquid diet with a standard sodium phosphate cathartic. *Aliment Pharmacol Ther* 2005; **21:** 1491-1495
5 **Zmora O,** Pikarsky AJ, Wexner SD. Bowel preparation for colorectal surgery. *Dis Colon Rectum* 2001; **44:** 1537-1549
6 **Donovan IA,** Arabi Y, Keighley MR, Alexander-Williams J. Modification of the physiological disturbances produced by whole gut irrigation by preliminary mannitol administration. *Br J Surg* 1980; **67:** 138-139
7 **Minervini S,** Alexander-Williams J, Donovan IA, Bentley S, Keighley MR. Comparison of three methods of whole bowel irrigation. *Am J Surg* 1980; **140:** 400-402
8 **Gründel K,** Schwenk W, Böhm B, Müller JM. **Improvements** in mechanical bowel preparation for elective colorectal surgery. *Dis Colon Rectum* 1997; **40:** 1348-1352
9 **Davis GR,** Santa Ana CA, Morawski SG, Fordtran JS. Development of a lavage solution associated with minimal water and electrolyte absorption or secretion. *Gastroenterology* 1980; **78:** 991-995
10 **DiPalma JA,** Brady CE, Stewart DL, Karlin DA, McKinney MK, Clement DJ, Coleman TW, Pierson WP. Comparison of colon cleansing methods in preparation for colonoscopy. *Gastroenterology* 1984; **86:** 856-860
11 **Bowden TA**, DiPiro JT, Michael KA. **Polyethylene glycol electrolyte** lavage solution (PEG-ELS). A rapid, safe mechanical bowel preparation for colorectal surgery. *Am Surg* 1987; **53:** 34-36
12 **Goldman J,** Reichelderfer M. Evaluation of rapid colonoscopy preparation using a new gut lavage solution. *Gastrointest Endosc* 1982; **28:** 9-11
13 **Beck DE**, Fazio VW. Current preoperative bowel cleansing methods. Results of a survey. *Dis Colon Rectum* 1990; **33**: 12-15
14 **Solla JA,** Rothenberger DA. Preoperative bowel preparation. A survey of colon and rectal surgeons. *Dis Colon Rectum* 1990; **33:** 154-159
15 **Nichols RL,** Smith JW, Garcia RY, Waterman RS, Holmes JW. Current practices of preoperative bowel preparation among North American colorectal surgeons. *Clin Infect Dis* 1997; **24:** 609-619
16 **Oliveira L,** Wexner SD, Daniel N, DeMarta D, Weiss EG, Nogueras JJ, Bernstein M. Mechanical bowel preparation for elective colorectal surgery. A prospective, randomized, surgeon-blinded trial comparing sodium phosphate and polyethylene glycol-based oral lavage solutions. *Dis Colon Rectum* 1997; **40:** 585-591
17 **Cohen SM,** Wexner SD, Binderow SR, Nogueras JJ, Daniel N, Ehrenpreis ED, Jensen J, Bonner GF, Ruderman WB. **Prospective,** randomized, endoscopic-blinded trial comparing precolo-

noscopy bowel cleansing methods. *Dis Colon Rectum* 1994; **37:** 689-696
18 **Frommer D.** Cleansing ability and tolerance of three bowel preparations for colonoscopy. *Dis Colon Rectum* 1997; **40:** 100-104
19 **Vanner SJ,** MacDonald PH, Paterson WG, Prentice RS, Da Costa LR, Beck IT. A randomized prospective trial comparing oral sodium phosphate with standard polyethylene glycol-based lavage solution (Golytely) in the preparation of patients for colonoscopy. *Am J Gastroenterol* 1990; **85:** 422-427
20 **Curran MP,** Plosker GL. Oral sodium phosphate solution: a review of its use as a colorectal cleanser. *Drugs* 2004; **64:** 1697-1714
21 **Golub RW,** Kerner BA, Wise WE, Meesig DM, Hartmann RF, Khanduja KS, Aguilar PS. Colonoscopic bowel preparations--which one? A blinded, prospective, randomized trial. *Dis Colon Rectum* 1995; **38:** 594-599
22 **Kolts BE,** Lyles WE, Achem SR, Burton L, Geller AJ, MacMath T. A comparison of the effectiveness and patient tolerance of oral sodium phosphate, castor oil, and standard electrolyte lavage for colonoscopy or sigmoidoscopy preparation. *Am J Gastroenterol* 1993; **88:** 1218-1223
23 **Hsu CW,** Imperiale TF. Meta-analysis and cost comparison of polyethylene glycol lavage versus sodium phosphate for colonoscopy preparation. *Gastrointest Endosc* 1998; **48:** 276-282
24 **Chia YW,** Cheng LC, Goh PM, Ngoi SS, Isaac J, Chan ST, Ti TK. Role of oral sodium phosphate and its effectiveness in large bowel preparation for out-patient colonoscopy. *J R Coll Surg Edinb* 1995; **40:** 374-376
25 **Law WL,** Choi HK, Chu KW, Ho JW, Wong L. Bowel preparation for colonoscopy: a randomized controlled trial comparing polyethylene glycol solution, one dose and two doses of oral sodium phosphate solution. *Asian J Surg* 2004; **27:** 120-124
26 **Poon CM,** Lee DW, Mak SK, Ko CW, Chan KC, Chan KW, Sin KS, Chan AC. Two liters of polyethylene glycol-electrolyte lavage solution versus sodium phosphate as bowel cleansing regimen for colonoscopy: a prospective randomized controlled trial. *Endoscopy* 2002; **34:** 560-563
27 **Kastenberg D,** Chasen R, Choudhary C, Riff D, Steinberg S, Weiss E, Wruble L. Efficacy and safety of sodium phosphate tablets compared with PEG solution in colon cleansing: two identically designed, randomized, controlled, parallel group, multicenter phase III trials. *Gastrointest Endosc* 2001; **54:** 705-713
28 **Ell C,** Fischbach W, Keller R, Dehe M, Mayer G, Schneider B, Albrecht U, Schuette W. A randomized, blinded, prospective trial to compare the safety and efficacy of three bowel-cleansing solutions for colonoscopy (HSG-01*). *Endoscopy* 2003; **35:** 300-304
29 **Reddy DN,** Rao GV, Sriram PV. Efficacy and safety of oral sodium phosphate versus polyethylene glycol solution for bowel preparation for colonoscopy. *Indian J Gastroenterol* 2002; **21:** 219-221
30 **Huynh T,** Vanner S, Paterson W. Safety profile of 5-h oral sodium phosphate regimen for colonoscopy cleansing: lack of clinically significant hypocalcemia or hypovolemia. *Am J Gastroenterol* 1995; **90:** 104-107
31 **Seinelä L,** Pehkonen E, Laasanen T, Ahvenainen J. Bowel preparation for colonoscopy in very old patients: a randomized prospective trial comparing oral sodium phosphate and polyethylene glycol electrolyte lavage solution. *Scand J Gastroenterol* 2003; **38:** 216-220
32 **Azzam I,** Kovalev Y, Storch S, Elias N. Life threatening hyperphosphataemia after administration of sodium phosphate in preparation for colonoscopy. *Postgrad Med J* 2004; **80:** 487-488
33 **Hookey LC,** Vanner S. Recognizing the clinical contraindications to the use of oral sodium phosphate for colon cleansing: a case study. *Can J Gastroenterol* 2004; **18:** 455-458
34 **Afridi SA,** Barthel JS, King PD, Pineda JJ, Marshall JB. Prospective, randomized trial comparing a new sodium phosphate-bisacodyl regimen with conventional PEG-ES lavage for outpatient colonoscopy preparation. *Gastrointest Endosc* 1995; **41:** 485-489
35 **Aradhye S,** Brensilver JM. Sodium phosphate-induced hypernatremia in an elderly patient: a complex pathophysiologic state. *Am J Kidney Dis* 1991; **18:** 609-611
36 **Gupta SC,** Gopalswamy N, Sarkar A, Suryaprasad AG, Markert RJ. Cardiac arrhythmias and electrocardiographic changes during upper and lower gastrointestinal endoscopy. *Mil Med* 1990; **155:** 9-11

Science Editor Pravda J and Guo SY **Language Editor** Elsevier HK

PO Box 2345, Beijing 100023, China
www.wjgnet.com
wjg@wjgnet.com

ELSEVIER

World J Gastroenterol 2005;11(47):7494-7498
World Journal of Gastroenterology ISSN 1007-9327

Health-related quality of life and impact of antiviral treatment in Chinese patients with chronic hepatitis C in Taiwan

Shih-Chao Kang, Shinn-Jang Hwang, Shiang-Ho Lee, Full-Young Chang, Shou-Dong Lee

Shih-Chao Kang, Division of Family Medicine, I-Lan Hospital, Department of Health, I-Lan, Taiwan, China
Shinn-Jang Hwang, Department of Family Medicine, Taipei Veterans General Hospital and National Yang-Ming University School of Medicine, Taipei, Taiwan, China
Shiang-Ho Lee, Shiang-Ho Clinic, Taipei, Taiwan, China
Full-Young Chang, Shou-Dong Lee, Division of Gastroenterology, Department of Medicine, Taipei Veterans General Hospital and National Yang-Ming University School of Medicine, Taipei, Taiwan, China
Supported by the National Science Council, Taiwan, China, NSC 89-2314-B-010-475
Co-first-authors: Shih-Chao Kang
Correspondence to: Shinn-Jang Hwang, MD, F.A.C.G., Department of Family Medicine, Taipei Veterans General Hospital, No. 201, Shih-Pai Road Sec. 2, Taipei 112, Taiwan, China. sjhwang@vghtpe.gov.tw
Telephone: +886-2-28757460 Fax: +886-2-28737901
Received: 2005-04-29 Accepted: 2005-07-08

Abstract

AIM: To evaluate health-related quality of life (HRQOL) in Chinese patients with chronic hepatitis C (CH-C), and the impact of antiviral treatment.

METHODS: Short Form 36 (SF-36) Health-related Quality of Life Questionnaires to interview CH-C patients, and age- and sex-matched control subjects at outpatient clinics of a medical center in Taiwan were used. Data were transformed to scores for comparisons of eight major SF-36 domains. We also enrolled consecutive CH-C patients who completed one course of antiviral treatment (interferon α with ribavirin), and measured the HRQOL before, at the 12th wk of treatment, at the end of treatment, and at mo 6, after stopping the treatment to evaluate the impact of antiviral treatment.

RESULTS: A total of 371 outpatients were enrolled, including 182 with CH-C and 189 age- and sex-matched subjects without CH-C. CH-C subjects had obviously lower educational status ($P<0.01$). Mean scores of domains in general health, physical functioning, role-physical, role-emotional, vitality, and mental health of the SF-36 were significantly lower in subjects with CH-C than those without CH-C ($P<0.05$). In an analysis of 47 CH-C patients who received and completed the whole course of antiviral treatment, mean scores of all domains were significantly lower at wk 12 of treatment compared to baseline. The scores returned to pretreatment values by the end of treatment, but were significantly increased at mo 6 after stopping the treatment. Among the 47 CH-C patients, 21 had sustained responses and 26 had non-sustained responses to antiviral treatment. Compared to pretreatment values, subjects with sustained responses had significantly lower social functioning scores at wk 12 of treatment, and scores for all SF-36 domains returned to pretreatment values, and increased significantly at mo 6 after stopping the treatment. For non-sustained virological responders, scores of all SF-36 domains significantly decreased at wk 12 of treatment, and did not increase significantly by the end of treatment, or at mo 6 after stopping the treatment when compared to the pretreatment values.

CONCLUSION: HRQOL in CH-C patients is significantly impaired in most SF-36 domains. Antiviral treatment impaired HRQOL of CH-C subjects during early treatment, mainly in non-sustained virological responders, and improved at mo 6 after stopping the treatment, mainly in sustained virological responders.

Key words: Hepatitis C; Quality of life; Questionnaire

Kang SC, Hwang SJ, Lee SH, Chang FY, Lee SD. Health-related quality of life and impact of antiviral treatment in Chinese patients with chronic hepatitis C in Taiwan. *World J Gastroenterol* 2005; 11(47): 7494-7498
http://www.wjgnet.com/1007-9327/11/7494.asp

INTRODUCTION

Hepatitis C virus infection (HCV), previously known as non-A, non-B hepatitis, has become an important health issue worldwide in the last 15 years. Its chronic sequelae, liver cirrhosis and hepatocellular carcinoma, have had a significant impact on the health of the population worldwide[1,2]. Antiviral treatments, including interferon with or without ribavirin, have been used in treating chronic hepatitis C (CH-C) patients to prevent the development of liver cirrhosis and hepatocellular carcinoma. In Taiwan, the prevalence of CH-C has been reported to be around 2-5% in urban populations. High HCV endemic villages with 20-60% positive rates of serum antibody to HCV have been found in central and southern parts of Taiwan[3,4]. Interferon α therapy with and without ribavirin for 6 mo has been used to treat CH-C patients since 1991 in Taiwan. The sustained virological response rate at the end of

the treatment ranged from 12% to 76%, but the sustained virological response rate at the 6th mo after stopping the treatment ranged only from 12% to 43%[5-8].

Health-related quality of life (HRQOL), which reflects what patients are concerned with and what they experience, has been widely researched in patients with CH-C in the West. Indeed, the impact on HRQOL and the adverse effects of antiviral treatment have been documented for Western populations. However, to our knowledge, such studies have not been done for HRQOL in Chinese patients with CH-C.

For evaluation of HRQOL in Chinese CH-C patients, the Short Form 36 (SF-36) Questionnaire is most commonly used. The aims of our study were to understand the characteristics of HRQOL in Chinese CH-C patients compared with age- and sex-matched subjects without CH-C, and to evaluate the impact of antiviral treatment on HRQOL in Chinese CH-C patients.

MATERIALS AND METHODS

We used questionnaires to conduct interviews of CH-C patients at the Outpatient Clinics of Taipei Veterans General Hospital, a medical center in Taipei City, Taiwan. CH-C patients were defined as those who had sustained elevation of serum transaminase and positive tests for serum antibody to HCV for more than 6 mo, and/or pathological changes consistent with the diagnosis of CH-C on liver biopsies. CH-C patients who showed decompensated cirrhosis or hepatocellular carcinoma were excluded from the study. Age- and sex-matched subjects without CH-C were interviewed at the same places and at the same times as CH-C patients. The enrolled outpatients were randomly selected and interviewed from January 1, 2002 to December 31, 2002. Demographic data, including subjective difficulty in completing the questionnaire, acute illness within the last 2 wk, combined chronic systemic diseases such as hypertension, coronary artery disease, chronic obstructive pulmonary disease, diabetes mellitus and osteoarthritis, were obtained for each subject. We trained senior-grade medical students and nurses to interview the subjects and to assist them in filling out the questionnaire.

We used the SF-36 HRQOL questionnaire, Taiwan version, as a tool for our study. The SF-36, developed by John E. Ware Jr. in late 1980s, has been widely used in different fields for health evaluations all over the world. Translated into several languages, the SF-36 has shown similar reliability and validity in studies conducted in different countries[9-15]. For the SF-36 Taiwan version, the norms and internal consistency have been validated by local researchers[16,17]. It measures eight main domains: (a) general health (GH); (b) physical functioning (PF); (c) limitation of roles due to physical problems, known as role-physical (RP); (d) limitation of roles due to emotional problems, known as role-emotional (RE); (e) social functioning (SF); (f) bodily pain (BP); (g) vitality (VT); and (h) mental health (MH). We recorded demographic data, summarized the original scores of each SF-36 domain, and translated them into final scores from 0 to 100 linearly via the formulas of the SF-36. A score of "0" indicates the least favorable health status; a score of "100", the most favorable health status.

Table 1 Demographic characteristics of 371 study subjects with and without chronic hepatitis C (CH-C)

	CH-C patients (n = 182)	Controls (n = 189)	P
Mean age (yr)	59.9±12.9	58.8±13.9	0.302
Sex (male:female)	91:91	106:83	0.254
Educational status (below high school:high school or above)	97:85	62:127	<0.001
Subjective difficulty to questionnaire(difficult: non difference:easy)	0.146	0.362	0.118
Acute illness during recent two weeks (yes:no)	47:135	47:142	0.905
Combined chronic diseases (yes:no)	94:88	115:74	0.076

[1]Mann-Whitney U test or χ^2 test.

We also enrolled and collected data from 47 consecutive CH-C patients who had completed one course of antiviral treatment. This included: (a) 24 patients who received pegylated interferon α-2a subcutaneously at a dose of 180 μg per week plus oral ribavirin (1 000 mg/d if body weight <75 kg, and 1 200 mg/d if body weight ⩾75 kg) for 6 mo; and (b) 23 patients receiving interferon α-2b subcutaneously 3 million units thrice a week plus oral ribavirin (1 000 mg/d if body weight <75 kg, and 1 200 mg/d if body weight ⩾75 kg) for 6 mo. We interviewed the subjects and recorded their SF-36 scores before the initiation of treatment, at the 12th wk of treatment, at the end of treatment, and at the 6th mo after the stopping treatment. The sustained virological responders were defined as those whose serum HCV RNA was detected to be negative by branched chain signal amplification assay (VERSANT HCV RNA 3.0 Quantitative Assay, Chiron Corporation, Tarrytown, NJ, USA) with a sensitivity of 3 200 copies/mL and reverse transcription-nested polymerase chain reaction with a sensitivity of 100 copies/mL at the 6th mo after stopping the treatment[18-21].

The data in the text and tables are expressed as mean ±SD. Mann-Whitney U tests, χ^2 tests, Fisher's exact tests, and paired t- tests were done appropriately depending on the type of data analyzed by using SPSS software (SPSS version 11.0, SPSS Inc., Chicago, IL, USA). Cronbach's α expressed both internal consistency of each domain and overall consistency of the SF-36. A two-tailed P<0.05 was considered statistically significant.

RESULTS

Three hundred and seventy-one subjects, including 182 CH-C patients and 189 age- and sex-matched control subjects without CH-C, received interviews and filled out questionnaires during the period of study. The internal consistency of each domain of the SF-36 shown by Cronbach's α was greater than 0.6 (GH: 0.75, PF: 0.87, RP: 0.90, RE: 0.88, SF: 0.69, BP: 0.81, VT: 0.83, MH: 0.67), and the

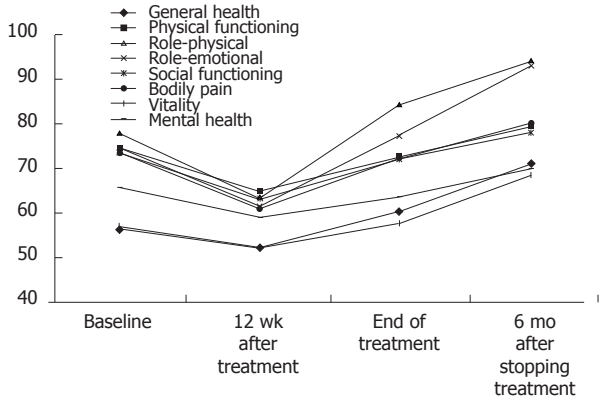

Figure 1 Impacts of antiviral treatment on mean scores of all domains of Short Form 36 (SF-36) Health-related Quality of Life Questionnaire in 47 chronic hepatitis C patients.

Table 2 Mean scores of eight domains of Short Form 36 (SF-36) Health-related Quality of Life (HRQOL) Questionnaire in subjects with and without chronic hepatitis C (CH-C)

SF-36 domains	CH-C patients (n = 182)	Non CH-C control group (n = 189)	P
General health	49.0±19.9	59.7±19.4	<0.001
Physical functioning	63.1±18.9	82.7±18.4	<0.001
Role-physical	58.0±43.9	69.6±40.3	0.008
Role-emotional	62.4±44.3	72.5±40.6	0.03
Social functioning	81.0±17.2	82.9±14.2	0.568
Body pain	72.3±16.9	70.5±17.6	0.319
Vitality	56.2±19.9	64.4±17.0	<0.001
Mental health	66.2±14.9	70.1±14.4	0.008

[1]Mann–Whitney *U* test.

Table 3 Characteristics and mean scores of Short Form 36 (SF-36) Health-related Quality of Life (HRQOL) Questionnaire in 47 CH-C subjects before initiation of antiviral treatment

Items	Overall subjects (n = 47)	Non-sustained virological responder (n = 26)	Sustained virological responder (n = 21)	P
Age (yr)	48.6±10.9	48.9±11.6	48.1±10.2	0.974
Sex (male:female)	41:06:00	24:02:00	17:04	0.386
General health	56.3±18.1	54.2±20.2	58.9±15.1	0.577
Physical functioning	74.6±15.8	75.0±11.3	74.0±20.3	0.352
Role-physical	77.7±34.7	76.9±30.8	78.6±39.8	0.343
Role-emotional	74.5±38.2	73.1±37.7	76.2±39.6	0.631
Social functioning	73.4±14.6	69.7±14.7	78.1±13.4	0.072
Body pain	73.5±18.8	71.5±19.8	75.9±17.6	0.322
Vitality	56.8±17.0	52.9±15.9	61.7±17.4	0.067
Mental health	65.6±15.8	61.5±13.6	70.7±17.2	0.024

[1]Mann–Whitney *U* test and Fisher's exact test.

overall consistency of the SF-36 (Cronbach's α) was 0.91. The demographic data for the 371 study subjects are listed in Table 1. Subjects with CH-C showed lower educational status than those without CH-C (P<0.01). The subjects with subjective difficulty in completing the questionnaire, with acute illness within the previous 2 wk, or combined chronic diseases showed no significant differences than the subjects without these characteristics.

The original scores of the SF-36 in 371 study subjects were translated to linear scores from 0 to 100, which are listed in Table 2. Subjects with CH-C had significantly lower scores in GH, PF, RP, RE, VT, and MH domains than those without CH-C (P<0.05). The domains of SF and BP showed no significant differences between subjects with or without CH-C.

Of the 47 CH-C patients who received antiviral treatment and completed the whole course of therapy, all had significantly lower mean HRQOL scores in all SF-36 domains at the 12th wk of treatment as compared with pretreatment values, but mean scores returned to pretreatment values by the end of treatment and significantly increased at the 6th mo after stopping the treatment (Figure 1). Among the 47 CH-C patients who received antiviral treatment, 21 were sustained virological responders and 26 were non-sustained virological responders. Sustained virological responders and non-sustained virological responders showed no significant difference for mean age, gender, and treatment modality. Mean scores for the SF-36 in all domains before antiviral treatment showed no significant difference between the two groups except that mean scores for MH was significantly higher in sustained virological responders than in non-sustained virological responders (Table 3).

Mean SF-36 scores at different time points of antiviral treatment in both sustained virological responders and non-sustained virological responders are listed in Tables 4 and 5, respectively. Compared to pretreatment values, subjects with sustained virological response showed significantly lower SF scores at the 12th wk of treatment. Mean scores of all SF-36 domains returned to pretreatment values by the end of treatment, and increased significantly by the 6th mo after stopping the treatment (P<0.05). For non-sustained virological responders, mean scores for all domains of the SF-36 significantly decreased at the 12th wk of treatment compared to pretreatment values, and did not increase significantly at the end of treatment and at the 6th mo after stopping the treatment.

DISCUSSION

Chronic HCV infection has become an important health issue in Taiwan and worldwide. Moreover, the chronic sequelae of liver cirrhosis and hepatocellular carcinoma have led to considerable morbidity and mortality in CH-C patients, and a negative impact on HRQOL in CH-C patients has been well documented for Western populations[22,23]. In Asia, impaired HRQOL in Korean patients with chronic viral hepatitis has been reported[24]. Till now, however, there have been no reports on HRQOL in Chinese patients with CH-C.

To the best of our knowledge, our study is the first study investigating HRQOL and the impact of antiviral treatment in Chinese CH-C patients. Our results showed

Table 4 Comparison of mean scores of Short Form 36 (SF-36) Health-related Quality of Life (HRQOL) Questionnaire in 21 sustained virological responders at different time points of antiviral treatment[1]

SF-36 domains/stages	Before treatment	At 12th wk of treatment	At the end of Treatment	At the 6th mo after stopping treatment
General health	58.9±19.1	59.1±19.5	67.9±11.5[a]	86.9±12.9[b]
Physical functioning	74.0±20.3	71.9±19.0	76.0±17.4	83.9±3.6[a]
Role-physical	78.6±39.8	77.4±40.2	91.7±24.1	100.0±0[a]
Role-emotional	76.2±39.6	74.6±43.3	87.3±30.7	98.2±7.6[a]
Social functioning	78.1±13.4	67.5±12.4[a]	72.0±11.8	89.9±10.9[b]
Body pain	75.9±17.6	67.4±21.3	77.1±15.3	94.1±10.9[b]
Vitality	61.7±17.4	60.0±14.0	63.1±16.0	81.0±8.5[b]
Mental health	70.7±17.2	65.7±11.0	67.0±16.0	82.9±6.7[b]

[1]By paired *t*- test; [a]$P<0.05$; [b]$P<0.01$.

Table 5 Comparison of mean scores of Short Form 36 (SF-36) Health-related Quality of Life (HRQOL) Questionnaire in 26 non-sustained virological responders at different time points of antiviral treatment[1]

SF-36 domains/stages	Before treatment	At the 12th wk of treatment	At the end of treatment	At the 6th mo after stopping treatment
General health	54.2±20.2	46.2±16.2[b]	53.1±19.7	54.1±19.3
Physical functioning	75.0±11.3	59.2±17.8[b]	68.9±12.7	75.7±8.7
Role-physical	76.9±30.8	51.9±43.0[b]	77.2±31.9	76.1±31.5
Role-emotional	73.1±37.7	51.3±45.4[a]	68.1±39.5	65.2±42.0
Social functioning	69.7±14.7	60.1±19.0[b]	71.7±15.6	69.0±17.6
Body pain	71.5±19.8	55.8±24.4[b]	67.2±17.1	67.7±24.0
Vitality	52.9±15.9	46.0±17.4[a]	52.8±18.0	55.0±14.5
Mental health	61.5±13.6	53.5±15.3[a]	60.5±14.6	61.7±15.3

[1]By paired *t*- test; [a]$P<0.05$; [b]$P<0.01$.

that HRQOL in Chinese CH-C patients in outpatient clinics was significantly impaired compared to non-CH-C subjects. This finding may reflect the fact that chronic viral hepatitis is more commonly seen in Chinese nationals than in Caucasians and the chronic sequelae of chronic viral hepatitis, such as cirrhosis and hepatocellular carcinoma, may have greatly affected the health of Chinese patients. We propose that Chinese patients with CH-C should be paid more attention regarding their HRQOL, health education and disease management.

Interferon was introduced for the antiviral treatment of CH-C in the late 1980s[25,26]. Due to the poorer sustained response rate using interferon therapy alone, combined treatment of interferon and ribavirin has been widely used in treating CH-C patients, which recently had 40-60% sustained virological response rate. However, the side effects of interferon with or without ribavirin, such as fatigue, malaise, flu-like symptoms, anemia, itching, skin rash or eruption, arthralgia, myalgia, depression, impaired sleeping quality, and loss of concentration, have been notable and have bothered CH-C patients during antiviral treatment[27]. Previous reports from Western countries had focused on comparison of HRQOL before and after antiviral therapy in CH-C patients, and they revealed that the HRQOL of CH-C patients could be improved through aggressive antiviral therapy, and sustained virological responders showed greater improvement[28-32]. Our results for Chinese CH-C patients were consistent with reports from Western countries that sustained virological responders to antiviral treatment have improved HRQOL.

Our results also revealed that all regimens of antiviral therapy impaired HRQOL of the subjects at early therapeutic stages, and especially bothered non-sustained virological responders. Initially therapeutic discomfort would impair patients' compliance and willingness to continue antiviral therapy. We suggest that active explanations of possible side effects and discomforts to patients before antiviral therapy are needed. If patients have insights into and are aware of possible adverse side effects, the compliance and continuity of antiviral therapy should be improved.

The limitations of our research are the different regimens of antiviral treatment. Therefore, we did not perform comparisons of the therapeutic effects and impact on HRQOL among the different kinds of antiviral regimens. Further evaluations and comparisons of the impact of different therapeutic regimens on HRQOL in CH-C patients are now indicated.

In conclusion, our study suggests that CH-C patients have a lower HRQOL than those without CH-C in Chinese populations visiting outpatient clinics. Antiviral treatment reduced HRQOL of CH-C patients at the early phase of treatment, mainly in non-sustained virological responders. The HRQOL may return to pretreatment values at the end of treatment and improve significantly at the 6th mo after stopping the treatment, mainly in sustained virological responders.

ACKNOWLEDGMENTS

The author wishes to thank Miss Jia-Ling Lin, Wei-Lin Chen, and senior students of the Department of Medicine, National Yang Ming University for selection of the subjects. The author especially expresses his thanks to Dr. Ming-Wei Lin for statistical assistance and Dr. Jui-Feng Rachel Lu for allowing us to use the SF-36 HRQOL Questionnaire, Taiwan version.

REFERENCES

1 **Hwang SJ**. Hepatitis C virus infection: an overview. *J Microbiol Immunol Infect* 2001; **34**: 227-234
2 **Seeff LB.** The natural history of chronic hepatitis C virus infection. *Clin Liver Dis* 1997; **1**: 587-602
3 **Lu SN**, Chue PY, Chen IL, Wang JH, Huang JF, Peng CF, Shih CH, Chang WY. Incidence of hepatitis C infection in a hepatitis C endemic township in southern Taiwan. *Kaohsiung J Med Sci* 1997**; 13**: 605-608
4 **Lin CC**, Hwang SJ, Chiou ST, Kuan CL, Chen LW, Lee TC, Lee MB, Lee HH, Hsu PS, Tsai ST. The prevalence and risk factors analysis of serum antibody to hepatitis C virus in the elders in northeast Taiwan. *J Chin Med Assoc* 2003; **66**: 103-108
5 **Hwang SJ**, Lee SD, Chan CY, Lu RH, Chang FY. A random-

ized, double blind, controlled trial of consensus interferon in the treatment of Chinese patients with chronic hepatitis C. *Am J Gastroenterol* 1999; **94**: 2496-2500

6 **Hwang S,** Lee S, Chu C, Lu R, Chang F. An open-label trial of consensus interferon 15 μg in the treatment of Chinese patients with chronic hepatitis C. *Hepatol Res* 2001; **19**:284-293

7 **Hwang SJ,** Chan CY, Lu RH, Wu JC, Lee SD. Randomized controlled trial of recombinant interferon-alpha 2b in the treatment of Chinese patients with chronic hepatitis C. *J Interferon Cytokine Res* 1995; **15:** 611-616

8 **Lai MY,** Kao JH, Yang PM, Wang JT, Chen PJ, Chan KW, Chu JS, Chen DS. Long-term efficacy of ribavirin plus interferon alfa in the treatment of chronic hepatitis C. *Gastroenterology* 1996; **111**: 1307-1312

9 **Ware JE**. John E. Ware Jr. on health status and quality of life assessment and the next generation of outcomes measurement. Interview by Marcia Stevic and Katie Berry. *J Healthc Qual* 1999; **21**: 12-17

10 **Keller SD**, Ware JE, Bentler PM, Aaronson NK, Alonso J, Apolone G, Bjorner JB, Brazier J, Bullinger M, Kaasa S, Leplège A, Sullivan M, Gandek B. Use of structural equation modeling to test the construct validity of the SF-36 Health Survey in ten countries: results from the IQOLA Project. International Quality of Life Assessment. *J Clin Epidemiol* 1998; **51**: 1179-1188

11 **Ware JE**, Gandek B, Kosinski M, Aaronson NK, Apolone G, Brazier J, Bullinger M, Kaasa S, Leplège A, Prieto L, Sullivan M, Thunedborg K. The equivalence of SF-36 summary health scores estimated using standard and country-specific algorithms in 10 countries: results from the IQOLA Project. International Quality of Life Assessment. *J Clin Epidemiol* 1998; **51**: 1167-1170

12 **Ware JE**, Kosinski M, Gandek B, Aaronson NK, Apolone G, Bech P, Brazier J, Bullinger M, Kaasa S, Leplège A, Prieto L, Sullivan M. The factor structure of the SF-36 Health Survey in 10 countries: results from the IQOLA Project. International Quality of Life Assessment. *J Clin Epidemiol* 1998; **51**: 1159-1165

13 **Gandek B**, Ware JE, Aaronson NK, Alonso J, Apolone G, Bjorner J, Brazier J, Bullinger M, Fukuhara S, Kaasa S, Leplège A, Sullivan M. Tests of data quality, scaling assumptions, and reliability of the SF-36 in eleven countries: results from the IQOLA Project. International Quality of Life Assessment. *J Clin Epidemiol* 1998; **51**: 1149-1158

14 **Wagner AK**, Gandek B, Aaronson NK, Acquadro C, Alonso J, Apolone G, Bullinger M, Bjorner J, Fukuhara S, Kaasa S, Leplège A, Sullivan M, Wood-Dauphinee S, Ware JE. Cross-cultural comparisons of the content of SF-36 translations across 10 countries: results from the IQOLA Project. International Quality of Life Assessment. *J Clin Epidemiol* 1998; **51**: 925-932

15 **Ware JE Jr**, Gandek B. Overview of the SF-36 Health Survey and the International Quality of Life Assessment (IQOLA) Project. *J Clin Epidemiol* 1998; **51**: 903-912

16 **Lu JFR**, Tseng HM, Tsai YJ. Assessment of health-related quality of life in Taiwan (I): development and psychometric testing of SF-36 Taiwan version. *Taiwan J. Public Health* 2003; **22**:501-511

17 **Tseng HM**, Lu JFR, Tsai YJ. Assessment of health-related quality of life in Taiwan (II): norming and validation of SF-36 Taiwan version. *Taiwan J. Public Health* 2003; **22**: 512-518

18 **Lu RH,** Hwang SJ, Chan CY, Chang FY, Lee SD. Quantitative measurement of serum HCV RNA in patients with chronic hepatitis C: comparison between Amplicor HCV monitor system and branched DNA signal amplification assay. *J Clin Lab Anal* 1998; **12**: 121-125

19 **Elbeik T**, Surtihadi J, Destree M, Gorlin J, Holodniy M, Jortani SA, Kuramoto K, Ng V, Valdes R, Valsamakis A, Terrault NA. Multicenter evaluation of the performance characteristics of the bayer VERSANT HCV RNA 3.0 assay (bDNA). *J Clin Microbiol* 2004; **42**: 563-569

20 **Hwang SJ**, Lee SD, Chan CY, Lu RH, Lo KJ. A randomized controlled trial of recombinant interferon alpha-2b in the treatment of Chinese patients with acute post-transfusion hepatitis C. *J Hepatol* 1994; **21**: 831-836

21 **Kao JH,** Chen PJ, Lai MY, Yang PM, Sheu JC, Wang TH, Chen DS. Mixed infections of hepatitis C virus as a factor in acute exacerbations of chronic type C hepatitis. *J Infect Dis* 1994; **170**: 1128-1133

22 **Ware JE Jr**, Bayliss MS, Mannocchia M, Davis GL. Health-related quality of life in chronic hepatitis C: impact of disease and treatment response. The Interventional Therapy Group. *Hepatology* 1999; **30**: 550-555

23 **Foster GR**, Goldin RD, Thomas HC. Chronic hepatitis C virus infection causes a significant reduction in quality of life in the absence of cirrhosis. *Hepatology* 1998; **27**: 209-212

24 **Park CK,** Park SY, Kim ES, Park JH, Hyun DW, Yun YM, Jo CM, Tak WY, Kweon YO, Kim SK, Choi YH, Park SG. [Assessment of quality of life and associated factors in patients with chronic viral liver disease] *Taehan Kan Hakhoe Chi* 2003; **9**: 212-221

25 **Davis GL,** Balart LA, Schiff ER, Lindsay K, Bodenheimer HC, Perrillo RP, Carey W, Jacobson IM, Payne J, Dienstag JL. Treatment of chronic hepatitis C with recombinant interferon alfa. A multicenter randomized, controlled trial. Hepatitis Interventional Therapy Group. *N Engl J Med* 1989; **321**: 1501-1506

26 **Di Bisceglie AM,** Martin P, Kassianides C, Lisker-Melman M, Murray L, Waggoner J, Goodman Z, Banks SM, Hoofnagle JH. Recombinant interferon alfa therapy for chronic hepatitis C. A randomized, double-blind, placebo-controlled trial. *N Engl J Med* 1989; **321**: 1506-1510

27 **Bonkovsky HL**, Woolley JM. Reduction of health-related quality of life in chronic hepatitis C and improvement with interferon therapy.The Consensus Interferon Study Group. *Hepatology* 1999; **29**: 264-270

28 **Kuehne FC**, Bethe U, Freedberg K, Goldie SJ. Treatment for hepatitis C virus in human immunodeficiency virus-infected patients: clinical benefits and cost-effectiveness. *Arch Intern Med* 2002; **162**: 2545-2556

29 **Michielsen P**, Brenard R, Reynaert H. Treatment of hepatitis C: impact on the virus, quality of life and the natural history. *Acta Gastroenterol Belg* 2002; **65**: 90-94

30 **Bernstein D**, Kleinman L, Barker CM, Revicki DA, Green J. Relationship of health-related quality of life to treatment adherence and sustained response in chronic hepatitis C patients. *Hepatology* 2002; **35**: 704-708

31 **Teuber G**, Berg T, Naumann U, Raedle J, Brinkmann S, Hopf U, Zeuzem S. Randomized, placebo-controlled, double-blind trial with interferon-alpha with and without amantadine sulphate in primary interferon-alpha nonresponders with chronic hepatitis C. *J Viral Hepat* 2001; **8**: 276-283

32 **McHutchison JG**, Ware JE, Bayliss MS, Pianko S, Albrecht JK, Cort S, Yang I, Neary MP.The effects of interferon alpha-2b in combination with ribavirin on health related quality of life and work productivity. *J Hepatol* 2001; **34**: 140-147

Science Editor Kumar M and Guo SY **Language Editor** Elsevier HK

PO Box 2345, Beijing 100023, China
www.wjgnet.com
wjg@wjgnet.com

ELSEVIER

World J Gastroenterol 2005;11(47):7499-7507
World Journal of Gastroenterology ISSN 1007-9327

Bactericidal and anti-adhesive properties of culinary and medicinal plants against *Helicobacter pylori*

Rachel O'Mahony, Huda Al-Khtheeri, Deepaka Weerasekera, Neluka Fernando, Dino Vaira, John Holton, Christelle Basset

Rachel O'Mahony, Huda Al-Khtheeri, John Holton, Centre for Infectious Diseases and International Health, Royal Free and University College London Medical School, London, United Kingdom
Deepeka Weerasekera, Department of Surgery, University of Sri Jayewardenapura, Colombo, Sri Lanka
Neluka Fernando, Department of Microbiology, University of Sri Jayewardenapura, Colombo, Sri Lanka
Dino Vaira, Department of Internal Medicine and Gastroenterology, University of Bologna, Bologna, Italy
Christelle Basset, INSERM 0114, Physiopathologie des Maladies Inflammatoires Intestinales, CHU Lille, France
Supported by the European Union on EC contract QLK2-CT-2001-01216 (ADRI)
Correspondence to: Rachel O'Mahony, Centre for Infectious Diseases and International Health, Royal Free and University College London Medical School, Windeyer Building, 46 Cleveland Street, London, W1P 6DB, United Kingdom. rachelomahony@hotmail.com
Telephone: +44-20-76799485
Received: 2005-03-02 Accepted: 2005-04-28

Abstract

AIM: To investigate the bactericidal and anti-adhesive properties of 25 plants against *Helicobacter pylori* (*H pylori*).

METHODS: Twenty-five plants were boiled in water to produce aqueous extracts that simulate the effect of cooking. The bactericidal activity of the extracts was assessed by a standard kill-curve with seven strains of *H pylori*. The anti-adhesive property was assessed by the inhibition of binding of four strains of FITC-labeled *H pylori* to stomach sections.

RESULTS: Of all the plants tested, eight plants, including Bengal quince, nightshade, garlic, dill, black pepper, coriander, fenugreek and black tea, were found to have no bactericidal effect on any of the isolates. Columbo weed, long pepper, parsley, tarragon, nutmeg, yellow-berried nightshade, threadstem carpetweed, sage and cinnamon had bactericidal activities against *H pylori*, but total inhibition of growth was not achieved in this study. Among the plants that killed *H pylori*, turmeric was the most efficient, followed by cumin, ginger, chilli, borage, black caraway, oregano and liquorice. Moreover, extracts of turmeric, borage and parsley were able to inhibit the adhesion of *H pylori* strains to the stomach sections.

CONCLUSION: Several plants that were tested in our study had bactericidal and/or anti-adhesive effects on *H pylori*. Ingestion of the plants with anti-adhesive properties could therefore provide a potent alternative therapy for *H pylori* infection, which overcomes the problem of resistance associated with current antibiotic treatment.

Key words: *H pylori*; Inhibition; Adhesion; Killing; Plants

O'Mahony R, Al-Khtheeri H, Weerasekera D, Fernando N, Vaira D, Holton J, Basset C. Bactericidal and anti-adhesive properties of culinary and medicinal plants against *Helicobacter pylori*. *World J Gastroenterol* 2005; 11(47): 7499-7507
http://www.wjgnet.com/1007-9327/11/7499.asp

INTRODUCTION

Over half the human population is colonized by *Helicobacter pylori* (*H pylori*), a Gram-negative, microaerophilic bacterium. If untreated, infection is usually life-long and leads to chronic active disease[1]. Although most infected people are asymptomatic, 5-10% of those infected with this bacterium develop severe gastroduodenal diseases, including gastric and duodenal ulcers, gastric lymphomas, and gastric adenocarcinomas[2].

The current and most effective treatment for peptic ulcer disease is a triple therapy regimen consisting of a proton pump inhibitor, such as omeprazole, and two antibiotics, clarithromycin and either amoxicillin or metronidazole. However, there is an increase that disturbs due to the prevalence of antibiotic resistance, which is high in some areas of the world. Metronidazole resistance is more common than clarithromycin, the latter particularly having an adverse effect on the eradication rate. Second line therapies following failure of one of the initial regimes include triple and quadruple regimens containing antibiotics, such as levofloxacin or furazolidone, or even regimens containing five agents. Although the use of molecular methods can rapidly detect antibiotic resistance and host polymorphisms, which may lead to reduced efficacy of treatment and thus eradication failure[3,4], this is not a long-term solution to the rising trend of antibiotic resistance.

Resistance to antibiotics is not limited to *H pylori* and has been an increasing problem for many years. There is therefore a constant need for new antimicrobial agents and novel approaches to treatment, ideally preventing disease, such as inhibition of adhesion or vaccination[5]. Plants are known to be the source of phytochemicals which are beneficial for health and could also prevent diseases[6]. Among these phytochemicals, two are of particular interest in the case of infectious diseases: antimicrobial and anti-adhesive agents.

Numerous studies have been undertaken in order to find antimicrobial agents from plants against organisms ranging from viruses to protozoa[7]. The major concern is the validation in human beings with well-designed clinical trials, and this has also been true for *H pylori* infection. Several *in vitro* studies have looked at the effect of plant extracts on *H pylori*. Anti-microbial effects have been reported for garlic[8,9], green tea[10], honey[11], thyme[12], some Iranian plants[13] and the essential oils from several species of mint[13]. Some of these studies have been validated in animals and confirmed the potential benefit of using plants as the source of anti-microbial agents against *H pylori*. Although garlic and cinnamon have been tested in human clinical trials with no significant effect[14], a recent study has shown that consumption of broccoli sprouts is associated with the eradication of *H pylori* in some patients[15], but more work needs to be done in determining the active ingredients of broccoli as well as performing studies on a larger number of patients.

The search for anti-adhesive agents represents the second alternative to antibiotic therapy, which has received less interest, although studies in animals and human beings have proved its potential as a new therapy[16]. Successful inhibition of adhesion has been shown *in vitro* with cranberry juice against *H pylori*[17] and for the seaweed *Cladosiphon fucoidan*[18]. Recently, Shibata *et al*.[19] have demonstrated that *Cladosiphon fucoidan* inhibits adhesion of *H pylori* to porcine gastric mucin. By adding the plant to the drinking water of infected Mongolian gerbils, the prevalence of animals with infection was shown to be markedly reduced. Lengsfeld *et al*.[20] have shown that adhesion of *H pylori* to human stomach sections was almost completely inhibited by pre-incubating *H pylori* with a fresh juice preparation of the fruit of the okra plant [*Abelmoschus esculentus* (L.) Moench]. Lengsfeld *et al*.[21] have also demonstrated that acidic high molecular weight galactans from blackcurrant seeds could inhibit adhesion of *H pylori* to human gastric mucosa tissue sections. Moreover, Lee *et al*.[22] have demonstrated the inhibition of *H pylori* adhesion by polysaccharide fractions of *Panax ginseng* and *Artemisia capillaris* to a human gastric adenocarcinoma epithelial cell line.

As mentioned earlier, many plants have been shown to kill microorganisms but rarely have been studied for their anti-adhesive properties. We have therefore investigated both the bactericidal and anti-adhesive properties of 25 plants against *H pylori*. Sixteen of them have never been tested before against *H pylori* and are plants that are frequently used in cooking as well as in medicine in Sri Lanka, Iran, and the Middle East. Moreover, we have used an *in situ* adhesion assay[23], with stomach tissues expressing either the Lewis a (Le a) or Lewis b (Le b) antigen, in order to determine whether the plant extracts inhibit adhesion by blocking the major *H pylori* adhesin BabA (which binds to Le b) or have an effect on other adhesins.

MATERIALS AND METHODS

H pylori isolates

H pylori NCTC 11637 and six fresh clinical strains from Italian patients with peptic ulcer disease [obtained by one of the authors (DV)] were used in the study. All strains were stored on beads at -80 ℃ until use. Bacteria were grown for 2 d on Columbia agar plates supplemented with 5% horse blood (Oxoid, UK) at 37 ℃ under microaerobic conditions. The number of bacterial cells was determined by obtaining viable counts of serial dilutions and measurement of the optical absorbance at 600 nm (Ultrospec II, LKB, UK) of a suspension of bacterial cells to prepare a standard curve for *H pylori*. All studies thereafter used the same concentration of organism based upon its absorbance.

Fluorescent labeling of H pylori isolates

Suspensions of 1×10^9 cells/mL were prepared from 1 mL carbonate buffer (0.15 mol/L NaCl/0.1 mol/L Na_2CO_3, pH 9.0). Five microliters of a 10 mg/mL fluorescein isothiocyanate (FITC, Isomer I, Sigma, UK) solution in dimethyl sulfoxide (DMSO, Sigma, UK) was added to each bacterial suspension and then incubated for 1 h with continuous shaking. The suspensions were then washed three times with phosphate buffered saline (PBS, 8.0 g/L NaCl; 1.21 g/L K_2HPO_4; 0.34 g/L KH_2PO_4, pH 7.4) containing 0.5 g/L Tween 20 (PBST; Sigma, UK), and resuspended in PBS. Labeling was confirmed by using flow cytometry (FACSCalibur, Becton Dickinson, UK). All incubation and washing steps were carried out in the dark at room temperature.

Plants

Twenty-five plants were obtained from different sources and are described in Table 1. Extracts from the plants were prepared as follows: for turmeric, ginger, fenugreek, cumin, fennel, coriander, and chilli, plants were boiled to 100 ℃ in sterile distilled water (100 mg/mL), filtered through sterile gauze, neutralized to pH 7.0 and then sterilized. Extracts from all the other plants were prepared as follows: plants were boiled in sterile distilled water (100 mg/mL) for 10 min, allowed to cool and filtered through sterile filter paper (Grade 1, Whatman, UK). Fresh garlic, black peppercorns and cinnamon sticks were finely chopped before being boiled. All extracts were stored in the dark at -20 ℃ until use. Before the experiments of adhesion, plant extracts were filtered again (Grade 1 filter paper, Whatman, UK).

Stomach sections

H pylori-negative biopsies of human stomach were obtained by one of the authors (DV), with the consent of the Ethics Committee, St Orsola Hospital, Bologna. Two

Table 1 Plants used in the study

English name	Sri Lankan name	Scientific name	Part of the plant used	Source	Use
Bengal quince	Belly	*Aegle marmelos*	Root	Sri Lanka	In cooking & medicine
Black caraway (Europe)/Black Cumin (USA)		*Nigella sativa*	Seeds	UK, Supermarket	In cooking & medicine
Black pepper	Gammiris	*Piper nigrum*	Seed berries/fruit	UK, Supermarket	In cooking & medicine
Black tea	Thee	*Camellia sinensis*	Leaves and shoots	Sri Lanka	In cooking
Borage (Starflower)		*Borago officinalis*	Flowers	Iran	In cooking & medicine
Chilli	Mirise	*Capsicum anunum*	Fruit	Sri Lanka	In cooking & medicine
Cinnamon	Curundu	*Cinnamomum verum*	Bark	UK, Supermarket	In cooking & medicine
Columbo weed	Veneval	*Coscinium fenestratum*	climbing root	Sri Lanka	In medicine
Coriander	Kottamalli	*Coriandrum sativum*	Seeds	Sri Lanka	In cooking & medicine
Cumin (small cumin)	Suduru	*Cuminum cyminum*	Seeds	Sri Lanka	In cooking & medicine
Dilla	Sududurru	*Anthum graveolens*	Leaves	UK, Supermarket	In cooking & medicine
Fenugreek	Mathe seeds	*Trigonella foenum-graecum*	Seeds	Sri Lanka	In cooking & medicine
Garlica	Sudulunu	*Allium sativum*	Bulb	UK, Supermarket	In cooking & medicine
Ginger	E'guru	*Zingiber officinale*	Rhizome	Sri Lanka	In cooking & medicine
Liquorice	Val'mee	*Glycyrrhiza glabra apofosa*	Stem	Sri Lanka	In cooking & medicine
Long pepper	Tiphili	*Piper longum*	Seeds	Sri Lanka	In cooking & medicine
Nightshade	Ela battu	*Solanum surattense*	Fruit and root	Sri Lanka	In medicine
Nutmeg	Sadikka	*Myristica fragans*	Kernel	UK, Supermarket	In cooking & medicine
Oreganoa	Oregano	*Origanum vulgare*	Leaves	UK, Supermarket	In cooking & medicine
Parsleya	Parsley	*Petroselinum crispum*	Leaves	UK, Supermarket	In cooking & medicine
Sagea	Minchi	*Salvia officinalis*	Leaves	UK, Supermarket	In cooking & medicine
Tarragona	Tarragon Path	*Artemisia dracunculoses/ dracunculus*	Leaves	UK, Supermarket	In cooking & medicine
Threadstem carpetweed	Paradagam	*Mollugo cerviana*	Seeds	Sri Lanka	In medicine
Turmeric	Kaha	*Curcuma longa*	Rhizome	Sri Lanka	In cooking & medicine
Yellow-berried nightshade	Katu val batu	*Solanum xanthocarpum*	Whole plant	Sri Lanka	In medicine

These plants were bought as both fresh and dried material.

sets of formalin-fixed stomach biopsies were used: those whose epithelial cells expressed the Lewis a blood group antigen (Le a stomach) and those expressing the Lewis b blood group antigen (Le b stomach). Five-micrometer thick sections of the stomach were cut using a Leica SM2400 rocking microtome. Sections were collected on polished glass slides coated with Vectabond (Vector Laboratories, UK). An antigen retrieval step was used by boiling for 5 min in an 800-W microwave in plastic Coplin jars containing 15 mL of citrate buffer (pH 6.0, 100 mol/L sodium citrate tribasic dihydrate, Sigma, UK). The Lewis phenotype of the tissue was determined by standard immunohistochemical staining using the DAKO EnVision Plus HRP kit (DAKO, UK) with anti-Le a and anti-Le b antibodies generously donated by Dr. J Bara, Hôpital St-Antoine, Paris, France. Both antibodies were supplied at a concentration between 1 and 5 μg/mL and diluted 1:10 for the anti-Le a antibodies and 1:50 for the anti-Le b antibodies.

Viable colony count

Bactericidal activity of the plant extracts was determined by a viable colony count. One hundred microliters of a suspension of 10^8 bacteria/mL was added to 900 μL of plant extract for 60 min. The control consisted of *H pylori* incubated with sterile distilled water. Serial 10-fold dilutions were made, and 100 μL of each dilution was plated onto 50 g/L horse blood agar (Oxoid, UK). These were incubated in gas jars under microaerophilic conditions using CampyPak (Oxoid, UK) for 3 d, and colonies were counted (colony forming units per milliliter, CFU/mL). Plant extracts that killed 100% of *H pylori* cells at 60 min (i.e. no colonies grew) were further tested at 0-, 15-, 30-, and 60-min intervals. All experiments were performed three times. The effectiveness of the plants at killing *H pylori* was expressed as percentage inhibition of colony growth (i.e. percentage of bacteria killed) compared to the control.

Microscopic examination

In order to validate the inhibition of adhesion by the plant extracts, any lytic effect of the extracts on the bacterial cells was first examined. FITC-labelled and non-labelled bacteria (1×10^8 cells/mL) were centrifuged (9 000 *g* for 3 min), re-suspended in 500 μL of undiluted plant extract (100 mg/mL) and incubated with continuous shaking for 1 h at room temperature in the dark. After incubation, bacteria were centrifuged, washed in PBST and re-suspended in 500 μL sterile distilled water. One drop of the bacterial suspension was Gram stained. Using a Zeiss light microscope, the slides were observed for bacterial lysis. All the plant extracts were examined, except long pepper and threadstem carpetweed, which were not tested due to their limited supply. The negative control consisted of *H pylori* incubated with sterile distilled water and the positive control of *H pylori* incubated with Puregene PCR

Table 2 Bactericidal activity of plants against *Helicobacter pylori*, determined using viable colony count. '% inhibition of growth' indicates the percentage of bacteria that were killed by the plants, (i.e. the colonies did not grow), compared to the control.

Plant name		*H pylori* clinical strains						
		NCTC strain	1	2	3	4	5	6
Turmeric	% inhibition of growth	100	100	100	100	100	100	100
	Minimum of time (min)	15	15	15	15	15	15	15
Ginger	% inhibition of growth	100	100	100	100	100	100	100
	Minimum of time (min)	30	30	30	30	30	30	30
Fenugreek	% inhibition of growth	0	0	0	0	0	0	0
	Minimum of time (min)	60	60	60	60	60	60	60
Cumin (small cumin)	% inhibition of growth	100	100	100	100	100	100	100
	Minimum of time (min)	30	30	30	30	30	30	30
Coriander	% inhibition of growth	0	0	0	0	0	0	0
	Minimum of time (min)	60	60	60	60	60	60	60
Chilli	% inhibition of growth	100	100	100	100	100	100	100
	Minimum of time (min)	30	30	30	30	30	30	30
Bengal quince	% inhibition of growth	0	0	0	0	0	0	0
	Minimum of time (min)	60	60	60	60	60	60	60
Columbo weed	% inhibition of growth	99.9	99.9	99.9	99.5	99.8	99.9	99.8
	Minimum of time (min)	60	60	60	60	60	60	60
Yellow-berried nightshade	% inhibition of growth	99.9	99.7	99.5	99.9	99.9	99.9	99.9
	Minimum of time (min)	60	60	60	60	60	60	60
Liquorice	% inhibition of growth	100	100	100	100	100	100	100
	Minimum of time (min)	60	60	60	60	60	60	30
Nightshade	% inhibition of growth	0	0	0	0	0	0	0
	Minimum of time (min)	60	60	60	60	60	60	60
Long pepper	% inhibition of growth	99.9	99.9	100	99.3	99.7	99.9	99.9
	Minimum of time (min)	60	60	60	60	60	60	60
Threadstem carpetweed	% inhibition of growth	99.9	99.7	99.9	99.9	99.9	99.9	99.9
	Minimum of time (min)	60	60	60	60	60	60	60
Garlic	% inhibition of growth	0	0	0	0	0	0	0
	Minimum of time (min)	60	60	60	60	60	60	60
Parsley	% inhibition of growth	99.6	99.3	99.9	99.6	99.9	99.99	99.8
	Minimum of time (min)	60	60	60	60	60	60	60
Dill	% inhibition of growth	0	0	0	0	0	0	0
	Minimum of time (min)	60	60	60	60	60	60	60
Sage	% inhibition of growth	99.9	99.9	99.7	99.5	99.9	99.9	99.9
	Minimum of time (min)	60	60	60	60	60	60	60
Oregano	% inhibition of growth	100	100	100	100	100	100	100
	Minimum of time (min)	30	30	30	30	60	30	30
Tarragon	% inhibition of growth	96.9	99.4	99.2	99.9	99.9	99.9	99.9
	Minimum of time (min)	60	60	60	60	60	60	60
Nutmeg	% inhibition of growth	95.9	95.6	99.5	99.4	99.2	96.1	98.9
	Minimum of time (min)	60	60	60	60	60	60	60
Black pepper	% inhibition of growth	0	0	0	0	0	0	0
	Minimum of time (min)	60	60	60	60	60	60	60
Cinnamon	% inhibition of growth	100	100	100	100	99.9	99.9	100
	Minimum of time (min)	60	30	30	30	60	60	60
Black caraway (Europe)/ Black cumin (USA)	% inhibition of growth	100	100	100	100	100	100	100
	Minimum of time (min)	60	60	60	60	60	60	60
Borage (Starflower)	% inhibition of growth	100	100	100	100	100	100	100
	Minimum of time (min)	60	60	60	60	60	60	60
Black tea	% inhibition of growth	0	0	0	0	0	0	0
	Minimum of time (min)	60	60	60	60	60	60	60

cell lysis solution (Flowgen, UK). The lysis experiments were performed twice.

Adhesion and adhesion-inhibition assay

Tissue sections were incubated for 30 min in a humidified atmosphere with 200 μL of blocking buffer (PBST+20 g/L BSA) per slide. Next, the sections were washed three times, by placing in a slide rack in a glass trough containing 350 mL of PBST, on a rotator for 10 min. Suspensions of FITC-*H pylori* were centrifuged and re-

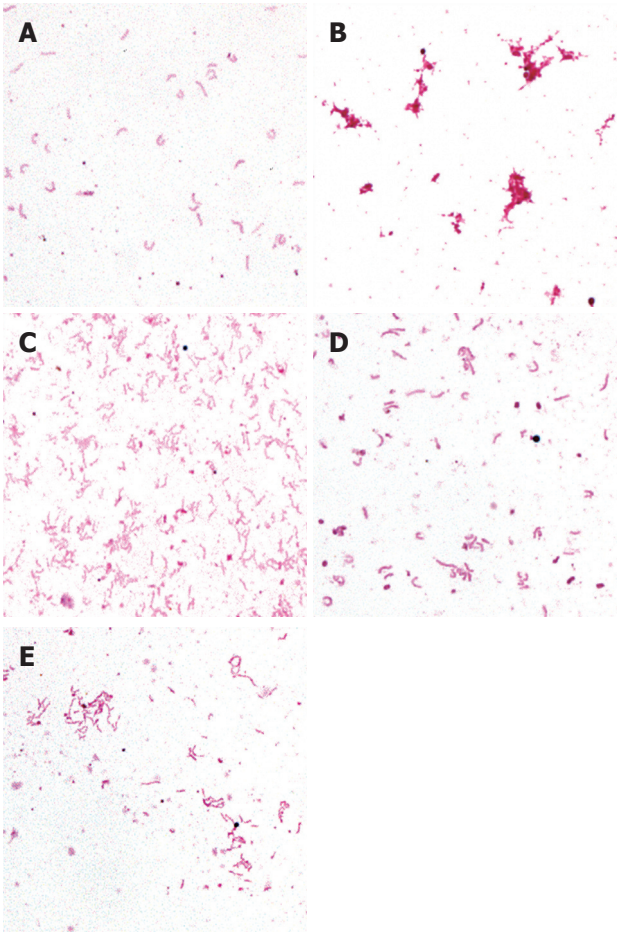

Figure 1 Bright-field images showing *H pylori* lysis experiment. **A**: negative control (*H pylori* + distilled water); **B**: positive control (*H pylori* + cell lysis solution); **C**: *H pylori* + 0.05 g/mL turmeric; **D**: *H pylori* + 0.05 g/mL borage; **E**: *H pylorii* + 0.05 g/mL parsley. Images taken using x100 objective.

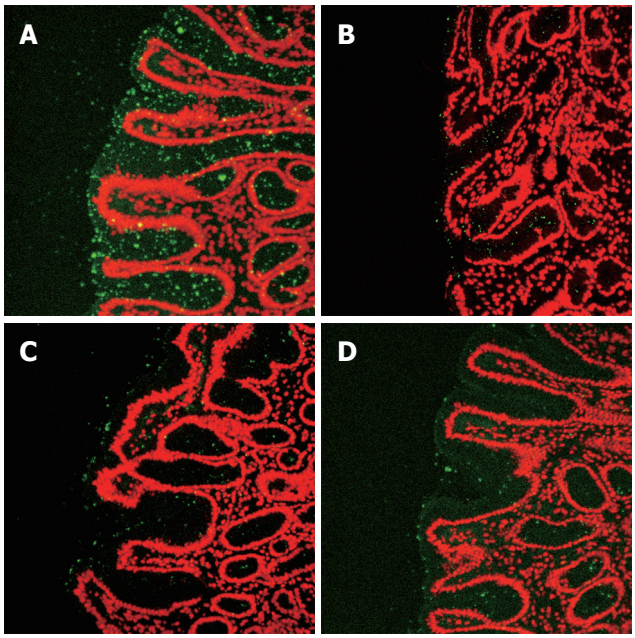

Figure 2 Confocal images showing inhibition of *H pylori* adhesion by **A**: distilled water (control); **B**: turmeric (0.05 g/mL); **C**: borage (0.05 g/mL) and **D**: parsley (0.05 g/mL); to stomach sections expressing the Lewis b blood group antigen.

suspended in plant extract to give 1×10^8 bacteria/mL. This was incubated with continuous shaking for 2 h, and then washed with the blocking buffer. For the controls, bacteria were re-suspended in sterile distilled water. The bacterial suspension (200 μL) was then added to each of the stomach sections and incubated in a humidified atmosphere for 1 h. After incubation, slides were washed in PBST as previously, and 200 μL of propidium iodide (PI, 5 μg/mL, Sigma, UK) was added and each slide was incubated for 3 min. Slides were then washed twice in PBST, air-dried and mounted with Vectashield (V-1000, Vector Laboratories, UK). All incubation and washing steps were carried out in the dark at room temperature. Two tissue sections were used for each plant that was tested.

All plant extracts were initially screened for inhibition of adhesion properties at a concentration of 50 mg/mL (diluted in sterile distilled water) and incubated with *H pylori* strain 11 637 and Le b stomach sections. For those plants which had an anti-adhesive effect, the inhibition assay was repeated using Le a and Le b stomach sections, and the plants were diluted to concentrations of 5, 10, and 50 mg/mL. Because 50 mg/mL was found to give a good inhibition of adhesion, for all further inhibition experiments, all plants were used at this concentration. Inhibition of adhesion experiments were then performed on three clinical strains. All experiments were performed three times.

Quantification of binding

Sections were observed using a Laser Scanning Confocal Microscope (Zeiss: Axiovert 100 TV) with a ×20 Zeiss LD-ACHR objective. The excitation wavelengths were 488 nm (for FITC) and 568 nm (for PI). We used 522- and 605-nm band-pass filters to acquire FITC emission and PI emission, respectively. Digital images (512×512 pixels) of the sections were captured using a Biorad Lasersharp 2000 Confocal Laser Scanning System. Images were converted to TIF files for processing. Two photographs showing adjacent areas of the tissue were taken for each tissue section. Using these digital images, the number of adherent *H pylori* were quantified as previously reported (Region of Interest method with standard area method of counting) using Metamorph Image analysis software (version 4.5r, Universal Imaging Corporation, USA)[23]. Using the Mann-Whitney (non-parametric) test, the difference between the number of adherent cells for each plant was compared statistically to the controls (0 μg/mL plant extract).

RESULTS

Bactericidal properties of plants

Among the 25 plants tested for their bactericidal activity against *H pylori*, eight showed no activity after 60 min of incubation, these were Bengal quince, nightshade, garlic, dill, black pepper, coriander, fenugreek and tea (data

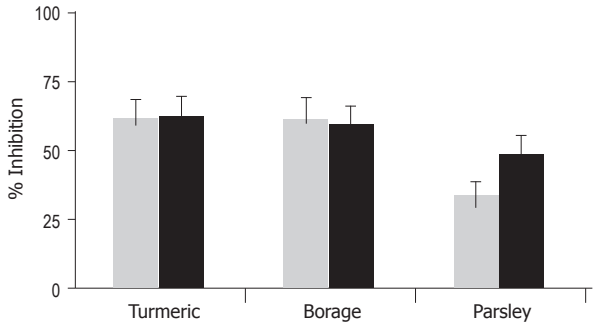

Figure 3 Inhibition of *H pylori* adhesion by turmeric, borage and parsley to stomach sections expressing either the Lewis a or Lewis b blood group antigen. Experiments were performed three times using four strains of *H pylori*. Mean percentage of inhibition is shown for each plant. Gray bar, Lewis a stomach; Black bar, Lewis b stomach.

not shown). The other 17 plants had activity (results are summarized in Table 2). Turmeric was the most efficient in killing the seven strains within 15 min. Ginger, cumin, and chilli were able to kill all the strains within 30 min, whereas liquorice, oregano, black caraway, and borage killed the strains within 60 min. Cinnamon had a bactericidal activity against *H pylori,* although the seven bacterial strains differed in their sensitivity. Moreover, the bacterial colonies were very small, reflecting some resistance to cinnamon. Finally, the following plants showed a bactericidal activity against *H pylori* but without achieving a complete inhibition of growth (i.e., killing all the colonies) within 60 min: columbo weed, yellow-berried nightshade, long pepper, threadstem carpetweed, sage, tarragon, nutmeg, and parsley. Small colonies were seen with yellow-berried nightshade, threadstem carpetweed, and sage.

Morphological studies

None of the 23 plant extracts that were tested caused lysis of *H pylori* cells, as the organisms that remained were spiral and intact like the negative control. Bacterial cells incubated with Puregene PCR cell lysis solution were lysed and no intact spiral shaped bacteria could be observed (Figure 1).

Anti-adhesive properties of plants

Of the 23 plants screened for anti-adhesive properties, turmeric, borage, and fresh parsley (50 mg/mL) were found to inhibit adhesion of *H pylori* 11637 to the stomach sections expressing the Le b antigen (Figure 2). Further testing of these three plant extracts using *H pylori* 11637 and three clinical isolates confirmed that they were able to inhibit *H pylori* adhesion to stomach sections expressing either the Le b antigen or the Le a antigen (Figure 3). Mean inhibition rates of the four strains to the stomach sections expressing the Le a antigen were 61.9%, 61.1%, and 33.9% for turmeric, borage and parsley, respectively. The differences between the number of adherent bacteria compared to the controls (0 μg/mL) were: highly significant ($P<0.01$) for turmeric; not quite significant ($P = 0.07$) for borage; and not significant ($P>0.05$) for parsley. For sections expressing the Le b antigen, inhibition rates were 62.3%, 59.5%, and 48.5% for turmeric, borage and parsley, respectively. The differences between the number of adherent bacteria compared to the control (0 μg/mL) were: not quite significant ($P = 0.07$) for turmeric; significant ($P<0.05$) for borage; and not significant ($P>0.05$) for parsley. There was no significant difference between the number of adherent bacteria (to Le a or Le b stomach sections) when comparing each of the plant-treatments, except for adhesion of bacteria to Le a sections where there was a highly significant difference ($P<0.001$) between turmeric and parsley.

DISCUSSION

Investigations into plant materials as alternative sources of antimicrobials have become more common over the past few years, due to the increased rate of development of antibiotic resistant organisms. New strategies to combat infection are also being sought and one such strategy is the use of 'anti-adhesive' molecules, targeting the primary step of infection - adhesion of the organism to host tissue[5]. In this study, we therefore examined both the anti-microbial and anti-adhesive properties of 25 plant extracts against *H pylori*, obtained simply by boiling, as would occur during the normal cooking process.

Of the eight plants that were not able to kill *H pylori* after 60 min of incubation (Bengal quince, nightshade, garlic, dill, black pepper, coriander, fenugreek, and black tea), two had been tested previously against *H pylori*. Several studies have shown that garlic does kill *H pylori in vitro* and *in vivo*[8,9]. It is probably due to the boiling method of extraction that this effect was not observed in this study, since boiling has been shown to reduce the inhibitory activity of garlic against *H pylori*[24,25]. Fenugreek sprouts have been shown to have high anti-microbial activity against *H pylori*[26]. In the present study, fenugreek appeared inactive but the seeds were examined rather than sprouts, which may account for the difference in results. Green tea catechins have previously been reported to have antibacterial effect against *H pylori*, which was confirmed in Mongolian gerbils[27]. Moreover, Chinese tea has been shown to reduce *H pylori* infection in patients[28]. In this study, black tea was tested, but no bactericidal activity against *H pylori* was observed.

Columbo weed, long pepper, parsley, tarragon, nutmeg, yellow-berried nightshade, threadstem carpetweed, sage, and cinnamon had bactericidal activity against *H pylori*, but total inhibition of growth was not achieved within 60 min. Moreover, a reduced colony size was observed with some of them, such as yellow-berried nightshade, threadstem carpetweed, sage, and cinnamon. Nutmeg[29], tarragon[30], and cinnamon[31] have previously been reported to inhibit the growth of *H pylori in vitro*. When tested in clinical trials, however, cinnamon was found to be ineffective at eradicating *H pylori*[32].

Among the plants that killed *H pylori*, turmeric was the most efficient, followed by cumin, ginger, and chilli. These results confirmed what has been published before

regarding turmeric[33], chilli[34], and ginger[35], but cumin has not been previously tested. Other plants, such as borage, black caraway, and oregano, which have never been tested before against *H pylori*, were also found to have bactericidal effects. Finally, the previous reported bactericidal effect of liquorice has been confirmed[36,37].

As well as looking at their bactericidal activity, all these plants were also tested for their anti-adhesive effects, using an *in situ* adhesion assay. Stomach tissues expressing either the Le a or Le b antigen were used. This was in order to determine whether the plant extracts inhibit adhesion by blocking the major *H pylori* adhesin BabA, which binds to Le b, or have an effect on other adhesins. Most studies have not attempted to determine which adhesin is being blocked, and this may be important because combinations of plants targeting several different adhesins may provide a more potent therapeutic treatment.

Extracts of turmeric, borage, and parsley were able to inhibit the adhesion of *H pylori* strains to both Le a and Le b stomach sections. Turmeric was the most effective at inhibiting *H pylori* adhesion to both Le a and Le b stomach sections, followed by borage and fresh parsley. From these results, it seems that both turmeric and borage could inhibit adhesins other than BabA, because the percentage of inhibition was almost exactly the same for Le a and Le b stomach sections. Parsley possibly inhibited BabA as well as other adhesins, because inhibition occurred on Le a and Le b stomach sections, but was higher for Le b stomach sections, indicating that it had a greater effect at inhibiting BabA. The morphological studies demonstrated that the reduction in adhesion caused by these plant extracts was due to the true inhibition of adhesion, but not because the plants caused the bacteria to lyse. Tarragon is the only plant in this study that has been tested previously for its anti-adhesive effects, where it was found to inhibit *H pylori* adhesion to human gastric adenocarcinoma cells[22]. However, in the present study, tarragon failed to inhibit *H pylori* adhesion to human stomach sections. This discrepancy is probably due to the differences between using cell-lines and whole-tissue.

Plants contain multiple organic components including phenols, quinones, flavones, tannins, terpenoids, and alkaloids all of which are known to have bactericidal effects[7]. These substances are also water-soluble and therefore very likely to be present in the plant extracts produced in this study, and are likely candidates responsible for the killing effect of the extracts on *H pylori*. Plants also contain many water-soluble proteins, lectins and carbohydrates which may bind specifically to sugar residues, polysaccharides, glycoproteins or glycolipids, such as the adhesins present on the cell surface of *H pylori*. In the event of such interactions occurring, the result would be to block the availability of the adhesin to its receptor and hence prevent adhesion of the bacterium to the stomach sections.

Despite the success of many plant materials at killing organisms, resistance can develop to these too, as shown in this study. The present work is of importance because plant extracts were shown to inhibit adhesion of *H pylori* to the stomach - an alternative strategy to bactericidal compounds. Because inhibition of adhesion works on the principle of sterically blocking bacteria from attaching to host tissue, the likelihood of resistance developing in organisms, which occurs when the organism is killed, is less likely.

Although the majority of individuals colonized by *H pylori* are asymptomatic, a proportion of patients develop peptic ulcers (duodenal and gastric), and an even smaller proportion develop gastric cancer. Globally, *H pylori* is the major cause of gastric cancer and has been classified as a Class I carcinogen by the WHO. Some plants are known to have anti-ulcerogenic and anti-cancer effects. Most of the plants tested here, which have bactericidal and/or anti-adhesive properties, also have anti-ulcerogenic or anti-cancer effects, for example, turmeric[38,39], ginger[40,41], cumin[42,43], borage[44], liquorice[45], and parsley[46]. Chilli has recently been shown to have detrimental effects on the gastric mucosa[47]. The anti-cancer and anti-ulcerogenic effects of ginger, cumin, liquorice, parsley, turmeric, and borage combined with their bactericidal and anti-adhesive properties, as shown in this study, suggests that ingestion of these six plants could have important therapeutic implications for patients with *H pylori*-induced peptic ulcer disease or gastric cancer. As turmeric killed 100% of organisms within 15 min, it could therefore be a useful anti-*Helicobacter* agent *in vivo*, because, if given orally, it would be able to kill *H pylori* despite the short amount of time that it would remain in the stomach during digestion. Moreover, these plants could be used in combination with antibiotics, possibly increasing the success of eradication, as has been shown *in vitro* for cranberry juice[48].

Most studies have used plant extracts that are obtained by chemical processing, for example, ethanol extracts. In developing countries where antibiotics are less freely available, such processing methods of plants would be impractical and/or expensive. This present study is therefore of importance because it has demonstrated that several plant extracts are effective against *H pylori* and are obtained simply by boiling the plants. Such a method may provide a treatment that is simple, relatively inexpensive and could be incorporated into the normal diet of the patient, which is highly favorable. Herbal treatments are usually unregulated and the safety of plants consumed is often unknown. The plants used and shown to be effective in this study are already commonly consumed, and thus they are already known to be safe.

Although the cidal and anti-adhesive effects of ginger, cumin, liquorice, parsley, turmeric, and borage have been shown *in vitro,* further studies are needed to be carried out to investigate their effects *in vivo,* to see whether the extracts are able to remain effective despite the harsh process of digestion.

ACKNOWLEDGMENTS

We are grateful to Martin Avedian for the idea of testing borage and for its supply and Ms A. Al-Dossary (School of Hygiene and Tropical Medicine, UK) for providing black caraway.

REFERENCES

1 **Achtman M,** Suerbaum S. Helicobacter pylori: Molecular and Cellular Biology. *Horizon scientific, Norfolk* 2001; 61
2 **Montecucco C,** Rappuoli R. Living dangerously: how Helicobacter pylori survives in the human stomach. *Nat Rev Mol Cell Biol* 2001; **2:** 457-466
3 **Basset C,** Holton J, Gatta L, Ricci C, Bernabucci V, Liuzzi G, Vaira D. *Helicobacter pylori* infection: anything new should we know? *Aliment Pharmacol Ther* 2004; **20** Suppl 2: 31-41
4 **Mégraud F**. H pylori antibiotic resistance: prevalence, importance, and advances in testing. *Gut 2004;* **53:** 1374-1384
5 **Basset C,** Holton J, O'Mahony R, Roitt I. Innate immunity and pathogen-host interaction. *Vaccine* 2003; **21** Suppl 2: S12-S23
6 **Lampe JW**. Health effects of vegetables and fruit: assessing mechanisms of action in human experimental studies. *Am J Clin Nutr* 1999; **70:** 475S-490S
7 **Cowan MM**. Plant products as antimicrobial agents. *Clin Microbiol Rev* 1999; **12:** 564-582
8 **Jonkers D,** van den Broek E, van Dooren I, Thijs C, Dorant E, Hageman G, Stobberingh E. Antibacterial effect of garlic and omeprazole on Helicobacter pylori. *J Antimicrob Chemother* 1999; **43:** 837-839
9 **Iimuro M,** Shibata H, Kawamori T, Matsumoto T, Arakawa T, Sugimura T, Wakabayashi K. Suppressive effects of garlic extract on Helicobacter pylori-induced gastritis in Mongolian gerbils. *Cancer Lett* 2002; **187:** 61-68
10 **Matsubara S,** Shibata H, Ishikawa F, Yokokura T, Takahashi M, Sugimura T, Wakabayashi K. Suppression of Helicobacter pylori-induced gastritis by green tea extract in Mongolian gerbils. *Biochem Biophys Res Commun* 2003; **310:** 715-719
11 **al Somal N,** Coley KE, Molan PC, Hancock BM. Susceptibility of Helicobacter pylori to the antibacterial activity of manuka honey. *J R Soc Med* 1994; **87:** 9-12
12 **Tabak M,** Armon R, Potasman I, Neeman I. In vitro inhibition of Helicobacter pylori by extracts of thyme. *J Appl Bacteriol* 1996; **80:** 667-672
13 **Nariman F,** Eftekhar F, Habibi Z, Falsafi T. Anti-Helicobacter pylori activities of six Iranian plants. *Helicobacter* 2004; **9:** 146-151
14 **Martin KW,** Ernst E. Herbal medicines for treatment of bacterial infections: a review of controlled clinical trials. *J Antimicrob Chemother* 2003; **51:** 241-246
15 **Galan MV,** Kishan AA, Silverman AL. Oral broccoli sprouts for the treatment of Helicobacter pylori infection: a preliminary report. *Dig Dis Sci* 2004; **49:** 1088-1090
16 **Ofek I,** Hasty DL, Sharon N. Anti-adhesion therapy of bacterial diseases: prospects and problems. *FEMS Immunol Med Microbiol* 2003; **38:** 181-191
17 **Burger O**, Ofek I, Tabak M, Weiss EI, Sharon N, Neeman I. A high molecular mass constituent of cranberry juice inhibits helicobacter pylori adhesion to human gastric mucus. *FEMS Immunol Med Microbiol* 2000; **29:** 295-301
18 **Shibata H,** KimuraTakagi I, Nagaoka M, Hashimoto S, Sawada H, Ueyama S, Yokokura T. Inhibitory effect of Cladosiphon fucoidan on the adhesion of Helicobacter pylori to human gastric cells. *J Nutr Sci Vitaminol (Tokyo)* 1999; **45:** 325-336
19 **Shibata H,** Iimuro M, Uchiya N, Kawamori T, Nagaoka M, Ueyama S, Hashimoto S, Yokokura T, Sugimura T, Wakabayashi K. Preventive effects of Cladosiphon fucoidan against Helicobacter pylori infection in Mongolian gerbils. *Helicobacter* 2003; **8:** 59-65
20 **Lengsfeld C**, Titgemeyer F, Faller G, Hensel A. Glycosylated compounds from okra inhibit adhesion of Helicobacter pylori to human gastric mucosa. *J Agric Food Chem* 2004; **52:** 1495-1503
21 **Lengsfeld C,** Deters A, Faller G, Hensel A. High molecular weight polysaccharides from black currant seeds inhibit adhesion of Helicobacter pylori to human gastric mucosa. *Planta Med* 2004; **70:** 620-626
22 **Lee JH,** Park EK, Uhm CS, Chung MS, Kim KH. Inhibition of Helicobacter pylori adhesion to human gastric adenocarcinoma epithelial cells by acidic polysaccharides from Artemisia capillaris and Panax ginseng. *Planta Med* 2004; **70:** 615-619
23 **O'Mahony R,** Basset C, Holton J, Vaira D, Roitt I. Comparison of image analysis software packages in the assessment of adhesion of microorganisms to mucosal epithelium using confocal laser scanning microscopy. *J Microbiol Methods* 2005; **61:** 105-126
24 **Cañizares P,** Gracia I,Gómez LA, García A, Martín De Argila C, Boixeda D, de Rafael L. Thermal degradation of allicin in garlic extracts and its implication on the inhibition of the in-vitro growth of Helicobacter pylori. *Biotechnol Prog* 2004; **20:** 32-37
25 **Cañizares P,** Gracia I, Gómez LA, Martín de Argila C, Boixeda D, García A, de Rafael L. Allyl-thiosulfinates, the bacteriostatic compounds of garlic against Helicobacter pylori. *Biotechnol Prog* 2004; **20:** 397-401
26 **Randhir R,** Lin YT, Shetty K. Phenolics, their antioxidant and antimicrobial activity in dark germinated fenugreek sprouts in response to peptide and phytochemical elicitors. *Asia Pac J Clin Nutr* 2004; **13:** 295-307
27 **Takabayashi F,** Harada N, Yamada M, Murohisa B, Oguni I. Inhibitory effect of green tea catechins in combination with sucralfate on Helicobacter pylori infection in Mongolian gerbils. *J Gastroenterol* 2004; **39:** 61-63
28 **Yee YK,** Koo MW, Szeto ML. Chinese tea consumption and lower risk of Helicobacter infection. *J Gastroenterol Hepatol* 2002; **17:** 552-555
29 **Bhamarapravati S,** Pendland SL, Mahady GB. Extracts of spice and food plants from Thai traditional medicine inhibit the growth of the human carcinogen Helicobacter pylori. *In Vivo* 2003; **17:** 541-544
30 **Wang YC,** Huang TL. Screening of anti-Helicobacter pylori herbs deriving from Taiwanese folk medicinal plants. *FEMS Immunol Med Microbiol* 2005; **43:** 295-300
31 **Tabak M,** Armon R, Neeman I. Cinnamon extracts' inhibitory effect on Helicobacter pylori. *J Ethnopharmacol* 1999; **67:** 269-277
32 **Nir Y,** Potasman I, Stermer E, Tabak M, Neeman I. Controlled trial of the effect of cinnamon extract on Helicobacter pylori. *Helicobacter* 2000; **5:** 94-97
33 **Mahady GB,** Pendland SL, Yun G, Lu ZZ. Turmeric (Curcuma longa) and curcumin inhibit the growth of Helicobacter pylori, a group 1 carcinogen. *Anticancer Res* 2002; **22:** 4179-4181
34 **Jones NL,** Shabib S, Sherman PM. Capsaicin as an inhibitor of the growth of the gastric pathogen Helicobacter pylori. *FEMS Microbiol Lett* 1997; **146:** 223-227
35 **Mahady GB,** Pendland SL, Yun GS, Lu ZZ, Stoia A. Ginger (Zingiber officinale Roscoe) and the gingerols inhibit the growth of Cag A+ strains of Helicobacter pylori. *Anticancer Res* 2003; **23:** 3699-3702
36 **Fukai T,** Marumo A, Kaitou K, Kanda T, Terada S, Nomura T. Anti-Helicobacter pylori flavonoids from licorice extract. *Life Sci* 2002; **71:** 1449-1463
37 **Krausse R,** Bielenberg J, Blaschek W, Ullmann U. *In vitro* anti-Helicobacter pylori activity of Extractum liquiritiae, glycyrrhizin and its metabolites. *J Antimicrob Chemother* 2004; **54:** 243-246
38 **Azuine MA,** Bhide SV. Chemopreventive effect of turmeric against stomach and skin tumors induced by chemical carcinogens in Swiss mice. *Nutr Cancer* 1992; **17:** 77-83
39 **Huang MT,** Lou YR, Ma W, Newmark HL, Reuhl KR, Conney AH. Inhibitory effects of dietary curcumin on forestomach, duodenal, and colon carcinogenesis in mice. *Cancer Res* 1994; **54:** 5841-5847
40 **Yamahara J,** Mochizuki M, Rong HQ, Matsuda H, Fujimura H. The anti-ulcer effect in rats of ginger constituents. *J Ethnopharmacol* 1988; **23:** 299-304
41 **Yoshikawa M,** Yamaguchi S, Kunimi K, Matsuda H, Okuno Y, Yamahara J, Murakami N. Stomachic principles in ginger. III. An anti-ulcer principle, 6-gingesulfonic acid, and three monoacyldigalactosylglycerols, gingerglycolipids A, B, and C, from

Zingiberis Rhizoma originating in Taiwan. *Chem Pharm Bull (Tokyo)* 1994; **42:** 1226-1230

42 **Aruna K,** Sivaramakrishnan VM. Anticarcinogenic effects of some Indian plant products. *Food Chem Toxicol* 1992; **30:** 953-956

43 **Gagandeep** S, Méndiz E, Rao AR, Kale RK. **Chemopreventive** effects of Cuminum cyminum in chemically induced forestomach and uterine cervix tumors in murine model systems. *Nutr Cancer* 2003; **47:** 171-180

44 **González CA,** Sanz JM, Marcos G, Pita S, Brullet E, Saigi E, Badia A, Agudo A, Riboli E. Borage consumption as a possible gastric cancer protective factor. *Cancer Epidemiol Biomarkers Prev* 1993; **2:** 157-158

45 **Dehpour AR,** Zolfaghari ME, Samadian T, Vahedi Y. The protective effect of liquorice components and their derivatives against gastric ulcer induced by aspirin in rats. *J Pharm Pharmacol* 1994; **46:** 148-149

46 **Al-Howiriny T,** Al-Sohaibani M, El-Tahir K, Rafatullah S. Prevention of experimentally-induced gastric ulcers in rats by an ethanolic extract of **"Parsley" Petroselinum crispum.** *Am J Chin Med* 2003; **31:** 699-711

47 **López-Carrillo L, López**-Cervantes M, Robles-Díaz G, Ramírez-Espitia A, Mohar-Betancourt A, Meneses-García A, López-Vidal Y, Blair A. Capsaicin consumption, Helicobacter pylori positivity and gastric cancer in Mexico. *Int J Cancer* 2003; **106:** 277-282

48 **Shmuely H,** Burger O, Neeman I, Yahav J, Samra Z, Niv Y, Sharon N, Weiss E, Athamna A, Tabak M, Ofek I. Susceptibility of Helicobacter pylori isolates to the antiadhesion activity of a high-molecular-weight constituent of cranberry. *Diagn Microbiol Infect Dis* 2004; **50:** 231-235

Science Editor Kumar M **Language Editor** Elsevier HK

PO Box 2345, Beijing 100023, China
www.wjgnet.com
wjg@wjgnet.com

ELSEVIER

World J Gastroenterol 2005;11(47):7508-7511
World Journal of Gastroenterology ISSN 1007-9327

• *RAPID COMMUNICATION* •

Learning curve of laparoscopy-assisted distal gastrectomy with systemic lymphadenectomy for early gastric cancer

Min-Chan Kim, Ghap-Joong Jung, Hyung-Ho Kim

Min-Chan Kim, Ghap-Joong Jung, Department of Surgery, Dong-A University College of Medicine, Busan, Korea
Hyung-Ho Kim, Department of Surgery, Seoul National University Bundang Hospital, Gyeonggi-do, Korea
Correspondence to: Hyung-Ho Kim, Department of Surgery, Seoul National University Bundang Hospital 300 Gumi-dong Bundang-gu, Seongnam-si, Gyeonggi-do 463-707 Korea. hhkim@snubh.org
Telephone: +82-31-787-7095 Fax: +82-31-787-4055
Received: 2005-04-27 Accepted: 2005-07-15

Abstract

AIM: To evaluate the nature of the "learning curve" for laparoscopy-assisted distal gastrectomy (LADG) with systemic lymphadenectomy for early gastric cancer.

METHODS: The data of 90 consecutive patients with early gastric cancer who underwent LADG with systemic lymphadenectomy between April 2003 and November 2004 were reviewed. The 90 patients were divided into 9 sequential groups of 10 cases in each group and the average operative time of these 9 groups were determined. Other learning indicators, such as transfusion requirements, conversion rates to open surgery, postoperative complication, time to first flatus, and postoperative hospital stay, were evaluated.

RESULTS: After the first 10 LADGs, the operative time reached its first plateau (230-240 min/operation) and then reached a second plateau (<200 min/operation) for the final 30 cases. Although a significant improvement in the operative time was noted after the first 50 cases, there were no significant differences in transfusion requirements, conversion rates to open surgery, postoperative complications, time to first flatus, or postoperative hospital stay between the groups.

CONCLUSION: Based on operative time analysis, this study show that experience of 50 cases of LADG with systemic lymphadenectomy for early gastric cancer is required to achieve optimum proficiency.

Key words: Laparoscopic gastrectomy; Systemic lymphadenectomy; Learning curve

Kim MC, Jung GJ, Kim HH. Learning curve of laparoscopy-assisted distal gastrectomy with systemic lymphadenectomy for early gastric cancer. *World J Gastroenterol* 2005; 11(47): 7508-7511
http://www.wjgnet.com/1007-9327/11/7508.asp

INTRODUCTION

In Korea, an aggressive surgical approach of gastrectomy with systemic lymphadenectomy has long been the standard treatment, even for superficial cancers, because of the limitations of preoperative assessment for the depth of tumor invasion[1,2] and imaging technique for the detection of regional lymph node metastasis[3-5]. Since its introduction in 1992, laparoscopy-assisted distal gastrectomy (LADG) has become a viable treatment alternative for patients with early gastric cancer[6-8]. Many studies have been conducted on the safety, efficacy, and feasibility of this procedure[9-14]. Surgeons who are seeking to undertake, or who are currently practicing this procedure, should be aware that it is considered as an advanced laparoscopic procedure and it is associated with a significant learning curve. Although many reports have been issued on the learning curves of laparoscopic cholecystectomy[15], laparoscopy-assisted colectomy[16], and laparoscopic urologic procedures[17], no report has been issued on the learning curve of LADG with systemic lymphadenectomy for early gastric cancer.

We hypothesized that the point at which proficiency is reached (as defined as the learning curve plateau) would be associated with improvements in perioperative outcomes, including transfusion requirement, conversion rates to open surgery, postoperative complications, time to first flatus, and postoperative hospital stay. The purpose of this study was to define the nature of the "learning curve" for LADG with systemic lymphadenectomy for early gastric cancer.

MATERIALS AND METHODS

Patients

The Dong-A University Medical Center's stomach cancer database and the medical records of 90 consecutive patients with early gastric cancer who underwent LADG with systemic lymphadenectomy by a single surgeon (MC Kim) between April 2003 and November 2004 were reviewed. The review board of the Dong-A University Medical Center approved the protocol used for LADG with systemic lymphadenectomy in early gastric cancer patients and written informed consent was obtained from every patient that

agreed to LADG with systemic lymphadenectomy.

Patients' characteristics, pathologic findings, and postoperative outcomes were evaluated. Cases with mucosal lesions suitable for endoscopic mucosal resection (EMR) and with a history of upper abdominal surgery were excluded. The indication for EMR at our hospital is a Tm lesion with a size of <2 cm with no ulcer.

Surgical technique

A periumbilical trocar (10 mm) was inserted using the open surgical method, and four trocars were introduced under laparoscopic guidance. A rigid electrolaparoscope (25 °, Panoview plus telescope, Richard Wolf, Germany) was then introduced through the umbilical port. Under pneumoperitoneum of 10-14 mmHg, the greater omentum was divided proximally at about 4 cm from the gastroepiploic arcade towards the lower pole of the spleen, using a new hemostatic device (The Ligasure™ Vessel Sealing System, Valleylab, Boulder, CO, USA). The roots of the left gastroepiploic vessels were then exposed using an ultrasonic dissector (Autosonix™, Tyco/US Surgical Inc., Norwalk, CT, USA) and a hook-type bovie, and divided with double Ligasure™ clamps. Their perforating branches were dissected away from the greater curvature using an ultrasonic dissector (Autosonix™, Tyco/US Surgical Inc., Norwalk, CT, USA), and the right gastroepiploic vein and artery were divided individually at their roots with double clips. The right gastric artery was then exposed and divided at its origin with double clips, thus creating room for the dissection of the suprapyloric lymph nodes (No. 5 lymph nodes). The duodenum was then transected 1 cm distal to the pylorus, using an endoscopic stapling device (Endo cutter 45 staple; Ethicon, OH, USA). After switching to an electrolaparoscope (50°, Panoview plus telescope, Richard Wolf, Germany), no. 8a (the common hepatic artery, anterosuperior group), and no. 9 (the celiac axis) lymph nodes were dissected along each artery, by using ultrasonic dissection and a hook-type bovie. In some cases, no. 11p (the proximal splenic artery), 12a (the hepatic artery), and 14v (the superior mesenteric vein) lymph nodes were dissected. The left gastric vein was then divided, and the root of the left gastric artery was exposed and divided with double clips, allowing dissection of the left gastric artery (No. 7 lymph nodes). The perigastric lymph nodes were dissected along the upper lesser curvature up to the esophagogastric junction. A 5-cm upper transverse skin incision that separated three fingers from the substernal angle, was made from the midline to the right side for the Billroth I reconstruction or to the left side for the Billroth II reconstruction. The distal two-thirds of the stomach were resected using a stapler (Proximate linear cutter 100 mm; Ethicon, OH, USA). Billroth I gastroduodenostomy was performed using a circular stapler (Proximate CDH 25; Ethicon, OH, USA), and Billroth II gastrojejunostomy with side to side jejunojejunostomy using two endoscopic stapling devices (Endo cutter 45 staple; Ethicon, OH, USA) or by hand sewing. Irrigation and observation of the operative field were achieved under pneumoperitoneum after closing the 5-cm minilaparotomy wound. Each trocar wound was closed after a closed suction drain had been placed around the anastomosis.

Table 1 Characteristics and pathologic results of patients

	Total	1–50 cases	51–90 cases	*P*
Total number of patients	90	50	40	
Age (yr, mean±SD)	55.7±12.0	56.3±11.3	54.9±12.9	0.6907
Sex ratio (male:female)	50:40	26:24	24:16	0.5854
Body mass index (kg/m^2, mean±SD)	22.8±2.7	23.1±2.5	22.5±2.9	0.1700
Comorbidity (%)	29 (32.2)	13 (26.0)	16 (40.0)	0.2359
Method of reconstruction				0.5343
B-I	67	39	28	
B-II	23	11	12	
T stage				0.1758
Tis	2	1	1	
Tm	66	33	33	
Tsm	22	16	6	
N stage				0.8439
N0	87	49	38	
N1	3	1	2	
Extent of lymphadenectomy				0.4709
D1+α	11	8	3	
D1+β	68	36	32	
D2	11	6	5	
Retrieved LN number (mean±SD)	27.0±9.7	25.4±10.0	28.9±8.9	0.1330
Resection margin (cm, mean±SD)				
Proximal	4.2±2.6	3.8±2.4	4.7±2.7	0.1472
Distal	5.1±3.1	5.0±3.1	5.3±3.0	0.5752

LN, lymph node; D1+α: D1+no. 7 LN; D1+β: D1+no. 7, 8a, 9 LN; D2: D1+β+no. 11p, 12a, 14v LN.

Perioperative management

All patients were managed routinely using a standardized postoperative protocol as follows: (1) No nasogastric intubation or preoperative mechanical bowel preparation; (2) the use of one closed suction drain; (3) sips of water at 48 h after the operation; (4) clear liquid diet after first flatus; (5) the discharge of the patients after tolerance of a soft diet for 2 d; and (6) no postoperative transfusion unless the hemoglobin level fell to or below 80 g/L and the patient complains of anemic symptoms. All patients received a continuous intravenous infusion of mixed analgesics (butorphanol 20 mg, ketorolac 300 mg, metoclopramide 30 mg, saline 100 mL) at 1 mL/h for 3-4 d after surgery.

Calculation of the learning curve

To define the learning curve, the 90 patients were divided into 9 sequential groups of 10 cases in each group and the average operative time of these 9 groups were determined. Other learning indicators, such as transfusion requirements, conversion rates to open surgery, postoperative complication, time to first flatus, and postoperative hospital stay, were evaluated for statistical significance. Statistical analysis was performed using the unpaired Student's *t*-test and the Mann-Whitney *U*-test for continuous variables, and the χ^2 and ANOVA tests for categorical variables. For all the three tests, $P<0.05$ was considered statistically significant. Data were expressed as mean±SD.

Table 2 Overall postoperative outcomes

	Total	1–50 cases	51–90 cases	*P*
Operative time (min, mean±SD)	227.2±48.0	251.3±47.3	227.2±48.0	<0.0001
No. of transfused patients (%)	5 (5.6)	3 (6.0)	2 (5.0)	0.837
Time to first flatus (d, mean±SD)	3.1±0.8	3.1±0.9	3.1±0.6	0.805
Postoperative hospital stay (d, mean±SD)	7.5±1.2	7.6±1.4	7.4±1.0	0.610
Postoperative complication (%)	13 (14.4)	6 (12.0)	7 (17.5)	0.663

Table 3 Comparison of postoperative outcomes (first 50 patients *vs* last 40 patients)

	Operative time (min)	Open conversion	Transfusion requirement	Time to first flatus (d)	Hospital stay (d)	Complication (patients)
First 50 patients	251.3±47.3	1	3	3.1±0.9	7.6±1.4	7
Last 40 patients	197.0±27.7	1	2	3.1±0.6	7.4±1.0	6

P<0.0001

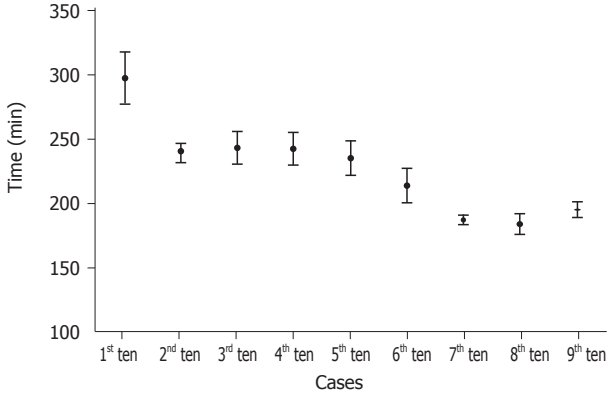

Figure 1 LADG with systemic lymphadenectomy (operative time *vs* number of cases experienced).

RESULTS

Patients' characteristics and pathologic findings are summarized in Table 1. The mean patient body mass index was 22.8 kg/m^2. Of the 22 patients with a submucosal lesion, two patients had one metastatic lymph node. There were no significant differences in patients' characteristics, oncological radicality, and pathology between the two groups.

Mean operative time was 227.2 min (Table 2). Open conversion was required intraoperatively in two cases due to excessive intra-abdominal fat (n = 1) or intra-abdominal adhesion (n = 1). The body mass index of the patient with excessive intra-abdominal fat was 29.3 kg/m^2. Fifteen complications occurred in 13 patients. These complications included wound complications, intra-abdominal bleeding, anastomotic bleeding, dumping syndrome, subcutaneous emphysema, intra-abdominal abscess, and anastomotic stricture. All these complications were treated by conservative management without reoperation. No deaths occurred in this series.

Defining the learning curve

Figure 1 shows two plateaus in operative time *vs* cumulative case number plot for LADG with systemic lymphadenectomy. After the first 10 LADGs, the operative time reached its first plateau (230-240 min/operation) and then reached a second plateau (<200 min/operation) for the final 30 cases, which was between 30 and 40 min/operation faster than that for the first 10-50 cases. We considered that learning was complete at the second plateau, and not at the first. When we compared the postoperative outcomes of the first 50 cases with the last 40 cases, no significant difference was observed despite the fact that mean operative time had been obviously reduced for the last 40 cases (Table 3).

DISCUSSION

The proportion of cancers invading the mucosa or submucosa represents about a half of surgical gastric cancer cases in Korea. Recently, many gastric surgeons have expressed a high level of interest in laparoscopic surgery for early gastric cancer, because laparoscopic surgery has been proven to have substantial advantages over conventional open surgery[14,18-20]. However, LADG with systemic lymphadenectomy is considered technically more complicated than other laparoscopic procedures (e.g., cholecystectomy, Nissen fundoplication, colon resection, or splenectomy) because many great vessels must be identified and extensive lymph node dissection is necessary for radical gastrectomy.

The definition of the completion of learning is clearly arbitrary. To determine that learning has occurred, some have used the minimization of operative complications or the reaching of a steady mean operative time as measures. According to the learning curves of other laparoscopic procedures, surgeons who have performed more than 20 laparoscopic cholecystectomies[15] or 8 laparoscopic urologic procedures[17] have lower complication rates. As for colorectal surgery, approximately 11-15 completed laparoscopic colectomies were found to be needed to comfortably learn this procedure[21]. We hypothesized that the point at which learning has been achieved (as defined by the operative time plateau) would be associated with an improved postoperative outcome. However, though a significant improvement in operative time was noted after the first 50

cases, this did not correspond with a significant reduction in other postoperative outcomes, including transfusion requirements, conversion rates to open surgery, postoperative complications, time to first flatus, or postoperative hospital stay. This finding may be attributed to, firstly, regardless of operative time, transfusion requirement or conversion to open surgery which was rare, and postoperative complications occurred evenly in each of the nine groups. Second, time to first flatus was not proportioned to operative time. The mean time to first flatus in the present study was 3.1 d, although flatus has been reported to return at a mean 2.5 d after laparoscopic gastrectomy and 3.5 d after conventional open gastrectomy[22,23]. However, the previous result of 2.6 d may have been caused by less extensive lymphadenectomy (D1+α).

Although Kitano *et al*.[11] reported that the mean operative time of 116 cases for LADG with D1+α lymphadenectomy (perigastric and no. 7 lymph nodes dissection) was 234 min, Noshiro *et al*.[13] found a mean operative time for 79 cases of LADG with D1+β lymphadenectomy of over 300 min. In another study of 43 LADGs was performed for 2 years, the mean operative time was 225 min despite LADG with D1+β lymphadenectomy[24]. We performed 90 LADGs with D1+β lymphadenectomy for 20 mo, and mean operative time of the present study was 227.2 min. We believe that the operative time required for LADG in gastric cancer is related to the extent of the lymphadenectomy, constant LADG practice, the experience of open radical gastrectomy, information and familiarity with the laparoscopic system and instruments, and the skill of the operative team.

In conclusion, based on operative time analysis, our study shows that experience of 50 cases of LADG with systemic lymphadenectomy for early gastric cancer is required to achieve optimum proficiency.

REFERENCES

1 **Polkowski M**, Palucki J, Wronska E, Szawlowski A, Nasierowska-Guttmejer A, Butruk E. Endosonography versus helical computed tomography for locoregional staging of gastric cancer. *Endoscopy* 2004; **36**: 617-623

2 **Ishigami S**, Yoshinaka H, Sakamoto F, Natsugoe S, Tokuda K, Nakajo A, Matsumoto M, Okumura H, Hokita S, Aikou T. Preoperative assessment of the depth of early gastric cancer invasion by transabdominal ultrasound sonography (TUS): a comparison with endoscopic ultrasound sonography (EUS). *Hepatogastroenterology* 2004; **51**: 1202-1205

3 **Kim MC**, Kim HH, Jung GJ, Lee JH, Choi SR, Kang DY, Roh MS, Jeong JS. Lymphatic mapping and sentinel node biopsy using 99mTc tin colloid in gastric cancer. *Ann Surg* 2004; **239**: 383-387

4 **Hayes N**, Karat D, Scott DJ, Raimes SA, Griffin SM. Radical lymphadenectomy in the management of early gastric cancer. *Br J Surg* 1996; **83**: 1421-1423

5 **Maruyama K**, Sasako M, Kinoshita T, Sano T, Katai H. Can sentinel node biopsy indicate rational extent of lymphadenectomy in gastric cancer surgery? Fundamental and new information on lymph-node dissection. *Langenbecks Arch Surg* 1999; **384**: 149-157

6 **Huscher CG**, Mingoli A, Sgarzini G, Sansonetti A, Di Paola M, Recher A, Ponzano C. Laparoscopic versus open subtotal gastrectomy for distal gastric cancer: five-year results of a randomized prospective trial. *Ann Surg* 2005; **241**: 232-237

7 **Adrales GL**, Gandsas A, Mastrangelo MJ, Schwartz R. An introduction to laparoscopic gastric resection. *Curr Surg* 2003; **60**: 385-389

8 **Kitano S**, Shiraishi N. Current status of laparoscopic gastrectomy for cancer in Japan. *Surg Endosc* 2004; **18**: 182-185

9 **Huscher CG**, Mingoli A, Sgarzini G, Sansonetti A, Lirici MM, Napolitano C, Piro F. Videolaparoscopic total and subtotal gastrectomy with extended lymph node dissection for gastric cancer. *Am J Surg*. 2004; **188**: 728-735

10 **Shimizu S**, Noshiro H, Nagai E, Uchiyama A, Tanaka M. Laparoscopic gastric surgery in a Japanese institution: analysis of the initial 100 procedures. *J Am Coll Surg* 2003; **197**: 372-378

11 **Kitano S**, Shiraishi N, Kakisako K, Yasuda K, Inomata M, Adachi Y. Laparoscopy-assisted Billroth-I gastrectomy (LADG) for cancer: our 10 years' experience. *Surg Laparosc Endosc Percutan Tech* 2002; **12**: 204-207

12 **Uyama I**, Sugioka A, Fujita J, Komori Y, Matsui H, Soga R, Wakayama A, Okamoto K, Ohyama A, Hasumi A. Completely laparoscopic extra**perigastric lymph node dissection for gastric** malignancies located in the middle or lower third of the stomach. *Gastric Cancer* 1999; **2**: 186-190

13 **Noshiro H**, Shimizu S, Nagai E, Ohuchida K, Tanaka M. Laparoscopy-assisted distal gastrectomy for early gastric cancer: is it beneficial for patients of heavier weight? *Ann Surg* 2003; **238**: 680-685

14 **Adachi Y**, Suematsu T, Shiraishi N, Katsuta T, Morimoto A, Kitano S, Akazawa K. Quality of life after laparoscopy-assisted Billroth I gastrectomy. *Ann Surg* 1999; **229**: 49-54

15 **Moore MJ**, Bennett CL. The learning curve for laparoscopic cholecystectomy. The Southern Surgeons Club. *Am J Surg* 1995; **170**: 55-59

16 **Bennett CL**, Stryker SJ, Ferreira MR, Adams J, Beart RW. The learning curve for laparoscopic colorectal surgery. Preliminary results from a prospective analysis of 1194 laparoscopic-assisted colectomies. *Arch Surg* 1997; **132**: 41-44; discussion 45

17 **See WA**, Cooper CS, Fisher RJ. Predictors of laparoscopic complications after formal training in laparoscopic surgery. *JAMA* 1993 ; **270**: 2689-2692

18 **Kitano S**, Shiraishi N, Fujii K, Yasuda K, Inomata M, Adachi Y. A randomized controlled trial comparing open vs laparoscopy-assisted distal gastrec**tomy for the treatment of early** gastric cancer: an interim report. *Surgery* 2002; **131**: S306-S311

19 **Adachi Y**, Shiraishi N, Shiromizu A, Bandoh T, Aramaki M, Kitano S. Laparoscopy-assisted Billroth I gastrectomy compared with conventional open gastrectomy. *Arch Surg* 2000; **135**: 806-810

20 **Weber KJ**, Reyes CD, Gagner M, Divino CM. Comparison of laparoscopic and open gastrectomy for malignant disease. *Surg Endosc* 2003; **17**: 968-971

21 **Simons AJ**, Anthone GJ, Ortega AE, Franklin M, Fleshman J, Geis WP, Beart RW. Laparoscopic-assisted colectomy learning curve. *Dis Colon Rectum* 1995; **38**: 600-603

22 **Kim MC**, Park SY, Jung GJ, Kim HH, Noh SH. **The usefulness** of intraoperative needle decompression of the colon during radical gastrectomy**--a prospective and randomized trial.** *Hepatogastroenterology* 2004; **51**: 97-99

23 **Mochiki E**, Nakabayashi T, Kamimura H, Haga N, Asao T, Kuwano H. Gastrointestinal recovery and outcome after laparoscopy-assisted versus conventional open distal gastrectomy for early gastric cancer. *World J Surg* 2002; **26**: 1145-1149

24 **Fujiwara M**, Kodera Y, Kasai Y, Kanyama Y, Hibi K, Ito K, Akiyama S, Nakao A. Laparoscopy-assisted distal gastrectomy with systemic lymph node dissection for early gastric carcinoma: a review of 43 cases. *J Am Coll Surg* 2003; **196**: 75-81

Science Editor Wang XL and Guo SY **Language Editor** Elsevier HK

PO Box 2345, Beijing 100023, China
www.wjgnet.com
wjg@wjgnet.com

ELSEVIER

World J Gastroenterol 2005;11(47):7512-7514
World Journal of Gastroenterology ISSN 1007-9327

• *RAPID COMMUNICATION* •

Baseline characterization of patients aged 70 years and above with hepatocellular carcinoma

Makoto Nakamuta, Shusuke Morizono, Motoyuki Kohjima, Kazuhiro Kotoh, Munechika Enjoji

Makoto Nakamuta, Shusuke Morizono, Motoyuki Kohjima, Kazuhiro Kotoh, Munechika Enjoji, Department of Medicine and Bioregulatory Science, Graduate School of Medical Sciences, Kyushu University, Fukuoka 812-8582, Japan
Correspondence to: Makoto Nakamuta, Department of Medicine and Bioregulatory Science, Graduate School of Medical Sciences, Kyushu University, 3-1-1 Maidashi, Higashi-ku, Fukuoka 812-5282, Japan. nakamuta@intmed3.med.kyushu-u.ac.jp
Telephone: +81-92-642-5282 Fax: +81-92-642-5287
Received: 2005-03-28 Accepted: 2005-05-24

Abstract

AIM: To characterize the baseline profiles of patients aged 70 years and above with hepatocellular carcinoma (HCC).

METHODS: A series of 127 consecutive patients with HCC were enrolled between 2000 and 2004, and none of them had been diagnosed as having HCC previously. Baseline profiles, including parameters of hepatic function such as serum transaminase and prothrombin time [PT (% activity)] were compared between patients aged ⩾70 and <70 years.

RESULTS: Patients ⩾70 years old showed significantly lower levels of aspartate aminotransferase ($P = 0.04$) and alanine aminotransferase ($P = 0.01$), and significantly higher PTs ($P = 0.04$) and platelet counts ($P = 0.02$). Concomitantly, among ⩾70-year-old patients, HCC was more common in non-cirrhotics, whereas among patients <70 years old, HCC was more common in cirrhotics. There was no significant difference between the groups in the number or size of tumors.

CONCLUSION: Older HCC patients showed less inflammation and better preservation of hepatic function, indicating that not only cirrhotic patients but also non-cirrhotic patients should be considered as a high-risk group among the elderly.

Key words: Hepatocellular carcinoma; Elderly patients; Baseline profile; Non-cirrhosis

Nakamuta M, Morizono S, Kohjima M, Kotoh K, Enjoji M. Baseline characterization of patients aged 70 years and above with hepatocellular carcinoma. *World J Gastroenterol* 2005; 11(47): 7512-7514
http://www.wjgnet.com/1007-9327/11/7512.asp

INTRODUCTION

Hepatocellular carcinoma (HCC), one of the most common forms of tumors, is increasing in frequency worldwide[1-4]. The increase is attributable to the spread of hepatitis C virus (HCV) infection in the population. HCV-related HCC is more common among the elderly patients, whereas hepatitis B virus (HBV)-related HCC is more common among the younger patients[3,5]. In Japan, fatalities from HCC are higher among patients who are aged 70 years and above[3]. However, the baseline profiles of such patients, including various parameters of hepatic function, have not been thoroughly investigated. In this study, we have evaluated the baseline profiles, including parameters of hepatic function such as alanine aminotransferase (ALT), aspartate aminotransferase (AST), and prothrombin time [PT (% activity)] in HCC patients aged ⩾70 and <70 years.

MATERIALS AND METHODS

A total of 127 consecutive patients with HCC, who had not been diagnosed with HCC previously, were admitted to our department at Kyushu University Hospital between 2000 and 2004 (Table 1). HCC was diagnosed by computed tomography (CT), ultrasonography, angiography and tumor biopsy, and treated with transcatheter arterial chemoembolization (TACE), percutaneous ablation [percutaneous ethanol injection therapy (PEIT) or radio frequency ablation (RFA)], and/or hepatic resection. Liver cirrhosis (LC) was diagnosed based on liver biopsy, laboratory data, ultrasonography, and/or computed tomography. Variables were compared between patients aged ⩾70 and <70 years, which included parameters of hepatic function (albumin, total bilirubin, AST, ALT, PT, and platelet number), serum levels of alpha-fetoprotein (AFP), tumor size and number (solitary or multiple), existence of liver cirrhosis, etiology [HBV, HCV, or non-HBV-non-HCV (NBNC)], and treatment.

Data were presented as mean±SE for quantitative variables. Differences in characteristics between patients aged ⩾70 and <70 years were analyzed by Wilcoxon rank sum test and Fisher's exact test for qualitative variables.

RESULTS

The number of older patients (aged ⩾70 years) and younger patients (aged <70 years) with HCC was 49 and 78, respectively. There was no difference in the proportion

Table 1 Comparison of baseline profiles between elderly patients and younger patients with HCC

Age (yr)	<70	≥70	*P*
n	78	49	
Male/female	56/22	34/15	0.772
Age (yr)	60.4±0.8	74.3±0.5	0.002
Platelet (mm^3)	10.3±0.7	13.9±0.9	0.002
PT (%)	66.8±3.2	76.6±3.1	0.036
Albumin (g/dL)	3.6±0.1	3.8±0.1	0.146
TBil (mg/dL)	1.5±0.2	1.2±0.2	0.298
AST (U/L)	86.4±6.0	66.3±7.9	0.044
ALT (U/L)	79.6±7.1	53.0±6.1	0.010
AFP (ng/mL)	1 651±839	1 006±390	0.562
HBV/HCV/NBNC	11/69/5	2/42/3	0.629
Non-LC/LC	35/44	36/13	0.001
HCC: solitary/multi	61/17	39/10	0.868
HCC: size diameter (mm)	36.0±4.0	28.6±3.0	0.184

of males and females between the two groups (Table 1). The prevalence of HBV and HCV in older and younger patients was 4% and 86%, and 14% and 88%, respectively. A comparison of hepatic function parameters showed differences in the platelet counts, PT (%), and the levels of AST and ALT (Table 1). Platelet counts and PT were significantly higher in older patients ($P = 0.016$ and $P = 0.0355$, respectively). The serum levels of AST and ALT were significantly lower in older patients ($P = 0.0443$ and $P = 0.0100$, respectively). The incidence of HCC among older patients was higher in those without LC than in those with LC, whereas in the younger patients, HCC developed more frequently in those with LC than in those without LC. There was no difference between the age groups in tumor number (solitary or multiple), tumor size, or serum levels of AFP. Resection was performed in 14% of the patients aged ≥70 years and in 13% of those aged <70 years. There was no difference between the groups in the types of treatment received.

DISCUSSION

This study demonstrated that older patients (aged ≥70 years) had higher PTs and platelet counts, and lower levels of AST and ALT as compared with younger patients (aged <70 years). The higher platelet counts and PTs indicate that liver function was better preserved, since platelet counts have been reported to correlate inversely with the degree of liver fibrosis[6]. In our study, 73% (36/49) of the older patients were diagnosed as having chronic hepatitis (non-LC), whereas only 45% (35/78) of the younger patients were diagnosed as having non-LC. Furthermore, the lower levels of AST and ALT indicate that hepatitis (inflammation) was less active. These results indicate that HCC in elderly patients tends to occur more frequently among those with non-LC and mild hepatic inflammation.

HCC is generally thought to be more common among LC patients, and the prevalence of cirrhosis in those with HCC is estima e EUROHEP group demonstrated that the 5-year risk of HCC was increased by 25% for a 60-year-old man with cirrhosis, mild elevation in total bilirubin (TBil) levels, and a low platelet count, whereas the risk was only increased by 3% for a 50-year-old man with cirrhosis, normal TBil levels, and normal platelet counts[8]. Tarao *et al*. also reported that the incidence of HCC in LC patients with ALT ≥80 U/L was much higher than in those with ALT <80 (13%/year *vs* 3%/year)[9]. These results are similar to our observations in patients <70 years old. However, in contrast with the previous studies, we found that the development of HCC in older patients was not strongly associated with LC, ALT levels, or the duration of disease. Although the precise reasons for this difference remain unknown, aging itself might be an important factor, independent of the duration of disease, since older people generally have a higher risk of cancer, regardless of the type[10]. It is possible that the patients with cirrhosis and HCC have died before reaching the age of 70 and those survived patients had well preserved hepatic function. To clarify this point, a Kaplan-Meier survival analysis of the two groups over the 5-year period of observation is needed. Comparison of the two groups of patients (<70 and ≥70 years) with chronic viral liver disease without HCC is also needed to know whether our present findings are indeed unique for HCC patients or a common profile in all patients with chronic viral disease.

Recently, the importance of surveillance for HCC among older LC patients has been recognized[11], due to the increasing life expectancy of cirrhotic patients as well as of the general population[1,12], and because surveillance among the older subjects can facilitate early detection and more effective treatment[13-15]. Trevisani *et al*. reported that surveillance for HCC in elderly LC patients improves their survival by identifying certain cancers earlier when they are more amenable to the treatment[11]. Better preservation of hepatic function as well as an early diagnosis can allow for more effective treatment such as hepatic resection. In our study, 14% of older patients received hepatic resection, which was similar to the percentage among younger patients. Therefore, we suggest that elderly non-LC patients should also be included in the surveillance to facilitate both early diagnosis and effective treatment.

Another significant finding in our study is that most of the patients (86%) suffered from HCV infection. It was recently reported that interferon treatment lowered the incidence of HCC[16,17], suggesting that interferon therapy would be advisable for preventing the development of HCC, even in elderly patients.

In conclusion, our study demonstrated that patients ≥ 70 years old with HCC had baseline clinical profiles that differed considerably from those of patients <70 years old; that is, HCC was more likely to develop among non-LC patients with well-preserved hepatic function and mild inflammation. Our results suggest that elderly non-LC patients, as well as LC patients, should be recognized as a high-risk group for HCC.

REFERENCES

1 **Deuffic S**, Poynard T, Buffat L, Valleron AJ. Trends in primary liver cancer. *Lancet* 1998; **351**: 214-215

2 **Fattovich G**, Stroffolini T, Zagni I, Donato F. Hepatocellular carcinoma in cirrhosis: incidence and risk factors. *Gastroenterology* 2004; **127**: S35-S50

3 **Kiyosawa K**, Umemura T, Ichijo T, Matsumoto A, Yoshizawa K, Gad A, Tanaka E. Hepatocellular carcinoma: recent trends in Japan. *Gastroenterology* 2004; **127**: S17-S26
4 **Tang ZY**. Hepatocellular carcinoma--cause, treatment and metastasis. *World J Gastroenterol* 2001; **7**: 445-454
5 **Shiratori Y**, Shiina S, Imamura M, Kato N, Kanai F, Okudaira T, Teratani T, Tohgo G, Toda N, Ohashi M. Characteristic difference of hepatocellular carcinoma between hepatitis B- and C-viral infection in Japan. *Hepatology* 1995; **22**: 1027-1033
6 **Pohl A**, Behling C, Oliver D, Kilani M, Monson P, Hassanein T. Serum aminotransferase levels and platelet counts as predictors of degree of fibrosis in chronic hepatitis C virus infection. *Am J Gastroenterol* 2001; **96**: 3142-3146
7 **Simonetti RG**, Cammà C, Fiorello F, Politi F, D'Amico G, Pagliaro L. Hepatocellular carcinoma. A worldwide problem and the major risk factors. *Dig Dis Sci* 1991; **36**: 962-972
8 **Fattovich G**, Schaim SW. Hepatitis and cirrhosis. In: Liang TJ, Hoofnagel JH, eds. Hepatitis C. San Diego: Academic Press, 2000; 241-263
9 **Tarao K**, Rino Y, Ohkawa S, Tamai S, Miyakawa K, Takakura H, Endo. O, Yoshitsugu M, Watanabe N, Matsuzaki S. Close association between high serum alanine aminotransferase levels and multicentric hepatocarcinogenesis in patients with hepatitis C virus-associated cirrhosis. *Cancer* 2002; **94**: 1787-1795
10 **Denduluri N**, Ershler WB. Aging biology and cancer. *Semin Oncol* 2004; **31**: 137-148
11 **Trevisani F**, Cantarini MC, Labate AM, De Notariis S, Rapaccini G, Farinati F, Del Poggio P, Di Nolfo MA, Benvegnu L, Zoli M, Borzio F, Bernardi M. Surveillance for hepatocellular carcinoma in elderly Italian patients with cirrhosis: effects on cancer staging and patient survival. *Am J Gastroenterol* 2004; **99**: 1470-1476
12 **La Vecchia C**, Negri E, Pelucchi C. The rise and fall in primary Liver cancer mortality in Italy. *Dig liver Dis* 2002; **34**: 169-171
13 **Poon RT**, Fan ST, Lo CM, Liu CL, Ngan H, Ng IO, Wong J. Hepatocellular carcinoma in the elderly: results of surgical and nonsurgical management. *Am J Gastroenterol* 1999; **94**: 2460-2466
14 **Teratani T**, Ishikawa T, Shiratori Y, Shiina S, Yoshida H, Imamura M, Obi S, Sato S, Hamamura K, Omata M. Hepatocellular carcinoma in elderly patients: beneficial therapeutic efficacy using percutaneous ethanol injection therapy. *Cancer* 2002; **95**: 816-823
15 **Qin LX**, Tang ZY. The prognostic significance of clinical and pathological features in hepatocellular carcinoma. *World J Gastroenterol* 2002; **8**: 193-199
16 **Shiratori Y**, Ito Y, Yokosuka O, Imazeki F, Nakata R, Tanaka N, Arakawa Y, Hashimoto E, Hirota K, Yoshida H, Ohashi Y, Omata M. Antiviral therapy for cirrhotic hepatitis C: association with reduced hepatocellular carcinoma development and improved survival. *Ann Intern Med* 2005; **142**: 105-114
17 **Azzaroli F**, Accogli E, Nigro G, Trere D, Giovanelli S, Miracolo A, Lodato F, Montagnani M, Tamé M, Colecchia A, Mwangemi C, Festi D, Roda E, Derenzini M, Mazzella G. Interferon plus ribavirin and interferon alone in preventing hepatocellular carcinoma: a prospective study on patients with HCV related cirrhosis. *World J Gastroenterol* 2004; **10**: 3099-3102

Science Editor Ma JY and Guo SY **Language Editor** Elsevier HK

PO Box 2345, Beijing 100023, China
www.wjgnet.com
wjg@wjgnet.com

ELSEVIER

World J Gastroenterol 2005;11(47):7515-7519
World Journal of Gastroenterology ISSN 1007-9327

• *RAPID COMMUNICATION* •

CT-maximum intensity projection is a clinically useful modality for the detection of gastric varices

Toru Ishikawa, Takashi Ushiki, Ken-ichi Mizuno, Tadayuki Togashi, Kouji Watanabe, Kei-ichi Seki, Hironobu Ohta, Toshiaki Yoshida, Keiko Takeda, Tomoteru Kamimura

Toru Ishikawa, Takashi Ushiki, Ken-ichi Mizuno, Tadayuki Togashi, Kouji Watanabe, Kei-ichi Seki, Hironobu Ohta, Toshiaki Yoshida, Tomoteru Kamimura, Department of Gastroenterology, Saiseikai Niigata Second Hospital, Niigata, Japan
Keiko Takeda, Department of Radiology, Saiseikai Niigata Second Hospital, Niigata, Japan
Correspondence to: Toru Ishikawa, Department of Gastroenterology, Saiseikai Niigata Second Hospital, Teraji 280-7, Niigata 950-1104, Japan. toruishi@ngt.saiseikai.or.jp
Telephone: +81-25-233-6161 Fax: +81-25-233-8880
Received: 2005-03-08 Accepted: 2005-07-28

Abstract

AIM: To evaluate the efficacy of CT-maximum intensity projection (CT-MIP) in the detection of gastric varices and their inflowing and outflowing vessels in patients with gastric varices scheduled to undergo balloon-occluded retrograde transvenous obliteration (B-RTO).

METHODS: Sixteen patients with endoscopically confirmed gastric varices were included in this study. All patients were evaluated with CT-MIP using three-dimensional reconstructions, before and after B-RTO.

RESULTS: CT-MIP clearly depicted gastric varices in 16 patients (100%), the left gastric vein in 6 (32.5%), the posterior gastric vein in 12 (75.0%), the short gastric veins in 13 (81.3%), gastrorenal shunts in 16 (100%), the hemiazygos vein (HAZV) in 4 (25.0%), the pericardiophrenic vein (PCPV) in 9 (56.3%), and the left inferior phrenic vein in 9 patients (56.3%). Although flow direction itself cannot be determined from CT-MIP, this modality provided clear images of the inflowing and the outflowing vessels. Moreover, in one patient, short gastric veins were not seen on conventional angiographic portography images of the spleen, but were clearly revealed on CT-MIP.

CONCLUSION: We suggest that CT-MIP should be considered as a routine method for detecting and diagnosing collateral veins in patients with gastric varices scheduled for B-RTO. Furthermore, CT-MIP is more useful than endoscopy in verifying the early therapeutic effects of B-RTO.

Key words: Gastric varices; CT-MIP; Portal hypertension

Ishikawa T, Ushiki T, Mizuno K, Togashi T, Watanabe K, Seki K, Ohta H, Yoshida T, Takeda K, Kamimura T. CT-maximum intensity projection is a clinically useful modality for the detection of gastric varices. *World J Gastroenterol* 2005; 11(47): 7515-7519
http://www.wjgnet.com/1007-9327/11/7515.asp

INTRODUCTION

Gastric varices have been increasingly recognized as a major cause of gastrointestinal bleeding in patients with portal hypertension[1,2]. These varices are appreciably less common than their more usual esophageal counterparts, but are associated with a poor prognosis.

Recent technical advances offer us increasingly greater imaging clarity of gastric varices. However, diagnosing this type of varices is problematic, mostly due to the absence of data on the hemodynamic features of such patients. Moreover, a non-invasive imaging modality is preferable in these high-risk patients. CT is currently reported to be superior to angiography in the detection of paraumbilical and retroperitoneal varices[3]. Furthermore, CT-MIP as a rendering method for visualizing the portal system provides superior visualization of portal collaterals.

The purpose of this study was to assess the accuracy and utility of CT-MIP in evaluating the collateral veins in patients with gastric varices before and after B-RTO. We also evaluated the detection of gastric varices and their inflowing and outflowing vessels by CT-MIP.

MATERIALS AND METHODS

Patients

Sixteen consecutive patients with gastric varices confirmed by endoscopy at the Saiseikai Niigata Second Hospital were enrolled in this study between April 1999 and April 2004. Both CT-MIP and transarterial portography were performed in these patients before and after B-RTO. Patients [8 men and 8 women, aged 45-72 years (mean 59.31 years)] were selected for routine endoscopic screening for esophago-gastric varices. The cause of portal hypertension was liver cirrhosis in 14 patients, and cirrhosis coupled with hepatocellular carcinoma in two patients. Cirrhosis was diagnosed through imaging, and regarding stage, 13 patients were classified as Child-Pugh class B and 3 as Child-Pugh class C. The etiology of liver disease was hepatitis B virus (HBV); in 1 patient

Table 1 Clinical features

Case	Age	Gender	Etiology	GV	Child	HCC
1	59	M	HBV	Lg f F3	C	+
2	69	F	AIH	Lg cf F2	B	−
3	56	F	ALC	Lg f F2	B	−
4	69	F	HCV	Lg f F3	B	−
5	53	F	AIH	Lg f F3	B	−
6	54	M	HCV	Lg f F2	B	+
7	64	M	HCV	Lg cf F3	B	−
8	53	F	HCV	Lg cf F2	B	−
9	45	M	ALC	Lg f F3	B	−
10	50	M	ALC	Lg cf F3	B	−
11	56	F	ALC	Lg f F3	B	−
12	72	F	HCV	Lg c F3	B	−
13	65	M	HCV	Lg c F3	C	−
14	62	F	AIH	Lg f F2	B	−
15	72	M	HCV	Lg c F2	B	−
16	50	M	ALC	Lg cf F2	C	−

(surface antigen (HBs)-positive), hepatitis C virus (HCV) in 7 (anti-HCV antibody-positive), alcoholic liver disease in 5, and autoimmune hepatitis in 3. Endoscopic findings of gastric varices were evaluated according to the general rules proposed by the Japanese Research Society for Portal Hypertension. Variceal form (F) was classified as small and straight (F1, n = 0); enlarged and tortuous (F2, n = 7), or large and coil-shaped (F3, n = 9). Variceal location (L) was classified as: cardiac (Lg-c; located adjacent to the cardiac orifice, n = 0); fundal (Lg-f; located far from the cardiac orifice, n = 11); or cardiofornical (Lg-cf; located between the cardiac orifice and the fornix, n = 5). Patient parameters and characteristics of varices are shown in Table 1.

Follow-up endoscopic examination was performed to evaluate the size of gastric varices at 1 wk, 1 mo, and 3 mo after B-RTO, with CT-MIP also performed at these times together.

Computed tomography

All CT studies were performed using an SD-CT scanner (HiSpeed LX/i; General Electric Medical Systems, Milwaukee, WI, USA). Gantry rotation time was 0.8 s. Initially, non-contrast enhanced images were obtained for localization with 10.0 mm beam collimation. Subsequently, after placing a 20-gauge plastic cannula in an antecubital vein, a bolus of 100 mL of iopamidol (Omnipaque; Daiichi Pharmacy Co., Ltd, Tokyo, Japan) was injected with an automated power injector (Auto Enhance A-50; Nemoto Kyorindo, Tokyo) at the rate of 3 mL/s. Scan delays were empirically set at 25, 50, and 200 s after contrast material injection for the arterial, portal, and equilibrium phases, respectively. The entire liver was scanned with a slice thickness of 2.5 mm and table feed of 15 mm (pitch of 6) in a cranio-caudal direction in the arterial phase. In the portal phase, scanning was performed at a slice thickness of 2.5 mm and table feed of 7.5 mm (pitch of 3) in a cranio-caudal direction. In the equilibrium phase, slice thickness was set at 5 mm and table feed at 15 mm (pitch of 3) in a cranio-caudal direction.

Three-dimensional reconstructions

Sources with 50% overlap were obtained from the raw data of the portal phase, and a total of 250-350 images were generated. These images were transferred to a workstation [Advantage Workstation 3.1; General Electric Medical Systems, Milwaukee, WI, USA), and three CT portographic models (volume rendering [VR], MIP, and surface shade display (SSD)] were reconstructed. In MIP and VR, voxels over -200 HU were selected. CT portography was reconstructed using the VR algorithm with lower thresholds of 70-90 HU. Display parameters including width, level, opacity, and brightness were chosen subjectively to best visualize the portal vasculature. For MIP, a slab of some 3-10 cm was applied to avoid interference of the vertebral bodies, and the overlying skeletal structures were carefully removed if necessary. Voxel data over the threshold level of 70-90 HU were extracted and applied for SSD images.

Transarterial portography

Transarterial portography was performed with the digital subtraction angiography technique (DSA, General Electric Medical Systems, Milwaukee, WI, USA) in all the 16 patients to evaluate portosystemic collaterals by the Seldinger method. In all cases, transarterial portography was performed through both the superior mesenteric and splenic arteries using the standard angiographic technique. After the administration of prostaglandin E1 (Palcus, Taisho Pharmacy Co., Ltd, Tokyo), a total of 25 mL of contrast material was injected by power injector at a rate of 5 mL/s via the superior mesenteric artery. Portography via the splenic artery was also obtained with 20 mL of contrast material at a rate of 5 mL/s. Balloon-occluded retrograde transvenous venography (B-RTV) was performed using a DSA device, and was done with selective injection of contrast material into the gastrorenal shunt in all the patients.

After confirming complete visualization of the gastric varices, the sclerotic agent (a mixture of equal amounts of 10% ethanolamine oleate and contrast medium) was injected through the balloon catheter until stasis was obtained in the gastric varices. Eradication of all gastric varices was achieved in all the patients.

RESULTS

All CT-MIP studies were of diagnostic quality, identifying the main portal veins and clearly delineating gastric varices in all the 16 patients (100%). Inflowing vessels to gastric varices were revealed by CT-MIP in all the patients (100%) and comprised the left gastric vein in 6 (32.5%), the posterior gastric vein in 12 (75.0%), and short gastric veins in 13 (81.3%) (Table 2). Regarding outflowing vessels from gastric varices, CT-MIP identified gastrorenal shunts in 16 patients (100%), the hemiazygos vein (HAZV) in 4 (25.0%), the pericardiophrenic vein (PCPV) in 9 (56.3%), and the left inferior phrenic veins in 9 patients (56.3%) (Table 2).

Table 2 Hemodynamics features of gastric varices

Case	Inflowing Vessels			Outflowing Vessels			
	LGV	PGV	SGV	G-R shunt	PCPV	HAZV	LIPV
1	−	+	−	+	+	−	+
2.	−	−	+	+	−	−	+
3	−	+	+	+	−	−	+
4	+	+	+	+	+	−	+
5	−	+	+	+	−	−	+
6	−	−	+	+	−	−	−
7	−	+	+	+	+	−	−
8	+	+	+	+	−	−	+
9	−	+	+	+	+	+	−
10	+	+	+	+	+	+	+
11	−	+	+	+	+	+	+
12	−	+	+	+	+	−	−
13	+	+	+	+	+	+	+
14	+	−	−	+	−	−	−
15	+	−	−	+	−	−	−
16	−	+	+	+	+	−	−

Pericardiophrenic V. (PCPV); hemiazygos V. (HAZV); Lt. inferior phrenic V. (LIPV); retroperitoneal V. (RPV) Lt. gastric V. (LGV); posterior gastric V. (PGV); short gastric V. (SGV)

Table 3 CT-MIP compared with conventional angiographic portography for inflowing vessels of gastric varices

Inflowing vessels	CT-MIP imaging	Conventional DSA
LGV	6	6
PGV	12	12
SGV	13	11

Lt. gastric V. (LGV); posterior gastric V. (PGV); short gastric V. (SGV)

Table 4 CT-MIP compared with conventional angiographic portography for outflowing vessels of gastric varices

Outflowing vessels	CT-MIP imaging	Conventional DSA
G-R shunt	16	16
PCPV	8	9
LIPV	8	9
HAZV	4	4

Pericardiophrenic V. (PCPV); hemiazygos V. (HAZV); Lt. inferior phrenic V. (LIPV); gastrorenal shunt (G-R shunt)

We then investigated collateral imaging, comparing CT-MIP with angiographic findings (conventional arterial portography) in all the patients. Gastric varices were delineated in all the 16 patients by both CT-MIP and angiography. Both CT-MIP and angiography depicted the gastrorenal shunt in all patients who were studied. Findings of CT-MIP and angiography agreed for the left gastric vein in six patients, for the short gastric vein in one, for the left gastric vein and short gastric vein in one, and for the left gastric vein and the posterior gastric vein in one. In two patients, CT-MIP revealed the short gastric vein as an inflowing vessel to gastric varices, while angiography failed to identify these veins (Table 3). However, CT-MIP failed to reveal the outflowing blood vessels in two patients, while angiography identified the left inferior phrenic vein and PCPV as outflowing vessels in these cases (Table 4). No statistically significant difference between CT-MIP and conventional angiography was apparent in the detection rates of gastric varices and their inflowing/outflowing vessels.

In case 5, in a 53-year-old woman, the endoscopic view revealed Lg-f, F3 type varices (Figure 1A). Using CT-MIP, clear images of gastric varices were obtained and agreed with those of angiographic findings (Figures 2A and B). The short gastric vein and the posterior gastric vein were identified as inflowing, and the gastrorenal shunt and left inferior phrenic vein as outflowing. One week after the procedure, endoscopy revealed unchanged variceal size, although the gastric varices had developed bronze discoloration (Figure 1B). One month after B-RTO therapy, complete disappearance of the varices was observed and this persisted for about 3 mo (Figure 1C).

CT-MIP at 1 wk after the treatment revealed disappearance of the gastrorenal shunt (Figure 2C). CT-MIP was therefore superior to conventional angiography in evaluating treatment of gastric varices in all cases.

DISCUSSION

The increasing numbers of patients being treated for portal hypertension has led to a growing demand for radiographic examination of the portal venous system. Several methods including endoscopy and intravascular interventional techniques such as balloon-occluded retrograde transvenous obliteration (B-RTO) are available for treating esophageal and gastric varices[4]. Evaluation of the portosystemic collateral pathways in patients with portal hypertension is essential and potentially helpful for clinical management.

For many years, transcatheter portography via the superior mesenteric or splenic arteries has been considered as a standard technique for visualizing the portal vein. However, it is gradually being challenged by non-invasive means of portal venous assessment. Several reports have demonstrated the usefulness of CT for examining the patency of the portal venous system for assessing portosystemic collaterals and evaluating the presence and patency of portosystemic shunts[5,6]. Studies have shown the clinical usefulness of CT-MIP in various diagnostic fields. Particularly in assessing intracranial vessels, CT-MIP has become a non-invasive alternative to conventional angiography for depicting aneurysms and arteriovenous malformations[7]. In contrast, CT-MIP has seldom been used in evaluating abdominal veins, particularly portosystemic collaterals. Recently, however, CT-MIP has been reported to be useful for evaluating the portal venous system in patients with portal hypertension[8] and it is possible that this modality is more sensitive than conventional angiography in detecting esophageal and gastric varices. To the best of our knowledge, no attempt has been made to evaluate whether CT-MIP might yield useful information on gastric varices, and only a few

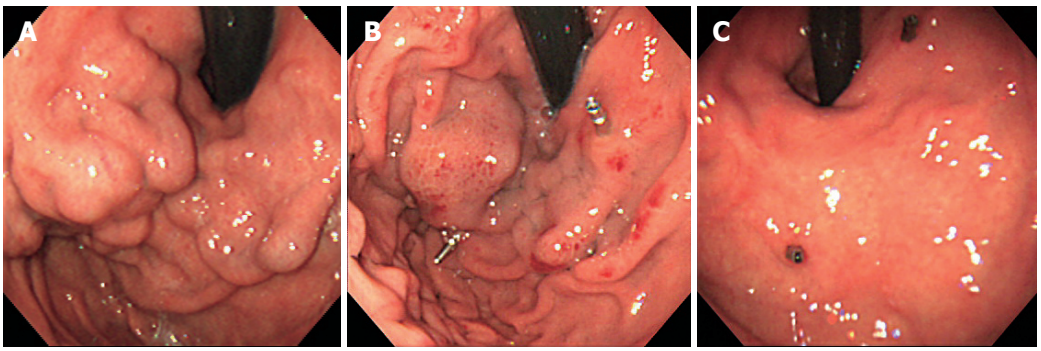

Figure 1 Case 5, a 53-year-old woman. (**A**) The endoscopic view revealed Lg-f F3 type varices. (**B**) One week after the procedure, endoscopic findings revealed varices to be unchanged in size, although the gastric varices had developed bronze discoloration. (**C**) One month after B-RTO therapy, complete disappearance of the varices was observed, and this persisted for about 3 mo.

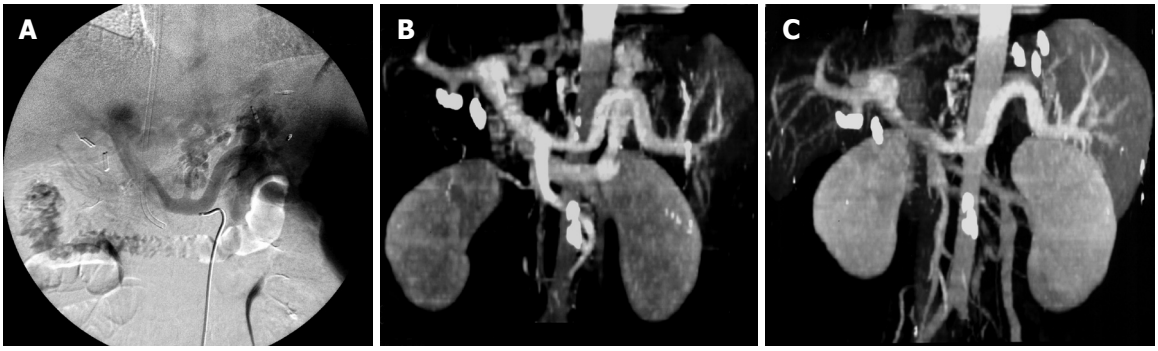

Figure 2 Case 5, a 53-year-old woman. (**A**) Angiographic findings (conventional arterial portography) the short gastric vein and the posterior gastric vein were revealed as inflowing, and the gastrorenal shunt and left inferior phrenic vein as outflowing. (**B**) Using CT-MIP, clear images of gastric varices were obtained. (**C**) CT-MIP 1 wk after the treatment revealed disappearance of the gastrorenal shunt.

reports have compared the results of CT-MIP with those of conventional angiographic portography regarding visualization of portosystemic collaterals[9].

We compared CT-MIP for portal venous phase images and DSA. We observed the hemodynamics of the gastric varices before and after B-RTO by means of CT-MIP. The inflowing vessels to gastric varices generally consist of the short gastric veins, the posterior gastric vein, and the left gastric vein, while the outflowing vessels are commonly gastrorenal shunts. In this study, CT-MIP more thoroughly delineated gastrorenal shunts, the left gastric vein, and gastric varices than did angiography and CT. Unlike DSA, CT-MIP is unable to demonstrate direction of the flow within the portal venous system. However, CT-MIP proved so effective that it can be considered as a less invasive alternative to conventional angiographic portography for assessing portosystemic collaterals.

CT-MIP was associated with the following limitations. Small vessels were not defined as well with CT-MIP as with retrograde venography performed during balloon occlusion. The modality is also prone to certain artifacts, such as those due to surrounding tissue and marking clips. In addition, it was difficult to distinguish between intramural gastric varices and extramural collateral veins using CT-MIP.

On the other hand CT-MIP has certain advantages. Firstly, it is a non-invasive modality. Furthermore, CT-MIP is useful for detecting the entire length of gastric varices, which is not always possible with B-RTV due to the limitations of venography. This study has emphasized that CT-MIP may be useful for the treatment of patients with gastric varices[10]. Moreover, the technique may be useful for evaluating the effect of embolization therapy[11]. Endoscopic findings of gastric varices after B-RTO are particularly limited, owing to the depth of submucosal or extramural collateral veins. On endoscopic findings following B-RTO, gastric varices gradually become reduced in size, disappearing completely after some months. Hence, CT-MIP revealed disappearance of gastrorenal shunts and gastric varices after B-RTO.

CT-MIP enabled us to detect the blood flow from gastric varices to other collateral shunts and is therefore useful in the follow-up after therapeutic procedures[12].

We suggest that CT-MIP can be used as a routine method for detecting and diagnosing collateral veins in patients with gastric varices and that it is effective for use with embolization therapy for gastric varices. Moreover, CT-MIP may also be useful for the assessment of therapeutic effect of B-RTO and could potentially demonstrate residual gastric varices after B-RTO, better than endoscopy.

We conclude that CT-MIP is a useful method for the

assessment of therapeutic effect following treatment of gastric varices. Although further evaluation and the development of alternative therapies for the treatment of gastric varices are warranted, it would seem that CT-MIP has a valuable role in this situation.

When considering B-RTO for the treatment of patients with gastric varices, CT-MIP is useful for selecting the patients as candidates, for planning the procedure, and finally for evaluating the results. Furthermore, CT-MIP may be useful for detecting collateral vessels by portal hypertension.

REFERENCES

1 **Sarin SK,** Lahoti D, Saxena SP, Murthy NS, Makwana UK. Prevalence, classification and natural history of gastric varices: a long-term follow-up study in 568 portal hypertension patients. *Hepatology* 1992; **16:** 1343-1349

2 **Ide K,** Nagasaki Y, Tomimatsu H, Nakashima T, Arakawa M, Kojiro M. Pathomorphologic and angio-architectural studies of oesophagogastric varices. *J Gastroenterol Hepatol* 1989; **4** Suppl 1: 204-207

3 **McCain AH,** Bernardino ME, Sones PJ Jr, Berkman WA, Casarella WJ. Varices from portal hypertension: correlation of CT and angiography. *Radiology* 1985; **154:** 63-69

4 **Koito K,** Namieno T, Nagakawa T, Morita K. Balloon-occluded retrograde transvenous obliteration for gastric varices with gastrorenal or gastrocaval collaterals. *Am J Roentgenol* 1996; **167:** 1317-1320

5 **Bernardino ME,** Steinberg HV, Pearson TC, Gedgaudas-McClees RK, Torres WE, Henderson JM. Shunts for portal hypertension: MR and angiography for determination of patency. *Radiology* 1986; **158:** 57-61

6 **Finn JP,** Kane RA, Edelman RR, Jenkins RL, Lewis WD, Muller M, Longmaid HE. Imaging of the portal venous system in patients with cirrhosis: MR angiography vs duplex Doppler sonography. *Am J Roentgenol* 1993; **161:** 989-994

7 **Korogi Y,** Takahashi M, Katada K, Ogura Y, Hasuo K, Ochi M, Utsunomiya H, Abe T, Imakita S. Intracranial aneurysms: detection with three-dimensional CT angiography with volume rendering--comparison with conventional angiographic and surgical findings. *Radiology* 1999; **211:** 497-506

8 **Hughes LA,** Hartnell GG, Finn JP, Longmaid HE, Volpe J, Wheeler HG, Clouse ME. Time-of-flight MR angiography of the portal venous system: value compared with other imaging procedures. *Am J Roentgenol* 1996; **166:** 375-378

9 **Horton KM,** Fishman EK. Paraumbilical vein in the cirrhotic patient: imaging with 3D CT angiography. *Abdom Imaging* 1998; **23:** 404-408

10 **Leyendecker JR,** Rivera E Jr, Washburn WK, Johnson SP, Diffin DC, Eason JD. MR angiography of the portal venous system: techniques, interpretation, and clinical applications. *Radiographics* 1997; **17:** 1425-1443

11 **Ono N,** Toyonaga A, Nishimura H, Hayabuchi N, Tanikawa K. Evaluation of magnetic resonance angiography on portosystemic collaterals in cirrhotic patients. *Am J Gastroenterol* 1997; **92:** 1515-1519

12 **Pieters PC,** Miller WJ, DeMeo JH. **Evaluation of the portal** venous system: complementary roles of invasive and noninvasive imaging strategies. *Radiographics* 1997; **17:** 879-895

Science Editor Guo SY **Language Editor** Elsevier HK

PO Box 2345, Beijing 100023, China
www.wjgnet.com
wjg@wjgnet.com

ELSEVIER

World J Gastroenterol 2005;11(47):7520-7524
World Journal of Gastroenterology ISSN 1007-9327

• *RAPID COMMUNICATION* •

Effect of *Clostridium butyricum* on fecal flora in *Helicobacter pylori* eradication therapy

Izumi Shimbo, Taketo Yamaguchi, Takeo Odaka, Kenichi Nakajima, Akinori Koide, Hidehiko Koyama, Hiromitsu Saisho

Izumi Shimbo, Taketo Yamaguchi, Takeo Odaka, Hiromitsu Saisho, Department of Medicine and Clinical Oncology, Graduate School of Medicine, Chiba University, 1-8-1 Inohana, Chuo-ku, Chiba-City, Chiba, 260-0856, Japan
Kenichi Nakajima, Tako Chuo Hospital, Tako-machi Katori-Country, Chiba, 289-2241, Japan
Akinori Koide, Kawasaki Chiba Hospital, Minami-cho, Chuo-ku, Chiba-City, Chiba, 260-0842, Japan
Hidehiko Koyama, International University of Health and Welfare, Mita Hospital, Mita Minato-ku Tokyo, 108-8329, Japan
Co-first-authors: Izumi Shimbo, and Taketo Yamaguchi
Co-correspondents: Taketo Yamaguchi
Correspondence to: Yamaguchi, PhD, Department of Medicine and Clinical Oncology, Graduate School of Medicine, Chiba University, 1-8-1 Inohana, Chuo-ku, Chiba-City, Chiba, 260-0856, Japan. yama.take@faculty.chiba-u.jp
Telephone: +81-43-226-2083 Fax: +81-43-226-2088
Received: 2005-04-27 Accepted: 2005-06-02

Abstract

AIM: To investigate the effect of probiotic bacterium, *Clostridium butyricum* MIYAIRI 588 strain (CBM) on the changes of the fecal flora in *Helicobacter pylori* (*H pylori*) treatment.

METHODS: Thirty-five patients with gastric or duodenal ulcers positive for *H pylori* were randomized either to 1 wk amoxicillin, clarithromycin, lansoprazole (Group 1) or to the same regimen supplemented with CBM 7 d ahead of the triple therapy (Group 2). Stool samples were collected before and 2, 4, 7, 15, and 22 d after the starting eradication therapy, and were examined intestinal flora. Patients were required to keep a diary record of their condition.

RESULTS: Obligate anaerobes decreased significantly on d 2, 4, 8 and 15 in Group 1. On the other hand, they did not decrease significantly in Group 2. The *Escherichia coli* was dominant bacterium in *Enterobacteriaceae*, but that was replaced by other species such as *Klebsiella* and *Enterobacter* after eradication in Group 1. The change was suppressed in Group 2. Abdominal symptoms were less frequent in Group 2 than in Group 1.

CONCLUSION: The combined use of CBM reduced the changes in the intestinal flora and decreased the incidence of gastrointestinal side effects.

Key words: *Clostridium butyricum*; Intestinal flora; *Helicobacter pylori*; Eradication

Shimbo I, Yamaguchi T, Odaka T, Nakajima K, Koide A, Koyama H, Saisho H. Effect of *Clostridium butyricum* on fecal flora in *Helicobacter pylori* eradication therapy. *World J Gastroenterol* 2005; 11(47): 7520-7524
http://www.wjgnet.com/1007-9327/11/7520.asp

INTRODUCTION

Antibiotic therapy causes loose stools and/or diarrhea quite frequently, probably because of changes in the intestinal flora. Super infection arising from the alterations of the normal intestinal flora is a factor in the onset of infectious enteritis.

Helicobacter pylori (*H pylori*) is deeply involved in gastroduodenal ulcer disease and *H pylori* -positive patients are generally treated with antibiotics to eradicate this bacterium[1]. Triple therapy with a proton pump inhibitor and two antibiotics selected from among the following three: amoxicillin, clarithromycin and metronidazole, is now considered to be the standard therapy, and it is reported that a bacterial eradication rate of about 80-90% can be achieved[2-4]. Although such therapy causes few serious adverse reactions, gastrointestinal side effects like diarrhea and loose stools occur at a high incidence[5].

It is known that probiotic supplementation prevents or reduces of antibiotics-induced diarrhea. Recent studies have shown that probiotics were effective against gastrointestinal symptoms associated with *H pylori* eradication therapy[6]. Probiotics are defined as viable microorganisms which, when ingested, have a beneficial effect on human health, including amelioration or prevention of specific pathologic conditions[7].

Clostridium butyricum is a butyric acid producing Gram-positive anaerobe which is found in soil and the intestines of healthy animals and humans, and the MIYAIRI 588 strain of *C. butyricum* (CBM) has been used as probiotics for treating and preventing non-antimicrobial induced diarrhea, antimicrobial associated diarrhea and constipation in human beings[8-10]. MIYA-BM® tablets (Miyarisan pharmaceutical Co., Ltd., Tokyo, Japan) containing CBM were approved from Japanese Ministry of Health and

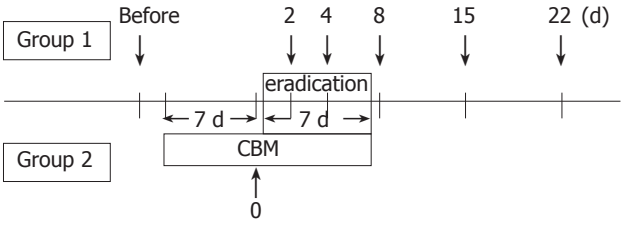

Figure 1 Study design. Fecal sample collection(↓).

Welfare for human clinical use since 1970 in Japan.

However, the preventive effect of CBM preparation on the abnormalities of intestinal microflora due to *H pylori* eradication therapy was unknown. Therefore, in the present study, we have examined the changes of fecal flora and gastrointestinal symptoms frequently during *H pylori* eradication therapy, and evaluated the utility of CBM supplementation to prevent the disturbance of the intestinal flora.

MATERIALS AND METHODS

Patients

Of the patients diagnosed as having gastric or duodenal ulcers at the outpatient clinic of the First Department of Medicine of Chiba University, 35 patients (male/female: 28/7; mean age 52.7±11.3 years) were enrolled in this study. They were all positive for *H pylori* by culture method, microscopical examination and the rapid urease test (PyloriTek® test kit, Serim Research Corp., Elkhart, IN, USA).

The patients were blindly and randomly allocated to two groups. Seventeen patients were assigned the 1 wk triple therapy consisting of amoxicillin 1 500 mg b.i.d., clarithromycin 400 mg b.i.d. and lansoprazole 60 mg b.i.d. (Group 1). Alternatively, eighteen were assigned to the same regimen supplemented with CBM (120 mg t.i.d.), which was started 1 wk prior to the eradication therapy for 14 d (Group 2). The patients had not been treated with any drugs that might have influenced intestinal bacteria, and had no known underlying gastrointestinal disorders. They were all given a full explanation of the contents of the study and they provided their informed consent in writing.

Six weeks after the completion of the therapy, the ^{13}C-urea breath test was performed to check whether eradication had been achieved.

Collection of stool samples

Stool samples were collected the day before the start of the therapy, and on d 2, 4, 8, 15, and 22 after the start of *H pylori* eradication therapy in Group 1. In Group 2, stools were also collected 1 wk after the administration of CBM (Figure 1). Fresh samples were placed in a transporter filled with CO_2 (Kenkiporter® II, Clinical Supply, Gifu, Japan), and were transferred under refrigeration for culture within 24 h of the collection.

Examination of intestinal flora

Intestinal flora was investigated according to Mitsuoka's method[8]. Any bacterium detected was identified at the level of species or genus, and counted. The microorganisms were classified into sub groups of bacteria according to morphology of the colonies, Gram staining and cell shapes. Isolation of *Clostridium difficile* was also attempted.

The nonselective media used for isolation included TS, EG, and BL agar, while selective media included DHL, TATAC, P, PEES, LBS, NBGT, ES, BS, and CCMA agar. A stool sample (0.5 g) was placed into an anaerobic glove box (N_2 80%, H_2 10%, CO_2 10%) and was diluted with a diluent for anaerobic bacteria from 10-fold to 10^8-fold in 10 steps. Aliquots (0.05 mL) of each dilution were cultured anaerobically in an incubator in the glove box at 37 ℃ for 3 d. When TS, DHL, TATAC, P, or PEES agar was used the culture plates were removed from the glove box after the bacteria were seeded and were cultured aerobically at 37 ℃ for 1 to 2 d. Any colony that grew during anaerobic culture was also examined for aerobic growth. Smears were prepared on slide glasses for any colony that grew and the smears were subjected to Gram staining for microscopic observation. Then each organism was classified on the basis of its characteristics, including colony morphology, growth under aerobic conditions, and growth in selective culture media. The number of live bacteria of each genus per 1 g of feces was calculated from the number of colonies and converted into a logarithmic equivalent for each bacterial species identified; log colony forming unit/g feces (logCFU/g feces). The detection limit was 2.3 logCFU/g feces. The total count of viable bacteria was calculated from the sum of the counts of each bacterial species. Species in the Enterobacteriaceae were identified by the kit of Enterotube® Ⅱ (Becton Dickinson, USA).

Assessment of symptoms

Each patient was required to keep a daily record of the conditions of their stools and any abdominal symptoms, from before the therapy to 2 wk after the completion of *H pylori* eradication therapy.

Statistical analysis

Bacterial counts were expressed as the mean±SD. Statistical evaluation of changes within groups was carried out using the Wilcoxon signed-rank test. The Mann-Whitney *U* test was used for comparison between groups. Fisher's exact test was performed to compare the detection rates. Differences of $P<0.05$ were considered to be statistically significant.

RESULTS

Intestinal flora before H pylori eradication therapy

The levels of obligate and facultative anaerobes in the groups did not differ significantly. The predominant bacteria were obligate anaerobes, such as Bacteroidaceae,

Table1 Level of obligate and facultative anaerobes in Group1 and Group2, before *H pylori* eradication therapy (mean±SD)

Population	LogCFU/g			
	Group 1 (n = 17)		Group 2 (n = 18)	
Total counts	10.4±0.4		10.2±0.5	
Obligate anaerobes	10.4±0.4		102±0.6	
Bacteroidaceae	10.1±0.4	(100)	9.3±1.6	(100)
Bifidobacteria	9.8±0.6	(93.8)	9.6±0.6	(93.8)
Peptococci	8.9±0.8	(62.5)	9.0±0.5	(62.5)
Clostridia	7.5±1.9	(93.8)	7.9±1.5	(100)
Micrococci	3.0±1.2	(25)	3.5±1.8	(37.5)
Facultative anaerobes	8.3±0.7		8.1±1.0	
Enterobacteriaceae	7.2±1.7	(93.8)	6.7±1.5	(100)
E.coli	7.3±1.4	(81.3)	6.4±1.6	(93.8)
Others	6.9±1.8	(18.8)	5.7±1.0	(31.3)
Enterococci	7.3±1.1	(93.8)	7.9±1.0	(93.8)
Lactobacilli	7.2±1.6	(100)	6.9±1.0	(93.8)
Bacilli	7.6±0.9	(37.5)	7.4±0.6	(25)
Yeasts	5.0±2.0	(75)	4.8±1.8	(56.3)

There are no significant differences between the two groups using Mann-Whitney *U* test. Figures in parentheses are detection rates.

Table 2 Detection rates of fecal flora

			Detection rates (%)				
Population	Group	Before	D2	D4	D8	D15	D22
Bacteroidaceae	1	100	100	93.8	100	100	93.3
	2	100	94.4	100	100	100	94.4
Bifidobacteria	1	93.8	62.5[a]	50.0[b]	62.5[a]	68.8	73.3
	2	93.8	66.7	44.4[b]	72.2	66.7	66.7
Clostridia	1	93.8	93.8	75	100	100	100
	2	100	94.4	94.4	94.4	100	100
Enterobacteriaceae	1	93.8	93.8	100	93.8	100	100
	2	100	94.4	100	94.4	100	100
E.coli	1	81.3	62.5	25	37.5[a]	87.5	93.3
	2	93.8	72.2	94.4	66.7[b]	88.9	77.8
Others	1	18.8	75.0[b]	81.3[d]	75	81.3[d]	46.7
	2	31.3	27.8	16.7	38.9	33.3	50
Enterococci	1	93.8	87.5	81.3	100	100	100
	2	93.8	100	100	100	100	100
Lactobacilli	1	100	87.5	68.8[a]	43.8[d]	93.8	93.3
	2	93.8	61.1[a]	61.1[a]	44.4[b]	100	88.9
Yeasts	1	75	93.8	100.0[a]	93.8	87.5	86.7
	2	56.3	61.1	72.2	83.3	44.4	66.7

[a]P<0.05, [b]P<0.01, [d]P<0.001 *vs* before, Fisher's exact test.

Bifidobacteria and in both groups (Table 1). As for the viable counts and detection rates of all species, there was not significant difference between the two groups. The viable counts and detection rates of all species did not change significantly between before and 1 wk after CBM administration in Group 2 (data not shown). None of the patients was positive for *C. difficile* as assessed by culture.

Counts of CBM and detection rate

Counts of CBM increased and averaged 6.7 logCFU/g on the day before eradication therapy. The detection rate was the highest on d 2 (90%); it gradually decreased. On d 15, CBM became under detectable.

Table 3 Clinical symptoms observed during and after *H pylori* eradication therapy

	Group 1 (n = 17, %)		Group 2 (n = 18, %)	
Loose stool	8	(47.1)	4	(22.2)
Water diarrhea	2	(11.8)	1	(5.6)
Abdominal pain	2	(11.8)	0	(0)
Abdominal distention	2	(11.8)	0	(0)

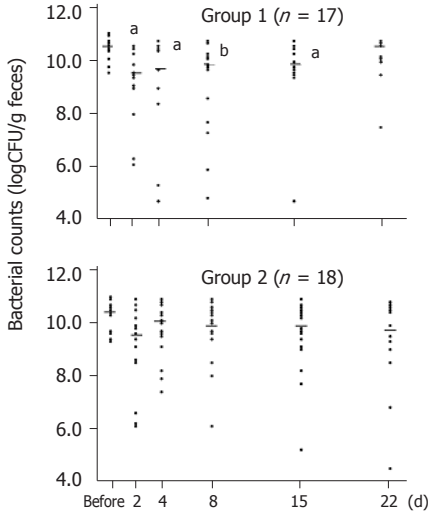

Figure 2 Obligate anaerobes during and after *H pylori* eradication therapy There are no significant differences between the two groups before therapy. Statistically significant changes are noted as [a]P<0.05, [b]P<0.01 before using the Wilcoxon's signed-rank test.

Intestinal flora after starting H pylori eradication therapy

Obligate anaerobes decreased significantly on d 2, 4, 8, and 15, and returned to their pretreatment levels on d 22 in Group 1. On the other hand, the number of obligate anaerobes did not change significantly at any time in Group 2 (Figure 2). The number of facultative anaerobes did not decrease significantly in either group.

The detection rates of intestinal flora are shown in Table 2. Bacteroidaceae, the dominant bacteria, did not change after starting eradication of *H pylori* in either group. *Bifidobacterium* was significantly lower on d 2, 4, and 8 in Group 1, in the other, only on d 4 in Group 2. As for each group of facultative anaerobes, *E.coli* was significantly lower on d 4, 8 and other species such as *Klebsiella* and Enterobacter in Enterobacteriaceae were significantly higher on d 2, 4, 8, and 15 in Group 1. On the other hand, either Enterobacteriaceae did not change significantly in Group 2. Lactobacilli significantly lower in either group.

Yeasts was significantly higher on d 4 in Group 1. No significant alterations in Yeasts were observed in Group 2. All bacterial groups recovered to pretreatment levels d 22 after completion of the drug administration. No patients were colonized with *C.difficile* at any time.

Clinical symptoms

As for abdominal symptoms, in Group 1, loose stools were noted in 8 of 17 patients (47.1%): diarrhea in 2 of 17 patients (11.8%): abdominal pain and distention in 2 of 17 patients (11.8%), each. In Group 2, loose stools were noted in 4 of 18 patients (22.2%) and diarrhea in 1 of 17 patients (5.6%). The rates were lower in Group 2, although the differences were not significant (Table 3). Treatment was successful in 13 out of 17 patients in Group 1 (76.5%) and in 17 out of 18 patients in Group 2 (94.4%).

DISCUSSION

The intestinal flora in our subjects before the treatment was similar to that detected in normal adults by Mitsuoka[11]. It is known that the normal fecal flora is almost the same as that of the recto-sigmoid colon. Intestinal flora is reported to remain stable in each individual, although it differs among individuals[12-13]. However, it has been shown that the administration of antimicrobial agents, which are excreted in the bile, in the intestinal mucosa or are incompletely absorbed, causes changes in the normal intestinal flora.

Buhling *et al*[14]. have shown that infrequent detection of Clostridia, *Veillonela, Eubacteria, Actinomyces,* Bifidobacteria and *E.coli* with simultaneous more frequent growth of other Enterobacteria and *Yeasts* on d 8 of starting *H pylori* treatment, and after 4 wk of therapy, the microflora returned to normal.

When they collected stool samples for three times (d 0, 8, 35-40), we examined the chronological changes of the intestinal flora were followed 6 or 7 times at short intervals during and after *H pylori* treatment in this study.

Then we found that the total bacterial counts started to decrease as early as on d 2 of therapy. Especially, obligate anaerobes, which are the dominant bacteria, were markedly reduced. And it took 3 wk for them to return to their pretreatment levels after starting of therapy.

These bacteria are known to produce short-chain fatty acids (SCFA). Such SCFA are considered to promote proliferation of colonic epithelial cells, provide energy for colonic epithelial cells and to stimulate the absorption of water and sodium[15-19].

Previous studies have demonstrated a close correlation between a decrease in the viable count of anaerobes and a reduction in SCFA content. The drastic reduction of intestinal SCFA associated with the decrease in anaerobes during the diarrheal stage and the increase of the pH thought to be due to these changes, result in increase of the fecal water content[20-22].

Probiotics are known to prevent or lower the antibiotic-related gastrointestinal side effects. It is reported that CBM together with germinated barley foodstuff effectively increased the level of SCFA in feces and suppressed dextran sulfate sodium-induced experimental colitis in rats[23]. Butyric acids, which is produced by CBM has stronger stimulatory effects on epithelial cell proliferation than other SCFA, such as acetic acid or propionic acid[24].

Tanaka *et al*[25]. reported that the effect of CBM on the side effect of *H pylori* eradication triple therapy *in vivo*. These results have shown that obligate anaerobe and Lactobacillus decreased in the rat intestine and then SCFA in intestinal contents were decreased. However, administration of CBM preparation with *H pylori* eradication triple therapy was increased SCFA and resident fusiform bacteria in the mucous layer were more frequently observed in rats administered with CBM preparation than *H pylori* eradication triple therapy.

Our present findings show that CBM preparations prevent the decrease of obligate anaerobes and reduce the frequency of gastrointestinal side effects. These result similar to the pervious *in vivo* result. However, we did not examine the concentration of SCFA in this study but it is possible that the one of mechanism of action of CBM preparation to prevent the side effect induced by not only maintenance of intestinal flora but also increased SCFA contents by CBM.

In our study, *H pylori* eradication therapy caused a significantly greater decrease of *E.coli* , as a results, Enterobacteriaceae, except of *E.coli,* such as *Klebsiella* and *Enterobacter* that are known to potential cause of diarrhea was rising in Group 1.

Our results showed that CBM suppressed the replacement of *E.coli* by other species in Entero-bacteriaceae and superinfection.

In conclusion, intestinal flora with an eradication treatment of *H pylori* not a little changed. The change was reduced by supplementation of CBM, and the frequency of gastrointestinal side effects decreased. Furthermore CBM may have some beneficial effects on *H pylori* infection.

ACKNOWLEDGMENT

We would like to express our gratitude to Mamoru Tanaka, Miyarisan pharmaceutical Co., Ltd. for his technical help.

REFERENCES

1 **Bakir AA,** Levy PS, Dunea G. The prognosis of lupus nephritis in African-Americans: a retrospective analysis. *Am J Kidney Dis* 1994; **24**: 159-171

2 **Miwa H**, Nagahara A, Sato K, Ohkura R, Murai T, Shimizu H, Watanabe S, Sato N. Efficacy of 1 week omeprazole or lansoprazole-amoxycillin-clarithromycin therapy for *Helicobacter pylori* infection in the Japanese population. *J Gastroenterol Hepatol* 1999; **14**: 317-321

3 **Labenz J**, Stolte M, Peitz U, Tillenburg B, Becker T, Börsch G. One-week triple therapy with omeprazole, amoxycillin and either clarithromycin or metronidazole for cure of *Helicobacter pylori* infection. *Aliment Pharmacol Ther* 1996; **10**: 207-210

4 **Wurzer H**, Rodrigo L, Stamler D, Archambault A, Rokkas T, Skandalis N, Fedorak R, Bazzoli F, Hentschel E, Mora P, Archimandritis A, Megraud F. Short-course therapy with amoxycillin-clarithromycin triple therapy for 10 days (ACT-10) eradicates *Helicobacter pylori* and heals duodenal ulcer. *ACT-10 Study Group. Aliment Pharmacol Ther* 1997; **11**: 943-952

5 **Lind T,** Veldhuyzen van Zanten S, Unge P, Spiller R, Bayerdorffer E, O'Morain C, Bardhan KD, Bradette M, Chiba N, Wrangstadh M, Cederberg C, Idstrom JP. Eradication of *Helicobacter pylori* using one-week triple therapies combining omeprazole with two antimicrobials: the MACH I Study. *Helicobacter* 1996; **1**: 138-144

6 **Armuzzi A**, Cremonini F, Bartolozzi F, Canducci F, Candelli M, Ojetti V, Cammarota G, Anti M, De Lorenzo A, Pola P, Gasbarrini G, Gasbarrini A. The effect of oral administration of *Lactobacillus* GG on antibiotic-associated gastrointestinal side-effects during *Helicobacter pylori* eradication therapy. *Aliment Pharmacol Ther* 2001; **15**: 163-169

7 **Gorbach SL**. Lactic acid bacteria and human health. *Ann Med* 1990; **22**: 37-41

8 **Seki H**, Shiohara M, Matsumura T, Miyagawa N, Tanaka M, Komiyama A, Kurata S. Prevention of antibiotic-associated diarrhea in children by *Clostridium butyricum* MIYAIRI. *Pediatr Int* 2003; **45**: 86-90

9 **Kamiya S**, Taguchi H, Yamaguchi H, Osaki T, Takahashi M, Nakamura S. Bacterioprophylaxis using *Clostridium butyricum* for lethal caecitis by *Clostridium difficile*. *Rev. Med. Miclobiol.* 1997; **8**: S57-S59.

10 **Okamoto T**, Sasaki M, Tsujikawa T, Fujiyama Y, Bamba T, Kusunoki M. Preventive efficacy of butyrate enemas and oral administration of *Clostridium butyricum* M588 in dextran sodium sulfate-induced colitis in rats. *J Gastroenterol* 2000; **35**: 341-346

11 **Mitsuoka T**. Cultivation of intestinal bacteria. In: Mitsuoka T, ed. Intestinal bacteria and health. Tokyo: Harcourt Brace Jovanovich Japan;1978.19-36.

12 **Sanders WE**, Sanders CC. Modification of Normal Fora by Antibiotics: Effects on Individuals and the Environment. In: Root RK, Sande MA, eds. New dimensions in antimicrobial therapy. New York: Churchill Livingstone, 1984:217-41

13 **Simon GL,** Gorbach SL. The human intestinal microflora. *Dig Dis Sci* 1986; **31**: 147S-162S

14 **Bühling A,** Radun D, Müller WA, Malfertheiner P. Influence of anti-*Helicobacter* triple-therapy with metronidazole, omeprazole and clarithromycin on intestinal microflora. *Aliment Pharmacol Ther* 2001; **15**: 1445-1452

15 **Sakata T**, von Engelhardt W. Stimulatory effect of short chain fatty acids on the epithelial cell proliferation in rat large intestine. *Comp Biochem Physiol* A *Comp Physiol* 1983; **74**: 459-462

16 **Roediger WE**. Utilization of nutrients by isolated epithelial cells of the rat colon. *Gastroenterology* 1982; **83**: 424-429

17 **Ruppin H**, Bar-Meir S, Soergel KH, Wood CM, Schmitt MG. Absorption of short-chain fatty acids by the colon. *Gastroenterology* 1980; **78**: 1500-1507

18 **Koruda MJ,** Rolandelli RH, Settle RG, Saul SH, Rombeau JL. Harry M. Vars award. The effect of a pectin-supplemented elemental diet on intestinal adaptation to massive small bowel resection. *JPEN J Parenter Enteral Nutr* 1986; **10**: 343-350

19 **Crump MH**, Argenzio RA, Whipp SC. Effects of acetate on absorption of solute and water from the pig colon. *Am J Vet Res* 1980; **41**: 1565-1568

20 **Tazume S**, Ozawa A, Yamamoto T, Takahashi Y, Takeshi K, Saidi SM, Ichoroh CG, Waiyaki PG. Ecological study on the intestinal bacteria flora of patients with diarrhea. *Clin Infect Dis* 1993; **16 Suppl 2**: S77-S82

21 **Fujita K**, Kaku M, Yanagase Y, Ezaki T, Furuse K, Ozawa A, Saidi SM, Sang WK, Waiyaki PG. Physicochemical characteristics and flora of diarrhoeal and recovery faeces in children with acute gastro-enteritis in Kenya. *Ann Trop Paediatr* 1990; **10**: 339-345

22 **Takahashi M**, Taguchi H, Yamaguchi H, Osaki T, Komatsu A, Kamiya S. The effect of probiotic treatment with *Clostridium butyricum* on enterohemorrhagic *Escherichia coli* O157:H7 infection in mice. *FEMS Immunol Med Microbiol* 2004; **41**: 219-226

23 **Araki Y**, Fujiyama Y, Andoh A, Koyama S, Kanauchi O, Bamba T. The dietary combination of germinated barley foodstuff plus *Clostridium butyricum* suppresses the dextran sulfate sodium-induced experimental colitis in rats. *Scand J Gastroenterol* 2000; **35**: 1060-1067

24 **Kripke SA**, Fox AD, Berman JM, Settle RG, Rombeau JL. Stimulation of intestinal mucosal growth with intracolonic infusion of short-chain fatty acids. *JPEN J Parenter Enteral Nutr* 1989; **13**: 109-116

25 **Tanaka M**, Miyagawa N, Tsutsumi Y Preventive effect of *Clostridium butyricum* on the side effect of the *Helicobacter pylori* eradication. *Chin J Gastroenterol* 2000; **5**: Suppl A116

Science Editor Guo SY **Language Editor** Elsevier HK

PO Box 2345, Beijing 100023, China
www.wjgnet.com
wjg@wjgnet.com

ELSEVIER

World J Gastroenterol 2005;11(47):7525-7530
World Journal of Gastroenterology ISSN 1007-9327

• *RAPID COMMUNICATION* •

Single nucleotide polymorphisms of *OCTN1*, *OCTN2*, and *DLG5* genes in Greek patients with Crohn's disease

Maria Gazouli, Gerassimos Mantzaris, Athanassios J Archimandritis, George Nasioulas, Nicholas P Anagnou

Maria Gazouli, Nicholas P Anagnou, Department of Biology, School of Medicine, University of Athens, Athens 11725, Greece
Gerassimos Mantzaris, Department of Gastroenterology, Evagelismos Hospital, Athens 11521, Greece
Athanassios J Archimandritis, Department of Internal Medicine, Hippokration General Hospital, School of Medicine, University of Athens, Athens 11527, Greece
George Nasioulas, Molecular Biology Department Research Center HYGEIA "Antonis Papayiannis", Athens, Greece
Correspondence to: Dr N.P. Anagnou, Department of Biology, School of Medicine, University of Athens, M. Asias 75, Athens 11527, Greece. anagnou@med.uoa.gr
Telephone: +30-2107462341 Fax: +30-2107462340
Received: 2005-02-23 Accepted: 2005-06-24

Abstract

AIM: To validate novel single nucleotide polymorphisms (SNPs) in Greek patients with Crohn's disease (CD).

METHODS: A total of 120 patients with CD, 85 patients with UC, and 100 unrelated healthy controls were genotyped. Genotyping was performed by allele-specific PCR or by PCR-RFLP analysis.

RESULTS: Our results showed that the 1672T and -207C alleles were obviously over-represented in CD patients only ($P<0.01$ and $P<0.05$, respectively) compared to the control population. The G113A polymorphism was completely absent in our studied population. The odds ratio for the carriage of the TC haplotype was 2.21 for CD patients as compared with controls. Additionally, the frequency of the TC haplotype was increased in patients with ileocolitis or colitis, and was mainly associated with the fibrostenotic phenotype of the disease. Furthermore, when the TC haplotype was compared jointly with the carriage of at least one mutation of the *NOD*2/*CARD*15 gene, there was an increased risk for CD, but not for UC, compared to controls. Regarding the location of the disease, the concomitant presence of the TC haplotype and *NOD*2/*CARD*15 mutations was mainly associated with ileocolitis or ileitis.

CONCLUSION: Collectively, our results suggest that the 1672T variant of the *OCTN*1 gene and the -207C variant of the *OCTN2* gene represent risk factors for CD in the Greek population.

Key words: Crohn's disease; SNPs; *OCTN1*; *OCTN2*; *DLG5*

Gazouli M, Mantzaris G, Archimandritis AJ, Nasioulas G, Anagnou NP. Single nucleotide polymorphisms of the *OCTN1*, *OCTN2*, and *DLG5* genes in Greek patients with Crohn's disease. *World J Gastroenterol* 2005; 11(47): 7525-7530
http://www.wjgnet.com/1007-9327/11/7525.asp

INTRODUCTION

The inflammatory bowel diseases (IBD), Crohn's disease (CD) and ulcerative colitis (UC), represent common chronic relapsing and remitting inflammatory disorders of the intestine. The pathogenesis of IBD is complex and both environmental and genetic factors contribute to its etiology. A series of genetic and epidemiologic studies have provided conclusive evidence for the presence of genetic determinants of disease susceptibility and progression[1]. Genome-wide linkage studies of IBD families that were affected by multiple factors have been remarkably successful in identifying a number of susceptibility loci, with convincing replication shown for at least 7 loci (IBD1-7)[2]. In 1996, Hugot *et al*[3]. identified the first susceptibility locus for CD adjacent to the centromere on chromosome 16 (IBD1)[3]. This has been further corroborated in several independent Caucasian populations[4-6]. In 2001, three independent CD mutations within the *NOD*2/*CARD*15 gene, mapping to chromosome 16, were discovered. These mutations are strongly associated with CD in populations of European descent[7-11].

Very recently, Peltekova *et al*[12]. reported on two novel functional single nucleotide polymorphisms (SNPs) in the carnitine/organic cation transporter (OCTN) cluster on 5q31 (designated as the IBD5 locus) that were associated with CD[12]. The cation transporters are expressed in the liver, kidney, intestine, brain, heart and placenta, and maintain physiological cation environments in the organism.

A C1672T substitution in exon 9 of the *OCTN*1 gene and a G-207C in the *OCTN*2 promoter region have been suggested as causative mutations to increase susceptibility to CD. Additionally, Stoll *et al*[13]. reported that a G113A SNP in exon 3 of the *DLG*5 gene was also associated with susceptibility to IBD. This gene is located on the long arm of chromosome 10 (10q23) and encodes a scaffolding protein involved in the maintenance of epithelial integrity. Genetic variants in *DLG*5 could therefore interfere with the epithelial barrier.

Table 1 Demographic characteristics and clinical features of 120 patients with Crohn's disease and of 85 patients with ulcerative colitis

	Crohn's disease	Ulcerative colitis
Total number	120	85
Sex (male/female)	58/62	42/43
Age of diagnosis (mean±SD yr)	29.82±14.00	33.36±14.24
Family history in first-degree relative (%)	4 (3.3 %)	5 (5.9%)
Smoking habit (%)		
Never	50 (41.7%)	48 (56.5%)
Ex-smoker	11 (9.2%)	14 (16.5%)
Current	59 (49.2%)	23 (27.1%)
Localization of disease		
Ileal	39 (32.5%)	
Colonic	11 (9.2%)	
Ileocolitis	67 (55.8%)	
Upper gastroenteric	3 (2.5%)	
Disease features		
Inflammatory	78 (65%)	
Fibrostenotic	32 (26.7%)	
Fistulizing	10 (8.3%)	
Extra-intestinal manifestations		
Arthritis	16 (13.3%)	
Erythema nodosum	5 (4.2%)	

To investigate whether the above mentioned SNPs in *OCTN*1, *OCTN*2, and *DLG*5 genes contribute to the predisposition to IBD, as well as whether the interaction of specific haplotypes of the *NOD*2/*CARD15*, *OCTN*1, *OCTN*2, and *DLG*5 genes could increase the risk for IBD in the Greek population, we genotyped 120 patients with CD, 85 patients with UC, and 100 healthy controls. Our studies documented that mutations of the *OCTN1* and *OCTN*2 genes were obviously associated with CD. Furthermore, the combination of the OCTN-TC haplotype was found to be significantly associated with ileocolitis or colitis and the fibrostenotic phenotype, while the combination of the TC haplotype with the *NOD*2/*CARD15* variants was associated with ileocolitis or ileitis.

MATERIALS AND METHODS

Subjects

Blood samples from 120 patients with CD, 85 patients with UC and 100 age- and sex-matched healthy individuals were collected at the IBD Outpatient Clinic of the Evagelismos Hospital, between September 2002 and February 2003. The vast majority of these patients had been diagnosed at our institutions (open-access visit to the IBD Outpatients Clinic or as emergency cases), but there were also some referrals by other physicians. All groups were matched with regard to sex and age, and all subjects were of Greek origin. The diagnosis of either CD or UC was based on standard clinical, endoscopic, radiological, and histological criteria[7,14]. For CD, the vast majority of the patients (102, 85%) had newly diagnosed disease that was classified according to the Vienna System. The records of CD patients were systematically reviewed for the following demographic and clinical characteristics: age, sex, smoking habits, age at diagnosis, disease localization (ileal, colonic, ileocolonic or upper gastroenteric), disease behavior (inflammatory, fibrostenotic or fistulizing), presence of extra-intestinal clinical manifestations (e.g., arthritis, erythema nodosum), and familial IBD (Table 1). Before the commencement of the study, the ethics committee at the participating centers had approved the recruitment protocols. Informed consent was obtained from all the participants.

Genotyping

DNA was isolated from blood with the NucleoSpin blood kit (Macherey-Nagel, Germany). To confirm the integrity of DNA, initially a 430-bp sequence in the human glyceraldehyde-3-phosphatate dehydrogenase gene was amplified.

The genotyping for the three casual *NOD*2/*CARD*15 variants (L1007fsinsC, R702W, and G908R) in the studied group of patients and controls has been previously performed[7].

The C1672T substitution in exon 9 of the *OCTN*1 was genotyped by a PCR amplification of specific allele assay, using two allele-specific reverse primers: octn1C, 5' TCTGACTGTCCTGATTGGAATCC 3' for the wild type allele and octn1T: 5' TCTGACTGTCCTGATTGGAATCT 3' for the mutant allele, in combination with a common forward primer octn1F: 5' AGATGAGGTTTCACTATGTTGGC 3' in two separate PCR reactions. The 3'-ends of the reverse primers were able to anneal to the regions that differed between the two alleles. The PCR profile included initial denaturation at 95 ℃ for 5 min, followed by 35 amplification cycles of denaturation at 94 ℃ for 45 s, annealing at 58 ℃ for 40 s and extension at 72 ℃ for 30 s and a final incubation at 72 ℃ for 10 min.

The mutation G-207C in the *OCTN*2 promoter region resulted in the abolishment of a restriction site for NlaIV and was genotyped by a combined PCR-RFLP method using primers 5' TCAGGTGCACTCCCGGCCCG 3' (forward) and 5' GACCAGGCAAGCCAGGCAGC 3' (reverse). The presence of a wild-type allele resulted in the generation of three fragments (42, 44, and 122 bp), whereas the RFLP profile of the -207C variant was characterized by two fragments of 42 and 167 bp, analyzed by 30 g/L agarose gel electrophoresis. The PCR conditions included initial denaturation at 95 ℃ for 5 min, followed by three cycles of denaturation at 94 ℃ for 40 s, annealing at 58 ℃ for 1 min and extension at 72 ℃ for 2 min, by two cycles of denaturation at 94 ℃ for 40 s, annealing at 56 ℃ for 1 min and extension at 72 ℃ for 2 min, and by 28 cycles of denaturation at 94 ℃ for 40 s, annealing at 54 ℃ for 1 min and extension at 72 ℃ for 2 min, and a final incubation at 72 ℃ for 10 min.

The G113A SNP in exon 3 of the *DLG*5 gene creates a restriction site for *Msp*I and was also genotyped by a combined PCR-RFLP method using a primers 5' TCACTTTCAGTTCTACCTGCTAC 3' (forward) and 5' TCTAGGAGACAGTGGTAGGG 3' (reverse). The

Table 2 Allele and genotype frequencies of C1672T SNP in *OCTN*1 gene in CD and UC patients and in healthy controls

	Alleles				Genotypes				
	C	T	T allele frequencies (%)	*P* [odds ratio (95%CI)]	CC	CT	TT	TT genotype frequencies (%)	*P* [odds ratio (95%CI)]
CD	180	60	25	0.01 [1.89 (1.16–3.07)]	70	40	10	8.33	0.095 [2.94 (0.78–10.99)]
UC	151	19	11.17	0.28 [0.71 (0.38–1.32)]	67	17	1	1.17	0.39 [0.38 (0.04–3.77)]
Controls	170	30	15		73	24	3	3	

Table 3 Allele and genotype frequencies of G-207C SNP in OCTN2 gene in CD and UC patients and in healthy controls

	Alleles				Genotypes				
	G	C	C allele frequencies (%)	*P* [odds ratio (95%CI)]	GG	GC	CC	CC genotype frequencies (%)	*P* [odds ratio (95%CI)]
CD	188	52	21.67	0.038 [1.69 (1.02–2.81)]	75	38	7	5.83	0.53 [1.49 (0.42–5.23)]
UC	152	18	10.58	0.32 [0.73 (0.39–1.37)]	69	14	2	2.35	0.53 [0.58 (0.10–3.24)]
Controls	172	28	14		76	20	4	4	

Table 4 Linkage disequilibrium (*D'* and r^2 between 1672T and -207C are indicated), and TC haplotype frequencies in patients with CD, UC and in healthy individuals

	Number of patients	*D'*	r^2	TC haplotype frequencies (%)	*P* [odds ratio (95%CI)]
CD	120	0.51	0.22	13.3	0.018 [2.21 (1.12–4.43)]
UC	85	0.5	0.23	5.9	0.81 [0.89 (0.37–2.15)]
Controls	100	0.34	0.1	6.5	

Table 5 Odds ratios for susceptibility to CD and UC of a *NOD*2/*CARD*15 mutation, and for the joint TC- NOD2/CARD15 effect

	Odds ratios		
	TC	*NOD*2/*CARD*15	Joint TC- *NOD*2/*CARD*15
CD	2.21 (1.12–4.43) *P* = 0.018	16.8 (8.6–32.7) *P* < 0.0001	9.22 (2.1–40.6) *P* = 0.0005
UC	0.89 (0.37–2.15) *P* = 0.79	3.34 (1.76–6.36) *P* = 0.0002	3.06 (0.58–16.21) *P* = 0.17

presence of a wild-type allele resulted in five fragments of 40, 51, 65, 124, and 360 bp, whereas the RFLP profile of the 113A variant was characterized by four bands of 65, 91, 124, and 360 bp. The PCR conditions included initial denaturation at 95 ℃ for 5 min, followed by 35 cycles of denaturation at 94 ℃ for 45 s, annealing at 58 ℃ for 40 s and extension at 72 ℃ for 30 s, and a final incubation at 72 ℃ for 10 min.

All PCR assays were performed in a 50-μL volume reaction containing 10 mmol/L Tris-HCl (pH 8.3), 50 mmol/L KCl, 2 mmol/L $MgCl_2$, 250 μmol/L dNTPs, 0.20 μmol/L of each primer, 200 ng of genomic DNA and 2.5 U of Taq DNA polymerase (Platinum Invitrogen). The specificity of PCR products was confirmed by sequencing analysis using a Dye Terminator Cycle Sequencing Ready Reaction kit (Applied Biosystems, Darmstadt, Germany), and an ABI 377 automated sequencer.

Statistical analysis

Frequency and susceptibilities of mutations among the patients and controls were compared using χ^2 test. Odds ratios (OR) were calculated with the corresponding χ^2 distribution test and 95% confidence intervals (95%CI). The two-tailed $P<0.05$ were considered statistically significant. Hardy-Weinberg equilibrium was verified by the calculation of expected frequencies and numbers, and significance testing was based on the 1 df χ^2. The hypothesis that there is no linkage disequilibrium (LD) was also tested using the 1 df χ^2. Allele frequency independent estimators of LD were used: the $D' = D/D_{max}$, where D_{max} is the maximum possible D (i.e., for border frequencies p_1, p_2, q_1, q_2, the lesser of p_1q_2 or p_2q_1 if D is positive or lesser of p_1q_1 or p_2q_2 if D is negative). Inference was aided by GraphPad InStat (version 3.00, GraphPad Software, Inc., San Diego, CA, USA).

RESULTS

We genotyped 120 patients with CD, 85 patients with UC and 100 healthy individuals in order to investigate a possible association of the genetic substitutions in the *OCTN*1, *OCTN*2 and *DLG5* genes with a susceptibility to CD in the Greek population. These mutations were reported to have significant association with CD in the Caucasian population[13,14].

The C1672T of the *OCTN*1 genotype carrier frequencies are summarized in Table 2. The distribution of genotypes was consistent with the Hardy-Weinberg equilibrium. The 1672T allele frequencies were 25%, 11.17%, and 15% in CD, UC and healthy controls, respectively. The frequency of the 1672T allele was significantly higher in CD patients compared to the controls ($P<0.05$). The 1672T allele was not found to be significantly associated with UC.

Allele and genotype frequencies of the mutations G-207C of the *OCTN*2 gene are presented in Table 3. The

distribution of genotypes was consistent with the Hardy-Weinberg equilibrium. C allele frequencies were markedly increased in only CD patients compared to the controls ($P<0.05$).

The G113A SNP of the *DLG5* gene was completely absent in the Greek IBD cases as well as in the Greek healthy population.

The C1672T and G-207C were in strong linkage disequilibrium and created a two-allele risk haplotype (TC) (Table 3). The TC haplotype was significantly overrepresented in patients with CD (13.3%) as compared to the controls (6.5%) ($P<0.05$, Table 4). Odds ratios conferred by allele 1672T, allele -207C or the TC haplotype were similar. The risk for CD was much greater in the presence of both the TC haplotype and at least one of the three main alleles of *NOD*2/*CARD*15 gene (Table 5).

A significant association was found between ileocolitis and colitis and possession of TC haplotype. Twenty-three out of the thirty carriers of the TC haplotype had ileocolitis or colitis, whereas only seven TC carriers had exclusively ileal disease ($P<0.01$). Notably, when the presence of TC haplotype was evaluated jointly with the presence of one or more of the common *NOD*2/*CARD*15 variants, a significant association was observed with ileocolitis and ileitis. Seventeen of the nineteen carriers of both TC haplotype and at least one of the *NOD*2/*CARD*15 variants had ileocolitis or ileitis, whereas only two patients presented exclusively colitis ($P<0.05$).

In CD patients, disease behavior in 32 (26.7%) was defined as fibrostenotic, in 10 (8.3%) as fistulizing and in 78 (65%) as inflammatory. A significant association was observed between the presence of the TC haplotype and fibrostenotic *vs* inflammatory phenotype of disease in our population. Twenty out of the thirty TC carriers presented a fibrostenotic phenotype since only 10 patients had inflammatory disease ($P<0.05$).

DISCUSSION

The precise etiology of CD and UC is uncertain, although it is widely accepted that IBD develops in a genetically predisposed individual following exposure to environmental stimuli[15]. The genetic basis of IBD is adequately documented, since genetic factors that affect susceptibility to IBD have been disclosed through genetic linkage and population-based association studies[9-11]. *NOD*2/*CARD*15 was the first gene which was found to be associated with IBD, specifically with CD[9,10]. Through the candidate gene approach, various genes were identified as candidate genes to predispose to IBD in some populations[16]. Very recently Peltekova *et al*[12]. reported on two functional mutations in the *OCTN* cluster on 5q31 (the IBD5 locus) that were associated with CD, while Stoll *et al*[13]. reported the association of IBD with mutations in the *DLG*5 gene.

Regarding the *OCTN*1 and *OCTN*2, it has been recently shown that mutations in these genes are associated with lower carnitine uptake rate and increased transport of xenobiotics[14,17]. It is known that carnitine deficiency could be related with a disorder of fatty acid oxidation and consequently with insufficient fatty acid β-oxidation[17]. On the other hand, there are some evidences that the inhibition of fatty acid oxidation in the epithelium of the colonic mucosa is associated with UC and inflammation[18]. Taking all these into consideration, it seems reasonable that the *OCTN* cluster might have an active role in IBD pathogenesis.

Our case-control study for *OCTN*1 and *OCTN2* genes showed that the frequency of the 1672T and -207C alleles was significantly higher in CD patients compared to UC patients and controls. Both mutations were, as expected from the previous studies on IBD5 haplotype, in strong linkage disequilibrium (LD) and created a two-allele risk haplotype, i.e. TC which in our cases had a frequency of 13.3% in CD patients compared to 6.5% in healthy individuals. Although the TC haplotype frequency that was observed was lower than that reported by Peltekova *et al*[12]. our results confirmed an association between the *OCTN* cluster and CD. The TC haplotype was not increased in UC in our population, which was in agreement with Peltekova *et al*[12]. but in contrast with several previous studies on IBD5[19,20]. It has to be pointed out that our results differed from those of a recent study in CD patients in a Japanese population, where other genetic variants have been associated with CD pathogenesis[21]. Furthermore, it is known that variants in the IBD5 haplotype appear to be very rare in the Japanese population[19].

It has been hypothesized that the third member of the *OCTN* cluster, the *OCTN*3 gene, in the *OCTN*1-*OCTN*2 interval, is also associated with IBD[22]. The *OCTN*3 gene might represent a homolog to the mouse gene Slc22a9 and several research groups were unable to identify a human counterpart or any other gene within this region[12,22].

Interestingly, the risk for CD was even greater in the presence of both TC haplotype and at least one of the *NOD*2/*CARD*15 variants, confirming the previously reported interaction between IBD5 haplotype and *NOD*2/*CARD*15[23]. Notably, in agreement with our results, very recently, Torok *et al*[24]. reported that TC haplotype was associated with an increased CD risk, which increases even more in the presence of *NOD*2/*CARD*15 mutations.

Patients with CD clinically present heterogeneous disease characteristics, including differences in disease behavior, localization and severity. Defining the relationship between *OCTN*-TC haplotype and disease phenotypic variation is not only crucial in probing the clinical diversity in disease presentation and behavior, but may also assist in defining rational treatment strategies. Concerning the disease location in the intestine, we found that the possession of the TC haplotype was associated mainly with colitis or ileocolitis, which was in agreement with previous findings that demonstrated the IBD5 association with colonic CD[24-27]. However, when the TC haplotype was combined with the presence of at least one of the *NOD*2/*CARD*15 variants, a significant association with ileitis or ileocolitis was observed, which was in agreement with the results of a recent study by Newman *et al*[28]. This observation suggests that these variants have a

biological involvement in CD pathogenesis. When disease behavior was examined, the presence of the TC haplotype was found to be associated with the fibrostenotic phenotype.

Concerning the *DLG*5 gene, which is important in maintaining the epithelial structure, the 113A variant was completely absent in our studied population. Our observations concerning the *DLG*5 gene were strongly in contrast with previous data reported by Stoll *et al*[13]. but were in full agreement with the studies by Torok *et al*[24]. and Noble *et al*[29]. in German and Scottish populations, respectively. These findings are not unexpected in a polygenic disease model, and imply significant differences in the genetic background for CD susceptibility among the different populations.

Collectively, our study confirms recent findings suggesting that the mutations in *OCTN*1 and *OCTN*2 genes are associated with CD[12]. Additionally, our results indicate that the carriage of the *OCTN*-TC haplotype is significantly associated with ileocolitis or colitis and the fibrostenotic phenotype, but the TC haplotype combined with the presence of *NOD*2/*CARD*15 variants, associates with ileocolitis or ileitis. However, further studies involving a larger number of cases and controls in a worldwide scale are needed to elucidate the complex biological mechanisms underlying IBD susceptibility.

REFERENCES

1 **Bonen DK**, Cho JH. The genetics of inflammatory bowel disease. *Gastroenterology* 2003; **124**: 521-536

2 **Ahmad T**, Tamboli CP, Jewell D, Colombel JF. Clinical relevance of advances in genetics and pharmacogenetics of IBD. *Gastroenterology* 2004; **126**: 1533-1549

3 **Hugot JP**, Laurent-Puig P, Gower-Rousseau C, Olson JM, Lee JC, Beaugerie L, Naom I, Dupas JL, Van Gossum A, Orholm M, Bonaiti-Pellie C, Weissenbach J, Mathew CG, Lennard-Jones JE, Cortot A, Colombel JF, Thomas G. Mapping of a susceptibility locus for Crohn's disease on chromosome 16. *Nature* 1996; **379**: 821-823

4 **Cavanaugh J**. International collaboration provides convincing linkage replication in complex disease through analysis of a large pooled data set: **Crohn disease and chromosome 16.** *Am J Hum Genet* 2001; **68**: 1165-1171

5 **Zouali H**, Chamaillard M, Lesage S, Cézard JP, Colombel JF, Belaiche J, Almer S, Tysk C, Montague S, Gassull M, Christensen S, Finkel Y, Gower-Rousseau C, Modigliani R, Macry J, Selinger-Leneman H, Thomas G, Hugot JP. Genetic refinement and physical mapping of a chromosome 16q candidate region for inflammatory bowel disease. *Eur J Hum Genet* 2001; **9**: 731-742

6 **Brant SR**, Panhuysen CI, Bailey-Wilson JE, Rohal PM, Lee S, Mann J, Ravenhill G, Kirschner BS, Hanauer SB, Cho JH, Bayless TM. Linkage heterogeneity for the IBD1 locus in Crohn's disease pedigrees by disease onset and severity. *Gastroenterology* 2000; **119**: 1483-1490

7 **Gazouli M**, Zacharatos P, Mantzaris GJ, Barbatis C, Ikonomopoulos I, Archimandritis AJ, Lukas JC, Papalambros E, Gorgoulis V. Association of NOD2/CARD15 variants with Crohn' s disease in a Greek population. *Eur J Gastroenterol Hepatol* 2004; **16**: 1177-1182

8 **Gazouli M**, Mantzaris G, Kotsinas A, Zacharatos P, Papalambros E, Archimandritis A, Ikonomopoulos J, Gorgoulis VG. Association between polymorphisms in the Toll-like receptor 4, CD14, and CARD15/NOD2 and inflammatory bowel disease in the Greek population. *World J Gastroenterol* 2005; **11**: 681-685

9 **Ogura Y**, Bonen DK, Inohara N, Nicolae DL, Chen FF, Ramos R, Britton H, Moran T, Karaliuskas R, Duerr RH, Achkar JP, Brant SR, Bayless TM, Kirschner BS, Hanauer SB, Nuñez G, Cho JH. A frameshift mutation in NOD2 associated with susceptibility to Crohn's disease. *Nature* 2001; **411**: 603-606

10 **Hugot JP**, Chamaillard M, Zouali H, Lesage S, Cézard JP, Belaiche J, Almer S, Tysk C, O'Morain CA, Gassull M, Binder V, Finkel Y, Cortot A, Modigliani R, Laurent-Puig P, Gower-Rousseau C, Macry J, Colombel JF, Sahbatou M, Thomas G. Association of NOD2 leucine-rich repeat variants with susceptibility to Crohn's disease. *Nature* 2001; **411**: 599-603

11 **Hampe J**, Cuthbert A, Croucher PJ, Mirza MM, Mascheretti S, Fisher S, Frenzel H, King K, Hasselmeyer A, MacPherson AJ, Bridger S, van Deventer S, Forbes A, Nikolaus S, Lennard-Jones JE, Foelsch UR, Krawczak M, Lewis C, Schreiber S, Mathew CG. Association between insertion mutation in NOD2 gene and Crohn's disease in German and British populations. *Lancet* 2001; **357**: 1925-1928

12 **Peltekova VD**, Wintle **RF, Rubin LA, Amos CI, Huang Q, Gu** X, Newman B, Van Oene M, Cescon D, Greenberg G, Griffiths AM, St George-Hyslop PH, Siminovitch KA. Functional variants of OCTN cation transporter genes are associated with Crohn disease. *Nat Genet* 2004; **36:** 471-475

13 **Stoll M**, Corneliussen B, Costello CM, Waetzig GH, Mellgard B, Koch WA, Rosenstiel P, Albrecht M, Croucher PJ, Seegert D, Nikolaus S, Hampe J, Lengauer T, Pierrou S, Foelsch UR, Mathew CG, Lagerstrom-Fermer M, Schreiber S. Genetic variation in DLG5 is associated with inflammatory bowel disease. *Nat Genet* 2004; **36**: 476-480

14 **Podolsky DK**. Inflammatory bowel disease 2. *N Engl J Med* 1991; **325**: 928-937

15 **Orchard TR**, Satsangi J, Van Heel D, Jewell DP. Genetics of inflammatory bowel disease: a reappraisal. *Scand J Immunol* 2000; **51**: 10-17

16 **Wild GE**, Rioux JD. Genome scan analyses and positional cloning strategy in IBD: successes and limitations. *Best Pract Res Clin Gastroenterol* 2004; **18**: 541-553

17 **Lahjouji K**, Mitchell GA, Qureshi IA. Carnitine transport by organic cation transporters and systemic carnitine deficiency. *Mol Genet Metab* 2001; **73**: 287-297

18 **Roediger WE**, Nance S. Metabolic induction of experimental ulcerative colitis by inhibition of fatty acid oxidation. *Br J Exp Pathol* 1986; **67**: 773-782

19 **Giallourakis C,** Stoll M, Miller K, Hampe J, Lander ES, Daly MJ, Schreiber S, Rioux JD. **IBD5 is a general risk factor for** inflammatory bowel disease: replication of association with Crohn disease and identification of a novel association with ulcerative colitis. *Am J Hum Genet* 2003; **73**: 205-**211**

20 **McGovern DP**, Van Heel DA, Negoro K, Ahmad T, Jewell DP. Further evidence of IBD5/CARD15 (NOD2) epista**sis in the** susceptibility to ulcerative colitis. *Am J Hum Genet* 2003; **73**: 1465-1466

21 **Yamazaki K**, Takazoe M, Tanaka T, Ichimori T, Saito S, Iida A, Onouchi Y, Hata A, Nakamura Y. Association analysis of SLC22A4, SLC22A5 and DLG5 in Japanese patients with Crohn disease. *J Hum Genet* 2004; **49**: 664-668

22 **Lamhonwah AM**, Skaug J, Scherer SW, Tein I. A third human carnitine/organic cation transporter (OCTN3) as a candidate for the 5q31 Crohn's disease locus (IBD5). *Biochem Biophys Res Commun* 2003; **301**: 98-101

23 **Mirza MM**, Fisher SA, King K, Cuthbert AP, Hampe J, Sanderson J, Mansfield J, Donaldson P, Macpherson AJ, Forbes A, Schreiber S, Lewis CM, Mathew CG. Genetic evidence for interaction of the 5q31 cytokine locus and the CARD15 gene in Crohn disease. *Am J Hum Genet* 2003; **72**: 1018-1022

24 **Török HP**, Glas J, Tonenchi L, Lohse P, Müller-Myhsok B, Limbersky O, Neugebauer C, Schnitzler F, Seiderer J, Tillack C, Brand S, Brünnler G, Jagiello P, Epplen JT, Griga T, Klein W, Sc**hiemann U, Folwaczny M, Ochsenkühn T, Folwaczny** C. Polymorphisms in the DLG5 and OCTN cation transporter

genes in Crohn's disease. *Gut* 2005; **54**: 1421-1427

25 **Armuzzi A**, Ahmad T, Ling KL, de Silva A, Cullen S, van Heel D, Orchard TR, Welsh KI, Marshall SE, Jewell DP. Genotype-phenotype analysis of the Crohn's disease susceptibility haplotype on chromosome 5q31. *Gut* 2003; **52**: 1133-1139

26 **Rioux JD**, Daly MJ, Silverberg MS, Lindblad K, Steinhart H, Cohen Z, Delmonte T, Kocher K, Miller K, Guschwan S, Kulbokas EJ, O'Leary S, Winchester E, Dewar K, Green T, Stone V, Chow C, Cohen A, Langelier D, Lapointe G, Gaudet D, Faith J, Branco N, Bull SB, McLeod RS, Griffiths AM, Bitton A, Greenberg GR, Lander ES, Siminovitch KA, Hudson TJ. Genetic variation in the 5q31 cytokine gene cluster confers susceptibility to Crohn disease. *Nat Genet* 2001; **29**: 223-228

27 **Crawford NP**, Colliver DW, Funke AA, Young MN, Kelley S, Cobbs GA, Petras RE, Galandiuk S. Characterization of genotype-phenotype relationships and stratification by the CARD15 variant genotype for inflammatory bowel disease susceptibility loci using multiple short tandem repeat genetic markers. *Hum Mutat* 2005; **25**: 156-166

28 **Newman B**, Gu X, Wintle R, Cescon D, Yazdanpanah M, Liu X, Peltekova V, Van Oene M, Amos CI, Siminovitch KA. A risk haplotype in the Solute Carrier Family 22A4/22A5 gene cluster influences phenotypic expression of Crohn's disease. *Gastroenterology* 2005; **128**: 260-269

29 **Noble CL,** Nimmo ER, Drummond H, Smith L, Arnott ID, Satsangi J. DLG5 variants do not influence susceptibility to inflammatory bowel disease in the Scottish population. *Gut* 2005; **54**: 1416-1420

Science Editor Kumar M and Guo SY **Language Editor** Elsevier HK

PO Box 2345, Beijing 100023, China
www.wjgnet.com
wjg@wjgnet.com

ELSEVIER

World J Gastroenterol 2005;11(47):7531-7535
World Journal of Gastroenterology ISSN 1007-9327

• *RAPID COMMUNICATION* •

Bleeding gastric varices: Results of endoscopic injection with cyanoacrylate at King Chulalongkorn Memorial Hospital

Phadet Noophun, Pradermchai Kongkam, Sutep Gonlachanvit, Rungsun Rerknimitr

Phadet Noophun, Pradermchai Kongkam, Sutep Gonlachanvit, Rungsun Rerknimitr, Division of Gastroenterology, Department of Internal Medicine, King Chulalongkorn Memorial Hospital, Chulalongkorn University, Bangkok, Thailand
Correspondence to: Pradermchai Kongkam, MD, Division of Gastroenterology, Department of Internal Medicine, King Chulalongkorn Memorial Hospital, Chulalongkorn University, Bangkok, Thailand. kongkam@hotmail.com
Received:2005-05-03 Accepted:2005-06-09

Key words: Bleeding gastric varices; Cyanoacrylate injection

Noophun P, Kongkam P, Gonlachanvit S, Rerknimitr R. Bleeding gastric varices: Results of endoscopic injection with cyanoacrylate at King Chulalongkorn Memorial Hospital. *World J Gastroenterol* 2005; 11(47): 7531-7535
http://www.wjgnet.com/1007-9327/11/7531.asp

Abstract

AIM: To evaluate the efficacy and safety of gastric varices injection with cyanoacrylate in patients with gastric variceal bleeding.

METHODS: Twenty-four patients (15 males, 9 females) with gastric variceal bleeding underwent endoscopic treatment with cyanoacrylate injection. Successful hemostasis, rebleeding rate, and complications were retrospectively reviewed. Followed up endoscopy was performed and repeat cyanoacrylate injection was given until gastric varices were obliterated.

RESULTS: Seventeen patients achieved definite hemostasis. Of these, 14 patients had primary success after initial endoscopic therapy. Ten patients developed recurrent bleeding. Repeated cyanoacrylate injection stopped rebleeding in three patients. Transjugular intrahepatic portosystemic shunt (TIPS) was performed to control rebleeding in one patient which occured after repeat endoscopic therapy. Six patients died (three from uncontrolled bleeding, two from sepsis, and one from mesenteric vein thrombosis). Minor complications occurred in 11 patients (six epigastric discomfort and five post injection ulcers). Cyanoacrylate embolism developed in two patients. One of these patients died from mesenteric vein thrombosis. The other had pulmonary embolism which resolved spontaneously. Advanced cirrhosis and hepatocellular carcinoma (HCC) were major risk factors for uncontrolled bleeding.

CONCLUSION: Endoscopic treatment for bleeding gastric varices with cyanoacrylate injection is effective for immediate hemostasis. Repeat cyanoacrylate injection has a lower success rate than the initial injection. Cyanoacrylate embolism is not a common serious complication.

INTRODUCTION

The source of variceal bleeding can be esophageal varices (EVs) or gastric varices (GVs). Generally, about 20% of patients with portal hypertension harbor GVs, but only a few bleed from these[1-3]. Unfortunately, bleeding GVs is catastrophic and usually present with massive UGI bleeding. Many endoscopic techniques have been applied to control GVs related bleeding. Rubber band ligation and sclerotherapy are the most preferred procedures for EVs treatment but neither of them seem to be effective enough to control GVs related bleeding[8-11]. Unlike EVs, GVs related bleeding is very difficult to control by routine band ligation since retroflex position of the scope has to be used in order to reach GVs. This in turn leads to difficult band deployment. Non-endoscopic methods, such as transjugular intrahepatic portosystemic shunt (TIPS) and surgical portosystemic shunts are effective but require experienced specialists[4-7]. Moreover emergency shunt carries a high rate of post operative mortality[6,7]. The discovery of tissue adhesive chemical has changed the management of gastric variceal bleeding. Cyanoacrylate (Histoacryl^{TM}), a tissue adhesive, was first applied for endoscopic treatment of bleeding GVs in 1980s. Thereafter, cyanoacrylate has become popular for this purpose in many countries. However, it is not available for use in the United States. We have retrospectively reviewed the safety and efficacy of endoscopic injection of cyanoacrylate for the treatment of UGI bleeding from GVs at King Chulalongkorn Memorial Hospital.

Patients

There were 143 patients who presented with esophagogastric varices bleeding identified by endoscopy at King Chulalongkorn Memorial Hospital between January 2000 and 2003. Twenty-four patients (15 men and 9 women), mean age 48 years (29-75 years), had gastric variceal bleeding and all underwent endoscopic injection

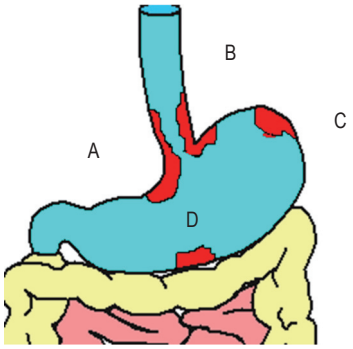

Figure 1 Classification of GVs on the basis of location and relationship with EVs (A and B: GOV, gastroesophageal varices, type 1 and 2 respectively. C and D: IGV, isolated GVs, type 1 and 2 respectively).

Table 1 Clinical characteristics of patients with bleeding gastric varices

	No. of patients	%
Total	24	100
Males:females	15:9	62:38
Mean age (Yr)	48	
Age range (Yr)	29-75	
Etiology of gastric varices		
- Cirrhosis	20	83.3
1. Viral hepatitis B	6	25.0
2. Viral hepatitis C	2	8.3
3. Alcoholism	9	37.5
4. Alcoholism and hepatitis B	2	8.3
5. Alcoholism and hepatitis C	1	4.2
- Primary biliary cirrhosis	1	4.2
- Idiopathic portal hypertension	3	12.5
Bleeding status		
- Active bleeding	9	38.0
- Recent bleeding	15	62.0
Child-Pugh classification		
A	6	25.0
B	11	45.8
C	7	29.2
Gastric varices classification		
GOV1	1	4.2
GOV2	17	70.8
IGV1	6	25.0
IGV2	0	0
Association with		
Hepatocellular carcinoma	6	25.0
Portal vein thrombosis	1	4.2
Hepatocellular carcinoma with portal vein thrombosis	1	4.2

of N-butyl-2-cyanoacrylate for hemostasis. Among these patients, nine had active bleeding (spurting or oozing) and the remaining 15 patients had evidence of recent variceal bleeding by demonstrating clot on gastric varices without any other potential source of bleeding.

Methods

Commercially flexible sclerotherapy injectors with a 6 mm/21-guage needle were used for gastric variceal injection. *N*-butyl-2-cyanoacrylate (Histoacryl™, B. Braun, Melsungen, Germany), was mixed with Lipiodal ™ (Laboratoire Guerbet, Aulnay-Sous-Bois, France) in 5:8 ratio and injected as a bolus dose of 2.6-5.2 cc, depending on the size of the GVs. Lipiodal was used to flush the needle before and after each injection. Generally injections

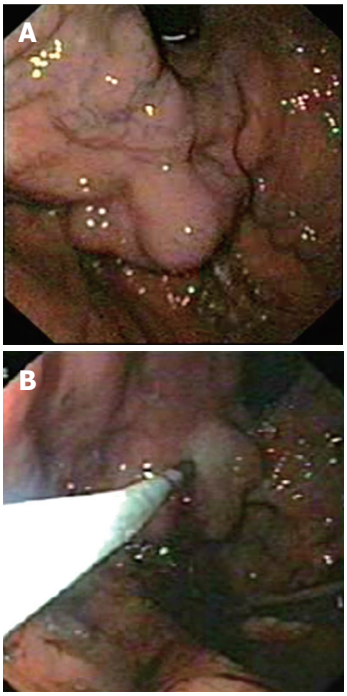

Figure 2 (**A**) (top) GVs at fundus, (**B**) (bottom) cyanoacrylate injection into the GV.

were directly delivered into gastric varices with active bleeding or containing stigmata of recent bleeding. Most procedures were performed by senior gastroenterologists under the supervision by experienced staff. At two week-follow-up endoscopy, reinjection was performed, if GVs were still detectable by palpation with the tip of biopsy forceps. An X-ray was taken after the injection to check the contour of the cyanoacrylate cast only in patients whom were suspected to have cyanoacrylate embolism. If there was recurrent bleeding during the follow-up period, reinjection with cyanoacrylate was also performed. Follow up endoscopy was performed in all the patients every two weeks and were followed up for a minimum of 4 wk. All patients who underwent endoscopic therapy received intravenous broad spectrum antibiotics prophylactically. Primary success was defined as an absence of recurrent bleeding after the first cyanoacrylate injection and during the follow-up period. Secondary success was defined as an absence of recurrent bleeding after reinjection of cyanoacrylate for recurrent bleeding. Definite hemostasis denotes primary or secondary success. A failure to achieve definite hemostasis was considered to be endoscopic failure. According to the classification proposed by Sarin *et al*[2]. (Figure 1) gastric varices were classified by their location: varices in the esophagus and lesser curvature (GOV1); varices in the esophagus and gastric fundus (GOV2); varices in the fundus only (IGV1); or varices at other sites in the stomach or in the first part of the duodenum (IGV2). Status of cirrhosis was classified according to Child-Pugh classification[12].

Statistical analysis

Data were expressed as percent, mean±SD, or median and range as appropriate. The prevalence of HCC and

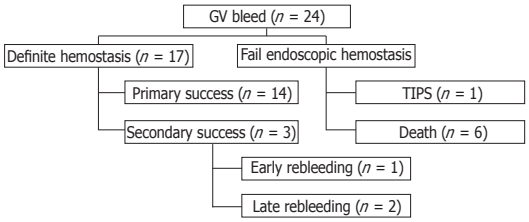

Early rebleeding: rebleeding occurred within 24 h after endoscopic treatment. Late rebleeding: rebleeding occurred after 24 h after endoscopic treatment.

Figure 3 Diagram demonstrating efficacy of cyanoacrylate glue for the treatment of GV bleeding.

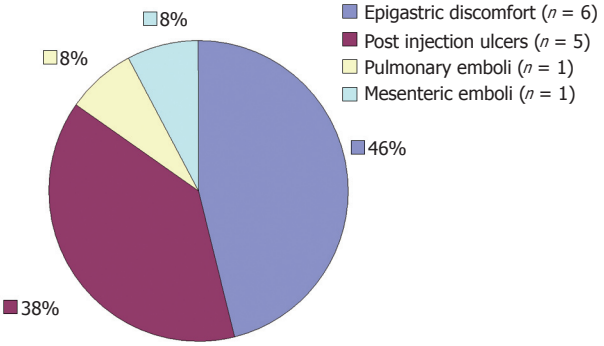

Figure 4 Complications of cyanoacrylate glue injection.

Child A, B or C cirrhosis in definite hemostasis group was compared to failed hemostasis group using Fisher's exact test. $P<0.05$ was considered statistically significant.

RESULTS

All patients who had gastric varices bleeding underwent endoscopic injection of *N*-butyl-2-cyanoacrylate. Patients characteristics are shown in Table 1 (The mean duration of follow-up was 8.3 mo, range 1-34 mo). Figure 2 shows gastric varices in one of the patients. Intra gastric variceal cyanoacrylate injection was performed (Figure 2B) and the GV was disappeared at 4-wk follow up endoscopy. Seventeen patients (71%) achieved definite hemostasis. Primary success was achieved in 14 patients (58%) (Figure 3). The remaining three (12%) were classified as secondary success after repeat endoscopic injection of cyanoacrylate. The mean number of sessions to achieve definite treatment was 1.4. Seven patients (29%) failed to achieve definite hemostasis despite multiple sessions of endoscopic treatment (1 IGV 1, 2 GOV 2). In one patient, the bleeding was successfully controlled by TIPS procedure. The remaining six patients had conditions unsuitable for TIPS procedure. None of them were treated with sclerotherapy. Three patients died from refractory gastrointestinal hemorrhage with severe coagulopathy, two died from sepsis, and another died from cyanoacrylate induced mesenteric embolism and bowel infarction (Table 2). Six of the seven patients (85.7%) who failed to achieve definite hemostasis had higher prevalence of

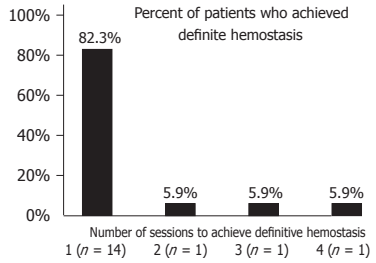

Figure 5 Number of sessions and percent of patients who achieved definite hemostasis ($n = 17$).

Table 2 Causes of death in patients who were unsuitable for TIPs

Causes of death	Number of patients
Uncontrolled GI bleeding	3
Sepsis	2
Mesenteric emboli and peritonitis	1

Table 3 Clinical comparisons of patients who achieved and failed definite hemostasis

	Definite hemostasis ($n = 17$)	Failed hemostasis ($n = 7$)
Hepatocellular carcinoma	1 (5.8%)	6 (85.7%)[1]
Cirrhosis Child A	5 (29.5%)	1 (14.2%)
Cirrhosis Child B	10 (58.8%)	1 (14.2%)
Cirrhosis Child C	2 (11.7%)	5 (71.6%)[2]

[1]Fisher's exact test, $P<0.01$. [2]Fisher's exact test of Child C *vs* non Child C between two groups, $P<0.01$.

HCC compared to patients who had definite hemostasis ($P<0.01$) (Table 3). Child C cirrhosis was presented more often in patients who failed definite hemostasis (71.6%) compared to patients who achieved hemostasis (11.7%, $P<0.01$) (Table 3). Eighteen patients did not have serious adverse effects from cyanoacrylate injection. Six patients complained of epigastric discomfort which resolved spontaneously. Follow up endoscopy in five patients revealed asymptomatic post-injection ulcers at injection site from cyanoacrylate. Two patients developed serious complication from cyanoacrylate emboli. One patient died from small bowel infarction and peritonitis. This was found to be related to cyanoacrylate emboli since lipiodal stain was detected in the territory of mesenteric vein. The other patient developed chest pain and tachypnea 2 h after endoscopic treatment. Lipiodal stain was detected by a chest film. Fortunately, this patient survived after conservative treatment (Figure 4).

DISCUSSION

In asymptomatic portal hypertensive patients who underwent endoscopic surveillance for varices, GVs were detected less commonly than esophageal varices (EVs). The risk of GVs bleeding is also less but whenever bleeding occurs, it is dangerous and may be fatal[2]. Unlike

EVs, endoscopic technique to control gastric variceal bleeding is very difficult due to the awkward position of the scope. All therapeutic devices have to come from retroflex position. In addition, blood in the fundus may obscure the view. Apart from endoscopic treatment, TIPS is the best alternative treatment for gastric variceal bleeding. Unfortunately, TIPS is not widely available. Endoscopic obliteration of bleeding gastric varices to achieve hemostasis has been reported from many centers around the world. Variety of sclerosing agents were used including alcohol, tissue thrombin, and cyanoacrylate. There have been reports that cyanoacrylate injection could control GV bleeding with excellent results[13]. Generally, endoscopic variceal ligation (EVL) is one of the preferred treatments for EVs. Applying this technique for GVs is possible. However, there is a significant limitation due to the position of the scope and size of GVs. Gastric varix that is larger than 2 cm in diameter may be difficult to suck in to the tip of the scope while performing EVL. Therefore, incomplete endoscopic ligation may occur. The residual varix with high pressure may be prone to recurrent bleeding. A recent study reported by Lo *et al*[14]. concluded that endoscopic obliteration using band ligation is less effective and more difficult than cyanoacrylate injection in the management of bleeding gastric varices. Endoscopic variceal injection by other agents beside cyanoacrylate such as alcohol appeared to be less effective. This has been confirmed by Sarin *et al*[15]. who showed that cyanoacrylate injection was significantly more effective in achieving variceal obliteration than alcohol injection. Furthermore, complete obliteration was achieved within a few weeks by injection of a smaller volume of the agent. In addition they also found that cyanoacrylate injection was able to stop acute GV bleeding more often than alcohol injection and the need for rescue surgery was less.

Our study has shown that bleeding GVs was controlled by the first session of cyanoacrylate injection in 14 of 17 patients (82.3%) who achieved definite hemostasis (Figure 5). Second injection was less effective resulting in definite hemostasis in only 30% of patients (3/10) who failed initial injection. The mean number of session for endoscopic therapy to achieve hemostasis in our series was lesser than a series from UK (1.4 *vs* 2±1)[16]. In our series, large volume of cyanoacrylate injection was used during the initial treatment and majority of GVs were obliterated. This in turn may lead to a less number of endoscopic sessions. The overall success rate is usually determined by definite hemostasis. Our success on definite hemostasis is lower than the previous study by Lo *et al*[14]. (71% *vs* 87%).

We found that patients who failed definite hemostasis had more advanced stage of liver disease than patients who achieved definite hemostasis. In addition, HCC was found more often in failure group (6 of 7 patients) compared to success group (1 of 17 patients) (Table 3). Endoscopic related complications from cyanoacrylate injection are generally minor and spontaneously resolved such as epigastric discomfort, nausea, vomiting, and ulcer at the injected site.

However, fatal complication may occur. The most dangerous complication is glue embolism. There have been many reports regarding this type of complication. For example, there was a case report of cerebral embolism after glue injection. Glue was found in the left atrium by echocardiography. Cardiac surgery was performed and intracardiac glue was removed[17]. A retrospective study from UK reported pulmonary embolism after glue injection in 1 of 23 cases[16]. Another larger study from Taiwan reported no case of pulmonary embolism after glue injection in 90 patients with bleeding gastric varices[18]. Unfortunately, one of the patients in our series developed generalized peritonitis, 8 h after glue injection. The lipiodal stain was detected from abdominal X-ray. This patient expired 2 d later without undergoing laparotomy due to his poor condition. During the period of our study, all patients received prophylactic antibiotics. Despite this protocol, there were two patients who died from septicemia. Sarin *et al*[15]. reported that 9 of 17 patients developed fever following glue injection for GVs. A case report from Malaysia showed that a patient developed multiple systemic emboli with septicemia after elective glue injection for fundic varices[19]. Fortunately, the patient recovered completely after intensified supportive treatment. Prophylactic administration is becoming a standard protocol for cirrhotic patient with active upper gastrointestinal hemorrhage[20]. However, antibiotic prophylaxis for elective glue injection is still controversial. Our recent unpublished data did not discover any bacteremia in the patient who underwent elective glue injection for GVs.

In conclusion, the results of the present study demonstrated that endoscopic injection of cyanoacrylate is effective to control majority of GVs related bleeding within the first session of treatment. Repeat endoscopic treatment is less effective than the initial injection. Advanced staged cirrhosis and HCC are major risk factors for failed hemostasis after cyanoacrylate injection of GVs.

REFERENCES

1 **Kim T**, Shijo H, Kokawa H, Tokumitsu H, Kubara K, Ota K, Akiyoshi N, Iida T, Yokoyama M, Okumura M. Risk factors for hemorrhage from gastric fundal varices. *Hepatology* 1997; **25**: 307-312

2 **Sarin SK**, Lahoti D, Saxena SP, Murthy NS, Makwana UK. Prevalence, classification and natural history of gastric varices: a long-term follow-up study in 568 portal hypertension patients. *Hepatology* 1992; **16**: 1343-1349

3 **Thakeb F**, Salem SA, Abdallah M, el Batanouny M. Endoscopic diagnosis of gastric varices. *Endoscopy* 1994; **26**: 287-291

4 **Skeens J**, Semba C, Dake M. Transjugular intrahepatic portosystemic shunts. *Annu Rev Med* 1995; **46**: 95-102

5 **Sanyal AJ**, Freedman AM, Luketic VA, Purdum PP, Shiffman ML, Tisnado J, Cole PE. Transjugular intrahepatic portosystemic shunts for patients with active variceal hemorrhage unresponsive to sclerotherapy. *Gastroenterology* 1996; **111**: 138-146

6 **Sanyal AJ**, Purdum PP, Luketic VA, Shiffman ML. Bleeding gastroesophageal varices. *Semin Liver Dis* 1993; **13**: 328-342

7 **Bornman PC**, Krige JE, Terblanche J. Management of oesophageal varices. *Lancet* **1994; 343**: 1079-1084

8 **Jutabha R**, Jensen DM, Egan J, Machicado GA, Hirabayashi K. Randomized, prospective study of cyanoacrylate injection, sclerotherapy, or rubber band ligation for endoscopic hemostasis of bleeding canine gastric varices. *Gastrointest Endosc* 1995; **41**: 201-205
9 **Chang KY**, Wu CS, Chen PC. **Endoscopic treatment of** bleeding fundic varices with 50% glucose injection. *Endoscopy* 1996; **28:** 398
10 **Chun HJ**, Hyun JH. A new method of endoscopic variceal ligation-injection sclerotherapy (EVLIS) for gastric varices. *Korean J Intern Med* 1995; **10**: 108-119
11 **Yoshida T**, Hayashi N, Suzumi N, Miyazaki S, Terai S, Itoh T, Nishimura S, Noguchi T, Hino K, Yasunaga M. Endoscopic ligation of gastric varices using a detachable snare. *Endoscopy* 1994; **26**: 502-505
12 **Pugh RN**, Murray-Lyon IM, Dawson JL, Pietroni MC, Williams R. Transection of the oesophagus for bleeding oesophageal varices. *Br J Surg* 1973; **60**: 646-649
13 **Sarin SK**. Long-term follow-up of gastric variceal sclerotherapy: an eleven-year experience. *Gastrointest Endosc* 1997; **46**: 8-14
14 **Lo GH**, Lai KH, Cheng JS, Chen MH, Chiang HT. A prospective, randomized trial of butyl cyanoacrylate injection versus band ligation in the management of bleeding gastric varices. *Hepatology* 2001; **33**: 1060-1064
15 **Sarin SK**, Jain AK, Jain M, Gupta R. A randomized controlled trial of cyanoacrylate versus alcohol injection in patients with isolated fundic varices. *Am J Gastroenterol* 2002; **97**: 1010-1015
16 **Mahadeva S**, Bellamy MC, Kessel D, Davies MH, Millson CE. Cost-effectiveness of N butyl-2-cyanoacrylate (histoacryl) glue injections versus transjugular intrahepatic portosystemic shunt in the management of acute gastric variceal bleeding. *Am J Gastroenterol* 2003; **98**: 2688-2693
17 **Gallet B**, Zemour G, Saudemont JP, Renard P, Hillion ML, Hiltgen M. Echocardiographic demonstration of intracardiac glue after endoscopic obturation of gastroesophageal varices. *J Am Soc Echocardiogr* 1995; **8**: 759-761
18 **Huang YH**, Yeh HZ, Chen GH, Chang CS, Wu CY, Poon SK, Lien HC, Yang SS. Endoscopic treatment of bleeding gastric varices by N-butyl-2-cyanoacrylate (Histoacryl) injection: long-term efficacy and safety. *Gastrointest Endosc* 2000; **52**: 160-167
19 **Tan YM**, Goh KL, Kamarulzaman A, Tan PS, Ranjeev P, Salem O, Vasudevan AE, Rosaida MS, Rosmawati M, Tan LH. Multiple systemic embolisms with septicemia after gastric variceal obliteration with cyanoacrylate. *Gastrointest Endosc* 2002; **55**: 276-278
20 **Bernard B**, Grangé JD, Khac EN, Amiot X, Opolon P, Poynard T. Antibiotic prophylaxis for the prevention of bacterial infections in cirrhotic patients with gastrointestinal bleeding: a meta-analysis. *Hepatology* 1999; **29**: 1655-1661

Science Editor Pravada J **Language Editor** Elsevier HK

PO Box 2345, Beijing 100023, China
www.wjgnet.com
wjg@wjgnet.com

ELSEVIER

World J Gastroenterol 2005;11(47):7536-7540
World Journal of Gastroenterology ISSN 1007-9327

• *RAPID COMMUNICATION* •

Apoptosis mechanisms of human gastric cancer cell line MKN-45 infected with human mutant p27

Jin-Shui Zhu, Long Wang, Guo-Qiang Cheng, Qin Li, Zu-Ming Zhu, Li Zhu

Jin-Shui Zhu, Long Wang, Guo-Qiang Cheng, Qin Li, Zu-Ming Zhu, Li Zhu, Department of Gastroenterology, Affiliated Sixth People's Hospital, Shanghai Jiaotong University, Shanghai 200233, China
Supported by the Natural Science Foundation of Shanghai, No. 04ZB14072
Correspondence to: Prof. Jin-Shui Zhu, Department of Gastroenterology, Affiliated Sixth People's Hospital, Shanghai Jiaotong University, Shanghai 200233, China. zhujs1803@hotmail.com
Telephone: +86-21-64837019 Fax: +86-21-64837019
Received: 2005-02-15 Accepted: 2005-04-02

Abstract

AIM: To explore the inducing effect of human mutant p27 gene on the apoptosis of the human gastric cancer cell line MKN-45 and its associated mechanisms.

METHODS: The recombinant adenovirus Ad-p27mt was constructed to infect the human gastric cancer cell line MKN-45. Using flow cytometry, TUNEL assay and DNA fragment analysis, we measured the apoptotic effect of Ad-p27mt on the human gastric cancer cells.

RESULTS: Ad-p27mt was successfully constructed and the infection efficiency reached 100%. After 18 h of infection, we observed an apoptotic hypodiploid peak on the flow cytometer before G_1-S and apoptotic characteristic bands in the DNA electrophoresis. The apoptotic rate detected by TUNEL method was significantly higher in the Ad-p27mt group (89.4±3.12%) compared to the control group (3.12±0.13%, $P < 0.01$).

CONCLUSION: Human mutant p27 can induce apoptosis of the human gastric cancer cells *in vitro*.

Key words: Gastric cancer; Human mutant p27; Cell line MKN-45

Zhu JS, Wang L, Cheng GQ, Li Q, Zhu ZM, Zhu L. Apoptosis mechanisms of human gastric cancer cell line MKN-45 infected with human mutant p27. *World J Gastroenterol* 2005; 11(47): 7536-7540
http://www.wjgnet.com/1007-9327/11/7536.asp

INTRODUCTION

Apoptosis plays a crucial role in the proliferation and turnover of cells in various malignant tumors. Studies have proved that apoptosis is enhanced in tumor by many anticancer drugs, such as cytotoxic drug, hormone, or some recombinant gene, medicine, etc. However, there is a lack of an effective therapy for advanced gastric cancer at present. Gastric cancer is a disease with not only abnormal cell proliferation and differentiation, but also abnormal apoptosis. So, the enhanced induction of apoptosis in human gastric cancer cell needs to be explored. Human mutant p27 gene is a kind of multifunctional cyclin-dependent kinase inhibitor, playing a negative role in cell cycle regulation by inhibiting transformation from G_0/G_1 phase to S phase. Similarly, a recombinant p27mt presents cell proliferation and tumorigenesis. Based on the previous studies, we examined the apoptotic effect and its associated mechanisms in human gastric cancer implanted into nude mice after the treatment with human mutant p27 gene.

MATERIALS AND METHODS

Materials

BALB/C-nu/nu mice (weight 18-22 g, 36-37 wk old) and human gastric carcinoma cell line MKN-45 were obtained from Shanghai Tumor Institution (No. 01842). The animals were subcutaneously grafted with the MKN-45 cell line.

RPMI 1640 culture medium and TRIzol total RNA isolation kit were purchased from Gibco BRL. The rat anti-human p27 kip1 multi-antibody was purchased from Santa Cruz Co. The liposome, trypsin, DMEM culture medium, Hepes and Csc1, 200-bp DNA ladder, dNTP, tag enzyme and the restriction endonuclease were obtained from Sigma Co. PORF9-hp27mt plasmid (human mutant p27 gene) was obtained from InvivoGen Co. The recombinant adenovirus (Ad-lac2) and Ad-LacZ (medium of the recombinant adenovirus) were provided by Dr. Robert, Huston University, USA.

Cell culture

Human gastric cancer cell line MKN-45 was routinely cultured in RPMI 1640 medium supplemented with heat-inactivated 100 mL/L fetal calf serum, 100 kU/L penicillin, 100 mg/L streptomycin and 2 mmol/L glutamine, and incubated at 37 ℃ in a humidified atmosphere containing 50 mL/L CO_2 in air until the gastric carcinoma cells were 80-90% confluent.

Construction and identification of human mutant p27 recombinant adenovirus

After pORF9-hp27mt was digested with *Age*I and *Nhe*I

enzymes, the 619-bp fragment was recycled and subcloned into pBluescript II SK (+), which was digested with *Xma*I and *Xba*I enzymes, resulting in pBluescript-hp27mt. pBluescript-hp27mt was digested with *Not*I and *Kpn*I enzymes, and then the 699-bp fragment was recycled and inserted into shuttle plasmid vector pShuttle-CMV-hp27mt, which was digested with the same enzyme, resulting in the transfer plasmid vector pShuttle-CMV-hp27mt. The competence *E. coli* was transformed by adenoviral framework plasmid pAdeasy-1. According to ampicillin-resistant gene, the BJ5183 containing pAdeasy-1 was picked out and prepared as the ultra-competent BJ5183 containing pAdeasy-1. Then the ultra-competence BJ5183 containing pAdeasy-1 was transformed by transfer plasmid pShuttle-CMV-hp27mt, which was digested with *Pme*I enzyme and dephosphorylated by alkaline phosphatase. A little DNA of the transformed clone bacterial plasmid was taken out and the suspect DNA of the recombinant adenovirus plasmid was chosen according to the size of plasmid on agarose electrophoresis. If the chosen DNA was identified as the proper DNA by digestion with *Pac*I enzyme, the recombinant adenovirus plasmid pAdeasy-1-hp27mt could be massively prepared, and then used to perform liposome PolyFect-mediated infection of Ad293 cells, thereby resulting in the preparation of human p27mt recombinant adenovirus (Ad-p27mt). The amplification, identification and titer determination of the recombinant adenovirus were carried out as previously described[3].

Chemical staining of X-gal

The MNK-45 cells taken from the 15-cm culture flask was infected with Ad-lacZ according to MOI of 20, 40, 50, and 100 and then incubated for another 48 h. After the cells were fixed by 0.5% glutaral pentanediol for 15 min and washed thrice with PBS, X-gal staining solution (20:1) was added, followed by incubation at 37 ℃ for 4-25 h in a humidified atmosphere containing 50 mL/L CO_2 in air. The blue-staining cells, i.e. the positive cells in which LacZ gene was expressed, were observed under microscope and the percentage of the positive cells was calculated.

Detection of expression of p27mt gene

The MKN-45 cells taken from the 75-cm culture flask was infected with Ad-p27mt (MOI) and Ad-LacZ (MOI), respectively. After being incubated at 37 ℃ for 48 h in a humidified atmosphere containing 50 mL/L CO_2 in air, all cells were digested with 0.5 g/L trypsin. The cells were collected and washed twice with PBS. After the cells were lysed with 500 μL of SDS-PAGE cell lysis solution and boiled for 5 min, they were centrifuged and the supernatant was collected for Western blot detection.

Flow cytometric detection of cells infected by Ad-p27mt

The MKN-45 cells taken from the 75-cm culture flask was infected with Ad-p27mt (MOI 100). After incubation for 48 h, they were digested with 0.5 g/L trypsin. The cells were collected and washed twice with PBS. Proper amount of PBS was added, until the cell concentration reached 10^9/L. Then 100 μL of cell suspension was mixed with 200 μL of DNA-PREP™ LPR, followed by detection using Coulter Epics XL flow cytometer after 15 min. The cell cycle and cell apoptosis rate were analyzed. The Ad-LacZ (MOI 100) group and the normal control group (MKN-45 cells cultivated without adenovirus) were used as control groups.

DNA fragment analysis

MKN-45 cells, after being infected with Ad-p27mt and Ad-LacZ for 48 h, and the normal control cells were separately collected and centrifugated at 1 000 r/min for 5 min. The supernatant was thrown away, and 500 μL of cell lysis solution [10 g/L NP40, 20 mmol/L EDTA, 50 mmol/L Tris-HCl (pH 7.5)] and 10 μL of protease K were added into the cell sediment, followed by heating in 56 ℃ water bath for 1-2 h and then extraction with phenol/chloroform and DNA precipitation with dehydrated alcohol. After the DNA precipitate was washed once with 700 mL/L alcohol, 200 μL of TE was added to lyse the DNA, followed by incubation with RNase (final concentration 50 mL/L) overnight at 37 ℃. The final DNA was electrophoresed on 10 g/L agarose gel and observed with the aid of an ultraviolet light lamp.

Detection of cell apoptosis by TUNEL method

Cell suspensions ($1x10^4$ cells) of each Ad-p27mt group and normal control group were inoculated separately into 60-mm dishes containing six cover glasses (washed and high-pressure sterilized), followed by incubation for 24 h. Then the glasses were taken out and washed twice with 1× PBS and fixed in methanol:freezing acetic acid (3:1) for 30 min. The following procedures were carried out according to the instructions of the kit. The average number of apoptotic cells was determined by counting 1 000 cells on each glass. Then the apoptotic index (AI), i.e. the number of apoptotic cells per 100 cancer cells, was calculated.

Statistical analysis

All statistical analyses were performed using SPSS 11.5 for Windows. The data were analyzed using *t*-test. A $P<0.05$ was considered statistically significant.

RESULTS

PCR identification of recombinant adenovirus Ad-p27mt

The pathological change of multi-drug resistant MKN-45 cells and their culture fluid were collected and centrifuged. Five milliliters of the supernatant was mixed with 1 mg of protease K, 2 mL of 10 g/L SDS, 10 mmol/L EDTA, and 20 mmol/L Tris-HCl to digest for 2 h. After being precipitated by dehydrated alcohol, the viral DNA was collected. PCR reaction was carried out after adding the forward and reverse primers. Finally, a 275-bp target gene was amplified, which showed that the recombinant adenovirus had already possessed p27mt target gene.

Detection of gene transfer rate by X-gal chemical staining

The adenovirus-mediated gene transfer rate was evaluated

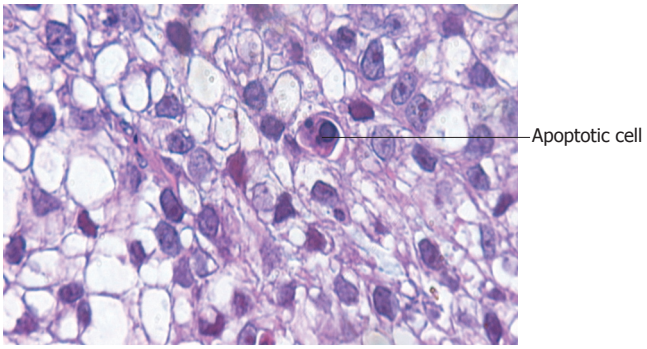

Figure 1 Detection of apoptotic cells by TUNEL method. The nuclei of apoptotic cells appeared blue in Ad-p27mt group.

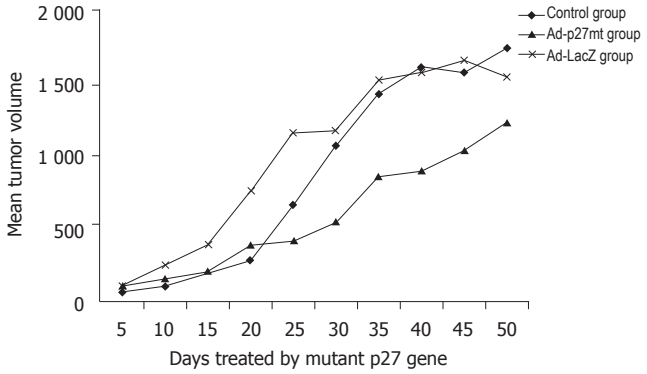

Figure 2 Growth curves of human gastric cancer implanted in nude mice.

by X-gal staining. The results showed that the infection efficiency could reach 100% when MOI was larger than 50, which indicated that recombinant adenovirus could effectively transfer to MKN-45 cells *in vitro*.

The expression of p27 protein was evaluated after MKN-45 was infected with human mutant p27 recombinant adenovirus *in vitro*. After MKN-45 cells were infected with Ad-p27mt (MOI 100) for 24 h, the cells were collected and lysed with 1x SDS-PAGE cell lysis solution, boiled at 100 ℃ for 5 min, and then centrifuged. The supernatant was collected and the protein was detected by using TMB system Western blot kit (KPL, USA). We found a high expression of 27-ku protein in Ad-p27mt group, while only slight trace expression (endogenous expression) in Ad-LacZ group and normal control group, indicating that the human mutant p27 recombinant adenovirus constructed in the present study could express p27 gene properly in MKN-45 cells and the protein product could be expressed at a high level in the cells.

After the MKN-45 cells were treated with Ad-p27mt, Ad-LacZ and without virus for 24 h, the apoptosis rate was detected in the different groups using flow cytometry. Reproducibility was confirmed by processing all samples at least six times. The average values of hypodiploid in Ad-p27mt, Ad-LacZ, and non-infected groups were 41.0%, 4.67%, and 1.96%, respectively, showing significant differences between these three groups.

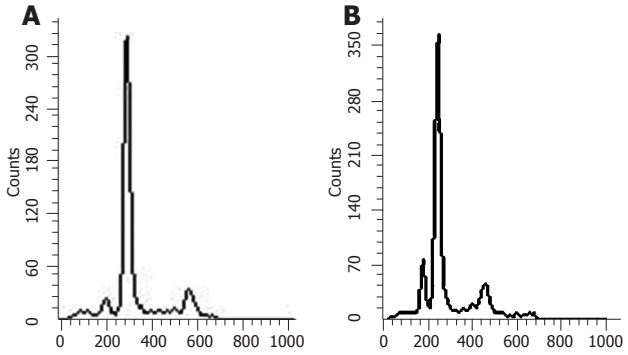

Figure 3 Detection of multi-drug resistant MKN-45 cells' apoptosis by flow cytometry. **A**: Non-infected MKN-45 cells; **B**: Ad-p27mt-infected MKN-45 cells.

Table 1 Effect of Ad-p27mt on the cell cycle of MKN-45 cells (mean ±SD)

Groups	G_0/G_1	S	G_2/M
Control	25.29±1.04	41.12±1.19	33.34±1.55
Ad-LacZ	27.57±0.45[a]	38.21±0.44[a]	34.22±0.92[a]
Ad-P27mt	77.96±2.20[b]	8.98±0.17[b]	13.06±2.35[b]

[1]$P>0.05$ *vs* control group; [b]$P<0.01$ *vs* Ad-LacZ group.

Detection of DNA fragment

The result of DNA electrophoresis showed that the gene bands were intact in Ad-LacZ group and normal control group, while there were obvious 180-200 bp diploid 'trapezia' bands in Ad-p27mt group, which was in concordance with the characteristic changes of apoptosis (Figures 1 and 2).

Detection of cell apoptosis by TUNEL method

The apoptotic cells had concentrated cytoplasm with shrunk and dark-stained nuclei. AI of Ad-p27mt group (82.6±3.2%) was significantly higher compared to the control group (5.0±3.5%, $P<0.05$), showing that Ad-p27mt could obviously induce apoptosis of gastric cancer cells (Figure 3).

The cell cycles of different groups of MKN-45 cells are shown in Table 1. We found that the number of G_0/G_1 phase cells decreased gradually and the percentage of S-phase cells increased in Ad-LacZ group and control group, which indicated that the transition time of cell cycle was shortened and cell proliferation was active. However, the percentage of G_0/G_1 phase cells significantly increased and the cell cycle was obviously arrested in G_0/G_1 phase in Ad-p27mt group as compared to the control group and Ad-LacZ group ($P<0.01$).

DISCUSSION

Human mutant p27 protein is a kind of heat stable protein, which was first found by Polyak and colleagues in a research on cell contact inhibition with TGF-β[4]. It has been found that p27 mainly inhibited the activity of cyclin E-CDK2, cyclin D-CDK4, and cyclin A-CDK2

complexes. In addition, the arrest of cells at G_0/G_1 phase was mainly caused by p27 accumulation induced by exogenous signal, and tumorigenesis was closely correlated with translocation, deletion and mutation of p27 gene and changes of expression and activity of p27 protein[5]. If the expression level of p27mt was downregulated, the inhibition of cyclin E-CDK2 complex by p27 would decrease and thus the DNA damaged cells could transform from G_1 to S phase directly.

The degradation of p27 protein is mainly caused by phosphorylation of the 187th threonine of p27 which is mediated by ubiquitin[6-8]. Kudo *et al*[9]. found that the 187th threonine of p27 was mediated by p27 protein, and thereby obviously inhibited the cell growth, and these inhibitive effects were more obvious on mutant p27 (T187A) than on wild-type p27.

In this study, we constructed a replication-deficient recombinant adenovirus, which carried p27mt, to investigate the apoptotic rate of gastric cancer cell line MKN-45, expecting for a more effective p27 gene to treat gastric cancer. Koguchi *et al*[11]. reported the prohibition of the viability of astrocytes, resulting from transfection with adenovirus-mediated exogenous p27 gene. Zhang *et al*[12]. reported that the upregulation of p27 expression by retinoic acid significantly inhibited the growth of the oophoroma cells. In addition, Koh *et al*[13]. found that high expression of p27 and raised expressions of cyclin D1 and cyclin E in cephalocervical squamous cell carcinoma cell lines SUN-1066, SUN-1041, and SUN-1076 after transfection with adenovirus-mediated p27kip1 could significantly inhibit the proliferation of the cancer cells by arresting the cells mainly at G_1-S stage. All these data showed that p27 gene might have a significant impact on the onset, development and prognosis of tumor.

Nowadays, functional reconstruction of anti-oncogene has been a reasonable strategy of gene therapy for tumor. Sasaki *et al*[14]. showed that compared with p27wt, p27mt had stronger inhibitive effects on the apoptosis of cholangiocarcinoma cells. Park *et al*[15,16]. reported similar results when they performed adenovirus-mediated transfection of p27mt and p27wt genes into lung cancer cell lines NCI H460, NCI H1264, NCI H358, and NCI H157. In our study, adenovirus-mediated transfection of mutant p27 gene could upregulate its expression in gastric cancer cell line MKN-45, suggesting that adenovirus with reconstructed p27mt can transfect the target gene into tumor cells. We also observed that the apoptotic rate was markedly higher in Ad-p27mt group as compared to the control group. DNA analysis showed 180-200 bp DNA ladder. Moreover, TUNEL assay showed obviously higher AI up to 82.6% in Ad-p27mt group as compared to the control group. These results revealed that p27 gene might play an important role in gastric carcinoma and its downregulation may be the main cause of cell differentiation dysfunction and apoptosis dysfunction. Thus, upregulating the expression of p27 by transfection of mutant p27 may serve as a new therapy on gastric carcinoma by exerting its apoptosis-inducing effect. The cell cycle analysis showed that the cleavage of tumor cells was stopped at G_1 stage via suppressing the activity of the cyclin/CDK kinase by p27mt. Winteringham *et al*[17]. have found that the accumulation of p27 plays a crucial role in the gastric cell cycle arrest at the initiation of cell differentiation.

In recent studies[18], although the gastric cancer cells apoptosis was successfully induced by the application of NM-3 and other gene therapies, Ad-p27mt-induced apoptosis of human gastric cancer cell line MKN-45 has not yet been reported in nude mice model. Our study showed a very useful experimental evidence for human gastric cancer suppression by using p27 gene therapy *in vivo*. The efficacy of p27 gene therapy and the mechanisms of apoptosis may provide an important theoretical evidence in the treatment of advanced gastric cancer.

REFERENCES

1 **Nan KJ,** Jing Z, Gong L. Expression and altered subcellular localization of the cyclin-dependent kinase inhibitor p27Kip1 in hepatocellular carcinoma. *World J Gastroenterol* 2004; **10**: 1425-1430

2 **Bryja V,** Pacherník J, Faldíková L, Krejcí P, Pogue R, Nevrivá I, Dvorák P, Hampl A. The role of p27(Kip1) in maintaining the levels of D-type cyclins in vivo. *Biochim Biophys Acta* 2004; **1691**: 105-116

3 **Chen J,** Xu SY, Deng CS, Wang JN, Huang YZ. **Efficient** generation of human mutant p27 gene recombinant adenovirus by homologous recombination in bacteria. *J Fourth Mil Med Univ* 2004; **5:** 406-409

4 **Polyak K,** Kato JY, Solomon MJ, Sherr CJ, Massague J, Roberts JM, Koff A. p27Kip1, a cyclin-Cdk inhibitor, links transforming growth factor-beta and contact inhibition to cell cycle arrest. *Genes Dev* 1994; **8**: 9-22

5 **Liu E,** Li X, Yan F, Zhao Q, Wu X. Cyclin-dependent kinases phosphorylate human Cdt1 and induce its degradation. *J Biol Chem* 2004; **279**: 17283-17288

6 **Takeda A,** Osaki M, Adachi K, Honjo S, Ito H. Role of the phosphatidylinositol 3'-kinase-Akt signal pathway in the proliferation of human pancreatic ductal carcinoma cell lines. *Pancreas* 2004; **28**: 353-358

7 **Guo W,** Shang F, Liu Q, Urim L, West-Mays J, Taylor A. Differential regulation of components of the ubiquitin-proteasome pathway during lens cell differentiation. *Invest Ophthalmol Vis Sci* 2004; **45**: 1194-1201

8 **Wei W,** Ayad NG, Wan Y, Zhang GJ, Kirschner MW, Kaelin WG. **Degradation of the SCF component Skp2 in cell-cycle** phase G1 by the anaphase-promoting complex. *Nature* 2004; **428**: 194-198

9 **Kudo Y,** Kitajima S, Sato S, Ogawa I, Miyauchi M, Takata T. Transfection of p27(Kip1) threonine residue 187 mutant type gene, which is not influenced by ubiquitin-mediated degradation, induces cell cycle arrest in oral squamous cell carcinoma cells. *Oncology* 2002; **63**: 398-404

10 **Hurteau JA,** Brutkiewicz SA, Wang Q, Allison BM, Goebl MG, Harrington MA. **Overexpression of a stabilized mutant form** of the cyclin-dependent kinase inhibitor p27(Kip1) inhibits cell growth. *Gynecol Oncol* 2002; **86**: 19-23

11 **Koguchi K,** Nakatsuji Y, Nakayama K, Sakoda S. Modulation of astrocyte proliferation by cyclin-dependent kinase inhibitor p27(Kip1). *Glia* 2002; **37**: 93-104

12 **Zhang D,** Holmes WF, Wu S, Soprano DR, Soprano KJ. Retinoids and ovarian cancer. *J Cell Physiol* 2000; **185**: 1-20

13 **Koh TY,** Park SW, Park KH, Lee SG, Seol JG, Lee DW, Lee CT, Heo DS, Kim KH, Sung MW. Inhibitory effect of p27KIP1 gene transfer on head and neck squamous cell carcinoma cell lines. *Head Neck* 2003; **25**: 44-49

14 **Sasaki T,** Katayose Y, Suzuki M, Yamamoto K, Shiraso

S, Mizuma M, Unno M, Takeuchi H, Lee CT, Matsuno S. Adenovirus expressing mutant p27kip1 enhanced apoptosis against cholangiocarcinoma than adenovirus-p27kip1 wild type. *Hepatogastroenterology* 2004; **51**: 68-75

15 **Park KH,** Seol JY, Kim TY, Yoo CG, Kim YW, Han SK, Shim YS, Lee CT. An adenovirus expressing mutant p27 showed more potent antitumor effects than adenovirus-p27 wild type. *Cancer Res* 2001; **61**: 6163-6169

16 **Park KH,** Lee J, Yoo CG, Kim YW, Han SK, Shim YS, Kim SK, Wang KC, Cho BK, Lee CT. Application of p27 gene therapy for human malignant glioma potentiated by using mutant p27. *J Neurosurg* 2004; **101**: 505-510

17 **Winteringham LN,** Kobelke S, Williams JH, Ingley E, Klinken SP. **Myeloid Leukemia Factor 1 inhibits erythropoietin-**induced differentiation, cell cycle exit and p27Kip1 accumulation. *Oncogene* 2004; **23**: 5105-5109

18 **Kumagai H,** Masuda T, Ohsono M, Hattori S, Naganawa H, Sawa T, Hamada M, Ishizuka M, Takeuchi T. Cytogenin, a novel antitumor substance. *J Antibiot (Tokyo)* 1990; **43**: 1505-1507

Science Editor Kumar M **Language Editor** Elsevier HK

PO Box 2345, Beijing 100023, China
www.wjgnet.com
wjg@wjgnet.com

ELSEVIER

World J Gastroenterol 2005;11(47):7541-7544
World Journal of Gastroenterology ISSN 1007-9327

• *CASE REPORT* •

Is colonoscopy sufficient for colorectal cancer surveillance in all HNPCC patients?

Vito D Corleto, Ermira Zykaj, Paolo Mercantini, Emanuela Pilozzi, Michele Rossi, Antonella Carnuccio, Emilio Di Giulio, Vincenzo Ziparo, Gianfranco Delle Fave

Vito D Corleto, Department of Digestive and Liver Diseases, II School of Medicine, University "La Sapienza", Centro Ricerche S. Pietro FBF, Rome, Italy
Ermira Zykaj, Antonella Carnuccio, Emilio Di Giulio, Gianfranco Delle Fave, Department of Digestive and Liver Diseases, II School of Medicine, University "La Sapienza", Rome, Italy
Paolo Mercantini, Vincenzo Ziparo, Department of Surgery, II School of Medicine, University "La Sapienza", Rome, Italy
Emanuela Pilozzi, Department of Pathology, II School of Medicine, University "La Sapienza", Rome, Italy
Michele Rossi, Department of Radiology, II School of Medicine, University "La Sapienza", Rome, Italy
Supported by Ricerche Ateneo 2004 n. C26A044873, University "La Sapienza", Rome, and PRIN 2003, n. 2003063877_002
Correspondence to: Vito D Corleto, MD, Department of Digestive and Liver Diseases, II School of Medicine, University "La Sapienza", Sant'Andrea Hospital, Via di Grottarossa 1035-1037, 00189 Rome, Italy. corleto@bce.uniroma1.it
Telephone: +39-06-80345289 Fax: +39-06-33251278
Received: 2005-04-07 Accepted: 2005-04-26

Abstract

A 34-year-old male with hereditary non-polyposis colon cancer with a mutation in hMSH2 line is reported. Despite regular colonoscopic follow-up, he developed cecal cancer involving the extraluminal area. Due to sub-occlusive symptoms, the patient was submitted to further colonoscopy, however with no clear evidence of neoplasia. Thin slice multiplanar reconstruction computed tomography CT scan performed thereafter revealed a transmural mass 2.5 cm in size localized near the cecal valve. Discussion is made on the reliability of colonoscopic examinations as well as the need for further investigations in the follow-up of patients at very high risk of right-sided colon cancer, such as male hMSH2 carrier affected by hereditary non-polyposis colon cancer.

Key words: Hereditary non-polyposis colon cancer; Spiral CT scan; Colonoscopy; hMSH2 carrier

Corleto VD, Zykaj E, Mercantini P, Pilozzi E, Rossi M, Carnuccio A, Giulio ED, Ziparo V, Fave GD. Is colonoscopy sufficient for colorectal cancer surveillance in all HNPCC patients? *World J Gastroenterol* 2005; 11(47): 7541-7544
http://www.wjgnet.com/1007-9327/11/7541.asp

INTRODUCTION

Hereditary non-polyposis colorectal cancer (HNPCC or Lynch syndrome) is a disease of autosomal dominant inheritance, accounting for 3-5% of all colorectal cancers[1]. This disorder predisposes to the development of colorectal cancer (CRC) at an early age (mean age 45 years), as well as other cancers mainly of the gastrointestinal and genitourinary tract. HNPCC is caused by defects in one of the mismatch repair (MMR) genes such as hMLH1, hMSH2, hMSH6, hPMS1 or hPMS2, all of which are important in the detection and repair of base pair mismatches during DNA replication[2]. The presence of this syndrome is suspected on the basis of specific diagnostic guidelines known as "Amsterdam I and II, original Bethesda and revised Bethesda criteria" and on the clinical features of colorectal adenomas and/or cancers[1]. Genetic tests, to detect MMR gene mutations, are usually used to confirm the diagnosis.

Even when the more stringent clinical criteria are met, germline mutations are detected only in 40-60%[3-5]. Patients who met the family history and clinical criteria or who have inherited MMR gene mutations are at high risk of developing cancer and should undergo specific surveillance and follow-up, particularly colonic endoscopic surveillance[6,7].

Herein, we describe a case of a man with HNPCC who developed a right-sided colon cancer at the age of 34 despite regular colonoscopic examinations.

CASE REPORT

A 34-year-old man was admitted to our department with pain in the right lower quadrant of the abdomen, abdominal distension, and signs of pseudo-obstruction. The patient, with a family history of HNPCC, was regularly attended for surveillance at a well-known international center for diagnosis, treatment, and surveillance of HNPCC patients. A germline mutation in the hMSH2 gene was detected at the age of 17. A substitution at codon 383, changing CGA (Arg) to TGA (stop codon), was found which resulted in the formation of a truncated protein. No alteration was identified in the hMLH1 line. The last full endoscopic colon examination was carried out almost 2 years before and the colonic mucosa was reported with no alteration. The patient's family pedigree is outlined in Figure 1. His father was diagnosed as having CRC at the age of 37, jejunum cancer at the age of 48 and at the age of 58 he died of cholangiocarcinoma. His older

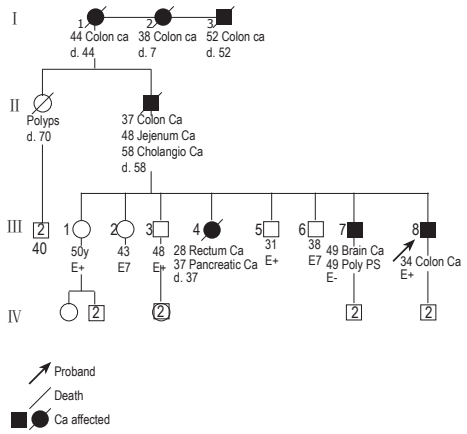

Figure 1 Pedigree of proband. d indicates age at death. E indicates evaluation for hMSH2 mutations.

sister presented rectal carcinoma at the age of 28 and died of pancreatic cancer at the age of 37. His older brother developed colonic polyps, three times consecutively, diagnosed during colonoscopic surveillance and also presented a glioblastoma at the age of 49, although he was negative for hMSH2 mutations upon DNA analysis.

This patient had been on a semi-liquid diet for 2 d, and was treated with 20 mg of i.v. *N*-butylbromide for the abdominal pain. Laboratory data revealed no abnormality. Complete blood count, hemoglobin, hematocrit, ferritin, urinalysis and electrolyte panel were all within the normal range. Liver function tests, carcinoembryonic antigen (CEA) and tissue polypeptide antigen (TPA) were also normal. An abdominal X-ray showed mild colonic and ileal distension in the absence of air-fluid levels or free air below the diaphragm. Complete abdominal ultrasonic investigations revealed normal kidney, urinary tract, liver, and biliary system. A chest X-ray was also negative.

The next day colonoscopy was performed. No alteration was detected, except in the mucosa around the ileocecal valve, an irregular and protuberant appearance, above which a small sessile polyp, 7 mm in diameter was visible. Multiple biopsies were collected. Histological examination revealed only the presence of a non-specific inflammatory submucosal infiltration.

A routine spiral-CT scanning (16 slices-Mx8000 IDT, Philips, Cleveland, OH, USA) was performed and simple axial reconstructions 5 mm thick were obtained. No alterations were detected at the first examination. However, after consultation with the radiologist, a thin slice (2 mm) multiplanar reconstruction (MPR) of the right colon was performed and a 2.5-cm mass was revealed extrinsically localized to the fundus of the cecum, well visualized in the coronal planes (Figures 2A and B). Before the surgery, the patient was informed about the surgical options and the related risks and/or potential benefits. The patient agreed to undergo a right hemicolectomy, but not total colectomy. At surgery, ascites was found locally and the mass was macroscopically transmural. The surgeon, therefore, had no choice but to carry out terminal ileum resection, resection of the ileocecal valve, hepatic flexure, part of the transverse colon and dissection of related lymph nodes.

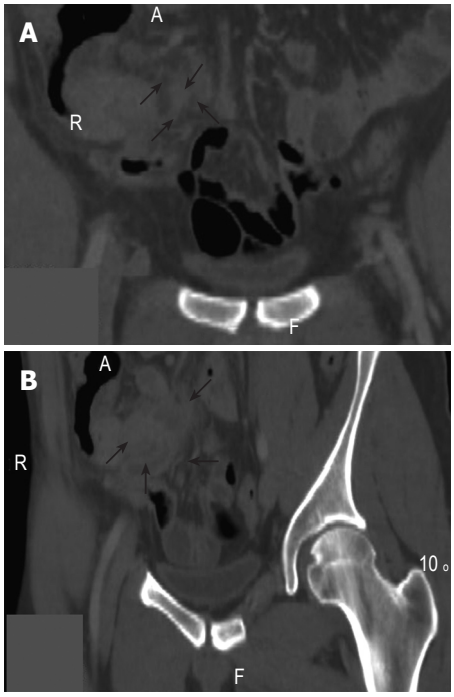

Figure 2 Spiral CT scan with multiple planar reconstruction, in coronal (**2A**) and oblique (**2B**) views, showing extrinsic localization of neoplasia. Soft tissue density mass is visible attached to the wall of cecum (black arrows) which is compressed without clear evidence of mucosal infiltration. Air distension of cecum (**A**) contributes to better visualization of the mass.

Upon histological examination, the neoplasia was found to contain moderately differentiated adenocarcinoma with transmural involvement and mucinous foci, covering 30% of the entire mass. The neoplasia was classified as T3N1MX, corresponding to Dukes' stage C. The patient rapidly recovered after surgery.

DISCUSSION

CRC is the third most frequently diagnosed cancer and the second leading cause of cancer-related deaths in the world. The lifetime risk, in the general population, is approximately 5-6%. The cancer develops sporadically in 80% of these patients, while 20% have an inherited predisposition to the disease[8,9]. HNPCC is the most common hereditary form of CRC accounting for 3-5% of all CRCs[10,11].

HNPCC is an autosomal dominant condition that predisposes to a lifetime risk of approximately 80% of the development of CRC, localized predominantly in the proximal colon. Adenomas, in these patients, tend to have a villous component and most of them present dysplasia, compared with the more common sporadic type. The aggressive behavior of HNPCC adenomas has been demonstrated with an accelerated adenoma-carcinoma sequence (2-3 years) compared to the sporadic forms[12], which are diagnosed at a mean age of 45 and are characteristically localized in the right colon in 60-70% of these patients[13]. HNPCC mutation carriers also have a 60% lifetime risk of developing cancers in other sites of the body, predominantly the uterus, ovary, urinary tract, small bowel, and bile duct[13]. Germline mutations in hMSH2

and hMLH1 account for 90% of the mutations identified in HNPCC patients. These are scattered throughout the entire coding region without a clear phenotype-genotype correlation. However, specific sex and genotype/phenotype associations in HNPCC mutation carriers have been reported. In fact, CRC risk is reported to be higher in males than in females[14]. In one study, the CRC risk is reported to be 96% in males with a hMSH2 mutation compared with 39% in females with the same mutation[15], whereas the risk of extracolonic cancers is reported to be 48% as compared with 11% reported in hMLH1 mutation carriers[14,15]. Based on these considerations, male hMSH2 mutation carriers should receive a tailored program of cancer surveillance. Colonoscopy is the most important tool in the surveillance for CRC; in all individuals, especially patients who are at high risk of developing a CRC, complete colonoscopy in examinations with scrupulous exploration of the cecum is always recommended[16]. Although, colonoscopy is a method of choice in colon cancer surveillance, concerns about its sensitivity and specificity in many clinical settings still remain. Complete colonoscopy refers to the passage of the colonoscope to the cecum and can be assessed by various landmarks[17]. The most reliable are the identification of the cecal valve and/or intubation of the terminal ileum[17]. The rate of colonoscopies considered to be complete decreases significantly (56.9%) when either or both of these landmarks are applied[17]. Moreover, it has been reported that only experienced endoscopists can reach the cecum in almost 97% of colonoscopies, whereas completion of the colonoscopic procedure, by self-trained endoscopists, is reported to be as low as 54%[18,19]. Various factors may cause this discrepancy, one of which might be related to the professional experience of the endoscopist who may erroneously believe that the cecum has been reached. The other factor may be related to bowel preparation that may not offer clear visualization of the cecum. The size of the cancer is also an important factor. If the neoplastic mass is very small or located in close proximity to the ileocecal valve, in an area which is difficult to explore, the cancer can be very easily missed. However, even if colonoscopy is complete, the extension of the neoplasia may be mainly extraluminal, as in the case described here.

All these factors suggest that additional diagnostic examinations, besides colonoscopy, should be made in the follow-up of very high-risk patients, such as the hMSH2 male mutation carriers, in order to complete right colon evaluation, in the event of incomplete or dubious colonoscopy. Spiral CT scan is currently used for the detection of extra-colonic cancers, which is frequently encountered in HNPCC patients. In this particularly high-risk patient, due to the specific sub-occlusive symptoms, a spiral CT scan, with thin slice multiplanar reconstruction, was used for complete visualization of the right colon, detecting a cecal cancer lesion with a predominantly extraluminal development missed at colonoscopy.

In conclusion, given the very high risk of developing a right-sided colon cancer in hMSH2 male carrier HNPCC patients and the possibility that colonoscopy may not completely visualize the cecal region, spiral CT scan should, in our opinion, be included in the follow-up of these patients. At present, due to the relative rarity of this disease, it is difficult to evaluate when, for these specific reasons, a spiral CT scan should be performed. However, besides evaluation of the clinical symptoms, surveillance of right colonic cancer with a thin slice multiplanar reconstruction spiral CT scan is advisable and should always be performed in hMSH2 male carriers in dubious cases or when colonoscopy is thought to be incomplete for any reason.

ACKNOWLEDGMENT

A special thanks to Mrs. Marian E. Shields for her English revision.

REFERENCES

1 **Lynch HT**, de la Chapelle A. Hereditary colorectal cancer. *N Engl J Med* 2003; **348**: 919-932
2 **Samowitz WS**, Curtin K, Lin HH, Robertson MA, Schaffer D, Nichols M, Gruenthal K, Leppert MF, Slattery ML. The colon cancer burden of genetically defined hereditary nonpolyposis colon cancer. *Gastroenterology* 2001; **121**: 830-838
3 **Ponz de Leon M**, Benatti P, Di Gregorio C, Pedroni M, Losi L, Genuardi M, Viel A, Fornasarig M, Lucci-Cordisco E, Anti M, Ponti G, Borghi F, Lamberti I, Roncucci L. Genetic testing among high-risk individuals in families with hereditary nonpolyposis colorectal cancer. *Br J Cancer* 2004; **90**: 882-887
4 **Terdiman JP**, Gum JR, Conrad PG, Miller GA, Weinberg V, Crawley SC, Levin TR, Reeves C, Schmitt A, Hepburn M, Sleisenger MH, Kim YS. Efficient detection of hereditary nonpolyposis colorectal cancer gene carriers by screening for tumor microsatellite instability before germline genetic testing. *Gastroenterology* 2001; **120**: 21-30
5 **Lackner C**, Hoefler G. Critical issues in the identification and management of patients with hereditary non-polyposis colorectal cancer. *Eur J Gastroenterol Hepatol* 2005; **17**: 317-322
6 American Gastroenterological Association medical position statement: hereditary colorectal cancer and genetic testing. *Gastroenterology* 2001; **121**: 195-197
7 **Grady WM**. Genetic testing for high-risk colon cancer patients. *Gastroenterology* 2003; **124**: 1574-1594
8 **Giardiello FM**, Brensinger JD, Petersen GM. AGA technical review on hereditary colorectal cancer and genetic testing. *Gastroenterology* 2001; **121**: 198-213
9 **Annie Yu HJ**, Lin KM, Ota DM, Lynch HT. Hereditary nonpolyposis colorectal cancer: preventive management. *Cancer Treat Rev* 2003; **29**: 461-470
10 **Lynch HT**, Lynch JF. Hereditary nonpolyposis colorectal cancer. *Semin Surg Oncol* 2000; **18**: 305-313
11 **Loukola A,** Eklin K, Laiho P, Salovaara R, Kristo P, Järvinen H, Mecklin JP, Launonen V, Aaltonen LA. Microsatellite marker analysis in screening for hereditary nonpolyposis colorectal cancer (HNPCC). *Cancer Res* 2001; **61**: 4545-4549
12 **Lynch HT,** Riley BD, Weissman SM, Coronel SM, Kinarsky Y, Lynch JF, Shaw TG, Rubinstein WS. Hereditary nonpolyposis colorectal carcinoma (HNPCC) and HNPCC-like families: Problems in diagnosis, surveillance, and management. *Cancer* 2004; **100**: 53-64
13 **Umar A**, Risinger JI, Hawk ET, Barrett JC. Testing guidelines for hereditary non-polyposis colorectal cancer. *Nat Rev Cancer* 2004; **4**: 153-158
14 **Dunlop MG**, Farrington SM, Carothers AD, Wyllie AH, Sharp L, Burn J, Liu B, Kinzler KW, Vogelstein B. Cancer risk associated with germline DNA mismatch repair gene mutations. *Hum Mol Genet* 1997; **6**: 105-110
15 **Lin KM,** Shashidharan M, Thorson AG, Ternent CA, Blatchford GJ, Christensen MA, Watson P, Lemon SJ, Franklin B, Karr B, Lynch J, Lynch HT. Cumulative incidence of

colorectal and extracolonic cancers in MLH1 and MSH2 mutation carriers of hereditary nonpolyposis colorectal cancer. *J Gastrointest Surg* 1998; **2**: 67-71

16 **Bradshaw N,** Holloway S, Penman I, Dunlop MG, Porteous ME. Colonoscopy surveillance of individuals at risk of familial colorectal cancer. *Gut* 2003; **52**: 1748-1751

17 **Bowles CJ,** Leicester R, Romaya C, Swarbrick E, Williams CB, Epstein O. A prospective study of colonoscopy practice in the UK today: are we adequately prepared for national colorectal cancer screening tomorrow? *Gut* 2004; **53**: 277-283

18 **Lieberman DA,** Weiss DG, Bond JH, Ahnen DJ, Garewal H, Chejfec G. Use of colonoscopy to screen asymptomatic adults for colorectal cancer. Veterans Affairs Cooperative Study Group 380. *N Engl J Med* 2000; **343**: 162-168

19 **Imperiale TF**, Wagner DR, Lin CY, Larkin GN, Rogge JD, Ransohoff DF. Risk of advanced proximal neoplasms in asymptomatic adults according to the distal colorectal findings. *N Engl J Med* 2000; **343**: 169-174

Science Editor Ma JY and Guo SY **Language Editor** Elsevier HK

PO Box 2345, Beijing 100023, China
www.wjgnet.com
wjg@wjgnet.com

ELSEVIER

World J Gastroenterol 2005;11(47):7545-7546
World Journal of Gastroenterology ISSN 1007-9327

• *CASE REPORT* •

Remission of bronchial asthma after viral clearance in chronic hepatitis C

Norihiko Yamamoto, Kazumoto Murata, Takeshi Nakano

Norihiko Yamamoto, Kazumoto Murata, Takeshi Nakano, The First Department of Internal Medicine, Mie University School of Medicine, Tsu, Mie, Japan
Correspondence to: Kazumoto Murata, MD, PhD, The First Department of Internal Medicine, Mie University School of Medicine, 2-174 Edobashi, Tsu, Mie, 514-8507, Japan. atarum@clin.medic.mie-u.ac.jp
Telephone: +81-59-231-5015 Fax: +81-59-231-5201
Received: 2005-04-11 Accepted: 2005-06-21

Abstract

A 53-year-old man with a history of blood transfusion at the age of 20 was admitted to our hospital because of liver dysfunction. He had bronchial asthma when he was 18 years old, which naturally resolved within 2 years. However, his bronchial asthma recurred at the age of 45 and was treated with oral theophylline. He was diagnosed as having chronic hepatitis C based on the histological and clinical findings, and then interferon (IFN) therapy was administered. The frequency of bronchial asthma attack was gradually decreasing after IFN therapy with marked improvement of hypereosinophilia. He achieved sustained viral response (SVR) and his bronchial asthma did not worsen even after the cessation of IFN. Hepatitis C virus (HCV) infection and IFN therapy were considered in the remission of asthma in this case. HCV infection could be the cause of bronchial asthma, especially in patients with late appearance of asthma.

Key words: Bronchial asthma; Chronic hepatitis C; IFN therapy

Yamamoto N, Murata K, Nakano T. Remission of bronchial asthma after viral clearance in chronic hepatitis C. *World J Gastroenterol* 2005; 11(47): 7545-7546
http://www.wjgnet.com/1007-9327/11/7545.asp

INTRODUCTION

Hepatitis C virus (HCV) infection is sometimes associated with extrahepatic diseases, such as cryoglobulinemia[1,2] and lichen planus[2,3]. These extrahepatic diseases are considered as part of immune responses against HCV. We have presented a case of chronic hepatitis C with bronchial asthma which improved after interferon (IFN) therapy.

CASE REPORT

A 53-year-old man with a history of blood transfusion at the age of 20 was admitted to our hospital because of liver dysfunction. He had bronchial asthma when he was 18 years old, which naturally resolved within 2 years. However, his bronchial asthma recurred at the age of 45 and has been treated with oral theophylline. Asthma occurred 5-10 times a week before IFN therapy which needed inhalation of β_2 stimulators in addition to daily treatment of theophylline therapy. They were all minor attacks and the patient was easily relieved after a few inhalations of β_2 stimulators. On admission, physical examinations revealed mild wheezing at bilateral lung fields, but no hepatosplenomegaly was observed. Laboratory findings were as follows; white blood cell counts: 5 500/mm^3 (eosinophils 11.2%); platelet counts: 169 000/mm^3, alanine aminotransferase (ALT): 171 IU/L; and aspartate aminotransferase (AST): 81 IU/L, albumin: 42 g/L. HCV-RNA (Genotype 1b, 500 KIU/mL) was positive, but HBsAg, anti-HBc and anti nuclear antibody were all negative. IgE level was within the normal limit (55 IU/mL) and immune complex was negative (Table 1). Abdominal ultrasonography showed chronic liver injury. Liver biopsy revealed moderate portal inflammation and fibrous expansion (A2F2). Based on these findings, he was diagnosed as having chronic hepatitis C. IFN-α2b (10 MU daily for 2 wk, followed by 10 MU thrice a week for another 22 wk) was started on September 2000 with careful observation because asthma exacerbation during IFN therapy was reported[4]. Surprisingly, the frequency of asthma attack was gradually decreasing after IFN therapy with marked improvement of hypereosinophilia (Figure 1). Furthermore, during IFN therapy, asthma attack never recurred even after the cessation of daily theophylline. HCV-RNA became negative after IFN therapy and he achieved sustained virological response (SVR). After the cessation of IFN therapy, he needed inhalation of β_2 stimulators for asthma occasionally. However, he did not require theophylline or steroid any more since the frequency of attack per month was well reduced and the degree of asthma attack was very mild. Interestingly, the eosinophil counts slightly increased after the cessation of IFN, but remained within the normal level (Figure 1).

DISCUSSION

Chronic HCV infection can be associated with various immune mediated extrahepatic manifestations, including porphyria cutanea tarda[1,2], membranoproliferative

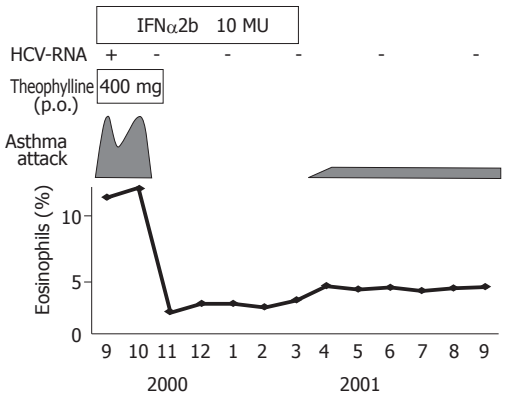

Figure 1 A clinical course of the 53-year-old man.

Table 1 Laboratory data on admission

Peripheral blood		Coagulation test	
WBC	5 500/μL (Eo:11.2%)	PT	149 %
RBC	456× 10^4 /μL	HPT	139 %
Hb	14.7 g/dL	Biochemistry	
Hct	43.6 %	TP	7.0 g/dL
Plt	16.9×10^4/mm^3	Alb	4.2 g/dL
Serological study		T-Bi	0.6 mg/dL
IgG	1236 mg/dL	AST	81 IU/L
IgA	240 mg/dL	ALT	171 IU/L
IgM	41 mg/dL	LDH	203 IU/L
CH50	55 U/mL	ALP	298 IU/L
Cryoglobulin	-	γGTP	65 IU/L
Immune complex	-	T.chol	176 mg/dL
Virology		Amy	104 IU/L
HCV genotype	Ⅰb	BUN	11.1 mg/dL
HCV RNA	500KIU/mL	Cre	0.8 mg/dL

glomerulonephritis[1,2], oral lichen planus[2,3], mixed cryoglobulinemias[1,2], vitiligo[2], B-cell non-Hodgkin lymphoma[2], etc. The response of bronchodilator against asthma was significantly better in the IFN responder group than in the IFN non-responder group[5]. Remission of asthma after the clearance of HCV by IFN therapy in our case could be considered from two points of view. Cytotoxic T cells induced by chronic HCV infection might be a trigger for the development of airway inflammation in patients with bronchial asthma[5] since latent viral infections may be an important cofactor causing airway inflammation[6]. In patients with chronic hepatitis C, the responses of inhaled corticosteroid therapy[5] or bronchodilator for bronchial asthma are impaired, which are recovered in IFN responders[5]. Peripheral B-cell markers such as CD81 and CD5 are correlated with HCV viral load and autoimmunity[7]. The response of antiviral therapy is correlated with the downregulation of these markers. These observations suggest that immune responses by HCV, including cytokines from lymphocytes, may contribute to chronic airway inflammation, and the clearance of HCV by IFN may improve it. The other cause is IFN itself. Injected IFN or released IFN induced by cytotoxic T cells against HCV may improve bronchial asthma by suppressing the chronic airway inflammation since IFN-γ acts as Th1 paracrine inflammatory cytokine. On the contrary, IFN-γ producing T cells may induce the migration of Th2 cells to the airways and IFN may worsen bronchial asthma[8]. Furthermore, IFN increases histamine release from basophilic cells, which is an important trigger for asthma attack[9]. The effect of IFN on bronchial asthma is still controversial.

This is, to our knowledge, the first case in which bronchial asthma improved after the clearance of HCV by IFN. HCV infection could be the cause of bronchial asthma, especially in patients with late onset of asthma.

REFERENCES

1 **Gumber SC**, Chopra S. Hepatitis C: a multifaceted disease. Review of extrahepatic manifestations. *Ann Intern Med* 1995; **123**: 615-620

2 **El-Serag HB**, Hampel H, Yeh C, Rabeneck L. Extrahepatic manifestations of hepatitis C among United States male veterans. *Hepatology* 2002; **36**: 1439-1445

3 **Pilli M**, Penna A, Zerbini A, Vescovi P, Manfredi M, Negro F, Carrozzo M, Mori C, Giuberti T, Ferrari C, Missale G. Oral lichen planus pathogenesis: A role for the HCV-specific cellular immune response. *Hepatology* 2002; **36**: 1446-1452

4 **Bini EJ**, Weinshel EH. Severe exacerbation of asthma: a new side effect of interferon-alpha in patients with asthma and chronic hepatitis C. *Mayo Clin Proc* 1999; **74**: 367-370

5 **Kanazawa H,** Mamoto T, Hirata K, Yoshikawa J. Interferon therapy induces the improvement of lung function by inhaled corticosteroid therapy in asthmatic patients with chronic hepatitis C virus infection: a preliminary study. *Chest* 2003; **123**: 600-603

6 **Keicho N**, Elliott WM, Hogg JC, Hayashi S. Adenovirus E1A upregulates interleukin-8 expression induced by endotoxin in pulmonary epithelial cells. *Am J Physiol* 1997; **272**: L1046-L1052

7 **Zuckerman E,** Kessel A, Slobodin G, Sabo E, Yeshurun D, Toubi E. Antiviral treatment down-regulates peripheral B-cell CD81 expression and CD5 expansion in chronic hepatitis C virus infection. *J Virol* 2003; **77**: 10432-10436

8 **Krouwels FH**, Hol BE, Bruinier B, Lutter R, Jansen HM, Out TA. Cytokine production by T-cell clones from bronchoalveolar lavage fluid of patients with asthma and healthy subjects. *Eur Respir J Suppl* 1996; **22**: 95s-103s

9 **Krasnowska M,** Małolepszy J, Liebhart E, Inglot AD. Inhaled natural human interferon alpha induces bronchospastic reactions in asthmatics. *Arch Immunol Ther Exp (Warsz)* 1992; **40**: 75-78

Science Editor Ma JY and Guo SY **Language Editor** Elsevier HK

PO Box 2345, Beijing 100023, China
www.wjgnet.com
wjg@wjgnet.com

ELSEVIER

World J Gastroenterol 2005;11(47):7547-7549
World Journal of Gastroenterology ISSN 1007-9327

• *CASE REPORT* •

Concordance of ulcerative colitis in monozygotic twin sisters

Madoka Horiya, Satoru Kakizaki, Katsunobu Teshigawara, Yuki Kikuchi, Tetsu Hashida, Yoshio Tomizawa, Tomohiro Iida, Takashige Masuo, Hitoshi Takagi, Masatomo Mori

Madoka Horiya, Satoru Kakizaki, Katsunobu Teshigawara, Yuki Kikuchi, Tetsu Hashida, Yoshio Tomizawa, Tomohiro Iida, Takashige Masuo, Hitoshi Takagi, Masatomo Mori, Department of Medicine and Molecular Science, Gunma University Graduate School of Medicine, Maebashi, Gunma 371-8511, Japan
Correspondence to: Satoru Kakizaki, **MD, PhD, Department** of Medicine and Molecular Science, Gunma University Graduate School of Medicine, 3-39-15 Showa-machi, Maebashi, Gunma 371-8511, Japan. **kakizaki@showa.gunma-u.ac.jp**
Telephone: +81-27-220-8127 **Fax:** +81-27-220-8136
Received: 2005-04-27 **Accepted:** 2005-05-12

Abstract

The etiology of inflammatory bowel disease is multifactorial and appears to combine both genetic and environmental factors. We experienced here a rare occurrence of woman monozygotic twins with ulcerative colitis (UC). A 45-year-old woman (the elder monozygotic twin) was admitted to our hospital because of bloody diarrhea occurring over 10 times per day, abdominal pain and fever. She was diagnosed as UC at the age of 22, and repeated the relapse and remission. She was diagnosed as relapse of UC and total colitis type. Her younger monozygotic twin sister also suffered from UC at the age of 22. Human leukocyte antigen was examined serologically with DNA type in both patients. DRB1*1502, which was previously shown to be dominant in Japanese patients with UC, was not observed in this case. Although the concordance in monozygotic twin in UC is reported to be 6.3-18.8%, the concordant case like this is relatively rare. We report this rare case of UC and the previously reported cases are also discussed.

Key words: Ulcerative colitis; Inflammatory bowel disease; Monozygotic twin; Human leukocyte antigen

Horiya M, Kakizaki S, Teshigawara K, Kikuchi Y, Hashida T, Tomizawa Y, Iida T, Masuo T, Takagi H, Mori M. Concordance of ulcerative colitis in monozygotic twin sisters. *World J Gastroenterol* 2005; 11(47): 7547-7549
http://www.wjgnet.com/1007-9327/11/7547.asp

INTRODUCTION

Ulcerative colitis (UC) is an idiopathic inflammatory bowel disease, which is thought to be multifactorial and appears to combine both genetic and environmental factors. A number of studies have demonstrated aggregation of cases of UC in families, suggesting that patients share a genetic background. The concordance in monozygotic twin in UC is reported to be 6.3-18.8%[1-4]. Although the concordance rate is not so low, patients with twin pairs suffering from UC are relatively rare[5-9] and few observations of the twin pairs with UC have been reported[10-14]. In addition, although previous studies on the associations of UC and human leukocyte antigen (HLA) genes suggest that HLA play a role in this disease, the associations of various HLA loci with UC have yet to be fully elucidated. We experienced here a rare monozygotic twin with UC and determined their HLA serological and DNA type.

CASE REPORT

A 45-year-old Japanese woman (the elder monozygotic twin) was admitted to Gunma University Hospital with episodes of bloody mucous diarrhea occurring over 10 times per day and associated crampy lower abdominal pain and fever. She had a past history of UC at the age of 22, and was followed up by her primary physician. UC repeated the relapse and remission. Bloody diarrhea, abdominal pain and fever worsened from September 2004, and caused the admission. Physical examination was unremarkable and laboratory examination showed 105 g/L hemoglobin, 7 200 /mm^3 WBC count, 15.7×10^4/mm^3 platelets, 56 mm/h erythrocyte sedimentation rate, 52 g/dL serum total protein, 27 g/L albumin, 33 U/L alanine transaminase, 35 U/L aspartate transaminase, 67 U/L γ-glutamyl transferase, and 5.3 mg/L C-reactive protein. Perinuclear pattern of antineutrophil cytoplasmic antibodies (p-ANCA) was negative. Stool cultures for bacteria showed negative findings. Computed tomography of abdomen showed no abnormalities of liver, pancreas or biliary tract. Colonoscopy revealed a total colitis with diffusely reddish, edematous and erosive lesions, being consistent with the relapse of UC (Figure 1). Histological examination of biopsy specimen revealed depletion of goblet cells, crypt abscesses and severe lymphoplasmacytic infiltration in the mucosa, which was also consistent with UC. There were no extra-bowel complications such as primary sclerosing cholangitis. Because sulfasalazine failed to control her colitis, she was treated with intravenous prednisolone and granulocyte and monocyte adsorptive apheresis, which led her to a remission state.

Her younger sister was also diagnosed as UC at the age of 22, and was followed-up by her primary physician. She had a similar course of UC disease as her elder

Table 1 HLA alleles in the case

Serological typing		
A Locus	A2	A33
B Locus	B44	B75
DR Locus	DR13	DR15
DQ Locus	DQ1	
DNA typing		
DRB1	1302	1501
DQB1	0602	0604

sister. Although she was not admitted to the hospital, her colitis worsened in October 2004, and was treated at the outpatient clinic. She was also negative for p-ANCA and had no extra-bowel complications.

The twins were born as full-term normal deliveries and the pregnancy was not complicated. No differences in dietary habits were observed between the twins. They were non-smokers. Their parents, husbands, and daughters had no history of UC or chronic diarrheal diseases. Both twins shared the same home for 24 years, but they lived in different places since the younger sister was married and left home. For the purpose of genetic search, HLA was revealed with serological and DNA types after informed consent was obtained from each patient. HLA was identical and A2, A33, B44, B75, DR13, DR15, DQ1 were detected serologically. DRB1*1501, *1302, DQB1*0602, *0604 were observed by DNA typing (Table 1).

DISCUSSION

The pathogenesis of UC and Crohn's disease is still unknown, but the importance of genetic susceptibility has been clearly shown by epidemiological data from family and twin studies[1-4]. Several twin studies reported that the concordance rate in monozygotic twin with UC is 6.3-18.8%[1-4]. Tysk *et al*[1]. used the Swedish twin registry and inpatient hospital records to identify twins affected by inflammatory bowel disease. Among 25 000 pairs of twins identified from the Swedish twin registry, 80 twin pairs suffering from inflammatory bowel disease were found. In the UC group, 1 of 16 monozygotic pairs was concordant with the disease and the proband concordance rate among monozygotic twins was 6.3% for UC. It was reported that the pair concordance rate in monozygotic twins increases from 6.3% to 18.8% in a Swedish study[2]. Thompson *et al*[3]. also traced 144 twin pairs with inflammatory bowel disease from 16 000 members of the National Association for Colitis and Crohn's Disease, and found that 15.8% monozygotic twins with UC are concordant with the disease. These studies and case reports all indicate a higher concordance with inflammatory bowel disease in monozygotic twins than in dizygotic twins[1-4]. The prevalence and incidence of UC are much lower in Japan than in Europe and North America[15]. Although inflammatory bowel diseases are increasing also in Japan as in European countries, hospital-based investigation in 1991 revealed that the prevalence of UC is 18.12/100 000 and

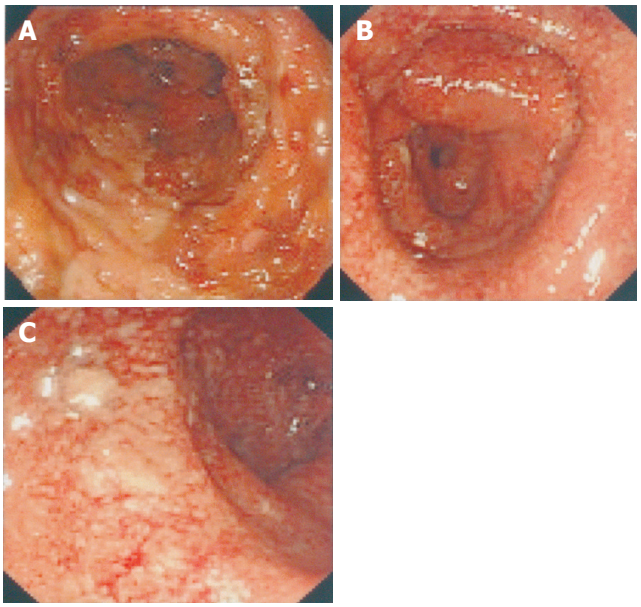

Figure 1 Colonoscopic findings in elder twin sister with UC.

the incidence is 1.95/100 000 in Japan[15]. Delivery with monozygotic twins is reported to be about 4/1 000. The twin study with UC reported that the concordance rate in monozygotic twins with UC is 6.3-18.8%[1-4]. If prevalence of UC is estimated to be 18.12/100 000, concordance rate to be 18.8% and twin delivery rate to be 4/1 000, concordance twin with UC like this case is estimated to be about 13.6/100 000 000. Thus, concordance twins with UC like this case are about only 13.6 cases in Japan. We searched concordant twins with UC using PubMed by key words ulcerative colitis and twin, and found only 22 cases (Table 2) including our case which was reported.

The apparently conflicting data on the HLA system in different studies from around the world may be explained by differences in ethnics, cases and genetic heterogeneity[16]. Replicated class II HLA includes HLA DRB1*0103 and DR2 (DRB1*1502) involved in UC susceptibility, and HLA DRB1*03 and DR4 as resistant alleles for Crohn's disease and UC respectively[16]. The strong association between HLA DR2 and UC has been reported in Japan[17], India[18], and Israel[19]. However, these alleles were not observed in our case. HLA could not explain the occurrence of UC in our case.

The role of environmental factors in the pathogenesis of inflammatory bowel disease is still controversial. The lack of complete concordance in monozygotic twin studies underlines the crucial role played by external factors in the determination of disease expression in patients with genetic susceptibility to inflammatory bowel disease. Non-smoking or a cessation of smoking is a proven risk factor for developing UC[20]. Neither of the twins in our case has ever smoked. Inversely, it has been suggested that appendectomy offers protection against the development of UC[21]. Neither of the twins in our case has received appendectomy.

Table 2 Previously reported cases and prevalence of concordant twins with UC

Author (country)	Total number of twin	IBD[1]	Ulcerative colitis[2]	Number of concordant cases	Concordance (%)	Referrence
Tysk,Halfvarson	25 000	80	16 (Monozygotic)	1 (3)	6.3 (18.8)	*Gut* 1988;29:990-996
(Sweden)			26 (Dizygotic)	0	0	*Gastroenterology*. 2003;124:1767-73
Thompson		128	38 (Monozygotic)	6	15.8	*BMJ* 1996;312:95-96
(UK)			34 (Dizygotic)	1 (Dizygotic)	2.9	
Orholm	29 421	103	21 (Monozygotic)	3	14.3	*Scand J Gastroenterol*. 2000;35:1075-81
(Denmark)			44 (Dizygotic)	2 (Dizygotic)	4.5	
Lyons (USA)	Case report			1		*Gastroenterology*. 1948;10:545
Webb (USA)	Case report			1		*Gastroenterology*. 1950;15:523-4
Bacon	Case report			1 (Dizygotic)		*Ulcerative colitis*. 1958, pp3 J.B.Lippincott Co.
Sleight	Case report			1		*Gastroenterology*. 1971;61:507-12
Sanford	Case report			1		*Am Surg*. 1971;37:512-7.
Fausa	Case report			1		*Scand J Gastroenterol*. 1972;16 (Suppl):38
Quigley (USA)	Case report			1		*Postgrad Med J*. 1982;58:112-4
Mayberry (UK)	Case report			1		*Gastroenterology*. 1983;85:1160-5
Masuichi (Japan)	Case report			1		*Nippon Shokakibyo Gakkai Zasshi*. 1995;92:1966-70
Iwaizumi (Japan)	Case report			1		*Intern Med*. 2002;41:629-32
Our case (Japan)	Case report			1		

Total number of concordant cases of ulcerative colitis in monozygotic twins. IBD[1]: number of twins, one or both pair suffered from inflammatory bowel disease Ulcerative colitis[2]: number of twins, one or both pair suffered from ulcerative colitis. UK: United Kingdom, USA: United States of America.

In summary, we have explained here a rare monozygotic twin with UC. HLA serological and DNA typing were determined. Similar twins are reported to be concordant with inflammatory bowel disease; however the concordant rate is only 6.3-18.8% and the accurate number of these cases is rare. Further accumulations of these cases are needed to clarify the contribution of genetic factors to the development of UC.

REFERENCES

1 **Tysk C,** Lindberg E, Järnerot G, Flodérus-Myrhed B. Ulcerative colitis and Crohn's disease in an unselected population of monozygotic and dizygotic twins. A study of heritability and the influence of smoking. *Gut* 1988; **29:** 990-996

2 **Halfvarson J,** Bodin L, Tysk C, Lindberg E, Järnerot G. Inflammatory bowel disease in a Swedish twin cohort: a long-term follow-up of concordance and clinical characteristics. *Gastroenterology* 2003; **124:** 1767-1773

3 **Thompson NP,** Driscoll R, Pounder RE, Wakefield AJ. Genetics versus environment in inflammatory bowel disease: results of a British twin study. *BMJ* 1996; **312:** 95-96

4 **Orholm M,** Binder V, Sørensen TI, Rasmussen LP, Kyvik KO. Concordance of inflammatory bowel disease among Danish twins. Results of a nationwide study. *Scand J Gastroenterol* 2000; **35:** 1075-1081

5 **Lyons CK,** Postlethwait RW. Chronic ulcerative colitis in twins; case report. *Gastroenterology* 1948; **10:** 545-550

6 **Webb LR.** The occurrence of chronic ulcerative colitis in twin males. *Gastroenterology* 1950; **15:** 523-524

7 **Bacon HE.** Ulcerative colitis: *J B Lippincott Co* 1958: 3

8 **Sanford GE.** Genetic implications in ulcerative colitis. *Am Surg* 1971; **37:** 512-517

9 **Sleight DR,** Galpin JE, Condon RE. Ulcerative colitis in female monozygotic twins and a female sibling. *Gastroenterology* 1971; **61:** 507-512

10 **Fausa O,** Fretheim B, Flatmark A, Froland S, Gjone E. Ulcerative twins in monozygotic twins. *Scand J Gastroenterol* 1972; **16** (Suppl): 38

11 **Quigley EM,** LaRusso NF, Ludwig J, MacSween RN, Birnie GG, Watkinson G. Familial occurrence of primary sclerosing cholangitis and ulcerative colitis. *Gastroenterology* 1983; **85:** 1160-1165

12 **Mayberry JF,** Dew MJ, Morris JS. Monozygotic twins with ulcerative colitis. *Postgrad Med J* 1982; **58:** 112-114

13 **Masuichi H,** Okawa K, Oka H, Ohba H, Watanabe K, Moriyoshi Y, Kioka K, Nebiki H, So K, Yamada H. Ulcerative colitis in female monozygotic twins. *Nihon Shokakibyo Gakkai Zasshi* 1995; **92:** 1966-1970

14 **Iwaizumi M,** Yamada M, Kitagawa M, Takehira Y, Hanajima K, Murohisa G, Kawamura M, Iwaoka Y, Wada T, Morita S, Kawata K. Ulcerative colitis in monozygotic twin sisters. *Intern Med* 2002; **41:** 629-632

15 **Matsumoto T,** Fujishima M. Epidemiologic aspects of ulcerative colitis in Japan--comparison with other countries. *Nihon Rinsho* 1999; **57:** 2443-2448

16 **van Heel DA,** Satsangi J, Carey AH, Jewell DP. Inflammatory bowel disease: progress toward a gene. *Can J Gastroenterol* 2000; **14:** 207-218

17 **Asakura H,** Tsuchiya M, Aiso S, Watanabe M, Kobayashi K, Hibi T, Ando K, Takata H, Sekiguchi S. Association of the human lymphocyte-DR2 antigen with Japanese ulcerative colitis. *Gastroenterology* 1982; **82:** 413-418

18 **Habeeb MA,** Rajalingam R, Dhar A, Kumar A, Sharma MP, Mehra NK. HLA association and occurrence of autoantibodies in Asian-Indian patients with ulcerative colitis. *Am J Gastroenterol* 1997; **92:** 772-776

19 **Delpre G,** Kadish U, Gazit E, Joshua H, Zamir R. HLA antigens in ulcerative colitis and Crohn's disease in Israel. *Gastroenterology* 1980; **78:** 1452-1457

20 **Harries AD,** Baird A, Rhodes J. Non-smoking: a feature of ulcerative colitis. *Br Med J (Clin Res Ed)* 1982; **284:** 706

21 **Rutgeerts P,** D'Haens G, Hiele M, Geboes K, Vantrappen G. Appendectomy protects against ulcerative colitis. *Gastroenterology* 1994; **106:** 1251-1253

Science Editor Wang XL and Guo SY **Language Editor** Elsevier HK

World Journal of Gastroenterology ®

Volume 11 Number 48
December 28, 2005

Supported by NSFC
2005-2006

National Journal Award
2005

ELSEVIER

The WJG Press and Elsevier Inc.

The WJG Press, Apartment 1066 Yishou Garden, 58 North
Langxinzhuang Road, PO Box 2345, Beijing 100023, China
Telephone: +86-(0)10-85381901-1023
Fax: +86-10-85381893
E-mail: wjg@wjgnet.com
http: //www.wjgnet.com

ISSN 1007-9327 CN 14-1219/R Local Post Offices Code No. 82-261

World Journal of Gastroenterology
www.wjgnet.com
Volume 11
Number 48
Dec 28
2005

ISSN 1007-9327
CN 14-1219/R

WJG

World Journal of Gastroenterology ®

Indexed and Abstracted in:
Index Medicus, MEDLINE, PubMed, Chemical Abstracts, EMBASE/Excerpta Medica, Abstracts Journals, Nature Clinical Practice Gastroenterology and Hepatology, CAB Abstracts and Global Health.

Volume 11 Number 48
December 28, 2005

World J Gastroenterol
2005 December 28; 11(48): 7555-7718
Online Submissions
www.wjgnet.com/wjg/index.jsp
www.wjgnet.com
Printed on Acid-free Paper

ELSEVIER

A Weekly Journal of Gastroenterology and Hepatology

ELSEVIER

World Journal of Gastroenterology®

Supported by NSFC 2005-2006

Volume 11 Number 48
December 28, 2005

National Journal Award 2005

Contents

World Journal of Gastroenterology®
Volume 11 **Number** 48 **December 28**, 2005

Contents

World Journal of Gastroenterology®
Volume 11 **Number** 48 **December 28**, 2005

Contents

Editorial Coordinator for this issue: Anitha Kumaran

World Journal of Gastroenterology (*World J Gastroenterol , WJG*), a leading international journal in gastroenterology and hepatology, has an established reputation for publishing first class research on esophageal cancer, gastric cancer, liver cancer, viral hepatitis, colorectal cancer, and *Helicobacter pylori* infection, providing a forum for both clinicians and scientists, and has been indexed and abstracted in Index Medicus, MEDLINE, PubMed, Chemical Abstracts, EMBASE, Abstracts Journals, Nature Clinical Practice Gastroenterology and Hepatology, CAB Abstracts and Global Health. *WJG* is a weekly journal published jointly by The *WJG* Press and Elsevier Inc. The publication date is on 7th, 14th, 21st, and 28th every month. The *WJG* is supported by The National Natural Science Foundation of China, No. 30224801 and No.30424812, which was founded with a name of *China National Journal of New Gastroenterology* on October 1,1995, and renamed as *WJG* on January 25, 1998.

PUBLISHED JOINTLY BY
The WJG Press and Elsevier Inc.

PRINTING GROUP
Printed in Beijing on acid-free paper by Beijing Kexin Printing House

 Print ISSN 1007-9327 CN 14-1219/R.

EDITORIAL OFFICE
Editor: *World Journal of Gastroenterology*,
The WJG Press, Apartment 1066 Yishou Garden, 58 North Langxinzhuang Road, PO Box 2345, Beijing 100023, China
Telephone: +86-(0)10-85381901-1023
Fax: +86-10-85381893
E-mail: wjg@wjgnet.com
http://www.wjgnet.com

Public Relationship Manager
Jing Wang
The WJG Press, Apartment 1066 Yishou Garden, 58 North Langxinzhuang Road, PO Box 2345, Beijing 100023, China
Telephone: +86-(0)10-85381901-1023
Fax: +86-10-8538 1893
E-mail: s.y.guo@wjgnet.com
http://www.wjgnet.com

SUBSCRIPTION INFORMATION
Foreign
Elsevier (Singapore) Pte Ltd, 3 Killiney Road
#08-01, Winsland House I, Singapore 239519
Telephone: +65-6349 0200
Fax: +65-6733 1817
E-mail: r.garcia@elsevier.com
http://asia.elsevierhealth.com
Institutional Rates Print-2005 rates: USD1 500.00
Personal Rates Print-2005 rates: USD700.00

Domestic
Local Post Offices Code No. BM 82-261

Author Reprints
The WJG Press, Apartment 1066 Yishou Garden, 58 North Langxinzhuang Road, PO Box 2345, Beijing 100023, China
Telephone: +86-(0)10-85381901-1023
Fax: +86-10-85381893
E-mail: wjg@wjgnet.com
http://www.wjgnet.com

ADVERTISING
Rosalia Da Carcia
Elsevier Science
Journals Marketing & Society Relations Health Science Asia
3 Killiney Road #08-01, Winsland House 1
Singapore 239519
Telephone: +65-6349 0200
Fax +65- 6733 1817
E-mail: r.garcia@elsevier.com
http://asia.elsevierhealth.com

INSTRUCTIONS TO AUTHORS
Full instructions are available online at http://www.wjgnet.com/wjg/help/instructions.jsp If you do not have web access please contact the editorial office.

PO Box 2345, Beijing 100023, China
www.wjgnet.com
wjg@wjgnet.com

ELSEVIER

World J Gastroenterol 2005;11(48):7555-7559
World Journal of Gastroenterology ISSN 1007-9327

• *GASTRIC CANCER* •

Effect of pseudolaric acid B on gastric cancer cells: Inhibition of proliferation and induction of apoptosis

Ke-Shen Li, Xue-Feng Gu, Ping Li, Yong Zhang, Ya-Shuang Zhao, Zhen-Jiang Yao, Nai-Qiang Qu, Bin-You Wang

Ke-Shen Li, Ya-Shuang Zhao, Zhen-Jiang Yao, Nai-Qiang Qu, Bin-You Wang, Department of Epidemiology, Harbin Medical University, Harbin 150086, Heilongjiang Province, China
Xue-feng Gu, Ping Li, Yong Zhang, Department of Biotechnology and Engineering, Harbin Institute of Technology, Harbin 150001, Heilongjiang Province, China
Supported by the National Natural Science Foundation of China, No. 30371243
Correspondence to: Dr Bin-You Wang, Department of Epidemiology, Harbin Medical University, Harbin 150086, Heilongjiang Province, China. wangby@public.hr.hl.cn
Telephone: +86-451-86842915 Fax: +86-451-86842915
Received: 2005-04-29 Accepted: 2005-07-12

Abstract

AIM: To examine the effect of pseudolaric acid B on the growth of human gastric cancer cell line, AGS, and its possible mechanism of action.

METHODS: Growth inhibition by pseudolaric acid B was analyzed using MTT assay. Apoptotic cells were detected using Hoechst 33258 staining, and confirmed by DNA fragmentation analysis. Western blot was used to detect the expression of apoptosis-regulated gene Bcl-2, caspase 3, and cleavage of poly (ADP-ribose) polymerase-1 (PARP-1).

RESULTS: Pseudolaric acid B inhibited the growth of AGS cells in a time- and dose-dependent manner by arresting the cells at G_2/M phase, which was accompanied with a decrease in the levels of cdc2. AGS cells treated with pseudolaric acid B showed typical characteristics of apoptosis including chromatin condensation and DNA fragmentation. Moreover, treatment of AGS cells with pseudolaric acid B was also associated with decreased levels of the anti-apoptotic protein Bcl-2, activation of caspase-3, and proteolytic cleavage of PARP-1.

CONCLUSION: Pseudolaric acid B can dramatically suppress the AGS cell growth by inducing apoptosis after G_2/M phase arrest. These findings are consistent with the possibility that G_2/M phase arrest is mediated by the down-regulation of cdc2 levels. The data also suggest that pseudolaric acid B can trigger apoptosis by decreasing Bcl-2 levels and activating caspase-3 protease.

Key words: Pseudolaric acid B; Apoptosis; AGS cells

Li KS, Gu XF, Li P, Zhang Y, Qu NQ, Yao ZJ, Zhao YS, Wang BY. Effect of pseudolaric acid B on gastric cancer cells: Inhibition of proliferation and induction of apoptosis. *World J Gastroenterol* 2005; 11(48): 7555-7559
http://www.wjgnet.com/1007-9327/11/7555.asp

INTRODUCTION

Extracts from the root and trunk barks of the Chinese tree *Pseudolarix kaempferi* containing pseudolaric acids are used in traditional Chinese medicine for the treatment of fungal infections[1]. Pseudolaric acid B is the major cell-permeable constituent that displays potent antifungal, antifertil, and anti-angiogenic properties[2-7]. Pseudolaric acid B has cancer chemopreventive activity and inhibits *in vitro* growth of a number of human cancer cell lines, including KB, A-549, HCT-8, P-388, and L-1210 tumor cells[8]. However, no information is at present available on the chemopreventive potentials of pseudolaric acid B on gastric carcinoma.

Apoptosis, a mode of cell death, is a physiologic event that regulates cell number and eliminates damaged cells. Recent studies implicated that apoptosis is a common mechanism through by which chemotherapeutic agents exert their cytotoxicity and that the efficiency of anti-tumor agents is related to the intrinsic propensity of target tumor cells to respond to these agents by apoptosis[9]. *In vitro* studies have shown that pseudolaric acid B treatment can induce apoptosis in human HeLa cells via the activation of c-Jun N-terminal kinase and caspase-3[10]. In order to exploit the chemotherapeutic potentials of pseudolaric acid B on gastric carcinoma, we treated human gastric cancer cell line, AGS, with pseudolaric acid B to examine its antiproliferative effect and apoptosis-inducing activity. Our results suggest that pseudolaric acid B can inhibit the growth of AGS human gastric cancer cells by inducing cell cycle arrest, which correlates with a marked decrease in the expression of key G_2/M-regulating proteins cdc2. The data also suggest that pseudolaric acid B can trigger apoptosis by decreasing Bcl-2 levels and activating caspase-3 protease. Pseudolaric acid B may be used as an effective chemotherapeutic agent against gastric carcinoma.

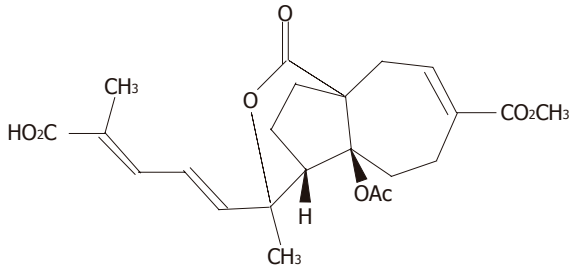

Figure 1 Chemical structure of pseudolaric acid B ($C_{23}H_{28}O_8$, MW = 432.5).

MATERIALS AND METHODS

Materials

Gastric adenocarcinoma cell line (AGS) was obtained from the Shanghai Institute of Cancer Research. Pseudolaric acid B was purchased from Calbiochem Company (La Jolla, CA, USA). The chemical structure of pseudolaric acid B is shown in Figure 1. Hoechst 33258, RNase A, proteinase K and MTT [3'-(4,5-dimethylthiazol-2-yl)-2,5-diphenyl tetrazolium bromide] were purchased from Sigma Chemical Company (St. Louis, USA). Monoclonal antibodies to Cdc2, Bcl-2, caspase-3, and PARP were purchased from Santa Cruz Biotechnology Incorporation (Santa Cruz, CA, USA). PVDF membrane was obtained from Bio-Rad (CA, USA).

Cell culture and treatment with pseudolaric acid B

AGS was maintained in RPMI 1640 supplemented with 10% fetal calf serum, penicillin G (100 kU/L) and kanamycin (0.1 g/L) in a humidified atmosphere of 95% air and 50 mL/L CO_2 at 37 °C. The medium was changed twice a week. A 10 mmol/L stock solution of pseudolaric acid B was prepared in DMSO and stored at -20 °C. Final concentrations of pseudolaric acid B used for different experiments were prepared by diluting the stock with DMEM.

Assay for cell proliferation inhibition (MTT assay)

AGS cells were subcultured in a 96-well plate with 1×10^4 cells/well in 100 μL medium. After 24-h incubation at 37 °C, the medium in each well was discarded and replaced with a fresh medium at various concentrations of pseudolaric acid B in a final volume of 200 μL. Cells were incubated at 37 °C for 6, 12, 24, and 48 h, respectively. At the end of incubation, 50 μL of PBS solution containing 1 mg/mL MTT was added to each well, and further incubated for 4 h. The cell suspension was then centrifuged at 720 r/min for 5 min, and the formazan precipitate in each well was dissolved in 100 μL DMSO for optical density reading at 570 nm.

Flow cytometric analysis

Control and pseudolaric acid B-treated cells were harvested by trypsinization (0.5% trypsin/2.6 mmol/L EDTA), washed twice with ice-cold PBS and fixed in methanol/PBS (9/1, v/v) at 22 °C for at least 30 min. The fixed cells were then washed twice with ice-cold PBS and stained with 50 mg/mL of propidium iodide in the presence of 25 mg/mL of RNase A. Cell cycle phase distribution was determined by flow cytometry (FACSCalibur, Becton Dickinson) and the data were analyzed by multicycle DNA content and cell cycle analysis software (Modfit LT 2.0).

Nuclear damage observed with Hoechst 33258 staining

After being treated with pseudolaric acid B, AGS cells were collected by centrifugation at 1 000 r/min for 5 min and washed twice with PBS. The cells were fixed with 3.7% paraformaldehyde at room temperature for 2 h, centrifuged and washed with PBS, stained with Hoechst 33258 (167 μmol/L) for 30 min at 37 °C. At the end of incubation, the cells were washed and resuspended in PBS for the observation of nuclear morphology under fluorescence microscope (Nikon, Japan).

DNA fragmentation analysis

After being treated with pseudolaric acid B for 12, 24, or 48 h, the cells were harvested and incubated in 0.2 mL lysis buffer containing 10 mmol/L Tris–HCl (pH 8.0), 1 mmol/L EDTA, 1% sodium dodecyl sulfate, and 100 μg/mL proteinase K at 37 °C for 24 h. RNase A (0.5 mg/mL) was added and further incubated at 55 °C for 18 h. Genomic DNA was extracted by phenol/chloroform, precipitated with ethanol and dissolved in TE. Integrity of the DNA was analyzed by electrophoresis on 1.7% agarose gels with ethidium bromide staining.

Western blot analysis

After being treated with pseudolaric acid B for the indicated periods, the cells were washed with PBS and lysed in a buffer containing 20 mmol/L Tris–HCl, 150 mmol/L NaCl, 1% Triton X-100, 1.5 mmol/L $MgCl_2$, 1 mmol/L $NaVO_3$, 100 mmol/L NaF, 10% glycerol, 1 mmol/L EGTA, 10 mmol/L sodium pyrophosphate, and 1 mmol/L phenylmethylsulfonyl fluoride, pH 7.5. Cell lysates were centrifuged at 12 000 *g* for 125 min at 4 °C. The protein concentrations were determined using Bio-Rad protein assay (Bio-Rad Laboratories, USA). After SDS-PAGE, proteins were transferred to PVDF membranes for 2 h at 80 mA. Blots were probed with mouse monoclonal antihuman anti-Bcl-2, anti-caspase-3, and rabbit monoclonal anti-human anti-PARP antibodies. Immunoreactivity was detected using either an anti-mouse (Santa Cruz) or an anti-rabbit (Amersham) peroxidase-conjugated secondary immunoglobulin G antibody followed by enhanced chemiluminescence (ECL, Amersham). Experiments were repeated at least thrice.

Statistical analysis

Data analysis was performed using Student's *t* test. $P<0.05$ was considered statistically significant.

RESULTS

Pseudolaric acid B inhibited AGS cell proliferation

The effects of pseudolaric acid B on cell growth in AGS cell lines were tested. As shown in Figure 2, pseudolaric

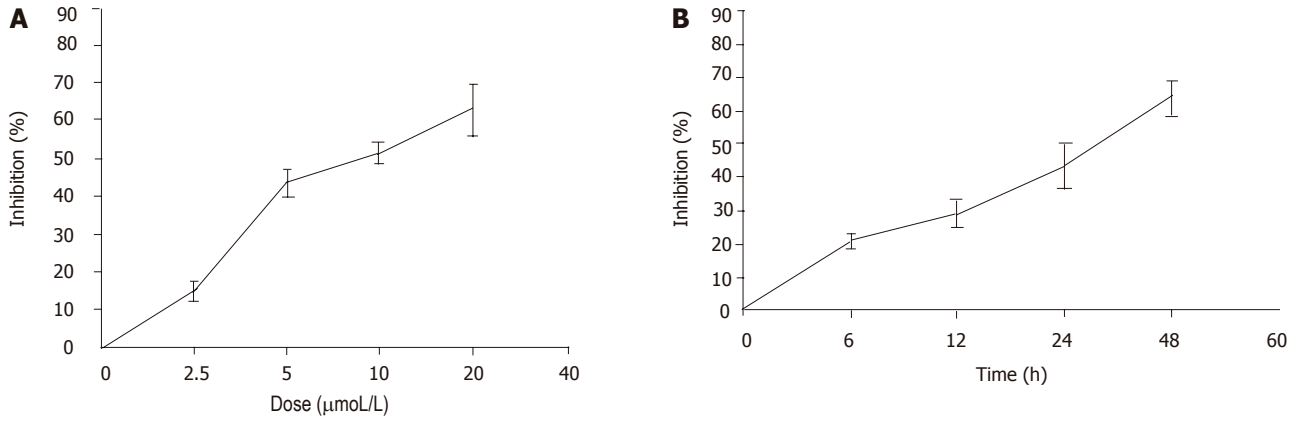

Figure 2 Dose- and time-dependent inhibitory effect of pseudolaric acid B on growth of AGS cells. **A:** AGS cells were treated with various doses of pseudolaric acid B for 24 h; **B**: AGS cells were treated with 5 μmol/L pseudolaric acid B for various time periods. Each point indicates mean±SD of three independent experiments.

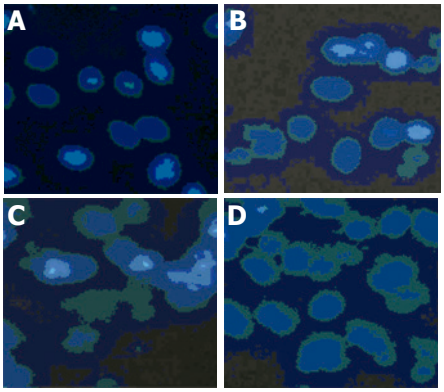

Figure 3 Time-dependent effect of 5 μmol/L pseudolaric acid B on morphological changes in AGS cells. **A:** 0; **B:** 12; **C:** 24; **D:** 48 h.

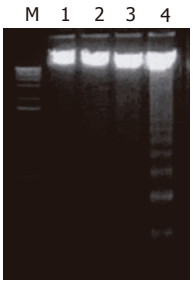

Figure 4 Time-dependent effect of 5 μmol/L pseudolaric acid B on internucleosomal DNA fragmentation in AGS cells. M: Marker; lane 1: 0 h; lane 2: 12 h; lane 3: 24 h; lane 4: 48 h.

acid B inhibited AGS cell proliferation in a time- and dose-dependent manner. Only a minor inhibition of AGS cell growth was observed in the presence of 2.5 μmol/L pseudolaric acid B. Growth was inhibited by more than 40% in cells exposed to 5 μmol/L pseudolaric acid B after 24 h. A concentration of 5 μmol/L pseudolaric acid B was used in all further experiments.

Changes of cell cycle detected by flow cytometric analysis

We further investigated the effects of pseudolaric acid B on the progression of AGS cells throughout the cell cycle. AGS cells were cultured for various lengths of time in the presence or absence of 5 μmol/L pseudolaric acid B and analyzed by flow cytometry. As shown in Table 1, pseudolaric acid B induced a time-dependent accumulation of AGS cells in the G_2/M phase accompanied with a decreased percentage of cells in S and G_0/G_1 phases of the cell cycle.

Table 1 Time course analysis of the cell cycle in pseudolaric acid B-treated cells

Time (h)	G_0/G_1 (%)	S (%)	G_2/M (%)
0 (control)	56.23	33.42	10.35
12	50.64	31.49	17.87[a]
24	43.56	30.81	25.63[b]
48	33.54	28.45	38.01[b]

[a]P<0.05 , [b]P<0.01 *vs* control. Results were representative of three independent experiments.

Morphological changes and DNA fragmentation in AGS cells

To determine the mode of cell death induced by pseudolaric acid B, morphologic alterations in the AGS cells after treatment with 5 μmol/L pseudolaric acid B for up to 48 h were examined under fluorescent microscope after Hoechst 33342 staining. In the control group, AGS cells were round in shape and stained homogeneously. After 24 h of treatment with pseudolaric acid B, blebbing nuclei and granular apoptotic bodies appeared (Figure 3). We analyzed chromosomal DNA from control and pseudolaric acid B-treated cells. Compared to DNA from control cells, treatment with pseudolaric acid B induced apoptosis, as shown by the formation of distinct internucleosomal DNA fragments (Figure 4). The intensity of the DNA banding ladder progressively increased in a time-dependent manner. An early DNA fragmentation was observed after 12 h of incubation with pseudolaric acid B.

Down-regulation of cdc2 levels in response to pseudolaric acid B

Because pseudolaric acid B arrested AGS cells at the

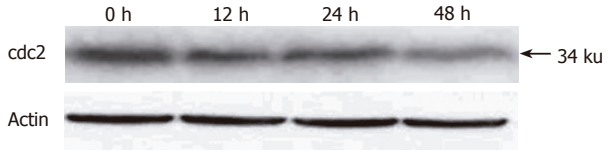

Figure 5 cdc2 levels in AGS cells down-regulated by pseudolaric acid B treatment.

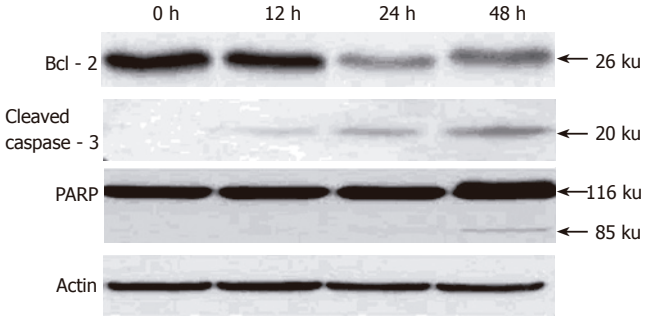

Figure 6 Time-dependent down-regulation of Bcl-2, activation of caspase-3, and PARP cleavage in cultured AGS cells induced by pseudolaric acid B.

G_2/M phase, it was of interest to test the effect of this compound on cdc2 levels, which plays an important role in the G_2 to M progression of the cell cycle. A time-dependent reduction in cdc2 protein level was evident in cells treated with pseudolaric acid B for 48 h (Figure 5).

Down-regulation of Bcl-2, activation of caspase-3, and cleavage of PARP induced by pseudolaric acid B treatment

To investigate the mechanism underlying apoptosis induced by pseudolaric acid B, we tested the effect of this compound on Bcl-2 level, an important regulator of apoptotic signaling pathways[19]. As shown in Figure 5, Western blot analysis revealed that pseudolaric acid B treatment decreased Bcl-2 protein levels. We also found that pseudolaric acid B induced proteolytic processing of caspase-3 in a time-dependent manner. Activation of caspase-3 led to the cleavage of a number of proteins, including PARP-1. Pseudolaric acid B treatment also induced a time-dependent proteolytic cleavage of PARP-1, with concomitant accumulation of the 85 ku and the disappearance of the full-size 116 ku molecule (Figure 6). These findings suggested that pseudolaric acid B could induce apoptosis by down-regulating Bcl-2 and activating caspase-3.

DISCUSSION

Gastric cancer is the second most common cause of cancer death worldwide. Though extensive clinical research has been carried out with numerous combinations of cytotoxic agents, the overall prognosis of advanced gastric cancer still remains poor[11]. Thus, there is considerable interest in identifying more effective cancer chemotherapeutic agents. Pseudolaric acid B, the diterpenoid isolated from the root and trunk bark of *Pseudolarix kaempferi* Gordon tree, has been recently reported to exert an antiproliferative effect on several cancer cell lines[10,12,13]. Since there is no report about its effect on human gastric cancer, we treated human gastric cancer cell line, AGS, with pseudolaric acid B to examine its antiproliferative effect and apoptosis-inducting activity. MTT assay showed that pseudolaric acid B could significantly inhibit growth of AGS cells in a dose- and time-dependent manner. In addition, flow cytometric analysis further revealed that pseudolaric acid B induced a time-dependent accumulation of AGS cells in the G_2/M phase which was coupled with a parallel depletion of the S and G_0/G_1 phase. To further analyze the molecular mechanism by which pseudolaric acid B causes cell cycle arrest, we evaluated cdc2 protein levels. The cdc2/cyclin B complex is one of the major regulatory elements governing the G_2 to M progression[14]. Cdc2 is activated by phosphorylation of and binding to cyclin B, which is synthesized during the S and G_2 phases of the cell cycle[15]. In our study, pseudolaric acid B treatment reduced cdc2 protein levels, suggesting that cell cycle arrest is mediated by the limitation of the supply of cdc2 to cdc2/cyclin B complex formation, which is an essential step in regulating passage into mitosis.

Cell cycle checkpoints are activated to ensure orderly and timely completion of critical events such as DNA replication and chromosome segregation. It is widely accepted that activation of checkpoints in response to DNA damage leads to cell cycle arrest, but in the case of severe damage, the cell cycle arrest leads to cell apoptosis[16,17]. The effects of pseudolaric acid B are compatible with this model. Our present investigation clearly demonstrated that pseudolaric acid B could induce apoptosis of AGS cells, which appears to account for its growth inhibitory and antiproliferative activities. The induction of cell apoptosis was accompanied with characteristic morphological changes, such as chromatin condensation and nuclear fragmentation. Internucleosomal DNA fragmentation as determined by agarose gel electrophoresis also supported the progress of apoptosis of pseudolaric acid B-treated AGS cells.

Apoptosis is a closely regulated process, involving changes in the expression of distinct genes. One of the major genes involved in regulating apoptosis is the protooncogene Bcl-2 encoding a 26-ku mitochondria-associated protein[18,19]. Bcl-2 functions as an intracellular apoptosis suppressor by controlling the mitochondrial membrane permeability with its pro-apoptotic relative, Bax. Diminished expression of Bcl-2 has been observed in certain types of cells undergoing apoptosis[20]. In line with these findings, pseudolaric acid B treatment decreased Bcl-2 protein levels in AGS cells, suggesting that down-regulation of Bcl-2 may be required for AGS cell apoptosis induced by pseudolaric acid B, thus increasing mitochondrial permeability and cytochrome *c* release, which initiates the progress of apoptosis. In addition, involvement of caspase 3 was also examined in pseudolaric acid B-induced AGS cell apoptosis. Caspase-3, a cysteine protease that exists as an inactive proenzyme in cells, is activated by proteolytic processing at internal aspartic

acid residue when cells receive an apoptosis-inducing signal[21]. Activation of caspase-3 leads to degradation and inactivation of key cellular proteins such as DNA repair, signaling, and structural proteins[22,23]. Among these, the cleavage of PARP represents a well described response of cells undergoing caspase-mediated apoptosis[24]. AGS cells treated with pseudolaric acid B exhibited time-dependent activation of caspase-3 and proteolytic cleavage of PARP, indicating that apoptosis of AGS cells is induced by pseudolaric acid B and caspase cascade process.

In conclusion, naturally occurring diterpenoid, pseudolaric acid B, is a potent inhibitor of the growth of human gastric cancer cells. Growth inhibition of the compound is highly related to the induction of cell cycle arrest and apoptosis.

REFERENCES

1 **Li E,** Clark AM, Hufford CD. Antifungal evaluation of pseudolaric acid B, a major constituent of Pseudolarix kaempferi. *J Nat Prod* 1995; **58:** 57-67

2 **Yang SP,** Dong L, Wang Y, Wu Y, Yue JM. Antifungal diterpenoids of Pseudolarix kaempferi, and their structure-activity relationship study. *Bioorg Med Chem* 2003; **11:** 4577-4584

3 **Wang WC,** Lu RF, Zhao SX, Zhu YZ. [Antifertility effect of pseudolaric acid B] *Zhongguo Yao Li Xue Bao* 1982; **3:** 188-192

4 **Zhang YL,** Lu RZ, Yan AL. [Inhibition of ova fertilizability by pseudolaric acid B in hamster] *Zhongguo Yao Li Xue Bao* 1990; **11:** 60-62

5 **Wang WC**, Gu ZP, Koo A, Chen WS. Effects of pseudolaric acid B on blood flows of endometrium and myometrium in pregnant rats. *Zhongguo Yao Li Xue Bao* 1991; **12:** 423-425

6 **Tan WF,** Zhang XW, Li MH, Yue JM, Chen Y, Lin LP, Ding J. Pseudolarix acid B inhibits angiogenesis by antagonizing the vascular endothelial growth factor-mediated anti-apoptotic effect. *Eur J Pharmacol* 2004; **499:** 219-228

7 **Li MH,** Miao ZH, Tan WF, Yue JM, Zhang C, Lin LP, Zhang XW, Ding J. Pseudolaric acid B inhibits angiogenesis and reduces hypoxia-inducible factor 1alpha by promoting proteasome-mediated degradation. *Clin Cancer Res* 2004; **10:** 8266-8274

8 **Pan DJ,** Li ZL, Hu CQ, Chen K, Chang JJ, Lee KH. The cytotoxic principles of Pseudolarix kaempferi: pseudolaric acid-A and -B and related derivatives. *Planta Med* 1990; **56:** 383-385

9 **Kim R,** Tanabe K, Uchida Y, Emi M, Inoue H, Toge T. Current status of the molecular mechanisms of anticancer drug-induced apoptosis. The contribution of molecular-level analysis to cancer chemotherapy. *Cancer Chemother Pharmacol* 2002; **50:** 343-352

10 **Gong X,** Wang M, Wu Z, Tashiro S, Onodera S, Ikejima T. Pseudolaric acid B induces apoptosis via activation of c-Jun N-terminal kinase and caspase-3 in HeLa cells. *Exp Mol Med* 2004; **36:** 551-556

11 **Parkin DM,** Pisani P, Ferlay J. Estimates of the worldwide incidence of 25 major cancers in 1990. *Int J Cancer* 1999; **80:** 827-841

12 **Gong XF,** Wang MW, Tashiro S, Onodera S, Ikejima T. Pseudolaric acid B induces human melanoma A375-S2 cell apoptosis in vitro. *Zhongguo Zhong Yao Za Zhi* 2005; **30:** 55-57

13 **Gong XF,** Wang MW, Tashiro S, Onodera S, Ikejima T. Pseudolaric acid B induces apoptosis through p53 and Bax/Bcl-2 pathways in human melanoma A375-S2 cells. *Arch Pharm Res* 2005; **28:** 68-72

14 **Nurse P.** Universal control mechanism regulating onset of M-phase. *Nature* 1990; **344:** 503-508

15 F**ang F,** Newport JW. Evidence that the G1-S and G2-M transitions are controlled by different cdc2 proteins in higher eukaryotes. *Cell* 1991; **66:** 731-742

16 **Orren DK**, Petersen LN, Bohr VA. Persistent DNA damage inhibits S-phase and G2 progression, and results in apoptosis. *Mol Biol Cell* 1997; **8:** 1129-1142

17 **Smith ML**, Fornace AJ Jr. Mammalian DNA damage-inducible genes associated with growth arrest and apoptosis. *Mutat Res* 1996; **340:** 109-124

18 **Adams JM**, Cory S. The Bcl-2 protein family: arbiters of cell survival. *Science* 1998; **281:** 1322-1326

19 **Burlacu A**. Regulation of apoptosis by Bcl-2 family proteins. *J Cell Mol Med* 2003; **7:** 249-257

20 **Oltvai ZN,** Milliman CL, Korsmeyer SJ. Bcl-2 heterodimerizes in vivo with a conserved homolog, Bax, that accelerates programmed cell death. *Cell* 1993; **74:** 609-619

21 **Nicholson DW**. Caspase structure, proteolytic substrates, and function during apoptotic cell death. *Cell Death Differ* 1999; **6:** 1028-1042

22 **Wolf BB,** Schuler M, Echeverri F, Green DR. Caspase-3 is the primary activator of apoptotic DNA fragmentation via DNA fragmentation factor-45/inhibitor of caspase-activated DNase inactivation. *J Biol Chem* 1999; **274:** 30651-30656

23 **Enari M**, Sakahira H, Yokoyama H, Okawa K, Iwamatsu A, Nagata S. A caspase-activated DNase that degrades DNA during apoptosis, and its inhibitor ICAD. *Nature* 1998; **391:** 43-50

24 **Kaufmann SH,** Desnoyers S, Ottaviano Y, Davidson NE, Poirier GG. Specific proteolytic cleavage of poly(ADP-ribose) polymerase: an early marker of chemotherapy-induced apoptosis. *Cancer Res* 1993; **53:** 3976-3985

Science Editors Wang XL and Guo SY **Language Editor** Elsevier HK

PO Box 2345, Beijing 100023, China
www.wjgnet.com
wjg@wjgnet.com

ELSEVIER

World J Gastroenterol 2005;11(48):7560-7563
World Journal of Gastroenterology ISSN 1007-9327

Effects of six months losartan administration on liver fibrosis in chronic hepatitis C patients: A pilot study

Silvia Sookoian, María Alejandra Fernández, Gustavo Castaño

Silvia Sookoian, Cardiología Molecular, Instituto de Investigaciones Médicas A. Lanari, University of Buenos Aires, Buenos Aires, Argentina
María Alejandra Fernández, Cathedra of Physiopathology, School of Pharmacy and Biochemistry, University of Buenos Aires, Buenos Aires, Argentina
Gustavo Castaño, Gastroenterology Section, Hospital José M. Penna. & Consejo de Investigación, Government of the City of Buenos Aires, Buenos Aires, Argentina
Correspondence to: Silvia Sookoian, MD, PhD, Instituto de Investigaciones Médicas, A Lanari. Cardiología Molecular, Combatientes de Malvinas 3150, Buenos Aires 1427, Argentina. ssookoian@intramed.net
Telephone: +54-11-45148701-04 Fax: +54-11-45238947
Received: 2005-03-28 Accepted: 2005-04-30

Abstract

AIM: To evaluate the safety and efficacy of chronic administration of losartan on hepatic fibrosis in chronic hepatitis C patients.

METHODS: Fourteen patients with chronic hepatitis C non-responders (n = 10), with contraindications (n = 2) or lack of compliance (n = 2) to interferon plus ribavirin therapy and liver fibrosis were enrolled. Liver and renal function test, clinical evaluation, and liver biopsies were performed at baseline and after losartan administration at a dose of 50 mg/d during the 6 mo. The control group composed of nine patients with the same inclusion criteria and paired liver biopsies (interval 6-14 mo). Histological activity index (HAI) with fibrosis stage was assessed under blind conditions by means of Ishak's score. Subendothelial fibrosis was evaluated by digital image analyses.

RESULTS: The changes in the fibrosis stage were significantly different between losartan group (decrease of 0.5±1.3) and controls (increase of 0.89±1.27; P<0.03). In the treated patients, a decrease in fibrosis stage was observed in 7/14 patients *vs* 1/9 control patients (P<0.04). A decrease in sub-endothelial fibrosis was observed in the losartan group. No differences were found in HAI after losartan administration. Acute and chronic decreases in systolic arterial pressures (P<0.05) were observed after the losartan administration, without changes in mean arterial pressure or renal function.

CONCLUSION: Chronic AT-II type 1 receptor (AT1R) blockade may reduce liver fibrosis in patients with chronic hepatitis C.

Key words: Hepatitis C; Liver fibrosis; Losartan; AT1R; Chronic liver disease; Angiotensin II

Sookoian S, Fernández MA, Castaño G. Effects of six months losartan administration on liver fibrosis in chronic hepatitis C patients: A pilot study. *World J Gastroenterol* 2005; 11(48):7560-7563
http://www.wjgnet.com/1007-9327/11/7560.asp

INTRODUCTION

The hepatitis C virus (HCV) is one of the leading causes of chronic hepatitis, liver cirrhosis, and hepatocellular carcinoma. Although major progress has been made in the treatment of chronic HCV infection, the current treatment regimens, including Peginterferons in association with ribavirin, appear capable of eradicating HCV in only 30-50% of the treated patients[1]. In this scenario, alternative medical strategies to reduce hepatic fibrosis are under investigation, since drugs with antifibrotic effects may be an option in the treatment of patients with chronic hepatitis C who do not respond to the standard antiviral therapy.

Much evidence suggests that hepatic stellate cells (HSCs) play important roles in the pathogenesis of liver fibrosis, since they were shown to undergo a transformation during the injury that is termed as activation[2]. Furthermore, *in vitro* studies have shown that angiotensin II (ANGII) is a mitogenic protein for a number of cell types and between them the HSCs undergo a MAPK-dependent pathway. In these cells, ANGII upregulates the transforming growth factor beta 1 expression *via* AT-II type 1 receptor (AT1R) *in vitro*. Additionally, proliferation of activated HSCs was found in chronic liver diseases taking part in the development of liver fibrosis[3]. The fact that the actions of ANGII are mediated through AT1R is related to the therapeutic interventions, since AT1R can be completely blocked by losartan, a specific ANGII receptor antagonist. For instance, ANGII stimulated mRNA expression of TGF-beta and fibronectin can be reversed by saralasin and losartan, a nonselective and specific antagonists for AT1R receptors, respectively[4]. Lastly, in animal

Table 1 Presenting features of the studied patients

	Treated group (n = 14)		Untreated group (n = 9)	
	Baseline	Post losartan	Baseline	Second biopsy
Females/males	4/14		1/8	
Age (yr)	49.6±13		51.4±9.6	
Hematocrit	45.2±3.59	44.1±3.85	48.8±4.66	47.8±4.15
White blood cells (K/mm^3)	6.66±1.41	6.71±1.67	5.98±0.95	5.78±1.19
Platelets (K/mm^3)	227±80.8	246±90.7[b]	223±68	209±78.4
Glucose (g/L)	0.99±0.38	1±0.29	0.95±0.1	1.01±0.06
Blood urea nitrogen (g/L)	0.31±0.06	0.32±0.06	0.28±0.07	0.25±0.04
Creatinine (mg/dL)	0.88±0.07	0.95±0.11	0.99±0.07	0.96±0.12
Total bilirubin (mg/dL)	1±0.53	1.08±0.63	1.35±0.58	1.19±0.58
Alkaline phosphatase (IU/L)	253±118	269±68.9	264±93.4	349±134
Alanine aminotransferase (IU/L)	90.5±66	91.9±47.6	264±167[a]	169±124
Aspartate aminotransferase (IU/L)	65.3±41	67±40.9	161±97.8[a]	130±84.5
Cholesterol (mg/dL)	157±36.4	161±42.6	166±38.1	169±39.2
Albumin (g/dL)	4.12±0.32	4.43±0.24[b]	4.32±0.56	4.32±0.5
Globulins (g/dL)	3.64±0.53	3.77±0.45	3.74±0.63	3.91±0.63
G glutamyl transpeptidase (IU/ L)	63.2±47.9	74.5±53.7	194±178[a]	217±214
Prothrombin time (%)	103±19.3	106±17.4	107±8.19	97±9.83
KPTT (s)	32.6±3.38	39.6±18.7	37.8±6.99	34.5±2.38

Results are expressed as mean±SD. [a]P<0.05 in comparison with baseline measurements in the treated group. [b]P<0.01 in comparison with baseline measurements in the treated group.

models of fibrosis, chronic administration of losartan prevented the development of hepatic fibrosis and portal hypertension[3,5,6].

The purpose of this study was to investigate the safety and efficacy of chronic administration of losartan on hepatic fibrosis in chronic hepatitis C patients.

MATERIALS AND METHODS

Fourteen outpatients (10 men and 4 women) aged 49.6±13 years, with both chronic hepatitis C infection and biopsy proven liver fibrosis, were enrolled in a pilot study.

Ten patients were previous non-responders to a 12-mo combined therapy of interferon and ribavirin, two had contraindications and two showed lack of compliance to the mentioned treatment.

In the control group, nine sex- and age-matched untreated chronic hepatitis C patients with the same inclusion and exclusion criteria who underwent paired liver biopsies (interval 6-14 mo) were included. No patient had a previous history of autoimmune disease, alcohol intake, current intravenous drug use or other chronic liver diseases. All were negative for hepatitis B surface antigen and anti-human immunodeficiency virus. Their clinical characteristics are shown in Table 1.

Written informed consent was obtained from all patients, and the local ethical committee approved the study protocol, based on the 1975 Declaration of Helsinki.

Systolic, diastolic, and mean arterial blood pressures were taken by an automatic sphygmomanometer (VR 12, Electronics for Medicine). Liver and renal function tests and liver biopsies were performed at baseline and after the losartan administration at a dose of 50 mg/d during 6 mo (Losacor, kindly donated by Roemmers, Buenos Aires, Argentina). During the losartan administration, patients did not receive any other medication. Clinical and biochemical follow-ups were assessed and blood pressure was monitored during the first hours, at 1 wk and monthly after the losartan administration.

Liver histology

Ultrasound-assisted liver biopsy was performed using modified Menghini needle of 1.4 mm diameter (Hepafix, Braun, Germany). Liver specimens, previously fixed in formalin, were stained with hematoxylin and eosin, Masson trichrome, silver impregnation for reticular fibers, Perls blue and Prussian blue, and examined by a liver pathologist who was blinded to the clinical data of the patients. Histological activity index (HAI) and fibrosis stage were assessed by means of Ishak's score.

Digital image analysis

Selected areas for fibrosis quantification included the hepatic lobule but without the portal, periportal, septal, and pericentral vein areas. Histological slides stained for reticular fibers were evaluated for sub-endothelial deposit of types III collagen[7] by a digital image analysis. A previous study of our group using this method showed a high correlation between image analysis and fibrosis stage[8]. Images were obtained using a video camera (Sony CCD Iris camera) attached to a light microscope and converted to digital format on a computer by CAP VIEW Leadtek Winfast 2000 PAL device (Leadtek Research Inc.). Standardization of the images was performed with software Adobe Photoshop 7.0 (Adobe Systems Inc.). The quantification of the selected color areas of the digitalized, standardized, and processed images was performed in a 256 gray tones scale with software Scion image for Windows (2000 Scion Corporation), and expressed in pixels/inch^2.

Statistical analysis

Results were expressed as mean±SD. Differences between

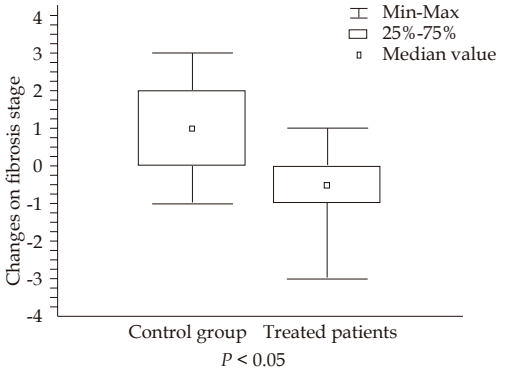

Figure 1 Changes in fibrosis stage in control group and treated patients.

Table 2 Histological changes in liver biopsies

	Treated group (n = 14)		Untreated group (n = 9)	
	Baseline	Post losartan	Baseline	Second biopsy
Histology activity index	8.08±2.56	8.54±1.51	7.0±2.12	7.6±2.3
Fibrosis stage	3.29±1.44	2.64±1.22	2.67±2	3.56±2.13
Sub-endothelial fibrosis (pixels/inch^2)	2.48±1.04	1.00±0.53[a]	1.65±0.43	1.55±0.27

Results are expressed as mean±SD. [a]P<0.01 *vs* baseline.

Table 3 Changes in arterial pressure after losartan administration

	Baseline	3 h	1 mo
Systolic arterial pressure (mmHg)	134±22.7	125±17.4[a]	124±18.1[a]
Diastolic arterial pressure (mmHg)	80.8±14	81.2±14.2	82.5±13.7
Mean arterial pressure (mmHg)	98.4±16.3	95.7±14.8	100±15.8

Results are expressed as mean±SD. [a]P<0.05 *vs* baseline.

Table 4 Orthostatic variations in arterial pressure after losartan administration

	Supine position	Sitting position	
Baseline (10:00 am)			
Systolic arterial pressure (mmHg)	132.7±22.1	132.2±16.8	
Diastolic arterial pressure (mmHg)	80.7±13.4	87.8±8.93	(P<0.0001)
Mean arterial pressure (mmHg)	98±15.7	102.6±11.1	(P<0.01)
Three hours post losartan			
Systolic arterial pressure (mmHg)	124. 7±17.4	127.3±14.9	
Diastolic arterial pressure (mmHg)	81.1±14.2	83.5±11.1	
Mean arterial pressure (mmHg)	95. 7±14.8	98.1±12	

proportions were analyzed by χ^2 test and the Fisher's exact test. Differences between the groups were analyzed by paired and unpaired Student's t- test, by Mann–Whitney U or Wilcoxon matched paired tests, according to the distribution and the scale of measurement. Spearman's ρ coefficient was utilized for correlations. Significance was established at P<0.05.

RESULTS

Effects of losartan

The changes in fibrosis stage were significantly different between losartan group and controls (a decrease of 0.64± 1.3 *vs* an increase of 0.89±1.27, respectively; P<0.02) (Table 2). In the treated patients, a decrease in fibrosis stage was observed in 7/14 patients *vs* 1/9 control patients (P<0.04). Three of the seven patients showed a reduction of two or more points in fibrosis stage. No differences were observed in HAI after losartan administration. Sub-endothelial fibrosis evaluated by image analysis of lobular areas was significantly reduced after losartan administration, without changes in the control group (Table 2 and Figure 1). A significant correlation was found between fibrosis stage and sub-endothelial fibrosis (Spearman's ρ 0.36, P<0.03). A significant increase was observed in albumin level and platelet counts in the treated patients.

Additionally, no significant differences were found in any clinical or biochemical parameters between responders and non-responders to losartan, except that patients who responded to losartan had higher baseline serum alkaline phosphatase than non-responders (309±132 IU/L *vs* 194± 25 IU/L, P = 0.009).

Safety

Acute (3 h) and chronic (1 mo) decreases in systolic arterial pressures in supine position, and a loss of physiologic increase in diastolic pressures from supine to sitting position were observed after losartan administration (Tables 3 and 4). Nevertheless, only one treated patient had a single episode of mild orthostatic hypotension. No differences were observed in renal function tests after losartan administration.

DISCUSSION

It is well known that, at present, the most effective therapy for treating hepatic fibrosis is the removal of the causative agent. In chronic hepatitis C, this goal may be achieved with standard antiviral therapy in a great proportion of patients. Nevertheless, non-responder patients may obtain a benefit from the emerging antifibrotic therapies.

Since renin-angiotensin system blockers are promising drugs in reducing the accumulation of scar tissue in experimental models of chronic liver injury, we performed a pilot study with chronic losartan administration in 14 chronic HCV non-responder patients or with contraindications to interferon plus ribavirin regimen.

Liver biopsy is considered the gold-standard method for the assessment of liver fibrosis[9]. In our study, paired biopsy specimens taken at baseline and at the study completion were compared by means of the standard Ishak score and by an image analysis method for quantification of liver fibrosis. Histopathological scores showed that losartan had an inhibitory effect on the progression of hepatic fibrosis stage. Subendothelial fibrosis evaluated by image analysis of lobular areas was significantly decreased after losartan administration in comparison with the untreated control group.

Regarding biochemical evaluation of the patients, liver

and renal function tests, and blood cells content did not change in either group, except for the platelet content and the albumin concentration in the losartan treated patients, who evidenced a significant improvement in comparison with the control group. Additionally, serum HCV-RNA levels had no change after the study in both groups (data not shown).

Several authors, including us, demonstrated in randomized controlled trials that losartan had equal or greater effects in lowering portal pressure than propranolol, without serious adverse effects[10-13]. The effects of losartan on portal pressure may be explained by the effect of the blockade of AT1R on the contractility of hepatic activated stellate cells, by means of a decrease in intrahepatic vascular resistance. In addition to these events, antifibrotic effects of AT1 blockade may have actions on the structural component of portal hypertension.

With regard to the safety of this treatment, no serious side effects were noted during the study. Nonetheless, an overall decrease was observed in systolic arterial pressures in supine position.

The pathogenesis of HCV-induced liver fibrosis is poorly understood due to the lack of a rodent model of persistent HCV infection. However, since liver fibrosis is the excessive accumulation of extracellular matrix proteins including collagen, it is rational to assume that any chronic damage of the liver may lead to the same final outcome.

Experimental and human studies have consistently shown that ANGII is involved in the development of fibrosis in cardiac and renal tissues in conditions associated with chronic inflammation. Besides, *in vivo* studies have shown that ACE inhibitors and AT1 receptors antagonists can limit the progression of cardiac, renal and pulmonary fibrosis.

In human beings, their efficacy has been tested in a few preliminary pilot studies in patients with NASH[14] and in chronic HCV infection[15], suggesting that renin–angiotensin blocking agents may have beneficial effects on fibrosis progression.

In conclusion, this study shows that administration of an AT1R antagonist may improve liver scores of fibrosis stage in patients with chronic hepatitis C, suggesting that losartan may provide an effective new approach to the treatment of non-responders to antiviral therapy. However, a randomized, controlled trial seems to be necessary in order to confirm the benefit of AT1R blocking for hepatic fibrosis in chronic HCV infection. Lastly, one may speculate that the combination treatment of the clinically used Peginterferons and AT1R blocker may provide a new strategy for anti-liver fibrosis treatment in HCV.

REFERENCES

1 NIH Consensus Statement on Management of Hepatitis C: 2002. *NIH Consens State Sci Statements 2002*; **19**: 1-46

2 **Bataller R**, Sancho-Bru P, Gines P, Lora JM, Al-Garawi A, Sole M, Colmenero J, Nicolas JM, Jimenez W, Weich N, Gutierrez-Ramos JC, Arroyo V, Rodes J. Activated human hepatic stellate cells express the renin-angiotensin system and synthesize angiotensin II. *Gastroenterology* 2003; **125**: 117-125

3 **Yoshiji H**, Kuriyama S, Yoshii J, Ikenaka Y, Noguchi R, Nakatani T, Tsujinoue H,Fukui H. Angiotensin-II type 1 receptor interaction is a major regulator for liver fibrosis development in rats. *Hepatology* 2001; **34**: 745-750

4 **Leung PS**, Suen PM, Ip SP, Yip CK, Chen G, Lai PB. Expression and localization of AT1 receptors in hepatic Kupffer cells: its potential role in regulating a fibrogenic response. *Regul Pept* 2003; **116**: 61-69

5 **Croquet V**, Moal F, Veal N, Wang J, Oberti F, Roux J, Vuillemin E, Gallois Y, Douay O, Chappard D, Cales P. Hemodynamic and antifibrotic effects of losartan in rats with liver fibrosis and/or portal hypertension. *J Hepatol* 2002; **37**: 773-780

6 **Yoshiji H**, Noguchi R, Kuriyama S, Yoshii J, Ikenaka Y. Combination of interferon and angiotensin-converting enzyme inhibitor, perindopril, suppresses liver carcinogenesis and angiogenesis in mice. *Oncol Rep* 2005; **13**: 491-495

7 **Ushiki T**. Collagen fibers, reticular fibers and elastic fibers. A comprehensive understanding from a morphological viewpoint. *Arch Histol Cytol* 2002; **65**: 109-126

8 **Fernadez A**, Castano G, Sookoian S, Lemberg A, Amante M, Parisi C,Perazzo J. A new image analysis method for quantification of liver fibrosis. *J Hepatol* 2003; **38**: 216-Abs .

9 Afdhal NH, Nunes D. Evaluation of liver fibrosis: a concise review. *Am J Gastroenterol* 2004; **99**: 1160-1174

10 **Schneider AW**, Kalk JF,Klein CP. Effect of losartan, an angiotensin II receptor antagonist, on portal pressure in cirrhosis. *Hepatology* 1999; **29**: 334-339

11 **Castano G**, Viudez P, Frider B, Sookoian S. Discussion on randomized comparison of long-term losartan versus propranolol in lowering portal pressure in cirrhosis. *Gastroenterology* 2002; **122**: 1544-1545

12 **Sookoian S,** Castano G, Garcia SI, Viudez P, Gonzalez C, Pirola CJ. A1166C angiotensin II type 1 receptor gene polymorphism may predict hemodynamic response to losartan in patients with cirrhosis and portal hypertension. *Am J Gastroenterol* 2005; **100**: 636-642

13 **De BK**, Bandyopadhyay K, Das TK, Das D, Biswas PK, Majumdar D, Mandal SK, Ray S, Dasgupta S. Portal pressure response to losartan compared with propranolol in patients with cirrhosis. *Am J Gastroenterol* 2003; **98**: 1371-1376

14 **Yokohama S**, Yoneda M, Haneda M, Okamoto S, Okada M, Aso K, Hasegawa T, Tokusashi Y, Miyokawa N, Nakamura K. Therapeutic efficacy of an angiotensin II receptor antagonist in patients with nonalcoholic steatohepatitis. *Hepatology* 2004; **40**: 1222-1225

15 **Terui Y**, Saito T, Watanabe H, Togashi H, Kawata S, Kamada Y, Sakuta S. Effect of angiotensin receptor antagonist on liver fibrosis in early stages of chronic hepatitis C. *Hepatology* 2002; **36**: 1022

Science Editor Ma JY and Guo SY **Language Editor** Elsevier HK

PO Box 2345, Beijing 100023, China
www.wjgnet.com
wjg@wjgnet.com

ELSEVIER

World J Gastroenterol 2005;11(48):7564-7568
World Journal of Gastroenterology ISSN 1007-9327

Tumor necrosis factor-α-induced protein 1 and immunity to hepatitis B virus

Marie C Lin, Nikki P Lee, Ning Zheng, Pai-Hao Yang, Oscar G Wong, Hsiang-Fu Kung, Chee-Kin Hui, John M Luk, George Ka-Kit Lau

Marie C Lin, Pai-Hao Yang, Oscar G Wong, Hsiang-Fu Kung, Institute of Molecular Biology, The University of Hong Kong, Hong Kong SAR, China
Nikki P Lee, John M Luk, Department of Surgery, The University of Hong Kong, Hong Kong SAR, China
Nikki P Lee, John M Luk, George Ka-Kit Lau, Center for the Study of Liver Diseases, The University of Hong Kong, Hong Kong SAR, China
Ning Zheng, Chee-Kin Hui, George Ka-Kit Lau, Department of Medicine, The University of Hong Kong, Hong Kong SAR, China
Correspondence to: George KK Lau, M.D. , Department of Medicine Rm 1838, Queen Mary Hospital 102 Pokfulum Road, Hong Kong SAR, China. gkklau@netvigator.com
Fax: +852-28184030
Received: 2004-10-06 Accepted: 2005-01-05

Abstract

AIM: To compare the gene expression profile in a pair of HBV-infected twins.

METHODS: The gene expression profile was compared in a pair of HBV-infected twins.

RESULTS: The twins displayed different disease outcomes. One acquired natural immunity against HBV, whereas the other became a chronic HBV carrier. Eighty-eight and forty-six genes were found to be up- or down-regulated in their PBMCs, respectively. Tumor necrosis factor-alpha-induced protein 1 (TNF-αIP1) that expressed at a higher level in the HBV-immune twins was identified and four pairs of siblings with HBV immunity by RT-PCR. However, upon HBV core antigen stimulation, TNF-αIP1 was downregulated in PBMCs from subjects with immunity, whereas it was slightly upregulated in HBV carriers. Bioinformatics analysis revealed a K+ channel tetramerization domain in TNF-αIP1 that shares a significant homology with some human, mouse, and *C elegan* proteins.

CONCLUSION: TNF-αIP1 may play a role in the innate immunity against HBV.

Key words: TNF-α; HBV; Immunity

Lin MC, Lee NP, Zheng N, Yang PH, Wong OG, Kung HF, Hui CK, Luk JM, Lau GKK. Tumor necrosis factor-α-induced protein 1 and immunity to hepatitis B virus. *World J Gastroenterol* 2005;11(48):7564-7568
http://www.wjgnet.com/1007-9327/11/7564.asp

INTRODUCTION

Though substantial advances have been made in understanding of the pathogenesis of hepatitis B virus (HBV), HBV infection remains a global health threat with currently more than 350 million carriers and causes about one million deaths worldwide. The situation is particularly severe in high-endemic areas like southeastern Asia. For instance, a study of 16 334 subjects in 1978-1979 in Hong Kong suggested that 43% of the local population have evidence of past infection and 10% are HBs Ag carriers[1].

The major spread mode of HBV in most high endemic areas, such as Hong Kong and China, is perinatal transmission, which accounts for 40%-50% of chronic HBV infection[2,3]. The reason for the preponderance of perinatal transmission among Orientals is at least in part related to the high prevalence of HBV infection among the Asian carriers of reproductive age[2]. Though the incidence of perinatal transmission is high in China, not all siblings in the same family with HBV-infected mothers remain persistently infected with HBV as some acquired natural immunity against the virus. We are among the first group to demonstrate that the use of HLA-matched donor marrow from siblings with natural immunity could enable serological clearance of HBV in their HBsAg positive recipient siblings[4-7]. This indicates that the transfer of certain molecules from the donor's immune system is sufficient to confer the recipient immunity against HBV. However, the identities of these molecules are unknown.

In this study, Affymetrix cDNA mircroarray was employed to investigate the differential gene expression patterns in PBMCs in an identical twin pair who had different outcomes to HBV infection. Use of the twin pair could eliminate the potential confounding factors like age, gender, and living environment, etc. A novel cytokine signaling-related gene, TNF-αIP1, is significantly downregulated in chronic HBV carriers. Moreover, we have confirmed that this gene is indeed differentially expressed in several groups of HBV-infected siblings who display different disease outcomes by reverse transcription-polymerase chain reaction (RT-PCR). We also found that upon HBcAg stimulation, TNF-αIP1 exhibited different

responses between PBMC isolated from subjects with immunity and chronic infection. These results suggest that TNF-αIP1 may be involved in immunity against HBV infection. An understanding of the immunological and genetic differences in PBMCs of these sibling pairs should provide insight into the molecular mechanisms of the protection and enable a more rationale design of therapeutic regimen for chronic HBV infection in Chinese.

MATERIALS AND METHODS

Patient sample information

Eight groups of HLA-A, B and DR identical Chinese siblings (including pair of identical twins) who differed in their outcomes to HBV infection were used in this study. RNA was isolated from PBMC of the siblings with spontaneous recovery (anti-HBs and anti-HBc positive) and their corresponding HLA-matched HBV-infected siblings (HBsAg positive).

PBMC preparation, RNA extraction, and labeling

Heparinized venous blood was collected and PBMC was separated by density-gradient centrifugation over Ficoll-Hypaque. Total RNA was extracted from PBMC using RNeasy kit (Qiagen, Valencia, CA, USA) following manufacturer's instructions. For each sample, 60 mg of total RNA was reverse transcribed using Superscript II (Invitrogen, Carlsbad, CA, USA) according to manufacturer's instructions.

DNA microarray

Generation of antisense RNA (aRNA) probe for cDNA microarray analysis was carried out as described previously[8]. Briefly, mRNA was amplified using two or three rounds of cDNA synthesis followed by aRNA synthesis. T7-promoter-oligo-dT [5'-GCCAGTGAATTGTAATAC GACTCACTATAGGGAGGCGG-$(dT)_{24}$-3'] was used for cDNA synthesis and T7 RNA polymerase was used for aRNA synthesis. Ten micrograms of starting total RNA was used to obtain 10 mg of final aRNA. During the process of the final aRNA synthesis, biotinylated UTP and CTP were used for labeling purpose (Enzo, Farmingdale, NY, USA). Detection of the hybridized probe using streptavidin-phycoerythrin fluorescent conjugate was done according to manufacturer's protocol (Molecular Probes, Eugene, OR, USA).

The labeled aRNA probe from PBMC was hybridized to a HU 95A gene chip representing 12 000 full-length human genes (Affymetrix, Santa Clara, CA, USA). The threshold for significant up- or down-regulation was 2.0- and 0.5-fold, respectively. Hybridizations were typically carried out for 16 h at 45 ℃ followed by washing, staining and using Affymetrix fluidic stations. Stained arrays were scanned in the G2500 A Hewlett-Packard Gene Array Scanner (Hewlett-Packard, Palo Alto, CA, USA) at the excitation wavelength of 488 nm. The amount of emitted light was proportional to the bound target at each location on the probe arrays.

RT-PCR

Total RNA was reverse transcribed using the Superscript II (Invitrogen) according to the manufacturer's instructions. PCR conditions for pre-B-cell colony-enhancing factor (PBEF), IL-18 receptor accessory protein (IL-18 RAP), TNF-αIP1 and GADPH were as follows: at 94 ℃ for 30 s, at 57 ℃ for 30 s, at 72 ℃ for 1 min for 35, 35, 35, and 32 cycles, respectively. The primer sequences of the genes tested were PBEF (sense: 5'-AAAAGCTGTTCCTGAGG GCTTTG-3'; anti-sense: 5'-TGACCACAGATACAGGCA CTGATG-3'); IL-18RAP (sense 5'-CCAGAGCCACAGA AATCACATTTC-3'; anti-sense 5'-CAAGAAATAGAGCC AGTGCTCCCA-3'); TNF-αIP1 (sense: 5'- TTACCTCCG AGATGACACCATCAC-3'; anti-sense: 5'-TCCTCATCTT CACTGGGGGAA-3').

RESULTS AND DISCUSSION

Perinatal transmission is the most common spread mode of hepatitis B infection in Chinese. Yet not all the siblings infected with HBV from mothers become chronic HBV carriers. It appears that different disease outcomes of these siblings represent success and failure of their immune systems in controlling HBV infection. In this study, we attempted to explore this phenomenon by investigating gene expression profiles in PBMCs of two identical twins who displayed diverse disease outcomes.

The differences in PBMC gene expression between two identical twins were analyzed using a DNA microarray chip containing 12 000 human expressed genes. Eighty-eight genes were expressed at a higher level and 46 genes were expressed at a lower level in twins with immunity (HBV resistant) compared to the HBV carrier twins [HBV susceptible). These genes were grouped on the basis of their predicted functions into 12 major groups (metabolism, cell signaling, transcription, transport physiology, growth, and differentiation, immune system, cell adhesion, house keeping, cell cycle, translation, apoptosis, and unknown genes (ESTs)] (Figure 1). We found that genes with unknown functions represented the major portion of genes with altered expression levels in the HBV immune twin.

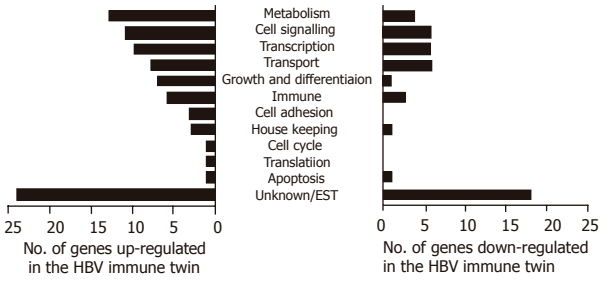

Figure 1 Number of genes upregulated or downregulated in the immune twin compared to the HBV carrier twin. PBMCs from two HBV infected twins with different disease outcomes were analyzed for gene expression using DNA microarray. Eighty-eight genes were identified as upregulated and 46 downregulated. They were further divided into 12 groups based on their presumed functions.

Table 1 Differential expression of immunity-related genes in PBMCs of HBV identical twin patients

UniGene ID	Gene name	Known function(s)	Fold change
Hs.244613	Signal transducer and activator of transcription 5b (STAT 5b)	Signal transducer of IL-2, IL-4, CSF1, and different growth hormones. I mportant for TCR signaling, apoptosis, adult mammary gland development, and sexual dimorphism of liver gene expression	–4.2
Hs.239138	Pre-B-cell colony-enhancing factor (PBEF)	A cytokine that increases the expression of IL-6 and IL-8 in fetal membrane and may be important in both normal spontaneous labor and infection-induced preterm labor	2.2
Hs.158315	Interleukin 18 receptor accessory protein (IL-18RAP)	An accessory subunit of the heterodimeric receptor for IL-18 enhances the IL-18 binding a ligand binding subunit of IL-18 receptor. The coexpression of IL-18R1 and this protein is required for the activation of NF-κB and MAPK8 (JNK) in response to IL-18	3.0
Hs.76090	Tumor necrosis factor-alpha-induced protein 1 (endothelial) (TNF-αIP1)	Unknown	2.3
Hs.225948	Chemokine (C-C motif) ligand 27 (CCL27)	Cytokine that plays a role in mediatinghoming of lymphocytes to cutaneous sites. It specifically binds to chemokine receptor 10 (CCR10). Studies of murine protein indicate that these protein-receptor interactions have a pivotal role in T-cell-mediated skin inflammation	-2.5
Hs.301921	C-C chemokine receptor type 1 (C-C CKR-1)	Cytokine receptor important for host protection from inflammatory response and susceptibility to virus and parasite	-2.7
Hs.57735	Scavenger receptor class F, member 1 (SCARF1)	Scavenger receptor that has roles in the binding and degradation of acetylated low density lipoprotein and may be involved in atherosclerosis	-2.2
Hs.4930	Low density lipoprotein receptor-related protein 4 (LRP4)	A membrane protein which may be involved in calcium ion binding	-2.8

[1]Fold changes between the HBV immune twin pair. Positive number indicates upregulation, whereas negative number denotes downregulation.

We are interested in the immune system-related genes that are putative candidates for conferring HBV immunity. Among the up- or down-regulated genes, eight genes were related to immune responses including several cytokine/chemokine signaling-related genes (Table 1). Three genes, namely cytokine PBEF, interleukin IL-18 receptor (R) accessory protein and TNF-αIP1 were upregulated in the immunity twin. PBEF is a cytokine transcribed in human bone marrow, liver tissue and muscle[9,10] and synergized with stem cell factor (SCF) and IL-7 activating pre-B-cell colony formation[11]. IL-18R accessory protein enhances the IL-18 binding activity of IL-18R1 and is required for the activation of nuclear factor-kappa B (NF-κB) and mitogen-activated protein kinase 8 (MAPK 8) in response to IL-18. TNF-αIP1 is first identified as a primary response gene in human umbilical vein endothelial cells towards TNF-α stimulation[12], but yet with no known function.

Five genes were downregulated in the HBV-immuned twins. They are the signal transducer and activator of transcription 5b (Stat5b), which is crucial for normal immune function and T-cell-mediated mitogenic signals and is a key signal transducer of T-cell receptor[13]. The chemokine (C-C motif) ligand 27 (CCL27) and C-C chemokine receptor type 1 (C-C CKR-1) are important for host inflammatory response. We also observed the downregulation of the scavenger receptor class F member 1 (SCARF1) and low-density lipoprotein receptor-related protein 4. Scavenger receptors encompass a broad range of molecules involved in receptor-mediated endocytosis of selected polyanionic ligands, including modified low-density lipoproteins (LDL)[14]. Further investigating the role of these genes and the molecular differences between immune siblings and HBV chronic carrier siblings may help us in designing therapeutic measures that modulate the immune system of patients in controlling HBV infection.

Of the eight immune system-related genes, TNF-αIP1 demonstrated the highest frequency of differential expression among the other groups of HBV-infected HLA-matched siblings with different disease outcomes as determined by semi-quantitative RT-PCR (Figure 2A). As shown in Figure 2B, the expression level of TNF-αIP1 was

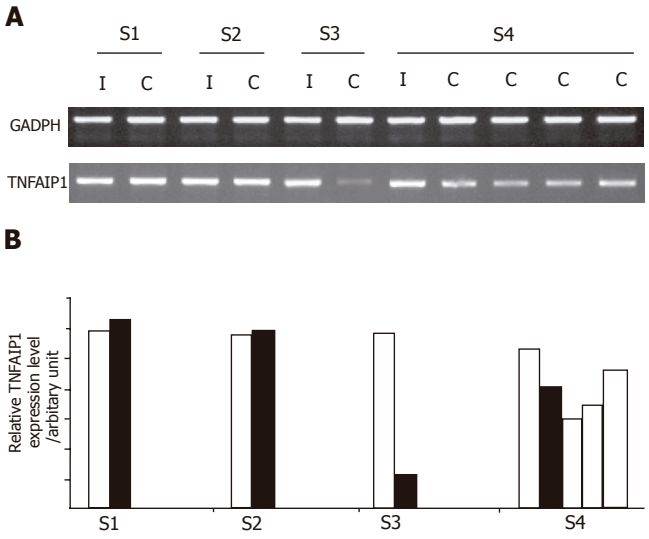

Figure 2 Expression levels of TNF-αIP1 gene in HBV-infected siblings with different disease outcomes. **A:** RT-PCR analysis of TNF-αIP1 in four sibling pairs; **B:** Fold changes of band intensity of TNF-αIP1 in different sibling groups. Open bar: HBV immune patients; black or patterned bars: HBV carrier; S1: sibling group 1; S2: sibling group 2; S3: sibling group 3; S4: sibling group 4.

lower in HBV carriers than in their HBV immune siblings in two siblings groups. Noticeably, the expression of TNF-αIP1 was significantly downregulated in HBV carrier siblings of group 3 and all four carrier siblings displayed down-regulation of TNF-αIP1. Suggesting that TNF-αIP1 may be a gene differentially expressed in PBMCs of HBV immune and carrier patients.

Recent studies suggest that cytokine response plays an important role in successful host defense against HBV infection. In transgenic mouse and chimpanzee model, cytotoxic T lymphocytes do not directly kill HBV-infected hepatocytes, but inhibit the viral replication through the actions of TNF-α and interferon (IFN-γ)[15,16]. Romero and Lavine[17] demonstrated that TNF-α and IFNs can downregulate the activity of HBV core/pregenomic (C/P) promoter, hence contributing to viral clearance. Moreover, activated intrahepatic antigen-presenting cells can inhibit liver HBV replication by secreting IL-12 and TNF-α[18]. One of the downstream mechanisms of how TNF-α modulates HBV infection is via the activation of NF-κB, which can inhibit HBV replication[19]. Interestingly, we have shown that TNF-αIP1 (a TNF-α inducible gene) expresses at a higher level in HBV immunized twin. TNF-αIP1 was first identified as an endothelial primary response gene towards TNF-α (then named B12), which induces TNF-αIP1 expression rapidly and transiently. Biochemical characterization suggests that TNF-αIP1 is a 36 ku protein, which may play a regulatory role and locate intracellularly[12]. The role of TNF-αIP1 in TNF-α-mediated NF-κB activation and HBV replication inhibition is of interest for further study.

Phylogenetic analysis showed that TNF-αIP1 could evolve into human and mouse endothelial protein 1 (Edp1), reflecting the fact that Edp1 is likely the mouse ortholog of TNF-αIP1 (Figure 3A). Predicted from the

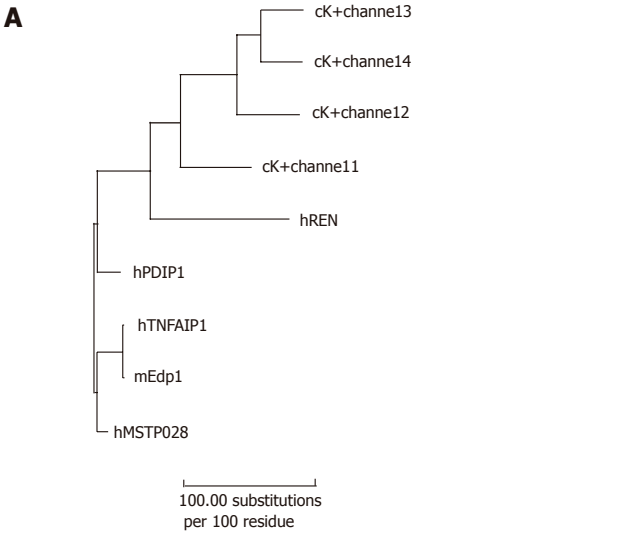

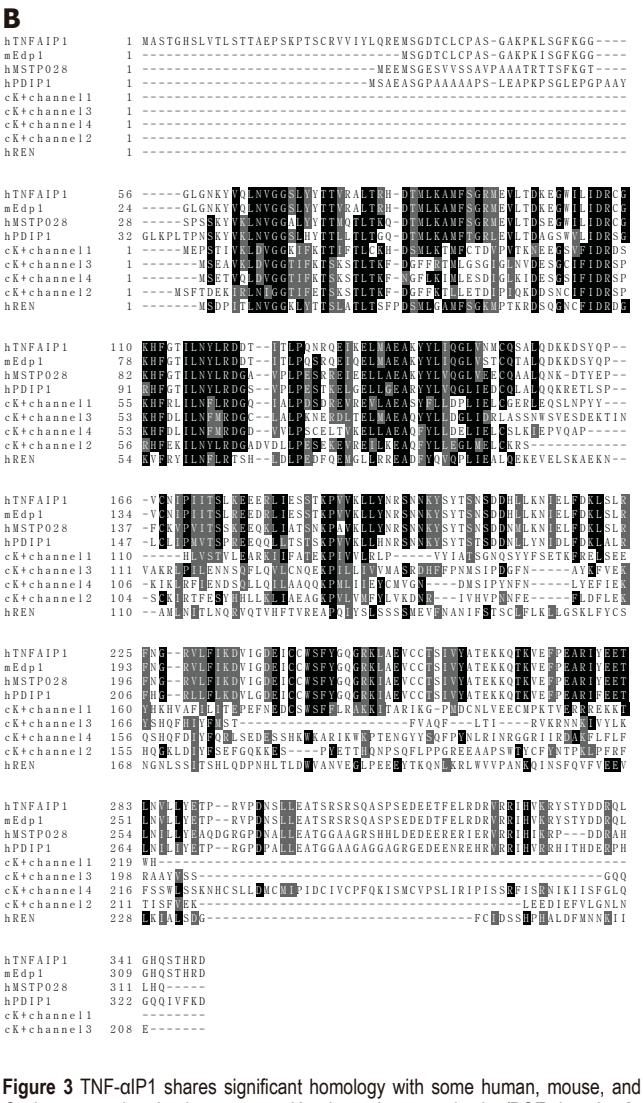

Figure 3 TNF-αIP1 shares significant homology with some human, mouse, and *C elegan* proteins, having common K+ channel tetramerization/POZ domain. **A:** Phylogenetic analysis of evolutionary distance of the protein sequences. The protein sequences were analyzed by the Growtree program provided by the GCG package. Kimura distance was adopted as the distance correction method. **B:** Amino acid sequence alignment of TNF-αIP1 (A41784) with mouse Edp1 protein (AAC78826), human MSTP028 protein (NP_114160), PDIP1 (AAL14962), human REN protein (XP_208568), and four C elegan K+ channel family members and with highest homology to TNF-αIP1 (NP_499312, NP_494320, NP_494476 and NP_494315). Black line: K+ channel tetramerization/POZ domain.

amino acid sequence of TNF-αIP1 (A41784), there is a K+ channel tetramerization domain in the middle of the sequence. This N-terminal, cytoplasmic tetramerization domain (T1) of voltage-gated K+ channels encodes molecular determinants for subfamily-specific assembly of alpha-subunits into functional tetrameric channels[20]. It is distantly related to the BTB/POZ domain which plays an oligomerization role in the function of this protein. Interestingly, the K+ channel tetramerization domain is the common domain feature shared by many TNF-α inducible proteins. For instance, mouse TNF-α inducible proteins such as Edp1 share high homology with the entire amino acid sequence of TNF-αIP1 (97% identity) (Figures 3A and B). It is also noticed that there was a group of C elegan proteins containing the K+ channel tetramerization domain. However, the function of this group of proteins is unknown.

Among the proteins containing K+ channel tetramerization domain, polymerase delta-interacting protein 1 (PDIP1) is best characterized[21]. PDIP1 is a TNF-α inducible protein and plays a role in linking cytokine activation and DNA replication in the liver as well as in other tissues. It localizes inside the nuclei and interacts with DNA polymerase δ small subunit (p50) and proliferating cell nuclear antigen (PCNA). In addition, it modulates DNA polymerase δ activity in a PCNA dependent manner. Importantly, it shares high homology (62% identity) with TNF-αIP1 (B12). PDIP1 is involved in TNF-α-mediated hepatocyte regeneration and stimulates hepatocyte proliferation upon TNF-α signal[21]. It is of interest to know whether this is also true for TNF-αIP1 using cell proliferation assay.

REFERENCES

1 **Yeoh EK,** Chang WK, Kwan JPW. Epidemiology of viral hepatitis B infection in Hong Kong. In Lam SK, Lai CL, Yeoh EK (editors): Viral hepatitis B infection: Vaccine and control. Singapore: *World Scientific* **1984:** 33-41

2 **Lok AS,** Lai CL, Wu PC, Wong VC, Yeoh EK, Lin HJ. Hepatitis B virus infection in Chinese families in Hong Kong. *Am J Epidemiol* 1987; **126:** 492-499

3 **Stevens CE,** Beasley RP, Tsui J, Lee WC. Vertical transmission of hepatitis B antigen in Taiwan. *N Engl J Med* 1975; **292:** 771-774

4 **Lok AS,** Liang RH, Chung HT. Recovery from chronic hepatitis B. *Ann Intern Med* 1992; **116:** 957-958

5 **Lau GK,** Lok AS, Liang RH, Lai CL, Chiu EK, Lau YL, Lam SK. Clearance of hepatitis B surface antigen after bone marrow transplantation: role of adoptive immunity transfer. *Hepatology* 1997; **25:** 1497-1501

6 **Lau GK,** Liang R, Lee CK, Yuen ST, Hou J, Lim WL, Williams R. Clearance of persistent hepatitis B virus infection in Chinese bone marrow transplant recipients whose donors were anti-hepatitis B core- and anti-hepatitis B surface antibody-positive. *J Infect Dis* 1998; **178:** 1585-1591

7 **Lau GK,** Lie AKW, Kwong YL, Lee CK, Hou J, Lau YL, Lim WL, Liang R. A case-controlled study on the use of HBsAg-positive donors for allogeneic hematopoietic cell transplantation. *Blood* 2000; **96:** 452-458

8 **Luo L,** Salunga RC, Guo H, Bittner A, Joy KC, Galindo JE, Xiao H, Rogers KE, Wan JS, Jackson MR, Erlander MG. Gene expression profiles of laser-captured adjacent neuronal subtypes. *Nat Med* 1999; **5:** 117-122

9 **Samal B,** Sun Y, Stearns G, Xie C, Suggs S, McNiece I. Cloning and characterization of the cDNA encoding a novel human pre-B-cell colony-enhancing factor. *Mol Cell Biol* 1994; **14:** 1431-1437

10 **Ognjanovic S,** Bryant-Greenwood GD. Pre-B-cell colony-enhancing factor, a novel cytokine of human fetal membranes. *Am J Obstet Gynecol* 2002; **187:** 1051-1058

11 **Rongvaux A,** Shea RJ, Mulks MH, Gigot D, Urbain J, Leo O, Andris F. Pre-B-cell colony-enhancing factor, whose expression is up-regulated in activated lymphocytes, is a nicotinamide ph osphoribosyltransferase, a cytosolic enzyme involved in NAD biosynthesis. *Eur J Immunol* 2002; **32:** 3225-3234

12 **Wolf FW,** Marks RM, Sarma V, Byers MG, Katz RW, Shows TB, Dixit VM. Characterization of a novel tumor necrosis factor-a-induced endothelial primary response gene. *J Biol Chem* 1992; **267:** 1317-1326

13 **Welte T,** Leitenberg D, Dittel BN, al-Ramadi BK, Xie B, Chin YE, Janeway Jr CA, Bothwell ALM, Bottomly K, Fu XY. STAT5 interaction with the T cell receptor complex and stimulation of T cell proliferation. *Science* 1999; **283:** 222-225

14 **Peiser L,** Mukhopadhyay S, Gordon S. Scavenger receptors in innate immunity. *Curr Opin Immunol* 2002; **14:** 123-128

15 **Guidotti LG,** Ishikawa T, Hobbs MV, Matzke B, Schreiber R, Chisari FV. Intracellular inactivation of the hepatitis B virus by cytotoxic T lymphocytes. *Immunity* 1996; **4:** 25-36

16 **Guidotti LG,** Rochford R, Chung J, Shapiro M, Purcell R, Chisari FV. Viral clearance without destruction of infected cells during acute HBV infection. *Science* 1999; **284:** 825-829

17 **Romero R,** Lavine JE. Cytokine inhibition of the hepatitis B virus core promoter. *Hepatology* 1996; **23:** 17-23

18 **Kimura K,** Kakimi K, Wieland S, Guidotti LG, Chisari FV. Activated intrahepatic antigen-presenting cells inhibit hepatitis B virus replication in the liver of transgenic mice. *J Immunol* 2002; **169:** 5188-5195

19 **Biermer M,** Puro R, Schneider RJ. Tumor necrosis factor alpha inhibition of hepatitis B virus replication involves disruption of capsid integrity through activation of NF-kB. *J Virol* 2003; **77:** 4033-4042

20 **Bixby KA,** Nanao MH, Shen NV, Kreusch A, Bellamy H, Pfaffinger PJ, Choe S. Zn2+-binding and molecular determinants of tetramerization in voltage-gated K+ channels. *Nat Struct Biol* 1999; **6:** 38-43

21 **He H,** Tan CK, Downey KM, So AG. A tumor necrosis factor a-and interleukin 6-inducible protein that interacts with the small subunit of DNA polymerase d and proliferating cell nuclear antigen. *PNAS* 2001; **98:** 11979-11984

Science Editors Wang XL and Guo SY **Language Editor** Elsevier HK

PO Box 2345, Beijing 100023, China
www.wjgnet.com
wjg@wjgnet.com

ELSEVIER

World J Gastroenterol 2005;11(48):7569-7578
World Journal of Gastroenterology ISSN 1007-9327

High affinity mouse-human chimeric Fab against Hepatitis B surface antigen

Biplab Bose, Navin Khanna, Subrat K Acharya, Subrata Sinha

Biplab Bose, Subrata Sinha, Department of Biochemistry, All India Institute of Medical Sciences, New Delhi, India
Navin Khanna, International Center for Genetic Engineering and Biotechnology, New Delhi, India
Subrat K. Acharya, Department of Gastroenterology, All India Institute of Medical Sciences, New Delhi, India
Supported by the Department of Biotechnology (DBT), Govt. of India, NO. BT/PR2540/PID/25/101/2001
Correspondence to: Professor Subrata Sinha, Department of Biochemistry, All India Institute of Medical Sciences, Ansari Nagar, New Delhi, PIN-110029,
India. sub_sinha2004@yahoo.co.in
Telephone: +91-11-26594483
Fax: +91-11-26588663 / +91-11-26588641
Received: 2005-04-06 Accepted: 2005-04-26

Abstract

AIM: Passive immunotherapy using antibody against hepatitis B surface antigen (HBsAg) has been advocated in certain cases of Hepatitis B infection. We had earlier reported on the cloning and expression of a high affinity scFv derived from a mouse monoclonal (5S) against HBsAg. However this mouse antibody cannot be used for therapeutic purposes as it may elicit anti-mouse immune responses. Chimerization by replacing mouse constant domains with human ones can reduce the immunogenicity of this antibody.

METHODS: We cloned the V_H and V_L genes of this mouse antibody, and fused them with CH1 domain of human IgG1 and C_L domain of human kappa chain respectively. These chimeric genes were cloned into a phagemid vector. After initial screening using the phage display system, the chimeric Fab was expressed in soluble form in *E. coli*.

RESULTS: The chimeric Fab was purified from the bacterial periplasmic extract. We characterized the chimeric Fab using several *in vitro* techniques and it was observed that the chimeric molecule retained the high affinity and specificity of the original mouse monoclonal. This chimeric antibody fragment was further expressed in different strains of *E. coli* to increase the yield.

CONCLUSION: We have generated a mouse-human chimeric Fab against HBsAg without any significant loss in binding and epitope specificity. This chimeric Fab fragment can be further modified to generate a full-length chimeric antibody for therapeutic uses.

Key words: Chimeric Fab; Hepatitis B surface antigen; Phage display

Bose B, Khanna N, Acharya SK, Sinha S. High affinity mouse-human chimeric Fab against Hepatitis B surface antigen. *World J Gastroenterol* 2005; 11(48): 7569-7578
http://www.wjgnet.com/1007-9327/11/7569.asp

INTRODUCTION

Hepatitis B virus (HBV) infection is the 10th leading cause of death worldwide, with 2 billion people infected by it and 350 million suffering from chronic HBV infection[1]. Protective antibodies that appear after natural infection are mostly directed against the major antigenic 'a'determinant of Hepatitis B surface antigen (HBsAg)[2]. The immunodominant 'a' epitope is a part of a large antigenic area of HBsAg, called the major hydrophilic region[3] and this epitope is present in all serotypes[4]. Antibodies against HBsAg are thus advocated for passive immunotherapy against Hepatitis B infection in cases of accidental needle stick injuries, for liver transplant patients and to prevent vertical transfer of HBV infection from mother to child[5-8]. Presently, human anti-HBs immune globulin (HBIG) collected from the blood of hyperimmune donors is used for postexposure prophylaxis. Being a blood derived product anti-HBs HBIG is costly and can cause cross-contamination. Therefore a recombinant antibody to HBsAg can be a suitable alternative to such a practice.

Although several recombinant antibodies against HBsAg have been reported in literature, none is available for clinical use[9–12]. In our previous work we had expressed and characterized a recombinant anti-HBs scFv cloned from a mouse monoclonal 5S[13]. This antibody binds to HBsAg with high affinity (K_D = 0.889 nmol/L). It tested positive in an *in vitro* surrogate test for seroconversion and protective antibodies (Hepanostika anti-HBs kit, Organon Teknika, The Netherlands). The scFv generated from this hybridoma retained the high affinity and epitope specificity[13]. However this mouse monoclonal cannot be used for therapeutic purposes as it may trigger human anti-mouse antibody response, especially when multiple infusions are required to obtain therapeutic efficacy[14,15]. It is well known that immunogenic reactions are predominantly directed towards constant domains of

Table 1 Oligonucleotide primers used for generation of the chimeric Fd and light chain

Primer	Sequence
5′ primer for V_H (5H23M)	5′- AG GTC CAG CTT CTC GAG CCC GGG GC -3′
3′ primer for V_H (Fd3)	5′-CGA TGG GCC CTT GGT GGA GGC TGA AGA GAC AGT GAC TGA GGT TCC-3′
5′ primer for C_H1 of human IgG1 (Fd5)	5′-GGA ACC TCA GTC ACT GTC TCT TCA GCC TCC ACC AAG GGC CCA TCG-3′
3′ primer for C_H1 of human IgG1 (CG1Z)	5′- GCA TGT ACT AGT TTT GTC ACA AGA TTT GGG -3′
5′ primer for V_L (5L35)	5′-CCA GAT GTG AGC TCG TGA TGA CCC AGA CTC CA-3′
3′ primer for V_L (K3)	5′-CAG ATG GTG CAG CCA CAG TCC GTT TGA GTT CCA GCT TGG-3′
5′ primer for C_L of human κ chain (K5)	5′-CCA AGC TGG AAC TCA AAC GGA CTG TGG CTG CAC CAT CTG-3′
3′ primer for C_L of human κ chain (Ck1d)	5′- GCG CCG TCT AGA ATT AAC ACT CTC CCC TGT TGA AGC TCT TTG TGA CGG GCG AAC TCA G -3′

Primer names are given in parenthesis. Sites for restriction enzymes are shown as underlined. Complementary overhangs are shown in bold letters.

murine antibodies[16]. Problems associated with the HAMA response can be reduced by creating mouse-human chimeric antibodies, where mouse constant regions are replaced by human ones[17-19].

The exact mechanisms of antibody-mediated virus neutralization are not clear till date. A few of the principal mechanisms, which have been postulated for virus neutralization, are virus aggregation, inhibition of attachment of virus to cell receptors and inhibition of events after attachment to cell receptors[20,21]. Though high affinity binding to viral epitopes is a pre-requisite for antibody-mediated virus neutralization, the importance of antibody constant domains is not clear. Apart from full-length antibodies, antibody Fab fragments have been shown to neutralize viruses[22-26]. It has been shown that $F(ab)_2$ fragments derived from HBIG is effective for the prevention of vertical transfer of HBV infection in neonates[27]. In comparison to a full-length antibody, a Fab fragment can be easily expressed in bacterial expression systems[28]. A recombinant Fab can be further modified for increase in affinity[29], for chimerization/humanization[30] and can be linked with antibody Fc region to generate a full-length antibody[31,32].

In the present work, we have fused the variable regions of the mouse monoclonal 5S (IgG1/κ) with the corresponding human constant regions (C_H1 of IgG1/C_L of κ) to generate a mouse-human chimeric Fab. This chimeric Fab was expressed using a phage display expression system. After initial screening of functional clones, the chimeric Fab was expressed in *E. coli* in soluble form. It was purified by affinity chromatography and characterized for antigen binding. We observed that the chimeric Fab fragment retained the high affinity binding and epitope specificity of the original mouse monoclonal. This chimeric molecule can be further modified for generation of a therapeutically useful full-length chimeric antibody.

MATERIALS AND METHODS

Materials

The phagemid vector pCOMB3H was provided by The Scripps Research Institute, La Jolla, USA. Shanta Biotech (India) provided purified recombinant HBsAg expressed in a *Pichia* system. *E. coli* XL1-Blue and TG1 cells and helper phage M13 KO7 were obtained from MRC, Cambridge, UK. *E. coli* strains AD494 and BL 21 CodonPlus were procured from Novagen. 5S hybridoma cells were maintained in RPMI (Sigma, USA) with 10% FCS (Sigma, USA). Anti-M13 mouse antibody was provided by Dr. Vijay Chaudhary, University of Delhi, South Campus, New Delhi, India.

Construction of the chimeric light chain and Fd fragment

The strategy for generation of the chimeric Fd and light chain is shown in Figure 1. The variable region genes of 5S hybridoma were amplified by reverse transcription followed by PCR. Primers used for all reverse transcriptions and PCRs are listed in Table 1. Total RNA was isolated from 5S cells using TRI reagent (Sigma, USA) and cDNAs for the V_H and V_L fragments were generated by reverse transcription using Omniscript RTase (Qiagen). Primers used for reverse transcriptions were Fd3 and K3 for V_H and V_L respectively. These primers have overhangs complementary to the 5' regions of the respective human constant domains. The V_H fragment was further amplified by PCR using primers 5H23M and Fd3. Similarly, the V_L fragment was amplified by PCR using primers 5L35 and K3. Conditions for both the PCRs were: 30 cycles at 94 °C for 1 min, 50 °C for 1 min, 72 °C for 2 min, followed by a final extension for 10 min at 72 °C.

For amplification of human constant domains, RNA was isolated from human peripheral blood lymphocytes (PBLs) using TRI reagent. cDNAs for the C_H1 region of human IgG1 and the C_L region of human kappa chain were generated by reverse transcription using Omniscript RTase (Qiagen). Primers used for reverse transcriptions were CG1Z and Ck1d for C_H1 and C_L respectively. The C_H1 fragment was further amplified by PCR using primers Fd5 and CG1Z. Human C_L was amplified by PCR using primers K5 and Ck1d. Fd5 and K5 carry overhangs complementary to the 3' end of variable regions of 5S. Conditions for both these PCRs were: 30 cycles at 94 °C for 1 min, 60 °C for 1 min, 72 °C for 2 min, followed by a final extension for 10 min at 72 °C.

PCR amplified fragments were resolved in 1.5% agarose gel and respective bands were eluted out using QIAquick gel extraction kit (Qiagen). PCR amplified C_H1 (human IgG1) and mouse V_H were used as templates for generation of the chimeric Fd by overlap PCR. Initial assembly of equimolar amounts of the mouse V_H and human C_H1 was done by PCR for 20 cycles at 94 °C for

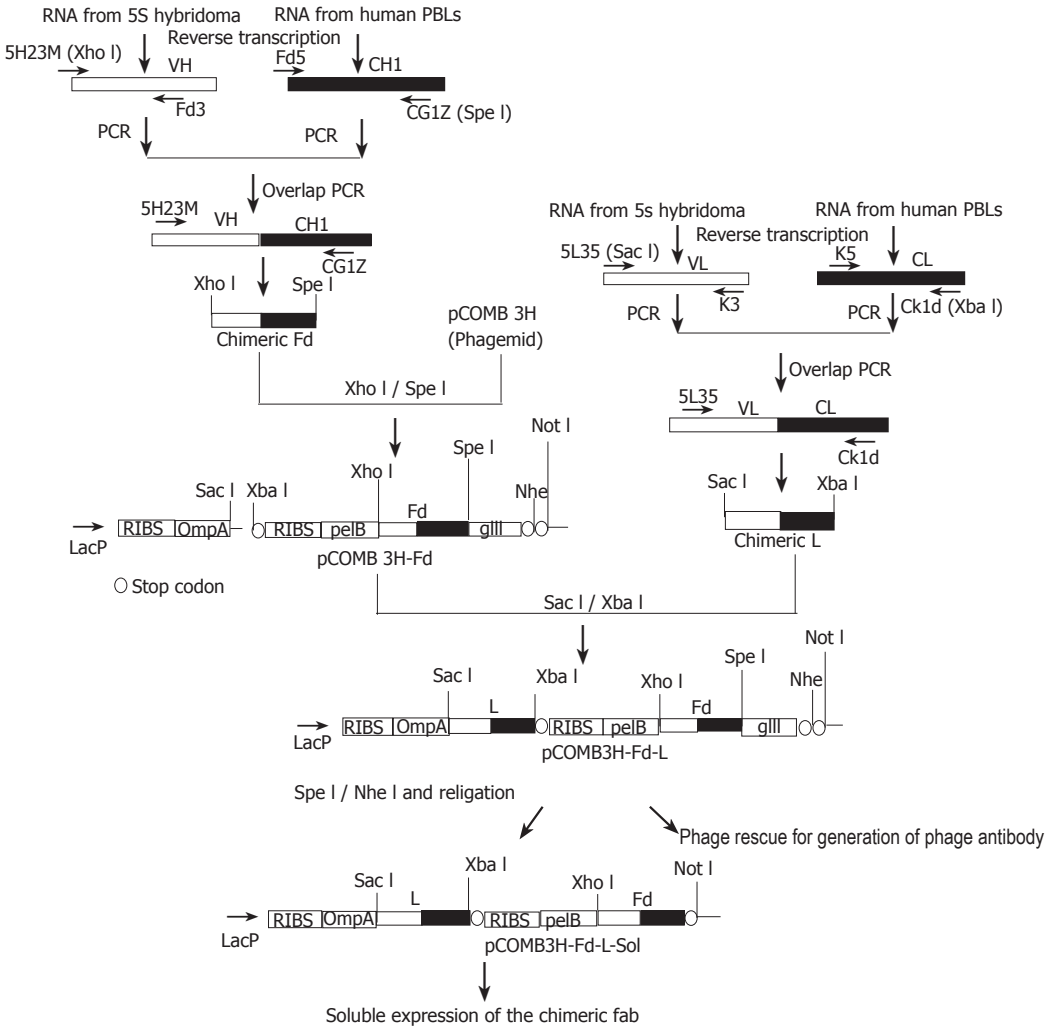

Figure 1 Schematic representation of the strategy for cloning and expression of the anti-HBs chimeric Fab. The V_H and V_L fragments of 5S hybridoma were fused with human C_H1 and C_L by overlap PCR. The resulting chimeric fragments were cloned in the bi-cistronic phagemid vector pCOMB3H. Both the fragments are under the control of a single *LacZ* promoter. *ompA* and *pelB* are two leader sequences, provided for directing the light chain and Fd fragment to the bacterial periplasm. Two ribosome-binding sites are present in the vector for stable expression of both the fragments. The Fd fragment was cloned upstream to the phage gIII sequence, for surface display of the chimeric Fab. This *gIII* fragment was removed by digestion with *Spe I/Nhe I* and after self-ligation of the vector, the Fab fragment was expressed in soluble form.

1 min, 60 °C for 1 min and 72 °C for 2 min, followed by final extension of 10 min at 72 °C. The product of the initial assembly reaction was diluted 10 times and used as the template for pull through PCR using primers 5H23M and CG1Z. Similarly human kappa C_L and mouse V_L fragment were joined to generate the chimeric light chain. Primers used for this reaction were 5L35 and Ck1d.

Construction of the phagemid construct

We used the bi-cistronic phagemid vector pCOMB3H, a variant of the phagemid pComb3[33], for the expression of the chimeric Fab. The essential features of this vector system and our cloning strategy are shown in Figure 1. The chimeric Fd was digested with *Xho1* and *Spe1* and cloned into the phagemid vector pCOMB3H. The resulting construct (pCOMB3H-Fd) was transformed into chemically competent *E. coli* XL1-Blue cells by standard chemical method ($CaCl_2$/heat shock)[34]. Transformed cells were grown on Amp-Agar plates. Colonies were picked up after overnight incubation and screened for the presence of the insert by colony PCR and restriction digestion (*Xho1*/*Spe1*). The recombinant phagemid pCOMB3H-Fd was isolated by alkali-lysis method and digested with *Sac1* and *Xba1*. The chimeric light chain digested with these two enzymes was cloned into pCOMB3H-Fd to generate the phagemid construct pCOMB3H-Fd-L. This construct was transformed into chemically competent XL1-Blue cells by standard chemical transformation method and after overnight incubation, recombinant clones were checked for the presence of the chimeric light chain by colony PCR and by restriction digestion (*Sac1*/*Xba1*).

Expression of the phage antibody and selection of antigen binding clones

Cells transformed with the construct pCOMB3H-Fd-L were used for expression of the chimeric Fab on phage surface. Phage displaying chimeric Fab was rescued by infection with helper phage M13-KO7 as described by

Barbas *et al*.[33]. Phage was precipitated from the culture supernatant by incubating with PEG/NaCl (20% PEG/2.5 mol/L NaCl) for 8 h on ice. After centrifugation, precipitated phage was resuspended in PBS and titrated to determine phage concentration[35].

Clones displaying functional Fab fragment were selected by biopanning over antigen-coated plates. The method for biopanning has been discussed in detail in our earlier article[13]. Essentially this method involves incubation of phage in uncoated ELISA plate followed by incubation of unbound phage in antigen-coated plate. After thorough washing, bound phage was eluted out at low pH. Eluted phage was passed through two more rounds of selection over coated and uncoated wells with increasing number of washing.

Identification of antigen binding clones by phage-ELISA

Phage obtained after three rounds of selection, was reinfected in XL1-Blue cells and amplified by standard phage rescue protocol as mentioned earlier. Antigen binding clones were identified by phage-ELISA. Maxisorp ELISA plates were coated with HBsAg (250 ng/well) in bicarbonate buffer (pH 9.5). After blocking with 2% non-fat milk in PBS (MPBS), phage (~10^{12}/well) was added and incubated for 1 h at room temperature. Bound phage was detected by incubation with 1:1 000 dilution of anti-M13 mouse antibody for 1 h at room temperature, followed by 1 h incubation with 1:2 000 dilution of anti-mouse antibody-HRP conjugate (Promega, USA). ELISA was developed by using 100 μL of 0.4 mg/mL *o*-phenylenediamine and 0.8 μL/mL of H_2O_2 in citrate-phosphate buffer (pH 5). The same amount of helper phage (M13-KO7) was used as negative control in phage-ELISA.

The phagemid construct was isolated from the clone showing maximum binding and the nucleotide sequences of the chimeric Fd and light chain were determined by sequencing using ABI-Prism automatic DNA sequencer. Primers used for sequencing the light chain were 5'-ATGAAAAAGACAGCTATCGC-3' and 5'-TAATAAC AATCCAGCGGCTG-3'. Primers used for sequencing the Fd fragment were 5'-TCTTTTCATAATCAAAATCACC G-3' and 5'-AAATGAAATACCTATTGCC-3'.

Soluble expression of the chimeric Fab

The antigen binding clone selected by phage ELISA was further processed for soluble expression of the anti-HBs chimeric Fab. For soluble expression of the chimeric Fab, the phage *gIII* sequence was removed from the recombinant phagemid construct pCOMB3H-Fd-L by double digestion with *Spe I* and *Nhe I*. Digestion by these two enzymes provides compatible ends for self-ligation of the vector. Double digested phagemid was self-ligated to generate the construct pCOMB3H-Fd-L-Sol and transformed in chemically competent XL1-Blue cells. For soluble expression of recombinant chimeric Fab, 1 L Super Broth with 20 mmol/L $MgCl_2$ and ampicillin (100 μg/mL) was inoculated with 10 mL of overnight culture of the recombinant clone and grown at 37 °C till the A_{600} reached approximately 0.6, when overexpression of the chimeric Fab was induced by 1 mmol/L IPTG. After overnight growth at 30 °C, cells were harvested by centrifugation at 4 000 r/min. Cell pellet was re-suspended in 20 mL PBS/ 1 mmol/L EDTA and kept on ice for 40 min. Clarified periplasmic extract was obtained by centrifugation of the re-suspended product at 10 000 *g*. The same method was used to express the soluble chimeric Fab in three other *E. coli* strains (AD494, BL21 CodonPlus and TG1).

Purification of the recombinant chimeric Fab

The periplasmic extract was concentrated (~10 times) using Centriprep YM-30 centrifugal filter (Millipore, USA). The recombinant chimeric Fab was purified from the periplasmic extract by affinity chromatography using HiTrap Protein G HP column (Amersham) as per the manufacturer's protocol. In brief, the protein G column (1 mL) was washed thoroughly with double distilled water (five column volumes) and equilibrated with five column volumes of equilibration buffer (pH 7.0). The concentrated periplasmic extract was allowed to pass through the column using a syringe at a speed of 2 mL/min. The column was washed thoroughly by 10 volume of equilibration buffer and bound chimeric Fab was eluted out by 5 volume of elution buffer (pH 2.7). Eluted fractions were immediately neutralized using neutralization buffer (77 μL/mL, pH 9). The eluted fractions were concentrated by Centriprep YM-30 centrifugal filter and checked on SDS-PAGE.

Electrophoresis and Western blot analysis

The purified chimeric Fab was resolved by 12% SDS-PAGE, separately in reducing (with βME) and non-reducing conditions (without βME or DTT). The resolved protein was stained by silver staining.

For Western blot analysis, the concentrated periplasmic extract was resolved by 12% SDS-PAGE in non-reducing conditions and electroblotted on nitrocellulose membrane. After blocking with 4% MPBS for 2 h, the chimeric Fab was detected by Rabbit anti-Human IgG-HRP conjugate (1:1 000 dilution; Dako). The blot was developed using DAB/H_2O_2 system. An equal amount of concentrated periplasmic extract of untransformed XL1-Blue cells was used as the negative control for the Western blot experiment. A separate Western blot experiment was performed under reducing conditions for the detection of the monomeric Fd and light chain. Whenever required, intensity of bands in Western blots was measured densitometrically using ChemiImager 4400 (Alpha Innotech Corp., USA).

Antigen binding assays for the chimeric Fab

Binding of the chimeric Fab was checked by solid phase ELISA. Maxisorp ELISA plate was coated with 250 ng/well of HBsAg in bicarbonate buffer (pH 9.5). After blocking with 4% MPBS, different dilutions of the chimeric Fab was added to antigen coated wells and bound antibodies were detected by Rabbit anti-Human IgG-HRP conjugate (1:2 000 dilution; Dako). Hybridoma supernatant of the original mouse monoclonal 5S was

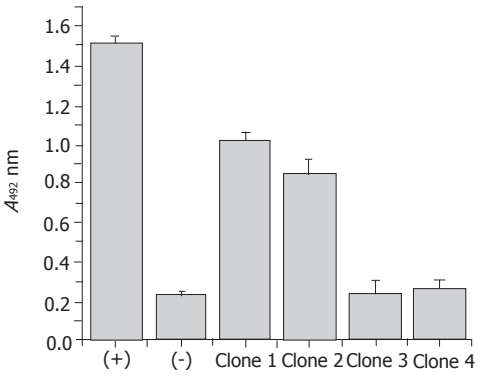

Figure 2 Phage ELISA to identify antigen binding clones. After three rounds of biopanning, selected phage was rescued and antigen-binding clones were detected by phage ELISA. In this experiment 5S hybridoma supernatant and helper phage M13 KO7 were used as positive (+) and negative (–) control respectively. Clone 1 was used for soluble expression of the chimeric Fab.

used as a positive control for this experiment. The extract of untransformed XL1-Blue cells was used as a negative control and corresponding readings were deducted from the readings of the chimeric Fab. This ELISA method was also used to study the levels of expression the chimeric Fab in different *E. coli* strains.

For competitive ELISA, plates were coated with HBsAg (100 ng/well) in bicarbonate buffer and blocked with 4% MPBS. Different amounts of the chimeric Fab were mixed with 1:80 dilution of 5S hybridoma supernatant and added to antigen-coated wells. After one hour incubation at room temperature, bound mouse antibody was detected by anti-mouse-HRP conjugate (Bangalore Genei, India). Periplasmic extract of untransformed XL1-Blue cells was used as the negative control and binding of the mouse monoclonal in its presence was taken as the maximum binding to calculate the percent inhibition.

Determination of the dissociation constant of the chimeric Fab

The dissociation constant (K_D) of HBsAg and chimeric Fab interaction was determined in solution phase by an ELISA method as described by Friguet *et al*.[36]. Essentially the technique involves incubation of a fixed amount of the antibody with different amounts of the antigen in solution phase for a prolonged period so that the equilibrium is reached. This is followed by detection of unbound antibody by conventional ELISA. This ELISA data is then used to calculate the K_D value, by using an equation derived from the law of mass action. The advantage of this technique is that it can be used to determine the affinity of an antibody without prior purification.

For this experiment we used crude periplasmic extract of the clone expressing the chimeric Fab in soluble form. A fixed amount of the periplasmic extract (1:300 dilution, in 100 μL of 4% MPBS) was incubated with varying concentrations of HBsAg (3-10 nmol/L) for 16 h at 4 °C. This equilibrated solution was incubated in antigen coated ELISA plates (250 ng antigen/well) for 20 min at room temperature to capture the free Fab. Bound chimeric Fab was detected by Rabbit anti-human IgG-HRP conjugate (Dako).

Protein estimation

Protein concentrations were estimated by Bradford assay[37].

RESULTS

Generation of a phagemid construct for the expression of phage antibody: Variable regions of the light chain and heavy chain of the mouse monoclonal 5S were amplified by RT-PCR. The $C_{H}1$ region of human IgG1 and C_L of human kappa chain were amplified by RT-PCR using RNA extracted from human PBLs. After the fusion of the mouse V_H and human $C_{H}1$, resulting chimeric Fd was cloned into the phagemid vector pCOMB3H to generate the recombinant construct pCOMB3H-Fd. Similarly, the chimeric light chain, generated by joining the mouse V_L and human C_L, was cloned into pCOMB3H-Fd to generate the recombinant construct pCOMB3H-Fd-L. This construct was transformed in XL1-Blue cells and phage displaying the chimeric Fab was generated by phage rescue using helper phage.

Selection of antigen binding clones and phage ELISA: The anti-HBs chimeric Fab was first expressed as phage antibody and antigen-binding clones were enriched by bio-panning over antigen coated plate. Selection was done on uncoated and antigen coated wells alternatively, thereby removing plastic binding clones, which can interfere in subsequent ELISAs. After three rounds of selection, functional clones were amplified and rescued to generate phage particles displaying the chimeric Fab and antigen-binding clones were detected by phage ELISA (Figure 2). As shown in Figure 2, clone 1 had the maximum binding and was used for soluble expression of the chimeric Fab. Nucleotide sequences of the chimeric Fd and light chain of this clone were submitted to the EMBL Nucleotide Sequence Database (EMBL accession numbers: AJ878860 and AJ878861). Sequence analysis indicated that the variable regions in these chimeric genes are identical to the variable regions of the mouse monoclonal 5S (data not shown).

Soluble expression of the chimeric Fab: Phage *gIII* sequence was removed from pCOMB3H-Fd-L for soluble expression of the chimeric Fab. The anti-HBs chimeric Fab was expressed in *E. coli* XL1-Blue cells by inducing overnight with 1 mmol/L IPTG. The leader sequences, present upstream to the chimeric genes, drag both the chains to the bacterial periplasm, where they form inter- and intra-chain disulphide bonds. The periplasmic extract was concentrated and the chimeric Fab was purified using Protein G column. Yield of the purified chimeric Fab when expressed in XL1-Blue cells was ~40 μg/L of culture. The purified product was resolved by SDS-PAGE in non-reducing (without βME/DTT) as well as in reducing conditions (with βME). As shown in Figure 3A, the chimeric Fab is expressed as a heterodimer (~50 ku) of the chimeric Fd and light chain. In reducing conditions, both the chains were detected in monomeric form (~25 ku).

Expression of the heterodimeric chimeric Fab was further confirmed by Western blot in non-reducing

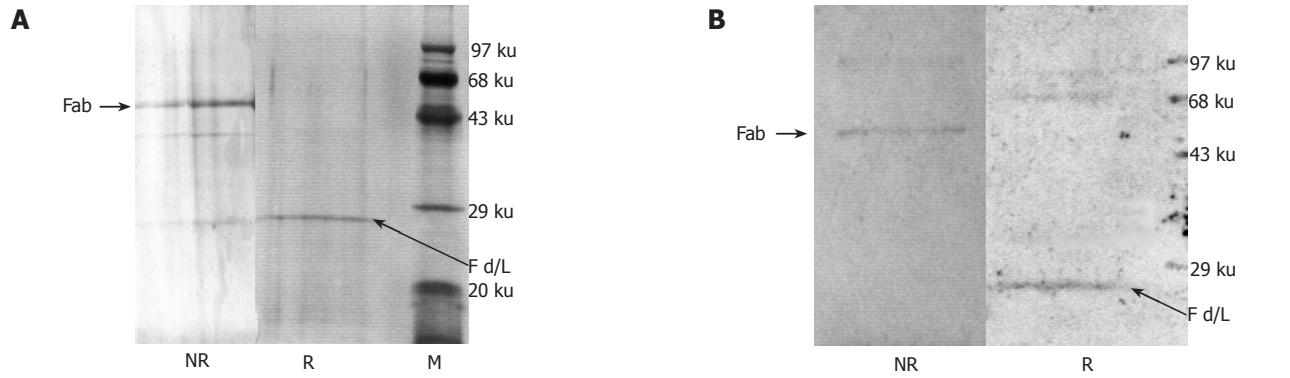

Figure 3 SDS-PAGE (**A**) and Western Blot (**B**) analysis of the chimeric Fab. The purified chimeric Fab was resolved in 12% SDS-PAGE under reducing (R) and non-reducing conditions (NR). In non-reducing conditions the Fab is a heterodimer of molecular weight ~50 ku. In reducing conditions the heterodimer dissociates into chimeric light chain (~25 ku) and Fd (~25 ku). Both the gels were stained by silver staining. M is the lane for the protein marker. Similar observations were made in Western Blots (**B**) of the chimeric Fab in reducing (R) and non-reducing (NR) conditions. Electroblotted antibody fragments were detected by Rabbit anti-Human IgG-HRP conjugate (1:1 000 dilution; Dako).

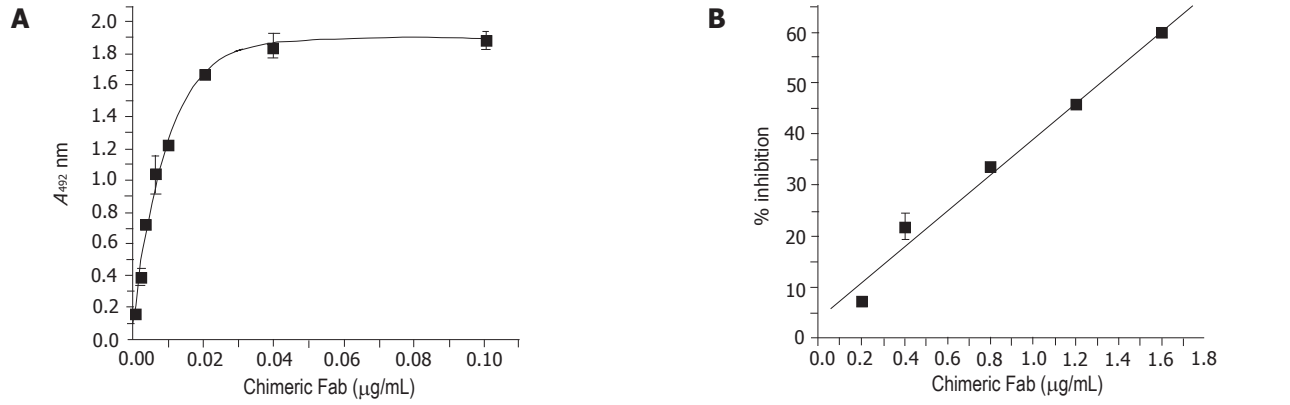

Figure 4 Binding properties of the anti-HBs chimeric Fab. 1 Solid phase ELISA was performed with different dilutions of the soluble chimeric Fab. The result of the competitive ELISA between the chimeric Fab and the mouse monoclonal 5S is shown in Figure (**B**). Different amounts of the chimeric Fab were allowed to compete with 1:80 dilution of the 5S-hybridoma culture supernatant for binding to HBsAg. Bound mouse monoclonal was detected with anti-mouse HRP and the % inhibition of binding was calculated.

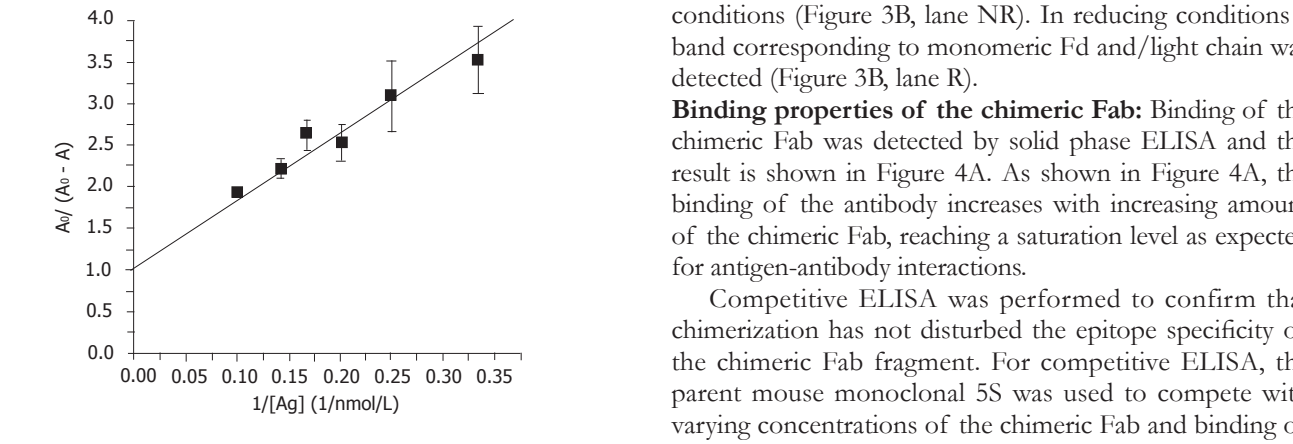

Figure 5 Dissociation constant (K_D) of the chimeric Fab. The K_D was determined using an ELISA based method. Different amounts of HBsAg were incubated with concentrated periplasmic extract of the clone expressing the anti-HBs chimeric Fab for 16 h and unbound antibody was detected by ELISA using rabbit anti-human antibody-HRP (Dako). The data was fitted to the equation $A_0/(A_0–A) = K_D*1/[Ag]+1$, where Ao = absorbance when the antibody was incubated without any antigen, A = absorbance corresponding to free antibody after incubation with the antigen. Dissociation constant of the chimeric Fab was determined from the slope of the straight line (K_D = 8.166±0.14 nmol/L).

conditions (Figure 3B, lane NR). In reducing conditions a band corresponding to monomeric Fd and/light chain was detected (Figure 3B, lane R).

Binding properties of the chimeric Fab: Binding of the chimeric Fab was detected by solid phase ELISA and the result is shown in Figure 4A. As shown in Figure 4A, the binding of the antibody increases with increasing amount of the chimeric Fab, reaching a saturation level as expected for antigen-antibody interactions.

Competitive ELISA was performed to confirm that chimerization has not disturbed the epitope specificity of the chimeric Fab fragment. For competitive ELISA, the parent mouse monoclonal 5S was used to compete with varying concentrations of the chimeric Fab and binding of the mouse antibody was detected using anti-mouse-HRP conjugate. Figure 4B shows that the chimeric Fab inhibits the binding of the mouse antibody, indicating that both of these bind to the same epitope.

Dissociation constant of the chimeric Fab: The dissociation constant of the chimeric Fab in solution phase was determined using an ELISA based technique developed by Friguet *et al.*[36]. As calculated from the slope

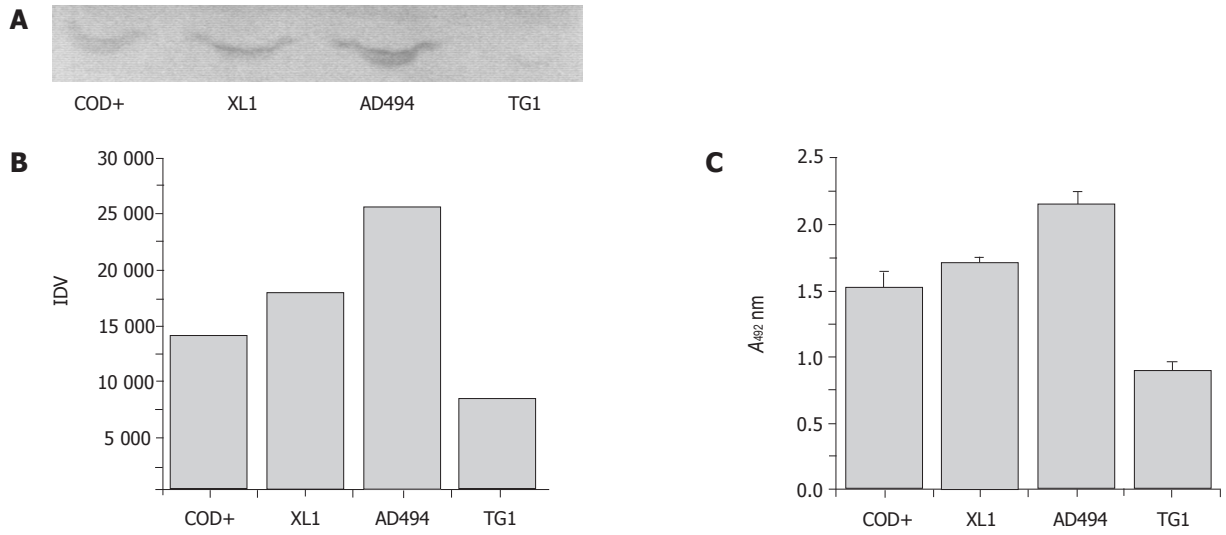

Figure 6 Expression profile of the chimeric Fab in different strains of *E. coli*. The chimeric Fab was expressed in soluble form in different *E. coli* strains in identical conditions. Levels of expression of the chimeric Fab were checked by Western blot in non-reducing conditions (**A**). Intensities of bands were measured densitometrically (**B**). Levels of expression were also checked by ELISA (**C**). Equal amount of the periplasmic extracts were allowed to bind to HBsAg coated on ELISA plate and bound chimeric Fab was detected. (XL1 = XL1-Blue, AD494 = AD494, COD+ = BL21 Codon Plus, TG1 = TG1, IDV = integrated density value).

Table 2 Yields of the anti-HBs chimeric Fab in different *E. coli* strains

E. coli strain	Yield (μg/L)[1]
XL1-Blue	40
AD494	62
BL21 Codon Plus	40
TG1	8

[1]Estimated by Bradford assay, after purification by protein G column

of the line in Figure 5, the K_D of the chimeric anti-HBs Fab is 8.166±0.14 nmol/L, (r^2 = 0.914).

Expression of the chimeric Fab in different *E.coli* strains: Yield of this chimeric Fab in *E. coli* XL1-Blue cells was found to be low (~40 μg/L). The recombinant construct pCOMB3H-Fd-L-Sol was transformed into three other strains of *E. coli*, (AD494, BL21 CodonPlus and TG1) to check the yield of the chimeric Fab in soluble form. The chimeric Fab was expressed in these cells in the same fashion as stated above for XL1-Blue cells. The levels of expression of the chimeric Fab in different *E. coli* strains were checked by Western Blot and compared densitometrically (Figures 6A and B). The levels of expression of the chimeric Fab in different strains of *E. coli* were further confirmed by ELISA using crude periplasmic extracts. The result of the ELISA is shown in Figure 6C. Yields of the purified chimeric Fab expressed in different *E. coli* strains are shown in Table 2. As shown in Figure 6 and Table 2, maximum yield of the chimeric Fab was observed in case of *E. coli* AD494 cells.

DISCUSSION

5S is a mouse monoclonal that binds to HBsAg with high affinity[13]. However, like any other mouse monoclonal, this antibody can give rise to HAMA response and cannot be used clinically. HAMA may neutralize the injected mouse antibody directly by immune complex formation, which could lead to rapid clearance or to hypersensitivity reactions[38,39]. As immunogenic reactions are predominantly directed towards the Fc region of murine antibodies[16], creation of mouse-human chimeric antibodies by swapping murine constant regions with the human ones can address the problem of HAMA response, at least in part[17-19]. But such domain swapping can alter the immunological and pharmacokinetic properties of an antibody, making the task of generation of chimeric antibodies quite tricky[40].

One of the crucial aspects in generation of chimeric antibodies is the selection of human isotypes for domain swapping. Effector functions of antibody constant domains are broadly dependent on the antibody classes and subclasses[41]. Usually human IgG1 is the preferred choice for chimeric antibodies in situations where activation of effector functions is the desired outcome[42]. Rath and Devey[43] had observed that the subclasses of antibodies associated with HBsAg in circulating immune complexes of patients with either acute or chronic HBV infections were predominantly IgG1 and IgG4. A study involving children, who have recovered from acute hepatitis B, has shown that after natural seroconversion, specific antibodies were highly restricted to IgG1[44]. It has also been observed that anti-HBs IgG1 is predominant after vaccination with recombinant vaccines[44,45].

Apart from being important for effector functions, the choice of isotype can also affect the antigen binding of a chimeric molecule. It has been observed that changes in constant domains can affect the functional affinity and specificity of antibodies[46]. Pritsch *et al*.[47] have shown that Fab fragments of antibodies sharing identical variable regions but C_H1 of different isotypes have significant differences in affinities. A molecular dynamic study

involving anti-HEL Fab has shown that, the interactions between C_L and C_H1 domains may have influence not only around the local interface between C_L and C_H1 but also around the interacting regions between HEL and Fv[48].

In the present work, the variable region genes of 5S (IgG1/κ) were fused with the C_H1 region of human IgG1 and human kappa chain constant region, to generate a mouse-human chimeric Fab. The C_H1 region of IgG1 and kappa C_L were amplified using RNA extracted from human PBLs and linked with respective variable regions of 5S hybridoma by overlap PCR. The chimeric fragments were subsequently cloned into the phagemid vector pCOMB3H and phage antibodies were expressed. Functional clones were selected by biopanning over antigen coated plate and selected clones were checked for binding by phage ELISA. It is well known that cloning of antibody genes by PCR may introduce mutations and may amplify truncated antibody genes, generating clones that are non-functional[49,50]. Use of a phagemid expression system allows the initial expression of antibody molecules as phage antibodies, which can be easily selected for antigen binding and then be further processed for soluble expression. As shown in Figure 2, two of the four clones checked by phage ELISA after three rounds of biopanning showed high binding. Clone 1 was further processed for soluble expression of the chimeric Fab. SDS-PAGE and Western blot in both reducing and non-reducing conditions confirmed that the chimeric Fab was expressed in the form of a heterodimer (Figures 3A and B). The chimeric Fab was further characterized by ELISA and competitive ELISA. Competitive ELISA confirmed that the chimeric Fab and the original mouse monoclonal bind to the same epitope (Figure 4B). The dissociation constant of the chimeric Fab as determined by the ELISA based method was found to be high (8.166±0.14 nmol/L). The dissociation constant for the original mouse monoclonal is 0.8899 nmol/L[13]. Given the level of accuracy of the method used for the determination of K_D values, one can consider both of these values to be in the same broad range. An anti-human antibody was used in the ELISA to calculate the K_D of the chimeric Fab; whereas an anti-mouse antibody was used in case of the mouse monoclonal. Such a difference in experimental setup can also be attributed for the difference in K_D values.

Though it seems simple, high yield expression of heterologous proteins in bacterial systems sometimes proves to be problematic. Multiple factors like codon usage[51], DNA/RNA/Protein interaction[52], regulatory factors for transcription and translation and nucleotide usage in the leader peptide[53] affect the yield of heterologous proteins in bacteria. The yield of Fab depends upon the relative levels of expression of the light chain and Fd. The light chain-heavy chain balance depends upon codon usage in the signal peptides and 5' sequence of coding regions[54]. In this present work, the yield of soluble recombinant Fab in XL1-Blue cells was low (~40 μg/L). Such a low yield of Fab fragment expressed in *E. coli* using pCOMB3H vector system has been reported earlier[55]. To optimize the yield of the soluble chimeric Fab, the recombinant construct was transformed in different *E. coli* strains — TG1, AD 494 and BL21 CodonPlus. *E. coli* BL21 CodonPlus-RP (Novagen) cells contain extra copies of the *argU* and *proL* genes. These genes encode tRNAs that recognize the arginine codons AGA, AGG and the proline codon CCC, respectively. *E. coli* BL21 has been used for high-level expression of several antibody fragments[56,57]. *E. coli* AD494 cells are thioredoxin negative (*trxB*$^-$), thereby providing an oxidizing environment in the cytoplasm. Proper folding and assembly of antibody domains require inter- and intra-chain disulphide bond formation. Therefore bacterial periplasm is suitable for the assembly of functional Fab fragments. An oxidizing environment in the cytoplasm may also help to increase the yield of properly folded soluble antibody fragments. We expressed the anti-HBs chimeric Fab in soluble form in different *E. coli* strains under identical conditions. As shown in Figure 6 and Table 2, there was a slight increase in the expression of the chimeric Fab in AD494 cells; whereas the expression in BL21 was equivalent to that in XL1-Blue cells. Though Raffai *et al*.[55] had observed increased yield of soluble Fab fragment in TG1 in comparison to XL1-Blue cells, we could not detect any such increase in yield.

Though chimerization and humanization are essential to reduce immunogenicity of non-human antibodies before they can be used clinically such genetic engineering can alter functional capabilities of the molecule, often leading to loss of binding or reduction in affinity. Our results show that the chimerization of the 5S mouse monoclonal did not disturb its binding to the antigen and the chimeric Fab binds to the same epitope as that of the original mouse monoclonal. Though chimeric and monovalent in nature, the affinity of the recombinant chimeric Fab remained in the same range as the mouse monoclonal 5S. The high affinity binding of this chimeric Fab fragment indicates that it can be further modified to generate a clinically applicable full-length chimeric anti-HBs antibody, with out any significant loss of binding affinity.

ACKNOWLEDGMENTS

We are thankful to Dr. Dennis R. Burton and The Scripps Research Institute, La Jolla, USA for providing the vector pCOM3H. We thank Dr. Vijay Chaudhary for his gift of anti-M13 antibody. We are also thankful to M/s. Mathura Prasad and Satish for their technical and secretarial assistance.

REFERENCES

1 **Lavanchy D**. Hepatitis B virus epidemiology, disease burden, treatment, and current and emerging prevention and control measures. *J Viral Hepat* 2004; **11:** 97-107
2 **Chisari FV**, Ferrari C. Hepatitis B virus immunopathology. *Springer Semin Immunopathol* 1995; **17:** 261-281
3 **Milich DR**, Chen M, Schodel F, Peterson DL, Jones JE, Hughes JL. Role of B cells in antigen presentation of the hepatitis B core. *Proc Natl Acad Sci USA* 1997; **94:** 14648-14653
4 **Magnius LO**, Norder H. Subtypes, genotypes and molecular epidemiology of the hepatitis B virus as reflected by sequence

variability of the S-gene. *Intervirology* 1995; **38:** 24-34
5 **Prince AM**, Szmuness W, Woods KR, Grady GF. Antibody against serum-hepatitis antigen. Prevalence and potential use as immune serum globulin in prevention of serum-hepatitis infections. *N Engl J Med* 1971; **285:** 933-938
6 **Karasu Z**, Ozacar T, Akyildiz M, Demirbas T, Arikan C, Kobat A, Akarca U, Ersoz G, Gunsar F, Batur Y, Kilic M, Tokat Y. Low-dose hepatitis B immune globulin and higher-dose lamivudine combination to prevent hepatitis B virus recurrence after liver transplantation. *Antivir Ther* 2004; **9:** 921-927
7 **Beasley RP**, Hwang LY, Lee GC, Lan CC, Roan CH, Huang FY, Chen CL. Prevention of perinatally transmitted hepatitis B virus infections with hepatitis B virus infections with hepatitis B immune globulin and hepatitis B vaccine. *Lancet* 1983; **2:** 1099-1102
8 **Li XM**, Yang YB, Hou HY, Shi ZJ, Shen HM, Teng BQ, Li AM, Shi MF, Zou L. Interruption of HBV intrauterine transmission: a clinical study. *World J Gastroenterol* 2003; **9:** 1501-1503
9 **Li YW**, Lawrie DK, Thammana P, Moore GP, Shearman CW. Construction, expression and characterization of a murine/human chimeric antibody with specificity for hepatitis B surface antigen. *Mol Immunol* 1990; **27:** 303-311
10 **Zheng W**, Tan H, Song S, Lu H, Wang Y, Yu Y, Yin R. The construction and expression of a fusion protein consisting anti-HBsAg antibody fragment Fab and interferon-a in E.coli. *World J Gastroenterol* 2000; **6(Suppl 3):** tk 83a
11 **Sanchez L**, Ayala M, Freyre F, Pedroso I, Bell H, Falcon V, Gavilondo JV. High cytoplasmic expression in E. coli, purification, and in vitro refolding of a single chain Fv antibody fragment against the hepatitis B surface antigen. *J Biotechnol* 1999; **72:** 13-20
12 **Maeda F**, Nagatsuka Y, Ihara S, Aotsuka S, Ono Y, Inoko H, Takekoshi M. Bacterial expression of a human recombinant monoclonal antibody fab fragment against hepatitis B surface antigen. *J Med Virol* 1999; **58:** 338-345
13 **Bose B**, Chugh DA, Kala M, Acharya SK, Khanna N, Sinha S. Characterization and molecular modeling of a highly stable anti-Hepatitis B surface antigen scFv. *Mol Immunol* 2003; **40:** 617-631
14 **Schroff RW**, Foon KA, Beatty SM, Oldham RK, Morgan AC Jr. Human anti-murine immunoglobulin responses in patients receiving monoclonal antibody therapy. *Cancer Res* 1985; **45:** 879-885
15 **Shawler DL**, Bartholomew RM, Smith LM, Dillman RO. Human immune response to multiple injections of murine monoclonal IgG. *J Immunol* 1985; **135:** 1530-1535
16 **Spiegelberg HL**, Weigle WO. Studies on the catabolism of gamma- G subunits and chains. *J Immunol* 1965; **95:** 1034-1040
17 **Reist CJ**, Bigner DD, Zalutsky MR. Human IgG2 constant region enhances in vivo stability of anti-tenascin antibody 81C6 compared with its murine parent. *Clin Cancer Res* 1998; **4:** 2495-2502
18 **Colcher D**, Milenic D, Roselli M, Raubitschek A, Yarranton G, King D, Adair J, Whittle N, Bodmer M, Schlom J. Characterization and biodistribution of recombinant and recombinant/chimeric constructs of monoclonal antibody B72.3. *Cancer Res* 1989; **49:** 1738-1745
19 **Yata Y**, Otsuji E, Okamoto K, Tsuruta H, Kobayashi S, Toma A, Yamagishi H. Decreased production of anti-mouse antibody after administration of human/mouse chimeric monoclonal antibody-neocarzinostatin conjugate to human. *Hepatogastroenterology* 2003; **50:** 80-84
20 **Dimmock NJ.** Mechanisms of neutralization of animal viruses. *J Gen Virol* 1984; **65 (Pt 6):** 1015-1022
21 **Burton DR**, Williamson RA, Parren PW. Antibody and virus: binding and neutralization. *Virology* 2000; **270:** 1-3
22 **Cheung SC**, Dietzschold B, Koprowski H, Notkins AL, Rando RF. A recombinant human Fab expressed in Escherichia coli neutralizes rabies virus. *J Virol* 1992; **66:** 6714-6720
23 **Barbas CF 3rd,** Bjorling E, Chiodi F, Dunlop N, Cababa D, Jones TM, Zebedee SL, Persson MA, Nara PL, Norrby E. Recombinant human Fab fragments neutralize human type 1 immunodeficiency virus in vitro. *Proc Natl Acad Sci USA* 1992; **89:** 9339-9343
24 **Barbas CF 3rd,** Crowe JE Jr, Cababa D, Jones TM, Zebedee SL, Murphy BR, Chanock RM, Burton DR. Human monoclonal Fab fragments derived from a combinatorial library bind to respiratory syncytial virus F glycoprotein and neutralize infectivity. *Proc Natl Acad Sci USA* 1992; **89:** 10164-10168
25 **Lamarre A**, Talbot PJ. Protection from lethal coronavirus infection by immunoglobulin fragments. *J Immunol* 1995; **154:** 3975-3984
26 **Thullier P**, Lafaye P, Megret F, Deubel V, Jouan A, Mazie JC. A recombinant Fab neutralizes dengue virus in vitro. *J Biotechnol* 1999; **69:** 183-190
27 **Tada H**, Yanagida M, Mishina J, Fujii T, Baba K, Ishikawa S, Aihara S, Tsuda F, Miyakawa Y, Mayumi M. Combined passive and active immunization for preventing perinatal transmission of hepatitis B virus carrier state. *Pediatrics* 1982; **70:** 613-619
28 **Skerra A**. Bacterial expression of immunoglobulin fragments. *Curr Opin Immunol* 1993; **5:** 256-262
29 **Gram H**, Marconi LA, Barbas CF 3rd, Collet TA, Lerner RA, Kang AS. In vitro selection and affinity maturation of antibodies from a naive combinatorial immunoglobulin library. *Proc Natl Acad Sci USA* 1992; **89:** 3576-3580
30 **Rosok MJ**, Yelton DE, Harris LJ, Bajorath J, Hellstrom KE, Hellstrom I, Cruz GA, Kristensson K, Lin H, Huse WD, Glaser SM. A combinatorial library strategy for the rapid humanization of anticarcinoma BR96 Fab. *J Biol Chem* 1996; **271:** 22611-22618
31 **Ames RS**, Tornetta MA, Deen K, Jones CS, Swift AM, Ganguly S. Conversion of murine Fabs isolated from a combinatorial phage display library to full length immunoglobulins. *J Immunol Methods* 1995; **184:** 177-186
32 **Bender E**, Woof JM, Atkin JD, Barker MD, Bebbington CR, Burton DR. Recombinant human antibodies: linkage of an Fab fragment from a combinatorial library to an Fc fragment for expression in mammalian cell culture. *Hum Antibodies Hybridomas* 1993; **4:** 74-79
33 **Barbas CF 3rd**, Kang AS, Lerner RA, Benkovic SJ. Assembly of combinatorial antibody libraries on phage surfaces: the gene III site. *Proc Natl Acad Sci USA* 1991; **88**: 7978-7982
34 **Sambrook J**, Russell DW. Molecular Cloning: A Laboratory Manual. 3rd ed. Cold Spring Harbor, New York: Cold Spring Harbor Laboratory Press, 2001: 1.116-1.118
35 **Barbas CF 3rd**, Burton DR, Scott JK, Silverman GJ. Phage Display: A Laboratory Manual. 1st ed. Cold Spring Harbor, NY: Cold Spring Harbor Laboratory Press, 2001: 23.11-23.12
36 **Friguet B**, Chaffotte AF, Djavadi-Ohaniance L, Goldberg ME. Measurements of the true affinity constant in solution of antigen-antibody complexes by enzyme-linked immunosorbent assay. *J Immunol Methods* 1985; **77:** 305-319
37 **Bradford MM**. A rapid and sensitive method for the quantitation of microgram quantities of protein utilizing the principle of protein-dye binding. *Anal Biochem* 1976; **72:** 248-254
38 **Sakahara H**, Reynolds JC, Carrasquillo JA, Lora ME, Maloney PJ, Lotze MT, Larson SM, Neumann RD. In vitro complex formation and biodistribution of mouse antitumor monoclonal antibody in cancer patients. *J Nucl Med* 1989; **30:** 1311-1317
39 **Rettenbacher L**, Galvan G. [Anaphylactic shock after repeated injection of 99mTc-labeled CEA antibody] *Nuklearmedizin* 1994; **33**: 127-128
40 **Colcher D**, Goel A, Pavlinkova G, Beresford G, Booth B, Batra SK. Effects of genetic engineering on the pharmacokinetics of antibodies. *Q J Nucl Med* 1999; **43:** 132-139
41 **Clark MR**. IgG effector mechanisms. *Chem Immunol* 1997; **65:** 88-110
42 **Steplewski Z**, Sun LK, Shearman CW, Ghrayeb J, Daddona

P, Koprowski H. Biological activity of human-mouse IgG1, IgG2, IgG3, and IgG4 chimeric monoclonal antibodies with antitumor specificity. *Proc Natl Acad Sci USA* 1988; **85:** 4852-4856

43 **Rath S**, Devey ME. IgG subclass composition of antibodies to HBsAg in circulating immune complexes from patients with hepatitis B virus infections. *Clin Exp Immunol* 1988; **72:** 164-167

44 **Gregorek H**, Madalinski K, Woynarowski M, Mikolajewicz J, Syczewska M, Socha J. The IgG subclass profile of anti-HBs response in vaccinated children and children seroconverted after natural infection. *Vaccine* 2000; **18:** 1210-1217

45 **Honorati MC**, Borzi RM, Dolzani P, Toneguzzi S, Facchini A. Distribution of IgG subclasses after anti-hepatitis B virus immunization with a recombinant vaccine. *Int J Clin Lab Res* 1997; **27:** 202-206

46 **Cooper LJ**, Robertson D, Granzow R, Greenspan NS. Variable domain-identical antibodies exhibit IgG subclass-related differences in affinity and kinetic constants as determined by surface plasmon resonance. *Mol Immunol* 1994; **31:** 577-584

47 **Pritsch O**, Hudry-Clergeon G, Buckle M, Petillot Y, Bouvet JP, Gagnon J, Dighiero G. Can immunoglobulin C(H)1 constant region domain modulate antigen binding affinity of antibodies? *J Clin Invest* 1996; **98:** 2235-2243

48 **Adachi M**, Kurihara Y, Nojima H, Takeda-Shitaka M, Kamiya K, Umeyama H. Interaction between the antigen and antibody is controlled by the constant domains: normal mode dynamics of the HEL-HyHEL-10 complex. *Protein Sci* 2003; **12:** 2125-2131

49 **Strohal R**, Kroemer G, Wick G, Kofler R. Complete variable region sequence of a nonfunctionally rearranged kappa light chain transcribed in the nonsecretor P3-X63-Ag8.653 myeloma cell line. *Nucleic Acids Res* 1987; **15:** 2771

50 **Duan L**, Pomerantz RJ. Elimination of endogenous aberrant kappa chain transcripts from sp2/0-derived hybridoma cells by specific ribozyme cleavage: utility in genetic therapy of HIV-1 infections. *Nucleic Acids Res* 1994; **22:** 5433-5438

51 **Andersson SG**, Kurland CG. Codon preferences in free-living microorganisms. *Microbiol Rev* 1990; **54:** 198-210

52 **Jacques N**, Dreyfus M. Translation initiation in Escherichia coli: old and new questions. *Mol Microbiol* 1990; **4:** 1063-1067

53 **Stemmer WP**, Morris SK, Kautzer CR, Wilson BS. Increased antibody expression from Escherichia coli through wobble-base library mutagenesis by enzymatic inverse PCR. *Gene* 1993; **123:** 1-7

54 **Humphreys DP**, Carrington B, Bowering LC, Ganesh R, Sehdev M, Smith BJ, King LM, Reeks DG, Lawson A, Popplewell AG. A plasmid system for optimization of Fab' production in Escherichia coli: importance of balance of heavy chain and light chain synthesis. *Protein Expr Purif* 2002; **26:** 309-320

55 **Raffai R**, Vukmirica J, Weisgraber KH, Rassart E, Innerarity TL, Milne R. Bacterial expression and purification of the Fab fragment of a monoclonal antibody specific for the low-density lipoprotein receptor-binding site of human apolipoprotein E. *Protein Expr Purif* 1999; **16:** 84-90

56 **Fan JY**, Wang G, Li W, Wu YM, Liu YF. [Expression of human Fab antibody against keratin in E.coli and its renaturation] *Xi Bao Yu Fen Zi Mian Yi Xue Za Zhi* 2004; **20:** 441-443

57 **Wang C**, Hou LH, Zhang YM, Li JM, Liao ZL, Du GX, Chen W, Sun QH, Tong YG. Construction and expression of anti-human integrin alphavbeta3 scFv. *Xi Bao Yu Fen Zi Mian Yi Xue Za Zhi* 2004; **20:** 159-162

Science Editor Guo SY **Language Editor** Elsevier HK

PO Box 2345, Beijing 100023, China
www.wjgnet.com
wjg@wjgnet.com

ELSEVIER

World J Gastroenterol 2005;11(48):7579-7584
World Journal of Gastroenterology ISSN 1007-9327

Application of restriction display PCR technique in the preparation of cDNA microarray probes

Zhao-Hui Sun, Wen-Li Ma, Bao Zhang, Yi-Fei Peng, Wen-Ling Zheng

Zhao-Hui Sun, Wen-Li MA, Bao Zhang, Yi-Fei Peng, Institute of Genetic Engineering, Southern Medical University, Guangzhou 510515, Guangdong Province, China
Wen-Ling Zheng, Institute of Molecular Oncology, Guangzhou General Hospital of Guangzhou Military Area Command, Guangzhou 510010, Guangdong Province, China
Supported by the National Natural Science Foundation of China, No. 39880032; Major Programs for Science and Technology Development of Guangzhou, No. 01-Z-005-01
Co-first-authors: Wen-Li Ma and Zhao-Hui Sun
Correspondence to: Professor Wen-Li Ma, Institute of Genetic Engineering, Southern Medical University, Guangzhou 510515, Guangdong Province, China. wenli@fimmu.com
Telephone: +86-20-61648210 Fax: +86-20-61647755
Received: 2005-04-14 Accepted: 2005-07-15

Abstract

AIM: To develop a simplified and efficient method for the preparation of hepatitis C virus (HCV) cDNA microarray probes.

METHODS: With the technique of restriction display PCR (RD-PCR), restriction enzyme *Sau3A* I was chosen to digest the full-length HCV cDNAs. The products were classified and re-amplified by RD-PCR. We separated the differential genes by polyacrylamide gel electrophoresis and silver staining. Single bands cut out from the polyacrylamide gel were isolated. The third-round PCR was performed using the single bands as PCR template. The RD-PCR fragments were purified and cloned into the pMD18-T vector. The recombinant plasmids were extracted from positive clones, and the target gene fragments were sequenced. The cDNA microarray was prepared by spotting RD-PCR products to the surface of amino-modified glass slides using a robot. We validated the detection of microarray by hybridization and sequence analysis.

RESULTS: A total of 24 different cDNA fragments ranging from 200 to 800 bp were isolated and sequenced, which were the specific gene fragments of HCV. These fragments could be further used as probes in microarray preparation. The diagnostic capability of the microarray was evaluated after the washing and scanning steps. The results of hybridization and sequence analysis showed that the specificity, sensitivity, accuracy, reproducibility, and linearity in detecting HCV RNA were satisfactory.

CONCLUSION: The RD-PCR technique is of great value in obtaining a large number of size-comparable gene probes, which provides a speedy protocol in generating probes for the preparation of microarrays. Microarray prepared as such could be further optimized and applied in the clinical diagnosis of HCV.

Key words: Restriction display PCR; HCV; Microarray; Probes

Sun ZH, Ma WL, Zhang B, Peng YF, Zheng WL. Application of restriction display PCR technique in the preparation of cDNA microarray probes. *World J Gastroenterol* 2005; 11(48): 7579-7584
http://www.wjgnet.com/1007-9327/11/7579.asp

INTRODUCTION

Hepatitis C virus (HCV) is a RNA virus with a high rate of genetic mutation[1]. HCV has a linear genome approximately 10 kb in length, which consists of a positive sense single-stranded RNA (ssRNA)[2]. Consistent with related members of the family *Flaviviridae,* HCV demonstrates a high degree of sequence variation throughout its genome. Sequence analysis of multiple strains of HCV has demonstrated that the nucleotide sequence can differ by as high as 30%[3]. Infection with HCV has been identified as the major cause of post-transfusion non-A, non-B hepatitis, and is a major public health problem in most areas of the world, raising the issues of its diagnosis, treatment, and prevention[4-6].

In the present study, we utilized the technique of restriction display PCR (RD-PCR) to prepare HCV cDNA chip probes. Restriction enzyme *Sau3A* I was chosen to digest the full-length HCV cDNAs. The products were classified and re-amplified by RD-PCR. We separated the differential genes by polyacrylamide gel electrophoresis and silver staining. The cDNA microarray was prepared by spotting RD-PCR products to the surface of amino-modified glass slides using a robot. The specificity, sensitivity, accuracy, reproducibility, and linearity in detecting HCV RNA were evaluated.

MATERIALS AND METHODS

Probe template

The full-length plasmid of HCV pCV-J4L6S was presented

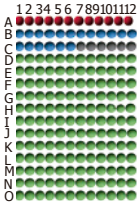

Figure 1 Arrangement of all spots on gene chip. Positive controls, negative controls, empty controls, HCV probes.

by Dr Jens Bukh of NIH (USA)[7].

Chemicals and reagents

Premix Taq, dNTP, *Eco*RI, *Not*I, *Xba*I, *Sau*3A I, pMD18-T vector, and T4 DNA ligase were obtained from Takara Corp. (Japan). Dimethyl sulfoxide (DMSO) was bought from Sangon (Shanghai, China). Plasmid Miniprep kits, 3S PCR purification kit V20 were purchased from Shen Neng Bo Cai Corp. (China). PCR primers of HCV and the primers in pMD18-T vector were synthesized by BioAsia Corp. (China). Universal primer (U) cy3-GTTTG GCTGGTGT GGATC, selective primers (similar with U but with one "nesting" base overhanging at 3'-end, UA, UT, UC, UG) and the adapter (SIP, SIR) were purchased from GIBCO Corp. (USA).

Instruments

GenePix 4000B scanner and ScanArray Lite were provided by GSI Lumonics (Billerica, USA). GS Gene Linker ultraviolet chamber was obtained from BioRad (Hercules, USA). PixSys 5500 gene chip printing machine was purchased from Cartesian Technologies (Irvine, USA). CMT-GAPSTM coated slides and Corning CMT-Hybridization™ chambers were ordered from Corning Microarray Technology (Acton, USA).

Bacterial strains

The *E. coli* strain XL-1 used in experiments was maintained in our laboratory.

Probe preparation

To isolate HCV genomes, plasmid pCV-J4L6S was digested with *Not*I and *Xba*I. The plasmid (1-2 μg) was added to a total volume of 20 μL mixture at 37 °C for 4 h. The target HCV gene was isolated and recovered with UNIQ-5 column DNA extraction kit (Sangon, China). RD-PCR was performed as previously described[8-10]. The recovered HCV cDNAs were digested with 2 μL *Sau*3A1 (5'↓ GATC3') (10 U/μL) in a total volume of 20 μL mixture at 37 °C for 3 h. The two ends of each *Sau*3AI-digested fragment were linked to an adapter that was prepared by annealing the 2 oligonucleotides containing the sequences of 5'-GATCCACACCAGCCAAACC CA (SIP) and 5' -GGTTTGGCTGGTGTG (SIR) in a ligation reaction containing 1 μL T4 DNA ligase (350 U/μL), 1 μL 10× DNA ligation buffer, 1 μL adapter (50 μmol/L), 20 pmol of digested HCV cDNA fragments of *Sau*3AI, and then UPW was added for a total of 10 μL. After 4 h of ligation at 16 °C, PCR was performed in a 9700 thermocycler with an initial denaturation at 94 °C for 5 min, followed by 35 cycles at 94 °C for 30 s, at 60 °C for 30 s, at 72 °C for 1 min, and a final extension at 72 °C for 7 min. PCR primers were designed to match the universal adapters, including the restriction site sequence, but with one "nesting" base overhanging at the 3'-end, and the reactions were divided into 10 subgroups. To check for positive PCR results, 7 μL of the PCR products was loaded onto 5% polyacrylamide (Takara, Japan) gel electrophoresis at 90 V for 5-6 h and the technique of DNA silver staining[11] was used to separate different target gene fragments.

DNA microarray printing

The final concentration of each probe was adjusted to 0.3 mg/mL with DMSO and water. The DMSO concentration was 50% (v/v). The probes were spotted onto a CMT-GAPS aminosilane-coated glass microscope slide at 25 °C and 60% relative humidity, using the ArrayIt ChipMaker2™ microspotting pins (TeleChem International, Sunnyvale, USA) and a Cartesian PixSys 5500 robot. A microarray of 12×15 spots was printed. The arrangement of all spots on the gene chip is shown in Figure 1. After printing, the slide was rehybridized and snap-dried in a plate at 80 °C for 5 min. A BioRad UV crosslinker was used to immobilize the DNAs onto the slide with 125 mJ of energy. The slide was treated with blocking solution (335 mL 1-methyl-2-pyrrolidinone, 6 g succinic anhydride and 15 mL 1 mol/L sodium borate, pH 8) and stored for later use.

Fluorescent labeling

The samples of HCV were digested at 37 °C with the restriction enzyme *Sau*3AI. T4 DNA ligase was used to link gene fragments with universal adapters (SIP, SIR). After 3 h of ligation at 16 °C, 25 μL 2×premix, 2 μL of linkage products, 2 μL of Cy3 labeled universal primer matched with the adapter, and 21 μL of water were added for a total volume of 50 μL. Reactions were performed in a GeneAmp PCR 9700 system with an initial denaturation at 94 °C for 10 min, and then subjected to 30 thermal cycles at 94 °C for 30 s, at 60 °C for 30 s, at 72 °C for 1 min, followed by a final incubation at 72 °C for 5 min. Finally, the reaction was stopped by cooling down the solution to 4 °C. After this labeling reaction, the sample DNA fragments of hundreds of base pairs were labeled with fluorescent Cy3. The labeled PCR products were further purified using a 3S PCR product purification kit V20. Of the 30 μL purified products, 5 μL was used for hybridization with the microarray probes.

Pre-hybridization and hybridization

The slide was incubated in 25% formamide, 5×SSC, 0.1% sodium dodecyl sulfate (SDS) in a jar for 45 min at 42 °C, rinsed 5 times in distilled water, immersed in isopropyl alcohol for 1 s, and then dried in the air. Five microliters of Cy3 labeled samples was mixed with 1 μL Cot-1 DNA (20 μg/μL, Life Technologies) and 6 μL 2×hybridization

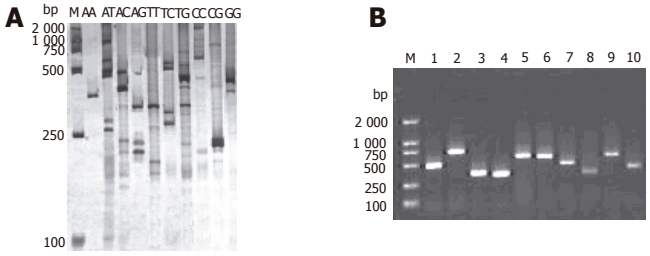

Figure 2 RD-PCR patterns of HCV genes (**A**) and 1.5% agarose gel electrophoresis of RD-PCR products from the white clones of HCV genomic fragments (**B**). M: MDL2 000 standard DNA ladder; lanes 1-10: PCR products of positive clones.

buffer (50% formamide, 10×SSC, 0.2% SDS) that was preheated at 42 °C, then heated to 95 °C for 5 min and centrifuged at 14 000 *g* for 2 min. This mixture was completely pipetted onto the pre-hybridized lambda phage DNA microarray slide and covered with a glass coverslip pretreated with Sigmacote® (Sigma, St. Louis, USA) to keep the sample from evaporating. The slide was put into a sealed hybridization box, 10 μL UPW was added to each well at the two ends of the chamber. The sealed chamber containing the DNA microarray slide was placed in a 42 °C water bath. After 4 h of incubation, the slide was taken out and washed in low-stringency washing buffer containing 1 ×SSC and 0.2% SDS at 42 °C for 5 min, in high-stringency washing buffer containing 0.1×SSC and 0.2% SDS at room temperature for 10 min, in 0.1×SSC and Milli Q water and ethanol, respectively. Finally, the air-dried slide was scanned using the ScanArray® Lite MicroArray Analysis System.

Scanning and analysis

The hybridized microarrays were scanned using GenePix 4000B scanner under the conditions of 90% laser power and 70% photo-multiplier tube (PMT). The results were analyzed using the QuantArray array analysis software. The criteria for positivity included the average fluorescence signal of Cy3 being three times as great as the value of the negative point, with a retro value of 2.7-3.3.

Probe optimization and printing

Ten HCV gene fragments were selected from the high value of the hybridized fluorescence signals to low fluorescence signals as microarray probes. The probes were spotted onto a CMT-GAPS aminosilane-coated glass microscope slide at 25 °C and 60% relative humidity, using the ArrayIt ChipMaker2™ microspotting pins and a Cartesian PixSys 5500 robot. A microarray of 12×8 spots was printed. The arrangement of all spots on the gene chip was similar to that shown in Figure 1. After printing, the slide was rehybridized and snap-dried in a plate at 80 °C for 5 min. A BioRad UV crosslinker was used to immobilize the DNAs onto the slide with 125 mJ of energy. The slide was treated with blocking solution and stored for later use.

Evaluation of microarray in sample detection

The specificity, sensitivity, accuracy, reproducibility, and linearity of this assay system were evaluated.

Identification of microarray probes and positive serum samples

After purification using the 3S PCR purification kit V20, the RD-PCR products (for probe preparation) and real-time RT-PCR products (for clinical serum sample detection) were inserted into the pMD18-T vector. The ligation mixture containing 4 μL of PCR products, 1 μL of pMD18-T vector (50 ng/μL) and 5 μL of loading buffer solution was incubated at 16 °C for 3 h, and then transferred into 100 μL of XL-1 *E. coli* competent cells treated with solutions containing Ca^{2+} ions (0.1 mol/L). To transform *E. coli*, the mixture of DNA formed in a ligation reaction was combined with a suspension of competent cells for 30 min, then heat-shocked at 42 °C for 1-2 min. The cells were then incubated in a growth medium and finally spread on an agar plate and incubated until single bacterial colonies were grown. Then the clones containing target fragments were selected and identified with the pMD18-T vector primer (primer A 5'-GTAAAACGACGGCC AGT-3', primer B 5'-CAGGAAACAGCTATGAC-3'). To check for positive PCR results, 5 μL of the PCR products was analyzed by 1.5% agarose (Takara, Japan) gel electrophoresis at 75 V for 45 min with a DNA marker DL2000 (Takara, Japan) as reference. Then the sequence was analyzed with ABI Prism™ 3730 DNA sequencer, and GenBank Blast sequence alignments were done.

RESULTS

Probe preparation

Twenty-four gene fragments of HCV were found in each subgroup by RD-PCR amplification with the expected size. The products were separated by electrophoresis on 5% polyacrylamide gel, and cDNA bands were stained with a silver solution (Figure 2A). Each subgroup produced 1-5 single cDNA bands with their length ranging from 200 to 800 bp. These bands could be used as probes for chip manufacture. Figure 2B shows the 1.5% agarose gel electrophoresis results of the clones.

Microarray design

The clinical diagnostic microarray was prepared by immobilizing the captured target genes of pathogens on a slide specifically treated. The DNA or RNA extracted from the patient's serum was labeled with fluorochrome and hybridized to the target DNA. In this study, the microarray was prepared by spotting RD-PCR products of HCV onto the surfaces of glass slides using a Cartesian 5500 MicroArrayer. Controls were immobilized at the same time. The control system was composed of empty controls which were DMSO without gene fragments, negative controls which were gene fragments of plants (rice) (B1-6) and an eukaryocyte (K562 cell) (B7-12) and a prokaryocyte (*E. coli*) (C1-6) not homologous with HCV, positive controls which were the reconstructed gene fragments.

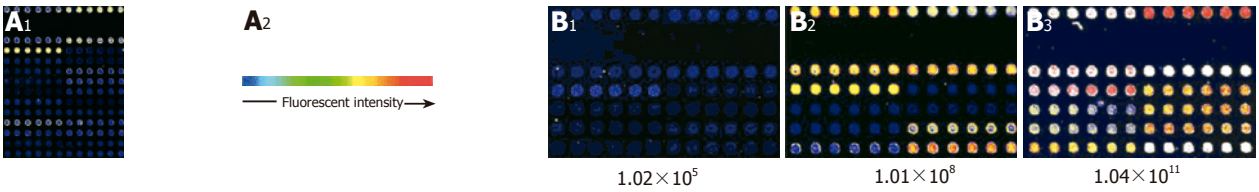

Figure 3 Scanning plots of hybridizing signals on gene chip of HCV (**A**) and modified gene chip (**B**). The samples were serially diluted (1.02×10^5, 1.01×10^8, 1.04×10^{11} copies/mL) and used in microarray analysis.

Eight of the 12×15 microarrays could be simultaneously immobilized on a glass slide.

Detection and analysis of hybridization

Based on the hybridizing signals under 90% laser energy and 70% GMT on the gene chip, the specificity and sensitivity in detecting HCV were satisfactory (Figure 3A). There was no signal on the empty control spots (printing 50% DMSO) and negative control spots (printing gene fragments of eukaryotic cells). The signal of spots hybridized to HCV positive controls and samples of HCV was strong and clear, but the analysis of variance showed that the density of signal was different in different probes (F = 8.325, P<0.001).

Optimization of microarray probes

Ten HCV gene fragments selected from the high- to low-density signals of hybridization were prepared for HCV gene chip probes. To obtain further information about the ten probes, we sequenced and analyzed the probes and found that nearly all of them had a similar length ranging 250-700 bp and a high GC content (≥40%) and T_m values (≥82 °C). The microarray was prepared by spotting the probes with Cartesian 5500 MicroArrayer. A microarray of 12×8 spots was printed. The arrangement of all spots on the gene chip is shown in Figure 1. The hybridization results indicated that the positive signal was strong compared to the hybridization signal (Figure 3B). There was no signal on the empty control spots and negative control spots.

Evaluation of microarray in sample detection

There was a strong linear relation between the concentrations of target cDNA and the fluorescence intensities obtained from microarray assay (r = 0.9819). The detection range of the microarray was 10^4-10^{11} copies/mL. The lower detection limit of HCV cDNA by microarray was 1.03×10^4 copies/mL, which was 2 log units lower than that by real-time RT-PCR. The reproducibility and accuracy of this assay system were evaluated by repeated measurement, and the within-run coefficient of validation was 6.6%, while the between-run coefficient of validation was 7.6%. Seventeen serum samples from hepatitis C patients (positive for anti-HCV, ALT≥80) were analyzed, and 15 patients (88.2%) were positive by microarray assay. Ten serum samples from healthy people were also evaluated and the results were all negative. The obtained sequences were verified and each sequenced PCR product was confirmed to be a HCV genome fragment using the basic local alignment search tool (BLAST) and the GenBank database.

DISCUSSION

HCV is the most important cause of transfusion-associated and community-acquired non-A, non-B hepatitis. Chronically infected individuals have a relatively high risk of developing chronic hepatitis, liver cirrhosis, and hepatocellular carcinoma. No effective vaccine therapy is available at present for HCV. Detection of HCV is essential for the correct diagnosis of HCV infection. Antibody-based methods have been considered as a practical way to detect infection of HCV. However, these methods cannot diagnose patients with hypoimmunity. Nucleic acid hybridization may have an excellent specificity, but its sensitivity is not satisfactory. In the protocol of PCR, cross contamination and false negative and positive incidents often occur. DNA microarray offers a solution to these problems and has the potential for the diagnosis of HCV infection. Compared to traditional diagnostic techniques, it has a number of advantages such as integration, micromation, and automatization[12,13]. The use of multiple independent gene fragments with a suitable size (ranging from 200 to 800 bp) for the probes to detect the same molecular targets can greatly enhance the signal-to-noise ratio and reduce the false-positive rate[14]. The gene chip also offers a dependable basis for the diagnosis and treatment of hepatotropic viral infections[15-17].

Probe preparation is a key step for microarray. One of the major difficulties in the development of microarray is to collect or prepare sufficient probes[18]. A few methods can be used to prepare microarray probes, including PCR amplification of DNA fragments with a molecular clone[19], artificial synthesis of oligonucleotide arrays by a DNA synthesizing machine[20] and light direction of *in situ* synthesis[21]. We prefer the first method because of its rapidity, simplicity, and effectiveness. However, conventional PCR is conducted with specific primers. RD-PCR provides an efficient and a simple way to obtain probes, since cDNA gene fragments digested by 4-cutter restriction endonuclease can be ligated with adapters at the same restriction site. In the present study, a PCR universal primer (U) was designed to match the sequence of both the adapters and the restriction site, but there were too many fragments amplified with universal primers (U). Using the selective primers with one or more

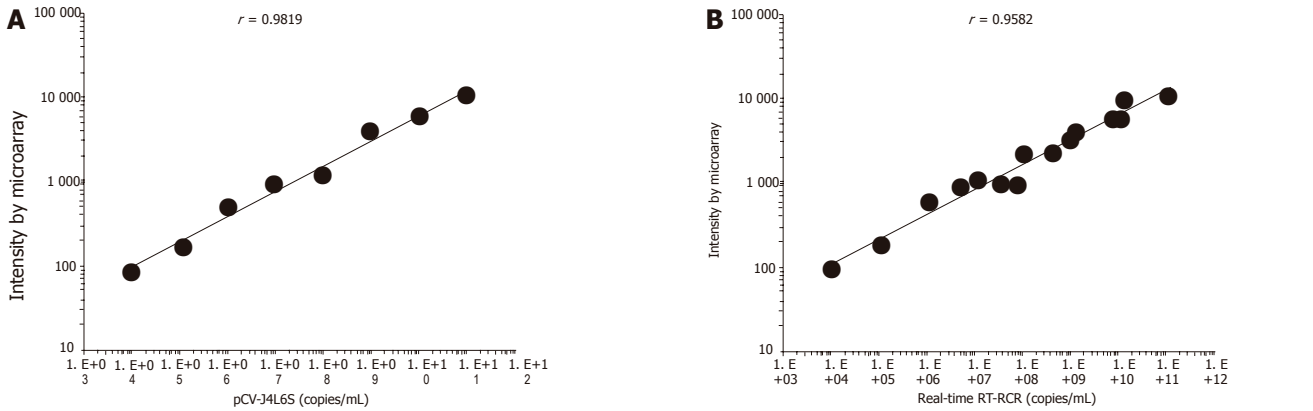

Figure 4 Fluorescence intensity from cDNA microarray analysis as a function of serial dilution from 10^4 to 10^{11} copies of plasmid pCV-J4L6S (r = 0.9819, ^bP<0.01)/mL (**A**) and comparison of the HCV RNA levels in 15 serum samples determined by cDNA microarray analysis and RT-PCR (Taqman) assays (**B**).

"nesting" bases at the 3'-end of universal primer, 10 or more subgroups of PCR reaction were performed for various single selective primers or primer combination, in which gene fragments were widely distributed in different groups and their isolation was achieved. We separated the differential genes by polyacrylamide gel electrophoresis and silver staining. Single bands cut out from polyacrylamide gel were isolated. Using the single bands as PCR template, we performed the third-round PCR and a total of 24 different cDNA fragments ranging from 200 to 800 bp were obtained and sequenced, which were the specific gene fragments of HCV. These fragments could be further used as probes in microarray preparation, suggesting that RD-PCR technique is of great value in obtaining a large number of size-comparable gene probes, thus providing a swift protocol in generating probes for the preparation of microarrays.

In general, the density of hybridization signal is correlative to the length of probes, GC contents and T_m value under the same experimental conditions. A further sequence analysis of the 10 probes, GC contents, and T_m value showed that these probes were 250-700 bp in length, and had a high GC content (≥40%) and T_m values (≥82 °C).The probes were widely distributed in the full HCV genome. The results of hybridization and sequence analysis showed that the specificity, sensitivity, accuracy, reproducibility, and linearity in detecting HCV RNA were satisfactory. There was a linear correlation between the concentrations of pCV-J4L6S target cDNA and the signal intensities (correlation coefficient = 0.9819). The detection range of the microarray was 10^4-10^{11} copies/mL. The lower detection limit of HCV RNA was 1.03×10^4 copies/mL, which was 2 log higher than that by RT-PCR (Taqman method). But the assay was as sensitive as the conventional RT-PCR in HCV detection. The chip we developed is cost-effective, and the procedure required to prepare the chip is straightforward and convenient. When results are verified by molecular hybridization, PCR cross contamination can be overcome. By incorporating negative and positive controls, the detection results can be reduced greatly using analytic software[22]. Seventeen serum samples from hepatitis C patients (positive for anti-HCV, ALT≥80) were analyzed, and fifteen patients (88.2%) were positive by microarray assay. Within the detection range of 10^4-10^{11} copies/mL, there was a good correlation between the two assay systems (n = 15, r = 0.9582) (Figure 4B). Ten serum samples from healthy people were also detected by this assay and no specific signal intensities were obtained from the samples. Finally, the reproducibility and accuracy of this assay system were evaluated by repeated measurement, and the within-run coefficient of validation was 6.6%, while the between-run coefficient of validation was 7.6%. However, further work should be done. It took about 10 h to complete our assay. Modifying the DNA extraction procedure could reduce this time. The sensitivity of the assay could be enhanced by increasing the amount of captured cDNA on the slide, or by pretreatment of the sample RNA. A large number of serum samples should be tested to verify the reliability of microarray assay in the detection of HCV.

In conclusion, cDNA microarray technology can be applied to other pathogens and is a useful diagnostic method for HCV infection.

ACKNOWLEDGMENTS

The authors thank Dr Jens Bukh for the presentation of HCV plasmid and Drs Zhang Bao and Shi Rong for critical technical assistance.

REFERENCES

1 **Ogata N**, Alter HJ, Miller RH, Purcell RH. Nucleotide sequence and mutation rate of the H strain of hepatitis C virus. *Proc Natl Acad Sci USA* 1991; **88:** 3392-3396

2 **Choo QL**, Kuo G, Weiner AJ, Overby LR, Bradley DW, Houghton M. Isolation of a cDNA clone derived from a blood-borne non-A, non-B viral hepatitis genome. *Science* 1989; **244:** 359-362

3 **Simmonds P**. Variability of hepatitis C virus. *Hepatology* 1995; **21:** 570-583

4 **Alter HJ**, Purcell RH, Shih JW, Melpolder JC, Houghton M, Choo QL, Kuo G. Detection of antibody to hepatitis C virus

in prospectively followed transfusion recipients with acute and chronic non-A, non-B hepatitis. *N Engl J Med* 1989; **321:** 1494-1500

5 **Hoofnagle JH**, di Bisceglie AM. The treatment of chronic viral hepatitis. *N Engl J Med* 1997; **336:** 347-356

6 **Cui J**, Dong BW, Liang P, Yu XL, Yu DJ. Construction and clinical significance of a predictive system for prognosis of hepatocellular carcinoma. *World J Gastroenterol* 2005; **11:** 3027-3033

7 **Yanagi M**, Purcell RH, Emerson SU, Bukh J. Hepatitis C virus: an infectious molecular clone of a second major genotype (2a) and lack of viability of intertypic 1a and 2a chimeras. *Virology* 1999; **262:** 250-263

8 **Ma WL**, Zheng WL. The research and development of DNA microarray technology. *Sci Found China* 1999; **13**: 270-273

9 **Ma WL**, Zheng WL, James FB. RD-PCR: A new technique of differential display.*In*:Sun yixian(ed).The development of biochemistry and molecular biology in PLA.vol.1. *Beijing: Uniform Medical Publishing*, 1998: 99-113

10 **Zheng WL**, Ma WL, Waes CV. The differential display of poly A polymerase in tumor cells of differential malignancy. *In:* Ye XS(ed). Investigation on cell modulation. vol.1. *Beijing: Uniform Medical Publishinghouse*, 1998: 73-79

11 **Zhao F**, Zhang SJ, Jiang SH. Modification of the technique of staining and the PAGE. *J Clin Exp Patho*l 1999; **15:** 401-402

12 **Sun ZH**, Ma WL, Zheng WL. Microarrays development in the diagnosis of HBV and HCV. *Med J Chin PLA* 2003; **28**: 375-376

13 **Sun ZH**, Zheng WL, Ma WL. The development of molecular diagnosis of viral hepatitis. *Guangdong med J* 2003; **24:** 440-442

14 **Lipshutz RJ**, Fodor SP, Gingeras TR, Lockhart DJ. High density synthetic oligonucleotide arrays. *Nat Genet* 1999; **21:** 20-24

15 **Petrik J**. Microarray technology: the future of blood testing? *Vox Sang* 2001; **80**: 1-11

16 **Zhaohui S**, Wenling Z, Bao Z, Rong S, Wenli M. Microarrays for the detection of HBV and HDV. *J Biochem Mol Biol* 2004; **37:** 546-551

17 **Livache T**, Fouque B, Roget A, Marchand J, Bidan G, Teoule R, Mathis G. Polypyrrole DNA chip on a silicon device: example of hepatitis C virus genotyping. *Anal Biochem* 1998; **255:** 188-194

18 **Stewart DJ**. Making and using DNA microarrays: a short course at Cold Spring Harbor Laboratory. *Genome Res* 2000; **10:** 1-3

19 **Sun ZH**, Zheng WL, Mao XM, Zhang B, Lu L, Ma XD, Shi R, Ma WL. Rapid preparation of DNA microarray using PCR for hepatitis B and D virus detection. *Di Yi Jun Yi Da Xue Xue Bao* 2003; **23:** 677-679

20 **Wang HY**, Malek RL, Kwitek AE, Greene AS, Luu TV, Behbahani B, Frank B, Quackenbush J, Lee NH. Assessing unmodified 70-mer oligonucleotide probe performancs. *Orv Hetil* 1998; **139:** 957-960

Science Editors Wang XL and Guo SY **Language Editor** Elsevier HK

PO Box 2345, Beijing 100023, China
www.wjgnet.com
wjg@wjgnet.com

ELSEVIER

World J Gastroenterol 2005;11(48):7585-7590
World Journal of Gastroenterology ISSN 1007-9327

Response of porcine hepatocytes in primary culture to plasma from severe viral hepatitis patients

Yong-Bo Cheng, Ying-Jie Wang, Shi-Chang Zhang, Jun Liu, Zhi Chen, Jia-Jia Li

Yong-Bo Cheng, Ying-Jie Wang, Shi-Chang Zhang, Jun Liu, Zhi Chen, Jia-Jia Li, Institute of Infectious Diseases, Southwest Hospital, Third Military Medical University, Chongqing 400038, China
Supported by National Natural Science Foundation of China, No. 30470458
Correspondence to: Ying-Jie Wang, MD, Institute of Infectious Diseases, Southwest Hospital, Third Military Medical University, Chongqing 400038, China. wangyj103@263.net
Telephone: +86-23-68754479-8062
Received: 2005-04-14 Accepted: 2005-06-24

Abstract

AIM: To observe the effects of plasma from patients with severe viral hepatitis (SVHP) on the growth and metabolism of porcine hepatocytes and the clinical efficiency of bioartificial liver device.

METHODS: Hepatocytes were isolated from male porcines by collagenase perfusion. The synthesis of DNA and total protein, leakages of AST and LDH, changes in glutathione (GSH), catalase and morphology of porcine hepatocytes exposed to SVHP were investigated to indicate the effect of plasma from patients with severe hepatitis on the growth, injury, detoxification, and morphology of porcine hepatocytes.

RESULTS: The synthesis of DNA and protein was inhibited in the medium containing 100% SVHP compared to the controls. The leakages of LDH and AST increased in porcine hepatocytes following exposure to 100% SVHP for 5 h. The difference between 100% SVHP and 10% newborn calf serum (NCS) was significant in t-test (LDH: t = 24.552, P = 0.001; AST: t = 4.169, P = 0.014). After exposure to SVHP for 24 h, alterations in GSH status were significant (F = 2.746, P<0.05) between porcine hepatocytes in 100% SVHP and 10% NCS, but no alteration occurred in the culture medium after 48 h (F = 4.378, P<0.05). A similar profile was observed in catalase activity. Many round vacuoles were observed in porcine hepatocytes cultured in SVHP. The membranes of these cells became indistinct and almost all the cells died on d 5.

CONCLUSION: Plasma from patients with severe hepatitis inhibits the growth, injures membrane, disturbs GSH homeostasis and induces morphological changes of porcine hepatocytes. It is suggested that SVHP should be pretreated to reduce the toxin load and improve the performance of porcine hepatocytes in extracorporeal liver-support devices.

Key words: Bioartificial liver; Porcine hepatocytes; Cell culture; Plasma toxicity

Cheng YB, Wang YJ, Zhang SC, Liu J, Chen Z, Li JJ. Response of porcine hepatocytes in primary culture to plasma from severe viral hepatitis patients. *World J Gastroenterol* 2005; 11(48):7585-7590
http://www.wjgnet.com/1007-9327/11/7585.asp

INTRODUCTION

A bioartificial liver (BAL) support system, composed of artificial materials and biological components such as hepatocytes, acts as a bridge to provide patients with prolonged time of survival until a donor organ becomes available for the transplantation or their own liver can regenerate[1]. The performance of a BAL depends on the viability and functional activities of hepatocytes in the system. Many laboratories are currently investigating the factors influencing the viability and functional activities of hepatocytes. It has been demonstrated that serum or plasma from liver failure patients interferes extensively with cellular metabolism[2-6]. When the patient's blood is detoxified by the BAL device, there is contact between the patient's plasma and cells in the device. It is thus important to assess the direct interactions between plasma and hepatocytes.

Porcine and human hepatocytes have similar physiological characteristics and metabolic functions and are considered to be the best candidate for use in a BAL[7-11]. They have been applied in clinical trials based on their easy source and excellent functions for the synthesis of protein, glucose, and urea as well as lower lactate dehydrogenase release. *In vitro*, porcine hepatocytes in the bioreactor can clear most conjugated bile acid species from pooled patient plasma[6]. Furthermore, it can be immobilized on a "hepatocyte/gold colloid" interface at which hepatocytes proliferate quickly[12].

In China, HBV infection rate has been estimated to be 10% or higher, and severe hepatitis caused by HBV is common[13,14]. BAL also provides temporary support for these patients when acute or chronic severe viral hepatitis (SVHP) develops. However, there are few reports on

how SVHP interferes with the growth and function of hepatocytes in primary culture. Therefore, we investigated the direct interactions between SVHP and porcine hepatocytes.

MATERIALS AND METHODS

Materials

Cell culture reagents, including RPMI-1640, sodium pyruvate, and L-glutamine were purchased from GIBCO, Life Technologies, Ltd. (Paisley, Scotland, UK). Type IV collagenase was a product of Sigma Chemical Co, Ltd (St. Louis, MO, USA). Reagents for the measurement of reduced glutathione (GSH), catalase (CAT) and total protein (TP) were from Nanjing Biological Technology Co, Ltd. Methyl thiazolyl tetrazolium (MTT) was from Fluka Chemic AG (Switzerland). TriPure isolation reagent was from Roche (Switzerland). Plasticware was from Nunc (Denmark). All solutions were prepared with twice-distilled water.

Hepatocyte preparation

Healthy Chinese experimental miniature male pigs aged 1-4 d were provided by Experimental Animal Center of Third Military Medical University. The research protocol was in compliance with Chinese guidelines for the humane care of experimental animals. Porcine hepatocytes were isolated by modified two-step *in situ* collagenase perfusion method[15,16]. The viability of freshly isolated suspensions determined by trypan blue exclusion was 85-95%. Porcine hepatocytes were cultured at 37 °C for 24 h in RPMI-1640 medium supplemented with 10% (vol/vol) newborn calf serum (NCS) at a density of 2×10^5 cells/mL in a 50 mL/L CO_2 incubator. The cultures were washed twice in warm phosphate-buffered saline (PBS) and cultured in a medium containing 10% (vol/vol) NCS, normal plasma (NP) anti-coagulated by heparin, and SVHP. Porcine hepatocytes were prepared for assay as described below.

Plasma from patients with severe virus hepatitis

Plasma was obtained from six patients with SVHP (3 females, 3 males, aged 34-60 years) at the onset of plasmapheresis and stored at -80 °C until use. Diagnosis of these patients was in accordance with the criteria of severe hepatitis described in the Viral Hepatitis Protection and Cure Guideline established by the Chinese Infection and Hepatology Association. In these six patients, total bilirubin (TB) averaged 611.8 μmol/L, prothrombin time (PT) averaged 32 s, total bile acids (TBA) averaged 309.8 μmol/L and PTa averaged 29%. Hepatitis B surface antigen (HBsAg) was positive and HBV-DNA was greater than 10^5 copies/mL in all the 6 patients. All patients suffered from hepatic encephalopathy, grade II in two patients, grade III in three patients, and grade IV in one patient. Normal serum was obtained from normal individuals.

Cell viability determination

Cells were seeded in 24-well plates in 500 μL medium. The viability was assessed by tetrazolium bromide assay (MTT) on d 0-5 after exposure to the culture medium containing 10% (vol/vol) NCS, 100% NP, and 100% SVHP.

DNA synthesis

After being cultured in six-well plates for 24 h, the media were discarded, and DNA was isolated as the procedures of TriPure isolation reagent description. DNA content was determined using a spectrophotometer (SmartSpec 3000, BioRad, USA).

Protein content

After being incubated for 24 and 48 h, monolayer cells were washed and dissolved. Total cellular protein was digested in 0.5 mol/L NaOH and measured by micromodification as previously described[17].

Leakage of LDH and AST

Porcine hepatocytes were exposed to 100% SVHP and 10% (vol/vol) NCS in RPMI-1640 for 5 h. The media were washed thrice with PBS and replaced with RPMI-1640 without plasma and serum. After 24 h of culture, the leakage of LDH and AST from hepatocytes into the supernatant was measured using an automated chemical analyzer (Model 7020 Hitachi Co., Tokyo, Japan)[18].

Oxidative status

After being incubated for 24 and 48 h, the medium containing 10% NCS, 100% NP, 100% SVHP was removed, the wells were washed with PBS, and GSH was added into 0.2 mL 10% (w/v) trichloroacetic acid for 10 min at room temperature. Samples were frozen at -20 °C until measurement of GSH by fluorimetry. CAT activity was measured.

Morphology

Cultured hepatocytes were observed daily under phase contrast microscope (IX70, Olympus, Tokyo, Japan), and the morphological changes were compared.

Statistical analysis

Data were expressed as mean±SD. Statistical analysis was carried out by analysis of variance and *t*-test. $P<0.05$ was considered statistically significant.

RESULTS

Viability of porcine hepatocytes cultured in SVHP

The viability of porcine hepatocytes cultured in 100% SVHP was significantly lower than that cultured in the medium containing 10% NCS ($F = 6.328$, $P<0.01$). The viability of porcine hepatocytes in 100% NP group was not higher than that in 10% NCS group. The viability of porcine hepatocytes in all the groups tended to decrease from the third day (Figure 1).

DNA content

After being cultured for 24 h, the DNA level in three

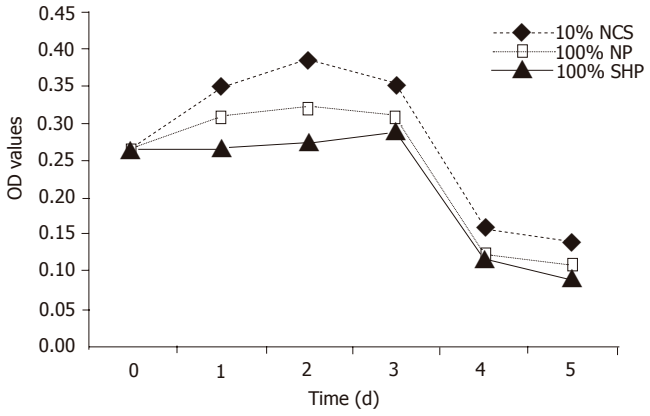

Figure 1 Viability of porcine hepatocytes cultured in ♦ medium containing 10% NCS, □ 100% NP, ▲ 100% SVHP. Results were expressed as mean±SD for six samples.

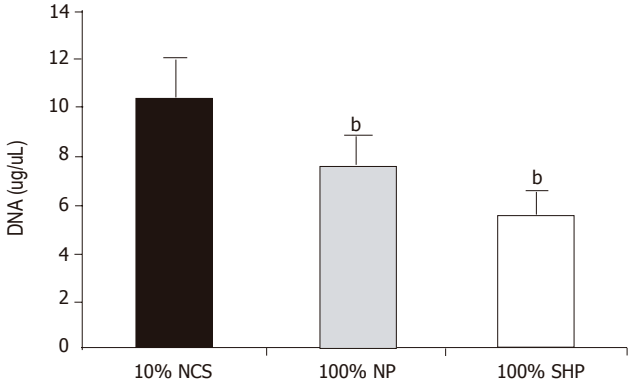

Figure 2 DNA content in porcine hepatocytes grown in three different media. DNA synthesis in 100% SVHP and normal plasma was compared to that in the medium containing 10% NCS (^bP<0.01 *vs* 10% NCS group, by ANOVA followed by multiple comparisons). Results were expressed as mean±SD for six samples Black oblique line: 10% NCS, black small point: 100% NP; black small square: 100% SVHP.

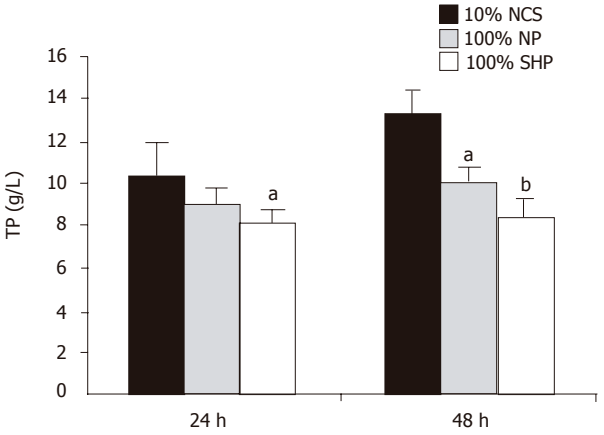

Figure 3 TP content in porcine hepatocytes grown in three different media. TP synthesis in 100% SVHP and NP was compared to that in the medium containing 10% NCS (^aP<0.05, ^bP<0.01 *vs* 10% NCS group, by two-way variance analysis). Results were expressed as mean±SD for six samples. Black bar: 10% NCS; gray bar: 100% NP; white bar: 100% SVHP.

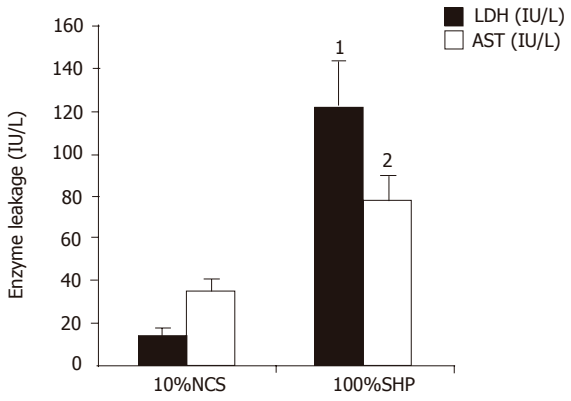

Figure 4 Leakage of LDH and AST after 5 h of culture (black bar: LDH; white bar: AST). The levels of LDH and AST in 100% SVHP were significantly higher than those in the medium containing 10% NCS. Results were expressed as mean±SD (1: t = 24.552, P = 0.001 and 2: t = 4.169, P = 0.014, compared to the10% NCS group, n = 6).

different media was significantly different (F = 20.107, P<0.01). The level was the lowest in 100% SVHP and lower in 100% NP than in 10% NCS. The inhibitory effect of porcine hepatocytes on DNA synthesis is shown in Figure 2.

Total protein synthesis

During the course of culture, the amount of TP in three different media was significantly different (F = 9.281, P<0.01, Figure 3). Multiple comparison showed that the TP level in 100% SVHP was lower than that in 10% NCS (P<0.01). The TP level in 100% NP was also significantly lower than that in 10% NCS (P<0.05).

Leakage of LDH and AST

LDH and AST elevations were observed in 100% SVHP group after 5 h of culture. The LDH level in 100% SVHP group was significantly higher than that in 10% NCS group (t = 24.552, P = 0.001). The AST level in 100% SVHP group was also significantly higher than that in 10% NCS group (t = 4.169, P = 0.014, Figure 4), indicating that hepatocytes cultured in plasma from patients with SVHP had damage in the cell membrane.

GSH content and CAT activity

GSH concentration in porcine hepatocytes decreased in SVHP and NP as compared to that in the culture medium containing 10% NCS (Figure 5A). A significant decrease in GSH content was observed in SVHP compared to that in the medium containing 10% NCS within 24 h (F = 2.746, P<0.05). After 48 h the GSH level declined slightly. There was no difference between 100% SVHP and 10% NCS (F = 4.378, P>0.05). A similar profile was observed in CAT levels following incubation with SVHP and NP (Figure 5B). The only difference between GSH and CAT was that the CAT content was dramatically decreased after being cultured for 48 h.

Morphological study

The dramatic change of porcine hepatocyte morphology

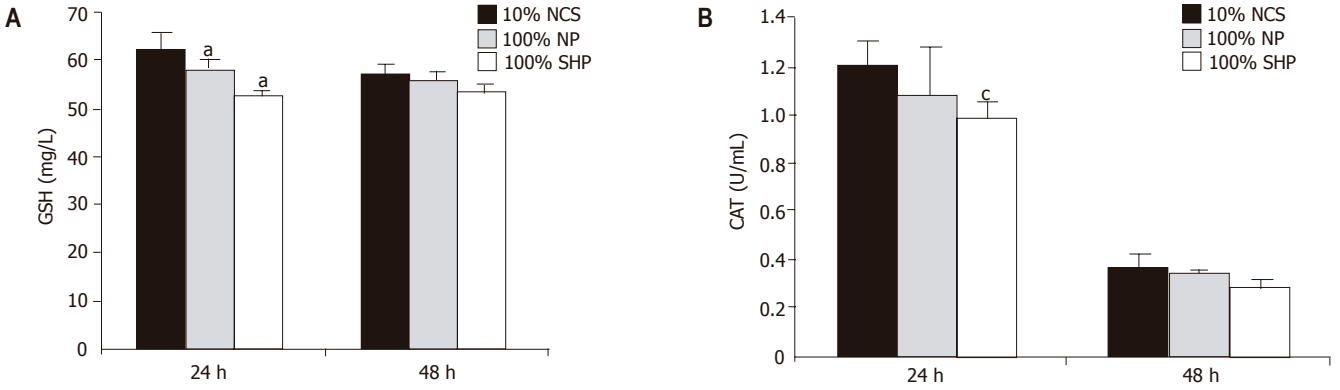

Figure 5 GSH content in porcine hepatocytes grown in three different cultures (**A**) ($^{a}P<0.05$ *vs* 10% NCS, by two-way variance analysis, compared to 10% NCS) and CAT activity of porcine hepatocytes grown in the three different cultures (**B**) ($^{c}P<0.05$ *vs* 10% NCS by two-way variance analysis, compared to 10% NCS). Black bar: 10% NCS, gray bar: 100% NP; white bar: 100% SVHP.

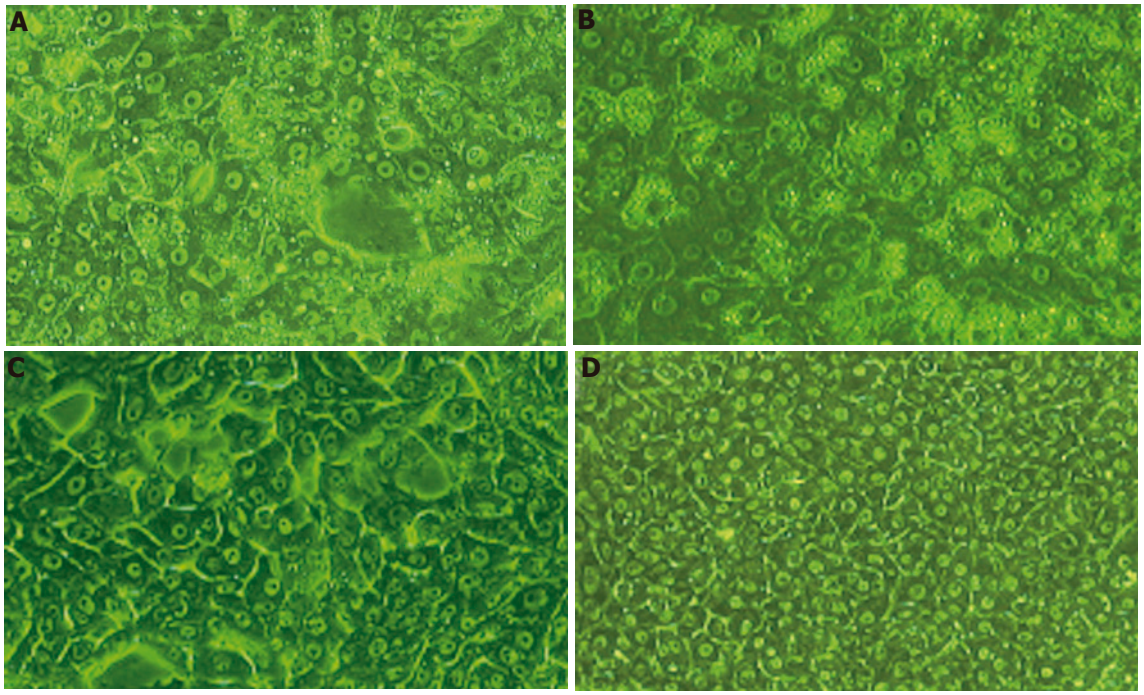

Figure 6 Morphological changes of porcine hepatocytes cultured in 100% SVHP **(A** and **B**) and media containing 10% NCS (**C** and **D**). After 24 h of culture, hepatocytes in the100% SVHP group were detached from the dishes, vacuolization in the cytoplasm and deformities were more commonly observed. The membranes of cells became indistinct (**A**); after 48 h of culture, vacuoles were more and mainly concentrated around cell nuclei (**B**); after 24 h of culture, hepatocytes in the 10% NCS group constituted confluent monolayers with an intact morphology throughout the culture (**C**); after 48 h of culture, hepatocytes in the 10% NCS group constituted confluent monolayers with an intact morphology throughout the culture (**D**).

after 24 h exposure to 100% SVHP was observed under phase contrast microscope. As shown in Figures 6A-D, most of the cells became detached and deformed. Vacuolization in cytoplasm and necrosis were more commonly observed. Membranes of the cells became indistinct. These morphological changes became marked after 48 h of culture. Vacuoles were mainly concentrated around cell nuclei and detached from their dishes. During the 48-h culture, hepatocytes in groups of 100% NP and 10% NCS spread and formed a clear confluent monolayer. Detachment, deformity, and vacuolization were not observed in the cytoplasm. There was no obvious difference between the two groups. After 5 d of culture, necrosis was observed in the two groups and almost all hepatocytes were dead in 100% SVHP group.

DISCUSSION

Experimental studies[3-5] have demonstrated that plasma from patients with fulminant hepatic failure (FHF) or liver failure (LF) can inhibit the growth of hepatocytes and synthesis of macromolecules in hepatocytes. McCloskey *et al*.[5] found that plasma from patients with liver failure could diminish DNA and protein synthesis.

Shi *et al*.[4] reported that serum from patients with FHF inhibits the growth rate and synthesis of DNA, RNA, and protein. In our study, the plasma was from patients with SVHP. Inhibition of growth and macromolecule synthesis, reduction of viability of porcine hepatocytes were demonstrated. The inhibition mechanism might be related to endogenic materials such as bile acids, growth factors, and cytokines in SVHP. There are more bile acids, hepatic growth factor (HGF) and tumor growth factor-β (TGF-β)[19] in SVHP. Accumulation of intracellular bile acids causes damage to intracellular organelles, such as mitochondria[20]. Bile acids in nuclei cause DNA injury by changing chromatin structure or by activating nuclear nuclease, thus resulting in conversion into a metabolite that could directly damage DNA[21,22]. HGF does not always accelerate the growth of hepatocytes. Sometimes there are converse results[23]. It was reported that HGF inhibits cell growth at a cell cycle phase and growth of cells is impaired with the increasing HGF concentration, while elevated serum TGF may lead to an increase in p21, a cyclin-dependent kinase inhibitor that can inhibit the activation of G1-associated cyclins such as Cdk2[24,25]. In this study, the viability of porcine hepatocytes cultured in 100% NP was decreased compared to that in 10% NCS, which may result from cytokine- and antibody-mediated damage.

Membrane damage and enzyme leakage have been detected in the culture medium[5,26,27]. McCloskey *et al*.[5] reported that after HHY41 hepatocytes are exposed to plasma from patients with LF containing $Na_2{}^{51}CrO_4$ for 16 h, the leakage of ^{51}Cr is about 20 times higher than that in controls. However, Uchino *et al*.[28] demonstrated that the function of pig hepatocytes does not deteriorate when they are exposed to the serum from the patients with FHF[28]. In this study, LDH and AST leakage from porcine hepatocytes cultured in SVHP was significantly higher than that from porcine hepatocytes cultured in 10% NCS. Morphological changes of hepatocytes also suggested severe cell membrane damage, indicating that SVHP can lead to hepatocellular membrane impairment. Endogenic toxins may originate either from cellular necrosis debris and breakdown products released into the blood stream or from accumulation of an agent that is normally eliminated by metabolism in hepatocytes. Bile acids play an important role in the toxicities and can form micelles with cholesterol and phospholipids on the surface of hepatocyte membranes, which produce apparent hepatocellular membrane injury[22]. Virus-mediated damage involves immune-mediated and direct viral cytopathic effects.

The highest cytotoxicity values have been found in the plasma from patients with FHF, indicating the utmost importance of detoxification by BAL. Intracellular GSH content often reflects the fate of potentially harmful substances, and examination of GSH status may provide information on the mechanisms of toxicity. Previous experimental studies revealed that exposure of hepatocytes to the serum from patient with FHF results in increase or decrease in GSH content. The changes are related to plasma concentration, culture time, hepatocyte type[4,5]. Previous studies have shown that Hep G2 cells respond to abnormal culture conditions and toxic concentrations of bile. GSH of HHY41 in plasma from patients with LF is decreased[5]. In our study, the pronounced decrease in GSH levels was observed following incubation with SVHP. As a main member of anti-oxidizing system, GSH plays an important role in relieving the tissue depression due to electrophilic reactive toxins or oxidative stress because it can react directly with reactive oxygen free-radicals and conjugate bile acids[29].These factors lead to a depletion of cellular GSH store. The activity of CAT changes as GSH, which requires further investigation.

REFERENCES

1 **Hui T**, Rozga J, Demetriou AA. Bioartificial liver support. *J Hepatobiliary Pancreat Surg* 2001; 8: 1-15

2 **Hughes RD**, Cochrane AM, Thomson AD, Murray-Lyon IM, Williams R. The cytotoxicity of plasma from patients with acute hepatic failure to isolated rabbit hepatocytes. *Br J Exp Pathol* 1976; **57:** 348 348-353

3 **Gove CD,** Hughes RD, Williams R. Rapid inhibition of DNA synthesis in hepatocytes from regenerating rat liver by serum from patients with fulminant hepatic failure. *Br J Exp Pathol* 1982; **63:** 547-553

4 **Shi Q,** Gaylor JD, Cousins R, Plevris J, Hayes PC, Grant MH. The effects of serum from patients with acute liver failure on the growth and metabolism of Hep G2 cells. *Artif Organs* 1998; **22:** 1023-1030

5 **McCloskey P**, Tootle R, Selden C, Larsen F, Roberts E, Hodgson HJ. Modulation of hepatocyte function in an immortalized human hepatocyte cell line following exposure to liver-failure plasma. *Artif Organs* 2002; **26:** 340-348

6 **Pazzi P**, Morsiani E, Vilei MT, Granato A, Rozga J, Demetriou AA, Muraca M. Serum bile acids in patients with liver failure supported with a bioartificial liver. *Aliment Pharmacol Ther* 2002; **16:** 1547-1554

7 **Rozga J**, Williams F, Ro MS, Neuzil DF, Giorgio TD, Backfisch G, Moscioni AD, Hakim R, Demetriou AA. Development of a bioarti.cial liver: properties and function of a hollow module inoculated with livers cells. *Hepatology* 1993; **17:** 258–265

8 **Watanabe FD**, Mullon CJ, Hewitt WR, Arkadopoulos N, Kahaku E, Eguchi S, Khalili T, Arnaout W, Shackleton CR, Rozga J, Solomon B, Demetriou AA. Clinical experience with a bioartificial liver in the treatment of severe liver failure. A phase I clinical trial. *Ann Surg* 1997; **225:** 484-91; discussion 491-494

9 **Khalili TM**, Navarro A, Ting P, Kamohara Y, Arkadopoulos N, Solomon BA, Demetriou AA, Rozga J. Bioarti.cial liver treatment prolongs survival and lowers incranial pressure in pigs with fulminant hepatic failure. *Artif Organs* 2001; **25:** 566–570

10 **Nagaki M**, Miki K, Kim YI, Ishiyama H, Hirahara I, Takahashi H, Sugiyama A, Muto Y, Moriwaki H. Development and characterization of a hybrid bioartificial liver using primary hepatocytes entrapped in a basement membrane matrix. *Dig Dis Sci* 2001; **46:** 1046-1056

11 **Mears DC**, Stewart G, Sun J, Woodman K, Bourne R, Wang L, Sheil AG. Experience with a porcine hepatocyte-based bioartificial liver support system. *Transplant Proc* 2003; **35:** 441 –442

12 **Gu HY**, Chen Z, Sa RX, Yuan SS, Chen HY, Ding YT, Yu AM. The immobilization of hepatocytes on 24 nm-sized gold colloid for enhanced hepatocytes proliferation. *Biomaterials* 2004; **25:** 3445-3451

13 **Merican I**, Guan R, Amarapuka D. Chronic hepatitis B virus infection in Asian countries. *J Gastroenterol Hepatol* 2000; **15:** 1356-1361

14 **Pokorski RJ**, Ohlmer U. Long-term morbidity and mortality

in Chinese insurance applicants infected with the hepatitis B virus. *J Insur Med* 2001; **33:** 143-164
15 **Chen Z**, Ding Y, Zhang H. Cryopreservation of suckling pig hepatocytes. *Ann Clin Lab Sci* 2001; **31:** 391-398
16 **Wang YJ**, Liu HL. Mass isolation and cryopreservation of hepatocytes. In: Wang YJ, eds. Bioartificial Liver. *Beijing-China: People's Health Publishing House* 2000: 207-2009.
17 **Lowry OH**, Rosebrough NJ, Farr AL, Randall RJ. Protein measurement with the Folin phenol reagent. *J Biol Chem* 1951; **193:** 265-275
18 **Flendrig LM**, la Soe JW, Jorning GG, Steenbeek A, Karlsen OT, Bovee WM, Ladiges NC, te Velde AA, Chamuleau RA. In vitro evaluation of a novel bioreactor based on an integral oxygenator and a spirally wound nonwoven polyester matrix for hepatocyte culture as small aggregates. *J Hepatol* 1997; **26:** 1379-1392
19 **Nozato E**, Shiraishi M, Nishimaki T. Up-regulation of hepatocyte growth factor caused by an over-expression of transforming growth factor beta, in the rat model of fulminant hepatic failure. *J Surg Res* 2003; **115:** 226-234
20 **Hoshino M**, Ohiwa T, Hayakawa T, Kamiya Y, Tanaka A, Hirano A, Kumai T, Katagiri K, Miyaji M, Takeuchi T. Effects of dibutyryl cyclic AMP and papaverine on intrahepatocytic bile acid transport. Role of vesicle transport. *Scand J Gastroenterol* 1993; **28:** 833-838
21 **Russo P**, Taningher M, Pala M, Pisano V, Pedemonte P, De Angeli MT, Carlone S, Santi L, Parodi S. Characterization of the effects induced on DNA in mouse and hamster cells by lithocholic acid. *Cancer Res* 1987; **47:** 2866-2874
22 **Kulkarni MS**, Cox BA, Yielding KL. Requirements for induction of DNA strand breaks by lithocholic acid. *Cancer Res* 1982; **42:** 2792-2795
23 **Drixler TA**, Vogten MJ, Ritchie ED. Liver regeneration is an angiogenesis associated phenomenon. *Ann Surg* 2002; **236:** 703-711
24 **Albrecht JH**, Meyer AH, Hu MY. Regulation of cyclin-dependent kinase inhibitor p21(WAF1/Cip1/Sdi1) gene expression in hepatic regeneration. *Hepatology* 1997; **25:** 557-563
25 **Sugiyama A**, Nagaki M, Shidoji Y, Moriwaki H, Muto Y. Regulation of cell cycle-related genes in rat hepatocytes by transforming growth factor beta1. *Biochem Biophys Res Commun* 1997; **238:** 539-543
26 **Ohiwa T**, Katagiri K, Hoshino M, Hayakawa T, Nakai T. Tauroursodeoxycholate and tauro-beta-muricholate exert cytoprotection by reducing intrahepatocyte taurochenodeoxycholate content. *Hepatology* 1993; **17:** 470-476
27 **Heuman DM**, Pandak WM, Hylemon PB, Vlahcevic ZR. Conjugates of ursodeoxycholate protect against cytotoxicity of more hydrophobic bile salts: in vitro studies in rat hepatocytes and human erythrocytes. *Hepatology* 1991; **14:** 920-926
28 **Uchino J**, Matsue H, Takahashi M, Nakajima Y, Matsushita M, Hamada T, Hashimura E. A hybrid artificial liver system. Function of cultured monolayer pig hepatocytes in plasma from hepatic failure patients. *ASAIO Trans* 1991; **37:** M337-M338
29 **Smirthwaite AD**, Gaylor JD, Cousins RB, Grant MH. Cytotoxicity of bile in human Hep G2 cells and in primary cultures of rat hepatocytes. *Artif Organs* 1998; **22:** 831-836

Science Editors Wang XL and Guo SY **Language Editor** Elsevier HK

PO Box 2345, Beijing 100023, China
www.wjgnet.com
wjg@wjgnet.com

ELSEVIER

World J Gastroenterol 2005;11(48):7591-7596
World Journal of Gastroenterology ISSN 1007-9327

Hepatitis C virus infection down-regulates the expression of peroxisome proliferator-activated receptor α and carnitine palmitoyl acyl-CoA transferase 1A

Yang Cheng, Sébastien Dharancy, Mathilde Malapel, Pierre Desreumaux

Yang Cheng, Sébastien Dharancy, Mathilde Malapel, Pierre Desreumaux, Equipe mixte INSERM 0114, Université de Lille, CHU, Lille 59037, France
Supported by the National Natural Science Foundation of China, No.30300458
Correspondence to: Yang Cheng, Institute of Liver Diseases, Shanghai University of TCM, Shanghai 201203, China. yangcheng@myrealbox.com
Telephone: +86-21-51322444 Fax: +86-21-51322445
Received: 2005-03-31 Accepted: 2005-04-18

Abstract

AIM: To elucidate the role of the peroxisome proliferator-activated receptor α (PPARα) and its target gene carnitine palmitoyl acyl-CoA transferase 1A (CPT1A) in the pathogenesis of hepatitis C virus (HCV) infection.

METHODS: Liver samples were collected from the patients with chronic HCV infection and controls. HepG2 cells were transfected with vector pEF352neo carrying. Two independent clones (clone N3 and N4) stably expressing HCV core protein were analyzed. Total RNA was extracted from cells and liver tissues. PPARα and CPT1A mRNAs were quantified by real-time polymerase chain reaction (PCR) using SYBR Green Master. Total extracted proteins were separated by polyacrylamide gel electrophoresis, and electroblotted. Membranes were incubated with the anti-PPARα antibody, then with a swine anti-rabbit IgG conjugated to horseradish peroxidase for PPARα. Protein bands were revealed by an enhanced chemiluminescence reaction for PPARα. For immunohistochemical staining of PPARα, sections were incubated with the primary goat polyclonal antibody directed against PPARα at room temperature.

RESULTS: Real-time PCR indicated that the PPARα level and expression level of CPT1A gene in hepatitis C patients lowered significantly as compared with the controls (1.8±2.8 *vs* 13±3.4, $P = 0.0002$; 1.1±1.5 *vs* 7.4±1, $P = 0.004$). Western blot results showed that the level of PPARα protein in the livers of hepatitis C patients was lower than that in controls (2.3±0.3 *vs* 3.6±0.2, $P = 0.009$). The immunohistochemical staining results in chronic hepatitis C patients indicated a decrease in PPARα staining in hepatocytes compared with those in the control livers. The *in vitro* studies found that in the N3 and N4 colon stably expressing HCV core protein, the PPARα mRNA levels were significantly lower than that in the controls.

CONCLUSION: The impaired intrahepatic PPARα expression is associated with the pathogenic mechanism in hepatic injury during chronic HCV infection. HCV infection reduced the expression of PPARα and CPT1A at the level of not only mRNAs but also proteins. PPARα plays an important role in the pathogenesis of chronic HCV infection, but the impaired function of this nuclear receptor in HCV infection needs further studies.

Key words: Hepatitis C virus; Infection; PPARα; CPT1A

Cheng Y, Dharancy S, Malapel M, Desreumaux P. Hepatitis C virus infection down-regulates the expression of peroxisome proliferator-activated receptor α and carnitine palmitoyl acyl-CoA transferase 1A. *World J Gastroenterol* 2005; 11(48): 7591-7596
http://www.wjgnet.com/1007-9327/11/7591.asp

INTRODUCTION

Hepatitis C virus (HCV) infection is a major health care problem around the world[1]. It is estimated that there are about 170 million chronic carriers worldwide with four million in the USA[2-4] and five million in the western Europe[5-6]. HCV infection accounts for 20% of cases of acute hepatitis, 70% of chronic hepatitis, 40% of end-stage cirrhosis, 60% of cases of hepatocellular carcinoma, and 30% of liver transplantation[7-10]. Liver lesions are thought to be mainly related to immune-mediated mechanisms[5] but the exact mechanisms during HCV infection are still unclear[8,9,11]. However, the HCV core protein is a major component of viral nucleocapsid and it is a multifunctional protein that affects transcription and cell growth[12]. HCV core protein plays an important role in the HCV pathogenesis[13].

The ability of peroxisome proliferators to activate a receptor in the steroid receptor superfamily was first discovered in 1990[14], and the cognate protein was designated as peroxisome proliferator-activated receptors (PPARs). The PPARs are soluble transcription factors that are activated by a diverse class of lipophilic compounds[15].

With the activation of PPAR, a concomitant induction of a number of genes that code for peroxisomal fatty acid metabolizing enzymes was observed in mouse liver. There are three PPAR subtypes: PPARα (NR1C1), PPARβ (NR1C2), and PPARγ (NR1C3); and each subtype is capable of binding to DNA after heterodimerizing with RXR (NR2B1). PPARα is highly expressed in the liver, kidney, and cardiac smooth muscles. Many of the genes regulated by PPARα are involved in fatty acid metabolism[16]. PPARα could influence fatty acid import into hepatocyte mitochondria by up-regulating the expression of the liver-predominant mitochondrial carnitine palmtoylacyl-CoA transferase 1 (CPT1) gene[17].

Three CPT1 isoforms with various tissue distributions and encoded by distinct genes have been identified: CPT1A or L-CPT1 (liver isoform), CPT1B or M-CPT1 (muscle isoform), and CPT1C (brain isoform). CPT1A is expressed in the liver, the neonatal heart, and a number of other tissues, and has been the most investigated member of the acyltransferase family. It is anchored in the mitochondrial outer membrane by two transmembrane segments (TM1 and TM2), its N terminus (residues 1-47) and C-terminal catalytic domain (residues 123-773) being located on the cytosolic face of mitochondria. The N-terminal domain (1-147 residues) was shown to be essential for mitochondrial import and for the maintenance of a folded active and malonyl-CoA-sensitive conformation[18].

Until now, the role of PPARα and its target gene CPT1A in liver diseases is still limited to animal studies. In order to elucidate the mechanism of PPARα during the pathogenesis of HCV infection, PPARα and CPT1A expression levels were studied *ex vivo* and *in vitro,* respectively in this study.

MATERIALS AND METHODS

Subjects and liver samples processing

Chronic hepatitis C infection was defined by increased serum alanine transaminase activity (>35 IU/L), positive serum HCV replication determined by polymerase chain reaction (PCR; Amplicor Monitor v2.0; Roche, Indianapolis, IN, USA), and histological hepatic injury quantified by the METAVIR score evaluating the intensity of fibrosis (F1-F4) and necroinflammatory activity (A1-A3)[19]. The subjects were excluded if their body mass index was greater than 30 or if they suffered from diabetes or dyslipidemia.

Patient liver samples were collected from 46 patients with chronic HCV infection (41 transcutaneous needle liver biopsy samples from chronic hepatitis C patients and 5 surgical liver samples from HCV-related cirrhotic patients when they underwent transplantation). Non-HCV-infected liver tissues as controls were collected from 40 patients (29 normal tissue samples from patients who underwent surgery because of hepatic carcinoma, 5 biopsy samples from patients with alcoholic cirrhosis, and 6 samples from patients with alcoholic hepatitis). Both patients and controls did not receive any therapy (antiviral therapy, hepatotoxic drugs, corticosteroids, or immunosuppressive drugs) before or during liver sample collection.

The liver samples collected from hepatitis C patients or controls were divided into two parts: one part was fixed in 4% paraformaldehyde/phosphate-buffered saline and embedded in paraffin wax, and routinely processed for pathological analysis and for immunostaining[20]. Specimen slides were incubated for 48 h at 37 °C and then deparaffinized by dimethylbenzene and rehydrated by graded alcohol series, then stained with H&E, safran, and Masson's trichrome. The other part was frozen immediately in the liquid nitrogen and stored at -80 °C for mRNA and protein analysis.

HepG2 cell culture and transfection

Human hepatocellular carcinoma cell line HepG2 was used for this study. Cells were maintained in Dulbecco's modified Eagle's medium (Sigma-Aldrich, St. Louis, MO, USA) supplemented with 10% heat-inactivated fetal bovine serum (Eurobio, Les Ulis, France) in a humidified atmosphere of 50 mL/L CO_2 in air at 37 °C.

In order to analyze the effect of the HCV core protein on PPARα expression, HepG2 cells were transfected with vector pEF352neo carrying, under the control of the elongation factor-1α promoter, an HCV complementary DNA including 1b HCV sequences from core to NS3 region as previously described[21]. Two independent clones (clone N3 and N4) stably expressing HCV core protein were analyzed. The clone transfected with the empty vector acted as negative control. Cells were resuspended in lysis buffer with 10% β-mercaptoethanol for RNA isolation[22]. All studies were performed in triplicate samples for three separate experiments.

RNA extraction and the real-time PCR analysis

Total RNA was extracted from cells and liver tissues by RNeasy kit (Macherey Nagel, Hoerdt, France) and TRIzol reagent (Life Technologies, Cergy Pontoise, France) following the protocols provided by the manufacturers with some modification[20]. RNA quantification was performed using spectrophotometry. After treatment at 37 °C for 30 min with 20-50 U of RNase-free DNase I (Roche Diagnostics Corporation), oligo-dT primers (Roche Diagnostics Corporation) were used to synthesize single-stranded complementary DNA. PPARα and CPT1A mRNAs were quantified using SYBR Green Master Mix (Applera, Courtaboeuf, France) with specific primers in a GeneAmp ABI prism 7000 (Applera). The primers used were as follows: PPARα anti-sense 5'-CCA CCA TCG CGA CCA GAT-3', PPARα sense 5'-GAC GTG CTT CCT GCT TCA TAG A-3'; CPT1A anti-sense 5'-TGT GCT GGA TGG TGT CTG TCT C-3', CPT1A sense 5' -CGT CTT TTG GGA TCC ACG ATT-3'; TBP anti-sense 5'-TTT TCT TGC TGC CAG TCT GGA C-3', TBP sense 5'-CAC GAA CCA CGG CAC TGA TT-3'. Calibrated and nontemplate controls were included in each assay. Each sample was run in triplicate. SYBR Green dye intensity was analyzed using the ABI prism 7000 SDS software (Applera). All results were normalized to the

TATA box-binding protein, an unaffected housekeeping gene[23]. All quantifications were performed in triplicate samples for three separate experiments.

Western blotting analysis

Protein preparation and immunoblotting were performed in liver specimens as described before. Total protein extracts were obtained by homogenization of tissues in an extraction buffer containing phosphate-buffered saline with 1% tergitol NP-40, 0.5% sodium desoxycholate, 0.1% sodium dodecyl sulfate, and a classic protease inhibitor cocktail. One hundred micrograms of total proteins were then separated by 10% polyacrylamide gel electrophoresis and electroblotted. Blots were blocked for 1 h at 4 °C with 5% milk Tris-Tween buffered saline 1×, and were incubated overnight at 1:1 000 with the anti-PPARα (Geneka Biotechnology Inc., Montreal, Canada). Membranes were incubated for 1 h with a swine anti-rabbit IgG conjugated to horseradish peroxidase for PPARα (dilution 1:1 000, Dako Laboratories, Trappes, France). Protein bands were revealed by an enhanced chemiluminescence reaction for PPARα. The results were expressed as units of optical density per quantity of total protein[20,24,25].

Immunohistochemical staining in liver tissues

Serial sections of paraffin embedded liver tissues were cut at 4 μm by Leica RM2145 rotary microtome (Leica Instruments GmbH, Germany). Glass slides were treated with poly-L-lysine in advance. Specimen slides were incubated for 48 h at 37 °C and then deparaffinized by xylene and rehydrated by graded alcohol series. An immunohistochemical staining was performed[20,24,25] for the detection of PPARγ expression. Liver sections were incubated in 3% H_2O_2 in methanol to deactivate endogenous peroxidase activity for 20 min. Then slides were incubated with 0.05% Saponin (ICN Biomedicals, OH, USA) for 30 min at room temperature to permeablize the tissues. After being washed, sections were pre-treated with Avidin D, followed by Biotin (Vector Laboratories) to block non-specific binding of Biotin/Avidin system reagents. Non-specific antibody binding was blocked with 1.5% goat serum in PBS for 15 min. Slides were incubated with 5% milk and 0.1% bovine serum albumin (BSA) in PBS for 15 min. Sections were incubated with the primary goat polyclonal antibody directed against PPARγ at room temperature (dilution 1:50, TEBU International) for 30 min, and were processed for peroxidase immunostaining using the Dako Laboratories system following the manufacturer's instructions. Sections were incubated for 30 min at room temperature in rabbit anti-goat IgG (dilution 1:100, Dako Laboratories), and then under the same conditions in an avidin-biotinylated peroxidase complex (Dako, Denmark) that was prepared at least 30 min before use. Staining was developed with 3,3'-diaminobenzidine in chromogen solution for 1 min, and the reaction was stopped in distilled water. Sections were counterstained with hematoxylin. As a negative control experiment, the primary antibody was omitted and replaced with a non-specific antibody[20].

Statistical analysis

All results were expressed as mean±SD. Comparisons were analyzed by the nonparametric Mann-Whitney *U* test. Differences were considered statistically significant, if the *P* value was less than 0.05.

RESULTS

Patients' ALT, HCV load, histological scores, and genotype

In this study, the body weights of the chronic hepatitis C patients were within the normal range and homogeneous. Before and during the study, they did not receive any treatment which could have influenced the results. Their mean serum alanine transaminase value was 119±27 IU/L, mean peripheral blood HCV RNA level was $747\pm267\times10^3$ IU/mL, and their histological lesions were consistent at the time of liver biopsy examination. Half of the patients had fibrosis scored F1, 24% F2, and 26% F3-F4. Seventy-two percent of the cases had an inflammatory activity scored A1 and 28% A2. Fifty-two percent of patients were genotype 1, 31% were genotype 3, 12% were genotype 2, and 5% were genotype 4.

HCV infection reduced the expression of PPARα and CPT1A

The real-time PCR analysis indicated that the housekeeping gene TATA box-binding protein concentrations were similar in patients and controls. But the level of PPARα in hepatitis C patient livers lowered by 86% compared with controls (1.8±2.8 *vs* 13±3.4, $P = 0.0002$) (Figure 1A). And the reduction in CPT1A mRNA was similar to the reduction in PPARα in the livers of patients in the study (Figure 1B). Compared with the 40 controls, the expression level of the CPT1A gene in the 46 hepatitis C patients lowered by more than 80% (1.1±1.5 *vs* 7.4±1, $P = 0.004$).

In a similar pattern, the Western blot also proved the results of real-time PCR analysis. Because of the limited amount of the liver biopsy samples, the Western blot analysis of PPARα was performed only in the surgically obtained liver specimens of patients with HCV infection ($n = 5$) and controls ($n = 7$). The analysis revealed a band with a molecular weight of approximately 55 ku corresponding to PPARα in all surgical liver specimens, and significantly lower levels of PPARα protein in HCV patients than in controls (2.3±0.3 *vs* 3.6±0.2 OD of PPARα protein/5 ng total protein, $P = 0.009$) (Figure 1C).

PPARα protein expression decreased in hepatocytes

The immunohistochemical staining was performed in all hepatitis C patients' and controls. Cell staining was positive for PPARα mainly in hepatocytes and by perinuclear staining (Figure 2, left). However, the results of stained cells in chronic hepatitis C patients indicated a decrease in PPARα staining in hepatocytes compared to those in control livers (Figure 2, right). Negative control staining was performed by omitting the primary antibody or the use of an irrelevant antibody. These results suggested that hepatocytes were the major sources of PPARα and they expressed low levels of PPARγ during HCV infection.

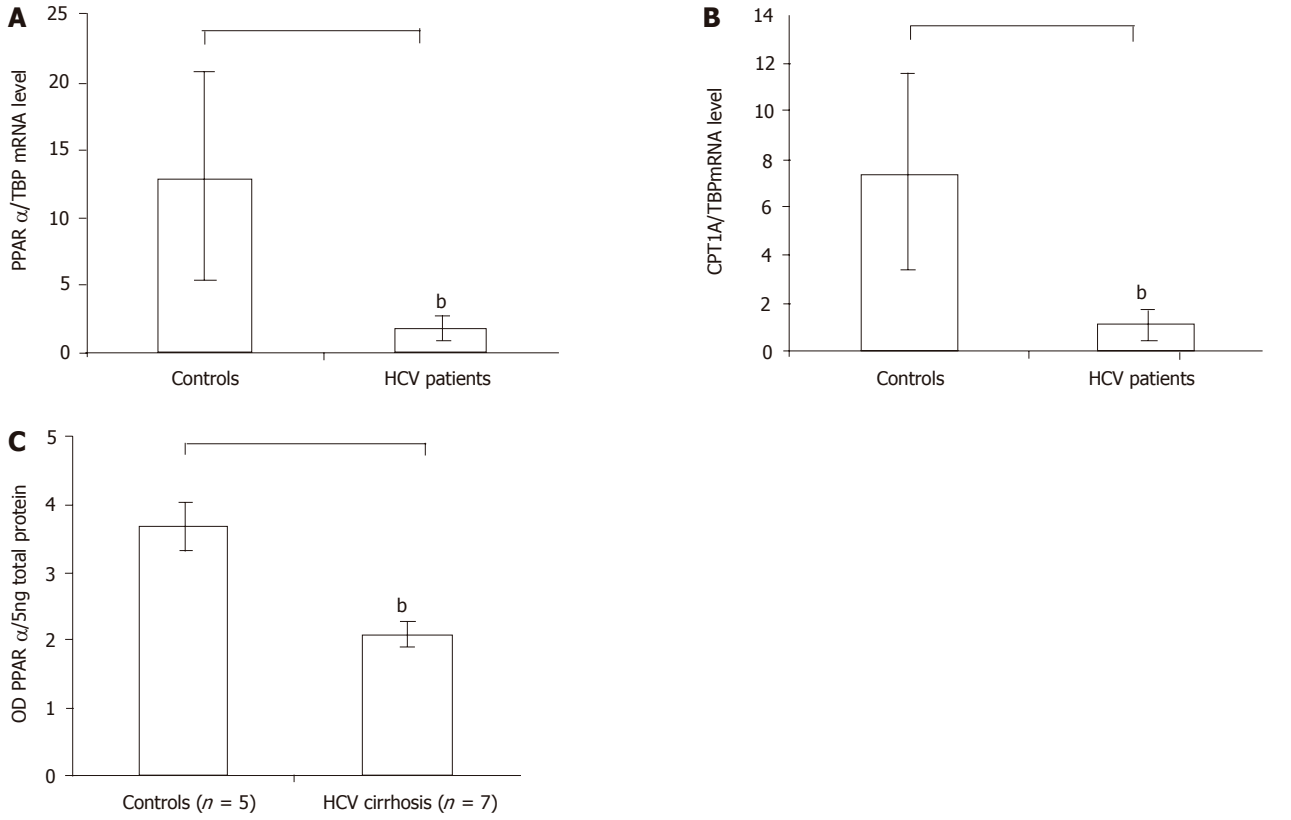

Figure 1 **A:** The PPARα mRNA level in the HCV patients reduced compared with controls by real-time RT-PCR, $^{b}P<0.01$ *vs* control; **B:** The PPARα target gene CPT1A mRNA level in the HCV patients also reduced compared with controls by real-time RT-PCR, $^{b}P<0.01$ *vs* control; **C:** The PPARα protein level in the HCV cirrhotic patients reduced compared with controls by Western blot. Results were expressed as mean±SD, $^{b}P<0.01$ *vs* control.

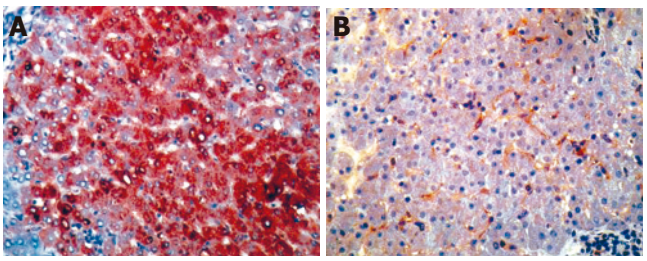

Figure 2 Representative PPARα immunostainings in liver specimens. The left: a control liver, PPARα staining was detected in the majority of hepatocytes (magnification ×160); The right: a severe hepatitis patient liver, the number of PPARα-stained hepatocytes was decreased markedly (magnification ×160).

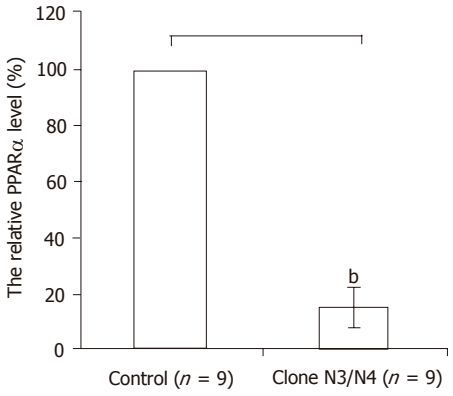

Figure 3 In the N3 colon and N4 colon which were stably expressing the HCV core protein PPARα mRNA levels decreased more than 80% compared with controls by real-time RT-PCR. Results were expressed as mean±SD, $^{b}P<0.01$ *vs* control.

HCV core protein reduced the expression of PPARα

Because hepatocytes were the parenchymal component in the liver that were prone to be infected by HCV, and HCV core protein regulated the transcriptional activity of several genes, the PPARα expression in HepG2 cells stably expressing HCV core protein were also quantified with the real-time PCR. In the N3 and N4 colons which were stably expressing the HCV core protein, PPARα mRNA levels were found to be similar, but decreased more than 80% compared with controls (Figure 3).

DISCUSSION

Because the morbidity and mortality of hepatitis C is high and the natural history is generally long and slow, many patients develop complications[6-8]. It is difficult to find an effective treatment if the exact mechanism of HCV is not clear, so it is a very important task to elucidate the pathogenesis of hepatitis C[2,4]. The results in this study demonstrated for the first time that the expression of PPARα was impaired in the livers of chronic hepatitis C patients. Both *in vitro* studies and the transgenic mouse model suggested that the HCV core protein is possibly responsible for lipid accumulation[12,26]. It was reported

that HCV core protein expression in transgenic mice could inhibit microsomal triglyceride transfer protein activity and very low density lipoprotein secretion causing steatosis[13]; and the mechanism postulated seemed to be related to mitochondrial toxicity with the production of reactive oxygen species. In this study, it was also found that in the N3 colon and N4 colon stably expressing the HCV core protein, the PPARα mRNA levels lowered significantly compared with controls. These results indicated the involvement of the HCV protein in the regulation of PPARα expression and activation.

PPARα plays a fundamental role in regulating energy homeostasis through controlling lipid metabolism[14]. PPARs belong to the type II steroid receptor family, including members such as RXR and thyroid hormone receptor[27]. These receptors are generally considered to localize to the nucleus and appear not to be bound to other proteins in inactive complexes, as has been extensively described for type I receptors (e.g. glucocorticoid receptor, progesterone receptor, androgen receptor). PPARα is a fatty acid-activated transcription factor that up-regulates the expression of a variety of genes encoding proteins involved in β-oxidation and lipoprotein metabolism[16]. PPARα plays a central role in fatty acid homeostasis by regulating the degradation of fatty acids by mitochondrial as well as by peroxisomal and microsomal fatty acid oxidation[28]. In addition, PPARα contributes to the maintenance of energy balance by regulating the expression of enzymes that participate in mitochondrial fatty acid oxidation and the formation of ketone bodies from fatty acids. Lack of this transcriptional factor in PPARα–/– mice results in the inability to up-regulate hepatic fatty acid oxidation and ketogenesis in the face of increased concentrations of free fatty acids in the circulation[15]. In this study, both the real-time PCR and Western blot analysis indicated that PPARα expression level was down-regulated in HCV infection; and the immunohistochemical staining also showed that the decreased expression was mainly in hepatocytes. So it suggests that HCV injures the liver partly through down-regulation of PPARα.

The PPARα-responsive human genes include CPT1A, the long chain fatty acyl-CoA synthase (ACS), and the mitochondrial HMG-CoA synthase (HMGCS2). Several aspects of fatty acid oxidation are disrupted in PPARα null mice that include a diminished, constitutive expression of several components of the mitochondrial fatty acid oxidation pathway. These results suggest that in mice, PPARα is a significant regulator of the mitochondrial capacity for fatty acid β-oxidation. The flux of long chain fatty acids through the mitochondrial γ-oxidation pathway is regulated by CPT1, a component of the long chain fatty acylcarnitine translocases. The activity of CPT1 is modulated by the concentration of malonyl-CoA, a potent inhibitor of the enzyme formed in the first committed step of fatty acid synthesis. Because CPT1 is induced by peroxisome proliferators in the liver, the target gene CPT1A of PPARα was also studied in order to understand the possible mechanisms of reduced expression of PPARα in the HCV infection. The human CPT1A gene is PPARα-responsive[17,18,29-31]. The fatty acyl-CoA substrates for CPT1 are formed by the esterification of free fatty acids to CoA by ACS. ACS is induced by peroxisome proliferators in rat liver, and PPRE has been identified in the promoter of the rat gene. In this study, the expression levels of the CPT1A gene in the livers of hepatitis C patients decreased significantly. It indicated that HCV core protein was possibly responsible for lipid accumulation by CPT1A, which was regulated by the transcriptional factor PPARα that was also the major isoform required for mediating the responses resulting from the actions of peroxisome proliferators in liver.

It was reported that human genes encoding key enzymes for mitochondrial fatty acid oxidation and ketogenesis could be regulated by human PPARα. In these tissues malonyl-CoA may act as a sensor or hormone and fuel through its ability to inhibit mitochondrial outer membrane CPT I[17]. This enzyme catalyzes the transesterification of long-chain fatty acyl-CoAs to long-chain acylcarnitines, which are carried into the mitochondrial matrix where acyl-CoA is regenerated for β-oxidation[18,30,31]. The role of PPARα in cell proliferation[32,33], tumor promotion[34,35] and in the prevention/reversal of liver injury has been studied by different researchers before[34-36].

To sum up, this report showed that the reduced intrahepatic PPARα expression level was associated with the HCV core protein. HCV infection down-regulated the expression of PPARα and CPT1A not only at mRNA level but also at the protein level. Correspondingly, the reduced PPARα level induced the low expression of CPT1A. The immunohistochemical analysis also proved that expression level of PPARα decreased in the hepatocytes. The function impairment of PPARα and CPT1A during the HCV infection still needs further investigation. The results in this study indicated that PPARα played an important role in the pathogenesis of chronic HCV infection, and this nuclear receptor could be a potential therapeutic target[34-36] in the treatment of HCV infection in the future.

REFERENCES

1 **Cohen J**. The scientific challenge of hepatitis C. *Science* 1999; **285**: 26-30

2 **Burroughs AK**, Groszmann R, Bosch J, Grace N, Garcia-Tsao G, Patch D, Garcia-Pagan J C, Dagher L. Assessment of therapeutic benefit of antiviral therapy in chronic hepatitis C: is hepatic venous pressure gradient a better end point? *Gut* 2002; **50**: 425-427

3 **Hickman IJ**, Clouston AD, Macdonald GA, Purdie DM, Prins JB, Ash S, Jonsson JR, Powell EE. Effect of weight reduction on liver histology and biochemistry in patients with chronic hepatitis C. *Gut* 2002; **51**: 89-94

4 **Siebert U**, Sroczynski G, Rossol S, Wasem J, Ravens-Sieberer U, Kurth BM, Manns MP, McHutchison JG, Wong JB. Cost effectiveness of peginterferon alpha-2b plus ribavirin versus interferon alpha-2b plus ribavirin for initial treatment of chronic hepatitis C. *Gut* 2003; **52:** 425-432

5 **Asselah T**, Boyer N, Guimont MC, Cazals-Hatem D, Tubach F, Nahon K, Daikha H, Vidaud D, Martinot M, Vidaud M, Degott C, Valla D, Marcellin P. Liver fibrosis is not associated

with steatosis but with necroinflammation in French patients with chronic hepatitis C. *Gut* 2003; **52**: 1638-1643
6 **Hoofnagle JH**. Hepatitis C: the clinical spectrum of disease. *Hepatology* 1997; **26**: 15S-20S
7 **Pagliaro L**, Peri V, Linea C, Camma C, Giunta M, Magrin S. Natural history of chronic hepatitis C. *Ital J Gastroenterol Hepatol* 1999; **31**: 28-44
8 **Desmet VJ**, Gerber M, Hoofnagle JH, Manns M, Scheuer PJ. Classification of chronic hepatitis: diagnosis, grading and staging. *Hepatology* 1994; **19**: 1513-1520
9 **Kage M**, Shimamatu K, Nakashima E, Kojiro M, Inoue O, Yano M. Long-term evolution of fibrosis from chronic hepatitis to cirrhosis in patients with hepatitis C: morphometric analysis of repeated biopsies. *Hepatology* 1997; **25**: 1028-1031
10 **Yano M**, Kumada H, Kage M, Ikeda K, Shimamatsu K, Inoue O, Hashimoto E, Lefkowitch JH, Ludwig J, Okuda K. The long-term pathological evolution of chronic hepatitis C. *Hepatology* 1996; **23**: 1334-1340
11 **Zaitoun AM**, Al Mardini H, Awad S, Ukabam S, Makadisi S, Record CO. Quantitative assessment of fibrosis and steatosis in liver biopsies from patients with chronic hepatitis C. *J Clin Pathol* 2001; **54**: 461-465
12 **Moriya K**, Fujie H, Shintani Y, Yotsuyanagi H, Tsutsumi T, Ishibashi K, Matsuura Y, Kimura S, Miyamura T, Koike K. The core protein of hepatitis C virus induces hepatocellular carcinoma in transgenic mice. *Nat Med* 1998; **4**: 1065-1067
13 **Perlemuter G**, Sabile A, Letteron P, Vona G, Topilco A, Chretien Y, Koike K, Pessayre D, Chapman J, Barba G, Brechot C. Hepatitis C virus core protein inhibits microsomal triglyceride transfer protein activity and very low density lipoprotein secretion: a model of viral-related steatosis. *FASEB J* 2002; **16**: 185-194
14 **Issemann I**, Green S. Activation of a member of the steroid hormone receptor superfamily by peroxisome proliferators. *Nature* 1990; **347:** 645-650
15 **Bandsma RH**, Van Dijk TH, Harmsel At A, Kok T, Reijngoud DJ, Staels B, Kuipers F. Hepatic de novo synthesis of glucose 6-phosphate is not affected in peroxisome proliferator-activated receptor alpha-deficient mice but is preferentially directed toward hepatic glycogen stores after a short term fast. *J Biol Chem* 2004; **279**: 8930-8937
16 **Gilde AJ**, van der Lee KA, Willemsen PH, Chinetti G, van der Leij FR, van der Vusse GJ, Staels B, van Bilsen M. Peroxisome proliferator-activated receptor (PPAR) alpha and PPARbeta/delta, but not PPARgamma, modulate the expression of genes involved in cardiac lipid metabolism. *Circ Res* 2003; **92:** 518-524
17 **van der Leij FR**, Cox KB, Jackson VN, Huijkman NC, Bartelds B, Kuipers JR, Dijkhuizen T, Terpstra P, Wood PA, Zammit VA, Price NT. Structural and functional genomics of the CPT1B gene for muscle-type carnitine palmitoyltransferase I in mammals. *J Biol Chem* 2002; **277:** 26994-27005
18 **Gobin S**, Thuillier L, Jogl G, Faye A, Tong L, Chi M, Bonnefont JP, Girard J, Prip-Buus C. Functional and structural basis of carnitine palmitoyltransferase 1A deficiency. *J Biol Chem* 2003; **278:** 50428-50434
19 **Bedossa P**, Poynard T. An algorithm for the grading of activity in chronic hepatitis C. The METAVIR Cooperative Study Group. *Hepatology* 1996; **24**: 289-293
20 **Desreumaux P**, Dubuquoy L, Nutten S, Peuchmaur M, Englaro W, Schoonjans K, Derijard B, Desvergne B, Wahli W, Chambon P, Leibowitz MD, Colombel JF, Auwerx J. Attenuation of colon inflammation through activators of the retinoid X receptor (RXR)/peroxisome proliferator-activated receptor gamma (PPARgamma) heterodimer. A basis for new therapeutic strategies. *J Exp Med* 2001; **193**: 827-838
21 **Barba G**, Harper F, Harada T, Kohara M, Goulinet S, Matsuura Y, Eder G, Schaff Z, Chapman MJ, Miyamura T, Brechot C. Hepatitis C virus core protein shows a cytoplasmic localization and associates to cellular lipid storage droplets. *Proc Natl Acad Sci USA* 1997; **94:** 1200-1205
22 **Martin G**, Schoonjans K, Lefebvre AM, Staels B, Auwerx J. Coordinate regulation of the expression of the fatty acid transport protein and acyl-CoA synthetase genes by PPARalpha and PPARgamma activators. *J Biol Chem* 1997; **272**: 28210-28217
23 **Bieche I**, Onody P, Laurendeau I, Olivi M, Vidaud D, Lidereau R, Vidaud M. Real-time reverse transcription-PCR assay for future management of ERBB2-based clinical applications. *Clin Chem* 1999; **45**: 1148-1156
24 **Dubuquoy L**, Jansson EA, Deeb S, Rakotobe S, Karoui M, Colombel JF, Auwerx J, Pettersson S, Desreumaux P. Impaired expression of peroxisome proliferator-activated receptor gamma in ulcerative colitis. *Gastroenterology* 2003; **124**: 1265-1276
25 **Philippe D**, Dubuquoy L, Groux H, Brun V, Chuoi-Mariot MT, Gaveriaux-Ruff C, Colombel JF, Kieffer BL, Desreumaux P. Anti-inflammatory properties of the mu opioid receptor support its use in the treatment of colon inflammation. *J Clin Invest* 2003; **111**: 1329-1338
26 **Otani K**, Korenaga M, Beard MR, Li K, Qian T, Showalter LA, Singh AK, Wang T, Weinman SA. Hepatitis C virus core protein, cytochrome P450 2E1, and alcohol produce combined mitochondrial injury and cytotoxicity in hepatoma cells. *Gastroenterology* 2005; **128**: 96-107
27 **McCarthy TC**, Pollak PT, Hanniman EA, Sinal CJ. Disruption of hepatic lipid homeostasis in mice after amiodarone treatment is associated with peroxisome proliferator-activated receptor-alpha target gene activation. *J Pharmacol Exp Ther* 2004; **311**: 864-873
28 **Mehendale HM**. PPAR-alpha: a key to the mechanism of hepatoprotection by clofibrate. *Toxicol Sci* 2000; **57**: 187-190
29 **Hsu MH**, Savas U, Griffin KJ, Johnson EF. Identification of peroxisome proliferator-responsive human genes by elevated expression of the peroxisome proliferator-activated receptor alpha in HepG2 cells. *J Biol Chem* 2001; **276**: 27950-27958
30 **Bonnefont JP**, Djouadi F, Prip-Buus C, Gobin S, Munnich A, Bastin J. Carnitine palmitoyltransferases 1 and 2: biochemical, molecular and medical aspects. *Mol Aspects Med* 2004; **25**: 495-520
31 **Price NT**, Jackson VN, van der Leij FR, Cameron JM, Travers MT, Bartelds B, Huijkman NC, Zammit VA. Cloning and expression of the liver and muscle isoforms of ovine carnitine palmitoyltransferase 1: residues within the N-terminus of the muscle isoform influence the kinetic properties of the enzyme. *Biochem J* 2003; **372**: 871-879
32 **Reddy JK**. Nonalcoholic steatosis and steatohepatitis. III. Peroxisomal beta-oxidation, PPAR alpha, and steatohepatitis. *Am J Physiol Gastrointest Liver Physiol* 2001; **281**: G1333- G1339
33 **Chakrabarti R**, Vikramadithyan RK, Misra P, Hiriyan J, Raichur S, Damarla RK, Gershome C, Suresh J, Rajagopalan R. Ragaglitazar: a novel PPAR alpha PPAR gamma agonist with potent lipid-lowering and insulin-sensitizing efficacy in animal models. *Br J Pharmacol* 2003; **140**: 527-537
34 **Rao MS**, Papreddy K, Musunuri S, Okonkwo A. Prevention/reversal of choline deficiency-induced steatohepatitis by a peroxisome proliferator-activated receptor alpha ligand in rats. *In Vivo* 2002; **16**: 145-152
35 **Karlic H**, Lohninger S, Koeck T, Lohninger A. Dietary l-carnitine stimulates carnitine acyltransferases in the liver of aged rats. *J Histochem Cytochem* 2002; **50**: 205-12
36 **Sumanasekera WK**, Tien ES, Turpey R, Vanden Heuvel JP, Perdew GH. Evidence that peroxisome proliferator-activated receptor alpha is complexed with the 90-kDa heat shock protein and the hepatitis virus B X-associated protein 2. *J Biol Chem* 2003; **278**: 4467-4473

Science Editors Ma JY and Guo SY **Language Editor** Elsevier HK

PO Box 2345, Beijing 100023, China
www.wjgnet.com
wjg@wjgnet.com

ELSEVIER

World J Gastroenterol 2005;11(48):7597-7601
World Journal of Gastroenterology ISSN 1007-9327

• *BASIC RESEARCH* •

Cytoskeleton reorganization and ultrastructural damage induced by gliadin in a three-dimensional *in vitro* model

Ersilia Dolfini, Leda Roncoroni, Luca Elli, Chiara Fumagalli, Roberto Colombo, Simona Ramponi, Fabio Forlani, Maria Teresa Bardella

Ersilia Dolfini, Leda Roncoroni, Chiara Fumagalli, Department of Biology and Genetics for Health Sciences, University of Milan, Milan, Italy
Luca Elli, Maria Teresa Bardella, Department of Digestive Diseases and Endocrinology, IRCCS Ospedale Maggiore di Milano, University of Milan, Milan, Italy
Roberto Colombo, Department of Biology, University of Milan, Milan, Italy
Simona Ramponi, Milan Research Imaging Centre, Bracco SpA, Milan, Italy
Fabio Forlani, Department of Agrifood Molecular Sciences, University of Milan, Milan, Italy
Supported by the "Fondazione San Paolo" grant to "Centro per lo Studio della Celiachia"
Correspondence to: Dr Ersilia Dolfini, Department of Biology and Genetics for Health Sciences, Via Viotti 3/5, 20131 Milano, Italy. ersilia.dolfini@unimi.it
Telephone: +39-02-50315837 Fax: +39-02-50315864
Received: 2005-03-01 Accepted: 2005-07-08

Abstract

AIM: To evaluate the interplay between gliadin and LoVo cells and the direct effect of gliadin on cytoskeletal patterns.

METHODS: We treated LoVo multicellular spheroids with digested bread wheat gliadin in order to investigate their morphology and ultrastructure (by means of light microscopy and scanning electron microscopy), and the effect of gliadin on actin (phalloidin fluorescence) and the tight-junction protein occludin and zonula occluden-1.

RESULTS: The treated spheroids had deep holes and surface blebs, whereas the controls were smoothly surfaced ovoids. The incubation of LoVo spheroids with gliadin decreased the number of intracellular actin filaments, impaired and disassembled the integrity of the tight-junction system.

CONCLUSION: Our data obtained from an "*in vivo*-like" polarized culture system confirm the direct noxious effect of gliadin on the cytoskeleton and tight junctions of epithelial cells. Unlike two-dimensional cell culture systems, the use of multicellular spheroids seems to provide a suitable model for studying cell-cell interactions.

Key words: Celiac disease; Gliadin; Cytoskeleton; Multicellular spheroids

Dolfini E, Roncoroni L, Elli L, Fumagalli C, Colombo R, Ramponi S, Forlani F, Bardella MT. Cytoskeleton reorganization and ultrastructural damage induced by gliadin in a three-dimensional *in vitro* model. *World J Gastroenterol* 2005; 11(48): 7597-7601
http://www.wjgnet.com/1007-9327/11/7597.asp

INTRODUCTION

Celiac disease (CD) is an immunomediated intestinal disorder that is triggered by dietary gluten and related cereal proteins in genetically susceptible individuals[1,2]. Gluten consists of a complex mixture of gliadin monomers and large polymeric glutenin polypetides. A number of *in vitro* studies of two-dimensional cell cultures have shown that gliadin has direct cytotoxic effects on epithelial cells[3], but the early steps allowing the start of the immunoreaction are largely unknown.

CD is characterized by enhanced paracellular permeability across the intestinal epithelium, a "leaky gut" condition that allows the passage of macromolecules through the paracellular spaces[4-6]. Moreover, it has also been demonstrated that cytoskeleton involved in the pathogenesis of CD as a gluten challenge rapidly causes the disappearance and disorganization of actin filaments in the intestinal mucosa of CD patients[7]. The actin filaments in epithelial cells are associated with tight junctions (TJs), appearing as a series of discrete sites of apparent membrane fusion (so called "kissing points") involving the outer leaflets of the plasma membranes of adjacent cells. The integrity of the barrier function is important for the separation of two different compartments, and TJs play a major role in controlling paracellular transport between the luminal and basolateral fluid compartments[8].

Almost all the proteins associated with TJs are peripheral membrane proteins that form part of the submembrane plaque (Figure 1). The first TJ-associated protein to be identified is zonula occluden-1 (ZO-1) whose C-terminal half contains an actin-binding site and mediates interactions between transmembrane proteins and cytoskeleton elements[9]. Occludin, a 60 ku integral membrane protein in TJ strands[10], is involved in TJ barrier and fence functions through its four transmembrane domains, three cytoplasmic domains and two extracellular

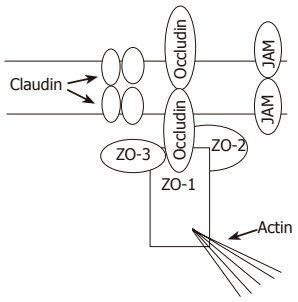

Figure 1 Tight junction (TJ) structure with emphasis on proteins of the TJ membrane domain: ZO family members and their interaction with actin filaments.

loops[8]. Claudin-1 and claudin-2 are 23 ku integral membrane proteins that function as major structural components of TJ strands[11]. Junctional adhesion molecules (JAMs) have only one putative transmembrane sequence. The intracellular domain consists of 45 residues, and the extracellular portion (215 residues) contains two domains with intra chain disulfide bonds[12].

The cytoskeletal network generates tension and transmits stress within and among the cells[13]. The formation of multicellular tumor spheroids (MCTSs) involves cell translocations and morphological changes that are indicative of the organization of the cytoskeleton. The cells grown in MCTSs are interconnected by the means of TJs that form a seal between adjacent cells, thus defining their apical and basolateral surfaces, and creating a model similar to *in vivo* tissue. This is very different from the organization of two-dimensional cell cultures[14,15].

The aim of this study was to evaluate the interplay between gliadin and LoVo MCTSs, with specific emphasis on the direct effect of gliadin on cytoskeleton patterns and reorganization.

MATERIALS AND METHODS

Cell line

Cells from the human colon adenocarcinoma cell line (LoVo, ATCC, Rockville, USA) were grown in T75 flasks (PBI, Italy) at 37 °C in an atmosphere containing 95% air and 50 mL/L CO_2. The medium consisted of Ham's F-12 medium (GIBCO, Italy), supplemented with 10% fetal bovine serum (GIBCO, Italy), 1% MEM vitamin solution 100× (GIBCO, Italy), and 3% L-glutamine 200 mmol/L (GIBCO, Italy).

After one week, the cells were removed using solution containing 0.25% (w/v) trypsin and 0.02% (w/v) EDTA (Sigma-Aldrich, Italy), and the cell suspensions were cultured again. Mycoplasma contamination was regularly searched for and excluded using the Hoechst method[16].

Gliadin digestion

Gliadin was purified from *Triticum aestivum* flour (Hereward Cultivar, UK) according to Capelli[17]. Pepsin (3.2-4.5 U/mg) was supplied by Sigma (Italy), and the pancreatin (0.1 mAnson/mg) by Merck (USA). All the chemicals were of analytical grade. Digestion was performed as previously described by our group[18]. Briefly, the gliadin was first incubated with pepsin at 37 °C for 24 h, and then with pancreatin at 37 °C for 3 h, adjusting to a pH of 8. The digested protein was analytically controlled by means of RP-HPLC, SE-HPLC, and SDS-PAGE, freeze-dried and stored.

Three-dimensional cell cultures and gliadin treatment

Three-dimensional cell cultures were initiated by seeding 4×10^5 cells/mL in 25 mL of complete medium supplemented with penicillin (100 U/mL) and streptomycin (100 Ug/mL) (GIBCO, Italy) in Erlenmeyer flasks (Corning, Italy), and incubated in a gyratory rotation incubator (60 rev/min) at 37 °C in air (Colaver, Italy). Homotypical aggregations were visible after 4 d of culture, and the MCTSs were usually complete within 7 d (average diameter±SD, 370±48.5 μm).

On the seventh day, the MCTSs were exposed to PT-digested gliadin (500 μg/mL) in a completely renewed medium for further 4 d and subsequently taken for microscopic examination. The PT-digested gliadin greatly inhibited cell growth (50% inhibitory concentration: 390 μg/mL) and the dose used was selected from four different concentrations (125, 500, 750, 1 000 μg/mL) on the basis of previous data obtained in our laboratory[18,19].

Scanning electron microscopy (SEM)

Three-dimensional cell cultures were washed twice in PBS, and then fixed in 2.5% glutaraldehyde in phosphate buffer at room temperature for 24 h at 4 °C. At the time of analysis, a representative sample of spheroids was recovered, immediately placed on a paper filter and observed in low vacuum modality at a high voltage of 10 kV. SEM analysis was performed using a Philips Scanning Electron Microscope (Mod. ×L20).

Confocal laser scanning microscopy of intracellular F-actin

LoVo MCTSs were washed twice in PBS, fixed in 4% paraformaldeyde for 1 h, permeabilized with 0.4% Triton X-100 (Sigma-Aldrich, Italy) for 20 min, washed thrice for 5 min in PBS and stained for immunocytochemistry by means of incubation with fluorescein TRITC-phalloidin (Sigma-Aldrich, Italy) (1:200 PBS) in a humid chamber at room temperature for 6 h. After washing thrice in PBS each for 5 min, 10 spheroids were transferred onto slides, and each slide was mounted with 90% glycerol in PBS. The results were analyzed using a confocal laser scanning microscope (Leica TCSNT, Germany).

Confocal laser scanning microscopy of occludin

LoVo MCTSs were washed twice in PBS and fixed in ethanol for 30 min at 4 °C. After the first incubation, the samples were incubated with acetone (previously stored at -20 °C) for an additional 3 min at room temperature. They were then blocked and incubated for immunocytochemistry overnight with anti-occludin-FITC (Zymed, CA, USA) before being analyzed by means of confocal laser scanning microscopy (Leica TCSNT, Germany).

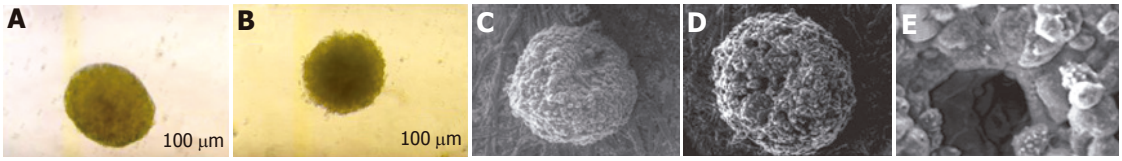

Figure 2 Phase-contrast micrographs (10×) showing control (**A**) and gliadin-treated multicellular tumor spheroids of the human colon adenocarcinoma LoVo cell line (**B**) after 11 d of culture; Scanning electron micrographs: showing the ovoid control spheroids (**C**) and their very compact, densely organized and tightly packed structure that they can be clearly distinguished from each other; The surface of gliadin-treated spheroids (**D**) focally interrupted by irregularly distributed holes, and loss of their structural thickness and organization (**E**).

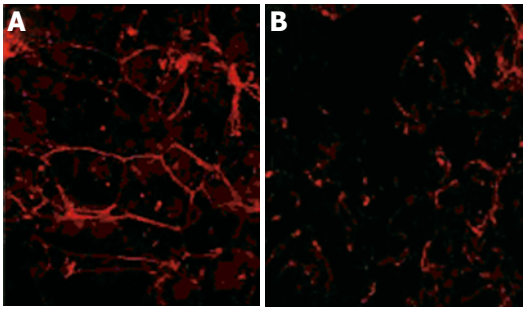

Figure 3 Confocal laser scanning micrograph in which TRICT-phalloidin highlights the organization of F-actin in multicellular tumor spheroids. The control spheroids (**A**) have a "chicken-wire" distribution under the plasma membrane, whereas the treated spheroids (**B**) show a reorganized actin cytoskeleton.

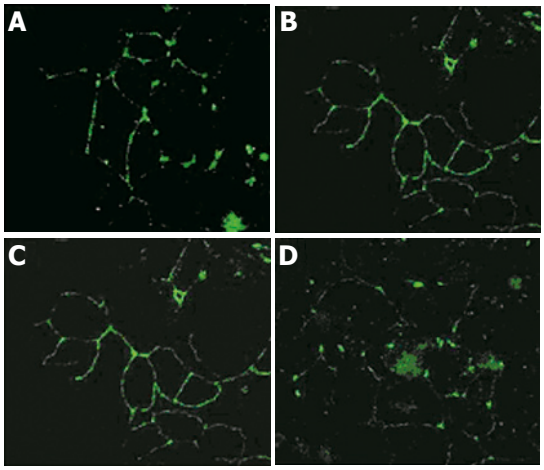

Figure 4 Confocal microscopy immunolocalization of occludin and zonula occluden-1 (ZO-1) in LoVo multicellular tumor spheroids. In the control spheroids, occludin and ZO-1 localized sharply in the apical region of the lateral membrane are visualized en face as a ring pattern (**A** and **C**), whereas the distribution of occludin and ZO-1 in the spheroids exposed to gliadin for 4 d is far from the lateral TJ membrane (**B** and **D**).

Confocal laser scanning microscopy of zonula occluden-1

LoVo MCTSs were washed twice in PBS and fixed in ethanol for 30 min at 4 °C. After the first incubation, the samples were incubated with acetone (previously stored at -20 °C) for an additional 3 min at room temperature. They were then blocked and incubated overnight with anti-ZO-1-FITC (Zymed, CA, USA) before being analyzed by means of confocal laser scanning microscopy (Leica TCSNT, Germany).

RESULTS

Light microscopy and SEM

The untreated MCTSs appeared bright and round at phase-contrast microscopy (Figure 2A). SEM showed that they were well-defined and compact, with smooth boundaries and a regular surface. Their structure was compact, densely organized and tightly packed (Figure 2C).

The MCTSs treated with PT-digested gliadin were loosely connected and irregularly shaped (Figure 2B). They were less bright than the controls and had frayed borders. SEM revealed an altered surface, with deep and irregularly distributed holes (Figures 2D and E).

Confocal laser scanning microscopy

The untreated MCTSs stained with TRITC-phalloidin had regular perijunctional actin rings and showed organized distribution at the cell boundaries (Figure 3A), whereas those treated with PT-digested gliadin had reorganized intracellular actin filaments and disassembled F-actin (Figure 3B).

In comparison with the normal subapical honeycomb pattern typical of TJs (Figures 4A and C), treatment with PT-digested gliadin led to their structural dissociation (Figures 4B and D). The morphologically characteristic ring structure of occludin and ZO-1 immunolocalization in the en face confocal images had sharp boundaries in the untreated spheroids, but was partially or completely lost in the treated spheroids.

DISCUSSION

CD is a chronic intestinal inflammatory disorder characterized by mucosal changes including lymphocyte infiltration, crypt hyperplasia and villous atrophy. Furthermore, intestinal permeability is increased and TJs appear open[20]. As TJs form a barrier against the diffusion of molecules from the lumen to the tissue parenchyma (barrier function), and restrict the diffusion of lipids and proteins between the apical and basolateral plasma membranes (fence function)[21], the loss of permeability allows the translocation of antigenic molecules from the intestinal lumen to the lamina propria, thus creating a condition for an immune response.

Traditional tissue culture methods have been based on growing cell lines as monolayers, but a new three-

dimensional culture system (Figure 2A) has been investigated as a mean of modeling a solid tumor under *in vitro* conditions that simulates its *in vivo* biological properties. Given the fundamental differences between monolayer and three-dimensional cultures, spheroids should become mandatory test systems in oncological therapeutic screening programs[22]. Furthermore, cells grown in three-dimensional cultures are oriented and polarized[23,24], and often express a gene repertoire that is different from that of the monolayer cultures[25]. Previous studies from our laboratory have confirmed the polarized structure, and the presence of microvilli and tightly connected epithelial junctional complexes[18].

The interaction between TJ proteins and actomyosin cytoskeleton in MCTSs is a primary target for physiological and pathological signals. Circumferential actomyosin contraction and cytoskeleton interaction modulate TJ permeability, thus contributing to the formation of the TJ fence[21]. Pizzuti *et al*.[26] have recently demonstrated that the intestinal mucosa of celiac patients has an altered TJ system during gluten exposure, and decreased ZO-1 expression is associated with a disrupted F-actin organization and the loss of normal distribution at cell-cell contact sites.

Our SEM morphological examinations confirmed that gliadin treatment could affect spheroid structure, causing a loss of cell thickness and organization, and the formation of hole-like surface structures (Figures 2C-E). Confocal laser scanning microscopy showed that gliadin could induce cytoskeleton reorganization (Figures 3A and B), and specifically act on TJ structural proteins.

Though our results have confirmed that the expression of occludin correlates with barrier properties, the decreased intensity or disappearance of occludin staining at cell–cell borders in gliadin-treated spheroids (Figures 4A and B) do not presuppose the absence of TJ structural integrity. Knockout experiments in mouse embryonic stem cells have demonstrated that occludin is not necessary to form functionally competent TJs[27], and ZO-1 has a wild-type localization in apical junctional regions of the outermost layer of epithelial cells in the absence of occludin[28]. We found that the immunolocalization of ZO-1 in TJ ring structures was severely disrupted by gliadin exposure, leading to almost complete lack of continuity, and *en face* confocal images showed a breakdown of junctional complexes (Figures 4C and D). Taken together, these findings suggest that ZO-1 lies at the centre of a network of protein–protein interactions and may be critical in recruiting the proteins necessary to establish TJs.

Our preliminary data showed that TJ permeability might be regulated directly as a result of TJ protein modifications, or indirectly as a result of the effects of xenobiotics on the cytoskeleton. New insights into the molecular architecture of TJs and their regulation have given rise to a new concept of TJ modulation based on peptides from the first extracellular domain of occludin[29]. We can speculate that gliadin peptides also act as modulators on the extracellular loops of TJ transmembrane proteins, mediating TJ opening and the consequent cytoskeletal redistribution. According to the "tensegrity model"[30,31], the cells are in prestressed structures in which cytoskeletal elements are major determinants of deformability, and so a local stress can cause global structural rearrangements. The cell response to xenobiotic exposure leads to the retraction of submembranous actin filaments from junctional complexes, thus determining the disappearance of organized TJs. Furthermore, this alteration of internal balance of tensile stress compromises the stability of cell shape: the cells become rounded and stimulate an apoptotic process. The correlation of apoptosis with a disrupted cytoskeleton and junctional system may explain the SEM images: the blebs and holes visible on the surface of treated spheroids are the results of an apoptotic process initiated by the deregulation of internal cell balance. Ojakian *et al*.[32] reported that gliadin has an apoptotic effect on Caco-2 colon carcinoma cells directly stimulated by digested gliadin.

Understanding the events of this process will throw light onto the changes in paracellular permeability caused by gliadin and identify novel therapeutic targets in celiac disease. Though the intricacies of this process *in vivo* have not yet been fully elucidated, our results indicate that a pivotal role is played by the disarrangement of the "belt-like" structure of perijunctional F-actin affiliated with TJs. This highlights the importance of the cytoskeleton network in the ultrastructural architecture of enterocytes, given that a gluten challenge in CD patients rapidly distorts the microvillous structure, thus disorganizing the actin network on the intestinal mucosa.

If the early steps of gliadin-induced mucosal damage in patients with CD concern intestinal permeability, which is directly altered by gliadin before the immunological response, MCTSs could become essential for testing the cytotoxic effects of new chemically, enzymatically or genetically modified gliadins studied as alternative therapies to a gluten-free diet.

ACKNOWLEDGMENTS

The authors would like to thank Kevin Smart (Link srl, Milan), "Centro per lo Studio della Celiachia" of the University of Milan, for his help in preparing the English version of the manuscript, Maria Letizia Falini and Rosita Caramanico for their help in preparing peptides, and San Paolo Bank for financial support.

The study was conceived and designed by E. Dolfini, R. Colombo, L. Roncoroni, C. Fumagalli, L. Elli, and M.T. Bardella. L. Roncoroni and C. Fumagalli were responsible for the cell cultures. V. Lorusso and S. Ramponi undertook the morphological investigations and F. Forlani prepared the digested gliadin.

REFERENCES

1 **Fasano A**, Catassi C. Current approaches to diagnosis and treatment of celiac disease: an evolving spectrum. *Gastroenterology* 2001; **120**: 636-651

2 **Green PH**, Jabri B. Coeliac disease. *Lancet* 2003; **362**: 383-391
3 **Elli L**, Dolfini E, Bardella MT. Gliadin cytotoxicity and in vitro cell cultures. *Toxicol Lett* 2003; **146**: 1-8
4 **Cooper BT.** Intestinal permeability in coeliac disease. *Lancet* 1983; **1**: 658-659
5 **Bjarnason I**, Peters TJ, Veall N. Intestinal permeability defect in coeliac disease. *Lancet* 1983; **1**: 1284-1285
6 **Schulzke JD**, Bentzel CJ, Schulzke I, Riecken EO, Fromm M. Epithelial tight junction structure in the jejunum of children with acute and treated celiac sprue. *Pediatr Res* 1998; **43:** 435-441
7 **Sjolander A**, Magnusson KE. Effects of wheat germ agglutinin on the cellular content of filamentous actin In intestine 407 cells. *Eur J Cell Biol* 1988; **47**: 32-35
8 **Tsukita S**, Furuse M. Occludin and claudins in tight-junction strands: leading or supporting players? *Trends Cell Biol* 1999; **9**: 268-273
9 **Stevenson BR**, Siliciano JD, Mooseker MS, Goodenough DA. Identification of ZO-1: a high molecular weight polypeptide associated with the tight junction (zonula occludens) in a variety of epithelia. *J Cell Biol* 1986; **103:** 755-766
10 **Furuse M**, Hirase T, Itoh M, Nagafuchi A, Yonemura S, Tsukita S, Tsukita S. Occludin: a novel integral membrane protein localizing at tight junctions. *J Cell Biol* 1993; **123**: 1777-1788
11 **Furuse M**, Fujita K, Hiiragi T, Fujimoto K, Tsukita S. Claudin-1 and -2: novel integral membrane proteins localizing at tight junctions with no sequence similarity to occludin. *J Cell Biol* 1998; **141**: 1539-1550
12 **Martin-Padura I**, Lostaglio S, Schneemann M, Williams L, Romano M, Fruscella P, Panzeri C, Stoppacciaro A, Ruco L, Villa A, Simmons D, Dejana E. Junctional adhesion molecule, a novel member of the immunoglobulin superfamily that distributes at intercellular junctions and modulates monocyte transmigration. *J Cell Biol* 1998; **142**: 117-127
13 **Bates RC**, Buret A, van Helden DF, Horton MA, Burns GF. Apoptosis induced by inhibition of intercellular contact. *J Cell Biol* 1994; **125:** 403-415
14 **Conforti G**, Codegoni AM, Scanziani E, Dolfini E, Dasdia T, Calza M, Caniatti M, Broggini M. Different vimentin expression in two clones derived from a human colocarcinoma cell line (LoVo) showing different sensitivity to doxorubicin. *Br J Cancer* 1995; **71:** 505-511
15 **Matsubara S**, Ozawa M. Expression of alpha-catenin in alpha-catenin-deficient cells results in a reduced proliferation in three-dimensional multicellular spheroids but not in two-dimensional monolayer cultures. *Oncogene* 2004; **23**: 2694-2702
16 **La Porta CA**, Dolfini E, Comolli R. Inhibition of protein kinase C-alpha isoform enhances the P-glycoprotein expression and the survival of LoVo human colon adenocarcinoma cells to doxorubicin exposure. *Br J Cancer* 1998; **78**: 1283-1287
17 **Capelli L**, Forlani F, Perini F, Guerrieri N, Cerletti P, Righetti PG. Wheat cultivar discrimination by capillary electrophoresis of gliadins in isoelectric buffers. *Electrophoresis* 1998; **19:** 311-318
18 **Dolfini E**, Elli L, Ferrero S, Braidotti P, Roncoroni L, Dasdia T, Falini ML, Forlani F, Bardella MT. Bread wheat gliadin cytotoxicity: a new three-dimensional cell model. *Scand J Clin Lab Invest* 2003; **63:** 135-141
19 **Dolfini E**, Elli L, Dasdia T, Bufardeci B, Colleoni MP, Costa B, Floriani I, Falini ML, Guerrieri N, Forlani F, Bardella MT. In vitro cytotoxic effect of bread wheat gliadin on the LoVo human adenocarcinoma cell line. *Toxicol In Vitro* 2002; **16**: 331-337
20 **Clemente MG**, De Virgiliis S, Kang JS, Macatagney R, Musu MP, Di Pierro MR, Drago S, Congia M, Fasano A. Early effects of gliadin on enterocyte intracellular signalling involved in intestinal barrier function. *Gut* 2003; **52**: 218-223
21 **Schneeberger EE**, Lynch RD. The tight junction: a multifunctional complex. *Am J Physiol Cell Physiol* 2004; **286**: C1213-C1228
22 **Desoize B.** Contribution of three-dimensional culture to cancer research. *Crit Rev Oncol Hematol* 2000; **36**: 59-60
23 **Ojakian GK**, Schwimmer R. Regulation of epithelial cell surface polarity reversal by β-1 integrins. *J Cell Sci* 1994; **107**: 561-576
24 **Laderoute KR**, Murphy BJ, Short SM, Grant TD, Knapp AM, Sutherland RM. Enhancement of transforming growth factor-alpha synthesis in multicellular tumour spheroids of A431 squamous carcinoma cells. *Br J Cancer* 1992; **65:** 157-162
25 **Murphy BJ**, Laderoute KR, Vreman HJ, Grant TD, Gill NS, Stevenson DK, Sutherland RM. Enhancement of heme oxygenase expression and activity in A431 squamous carcinoma multicellular tumor spheroids. *Cancer Res* 1993; **53:** 2700-2703
26 **Pizzuti D**, Bortolami M, Mazzon E, Buda A, Guariso G, D' Odorico A, Chiarelli S, D'Inca R, De Lazzari F, Martines D. Transcriptional downregulation of tight junction protein ZO-1 in active coeliac disease is reversed after a gluten-free diet. *Dig Liver Dis* 2004; **36**: 337-341
27 **Saitou M**, Ando-Akatsuka Y, Itoh M, Furuse M, Inazawa J, Fujimoto K, Tsukita S. Mammalian occludin in epithelial cells: its expression and subcellular distribution. *Eur J Cell Biol* 1997; **73**: 222-231
28 **Harhaj NS**, Antonetti DA. Regulation of tight junctions and loss of barrier function in pathophysiology. *Int J Biochem Cell Biol* 2004; **36**: 1206-1237
29 **Tavelin S**, Hashimoto K, Malkinson J, Lazorova L, Toth I, Artursson P. A new principle for tight junction modulation based on occludin peptides. *Mol Pharmacol* 2003; **64**: 1530-1540
30 **Ingber DE**. Tensegrity I. Cell structure and hierarchical systems biology. *J Cell Sci* 2003; **116:** 1157-1173
31 **Ingber DE.** Tensegrity II. How structural networks influence cellular information processing networks. *J Cell Sci* 2003; **116**: 1397-1408
32 **Ojakian GK**, Schwimmer R. Regulation of epithelial cell surface polarity reversal by beta 1 integrins. *J Cell Sci* 1994; **107 (Pt 3):** 63-71

Science Editor Wang XL and Guo SY **Language Editor** Elsevier HK

PO Box 2345, Beijing 100023, China
www.wjgnet.com
wjg@wjgnet.com

ELSEVIER

World J Gastroenterol 2005;11(48):7602-7605
World Journal of Gastroenterology ISSN 1007-9327

• *BASIC RESEARCH* •

Cyclosporine A, FK-506, 40-0-[2-hydroxyethyl]rapamycin and mycophenolate mofetil inhibit proliferation of human intrahepatic biliary epithelial cells *in vitro*

Chao Liu, Thomas Schreiter, Andrea Frilling, Uta Dahmen, Christoph E Broelsch, Guido Gerken, Ulrich Treichel

Chao Liu, Thomas Schreiter, Guido Gerken, Ulrich Treichel, Department of Gastroenterology and Hepatology, University Hospital Essen, Germany
Andrea Frilling, Uta Dahmen, Christoph E Broelsch, Department of General Surgery and Transplantation, University Hospital Essen, Germany
Chao Liu, Department of General Surgery, Sun Yat-Sen Memorial Hospital, Sun Yat-Sen University, No. 107 West Yan Jiang Road, 510120 Guangzhou, Guangdong Province, China. mdliuchao@hotmail.com,
Telephone: +86-20-3407-0891
Correspondence to: Ulrich Treichel, MD, Department of Gastroenterology and Hepatology, University Hospital Essen, Hufelandstr. 55, 45122 Essen, Germany. ulrich.treichel@uni-essen.de
Telephone: +49-201-723-3612 Fax: +49-201-723-5970
Received: 2004-12-30 Accepted: 2005-02-18

Abstract

AIM: To investigate the effect of cyclosporine A (CsA), FK-506, and mycophenolate mofetil (MMF) and 40-0-[2-hydroxyethyl]rapamycin (RAD) on proliferation of human intrahepatic biliary epithelial cells (BECs) *in vitro*.

METHODS: BECs were isolated from six human liver tissuespecimens with the immunomagnetic separation method and treated with different concentrations of CsA, FK-506, RAD, and MMF *in vitro*. Proliferation of the cells was measured by MTT assay at 24 and 48 h after treatment, respectively. One-way analysis of variance was used to analyze the results. Expression of CK 19 in BECs was monitored by flow cytometry and Western blot.

RESULTS: Six lines of BECs were established. They survived for 4-18 wk *in vitro*. Flow cytometry analysis showed that these cells always expressed CK19. CsA, FK-506, RAD, and MMF inhibited proliferation of BECs in a dose-dependent manner. The lowest concentration of CsA, FK-506, RAD, and MMF to inhibit proliferation of BECs ($P<0.05$) was 500, 100, 0.25, and 100 μg/L, respectively. However, the expression of CK19 by BECs was not changed.

CONCLUSION: CsA, FK-506, RAD, and MMF have an antiproliferative effect on human intrahepatic BECs *in vitro*, while RAD has the strongest growth-inhibitory effect. Their possible effects on liver regeneration and bile duct injury in transplant patients should be further investigated.

Key words: Cyclosporine A; FK-506, Rapamycin; Mycophenolate mofetil; Biliary epithelial cells

Liu C, Schreiter T, Frilling A, Dahmen U, Broelsch CE, Gerken G, Treichel U. Cyclosporine A, FK-506, 40-0-[2-hydroxyethyl]rapamycin and mycophenolate mofetil inhibit proliferation of human intrahepatic biliary epithelial cells *in vitro*. *World J Gastroenterol*; 2005: 11(48): 7602-7605
http://www.wjgnet.com/1007-9327/11/7602.asp

INTRODUCTION

Within the last decade, living donor liver transplantation (LDLT) has become an accepted treatment for adult patients with end-staged liver disease and it provides a viable alternative to many recipients who would otherwise die while on the waiting lists. Part of the donor liver used for adult LDLT is small in size when transplanted into the recipient. The liver has the unique ability to regenerate and adjust its size according to the requirement of the recipient. Therefore, liver regeneration is crucial for a successful LDLT. The volume and quality of the graft, ischemic time, portal flow, venous outflow, and immunosuppressive agents are among the factors affecting liver regeneration after adult LDLT.

Cyclosporine A (CsA), FK-506, and MMF can augment liver regeneration after hepatectomy or orthotopic liver transplantation in rats[1-6]. However, in vitro experiments indicate that CsA and FK-506 have an antiproliferative or cytotoxic effect on adult human hepatocytes[7,8]. During liver regeneration after partial hepatectomy, both mature hepatocytes and BECs are induced to proliferate. Human hepatocytes and intrahepatic BECs can be isolated from the liver tissue and maintained *in vitro* for a certain time. *In vitro*, mature hepatocytes have a very limited ability to replicate, while BECs have a great potential to proliferate[9,10]. In this study, the effect of CsA, FK-506, MMF, and 40-0-[2-hydroxyethyl]rapamycin (RAD) on the proliferation of human intrahepatic BECs *in vitro* was investigated.

MATERIALS AND METHODS

Liver tissue

All liver specimens were taken from the patients who

underwent hepatectomy or liver transplantation at University Hospital Essen, Germany. The procedure confirmed to the local ethical guidelines and followed the ethical guidelines of the 1975 Declaration of Helsinki. All patients or their relatives gave informed consents. Three diseased liver tissues were obtained from explanted livers, including one case of primary biliary cirrhosis (64 years old), one case of oxalosis (one year old) and one case of carbamoyl-phosphate-synthetase deficiency (one year old). Two normal liver tissues were obtained during hepatectomy, including one case of hepatoblastoma (1.5 years old) and one case of hepatocellular carcinoma (67 years old). Another normal liver tissue was obtained from a donor (10 years old) when the graft exceeded surgical requirement. All tissues were stored in Dulbecco' s minimum essential medium (PAA Laboratories, Coelbe, Germany) at 4 ºC and used within 36 h after hepatectomy.

Isolation and culture of human intrahepatic BECs

Human intrahepatic BECs were isolated with an immunomagnetic separation method employing an antibody against human epithelial antigen (HEA) as reported[11,12]. BECs were cultured with the plating medium in a 25-cm^2 flask (Greiner, Frickenhausen, Germany) pre-coated with collagen G (Biochrom KG, Berlin). The cell culture was maintained in a humidified atmosphere composed of 95% air and 50 mL/L CO_2. About 24-72 h after plating, the growth medium containing hepatocyte growth factor (HGF, R&D systems, UK) was used to culture the cells. The composition of the plating medium and growth medium was similar to the reported[13]. At confluence, BECs were detached with a solution containing 0.1 g/L trypsin and 1.0 g/L EDTA (Sigma, Taufkirchen, Germany) and maintained in a culture or used for the experiment.

Flow cytometry analysis of cytokeratin (CK) 19 expression

The expression of CK19 by BECs was investigated using flow cytometry with a FACS-Scan machine (Becton Dickinson, Heidelberg, Germany). Cells were pre-treated with the Fix & Perm cell permeabilization kit (Dianova, Hamburg, Germany). The monoclonal antibody against CK19 (IgG2b, Progen, Heidelberg, Germany) was used in a three times dilution according to the manufacturer's instructions. The FITC-labeled second antibody (Dianova, Hamburg, Germany) was diluted fifty times.

In vitro exposure to drugs

During passage, BECs were seeded at the density of 1×104 viable cells/well in 24-well plates with the plating medium. One day later, the medium was changed to the growth medium containing the drugs. CsA (MW 1203, Sandoz, Switzerland), FK 506 (MW 822, Fujisawa, Japan), RAD (MW 958.25, Sandoz, Switzerland) and MMF (MW 433.5, Sandoz, Switzerland) were diluted with a phosphate-buffered solution (PBS, PAA Laboratories, Coelbe, Germany). The concentrations of CsA, FK 506, RAD, and MMF in the medium ranged from 10 to 1 000 μg/L, 10 to 1 000 μg/L, 0.05 to 10 μg/L, 0.05 to 500 μg/L, respectively. Each concentration of the drug was determined in eight wells per experiment. The vigorously proliferating BECs derived from each liver tissue were used in the study and each drug was investigated eight times. Negative control cultures only received the growth medium.

MTT assay of cell growth

Dimethylthiazol-diphenyl-tetrazolium (MTT) assay was performed at 24 and 48 h after addition of the drugs, respectively. Fifty microliters of 4 mg/mL MTT (Sigma, Taufkirchen, Germany) was given to each well (containing 0.5 mL medium) in the 24-well plate. Four hours later, the medium was removed and 250 μL dimethyl sulfoxide (DMSO) was added into each well to solubilize the formazan dye converted from MTT by the cells. Five minutes later, the plates were shaken to make a homogenous dye solution and measured immediately with an ELISA reader (Lambda E, MWG-Biotech, Ebersberg, Germany) at a wavelength of 550 nm minus 690 nm. The cell number in each well was recorded in the form of optical density (OD).

Western blot analysis of CK19 expression

BECs were passaged into six-well plates pre-coated with collagen G. After 24 h, CsA or FK-506 was added into the growth medium and the cells were cultured for 48 h. The concentrations of both CsA and FK-506 in the medium were 500, 1 000 and 2 000 μg/L, respectively. BECs were detached by the use of 0.05% collagenase XI (Sigma, Taufkirchen, Germany), washed with PBS and stored at –20 °C. Protein amount was determined with the Bradford method (Biorad, Munich, Germany) after the cell pellet was boiled 10 times with 40 μL of 0.1% Triton/PBS. Extracted protein (1 μg/lane) was electrophoretically separated on a 10% SDS-PAGE and transferred to nitrocellulose. For the staining, blots were blocked with 1.2% gelatin in PBS and washed with 0.05% Tween 20 in PBS. First antibody against CK19 (IgG2b, Progen, Heidelberg, Germany) was diluted 1:80 in PBS and incubated for 1 h at room temperature. Anti-mouse Ig AP-conjugate as second antibody was diluted 1:1 000 in PBS and also incubated for 1 h at room temperature. Finally, the color was developed using BCIP and NBT (Gerbu, Gaiberg, Germany).

Statistical analysis

The average OD measured at different concentrations of each drug was compared using one-way analysis of variance (ANOVA) with the software SPSS 11.0 (SPSS, Inc., Chicago, IL, USA). Proliferation of the cells exposed to the drugs was compared to the negative control. $P<0.05$ was considered statistically significant.

RESULTS

Isolation and culture of intrahepatic BECs

The freshly isolated cells were small and round in shape and most of them formed clusters. Magnetic beads could

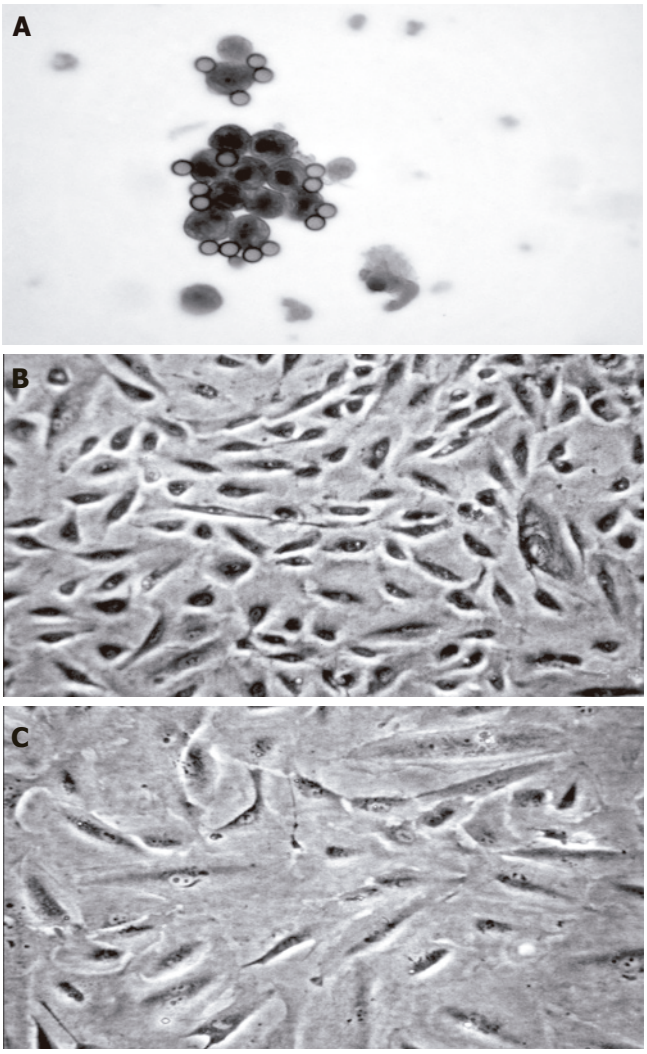

Figure 1 Freshly isolated (**A**) and proliferating human intrahepatic BECs (**B**) as well as BECs exposed to immunosuppressive agents (**C**).

be seen on the cell surface (Figure 1A). Intrahepatic BECs isolated from six liver tissues proliferated for 4-18 wk *in vitro* and were passaged 3-12 times. The proliferating BECs were small and oval in shape (Figure 1B). Flow cytometry analysis showed that the proliferating BECs consistently expressed CK19 (Figure 2).

Growth of intrahepatic BECs exposed to drugs

The vigorously proliferating BECs which represented passage (P) 1–6 BECs derived from different liver tissues, were exposed to the drugs. In this set of experiments, all the four immunosuppressive agents had no growth-promoting effect on BECs at any concentration *in vitro*. On the contrary, they inhibited the proliferation of BECs and this could be clearly shown at 48 h after the addition of the drugs (Figure 3A). All the four drugs inhibited the proliferation of BECs in a dose-dependent manner (Figure 3B) and this was repeatedly demonstrated with BECs derived from different liver tissues and in different passages. The lowest concentration for CsA, FK-506,

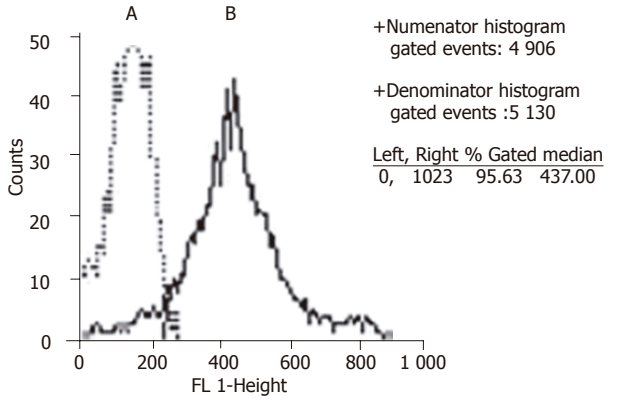

Figure 2 Flow cytometry analysis of CK19 expression. **A:** negative control. **B:** with antibody against CK19.

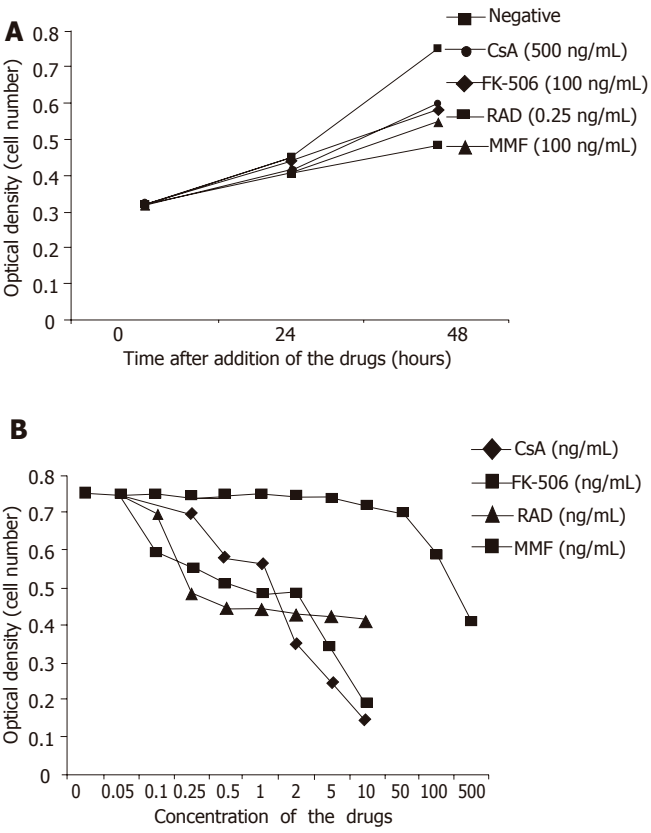

Figure 3 MTT analysis of proliferation of BECs exposed to drugs. **A:** BECs exposed to the drugs for 24 and 48 h. At 48 h, CsA (500 μg/L), FK-506 (100 μg/L), RAD (0.25 μg/L), and MMF (100 μg/L) inhibited proliferation of BECs (P<0.05). **B:** BECs exposed to the drugs for 48 h. CsA, FK-506, RAD, and MMF inhibited the proliferation of BECs in a dose-dependent manner.

RAD, and MMF to inhibit the proliferation of BECs (P<0.05) was 500, 100, 0.25, and 100 μg/L, respectively (Figures 3A and B). RAD had the strongest growth-inhibiting effect. Microscopically, the BECs treated with the drugs became larger than the cells in negative control (Figure 1C). However, Western blot analysis showed that CsA and FK-506 did not change CK19 protein expression by BECs (Figure 4).

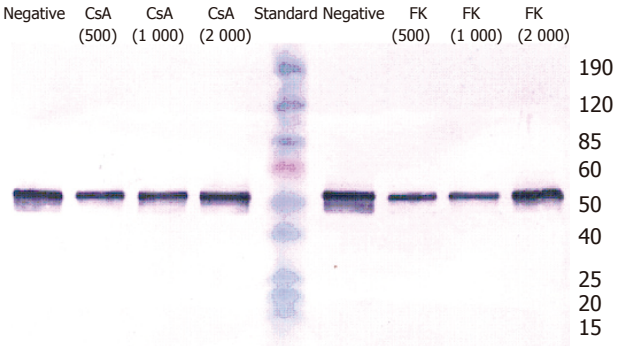

Figure 4 Western blot analysis of CK19 expression. BECs were treated with 500, 1 000, 2 000 μg/L CSA, and FK-506, respectively for 48 h. CsA and FK-506 did not change the protein expression of CK19 in BECs.

DISCUSSION

Intrahepatic BECs represent about 5% of total cell population in the liver. In the human liver, human epithelial antigen (HEA) is the cell surface antigen that only exists in intrahepatic BECs. With the immunomagnetic isolation technique employing anti-HEA monoclonal antibody, intrahepatic BECs can be purified after density-gradient centrifugation[11]. The purity of isolated human intrahepatic BECs is more than 99%[12]. The specific markers for biliary cells include CK7 and CK19. All the cells used in this experiment expressed CK19 (Figure 2), indicating that they are intrahepatic BECs.

In liver transplantation, the damaged liver cells caused by ischemia-reperfusion injury are repaired by liver regeneration. In adult LDLT, liver regeneration is of particular importance to meet the necessary metabolism requirement of the recipient. An immunosuppressive agent is one of the factors affecting liver regeneration after liver transplantation.

Generally speaking, CsA and FK-506 exert their immunosuppressive effect by blocking the production of interleukin-2 (IL-2) by T helper cells, while MMF and RAD exert their immunosuppressive effect by inhibiting proliferation of lymphocytes. CsA, FK-506, and MMF can enhance liver regeneration after hepatectomy or small-for-size liver transplantation in animals. The augmented liver regeneration might be an indirect effect, as CsA and FK-506 have anti-proliferative or cytotoxic effect on hepatocytes[7,8]. The possible mechanism for CsA and FK-506 on enhanced liver regeneration is through inhibition of production of IL-2 production and activation of natural killer (NK) cells[6]. The mechanism of MMF underlying accelerated liver regeneration is not fully understood.

In this study, all the four immunosuppressive agents inhibited human intrahepatic BECs in a dose-dependent manner *in vitro*, indicating that they have a direct inhibiting effect on liver regeneration and this direct effect should not be neglected, especially in adult LDLT. Our results showed that RAD had the strongest inhibiting effect on human intrahepatic BECs *in vitro*. The minimal concentration of RAD to inhibit proliferation of BECs (0.25 μg/L) *in vitro* was much lower than that of target serum through RAD level in patients undergoing immunosuppression (8-12 μg/L) after liver transplantation. Though the results obtained from an *in vitro* experiment were not identical to the results *in vivo*, it may indicate the importance of the direct effect of RAD on liver regeneration. Also, as an immunosuppressive agent, RAD has been reported to attenuate liver regeneration in a rat hepatectomy model[14]. Moreover, immunosuppressant-induced bile duct damage has been reported in azathioprine[15-18]. RAD and azathioprine share the similar immunosuppressive mechanism and it should be alerted that RAD might also cause bile duct damage in transplant patients.

In conclusion, CsA, FK-506, RAD, and MMF have an anti-proliferative effect on human intrahepatic BECs *in vitro*, while RAD has the strongest growth-inhibitory effect. Their possible effects on liver regeneration and bile duct injury in transplant patients should be further investigated.

REFERENCES

1 **Motale P,** Mall A, Spearman CW, Lotz Z, Tyler M, Shepherd E, Kahn D. The effect of mycophenolate mofetil on liver regeneration. *Transplant Proc* 2001; **33:** 1054-1055
2 **Mazzaferro V,** Porter KA, Scotti-Foglieni CL, Venkataramanan R, Makowka L, RossaroL, Francavilla A, Todo S, Van Thiel DH, Starzl TE. The hepatotropic influence of cyclosporine. *Surgery* 1990; **107:** 533-539
3 **Starzl TE,** Porter KA, Mazzaferro V, Todo S, Fung J, Francavilla A. Hepatotrophic effects of FK506 in dogs. *Transplantation* 1991; **51:** 67-70
4 **Kikuchi N,** Yamaguchi Y, Mori K, Takata N, Goto M, Makino Y, Hamaguchi H, Hisama N, Ogawa M. Effect of cyclosporine on liver regeneration after orthotopic reduced-size hepatic transplantation in the rat. *Dig Dis Sci* 1993; **38:** 1492-1499
5 **Kahn D,** Makowka L, Lai H, Eagon PK, Dindzans V, Starzl TE, Van Thiel DH.Cyclosporine augments hepatic regenerative response in rats. *Dig Dis Sci* 1990; **35:** 392-398
6 **Francavilla A,** Barone M, Todo S, Zeng Q, Porter KA, Starzl TE. Augmentation of rat liver regeneration by FK 506 compared with cyclosporin. *Lancet* 1989; **2:** 1248-1249
7 **Loreal O,** Fautrel A, Meunier B, Guyomard C, Guillouzo A, Launois B. FK 506 is less cytotoxic than cyclosporine to human and rat hepatocytes in vitro. *Transplant Proc* 1991; **23:** 2825-2828
8 **Blanc P,** Etienne H, Daujat M, Fabre I, Pichard L, Domergue J, Joyeux H, Fourtanier G, Maurel P. Antiproliferative effect of FK 506 and cyclosporine on adult humanhepatocytes in culture. *Transplant Proc* 1991; **23:** 2821-2824
9 **Strain AJ.** Isolated hepatocytes: use in experimental and clinical hepatology. *Gut* 1994; **35:** 433-436
10 **Joplin R.** Isolation and culture of biliary epithelial cells. *Gut* 1994; **35:** 875-878
11 **Joplin R,** Strain AJ, Neuberger JM. Immuno-isolation and culture of biliary epithelialcells from normal human liver. *In Vitro Cell Dev Biol* 1989; **25:** 1189-1192
12 **Joplin R,** Strain AJ, Neuberger JM. Biliary epithelial cells from the liver of patients withprimary biliary cirrhosis: isolation, characterization, and short-term culture. *J Pathol* 1990; **162:** 255-260
13 **Joplin R,** Hishida T, Tsubouchi H, Daikuhara Y, Ayres R, Neuberger JM, Strain AJ.Human intrahepatic biliary epithelial cells proliferate in vitro in response to human hepatocyte growth factor. *J Clin Invest* 1992; **90:** 1284-1289
14 **Chavez R,** Jamieson N, Takamori S, Nivatvongs S, Pino G, Metcalfe A, Watson C,14 Romero D, Metcalfe S. Hepatotrophic

effect of cyclosporine and FK 506 is not mimicked by rapamycin. *Transplant Proc* 1999; **31:** 2429

15 **Sobesky R,** Dusoleil A, Condat B, Bedossa P, Buffet C, Pelletier G. Azathioprine-induced destructive cholangitis. *Am J Gastroenterol* 2001; **96:** 616-617

16 **Horsmans Y,** Rahier J, Geubel AP. Reversible cholestasis with bile duct injury following azathioprine therapy. *A case report. Liver* 1991; **11:** 89-93

17 **DePinho RA,** Goldberg CS, Lefkowitch JH. Azathioprine and the liver. Evidence favoring idiosyncratic, mixed cholestatic-hepatocellular injury in humans. *Gastroenterology* 1984; **86:** 162-165

18 **Desmet VJ.** Vanishing bile duct syndrome in drug-induced liver disease. *J Hepatol* 1997; **26** Suppl 1: 31-35

Science Editor Wang XL and Guo SY **Language Editor** Elsevier HK

PO Box 2345, Beijing 100023, China
www.wjgnet.com
wjg@wjgnet.com

ELSEVIER

World J Gastroenterol 2005;11(48):7607-7614
World Journal of Gastroenterology ISSN 1007-9327

• *BASIC RESEARCH* •

Protective effects of Asian green vegetables against oxidant induced cytotoxicity

Peter Rose, Choon Nam Ong, Matt Whiteman

Peter Rose, Matt Whiteman, Department of Biochemistry, Faculty of Medicine, Yong Loo Lin School of Medicine, National University of Singapore, 8 Medical Drive, Singapore 117597, Singapore
Choon Nam Ong, Department of Community, Occupational and Family Medicine, Faculty of Medicine, Yong Loo Lin School of Medicine, National University of Singapore, 8 Medical Drive, Singapore 117597, Singapore
Correspondence to: Dr Peter Rose, Department of Biochemistry, National University of Singapore, 8 Medical Drive, 117597 Singapore. bchpcr@nus.edu.sg
Telephone: +65-6874-4996
Received: 2004-09-02 Accepted: 2005-02-01

Abstract

AIM: To evaluate the antioxidant and phase II detoxification enzyme inducing ability of green leaf vegetables consumed in Asia.

METHODS: The antioxidant properties of six commonly consumed Asian vegetables were determined using the ABTS, DPPH, deoxyribose, PR bleaching and iron-ascorbate induced lipid peroxidation assay. Induce of phase II detoxification enzymes was also determined for each respective vegetable extract. Protection against authentic ONOO- and HOCl mediated cytotoxicity in human colon HCT116 cells was determined using the MTT 3-(4,5-dimethylthiazol-2-yl)-2,5-diphenyl tetrasodium bromide) viability assay.

RESULTS: All of the extracts derived from green leaf vegetables exhibited antioxidant properties, while also having cytoprotective effects against ONOO- and HOCl mediated cytotoxicity. In addition, evaluation of the phase II enzyme inducing ability of each extract, as assessed by quinone reductase and glutathione-S-transferase activities, showed significant variation between the vegetables analyzed.

CONCLUSION: Green leaf vegetables are potential sources of antioxidants and phase II detoxification enzyme inducers in the Asian diet. It is likely that consumption of such vegetables is a major source of beneficial phytochemical constituents that may protect against colonic damage.

Key Words: Cruciferous vegetables; Lipid peroxidation; Free radicals; Isothiocyanates

Rose P, Ong CN, Whiteman M. Protective effects of Asian green vegetables against oxidant induced cytotoxicity. *World J Gastroenterol* 2005; 11(48): 7607-7614
http://www.wjgnet.com/1007-9327/11/7607.asp

INTRODUCTION

Reactive oxygen, nitrogen and chlorine species are generated *in vivo* by a diverse array of mechanisms including inflammatory responses, aerobic metabolism, and exposure to ionizing radiation. For example, the interaction of nitrogen monoxide (·NO) and superoxide ($O_2^{\cdot -}$) forms the cytotoxic product peroxynitrite, ($ONOO^-$) (Eq. 1)[1]. $NO + O_2^{\cdot -} \rightarrow ONOO^-$ (1)

Under physiological conditions ONOO- is converted to its protonated form peroxynitrous acid, ONOOH, which in turn decays to generate multiple toxic products with reactivities resembling those of the nitryl cation (NO_2^+), nitrogen dioxide radical ($^{\cdot}NO_2$), and hydroxyl radical (·OH). Similarly, at sites of chronic inflammation, neutrophils secrete hydrogen peroxide (H_2O_2) and the enzyme myeloperoxidase (MPO) which catalyzes the formation of hypochlorous acid (HOCl) (equation 2).

$H_2O_2 + Cl^- \rightarrow HOCl + OH^-$ (2)

Up to 80% of the H_2O_2 generated by activated neutrophils is used to form 20-400 μmol/L HOCl an hour[2-4]. Throughout this paper we use the term "hypochlorous acid" (pKa = 7.46) to refer to the approximately 50% ionized mixture of HOCl and OCl- species that exists at physiological pH 6[5]. Both peroxynitrite and HOCl and species derived from it can oxidize lipids, proteins, DNA, and carbohydrates[6-11]. Indeed, the addition of ONOO- or HOCl to biological fluids leads to the depletion of antioxidants including ascorbate, urate, and thiols. Depletion of *in vivo* antioxidant level by RS can initiate and promote cellular damage leading to genotoxicity and disease progression[12]. For example, RS may participate in the carcinogenesis by inducing genetic mutations. Therefore, due to the cytotoxicity of RS considerable interest in identifying chemical agents or dietary constituents that can interfere with RS mediated damage has been sought[13,14]. Plant derived antioxidants have been proposed to fulfill this role[15,16] and much research has focused on the potential antioxidant and cytoprotective or anti-carcinogenic properties of numerous phytochemical compounds[17,18]. These studies have been further supported by epidemiological investigations indicating that dietary habits

Table 1 Total phenolic content and inhibition of PR bleaching mediated by ONOO- and HOCl by green leaf vegetables used in this study.

Common name	Latin name	Total phenoliccontent (GAE mg/g Dwt)	% Inhibition of PR bleaching
Watercress "Rorripa"	*Rorripa nasturtium aquaticum*	133.6±15.1	75.6±3.2[a] 68.6±3.4
Broccoli	*Brassica oleracea var. italica*	61.03±13.1	85.7±10.36[a] 0.6±0.5
Choi Sum	*B.chinensis var. parachinensis*	163.7±2.11	104±6.6[a] 53.3±1.2
Pa Po	*B. chinensis var. parachinensis*	65.7±3.6	91.1±7.2[a] 50.1±1.6
Pheuy leng	*Amaranthus tricolor*	56.2±3.0	102±3.5[a] 50.7±0.2
SioPek	*B. chinensis*	111.0±11.9	76.9±7.8[a] 58.3±0.6

[a]$P<0.05$ *vs* others.

play a significant role in the risk of developing cancer[19]. High consumption of fruits and vegetables, reduced red meat intake and low alcohol consumption appears to be inversely correlated with colon cancer development. In Asia the lower prevalence of degenerative disease like cancer and heart disease are thought to be due to the high consumption of fruits and vegetables[20]. However, little information is available on the antioxidant properties of green vegetables that are widely consumed in Asia. These food stuffs are perhaps a major source of antioxidants and antioxidant like compounds in the Asian diet. Therefore, in this report, we determined the antioxidant properties and phase II enzyme inducing the ability of several green vegetables commonly consumed in Asia. In addition, each vegetable was evaluated for its protective effects against both authentic ONOO- and HOCl mediated cellular toxicity in human colon cells.

MATERIALS AND METHODS

Chemicals

Glutathione (GSH, reduced form), 4-nitrobenzaldehyde (4-NBA), h-nicotinamide adenine dinucleotide (NAD), NADP, NADPH, NADH, 1-chloro-2,4-dinitrobenzene (CDNB), flavin adenine dinucleotide (FAD), 2,6-dichloroindophenol (2,6-DCIP), were purchased from Sigma Chemical Co. (St. Louis, MO, USA). Protein assay kit was purchased from Bio-Rad labs (Hercules, CA, USA).

Plant material and extract preparation

Individual vegetables, broccoli (B), *Rorripa* (R), Sio Pek (SP), Pa Po (PP), Pheuy leng (PL) and Choi Sum (CS) were collected over a 3 mo period from the local supermarkets (Table 1). *Rorripa* and watercress are used interchangeably through the current text. All individual varieties were placed on dry ice and freeze dried immediately to preserve freshness. All individual representative vegetable samples were then pooled, this being conducted to eliminate variation. Extracts were then prepared using the procedure detailed[23,24]. In brief, 100 mg of freeze-dried tissue was weighed into a 50 mL polypropylene tube, hydrated with 2.0 mL of deionised water and homogenized for 15 s (Ultraturrax homogeniser) and left at room temperature for 1 h with occasional vortexing. Boiling 700 mL/L methanol (3.0 mL) was added to the mix and incubated for a further 15 min at +70 °C. The mixture was cooled to room temperature, and centrifuged at 3 000 r/min for 5 min. After centrifugation 1 mL aliquots were removed and vacuum condensed to 200 μL volumes. The resultant concentrates were filtered through sterile non-pyrogenic filters (0.2 μm; Millipore) and stored at -70 °C prior to testing. Extracts gave an equivalent concentration of 100 mg/mL for each sample. All extracts were analyzed for their respective ITC composition using a Finnigan- LCQ LC-MS system using the method previously described.

Cell culture and treatments

Human HCT116 cells were obtained from the American Type Culture Collection (ATCC, Manassas, VA, USA). Cells were grown in complete DMEM (containing 100 mL/L FBS, 100 000 U/L penicillin, 100 mg/L streptomycin, pH 7.4) in 75/cm^2 culture flasks at 37 °C in 50 mL/L CO_2. HOCl concentration was quantified immediately before use spectrophotometrically at 290 nm (pH 12, ε = 350 mol/L/cm). HOCl was diluted in ice cold EBSS to a concentration of 10 mmoL/L and stored on ice for no longer than 1 min. To expose the cells to HOCl, cells were washed twice with PBS and once with EBSS warmed to 37 °C. Fresh EBSS was then added followed by oxidant addition as described. The addition of HOCl did not significantly alter the pH of the reaction mixture. Hydrogen peroxide-free peroxynitrite (ONOO-) was synthesized as described[24], respectively. ONOO- solution was quantified immediately before use using a molar absorption coefficient of 1670/cm/mol/L[5].

ABTS assay

This was carried out as described in Ref.[25] 2,2'-Azinobis[3-ethylbenzothiazoline-6-sulfonate] (ABTS) in water (7 mmol/L final concentration) was oxidized using potassium persulfate (2.45 mmol/L final concentration) for at least 12 h in the dark. The ABTS$^+$ solution was diluted to an absorbance of 0.8±0.05 at 734 nm (Beckman UV-VIS spectrophotometer, Model DU640B) with phosphate-buffered saline (PBS). Absorbance was measured every 1 min for 5 min after initial mixing of extracts of different concentrations or Trolox standard with 1 mL of ABTS$^+$ solution. Trolox was used as a reference standard. Antioxidant properties of extracts were expressed as Trolox equivalent antioxidant capacity (TEAC).

Ascorbate-iron induced lipid peroxidation

Peroxidation of bovine brain extract was performed as described[26]. Briefly, bovine brain extract (BBE, 100 mg) was dissolved with PBS, and sonicated in an ice bath until dissolved. The BBE (0.2 mL) was preincubated with vegetable extracts in the presence of PBS and $FeCl_3$ (1 mmol/L). Lipid peroxidation was initiated by adding ascorbate (1 mmol/L), and the mixture was then incubated

for 1 h at 37 °C. The reaction was stopped by adding butylated hydroxytoluene (2 g/L in 950 mL/L ethanol), followed by the addition of trichloroacetic acid (28 g/L) and 2-thiobarbituric acid (TBA, 1 g/L). The mixture was heated at 80 °C for 20 min in a water bath. The (TBA) 2-MDA (malondialdehyde) chromogen formed was measured at 532 nm after extraction into 1-butanol using a SpectraMax190 microplate reader (Molecular Devices). Results were expressed as percentages of control.

Scavenging of 2,2-diphenyl-1-picrylhydrazyl

Scavenging activity was determined as described in Ref.[27]. DPPH solution (200 µmol/L in 800 mL/L ethanol) was mixed with an equal volume of extracts, and the absorbance at 520 nm was measured after 20 min at room temperature using the microplate reader. Results were expressed as percentages of control (100%).

Assessment of pyrogallol red bleaching by peroxynitrite

Bleaching of PR was performed as described in Ref.[28], respectively. PR (100 µmol/L final concentration) was dissolved in K_2HPO_4-KH_2PO_4 buffer. Compounds to be tested were added into the PR solution and incubated at room temperature for 10 min; addition of ONOO- (200 µmol/L) or HOCl (125 µmol/L) followed and the mixture was vortexed immediately for 10 s. The decrease in absorbance at 542 nm was determined using a microplate reader.

Total phenolic content

Total phenolic content of extracts was assessed approximately by using the Folin-Ciocalteu phenol reagent as described in Ref.[29]. The extracts (100 µL) were mixed with the Folin-Ciocalteu phenol reagent (0.2 mL), water (2 mL), and Na_2CO_3 (15 g/L, 1 mL), and absorbance at 765 nm was measured 2 h after incubation at room temperature using the microplate reader specified above. Gallic acid was used as a reference standard, and the total phenolics were expressed as milligrams per milliliter of gallic acid equivalents (GAEs).

Determination of phase II enzymatic induction and cellular glutathione

Glutathione-S-transferase and quinone reductase activities were determined as previously described[30]. Reduced glutathione levels in HCT116 cells were determined using the procedure described[31]. The formation of the GSH-phthalaldehyde conjugate was measured fluorometrically (excited at a wavelength of 350 nm, and the fluorescence measured at 420 nm).

Statistical analysis

All statistical analysis of data was conducted using MINITAB version 10.1 software package. ANOVA analysis was performed to determine the variation within and between selected populations.

RESULTS

Total phenolic content

The amounts of total phenolics varied widely in the vegetable extracts evaluated, these ranging between 56.2 to 163.7 mg GAE/g dry weight material (Table 1). Among the vegetable extracts, Choi Sum (*B. chinensis var. parachinensis*) contained the highest total amount of phenolics (163.2 mg GAE/g), whereas lower levels were found in Pa Po (*B. chinensis*), broccoli (*Brassica oleracea. var. italica*), and Pheuy leng (*Amaranthus tricolor*), (65.7, 61.0, and 56.2, respectively).

An additional assay, pyrogallol red (PR) bleaching, was used as an initial screening for the protective effects of each vegetable extract (10 mg/mL concentration) against ONOO- and HOCl induced PR bleaching. As shown in Table 1, all extracts showed some degree in preventing both ONOO- and HOCl mediated bleaching.

Radical scavenging by Asian green leaf vegetable extracts

The antioxidant activities of each vegetable extract were determined using four different chemical assays, ABTS, DPPH, deoxyribose and iron ascorbate lipid peroxidation assay. All the methods have been extensively used for the screening of antiradical activities of fruit and vegetable juices and extracts.

The antioxidant properties of each individual vegetable extract are represented in Figure 1A and F. Extracts of each vegetable were examined and compared for their free radical scavenging activities against radical cation ABTS+. The ABTS assay has been widely used to determine the radical scavenging ability of both synthetic chemicals and plant extracts. All extracts showed ABTS+ scavenging capacity as determined by the reduction in absorbance at 734 nm, as previously reported (Figures 1A and B). In addition, comparison with the water soluble analog Trolox allowed us to determine the total antioxidant capacity TEAC value for each extract, none of the extracts were more effective than Trolox alone (Figure 1C). Likewise, as demonstrated in Figure 1D, all vegetable extracts showed antioxidant scavenging potential in the DPPH assay. In additional assays, we also examined the effects of extracts on hydroxyl radicals and lipid peroxidation (Figures 1E and F). Again all extracts showed some positive inhibition in each assay however, we were unable to show any correlation between phenolic acid content and scavenging ability. Kahkonen *et al.* and Shahidi *et al.* reported that differences in antioxidant activities of plant extracts are a likely result of differences in the types of phenolic acids and flavonoid compounds and their derivatives present with in the plant extracts[32,33]. For example, the antioxidant activities of phenolic acids and their esters are dependant on the number of hydroxy groups in the molecules. Perhaps such limitations are also apparent in our study.

Protection Against ONOO- and HOCl mediated cytotoxicity in HCT116 cells by asian green leaf vegetables

Incubating HCT116 colon cells in the presence of each vegetable extract (0.2-10 mg/mL extract) for 1 h did not result in any significant cytotoxicity measured using the MTT assay (data not shown) whereas the addition of 200 µmol/L ONOO- or 125 µmol/L HOCl led to

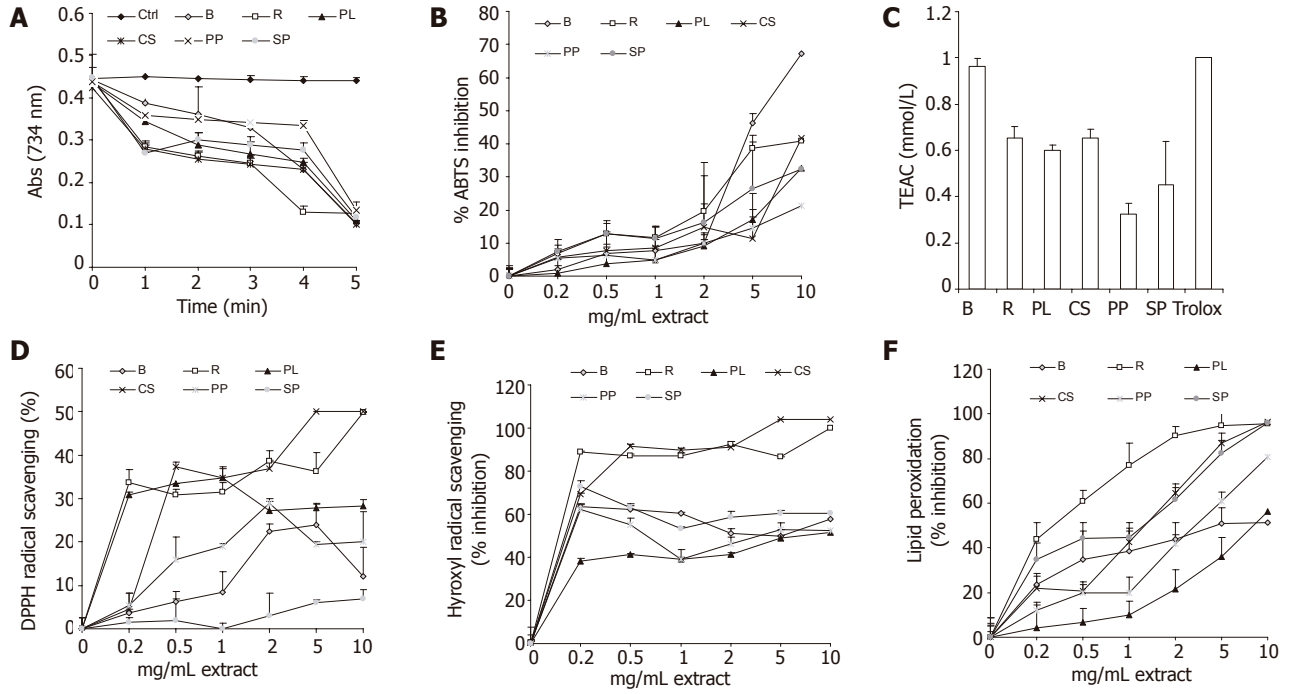

Figure 1 Kinetics of reactions of ABTS radicals in the presence of 10 mg/mL of each vegetable extract (**A**), (**B**) the effects of increased concentration of the vegetable extracts on the inhibition of the ABTS radical represented as % ABTS inhibition, (**C**) total antioxidant activity of extracts from green leaf vegetables as compared to trolox, (**D**) DPPH radical scavenging, (**E**) hydroxyl radical scavenging, and (**F**) iron-ascorbate induced lipid peroxidation. Values are presented as means±SD (n = 6).

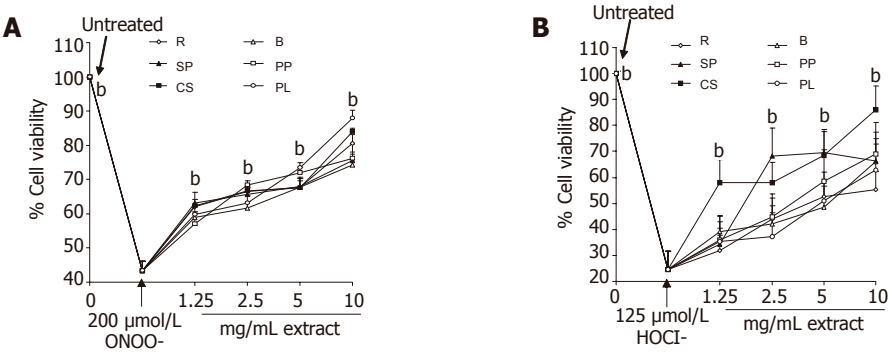

Figure 2 Concentration dependant inhibition of ONOO–- and HOCl mediated cytotoxicity by green leaf vegetable extracts. HCT116 cells were treated with each extract for 5 min and ONOO– or HOCl added. Cell viability was assayed using MTT and measurement of the solubilized formazan dye at Abs 595 nm. Experiments were conducted as described in Materials and methods and data are expressed as mean±SD (n = 6). ^{b}P<0.01 comparing extracts to ONOO– or HOCl treatment alone.

substantial decrease in viability (Figures 3A and B). All extracts significantly inhibited ONOO–- and HOCl mediated cytotoxicity in a concentration-dependent manner.

Induction of phase II detoxification enzymes by Asian green leaf vegetable extracts inhibits ONOO- and HOCl mediated cytotoxicity

The induction of phase II detoxification enzymes QR and GST varied widely among the vegetable extracts evaluated. As shown in Figures 3A and B, both the broccoli and watercress extracts, two species previously been shown as potent inducers of phase II enzymes, showed the most significant induction of QR and GST at 0.02-0.1 mg/mL extract in human HCT116 cells. In contrast, only extracts of Choi Sum (*B. chinensis var. parachinensis*) and Pheuy leng (*Amaranthus tricolor*), showed any potential in inducing QR and GSTs in the current study, all be it at a 10 fold higher concentration (0.1-10 mg/mL extract) than that of broccoli or watercress. Neither Pa Po (*B. chinensis var. parachinensis*) nor Sio Pek (*B. chinensis var. parachinensis*) showed any ability to induce QR or GST (Figure 3C and D). In addition, analysis of each vegetable extract using LC-MS, we were unable to find any putative ITCs present except in any extracts except for broccoli (4-methylsulfinylbutyl ITC) and *Rorripa* (7-methylsulfinylheptyl ITC), respectively. All LC-MS data corresponded to that previously published[23-24]. This may suggest that the other vegetable extracts did not contain any ITCs or that the levels were below the level of detection in our method (Figures 3E and F). To

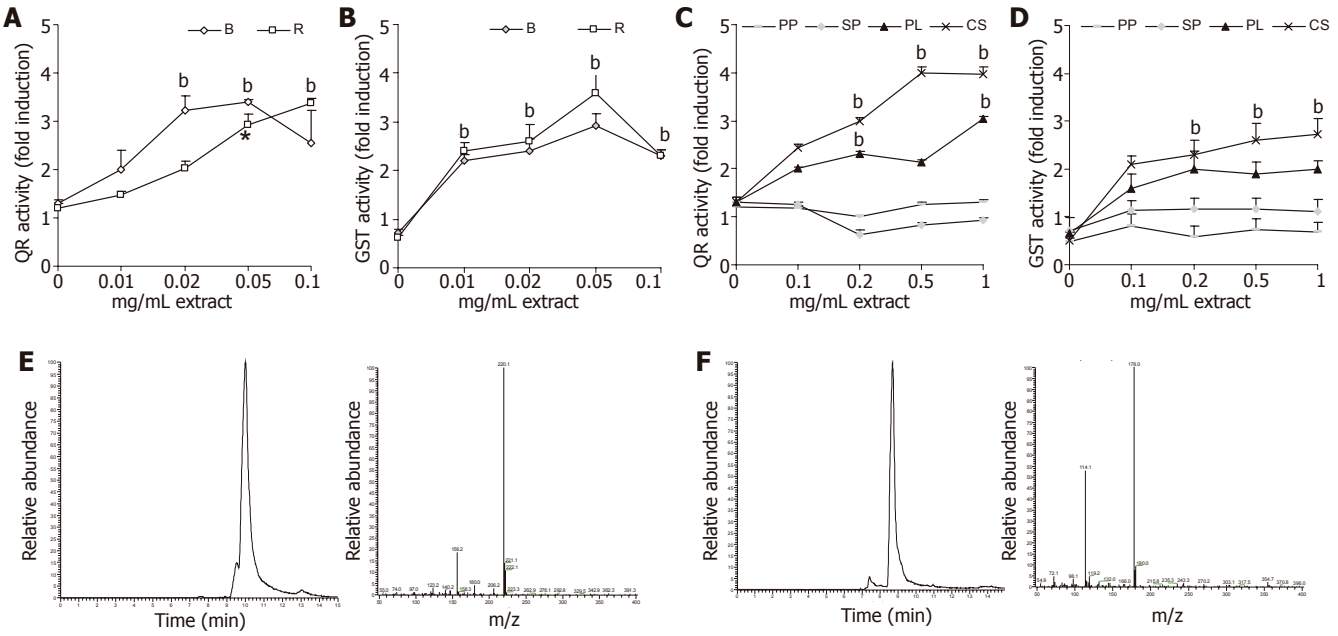

Figure 3 Effect of green vegetable extracts on QR and GST induction in the human colon HCT116 cell line. Cells were treated with each respective extract at 0.01-1 mg/mL (broccoli and *Rorripa*) and 1-10 mg/mL Choi Sum, Pa Po, Pheuy leng and Sio Pek for 24 h. (**A**) induction of QR and (**B**) GST induction by broccoli and *Rorripa*, (**C**) and (**D**) induction of QR and GST by Choi Sum, Pa Po, Pheuy leng and Sio Pek, (**E**) *Rorripa* ITC, 7-methylsulfinylheptyl ITC and (**F**) broccoli ITC, 4-methylsulfinylbutyl ITC as determined using LC-MS. Each data point represents the mean±SD for four separate experiments. $^{b}P<0.001$ *vs* the control cells.

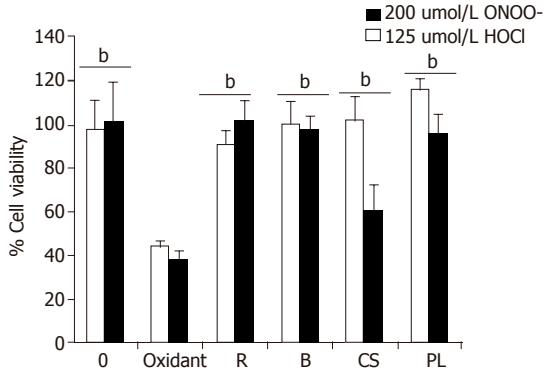

Figure 4 Protective effects of vegetable extracts on ONOO-- and HOCl mediated cytotoxicity in HCT116 cells. Cells were pre-treated with each extract for 24 h to induce phase II detoxification enzymes prior to the addition of ONOO- or HOCl for 30 min. Cell viability was assayed using MTT and measurement of the solubilized formazan dye at Abs 595 nm. Experiments were conducted as described in Materials and methods and data are expressed as mean±SD (n = 6). $^{b}P<0.001$ *vs* extracts to ONOO- or HOCl treatment alone.

examine whether the induction of phase II enzymes could protect against oxidative stress, human HCT116 cell were pre-incubated for 24 h with each respective extract at a concentration that induced a 2 fold induction of QR and GST [(0.01mg/mL) broccoli or *Rorripa* and 1 mg/mL for Pheuy leng, and Choi Sum)], respectively. Consequently, intracellular glutathione was determined prior to the addition of the oxidants ONOO- and HOCl. In all the treatment groups particularly broccoli, Rorripa and Choi Sum, intracellular GSH was elevated (Table 2). Moreover, pre-treated cells were more resistant against ONOO- and HOCl mediated toxicity (Figure 4A).

Table 2 Pre-treatment with green leaf vegetables increases intracellular glutathione levels in HCT116 cells. $^{b}P<0.01$ comparing treated to control cells (mean±SD).

Vegetable	Total GSH ($nmol^{-1}/mg^{-1}$protein)
Ctrl	15.2±0.4
Watercress "*Rorripa*"	33.2±2.7^{b}
Broccoli	28.7±0.5^{b}
Choi Sum	25.1±1.9^{b}
Pheuy leng	25.2±2.2^{b}

DISCUSSION

In the present investigation we evaluated green leaf vegetables that are commonly consumed in Singapore, this being a representative group of vegetables commonly consumed in the region. Recent epidemiological studies have highlighted a protective effect of vegetable consumption, particularly cruciferous vegetables, on colon cancer development[34-37]. Thus, knowledge of the antioxidant properties of local vegetables may partly explain their beneficial health effects.

The generation of $ONOO^{-}$ and HOCl *in vivo* is implicated in a wide range of human diseases ranging from cancer and cardiovascular diseases to chronic inflammation[12]. The *in vivo* formation of ONOO- in patients with colorectal cancer and a corresponding reduction in plasma antioxidant status has been reported[38]. While increased expression levels of inducible nitric oxide sythase and the formation of ONOO- is observed in patients with ulcerative colitis[39]. Similarly, HOCl produced by inflammatory phagocytic leukocytes reportedly contribute to gastrointestinal mucosal damage[40]. These data being suggestive that

oxidative stress contributes to the pathogenesis of colonic inflammation and cancers. Indeed, supplementation with antioxidants in numerous gastrointestinal model systems has been shown to reduce oxidant induced damage[41-45]. Therefore, agents that are able to protect against ONOO- and HOCl dependent damage may be particularly useful in the diet.

Till date, much is known about the dietary sources and antioxidant properties of vegetables commonly consumed in the Western diet however, much less is known about the antioxidant properties of green leaf vegetables consumed in Asia. In our study, we examined six local vegetables, five being members of the family Cruciferae, and an additional specimen being a spinach substitute used in the region, a member of the genus *Amaranthus* (Table 1). Analysis of total phenolic content using the Folin–Ciocalteu phenol reagent method showed considerable variation among the vegetables studied. Chye Sim had the highest total phenolic content (163.7±2.1 mg/g sample) whereas Pheuy leng had the lowest (56.2±3.0 mg/g sample). Dietary derived phenolic compounds like flavonoids, phenolic acids and condensed tannins are all reported to function as antioxidants. Indeed, in all the antioxidant assays used in the current study, PR bleaching, lipid peroxidation, ABTS, DPPH and hydroxyl radical scavenging; all vegetable extracts, to a varying degree, possessed antioxidant properties. Moreover, co-treatment of human colon cancer HCT116 cell line with individual vegetable extract inhibited both ONOO- and HOCl mediated toxicities in a concentration dependant manner. Several investigators have correlated the antioxidant potential of plant extracts with the content of individual compounds. As well as phenolic constituents many vegetables also contain fat-soluble vitamins and precursors, such as tocopherols and carotenoids, along with the water-soluble vitamin ascorbic acid that also poses antioxidant properties. Indeed, the antioxidant potential of Broccoli has been partially attributed to both flavonoid as well as hydroxycinnamic acid constituents[46]. Flavonoids along with other phenolic constituents are widely distributed in higher plants and exhibit diverse biological activities. For example, the antioxidant action of flavonoids in the GI tract could be mediated by the suppression of ROS formation either by inhibition of enzymes or chelating trace elements involved in free radical production, direct scavenging ROS or the upregulation of antioxidant defense system. Structure function analysis has revealed that the antioxidant properties are dependant upon the extent, type and position of functional group substitutions on the ring structures. In our study we were unable to find any correlation between the antioxidant potential of individual vegetable extracts and their total phenolic content. Our findings are in-agreement with that of Kurilich *et al.* 2002, who demonstrated that the antioxidant properties of different broccoli cultivars did not correlate with their respective ascorbic acid or flavonoid composition[47]. We propose that such discrepancies are a likely result of differences in the chemical composition of each vegetable and that such effects may influence the antioxidant properties as observed in the current study. Also, given that recent evidence suggests that many phenolic compounds such as flavonoids are not absorbed to any appreciable levels *in vivo*, perhaps the major site of action is in the lumen of the GI tract as has previously been suggested[48]. We assume that the observed variation in antioxidant properties and cytoprotective effects are perhaps due to the composition of phenolic compounds present in each vegetable, although this requires further study.

In contrast to direct antioxidant scavenging properties, a secondary mechanism that may protect against oxidative stress is the stimulation of cellular protective pathways. The co-ordinate induction of phase 2 detoxification enzymes provides protection against electrophilic and oxidant induced cellular damage. Interestingly, cruciferous vegetables contain phytochemicals known as glucosinolates that under the action of plant or bacterial myrosinases (thioglucoside glucohydrolase; EC 3.2.3.1) following tissue disruption, are converted to bioactive isothiocyanates (ITC)[49]. ITCs are potent inducers of phase II detoxification enzymes in mammals[23-52]. Indeed, induction of phase II enzymes by the ITC sulforaphane has recently been shown to protect human adult retinal pigment cells, epithelial keratinocytes and murine leukemia cells against oxidant induced damage[50]. Mechanistic studies have also indicated that, depending upon the specific structure of the ITC, these compounds can act at three stages of carcinogenesis. Firstly, they can prevent carcinogen activation through inhibition of phase I enzymes such as cytochrome P450s[51]. Secondly they can induce phase II enzymes such as quinone reductase (QR) [NAD(P)H: (quinone-acceptor) oxidoreductase, EC 1.6.99.2], glutathione S-transferases (GSTs) [EC 2.5.1.18] and UDP-glucuronosyltransferases [EC 2.4.1.17] , resulting ultimately in the excretion of the potential carcinogens[52]. Thirdly, they can induce apoptosis[53-56]. The putative anticarcinogenic activity of ITCs is consistent with the results of epidemiological studies, which have suggested a reduction in risk of cancer, particularly of the gastrointestinal tract, through the consumption of cruciferous vegetables[34,36]. In our, study, we found a 10 fold difference in the ability of the vegetables examined to induce both QR and GSTs in human colon HCT116 cells. Both broccoli and *Rorripa* were the strongest enzyme inducers, this previously being attributed to there ITC composition[23-24]. Of the local vegetables only Choi Sum and Pheuy leng induced any significant increase in QR and GST activity. We assume that such variation in phase II enzyme induction is likely to be a result of the composition and content of ITCs present within each vegetable. Jiao *et al.* 1998, previously demonstrated that considerable variation exists between local cruciferous asian vegetables (low ITC content) when compared to broccoli or *Rorripa* (High ITC content)[57]. Moreover, Hecht *et al.* 2004, also reported that cruciferous vegetables collected in Singapore contained high levels of glucobrassicins (70-90%) and relatively low levels of alkyl GSLs, the progenitor compounds of chemicals like sulforaphane[58]. Glucobrassicins, upon tissue disruption form indole-3-carbinols, these compounds have previously been shown to be poor inducers of phase II detoxification enzymes[59].

In summary, our data supports the finds that cruciferous vegetables can decrease *in vitro* and *in vivo* oxidant induced genotoxicity[60] by being potent source of antioxidants that may offer protection against oxidant induced damage in human beings. Moreover, we also found that the phase II enzyme inducing ability varied considerably among the vegetables analyzed, these data suggesting that biomarkers of exposure to cruciferous vegetables may be a more important inclusion into epidemiological studies than previously thought.

REFERENCES

1 **Beckman JS,** Chen J, Ischiropoulos H, Crow JP. Oxidative chemistry of peroxynitrite. *Methods Enzymol* 1994; **233**: 229-240
2 **Foote CS**, Goyne TE, Lehrer RI. Assessment of chlorination by human neutrophils. *Nature* 1983; **301:** 715-716
3 **Weiss SJ,** Klein R, Slivka A, Wei M. Chlorination of taurine by human neutrophils. Evidence for hypochlorous acid generation. *J Clin Invest* 1982; **70:** 598-607
4 **Babior BM.** Phagocytes and oxidative stress. *Am J Med* 2000; **109:** 33-44
5 **Morris JC.** The acid ionization constant of hypochlorous acid from 5 to 35 degrees. *J Phys Chem* 1966; **70:** 3798–3805.
6 **Schraufstatter IU,** Browne K, Harris A, Hyslop PA, Jackson JH, Quehenberger O, Cochrane CG. Mechanisms of hypochlorite injury of target cells. *J Clin Invest* 1990; **85:** 554-562
7 **Prutz WA.** Hypochlorous acid interactions with thiols, nucleotides, DNA, and other biological substrates. *Arch Biochem Biophys* 1996; **332:** 110-120
8 **Spickett CM,** Jerlich A, Panasenko OM, Arnhold J, Pitt AR, Stelmaszynska T, Schaur RJ. The reactions of hypochlorous acid, the reactive oxygen species produced by myeloperoxidase, with lipids. *Acta Biochim Pol* 2000; **47:** 889-899
9 **Radi R,** Beckman JS, Bush KM, Freeman BA. Peroxynitrite-induced membrane lipid peroxidation: the cytotoxic potential of superoxide and nitric oxide. *Arch Biochem Biophys* 1991; **288:** 481-487
10 **Ischiropoulos H,** al-Mehdi AB. Peroxynitrite-mediated oxidative protein modifications. *FEBS Lett* 1995; **364:** 279-282
11 **Beckman JS,** Beckman TW, Chen J, Marshall PA, Freeman BA. Apparent hydroxyl radical production by peroxynitrite: implications for endothelial injury from nitric oxide and superoxide. *Proc Natl Acad Sci USA* 1990; **87:** 1620-1624
12 **Halliwell B,** Gutteridge JMC. Free radicals in biology and medicine, 3rd ed., Oxford: Oxford Univ. Press; 1999
13 **Whiteman M,** Halliwell B. Protection against peroxynitrite dependent tyrosine nitration and alpha 1-antiproteinase inactivation by ascorbic acid A comparison with other biological antioxidants. *Free Radic Res* 1996; **25:** 275-283
14 **Hooper DC,** Spitsin S, Kean RB, Champion JM, Dickson GM, Chaudhry I, Koprowski H. Uric acid, a natural scavenger of peroxynitrite, in experimental allergic encephalomyelitis and multiple sclerosis. *Proc Natl Acad Sci USA* 1998; **95:** 675-680
15 **Choi JS,** Chung HY, Kang SS, Jung MJ, Kim JW, No JK, Jung HA. The structure-activity relationship of flavonoids as scavengers of peroxynitrite. *Phytother Res* 2002; **16:** 232-235
16 **Heijnen CG,** Haenen GR, van Acker FA, Van der Vijgh WJ, Bast A. Flavonoids as peroxynitrite scavengers: the role of the hydroxyl groups. *Toxicol In Vitro* 2001; **15:** 3-6
17 **Harborne JB,** Williams CA. Advances in flavonoid research since 1992. *Phytochemistry* 2000; **55:** 481-504
18 **Nijveldt RJ,** van Nood E, van Hoorn DE, Boelens PG, van Norren K, van Leeuwen PA. Flavonoids: a review of probable mechanisms of action and potential applications. *Am J Clin Nutr* 2001; **74:** 418-425
19 **Hertog MG,** Kromhout D, Aravanis C, Blackburn H, Buzina R, Fidanza F, Giampaoli S, Jansen A, Menotti A, Nedeljkovic S. Flavonoid intake and long-term risk of coronary heart disease and cancer in the seven countries study. *Arch Intern Med* 1995; **155:** 381-386
20 **Mason JB.** Nutritional chemoprevention of colon cancer. *Semin Gastrointest Dis* 2002; **13:** 143-153
21 **Miller AB,** Howe GR, Jain M, Craib KJ, Harrison L. Food items and food groups as risk factors in a case-control study of diet and colo-rectal cancer. *Int J Cancer* 1983; **32:** 155-161
22 **Tarwadi K,** Agte V. Potential of commonly consumed green leafy vegetables for their antioxidant capacity and its linkage with the micronutrient profile. *Int J Food Sci Nutr* 2003; **54:** 417-425
23 **Rose P,** Faulkner K, Williamson G, Mithen R. 7-Methylsulfinylheptyl and 8-methylsulfinyloctyl isothiocyanates from watercress are potent inducers of phase II enzymes. *Carcinogenesis* 2000; **21**: 1983-1988
24 **Mithen R,** Faulkner K, Magrath R, Rose P, Williamson G, Marquez J. Development of isothiocyanate-enriched broccoli, and its enhanced ability to induce phase 2 detoxification enzymes in mammalian cells. *Theor Appl Genet* 2003; **106:** 727-734
25 **Re R,** Pellegrini N, Proteggente A, Pannala A, Yang M, Rice-Evans C. Antioxidant activity applying an improved ABTS radical cation decolorization assay. *Free Radic Biol Med* 1999; **26:** 1231-1237
26 **Gutteridge JM,** Halliwell B. The measurement and mechanism of lipid peroxidation in biological systems. *Trends Biochem Sci* 1990; **15:** 129-135
27 **Gao X,** Ohlander M, Jeppsson N, Bjork L, Trajkovski V. Changes in antioxidant effects and their relationship to phytonutrients in fruits of sea buckthorn (*Hippophae rhamnoides L.*) during maturation. *J Agric Food Chem* 2000; **48:** 1485-1490
28 **Balavoine GG,** Geletii YV. Peroxynitrite scavenging by different antioxidants. Part I: convenient assay. *Nitric Oxide Biol Chem* 1999; **3:** 40- 54
29 **Singleton VL,** Orthofer R, Lamuela-Raventos RM. Analysis of total phenols and other oxidation substrates and antioxidants by means of Folin– Ciocalteu reagent. *Methods Enzymol* 1999; **299:** 152-178
30 **Jiang ZQ,** Chen C, Yang B, Hebbar V, Kong AN. Differential responses from seven mammalian cell lines to the treatments of detoxifying enzyme inducers. *Life Sci* 2003; **72:** 2243-2253
31 **Hissin PJ,** Hilf R. A fluorometric method for determination of oxidized and reduced glutathione in tissues. *Anal Biochem* 1976; **74:** 214-226
32 **Kahkonen MP,** Hopia AI, Heinonen M. Berry phenolics and their antioxidant activity. *J Agric Food Chem* 2001; **49:** 4076-4082
33 **Sahidi F.** Antioxidant factors in plant foods and selected oilseeds. *Biofactors* 2000; **13:** 179-185
34 **Lee HP,** Gourley L, Duffy SW, Esteve J, Lee J, Day NE. Colorectal cancer and diet in an Asian population--a case-control study among Singapore Chinese. *Int J Cancer* 1989; **43:** 1007-1016
35 **Voorrips LE,** Goldbohm RA, van Poppel G, Sturmans F, Hermus RJ, van den Brandt PA. Vegetable and fruit consumption and risks of colon and rectal cancer in a prospective cohort study: The Netherlands Cohort Study on Diet and Cancer. *Am J Epidemiol* 2000; **152:** 1081-1092
36 **Seow A,** Yuan JM, Sun CL, Van Den Berg D, Lee HP, Yu MC. Dietary isothiocyanates, glutathione S-transferase polymorphisms and colorectal cancer risk in the Singapore Chinese Health Study. *Carcinogenesis* 2002; **23:** 2055-2061
37 **Witte JS,** Longnecker MP, Bird CL, Lee ER, Frankl HD, Haile RW. Relation of vegetable, fruit, and grain consumption to colorectal adenomatous polyps. *Am J Epidemiol* 1996; **144:** 1015-1025
38 **Szaleczky E,** Pronai L, Nakazawa H, Tulassay Z. Evidence of in vivo peroxynitrite formation in patients with colorectal

carcinoma, higher plasma nitrate/nitrite levels, and lower protection against oxygen free radicals. *J Clin Gastroenterol* 2000; **30:** 47-51

39 **Kimura H,** Hokari R, Miura S, Shigematsu T, Hirokawa M, Akiba Y, Kurose I, Higuchi H, Fujimori H, Tsuzuki Y, Serizawa H, Ishii H. Increased expression of an inducible isoform of nitric oxide synthase and the formation of peroxynitrite in colonic mucosa of patients with active ulcerative colitis. *Gut* 1998; **42:** 180-187

40 **Yamada T**, Grisham MB. Role of neutrophil-derived oxidants in the pathogenesis of intestinal inflammation. *Klin Wochenschr* 1991; **69:** 988-994

41 **Martin AR,** Villegas I, La Casa C, de la Lastra CA. Resveratrol, a polyphenol found in grapes, suppresses oxidative damage and stimulates apoptosis during early colonic inflammation in rats. *Biochem Pharmacol* 2004; **67:** 1399-1410

42 **Loguercio C,** D'Argenio G, Delle Cave M, Cosenza V, Della Valle N, Mazzacca G, Del Vecchio Blanco C. Glutathione supplementation improves oxidative damage in experimental colitis. *Dig Liver Dis* 2003; **35:** 635-641

43 **Oliveira CP,** Kassab P, Lopasso FP, Souza HP, Janiszewski M, Laurindo FR, Iriya K, Laudanna AA. Protective effect of ascorbic acid in experimental gastric cancer: reduction of oxidative stress. *World J Gastroenterol* 2003; **9:** 446-448

44 **Rotting AK,** Freeman DE, Eurell JA, Constable PD, Wallig M. Effects of acetylcysteine and migration of resident eosinophils in an in vitro model of mucosal injury and restitution in equine right dorsal colon. *Am J Vet Res* 2003; **64:** 1205-1212

45 **Tamai H,** Kachur JF, Grisham MB, Gaginella TS. Scavenging effect of 5-aminosalicylic acid on neutrophil-derived oxidants. Possible contribution to the mechanism of action in inflammatory bowel disease. *Biochem Pharmacol* 1991; **41:** 1001-1006

46 **Plumb GW.** Price KR. Rhodes MJ. Williamson G. Antioxidant properties of the major polyphenolic compounds in broccoli. *Free Radic Res* 1997; **27:** 429-435

47 **Kurilich AC,** Jeffery EH, Juvik JA, Wallig MA, Klein BP. Antioxidant capacity of different broccoli (*Brassica oleracea*) genotypes using the oxygen radical absorbance capacity (ORAC) assay. *J Agric Food Chem* 2002; **50:** 5053-5057

48 **Halliwell B,** Zhao K, Whiteman M. The Gastrointestinal Tract: A Major Site of Antioxidant Action? *Free Radic Res* 2001; **33:** 819-830

49 **Rask L,** Andreasson E, Ekbom B, Eriksson S, Pontoppidan B, Meijer J. Myrosinase: gene family evolution and herbivore defense in Brassicaceae. *Plant Mol Biol* 2000; **42:** 93-113

50 **Gao X,** Dinkova-Kostova AT, Talalay P. Powerful and prolonged protection of human retinal pigment epithelial cells, keratinocytes, and mouse leukemia cells against oxidative damage: the indirect antioxidant effects of sulforaphane. *Proc Natl Acad Sci USA* 2001; **98:** 15221-15226

51 **Conaway CC,** Jiao D, Chung FL. Inhibition of rat liver cytochrome P450 isozymes by isothiocyanates and their conjugates: a structure-activity relationship study. *Carcinogenesis* 1996; **17:** 2423-2427

52 **Zhang Y,** Talalay P. Mechanism of differential potencies of isothiocyanates as inducers of anticarcinogenic Phase 2 enzymes. *Cancer Res* 1998; **58:** 4632-4639

53 **Gamet-Payrastre L,** Li P, Lumeau S, Cassar G, Dupont MA, Chevolleau S, Gasc N, Tulliez J, Terce F. Sulforaphane, a naturally occurring isothiocyanate, induces cell cycle arrest and apoptosis in HT29 human colon cancer cells. *Cancer Res* 2000; **60:** 1426-1433

54 **Rose P,** Whiteman M, Huang SH, Halliwell B, Ong CN. beta-Phenylethyl isothiocyanate-mediated apoptosis in hepatoma HepG2 cells. *Cell Mol Life Sci* 2003; **60:** 1489-1503

55 **Rose P,** Armstrong JS, Chua YL, Ong CN, and Whiteman M. Beta-phenylethyl isothiocyanate mediated apoptosis; contribution of Bax and the mitochondrial death pathway. *Int J Biochem Cell Biol* 2005; **37:** 100-119

56 **Xu K,** Thornalley PJ. Studies on the mechanism of the inhibition of human leukaemia cell growth by dietary isothiocyanates and their cysteine adducts in vitro. *Biochemical Pharmacol* 2000; **60:** 221-231

57 **Jiao D,** Yu MC, Hankin JH, Low SH, and Chung FL. Total Isothiocyanate Contents in Cooked Vegetables Frequently Consumed in Singapore. *J Agric Food Chem* 1998; **46:** 1055-1058

58 **Hecht SS,** Carmella SG, Kenney PM, Low SH, Arakawa K, Yu MC. Effects of cruciferous vegetable consumption on urinary metabolites of the tobacco-specific lung carcinogen 4-(methylnitrosamino)-1-(3-pyridyl)-1-butanone in singapore chinese. *Cancer Epidemiol Biomarkers Prev* 2004; **13:** 997-1004

59 **Chen YH,** Yang D. Differential effects of vegetable-derived indoles on the induction of quinone reductase in hepatoma cells. *J Nutr Sci Vitaminol* (Tokyo) 2002; **48:** 477-482

60 **Gill CI,** Haldar S, Porter S, Matthews S, Sullivan S, Coulter J, McGlynn H, Rowland I. The effect of cruciferous and leguminous sprouts on genotoxicity, in vitro and in vivo. *Cancer Epidemiol Biomarkers Prev* 2004; **13:** 1199-1205

Science Editor Li WZ **Language Editor** Elsevier HK

PO Box 2345, Beijing 100023, China
www.wjgnet.com
wjg@wjgnet.com

ELSEVIER

World J Gastroenterol 2005;11(48):7615-7619
World Journal of Gastroenterology ISSN 1007-9327

• *BASIC RESEARCH* •

Detection and identification of intestinal pathogenic bacteria by hybridization to oligonucleotide microarrays

Lian-Qun Jin, Jun-Wen Li, Sheng-Qi Wang, Fu-Huan Chao, Xin-Wei Wang, Zheng-Quan Yuan

Lian-Qun Jin, Zheng-Quan Yuan, PLA Center of Disease Control and Prevention, Beijing 100039, China
Jun-Wen Li, Fu-Huan Chao, Xin-Wei Wang, Tianjin Institute of Hygiene and Environmental Medicine, Tianjin 300050, China
Sheng-Qi Wang, Beijing Institute of Radiation Medicine, Beijing 100850, China
Supported by the National High Technology Research and Development Program of China (863 Program), No. 2002AA2Z2011
Correspondence to: Dr Jun-Wen Li, Tianjin Institute of Hygiene and Environmental Medicine, 1, Da Li Road, Tianjin 300050, China. jinlianqun@sina.com
Telephone: +86-22-84655345 Fax: +86-22-23328809
Received: 2005-01-14 Accepted: 2005-06-06

Abstract

AIM: To detect the common intestinal pathogenic bacteria quickly and accurately.

METHODS: A rapid (<3 h) experimental procedure was set up based upon the gene chip technology. Target genes were amplified and hybridized by oligonucleotide microarrays.

RESULTS: One hundred and seventy strains of bacteria in pure culture belonging to 11 genera were successfully discriminated under comparatively same conditions, and a series of specific hybridization maps corresponding to each kind of bacteria were obtained. When this method was applied to 26 divided cultures, 25 (96.2%) were identified.

CONCLUSION: *Salmonella sp*., *Escherichia coli*, *Shigella sp*., *Listeria monocytogenes*, *Vibrio parahaemolyticus*, *Staphylococcus aureus*, *Proteus* sp., *Bacillus cereus*, *Vibrio cholerae*, *Enterococcus faecalis*, *Yersinia enterocolitica*, and *Campylobacter jejuni* can be detected and identified by our microarrays. The accuracy, range, and discrimination power of this assay can be continually improved by adding further oligonucleotides to the arrays without any significant increase of complexity or cost.

Key words: Oligonucleotide array; Sequence analysis; Gene chip; Intestines; Microbiology

Jin LQ, Li JW, Wang SQ, Chao FH, Wang XW, Yuan ZQ. Detection and identification of intestinal pathogenic bacteria by hybridization to oligonucleotide microarrays. *World J Gastroenterol* 2005; 11(48): 7615-7619
http://www.wjgnet.com/1007-9327/11/7615.asp

INTRODUCTION

Intestinal pathogenic bacteria exert a great threat upon human health. It is still a challenge to detect and identify bacterial pathogens quickly and accurately from the samples. Since intestinal bacterial pathogens involve a wide range of genera and species, few existing methods can meet the requirement of quick and parallel detection of these bacterial pathogens. Classical diagnostic methods, including culture and biochemical identification, immunological assay, nucleotide probe hybridization, and PCR amplification, share a common shortcoming: only one or few kinds of bacteria can be identified in a complete cycle of experiment. These serial procedures are hard to use for quick and simultaneous detection of multiple pathogenic bacteria. To meet the demands of rapid and parallel detection and identification of many common pathogenic bacteria in one experiment, we present here a new approach based on the epoch-making gene-chip (microarray) technology.

Gene chip technology is based upon the reversed solid hybridization of oligonucleotides[1,2]. The major advantages of gene chip technology, including miniature, high performance, parallelism, automation, have expanded its application in this decade[3]. Since the efficacy of gene chip technology depends heavily upon the oligonucleotide probes, careful selection of target genes and wise design of oligonucleotide probes with variable kind, sequence and amount, are cardinal factors for a good gene chip. The target genes may be species-specific. For example, the pathogenic genes[4] can be easily identified by simple PCR. However, it is impractical to use different primers for different species in gene chip technology, especially in the case where a specimen of one or more possible bacteria is given. Either a complex PCR with a mixture of many primers or a series of PCRs performed in parallel or sequential are necessary to amplify the target genes. However, the time, complexity and expense of experiment will also increase. On the contrary, if a consensus gene among many pathogenic bacteria is chosen, a single pair of carefully designed universal primers may be used to amplify the conserved stretches of DNA, which are then detected and identified by the wisely designed oligonucleotide probes. The conserved consensus genes usually chosen by many researchers are 16S ribosomal DNA (rDNA),

Table 1 Standard strains used in the present study

Genus or species	Standard strain(s)[1]
Salmonella	50 001, 50 004, 50 009, 50 013, 50 014, 50 018, 50 019, 50 020, 50 021, 50 023, 50 029, 50 041, 50 042, 50 043, 50 047, 50 051, 50 073, 50 082, 50 083, 50 086, 50 093, 50 096, 50 098, 50 099, 50 100, 50 104, 50 105, 50 106, 50 109, 50 112, 50 115, 50 120, 50 124, 50 128, 50 145, 50 191, 50 200, 50 201, 50 220, 50 304, 50 306, 50 307, 50 309, 50 310, 50 313, 50 315, 50 320, 50 321, 50 322, 50 326, 50 327, 50 333, 50 335, 50 337, 50 338, 50 354, 50 355, 50 358, 50 360, 50 362, 50 402, 50 707, 50 708, 50 709, 50 710, 50 711, 50 712, 50 718, 50 719, 50 730, 50 731, 50 732, 50 733, 50 735, 50 736, 50 739, 50 746, 50 761, 50 774, 50 783, 50 825, 50 835, 50 846, 50 853, 50 854, 50 864, 50 913
Shigella	51 081, 51 100, 51 207, 51 227, 51 233, 51 252, 51 253, 51 255, 51 258, 51 259, 51 262, 51 307, 51 315, 51 334, 51 335, 51 336, 51 424, 51 464, 51 570, 51 571, 51 572, 51 573, 51 575, 51 582, 51 583, 51 584, 51 585, 51 610
Escherichia coli	44 102, 44 105, 44 109, 44 110, 44 113, 44 126, 44 127, 44 149, 44 155, 44 156, 44 186, 44 216, 44 336, 44 338, 44 344, 44 505, 44 710, 44 719, 44 752, 44 813, 44 824, 44 825
Proteus	49 027, 49 101, 49 102, 49 103
Staphylococcus	26 001, 26 003, 26 005, 26 101, 26 111, 26 113, 26 517
Yersinia enterocolitica	52 202, 52 203, 52 206, 52 207, 52 211, 52 215, 52 217, 52 219, 52 302
Listeria monocytogenes	54 003, 54 005, 54 006, 54 007
Vibrio	20 502, 20 506, 20 507, 20 511, 02-12
Enterococcus faecalis	32 221, 32 223
Campylobacter jejuni	26 277
Bacillus cereus	63 301

[1]Except that one strain of Vibrio sp. was obtained from the Beijing Institute of Microbiology and Epidemiology, all other strains used in the present study were purchased from the National Center for Medical Culture Collection.

23S rDNA[5,6], 16S-23S rDNA spacer region[7], ERIC, while 16S rDNA[8] is the most popular one. Among the eubacterial 16S rDNA genes, the highly conserved sequences compose the constant regions, and the relatively less conserved sequences compose the variable regions, both interlace along the linear genes. Therefore, the pair of universal primers was carefully designed based upon the constant regions of 16S rDNA, so that they were capable of amplifying the 16S rDNA genes of all bacteria under certain circumstances. Meanwhile, the oligonucleotide probes were wisely designed based upon the variable regions of 16S rDNA at the species or genera level.

MATERIALS AND METHODS

Materials

The standard strains used in this study including a wide range of species and many of the common organisms causing intestinal disease are listed in Table 1. These organisms were identified by conventional methods.

Extraction of bacterial DNA from standard cultures

One colony from a fresh culture was resuspended in 100 μL distilled water in Eppendorf tubes. Then the tubes were transferred to a thermal cycler (Techgene, Techne Ltd.) and heated to 95 °C for 10 min. Finally, they were spun at 10 000 *g* for 1 min in a microcentrifuge, and 2 μL of the supernatant was used in PCR described below.

Sample preparation

Strains divided from Hai River, Luan River, municipal sewage, and food samples from markets were used in this study. All the divided strains were identified by conventional methods and the VITEK test system (BioMerieux SA, France). Extraction of DNA from divided bacterial cultures was performed as above.

Design of primers to amply bacterial 16S rDNA

We downloaded 113 bacterial 16S rDNA sequences from the GenBank database. Then, we used the program ClustalW alignment of the software MacVector 6.5.1 to analyze these sequences and showed the conserved regions of 16S rDNA. The primers were based on the conserved regions 8 and 10 of the 16S rDNA. The sequences of forward primer 1169U20 (5'-AACTGGAGGAAGGTGGGGAT) and reverse primer 1521L19 (5'-AGGAGGTGATCCAACCGCA) were used to amply bacterial 16S rDNA. The forward primer 1169U20 was labeled with 5'-Cy3 fluorescence.

Design of primers to amply specific pathogenic genes of Salmonella and Shigella

Sequences of forward primer invA-139 (5'-GTGAAA TTATCGCCACGTTCGGGCAA) and reverse primer invA-141 (5'-TCATCGCACCGTCAAAGGAACC) were used to amplify the invA gene of *Salmonella*. Sequences of forward primer virA-1 (5'-CTGCATTCTGGCAATCTC TTCACATC) and reverse primer virA-2 (5'-TGATGAG CTAACTTCGTAAGCCCTCC) were used to amplify the virA gene of *Shigella*. The forward primers invA-139 and virA-1 were labeled with 5'-Cy3 fluorescence.

PCR amplification to get hybridization targets

Each 50 μL reaction contained 33 μL sterile water, 5 μL 10 ×buffer (Takara Biotechnology Co., Ltd.), 2 μL supernatant from the extraction of bacterial DNA, 200 μmol/L dNTP mixture (Takara), 0.02 U/μL Takara Taq (Takara, 5 U/mL) and 0.1 μmol/L each primer (1169U20, 1521L19, invA-139, invA-141, virA-1, and virA-2). The PCR mixtures were subjected to 95 °C for 5 min, followed by 35 cycles at 94 °C for 25 s, at 55 °C for 30 s, and at 72 °C for 25 s. The PCR products were checked using 2% agarose electrophoresis and visualized with ethidium bromide staining.

Making oligonucleotide microarrays

All the oligonucleotide probes were chosen based on the variable regions between PCR primers using the alignment information. They were synthesized and modified with

Table 2 Oligonucleotide probes used in the present study

No.	Sequence (5' to 3')	Target
1	gtacaaggcccgggaacgtattcacc	All known eubacteria (universal bacterial probe)
2	gacataaggggcatgatgatttgacgt	All Gram-positive bacteria
3	gtcgtaagggccatgatgacttgacgt	All Gram-negative bacteria
4	gtcatgaatcacaaagtggtaagcgc	All enteric bacterial
5	acgacgcactttatgaggtccgcttg	*Escherichia coli, Shigella sp.* and *Salmonella sp.*
6	gctcctaaaaggttactccaccggct	*Staphylococcus aureus*
7	cgacggctagctccaaatggttactg	Coagulase-negative *Staphylococcus*
9	tcacggtcttgcgtcttattgtacctac	*Clostridium botulinum*
11	gaactgagactggtttttaagtttggct	*Clostridium perfringens*
15	cgaactgggacatattttatagatttgc	*Campylobacter jejuni*
16	aggtcgccccttcgccgccctctgtatc	*Legionella pneumophila*
17	cgatccgaactgagaccggcttttaagg	*Mycobacterium tuberculosis*
18	tactcgtaagggccatgatacgacttaa	*Proteus sp.*
19	cgcggcttggcaacccttttgtaccgacc	*Pseudomonas aeruginosa*
20	actgagaatagttttatgggattagg	*Listeria monocytogenes*
21	gctccaccttcgcggtattcgctgccct	*Vibrio cholerae*
22	tcactttcgcaagttggccgccctctgt	*Vibrio fluvialis*
23	tggtaagcgtccccccgtagttgaaac	*Vibrio parahaemolyticus*
24	tacgacagactttatgtggtccgcttgc	*Yersinia enterocolitica*
25	cctcgcggtctagcagctcgttgtgctt	*Enterococcus faecalis*
26	ggattcgctcactatcgctagcttgcag	*Aeromonas hydrophila*
27	ccgacttcgggtgttacaaactctcg	*Bacillus cereus, P.*
28	gcttcatgcactcgagttgcagagtg	*cocovenenans subsp. farinofermentans*
30	atccccaccttcctccagtt	Positive control
31	cccccagaggcagagattgca	virA gene of *Shigella* sp.
32	cgccaataacgaattgcccga	invA gene of *Salmonella* sp.

3'-NH_2 in order to increase their binding to the glass slide surface and their hybridization intensity.

Before use, the glass slides for microscopy must be cleaned as described by Brown (http://cmgm.stanford.edu/pbrown/protocols.html). Then the oligonucleotide probes were bound to the slides as follows: 5 μL of 50 μmol/L oligonucleotide drop was spotted on the glass slide by an arrayer (PixSys 5500 Workstation, Cartesian Technologies), 5 mm between each oligonucleotide spot. When all the oligonucleotide probes were applied, the glass slides were left at room temperature for 24 h to permit thorough drying of the DNA on the slide surface. After drying, the slides were washed twice in 0.2% SDS for 5 min each and twice in distilled water for 5 min each. Subsequently, the slides were washed in sodium borohydride solution (1.3 g Na_2BH_4 was dissolved in 375 mL phosphate buffered saline, and then 125 mL pure ethanol was added) for 5 min, in 0.2% SDS for 2 min, and twice in distilled water for 2 min each.

Hybridization

The fluorescent-labeled amplicons were hybridized to the oligonucleotide microarrays using the following protocol: 1 μL of amplicons was added into a tube containing 4 μL hybridization solution (UniHyb™, TeleChem International, Inc.), and the tube was heated to 95 °C for 10 min and was put on ice immediately. Mixture in the tube was then transferred onto the microarray, kept at 50 °C for 1 h in a hybridization cassette (TeleChem International, Inc.). After hybridization, unbound fluorescent amplicons were washed with washing buffer A (1×SSC+0.2% SDS) for 1 min, B (0.1×SSC+0.2% SDS) for 1 min, C (0.1×SSC) for 1 min, respectively.

Scanning the microarray for fluorescent signals

We used the ScanArray 3000 (GSI Lumonics) to scan the area of the slide containing the microarray. The laser power and PMT were set at 80%.

Scoring hybridization results

The resolution of the ScanArray 3000 scanner is 10 μm, and the fluorescent density of each pixel is saved into the TIFF image file, facilitating further process and analysis of software. We uploaded the scanned image TIFF file into the ImaGene 4.0 software (BioDiscovery) to examine each feature for fluorescence intensity.

RESULTS

Under the same conditions for PCR amplification and hybridization, all the 170 strains produced PCR products, showing bands at approximately 370 bp, being equivalent to the fragment of 16s rDNA. Besides, strains belonging to *Salmonella* sp. produced another band of 285 bp, and strains belonging to *Shigella* sp. produced a 215-bp band. After the hybridization between PCR products and oligonucleotide probes, respective hybridization maps were built through the signal acquisition step using the ScanArray 3000 scanner. The original images generated by ScanArray 3000 scanner are shown in Figure 1. Monochrome fluorescent signals were mapped into pseudocolor spectrum according to their density in ascending order, e.g. black, dark blue, blue, green, yellow, red, white. Twelve typical hybridization maps corresponded to nine genera or species of bacteria, specifically.

The wisely designed oligonucleotide probes could be classified by their efficacy into six categories (Table 2).

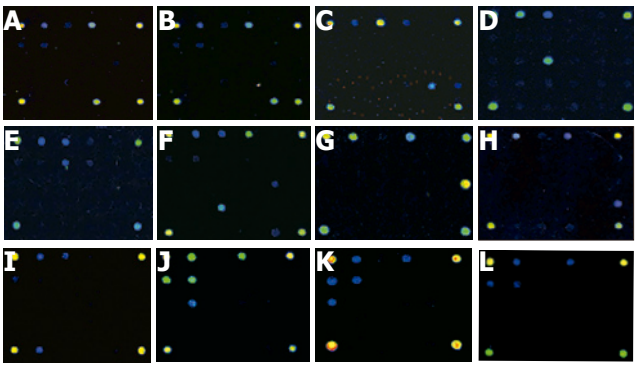

Figure 1 Typical hybridization results from *Vibrio parahaemolyticus* (**A**), *Yersinia enterocolitica* (**B**), *Listeria monocytogenes* (**C**), *Bacillus cereus* (D), *Staphylococcus aureus* (**E**), *Proteus sp.* (**F**), *Campylobacter jejuni* (**G**), *Vibrio cholerae* (**H**), *Enterococcus faecalis* (**I**), *Salmonella sp.* (**J**), *Shigella sp.* (**K**) and *Escherichia coli* (**L**).

	1	2	3	4	5	6
A	30	1	2	3	–[1]	30
B	4	5	6	7	28	9
C	31	32	27	11	26	15
D	16	17	18	19	20	21
E	30	25	22	23	24	30

[1]Negative control (3×SSC).

Figure 2 Layout of oligonucleotide probes.

Category one, including oligonucleotide probe 1, a universal probe targeting the portion of 16S rDNA shared by all known eubacteria, was used to detect all kinds of known eubacteria. Category two, including oligonucleotide probes 2 and 3, the specific probes targeting the portion of 16S rDNA shared by both Gram-positive (G^+) and negative (G^-) bacteria, was used to distinguish between G^+ and G^- bacteria. Category three, including oligonucleotide probes 4 and 5, targeting the portion of 16S rDNA shared by all enteric bacteria, was used to identify intestinal bacteria at the family level. Category four, including oligonucleotide probes 6, 7, 9, 11, and 15-28, a cluster of genus or species-specific probes targeting the portion of 16S rDNA shared by their respective bacteria, was used to identify bacteria at genus or species level. Category five, including oligonucleotide probes 31 and 32, targeting the portion of the specific pathogenic genes of *Shigella* and *Salmonella*, was used to discriminate between bacteria of these two genera. Category six, including oligonucleotide probe 30, a positive control probe, was used both as a gauge to reflect the effectiveness of this hybridization system and as a reference coordinate for scanning. From hybridization signals of the five categories of oligonucleotide probes, it was easy to identify the target pathogenic bacteria in a given specimen. For instance, strong hybridization signals at the sites corresponding to the oligonucleotide probes 1, 3, and 23 were found, so the pathogenic bacteria in the given specimen could be sequentially identified as eubacteria, G^- bacteria, and strains of *Vibrio parahaemolyticus* (Figure 1G). Some slightly weaker signals due to unspecific hybridization were also found. By means of multiple experiments, a hybridization signal was regarded as a specific signal if it meets the following criterion: the foreground fluorescent signal at an oligonucleotide probe spot was stronger than its background fluorescent signal with a signal-noise ratio larger than 100 calculated by ImaGene 4.0. Since the fluorescent signals of specific hybridization were three-fold stronger compared to those of unspecific hybridization, it was easy to identify the specific hybridization signals from the hybridization maps directly (Figure 2).

Twenty-six unselected divided cultures were also processed and hybridized as described above, and then identified according to the specific hybridization maps (Table 3). Among them, 25 strains were distinguished according to their hybridization maps, but only one strain was indistinguishable due to its weak signal. The comprehensive identification results by classical methods were regarded as the final standards. Except for sample 7, all other results were consistent with those detected by hybridization assay and conventional method, the consistency was 96.2% (25/26).

DISCUSSION

Our study showed that the gene chip-based method could identify a wide range of intestinal pathogenic bacterial species. The genus or species specific probes on the microarray are targeted at the 16S rDNA, while two discriminative probes are targeted at special pathogenic genes. Sample DNA was labeled with fluorescence by PCR, then hybridized to the probes on the chip, thus a couple of genus or species-specific hybridization patterns could be generated and used to discriminate the bacteria[9].

When the oligonucleotide probes for 16S rDNA were designed, we preferred a longer oligonucleotide segment with multiple mutation sites over a shorter one, which is also suitable for detecting single-nucleotide mutation[10-12]. The advantages are obvious: the amount of essential oligonucleotides is less, the cost of experiment is lower, and the identification of hybridization map is easier. However, the shortcoming is somewhat less discriminative to those sequences where only minor differences are present.

The 16S rDNA sequences of *Shigella*, *Salmonella,* and *Escherichia coli* are similar, and share almost identical sequences of the target 16S rDNA genes. Thus, these three genera can hardly be identified by only 16S rDNA[13,14].

Besides, intestinal pathogenic bacteria belonging to *Listeria monocytogenes*, *Vibrio parahaemolyticus*, *Proteus* sp., *Vibrio cholerae*, *Enterococcus faecalis*, *Yersinia enterocolitica,* and *Campylobacter jejuni*, could be detected and identified using the gene chip.

Compared to the classic microbial assay, immunological assay, PCR-based assay, the method based upon the gene chip technology could detect and identify a given strain of bacterium within 3 h. It is a fundamental start point to develop other methods for a large-scale assay. The target spectrum of this gene chip may be gradually expanded

Table 3 Comparison of identifications based on hybridization assay and conventional methods for 26 cultures

No.	Hybridization assay	Conventional methods	Consistency
1	*Staphylococcus aureus*	*Staphylococcus aureus*	Y[1]
2	Coagulase-negative *Staphylococcus*	*Staphylococcus epidermidis*	Y
3	*Staphylococcus aureus*	*Staphylococcus aureus*	Y
4	*Staphylococcus aureus*	*Staphylococcus aureus*	Y
5	*Staphylococcus aureus*	*Staphylococcus aureus*	Y
6	*Pseudomonas aeruginosa*	*Pseudomonas aeruginosa*	Y
7	-[3]	*Salmonella typhimurium*	-[2]
8	*Escherichia coli*	*Escherichia coli*	Y
9	*Staphylococcus aureus*	*Staphylococcus aureus*	Y
10	*Pseudomonas aeruginosa*	*Pseudomonas aeruginosa*	Y
11	*Shigella* sp.	*Shigella flexneri*	Y
12	*Shigella* sp.	*Shigella flexneri*	Y
13	*Shigella* sp.	*Shigella flexneri*	Y
14	*Shigella* sp.	*Shigella flexneri*	Y
15	*Vibrio parahaemolyticus*	*Vibrio parahaemolyticus*	Y
16	*Yersinia enterocolitica*	*Yersinia enterocolitica*	Y
17	*Pseudomonas aeruginosa*	*Pseudomonas aeruginosa*	Y
18	*Shigella* sp.	*Shigella flexneri*	Y
19	*Shigella* sp.	*Shigella flexneri*	Y
20	*Vibrio parahaemolyticus*	*Vibrio parahaemolyticus*	Y
21	*Escherichia coli*	*Escherichia coli*	Y
22	*Escherichia coli*	*Escherichia coli*	Y
23	*Salmonella* sp.	*Salmonella typhimurium*	Y
24	*Campylobacter jejuni*	*Campylobacter jejuni*	Y
25	*Salmonella* sp.	*Salmonella typhimurium*	Y
26	*Salmonella* sp.	*Salmonella typhimurium*	Y

[1]The results from hybridization assay and conventional methods are consistent. [2]The results are inconsistent. [3]No signal was detected.

by adding newly designed oligonucleotide probes into the oligonucleotide microarray, and the accuracy may also be improved by increasing and readjusting the oligonucleotide probes in the oligonucleotide microarray. The arrangement of the oligonucleotide microarray may be rearranged according to its end usage. This method for intestinal pathogen assay using gene chip technology can be used for the diagnosis of infectious diseases, environmental supervision, food quality surveillance, etc.

REFERENCES

1 **Cheung VG**, Morley M, Aguilar F, Massimi A, Kucherlapati R, Childs G. Making and reading microarrays. *Nat Genet* 1999; **21:** 15-19

2 **Bowtell DD**. Options available--from start to finish--for obtaining expression data by microarray. *Nat Genet* 1999; **21:** 25-32

3 **Holloway AJ**, van Laar RK, Tothill RW, Bowtell DD. Options available--from start to finish--for obtaining data from DNA microarrays II. *Nat Genet* 2002; **32 Suppl:** 481-489

4 **Chizhikov V**, Rasooly A, Chumakov K, Levy DD. Microarray analysis of microbial virulence factors. *Appl Environ Microbiol* 2001; **67:** 3258-3263

5 **Ludwig W**, Schleifer KH. Bacterial phylogeny based on 16S and 23S rRNA sequence analysis. *FEMS Microbiol Rev* 1994; **15:** 155-173

6 **Anthony RM**, Brown TJ, French GL. Rapid diagnosis of bacteremia by universal amplification of 23S ribosomal DNA followed by hybridization to an oligonucleotide array. *J Clin Microbiol* 2000; **38:** 781-788

7 **Sharples GJ**, Lloyd RG. A novel repeated DNA sequence located in the intergenic regions of bacterial chromosomes. *Nucleic Acids Res* 1990; **18:** 6503-6508

8 **Dams E**, Hendriks L, Van de Peer Y, Neefs JM, Smits G, Vandenbempt I, De Wachter R. Compilation of small ribosomal subunit RNA sequences. *Nucleic Acids Res* 1988; **16 Suppl:** r87-173

9 **Call DR**, Borucki MK, Loge FJ. Detection of bacterial pathogens in environmental samples using DNA microarrays. *J Microbiol Methods* 2003; **53:** 235-243

10 **Noller HF**, Green R, Heilek G, Hoffarth V, Huttenhofer A, Joseph S, Lee I, Lieberman K, Mankin A, Merryman C. Structure and function of ribosomal RNA. *Biochem Cell Biol* 1995; **73:** 997-1009

11 **Boyer SL**, Flechtner VR, Johansen JR. Is the 16S-23S rRNA internal transcribed spacer region a good tool for use in molecular systematics and population genetics? A case study in cyanobacteria. *Mol Biol Evol* 2001; **18:** 1057-1069

12 **Hacia JG**. Resequencing and mutational analysis using oligonucleotide microarrays. *Nat Genet* 1999; **21:** 42-47

13 **Villalobo E**, Torres A. PCR for detection of Shigella spp. in mayonnaise. *Appl Environ Microbiol* 1998; **64:** 1242-1245

14 **Rahn K**, De Grandis SA, Clarke RC, McEwen SA, Galan JE, Ginocchio C, Curtiss R 3rd, Gyles CL. Amplification of an invA gene sequence of Salmonella typhimurium by polymerase chain reaction as a specific method of detection of Salmonella. *Mol Cell Probes* 1992; **6:** 271-279

Science Editor Wang XL and Guo SY **Language Editor** Elsevier HK

PO Box 2345, Beijing 100023, China
www.wjgnet.com
wjg@wjgnet.com

ELSEVIER

World J Gastroenterol 2005;11(48):7620-7624
World Journal of Gastroenterology ISSN 1007-9327

• *BASIC RESEARCH* •

Morphological and serum hyaluronic acid, laminin and type IV collagen changes in dimethylnitrosamine-induced hepatic fibrosis of rats

Chun-Hui Li, Dong-Ming Piao, Wen-Xie Xu, Zheng-Ri Yin, Jing-Shun Jin, Zhe-Shi Shen

Chun-Hui Li, Dong-Ming Piao, Zheng-Ri Yin, Jing-Shun Jin, Zhe-Shi Shen, Department of Pathology, Affiliated Hospital of Yanbian University College of Medicine, Yanji 133000, Jilin Province, China
Wen-Xie Xu, Department of Physiology, College of Medicine, Shanghai Jiaotong University, Shanghai 200030, China
Chun-Hui Li, Affiliated Hospital of Chengde Medical College, Chengde 067000, Hebei Province, China
Correspondence to: Dong-Ming Piao, Department of Pathology, Affiliated Hospital of Yanbian University College of Medicine, Yanji 133000, Jilin Province,
China. pdm11172000@yahoo.con.cn
Telephone: +86-0433-2660203 Fax: +86-0433-2513610
Received: 2005-05-18 Accepted: 2005-06-18

Abstract

AIM: To study the morphological and serum hyaluronic acid (HA), laminin (LN), and type IV collagen changes in hepatic fibrosis of rats induced by dimethylnitrosamine (DMN).

METHODS: The rat model of liver fibrosis was induced by DMN. Serum HA, type IV collagen, and LN were measured by ELISA. The liver/weight index and morphological changes were examined under electron microscope on d 7, 14, 21, and 28 by immunohistochemical alpha smooth muscle actin α-SMA staining as well as Sirius-red and HE staining.

RESULTS: The levels of serum HA, type IV collagen and LN significantly increased from d 7 to d 28 (P = 0.043). The liver/weight index increased on d 7 and decreased on d 28. In the model group, the rat liver stained with HE and Sirius-red showed evident hemorrhage and necrosis in the central vein of hepatic 10 lobules on d 7. Thin fibrotic septa were formed joining central areas of the liver on d 14. The number of α-SMA positive cells was markedly increased in the model group. Transitional hepatic stellate cells were observed under electron microscope. All rats in the model group showed micronodular fibrosis in the hepatic parenchyma and a network of α-SMA positive cells. Typical myofibroblasts were embedded in the core of a fibrous septum. Compared to the control group, the area-density percentage of collagen fibrosis and pathologic grading were significantly different in the model group (P<0.05) on different d (7, 14, and 28). The area-density percentage of collagen fibrosis in hepatic tissue had a positive correlation with the levels of serum HA, LN, and type IV collagen.

CONCLUSION: The morphological and serum HA, type IV collagen, and LN are changed in DMN-induced liver fibrosis in rats.

Key words: Rat; Hepatic fibrosis; DMN; Morphological change; Serum; Experimental studies

Li CH, Piao DM, Xu WX, Yin ZR, Jin JS, Shen ZS. Morphological and serum hyaluronic acid, laminin and type IV collagen changes in dimethylnitrosamine-induced hepatic fibrosis of rats. *World J Gastroenterol* 2005; 11(48): 7620-7624
http://www.wjgnet.com/1007-9327/11/7620.asp

INTRODUCTION

In China, the incidence of liver cirrhosis is still high[1]. Hepatic cirrhosis results from fibrosis[2-4]. Many factors can lead to chronic liver disease and hepatic fibrosis[5-9]. Hepatic fibrosis is associated with a number of morphological and biochemical changes leading to structural and metabolic abnormalities in the liver. Hepatic stellate cells (HSCs) play a major role in various types of liver fibrosis through initial myofibroblast transformation. Transformed HSCs can actively synthesize extracellular matrix and then change morphology and function of the liver. Dimethylnitrosamine (DMN)-induced hepatic fibrosis in rats appears to be a good and reproducible model with decompensating features of human disease[10,11]. This study was to observe the morphological and serum hyaluronic acid (HA), laminin (LN), and type IV collagen changes in DMN-induced hepatic fibrosis of rats.

MATERIALS AND METHODS

Animals and experiment protocol

Male Wistar rats weighing 175-200 g were obtained from the Experimental Animal Center of Yanbian University College of Medicine. The rats were divided into two groups. The model group (n = 40) received 1% DMN (10 μL/kg

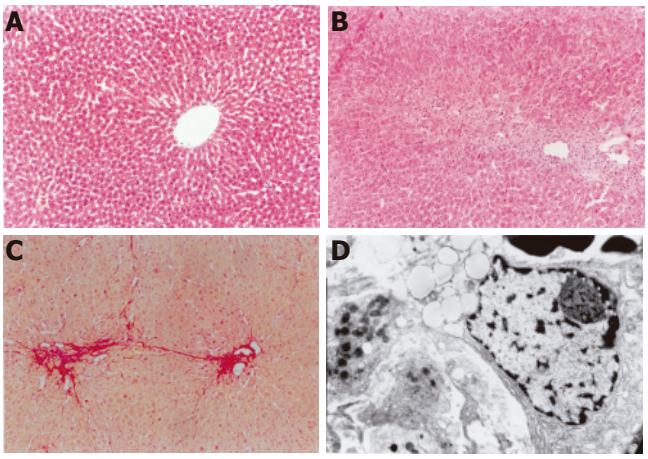

Figure 1 Changes after DMN treatment. **A:** Livers in the control group showed normal lobular architecture with central veins; **B:** after 7 d of DMN treatment, extensive necrosis was observed in portal areas; **C:** after 14 d of DMN treatment, thin fibrotic septa were formed joining central areas; **D:** after 21 or 28 d of DMN treatment, thick intralobular septa were evident.

body weight, i.p.) thrice a week for 4 wk, while the control group (n = 12) received an equivalent amount of saline. The animals were killed on d 7, 14, 21, and 28 (10 treated with DMN at each time interval). Blood was taken from the left ventricle. Serum samples obtained from all study subjects were frozen at -70 °C and aliquots were thawed when needed for specific tests. The liver was examined by light and electron microscopy.

Serum HA, type IV collagen, and LN levels testing

A quantitative ELISA was used to determine serum HA, type IV collagen, and LN levels according to the manufacturer's instructions.

Sirius-red and HE staining

Formalin-fixed tissues were paraffin-embedded and cut into 4-μm thick sections from the right lobe of rat's liver for HE and Sirius-red staining. HE staining was used to observe liver pathologic structures, Sirius-red staining was used to grade liver fibrosis from 0 to 4[16]: grade 0 = no fibrosis, grade 1 = portal area fibrosis, grade 2 = fibrotic septa between portal tracts, grade 3 = fibrosis septa and structure disturbance of hepatic lobule, grade 4 = cirrhosis. At the same time, Sirius-red staining and CMIAS image analysis system (Beijing, China) were used to determine the area-density percentage of collagen fibrosis in hepatic tissue. At least five high-power (×400 field) fields were chosen and positive collagen fibrosis (red staining) was determined. Area-density percentage of collagen fibrosis was calculated by dividing the number of positive collagen fibroses (positive optical density) over the total number of collagen fibroses (integrated optical density).

Immunohistochemical staining

α-SMA for the detection of activated HSCs was studied by immunohistochemical staining. Sections (5-μm) were deparaffinized, rehydrated and incubated with 0.3% hydrogen peroxidase in methanol for 15 min at room temperature to block endogenous peroxidase activity. After being washed twice with phosphate-buffered saline (PBS) for 5 min, tissue sections were incubated at 37 °C for 20 min with blocking solution, then incubated at 37 °C for 2 h with rabbit anti-rat α-SMA antibody (Dako, Denmark) at dilution 1:100. After being washed twice with PBS (0.01 mol/L, PH 7.4) for 10 min, tissue sections were incubated at 37 °C for 30 min with biotin-anti-rabbit IgG. After being washed twice with PBS for 5 min, the sections were incubated with streptavidin-HRP for 30 min. Then the sections were washed twice with PBS for 5 min and incubated with metal-enhanced 3, 3-diaminobenzidine solution for 15 min, washed twice in distilled waster and counterstained with hematoxylin. Negative control sections were incubated with normal rabbit serum instead of primary antibody. The positive staining for α-SMA positive cells was expressed as red brown granules and photomicrographed (Olympus PM-10AD).

Electron microscopy

Fresh fragments of 1 mm^3 liver tissue were fixed in 10% paraffin, dehydrated and embedded in Epon-812 resin. Sections were stained with uranyl acetate for 15 min and then lead citrate for 15 min. Transitional HSCs were observed under JEM-1200EX, 80 kV electron microscope (JEOL, Japan).

Statistical analysis

Data were expressed as mean±SD. The two-tailed χ^2 test was used to examine the correlation between the area-density percentage of collagen fibrosis in hepatic tissue and serum HA, LN, and type IV collagen levels. Statistical significance was estimated by t-test. $P<0.05$ was considered statistically significant. All calculations were made by SPSS 11.0 for Windows.

RESULTS

Serum HA, type IV collagen, and LN levels change

When compared to control values, a significant increase ($P<0.05$) was observed in serum levels of HA, LN, and type IV collagen on d 7, 14, 21, and 28 after administration of DMN. The maximum increase in serum levels of HA, LN, and type IV collagen was observed on d 28 after DMN treatment (Figure 3).

Change in the weight of body and liver as well as liver and body ratio

An increase in liver weight was observed on d 7 after DMN treatment, with a decreased liver weight on d 28. The maximum liver and body weight ratio increased on d 14 and decreased on d 28 (Table 1).

Changes after DMN treatment

The rat liver stained with Sirius-red and HE showed an extensive accumulation of collagens. Fibrotic septum increased from port to port and from port to central

Table 1 Changes in the weight of body and liver as well as liver/body ratio of rats during DMN treatment (mean±SD)

Group	*n*	Body weight	Liver weight	Liver/body ratio
Control	10 (0)	192.50±9.0446	6.2260±0.3848	3.2191±0.2829
Day 7	6 (4)	207.85±5.3293	7.8114±0.3869	3.7492±0.1195
Day 14	9 (1)	167.27±11.9157[a]	6.9164±0.6229[a]	4.1059±0.1636[a,c]
Day 21	9 (1)	181.11±13.3536[a]	6.5122±0.6200[a]	3.5671±0.1437[a]
Day 28	10 (0)	186.42±10.7301[a]	6.3657±0.5306[a]	3.3903±0.1096[a,c]

[a]*P*<0.05 *vs* control; [c]*P*<0.05 *vs* day 7; ( ): number of deaths.

Table 2 Pathologic grading of DMN-induced hepatic fibrosis in rats (mean±SD)

Groups	*n*	Grading of hepatic fibrosis				
		–	+	++	+++	++++
Control	10 (0)	10	0	0	0	0
Day 7	6 (4)	0	3	3	0	0
Day 14	9 (1)	0	2	4	3	0
Day 21	9 (1)	0	0	2	4	3
Day 28	10 (0)	0	0	2	4	4

P<0.001 *vs* control; *P*<0.001 *vs* d 7; ( ): number of deaths.

vein in some parts of lobules. The livers of the rats in the control group showed normal lobular architecture with central veins and radiating hepatic cords (Figure 1A). After 7 d of DMN treatment, extensive necrosis occurred in portal area and hemorrhage was prominent (Figure 1B). After 14 d, hemorrhagic necrosis and formation of thin fibrotic septa joining central areas were found (Figure 1C). After 21 d, thick intralobular septa were evident (Figure 1D). After 28 d, the pattern was similar with that after 21 d. At the same time, fibrotic septum increased the area-density percentage of collagen fibrosis in hepatic fibrosis. Compared to control values, a significant increase ($P<0.05$) was observed in area-density percentage of collagen fibrosis on d 7, 14, 21, and 28 after administration of DMN. The maximum increase in the levels of the area-density percentage of collagen fibrosis was observed on d 28 after DMN treatment (Figure 2). Liver fibrosis was graded from 0 to 4 (Table 2)

Distribution of α-SMA positive cells

Activated HSCs characterized by the expression of α-SMA increased in the liver of rats that received DMN. The distribution of α-SMA positive cells was similar to that of collagen in the liver. After 14 d, linear immunoreaction for α-SMA was scattered along the sinusoidal wall (Figure 4A). After 21 d, a network of α-SMA cells was evident (Figure 4B). After 28 d, a dense network of α-SMA cells was evident (Figure 4C). Transitional HSCs were observed under electron microscope, showing features of lipid-containing myofibroblasts and bundles of connective tissue after 14 d of DMN treatment (Figure 4D). Typical myofibroblasts were embedded in the core of fibrous septa after 21–28 d of DMN treatment. The elongated cell body contained a nucleus and numerous microfilaments outlined by a lamina-like structure. Collagen fibers of variable size were seen around the myofibroblasts (Figure 4E).

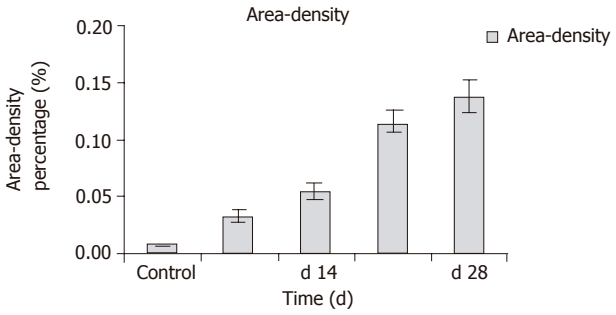

Figure 2 Area–density percentage of collagen fibrosis in hepatic tissue. *P*<0.05 *vs* control; *P*<0.05 *vs* d 7.

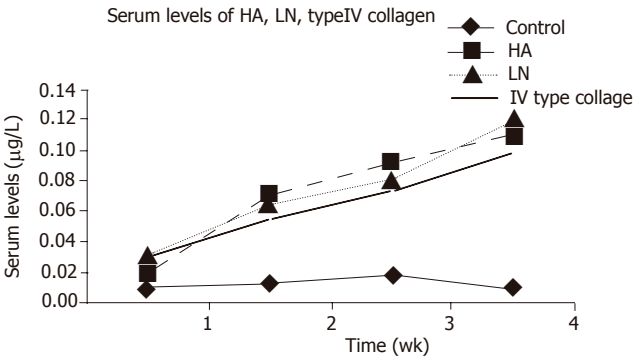

Figure 3 Serum levels of HA, LN, and Type IV collagen in DMN-induced fibrosis of rats and control, *P*<0.05 *vs* control.

Relationship between area-density percentage of collagen fibrosis and serum HA, type IV collagen, and LN levels

A positive correlation ($r = 0.707$, $P<0.01$) was noticed between the area-density percentage of collagen fibrosis and serum levels of HA, LN, and type IV collagen during the course of DMN administration.

DISCUSSION

Liver fibrosis is common in most chronic liver diseases regardless of their etiology[12-15]. The incidence rate of chronic liver disease in China is high[16]. Hepatic fibrosis is the intermediate and crucial stage of cirrhosis. If treated properly in this stage, cirrhosis could be successfully prevented[17], but it remains a problem to prevent cirrhosis or to control its progression in patients with chronic liver disease[18]. HSCs play a central role in the pathogenesis of liver fibrosis. After liver injury, HSCs become activated and express a wide variety of extracellular matrixes. It was reported that hepatic fibrosis is induced in rats by low doses of DMN and morphological changes of hepatic fibrosis are associated with cells bearing 'transitional' features of HSCs, myofibroblasts and fibroblasts[19]. Activated but not quiescent HSCs have a high level of collagen and express α-SMA. HSCs play a key role in the pathogenesis of hepatic fibrosis[20]. To evaluate the distribution of α-SMA positive cells in various liver diseases, Yu *et al*.[21] undertook an immunohistochemical

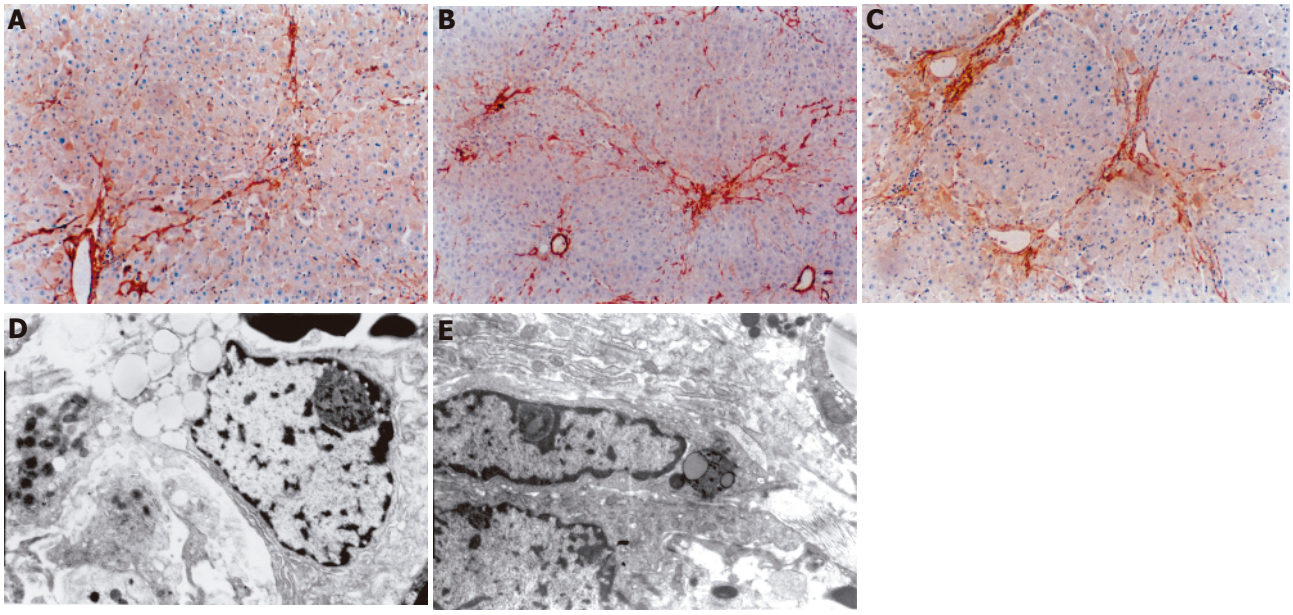

Figure 4 Distribution of α-SMA positive cells after DMN treatment. **A:** After 14 d, linear immunoreaction for α-SMA was scattered along the sinusoidal wall; **B:** after 21 d, a network of α-SMA cells was evident; **C:** after 28 d, a dense network of α-SMA cells was evident; **D:** after 14 d, transitional hepatic stellate cells were observed under electron microscope; **E:** after 21 or 28 d, typical myofibroblasts were embedded in the core of fibrous septa.

study of liver diseases including chronic persistent hepatitis, chronic active hepatitis, liver cirrhosis, intrahepatic cholelithiasis and hepatocellular carcinoma, and found that expression of α-SMA may be related to the fibrotic process[22]. DMN-induced experimental model may contribute to the understanding of the relationship between liver injury and hepatic fibrosis[23] and is used to detect different degrees of hepatic fibrosis[24,25]. In our study, serum levels of HA, LN, and type IV collagen increased significantly in hepatic fibrosis, suggesting that detection of HA, LN, and type IV collagen level is an optimal choice[26]. In this study, a positive correlation was noticed between the area-density percentage of collagen fibrosis and serum levels of LN, HA, and type IV collagen during the course of DMN administration, indicating that DMN is a potent hepatotoxin that can cause fibrosis of the liver. DMN can be administered to adult male albino rats in order to document sequential pathological and biochemical alterations[27].

In conclusion, HSCs play a central role in the pathogenesis of liver fibrosis and can regulate degradation of matrix in the liver.

REFERENCES

1 **Du WD**, Zhang YE, Zhai WR, Zhou XM. Dynamic changes of type I,III and IV collagen synthesis and distribution of collagen-producing cells in carbon tetrachloride-induced rat liver fibrosis. *World J Gastroenterol* 1999; **5:** 397-403

2 **Canturk NZ,** Canturk Z, Ozden M, Dalcik H, Yardimoglu M, Tulubas F. Protective effect of IGF-1 on experimental liver cirrhosis-induced common bile duct ligation. *Hepatogastroenterology* 2003; **50:** 2061-2066

3 **Xu LX**, Xie XC, Jin R, Ji ZH, Wu ZZ, Wang ZS. Protein deficiency and muscle damage in carbon tetrachloride induced liver cirrhosis. *Food Chem Toxicol* 2003; **41:** 1789-1797

4 **Pan NS**, Li ST, Wang Y, Li MF, Han Z. [Therapeutic effect of "anti-hepatic-fibrosis 268" on hepatic fibrosis in rats] *Sichuan Da Xue Xue Bao Yi Xue Ban* 2004; **35:** 528-531

5 **Kuroki T,** Seki S, Kawakita N, Nakatani K, Hisa T, Kitada T, Sakaguchi H.Expression of antigens related to apoptosis and cell proliferation in chronic nonsuppurative destructive cholangitis in primary biliary cirrhosis. *Virchows Arch* 1996; **429:** 119-129

6 **Jia JD.** Further systematize and standardize the diagnosis and treatment of liver cirrhosis. *Zhonghua Ganzangbing Zazhi* 2005; **13:** 401-402

7 **Jaster R**. Molecular regulation of pancreatic stellate cell function. *Mol Cancer* 2004; **3:** 26

8 **Breitkopf K**, Sawitza I, Gressner AM. Characterization of intracellular pathways leading to coinduction of thrombospondin-1 and TGF-beta1 expression in rat hepatic stellate cells. *Growth Factors* 2005; **23:** 77-85

9 **Tox U**, Goeser T. [Therapy of complications of hepatic cirrhosis] *Schweiz Rundsch Med Prax* 2005; **94:** 727-733

10 **Jenkins SA**, Grandison A, Baxter JN, Day DW, Taylor I, Shields R. A dimethylnitrosamine-induced model of cirrhosis and portal hypertension in the rat. *J Hepatol* 1985; **1:** 489-499

11 **Veal N**, Auduberteau H, Lemarie C, Oberti F, Cales P. Effects of octreotide on intestinal transit and bacterial translocation in conscious rats with portal hypertension and liver fibrosis. *Dig Dis Sci* 2001; **46:** 2367-2673

12 **McCaughan GW**, Gorrell MD, Bishop GA, Abbott CA, Shackel NA, McGuinness PH, Levy MT, Sharland AF, Bowen DG, Yu D, Slaitini L, Church WB, Napoli J. Molecular pathogenesis of liver disease: an approach to hepatic inflammation, cirrhosis and liver transplant tolerance. *Immunol Rev* 2000; **174:** 172-191

13 **Jung SA**, Chung YH, Park NH, Lee SS, Kim JA, Yang SH, Song IH, Lee YS, Suh DJ, Moon IH. Experimental model of hepatic fibrosis following repeated periportal necrosis induced by allylalcohol. *Scand J Gastroenterol* 2000; **35:** 969-975

14 **Plummer JL**, Ossowicz CJ, Whibley C, Ilsley AH, Hall PD. Influence of intestinal flora on the development of fibrosis and cirrhosis in a rat model. *J Gastroenterol Hepatol* 2000; **15:** 1307-1311

15 **Ramalho F**. Hepatitis C virus infection and liver steatosis. *Antiviral Res* 2003; **60:** 125-127

16 **Lamireau T**, Desmouliere A, Bioulac-Sage P, Rosenbaum J. Mechanisms of hepatic fibrogenesis. *Arch Pediatr* 2002; **9:** 392-405

17 **Riley TR 3rd**, Bhatti AM. Preventive strategies in chronic liver disease: part II. Cirrhosis. *Am Fam Physician* 2001; **64:** 1735-1740

18 **Murphy F**, Arthur M, Iredale J. Developing strategies for liver fibrosis treatment. *Expert Opin Investig Drugs* 2002; **11:** 1575-1585

19 **Jezequel AM,** Mancini R, Rinaldesi ML, Macarri G, Venturini C, Orlandi F. A morphological study of the early stages of hepatic fibrosis induced by low doses of dimethylnitrosamine in the rat**.** *J Hepatol* 1987; 5: 174-187

20 **Lee KS,** Lee SJ, Park HJ, Chung JP, Han KH, Chon CY, Lee SI, Moon YM. Oxidative stress effect on the activation of hepatic stellate cells. *Yonsei Med J* 2001; **42:** 1-8

21 **Yu E**, Choe G, Gong G, Lee I. Expression of alpha-smooth muscle actin in liver diseases. *J Korean Med Sci* 1993; **8:** 367-373

22 **Tanaka Y**, Nouchi T, Yamane M, Irie T, Miyakawa H, Sato C, Marumo F. Phenotypic modulation in lipocytes in experimental liver fibrosis. *J Pathol* 1991; **164:** 273-278

23 **Jezequel AM,** Mancini R, Rinaldesi ML, Ballardini G, Fallani M, Bianchi F, Orlandi F. Dimethylnitrosamine-induced cirrhosis. Evidence for an immunological mechanism**.** *J Hepatol* 1989 ; **8:** 42-52

24 **Lee MH,** Yoon S, Moon JO. The flavonoid naringenin inhibits dimethylnitrosamine-induced liver damage in rats**.** *Biol Pharm Bull* 2004; **27:** 72-76

25 **Hsu YC,** Chiu YT, Lee CY, Lin YL, Huang YT. Increases in fibrosis-related gene transcripts in livers of dimethylnitrosamine-intoxicated rats**.** *J Biomed Sci* 2004; **11:** 408-417

26 **Liang XH,** Zheng H. Value of simultaneous determination of serum hyaluronic acid, collagen type IV and the laminin level in diagnosing liver fibrosis. *Hunan Yike Daxue Xuebao* 2002; **27:** 67-68

27 **Madden JW**, Gertman PM, Peacock EE. Dimethylnitrosamine-induced hepatic cirrhosis:a new canine model of an ancient human disease. *Surgery* 1970; **68:** 260-268

Science Editor Wang XL and Guo SY **Language Editor** Elsevier HK

PO Box 2345, Beijing 100023, China
www.wjgnet.com
wjg@wjgnet.com

ELSEVIER

World J Gastroenterol 2005;11(48):7625-7630
World Journal of Gastroenterology ISSN 1007-9327

• *CLINICAL RESEARCH* •

Management of hilar cholangiocarcinoma in the North of England: Pathology, treatment, and outcome

SD Mansfield, O Barakat, RM Charnley, BC Jaques, CB O'Suilleabhain, PJ Atherton, D Manas

SD Mansfield, O Barakat, RM Charnley, BC Jaques, CB O' Suilleabhain, PJ Atherton, D Manas, Department of Hepato-Pancreatico-Biliary Surgery, Liver Transplantation, and Oncology, Freeman Hospital, Newcastle upon Tyne, United kingdom
Correspondence to: Derek Manas, Hepato-Pancreatico-Biliary Surgery Unit, Freeman Hospital, High Heaton, Newcastle upon Tyne, Tyne and Wear NE7 7DN,
United kingdom. derek.manas@nuth.northy.nhs.uk
Telephone: +44-191-2336161 Fax: +44-191-2231483
Received: 2004-04-30 Accepted: 2004-07-15

Key words: Hilar cholangiocarcinoma; Pathology; Treatment; Outcome; England

Mansfield SD, Barakat O, Charnley RM, Jaques BC, O' Suilleabhain CB, Atherton PJ, Manas D. Management of hilar cholangiocarcinoma in the North of England: Pathology, treatment, and outcome. *World J Gastroenterol* 2005; 11(48): 7625-7630
http://www.wignet.com/1007-9327/11/7625.asp

Abstract

AIM: To assess the management and outcome of hilar cholangiocarcinoma (Klatskin tumor) in a single tertiary referral center.

METHODS: The notes of all patients with a diagnosis of hilar cholangiocarcinoma referred to our unit for over an 8-year period were identified and retrospectively reviewed. Presentation, management and outcome were assessed.

RESULTS: Seventy-five patients were identified. The median age was 64 years (range 34-84 years). Male to female ratio was 1:1. Eighty-nine percent of patients presented with jaundice. Most patients referred were under Bismuth classification 3a, 3b or 4. Seventy patients required biliary drainage, 65 patients required 152 percutaneous drainage procedures, and 25 had other complications. Forty-one patients had 51 endoscopic drainage procedures performed (15 failed). Of these, 36 subsequently required percutaneous drainage. The median number of drainage procedures for all patients was three, 18 patients underwent resection (24%), nine had major complications and three died post-operatively. The 5-year survival rate was 4.2% for all patients, 21% for resected patients and 0% for those who did not undergo resection (P = 0.0021). The median number of admissions after diagnosis in resected patients was two and three in non-resected patients (P<0.05). Twelve patients had external-beam radiotherapy, seven brachytherapy, and eight chemotherapy. There was no significant benefit in terms of survival (P = 0.46) or hospital admissions.

CONCLUSION: Resection increases survival but carries the risk of significant morbidity and mortality. Percutaneous biliary drainage is almost always necessary and endoscopic drainage should be avoided if possible.

INTRODUCTION

Cholangiocarcinoma is a relatively rare tumor, accounting for approximately 2% of all diagnosed cancers. Its prevalence in England and Wales is approximately 2.0/100 000; however, the mortality rate has risen sharply in the past 30 years[1]. Upper third or perihilar (Klatskin) tumors make up 40-60% of cases[2,3] and are the main subjects of this paper. Klatskin tumors may be categorized as suggested by Bismuth classification into:

- Type I: tumors below the bifurcation of the common hepatic duct;
- Type II: tumors involving the bifurcation, but not extending into the main right or left duct;
- Type III: tumors infiltrating the right (IIIa) or the left (IIIb) hepatic duct;
- Type IV: tumors involving both the right and left hepatic ducts.

Cholangiocarcinoma is a slowly growing tumor and tends to spread longitudinally along the bile ducts with neural, perineural, and subepithelial extensions[4]. Lymph node invasion, particularly to the portal and peripancreatic regions, can be found in 46% of patients at the time of diagnosis[5]. Blood-born metastasis is rare and occurs at later stages of the disease. The prognosis for patients with unresectable tumors is poor and the majority of them die within 6 mo to a year of diagnosis[3].

Most patients present with obstructive jaundice. Preoperative investigations help establish the cause of obstruction, determine the extent of local disease and any evidence of distant metastasis, and evaluate the hepatic vasculature.

Treatment options for Klatskin tumors may be primarily surgical - either curative resection or palliative bypass, or non-surgical using modalities such as chemotherapy,

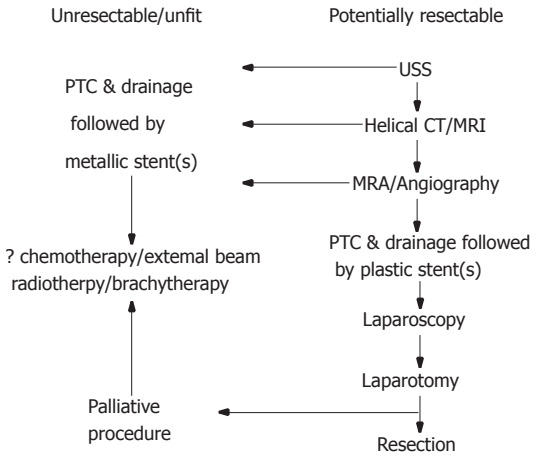

Figure 1 Flow chart demonstrating management options for hilar cholangiocarcinoma. USS, ultrasound scan; CT, computed tomography; MRI, magnetic resonance imaging; MRA, magnetic resonance angiography; PTC, percutaneous transhepatic cholangiography.

radiotherapy (external or endoluminal), a combination of the two or more recently photodynamic therapy and gene therapy. The use of biliary endoprosthesis is common either as the primary modality in palliation or for relieving jaundice or sepsis prior to more definitive treatment.

The aim of our study was to assess the management and outcome of hilar cholangiocarcinoma in a single tertiary referral center in the United Kingdom.

MATERIALS AND METHODS

Patients

Our unit is a cancer center recognized for the treatment of hepatobiliary malignancy and covers a population of approximately 3.5 million people across the North of England. The notes of all patients with hilar cholangiocarcinoma presenting to our unit during an 8-year period from June 1995 to June 2003 were identified and assessed retrospectively. Seventy-five patients were identified. Male to female ratio was 1:1 with a median age of 64 years (range 34-84 years). Thirty-seven patients had confirmed histological diagnoses with the remainder being diagnosed on strong radiological evidence. In each case, tumors were categorized using the Bismuth classification. A schematic representation for the treatment of these patients is shown in Figure 1.

Investigations

All patients were assessed using triple phase helical CT or magnetic resonance imaging. Scans performed at referring hospitals were repeated, if deemed to be of insufficient quality. Vascular involvement of hilar vessels by tumors was assessed using magnetic resonance angiography (MRA) or transfemoral angiography if MRA could not be performed or was inadequate for accurate assessment. No percutaneous or endoscopic cholangiography was performed for purely diagnostic reasons. Further imaging and laparoscopic assessment were performed if clinically indicated. Staging procedures were completed, wherever possible, before biliary drainage.

Biliary drainage

It is our policy, to drain all obstructed segments of the bile ducts in all jaundiced patients with hilar cholangiocarcinoma wherever possible. Many patients referred from other units attempted endoscopic stenting of hilar strictures. In our experience, this is often inadequate and therefore staged percutaneous drainage was performed in the majority of cases with the initial placement of internal/external or external biliary catheters being followed by the placement of single or multiple stents. When the possibility of resection was excluded, self-expanding metallic stents were used, otherwise plastic stents were inserted.

Surgical procedures

Tumors were deemed to be unresectable on pre-operative staging in the presence of extra-hepatic metastases, occlusion of main hepatic vessels, or bilateral invasion of secondary biliary radicals into the liver parenchyma. On laparotomy or laparoscopic assessment, evidence of extensive lymph node involvement and peritoneal deposits were also taken to indicate unresectability. Curative resections involved complete removal of all gross and microscopic diseases to achieve negative histological margins with eradication of all metastatic lymph nodes restricted to the scope of dissection (Ro) and restoration of bilio-enteric continuity. Caudate lobectomy was also performed in the majority of cases. For all surgical procedures, duration, blood loss, utilization of critical care beds, and complications were recorded.

Other treatment modalities

Palliative chemotherapy, external beam radiotherapy, and brachytherapy were utilized in selected cases after consultation with clinical oncologists.

Follow-up

For all patients, the last consultation date as well as dates and causes of death were recovered from patient records. For those who lost their follow-up, data were completed by consulting the patients' general practitioners or collected from the local health authority records.

Statistical analysis

Data were analyzed using Minitab statistical software. Numbers of admissions and drainage procedures were compared using the Student's *t*-test and Bismuth classification. Breakdown was made using the χ^2 test. Survival analysis was made using the log-rank test. In all cases, $P<0.05$ was considered statistically significant.

RESULTS

Management for the 75 patients is shown in Figure 2. Of these, 67 (89%) patients presented with obstructive jaundice. Although there was an incidence of type IV tumors in the non-resected group, there was no significant difference in Bismuth classification between resected and

Table 1 Bismuth classification

Bismuth classification	All patients	Resected	Not resected
1	5	0	5
2	14	4	10
3a	12	6	6
3b	13	4	9
4	24	4	20
Not recorded	6	0	6

Table 2 Surgical procedures

Procedure	*n*
Extend right hemihepatectomy and excision of extrahepatic biliary tree	7
Right hemihepatectomy and excision of extrahepatic biliary tree	4
Left hemihepatectomy and excision of extrahepatic biliary tree	6
Segment 4 resection and excision of extrahepatic biliary tree	1
Roux-en-Y segment 2,3,5 bypass	1
Roux-en-Y hepaticojejunostomy and U-tube insertion	1
U-tube insertion	1
Choledochojejunostomy	3
Laparoscopy and lateral segmentectomy (due to hemorrhage)	1
Open/close	2

non-resected groups (χ^2 test, Table 1).

Investigations

All patients received transcutaneous ultrasonography, of them 72 patients (96%) underwent assessment with CT scanning, 42 (56%) had MRI scans, and 18 (24%) received transfemoral angiography.

Biliary drainage

Biliary drainage was necessary in 70 patients, of them 65 (93%) required percutaneous drainage. A total of 51 endoscopic biliary drainages were performed in 41 patients, of which 15 (29%) failed. Percutaneous drainage was subsequently required in 36 of the 41 patients who underwent ERCP, due to failure or inadequate drainage or stent occlusion. Of the 199 drainage procedures performed, 49 (24.6%) had complications including 20 failures, 20 episodes of biliary sepsis, and 3 cases of pancreatitis. The median number of drainage procedures for all patients was three.

Surgical procedures and complications

A total of 27 surgical procedures were performed in 26 patients (Table 2). Eighteen patients underwent resection (24%) and three underwent portal vein resection. Major complications occurred in nine (50%) including three post-operative deaths (16.7%). The breakdown of complications is shown in Table 3. The median blood loss (range) in resected cases was 2.4 L (range 1-12 L), the median duration of procedure was 8 h (6-18) and the median critical care stay was 6 d (range 2-40d).

Follow-up

The median follow-up time was 9 mo. The 5-year survival rate was 4.2% for all patients, 21% for resected patients and 0% for those who did not undergo resection (P = 0.0021, log-rank test, Figure 2). The number of admissions after diagnosis was significantly lower (P<0.05, Student's t-test) in resected patients (median = 2) than in non-resected patients (median = 3).

Table 3 Complications of resection

Complication	*n*
Death	3 (17%)
Sepsis	9 (50%)
Bile leak	6 (33%)
Collection	6 (33%)
Chest infection	5 (28%)
Liver failure	5 (28%)
Wound infection	4 (22%)
Bleeding	3 (17%)
ARDS	1 (6%)
Hepatic artery thrombosis	1 (6%)
GI obstruction	1 (6%)
Pleural effusion	1 (6%)
Renal failure	1 (6%)
Respiratory arrest	1 (6%)
Wound dehiscence	1 (6%)

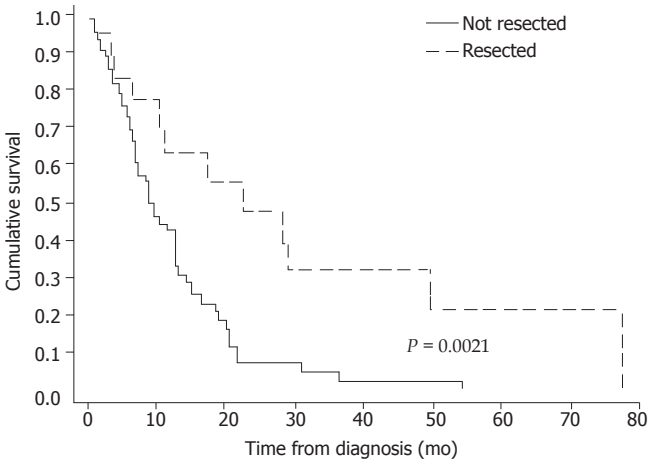

Figure 3 Kaplan–Meier survival plots for all patients with breakdown in resected and non-resected groups.

Other treatment modalities

In 23 patients who did not undergo resection, radiotherapy or chemotherapy was employed (Figure 3). These conferred no significant benefit in terms of survival (P = 0.46, log-rank test) (Figure 4), number of drainage procedures, or total hospital admissions.

Resected specimen pathology and staging

R0 resections were reported in 13 of 18 resected cases (72%). The pathological breakdown of resected cases by

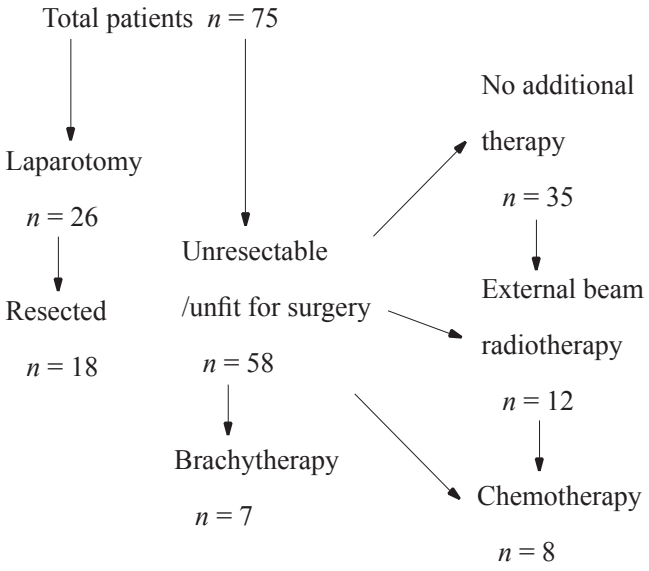

Figure 2 Flow chart showing management outcomes.

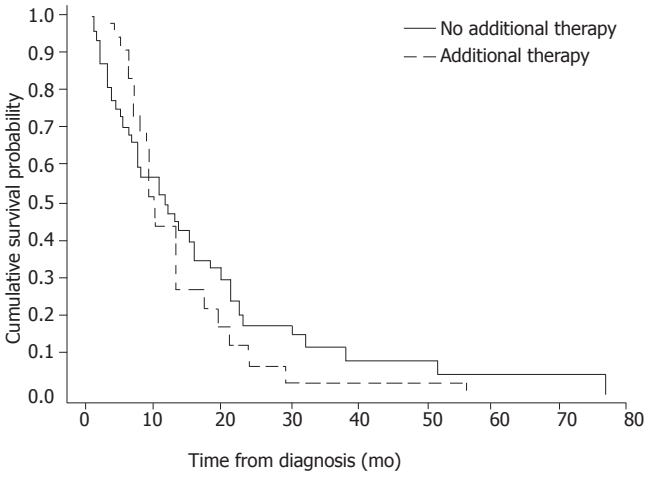

Figure 4 Kaplan-Meier survival plots for non-surgical therapeutic modalities in non-resected patients.

TNM classification is shown in Table 4. Vascular invasion was present in 9 cases (50%), perineural invasion in 13 cases (72%) and lymphatic invasion in 7 cases (39%). Patients who had node-negative resections tended to have a better survival than those who had node-positive resections (Figure 5) but this did not reach statistical significance ($P = 0.1$, log-rank test).

DISCUSSION

Our study is one of the few UK studies, documenting experienc-es in the management of hilar cholangiocarcinoma. The disease generally has a dismal prognosis; however, our findings demonstrate that an aggressive approach to the resection of these tumors results in prolonged survival. Resection is the only potentially curative treatment, and many patients do develop recurrence; however, these still benefit in terms of survival, fewer hospital admissions and decreased necessity for

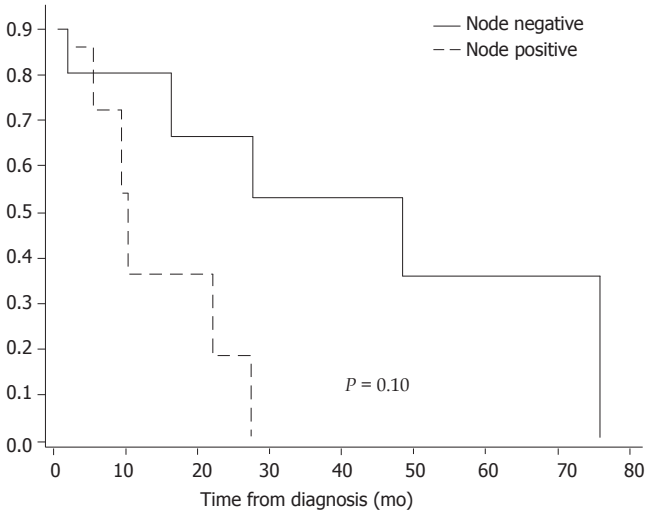

Figure 5 Kaplan-Meier survival plots for node positive and node negative resections.

Table 4 Pathological breakdown for resected cases

TNM classification	*n*
T1 N0	0
T1 N1	1
T2 N0	7
T2 N1	3
T3 N0	3
T3 N1	2
T3 N2	1
T4 N1	1

biliary drainage. Our results are comparable with several reported series of surgical resections for Klatskin tumors, with 5-year survival of 8-56%, in-hospital mortality of 6-17% and morbidity of 30-50%[2,3,6-11]. Negative resection margins have been shown to be important in prolonging survival although this could not be independently assessed in our study due to small numbers[3,8,12-14].

Major resection of a cholestatic liver is associated with an increased risk of serious complications due to impairment of liver function, including reticuloendothelial cells, mitochondrial and microsomal functions, impaired protein synthesis, wound healing and cell medicated immunity. All obstructed segments of the bile ducts in all patients undergoing preoperative assessment for surgical resection are therefore drained in our center. This facilitates not only the relief of jaundice, but also provides valuable information regarding the proximal extent of the tumor. In addition, it identifies the most common organisms isolated from the bile cultures to formulate the most appropriate perioperative antibiotic regimen.

In our study, endoscopic biliary drainage of hilar lesions had a high failure rate and almost all patients had to have subsequent percutaneous procedures in order to achieve adequate drainage. This is comparable with previously published data. Success rates for adequate endoscopic

biliary drainage for hilar tumors has been reported to be between 55% and 81%[15-18]. Even in studies supporting this modality, stent occlusion requiring further drainage procedures has been reported between 33% and 94% with morbidity of 22% and 44%[15,20]. Rerknimitr[15] describes an 81% rate for successful endoscopic drainage for Bismuth type II, III or IV tumors; however, 54% developed cholangitis and 30 of the 32 who did not undergo resection required further procedures within a mean of 47 d from initial drainage. Liu[18]describes a cohort of 55 patients undergoing endoscopic biliary drainage. Of these, only 73% had successful prosthesis insertion (16% required multiple procedures) with only 20 having satisfactory drainage. Of the 16 patients treated with palliative intent only, only 3 were successfully palliated by endoscopic means with the remainder requiring percutaneous drainage. Finally, Nomura[20]describes a significantly higher risk of cholangitis in patients treated endoscopically when compared to percutaneous drainage. Biliary obstruction due to hilar cholangiocarcinoma should therefore be ideally managed with percutaneous biliary drainage. Plastic internal-external catheters are placed initially and are then internalized. The majority of patients present with unresectable disease and in these cases, effective and reliable relief of the primary symptom - usually obstructive jaundice is paramount. For these patients also, percutaneous drainage is the method of choice. Self-expanding metallic Wallstents are preferred over plastic stents that have been shown to have longer duration of patency (6-8 mo), are more cost-effective, and are associated with a shorter hospital stay[21-23].

The use of palliative non-surgical treatment modalities conferred no benefit in our study. To date, there is no chemotherapeutic regimen that markedly improves survival in patients with advanced Klatskin tumors. Almost all phase II trials using single agents failed to demonstrate any beneficial effects with partial response rate of less than 10%[24-27]. Using combination therapy, however, the overall response rate has generally been shown to be slightly better at around 27%[28-32]. Radiotherapy may be delivered as an external beam irradiation using linear accelerator or by intraluminal brachytherapy. Trials assessing the palliative radiotherapy have generally been disappointing although a few have shown promising results. Shinchi *et al*. have shown in a retrospective review of 51 patients that external radiotherapy combined with metallic stents can offer a mean survival rate of 10.6% mo, which was significantly longer than stenting alone (4-6 mo), with a much improved quality of life[33]. Kuvshinoff *et al*. also reported similar encouraging results in 12 patients managed with intra-ductal brachytherapy and external beam radiation; the mean survival being 14.5 mo[34].

In conclusion, resection of hilar cholangiocarcinoma, when possible, increases survival although it carries the risk of significant morbidity and mortality. Percutaneous biliary drainage is almost always necessary and ERCP should be avoided. There is no evidence of benefit from chemotherapy or radiotherapy in non-resected patients, although there is data from other studies suggesting some beneficial effects.

REFERENCES

1 **Taylor-Robison SD,** Toledano MB, Arora S, Keegan TJ,Hargreaves S, Beck A, Khan SA, Elliott P, Thomas HC. Increase in mortality rates from intrahepatic cholangiocarcinoma in England and Wales 1968-1998. *Gut* 2001; **48**: 816-820

2 **Nakeeb A,** Pitt HA, Sohn TA, Coleman J, Abrams RA, Piantadosi S, Hruban RH, Lillemoe KD, Yeo CJ, Cameron JL. Cholangiocarcinoma A spectrum of intrahepatic, perihilar, and distal tumours. *Ann Surg* 1996. **224**: 463-447

3 **Burke EC,** Jarnagin WR, Hochwald SN, Pisters PW, Fong Y, Blumgart LH. Hilar Cholangiocarcinoma: patterns of spread, the importance of hepatic resection for curative operation, and a pre-surgical clinical staging system. *Ann Surg* 1998; **228**: 385-394

4 **Weinbren K,** Mutum SS. Pathological aspects of cholangiocarcinoma. *J Pathol* 1983; **139**: 217-238

5 **Chamberlain RS,** Blumgart LH. Hilar cholangiocarcinoma: a review and commentary. *Ann Surg Oncol* 2000; **7**: 55-66

6 **Lee SG,** Lee YJ, Park KM, Hwang S, Min PC. One hundred and eleven liver resections for hilar bile duct cancer. *J Hepatobiliary Pancreat Surg* 2000; **7**: 135-141

7 **Gazzaniga GM,** Filauro M, Bagarolo C, Mori L. Surgery for hilar cholangiocarcinoma: an Italian experience. *J Hepatobiliary Pancreat Surg* 2000; **7**: 122-127

8 **Pichlmayr R,** Weimann A, Ringe B. Indications for liver transplantation in hepatobiliary malignancy. *Hepatology* 1994; **20**: 33S-40S

9 **Madariaga JR,** Iwatsuki S, Todo S, Lee RG, Irish W, Starzl TE.Liver resection for hilar and peripheral cholangiocarcinomas: a study of 62 cases. *Ann Surg* 1998; **227**: 70-79

10 **Launois B, Reding R,** Lebeau G, Buard JL. Surgery for hilar cholangiocarcinoma: French experience in a collective surveyof 552 extrahepatic bile duct cancers. *J Hepatobiliary Pancreat Surg* 2000; **7**: 128-134

11 **Klempnauer J,** Ridder GJ, Werner M, Weimann A, Pichlmayr R. What constitutes long-term survival after surgery for hilar cholangiocarcinoma? *Cancer* 1997; **79**: 26-34

12 **Tabata M,** Kawarada Y, Yokoi H, Higashiguchi T, IsajiS. Surgical treatment for hilar cholangiocarcinoma. *J Hepatobiliary Pancreat Surg* 2000; **7**: 148-154

13 **Lillemoe KD,** Cameron JL. Surgery for hilar cholangiocarcinoma: the Johns Hopkins approach. *J Hepatobiliary Pancreat Surg* 2000; **7**: 115-121

14 **Tsao JI,** Nimura Y, Kamiya J, Hayakawa N, Kondo S, Nagino M, Miyachi M, Kanai M, Uesaka K, Oda K, Rossi RL, Braasch JW, Dugan JM. Management of hilar cholangiocarcinoma: comparison of an American and a Japanese experience. *Ann Surg* 2000; **232**: 166-174

15 **Rerknimitr R,** Kladcharoen N, Mahachai V, Kullavanijaya P. Result of endoscopic biliary drainage in hilar cholangiocarcinoma. *J Clin Gastroenterol* 2004; **38**: 518-523

16 **Born P,** Rosch T, Bruhl K, Sandschin W, Weigert N, Ott R,Frimberger E, Allescher HD, Hoffmann W, Neuhaus H, Classen M. Long-term outcome in patients with advanced hilar bile duct tumors undergoing palliative endoscopic or percutaneous drainage. *Z Gastroentero l* 2000; **38**: 483-489

17 **Lai EC,** Mok FP, Fan ST, Lo CM, Chu KM, Liu CL, Wong J. Preoperative endoscopic drainage for malignant obstructive jaundice *Br J Surg* 1994; **81**: 1195-1198

18 **Liu CL,** Lo CM, Lai EC, Fan ST. Endoscopic retrogra-de cholangiopancreatography and endoscopic endoprosthesis insertion in patients with Klatskin tumors. *Arch Surg* 1998; **133**: 293-296

19 **De Palma GD,** Galloro, G, Siciliano S, IovinoP, Catanzano C. Unilateral versus bilateral endoscopic hepatic duct drainage in patients with malignant hilar biliary obstruction: results of a prospective, randomized, and controlled study. *Gastrointest*

Endosc 2001; **53**: 547-553

20 **Nomura T,** Shirai Y, Hatakeyama K. Cholangitisafter endoscopic biliary drainage for hilar lesions. *Hepatogastroenterology* 1997; **44**: 1267-1270

21 **Jarngian WR,** Burke E, Powers C, Fong Y, Blumgart LH. Intrahepatic biliary enteric bypass provides effective palliation in selected patients with malignant obstruction at the hepatic duct confluence. *Am J Surg* 1998; **175**: 453-460

22 **Prat F,** Chapat O, Ducot B, Ponchon T, Pelletier G, Fritsch J, Choury AD, Buffet C. A randomized trial of endoscopic drainage methods for inoperable malignant strictures of the common bile duct. *Gastrointest Endosc* 1998; **47**: 1-7

23 **Lammer J,** Hausegger KA, Fluckiger F, Winkelbauer FW, Wildling R, Klein GE, Thurnher SA, Havelec L. Common bile duct obstruction due to malignancy: treatment with plastic versus metal stents. *Radiology* 1996; **201**: 167-172

24 **Falkson G,** MacIntyre JM, Moertel CG. Eastern CooperativeOncology Group experience with chemotherapy for inoperable gallbladder and bile duct cancer. *Cancer* 1984; **54:** 965-969

25 **Taal BG,** Audiso RA, Bleiberg H, Blijham GH, Neijt JP, Veenhof CH, Duez N, Sahmoud T. Phase II trial of mitomycin C (MMC) in advanced gallbladder and biliary tree carcinoma. An EORTC Gastrointestinal Tract Cancer CooperativeGroup Study. *Ann Oncol* 1993; **4**: 607-609

26 **Sali A,** McQuillan T, Read A, Kune G. Rifampicin as cytotoxic agent for cholangiocarcinoma: preliminary report of seven cases. *J Cancer Res Clin Oncol* 1991; **11**: 7: 503-504

27 **Jones DV Jr,** Lozano R, Hoque A, Markowitz A, Patt YZ. PhaseII study of paclitaxel therapy for unresectable biliary tree carcinomas. *J Clin Oncol* 1996; **14**: 2306-2310

28 **Ekstrom K,** Hoffman K, Linne T, Eriksson B, Glimelius B.Single-dose etoposide in advanced pancreatic and biliary cancer, a phase II study. *Oncol Rep* 1998; **5**: 931-934

29 **Ellis PA,** Hill NA, O'Brien ME, Nicolson M, Hickish T, Cunningham D. Epirubicin, Cisplatin and infusional 5-fluorouracil (5-FU) (ECF) in hepatobiliary tumour. *Eur J Cancer* 1995; **31A**: 1594-1598

30 **Kajanti M,** Pyrhonen S. Epirubicin-sequential methotrexate-5fluorouracil-leucovorin treatment in advanced cancer of the extrahepatic biliary system. A phase II sturdy. *Am J Clin Oncol* 1994; **17**: 223-226

31 **Patt YZ,** Jones DV Jr, Hoque A, Lozano R, Markowitz A, Raijman I, Lynch P, Charnsangavej C. Phase II trial of intravenous fluorouracil and subcutaneous interferon alfa-2b for biliary tract cancer. *J Clin Oncol* 1996; **14**: 2311-2315

32 **Sanz-Altamira PM,** Ferrante K, Jenkins RL, Lewis WD, Huberman MS, Stuart KE. A phase II trial of 5-fluorouracil, leucovorin, and carboplatin in patients with unresectable biliary tree carcinoma. *Cancer* 1998; **82**: 2321-2325

33 **Shinchi H,** Takao S, Nishida H, Aikou T. Length and quality of survival following external beam radiotherapy combined with expandable metallic stent for unresectable hilar cholangiocarcinoma. *J Surg Oncol* 2000; **75**: 89-94

34 **Kuvshinoff BW,** Armstrong JG, Fong Y, Schupak K, Getradjman G, Heffernan N, Blumgart LH. Palliation of irresectable hilar cholangiocarcinoma with biliary drainage and radiotherapy. *Br J Surg* 1995; **82**: 1522-1525

Science Editor Wang XL and Guo SY **Language Editor** Elsevier HK

PO Box 2345, Beijing 100023, China
www.wjgnet.com
wjg@wjgnet.com

ELSEVIER

World J Gastroenterol 2005;11(48):7631-7638
World Journal of Gastroenterology ISSN 1007-9327

• *CLINICAL RESEARCH* •

Distribution and effects of polymorphic RANTES gene alleles in HIV/HCV coinfection – A prospective cross-sectional study

Golo Ahlenstiel, Agathe Iwan, Jacob Nattermann, Karin Bueren, Jürgen K Rockstroh, Hans H Brackmann, Bernd Kupfer, Olfert Landt, Amnon Peled, Tilman Sauerbruch, Ulrich Spengler, Rainer P Woitas

Golo Ahlenstiel, Agathe Iwan, Jacob Nattermann, Karin Bueren, Jürgen K Rockstroh, Tilman Sauerbruch, Ulrich Spengler, Rainer P Woitas, Department of Internal Medicine 1, University of Bonn, 53105 Bonn, Germany
Hans H Brackmann, Institute of Experimental Hematology, University of Bonn, 53105 Bonn, Germany
Bernd Kupfer, Institute of Medical Microbiology and Immunology, University of Bonn, 53105 Bonn, Germany
Olfert Landt, TIB MOLBIOL Synthesis Laboratory, 12103 Berlin, Germany
Amnon Peled, Goldyne Savad Institute of Gene Therapy, Hadassah University Hospital, Jerusalem 91120, Israel
Correspondence to: RP Woitas, Medizinische Klinik u Poliklinik 1, Universitätsklinikum Bonn, Sigmund-Freud-Straße 25, D-53105 Bonn, Germany. rainer.woitas@ukb.uni-bonn.de
Telephone: +49-228-2875507 Fax: +49-228-287-6643
Received: 2005-04-01 Accepted: 2005-06-18

Abstract

AIM: Chemokines and their receptors are crucial for immune responses in HCV and HIV infection. RANTES gene polymorphisms lead to altered gene expression and influence the natural course of HIV infection. Therefore, these mutations may also affect the course of HIV/HCV coinfection.

METHODS: We determined allele frequencies of RANTES-403 (G→A), RANTES-28 (C→G) and RANTES-IN1.1 (T→C) polymorphisms using real-time PCR and hybridization probes in patients with HIV (n = 85), HCV (n = 112), HIV/HCV coinfection (n = 121), and 109 healthy controls. Furthermore, HIV and HCV loads as well as CD4+ and CD8+ cell counts were compared between different RANTES genotypes.

RESULTS: Frequencies of RANTES-403 A, RANTES-28 G and RANTES-IN1.1 C alleles were higher in HIV infected patients than in healthy controls (-403: 28.2% *vs* 15.1%, P = 0.002; -28: 5.4% *vs* 2.8%, not significant; IN1.1: 19.0% *vs* 11.0%, P = 0.038). In HIV/HCV coinfected patients, these RANTES alleles were less frequent than in patients with HIV infection alone (15.4% P = 0.002; 1.7%; P = 0.048; 12.0%; not significant). Frequencies of these alleles were not significantly different between HIV/HCV positive patients, HCV positive patients and healthy controls.

CONCLUSION: All three RANTES polymorphisms showed increased frequencies of the variant allele exclusively in patients with HIV monoinfection. The finding that the frequencies of these alleles remained unaltered in HIV/HCV coinfected patients suggests that HCV coinfection interferes with selection processes associated with these alleles in HIV infection.

Key words: RANTES polymorphism; HIV/HCV-coinfection; HCV

Ahlenstiel G, Iwan A, Nattermann J, Bueren K, Rockstroh JK, Brackmann HH, Kupfer B, Landt O, Peled A, Sauerbruch T, Spengler U, Woitas RP. Distribution and effects of polymorphic RANTES gene alleles in HIV/HCV coinfection – A prospective cross-sectional study. *World J Gastroenterol* 2005; 11(48): 7631-7638
http://www.wjgnet.com/1007-9327/11/7631.asp

INTRODUCTION

Coinfection with human immunodeficiency virus (HIV) and hepatitis C virus (HCV) is common among certain risk groups such as hemophiliacs and intravenous drug abusers (IVDA)[1]. Unfortunately, HIV/HCV coinfection is associated with an accelerated course of HCV infection leading to progressive liver disease, cirrhosis, and hepatic failure[2,3].

Chemokines and their receptors play a central role in HIV infection. During the initial steps of viral infection chemokine receptors, such as the chemokine receptor 5 (CCR5), are used as co-receptors by HIV to enter monocytes and CD4 positive T-helper cells. A mutation in the encoding region of CCR5, CCR5-△32, abrogates HIV cell entry of m-tropic HIV strains, and thus prevents HIV infection in CCR5-△32 homozygous patients[4]. Heterozygosity for the CCR5-△32 mutation is associated with delayed progression of HIV infection to AIDS[4]. Recently, we have reported that the CCR5-△32 mutation was more prevalent in hemophiliac patients with chronic hepatitis C virus infection and was associated with increased hepatitis C viral loads[5]. A study on liver biopsies of patients with chronic hepatitis C revealed that this mutation may be associated with reduced portal inflammation and fibrosis[6]. Furthermore, we have found epidemiological evidence that the CCR5-△32 mutation is a predictor of treatment failure in interferon-α monotherapy

of chronic HCV infection, possibly indicating that the CCR5 receptor may also play an important role in the immune response to HCV infection[7].

The natural ligands of CCR5 are the chemokines RANTES (regulated on activation normal T cell expressed and secreted; CCL5), MIP-1α (macrophage inhibitory protein-1α; CCL3) and MIP-1β (macrophage inhibitory protein-1β; CCL4), all of which are potent inhibitors of HIV-1 cell entry[8]. Importantly, RANTES blocks the CCR5 receptor via receptor binding and down-regulation of CCR5 on T cells and macrophages. Furthermore, RANTES was reported to be critically involved in the recruitment of T cells to the liver[9]. Several single nucleotide polymorphisms in the RANTES gene have been reported to influence the natural course of HIV infection by up- or down-regulating RANTES gene activity. The most frequent of those polymorphic sites comprise RANTES-403 (G→A) and RANTES-28 (C→G) in the promoter region and RANTES-IN1.1 (T→C) in the first intron region[10,11]. Both promoter polymorphisms increase RANTES transcription and may delay HIV disease progression[11,12]. Conversely, the RANTES-IN1.1 C allele seems to decrease RANTES transcriptional activity and is probably associated with an increased risk for HIV infection and progression to AIDS[10].

Since RANTES seems to be involved in the pathogenesis of both HIV and HCV infection, we studied the effects of the RANTES gene polymorphisms in patients with HIV/HCV coinfection as compared to patients with HIV infection. To exclude that HCV infection or allele frequency in the background population contributed to our results we also included patients with HCV monoinfection as well as a group of healthy blood donors into the study.

MATERIALS AND METHODS

Design and study populations

All anti-HCV or anti-HIV positive patients of Caucasian descent attending our outpatient department between May 1999 and August 2000 were enrolled into one of the three study groups (HCV monoinfection = group I, HIV monoinfection = group II, HIV/HCV double infection = group III). None of the anti-HCV positive and anti-HIV/HCV positive patients had received interferon therapy at the time of the study. Type and duration of antiretroviral therapy and risk factors for infection were recorded in groups II and III. One hundred and nine healthy Caucasian blood donors of the Bonn University transfusion center (females 37, males 72, median age 27 years, range: 12-58 years) served as a reference group. In this reference group, HIV and HCV infection had been excluded by serology and PCR.

EDTA blood samples were obtained from each patient for genotyping of RANTES-403, -28 and -IN1.1 alleles. HCV genotype, HCV, and HIV viral loads, aminotransferase serum levels, CD4+ and CD8+ cell counts were determined in HIV, HCV, and HIV/HCV coinfected patients, respectively.

Serum aminotransferase levels were determined by routine biochemical procedures. Serologic markers of hepatitis B virus infection (HBs antigen, anti-HBs, and anti-HBc) were assessed by commercially available assays according to the manufacturer's instructions (Abbott, Wiesbaden, Germany). CD4 and CD8 cell counts were analyzed on a FACSort™ (Becton Dickinson, Heidelberg, Germany) flow cytometer using the Simulset™ test kit (Becton Dickinson, Heidelberg, Germany). The study conformed to the ethical guidelines of the Helsinki declaration as approved by the local ethics committee.

Diagnosis of HIV infection

Serum samples were analyzed for anti-HIV antibodies and p24 antigen with commercially available test kits (Abbott, Wiesbaden and Coulter, Hamburg, Germany) according to the manufacturer's instructions. A positive ELISA result was confirmed by immunoblot (Biorad, Munich, Germany).

HIV DNA was amplified from peripheral blood leukocytes by nested PCR according to Saiki *et al*.[13]. Amplification of the HIV-1 proviral DNA was carried out as nested PCR with the following primers for the first PCR (sense: 5-ATTTGTCATCCATCCTATTTGTTCCTGAA GGGT-3, antisense: 5-AGTGGGGGGGACATCAAGC AGCCATGCAAAT-3) and with the following primers for the second PCR (sense: 5-TGCTATGTCACTTCCCCTT GGTTCTCT-3, antisense: 5-GAGACTATCAATGAGGA AGCTGCAGAATGGGAT-3). The amplified product was detected by agarose gel electrophoresis.

HIV load was determined quantitatively using the NucliSens HIV-QT assay (Organon Teknika, Boxtel, the Netherlands). Amplified patient and calibrator RNA were quantified with different electrochemiluminescent probes in the NASBA QR system (Organon Teknika, Boxtel, the Netherlands) based on competitive internal linear standard curves[14]. This assay had a detection limit of 80 copies/mL.

Diagnosis of HCV infection

HCV antibodies were detected with a microparticle enzyme immunoassay (MEIA, Axsym, Abbott, Wiesbaden, Germany). Positive results were confirmed by dot immunoassay (Matrix, Abbott, Wiesbaden, Germany). HCV RNA was detected after nucleic acid purification kit (Viral Kit, Qiagen, Hilden, Germany) followed by reverse transcription and nested polymerase chain reaction as described elsewhere[15]. The detection limit was 100 copies/mL. Quantitative determination of HCV load was done via branched DNA technology (Quantiplex HCV RNA 2.0 assay, Chiron, Emeryville, CA, USA), which has good linearity for all genotypes above its detection limit of 200 000 copies/mL serum. HCV genotypes were determined by the Innolipa II line probe assay (Innogenetics, Zwijndrecht, Belgium) according to the manufacturer's instructions.

Genotyping of the RANTES-403, -IN1.1, and -28 single nucleotide polymorphisms

Genomic DNA was extracted from 200 μL EDTA-

treated blood samples using the QIAamp Blood Mini Kit (Qiagen, Hilden, Germany) according to the manufacturer's protocol.

Light Cycler PCR and hybridization probes: RANTES genotyping was performed using lightcycler and "fluorescence resonance energy transfer" (FRET) technology[16,17]. For amplification 2 μL light cycler-DNA master hybridization probes (Roche Diagnostics, Mannheim, Germany), 2 μL $MgCl_2$ (25 mmol/L), 8 μL PCR-grade water were used. For genotyping of the amplified DNA, 4 pmol of each hybridization probe (TIB MolBiol, Germany) was added to the reaction mixture. Sequences of oligonucleotide primers and hybridization probes for RANTES-403 were: sense *CACCTCCTTTGGGGACTGTA* and antisense *CCTCCGGAAATTCGAGTCTC*, anchor *GAGTCACTG AGTCTTCAAAGTTCCTGCTTA-F* and sensor *LC640-CATTACAgATCTTACCTCCTTTCCp*. The sensor hybridization probe was specific for the RANTES-403G allele at a melting temperature of 62.5 ℃.

Sequences of oligonucleotide primers and hybridization probes for RANTES-28 were: sense *CACCTCCTTTGGGGACTgTA* and antisense *TGGGATGGGGTAGGCATTCTA*, anchor probe *GTTGCTATTTTGGAAACTCCCCTTAGG-F* and sensor probe *LC705-ATGCCCCTGAACTGGCCp*. The sensor hybridization probe was specific for the RANTES-28G allele at a melting temperature of 60.0 ℃. Sequences of oligonucleotide primers and hybridization probes for RANTES-IN1.1 were: sense *CCTGGTCTTGACCACCACA* and antisense *GCTGACAGGCATGAGTCAGA*, anchor probe *LC640-CCCTCAAGGCCTACAGGTGTTCACp* and sensor probe *TCAGTTTTTCTGTCTTCAAGTCTAC-F*. The sensor probe was specific for the C allele at a melting temperature of 65 ℃.

An initial denaturation step at 95 ℃ (60 s, ramp rate 20 ℃/s) was followed by amplification for 40 cycles of denaturation (95 ℃, 0 s, ramp rate 20 ℃/s), annealing (63 ℃, 10 s, ramp rate 20 ℃/s) and extension (72 ℃, 15 s, ramp rate 20 ℃/s). For RANTES-IN1.1, the annealing temperature was lowered to 55 ℃. After DNA amplification a melting curve was generated at 95 ℃ (5 s, ramp rate 20 ℃/s) followed by 45 ℃ (15 s, ramp rate 20 ℃/s) and 75 ℃ (0 s, ramp rate 0.1 ℃/s, acquisition mode: continuous) for RANTES-403 and RANTES-IN1.1 and 95 ℃, 35 ℃, and 70 ℃ for RANTES-28. After a final cooling step for 30 s at 40 ℃ melting curve analysis could be performed. Representative genotyping results are given in Figures 1A-C.

Statistical analysis

RANTES genotypes and allele frequencies were compared to the healthy reference population via contingency tables using χ^2 statistics and Fisher's exact test where appropriate. Based on gene frequencies, the expected phenotype frequencies were calculated according to the Hardy–Weinberg equation and compared to the observed frequencies using χ^2statistics[18]. Haplotype analysis for combined RANTES-403 and -28 genotypes as in Table 3 was performed according to Gonzalez *et al*.[19]. In each group, different genotypes of each RANTES polymorphism were compared with respect to HIV and HCV loads, CD4+ and CD8+ cell counts using parametric (unifactorial ANOVA with Bonferroni's correction) or non-parametric statistical analysis as appropriate (Kruskal-Wallis test followed by the Mann-Whitney test for pairwise comparison of the groups), if the number of patients with the particular genotype exceeded five. Results are given as median and range unless indicated otherwise.

In all statistical tests, $P<0.05$ were regarded as significant. All calculations were performed on a personal computer with SPSS 11.0 software (SPSS, Chicago, IL, USA).

RESULTS

Patient groups

One hundred and twelve anti-HCV positive, 85 anti-HIV positive, and 121 anti-HIV/HCV double-positive Caucasian patients were recruited into this study. The characteristics of these patient groups are summarized in Table 1. Hemophilia was the major risk factor for infection in HCV and HIV/HCV coinfected patients, whereas sexual transmission was the main risk factor in HIV infected patients. Rates of persistent HBs antigenemia was low in each study group (<5%), although the high prevalence of anti-HBc antibodies in the anti-HCV and the double infected groups indicated significant exposure to HBV (Table 1).

Distribution of RANTES-403, -28, and -IN1.1 genotypes

The distribution of RANTES-403, -28, and -IN1.1 alleles is shown in Table 2. The RANTES-403 A, RANTES-28 G, and RANTES-IN1.1 C alleles were more frequent in HIV monoinfected patients than in healthy controls as has been previously described[10]. The distribution of RANTES-403 genotypes in HIV infected patients differed significantly from controls ($P = 0.004$), whereas the RANTES-28 and RANTES-IN1.1 genotypes did not differ between the groups.

Unexpectedly, these higher frequencies of distinct RANTES alleles and genotypes were not observed in patients with HIV/HCV coinfection. RANTES-403 A, RANTES-28 G, and RANTES-IN1.1 C alleles were significantly less frequent than in HIV monoinfected patients ($P = 0.002$; $P = 0.048$; not significant). In contrast, the frequencies of the different RANTES alleles did not differ between HIV/HCV coinfected and HCV infected patients or healthy controls. This also held true for RANTES-403, -28, and IN1.1 genotype distribution ($P = 0.005$; $P = 0.045$; not significant). There was no deviation from the Hardy-Weinberg equilibrium in any of the groups.

Interestingly, the frequency of the combined RANTES wildtype (-403 G/G; -28 C/C; IN1.1 T/T) was lowest in HIV infected patients (49.4%) compared to healthy

Table 1 Patient Characteristics [data given as number (%) or median (range)]

	HCV-infection (Group I)	HIV-infection (Group II)	HCV/HIV-coinfection (Group III)	Statistical significance
Number	112	85	121	
Sex (Male / female)	108 / 4	73 / 12	117 / 4	Group I *vs* II $P = 0.009$*; group II *vs* III $P = 0.007$*
Age (median, range)	39 (13 - 77)	38 (23 - 70)	37 (21 - 62)	
Risk factors (%)				
Sexual	- - -	62 (72.9)	1 (0.8)	Group I *vs* II and II *vs* III $P < 0.001$*
Endemic	- - -	5 (5.9)	- - -	Group I *vs* II $P = 0.009$*; group II *vs* III $P = 0.011$*
I.V. drugs	- - -	4 (4.7)	3 (2.4)	Group I *vs* II $P = 0.023$*
Blood transfusion	- - -	1 (1.2)	- - -	
Hemophilia	110 (98.2)	- - -	115 (95.0)	Group I *vs* II $P < 0.001$*; group II *vs* III $P < 0.001$*
Unknown	2 (1.8)	13 (15.3)	2 (1.7)	Group I *vs* II $P < 0.001$*; group II *vs* III $P < 0.001$*
Aminotransferase activities				
ALT U/L (median, range)	34.0 (5.2 - 226.0)	17.0 (7.0 - 84.0)	38.5 (1.0 - 214.0)	Group I *vs* II and II *vs* III $P < 0.001$
AST U/L (median, range)	19.0 (5.8 - 157.0)	12.0 (4.3 - 106.0)	26.1 (7.8 - 168.0)	Group I *vs* II $P = 0.002$; group I *vs* III $P = 0.030$; Group II *vs* III $P < 0.001$
GGT U/L (median, range)	25.2 (5.2 - 350.9)	17.0 (6.2 - 149.0)	42.0 (2.9 - 254.6)	Group II *vs* III $P < 0.001$
HIV-status				
CD4 count (median, range)	668 (171 - 2 039)/μL	350 (5 - 1 142)/μL	292.5 (6 - 1 219)/μL	Group I *vs* II and I *vs* III $P < 0.001$
CD8 count (median, range)	499 (62 - 1 653)/μL	931 (88 - 2 152)/μL	804 (39 - 3 056)/μL	Group I *vs* II and I *vs* III $P < 0.001$
HIV load (median, range)	- - -	300 (<80 - 830 000)	725 (<80 - 210,000)	
HIV-viremia < 80 copies/mL	- - -	47 (55.3%)	80 (66.1%)	
Type of antiretroviral Therapy (%)				
Protease inhibitor-based HAART	- - -	62 (72.9)	58 (47.9)	Group II *vs* III $P = 0.001$
NNRTI-based HAART	- - -	11 (12.9)	25 (20.7)	
Total	- - -	73 (85.9)	83 (68.6)	Group II *vs* III $P = 0.007$
HCV-status				
HCV load (copies/mL)	8 888 000 (n.d.-126,500,000)	- - -	13 535 000 (n.d.-178 900 000)	Group I *vs* III $P = 0.012$
HCV load (IU/mL)	1 410 794 (n.d.-20,079,365)	- - -	2 148 413 (n.d.-28 396 825)	
HCV-genotypes (%)				
Genotype 1	70 (62.5)	- - -	76 (62.8)	
Genotype 2	14 (12.5)	- - -	11 (9.1)	
Genotype 3	8 (7.1)	- - -	21 (17.4)	Goups I *vs* III $P = 0.028$*
Genotype 4	6 (5.4)	- - -	5 (4.1)	
Multiple genotypes	1 (0.9)	- - -	1 (0.8)	
Undeterminded genotype	13 (11.6)	- - -	7 (5.8)	
HBV-status (%)				
Anti-HBs+ and anti-HBc+	52 (46.4)	15 (17.6)	43 (35.5)	Group I *vs* II $P < 0.001$; group II *vs* III $P = 0.008$
Anti-HBc+ alone	10 (8.9)	5 (5.9)	34 (28.1)	Group I *vs* III $P < 0.001$; group II *vs* III $P < 0.001$*
HBs-Ag+	1 (0.9)	3 (3.5)	6 (5.0)	

* Fisher´s exact test; n.d. = not detected.

controls (69.9%; $P = 0.007$), but also compared to HCV (63.4%; not significant) and HIV/HCV coinfected patients (70.4%; $P = 0.004$). The [-403 G/A; -28 C/G; IN1.1 T/C] combination genotype had the highest prevalence in HIV infected patients (9.6%) differing significantly from HCV (0.9%; $P = 0.005$) and HIV/HCV coinfected patients (1.7%; $P = 0.015$) as well as controls (4.9%; not significant).

When haplotype analysis for RANTES promoter polymorphisms was performed as described previously by Gonzalez *et al*.[19], the RANTES high producer haplotype (-403A, -28G) was most frequent in HIV monoinfected patients, whereas in HIV/HCV coinfected patients the frequency of this haplotype was similar in HCV infected patients and healthy controls (Table 3). The same finding also applies when the frequency of the (-403A, -28G) haplotype was compared between HIV and HIV/HCV infected patients ($P = 0.006$), between HIV and HCV infected patients ($P = 0.002$) and between HIV infected patients and controls ($P = 0.019$).

Effects of the RANTES-403, -28 and -IN1.1 mutations on parameters of HIV and HCV infection

HCV and HIV viral loads as well as the numbers of CD4+ and CD8+ cell counts are given in Table 4 stratified according to RANTES genotypes. There was a trend towards higher HIV loads in HIV infected patients with the RANTES-403 G/G genotype (wildtype) compared to subjects with the G/A and A/A genotype. Furthermore, HIV infected patients with the RANTES-28 C/G genotype tended to have lower HIV loads than patients with the C/C genotype (wildtype), whereas the RANTES-IN1.1 polymorphism did not affect HIV or HCV viral loads. However, statistical analysis could not be performed for RANTES-403 A/A and RANTES-IN1.1 C/C genotypes in HCV and HCV/HIV coinfection, because these genotypes were rare in each of the groups. CD4+ and CD8+ cell counts were not affected by any of the different RANTES genotypes. Finally, HIV and HCV viral loads did not differ significantly between the different haplotypes (Figure 1).

Table 2 Distribution of RANTES-403, RANTES-28 and RANTES IN1.1 genotypes and allele frequencies

RANTES-403 (%)	G/G	G/A	A/A	Statistics	[A]-allele frequency (%)	Statistics
HCV (n = 112)	71 (63.4)	39 (34.8)	2 (1.8)	*vs* HIV P = 0.077	19.2	*vs* HIV P = 0.047
HIV (n = 85)	42 (49.4)	38 (44.7)	5 (5.9)		28.2	
HCV/HIV (n = 120)	86 (71.7)	31 (25.8)	3 (2.5)	*vs* HIV P = 0.005	15.4	*vs* HIV P = 0.002
Controls (n = 109)	77 (70.6)	31 (28.4)	1 (0.9)	*vs* HIV P = 0.004	15.1	*vs* HIV P = 0.002
RANTES-28 (%)	**C/C**	**C/G**	**G/G**	**Statistics**	**[G]-allele frequency**	**Statistics**
HCV (n = 112)	108 (96.4)	4 (3.6)	0 (0.0)	*vs* HIV P = 0.078	1.8	*vs* HIV P = 0.083
HIV (n = 83)	74 (89.2)	9 (10.8)	0 (0.0)		5.4	
HCV/HIV (n = 116)	112 (96.6)	4 (3.4)	0 (0.0)	*vs* HIV P = 0.045	1.7	*vs* HIV P = 0.048
Controls (n = 109)	103 (94.5)	6 (5.5)	0 (0.0)	*vs* HIV P = 0.186	2.8	*vs* HIV P = 0.195
RANTES-In1.1 (%)	**T/T**	**T/C**	**C/C**	**Statistics**	**[C]-allele frequency**	**Statistics**
HCV (n = 112)	87 (77.7)	25 (22.3)	0 (0.0)	*vs* HIV P = 0.054	12.6	*vs* HIV P = 0.041
HIV (n = 84)	53 (63.1)	30 (35.7)	1 (1.2)		19	
HCV/HIV (n = 121)	93 (76.9)	27 (22.3)	1 (0.8)	*vs* HIV P = 0.101	12	*vs* HIV P = 0.066
Controls (n = 109)	86 (78.9)	22 (20.2)	1 (0.9)	*vs* HIV P = 0.052	11	*vs* HIV P = 0.038

Table 3 Distribution of RANTES-403/-28 haplotypes

Haplotype 403	28	HIV	HIV/HCV	HCV	Controls
G	C	71.7%	84.0%	80.8%	84.2%
A	G	5.4%	1.3%	1.8%	2.9%
A	C	22.9%	14.2%	17.4%	12.9%
G	G	- - -	0.5%	- - -	- - -

Haplotype pair (-403/-28)		HIV[1,2,3]	HIV/HCV	HCV	Controls
G/C	G/C	41 (49.4%)	82 (70.7%)	71 (63.4%)	73 (69.5%)
G/C	G/G	- - -	1 (0.9%)	- - -	- - -
G/C	A/C	28 (33.7%)	28 (24.1%)	37 (33.0%)	25 (23.8%)
G/C	A/G	9 (10.8%)	2 (1.7%)	2 (1.8%)	6 (5.7%)
A/C	A/C	5 (6.0%)	2 (1.7%)	- - -	1 (1.0%)
A/C	A/G	- - -	1 (0.9%)	2 (1.8%)	- - -

[1] *vs* HIV P = 0.002; [2] *vs* HIV/HCV P = 0.006; [3] *vs* controls P = 0.019.

DISCUSSION

RANTES polymorphisms have been proposed to modify susceptibility to HIV infection and progression to AIDS[10,11,19]. In this study, the prevalence of all three polymorphic RANTES alleles (RANTES-403 A, RANTES-28 G, and RANTES-IN1.1 C) was higher in HIV monoinfected patients compared to healthy blood donors. In contrast, in HIV/HCV coinfection the frequency of the studied RANTES alleles did not differ from HCV monoinfection or healthy controls. Since we included patients with HCV monoinfection as well as a cohort of healthy blood donors into the study to exclude biased results as a consequence of HCV infection or allele frequency of the background population, the influence of RANTES alleles on HIV infection seems to be neutralized by concomitant HCV infection.

The increased frequency of distinct polymorphic RANTES alleles in HIV infection is in line with McDermott *et al*., who observed increased susceptibility to HIV infection in patients with RANTES-403 G/A -28 C/C haplotypes[20]. The prevalence of the RANTES-28 G allele in all groups was as low as previously described by An *et al*.[10], and none of our patients was homozygous for the RANTES-28 G allele[11].

The RANTES-IN1.1 C allele has been reported to be associated with an increased susceptibility for infection with HIV, which would explain the significantly increased frequency of the C allele in our HIV monoinfected patients[10]. However, none of the different RANTES alleles was significantly associated with altered HIV viral loads or CD4+ cells counts. In this context, we cannot rule out that we have missed an association between viral loads or CD4 counts and the polymorphic RANTES alleles, because our study group was rather small and not well balanced for antiviral therapy. To exclude that the presence of the CCR5-△32 allele which probably also affects susceptibility to HCV infection has influenced our findings, we tested whether any of the RANTES polymorphisms was associated or in linkage disequilibirum with CCR5-△32[5]. However, we could not find any associations between CCR5-△32 and the RANTES alleles.

The low frequency of the RANTES alleles -403A and -28G in our HCV infected patients is in accordance with Promrat *et al*., who also could not find any association of RANTES-403 and –28 polymorphisms with susceptibility to HCV infection or laboratory parameters of chronic

Table 4 Viral loads and immunological data in different RANTES-403, RANTES-28 and RANTES-IN1.1 genoytpes. Data are given as [median (range)]. Statistically significant differences are indicated by index numbers

	HCV-Infection			HIV-Infection			HIV/HCV-Infection		
RANTES-403	G/G	G/A	A/A	G/G	G/A	A/A	G/G	G/A	A/A
	(*N* = 71)	(*N* = 39)	(*N*= 2)	(*N*= 42)	(*N* = 38)	(*N* = 5)	(*N* = 86)	(*N* = 31)	(*N* = 3)
HCV-Load	10.8	4.2	39.0	- - -	- - -	- - -	13.8	14.0	1.6
x 10^6 copies/mL	(n.d.-126.5)	(n.d.-56.6)	(n.d.-39.8)				(0.2-178.9)	(0.6-150.5)	(0.4-6.8)
HIV-Load	- - -	- - -	- - -	455	380	<80	550	770	9900
x 10^3 copies/mL				(<80-830 000)	(<80-50 000)	(<80-990)	(<80-210 000)	(<80-50 000)	(2 400-27 000)
CD4 count	683	621	916	353.5	348.5	300	302	279	293
cells/μL	(171-2 039)	(282-1 544)	(787-1 045)	(51-1 111)	(5-1 142)	(28-629)	(6-1 219)	(106-651)	(149-331)
CD8 count	496.5	499	581.5	918.5	927	1 099	792	968.5	675
cells/μL	(62-1 653)	(185-1 183)	(425-738)	(202-1 717)	(88-2 152)	(382-1 421)	(39-2 466)	(319-3 056)	(465-895)
RANTES-28	C/C	C/G	G/G	C/C	C/G	G/G	C/C	C/G	G/G
	(*N* = 108)	(*N* = 4)	(*N* = 0)	(*N* = 74)	(*N* = 9)	(*N* = 0)	(*N* = 112)	(*N* = 4)	(*N* = 0)
HCV-Load	8.4	38.3	- - -	- - -	- - -	- - -	13.5	22.3	- - -
x 10^6 copies/mL	(n.d.-126.5)	(29.9-39.8)					(0.2-178.9)	(0.4-45.8)	
HIV-Load	- - -	- - -	- - -	310	<80	- - -	560	2 150	- - -
x 10^3 copies/mL				(<80-830 000)	(<80-3 700)		(<80-210 000)	(400-91 000)	
CD4 count	662	916	- - -	355	330	- - -	293	220	- - -
cells/μL	(171-2 039)	(443-1 305)		(10-1 142)	(141-637)		(13-1 219)	(149-651)	
CD8 count	499	581.5	- - -	942.5	636	- - -	828	602.5	- - -
cells/μL	(62-1 653)	(338-739)		(202-2 152)	(362-1 997)		(39-3 056)	(397-2 401)	
RANTES-IN1.1	T/T	T/C	C/C	T/T	T/C	C/C	T/T	T/C	C/C
	(*N* = 87)	(*N* = 25)	(*N* = 0)	(*N* = 53)	(*N* = 30)	(*N* = 1)	(*N* = 93)	(*N* = 27)	(*N* = 1)
HCV-Load	9.6	6.2	- - -	- - -	- - -	- - -	13.5	14.2	1.6
x 10^6 copies/mL	(n.d.-126.5)	(0.4-56.6)					(0.2-178.9)	(0.4-150.5)	
HIV-Load	- - -	- - -	- - -	600	<80	990	735	560	9 900
x 10^3 copies/mL				(<80-830 000)	(<80-38 000)		(<80-210 000)	(<80-91 000)	
CD4 count	662	702	- - -	353	342	629	294	242	331
cells/μL	(171-2 039)	(392-1 305)		(51-1 142)	(10-1 028)		(6-1 219)	(110-651)	
CD8 count	501	497	- - -	936.5	927	1 421	792	1 034	675
cells/μL	(62-1 653)	(191-1 119)		(202-1 717)	(362-2 152)		(39-2 466)	(319-3 056)	

n.d. = not detectable

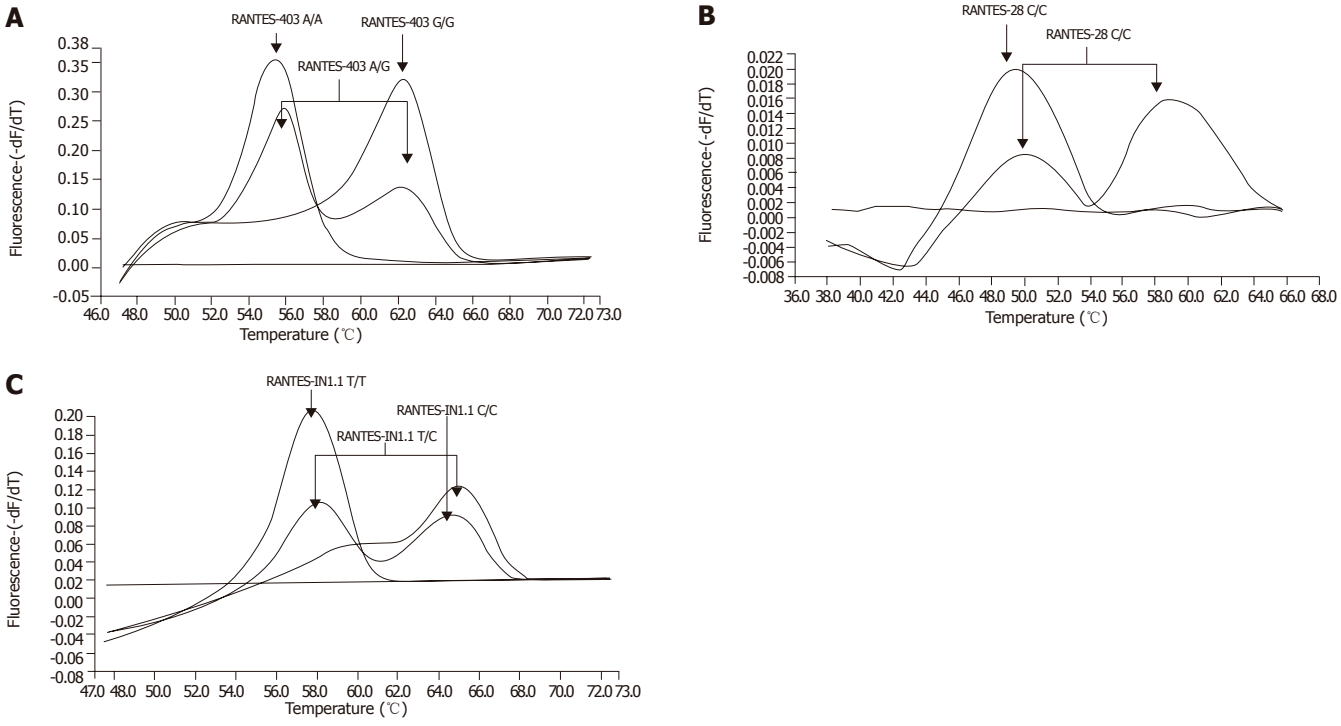

Figure 1 Shows the melting curve analysis (first order derivate) for different genotypes of the RANTES-403 (**A**), RANTES-28 (**B**), and RANTES-IN1.1 (**C**) polymorphisms. When the PCR product is melted, the probe-DNA binding will break up at a hybridization probe-specific temperature, which causes a loss in emitted fluorescence energy. This can be seen as a peak in the first order derivate of the melting curve. As the sensor probe is specific for only one of the two possible alleles in each PCR, binding of the probe to the other allele will cause a mismatch and therefore a weaker coupling and disengagement of probe and DNA at lower temperatures.

hepatitis C[21]. In contrast, Hellier *et al*. reported the RANTES-403 A/A genotype to be associated with mild portal inflammation[6]. However, the frequency of the A/A genotype in the study of Hellier (1.9%) was not different from the frequency in our patients[6]. Therefore, it was unexpected that the prevalence of RANTES alleles known to be increased in patients with HIV monoinfection was significantly lower in our HIV/HCV coinfected patients. Additionally, prevalence of these alleles was similar to HCV monoinfected patients and controls.

Several explanations may account for these divergent results: First, none of the studies so far was controlled for differences in transmission routes. Therefore, it is unclear whether disease modifying effects of the RANTES polymorphisms are equally operative in patients with sexual transmission *vs* parenteral transmission.

Alternatively, our patients with HIV/HCV coinfection could represent long time survivors: The RANTES-IN1.1 C allele has been described to be associated with rapid progression to AIDS, whereas both the RANTES-403 A and the RANTES-28 G allele have been reported to delay HIV disease progression[10,11,19]. However, frequency of these polymorphic RANTES alleles did not differ from our background population. Finally, differences in genotype and allele frequencies between HIV and HIV/HCV coinfected patients might reflect differences in the physiological roles of the single polymorphisms. RANTES-403 A and RANTES-28 G alleles have been shown to up-regulate RANTES transcription, whereas RANTES-IN1.1 C has been reported to be associated with the down-regulation of RANTES promoter activity[10-12]. Thus, RANTES expression should be characterized in terms of haplotypes, defined by the combination of the various alleles, giving the possibility to explain selection effects on the course of HIV infection[10]. However, only haplotypes AC and AG were more prevalent in patients with HIV infection, whereas their frequencies in patients with HCV and HIV/HCV coinfection were identical to the healthy background population.

The selection effect of the RANTES alleles in HIV infection may be lost in patients with HCV coinfection, because interactions of HCV-specific proteins such as core and NS5A may interact with host genes to augment RANTES promotor activity[22]. Binding of the HCV-specific protein E2 to CD81 is associated with increased RANTES serum levels resulting in CCR5 internalization[23]. Therefore, HCV infection is likely to trigger increased RANTES serum levels, which in turn decrease CCR5 expression on the cell surface due to receptor internalization. This hypothesis is further supported by a recent study that shows reduced CCR1 and CCR5 surface expression on peripheral blood cells in chronic HCV infection[24]. Thus, it is intriguing to speculate that the effects of RANTES polymorphisms on RANTES expression in HIV infection are abrogated in HIV/HCV coinfection due to induction of RANTES by HCV-specific proteins. In line with this assumption, we observed reduced frequencies of patients carrying the putatively up-regulating (RANTES-403 and RANTES-28) as well as down-regulating RANTES polymorphisms (RANTES-IN1.1) in our patients with HCV and HIV/HCV coinfection.

In summary, deviations in polymorphic RANTES allele frequencies seen in HIV infection could not be confirmed in HIV/HCV coinfection. Functional studies will be required to further analyze the differences in RANTES regulation between HIV and HIV/HCV coinfection at a molecular level.

REFERENCES

1 **Rockstroh JK**, Spengler U. HIV and hepatitis C virus co-infection. *Lancet Infect Dis* 2004; **4:** 437-444

2 **Soto B**, Sanchez-Quijano A, Rodrigo L, del Olmo JA, Garcia-Bengoechea M, Hernandez-Quero J, Rey C, Abad MA, Rodriguez M, Sales Gilabert M, Gonzalez F, Miron P, Caruz A, Relimpio F, Torronteras R, Leal M, Lissen E. Human immunodeficiency virus infection modifies the natural history of chronic parenterally-acquired hepatitis C with an unusually rapid progression to cirrhosis. *J Hepatol* 1997; **26:** 1-5

3 **Telfer P**, Sabin C, Devereux H, Scott F, Dusheiko G, Lee C. The progression of HCV-associated liver disease in a cohort of haemophilic patients. *Br J Haematol* 1994; **87:** 555-561

4 **Dean M**, Carrington M, Winkler C, Huttley GA, Smith MW, Allikmets R, Goedert JJ, Buchbinder SP, Vittinghoff E, Gomperts E, Donfield S, Vlahov D, Kaslow R, Saah A, Rinaldo C, Detels R, O'Brien SJ. Genetic restriction of HIV-1 infection and progression to AIDS by a deletion allele of the CKR5 structural gene. Hemophilia Growth and Development Study, Multicenter AIDS Cohort Study, Multicenter Hemophilia Cohort Study, San Francisco City Cohort, ALIVE Study. *Science* 1996; **273:** 1856-1862

5 **Woitas RP**, Ahlenstiel G, Iwan A, Rockstroh JK, Brackmann HH, Kupfer B, Matz B, Offergeld R, Sauerbruch T, Spengler U. Frequency of the HIV-protective CC chemokine receptor 5-Delta32/Delta32 genotype is increased in hepatitis C. *Gastroenterology* 2002; **122:** 1721-1728

6 **Hellier S**, Frodsham AJ, Hennig BJ, Klenerman P, Knapp S, Ramaley P, Satsangi J, Wright M, Zhang L, Thomas HC, Thursz M, Hill AV. Association of genetic variants of the chemokine receptor CCR5 and its ligands, RANTES and MCP-2, with outcome of HCV infection. *Hepatology* 2003; **38:** 1468-1476

7 **Ahlenstiel G**, Berg T, Woitas RP, Grunhage F, Iwan A, Hess L, Brackmann HH, Kupfer B, Schernick A, Sauerbruch T, Spengler U. Effects of the CCR5-Delta32 mutation on antiviral treatment in chronic hepatitis C. *J Hepatol* 2003; **39:** 245-252

8 **Berger EA**, Murphy PM, Farber JM. Chemokine receptors as HIV-1 coreceptors: roles in viral entry, tropism, and disease. *Annu Rev Immunol* 1999; **17:** 657-700

9 **Apolinario A**, Majano PL, Alvarez-Perez E, Saez A, Lozano C, Vargas J, Garcia-Monzon C. Increased expression of T cell chemokines and their receptors in chronic hepatitis C: relationship with the histological activity of liver disease. *Am J Gastroenterol* 2002; **97:** 2861-2870

10 **An P**, Nelson GW, Wang L, Donfield S, Goedert JJ, Phair J, Vlahov D, Buchbinder S, Farrar WL, Modi W, O'Brien SJ, Winkler CA. Modulating influence on HIV/AIDS by interacting RANTES gene variants. *Proc Natl Acad Sci USA* 2002; **99:** 10002-10007

11 **Liu H**, Chao D, Nakayama EE, Taguchi H, Goto M, Xin X, Takamatsu JK, Saito H, Ishikawa Y, Akaza T, Juji T, Takebe Y, Ohishi T, Fukutake K, Maruyama Y, Yashiki S, Sonoda S, Nakamura T, Nagai Y, Iwamoto A, Shioda T. Polymorphism

in RANTES chemokine promoter affects HIV-1 disease progression. *Proc Natl Acad Sci USA* 1999; **96:** 4581-4585

12 **Nickel RG**, Casolaro V, Wahn U, Beyer K, Barnes KC, Plunkett BS, Freidhoff LR, Sengler C, Plitt JR, Schleimer RP, Caraballo L, Naidu RP, Levett PN, Beaty TH, Huang SK. Atopic dermatitis is associated with a functional mutation in the promoter of the C-C chemokine RANTES. *J Immunol* 2000; **164:** 1612-1616

13 **Saiki RK**, Gelfand DH, Stoffel S, Scharf SJ, Higuchi R, Horn GT, Mullis KB, Erlich HA. Primer-directed enzymatic amplification of DNA with a thermostable DNA polymerase. *Science* 1988; **239:** 487-491

14 **van Gemen B**, Kievits T, Schukkink R, van Strijp D, Malek LT, Sooknanan R, Huisman HG, Lens P. Quantification of HIV-1 RNA in plasma using NASBA during HIV-1 primary infection. *J Virol Methods* 1993; **43:** 177-187

15 **Imberti L**, Cariani E, Bettinardi A, Zonaro A, Albertini A, Primi D. An immunoassay for specific amplified HCV sequences. *J Virol Methods* 1991; **34:** 233-243

16 **Morrison LE**, Halder TC, Stols LM. Solution-phase detection of polynucleotides using interacting fluorescent labels and competitive hybridization. *Anal Biochem* 1989; **183:** 231-244.

17 **Morrison LE**, Stols LM. Sensitive fluorescence-based thermodynamic and kinetic measurements of DNA hybridization in solution. *Biochemistry* 1993; **32:** 3095-3104

18 **Emery AEH**. An Introduction to Statistical Methods. Methodology in medical genetics. 2nd ed. London, New York: *Churchill Livingstone* 1986

19 **Gonzalez E**, Dhanda R, Bamshad M, Mummidi S, Geevarghese R, Catano G, Anderson SA, Walter EA, Stephan KT, Hammer MF, Mangano A, Sen L, Clark RA, Ahuja SS, Dolan MJ, Ahuja SK. Global survey of genetic variation in CCR5, RANTES, and MIP-1alpha: impact on the epidemiology of the HIV-1 pandemic. *Proc Natl Acad Sci USA* 2001; **98:** 5199-5204

20 **McDermott DH**, Beecroft MJ, Kleeberger CA, Al-Sharif FM, Ollier WE, Zimmerman PA, Boatin BA, Leitman SF, Detels R, Hajeer AH, Murphy PM. Chemokine RANTES promoter polymorphism affects risk of both HIV infection and disease progression in the Multicenter AIDS Cohort Study. *AIDS* 2000; **14:** 2671-2678

21 **Promrat K**, McDermott DH, Gonzalez CM, Kleiner DE, Koziol DE, Lessie M, Merrell M, Soza A, Heller T, Ghany M, Park Y, Alter HJ, Hoofnagle JH, Murphy PM, Liang TJ. Associations of chemokine system polymorphisms with clinical outcomes and treatment responses of chronic hepatitis C. *Gastroenterology* 2003; **124:** 352-360

22 **Soo HM**, Garzino-Demo A, Hong W, Tan YH, Tan YJ, Goh PY, Lim SG, Lim SP. Expression of a full-length hepatitis C virus cDNA up-regulates the expression of CC chemokines MCP-1 and RANTES. *Virology* 2002; **303:** 253-277

23 **Nattermann J**, Nischalke HD, Feldmann G, Ahlenstiel G, Sauerbruch T, Spengler U. Binding of HCV E2 to CD81 induces RANTES secretion and internalization of CC chemokine receptor 5. *J Viral Hepat* 2004; **11:** 519-526

24 **Lichterfeld M**, Leifeld L, Nischalke HD, Rockstroh JK, Hess L, Sauerbruch T, Spengler U. Reduced CC chemokine receptor (CCR) 1 and CCR5 surface expression on peripheral blood T lymphocytes from patients with chronic hepatitis C infection. *J Infect Dis* 2002; **185:** 1803-1807

Science Editor Guo SY **Language Editor** Elsevier HK

PO Box 2345, Beijing 100023, China
www.wjgnet.com
wjg@wjgnet.com

ELSEVIER

World J Gastroenterol 2005;11(48):7639-7645
World Journal of Gastroenterology ISSN 1007-9327

• *CLINICAL RESEARCH* •

Elevated plasma von Willebrand factor levels in patients with active ulcerative colitis reflect endothelial perturbation due to systemic inflammation

Petros Zezos, Georgia Papaioannou, Nikolaos Nikolaidis, Themistoclis Vasiliadis, Olga Giouleme, Nikolaos Evgenidis

Petros Zezos, Nikolaos Nikolaidis, Themistoclis Vasiliadis, Olga Giouleme, Nikolaos Evgenidis, Division of Gastroenterology, 2nd Propaedeutic Department of Internal Medicine, Hippokration General Hospital, Aristotle University of Thessaloniki, Greece
Georgia Papaioannou, Department of Haematology, Papageorgiou General Hospital of Thessaloniki, Greece
Correspondence to: Associate Professor Nikolaos Evgenidis, Division of Gastroenterology, 2nd Propaedeutic Department of Internal Medicine, Aristotle University of Thessaloniki, Hippokration General Hospital, 49 Konstantinoupoleos Str., 54642 Thessaloniki, Greece. zezosp@hol.gr
Telephone: +302310892073 Fax: +302310848354
Received: 2005-01-22 Accepted: 2005-04-09

Abstract

AIM: To evaluate the plasma von Willebrand factor (vWF) levels in patients with ulcerative colitis (UC) and to investigate their relationship with disease activity, systemic inflammation and coagulation activation.

METHODS: In 46 patients with ulcerative colitis (active in 34 patients), clinical data were gathered and plasma vWF levels, markers of inflammation (ESR, CRP, and fibrinogen) and thrombin generation (TAT, F1+2, and D-dimers) were measured at baseline and after 12 wk of treatment. Plasma vWF levels were also determined in 52 healthy controls (HC). The relationship of plasma vWF levels with disease activity, disease extent, response to therapy, acute-phase reactants (APRs) and coagulation markers (COAGs) was assessed.

RESULTS: The mean plasma vWF concentrations were significantly higher in active UC patients (143.38 ±63.73%) than in HC (100.75±29.65%, P = 0.001) and inactive UC patients (98.92±43.6%, P = 0.031). ESR, CRP and fibrinogen mean levels were significantly higher in active UC patients than in inactive UC patients, whereas there were no significant differences in plasma levels of D-dimers, F1+2, and TAT. UC patients with raised APRs had significantly higher mean plasma vWF levels than those with normal APRs (144.3% *vs* 96.2%, P = 0.019), regardless of disease activity. Although the mean plasma vWF levels were higher in UC patients with raised COAGs than in those with normal COAGs, irrespective of disease activity, the difference was not significant (141.3% *vs* 118.2%, P = 0.216). No correlation was noted between plasma vWF levels and disease extent. After 12 wk of treatment, significant decreases of fibrinogen, ESR, F1+2, D-dimers and vWF levels were noted only in UC patients with clinical and endoscopic improvement.

CONCLUSION: Our data indicate that increased plasma vWF levels correlate with active ulcerative colitis and increased acute-phase proteins. Elevated plasma vWF levels in ulcerative colitis possibly reflect an acute-phase response of the perturbed endothelium due to inflammation. In UC patients, plasma vWF levels may be another useful marker of disease activity or response to therapy.

Key words: Coagulation; Endothelial injury; Inflammation; Inflammatory bowel disease; Ulcerative colitis; von Willebrand factor

Zezos P, Papaioannou G, Nikolaidis N, Vasiliadis T, Giouleme O, Evgenidis N. Elevated plasma von Willebrand factor levels in patients with active ulcerative colitis reflect endothelial perturbation due to systemic inflammation. *World J Gastroenterol* 2005; 11(48): 7639-7645
http://www.wjgnet.com/1007-9327/11/7639.asp

INTRODUCTION

The etiology and pathogenesis of inflammatory bowel diseases (IBD), ulcerative colitis (UC) and Crohn's disease (CD), are still unclear[1]. "Vascular" theory supports that intestinal vascular injury is involved in CD and UC pathogenesis[2,3].

There is evidence that a hypercoagulable state exists in IBD, which might play a role in IBD pathogenesis[3-5]. This theory is further supported by the observation of Gaffney *et al*.[6] that patients with hemophilia and von Willebrand's disease have a lower risk in developing IBD and by the beneficial effects of heparin in the treatment of refractory ulcerative colitis[7,8]. The hypercoagulable state has been found to exist both in active and in inactive disease[9-15]. Furthermore, endothelial dysfunction, due to effects of

increased proinflammatory cytokines (IL-1, TNF-α), seems to play a central role in the hypercoagulant state production in IBD and also provides an evidence of interrelation between coagulation and inflammation pathways[16-18].

von Willebrand factor (vWF) is a large glycoprotein which circulates in human plasma or is deposited into the vascular subendothelium. Approximately 85% of circulating vWF is synthesized by the vascular endothelial cells, which are the main source of synthesis and secretion of this coagulation factor. vWF is also synthesized by megakaryocytes and is contained in platelets, which derive the remaining 15% of the circulating protein in blood. vWF serves as a stabilizing carrier protein of the coagulation factor VIII in circulation. vWF also mediates platelet to platelet interactions and platelet adhesion to the subendothelium in response to endothelial injury during the first step of thrombus formation[19]. Increased circulating levels of vWF in serum are considered as a marker of endothelial dysfunction or injury[19,20]. Increased levels of vWF are also observed as an acute-phase response in various inflammatory conditions[21].

vWF serum levels have been reported to be increased in patients with IBD, but it is not clear whether they reflect primary endothelial damage[17,22–25] or they are a manifestation of acute-phase response due to inflammation[22,23,26].

In this study, in order to clarify the meaning of elevated vWF levels in ulcerative colitis, we measured the circulating plasma vWF levels in a group of patients with ulcerative colitis and investigated their relationship with clinical activity and endoscopic severity of disease, markers of systemic inflammation and thrombin generation. We also monitored the changes of these variables during 12 wk of therapy and estimated their relationship with the clinical outcome.

MATERIALS AND METHODS

Patients and controls

Forty-six patients with ulcerative colitis (30 males and 16 females, mean age 41.8 years, range 17-73 years) and 52 healthy individuals (healthy controls, HC) (30 males and 22 females, mean age 40.9 years, range 19-65 years) were consecutively included in the study. All patients and controls were from the same geographical area (Northern Greece) and had a Greek ancestry.

Methods

The diagnosis of UC was based on the standard clinical, endoscopic and histological criteria. A complete medical history was obtained and physical examination was performed in all UC patients. During baseline evaluation, disease activity in patients with UC (active or inactive) was assessed with the simple clinical colitis activity index (SCCAI), taking into account five clinical criteria: day and night stool frequency, urgency of defecation, blood in the stool, general well being and presence of extracolonic manifestations[27]. A SCCAI score of ≤2 points was defined as clinical remission. Baseline colonoscopy with biopsy sampling was performed in all patients with UC, in order to assess the endoscopic severity and extent of disease. Endoscopic severity was measured by a modified endoscopic score with an 18-point scale[28] involving nine parameters: erythema, vascular pattern, friability, granularity, spontaneous bleeding, occurrence and severity of ulcers, extent of ulcerated surface, and presence of mucopurulent exudates. All parameters were scored from 0 to 2 points. Four grades of activity were considered according to the sum of all parameters: inactive disease (0-3), mild disease (4-7), moderate disease (8-12), and severe disease (13-18). Grading of endoscopic severity was done from the most inflamed part of the bowel. The extent of disease was recorded as rectosigmoiditis, left-sided colitis, and pancolitis. Patients with severe hepatic, renal and cardiac disease were excluded from the study.

Healthy control subjects were visitors in the outpatient clinic of Haematology Department and had no known diseases, or clinical or laboratory evidence of metabolic, neoplastic or inflammatory disease. They also had no history of thromboembolic disease.

All patients and control subjects gave their informed consent to participate in the study, which was approved by the Hospital's Scientific Committee.

Laboratory studies

Blood samples were collected at baseline from UC patients and control subjects for the quantitative determination of von Willebrand factor antigen (vWFAg) in plasma with an immuno-turbidimetric assay (STA-Liatest vWF, Diagnostica Stago, France; normal values 50-160%). Additional blood samples were obtained from UC patients in order to determine variables of inflammation (ESR, CRP and fibrinogen) and parameters reflecting thrombin generation (thrombin–antithrombin complex [TAT], prothrombin fragments 1+2 [F1+2], and D-dimers [D-Di]).

ESR was measured by standard laboratory technique (normal values <20 mm/h) and CRP was measured with ELISA (normal values <5 mg/L). Plasma fibrinogen concentration was measured by the Claus method using bovine thrombin (bioMerieux sa, France) on OPTION coagulation analyzer (normal values 2-4 g/L).

TAT levels in plasma were measured by sandwich enzyme immunoassay (Enzygnost TAT micro, Dade Behring, Marburg, Germany; normal values 1-4.1 μg/L). F1+2 levels in plasma were measured by sandwich enzyme immunoassay (Enzygnost F1+2 micro, Dade Behring, Marburg, Germany; normal values 0.4-1.1 nmol/L). D-dimers levels in plasma were measured by immuno-turbidimetric assay (STA-Liatest D-Di, Diagnostica Stago, France; normal values <500 μg/L).

All venipunctures were performed using a butterfly 18-gauge needle between 08:00 and 10:00 a.m. The first 10 mL of blood was not used for determination of hemostatic variables. Venous blood samples for hemostatic variables were collected in trisodium citrate tubes and platelet-poor plasma was prepared by one-stage centrifugation at 2 000 r/min for 20 min at 4 °C. Plasma was removed and assayed immediately for fibrinogen and stored at -20 °C until assayed, within one month, for vWF, TAT, F1+2, and D-dimers.

All UC patients were considered to have increased acute-phase reactants (APRs) if an increase in at least one of the two inflammation variables (ESR, CRP) was noted, as previously described[26]. Likewise, all UC patients were considered to have increased coagulation markers (COAGs) if an increase in at least one of the three hemostatic variables (TAT, F1+2, and D-dimers) was noted.

Treatment and course

Patients with active UC were treated for attenuation of disease activity with high-dose corticosteroids and mesalazine orally and rectally. Azathioprine was continued if already used. Patients were set into a follow-up program with regular visits every 2nd wk for 12 wk. Corticosteroids were tapered off with a weekly based schedule throughout the study period. At the end of the study (12th wk), complete clinical, endoscopic and laboratory evaluation, similar to baseline week, was performed in all patients with active colitis. Complete response to therapy (remission) was considered, if a SCCAI score of ≤2 and endoscopic remission was achieved after 12 wk of therapy. Partial response was considered if a 50% reduction of SCCAI score was noted together with a reduction of endoscopic activity by at least one grade.

Statistical analysis

Statistical analysis was performed using the SPSS for Windows package (version 11.0, SPSS, Chicago, IL, USA). Data were presented as mean±SD. Baseline comparisons were performed between the three main groups (healthy controls, patients with inactive UC and patients with active UC). A detailed analysis and multiple comparisons were performed between different subgroups of patients with UC according to disease activity, raised APRs or raised COAGs. Comparisons between groups were performed with Student's *t* test or ANOVA when appropriate. Student's *t* test for paired samples was used to compare baseline and follow-up measurements in patients with active disease. Associations between continuous variables were tested with Pearson's correlation. Differences in frequencies were studied with Fisher's exact test. $P<0.05$ was considered statistically significant.

RESULTS

During baseline evaluation, 12 patients with ulcerative colitis were found to be in remission and 34 patients had active disease. Demographic and clinical data of patients are shown in Table 1. There were no significant differences in sex, age and extent of disease between patients with active and inactive disease.

Table 1 Demographic and clinical data of ulcerative colitis patients (mean±SD)

	Active UC (n = 34)	Inactive UC (n = 12)
Male/female	22/12	8/4
Age (yr)	41.5±14.6 (17–73)	42.8±15.2 (18–65)
Extent of disease		
Rectosigmoiditis	6	3
Left-sided colitis	20	6
Pancolitis	8	3
SCCAI score	8±3 (3–12)	0±1 (0–2)
Endoscopic score	16±2 (12–18)	2±1 (0–3)
Treatment		
Oral steroids	15	0
5-ASA compounds	30	12
Azathioprine	11	2
None	2	0
Smoking	7	5

SCCAI: simple clinical colitis activity index; 5-ASA: 5-aminosalicylates.

Elevated plasma vWF concentrations were found in 1 patient with ulcerative colitis in remission and in 11 patients with active disease. None of the healthy subjects had an elevated value of plasma vWF. Mean plasma vWF concentrations were significantly higher in active ulcerative colitis patients (143.38±63.73%) than in healthy controls (100.75±29.65%, $P = 0.001$) and inactive UC patients (98.92 ±43.6%, $P = 0.031$). There was no difference in mean plasma vWF concentrations between HC and inactive UC patients (Table 2).

Mean levels of ESR, CRP and fibrinogen were significantly higher in active UC patients than in inactive UC patients. There were no significant differences in plasma levels of coagulation markers (D-dimers, F1+2 and TAT) between patients with active and inactive UC (Table 2).

UC patients with raised APRs (n = 34), irrespective of disease activity, had significantly higher mean plasma vWF levels than those with normal APRs (n = 12) (144.3 ±62.4% *vs* 96.2±45.8%, $P = 0.019$). Mean plasma vWF levels were also higher in UC patients with raised COAGs (n = 27), irrespective of disease activity, than in those with normal COAGs (n = 19), but did not reach statistical significance (141.3±64.8% *vs* 118.2±56.3%, $P = 0.216$). However, when all UC patients were divided into four subgroups according to raised or normal APRs and COAGs,

Table 2 Acute phase reactants and coagulation factors in patients with ulcerative colitis and healthy controls (mean±SD)

	Active UC (n = 34)	Inactive UC (n = 12)	Healthy controls (n = 52)
vWF (%)	143.38±63.73 (49-278)	98.92±43.6[a] (25-188)	100.75±29.65[b] (51–160)
ESR (mm/h)	40±21 (10-97)	16±12[a] (4-40)	
CRP (mg/L)	24.7±40.2 (3.1-175.5)	4.1±1.7[a] (3.1-7.3)	
Fibrinogen (g/L)	4.86±1.21 (2.93-7.3)	3.48±1.14[a] (1.25-5.61)	
D-dimers (μg/L)	873±1 308 (32-3 993)	608±1 149 (19-4 038)	
F1+2 (nmol/L)	3.71±6.09 (0.21–22.53)	3.72±6.41 (0.28-21.52)	
TAT (μg/L)	6.91±15.18 (0.09–85.9)	3.99±4.2 (0.85-13.2)	

vWF: von Willebrand factor; ESR: erythrocyte sedimentation rate; CRP: C-reactive protein; F1+2: prothrombin fragments 1+2; TAT: thrombin–antithrombin complexes. [a]$P<0.05$ active UC *vs* inactive UC. [b]$P<0.001$ active UC *vs* HC.

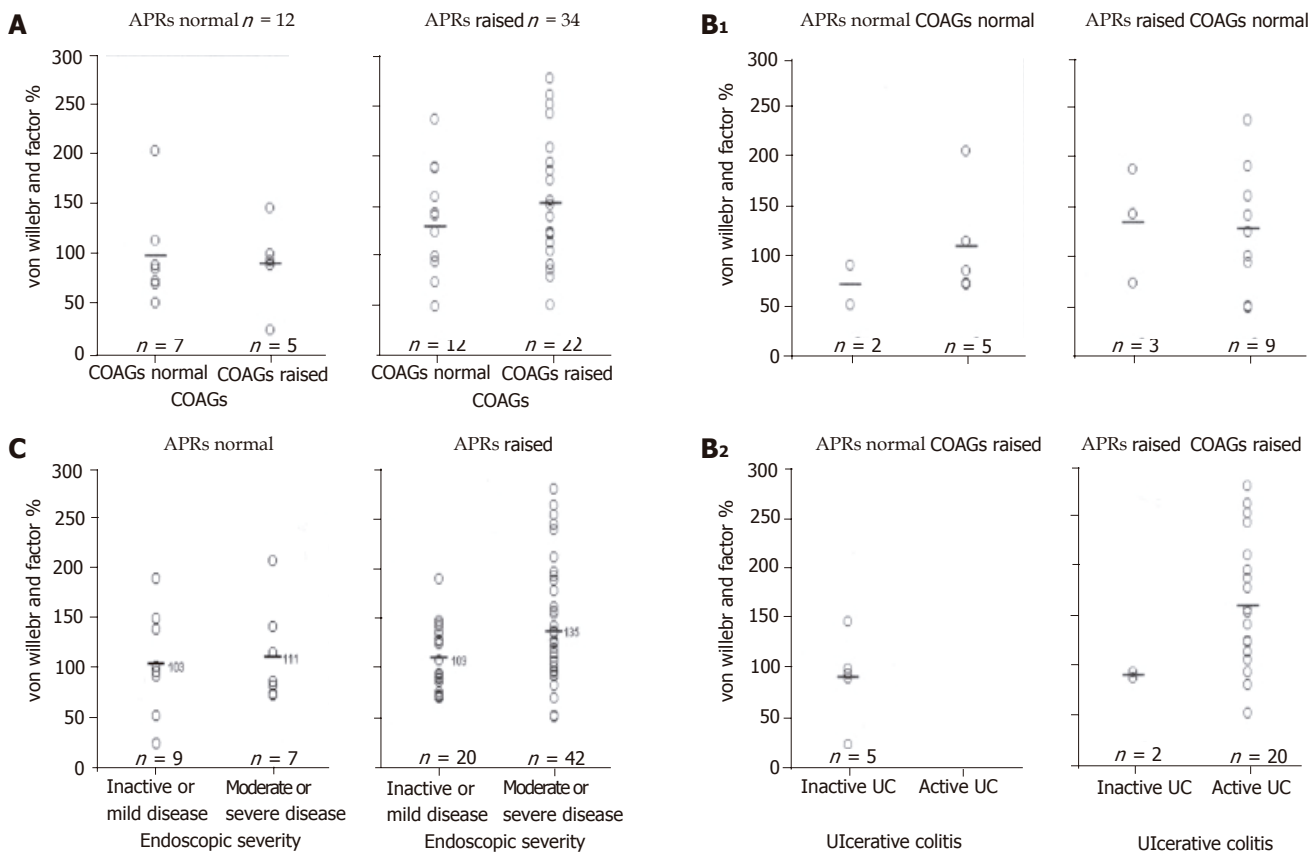

Figure 1 Mean plasma von Willebrand factor (vWF) levels in UC patients (**A**), their subgroups were divided according to disease activity, APRs and COAGs (**B1**, **B2**), as well as according to endoscopic severity and APRs(**C**). Open circle black dots (o) represent individual values and horizontal black lines (-) represent mean values. APRs: acute-phase reactants; COAGs: thrombin generation coagulation markers.

irrespective of disease activity, it was noted that patients with raised APRs had significantly higher mean plasma vWF levels than those with normal APRs, regardless of COAGs status (Figure 1A).

Furthermore, when UC patients were divided into subgroups according to disease activity and raised or not APRs and COAGs, there was a trend towards higher mean plasma vWF levels in almost all subgroups of patients with raised APRs (especially to those with active disease) compared to the patients with normal APRs. However, there were no significant differences between subgroups (Figure 1B1, B2).

In patients with ulcerative colitis (active and inactive), Pearson's correlation analysis revealed that there was a significant positive correlation of plasma vWF levels with clinical activity index (SCCAI) (r = 0.41, P = 0.004), endoscopic score (r = 0.3, P = 0.041), ESR (r = 0.39, P = 0.006), fibrinogen (r = 0.42, P = 0.003) and D-dimers (r = 0.36, P = 0.015). No correlation was noted between plasma vWF levels and extent of the disease or smoking status.

In all patients with UC, analysis of the percentages of high plasma vWF levels between subgroups revealed that raised APRs were the main factors influencing the plasma vWF levels (data not shown).

Thirty-two patients with active UC completed the study after 12 wk of treatment. Two patients did not show up at the final date of the follow-up schedule (12th week). There were no complications of the disease or adverse events from the treatment during the study period. Twenty-two patients showed response to therapy (complete or partial) and 10 patients were non-responders. A significant decrease of the inflammatory parameters (fibrinogen and ESR), the coagulation markers (F1+2 and D-dimers) and von Willebrand factor levels was noted only in the "responders" group (Table 3).

We pooled all patients in respect of endoscopic severity, before and after the therapy for active disease plus patients in remission at baseline week, and found that mean plasma vWF levels in patients with active disease at endoscopy (n = 54, 131.2±56.2%) were significantly higher than those in patients with endoscopic remission (n = 24, 103.1±36.7%, P = 0.028). There were no significant differences in plasma vWF levels between the groups of endoscopic severity grades (mild to severe) in patients with active disease. However, when we divided the patients in respect of APR status, we found that patients with raised APRs and moderate or severe endoscopic activity had significantly higher mean plasma vWF levels than the other subgroups (Figure 1C).

DISCUSSION

This study showed that mean plasma vWF levels were significantly raised in patients with active UC compared

Table 3 Laboratory parameters at baseline and after 12 wk of therapy in active UC patients who completed the study (*n* = 32) (mean±SD)

	Weeks of follow-up	Responders	Non-responders
	Paired samples *t* test	*n* = 22	*n* = 10
ESR (mm/h)	Baseline	43±24	34±13
	12th week	32±18	27±12
	P	0.055	0.206
CRP (mg/L)	Baseline	27.21±42.13	22.24±41.2
	12th week	11.11±25.57	11.42±13.29
	P	0.106	0.460
Fibrinogen (g/L)	Baseline	4.9±1.13	4.98±1.48
	12th week	4.05±0.68	4.55±0.82
	P	0.001	0.372
vWF (%)	Baseline	153.91±69.53	129.3±50.35
	12th week	111.14±30.65	105.4±32.87
	P	0.005	0.153
F1+2 (nmol/L)	Baseline	3.73±5.73	4.21±7.26
	12th week	1.23±1.12	0.71±0.26
	P	0.043	0.186
D-dimers (μg/L)	Baseline	1 202±1 522	302±329
	12th week	251±288	683±1 286
	P	0.005	0.381
TAT (μg/L)	Baseline	4.39±4.6	13.43±26.94
	12th week	5.41±13.1	1.97±1.57
	P	0.733	0.211

vWF: von Willebrand factor; ESR: erythrocyte sedimentation rate; CRP: C-reactive protein; F1+2: prothrombin fragments 1+2; TAT: thrombin–antithrombin complexes.

to healthy controls and patients with UC in remission. Since elevated circulating von Willebrand factor levels are regarded as markers of both endothelial dysfunction and acute phase response to inflammation, we tried to investigate the relationship between vWF and markers of inflammation and coagulation, in order to clarify the meaning of elevated vWF levels in our patients with active ulcerative colitis. APRs were significantly higher in patients with active UC than in those with inactive disease. On the other hand, there were no significant differences in markers of thrombin generation between patients with active and inactive UC (Table 2). These observations are in accordance with previous studies, suggesting that a hypercoagulable state exists in both active and inactive UC[29-31]. In contrast, intense inflammatory response to elevated APRs is a prominent feature of active UC[32,33].

In our study, UC patients were divided into subgroups according to disease activity (active and inactive) and APRs or COAGs status (raised or not). The analysis of data revealed two main findings. The mean plasma vWF levels were significantly higher in patients with active disease (Table 2) and higher in patients with raised APRs irrespective of disease activity or COAGs status (Figure 1).

In a recent study, Meucci *et al*.[26] reported that elevated vWF levels in a group of patients with IBD are related to increased APRs, regardless of disease activity and concluded that elevated plasma vWF levels are a secondary manifestation due to systemic inflammation. In our study, we had similar findings with Meucci *et al*.[26], suggesting that elevated plasma vWF levels in patients with UC correlate mainly with the inflammatory response and to a lesser degree with hypercoagulability. However, in the most recent study, Xu *et al*.[25] had the opposite findings in a group of patients with UC, reporting that plasma vWF levels are significantly higher in patients with ulcerative colitis than in controls, with no differences between active and inactive disease. They also reported that D-dimers levels are higher in patients with active disease than in those in remission and D-dimers levels are positively correlated with vWF levels. The authors concluded that elevated vWF levels both in active and inactive UC reflect the fact that endothelial cell damage is a feature of UC and that D-dimers levels can be used as a marker of inflammation to distinguish active from inactive UC.

Inflammation, coagulation and endothelial dysfunction correlations have been studied in many other clinical conditions[34-37]. Inflammation as measured by CRP has been found to be associated with prothrombotic status and endothelial dysfunction as reflected by elevated vWF in acute coronary syndromes[38]. Plasma vWF has been reported as an APR in patients with acute infectious diseases which parallels CRP levels during illness and recovery phase[21]. The inflammatory and coagulation abnormalities observed in patients with ulcerative colitis possibly represent combined and cross-linked manifestations of the inflammation and coagulation systems, which are interrelated in a bidirectional way with the endothelium being the interface between inflammation and coagulation[18].

Inflammation is undoubtedly a key component in the pathogenesis of ulcerative colitis[39] and proinflammatory cytokines (IL-1, IL-6, IL-8, TNF-α, and IFN-γ) operate as a cascade and network in stimulating the production of acute-phase proteins and induction of acute-phase manifestations[40]. Inflammation can also lead to activation of coagulation system with the endothelium playing a central role in all major pathways involved in the pathogenesis of hemostatic derangement[18]. Proinflammatory cytokines induce a procoagulant profile with thrombin production,

through their effects on the vascular endothelial cells[18] and can also stimulate vWF secretion from Weibel-Palade storage granules of the endothelial cells[19,41,42]. A small fraction of the elevated plasma vWF levels can also be derived from platelets, since reactive thrombocytosis and *in vivo* activation of platelets are observed in active ulcerative colitis[15], consisting acute-phase phenomena due to systemic inflammation[40], but it seems that the contribution of platelet-derived vWF to elevated plasma levels is minor[23]. We can assume that, like other coagulation factors which are synthesized in liver cells and behave as acute-phase proteins (fibrinogen, factor VIII) during inflammation, elevated plasma vWF concentrations represent an endothelial component of the acute-phase response[23].

Glucocorticoids are known to increase plasma concentrations of factor VIII (FVIII) and von Willebrand factor (vWF), and their administration is associated with an increased thrombotic tendency[43,44]. In our study, patients with active ulcerative colitis were treated with high doses of corticosteroids for attenuation of disease activity and had no thromboembolic complications during the study period. Follow-up measurements after 12 wk of treatment showed that patients who responded to therapy had a significant improvement of all the variables of inflammation and hemostasis, including von Willebrand factor. Inflammation is undoubtedly the main feature of UC and the attenuation of inflammatory process due to the potent anti-inflammatory properties of corticosteroids is the principal mechanism that contributes to the improvement of disease severity and its clinical or laboratory manifestations. It is likely that hepatic and endothelial acute-phase responses have a parallel course during inflammatory process since they may be regulated in a similar manner by the same cytokines.

In our study, we investigated the relationship of plasma vWF levels with disease activity, parameters of inflammation and hemostasis in a group of patients with ulcerative colitis (active and inactive), before and after therapy. It is the first study to our knowledge which combines the assessment of all these variables in a time course manner and represents an extension of the two most recent studies[25,26]. The small number of patients in our study did not allow us to generalize our findings and give a possible explanation for any discrepancies of data among all relative studies. However, the general trend from the data is that plasma vWF levels are correlated with systemic inflammation.

In conclusion, increased plasma vWF levels in ulcerative colitis patients correlate with disease activity and increased acute-phase proteins. It seems that elevated plasma vWF levels in active ulcerative colitis patients reflect an acute-phase response of the perturbed endothelium due to inflammation and von Willebrand factor can be regarded as an endothelial APR. Further and larger studies are needed to show if plasma von Willebrand factor levels can be a useful and sensitive marker of disease activity or response to therapy.

REFERENCES

1 **Oliva-Hemker M,** Fiocchi C. Etiopathogenesis of inflammatory bowel disease: the importance of the pediatric perspective. *Inflamm Bowel Dis* 2002; **8:** 112-128
2 **Hamilton MI**, Dick R, Crawford L, Thompson NP, Pounder RE, Wakefield AJ. Is proximal demarcation of ulcerative colitis determined by the territory of the inferior mesenteric artery? *Lancet* 1995; **345:** 688-690
3 **Wakefield AJ**, Sawyerr AM, Dhillon AP, Pittilo RM, Rowles PM, Lewis AA, Pounder RE. Pathogenesis of Crohn's disease: multifocal gastrointestinal infarction. *Lancet* 1989; **2:** 1057-1062
4 **Juhlin L**, Krause U, Shelley WB. Endotoxin-induced microclots in ulcerative colitis and Crohn's disease. *Scand J Gastroenterol* 1980; **15:** 311-314
5 **Dhillon AP**, Anthony A, Sim R, Wakefield AJ, Sankey EA, Hudson M, Allison MC, Pounder RE. Mucosal capillary thrombi in rectal biopsies. *Histopathology* 1992; **21:** 127-133
6 **Thompson NP,** Wakefield AJ, Pounder RE. Inherited disorders of coagulation appear to protect against inflammatory bowel disease. *Gastroenterology* 1995; **108**: 1011-1015
7 **Gaffney PR**, Doyle CT, Gaffney A, Hogan J, Heys DP, Annis P. Paradoxical response to heparin in 10 patients with ulcerative colitis. *Am J Gastronterol* 1995; **90:** 220-223
8 **Torkvist L**, Thorlacius H, Sjoqvist U, Bohman L, Lapidus A, Flood L, Agren B, Raud J, Lofberg R. Low molecular weight heparin as adjuvant therapy in active ulcerative colitis. *Aliment Pharmacol Ther* 1999; **13:** 1323-1328
9 **Lee LC**, Spittell JA Jr, Sauer WG, Owen CA Jr, Thompson JH Jr. Hypercoagulability associated with chronic ulcerative colitis: changes in blood coagulation factors. *Gastroenterology* 1968; **54:** 76-85
10 **Lam A**, Borda IT, Inwood MJ, Thomson S. Coagulation studies in ulcerative colitis and Crohn's disease. *Gastroenterology* 1975; **68:** 245-251
11 **de Jong E**, Porte RJ, Knot EA, Verheijen JH, Dees J. Disturbed fibrinolysis in patients with inflammatory bowel disease. A study in blood plasma, colon mucosa, and faeces. *Gut* 1989; **30:** 188-194
12 **Conlan MG**, Haire WD, Burnett DA. Prothrombotic abnormalities in inflammatory bowel disease. *Dig Dis Sci* 1989; **34:** 1089-1093
13 **Vecchi M**, Cattaneo M, de Franchis R, Mannucci PM. Risk of thromboembolic complications in patients with inflammatory bowel disease. Study of hemostasis measurements. *Int J Clin Lab Res* 1991; **21:** 165-170
14 **Hudson M**, Hutton RA, Wakefield AJ, Sawyerr AM, Pounder RE. Evidence for activation of coagulation in Crohn's disease. *Blood Coagul Fibrinolysis* 1992; **3:** 773-778
15 **Collins CE**, Cahill MR, Newland AC, Rampton DS. Platelets circulate in an activated state in inflammatory bowel disease. *Gastroenterology* 1994; **106:** 840-845
16 **Bevilacqua MP**, Gimbrone MA Jr. Inducible endothelial functions in inflammation and coagulation. *Semin Thromb Hemost* 1987; **13:** 425-433
17 **Souto JC**, Martinez E, Roca M, Mateo J, Pujol J, Gonzalez D, Fontcuberta J. Prothrombotic state and signs of endothelial lesion in plasma of patients with inflammatory bowel disease. *Dig Dis Sci* 1995; **40:** 1883-1889
18 **Levi M**, ten Cate H, van der Poll T. Endothelium: interface between coagulation and inflammation. *Crit Care Med* 2002; **30:** S220- S224
19 **Mannucci PM**. von Willebrand factor: a marker of endothelial damage? *Arterioscler Thromb Vasc Biol* 1998; **18:** 1359-1362
20 **Goldsmith I**, Kumar P, Carter P, Blann AD, Patel RL, Lip GY. Atrial endocardial changes in mitral valve disease: a scanning electron microscopy study. *Am Heart J* 2000; **140:** 777-784
21 **Pottinger BE**, Read RC, Paleolog EM, Higgins PG, Pearson JD. von Willebrand factor is an acute phase reactant in man. *Thromb Res* 1989; **5:** 387-394
22 **Stevens TR**, James JP, Simmonds NJ, McCarthy DA, Lauren-

son IF, Maddison PJ, Rampton DS. Circulating von Willebrand factor in inflammatory bowel disease. *Gut* 1992; **33:** 502-506
23 **Sawyerr AM**, Smith MS, Hall A, Hudson M, Hay CR, Wakefield AJ, Brook MG, Tomura H, Pounder RE. Serum concentrations of von Willebrand factor and soluble thrombomodulin indicate alteration of the endothelial function in inflammatory bowel disease. *Dig Dis Sci* 1995; **40:** 793–799
24 **Stevens TR**, Harley SL, Groom JS, Cambridge G, Leaker B, Blake DR, Rampton DS. Anti-endothelial cell antibodies in inflammatory bowel disease. *Dig Dis Sci* 1993; **38:** 426-432
25 **Xu G**, Tian KL, Liu GP, Zhong XJ, Tang SL, Sun YP. Clinical significance of plasma D-dimer and von Willebrand factor levels in patients with ulcer colitis. *World J Gastroenterol* 2002; **8:** 575-576
26 **Meucci G**, Pareti F, Vecchi M, Saibeni S, Bressi C, de Franchis R. Serum von Willebrand factor levels in patients with inflammatory bowel disease are related to systemic inflammation. *Scand J Gastroenterol* 1999; **34:** 287-290
27 **Walmsley RS**, Ayres RC, Pounder RE, Allan RN. A simple clinical colitis activity index. *Gut* 1998; **43:** 29-32
28 **van der Heide H**, van der Brandt-Gradel V, Tytgat GN, Endert E, Wiltink EH, Schipper ME, Dekker W. Comparison of beclomethasone diproprionate and pednisolone 21-phosphate enemas in the treatment of ulcerative colitis. *J Clin Gastroenterol* 1988; **10:** 169-172
29 **van Bodegraven AA**, Schoorl M, Baak JPA, Linskens RK, Bartels PC, Tuynman HA. Hemostatic imbalance in active and quiescent ulcerative colitis. *Am J Gastroenterol* 2001; **96:** 487-493
30 **van Bodegraven AA**, Schoorl M, Linskens RK, Bartels PC, Tuynman HA. Persistent activation of coagulation and fibrinolysis after treatment of active ulcerative colitis. *Eur J Gastroenterol Hepatol* 2002; **14:** 413-418
31 **Kjeldsen J**, Lassen JF, Brandslund I, Schaffalitzky de Muckadell OB. Markers of coagulation and fibrinolysis as measures of disease activity in inflammatory bowel disease. *Scand J Gastroenterol* 1998; **33:** 637-643
32 **Niederau C**, Backmerhoff F, Schumacher B, Niederau C. Inflammatory mediators and acute phase proteins in patients with Crohn's disease and ulcerative colitis. *Hepatogastroenterology* 1997; **44:** 90-107
33 **Vermeire S**, Van Assche G, Rutgeerts P. C-reactive protein as a marker for inflammatory bowel disease. *Inflamm Bowel Dis* 2004; **10:** 661-665
34 **Thor M**, Yu A, Swedenborg J. Markers of inflammation and hypercoagulability in diabetic and nondiabetic patients with lower extremity ischemia. *Thromb Res* 2002; **105:** 379-383
35 **Conway DS**, Buggins P, Hughes E, Lip GY. Predictive value of indexes of inflammation and hypercoagulability on success of cardioversion of persistent atrial fibrillation. *Am J Cardiol* 2004; **94:** 508–510
36 **Paisley KE**, Beaman M, Tooke JE, Mohamed-Ali V, Lowe GD, Shore AC. Endothelial dysfunction and inflammation in asymptomatic proteinuria. *Kidney Int* 2003; **63:** 624-633
37 **Hurlimann D**, Enseleit F, Ruschitzka F. Rheumatoid arthritis, inflammation, and atherosclerosis. *Herz* 2004; **29:** 760-768
38 **Apetrei E**, Ciobanu-Jurcut R, Rugina M, Gavrila A, Uscatescu V. C-reactive protein, prothrombotic imbalance and endothelial dysfunction in acute coronary syndromes without ST elevation. *Rom J Intern Med* 2004; **42:** 95-102
39 **Podolsky DK**. Inflammatory bowel disease. *N Engl J Med* 2002; **347:** 417-429
40 **Gabay C**, Kushner I. Acute-phase proteins and other systemic responses to inflammation. *N Engl J Med* 1999; **340:** 448-54
41 **van der Poll T**, van Deventer SJ, Pasterkamp G, van Mourik JA, Buller HR, tenCate JW. Tumor necrosis factor induces von Willebrand factor release in healthy humans. *Thromb Haemost* 1992; **67:** 623-626
42 **Paleolog EM**, Crossman DC, McVey JH, Pearson JD. Differential regulation by cytokines of constitutive and stimulated secretion of von Willebrand factor from endothelial cells. *Blood* 1990; **75:** 688-695
43 **Casonato A**, Pontara E, Boscaro M, Sonino N, Sartorello F, Ferasin S, Girolami A. Abmormalities of von Willebrand factor are also part of the prothrombotic state of Cushing's syndrome. *Blood Coagul Fibrinolysis* 1999; **10:** 145-151
44 **Boscaro M**, Sonino N, Scarda A, Barzon L, Fallo F, Sartori MT, Patrassi GM, Girolami A. Anticoagulant prophylaxis markedly reduces thromboembolic complications in Cushing's syndrome. *J Clin Endocrinol Metab* 2002; **87:** 3662-3666

Science Editor Wang XL and Guo SY **Language Editor** Elsevier HK

PO Box 2345, Beijing 100023, China
www.wjgnet.com
wjg@wjgnet.com

ELSEVIER

World J Gastroenterol 2005;11(48):7646-7650
World Journal of Gastroenterology ISSN 1007-9327

• *CLINICAL RESEARCH* •

Involvement of serum retinoids and Leiden mutation in patients with esophageal, gastric, liver, pancreatic, and colorectal cancers in Hungary

Gyula Mózsik, György Rumi, András Dömötör, Mária Figler, Beáta Gasztonyi, Előd Papp, Alajos Pár, Gabriella Pár, József Belágyi, Zoltán Matus, Béla Melegh

Gyula Mózsik, György Rumi, András Dömötör, Beáta Gasztonyi, Előd Papp, Alajos Pár, Gabriella Pár, First Department of Medicine, Medical Faculty, Medical and Health Centre, University of Pécs, Hungary
Zoltán Matus, Department of Biochemistry and Medical Chemistry, Medical Faculty, Medical and Health Centre, University of Pécs, Hungary
Béla Melegh, Department of Medical Genetics and Child Development, Medical Faculty, Medical and Health Centre, University of Pécs, Hungary
József Belágyi, Department of Bioanalysis, Medical Faculty, Medical and Health Centre, University of Pécs, Hungary
Mária Figler, Department of Human Clinical Nutrition and Dietetics, Faculty of Health Sciences, Medical and Health Centre, University of Pécs, Hungary
Supported by the grant from the Hungarian Ministry of Health (ETT 595/2003)
Correspondence to: Professor. Gyula Mózsik, MD, First Department of Medicine, Medical and Health Centre, University of Pécs, Hungary. gyula.mozsik@aok.pte.hu
Telephone: +36-72-536-494 Fax: +36-72-536-495
Received: 2005-03-10 Accepted: 2005-08-03

Abstract

AIM: To analyze the serum levels of retinoids and Leiden mutation in patients with esophageal, gastric, liver, pancreatic, and colorectal cancers.

METHODS: The changes in serum levels of retinoids (vitamin A, α- and β-carotene, α- and β-cryptoxanthin, zeaxanthin, lutein) and Leiden mutation were measured by high liquid performance chromatography (HPLC) and polymerase chain reaction (PCR) in 107 patients (70 males/37 females) with esophageal (0/8), gastric (16/5), liver (8/7), pancreatic (6/4), and colorectal (30/21 including 9 patients suffering from *in situ* colon cancer) cancer. Fifty-seven healthy subjects (in matched groups) for controls of serum retinoids and 600 healthy blood donors for Leiden mutation were used.

RESULTS: The serum levels of vitamin A and zeaxanthin were decreased significantly in all groups of patients with gastrointestinal (GI) tumors except for vitamin A in patients with pancreatic cancer. No changes were obtained in the serum levels of α- and β-carotene, α- and β-cryptoxanthin, zeaxanthin, lutein in patients with GI cancer. The prevalence of Leiden mutation significantly increased in all groups of patients with GI cancer.

CONCLUSION: Retinoids (as environmental factors) are decreased significantly with increased prevalence of Leiden mutation (as a genetic factor) in patients before the clinical manifestation of histologically different (planocellular and hepatocellular carcinoma, and adenocarcinoma) GI cancer.

Key words: Human gastrointestinal cancer; Leiden mutation; Retinoids; Vitamin A; Zeaxanthin

Mózsik G, Rumi G, Dömötör A, Figler M, Gasztonyi B, Papp E, Pár A, Pár G, Belágyi J, Matus Z, Melegh B. Involvement of serum retinoids and Leiden mutation in patients with esophageal, gastric, liver, pancreatic, and colorectal cancers in Hungary. *World J Gastroenterol* 2005; 11(48): 7646-7650
http://www.wjgnet.com/1007-9327/11/7646.asp

INTRODUCTION

The number of patients with different gastrointestinal (esophageal, gastric, liver, pancreatic, and colorectal) cancer has increased about two- to threefolds in the last decades (except for gastric cancer which has decreased 50%) in Hungary. The number of patients who died of these malignant diseases represents the second highest population of the total mortality of patients in Hungary. The second highest mortality rate of gastrointestinal (GI) tumor takes place at the second place in our country.

The causes of GI tumors are not known. However, different genetic and environmental factors play a role in the development of GI cancer. It is generally accepted that different diseases such as acute and chronic inflammatory diseases, polyposis, can be taken as precancerous states of GI cancer.

Since the year of l980, we have studied the role of retinoids in protecting gastrointestinal mucosa in animal experiments and human observations[1-4]. Retinoids are chemical compounds of color materials from plants and are built up from C-20 and four isoprene units, while carotenoids are built up from C-40 and eight isoprene units located in about 600 plants, and about 50 from 600

Table 1 Patients with different gastrointestinal tumors

	Number of patients			
Types of tumors	Male	Female	Total	Histology
Esophageal	8 (60±10 yr)[1]	–	8	Planocellular carcinoma
Gastric	16 (64±12 yr)[1]	5 (68±10 yr)[1]	21	Adenocarcinoma
Liver	8 (60±8 yr)[1]	7 (57±13 yr)[1]	15	Hepatocellular carcinoma
Pancreas	6 (56±11 yr)[1]	4 (63±9 yr)[1]	10	Adenocarcinoma
Colorectal	30 (66±10 yr)[1]	23 (65±11 yr)[1]	53	Adenocarcinoma
In situ carcinoma in colon polyps	4 (60±5 yr)[1]	5 (61±5 yr)[1]	9	Adenocarcinoma
Total	70	37	107	
Healthy subjects	29 (50±12 yr)[1]	28 (49±10 yr)[1]	57	

600 blood donors (healthy controls) for Leiden mutation study. [1]Age of patients (mean±SD).

isolated compounds are precursors of vitamin A.

Vitamin A and β-carotene (and other retinoids) have gastric mucosal protective effects in rats provoked by intragastric administration of 1 mL from 0.6 mol/L HCl, 25% NaCl, 0.2 NaOH, and 960 mL/L ethanol, without the presence of any inhibition of gastric acid secretion[1]. Vitamin A has a higher ulcer healing effect than atropine, cimetidine DE-NOL (tripotassio–dicitrato) in patients with gastric ulcer[2-4] .The serum level of retinoids is decreased in patients with inflammatory bowel disease[5-8]. It was also demonstrated that the serum levels of vitamin A and zeaxanthin are also decreased in patients with GI cancer[9], but the possible correlation between the changes in other serum retinoids and the prevalence of Leiden mutation has not been studied.

The presence of Leiden mutation (replacement of Arg by Glu of residue 506 in the factor V molecule, FVR, 506 Q) has been proven in thrombophylia[10-13] as well as in Crohn's disease and ulcerative colitis[14-18], meanwhile no higher prevalence of Leiden mutation has been obtained in patients with acute gastritis and hepatitis[17]. The significant presence of Leiden mutation (APC) is responsible for blood coagulation abnormality in thrombophylia.

The aims of our present study were to evaluate the changes in serum levels of retinoids (as nutritional components of vitamin A, β-carotene, α-carotene, α- and β-cryptoxanthin, zeaxanthin, lutein) in patients with different gastrointestinal (esophageal, gastric, liver, pancreatic, and colorectal) cancer, to study the prevalence of Leiden mutation in the above mentioned patients, to find some correlation between the changes in Leiden mutation and serum level of vitamin A and zeaxanthin in GI cancer patients as well as between GI cancer development and chemical structure of retinoids, to obtain some correlation between serum levels of vitamin A and zeaxanthin in patients with different GI tumors.

MATERIALS AND METHODS

Observations were carried in 107 patients with esophageal (n = 8), gastric (n = 21), liver (n = 15), pancreatic (n = 10), colorectal (n = 53), and *in situ* colon (n = 9) cancer, including 70 males (50±12 years) and 37 females (49± 10 years). Fifty-seven healthy persons (in matched group) were used as control, and 600 healthy blood donors were used for the control of Leiden mutation (Table 1). A total of 764 patients with gastrointestinal cancer and healthy subjects were included in this study. The studies were approved by the Ethical Committee of University of Pécs, Hungary. Written informed consent was obtained from all participants and the nature of the study was fully explained (Table 1).

Physical, laboratory, iconographic, and histological examinations were carried out in the patients with gastrointestinal tumor. The diagnostic histology indicated planocellular carcinoma in esophagus, hepatocellular carcinoma in liver and adenocarcinoma in stomach, pancreas and colorectum. The control (healthy subjects) persons received physical and laboratory screening, and the medical histories were found to be negative (including the genetic backgrounds).

Measurement of serum retinoid levels

The serum levels of retinoids were measured by high performance liquid chromatography (HPLC). The serum levels of vitamin A, α- and β-carotene, α- and β-cryptoxanthin, zeaxanthin and lutein both in the control (healthy subjects) and in patients with GI tumors were measured. Blood samples were prepared for HPLC measurements: 2 mL of serum sample was shaken with 2 mL/L ethanol for 2 min, and extracted with 3 mL hexane for 2 min. The mixture was centrifuged for 5 min. As an internal standard, canthaxanthin was added to the removed homogenous organic phase, evaporated in vacuum. The residue was dissolved in 0.2 mL 1:4 dichloromethane/methanol and 0.125 mL of this solution was injected. The chromatographic system consists of a gradient former Model 250 B Glenco injector (Glycotec, Germany) and a time programmable UV-vis detector Model 166-2, equipped with Gold chromatography software (Beckmann, USA).The column is 150 mm× 4.6 mm in size packed with Chromsil-C 0.186 mm. The eluent was 30 mL/L water in methanol (A), methanol (B) and 20 v/v dichloromethane in methanol. The flow rate was 1.5 mL/min. The gradient program was 100% A for 30 s, 100% B for 3 min, to 100% for 4 min (linear steps). The time program of wavelength was 323 mm for 3.5 min (detecting vitamin A), then 450 mm (detecting other retinoids). The chromatograms were evaluated quantitatively by relating the peak areas of the individual components to canthaxanthin used as internal standard. The ratio of the molar extinctions of the authentic

Table 2 Serum retinoid level in patients with different gastrointestinal cancer (mean±SE, μmol/L)

Retinoids	Healthy subjects	Esophageal cancer	Gastric cancer	Liver cancer	Pancreatic cancer	Colon cancer	*In situ* colon cancer
Vitamin A	2.07±0.12	0.14±0.04[b]	1.02±0.10[b]	0.75±0.07[c]	1.68±0.10[NS]	0.35±0.02[c]	0.30±002[c]
α-Carotene	3.93±0.40	3.81±0.50[NS]	3.85±0.60[NS]	3.82±0.50[NS]	3.90±0.40[NS]	3.80±0.70[NS]	3.80±0.70[NS]
β-Carotene	8.59±0.40	7.50±0.30[NS]	8.01±0.35[NS]	8.10±0.30[NS]	8.40±0.40[NS]	6.80±0.40[NS]	7.90±0.30[NS]
α-Cryptoxanthin	4.10±0.50	4.00±0.60[NS]	3.90±0.50[NS]	4.00±0.40[NS]	3.90±0.40[NS]	4.00±0.30[NS]	4.00±0.30[NS]
β-Cryptoxanthin	6.00±0.60	5.90±0.40[NS]	6.00±0.50[NS]	5.90±0.40[NS]	5.90±0.50[NS]	4.95±0.40[NS]	4.90±0.30[NS]
Zeaxanthin	0.14±0.01	0.074±0.007[b]	0.08±0.004[a]	0.05±0.005[c]	0.03±0.002[c]	0.07±0.004[c]	0.03±0.002[c]
Lutein	0.11±0.007	0.10±0.04[NS]	0.10±0.02[NS]	0.08±0.007[NS]	0.06±0.004[b]	0.010±0.04[NS]	0.10±0.04[NS]

NS: not significant, [a]P<0.05, [b]P<0.01, [c]P<0.001 *vs* each group.

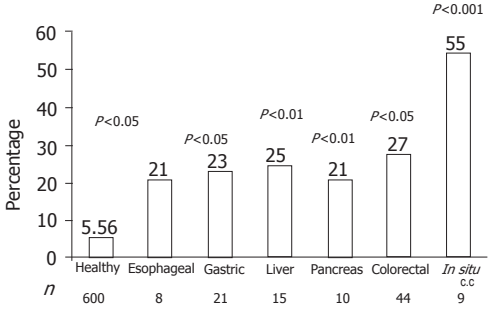

Figure 1 Prevalence of Leiden mutation in patients with different gastrointestinal tumors. The number in abscissa indicates the number of patients (600 healthy blood donors used as control).

samples to that of canthaxanthin was employed as a correction factor of the detector signals. The results were given in μmol/L, and expressed as mean±SE.

Determination of Leiden mutation

Leiden mutation was detected by polymerase-chain reaction (PCR)[12]. The DNA was isolated from 3 mL EDTA blood.

Statistical analysis

The changes in serum levels of retinoids were detected by the method of ANOVA. The prevalence of Leiden mutation was statistically analyzed by χ^2 test. P<0.05 (in the changes of serum retinoids and prevalence of Leiden mutation) was considered statistically significant.

RESULTS

The serum levels of vitamin A were decreased in all groups of patients with esophageal, gastric, hepatocellular and colorectal cancer meanwhile its level remained normal in patients with pancreatic cancer. The serum levels of α- and β-carotene, as provitamins of vitamin A, were normal in different groups of patients with GI cancer. Zeaxanthin level (without presence of any vitamin A property) was decreased significantly in patients with esophageal, gastric, hepatocellular, pancreatic, and colorectal cancer. No changes were obtained in the serum levels of α- and β-cryptoxanthin and lutein in the studied cancer patients (Table 2).

Prevalence of Leiden mutation accounted for 5.56% in 600 healthy blood donors, which was significantly higher in patients with esophageal (P<0.05), gastric (P<0.01), liver (P<0.01), pancreatic (P<0.05), colorectal (P<0.001) cancer. The higher prevalence of Leiden mutation (55%) was found *in situ* colorectal cancer (P<0.001, Figures 1 and 2).

DISCUSSION

Retinoids are chemical compounds of color materials from plants. Increased intake of plant foods can prevent different types of GI cancer. We studied the possible role of different retinoids (vitamin A, α- and β-carotene, α- and β-cryptoxanthin, zeaxanthin, and lutein) in patients with different GI cancer based on previous studies[5–9,19,20]. The location of GI tumor differed in organs (esophagus, stomach, pancreas, liver, and colon), suggesting that different etiological factors are involved in the development of different GI cancer (Barrett's esophageal metaplasia, chronic atrophic gastritis, viral infection in liver, chronic inflammatory bowel disease) in our everyday medical practice.

The serum levels of vitamin A and zeaxanthin were decreased significantly in all groups of GI cancer patients (not in patients with pancreatic cancer). Surprisingly the serum levels of provitamins were normal in patients with different GI tumor. These results indicate that transformation of provitamins into vitamin A is impaired by some factors at the level of liver, suggesting that the liver plays a key role in the development of tumor. Similar changes were observed in the serum levels of retinoids in patients with hepatocellular cancer, which offers a further proof for this hypothesis.

It is also interesting to evaluate the possible correlation between the terminal chemical structure, vitamin A activity and GI mucosal protection. Our results have clearly proved that there is no close correlation between the terminal chemical structure, vitamin A activity and GI mucosal protection (Table 3).

Similar results have been obtained in animal experiments[1,21-24] (Table 4). At present, no information is available on the correlation between the serum and tissue levels of retinoids in patients with different GI tumor. These observations cannot be done due to the obligatory necessity of histological evaluation of tumor tissues.

In animal experiments, β-carotene has been found in gastric mucosa of indomethacin-treated rats after

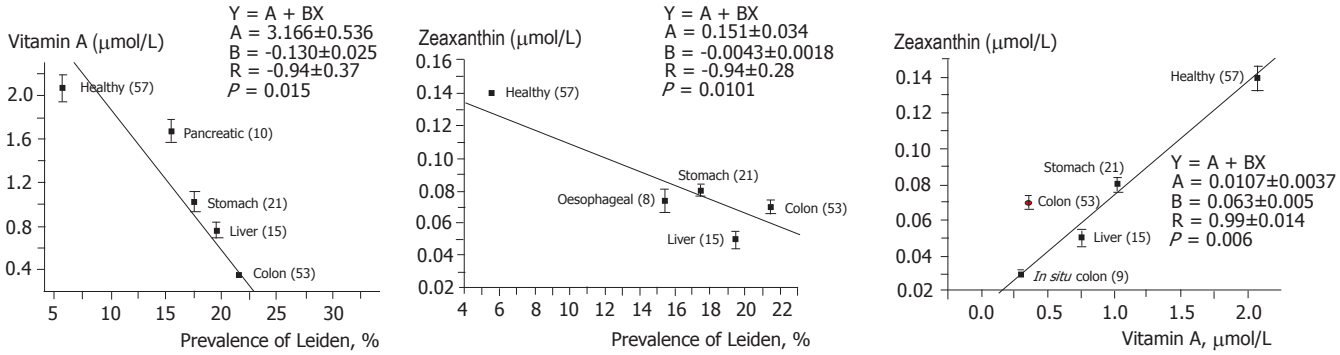

Figure 2 Correlation between the prevalence of Leiden mutation and serum level of vitamin A (**A**) and zeaxanthin (**B**) as well as between serum levels of vitamin A and zeaxanthin (**C**) in patients with different GI tumors. *n* indicates the number (in parenthesis) of examined patients.

Table 3 Changes of serum level of retinoids in patients with different gastrointestinal cancer

	Esophageal cancer	Gastric cancer	Hepatocellular cancer	Pancreatic cancer	Colorectal cancer	*In situ* colon cancer
Patients	8	21	15	10	44	9
Vitamin A	↓↓	↓↓	↓↓↓	NS	↓↓↓	↓↓↓
α-Carotene	NS	NS	NS	NS	NS	NS
β-Carotene	NS	NS	NS	NS	NS	NS
α-Cryptoxantin	NS	NS	NS	NS	NS	NS
β-Cryptoxantin	NS	NS	NS	NS	NS	NS
Zeaxantin	↓↓	↓	↓↓↓	↓↓↓	↓↓↓	↓↓↓
Lutein	NS	NS	NS	↓↓	NS	NS

P values: between healthy controls *vs* each group; ↓= $P<0.05$ ↓↓ = $P<0.01$ ↓↓↓ = $P<0.01$.

Table 4 Correlation between gastric cytoprotective effects of retinoids, their chemical structure and vitamin A activity in rats

Retinoids	Terminal chemical structure	Vitamin A activity	Gastric mucosal prevention
Vitamin A	*R* = *a*	Yes	Yes
β-Carotene	*X* = *Y* = *a*	Yes	Yes
β-Cryptoxanthin	*X* = a, *Y* = b	Yes	Yes
Zeaxanthin	*X* = *Y* = b	None	Yes
Lutein	*X* = b, *Y* = c	None	Yes
Capsorubin	*X* = *Y* = d	None	None
Capsanthin	*X* = b, *Y* = d	None	None
Capsanthol	*X* = b, *Y* = e	None	None
Lycopene	*X* = *Y* = f	None	None

acute surgical vagatomy[25,26], however no gastric mucosal protection is found, indicating that intact vagal nerve is necessary for the development of β-carotene-induced gastric cytoprotection[26]. The mechanism of retinoids is very complex. Our earlier observations indicate that the GI mucosal protective effect of retinoids depends on intact vagal nerve and adrenals as well as on gastric mucosal biochemical changes (retinoids produce a dose-dependent inhibition on the extent of ATP-transformation into ADP in association with a simultaneous increase in the transformation of ATP into cAMP), intact function of sulfhydryl groups and scavenger properties[9,19-28].

Retinoid-induced GI mucosal protection does not depend on the inhibition of gastric acid secretory responses, vitamin A activity, number of unsaturated double bonds, presence of a characteristic chemical structure of their terminal components and modification of vascular permeability[20]. These results clearly indicate that the beneficial effect of retinoids is much more complex than that of their scavengers. The results of biochemical observations suggest that different cAMP-dependent cellular regulatory mechanisms exist (including the functions of retinoid receptors, gene expressions)[7,20,27].

The involvement of vascular events is suggested in the development of different acute inflammatory processes in the GI tract[20]. That is the reason why we studied the potential role of Leiden mutation in acute and chronic gastrointestinal inflammatory processes (*Helicobacter pylori*-induced gastritis, viral hepatitis, Crohn's disease, ulcerative colitis). The prevalence of Leiden mutation increased in chronic inflammatory bowel diseases, but no changes were obtained in gastritis and hepatitis. The prevalence of Leiden mutation was also significantly higher in patients with esophageal, gastric, hepatocellular, pancreatic, and colorectal cancer. These results indicate that only the increased prevalence of Leiden mutation does not take place directly in the tumor genesis of human GI cancer. We compared the different results in the examined parameters in patients with acute and chronic gastrointestinal inflammatory diseases, and found a time-sequence process between the inflammatory diseases and GI cancer in patients, suggesting that retinoids play a key role in the development of precancerous state to cancerous state[5,8,20].

In conclusion, the prevalence of Leiden mutation is significantly correlated with decrease in serum levels of vitamin A and zeaxanthin, suggesting that retinoids play a role in the human GI tumor genesis.

ACKNOWLEDGMENTS

The authors express their thanks to Ms. Katalin Vincze and Ms. Erika Kispap for the careful preparation of the manuscript.

REFERENCES

1 **Javor T**, Bata M, Lovasz L, Moron F, Nagy L, Patty I, Szabolcs J, Tarnok F, Toth G, Mozsik G. Gastric cytoprotective effects of vitamin A and other carotenoids. *Int J Tissue React* 1983; **5:** 89-296

2 **Patty I**, Benedek S, Deak G, Javor T, Kenez P, Nagy L, Simon L, Tarnok F, Mozsik G. Controlled trial of vitamin A therapy in gastric ulcer. *Lancet* 1982; **2:** 876

3 **Patty I**, Benedek S, Deak G, Javor T, Kenez P, Moron F, Nagy L, Simon L, Tarnok F, Mozsik G. Cytoprotective effect of vitamin A and its clinical importance in the treatment of patients with chronic gastric ulcer. *Int J Tissue React* 1983; **5:** 301-307

4 **Patty I**, Tarnok F, Simon L, Javor T, Deak G, Benedek S, Kenez P, Nagy L, Mozsik G. A comparative dynamic study of the effectiveness of gastric cytoprotection by vitamin A, De-Nol, sucralfate and ulcer healing by pirenzepine in patients with chronic gastric ulcer (a multiclinical and randomized study). *Acta Physiol Hung* 1984; **64:** 379-384

5 **Rumi G Jr,** Szabo I, Vincze A, Matus Z, Toth G, Rumi G, Mozsik G. Decrease in serum levels of vitamin A and zeaxanthin in patients with colorectal polyp. *Eur J Gastroenterol Hepatol* 1999; **11:** 305-308

6 **Rumi Gy,** Szabó I, Matus Z, Vincze Á, Tóth Gy, Rumi Gy, Mózsik Gy Decrease of serum carotenoids in Crohn's disease. *J Physiol (Paris)* 2000; **94:** 159-161

7 **Mózsik Gy,** Bódis B, Karádi O, Király Á, Rumi Gy, Sütő G, Szabó I, Vincze Á Cellular Mechanisms of ß-carotene induced gastric cytoprotection in indomethacine treated rats. *Inflammopharmacology* 1998; **6**: 27-40

8 **Mozsik G**, Nagy Z, Nagy A, Rumi G, Karadi O, Czimmer J, Matus Z, Toth G, Par A. Leiden mutation (as genetic) and environmental (retinoids) sequences in the acute and chronic inflammatory and premalignant colon disease in human gastrointestinal tract. *J Physiol Paris* 2001; **95:** 489-494

9 **Rumi Gy,** Pár A, Matus Z, Rumi Gy, Mózsik Gy The Defensive Effects of Retinoids in the Gastrointestinal Tract (Animal Experiments and Human Observations). *Budapest, Akadémiai Kiadó* 2001: 1-79

10 **Bargen JA,** Barker NW Extensive arterial and venous thrombosis complicating chronic ulcerative colitis. *Arch Intern Med* 1936; **58:** 17-31

11 **Dahlback B,** Carlsson M, Svensson PJ. Familial thrombophilia due to a previously unrecognized mechanism characterized by poor anticoagulant response to activated protein C: prediction of a cofactor to activated protein C. *Proc Natl Acad Sci USA* 1993; **90:** 1004-1008

12 **Bertina RM,** Koeleman BP Koster T, Rosendaal FR, Dirven RJ, Ronde de H, Velden van der PA. Reitsma PH. Mutation in blood coagulation factor V associated with resistance to activated protein C resistance resistance. *Nature* 1994; **369**: 64-67

13 **Dahlback B**. New molecular insights into the genetics of thrombophilia. Resistance to activated protein C caused by Arg506 to Gln mutation in factor V as a pathogenic risk factor for venous thrombosis. *Thromb Haemost* 1995; **74:** 139-148

14 **Talbot RW**, Heppell J, Dozois RR, Beart RW Jr. Vascular complications of inflammatory bowel disease. *Mayo Clin Proc* 1986; 61: 140-145

15 **Best WR**, Becktel JM, Singleton JW, Kern F Jr. Development of a Crohn's disease activity index. National Cooperative Crohn's Disease Study. *Gastroenterology* 1976; **70:** 439-444

16 **Nagy Z,** Nagy A, Karadi O, Par A, Mozsik G. The high prevalence of the factor V Leiden mutation in central European inflammatory bowel disease patients. *Am J Gastroenterol* 2000; **95:** 3013-3014

17 **Nagy Z**, Nagy A, Karadi O, Figler M, Rumi G Jr, Suto G, Vincze A, Par A, Mozsik G. Prevalence of the factor V Leiden mutation in human inflammatory bowel disease with different activity. *J Physiol Paris* 2001; **95:** 483-487

18 **Papa A**, Danese S, Grillo A, Gasbarrini G, Gasbarrini A. Review article: inherited thrombophilia in inflammatory bowel disease. *Am J Gastroenterol* 2003; **98:** 1247-1251

19 **Mózsik Gy,** Pár A, Pár G, Gasztonyi B, Figler M Nutritional gastrointestinal mucosal protection: an update overview. In: Sikiric P, Seiwerth S., *Mózsik Gy., Arakava T., Takeuchi K.,* Ulcer Research, *Bologna Monduzzi Editore,* 1994: 155-162

20 **Mózsik Gy,** Neural, hormonal and pharmacological regulations of retinoids-induced gastrointestinal musocal protection. *Recent Res Develop in Life Sci* 2005; **3:** 131-202

21 **Mózsik Gy,** Garamszegi M, Jávor T, Sütő G, Vincze Á, Tóth Gy, Zsoldos T Correlations between the oxygen free radicals, membrane-bound ATP-dependent energy systems in relation of development of ethanol- and HCl- induced gastric mucosal damage and of β-carotene-induced gastric cytorprotection. In: Tsuchiya M, Kawai K, Kondo M, Yoshikawa T, eds. Free Radicals in Digestive Diseases. *Amsterdam: Elsevier Science Publisher Co., Inc,* 1988: 111-116

22 **Mózsik Gy,** Figler M, Garamszegi M, Jávor T, Nagy L, Sütő G, Vincze Á, Zsoldos T Mechanism of gastric mucosal cytoprotection. I. Time-sequence analysis of gastric mucosal membrane-bound ATP-dependent energy systems, oxygen free radicals and macroscopically appearance of gastric cytoprotection by PGI_2 and β-carotene in HCL- model of rats. In: Hayashi E, Niki M, Kondo M, Yoshikawa T eds. Medical, Biochemical, and Chemical Aspects of Free Radicals. *Amsterdam: Elsevier Science Publishers Co, Inc,* 1989: 1421 -1425

23 **Mózsik Gy,** Figler M, Garamszegi M, Jávor T, Nagy L, Sütő G, Vincze Á, Zsoldos T Mechanism of gastric mucosal cytoprotection. II. Time-sequence analysis of gastric mucosal membrane-bound ATP-dependent energy systems, oxygen free radicals and appearance of gastric mucosal damage. In: Hayashi E, Niki M, Kondo M, Yoshikawa T eds. Medical, Biochemical, and Chemical Aspects of Free Radicals. *Amsterdam Elsevier Science Publishers, Co, Inc* 1989: 1427-1431

24 **Mózsik Gy,**. Jávor T Therapy of ulcers with sulfhydryl and nonsulfhydryl antioxidants. In: Swabb A, Szabo S eds. Ulcer Disease. Investigation and Basis for Therapy. *New York, Basel, Hong Kong Marcel Dekker Inc,* 1991: 321-341

25 **Mozsik G**, Kiraly A, Garamszegi M, Javor T, Nagy L, Suto G, Toth G, Vincze A. Failure of prostacyclin, beta-carotene, atropine and cimetidine to produce gastric cyto- and general mucosal protection in surgically vagotomized rats. *Life Sci* 1991; **49:** 1383-1389

26 **Mozsik G**, Nagy Z, Nagy A, Rumi G, Karadi O, Czimmer J, Matus Z, Toth G, Par A. Leiden mutation (as genetic) and environmental (retinoids) sequences in the acute and chronic inflammatory and premalignant colon disease in human gastrointestinal tract. *J Physiol Paris* 2001; **95:** 229-239

27 **Mozsik G,** Bodis B, Figler M, Kiraly A, Karadi O, Par A, Rumi G, Suto G, Toth G, Vincze A. Mechanisms of action of retinoids in gastrointestinal mucosal protection in animals, human healthy subjects and patients. *Life Sci* 2001; **69:** 3103-3112

28 **Mózsik Gy,** Bódis B, Garamszegi M, Karádi O, Király Á, Nagy L, Sütő G, Tóth Gy, Vincze Á Role of vagal nerve in the development of gastric mucosal injury and its prevention by atropine, cimetidine, β-carotene and prostacyclin in rats. In: Szabo S, Tache Y, Neuroendocrinology of Gastrointestinal Ulceration. *New York Plenum Press,* 1995: 175-190

Science Editor Wang XL and Guo SY **Language Editor** Elsevier HK

PO Box 2345, Beijing 100023, China
www.wjgnet.com
wjg@wjgnet.com

ELSEVIER

World J Gastroenterol 2005;11(48):7651-7656
World Journal of Gastroenterology ISSN 1007-9327

• *RAPID COMMUNICATION* •

Helicobacter pylori upregulates prion protein expression in gastric mucosa: A possible link to prion disease

Peter C Konturek, Karolina Bazela, Vitaliy Kukharskyy, Michael Bauer, Eckhart G Hahn, Detlef Schuppan

Peter C Konturek, Karolina Bazela, Vitaliy Kukharskyy, Michael Bauer, Eckhart G Hahn, Detlef Schuppan, Department of Medicine, University of Erlangen-Nuernberg, 91054 Erlangen, Germany
Supported by Bavarian Ministry of Health, Germany
Co-correspondents: Eckhart G Hahn
Correspondence to: Assistant Professor Dr Peter C Konturek, Department of Medicine I, University Erlangen-Nuremberg, Germany. peter.konturek@med1.imed.uni-erlangen.de
Telephone: +49-9131-8535210 Fax: +49-9131-8535212
Received: 2005-01-18 Accepted: 2005-07-08

Abstract

AIM: Pathological prion protein (PrP^{sc}) is responsible for the development of transmissible spongiform encephalopathies (TSE). While PrPc enters the organism via the oral route, less data is available to know about its uptake and the role of gastrointestinal inflammation on the expression of prion precursor PrPc, which is constitutively expressed in the gastric mucosa.

METHODS: We studied PrPc expression in the gastric mucosa of 10 *Helicobacter pylori*-positive patients before and after successful *H pylori* eradication compared to non-infected controls using RT-PCR and Western blotting. The effect of central mediators of gastric inflammation, i.e., gastrin, prostaglandin E_2 (PGE_2), tumor necrosis factor alpha (TNF-α) and interleukin 1 beta (IL-1β) on PrPc expression was analyzed in gastric cell lines.

RESULTS: PrPc expression was increased in *H pylori*-infection compared with non-infected controls and decreased to normal after successful eradication. Gastrin, PGE_2, and IL-1β dose-dependently upregulated PrPc in gastric cells, while TNF-α had no effect.

CONCLUSION: *H pylori* infection leads to the upregulation of gastric PrPc expression. This can be linked to *H pylori* induced hypergastrinemia and increased mucosal PGE_2 and IL-1β synthesis. *H pylori* creates a milieu for enhanced propagation of prions in the gastrointestinal tract.

Key words: Prions; *Helicobacter pylori*; Gastrin; Pro-inflammatory cytokines

Konturek PC, Bazela K, Kukharskyy V, Bauer M, Hahn EG, Schuppan D. *Helicobacter pylori* upregulates prion protein expression in gastric mucosa: A possible link to prion disease. *World J Gastroenterol* 2005; 11(48): 7651-7656
http://www.wjgnet.com/1007-9327/11/7651.asp

INTRODUCTION

Transmissible spongiform encephalopathies (TSE) are fatal neurodegenerative diseases affecting both animals and human beings[1]. They are characterized by typical cerebral histopathological findings such as amyloid deposition, neuronal loss, and spongiform changes. The prion protein (PrP) can exist in the normal cellular form (PrPc) or in an "infectious" form (PrP^{sc}) that causes disease by converting apathogenic PrPc into pathogenic PrP^{sc}[2]. Previous studies have demonstrated that PrPc is required for prion infection propagation and infectivity has been suggested to be a consequence of conformational modification of PrPc by the infectious PrP^{sc}. Experiment on animals shows that animals lacking the PrPc gene are not able to propagate prion infectivity and are not able to develop the disease[3]. Both the prion isoforms differ dramatically in their physicochemical properties. Whereas PrPc is soluble and easily digested by proteinase K, PrP^{sc} is rich in β-sheet structure, aggregates into fibrils, and is resistant to proteinase K.

The main entry for prions is the gastrointestinal tract. Recent animal studies have shown that after oral exposure to pathogenic prions, PrP^{sc} accumulates in gut lymphoid tissues or in the enteric nervous system prior to its appearance in the central nervous system[4,5]. It has been postulated that prions then propagate from the enteric nervous system along the nerve pathways to ventral and dorsal root ganglia and further through the spinal cord into the brain cortex[4-6].

However, the mechanisms of propagation of prions from the gut lumen, before they reach intestinal lymph follicles or the enteric nervous system remain unexplained. Recently, the 67-ku laminin, binding protein, which can act as a PrP^{sc} receptor was demonstrated on small intestinal epithelial cells[7-9], suggesting that individuals with a high expression of this receptor could be at greater risk of developing TSE after oral challenge with PrP^{sc}. There is also evidence of transepithelial transport of pathogenic prions via intestinal M cells to adjacent lymph follicles (Peyer's patches)[10]. However, it is unknown if and how far gastrointestinal inflammation may influence PrPc expression

and thus potentially PrP^{sc} propagation in the GI tract.

MATERIALS AND METHODS

Patients

Ten *H pylori* positive patients with non-ulcer dyspepsia (mean age 47 years, range 20-79 years) were included in this study. All patients underwent upper gastrointestinal endoscopy during which four biopsies from the antrum and corpus were obtained. Patients with *H pylori* gastritis were graded according to the updated Sydney classification[11]. All patients underwent a second endoscopy 4 wk after completing successful eradication therapy consisting of clarithromycine 500 mg twice daily, amoxicillin 1 000 mg twice daily and omeprazole 40 mg twice daily for 1 wk. *H pylori* was considered to be successfully eradicated, if histology was normal and silver stainable organisms were not detected anymore in the follow-up endoscopy, during which again four biopsies from the antrum and corpus were obtained.

Cell culture

MKN45 and KATO III cell lines were obtained from the American Type Culture Collection. Cells were cultured in RPMI medium containing 10% of fetal calf serum (FCS), 2 mmol/L L-glutamine and antibiotics (1% penicillin-streptomycin, 0.5% gentamycin) at 37 ℃ in a water-saturated atmosphere of 95% air and 50 mL/L CO_2. Subconfluent MKN45 cells were incubated in RPMI without FCS and antibiotics for 24 h. Following serum starvation, cells were exposed to the increasing amounts of gastrin (Clinalfa, Switzerland, C-210), prostaglandin E_2 (PGE_2), interleukin 1 beta (IL-1β) or tumor necrosis factor alpha (TNF-α) (all from Calbiochem, Bad Soden, Germany).

Extraction of mRNA and RT-PCR analysis

Total RNA was extracted from biopsy specimens and cultured cells using TRIzol reagent (Gibco, Karlsruhe, Germany). Single stranded cDNA was generated from 5 μg RNA using Moloney murine leukemia virus reverse transcriptase (MMLV-RT) and oligo-(dT)-primers (both Stratagene, Heidelberg, Germany). Briefly, 5 μg of total RNA was uncoiled by heating (65 ℃ for 5 min) and then reverse transcribed (37 ℃ for 1 h) into complementary DNA (cDNA) in a 50 μL reaction mixture that contained 50 U MMLV-RT, 0.3 μg oligo-(dT)-primer, 40 U RNase Block Ribonuclease Inhibitor, 2 μL of a 100 mmol/L mixture of dNTPs, and 5 μL of buffer (10 mmol/L Tris-HCl, 50 mmol/L KCl, 5 mmol/L $MgCl_2$, pH 8.3). The resultant cDNA (2 μL) was amplified in a 50 μL reaction volume containing 2 U Taq polymerase, dNTP (200 μmol/L each), 1.5 mmol/L $MgCl_2$, 5 μL 10× PCR buffer (50 mmol/L KCl, 10 mmol/L Tris-HCl, pH 8.3) and specific primers at a final concentration of 1 mmol/L (all reagents from Takara, Shiga, Japan). Reactions were carried out at the following conditions: denaturation at 94 ℃ for 45 s, annealing at 60 °C (for GAPDH) and 67 ℃ (for PrPc) for 45 s and extension at 72 ℃ for 2 min. Polymerase chain reaction (PCR) products were detected by electrophoresis on a 1.5% agarose gel containing ethidium bromide. Product size was confirmed by using a 100-bp ladder (Takara, Shiga, Japan) as standard. The gel was photographed under UV transillumination and the intensity of PCR products were measured using a video image analysis system (Kodak Digital Science). The signal for PrPc mRNAs was standardized against that of the GAPDH mRNA from each sample and the results were expressed as PrPc/GAPDH mRNA ratio. The following PCR primers were used based on published sequences: PrPc (sense) 5`- GGCAGTG ACTATGAGGACCGTTAC-3´; PrPc (antisense) 5´-GG CTTGACCAGCATCTCAGGTCTA-3´; GAPDH (sense) 5´-GTCTTCACCACCATGGAGAAGGCT-3´; GAPDH (antisense) 5´-CATGCCAGTGAGCTTCCCGTTCA-3´. Expected product lengths were 528 bp for PrPc and 392 bp for GAPDH. All primer sequences were based on the sequences of the published cDNAs[12,13] and synthesized by GIBCO BRL/Life Technologies (Eggenstein, Germany).

Real-time RT-PCR

PrPc transcript levels were quantified by real-time RT-PCR. Using the Primer Express software (Perkin Elmer, Tokyo, Japan) TaqMan probe and primer set were designed based on published sequences of human PrPc (GenBank accession no.: GI 11079225); PrPc sense (5´ -CGCGAGCTTCTCCTCTCCTC-3´), PrPc antisense (5´ -GCCCAGGTCACTCCATGT-3´) and beta-2-microglobulin (β2M, GenBank accession no.: XM_007650), β2M sense 5 ´-TGACTTTGT-CACAGCCCAAGATA-3´, β2M antisense primer 5´-AATCCA-AATGCGGCATCTTC-3´. Probes for PrPc (5´-TCGCCATAA-TGACTGCTCTGCCTCGGT-3´) and β2M (5´-TGATGCTG-CTTACAT GTCTCGATCCCA-3´) were synthesized and labeled with a reporter dye (FAM) at the 5' end and quencher dye (TAMRA) at the 3´-end at MWG Biotech AG (Ebersberg, Germany). For normalization of differences in RNA amounts and efficiencies in the reverse transcription reactions, the housekeeping gene β2M was amplified under the same conditions as PrPc. Real-time RT-PCR was performed on a LightCycler (Roche, Mannheim, Germany) in a reaction volume of 15 μL using the LightCycler FastStart DNA Master Hybridization Probes Kit (Roche Molecular Biochemicals, Mannheim, Germany). The reaction mix included FastStart Taq DNA-Polymerase, dNTP-mix, reaction buffer, $MgCl_2$ (3.0 mmol/L), primers (2 μmol/L of each) and probe (0.5 μmol/L). After pippeting 13.5 μL of this mixture into LC-capillaries and 1.5 μL template cDNA was added. The capillaries were sealed and placed into the thermal chamber of the LightCycler. Samples were amplified with a pre-cycling step at 95 ℃ for 10 min, followed by 40 cycles of denaturation at 95 ℃ for 10 s, annealing at 60 ℃ for 15 s and extension at 72 ℃ for 6 s.

Immunoblot

MKN45 cells were incubated with Gastrin 1-1 000 nmol/L, PGE_2 1-100 nmol/L, TNF-α 1-10 ng/mL or IL-1β 1-10 ng/mL) for 24 h. Cells were collected, washed

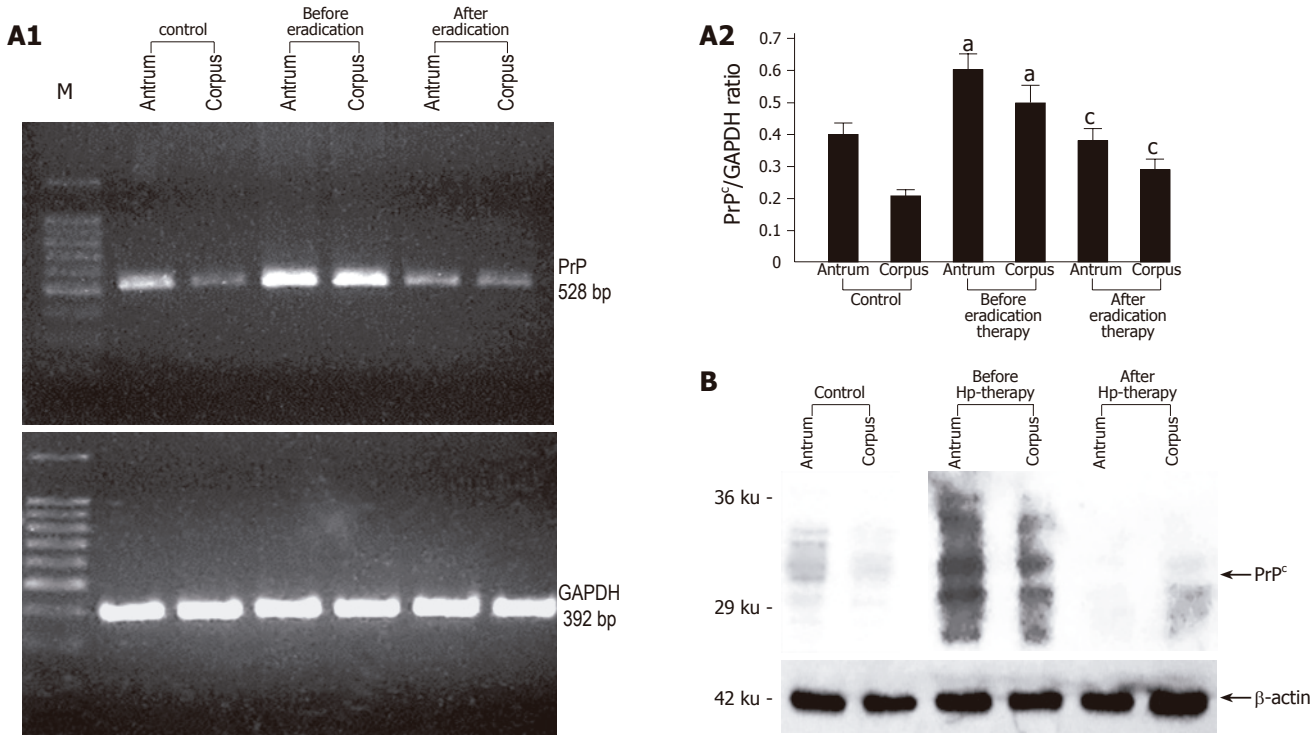

Figure 1 A: Representative RT-PCR and densitometric analysis showing PrPc mRNA expression in the gastric mucosa colonized with *H pylori* before and after successful eradication therapy (n = 10). Data are expressed as means ± SE. $^{a}P<0.05$ *vs* the control group, $^{c}P<0.05$ *vs* the expression before eradication therapy; **B**: Representative immunoblot analysis showing PrPc protein expression in the gastric mucosa colonized with *H pylori* before and after successful eradication therapy.

twice with PBS, and lysed in 0.4 mL of lysis buffer (0.06 mol/L Tris-HCl, pH 6.8, 10% glycerol, 2% SDS, 5% beta-mercaptoethanol, 0.0025% bromophenol blue). DNA was sheared by a needle, the solution heated at 95 ℃ for 5 min and centrifuged at 15 000 *g* for 2 min at 4 ℃. Twenty-five micrograms of the total protein was loaded on SDS-polyacrylamide gel, run at 40 mA and transferred to nitrocellulose (Protran, Schleicher&Schuell, Germany) by electroblotting. Filters were blocked with 3% bovine serum albumin (BSA, Sigma Aldrich, Germany) in TBS/Tween-20 buffer (137 mmol NaCl, 20 mmol Tris-HCl, pH 7.4, 0.1% Tween-20) before incubation with antibodies against PrPc (mouse monoclonal anti-PrP antibody 6H4, 1:2 000 dilution; Prionics, Switzerland), or β-actin (mouse monoclonal, dilution 1:5 000; Sigma Aldrich, Germany), followed by horseradish peroxidase-conjugated anti-mouse or anti-rabbit-IgG secondary antibody (dilution 1:20.000; Promega, WI, USA) dissolved in 1% non-fat milk in TBS/Tween-20. Immune complexes were detected by the SuperSignal West Pico Chemiluminescent Kit (Pierce, USA) and exposed to an X-ray film (Kodak, Wiesbaden, Germany).

Statistical analysis

Statistical analysis was performed using the Mann-Whitney Wilcoxon's test. The level of significance was set at $P<0.05$.

RESULTS

Analysis of gastric biopsy samples obtained endoscopically from patients infected with *H pylori*, which is found in approximately 50% of the world's population[14] and which causes gastric inflammation and ulceration[15] demonstrated highly increased PrPc expression compared to uninfected controls. After treatment with antibiotics which usually lead to *H pylori* eradication, PrPc mRNA and protein expression decreased to control levels (Figures 1A and B).

Using RT-PCR and immunoblotting we demonstrated the expression of PrPc mRNA and protein in two different gastric cell lines (MKN45 and KATO III) (Figure 2). In order to assess possible mechanisms responsible for the upregulation of PrPc during chronic *H pylori* gastritis, we analyzed the effect of increasing doses of key physiological modulators of the gastric mucosa on PrPc expression in these gastric cell lines. These modulators included gastrin (hypergastrinemia is a hallmark of chronic *H pylori* infection[16,17], PGE_2 chronic *H pylori* infection is accompanied by an increased mucosal production of PGE_2[18], and the pro-inflammatory cytokines TNF-α and IL-1β, which are implicated as key promoters of *H pylori*-induced gastritis and ulceration. When exposed to gastrin, cellular PrPc expression increased in a dose-dependent manner, reaching a peak value of 100 nmol/L (Figure 3A). Similarly, PGE_2 induced maximal PrPc mRNA and protein expression at 10 μmol/L (Figure 3B). While IL-1β increased PrPc expression in a dose-dependent manner at the mRNA and protein level (Figures 3C and D), TNF-α showed no effect (Figure 3E).

DISCUSSION

Considering the importance of the human gastrointestinal

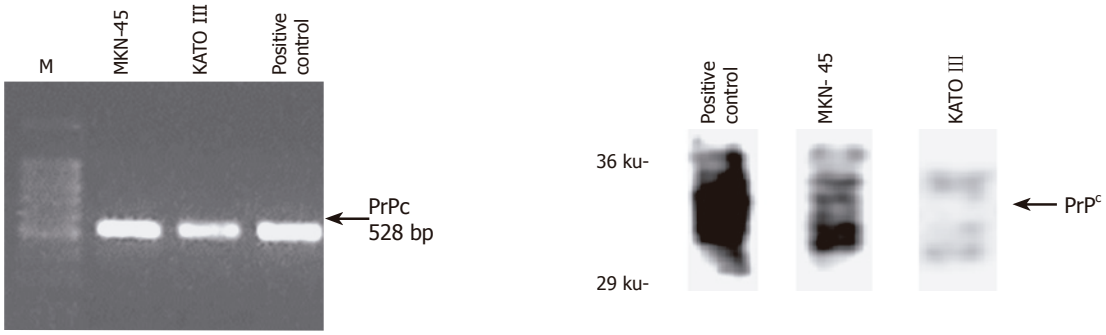

Figure 2 Protein expression of PrPc in two gastric cell lines (MKN45 and KATO III); the positive control is from bovine brain.

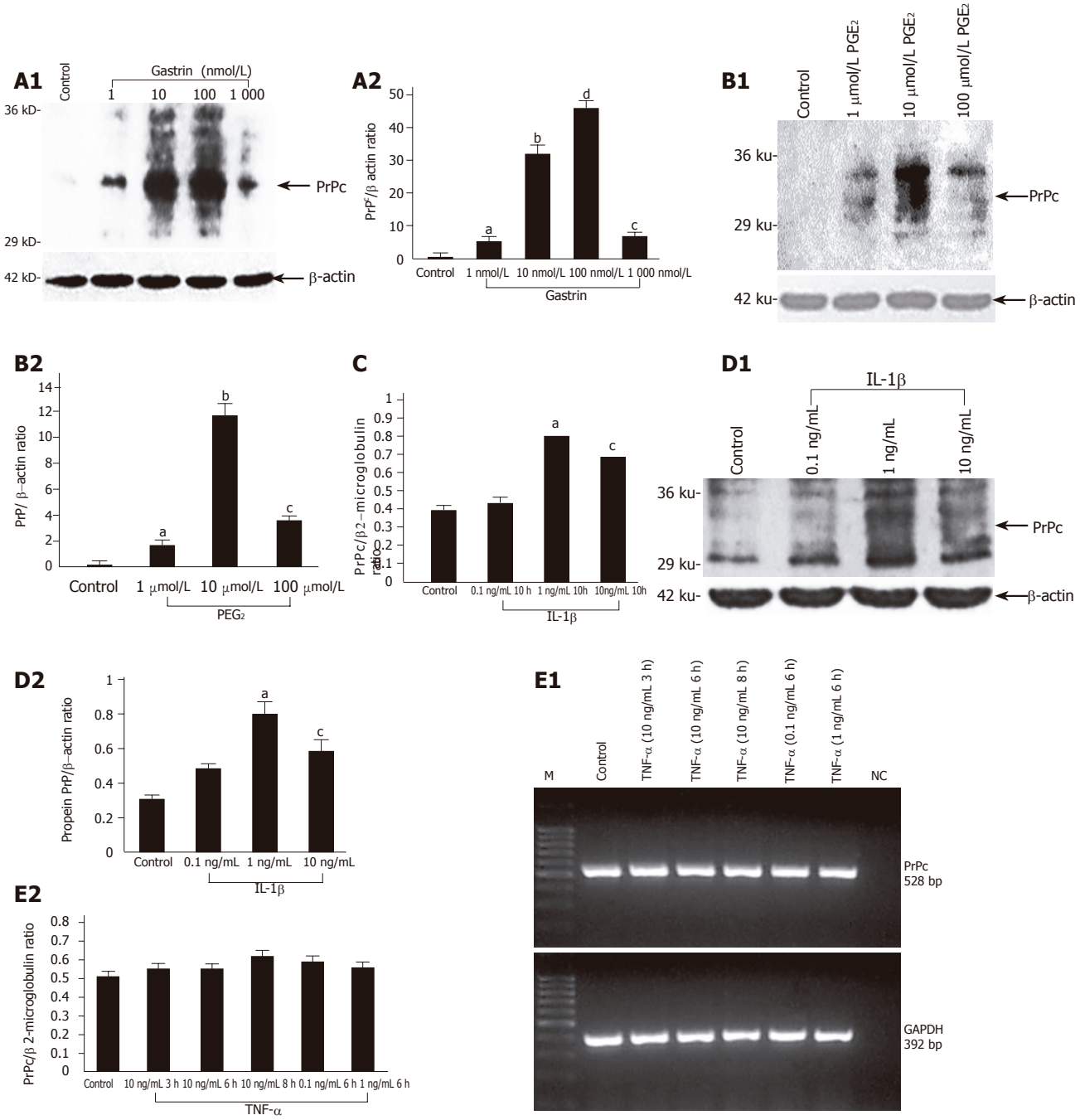

Figure 3 PrPc protein and mRNA expression in MKN45 cells incubated with increasing doses of gastrin (1-1 000 nmol/L) (**A**), PGE_2 (1-100 μmol/L) [a]*P*<0.05 *vs* control, [b]*P*<0.001 *vs* control, [c]*P*<0.05 *vs* control, [d]*P*<0.001 *vs* control (**B**), interleukin 1β (0.1-10 ng/mL) (**C** and **D**) or TNF-α (0.1-10 ng/mL) [a]*P*<0.05 *vs* control, [b]*P*<0.001 *vs* control, [c]*P*<0.05 *vs* control (**E**). Data represent means±SE of three independent experiments. At the mRNA level, the expression of PrPc was normalized to β2-microglobulin and at the protein level to β-actin.

tract for the propagation of prions from the gut to the central nervous system, we analyzed the expression of PrPc in human beings with *H pylori* infection (determined by histology) before and after eradication therapy. This study provides the first *in vitro* and *in vivo* evidence that *H pylori* infection is accompanied by a dramatic upregulation of PrPc expression in the gastric mucosa. The physiological importance of the observed PrPc overexpression in *H pylori* infected gastric mucosa remains elusive. However, multiple physiological functions of PrPc were identified only recently. Thus, PrPc is involved in signal transduction, from the extracellular space to cells, participates in intracellular signaling and regulation of cell survival, protects against oxidative stress, and interacts preferentially with some of the heat-shock-proteins[19-20]. Therefore, the main role of increased PrPc expression in the stomach appears to be the protection of the gastric mucosa against oxidative stress induced, for example by chronic *H pylori* infection[21]. This assumption is further supported by a previous study demonstrating that PrPc upregulates antioxidant enzyme activities[22]. Another possible role of PrPc in the gastric mucosa could be the modulation of apoptosis induced by *H pylori*[23], since PrPc was shown to protect cells against Bax-mediated cell death[24,25]. But this issue remains controversial, as other investigators demonstrated that PrPc may sensitize cells to apoptosis[26,27]. An explanation could be the preferential use of various neuronal cell lines[28] *in vitro* which necessitates further *in vitro* and *in vivo* studies on modulation of apoptosis gastric epithelial cells by PrPc.

In the present study, using quantitative RT-PCR and Western blot analysis we demonstrated an increased PrPc expression in the *H pylori* infected mucosa which significantly decreased after a successful eradication therapy. The mechanisms behind this phenomenon appears to be linked to the hypergastrinemia observed during *H pylori* infection which is supported by our *in vitro* data showing a dose-dependent increase in PrPc expression in gastric epithelial MKN45 cells after incubation with gastrin. According to previous studies, this finding shows that PrPc expression may be modulated by different growth factors[29,30].

Since *H pylori* infection is associated with an increased generation of prostaglandins in the gastric mucosa[18], we analyzed the effect of prostaglandin PGE_2 on PrPc expression in MKN45 cells. At the protein level, we observed a dose-dependent increase in PrPc expression which reached its maximum at the physiological concentration of 10 μmol/L. This could represent another mechanism by which the *H pylori*-induced inflammatory response triggers protective mechanisms in the gastric mucosa.

According to previous studies, chronic infection with *H pylori* is accompanied by a significantly increased generation of pro-inflammatory cytokines, especially IL-1β and TNF-α, in the gastric mucosa. Thus, both cytokines could be responsible for the upregulation of PrPc in the gastric mucosa colonized by *H pylori*. Here we have demonstrated a significant dose-dependent increase of PrPc expression in MKN45 cells incubated with IL-1β, while in contrast, TNF-α showed no effect. We did not further analyze the difference in the action of these two cytokines, but it has been shown by others that these two cytokines evoke different signaling cascades in gastric epithelial cells[31,32].

Gastrin, IL-1β and prostaglandins are not the sole candidates for stimulation of PrPc expression in *H pylori* infected gastric mucosa. Although not investigated in this study, heat shock proteins could represent additional important factors responsible for the upregulation of PrPc. Previous studies demonstrated that exposure of the gastric mucosa to *H pylori* lipopolysaccharide leads to a strong upregulation of heat shock proteins which could in turn stimulate the PrPc expression in gastric epithelial cells[33]. In a previous study, it was found that cellular stress upregulates PrPc expression through its interaction with the heat shock elements (HSE) on the PrPc gene promoter[34]. Together these findings suggest a regulation of PrPc expression by heat shock proteins. All these findings demonstrate the complexicity of the regulation PrPc expression and underscore the need to further analyze the precise link between *H pylori* infection and PrPc expression.

In conclusion, our results indicate that (1) *H pylori* infection is accompanied by a dramatic upregulation of PrPc expression in the gastric mucosa; (2) this is linked to *H pylori*-induced hypergastrinemia, increased mucosal prostaglandin synthesis and enhanced mucosal generation of IL-1β; (3) Thus, *H pylori* infection may promote uptake and propagation of alimentary prions from the gastrointestinal tract by upregulation of PrPc expression.

REFERENCES

1 **Prusiner SB.** Prions. *Proc Natl Acad Sci USA* 1998; **95**: 13363-13383
2 **Raeber AJ,** Brandner S, Klein MA, Benninger Y, Musahl C, Frigg R, Roeckl C, Fischer MB, Weissmann C, Aguzzi A. Transgenic and knockout mice in research on prion diseases. *Brain Pathol* 2002; **98**: 715-733
3 **Weissmann C,** Bueler H, Fischer M, Sailer A, Aguzzi A, Aguet M. PrP-deficient mice are resistant to scrapie. *Ann NY Acad Sci* 1994; **724**: 235-240
4 **Beekes M,** McBride PA. Early accumulation of pathological PrP in the enteric nervous system and gut-associated lymphoid tissue of hamsters orally infected with scrapie. *Neurosci Lett* 2000; **278**: 181-184
5 **Shmakov AN,** Ghosh S. Prion proteins and the gut: une liaison dangereuse? *Gut* 2001; **48**: 443-447
6 **Shmakov AN,** McLennan NF, McBride P, Farquhar CF, Bode J, Rennison KA, Ghosh S. Cellular prion protein is expressed in the human enteric nervous system. *Nat Med* 2000; **6**: 840-841
7 **Gauczynski S,** Peyrin JM, Haik S, Leucht C, Hundt C, Rieger R, Krasemann S, Deslys JP, Dormont D, Lasmezas CI, Weiss S. The 37-kDa/67-kDa laminin receptor acts as the cell surface receptor for the cellular prion protein. *EMBO J* 2001; **20**: 5863-5875
8 **Rieger R,** Edenhofer F, Lasmezas CI , Weiss S. The human 37-kDa laminin receptor precursor interacts with the prion protein in eucaryotic cells. *Nature Med* 1997; **3**: 383-1388
9 **Shmakov AN,** Bode J, Kilshaw PJ, Ghosh S. Diverse patterns of expression of the 67-kD laminin receptor in human small intestinal mucosa: potential binding sites for prion proteins? *J Pathol* 2000; **191**: 318-322
10 **Heppner FL,** C.A., Klein MA, Prinz M, Fried M, Kraehenbuhl

JP, Aguzzi A. Transepithelial prion transport by M cells. *Nature Med* 2001; **7**: 976-977

11 **Dixon MF,** Genta RM, Yardley JH , Correa P. Classification and grading of gastritis. The updated Sydney System. International Workshop on the Histopathology of Gastritis, Houston 1994. *Am J Surg Pathol* 1996; **20**: 1161-1181

12 **Burthem J,** Urban B, Pain A, Roberts DJ. The normal cellular prion protein is strongly expressed by myeloid dendritic cells. *Blood* 2001; **98**: 3733-3738

13 **Konturek PC,** Konturek SJ, Sulekova Z, Meixner H, Bielanski W, Starzynska T, Karczewska E, Marlicz K, Stachura J, Hahn EG. Expression of hepatocyte growth factor, transforming growth factor alpha, apoptosis related proteins Bax and Bcl-2, and gastrin in human gastric cancer. *Aliment Pharmacol Ther* 2001; **15**: 989-999

14 **Brown LM.** Helicobacter pylori: epidemiology and routes of transmission. *Epidemiol Rev* 2002; ***200***: 283-297

15 **Marshall BJ,** Warren JR. Unidentified curved bacilli in the stomach of patients with gastritis and peptic ulceration. *Lancet* 1984; **1**: 1311-1315

16 **Levi S,** Beardshall K, Swift I, Foulkes W, Playford R, Ghosh P, Calam J. Antral Helicobacter pylori, hypergastrinaemia, and duodenal ulcers: effect of eradicating the organism. *BMJ* 1989; **299**: 1504-1505

17 **Smith JT,** Pounder RE, Nwokolo CU. Inappropriate hypergastrinaemia in asymptomatic healthy subjects infected with Helicobacter pylori. *Gut* 1990; **28**, 522-525

18 **Hudson N,** Balsitis M, Filipowicz F, Hawkey CJ. Effect of Helicobacter pylori colonisation on gastric mucosal eicosanoid synthesis in patients taking non-steroidal anti-inflammatory drugs. *Gut* 1993; **34**: 748-7512

19 **Lasmezas CI.** Putative functions of PrPc. *Br Med Bull* 2003; **66**: 61-70

20 **Derrington EA,** Darlix JL. The Enigmatic Multifunctionality of the Prion Protein. *Drug News Perspect* 2002; **15**: 206-219

21 **Felley CP,** Pignatelli B, Van Melle GD, Crabtree JE, Stolte M, Diezi J, Corthesy-Theulaz I, Michetti P, Bancel B, Patricot LM, Ohshima H, Felley-Bosco E. Oxidative stress in gastric mucosa of asymptomatic humans infected with Helicobacter pylori: effect of bacterial eradication. *Helicobacter* 2002; **7**: 342-348

22 **Rachidi W,** Vilette D, Guiraud P, Arlotto M, Riondel J, Laude H, Lehmann S, Favier A . Expression of prion protein increases cellular copper binding and antioxidant enzyme activities but not copper delivery. *J Biol Chem* 2003; **278**: 9064-9072

23 **Konturek PC,** Pierzchalski P, Konturek SJ, Meixner H, Faller G, Kirchner T, Hahn EG. *Helicobacter pylori* induces apoptosis in gastric mucosa through an upregulation of Bax expression in humans. *Scand J Gastroenterol* 1999; **34**: 375-383

24 **Kuwahara C,** Takeuchi AM, Nishimura T , Haraguchi K, Kubosaki A, Matsumoto Y, Saeki K, Matsumoto Y, Yokoyama T, Itohara S, Onodera T. Prions prevent neuronal cell-line death. *Nature* 1999; **400**: 225-226

25 **Bounhar Y,** Zhang Y, Goodyer CG, LeBlanc A. Prion protein protects human neurons against Bax-mediated apoptosis. *J Biol Chem* 2001; **276**: 39145-39149

26 **Paitel E,** Alves da Costa C, Vilette D, Grassi J, Checler F. Overexpression of PrPc triggers caspase 3 activation: potentiation by proteasome inhibitors and blockade by anti-PrP antibodies. *J Neurochem* 2002; **83**: 1208.1214

27 **Paitel E,** Fahraeus R, Checler F. Cellular prion protein sensitizes neurons to apoptotic stimuli through Mdm2-regulated and p53-dependent caspase 3-like activation. *J Biol Chem* 2003; **278**: 10061-10066

28 **Satoh J,** Kurohara K, Yukitake M, Kuroda Y. Constitutive and cytokine-inducible expression of prion protein gene in human neural cell lines. *J Neuropathol Exp Neurol* 1998; **57**: 131-139

29 **Sauer H,** Wefer K, Vetrugno V, Pocchiari M, Gissel C, Sachinidis A, Hescheler J, Wartenberg M. Regulation of intrinsic prion protein by growth factors and TNF-alpha: the role of intracellular reactive oxygen species. *Free Radic Biol Med* 2003; **35**: 586-594

30 **Kuwahara C,** Kubosaki A, Nishimura T, Nasu Y, Nakamura Y, Saeki K, Matsumoto Y, Onodera T. Enhanced expression of cellular prion protein gene by insulin or nerve growth factor in immortalized mouse neuronal precursor cell lines. *Biochem Biophys Res Commun* 2000; **268**: 763-766

31 **Clerk A,** Harrison JG, Long CS, Sugden PH. Pro-inflammatory cytokines stimulate mitogen-activated protein kinase subfamilies, increase phosphorylation of c-Jun and ATF2 and upregulate c-Jun protein in neonatal rat ventricular myocytes. *J Mol Cell Cardiol* 1999; **31**: 2087-2099

32 **Wang H,** Xu L, Venkatachalam S, Trzaskos JM, Friedman SM, Feuerstein GZ, Wang X. Differential regulation of IL-1beta and TNF-alpha RNA expression by MEK1 inhibitor after focal cerebral ischemia in mice. *Biochem Biophys Res Commun* 2001; **286**: 869-874

33 **Brzozowski T,** Konturek PC, Moran AP, et al. Enhanced expression of gastric mucosa to damaging agents in the rat stomach adapted to Helicobacter pylori lipopolysaccharide. *Digestion* 2003; **67**: 195-208

34 **Shyu WC,** Harn HJ, Saeki K, Kubosaki A, Matsumoto Y, Onodera T, Chen CJ, Hsu YD, Chiang YH. Molecular modulation of expression of prion proteins by heat shock. *Mol Neurobiol* 2002; **26**; 1-12

Science Editor Xia HHX and Guo SY **Language Editor** Elsevier HK

PO Box 2345, Beijing 100023, China
www.wjgnet.com
wjg@wjgnet.com

ELSEVIER

World J Gastroenterol 2005;11(48):7657-7660
World Journal of Gastroenterology ISSN 1007-9327

• *RAPID COMMUNICATION* •

Asthma and gastroesophageal reflux disease: Effect of long-term pantoprazole therapy

Calabrese Carlo, Fabbri Anna, Areni Alessandra, Scialpi Carlo, Zahlane Desiree, Di Febo Giulio

Calabrese Carlo, Fabbri Anna, Areni Alessandra, Scialpi Carlo, Zahlane Desiree, Di Febo Giulio, Department of Internal Medicine and Gastroenterology, University of Bologna, Italy
Supported by grants from Altana-Pharma Italia
Correspondence to: Carlo Calabrese, Department of Internal Medicine and Gastroenterology, Policlinico S. Orsola-Malpighi, Via Massarenti 9, 40138 Bologna, Italy. calabrese.c@med.unibo.it
Telephone: +390516364191 Fax: +390516364138
Received: 2005-03-01 Accepted: 2005-08-03

Abstract

AIM: To define the prevalence of gastroesophageal reflux disease (GERD) in mild persistent asthma and to value the effect of pantoprazole therapy on asthmatic symptoms.

METHODS: Seven of thirty-four asthmatic patients without GERD served as the non-GERD control group. Twenty-seven of thirty-four asthmatic patients had GERD (7/27 also had erosive esophagitis, sixteen of them presented GERD symptoms. An upper gastrointestinal endoscopy was performed in all the subjects to obtain five biopsy specimens from the lower 5 cm of the esophagus. Patients were considered to have GERD when they had a dilation of intercellular space (DIS)>0.74 μm at transmission electron microscopy. Patients with GERD were treated with pantoprazole, 80 mg/day. Forced expiratory volume in one second (FEV1) was performed at entry and after 6 mo of treatment. Asthmatic symptoms were recorded. The required frequency of inhaling rapid acting β2-agonists was self-recorded in the patients' diaries.

RESULTS: Seven symptomatic patients presented erosive esophagitis. Among the 18 asymptomatic patients, 11 presented DIS, while all symptomatic patients showed ultrastructural esophageal damage. Seven asymptomatic patients did not present DIS. At entry the mean of FEV_1 was 1.91 L in symptomatic GERD patients and 1.88 L in asymptomatic GERD patients. After the treatment, 25 patients had a complete recovery of DIS and reflux symptoms. Twenty-three patients presented a regression of asthmatic symptoms with normalization of FEV1. Four patients reported a significant improvement of symptoms and their FEV1 was over 80%.

CONCLUSION: GERD is a highly prevalent condition in asthma patients. Treatment with pantoprazole (80 mg/day) determines their improvement and complete regression.

Key words: Asthma; Gastroesophageal reflux disease; Pantoprazole; NERD; ERD; Dilated intercellular spaces; TEM

Carlo C, Anna F, Alessandra A, Carlo S, Desiree Z, Giulio DF. Asthma and gastroesophageal reflux disease: Effect of long term pantoprazole therapy. *World J Gastroenterol* 2005; 11(48): 7657-7660
http://www.wjgnet.com/1007-9327/11/7657.asp

INTRODUCTION

The association of asthma with GERD has attracted particular attention because about half of the patients with asthma also have GERD[1–3]. Mechanisms by which esophageal reflux triggers asthma include acid aspiration, direct acid stimulation of the esophagus, or stimulation of vagal nerves which heightens bronchial responsiveness to extrinsic allergens. Clinicians are advised to treat GERD to improve and control asthma[1]. Endoscopic findings of the esophageal erosions (ERD) confirm the diagnosis of GERD. However, absence of macroscopic signs of damage does not rule out an endoscopy negative esophagitis (NERD) that may also be associated with asthma[4]. Recently, we have shown the presence of a highly sensitive and specific marker of damage, the dilation of intercellular spaces (DIS) in GERD with or without erosions, which permits us to define NERD with a strong accuracy[5].

The prevalence of GERD and effects of proton pump inhibitor (PPI) treatment on the decors of asthma are still uncertain and results obtained are often conflicting[6,7]. Bias in the selection of asthma patients or during PPI treatment and absence of highly sensitive parameters of morphology to define the presence of esophageal mucosa damage, may affect the reported results of studies. Moreover, several studies have a non-randomized poor quality design which leads to a further potential error on definition of treatment effects[8,9].

For this reason, the aim of the present study was to define the prevalence of GERD in patients with mild persistent intrinsic asthma and to estimate the effect of pantoprazole in relation with GERD, asthmatic symptoms and respiratory function in this subset of patients.

Table 1 Demographic data of 34 asthmatic patients with or without GERD symptoms

	Symptomatic	Asymptomatic	
		GERD	Non-GERD
Number	16	11	7
Male/female	6/10	5/6	4/3
ERD	7	0	0
NERD	9	11	7
Age (mean±SD) (yrs)	33.75±10	38.27±5.68	36.14±8.76
DIS (mean±SD) (μm)	2.105±0.262	2.08±0.24	0.5±0.08
FEV1 (mean±SD) (L)	1.87±0.05	1.95±0.04	1.88±0.02

Table 2 Comparison of background characteristics of asthmatic patients with GERD and controls

	GERD (27)	Controls (7)	*t*-Test
Age (yrs) (mean±SD)	35.59±8.67	36.14±8.76	NS
Male/female	11/16	4/3	NS
QUEST score	8.8±4.5	0.12±0.8	$P<0.0001$
Erosive esophagitis	7 (4B, 2C, 1D)	0	$P<0.05$
DIS (mean±SD) (μm)	2.09±0.24	0.5±0.08	$P<0.001$
FEV_1 (L)	1.91±0.045	1.88±0.02	NS

MATERIALS AND METHODS

Among the 301 asthma patients, 34 consecutive asthma patients with intrinsic, mild persistent asthma[10] were enrolled and their diagnosis was made according to the diagnostic criteria recommended by American Thoracic Society (ATS). Patients were excluded if they had any of the following: past or present smoker, unequivocally extrinsic and/or occupational asthma, acids suppression therapy within 4 wk prior to recruitment, previous gastroesophageal surgery, professional voice users, previous glottal surgery or radiotherapy or malignancy, immune suppression therapy, age above 50 years.

For evaluation of ventilation function, FEV_1 was performed using the Jaeger Masterlab spirometer based on the guidelines of ATS[14]. Symptoms were recorded in each patient to rate the frequency and severity of asthmatic episodes. Symptom severity was rated on a scale of 0 (none) to 6 (severe). The required frequency of inhaling rapid acting β2-agonists was self-recorded in the patients' diaries. All the patients did not use systemic bronchodilators or corticosteroids.

For the diagnosis of GERD, the patients underwent gastrointestinal endoscopic (GE) examination and interviews according to the QUEST questionnaire[11]. Reflux esophagitis was graded according to the Los Angeles classification[12,13]. During endoscopy, five biopsy specimens were taken from the lower 5 cm of esophagus for ultrastructural evaluation. At transmission electron microscopy (TEM), ultrastructural signs of mucosal damage were considered to be the DIS>0.74 μm[5]. To obtain this measure, 10 photomicrographs of biopsy specimens of the supra-basal layer of the esophageal mucosa from each patient were taken. At least 10 randomly selected perpendicular trans-sections to adjacent membranes were drawn and measured in each image for a total of 100 measurements in each case. Measurements obtained were used to calculate the mean DIS score.

The endoscopists, pneumologists and pathologists were unaware of the clinical history of the patients. Data were collected separately by another physician (DZ) who assigned patients to different groups and established the therapy. Symptomatic and asymptomatic patients with or without endoscopic signs, were considered to have GERD when they had ultrastructural evidence of esophageal damage. Patients so defined with GERD were treated with pantoprazole, 80 mg once daily for 6 mo. After 6 mo, a new endoscopy with biopsies was performed and DIS was evaluated. Improvements in GERD symptoms according to the QUEST questionnaire were recorded. FEV_1 was valued.

Asthma patients without GERD were followed up for 6 mo and the use of anti-asthmatic treatment (inhaled glucocorticosteroid 200–1 000 μg BDP or rapid acting β_2-agonists) and symptoms were recorded. We considered them as the control group for the evaluation of asthmatic symptoms, respiratory function and drug assumption with time.

The study was conducted in accordance with the guidelines of the Declaration of Helsinki. The local research ethical committee approved the study protocol in 2002. The objective of the study was explained to each patient and written informed consent was obtained from each one.

For statistical analysis, one-way analysis of variance, paired and unpaired *t* test were performed. The results of the treatment were compared by χ^2 test or Fisher' s exact test. All statistical analyses were two-tailed. Data were analyzed with SPSS software. $P<0.05$ was considered statistically significant.

RESULTS

Among the 34 patients evaluated, 16 presented GERD symptoms (heartburn and/or acid regurgitation) and 18 were asymptomatic for reflux disease. At endoscopy, all asymptomatic subjects had no macroscopic signs of esophagitis. Seven symptomatic patients (43.75%) presented erosive esophagitis (ERD).

Among the 18 asymptomatic patients, 11 (61%) presented DIS, while all symptomatic patients showed ultrastructural esophageal damage. Seven asymptomatic patients (38.9%) did not present DIS (Table 1). At entry the mean of FEV_1 was 1.91 L in symptomatic GERD patients and 1.88 L in asymptomatic GERD patients. The two groups at baseline were not significantly different (P = NS) (Table 2).

All the 27 patients with GERD (79.4%) completed the study. They were treated for 6 mo with pantoprazole. At the end of this period erosive esophagitis was healed in seven patients with ERD. Among the 25 patients (92.6%), 6 with ERD and 19 with NERD, had a complete recovery of DIS and reflux symptoms (Table 3 and Figure 1A).

Twenty-three patients (85.18%) presented a regression of asthmatic symptoms (Table 4 and Figure 1B), including nocturnal asthma and FEV_1 (2.75 L, $P<0.01$), but there

Table 3 Effect of treatment on dilation of intercellular space (DIS) in 25 responders to pantoprazole (mean±SD)

		Value (μm)	*t*-Test
Symptomatic	Baseline	2.105±0.261	*P*<0.001
	After therapy	0.592±0.194	
Asymptomatic	Baseline	2.081±0.242	*P*<0.001
	After therapy	0.517±0.072	

Table 4 Effect of therapy on asthma symptom score in GERD patients (mean±SD)

		Baseline	After therapy	*t*-test
Patients	GERD	4.37±0.97	0.33±0.83	*P*<0.001
	Controls	4.57±0.79	4.14±0.38	*P* = NS

was no statistical difference in respiratory parameters between patients with ERD and those with NERD. After 3 wk of treatment no more asthmatic symptoms occurred and no inhaler was needed.

Four patients (14.8%) reported a significant improvement in symptoms, including dyspnea, cough, wheeze, and expectoration with a significant reduction in the consumption of inhalers and FEV_1 over 80%.

DISCUSSION

Physicians mostly focus on the effects induced by gastroesophageal reflux into the esophagus. The anatomic proximity of the esophagus to the respiratory tract in some patients also leads to his involvement. Thus, the spectrum of symptoms of GERD includes also respiratory complications like chronic cough, laryngeal disorders, chest pain, and asthma. In this contest, GERD gains an additional fraction of significance and has been reported to occur in 30-89% of asthma patients[13,15-18].

Treatment with PPI can relieve the symptoms of GERD in up to 90% of patients. It has been tempted to investigate if treatment of GERD with PPI could improve also the respiratory symptoms of asthma patients[19].

It seems obvious that to achieve improvement in asthma symptoms and lung function, the treatment needs to be effective in controlling reflux as well as reducing acidity. However, this has been only objectively confirmed in few studies using high doses of omeprazole[19]. An optimal study design would establish if the esophageal damage is adequately treated as a prerequisite to assess the effects on asthma.

In this study, we analyzed the esophageal specimens from 31 consecutive asthmatic patients, 16 of them were symptomatic for GERD. We found that all symptomatic patients presented an ultrastructural pattern of damage and 73% of asymptomatic GERD patients had esophageal signs of ultrastructural damage, suggesting that GERD is a highly prevalent condition even in asymptomatic patients. Acid stress might initiate or exacerbate asthma in this contest. Electron microscopy is able to find out esophageal damage, especially in asymptomatic patients with NERD.

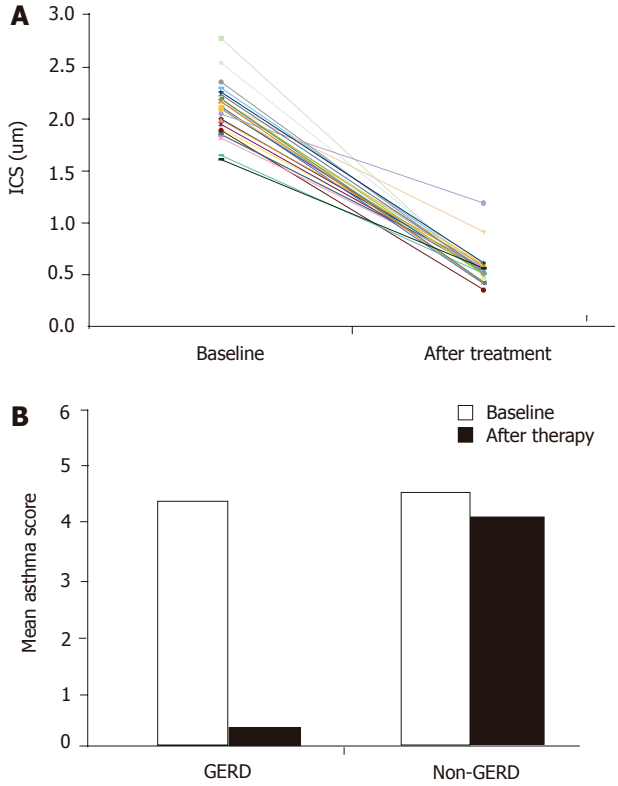

Figure 1 Effect of pantoprazole treatment on dilation of DIS (**A**) and asthma symptom scores (**B**) in GERD patients. The dashed line in Figure 1A corresponds to the mean score of DIS; its cut-off (0.74 μm) represents the presence of damage. Graphic is based on the data analyzed as mean value.

All patients with GERD so defined in our study were treated with a high dosage of pantoprazole for 6 mo. We observed that 93% of patients recovered DIS, 85% of them presented a regression of asthmatic symptoms with normalization of FEV_1, with no statistical difference in respiratory parameters between patients with ERD or NERD. Other patients improved markedly their symptoms and pulmonary function but sporadically presented asthmatic episodes.

We believe that the strong efficacy of PPI treatment in these patients is related to the characteristics of the carefully defined population. The young age of subjects and the mild-moderate asthma let us suppose the existence of an early "action" of treatment before the chronicity of the illness or the worsening to a severe status of asthma. In other words, PPI can suppress or delay the potential development of pulmonary tissue injury.

In conclusion, GERD-related asthma complications are highly prevalent in patients with mild-moderate intrinsic asthma. Treatment with pantoprazole (80 mg once daily for 6 mo) determines the improvement and complete regression of asthmatic symptoms and respiratory function in most patients.

REFERENCES

1 **Harding SM**, Richter JE. The role of gastroesophageal reflux

in chronic cough and asthma. *Chest* 1997; **111:** 1389-1402
2 **Field SK**, Sutherland LR. Does medical antireflux therapy improve asthma in asthmatics with gastroesophageal reflux? *Chest* 1998; **114:** 275-283
3 **Harding SM**, Guzzo MR, Richter JE. 24-h esophageal pH testing in asthmatics: respiratory symptom correlation with esophageal acid events. *Chest* 1999; **115:** 654-659
4 **Jaspersen D**, Kulig M, Labenz J, Leodolter A, Lind T, Meyer-Sabellek W, Vieth M, Willich SN, Lindner D, Stolte M, Malfertheiner P. Prevalence of extra-oesophageal manifestations in gastro-oesophageal reflux disease: an analysis based on the ProGERD Study. *Aliment Pharmacol Ther* 2003; **17:** 1515-1520
5 **Calabrese C**, Fabbri A, Bortolotti M, Cenacchi G, Areni A, Scialpi C, Miglioli M, Di Febo G. Dilated intercellular spaces as a marker of oesophageal damage: comparative results in gastro-oesophageal reflux disease with or without bile reflux. *Aliment Pharmacol Ther* 2003; **18:** 525-532
6 **Harding SM**, Sontag SJ. Asthma and gastroesophageal reflux. *Am J Gastroenterol* 2000; **95:** S23 - S32
7 **Hogan WJ,** Shaker R. Medical treatment of supraesophageal complications of gastroesophageal reflux disease. *Am J Med* 2001; **111 Suppl 8A:** 197S-201S
8 **Levin TR**, Sperling RM, McQuaid KR. Omeprazole improves peak expiratory flow rate and quality of life in asthmatics with gastroesophageal reflux. *Am J Gastroenterol* 1998; **93:** 1060-1063
9 **Teichtahl H**, Kronborg IJ, Yeomans ND, Robinson P. Adult asthma and gastro-oesophageal reflux: the effects of omeprazole therapy on asthma. *Aust NZJ Med* 1996; **26:** 671-676
10 National Institute of Health NHLBI. Burden of asthma. In: Global Strategy for Asthma Management and Prevention. *NIH Publication*, 2002: 11-27
11 **Carlsson R**, Dent J, Bolling-Sternevald E, Johnsson F, Junghard O, Lauritsen K, Riley S, Lundell L. The usefulness of a structured questionnaire in the assessment of symptomatic gastroesophageal reflux disease. *Scand J Gastroenterol* 1998; **33:** 1023-1029
12 **Armstrong D**, Bennett JR, Blum AL, Dent J, De Dombal FT, Galmiche JP, Lundell L, Margulies M, Richter JE, Spechler SJ, Tytgat GN, Wallin L. The endoscopic assessment of esophagitis: a progress report on observer agreement. *Gastroenterology* 1996; **111:** 85-92
13 **Lundell LR**, Dent J, Bennett JR, Blum AL, Armstrong D, Galmiche JP, Johnson F, Hongo M, Richter JE, Spechler SJ, Tytgat GN, Wallin L. Endoscopic assessment of oesophagitis: clinical and functional correlates and further validation of the Los Angeles classification. *Gut* 1999; **45:** 172-180
14 Standardization of Spirometry, 1994 Update. American Thoracic Society. *Am J Respir Crit Care Med* 1995; **152:** 1107-1136
15 **Buts JP**, Barudi C, Moulin D, Claus D, Cornu G, Otte JB. Prevalence and treatment of silent gastro-oesophageal reflux in children with recurrent respiratory disorders. *Eur J Pediatr* 1986; **145:** 396-400
16 **Ducolone A**, Vandevenne A, Jouin H, Grob JC, Coumaros D, Meyer C, Burghard G, Methlin G, Hollender L. Gastroesophageal reflux in patients with asthma and chronic bronchitis. *Am Rev Respir Dis* 1987; **135:** 327-332
17 **Perrin-Fayolle M**, Bel A, Braillon G, Lombard-Platet R, Kofman J, Harf R, Montagnon B, Pacheco Y, Perpoint B. [Asthma and gastro-esophagal reflux (GER). Results of surgical treatment of reflux in 50 patients (author's transl)] *Poumon Coeur* 1980; **36:** 231-237
18 **Sontag SJ,** O'Connell S, Miller TQ, Bernsen M, Seidel J. Asthmatics have more nocturnal gasping and reflux symptoms than nonasthmatics, and they are related to bedtime eating. *Am J Gastroenterol* 2004; **99:** 789-796
19 **Sontag S**, O'Connell S, Khandelwal S, et al. Most asthmatics have gastroesophageal reflux with or without bronchodilator therapy. *Gastroenterology* 1990; **99:** 613-620
20 **Kiljander TO**. The role of proton pump inhibitors in the management of gastroesophageal reflux disease-related asthma and chronic cough. *Am J Med* 2003; **115 Suppl 3A:** 65S-71S
21 **Chiba N**, De Gara CJ, Wilkinson JM, Hunt RH. Speed of healing and symptom relief in grade II to IV gastroesophageal reflux disease: a meta-analysis. *Gastroenterology* 1997; **112:** 1798-1810

Science Editor Wang XL and Guo SY **Language Editor** Elsevier HK

PO Box 2345, Beijing 100023, China
www.wjgnet.com
wjg@wjgnet.com

ELSEVIER

World J Gastroenterol 2005;11(48):7661-7665
World Journal of Gastroenterology ISSN 1007-9327

• *RAPID COMMUNICATION* •

Phagocytic and oxidative burst activity of neutrophils in the end stage of liver cirrhosis

Anatol Panasiuk, Jolanta Wysocka, Elzbieta Maciorkowska, Bozena Panasiuk, Danuta Prokopowicz, Janusz Zak, Karol Radomski

Anatol Panasiuk, Bozena Panasiuk, Danuta Prokopowicz, Department of Infectious Diseases, Medical University of Bialystok, Poland
Jolanta Wysocka, Janusz Zak, Karol Radomski, Department of Pediatrics Diagnostics, Medical University of Bialystok, Poland
Elzbieta Maciorkowska, Department of Pediatric Nursing, Medical University of Bialystok, Poland
Correspondence to: Anatol Panasiuk, MD, Department of Infectious Diseases, Medical University of Bialystok, Zurawia Str, 14, 15-540 Bialystok, Poland. anatol@panasiuk.pl
Telephone: +4885-7416-921 Fax: +4885-7416-921
Received: 2005-03-01 Accepted: 2005-04-18

Abstract

AIM: To evaluate the phagocytic activity and neutrophil oxidative burst in liver cirrhosis.

METHODS: In 45 patients with advanced postalcoholic liver cirrhosis (aged 45±14 years) and in 25 healthy volunteers (aged 38±5 years), the percentage of phagocytizing cells after *in vitro* incubation with *E. coli* (Phagotest Kit), phagocytic activity (mean intensity of fluorescence, MIF) and the percentage of neutrophil oxidative burst (Bursttest Kit), and the level of free oxygen radical production (MIF of Rodamine 123) were analyzed by flow cytometry. The levels of soluble sICAM-1, sVCAM-1, sP-selectin, sE-selectin, sL-selectin, and TNF-α were determined in blood serum.

RESULTS: The percentage of *E. coli* phagocytizing neutrophils in liver cirrhosis patients was comparable to that in healthy subjects. MIF of neutrophil - ingested *E. coli* was higher in patients with liver cirrhosis. The oxidative burst in *E. coli* phagocytizing neutrophils generated less amount of active oxygen compounds in liver cirrhosis patients (MIF of R123: 24.7±7.1 and 29.7±6.6 in healthy, $P<0.01$). Phorbol myristate acetate (PMA) - stimulated neutrophilsproduced less reactive oxidants in liver cirrhosis patients than in healthy subjects (MIF of R123: 42.7± 14.6 *vs* 50.2±13.3, $P<0.01$). A negative correlation was observed between oxidative burst MIF of PMA-stimulated neutrophils and ALT and AST levels (r -0.35, $P<0.05$; r-0.4, $P<0.03$). sVCAM-1, sICAM-1, sE-selectin concentrations correlated negatively with the oxygen free radical production (MIF of R123) in neutrophils after PMA stimulation in liver cirrhosis patients (r-0.45, $P<0.05$; r-0.41, $P<0.05$; r-0.39, $P<0.05$, respectively).

CONCLUSION: Neutrophil metabolic activity diminishes together with the intensification of liver failure. The metabolic potential of phagocytizing neutrophils is significantly lower in liver cirrhosis patients, which can be one of the causes of immune mechanism damage. The evaluation of oxygen metabolism of *E. coli*-stimulated neutrophils reveals that the amount of released oxygen metabolites is smaller in liver cirrhosis patients than in healthy subjects.

Key words: Neutrophil; Phagocytosis; Oxidative burst; Liver cirrhosis; Flow cytometry

Panasiuk A, Wysocka J, Maciorkowska E, Panasiuk B, Prokopowicz D, Zak J, Radomski K. Phagocytic and oxidative burst activity of neutrophils in the end stage of liver cirrhosis. *World J Gastroenterol* 2005; 11(48): 7661-7665
http://www.wjgnet.com/1007-9327/11/7661.asp

INTRODUCTION

Neutrophils play an important role in non-specific immune response and organism resistance, specifically in anti-bacterial resistance as effectors, inducing and regulating cells[1,2]. They reveal many features which are crucial in organism immunity: to produce and adhere towards vascular endothelial cells, migrate to inflammatory sites through the vessel walls, recognize and phagocytize opsonized molecules, and degradate and release proteins from granules[3,4]. These features are possible due to the presence of receptors distributed on the surface and inside of the cells such as cytokine-, neuromediator-, autocoid-, hormone receptors. Neutrophil chemotaxis occurs towards stimulus gradient, in response to chemotactic factors (chemotaxins) produced at the inflammatory site. Moreover, chemotaxins increase neutrophil metabolism, aggregation, and bactericidal abilities[5-7].

Phagocytosis is facilitated by specific (immunoglobulins IgG) and non-specific (complement components) opsonins, circulating in the plasma. On their surface, granulocytes have receptors that bind to Fc fragment of IgG1 and IgG2 immunoglobulins, and complement C3b fragment receptors[8]. Absorbed opsonized microorganisms are killed through both oxygen-dependent and independent mechanisms. Free oxygen radicals kill

absorbed bacteria in phagosomes and partially are released into the environment, intensifying killing microorganisms and simultaneously injuring the surrounding tissues. It is specifically intensified in acute inflammation, less in chronic course of the disease[1]. Microorganism killing is also possible by proteins present in azurophil granules, such as cathepsin G, lysozyme, interferons, and others.

Inflammatory mediators, cytokines (e.g. TNFα) and selectins increase the ability of granulocytes to localize at the site of inflammation. Phagocytic ability is elevated by intensification of hydroxylic radical production and lysosomal enzyme release[9,10]. TNFα is an important factor strengthening granulocyte phagocytic and cytotoxic activity. Activated granulocytes secrete cytokines. IL-1, which stimulates monocytes, endothelial cells, and fibroblasts to secrete IL-8, in turn increases the expression of CD11b/CD18 adhesive molecules and granulocyte oxygen metabolism[11]. Interferon gamma is a strong cytokine, which intensifies Fc receptor expression, stimulates oxygen changes, and strengthens granulocytic granule release.

The aim of the study was to evaluate the metabolic activity of oxidative burst *in vitro* and the production of active oxygen compounds stimulated by *E. coli* and phorbol myristate acetate (PMA). Determination of the percentage of phagocytizing cells and their ability to phagocytize opsonized bacteria is of great importance in the estimation of neutrophil functioning. We evaluated the neutrophil ability to phagocytize *E. coli in vitro* in advanced liver cirrhosis. We also tried to establish the relationship between the neutrophil ability and the concentration of soluble adhesive molecules in peripheral blood.

MATERIALS AND METHODS

Patients

The studies were conducted in the group of 45 patients with advanced postalcoholic liver cirrhosis (30 men and 15 women, aged 45±14 years) (Table 1). Liver cirrhosis was confirmed clinically and histologically. Patients with acute viral or bacterial disease and those in the course of corticosteroid therapy who did not drink alcohol for at least 6 mo were excluded from the study. Patients with liver cirrhosis were divided into groups B and C in accordance with the classification of liver failure according to Child-Pugh[12]. The control group consisted of 25 healthy volunteers (12 women and 13 men, aged 38±5 years), who had never suffered from liver diseases and those without registered immunity disorders. Ethical approval for research was obtained from local Ethics Committee in the Medical University.

Methods

Blood was collected in plastic testing tubes with EDTA K2 and the absolute number of leukocytes and neutrophils was evaluated. The blood was collected in lithium heparin plastic testing tubes for the evaluation of phagocytizing cells and phagocytic activity and the percentage of bursting cells as well as neutrophil oxygen metabolism.

Table 1 Clinical characteristics of patients with liver cirrhosis (mean±SD)

	Child–Pugh B	Child–Pugh C
Age, year	43±12	46±13
Male/female	15/10	15/5
Albumin, g/dL	3.2±0.3	2.8±0.6
AST/ALT, IU/mL	98±65/87±98	110±45/97±45
Bilirubin, mg/dL	4.5±3.8	9.7±6.5

The assessment of phagocytosis was performed using the Phagotest Kit (ORPEGEN Pharma, Germany) containing fluorescein-labeled opsonized Escherichia coli (*E. coli* - FITC). Samples of 100 μL of blood with heparin were cooled in an ice bath for 15 min mixed with 2×10^7 FITC-labeled *E. coli* and then put in a chamber thermostat at 37 °C for 10 min. Simultaneously, the control samples were put into an ice bath to inhibit phagocytosis. Afterwards, 100 μL of brilliant blue (Quenching solution) was added in order to suppress the fluorescence of bacteria connected to the leukocyte surface. After two washing steps (with 2 mL of washing solution, centrifuged at 2 000 r/min, supernatant was pumped out), erythrocytes were lysed using lysis fluid for 20 min at room temperature. At the end, 50 μL propidyne iodide was added to stain leukocytes and bacterial DNA.

Oxidative burst

Granulocyte oxidative burst was determined quantitatively with Bursttest Kit (ORPEGEN Pharma, Germany). Fresh heparinized blood was put in a water bath for 15 min. Then, four testing tubes were filled with 100 μL of blood each and 2×10^7 unlabeled opsonized bacteria *E. coli*, 20 μL of substrate solution (negative control), 20 μL fMLP (peptide *N*-formyl-MetLeuPhe) as chemotactic low physiological stimulus (low control) and 20. μL phorbol 12-myristate 13-acetate (PMA), a strong non-receptor activator (high control). All the samples were incubated for 10 min at 37.0 °C in a water bath, dihydrorhodamine (DHR) 123 as a fluorogenic substrate was added and incubated again in the same conditions. The oxidative burst occurred with the production of reactive oxygen substrates (ROS) (superoxide anion, hydrogen peroxide) in granulocytes stimulated *in vitro*. In ROS-stimulated granulocytes, nonfluorescent DHR 123 underwent conversion to fluorescent rhodamine (R) 123 registered in the flow cytometer. Erythrocytes were removed using lysing solution for 20 min at room temperature, centrifuged (5 min, 250 r/min, 4 °C), and supernatant was discarded. Samples were washed again (washing solution), centrifuged (5 min, 250 r/min, 4 °C) and the supernatant was decanted. An amount of 200 μL of DNA staining solution (centrifuged and incubated for 10 min at 0 °C in a dark place) was added to discriminate and exclude aggregation artifacts of bacteria and/or cells in cytometric flow analysis.

Cytometric analysis

The flow cytometer EPICS XL (Coulter, USA) equipped

with 488 nm argon-ion laser was used. The apparatus was calibrated every day using DNA check. Neutrophil populations were identified by the use of forward and right angle light scatter, and the fluorescence emission of 10^4 cells per sample was recorded on a logarithmic scale. Fluorescent measurements were conducted with identical settings as for the standard determination of cell phenotype with fluorochrome-stained mAb.

Phagocytic activity was determined as the percentage of phagocytizing neutrophils (one or more bacteria ingestion) and as the mean intensity of fluorescence (MIF) value, which equaled the mean number of bacteria phagocytized by the cells.

Granulocyte oxygen metabolism was determined with the percentage of cells phagocytizing *E. coli* producing reactive oxidants (cells undergoing bursts, the change from DHR 123 to R 123), and with the evaluation of granulocyte enzymatic activity (the amount of released active oxygen compounds – the amount of MIF R 123 per cell).

Adhesive molecules and TNFα

ELISA tests were used to determine the level of sICAM-1 (Human sICAM-1, R&D, UK), sVCAM-1 (Human sVCAM-1, R&D), and the level of tumor necrosis factor alpha (Human TNFα, R&D) in blood serum. Soluble forms of P- (Human soluble P-Selectin, R&D), E- (Human sE-Selectin, R&D), and L-selectins (Human sL-Selectin, R&D) were determined by ELISA tests simultaneously in blood serum.

Statistical analysis

The results were presented as mean±SD. Statistical analysis was performed by non-parametrical *U* (Mann-Whitney) test. The result of correlation was calculated by Spearman's correlation test. $P<0.05$ was considered statistically significant.

RESULTS

Phagocytic activity of neutrophils

The ability of neutrophils to phagocytize opsonized *E. coli* was assessed. No significant differences were found in phagocytizing neutrophils both in liver cirrhosis patients and in healthy subjects (Table 2). The MIF of absorbed *E. coli* was slightly higher in patients with liver cirrhosis (differences being statistically insignificant). A positive correlation was observed between the percentage of neutrophils-phagocytized *E. coli* and the percentage of neutrophils with oxidative burst after *E. coli* stimulation *in vitro* ($r = 0.37$, $P<0.05$, Table 3).

Neutrophil oxidative burst

Stimulation *in vitro* with a strong activator PMA causes a markedly lower production of reactive oxidants in neutrophils in liver cirrhosis patients than in healthy individuals (MIF 42.7±14.6 *vs* 50.2±13.3, $P<0.01$, Table 2). Incubation of neutrophils with non-opsonized *E. coli* induced oxidative burst in more neutrophils in patients with liver cirrhosis than in the control group. However, neutrophils phagocytizing *E. coli* showed markedly lower metabolic potential in liver cirrhosis patients than that in healthy subjects. The oxidative burst in neutrophils phagocytizing *E. coli* caused generation of smaller amounts of active oxygen compounds in the cells of patients with liver cirrhosis. Neutrophils with oxidative burst (MIF of rhodamine 123) were statistically lower in liver cirrhosis patients (24.7±7.1) than in healthy subjects (29.7±6.6, $P<0.01$). PMA neutrophil stimulation *in vitro* was more effective than a direct contact with *E. coli*.

The decrease in neutrophil metabolic and phagocytic activities was observed together with the intensification of liver damage. We noted a negative correlation of MIF of neutrophil oxidative burst after PMA stimulation and ALT and AST, which was $r = -0.35$, $P<0.05$ and $r = -0.4$, $P<0.03$, respectively.

Adhesive molecules and TNFα

The concentrations of adhesive molecules sVCAM-1 and sICAM-1 in blood serum were several times higher in patients with liver cirrhosis ($P<0.01$, Table 2). Soluble E-selectin concentrations in liver cirrhosis patients were also significantly higher than in healthy subjects ($P<0.01$). However, significant differences of sL-selectin concentrations were not present, while sP-selectin concentrations were lower in liver cirrhosis patients. The level of sVCAM-1, sICAM-1, sE-selectin correlated negatively with the activity of oxygen radical production (MIF) after PMA neutrophil simulation ($r = -0.45$, $P<0.05$, $r = -0.41$, $P<0.05$, $r = -0.39$, $P<0.05$, respectively). The concentration of TNFα was markedly higher in liver cirrhosis patients than in healthy individuals ($P<0.01$). No correlation was observed between neutrophil metabolic and phagocytic activities and TNFα concentration. On the other hand, there was a positive correlation between sVCAM-1 and sE-selectin concentration ($r = 0.4$, $P<0.05$) and between sL-selectin concentration and the production of free oxygen radicals in neutrophils (MIF of R123) ($r = 0.35$, $P< 0.05$).

DISCUSSION

Infectious and toxic factors and over reactivity of the immune system are crucial in the pathogenesis of chronic liver diseases. The essence of the disease is accumulation of natural killer cells and inflammatory cells as well as intensified fibrosis in the liver. Chronic failure of endothelial cells of hepatic vessels increases expression and concentration of adhesive molecules. It facilitates inflammatory cell activation, margination and accumulation of leukocytes in the liver[4,13-15]. Neutrophils are professionally phagocytizing cells, which play an important role in immunological processes of the organism. They participate mainly in non-specific response as they do not possess the properties for precise recognition of antigens. Chemotactic factors and cytokines (IL-1, IL-8, TNFα, TGF-β) induce migration of granulocytes and other cells to the inflammatory site.

Table 2 Phagocytic and oxidative burst activity of neutrophils, level of soluble form of adhesive molecules and TNFα in liver cirrhosis patients (mean±SD)

		Liver cirrhosis		Healthy
	Total	Child–Pugh B	Child–Pugh C	
Oxidative burst				
Percentage of neutrophils with oxidative burst after PMA stimulation (%)	98.3±1.2	98.4±1.5	98.2±1.6	98.8±2.8
MIF oxidative burst after PMA stimulation	42.7±14.6[b]	44.3±10.1[b]	41.1±12.6[b]	50.2±13.3
Percentage of neutrophils with oxidative burst after *E. coli* stimulation (%)	94.0±4.8	93.0±4.1	94.0±3.8	92.2±3.7
MIF oxidative burst after *E. coli* stimulation	24.7±7.1[b]	25.1±8.1[b]	22.2±5.1[b]	29.7±6.6
Phagocytic activity				
Percentage of neutrophils phagocytizing of *E. coli*	93.0±3.3	92.9±4.3	93.8±2.3	92.5±4.3
MIF phagocytosis *E. coli*	20.0±3.9	19.8±4.1	21.0±2.8	19.0±5.8
Soluble form of adhesion molecules and TNFα				
sICAM-1 (ng/mL)	852±331[b]	788±343[b]	892±293[b]	254±74
sVCAM-1 (ng/mL)	2 937±1 591[b]	2 637±1 291[b]	3 297±1 490[b]	510±248
sP-selectin (ng/mL)	101±180[b]	98±140[b]	104±162[b]	124±58
sE-selectin (ng/mL)	136±89[b]	120±68[b]	148±58[b]	49±21
sL-selectin (ng/mL)	1 209±364	1 206±314	1 211±344	1 209±291
TNFα (pg/mL)	2.94±1.43[b]	2.64±1.33[b]	2.99±1.02[b]	1.58±0.22

[b]$P<0.01$ *vs* healthy subjects (Mann–Whitney *U* test).

Table 3 Correlation (*r*) of phagocytic activity of neutrophils with their oxidative burst level and biochemical tests of liver dysfunction (Spearman test)

Correlations	*r*	*P*
MIF oxidative burst neutrophils after PMA stimulation with ALT level	-035	0.05
MIF phagocytizing *E. coli* with prothrombin time	-0.47	0.03
Percentage of neutrophils phagocytizing *E. coli* with leukocyte number	0.35	0.05
Percentage of oxidative burst neutrophils after *E. coli* stimulation with MIF phagocytosis *E. coli*	0.37	0.05

The study showed a significant impairment of neutrophil immune mechanisms in liver cirrhosis as well as oxidative burst damage with diminished amount of generated free oxygen form in neutrophils. Stimulation *in vitro* with the strong stimulant PMA and non-opsonized *E. coli* induces less amount of released active oxygen compounds in neutrophils in liver cirrhosis patients than in healthy subjects. It should be assumed that it is a result of permanent stimulation of neutrophils by inflammatory factors or lipopolysaccarides (LPS). Observed disorders can be treated as dysfunctions of exhausted neutrophils, and oxygen exchange impairment (processes being important in the maintenance of organism immunity) has been confirmed in other studies[16,17]. The higher release of oxygen metabolites observed after PMA is probably due to different stimulation mechanisms. The neutrophil phagocytic activity in both groups was comparable. Cytometric examinations of the percentage of phagocytizing neutrophils and MIF of absorbed opsonized *E. coli* did not show differences in both groups.

Vascular endothelium has many important functions, and is a barrier against pathogens as well as the site of immunological and inflammatory process initiation with participating neutrophils[18]. Neutrophil accumulation at the site of inflammation depends on the adhesive molecule expression in endothelial cells. Neutrophil stimulation leads to activation of L-selectin and other molecules (β2-integrines) that participate in adhesion to the endothelium. In addition, increase in adhesive molecule expression directly activates antibacterial mechanisms, granule secretion and neutrophil oxygen metabolism. Activation of neutrophils (the main generators of free oxygen radicals in inflammatory processes) leads to elevation of active oxygen metabolites responsible for killing microorganisms[19]. In patients with end-stage liver disease, the ability of neutrophils to migrate to the inflammatory sites is impaired. It was observed that neutrophils present there have their phagocytizing activity reduced[16].

Adhesive molecules (ICAM-1, VCAM-1, selectins) play an important role in keeping neutrophils in liver sinusoids. Antibodies against anti-ICAM-1 and anti-VCAM-1 inhibit neutrophil accumulation in liver tissues and diminish their damage[9,20]. P- and E-selectin expressions in endothelial cells and L-selectin – in leukocytes – lead to slower flow of leukocytes and blood platelets in bloodstream, activation, rolling, and adhesion of these cells. In liver cirrhosis patients, adhesive molecule expression increases due to tissue hypoxia, deposits of immunological complexes, endogenic toxic compounds, LPS, bacteria, and viruses[21-23].

Fiuza *et al.*[16] have suggested that, in the end-stage liver disease, neutrophils have injured ability to migrate to the inflammatory sites and their phagocytic activity is diminished, which in turn, correlates with the severity of liver disease. It has been shown that chronic intravascular peripheral neutrophil activation occurs in vessels. Their results point to the fact that antibacterial early inflammatory immune response is damaged in liver cirrhosis. The increase in bacterial translocation and endotoxin absorption from the bowel is a stimulus for the reticuloendothelial system to produce proinflammatory cytokines[24,25]. Neutrophil activity and phagocytic ability failure may result in ascitic fluid microinfection and

subclinical SBP. On the other hand, a persistent stimulation of neutrophils by inflammatory factors can lead to the exhaustion of their functional potential. Proinflammatory factor elimination from peripheral blood is impaired in liver cirrhosis which facilitates persistent stimulation of peripheral blood neutrophils[25].

We observed high concentrations of soluble adhesive molecules VCAM-1, ICAM-1, and E-selectin, which can account for a marked vascular endothelium damage in liver cirrhosis. Endothelial cell failure or stimulation can occur due to high levels of proinflammatory cytokines (e.g. TNFα). Chronic endotoxemia may also stimulate adhesive molecule expression. High concentrations of VCAM-1, ICAM-1 and E-selectin stimulate inflammatory site to accumulate in terminal capillaries of the liver and other organs. In our studies, the increased expression and concentration of soluble adhesive molecules might result in exhaustion of oxygen metabolism of neutrophils in liver cirrhosis.

Neutrophils are an important host immune barrier against bacterial infections. A persistent stimulation of leukocytes that flow through the liver affected by inflammation leads to the exhaustion of mechanisms responsible for their immune properties.

REFERENCES

1 **Chishti AD,** Shenton BK, Kirby JA, Baudouin SV. Neutrophil chemotaxis and receptor expression in clinical septic shock. *Intensive Care Med* 2004; **30**: 605-611

2 **Tanji-Matsuba K,** van Eeden SF, Saito Y, Okazawa M, Klut ME, Hayashi S, Hogg JC. Functional changes in aging polymorphonuclear leukocytes. *Circulation* 1998; **97**: 91-98

3 **Gregory SH,** Sagnimeni AJ, Wing EJ. Bacteria in the bloodstream are trapped in the liver and killed by immigrating neutrophils. *J Immunol* 1996; **157:** 2514-2520

4 **Jaeschke H,** Smith CW. Cell adhesion and migration. III. Leukocyte adhesion and transmigration in the liver vasculature. *Am J Physiol* 1997; **273:** G1169-G1173

5 **Charo IF,** Taubman MB. Chemokines in the pathogenesis of vascular disease. *Circ Res* 2004; **95**: 858-866

6 **Liu L,** Cara DC, Kaur J, Raharjo E, Mullaly SC, Jongstra-Bilen J, Jongstra J, Kubes P. LSP1 is an endothelial gatekeeper of leukocyte transendothelial migration. *J Exp Med* 2005; **201**: 409-418

7 **Speyer CL,** Gao H, Rancilio NJ, Neff TA, Huffnagle GB, Sarma JV, Ward PA. Novel chemokine responsiveness and mobilization of neutrophils during sepsis. *Am J Pathol* 2004; **165**: 2187-2196

8 **Gomez F,** Ruiz P, Schreiber AD. Impaired function of macrophage Fc gamma receptors and bacterial infection in alcoholic cirrhosis. *N Engl J Med* 1994; **331**: 1122-1128

9 **Jaeschke H,** Farhood A, Fisher MA, Smith CW. Sequestration of neutrophils in the hepatic vasculature during endotoxemia is independent of beta 2 integrins and intercellular adhesion molecule-1. *Shock* 1996; **6***:* 351-356

10 **Laffi G,** Foschi M, Masini E, Simoni A, Mugnai L, La Villa G, Barletta G, Mannaioni PF, Gentilini P. Increased production of nitric oxide by neutrophils and monocytes from cirrhotic patients with ascites and hyperdynamic circulation. *Hepatology* 1995; **22**: 1666-1673

11 **Li CP,** Lee FY, Tsai YT, Lin HC, Lu RH, Hou MC, Wang TF, Chen LS, Wang SS, Lee SD. Plasma interleukin-8 levels in patients with post-hepatitic cirrhosis: relationship to severity of liver disease, portal hypertension and hyperdynamic circulation. *J Gastroenterol Hepatol* 1996; 11: 635-640

12 **Pugh RN,** Murray-Lyon IM, Dawson JL, Pietroni MC, Williams R. Transection of the oesophagus for bleeding oesophageal varices. *Br J Surg* 1973; **60:** 646-649

13 **Chosay JG,** Essani NA, Dunn CJ, Jaeschke H. Neutrophil margination and extravastaion in sinusoids and venules of liver during endotoxin-induced injury. *Am J Physiol 1997;* **272***:* G1195-G1200

14 **Moulin F,** Copple BL, Ganey PE, Roth RA. Hepatic and extrahepatic factors critical for liver injury during lipopolysaccharide exposure. *Am J Physiol Gastrointest Liver Physiol* 2001; **281:** G1423-G1431

15 **Rosenbloom AJ,** Pinsky MR, Bryant JL, Shin A, Tran T, Whiteside T. Leukocyte activation in the peripheral blood of patients with cirrhosis of the liver and SIRS. Correlation with serum interleukin-6 levels and organ dysfunction. *JAMA* 1995; **274**: 58-65

16 **Fiuza C,** Salcedo M, Clemente G, Tellado JM. In vivo neutrophil dysfunction in cirrhotic patients with advanced liver disease. *J Infect Dis* 2000; **182**: 526-533

17 **Rajkovic IA,** Williams R. Abnormalities of neutrophil phagocytosis, intracellular killing and metabolic activity in alcoholic cirrhosis and hepatitis. *Hepatology* 1986; **6**: 252-262

18 **Hippenstiel S,** Suttorp N. Interaction of pathogens with the endothelium. *Thromb Haemost* 2003; **89:** 18-24

19 **Aratani Y,** Kura F, Watanabe H, Akagawa H, Takano Y, Suzuki K, Dinauer MC, Maeda N, Koyama H. In vivo role of myeloperoxidase for the host defense. *Jpn J Infect Dis* 2004; **57**: S15

20 **Essani NA,** Bajt ML, Farhood A, Vonderfecht SL, Jaeschke H. Transcriptional activation of vascular cell adhesion molecule-1 gene in vivo and its role in the pathophysiology of neutrophil-induced liver injury in murine endotoxin shock. *J Immunol* 1997; **158:** 5941-5948

21 **Lautenschlager I,** Hockerstedt K, Taskinen E, von Willebrand E. Expression of adhesion molecules and their ligands in liver allografts during cytomegalovirus (CMV) infection and acute rejection. *Transpl Int* 1996; **9** Suppl 1: S213-S215

22 **Panasiuk A,** Prokopowicz D, Zak J, Matowicka-Karna J, Osada J, Wysocka J. Activation of blood platelets in chronic hepatitis and liver cirrhosis P-selectin expression on blood platelets and secretory activity of beta-thromboglobulin and platelet factor-4. *Hepatogastroenterology* 2001; **48**: 818-822

23 **Pata C,** Yazar A, Altintas E, Polat G, Aydin O, Tiftik N, Konca K. Serum levels of intercellular adhesion molecule-1 and nitric oxide in patients with chronic hepatitis related to hepatitis C virus: connection fibrosis. *Hepatogastroenterology* 2003; **50:** 794-797

24 **Runyon BA,** Squier S, Borzio M. Translocation of gut bacteria in rats with cirrhosis to mesenteric lymph nodes partially explains the pathogenesis of spontaneous bacterial peritonitis. *J Hepatol* 1994; **21***:* 792-796

25 **Saitoh O,** Sugi K, Lojima K, Matsumoto H, Nakagawa K, Kayazawa M, Tanaka S, Teranishi T, Hirata I, Katsu Ki K. Increased prevalence of intestinal inflammation in patients with liver cirrhosis. *World J Gastroenterol* 1999; **5**: 391-396

Science Editor Wang XL and Guo SY **Language Editor** Elsevier HK

PO Box 2345, Beijing 100023, China
www.wjgnet.com
wjg@wjgnet.com

ELSEVIER

World J Gastroenterol 2005;11(48):7666-7670
World Journal of Gastroenterology ISSN 1007-9327

• *RAPID COMMUNICATION* •

Possible involvement of leptin and leptin receptor in developing gastric adenocarcinoma

Liang Zhao, Zhi-Xiang Shen, He-Sheng Luo, Lei Shen

Liang Zhao, Zhi-Xiang Shen, He-Sheng Luo, Lei Shen, Department of Gastroenterology, Renmin Hospital, Wuhan University, Wuhan 430060, Hubei Province, China
Correspondence to: Liang Zhao, MD, Department of Gastroenterology, Renmin Hospital, Wuhan University, Wuhan 430060, Hubei Province, China. airman-zhao@tom.com
Telephone: +86-27-88041919-2135
Received: 2005-01-31 Accepted: 2005-04-11

Abstract

AIM: To investigate the expression of leptin and leptin receptor (ob-R) in intestinal-type gastric cancer and precancerous lesions, and to explore the possible mechanism and role of the leptin system in developing intestinal-type gastric adenocarcinoma.

METHODS: Immunohistochemistry was performed to examine the expression of leptin and leptin receptor in archival samples of gastric adenocarcinoma and preneoplastic lesions, including intestinal metaplasia and mild to severe gastric epithelial dysplasia. Positive staining was identified and percentage of positive staining was graded.

RESULTS: Dual expression of leptin and leptin receptor were detected in 80% (16/20) intestinal metaplasia, 86.3% (25/30) mild gastric epithelial dysplasia, 86.7% (26/30) moderate gastric epithelial dysplasia, 93.3% (28/30) severe gastric epithelial dysplasia, 91.3% (55/60) intestinal-type gastric adenocarcinoma and 30.0% (9/30) diffuse-type gastric carcinoma. The percentage of dual expression of leptin and leptin receptor in intestinal-type gastric adenocarcinoma was significantly higher than that in diffuse-type gastric adenocarcinoma ($\chi^2 = 37.022$, $P<0.01$).

CONCLUSION: Our results indicate the presence of an autocrine loop of leptin system in the development of intestinal-type gastric adenocarcinoma.

Key words: Leptin; Leptin receptor (ob-R); Intestinal-type gastric adenocarcinoma; Intestinal metaplasia; Gastric epithelial dysplasia

Zhao L, Shen ZX, Luo HS, Shen L. Possible involvement of leptin and leptin receptor in developing gastric adenocarcinoma. *World J Gastroenterol* 2005; 11(48): 7666-7670
http://www.wjgnet.com/1007-9327/11/7666.asp

INTRODUCTION

Leptin, the product of the obesity gene (ob gene), is a cytokine-like peptide capable of signal transduction via interaction with its specific receptor (ob-R). It was initially found to be synthesized by adipocytes and act centrally in the hypothalamus to regulate food intake and energy expenditure[1]. Subsequently, expressions of leptin or ob-R were detected in a wide variety of tissues with multiple role in hematopoiesis, reproductive control, angiogenesis, cardiovascular medication, immunomodulation and carcinogenesis[2–6]. Recently, the presence of leptin has also been demonstrated in stomach and thought to be stomach-derived. This endogenous gastric leptin acts as a gastrointestinal hormone via autocrine and/or paracrine pathway in gastrointestinal tract and plays an important role in digestive physiological activities, including short-term meal size control, gastric mucosal cytoprotection and nutrition, regulation of gastric acid and gastric hormone secretion, and modulation of intestinal transport[7].

According to Lauren, gastric cancer can be divided into two histological types: diffuse and intestinal[8]. During the carcinogenesis of intestinal-type gastric adenocarcinoma, a stepwise process proposed by Correa has been widely accepted, which suggested that prolonged *H pylori* infection leads to atrophic gastritis, then with further mutational events leads to the development of intestinal metaplasia, epithelial dysplasia and finally intestinal-type gastric adenocarcinoma[9]. Gastrointestinal hormones and cytokines, including gastrin, epithelial growth factor, vasoactive intestinal peptide and IL-6, seem to play important roles in this transformation processes[10–16]. However, whether leptin, a cytokine-like gastrointestinal hormone that share similarity with aforementioned hormones or cytokines, is involved in the development of intestinal-type gastric adenocarcinoma remains unclear. In the present study, using immunohistochemistry, we examined the expression of leptin and ob-R protein in the tissues of intestinal metaplasia, gastric epithelial dysplasia and intestinal-type gastric adenocarcinoma. Their presence may suggest an autocrine/paracrine pathway of leptin system in gastric carcinogenesis.

MATERIALS AND METHODS

Samples

Formalin-fixed samples of 30 cases of intestinal

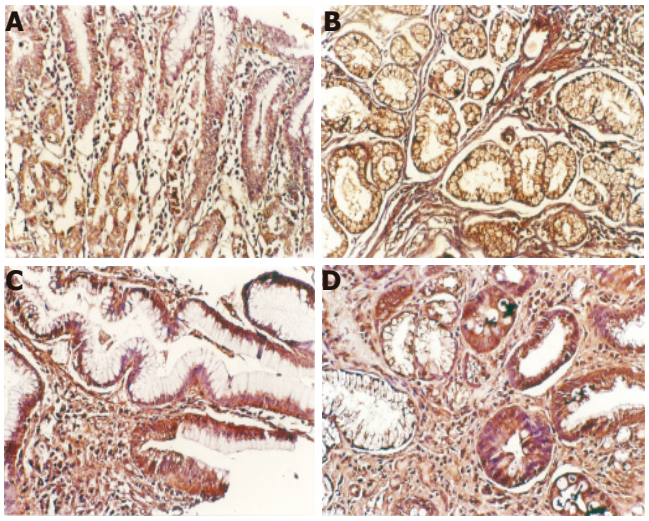

Figure 1 Immunohistochemical stainings of leptin located in cytoplasm (×200). **A:** Normal gastric mucosa; **B:** intestinal metaplasia; **C:** gastric dysplasia; **D:** intestinal-type gastric adenocarcinoma.

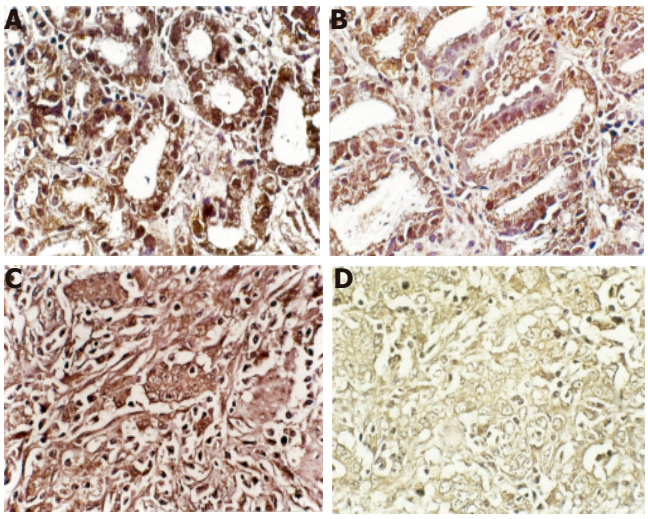

Figure 2 Immunohistochemical stainings of leptin receptor located at cell membrane (×200). **A:** Normal gastric mucosa; **B:** intestinal metaplasia; **C:** gastric dysplasia; **D:** intestinal-type gastric adenocarcinoma.

metaplasia, 90 cases of epithelial dysplasia (mild dysplasia, moderate dysplasia and severe dysplasia, each 30 cases), and 90 cases of gastric adenocarcinoma (60 intestinal-type, 30 diffuse-type) were obtained from pathology archives during 1995-2004 from Renmin Hospital, Wuhan University, Wuhan, China. Those patients had never received chemotherapy, radiation therapy or *H pylori* eradiation. For each case, a paraffin-embedded section with hematoxylin-eosin-safran staining was subjected to pathological identification by a consultant histopathologist on the basis of the Lauren's classification and WHO classification.

Immunohistochemistry

For immunohistochemistry analysis, paraffin-embedded tissue blocks were serially sectioned (4-μm thickness) and mounted onto histostick-coated slides and kept in an oven at 72 °C for 2 h. Sections were deparaffinized in xylene and rehydrated before analysis. Endogenous peroxides was quenched with 30 mL/L hydrogen peroxide in methanol for 10 min. Antigen retrieval was performed by means of microwave irradiation for 15 min and blocked for 15 min with normal goat serum, followed by incubation overnight at 4 °C with a rabbit polyclonal antibody (SC-842) against human leptin (Santa Cruz Biotechnology) and a rabbit polyclonal antibody (SC-1834) against human leptin receptor (Santa Cruz Biotechnology) both at a dilution of 1:70. Replacement of the primary antibodies by PBS solution was used as a negative control. Sections of normal gastric fundus mucosa that had previously shown expression of leptin and ob-R were used as positive

Table 1 Expression of leptin and ob-R in gastric cancer and precancerous lesions

	n	Leptin						Ob-R						Dual expression of leptinand ob-R	
		–	+	+ +	++ +	++ ++		–	+	++	++ +	+++ +		*n*	(%)
Intestinal metaplasia	30	5	4	5	17	0		4	5	7	14	0		25	(83.3)
Gastric dysolasia	90	6	12	28	39	0		9	15	25	35	4		79	(87.7)
Gastric cancer	90	25	9	16	16	24		24	9	22	12	25		75	(83.3)

For comparison of positive percentage for dusl expression of loptin and ob-R among (1) intestinal metaplsia (2) gastric dysplasia (3) gastric carcinoma, (1) *vs* (2) $\chi^2 = 0.3864$, P=0.5351; (1) *vs* (3) $\chi^2 = 0.3864$, $P = 1.000$; (2) *vs* (3) $\chi^2 = 0.7193$, $P = 0.3964$

Table 2 Expression of leptin and ob-R in mild, moderate, and severe gastric

	n	Leptin						Ob-R						Dual expression of leptinand ob-R	
		–	+	+ +	++ +	++ ++		–	+	++	++ +	+++ +		*n*	(%)
Mild dysplasia	30	3	6	9	12	0		4	8	9	9	0		25	(83.3)
Moderate dysplasia	30	3	2	12	10	3		3	3	9	13	2		26	(86.7)
Severe dysplasia	30	0	4	7	17	2		2	4	7	15	2		28	(93.3)

For comparison of positive percentage for dusl expression of loptin and ob-R among (1) mild gastric dysplasia (2) moderate gastric dysplasia (3) severe gastric dysplasia, (1) *vs* (2) $\chi^2 = 0.1307$, $P = 0.7177$; (1) *vs* (3) $\chi^2 = 1.456$, $P = 0.2276$; (2) *vs* (3) $\chi^2 = 0.7407$, $P = 0.3894$

Table 3 Expression of leptin and ob-R in intestinal-type and diffuse-type gastric cancer

	n	Leptin					Ob-R					Dual expression of leptinand ob-R	
		-	+	++	++	++	-	+	++	++	+++	*n*	(%)
				+	+	++				+	+		
Intestinal-type GC[1]	60	4	6	11	15	24	5	7	15	10	25	55	(91.7)
Diffuse-type GC[1]	30	21	3	5	1	0	19	2	7	2	0	9	(30)

[1]GC-gastric cancer for comparison of positive percentage for dual expression of leptin and ob-R between intestinal-type gastric carcinoma and diffuse-type gastric carcinoma, $\chi^2 = 37.022$, $P<0.001$.

controls. Sections were washed thrice with PBS for 2 min each and incubated with biotin-labeled anti-rabbit IgG at room temperature for 1 h. After washing thrice with PBS for 2 min each, sections were stained by streptavidin-peroxidase detection system. Antibody binding was visualized using the diaminobenzidine as chromogen and counterstained with hematoxylin. The positive cells were counted in ten randomly selected fields under ×200 or × 400 microscopic magnification for each specimen and the mean positive percentage was calculated as the density of positive cells. Immunoreactivity was performed by two experienced histopathologists without knowledge of the background features. The abundance of positive stains was graded as follows: -, no cell stained; +, <25% of cells stained; ++, 25–50% of cells stained; +++, 50–75% of cells stained; and ++++, >75% of cells stained.

Statistical analysis

Data were analyzed using SPSS 10.0 software. The χ^2 test was used to compare binomial proportions. A P value less than 0.05 was considered statistically significant.

RESULTS

Immunostainings of leptin and ob-R in normal gastric mucosa, intestinal metaplasia, gastric epithelial dysplasia, intestinal-type gastric adenocarcinoma, diffuse-type gastric carcinoma are shown in Figures 1 and 2. Positive staining of leptin was identified as brownish-yellow granules in cytoplasm. Positive staining of ob-R was identified as brownish-yellow granule at cell membrane.

DISCUSSION

In the present study, the expressions of leptin and ob-R in intestinal metaplasia, gastric epithelial dysplasia, intestinal-type gastric adenocarcinoma and diffuse-type gastric cancer were determined using immunohistochemistry. Our results demonstrated that dual expressions of leptin and leptin receptor were detected in 83.3% (25/30) intestinal metaplasia, 87.7% (79/90) gastric epithelial dysplasia, and 83.3% (75/90) intestinal-type gastric adenocarcinoma without statistically significant difference among those groups. Moreover, no obvious difference among mild gastric dysplasia (83.3%, 25/30), moderate gastric dysplasia (86.7%, 26/30) and severe gastric dysplasia (93.3%, 28/30) was observed. The percentage of dual expression in intestinal-type gastric adenocarcinoma (91.7%, 55/60) was significantly higher than that in diffuse-type gastric carcinoma (30.0%, 9/30). These results indicated that dual expression of leptin and ob-R might be a tumor-specific phenomenon in the transformation from intestinal metaplasia to intestinal-type gastric adenocarcinoma. To the best of our knowledge, our study may be the first study demonstrating dual expression of leptin and ob-R in intestinal metaplasia, gastric epithelial dysplasia and intestinal-type gastric adenocarcinoma, which may play important roles in this transformation process.

As a growth factor, leptin exhibited simulative effect on the proliferation of a variety of malignant cell lines, including leukemia, breast cancer, esophagus adenocarcinoma, prostate cancer, colon cancer, and pituitary adenomas[6,17–21]. In addition, there had been increasing evidence that leptin plays an important role in tumor invasion, metastases, angiogenesis and resistance to chemotherapy[22–26]. Based on these results, leptin is considered to serve as a multi-functional growth factor in tumorigenesis and is capable of promoting an aggressive cancer phenotype. Recently, it has been shown that leptin induced the proliferation of human gastric adenocarcinoma AGS cell line in a dose-dependent fashion[27]. Therefore, it is reasonable to speculate that dual expression of leptin and ob-R may form an autocrine/paracrine stimulatory loop based on intestinal-type gastric adenocarcinoma and precancerous lesions, and play an important role in gastric carcinogenesis.

As a member of the class I cytokine receptor family, ob-R is identified as a single membrane-spanning protein with multiple isoforms (ob-Ra, ob-Rb, ob-Rc, ob-Rd). ob-Rb contains sequence motifs of janus-kinase (JAK)/signal transduction and activation of transcription signal transduction pathways. In addition, leptin activates mitogen-activated protein kinase (MAPK) signal transduction pathways through the ob-Rb receptor and also through the ob-Ra receptor in some cases[18,28]. Those downstream signal pathways of leptin system were verified to be implicated in the formation and progression of tumor. Proliferation of prostate cancer cells appeared to be working through the PI3K and MAPK leptin receptor-activated pathways, depending on cell type[21]. In colon cancer cell line, leptin was demonstrated to stimulate proliferation via P42/44 MAPK signal pathway and induce invasion via JAK/PI3K signal pathway[18,23]. Recently, Schneilder et al.[27] have also reported that leptin caused a moderate, significant proliferative effect on gastric adenocarcinoma cell line AGS proliferation through MAPK signal pathways.

On the other hand, the expression of leptin protein in intestinal-type gastric adenocarcinoma and precancerous lesions in our study can be viewed as "ectopic secretion"

of gastric leptin in those tissues. Similar "ectopic secretion" of gastrointestinal hormone such as gastrin, epithelial growth factor, cholecystokinin, vasoactive intestinal peptide in gastrointestinal tumors has been well documented in previous studies[13–16]. Those "ectopic secretion" of gastrointestinal hormone acted as a growth factor and promoter of angiogenesis in gastrointestinal tumors via interaction with its specific receptor in tumors. Taking into account that those ectopic-secreting gastrointestinal hormones exert similar function in gastrointestinal tumors to their physiological functions to normal gastrointestinal tract, we hypothesized that the ectopic-secreting leptin in intestinal-type gastric adenocarcinoma and precancerous lesions may have similar function with gastric leptin[13–16]. As gastric leptin has been found to mediate gastric cytoprotection and increase mucosal blood flow via overexpression of growth factors, such as EGF, TGF-α and VEGF[29,30], it can be anticipated that leptin may enhance growth and angiogenesis of intestinal-type gastric cancer via similar mechanism mentioned above.

What activates leptin expression in gastric adenocarcinoma remains unclear. Recently, it has been reported that *H pylori* infection significantly increases gastric leptin expression[31]. In addition, leptin expression and secretion were induced by chronic inflammation of inflammatory bowel disease in colonic epithelial cells that were unable to express leptin physiologically[32]. Therefore, we postulated that leptin might be induced as a pro-inflammatory mediator in chronic gastrointestinal inflammation, including *H pylori*-associated chronic gastritis. In addition, previous reports demonstrated that K-ras mutation or amplification of chromosome 17q12-q21 induced the amplification of gastrin gene in colon or gastric cancer[33,34]. Whether *H pylori* infection and chronic gastritis might induce some special biomolecular alterations to amplify leptin expression and its downstream signal pathways during gastric carcinogenesis needs further investigation.

In conclusion, our study demonstrates constitutive dual expression of leptin and ob-R in intestinal-type gastric adenocarcinoma and precancerous lesions. Based on these results, we suggest that leptin system might act as a growth factor and angiogenesis promoter via autocrine and/or paracrine pathway in gastric carcinogenesis. Further investigations are warranted to identify the exact role of leptin system and exact mechanism of its activation in gastric carcinogenesis.

REFERENCES

1 **Zhang YR,** Proenca M, Maffei M, Barone M, Leopold L, Friedman JM. Positional cloning of the mouse ob gene and its human homlogue. *Nature* 1994; **372:** 425-432
2 **Wauters M,** Van Gaal L. Gender differences in leptin levels and physiology: a role for leptin in human reproduction. *J Gend Specif Med* 1999; **2:** 46-51
3 **Baratta M.** Leptin--from a signal of adiposity to a hormonal mediator in peripheral tissues. Med Sci Monit 2002; **8:** 282-292
4 **Fantuzzi G,** Faggioni R. Leptin in the regulation of immunity, inflammation, and hematopoiesis. *J Leukoc Biol* 2000; **68:** 437-446
5 **Rahmouni K,** Haynes WG. Leptin and the cardiovascular system. *Recent Prog Horm Res* 2004; **59:** 225-244
6 **Somasundar P,** McFadden DW, Hileman SM, Vona-Davis L. Leptin is a growth factor in cancer. *J Surg Res* 2004; **116:** 337-349
7 **Lewin MJ,** Bado A. Gastric leptin. *Microsc Res Tech* 2001; **53:** 372-376
8 **Lauren P.** The two histological main types of gastric carcinoma: diffuse and so-called intestinal-type carcinoma. *Acta pathol Microbiol Sacnd* 1965; **64:** 31-49
9 **Correa P.** A human model of gastric carcinogenesis. *Cancer Res* 1988; **48:** 3354-3360
10 **Tanahashi T,** Kita M, Kodama T, Yamaoka Y, Sawai N, Ohno T, Mitsufuji S, Wei YP, Kashima K, Imanishi J. Cytokine expression and production by purified Helicobacter pylori urease in human gastric epithelial cells. *Infect Immun* 2000; **68:** 664-671
11 **Coyle WJ,** Sedlack RE, Nemec R, Peterson R, Duntemann T, Murphy M, Lawson JM. Eradication of Helicobacter pylori normalizes elevated mucosal levels of epidermal growth factor and its receptor. *Am J Gastroenterol* 1999; **94:** 2885-2889
12 **Jonjic N,** Kovac K, Krasevic M, Valkovic T, Ernjak N, Sasso F, Melato M. Epidermal growth factor-receptor expression correlates with tumor cell proliferation and prognosis in gastric cancer. *Anticancer Res* 1997; **17:** 3883-3888
13 **Zhou JJ,** Chen ML, Zhang QZ, Hu JK, Wang WL. Coexpression of cholecystokinin-B/gastrin receptor and gastrin gene in human gastric tissues and gastric cancer cell line. *World J Gastroenterol*. 2004; **10:** 791-794
14 **Okada N,** Kubota A, Imamura T, Suwa H, Kawaguchi Y, Ohshio G, Seino Y, Imamura M. Evaluation of cholecystokinin, gastrin, CCK-A receptor, and CCK-B/gastrin receptor gene expressions in gastric cancer. *Cancer Lett*. 1996; **106:** 257-262
15 **Heasley LE.** Autocrine and paracrine signaling through neuropeptide receptors in human cancer. *Oncogene* 2001; **20:** 1563-1569
16 **Reubi JC,** Laderach U, Waser B, Gebbers JO, Robberecht P, Laissue JA. Vasoactive intestinal peptide/pituitary adenylate cyclase-activating peptide receptor subtypes in human tumors and their tissues of origin. *Cancer Res* 2000; **60:** 3105-3112
17 **Hu X,** Juneja SC, Maihle MJ, Cleary MP. Leptin-a growth factor in normal and malignant breast cells and for normal mammary gland development. *J Natl Cancer Inst* 2002; **94:** 1704-1711
18 **Isono M,** Inoue R, Kamida T ,Kobayashi H, Matsuyama J. Significance of leptin expression in invasive potential of pituitary adenomas. *Clin Neurol Neurosurg* 2003; **105:** 111-116
19 **Hardwick JC,**VanDen Brink GR, Offerhaus GJ, Van Deventer SJ, Peppelenbosch MP. Leptin is a growth factor for colonic epithelial cells. *Gastroenterology* 2001; **121:** 79-90
20 **Somasundar P,** Riggs D, Jackson B, Vona-Davis L, McFadden DW. Leptin stimulates esophageal adenocarcinoma growth by nonapoptotic mechanisms. *Am J Surg* 2003; **186:** 575-578
21 **Somasundar P,** Frankenberry KA, Skinner H, Vedula G, McFadden DW, Riggs D, Jackson B, Vangilder R, Hileman SM, Vona-Davis LC. Prostate cancer cell proliferation is influenced by leptin. *J Surg Res* 2004; **118 :** 71-82
22 **Mareel M,** Leroy A. Clinical, cellular, and molecular aspects of cancer invasion. *Physiol Rev* 2003; **83:** 337-376
23 **Attoub S,** Noe V, Pirola L, Bruyneel E, Chastre E, Mareel M, Wymann MP, Gespach C. Leptin promotes invasiveness of kidney and colonic epithelial cells via phosphoinositide 3-kinase-, rho-, and rac-dependent signaling pathways. *FASEB J* 2000; **14:** 2329-2338
24 **Beecken WD,** Kramer W, Jonas D. New molecular mediators in tumor angiogenesis. *J Cell Mol Med* 2000; **4:** 262-269
25 **Iversen PO,** Drevon CA, Reseland JE. Prevention of leptin binding to its receptor suppresses rat leukemic cell growth by

inhibiting angiogenesis. *Blood* 2002; **100:** 4123-4128

26 **Efferth T,** Fabry U, Osieka R. Leptin contributes to the protection of human leukemic cells from cisplatinum cytoxicity. *Anticancer Res* 2000; **20:** 2541-2546

27 **Schneilder R,** Bomstein SR, Chrousos GP, Boxberger S, Ehninger G, Breidert M. leptin mediates a proliferative response in human gastric mucosa cells with functonal receptor. *Horm Metab Res* 2001; **33:** 1-6

28 **Hegyi K,** Fulop K, Kovacs K, Toth S, Falus A. Leptin-induced signal transduction pathways. *Cell Biol Int* 2004; **28:** 159-169

29 **Konturek SJ,** Bielanski W ,Karcze wska E,Pierzchalski P, Hahn EG, Hartwich A. Role of gastrin in gastric cancerogenesis in Helicobacter pylori infecsed humans . *J Physiol Pharmacol* 1999; **50:** 857-873

30 **Konturek PC,** Brzozowski T, Sulekova Z, Meixner H, Hahn EG, Konturek SJ. Enhanced expression of leptin following acute gastric injury in rat. 1999; **50:** 587-595

31 **Azuma T,** Suto H, Ito Y, Ohtani M, Dojo M, Kuriyama M, Kato T. Gastric leptin and *Helicobacter pylori* infection. *Gut* 2001; **49:** 324-329

32 **Sitaraman S,** Liu X, Charrier L, Ziegler TR, Gewirtz A, Merlin D. Colonic leptin: source of a novel proinflammatory cytokine involved in IBD. *FASEB J* 2004; **18:** 696-69833

33 **Nakata H,** Wang Sl, Chung DC ,Westwick JK, Tilotson LG. Oncogenic ras induces gastrin gene expression in colon cancer. *Gastroentrology* 1998; **115:** 1144-1153

34 **Vidgren V,** Varis A, Kokkola A, Monni O, PurlakkainenP, Nordling S, Fonzan F, Kallioniemi A, Vakkari ML, Kirilaakso E, Knmntilas. Concomitant gastrin and ERBB2 gene amplifications at 17q12-q21 in the intestinal type of gastric cancer. : *Genes Chromosomes Cancer* 1999; **24:** 24-29

Science Editor Kumar M and Guo SY **Language Editor** Elsevier HK

PO Box 2345, Beijing 100023, China
www.wjgnet.com
wjg@wjgnet.com

ELSEVIER

World J Gastroenterol 2005;11(48):7671-7675
World Journal of Gastroenterology ISSN 1007-9327

• *RAPID COMMUNICATION* •

New tumor-associated antigen SC6 in pancreatic cancer

Min-Pei Liu, Xiao-Zhong Guo, Jian-Hua Xu, Di Wang, Hong-Yu Li, Zhong-Min Cui, Jia-Jun Zhao, Li-Nan Ren

Min-Pei Liu, Xiao-Zhong Guo, Jian-Hua Xu, Di Wang, Hong-Yu Li, Zhong-Min Cui, Jia-Jun Zhao, Li-Nan Ren, Department of Experimental Medicine, Northern Hospital, Shenyang, Liaoning Province, China
Correspondence to: Dr. Min-Pei Liu, Department of Experimental Medicine, Northern Hospital, No. 83, Wenhua Road, Shenhe District, Shenyang 110016, Liaoning Province, China. liuminp@yahoo.com.cn
Telephone: +86-24-2305-6274 Fax: +86-24-2450-8052
Received: 2005-01-28 Accepted: 2005-04-30

Abstract

AIM: To examine the concentration of a new antigen SC6 (SC6-Ag) recognized by monoclonal antibody (MAb) in patients with pancreatic cancer and other malignant or benign diseases and to understand whether SC6-Ag has any clinical significance in distinguishing pancreatic cancer from other gastrointestinal diseases.

METHODS: Six hundred and ninety-five serum specimens obtained from 115 patients with pancreatic cancer, 154 patients with digestive cancer and 95 patients with non-digestive cancer were used and classified in this study. Serum specimens obtained from 140 patients with benign digestive disease and 89 patients with non-benign digestive disease served as controls. Ascites was tapped from 16 pancreatic cancer patients, 19 hepatic cancer patients, 16 colonic cancer patients, 10 gastric cancer and 6 severe necrotic pancreatitis patients. The samples were quantitated by solid-phase radioimmunoassay. The cut-off values (CV) of 41, 80, and 118 U/mL were used.

RESULTS: The average intra- and interassay CV detected by immunoradiometric assay of SC6-Ag was 5.4% and 8.7%, respectively. The sensitivity and specificity were 73.0% and 90.9% respectively. The levels in most malignant and benign cases were within the normal upper limit. Among the 16 pancreatic cancer cases, the concentration of SC6-Ag in ascites was over the normal range in 93.8% patients. There was no significant difference in the concentration of SC6-Ag. Decreased expression of SC6-Ag in sera was significantly related to tumor differentiation. The concentration of SC6-Ag was higher in patients before surgery than after surgery. The specificity of SC6-Ag and CA19-9 was significantly higher than that of ultrasound and computer tomography (CT) in pancreatic cancer patients. Higher positive predictive values were indicated in 92.3% SC6-Ag and 88.5% CA19-9, but lower in 73.8% ultrasound and 76.2% CT.

CONCLUSION: The combined test of SC6-Ag and CA19-9 may improve the diagnostic rate of primary cancer. The detection of SC6-Ag is valuable in the diagnosis of pancreatic cancer before and after surgery.

Key words: Tumor antigen SC6; Pancreatic neoplasm; Immunoradiometric assay

Liu MP, Guo XZ, Xu JH, Wang D, Li HY, Cui ZM, Zhao JJ, Ren LN. New tumor-associated antigen SC6 in pancreatic cancer. *World J Gastroenterol* 2005; 11(48): 7671-7675
http://www.wjgnet.com/1007-9327/11/7671.asp

INTRODUCTION

Pancreatic cancer is the fourth or the fifth leading cause of cancer-related deaths in the Western world[1,2]. Approximately 50% of pancreatic cancer patients have metastatic disease at the time of diagnosis with a median survival of 3-6 mo[2,3]. However, even 70-80% of patients, whose tumor could be completely removed, suffer from an incurable local relapse, distant metastases, or peritoneal carcinosis[4,5]. The overall 5-year survival rate of pancreatic cancer patients is only 1%[6,7]. Ultrasound, computer tomography (CT), magnetic resonance imaging and other methods have made it easier to define the late-stage disease and to establish its diagnosis. Unfortunately, these imaging and diagnostic methods cannot detect the early-stage disease[8-11].

In recent years, there has been an increasing clinical attention to the role of tumor markers in the pathogenesis of pancreatic cancer[12-14]. The most widely used marker for pancreatic cancer is CA19-9[15-18]. CA19-9 has a mean sensitivity of 81% and a mean specificity of 90% for pancreatic cancer[19-23]. Other mucin-type markers such as CA50, CA242, DU-PAN2, CA195 and CAM17.1/WGA have also been described for pancreatic cancer[24-28]. These markers have been investigated less widely than CA19-9 but available evidence appears to provide similar data[29-33]. CA19-9 remains as the "gold standard marker"[10] against which tumor markers for pancreatic cancer are evaluated.

Antigen SC6 (SC6-Ag) recognized by monoclonal antibody SC6 (MAb SC6) against human colonic cancer is a relatively new marker compared with CA19-9, CA242, CEA, AFP, DU-PAN-2 and β_2-MG[34-36]. The antigen was purified by immunoaffinity chromatography using the MAb SC6 at our laboratory. The results of SDS-

PAGE, Western blotting and amino acid analysis indicate that SC6-Ag is a glycoprotein with a molecular weight of 67 kμ and contains 18 amino acids. An immunoradiometric sandwich assay of SC6-Ag has been established by us[37]. The diagnostic value of SC6-Ag was evaluated in patients with pancreatic cancer. The sensitivity and specificity of SC6Ag for patients with pancreatic cancer are similar to those of CA 19-9 detected by radioimmunodetection[38]. Therefore, in the present study, we analyzed and compared the pattern of SC6Ag expression in pancreatic cancer and other gastrointestinal cancers to evaluate whether it might be also of high biological strategy in the diagnosis of pancreatic cancer.

MATERIALS AND METHODS

Patients

Serum specimens were obtained from 115 patients with pancreatic cancer (41 females and 74 males, mean age 61 years, with a range of 39-80 years). Among them, 39 had well-and moderately-differentiated tumor, 55 had poorly-differentiated tumor and 21 had differentiated tumor with unknown reason. According to International Union Against Cancer criteria, 9 patients had stage I disease, 33 stage II, 46 stage III and 6 stage IV. Fifteen primary esophageal cancer specimens, 43 gastric cancers specimens, 11 specimens of cancer of papilla of Vater, 39 hepatocellular carcinoma specimens and 46 colonic cancer specimens were classified. Fifteen esophagitis patients (5 females and 10 males; mean age 41 years), 27 gastritis patients (11 females and 16 males; mean age 38 years), 16 papilla of Vater cancer patients (7 females and 9 males; mean age 43 years), 28 pancreatitis patients (15 females and 13 males; mean age 35 years), 23 cirrhosis patients (10 females and 13 males; mean age 44 years) and 31 colitis patients (17 females and 14 males; mean age 35 years) were obtained. The diagnosis of pancreatic cancer was made based on histology and clinical and radiological findings. We noted weight loss, duration of symptoms and tumor position. Other cancers were diagnosed by abdominal ultrasound and CT scan, surgery and pathology. Ninety-five cancers involving lung and bladder were determined. Fifteen out of 42 suspicious patients before surgery were diagnosed having pancreatic cancer after surgery. CA 19-9 was examined in the same samples. Ascites was tapped from 16 pancreatic cancer patients, 19 hepatic cancer patients, 16 colonic cancer patients, 10 gastric cancer and 6 severe necrotic pancreatitis patients.

Sample collection

Blood samples were obtained from all the subjects after an overnight fast. The plasma was immediately separated by centrifugation. The samples were frozen and stored at -20 °C until assay.

Radiolabeling of MAb SC6

MAb SC6 is a murine MAb of the IgG1 isotype against purified antigen SC6 from human colonic cancer tissues as described previously[34-36]. MAb SC6 was isolated from the ascitic fluid of BALB/C mice in which hybridoma cell line SC6 was injected intraperitoneally and purified by protein A-Sepharose 4B columns (Bioinstitute, Shanghai, China). Normal murine immunoglobulin (IgG1, Bioinstitute, Beijing, China) was used as nonspecific control antibody. The MAb was labeled with $Na^{125}I$ by the iodogen method. The average intra- and interassay CV of the method was 5.4% and 8.7% respectively. The recovery rate was 96.5-108.0%, average 102.3%.

Sandwich measurement by radioimmunoassay

After the MAb SC6 was labeled, ^{125}I uncombined with MAb SC6 was separated from bound iodine by gel filtration on a Sephadex G-25 column. Microtiterplates (96-well) were coated with MAb SC6 (20 ng/mL, 100 μL/well) overnight and then incubated with 100 μL/well of 3% bovine albumin in phosphate-buffered saline at 37 °C for 2.5 h. Standard SC6-Ag, various sera, quantity control sera and nonspecific control were incubated at 37 °C for 1 h. ^{125}I-MAb SC6 (25 ng/mL, 100 μL/well) was coated at 37 °C for 3 h and the radioactivity of each well was determined with a Gamma counter (Instrument Factory, Xian, China). After each step, the wells were washed four times with phosphate-buffered saline.

The cut-off values (CV) of SC6-Ag were determined and expressed as mean±SD. The SC6-Ag concentration in sera of controls was lower than CV. The CV of 41 U was mean±2SD, 80 U was mean±3SD, 118 U was mean±4SD. CA 19-9 kit (Abbott Diagnostics, USA) was quantitated by solid-phase radioimmunoassay, CV of 37 U/mL were used.

Statistical analysis

Analysis was performed using SPSS 10.0 software package. For the comparison of various tumor markers, CV representing 90% and 95% specificity levels in patients with relevant benign diseases were determined. The correlation between SC6-Ag and CA 19-9 concentrations was calculated by linear regression using the logarithms of the serum levels. The statistical comparison of multifactors was made and results were significant ($P<0.05$).

RESULTS

SC6-Ag levels in pancreatic cancer and other diseases

The characteristics of the 695 patients are presented in Table 1. Low concentration SC6-Ag was found in the sera from 102 healthy individuals and the cut-off of its normal upper limit was 41 U/mL (20.7±9.8). Among the 115 patients with pancreatic cancer, the cut-off was over the normal range in 73.3% patients, more than 118 U/mL in 48.7% patients and over 41 U/mL in 29.9% patients. The SC6-Ag level was mainly elevated in colonic cancer, hepatic carcinoma and gall bladder tract/bile duct cancers. Non-digestive cancers were mainly non-small cell lung cancer and renal carcinoma. Lower levels of SC6-Ag were observed in benign digestive and non-digestive diseases

Table 1 SC6-Ag levels in patients with malignant and benign disease

Groups	Cases	>41 U/mL	>80 U/mL	>118 U/mL
		n (%)	*n* (%)	*n* (%)
Control	102	7 (6.9)	2 (2.0)	0 (0.0)
Pancreatic Ca	115	84 (73.0)	68 (59.1)	56 (48.7)
Digestive Ca	154	46 (29.9)	24 (15.6)	11 (7.1)
Non-digestive Ca	95	11 (11.6)	8 (8.4)	4 (4.2)
Benign digestive Diseases	140	13 (9.3)	9 (6.4)	2 (1.4)
Non-benign digestive Diseases	89	8 (9.0)	4 (4.5)	0 (0.0)

Table 2 SC6-Ag concentration in ascites from patients with different digestive diseases (mean±SD)

Groups	Cases	SC6-Ag (U/mL) Concentration	>41	>80	>118
			n (%)	*n* (%)	*n* (%)
Pancreatic Ca	16	120.9±109.1	15 (93.8)	11 (68.8)	7 (43.8)
Hepatic Ca	19	55.7±33.4	10 (52.6)	3 (15.8)	1 (5.3)
Colonic Ca	16	54.9±36.7	9 (56.3)	4 (25.0)	1 (6.3)
Gastric Ca	10	38.1±23.4	3 (30.0)	1 (10.0)	0 (0.0)
Several pancreatitis	6	30.9±26.3	2 (33.3)	0 (0.0)	0 (0.0)

mainly including acute pancreatitis and obstruction of gall bladder/bile duct and acute renal impairment.

Relationship between SC6-Ag and clinicopathological factors

SC6-Ag was not significantly related with clinicopathological factors in patients with pancreatic cancer. Decrease of SC6-Ag in the pancreatic head was compared with that in its body and tail. However, the difference failed to reach statistical significance ($P>0.05$).

SC6-Ag concentration in ascites from patients with different digestive diseases

Among the 16 patients with pancreatic cancer, the concentration of SC6-Ag in ascites was over the normal range in 93.8% patients, over 41 U/mL in 33.3-52.6% patients and more than 118 U/mL in 43.8% patients (Table 2).

Parameters for SC6-Ag, CA19-9, ultrasound and CT in patients with pancreatic cancer

The sensitivity of SC6-Ag and CA19-9 was similar to that of ultrasound and CT, while the specificity of SC6-Ag and CA19-9 was significantly higher than that of ultrasound and CT in patients with pancreatic cancer. Higher positive predictive values were found in 92.3% SC6-Ag and 88.5% CA19-9, but lower positive predictive values were found in 73.8% ultrasound and 76.2% CT (Table 3).

Table 3 Comparison of parameters for SC6-Ag, CA19-9, ultrasound and CT in patients with pancreatic cancer

	SC6-Ag (%)	CA19-9 (%)	Ultrasound (%)	CT (%)
Sensitivity	73.0 (84/115)	84.3 (97/115)	82.6 (95/115)	83.5 (96/115)
Specificity	90.9 (70/77)	84.4 (65/77)	55.8 (43/77)	59.7 (46/77)
Positive predictive value	92.3 (84/91)	88.5 (92/104)	73.8 (96/130)	76.2 (99/130)
Negative predictive value	69.3 (70/101)	73.9 (65/88)	69.4 (43/62)	74.2 (46/62)

DISCUSSION

It is obvious that early diagnosis has the greatest impact on the survival of patients with pancreatic cancer. Clinically, fast spiral CT using dynamic intravenous contrast and the potential for improved MRI can provide high-resolution images of small masses[9-13]. Endoscopic retrograde cholangiopancreatography with improved cytology, brushes, and biopsy forceps should enhance preoperative diagnosis of this malignancy. Endoscopic ultrasound also may help detect small lesions and determine the depth of invasion and vascular involvement. Tumor markers are normally produced in low quantities by cells in the body. Detection of a higher serum level of tumor markers by radioimmunoassay or immunohistochemical techniques usually indicates the presence of a certain type of cancer. In some types of cancer, tumor marker levels may reflect the extent or stage of the disease and can be useful in its diagnosis. Recently, the most widely used marker for pancreatic carcinoma is CA19-9, but SC6-Ag has also been found in China[34-38].

In the present study, high levels of SC6-Ag over the normal upper limit (41 U/mL) were found in 73.0% patients with pancreatic cancer, and in 29.8% patients with other digestive tumors. Using a cut-off point of 80 U/mL, the proportion of patients with elevated levels was 59.2%. But over 118 U/mL SC6-Ag was detected in 48.7% patients with pancreatic cancer, in 5.8% patients with digestive cancers, in 4.2% patients with non-digestive carcinoma and in 2% patients with benign digestive diseases. Furthermore, patients with certain benign diseases such as jaundice and pancreatitis, may present with elevated levels of CA19-9[12-14], suggesting that SC6-Ag and CA19-9 may have similar value in the diagnosis of pancreatic cancer.

Increased SC6-Ag concentrations in ascites are not specific for adenocarcinoma of the pancreas when the CV is 41 U/mL, which was evaluated in other digestive tumors and pancreatitis in our study (Table 2). With a cut-off point of 118 U/mL, the respective specificities for patients with pancreatic cancer were high compared to patients with gastric cancer or pancreatitis, indicating that high SC6-Ag level can be used to distinguish pancreatic cancer from benign disorders. However, decreased level of SC-Ag in pancreatic head compared to that in its body and tail failed to reach statistical significance, and there was no relationship between SC-Ag and tumor stage, size and duration ($P>0.05$).

Up to now, it is difficult to diagnose pancreatic cancer using one of the tumor markers because tumor marker levels can be elevated in patients with benign conditions.

In the recent study, the sensitivity, specificity and positive predictive value of SC6-Ag were found to be 73.0%, 90.9% and 92.3%, respectively. By analyzing the four factors, we found that the sensitivity of SC6 and CA19-9 was lower than that of ultrasound and CT, but their specificity was significantly higher (Table 3). Positive predictive values in SC6-Ag and CA19-9 were 92.3% and 88.5%, which were distinctly higher than those of ultrasound (73.8%) and CT (76.2%). The lack of sensitivity and specificity also limits the diagnosis of pancreatic cancer although CA19-9 and SC6-Ag may be useful in differentiating benign from malignant pancreatic disease in non-jaundiced patients. However, combined measures are more useful in the diagnosis of pancreatic cancer.

In conclusion, detection of SC6-Ag is valuable in the diagnosis of pancreatic cancer before and after surgery. The combined test of SC6-Ag and CA19-9 may improve the diagnostic rate of primary cancer.

REFERENCES

1 **Jemal A,** Thomas A, Murray T, Thun M. Cancer statistics, 2002. *CA Cancer J Clin* 2002; **52:** 23-47
2 **Liu MP,** Ma JY, Pan BR, Ma LS, Study of pancreatic cancer in China. *Shijie Huaren Xiaohua Zazhi* 2001; **9:** 1103-1109
3 **Rocha Lima CM,** Centeno B. Update on pancreatic cancer. *Curr Opin Oncol* 2002; **14:** 424-430
4 **Sawabu N,** Watanabe H, Yamaguchi Y, Ohtsubo K, Motoo Y. Serum tumor markers and molecular biological diagnosis in pancreatic cancer. *Pancreas* 2004; **28:** 263-267
5 **Iacobuzio-Donahue CA,** Hruban RH. Gene expression in neoplasms of the pancreas: applications to diagnostic pathology. *Adv Anat Pathol* 2003; **10:** 125-134
6 **Coppola D.** Molecular prognostic markers in pancreatic cancer. *Cancer Control* 2000; **7:** 421-427
7 **Schlieman MG,** Ho HS, Bold RJ. Utility of tumor markers in determining resectability of pancreatic cancer. *Arch Surg* 2003; **138:** 951-955; discussion 955-956
8 **Cohen-Scali F,** Vilgrain V, Brancatelli G, Hammel P, Vullierme MP, Sauvanet A, Menu Y. Discrimination of unilocular macrocystic serous cystadenoma from pancreatic pseudocyst and mucinous cystadenoma with CT: initial observations. *Radiology* 2003; **228:** 727-733
9 **Zhao XY,** Yu SY, Da SP, Bai L, Guo XZ, Dai XJ, Wang YM. A clinical evaluation of serological diagnosis for pancreatic cancer. *World J Gastroenterol* 1998; **4:** 147-149
10 **Rosty C,** Goggins M. Early detection of pancreatic carcinoma. *Hematol Oncol Clin North Am* 2002; **16:** 37-52
11 **Furukawa H.** Diagnostic clues for early pancreatic cancer. *Jpn J Clin Oncol* 2002; **32:** 391-392
12 **Bassi C,** Salvia R, Gumbs AA, Butturini G, Falconi M, Pederzoli P. The value of standard serum tumor markers in differentiating mucinous from serous cystic tumors of the pancreas: CEA, Ca 19-9, Ca 125, Ca 15-3. *Langenbecks Arch Surg* 2002; **387:** 281-285
13 **Carpelan-Holmstrom M,** Louhimo J, Stenman UH, Alfthan H, Haglund C. CEA, CA 19-9 and CA 72-4 improve the diagnostic accuracy in gastrointestinal cancers. *Anticancer Res* 2002; **22:** 2311-2316
14 **Schneider J,** Schulze G. Comparison of tumor M2-pyruvate kinase (tumor M2-PK), carcinoembryonic antigen (CEA), carbohydrate antigens CA 19-9 and CA 72-4 in the diagnosis of gastrointestinal cancer. *Anticancer Res* 2003; **23:** 5089-5093
15 **Crnogorac-Jurcevic T,** Missiaglia E, Blaveri E, Gangeswaran R, Jones M, Terris B, Costello E, Neoptolemos JP, Lemoine NR. Molecular alterations in pancreatic carcinoma: expression profiling shows that dysregulated expression of S100 genes is highly prevalent. *J Pathol* 2003; **201:** 63-74
16 **Kuwahara K,** Sasaki T, Kuwada Y, Murakami M, Yamasaki S, Chayama K. Expressions of angiogenic factors in pancreatic ductal carcinoma: a correlative study with clinicopathologic parameters and patient survival. *Pancreas* 2003; **26:** 344-349
17 **Akashi T,** Oimomi H, Nishiyama K, Nakashima M, Arita Y, Sumii T, Kimura T, Ito T, Nawata H, Watanabe T. Expression and diagnostic evaluation of the human tumor-associated antigen RCAS1 in pancreatic cancer. *Pancreas* 2003; **26:** 49-55
18 **Ji H,** Isacson C, Seidman JD, Kurman RJ, Ronnett BM. Cytokeratins 7 and 20, Dpc4, and MUC5AC in the distinction of metastatic mucinous carcinomas in the ovary from primary ovarian mucinous tumors: Dpc4 assists in identifying metastatic pancreatic carcinomas. *Int J Gynecol Pathol* 2002; **21:** 391-400
19 **Palumbo KS,** Wands JR, Safran H, King T, Carlson RI, de la Monte SM. Human aspartyl (asparaginyl) beta-hydroxylase monoclonal antibodies: potential biomarkers for pancreatic carcinoma. *Pancreas* 2002; **25:** 39-44
20 **Mizumoto K,** Tanaka M. Genetic diagnosis of pancreatic cancer. *J Hepatobiliary Pancreat Surg* 2002; **9:** 39-44
21 **Ghaneh P,** Kawesha A, Evans JD, Neoptolemos JP. Molecular prognostic markers in pancreatic cancer. *J Hepatobiliary Pancreat Surg* 2002; **9:** 1-11
22 **Boltze C,** Schneider-Stock R, Aust G, Mawrin C, Dralle H, Roessner A, Hoang-Vu C. CD97, CD95 and Fas-L clearly discriminate between chronic pancreatitis and pancreatic ductal adenocarcinoma in perioperative evaluation of cryocut sections. *Pathol Int* 2002; **52:** 83-88
23 **Maacke H,** Hundertmark C, Miska S, Voss M, Kalthoff H, Sturzbecher HW. Autoantibodies in sera of pancreatic cancer patients identify recombination factor Rad51 as a tumour-associated antigen. *J Cancer Res Clin Oncol* 2002; **128:** 219-222
24 **Tempia-Caliera AA,** Horvath LZ, Zimmermann A, Tihanyi TT, Korc M, Friess H, Buchler MW. Adhesion molecules in human pancreatic cancer. *J Surg Oncol* 2002; **79:** 93-100
25 **Kunzli BM,** Berberat PO, Zhu ZW, Martignoni M, Kleeff J, Tempia-Caliera AA, Fukuda M, Zimmermann A, Friess H, Buchler MW. Influences of the lysosomal associated membrane proteins (Lamp-1, Lamp-2) and Mac-2 binding protein (Mac-2-BP) on the prognosis of pancreatic carcinoma. *Cancer* 2002; **94:** 228-239
26 **Gerdes B,** Ramaswamy A, Ziegler A, Lang SA, Kersting M, Baumann R, Wild A, Moll R, Rothmund M, Bartsch DK. p16INK4a is a prognostic marker in resected ductal pancreatic cancer: an analysis of p16INK4a, p53, MDM2, an Rb. *Ann Surg* 2002; **235**: 51-59
27 **Kim GE,** Bae HI, Park HU, Kuan SF, Crawley SC, Ho JJ, Kim YS. Aberrant expression of MUC5AC and MUC6 gastric mucins and sialyl Tn antigen in intraepithelial neoplasms of the pancreas. *Gastroenterology* 2002; **123**: 1052-1060
28 **Hamanaka Y**, Suehiro Y, Fukui M, Shikichi K, Imai K, Hinoda Y. Circulating anti-MUC1 IgG antibodies as a favorable prognostic factor for pancreatic cancer. *Int J Cancer* 2003; **103**: 97-100
29 **Yiannakou JY,** Newland P, Calder F, Kingsnorth AN, Rhodes JM. Prospective study of CAM 17.1/WGA mucin assay for serological diagnosis of pancreatic cancer. *Lancet* 1997; **349:** 389-392
30 **Levi E,** Klimstra DS, Andea A, Basturk O, Adsay NV. MUC1 and MUC2 in pancreatic neoplasia. *J Clin Pathol* 2004; **57**: 456-462
31 **Swierczynski SL,** Maitra A, Abraham SC, Iacobuzio-Donahue CA, Ashfaq R, Cameron JL, Schulick RD, Yeo CJ, Rahman A, Hinkle DA, Hruban RH, Argani P. Analysis of novel tumor markers in pancreatic and biliary carcinomas using tissue microarrays. *Hum Pathol* 2004; **35:** 357-366
32 **Koopmann J,** Fedarko NS, Jain A, Maitra A, Iacobuzio-Donahue C, Rahman A, Hruban RH, Yeo CJ, Goggins M. Evaluation of osteopontin as biomarker for pancreatic

adenocarcinoma. *Cancer Epidemiol Biomarkers Prev* 2004; **13:** 487-491

33 **Grutzmann R,** Luttges J, Sipos B, Ammerpohl O, Dobrowolski F, Alldinger I, Kersting S, Ockert D, Koch R, Kalthoff H, Schackert HK, Saeger HD, Kloppel G, Pilarsky C. ADAM9 expression in pancreatic cancer is associated with tumour type and is a prognostic factor in ductal adenocarcinoma. *Br J Cancer* 2004; **90:** 1053-1058

34 **Liu MP**,Characteristics and reactivities of a panel of monoclonal antibodies (McAbs) recognizing human colon cancer associated antigens. *Zhonghua Zhongliu Zazhi* 1992; **14:** 91-93

35 **Liu MP,** Immunohistochemical analysis of physicochemical properties of target antigens with anti-tumor monoclonal antibodies. *Zhonghua Zhongliu Zazhi* 1992; **14:** 6-9

36 **Liu MP**, Zhou JC, Guo XZ, Chen W, Dai B,An TY, Ma SY. Purification and charaterization of antigen SC6 for pancreatic cancer. *Shijie Huaren Xiaohua Zazhi* 1999; **7:** 593-595

37 **Guo XZ**, Liu MP, Li XX, An R, Ma SY, Liu ZF, Zhao XL, Li RP. Evaluation of serum antigen SC6 using immunoradiomrtric assay for diagnosis of pancreatic cancer. *Zhonghua Neike Zazhi* 1992; **31:** 84-86

38 **Guo XZ,** Liu ZF, An R, Zhao XL, Li FH, Wang KG.antigen SC6 for the dia gnosis of pancreatic cancer before operation. *Zhonghua Yixue Zazhi* 1993; **73:** 26-28

Science Editor Wang XL and Guo SY **Language Editor** Elsevier HK

PO Box 2345, Beijing 100023, China
www.wjgnet.com
wjg@wjgnet.com

ELSEVIER

World J Gastroenterol 2005;11(48):7676-7683
World Journal of Gastroenterology ISSN 1007-9327

• *CASE REPORT* •

Liver transplantation for metastatic neuroendocrine tumor: A case report and review of the literature

Wojciech C Blonski, K Rajender Reddy, Abraham Shaked, Evan Siegelman, David C Metz

Wojciech C Blonski, Department of Gastroenterology and Hepatology, Wroclaw Medical University, Wroclaw, Poland
Wojciech C Blonski, the Kosciuszko Foundation Awardee in the Division of Gastroenterology at the University of Pennsylvania, Philadelphia, United States
K Rajender Reddy, Division of Gastroenterology, University of Pennsylvania, Philadelphia, PA, United States
Abraham Shaked, Department of Surgery, University of Pennsylvania, Philadelphia, PA, United States
Evan Siegelman, Department of Magnetic Resonance Imaging Division, University of Pennsylvania, Philadelphia, PA, United States
David C Metz, Division of Gastroenterology, University of Pennsylvania, Philadelphia, PA, United States
Correspondence to: Dr. David C. Metz, 3400 Spruce Street, 3 Ravdin Building, Gastroenterology Division, University of Pennsylvania Health System, Philadelphia, PA 19104, United States. david.metz@uphs.upenn.edu
Telephone: +1-215-662-3541 Fax: +1-215-349-5815
Received: 2005-04-09 Accepted: 2005-04-30

Abstract

Neuroendocrine tumors are divided into gastrointestinal carcinoids and pancreatic neuroendocrine tumors. The WHO has updated the classification of these lesions and has abandoned the term "carcinoid". Both types of tumors are divided into functional and non-functional tumors. They are characterized by slow growth and frequent metastasis to the liver and may be limited to the liver for long periods. The therapeutic approach to hepatic metastases should consider the number and distribution of the liver metastases as well as the severity of symptoms related to hormone production and tumor bulk. Surgery is generally considered as the first line therapy. In patients with unresectable liver metastases, alternative treatments are dependent on the type and the growth rate. Initial treatments consist of long acting somatostatin analogs and/or interferon. Streptozocin-based chemotherapy is usually reserved for symptomatic patients with rapidly advancing disease, but generally the therapy is poorly tolerated and its effects are short-lived. Locoregional therapy directed such as hepatic-artery embolization and chemoembolization, radiofrequency thermal ablation and cryosurgery, is often used instead of systemic therapy, if the disease is limited to the liver. However, liver transplantation should be considered in patients with neuroendocrine metastases to the liver that are not accessible to curative or cytoreductive surgery and if medical or locoregional treatment has failed and if there are life threatening hormonal symptoms. We report a case of liver transplantation for metastatic neuroendocrine tumor of unknown primary source and provide a detailed review of the world literature on this controversial topic.

Key words: Liver metastases; Neuroendocrine tumors; Liver transplantation

Blonski WC, Reddy KR, Shaked A, Siegelman E, Metz DC. Liver transplantation for metastatic neuroendocrine tumor: A case report and review of the literature. *World J Gastroenterol* 2005;11(48): 7676-7683
http://www.wjgnet.com/1007-9327/11/7676.asp

INTRODUCTION

Neuroendocrine tumors are divided into gastrointestinal carcinoids and pancreatic neuroendocrine tumors[1]. However, it is suggested that they may be grouped together and be categorized into functional and non-functional tumors[2] to indicate the clinical manifestations of syndromes caused by hypersecretion of neuropeptides and biogenic amines at supraphysiologic levels[2,3]. These tumors are very rare and occur with an incidence of 2 per 100 000/year (with a slight female predominance) for carcinoids[4-6] and 1-1.5 per 100 000/year for pancreatic neuroendocrine tumors[7].

Gastrointestinal carcinoid tumors originate from cells of the diffuse neuroendocrine system, which is composed of amine-and peptide-producing cells[1]. These cells are scattered throughout the body and predominantly occur in the submucosa of the large and small intestine, stomach and larger bronchi[1]. In 85% of all cases they arise in the lung, stomach, ileum, appendix and rectum[1]. Although the majority of these tumors are nonfunctional, certain primary site locations, such as the ileum and bronchi, have a predilection for producing the carcinoid syndrome[1]. This syndrome is characterized by flushing, diarrhea, abdominal pain and less often by wheezing and heart disease and is predominantly caused by the production of serotonin[1,8]. Other biological substances, produced by carcinoid tumors, such as kalikrein and prostaglandins also take part in the pathogenesis of the carcinoid syndrome[1]. Overall, the carcinoid syndrome develops in only 5% of all carcinoid tumor patients, but this figure rises to approximately 60% in cases with liver metastases[1]. Prior to metastasizing to the liver, carcinoid tumors are usually

silent because their secretory products are inactivated in the liver[1,8,9].

Pancreatic endocrine tumors arise from pleuropotential stem cells within the pancreas[9,10] and those that are functional produce biologically active peptides such as gastrin, insulin, glucagon, vasoactive intestinal polypeptide, somatostatin, growth hormone releasing factor, and pancreatic polypeptide which are responsible for distinct clinical syndromes[1,11]. Gastrinomas and the insulinomas are the most common functional pancreatic endocrine tumors whereas all others are rare[1,11]. Non-functional pancreatic neuroendocrine tumors (45-50% of all pancreatic neuroendocrine tumors) exhibit no specific syndromes; such tumors present only with symptoms due to tumor mass[3,11].

Liver metastases develop in 46-93% of patients with neuroendocrine tumors and can involve large portions of the liver before becoming symptomatic[12]. They exhibit a slow growth despite their multilocular and bilateral occurrence in most cases[13] and may be limited to the liver for long periods[14]. Surgery is generally the first line therapy for patients with liver metastases due to neuroendocrine tumors[15-17]. Potentially curative resection is considered in patients with solitary or unilobar hepatic metastases and without radiological evidence of systemic disease[18]. However, curative resection is possible only in approximately 20% of patients[19], because liver metastases frequently diffuse at the time of diagnosis[8]. In patients with bulky disease, preoperative hepatic artery embolization is recommended in order to decrease the blood flow and shrink tumors[18]. In patients with previously resected or resectable primary tumors, regional nodal disease and metastases confined to the liver, cytoreductive surgery is recommended, provided that preoperative imaging confirms that the primary and regional diseases are controlled or controllable and 90% or more of the bulk of the tumor can be removed[14]. In patients with unresectable liver metastases alternative treatments that can be considered include immunotherapy (somatostatin analogs and/or alpha-interferon) and chemotherapy (usually streptozocin-based). Additional therapy such as hepatic-artery embolization or chemoembolization, radiofrequency ablation and cryosurgery are pursued as needed[8,11,18,20]. Some studies report a tumoristatic effect of somatostatin analogs such as octreotide and lanreotide in 36.5-75% of treated patients lasting for 3-12 months[21-24]. Furthermore, treatment with high-dose somatostatin analogs may induce apoptosis in neuroendocrine tumors[25]. In addition, small liver metastases (diameter less than 1-2 cm) may respond to radiopharmaceutical agents such as Y (90)- and In (131)-labeled octreotide which involve insertion of radiotherapeutic agents directly into the tumor[26]. A recent study suggested that the administration of combinations of Y (90)- and Lu (177)-labeled octreotide in patients with tumors of different sizes may allow wider tumor penetration[27]. In patients with bilobar hepatic tumors, hepatic artery embolization combined with octreotide treatment has also been proposed[28].

Liver transplantation is considered in patients with neuroendocrine metastases to the liver which are not accessible to curative or cytoreductive surgery, tumors which do not respond to medical or interventional treatment and in tumors causing uncontrollable life-threatening hormonal symptoms (severe hypoglycemia, gastrointestinal hemorrhage, severe diarrhea, valvulopathy)[29,30] providing the disease has not extended beyond the liver, although certain hormonal symptoms (e.g. insulinoma) may be less amenable to transplantation than others.

We report herein a case of liver transplantation due to metastatic neuroendocrine tumor of unknown primary source. In addition, we present a comprehensive review of liver transplantation in patients with metastatic neuroendocrine tumors.

CASE REPORT

A 61-year-old white male with a prior history of hypertension and arteriosclerotic heart disease was referred in May 1999 for evaluation of multiple liver metastases from an unclear primary source. In the 4-5 years prior to referral, he described that he had flushing and cough. The flushing was primarily on his face, lasted for about an hour at a time and was precipitated by heat. In the few months prior to referral he developed episodes of fevers, chills and lassitude and had been treated briefly with antibiotics with a good response. The patient had lost about 16 pounds, which was attributed to dieting and anxiety. Physical examination revealed hepatomegaly. Ultrasound of the right upper quadrant and CT scanning of the chest and abdomen revealed multiple metastases in the liver but no other obvious primary tumor (Figure 1A). Laboratory data included a urinalysis which was negative, a serum albumin of 2.9 gm/dL (n.: 3.5-5.0), an elevated alkaline phosphatase of 197 IU/L (n.: 42-121), an ALT of 96 IU/L (n.: 10-60), an AST of 57 IU/L (n.: 10-42), a BUN of 18 mg/dL (n.: 6-20), a normal serum calcium and normal chloride and electrolytes. His total bilirubin was 1.0 mg/dL (n.: 0.2-1.0) and his total protein was 6.7 gm/dL (n.: 6.4-8.2). His CBC was within normal limits.

His serum gastrin level was 38 pg/mL (n.: 0-100), serum chromogranin A level was 275 ng/mL (n.<50) and serum pancreatic polypeptide was 258 pg/mL (n.<312). 24-h urine analysis for 5-hydroxydinoloacetic acid was normal. A transcutaneous liver biopsy was positive for neuroendocrine tumor. The tumor was strongly positive for neuron specific enolase, synaptophysin, insulin, S100 and chromogranin. An OctreoScan showed liver and midline abdominal foci of increased radiotracer uptake compatible with neuroendocrine lesions. There were no neuroendocrine lesions within the lungs and mediastinum. His small bowel enema was normal. An upper endoscopy revealed a few small prepyloric ulcers with no evidence of *Helicobacter pylori*. In addition, there was evidence of extrinsic antral compression from the left lobe of the liver. An echocardiogram was performed which showed a thickened and calcified aortic valve and mitral valve with mild mitral regurgitation. A diagnosis of metastatic

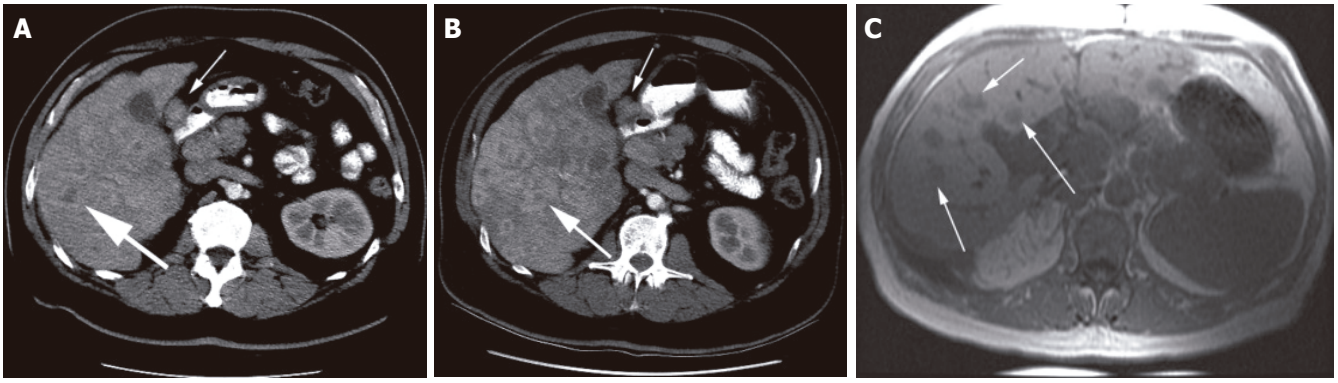

Figure 1 (A) Enhanced CT of the abdomen shows multiple hepatic metastases (big arrow) and lymphadenopathy of the gastrohepatic ligament (small arrow). **(B)** Follow-up CT, 2 mo later reveals an increase in size and number of liver metastases (big arrow) and persistent gastrohepatic ligament adenopathy (small arrow). **(C)** T1-weighed MR image performed 9 mo after transplantation shows the interval development of multiple liver metastases (arrows).

nonfunctional neuroendocrine tumor was eventually made. For the next six months the patient received somatostatin maintenance therapy at which point recurrent upper respiratory symptoms and severe abdominal discomfort developed. There were no carcinoid symptoms and the patient continued to work. A follow up CT scan of the abdomen revealed innumerable metastases throughout the liver (which had coalesced when compared to an examination performed 2 mo earlier) and increasing adenopathy within the gastrohepatic ligament (Figure 1B). Six months later, while on depot octreotide maintenance, he presented with bleeding esophageal varices, and frank hepatic encephalopathy. A metastatic work-up at that time revealed disease predominantly in the liver with additional sites of involvement in the pancreas (possibly an enlarging primary site) and questionable lesions in the chest.

His most recent MRI scan showed no change in tumor size although possibly there was more inferior vena cava obstruction.

The patient underwent orthotopic liver transplantation (OLT) without a pancreatic resection. His explant revealed a liver diffusely involved (approximately 60%) by low grade, neuroendocrine carcinoma with metastasis involving perihilar lymph nodes and cirrhosis. The patient was placed on Prograf and Ganciclovir. Octreotide was discontinued. The patient remained healthy for several months after the transplant and a follow up MRI at 3 mo did not reveal any malignancy until 12 mo later when he presented with pruritus, generalized fatigue and profound diminution in stamina. MRI of the liver confirmed metastasis (Figure 1C) as well as multiple pulmonary nodules and spinal lesions. He was retreated with somatostatin, initially subcutaneously and later by depot injections. However over the next 12 mo his condition deteriorated and despite treatment with Ytrium octreotide in an experimental protocol he ultimately expired 27 mo after liver transplantation.

DISCUSSION

Neuroendocrine tumors represent an unusual group of rare tumors due to their slow growth and ability to produce and secrete a multitude of peptide hormones and amines[30,31]. These substances give rise to different clinical syndromes related to the peptide production, such as the carcinoid syndrome, insulinoma syndrome, Zollinger-Ellison syndrome, glucagonoma syndrome, WDHA syndrome and somatostatinoma syndrome[31]. However, as in this case, many patients have nonfunctional tumors and present with hepatic metastases[30]. In most cases neuroendocrine metastases to the liver are located in both lobes. Gastrointestinal carcinoid tumors, especially those located in the small intestine or ascending colon, are the most common neuroendocrine tumors presenting with liver metastases. Gastrointestinal carcinoids and pancreatic neuroendocrine tumors have different degrees of malignant potential and frequency of liver metastases[32].

The therapeutic approach to hepatic metastases should consider the natural history of the disease and the progression and severity of symptoms caused by both hormone production and tumor mass[33]. In contrast to nonendocrine tumors, therapy for hepatic metastases from neuroendocrine tumors with liver transplantation is reasonable because the disease may be confined to the liver for extended periods and the growth is slow[13,34-36]. The presence of liver metastases from neuroendocrine tumors is a very important prognostic factor for decreased survival[37]. The 5-year survival rate in untreated patients is approximately 30%[38,39] and chemotherapy only prolongs life by a mean of 12-24 mo[40,41].

There have been several single-center (Table1) retrospective analyses and three multicenter restrospective studies[43,46,49] of liver transplantation in patients with liver metastases from neuroendocrine tumors. They are summarized in Table 1. However closer review of these reports reveals that some of the patients were part of more than one publication. Several tumor and patient characteristics influence the outcome following liver transplantation. A large retrospective study of 637 patients who underwent OLT between 1968 and 1991, observed that 67% of patients with carcinoid tumors had recurrence[42]. The authors concluded that patients with slowly growing metastatic neuroendocrine tumors might be suitable candidates for liver transplantation[42].

Table 1 Liver transplantation for metastatic neuroendocrine tumors

Author	Year	Number of patients	Actuarial survival (%)					Comments	Ref. no
			1 (yr)	2 (yr)	3 (yr)	4 (yr)	5 (yr)		
O'Grady	1987	2	nr	nr	nr	nr	nr	2 carcinoids, 1 death at 7 mo, 1 symptom free at 12 mo after LT	53
Makowka	1989	5	nr	nr	nr	nr	nr	3 alive 7, 16 and 34 mo after LT	35
Arnold	1989	4	nr	nr	nr	nr	nr	2 no recurrence 20, 38 moths after LT, 2 deaths 7, 8 mo (chronic rejection)	54
Bramley	1990	1	nr	nr	nr	nr	nr	VIP-oma, no tumor 12 mo after LT	55
Alsina	1990	2	nr	nr	nr	nr	nr	1 carcinoid and 1 PNT no symptoms 5, 13 mo after LT	56
Penn	1991	13	nr	nr	nr	nr	nr	9 carcinoids, 4PNT; 67%recurrence for carcinoids	42
Bechstein	1994	30	52	52	52	nr	nr	multicenter study; at the time of report: 57% alive, 43% dead, 30% recurrence, 70% no evidence of disease	43
Allessiani	1995	14	nr	nr	64	nr	nr	cluster transplantation, recurrence rate 45.5%	44
Routley	1995	11	82	nr	nr	nr	57	7 carcinoids, 2 PNT, 2 ET-primary unknown;6 alive (2 carcinoids) 8–106 mo after LT; 5 deaths(3 carcinoids) in 8–67 mo after LT	45
Curtiss	1995	3	nr	nr	nr	nr	nr	3 alive 12, 20, 30 mo after LT	57
Anthuber	1996	4	nr	nr	nr	nr	nr	4 deaths 10 days and 4, 8, 33 mo after LT	58
Dousset	1996	9	nr	nr	nr	nr	nr	4 carcinoids, 5 PNT; 3 (carcinoids) alive 15, 24, 62 mo after LT, 6 deaths 6, 7, 12, 83 days and 7, 8 mo after LT	59
Le Treut	1997	31	58	51	47	36	36	multicenter study, 11 centers in Europe; disease free survival: 45% at 1 yr, 29% at 3 yr, 17% at 5 yr after LT; higher survival for carcinoids (69% at 5 yr) than for non-carcinoids (8% at 4 yr)	46
Le Treut	1997	37	66	56	46	46	46	literature review, 14 centers, higher survival for non-carcinoids (83% at 2 yr) than carcinoids (34% at 2 yr)	46
Lang	1997	12	nr	nr	nr	nr	nr	9 alive-median survival 55 mo (4 no recurrence 2, 57, 58, 103.5 mo after LT)	47
Lehnert	1998	103	68	60	53	47	47	multicenter study; disease-free survival:60% at 1 yr, 48% at 2 yr, 42% at 3 yr, 42% at 3 yr,33% at 4 yr, 24% at 5 yr. favorable prognostic factors: age>50yr, limited operation (survival 65% at 5 yr).	48
Pilchmayr	1998	15	nr	nr	nr	nr	86.7	11 alive, 4 with no recurrence, the longest survival 10 yr after LT	49
Gottwald	1998	1	nr	nr	nr	nr	nr	Gastrinoma, alive with good liver function after LT	60
Frilling	1998	4	nr	nr	nr	nr	nr	3 carcinoids (2 alive,1 dead 32 d after LT), 1PNT(death 4 days after LT); 1 recurrence-free	61
Pascher	2000	4	nr	nr	nr	nr	nr	4 carcinoids; 2 deaths 14, 42 mo after LT, 2 alive 36, 76 mo after LT	62
Claure	2000	1	nr	nr	nr	nr	nr	1 carcinoid	63
Coppa	2001	9	100	100	100	70	70	Disease-free survival 53% at 5 yr	19
Ringe	2001	5	nr	nr	nr	nr	nr	4 alive (2 tumor-free survivals 4–25 mo after LT); 1 death 0.2 month after LT	64
Olausson	2002	9	89	nr	nr	nr	nr	5 PNT, 4 carcinoids; 7 OLT,2 MVT; 8 alive, 6 no evidence of disease, 4 recurrent tumors 9–36 mo after LT	29
Rosenau	2002	19	89	nr	nr	nr	80	Survival at 10 yr 50%;recurrence free survival 56% at 1 yr, 21% at 5 and 10 yr; survival 100% at 7 yr with Ki67<5% and regular E-cadherin staining; survival 0% at 7 yr with Ki67>5% and E-cadherin aberrant staining	50
Fernandez	2003	5	nr	nr	nr	nr	nr	2 alive and recurrence free 3, 6 yr after LT; 3 deaths 4, 10, 17 mo after LT	65
Amarapurkar	2003	14	nr	nr	nr	nr	nr	MIB-1 index >5%: recurrence at median 11 mo, survival median 13 mo MIB-1 index <5%: recurrence at median 69 mo, survival median 80.5 mo	66
Cahlin	2003	10	nr	80	nr	nr	nr	7 OLT, 3 MVT; 2 yr survival 100% for carcinoids; 67% for PNT; 2 yr disease-free survival 75% for carcinoids and 33% for PNT	51
Florman	2004	11	73	nr	nr	nr	36	1 patients disease-free at 5 yr after LT	52
Ahlman	2004	12	nr	nr	nr	nr	nr	8 after OLT alive at time of study, 2 after MVT died 4 mo after LT; other 2 after MVT with no recurrence at 8, 36 mo.	14

LT: liver transplantation; OLT: orthotopic liver transplantation; MVT: multivisceral transplantation; PNT: pancreatic endocrine tumors, nr: results not reported

These data were further supported by another experience on 30 patients from 14 centers who underwent OLT for metastatic neuroendocrine tumors[43]. It was noted that the actuarial survival, often combined with other upper abdominal resective procedures, for the entire group of patients was 52% after 1 year and remained stable for another 24 mo[43]. Overall, mortality during the first year after transplantation due to recurrent tumor was 17%[43]. The longest survival, 42 mo, was in a patient who died from recurrent carcinoid tumor[43]. Overall, at the time of this study 57% of patients were alive, 30% had developed recurrence, 43% had died and 70% did not have evidence of disease recurrence. Based on their observations they proposed that extrapancreatic primary neuroendocrine tumors be treated with radical hepatic resection followed by medical therapy and that the tumor response should be evaluated before considering liver transplantation[43]. Even the primary pancreatic primary tumors with slow growth that do not respond to medical therapy can be considered for liver transplantation but with a combination of a pancreatic resection procedure[43].

The role of abdominal cluster transplantation was best described in 57 patients presenting with primary or metastatic liver tumors[44]. Abdominal cluster transplantation for metastatic neuroendocrine liver tumors had a better 3-year survival rate (64%) than for patients who underwent this procedure due to sarcoma (44%), hepatocellular carcinoma (25%), cholangiocarcinoma (20%) and other adenocarcinomas (20%)[44]. OLT was found to be effective in controlling symptoms that were caused by carcinoid metastases to the liver[45]. The tumor recurrence was not necessarily associated with early recurrence of symptoms[45]. The patients with non-carcinoid tumors were found to have a higher likelihood of prolonged disease-free survival than those with carcinoid tumors[45]. On the other hand Le Treut *et al.* found significantly higher survival in patients with metastatic carcinoid tumors (80% after 1 year and 69% after 5 years) than in patients with non-carcinoid neuroendocrine tumors who underwent OLT (38% after 1 year and 8% after 4 years)[46]. However additional analysis of 37 cases of OLT for metastatic neuroendocrine tumors presented in the literature revealed significantly higher survival rates in patients with non carcinoid apudomas (83% after 2 years) than in patients with carcinoids (34% after 2 years)[46].

When liver transplantation was done only in cases with unresectable liver tumor, untreatable hormonal symptoms or massive tumor bulk[47] and without extrahepatic tumors at the time of transplantation, patients were observed to derive benefit from OLT[47]. A characteristic of the patients who did not have recurrence during follow up was that they had less than 40–50% tumor bulk in the explant. Thus, it has been suggested that OLT may be also regarded as curative treatment in some patients with neuroendocrine metastases who have relatively low tumor burden[47]. In contrast, Florman found only 1 rare case of 5-year disease free survival among 11 transplanted patients. Moreover, it was claimed that due to only few reports in the literature of 5-year disease free survival (4.6%), OLT cannot be considered as a curative procedure[48].

Other prognostic indicators that have been suggested include a limited operation and age of <50 years. Patients with such features had an overall 5-year survival of 65% and median survival of more than 8 years[49]. On the other hand, patients who underwent extended operations including upper abdominal exenteration or Whipple's operation had 1-year survival of 50% and 5-year survival of 31%[49]. Therefore, an extended operation (Whipple's operation, abdominal exenteration) and age≥50 years were considered as independent indicators of poor outcome and thus extensive surgery does not translate into better outcomes perhaps because of the high rate of post operative morbidity and mortality (10 of 11 patients with such features died after a median of 7 mo)[49]. Interestingly, location of the primary tumor, tumor histology and treatment with somatostatin were not found to be prognostic factors, although patients with primary tumors located in the pancreas or gastrinoma seemed to have poorer outcomes[49]. The outcome of liver transplantation showed a highly significant survival difference between patients with metastases from neuroendocrine tumors and other tumors such as colorectal carcinoma, melanoma, choriocarcinoma or pancreatic carcinoma[50]. The 5-year survival was 86.7% in patients with neuroendocrine metastases and 0% in patients with other malignancies[50].

Little is known about tumor markers as prognostic factors. It has been demonstrated that low tumor expression of the immunohistochemical marker, Ki67(<5%), and the adhesion molecule, E-cadherin, might be associated with a favorable outcome after liver transplantation for metastatic neuroendocrine tumors[51]. Patients (n = 12) with an increased expression of the markers, (Ki67≥5% positive cells and/or E-cadherin staining) showed decreased survival (median 46 mo) whereas patients (n = 5) with low expression of these markers showed increased survival (median 90 mo)[51]. It was also suggested that the combination of these two markers had an excellent specificity and sensitivity to predict a survival of 7 years after liver transplantation[51]. Further study showed that liver transplantation for metastatic well-differentiated neuroendocrine tumors with a low expression of protein Ki67 (Ki67<10%) resulted in relief of hormonal symptoms and long disease-free periods[14]. Another study suggested that MIB-1 antibody expression might have prognostic value in patients undergoing liver transplantation for metastatic carcinoid tumors[66]. The authors assessed the cell proliferative activity by MIB-1 antibody labeling in 14 patients with metastatic neuroendocrine liver tumors (7 carcinoids, 7 non-carcinoids) who underwent liver transplantation[66]. In this group, two patients remained alive and disease-free at 96 and 192 mo after liver transplantation[66]. MIB-1 index was calculated by dividing the number of tumor cells with positive staining for MIB-1 antibody by the total number of tumor cells[66]. It was shown that patients with a MIB-1 index of greater than 5% showed early tumor recurrence (median 11 mo) and shorter survival (median 13 mo)

whereas patients with a MIB-1 index of less than 5% showed late tumor recurrence (median 69 mo) and longer survival (median 80.5 mo)[66]. The low MIB-1 index (<5%) was found to have a sensitivity of 71% and a specificity of 83% for predicting survival of greater than 2 years[66].

Current knowledge about the role of liver transplantation for patients with neuroendocrine liver metastases indicates that liver transplantation should be considered only in selected individuals. Coppa *et al*. proposed that selection of patients with non-resectable metastatic neuroendocrine tumors for liver transplantation should be based on the Milan criteria: young patients (less than 50 years) with carcinoids confirmed by histology, with less than 50% of the liver replaced by metastases, with a primary tumor (originating from the gastrointestinal tract) drained by the portal venous system, an absence of extrahepatic disease and stable disease during the pretransplantation period[19]. In a group of nine patients who underwent liver transplantation based on these criteria the 5-year survival was 70% and the 5-year disease-free survival was 53%[19]. On the other hand, in the group of 20 patients who were treated by liver resection due to less advanced liver metastases, the 5-year survival was 67% and the 5 year disease-free survival was 29%[19]. Our patient had a 27 mo survival and the less than ideal outcome may have been because of some of the poor prognostic factors of age>50, tumor bulk exceeding 50%, and regional metastasis. Furthermore, whether immunosuppression after OLT has any effect on the rate of tumor recurrence or not is pure speculation. Thus, given the shortage of donor organs and the high rate of tumor recurrence, we currently believe that OLT should only be undertaken, when other therapeutic approaches including combinations of regional or systemic chemotherapy and hormone inhibitors together with partial hepatectomy have failed[64]. There is a need for prospective studies in large numbers of patients to fully evaluate the role of liver transplantation in patients with metastatic neuroendocrine tumors who may gain many years of effective palliation with careful selection. However, suboptimal outcomes may occur if case selection is compromised.

REFERENCES

1 **Metz DC,** Jensen RT. Endocrine tumors of the gastrointestinal tract and pancreas. In: Rustgi AK, ed. Gastrointestinal cancers. A companion to Sleisenger and Fordtran's Gastrointestinal and Liver Disease. *Edinburgh: Elsevier Science Ltd* 2003; 681-719

2 **Kloppel G,** Perren A, Heitz PU. The gastroenteropancreatic neuroendocrine cell system and its tumors: the WHO classification. *Ann N Y Acad Sci* 2004; **1014:** 13-27

3 **Oberg K,** Kvols L, Caplin M, Delle Fave G, de Herder W, Rindi G, Ruszniewski P, Woltering EA, Wiedenmann B. Consensus report on the use of somatostatin analogs for the management of neuroendocrine tumors of the gastroenteropancreatic system. *Ann Oncol* 2004; **15:** 966-973

4 **Modlin IM,** Sandor A. An analysis of 8305 cases of carcinoid tumors. *Cancer* 1997; **79:** 813-829

5 **Levi F,** Te VC, Randimbison L, Rindi G, La Vecchia C. Epidemiology of carcinoid neoplasms in Vaud, Switzerland, 1974-97. *Br J Cancer* 2000; **83:** 952-955

6 **Quaedvlieg PF,** Visser O, Lamers CB, Janssen-Heijen ML, Taal BG. Epidemiology and survival in patients with carcinoid disease in The Netherlands. An epidemiological study with 2391 patients. *Ann Oncol* 2001; **12:** 1295-1300

7 **Delcore R,** Friesen SR. Gastrointestinal neuroendocrine tumors. *J Am Coll Surg* 1994; **178:** 187-211

8 **McStay MKG,** Caplin ME: Carcinoid tumor. *Minerva Med* 2002; **93:** 389-401

9 **Norheim I,** Oberg K, Theodorsson-Norheim E, Lindgren PG, Lundqvist G, Magnusson A, Wide L, Wilander E. Malignant carcinoid tumors. An analysis of 103 patients with regard to tumor localization, hormone production, and survival. *Ann Surg* 1987; **206:** 115-125

10 **Jensen RT,** Norton JA. Pancreatic endocrine tumors. In: Feldman M, Friedman LS, Sleisenger MH, eds. Sleisenger and Fordtran's Gastrointestinal and liver disease. 7th ed. *Philadelphia: Saunders,* 2002: 988-1016

11 **McLoughlin JM,** Kuhn JA, Lamont JT. Neuroendocrine tumors of the pancreas. *Curr Treat Opin in Gastroenterol* 2004; **7:** 355-364

12 **Chamberlain RS,** Canes D, Brown KT, Saltz L, Jarnagin W, Fong Y, Blumgart LH. Hepatic neuroendocrine metastases: does intervention alter outcomes? *J Am Coll Surg* 2000; **190:** 432-445

13 **Frilling A,** Rogiers X, Malago M, Liedke O, Kaun M, Broelsch CE. Liver transplantation in patients with liver metastases of neuroendocrine tumors. *Transplant Proc* 1998; **30:** 3298-3300

14 **Ahlman H,** Friman S, Cahlin C, Nilsson O, Jansson S, Wangberg B, Olausson M. Liver transplantation for treatment of metastatic neuroendocrine tumors. *Ann N.Y Acad Sci* 2004; **1014:** 265-269

15 **Que F,** Nagorney DM, Batts KP, Linz LJ, Kvols LK. Hepatic resection for metastatic neuroendocrine carcinomas. *Am J Surg* 1995; **169:** 36-43

16 **Benevento A,** Boni L, Frediani L, Ferrari A, Dionigi R. Results of liver resection as treatment for metastases from noncolorectal cancer. *J Surg Oncol* 2000; **74:** 24-29

17 **Norton JA,** Warren RS, Kelly MC, Zuraek MB, Jensen RT. Aggresive surgery for metastatic neuroendocrine tumors. *Surgery* 2003; **134:** 1057-1065

18 **Sutcliffe R,** Maguire D, Ramage J, Rela M, Heaton N. Management of neuroendocrine liver metastases. *Am J Surg* 2004; **187**: 39-46

19 **Coppa J,** Pulvirent A, Schiavio M, Romito R, Collini P, Di Bartolomeo M, Fabbri A, Regalia E, Mazzaferro V. Resection versus transplantation for liver metastases from neuroendocrine tumors. *Transpl Proc* 2001; **33:** 1537-1539

20 **Miller CA,** Ellison EC. Therapeutic alternatives in metastatic neuroendocrine tumors. *Surg Oncol Clin N Am* 1998; **7:** 863-879

21 **Eriksson B,** Renstrup J, Imam H, Oberg K. High-dose treatment with lanreotide of patients with advanced neuroendocrine gastrointestinal tumors: clinical and biological effects. *Ann Oncol* 1997; **8:** 1041-1044

22 **Saltz L,** Trochanowski B, Buckley M, Heffernan B, Niedzwiecki D, Tao Y, Kelsen D. Octreotide as an antineoplastic agent in the treatment of functional and nonfunctional neuroendocrine tumors. *Cancer* 1993; **72:** 244-248

23 **Welin SV,** Janson ET, Sundin A, Stridsberg M, Lavenius E, Granberg D, Skogseid B, Oberg KE, Eriksson BK High-dose treatment with a long-acting somatostatin analogue in patients with advanced midgut carcinoid tumours. *Eur J Endocrinol* 2004; **151:** 107-112

24 **Arnold R,** Trautmann ME, Creutzfeldt W, Benning R, Benning M, Neuhaus C, Jurgensen R, Stein K, Schafer H, Bruns C, Dennler HJ. Somatostatin analogue octreotide and inhibition of tumour growth in metastatic endocrine gastroenteropancreatic tumours. *Gut* 1996; **38:** 430-438

25 **Imam H,** Eriksson B, Lukinius A, Janson ET, Lindgren PG, Wilander E, Oberg K. Induction of apoptosis in neuroendocrine tumors of the digestive system during treatment with somatostatin analogs.*Acta Oncol* 1997; **36:**

607-614
26 **Chatal JF,** Le Bodic MF, Kraeber-Bodere F, Rousseau C, Resche I. Nuclear medicine applications for neuroendocrine tumors. *World J Surg* 2000; **24:** 1285-1289
27 **De Jong M,** Valkema R, Jamar F, Kvols LK, Kwekkeboom DJ, Breeman WA, Bakker WH, Smith C, Pauwels S, Krenning EP. Somatostatin receptor-targeted radionuclide therapy of tumors: preclinical and clinical findings. *Semin Nucl Med* 2002; **32:** 133-140
28 **Wangberg B,** Wetsberg G, Tylen U, Tisell LE, Jansson S, Nilsson O, Johansson V, Schersten T, Ahlman H. Survival of patients with disseminated midgut carcinoid tumors after aggressive tumor reduction. *World J Surg* 1996; **20:** 892-896
29 **Olausson M,** Friman S, Cahlin C, Nilsson O, Jansson S, Wangberg B, Ahlman H: Indications and resuls of liver transplantation in patients with neuroendocrine tumors. *World J Surg* 2002; **26:** 998-1004
30 **Sarmiento JM,** Que FG. Hepatic surgery for metastases from neuroendocrine tumors. *Surg Oncol Clin N Am* 2003; **12:** 231-242
31 **Eriksson B,** Oberg K, Stridsberg M. Tumor markers in neuroendocrine tumors. *Digestion* 2000; **62**(suppl1):33-38
32 **Ihse I,** Persson B, Tibblin S: Neuroendocrine metastases of the liver. *World J Surg* 1995; **19:** 76-82
33 **Lang H,** Schlitt HJ, Schmidt H, Flemming P, Nashan B, Scheumann GFW, Oldhafer KJ, Manns MP, Raab R. Total hepatectomy and liver transplantation for metastatic neuroendocrine tumors of the pancreas- a single center experience with ten patients. *Langenbecks Arch Surg* 1999; **384:** 370-377
34 **Rosado B,** Gores GJ. Liver transplantation for neuroendocrine tumors:progress and uncertainty. *Liver Transplantation* 2004; **10:** 712-713
35 **Makowka L,** Tzakis AG, Mazzaferro V, Teperman L, Demetris J, Iwatsuki S, Starzl TE. Transplantation of the liver for metastatic endocrine tumors of the intestine and pancreas. *Surg Gynec Obst* 1989; **168:** 107-111
36 **El Rassi ZS,** Ferdinand L, Mohsine RM, Berger F, Lombard-Bohas C, Boillot O, Partensky CCM. Primary and secondary liver endocrine tumors:clinical presentation, surgical approach and outcome. *Hepato-Gastroenterology* 2002; **49:** 1340-1346
37 **Weber C,** Venzon DJ, Lin JT, Fishbein VA, Orbuch M, Strader DB, Gibril F, Metz DC, Fraker DL, Norton JA, Jensen RT. Determinants of metastatic rate and survival in patients with Zollinger-Ellison syndrome: a propsective long-term study. *Gastroenterology* 1995; **108:** 1637-1649
38 **Moertel CG.** Karnofsky memorial lecture. An odyssey in the land of small tumors. *J Clin Oncol* 1987; **5:** 1503-1522
39 **Soreide O,** Berstad T, Bakka A, Schrumpf E, Hanssen LE, Engh V, Bergan A, Flatmark A. Surgical treatment as a principle in patients with advanced abdominal carcinoid tumors. *Surgery* 1992; **111:** 48-54
40 **Moertel CG,** Kvols LK, O'Connell MJ, Rubin J. Treatment of neuroendocrine carcinomas with combined etoposide and cisplatin. Evidence of major therapeutic activity in the anaplastic variants of these neoplasms. *Cancer* 1991; **68:** 227-232
41 **Moertel CG,** Lefkopoulo M, Lipsitz S, Hahn RG, Klaassen D. Streptozocin-doxorubicin, streptozocin-fluorouracil or chlorozotocin in the treatment of advanced islet-cell carcinoma. *N Engl J Med* 1992; **326:** 519-523
42 **Penn I.** Hepatic transplantation for primary and metastatic cancers of the liver. *Surgery* 1991; **110:** 726-734
43 **Bechstein WO,** Neuhaus P. Liver transplantation for hepatic metastases of neuroendocrine tumors. *Ann N Y Ac Sci* 1994; **733:** 507-514
44 **Alessiani M,** Tzakis A, Todo S, Demetris AJ, Fung JJ, Starzl TE.Assessment of five-year experience with abdominal organ cluster transplantation. *J Am Coll Surg* 1995; **180:** 1-9
45 **Routley D,** Ramage JK, McPeake J, Tan KC, Williams R. Orthotopic liver transplantation in the treatment of metastatic neuroendocrine tumors of the liver. *Liver Transpl Surg* 1995; **1:** 118-121
46 **Le Treut YP,** Delpero JR, Dousset B, Cherqui D, Segol P, Mantion G, Hannoun L, Benhamou G, Launois B, Boillot O, Domergue J, Bismuth H. Results of liver transplantation in the treatment of metastatic neuroendocrine tumors. A 31-case French multicenter report. *Ann Surg* 1997; **225:** 355-364
47 **Lang H,** Oldhafer KJ, Weimann A,Schlitt HJ, Scheumann GFW, Flemming P, Ringe B, Pichlmayr R. Liver transplantation for metastatic neuroendocrine tumors. *Ann Surg* 1997; **225:** 347-354
48 **Florman S,** Toure B, Kim L, Gondolesi G, Roayaie S, Krieger N, Fishhein T, Emre S, Miller C, Schwartz M. Liver transplantation for neuroendocrine tumors. *J Gastrointest Surg* 2004; **8:** 208-212
49 ***Lehnert T.*** Liver transplantation for metastatic neuroendocrine carcinoma: An analysis of 103 patients. *Transplantation* 1998; **66:** 1307-1312
50 **Pichlmayr R,** Weimann A, Oldhafer KJ, Schlitt HJ, Tusch G, Raab R. Appraisal of transplantation for malignant tumors of the liver with special reference to early stage hepatocellular carcinoma. *Eur J Surg Oncol* 1998; **24:** 60-67
51 **Rosenau J,** Bahr MJ, von Wasielewski R, Mengel M, Schmidt HHJ, Nashan B, Lang H, Klempnauer J, Manns MP, Boeker KH. Ki67, e-cadherin, and p53 as prognostic indicators of long-term outcome after liver transplantation for metastatic neuroendocrine tumors. *Transplantation* 2002; **73:** 386-394
52 **Cahlin C,** Friman S, Ahlman H, Backman L, Mjornstedt L, Lindner P, Herlenius G, Olausson M. Liver transplantation for metastatic neuroendocrine tumor disease. *Transplant Proc* 2003; **35:** 809-810
53 **O'Grady JG,** Polson RJ, Rolles K, Calne RY, Williams R. Liver transplantation for malignant disease. Results in 93 consecutive patients. *Ann Surg* 1988; **207:** 373-379
54 **Arnold JC,** O'Grady JG, Bird GL, Calne RY, Williams R. Liver transplantation for primary and secondary hepatic apudomas. *Br J Surg* 1989; **76:** 248-249
55 **Bramley PN,** Lodge JP, Losowsky MS, Giles GR. Treatment of metastatic Vipoma by liver transplantation. *Clin Transplant* 1990; **4:** 276-278
56 **Alsina AE,** Bartus S, Hull D, Rosson R, Schweizer RT. Liver transplant for metastatic neuroendocrine tumor. *J Clin Gastroenterol* 1990; **12:** 533-537
57 **Curtiss SI,** Mor E, Schwartz ME, Sung MW, Hytiroglou P, Thung SN, Sheiner PA, Emre S, Miller CM. A rational approach to the use of hepatic transplantation in the treatment of metastatic neuroendocrine tumors. *J Am Coll Surg* 1995; **180:** 184-187
58 **Anthuber M,** Jauch KW, Briegel J, Groh J, Schildberg FW. Results of liver transplantation for gastroenteropancreatic tumor metastases. *World J Surg* 1996; **20:** 73-76
59 **Dousset B,** Saint-Marc O, Pitre J, Soubrane O, Houssin D, Chapuis Y. Metastatic endocrine tumors: medical treatment, surgical resection, or liver transplantation. *World J Surg* 1996; **20:** 908-914
60 **Gottwald T,** Koveker G, Busing M, Lauchart W, Becker HD. Diagnosis and management of metastatic gastrinoma by multimodality treatment including liver transplantation: report of a case. *Surg Today* 1998; **28:** 551-558
61 **Frilling A,** Rogiers X, Malago M, Liedke O, Kaun M, Broelsch CE. Liver transplantation in patients with liver metastases of neuroendocrine tumors. *Transplant Proc* 1998; **30:** 3298-3300
62 **Pascher A,** Steinmuller T, Radke C, Hosten N, Wiedenmann B, Neuhaus P, Bechstein WO. Primary and secondary hepatic manifestation of neuroendocrine tumors. *Langenbecks Arch Surg* 2000; **385:** 265-270
63 **Claure RE,** Drover DD, Haddow GR, Esquivel CO, Angst MS. Orthotopic liver transplantation for carcinoid tumour

metastatic to the liver: anesthetic management. *Can J Anaesth* 2000; **47:** 334-337

64 **Ringe B, Lorf T,** Dopkens K, Canelo R. Treatment of hepatic metastases from gastroenteropancreatic neuroendocrine tumors: Role of liver transplantation. *World J Surg* 2001; **25:** 697-699

65 **Fernandez JA,** Robles R, Marin C, Hernandez Q, Sanchez Bueno F, Ramirez P, Rodriguez JM, Lujan JA, Navalon JC, Parrilla P. Role of liver transplantation in the management of metastatic neuroendocrine tumors.*Transplant Proc* 2003; **35:** 1832-1833

66 **Amarapurkar AD,** Davies A, Ramage JK, Stangou AJ, Wight DGD, Portmann BD. Proliferation of antigen MIB-1 in metastatic carcinoid tumours removed at liver transplantation: revelance to prognosis. *Eur J Gastroenterol Hepatol* 2003; **15:** 139-143

Science Editor Guo SY **Language Editor** ELsevier HK

PO Box 2345, Beijing 100023, China
www.wjgnet.com
wjg@wjgnet.com

ELSEVIER

World J Gastroenterol 2005;11(48):7684-7685
World Journal of Gastroenterology ISSN 1007-9327

• *CASE REPORT* •

Successful outcome following resection of a pancreatic liposarcoma with solitary metastasis

IM Dodo, JA Adamthwaite, P Jain, A Roy, PJ Guillou, KV Menon

IM Dodo, JA Adamthwaite, P Jain, A Roy, PJ Guillou, KV Menon, Department of Academic Surgery, St James's University Hospital, Leeds, West Yorkshire LS9 7TF, United Kingdom
Correspondence to: Mr KV Menon, Consultant Hepatobiliary Surgeon, St James's University Hospital, Leeds LS9 7TF, United Kingdom. kvmenon@aol.com
Telephone: +44-113-2064036 Fax: +44-113-2066416
Received: 2004-12-30 Accepted: 2005-02-18

Abstract

Liposarcomas are rare soft tissue tumors, commonly affecting the lower limbs and less commonly the retroperitoneum. Although other organs can be affected, the pancreas is one of the rarest, and metastasis at presentation has never been reported. We describe the case of a 76-year-old gentleman presenting with abdominal pain and an abdominal mass. Imaging confirmed a primary tumor in the body and tail of the pancreas, with a metastatic deposit in the mesentery adjacent to the second part of the duodenum. Biopsy confirmed a liposarcoma, and subsequently a complete surgical excision was achieved. He then received adjuvant radiotherapy and has remained disease free for the next 26 mo.

Key words: Pancreas; Liposarcoma; Metastasis

Dodo IM, Adamthwaite JA, Jain P, Roy A, Guillou PJ, Menon KV. Successful outcome following resection of a pancreatic liposarcoma with solitary metastasis. *World J Gastroenterol* 2005; 11(48): 7684-7685
http://www.wjgnet.com/1007-9327/11/7684.asp

INTRODUCTION

Primary retroperitoneal neoplasms account for only 0.1-0.2% of all malignancies. Liposarcoma is a rare mesenchymal tumor that occurs most commonly in the soft tissues of the extremities, but other sites such as the retroperitoneum can also be involved. Retroperitoneal liposarcomas grow slowly and silently. Prognosis is poor due to relapse, so only complete excision, which is often difficult, produces a 'cure'[1]. There are only four cases of pancreatic liposarcoma in the literature. To our knowledge, this is the first reported case of metastatic pancreatic liposarcoma at the time of presentation, with successful outcome following surgery.

CASE REPORT

A 76-year-old retired civil engineer presented with a 1-mo history of abdominal pain. He had anorexia associated with significant weight loss. His medical history was unremarkable. He was a smoker and drank a moderate amount of alcohol. On examination he was cachectic and had a large, firm, but non-tender, upper abdominal mass. All blood results including tumor markers (CEA, CA 19.9, AFP, CA125) were within the normal limits. Abdominal ultrasound showed two large masses adjacent to the pancreas. CT scan revealed a 20-cm mass in the mesentery adjacent to the second part of the duodenum, and an 8-cm tumor of the body and tail of the pancreas (Figure 1). The appearances were suggestive of liposarcoma, and this was confirmed by CT-guided core biopsy.

At laparotomy, he had a primary tumor (9 cm×6 cm ×2.5 cm) (Figure 2A) in the distal body and tail of the pancreas attached to the spleen and a further tumor (27 cm ×20 cm×10 cm) (Figure 2B) adjacent to the second part of the duodenum, not infiltrating the bowel or the pancreas. He underwent distal pancreatectomy with splenectomy and the second lesion, which was encapsulated, was completely enucleated. His post-operative recovery was slow with the development of sepsis and a pancreatic fistula, which was managed conservatively with drainage.

Histology of both masses demonstrated a well differentiated sclerosing liposarcoma (Figure 3A) with an area within the primary mass of dedifferentiation (Trojani grade 3) (Figure 3B). The patient received adjuvant radiotherapy and was under follow-up with abdominal CT every 6 mo. At 26 mo, there was no evidence of recurrence and he remained asymptomatic.

DISCUSSION

Liposarcomas are intermediate (locally aggressive) malignant mesenchymal tumor comprising 16-18% of all malignant soft tissue tumors in adults[2]. The incidence is the same in the USA and Europe, with a slight male preponderance[2]. These tumors can grow slowly by direct invasion and can metastasize to the lungs, liver and other viscera[3]. Histologically they can be classified into well differentiated (WD), myxoid, round cell poorly differentiated myxoid and pleomorphic[4,5].

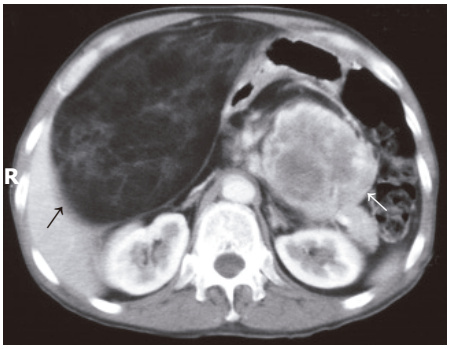

Figure 1 Abdominal CT showing the primary tumor in the body and tail of the pancreas (white arrow) and the solitary metastasis in the mesentery adjacent to the duodenum (black arrow).

Figure 2 The primary tumor (right) and its solitary metastasis (left) after removal.

WD liposarcomas are the commonest, accounting for approximately 40-45%[6]. WD liposarcomas can in turn be subdivided morphologically into four main subtypes: adipocytic, sclerosing, inflammatory and spindle cell. This case was a WD sclerosing liposarcoma, which ranks second in frequency, and is most often seen in retroperitoneal and paratesticular lesions[6].

WD liposarcomas show no potential for metastasis unless they undergo dedifferentiation. Dedifferentiation occurs in up to 10%, with 90% arising *de novo* and the rest in recurrences. Risk of dedifferentiation appears higher with deep-seated (particularly retroperitoneal) lesions and is markedly less in the limbs. This is probably a time-dependant phenomenon. However, it is often impossible to obtain a wide surgical resection margin and local recurrence is almost inevitable and often leads to death[6].

Retroperitoneal liposarcomas produce non-specific symptoms and are often extensive on diagnosis[1]. Most tumors occur at 40-60 years of age, though they may appear at any time. The etiology of these tumors is unknown, although trauma or radiation exposure has been suggested. CT scan is good at characterizing the lesions and aspiration cytology is recommended to differentiate from other pancreatic neoplasms[2]. Pancreatic liposarcomas are very rare with eventual metastases reported in 30-60% of cases[3]. Regardless of cell type, aggressive surgical excision offers the best chance of cure[3]. Some patients may benefit from adjuvant radiotherapy and less commonly chemotherapy. This patient had successful resection of the primary tumor and a giant metastasis followed by adjuvant radiotherapy, and had remained disease free. Prognosis depends on tumor location and histological type[2]. Reported 5-year survival following surgical excision varies from 41%[3] to 50%[4]. Radiotherapy can increase the duration of remission after incomplete excision and possibly achieve clinical cure[3].

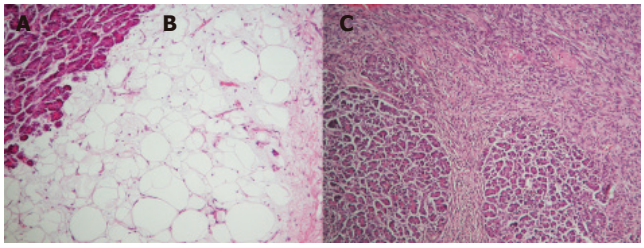

Figure 3 Microphotographs of the primary tumor. **A:** Normal pancreatic tissue; **B:** well-differentiated sclerosing liposarcoma; **C:** area of dedifferentiation.

CONCLUSION

Aggressive resection combined with adjuvant radiotherapy should be considered for metastatic pancreatic liposarcomas when feasible as this offers the best chance of cure and follow-up is essential.

REFERENCES

1 **Osmanagaoglu MA,** Bozkaya H, Ozeren M, Cobanoglu U. Primary retroperitoneal liposarcoma. *Eur J Obstet Gynecol Reprod Biol* 2003; **109:** 228-230
2 **Amano H,** Harima K, Aibe T, Nagatomi Y, Kawashima M, Maetani N, Azuma M, Ariyama S, Fuji T, Kawamura S, Takemoto T. A case of pancreatic liposarcoma (author's transl). *Nippon Shokakibyo Gakkai Zasshi* 1981; **78:** 1475-1479
3 **Elliott TE,** Albertazzi VJ, Danto LA. Pancreatic liposarcoma: case report with review of retroperitoneal liposarcomas. *Cancer* 1980; **45:** 1720-1723
4 **Milano C,** Colombato LA, Fleischer I, Boffi A. Liposarcoma of the pancreas. Report of a clinical case and review of the literature. *Acta Gastroenterol Latinoam* 1988; **18:** 133-138
5 **Choux R,** Andrac L, Rodriguez M, Masselot R, Hassoun J. Liposarcoma of the pancreas. Study of a case including ultrastructure. *Ann Anat Pathol (Paris)* 1979; **24:** 251-259
6 **Dei Tos AP, Pedeutour F.** Atypical lipomatous tumor/Well differentiated liposarcoma and Dedifferentiated liposarcoma. In: Fletcher CDM, Unni K, Mertens K eds. *Pathology and genetics of tumors of soft tissue and bone*. Lyon: IARC Press 2000: 35-39

Science Editor Wang XL and Guo SY **Language Editor** Elsevier HK

PO Box 2345, Beijing 100023, China
www.wjgnet.com
wjg@wjgnet.com

ELSEVIER

World J Gastroenterol 2005;11(48):7686-7687
World Journal of Gastroenterology ISSN 1007-9327

• *CASE REPORT* •

Recurrent severe gastrointestinal bleeding and malabsorption due to extensive habitual megacolon

Ingo Mecklenburg, Markus Leibig, Christof Weber, Stefan Schmidbauer, Christian Folwaczny

Ingo Mecklenburg, Christian Folwaczny, Department of Gastroenterology and Endoscopy, Medizinische Poliklinik, Ludwig-Maximilians-University, Munich, Germany
Markus Leibig, Department of Cardiology, Medizinische Poliklinik, Ludwig-Maximilians-University, Munich, Germany
Christof Weber, Institute for Clinical Radiology, Klinikum Innenstadt, Ludwig-Maximilians-University, Munich, Germany
Stefan Schmidbauer, Department of Surgery, Klinikum Innenstadt, Ludwig-Maximilians-University, Munich, Germany
Correspondence to: Dr. Christian Folwaczny, Medizinische Poliklinik, Klinikum Innenstadt, Ludwig-Maximilians-University, Pettenkoferstr. 8a, 80336 Munich, Germany. christian.folwaczny@med.uni-muenchen.de
Telephone: +49-89-5160-2625 Fax: +49-89-5160-4187
Received: 2005-03-01 Accepted: 2005-08-03

Abstract

Dilatation of the colon and the rectum, which is not attributable to aganglionosis, is a rare finding and can be the result of intractable chronic constipation. We report a rare case of a 29-year-old male patient with impressive megacolon, in whom Hirschsprung's or Chagas disease was ruled out. In the present case, dilatation of the colon was most likely due to a behavioral disorder with habitual failure of defecation. Chronic stool retention led to a bizarre bulging of the large bowel with displacement of the other abdominal organs and severe occult blood loss. Because of two episodes of life-threatening gastrointestinal bleeding despite conventional treatment of constipation, a surgical approach for bowel restoration was necessary. Temporary loop ileostomy had to be performed for depressurization of the large bowel and the subsequent possibility for effective antegrade colonic lavage to remove impacted stools. Shortly after the operation, the patient was healthy and could easily manage the handling of the ileostomy. However, the course of the megacolon in this young adult cannot be predicted and the follow-up will have to reveal if regression of this extreme colonic distension with reestablishment of regular rectal perception will occur.

Key words: Gastrointestinal bleeding; Malabsorption; Habitual megacolon

Mecklenburg I, Leibig M, Weber C, Schmidbauer S, Folwaczny C. Recurrent severe gastrointestinal bleeding and malabsorption due to extensive habitual megacolon. *World J Gastroenterol* 2005; 11(48): 7686-7687
http://www.wjgnet.com/1007-9327/11/7686.asp

INTRODUCTION

Occult gastrointestinal bleeding is a frequent actuality in human beings, likewise is a temporary absence after drinking beer on the "Oktoberfest" in Munich. We report the case of a young male with the unusual combination of both conditions.

CASE REPORT

A 29-year-old male patient collapsed at the "Oktoberfest" after consumption of a small beer and was admitted to our emergency department. The patient was pale and displayed hemoglobin of 30 g/L despite normal blood pressure and heart rate. On clinical examination, cachexia and an obvious distension of the abdomen with slight pain in the epigastrium and the periumbilical region were noted. The digital rectal exam revealed black stools with positive guaiac testing, but the patient denied gross rectal bleeding in the past. The patient has seldom bowel movements (every third day) and denotes the absence of the urge for defecation. He has recently lost his job as a janitor because of permanent fatigue and decreasing tolerance to work. Furthermore, he reported an unclassified "bowel disease" since early childhood and a "dilatation" of the colon which had been performed during infancy. Two years ago, iron deficiency anemia had been treated at another hospital but repeated attempts for colonoscopy had failed because of stool residues in the colon despite lavage for several days at that time.

After transfusion, a diagnostic procedure was performed in addition to the severe anemia and the laboratory tests revealed significant iron deficiency with a ferritin level of 6 μg/L and transferrin saturation of 4.5%. Serum potassium and albumin were decreased to 2.13 mmol/L and 28 g/L, respectively. The abdominal CT scan showed massive dilatation of the rectum and the left-sided colon (Figures 1A and B) with displacement of the other organs. A colonoscopy could not be performed because of persistent masses of stools in the colon even after prolonged bowel lavage. An upper gastrointestinal endoscopy demonstrated regular mucosa without evidence for celiac disease or a bleeding source in the proximal gastrointestinal tract. A radionuclide bleeding

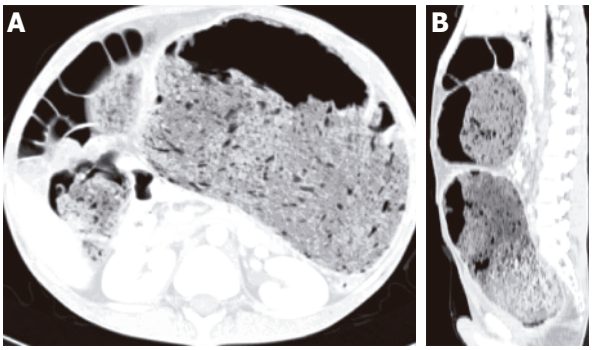

Figure 1 A: Axial CT image of the abdomen; **B:** Saggital CT reconstruction of the abdomen.

scan was negative for an apparent bleeding source. Rectal manometry demonstrated regular arbitrary contraction and a normal reflectory relaxation of the anal sphincter. A dynamic MR defecography revealed again a massive dilatation of the distal colon with complete failure of emptying on command. The histological examination of a rectal biopsy demonstrated chronic proctitis with pseudomelanosis and explicit verification of submucous ganglions excluding Hirschsprung's disease (aganglionosis). Chagas' disease was ruled out by serology. A pathological H2-glucose breath test showed signs for a bacterial overgrowth of the small bowel and significant osteopenia was documented by measurement of the bone density by dual X-ray densitometry.

Initially, we aimed at relieving the chronic constipation by regular administration of polyethylene glycol. However, distention of the colon was even progressive and gastrointestinal bleeding continued. Therefore, a temporary loop ileostomy was performed and about 12 kg of stools could be removed by antegrade colonic lavage. A CT scan 3 wk after surgery demonstrated declining of the colonic dilatation with a marked decrease of abdominal distension. The postoperative course was uneventful and the patient's fitness improved significantly. He received intravenous iron and vitamin supplementation and due to the bacterial overgrowth antibiotic treatment with metronidazole was initiated. Subsequently lower gastrointestinal bleeding subsided and a repeat colonoscopy showed regular mucosa in the right colon with atrophic appearance of the mucosa in the left colon. The patient was motivated to perform stool training aiming at the establishment of a normal rectal perception.

DISCUSSION

Dilatation of the colon and the rectum, which is not attributable to aganglionosis[1] is a rare finding and can be the result of intractable chronic constipation[2]. Herein we report a rare case of a young adult with impressive megacolon, in whom Hirschsprung's or Chagas disease was ruled out. In the present case dilatation of the colon is likely to be due to a behavioral disorder with habitual failure of defecation. Chronic stool retention led to a bizarre bulging of the large bowel with displacement of the other abdominal organs. Occult gastrointestinal bleeding has not been described in patients with megacolon, but in our patient dilation of the colonic wall presumably resulted in occult blood loss. The exact bleeding source could not be localized by a radionuclide bleeding scan, thus the intensity of bleeding was supposed to be low. The low hemoglobin value was well tolerated by the patient; therefore, the anemia was most likely due to a chronic blood loss. However, the patient had previously experienced two episodes of life-threatening gastrointestinal bleeding despite conventional treatment of constipation; consequently, a surgical approach for bowel restoration appeared feasible.

A further concern in this patient was the apparent malabsorption with low levels of albumin, severe iron deficiency and osteoporosis. Distension of the colon with subsequent stasis can lead to small bowel bacterial overgrowth, as demonstrated in patients with megacolon due to Chagas disease[3]. Restoration of the small bowel by antibiotic treatment would be a futile approach as long as the underlying stasis of the bowel is not corrected. Therefore, a temporary loop ileostomy was performed for depressurization of the large bowel and the subsequent possibility for effective antegrade colonic lavage to remove impacted stools[4].

In the present case, the indication for surgical intervention was delicate, because ileostomy does not affect the underlying behavioral disorder and includes the risk for a complete unlearning of defecation. Furthermore, the development of a diversion colitis is a possible sequelae[5]. Nevertheless, shortly after the operation the patient was healthy and could easily manage the handling of the ileostomy. However, the course of the megacolon in this young adult cannot be predicted and the follow-up will have to reveal if regression of this extreme colonic distension with re-establishment of regular rectal perception will occur.

REFERENCES

1 **Puri P**, Shinkai T. Pathogenesis of Hirschsprung's disease and its variants: recent progress. *Semin Pediatr Surg* 2004; **13:** 18-24
2 **Rajagopal A**, Martin J. Giant fecaloma with idiopathic sigmoid megacolon: report of a case and review of the literature. *Dis Colon Rectum* 2002; **45**: 833-835
3 **Guimaraes Quintanilha AG**, Azevedo dos Santos MA, Avila-Campos MJ, Saad WA, Pinotti HW, Zilberstein B. Chagasic megacolon and proximal jejunum microbiota. *Scand J Gastroenterol* 2000; **35**: 632-636
4 **Stabile G**, Kamm MA, Hawley PR, Lennard-Jones JE. Results of stoma formation for idiopathic megarectum and megacolon. *Int J Colorectal Dis* 1992; **7:** 82-84
5 **Edwards CM**, George B, Warren B. Diversion colitis--new light through old windows. *Histopathology* 1999; **34:** 1-5

Science Editor Guo SY **Language Editor** Elsevier HK

PO Box 2345, Beijing 100023, China
www.wjgnet.com
wjg@wjgnet.com

ELSEVIER

World J Gastroenterol 2005;11(48):7688-7689
World Journal of Gastroenterology ISSN 1007-9327

• *CASE REPORT* •

Does *Fasciola hepatica* infection modify the response of acute hepatitis C virus infection to IFN-α treatment?

Mehmet Sahin, Mehmet Isler, Altug Senol, Mustafa Demirci, Zeynep Dilek Aydın

Mehmet Sahin, Altug Senol, Zeynep Dilek Aydın, Department of Internal Medicine, Suleyman Demirel University, School of Medicine, Isparta, Turkey
Mehmet Isler, Department of Internal Medicine, Division of Gastroenterology, Suleyman Demirel University, School of Medicine, Isparta, Turkey
Mustafa Demirci, Department of Microbiology and Parasitology, Suleyman Demirel University, School of Medicine, Isparta, Turkey
Correspondence to: Mehmet Sahin, MD, SDU Tıp Fakultesi, Ic Hastalıkları BD, Isparta, Turkey. mehmetsahin66@hotmail.com
Telephone: +90-246-211-26-13 Fax: +90-246-237-02-40
Received: 2004-09-21 Accepted: 2004-12-01

Abstract

Immunologic response to acute hepatitis C is mainly a Th1 response, whereas fasciolopsiasis is associated with a diverse T-cell response. Interferon-alpha has immunomodulatory effects and enhances Th1 immune response. Fasciola infection could theoretically interfere with the Th1 immune response, even when acquired after an initial response to interferon-alpha treatment for acute hepatitis C virus (HCV) infection. We report here the case of a male patient who acquired *Fasciola hepatica* infection after an initial response to IFN-alpha therapy with a favorable outcome

Key words: Hepatitis C; Interferon; *Fasciola hepatica*

Sahin M, Isler M, Senol A, Demirci M, Aydın ZD. Does *Fasciola hepatica* infection modify the response of acute hepatitis C virus infection to IFN-α treatment? *World J Gastroenterol* 2005; 11(48): 7688-7689
http://www.wjgnet.com/1007-9327/11/7688.asp

INTRODUCTION

Hepatitis C virus (HCV) infection is a common cause of hepatocellular injury associated with complex immunologic mechanisms including both humoral and cell-mediated responses. Acute hepatitis C infection especially produces a Th1 response[1]. Fasciolopsiasis, like other helminth infections, is associated with the induction of T-cell responses particularly the Th2 subtype[2]. Enhanced induction of Th2 cytokines and downregulation of Th1 responses during infection with *Fasciola hepatica* could be expected to interfere with the natural course of and the response to the treatment of acute viral hepatitis C. The concurrence of HCV and *F. hepatica* infection is uncommon and whether *F. hepatica* infection acquired during IFN-α therapy has any effect on HCV replication is unknown.

CASE REPORT

A 50-year-old male patient, with chronic renal failure began hemodialysis 3 mo ago. Prior to initiation of hemodialysis, liver function tests were normal and serological tests for hepatitis B and C were negative. During the 3rd mo of hemodialysis, laboratory evaluation showed elevations of 183 IU/L AST (normal, 5-45 IU/L), 394 IU/L ALT (normal, 5-45 IU/L), 141 IU/L GGT (normal, 0-50 IU/L), and 90 IU/L ALP (normal, 53-128 IU/L). Physical examination was normal. Abdominal ultrasonography showed normal liver size with grade II heterogeneity, normal portal vein size and no ascites. Anti-HCV antibody and HCV RNA were positive. Anti-HAV IgM, HBs Ag, and anti HIV were negative.

The patient was diagnosed with acute viral hepatitis C. IFN-α 2b (Intron A; Schering Plough Corporation, Kenilworth, NJ, USA) was started 3 MU thrice weekly subcutaneously for 12 mo. ALT levels normalized during the 4th wk of the therapy. HCV RNA was negative after 6 mo.

After 6 mo of treatment with IFN-α, the patient reported marked malaise and right upper quadrant abdominal pain. Physical examination revealed right hypochondrium tenderness. Repeated liver function tests showed elevations of ALT (51 IU/L), ALP (196 IU/L), and GGT (272 IU/L). WBC were 6 800/mm^3 with marked eosinophilia (20%). Abdominal ultrasonography showed hepatomegaly and a well-defined 9-mm hyperechoic round mass in the anterior–superior segment of the right hepatic lobe which raised the suspicion of hemangioma and the possibility of *F. hepatica*. The causes of eosinophilia were investigated in the 9th mo of IFN-α therapy. Serology for fasciolopsiasis revealed positivity by enzyme-linked immunosorbent assay (ELISA) prepared against a secretory antigen according to Carnevale *et al*.[3]. The assay was reported to have 100% sensitivity and 100% specificity. ELISA absorbance value of the patient's sera was 2 900 units, while the cut-off value was 380. Stool specimens were negative for ova and parasites of *F. hepatica*. Oral triclabendazole (10 mg/kg), twice daily

doses was initiated for fasciolopsiasis. One week after the initiation of triclabendazole (10th mo of IFN therapy), the patient reported to have right upper abdominal pain and was hospitalized. Physical examination showed abdominal tenderness on the upper right quadrant and a positive Murphy's sign. Laboratory tests showed elevations of serum total and direct bilirubin which were 2.28 mg/L (normal, 0.2-1 mg/L) and 2.24 mg/L (normal, 0.1-0.5 mg/L), respectively in addition to elevations of ALT (58 IU/L), AST (53 IU/L), GGT (333 IU/L), and ALP (399 IU/L). WBC were 11 700/mm^3 with 10% eosinophilia. Abdominal ultrasonography revealed no intraparenchymal lesion in the liver, thickening of gallbladder wall and a hyperechoic round mass measured 10 mm in the gallbladder. Intra and extrahepatic bile ducts were normal. The patient's condition improved after 48 h of intravenous fluids and antibiotics.

Twenty-four months after the initiation of IFN-α treatment, liver function tests and complete blood count were normal with 2% eosinophilia. Stool specimen for fasciola was negative. HCV RNA was negative. The patient continued his regular hemodialysis schedule.

DISCUSSION

An effective host response against a viral infection requires coordinated efforts by both nonspecific and antigen-specific immune responses. Cytokines play a key role in the cell-to-cell communication necessary for this process. Immediately after viral infection, several antigen nonspecific effector mechanisms are activated[4].

Among the individuals who recover from acute HCV infection, Th1 subtype responses predominate and are necessary for complete recovery in acute HCV infection[5,6]. Lechmann *et al*.[7] found that cellular immune responses against a panel of HCV core-derived peptides are stronger than humoral immune responses in individuals who have recovered from acute HCV infection. Also, experimental models reveal that rats with resolved acute hepatitis C have a higher proportion of cells producing Th1 subtype cytokines. Parasitic infections are frequently accompanied with a downregulation of cell-mediated immunity. Parasitic infections can exert bystander suppression of protective Th1 responses to infection and liver flukes may secrete molecules that down-regulate Th1 responses[2]. In an experimental model, Miriam *et al*.[8] showed that Th1 response to *Bordetella pertussis* antigens is markedly suppressed following infection with *F. hepatica*. Kamal *et al*.[9] showed that patients with acute hepatitis C and schistosomiasis coinfection cannot clear viremia and show rapid progression once chronic infection is established. In contrast, in the present case, the clinical and serological response marked by the clearance of HCV-RNA was maintained though the acquisition of *F. Hepatica*. This favorable outcome may be related to immunomodulatory effects of IFN-α therapy. IFN-α induces the production of certain cytokines and has been recognized as a cytokine promoting Th1 differentiation[10,11]. In addition, it increases cytotoxic activity of natural killer cells, cytotoxic T lymphocytes and macrophages[12]. Recent data suggest that early treatment of acute HCV infection with IFN-α may be highly effective in preventing chronic hepatitis C infection[13].

In conclusion, the present case illustrates that acute hepatitis C is responsive to the treatment even in the coexistence of fasciolopsiasis.

REFERENCES

1 **Jacobson Brown PM**, Neuman MG. Immunopathogenesis of hepatitis C viral infection: Th1/Th2 responses and the role of cytokines. *Clin Biochem* 2001; **34:** 167-171

2 **O'Neill SM**, Brady MT, Callanan JJ, Mulcahy G, Joyce P, Mills KH, Dalton JP. Fasciola hepatica infection downregulates Th1 responses in mice. *Parasite Immunol* 2000; **22:** 147-155

3 **Carnevale S**, Rodriguez MI, Santillan G, Labbe JH, Cabrera MG, Bellegarde EJ, Velasquez JN, Trgovcic JE, Guarnera EA. Immunodiagnosis of human fascioliasis by an enzyme-linked immunosorbent assay (ELISA) and a micro-ELISA. *Clin Diagn Lab Immunol* 2001; **8:** 174-177

4 **Foster GR**. Interferons in host defense. *Semin Liver Dis* 1997; **17**: 287-295

5 **Koziel MJ**. The role of immune responses in the pathogenesis of hepatitis C virus infection. *J Viral Hepat* 1997; **4 Suppl 2:** 31-41

6 **Woitas RP**, Lechmann M, Jung G, Kaiser R, Sauerbruch T, Spengler U. CD30 induction and cytokine profiles in hepatitis C virus core-specific peripheral blood T lymphocytes. *J Immunol* 1997; **159**: 1012-1018

7 **Lechmann M**, Ihlenfeldt HG, Braunschweiger I, Giers G, Jung G, Matz B, Kaiser R, Sauerbruch T, Spengler U. T- and B-cell responses to different hepatitis C virus antigens in patients with chronic hepatitis C infection and in healthy anti-hepatitis C virus--positive blood donors without viremia. *Hepatology* 1996; **24:** 790-795

8 **Brady MT**, O'Neill SM, Dalton JP, Mills KH. Fasciola hepatica suppresses a protective Th1 response against Bordetella pertussis. *Infect Immun* 1999; **67:** 5372-5378

9 **Kamal SM**, Rasenack JW, Bianchi L, Al Tawil A, El Sayed Khalifa K, Peter T, Mansour H, Ezzat W, Koziel M. Acute hepatitis C without and with schistosomiasis: correlation with hepatitis C-specific CD4(+) T-cell and cytokine response. *Gastroenterology* 2001; **121**: 646-656

10 **Dianzani F**. Biological basis for the clinical use of interferon. *Gut* 1993; **34**: 74-76

11 **Eui-Young So**, Hyun-Hee Park and Choong-Eun Lee. IFN-gamma and IFN-α posttranscriptionally down-regulate the IL-4 induced IL-4 receptor gen expression. *J Immunol* 2000; **165**: 5472-5479

12 **Rook G**. Immunity to viruses, bacteria and fungi. In:Roitt I, Brostoff J, Male D, eds. *Immunology. London: Mosby* 1993; **3**: 15-22

13 **Jaeckel E**, Cornberg M, Wedemeyer H, Santantonio T, Mayer J, Zankel M, Pastore G, Dietrich M, Trautwein C, Manns MP. Treatment of acute hepatitis C with interferon alfa-2b. *N Engl J Med* 2001; **345:** 1452-1457

Science Editor Wang XL and Guo SY **Language Editor** Elsevier HK

PO Box 2345, Beijing 100023, China
www.wjgnet.com
wjg@wjgnet.com

ELSEVIER

World J Gastroenterol 2005;11(48):7690-7693
World Journal of Gastroenterology ISSN 1007-9327

• *CASE REPORT* •

Autosomal dominant polycystic liver disease in a family without polycystic kidney disease associated with a novel missense protein kinase C substrate 80K-H mutation

Ramón Peces, Joost PH Drenth, Rene HM te Morsche, Pedro González, Carlos Peces

Ramón Peces, Section of Nephrology, Hospital General La Mancha-Centro, Alcázar de San Juan, Ciudad Real and Service of Nephrology, Hospital Universitario La Paz, Madrid, Spain
Joost PH Drenth, Rene HM te Morsche, Department of Medicine, Division of Gastroenterology and Hepatology, Radboud University Nijmegen Medical Center, Nijmegen, The Netherlands
Pedro González, Section of Digestive Hospital General La Mancha-Centro, Alcázar de San Juan, Ciudad Real, Spain
Carlos Peces, Computer Science Superior School, Castilla La Mancha University and Technology Area of the Castilla La Mancha Health Service (SESCAM), Ciudad Real, Spain
Supported by a grant from the Instituto de Ciencias de la Salud, Consejería de Sanidad de Castilla La Mancha (Grant EQ03016). Joost PH Drenth is a recipient of a NOW-VIDI grant
Correspondence to: Dr Ramón Peces, Servicio de Nefrología, Hospital Universitario La Paz, Paseo de la Castellana 261, 28046 Madrid, Spain. cpeces@varnet.com
Telephone: +34-917277224 Fax: +34-917277133
Received: 2004-12-12 Accepted: 2005-06-16

Abstract

Polycystic liver disease (PLD) is characterized by the presence of multiple bile duct-derived epithelial cysts scattered in the liver parenchyma. PLD can manifest itself in patients with severe autosomal dominant polycystic kidney disease (ADPKD). Isolated autosomal dominant polycystic liver disease (ADPLD) is genetically distinct from PLD associated with ADPKD, although it may have similar pathogenesis and clinical manifestations. Recently, mutations in two causative genes for ADPLD, independently from ADPKD, have been identified. We report here a family (a mother and her daughter) with a severe form of ADPLD not associated with ADPKD produced by a novel missense protein kinase C substrate 80K-H (PRKCSH) mutation (R281W). This mutation causes a severe phenotype, since the two affected subjects manifested signs of portal hypertension. Doppler sonography, computed tomography (CT) and magnetic resonance (MR) imaging are effective in documenting the underlying lesions in a non-invasive way.

Key words: ADPLD; Hepatic cysts; Hepatocystin; Inferior vena cava compression; Polycystic liver disease; Portal hypertension

Peces R, Drenth JPH, te Morsche RHM, González P, Peces C. Autosomal dominant polycystic liver disease in a family without polycystic kidney disease associated with a novel missense protein kinase C substrate 80K-H mutation. *World J Gastroenterol* 2005; 11(48): 7690-7693
http://www.wjgnet.com/1007-9327/11/7690.asp

INTRODUCTION

Proof of existence of autosomal dominant polycystic liver disease (ADPLD) as a distinct genetic entity, independently from autosomal dominant polycystic kidney disease (ADPKD), stems from three studies in which isolated familial polycystic liver disease (PLD) was shown to be unlinked to the PKD1 or PKD2 loci[1-3]. In 2000, Reynolds *et al*.[4] identified a locus for ADPLD on chromosome 19p13.2-13.1. In 2003, two independent groups demonstrated that mutations in *PRKCSH*, encoding the β-subunit of glucosidase II, a N-linked glycan-processing enzyme in the endoplasmic reticulum, cause isolated ADPLD[5,6]. Given its role in the pathogenesis of ADPLD, this protein has been renamed as hepatocystin[5]. Very recently, Davila *et al*.[7] found that mutations in *SEC63* (chromosome 6q21), encoding a component of the protein translocation machinery in the endoplasmic reticulum, also cause ADPLD. Mutations in *PRKCSH* and *SEC63* probably account for less than one-third of ADPLD cases, indicating that there is at least one more locus associated with this disease[7,8].

We have reported here the first Spanish family with a severe form of ADPLD not associated with ADPKD. The proband manifested displacement of abdominal structures by a massively enlarged liver causing portal hypertension and inferior vena cava compression.

CASE REPORT

A 36-year-old woman presented with a long history of abdominal enlargement. She had two pregnancies and live births at 29 and 34 years of age, respectively. Physical examination showed a bulging abdomen with a palpable mass extending from the right hemiabdomen to the left quadrant reaching 10 cm below the umbilicus. Laboratory data showed 0.9 mg/dL creatinine (normal range 0.6-1.2 mg/dL), 7.2 g/dL total proteins (normal range 6-8 g/dL), 137 mg/dL total cholesterol (normal range 140-220 mg/dL), 30 mg/dL triglycerides (normal range 50-128 mg/dL), 29 IU/L aspartate

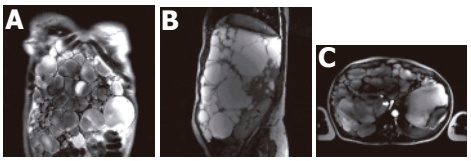

Figure 1 Massive polycystic liver disease on coronal MR imaging (**A**), caudal and posterior displacement of abdominal organs by the massively enlarged liver on sagittal MR imaging (**B**), and compression of the inferior vena cava (arrow) produced by the massively enlarged liver (**C**) on MR angiograph.

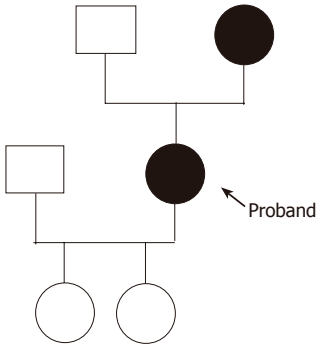

Figure 2 Family pedigree of the patient.

aminotransferase (normal range 10-40 IU/L), 22 IU/L alanine aminotransferase (normal range 10-40 IU/L), 135 IU/L gamma glutamyl transpeptidase (normal range 10-40 IU/L), 117 IU/L alkaline phosphatase (normal range 40-105 IU/L), 1.1 mg/dL total bilirubin (normal range 0.1-1.0 mg/dL), 82% prothrombin time and 394 mg/dL fibrinogen (normal range 200-400 mg/dL). Sonography and computed tomography (CT) of the abdomen were compatible with an increased liver volume caused by numerous hepatic cysts of various sizes. Magnetic resonance (MR) imaging of the abdomen revealed a massive polycystic liver with caudal and posterior displacement of the abdominal organs (Figures 1A and B). Doppler sonography and MR angiography demonstrated displacement of the kidneys and their vascular structures by the massively enlarged polycystic liver. The celiac axis was also displaced and the portal vein and a segment of the inferior vena cava below the hepatic veins were compressed by the hepatic cysts (Figure 1C). The kidneys were normal except for two small cortical cysts on the left kidney. There were signs of moderate portal hypertension with varices in the hepatic hilum. Seven years after the diagnosis, the patient was healthy and free of complications. Currently she is awaiting a liver transplantation.

Family history revealed that the patient's mother also had PLD without kidney disease. The father was not known to suffer from liver or kidney disease. The proband's daughters had no renal or hepatic cysts. The family pedigree is represented in Figure 2. The proband's mother (age 72 years) had a history of cholecystectomy in 1983 (performed in another hospital) and a diagnosis of heterozygous beta thalassemia minor in 1990. She had one daughter. Laboratory data showed 37% hematocrit (normal range 36-46%), 12.2 g/dL hemoglobin (normal range

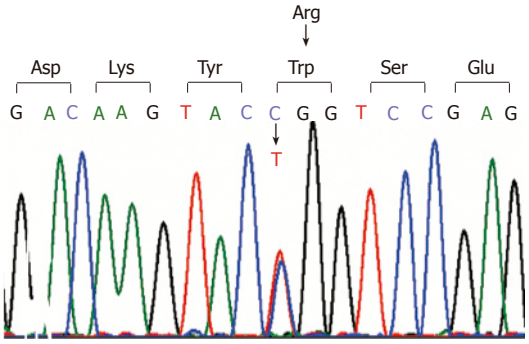

Figure 3 Sequence identification of the C>T changes in exon 10. This mutation, C841T which is predicted to change the amino acid composition of hepatocystin, changes arginine to tryptophan at codon 281 (R281W).

12-16 g/dL), 66.6 fL MCV (80-100 fL), 21.8 pg MCH (normal range 26-34 pg), 5.9% hemoglobin A2 (normal range 2-3.5%), 3 500/μL white blood cell with normal differentiation, 105 000/mm^3 platelet count, 0.6 mg/dL creatinine, 6.9 g/dL total proteins, 177 mg/dL total cholesterol, 101 mg/dL triglycerides, 31 IU/L aspartate aminotransferase, 19 IU/L alanine aminotransferase, 14 IU/L gamma glutamyl transpeptidase, 109 IU/L alkaline phosphatase, 2.1 mg/dL total bilirubin, 79% prothrombin time and 362 mg/dL fibrinogen. Ultrasonography and CT of the abdomen demonstrated PLD. There were signs of portal hypertension with varices in the hepatic hilum, gastrohepatic ligament, and lower esophagus. The spleen was enlarged, measuring 17.6 cm in length. The kidneys were normal. The patient was healthy and had no variceal bleeding. She refused any invasive procedure.

DNA sequencing and mutation detection

DNA was isolated from peripheral blood leukocytes by standard procedures. We performed polymerase chain reaction amplification using specific primer sets for all the 18 exons that constitute the open reading frame of *PRKCSH*. We determined the nucleotide sequences of the amplified fragments by fluorescence sequencing with dye-terminator chemistry on an ABI3700 capillary sequencer (Perkin-Elmer Applied Biosystems).

RESULTS

Sequence analysis of PRKCSH gene from DNA isolated from the proband demonstrated a base pair change (C>T) on one allele at position 841 (Figure 3). This mutation located in exon 10 resulted in a change of the amino acid composition of hepatocystin with the replacement of arginine to tryptophan at codon (R281W). The missense mutation was also present in the affected mother of the proband but not in her two children. Within hepatocystin, the mutation was located between the EF-hand calcium-binding domain, ending at codon 234 and the glutamic acid-rich region which starts at codon 299 (Figure 4). Hepatocystin, the protein product of PRKCSH, comprises 528 amino acid residues and has a predicted molecular mass of approximately 59 ku. This protein contains a signal peptide for translocation across the endoplasmic

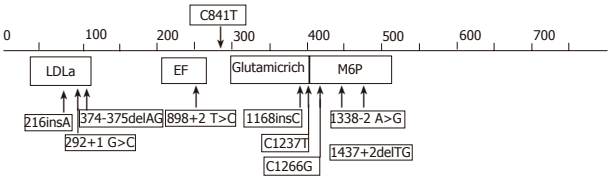

Figure 4 Schematic representation of hepatocystin. The position of *PRKCSH* mutations that have been associated with PCLD are superimposed on the structure of hepatocystin. The new mutation detected in our family is indicated on top. The numbers reflect the amino acid numbering of hepatocystin. LDLa: low-density lipoprotein receptor domain A; EF: EF-hand calcium-binding domains; MPR: mannose 6-phosphate receptor domain.

Table 1 Missense PRKCSH mutation detected in our family

	278			279			280			281		
Species	Asp			Lys			Tyr			Arg		
HS	G	A	C	A	A	G	T	A	C	C	G	G
BT	G	A	C	A	A	G	T	A	C	C	G	G
MM	G	A	C	A	A	G	T	A	C	C	G	C
RN	G	A	C	A	A	G	T	A	C	C	G	C
Patients	G	A	C	A	A	G	T	A	C	**T**	G	G

HS: *Homo sapiens*; BT: *Bos Taurus*; MM: *Mus musculus*, RN: *Rattus norvegicus*. The C841T *PRKCSH* mutation detected in this study is indicated in bold, and for comparison the corresponding nucleotides from various species are included. The numbers on top correspond with the codon numbering of hepatocystin, while Asp is aspartic acid; Lys is lysine; Tyr is tyrosine; Arg is arginine. Note that the C at position 841 is highly conserved among the species.

reticulum membrane, a low-density lipoprotein receptor domain class A (LDLa) domain, two EF-hand domains, a glutamic-acid-rich region, a mannose-6-phosphate receptor domain and a conserved C-terminal HDEL amino acid sequence for endoplasmic reticulum retention. Hepatocystin is an endoplasmic reticulum-resident enzyme that is involved in carbohydrate processing and quality control of newly synthesized glycoproteins.

DISCUSSION

ADPLD is a rare autosomal dominant disorder that has been described in fewer than 50 families from Finnish[8], Dutch[5], American[4], Belgian[2], and Spanish-Belgian[3] ancestry. The pathology of ADPLD consists of numerous cysts of biliary epithelial origin spread throughout the liver parenchyma. This disease is distinct from ADPKD1 and ADPKD2, in which affected individuals develop bilateral renal cysts and liver and pancreatic cysts in advanced cases[9-11]. Cystic liver disease occurs in a substantial portion of patients with ADPKD and end-stage renal disease. Factors influencing the prevalence of PLD in ADPKD include female sex, age (prevalence of PLD is 10% in the third decade, but 60% in patients older than 60 years), and pregnancy (multiparity is associated with increased size and number of cysts in ADPKD)[12].

The recent cloning of the gene involved in ADPLD has greatly facilitated the possibility of a firm molecular diagnosis in our family. Up to now, a total of nine different *PRKCSH* mutations have been described[13,14]. We detected a novel missense *PRKCSH* mutation (R281W) in our family. Several lines of evidence suggest that the R281W represents a bona fide disease causing mutation. First, there is segregation of the mutation with the disease in our family. Second, arginine, a positively charged amino acid is replaced by tryptophan which is neutral. Lastly, the C at position 841 is highly conserved among the species (Table 1).

As is the case for ADPKD, ADPLD is clinically and genetically heterogeneous[8-14]. Although isolated PLD is genetically distinct from PLD associated with ADPKD, both diseases may have similar pathogenesis and clinical manifestations. If ADPLD, like ADPKD[15], occurs by a cellular recessive, two-hit mechanism, then mutations in either *PRKCSH* or *SEC63* will result in loss of proper folding of integral membrane or secreted glycoproteins in bile duct cells that have undergone somatic second hits[7,13,14]. However, the two-hit model has not been investigated in isolated PLD.

The clinical profile of PLD has been defined by Qian *et al*.[16] who on the basis of a small series concluded that extra hepatic manifestations are infrequent but may include simple renal cysts, intracranial aneurysms, and mitral valve abnormalities. Genotype-phenotype relations remain speculative at this point. Liver cysts are usually asymptomatic, and as a consequence, the disease may go undetected and is likely to be underdiagnosed in the general population[17]. Symptoms occurred are caused by the mass effect of the cysts, or the development of complications such as hemorrhage, infection, or rupture of cysts. Symptoms caused by the mass effect of the cysts include vague abdominal distension, early satiety, dyspnea, and back pain. Rarely, ascites can form because of hepatic venous outflow obstruction by cysts. Lower extremity edema is secondary to extrinsic compression of the inferior vena cava, hepatic veins, or portal vein by large or by many small or medium size hepatic cysts. Compression of the bile ducts can cause jaundice. The symptoms of compression or thrombosis of the inferior vena cava may be obscure and a high index of suspicion is required for the diagnosis[18]. Liver metabolic and synthetic functions remain normal, although an increase in serum levels of alkaline phosphatase, bilirubin and gamma glutamyl transpeptidase, and a decrease in serum levels of total cholesterol and triglycerides have been described in some cases[16]. The factors that affect disease progression are unclear. However, some risk factors for the progression of the disease are age, sex, number of pregnancies, and use of estrogen[14,16].

The proband manifested a massively enlarged liver, which caused abdominal heaviness and progressive hemodynamic changes. She presented displacement of abdominal structures by the massively enlarged liver and hepatic cysts not only caused extrinsic compression of the inferior vena cava, but also were responsible for portal hypertension. Whereas laboratory studies in the proband disclosed a slight increase in the serum levels of alkaline phosphatase and gamma glutamyl transpeptidase, and a decrease in serum levels of total cholesterol and triglycerides, the proband's mother presented thrombocytopenia and a slight increase in total bilirubin.

As the proband's history shows, the disease may become highly symptomatic in young women. The more severe extensive development of the condition in the proband than in her affected mother contrasts with the reported greater severity of the liver involvement with age. The increased severity of the disease in the proband could be in relation, at least in part, with repeated pregnancies in this patient. However, other possible factors for the progression of the disease remain unknown. Screening of the at-risk members of the families of other affected patients could help to answer this question.

The presence of (few) renal cysts, as demonstrated in our proband who had 2 renal cysts does not preclude the diagnosis ADPLD. This is in accord with the data from another study that demonstrated *PRKCSH* mutations in four patients with polycystic livers who possessed at least one renal cyst[14].

Most patients with PLD require no treatment. In highly symptomatic patients, percutaneous cyst aspiration, sclerosis and cyst fenestration may be indicated[16]. In patients with diffuse cystic liver, hepatic resection[19] is often the only possibility but entails a high mortality rate. Stent placement in the inferior vena cava has been successfully applied in a few well-selected patients with only inferior vena cava compression. In patients with severe phenotype, liver transplantation should be considered[20]. In our patients, due to the size of their liver, resection of the lobes of their livers for decompression was deemed to be problematic and liver transplantation was considered as the better option in the proband.

In summary, we have described here a family with a severe form of ADPLD not associated with ADPKD, and a novel *PRKCSH* mutation that was vertically transmitted. The two affected subjects manifested signs of portal hypertension. This family underlines the need for a careful investigation of patients with otherwise unexplained liver cystic disease, focusing on whether other organ systems are involved. It also stresses the importance of accurate family investigation whenever possible. Doppler sonography, CT, and MR are effective in documenting the underlying lesions non-invasively.

ACKNOWLEDGMENTS

We thank the family members for their great cooperation.

REFERENCES

1 **Somlo S**, Torres VE, Reynolds D, King BF, Nagorney DM. Autosomal dominant polycystic liver disease without polycystic kidney disease is not linked to either the PKD1 or PKD2 gene loci [abstract]. *J Am Soc Nephrol* 1995; **6:** 727A

2 **Pirson Y**, Lannoy N, Peters D, Geubel A, Gigot JF, Breuning M, Verellen-Dumoulin C. Isolated polycystic liver disease as a distinct genetic disease, unlinked to polycystic kidney disease 1 and polycystic kidney disease 2. *Hepatology* 1996; **23:** 249-252

3 **Iglesias DM**, Palmitano JA, Arrizurieta E, Kornblihtt AR, Herrera M, Bernath V, Martin RS. Isolated polycystic liver disease not linked to polycystic kidney disease 1 and 2. *Dig Dis Sci* 1999; **44:** 385-388

4 **Reynolds DM**, Falk CT, Li A, King BF, Kamath PS, Huston J 3rd, Shub C, Iglesias DM, Martin RS, Pirson Y, Torres VE, Somlo S. Identification of a locus for autosomal dominant polycystic liver disease, on chromosome 19p13.2-13.1. *Am J Hum Genet* 2000; **67:** 1598-1604

5 **Drenth JP**, te Morsche RH, Smink R, Bonifacino JS, Jansen JB. Germline mutations in PRKCSH are associated with autosomal dominant polycystic liver disease. *Nat Genet* 2003; **33:** 345-347

6 **Li A**, Davila S, Furu L, Qian Q, Tian X, Kamath PS, King BF, Torres VE, Somlo S. Mutations in PRKCSH cause isolated autosomal dominant polycystic liver disease. *Am J Hum Genet* 2003; **72:** 691-703

7 **Davila S**, Furu L, Gharavi AG, Tian X, Onoe T, Qian Q, Li A, Cai Y, Kamath PS, King BF, Azurmendi PJ, Tahvanainen P, Kaariainen H, Hockerstedt K, Devuyst O, Pirson Y, Martin RS, Lifton RP, Tahvanainen E, Torres VE, Somlo S. Mutations in SEC63 cause autosomal dominant polycystic liver disease. *Nat Genet* 2004; **36:** 575-577

8 **Tahvanainen P**, Tahvanainen E, Reijonen H, Halme L, Kaariainen H, Hockerstedt K. Polycystic liver disease is genetically heterogeneous: clinical and linkage studies in eight Finnish families. *J Hepatol* 2003; **38:** 39-43

9 **Coto E**, Sanz de Castro S, Aguado S, Alvarez J, Arias M, Menendez MJ, Lopez-Larrea C. DNA microsatellite analysis of families with autosomal dominant polycystic kidney disease types 1 and 2: evaluation of clinical heterogeneity between both forms of the disease. *J Med Genet* 1995; **32:** 442-445

10 **Ariza M**, Alvarez V, Marin R, Aguado S, Lopez-Larrea C, Alvarez J, Menendez MJ, Coto E. A family with a milder form of adult dominant polycystic kidney disease not linked to the PKD1 (16p) or PKD2 (4q) genes. *J Med Genet* 1997; **34:** 587-589

11 **Torres VE**, Harris PC. Autosomal dominant polycystic kidney disease. *Nefrologia* 2003; **23 Suppl 1:** 14-22

12 **Everson GT**, Taylor MR, Doctor RB. Polycystic disease of the liver. *Hepatology* 2004; **40:** 774-782

13 **Drenth JP**, Martina JA, Te Morsche RH, Jansen JB, Bonifacino JS. Molecular characterization of hepatocystin, the protein that is defective in autosomal dominant polycystic liver disease. *Gastroenterology* 2004; **126:** 1819-1827

14 **Drenth JP**, Tahvanainen E, te Morsche RH, Tahvanainen P, Kaariainen H, Hockerstedt K, van de Kamp JM, Breuning MH, Jansen JB. Abnormal hepatocystin caused by truncating PRKCSH mutations leads to autosomal dominant polycystic liver disease. *Hepatology* 2004; **39:** 924-931

15 **Watnick TJ**, Torres VE, Gandolph MA, Qian F, Onuchic LF, Klinger KW, Landes G, Germino GG. Somatic mutation in individual liver cysts supports a two-hit model of cystogenesis in autosomal dominant polycystic kidney disease. *Mol Cell* 1998; **2:** 247-251

16 **Qian Q**, Li A, King BF, Kamath PS, Lager DJ, Huston J 3rd, Shub C, Davila S, Somlo S, Torres VE. Clinical profile of autosomal dominant polycystic liver disease. *Hepatology* 2003; **37:** 164-171

17 **Peces R**, González P, Venegas JL. Enfermedad poliquística hepática no asociada a poliquistosis renal autosómica dominante. *Nefrología* 2003; **23:** 454-458

18 **Peces R**, Gil F, Costero O, Pobes A. Trombosis masiva de la vena cava inferior secundaria a compresión por quistes hepáticos en un paciente con poliquistosis renal autosómica dominante. *Nefrología* 2002; **22:** 75-78

19 **Yang GS**, Li QG, Lu JH, Yang N, Zhang HB, Zhou XP. Combined hepatic resection with fenestration for highly symptomatic polycystic liver disease: A report on seven patients. *World J Gastroenterol* 2004; **10:** 2598-2601

20 **Gustafsson BI**, Friman S, Mjornstedt L, Olausson M, Backman L. Liver transplantation for polycystic liver disease--indications and outcome. *Transplant Proc* 2003; **35:** 813-814

Science Editor Wang XL and Guo SY **Language Editor** Elsevier HK

PO Box 2345, Beijing 100023, China
www.wjgnet.com
wjg@wjgnet.com

ELSEVIER

World J Gastroenterol 2005;11(48):7694-7696
World Journal of Gastroenterology ISSN 1007-9327

• *CASE REPORT* •

Robotic-assisted laparoscopic resection of ectopic pancreas in the posterior wall of gastric high body: Case report and review of the literature

Sheng-Der Hsu, Hurng-Sheng Wu, Chien-Long Kuo, Yueh-Tsung Lee

Sheng-Der Hsu, Division of General Surgery, Department of Surgery, Tri-Service General Hospital, National Defense Medical Center, Taipei, Taiwan, China
Chien-Long Kuo, Department of Pathology, Show-Chwan Memorial Hospital, Changhua, Taiwan, China
Hurng-Sheng Wu, Division of General Surgery, Department of Surgery, Tri-Service General Hospital, National Defense Medical Center, Taipei, Taiwan; Division of General Surgery, Department of Surgery, Show-Chwan Memorial Hospital, Changhua, Taiwan, China
Yueh-Tsung Lee, Division of General Surgery, Department of Surgery, Show-Chwan Memorial Hospital, Changhua, Taiwan, China
Correspondence to: Dr Yueh-Tsung Lee, Division of General Surgery, Department of Surgery, Show-Chwan Memorial Hospital, No. 325, Sec. 2, Cheng-Kung Road, Neihu 114, Taipei, Taiwan, China. f1233j@yahoo.com.tw
Telephone: +886-2-8792-7191
Received: 2005-01-24 Accepted: 2005-06-18

Abstract

Minimally invasive surgery has revolutionized the treatment of gastrointestinal tumors. Submucosal tumors of the stomach can be resected using laparoscopic techniques. We report here a case of ectopic pancreas tissue in the gastric wall that was removed using robotic-assisted laparoscopic resection. The patient was a 15-year-old female who presented with abdominal discomfort and tarry stools. Laboratory analysis showed iron deficiency anemia. Preoperative endoscopy revealed a submucosal lesion in the posterior wall of the gastric high body. Intraoperative upper endoscopy clearly located the lesion. A robotic-assisted laparoscopic wedge resection of the putative gastric submucosal tumor was performed. The pathology results showed an ectopic pancreas. The patient had an uneventful recovery and we believe that this is a valid treatment option for this benign condition.

Key words: Robotic surgery; Ectopic pancreas

Hsu SD, Wu HS, Kuo CL, Lee YT. Robotic-assisted laparoscopic resection of ectopic pancreas in the posterior wall of gastric high body: Case report and review of the literature. *World J Gastroenterol* 2005; 11(48): 7694-7696
http://www.wjgnet.com/1007-9327/11/7694.asp

INTRODUCTION

Ectopic pancreas is relatively rare and is definite as abnormally situated pancreatic tissue has no contact with the normal pancreas, and has its own ductal system and blood supply[1]. It is a rare entity and is usually an incidental finding in clinical practice. Most patients with an ectopic pancreas are asymptomatic, and if present, symptoms are nonspecific and depend upon the site of the lesion and different complications are encountered. Heterotopic pancreatic tissue has been found in several abdominal and intrathoracic locations, most frequently in the stomach (25-60%) or duodenum (25-35%)[2]. We report here a successful robotic-assisted laparoscopic wedge resection of a putative gastric submucosal tumor in a 15-year-old female.

CASE REPORT

A 15-year-old adolescent girl presented with intermittent epigastric pain with tarry stools for about 10 mo. She did not have any history of gastrointestinal cancer. The familial and personal history was nothing special. Laboratory findings showed iron deficiency anemia that prompted further gastrointestinal evaluation. The results of abdominal sonography and colonoscopy were negative. Panendoscopy revealed a submucosal lesion in the posterior wall of the gastric high body (Figure 1). The submucosal lesion measured about 1.5 cm in diameter. Pathological evaluation of a biopsy sample revealed chronic gastritis and mucosal hyperplasia. Biopsies collected with endoscopic techniques often do not provide the representative histologic sample needed for further therapeutic decisions. Because a malignant etiology could not be ruled out, a laparoscopic-endoscopic approach was considered to be appropriate for a curative and definitive diagnosis and minimally invasive for the resection of a localized gastric submucosal tumor.

The initial trocar was inserted at the umbilicus, using the Hasson technique. A pneumoperitoneum was created with carbon dioxide. In total, four trocars were inserted in the upper abdomen. The abdominal cavity was fully explored, during which robotic-assisted laparoscopic procedures were performed using the Zeus robot system. The greater omentum was detached from the greater curvature of the stomach with a harmonic scalpel, and the lesser sac was entered (Figure 2).

A clearly localized tumor mass was identified with

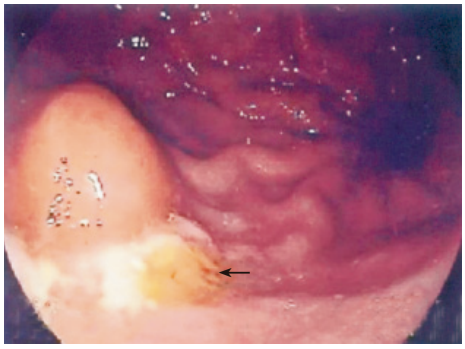

Figure 1 One submucosal lesion about 1.5 cm in diameter with a round surface on the area of the posterior wall of gastric high body with mucosal ulceration (arrow).

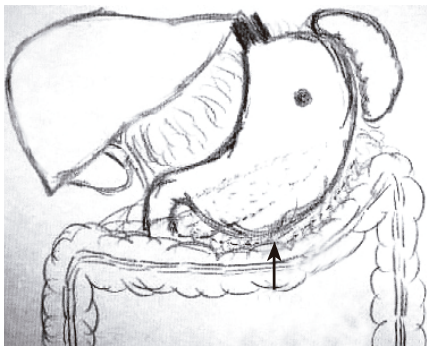

Figure 2 Detachment of greater omentum from the greater curvature of the stomach with a harmonic scalpel.

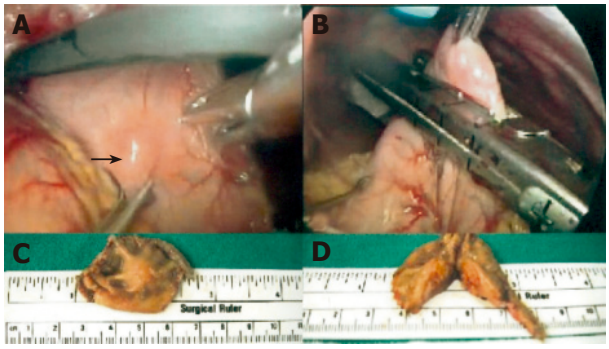

Figure 3 Localization of the tumor mass by intra-operative upper tract endoscopy. **A:** Tumor lesion in the posterior wall of gastric high body; **B:** robotic-assisted laparoscopic wedge resection of the gastric high body; **C:** submucosal tumor with tumor-free margin; **D:** cutting surface with firm, yellow, well-circumscribed, lobulated nodules.

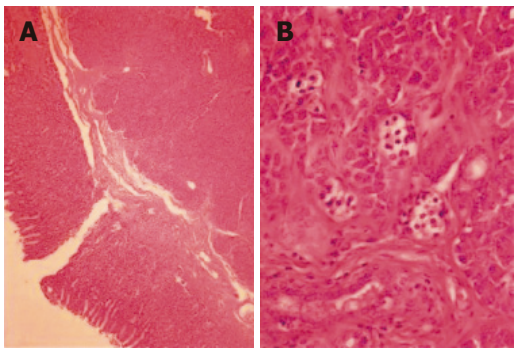

Figure 4 Pancreatic acinar cells and ducts shown in the low power view of gastric submucosal tumor (**A**) and in the high power view of ectopic pancreas (**B**).

the assistance of intraoperative upper-tract endoscopy. A robotic-assisted laparoscopic wedge resection of the gastric high body was performed using the Endo-GIA roticulator (Figure 3). The resection margins were clear and the specimen was sent for pathological analysis. A layer of interrupted silk sutures was placed in the serosa surface to ensure the integrity of the staple line. A nasogastric tube was inserted into the stomach and a drain tube was placed near the staple line. The abdominal cavity was deflated and the trocar sites were closed.

The final pathology report revealed that the resected specimen was an ectopic pancreas (Figure 4). The patient was discharged on postoperative d 6, with no complications and normal gastrointestinal motility. She had an uneventful recovery.

DISCUSSION

Ectopic pancreas is a rare entity and is usually an incidental finding in clinical practice. Most patients with an ectopic pancreas are asymptomatic, and if present, symptoms are nonspecific and depend on the site of the lesion and the different complications are encountered[3-5]. About 75% of all pancreatic rests are located in the stomach, duodenum, or jejunum[6]. However, they have also been found in the ileum, Meckel's diverticulum, gall bladder, common bile duct, splenic hilum, umbilicus, lung, and in perigastric and periduodenal tissues[7]. In autopsy series, the frequency of ectopic pancreas is between 1% and 2%. The rate of recognition at the time of laparotomy is 0.2%.

A preoperative diagnosis of ectopic pancreas in the gastric wall is not easy. Although a radiological diagnosis of gastric ectopic pancreatic tissue is difficult, double-contrast barium meal may show a characteristic focally raised mucosal area with associated superficial ulceration. The role of endoscopic biopsies in identifying ectopic pancreas remains questionable because normal gastric mucosa covers the lesion. Recently, endoscopic ultrasound combined with fine-needle aspiration cytology has been reported to facilitate a definitive diagnosis by histological examination[8]. Surgical excision, either endoscopically or laparoscopically, provides symptomatic relief and is recommended if the diagnosis remains uncertain. Laparoscopic wedge resection of a presumed gastric submucosal tumor appears to have been a suitable treatment for our patient. This approach is more advantageous over a laparotomy because recovery is easier and morbidity is less.

With the advent of laparoscopy at the end of the 1980s, surgery has entered the computer age[9]. More recently, robotic-assisted laparoscopy has joined the general surgeon's armory to address some of the shortcomings of laparoscopic surgery. Magnified and computer-enhanced

video images provide surgeons with much better access to and visualization of the abdomen. The main advantages of robot-assisted laparoscopic surgery are the availability of three-dimensional visibility and easier instrument manipulation compared to standard laparoscopy. Initially, robotic-assisted laparoscopic cholecystectomy was deemed safe, and has been proved to be safe in foregut procedures.

In conclusion, ectopic pancreas in the posterior wall of gastric high body can be resected by robotic-assisted laparotomy. This procedure is minimally invasive for such benign lesions.

REFERENCES

1 **Guillou L**, Nordback P, Gerber C, Schneider RP. Ductal adenocarcinoma arising in a heterotopic pancreas situated in a hiatal hernia. *Arch Pathol Lab Med* 1994; **118**: 568-571

2 **Moen J**, Mack E. Small-bowel obstruction caused by heterotopic pancreas in an adult. *Am Surg* 1989; **55**: 503-504

3 **Mulholland MW**, Simeone DM. Pancreas: Anatomy and structural anomalies: Congenital anomalies: Heterotopic pancreas. In: Yamada T, Alpers DH, Laine L, Owyang CH, Powell DW (eds): Textbook of Gastroenterology, ed 3. Philadelphia: Lippincott Williams & Wilkins, 1999; 2115-2119

4 **Abrahams JI**. Heterotopic pancreas simulating peptic ulceration. *Arch Surg* 1966; **93**: 589-592

5 **Armstrong CP**, King PM, Dixon JM, Macleod IB. The clinical significance of heterotopic pancreas in the gastrointestinal tract. *Br J Surg* 1981; **68**: 384-387

6 **Grendell JH**, Ermak TH. Anatomy, Histology, Embriology, and Developmental Anomalies of the Pancreas. In: Sleisenger & Fordtran's Gastrointestinal and Liver Disease, Philadelphia: WBSaunders, 1998: 761-771

7 **Kopelman HR**. The pancreas: Congenital anomalies. In: Walker WA¸ Durie PR¸ Hamilton RJ¸ Walker-Smith JW¸ Watkins JB. Pediatric Gastrointestinal Disease. St.Lous: Mosb, 1996; 1426-1427

8 **Riyaz A**, Cohen H. Ectopic pancreas presenting as a submucosal gastric antral tumor that was cystic on EUS. *Gastrointest Endosc* 2001; **53**: 675-677

9 **Chapman WH 3rd**, Albrecht RJ, Kim VB, Young JA, Chitwood WR Jr. Computer-assisted laparoscopic splenectomy with the da Vinci surgical robot. *J Laparoendosc Adv Surg Tech A* 2002; **12**: 155-159

Science Editors Wang XL and Guo SY **Language Editor** Elsevier HK

PO Box 2345, Beijing 100023, China
www.wjgnet.com
wjg@wjgnet.com

ELSEVIER

World J Gastroenterol 2005;11(48):7697-7699
World Journal of Gastroenterology ISSN 1007-9327

• *CASE REPORT* •

Isolated rectal diverticulum complicating with rectal prolapse and outlet obstruction: Case report

Chuang-Wei Chen, Shu-Wen Jao, Huang-Jen Lai, Ying-Chun Chiu, Jung-Cheng Kang

Chuang-Wei Chen, Shu-Wen Jao, Huang-Jen Lai, Ying-Chun Chiu, Jung-Cheng Kang, Division of Colon and Rectal Surgery, Department of Surgery; Department of Radiology, Tri-Service General Hospital, Taipei, Taiwan, China
Correspondence to: Dr Jung-Cheng Kang, Division of Colon and Rectal Surgery, Department of Surgery, Tri-Service General Hospital, No. 325, Cheng-Gong Road, Section 2, Taipei, Taiwan, China. docallen.tw@yahoo.com.tw
Telephone: +886-2-87923311-16049 Fax: +886-2-87927411
Received: 2005-04-12 Accepted: 2005-07-28

Abstract

The occurrence of rectal diverticula is very rare, with only sporadic reports in the literature since 1911. Symptomatic rectal diverticula are encountered even less frequently. Treatments of these complicated events range from conservative treatments to major surgical interventions. We present a hitherto unreported occurrence of isolated rectal diverticulum complicated with rectal prolapse and outlet obstruction. Delorme's procedure resulted in subsidence of symptoms and resolution of the diverticulum. It provides a minimal invasive surgical technique to successfully address the reported malady.

Key words: Rectal diverticula; Rectal prolapse; Delorme's procedure

Chen CW, Jao SW, Lai HJ, Chiu YC, Kang JC. Isolated rectal diverticulum complicating with rectal prolapse and outlet obstruction: Case report. *World J Gastroenterol* 2005; 11(48): 7697-7699
http://www.wjgnet.com/1007-9327/11/7697.asp

INTRODUCTION

Cases involving complicated rectal diverticula are extremely rare[1]. But when they occur, they usually present with rectal pain and bleeding, or inflammatory lesions such as abscess formation[3,4]. The following report documents a patient who experienced outlet obstruction during defecation and episodic rectal prolapse as the initial presentation. Eventual diagnosis was complication arising from a rectal diverticulum. Surgical intervention utilizing Delorme's procedure was successful, and is novel for the treatment of this rare and complicated event.

CASE REPORT

A 71-year-old female was admitted with a chief complaint of the sudden onset of a prolapsed mucosa through the anus during defecation on the night before admission. The protruding mucosa was reduced manually. She was nulliparous and had undergone surgical intervention for a benign tumor of unknown origin within the pelvis by a gynecologist 35 years before. Records had been lost during the subsequent postoperative period. She had experienced chronic constipation for 20 years, primarily involving an outlet obstruction for the passage of stools. She had to push her left buttock manually with her fingers to let the stool pass through the anal canal.

Upon admission, the patient was normal in general appearance except for a longitudinal surgical scar at the lower abdomen courtesy of the previous surgery. Results of physical examination were essentially normal except for the rectum. A large out-pouched pocket situated at the left lateral aspect of the rectal wall approximately 3 cm from the anal verge was digitally palpable. Sigmoidoscopy was negative. Barium enema examination showed a marked solitary 5 cm diameter diverticulum with wide-orifice neck arising from the rectal wall (Figure 1). Thus, we considered that the rectal diverticulum resulted in the accumulation of stools, causing the symptom of outlet obstruction, and subsequently had appeared as a prolapsed rectum due to the inverted rectal diverticulum protruding through the anus after excessive straining during defecation. The diagnosis of rectal diverticulum complicating with rectal prolapse and outlet obstruction was made.

The patient underwent a 50-min Delorme's procedure under intravenous anesthesia. A circumferential incision was made through the mucosa near the dentate line. Using electrocautery, the mucosa was stripped to the apex of the prolapsed lump and excised. The denuded prolapsed muscle was then pleated with 2-0 prolene sutures and reefed up. The transected edges of the mucosa were sutured together using 3-0 chromic catgut (Ethicon, Johnson & Johnson, Medical Taiwan). The excised specimen consisted of the resected rectal mucosa with an out-pouched sacculation measuring 50 mm×70 mm in size.

Postoperatively, bowel movements occurred more than 10 times a day initially but rapidly improved to 3-4 times per day in the following days. She recovered uneventfully and obtained relief from the outlet obstruction. Repeated

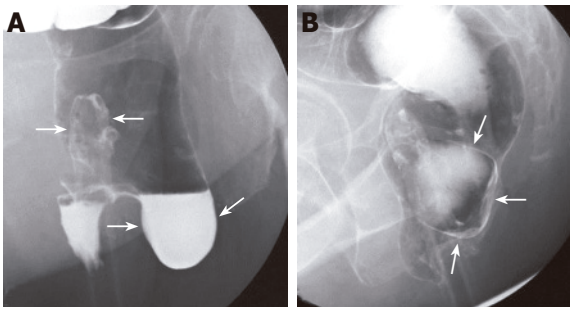

Figure 1 A and **B**. Double-contrast barium enema examination demonstrates a large diverticulum with wide-orifice arising from the left lateral rectal wall (large arrows). The rectal catheter is also seen (small arrows).

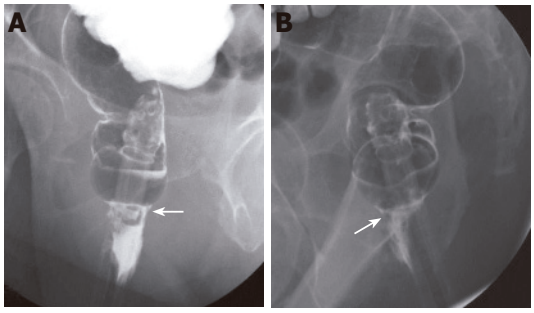

Figure 2 A and **B**. Postoperative barium study revealed the subsidence of the rectal diverticulum (arrows).

rectal examination revealed that the wide-orifice neck of the diverticular out-pouching had been tightly closed. She was discharged 6 d after the operation. A barium enema was repeated 2 mo later. (Figure 2) She defecated normally with 1–2 bowel movements per day during the 12 mo following the operation.

DISCUSSION

Diverticular disease occurs in the colon with great frequency. However, rectal involvement is very rare; being estimated to occur in less than 0.1% of cases[1,2]. Most patients with rectal diverticula are diagnosed by accident, as the malady is asymptomatic. Such uncomplicated rectal diverticula are clinically insignificant. However, complications associated with rectal diverticula can include rectal diverticulitis with perforation and abscess formation, diverticulitis of the midrectum, and a prolapsed rectum from an inverted rectal diverticulum[3-5]. Postinflammatory stenosis of the rectum, a rectal-vesical fistula, and an enormous fecaloma within a rectal diverticulum have also been reported as complications of rectal diverticula[6,7]. Erroneous diagnosis of carcinoma can prompt abdominal perineal resection[8].

Diverticulosis of the rectum typically occurs in the presence of colonic diverticula, especially the sigmoid segment. The factors that may contribute to rectal diverticula are still not completely understood. Possible predisposing factors include congenital anomalies such as weakness in the circumferential muscle that surrounds the rectum, primary muscle atrophy, or the absence of supporting structures such as the coccyx. Other acquired causes include relaxed rectal-vaginal septum, recurrent fecal impactions that exert pressure and cause distension of the rectum and pelvic trauma or infections leading to the weakening of the rectal wall[8,9]. In addition, Plavsic *et al*.[2] reported in 1995 that 2 of 27 patients with scleroderma had rectal diverticulosis without other diverticula in the rest of the colon. Loss of colonic haustrations has been reported in scleroderma and likely results in the development of colonic diverticula[10]. To our knowledge, the case we present is only the third reported case of isolated rectal diverticulum.

Rectal diverticula are typically situated along the lateral aspects of the rectum, since the complete longitudinal muscular layer of the rectum is thicker anteriorly and posteriorly compared to the lateral aspects of the wall[9]. Additionally, most rectal diverticula thus far described include all layers of the colonic wall as opposed to the more pseudodiverticula of the colon, suggesting the possibility that they occur at areas of focal weakness in the rectal wall caused by congenital or acquired origin[11]. The number of rectal diverticula per patient ranges from one to three with a diameter of 20 mm or greater compared with the remaining colonic diverticula, which typically measures less than 15 mm[9]. Rectal diverticula may also vary greatly in size with changes in intra-abdominal pressure[11].

Surgical treatments of the complicated rectal diverticula include drainage of the abscess, diverting colostomy, resection of the diverticular mass or abdominal perineal resection of the rectum. However, the Delorme's procedure has never been reported for these complicated events. This procedure is often used for small rectal prolapse but may also be used for large ones. Our case presented with rectal prolapse, which was considered to be the result of an inverted rectal diverticulum protruding through the anal canal. Delorme's procedure carries the advantage of a less invasive procedure that shortens the hospital stay. The patient recovered rapidly and uneventfully. Recurrence is the most common complication of this operation with an average incidence of 12% in different series[12]. Other complications such as hemorrhage, suture line dehiscence, stricture, and incontinence had ever been reported[13].

In conclusion, rectal diverticula are rare and can be easily missed by proctoscopy. They typically require no treatment because they are asymptomatic in most patients. Surgical intervention is only necessary in such patients with complicated events. Various approaches had been described in the management of different complications. Correct diagnosis preoperatively is required to prevent unnecessary surgery. In our presenting case, solitary rectal diverticulum was diagnosed by digital examination and barium enema preoperatively. Delorme's procedure provides a minimal invasive surgery and produces excellent results.

REFERENCES

1 **Walstad PM**, Sahibzada AR. Diverticula of the rectum. *Am J Surg* 1968; **116:** 937-939
2 **Plavsic BM**, Raider L, Drnovsek VH, Kogutt MS. Association of rectal diverticula and scleroderma. *Acta Radiol* 1995; **36:** 96-99
3 **Giustra PE**, Root JA, Killoran PJ. Rectal diverticulitis with perforation. *Radiology* 1972; **105**: 23-24
4 **Chiu TC**, Bailey HR, Hernandez AJ Jr. Diverticulitis of the midrectum. *Dis Colon Rectum* 1983; **26:** 59-60
5 **Edwards VH**, Chen MY, Ott DJ, King GT. Rectal diverticulum appearing as a prolapsed rectum. *J Clin Gastroenterol* 1994; **18**: 254-255
6 **Wilson LB**. Diverticula of the lower bowel: their development and relationship to carcinoma. *Ann Surg* 1911; **53**: 223-231
7 **Govoni AF**, Smulewicz JJ. Large diverticulum of the anal canal: case report and review of the literature on anal canal and rectal diverticula. *Am J Roentgenol* 1974; **121**: 344-7
8 **Weston SD**, Schlachter IS. Diverticulum of the rectum. *Dis Colon Rectum* 1959; **2:** 458-464
9 **Damron JR**, Lieber A, Simmons T. Rectal diverticula. *Radiology* 1975; **115**: 599-601
10 **Martel W**, Chang SF, Abell MR. Loss of colonic haustration in progressive systemic sclerosis. *Am J Roentgenol* 1976; **126**: 704
11 **Halpert RD**, Crnkovich FM, Schreiber MH. Rectal diverticulosis: a case report and review of the literature. *Gastrointest Radiol* 1989; **14:** 274-276
12 **Nay HR**, Blair CR. Perineal surgical repair of rectal prolapse. *Am J Surg* 1972; **123**: 577-579
13 **Senapati A**, Nicholls RJ, Thomson JP, Phillips RK. Results of Delorme's procedure for rectal prolapse. *Dis Colon Rectum* 1994; **37:** 456-460

Science Editor Guo SY **Language Editor** Elsevier HK

PO Box 2345, Beijing 100023, China
www.wjgnet.com
wjg@wjgnet.com

ELSEVIER

World J Gastroenterol 2005;11(48):7700-7701
World Journal of Gastroenterology ISSN 1007-9327

Mesenteric and portal vein thrombosis associated with hyperhomocysteinemia and heterozygosity for factor V Leiden mutation

Giuseppe Famularo, Giovanni Minisola, Giulio Cesare Nicotra, Claudio De Simone

Giuseppe Famularo, Giovanni Minisola, Giulio Cesare Nicotra, Department of Internal Medicine, San Camillo Hospital, Rome
Claudio De Simone, Department of Experimental Medicine, University of L'Aquila, L'Aquila, Italy
Correspondence to: Dr. Giuseppe Famularo, Department of Internal Medicine, San Camillo Hospital, Circonvallazione Gianicoense, 00152 Rome,
Italy. gfamularo@scamilloforlanini.rm.it
Telephone: + 39-6-58704325 Fax: + 39-6-58704325
Received: 2005-04-21 Accepted: 2005-07-14

Key words: Portal; Mesenteric; Thrombosis hyperhomocysteinemia; Factor V Leiden heterozygosity

Famularo G, Minisola G, Nicotra GC, Simone CD. Mesenteric and portal vein thrombosis associated with hyperhomocysteinemia and heterozygosity for factor V Leiden mutation. *World J Gastroenterol* 2005; 11(48): 7700-7701
http://www.wjgnet.com/1007-9327/11/7700.asp

TO THE EDITOR

A 79-year-old man was hospitalized because of worsening upper abdominal pain which started two days before admission and was continuously present. His personal and family history was uneventful, he did not smoke and denied toxic habits or using any medications, including over-the-counter medications, herbal remedies or any vitamin supplements.

At admission, the patient was fully alert and oriented, afebrile, but distressed due to severe abdominal pain; his vital parameters were normal. On physical examination, there was abdominal guarding and rebound with hypoactive bowel sounds, rectal examination revealed no masses, liver and spleen were normal, and a stool sample was guaiac negative. The remaining physical examination was unrevealing.

Laboratory tests showed a leukocyte count of 12×10^9 cells/L, 90% of which were neutrophils; electrolytes, amylase, lipase, and liver and renal function tests were normal. An electrocardiogram and a chest X-ray were also normal. A color Doppler ultrasonography and an emergency contrast-enhanced computed tomography disclosed thrombosis with complete occlusion of both intra- and extra-hepatic branches of the portal vein and partial obstruction of the superior mesenteric vein; abundant intraperitoneal fluid was observed with no collateral venous vessels or any direct or indirect evidence of transmural intestinal infarction. Endoscopy of both the upper and lower gastrointestinal tract was negative.

A thrombophilic screening showed extremely elevated blood levels of homocysteine (91 and 88 μmol/L on the 1st and 5th d of hospital stay; normal values < 15); search for antiphospholipid antibody and lupus anticoagulant was negative and blood levels of antithrombin and protein C and S were normal. Circulating vitamin B_6, B_{12}, and folate concentrations were also normal.

The patient was treated with bowel rest, intravenous fluids, antibiotics, and enoxaparin (100 IU/kg twice daily) and he reported complete recovery from abdominal pain on the 2nd d after admission. We added folate and vitamin B_6 to his regimen and the patient was discharged free of symptoms on the 15th d; at this time blood homocysteine was 75 μmol/L. At a follow-up visit 2 mo later, while still on enoxaparin and folate, he was doing well with no clinical or laboratory evidence of active thrombosis. We received the results of molecular studies performed on blood samples taken at admission, which showed heterozygosity for factor V Leiden mutation; search for prothrombin G20210A and MTHFR C677T mutations was negative. Blood homocysteine concentration was < 15 μmol/L and imaging studies showed normal flow in the superior mesenteric vein along with a complete occlusion of the portal vein, which was unchanged; there were venous collaterals in the hilar area of the liver. Anticoagulant therapy was shifted to warfarin with a targeted international normalized ratio (INR) 2-3 and, when last seen six months after discharge, the patient was asymptomatic with INR 2.6, normal blood homocysteine and no active thrombosis.

Combined thrombosis involving one mesenteric vein and the portal vein is rare, difficult to diagnose and can be fatal, with diffuse abdominal pain, distension and tenderness being the most common symptoms and physical findings[1,2]. Stricture and bowel necrosis with peritonitis due to transmural intestinal infarction may complicate the course and are important causes of mortality among those patients[1,2]. The early initiation of anticoagulation using unfractionated heparin or low

molecular weight heparin has been shown to minimize the risk of serious complications [1,2], nonetheless spontaneous resolution of extensive superior mesenteric and portal vein thrombosis has been also reported [3]. Common causes include liver disease, pancreatitis, inflammatory bowel disease, cancer, sepsis, an underlying myeloproliferative disorder, surgery or trauma, and systemic thrombophilia [4,5].

The association of hyperhomocysteinemia with extremely elevated blood levels of homocysteine and heterozygosity for factor V Leiden mutation was the cause of such a severe abdominal venous thrombosis in the case we report on. No precipitating events of venous thromboembolism were recognized and the patient had none of the abdominal disorders that may trigger thrombosis of the mesenteric veins or the portal vein or any other inherited or acquired prothrombotic condition. Available data consistently suggest a moderate, positive, and dose-related relationship between blood levels of homocysteine and the risk of portal or mesenteric venous thrombosis [6]. However, almost all the patients so far described in whom portal or mesenteric venous thrombosis was linked with hyperhomocysteinemia also had at least one additional prothrombotic disorder [7-10]. Our Medline search yielded no case of combined mesenteric-portal vein thrombosis associated only with hyperhomocysteinemia and no other risk factors for venous thromboembolism. It is not surprising in our opinion that, despite being heterozygous for factor V Leiden mutation, our patient did not experience any thrombotic disorders until severe hyperhomocysteinemia developed. This adds weight to the relevance of hyperhomocysteinemia in the pathophysiological mechanisms as a trigger of venous thrombosis in this case.

The mechanisms of hyperhomocysteinemia in our patient remain unclear. The patient was not exposed before presentation to any folate or vitamin B_6 antagonists, i.e. methotrexate, phenytoin, estrogens, or theophylline, and we ruled out upon history and clinical examination atherosclerosis, smoking or elevated blood pressure, which are also associated with raised circulating concentrations of homocysteine [11]. An acquired nutritional deficiency of folate also sounds a non reliable cause. Even though blood levels of folate, vitamin B6 and vitamin B12 were normal, homocysteine concentrations returned to the normal range after eight weeks of treatment with folate and vitamin supplements. This apparent discrepancy is difficult to explain, however we could reasonably speculate that the exogenous supplementation of folate and vitamins did ultimately correct a subtle age-dependent impairment of folate metabolism.

We claim that patients with apparently unexplained combined thrombosis involving both one mesenteric vein and the portal vein should be screened for hyperhomocysteinemia. Outcome could be favorable, even in those carrying other prothrombotic conditions such as factor V Leiden mutation, with a complete recovery if appropriate treatment with anticoagulants, folate and vitamin supplements is timely started.

REFERENCES

1 **Acosta S**, Ogren M, Sternby NH, Bergqvist D, Bjorck M. Mesenteric venous thrombosis with transmural intestinal infarction: a population-based study. *J Vasc Surg* 2005; **41**: 59-63

2 **Joh JH**, Kim DI. Mesenteric and portal vein thrombosis: treated with early initiation of anticoagulation. *Eur J Vasc Endovasc Surg* 2005; **29**: 204-208

3 **Fernandez-Marcote Menor EM**, Opio Maestro VA. [Spontaneous resolution of extensive superior mesenteric and portal vein thrombosis. A case report] *Gastroenterol Hepatol* 2004; **27:** 470-472

4 **Valla DC**, Condat B. Portal vein thrombosis in adults: pathophysiology, pathogenesis and management. *J Hepatol* 2000; **32**: 865-871

5 **Kumar S**, Kamath PS. Acute superior mesenteric venous thrombosis: one disease or two? *Am J Gastroenterol* 2003; **98**: 1299-1304

6 **Primignani M**, Martinelli I, Bucciarelli P, Battaglioli T, Reati R, Fabris F, Dell'era A, Pappalardo E, Mannucci PM. Risk factors for thrombophilia in extrahepatic portal vein obstruction. *Hepatology* 2005; **41:** 603-608

7 **Elhajj II**, Salem ZM, Birjawi GA, Taher AT, Soweid AM. Heterozygous prothrombin 20210G/A mutation, associated with hyperhomocysteinemia, and homozygous methylenete trahydrofolate reductase 677C/T mutation, in a patient with portal and mesenteric venous thrombosis. *Hematol J* 2004; **5:** 540-542

8 **Silingardi M**, Ghirarduzzi A, Galimberti D, Iorio A, Iori I. Mesenteric-portal vein thrombosis in a patient with hyperhomocysteinemia and heterozygous for 20210A prothrombin allele. *Thromb Haemost* 2000; **84**: 358-359

9 **Audemar F**, Denis B, Blaison G, Mazurier I, Peter A, Serbout R. Left branch portal vein thrombosis associated with hyperhomocysteinemia. *Gastroenterol Clin Biol* 1999; **23:** 1388-1391

10 **Spanier BW**, Frederiks J. Aetiology of extrahepatic portal vein thrombosis. *Gut* 2002; **51:** 755-756; author reply 756

11 **Hankey GJ**, Eikelboom JW. Homocysteine and vascular disease. *Lancet* 1999; **354**: 407-413

Science Editor Guo SY **Language Editor** ELsevier HK

PO Box 2345, Beijing 100023, China
www.wjgnet.com
wjg@wjgnet.com

ELSEVIER

World J Gastroenterol 2005;11(48):7702-7703
World Journal of Gastroenterology ISSN 1007-9327

Fenofibrate-induced liver injury

Kazufumi Dohmen, Chun Yang Wen, Shinya Nagaoka, Koji Yano, Seigo Abiru, Toshihito Ueki, Atsumasa Komori, Manabu Daikoku, Hiroshi Yatsuhashi, Hiromi Ishibashi

Kazufumi Dohmen, Internal Medicine, Okabe Hospital, 1-2-1 Myojinzaka Umi-machi Kasuya-gun Fukuoka 811-2122, Japan
Chun Yang Wen, Shinya Nagaoka, Koji Yano, Seigo Abiru, Toshihito Ueki, Atsumasa Komori, Manabu Daikoku, Hiroshi Yatsuhashi, Hiromi Ishibashi, Clinical Research Center, National Nagasaki Medical Center, Omura 856-8562, Japan
Correspondence to: Dr. Kazufumi Dohmen, Internal Medicine, Okabe Hospital, 1-2-1 Myojinzaka Umi-machi Kasuya-gun Fukuoka 811-2122,
Japan. dohmenk@par.odn.ne.jp
Telephone: +81-92-9322-0025 Fax: +81-92-933-7253
Received: 2005-04-12 Accepted: 2005-04-25

Dohmen K, Wen CY, Nagaoka S, Yano K, Abiru S, Ueki T, Komori A, Daikoku M, Yatsuhashi H, Ishibashi H. Fenofibrate-induced liver injury. *World J Gastroenterol* 2005; 11(48):7702-7703
http://www.wjgnet.com/1007-9327/11/7702.asp

TO THE EDITOR

Fenofibrate is a member of such fibrate class agents as bezafibrate and it work as a ligand of PPARα, and also shows a potent triglyceride-lowering effect. The elevation of aminotransferase levels has been frequently observed after the administration of fenofibrate and this phenomenon is considered to be non-pathological because fenofibrate activates the gene expression of the aminotransferases. Recently, fenofibrate has been used not only for hypercholesterolemia but also for primary biliary cirrhosis (PBC)[1, 2]. However, the occurrence of liver injury induced by fenofibrate has not yet been reported written in the English literature. We herein report a rare case of liver injury due to the oral use of this drug.

A 66-year-old Japanese female patient was admitted to undergo a further examination with a nearly 20-year history of liver dysfunction. She had been previously treated with 600 mg of ursodeoxycholic acid (UDCA) for nearly 6 mo at another clinic. On admission her conjunctiva was neither anemic nor icteric. The laboratory data revealed white blood cell counts of 6 600/μL with a differential of neutrophils 50%, lymphocyte 38%, monocytes 6%, basophils 1%, eosinophils 5%. The C reactive protein level was less than 0.3 mg/dL. The hepatic function profiles showed the total bilirubin to be 0.8 mg/dL, aspartate aminotransferase (AST) 40 IU/L, alanine aminotransferase (ALT) 29 IU/L, lactate dehydrogenase (LDH) 183 IU/L, alkaline phosphatase (ALP) 367 IU/L and gamma-glutamil transpeptidase (γ-GTP) 272 IU/L. Regarding the hepatitis virus, hepatitis B virus surface antigen and hepatitis C virus antibody were both negative. Serology revealed a high level of IgM of 393 mg/dL, and the antinuclear antibody of 80-fold and antimitochondrial antibody (AMA) of 320-fold each and antibody of 176 U/mL were positive for pyruvate dehydrogenase complex-E2. Histopathologically, a damaged bile duct with aggregates of lymphocytes with a nonsuppurative inflammatory destruction of the small bile duct and granuloma was seen in the portal area, which was compatible with those of Scheuer's stage 1 of primary biliary cirrhosis.

Based on the diagnosis of primary biliary cirrhosis, the administration of fenofibrate 150 mg per day was initiated in addition to 600 mg of UDCA. A fever of over 37.5 ℃, anorexia and discomfort in the right hypochondrium appeared 11 d after the administration of fenofibrate. Liver injury such as elevations of total bilirubin of 1.8 mg/dL, AST 268, ALT 216, ALP 537, and γ-GTP 660 IU/L was confirmed, and both the CRP level and the ratio of eosinophils in the peripheral blood increased to 5.14 mg/dL and 14.4 %, respectively. She was diagnosed to have fenofibrate-induced liver injury based on the laboratory data and the clinical course. Therefore, fenofibrate was discontinued, however, UDCA continued to be administered continuously. Thereafter, the serum concentrations of AST, ALT, ALP, γ-GTP, CRP, and the rate of eosinophils rapidly returned to the pretreatment levels of 30, 27, 457, 399 IU/L, less than 0.3 mg/dL and 4.6 %, respectively, 12 d after the discontinuation of fenofibrate (Figure 1). Later, the lymphocyte stimulation index for fenofibrate for this patient was found to be positive, while showing a stimulation index of 212 % in comparison to normal samples.

Several clinical studies on lipoprotein-lowering agents such as simvastatin[3] and bezafibrate[4-7] on PBC patients who failed to respond to UDCA have so far been conducted, and the results have been found to be of value. In addition, fenofibrate, a member of such fibrate class agents as bezafibrate, has also recently been found to be a likely agent for PBC because of its stronger anti-inflammatory effect via PPARα, and its greater ability to reduce the levels of TG and LDL-C than that of bezafibrate. We previously found fenofibrate to effectively treat UDCA-resistant PBC in nine cases without any adverse effect[2].

Regarding the adverse effect of fenofibrate, a Diabetes Arteriosclerosis Intervention Study (DAIS) showed that micronized fenofibrate at 200 mg (equivalent to 300 mg of

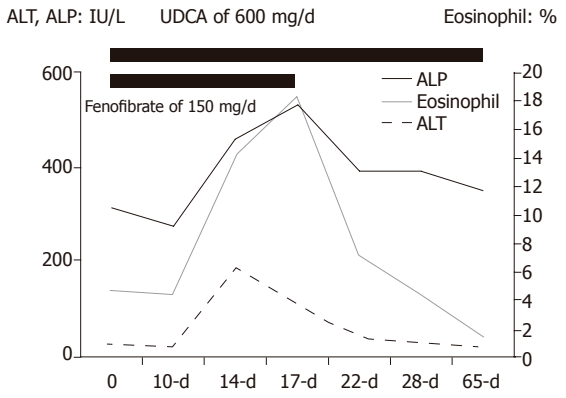

Figure 1 Clinical course.

the standard formulation) was administered for 3 years to type 2 diabetic patients in order to observe the inhibitory effect in the progression of coronary arterial stenosis. As a result, no difference in the safety between fenofibrate and placebo was observed[8]. In addition, studies of human first-generation cultured cells and HepG2 cells suggested the serum aminotransferase levels to be transiently elevated and normalized or returned to pretreatment levels[9]. The increase in the aminotransferase level which occurs after treatment with fenofibrate is not considered to be clinically significant although fenofibrate activates the aminotransferase gene expression, thus leading to a mild and transient elevation of aminotransferase via PPARα through mechanisms involving increased levels of reactive oxygen species and intracellular glutathion depletion, thus leading to mitochondrial dysfunction and a perturbation of intracellular Ca^{++} homeostasis and also cell death[9].

Since fenofibrate is a widely prescribed therapeutic agent world-wide for patients with hypercholesterolemia and recently for those with PBC[1, 2], the early recognition of any possible liver dysfunction especially in the case of PBC, and the immediate cessation of its administration, when positively identified are thus called for to avoid any dangerous clinical complications. Furthermore, our case shows that fenofibrate-induced liver injury might occur in addition to the transient elevations in the AST and ALT levels via PPARα.

REFERENCES

1 **Ohira H,** Sato Y, Ueno T, Sata M. Fenofibrate treatment in patients with primary biliary cirrhosis. *Am J Gastroenterol* 2002; **97:** 2147-2149
2 **Dohmen K,** Mizuta T, Nakamuta M, Shimohashi N, Ishibashi H, Yamamoto K. Fenofibrate for patients with asymptomatic primary biliary cirrhosis. *World J Gastroenterol* 2004; **10:** 894-898
3 **Ritzel U,** Leonhardt U, Nather M, Schafer G, Armstrong VW, Ramadori G. Simvastatin in primary biliary cirrhosis: effects on serum lipids and distinct disease markers. *J Hepatol* 2002; **36:** 454-458
4 **Nakai S,** Masaki T, Kurokohchi K, Deguchi A, Nishioka M. Combination therapy of bezafibrate and ursodeoxycholic acid in primary biliary cirrhosis: a preliminary study. *Am J Gastroenterol* 2000; **95:** 326-327
5 **Miyaguchi S,** Ebinuma H, Imaeda H, Nitta Y, Watanabe T, Saito H, Ishii H. A novel treatment for refractory primary biliary cirrhosis? *Hepatogastroenterology* 2000; **47:** 1518-1521
6 **Kurihara T,** Niimi A, Maeda A, Shigemoto M, Yamashita K. Bezafibrate in the treatment of primary biliary cirrhosis: comparison with ursodeoxycholic acid. *Am J Gastroenterol* 2000; **95:** 2990-2992
7 **Yano K,** Kato H, Morita S, Takahara O, Ishibashi H, Furukawa R. Is bezafibrate histologically effective for primary biliary cirrhosis? *Am J Gastroenterol* 2002; **97:** 1075-1077
8 Diabetes Arteriosclerosis Intervention Study Investigators. Effect of fenofibrate on progression of coronary–artery disease in type 2 diabetes: the Diabetes Arteriosclerosis Intervention Study, a randomized study. *Lancet* 2001; **357:** 905–910
9 **Edgar AD,** Tomkiewicz C, Costet P, Legendre C, Aggerbeck M, Bouguet J, Staels B, Guyomard C, Pineau T, Barouki R. Fenofibrate modifies transaminase gene expression via a peroxisome proliferator activated receptor alpha-dependent pathway. *Toxicol Lett* 1998; **98:** 13-23

Science Editor Guo SY **Language Editor** Elsevier HK

PO Box 2345, Beijing 100023, China
www.wjgnet.com
wjg@wjgnet.com

ELSEVIER

World J Gastroenterol 2005;11(48):7704-7714
World Journal of Gastroenterology ISSN 1007-9327

Acknowledgments to Reviewers of *World Journal of Gastroenterology*

Many reviewers have contributed their expertise and time to the peer review, a critical process to ensure the quality of *World Journal of Gastroenterology*. The editors and authors of the articles submitted to the journal are grateful to the following reviewers for evaluating the articles (including those were published and those were rejected in this issue) during the last editing period of time. Arabic number in parenthesis stands for the number of the reviewer have reviewed this year.

1 **Christian Cormac Abnet, PhD, MPH**
Investigator, tritional Epidemiology Branch Division of Cancer Epidemiology and Genetics, 6120 Executive Blvd, EPS/320, MSC 7232 Rockville, MD 20852, United States

2 **Kyoichi Adachi, MD (12)**
Department of Gastroenterology and Hepatology, Shimane University, School of Medicine Shimane, 89-1 Enya-cho, Izumo-shi Shimane 693-8501, Japan

3 **Yasushi Adachi, Dr**
First Department of Internal Medicine, Sapporo Medical University, South-1, West-16, Chuo-ku, Sapporo, 060-8543, Japan

4 **Taiji Akamatsu, Associate Professor (6)**
Department of Endoscopy, Shinshu University Hospital, 3-1-1 Asahi, Matsumoto 390-8621, Japan

5 **Gianfranco D Alpini, Professor (4)**
Internao Medicine and Medical Physiology, Scoh Whot Hospital, 702 SW H.K. dod genloop MRB rm316B, Temple 76504, United States

6 **Domenico Alvaro, MD (2)**
Division of Gastroenterology, Department of Clinical MedicineUniversity of Rome La Sapienza, Viale Università 37, Rome 00185, Italy

7 **Takafumi Ando, MD (5)**
Nagoya University Graduate School of Medicine, Therapeutic Medicine, 65 Tsurumai-cho, Showa-ku, Nagoya 466-8550, Japan

8 **Hisataka S Moriwaki, Professor**
Department Of Medicine, Gifu University, 1-1 Yanagido, Gifu 501-1194, Japan

9 **Akira Andoh, MD (5)**
Department of Internal Medicine, Shiga University of Medical Science, Seta Tukinowa, Otsu 520-2192, Japan

10 **Vito Annese, MD (2)**
Department of Internal Medicine, Unit of Gastroenterology, Hospital, Viale Cappuccini, 1, San Giovanni Rotondo 71013, Italy

11 **Bruno Annibale, Professor (2)**
Digestive and Liver Disease Unit, University " La Sapienza" II School of Medicine, Via di Grottarossa 1035, Roma 00189, Italy

12 **Taku Aoki, MD (5)**
Division of Hepato-Biliary-Pancreatic and Transplantation Surgery, Department of Surgery, Graduate School of Medicine, University of Tokyo,7-3-1 Hongo, Bunkyo-ku, Tokyo, 113-8655, Japan

13 **Masahiro Arai, MD, PhD (11)**
Department of Gastroenterology, Toshiba General Hospital, 6-3-22 Higashi-ooi, Shinagawa-ku,Tokyo 140-8522, Japan

14 **Tetsuo Arakawa, Professor**
Department of Gastroenterology, Osaka City University Medical School,1-4-3, Asahi-machi, Abeno-ku, Osaka 545-8585, Japan

15 **Yasuji Arase, MD (5)**
Department of Gastroenterology, Toranomon Hospital, 2-2-2Toranomonminato-ku, Tokyo 105-8470, Japan

16 **Rudolf Arnold, Professor**
Department of Internal Medicine, Philipps University Marburg, Baldingerstraße, Marburg D-35043, Germany

17 **Hitoshi Asakura, Director**
Emeritus Professor (2), International Medical Information Center, Shinanomachi Renga BLDG.35, Shinanomachi, Shinjukuku, Tokyo 160-0016, Japan

18 **Fernando Azpiroz, MD**
Digestive System Research Unit, University Hospital Vall d' Hebron, Paseo Vall d'Hebron, 119-129, Barcelona 08035, Spain

19 **Takeshi Azuma, Associate Professor**
Second Department of Internal Medicine, University of Fukui, Faculty of Medical Sciences, Matsuoka-cho, YoshIDa-gun, Fukui 910-1193, Japan

20 **Jasmohan Singh Bajaj, Assistant Professor**
Division of Gastroenterology and Hepatology, Medical College of Wisconsin, 9200 W Wisconsin Ave, Milwaukee WI 53212, United States

21 **Giovanni Barbara, Professor**
Internal Medicine and Gastroenterology, University of Bologna, St.Orsola Hospital - Building No. 5Via Massarenti, 9 -40138, Bologna 40138

22 **Jamie S Barkin, MD (2)**
Professor of Medicine, Chief, Sinai Medical Center Division of Gastroenterology, Mt. Sinai Medical Center, University of Miami, School of Medicine, 4300 Alton Road, Miami Beach, FL 33140, United States

23 **Kim Elaine Barrett, Professor (6)**
Department of Medicine, UCSD School of Medicine, UCSD Medical Center 8414, 200 West Arbor Drive, San Diego CA 92103, United States

24 Gabrio Bassotti, MD (2)
Department of Clinical and Experimental Medicine, University of Perugia, Via Enrico dal Pozzo, Padiglione W, Perugia 06100, Italy

25 **Ramon Bataller, MD, (4)**,
Liver Unit, Hospital Clinic,Villarroel 170, Barcelona 08036, Spain

26 **Daniel C Baumgart, MD, PhD, FEBG**
Division of Hepatology and Gastroenterology, Department of

Medicine, Charité Medical School，Humboldt-University of Berlin , Virchow Hospital, Berlin D-13344, Germany

27 **Yusuf Bayraktar, Professor (3)**
Department of Gastroenterology, School of Medicine, Hacettepe University, Ankara 06100, Turkey

28 **Christoph Beglinger, Professor**
University Hospital, Division of Gastroenterology, University of Basel, Petersgraben 4, Basel CH-4031, Switzerland

29 **Antomio Benedetti, Professor (2)**
epartment of Gastroenterology, University of Politecnica Melle Marche, Via Conca 71, Ancona 60020, Italy

30 **Trond Berg, Professor (2)**
Department of Molecular Biosciences, University of Oslo, PO Box 1041 Blindern, Oslo 0316, Norway

31 **Mauro Bernardi, Professor**
Internal Medicine,Cardioangiology,Hepatology, University of Bologna, Semeiotica Medica - Policlinico S. Orsola-Malpighi - Via Massarenti, 9, Bologna 40138, Italy

32 **Jennifer D Black, MD (2)**
Roswell Park Cancer Institute, Department of Pharmacology and Therapeutics, Roswell Park Cancer Institute, Elm and Carlton Streets, Buffalo 14263, United States

33 **Hubert Blum, Professor**
University of Freiburg, Hugastetter Strasse 55, Freiburg L-79106, Germany

34 **Luigi Bonavina, Professor**
Department of Surgery, Policlinico San Donato, University of Milano, via Morandi 30, Milano 20097, Italy

35 **Joseph Daoud Boujaoude, Assistant Professor**
Department of Gastroenterology, Hotel-Dieu de FranceHospital, aint-Joseph University, Beirut 961, Lebanon

36 **Lee Bouwman, Dr** Leiden University Medical Centre, department of surgery, Albinusdreef 2 PO Box 9600, 230 RC Leiden, The Netherlands

37 **Filip Braet, Associate Professor (3)**
Australian Key Centre for Microscopy and Microanalysis, Madsen Building (F09), The University of Sydney, Sydney NSW 2006, Australia

38 **Reinhard Buettner Professor** Institute of Pathology
University Hospital Bonn, Sigmund-Freud-Str. 25, D-53127 Bonn, Germany

39 **Michael F Byrne , MD**
Clinical Associate Professor, Division of Gastroenterology Vancouver General Hospital, 100-2647 Willow Street Vancouver BC V5Z 3P1, Canada

40 **Giovanni Cammarota, MD**
Department of Internal Medicine and Gastroent, Catholic University of Medicine and Surgery, Rome, Policlinico A. Gemelli; Istituto di Medicina Interna; Largo A. Gemlli, 8, Roma 00168, Italy

41 **Elke Cario, MD**
Division of Gastroenterology and Hepatology, University Hospital of Essen, Institutsgruppe I, Virchowstr. 171, Essen D-45147, Germany

42 **Julio Horacio Carri, Professor**
Internal Medicine – Gastroenterology, Universidad Nacional de Córdoba, Av.Estrada 160-P 5-Department D, Córdoba 5000, Argentina

43 **David L Carr-Locke, MD**
Director of Endoscopy, Brigham and Women's Hospital, Endoscopy Center, Brigham and Women's Hospital, 75 Francis St, Boston MA 02115, United States

44 **Antoni Castells, MD (3)**
Gastroenterology Department, Hospital Clínic, University of Barcelona, Villarroel 170, Barcelona 08036, Spain

45 **Yogesh K Chawla, Dr, Professor (2)**
Department of Hepatology, Postgraduate Institute of Medical Education and Research, Chandigarh 160012, India

46 **Wang-Xue Chen, Dr (3)**
Institute for Biological Sciences, National Research Concil Canada, 100 Sussex Drive, Room 3100, Ottawa, Ontario K1A 0R6, Canada

47 **Xian-Ming Chen, MD (3)**
Center for Basic Research in Digestive Diseases, Division of Gastroenterology and Hepatology, Mayo Clinic College of Medicine, 200 First Street, SW, Rochester, MN 55905, United States

48 **Xiao-Ping Chen, Professor (5)**
Institute of Hepato-Pancreato-Biliary Surgery, Tongji Hospital, 1095# Jie-fang Da-dao, Wuhan 430030, China

49 **Jun Cheng, Professor,**
Dean Assistant, Beijing Earth Altar Hospital Dean 13 Earth Altar Park, Anwai Avenue, East District, Beijing 100011, China

50 **Giuseppe Chiarioni, Dr (2)**
Gastroenterological Rehabilitation Division of the University of Verona, Valeggio sul Mincio Hospital, Azienda Ospedale di Valeggio s/M, Valeggio s/M 37067, Italy

51 **Yoichi Chida, Assistant professor (2)**
Department of Psychosomatic Medicine, Graduate School of Medical Sciences, Kyushu University, 3-1-1 Maidashi, Higashi-ku, Fukuoka 812-8582, Japan

52 **Andrew Seng Boon Chua, MD**
Department of Gastroenterology, Gastro Centre Ipoh, 1, lorong Rani, 31, lebuhraya Tmn Ipoh, Ipoh Garden South, IPOH 30350, Malaysia

53 **James M Church, MD**
Colorectal Surgery, Cleveland Clinic Foundation, Desk A 30, 9500 EuclID Ave, Cleveland 44195, United States

54 **Paul Jonathan Ciclitira, Professor (2)**
The Rayne Institute (GKT), St Thomas' hospital, London NW32QG, United Kingdom

55 **Andrew D Clouston, Associate Professor**
Histopath Laboratories, Suite 4, Level 9, Strathfield Plaza, Strathfield, Sydney, 2135, Australia

56 **Dario Conte, Professor (3)**
GI Unit - IRCCS Osp. Maggiore, Chair of Gastroenterology, Via F. Sforza, 35, Milano 20122, Italy

57 **Gino Roberto Corazza, Professor (5)**
Department of Internal Medicine, University of Pavia, Gastroenterology Unit - I.R.C.C.S. Policlinico San Matteo - Piazzale Golgi n.5, Pavia 27100, Italy

58 **Chi-Hin Cho, Chair and Professor**

90 Karel Geboes, Professor
Laboratory of Histo- and Cytochemistry; University Hospital K.U.Leuven, Capucienenvoer 33, 3000 Leuven, Belgium

91 John P Geibel, MD
Professor of Surgery and Cellular and Molecular Physiology, Director of Surgical Research, Yale University School of Medicine, BML 265, New Haven, CT 06520, United States

92 Alexander L Gerbes, Professor (3)
Medizinische Klinik II, Munich, Germany, Marchioninistr 15, Munich D-81377, Germany

93 Subrata Ghosh, Professor (2)
Department of Gastroenterology, Imperial College London, Hammersmith Hospital, 9 Lady Aylesford Avenue, Stanmore, Middlesex, London HA7 4FG, United Kingdom

94 Edoardo G Giannini, Assistant Professor (3)
Department of Internal Medicine, Gastroenterology Unit, Viale Benedetto XV, no. 6, Genoa, 16132, Italy

95 Ignacio Gil-Bazo, MD, PhD (2)
Cancer Biology and Genetics Program, Memorial-Sloan Kettering Cancer Center, 1275 York Avenue. Box 241, New York 10021, United States

96 Roberto De Giorgio, MD
Department of Internal Medicine and Gastroenterology, University of Bologna, St.Orsola-Malpighi Hospital, Via Massarenti, 9, Bologna 40138, Italy

97 Dieter Glebe, PhD
Institute for Medical Virology, Justus Liebig University Giessen, Frankfurter Str. 107, Giessen 35392, Germany

98 David Y Graham, Professor (6)
Department of Medicine, Michael E. DeBakey VAMC, Rm 3A-320 (111D), 2002 Holcombe Blvd, Houston, TX 77030, United States

99 William Greenhalf, PhD Division of Surgery and Oncology, University of Liverpool, UCD Building, 5th Floor, Royal Liverpool University Hospital, Daulby Street, Liverpool, L69 3GA, United Kingdom

100 Hans Gregersen, Professor
The Research Administration, Aalborg Hospital, Hobrovej 42 A, Aalborg 9000, Denmark

101 Axel M Gressner, Professor (4)
Institut für Klinische Chemie und Pathobiochemie sowie Klinisch-Chemisches Zentrallaboratorium, Universitätsklinikum Aachen, Pauwelsstr. 30, Aachen 52074, Germany

102 Rick Greupink, Dr (2)
University of Groningen, A. Deusinglaan 1, Groningen 9713AV, The Netherlands

103 Jin Gu, Professor (2)
Peking University School of Oncology, Beijing Cancer Hospital, Beijing 100036, China

104 Hallgrimur Gudjonsson, MD
Gastroenterolog, University Hospital, University Hospital, Landspitali,Hringbraut, Reykjavik 101, Iceland

105 Anna S Gukovskaya, Professor (2)
VA Greater Los Angeles Health Care System ,University of California, Los Angeles, 11301 Wilshire Blvd, Los Angeles 91301, United States

106 De-Wu Han, Professor (4)
Institute of Hepatology, Shanxi Medical University, 86 Xinjian South Road, Taiyuan 030001, China

107 Kazuhiro Hanazaki, MD, (11)
Department of Surgery, Shinonoi General Hospital, 666-1 Ai, Shinonoi, Nagano 388-8004, Japan

108 Naohiko Harada, PhD
Department of Gastroenterology, Fukuoka Higashi Medical Center, Chidori 1-1-1, Koga, Fukuoka 811-3195, Japan

109 Tetsuo Hayakawa, Emeritus Professor (3)
Director general, Meijo Hospital, Meijo Hospital, Sannomaru 1-3-1, Naka-ku, Nagoya 460-0001, Japan

110 Peter Clive Hayes, Professor
Liver Unit, Royal Infirmary, Si Little France Crescent, EH16 4SA, United Kingdom

111 Ming-Liang He, Associate Professsor (2)
Faculty of Medicine , The Center for Emerging Infectious Diseases, The Chinese University of Hong Kong, Hong Kong, China

112 Stephan Hellmig, Dr (2)
Department of General Internal Medicine, University Hospital Schleswig-Holstein, Campus Kiel, Schittenhelmstra 12, Kiel 24105, Germany

113 Alan W Hemming MD, MSc, FRCSC, FACS
Professor of Surgery, Director of Hepatobiliary Surgery, Department of Surgery, Division of Transplantation, PO Box 100286, University of Florida,Gainesville, FL, 32610
United States

114 Kazuhide Higuchi, Associate Professor (2)
Department of Gastroenterology, Graduate School of Medicine, Osaka City University, 1-4-3 Asahi-machi, Abeno-ku, Osaka 545-8585, Japan

115 Keiji Hirata, MD
Surgery 1, University of Occupational and Environmental Health, 1-1 Iseigaoka, Yahatanishi-ku, Kitakyushu 807-8555, Japan

116 Yik-Hong Ho, Professor (3)
Department of Surgery, School of Medicine, James Cook University, Townsville 4811, Australia

117 Anthony R Hobson, Dr (2)
Section of Gastrointestinal Sciences, University of Manchester, Eccles Old Road, Hope Hospital, Clinical Sciences Building, Salford M6 8HD, United Kingdom

118 Werner Hohenberger, Professor,
Chirurgische Klinik und Poliklinik, Krankenhausstrasse 12, Erlangen D-91054, Germany

119 Joerg C Hoffmann, Dr
Medizinische Klinik I, Charité - Universitätsmedizin Berlin, Campus Benjamin Franklin, Hindenburgdamm 30, Berlin D12200, Germany

120 Michael Horowitz, Professor (2)
Department of Medicine, University of Adelaide and Director, Endocrine and Metabolic Unit, Royal Adelaide Hospital, Level 6, Eleanor Harrald Bullding, North Terrace, Adelaide 5000, Australia

121 Yves J Horsmans, Professor

153 Jin-Hong Kim, Professor
Department of Gastroenterology, Ajou University Hospital, San 5, Wonchon-dong, Yeongtong-gu, Suwon 442-721, South Korea

154 Myung-Hwan Kim, Professor (10)
College of Medicine, Asan Medical Center, 388-1 Pungnap-dong, Songpa-gu, Seoul 138-736, South Korea

155 Tsuneo Kitamura, Associate Professor (5)
Department of Gastroenterology, Juntendo University Urayasu Hospital, Juntendo University School of Medicine, 2-1-1 Tomioka, Urayasu-shi, Chiba 279-0021, Japan

156 Seigo Kitano, Professor (5)
Department of Surgery I, Oita University Faculty of Medicine, 1-1 Idaigaoka Hasama-machi, Oita 879-5593, Japan

157 Burton I Korelitz, MD
Department of Gastroenterology, Lenox Hill Hospital, 100 East 77th Street, 3 Achelis, New York, N.Y 10032, United States

158 Robert J Korst, MD (3)
Department of Cardiothoracic Surgery, Weill Medical College of Cornell University, Room M404, 525 East 68th Street, New York 10032, United States

159 Elias A Kouroumalis, Professor (2)
Department of Gastroenterology, University of Crete, Medical School, Department of Gastroenterology, University Hospital, PO Box 1352, Heraklion, Crete 71110, Greece

160 Shoji Kubo, MD (3)
Hepato-Billiary-Pancreatic Surgery, Osaka City University Graduate School of Medicine, 1-4-3 Asahimachi, Abeno-ku, Osaka 545-8585, Japan

161 Gerd A Kullak-Ublick, Professor
Laboratory of Molecular Gastroenterology and Hepatology, Department of Internal Medicine, University Hospital Zurich, Zurich CH-8091, Switzerland

162 Shiu-Ming Kuo, MD (3)
University at Buffalo, 15 Farber Hall, 3435 Main Street, Buffalo 14214, United States

163 Shigeki Kuriyama, MD
Kagawa University School of Medicine, Third Department of InternalMedicine, 1750-1 Ikenobe, Miki-cho, Kita-gun, Kagawa 761-0793, Japan

164 Masato Kusunoki, Professor and Chairman (2)
Second Department of Surgery, Mie University School of Medicine, Mie, 2-174 Edobashi, Tsu MIE 514-8507, Japan

165 Joachim Labenz, Associate Professor (2)
Jung-Stilling Hospital, Wichernstr. 40, Siegen 57074, Germany

166 Giacomo Laffi, Professor (2)
University of Florence, Viale Morgagni 85, Firenze I-50134, Italy

167 Kam Chuen Lai, MD (2)
Department of Medicine, The University of Hong Kong, Queen Mary Hospital, Hong Kong, China

168 Peter Laszlo Lakatos, MD, PhD, Assistant Professor (4)
1st Department of Medicine, Semmelweis University, Koranyi S 2A, Budapest H1083, Hungary

169 Rene Lambert, Professor (8)
International Agency for Research on Cancer, 150 Cours Albert Thomas, Lyon 69372 cedex 8, France

170 Angel Lanas, Professor
Service of Gastroenterology, Hospital Clinico Universitario, Service of GastroenterologyUniversity HospitalC/ San Juan Bosco 15, Zaragoza 50009, Spain

171 Samuel S Lee, Professor
Department of Medicine, University of Calgary, Health Science Centre, Rm 1721, 3330 Hospital Dr NW, Calgary, AB, T2N 4N1, Canada

172 Jong Kyun Lee, Associate Professor (2)
Department of Gastroenterology, Sungkyunkwan University School of Medicine, Ilwom-Dong 50,Gangnam-GU, Seoul 135-710, South Korea

173 Samuel S Lee, Professor
Department of Medicine, University of Calgary, Health Science Centre, Rm 1721, 3330 Hospital Dr NW, Calgary, AB, T2N 4N1, Canada

174 Lee Shou-Dong Lee, Professor (6)
Department of Medicine, Taipei Veterans General Hospital, 201 Shih-Pai Road, Sec. 2. Taipei 112, Taiwan, China

175 Yuk Tong Lee, MD
Department of Medicine and Therapeutics, Prince of Wales Hospital, Shatin, New Territories, Hong Kong, China

176 Kurt Lenz, Professor
Department of Internal Medicine, Konventhospital Barmherzige Brueder, A-4020 Linz, Austria

177 Andreas Leodolter, Professor (10)
Department of Gastroenterology, Otto-von-Guericke University, c/o The Burnham Institute, Caner Genetics and Epigentics, 10901 N. Torrey Pines Road, La Jolla 92037, United States

178 Gene LeSage, Dr
Medicine, University of Texas Houston Medical School, 6431 Fannin Street, MSB 4.234, Houston, TX 77030, United States

179 Ming Li, Associate Professor
Tulane University Health Sciences Center, 1430 Tulane Ave Sl-83, New Orleans 70112, United States

180 Geng-Tao Liu, Professor
Department of Pharmacology, Institute of Materia Medica, Chinese Academy of Medical Sciences and Peking Union Medical College, Beijing 100050, China

181 Hong-Xiang Liu, PhD (2)
Department of Pathology, Division of Molecular Histopathology, University of Cambridge, Box 231, Level 3, Lab Block, Addenbrooke's Hospital, Hills Road, Cambridge CB2 2QQ, United Kingdom

182 Zhi-Hua Liu, Professor (2)
Cancer Institute, Chinese Academy of Medical Sciences, 17 Panjiayuan Nanli, Beijing 100021, China

183 Walter Edwin Longo, Professor
Department of Surgery, Yale University School of Medicine, 205 Cedar Street, New Haven 06510, United States

184 María Isabel Torres López, Professor (2)
Experimental Biology, University of Jaen, araje de las Lagunillas s/n, Jaén 23071, Spain

185 Robin G Lorenz, Associate Professor (6)
Department of Pathology, University of Alabama at Birmingham, 845 19th Street South BBRB 730, Birmingham, AL 35294-2170, United States

Minato-ku, Tokyo 105-8461, Japan

219 Hisato Nakajima, MD
Department of Gastroenterology and Hepatology, The Jikei University School of Medicine, 3-25-8, Nishi-Shinbashi, Minato-ku, Tokyo 105-8461, Japan

220 Hiroki Nakamura, MD (2)
Department of Gastroenterology and Hepatology, 1-1-1, Minami Kogushi, Ube, Yamaguchi 755-8505, Japan

221 Shotaro Nakamura, MD (6)
Department of Medicine and Clinical Science, Kyushu University, Maidashi 3-1-1, Higashi-ku, Fukuoka 812-8582, Japan

222 Nikolai V Naoumov, Professor
Department of Medicine, Institute of Hepatology University College London, 69-75 Chenies Mews, London WC1E 6HX, United Kingdom

223 John P Neoptolemos, Professor (2)
Divison of Surgery and Oncology, University of Liverpool, Royal Liverpool University Hospital, Daulby Street, Liverpool, L69 3GA, United Kingdom

224 James Neuberger, Professor (9)
Liver Unit, Queen Elizabeth Hospital, Birmingham B15 2TH, United Kingdom

225 Yaron Niv, Professor (3)
Department of Gastroenterology, Rabin Medical Center, Beilinson Campus, Tel Aviv University, 2 Hadekel St., Pardesia 42815, Israel

226 Masayuki Ohta, MD (7)
Department of Surgery I, Oita University Faculty of Medicine, 1-1 Idaigaoka, Hasama-machi, Oita 879-5593, Japan

227 Tetsuo Ohta, MD (2)
Department of Gastroenterologic Surgery, Kanazawa University Hospital, Takara-machi 13-1, Kanazawa 920-0934, Japan

228 Katsuhisa Omagari, MD (3)
Second Department of Internal Medicine, Nagasaki University School of Medicine, 1-7-1 Sakamoto, Nagasaki-city 852-8501, Japan

229 Giovanni D De Palma, Professor
Department of Surgery and Advanced Technologies, University of Naples Federico II, School of Medicine, Naples 80131, Italy

230 Bo-Rong Pan, Professor (2)
Departmant of Oncology, Xijing Hospital, Fourth Military Medical University, No.1, F. 8, Bldg 10, 97 Changying East Road, Xi'an 710032, Shaanxi Province, China

231 Julian Panes, Professor (2)
Department of Gastroenterology, Hospital Clinic of Barcelona, Villarroel 170, Barcelona 08036, Spain

232 Fabrizio R Parente, MD (2)
Department of Gastroenterology, L.Sacco University Hospital Via GB Grassi, 74, Milan 20157, Italy

233 Jae-Gahb Park, Professor (4)
Seoul National University College of Medicine, 28 Yongon-dong, Chongno-gu, Seoul 110-744, South Korea

234 Zhiheng Pei, Assistant Professor (3)
Department of Pathology and Medicine, New York University School of Medicine, Department of Veterans Affairs, New York Harbor Healthcare System, 6001W, 423 East 23rd street, New York NY 10010, United States

235 Amado Salvador Peña, Professor (2)
Department of Pathology, Immunogenetics, VU University Medical Centre, De Boelelaan 1117, PO Box 7057, Amsterdam 1007 MB, The Netherlands

236 Miguel Perez-Mateo, Professor (4)
Liver Unit, Hospital General Universitario Alicante, Pintor Baeza s/n, Alicante 03004, Spain

237 Raffaele Pezzilli, MD (6)
Department of Internal Medicine and Gastroenterology, Sant' Orsola-Malpighi Hospital, Via Massarenti, 9, Bologna 40138, Italy

238 Josep M Pique, MD
Department of Gastroenterology, Hospital Clínic of Barcelona, Villarroel, 170, Barcelona 08036, Spain

239 Gabriele Bianchi Porro, Professor
Gastroenterology Unit, "L. Sacco" University Hospital, Via G.B. Grassi 74, Milano 20157, Italy

240 Piero Portincasa, Professor
Internal Medicine – DIMIMP, University of Bari Medical School, Hospital Policlinico Piazza G. Cesare 11, Bari 70124, Italy

241 Jesus Prieto, Professor (5)
Clinica Universitaria, University of Navarra, Avda, Pio XII, 36, Pamplona 31080, Spain

242 Lun-Xiu Qin, Professor (3)
Liver Cancer Institute and Zhongshan Hospital, Fudan University, 180 Feng Lin Road, Shanghai 200032, China

243 Eamonn M Quigley, Professor (2)
Department of Medicine National University of Ireland, Cork, Cork University Hospital Clinical Sciences Building Wilton, Cork, Ireland

244 Massimo Raimondo, Dr
Division of Gastroenterology and Hepatology, Mayo Clinic, 4500 San Pablo Road, Jacksonville, FL 32224, United States

245 Bernardino Rampone, Dr
Department of General Surgery and Surgical Oncology, University of Siena, viale Bracci, Siena 53100, Italy

246 David S Rampton, Professor
Centre for Gastroenterology, Institute of Cell and Molecular Science, Queen Mary School of Medicine and Dentistry, London E1 2AD, United Kingdom

247 Vasiliy Ivanovich Reshetnyak, Professor (3)
Institute of General Reanimatology, 25-2, Petrovka Str., Moscow 107031, Russian

248 Sabino Riestra, Servicio Aparato Digestivo
Hospital Universitario Central de Asturias, Hermanos Felgueroso 4-3?b., Pola De Siero 33510, Spain

249 Enrico Roda, Professor
Director of Digestive Disease, Metabolism and Infectious Diseases, University of Bologna, Policlinico S.Orsola-Malpighi, Via Massarenti 9, 40138 Bologna, Italy

250 Luis Rodrigo, Professor (4)
Gastroenterology Service, Hospital Central de Asturias, c/ Celestino Villamil, s.n., Oviedo 33.006, Spain

Surgery, Graduate School of Medicine University of Tokyo, Tokyo, Japan

286 Hidekazu Suzuki, Assistant Professor (2)
Department of Internal Medicine, Keio University School of Medicine, 35 Shinanomachi, Shinjuku-ku, Tokyo 160-8582, Japan

287 Yvette Taché, PhD
Digestive Diseases Research Center and Center for Neurovisceral Sciences and Women's Health, Division of Digestive Diseases, Department of Medicine, David Geffen School of Medicine at UCLA, University of California, Los Angeles and VA Greater Los Angeles Healthcare System; 11301 Wilshire Boulevard, CURE Building 115, Room 117, Los Angeles, CA, 90073, United States

288 Seyed Alireza Taghavi, Associate Professor
Department of Internal Medicine, Nemazee Hospital, No.23, 59th Alley, Ghasrodasht St., Shiraz 71838-95453, Iran

289 Tadatoshi Takayama, Professor (2)
Department of Digestive Surgery, Nihon University School of Medicine, 30-1 Oyaguchikami-machi, Itabashi-ku, Tokyo 173-8610, Japan

290 Tadashi Takeda, MD (3)
Department of Hepatology, Osaka City University, 1-4-3 Asahimachi, Abeno-ku, Osaka 545-8585, Japan

291 Nicholas J Talley, MD, PhD, Professor of Medicine
Division of Gastroenterology and Hepatology, Mayo Clinic College of Medicine, 200 First Street S.W., PL-6-56, Rochester, MN 55905, United States

292 Kiichi Tamada, MD (4)
Department of Gastroenterology, Jichi Medical Shool, 3311-1 Yakushiji,Minamikawachi,Kawachigun, Tochigi 329-0498, Japan

293 Tanaka Noriaki Tanaka, Professor (3)
Department of Gastroenterological Surgery, Transplant and Surgical Oncology, Okayama University Graduate School of Medicine and Dentistry, 2-5-1, Shikata-cho, Okayama 700-8558, Japan

294 Shinji Tanaka, Director (5)
Department of Endoscopy, Hiroshima University Hospital, 1-2-3 Kasumi, Minami-ku, Hiroshima 734-8551, Japan

295 Wei Tang, MD, EngD, Assistant Professor (5)
H-B-P Surgery Division, Artificial Organ and Transplantation Division, Department of surgery, Graduate School of Medicine, The University of Tokyo, Tokyo 113-8655, Japan

296 Kyuichi Tanikawa, Professor
International Institute for Liver Research, 1-1 Hyakunen Kouen, Kurume 839-0864, Japan

297 Simon D Taylor-Robinson, MD
Department of Medicine A, Imperial College London, Hammersmith Hospital, Du Cane Road, London W12 0HS, United Kingdom

298 Simon D Taylor-Robinson, MD (4)
Department of Medicine A, Imperial College London, Hammersmith Hospital, Du Cane Road, London W12 0HS, United Kingdom

299 Akira Terano, Professor
Dokkyo University School of Medicine, Mibu, Shimotsugagun Tochigi 321-0293, Japan

300 Roberto Testa, Professor
Department of Internal Medicine, University of Genoa, Viale Benedetto XV 6, Genoa 16132, Italy

301 Paul Joseph Thuluvath, Professor
Department of Gastroenterology and Hepatology, The Johns Hopkins Hospital, 1830 E. Monument St, Baltimore MD 21205, United States

302 Swan Nio Thung, Professor
Department of Pathology, Mount Sinai School of Medicine, One Gustave L. Levy Place, New York 10029, United States

303 Hans Ludger Tillmann, Professor (4)
Medizinische Klinik und Poliklinik II, University Leipzig, Philipp Rosenthal, Str. 27, Leipzig 04103, Germany

304 Michael Trauner, Professor
Medical University Graz, Auenbruggerplatz 15, Graz A-8036, Austria

305 Chung-Jyi Tsai, MD
Division of Digestive Diseases and Nutrition, University of Kentucky Medical Center, 800 Rose Street, Lexington 40536-0298, Kentucky, United States

306 Akihito Tsubota, Assistant Professor (5)
Institute of Clinical Medicine and Research , Jikei University School of Medicine, 163-1 Kashiwa-shita, Kashiwa, Chiba 277-8567, Japan

307 Tung-Yu Tsui, Dr
Department of Surgery, University of Regensburg Medical Centre, Franz-Josef-Strauss-Allee 11, 93053 Regensburg, Germany

308 Shingo Tsuji, Professor
Department of Internal Medicine and Therapeutics, Osaka University Graduate School of Medicine(A8), 2-2 Yamadaoka, Suita, Osaka 565-0871, Japan

309 Ueno Takato Ueno, Professor (3)
Research Center for Innovative Cancer Therapy, Kurume University, 67 Asahi-machi, Kurume 830-0011, Japan

310 Yvan Vandenplas, Professor (5)
Department of Pediatrics, AZ-VUB, Laarbeeklaan 101, Brussels 1090, Belgium

311 Hugo E Vargas, Associate Professor of Medicine
Division of Transplantation Medicine, Mayo Clinic, 5777 E. Mayo Blvd, 5E, Scottsdale AZ 85054, United States

312 Patrick Veit, MD
Department of Diagnostic an Interventional Radiology and Neuroradiology University Hospital Essen Hufelandstrasse 55 45121 Essen, Germany

313 Saúl Villa-Trevi?o, MD, PhD
Departamento de Biología Celular, Centro de Investigación y de Estudios Avanzados del IPN (Cinvestav), Ave. IPN No. 2508. Col. San Pedro, Zacatenco, C.P. 07360, México, DF, Mexico

314 Shinichi Wada, MD (6)
Department of Gastroenterology, Jichi Medical School, Minamikawachimachi,Kwachi-gun, Tochigi-ken, Tochigi 329-0498, Japan

315 Siegfried Wagner, Professor (3)
Medizinische Klinik II, Klinikum Deggendorf, Perlasberger Str. 41, Deggendorf 94469, Germany

PO Box 2345, Beijing 100023, China
www.wjgnet.com
wjg@wjgnet.com

ELSEVIER

World J Gastroenterol 2005;11(48):7715
World Journal of Gastroenterology ISSN 1007-9327

Meetings

MAJOR MEETINGS COMING UP

American College of Gastroenterology Annual Scientific Meeting
October 28 -November 2, 2005
annualmeeting@acg.gi.org
www.acg.gi.org

EVENTS AND MEETINGS IN THE UPCOMING 6 MONTHS

ISGCON2005
November 11-15, 2005
isgcon2005@yahoo.co.in
isgcon2005.com

II Latvian Gastroenterology Congress
November 29, 2005
gec@stradini.lv
www.gastroenterologs.lv

70th ACG Annual Scientific Meeting and Postgraduate Course
October 28-November 2, 2005

Advanced Capsule Endoscopy Users Course
November 18-19, 2005
www.asge.org/education

2005 CCFA National Research and Clinical Conference - 4th Annual Advances in the Inflammatory Bowel Diseases
December 1-3, 2005
c.chase@imedex.com
www.imedex.com/calendars/therapeutic.htm

EVENTS AND MEETINGS IN 2005

XIII Argentine Hepatology Congress
XIII Congreso Argentino de HepatologÃa
June 10-13, 2005
mci@mcimeetings.com
www.hepatologia.org

9th Annual Coolum Update in Gastroenterology & Hepatology
June 11-13, 2005
info@e-Kiddna.com.au

Canadian Digestive Disease Week Conference
February 26-March 6, 2005
www.cag-acg.org

2005 World Congress of Gastroenterology
September 12-14, 2005
wcog2005@congrex.nl

International Colorectal Disease Symposium 2005
February 3-5, 2005
info@icds-hk.org

15th World Congress of the International Association of Surgeons and Gastroenterologists
September 7-10, 2005
iasg2005@guarant.cz
www.iasg2005.cz

7th International Workshop on Therapeutic Endoscopy
September 10-12, 2005
alfa@alfamedical.com
www.alfamedical.com

EASL 2005 the 40th annual meeting
April 13-17, 2005
www.easl.ch/easl2005/

ISGCON2005
November 11-15, 2005
isgcon2005@yahoo.co.in
isgcon2005.com

Pediatric Gastroenterology, Hepatology and Nutrition
March 13, 2005

II Latvian Gastroenterology Congress
November 29, 2005
gec@stradini.lv
www.gastroenterologs.lv

21st annual international congress of Pakistan society of Gastroenterology & GI Endoscopy
March 25-27, 2005
psgc05@hotmail.com
www.psgc2005.com

8th Congress of the Asian Society of HepatoBiliary Pancreatic Surgery
February 10-13, 2005

1º Workshop de Gastrenterologia para Clínica Geral
April 29, 2005
luis.m.lopes@sapo.pt

APDW 2005 - Asia Pacific Digestive Week 2005
September 25-28, 2005
asiapdw@kornet.net
www.apdw2005.org

World Congress on Gastrointestinal Cancer
June 15-18, 2005
meetings@imedex.com

British Society of Gastroenterology Conference
March 14-17, 2005
www.bsg.org.uk

Training Director's Workshop:Developing and Teaching Principles in the New Era of GI Training
February 4-6, 2005
www.asge.org/education

The Pharmacological, Surgical and Endoscopic Management of GERD
April 8-9, 2005
www.asge.org/education

Digestive Disease Week
DDW 106th Annual Meeting
May 15-18, 2005
ddwadmin@gastr.org
www.ddw.org

ASGE Advanced Endscopy Skills Hands-on Sessions
May 15, 2005
www.asge.org/education

ASGE GERD Hands-on Session
May 17, 2005
www.asge.org/education

Annual Postgraduate Course
May 18-19, 2005
www.asge.org/education

Advanced Capsule Endoscopy Users Course
June 4-5, 2005
www.asge.org/education

Advanced Capsule Endoscopy Users Course
August 12-13, 2005
www.asge.org/education

GI Practice Management Symposium: Solutions for a Successful Practice
August 18, 2005
www.asge.org/education

70th ACG Annual Scientific Meeting and Postgraduate Course
October 28-November 2, 2005

Advanced Capsule Endoscopy Users Course
November 18-19, 2005
www.asge.org/education

2005 CCFA National Research and Clinical Conference - 4th Annual Advances in the Inflammatory Bowel Diseases
December 1-3, 2005
c.chase@imedex.com
www.imedex.com/calendars/therapeutic.htm

EVENTS AND MEETINGS IN 2006

10th World Congress of the International Society for Diseases of the Esophagus
February 22-25, 2006
isde@sapmea.asn.au
www.isde.net

Easl 2006 - The 41st Annual Meeting
April 26-30, 2006

Canadian Digestive Disease Week Conference
March 4-12, 2006
www.cag-acg.org

XXX pan-american congress of digestive diseases
XXX congreso panamericano de anfermedades digestivas
November 25-December 1, 2006
amg@gastro.org.mx
www.gastro.org.mx

World Congress on Gastrointestinal Cancer
June 14-17, 2006
c.chase@imedex.com

7th World Congress of the International Hepato-Pancreato-Biliary Association
September 3-7, 2006
convention@edinburgh.org
www.edinburgh.org/conference

Annual Postgraduate Course
May 25-26, 2006
www.asge.org/education

71st ACG Annual Scientific Meeting and Postgraduate Course
October 20-25, 2006

PO Box 2345, Beijing 100023, China
www.wjgnet.com
wjg@wjgnet.com

ELSEVIER

World J Gastroenterol 2005;11(48):7716-7717
World Journal of Gastroenterology ISSN 1007-9327

Instructions to authors

GENERAL INFORMATION

World Journal of Gastroenterology (*WJG,* ISSN 1007-9327 CN 14-1219/R) is a weekly journal of more than 48 000 circulation, published on the 7th, 14th, 21st and 28th of every month.

Original Research, Clinical Trials, Reviews, Comments, and Case Reports in esophageal cancer, gastric cancer, colon cancer, liver cancer, viral liver diseases, *etc*., from all over the world are welcome on the condition that they have not been published previously and have not been submitted simultaneously elsewhere.

Published jointly by
The WJG Press and Elsevier Inc.

SUBMISSION OF MANUSCRIPTS

Manuscripts should be typed double-spaced on A4 (297×210 mm) white paper with outer margins of 2.5 cm. Number all pages consecutively, and start each of the following sections on a new page: Title Page , Abstract, Introduction, Materials and Methods, Results, Discussion, Acknowledgements, References, Tables, Figures and Figure Legends. Neither the Editors nor the Publisher is responsible for the opinions expressed by contributors. Manuscripts formally accepted for publication become the permanent property of The WJG Press and Elsevier Inc., and may not be reproduced by any means, in whole or in part without the written permission of both the Authors and the Publisher. We reserve the right to put onto our website and copy-edit accepted manuscripts. Authors should also follow the guidelines for the care and use of laboratory animals of their institution or national animal welfare committee.

Authors should retain one copy of the text, tables, photographs and illustrations, as rejected manuscripts will not be returned to the author(s) and the editors will not be responsible for the loss or damage to photographs and illustrations.

Online submission
Online submission is strongly advised. Manuscripts should be submitted through the Online Submission System at: http://www.wjgnet.com/index.jsp. Authors are highly recommended to consult the ONLINE INSTRUCTIONS TO AUTHORS (http://www.wjgnet.com/wjg/help/instructions.jsp) before attempting to submit online. Authors encountering problems with the Online Submission System may send an email describing the problem to wjg@wjgnet.com for assistance. If you submit manuscript online, do not make a postal contribution. A repeated online submission for the same manuscript is strictly prohibited.

Postal submission
Send 3 duplicate hard copies of the full-text manuscript typed double-spaced on A4(297×210 mm) white paper together with any original photographs or illustrations and a 3.5 inch computer diskette or CD-ROM containing an electronic copy of the manuscript including all the figures, graphs and tables in native Microsoft Word format or *.rtf format to:

World Journal of Gastroenterology
Apartment 1066 Yishou Garden,
58 North Langxinzhuang Road,
PO Box 2345, Beijing 100023, China
E-mail: wjg@wjgnet.com
http: //www.wjgnet.com

MANUSCRIPT PREPARATION

All contributions should be written in English. All articles must be submitted using a word-processing software. All submissions must be typed in 1.5 line spacing and in word size 12 with ample margins. The letter font is Tahoma. For authors originating from China, one copy of the Chinese translation of the manuscript is also required (excluding references). Style should conform to our house format. Required information for each of the manuscript sections is as follows:

Title page
Full manuscript title, running title, all author(s) name(s), affiliations, institution(s) and/or department(s) where the work was accomplished, disclosure of any financial support for the research, and the name, full address, telephone and fax numbers and email address of the corresponding author should be involved. Titles should be concise and informative (removing all unnecessary words), emphasize what is NEW, and avoid abbreviations. A short running title of less than 40 letters should be provided. List the author(s)' name(s) as follows: initials and/or first name, middle name or initial(s) and full family name.

Abstract
An informative, structured abstract of no more than 250 words should accompany each manuscript. Abstracts for original contributions should be structured into the following sections: AIM: Only the purpose should be included. METHODS: The materials, techniques, instruments and equipments, and the experimental procedures should be included. RESULTS: The observatory and experimental results, including data, effects, outcome, *etc*. should be included. Authors should present *P* value where necessary, and the significant data should accompany. CONCLUSION: Accurate view and the value of the results should be included.

The format of structured abstracts is at: http://www.wjgnet.com/wjg/help/11.doc

Key words
Please list 3-10 key words that could reflect content of the study.

Text
For most article types, the main text should be structured into the following sections: INTRODUCTION, MATERIALS AND METHODS, RESULTS and DISCUSSION, and should include appropriate Figures and Tables. Data should be presented in the body text or Figures and Tables, not both.

Illustrations
Figures should be numbered as 1, 2, 3 and so on, and mentioned clearly in the main text. Provide a brief title for each figure on a separate page. No detailed legend should be involved under the figures. This part should add into the text where the figures are applicable. Digital images: black and white photographs should be scanned and saved in TIFF format at a resolution of 300 dpi; color images should be saved as CMYK (print files) and not RGB (screen-viewing files). Place each photograph in a separate file. Print images: supply images of size no smaller than 126× 76 mm printed on smooth surface paper; label the image by writing the Figure number and orientation using an arrow. Photomicrographs: indicate the original magnification and stain in the legend. Digital Drawings: supply files in EPS if created by Freehand and Illustrator, or TIFF from Photoshop. EPS files must be accompanied by a version in native file format for editing purposes. Scans of existing line drawings should be scanned at a resolution of 1200 dpi and as close as possible to the size at which they will appear when printed, not smaller. Please use uniform legends for the same subjects. For example: Figure 1 Pathological changes of atrophic gastritis after treatment. A: ...; B: ...;C: ...; D: ...; E: ...; F: ...; G: ...

Tables
Three-line tables should be numbered as 1, 2, 3 and so on, and mentioned clearly in the main text. Provide a brief title for each table. No detailed legend should be involved under the tables. This part should add into the text where the tables are applicable. The information should complement but not duplicate that contained in the text. Use one horizontal line under the title, a second under the column heads, and a third below the Table, above any footnotes. Vertical and italic lines should be omitted.

Notes in tables and illustrations
Data which is not statistically significant should not be noted. $^{a}P<0.05$, $^{b}P<0.01$ ($P>0.05$ should not be noted). If there are other series of *P* values, $^{c}P<0.05$ and $^{d}P<0.01$ are used; Third series of *P* values can be expressed as $^{e}P<0.05$ and $^{f}P<0.01$. Other notes in tables or under illustrations should be expressed as ^{1}F, ^{2}F, ^{3}F; or some other symbols with a superscript (Arabic

numerals) in the upper left corner. In a multi-curve illustration, each curve should be labeled with ●, ○, ■, □, ▲, △, *etc*. in a certain sequence.

Acknowledgments

Brief acknowledgments of persons who have made genuine contributions to the manuscripts and who endorse the data and conclusions are included. Authors are responsible for obtaining written permission to use any copyrighted text and/or illustrations.

References

Cited references should mainly be drawn from journals covered in the Science Citation Index (http://www.isinet.com) and/or Index Medicus (http://www.ncbi.nlm.nih.gov/PubMed) databases. Mention all references in the text, tables and figure legends, and set off by consecutive, superscripted Arabic numerals. References should be numbered consecutively in the order in which they appear in the text. Abbreviate journal title names according to the Index Medicus style (http://www.ncbi.nlm.nih.gov/entrez/query.fcgi?db=journals). Unpublished observations and personal communications are not listed as references. The style and punctuation of the references conform to ISO standard and the Vancouver style (5th edition); see examples below. Reference lists not conforming to this style could lead to delayed or even rejected publication status. Examples:

Standard jounal article (list all authors and include the PubMed ID [PMID] where applicable)

1 **Das KM,** Farag SA. Current medical therapy of inflammatory bowel disease. *World J Gastroenterol* 2000; 6: 483-489 [PMID: 11819634]

2 **Pan BR**, Hodgson HJF, Kalsi J. Hyperglobulinemia in chronic liver disease: Relationships between *in vitro* immunoglobulin synthesis, short lived suppressor cell activity and serum immunoglobulin levels. *Clin Exp Immunol* 1984; 55: 546-551 [PMID: 6231144]

3 **Lin GZ,** Wang XZ, Wang P, Lin J, Yang FD. Immunologic effect of Jianpi Yishen decoction in treatment of Pixu-diarrhoea. *Shijie Huaren Xiaohua Zazhi* 1999; 7: 285-287 [CMFAID:1082371101835979]

Books and other monographs (list all authors)

4 **Sherlock S,** Dooley J. Diseases of the liver and billiary system. 9th ed. Oxford: Blackwell Sci Pub, 1993: 258-296

Chapter in a book (list all authors)

5 **Lam SK.** Academic investigator's perspectives of medical treatment for peptic ulcer. In: Swabb EA, Azabo S. Ulcer disease: investigation and basis for therapy. New York: Marcel Dekker, 1991: 431-450

Electronic journal (list all authors)

6 **Morse SS.** Factors in the emergence of infectious diseases. Emerg Infect Dis serial online, 1995-01-03, cited 1996-06-05; 1(1):24 screens. Available from: URL: http//www.cdc.gov/ncidod/EID/eid.htm

PMID requirement

From the full reference list, please submit a separate list of those references embodied in PubMed, keeping the same order as in the full reference list, with the following information only: (1) abbreviated journal name and citation (e.g. *World J Gastroenterol* 2003;9(11):2400-2403; (2) article title (e.g. Epidemiology of gastroenterologic cancer in Henan Province, China; (3) full author list (e.g. Lu JB, Sun XB, Dai DX, Zhu SK, Chang QL, Liu SZ, Duan WJ; (4) PMID (e.g. 14606064). Provide the full abstracts of these references, as quoted from PubMed on a 3.5 inch disk or CD-ROM in Microsoft Word format and send by post to The *WJG* Press. For those references taken from journals not indexed by *Index Medicus*, a printed copy of the first page of the full reference should be submitted. Attach these references to the end of the manuscript in their order of appearance in the text.

Inappropriate references

Authors should always cite references that are relevant to their article, and avoid any inappropriate references. Inappropriate references include those that are linked with a hyphen and the difference between the two numbers at two sides of the hyphen is more than 5. For example, [1-6], [2-14] and [1, 3, 4-10, 22] are all considered as inappropriate references. Authors should not cite their own unrelated published articles.

Statistical data

Present as mean±SD and mean±SE.

Statistical expression

Express *t* test as *t*(in italics), *F* test as *F*(in italics), chi square test as χ^2(in Greek), related coefficient as *r*(in italics), degree of freedom as γ (in Greek), sample number as *n*(in italics), and probability as *P*(in italics).

Units

Use SI units. For example: body mass, m(B) = 78 kg; blood pressure, p(B)=16.2/12.3 kPa; incubation time, t(incubation)=96 h, blood glucose concentration, c(glucose) 6.4±2.1 mmol/L; blood CEA mass concentration, p(CEA) = 8.6 24.5 μg/L; CO_2 volume fraction, 50 mL/L CO_2 not 5% CO_2; likewise for 40 g/L formaldehyde, not 10% formalin; and mass fraction, 8 ng/g, *etc*. Arabic numerals such as 23,243,641 should be read 23 243 641.

The format about how to accurately write common units and quantum is at: http://www.wjgnet.com/wjg/help/15.doc

Abbreviations

Standard abbreviations should be defined in the abstract and on first mention in the text. In general, terms should not be abbreviated unless they are used repeatedly and the abbreviation is helpful to the reader. Permissible abbreviations are listed in Units, Symbols and Abbreviations: A Guide for Biological and Medical Editors and Authors (Ed. Baron DN, 1988) published by The Royal Society of Medicine, London. Certain commonly used abbreviations, such as DNA, RNA, HIV, LD50, PCR, HBV, ECG, WBC, RBC, CT, ESR, CSF, IgG, ELISA, PBS, ATP, EDTA, mAb, can be used directly without further mention.

Italicization

Quantities: *t* time or temperature, *c* concentration, *A* area, *l* length, *m* mass, *V* volume.

Genotypes: *gyr*A, *arg* 1, *c myc*, *c fos*, *etc*.

Restriction enzymes: *Eco*RI, *Hin*dI, *Bam*HI, *Kbo* I, *Kpn* I, *etc*.

Biology: *Helicobacter pylori, H pylori, E coli, etc*.

SUBMISSION OF THE REVISED MANUSCRIPTS AFTER ACCEPTED

Please revise your article according to the revision policies of *WJG*. The revised version including manuscript and high-resolution image figures (if any) should be copied on a floppy or compact disk. Author should send the revised manuscript, along with printed high-resolution color or black and white photos, copyright transfer letter, the final check list for authors, and responses to reviewers by a courier (such as EMS) (submission of revised manuscript by e-mail or on the WJG Editorial Office Online System is NOT available at present).

Language evaluation

The language of a manuscript will be graded before sending for revision. (1) Grade A: priority publishing; (2) Grade B: minor language polishing; (3) Grade C: a great deal of language polishing; (4) Grade D: rejected. The revised articles should be in grade B or grade A.

Copyright assignment form

It is the policy of WJG to acquire copyright in all contributions. Papers accepted for publication become the copyright of WJG and authors will be asked to sign a transfer of copyright form. All authors must read and agree to the conditions outlined in the Copyright Assignment Form (which can be downloaded from http://www.wjgnet.com/wjg/help/9.doc).

Final check list for authors

The format is at: http://www.wjgnet.com/wjg/help/13.doc

Responses to reviewers

Please revise your article according to the comments/suggestions of reviewers. The format for responses to the reviewers' comments is at: http://www.wjgnet.com/wjg/help/10.doc

Proof of financial support

For paper supported by a foundation, authors should provide a copy of the document and serial number of the foundation.

Publication fee

Authors of accepted articles must pay publication fee.

PO Box 2345, Beijing 100023, China
www.wjgnet.com
wjg@wjgnet.com

ELSEVIER

World J Gastroenterol 2005;11(48):7718
World Journal of Gastroenterology ISSN 1007-9327

World Journal of Gastroenterology standard of quantities and units

Number	Nonstandard	Standard	Notice
1	4 days	4 d	In figures, tables and numerical narration
2	4 days	four days	In text narration
3	day	d	After Arabic numerals
4	Four d	Four days	At the beginning of a sentence
5	2 hours	2 h	After Arabic numerals
6	2 hs	2 h	After Arabic numerals
7	hr, hrs,	h	After Arabic numerals
8	10 seconds	10 s	After Arabic numerals
9	10 year	10 years	In text narration
10	Ten yr	Ten years	At the beginning of a sentence
11	0,1,2 years	0,1,2 yr	In figures and tables
12	0,1,2 year	0,1,2 yr	In figures and tables
13	4 weeks	4 wk	
14	Four wk	Four weeks	At the beginning of a sentence
15	2 months	2 mo	In figures and tables
16	Two mo	Two months	At the beginning of a sentence
17	10 minutes	10 min	
18	Ten min	Ten minutes	At the beginning of a sentence
19	50% (*V/V*)	500 mL/L	
20	50% (m/*V*)	500 g/L	
21	1 M	1 mol/L	
22	10 μM	10 μmol/L	
23	1N HCl	1 mol/L HCl	
24	1N H_2SO_4	0.5 mol/L H_2SO_4	
25	4rd edition	4^{th} edition	
26	15 year experience	15- year experience	
27	18.5 kDa	18.5 ku,18 500u or M_r18 500	
28	25 $g.kg^{-1}/d^{-1}$	25 g/(kg·d) or 25 g/kg per day	
29	6900	6 900	
30	1000 rpm	1 000 r/min	
31	sec	s	After Arabic numerals
32	1 pg $\cdot L^{-1}$	1 pg/L	
33	10 kilograms	10 kg	
34	13 000 rpm	13 000 *g*	High speed; *g* should be in italic and suitable conversion.
35	1000 *g*	1 000 r/min	Low speed. *g* cannot be used.
36	Gene bank	GenBank	International classified genetic materials collection bank
37	Ten L	Ten liters	At the beginning of a sentence
38	Ten mL	Ten milliliters	At the beginning of a sentence
39	umol	μmol	
40	30 sec	30 s	
41	1 g/dl	10 g/L	10-fold conversion
42	OD_{260}	A_{260}	"OD" has been abandoned.
43	One g/L	One microgram per liter	At the beginning of a sentence
44	*A*260 nm	A_{260} nm	*A* should be in italic.
	$^bP<0.05$	$^aP<0.05$	In Table, no note is needed if there is no significance in statistics: $^aP<0.05$, $^bP<0.01$ (no note if $P>0.05$). If there is a second set of *P* value in the same table, $^cP<0.05$ and $^dP<0.01$ are used for a third set: $^eP<0.05$, $^fP<0.01$.
45	**F*=9.87, $^§F$=25.9, $^{\#}F$=67.4	^1F=9.87,^2F=25.9, ^3F=67.4	Notices in or under a table
46	KM	km	kilometer
47	CM	cm	centimeter
48	MM	mm	millimeter
49	Kg, KG	kg	kilogram
50	Gm, gr	g	gram
51	nt	N	newton
52	l	L	liter
53	db	dB	decibel
54	rpm	r/min	rotation per minute
55	bq	Bq	becquerel, a unit symbol
56	amp	A	ampere
57	coul	C	coulomb
58	HZ	Hz	
59	w	W	watt
60	KPa	kPa	kilo-pascal
61	p	Pa	pascal
62	ev	EV	volt (electronic unit)
63	Jonle	J	joule
64	J/mmol	kJ/mol	kilojoule per mole
65	10×10×10cm^3	10 cm×10 cm×10 cm	
66	N·km	KN·m	moment
67	$\bar{x}\pm s$	mean±SD	In figures, tables or text narration
68	– Mean±SEM	mean±SE	In figures, tables or text narration
69	*im*	im	intramuscular injection
70	*iv*	iv	intravenous injection
71	Wang et al	Wang *et al.*	
72	EcoRI	*Eco*RI	*Eco* in italic and RI in positive. Restriction endonuclease has its prescript form of writing.
73	Ecoli	*E.coli*	Bacteria and other biologic terms have their specific expression.
74	Hp	*H pylori*	
75	Iga	*Iga*	writing form of genes
76	*igA*	IgA	writing form of proteins
77	-70 kDa	~70 ku	